

• REVIEW •

Role of *Helicobacter pylori* eradication in aspirin or non-steroidal anti-inflammatory drug users

George V. Papatheodoridis, Athanasios J. Archimandritis

George V. Papatheodoridis, Athanasios J. Archimandritis, Second Academic Department of Internal Medicine, Medical School of Athens University, Hippokraton General Hospital, Athens, Greece
Correspondence to: George V. Papatheodoridis, MD, Assistant Professor in Medicine and Gastroenterology, Second Academic Department of Internal Medicine, Medical School of Athens University, Hippokraton General Hospital of Athens, 114 Vas. Sophias Ave., Athens 115 27, Greece. gpath@cc.uoa.gr
Telephone: +30-210-7774742 Fax: +30-210-7706871
Received: 2004-07-09 Accepted: 2004-11-04

Abstract

Helicobacter pylori (*H pylori*) infection and the use of non-steroidal anti-inflammatory drugs (NSAIDs) including aspirin at any dosage and formulation represent well-established risk factors for the development of uncomplicated and complicated peptic ulcer disease accounting for the majority of such cases. Although the interaction between *H pylori* and NSAID/aspirin use in the same individuals was questioned in some epidemiological studies, it has now become widely accepted that they are at least independent risk factors for peptic ulcer disease. According to data from randomized intervention trials, naive NSAID users certainly benefit from testing for *H pylori* infection and, if positive, *H pylori* eradication therapy prior to the initiation of NSAID. A similar strategy is also suggested for naive aspirin users, although the efficacy of such an approach has not been evaluated yet. Strong data also support that chronic aspirin users with a recent ulcer complication should be tested for *H pylori* infection and, if positive, receive *H pylori* eradication therapy after ulcer healing, while they appear to benefit from additional long-term therapy with a proton pump inhibitor (PPI). A similar approach is often recommended to chronic aspirin users at a high risk of ulcer complication. *H pylori* eradication alone does not efficiently protect chronic NSAID users with a recent ulcer complication or those at a high-risk, who certainly should be treated with long-term PPI therapy, but *H pylori* eradication may be additionally offered even in this setting. In contrast, testing for *H pylori* or PPI therapy is not recommended for chronic NSAID/aspirin users with no ulcer complications or those at a low risk of complications.

© 2005 The WJG Press and Elsevier Inc. All rights reserved.

Key words: *Helicobacter pylori*; Aspirin

Papatheodoridis GV, Archimandritis AJ. Role of *Helicobacter pylori* eradication in aspirin or non-steroidal anti-inflammatory

drug users. *World J Gastroenterol* 2005; 11(25): 3811-3816
<http://www.wjgnet.com/1007-9327/11/3811.asp>

INTRODUCTION

Salicylates have been used in therapeutic medicine since the Hippocrates' era and their use is still growing. During the last 50 years, there is a continuously increasing consumption of aspirin for cardioprotection and for secondary prophylaxis of recurrent stroke or other vascular occlusion, while the drug seems to have a possible role in chemoprevention of cancer and Alzheimer's disease^[1-4]. Non-steroidal anti-inflammatory drugs (NSAIDs) are also widely used agents^[5]. In the USA, it is estimated that more than 50% of the population over 65 years take aspirin or NSAIDs frequently^[6].

The increasing widespread consumption of aspirin/NSAIDs, however, is associated with an increasing incidence of their well-known gastrointestinal complications, which include dyspepsia, gastric and/or duodenal erosions and ulcers and peptic ulcer complications. Peptic ulcer complications, usually bleeding, represent the most frequent serious adverse events of the use of aspirin/NSAIDs^[1,7]. Peptic ulcer(s) may be found at endoscopy in up to 20-25% and ulcer complications requiring hospital admission develop in 2-5% of chronic users of NSAIDs^[7-12]. Use of NSAIDs has also been shown to increase the risk of lower gastrointestinal bleeding^[13]. The damaging effect of aspirin on the gastric mucosa may be less potent than the effect of NSAIDs^[14]. Thus, it is estimated that the chronic use of aspirin increases the absolute annual risk of gastrointestinal bleeding by 0.04% (absolute annual risk of bleeding with and without aspirin: 0.09% and 0.05% respectively)^[15]. Nevertheless, despite the relatively low absolute risk of bleeding in aspirin users, the numbers of aspirin related acute gastrointestinal bleeding episodes are rather high probably due to the huge numbers of individuals who take the drug regularly for long periods often having additional factors with increased risk for bleeding, such as old age and history of peptic ulcer disease. The use of selective NSAIDs, such as selective cyclooxygenase 2 (COX-2) inhibitors, significantly reduces but does not completely eliminate the risk of gastrointestinal complications^[11,12,16], while their gastrointestinal benefit appears to be significantly restricted in cases of concomitant use of aspirin, even at low doses^[11,17].

Helicobacter pylori (*H pylori*) is undoubtedly associated with the development of gastritis and uncomplicated and complicated peptic ulcer diseases^[18]. Although the presence of two factors that can damage the gastric mucosa, such as *H pylori* and aspirin/NSAIDs, would be reasonably considered

to increase the risk for development of uncomplicated and complicated peptic ulcer, data from several, mainly epidemiological, studies appear to be controversial and do not always confirm such an assumption^[19]. This review focuses on the role of *H pylori* infection and the need for its eradication for prevention of gastrointestinal complications among aspirin/NSAIDs users by evaluating the relevant pathophysiological and epidemiological data as well as the results of the randomized, controlled clinical trials of therapeutic intervention.

PATHOPHYSIOLOGY

Aspirin or NSAIDs use is associated with the development of peptic erosions or ulcers through several mechanisms. First, aspirin acts locally through the release of salicylic acid in the stomach, which is not ionized by the gastric acid. Salicylic acid enters and accumulates within the gastric epithelial cells, is ionized intracellularly and disrupts cell metabolic functions increasing mucosal permeability and permitting the back diffusion of H⁺ ions^[20]. Moreover, aspirin promotes topical inflammation by inducing recruitment of leukocytes, which eventually results in capillary constriction and topical ischemia. The topical gastrototoxic effect of aspirin, however, does not seem to be particularly important, since it is associated only with superficial ulcerations that often resolve spontaneously despite the continued aspirin use^[20]. The systemic gastrototoxic effect of aspirin is related to the inhibition of cyclo-oxygenase-1 (COX-1) and the subsequent disruption of prostaglandin synthesis and to the antiplatelet function that promotes bleeding complications^[20]. The key role of the systemic effects of aspirin in the development of gastrointestinal complications is strongly supported by the data showing that the risk of such complications is independent of the drug formulation^[17,21,22]. Even low doses of aspirin, such as 75 mg/d, have been shown to increase the risk of gastroduodenal ulcerations^[21,22]. Inhibition of COX-1 with disruption of prostaglandin production is also the main mechanism of NSAIDs induced gastroduodenal complications^[11-13].

H pylori infection induces a substantial inflammatory reaction in the gastric mucosa with recruitment of leukocytes and production of several inflammatory cytokines, which eventually result in attenuation of mucosal defense mechanisms^[18]. Thus, *H pylori* infection and aspirin/NSAID use impaired gastric mucosal defense by different mechanisms and therefore an interaction between these two factors is biologically plausible.

EPIDEMIOLOGICAL STUDIES

The interaction between *H pylori* infection and aspirin/NSAIDs use in the development of ulcer and ulcer complications has been initially evaluated in several cohort or case-control studies. The findings of these studies, however, have been controversial, since some studies suggested an independent or additive role of *H pylori* infection and aspirin/NSAIDs use in gastrointestinal complications^[21-30] and others proposed no association or even a protective role of *H pylori* infection in users of aspirin/NSAIDs^[31-33]. Moreover, in one study, *H pylori* infection was found to increase the risk of gastric but not of duodenal ulceration in this setting^[34]. The

heterogeneity in study design and methodology, definitions, power, outcome, and selection of controls have been suggested to be responsible for such conflicting results^[19].

In a systemic review published in 2002, the combined analysis of the data available up to October 2000 showed that there is synergism for the development of peptic ulcer and ulcer bleeding between *H pylori* infection and aspirin/NSAID use^[35]. In particular, the presence of *H pylori* infection was found to increase 3-5-fold the risk of peptic ulcer in aspirin/NSAID users (prevalence of peptic ulcer in *H pylori* positive: 53% and *H pylori* negative: 21%, OR: 3.5) and 18-fold in subjects not taking aspirin/NSAID (prevalence of peptic ulcer in *H pylori* positive: 18% and *H pylori* negative: 0%, OR: 18.1)^[35]. Thus, the risk of peptic ulcer is approximately 60-fold higher in *H pylori* positive aspirin/NSAID users compared with *H pylori* negative subjects not taking aspirin/NSAID^[35]. Moreover, *H pylori* infection was shown to increase the risk of ulcer bleeding 1.8-fold, aspirin/NSAID use 4.85-fold, and the presence of both factors 6.1-fold compared with the risk of bleeding among *H pylori* negative subjects not taking aspirin/NSAID^[35]. *H pylori* infection has also been found to increase the risk of upper gastrointestinal bleeding even in chronic users of low dose aspirin^[27]. In a more recent case-control study from our group, *H pylori* infection was again found to increase the risk for upper gastrointestinal bleeding in aspirin/NSAID users 2.9-fold, or 1.7-fold when adjustment for other risk factors for bleeding was performed^[28]. Taking all together, it seems that aspirin/NSAID use and presence of *H pylori* infection are at least independent risk factors for peptic ulcer and bleeding from peptic ulcer.

RANDOMIZED CLINICAL TRIALS

***H pylori* eradication in naive aspirin/NSAID users**

If *H pylori* gastritis does enhance the risk for ulcer bleeding in aspirin/NSAID users, then *H pylori* eradication should substantially reduce such a risk in this setting. Since the risk of bleeding in aspirin/NSAID users is strongly related to the duration of drug use, being higher in subjects with new or recent drug onset (<1-3 mo) than in chronic drug users (>1-3 mo)^[36-38], the possible beneficial effect of *H pylori* eradication on naive aspirin/NSAID users was initially evaluated. In fact, only naive users of non-aspirin NSAIDs have been included in the relevant clinical trials to date, while the possible benefit of *H pylori* eradication in naive users of aspirin has not been evaluated yet.

H pylori eradication before NSAID use was found to significantly reduce the occurrence of peptic ulcers in 92 *H pylori* positive, NSAID naive patients with musculoskeletal pain treated with an 8-wk course of naproxen at a daily dose of 750 mg (peptic ulcers: 3/45 or 7% of patients in the *H pylori* eradication group *vs* 12/47 or 26% of patients in the placebo group, $P = 0.01$)^[39]. In a longer trial with a similar design, *H pylori* eradication before NSAID use was again found to significantly reduce the risk of peptic ulcers in 100 *H pylori* positive, NSAID naive, patients with arthritis and a history of peptic ulcer or dyspepsia treated with a 6-mo course of diclofenac slow release at a daily dose of 100 mg (peptic ulcers: 5/51 or 12% *vs* 15/49 or 34%, $P = 0.0085$)^[40]. In the latter trial, *H pylori* eradication

was also found to significantly reduce the risk of ulcer complications as well [6-mo probability: 4.2% (1.3-9.7) *vs* 27.1% (14.7-39.5), $P = 0.0026$]^[40].

***H pylori* eradication in chronic aspirin/NSAID users without a history of peptic ulcer complications**

The results of the first large clinical trial of *H pylori* eradication in chronic NSAID users raised several questions for the benefit of such an intervention. In this trial^[41], 285 *H pylori* positive chronic NSAID users with past or current peptic ulcers or NSAID-associated dyspepsia who continued a minimum dosage of NSAID for at least 6 mo were randomized to receive *H pylori* eradication therapy with omeprazole, amoxicillin and clarithromycin ($n = 142$) or omeprazole plus placebo antibiotics ($n = 143$) for 1 wk. Subsequently, all patients received omeprazole 20 mg daily for 3 wk followed by an additional 4-wk omeprazole course in cases with endoscopically detected peptic ulcers at 4th wk. The probability of being peptic ulcer free at 6th mo was similar in the *H pylori* eradication [0.56 (95%CI: 0.47-0.65)] and the omeprazole-control group [0.53 (95%CI: 0.44-0.62)], while healing of gastric ulcers was significantly impaired in the *H pylori* eradication group (gastric ulcers healed at 8th wk: 72% in the *H pylori* eradication group *vs* 100% in the omeprazole-control group, $P = 0.006$)^[41].

The design of the latter trial, however, was different from the design of the trials in naive NSAID users, since *H pylori* eradication therapy was given to subjects with ulcers or at high-risk of ulcers, who had already been on long-term NSAID consumption. Moreover, both the *H pylori* eradication and control groups were treated with 4-8 wk of omeprazole for ulcer healing. The lower probability of gastric ulcer healing at 8th wk in the *H pylori* eradication group should be associated with the more potent antisecretory activity of the PPIs including omeprazole in the presence than absence of *H pylori* infection^[42]. Similar findings have also been observed in another large study including 692 chronic NSAID users, in which gastric ulcer healing with ranitidine or lansoprazole was shown to be significantly enhanced in the presence of *H pylori* infection (healing of gastric ulcers at 8th wk: 70% in *H pylori* positive *vs* 61% in *H pylori* negative, $P < 0.05$)^[43]. According to these data, it has been reasonably suggested that any attempt to eradicate *H pylori* infection should follow ulcer healing in the management of chronic NSAID users, although the efficacy of such an approach remains to be tested. The efficacy of *H pylori* eradication in chronic aspirin users has not been evaluated yet.

***H pylori* eradication in chronic aspirin/NSAID users with a recent peptic ulcer complication**

Subjects with a history of upper gastrointestinal bleeding or other peptic ulcer complications represent a particular subgroup of aspirin/NSAID users who are at a high risk for recurrent bleeding during continued aspirin/NSAID use^[44,45]. Strategies that may prevent bleeding in this setting include concurrent therapy with a PPI or eradication of *H pylori* infection in *H pylori* positive subjects. The efficacy of these two strategies was evaluated in a large clinical trial including 400 *H pylori* positive aspirin/NSAID users with a history of upper gastrointestinal bleeding^[46]. All patients initially discontinued

aspirin or NSAID therapy and were treated with omeprazole 20 mg daily for at least 8 wk to promote ulcer healing. Once the healing of ulcer was confirmed, 250 patients who were given 80 mg of aspirin daily for heart disease or stroke and 150 patients who were given 500 mg of naproxen twice daily for arthritis, both for at least 6 mo, were separately randomized to receive 20 mg of omeprazole daily for 6 mo or a 7-d course of *H pylori* eradication therapy followed by placebo once daily for 6 mo. In patients taking aspirin, no significant difference in the probability of recurrent bleeding during the 6-mo follow-up period was observed between those who received *H pylori* eradication therapy (1.9%) and those who received omeprazole (0.9%) (absolute difference: 1%, 95%CI: -1.9-3.9%). In contrast, in patients taking naproxen, the 6-mo probability of recurrent bleeding was significantly lower in the omeprazole (4.4%) than in the *H pylori* eradication group (18.8%) (absolute difference: 14.4%, 95%CI: 4.4-24.4%, $P = 0.005$)^[46]. According to these data, it seems that, after ulcer healing, *H pylori* eradication may be effective in preventing recurrence of upper gastrointestinal bleeding in chronic aspirin users, but not in chronic NSAID users, who require long-term potent antisecretory therapy with a PPI.

Whether the combination of *H pylori* eradication and long-term use of PPIs may further decrease the risk of recurrence of peptic ulcer complications in chronic aspirin users was evaluated in a recent clinical trial^[47]. Thus, 123 *H pylori* positive patients with a history of an aspirin-related peptic ulcer complication and current peptic ulcer were initially treated with a 7-d *H pylori* eradication therapy followed by 40 mg of famotidine daily for 5 or 13 additional weeks until ulcer healing. Then, they all restarted taking 100 mg of aspirin daily and randomized to receive 30 mg of lansoprazole daily or placebo. During a median follow-up of 12 mo, recurrence of ulcer complications was observed in 9 (14.8%) of 61 patients in the placebo group and in only 1 (1.6%) of 62 patients in the lansoprazole group (adjusted hazard ratio: 9.6, 95%CI: 1.2-76.1, $P = 0.008$)^[47]. It should be noted, however, that four of the nine placebo treated patients with a recurrence of ulcer complications were reinfected with *H pylori* and an additional two patients of this group took other NSAIDs. Despite these problems in the latter trial, it is becoming widely accepted that long-term therapy with a PPI after *H pylori* eradication offers additional benefit in preventing peptic ulcer complications in high risk *H pylori* positive chronic aspirin users^[19].

DISCUSSION

All existing data suggest that the presence of *H pylori* infection represents an additional risk factor for peptic ulcer complications in aspirin/NSAID users^[19,48]. However, in current clinical practice which should be guided by the evidence-based medicine and should take into account the cost/benefit analysis of any major intervention, the management of *H pylori* infection and generally the gastrointestinal prevention in aspirin/NSAID users should probably be individualized (Table 1). Thus, the optimal management of such subjects appears to depend on the main factors affecting the risk of ulcer complications, which are: (1) whether the subject is a

Table 1 Recommendations^[19,48] and evidence for the *H pylori* test-and-treat approach and/or the long-term therapy with a proton pump inhibitor (PPI) in users of aspirin or non-steroidal anti-inflammatory drugs (NSAIDs)

	<i>H pylori</i> test-and-treat approach	Long-term PPI therapy
Naive aspirin users	Recommendation	No
Naive NSAIDs users	Recommendation-evidence ^[39,40]	No
Chronic aspirin users		
With a recent ulcer complication	Recommendation ¹ -evidence ^[46,47]	Recommendation-evidence ^[47]
At high risk for ulcer complication	Recommendation ¹	Recommendation
At low risk for ulcer complication	No	No
Chronic NSAIDs users		
With a recent ulcer complication	Potential benefit ^{1,2}	Recommendation-evidence ^[46]
At high risk for ulcer complication	Potential benefit ^{1,2}	Recommendation
At low risk for ulcer complication	No	No

¹*H pylori* eradication therapy in chronic users of aspirin or NSAIDs with a recent ulcer complication or those at a high-risk should be administered after confirmation of ulcer healing. ²*H pylori* eradication therapy in chronic NSAIDs users with a recent ulcer complication or those at a high-risk may be given as a potentially beneficial intervention in addition to the long-term PPI therapy.

naive aspirin/NSAID user or already on long-term (>1-3 mo) or chronic drug use^[36-38]; (2) whether the subject is at high risk for bleeding or other complication of peptic ulcer (history of complicated or uncomplicated peptic ulcer, age older than 60-65 years, recent dyspepsia, treatment with anticoagulants)^[6,36-38,49]; and (3) perhaps whether they take aspirin or non-aspirin NSAID^[19,48].

In naive NSAID users, it is well accepted and supported by strong data^[39,40] that they should be tested for the presence of *H pylori* infection and, if positive, receive *H pylori* eradication therapy before NSAID use^[19-48]. A similar strategy is also suggested for naive aspirin users^[19], although the efficacy of such an approach has not been evaluated yet.

In chronic aspirin/NSAIDs users, the recommendations may depend on the risk for peptic ulcer complications^[6] and the type of drug. The indication for use of aspirin or NSAIDs should be first evaluated in all such users at high risk for peptic ulcer complications. Moreover, the probability and the cost/benefit of replacement of aspirin or NSAID with a less gastrototoxic antiplatelet agent or a selective COX-2 inhibitor respectively may be considered^[6,11,12].

All individuals, who should continue taking aspirin after development of a peptic ulcer complication, should be tested for the presence of *H pylori* infection and, if positive, receive *H pylori* eradication therapy after peptic ulcer healing. In addition, they should subsequently receive long-term therapy with a PPI^[19,47]. A similar approach may be recommended in chronic aspirin users without a recent ulcer complication but at high risk for ulcer complication, such as those with a history of peptic ulcer^[19]. It should be noted, however, that there are no strong data to support the combined prophylactic approach with both *H pylori* eradication and long-term PPI therapy in this setting.

All individuals, who should continue taking NSAIDs being at high-risk for peptic ulcer complication, certainly benefit from long-term therapy with a PPI^[19,46,48]. The risk of relapse of ulcer complication in chronic NSAIDs users taking PPI, however, is higher than the risk of such a relapse in aspirin users irrespective of the type of gastroprotection^[46]. Thus, given that *H pylori* infection represents an independent risk factor for gastrointestinal bleeding in chronic NSAIDs

users^[35], it is often recommended that testing for *H pylori* infection and, if positive, *H pylori* eradication therapy should be offered to high-risk chronic NSAIDs users in addition to the long-term PPI therapy^[19], despite that there are no strong data to support such an approach.

Finally, testing for *H pylori* infection or PPI therapy is not recommended for chronic users of aspirin or NSAIDs with no peptic ulcer or complication or those at a low risk of the same^[19].

REFERENCES

- Lauer MS. Aspirin for primary prevention of coronary events. *N Engl J Med* 2002; **346**: 1468-1474
- Antiplatelet Trialists' Collaboration. Collaborative overview of randomised trials of antiplatelet therapy prevention of death, myocardial infarction, and stroke by prolonged antiplatelet therapy in various categories. *Br Med J* 1994; **308**: 81-106
- Giovannucci E, Egan KM, Hunter DJ, Stampfer MJ, Colditz GA, Willett WC, Speizer FE. Aspirin and the risk of colorectal cancer in women. *N Engl J Med* 1995; **333**: 609-614
- Arber N, DuBois RN. Nonsteroidal anti-inflammatory drugs and prevention of colorectal cancer. *Curr Gastroenterol Rep* 1999; **1**: 441-448
- Baum C, Kennedy DL, Forbes MB. Utilization of nonsteroidal antiinflammatory drugs. *Arthritis Rheum* 1985; **28**: 686-692
- Laine L. Approaches to nonsteroidal anti-inflammatory drugs use in the high-risk patient. *Gastroenterology* 2001; **120**: 594-606
- Singh G, Ramey DR, Morfeld D, Shi H, Hatoum HT, Fries JF. Gastrointestinal tract complications of nonsteroidal anti-inflammatory drug treatment in rheumatoid arthritis. A prospective observational cohort study. *Arch Intern Med* 1996; **156**: 1530-1536
- Hawkey CJ, Laine L, Simon T, Quan H, Shingo S, Evans J. Incidence of gastroduodenal ulcers in patients with rheumatoid arthritis after 12 wk of rofecoxib, naproxen, or placebo: a multicentre, randomised, double blind study. *Gut* 2003; **52**: 820-826
- Geis GS. Update on clinical developments with celecoxib, a new specific COX-2 inhibitor: what can we expect? *J Rheumatol* 1999; **26** (Suppl 56): 31-36
- Silverstein FE, Graham DY, Senior JR, Davies HW, Struthers BJ, Bittman RM, Geis GS. Misoprostol reduces serious gastrointestinal complications in patients with rheumatoid ar-

- thritis receiving nonsteroidal anti-inflammatory drugs. A randomized, double-blind, placebo-controlled trial. *Ann Intern Med* 1995; **123**: 241-249
- 11 **Silverstein FE**, Faich G, Goldstein JL, Simon LS, Pincus T, Whelton A, Makuch R, Eisen G, Agrawal NM, Stenson WF, Burr AM, Zhao WW, Kent JD, Lefkowitz JB, Verburg KM, Geis GS. Gastrointestinal toxicity with celecoxib vs nonsteroidal anti-inflammatory drugs for osteoarthritis and rheumatoid arthritis: the CLASS study: A randomized controlled trial. Celecoxib Long-term Arthritis Safety Study. *JAMA* 2000; **284**: 1247-1255
 - 12 **Bombardier C**, Laine L, Reicin A, Shapiro D, Burgos-Vargas R, Davis B, Day R, Ferraz MB, Hawkey CJ, Hochberg MC, Kvien TK, Schnitzer TJ. Comparison of upper gastrointestinal toxicity of rofecoxib and naproxen in patients with rheumatoid arthritis. VIGOR Study Group. *N Engl J Med* 2000; **343**: 1520-1528
 - 13 **Laine L**, Connors LG, Reicin A, Hawkey CJ, Burgos-Vargas R, Schnitzer TJ, Yu Q, Bombardier C. Serious lower gastrointestinal clinical events with nonselective NSAID or coxib use. *Gastroenterology* 2003; **124**: 288-292
 - 14 **Singh G**, Ramey DR, Morfeld D, Fries JF. Comparative toxicity of non-steroidal anti-inflammatory agents. *Pharmacol Ther* 1994; **62**: 175-191
 - 15 **Sanmuganathan PS**, Ghahramani P, Jackson PR, Wallis EJ, Ramsay LE. Aspirin for primary prevention of coronary heart disease: safety and absolute benefit related to coronary risk derived from meta-analysis of randomised trials. *Heart* 2001; **85**: 265-271
 - 16 **Hawkey CJ**, Laine L, Harper SE, Quan HU, Bolognese JA, Mortensen E. Influence of risk factors on endoscopic and clinical ulcers in patients taking rofecoxib or ibuprofen in two randomized controlled trials. *Aliment Pharmacol Ther* 2001; **15**: 1593-1601
 - 17 **Sorensen HT**, Mellemejaer L, Blot WJ, Nielsen GL, Steffensen FH, McLaughlin JK, Olsen JH. Risk of upper gastrointestinal bleeding associated with use of low-dose aspirin. *Am J Gastroenterol* 2000; **95**: 2218-2224
 - 18 **Suerbaum S**, Michetti P. *Helicobacter pylori* infection. *N Engl J Med* 2002; **347**: 1175-1186
 - 19 **Hunt RH**, Bazzoli F. Should NSAID/low-dose aspirin takers be tested routinely for *H pylori* infection and treated if positive? Implications for primary risk of ulcer and ulcer relapse after initial healing. *Aliment Pharmacol Ther* 2004; **19** (Suppl 1): 9-16
 - 20 **Kaufman G**. Aspirin-induced gastric mucosal injury: lessons learned from animal models. *Gastroenterology* 1989; **96**: 606-614
 - 21 **Derry S**, Loke YK. Risk of gastrointestinal haemorrhage with long term use of aspirin: meta-analysis. *Br Med J* 2000; **321**: 1183-1187
 - 22 **Kelly JP**, Kaufman DW, Jurgelon JM, Sheehan J, Koff RS, Shapiro S. Risk of aspirin-associated major upper-gastrointestinal bleeding with enteric-coated or buffered product. *Lancet* 1996; **348**: 1413-1416
 - 23 **Lichtenstein DR**, Syngal S, Wolfe MM. Nonsteroidal anti-inflammatory drugs and the gastrointestinal tract. *Arthritis Rheum* 1995; **38**: 5-18
 - 24 **Labenz J**, Peitz U, Kohl H, Kaiser J, Malfertheiner P, Hackelsberger A, Borsch G. *Helicobacter pylori* increases the risk of peptic ulcer bleeding: a case-control study. *Ital J Gastroenterol Hepatol* 1999; **31**: 110-115
 - 25 **Aalykke C**, Lauritsen JM, Hallas J, Reinholdt S, Krogfelt K, Lauritsen K. *Helicobacter pylori* and risk of ulcer bleeding among users of nonsteroidal anti-inflammatory drugs: a case-control study. *Gastroenterology* 1999; **116**: 1305-1309
 - 26 **Ng TM**, Fock KM, Khor JL, Teo EK, Sim CS, Tan AL, Machin D. Non-steroidal anti-inflammatory drugs, *Helicobacter pylori* and bleeding gastric ulcer. *Aliment Pharmacol Ther* 2000; **14**: 203-209
 - 27 **Lanas A**, Fuentes J, Benito R, Serrano P, Bajador E, Sainz R. *Helicobacter pylori* increases the risk of upper gastrointestinal bleeding in patients taking low-dose aspirin. *Aliment Pharmacol Ther* 2002; **16**: 779-786
 - 28 **Papatheodoridis GV**, Papadelli D, Cholongitas E, Vassilopoulos D, Mentis A, Hadziyannis SJ. Effect of *Helicobacter pylori* infection on the risk of upper gastrointestinal bleeding in users of non-steroidal anti-inflammatory drugs: a prospective, case-control study. *Am J Med* 2004; **116**: 601-605
 - 29 **Laine L**, Marin-Sorensen M, Weinstein WM. Nonsteroidal anti-inflammatory drug associated gastric ulcers do not require *Helicobacter pylori* for their development. *Am J Gastroenterol* 1992; **87**: 1398-1402
 - 30 **Cullen DJ**, Hawkey GM, Greenwood DC, Humphreys H, Shepherd V, Logan RF, Hawkey CJ. Peptic ulcer bleeding in the elderly: relative roles of *Helicobacter pylori* and non-steroidal anti-inflammatory drugs. *Gut* 1997; **41**: 459-462
 - 31 **Loeb DS**, Talley NJ, Ahlquist DA, Carpenter HA, Zinsmeister AR. Long-term nonsteroidal anti-inflammatory drug use and gastroduodenal injury: the role of *Helicobacter pylori* infection. *Gastroenterology* 1992; **102**: 1899-1905
 - 32 **Pilotto A**, Leandro G, Di Mario F, Franceschi M, Bozzola L, Valerio G. Role of *Helicobacter pylori* infection on upper gastrointestinal bleeding in the elderly: a case-control study. *Dig Dis Sci* 1997; **42**: 586-591
 - 33 **Stack WA**, Atherton JC, Hawkey GM, Logan RF, Hawkey CJ. Interactions between *Helicobacter pylori* and other risk factors for peptic ulcer bleeding. *Aliment Pharmacol Ther* 2002; **16**: 497-506
 - 34 **Santolaria S**, Lanas A, Benito R, Perez-Aisa M, Montoro M, Sainz R. *Helicobacter pylori* infection is a protective factor for bleeding gastric ulcers but not for bleeding duodenal ulcers in NSAID users. *Aliment Pharmacol Ther* 1999; **13**: 1511-1518
 - 35 **Huang JQ**, Sridhar S, Hunt RH. Role of *Helicobacter pylori* infection and non-steroidal anti-inflammatory drugs in peptic-ulcer disease: a meta-analysis. *Lancet* 2002; **359**: 14-22
 - 36 **Gabriel SE**, Jaakkimainen L, Bombardier C. Risk for serious gastrointestinal complications related to use of nonsteroidal anti-inflammatory drugs. A meta-analysis. *Ann Intern Med* 1991; **115**: 787-796
 - 37 **Griffin MR**, Piper JM, Daugherty JR, Snowden M, Ray WA. Nonsteroidal anti-inflammatory drug use and increased risk for peptic ulcer disease in elderly persons. *Ann Intern Med* 1991; **114**: 257-263
 - 38 **Langman MJ**, Weil J, Wainwright P, Lawson DH, Rawlins MD, Logan RF, Murphy M, Vessey MP, Colin-Jones DG. Risks of bleeding peptic ulcer associated with individual non-steroidal anti-inflammatory drugs. *Lancet* 1994; **343**: 1075-1078
 - 39 **Chan FK**, Sung JJ, Chung SC, To KF, Yung MY, Leung VK, Lee YT, Chan CS, Li EK, Woo J. Randomised trial of eradication of *Helicobacter pylori* before non-steroidal anti-inflammatory drug therapy to prevent peptic ulcers. *Lancet* 1997; **350**: 975-979
 - 40 **Chan FK**, To KF, Wu JC, Yung MY, Leung WK, Kwok T, Hui Y, Chan HL, Chan CS, Hui E, Woo J, Sung JJ. Eradication of *Helicobacter pylori* and risk of peptic ulcers in patients starting long-term treatment with non-steroidal anti-inflammatory drugs: a randomised trial. *Lancet* 2002; **359**: 9-13
 - 41 **Hawkey CJ**, Tulassay Z, Szczepanski L, van Rensburg CJ, Filipowicz-Sosnowska A, Lanas A, Wason CM, Peacock RA, Gillon KR. Randomised controlled trial of *Helicobacter pylori* eradication in patients on non-steroidal anti-inflammatory drugs: HELP NSAIDs study. Helicobacter Eradication for Lesion Prevention. *Lancet* 1998; **352**: 1016-1021
 - 42 **van Herwaarden MA**, Samsom M, van Nispen CH, Mulder PG, Smout AJ. The effect of *Helicobacter pylori* eradication on intragastric pH during dosing with lansoprazole or ranitidine. *Aliment Pharmacol Ther* 1999; **13**: 731-740
 - 43 **Campbell DR**, Haber MM, Sheldon E, Collis C, Lukasik N, Huang B, Goldstein JL. Effect of *H pylori* status on

- gastric ulcer healing in patients continuing nonsteroidal anti-inflammatory therapy and receiving treatment with lansoprazole or ranitidine. *Am J Gastroenterol* 2002; **97**: 2208-2214
- 44 **Lanas A**, Bajador E, Serrano P, Fuentes J, Carreno S, Guardia J, Sanz M, Montoro M, Sainz R. Nitrovasodilators, low-dose aspirin, other nonsteroidal antiinflammatory drugs, and the risk of upper gastrointestinal bleeding. *N Engl J Med* 2000; **343**: 834-839
- 45 **Garcia Rodriguez LA**, Jick H. Risk of upper gastrointestinal bleeding and perforation associated with individual non-steroidal anti-inflammatory drugs. *Lancet* 1994; **343**: 769-772
- 46 **Chan FK**, Chung SC, Suen BY, Lee YT, Leung WK, Leung VK, Wu JC, Lau JY, Hui Y, Lai MS, Chan HL, Sung JJ. Preventing recurrent upper gastrointestinal bleeding in patients with *Helicobacter pylori* infection who are taking low-dose aspirin or naproxen. *N Engl J Med* 2001; **344**: 967-973
- 47 **Lai KC**, Lam SK, Chu KM, Wong BC, Hui WM, Hu WH, Lau GK, Wong WM, Yuen MF, Chan AO, Lai CL, Wong J. Lansoprazole for the prevention of recurrences of ulcer complications from long-term low-dose aspirin use. *N Engl J Med* 2002; **346**: 2033-2038
- 48 **Malfertheiner P**, Megraud F, O'Morain C, Hungin AP, Jones R, Axon A, Graham DY, Tytgat G. Current concepts in the management of *Helicobacter pylori* infection-the Maastricht 2-2000 Consensus Report. *Aliment Pharmacol Ther* 2002; **16**: 167-180
- 49 **Laine L**, Bombardier C, Hawkey CJ, Davis B, Shapiro D, Brett C, Reicin A. Stratifying the risk of NSAID-related upper gastrointestinal clinical events: results of a double-blind outcomes study in patients with rheumatoid arthritis. *Gastroenterology* 2002; **123**: 1006-1012

Science Editor Zhu LH and Guo SY Language Editor Elsevier HK

• REVIEW •

Current preventive treatment for recurrence after curative hepatectomy for liver metastases of colorectal carcinoma: A literature review of randomized control trials

Peng Wang, Zhen Chen, Wen-Xia Huang, Lu-Ming Liu

Peng Wang, Zhen Chen, Wen-Xia Huang, Lu-Ming Liu, Department of Oncology, Shanghai Medical College of Fudan University and Department of Liver Neoplasms, Cancer Hospital of Fudan University, Shanghai 200032, China
Correspondence to: Peng Wang, Department of Liver Neoplasms, Cancer Hospital of Fudan University, 270 Dong An Road, Shanghai 200032, China. wangp413@yahoo.com.cn
Telephone: +86-21-64175590-1304 Fax: +86-21-64434191
Received: 2004-09-18 Accepted: 2004-12-21

Metastatic colorectal cancer; Randomized control trials

Wang P, Chen Z, Huang WX, Liu LM. Current preventive treatment for recurrence after curative hepatectomy for liver metastases of colorectal carcinoma: A literature review of randomized control trials. *World J Gastroenterol* 2005; 11(25): 3817-3822
<http://www.wjgnet.com/1007-9327/11/3817.asp>

Abstract

To review the preventive approaches for recurrence after curative resection of hepatic metastases from colorectal carcinoma, we have summarized all available publications reporting randomized control trials (RCTs) covered in PubMed. The treatment approaches presented above include adjuvant intrahepatic arterial infusion chemotherapy, systemic chemotherapy, neoadjuvant chemotherapy, and immunotherapy. Although no standard treatment has been established, several approaches present promising results, which are both effective and tolerable in post-hepatectomy patients. Intrahepatic arterial infusion chemotherapy should be regarded as effective and tolerable and it increases overall survival (OS) and disease-free survival (DFS) of patients, while 5-fluorouracil-based systemic chemotherapy has not shown any significant survival benefit. Fortunately chemotherapy combined with hepatic arterial infusion and intravenous infusion has shown OS and DFS benefit in many researches. Few neoadjuvant RCT studies have been conducted to evaluate its effect on prolonging survivals although many retrospective studies and case reports are published in which unresectable colorectal liver metastases are downstaged and made resectable with neoadjuvant chemotherapy. Liver resection supplemented with immunotherapy is associated with optimal results; however, it is also questioned by others. In conclusion, several adjuvant approaches have been studied for their efficacy on recurrence after hepatectomy for liver metastases from colorectal cancer (CRC), but multi-centric RCT is still needed for further evaluation on their efficacy and systemic or local toxicities. In addition, new adjuvant treatment should be investigated to provide more effective and tolerable methods for the patients with resectable hepatic metastases from CRC.

INTRODUCTION

Although many approaches have been invented for the treatment of liver metastases from colorectal cancer (CRC)^[1], resection continues to be the only curative therapeutic option. Liver resection is today a safe procedure, with a low mortality rate of 0.8%^[2] and a morbidity of 7.2%^[3]. Though the 5- and 10-year overall survival (OS) rates are 37% and 22% respectively^[4], recurrence is already evidenced, either in the liver or with extrahepatic disease in about half of all resected patients within 18 mo after resection^[5]. Intrahepatic recurrence, alone or with other localization, is common. However, about 60% recurrences are seen in the remnant liver^[6]. In the last two decades people have tried a number of approaches to prevent recurrence, but only a few of them were designed as randomized control trials (RCTs), which provide evidence-based results for those treatment modalities. In this paper, we summarized the results from RCTs, attempting to find a more suitable treatment modality for prevention of recurrence.

LITERATURE REVIEWS OF RANDOMIZED CONTROL TRIALS TO PREVENT RECURRENCE AFTER CURATIVE HEPATECTOMY FOR LIVER METASTASES OF COLORECTAL CARCINOMA

Hepatic arterial infusion

Rationale for regional therapy after resection of liver metastases is that hepatic metastases are perfused almost exclusively by the hepatic artery, while normal hepatocytes derive their blood supply from the portal vein, which provides the basis for the use of regional hepatic arterial infusion (HAI) therapy after resection of hepatic metastases. Though favorable long-term results can be achieved after surgery for colorectal metastases to the liver, recurrences both intrahepatic and extrahepatic commonly occur^[5,6]. Tumor cells from colorectal carcinoma spread hematogenously

© 2005 The WJG Press and Elsevier Inc. All rights reserved.

Key words: Preventive treatment; Recurrence; Hepatectomy;

via the portal circulation, making liver the first site of metastases. The most common site of failure after resection is within the remnant liver. Hence, additional therapy, either regional or systemic or both, has potential as an adjunct treatment after surgery. Extraction of drugs from the hepatic arterial circulation ensures high drug concentrations to residual cancer cells while minimizing systemic toxicity, provided the agent used has a high first-pass extraction. Of the various chemotherapy agents, 5-fluoro-2-deoxyuridine (FUdR) is the most commonly used drug for this purpose, which demonstrates 95% hepatic extraction when given via HAI. FUdR via HAI markedly increases its estimated exposure up to 400-fold. 5-FU is the other agent used in this setting of regional therapy and its response rate can be expected higher when used in combination with concomitant leukovorin^[7]. Combining 5-FU with other agents by hepatic artery infusion has been proven to be an effective treatment for liver metastases from CRC.

Table 1 summarizes the randomized series of adjuvant intrahepatic therapy (with or without systemic therapy) after potentially curative hepatic resection of metastatic CRC.

A small study by Lygidakis *et al.*^[8], prospectively randomized 40 patients to hepatic surgery alone or surgery combined with post-operative regional chemoimmunotherapy via implanted splenic and gastroduodenal arterial catheters, and found that liver resection supplemented with postoperative targeted transarterial locoregional immunotherapy-chemotherapy is associated with optimal results.

Asahara *et al.*^[9], conducted a study to evaluate the efficacy of postoperative transarterial infusion chemotherapy for the prevention of recurrence after hepatectomy following curative surgery for colorectal carcinoma. The result showed that the 3- and 4-year survival rates are 100% in the experimental group, and 60% and 47% respectively in the control group.

Kemeny *et al.*^[12], tried to improve the outcomes by treating patients with HAI of floxuridine plus systemic

fluorouracil after liver resection, and found that a 2-year OS and DFS benefit in HAI group is 86% vs 72%, 57% vs 42%. After 2 years, the rate of survival free of hepatic recurrence is 90% in the HAI group and 60% in the monotherapy group, suggesting that for patients who undergo resection of liver metastases from CRC, postoperative treatment with a combination of HAI of floxuridine and intravenous fluorouracil improves the outcome.

Tono *et al.*^[13], divided 19 patients who underwent curative hepatectomy for metastatic colorectal carcinoma into HAI group and control group. Patients in HAI group received continuous intra-arterial infusion of 5-FU (500 mg/d), 4 d a week for 6 wk. The study showed a significant 1-, 2-, 3-year prolongation of DFS in the HAI group (77.8% vs 50.0%, 77.8% vs 30.0%, 66.7% vs 20.0%, $P = 0.045$). The 1-, 3-, and 5-year cumulative survival rates for the HAI group were 88.9%, 77.8%, and 77.8%, respectively, whereas those of the control group were 100.0%, 50.0%, and 50.0%, respectively. This randomized study reveals that short-term HAI of 5-FU after curative resection of colorectal hepatic metastases is effective in preventing the recurrence of disease and has no serious complications.

Kemeny *et al.*^[14], studied the effect of postoperative hepatic arterial floxuridine combined with intravenous continuous infusion of fluorouracil on the OS and DFS of patients, and found that the 4-year recurrence-free rate is 25% in the control group and 46% in the chemotherapy group, the median survival time of the 75 assessable patients is 49 mo in the control group and 63.7 mo in the chemotherapy group, demonstrating that adjuvant intra-arterial and intravenous chemotherapy is beneficial to the prevention of hepatic recurrence after hepatic resection of CRC.

However, in a German co-operative multicenter study^[11], patients were randomized to resection only or resection plus 6 mo of HAI of 5-FU/LV given as a 5-d continuous

Table 1 Randomized series of adjuvant intrahepatic arterial chemotherapy after surgical resection of hepatic metastases

Authors	Treatment protocol	Sample size (Tx/Ctl)	Observation time	DFS Tx vs Ctl	OS Tx vs Ctl	Conclusions
Lygidakis <i>et al.</i> ^[8]	Surgery+HAI chemoimmunotherapy vs surgery alone	40 (20/20)	3 yr	NA	Median 20 vs 11 (mo) ($P < 0.05$)	Beneficial
Asahara <i>et al.</i> ^[9]	Surgery+HAI chemotherapy vs surgery alone	38 (10/28)	NA	NA	3-yr 100% vs 60%, 4-yr 100% vs 47%, respectively ($P < 0.05$)	Beneficial
Rudroff <i>et al.</i> ^[10]	Surgery+HAI 5-FU/MMC vs surgery alone	30 (14/16)	5 yr	5-yr 15% vs 23% ($P > 0.05$)	5-yr 25% vs 31% ($P > 0.05$)	Not beneficial
Lorenz <i>et al.</i> ^[11]	Surgery+HAI 5-FU/LV vs surgery alone	226 (113/113)	NA	Median 14.2 vs 13.7 (mo) ($P > 0.05$)	Median 34.5 vs 40.8 (mo) ($P > 0.05$)	Not beneficial
Kemeny <i>et al.</i> ^[12]	Surgery+HAI FUdR/DEXA+IV 5-FU/LV vs surgery+IV 5-FU/LV	156 (74/82)	2 yr	2-yr 57% vs 42% ($P = 0.07$)	2-yr 86% vs 72% ($P = 0.03$)	Beneficial
Tono <i>et al.</i> ^[13]	Surgery+HAI 5-FU+oral 5-FU vs surgery+oral 5-FU	19 (9/10)	62.2 (mo) (mean)	1-, 2-, 3-yr 77.8%, 77.8%, 66.7% vs 50.0%, 30.0%, 20.0% respectively ($P = 0.045$)	1-, 2-, 3-yr 88.9%, 77.8%, 77.8% vs 100.0%, 50.0%, and 50.0% respectively ($P = 0.2686$)	Beneficial
Kemeny <i>et al.</i> ^[14]	Surgery+HAI FUdR+IV 5-FU vs surgery	109 (53/56)	NA	4-yr 46% vs 25% ($P = 0.04$)	Median 63.7 vs 49 (mo) ($P = 0.60$)	Beneficial

Tx: treatment; Ctl: control; DFS: disease-free survival; OS: overall survival; NA: not available.

infusion every 28 d. No differences in time-to-progression, time-to-hepatic progression, or median OS are noted in this study.

Rudroff *et al.*^[10], evaluated the preventive effect of adjuvant intra-arterial chemotherapy after R0 liver resection and found that there is no significant difference in either 5-year survival or long-term disease-free status between the two groups. They concluded that routine application of adjuvant regional chemotherapy after R0 liver resection is not warranted.

A recent meta-analysis^[15] also showed that hepatic artery chemotherapy after curative hepatectomy metastases cannot improve the OS.

The above data suggest that adjuvant intrahepatic arterial chemotherapy combined with or without intravenous chemotherapy can inhibit the recurrence, and that the toxicity and side effects are tolerable.

At present, the superior rates of response and survival reported with irinotecan- and oxaliplatin-based regimens^[16-19] provide a new standard first-line treatment of metastatic CRC, which have led to more clinical trials to re-evaluate the efficiency of HAI combining irinotecan or oxaliplatin on recurrence after curative hepatectomy for CRC. At the Memorial Sloan-Kettering Cancer Center (MSKCC), a phase I/II study used HAI with floxuridine and dexamethasone in combination with systemic irinotecan as adjuvant therapy following curative hepatectomy in 90 CRC patients. The maximum tolerable dose of combined HAI+systemic irinotecan is 0.12 mg/kg FUDR with systemic CPT-11 at 200 mg/m² every other week, the 2-year survival rate is 87%^[20-22]. Oxaliplatin, a new cytotoxic agent, when used in combination with 5-FU/LV (FOLFOX), can achieve more than 50% clinical response and a median survival time of 16.2 mo in untreated patients with metastatic CRC^[18,19], suggesting that oxaliplatin-based regimens combined with HAI of FUDR have a promising result.

HAI of FUDR plus systemic 5-FU/LV following resection of hepatic metastases decreases local recurrence and improves OS. It is necessary to further study the effect of HAI combining newer systemic agents, such as irinotecan and oxaliplatin and to make it clear which combination of regimens are the most effective and well-tolerated.

Systemic chemotherapy

While patients who undergo resection of liver metastases from CRC can prolong their survival time, the majority will have relapse not only intrahepatically but also extrahepatically. Therefore, the investigation of adjuvant

therapies designed to decrease relapse is warranted. Adjuvant chemotherapy via HAI after resection of liver metastases has shown its efficacy in terms of both disease-free survival (DFS) and OS. On the contrary, the role of “adjuvant” chemotherapy following liver resection for hepatic colorectal metastases remains unclear. Some retrospective trials about adjuvant 5-FU-based systemic chemotherapy have not shown any significant survival benefit^[18,19]. Few prospective randomized studies have been performed to answer the question whether postoperative chemotherapy improves survival in comparison to liver resection alone. However, the effects on survival of postoperative systemic chemotherapy are currently under evaluation. The following are recent RCT studies on systemic chemotherapy (Table 2).

Lopez-Ladron *et al.*^[24], studied the outcome of 38 patients with resection of liver metastases from CRC, and found that the median OS time of patients who did not receive CT is 15 mo, while patients who received CT after hepatic surgery have a median survival time of 30 mo. The actual OS of patients who received adjuvant CT seems to be higher, suggesting that these results should be confirmed in phase III studies.

An intergroup multicentric randomized study^[23] was performed to evaluate the value of FU/FA after complete resection of liver metastases compared to surgery alone. The result is in favor of patients who received systemic chemotherapy after resection of liver metastases.

At present, more studies are focused on the effect of HAI combined with systemic chemotherapy on the OS and DFS^[12,14] (Table 1).

In general, systemic chemotherapy alone cannot inhibit recurrence in patients after resection of hepatic colorectal metastases, although systemic 5-FU/LV and HAI of FUDR following resection of hepatic metastases decrease local recurrence and improve 2-year survival. Both hepatic and extrahepatic relapses remain a problem. Studies on newer systemic agents such as irinotecan and oxaliplatin are under way.

Neoadjuvant therapy

The application of neoadjuvant chemotherapy has a number of potential advantages in patients with resectable liver metastases. Firstly, it helps the selection of chemotherapeutic agents after resection. The degree of response gives information on the *in vivo* chemosensitivity of the tumor. In patients with fewer responses or severe toxicity, the same agents should be avoided and alternative agents should

Table 2 RCT studies on efficacy of systemic chemotherapy on prevention of recurrence

Authors	Treatment protocol	Sample size (Tx/Ctl)	Observation time	DFS Tx vs Ctl	OS Tx vs Ctl	Conclusions
Lopez-Ladron <i>et al.</i> ^[24]	Surgery+post-operative chemotherapy vs surgery alone	38 (28/10)	Median 15 (mo)	Median 15 vs 9 (mo) (P = 0.352)	Median 30 vs 15 (mo) (P = 0.066)	Not beneficial, needing further study
Portier <i>et al.</i> ^[23]	Surgery+post-operative chemotherapy (FU/FA) vs surgery alone	162 (81/81)	5 yr	5-yr 33% vs 24% (P>0.05)	5-yr 51% vs 44% (P>0.05)	Not beneficial

Tx: treatment; Ctl: control; DFS: disease-free survival; OS: overall survival; NA: not available.

Table 3 RCTs on efficacy of neoadjuvant chemotherapy

Authors	Treatment protocol	Sample size (Tx/Ctl)	Observation time	DFS Tx vs Ctl	OS Tx vs Ctl	Conclusions
Lorenz <i>et al.</i> ^[29]	Biweekly FOLFOX regimen×6 cycles vs biweekly FOLFOX regimen×3 cycles	40 (20/20)	NA	NA	NA	Induced significant remissions without increasing morbidity
Bathe <i>et al.</i> ^[90]	5-FU+leukovorin+CPT-11					Ongoing

Tx: treatment; Ctl: control; DFS: disease-free survival; OS: overall survival; NA: not available.

be considered after resection. Secondly, neoadjuvant chemotherapy may also help the selection of candidates for resection, which means patients who develop extrahepatic disease during a short course of chemotherapy are unsuitable for resection in the first place. Finally, neoadjuvant chemotherapy enhances resectability in some instances^[25-27]. Reduction of tumor volume may limit the amount of liver that needs to be removed to accomplish eradication of the tumor and preserve more normal hepatic tissues.

Most reports on neoadjuvant chemotherapy for liver metastasis focus on the strategies for unresectable tumors^[25,28]. The reported resectability rate ranges from 10% to 40% for unresectable colorectal liver metastases after preoperative chemotherapy.

Recently, Lorenz *et al.*^[29], conducted a prospective pilot study of neoadjuvant chemotherapy with 5-fluorouracil, folinic acid and oxaliplatin for resectable liver metastases of CRC, and found that neoadjuvant chemotherapy for resectable liver metastases induces significant remissions without increasing morbidity (Table 3).

Due to the potential advantage in patients with resectable liver metastases and new regimens using either oxaliplatin or irinotecan in combination with 5-FU, one phase II study^[30] of neoadjuvant 5-FU+leukovorin+CPT-11 in patients with resectable liver metastases from colorectal adenocarcinoma is under investigation. The general aim of this study is to determine the efficacy of neoadjuvant chemotherapy for patients with ablative liver metastases from CRC in reducing

recurrence rate. Response to the chemotherapy regimen will constitute an *in vivo* chemosensitivity test, and this will guide adjuvant chemotherapy following resection of liver metastases from CRC.

Immunotherapy

Since early 1990s, immunotherapy has become a very attractive cancer treatment modality. However, it is not so effective as expected in a number of clinical trials^[31,32]. Recently a series of clinical trials have begun to investigate the effect immunotherapy on recurrence of cancer after surgery. The summary of these RCTs are as follows (Table 4).

Lygidakis *et al.*^[8], compared the effect of liver resection combined with post-operative locoregional immunotherapy +chemotherapy on recurrence after curative hepatectomy of hepatic colorectal metastases, and found that the survival time of control group ranges from 4 to 25 mo (mean 11 mo), suggesting that liver resection in combination with postoperative targeted transarterial locoregional immunotherapy -chemotherapy is associated with good results. It is highly recommended as the procedure of choice for patients with liver metastasis of colorectal carcinoma.

Lygidakis *et al.*^[33], showed the same results, which support post-operatively locoregional chemotherapy for hepatic metastases of CRC. Lygidakis *et al.*^[34], reported that regional immunochemotherapy combined with systemic chemotherapy leads to a lower incidence of disease recurrence and a significant prolongation of the OS and DFS time.

Table 4 RCTs of immunotherapy

Authors	Treatment protocol	Sample size (Tx/Ctl)	Observation time	DFS Tx vs Ctl	OS Tx vs Ctl	Conclusions
Lygidakis <i>et al.</i> ^[8]	Surgery+post-operative HAI immunochemotherapy vs surgery alone	40 (20/20)	3 yr	NA	Median 20 vs 11 (mo) (P<0.05)	Beneficial
Lygidakis <i>et al.</i> ^[33]	Post-operatively locoregional immunochemotherapy vs post-operatively locoregional chemotherapy	45 (33/15)	NA	NA	Median 20.3 vs 9.9 (mo)	Beneficial
Lygidakis <i>et al.</i> ^[34]	Locoregional chemoimmunotherapy with systemic chemotherapy vs systemic immunochemotherapy	122 (62/60)	NA	2-yr 66% vs 48%	2-yr 92% vs 75% 5-yr 73% vs 60%	Beneficial
Elias <i>et al.</i> ^[35]	Preoperative rIL-2 continuous intravenous infusion	19 (12/7)	NA	NA	NA	Beneficial (well tolerated and reverse postoperative immunodepression)
Gardini <i>et al.</i> ^[36]	Post-operative TIL+IL-2 vs post-operative+chemotherapy	45 (25/22)	NA	1-, 3-, and 5- yr No difference	1-, 3-, and 5- yr No difference	Not beneficial

Tx: treatment; Ctl: control; DFS: disease-free survival; OS: overall survival; NA: not available.

Elias *et al.*^[35], investigated prehepatectomy immunostimulation with recombinant interleukin-2 (rIL-2) and evaluated the tolerance of rIL-2 in association with major hepatectomy to verify the effect of preoperative immunostimulation (neoadjuvant immunotherapy), and found that toxicity during rIL-2 infusion is acceptable, suggesting that infusion of rIL-2 before major hepatectomy for liver metastases of CRC is well tolerated and reverses postoperative immunodepression.

Gardini *et al.*^[36], also studied immunotherapy with tumor infiltrating lymphocytes (TIL) plus interleukin-2 (IL-2) as adjuvant treatment, and found that there are no significant differences in the actual and DFS rates after 1, 3, and 5 years, suggesting that whether TIL+IL-2 treatment is an effective adjuvant therapy needs to be further studied.

SUMMARY

Number of preventive treatment protocols for inhibiting recurrence after curative resection of liver metastases from colorectal origin have been evaluated by RCT. Although no standard treatment has been proven to be effective in all patients, several approaches present promising results, which are both effective and tolerable in post-operative patients. Generally intrahepatic arterial infusion chemotherapy is effective in preventing the recurrence of disease without serious complications, while systemic chemotherapy is not in favor of patients who receive systemic chemotherapy after liver metastases resection. Neoadjuvant chemotherapy has shown an advantage in patients with resectable liver metastases. Immunotherapy approaches can achieve a better outcome, but need more evidence before wide acceptance.

REFERENCES

- Liu LX, Zhang WH, Jiang HC. Current treatment for liver metastases from colorectal cancer. *World J Gastroenterol* 2003; **9**: 193-200
- Cavallari A, Vivarelli M, Bellusci R, Montalti R, De Ruvo N, Cucchetti A, De Vivo A, De Raffele E, Salone M, La Barba G. Liver metastases from colorectal cancer: present surgical approach. *Hepatogastroenterology* 2003; **50**: 2067-2071
- Teh CS, Ooi LL. Hepatic resection for colorectal metastases to the liver: the national cancer centre/singapore general hospital experience. *Ann Acad Med Singapore* 2003; **32**: 196-204
- Fong Y, Fortner J, Sun RL, Brennan MF, Blumgart LH. Clinical score for predicting recurrence after hepatic resection for metastatic colorectal cancer: analysis of 1001 consecutive cases. *Ann Surg* 1999; **230**: 309-318
- Topal B, Kaufman L, Aerts R, Penninckx F. Patterns of failure following curative resection of colorectal liver metastases. *Eur J Surg Oncol* 2003; **29**: 248-253
- Nakajima Y, Nagao M, Ko S, Kanehiro H, Hisanaga M, Aomatsu Y, Ikeda N, Shibaji T, Ogawa S, Nakano H. Clinical predictors of recurrence site after hepatectomy for metastatic colorectal cancer. *Hepatogastroenterology* 2001; **48**: 1680-1684
- Rustum YM, Harstrick A, Cao S, Vanhoefer U, Yin MB, Wilke H, Seeber S. Thymidylate synthase inhibitors in cancer therapy: direct and indirect inhibitors. *J Clin Oncol* 1997; **15**: 389-400
- Lygidakis NJ, Ziras N, Parissis J. Resection versus resection combined with adjuvant pre- and post-operative chemotherapy-immunotherapy for metastatic colorectal liver cancer. A new look at an old problem. *Hepatogastroenterology* 1995; **42**: 155-161
- Asahara T, Kikkawa M, Okajima M, Ojima Y, Toyota K, Nakahara H, Katayama K, Itamoto T, Marubayashi S, One E, Yahata H, Dohi K, Azuma K, Ito K. Studies of postoperative transarterial infusion chemotherapy for liver metastasis of colorectal carcinoma after hepatectomy. *Hepatogastroenterology* 1998; **45**: 805-811
- Rudroff C, Altendorf-Hoffmann A, Stangl R, Scheele J. Prospective randomised trial on adjuvant hepatic-artery infusion chemotherapy after R0 resection of colorectal-liver metastases. *Langenbecks Arch Surg* 1999; **384**: 243-249
- Lorenz M, Muller HH, Schramm H, Gassel HJ, Rau HG, Ridwelski K, Hauss J, Stieger R, Jauch KW, Bechstein WO, Encke A. Randomized trial of surgery versus surgery followed by adjuvant hepatic arterial infusion with 5-fluorouracil and folinic acid for liver metastases of colorectal cancer. German Cooperative on Liver Metastases (Arbeitsgruppe Lebermetastasen). *Ann Surg* 1998; **228**: 756-762
- Kemeny N, Huang Y, Cohen AM, Shi W, Conti JA, Brennan MF, Bertino JR, Turnbull AD, Sullivan D, Stockman J, Blumgart LH, Fong Y. Hepatic arterial infusion of chemotherapy after resection of hepatic metastases from colorectal cancer. *N Engl J Med* 1999; **341**: 2039-2048
- Tono T, Hasuike Y, Ohzato H, Takatsuka Y, Kikkawa N. Limited but definite efficacy of prophylactic hepatic arterial infusion chemotherapy after curative resection of colorectal liver metastases: A randomized study. *Cancer* 2000; **88**: 1549-1556
- Kemeny MM, Adak S, Gray B, Macdonald JS, Smith T, Lipsitz S, Sigurdson ER, O'Dwyer PJ, Benson AB 3rd. Combined-modality treatment for resectable metastatic colorectal carcinoma to the liver: surgical resection of hepatic metastases in combination with continuous infusion of chemotherapy-an intergroup study. *J Clin Oncol* 2002; **20**: 1499-1505
- Nelson RL, Freels S. A systematic review of hepatic artery chemotherapy after hepatic resection of colorectal cancer metastatic to the liver. *Dis Colon Rectum* 2004; **47**: 739-745
- Douillard JY, Cunningham D, Roth AD, Navarro M, James RD, Karasek P, Jandik P, Iveson T, Carmichael J, Alakl M, Gruia G, Awad L, Rougier P. Irinotecan combined with fluorouracil compared with fluorouracil alone as first-line treatment for metastatic colorectal cancer: a multicentre randomised trial. *Lancet* 2000; **355**: 1041-1047
- Saltz LB, Cox JV, Blanke C, Rosen LS, Fehrenbacher L, Moore MJ, Maroun JA, Ackland SP, Locker PK, Pirotta N, Elfring GL, Miller LL. Irinotecan plus fluorouracil and leucovorin for metastatic colorectal cancer. Irinotecan Study Group. *N Engl J Med* 2000; **343**: 905-914
- de Gramont A, Figuer A, Seymour M, Homerin M, Hmissi A, Cassidy J, Boni C, Cortes-Funes H, Cervantes A, Freyer G, Papamichael D, Le Bail N, Louvet C, Hendler D, de Braud F, Wilson C, Morvan F, Bonetti A. Leucovorin and fluorouracil with or without oxaliplatin as first-line treatment in advanced colorectal cancer. *J Clin Oncol* 2000; **18**: 2938-2947
- Tournigand C, Louvet C, Quinaux E, Andre T, Lledo G, Flesch M, Ganem G, Landi B, Colin P, Denet C, Mery-Mignard D, Risse ML, Buyse M, de Gramont A. FOLFIRI Followed by FOLFOX Versus FOLFOX Followed by FOLFIRI in Metastatic Colorectal Cancer (MCRC): Final Results of a Phase III Study. *Proc Am Soc Clin Oncol* 2001; abstr494. Available from: URL: http://www.asco.org/ac/1,1003,_12-002643-00_18-0010-00_19-00494,00.asp
- Jarnagin WR, Gonen M, Blumgart L, Sperber D, Koenigsberg A, Fong Y, Kemeny N. Completed phase I trial of hepatic arterial infusion with floxuridine and dexamethasone in combination with systemic irinotecan after resection of hepatic metastases from colorectal cancer. *Proc Am Soc Clin Oncol* 2003; abstr 1073. Available from: URL: http://www.asco.org/ac/1,1003,_12-002643-00_18-0023-00_19-00100969,00.asp
- Ruers T, Bleichrodt RP. Treatment of liver metastases, an update on the possibilities and results. *Eur J Cancer* 2002; **38**: 1023-1033
- Yap B, Sheen A, Eaton D, Swindell R, James R, Levine E, Valle J, Hawkins R, Sherlock D, Saunders M. A large single centre cohort of adjuvant chemotherapy following curative resec-

- tion of hepatic colorectal metastases. *Proc Am Soc Clin Oncol* 2002; abstr 2367. Available from: URL: http://www.asco.org/ac/1,1003,12-002643-00_18-0016-00_19-002367,00.asp
- 23 **Portier G**, Rougier P, Milan C, Bouché O, Gillet M, Bosset JF, Ducreux M, Saric J, Bugat R, Stremsdoerfer N, Nordlinger B, Bedenne L, Lazorthes F. Adjuvant systemic chemotherapy (CT) using 5-fluorouracil (FU) and folinic acid (FA) after resection of liver metastases (LM) from colorectal (CRC) origin. Results of an intergroup phase III study (trial FFCD - ACHBTH - AURC 9002). *Proc Am Soc Clin Oncol* 2002; abstr 528. Available from: URL: http://www.asco.org/ac/1,1003,12-002643-00_18-0016-00_19-00528,00.asp
- 24 **Lopez-Ladron A**, Salvador J, Bernabe R, Bernardos A, Arriola E, Serrano J, Reina JJ, Gomez MA, Barneto I, Moreno-Nogueira JA. Observation versus postoperative chemotherapy after resection of liver metastases in patients with advanced colorectal cancer. *Proc Am Soc Clin Oncol* 2003 abstr 1497. Available from: URL: http://www.asco.org/ac/1,1003,12-002643-00_18-0023-00_19-00104357,00.asp
- 25 **Bismuth H**, Adam R, Levi F, Farabos C, Waechter F, Castaing D, Majno P, Engerran L. Resection of nonresectable liver metastases from colorectal cancer after neoadjuvant chemotherapy. *Ann Surg* 1996; **224**: 509-520
- 26 **Meric F**, Patt YZ, Curley SA, Chase J, Roh MS, Vauthey JN, Ellis LM. Surgery after downstaging of unresectable hepatic tumors with intra-arterial chemotherapy. *Ann Surg Oncol* 2000; **7**: 490-495
- 27 **Adam R**, Hugué E, Azoulay D, Castaing D, Kunstlinger F, Levi F, Bismuth H. Hepatic resection after down-staging of unresectable hepatic colorectal metastases. *Surg Oncol Clin N Am* 2003; **12**: 211-220
- 28 **Clavien PA**, Selzner N, Morse M, Selzner M, Paulson E. Downstaging of hepatocellular carcinoma and liver metastases from colorectal cancer by selective intra-arterial chemotherapy. *Surgery* 2002; **131**: 433-442
- 29 **Lorenz M**, Staib-Sebler E, Gog C, Proschek D, Jauch KW, Ridwelski K, Hohenberger W, Gassel HJ, Lehmann U, Vestweber KH, Padberg W, Zamzow K, Muller HH. Prospective pilot study of neoadjuvant chemotherapy with 5-fluorouracil, folinic acid and oxaliplatin in resectable liver metastases of colorectal cancer. Analysis of 42 neoadjuvant chemotherapies. *Zentralbl Chir* 2003; **128**: 87-94
- 30 **Bathe OF**, Dowden S, Sutherland F, Dixon E, Butts C, Bigam D, Walley B, Ruether D, Ernst S. Phase II study of neoadjuvant 5-FU + leucovorin + CPT-11 in patients with resectable liver metastases from colorectal adenocarcinoma. *BMC Cancer* 2004; **4**: 32
- 31 **Hanna MG Jr**, Hoover HC Jr, Vermorken JB, Harris JE, Pinedo HM. Adjuvant active specific immunotherapy of stage II and stage III colon cancer with an autologous tumor cell vaccine: first randomized phase III trials show promise. *Vaccine* 2001; **19**: 2576-2582
- 32 **Huncharek M**, Caubet JF, McGarry R. Single-agent DTIC versus combination chemotherapy with or without immunotherapy in metastatic melanoma: a meta-analysis of 3273 patients from 20 randomized trials. *Melanoma Res* 2001; **11**: 75-81
- 33 **Lygidakis NJ**, Stringaris K, Kokinis K, Lyberopoulos K, Raptis S. Locoregional chemotherapy versus locoregional combined immuno-chemotherapy for patients with advanced metastatic liver disease of colorectal origin: a prospective randomized study. *Hepatogastroenterology* 1996; **43**: 212-220
- 34 **Lygidakis NJ**, Sgourakis G, Vlachos L, Raptis S, Safioleas M, Boura P, Kountouras J, Alamani M. Metastatic liver disease of colorectal origin: the value of locoregional immunotherapy combined with systemic chemotherapy following liver resection. Results of a prospective randomized study. *Hepatogastroenterology* 2001; **48**: 1685-1691
- 35 **Elias D**, Farace F, Triebel F, Hattchouel JM, Pignon JP, Lecesne A, Rougier P, Lasser P, Duvillard P, Escudier B. Phase I-II randomized study on prehepatectomy recombinant interleukin-2 immunotherapy in patients with metastatic carcinoma of the colon and rectum. *J Am Coll Surg* 1995; **181**: 303-310
- 36 **Gardini A**, Ercolani G, Riccobon A, Ravaioli M, Ridolfi L, Flamini E, Ridolfi R, Grazi GL, Cavallari A, Amadori D. Adjuvant, adoptive immunotherapy with tumor infiltrating lymphocytes plus interleukin-2 after radical hepatic resection for colorectal liver metastases: 5-year analysis. *J Surg Oncol* 2004; **87**: 46-52

• ESOPHAGEAL CANCER •

Impact of simultaneous assay, the PCNA, cyclinD1, and DNA content with specimens before and after preoperative radiotherapy on prognosis of esophageal cancer-possible incorporation into clinical TNM staging system

Shu-Chai Zhu, Ren Li, Yu-Xiang Wang, Wei Feng, Juan Li, Rong Qiu

Shu-Chai Zhu, Ren Li, Yu-Xiang Wang, Wei Feng, Juan Li, Rong Qiu, Department of Radiation Oncology, Fourth Hospital, Hebei Medical University, Shijiazhuang 050011, Hebei Province, China

Supported by the Distinguished Young Teacher Programs Foundation of Ministry of Education of China, No. 2001125

Co-first-author: Ren Li

Correspondence to: Professor Shu-Chai Zhu, Department of Radiation Oncology, Fourth Hospital, Hebei Medical University, Jiankanglu 12, Shijiazhuang 050011, Hebei Province, China. sczhu@heinfo.net

Telephone: +86-311-6033941-317 Fax: +86-311-6992121

Received: 2004-10-26 Accepted: 2004-12-26

Key words: Esophageal carcinoma; Radiotherapy; Cell proliferating marker

Zhu SC, Li R, Wang YX, Feng W, Li J, Qiu R. Impact of simultaneous assay, the PCNA, cyclinD1, and DNA content with specimens before and after preoperative radiotherapy on prognosis of esophageal cancer-possible incorporation into clinical TNM staging system. *World J Gastroenterol* 2005; 11(25): 3823-3829

<http://www.wjgnet.com/1007-9327/11/3823.asp>

Abstract

AIM: The aim of the present study is to use immunohistochemical methods to investigate the clinical implications of tumor markers in esophageal squamous cell carcinoma and evaluate their impact on prognosis.

METHODS: From November 1990 to December 1996, 47 patients were treated with preoperative radiation followed by radical esophagectomy. All patients were confirmed pathologically as suffering from squamous cell carcinoma. Immunohistochemical stain was done for PCNA, cyclinD1 protein expression and DNA content analyzed by image cytometry. Kaplan-Meier method for single prognostic factor and log-rank test was used to test the significant difference. Cox stepwise regression model and prognosis index model were used for survival analysis with multiple prognostic factors.

RESULTS: Radio-pathological change, T stage and N stage, as the traditional prognostic factors had statistical difference in 3-, 5- and 10-year survival rates. While, tumor cell proliferating marked PCNA, cyclinD1 and DNA content served as independent prognostic factors of esophageal carcinoma. There was definitely an identity between the single and multiple factor analyses. PI was more accurate to evaluate the prognosis of esophageal carcinoma.

CONCLUSION: It is possible that tumor cell proliferating marked PCNA, cyclinD1 and DNA content would become the endpoints for evaluating the prognosis of esophageal carcinoma.

INTRODUCTION

Esophageal cancer, the sixth most common cancer worldwide, is one of the most interesting cancers in terms of its geographic distribution, variety of environmental factors including tobacco, alcohol, nutritional deficiencies and nitrosamines^[1,2]. The ratio of the incidence rates between high-risk and low-risk areas can be as great as 500:1, e.g., Cixian, in Hebei Province of northern China, has received worldwide attention over the past decades because of its high esophageal cancer incidence. Results from earlier studies show that malignant transformation of human esophageal mucosa is a multistage process. An early indicator of abnormality in persons predisposed to squamous cell carcinoma (SCC) is the proliferation of esophageal epithelial cells, morphologically manifested as basal-cell hyperplasia (BCH) and dysplasia (DYS). However, key molecular changes in the esophageal carcinogenesis still remain to be characterized^[3].

Furthermore, genetic factors, such as the activation of oncogene and the inactivation of tumor suppressor genes, are believed to play important roles. Earlier studies have shown the PCNA (proliferating cell nuclear antigen) is a 36-ku, 261-amino acid non-histone polypeptide that is localized in the nucleus and is associated with cell proliferation with function as an auxiliary protein to DNA polymerase-delta. PCNA appears to be necessary for DNA replication and elevated level of this protein at the G₁/S phase transition are present in cells undergoing division^[4,5].

Recent evidence has suggested that cyclinD1 gene (also referred to as *prad1*) amplification might also be involved in the development of esophageal carcinoma. The cyclinD1 gene has been mapped to the chromosome 11q13 locus close to the *int2* and *hst1* genes. The complex of cyclinD1 protein and cyclin-dependent protein kinases (cdks) may

govern key transitions in the cell cycle. Zhang^[6] found that cyclinD1 gene was amplified and its protein expression increased in only one-third of the esophageal SCC. However, the knowledge of the role of cyclinD1 in esophageal carcinogenesis is not yet definite in detail, since the level of cyclinD1 protein in different stages of carcinogenesis of esophageal carcinoma has not been determined^[6].

In the current study, it is possible to use only cancer cells for analyzing the DNA patterns and ploidy in cytophotometry. Most investigators have shown in clinical esophageal SCC, high-ploidy tumors grow more rapidly than low-ploidy ones, and the duration from curative esophagectomy to recurrence decreases in proportion to the degree of DNA aneuploidy^[7].

Thus, despite aggressive therapy for esophageal cancer, the outcome is generally poor with a large number of patients developing rapid recurrence even after curative operation^[8,9]. If the prospect of prognosis and metastasis could be predicted preoperatively, it would be appropriate to select the most adequate treatment for individual cancer patient. Thus multi-disciplinary treatment including chemotherapy and irradiation would be reserved for patients predicted to have a poor prognosis while a less aggressive approach could be undertaken for those with better prognosis. Though most of the previous lectures showing DNA ploidy, AgNoRs and amplification of some oncogenes had been investigated to determine their prognostic value in esophageal cancer, the indication by PCNA, cyclinD1 protein expression combined with DNA ploidy have not been reported. It is expected to be of interest to evaluate them together as predictors of the malignant potential. In this report, we examined the cyclinD1, PCNA protein and DNA ploidy of esophageal carcinoma in 47 paired specimens from endoscopic biopsy and surgical resection tissue, with biologic features and prognostic value was also discussed.

MATERIALS AND METHODS

Patients

There are 47 patients (median age 62 years, range 33-74 years, 28 males and 19 females) with SCC of esophagus treated from November 1990 to December 1993 by preoperative radiotherapy followed by curative esophagectomy at the Fourth Hospital, Hebei Medical University, in northern China. All patients had been examined by gastrointestinal endoscopy, barium swallow, chest X-ray and liver ultrasound scans. Patients with stage IV disease shown by computed tomography were excluded. Pathological evaluation done according to the criteria established by the Chinese Society for Esophageal Disease (Henan, 1987), showed all patients were suffering from SCC. We had obtained two sets of specimens from each patient: endoscopic biopsy before preoperative radiotherapy and the surgical specimens of the same patient after esophagectomy of which the tumor markers in all 47 paired specimens were investigated. The maximum follow-up was 144 mo with a median of 56 mo.

Radiotherapy

All the 47 patients received preoperative radiotherapy, the external beam radiation was given by a 10-MV X-ray (Linear Accelerator, SIEMENS, PRIMUS) using the

conventional fractionated irradiation. The irradiated volume included the gross tumor with a safety margin of 5.0 cm both proximally and distally. Treatment was given through two opposing fields (anterior and posterior); 2.0 Gy was delivered daily for 5 d a wk to a total dose of 30-40 Gy in 15-20 fractions over 3-4 wk.

Esophagectomy

Transthoracic esophagectomy, the most common approach through a right or left thoracotomy incision depending on the preference of the surgeon and the location of the tumor was performed. Tumor located in the lower third of the esophagus usually was approached through a left thoracotomy. A left sixth interspace incision provides excellent exposure of the lower mediastinum. Gastrointestinal reconstruction was subsequently achieved by prepared esophageal substitute (usually the stomach), by passing of a prepared esophageal substitute, usually the stomach underneath the aortic arch and suture to the esophageal stump. Definite esophagectomy was undertaken 3 wk after radiotherapy.

Immunohistochemical stain

Biopsy and surgical specimens were fixed in 40 g/L formaldehyde and embedded in paraffin wax. Five-micron sections cut from each specimen, dewaxed in xylene, rehydrated through grading concentrations of ethanol were immersed in 3% hydrogen peroxide to block the endogenous peroxidase and washed in phosphate buffered saline. For cyclinD1 and PCNA immunohistochemical stain, tissue sections were heated in 10 mmol/L sodium citrate (pH 6.0) in a microwave oven for 10 min to expose the antigens, and, then, treated with normal goat serum (10%) before staining to reduce nonspecific antibody binding. Tissue sections were incubated at 4 °C overnight for cyclinD1. CyclinD1 and PCNA stain with the following antibodies: mouse monoclonal anti-cyclinD1 antibody (Novocastra Laboratories Ltd., UK) at 1:20 dilution and mouse monoclonal anti-PCNA antibody (PC-10, Dakopath, Glostrup, Denmark) at 1:100 dilution. The sections were then washed and incubated with biotinylated goat anti-rabbit IgG (Vector Laboratories, Burlingame, CA) at room temperature for 30 min. After washing, the sections were incubated with avidin-biotin-peroxidase complex at room temperature for 30 min with the vectastain Elite ABC kit (Vector Laboratories Burlingame, CA). Color developed with 3,3'-diaminobenzidine as the substrate. Sections were counter-stained with Harris acid hematoxylin to demonstrate the specificity of the immunostain and the primary antibodies were replaced with similar protein concentrations of normal rabbit IgG.

The PCNA, cyclinD1 protein expression of the endoscopic biopsy and surgical specimens were compared by two histopathologists by the double-blind arrangement in assessing the tumor response to radiotherapy. For cyclinD1 and PCNA, 1 000 tumor cells in five high-power fields were counted respectively. PCNA index was the percentage of nuclei stained positive. PCNA index greater than 25% was taken as PCNA positive. PCNA index lower than 25% was taken as PCNA-negative. For cyclinD1, positive cell nucleus not found was taken as negative. When the percentage of positive cell nucleus was greater than 30%, it was taken

as strongly positive. Between the two levels, it was positive. Therefore three grades were ascertained for cyclinD1 expression^[5,9,10].

Analysis of DNA content

Cellular DNA analysis was performed on paraffin sections cut 100 μm thick. The sections were stained with Feulgen stain and examined using a microspectrophotometer by two-wavelength method. Data processing was carried out with a personal computer (HP-85, Hewlett-Packard, Palo Alto, CA, USA). In each section, the mean DNA value of 20 stromal lymphocytes was used as a control of the normal diploid complement (2C). The relative DNA content as compared with the 2C value was determined in 100 tumor cells in each lesion as previously described^[11,12]. The DNA distribution patterns were then classified into four types, according to the degree of the peak and dispersion on the DNA histogram, as follows: Type I, a prominent peak in the 2C region with a dispersion to the 4C region, Type II, a relative high peak in the 2C-3C regions with a dispersion limited to the 6C region, Type III, a low peak beyond the 3C region with less than 20% of the cells beyond the 6C region and Type IV, multiple peaks with a broad dispersion and more than 20% of cells beyond the 6C region.

Statistical analysis

PCNA, cyclinD1 protein expression index and DNA distribution pattern were analyzed and regarded in the clinicopathological features as determined by the χ^2 test. Difference between the cumulative survival rates of patient groups were calculated by log-rank test for comparison of Kaplan-Meier survival curves. The significance of various parameters on survival were analyzed by multivariate Cox regression model. A *P* value of 0.05 or less was considered statistically significant (statistical software SPSS 10.0 for Windows).

RESULTS

Response to preoperative radiotherapy and the overall survival of patients

All the patients had received preoperative radiotherapy followed by definite surgical resection. The complete response rate as shown by pathology was 29.8% (14/47) for the entire group treated by preoperative radiotherapy and 5-year survival rate was 71.4% (10/14) for 14 patients with complete response by pathology. The overall survival rates of all these patients in the 3, 5 and 10-years were 54.3%, 46.2% and 38.8%, respectively.

Expression of PCNA, cyclinD1 immunoreactivity and DNA content in the tumor cells by histopathology

PCNA stain was almost entirely confined to the cell nuclei and showed diffuse and granular pattern or a mixture of both. While cyclinD1 stain was present in the cytoplasm around the cell nuclei in most parts, and a few parts in the tumor cell nuclei. At the same time, PCNA stain was observed in the basal layer of stratified squamous epithelium in normal tissue. In this study, all cyclinD1 present both in the stained nuclei and the cytoplasm around them were considered as protein expression positive carcinoma cells. We took both

Types I and II DNA content as the low ploidy pattern and Types III and IV as the high ploidy pattern.

Analysis of cyclinD1, PCNA expression and DNA distribution pattern with regard to clinicopathological features and prognosis

Kaplan-Meier method was used to analyze the single factors, including age, sex, irradiation dose, location of disease, length, and radiation response observed by pathology, T stage, N stage, PCNA index, cyclinD1 protein expression and DNA content pattern, e.g. Types I and II or Types III and IV influenced the prognosis of esophageal carcinoma obviously. The *P* value as checked by the log-rank test ≥ 0.05 was taken as significant. Only the four preoperative radiotherapy factors: radiation changes observed by pathology, T stage, N stage and cyclinD1 protein expression before radiation in the endoscopic biopsies; those observed in the surgery resected specimens showing PCNA index, cyclinD1 expression level, DNA content pattern, revealed significant difference ($P < 0.05$, Table 1), whereas age, sex, total tumor dose, location and length of disease possessed no value in prognosis.

Multiple varieties combined by Cox hazard risk model analysis

T stage, N stage, pathological changes after radiotherapy, pre-radiotherapy cyclinD1 protein expression and post-radiotherapy PCNA index, cyclinD1 protein expression and DNA content pattern with Cox hazard risk regression model were analyzed. The most significant factors were the post-radiotherapy PCNA index and DNA content pattern (specimens from surgical specimens). Furthermore, each factor by single parameter analysis gave the most marked prognostic difference, while multivariation considered by Cox model, clearly affected the prognosis of esophageal cancer patients (Table 2).

Analysis of esophageal squamous cell carcinoma by prognosis index model

According to the formulation of prognosis index (PI) model from statistic software, it was defined as 0 which had the least influence on prognosis. Number 2 had the greatest effect on prognosis. When the number was 1, the prognosis was between 0 and 2. For example, T stage divided by T₁, T₂, T₃ would show difference on patients survival and we gave them the number 0, 1, 2 respectively as shown in Table 2. The group's weight (0, 1, 2 or 0, 1) times the coefficient of Cox regression model (β value). Then by adding each group's data results would give each patient's PI value, e.g., different factors (T stage, N stage, PCNA, cyclinD1 expression, etc.) at the same weight number. For example, all number 0 patients, or number 1 patients, or number 2 patients would give the PI (prognosis index) value for each patient (Table 3).

Different PI values give different prognosis

According to the distribution of PI values in all patients, the four subgroups were divided according to different PI values. PI values lower than 2.0, between 2.0 and 5.0, between 5.0 and 7.0 or higher than 7.0 may go stepwise further with the median survival terms and 3-, 5-, 10-year survival rates of the four subgroup patients would reveal significant

Table 1 Relation between accumulated survival rates and clinicopathological and tumor cell protein expression pre- or post-radiotherapy

Factors	Patient number	Median (mo)	Mean (mo)	3 yr (%)	5 yr (%)	10 yr (%)	Log-rank	P
Sex								
Male	28	48	76	60.7	49.7	38.2		
Female	19	27	62	44.9	45.1	38.1	0.6705	0.2513
Age (yr)								
≤50	26	31	66.6	50.4	49.7	36.8		
>50	21	50	74.2	57.7	45.2	39.6	0.2317	0.4084
Total dose								
≤35 Gy	23	53	78.4	56.5	56.5	46.3		
>35 Gy	24	35.5	63.5	52.6	39.6	30.3	0.6470	0.2588
Site of lesion								
Upper-thoracic	10	69.5	81.5	70.0	70.0	46.7		
Middle-thoracic	37	31.0	67.9	50.2	41.7	35.4	0.8864	0.1877
Tumor length								
≤7.0 cm	39	48	77.1	58.1	50.1	41.4		
>7.0 cm	8	22.5	40.0	37.5	37.5	18.8	0.9653	0.1672
Pathological change after radiation								
Grade III	24	93	95.0	70.8	62.3	57.6		
Grade II	15	26	49.3	40.0	40.0	16.0		
Grade I	8	13	38.6	31.1	15.6	15.6	5.1450	0.0764
T stage								
T ₁	11	135	112.9	90.9	81.8	61.9		
T ₂	19	48	77.5	57.9	46.9	41.0		
T ₃	17	19	36.1	26.0	26.0	17.3	8.9800	0.0113
N stage								
N ₀	39	60	81.7	61.5	53.7	42.6		
N ₁	8	12	17.6	16.7	16.7	0	2.4170	0.0078
Pre-radiotherapy PCNA								
Low expression	21	35.5	67.4	50.0	42.0	32.9		
High expression	26	48	75.1	60.4	55.2	44.2	0.8880	0.1873
Pre-radiotherapy cyclinD1								
Negative	21	135	106.3	80.9	71.4	61.6		
Positive	20	19	46.2	32.5	32.5	24.4		
Strong positive	6	24	28.7	33.3	16.7	0	10.3990	0.0055
Pre-radiotherapy DNA content								
I+II Type	10	98.5	88.9	60.0	60.0	50.0		
III+IV Type	37	40.0	65.9	53.0	44.3	34.3	0.5158	0.3032
Post-radiotherapy PCNA								
Low expression	17	135	107.4	81.5	73.9	61.8		
High expression	30	18	21.4	16.1	9.8	0	4.1124	0.00002
Post-radiotherapy cyclinD1								
Negative	17	77	94.1	76.5	70.4	49.8		
Positive	22	30	64.4	53.1	43.1	37.8		
Strongly positive	8	21	39.0	12.5	12.5	12.5	7.9215	0.0191
Pre-radiotherapy DNA content								
I+II Type	23	135	110.7	87.0	78.3	60.2		
III+IV III+IV Type	24	20	32.5	22.0	16.6	16.6	3.7074	0.0001

Prognostic parameters in 47 patients with SCC of esophagus.

Table 2 Independent predictors of survival in 47 esophageal SCC patients according to multivariate Cox regression analysis

Factors	Group	Group value	β value	SD	P	Risk
Pathological radiation change's	III/II/I Grades	0/1/2	0.6405	0.2451	0.0090	0.1582
Surgical specimens T stage	T ₁ /T ₂ /T ₃	0/1/2	0.7678	0.2737	0.0050	0.1744
Surgical specimens N stage	N ₀ /N ₁	0/1	1.2957	0.4845	0.0075	0.1634
Pre-radiotherapy cyclinD	N/P/SP	0/1/2	0.8434	0.2564	0.0010	0.2139
Post-radiotherapy cyclinD1	N/P/SP	0/1/2	0.6538	0.2643	0.0134	0.1462
Post-radiotherapy PCNA	Low/high expression	0/1	2.0965	0.4720	0.0000	0.3032
Post-radiotherapy DNA	I+II Type/III+IV Type	0/1	1.5593	0.4287	0.0003	0.2413

Table 3 Formula for calculation of prognosis index with different indicator factors

Factors	Group	Group value (1)	β (2)	prognosis index (PI)1
Pathological radiation change's	III/II/I Grades	0/1/2	0.6405	(1)x(2)
Surgical specimens T stage	T ₁ /T ₂ /T ₃	0/1/2	0.7678	(1)x(2)
Surgical specimens N stage	N ₀ /N ₁	0/1	1.2957	(1)x(2)
Pre-radiotherapy cyclinD	N/P/SP	0/1/2	0.8434	(1)x(2)
Post-radiotherapy cyclinD1	N/P/SP	0/1/2	0.6538	(1)x(2)
Post-radiotherapy PCNA	low/high expression	0/1	2.0965	(1)x(2)
Post-radiotherapy DNA	I+II Type/III+IV Type	0/1	1.5593	(1)x(2)

Each prognosis indexes were added together.

differences (Table 4, Figure 1). It was multiple variety combined analysis, which showed a clear difference in survival among the four subgroups.

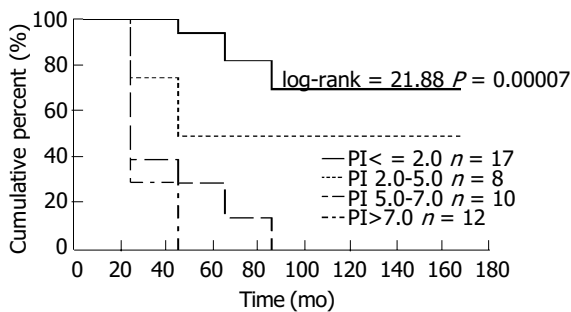


Figure 1 The survival curves with different PI value.

DISCUSSION

Cancer of the esophagus is the most common cancer in northern China, for which current consensus of treatment varies from surgery, radiotherapy, chemotherapy, and endoscopic laser surgery or their combination. The outcome, however, remains dismal because most patients are seen with advanced disease on diagnosis^[13-15]. Thus, what the majority of patients need is a multimodality program. Yet how to know which patients really need which modality is still an open focus. Nevertheless, traditional prognostic factors: T stage, N stage are basically the most important. Yet up to now, their application has merely been used by the surgically treated patients. For conservative treatment, besides the TNM classification system, additional variables such as biological staging for the intrinsic malignant potential of the tumor, are to be useful to determine the treatment and long-term survival^[16].

Recently, with rapid advance in biological and genetic studies, more and more tumor markers are being correlated

with tumor characteristics^[8]. The ability to predict, on the basis of immunocytochemical assessment of pretreatment biopsy, which patients are likely to respond to chemoradiotherapy would be a major advance in the management of cancer patients. Thus, it is possible to provide the most adequate protocol for different patients by combining traditional factors and the markers of tumor cells^[16].

Several studies^[8,9,15] have shown that high PCNA expression in esophageal tumor is associated with a worse prognosis in surgical patients and greater likelihood of recurrence. However, such a report on PCNA, and cyclinD1 protein expression examined simultaneously in biopsy and resected specimens of esophageal carcinoma has never been seen. Nor possible correlation between PCNA, cyclinD1 protein expression and the traditional prognostic factors (T stage, N stage) to chemoradiotherapy has never been investigated. Immunohistochemical detection of PCNA being simple and useful for the study of cell kinetics, allows the retrospective evaluation of the proliferating state of the tumor as it can be used in conventionally fixed materials. Many authors^[17,18] showed the higher PCNA index patients usually gave the worse prognosis with local recurrence. In the past years, it has been proved that the combination of PCNA index with the AgNOR count appears to be an effective means of identifying patients with poor prognosis. For patients with a PCNA index of ≥ 44 and AgNOR count of ≥ 6, multidisciplinary treatment should be recommended in an attempt to prolong survival. However, in this study, PCNA index as checked by endoscopic biopsies have not shown such influence on survival^[9].

Furthermore, we have found PCNA protein expression to be significantly high in surgically resected specimens with PCNA index 63.8% (30/47) compared to the endoscopic biopsy before radiation 55.3% (26/47). At the same time, patients with high PCNA index in the surgically resected specimens had the worse prognosis. PCNA protein expression examined after radiotherapy made a significant difference to esophageal cancer prognosis. The repopulation of tumor cells after radiation may exist which results in local recurrence of esophageal carcinoma after radiotherapy.

Table 4 Median survivals and survival rates with subgroups divided by prognosis index (%)

Prognosis indexes	Number patients	Median month	3 yr	5 yr	10 yr
<2.0	17	146	100	88.2	69.7
2.0-5.0	8	93.5	50	50	50
5.0-7.0	10	20	30	30	0
>7.0	12	13	9.6	0	0

The most important advantage of PCNA, cyclinD1 immunohistochemical assay is that the analysis changes are restricted to the tumor cells. In contrast, flow cytometry assay, all cells in the tissue block are measured and in DNA diploid cases, this means that SPF reflects the sum of cell proliferation that estimates the malignant and benign (stromal and inflammatory cells) components^[9].

Most studies^[6,19] reported patients with cyclinD1 amplification and protein expressions had a poor outcome and a higher incidence of distant metastasis than those in amplification-negative or protein expression-negative groups. The surgical survival rates and disease-free survival in the high cyclinD1 expression group were significantly shorter than in the cyclinD1 low or non-expression group. CyclinD1 amplification and protein expression in patients with SCC of the esophagus would mean a grave biological malignancy. Naiton *et al.*^[20], reported 55 esophageal cancer patients with a ratio of cyclinD1 protein-positive expression of 38% gave a 5-year survival rate of 7%, as compared with the 5-year survival rate of 59% in patients who showed cyclinD1 protein negative expression ($P < 0.01$). In 1998, Ishikawa^[21] studied cyclinD1 protein expression in esophageal SCC and observed similar results. Our checked results showing higher cyclinD1 protein expression both in endoscopic biopsy and surgical resected specimens also gave bad prognostic results (Table 1).

In our previous study, the clinical characteristics of patients with SCC of the esophagus, such as outcome and distant organ metastases, were found to be closely correlated with cyclinD1 amplification and protein expression in the tumor tissue. It was observed that parameters were independent from clinicopathological factors for the outcome and metastasis. It was the second highest partial regression coefficient after the pN factor in the life table with Cox proportional hazard model, and the probability rate was significant^[19,21]. In this study, the same results were obtained. From Table 2, it is apparent that both the cyclinD1 protein expression in biopsy and surgical specimens had a significant effect on the prognosis of SCC of the esophagus. Specially, cyclinD1 protein-positive expression in endoscopic biopsy was the third highest partial regression coefficient after the PCNA index and DNA content in the resected specimens in multivariate analysis using the Cox proportional hazard model. We speculate that the cyclinD1 protein prognostic value maybe relatively high as the most useful factor for predicting the outcome in SCC of the esophagus in the previous study, e.g., pN factor and pT. According to the results of both univariate and multivariate analyses, the fact that patients with cyclinD1 protein-positive had a poor outcome in every group implies this agent is a useful prognostic indicator in esophageal carcinoma. Hence, it may very well supplement the TNM classification for predicting clinical characteristics and outcome, especially for patients who are destined to undergo non-operative treatment. For these patients, TNM classification could hardly be of any assistance to offer an endpoint and select more appropriate protocol for patients with SCC of the esophagus. By checking cyclinD1 protein expression level, the ultimate combined TNM classification could thus be perfected.

The essence of cell division really is the DNA replication and changes of DNA distribution pattern which predict

tumor cell proliferation kinetics. Here cytophotometric technique is to analyze the DNA content pattern both in endoscopic biopsy and resected specimens. The most important advantage of DNA content checked by cytophotometric method is that the analysis is restricted to the tumor cells, as compared to flow cytometry, by which all cells in the tumor tissue are measured. It reflects the sum of cell proliferation which estimates both malignant and benign (stromal cell and inflammatory cell) components^[9]. In clinical esophageal carcinoma, high-ploidy tumors grow more rapidly than low-ploidy ones and the duration from curative esophagectomy to recurrence decreases in proportion to the degree of DNA aneuploidy, a view believed by many authors.

During early years, some authors^[9,11,22] reported the relationship between DNA content of a variety of human cancer cells and their malignant potential as measured by cytophotometric analysis, most of who reported that such measurement are useful in elucidating the pattern of tumor progression or the prognosis with most of the results being negative between DNA content and long-term survival. For example, Miun *et al.*^[22], reported 78 esophageal cancer patients who gave 5-year survival rate of 14% and 57% in high DNA content and low DNA content groups with statistical significance in the difference ($P = 0.03$). Matsuura^[11] found that not one patient survived over 5 years in DNA triploids or tetraploidy, but the 5-year survival rate was 70% in DNA diploidy patients. Our study shows no influence on survival or prognosis by biopsy DNA content measurement. The measured results may have been inaccurate due to the very small size of biopsy specimens. From Tables 1 and 2, the surgically resected specimens gave DNA content measurement showing significant correlation between the results and the prognosis of SCC of esophagus as assessed by univariate and multivariate analyses. This result conforms well to most of the studies reported so far^[9,11].

Through combination of the traditional prognostic factors and tumor cell markers, the radiation pathological changes, T stage, N stage, cyclinD1, PCNA protein expression and DNA content as analyzed by Cox proportional hazard model, it is found that patients with grade III pathological changes, T₁ stage, N₀ stage, cyclinD1 protein-negative, lower PCNA index and DNA content pattern Types I and II, give higher long-term survival than the control groups.

With the total patients divided into four subgroups according to the formulation of prognosis index model, prognosis is observed to be worse with higher prognosis index, giving significant difference in spite of the few patients allotted. This result clearly demonstrates the evaluation of SCC of esophagus by prognosis index model with multivariate factors is dependable and accurate.

ACKNOWLEDGMENTS

The authors wish to thank Ms Laura Kresty for her expert technical assistance and N Sugimoto (Sanwa Kagakau Co., Ltd, Nagoya, Japan) for his support in the statistical analysis.

REFERENCES

- 1 **Castellsague X**, Munoz N, De Stefani E, Victora CG, Castelletto R, Rolon PA, Quintana MJ. Independent and

- joint effects of tobacco smoking and alcohol drinking on the risk of esophageal cancer in men and women. *Int J Cancer* 1999; **82**: 657-664
- 2 **Zhao WX**, Shi TX, Gao XP, Zhang HX, Li SL. Association of p53, PCNA expression and trace element content in esophageal mucosa. *Aizheng* 2002; **21**: 757-760
 - 3 **Dong WL**, Bin Yue W, Zhou Y, Wei Feng C, Liu B, Zhou Q, Ying Jia Y, Zheng S, Gao SS, Ji Xie X, Min Fan Z, Min Niou H, Hao Zhuang Z, Yang CS, Min Bai Y, Jun Qi Y. Endoscopic screening and determination of p53 and proliferating cell nuclear antigen in esophageal multistage carcinogenesis: a comparative study between high- and low-risk populations in Henan, northern China. *Dis Esophagus* 2002; **15**: 80-84
 - 4 **Gelb AB**, Kamel OW, Le-Brun DP, Wamke RA. Estimation of tumor growth fractions in archival formalin-fixed, paraffin-embedded tissues using two anti-PCNA/Cyclin monoclonal antibodies. Factors affecting reactivity. *Am J Pathol* 1992; **141**: 1453-1458
 - 5 **Siitonen SM**, Kallioniemi OP, Isola JJ. Proliferating cell nuclear antigen immunohistochemistry using monoclonal antibody 19A2 and a new antigen retrieval technique has prognostic impact in archival paraffin-embedded node-negative breast cancer. *Amer J Pathol* 1993; **142**: 1081-1089
 - 6 **Zhang JH**, Li Y, Wang R, Wen D, Sarbia M, Kuang G, Wu M, Wei L, He M, Zhang L, Wang S. Association of cyclinD1 (G870A) polymorphism with susceptibility to esophageal and gastric cardiac carcinoma in a northern Chinese population. *Int J Cancer* 2003; **105**: 281-284
 - 7 **Morita M**, Kuwano H, Tsutsui S, Ohno S, Matsuda H, Sugimachi K. Cytophotometric DNA content and argyrophilic nucleolar organizer regions of oesophageal carcinoma. *Br J Cancer* 1993; **67**: 480-485
 - 8 **Ueno H**, Hirai T, Nishimoto N, Hihara J, Inoue H, Yoshida K, Yamashita Y, Toge T, Tsubota N. Prediction of lymph node metastasis by p53, p21(Waf1), and PCNA expression in esophageal cancer patients. *J Exp Clin Cancer Res* 2003; **22**: 239-245
 - 9 **Kuwano H**, Sumiyoshi K, Nozoe T, Yasuda M, Watanabe M, Sugimachi K. The prognostic significance of the cytophotometric DNA content and its relationship with the argyrophilic nucleolar organizer regions (AgNOR) and proliferating cell nuclear antigen (PCNA) in oesophageal cancer. *Eur J Surg Oncol* 1995; **21**: 368-373
 - 10 **Hagiwara N**, Tajiri T, Tajiri T, Miyashita M, Sasajima K, Makino H, Matsutani T, Tsuchiya Y, Takubo K, Yamashita K. Biological behavior of mucoepidermoid carcinoma of the esophagus. *J Nippon Med Sch* 2003; **70**: 401-407
 - 11 **Ma J**, Nicholas Terry HA, Lin SX, Patel N, Mai HG, Hong MH, Lu TX, Cui NJ, Min HQ. Prognostic significance of DNA ploidy and proliferative indices in patients with nasopharyngeal carcinoma. *Aizheng* 2002; **22**: 644-650
 - 12 **Korenaga D**, Okamura T, Saito A, Baba H, Sugimachi K. DNA ploidy is closely linked to tumor invasion, lymph node metastasis, and prognosis in clinical gastric cancer. *Cancer* 1988; **62**: 309-313
 - 13 **Michel P**, Magois K, Robert V, Chiron A, Lepessot F, Bodenat C, Roque I, Seng SK, Frebourg T, Paillet B. Prognostic value of TP53 transcriptional activity on p21 and bax in patients with esophageal squamous cell carcinomas treated by definitive chemoradiotherapy. *Int J Radiat Oncol Biol Phys* 2002; **54**: 379-385
 - 14 **Wang LS**, Chow KC, Chi KH, Liu CC, Li WY, Chiu JH, Huang MH. Prognosis of esophageal squamous cell carcinoma: analysis of clinicopathological and biological factors. *Am J Gastroenterol* 1999; **94**: 1933-1940
 - 15 **Yasunaga M**, Tabira Y, Nakano K, Iida S, Ichimaru N, Nagamoto N, Sakaguchi T. Accelerated growth signals and low tumor-infiltrating lymphocyte levels predict poor outcome in T4 esophageal squamous cell carcinoma. *Ann Thorac Surg* 2000; **70**: 1634-1640
 - 16 **Horii N**, Nishimura Y, Okuno Y, Kanamori S, Hiraoka M, Shimada Y, Imamura M. Impact of neoadjuvant chemotherapy on Ki-67 and PCNA labeling indices for esophageal squamous cell carcinomas. *Int J Radiat Oncol Biol Phys* 2001; **49**: 527-532
 - 17 **Dabrowski A**, Szumilo J, Brajerski G, Wallner G. Proliferating nuclear antigen (PCNA) as a prognostic factor of squamous cell carcinoma of the oesophagus. *Ann Univ Mariae Curie Sklodowska* 2001; **56**: 59-67
 - 18 **Shiozaki H**, Doki Y, Kawanishi K, Shamma A, Yano M, Inoue M, Monden M. Clinical application of malignancy potential grading as a prognostic factor of human esophageal cancers. *Surgery* 2000; **127**: 552-561
 - 19 **Shamma A**, Doki Y, Shiozaki H, Tsujinaka T, Yamamoto M, Inoue M, Yano M, Monden M. Cyclin D1 overexpression in esophageal dysplasia: a possible biomarker for carcinogenesis of esophageal squamous cell carcinoma. *Int J Oncol* 2000; **16**: 261-266
 - 20 **Naitoh H**, Shibata J, Kawaguchi A, Kodama M, Hattori T. Overexpression and localization of cyclin D1 mRNA and antigen in esophageal cancer. *Am J Pathol* 1995; **146**: 1161-1169
 - 21 **Ishikawa T**, Furihata M, Ohtsuki Y, Murakami H, Inoue A, Ogoshi S. Cyclin D1 overexpression related to retinoblastoma protein expression as a prognostic marker in human oesophageal squamous cell carcinoma. *Br J Cancer* 1998; **77**: 92-97
 - 22 **Minu AR**, Endo M, Sunagawa M. Role of DNA ploidy patterns in esophageal squamous cell carcinoma. An ultraviolet microspectrophotometric study. *Cancer* 1994; **74**: 578-585

Anti-cancer effect of iNOS inhibitor and its correlation with angiogenesis in gastric cancer

Guang-Yi Wang, Bai Ji, Xu Wang, Jian-Hua Gu

Guang-Yi Wang, Bai Ji, Xu Wang, Jian-Hua Gu, Department of General Surgery, the First Hospital, Jilin University, Changchun 130021, Jilin Province, China

Supported by the Natural Science Foundation of Jilin Province, No. 20010536

Correspondence to: Dr. Guang-Yi Wang, Department of General Surgery, the First Hospital, Jilin University, Changchun 130021, Jilin Province, China. wgynd@sina.com

Telephone: +86-431-5613331

Received: 2004-12-07 Accepted: 2005-01-05

Abstract

AIM: To observe the anti-cancer effect of iNOS selective inhibitor (aminoguanidine, AG) and investigate the relationship between iNOS inhibitor and angiogenesis, infiltration or metastasis in MFC gastric cancer xenografts.

METHODS: Fifty athymic mice xenograft models were established by inoculating gastric cancer cell MFC subcutaneously. Twenty-four hours later, 0.9% sodium chloride solution, mitomycin, low dosage AG, high dosage AG, mitomycin and AG were administered by intraperitoneal injection respectively. Thus these mice were divided into five groups of 10 each randomly: control group, MMC group, AG_L group, AG_H group, MMC+AG_H group. Two weeks later the mice were killed, and the tumor weight, inhibitory rate were evaluated. Greiss assay was used to detect the nitric oxide levels in plasma. HE and immunohistochemistry staining were used to examine microvessel density (MVD) and the expression of iNOS, VEGF, and PCNA. Apoptosis was detected by using TUNEL assay.

RESULTS: The inhibitory rates in MMC+AG_H group and AG_H group were 52.9% and 47.1% respectively, which is significant statistically compared with that of control group (0). In treatment groups, the cell proliferation index (PI) was lower and apoptosis index was higher than those of control group. Microvessel density, iNOS, and VEGF in MMC+AG_H group were 8.8±2.6, 2.4±1.1, and 2.1±1.4 respectively, which is significant statistically compared with those of control group (68.3±10.6, 11.3±1.3, and 10.3±1.6). The NO level in plasma of MMC+AG_H and AG_H group were 12.7±2.1 and 12.9±2.0 μmol/L. Compared with that of control group (46.6±2.3 μmol/L), the difference is statistically significant.

CONCLUSION: AG has anticancer effect on gastric cancer, and it has positive synergistic effect with chemotherapeutic drugs. It may play important inhibitory roles in angiogenesis of gastric cancer. The anticancer effect of iNOS inhibitors

may include inducing cell apoptosis, suppressing cell proliferation and reducing angiogenesis.

© 2005 The WJG Press and Elsevier Inc. All rights reserved.

Key words: Stomach neoplasms; Inducible nitric oxide synthase; Angiogenesis inhibitors; Vascular endothelial growth factor; Microvessel density

Wang GY, Ji B, Wang X, Gu JH. Anti-cancer effect of iNOS inhibitor and its correlation with angiogenesis in gastric cancer. *World J Gastroenterol* 2005; 11(25): 3830-3833
<http://www.wjgnet.com/1007-9327/11/3830.asp>

INTRODUCTION

The incidence of gastric cancer is high in China, and more than 170 000 people die of it each year^[1]. It is significant if certain drugs are found to lower its incidence, even prevent it.

To date, we know that carcinogenesis has intimate correlation with angiogenesis^[2-4]. So to reduce angiogenesis probably may inhibit the growth and development of tumors^[5]. It is well known that vascular endothelial growth factor (VEGF) is an important angiogenesis factor^[6,7]. We have proved that inducible nitric oxide synthase (iNOS) can induce the expression of VEGF in gastric cancer, and microvessel density (MVD) can increase with the enhancement of iNOS and VEGF^[8-10]. So VEGF and iNOS both can induce angiogenesis. So if the activity of iNOS is inhibited, tumor angiogenesis may be reduced. As a result the growth and development of tumors will be inhibited. Although the roles that iNOS inhibitors play in various tumors and their mechanisms are being widely studied recently, few people have gone deep into *in vivo* experiment. Based on *in vitro* cytologic experiments, this study went further into *in vivo* experiment to confirm the anticancer effect of iNOS inhibitor (aminoguanidine, AG).

MATERIALS AND METHODS

Animals and cell line

Fifty Kunming mice (25 females, 25 males) weighing 20-25 g were purchased from Experimental Animal Center of Jilin University. Mice were maintained under specific pathogen-free conditions and fed with sterilized food and autoclaved water. Human gastric cancer cell line MFC was purchased from Shanghai Tumor Cell Research Institute.

Agents

Greiss reagent and AG were purchased from Sigma (St.

Louis, USA). Immunohistochemical S-P kit and polyclonal antibodies to iNOS, VEGF, PCNA, and FVIIIIRag were all from Fuzhou Maxim Biotechnical Company (Fuzhou, China).

Animal experiment procedure

Each mouse was inoculated with a subcutaneous injection of MFC cells (2×10^6 in 0.2 mL PBS) into the left hind legs. Then these mice were divided into 5 groups of 10 each according to different agents which were administered to mice by intraperitoneal injection for 14 d. These agents included 0.9% sodium chloride solution (control group), mitomycin (MMC group, twice a week 0.7 mg/kg), low dosage of AG (AG_L group, 50 mg/(kg · d)), high dosage of AG (AG_H group, 150 mg/(kg · d)) and MMC+AG_H group (MMC twice a week 0.7 mg/kg, AG 150 mg/(kg · d)). On the 15th d the mice were killed. The blood was taken from abdominal aorta, then centrifuged for plasma to detect NO level by Greiss assay. All tumors were resected from the body and weighed. The inhibitory rate was deduced according to the formula: inhibitory rate (%) = (1-tumor weight of treatment group/tumor weight of control group) × 100%. Then the tumors were fixed in 40 g/L phosphate-buffered formaldehyde.

HE and immunohistochemical staining

Streptavidin-peroxidase (SP) method was used to detect MVD and the expression of iNOS, VEGF and PCNA. The formalin-fixed tissues were embedded in paraffin, and sectioned at a thickness of 4 μm. The sections were deparaffinized and hydrated gradually and examined by histology of HE staining, immunohistochemistry, and TUNEL technique respectively. Sections were heated in a microwave oven for 15 min to retrieve antigens. Endogenous peroxidase was blocked with 3 mL/L hydrogen peroxide methanol for 10 min at room temperature. After washing with phosphate-buffered saline (0.01 g/L, pH 7.4) for 3 min × 5 min, the tumor sections were incubated with normal non-immune serum from bull for 15 min at room temperature to eliminate non-specific staining. The sections were then incubated with the primary antibody against iNOS, VEGF, PCNA, and FVIIIIRag (dilution 1/100) for 60 min at room temperature, washed with PBS for 3 min × 5 min, and incubated with the secondary antibody for 15 min followed by avidin-biotin-peroxidase for 15 min at room temperature. Finally, the slides were washed for 3-15 min with PBS, visualized with DAB reagent and counterstained with hematoxylin. Negative and positive controls were used simultaneously to ensure specificity and reliability of the staining process. The negative controls were performed by substituting the primary antibody with PBS, and a positive section supplied by the manufacturer of the staining kit was taken as positive control. Sections were observed under microscope after being mounted. High vessel density was found in 100 × sights. Microvessels in 10 hot regions were counted in 400 × sights, and the average of microvessels with FVIIIIRag staining in 10 hot regions was calculated as MVD. Positive staining with iNOS, VEGF and PCNA were defined by brown staining of cytoplasm. The staining degree was calculated quantitatively with CIMA-400 Colorful Image Assay System which can calculate the percentages of positive staining region of the whole region.

The percentage of positive cells with PCNA staining in five 400 × sights was counted as proliferation index (PI).

Apoptosis detection by TUNEL method

The reagent kit for apoptosis detection, TdT-FragEL DNA fragmentation detection kit was bought from ONCOGENE. Test procedures consisting of the following sections were provided in the brochure of the kit. The specimens were deparaffinized and hydrated gradually, and rinsed with 1 × TBS, then incubated with proteinase K (20 μg/mL in 10 mmol/L Tris-HCl) for 20 min. After immersed in 30 mL/L H₂O₂ at room temperature for 5 min and in TdT labeling reaction mixture at 37 °C for 1.5 h, specimens were covered with 1 × conjugate for 30 min, visualized by DAB and counter-stained by hematoxylin afterwards. TBS took the place of primary antibodies as a negative control. After being mounted, sections were observed under microscope. The results of staining were analyzed and evaluated with American Image-Pro Plus software. The percentage of positive cells with TUNEL staining in five 400 × sights served as apoptosis index (AI).

Statistical analysis

All data were presented as mean ± SD. The results were compared by one-way analysis of variance (ANOVA). All statistical calculations were performed with the SPSS11.0 software package. A *P* value less than 0.05 was regarded as statistically significant.

RESULTS

Effect of AG on tumor growth

The tumor volume of MMC group on the 7th d was (383.4 ± 179.3) mm³, and on the 10th d those of AG_H and MMC+AG_H groups were (382.8 ± 132.8) mm³ and (50.0 ± 16.6) mm³ respectively. The tumor cell proliferation was almost completely suppressed. On the 14th d the tumor weight of control group was (1.7 ± 0.5) g, and those of MMC, AG_H and MMC+AG_H groups were (1.0 ± 0.2), (0.9 ± 0.3) and (0.8 ± 0.2) g, respectively. Compared with control group, the difference was significant statistically (*P* < 0.01). The NO level of plasma in AG_L, AG_H and MMC+AG_H groups were lower than that of the control group, and there was dose-effect relationship. The difference was significant statistically (*P* < 0.05, Table 1).

Table 1 Inhibitory effects of AG on transplanted stomach cancer in mice (*n* = 10, mean ± SD)

Group	Concentration of NO in plasma (μmol/L)	Weight of tumor (g)	Inhibition rate (%)
Control	46.6 ± 2.3	1.7 ± 0.5	-
MMC	42.1 ± 2.3	1.0 ± 0.2 ^b	41.2
AG _L	17.3 ± 2.0 ^b	1.1 ± 0.3 ^a	35.3
AG _H	12.9 ± 2.0 ^b	0.9 ± 0.3 ^b	47.1
MMC+AG _H	12.7 ± 2.1 ^b	0.8 ± 0.2 ^b	52.9

^a*P* < 0.05, ^b*P* < 0.01 vs control group.

Expression of iNOS and VEGF and their correlation with MVD

MVD has positive correlation with iNOS and VEGF

respectively. The coefficient of product-moment correlation $r_{\text{VEGF}} = 0.80$, $r_{\text{iNOS}} = 0.85$, $P < 0.05$. The linear regression equation is $Y_{\text{VEGF}} = 2.3565 + 0.1087X$, $n = 46$, $Y_{\text{iNOS}} = 1.8485 \pm 0.1227X$, $n = 46$. Student's t test, $P < 0.05$ (Table 2).

Table 2 Effects of AG on the microvessel density, the expression of iNOS and VEGF in tumor ($n = 10$, mean \pm SD)

Group	iNOS	VEGF	MVD
Control	11.3 \pm 1.3	10.3 \pm 1.6	68.3 \pm 10.6
MMC	9.3 \pm 1.8 ^a	8.9 \pm 2.1	56.9 \pm 10.3
AG _L	7.1 \pm 1.7 ^a	7.6 \pm 1.2 ^a	44.4 \pm 16.5 ^a
AG _H	3.8 \pm 0.9 ^b	4.8 \pm 1.6 ^b	21.2 \pm 12.4 ^b
MMC+AG _H	2.4 \pm 1.1 ^b	2.1 \pm 1.4 ^b	8.8 \pm 2.6 ^b

^a $P < 0.05$, ^b $P < 0.01$ vs control group.

HE staining

In AG and MMC+AG_H groups many necrotic cells were seen and many inflammatory cells were invasive. The tumor tissues were separated by necrosis regions. In MMC group diffusely necrotic tissues could be seen. However, in control group there were a few nuclear mitotic phases in tumor cells and in tumor tissues few muscle fibers could be seen (Figures 1A and B).

Immunohistochemical staining

MVD and the expression of iNOS and VEGF in AG groups were apparently lower than those in the control ($P < 0.01$). The difference was significant statistically. This revealed that AG could suppress angiogenesis of MFC xenografts. (Table 2, Figures 1C-H).

Cell proliferation and apoptosis

PI of control group was significantly higher than that of AG

group and MMC+AG_H group ($P < 0.05$), but the difference was not notable between treatment groups. AI in treatment groups was higher than that in the control group ($P < 0.05$), while there was also no difference between the treatment groups. The AI/PI value was calculated and compared among all groups. Consequently, it was apparently larger in treatment groups ($P < 0.01$), however no difference was shown between them (data not shown).

DISCUSSION

NO which has many biological functions is a cytokine in mammifer^[11]. It is synthesized from L-Arginine by iNOS which is the only rate-limiting enzyme^[12]. It involves a serial physiological and pathological process, such as carcinogenesis. NO can induce angiogenesis, but the mechanisms are not clear^[13-16]. However, several researches have revealed that NO can regulate the roles of VEGF in inducing angiogenesis by stimulating vascular endothelial cell proliferation and migration and improving vascular penetration^[17-20]. VEGF can increase the activity of iNOS^[6,7]. So iNOS and VEGF have positive correlation^[8-10]. It has been observed that iNOS is highly expressed in many human tumors, such as colon cancer, gastric cancer, ovarian cancer, breast cancer, *etc.*^[21]. In our previous study we have observed that the expression of VEGF and iNOS in gastric cancer presents positive correlation^[8-10]. This indicates that iNOS plays an important role in the expression and activity of VEGF. We also found that iNOS and VEGF have positive correlation with the clinicopathological characteristics of gastric cancer, such as infiltration, lymphatic or hematogenous metastasis, *etc.* At the same time MVD was higher with the enhancement of VEGF and iNOS. This revealed that iNOS and VEGF can induce angiogenesis in gastric cancer^[8-10,21].

To explore the anticancer mechanisms of iNOS inhibitor (aminoguanidine), in this study we evaluated the effect of

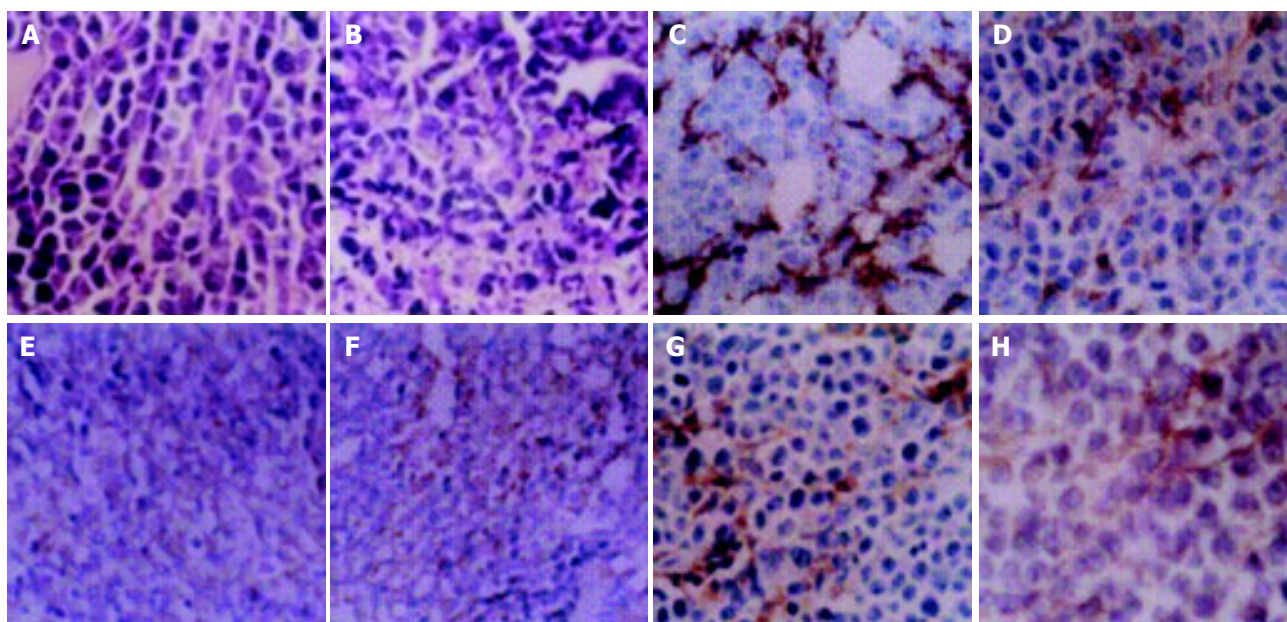


Figure 1 HE staining: morphology of tumor cells in AG group (A, original magnification x100) and control group (B, original magnification x200); immunohistochemical staining of tumor cells: the expression of FVIII Rag (C),

iNOS (E) and VEGF (G) in control group, and the expression of FVIII Rag (D), iNOS (F) and VEGF (H) in AG group. (original magnification, x400).

AG on tumor cell proliferation and apoptosis in xenografts. The AI/PI, a value reflecting cytokinetics, showed a more significant difference. Finally it is shown that compared with control group, the inhibitory rate of treatment groups are apparently higher. We also observed that AG obviously decreases the expression of iNOS and VEGF, and reduces MVD compared to that of control group. By immunohistochemistry (SP method) and Greiss assay we detected the NO level in plasma. The results indicate that the anticancer mechanisms of AG are mainly to inhibit the expression of iNOS and reduce the NO level in plasma. Therefore, the growth of tumor and angiogenesis are inhibited directly, and MVD and the expression of VEGF are suppressed indirectly. In this way the nutrition supply of the tumor is impaired, and further cell proliferation is inhibited and cell apoptosis is improved. These results are consistent with those of Koh *et al.*, They observed that AG could inhibit the activity of iNOS in gastric cancer, and suppressed carcinogenesis. At the same time AG and COX-2 selective inhibitors could obviously inhibit the activity of iNOS and COX-2. So, the primitive pathology of colon cancer (aberrant crypt foci, ACF) is prevented.

Compared with traditional anticancer therapy, antiangiogenesis therapy has many superiorities. In this study the effect of MMC group is similar to that of AG group. However, the target of chemotherapeutic drugs is tumor cells which have genetic instability and are apt to mutation and drug-resistance, so the drug-resistance incidence of chemotherapeutic drugs is 30%. And these drugs have many toxic effects. In MMC+AG_H group the anticancer effect is the best which indicates that the effect of AG depends on proper treatment opportunity and scheme. MMC and AG have positive synergy. So certain drugs which can reduce the NO level by inhibiting the expression and activity of iNOS at cellular or genetic level probably may regulate the NO level of tumor microvessel to inhibit carcinogenesis and angiogenesis. And if combined with radiotherapy or bioreactive modulators, it will play a more important role in anticancer effect. This is the first part of a serial study, and we will carry out the further study afterwards with molecular biological technology, such as Southern blotting, Northern blotting, RT-PCR, *etc.*

REFERENCES

- 1 Sun XD, Mu R, Zhou YS, Dai XD, Zhang SW, Huangfu XM, Sun J, Li LD, Lu FZ, Qiao YL. Analysis of mortality rate of stomach cancer and its trend in twenty years in China. *Zhonghua Zhongliu Zazhi* 2004; **26**: 4-9
- 2 Feng CW, Wang LD, Jiao LH, Liu B, Zhang S, Xie XJ. Expression of p53, inducible nitric oxide synthase and vascular endothelial growth factor in gastric precancerous and cancerous lesions: correlation with clinical features. *BMC Cancer* 2002; **2**: 8
- 3 Koh E, Noh SH, Lee YD, Lee HY, Han JW, Lee HW, Hong S. Differential expression of nitric oxide synthase in human stomach cancer. *Cancer Lett* 1999; **146**: 173-180
- 4 Doi C, Noguchi Y, Marat D, Saito A, Fukuzawa K, Yoshikawa T, Tsuburaya A, Ito T. Expression of nitric oxide synthase in gastric cancer. *Cancer Lett* 1999; **144**: 161-167
- 5 Eroglu A, Demirci S, Ayyildiz A, Kocaoglu H, Akbulut H, Akgul H, Elhan HA. Serum concentrations of vascular endothelial growth factor and nitrite as an estimate of *in vivo* nitric oxide in patients with gastric cancer. *Br J Cancer* 1999; **80**: 1630-1634
- 6 Lee JC, Chow NH, Wang ST, Huang SM. Prognostic value of vascular endothelial growth factor expression in colorectal cancer patients. *Eur J Cancer* 2000; **36**: 748-753
- 7 Mattern J, Koomagi R, Volm M. Coexpression of VEGF and bFGF in human epidermoid lung carcinoma is associated with increased vessel density. *Anticancer Res* 1997; **17**: 2249-2252
- 8 Wang GY, Gu JH, Lu GY, Meng XY. Effects of aminoguanidine on transplantation stomach cancer in mice. *J Jilin University* 2004; **30**: 409-412
- 9 Wang GY, Wang X. Relationship between tumor angiogenesis and expression of vascular endothelial growth factor and nitric oxide synthase in human gastric cancer. *Zhongguo Puwai Jichu Yu Linchuang Zazhi* 2004; **11**: 55-57
- 10 Wang X, Wang GY. Expression of vascular endothelial growth factor and nitric oxide synthase in human gastric cancer and its relation to angiogenesis and clinical pathology. *Zhonghua Weichang Waikao Zazhi* 2002; **5**: 145-148
- 11 Farsky SH, Borelli P, Fock RA, Proto SZ, Ferreira JM Jr, Mello SB. Chronic blockade of nitric oxide biosynthesis in rats: effect on leukocyte endothelial interaction and on leukocyte recruitment. *Inflamm Res* 2004; **53**: 442-452
- 12 Tong BC, Barbul A. Cellular and physiological effects of arginine. *Mini Rev Med Chem* 2004; **4**: 823-832
- 13 Lala PK, Orucevic A. Role of nitric oxide in tumor progression: lessons from human tumors. *Cancer Metastasis Rev* 1998; **17**: 91-106
- 14 Jenkins DC, Charles IG, Thomsen LL, Moss DW, Holmes LS, Baylis SA, Rhodes P, Westmore K, Emson PC, Moncadas S. Roles of nitric oxide in tumor growth. *Proc Natl Acad Sci USA* 1995; **92**: 4392-4396
- 15 Kitadai Y, Haruma K, Tokutomi T, Tanaka S, Sumii K, Carvalho M, Kuwabara M, Yoshida K, Hirai T, Kajiyama G, Tahara E. Significance of vessel count and vascular endothelial growth factor in human esophageal carcinoma. *Clin Cancer Res* 1998; **4**: 2195-2200
- 16 Salvucci O, Carsana M, Bersani I, Tragni G, Anichini A. Antiapoptotic role of endogenous nitric oxide in human melanoma cells. *Cancer Res* 2001; **61**: 318-326
- 17 Gallo O, Masini E, Morbidelli L, Franchi A, Fini-storchi I, Vergari WA, Ziche M. Role of nitric oxide in angiogenesis and tumor progression in head and neck cancer. *J Natl Cancer Inst* 1998; **90**: 587-596
- 18 Rieder G, Hofmann JA, Hatz RA, Stolte M, Enders GA. Up-regulation of inducible nitric oxide synthase in *Helicobacter pylori*-associated gastritis may represent an increased risk factor to develop gastric carcinoma of the intestinal type. *Int J Med Microbiol* 2003; **293**: 403-412
- 19 Rao CV, Indranie C, Simi B, Manning PT, Connor JR, Reddy BS. Chemopreventive properties of a selective inducible nitric oxide synthase inhibitor in colon carcinogenesis, administered alone or in combination with Celecoxib, a selective Cyclooxygenase-2 inhibitor. *Cancer Res* 2002; **62**: 165-170
- 20 Jung ID, Yang SY, Park CG, Lee KB, Kim JS, Lee SY, Han JW, Lee HW, Lee HY. 5-Fluorouracil inhibits nitric oxide production through the inactivation of I κ B kinase in stomach cancer cells. *Biochem Pharmacol* 2002; **64**: 1439-1445
- 21 Chen T, Nines RG, Peschke SM, Kresty LA, Stoner GD. Chemopreventive effects of a selective nitric oxide synthase inhibitor on carcinogen-induced rat esophageal tumorigenesis. *Cancer Res* 2004; **64**: 3714-3717

Effects of dietary intake and genetic factors on hypermethylation of the *hMLH1* gene promoter in gastric cancer

Hong-Mei Nan, Young-Jin Song, Hyo-Yung Yun, Joo-Seung Park, Heon Kim

Hong-Mei Nan, Heon Kim, Department of Preventive Medicine, College of Medicine, Chungbuk National University, Cheongju, Republic of Korea

Young-Jin Song, Hyo-Yung Yun, Departments of Surgery, College of Medicine, Chungbuk National University, Cheongju, Republic of Korea

Joo-Seung Park, Department of Surgery, Eulji University, School of Medicine, Daejeon, Republic of Korea

Supported by the Korea Health 21 R and D Project, Ministry of Health and Welfare, Republic of Korea. No. 00-PJ1-PG3-21900-0008

Correspondence to: Heon Kim, MD, PhD, Professor, Department of Preventive Medicine, College of Medicine, Chungbuk National University, 12 Kaeshin-dong, Hungdok-gu, Cheongju-si, Chungbuk 361-763, Republic of Korea. kimheon@cbu.ac.kr

Telephone: +82-43-261-2864 Fax: +82-43-274-2965

Received: 2004-10-9 Accepted: 2004-12-23

hypermethylated at the *hMLH1* promoter region. Hypermethylation of the *hMLH1* gene promoter was significantly inversely correlated with mutation of the *p53* gene.

CONCLUSION: These results suggest that cigarette smoking and alcohol consumption may influence the development of *hMLH1*-positive gastric cancer. Most dietary factors and polymorphisms of *GSTM1*, *GSTT1*, *CYP1A1*, *CYP2E1*, *ALDH2*, and *L-myc* genes are not independent risk factors for gastric cancer with hypermethylation of the *hMLH1* promoter. These data also suggest that there could be two or more different molecular pathways in the development of gastric cancer, perhaps involving tumor suppression mechanisms or DNA mismatch repair.

© 2005 The WJG Press and Elsevier Inc. All rights reserved.

Abstract

AIM: Hypermethylation of the promoter of the *hMLH1* gene, which plays an important role in mismatch repair during DNA replication, occurs in more than 30% of human gastric cancer tissues. The purpose of this study was to investigate the effects of environmental factors, genetic polymorphisms of major metabolic enzymes, and microsatellite instability on hypermethylation of the promoter of the *hMLH1* gene in gastric cancer.

METHODS: Data were obtained from a hospital-based, case-control study of gastric cancer. One hundred and ten gastric cancer patients and 220 age- and sex-matched control patients completed a structured questionnaire regarding their exposure to environmental risk factors. Hypermethylation of the *hMLH1* gene promoter, polymorphisms of the *GSTM1*, *GSTT1*, *CYP1A1*, *CYP2E1*, *ALDH2* and *L-myc* genes, microsatellite instability and mutations of *p53* and *Ki-ras* genes were investigated.

RESULTS: Both smoking and alcohol consumption were associated with a higher risk of gastric cancer with hypermethylation of the *hMLH1* gene promoter. High intake of vegetables and low intake of potato were associated with increased likelihood of gastric cancer with hypermethylation of the *hMLH1* gene promoter. Genetic polymorphisms of the *GSTM1*, *GSTT1*, *CYP1A1*, *CYP2E1*, *ALDH2*, and *L-myc* genes were not significantly associated with the risk of gastric cancer either with or without hypermethylation in the promoter of the *hMLH1* gene. Hypermethylation of the *hMLH1* promoter was significantly associated with microsatellite instability (MSI): 10 of the 14 (71.4%) MSI-positive tumors showed hypermethylation, whereas 28 of 94 (29.8%) the MSI-negative tumors were

Key words: Gastric cancer; Environmental carcinogens; Genetic polymorphisms; *hMLH1*; Microsatellite instability; *p53*; *Ki-ras*

Nan HM, Song YJ, Yun HY, Park JS, Kim H. Effects of dietary intake and genetic factors on hypermethylation of the *hMLH1* gene promoter in gastric cancer. *World J Gastroenterol* 2005; 11(25): 3834-3841

<http://www.wjgnet.com/1007-9327/11/3834.asp>

INTRODUCTION

Gastric cancer is the most common cancer among Koreans. Environmental factors including cigarette smoking and dietary intake have been implicated in the etiology of gastric cancer^[1-4]. Genetic polymorphisms of xenobiotic-metabolizing enzymes can also affect susceptibility to cancer. Several studies have reported that the genetic polymorphisms of metabolic enzymes, such as cytochrome p450 2E1 (*CYP2E1*)^[5], glutathione S-transferase mu 1 (*GSTM1*)^[6], glutathione S-transferase theta 1 (*GSTT1*)^[7], aldehyde dehydrogenase 2 (*ALDH2*)^[8], and *L-myc* proto-oncogene^[9], and mutations of *p53*^[10] and *Ki-ras*^[11] genes are associated with the development of gastric cancer.

Promoter hypermethylation is an alternative mechanism of gene inactivation in carcinogenesis^[12]. Several studies have suggested that aberrant methylation of the promoter causes transcriptional silencing of some important suppressor genes, such as *p16*^[13], *E-cadherin*^[14], and von Hippel Lindau (*VHL*) gene^[15], and this has been implicated in the carcinogenic process in many cancers^[12]. In addition, it was recently shown that hypermethylation of gene promoters increases along

the pathway of development from chronic gastritis, intestinal metaplasia, and adenomas to carcinomas of the stomach^[16,17].

The *hMLH1* protein, a mismatch repair enzyme, maintains the fidelity of the genome during cellular proliferation. It has no known enzymatic activity and probably acts as a 'molecular matchmaker', recruiting other DNA-repair proteins to the mismatch repair complex^[18]. Dysfunction of a mismatch repair system such as *hMLH1* and *hMSH2* could alter microsatellites, short tandem repetitive sequences^[19]. Several reports have suggested that hypermethylation of the *hMLH1* promoter correlates with a loss of expression of the gene, resulting in microsatellite instability in gastric cancer^[20,21].

There is evidence that diet may be associated with hypermethylation of the *hMLH1* gene promoter in gastric cancer. Aberrant hypermethylation of the *hMLH1* gene promoter is frequently observed in cancers of digestive organs such as the colon, rectum, and stomach^[21,22], and decreased levels of folate, vitamin C, and niacin can induce hypermethylation of gene promoters^[23]. These facts led us to hypothesize that genetic polymorphisms and environmental factors, such as cigarette smoking, alcohol consumption, and diet, may interact during the hypermethylation of the *hMLH1* gene promoter and in the carcinogenesis of gastric cancer. We studied the association between hypermethylation of the *hMLH1* gene promoter and environmental factors, genetic polymorphisms of major metabolic enzymes, genetic mutation of p53 and Ki-ras genes, and microsatellite instability in gastric cancer.

MATERIALS AND METHODS

Subjects

One hundred and ten individuals with gastric cancer and 220 age-matched (within 3 years) and sex-matched controls were enrolled in this study. Cases of cancer were all histologically confirmed from February 1997 to June 2002 at Chungbuk National University Hospital and Eulji University Hospital, Korea. Control subjects were selected from patients newly diagnosed with diseases other than cancer at the same hospitals or from individuals receiving routine medical examinations in Chungbuk National University Hospital. Table 1 shows the age and gender distribution of the subjects according to hypermethylation of the *hMLH1* gene promoter. The mean±SD ages were 59.81±11.23 years for cases and 59.60±11.03 years for controls. This study was conducted in accordance with the recommendations outlined in the Declaration of Helsinki and all subjects provided written informed consent.

Table 1 Gender and age distribution of cases and controls

	Cases	Controls
Gender		
Male	70	140
Female	40	80
Age (yr)		
<39	6	12
40-49	11	22
50-59	34	68
60-69	40	80
70-	19	38

Exposure to environmental factors

Trained interviewers interviewed subjects using a structured questionnaire within a month after the diagnosis of gastric cancer or benign diseases or at the time of the hospital visit for control subjects undergoing routine medical examination. The questionnaire included questions on demographic factors, smoking habits, alcohol consumption, and diet. Dietary data were collected using a semiquantitative food frequency table previously evaluated for validity and reliability^[24]. All subjects were asked about their average frequency of consumption and portion size of 89 common food items during the year preceding the interview. These items were classified into 21 food groups having similar ingredients. The 21 food groups were as follows: cereals; potato; nuts; noodles; breads and cakes; vegetables; mushrooms; fruits; meats; eggs; fishes and shellfishes; stews; chicken; kimchi; soybean foods; soybean pastes; milk and dairy products; butter, cheeses, and margarine; jams, honey, candies, and chocolates; coffee and tea; seaweeds; and alliums.

The amount of calories, nutrients, vitamins, and minerals consumed for each food item was estimated by multiplying the intake amount of the food item and its nutrient value. The total intake of calories, nutrients, vitamins, and minerals was calculated for each subject by summing the respective calories, nutrients, vitamins, and minerals for each food item^[25]. The intake amounts of these factors were adjusted for caloric intake using the method of Willett *et al.*^[26].

Analysis of genetic polymorphisms

Genomic DNA was isolated from peripheral leukocytes by proteinase K digestion and phenol-chloroform extraction. A multiplex polymerase chain reaction (PCR) method^[27] was used simultaneously to detect the presence or absence of the *GSTM1* and *GSTT1* genes with slight modification. The primers used were 5'-GAA GGT GGC CTC CTC CTT GG-3' and 5'-AAT TCT GGA TTG TAG CAG AT-3' for *GSTM1*, 5'-TTC CTT ACT GGT CCT CAC ATC TC-3' and 5'-TCA CCG GAT CAT GGC CAG CA-3' for *GSTT1*, and 5'-CAA CTT CAT CCA CGT TCA CC-3' and 5'-GAA GAG CCA AGG ACA GTT AC-3' for β -globin, the internal reference gene. The PCR reactions were performed in 25 μ L of a solution containing 50 ng of genomic DNA, 1 \times PCR buffer [50 mmol/L KCl, 10 mmol/L Tris-HCl (pH 9.0), 1.5 mmol/L MgCl₂, and 0.1% Triton X-100], 5 pmol of each primer, 80 μ mol/L each dNTP, and 2.0 units *Taq* polymerase (Promega, Madison, WI). Amplifications were carried out in a thermocycler (MJ Research, Watertown, MA) as follows: 5 min of denaturation at 94 °C, followed by 35 cycles consisting of denaturation at 94 °C for 1 min, annealing at 58 °C for 1 min, and extension at 74 °C for 1 min. PCR products were separated on 2% agarose gels with ethidium bromide. *GSTM1* and *GSTT1* genotypes were not scored unless the PCR product of the β -globin gene was evident.

The A4889G polymorphism in exon 7 of the *CYP1A1* gene was analyzed for each subject as described previously^[28]. Briefly, PCR was performed using the primers 5'-GAA CTG CCA CTT CAG CTG TC-3' and 5'-GAA AGA CCT CCC AGC GGT CA-3'. The temperature program for the PCR

reaction was slightly modified. After initial denaturation for 5 min at 94 °C, a thermal cycle consisting of denaturation for 90 s at 94 °C, annealing for 90 s at 53 °C, and extension for 30 s at 74 °C, was repeated 35 times. The PCR products (187-bp fragments) were digested with *HincII* restriction enzyme at 37 °C overnight and subjected to electrophoresis on 12% polyacrylamide gels. PCR analysis resulted in the following genotype classification: a predominant homozygote (Ile/Ile), a heterozygote (Ile/Val), and a rare homozygote (Val/Val).

The 5'-flanking region polymorphism of the *CYP2E1* gene was analyzed using procedures described previously^[29]. Briefly, PCR was performed using the primers 5'-CCA GTC GAG TCT ACA TTG TCA-3' and 5'-TTC ATT CTG TCT TCT AAC TGG-3'. Initial denaturation was performed at 94 °C for 5 min, followed by 35 thermal cycles consisting of denaturation for 1 min at 94 °C, annealing for 1 min at 53 °C, and extension for 30 s at 74 °C. The 410-bp PCR product was digested with *RsaI* at 37 °C overnight and subjected to electrophoresis on 2% agarose gels. The genotypes of *CYP2E1* were classified as follows: a predominant homozygote (c1/c1), a heterozygote (c1/c2), and a rare homozygote (c2/c2).

The *MboII* polymorphism of *ALDH2* was identified using a PCR-RFLP method^[30] with slight modification. Briefly, PCR was performed using the primers 5'-CCA CAC TCA CAG TTT TCT CTT-3' and 5'-AAA TTA CAG GGT CAA CTG CT-3'. We used the same PCR conditions as in the *CYP1A1* gene analysis. The 134-bp amplicon was digested with *MboII* restriction enzyme at 37 °C overnight and subjected to electrophoresis on 15% polyacrylamide gels. The genotypes of *ALDH2* were identified as the predominant homozygote (NN), the heterozygote (ND), and the rare homozygote (DD).

The polymorphism of the *L-myc* gene was analyzed using procedures described previously^[31]. Briefly, PCR was performed using the primers 5'-ACG GCT GGT GGA GTG GTA GA-3' and 5'-AAG CTT GAG CCC CTT TGT CA-3'. Initial denaturation was performed at 94 °C for 5 min, followed by 35 thermal cycles consisting of denaturation for 45 s at 95 °C, annealing for 40 s at 60 °C, and extension for 40 s at 74 °C. The amplified 613-bp PCR product was directly digested with the restriction enzyme *EcoRI* at 37 °C overnight and separated by electrophoresis on 2% agarose gels. The genotypes of *L-myc* were classified as follows: a predominant homozygote (LL), a heterozygote (LS), and a rare homozygote (SS).

Methylation-specific PCR for hMLH1 promoter

Tissue samples from gastric cancer patients were immediately frozen and stored in liquid nitrogen until analysis. DNA was extracted using a DNA extraction kit (Promega) according to the manufacturer's instructions.

The promoter methylation status of the *bMLH1* gene was determined by methylation-specific PCR (MSP), as described previously^[32]. MSP distinguishes unmethylated from hypermethylated alleles in a given gene based on sequence changes produced after bisulfite treatment of DNA, which converts unmethylated, but not methylated, cytosines to uracils. Briefly, 2 µg of genomic DNA was

denatured by treatment with NaOH and modified by sodium bisulfite. DNA samples were then purified using a Wizard DNA Purification Resin (Promega), treated again with NaOH, precipitated with ethanol, and resuspended in water. Modified DNA was amplified using the primer pairs as follows: 5'-TTT TGA TGT AGA TGT TTT ATT AGG GTT GT-3' and 5'-ACC ACC TCA TCA TAA CTA CCC ACA-3' for the unmethylated reaction (124-bp), and 5'-ACG TAG ACG TTT TAT TAG GGT CGC-3' and 5'-CCT CAT CGT AAC TAC CCG CG-3' for the methylated reaction (115-bp)^[32]. PCR was performed in a thermocycler (MJ Research) as follows: 5 min of denaturation at 95 °C, then 35 cycles consisting of denaturation at 95 °C for 30 s, annealing at 55 °C for 30 s, and extension at 72 °C for 30 s. PCR products were separated on 6% polyacrylamide gels with ethidium bromide. DNA from blood samples was used as a negative control for hypermethylated *bMLH1*.

Microsatellite instability

Microsatellite instability (MSI) was examined using BAT25 and BAT26 mononucleotide microsatellite markers. PCR was performed in a 25 µL reaction volume containing 50 ng of genomic DNA, 1× PCR buffer, 5 pmol of each primer, 80 µmol/L each dNTP, 2.0 units *Taq* polymerase (Takara, Shiga, Japan), and 0.2 µCi of α -³²P-labeled dCTP. Amplifications were carried out as follows: 5 min of denaturation at 95 °C, then 35 cycles consisting of denaturation at 95 °C for 50 s, annealing at 58 °C for 90 s, and extension at 72 °C for 90 s. Two microliters of PCR product was electrophoresed on 6% denaturing polyacrylamide gels containing 6 mol/L urea at room temperature. The gels were dried and autoradiographed on X-ray film. MSI-positive results were identified when the mobility of the microsatellite fragment amplified from tumor DNA differed from the corresponding blood DNA. Tumors were considered microsatellite instability-positive (MSI+) if they manifested instability at one or two loci or microsatellite instability-negative (MSI-) if no unstable microsatellite was found.

Sequencing of p53 and Ki-ras genes

Reverse transcription (RT)-PCR and direct sequencing methods were used to detect mutations in *p53* and *Ki-ras* genes. Briefly, tissues from gastric cancer patients were homogenized and RNA was isolated using TRIzol solution (Invitrogen Life Technologies, Grand Island, NY). RT-PCR to amplify *p53* and *Ki-ras* cDNA were performed using reagents purchased from Promega. Specific primers synthesized by Bioneer Company (Cheongju, South Korea), *Ex Taq* polymerase (Takara), dNTPs, MgCl₂, PCR buffer, and cDNA template were mixed and then amplified for 40 cycles at 95 °C for 30 s and at 72 °C for 1 min. The cDNA regions were amplified using primers 5'-TCT AGA GCC ACC GTC CAG GGA G-3' and 5'-AAC CTC AGG CGG CTC ATA GGG CA-3' for the +2-+810 region of *p53*, and 5'-ACC AGG GCA GCT ACG GTT TCC GT-3' and 5'-TCA GTC TGA ATC AGG CCC TTC TGT-3' for the +443-+1 317 region of *p53*. Exons 1 and 2 of the *Ki-ras* gene were amplified using primers 5'-GAC TGA ATA TAA ACG TGT GGT AG-3' and 5'-ACT GGT CCC TCA TTG

CAC TG-3'. Before the RT-PCR products were sequenced by cycle sequencing, a PCR purification kit (Boehringer Mannheim, Indianapolis, IN) was used to remove unwanted reagents from the PCR reaction. The purified PCR products were then directly cycle-sequenced using an ABI PRISM 3100 Avant Genetic Analyzer (Applied Biosystems, Foster City, CA) according to the manufacturer's instructions.

Data analysis

Calorie-adjusted intakes of foods, nutrients, vitamins, and minerals were categorized into low- and high-intake groups based on the median values of the control population. Alcohol consumption per week was calculated from questions about the types, frequency, and average amount of alcohol consumed. Alcohol consumption was categorized into three groups: none, ≤280 g of alcohol/week, and >280 g of alcohol/week. Subjects who had smoked 20 cigarettes or more during their life were classified as smokers and those who had not were considered nonsmokers. Pack-year was used as an index of cumulative smoking.

The purpose of the study was to determine if dietary factors, genetic polymorphisms, MSI, and mutations of *p53* and *Ki-ras* genes were associated with hypermethylation of

the *bMLH1* gene promoter. We used unconditional logistic analysis to compare the risk of exhibiting or not exhibiting hypermethylation of the *bMLH1* promoter in tumors and controls using the SAS System for Windows (Release 8.1). *P*-values less than 0.05 were considered significant.

RESULTS

There were significant differences according to the smoking history, pack-years, and higher weekly alcohol intake between patients with gastric cancers with hypermethylation of the *bMLH1* promoter and controls (Table 2). As the amount of cigarette smoking or alcohol drinking increased, the risk of gastric cancer with the *bMLH1* promoter hypermethylation (Table 3).

High consumption of potatoes and butter, cheese and margarine was associated with lower risk of gastric cancer with hypermethylation of the *bMLH1* promoter. In contrast, consumption of vegetables was associated with higher risk of gastric cancer with hypermethylation of the *bMLH1* promoter. High intake of mushrooms and fruits and low intake of cereals and butter, cheese and margarine were associated with higher risk of gastric cancer without hypermethylation of the *bMLH1* promoter (Table 4). Among the nutrients, vitamins, and minerals evaluated, high intake of protein, phosphorus, potassium, vitamin C, zinc, and calcium was associated with higher risk of gastric cancer without hypermethylation of the *bMLH1* gene promoter. However, the intake of nutrients, vitamins, and minerals

Table 2 Interaction between cigarette smoking and alcohol intake, and *hMLH1* gene promoter hypermethylation in gastric cancer

	Controls (n)	Cases without <i>hMLH1</i> promoter hypermethylation (n)	Cases with <i>hMLH1</i> promoter hypermethylation (n)	χ^2_{trend}
Smoking history				
Non-smoker	102	27	13	3.827
Smoker	117	42	24	
Odds ratio	Referent (1.00)	1.16 (0.62–2.17)	3.04 ^a (1.29–7.19)	
Alcohol drinking				
Never	95	26	15	1.327
Ever	124	43	22	
Odds ratio	Referent (1.00)	1.07 (0.57–2.01)	2.11 (0.90–4.98)	

Odds ratio was adjusted for age and sex. ^a*P*<0.05 vs others.

Table 3 Interaction between amount of cigarette smoking and alcohol intake, and *hMLH1* gene promoter hypermethylation in gastric cancer

	OR ¹ (95%CI ²)	
	Cases without <i>hMLH1</i> promoter hypermethylation vs controls	Cases with <i>hMLH1</i> promoter hypermethylation vs controls
Cumulative smoking		
0	1.00	1.00
1–15	0.96 (0.38–2.41)	0.86 (0.22–3.41)
16–34	0.92 (0.44–1.93)	0.75 (0.24–2.38)
35–	0.39 ^a (0.16–0.93)	3.17 ^a (1.20–8.42)
χ^2_{trend}	1.202	6.344 ^a
Ethanol uptake per week (g/wk)		
0	1.00	1.00
≤280	0.58 (0.29–1.14)	1.35 (0.51–3.55)
≥281	0.68 (0.30–1.53)	3.94 ^a (1.21–12.80)
χ^2_{trend}	0.830	5.419 ^a

¹Odds ratio estimated using a conditional logistic analysis. ²Confidence interval. ^a*P*<0.05 vs others.

Table 4 Distribution of controls and cases with or without promoter hypermethylation of the *hMLH1* gene according to their intake of food groups which were statistically significant

	Controls (n)	Cases without <i>hMLH1</i> promoter hypermethylation (n)	Cases with <i>hMLH1</i> promoter hypermethylation (n)
Cereal			
Low	110	45	17
High	109	24	20
Odds ratio	Referent (1.00)	0.56 ^a (0.32–0.99)	0.94 (0.45–1.96)
Potato			
Low	109	36	27
High	110	33	10
Odds ratio	Referent (1.00)	1.00 (0.57–1.74)	0.30 ^b (0.14–0.67)
Vegetable			
Low	110	29	12
High	109	40	25
Odds ratio	Referent (1.00)	1.42 (0.82–2.46)	2.17 ^a (1.03–4.58)
Mushroom			
Low	110	26	18
High	109	43	19
Odds ratio	Referent (1.00)	1.85 ^a (1.05–3.27)	0.89 (0.43–1.83)
Fruit			
Low	110	25	13
High	109	44	24
Odds ratio	Referent (1.00)	1.86 ^a (1.06–3.27)	1.69 (0.81–3.54)
Butter, cheese, and margarine			
Low	110	49	24
High	109	20	13
Odds ratio	Referent (1.00)	0.45 ^b (0.24–0.81)	0.44 ^a (0.20–0.93)

Odds ratio was adjusted for age and sex. ^a*P*<0.05. ^b*P*<0.01 vs others.

did not differ significantly between patients with gastric cancers with the *bMLH1* promoter hypermethylation, those with gastric cancers without it, or controls (Table 5).

Genetic polymorphism of *GSTM1*, *GSTT1*, *CYP1A1*, *CYP2E1*, *ALDH2* and *L-myc* was not associated with development of gastric cancers with the *bMLH1* promoter hypermethylation or those without it (Table 6).

Hypermethylation of the *bMLH1* gene promoter was detected in 35.2% of patients with gastric cancer, in 13.6% of those with MSI, in 28.2% of those with mutations of *p53*, and in 4.9% of those with the *Ki-ras* gene (data not shown). Hypermethylation of the *bMLH1* promoter occurred in 10 of 14 MSI+ cases (71.4%) and in 28 of 94 MSI- cases (29.8%). We found a striking association between hypermethylation of the *bMLH1* promoter and MSI (Table 7). Hypermethylation of the *bMLH1* gene promoter was significantly inversely correlated with mutation of the *p53* gene (Table 7).

DISCUSSION

Cigarette smoking and alcohol consumption have been identified as risk factors for gastric cancer in some studies^[33-36], although others have not found a causal relationship between these factors^[37,38]. Data from our unconditional logistic models showed that both cigarette smoking and alcohol consumption play dominant roles in the development of gastric cancer with hypermethylation of the *bMLH1* promoter, but not in the development of cancer without

Table 5 Distribution of controls and cases with or without promoter hypermethylation of the hMLH1 gene according to their intake of nutrients, vitamins, and minerals which were statistically significant

	Controls (n)	Cases without hMLH1 promoter hypermethylation (n)	Cases with hMLH1 promoter hypermethylation (n)
Protein			
Low	109	25	18
High	110	44	19
Odds ratio	Referent (1.00)	1.81 ^a (1.03-3.17)	1.00 (0.49-2.02)
Phosphorus			
Low	109	25	20
High	110	44	17
Odds ratio	Referent (1.00)	1.82 ^a (1.03-3.19)	0.77 (0.38-1.57)
Potassium			
Low	109	22	15
High	110	47	22
Odds ratio	Referent (1.00)	2.38 ^b (1.32-4.26)	1.24 (0.60-2.56)
Vitamin C			
Low	110	19	13
High	109	50	24
Odds ratio	Referent (1.00)	2.78 ^b (1.53-5.05)	1.74 (0.84-3.63)
Zinc			
Low	110	23	15
High	109	46	22
Odds ratio	Referent (1.00)	2.20 ^b (1.23-3.91)	1.31 (0.64-2.70)
Calcium			
Low	110	22	15
High	109	47	22
Odds ratio	Referent (1.00)	2.32 ^b (1.30-4.14)	1.34 (0.65-2.76)

Odds ratio was adjusted for age and sex. ^aP<0.05, ^bP<0.01 vs others.

hypermethylation of the promoter. This finding suggests that smoking- or alcohol-related biological pathways leading to the development of gastric cancer involve hypermethylation of the *bMLH1* promoter. Although it is unclear whether smoking induces hypermethylation of the *bMLH1* gene promoter in humans, recent reports indicate an association between DNA methylation and tobacco carcinogens in animal models^[39,40]. Previous studies have also shown that smoking and alcohol consumption increase the risk of developing microsatellite-unstable tumors^[41,42].

The exact mechanism of DNA hypermethylation by alcohol is unknown. However, it has been hypothesized that

Table 6 Distribution of controls and cases with or without promoter hypermethylation of the hMLH1 gene according to the genetic polymorphisms of *GSTM1*, *GSTT1*, *CYP1A1*, *CYP2E1*, *NAT2*, *ALDH2*, and *L-myc*

	Controls (n)	Cases without hMLH1 promoter hypermethylation (n)	Cases with hMLH1 promoter hypermethylation (n)
GSTM1			
Undeleted	90	21	13
Deleted	130	48	25
Odds ratio	Referent (1.00)	1.67 (0.93-3.00)	1.18 (0.56-2.47)
GSTT1			
Undeleted	117	32	17
Deleted	103	37	21
Odds ratio	Referent (1.00)	1.32 (0.76-2.29)	1.47 (0.72-2.98)
CYP1A1			
Ile/Ile	115	36	22
Ile/Val+Val/Val	104	33	15
Odds ratio	Referent (1.00)	1.02 (0.59-1.77)	0.74 (0.36-1.52)
CYP2E1			
c1/c1	129	44	25
c1/c2+c2/c2	88	26	13
Odds ratio	Referent (1.00)	0.89 (0.51-1.56)	0.76 (0.37-1.59)
ALDH2			
NN	139	38	26
ND+DD	79	31	11
Odds ratio	Referent (1.00)	1.45 (0.83-2.52)	0.73 (0.34-1.56)
L-myc			
Low	52	20	9
High	164	48	29
Odds ratio	Referent (1.00)	1.59 (0.86-2.92)	1.56 (0.61-3.99)

Odds ratio was adjusted for age and sex.

Table 7 Frequencies of mutations of the *p53* and *Ki-ras* genes, and microsatellite instability according to *bMLH1* promoter hypermethylation

Gene	<i>bMLH1</i> promoter hypermethylation		OR ¹ (95%CI ²)	χ^2	P
	Yes (%)	No (%)			
P53					
No	31 (81.58)	46 (65.71)	1.00	4.199	0.041
Yes	7 (18.42)	24 (34.29)	0.34 (0.12-0.95)		
Ki-ras					
No	37 (97.37)	58 (93.55)	1.00	0.407	0.524
Yes	1 (2.63)	4 (6.45)	0.47 (0.05-4.72)		
³MSI					
No	28 (73.68)	66 (92.86)	1.00	7.458	0.006
Yes	10 (26.32)	4 (7.14)	6.19 (1.67-22.88)		

¹Odds ratio was adjusted for age and sex. ²Confidence interval. ³Microsatellite instability.

alcohol could influence carcinogenesis by influencing mucosal cell proliferation and related histological changes^[43]. These changes have been associated with mucosal hyper-regeneration, which may make the mucosa more susceptible to the action of other carcinogens such as cigarette smoke^[43]. Therefore, alcohol consumption might increase the bio-availability of DNA-binding smoke components in the mucosa of the upper digestive tract, increasing the plasma levels of these compounds, or might modify the metabolism of pro-carcinogenic compounds by inducing specific metabolic pathways involving an aberrant mismatch repair system^[44].

Folate deficiency is associated with hypermethylation of the H-cadherin promoter^[45]. However, we found no significant association between folate intake and hypermethylation of the *bMLH1* promoter. Su and Arab reported that low folate intake is aggravated by high alcohol intake^[46], probably because folate is degraded by acetaldehyde, an intermediate metabolite of alcohol^[47]. van Engeland *et al.*, suggested that intake of folate and alcohol is associated with changes in promoter hypermethylation in colorectal cancer^[48]. Our data showing that alcohol intake increased the risk of gastric cancer with hypermethylation of the *bMLH1* promoter are consistent with these previous reports.

Most dietary factors, nutrients, vitamins, and minerals are not associated with gastric cancer with hypermethylation of the *bMLH1* promoter, although we found that a high intake of vegetables and low intake of potato and butter, cheese, and margarine were associated with increased likelihood of gastric cancer without hypermethylation of the *bMLH1* promoter, and high intake of mushrooms and fruits and low intake of cereals and butter, cheese and margarine were associated with higher risk of gastric cancer without hypermethylation of the *bMLH1* promoter. We cannot be certain that these results did not occur by chance, given the low number of comparisons. However, we observed that different dietary factors selectively affected the pathways to gastric cancer with or without hypermethylation of the *bMLH1* promoter. For example, a high intake of butter, cheese, and margarine was associated with a lower risk of gastric cancers either with or without hypermethylation of the *bMLH1* promoter. These findings agree with epidemiological data showing a relatively low incidence of gastric cancer in countries with consumption of high butter, cheese, and margarine^[49]. Based on these facts, it could be suggested that butter, cheese and margarine decrease the risk of gastric cancer regardless of the *hMLH1* promoter hypermethylation.

It has been reported that vitamin C can induce hypermethylation of gene promoters^[23]. However, a higher intake of vitamin C is associated with an increased risk of gastric cancer in this present study. One of the main vitamin C sources for Koreans is kimchi, which has been reported as a potent risk factor for gastric cancer in some Korean epidemiologic studies^[3]. Therefore, kimchi intake increases vitamin C intake amount, and, at the same time, the risk of gastric cancer.

Few epidemiological studies on gastric cancer have included genetic polymorphisms in the analysis or evaluated the association between genetic polymorphisms and

hypermethylation of the *bMLH1* gene promoter. Several studies have reported an independent, increased risk of gastric cancer for the *GSTM1* null^[7], *GSTT1* null^[6], *CYP2E1* c1/c2 or c2/c2^[50], *2-allele containing *ALDH2* genotypes^[9], and shorter (s) allele-containing *L-myc*^[10] genotypes. However, other studies have not found any association between gastric cancer and these genotypes^[51-53]. We found no significant association between polymorphisms of *GSTM1*, *GSTT1*, *CYP1A1*, *CYP2E1*, *ALDH2*, and *L-myc* and the risk of gastric cancer with or without hypermethylation of the *bMLH1* promoter. These findings suggest that the genetic polymorphisms of the *GSTM1*, *GSTT1*, *CYP1A1*, *CYP2E1*, *ALDH2*, and *L-myc* genes might not be independent risk factors, but could act as effect modifiers of the risk of gastric cancer through environmental factors, such as dietary intake.

We examined the mononucleotide repeats BAT25 and BAT26 to detect genuine MSI because these repeats are considered as ideal diagnostic markers. Mononucleotide repeats are sufficient for the diagnosis of true MSI^[54]. A consensus mononucleotide locus, BAT26 is altered in all tumors with genuine MSI^[55,56]. We found that 10 of the 14 MSI+ gastric cancer cases (71%) in our patients were hypermethylated in the promoter region of *bMLH1*. We found a significant association between hypermethylation of the *bMLH1* promoter and MSI+ gastric carcinoma ($P = 0.006$), which is consistent with previous reports^[21,57].

Point mutations in the *p53* tumor suppressor gene^[58,59] and *ras* oncogenes^[60,61] are frequently found in human and rodent tumors. Mutations of the *p53* and *Ki-ras* genes were detected in 28.2% and 4.9% of our patients with gastric cancer, respectively. We also found a significant inverse association between hypermethylation of the *bMLH1* gene promoter and *p53* mutations. Previous studies have reported a significantly lower incidence of *p53* gene alterations in MSI+ gastric cancer, in MSI+ colorectal cancers, and in colorectal cancer cell lines^[62,63] than in MSI- gastric cancer^[64,65]. Together, these data confirm the existence of alternative genetic pathways for gastric cancer, such as the classical 'tumor suppressor' pathway and the 'mismatch repair' pathway.

In conclusion, despite its limited size, this study suggests that cigarette smoking and alcohol consumption are significantly associated with higher risk of gastric cancer having hypermethylation of the *bMLH1* promoter. Polymorphisms of *GSTM1*, *GSTT1*, *CYP1A1*, *CYP2E1*, *ALDH2*, and *L-myc* genes were not associated with gastric cancers either with or without hypermethylation of the *bMLH1* promoter, suggesting that these polymorphisms operate along disease pathways other than those involving the mismatch repair system in gastric cancer. Our data also highlight the importance of aberrant methylation of the *bMLH1* promoter in causing MSI in gastric cancer. The negative association between hypermethylation of the *bMLH1* gene promoter and *p53* mutations suggests that there could be two or more different molecular pathways in the development of gastric cancer, such as tumor suppression mechanisms and DNA mismatch repair.

REFERENCES

- 1 Kim JP, Park JG, Lee MD, Han MD, Park ST, Lee BH, Jung

- SE. Co-carcinogenic effects of several Korean foods on gastric cancer induced by N-methyl-N'-nitro-N-nitrosoguanidine in rats. *Jpn J Surg* 1985; **15**: 427-437
- 2 **Yun TK**, Choi SY. Preventive effect of ginseng intake against various human cancers: a case-control study on 1987 pairs. *Cancer Epidemiol Biomarkers Prev* 1995; **4**: 401-408
- 3 **Lee JK**, Park BJ, Yoo KY, Ahn YO. Dietary factors and stomach cancer: a case-control study in Korea. *Int J Epidemiol* 1995; **24**: 33-41
- 4 **Ahn YO**. Diet and stomach cancer in Korea. *Int J Cancer* 1997; **10**: 7-9
- 5 **Nishimoto IN**, Hanaoka T, Sugimura H, Nagura K, Ihara M, Li XJ, Arai T, Hamada GS, Kowalski LP, Tsugane S. Cytochrome P450 2E1 polymorphism in gastric cancer in Brazil: case-control studies of Japanese Brazilians and non-Japanese Brazilians. *Cancer Epidemiol Biomarkers Prev* 2000; **9**: 675-680
- 6 **Setiawan VW**, Zhang ZF, Yu GP, Li YL, Lu ML, Tsai CJ, Cordova D, Wang MR, Guo CH, Yu SZ, Kurtz RC. GSTT1 and GSTM1 null genotypes and the risk of gastric cancer: a case-control study in a Chinese population. *Cancer Epidemiol Biomarkers Prev* 2000; **9**: 73-80
- 7 **Harada S**, Misawa S, Nakamura T, Tanaka N, Ueno E, Nozoe M. Detection of GST1 gene deletion by the polymerase chain reaction and its possible correlation with stomach cancer in Japanese. *Hum Genet* 1992; **90**: 62-64
- 8 **Yokoyama A**, Muramatsu T, Ohmori T, Yokoyama T, Okuyama K, Takahashi H, Hasegawa Y, Higuchi S, Maruyama K, Shirakura K, Ishii H. Alcohol-related cancers and aldehyde dehydrogenase-2 in Japanese alcoholics. *Carcinogenesis* 1998; **19**: 1383-1387
- 9 **Shibuta K**, Mori M, Haraguchi M, Yoshikawa K, Ueo H, Akiyoshi T. Association between restriction fragment length polymorphism of the L-myc gene and susceptibility to gastric cancer. *Br J Surg* 1998; **85**: 681-684
- 10 **Shiao YH**, Ruge M, Correa P, Lehmann HP, Scheer WD. p53 alteration in gastric precancerous lesions. *Am J Pathol* 1994; **144**: 511-517
- 11 **Craanen ME**, Blok P, Top B, Boerrieger L, Dekker W, Offerhaus GJ, Tytgat GN, Rodenhuis S. Absence of ras gene mutations in early gastric carcinomas. *Gut* 1995; **37**: 758-762
- 12 **Baylin SB**, Herman JG, Graff JR, Vertino PM, Issa JP. Alterations in DNA methylation: a fundamental aspect of neoplasia. *Adv Cancer Res* 1998; **72**: 141-196
- 13 **Merlo A**, Herman JG, Mao L, Lee DJ, Gabrielson E, Burger PC, Baylin SB, Sidransky D. 5' CpG island methylation is associated with transcriptional silencing of the tumour suppressor p16/CDKN2/MTS1 in human cancers. *Nat Med* 1995; **1**: 686-692
- 14 **Graff JR**, Herman JG, Lapidus RG, Chopra H, Xu R, Jarrard DF, Isaacs WB, Pitha PM, Davidson NE, Baylin SB. E-cadherin expression is silenced by DNA hypermethylation in human breast and prostate carcinomas. *Cancer Res* 1995; **55**: 5195-5199
- 15 **Herman JG**, Latif F, Weng Y, Lerman MI, Zbar B, Liu S, Samid D, Duan DS, Gnarr JR, Linehan WM, Baylin SB. Silencing of the VHL tumor-suppressor gene by DNA methylation in renal carcinoma. *Proc Natl Acad Sci USA* 1994; **91**: 9700-9704
- 16 **Kang GH**, Shim YH, Jung HY, Kim WH, Ro JY, Rhyu MG. CpG island methylation in premalignant stages of gastric carcinoma. *Cancer Res* 2001; **61**: 2847-2851
- 17 **Fleisher AS**, Esteller M, Tamura G, Rashid A, Stine OC, Yin J, Zou TT, Abraham JM, Kong D, Nishizuka S, James SP, Wilson KT, Herman JG, Meltzer SJ. Hypermethylation of the hMLH1 gene promoter is associated with microsatellite instability in early human gastric neoplasia. *Oncogene* 2001; **20**: 329-335
- 18 **Modrich P**. Mechanisms and biological effects of mismatch repair. *Annu Rev Genet* 1991; **25**: 229-253
- 19 **Thibodeau SN**, Bren G, Schaid D. Microsatellite instability in cancer of the proximal colon. *Science* 1993; **260**: 816-819
- 20 **Kang GH**, Shim YH, Ro JY. Correlation of methylation of the hMLH1 promoter with lack of expression of hMLH1 in sporadic gastric carcinomas with replication error. *Lab Invest* 1999; **79**: 903-909
- 21 **Fleisher AS**, Esteller M, Wang S, Tamura G, Suzuki H, Yin J, Zou TT, Abraham JM, Kong D, Smolinski KN, Shi YQ, Rhyu MG, Powell SM, James SP, Wilson KT, Herman JG, Meltzer SJ. Hypermethylation of the hMLH1 gene promoter in human gastric cancers with microsatellite instability. *Cancer Res* 1999; **59**: 1090-1095
- 22 **Cunningham JM**, Christensen ER, Tester DJ, Kim CY, Roche PC, Burgart LJ, Thibodeau SN. Hypermethylation of the hMLH1 promoter in colon cancer with microsatellite instability. *Cancer Res* 1998; **58**: 3455-3460
- 23 **Singh SM**, Murphy B, O'Reilly RL. Involvement of gene-diet/drug interaction in DNA methylation and its contribution to complex diseases: from cancer to schizophrenia. *Clin Genet* 2003; **64**: 451-460
- 24 **Kim MK**, Lee SS, Ahn YO. Reproducibility and validity of a self-administered semiquantitative food frequency questionnaire among middle-aged men in Seoul. *Korean J Commun Nutr* 1996; **1**: 376-394
- 25 The Korean Nutrition Society. Recommended dietary allowance for Koreans, 7th Revision. The Korean Nutrition Society, Seoul, 2000
- 26 **Willett W**, Stampfer MJ. Total energy intake: implications for epidemiologic analyses. *Am J Epidemiol* 1986; **124**: 17-27
- 27 **Chen H**, Sandler DP, Taylor JA, Shore DL, Liu E, Bloomfield CD, Bell DA. Increased risk for myelodysplastic syndromes in individuals with glutathione transferase theta 1 (GSTT1) gene defect. *Lancet* 1996; **347**: 295-297
- 28 **Oyama T**, Mitsudomi T, Kawamoto T, Ogami A, Osaki T, Kodama Y, Yasumoto K. Detection of CYP1A1 gene polymorphism using designed RFLP and distributions of CYP1A1 genotypes in Japanese. *Int Arch Occup Environ Health* 1995; **67**: 253-256
- 29 **Kawamoto T**, Koga M, Murata K, Matsuda S, Kodama Y. Effects of ALDH2, CYP1A1, and CYP2E1 genetic polymorphisms and smoking and drinking habits on toluene metabolism in humans. *Toxicol Appl Pharmacol* 1995; **133**: 295-304
- 30 **Harada S**, Zhang S. New strategy for detection of ALDH2 mutant. *Alcohol Alcohol Suppl* 1993; **1A**: 11-13
- 31 **Yaylim I**, Isbir T, Ozturk O, Turna A, Isitmangil T, Zonuzi F, Camlica H. Is there any correlation between restriction fragment length polymorphism of the L-MYC gene and metastasis of human nonsmall cell lung cancer? *Cancer Genet Cytogenet* 2002; **134**: 118-122
- 32 **Herman JG**, Graff JR, Myohanen S, Nelkin BD, Baylin SB. Methylation-specific PCR: a novel PCR assay for methylation status of CpG islands. *Proc Natl Acad Sci USA* 1996; **93**: 9821-9826
- 33 **Bjain M**, Choi NW, Fodor JG, Pfeiffer CJ, Howe GR, Harrison LW, Craib KJ, Miller AB. Dietary factors and the incidence of cancer of the stomach. *Am J Epidemiol* 1985; **122**: 947-959
- 34 **You WC**, Blot WJ, Chang YS, Ershow AG, Yang ZT, An Q, Henderson B, Xu GW, Fraumeni JF Jr, Wang TG. Diet and high risk of stomach cancer in Shandong, China. *Cancer Res* 1988; **48**: 3518-3523
- 35 **McLaughlin JK**, Hrubec Z, Blot WJ, Fraumeni JF Jr. Stomach cancer and cigarette smoking among U.S. veterans, 1954-1980. *Cancer Res* 1990; **50**: 3804
- 36 **Kabat GC**, Ng SK, Wynder EL. Tobacco, alcohol intake, and diet in relation to adenocarcinoma of the esophagus and gastric cardia. *Cancer Causes Control* 1993; **4**: 123-132
- 37 **Pollack ES**, Nomura AM, Heilbrun LK, Stemmermann GN, Green SB. Prospective study of alcohol consumption and cancer. *N Engl J Med* 1984; **310**: 617-621
- 38 **Nomura A**, Grove JS, Stemmermann GN, Severson RK. A prospective study of stomach cancer and its relation to diet, cigarettes, and alcohol consumption. *Cancer Res* 1990; **50**: 627-631
- 39 **Swafford DS**, Middleton SK, Palmisano WA, Nikula KJ, Tesfaigzi J, Baylin SB, Herman JG, Belinsky SA. Frequent

- aberrant methylation of p16INK4a in primary rat lung tumors. *Mol Cell Biol* 1997; **17**: 1366-1374
- 40 **Lee YW**, Klein CB, Kargacin B, Salnikow K, Kitahara J, Dowjat K, Zhitkovich A, Christie NT, Costa M. Carcinogenic nickel silences gene expression by chromatin condensation and DNA methylation: a new model for epigenetic carcinogens. *Mol Cell Biol* 1995; **15**: 2547-2557
- 41 **Slattery ML**, Curtin K, Anderson K, Ma KN, Ballard L, Edwards S, Schaffer D, Potter J, Leppert M, Samowitz WS. Associations between cigarette smoking, lifestyle factors, and microsatellite instability in colon tumors. *J Natl Cancer Inst* 2000; **92**: 1831-1836
- 42 **Slattery ML**, Anderson K, Curtin K, Ma KN, Schaffer D, Samowitz W. Dietary intake and microsatellite instability in colon tumors. *Int J Cancer* 2001; **93**: 601-607
- 43 **Kune GA**, Vitetta L. Alcohol consumption and the etiology of colorectal cancer: a review of the scientific evidence from 1957 to 1991. *Nutr Cancer* 1992; **18**: 97-111
- 44 **Izzotti A**, Balansky RM, Blagoeva PM, Mircheva ZI, Tulimiero L, Cartiglia C, De Flora S. DNA alterations in rat organs after chronic exposure to cigarette smoke and/or ethanol ingestion. *FASEB J* 1998; **12**: 753-758
- 45 **Jhaveri MS**, Wagner C, Trepel JB. Impact of extracellular folate levels on global gene expression. *Mol Pharmacol* 2001; **60**: 1288-1295
- 46 **Su LJ**, Arab L. Arab Nutritional status of folate and colon cancer risk: evidence from NHANES I epidemiologic follow-up study. *Ann Epidemiol* 2001; **11**: 65-72
- 47 **Homann N**, Tillonen J, Salaspuro M. Microbially produced acetaldehyde from ethanol may increase the risk of colon cancer via folate deficiency. *Int J Cancer* 2000; **86**: 169-173
- 48 **van Engeland M**, Weijenberg MP, Roemen GM, Brink M, de Bruine AP, Goldbohm RA, van den Brandt PA, Baylin SB, de Goeij AF, Herman JG. Effects of dietary folate and alcohol intake on promoter methylation in sporadic colorectal cancer: the Netherlands cohort study on diet and cancer. *Cancer Res* 2003; **63**: 3133-3137
- 49 **Stadtlander CT**, Waterbor JW. Molecular epidemiology, pathogenesis and prevention of gastric cancer. *Carcinogenesis* 1999; **20**: 2195-2208
- 50 **Gao C**, Takezaki T, Wu J, Li Z, Wang J, Ding J, Liu Y, Hu X, Xu T, Tajima K, Sugimura H. Interaction between cytochrome P-450 2E1 polymorphisms and environmental factors with risk of esophageal and stomach cancers in Chinese. *Cancer Epidemiol Biomarkers Prev* 2002; **11**: 29-34
- 51 **Kato S**, Onda M, Matsukura N, Tokunaga A, Matsuda N, Yamashita K, Shields PG. Genetic polymorphisms of the cancer related gene and *Helicobacter pylori* infection in Japanese gastric cancer patients. An age and gender matched case-control study. *Cancer* 1996; **77**: 1654-1661
- 52 **Deakin M**, Elder J, Hendrickse C, Peckham D, Baldwin D, Pantin C, Wild N, Leopard P, Bell DA, Jones P, Duncan H, Brannigan K, Alldersea J, Fryer AA, Strange RC. Glutathione S-transferase GSTT1 genotypes and susceptibility to cancer: studies of interactions with GSTM1 in lung, oral, gastric and colorectal cancers. *Carcinogenesis* 1996; **17**: 881-884
- 53 **Dlugosz A**, Adler G, Ciechanowicz A, Jaroszewicz-Heigelmann H, Starzynska T. EcoRI polymorphism of the L-myc gene in gastric cancer patients. *Eur J Gastroenterol Hepatol* 2002; **14**: 1231-1235
- 54 **Boland CR**, Thibodeau SN, Hamilton SR, Sidransky D, Eshleman JR, Burt RW, Meltzer SJ, Rodriguez-Bigas MA, Fodde R, Ranzani GN, Srivastava S. National Cancer Institute Workshop on Microsatellite Instability for cancer detection and familial predisposition: development of international criteria for the determination of microsatellite instability in colorectal cancer. *Cancer Res* 1998; **58**: 5248-5257
- 55 **Yamamoto H**, Itoh F, Fukushima H, Adachi Y, Itoh H, Hinoda Y, Imai K. Frequent Bax frameshift mutations in gastric cancer with high but not low microsatellite instability. *J Exp Clin Cancer Res* 1999; **18**: 103-106
- 56 **Yamamoto H**, Perez-Piteira J, Yoshida T, Terada M, Itoh F, Imai K, Perucho M. Gastric cancers of the microsatellite mutator phenotype display characteristic genetic and clinical features. *Gastroenterology* 1999; **116**: 1348-1357
- 57 **Leung SY**, Yuen ST, Chung LP, Chu KM, Chan AS, Ho JC. hMLH1 promoter methylation and lack of hMLH1 expression in sporadic gastric carcinomas with high-frequency microsatellite instability. *Cancer Res* 1999; **59**: 159-164
- 58 **Hollstein M**, Sidransky D, Vogelstein B, Harris CC. p53 mutations in human cancers. *Science* 1991; **253**: 49-53
- 59 **Levine AJ**, Momand J, Finlay CA. The p53 tumor suppressor gene. *Nature* 1991; **351**: 453-456
- 60 **Sukumar S**, Notario V, Martin-Zanca D, Barbacid M. Induction of mammary carcinomas in rats by nitroso-methylurea involves malignant activation of H-ras-1 locus by single point mutations. *Nature* 1983; **306**: 658-661
- 61 **Zarbl H**, Sukumar S, Arthur AV, Martin-Zanca D, Barbacid M. Direct mutagenesis of Ha-ras-1 oncogenes by N-nitroso-N-methylurea during initiation of mammary carcinogenesis in rats. *Nature* 1985; **315**: 382-385
- 62 **Olschwang S**, Hamelin R, Laurent-Puig P, Thuille B, De Rycke Y, Li YJ, Muzeau F, Girodet J, Salmon RJ, Thomas G. Alternative genetic pathways in colorectal carcinogenesis. *Proc Natl Acad Sci USA* 1997; **94**: 12122-12127
- 63 **Cottu PH**, Muzeau F, Estreicher A, Flejou JF, Iggo R, Thomas G, Hamelin R. Inverse correlation between RER+ status and p53 mutation in colorectal cancer cell lines. *Oncogene* 1996; **13**: 2727-2730
- 64 **Strickler JG**, Zheng J, Shu Q, Burgart LJ, Alberts SR, Shibata D. p53 mutations and microsatellite instability in sporadic gastric cancer: when guardians fail. *Cancer Res* 1994; **54**: 4750-4755
- 65 **Yamamoto H**, Perez-Piteira J, Yoshida T, Terada M, Itoh F, Imai K, Perucho M. Gastric cancers of the microsatellite mutator phenotype display characteristic genetic and clinical features. *Gastroenterology* 1999; **116**: 1348-1357

Use of Fourier-transform infrared spectroscopy to rapidly diagnose gastric endoscopic biopsies

Qing-Bo Li, Xue-Jun Sun, Yi-Zhuang Xu, Li-Min Yang, Yuan-Fu Zhang, Shi-Fu Weng, Jing-Sen Shi, Jin-Guang Wu

Qing-Bo Li, Yi-Zhuang Xu, Li-Min Yang, Yuan-Fu Zhang, Shi-Fu Weng, Jin-Guang Wu, The State Key Laboratory of Rare Earth Materials Chemistry and Applications, College of Chemistry and Molecular Engineering, Peking University, Beijing 100871, China
Xue-Jun Sun, Jing-Sen Shi, Department of General Surgery, First Hospital of Xi'an Jiaotong University, Xi'an 710061, Shaanxi Province, China

Supported by the National Natural Science Foundation of China, No. 30371604 and State Key Project of China, No. 2002CCA01900
Correspondence to: Jin-Guang Wu, the State Key Laboratory of Rare Earth Materials Chemistry and Applications, College of Chemistry and Molecular Engineering, Peking University, Beijing 100871, China. wujg@pku.edu.cn

Telephone: +86-10-62757951 Fax: +86-10-62751708

Received: 2004-07-09 Accepted: 2004-09-09

Abstract

AIM: To determine if Fourier-transform infrared (FT-IR) spectroscopy of endoscopic biopsies could accurately diagnose gastritis and malignancy.

METHODS: A total of 123 gastroscopic samples, including 11 cases of cancerous tissues, 63 cases of chronic atrophic gastritis tissues, 47 cases of chronic superficial gastritis tissues and 2 cases of normal tissues, were obtained from the First Hospital of Xi'an Jiaotong University, China. A modified attenuated total reflectance (ATR) accessory was linked to a WQD-500 FT-IR spectrometer for spectral measurement followed by submission of the samples for pathologic analysis. The spectral characteristics for different types of gastroscopic tissues were summarized and correlated with the corresponding pathologic results.

RESULTS: Distinct differences were observed in the FT-IR spectra of normal, atrophic gastritis, superficial gastritis and malignant gastric tissues. The sensitivity of FT-IR for detection of gastric cancer, chronic atrophic gastritis and superficial gastritis was 90.9%, 82.5%, 91.5%, and specificity was 97.3%, 91.7%, 89.5% respectively.

CONCLUSION: FT-IR spectroscopy can distinguish gastric inflammation from malignancy.

© 2005 The WJG Press and Elsevier Inc. All rights reserved.

Key words: Fourier-transform infrared spectroscopy; Gastric endoscope; Gastric cancer; Chronic gastritis; Spectral analysis; Infrared detection

Li QB, Sun XJ, Xu YZ, Yang LM, Zhang YF, Weng SF, Shi JS, Wu JG. Use of Fourier-transform infrared spectroscopy to

rapidly diagnose gastric endoscopic biopsies. *World J Gastroenterol* 2005; 11(25): 3842-3845

<http://www.wjgnet.com/1007-9327/11/3842.asp>

INTRODUCTION

Fourier-transform infrared (FT-IR) spectroscopy can effectively provide chemical variation information of the structure and composition of biologic materials at molecular level^[1]. Therefore, vibrational spectroscopy is becoming an increasingly powerful tool for the research on biochemistry of cancer^[2-5]. Our research group has successfully used FT-IR spectroscopy to diagnose carcinomas, such as carcinoma of stomach, colon, esophagus, lung, salivary gland since 1995^[6-9]. There are significant differences between the spectra of malignant and corresponding normal tissues^[10-12]. In addition, FT-IR spectroscopy could detect molecular abnormalities which occur before the change in morphology seen under light microscope^[13]. Therefore, FT-IR technology makes it possible to detect inflammatory and precancerous changes. Rapid, accurate and convenient detection of gastroscopic tissues can be performed using FT-IR spectroscopy if mid-infrared fiber optics technology and stomach endoscopy technology are combined, however the flexible mid-infrared optical fiber and mini probe are not yet available^[14].

MATERIALS AND METHODS

Patients and materials

Informed consent was obtained from each patient prior to the study. A total of 123 fresh surgically resected gastric tissue specimens were obtained from the First Hospital of Xi'an Jiaotong University, China. There were 47 women and 76 men, aged between 18 and 80 years (mean 50.3 years). One endoscopic pinch biopsy, 1-3 mm in diameter, was obtained from each patient. The detected samples consisted of 11 cases of cancerous tissues, 63 cases of chronic atrophic gastritis tissues, 47 cases of chronic superficial gastritis tissues and 2 cases of normal tissues.

Spectral measurement

As the size of samples was too small to obtain an FT-IR spectrum with high quality, the modified ATR accessory linked to a WQD-500 FT-IR spectrometer was used. The FT-IR spectrometer was equipped with a liquid nitrogen cooled mercury cadmium telluride (MCT) detector.

The fresh tissue specimens were obtained in gastroscopy detection, and then immediately and non-invasively measured using the mobile FT-IR spectrometer near the operation

room. The sample was put on ATR accessory to measure the spectrum. The background spectrum was collected. For the collection of each spectrum, 32 scans at a resolution of 4/cm, with a normal range from 4 000/cm to 800/cm were applied. It took about 1-2 min to non-invasively measure the spectrum. After measurement, the samples were stored in liquid nitrogen and sent for the pathologic examination of H&E staining as the reference in the spectral analysis.

RESULTS

The spectral differences among chronic superficial gastritis, atrophic gastritis and malignant gastric endoscopy samples were studied. For the sharper difference in the ratio of peak intensity, baseline corrections of the spectra were performed at first. Several typical spectra of malignant gastric tissues obtained by endoscopy are illustrated in Figure 1A. The spectral characteristics were similar to those of spectra of gastric tissues, which were obtained during surgical operation in our previous research^[15]. The spectral features of malignant gastric tissues were in good agreement with the criteria established in our previous work^[15]. For example, the broad -3 300/cm absorption band, assigned to N-H stretching vibration of protein and OH stretching vibration of water, was more intense in the malignant stomach samples because of the higher content of water in malignant tissues. C = O band near 1 741/cm was assigned to the fat in tissues, and C-H stretching vibration bands near 2 961, 2 927, and 2 853/cm were related to lipid and fat content and these bands usually disappeared in the spectra of malignant gastric tissues. -1 641/cm absorption peak belonged to amide I band of protein and H-O-H variable-angle vibration of water. In addition, amide II band of protein was located

near 1 550/cm. The intensity of amide II band decreased in the spectra of malignant gastric tissues. Thus, the ratio of intensity of -1 641/cm band to -1 550/cm band was higher in the malignant gastric samples. The intensity of -1 400/cm peak was stronger than that of -1 460/cm peak in the spectra of cancerous samples. According to the statistical results, the relative intensity of I_{1460}/I_{1400} was less than 1 for about 90% of malignant gastric samples. The intensity of absorption peak at about 1 308/cm increased. The peak position shifted to a low wave number. The peak position was lower than 1 310/cm for 72% of the malignant tissues. The intensity of -1 160/cm was often less than that of -1 120/cm in the spectra of stomach cancer samples.

The spectra of chronic atrophic gastritis were close to those of malignant gastric tissues (Figure 1B), and exhibited partial characteristic bands as those of malignant tissues. CH stretching vibrational band near 3 000-2 800/cm and C = O vibrational band about 1 740/cm were still weak in the spectra of atrophic gastritis samples. Compared with the spectra of malignant gastric tissues, the amide II band in the spectra of atrophic gastritis tissues was broader, and the relative intensity of amide II band to amide I band became higher. The decrease in the extent of the intensity of absorption peak near 1 460/cm was not significant, i.e., the intensity of band at about 1 460/cm became a little less than that at 1 400/cm in the spectra of atrophic gastritis samples. In the spectra of about 81% of atrophic gastritis samples, the relative intensity of I_{1460}/I_{1400} was less than or equal to 1. Compared with the spectra of malignant tissues, the absorption peak near 1 310/cm was weaker in the spectra of atrophic gastritis samples. Similar to gastric cancerous tissues, the peak position of this band at about 1 310/cm often shifted to a low wave number, which was different from the situation of chronic superficial gastritis, indicating that

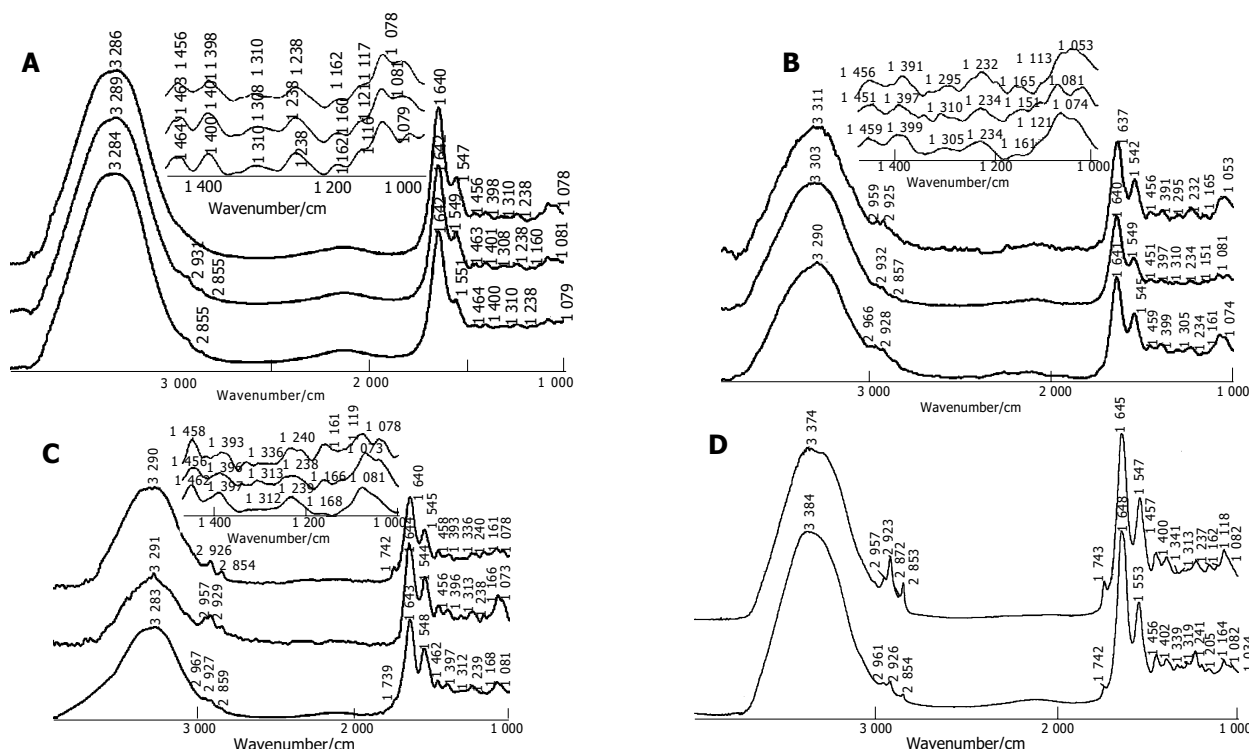


Figure 1 Typical FT-IR spectra of gastric endoscopy samples. A: Spectrum of malignant gastric tissue sample; B: spectrum of chronic atrophic gastritis tissue

sample; C: spectrum of chronic superficial gastritis tissue sample; D: spectrum of normal gastric tissue sample.

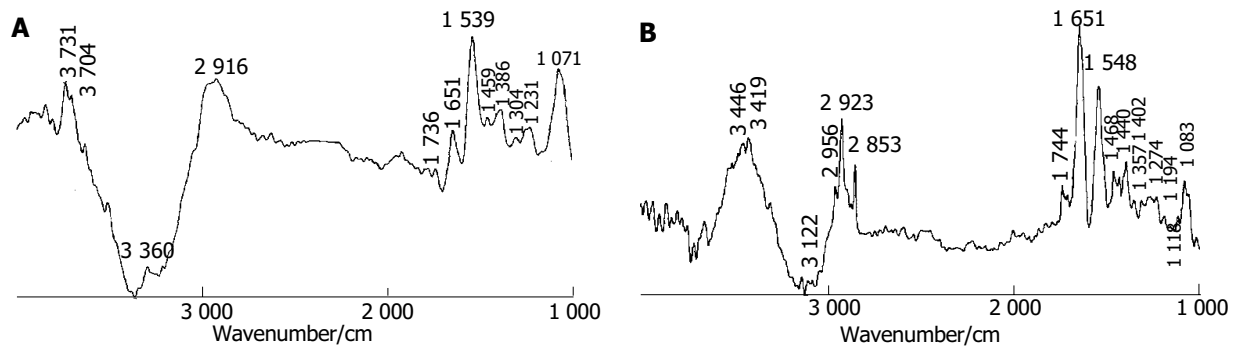


Figure 2 Subtraction spectra of gastric endoscopy samples. **A:** Spectrum of chronic atrophic gastritis tissue minus that of malignant gastric tissue; **B:** spectrum

of normal gastric tissue minus that of chronic superficial gastritis tissue.

the peak position was lower than 1 310/cm for 73% of atrophic gastritis tissues.

The spectra of chronic superficial gastritis tissues (Figure 1C) were similar to those of normal stomach tissues^[15] (Figure 1D). The spectral features were as follows. CH stretching vibrational band near 3 000-2 800/cm and C = O vibrational band at about 1 740/cm were strong in the spectra of superficial gastritis samples. In general, there existed strong and broad amide II bands in the spectra of superficial gastritis samples. The peak at 1 460/cm was stronger than that at 1 400/cm. The relative intensity of I_{1460}/I_{1400} was higher than 1 in about 78% of superficial gastritis samples. The peak at about 1 250/cm was stronger, and the band near 1 308/cm disappeared or became weak and the position of this band often shifted to a high wave number, indicating that the peak position was higher than 1 310/cm in 80% of superficial gastritis tissues. Similar to normal gastric tissues, the intensity of peak near 1 160/cm increased and often became stronger than that at about 1 120/cm.

DISCUSSION

To enhance our understanding, the subtraction technique was performed in the spectral analysis^[16]. The subtraction spectra (Figures 2A and B) could highlight spectral differences between chronic atrophic gastritis tissue and malignant gastric tissue, and between normal gastric tissue and chronic superficial gastritis tissue. From the two subtraction spectra, some new information could be observed.

Figure 2A illustrates the subtraction result of the spectrum of chronic atrophic gastritis tissue minus that of malignant gastric tissue. It verified that chronic atrophic gastritis tissues exhibited relatively stronger C-H stretching vibration, C = O stretching band, amide I, amide II than gastric cancer tissue. In addition, there was more water in gastric cancer tissue due to the strong negative band located near 3 360/cm in the spectrum of subtraction malignant tissue from chronic atrophic gastritis tissue.

Figure 2B shows the spectral differences between normal gastric tissue and chronic superficial gastritis tissue. The positive peaks in the region of 2 800-3 000/cm and near 1 740/cm were observed in the subtraction spectrum, suggesting that normal gastric tissue contains more components

of long-chain C-H and C = O bonds. However, these peaks often decrease and even disappear in the spectra of gastritis and malignant tissues. Because triglyceride contains a large proportion of methyl, methylene and carbonyl, and fat in the region of malignant tissue is consumed because of the necessary nutritional and energy requirement in the development of carcinoma. At the same time, amide I and amide II bands are stronger in the spectrum of normal gastric tissue than in that of chronic superficial gastritis tissue, indicating that normal gastric tissue has more regular protein secondary structures, such as α helical structure.

In conclusion, the results in our study demonstrate that the sensitivity of FT-IR detection to gastric cancer, chronic atrophic gastritis and superficial gastritis is 90.9%, 82.5%, 91.5%, and specificity is 97.3%, 91.7%, 89.5% respectively. FT-IR spectroscopy is effective in distinguishing gastric inflammation from malignancy.

REFERENCES

- 1 Wong PT, Wong RK, Caputo TA, Godwin TA, Rigas B. Infra-red spectroscopy of exfoliated human cervical cells: evidence of extensive structural changes during carcinogenesis. *Proc Natl Acad Sci USA* 1991; **88**: 10988-10992
- 2 Fujioka N, Morimoto Y, Arai T, Kikuchi M. Discrimination between normal and malignant human gastric tissues by Fourier transform infrared spectroscopy. *Cancer Detect Prev* 2004; **28**: 32-36
- 3 Wong PT, Lacelle S, Fung Kee Fung M, Senterman M, Mikhael NZ. Characterization of exfoliated cells and tissues from human endocervix and ectocervix by FTIR and ATR/FTIR spectroscopy. *Biospectroscopy* 1995; **1**: 357-364
- 4 Sindhuphak R, Issaravanich S, Udomprasertgul V, Srisookho P, Warakamin S, Sindhuphak S, Boonbundarlchai R, Dusitsin N. A new approach for the detection of cervical cancer in Thai women. *Gynecol Oncol* 2003; **90**: 10-14
- 5 Argov S, Ramesh J, Salman A, Sinelnikov I, Goldstein J, Guterman H, Mordechai S. Diagnostic potential of Fourier-transform infrared microscopy and advanced computational methods in colon cancer patients. *J Biomed Opt* 2002; **7**: 248-254
- 6 Ling XF, Xu YZ, Soloway RD, Xu Z, Zhang TI, Zhou XS, Li WH, Yang ZL, Weng SF, Xu DF, Wu JG. Identification of colorectal and gastric cancer by Fourier transform Infrared (FT-IR) spectroscopy and separation from normal tissue. *Gastroenterology* 2002; **122**: T1584
- 7 Li QB, Yang LM, Ling XF, Wang JS, Zhou XS, Shi JS, Wu JG. Application of the SIMCA method to cancer diagnosis with Fourier-transform infrared spectroscopy. *Guangpuxue Yu*

- Guangpu Fenxi* 2004; **24**: 414-417
- 8 **Ren Y**, Xu YZ, Wang J, Zhang YF, Wang F, Shi JS, Wu JG. FTIR spectroscopic and statistical studies on the lung tissues. *Guangpuxue Yu Guangpu Fenxi* 2003; **23**: 681-684
- 9 **Sun CW**, Xu YZ, Sun KH, Wu QG, Li WH, Xu ZH, Wu JG. A study of the diagnosis of salivary gland tumors by means of mid infrared optical fiber technique. *Guangpuxue Yu Guangpu Fenxi* 1996; **16**: 22-25
- 10 **Wu JG**, Xu YZ, Sun CW, Soloway RD, Xu DF, Wu QG, Sun KH, Weng SF, Xu GX. Distinguishing malignant from normal oral tissues using FTIR fiber-optic techniques. *Biopolymers* 2001; **62**: 185-192
- 11 **Xu YZ**, Soloway RD, Lin XF, Zhi X, Weng SF, Wu QG, Shi JS, Sun WX, Zhang TX, Wu JG, Xu DF, Xu GX. Fourier transform infrared (FT-IR) mid-IR spectroscopy separates normal and malignant tissue from the colon and stomach. *Gastroenterology* 2000; **118**: A6438
- 12 **Wang JS**, Xu YZ, Shi JS, Zhang L, Duan XY, Yang LM, Su YL, Weng SF, Xu DF, Wu JG. FTIR spectroscopic study on normal and cancerous tissues of esophagus. *Guangpuxue Yu Guangpu Fenxi* 2003; **23**: 863-865
- 13 **Zhang L**, Sun KH, Soloway RD, Ling XF, Xu YZ, Wu QG, Weng SF, Yang ZL, Zhang TL, Yao GQ, Chen HH, Zhou XS, Xu DF, Wu JG. Intraoperative Fourier transform infrared spectroscopy can guide individual resections in patients with gastric cancer. *Gastroenterology* 2004; **126**: A626
- 14 **Van Dam J**. Novel methods of enhanced endoscopic imaging. *Gut* 2003; **52**(Suppl 4): 12-16
- 15 **Peng Q**, Xu YZ, Li WH, Zhou XS, Wu JG. FTIR study on the normal and tumor gastrointestinal tissues. *Guangpuxue Yu Guangpu Fenxi* 1998; **18**: 528-531
- 16 **Ling XF**, Xu YZ, Weng SF, Li WH, Xu Z, Hammaker RM, Fateley WG, Wang F, Zhou XS, Soloway RD, Ferraro JR, Wu JG. Investigation of normal and malignant tissue samples from the human stomach using Fourier transform Raman spectroscopy. *Appl Spectrosc* 2002; **56**: 570-573

Science Editor Wang XL and Guo SY Language Editor Elsevier HK

Clinical significance of expression of apoptotic signal proteins in gastric carcinoma tissue

Xin-Han Zhao, Shan-Zhi Gu, Hong-Gang Tian, Ping Quan, Bo-Rong Pan

Xin-Han Zhao, Shan-Zhi Gu, Hong-Gang Tian, Ping Quan, Key Laboratory of Environment and Genes Related to Diseases of Ministry of Education, Department of Medical Oncology, First Hospital of Xi'an Jiaotong University, Xi'an 710061, Shaanxi Province, China
Bo-Rong Pan, Department of Oncology, Xijing Hospital, Fourth Military Medical University, Xi'an 710032, Shaanxi Province, China
Co-first-authors: Shan-Zhi Gu
Correspondence to: Dr. Xin-Han Zhao, Key Laboratory of Environment and Genes Related to Diseases of Ministry of Education, Department of Forensic Medicine, Medical College of Xi'an Jiaotong University, Xi'an 710061, Shaanxi Province, China. xashanshan@sohu.com
Telephone: +86-29-82655475 Fax: +86-29-82655472
Received: 2004-10-09 Accepted: 2004-11-26

Abstract

AIM: To evaluate the expressions of apoptotic signal proteins FADD, TRADD, FasL, Fas, and NF κ B in gastric carcinoma tissues and their clinical significance.

METHODS: Western blot immune trace method was adopted to detect the expressions of apoptotic signal proteins FADD, TRADD, FasL, Fas, and NF κ B in 55 tissue specimens of gastric carcinoma.

RESULTS: Five apoptotic signal proteins had different expressions in the gastric carcinoma samples and their expressions were not correlated to age ($P = 0.085$). Expressions of the FADD, FasL, Fas, and NF κ B proteins reduced with increase of the volume of tumor with the exception of increased expression the TRADD protein (64.7-71.1%, $P = 0.031$). With gradual increase of the malignancy of gastric carcinoma tissues, expressions of the FADD, FasL, and Fas proteins decreased (78.6-28.0%, $P = 0.008$; 78.6-65.9%, $P = 0.071$; 100.0-46.3%, $P = 0.014$), while expressions of the TRADD and NF κ B proteins increased (42.9-78.1%, $P = 0.063$; 78.6-79.1%, $P = 0.134$). With gradual increase of serum CEA, expression of the FADD protein decreased (62.5-34.0%, $P = 0.073$), but expressions of the TRADD, FasL, Fas, and NF κ B proteins increased (0.0-80.8%, $P = 0.005$; 62.5-70.2%, $P = 0.093$; 0.0-70.2%, $P = 0.003$; 62.5-80.9%, $P = 0.075$). When compared to the tissues of gastric carcinoma without metastasis, the positive rate of expressions of the FADD and FasL proteins increased, whereas expressions of the TRADD, FADD, and NF κ B proteins decreased. There was no significant difference between them ($P = 0.095$).

CONCLUSION: Gastric carcinoma is endurable to Fas-related apoptosis and apoptotic signal proteins are differently expressed in gastric carcinoma.

© 2005 The WJG Press and Elsevier Inc. All rights reserved.

Key words: Gastric cancer; Apoptosis; Signal protein; Western blot

Zhao XH, Gu SZ, Tian HG, Quan P, Pan BR. Clinical significance of expression of apoptotic signal proteins in gastric carcinoma tissue. *World J Gastroenterol* 2005; 11(25): 3846-3849
<http://www.wjgnet.com/1007-9327/11/3846.asp>

INTRODUCTION

Gastric carcinoma is one of the most common causes of malignancy-related death in China^[1-4]. Its therapy in clinics is a big challenge. Better remedial method possibly depends on advances in basic research^[5-7]. Recent evidence suggests that apoptosis of cells is closely related to occurrence, progress and metastasis of the tumor^[8-10]. At present, studies on the apoptosis of tumor cells are an important field of tumor therapy and tumor molecular biology^[11-14]. The abnormalities in expressions of apoptotic signal proteins always influence the gastrocellular apoptosis, thus leading to the incidence and development of gastric carcinoma^[15-17]. We adopted the Western blot immune trace method to detect the expressions of apoptotic signal proteins FADD, TRADD, FasL, Fas, and NF κ B in gastric carcinoma tissues and their significance in gastric carcinoma was assessed.

MATERIALS AND METHODS

Samples

A total of 55 cases were selected from patients with primary gastric carcinoma excision in our hospital from January 2000 to April 2001, who were pathologically diagnosed as adenocarcinoma. There were 35 male and 20 female cases aged 34-78 years with an average age of 54 years. According to Edmondson grading III, the samples were graded as I-II grade in 14 cases and III-IV grade in 41 cases. All samples were submerged in liquid nitrogen within half an hour after the excision and placed in a -80 °C refrigerator.

Protein extraction

Fifty-five tumor tissue specimens were homogenized, sonicated for 15 s twice in 500 μ L of lysis buffer containing 1 \times phosphate-buffered saline (PBS), 1% Nonidet-P40, 0.5% sodium deoxycholate, 0.1% SDS and 0.1 mg/mL phenylmethylsulfonyl fluoride, and placed on ice for 30 min. The lysate was centrifuged at 13 000 g for 15 min at 4 °C, the supernatant was collected (450 μ L) and the

Table 1 Expressions of FADD, TRADD, FasL, Fas and NFκB proteins in gastric carcinoma tissue specimens, *n* (%)

Sex	<i>n</i>	FADD	TRADD	FasL	Fas	NFκB
Male	35	12 (34.3)	26 (74.3)	25 (71.4)	21 (60.0)	28 (80.0)
Female	20	8 (40.0)	12 (60.0)	13 (65.0)	12 (60.0)	15 (75.0)
	55	20 (36.4)	38 (69.1)	38 (69.1)	33 (60.0)	43 (78.2)

protein concentration for each sample was determined by spectrophotometry (Pharmacia) and using a DC protein assay kit (Bio-Rad).

Reagents and methods

Sheep antihuman FADD, TRADD, FasL, and Fas polyclonal antibodies, rabbit antihuman NFκB polyclonal antibodies, alkaline phosphatase marking anti-sheep, anti-rabbit and protein molecular mass marker were also purchased from Santa Cruz Company. Western blot immune trace method was employed to determine the expression of apoptotic signal proteins. Twenty microliters of extracted protein for 120 g/L polyacrylamide gel electrophoresis. When it was semidry, electrical metastasis to the nitrocellulose film was made and enclosed with 100 mL/L bovine serum for 1 h. The first antibody (1:1 000) was put into PBST (1 g/L Tween20 in PBS) and stored overnight at 4 °C. After being washed, the sample was enclosed again with 100 mL/L bovine serum for 30 min, and then the second antibody was put in at room temperature for 1 h. After being washed with PBS for 1 h, NBTBCIP development method was performed for coloration.

Assessment standards

The protein molecular mass marker was taken as the standard. In the respective different molecular mass scope, the sample with black stripes was considered positive and vice versa negative. The molecular mass of FADD, TRADD, FasL, Fas, and NFκB proteins was 23, 34, 31, 48, and 65 ku respectively.

Statistical analysis

Chi squared test, accurate 4-chess table method and correlation analysis were used to analyze the correlation of protein expressions with sex, age, tumor size, pathological grading and tumor metastasis. $P < 0.05$ was considered statistically significant.

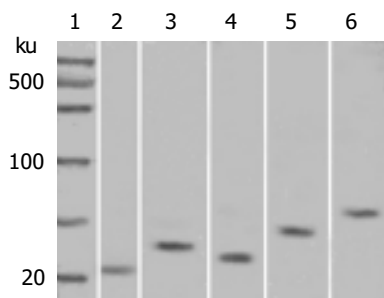


Figure 1 Western blot analysis of the accurate expression of apoptotic signal proteins. Lane 1: marker; lane 2: FADD; lane 3: TRADD; lane 4: FasL; lane 5: Fas; lane 6: NFκB.

RESULTS

Expression of apoptotic signal proteins in gastric carcinoma

The expression of FADD, TRADD, FasL, Fas, and NFκB proteins in gastric carcinoma tissue specimens was 36.4% (20/55), 69.1% (38/55), 69.1% (38/55), 60.0% (33/55) and 78.2% (43/55) respectively (Table 1). We carried out Western blot analysis to determine the accuracy of protein expression (Figure 1).

Relation between apoptotic signal proteins and clinical characteristics

Different expressions of the five apoptotic signal proteins were not correlated to age ($P = 0.085$, Figure 2A). Expressions of the FADD, TRADD, FasL, Fas, and NFκB proteins reduced with increase of the tumor volume, with the exception of increased expression of the TRADD protein (64.7-71.1%, $P = 0.031$). Among them, the positive rate of the expression of the Fas protein in the tissue of gastric carcinoma with a lump ≤ 5 cm was higher than that of gastric carcinoma > 5 cm and the difference was significant ($P = 0.037$, Table 2, Figure 2B).

With the increased of malignancy grade in adenocarcinoma tissues, expressions of the FADD, FasL, and Fas proteins decreased, while expressions of the TRADD and NFκB proteins increased. Expressions of the FADD and Fas

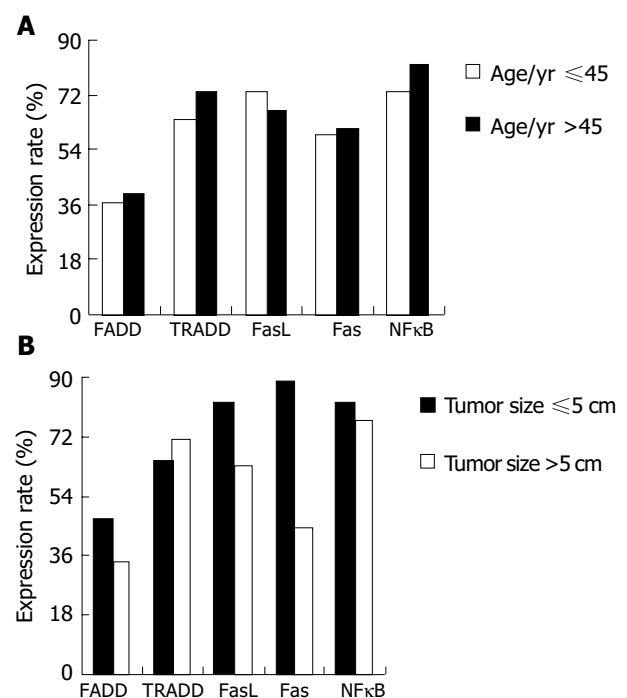


Figure 2 Different expressions of five proteins before and after 45 years (A) and different tumor size (B).

Table 2 Relationship between expressions of the FADD, TRADD, FasL, Fas, NFκB proteins and clinical characteristics, *n* (%)

Clinical characteristics	<i>n</i>	FADD	TRADD	FasL	Fas	NFκB
Male	35	12 (34.3)	26 (74.3)	25 (71.4)	21 (60.0)	28 (80.0)
Female	20	8 (40.0)	12 (60.0)	13 (65.0)	12 (60.0)	15 (75.0)
Age/yr ≤45	22	8 (36.4)	14 (63.6)	16 (72.7)	13 (59.1)	16 (72.7)
>45	33	13 (39.4)	24 (72.7)	22 (66.7)	20 (60.6)	27 (81.8)
Tumor						
Size ≤5 cm	17	8 (47.1)	11 (64.7)	14 (82.4)	15 (88.2) ^a	14 (82.4)
>5 cm	38	13 (34.2)	27 (71.1)	24 (63.2)	17 (44.7)	29 (76.3)
Grading I-II	14	11 (78.6) ^b	6 (42.9)	11 (78.6)	14 (100.0) ^c	11 (78.6)
III-IV	41	9 (22.0)	32 (78.1)	27 (65.9)	19 (46.3)	32 (78.1)
CEA ≤30 (μg/L)	8	5 (62.5)	0 (0.0)	5 (62.5)	0 (0.0)	5 (62.5)
>30 (μg/L)	47	16 (34.0)	38 (80.9) ^d	33 (70.2)	33 (70.2) ^d	38 (80.9)
Tumor transformation						
Yes	6	3 (50.0)	3 (50.0)	5 (83.3)	3 (50.0)	3 (50.0)
No	49	17 (34.2)	35 (71.4)	33 (67.4)	30 (61.2)	39 (79.6)

^a*P*<0.05 vs size >5 cm; ^b*P*<0.01, ^c*P*<0.05 vs grading III-IV; ^d*P*<0.01 vs CEA ≤30 (μg/L).

proteins were significantly different between the pathological grades (*P* = 0.008 and *P* = 0.014, Figure 3A). With the increase of serum CEA, expression of the FADD protein in gastric carcinoma tissues decreased, while expressions of the TRADD, FasL, Fas and NFκB proteins increased. Expression of the TRADD and Fas proteins were positively correlated with the serum CEA level (*r* = 0.700, *P* = 0.005) and the difference was very significant (*P* = 0.003, Figure 3B). When compared to the tissues of gastric carcinoma with metastasis, the positive expression rate of the FADD and FasL proteins increased, whereas expressions of the TRADD, FAS and NFκB proteins decreased. There was no significant difference between them (*P* = 0.095).

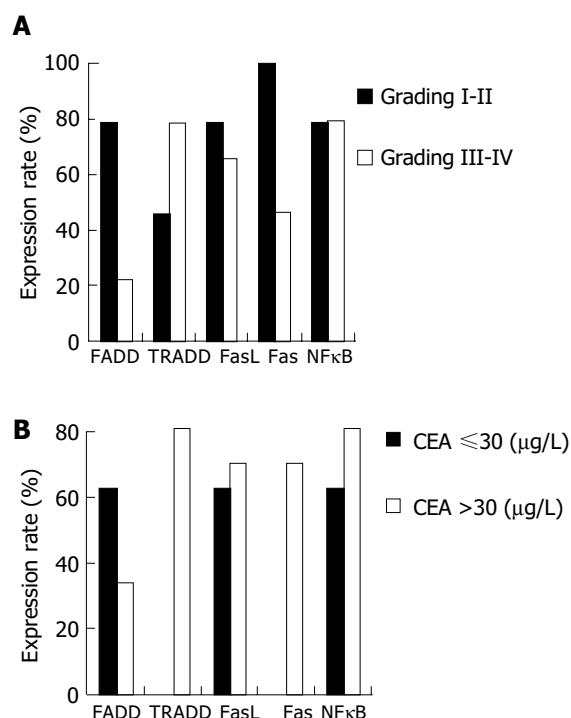


Figure 3 Different expressions of the five proteins with different pathological grading (A) and different serum CEA (B).

DISCUSSION

Apoptotic abnormality is considered as an important mechanism underlying the development of gastric carcinoma^[18,19] and even more crucial than the reproduction of cells of out control^[20,21]. The expression of apoptotic signal proteins play different roles in the death of gastric cancer cells. The current studies^[22,23] have denoted the main mechanism of the interaction of the apoptotic signal proteins to conduct down the apoptotic signal. FasL is polymerized with its corresponding Fas receptors^[24,25]. By activating the FADD and caspase family, the apoptosis of cancer cells ensues; and by activating TRADD, RIP is motivated, causing NFκB to be activated, thereby participating in gene transcription of the survival of cells. The balance between counter signals and paths eventually determines the survival or apoptosis of cells.

In this study, the expression of Fas protein was downregulated with increase of the gastric carcinoma volume and the malignancy degree and positively correlated with the expression of CEA. It was reported^[26] that gastric cancer cells inhibit expression of the downregulated FasL, thus escaping Fas-related apoptosis and immune monitoring of the host to enable cancer cells to reproduce continuously and increase their malignancy degree. Expression of the FADD protein is downregulated with increase of the malignancy degree of gastric carcinoma^[27]. Gastric cancer cells might through the expression of the downregulated FADD enable caspases 3 and 8 necessary for apoptosis of Fas-related cells to be devitalized, resulting in inhibition of the apoptosis of gastric cancer cells. If FADD is injected, such cells can become sensitive to Fas and induce Fas-related apoptosis, suggesting that the function of FADD is extremely crucial.

The TRADD protein is able to vitalize the NFκB transcription factor and prolong the survival of cells. In the present study, the TRADD protein expression was positively correlated with CEA only when CEA possessed the value of 30 μg/L, suggesting that both of them can be used as indexes to detect gastric carcinoma. However, this can be determined only after investigating a large size of samples^[28-30]. As the change of expressions of apoptotic

signal proteins is not much related to metastasis of gastric carcinoma, the abnormalities of the function of these proteins only contribute to the reproduction and rise of malignancy degree of gastric cancer cells, whereas metastasis of gastric carcinoma might correlate to other factors.

In summary, gastric carcinoma is a tumor endurable to Fas-related apoptosis. Apoptotic signal proteins are differently expressed in gastric carcinoma.

REFERENCES

- 1 **Duan LX**, Zhong DW, Hu FZ, Zhao H, Yang ZL, Yi WJ, Shu GS, Hua SW. Relationship between expression of VEGF, Flt1, bFGF and P53 and outcome in patients with gastric carcinoma. *Shijie Huaren Xiaohua Zazhi* 2004; **12**: 546-549
- 2 **Xia JG**, Ding YB, Chen GY. Expression of tyrosine kinase Syk and its clinical significance in gastric carcinoma. *Shijie Huaren Xiaohua Zazhi* 2004; **12**: 767-769
- 3 **Fukui T**, Matsui K, Kato H, Takao H, Sugiyama Y, Kunieda K, Saji S. Significance of apoptosis induced by tumor necrosis factor- α and/or interferon- γ against human gastric cancer cell lines and the role of the p53 gene. *Surg Today* 2003; **33**: 847-853
- 4 **Kojima N**, Kunieda K, Matsui K, Kato H, Saji S. Evaluation of carcinoembryonic antigen mRNA in living, necrotic, and apoptotic gastric cancer cells by reverse transcriptase-polymerase chain reaction. *Surg Today* 2003; **33**: 839-846
- 5 **Igarashi A**, Konno H, Tanaka T, Nakamura S, Sadzuka Y, Hirano T, Fujise Y. Liposomal photofrin enhances therapeutic efficacy of photodynamic therapy against the human gastric cancer. *Toxicol Lett* 2003; **145**: 133-141
- 6 **Kokura S**, Yoshida N, Ueda M, Imamoto E, Ishikawa T, Takagi T, Naito Y, Okanoue T, Yoshikawa T. Hyperthermia enhances tumor necrosis factor α -induced apoptosis of a human gastric cancer cell line. *Cancer Lett* 2003; **201**: 89-96
- 7 **Huang HL**, Wu BY, You WD, Shen MS, Wang WJ. Influence of dendritic cell infiltration on prognosis and biologic characteristics of progressing gastric cancer. *Zhonghua Zhongliu Zazhi* 2003; **25**: 468-471
- 8 **Wu YQ**, Wang MW, Wu BY, You WD, Zhu QF. Expression of apoptosis-related proteins and proliferating cell nuclear antigen during stomach canceration. *Shijie Huaren Xiaohua Zazhi* 2004; **12**: 770-773
- 9 **Nakashima S**, Hiraku Y, Tada-Oikawa S, Hishita T, Gabazza EC, Tamaki S, Imoto I, Adachi Y, Kawanishi S. Vacuolar H⁺-ATPase inhibitor induces apoptosis via lysosomal dysfunction in the human gastric cancer cell line MKN-1. *J Biochem* 2003; **134**: 359-364
- 10 **Zhan N**, Xiong YY, Lan J, Wang BC, Tian SF, Yu SP. Relationship between *Helicobacter pylori* infection and expression of c-myc, Bcl-2, and Bax protein in different gastric mucosa lesions. *Aizheng* 2003; **22**: 1034-1037
- 11 **Jiang XH**, Wong BC. Cyclooxygenase-2 inhibition and gastric cancer. *Curr Pharm Des* 2003; **9**: 2281-2288
- 12 **Suzuki H**, Masaoka T, Nomura S, Hoshino Y, Kurabayashi K, Minegishi Y, Suzuki M, Ishii H. Current consensus on the diagnosis and treatment of *H pylori*-associated gastroduodenal disease. *Keio J Med* 2003; **52**: 163-173
- 13 **Naidu KA**. Vitamin C in human health and disease is still a mystery? An overview. *Nutr J* 2003; **2**: 7
- 14 **Fukumoto H**, Tennis M, Locascio JJ, Hyman BT, Growdon JH, Irizarry MC. Age but not diagnosis is the main predictor of plasma amyloid β -protein levels. *Arch Neurol* 2003; **60**: 958-964
- 15 **Valbonesi P**, Sartor G, Fabbri E. Characterization of cholinesterase activity in three bivalves inhabiting the North Adriatic sea and their possible use as sentinel organisms for biosurveillance programmes. *Sci Total Environ* 2003; **312**: 79-88
- 16 **Bjorling-Poulsen M**, Seitz G, Guerra B, Issinger OG. The pro-apoptotic FAS-associated factor 1 is specifically reduced in human gastric carcinomas. *Int J Oncol* 2003; **23**: 1015-1023
- 17 **Ishii H**, Zanasi N, Vecchione A, Trapasso F, Yendamuri S, Sarti M, Baffa R, During MJ, Huebner K, Fong LY, Croce CM. Regression of upper gastric cancer in mice by FHIT gene delivery. *FASEB J* 2003; **17**: 1768-1770
- 18 **Hahm KB**, Kim DH, Lee KM, Lee JS, Surh YJ, Kim YB, Yoo BM, Kim JH, Joo HJ, Cho YK, Nam KT, Cho SW. Effect of long-term administration of rebamipide on *Helicobacter pylori* infection in mice. *Aliment Pharmacol Ther* 2003; **18**(Suppl 1): 24-38
- 19 **Kim DH**, Kim SW, Song YJ, Oh TY, Han SU, Kim YB, Joo HJ, Cho YK, Kim DY, Cho SW, Kim MW, Kim JH, Hahm KB. Long-term evaluation of mice model infected with *Helicobacter pylori*: focus on gastric pathology including gastric cancer. *Aliment Pharmacol Ther* 2003; **18**(Suppl 1): 14-23
- 20 **Jeong JH**, Park JS, Moon B, Kim MC, Kim JK, Lee S, Suh H, Kim ND, Kim JM, Park YC, Yoo YH. Orphan nuclear receptor Nur77 translocates to mitochondria in the early phase of apoptosis induced by synthetic chenodeoxycholic acid derivatives in human stomach cancer cell line SNU-1. *Ann N Y Acad Sci* 2003; **1010**: 171-177
- 21 **Ohno S**, Inagawa H, Dhar DK, Fujii T, Ueda S, Tachibana M, Suzuki N, Inoue M, Soma G, Nagasue N. The degree of macrophage infiltration into the cancer cell nest is a significant predictor of survival in gastric cancer patients. *Anticancer Res* 2003; **23**: 5015-5022
- 22 **Zhao Y**, Wu K, Yu Y, Li G. Roles of ERK1/2 MAPK in vitamin E succinate-induced apoptosis in human gastric cancer SGC-7901 cells. *Weisheng Yanjiu* 2003; **32**: 573-575
- 23 **Miyachi K**, Sasaki K, Onodera S, Taguchi T, Nagamachi M, Kaneko H, Sunagawa M. Correlation between survivin mRNA expression and lymph node metastasis in gastric cancer. *Gastric Cancer* 2003; **6**: 217-224
- 24 **Yamaguchi H**, Tanaka F, Sadanaga N, Ohta M, Inoue H, Mori M. Stimulation of CD40 inhibits Fas- or chemotherapy-mediated apoptosis and increases cell motility in human gastric carcinoma cells. *Int J Oncol* 2003; **23**: 1697-1702
- 25 **Li Z**, Wang Z, Zhao Z, Zhang Y, Ke Y. Expression of Fas, FasL and IFN- γ in gastric cancer. *Beijing Daxue Xuebao* 2003; **35**: 386-389
- 26 **Lim SC**. Fas-related apoptosis in gastric adenocarcinoma. *Oncol Rep* 2003; **10**: 57-63
- 27 **Katoh M**, Katoh M. FLJ10261 gene, located within the CCND1-EMS1 locus on human chromosome 11q13, encodes the eight-transmembrane protein homologous to C12orf3, C11orf25 and FLJ34272 gene products. *Int J Oncol* 2003; **22**: 1375-1381
- 28 **Dechant MJ**, Fellenberg J, Scheuerpflug CG, Ewerbeck V, Debatin KM. Mutation analysis of the apoptotic "death-receptors" and the adaptors TRADD and FADD/MORT-1 in osteosarcoma tumor samples and osteosarcoma cell lines. *Int J Cancer* 2004; **109**: 661-667
- 29 **Jamieson NB**, McMillan DC, Brown DJ, Wallace AM. Comparison of simple acid-ethanol precipitation with gel exclusion chromatography for measuring leptin binding in serum of normal subjects and cancer patients. *Ann Clin Biochem* 2003; **40**(Pt 2): 185-187
- 30 **El Yazidi-Belkoura I**, Adriaenssens E, Dolle L, Descamps S, Hondermarck H. Tumor necrosis factor receptor-associated death domain protein is involved in the neurotrophin receptor-mediated antiapoptotic activity of nerve growth factor in breast cancer cells. *J Biol Chem* 2003; **278**: 16952-16956

Expression and significance of tumor-related genes in HCC

Zi-Li Lü, Dian-Zhong Luo, Jian-Ming Wen

Zi-Li Lü, Dian-Zhong Luo, Department of Pathology, Guangxi Medical University, Nanning 530021, Guangxi Zhuang Autonomous Region, China

Jian-Ming Wen, Department of Pathology, Zhongshan Medical College, Sun Yat-Sen University, Guangzhou 510080, Guangdong Province, China

Supported by the National Natural Science Foundation of China, No. 39860079

Correspondence to: Dr. Dian-Zhong Luo, Department of Pathology, Guangxi Medical University, Nanning 530021, Guangxi Zhuang Autonomous Region, China. luodianzhong@yahoo.com.cn
Telephone: +86-771-5356534

Received: 2004-08-18 Accepted: 2004-11-24

Abstract

AIM: To investigate the expression and clinical significance of *DEK*, *cyclin D1*, insulin-like growth factor II (*IGF-II*), glypican 3 (*GPC3*), ribosomal phosphoprotein 0 (*rpP0*) mRNA in hepatocellular carcinoma (HCC) and its paraneoplastic tissues.

METHODS: The expression of mRNAs of *DEK*, *cyclin D1*, *IGF-II*, *GPC3* and *rpP0* mRNA was detected in HCC and its paraneoplastic tissues by multiplex RT-PCR.

RESULTS: By the simplex RT-PCR, the overexpression of mRNAs of *DEK*, *cyclin D1*, *IGF-II*, *GPC3*, *rpP0* mRNA in HCC and its paraneoplastic tissues was 78.1%, 87.5%, 87.5%, 75.0%, 81.3% and 15.6%, 40.6%, 37.5%, 21.9%, 31.3% respectively ($P < 0.05$). By the multiplex RT-PCR, at least one of the mRNAs was detected in all HCC samples and in 75.0% of paraneoplastic samples ($P > 0.05$). However, all these five mRNAs were found in 68.8% of HCC samples, but only in 9.4% of paraneoplastic tissues ($P < 0.05$). The positive expression of mRNAs of *DEK*, *cyclin D1*, *IGF-II*, *GPC3*, *rpP0* in well- and poorly-differentiated HCC was 89.0%, 66.7%, 66.7%, 66.7%, 77.8% and 73.9%, 95.7%, 95.7%, 82.6%, respectively ($P > 0.05$). The expression of these genes in HCCs with α -feto protein (AFP) negative and positive was 90.0%, 80.0%, 90.0%, 90.0%, 90.0% and 72.7%, 86.3%, 77.3%, 90.9%, 68.2% respectively ($P > 0.05$).

CONCLUSION: The expression of *DEK*, *cyclin D1*, *IGF-II*, *GPC3*, *rpP0* mRNA in HCC is much higher in HCC than in its paraneoplastic tissues. Multiplex RT-PCR assay is an effective, sensitive, accurate, and cost-effective diagnostic method of HCC.

© 2005 The WJG Press and Elsevier Inc. All rights reserved.

Key words: HCC; *DEK*; *Cyclin D1*; *IGF-II*; *GPC3*; *rpP0*

Lü ZL, Luo DZ, Wen JM. Expression and significance of tumor-related genes in HCC. *World J Gastroenterol* 2005; 11(25): 3850-3854

<http://www.wjgnet.com/1007-9327/11/3850.asp>

INTRODUCTION

Hepatocellular carcinoma (HCC) is an aggressive malignancy with poor prognosis and one of the most common tumors in humans. The development of HCC is a chronic process and involves many factors, including infection of hepatitis virus and contamination with aflatoxin B1^[1]. Recent advances in molecular genetics indicate that some tumor suppressor genes, oncogenes, and growth factors may play an important role in hepatocarcinogenesis^[2].

Several methods such as DDRT-PCR, cDNA screening^[3] are used to identify differential expression of mRNA in tumor and non-tumor tissues. It is reported that some genes, such as *DEK*, *rpP0*^[4], *cyclin D1*^[5], *IGF-II*^[6], and *GPC3*^[7], are overexpressed in HCC tissue. The expression of *DEK*, *IGF-II* and *rpP0* is higher in HCC than non-tumor tissues in our previous study.

RT-PCR is widely used to analyze gene expression in HCC and paraneoplastic liver tissue. However, the overexpressed genes are only relatively higher in HCC than in paraneoplastic liver tissue and the positive detection rate is relatively low. Moreover, RT-PCR can detect only a single gene once in the past, and the results obtained are fluctuant and less useful in clinics. In order to find a method to enhance the specificity and positive rate, multiplex PCR was used to detect several genes, such as *DEK*, *cyclin D1*, *IGF-II*, *GPC3*, *rpP0*.

MATERIALS AND METHODS

Tissue samples and patients

HCC and corresponding paraneoplastic tissues were obtained with informed consent from 32 patients who underwent hepatectomy at the First Affiliated Hospital of Guangxi Medical University and Guangxi Tumor Hospital. The profiles were obtained from medical records of 20 male and 12 female patients with an average age of 42.5 years. Twenty-two patients were positive for α -feto protein (AFP). HCC and paraneoplastic tissues were enucleated separately and immediately frozen in liquid nitrogen. Histological classification was performed according to the Edmondson's grading criteria.

Multiplex RT-PCR

Total RNA was isolated from 100 mg of frozen tissue according to the manufacturer's instructions using TRIzol

kit (Sagon Company, Shanghai, China), and then dissolved in water that was treated by DEPC. Four micrograms of total RNA was used to produce cDNA using oligo(dT) primer and MuLV reverse transcription (MBI Company) in a final volume of 20 μ L at 42 $^{\circ}$ C for 1 h. The reaction was terminated by incubation at 75 $^{\circ}$ C for 10 min. One microgram of products was PCR amplified with multiple primer sets (0.5 μ mol/L, Sagon Company, Shanghai, China), 0.75 units of Taq DNA polymerase (MBI), 0.5 μ L 10 mmol/L dNTPs, 2.5 μ L 10 \times buffer. The primers were as follows: *DEK*: 5'-AGG CAC TGT GTC CTC ATT AA and 5'-TCT GAC AGA ATT TCA GGA CA (332 bp); *cyclin D1*: 5'-TAT TTG CAT AAC CCT GAG CG and 5'-GTG ACT ACA TGC ATA TGA GC (350 bp); *IGF*: 5'-AGG AGC TCC TGG ATA ATT TC and 5'-AAT ATT TCA CGT GAC AGA AC (421 bp); *GPC3*: 5'-TGG ACA TCA ATG AGT GCC TC and 5'-CAC ATT CTG GTG AGC ATT CG (204 bp); *rpP0*: 5'-ATG TGA AGT CAC TGT GCC AG and 5'-CTT GGC TTC AAC CTT AGC TG (549 bp). GAPDH was used as control, the primers were 5'-TGA GTA CGT CGT GGA GTC CA and 5'-CAA AGT TGT CAT GGA TGA CC (230 bp). The conditions were initial denaturation at 94 $^{\circ}$ C for 5 min, 30 cycles of amplification, each cycle consisting of denaturation at 94 $^{\circ}$ C for 45 s, annealing at 58 $^{\circ}$ C for 30 s, extension at 72 $^{\circ}$ C for 30 s, final extension at 72 $^{\circ}$ C for 7 min. Because of the limitation by the length of PCR products, the primers of *cyclin D1* and *GPC3* were used together in a single reaction and the primers of *DEK*, *IGF-II*, and *rpP0* were used together in a single reaction.

Analysis by electrophoresis

The amplified products were electrophoresed on 1.2% agarose gel to detect the expression of the genes in HCC and paraneoplastic tissues. The images were analyzed by Quantity One software.

Statistical analysis

Results were analyzed by χ^2 test to compare the differences between the groups. $P < 0.05$ was considered statistically significant.

RESULTS

Expression of GAPDH mRNA

The expression of *GAPDH* mRNA was detected in all HCC and non-HCC tissues. There was no difference between the two groups (Figure 1A).

Expression of DEK, cyclin D1, IGF-II, GPC3, rpP0 mRNAs in HCC and adjacent noncancerous liver tissues

The expression of *DEK*, *cyclin D1*, *IGF-II*, *GPC3*, *rpP0* mRNAs in HCC and adjacent noncancerous liver tissues was 78.1%, 87.5%, 87.5%, 75.0%, 81.3%, and 15.6%, 40.6%, 37.5%, 21.9%, 31.3%, respectively ($P < 0.05$, Table 1), which were significantly higher in HCC tissues than in adjacent nontumorous tissue (Figures 1B and C). The density of the bands was also higher in HCC than in adjacent noncancerous liver tissues.

The expression of *DEK*, *cyclin D1*, *IGF-II*, *GPC3*, *rpP0* mRNAs in well- and poorly-differentiated HCC was 89.0%,

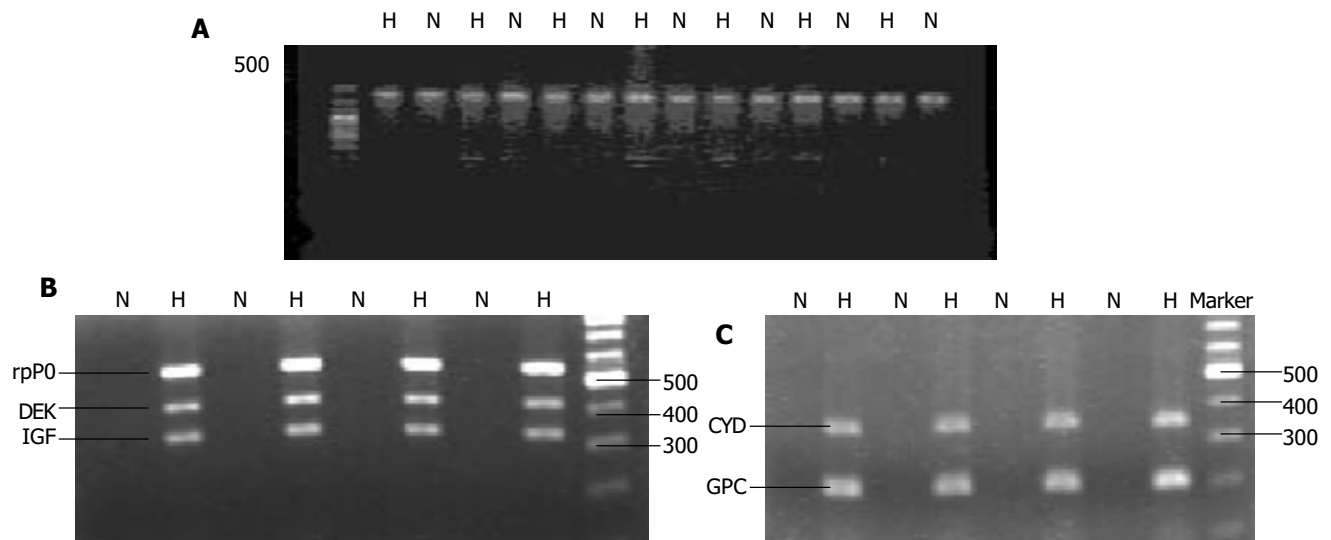


Figure 1 Expression of GAPDH (A), mRNA of rpP0, DEK, and IGF-II (B), mRNA of cyclin D1 and GPC3 (C) in HCC tissue (H) and adjacent nontumorous tissue (N).

Table 1 Expression of *DEK*, *cyclin D1*, *IGF-II*, *GPC3*, *rpP0* mRNAs in HCC and adjacent noncancerous liver tissues

	Cyclin D1 ^a		GPC3 ^c		DEK ^e		IGF ^g		rpP0 ⁱ	
	T	N	T	N	T	N	T	N	T	N
Positive	28	13	24	7	25	5	28	12	26	10
Negative	4	19	8	25	7	27	4	20	6	22

T, HCC tumor tissue; N, adjacent nontumorous tissue. χ^2 -test: ^a $P < 0.05$, ^c $P < 0.05$, ^e $P < 0.05$, ^g $P < 0.05$, ⁱ $P < 0.05$ vs others.

66.7%, 66.7%, 66.7%, 77.8% and 73.9%, 95.7%, 95.7%, 95.7%, 82.6%, respectively ($P>0.05$, Table 2).

The expression of *DEK*, *cyclin D1*, *IGF-II*, *GPC3*, *rpP0* mRNAs in HCC with AFP negative and positive was 90.0%, 80.0%, 90.0%, 90.0%, 90.0% and 72.7%, 86.3%, 77.3%, 90.9%, 68.2%, respectively ($P>0.05$, Table 3).

Expression of *DEK*, *cyclin D1*, *IGF-II*, *GPC3*, *rpP0* mRNAs in HCC and adjacent noncancerous liver tissues shown by multiplex RT-PCR

By multiplex RT-PCR, at least one of the mRNAs could be detected in all HCC tissues and in 75.0% of paraneoplastic tissues ($P>0.05$) (Table 4). However, all these five mRNAs were found in 68.8% of HCC tissue, but only in 9.4% of paraneoplastic tissues ($P<0.05$, Table 4).

DISCUSSION

The growth of cells depends on the regulation by many factors, including oncogenes, tumor suppressor genes, growth factors, signal transduction factors, and apoptosis factors, *etc.* The origin of tumor is related to the modification of these genes. Genes such as *DEK*, *cyclin D1*, *IGF-II*, *GPC3*, *rpP0*, are involved in the initiation and development of HCC, and the possible markers for the diagnosis of HCC in clinic. To identify whether these genes were generally involved in hepatocarcinogenesis, multiplex PCR was used in the present study. We found that these genes had an upregulated expression in HCC and multiplex PCR could enhance the detective positive rate.

Cyclin D1

Cyclin, cyclin-dependent kinases, and tumor suppressor gene

products interact and regulate the normal cell cycle. *Cyclin D1* and cyclin-dependent kinases are required for completion of the G₁/S transition in normal mammalian cells^[8]. *Cyclin D1* is located on chromosome 11q13 and exhibits many characteristics of cellular oncogenes. Overexpression of *cyclin D1* may be associated with actual gene amplification or transcriptional dysregulation in cancer. *Cyclin D1* is overexpressed in hyperplastic lesions, such as endometrioid adenocarcinoma^[9], mantle cell lymphoma^[10], and ovarian carcinoma^[11]. The results in our study showed that the expression of *cyclin D1* was significantly higher in HCC than in adjacent nontumorous tissue. The mechanism of *cyclin D1* dysregulation in HCC is not clear, but it is likely that the dysregulation contributes to increasing the proportion of cells in transition from G₁ to S phase. The overexpression of *cyclin D1* may be one of the several mechanisms involved in hyperplasia of liver cells.

DEK

DEK is a 43-ku phosphoprotein that was first isolated as part of a fusion protein expressed in a subtype of acute myeloid leukemias with t(6;9) chromosomal translocations^[12]. *DEK* was lately identified as an autoimmune antigen in patients with pauciarticular onset juvenile rheumatoid arthritis, systemic lupus erythematosus^[13], and other autoimmune diseases. In recent study, it was demonstrated that *DEK* was a site-specific DNA binding protein that was involved likely in transcriptional regulation and signal transduction and it had implications not only for HIV-2 transcription^[14] but also for multiple cellular processes involving with *DEK*. Recent data demonstrated that the major portion of *DEK* is associated with chromatin

Table 2 Expression of *DEK*, *cyclin D1*, *IGF-II*, *GPC3*, *rpP0* mRNAs in well- and poorly-differentiated HCC

	Cyclin D1		GPC3		DEK		IGF-II		rpP0	
	+	-	+	-	+	-	+	-	+	-
Well-differentiated HCC	6	3	6	3	8	1	6	3	7	2
Poor-differentiated HCC	22	1	18	5	17	6	22	1	19	4
Total	28	4	24	8	25	7	28	4	26	6

Table 3 Expression of *DEK*, *cyclin D1*, *IGF-II*, *GPC3*, *rpP0* mRNAs in HCC with AFP negative and positive HCC tissue

	<i>n</i>	Cyclin D1+	GPC3+	DEK+	IGF-II+	rpP0+
AFP(-)	10	8	9	9	9	9
AFP(+)	22	20	15	16	19	17
Total	32	28	24	25	28	26

χ^2 test, $P>0.05$, the group of APF(+) vs the group of APF(-).

Table 4 Expression of *DEK*, *cyclin D1*, *IGF-II*, *GPC3*, *rpP0* mRNAs in HCC and adjacent noncancerous liver tissues by multiplex RT-PCR

Groups	<i>n</i>	Positive reaction		Negative reaction	
		Anyone of the five mRNAs (%)	All of the five mRNAs (%)	Anyone of the five mRNAs (%)	All of the five mRNAs (%)
T	32	32 (100)	22 (68.8)	10 (31.3)	0 (0)
N	32	24 (75.0)	3 (9.4)	29 (90.6)	8 (25.0)
		$P>0.05$	$P>0.05$	$P>0.05$	$P>0.05$

in vivo and suggested that it might play a role in chromatin architecture^[15]. Our present experiment shows that the percentage of overexpression of mRNA of *DEK* (78.1%) in HCC was higher than in adjacent nontumorous tissues (15.6%). It indicates the overexpression of *DEK* may be involved in the transformation from normal liver tissue to HCC, perhaps by activating the oncogenes.

GPC3

GPC3 gene is located at Xq26, and mutated in the Simpson-Golabi-Behmel syndrome^[16]. It may be regulated by methylation of the inactive X in expressing tissues, and encodes a developmentally regulated heparin sulfate proteoglycan that is bound to the cell surface through a glycosylphosphatidylinositol anchor. Based on their localization on the cell surface, such glypicans are thought to regulate interactions between growth factor and their receptors. It is associated with apoptosis and cell signal transduction. It is reported that *GPC3* is a tissue-specific gene in breast tumor^[17], ovarian tumor^[18], and malignant mesothelioma^[19] in which it is downregulated by aberrant methylation of the *GPC3* promoter region, and upregulated in HCC. In the present study, *GPC3* was overexpressed in HCC tissue and the positive expression rate was 75.0%, which was higher than that in adjacent nontumorous tissue (21.9%). Although the role of overexpression of *GPC3* in the development of HCC is not known, it may break the balance between cell growth and death.

IGF-II

It was reported that IGF-II is positive in some benign neoplastic nodules and HCC^[20]. In the present study, the levels of IGF-II was higher in HCC than in adjacent nontumorous tissue, suggesting that the growth factor may act as an autocrine regulation of cell proliferation, *GPC3* may act as a positive regulator of IGF-II, although we have not detected a direct interaction between *GPC3* and IGF-II. It is possible that *GPC3* positively regulates IGF-II activity by interacting with the components of its signaling system.

rpP0

Ribosome acts as a place for protein synthesis. It is composed of rRNA and ribosomal phosphoproteins. In the family of ribosomal phosphoprotein, there are five members: P0, P1 α , P1 β , P2 α , and P2 β . Three functional domains can be defined in the rpP0: one involved in binding to rRNA, one connected to P1/P2 protein interaction, and one associated with elongation factors^[21]. It was reported that rpP0 expression increases in colon carcinoma cells^[22]. In the present study, rpP0 was overexpressed in HCC tumor tissue, suggesting that upregulation of rpP0 is associated with HCC, which may be a signal for increasing protein synthesis.

Multiplex RT-PCR and HCC

In this study, we used multiplex RT-PCR to detect the expression of mRNAs of *DEK*, *cyclin D1*, *IGF-II*, *GPC3*, *rpP0* in HCC and adjacent nontumorous liver tissue. We found that at least one of the mRNAs could be detected in all HCC tissues and 68.8% of HCC tissues expressed all these five mRNAs, while only 9.4% of paraneoplastic tissues

expressed all of them ($P < 0.05$), suggesting that multiplex RT-PCR enhances the detective sensitivity and specificity when combining several specific primers. The expression of anyone of these mRNAs in liver tissue could be regarded as a risk factor for HCC. The higher the expression of these mRNAs the greater the risk. When all these mRNAs are negative in tissues, the possibility of HCC is lower. Multiplex RT-PCR provides an easy and quick method to detect the expression of these genes in liver tissues.

ACKNOWLEDGMENTS

The authors thank Dr. Dang-Rong Li for practical and productive technical advice regarding the RT-PCR technique and Dr. Le-Qun Li for providing useful tissues.

REFERENCES

- 1 **Park US**, Su JJ, Ban KC, Qin L, Lee EH, Lee YI. Mutations in the p53 tumor suppressor gene in tree shrew hepatocellular carcinoma associated with hepatitis B virus infection and intake of aflatoxin B1. *Gene* 2000; **251**: 73-80
- 2 **Park DY**, Sol MY, Suh KS, Shin EC, Kim CH. Expressions of transforming growth factor (TGF)-beta1 and TGF-beta type II receptor and their relationship with apoptosis during chemical hepatocarcinogenesis in rats. *Hepatol Res* 2003; **27**: 205-213
- 3 **Sell S**. Mouse models to study the interaction of risk factors for human liver cancer. *Cancer Res* 2003; **63**: 7553-7562
- 4 **Kondoh N**, Wakatsuki T, Ryo A, Hada A, Aihara T, Horiuchi S, Goseki N, Matsubara O, Takenaka K, Shichita M, Tanaka K, Shuda M, Yamamoto M. Identification and characterization of genes associated with human hepatocellular carcinoma. *Cancer Res* 1999; **59**: 4990-4996
- 5 **Azechi H**, Nishida N, Fukuda Y, Nishimura T, Minata M, Katsuma H, Kuno M, Ito T, Komeda T, Kita R, Takahashi R, Nakao K. Disruption of the p16/cyclin D1/retinoblastoma protein pathway in the majority of human hepatocellular carcinoma. *Oncology* 2001; **60**: 346-354
- 6 **Tsai JF**, Jeng JE, Chuang LY, You HL, Ho MS, Lai CS, Wang LY, Hsieh MY, Chen SC, Chuang WL, Lin ZY, Yu ML, Dai CY. Serum insulin-like growth factor-II and alpha-fetoprotein as tumor markers of hepatocellular carcinoma. *Tumour Biol* 2003; **24**: 291-298
- 7 **Sung YK**, Hwang SY, Park MK, Farooq M, Han IS, Bae HI, Kim JC, Kim M. Glypican-3 is overexpressed in human hepatocellular carcinoma. *Cancer Sci* 2003; **94**: 259-262
- 8 **Jirstrom K**, Ringberg A, Ferno M, Anagnostaki L, Landberg G. Tissue microarray analyses of G1/S-regulatory proteins in ductal carcinoma *in situ* of the breast indicate that low cyclin D1 is associated with local recurrence. *Br J Cancer* 2003; **89**: 1920-1926
- 9 **Ruhul Quddus M**, Latkovich P, Castellani WJ, James Sung C, Steinhoff MM, Briggs RC, Miranda RN. Expression of cyclin D1 in normal, metaplastic, hyperplastic endometrium and endometrioid carcinoma suggests a role in endometrial carcinogenesis. *Arch Pathol Lab Med* 2002; **126**: 459-463
- 10 **Howe JG**, Crouch J, Cooper D, Smith BR. Real-time quantitative reverse transcription-PCR for cyclin D1 mRNA in blood, marrow, and tissue specimens for diagnosis of mantle cell lymphoma. *Clin Chem* 2004; **50**: 80-87
- 11 **Raju U**, Nakata E, Mason KA, Ang KK, Milas L. Flavopiridol, a cyclin-dependent kinase inhibitor, enhances radiosensitivity of ovarian carcinoma cells. *Cancer Res* 2003; **63**: 3263-3267
- 12 **Maeda T**, Kosugi S, Ujiie H, Osumi K, Fukui T, Yoshida H, Kashiwagi H, Ishikawa J, Tomiyama Y, Matsuzawa Y. Localized relapse in bone marrow in a posttransplantation patient with t(6;9) acute myeloid leukemia. *Int J Hematol* 2003; **77**: 522-525
- 13 **Wichmann I**, Respaldiza N, Garcia-Lozano JR, Montes M,

- Sanchez-Roman J, Nunez-Roldan A. Autoantibodies to DEK oncoprotein in systemic lupus erythematosus (SLE). *Clin Exp Immunol* 2000; **119**: 530-532
- 14 **Faulkner NE**, Hilfinger JM, Markovitz DM. Protein phosphatase 2A activates the HIV-2 promoter through enhancer elements that include the pTATA site. *J Biol Chem* 2001; **276**: 25804-25812
- 15 **Kappes F**, Burger K, Baack M, Fackelmayer FO, Gruss C. Subcellular localization of the human proto-oncogene protein DEK. *J Biol Chem* 2001; **276**: 26317-26323
- 16 **Veugelers M**, Cat BD, Muyldermans SY, Reekmans G, Delande N, Frints S, Legius E, Fryns JP, Schrandt-Stumpel C, Weidle B, Magdalena N, David G. Mutational analysis of the GPC3/GPC4 glypican gene cluster on Xq26 in patients with Simpson-Golabi-Behmel syndrome: identification of loss-of-function mutations in the GPC3 gene. *Hum Mol Genet* 2000; **9**: 1321-1328
- 17 **Xiang YY**, Ladeda V, Filmus J. Glypican-3 expression is silenced in human breast cancer. *Oncogene* 2001; **20**: 7408-7412
- 18 **Lin H**, Huber R, Schlessinger D, Morin PJ. Frequent silencing of the GPC3 gene in ovarian cancer cell lines. *Cancer Res* 1999; **59**: 807-810
- 19 **Murthy SS**, Shen T, De Rienzo A, Lee WC, Ferriola PC, Jhanwar SC, Mossman BT, Filmus J, Testa JR. Expression of GPC3, an X-linked recessive overgrowth gene, is silenced in malignant mesothelioma. *Oncogene* 2000; **19**: 410-416
- 20 **Tsai JF**, Jeng JE, Chuang LY, You HL, Ho MS, Lai CS, Wang LY, Hsieh MY, Chen SC, Chuang WL, Lin ZY, Yu ML, Dai CY. Serum insulin-like growth factor-II and alpha-Fetoprotein as tumor markers of hepatocellular carcinoma. *Tumour Biol* 2003; **24**: 291-298
- 21 **Rodriguez-Gabriel MA**, Remacha M, Ballesta JP. The RNA interacting domain but not the protein interacting domain is highly conserved in ribosomal protein P0. *J Biol Chem* 2000; **275**: 2130-2136
- 22 **Barnard GF**, Staniunas RJ, Bao S, Mafune K, Steele GD Jr, Gollan JL, Chen LB. Increased expression of human ribosomal phosphoprotein P0 messenger RNA in hepatocellular carcinoma and colon carcinoma. *Cancer Res* 1992; **52**: 3067-3072

Science Editor Wang XL and Guo SY Language Editor Elsevier HK

Expression and significance of new inhibitor of apoptosis protein survivin in hepatocellular carcinoma

Hong Zhu, Xiao-Ping Chen, Wan-Guang Zhang, Shun-Feng Luo, Bi-Xiang Zhang

Hong Zhu, Xiao-Ping Chen, Wan-Guang Zhang, Shun-Feng Luo, Bi-Xiang Zhang, Hepatic Surgery Center, Tongji Hospital Affiliated to Tongji Medical College, Huazhong University of Science and Technology, Wuhan 430030, Hubei Province, China
Supported by the Grants From Key Subsidy Project of Clinical Speciality of Chinese Ministry of Public Health from 2001 to 2003, No. 321[2001]
Correspondence to: Dr. Hong Zhu, Hepatic Surgery Center, Tongji Hospital Affiliated to Tongji Medical College, Huazhong University of Science and Technology, 1095 Jiefang Dadao, Wuhan 430030, Hubei Province, China. hong_jasmine@hotmail.com
Telephone: +86-27-83662599 Fax: +86-27-83662851
Received: 2003-07-04 Accepted: 2003-11-06

© 2005 The WJG Press and Elsevier Inc. All rights reserved.

Key words: Survivin; Vascular endothelial growth factor; Hepatocellular carcinoma

Zhu H, Chen XP, Zhang WG, Luo SF, Zhang BX. Expression and significance of new inhibitor of apoptosis protein survivin in hepatocellular carcinoma. *World J Gastroenterol* 2005; 11(25): 3855-3859
<http://www.wjgnet.com/1007-9327/11/3855.asp>

Abstract

AIM: To investigate expression and significance of inhibitor of apoptosis protein survivin in hepatocellular carcinoma (HCC).

METHODS: The expression of survivin and vascular endothelial growth factor (VEGF) was investigated in 38 cases of HCC tissues and 38 liver cirrhosis tissues by immunohistochemistry and Western blot. The relationship between the expression of survivin and clinicopathological factors of HCC was analyzed.

RESULTS: Survivin protein was detected in 23 (60.5%) of 38 HCCs and 3 (7.9%) of 38 liver cirrhosis tissues. In 23 cases of HCC which expressed survivin, the expression of VEGF was positive in 18 cases and slight positive or negative in 5 cases. While in 15 cases of HCC which did not express survivin, 12 cases did not express or slightly expressed, and 3 cases expressed VEGF. In liver cirrhosis tissues, the expression of VEGF was as follows: 24 cases were negative, 10 cases were weak positive and 4 cases were strong positive. The expression of survivin was coincident with the expression of VEGF in HCC ($P < 0.01$). The expression of survivin in HCC had no relationship with the patients' age, gender, tumor size and differentiation level of HCC, while it was related to the metastasis of HCC. The protein quantitative analysis by Western blot also showed that overexpression of survivin in HCC was closely correlated to the expression of VEGF ($P < 0.01$). Furthermore, stronger expression of survivin and VEGF was also found in patients with metastasis rather than in those with no metastasis ($P < 0.01$).

CONCLUSION: Survivin plays a pivotal role in the metastasis of HCC, and it has some correlation with tumorigenesis. The expression of survivin in the primary lesion is very useful as an indicator for metastasis and prognosis of HCC. It could become a new target of gene therapy of HCC.

INTRODUCTION

In organisms, cell death and cell cycle progression are two sides of the same coin, and these two different phenomena are regulated moderately to maintain the cellular homeostasis^[1]. On the other hand, gene mutation could be accumulated and cell growth cycle could be prolonged, thus finally facilitating the formation of tumor. At present, it has been confirmed that P53 and bcl-2 family are critical to the regulation of cell apoptosis. Survivin protein (M_r 16 500) is a recently described member of inhibitor of apoptosis protein (IAP) family of antiapoptotic proteins, which may act simultaneously with the bcl-2 family proteins, but has a different apoptosis inhibitory mechanism^[2]. Survivin is conserved across evolution with homologs found in both vertebrate and invertebrate animal species^[3]. The tissue distribution of survivin has obvious cell selectivity. Some research has found that survivin is undetectable in terminally differentiated adult tissues, yet it is abundantly expressed in fetal tissues and in a variety of human tumors including lung, colo-rectal, breast, prostate, melanoma, pancreatic, and gastric carcinoma as well as in high-grade lymphomas and neuroblastomas^[4-11]. However, the expression and implication of survivin in hepatocellular carcinoma are still unknown.

Vascular endothelial growth factor (VEGF) is considered to be the most primary factor prompting the angiogenesis in tumor tissue, which also holds the central position in the course of formation and metastasis of tumor. However, it is unclear how VEGF accelerates the metastasis of neoplasms.

To explore the role and mechanism of survivin in the progression of HCC and the relationship with VEGF, we adopted immunohistochemistry and Western-blot techniques to investigate the expression of survivin and VEGF in HCC.

MATERIALS AND METHODS

Patients and samples

A total of 38 cases of HCC was involved in this study. The

patients with HCC, who underwent potentially curative tumor resection at Hepatic Surgery Center of Tongji Hospital from 2001 to 2002, had received neither chemotherapy nor radiation therapy before surgery. Among them, there were 33 males and 5 females, and the mean age of the patients was 47.3 years (SD, 11.2 years; range, 18-76 years).

All the specimens were confirmed to be hepatocellular carcinoma by pathological diagnosis. Cell differentiation was graded by Edmondson-Steiner's criteria. Tumors with Edmondson-Steiner's grade I were regarded as moderate to well differentiation and those with grade II-IV were poorly differentiated. The criteria of metastasis included extrahepatic tissue or organ involvement; hilum or remote lymphoid nodule metastasis; tumor thrombus formation in the main portal trunk or hepatic vein or bile duct. Multifocal HCC was excluded from this study because it was a controversial issue^[12].

Routinely processed formalin-fixed, paraffin-embedded blocks containing principal tumor were selected. Serial sections of 2-4 μm were prepared from the cut surface of blocks at the maximum cross-section of the tumor.

Immunohistochemical staining for survivin and VEGF

Immunohistochemical staining for survivin and VEGF antigen was carried out by the standard streptavidin-peroxidase-biotin technique (SP technique) using SP kit (Zhongshan Company, Beijing, China). Rabbit-anti-human survivin monoclonal antibody and rat-anti-human VEGF monoclonal antibody were obtained from Neomarkers Company. Experimental procedure was conducted according to the SP kit specification. Primary antibody was diluted at 1:200. Antigen retrieval was done by microwave citrate salt method. 3,3'-diaminobenzidine and hematoxylin were used for color development and counterstaining respectively. Cells whose cytoplasm was dyed brown were regarded as positive ones. One case of stage III gastric cancer was stained intensively and reproducibly for survivin expression in >30% of tumor cells, and was used as a positive control throughout the study. Negative control slides processed without primary antibody were included for each staining. In brief, deparaffinized and rehydrated sections were bathed in a 10^{-3} mol/L sodium citrate buffer (pH 6.0) then the solution was put to a pressure cooker and boiled for 20 min while maintaining the pressure. After endogenous peroxidase was quenched in 3% hydrogen peroxide and blocked for 5 min, the sections were incubated overnight at 4 °C with primary polyclonal antibody at a 1:200 dilution. Biotinylated immunoglobulin and streptavidin conjugated to peroxidase were then added. Finally, 3,3'-diaminobenzidine was used for color development, and hematoxylin was used for counterstaining. The mean percentage of positive tumor cells was determined in at least five areas at 200-fold magnification for survivin and 100-fold magnification for VEGF and scaled as the following: (0) <5%; (1) 5-25%; (2) 25-50%; (3) 50-75%; and (4) >75%. The intensity of survivin immunostaining was scored as follows: 1+, weak; 2+, moderate; and 3+, intense. Because tumors showed heterogeneous staining, the dominant pattern was used for scoring. The scores indicating percentage of positive tumor cells and staining intensity were multiplied to produce a weighed score for each case. Cases with weighed

scores <1 were defined as negative; cases with weighed scores >2 were defined as strongly positive and those in between were defined as positive.

Western blot

Proteins were extracted from tissues and cells by detergent lysis using NP-40 lysis buffer (0.2% NP-40, 100 mmol/L Tris-HCl, pH 8.0, 200 mmol/L NaCl, 0.01% SDS). Proteins were fixed quantitatively by ultraviolet spectrophotometer analysis. A total of 20 μg of the proteins of HCC tissue was fractionated on a 75 g/L polyacrylamide slab gel containing 1 g/L SDS and then transferred onto a nitrocellulose filter by electroblotting. The filter was incubated for at least 1 h in 10 mmol/L Tris-HCl buffer (pH 8.0) containing 150 mmol/L NaCl, 0.05% Tween-20 and 50 g/L bovine serum albumin for survivin and in 10 mmol/L Tris-HCl buffer (pH 8.0) containing 150 mmol/L NaCl, 0.05% Tween-20 and 50 g/L milk powder for VEGF to prevent nonspecific binding of antibodies. Then it was incubated with primary antibody (survivin, 1:1 000; VEGF 1:2 000) for 12 h, and with second antibodies for 1 h at room temperature in the same buffer. Respectively, the second antibodies of survivin were goat-anti-rabbit polyclonal antibody labeled by alkaline phosphatase and those of VEGF were goat-anti-rat polyclonal antibody labeled by horseradish peroxidase. VEGF was dyed by 0.01% DAB/ H_2O_2 form 5 to 15 min and brown straps were viewed as positive results. Survivin was dyed by NBT/BCIP for 10 min or so and blue-black straps were positive. At the same time protein molecular weight marker (M_r 14 000-70 000) was used to identify destined straps. The expressed protein quantity was automatically analyzed by GIS gel image processing system (version 3.10, Tanon Technological Limited Company, Shanghai, China). The net area of strap represented the expressed protein quantity.

Statistical analysis

All statistical analyses were performed using the SPSS 10.0 J software package for Macintosh (SPSS, Inc., Chicago, IL). Variables associated with survivin expression were analyzed by the χ^2 test. The coincident expression of survivin and VEGF protein in HCC or liver cirrhosis tissues was analyzed by the paired *t*-test. The correlation between HCC metastasis and expression of survivin and VEGF protein was tested by bivariate correlation analysis. $P < 0.05$ was considered significant and $P < 0.01$ was considered remarkably significant.

RESULTS

Immunohistochemical staining

Twenty-three cases (60.5%) of 38 HCCs expressed survivin protein, among them, 8 cases strongly expressed, 12 cases positively expressed, and 3 cases slightly expressed. Survivin protein was detected in only 3 (7.9%) of 38 liver cirrhosis. The relationship between the expression of survivin and clinicopathological factors of HCC is shown in Table 1. In 23 cases of HCC which expressed survivin, the expression of VEGF was positive in 18 cases and slightly positive or negative in 5 cases. In 15 cases which did not express survivin

Table 1 Relationship of the expression of survivin and clinicopathological factors of HCC

	<i>n</i>	Survivin		<i>P</i>
		Positive (<i>n</i>)	Percent (%)	
Tissue				<0.01
Cirrhosis	38	3	7.9	
HCC	38	23	60.5	
Age (yr)				>0.05
<60	31	19	61.3	
≥60	7	4	57.1	
Sex				>0.05
Male	33	21	63.6	
Female	5	2	40.0	
Size (cm)				>0.05
≥5	17	12	70.6	
<5	21	11	52.4	
Differentiation				>0.05
Moderate to well	16	9	56.3	
Poor	22	14	63.6	
Metastasis				<0.05
Positive	14	12	85.7	
Negative	24	11	45.8	

protein, 12 cases of HCC did not express or slightly expressed VEGF and 3 cases expressed VEGF. In liver cirrhosis tissue,

the expression of VEGF was negative in 24 cases, weak positive in 10 cases and strong positive in 4 cases. The staining of both survivin and VEGF was mainly localized in cytoplasm.

By statistical analysis, there was a remarkable difference in survivin expression between the tumor tissue and liver cirrhosis tissues ($P<0.01$). The expression of survivin in HCC had no significant relation with the patients' age, gender, tumor size and differentiation level of HCC, while it was related to the metastasis of HCC ($P<0.05$). Furthermore, a high expression of survivin was coincident with the expression of VEGF in HCC ($P<0.01$) (Table 2 and Figures 1 and 2).

Western blot

By analysis with GIS gel image processing system, the values of net area indicating the expressed protein quantity are as shown in Tables 3 and 4, Figures 3 and 4.

DISCUSSION

It has been identified that bcl-2 family and IAPs family have close relations with cell apoptosis. So far six members of IAPs family (NAIP, c-IAP1, c-IAP2, XIAP, Survivin and Bruce) have been cloned^[13]. IAPs family expresses extensively among many species, which are of homology in their

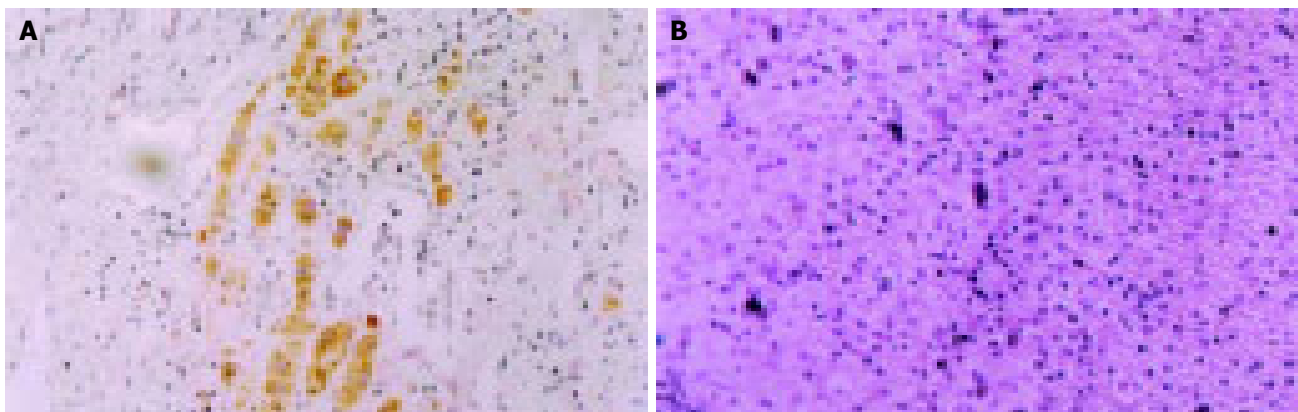


Figure 1 Expression of survivin in HCC and liver cirrhosis tissues (SP method, $\times 200$). **A:** The brown granules in the cytoplasm indicate survivin

protein in liver cancer cells; **B:** Survivin protein is not detected in liver cirrhosis tissues.

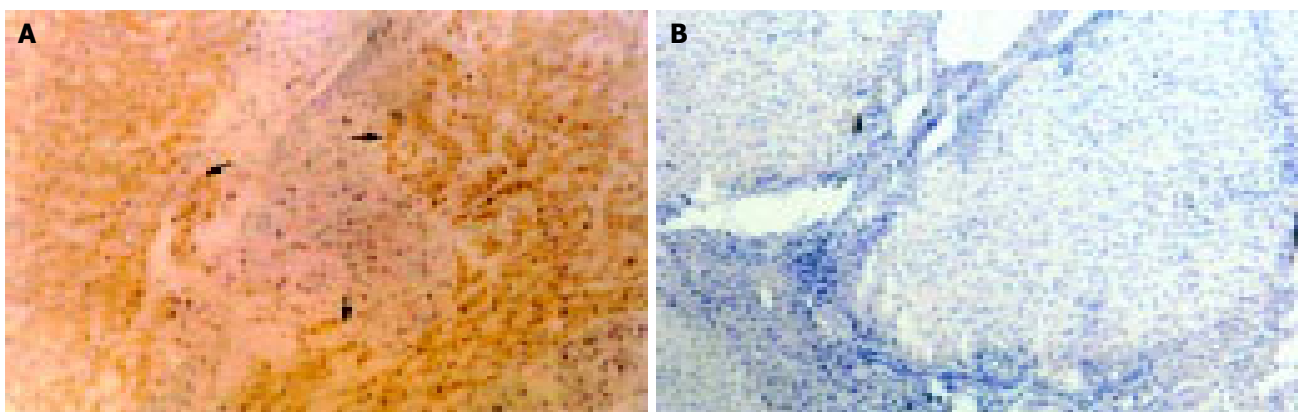


Figure 2 Expression of VEGF in HCC and liver cirrhosis tissues (SP method, $\times 100$). **A:** The brown granules in the cytoplasm indicate VEGF expression in

HCC; **B:** Expression of VEGF was weak positive in some liver cirrhosis tissues.

Table 2 Expression of survivin and VEGF protein in HCC tissues

	VEGF		P
	Positive	Negative	
Survivin			<0.01
Positive	18	5	
Negative	3	12	

Table 3 Coincident expression of survivin and VEGF protein in HCC or liver cirrhosis tissues

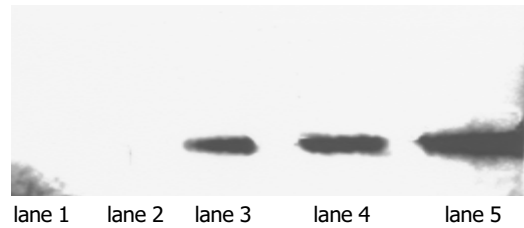
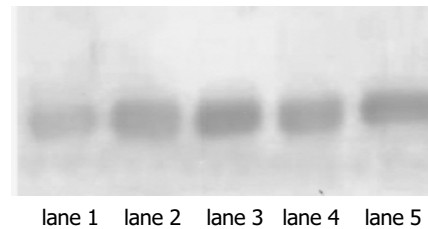
	HCC group (n = 38)	Cirrhosis group (n = 38)	P
Survivin	3229.3±1383.2	562.6±226.5	<0.01
VEGF	1134.8±862.2	445.4±322.6	

Table 4 Correlation between HCC metastasis and expression of survivin and VEGF protein

	Metastasis group (n = 14)	Non-metastasis group (n = 24)	P
Survivin	3841.4±1061.2	1253.8±725.3	<0.01
VEGF	1388.6±652.4	1081.3±773.5	<0.01

structures and the abilities of inhibiting apoptosis^[14]. Survivin is the smallest member among the IAPs family. Altieri of Yale University utilized EPR-1 (effector cell protease receptor-1) cDNA to screen and clone survivin from human GenBank in 1997^[3]. It has been suggested (but not proven) that EPR-1 may act as a natural anti-sense to survivin in cells^[15].

The expression of survivin depends on cell cycle. HeLa blocked tumor cells in G1, S, G2/M phase separately to detect survivin mRNA amount. Survivin mRNA was not detectable in G1 phase, increased 6.2 times in S phase and elevated 40 times in G2/M phase. Therefore, the expression of survivin was closely related to cell proliferation. Survivin can suppress apoptosis of NIH3T3 cell induced by Taxol and 293 cell induced by Fas and Bax^[16]. Survivin inhibits apoptosis mainly through targeting the terminal effectors caspase-3 and -7 activity in apoptotic protease cascade reaction^[17,18]. These caspases operate in the distal portions of apoptotic protease cascades, functioning as effectors rather than initiators of apoptosis. Survivin is characterized by a unique structure with a single BIR and no zinc-binding domain known as the RING finger, thus survivin cannot bind caspase-3 directly. Survivin is expressed in the G2-M phase of the cell cycle in a cell cycle-regulated manner and associates with microtubules of the mitotic spindle by the coiled spirals zone^[19-21]. Survivins are also called chromosomal passenger proteins: they associate with inner centromere regions during prophase, but subsequently relocate to the midzone of the central spindle and concentrate at the midbody^[22]. Survivin has the double function of controlling spindle checkpoint and apoptotic checkpoint. The over-expression of survivin in neoplasms may obliterate this apoptotic checkpoint and allow aberrant progression of transformed cells through mitosis. The disruption of survivin-microtubule interaction results in loss of antiapoptosis function of survivin and increases caspase-3 activity during mitosis^[21].

**Figure 3** Expression of survivin in HCC and liver cirrhosis tissues. Lanes 1 and 2: liver cirrhosis tissues; lanes 3-5: HCC tissues. M_r of survivin: 16 500.**Figure 4** Expression of VEGF in HCC and liver cirrhosis tissues. Lanes 1 and 2: liver cirrhosis tissues; lanes 3-5: HCC tissues. M_r of VEGF: 21 000.

The results revealed that survivin was highly expressed in HCC and seldom detected in liver cirrhosis tissues. The expression of survivin had no association with the patients' age, gender, tumor size and differentiation level of HCC. It suggests that survivin may play some role in tumorigenesis of HCC. Simultaneously, in our series, we found that high expression of survivin was significantly correlated to VEGF in HCC. More importantly, stronger expression of survivin and VEGF was found in patients with metastasis than in those without metastasis. Consequently the expression of survivin seems to be involved in metastatic capacity of HCC.

As we know, VEGF is considered to be the most cardinal vascular growth factor prompting angiogenesis in tumor tissue. The mechanism of liver cancer cell shift induced by VEGF is closely related to increased proliferation ability of liver cells. Emerging studies have implicated a marked induction of survivin by VEGF in vascular endothelial cells, which can facilitate tumor metastasis by controlling apoptosis during angiogenesis. VEGF binding to VEGF-R2 activates the phosphatidylinositol 3-kinase (PI3K) survival pathway, resulting in phosphorylation and activation of the serine/threonine kinase protein kinase B (PKB/Akt). VEGF induces the expression of several anti-apoptotic effector molecules in Ecs by PKB/Akt pathway, including bcl-2, A1, and two members of the IAP family, X-linked IAP (XIAP), and survivin^[23-26]. VEGF-dependent upregulation of survivin could be prevented by cell cycle arrest in the G1 and S phases and allows for the maintenance of the microtubule network to inhibit apoptosis of endothelial cells^[27-30]. Our results demonstrate that the expression of survivin is consistent with that of VEGF in HCC and both are closely correlated to infiltration and metastasis of HCC. This is similar to findings in endothelial cells. As such, we assume that VEGF probably promotes the expression of survivin in HCC tissues, then the latter inhibits apoptosis of hepatocarcinoma cells and enhances tumor cell ability of infiltration and invasion,

thus accelerating tumor metastasis. To clarify the interaction mechanism between survivin and VEGF in HCC, further studies are needed.

The cancer-specific expression of survivin, coupled with its importance in inhibiting cell death and in regulating cell division, makes it a useful diagnostic marker of cancer and a potential target for cancer treatment^[31]. Recently some studies have set about to evaluate the possibility of targeting survivin function *in vivo* as an anticancer strategy in which it is shown that inhibition of survivin could effectively inhibit *de novo* tumor formation and progression^[32,33]. In the light of the effect of survivin on the progression of HCC, it is possible that inhibiting the function of survivin can be a new treatment of HCC.

In conclusion, inhibitor of apoptosis protein survivin plays a pivotal role in the metastasis of HCC, and it has some correlation with tumorigenesis. It is associated with the progression of HCC as a late event in tumorigenesis. The expression of survivin in the primary lesion can be an indicator for metastasis and prognosis of HCC. It could become a new target of gene therapy of HCC.

REFERENCES

- 1 Suzuki A, Shiraki K. Tumor cell "dead or alive": caspase and survivin regulate cell death, cell cycle and cell survival. *Histol Histopathol* 2001; **16**: 583-593
- 2 Sela B. Survivin: anti-apoptosis protein and a prognostic marker for tumor progression and recurrence. *Harefuah* 2002; **141**: 103-107
- 3 Ambrosini G, Adida C, Altieri DC. A novel anti-apoptosis gene, survivin, expressed in cancer and lymphoma. *Nat Med* 1997; **3**: 917-921
- 4 Falleni M, Pellegrini C, Marchetti A, Oprandi B, Buttitta F, Barassi F, Santambrogio L, Coggi G, Bosari S. Survivin gene expression in early-stage non-small cell lung cancer. *J Pathol* 2003; **200**: 620-626
- 5 Tanaka K, Iwamoto S, Gon G. Expression of survivin and its relationship to loss of apoptosis in breast carcinomas. *Clin Cancer Res* 2000; **6**: 127-134
- 6 McEleny KR, Watson RW, Coffey RN, O'Neill AJ, Fitzpatrick JM. Inhibitors of apoptosis proteins in prostate cancer cell lines. *Prostate* 2002; **51**: 133-140
- 7 Sarela AI, Macadam RC, Farmery SM. Expression of the antiapoptosis gene, survivin, predicts death from recurrent colorectal carcinoma. *Gut* 2000; **46**: 645-650
- 8 Satoh K, Kaneko K, Hirota M. Expression of survivin is correlated with cancer cell apoptosis and is involved in the development of human pancreatic duct cell tumors. *Cancer* 2001; **92**: 271-278
- 9 Hussein MR, Haemel AK, Wood GS. Apoptosis and melanoma: molecular mechanisms. *J Pathol* 2003; **199**: 275-288
- 10 Garcia JF, Camacho FI, Morente M, Fraga M, Montalban C, Alvaro T, Bellas C, Castano A, Diez A, Flores T, Martin C, Martinez MA, Mazon F, Menarguez J, Mestre MJ, Mollejo M, Saez AI, Sanchez L, Piris MA. Spanish Hodgkin Lymphoma Study Group. Hodgkin and Reed-Sternberg cells harbor alterations in the major tumor suppressor pathways and cell-cycle checkpoints: analyses using tissue microarrays. *Blood* 2003; **101**: 681-689
- 11 Borriello A, Roberto R, Della Ragione F, Iolascon A. Proliferate and survive: cell division cycle and apoptosis in human neuroblastoma. *Haematologica* 2002; **87**: 196-214
- 12 Nakano S, Haratake J, Okamoto K, Takeda S. Investigation of resected multinodular hepatocellular carcinoma: assessment of unicentric or multicentric genesis from histological and prognosis viewpoint. *Am J Gastroenterol* 1994; **9**: 189-193
- 13 Liston P, Roy N, Tamai K. Suppression of apoptosis in mammalian cells by NAIP and a related family of IAP genes. *Nature* 1996; **379**: 349-353
- 14 Hay BA. Understanding IAP function and regulation: a view from Drosophila. *Cell Death Differ* 2000; **7**: 1045-1056
- 15 O'Driscoll L, Linehan R, Clynes M. Survivin: role in normal cells and in pathological conditions. *Curr Cancer Drug Targets* 2003; **3**: 131-152
- 16 Tamm I, Wang Y, Sausville E. IAP-family protein survivin inhibits caspase activity and apoptosis induced by Fas (CD95), Bax, caspases, and anticancer drugs. *Cancer Res* 1998; **58**: 5315-5320
- 17 Sambrook J, Fritsch EF, Maniatis T. Molecular Cloning: A Laboratory Manual. 2nd ed. USA: Cold Spring Harbor Laboratory Press 1989: 870-877
- 18 Johnson AL, Langer JS, Bridgham JT. Survivin as a cell cycle-related and antiapoptotic protein in granulosa cells. *Endocrinology* 2002; **143**: 3405-3413
- 19 Kobayashi K, Hatano M, Otaki M, Ogasawara T, Tokuhisa T. Expression of a murine homologue of the inhibitor of apoptosis protein is related to cell proliferation. *Proc Natl Acad Sci USA* 1999; **96**: 1457-1462
- 20 Verdecia MA, Huang H, Dutil E, Kaiser A, Hunter T, Noel JP. Structure of the human anti-apoptotic protein survivin reveals a dimeric arrangement. *Nat Struct Biol* 2000; **7**: 620-623
- 21 Li F, Ambrosini G, Chu EY, Plescia J, Tognin S, Marchisio PC, Altieri DC. Control of apoptosis and mitotic spindle checkpoint by survivin. *Nature* 1998; **396**: 580-584
- 22 Adams RR, Carmena M, Earnshaw WC. Chromosomal passengers and the (aurora) ABCs of mitosis. *Trends Cell Biol* 2001; **11**: 49-54
- 23 Gerber HP, McMurtrey A, Kowalski J, Yan M, Keyt BA, Dixit V, Ferrara N. Vascular endothelial growth factor regulates endothelial cell survival through the phosphatidylinositol 3'-kinase/Akt signal transduction pathway. Requirement for Flk-1/KDR activation. *J Biol Chem* 1998; **273**: 30336-30343
- 24 Gerber HP, Dixit V, Ferrara N. Vascular endothelial growth factor induces expression of the antiapoptotic proteins Bcl-2 and A1 in vascular endothelial cells. *J Biol Chem* 1998; **273**: 13313-13316
- 25 Nor JE, Christensen J, Liu J, Peters M, Mooney DJ, Strieter RM, Polverini PJ. Up-Regulation of Bcl-2 in microvascular endothelial cells enhances intratumoral angiogenesis and accelerates tumor growth. *Cancer Res* 2001; **61**: 2183-2188
- 26 Tran J, Rak J, Sheehan C, Saibil SD, LaCasse E, Korneluk RG, Kerbel RS. Marked induction of the IAP family antiapoptotic proteins survivin and XIAP by VEGF in vascular endothelial cells. *Biochem Biophys Res Commun* 1999; **264**: 781-788
- 27 O'Connor DS, Schechner JS, Adida C, Mesri M, Rothermel AL, Li F, Nath AK, Pober JS, Altieri DC. Control of apoptosis during angiogenesis by survivin expression in endothelial cells. *Am J Pathol* 2000; **156**: 393-398
- 28 Conway EM, Zwerts F, VanEygen V, DeVriese A, Nagai N, Luo W, Collen D. Survivin-dependent angiogenesis in ischemic brain: molecular mechanisms of hypoxia-induced up-regulation. *Am J Pathol* 2003; **163**: 935-946
- 29 Mesri M, Morales-Ruiz M, Ackermann EJ, Bennett CF, Pober JS, Sessa WC, Altieri DC. Suppression of vascular endothelial growth factor-mediated endothelial cell protection by survivin targeting. *Am J Pathol* 2001; **158**: 1757-1765
- 30 Tran J, Master Z, Yu JL, Rak J, Dumont DJ, Kerbel RS. A role for survivin in chemoresistance of endothelial cells mediated by VEGF. *Proc Natl Acad Sci USA* 2002; **99**: 4349-4354
- 31 Chiou SK, Jones MK, Tarnawski AS. Survivin-an anti-apoptosis protein: its biological roles and implications for cancer and beyond. *Med Sci Monit* 2003; **9**: PI25-29
- 32 Kanwar JR, Shen WP, Kanwar RK, Berg RW, Krissansen GW. Effects of survivin antagonists on growth of established tumors and B7-1 immunogene therapy. *J Nat Cancer Inst* 2001; **93**: 1541-1552
- 33 Mesri M, Wall NR, Li J, Kim RW, Altieri DC. Cancer gene therapy using a survivin mutant adenovirus. *J Clin Invest* 2001; **108**: 981-990

Activation of transcription factors NF-kappaB and AP-1 and their relations with apoptosis-associated proteins in hepatocellular carcinoma

Lin-Lang Guo, Sha Xiao, Ying Guo

Lin-Lang Guo, Sha Xiao, Ying Guo, Department of Pathology, Zhujiang Hospital, Guangzhou 210282, Guangdong Province, China
Lin-Lang Guo, University of California, Davis Cancer Center, CA 95817, the United States
Correspondence to: Lin-Lang Guo, MD, University of California, Davis Cancer Center, Suite 2300, Research Building III, 4645 Second Avenue, Sacramento, CA 95817, United States. linlangg@yahoo.com
Telephone: +916-734-1479 Fax: +916-734-2361
Received: 2004-08-18 Accepted: 2004-11-29

Abstract

AIM: To study the distribution pattern of transcription factors NF- κ B and AP-1 and their relations with the expression of apoptosis associated-proteins Fas/FasL and ICH-1L/S in human hepatocellular carcinoma (HCC).

METHODS: We performed *in situ* hybridization and immunohistochemical techniques for NF- κ B, AP-1, Fas/FasL and ICH-1 in 40 cases of human HCC along with corresponding nontumoral tissues and 7 cases of normal liver tissues.

RESULTS: Twenty-two (55%) and 25 (62.5%) of 40 cases for NF- κ B and AP-1 were presented for nuclear or both nuclear and cytoplasmic staining respectively, while less cases were presented for only cytoplasmic staining for NF- κ B (18%) and AP-1 (10%) in adjacent nontumoral tissues and negative staining in normal liver tissues. There was no statistically significant difference of NF- κ B or AP-1 activation between well differentiated tumors and poorly differentiated tumors ($P > 0.05$). NF- κ B activity is positively corresponded to AP-1 activation. The expression of ICH-1L/S was associated with the activation of NF- κ B and AP-1 ($P < 0.05$), but no significant relationship was found between Fas/FasL and NF- κ B or AP-1 ($P > 0.05$).

CONCLUSION: Activation of both NF- κ B and AP-1 may be required for ICH-1L/S-induced apoptosis in HCC, but not for Fas/FasL-mediated apoptosis. NF- κ B and AP-1 may play important roles in the pathogenesis of human HCC.

© 2005 The WJG Press and Elsevier Inc. All rights reserved.

Key words: Hepatocellular carcinoma (HCC); Transcription factors; Apoptosis; Protein

Guo LL, Xiao S, Guo Y. Activation of transcription factors

NF-kappaB and AP-1 and their relations with apoptosis-associated proteins in hepatocellular carcinoma. *World J Gastroenterol* 2005; 11(25): 3860-3865
<http://www.wjgnet.com/1007-9327/11/3860.asp>

INTRODUCTION

Hepatocellular carcinoma (HCC) is one of the most common cancers and cause of mortality in China. Much advanced progresses in the mechanism of hepatocarcinogenesis have been achieved for these years. Many genes such as proto-oncogenes, tumor suppressor genes, apoptosis genes and growth factors genes have been implicated and apoptosis genes may play an important effect in the process of hepatocarcinogenesis^[1-6]. Apoptosis-related genes such as bcl-2/bax, Fas/FasL and caspase are involved in the pathogenesis of HCC^[3-6]. However, more steps of apoptosis genes in this process remain unknown yet.

Activated protein-1 (AP-1) and nuclear factor κ B (NF- κ B), two of important transcription factors, play important roles in signal transduction pathways of cell differentiation, proliferation and apoptosis in response to a variety of physiological and pathological stimuli^[7-13]. AP-1 consists of homodimers and heterodimers of the Jun family (c-Jun, JunB, JunD), and the Fos family (c-Fos, FosB, Fra1, Fra2). NF- κ B is a heterodimeric complex composed of two subunits of the Rel/NF- κ B family, factors including NF- κ B1 (p50), NF- κ B2 (p52), c-Rel, RelA/p65, and RelB^[14]. Some investigators have presented aberrant DNA binding activity of AP-1 and NF- κ B in various types of human tumor such as HCC, gastric carcinoma, breast carcinoma and so on^[15-22]. These findings suggested that AP-1 and NF- κ B may be important in the control of cell proliferation and oncogenesis of these tumors.

The molecular mechanisms of NF- κ B and AP-1 in the regulation of Fas/FasL mediated apoptosis may be different in T cells, Jurkat cells, hepatocyte-derived cell lines and colon carcinoma cell^[23-27]. However, whether NF- κ B and AP-1 play important roles in regulation of Fas/FasL and ICH-1L/S expression in human HCC is still not known. In the present study, we undertook to investigate whether AP-1 and NF- κ B are constitutively activated in human HCC tissues and to evaluate the relationship between AP-1 or NF- κ B activity and the expression of apoptosis associated proteins (Fas/FasL and ICH-1L/S) by *in situ* hybridization and immunohistochemical techniques.

MATERIALS AND METHODS

Tissue preparation

Forty samples were obtained by surgical resection in our department. All samples were independently reviewed by two pathologists. The cases of HCC were classified according to the criteria described by Edmondson-Steiner and grouped as well differentiated (grade I-II; $n = 25$) or poorly differentiated (grade III-IV; $n = 15$). Seven undamaged liver tissues from surgical resection specimens of young adults with minor liver injury who underwent partial hepatectomy were used as normal control. All tissues were fixed in 40 g/L formaldehyde (pH 7.0) for 12-24 h and embedded in paraffin wax and then 4 μ m serial sections were cut and mounted on poly-L-lysine coated slides.

Immunohistochemistry staining

Sections were deparaffinized and rehydrated routinely. Antigen was retrieved by heating sections in a microwave oven at 700 W in 10 mmol/L citrate buffer (pH 6.0) for 10 min. After blocking with 0.3% H₂O₂ and swine serum, specimens were then incubated with the primary antibodies, directed against Fas, FasL, and ICH-1L/S (Santa Cruz product, dilution 1:100) at 4 °C overnight. Secondary antibodies were applied according to the manufacturer's recommendations (Amersham). The staining was performed by streptavidin-peroxidase enzyme conjugate method using a S-P kit (Zymed product). Reaction products were visualized by DAB (diaminobenzidine). The slides were counterstained with hematoxylin before mounting in paramount. Brown-yellow granules in cytoplasm were recognized as positive staining.

In situ hybridization

Sections were deparaffinized and rehydrated routinely. Oligonucleotides containing the consensus sequence of

AP-1 (5'-CGCTTGATGAGTCAGCCGGAA-3') and NF- κ B (5'-AGTTGAGGGGACTTCCAGGC-3') were respectively used as probes and 3'-labeled with biotin. Preparations were incubated with the labeled probes (37 °C, overnight). Non-specific antigen was blocked with 2% bovine serum and 0.3% Triton X-100, followed by incubation with anti-biotin antibody alkaline phosphates mixture for 1 h. Slides were then visualized with BCIP/NBT. Purple-blue granules were regarded as positive staining. In general, inactivated NF- κ B and AP-1 were located in cytoplasm and nuclei staining scored as activated NF- κ B and AP-1.

Negative controls

We used the following negative controls: (a) absence of probes, (b) mutant AP-1 or NF- κ B probes 5'-CGCTTGAT-AAATCAGCCGGAA-3', and 5'-AGTTGAGGCTC-CTTCCAGGC-3', respectively, labeled with biotin, (c) competition assays with a 100-fold excess of unlabeled AP-1 or NF- κ B probes, followed by incubation with its respective labeled probe.

Statistical analysis

Statistical significance was calculated by χ^2 test. The χ^2 test was used to analyze the association between NF- κ B/AP-1 and histopathological grades and Fas/FasL and ICH-1L/S. $P < 0.05$ was regarded as significant difference.

RESULTS

Detection of NF- κ B and AP-1 in HCC

In situ hybridization was performed to detect the activity status of NF- κ B and AP-1 in all 40 HCCs. NF- κ B and AP-1 distribution in nuclear or both nuclear and cytoplasm of cancer cells are illustrated in Figures 1 and 2. Of 40

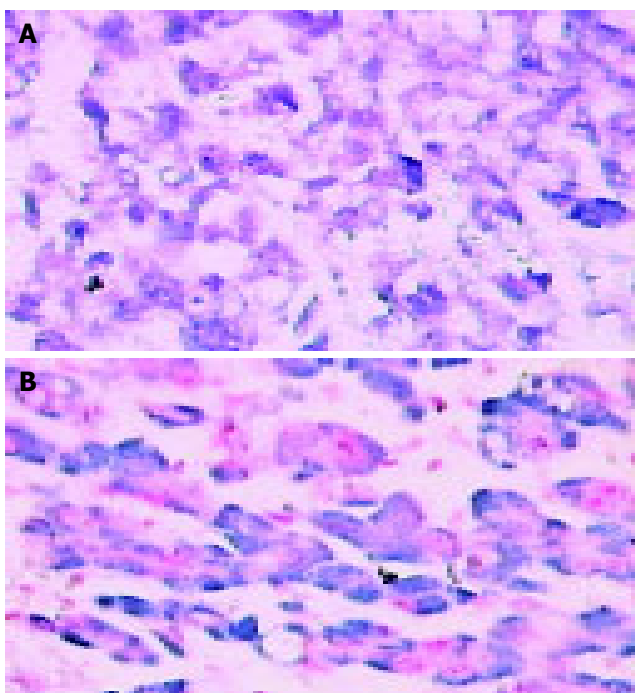


Figure 1 Hepatocellular carcinoma showing nuclear and cytoplasmic positivity for NF- κ B (A) and AP-1 (B). *In situ* hybridization (magnification $\times 200$).

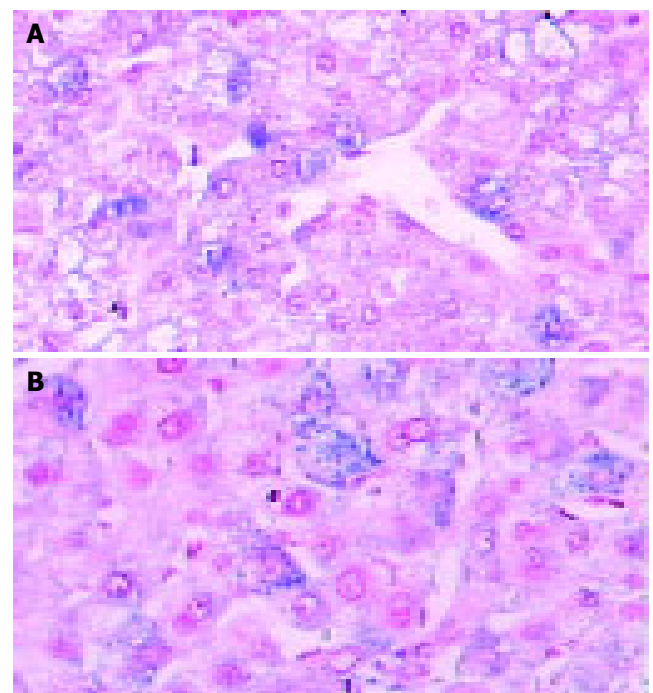


Figure 2 Nontumor liver tissue showing focal and weak cytoplasmic positivity for NF- κ B (A) and AP-1 (B). *In situ* hybridization (magnification $\times 200$).

HCCs, 22 (55%) presented nuclear or both nuclear and cytoplasmic staining of NF- κ B by *in situ* hybridization in which 13/25 (52%) were well differentiated tumors and 9/15 (60%) were poorly differentiated tumors. While 25 (62.5%) of 40 cases for AP-1 positive staining were shown in which 14/25 (56%) were well differentiated tumors and 10/15 (66.7%) were poorly differentiated tumors. There was no statistically significant difference of NF- κ B or AP-1 activation between well differentiated tumors and poorly differentiated tumors ($P>0.05$). In adjacent non-tumor tissues, cytoplasmic staining of NF- κ B or AP-1 was noted in 27(68%) and 23(58%) respectively. But lower nuclear staining for NF- κ B (17.5%) and AP-1 (10%) was found in non-tumor tissues than those in HCC with a statistical significance ($P<0.05$). Only few hepatocytes showed cytoplasmic staining for NF- κ B (1/7) and AP-1 (2/7) in normal liver tissues, but no staining in the nucleus. NF- κ B activity positively corresponded to AP-1 activation (Table 1).

Table 1 Detection of NF- κ B and AP-1 in HCC

Group	Cases	NF- κ B nucleus/cytoplasm + nucleus (+) (%)	AP-1 nucleus/cytoplasm + nucleus (+) (%)
Tumor tissue	40	22 (55) ^a	24 (60)
Well differentiated	25	13 (52)	14 (56)
Poorly differentiated	15	9 (60)	10 (66.7)
Nontumor tissue	40	7 (17.5)	4 (10)
Normal tissue	7	0	0

^a $P<0.05$ vs tumor tissue.

Expression of apoptosis proteins in HCC

Table 2 summarizes the results of immunohistochemical studies on apoptosis proteins including Fas, FasL, ICH-1L and ICH-1S. Fas, FasL, ICH-1L, and ICH-1S presented cytoplasmic reactivity in 7 (17.5%), 6 (15%), 15 (37.5%) and 21 (52.5%) of tumors, while in 21 (52.5%), 18 (45%),

29 (72.5%) and 31 (77.5%) of nontumor tissues, in 0%, 0%, 2/7 and 1/7 of normal liver tissues, respectively. There were statistically significant differences of the expression of Fas, FasL, ICH-1L, and ICH-1S between non-tumor tissues and tumor tissues ($P<0.05$). The differences of Fas and ICH-1S expression except FasL and ICH-1L were also statistically significant between nontumor tissues and normal liver tissues ($P<0.05$, Figure 3).

Table 2 Expression of Fas, FasL, ICH-1L, and ICH-1S in HCC

Group	Cases	Fas (%)	FasL (%)	ICH-1L (%)	ICH-1S (%)
Tumor tissue	40	7 (17.5) ^a	6 (15)	15 (37.5)	21 (52.5)
Nontumor tissue	40	21 (52.5) ¹	18 (45) ²	29 (72.5) ³	31 (77.5) ⁴
Normal tissue	7	0 ⁵	0 ⁶	2	1 ⁶

^a $P<0.05$ vs tumor tissue. ¹ $\chi^2 = 10.2692$, ² $\chi^2 = 8.5714$, ³ $\chi^2 = 9.8990$, ⁴ $\chi^2 = 5.4945$, ⁵ $\chi^2 = 4.6890$, ⁶ $\chi^2 = 8.2398$.

Relationship between activated NF- κ B and apoptosis proteins in HCC

The expression of Fas and FasL was more frequent in 22 cases of HCC with activated NF- κ B compared with 18 cases of HCC with inactivated NF- κ B, but the differences were not significant statistically between cases with activated NF- κ B group and with inactivated NF- κ B group ($P>0.05$). However, there was positive relationship between the expression of ICH-1L and ICH-1S in the cases with activated NF- κ B and those with inactivated NF- κ B ($P<0.05$, Table 3).

Relationship between activated AP-1 and apoptosis proteins in HCC

The expression of ICH-1L and ICH-1S in HCC with activated AP-1 was also more common with a statistical significance as compared with those with inactivated AP-1 respectively ($P<0.05$). But there was no significant difference between the expression of Fas and FasL in the cases with activated AP-1 and those with inactivated AP-1 ($P>0.05$, Table 4).

Table 3 Relationship between activated NF- κ B and apoptosis proteins in HCC

NF- κ B	Cases	Apoptosis protein							
		Fas		FasL		ICH-1L		ICH-1S	
		+	-	+	-	+	-	+	-
Activated	22	6	16	5	17	13	12	17	8
Inactivated	18	1	17	1	17	2	13	4	11
χ^2		1.9048		1.4495		4.4444		4.8722	
P		>0.05		>0.05		<0.05		<0.05	

Table 4 Relationship between activated AP-1 and apoptosis proteins in HCC

AP-1	Cases	Apoptosis protein							
		Fas		Fas L		ICH-1L		ICH-1S	
		+	-	+	-	+	-	+	-
Activated	25	7	18	6	19	13	12	16	9
Inactivated	15	0	15	0	15	2	13	3	12
χ^2		3.3362		2.5621		4.4444		5.6207	
P		>0.05		>0.05		<0.05		<0.025	

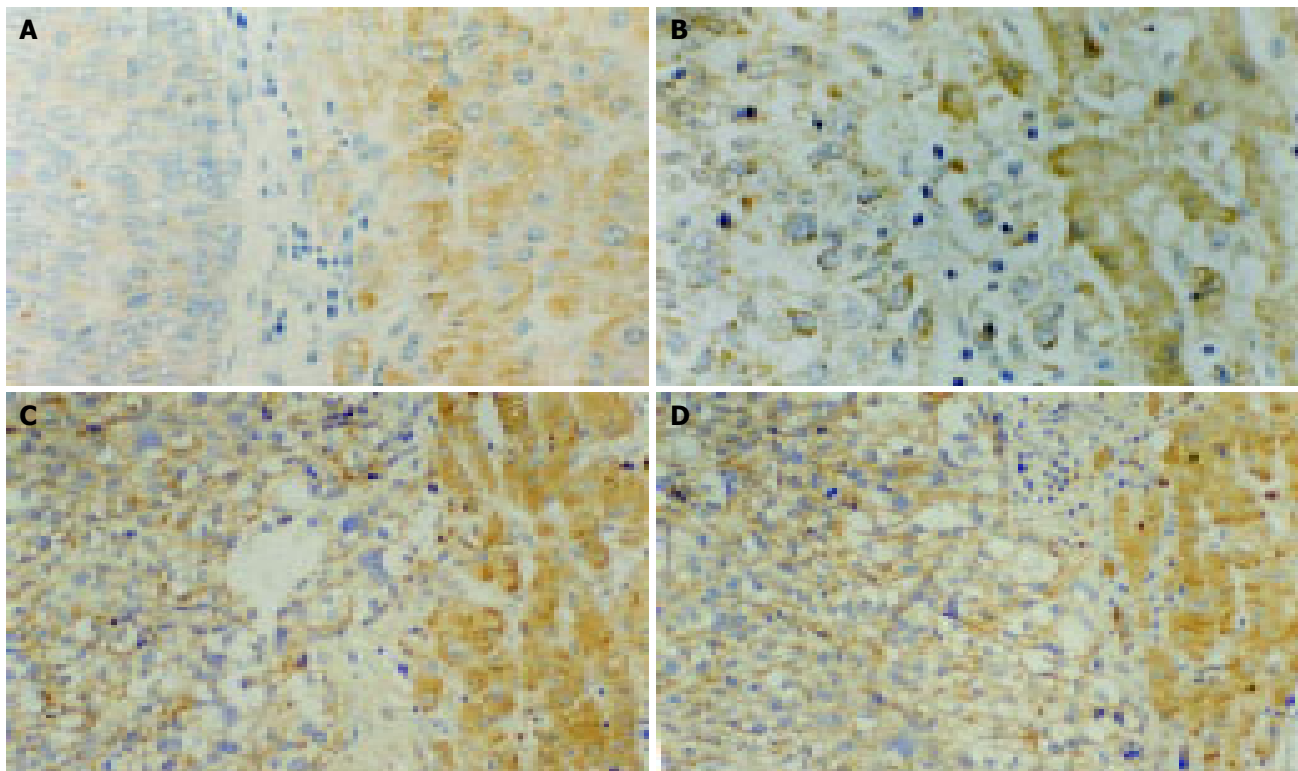


Figure 3 Immunohistochemistry staining showing strong cytoplasmic positivity in adjacent hepatocytes and weak positivity in HCC for Fas (A), FasL (B), ICH-

IL (C) and ICH-IS (D) (magnification ×200).

DISCUSSION

Electrophoretic mobility shift assays is a common and useful technique for studying transcription factors. However, the distribution of transcription factors either in nucleus or cytoplasm cannot be shown using this technique. *In situ* detection using nonradioactive oligonucleotides in paraffin wax-embedded tissues was successfully used for studying NF-κB and AP-1 activation in kidney and injured vessels^[28]. In this study, we performed this technique to detect NF-κB and AP-1 in HCC and obtained ideal results. The distribution of NF-κB and AP-1 was presented in nuclear and cytoplasmic types. Positive signals in HCC were mainly located both in nuclei and cytoplasm while cytoplasmic staining mainly in nontumor. We concluded that *in situ* hybridization is a convenient and efficient tool for studying transcription factors (Table 5).

Some studies have shown that DNA binding activity of NF-κB and AP-1 was aberrant in HCC^[15,16]. Liu *et al.*, measured the DNA binding activity of AP-1 and NF-κB in the peritumoral and the tumoral parts of 15 primary liver cancers. AP-1 and NF-κB binding activities were in 73%

and 87% of the cases in the peritumoral tissue respectively. A further activation of AP-1 and NF-κB binding in the tumoral parts was detected in 40% and 80% of the cases respectively. Early activation of AP-1 and NF-κB contributes probably to the acquisition of a transformed phenotype during hepatocarcinogenesis, whatever the etiology^[15]. Tai *et al.*, studied the NF-κB-DNA binding activity and its dimmer, active nuclear RelA and nuclear IκappaB-alpha proteins expression in HCC using electrophoretic mobility shift assay and Western blot analysis. The results showed that nuclear NF-κB DNA binding activity and nuclear RelA protein expression were greater in tumor tissue compared with nontumor tissue^[16]. Constitutive activation of NF-κB was found more frequently in tumor tissue compared with nontumor tissue. In our study, the results are similar to that by electrophoretic mobility shift assay. Furthermore, our findings presented positive staining for NF-κB and AP-1 distribution in cytoplasm (inactive form) at 68% and 58% in adjacent liver tissues, 1/7 and 2/7 in normal liver, and in nuclei (active form) at 55% and 62.5% in tumor tissues. The possible activation of NF-κB has been shown in some

Table 5 Relationship between activated NF-κB and apoptosis proteins in nontumor tissues

NF-κB	Cases	Adjacent nontumor tissues								Normal liver tissues								
		Fas		FasL		ICH-IL		ICH-IS		Fas		FasL		ICH-IL		ICH-IS		
		+	-	+	-	+	-	+	-	+	-	+	-	+	-	+	-	
Activated	7	15	7	13	9	19	3	21	1	0	0	0	0	0	0	0	0	0
Inactivated	33	6	12	5	13	10	8	10	8	7	0	7	0	7	2	5	1	6
χ^2		4.8211		3.9221		4.7130		6.8946			0		0		0		0	
P		<0.05		<0.05		<0.05		<0.05			>0.05		>0.05		>0.05		>0.05	

carcinoma tissues such as human pancreatic carcinoma, gastric carcinoma and breast carcinoma. NF- κ B activation was evaluated on the basis of nuclear translocation from inactive form with NF- κ B-I κ Bs complex in cytoplasm^[18,20-22]. However, the mechanism concerning AP-1 activation in carcinoma is not available. We further found that NF- κ B activity positively corresponded to AP-1 activation. Taken together, these results demonstrated that NF- κ B and AP-1 translocated from cytoplasm (inactive form) to nucleus (active form) during hepatocarcinogenesis and suggested that activation of both NF- κ B and AP-1 may be required to produce potential biological function and play important roles in the oncogenesis of human HCC.

Fas/FasL system is involved in apoptosis in human HCC^[5,6]. In this study, we further investigated whether there is a relationship between NF- κ B or AP-1 activity and Fas/FasL expression in HCC. The results showed that more expression of Fas and FasL was found in cases with activated NF- κ B or AP-1 than those with inactivated NF- κ B or AP-1 in HCC but the differences were not significant statistically ($P>0.05$). These data indicated that NF- κ B and AP-1 activation may not be required for Fas/FasL-induced apoptosis in HCC. Similar results have been reported in other different cells. Nagaki *et al.*, found NF- κ B blocks hepatocyte apoptosis mediated by the TNF receptor, but not by Fas^[23]. In T cells, NF- κ B signaling pathway is not required for activation-induced FasL expression^[24]. Lack of a requirement for AP-1 induction in Fas-mediated death was substantiated with Jurkat cell^[25]. However, the results contrary to those stated above have been implicated in some studies. Marusawae *et al.*, demonstrated that NF- κ B activity is related to Fas signaling in hepatocyte-derived cell lines, HepG2 and Huh-7 cells. Overexpression of kinase-inactive NF- κ B-inducing kinase (NIK) and IkappaB kinase (IKK) inhibited the activation of NF- κ B introduced by anti-Fas treatment in these cells. Inactivation of NF- κ B by the production of IkappaB-alpha protein made these cells more susceptible to apoptosis induced by Fas stimulation^[26]. NF- κ B and AP-1 are also found involving in the transcriptional regulation of FasL in Fas-mediated thymineless death of colon carcinoma cell^[27]. These results suggested NF- κ B and AP-1 may play different roles in the regulation of Fas/FasL-mediated apoptosis in different cells.

ICH-1, a gene related to the *C. elegans* cell death gene *ced-3* and the mammalian homolog of *ced-3*, interleukin-1 beta-converting enzyme (ICE). Alternative splicing results in two distinct ICH-1 mRNA species. One mRNA species encodes a protein product of 435 amino acids (ICH-1L) that is homologous to both the P20 and P10 subunits of ICE (27% identity) and the entire CED-3 protein (28% identity). The other mRNA encodes a 312 amino acid truncated version of ICH-1L protein (ICH-1S). Overexpression of ICH-1L induces programmed cell death, while ICH-1S suppresses Rat-1 cell death induced by serum deprivation. ICH-1 plays an important role in both positive and negative regulation of programmed cell death in vertebrate animals^[29]. In this study, we found that aberrant expression of ICH-1 in HCC and adjacent tissues compared to normal liver. The results also showed that there are statistical differences between expression of ICH-1L or ICH-1S and NF- κ B or AP-1

activation. These findings suggested that NF- κ B and AP-1 may play a role in mediating ICH-1L/S expression during pathogenesis of HCC.

REFERENCES

- 1 **Shao J**, Li Y, Li H, Wu Q, Hou J, Liew C. Deletion of chromosomes 9p and 17 associated with abnormal expression of p53, p16/MTS1 and p15/MTS2 gene protein in hepatocellular carcinomas. *Chin Med J* 2000; **113**: 817-822
- 2 **Staib F**, Hussain SP, Hofseth LJ, Wang XW, Harris CC. TP53 and liver carcinogenesis. *Hum Mutat* 2003; **21**: 201-216
- 3 **Yuen MF**, Wu PC, Lai VC, Lau JY, Lai CL. Expression of c-Myc, c-Fos, and c-jun in hepatocellular carcinoma. *Cancer* 2001; **91**: 106-112
- 4 **Ikeguchi M**, Hirooka Y, Kaibara N. Quantitative analysis of apoptosis-related gene expression in hepatocellular carcinoma. *Cancer* 2002; **95**: 1938-1945
- 5 **Lee SH**, Shin MS, Lee HS, Bae JH, Lee HK, Kim HS, Kim SY, Jang JJ, Joo M, Kang YK, Park WS, Park JY, Oh RR, Han SY, Lee JH, Kim SH, Lee JY, Yoo NJ. Expression of Fas and Fas-related molecules in human hepatocellular carcinoma. *Hum Pathol* 2001; **32**: 250-256
- 6 **Roskams T**, Libbrecht L, Van Damme B, Desmet V. Fas and Fas ligand: strong co-expression in human hepatocytes surrounding hepatocellular carcinoma; can cancer induce suicide in peritumoural cells? *J Pathol* 2000; **191**: 150-153
- 7 **Angel P**, Karin M. The role of Jun, Fos, and the AP-1 complex in cell-proliferation and transformation. *Biochim Biophys Acta* 1991; **1072**: 129-157
- 8 **Karin M**, Liu ZG, Zandi E. AP-1 function and regulation. *Curr Opin Cell Biol* 1997; **9**: 240-246
- 9 **Shaulian E**, Karin M. AP-1 in cell proliferation and survival. *Oncogene* 2001; **20**: 2390-2400
- 10 **Beg AA**, Sha WC, Bronson RT, Ghosh S, Baltimore D. Embryonic lethality and liver degeneration in mice lacking the RelA component of NF- κ B. *Nature* 1995; **376**: 167-170
- 11 **Van Antwerp DJ**, Martin SJ, Kafri T, Green DR, Verma IM. Suppression of TNF-alpha-induced apoptosis by NF-kappaB. *Science* 1996; **274**: 787-789
- 12 **Bellas RE**, FitzGerald MJ, Fausto N, Sonenshein GE. Inhibition of NF- κ B activity induces apoptosis in murine hepatocytes. *Am J Pathol* 1997; **151**: 891-896
- 13 **Beg AA**, Baltimore D. An essential role for NF-kappaB in preventing TNF-alpha-induced cell death. *Science* 1996; **274**: 782-784
- 14 **Siebenlist U**, Franzoso G, Brown K. Structure, regulation and function of NF-kappa B. *Annu Rev Cell Biol* 1994; **10**: 405-455
- 15 **Liu P**, Kimmoun E, Legrand A, Sauvanet A, Degott C, Lardeux B, Bernuau D. Activation of NF-kappaB, AP-1 and STAT transcription factors is a frequent and early event in human hepatocellular carcinomas. *J Hepatol* 2002; **37**: 63-71
- 16 **Tai DI**, Tsai SL, Chang YH, Huang SN, Chen TC, Chang KS, Liaw YF. Constitutive activation of nuclear factor kappaB in hepatocellular carcinoma. *Cancer* 2000; **89**: 2274-2281
- 17 **Fujikawa K**, Shiraki K, Sugimoto K, Ito T, Yamanaka T, Takase K, Nakano T. Reduced expression of ICE/caspase1 and CPP32/caspase3 in human hepatocellular carcinoma. *Anticancer Res* 2000; **20**: 1927-1932
- 18 **Sasaki N**, Morisaki T, Hashizume K, Yao T, Tsuneyoshi M, Noshiro H, Nakamura K, Yamanaka T, Uchiyama A, Tanaka M, Katano M. Nuclear factor-kappaB p65 (RelA) transcription factor is constitutively activated in human gastric carcinoma tissue. *Clin Cancer Res* 2001; **7**: 4136-4142
- 19 **Luque I**, Gelinas C. Rel/NF- κ B and I κ B factors in oncogenesis. *Semin Cancer Biol* 1997; **8**: 103-111
- 20 **Wang W**, Abbruzzese JL, Evans DB, Larry L, Cleary KR, Chiao PJ. The nuclear factor- κ B RelA transcription factor is constitutively activated in human pancreatic adenocarcinoma cells. *Clin Cancer Res* 1999; **5**: 119-127

- 21 **Sovak MA**, Bellas RE, Kim DW, Zanieski GJ, Rogers AE, Traish AM, Sonenshein GE. Aberrant nuclear factor- κ B/Rel expression and the pathogenesis of breast cancer. *J Clin Invest* 1997; **100**: 2952-2960
- 22 **Kim DW**, Sovak MA, Zanieski G, Nonet G, Romieu-Mourez R, Lau AW, Hafer LJ, Yaswen P, Stampfer M, Rogers AE, Russo J, Sonenshein GE. Activation of NF- κ B/Rel occurs early during neoplastic transformation of mammary cells. *Carcinogenesis* 2000; **21**: 871-879
- 23 **Nagaki M**, Naiki T, Brenner DA, Osawa Y, Imose M, Hayashi H, Banno Y, Nakashima S, Moriwaki H. Tumor necrosis factor alpha prevents tumor necrosis factor receptor-mediated mouse hepatocyte apoptosis, but not fas-mediated apoptosis: role of nuclear factor-kappaB. *Hepatology* 2000; **32**: 1272-1279
- 24 **Rivera-Walsh I**, Cvijic ME, Xiao G, Sun SC. The NF-kappa B signaling pathway is not required for Fas ligand gene induction but mediates protection from activation-induced cell death. *J Biol Chem* 2000; **275**: 25222-25230
- 25 **Lenczowski JM**, Dominguez L, Eder AM, King LB, Zacharchuk CM, Ashwell JD. Lack of a role for Jun kinase and AP-1 in Fas-induced apoptosis. *Mol Cell Biol* 1997; **17**: 170-181
- 26 **Marusawa H**, Hijikata M, Watashi K, Chiba T, Shimotohno K. Regulation of Fas-mediated apoptosis by NF-kappaB activity in human hepatocyte derived cell lines. *Microbiol Immunol* 2001; **45**: 483-489
- 27 **Harwood FG**, Kasibhatla S, Petak I, Vernes R, Green DR, Houghton JA. Regulation of FasL by NF-kappaB and AP-1 in Fas-dependent thymineless death of human colon carcinoma cells. *J Biol Chem* 2000; **275**: 10023-10029
- 28 **Hernandez-Presa MA**, Gomez-Guerrero C, Egido J. *In situ*-nonradioactive detection of nuclear factors in paraffin sections by Southwestern histochemistry. *Kidney Int* 1999; **55**: 209-214
- 29 **Wang L**, Miura M, Bergeron L, Zhu H, Yuan J. Ich-1, an Ice/ced-3-related gene, encodes both positive and negative regulators of programmed cell death. *Cell* 1994; **78**: 739-750

Science Editor Li WZ. Language Editor Elsevier HK

• COLORECTAL CANCER •

Assessment of spiral CT pneumocolon in preoperative colorectal carcinoma

Can-Hui Sun, Zi-Ping Li, Quan-Fei Meng, Shen-Ping Yu, Da-Sheng Xu

Can-Hui Sun, Zi-Ping Li, Quan-Fei Meng, Shen-Ping Yu, Da-Sheng Xu, Department of Radiology, First Affiliated Hospital, Sun Yat-Sen University, Guangzhou 510080, Guangdong Province, China

Supported by the Medical Science Foundation of Guangdong Province, No. A2002185

Correspondence to: Dr. Zi-Ping Li, Department of Radiology, First Affiliated Hospital, Sun Yat-Sen University, Guangzhou 510080, Guangdong Province, China. liziping163@163.net

Telephone: +86-20-87335415 Fax: +86-20-87750632

Received: 2004-10-09 Accepted: 2004-11-26

Abstract

AIM: To investigate the value of spiral CT pneumocolon in preoperative colorectal carcinoma.

METHODS: Spiral CT pneumocolon was performed prior to surgery in 64 patients with colorectal carcinoma. Spiral CT images were compared to specimens from the resected tumor.

RESULTS: Spiral CT depicted the tumor in all patients. Comparison of spiral CT and histologic results showed that the sensitivity and specificity were 95.2%, 40.9% in detection of local invasion, and 75.0%, 90.9% in detection of lymph node metastasis. Compared to the Dukes classification, the disease was correctly staged as A in 6 of 18 patients, as B in 18 of 23, as C in 10 of 15, and as D in 7 of 8. Overall, spiral CT correctly staged 64.1% of patients.

CONCLUSION: Spiral CT pneumocolon may be useful in the preoperative assessment of patients with colorectal carcinoma as a means for assisting surgical planning.

© 2005 The WJG Press and Elsevier Inc. All rights reserved.

Key words: Tomography; X-ray compute; Pneumocolon; Preoperative staging; Colorectal cancer

Sun CH, Li ZP, Meng QF, Yu SP, Xu DS. Assessment of spiral CT pneumocolon in preoperative colorectal carcinoma. *World J Gastroenterol* 2005; 11(25): 3866-3870
<http://www.wjgnet.com/1007-9327/11/3866.asp>

INTRODUCTION

With the development of high-resolution scanners, technical refinements in obtaining better quality studies, and the accumulated clinical experience leading to better interpretation,

the role, indications, and accuracy of CT of the colon have dramatically enlarged and improved^[1-3]. Reliable preoperative determination of the extent of spread of a colorectal carcinoma not only indicates the expected prognosis but also assists management. For obtaining reliable results from CT scan, preparation of the patients, especially complete distention of the colon using water or air as contrast agent, is the most important precondition. Otherwise, collapse of the colon and feces can easily be misinterpreted as tumor. Many studies have shown that water enema spiral CT is a useful modality for preoperative staging of patients with colorectal carcinoma^[4-7]. However, water enema can be difficult and distressing in frail elderly patients and has risk of water incontinence. Air insufflation for the colon can be achieved easily and rapidly and is well tolerated by the patients, and air provides an excellent CT contrast medium^[8]. There have been few reports concerning the preoperative staging of colorectal carcinoma with spiral CT pneumocolon. Therefore, this study aimed to assess the value of spiral CT pneumocolon in preoperative colorectal carcinoma.

MATERIALS AND METHODS

Patients

From August 1998 to December 2002, 64 patients with colorectal carcinoma, who were operated on at our institution, underwent spiral CT pneumocolon. There were 40 men and 24 women, ranging in age from 32 to 88 years (mean 59 years). Among the 64 patients who had a prior colonoscopy, 4 of 15 patients had an incomplete barium enema due to barium incontinence, and 19 of 64 patients had incomplete colonoscopy due to inability to cross a distal stricture.

Technique

All patients were fasted for at least 12 h before the study and given an oral colon cleansing preparation the night before CT scan. Nine-hundred milliliters of 3% diluted gastrografin solution was given orally 45 min before, so that small bowel loops were opacified. Anisodamine hydrochloride (10 mg, IM) was used to control peristaltic artifact and relax the colon. The patient was previously instructed not to void. As the study progressed, interpretation was more straightforward when the bladder was full.

The patients were positioned on the CT table in supine position. A Foley catheter was inserted into the rectum and 1 500-2 000 mL room air was administered per rectum to distend the colon. The enema was stopped if the patient experienced abdominal discomfort. Adequate distention of the whole colon was confirmed on the scanogram.

Studies were performed on a Toshiba Xpress/SX spiral

CT scanner with a 10-mm collimation and pitch of 1-2, at 120 kV and 200 mA. After plain scanning, 1.5 mL/kg of non-ionic iodinated contrast medium (iopromide, Ultravist 300; Schering, Berlin, Germany) was administered via the antecubital vein at a rate of 3 mL/s using an autoinjector, and scanning commenced 60 s after start of the injection from the dome of the liver to the anal verge. The time between CT scan and surgery ranged 1-8 d (mean 4.7 d).

Evaluating criteria

Based on previous reports^[5,7,8] and our own experience, the following three parameters were established and evaluated: (1) local extramural invasion (irregularly serrated or speculated outer contour, tumor mass or strands of soft tissue extending out, and/or indistinctly increased density of the pericolic fat), (2) lymph node involvement (lymph node short axis 1 cm or larger, or node less than 1 cm in diameter with obvious enhancement), and (3) distal and/or extensive disease (liver or lung metastases, direct extension into adjacent solid or hollow organs).

All patients with colorectal carcinoma were staged on CT according to the modified Dukes' classification^[7]: stage A, tumor limited to the colonic wall; stage B, tumor affecting the serosa or the pericolic fat; stage C, lymph node involvement; and stage D, tumor infiltrating adjacent organs and/or with metastases. The modified Dukes' classification was used because this system was currently used by surgeons at our institution.

Image interpretation

Two experienced radiologists, who were blind to the surgical and pathologic findings of each patient, interpreted the images as compared to above parameters, and any discrepant readings were solved by consensus. After a minimum of 4 wk, the same two radiologists reviewed the images for the second time. Intraobserver variability was evaluated by means of a weighed k -statistic^[9].

RESULTS

The overall results showed good agreement between the two reviews by the two radiologists. The k -statistic for the data was 0.77, representing good intraobserver agreement.

Normal findings and primary tumor

All patients tolerated the spiral CT pneumocolon well with no significant discomfort, and had good bowel preparation and no fluid levels or residual fecal material. The distended colon lumen and normal colonic wall were well seen on spiral CT (Figure 1). Using this technique the normal colonic wall represented a single layer which was 1-2-mm thick.

Spiral CT detected the tumor in all patients and the smallest mass was 0.7 cm×1.0 cm. The lesion was shown as an eccentric focal mass with irregular segmental or circumferential wall ranging 0.7-4.5 cm in thickness, and their extension ranged 1.0-10.0 cm (Figures 2A-C). Most lesions had an uneven, lobulated configuration and large masses had patchy areas of necrosis. Different degrees of distal colonic stricture were presented. The majority of the mass showed moderate to obvious enhancement.

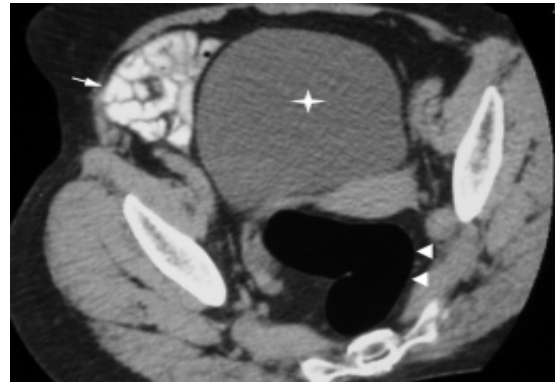


Figure 1 Optimal visualization of normal rectal wall (arrowheads), small intestine (arrow), and urinary bladder (star).

Local invasion

Tumor invasion of serosa and/or pericolic fat was correctly staged by spiral CT in 49 (76.6%) of 64 patients (Figures 2A and B). In the incorrectly staged group, spiral CT overstaged 12 patients (Figure 3A) and understaged 2 patients (Figure 3B). Spiral CT evaluation had a sensitivity of 95.2% and a specificity of 40.9%.

Lymph node involvement

Involvement of lymph nodes less than 5 mm in diameter was seen in 7 (35.0%) of 20 patients. Spiral CT correctly diagnosed lymph node metastasis in 15 of 20 patients (Figure 2C). In the correctly diagnosed group, seven patients showed nodal enhancement, and eight patients showed no enhancement of lymph nodes larger than 1 cm in diameter. Clusters of three or more smaller nodes (each less than 1 cm in diameter) were seen by CT in five patients, histology revealed no evidence of nodal involvement.

Nodal involvement was correctly staged by spiral CT in 55 (85.9%) of 64 patients. In the incorrectly staged group, spiral CT overstaged 3 (Figure 3C) and understaged 5 of 20 patients. Spiral CT evaluation had a sensitivity of 75.0% and a specificity of 90.9%.

Distal metastasis

Liver metastasis was presented in four patients (Figure 2D), lung metastasis in two patients, and abdominal wall metastasis in one patient. They were all correctly diagnosed by CT. Only one patient with peritoneal seeding was missed due to the small lesion.

Preoperative staging

Staging results are presented in Table 1. CT stage A was correct in 6 of 18, stage B in 18 of 23, stage C in 10 of 15, and stage D in 7 of 8 patients. Overall, the diagnostic accuracy was 64.1% (41/64).

DISCUSSION

Colonoscopy and barium enema are the main methods for diagnosis of colorectal tumors. However, both modalities do not permit a precise preoperative prediction as to whether a tumor is limited to the colonic wall or has spread into surrounding tissues. Patients with severe colonic stricture

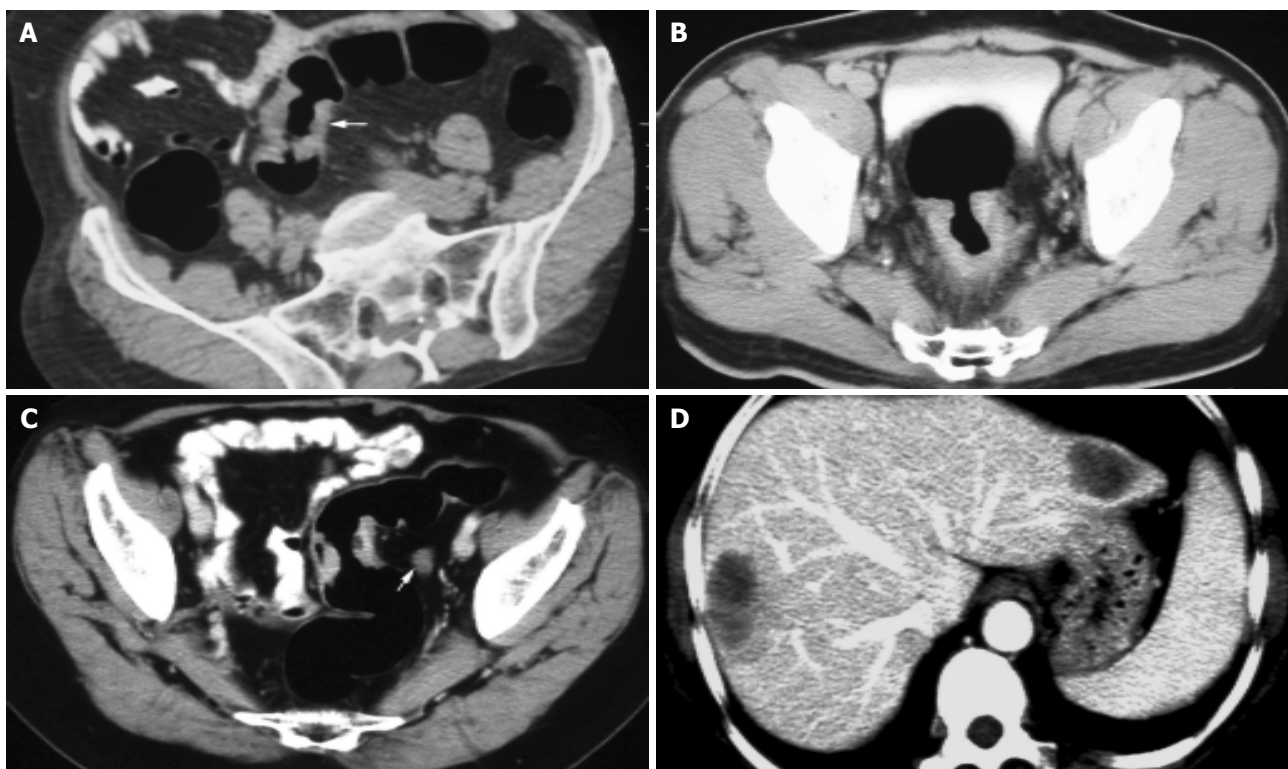


Figure 2 Correctly staged lesions. **A:** Dukes stage A carcinoma (arrow); **B:** Dukes stage B carcinoma; **C:** Dukes stage C carcinoma; **D:** Dukes stage D carcinoma.

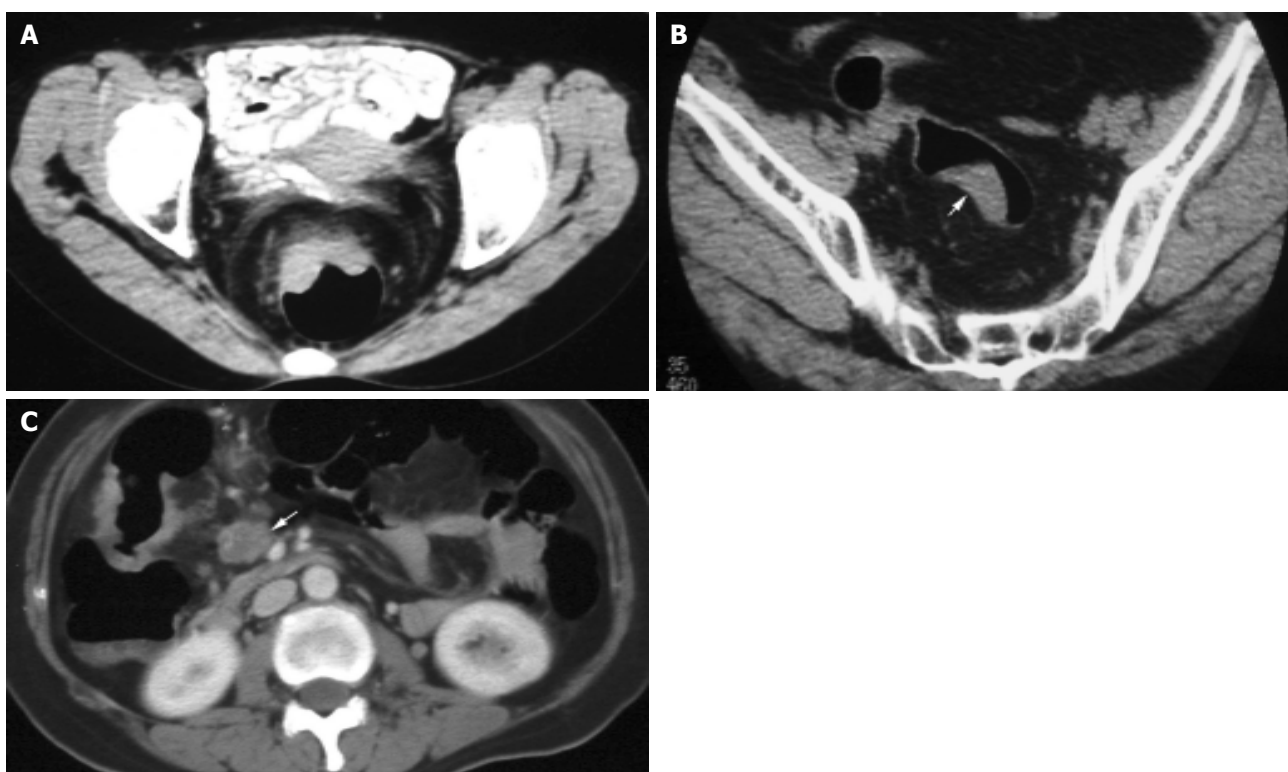


Figure 3 Incorrectly staged lesions. **A:** Dukes stage A carcinoma; **B:** Dukes stage B carcinoma (arrow); **C:** Dukes stage B carcinoma.

or barium incontinence may be poor candidates for the two examinations. Our study showed that CT pneumocolon had the potential utility as an adjunctive imaging technique for patients with colorectal carcinoma.

Imaging with spiral CT pneumocolon could clearly show the lumen and wall of the colon and colonic lesions. Normal colonic wall thickness should not exceed 3 mm in a well-distended segment, and the thickness greater than 6 mm is

Table 1 CT findings and pathologic staging

CT staging	Pathologic staging				Total
	A	B	C	D	
A	6	2	1		9
B	12	18	4		34
C		3	10	1	14
D				7	7
Total	18	23	15	8	64

considered abnormal^[1]. In our study with spiral CT pneumocolon technique, the thickness of the normal colonic wall ranged 1-2 mm, and the thickness of the lesion was greater than 6 mm. We were unable to identify the mucosal lining nor the different anatomic layers of the colonic wall as reported by others who used water enema technique^[6,7].

The sensitivity of CT detection depends mainly on the size of the lesion and on the quality of the CT examination. It varies from 68% if no special attempts are made to promote visualization of the colonic lumen to 95% when the colonic lumen is distended well. In this study, the overall detection rate was 100%, and masses with a diameter in 1 cm were identified. Our results corresponded favorably with previous reports^[10,11]. This may be due to the adequate preparation of patients and CT pneumocolon technique. CT colonography generated from CT pneumocolon has emerged in recent years. This technique can detect lesions less than 5 mm in diameter, and its sensitivity is over 85% in detection of polyps 10 mm or greater in size, 70-80% of polyps 5-9 mm in size and 60% of polyps smaller than 5 mm^[12,13]. It is a viable alternative for screening primary colorectal neoplasms and examining portions of the colon proximal to an obstructing lesion that cannot be traversed by colonoscopy or by barium^[3,10,13].

In our experience, CT has a sensitivity of 95.2% and an accuracy of 76.6% in evaluating the local invasion. However, the specificity is only 40.9%. Harvey *et al.*^[8], reported that its sensitivity is 100% and specificity is 33%. Zhou *et al.*^[2], reported that its sensitivity is 92.9% and specificity is 50.0%. The reasons for the low specificity in local extension may be that CT is not possible to distinguish the single layers comprising the wall and there is no simple CT criterion to differentiate inflammation of the serosa from tumor invasion^[2,8]. Matsuoka *et al.*^[14], reported that using sagittal or coronal sections improves diagnostic accuracy from 79.4% to 90.4% in assessing the depth of tumor invasion. Endoscopic ultrasonography (EUS) is superior to CT in detecting the exact depth of parietal invasion, and its accuracy is 84.9%^[15]. In our study, the accuracy of EUS was 87.5%, and its specificity was 100% in assessing the local extension.

Traditionally, CT detection of abnormal lymph nodes is based on imaging nodes greater than 1 cm in diameter or finding of clustered lymph nodes^[5,8]. However, lymph node metastasis in colon cancer occurs frequently in lymph nodes measuring less than 5 mm. Herrera-Ornelas *et al.*^[16], have reported a 65% incidence of lymph node metastasis. Whereas enlarged lymph nodes may be infiltrated by inflammatory or neoplastic cells. A relatively low sensitivity of CT in detecting nodal metastases is anticipated. Harvey *et al.*^[8], reported that its sensitivity is 56% and specificity is

95%. Gazelle *et al.*^[5], reported that its sensitivity is 60% and specificity is 79%. Hundt *et al.*^[4], reported that its sensitivity is 84.3%, its specificity being 60% and accuracy being 81.0%. In this present study, its sensitivity, specificity, and accuracy in detecting lymph node involvement were 75.0%, 90.9%, and 85.9%, respectively. The disparity in these reports is probably due to the different criteria used. In our study, five patients with clustered lymph nodes (<1 cm) had no pathologic evidence of nodal involvement, suggesting that this criterion is unreliable. Further investigation is needed.

The data in this series showed that compared to the Dukes classification, CT correctly staged 64.1% of all patients, which is consistent with previous reports^[2,8]. CT staging accuracy, however, showed significant variations in different Dukes categories. It correctly staged 6 (33.3%) of 18 patients with Dukes A lesion, 18 (78.3%) of 23 patients with Dukes B lesion, 10 (66.7%) of 15 patients with Dukes C tumor, and 7 (87.5%) of 8 patients with Dukes D tumor.

Colon cancer is potentially curable and decision on treatment is based on the extent of tumor. If extensive local spread of tumor is shown by CT or MRI, the patients can be treated with radiation therapy alone or undergo tumor resection after radiation therapy. The success of subsequent chemotherapy and irradiation can be determined in patients by follow-up CT or MRI, which can be compared to the base-line study before treatment. Recent studies showed that endorectal surface coil MR imaging is valuable in patients with rectal carcinoma to assess involvement of the levator ani^[1]. If involvement of the levator ani is demonstrated, an abdominoperineal resection is needed.

In conclusion, spiral CT pneumocolon is a quick and noninvasive method for detecting colorectal carcinoma, and can provide valuable information preoperatively. In addition, it may represent a useful adjunct to colonoscopy or barium enema in patients with colorectal carcinoma.

REFERENCES

- 1 Dobos N, Rubesin SE. Radiologic imaging modalities in the diagnosis and management of colorectal cancer. *Hematol Oncol Clin North Am* 2002; **16**: 875-895
- 2 Zhou C, Li J, Zhao X. Spiral CT in the preoperative staging of colorectal carcinoma-radiologic-pathologic correlation. *Zhonghua Zhongliu Zazhi* 2002; **24**: 274-277
- 3 Laghi A, Iannaccone R, Trenna S, Mangiapane F, Sinibaldi G, Piacentini F, Sammartino P, Stipa V, Passariello R. Multislice spiral CT colonography in the evaluation of colorectal neoplasms. *Radiol Med* 2002; **104**: 394-403
- 4 Hundt W, Braunschweig R, Reiser M. Evaluation of spiral CT in staging of colon and rectum carcinoma. *Eur Radiol* 1999; **9**: 78-84
- 5 Gazelle GS, Gaa J, Saini S, Shellito P. Staging of colon carcinoma using water enema CT. *J Comput Assist Tomogr* 1995; **19**: 87-91
- 6 Gossios KJ, Tsianos EV, Kontogiannis DS, Demou LL, Tatsis CK, Papakostas VP, Merkouropoulos MM, Tsimoyiannis EC. Water as contrast medium for computed tomography study of colonic wall lesions. *Gastrointest Radiol* 1992; **17**: 125-128
- 7 Angelelli G, Macarini L, Lupo L, Caputi-Jambrenghi O, Pannarale O, Memeo V. Rectal carcinoma: CT staging with water as contrast medium. *Radiology* 1990; **177**: 511-514
- 8 Harvey CJ, Amin Z, Hare CM, Gillams AR, Novelli MR, Boulos PB, Lees WR. Helical CT pneumocolon to assess colonic tumors: radiologic-pathologic correlation. *Am J Roentgenol* 1998; **170**: 1439-1443

- 9 **Song JH**, Francis IR, Platt JF, Cohan RH, Mohsin J, Kielb SJ, Korobkin M, Montie JE. Bladder tumor detection at virtual cystoscopy. *Radiology* 2001; **218**: 95-100
- 10 **Britton I**, Dover S, Vallance R. Immediate CT pneumocolon for failed colonoscopy; comparison with routine pneumocolon. *Clin Radiol* 2001; **56**: 89-93
- 11 **Miao YM**, Amin Z, Healy J, Burn P, Murugan N, Westaby D, Allen-Mersh TG. A prospective single centre study comparing computed tomography pneumocolon against colonoscopy in the detection of colorectal neoplasms. *Gut* 2000; **47**: 832-837
- 12 **Yee J**, Kumar NN, Hung RK, Akerkar GA, Kumar PR, Wall SD. Comparison of supine and prone scanning separately and in combination at CT colonography. *Radiology* 2003; **226**: 653-661
- 13 **Harvey CJ**, Renfrew I, Taylor S, Gillams AR, Lees WR. Spiral CT pneumocolon: applications, status and limitations. *Eur Radiol* 2001; **11**: 1612-1625
- 14 **Matsuoka H**, Nakamura A, Masaki T, Sugiyama M, Takahara T, Hachiya J, Atomi Y. Preoperative staging by multidetector-row computed tomography in patients with rectal carcinoma. *Am J Surg* 2002; **184**: 131-135
- 15 **Shimizu S**, Tada M, Kawai K. Use of endoscopic ultrasonography for the diagnosis of colorectal tumors. *Endoscopy* 1990; **22**: 31-34
- 16 **Herrera-Ornelas L**, Justiniano J, Castillo N, Petrelli NJ, Stulc JP, Mittelman A. Metastases in small lymph nodes from colon cancer. *Arch Surg* 1987; **122**: 1253-1256

Science Editor Wang XL and Guo SY Language Editor Elsevier HK

Urinary nucleosides as biological markers for patients with colorectal cancer

Yu-Fang Zheng, Jun Yang, Xin-Jie Zhao, Bo Feng, Hong-Wei Kong, Ying-Jie Chen, Shen Lv, Min-Hua Zheng, Guo-Wang Xu

Yu-Fang Zheng, Jun Yang, Xin-Jie Zhao, Hong-Wei Kong, Shen Lv, Guo-Wang Xu, National Chromatographic R&A Center, Dalian Institute of Chemical Physics, the Chinese Academy of Sciences, Dalian 116023, Liaoning Province, China
Bo Feng, Min-Hua Zheng, Department of Surgical, the Ruijin Affiliated Hospital of Shanghai Second Medical University, Shanghai 200025, China

Ying-Jie Chen, Shen Lv, Center of Experiment, the Second Affiliated Hospital of Dalian Medical University, Dalian 116023, Liaoning Province, China

Supported by the High-tech R and D Plan, No. 2003AA223061 and the Sociality Commonweal Project of State Ministry of Science and Technology of China, the Knowledge Innovation Program of the Chinese Academy of Sciences, No. K2003A16 and Liaoning Province Foundation of Science and Technology

Correspondence to: Professor Dr. Guo-Wang Xu, National Chromatographic R and A Center, Dalian Institute of Chemical Physics, Chinese Academy of Sciences, Dalian 116023, Liaoning Province, China. dicp402@mail.dlptt.ln.cn

Telephone: +86-411-84379530 Fax: +86-411-84379559

Received: 2004-10-02 Accepted: 2004-12-03

Abstract

AIM: Fourteen urinary nucleosides, primary degradation products of tRNA, were evaluated to know the potential as biological markers for patients with colorectal cancer.

METHODS: The concentrations of 14 kinds of urinary nucleosides from 52 patients with colorectal cancer, 10 patients with intestinal villous adenoma and 60 healthy adults were determined by column switching high performance liquid chromatography method.

RESULTS: The mean levels of 12 kinds of urinary nucleosides (except uridine and guanosine) in the patients with colorectal cancer were significantly higher than those in patients with intestinal villous adenoma or the healthy adults. Using the levels of 14 kinds of urinary nucleosides as the data vectors for principal component analysis, 71% (37/52) patients with colorectal cancer were correctly classified from healthy adults, in which the identification rate was much higher than that of CEA method (29%). Only 10% (1/10) of patients with intestinal villous adenoma were indistinguishable from patients with colorectal cancer. The levels of m1G, Pseu and m1A were positively related with tumor size and Duke's stages of colorectal cancer. When monitoring the changes in urinary nucleoside concentrations of patients with colorectal cancer associated with surgery, it was found that the overall correlations with clinical assessment were 84% (27/32) and 91% (10/11) in response group and progressive

group, respectively.

CONCLUSION: These findings indicate that urinary nucleosides determined by column switching high performance liquid chromatography method may be useful as biological markers for colorectal cancer.

© 2005 The WJG Press and Elsevier Inc. All rights reserved.

Key words: Nucleosides; Biological markers; Colorectal cancer; High performance liquid chromatography

Zheng YF, Yang J, Zhao XJ, Feng B, Kong HW, Chen YJ, Lv S, Zheng MH, Xu GW. Urinary nucleosides as biological markers for patients with colorectal cancer. *World J Gastroenterol* 2005; 11(25): 3871-3876

<http://www.wjgnet.com/1007-9327/11/3871.asp>

INTRODUCTION

Modified nucleosides, derived predominantly from transfer ribonucleic acid (tRNA)^[1-3], have been shown to be excreted in abnormal amounts in the urine of cancer patients^[4-7]. Interest in these materials as potential biological markers was stimulated following evidence that tRNA methyltransferase from cancer tissue had both increased activity and capacity when compared to the enzyme derived from the corresponding normal tissue of origin^[8]. Studies by Borek *et al.*^[9], also showed that tRNA from neoplastic tissue had a much more rapid turnover rate than the tRNA from the corresponding normal tissue. Evidence indicates that methylation of tRNA occurs only after synthesis of the intact macromolecule. Because there are no specific enzyme systems to incorporate the modified nucleosides into the macromolecular nucleic acid, these nucleosides once released in the process of tRNA turnover cannot be reutilized, nor are they further degraded, but are excreted in urine^[10]. Studies have also shown that urinary nucleosides excretion in human beings is little affected by diet, and when normalized to urinary creatinine the daily excretion rate is remarkably constant in a healthy individual^[11].

Methodically in most of the studies urinary nucleosides are isolated by phenylboronate affinity gel chromatography and separated by reverse-phase high performance liquid chromatography (HPLC)^[1,5,6,12,13]. But these methods still involve elaborate and manually performed sample-processing steps due to the complexity of the sample matrix. Among the various types of cancer, colorectal cancer is known to be one of the most prevalent and its early

detection is thus desirable. However, attempts were rarely made to measure the levels of urinary nucleosides from patients with colorectal cancer to date. In this study, we developed the automated column switching HPLC method to investigate the excretion pattern of urinary nucleosides associated with colorectal cancer and intestinal villous adenoma. Differences in 14 urinary nucleoside levels were quantified in 52 patients with colorectal cancer, 10 patients with intestinal villous adenoma and 60 healthy adults. The relationship of urinary excretion of these compounds from patients with colorectal cancer with the tumor size, Duke's stages and differentiation were studied. Changes in the levels of urinary nucleosides were examined preoperatively and postoperatively in patients with colorectal cancer. These data were collected to test the utility of urinary nucleosides as biological markers for colorectal cancer.

MATERIALS AND METHODS

Chemicals and equipment

The following 14 nucleoside standards including the internal standard 8-bromoguanosine hydrate (Br8G) were obtained from Sigma (St. Louis, MO, USA): pseudouridine (Pseu), cytidine (C), uridine (U), 1-methyladenosine (m1A), inosine (I), 5-methyluridine (m5U), guanosine (G), 1-methylinosine (m1I), 1-methylguanosine (m1G), N⁴-acetylcytidine (ac4C), N²-methylguanosine (m2G), adenosine (A), N², N²-methylguanosine (m22G), N⁶-methyladenosine (m6A). Methanol (MeOH) was HPLC-grade purchased from Tedia (Fairfield, OH, USA). Ammonium acetate (NH₄AC), ammonia (NH₃·H₂O) and potassium dihydrogenphosphate (KH₂PO₄) were all analytical reagents obtained from China. Water was deionized and purified by a Milli-Q system (Millipore, Bedford, MA, USA).

The HPLC system (Figure 1) consisted of three Shimadzu LC-10ATVP pumps (Kyoto, Japan), an autoinjector model SIL 10ADVP, an SPD-10AVP UV-Vis detector and an SCL 10AVP interface. An electric six-port valve (Rheodyne, USA) was used for the automated column switching. Valve switching and data acquisition were done on Shimadzu Class-VP version 6.10 software. The column 1 (40 mm×4.0 mm ID) was packed with a laboratory prepared boronic acid-substituted silica material. It can tolerate pH values of the buffers from 2 to 12 as well as the usual organic solvents. The column 2 (250 mm×4.6 mm ID) was packed with 5 μm Hypersil ODS₂ (Elite, Dalian, China).

Urine samples

Sixty healthy adults (31 males, 29 females, from 21 to 71 years, median age 52 years), who have the normal physical indices including hepatic function, renal function, chest X-ray and colonoscopy during a regular physical examination period in our institute, have been chosen as control material. Fifty-two patients with colorectal cancer and 10 patients with intestinal villous adenoma were from Ruijin Affiliated Hospital of Shanghai Second Medical University, the First and Second Affiliated Hospitals of Dalian Medical University of China. No patient had received chemotherapy or radiation therapy before surgery. Diagnoses of colorectal cancer and intestinal villous adenoma were made on the

basis of usual clinical and laboratory findings and were confirmed by histopathology. Table 1 shows the clinical pathological parameters of patients with colorectal cancer.

Spontaneous urine samples were collected from healthy adults, patients with colorectal cancer and intestinal villous adenoma. In 43 patients with colorectal cancer, urine samples were also obtained 2 wk after surgery. All persons had normal renal function and were free of bacterial infection at the time when the urine was collected. After collection the samples free of preservatives were frozen immediately and stored at -20 °C. Prior to analysis, the samples were thawed at room temperature and adjusted to pH 8.0 with 50 mL/L NH₃·H₂O and vortex for 3 min at 5 000 r/min. Aliquots of 1 mL centrifuged urine containing 30 μL of Br8G (0.30 mmol/L) were transferred to autosampler vials and samples of 150 μL were injected to a column-switching HPLC system.

Table 1 Clinicopathological parameters of 52 patients with colorectal carcinoma

Clinicopathological parameters		Numbers(%)
Gender	Male	29 (55.8)
	Female	23 (44.2)
Age (yr)	Range	26-87
	Mean	56.4
	Median	60.0
Primary site	Rectum	15 (28.8)
	Sigmoid colon	6 (11.5)
	Colon	31 (59.6)
Duke's stage	Duke's A	7 (13.5)
	Duke's B	23 (44.2)
	Duke's C	15 (28.8)
	Duke's D	7 (13.5)
Tumor size	≥5 cm	23 (44.2)
	<5 cm	29 (55.8)
Histological grade	Well differentiated tumor	9 (17.3)
	Moderately differentiated tumor	32 (61.5)
	Poorly differentiated tumor	11 (21.2)
CEA	≥5 mg/L	15 (28.8)
	<5 mg/L	37 (71.2)

Column switching HPLC method

Column 1 (Figure 1) was equilibrated for 5 min with the mobile phase delivered by pump 1. After sample injection (150 μL urine), column 1 was washed for 7 min with the same buffer. During that time, nucleosides were selectively retarded on the column 1 and the sample matrix was discharged. At the same time, column 2 was conditioned with the mobile phase delivered by pump 2 (position 1; Figure 1). After this clean-up step, column 1 was series-connected in front of the column 2. The group-specifically bound nucleosides on the column 1 were then eluted and concentrated on top of the column 2 over a period of 3 min (position 2; Figure 1). Separation of nucleosides on the column 2 was carried out with a linear gradient elution program over 40 min, while the column 1 was regenerated for a new extraction cycle (position 1; Figure 1). The nucleosides were detected at 260 nm and quantified using the internal standard method. Table 2 shows the time events

used for the analytical procedure.

Peak identification was performed on the basis of retention times. Standard solutions were run daily before and after the samples to monitor reproducibility of retention times. The standard addition method was also used to confirm peak identification. The levels of the urinary nucleosides were calculated by the calibration curves, and then were transformed into nmoL/ μ moL creatinine. Urinary creatinine levels were determined as described by Zheng *et al.*^[7].

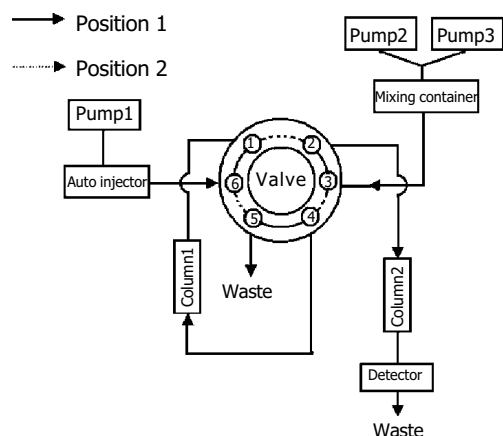


Figure 1 Schematic diagram of the column-switching HPLC system.

Data analysis

The mean excreted amounts of urinary nucleosides have been calculated using MS Excel software. Differences of urinary nucleoside concentrations of healthy adults, patients with intestinal villous adenoma and colorectal cancer were compared with SPSS 10.0 software. Spearman Correlation Analysis was used to examine the relationship of urinary nucleoside concentrations from patients of colorectal cancer with the tumor size, clinical stage and differentiation. Principal component analysis (PCA) software, a home-made pattern recognition software, was used to classify healthy controls, patients with intestinal villous adenoma and colorectal cancer. It was also used to monitor changes in the urinary excretion of nucleosides before and after surgery. Principal components plots were drawn on the basis of the first principal component analysis function (PC1) against

the second principal component analysis function (PC2) of the nucleosides for each urine specimen. The oblique rotational method used in the software is the Promax method^[6].

RESULTS

Analytical characteristics of the method

Figure 2A is a standard chromatogram showing the resolution of 14 nucleosides as well as the internal standard Br8G under the condition newly developed. The calibration curves for 14 nucleosides, linear responses in peak area ratios of nucleosides to the internal standard *vs* the nucleoside concentrations were obtained with the correlation coefficients varying from 0.995 to 0.9995. The intra- and inter-day precisions of the method were determined by five repetitive analyses of an aqueous solution of standard nucleosides on three nonconsecutive days. The relative standard deviation (RSD) of retention times was less than 1.70% (intraday) and 3.51% (interday), and that of peak areas was less than 3.84% (intraday) and 7.85% (interday). The limits of detection ranged from 0.05 to 0.56 μ mol/L, which are better than the previous reports^[13,15,16], thus being suitable for the quantitative analysis.

When applied to the urine specimens from 60 healthy adults, 10 patients with intestinal villous adenoma and 52 patients with colorectal cancer, a total of 14 nucleosides were positively identified. A typical chromatogram of urinary nucleosides from a normal person with peak identification is given in Figure 2B.

Comparison of urinary excretion of nucleosides in healthy adults, patients with intestinal villous adenoma and colorectal cancer

Fourteen nucleoside concentrations of healthy adults (group 1), patients with intestinal villous adenoma (group 2) and patients with colorectal cancer (group 3) are listed in Table 3. In the mean values of three groups, the most abundant nucleoside was Pseu, followed by m1A and m1I. Pseu level was elevated above the normal values plus two standard deviation (s) in the 58% (30/52) of patients with colorectal cancer, while 20% (2/10) of patients with intestinal villous adenoma was elevated. Clearly, the concentrations of 12 nucleosides (except U, G) were significantly elevated in patients with colorectal cancer ($P < 0.05$). Only four kinds of nucleoside concentrations of patients with intestinal villous adenoma were higher in comparing with those of

Table 2 Time events for the switching of column and of mobile phase¹

Time (min)	Pump	Event	Valve position
0.00–7.00	Pump 1 (eluent A)	Sample matrix are discharged by column 1	1
	Pump 2 (eluent B)	Conditioning of column 2	
7.00–10.00	Pump 2 (eluent B)	Analytes are transferred from column 1 to column 2	2
10.00–50.00	Pump 2 and Pump 3 (eluent B and C)	Analysis of nucleosides on column 2 by using a linear gradient elution program	1
	Pump 1 (eluent A)	Conditioning of column	1

¹Eluent A: 0.25 mol/L NH₄AC (pH 8.5); eluent B: 25 mmol/L KH₂PO₄ (pH 4.5); eluent C: methanol:water (3:2, v/v). Flow rate: pump 1, 0.2 mL/min; pump 2, 1.2 mL/min. Detection wavelength: 260 nm.

healthy adults. Using 14 nucleoside concentrations as the data vectors for PCA technique, 71% (37/52) patients with colorectal cancer was distinguishable from healthy adults, while healthy adults are correctly classified at 96% (58/60) specificity. Serum CEA is the tumor marker being used in clinic to diagnose colorectal cancer (cut-off level: 5 mg/L). But the sensitivity of CEA method is 29% (15/52) based on the data provided by the hospitals. Based on the equation of classification of patients with colorectal cancer and healthy adults, 14 urinary nucleoside concentrations of patients with intestinal villous adenoma were calculated and the results was marked into Figure 3A, it was found that 10% (1/10) of patients with intestinal villous adenoma were in the area of patients with colorectal cancer.

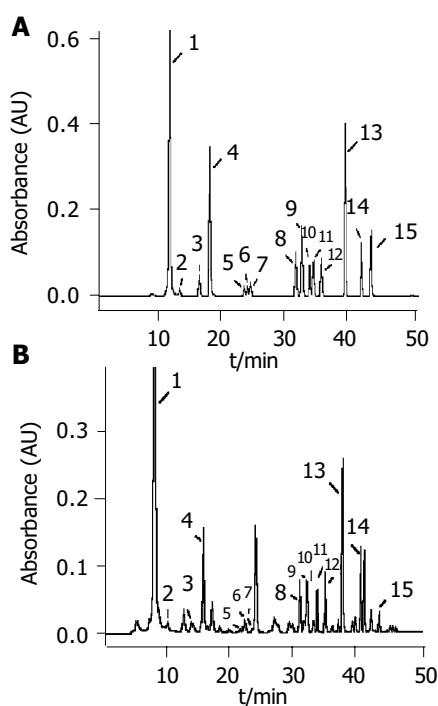


Figure 2 Typical chromatograms of (A) 14 standard nucleoside mixtures (B) urinary nucleosides of a normal urine obtained under the established analysis conditions. Column-switching HPLC conditions as Table 2. Peak identification: 1 Pseu; 2 C; 3 U; 4 m1A; 5 I; 6 m5U; 7 G; 8 m1I; 9 m1G; 10 ac4C; 11 m2G; 12 A; 13 m22G; 14 Br8G; 15 m6A.

Table 3 Comparison of levels of urinary nucleosides from healthy adults, patients with intestinal villous adenoma and colorectal cancer (mean \pm SD, nmol/ μ mol creatinine)

Nucleoside	Healthy adults	Patients with intestinal villous adenoma	Patients with colorectal cancer
Pseu	22.08 \pm 5.11	23.99 \pm 5.61	42.19 \pm 22.25 ^a
C	0.15 \pm 0.12	0.40 \pm 0.21 ^c	0.43 \pm 0.49 ^a
U	0.30 \pm 0.15	0.31 \pm 0.12	0.31 \pm 0.23
m1A	2.04 \pm 0.53	2.30 \pm 0.62	2.74 \pm 0.80 ^a
I	0.28 \pm 0.11	0.27 \pm 0.11	0.50 \pm 0.35 ^a
m5U	0.04 \pm 0.06	0.12 \pm 0.06 ^c	0.13 \pm 0.08 ^a
G	0.09 \pm 0.03	0.08 \pm 0.02	0.10 \pm 0.04
m1I	1.25 \pm 0.28	1.97 \pm 0.50 ^c	2.76 \pm 1.94 ^a
m1G	0.82 \pm 0.24	1.21 \pm 0.26 ^c	1.44 \pm 0.51 ^a
ac4C	0.69 \pm 0.20	0.70 \pm 0.19	0.84 \pm 0.30 ^a
m2G	0.55 \pm 0.14	0.52 \pm 0.28	0.63 \pm 0.26 ^a
A	0.52 \pm 0.16	0.59 \pm 0.25	0.66 \pm 0.30 ^a
m22G	1.25 \pm 0.23	1.43 \pm 0.27	1.81 \pm 0.55 ^a
m6A	0.04 \pm 0.02	0.06 \pm 0.05	0.07 \pm 0.05 ^a

^a P <0.05 patients with colorectal cancer vs healthy adults. ^c P <0.05 patients with intestinal villous adenoma vs healthy adults.

Urinary excretion of nucleosides and clinical pathological characteristics of colorectal cancer

We examined the relationship of urinary nucleoside concentrations from patients of colorectal cancer with the tumor size, Duke's stages and differentiation. These results are listed in Table 4. The level of m1G, Pseu and m1A were positively correlated with the tumor size and Duke's stages of colorectal cancer, respectively (P <0.05). No significant correlation was noted in observed values with regard to tumor differentiation.

Preoperative and postoperative urinary excretion of nucleosides

The changes in six urinary modified nucleoside concentrations (Pseu, m1A, m1I, m1G, ac4C, m22G) before and after surgery in 43 patients with colorectal cancer were studied. The patients were classified into two groups: response group (32 persons) and progressive disease group (11 persons). Using the paired t -test, these urinary modified nucleoside concentrations of response group before surgery were

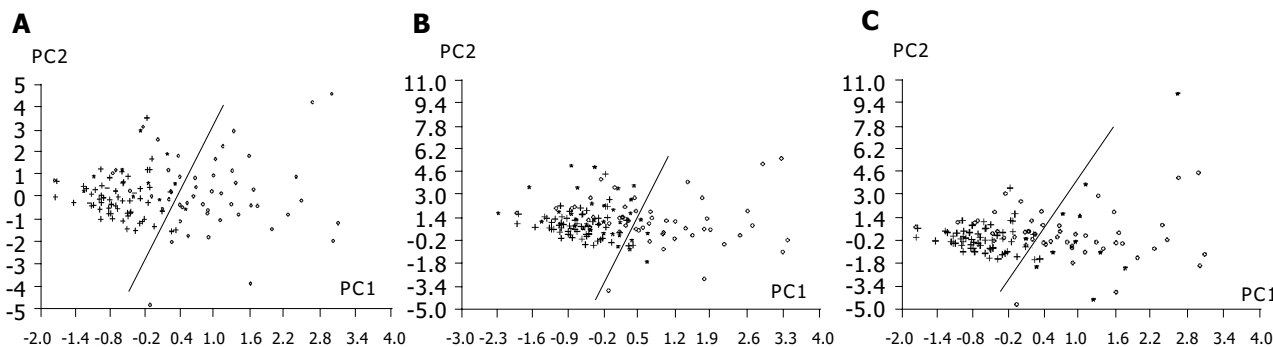


Figure 3 PCA based on 14 nucleoside concentrations from healthy controls (+) and patients with colorectal cancer (o). A: Positions of patients with intestinal villous adenoma (*) were marked into the figure based on classification equation from healthy controls and patients with colorectal cancer; B: Positions of 32 of responsive cases after surgery (*) were marked into the figure based on

classification equation from healthy controls and patients with colorectal cancer; C: Positions of 11 of progressive cases after surgery (*) were marked into the figure based on classification equation from healthy controls and patients with colorectal cancer.

Table 4 Relationship of the levels of urinary nucleosides from patients of colorectal cancer with the tumor size, Duke's stage and differentiation

Nucleoside	Tumor size R	Duke's stage R	Differentiation R
Pseu	0.192	0.325 ^a	-0.051
C	0.199	0.103	0.109
U	0.159	0.190	0.142
m1A	0.188	0.303 ^a	-0.014
I	0.241	0.198	-0.009
m5U	0.056	0.149	0.033
G	0.262	0.135	0.113
m1I	0.287	0.202	0.045
m1G	0.376 ^a	0.256	0.041
ac4C	0.053	0.189	0.008
m2G	0.275	0.261	0.091
A	0.068	0.224	0.023
m22G	0.287	0.270	0.051
m6A	0.097	0.157	0.201

R: relationship coefficient; ^a $P < 0.05$ nucleosides vs Duke's stage.

significantly higher than those of patients after surgery ($P < 0.05$). However, the pre- and post-surgery difference in levels of these nucleosides for progressive disease group had no significant changes.

PCA technique based on 14 nucleoside concentrations as the data vectors was used to monitor changes in the urinary excretion of nucleosides for patients with colorectal cancer before and after surgery. When urinary nucleoside concentrations of patients with colorectal cancer after surgery were fed to the principal component regression and marked to the space produced by the first two principal components (PC1, PC2) of healthy adults and patients with colorectal cancer before surgery (the process was similar to the position prediction of the patients with intestinal villous adenoma), it can be seen that points of 84% (27/32) patients with effective treatment have come back to the normal person area (Figure 3B). In the mean time, points of 91% (10/11) patients with ineffective treatment have entered into the area of colorectal cancer (Figure 3C).

DISCUSSION

Urinary nucleosides as biological markers of malignancy have previously been reported for a wide variety of cancers^[1-7,17,18]. However, only few reports existed regarding colorectal cancer. Our preliminary examination revealed that patients with colorectal cancer excreted in their urine significantly elevated amounts of nucleosides by HPLC method^[13]. But the method analysis of urinary nucleosides involves manual sample extraction steps, resulting in artificial error and time-consumption. In the current study, we developed the automated column switching HPLC method to examine the relationship between urinary nucleosides and pathological characteristics of colorectal cancer and the potential value of these compounds in monitoring progress of the disease during surgery. The method is simple and rapid, requiring a total analysis time of 50 min per sample, with no time involved for sample processing. Its application to routine urine samples suggests utility for mass patient screening.

The present study also confirmed that significantly elevated levels of urinary nucleosides were detected in patients with colorectal cancer by the column-switching HPLC method developed. Our data revealed that the mean nucleoside concentrations from patients with intestinal villous adenoma were significantly lower than those from patients with colorectal cancer. Only 10% (1/10) of patients with intestinal villous adenoma were in the area of patients with colorectal cancer. This is in accordance with the previous studies showing that patients with noncancerous diseases and acute infections^[19,20] do not excrete significantly elevated levels of urinary nucleosides. A current study on urinary nucleosides in colorectal cancer patients demonstrate that in the malignant disease not just one but several of the nucleosides is elevated. In such a multi-component alteration of the nucleoside levels, a pattern recognition method could reveal more information on difference among healthy adults, patients with intestinal villous adenoma and colorectal cancer than the evaluation of single components. The PCA method was applied for evaluation of the nucleoside levels in the three groups. The sensitivity of urinary nucleosides in patients with colorectal cancer was 71%, whereas the sensitivity of currently used tumor marker CEA is 29%. Urinary nucleosides may be a satisfactory biological marker for this disease.

It was also found that the level of m1G, Pseu and m1A were positively correlated with the tumor size and Duke's stages of colorectal cancer, respectively. These nucleosides may be useful as prognostic factors. Modified nucleosides have a much shorter half-life in the body than protein. A faster response to therapy and recurrence of disease is therefore feasible. Our results show that the changes in urinary nucleoside concentrations of patients with colorectal cancer almost paralleled with the change of disease status of patients after surgery (Figures 3B and C). The results are in agreement with the previous studies about urinary nucleosides being useful for monitoring progress of lymphoma and small cell carcinoma of the lung^[21,22]. These facts indicated that urinary nucleosides may be of value for a rapid assessment of disease course in monitoring colorectal cancer.

These studies have indicated the potential utility of urinary nucleosides as biological marker for colorectal cancer, especially when the column switching HPLC method developed is combined with the PCA data processing method. Because the whole-body RNA turnover correlates quite well with the protein turnover^[23], attention has to be paid to the alterations of urinary nucleosides under various catabolic conditions other than those occurring in malignancies, e.g. malnutrition, endocrine abnormalities, alcoholism and stress. More works are currently in progress to evaluate the usefulness of urinary nucleosides in differentiating cancer from other disease status.

ACKNOWLEDGMENTS

We are very grateful to Professor K.-S. Boos of Institute of Clinical Chemistry, University Hospital Grosshadern, Munich, Germany for the denotation of boronic acid-substituted silica column.

REFERENCES

- 1 **Xu G**, Di Stefano C, Liebich HM, Zhang Y, Lu P. Reversed-phase high-performance liquid chromatographic investigation of urinary normal and modified nucleosides of cancer patients. *J Chromatogr B* 1999; **732**: 307-313
- 2 **Liebich HM**, Xu G, Di Stefano C, Lehmann R. Capillary electrophoresis of urinary normal and modified nucleosides of cancer patients. *J Chromatogr A* 1998; **793**: 341-347
- 3 **Xu G**, Lu X, Zhang Y, Lu P, Di Stefano C, Lehmann R, Liebich HM. Two approaches to determining the urinary excretion patterns of nucleosides- HPLC and CE. *Se Pu* 1999; **17**: 97-101
- 4 **Zhao R**, Xu G, Yue B, Liebich HM, Zhang Y. Artificial neural network classification based on capillary electrophoresis of urinary nucleosides for the clinical diagnosis of tumors. *J Chromatogr A* 1998; **828**: 489-496
- 5 **Xu G**, Liebich HM, Lehmann R, Muller-Hagedorn S. Capillary electrophoresis of urinary normal and modified nucleosides of cancer patients. *Methods Mol Biol* 2001; **162**: 459-474
- 6 **Xu G**, Schmid HR, Lu X, Liebich HM, Lu P. Excretion pattern investigation of urinary normal and modified nucleosides of breast cancer patients by RP-HPLC and factor analysis method. *Biomed Chromatogr* 2000; **14**: 459-463
- 7 **Zheng YF**, Xu GW, Liu DY, Xiong JH, Zhang PD, Zhang C, Yang Q, Lv S. Study of urinary nucleosides as biological marker in cancer patients analyzed by micellar electrokinetic capillary chromatography. *Electrophoresis* 2002; **23**: 4104-4109
- 8 **Borek E**, Kerr SJ. A typical transfer RNA's and their origin in neoplastic cells. *Adv Cancer Res* 1972; **15**: 163-190
- 9 **Borek E**, Baliga BS, Gehrke CW, Kuo CW, Belman S, Troll W, Waalkes TP. High turnover rate of transfer RNA in tumor tissue. *Cancer Res* 1977; **37**: 3362-3366
- 10 **Mandel LR**, Srinivasan PR, Borek E. Origin of urinary methylated purines. *Nature* 1966; **209**: 586-588
- 11 **Sander G**, Topp H, Heller-Schoch G, Wieland J, Schoch G. Ribonucleic acid turnover in man: RNA catabolites in urine as measure for the metabolism of each of the three major species of RNA. *Clin Sci* 1986; **71**: 367-374
- 12 **Liebich HM**, Di Stefano C, Wixforth A, Schmid HR. Quantitation of urinary nucleosides by high-performance liquid chromatography. *J Chromatogr A* 1997; **763**: 193-197
- 13 **Zheng YF**, Chen YJ, Pang T, Shi XZ, Kong HW, Lu S, Yang Q, Xu GW. Investigation of urinary nucleosides excretion of intestinal cancer patients by reversed-phase high performance liquid chromatography. *Se Pu* 2002; **20**: 498-501
- 14 **Gehrke CW**, Kuo KC, Waalkes TP, Borek E. Patterns of urinary excretion of modified nucleosides. *Cancer Res* 197; **39**: 1150-1153
- 15 **Liebich HM**, Xu G, Di Stefano C, Lehmann R, Haring HU, Lu P, Zhang Y. Analysis of normal and modified nucleosides in Urine by Capillary Electrophoresis. *Chromatographia* 1997; **45**: 396-401
- 16 **Zheng YF**, Zhang Y, Liu DY, Guo XL, Mei SR, Xiong JH, Kong HW, Zhang C, Xu G. Analysis of Urinary Nucleosides by Micellar Electrokinetic Chromatography. *Chemical J Chinese Universities* 2001; **22**: 912-915
- 17 **Kim KR**, La S, Kim A, Kim JH, Liebich HM. Capillary electrophoretic profiling and pattern recognition analysis of urinary nucleosides from uterine myoma and cervical cancer patients. *J Chromatogr B* 2001; **754**: 97-106
- 18 **La S**, Cho JH, Kim JH, Kim KR. Capillary electrophoretic profiling and pattern recognition analysis of urinary nucleoside from thyroid cancer patients. *Anal Chim Acta* 2003; **486**: 171-182
- 19 **Borek E**, Sharma OK, Buschman FL, Cohn DL, Penley KA, Judson FN, Dobozin BS, Horsburgh CR Jr, Kirkpatrick CH. Altered excretion of modified nucleosides and beta-aminoisobutyric acid in subjects with acquired immunodeficiency syndrome or at risk for acquired immunodeficiency syndrome. *Cancer Res* 1986; **46**: 2557-2561
- 20 **Fischbein A**, Sharma OK, Selikoff IJ, Borek E. Urinary excretion of modified nucleosides in patients with malignant mesothelioma. *Cancer Res* 1983; **43**: 2971-2974
- 21 **Rasmuson T**, Bjork GR. Urinary excretion of pseudouridine and prognosis of patients with malignant lymphoma. *Acta Oncol* 1995; **34**: 61-67
- 22 **Waalkes TP**, Abeloff MD, Ettinger DS, Woo KB, Gehrke CW, Kuo KC, Borek E. Biological markers and small cell carcinoma of the lung: a clinical evaluation of urinary ribonucleosides. *Cancer* 1982; **50**: 2457-2464
- 23 **Sander G**, Hulsemann J, Topp H, Heller-Schoch G, Schoch G. Protein and RNA turnover in preterm infants and adults: a comparison based on urinary excretion of 3-methylhistidine and of modified one-way RNA catabolites. *Ann Nutr Metab* 1986; **30**: 137-142

Science Editor Guo SY Language Editor Elsevier HK

• COLORECTAL CANCER •

Effects of hepatocyte growth factor/scatter factor on the invasion of colorectal cancer cells *in vitro*

Hong-Wu Li, Ji-Xian Shan

Hong-Wu Li, Ji-Xian Shan, Department of Oncology, First Affiliated Hospital, China Medical University, Shenyang 110001, Liaoning Province, China

Correspondence to: Ji-Xian Shan, Department of Oncology, First Affiliated Hospital, China Medical University, Shenyang 110001, Liaoning Province, China. lhw-005@163.com

Telephone: +86-24-23256666-6227

Received: 2004-12-02 Accepted: 2005-01-05

Key words: HGF; Colorectal cancer cells; Invasion; MMPs

Li HW, Shan JX. Effects of hepatocyte growth factor/scatter factor on the invasion of colorectal cancer cells *in vitro*. *World J Gastroenterol* 2005; 11(25): 3877-3881

<http://www.wjgnet.com/1007-9327/11/3877.asp>

Abstract

AIM: Hepatocyte growth factor (HGF) is a multifunctional growth factor which has pleiotrophic biological effects on epithelial cells, such as proliferation, motogenesis, invasiveness and morphogenesis. There are few reports about the role of HGF played in the colorectal cancer invasion. In the present study, we tried to investigate the possible mechanism of HGF involved in the invasion of colorectal cancer cells *in vitro*.

METHODS: Matrigel migration assay was used to analyze the migrational ability of Caco-2 and Colo320 *in vitro*. We detected the mRNA expressive levels of MMP-2, MMP-9 and their natural inhibitors TIMP-1, TIMP-2 in Caco-2 cells by reverse-transcription polymerase chain reaction (PCR) technique.

RESULTS: After 48 h incubation, there were notable differences when we compared the migrational numbers of Caco-2 cells in the group of HGF and PD98059 (the inhibitor of p42/p44MAPK) with the control (104.40 ± 4.77 vs 126.80 ± 5.40 , $t = 7.17$, $P = 0.002 < 0.01$; 104.40 ± 4.77 vs 82.80 ± 4.15 , $t = 7.96$, $P = 0.001 < 0.01$). The deviation between the HGF and PD98059 was significant ($P < 0.01$). Compared with controls, MMP-2 and MMP-9 mRNA expressions were up-regulated by HGF (0.997 ± 0.011 vs 1.207 ± 0.003 , $t = 35.002$, $P = 0.001 < 0.01$; 0.387 ± 0.128 vs 0.971 ± 0.147 , $t = 106.036$, $P = 0.0000 < 0.01$, respectively); compared with controls, TIMP-1, TIMP-2 mRNA expressions were increased by PD98059 (1.344 ± 0.007 vs 1.905 ± 0.049 , $t = 17.541$, $P = 0.003 < 0.01$; 1.286 ± 0.020 vs 1.887 ± 0.022 , $t = 24.623$, $P = 0.002 < 0.01$, respectively).

CONCLUSION: HGF promoted Caco-2 migration mainly by p42/p44MAPK pathway; HGF/SF stimulated the expression of MMP-2, MMP-9 in Caco-2 and enabled tumoral cells to damage the ECM and reach the distant organ and develop metastasis; HGF played the function of promoted-invasion and promoted-metastasis, in which cellular selection was possible.

INTRODUCTION

Hepatocyte growth factor/scatter factor is a polypeptide growth factor, which enhances strong cellular disintegration, tissue formation, inducing the migration, invasion and angiogenesis of epithelial cells^[1]. The protein production of the c-met proto-oncogene encodes trans-membrane tyrosine kinase and is the receptor for hepatocyte growth factor, which regulates proliferation, differentiation, morphogenesis and motility in various cells after being activated by HGF. Thus, it relates with the genesis and progress in many types of human tumors. The mechanism for HGF-c-met in the invasion and metastasis of malignant tumor includes that they can promote cellular migration and increase the abilities of invasion, they also can trigger Ca⁺⁺-dependent signaling system, so activate the Ras, then activate extracellular-signal regulated kinase (Erk), thereby regulate the contraction and motion of cells and phosphorylate microfilament relating-protein, regulate cellular skeleton and reinforce the ability of cellular movement. HGF can coordinate other factors *in vivo* and therefore enlighten the abilities of migration and invasion in some malignant cells^[2]. Yi found that HGF could increase the invasion of 13 lung cancer cells in which the receptor of c-met was expressed^[3]. The motility of tumoral cells correlated closely with the metastasis in tumor.

Tumoral invasion occurs in three main steps: adhesion, degradation of basement membrane and movement, in which the degradation of basement membrane passes mainly through proteolytic kinases. Matrix metalloproteinases (MMPs) are part of these kinases, in which MMP-2 and MMP-9 correlated with the tumoral metastasis. The report showed that HGF could regulate the expression of MMPs.

Mitogen-activated protein kinases (MAPK) are the kinases between the receptors of cell membrane and the significant intracellular regulating-targets. Cells apply this system conducting extracellular stimulating-signal to the nucleus of cell so that the biological effects from the cells can be transmitted. The pathway of intracellular signal conduction for HGF-c-met induced-biological effects is not clear.

Cellular migration is the premise of tumoral metastasis. The characters of tumoral infiltration and metastasis are the key factors affecting the survival and prognosis in patients. To

confirm the conclusion that HGF can promote migration *in vitro*, regulate the expression of MMPs and exist the MAPK pathway during these processes, we applied the HGF together with the inhibitors of p42/p44MAPK(PD98059) and p38MAPK(SB203580) dealt with the colorectal cancer cells: in Caco-2 and Colo320, we also observed mRNA expression of MMP-2, MMP-9 and tissue inhibitor of metalloproteinase-1 (TIMP-1) and tissue inhibitor of metalloproteinase-2(TIMP-2) in order to investigate the function of HGF in the invasion of colorectal cancer cells *in vitro*.

MATERIALS AND METHODS

Materials

Cells and cell culture The human colorectal cancer cell lines Caco-2 and Colo320 were purchased from China Academy of Science in Shanghai Institute of Life Science, Caco-2 were cultured in DMEM supplemented with 10% fetal bovine serum, 100 U/mL penicillin and 100 µg/mL streptomycin at 37 °C in a 50 mL/L CO₂ atmosphere. Medium were exchanged every other day, when the cells reached confluence, we digested them with 0.02% EDTA+trypsin and delivered them according to 1:2 or 1:4. Colo320 were cultured in DMEM supplemented with 20% fetal bovine serum, others were identical with Caco-2.

Reagent and apparatus DMEM were purchased from Gibco; FBS from TBD; HGF from JingMei Biol in ShenZhen and were compounded with free serum medium, the concentration was 20 ng/mL. PD98059 and SB203580 were from Promega, they were compounded with DMSO and made up to 10 and 20 mmol/L for storage and the applicable concentration was 40 µmol/L combined with free serum, stored at 4 °C. Matrigel from Gene Company in ShenYang was compounded with DMEM according to 1:3, 0 °C fusion; 8 µmol/L polycarbonate size membrane and TRIzol were from HuaMei Company, Boyden chamber were from the Department of Oncology in China Medical University. RT-PCR kit was from Takara, the primers of MMP-2, MMP-9, TIMP-1, TIMP-2, β-actin were synthesized by BoYa Bio Company in Shanghai. Amplified sections were 307, 215, 285, 265, and 690 bp respectively. Autoradiography were purchased from Olympus and PCR amplification instrument were from PE Company in the USA.

Methods

Matrigel migration assay This assay is similar to that described previously^[5], Boyden chambers system whose upper and lower compartments were used to analyze the invasive ability of Caco-2 and Colo320. The chambers were washed, dried and irradiated under ultraviolet rays for 30 min, the experiments were divided into four groups DMEM, HGF, PD98059, and SB203580.

DMEM, 20 ng/mL HGF, 10% FBS (Caco-2) or 20% FBS (Colo320), 200 µL in the lower compartment with 50 µg Matrigel onto a polycarbonate membrane, and then 1 mL (about 3 ± 10^5 cell/mL) colorectal cancer cells were put in the upper compartment of the chamber, and the chambers were incubated at 37 °C in humidified air containing 50 mL/L CO₂ for 48 h, at the end of incubation, the cells on the upper side of polycarbonate membrane were wiped off with a cotton swab and the remaining cells that traversed

the Matrigel and spread on the lower surface of the membrane were rinsed using distilled water twice, the membrane were fixed for 30 min with 5 mL methanol, dried and stained with hematoxylin for 10 min, rinsed with 1% HCl+10% alcohol and distilled water for 1-5 min, rinsed with 1% ammonia water and distilled water for 1-5 min, stained with eosin 1-10 min, at last rinsed and fixed with gradient alcohol and xylene, enclosed and counted five fields of vision using light microscope. Results were expressed as the number of colorectal cancer cells invaded per filter. Experiments were done in triplicate and results are shown as mean±SD.

Effect of PD98059 on HGF-induced migration 40 µmol/L PD98059 were added to the upper compartment with 1 mL cells for 30 min before 20 ng/mL HGF was added to the lower side of chamber which was incubated at 37 °C in a 50 mL/L CO₂ atmosphere for 48 h. After incubation, similar treatment as the above-mentioned, was carried out.

Effect of SB203580 on HGF-induced migration: 40 µmol/L SB203580 were added to the upper compartment with 1 mL cells for 30 min before 20 ng/mL HGF was added to the lower side of chamber which was incubated at 37 °C in a 50 mL/L CO₂ atmosphere for 48 h. After incubation, the treatment was identical with the above-mentioned.

Detection of MMP-2, MMP-9, TIMP-1, TIMP-2 mRNA by RT-PCR

Total RNA was extracted from subconfluent cell layers according to Single-step method of RNA isolation by acid guanidinium thiocyanate-phenol-chloroform extraction, 2 µL RNA was reverse-transcribed using AMV, 3 µL of the reaction were used for amplification. The primers used are as follows:

MMP-2-F: 5'-TCAACGGTTCGGGAATACA-3'
MMP-2-R: 5'-CCCACAGTGGACATAGCG-3'
MMP-9-F: 5'-TCGAACCTTTGACAGCGACAAGAA-3'
MMP-9-R: 5'-TCAGGGCGAGGACCATAGAGG-3'
TIMP-1-F: 5'-CTTCCACAGGTCCCACAACC-3'
TIMP-1-R: 5'-CAGCCCTGGCTCCCGAGGC-3'
TIMP-2-F: 5'-AAACGACATTTATGGCAACCCT-ATC-3'
TIMP-2-R: 5'-ACAGGAGCCGTCACCTTCTCTTG-ATG-3'
β-actin-R: 5'-GATTGCCTCAGGACATTTCTG-3'
β-actin-F: 5'-GATTGCTCAGGACATTTCTG-3'

PCR reaction conditions were as follows: Thirty-five cycles of MMP-2 PCR were performed, each consisting of denaturation for 3 min and 45 s at 94 °C, annealing for 1 min at 55 °C and elongation for 1 and 7 min at 72 °C. Thirty-five cycles of MMP-9 PCR were performed, each consisting of denaturation for 3 min and 45 s at 94 °C, annealing for 1 min at 60.5 °C and elongation for 1 and 7 min at 72 °C. Thirty cycles of TIMP-1 PCR were performed, each consisting of denaturation for 3 min and 30 s at 94 °C, annealing for 1 min at 63 °C and elongation for 30 s and 7 min at 72 °C. Thirty cycles of TIMP-2 PCR were performed, each consisting of denaturation for 3 min and 45 s at 94 °C, annealing for 1 min at 65 °C and elongation for 30 s and 7 min at 72 °C. Agarose gel electrophoresis consisting of 20 g/L ethidium bromide (EB) was used to analyze the production of PCR. Electrophoresis zones were reserved for 1 D kodak autoradiography system, β-actin was for controls; measure values were counted/β-actin.

Statistical analysis

SPSS12.0 software was used, all values were expressed as mean±SD, *t*-test was used to determine the significance of differences in multiple comparisons. Values of $P<0.05$ were considered to be statistically significant.

RESULTS

Migration of *Caco-2*

After 48 h incubation, there were notable differences when we compared the migrational numbers of *Caco-2* cells in the group of HGF and PD98059 with the control ($P<0.01$). The deviation between the HGF and PD98059 was significant ($P<0.01$). The group of SB203580 had no implication. We did not find the phenomenon in the Colo320 cells. HGF increased the number of invading Matrigel cells, the more numbers, the more the invading ability. We found that PD98059 inhibited the migration of HGF-induced *Caco-2*. (Figure 1 and Table 1).

Table 1 Migrational numbers of *Caco-2* in different factors

The migrational numbers of <i>Caco-2</i> (mean±SD)	
Control	104.40±4.77
HGF/SF	126.80±5.40 ^b
PD98059	82.80±4.15 ^d
SB203580	108.4±14.38

^b $P<0.01$, $t=7.17$; ^d $P<0.01$, $t=7.96$.

Expression of MMP-2, MMP-9, TIMP-1, TIMP-2 mRNA in *Caco-2* cell conditions were identified with Matrigel migration assay. Examination of MMP-2, MMP-9, TIMP-1, TIMP-2 expression were by RT-PCR. DMEM was control, MMP-9 expressed all groups except control, MMP-2 was high expression in HGF group, TIMP-1 and TIMP-2 were high expression in the group of PD98059. HGF could stimulate the expression of MMP-2 and MMP-9, but the function was inhibited in the presence of PD98059 ($P<0.01$). There were different expressions of MMP-2, MMP-9 and TIMP-1, TIMP-2 in the group of PD98059, with no significance. Expression of MMP-2, MMP-9 and TIMP-1, TIMP-2 in the group of HGF were not divergent. (Figure 2 and Table 2).

Table 2 Expression of MMPs and its inhibitors in *Caco-2* (mean±SD)

	MMP-2	MMP-9	TIMP-1	TIMP-2
Control	0.997±0.011	0.387±0.128	1.344±0.007	1.286±0.020
HGF	1.207±0.003	0.971±0.147	0.846±0.075	0.992±0.009
PD98059	0.824±0.037	0.350±0.007	1.905±0.049	1.887±0.022

DISCUSSION

In vitro, HGF/SF has the function of strongly promoting mitogen and stimulating the growth of normal and malignant cells^[6]. HGF/SF could agitate directly cellular mobility and spreadable effects and colon formation gets diffused by it.

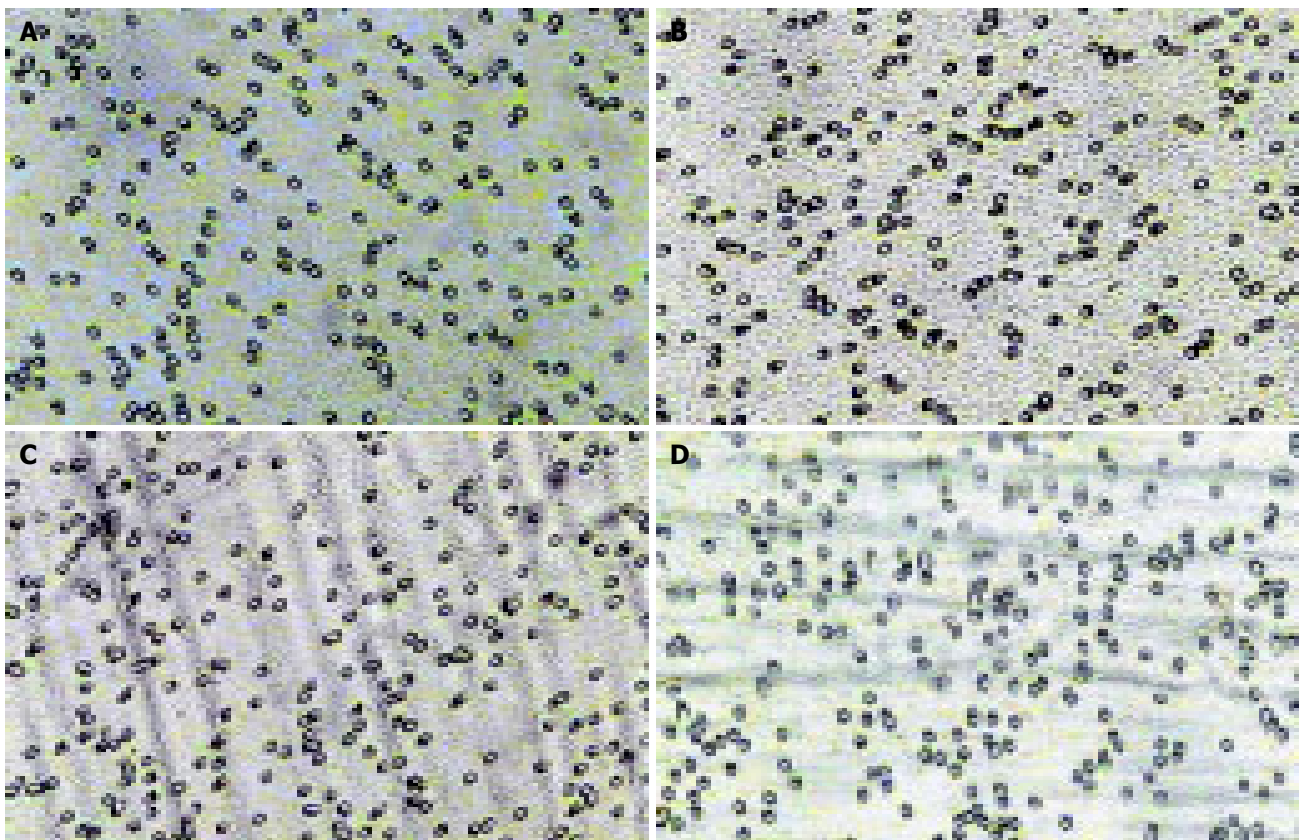


Figure 1 Migration of *Caco-2* in different factors: control (A), Effect of HGF (B),

PD98059 (C), and SB203580 (D).

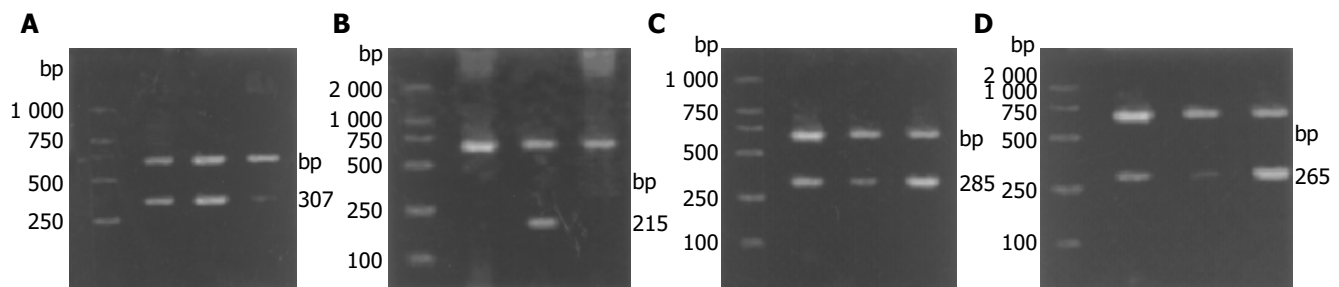


Figure 2 Expression of MMPs and TIMPs in Caco-2 cell: MMP-2 amplification section (A), MMP-9 amplification section (B), TIMP-1 amplification section (C),

TIMP-2 amplification section (D).

The activity of HGF-promoted motogen and morphogen could promote adhesion, migration and infiltration of the cancer cells^[7], as it enhanced Integrins-modulated adhesion so that lymphocyte invasion increased six-fold^[8]. About the mechanism of HGF-promoted tumoral metastasis, Fujisaki^[9] reported that the stimulation of CD44 could induce the expression of c-met; HGF/SF amplified CD44-induced adhesion of LFA-1 (lymphocyte function associated antigen-1), further amplified and agitated the Integrin-modulated adhesion, enabled the cancer cells to adhere blood vessel endothelium and pass through the vessel walls. The experiments of cotransfection for c-met and CD44 found that CD44, acted as the co-receptor of HGF, promoted the c-met tyrosine kinases phosphorylation and downstream signaling conduction protein kinases activation (activated MAPK), induced tumoral growth and metastasis^[10].

Recently, the research of extracellular-signal transduction has made great progress in the interior and exterior parts of the country. Extracellular stimulation entered from the cellular surface and activated the signaling transduction pathway in the cytoplasm, transduced the signaling to the nucleus through many pathways and promoted or inhibited special expression of the target-gene^[11], including the pathway of Ras-MAPK which played a main role in promoting cellular proliferation and regulating genetic transcription. The character of the cytokine receptor decided the manner of signaling transduction, many cytokines transmitted to the nucleus through mainly MAPK-cascades, induced the same genetic expression procedures, produced the same biological effects so that MAPK-cascades originated together or from the last pathway in which many membrane receptors transduced growth signaling to pass through the membrane^[12]. MAPK was the important intercellular signaling system, cells applied it to transmit stimulating extracellular signal to the nucleus and modulated biological effects produced by cells^[13]. It had decided four MAPK pathways in eukaryotic cell, including ERK, JNK, p38MAPK, and ERK5^[14]. MAPK was a kind of serine/threonine protein kinase, activated by phosphorylation^[15]. An extracellular stimulator could activate synchronously several members of MAPK families, Xia^[16] found if they removed neurogenic growth factor from incubation systems, and then induced the apoptosis of PCI2, there existed activation of p38MAPK, JNK and inhibition of ERK, the deduced apoptosis and survival were decided by the balance between ERK-activated by growth factor and p38MAPK, and JNK-activated by stress.

In our study, we found that PD98059, the inhibitor of p42/p44MAPK, could restrain the numbers of HGF-induced colorectal cancer cells passed Matrigel, as such, we confirmed that p42/p44MAPK was one of the pathways of HGF-promoted Caco-2 invasion.

The main components of extracellular matrix (ECM) including collagen, glucoprotein, proteoglycan and glycosamine existed as the form of basement membrane and intercellular tissues. There was a kind of anti-adhesion protein in extracellular matrix called basement membrane protein, the sections of these molecules degradation had chemotaxis so that promoted the mobility of the cancer cells^[13]. A lot of barriers were during the metastatic processes, it was of significance for the basement membrane beside tumoral cells and interstitial matrix to maintain tissue morphogenesis and biological specificity. Tumor cells might produce proteolytic ferment through autosecretion or stimulate host to cross basement membrane so that metastasis occurred. Therefore, the degradation of tumor to ECM was the prerequisite for tumoral invasion and metastasis^[14]. Matrix metalloproteinases (MMPs) were this kind of peptidase which Zn²⁺-dependently degraded ECM, at present, 20 members of MMPs families were determined. According to the different substrates, MMPs were divided as follows: interstitial collagenase, gelatinase, stromelysin, membrane-type MMPs^[17]. In the 1980s, it was first reported that MMPs related with the potency of cancer metastasis^[18]. The mechanism of tumor cells degraded ECM including the activation of MAPK, cells applied the pathway to promote the secretion of MT-MMPs and the rearrangement of microfilament skeleton formed by myoprotein and increased the ability of decomposing collage of ECM and migration, then, induced tumoral infiltration and metastasis. MMPs were the major kinases during the physiological and pathological processes in the rebuilding or degradation of ECM, they were the key to removing the barrier of cellular migration. Increasing activities of MMPs was one of the essential conditions in tumor invasion and metastasis, MMPs could affect cellular adhesion and migration directly. But the total degradation of ECM was controlled strictly by the balance between activated MMPs and TIMPs (inhibitors of MMPs)^[19]. Our results showed that HGF/SF up-regulated the expression of MMP-2, MMP-9 and TIMPs in Caco-2 compared with the control groups, we confirmed *in vitro* that HGF increased the numbers of migrational Caco-2, the results suggested that increasing activities of MMPs in the presence of HGF enabled tumoral cells to damage the

ECM and easily developed metastasis.

In conclusion, HGF promoted Caco-2 migration mainly by p42/p44MAPK pathway; HGF/SF up-regulated the expression of MMP-2, MMP-9 in Caco-2 and enabled tumoral cells to damage the ECM; HGF played the function of promoted-invasion and promoted-metastasis in cellular selection; HGF could play the biological effects by MAPK, therefore, it had a major significance for we studied the regulation about MAPK in tumoral metastasis to understand the relationship between the MAPK pathway and colorectal cancer, furthermore, it would provide the evidence for MAPK to become the target of tumoral treatment.

REFERENCES

- 1 **Zeng Q**, Chen S, You Z, Yang F, Carey TE, Saims D, Wang CY. Hepatocyte growth factor inhibits anoikis in head and neck squamous cell carcinoma cells by activation of ERK and Akt signaling independent of NF-KB. *J Biol Chem* 2002; **277**: 25203-25208
- 2 **Rosenthal EL**, Johnson TM, Allen ED, Apel II, Punturieri A, Weiss SJ. Role of the plasminogen activator matrix metalloproteinase systems in epidermal growth factor and scatter factor stimulated invasion of carcinoma cells. *Cancer Res* 1998; **58**: 5221-5230
- 3 **Yi S**, Chen JR, Viallet J, Schwall RH, Nakamura T, Tsao MS. Paracrine effects of hepatocyte growth factor/scatter factor on non-small-cell lung carcinoma cell lines. *Br J Cancer* 1998; **77**: 2162-2170
- 4 **Harvey P**, Clark IM, Jaurand MC, Warn RM, Edwards DR. Hepatocyte growth factor/scatter factor enhances the invasion of mesothelioma cell lines and the expression of matrix metalloproteinases. *Br J Cancer* 2000; **83**: 1147-1153
- 5 **Kundra V**, Anand-Apte B, Feig LA, Zetter BR. The chemotactic response to PDGF-BB: evidence of a role of ras. *J Cell Biol* 1995; **130**: 725-731
- 6 **Tamatani T**, Hattori K, Iyer A, Tamatani K, Oyasu R. Hepatocyte growth factor is an invasion/migration factor of rat urothelial carcinoma cells *in vitro*. *Carcinogenesis* 1999; **20**: 957-962
- 7 **Li XN**, Ding YQ. HGF/SF-met signaling pathway and tumoral metastasis. *Medical Recapitulate* 2001; **7**: 643-644
- 8 **Weimar IS**, de Jong D, Muller EJ, Nakamura T, van Gorp JM, de Gast GC, Gerritsen WR. Hepatocyte growth factor/scatter factor promotes adhesion of lymphoma cells to extracellular matrix molecules via alpha4 beta 1 and alpha 5 beta 1 integrins. *Blood* 1997; **89**: 990-1000
- 9 **Fujisaki T**, Tanaka Y, Fujii K, Mine S, Saito K, Yamada S, Yamashita U, Irimura T, Eto S. CD44 stimulation induces integrin-mediated adhesion of colon cancer cell lines to endothelial cells by up-regulation of integrins and c-Met and activation of integrins and c-Met and activation of integrins. *Cancer Res* 1999; **59**: 4427-4434
- 10 **van der Voort R**, Taher TE, Wielenga VJ, Spaargaren M, Prevo R, Smit L, David G, Hartmann G, Gherardi E, Pals ST. Heparan sulfate-modified CD44 promotes hepatocyte growth factor/scatter factor-induced signal transduction through the receptor tyrosine kinase c-Met. *J Biol Chem* 1999; **274**: 6499-6506
- 11 **Lenferink AE**, Busse D, Flanagan WM, Yakes FM, Arteaga CL. ErbB2/neu kinase modulates cellular p27(kip1) and cyclinD₁ through multiple signaling pathways. *Cancer Res* 2001; **61**: 6583-6591
- 12 **Donovan JC**, Milica A, Slingerland JM. Constitutive MEK/MAPK activation leads to p27(kip1) deregulation and antiestrogen resistance in human breast cancer cells. *J Biol Chem* 2001; **276**: 40888-40895
- 13 **Mao H**, Yuan AL, Zhao MF, Lai ZS. The effect of signal pathway of mitogen activated protein kinase on hepatocellular carcinoma metastasis induced by VEGF. *Chin J Di* 2000; **20**: 14-16
- 14 **Feng S**, Song JD. Extracellular matrix degradational kinases in tumoral invasion and metastasis. *Zhongliu Fangzhi Yanjiu* 1999; **26**: 72-73
- 15 **Dinev D**, Jordan BW, Neufeld B, Lee JD, Lindemann D, Rapp UR, Ludwig S. Extracellular signal regulated kinase 5(ERK5) is required for the differentiation of muscle cells. *EMBO Rep* 2001; **2**: 829-834
- 16 **Testa JE**, Quigley JP. Principle and Practice of Cancer- Oncology (volume one). Translator: Xu CG, Zhang MH, Yang XI. The Fifth Edition, Jinan: *Shandong Science and Technology Press* 2001: 146
- 17 **Yamamoto S**, Konishi I, Mandai M, Kuroda H, Komatsu T, Nanbu K, Sakahara H, Mori T. Expression of vascular endothelial growth factor (VEGF) in epithelial ovarian neoplasms: correlation with clinicopathology and patient survival, and analysis of serum VEGF levels. *Br J Cancer* 1997; **76**: 1221-1227
- 18 **Liotta LA**, Tryggvason K, Garbisa S, Hart I, Foltz CM, Shafie S. Metastatic potential correlates with enzymatic degradation of basement membrane collagen. *Nature* 1980; **284**: 67-68
- 19 **Kong LL**, Yang JW, Cui W. Progress of the relationship between matrix metalloproteinases and tumor. *J Jining Medical College* 2003; **26**: 64-66

• VIRAL HEPATITIS •

Natural history of major complications in hepatitis C virus-related cirrhosis evaluated by per-rectal portal scintigraphy

Etsushi Kawamura, Daiki Habu, Takehiro Hayashi, Ai Oe, Jin Kotani, Hirotaka Ishizu, Kenji Torii, Joji Kawabe, Wakaba Fukushima, Takashi Tanaka, Shuhei Nishiguchi, Susumu Shiomi

Etsushi Kawamura, Takehiro Hayashi, Ai Oe, Jin Kotani, Hirotaka Ishizu, Kenji Torii, Joji Kawabe, Susumu Shiomi, Department of Nuclear Medicine, Graduate School of Medicine, Osaka City University, 1-4-3, Asahimachi, Abenoku, Osaka 545-8585, Japan
Daiki Habu, Shuhei Nishiguchi, Department of Hepatology, Graduate School of Medicine, Osaka City University, 1-4-3, Asahimachi, Abenoku, Osaka 545-8585, Japan

Wakaba Fukushima, Takashi Tanaka, Department of Public Health, Graduate School of Medicine, Osaka City University, 1-4-3, Asahimachi, Abenoku, Osaka 545-8585, Japan

Supported by the Study Group of Portal Malcirculation supported by Ministry of Health, Labour and Welfare

Correspondence to: Dr. Etsushi Kawamura, Department of Nuclear Medicine, Graduate School of Medicine, Osaka City University, 1-4-3, Asahimachi, Abenoku, Osaka 545-8585,

Japan. etsushi-k@med.osaka-cu.ac.jp

Telephone: +81-6-66453885 Fax: +81-6-66460686

Received: 2004-12-07 Accepted: 2004-12-20

shunting and liver failure non-invasively. It indicates that PSI may play an important role in follow-up of the porto-systemic hypertension gradient for outpatients with LC unlike hepatic venous catheterization.

© 2005 The WJG Press and Elsevier Inc. All rights reserved.

Key words: Portal shunt index; Porto-systemic shunting; Per-rectal portal scintigraphy; Natural history; Liver cirrhosis; HCV; Hepatocellular carcinoma; Liver failure; Varix

Kawamura E, Habu D, Hayashi T, Oe A, Kotani J, Ishizu H, Torii K, Kawabe J, Fukushima W, Tanaka T, Nishiguchi S, Shiomi S. Natural history of major complications in hepatitis C virus-related cirrhosis evaluated by per-rectal portal scintigraphy. *World J Gastroenterol* 2005; 11(25): 3882-3886

<http://www.wjgnet.com/1007-9327/11/3882.asp>

Abstract

AIM: To examine the correlation between the porto-systemic hypertension evaluated by portal shunt index (PSI) and life-threatening complications, including hepatocellular carcinoma (HCC), liver failure (Child-Pugh stage progression), and esophagogastric varices.

METHODS: Two hundred and twelve consecutive subjects with HCV-related cirrhosis (LC-C) underwent per-rectal portal scintigraphy. They were allocated into three groups according to their PSI: group I, $PSI \leq 10\%$; group II, $10\% < PSI < 30\%$; and group III, $30\% \leq PSI$. Of these, selected 122 Child-Pugh stage A (Child A) subjects were included in analysis (a mean follow-up period of 5.9 ± 5.4 years, range 6 mo-21 years).

RESULTS: No significant correlation between PSI and cumulative probability of HCC incidence was observed. Cumulative probability of Child A to B progression was tended to be higher in group III than in group I, and significantly higher in group III than in group II (62% vs 34%, 62% vs 37%; $P = 0.060$, < 0.01 ; respectively). Cumulative probability of varices tended to be higher in group III than in group I (31% vs 12%, $P = 0.090$). On multivariate analyses, significant correlation between PSI and Child A to B progression was observed, and no significant correlation between PSI and HCC incidence or varices progression was observed.

CONCLUSION: Patients with LC-C of Child A will progress to Child B rapidly after their PSI reaches 30% or higher. PSI can be used to predict occult progressive porto-systemic

INTRODUCTION

Hepatitis C virus (HCV) is the most common cause of chronic liver disease in several countries, including Japan, and chronic hepatitis due to HCV (CH-C), which exhibits a variable natural course, is becoming a subject of worldwide interest. CH-C progresses to cirrhosis of the liver (LC), and may be complicated by hepatocellular carcinoma (HCC), hepatic decompensation, and esophagogastric varices^[1,2], although its clinical course has not been fully defined. Despite treatment such as injection of interferon plus oral ribavirin^[3], many patients with CH-C progress to cirrhosis^[4], and develop portal hypertension as CH-C advances to the early phase of LC^[5].

Portal hypertension evaluated by "invasive" hepatic venous pressure gradient (HVPG) is associated with progression of liver failure and death^[6-8]. Using the method described in this study, the extent of porto-systemic shunting (PSS) can be evaluated with the portal shunt index (PSI) using relatively "non-invasive" per-rectal portal scintigraphy with ^{99m}Tc pertechnetate, because PSI correlates strongly with portal pressure^[9,10]. This study monitored three life-threatening complications of LC, including the incidence of HCC, Child-Pugh stage progression, and progression of esophagogastric varices, and examined the correlation between PSI and these three complications.

MATERIALS AND METHODS

Patients

A retrospective cohort study was performed on 212 subjects with HCV-related cirrhosis (LC-C), who were admitted to

our hospital during the 24 years between March 1979 and June 2002, and who were evaluated with PSI obtained by per-rectal portal scintigraphy with ^{99m}Tc pertechnetate. These subjects were diagnosed by examination of liver specimens obtained by laparoscopy, or needle biopsy performed under ultrasonic guidance. Exclusion criteria for this study were as follows: other causes of cirrhosis such as HBV, autoimmune disease, any alcohol consumption; past treatment with interferon, endoscopic sclerotherapy or open surgery for varices; and trans-arterial embolization or open surgery for HCC. Within a week of hospitalization, all subjects underwent abdominal ultrasonography for detection of ascites, Child-Pugh staging as an index of liver failure and endoscopy for detection of esophagogastric varices^[11]. Three Child-Pugh stages were considered: stage A (score 5-6), stage B (7-9), and stage C (10-15). The 212 subjects with cirrhosis were distributed as follows: Child-Pugh stage A (Child A), 122; Child B, 73; and Child C, 17. At entry, we used other possible predictors of LC prognosis, including sex, age, serum albumin, total bilirubin (T-bil), prothrombin time (PT), and platelets^[12].

Longitudinal study

We selected 122 Child A subjects for a longitudinal study; these subjects gave their informed consent to participate, and agreed to return after discharge to our outpatient clinic for monitoring. The procedures were approved by the Ethics Committee of Graduate School of Medicine, Osaka City University. A total of 122 subjects were monitored for a mean period of 5.9 ± 5.4 years (range 6 mo to 21 years). Monitoring was maintained for each evaluation until confirmation of HCC, or Child A to B progression, or varices progression, or the end of the outcome observation period (June 2002). Subjects were excluded from the study if they were followed by another hospital, or their monitoring periods were less than 6 mo.

After excluding dropouts, we were able to monitor the following subjects for at least 6 mo: for HCC incidence, 108 subjects; for Child A to B progression, 107; and for varices progression, 109. A PSI value of 10% or higher is considered to be abnormal^[9], and a PSI of 30% or higher has an especially poor prognosis for chronic liver diseases^[5]. We defined three groups according to their PSI: group I, $\text{PSI} \leq 10\%$; group II, $10\% < \text{PSI} < 30\%$; and group III, $30\% \leq \text{PSI}$. The subjects were further divided as follows: for

HCC incidence, 108 subjects—group I, 33; group II, 41; and group III, 34; for Child A to B progression, 107 subjects—group I, 32; group II, 41; and group III, 34; for varices progression, 109 subjects—group I, 33; group II, 41; and group III, 35. These subjects underwent the following examinations: laboratory studies and physical assessment of the extent of hepatic encephalopathy for Child's staging, with a mean interval of 4.1 ± 0.8 mo; abdominal ultrasonography or dynamic CT for assessment of the extent of ascites or the existence of HCC, with a mean interval of 2.1 ± 0.6 mo; and endoscopy for varices, with a mean interval of 8.1 ± 2.1 mo. HCC was confirmed by histology obtained by needle biopsy performed under ultrasonic guidance, or confirmed by selective angiography. The extent of hepatic encephalopathy was defined from detection of tremor and/or disorientation by physicians. The extent of ascites was confirmed by abdominal ultrasonography and/or physical assessment. We defined progression (or incidence) of each complication as the first confirmation of HCC, or Child B or a new variceal factor^[13]. Figure 1 shows flow of participants through monitoring.

Measurement of the portal shunt index

The subjects fasted after the evening meal on the day before examination. In the morning, the rectum was emptied by administration of a laxative. First, 370 MBq of ^{99m}Tc pertechnetate (2 mL solution) was given per rectum through a polyethylene tube (Nélaton's catheter, French 16) into the upper rectum, followed by 15 mL of air. Time-activity curves for the heart and liver areas were obtained every 4 s using a large-field scintillation camera (Vertex-Plus, ADAC Laboratories, Silicon Valley, USA). It was equipped with a low-energy, multipurpose, parallel-hole collimator and was interfaced with a digital computer. The camera was positioned over the patient's abdomen so that the field of view included the heart, liver, and spleen. At the end of the 5-min examination, a 5-min summed color image was recorded. To measure the extent of PSS by PSI, we calculated the number of counts for the heart as a percentage of the counts for the heart and liver integrated for 24 s immediately after the appearance of the liver time-activity curve^[9].

Statistical analysis

Results were analyzed by SAS 8.12 statistical software (SAS

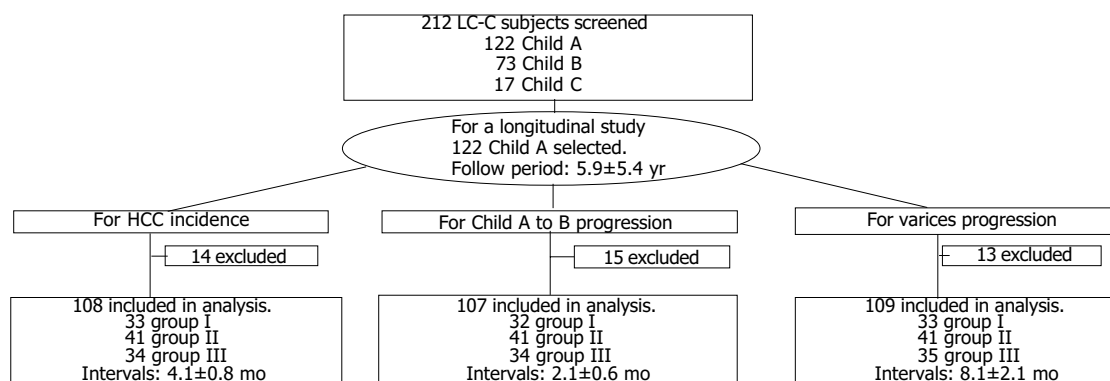


Figure 1 Flow of monitoring, group I, $\text{PSI} \leq 10\%$; group II, $10\% < \text{PSI} < 30\%$; group III, $30\% \leq \text{PSI}$. LC-C, HCV-related cirrhosis; Child A, Child-Pugh stage

A; PSI, portal shunt index.

Institute Inc., Cary, NC)^[14,15]. Data were expressed as mean±SD. Comparisons between PSI groups were made by the Kruskal-Wallis test, the Mantel-Haenszel test, or ANOVA. The cumulative progression rates were calculated and plotted by the Kaplan-Meier method, and were compared by the log-rank test. Any significant variable was considered suitable for the multivariate analysis using Cox's regression model. $P < 0.05$ was taken as statistically significant.

RESULTS

Patient characteristics at entry

Table 1 presents patient data at entry classified by PSI. The differences between the PSI groups were significant for the following parameters: age, albumin, T-bil, platelets ($P < 0.01$, < 0.01 , < 0.05 , and < 0.01 , respectively).

Cumulative progression

No significant correlation between PSI and cumulative probability of HCC incidence was observed (Figure 2A). Cumulative probability of Child A to B progression was tended to be higher in group III than in group I, and significantly higher in group III than in group II (62% vs 34%, 62% vs 37%; $P = 0.060$, < 0.01 ; respectively) (Figure 2B). Cumulative probability of esophagogastric varices tended to be higher in group III than in group I (31% vs 12%, $P = 0.090$) (Figure 2C).

Morbidity

Table 2 presents the proportions of Child A to B progression and relative risks as uni- and multivariates of possible

predictors, which were classified at the entry of the study. The total proportion of each predictor, except PSI, was divided into two between better (upper line) and worse (lower line) at a cut-off value according to Child staging, or reports by other authors: for instance, albumin, at 3.5 g/dL^[11,12,16].

Group III had the highest rate of Child A to B progression (21 of 34, 61.8%), followed by < 3.5 albumin (50.0%), and < 100 PT (48.8%) (Table 2). A significant relationship was found between group (I+II) and group III (crude RR = 2.44, 95%CI = 1.33-4.48, $P < 0.01$), and between group II and group III (2.95, 1.40-6.24, $P < 0.01$), with a trend of significance ($P < 0.05$). No significant increase of other predictors was revealed. PSI and the common useful predictors such as albumin and platelets were included in multivariate analysis; only group III remained significant (adjusted RR = 2.98, 95%CI = 1.29-6.87, $P < 0.05$).

The group with < 10 platelets had the highest incidence of HCC and the highest progression of varices (30.3%, 47.1%, respectively). On multivariate analyses, no significant associations were found between PSI and incidence of HCC or progression of esophagogastric varices.

DISCUSSION

Even if physical symptoms and serum biochemical tests indicate the early phase of LC-C, the patient may already have occult advanced hepatic damage. PSI is a possible predictor of occult progressive stages of LC-C for outcome patients. While PSI obtained by per-rectal portal scintigraphy has its own weaknesses (it emphasizes PSS via the inferior mesenteric vein, rather than via the superior mesenteric vein, and

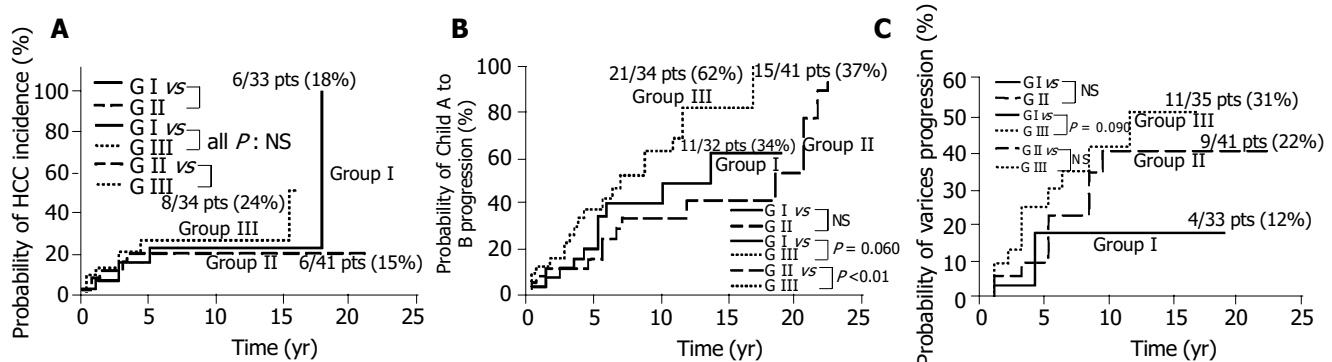


Figure 2 The probability of each life-threatening complication. **A:** The cumulative incidence rate of HCC ($n = 108$). **B:** The cumulative progression rate of Child A to B ($n = 107$). **C:** The cumulative progression rate of esophagogastric varices ($n = 109$). The continuous line shows group I (PSI $\leq 10\%$); the large dotted line

shows group II (10% $<$ PSI $<$ 30%); and the small dotted line shows group III (30% \leq PSI). Child A, Child-Pugh stage A; PSI, portal shunt index; pts, patients; GI, group I; GII, group II; GIII, group III; NS, not significant.

Table 1 Characteristics by portal shunt index at entry

	Group I PSI $\leq 10\%$	Group II 10% $<$ PSI $<$ 30%	Group III 30% \leq PSI	P	
Sex (Male/Female), n	25/13	31/15	30/8	NS	2
Age, yr	48.4 \pm 11.7	54.3 \pm 13.0	54.9 \pm 9.9	< 0.01	1
Albumin, g/dL	4.0 \pm 0.5	4.0 \pm 0.3	3.6 \pm 0.4	< 0.01	3
Total bilirubin, mg/dL	0.8 \pm 0.3	0.9 \pm 0.4	1.1 \pm 0.4	< 0.05	1
Prothrombin time, %	95.4 \pm 17.2	94.5 \pm 15.5	92.5 \pm 20.2	NS	1
Platelets, /mm ³	16.4 \pm 5.7	14.7 \pm 6.9	10.6 \pm 5.0	< 0.01	1

ANOVA: analysis of variance, PSI: portal shunt index, NS: not significant. Data are expressed as mean±SD. ¹Kruskal-Wallis test, ²Mantel-Haenszel test, ³ANOVA.

Table 2 Relative risks of possible predictors for Child-Pugh stage A to B progression

Classification of predictor at entry		Proportion of Child-Pugh stage A to B progression, n/N (%)	¹ Relative risks	
			Crude RR (95%CI)	² Adjusted RR (95%CI)
Sex	Female	16/34 (47.1)	1.00	
	Male	31/73 (42.5)	1.47 (0.76-2.84)	
Age (per 1 yr)			0.99 (0.96-1.01)	
Albumin, g/dL	3.5+	25/63 (39.7)	1.00	
	<3.5	22/44 (50.0)	1.49 (0.83-2.67)	0.98 (0.49-1.95)
Total bilirubin, mg/dL	<1.0	32/69 (46.4)	1.00	
	1.0+	15/38 (39.5)	1.27 (0.68-2.39)	
Prothrombin time, %	100+	27/66 (40.9)	1.00	
	<100	20/41 (48.8)	1.06 (0.59-1.91)	
Platelets, /mm ³	10+	32/73 (43.8)	1.00	
	<10	13/32 (40.6)	1.60 (0.81-3.16)	1.40 (0.68-2.86)
Portal shunt index	Group I	11/32 (34.4)	1.51 (0.65-3.51)	1.67 (0.70-3.99)
	Group II	15/41 (36.6)	1.00	
	Group III	21/34 (61.8)	2.95 (1.40-6.24) ^b	2.98 (1.29-6.87) ^a
			(<i>P</i> trend <0.05)	(<i>P</i> trend: NS)
	Group (I+II)	26/73 (35.6)	1.00	
	Group III	21/34 (61.8)	2.44 (1.33-4.48) ^d	2.36 (1.17-4.78) ^c

^a*P*<0.05 vs Group II PSI, ^b*P*<0.01 vs Group II PSI, ^c*P*<0.05 vs Group (I+II) PSI, ^d*P*<0.01 vs Group (I+II) PSI, NS: not significant. ¹RR and their 95% CI were determined by a Cox's regression model. ²This model includes albumin, platelets, PSI. Group I, PSI ≤10%; Group II, 10%<PSI<30%; Group III, 30% ≤PSI; Group (I+II), PSI <30%. CI: Confidence interval, RR: Relative risk, PSI: Portal shunt index, *n*, progression proportion, *N*; total proportion.

expresses the extent of PSS indirectly), it should be useful for the observation of LC-C because it is a simple and non-invasive technique unlike hepatic venous catheterization^[9].

In this study, we used ^{99m}Tc pertechnetate for per-rectal portal scintigraphy because of its short half-life and low cost^[17]. Our study had three major findings.

First, there was no correlation between the porto-systemic hypertension and HCC incidence. This finding suggests that HCC occurs independently of the decrease in hepatic blood flow due to the development of PSS.

Second, patients with LC-C of Child A will progress to Child B rapidly after their PSI reaches 30% or higher. Shiomi *et al.*^[5], have reported that changes in the portal hemodynamics of chronic liver disease subjects were not gradual. The development of PSS causes hepatic functional reserve to deteriorate rapidly. We propose that per-rectal portal scintigraphy is useful to predict occult progressive portal hypertension and liver failure in the early phase of LC-C, on the basis of the strong relationship between PSI and the Child-Pugh staging.

Third, the natural advance of PSS has relevance to esophagogastric varices progression in patients with the early phase of LC-C. Other authors have reported that the porto-systemic pressure gradient is a strong predictor for varices progression^[18,19]. But in this study, PSI showed no statistical advantage over platelets, albumin, or T-bil for detecting the progression of varices. The reason why PSI was worse than these laboratory data is because esophagogastric varices mainly reflect the flow of superior mesenteric vein.

Progressive viral hepatitis has been acknowledged as a major indication for liver transplantation^[20,21]. Kiuchi *et al.*^[22], have emphasized the need to evaluate the recipients preoperatively. One of the important recipient factors is the presence of collateral circulation^[23]. Bruix *et al.*^[24], have reported that LC patients with increased portal pressure are at high risk of hepatic decompensation after resection of HCC. We propose that preoperative per-rectal portal

scintigraphy would be useful for early detection of occult portal hypertension, to assess graft size requirement to prevent graft failure after liver transplantation, or to avoid liver failure after hepatectomy.

In summary, physicians can monitor the porto-systemic hypertension gradient in LC patient during the outcome observation period by using "non-invasive" per-rectal portal scintigraphy; on the other hand, measurement of HVPG needs hospitalization. In the early phase of LC-C, PSI can be used to predict occult progressive PSS and liver failure. Therefore, even for patients diagnosed as being in the early phase of LC-C on the basis of other indicators, those with an initial PSI ≥30% should be observed by keeping early liver transplantation, or liver failure after hepatectomy in mind; HCC should be watched for, regardless of PSI.

REFERENCES

- 1 Sorbi D, Gostout CJ, Peura D, Johnson D, Lanza F, Foutch PG, Schleck CD, Zinsmeister AR. An assessment of the management of acute bleeding varices: a multicenter prospective member-based study. *Am J Gastroenterol* 2003; **98**: 2424-2434
- 2 Davis GL, Albright JE, Cook SF, Rosenberg DM. Projecting future complications of chronic hepatitis C in the United States. *Liver Transpl* 2003; **9**: 331-338
- 3 Fattovich G, Zagni I, Minola E, Felder M, Rovere P, Carlotto A, Suppressa S, Miracolo A, Paternoster C, Rizzo C, Rossini A, Benedetti P, Capanni M, Ferrara C, Costa P, Bertin T, Pantalena M, Lomonaco L, Scattolini C, Mazzella G, Giusti M, Boccia S, Milani S, Marin R, Lisa Ribero M, Tagger A. A randomized trial of consensus interferon in combination with ribavirin as initial treatment for chronic hepatitis C. *J Hepatol* 2003; **39**: 843-849
- 4 Iino S. Natural history of hepatitis B and C virus infections. *Oncology* 2002; **62**: 18-23
- 5 Shiomi S, Sasaki N, Habu D, Takeda T, Nishiguchi S, Kuroki T, Tanaka T, Ochi H. Natural course of portal hemodynamics in patients with chronic liver diseases, evaluated by per-rectal portal scintigraphy with Tc-99m pertechnetate. *J Gastroenterol* 1998; **33**: 517-522
- 6 Debernardi-Venon W, Bandi JC, Garcia-Pagan JC, Moitinho

- E, Andreu V, Real M, Escorsell A, Montanya X, Bosch J. CO (2) wedged hepatic venography in the evaluation of portal hypertension. *Gut* 2000; **46**: 856-860
- 7 **Abraides JG**, Tarantino I, Turnes J, Garcia-Pagan JC, Rodes J, Bosch J. Hemodynamic response to pharmacological treatment of portal hypertension and long-term prognosis of cirrhosis. *Hepatology* 2003; **37**: 902-908
- 8 **Patch D**, Nikolopoulou V, McCormick A, Dick R, Armonis A, Wannamethee G, Burroughs A. Factors related to early mortality after transjugular intrahepatic portosystemic shunt for failed endoscopic therapy in acute variceal bleeding. *J Hepatol* 1998; **28**: 454-460
- 9 **Shiomi S**, Kuroki T, Kurai O, Kobayashi K, Ikeoka N, Monna T, Ochi H. Portal circulation by technetium-99m pertechnetate per-rectal portal scintigraphy. *J Nucl Med* 1988; **29**: 460-465
- 10 **Boldys H**, Hartleb M, Rudzki K, Nowak A, Nowak S. Effect of propranolol on portosystemic collateral circulation estimated by per-rectal portal scintigraphy with technetium-99m pertechnetate. *J Hepatol* 1995; **22**: 173-178
- 11 **Pugh RN**, Murray-Lyon IM, Dawson JL, Pietroni MC, Williams R. Transection of the oesophagus for bleeding oesophageal varices. *Br J Surg* 1973; **60**: 646-649
- 12 **Kusaka K**, Harihara Y, Torzilli G, Kubota K, Takayama T, Makuuchi M. Objective evaluation of liver consistency to estimate hepatic fibrosis and functional reserve for hepatectomy. *J Am Coll Surg* 2000; **191**: 47-53
- 13 **Idezuki Y**. General rules for recording endoscopic findings of esophagogastric varices. Japanese Society for Portal Hypertension. *World J Surg* 1995; **19**: 420-422
- 14 **Schlichting P**, Christensen E, Andersen PK, Fauerholdt L, Juhl E, Poulsen H, Tygstrup N. Prognostic factors in cirrhosis identified by Cox's regression model. *Hepatology* 1983; **3**: 889-895
- 15 **Holford TR**. Life tables with concomitant information. *Biometrics* 1976; **32**: 587-597
- 16 **Meijer K**, Haagsma EB, Kok T, Schirm J, Smid WM, van der Meer J. Natural history of hepatitis C in HIV-negative patients with congenital coagulation disorders. *J Hepatol* 1999; **31**: 400-406
- 17 **Urbain D**, Jeghers O, Ham HR. Per-rectal portal scintigraphy: comparison between technetium-99m, thallium-201, and iodine-123-HIPDM. *J Nucl Med* 1988; **29**: 2020-2021
- 18 **Vorobioff J**, Groszmann RJ, Picabea E, Gamen M, Villavicencio R, Bordato J, Morel I, Audano M, Tanno H, Lerner E, Passamonti M. Prognostic value of hepatic venous pressure gradient measurements in alcoholic cirrhosis: a 10-year prospective study. *Gastroenterology* 1996; **111**: 701-709
- 19 **Groszmann RJ**, Bosch J, Grace ND, Conn HO, Garcia-Tsao G, Navasa M, Alberts J, Rodes J, Fischer R, Bermann M. Hemodynamic events in a prospective randomized trial of propranolol versus placebo in the prevention of a first variceal hemorrhage. *Gastroenterology* 1990; **99**: 1401-1407
- 20 **Villeneuve JP**, Durantel D, Durantel S, Westland C, Xiong S, Brosgart CL, Gibbs CS, Parvaz P, Werle B, Trepo C, Zoulim F. Selection of a hepatitis B virus strain resistant to adefovir in a liver transplantation patient. *J Hepatol* 2003; **39**: 1085-1089
- 21 **Rosen HR**, Gretch D, Kaufman E, Quan S. Humoral immune response to hepatitis C after liver transplantation: assessment of a new recombinant immunoblot assay. *Am J Gastroenterol* 2000; **95**: 2035-2039
- 22 **Kiuchi T**, Tanaka K, Ito T, Oike F, Ogura Y, Fujimoto Y, Ogawa K. Small-for-size graft in living donor liver transplantation: how far should we go? *Liver Transpl* 2003; **9**: S29-35
- 23 **Feverly J**. Liver transplantation: problems and perspectives. *Hepatogastroenterology* 1998; **45**: 1039-1044
- 24 **Bruix J**, Castells A, Bosch J, Feu F, Fuster J, Garcia-Pagan JC, Visa J, Bru C, Rodes J. Surgical resection of hepatocellular carcinoma in cirrhotic patients: prognostic value of preoperative portal pressure. *Gastroenterology* 1996; **111**: 1018-1022

Science Editor Guo SY Language Editor Elsevier HK

C-terminal domain of hepatitis C virus core protein is essential for secretion

Soo-Ho Choi, Kyu-Jin Park, So-Yeon Kim, Dong-Hwa Choi, Jung-Min Park, Soon B. Hwang

Soo-Ho Choi, Kyu-Jin Park, So-Yeon Kim, Dong-Hwa Choi, Jung-Min Park, Soon B. Hwang, Ilsong Institute of Life Science, Hallym University, Chuncheon 200-702, South Korea
Supported by a grant from the Korean Ministry of Science and Technology (Korean Systems Biology Research Grant, M1-0309-06-0002) and partly by the research grant from Hallym University, Korea
Co-first-authors: Kyu-Jin Park

Correspondence to: Soon B. Hwang, Ilsong Institute of Life Science, Hallym University, 1 Ockcheon-dong, Chuncheon 200-702, South Korea. sbhwang@hallym.ac.kr
Telephone: +82-31-380-1732 Fax: +82-31-384-5395
Received: 2004-12-12 Accepted: 2005-01-05

Abstract

AIM: We have previously demonstrated that hepatitis C virus (HCV) core protein is efficiently released into the culture medium in insect cells. The objective of this study is to characterize the HCV core secretion in insect cells.

METHODS: We constructed recombinant baculoviruses expressing various-length of mutant core proteins, expressed these proteins in insect cells, and examined core protein secretion in insect cells.

RESULTS: Only wild type core was efficiently released into the culture medium, although the protein expression level of wild type core was lower than those of other mutant core proteins. We found that the shorter form of the core construct expressed the higher level of protein. However, if more than 18 amino acids of the core were truncated at the C-terminus, core proteins were no longer secreted into the culture medium. Membrane flotation data show that the secreted core proteins are associated with the cellular membrane protein, indicating that HCV core is secreted as a membrane complex.

CONCLUSION: The C-terminal 18 amino acids of HCV core were crucial for core secretion into the culture media. Since HCV replication occurs on lipid raft membrane structure, these results suggest that HCV may utilize a unique core release mechanism to escape immune surveillance, thereby potentially representing the feature of HCV morphogenesis.

© 2005 The WJG Press and Elsevier Inc. All rights reserved.

Key words: Hepatitis C virus; Core secretion; Morphogenesis; Virus assembly

Choi SH, Park KJ, Kim SY, Choi DH, Park JM, Hwang SB. C-terminal domain of hepatitis C virus core protein is essential for secretion. *World J Gastroenterol* 2005; 11(25): 3887-3892
<http://www.wjgnet.com/1007-9327/11/3887.asp>

INTRODUCTION

Hepatitis C virus (HCV) is the major etiologic agent of transfusion-associated hepatitis^[1-3] and is associated with a chronic infection that leads to liver cirrhosis and hepatocellular carcinoma^[4,5]. HCV is an enveloped virus and its virion size has been estimated at a diameter of 30-60 nm^[6]. The virion contains a single-stranded, positive-sense RNA genome of approximately 9 600 nucleotides^[7-10]. HCV belongs to the *Flaviviridae* family^[11,12] and its genomic sequence is related to the flaviviruses and the pestiviruses^[9,13]. The viral genome encodes a polyprotein precursor of 3 010-3 030 amino acids from one long open reading frame and is further processed into multiple viral proteins^[14-16]. The structural proteins are processed by a host signal peptidase into a core protein, envelope proteins E1 and E2, and p7^[13,16,17]. The viral nonstructural proteins are cleaved by viral proteinase into serine protease, helicase, RNA polymerase, and functionally undefined proteins. Biochemical properties of many structural and nonstructural proteins have been extensively characterized. However, studies on virion morphogenesis and viral replication have been hampered by the inability to propagate the viruses in a cell culture system.

The mechanism of HCV virion assembly is not yet known because the expression of the HCV structural gene in mammalian cells generates no detectable virion particles. However, it has been reported that either virus-like particles (VLPs) were produced in insect cells infected with recombinant baculoviruses expressing HCV structural proteins^[18] or nucleocapsid-like particles were self-assembled from recombinant proteins purified in *E. coli*^[19]. Furthermore, previous study showed that HCV core proteins were secreted in insect cells^[20] and in mammalian cell culture^[21]. In the present study, we have further characterized the HCV core secretion using recombinant baculovirus expression system in insect cells. We found that C-terminal 18 amino acids of the core were necessary for the secretion of core protein into the culture media. Furthermore, HCV core is efficiently released into the culture medium as a membrane-associated protein, which may represent a unique mechanism of HCV core assembly.

MATERIALS AND METHODS

Construction of recombinant baculovirus shuttle vector

HCV cDNA sequence corresponding to the core protein of the Korean isolate (genotype 1b)^[22] was subcloned into the baculovirus shuttle vector, pVL941, as described previously^[23]. Briefly, cDNAs corresponding to the both wild type and mutant forms of HCV core protein were amplified by polymerase chain reaction (PCR) using *Taq*

DNA polymerase (Boehringer Mannheim). Each primer contains a *Bam*HI or a *Bgl*II site and a protein initiation codon (ATG) at the front, and a stop codon (TGA) plus a *Bam*HI or a *Bgl*II endonuclease site at the end. The amplified PCR product was gel-purified and digested with either *Bam*HI or *Bgl*II and inserted into the *Bam*HI site of the pVL941 vector behind polyhedrin promoter.

Production of recombinant baculoviruses

Spodoptera frugiperda (Sf9) insect cells were co-transfected with wild type baculovirus (*Autographa californica* nuclear polyhedrosis virus, AcNPV) DNA and each recombinant transfer vector DNA as described previously^[23]. The supernatant was harvested at 4 d after transfection and used for plaque assays. Each virus isolated from a plaque was used to infect Sf9 cells to obtain high titer of recombinant viruses. Protein expression was examined either by SDS-PAGE and Coomassie blue staining or by Western blot analysis.

Purification of secreted core protein

Sf9 cells were infected with recombinant baculoviruses at a multiplicity of infection (m.o.i.) of 3 and incubated at 27 °C. The culture supernatant was collected at 3 d after infection and cell debris were removed by centrifugation at 3 500 r/min for 15 min. Supernatant was further subjected to centrifugation at 12 000 g for 30 min to eliminate the baculoviruses. The supernatant was pelleted through 300 g/L sucrose cushion for 90 min at 27 000 g using a SW 28 rotor. For velocity centrifugation, the pellet was resuspended in PBS and layered onto 200–600 g/L sucrose gradient and centrifuged at 38 000 g for 12 h at 4 °C using a SW 41 rotor. Twelve fractions were collected from the top, diluted in PBS, and subjected to centrifugation at 48 000 g for 90 min using a SW 55 Ti rotor. The peak fractions were pooled and pelleted as described above. The pellet was dissolved in sample buffer and analyzed by Western blot using HCV patient sera.

Western blot analysis

Recombinant baculovirus-infected Sf9 cells were harvested at 3 d after infection and washed twice in PBS. Either cell lysates or secreted proteins were separated by electrophoresis in 10–15% polyacrylamide gel containing 0.5% SDS and transferred to a nitrocellulose membrane for 1 h. The membrane was incubated with either HCV patient serum or rabbit anti-HCV core antibody and proteins were visualized as previously described^[23].

Membrane flotation analysis

Sf9 insect cells were infected with recombinant baculoviruses expressing full-length of HCV core protein. At 60 h after infection, the culture supernatant was collected and cell debris was removed by centrifugation at 3 500 r/min for 20 min. Culture supernatant was further subjected to centrifugation at 12 000 g for 30 min to eliminate the baculoviruses. The supernatant was pelleted through 300 g/L sucrose cushion for 90 min at 27 000 g using a SW 28 rotor. The secreted HCV core proteins were subjected to equilibrium density centrifugation and 1 mL of each fraction was analyzed by immunoblotting using rabbit anti-HCV core antibody as previously described^[23].

RESULTS

Expression of HCV core protein in insect cells

In order to understand the mechanism of HCV core secretion in culture media, we generated recombinant baculoviruses encoding full-length of HCV core protein and used them to infect insect cells with low m.o.i. (10^3). Cell lysates were prepared at 3 d after infection and analyzed for protein expression by immunoblotting with HCV patient sera. As shown in Figure 1A, recombinant baculovirus-infected cells expressed the corresponding HCV core protein (lane 3). Both wild type baculovirus (AcNPV)-infected and recombinant baculovirus expressing small hepatitis delta antigen (SHDAg)-infected cells^[24] were compared as controls. To examine whether HCV core proteins are released into the culture medium, Sf9 cells were infected with either wild type or recombinant baculoviruses and cell culture supernatants were harvested at d 3 postinfection. The supernatants were pelleted through a 300 g/L sucrose cushion and examined for core secretion using HCV patient serum. The result showed that the supernatant collected from the core-expressing cells contained the core protein reacting with HCV patient serum (Figure 1B, lane 3). Although SHDAg protein was highly expressed in insect cells^[24], this protein was not released into the culture medium (data not shown). We further looked for SHDAg release in the culture supernatant harvested from SHDAg-expressing cells at d 4 postinfection. Although cytolysis started to occur at d 4 postinfection in insect cells^[25], we were unable to detect SHDAg in supernatant collected from SHDAg-expressing cells (data not shown).

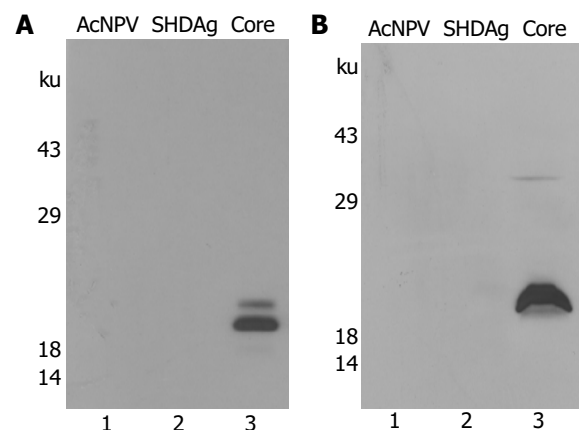


Figure 1 Core proteins are secreted into the culture medium in insect cells. **A:** Expression of HCV core protein in insect cells. cDNA corresponding to the HCV core was subcloned into the *Bam*HI site of the transfer vector pVL941 behind polyhedrin promoter. Recombinant baculoviruses expressing HCV core protein were produced as described in Materials and methods. Sf9 cells were infected with either wild type (AcNPV) or recombinant baculoviruses expressing SHDAg, or recombinant baculoviruses expressing HCV core protein and were harvested at d 3 postinfection. Cell lysates were separated by SDS-containing polyacrylamide gel electrophoresis, transferred to a nitrocellulose membrane. Proteins were detected by Western blotting using HCV patient sera. Lane 1, Sf9 cells infected with wild type baculoviruses; lane 2, Sf9 cells infected with recombinant baculovirus expressing SHDAg; lane 3, Sf9 cells infected with recombinant baculovirus expressing HCV core; **B:** The culture medium from (A) was centrifuged at 3 500 r/min for 15 min to remove cell debris. Supernatant was further centrifuged at 12 000 g for 30 min to remove baculoviruses. The resultant supernatant was then pelleted through a 300 g/L sucrose cushion for 90 min at 27 000 g. The pellet was dissolved in sample buffer and analyzed by Western blotting using HCV patient sera.

Characterization of secreted core proteins

To characterize the secreted core proteins, culture supernatant harvested from recombinant baculovirus-infected cells was pelleted through the 300 g/L sucrose cushion. The pellet was then further subjected to sucrose velocity gradient centrifugation. As shown in Figure 2, secreted core proteins were located in specific fractions. When the peak fractions were examined by electron microscopy, most of the released core proteins were heterogeneous in size as reported^[19] with amorphous structure (Choi *et al.*^[20], and data not shown). We observed that some of the core proteins were easily aggregated during preparation for electron microscopy. As we previously reported, these secreted proteins have a buoyant density of 1.25 g/mL in CsCl gradient separation^[20].

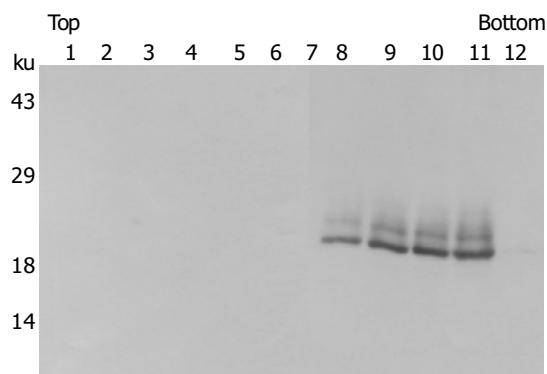


Figure 2 Isolation of core proteins from cell culture supernatant. Sf9 cells were infected with recombinant baculoviruses expressing HCV core protein. The culture supernatant was collected at d 3 postinfection. Following removal of cell debris and recombinant baculoviruses, the released core proteins were partially purified through a sucrose cushion and were subjected to velocity gradient centrifugation. Twelve fractions were collected and proteins were detected by Western blot analysis using HCV patient sera.

Kinetics of core secretion

The HCV core secretion in recombinant baculovirus-infected cells was examined over a 4-d period following infection. Sf9 cells were infected with recombinant baculovirus expressing full-length HCV core and kinetics of protein expression in cells and core secretion in culture media were examined. Cell lysates and secreted core protein were prepared from d 1 to d 4 after infection as described above. Two species of HCV core proteins, M_r 19 000 and M_r 21 000, were expressed in cells as early as d 1 (Figures 3A and C). Two days after virus infection, intracellular core levels reached plateau and gradually decreased thereafter. In contrast, secreted core proteins were detected 2 d after the infection, efficiently released into the culture medium and reached plateau on the 3rd d, and maintained the similar level for an additional day (Figures 3B and D). Trypan blue staining result indicated that most of the recombinant baculovirus-infected cells were viable for 4 d (data not shown).

C-terminal 18 amino acids of core protein are essential for core secretion

To examine which domain of the HCV core is required for core secretion in insect cells, we constructed a series of C-terminal-deleted mutants (Figure 4A) and generated

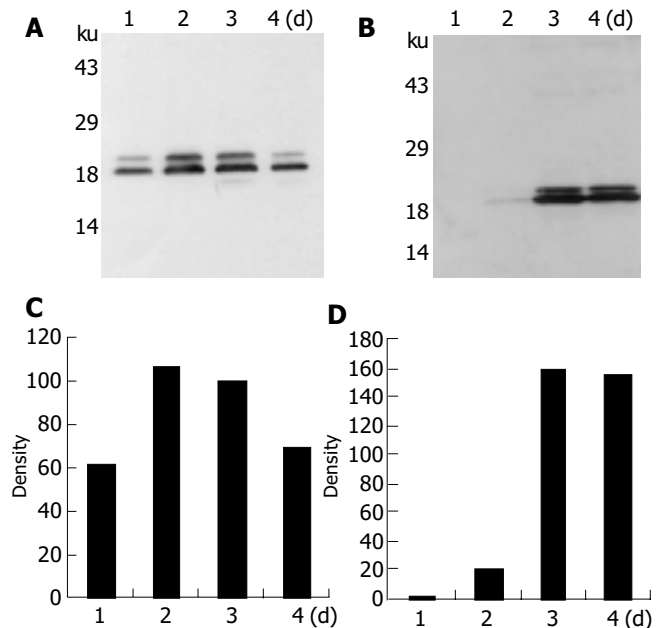


Figure 3 Kinetics of core protein secretion in culture medium of the recombinant baculovirus-infected insect cells. Sf9 insect cells were infected with recombinant baculoviruses expressing full-length core protein (A). Cell lysates were prepared from d 1 to d 4 postinfection, and separated by SDS-PAGE on a 15% gel and Western blotted with an HCV patient serum (B); Culture supernatants were harvested from d 1 to d 4 postinfection and secreted core proteins were detected by Western blot analysis. Kinetics of intracellular core protein (C) and extracellular core protein (D) productions were quantified using a densitometric scanner (Molecular Dynamics).

recombinant baculoviruses by co-transfecting insect cells with each mutant DNA and wild type baculovirus DNA. Using low titer (10^3 PFU/mL) of these recombinant baculoviruses, Sf9 insect cells were infected and protein expressions were determined using cell lysates. As shown in Figure 4B, all mutant viruses expressed the expected molecular mass of proteins. This was further confirmed by Western blot analysis (Figure 4C). It is noteworthy that the shorter form of the core construct expressed the higher level of protein. We proceeded to purify the secreted core from each culture supernatant in the same way as described above. Figure 4D showed that full-length core (C191) was efficiently released into the culture medium, although the protein expression level of C191 was lower than those of other mutant core proteins. However, if C-terminal 18 amino acids of the core were deleted, core proteins were no longer secreted into the culture medium, indicating that C-terminal 18 amino acids of HCV core were crucial for core secretion into the culture media. We next examined whether the C-terminal domain of HCV core could be replaced with the comparable domains of other related hepatitis viruses. For this purpose, we replaced C-terminal 18 aa of HCV core with either C-terminal 18 aa of hepatitis B virus surface antigen (HBsAg) or C-terminal 19 aa of large delta antigen of hepatitis delta virus^[24]. Although these chimera proteins were highly expressed in insect cells, none of these proteins were released into the culture medium (data not shown), suggesting that authentic core sequence is necessary for secretion.

Membrane association of the secreted core protein

Recently, we showed that HCV core and NS5A protein are

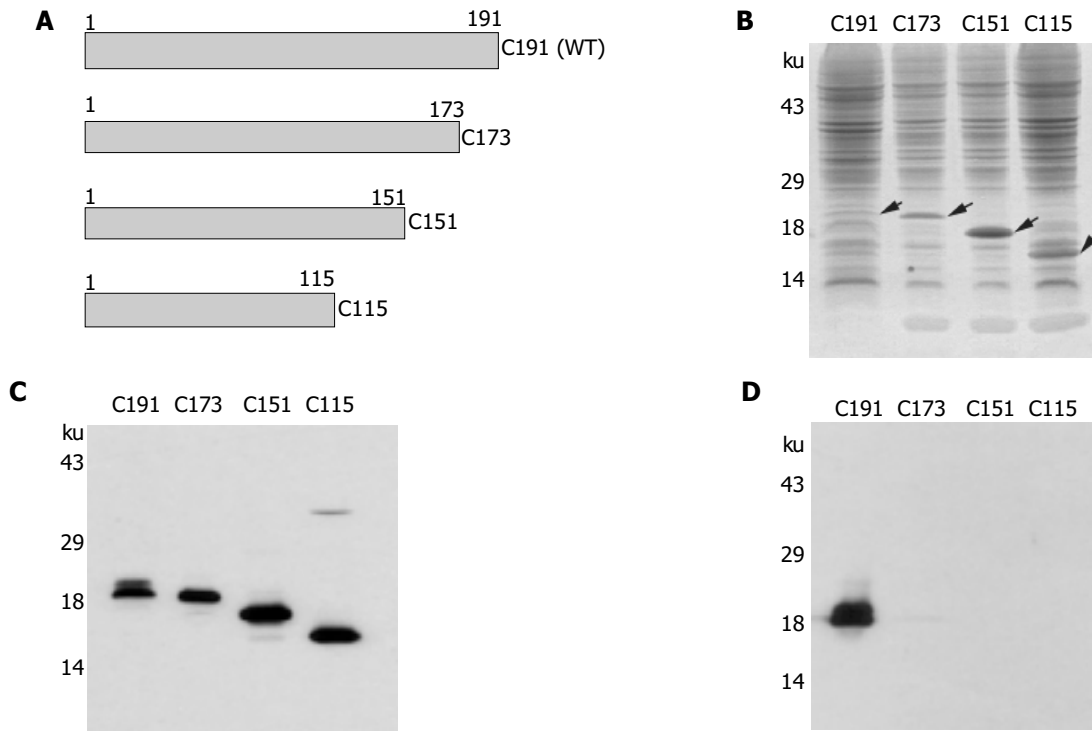


Figure 4 Effects of mutant core proteins on core secretion. (A) Schematic diagram illustrating the recombinant baculoviruses expressing truncated forms of core protein. Mutant core constructs were generated by PCR and the subsequent recombinant baculoviruses were made as described in Materials and methods. Protein expression of each mutant was confirmed by SDS-PAGE and Coomassie Brilliant Blue staining (B) and Western blot analysis by using HCV patient serum

(C). (D) Determination of extracellular core release among wild type and mutant core proteins. Insect cells were infected with recombinant baculoviruses expressing wild type and various mutant forms of core proteins and harvested at d 3 postinfection. Culture supernatants were partially purified and determined for core secretion by Western blot analysis as described in the legend to Figure 1B.

associated with cellular membrane^[26] and HCV replication occurs on lipid raft membrane structure^[27]. To investigate whether extracellular form of core proteins were secreted as a membrane complex, we separated the released core proteins into membrane and cytosol fractions using the membrane flotation method as previously described^[23]. The presence of the core protein in each fraction was determined by immunoblotting using a rabbit anti-core antibody. As shown in Figure 5, the secreted HCV core protein was found in both membranous and cytosolic fractions. This result indicates that the secreted core proteins are associated with some membranous materials.

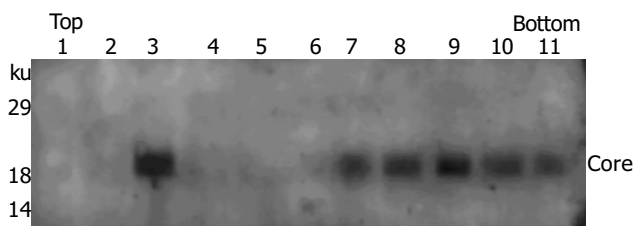


Figure 5 Membrane flotation analysis of secreted core proteins. Sf9 insect cells were infected with recombinant baculoviruses expressing full-length HCV core protein. Culture supernatant was collected at 60 h postinfection and secreted core proteins were partially purified as described in Materials and methods. The sample was then subjected to fractionation by equilibrium sucrose gradient centrifugation. Eleven fractions collected from the top were analyzed by Western blotting using rabbit anti-HCV core antibody.

DISCUSSION

It has been previously reported that HCV core without envelope proteins could form a capsid in an acellular assay^[19,28] and secreted core protein has also been detected in mammalian cells^[21]. Recently, we have demonstrated that HCV core protein is efficiently released into the culture medium in insect cells^[20]. To further understand the mechanisms of core assembly and HCV morphogenesis, we studied the HCV core secretion in insect cells using mutant forms of core protein. We constructed recombinant baculoviruses expressing various-length of HCV core proteins and were used to infect Sf9 insect cells. Culture supernatants harvested from recombinant baculovirus-infected cells were examined to see which domain of core protein is required for core secretion. As we previously reported^[20], full-length HCV core protein was efficiently released in cell culture media. However, C-terminal-truncated mutant core proteins were not able to be released into culture media although protein expression levels were higher than that of wild type core protein. This result suggests that C-terminal 18 amino acids are essential for core protein secretion in insect cells. We further showed that secreted core proteins are amorphous in structure and are released into the medium as a membrane complex. This result is consistent with the finding that both core and NS5A are associated with intracellular membranes^[27], which may play a role in the pathogenesis of HCV. Previously, it has been demonstrated that VLPs produced from recombinant baculoviruses expressing a part of the 5' UTR and structural proteins were retained in intracellular membrane vesicles

and were not released into the culture medium^[18]. In fact, transmembrane domains of E1 and E2 function as retention signals in the endoplasmic reticulum (ER) compartment. It has been reported that E1 and E2 of HCV formed a complex and were retained to the ER^[29,30]. Moreover, core protein co-localized with the E2 protein^[31]. This may be the reason why core protein alone, if envelope proteins were not present, was efficiently released into the culture media.

Previously, many capsid proteins of non-enveloped viruses were reported to assemble into VLPs, including B19 parvovirus^[32], Norwalk virus^[33], papillomavirus^[34], rotavirus^[35,36], and rabbit hemorrhagic disease virus^[37]. Similarly, HCV core protein without envelope proteins may be assembled into particle-like structure. HCV is an enveloped virus. How HCV core alone, in the absence of envelope proteins, could be assembled into particles is an intriguing question. Nevertheless, there are similar bodies of evidence that gag protein precursor of HIV-1^[38], HIV-2^[39], or simian immunodeficiency virus^[40] self-assembled into VLPs in recombinant baculovirus-infected insect cells. Budding of rabies virus particles also occurred in the absence of glycoprotein^[41]. Therefore, HCV seems to employ a similar assembly mechanism to those of retroviruses and rhabdoviruses. One study showed that VLPs were not produced from the Huh-7 cells carrying the full-length HCV genome^[42]. To date, it is uncertain how virions are assembled in HCV-infected patients.

It is not clear how HCV core protein itself can be efficiently secreted into insect culture media. In this study, core protein was released out of the cells as early as 2 d after infection. This result suggests that HCV core has the intrinsic capacity to be secreted in culture media. Kunkel *et al.*^[19], reported that N-terminal 124 aa residues of the core (genotype 1a) were sufficient for self-assembly into nucleocapsid-like particles. In contrast, our data suggest that full-length of core should be necessary for core assembly. The discrepancy between the two systems may be due to the different genotypes or different expression systems. However, it is consistent that C-terminal hydrophobic sequence (E1 peptidase signal) inhibits high level of protein expression in both prokaryotic and eukaryotic cell culture systems. In mammalian cells, the C-terminally truncated core 173 is translocated into the nucleus, whereas intact core is destined to the ER^[43,44]. This is why core 173 could not be released into the medium although its intracellular expression level was high. In this study we showed that only the full-length core was efficiently released into the culture medium, although the protein expression level of the full-length core was lower than those of other mutant core proteins. Furthermore, the comparable domains of other hepatitis viruses were unable to replace the function of C-terminal region of HCV core. It is hence conceivable that the C-terminal domain of HCV core, in addition to being a signal sequence for E1 protein, has intrinsic function in secretion. It is also possible that C-terminal domain of HCV core may interact with cellular proteins specifically.

We have compared the viability of cells infected with recombinant baculovirus expressing HCV core and those infected with wild type or recombinant baculoviruses expressing HCV 5A or 5B. All of these cells showed the similar level of viability after virus infection, indicating that HCV core

was not toxic to the insect cells (data not shown). We also used low titer of virus (m.o.i. of 3) to infect cells in order to prevent cells from baculovirus-induced cytolysis^[25]. Since most of the cells were alive at the time of harvest, the release of core protein in culture media is not due to cytolysis. It may represent a unique mechanism of the HCV core secretion. Indeed, it has been shown that HCV core protein was also secreted from mammalian cell lines in culture^[21]. Recently, Maillard *et al.*^[45], reported that nonenveloped HCV nucleocapsids were overproduced in the plasma of HCV patients and released into the bloodstream. They also found that nucleocapsid-like particles but not VLPs were produced in insect cells infected with recombinant baculovirus expressing entire structural proteins. Our study together with these reports strongly suggests that the production of nonenveloped HCV capsids may represent the feature of HCV morphogenesis. HCV may utilize a unique core release mechanism to escape immune surveillance and hence may play a role in HCV pathogenesis.

REFERENCES

- 1 **Alter HJ**, Purcell RH, Shih JW, Melpolder JC, Houghton M, Choo QL, Kuo G. Detection of antibody to hepatitis C virus in prospectively followed transfusion recipients with acute and chronic non-A, non-B hepatitis. *N Engl J Med* 1989; **321**: 1494-1500
- 2 **Kuo G**, Choo QL, Alter HJ, Gitnick GL, Redeker AG, Purcell RH, Miyamura T, Dienstag JL, Alter MJ, Tegtmeier CE, Bonino F, Colombo M, Lee WS, Kuo C, Berger K, Shuster RJ, Overby LR, Bradley DW, Houghton M. An assay for circulating antibodies to a major etiologic virus of human non-A, non-B hepatitis. *Science* 1989; **244**: 362-364
- 3 **Kato N**, Hijikata M, Ootsuyama Y, Nakagawa M, Ohkoshi S, Sugimura T, Shimotohno K. Molecular cloning of the human hepatitis C virus genome from Japanese patients with non-A, non-B hepatitis. *Proc Natl Acad Sci USA* 1990; **87**: 9524-9528
- 4 **Saito I**, Miyamura T, Ohbayashi A, Harada H, Katayama T, Kikuchi S, Watanabe Y, Koi S, Orji M, Ohta Y, Choo QL, Houghton M, Kuo G. Hepatitis C virus infection is associated with the development of hepatocellular carcinoma. *Proc Natl Acad Sci USA* 1990; **87**: 6547-6549
- 5 **Shimotohno K**. Hepatocellular carcinoma in Japan and its linkage to infection with hepatitis C virus. *Semin Virol* 1993; **4**: 305-312
- 6 **He LE**, Alling D, Popkin D, Shapiro M, Alter HJ, Purcell RH. Determining the size of non-A, non-B hepatitis virus by filtration. *J Infect Dis* 1987; **156**: 636-640
- 7 **Choo QL**, Kuo G, Weiner AJ, Overby LR, Bradley DW, Houghton M. Isolation of a cDNA clone derived from a blood-borne non-A, non-B hepatitis genome. *Science* 1989; **244**: 359-362
- 8 **Inchauspe G**, Zebedee S, Lee DH, Sugitani M, Nasoff M, Prince AM. Genomic structure of the human prototype strain H of hepatitis C virus: Comparison with American and Japanese isolates. *Proc Natl Acad Sci USA* 1991; **88**: 10292-10296
- 9 **Miller RH**, Purcell RH. Hepatitis C virus shares amino acids sequence similarity with pestiviruses and flaviviruses as well as members of two plant virus super groups. *Proc Natl Acad Sci USA* 1990; **87**: 2057-2061
- 10 **Takamizawa A**, Mori C, Fuke I, Manabe S, Murakami S, Fujita J, Onishi E, Andoh T, Yoshida I, Okayama H. Structure and organization of the hepatitis C virus genome isolated from human carriers. *J Virol* 1991; **65**: 1105-1113
- 11 **Francki RB**, Fauquet CM, Knudson DL, Brown F. Classification and nomenclature of viruses. Fifth report of the International Committee on Taxonomy of Viruses. *Arch Virol* 1991; **2** (Suppl): 223

- 12 **Rice CM.** *Flaviviridae*: The viruses and their replication. In: Fields BN, Knipe DM, Howley PM, eds. *Fields virology*, 3rd ed. Lippincott-Raven, Philadelphia, PA 1996: 931-959
- 13 **Hijikata M,** Kato N, Ootsuyama Y, Nakagawa M, Shimotohno K. Gene mapping of the putative structural region of the hepatitis C virus genome by in vitro processing analysis. *Proc Natl Acad Sci USA* 1991; **88**: 5547-5551
- 14 **Grakoui A,** Wychowski C, Lin C, Feinstone SM, Rice CM. Expression and identification of hepatitis C virus polyprotein cleavage products. *J Virol* 1993; **67**: 1385-1395
- 15 **Matsuura Y,** Miyamura T. The molecular biology of hepatitis C virus. *Semin Virol* 1993; **4**: 297-304
- 16 **Lin C,** Lindenbach BD, Pragai B, McCourt DW, Rice CM. Processing of the hepatitis C E2-NS2 region: identification of p7 and two distinct E2-specific products with different C termini. *J Virol* 1994; **68**: 5063-5073
- 17 **Mizushima H,** Hijikata M, Asabe SI, Hirota M, Kimura K, Shimotohno K. Two hepatitis C virus glycoprotein E2 products with different C termini. *J Virol* 1994; **68**: 6215-6222
- 18 **Baumert TF,** Ito S, Wong DT, Liang TJ. Hepatitis C virus structural proteins assemble into viruslike particles in insect cells. *J Virol* 1998; **72**: 3827-3836
- 19 **Kunkel M,** Lorinczi M, Rijnbrand R, Lemon SM, Watowich S. Self-assembly of nucleocapsid-like particles from recombinant hepatitis C virus core protein. *J Virol* 2001; **75**: 2119-2129
- 20 **Choi SH,** Kim SY, Park KJ, Kim YJ, Hwang SB. Hepatitis C virus core protein is efficiently released into the culture medium in insect cells. *J Biochem Mol Biol* 2004; **37**: 735-740
- 21 **Sabile A,** Perlemuter G, Bono F, Kohara K, Demaugre F, Kohara M, Matsuura Y, Miyamura T, Brechot C, Barba G. Hepatitis C virus core protein binds to apolipoprotein AII and its secretion is modulated by fibrates. *Hepatology* 1999; **30**: 1064-1076
- 22 **Cho YG,** Yoon JW, Jang KL, Kim CM, Sung YC. Full genome cloning and nucleotide sequence analysis of hepatitis C virus from sera of chronic hepatitis patients in Korea. *Mol Cells* 1993; **3**: 195-202
- 23 **Hwang SB,** Park KJ, Kim YS, Sung YC, Lai MMC. Hepatitis C virus NS5B protein is a membrane-associated phosphoprotein with a predominantly perinuclear localization. *Virology* 1997; **227**: 439-446
- 24 **Hwang SB,** Lai MMC. Hepatitis delta antigen expressed by recombinant baculoviruses: comparison of biochemical properties and post-translational modifications between the large and small forms. *Virology* 1992; **190**: 413-422
- 25 **Hwang SB,** Park KJ, Kim YS. Overexpression of hepatitis delta antigen protects insect cells from baculovirus-induced cytolysis. *Biochem Biophys Res Commun* 1998; **244**: 652-658
- 26 **Shi ST,** Polyak SJ, Tu H, Taylor DR, Gretch DR, Lai MMC. Hepatitis C virus NS5A colocalizes with the core protein on lipid droplets and interacts with apolipoproteins. *Virology* 2002; **292**: 198-210
- 27 **Shi ST,** Lee KJ, Aizaki H, Hwang SB, Lai MMC. Hepatitis C virus RNA replication occurs on a detergent-resistant membrane that cofractionates with caveolin-2. *J Virol* 2003; **77**: 4160-4168
- 28 **Klein KC,** Polyak SJ, Lingappa JR. Unique features of hepatitis C virus capsid formation revealed by de novo cell-free assembly. *J Virol* 2004; **78**: 9257-9269
- 29 **Cocquerel L,** Meunier JC, Pillez A, Wychoeski C, Dubuisson J. A retention signal necessary and sufficient for endoplasmic reticulum localization maps to the transmembrane domain of hepatitis C virus glycoprotein E2. *J Virol* 1998; **72**: 2183-2191
- 30 **Deleersnyder V,** Pillez A, Wychowski C, Blight K, Xu J, Hahn YS, Rice CM, Dubuisson J. Formation of native hepatitis C virus glycoprotein complexes. *J Virol* 1997; **71**: 697-704
- 31 **Santolini E,** Migliaccio G, La Monica N. Biosynthesis and biochemical properties of the hepatitis C virus core protein. *J Virol* 1994; **68**: 3631-3641
- 32 **Kajigaya S,** Fujii H, Field A, Anderson S, Rosenfeld S, Anderson LJ, Shimada T, Young NS. Self-assembled B19 parvovirus capsids, produced in a baculovirus system, are antigenically and immunogenically similar to native virions. *Proc Natl Acad Sci USA* 1991; **88**: 4646-4650
- 33 **Jiang X,** Wang M, Graham DY, Estes MK. Expression, self-assembly, and antigenicity of the norwalk virus capsid protein. *J Virol* 1992; **66**: 6527-6532
- 34 **Kirnbauer R,** Booy F, Cheng N, Lowy DR, Schiller JT. Papillomavirus L1 major capsid protein self-assembles into virus-like particles that are highly immunogenic. *Proc Natl Acad Sci USA* 1992; **89**: 12180-12184
- 35 **Crawford SE,** Labbe M, Cohen J, Burroughs MH, Zhou YJ, Estes MK. Characterization of virus-like particles produced by the expression of rotavirus capsid protein in insect cells. *J Virol* 1994; **68**: 5945-5952
- 36 **Zeng C,** QY, Wentz MJ, Cohen J, Estes MK, Ramig RF. Characterization and replicase activity of double-layered and single-layered rotavirus-like particles expressed from baculovirus recombinants. *J Virol* 1996; **70**: 2736-2742
- 37 **Sibilia M,** Boniotti MB, Angoscini P, Capucci L, Rossi C. Two independent pathways of expression lead to self-assembly of the rabbit hemorrhagic disease virus capsid protein. *J Virol* 1995; **69**: 5812-5815
- 38 **Gheysen D,** Jacobs E, de Foresta F, Thiriart C, Francotte M, Thines D, De Wilde M. Assembly and release of HIV-1 precursor pr55gag virus-like particles from recombinant baculovirus-infected insect cells. *Cell* 1989; **59**: 103-112
- 39 **Luo L,** Li Y, Kang CY. Expression of gag precursor protein and secretion of virus-like gag particles of HIV-2 from recombinant baculovirus-infected insect cells. *Virology* 1990; **179**: 874-880
- 40 **Delchambre M,** Gheysen D, Thines D, Thiriart C, Jacobs E, Verdin E, Horth M, Burny A, Bex F. The GAG precursor of simian immunodeficiency virus assembles into virus-like particles. *EMBO J* 1989; **8**: 2653-2660
- 41 **Mebatsion T,** Konig M, Conzelmann KK. Budding of rabies virus particles in the absence of the spike glycoprotein. *Cell* 1996; **84**: 941-951
- 42 **Pietschmann T,** Lohmann V, Kaul A, Krieger N, Rinck G, Rutter G, Strand D, Bartenschlager R. Persistent and transient replication of full-length hepatitis C virus genomes in cell culture. *J Virol* 2002; **76**: 4008-4021
- 43 **Liu Q,** Tackney C, Bhat RA, Prince AM, Zhang P. Regulated processing of hepatitis C virus core protein is linked to subcellular localization. *J Virol* 1997; **71**: 657-662
- 44 **Lo SY,** Masiarz F, Hwang SB, Lai MMC, Ou JH. Differential subcellular localization of hepatitis C virus core gene products. *Virology* 1995; **213**: 455-461
- 45 **Maillard P,** Krawczynski K, Nitkiewicz J, Bronnert C, Sidorkiewicz M, Gounon P, Dubuisson J, Faure G, Crainic R, Budkowska A. Nonenveloped nucleocapsids of hepatitis C virus in the serum of infected patients. *J Virol* 2001; **75**: 8240-8250

Transactivating effect of complete S protein of hepatitis B virus and cloning of genes transactivated by complete S protein using suppression subtractive hybridization technique

Gui-Qin Bai, Yan Liu, Jun Cheng, Shu-Lin Zhang, Ya-Fei Yue, Yan-Ping Huang, Li-Ying Zhang

Gui-Qin Bai, Shu-Lin Zhang, Ya-Fei Yue, Yan-Ping Huang, The First Hospital of Xi'an Jiaotong University, Xi'an 710004, Shaanxi Province, China

Yan Liu, Jun Cheng, Li-Ying Zhang, Gene Therapy Research Center, Institute of Infectious Diseases, 302 Hospital of PLA, 100 Xisihuanzhong Road, Beijing 100039, China

Supported by the National Natural Science Foundation of China, No. C03011402, No. C30070690; the Science and Technique Foundation of PLA during the 9th Five-year Plan period, No. 98D063; the Launching Foundation for Students Studying Abroad of PLA, No. 98H038; the Youth Science and Technique Foundation of PLA during the 10th Five-year plan period, No. 01Q138; and the Science and Technique Foundation of PLA during the 10th Five-year Plan period, No. 01MB135

Correspondence to: Dr. Gui-Qin Bai, Department of Obstetrics and Gynecology of First Hospital, Xi'an Jiaotong University, Jiankang Road 1, Xi'an 710061, Shaanxi Province, China
Telephone: +86-29-85213194 Fax: +86-29-85252812

Received: 2004-11-08 Accepted: 2004-12-26

Abstract

AIM: To investigate the transactivating effect of complete S protein of hepatitis B virus (HBV) and to construct a subtractive cDNA library of genes transactivated by complete S protein of HBV by suppression subtractive hybridization (SSH) technique and to clone genes associated with its transactivation activity, and to pave the way for elucidating the pathogenesis of hepatitis B virus infection.

METHODS: pcDNA3.1(-)-complete S containing full-length HBV S gene was constructed by insertion of HBV complete S gene into *BamH I/Kpn I* sites. HepG2 cells were cotransfected with pcDNA3.1(-)-complete S and pSV-lacZ. After 48 h, cells were collected and detected for the expression of β -galactosidase (β -gal). Suppression subtractive hybridization and bioinformatics techniques were used. The mRNA of HepG2 cells transfected with pcDNA3.1(-)-complete S and pcDNA3.1(-) empty vector was isolated, and detected for the expression of complete S protein by reverse transcription polymerase chain reaction (RT-PCR) method, and cDNA was synthesized. After digestion with restriction enzyme *RsaI*, cDNA fragments were obtained. Tester cDNA was then divided into two groups and ligated to the specific adaptors 1 and 2, respectively. After tester cDNA had been hybridized with driver cDNA twice and underwent nested PCR twice, amplified cDNA fragments were subcloned into pGEM-Teasy vectors to set up the subtractive library. Amplification of the library was carried out within *E. coli* strain DH5 α . The cDNA was sequenced

and analyzed in GenBank with BLAST search after polymerase chain reaction (PCR) amplification.

RESULTS: The complete S mRNA could be detected by RT-PCR in HepG2 cells transfected with the pcDNA3.1(-)-complete S. The activity of β -gal in HepG2 cells transfected with the pcDNA3.1(-)-complete S was 6.9 times higher than that of control plasmid. The subtractive library of genes transactivated by HBV complete S protein was constructed successfully. The amplified library contains 86 positive clones. Colony PCR showed that 86 clones contained DNA inserts of 200-1 000 bp, respectively. Sequence analysis was performed in 35 clones randomly, and the full length sequences were obtained with bioinformatics method and searched for homologous DNA sequence from GenBank, altogether 33 coding sequences were obtained. These cDNA sequences might be target genes transactivated by complete S protein of HBV. Moreover, two unknown genes were discovered, full length coding sequences were obtained by bioinformatics techniques, one of them was named complete S transactivated protein 1 (CSTP1) and registered in GenBank (AY553877).

CONCLUSION: The complete S gene of HBV has a transactivating effect on SV40 early promoter. A subtractive cDNA library of genes transactivated by HBV complete S protein using SSH technique has been constructed successfully. The obtained sequences may be target genes transactivated by HBV complete S protein among which some genes coding proteins are involved in cell cycle regulation, metabolism, immunity, signal transduction, cell apoptosis and formation mechanism of hepatic carcinoma.

© 2005 The WJG Press and Elsevier Inc. All rights reserved.

Key words: Complete S protein; Transactivated genes; Hepatitis virus B

Bai GQ, Liu Y, Cheng J, Zhang SL, Yue YF, Huang YP, Zhang LY. Transactivating effect of complete S protein of hepatitis B virus and cloning of genes transactivated by complete S protein using suppression subtractive hybridization technique. *World J Gastroenterol* 2005; 11(25): 3893-3898
<http://www.wjgnet.com/1007-9327/11/3893.asp>

INTRODUCTION

Hepatitis B virus (HBV) genome is defined as four open

read frames (ORFs), which are named as the regions of S, C, P, X, respectively. The region of S is divided into the sub-regions of pre-S1, pre-S2 and S according to different initial code ATG in frame. Dong *et al.*^[1], have shown that there is ORF before pre-S1 region in the genome of HBV from serum of patients with long and accurate polymerase chain reaction (LA-PCR). This region is 135 bp, which is named temporarily as pre-pre-S and its promoter activities are confirmed in 277 bp upstream nucleotide sequences before pre-S1 gene^[2]. Pre-pre-S, pre-S1, pre-S2 and S genes are translated in frame according to the same ORF. It is well-known that HBV causes acute and chronic infections of the liver, especially chronic infections may result in remarkable consequences^[3]. HBV is considered to be a major etiological factor in the development of human hepatocellular carcinoma (HCC)^[4-9]. Although the precise role of HBV in the etiology of HCC is not well understood, data have shown that some HBV proteins can exert a significant transactivating activity on both viral and cellular promoter^[10]. This mechanism may have a close relation with the formation of HCC.

Suppression subtractive hybridization (SSH) is a widely used new technique in the cloning of genes transactivated by viral proteins^[11]. Complete S of HBV includes pre-pre-S, pre-S1, pre-S2 and S regions, complete S protein functions as a transcriptional transactivator. In the present study, we have successfully constructed the subtractive library of genes transactivated by HBV complete S protein.

MATERIALS AND METHODS

Construction and identification of expression vector

The complete S gene was prepared by PCR amplification using plasmid G376 A7 (GenBank number: AF384371) as template^[1,12,13], sense (5'-GGA TCC ATG CAG TTA ATC ATT ACT TCC-3') and antisense (5'-GGT ACC AAT GTA TAC CCA AAG ACA AAA G-3') primers (Shanghai BioAsia Biotech Co., Ltd, China). As these primers contain *Bam*HI and *Kpn*I (Takara) recognition sites on their respective 5'-ends, the amplified 1 338 bp PCR fragment was subcloned into the *Bam*HI and *Kpn*I sites of pcDNA3.1(-) vector (Invitrogen Co., USA). The expression vector, pcDNA3.1 (-)-complete S which could directly express complete S fusion protein was obtained, then identified by PCR and digested by *Bam*HI/*Kpn*I.

Expression of pcDNA3.1 (-)-complete S in HepG2 cells

HepG2 cells were transiently transfected with pcDNA3.1 (-)-complete S. At the same time, empty vectors were also transfected into cells as controls. HepG2 cells were plated at a density of 1.5×10^6 in a 35 mm plate in Dulbecco's modified Eagle's medium (DMEM) supplemented with 100 mL/L heat-inactivated fetal bovine serum (FBS). After 24 h of growth to 40-50% confluence, the cells were transfected with plasmids using FuGENE6 transfection reagent following the manufacturer's protocol (Roche C, USA).

mRNA and cDNA isolation

The mRNA from HepG2 cells transfected with pcDNA3.1

(-)-complete S and pcDNA3.1(-) empty vector was isolated using micro mRNA purification kit (Amersham Biosciences, Co., USA). cDNAs were reverse-transcribed from total RNA. Identification was done by PCR with complete S sequence-specific primers.

Cotransfection with reporter vector pSV-lacZ

HepG2 cells were transfected with various concentrations of plasmid pSV-lacZ (0.1-1.8 μ g) (Promega Co., USA). Expression of β -gal was detected by a β -gal assay kit (Promega, Co., USA). In pSV-LacZ the LacZ gene was under the control of the SV40 early promoter element. The optimal concentration of pSV-lacZ plasmid DNA was selected, HepG2 cells was cotransfected with pSV-lacZ and pcDNA3.1 (-)-complete S (2.0 μ g). At the same time, cotransfected HepG2 cells transfected with empty pcDNA3.1(-) (2.0 μ g) and pSV-lacZ were used as controls. After 48 h, cells were collected and detected for the expression of β -gal.

Generation of subtractive cDNA library

Gene expression comparisons by suppression subtractive hybridization according to the manufacturer's instructions of PCR-selectTM cDNA subtraction kit (Clontech Co., USA). In brief, 2 μ g of mRNA from the tester and the driver was subjected to cDNA synthesis. Tester and driver cDNAs were digested with *Rsa*I. The tester cDNA was subdivided into two portions, and each was ligated with a different cDNA adapter. In the first hybridization reaction, an excess of driver cDNA was added to each sample of tester. The samples were heat denatured and allowed to anneal. Because of the second-order kinetics of hybridization, the concentration of high- and low-abundance sequences was equalized among the single-stranded tester molecules. At the same time single-stranded tester molecules were significantly enriched for differentially expressed sequences. During the second hybridization, two primary hybridization samples were mixed without denaturation. Only the remaining equalized and subtracted single-stranded tester cDNAs could re-associate forming double-stranded tester molecules with different ends. After filling in the ends with DNA polymerase, the entire population of molecules was subjected to nested PCR with two adapter-specific primer pairs.

PCR analysis of subtraction efficiency

PCR was performed on un-subtracted and subtracted secondary PCR products with the G3PDH 5'- and 3'-primers, respectively. From each reaction, 5 μ L sample was removed, and the rest of the reaction was put back into the thermal cycler for five more cycles. The above step was repeated thrice, and then 5 μ L sample (i.e., the aliquots were removed from each reaction after 18, 23, 28, and 33 cycles) was examined on 2.0% agarose gel.

Cloning subtractive library into pGEM-teasy vector

The amplified products containing a subtractive cDNA library (6 μ L) were cloned into a pGEM-teasy vector (Promega Co., USA). Subsequently, Plasmid DNA was transformed into *E. coli* strain DH5 α . Bacteria were taken up in 800 μ L of LB medium and incubated for 45 min at 37 $^{\circ}$ C. Bacteria were plated onto agar plates containing

ampicillin (100 µg/mL), 5-bromo-4-chloro-3-indolyl-β-D-galactoside (X-Gal; 20 µg/cm²), and isopropyl-β-D-thiogalactoside (IPTG; 12.1 µg/cm²) and incubated overnight at 37 °C. Positive (white) colonies were picked out and identified by PCR. Primers were T7/SP6 primer of pGEM-teasy vector. After the positive colonies were sequenced (Shanghai BioAsia Biotechnology Co., Ltd, China), nucleic acid sequence homology searches were performed using the BLAST (basic local alignment search tool) server at the National Center for Biotechnology Information.

RESULTS

Identification of expression vector

Restriction enzyme analysis of pcDNA3.1(-)-complete S plasmid cleaved with *Bam*HI and *Kpn*I yielded two bands: 5 396 bp empty pcDNA3.1(-) and 1 338 bp HBV complete S, and only one 6 734 bp band (5 396 bp+1 338 bp), it was cleaved with *Kpn*I. The plasmid by PCR amplification with complete S-specific primers got a clear band with the expected size (1 338 bp). The sequence of the PCR product was correct (Figure 1).

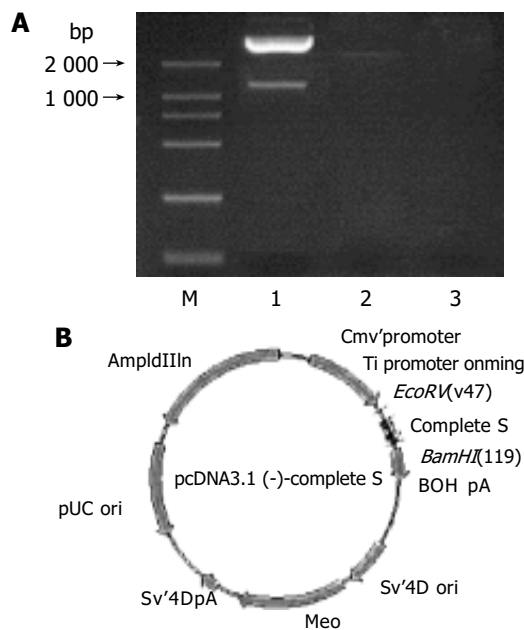


Figure 1 Electrophoresis of PCR products of pcDNA3-complete S and cleaved restriction enzyme (A). Structure of expression vector pcDNA3.1(-)-complete S plasmid(B).

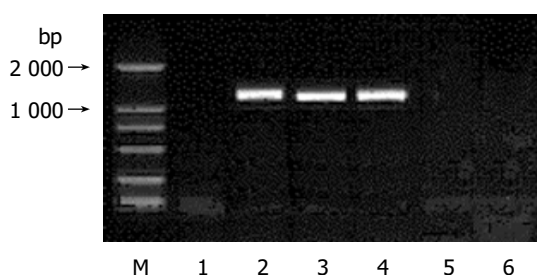


Figure 2 Electrophoresis of RT-PCR products in 0.9% agarose gel. Lane 1: negative control; lanes 2-4: mRNA isolated from pcDNA3.1(-)-complete S; lane 5: blank control; M: DNA marker (2 000 bp).

Identification of HBV complete S transient expression

Reverse-transcription by three different Oligo dT, identification of cDNA by PCR yielded a common 1.338 bp band (Figure 2).

The stable expression of pcDNA3.1(-)-complete S in HepG2 cells was also confirmed by Western blotting hybridization at a high level.

Result of cotransfection of pSV-lacZ and pcDNA3.1(-)-complete S

The best concentration was at 1.0 µg of pSV-lacZ. When cotransfected with pcDNA3.1(-)-complete S and pSV-lacZ, the *A* data about the expression of β-gal were 0.228. In contrast, the expression of β-gal cotransfected with empty pcDNA3.1(-) and pSV-lacZ was 0.033. Expression of β-gal was 6.9-fold higher when cotransfected with pcDNA3.1(-)-complete S and pSV-lacZ than when cotransfected with empty pcDNA3.1(-) and pSV-lacZ. The significant increase of expression of β-gal was attributed to the transactivating effect of HBV complete S protein on early promoter of SV40, thus increasing the expression of downstream gene lacZ (Figure 3).

Result of PCR analysis of subtraction efficiency

The G3PDH (a housekeeping gene) primers were used to confirm the reduced relative abundance of G3PDH following the PCR selection procedure. The result displayed that the G3PDH abundance of subtracted secondary PCR products significantly decreased compared to the un-subtracted one, indicating that the subtractive library had a high subtraction efficiency (Figure 4).

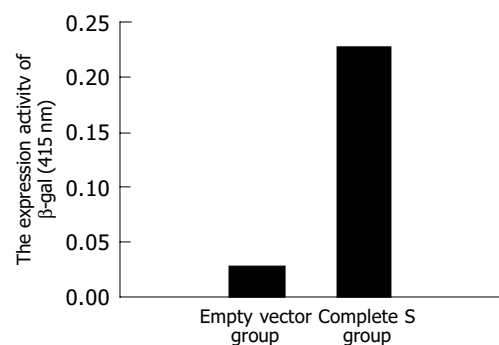


Figure 3 Result of β-galactosidase enzyme analysis.

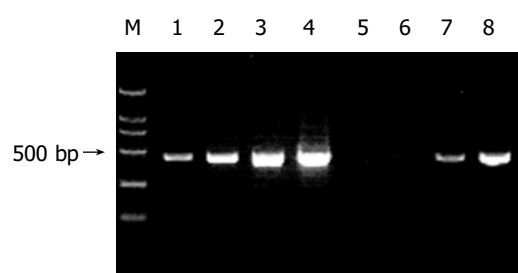


Figure 4 Reduction of G3PDH abundance by PCR-selection subtraction. Lanes 1 and 5: 18 cycles; lanes 2 and 6: 23 cycles; lanes 3 and 7: 28 cycles; lanes 4 and 8: 33 cycles. Lane M: marker (2 000 bp).

Analysis of subtractive library

Using suppression subtractive hybridization technique, we obtained a total of 86 positive clones. These clones were prescreened by PCR amplification to ensure that only clones with different inserts were subjected to sequencing analysis (Figure 5). Eighty-six clones contained 200-1 000 bp inserts. A total of 35 clones from cDNA library were randomly selected and sequenced, and 33 coding sequences were obtained. The data are presented in Table 1. The smear difference in subtractive library was displayed after electrophoresis of PCR products on 2% agarose gel (Figure 6).

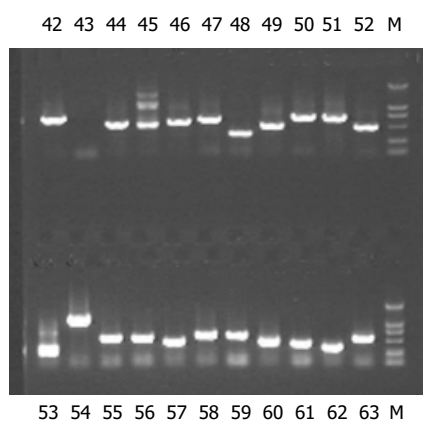


Figure 5 Electrophoresis of PCR products of part clones (42-63) on 0.9% agarose gel; M: marker (2 000 bp).

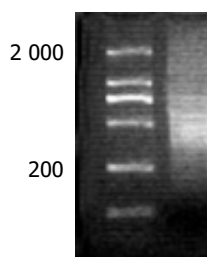


Figure 6 Smears of HBV complete S after PCR.

DISCUSSION

The open reading frame of HBV complete S gene consists of four coding regions: pre-pre-S, pre-S1, pre-S2 and S, each starting with an ATG codon in frame. Through in frame translational initiation at each of the four ATG codons, complete S (pre-pre-S +pre-S1+pre-S2+S), large (LHBs; pre-S1+pre-S2+S), middle (MHBs; pre-S2+S) and small (SHBs; S) envelope glycoproteins can be synthesized^[14-18]. The transactivator function of the surface protein requires the cytoplasmic orientation of the pre-S2 domain (the minimal functional unit) that occurs in the case of MHBs[†] and in a fraction of Labs^[19,20]. Some studies indicate the biological significance of the pre-S2 transactivators^[21]. But we firstly discussed the transactivator function of HBV complete S protein in the present study.

We cotransfected HepG2 cells with pcDNA3.1(-)-complete S and pSV-lacZ and demonstrated that the HBV

Table 1 Comparison between positive clones and GenBank homology sequences

High similarity between proteins and known genes	Number of similar clones
<i>Homo sapiens</i> amino acid transporter system A2 (ATA2)	2
<i>Homo sapiens</i> heat shock 90 ku protein 1, (HSPCA)	4
<i>Homo sapiens</i> fibrinogen	1
<i>Homo sapiens</i> CDK4	5
<i>Homo sapiens</i> ribosomal protein	1
<i>Homo sapiens</i> translational initiation factor	1
<i>Homo sapiens</i> synaptophysin-like protein	1
Human mRNA for cytosolic malate dehydrogenase	1
<i>Homo sapiens</i> cytochrome c oxidase subunit I	2
<i>Homo sapiens</i> adenylate kinase 2 (AK2)	1
<i>Homo sapiens</i> NADH dehydrogenase	1
Human complement component C3 mRNA	1
<i>Homo sapiens</i> insulin-like growth factor binding protein 1	1
<i>Homo sapiens</i> SMT3 suppressor of mif two 3 homolog 2	1
<i>Homo sapiens</i> succinate dehydrogenase complex	1
<i>Homo sapiens</i> apolipoprotein H (beta-2-glycoprotein I) (APOH)	1
<i>Homo sapiens</i> BRCA2 and Cip1/p21 interacting protein splice variant	1
<i>Homo sapiens</i> Sec23 homolog A	1
<i>Homo sapiens</i> glutamate dehydrogenase 1	1
<i>Homo sapiens</i> proteasome (prosome, macropain) subunit	2
<i>Homo sapiens</i> eukaryotic translation elongation factor 1	1
<i>Homo sapiens</i> polymerase (RNA) I polypeptide D	2

complete S protein was successfully expressed in transfected HepG2 cells. Expression of β -gal was 6.9-fold higher when cotransfected with pcDNA3.1(-)-complete S and pSV-lacZ than when cotransfected with empty pcDNA3.1(-) and pSV-lacZ. HBV complete S had significant transactivating effect on early promoter of SV40 virus, thus increasing the expression of downstream gene lacZ. This result indicates that the HBV complete S protein expressed in HepG2 cells retains its biological activity in terms of transcriptional activation.

To get insight into the transactivation mechanism of HBV complete S protein, SSH was used for identification of transactivating target genes of complete S protein, and subtractive library was set up successfully. Sequence analysis was performed for 35 clones, and 33 coding sequences were obtained. These genes can be divided into four groups:

(1) The genes involved in cell structure and cell cycle that possess the important ability to control cell growth, differentiation and adherence, such as ribosomal protein, mitochondrion, eukaryotic translation elongation factor.

(2) The genes related to cell energy or substance metabolism (i.e., NADH dehydrogenase 2, cytochrome C oxidase II, etc.).

(3) The genes involved in the mechanism underlying the development of hepatocellular carcinoma. Cyclin-dependent kinase 4 (CDK4) is a key regulator of cell cycle. It has been shown that a variety of cell cycle-related proteins play an important role in the process of hepatocarcinogenesis. CDK4 is related to the regulation of the cyclin G1 phase, and significantly elevates in HCC compared to surrounding cirrhotic tissues by Western blot and *in vitro* kinase assays. The enhanced cyclin D1-related kinase activity in HCC was accompanied with the up-regulation of CDK4 activity. In addition, the protein levels and kinase activities of CDK4 are higher in poorly differentiated and advanced HCC. In

conclusion, the increases of cyclin D1 and CDK4 play an important role in the development of HCC. CDK4 activation may be closely related to the histopathologic grade and progression of HCC^[22-24]. But CDK4 does not increase in children with hepatic carcinoma^[25]. Amino acid transporter system A2 (ATA2) is responsible for Na⁺-independent amino acid transporter system. When amino acid is starved, the expression of ATA2 increases, suggesting that this expression is directly related to the activity of amino acid transporter^[26]. Its mRNA increases in the biopsy of hepatocirrhosis and hepatic carcinoma^[27], especially in chorion after hepatectomy, suggesting that ATA2 is closely associated with hepatic regeneration^[26,28]. ATA2 is cloned in hepatic carcinoma HepG2, and increases in patients of hepatic carcinoma^[29].

(4) The genes controlling hepatic cell infection and apoptosis, such as adenylate kinase 2(AK2) protein. AK2 gene located at the right arm of the second chromosome may play a role in maintaining the levels of ADP/ATP by releasing two-molecule ADP from ATP to AMP^[30]. The release of two mitochondrial proteins, cytochrome C and apoptosis-inducing factor (AIF), into the soluble cytoplasm of cells undergoing apoptosis has been well established. Since only AK2 intermembrane proteins release from mitochondria during the early phase of the apoptotic process, AK2 is very important in cell apoptosis. AK2 and cytochrome C are translocated in cytoplasm gelatum in apoptosis model^[31]. Therefore AK2 plays a role in inducing cell apoptosis. Apolipoprotein H (APOH), is named as beta-2-glycoprotein I and anticoagulative serum protein. The polymorphous APOH gene is closely related to fat metabolism, coagulation and hypertension^[32]. It is the pre-S of HBsAg that results in HBsAg combination with APOH. Resecting phosphatide and oxygenated phosphatide could disturb this mutual action, suggesting that this action is involved in the ectoblastic phosphatide^[33]. Furthermore, it is restrained from rebuilding HBsAg, anti-HBsAg and APOH. APOH may be the vector of HBV and plays a role in HBV infection. APOH chiefly combines with complete Dane HBV particle with telescope, and the activity of APOH-HBsAg is the highest in patients with active duplication^[33]. This combination facilitates virus particle entrancing hepatic cells, and plays an important role in the beginning of HBV infection^[34].

We testified the transactivator ability of HBV complete S protein, and constructed the subtractive cDNA library of genes transactivated by complete S protein. These genes are closely correlated with carbohydrate metabolism, immunoregulation, occurrence and development of tumor. How these genes affect occurrence and development of chronic hepatitis B, hepatic fibrosis and hepatocarcinoma needs to be further studied.

REFERENCES

- Dong J, Cheng J. Study on definition of pre-per-s region in hepatitis B virus genome. *Shijie Huaren Xiaohua Zazhi* 2003; **8**: 1091-1096
- Yang Q, Dong J, Cheng J, Liu Y, Hong Y, Wang JJ, Zhuang SL. Definition of pre-pre-s promoter sequence from hepatitis B virus genome and identification of its transcription activity. *Jiefangjun Yixue Zazhi* 2003; **9**: 761-762
- Beasley RP. Hepatitis B virus. The major etiology of hepatocellular carcinoma. *Cancer* 1988; **61**: 1942-1956
- Dong J, Cheng J, Wang Q, Wang G, Shi S, Liu Y, Xia X, Li L, Zhang G, Si C. Quasispecies and variations of hepatitis B virus: core promoter region as an example. *Zhonghua Shiyan He Linchuang Bingduxue Zazhi* 2002; **16**: 264-266
- Dong J, Cheng J, Wang Q, Shi S, Wang G, Si C. Cloning and analysis of the genomic DNA sequence of augmenter of liver regeneration from rat. *Chin Med Sci J* 2002; **17**: 63-67
- Deng H, Dong J, Cheng J, Huangfu KJ, Shi SS, Hong Y, Ren XM, Li L. Quasispecies groups in the core promoter region of hepatitis B virus. *Hepatobiliary Pancreat Dis Int* 2002; **1**: 392-396
- Parkin DM, Pisani P, Ferlay J. Estimates of the worldwide incidence of 25 major cancers in 1990. *Int J Cancer* 1999; **80**: 827-841
- Dong J, Cheng J, Wang Q, Huangfu J, Shi S, Zhang G, Hong Y, Li L, Si C. The study on heterogeneity of hepatitis B virus DNA. *Zhonghua Yixue Zazhi* 2002; **82**: 81-85
- Xia X, Cheng J, Yang J, Zhong Y, Wang G, Fang H, Liu Y, Li K, Dong J. Construction and expression of humanized anti-HBsAg scFv targeting interferon-alpha in *Escherichia coli*. *Zhonghua Ganzhangbing Zazhi* 2002; **10**: 28-30
- Seeger C, Mason WS. Hepatitis B virus biology. *Microbiol Mol Biol Rev* 2000; **64**: 51-68
- Kuang WW, Thompson DA, Hoch RV, Weigel RJ. Differential screening and suppression subtractive hybridization identified genes differentially expressed in an estrogen receptor-positive breast carcinoma cell line. *Nucleic Acid Res* 1998; **26**: 1116-1123
- Liu Y, Cheng J, Shao DZ, Wang L, Zhong YW, Dong J, Li K, Li L. Synergetic transactivating effect of HCV core and HBV X proteins on SV40 early promoter/enhancer. *Zhonghua Shiyan He Linchuang Bingduxue Zazhi* 2003; **17**: 70-72
- Huangfu J, Dong J, Deng H, Cheng J, Shi S, Hong Y, Ren X, Li L. A preliminary study on the heterogeneity of preS2 region in hepatitis B virus. *Zhonghua Neike Zazhi* 2002; **41**: 233-236
- Borchani-Chabchoub I, Mokdad-Gargouri R, Gargouri A. Glucose dependent [correction of dependant] negative translational control of the heterologous expression of the pre-S2 HBV antigen in yeast. *Gene* 2003; **311**: 165-170
- Soussan P, Pol S, Garreau F, Brechet C, Kremsdorf D. Vaccination of chronic hepatitis B virus carriers with pre-S2/S envelope protein is not associated with the emergence of envelope escape mutants. *J Gen Virol* 2001; **82**: 367-371
- Park JH, Lee MK, Kim HS, Kim KL, Cho EW. Targeted destruction of the polymerized human serum albumin binding site within the preS2 region of the HBV surface antigen while retaining full immunogenicity for this epitope. *J Viral Hepat* 2003; **10**: 70-79
- Borchani-Chabchoub I, Gargouri A, Mokdad-Gargouri R. Genotyping of Tunisian hepatitis B virus isolates based on the sequencing of pre-S2 and S regions. *Microbes Infect* 2000; **2**: 607-612
- Tai PC, Suk FM, Gerlich WH, Neurath AR, Shih C. Hypermodification and immune escape of an internally deleted middle-envelope (M) protein of frequent and predominant hepatitis B virus variants. *Virology* 2002; **292**: 44-58
- Hildt E, Urban S, Hofschneider PH. Characterization of essential domains for the functionality of the MHBst transcriptional activator and identification of a minimal MHBst activator. *Oncogene* 1995; **11**: 2055-2066
- Bruss V, Lu X, Thomssen R, Gerlich WH. Post-translational alterations in transmembrane topology of the hepatitis B virus large envelope protein. *EMBO J* 1994; **13**: 2273-2279
- Hildt E, Munz B, Saher G, Reifenberg K, Hofschneider PH. The Pre-S2 activator MHBs (t) of hepatitis B virus activates c-raf-1/Erk2 signaling in transgenic mice. *EMBO J* 2002; **21**: 525-535
- Kita Y, Masaki T, Funakoshi F, Yoshida S, Tanaka M, Kurokohchi K, Uchida N, Watanabe S, Matsumoto K,

- Kuriyama S. Expression of G1 phase-related cell cycle molecules in naturally developing hepatocellular carcinoma of Long-Evans Cinnamon rats. *Int J Oncol* 2004; **24**: 1205-1211
- 23 **Edamoto Y**, Hara A, Biernat W, Terracciano L, Cathomas G, Riehle HM, Matsuda M, Fujii H, Scoazec JY, Ohgaki H. Alterations of RB1, p53 and Wnt pathways in hepatocellular carcinomas associated with hepatitis C, hepatitis B and alcoholic liver cirrhosis. *J Cancer* 2003; **106**: 334-341
- 24 **Masaki T**, Shiratori Y, Rengifo W, Igarashi K, Yamagata M, Kurokohchi K, Uchida N, Miyauchi Y, Yoshiji H, Watanabe S, Omata M, Kuriyama S. Cyclins and cyclin-dependent kinases: comparative study of hepatocellular carcinoma versus cirrhosis. *Hepatology* 2003; **37**: 534-543
- 25 **Kim H**, Lee MJ, Kim MR, Chung IP, Kim YM, Lee JY, Jang JJ. Expression of cyclin D1, cyclin E, cdk4 and loss of heterozygosity of 8p, 13q, 17p in hepatocellular carcinoma: comparison study of childhood and adult hepatocellular carcinoma. *Liver* 2000; **20**: 173-178
- 26 **Freeman TL**, Mailliard ME. Posttranscriptional regulation of ATA2 transport during liver regeneration. *Biochem Biophys Res Commun* 2000; **278**: 729-732
- 27 **Bode BP**, Fuchs BC, Hurley BP, Conroy JL, Suetterlin JE, Tanabe KK, Rhoads DB, Abcouwer SF, Souba WW. Molecular and functional analysis of glutamine uptake in human hepatoma and liver-derived cells. *Am J Physiol Gastrointest Liver Physiol* 2002; **283**: G1062-1673
- 28 **Freeman TL**, Thiele GM, Tuma DJ, Machu TK, Mailliard ME. ATA2-mediated amino acid uptake following partial hepatectomy is regulated by redistribution to the plasma membrane. *Arch Biochem Biophys* 2002; **400**: 215-222
- 29 **Hatanaka T**, Huang W, Wang H, Sugawara M, Prasad PD, Leibach FH, Ganapathy V. Primary structure, functional characteristics and tissue expression pattern of human ATA2, a subtype of amino acid transport system A. *Biochim Biophys Acta* 2000; **1467**: 1-6
- 30 **Villa H**, Perez-Pertejo Y, Garcia-Estrada C, Reguera RM, Requena JM, Tekwani BL, Balana-Fouce R, Ordonez D. Molecular and functional characterization of adenylate kinase 2 gene from *Leishmania donovani*. *Eur J Biochem* 2003; **270**: 4339-4347
- 31 **Kohler C**, Gahm A, Noma T, Nakazawa A, Orrenius S, Zhivotovsky B. Release of adenylate kinase 2 from the mitochondrial intermembrane space during apoptosis. *FEBS Lett* 1999; **447**: 10-12
- 32 **Xia J**, Yang QD, Yang QM, Xu HW, Liu YH, Zhang L, Zhou YH, Wu ZG, Cao GF. Apolipoprotein H gene polymorphisms and risk of primary cerebral hemorrhage in a Chinese population. *Cerebrovasc Dis* 2004; **17**: 197-203
- 33 **Stefas I**, Rucheton M, D'Angeac AD, Morel-Baccard C, Seigneurin JM, Zarski JP, Martin M, Cerutti M, Bossy JP, Misse D, Graafland H, Veas F. Hepatitis B virus Dane particles bind to human plasma apolipoprotein H. *Hepatology* 2001; **33**: 207-217
- 34 **Gao P**, Guo Y, Qu L, Shi T, Zhang H, Dong C, Yang H. Relation between Beta-2-glycoprotein I and hepatitis B virus surface antigen *Zhonghua Ganzangbing Zazhi* 2002; **10**: 31-33

Science Editor Wang XL and Guo SY Language Editor Elsevier HK

• VIRAL HEPATITIS •

Screening of hepatocyte proteins binding to complete S protein of hepatitis B virus by yeast-two hybrid system

Gui-Qin Bai, Jun Cheng, Shu-Lin Zhang, Yan-Ping Huang, Lin Wang, Yan Liu, Shu-Mei Lin

Gui-Qin Bai, Shu-Lin Zhang, Yan-Ping Huang, Shu-Mei Lin, First Hospital of Xi'an Jiaotong University, Xi'an 710004, Shaanxi Province, China

Jun Cheng, Lin Wang, Yan Liu, Institute of Infectious Diseases, Ditan Hospital, Anwai Street, Beijing 100011, China

Supported by the National Natural Science Foundation of China, No. C03011402, No. C30070690; the Science and Technique Foundation of PLA during the 9th Five-year plan period, No. 98D063; the Launching Foundation for Students Studying Abroad of PLA, No. 98H038; the Youth Science and Technique Foundation of PLA during the 10th Five-year plan period, No. 01Q138; and the Science & Technique Foundation of PLA during the 10th Five-year plan period, No. 01MB135

Correspondence to: Dr. Gui-Qin Bai, Department of Obstetrics and Gynecology of First Hospital, Xi'an Jiaotong University, Jiankang Road 1, Xi'an 710061, Shaanxi Province, China

Telephone: +86-29-85213194 Fax: +86-29-85252812

Received: 2004-11-08 Accepted: 2004-12-26

Abstract

AIM: To investigate the biological function of complete S protein and to look for proteins interacting with complete S protein in hepatocytes.

METHODS: We constructed bait plasmid expressing complete S protein of HBV by cloning the gene of complete S protein into pGBKT7, then the recombinant plasmid DNA was transformed into yeast AH109 (a type). The transformed yeast AH109 was mated with yeast Y187 (α type) containing liver cDNA library plasmid in 2×YPDA medium. Diploid yeast was plated on synthetic dropout nutrient medium (SD/-Trp-Leu-His-Ade) containing X- α -gal for selection and screening. After extracting and sequencing of plasmids from positive (blue) colonies, we underwent sequence analysis by bioinformatics.

RESULTS: Nineteen colonies were selected and sequenced. Among them, five colonies were *Homo sapiens* solute carrier family 25, member 23 (SLC25A23), one was *Homo sapiens* calreticulin, one was human serum albumin (ALB) gene, one was *Homo sapiens* metallothionein 2A, two were *Homo sapiens* betaine-homocysteine methyltransferase, three were *Homo sapiens* Na⁺ and H⁺ coupled amino acid transport system N, one was *Homo sapiens* CD81 antigen (target of anti-proliferative antibody 1) (CD81), three were *Homo sapiens* diazepam binding inhibitor, two colonies were new genes with unknown function.

CONCLUSION: The yeast-two hybrid system is an effective method for identifying hepatocyte proteins interacting with complete S protein of HBV. The complete

S protein may bind to different proteins i.e., its multiple functions *in vivo*.

© 2005 The WJG Press and Elsevier Inc. All rights reserved.

Key words: Complete S protein; Yeast-two hybrid system; Hepatitis B virus

Bai GQ, Cheng J, Zhang SL, Huang YP, Wang L, Liu Y, Lin SM. Screening of hepatocyte proteins binding to complete S protein of hepatitis B virus by yeast-two hybrid system. *World J Gastroenterol* 2005; 11(25): 3899-3904
<http://www.wjgnet.com/1007-9327/11/3899.asp>

INTRODUCTION

Hepatitis B virus (HBV) causes acute and chronic infections of the liver. Acute infections may produce serious diseases, and approximately 0.5% of the diseases will develop into fatal, fulminant hepatitis. Chronic infections may also have remarkable consequences^[1]. Thus HBV is considered to be a major etiological factor in the development of human hepatocellular carcinoma (HCC), one of the most frequent fatal malignancies worldwide, and worldwide deaths of HCC exceed one million per year^[2-7]. Epidemiological studies have demonstrated an approximately 10-fold increase in the relative risk of HCC among HBV carriers compared to non-carrier.

The precise role of HBV in the etiology of HCC is not well understood. Only occasionally, genes controlling cell growth and differentiation are disturbed by integration of HBV DNA sequences. An alternative mechanism of chronic infections and hepatocarcinogenesis may be the key steps to mutual interaction between viral proteins and hepatocellular proteins, this action may mediate virus to enter into the liver cells and affect the activities and function of these proteins. Moreover, the protein from hepatocytes infected with HBV inversely disturbs virus replication and reduces immunity of the host, resulting in chronic liver diseases and HCC. Elucidating this interaction between these proteins may help to bring some new clues for discovering the pathogenesis of viral hepatitis.

The first full length nucleotide sequence of HBV was published in 1979. Its length is 3 182 nt, and the serum type is ayw. The four open read frames (ORF) defined in HBV genome at that time, are named as the regions of S, C, P and X. The region of S is divided into the sub-regions of pre-S1, pre-S2 and S according to different initial code ATG in frame. Dong *et al.*^[8], have shown that there is an

open read frame (ORF) before pre-S1 region in the genome of HBV, amplified from serum of patients infected with HBV by long and accurate polymerase chain reaction (LA-PCR). This region is 135 bp, and named temporarily as pre-pre-S and its promoter activities have been confirmed in 277 bp upstream nucleotide sequences before pre-S1 gene^[9]. Pre-pre-S, pre-S1, pre-S2 and S genes are translated in frame according to the same ORF, complete S of HBV, including pre-pre-S, pre-S1, pre-S2 and S regions.

The function of the complete S protein in the life cycle of HBV remains unknown. To investigate the biological importance of the complete S protein, we screened and identified the proteins interacting with HBV complete S protein by yeast-two hybrid system to elucidate the biological functions of complete S protein of HBV genome.

MATERIALS AND METHODS

Bacterials, yeast strains and plasmids

All yeast strains and plasmids for yeast-two hybrid experiments were obtained from Clontech Co. (Palo Alto, CA, USA) as components of the MATCHMAKER two hybrid system 3. Yeast strain AH109 (MATa, *trp1-901*, *leu2-3,112*, *ura3-52*, *bis3-200*, *gal4*Δ, *gal80*Δ, *LYS2: GAL1_{UAS}-GAL1_{TATA}-HIS3*, *GAL2_{UAS}-GAL2_{TATA}-ADE2*, *URA3: MEL1_{UAS}-MEL1_{TATA}-LacZ*) containing pGBKT7-53, coding for DNA-BD/mouse p53 fusing protein was used for cloning of bait plasmid. Yeast strain Y187 (MATa *ura3-52*, *bis3-200*, *Ade2-101*, *trp1-901*, *leu2-3, 112*, *gal4*Δ, *gal80*Δ, *met-*, *URA3: GAL1_{UAS}-GAL1_{TATA}-lacZ MEL1*) containing pTD1-1, coding for AD/SV40 large T antigen fusing protein was used for cloning of library plasmids. Pre-transformed human cDNA liver cell library Y187 and bacterial strain DH5a were used for cloning of shuttle plasmids. Yeast-*Escherichia coli* shuttle plasmids, pGBKT7 DNA-BD cloning plasmid, pGADT7 AD cloning plasmid, pGBKT7-53 control plasmid, pGADT7, pGBKT7-Lam control plasmid, pCL1 plasmid were all from Clontech Co. (K1612-1). pGEM T vector was from Promega Co., USA.

Chemical agents and culture media

Taq DNA polymerase was purchased from MBI Co., T4 DNA ligase, *Eco*RI and *Bam*HI restriction endonuclease were from Takara Co., Japan. Anti-c-myc monoclonal antibody secreted by 1-9E10.2 hybridoma (ATCC) was prepared in our laboratory. Goat anti-mouse IgG conjugated with horseradish peroxidase was from Zhongshan Co., China. Lithium acetate, semi-sulfate adenine, acrylamide and N, N'-bis-acrylamide were from Sigma Co., and TEMED was from Boehringer Mannheim Co. Tryptone and yeast extracts were from OXOID Co. X-α-gal and culture media: YPDA, SD/-Trp SD/-Leu, SD/-Trp/-Leu, SD/-Trp/-Leu/-His, SD/-Trp/-Leu/-His/-Ade were from Clontech Co., protein-G agarose was from Roche Co., and pGEM-T vector was from Promega Co.

RT-PCR kit and TNT[®] coupled reticulocyte lysate systems were from Promega Co. [³⁵S]-methionine (1 000 Ci/mmol, 10 mCi/mL) was from Isotope Company of China. Amplification fluorographic reagent (#NAMP100) was from Amersham Life Sciences Co. Others reagents were from Sigma Co., USA.

Construction of "bait" plasmid and expression of HBV complete S protein

HBV-complete S sequences were generated by PCR amplification using the plasmid G376 A7 (GenBank number: AF384371^[8,10-13]) as template. The sequences of the primers containing the *Eco*RI and *Bam*HI restriction enzyme sites were: sense primer (*Eco*RI): 5'-GAA TTC ATG CAG TTA ATC ATT ACT TCC-3'; antisense primer (*Bam*HI): 5'-GGA TCC TCA AAT GTA TAC CCA AAG AC-3'. The PCR conditions were at 94 °C for 60 s, at 55 °C for 60 s, at 72 °C for 90 s. Ten nanograms of PCR product was cloned with pGEM-T vector. The primary structure of insert was confirmed by direct sequencing. The fragment of encoding complete S was released from the pGEM-T-complete S by digestion with *Eco*RI and *Bam*HI, and ligated to pGBKT7. Vector pGBKT7 expressing proteins were fused with amino acids 1-147 of the GAL4 DNA binding domain (DNA-BD), pGADT7 expressing proteins were fused with amino acids 768-881 of the GAL4 activation domain (AD). Plasmid pGBKT7-complete S (Figure 1) containing full-length HBV complete S gene could express DNA binding domain, c-myc and complete S fusion protein. The plasmid was transformed into yeast strain AH109 by lithium acetate method^[14]. Western blotting was performed to confirm the expression of the fusion protein using anti-c-myc monoclonal antibody. Transformed AH109 (bait) was cultured on quadruple dropout media to exclude the auto-activation activity.

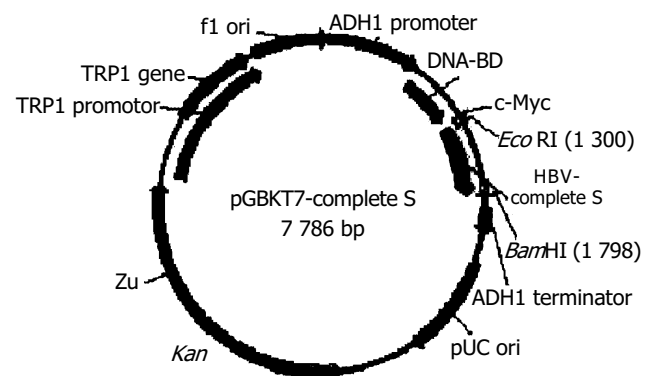


Figure 1 Structure of "bait" plasmid pGBKT7-complete S.

Yeast-two hybrid library screening using yeast mating

One large (2-3 mm), fresh (<2 mo old) colony of AH109 [bait] was inoculated into 50 mL of SD/-Trp and incubated at 30 °C overnight (16-24 h) and shaken at 250-270 r/min. Then the cells were spanned down by centrifuging the entire 50 mL culture at 1 000 r/min for 5 min. After the supernatant was decanted, the cell pellet was resuspended in the residual liquid by vortexing. A human liver cDNA library cloned into pACT2 and yeast reporter strain Y187 (Clontech Co., USA) were co-cultured. The entire AH109 [bait] culture and the 1 mL human liver cDNA library (1×10⁶ cfu/mL) were combined and cultured in a 2-L sterile flask and 45 mL of 2X YPDA/Kan was added and swirled gently. After 20 h of mating, the cells were spanned down and resuspended, and then spread on 50 large (150 mm) plates containing 100 mL of SD/-Ade/-His/-

Leu/-Trp (QDO). After 6-15 d of growth, the yeast colonies were transferred onto the plates containing X- α -gal to check for expression of the MEL1 reporter gene (blue colonies).

Plasmid isolation from yeast and transformation of *E. coli* with yeast plasmid

Approximately 1×10^6 colonies were screened and positive clones were identified. Yeast plasmid was isolated from positive yeast colonies with lysis method (Clontech Co., USA), and transformed into super-competence *E. coli* DH5 α using chemical method. Transformants were plated on ampicillin SOB selection media and grown under selection. Subsequently, pACT2-cDNA constructs were re-isolated, analyzed by restriction digestion and sequencing.

Bioinformatic analysis

After the positive colonies were sequenced, the sequences were blasted with GenBank to analyze the function of the genes (<http://www.ncbi.nlm.nih.gov/blast>).

Cell culture and new gene cloning

Hepatoblastoma cell line HepG2 was propagated in DMEM supplemented with 10% FBS, 200 μ mol/L L-glutamine, penicillin, and streptomycin. HepG2 cells were plated at a density of 1×10^6 /well in 35-mm dishes. Total cellular RNA was isolated using TRIzol (Invitrogen Co., USA) according to the manufacturer's instructions. cDNAs were reverse-transcribed from total RNA.

On the basis of liver cDNA library of genes of proteins interacting with HBV-complete S protein, the coding sequence of a new gene without known function, HBV CSBP1, was obtained by bioinformatics methods. The standard PCR cloning technique was used to amplify HBV CSBP1 gene. Total cell RNA was isolated from HepG2 cells. RNA was used for RT-PCR amplification. The PCR conditions were: 94 °C for 60 s, 58 °C for 60 s, and 72 °C for 60 s, for 35 cycles. The PCR product was cloned with pGEM-T vector (Promega Co., USA). The primary structure of insert was confirmed by direct sequencing. The gene fragment was cloned into yeast plasmids pGBKT7 and pGADT7.

Confirmation of the true interaction in yeast

To confirm the true protein-protein interaction and exclude false positives, the plasmids of positive colonies were transformed into yeast strain Y187, and then mating experiments were carried out by mating with yeast strain AH109 containing pGBKT7-complete S or pGBKT7-Lam. After mating, the diploids yeast was plated on SD/-Ade-His-Leu-Trp (QDO) covered with X- α -gal to test the specificity of interactions.

In vitro translation

Twenty-five microliter mixture of TNT[®] reticulocytes, 2 μ L TNT[®] reaction buffer, 1 μ L T7 TNT[®] RNA polymerase, 1 μ L amino acids mixture (minus methionine, 1 mol/L), 1 μ L [³⁵S]-methionine 2 μ L, RNasin RNase inhibitor (40 u/mL), 2 μ L DNA template (pGBKT7-complete S or pGADT7-library gene) (0.5 μ g/mL), 16 μ L ddH₂O, were incubated at 30 °C for 90 min.

Coimmunoprecipitation

The following reactants were combined in a 1.5 mL microce-

ntrifugation tube on ice: 5 μ L *in vitro*-translated bait protein, 5 μ L *in vitro*-translated library protein. The only control added was 10 μ L pGBKT7-complete S plasmid. The mixtures were incubated at 30 °C for 1 h. Then, the following reagents were added into the reaction tubes: 470 μ L coimmunoprecipitation buffer (20 mol/L Tris-HCl (pH 7.5), 150 mol/L NaCl, 1 mol/L DTT, 5 μ g/mL aprotinin, 0.5 mol/L PMSF, 0.1 % Tween 20, 10 μ L protein-G agarose beads, 10 μ L anti-c-myc monoclonal antibody. Incubation was done at 4 °C for 2 h with continuous shaking. The tubes were centrifuged at 14 000 *g* for 1-2 min. The supernatants were removed. Half a milliliter of TBST was added into the tubes. Rinse steps were repeated thrice. Fifteen microliters of SDS-loading buffer was added. The samples were heated at 80 °C for 5 min. The tubes were placed on ice and then briefly centrifuged, and 10 μ L was loaded onto a SDS-PAGE mini-gel to begin the electrophoretic separation. After electrophoresis, the gel was transferred onto a tray containing gel fixation solution, and placed on a rotary shaker for 10 min at room temperature. The gel was rinsed with H₂O, then amplification fluorographic reagent was added and shaken for 20 min at room temperature, then dried at 80 °C under constant vacuum. The gel was exposed to an X-ray film overnight at room temperature. The film was developed by standard techniques.

RESULTS

Identification of recombinant plasmid

The full length sequences of HBV complete S were generated by PCR amplification of the plasmid G376 A7 (GenBank number: AF384371)^[1,10-13], and a 942-bp fragment of HBV CSBP1 was amplified by RT-PCR after total RNA was prepared from HepG2 cells, sequenced and analyzed by comparing Vector NTI 6 and BLAST database homology search (<http://www.ncbi.nlm.nih.gov/blast>). After being cut by *EcoRI/BamHI*, the fragments were in-frame ligated, respectively into pGBKT7 and pGADT7 at the *EcoRI/BamHI* sites. Restriction enzyme analysis of pGBKT7-complete S, pGBKT7-CSBP1 and pGADT7-CSBP1 plasmids with *EcoRI/BamHI* yielded respectively two bands: 7 300 bp empty pGBKT7 and 1 338 bp HBV complete S, 7 300 bp empty pGBKT7 and 942 bp of HBV CSBP1, 7 900 bp empty pGADT7 and 942 bp HBV CSBP1. The products of plasmid were amplified by PCR. Analysis of the PCR amplified products by agarose gel electrophoresis showed the clear bands with the expected size (1 338 bp of complete S, 942 bp of CSBP1). Sequences of the PCR products were correct (Figures 2A-D).

Expression of "bait" fusion protein

Yeast strain AH109 transformed with pGBKT7-complete S and pGBKT7-CSBP1 could stably express the fusion protein at high level (Figure 3) and could only grow on SD/-Trp medium but not on QDO medium. Thus, the transformed yeast could be used for yeast hybrid analysis.

Screening of liver cell cDNA library

We isolated plasmids from the blue colonies containing only pGBKT7-complete S and one library plasmid other than other plasmids. Because plasmid pACT2-cDNA contains

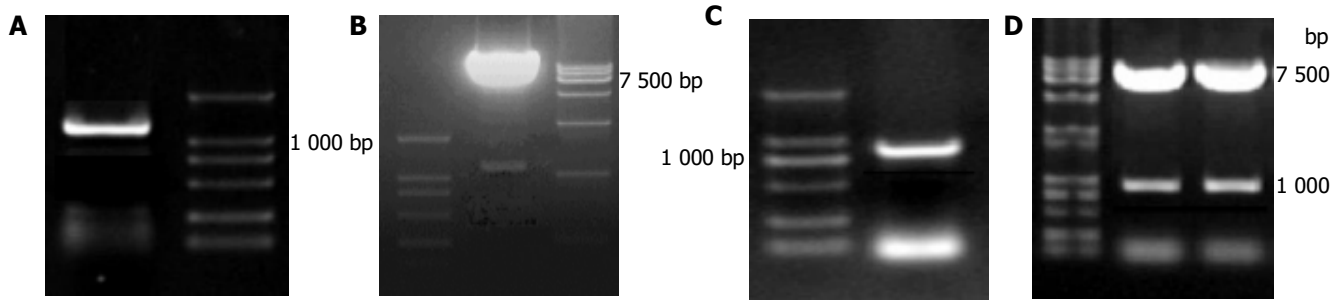


Figure 2 One thousand three hundred and thirty eight basepair fragment-complete S amplified by RT-PCR (A), pGBKT7-complete S cut by *EcoRI*

BamHI (B), a 945 bp fragment-CSBP1 amplified by RT-PCR (C), pGBKT7-CSBP1 and pGADT7-CSBP1 cut by *EcoRI*/*BamHI* (D).

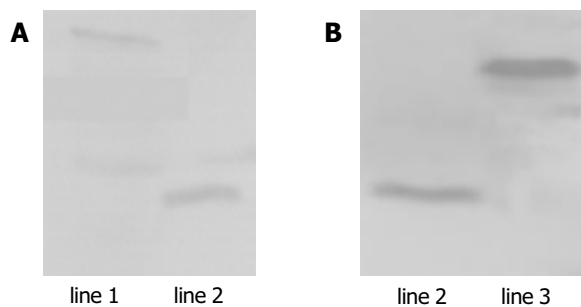


Figure 3 Expression of HBV complete S and HBV CSBP1 protein in yeast confirmed by Western blotting. Lane 1: HBV complete S protein; lane 2: positive control; lane 3: HBV CSBP1 protein.

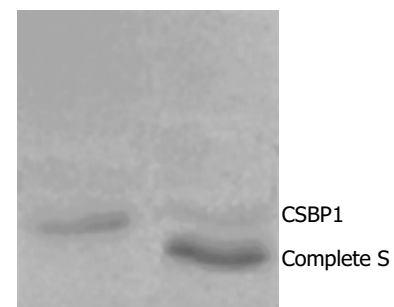


Figure 5 Interaction between HBV complete S protein and CSBP1 protein identified by coimmunoprecipitation. Lane 1: HBV complete S protein; lane 2: interaction with two proteins.

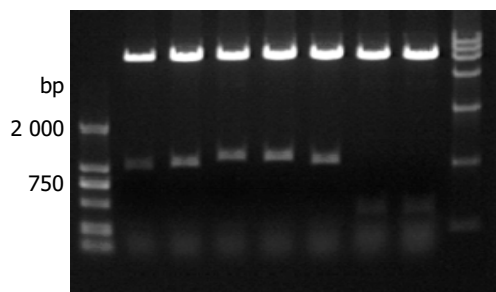


Figure 4 Identification of different colonies with *BglII* digestion.

two restriction endonuclease sites of *BglII* on both sides of multiple cloning sites, the gene fragments of the liver cell cDNA library (pACT2-cDNA) screened were released by *BglII* digestion (Figure 4). The gene fragments of different lengths in Figure 5 proved that these screened clones were positive colonies growing on SD/-Trp/-Leu/-His/-Ade culture medium after mating.

Analysis of cDNA sequencing and homology

We obtained a total of 19 positive colonies growing on the selective SD/-trp-leu-his-ade/ α -gal medium. These colonies were prescreened by *BglII* digestion to make sure that only colonies with different inserts were subjected to sequencing. Nineteen colonies from cDNA library were sequenced. Using the BLAST program at the National Center for Biotechnology Information, 17 sequences had a high similarity to known genes. The data are presented in Table 1.

Table 1 Comparison between positive clones and similar sequences in GenBank

High similarity to known genes	Number of similar (%)	Homology (%)
<i>Homo sapiens</i> calreticulin	1	99
<i>Homo sapiens</i> solute carrier family 25, member 23 (SLC25A23)	5	99
Human serum albumin (ALB) gene	1	100
<i>Homo sapiens</i> metallothionein 2A	1	98
<i>Homo sapiens</i> betaine-homocysteine methyltransferase, mRNA	2	98
<i>Homo sapiens</i> diazepam binding inhibitor	3	96
<i>Homo sapiens</i> Na ⁺ and H ⁺ coupled amino acid transport system N	3	100
<i>Homo sapiens</i> CD81 antigen (CD81)	1	100

In vitro coimmunoprecipitation

HBV complete S protein containing 447 aa, was smaller than CSBP1 containing 280 aa (Figure 5).

DISCUSSION

The open reading frame of HBV complete S gene consists of four coding regions: pre-pre-S, pre-S1, pre-S2 and S, each starting with an ATG codon in frame. Through in frame translational initiation at each of the four ATG codons, complete S (pre-pre-S+pre-S1+pre-S2+S), large (LHBs; pre-S1+pre-S2+S), middle (MHBs; pre-S2+S) and small (SHBs; S) envelope glycoproteins can be synthesized^[12,13,15-17]. Interactions between viral and hepatocellular proteins play an important role in the pathogenesis of the virus and may mediate virus

to enter into hepatocytes. Their network interactions can change normal biological functions of proteins, influence self-replication of virus, and result in diseases. Yeast-two hybrid system 3 is an effective gene analysis method to analyze the interactions between protein and protein, protein and DNA, protein and RNA in eukaryotic cells and a new genetics technique for studying interactions of proteins in physiologic conditions *in vivo*.

Yeast-two hybrid system 3 is based on the system originally designed by Fields and Song by taking advantage of the properties of the GAL4 protein of the yeast *Saccharomyces cerevisiae*. GAL4-yeast-two hybrid assay uses two expression vectors, one uses GAL4-DNA-binding domain (DBD) and the other uses GAL4-actibating domain (AD). The GAL4-DBD fused to protein 'X' and a GAL4-AD fused to protein 'Y' to form the bait and the target of the interaction trap, respectively. A selection of host cells with different reporter genes and different growth selection markers provides a means to detect and confirm protein-protein interactions and has significantly fewer false positives^[18-21].

In this study, the "bait" plasmid pGBKT7-complete S was transformed into yeast strain AH109. HBV complete S gene was expressed in yeast cells. After the "bait" plasmid pGBKT7-complete S yeast strain AH109s mated with liver cDNA library yeast strain Y187, the diploid yeast cells were plated on QDO media containing X- α -gal, 19 true positives were obtained. By sequencing analysis of isolated library plasmids, we got the sequences of the 17 genes with known functions and two genes with unknown functions, one of them was named as complete S-binding protein 1 (CSBP1). In order to further confirm the interaction between the expressed protein and HBV complete S protein, we performed the experiment of coimmunoprecipitation of both proteins. A strong interaction between HBV complete S protein and CSBP1 protein *in vitro* was observed.

We screened *Homo sapiens* metallothionein 2A (MT) interacting with complete S protein from liver cDNA library. Metallothionein is a low-molecular weight protein with pleiotropic functions and a family member of metal binding proteins. MT is localized in nuclei and/or cytoplasm of tumor cells^[22]. It may be involved in the regulation of carcinogenesis and apoptosis in addition to various physiological processes. Metallothionein is a small stress response protein that can be induced by exposure to heavy metal cations, oxidative stressors, and acute phase cytokines that mediate inflammation^[23]. In humans, there are four groups of MT proteins. MT-2A is highly expressed in epithelial cells of breast cancer, and differentially up-regulated in invasive breast cancer cells^[24]. Jin *et al.*^[25], reported that 26-100% of invasive ductal breast cancers express the MT protein, and are associated with cell proliferation and higher histological grade in invasive ductal breast cancer tissues. Rao *et al.*^[26], thought that the mechanism may be completed through interaction between protein kinase C (PKC) signal transduction and MT 2A. Therefore this protein plays an important role in maintaining transition metal ion homeostasis, redox balance in cells and fundamental cellular processes such as proliferation, apoptosis, and regulation of carcinogenesis^[27,28]. MT 2A is also involved in human prostate homeostasis and carcinogenesis^[29]. MT-2A is expressed in retinal pigment epithelial

(RPE) cells, photoreceptor cells, inner nuclear layer cells and ganglion cells, and can protect cells against oxidative stress and apoptosis^[30].

Another important protein interacting with complete S protein from liver cDNA library is *Homo sapiens* calreticulin. Yoon *et al.*^[31], have analyzed nuclear matrix proteins in 11 hepatocellular carcinomas and compared them with corresponding non-neoplastic liver tissue by two-dimensional gel electrophoresis. Calreticulin is also found in the nuclear matrices of various carcinoma cell lines. The formation and/or expansion of calreticulin-nuclear matrix may be related to the activated cell growth. Le Naour *et al.*^[32], showed that autoantibodies of calreticulin are detectable in patients with HCC (27%), suggesting that a distinct repertoire of autoantibodies is associated with HCC. Therefore it may play a role in early diagnosis of HCC.

HBV complete S protein also interacts with *Homo sapiens* CD81 antigen (CD81). The protein encoded by this gene is a member of the transmembrane four superfamily, also known as the tetraspanin family^[33]. Most of these members are cell-surface proteins characterized by the presence of four hydrophobic domains. CD81, a signal transducing molecule, significantly increases in peripheral blood and more dramatic in the liver of HCV-infected individuals^[34]. Recently, CD81 has been identified as a hepatitis C virus (HCV) receptor of B lymphocytes, the large extracellular loop of CD81 is a determinant combination position for viral entry^[35-39]. These data suggest a functional role for CD81 as a coreceptor for HCV glycoprotein-dependent viral cell entry, providing a mechanism by which B cells are infected with and activated by the virus. It has recently been shown that peripheral B-cell CD81 overexpression is associated with HCV viral load and development of HCV-related autoimmunity. The human CD81 (hCD81) molecule has been identified as a putative receptor in B lymphocytes for hepatitis C virus with murine fibroblast cell line NIH/3T3 model. CD81 chimeras could internalize recombinant E2 protein and E2-enveloped viral particles from serum of HCV-infected patients into Huh7 liver cells. The latter result in persistent positive-strand viral RNA and accumulation of replication, therefore CD81 represents one of the pathways by which HCV can infect hepatocytes. Although CD81 can bind to HCV E2 protein, its role as a receptor for HBV remains controversial. These questions need further study. Whether CD81 could be used as the receptor or co-receptor for hepatocytes, should be studied intensively. CD81 proteins mediate signal transduction events that play a role in the regulation of cell development, activation, growth and motility. This protein appears to promote muscle cell fusion and support myotube maintenance. Also it may be involved in signal transduction. This gene is localized in the tumor-suppressor gene region, thus it is a candidate gene for malignancies.

These interacting proteins screened by yeast-two hybrid are closely correlated with carbohydrate metabolism, immunoregulation, occurrence and development of tumor, and may provide a new study clue for revealing biological functions of HBV complete S protein, pathogenesis of HBV and causes of malignancy conversion. How the interactions between HBV complete S protein and the above-mentioned interacting proteins affect the occurrence and development

of chronic hepatitis B, hepatic fibrosis and hepatocarcinoma, needs to be further studied.

REFERENCES

- 1 **Beasley RP.** Hepatitis B virus. The major etiology of hepatocellular carcinoma. *Cancer* 1988; **61**: 1942-1956
- 2 **Xia X, Cheng J, Yang J, Zhong Y, Wang G, Fang H, Liu Y, Li K, Dong J.** Construction and expression of humanized anti-HBsAg scFv targeting interferon-alpha in *Escherichia coli*. *Zhonghua Ganzangbing Zazhi* 2002; **10**: 28-30
- 3 **Dong J, Cheng J, Wang Q, Huang FJ, Shi S, Zhang G, Hong Y, Li L, Si C.** The study on heterogeneity of hepatitis B virus DNA. *Zhonghua Yiyue Zazhi* 2002; **82**: 81-85
- 4 **Dong J, Cheng J, Wang Q, Wang G, Shi S, Liu Y, Xia X, Li L, Zhang G, Si C.** Quasispecies and variations of hepatitis B virus: core promoter region as an example. *Zhonghua Shiyan He Linchuang Bingduxue Zazhi* 2002; **16**: 264-266
- 5 **Dong J, Cheng J, Wang Q, Shi S, Wang G, Si C.** Cloning and analysis of the genomic DNA sequence of augments of liver regeneration from rat. *Chin Med Sci J* 2002; **17**: 63-67
- 6 **Deng H, Dong J, Cheng J, Huangfu KJ, Shi SS, Hong Y, Ren XM, Li L.** Quasispecies groups in the core promoter region of hepatitis B virus. *Hepatobiliary Pancreat Dis Int* 2002; **1**: 392-396
- 7 **Parkin DM, Pisani P, Ferlay J.** Estimates of the worldwide incidence of 25 major cancers in 1990. *Int J Cancer* 1999; **80**: 827-841
- 8 **Dong J, Cheng J.** Study on definition of pre-pre-S region in hepatitis B virus genome. *Shijie Huaren Xiaohua Zazhi* 2003; **8**: 1091-1096
- 9 **Yang Q, Dong J, Cheng J, Liu Y, Hong Y, Wang JJ, Zhuang SL.** Definition of pre-pre-S promoter sequence from hepatitis B virus genome and identification of its transcription activity. *Jiefangjun Yixue Zazhi* 2003; **9**: 761-762
- 10 **Liu Y, Cheng J, Shao DZ, Wang L, Zhong YW, Dong J, Li K, Li L.** Synergistic transactivating effect of HCV core and HBV X proteins on SV40 early promoter/enhancer. *Zhonghua Shiyan He Linchuang Bingduxue Zazhi* 2003; **17**: 70-72
- 11 **Huangfu J, Dong J, Deng H, Cheng J, Shi S, Hong Y, Ren X, Li L.** A preliminary study on the heterogeneity of preS2 region in hepatitis B virus. *Zhonghua Neike Zazhi* 2002; **41**: 233-236
- 12 **Borchani-Chabchoub I, Mokdad-Gargouri R, Gargouri A.** Glucose dependent [correction of dependant] negative translational control of the heterologous expression of the pre-S2 HBV antigen in yeast. *Gene* 2003; **311**: 165-170
- 13 **Soussan P, Pol S, Garreau F, Brechot C, Kremsdorf D.** Vaccination of chronic hepatitis B virus carriers with pre-S2/S envelope protein is not associated with the emergence of envelope escape mutants. *J Gen Virol* 2001; **82**: 367-371
- 14 **Matsumoto M, Hsieh TY, Zhu N, VanArsdale T, Hwang SB, Jeng KS, Goralbenya AE, Lo SY, Ou JH, Ware CF, Lai MM.** Hepatitis C virus core protein interacts with the cytoplasmic tail of lymphotoxin-beta receptor. *J Virol* 1997; **71**: 1301-1309
- 15 **Park JH, Lee MK, Kim HS, Kim KL, Cho EW.** Targeted destruction of the polymerized human serum albumin binding site within the preS2 region of the HBV surface antigen while retaining full immunogenicity for this epitope. *J Viral Hepat* 2003; **10**: 70-79
- 16 **Borchani-Chabchoub I, Gargouri A, Mokdad-Gargouri R.** Genotyping of Tunisian hepatitis B virus isolates based on the sequencing of preS2 and S regions. *Microbes Infect* 2000; **2**: 607-612
- 17 **Tai PC, Suk FM, Gerlich WH, Neurath AR, Shih C.** Hypermodification and immune escape of an internally deleted middle-envelope (M) protein of frequent and predominant hepatitis B virus variants. *Virology* 2002; **292**: 44-58
- 18 **Fields S, Song O.** A novel genetic system to detect protein-protein interactions. *Nature* 1989; **340**: 245-246
- 19 **Osman A.** Yeast two-hybrid assay for studying protein-protein interactions. *Methods Mol Biol* 2004; **270**: 403-422
- 20 **Gietz RD, Woods RA.** Screening for protein-protein interactions in the yeast two-hybrid system. *Methods MolBiol* 2002; **185**: 471-486
- 21 **Zhen Z.** Progress in proteomics. *Shengwu Gongcheng Xuebao* 2001; **17**: 491-493
- 22 **Yamamura Y, Ohta Y, Iguchi T, Matsuzawa A.** Metallothionein expression and apoptosis in pregnancy-dependent and -independent mouse mammary tumors. *Anticancer Res* 2001; **21**: 1145-1149
- 23 **Canpolat E, Lynes MA.** *In vivo* manipulation of endogenous metallothionein with a monoclonal antibody enhances a T-dependent humoral immune response. *Toxicol Sci* 2001; **62**: 61-70
- 24 **Jin R, Bay BH, Chow VT, Tan PH, Dheen T.** Significance of metallothionein expression in breast myoepithelial cells. *Cell Tissue Res* 2001; **303**: 221-226
- 25 **Jin R, Chow VT, Tan PH, Dheen ST, Duan W, Bay BH.** Metallothionein 2A expression is associated with cell proliferation in breast cancer. *Carcinogenesis* 2002; **23**: 81-86
- 26 **Rao PS, Jaggi M, Smith DJ, Hemstreet GP, Balaji KC.** Metallothionein 2A interacts with the kinase domain of PKCmu in prostate cancer. *Biochem Biophys Res Commun* 2003; **310**: 1032-1038
- 27 **Jin R, Huang J, Tan PH, Bay BH.** Clinicopathological significance of metallothioneins in breast cancer. *Pathol Oncol Res* 2004; **10**: 74-79
- 28 **Tai SK, Tan OJ, Chow VT, Jin R, Jones JL, Tan PH, Jayasurya A, Bay BH.** Differential expression of metallothionein 1 and 2 isoforms in breast cancer lines with different invasive potential: identification of a novel nonsilent metallothionein-1H mutant variant. *Am J Pathol* 2003; **163**: 2009-2019
- 29 **Hasumi M, Suzuki K, Matsui H, Koike H, Ito K, Yamanaka H.** Regulation of metallothionein and zinc transporter expression in human prostate cancer cells and tissues. *Cancer Lett* 2003; **200**: 187-195
- 30 **Lu H, Hunt DM, Ganti R, Davis A, Dutt K, Alam J, Hunt RC.** Metallothionein protects retinal pigment epithelial cells against apoptosis and oxidative stress. *Exp Eye Res* 2002; **74**: 83-92
- 31 **Yoon GS, Lee H, Jung Y, Yu E, Moon HB, Song K, Lee I.** Nuclear matrix of calreticulin in hepatocellular carcinoma. *Cancer Res* 2000; **60**: 1117-1120
- 32 **Le Naour F, Brichory F, Misek DE, Bréchet C, Hanash SM, Beretta L.** A distinct repertoire of autoantibodies in hepatocellular carcinoma identified by proteomic analysis. *Mol Cell Proteomics* 2004; **1**: 197-203
- 33 **Levy S, Todd SC, Maecker HT.** CD81 (TAPA-1): a molecule involved in signal transduction and cell adhesion in the immune system. *Annu Rev Immunol* 1998; **16**: 89-109
- 34 **Curry MP, Golden-Mason L, Doherty DG, Deignan T, Norris S, Duffy M, Nolan N, Hall W, Hegarty JE, O'Farrelly C.** Expansion of innate CD5pos B cells expressing high levels of CD81 in hepatitis C virus infected liver. *J Hepatol* 2003; **38**: 642-650
- 35 **Van Compernelle SE, Wiznycia AV, Rush JR, Dhanasekaran M, Baures PW, Todd SC.** Small molecule inhibition of hepatitis C virus E2 binding to CD81. *Virology* 2003; **314**: 371-380
- 36 **Cao J, Zhao P, Miao XH, Zhao LJ, Xue LJ, Qi Zt Z.** Phage display selection on whole cells yields a small peptide specific for HCV receptor human CD81. *Cell Res* 2003; **13**: 473-479
- 37 **Cao J, Zhao P, Zhao LJ, Wu SM, Zhu SY, Qi ZT.** Identification and expression of human CD81 gene on murine NIH/3T3 cell membrane. *J Microbiol Methods* 2003; **54**: 81-85
- 38 **Zhang J, Randall G, Higginbottom A, Monk P, Rice CM, McKeating JA.** CD81 is required for hepatitis C virus glycoprotein-mediated viral infection. *J Virol* 2004; **78**: 1448-1455
- 39 **Bartosch B, Vitelli A, Granier C, Goujon C, Dubuisson J, Pascale S, Scarselli E, Cortese R, Nicosia A, Cosset FL.** Cell entry of hepatitis C virus requires a set of co-receptors that include the CD81 tetraspanin and the SR-B1 scavenger receptor. *J Biol Chem* 2003; **278**: 41624-41630

• BRIEF REPORTS •

Prevalence of HFE mutations and relation to serum iron status in patients with chronic hepatitis C and patients with nonalcoholic fatty liver disease in Taiwan

Tsung-Jung Lin, Chih-Lin Lin, Chaur-Shine Wang, Shu-O Liu, Li-Ying Liao

Tsung-Jung Lin, Chih-Lin Lin, Chaur-Shine Wang, Shu-O Liu, Li-Ying Liao, Division of Gastroenterology, Department of Internal Medicine, Taipei Municipal Jen-Ai Hospital, Taipei, Taiwan, China
Correspondence to: Dr. Li-Ying Liao, Division of Gastroenterology, Department of Internal Medicine, Taipei Municipal Jen-Ai Hospital, 5F, No. 52, Lane 240, Guangfu S. Road, Da-an District Taipei City 106, Taiwan, China. ronlin@aptg.net
Telephone: +886-2-27093600 Fax: +886-2-27047859
Received: 2004-08-14 Accepted: 2004-10-05

Abstract

AIM: To assess the prevalence of the two mutations, C282Y and H63D of HFE gene, in healthy subjects, patients with chronic hepatitis C (CHC), and patients with nonalcoholic fatty liver disease (NAFLD) in Taiwan and to explore the contribution of the HFE mutation on serum iron stores in CHC and NAFLD groups.

METHODS: We examined C282Y and H63D mutations of HFE gene in 125 healthy subjects, 29 patients with CHC, and 33 patients with NAFLD. The serum iron markers, including ferritin, iron, and total iron binding capacity (TIBC), were assessed in all patients.

RESULTS: All of the healthy subjects and patients were free from C282Y mutation. The prevalence of H63D heterozygosity was 4/125 (3.20%) in healthy subjects, 2/29 (6.90%) in CHC group, and 1/33 (3.03%) in NAFLD group. The healthy subjects showed no significant difference in the prevalence of H63D mutation as compared with the CHC or NAFLD group. Increased serum iron store was found in 34.48% of CHC patients and 36.36% of NAFLD patients. In three patients of H63D heterozygosity, only one CHC patient had increased serum iron store. There was no significant difference in the prevalence of HFE mutations between patients with increased serum iron store and those without in CHC or NAFLD group.

CONCLUSION: The HFE mutations may not contribute to iron accumulation in the CHC or NAFLD group even when serum iron overload is observed in more than one-third of these patients in Taiwan.

© 2005 The WJG Press and Elsevier Inc. All rights reserved.

Key words: Hereditary hemochromatosis; HFE gene; Serum iron; Chronic hepatitis C; Nonalcoholic fatty liver disease

Lin TJ, Lin CL, Wang CS, Liu SO, Liao LY. Prevalence of HFE

mutations and relation to serum iron status in patients with chronic hepatitis C and patients with nonalcoholic fatty liver disease in Taiwan. *World J Gastroenterol* 2005; 11(25): 3905-3908
<http://www.wjgnet.com/1007-9327/11/3905.asp>

INTRODUCTION

Hereditary hemochromatosis is one of the most common inherited diseases among Caucasians. It occurs with a frequency of 1:200 to 1:400 and a carrier rate approaching 1:10^[1,2]. Hereditary hemochromatosis is an autosomal recessive condition in which excessive iron is absorbed by the intestine. Iron accumulation in many organs causes the clinical manifestations including heart failure, diabetes, and liver cirrhosis. Early diagnosis has been difficult because the tests based on measurement of serum transferrin saturation and serum ferritin concentration not only gave many false positive results but do not always identify patients in the early stage of iron accumulation^[3]. The excessive iron can be removed by venesection^[4]. Although venesection is a simple, effective and safe therapy, much of the organ damage is irreversible when hereditary hemochromatosis is diagnosed. Because the major clinical presentations are often non-specific, appropriate screening tests are important.

The gene responsible for hereditary hemochromatosis was identified and designated as HFE in 1996^[5]. The two recognized recessively-inherited missense mutations of the HFE gene result in amino acid substitutions at position 282 (cysteine to tyrosine, C282Y) and at position 63 (histidine to aspartic acid, H63D). A total of 64-100% patients of Western population with hereditary hemochromatosis were C282Y homozygotes^[6-10]. In individuals of the northern European descent, the frequency of C282Y homozygote was about 0.5%^[11]. The allele frequencies for C282Y mutation and H63D mutation were 5-10% and 6-30%, respectively^[1,2,11]. In Taiwan, a very low frequency of C282Y mutation in the general population (0.33% of carrier rate) was reported^[12]. The C282 heterozygote may have higher serum and hepatic iron levels than controls, but levels are only mildly elevated^[13]. The clinical significance of the H63D mutation still remains undetermined. It seems to be associated with hereditary hemochromatosis only when inherited together with the C282Y mutation (compound C282Y/H63D heterozygote).

Mild to moderate hepatic iron overload is common in patients with chronic hepatitis C (CHC)^[14-16] and in patients with nonalcoholic fatty liver disease (NAFLD)^[17,18]. Iron-induced oxidative stress may play an important role in the

exacerbation of liver cell injury^[19,20]. The HFE mutation may also be associated with elevated markers of iron store in the two disorders. This study was performed to assess the prevalence of the two mutations, C282Y and H63D of HFE gene, in healthy subjects, patients with CHC, and patients with NAFLD in Taiwan. We also checked the serum iron markers and explored the contribution of the HFE mutation on serum iron stores in patients with CHC and patients with NAFLD.

MATERIALS AND METHODS

Healthy subjects and patients

C282Y and H63D mutations of HFE gene were analyzed in 125 healthy subjects, 29 patients with CHC, and 33 patients with NAFLD. Local healthy subjects with normal liver function test, no history of liver disease, other severe chronic disease, heavy drinking (ethanol consumption >20 g/d), anemia or iron overload were collected from the health checkup at our hospital in 2003. The patients with CHC or NAFLD were collected at our out-patient department from 2002 to 2003. CHC was diagnosed by biochemical liver damage for more than 6 mo and positivity of serum antibody to hepatitis C virus (HCV). Patients with secondary causes of iron overload were excluded, including heavy drinking, ribavirin therapy, and multiple transfusions. Co-infection with HBV was also excluded. The diagnosis of NAFLD was made on the basis of the presence of elevated serum AST or ALT and fatty change of liver by sonography. No subject consumed alcohol more than 20 g/d. They were negative for hepatitis B surface antigen and HCV antibody. Their serum levels of ceruloplasmin were within normal range. Serological tests for autoimmune hepatitis (anti-nuclear antibody, anti-smooth muscle antibody) and for primary biliary cirrhosis (anti-mitochondrial antibody) were negative.

Serological evaluation

The serum aspartate aminotransferase (AST) and alanine aminotransferase (ALT) were determined using an Olympus 5000 analyzer. The upper limit of normal for ALT is 34 U/L. HCV antibody was tested by a commercially available ELISA (AxSYM, Abbott Diagnostic Corporation, USA). Total iron status of each patient was evaluated using biochemical tests. Serum iron (normal range, 60-160 µg/dL) was measured by the colorimetry and ferritin (normal range: 18-274 ng/mL

in men and 6-283 ng/mL in women) was measured by a commercially available ELISA (AxSYM, Abbott Diagnostic Corporation). Transferrin saturation was calculated as (the serum iron divided by the total iron binding capacity (TIBC)) ×100%. The increased serum iron store was defined by transferrin saturation >50% and/or ferritin >upper normal limit.

Mutational analysis of HFE gene

We used the method of polymerase chain reaction-restriction fragment length polymorphism (PCR-RFLP) to analyze the HFE mutations. Genomic DNA was isolated from whole peripheral blood using the High Pure Viral Nuclear Kit (Roche Diagnosis Corporation, USA). The DNA fragments of HFE gene were amplified by PCR using the following primers^[5]: 5'-TGGCAAGGGTAAACAGATCC and 5'-CTCAGGCACTCCTCTCAACC for C282Y; and 5'-ACATGGTTAAGGCCTGTTGC and 5'-GCCACATCTGGCTTGAATT for H63D. Restriction fragment length analysis was then performed by digesting the PCR products with *RsaI* for C282Y and *BclI* for H63D^[21].

Statistical analysis

Data are summarized as mean±SD. Categorical variables were compared with the χ^2 test or Fisher's exact test as required. Comparison between groups was performed using the unpaired *t*-test as appropriate.

RESULTS

The demographic and laboratory data of subjects are summarized in Table 1. CHC patients were older than healthy subjects (60.83±8.55 years *vs* 44.62±11.19 years, *P*<0.01) and NAFLD patients were not (49.48±14.58 years *vs* 44.62±11.19 years, *P* = 0.082). There was no significant difference in the male to female ratio between healthy subjects (44/81) and CHC (12/17) or NAFLD (16/17) group.

All of the healthy subjects and patients were free from C282Y mutation. Four healthy subjects (one man and three women) were heterozygotes of H63D, two CHC patients (one man and one woman) and one NAFLD patient (woman) were heterozygotes of H63D. The prevalence of H63D mutation was 4/125 (3.20%) in healthy subjects, 2/29 (6.90%) in CHC group, and 1/33 (3.03%) in NAFLD

Table 1 Demographic and laboratory data of healthy subjects, CHC and NAFLD (mean±SD)

	Reference range	Healthy subjects	Chronic hepatitis C	<i>P</i>	NAFLD	<i>P</i>
Age (yr)		44.62±11.19	60.83±8.55	<0.01	49.48±14.58	0.082
Sex (male:female)		44:81	12:17	0.533	16:17	0.162
AST (IU/L)	10-34		97.17±52.62		74.68±42.09	
ALT (IU/L)	7-33		114.28±61.87		108.52±65.07	
Iron (µg/dL)	60-160		146.39±48.19		108.73±31.06	
TIBC (µg/dL)	250-410		377.93±41.10		361.57±42.73	
Transferrin saturation (%)	20-50		39.01±13.20		30.53±9.80	
Ferritin (ng/mL)	Male: 18-294 Female: 6-283		225.95±178.24		331.20±283.82	
Increased serum iron store (%)			10/29 (34.48)		12/33 (36.36)	

CHC, chronic hepatitis C; NAFLD, nonalcoholic fatty liver disease. *P* value: comparing data obtained from healthy subjects with chronic hepatitis C or NAFLD. The increased serum iron store was defined by transferrin saturation >50% and/or ferritin >upper normal limit.

group. The healthy subjects showed no significant difference in the prevalence of H63D mutation as compared with the CHC or NAFLD group (Table 2).

Table 2 Statistical analysis of H63D mutation between healthy subjects and CHC, and healthy subjects and NAFLD

	Male	Female	Total
Healthy subjects:CHC	1/44:1/12	3/81:1/17	4/125:2/29
<i>P</i>	0.386	0.539	0.315
Healthy subjects:NAFLD	1/44:0/16	3/81:1/17	4/125:1/33
<i>P</i>	0.999	0.539	0.999

CHC, chronic hepatitis C; NAFLD, nonalcoholic fatty liver disease.

Ten CHC patients (4 men and 6 women) and 12 NAFLD patients (8 men and 4 women) had increased serum iron stores. The percentage was 34.48% and 36.36% in CHC and NAFLD patients, respectively. There was no gender-related difference in the frequency of increased serum iron stores in either the CHC or NAFLD group (Table 3). In the three patients of H63D heterozygosity, only one CHC patient had increased serum iron store. There was no significant difference in the prevalence of HFE mutations between patients with increased serum iron store and those without in the CHC or NAFLD group (Table 4).

Table 3 Statistical analysis of increased serum iron stores between male and female patients with CHC or NAFLD

	CHC	NAFLD
Male:female	4/12:6/17	8/16:4/17
<i>P</i>	0.913	0.114

CHC, chronic hepatitis C; NAFLD, nonalcoholic fatty liver disease.

Table 4 Statistical analysis of HFE mutation between patients with increased serum iron store and those without in CHC or NAFLD group

Increased serum iron store	CHC	NAFLD
With:without	1/10:1/19	0/12:1/21
<i>P</i>	0.999	0.999

CHC, chronic hepatitis C; NAFLD, nonalcoholic fatty liver disease.

DISCUSSION

A population study of global prevalence in HFE mutation showed that there were nine H63D heterozygotes in one Asian population of 242 cases and no other HFE genotypes were found^[1]. The H63D allele frequency was 1.9% (9/484). Similar results were reported in a Japanese population^[22]. All of the 151 healthy volunteers were free from C282Y mutation and only 8 subjects were H63D heterozygotes. The prevalence of chromosomes with H63D was 2.6% (8/302). We firstly found no C282Y mutation and an incidence of 1.6% (4/250) for H63D allele in 125 healthy subjects in Taiwan. The results were similar to that in other Asian area. No mutations of C282Y were found probably because of the limited number of subjects studied. The very low frequency

of HFE mutation in the Asians, especially C282Y, reflects the ethnic differences in the prevalence of hereditary hemochromatosis from Caucasians.

Similar prevalence of HFE mutations was found between controls and patients with CHC^[22-25]. Our findings were in lines with these studies. However, the equal distribution of HFE mutations does not allow the conclusion that HFE mutations play no or only a minor role in patients with CHC. It should depend on the contribution of HFE mutations on the iron stores. Either the prevalence of C282Y mutation^[18,26] or combined C282Y and H63D mutations^[27] was increased in nonalcoholic steatohepatitis (NASH) population. Because there was no pathological diagnosis of steatohepatitis in our patients, the patient group in our study is called NAFLD, instead of NASH. Our study showed no significant difference in the frequency of HFE mutations between healthy subjects and NAFLD patients. In another study of NAFLD, the prevalence of the two HFE mutations also was not significantly increased in NAFLD patients and matched those of the general population. These findings gave us a hint that HFE mutation may play a role in the progression of NAFLD.

Elevations in serum iron, ferritin, and transferrin saturation are common in patients with CHC or NASH, as are mild increases in hepatic iron concentration. In CHC, 40-46% of patients had elevated serum iron, ferritin, or transferrin saturation level^[14,15], and 10-36% of patients had increased hepatic iron concentration^[15,16]. In NASH, 58% of patients had elevated serum iron indices and in some cases increased hepatic iron stores^[18]. In our study, we found that 34.48% and 36.36% of patients had increased serum iron stores in CHC and NAFLD group, respectively. Normal or only mildly increased amounts of iron in the liver can be damaging because iron increases oxidative stress^[19,20]. It appears that iron overload may play a role in pathogenesis of some chronic liver diseases, especially when iron is combined with other hepatotoxic factors such as virus, free fatty acid, and alcohol^[17]. In addition to the effect of production of oxidative stress, the iron may enhance the rates of viral replication and mutation as well as cause impairment of the host immunity^[20]. However, the iron can be released from damaged hepatocytes in inflammatory conditions, and it has not been clear whether the iron accumulation is the cause or result of liver injury.

Our data demonstrated no significant difference in the prevalence of HFE mutations between the subgroup of HCV or NAFLD patients with increased serum iron store and the subgroup without. The findings suggested that HFE mutations played no or only a minor role in contribution to serum iron overload in patients with CHC or NAFLD in Taiwan. In addition to the reason of low prevalence of HFE mutations in Taiwan, the fact that only H63D heterozygote was found in our study may explain the results. The H63D heterozygosity usually does not lead to iron overload. Only in conjunction with the heterozygous C282Y mutation (compound C282Y/H63D heterozygote) has the H63D mutation been associated with an increased risk of iron overload^[5].

There were many reports suggesting that the C282Y mutation plays a role in the hepatic iron accumulation and favors the progression of CHC^[23-25]. However, the relationship

between HFE mutations, iron stores, and NASH still remains as a controversial area. Previous studies have found conflicting results. George *et al.*^[18], found that the C282Y mutation was responsible for most of the mild iron overload in NASH and had a significant association with hepatic damage in these patients. Bonkovsky *et al.*^[27], also found that C282Y heterozygotes were more likely to have advanced fibrosis. These authors did not adjust for potential confounders such as age, body mass index, and diabetes. After adjustment for these confounders, Chitturi *et al.*^[26], reported in NASH and Bugianesi *et al.*, reported in NAFLD patients that iron burden and HFE mutations did not contribute significantly to hepatic fibrosis. Therefore, we believe that continued exploration of the link between hepatic iron, HFE mutation, and NAFLD patients is warranted.

In conclusion, HFE mutations are infrequent in Taiwan. The prevalence of HFE mutations associated with hereditary hemochromatosis is not increased in the patients with CHC or NAFLD. The HFE mutations may not contribute to iron accumulation in the CHC or NAFLD group even when serum iron overload is observed in more than one-third of these patients in Taiwan.

REFERENCES

- Merryweather-Clarke AT, Pointon JJ, Shearman JD, Robson KJ. Global prevalence of putative haemochromatosis mutations. *J Med Genet* 1997; **34**: 275-278
- Edwards CQ, Griffen LM, Goldgar D, Drummond C, Skolnick MH, Kushner JP. Prevalence of hemochromatosis among 11,065 presumably healthy blood donors. *N Engl J Med* 1988; **318**: 1355-1362
- Powell LW, Halliday JW, Cowlshaw JL. Relationship between serum ferritin and total body iron stores in idiopathic hemochromatosis. *Gut* 1978; **19**: 538
- Niederau C, Fischer R, Purschel A, Stremmel W, Haussinger D, Strohmeyer G. Long-term survival in patients with hereditary hemochromatosis. *Gastroenterology* 1996; **110**: 1107-1119
- Feder JN, Ginirke A, Thomas W, Tsuchihashi Z, Ruddy DA, Basava A, Dormishian F, Domingo R Jr, Ellis MC, Fullan A, Hinton LM, Jones NL, Kimmel BE, Kronmal GS, Lauer P, Lee VK, Loeb DB, Mapa FA, McClelland E, Meyer NC, Mintier GA, Moeller N, Moore T, Morikang E, Prass CE, Quintana L, Starnes SM, Schatzman RC, Brunke KJ, Drayna DT, Risch NJ, Bacon BR, Wolff RK. A novel MHC class-like gene is mutated in patients with hereditary haemochromatosis. *Nat Genet* 1996; **13**: 399-408
- Jazwinska EC, Cullen LM, Busfield F, Pyper WR, Webb SI, Powell LW, Morris CP, Walsh TP. Haemochromatosis and HLA-H. *Nat Genet* 1996; **14**: 249
- Jouanolle AM, Gandon G, Jezequel P, Blayau M, Campion ML, Yaouanq J, Mosser J, Fergelot P, Chauvel B, Bouric P, Carn G, Andrieux N, Gicquel I, Le Gall JY, David V. Haemochromatosis and HLA-H. *Nat Genet* 1996; **14**: 251
- Consortium UH. A simple genetic test identifies 90% of UK patients with hemochromatosis. *Gut* 1997; **41**: 841-844
- Datz C, Lalloz MR, Vogel W, Graziadei I, Hackl F, Vautier G, Layton DM, Maier-Dobersberger TH, Ferenci P, Penner E, Sandhofer F, Bomford A, Paulweber B. Predominance of the HLA-H Cys282Tyr mutation in Austrian patients with genetic hemochromatosis. *J Hepatol* 1997; **27**: 773-779
- Piperno A, Sampietro M, Pietrangelo A, Arosio C, Lupica L, Montosi G, Vergani A, Fraquelli M, Girelli D, Pasquero P, Roetto A, Gasparini P, Fargion S, Conte D, Camaschella C. Heterogeneity of hemochromatosis in Italy. *Gastroenterology* 1998; **114**: 996-1002
- Olynyk JK, Cullen DJ, Aquilia S, Rossi E, Summerville L, Powell LW. A population-based study of the clinical expression of the hemochromatosis gene. *N Engl J Med* 1999; **341**: 718-724
- Chang JG, Liu TC, Lin SF. Rapid diagnosis of the HLA-H gene Cys 282 Tyr mutation in haemochromatosis by polymerase chain reaction-A very rare mutation in the Chinese population. *Blood* 1997; **89**: 3492
- Bulaj ZI, Griffen LM, Jorde LB, Edwards CQ, Kushner JP. Clinical and biochemical abnormalities in people heterozygous for hemochromatosis. *N Engl J Med* 1996; **335**: 1799-1805
- Di Bisceglie AM, Axiotis CA, Hoofnagle JH, Bacon BR. Measurements of iron status in patients with chronic hepatitis. *Gastroenterology* 1992; **102**: 2108-2113
- Riggio O, Montagnese F, Fiore P, Folino S, Giambartolomei S, Gandin C, Merli M, Quinti I, Violante N, Caroli S, Senofonte O, Capocaccia L. Iron overload in patients with chronic viral hepatitis: how common is it? *Am J Gastroenterol* 1997; **92**: 1298-1301
- Piperno A, D'Alba R, Fargion S, Roffi L, Sampietro M, Parma S, Arosio V, Fare M, Fiorelli G. Liver iron concentration in chronic viral hepatitis: a study of 98 patients. *Eur J Gastroenterol Hepatol* 1995; **7**: 1203-1208
- Bonkovsky HL, Banner BE, Lambrecht RW, Rubin RB. Iron in liver diseases other than hemochromatosis. *Semin Liver Dis* 1996; **16**: 65-82
- George DK, Goldwurm S, MacDonald GA, Cowley LL, Walker NI, Ward PJ, Jazwinska EC, Powell LW. Increased hepatic iron concentration in nonalcoholic steatohepatitis is associated with increased fibrosis. *Gastroenterology* 1998; **114**: 311-318
- Bacon BR, Britton RS. The pathology of hepatic iron overload: a free radical-mediated process? *Hepatology* 1990; **11**: 127-137
- Bonkovsky HL, Banner BF, Rothman AL. Iron and chronic viral hepatitis. *Hepatology* 1997; **25**: 759-768
- Caroline L. A cheaper and more rapid polymerase chain reaction-restriction fragment length polymorphism method for the detection of the HLA-H gene mutations occurring in hereditary hemochromatosis. *Blood* 2007; **90**: 4235
- Shiono Y, Ikeda R, Hayashi H, Wakusawa S, Sanae F, Takikawa T, Imaizumi Y, Yano M, Yoshioka K, Kawanaka M, Yamada G. C282Y and H63D mutations in the HFE gene have no effect on iron overload disorders in Japan. *Internal Medicine* 2001; **40**: 852-856
- Smith BC, Grove J, Guzail MA, Day CP, Daly AK, Burt AD, Bassendine MF. Heterozygosity for hereditary hemochromatosis is associated with more fibrosis in chronic hepatitis C. *Hepatology* 1998; **27**: 1695-1699
- Kazemi-Shirazi L, Datz C, Maier-Dobersberger T, Kaserer K, Hackl F, Polli C, Steindl PE, Penner E, Ferenci P. The relation of iron status and hemochromatosis gene mutations in patients with chronic hepatitis C. *Gastroenterology* 1999; **116**: 127-134
- Erhardt A, Maschner-Olberg A, Mellenthin C, Kappert G, Adams O, Donner A, Willers R, Niederau C, Haussinger D. HFE mutations and chronic hepatitis C: H63D and C282Y heterozygosity are independent risk factors for liver fibrosis and cirrhosis. *J Hepatol* 2003; **3**: 335-342
- Chitturi S, Weltman M, Farrell GC, McDonald D, Liddle C, Samarasinghe D, Lin R, Abeygunasekera S, George J. HFE mutations, hepatic iron, and fibrosis: ethnic-specific association of NASH with C282Y but not with fibrotic severity. *Hepatology* 2002; **36**: 142-149
- Bonkovsky HL, Jawaid Q, Tortorelli K, LeClair P, Cobb J, Lambrecht RW, Banner BF. Non-alcoholic steatohepatitis and iron: increased prevalence of mutations of the HFE gene in the non-alcoholic steatohepatitis. *J Hepatol* 1999; **31**: 421-429

• BRIEF REPORTS •

Polymerase chain reaction: A sensitive method for detecting *Helicobacter pylori* infection in bleeding peptic ulcers

Ching-Chu Lo, Kwok-Hung Lai, Nan-Jing Peng, Gin-Ho Lo, Hui-Hwa Tseng, Chiun-Ku Lin, Chang-Bih Shie, Chao-Ming Wu, Yu-Shan Chen, Wen-Keui Huang, Angela Chen, Ping-I Hsu

Ching-Chu Lo, Kwok-Hung Lai, Gin-Ho Lo, Chiun-Ku Lin, Chang-Bih Shie, Chao-Ming Wu, Yu-Shan Chen, Ping-I Hsu, Division of Gastroenterology, Department of Internal Medicine, Kaohsiung Veterans General Hospital, National Yang-Ming University, Taiwan, China

Nan-Jing Peng, Department of Nuclear Medicine, Kaohsiung Veterans General Hospital, National Yang-Ming University, Taiwan, China

Hui-Hwa Tseng, Department of Pathology, Kaohsiung Veterans General Hospital, National Yang-Ming University, Taiwan, China

Wen-Keui Huang, Division of Infectious Diseases, Department of Internal Medicine, Kaohsiung Veterans General Hospital, National Yang-Ming University, Taiwan, China

Angela Chen, Institute of Biomedical Sciences, National Sun Yat-Sen University, Kaohsiung, Taiwan, China

Supported by the Research Foundation of Kaohsiung Veterans General Hospital, No. VGHKS-91-35 and No. VTY88-G3-2, VGH-NYMU Joint Research Program, Taiwan, China

Correspondence to: Ping-I Hsu, Division of Gastroenterology, Department of Internal Medicine, Kaohsiung Veterans General Hospital, 386, Ta-Chung 1st Road, Kaohsiung, 813, Taiwan, China. williamhsup@yahoo.com.tw

Telephone: +886-7-3422121-2075 Fax: +886-7-3468237

Received: 2004-02-23 Accepted: 2004-04-14

Abstract

AIM: To assess the sensitivity and specificity of polymerase chain reaction (PCR) in detecting *Helicobacter pylori* (*H pylori*) infection in patients with bleeding peptic ulcers, and to compare its diagnostic efficacy with other invasive and non-invasive tests.

METHODS: From April to September 2002, *H pylori* status in 60 patients who consecutively presented with gastroduodenal ulcer bleeding was examined by rapid urease tests (RUT), histology, culture, PCR, serology and urea breath tests (UBT).

RESULTS: The sensitivity of PCR was significantly higher than that of RUT, histology and culture (91% vs 66%, 43% and 37%, respectively; $P = 0.01$, <0.001 , <0.001 , respectively), but similar to that of serology (94%) and UBT (94%). Additionally, PCR exhibited a greater specificity than serology (100% vs 65%, $P < 0.01$). However, the specificity of PCR did not differ from that of other tests. Further analysis revealed significant differences in the sensitivities of RUT, culture, histology and PCR between the patients with and those without blood in the stomach ($P < 0.01$, $P = 0.09$, $P < 0.05$, and $P < 0.05$, respectively).

CONCLUSION: PCR is the most accurate method among the biopsy-based tests to detect *H pylori* infection in patients with bleeding peptic ulcers. Blood may reduce the sensitivities of all biopsy-based tests.

© 2005 The WJG Press and Elsevier Inc. All rights reserved.

Key words: Polymerase chain reaction; *Helicobacter pylori*; Bleeding peptic ulcers

Lo CC, Lai KH, Peng NJ, Lo GH, Tseng HH, Lin CK, Shie CB, Wu CM, Chen YS, Huang WK, Chen A, Hsu PI. Polymerase chain reaction: A sensitive method for detecting *Helicobacter pylori* infection in bleeding peptic ulcers. *World J Gastroenterol* 2005; 11(25): 3909-3914

<http://www.wjgnet.com/1007-9327/11/3909.asp>

INTRODUCTION

Bleeding is a common and serious complication of peptic ulcer diseases. It is estimated that peptic ulcer bleeding accounts for approximately 150 000 hospitalizations per year in the USA^[1,2]. The prevalence of *Helicobacter pylori* (*H pylori*) in bleeding peptic ulcers has not been definitely determined, but it is estimated to be 70%^[3-5]. The accurate diagnosis of *H pylori* infection is crucial in the short-term and long-term management of patients with bleeding peptic ulcers^[6]. If a patient with a bleeding ulcer requires surgical intervention, knowledge of his or her *H pylori* status may guide the selection of procedures for the patient (i.e., a simple closure vs full-blown ulcer surgery)^[6]. Patients whose bleeding episodes cease in the short term, one-third of those who do not receive maintenance therapy, surgery or anti-*H pylori* therapy will experience recurrent bleeding within the next 1-2 years^[7]. However, numerous studies have demonstrated that eradicating *H pylori* can drastically reduce the incidence of rebleeding in patients with bleeding peptic ulcers, preventing the need for long-term antisecretory therapy or surgical intervention^[8-10]. Therefore, the *H pylori* status in a patient with bleeding peptic ulcers must be documented.

Currently, *H pylori* infection can be diagnosed by invasive assays, i.e., those requiring esophagogastroduodenoscopy (EGD), or by non-invasive assays in which EGD is not necessary. Invasive diagnostic tests include culture, histology, rapid urease test (RUT) and polymerase chain reaction (PCR). Non-invasive tests comprise serology, stool antigen test and urea breath test (UBT). The choice of a diagnostic test should depend on the clinical circumstances, sensitivity

and specificity of the tests, and the cost effectiveness of the testing strategy. Because of its simplicity, accuracy and rapid determination of *H pylori* status, RUT is generally considered to be the initial endoscopic test of choice for uncomplicated peptic ulcers^[11]. However, many studies have demonstrated that RUT lacks sensitivity in *H pylori* diagnosis when peptic ulcer diseases are presented with bleeding^[5,12]. Moreover, a recent study by Colin *et al.*^[13], indicated that all direct tests on *H pylori* including RUT, culture and histology reduced the sensitivity in the setting of ulcer bleeding. The sensitivities of aforementioned three tests were 31%, 25% and 26%, respectively.

PCR can diagnose *H pylori* infection under non-bleeding conditions much more accurately than histology or culture^[14,15]. The level of sensitivity of this test is extremely high and has a threshold of 10 to 100 *H pylori* strains per specimen^[14-16]. An accurate diagnosis of *H pylori* at the time of bleeding episode is essential, but few studies have addressed the application of PCR to bleeding ulcers. We performed this prospective study to evaluate the sensitivity, specificity and accuracy of PCR assay for detecting *H pylori* infection in patients with bleeding peptic ulcers and to compare its diagnostic efficacy with that of other invasive and non-invasive tests.

MATERIALS AND METHODS

Patients

From April to September 2002, 60 consecutive patients with hematemesis, melena, or both due to gastroduodenal ulcer bleeding, who underwent an EGD, were enrolled in this study. Exclusion criteria included: age <15 or >80 years; history of coagulopathy or other disorders contraindicated for EGD or biopsy sampling; previous history of anti-*H pylori* therapy. Data regarding age, sex, medical history, drug history, presenting symptoms, gastroduodenal lesions and presence or absence of blood in the stomach were recorded. Written informed consent was obtained from each subject. This study was approved by the Human Medical Research Committee of the Kaohsiung Veterans General Hospital, Kaohsiung, Taiwan.

Endoscopy and biopsy sampling

During endoscopy, gastric biopsy specimens were taken from the lesser curvature of the antrum and corpus for RUT (one antrum biopsy specimen), histology (one antrum and one corpus biopsy specimen), culture (one antrum biopsy specimen) and PCR (one antrum biopsy specimen). Endoscopes were cleaned by a mechanical wash and then washed in an Olympus washing machine. They were then air-dried and cleaned with 70% ethanol.

RUT

RUT was performed according to our previous study^[17,18]. A biopsy specimen from antrum was immediately placed in 1 mL of a 10% solution of urea in deionized water (pH 6.8) to which two drops of 1% phenol red solution was added and incubated at 37 °C for up to 24 h. If the yellowish color around the area of inserted specimen changed to bright pink within the 24-h limit, the urease test was considered

positive. In our laboratory, the sensitivity and specificity of RUT were 96% and 91%, respectively^[17].

Histological examination

Biopsy specimens were fixed in 10% buffered formalin, embedded in paraffin, and sectioned. One 4- μ m-thick section was cut and stained with hematoxylin-eosin to observe the presence of curved rod shaped bacteria on the mucosal surface^[19,20]. The specimens were interpreted by a histopathologist (H-H Tseng) blinded to the patient status and the results of other laboratory tests.

Culture

The specimen for culture was transferred with brain heart infusion on ice for microbiological examination and inoculated onto the CDC anaerobic blood agar (Becton Dickinson Microbiology System, Cockeysville, MD) according to our previous studies^[21,22]. The agar was incubated at 35 °C for two days in a micro-aerophilic gas mixture containing 5% O₂, 100 mL/L CO₂, and 85% N₂. Culture-positive patients were those with bacterial colonies grown in culture within 7 d. The organisms were identified as *H pylori* by Gram staining, colony morphology and positive oxidase, catalase and urease reaction.

PCR amplification

DNA extraction was performed using a commercially available kit (QIAamp Tissue kit, QIAGEN Inc., Valencia, CA) according to the manufacturer's instructions^[23]. The primers used were derived from the internal 411-bp fragment of the *urease A* gene as described by Clayton *et al.*^[24]: HPU1 (5'GCCAATGGTAAATTAGTT3') and HPU2 (5'CTCCT-TAATTGTTTTTAC3'). Reactions were performed in a 25 μ L volume in a thermal cycler 480 (Perkin Elmer Applied Biosystems, Foster City, CA). A reaction mixture contained 2.5 μ L of extracted DNA, 0.5 μ mol/L of each primer, 2.5 mmol/L of MgCl₂, 2.5 μ L of 10 \times PCR buffer, 1 U of *AmpliTag* DNA polymerase (Perkin-Elmer Corp., Foster City, CA) and 100 μ mol/L of each of dATP, dCTP, dGTP and dTTP. The amplification cycle consisted of an initial denaturation at 94 °C for 1 min, primer annealing at 45 °C for 1 min, and extension for 5 min at 72 °C to ensure a full extension of the products. Samples were amplified in 35 consecutive cycles. The final cycle included a 7-min extension step to ensure a full extension of the PCR products. PCR products were analyzed on a 2% agarose electrophoresis gel stained with ethidium bromide.

UBT

UBT was performed according to our previous studies^[21,25] within 1 d of EGD. The patients were fasted for at least 6 h. Fresh milk (1 000 mL) was taken to delay gastric emptying. The test consisted of a baseline breath sample and a second breath sample collected 15 min after oral administration of 100 mg of ¹³C-labeled urea (INER-Hp C-tester, Taiwan) dissolved in 50 mL sterile water. Values were expressed as an excess $\delta^{13}\text{CO}_2\text{‰}$ excretion. The $\delta^{13}\text{CO}_2$ was the ratio of ¹³C to ¹²C in the sample compared to the Pee Dee Belemnite (PDB) standard. The equation was given as: $\delta^{13}\text{CO}_2 = (R_{\text{samp}} - R_{\text{std}}) / R_{\text{std}} \times 1\,000$. R_{samp} and R_{std}

represented the ratio of ^{13}C to ^{12}C in samples and standard, respectively. If the value of $\delta^{13}\text{CO}_2$ was more than 4.8‰, this was considered as a positive result.

Serology

Blood samples for serological evaluation were obtained before EGD. A serological assay for IgG antibodies against *H pylori* was performed by an indirect solid-phase immunochromatographic assay using the ASSURE™ *H pylori* rapid test kit (Genelabs Diagnostics, Cavendish Singapore Science Park, Singapore). The sensitivity and specificity of the assay were 96% and 92%, respectively according to the manufacturer's instructions.

Gold standard definition

A patient was classified as being *H pylori*-positive on the basis of either a positive culture or a negative culture, at least three positive results of RUT, histology, UBT and serological tests.

Statistical analysis

Statistical tests were performed using the SPSS system. Sensitivity, specificity, accuracy, predictive values of positive and negative results were calculated in accordance with standard methods. χ^2 test and 95%CI were used to compare the sensitivity, specificity and accuracy of different diagnostic methods. Two-sample *t*-tests were used to compare the excess $\delta^{13}\text{CO}_2$ values of UBT between the true-positive and false-negative groups of various invasive tests. $P < 0.05$ was considered statistically significant.

RESULTS

Of the 60 patients initially enrolled in this study, five did not complete all the tests and were excluded from the statistical analysis. Table 1 presents the demographic data of the remaining 55 patients (37 males, 18 females; mean age: 62.2 ± 14.5 years) who finished all of the invasive and non-invasive assays. EGD of these subjects showed a gastric ulcer in 19 patients (35%), a duodenal ulcer in 13 (24%) and both gastric and duodenal ulcers in 23 (42%). According to the gold standard definition, 35 (63.6%) were *H pylori*-positive and 20 (36.4%) were *H pylori*-negative.

Comparison of various tests for detecting *H pylori* infection in bleeding peptic ulcers

Table 2 presents the sensitivity, specificity and accuracy of various tests in diagnosing *H pylori* infection. The sensitivities

of RUT, histology and culture were low (66%, 43% and 37%, respectively) although these assays exhibited a high specificity (95-100%). Their overall accuracies were 76%, 62% and 60%, respectively. Among the four biopsy-based methods, only PCR exhibited the satisfactory sensitivity (91%), specificity (100%), and accuracy (94%). Its sensitivity and accuracy were significantly higher than those of RUT, histology and culture (sensitivity: $P < 0.05$, $P < 0.001$ and $P < 0.001$, respectively; accuracy: $P < 0.05$, $P < 0.001$, $P < 0.001$, respectively).

Of the non-invasive assays, the serological test had a high sensitivity (95%) but its specificity (65%) was lower than that of PCR ($P < 0.05$). The sensitivity (94%), specificity (85%) and accuracy (91%) of UBT were similar to those of PCR. Among all of the tests investigated herein, PCR and UBT were the most accurate methods for diagnosing *H pylori* infection in patients with bleeding peptic ulcers.

Relationship between intragastric blood and sensitivity of various tests in diagnosis of *H pylori* infection

The patients were divided into two groups according to the presence or absence of blood in the stomach, to investigate the relationships between intragastric blood and sensitivities

Table 1 Baseline characteristics of patients with bleeding peptic ulcers ($n = 55$)

	Number of patients ($n = 55$)
Age (mean \pm SD)	62.2 (14.5)
Sex	
Male	37 (67)
Female	18 (33)
Smoking	13 (24)
Alcohol consumption	4 (7)
Coffee consumption	5 (9)
Ingestion of tea	18 (33)
Ingestion of NSAID ¹	26 (47)
Sites of ulcer	
Stomach	19 (35)
Duodenum	13 (24)
Stomach and duodenum	23 (42)
Ulcer lesions	
Bleeding visible vessel	2 (4)
Non-bleeding visible vessel	3 (6)
Adherent clot	15 (27)
Red or black spot	21 (38)
Clean base	14 (26)

¹NSAID: non-steroidal anti-inflammatory drugs.

Table 2 Sensitivity, specificity, and accuracy of various tests for diagnosis of *H pylori* infection in bleeding peptic ulcers ($n = 55$) [% (95%CI)]

	Sensitivity	Specificity	Accuracy	PPV	NPV
RUT	66 (49–82) ^b	95 (84–100)	76 (64–88) ^b	96 (87–100)	61 (43–79) ^a
Histology	43 (26–60) ^d	95 (84–100)	62 (48–75) ^d	100	48 (31–64) ^b
Culture	37 (20–54) ^d	100	60 (46–73) ^d	100	48 (32–63) ^b
PCR	91 (82–100)	100	95 (88–100)	100	87 (72–100)
Serology	94 (86–100)	65 (42–88) ^b	84 (73–93)	83 (70–95) ^a	87 (67–100)
UBT	94 (86–100)	85 (68–100)	91 (83–98)	92 (82–100)	90 (74–100)

^a $P < 0.05$ vs PCR; ^b $P < 0.01$ vs PCR; ^d $P < 0.001$ vs PCR.

of biopsy-based tests for *H pylori* infection. The sensitivities of RUT, histology, culture, PCR, serology and UBT were 29%, 21%, 21%, 79%, 93% and 100% in the patients with intragastric blood, respectively, and 90%, 57%, 48%, 100%, 95% and 91% in the patients without intragastric blood, respectively. There were statistically significant differences in the sensitivities of RUT, histology and PCR between the patients with and without blood in the stomach (Figure 1; $P < 0.01$, $P < 0.05$ and $P < 0.05$, respectively). Additionally, there was a trend towards decreased sensitivity of culture in the patients with blood in the stomach ($P = 0.09$).

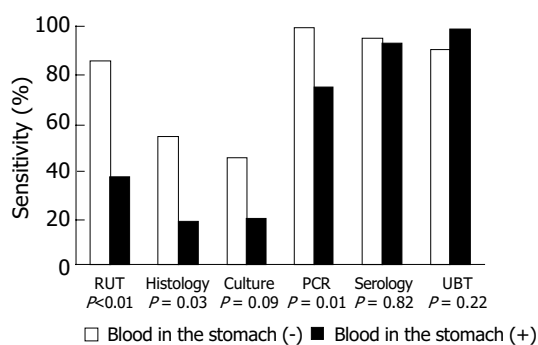


Figure 1 Sensitivities of various tests for detecting *H pylori* infection between the bleeding ulcer patients with and without blood in the stomach.

Comparison of bacterial loads between true-positive and false-negative groups of biopsy-based tests

Since the quantitative data obtained by UBT could reflect the intragastric bacterial load of *H pylori*, we further compared the excess $\delta^{13}\text{CO}_2$ values of UBT between the true-positive and false-negative groups in biopsy-based tests. The excess $\delta^{13}\text{CO}_2$ values of RUT, histology, culture and PCR were 26.7 ± 18.1 , 31.5 ± 21.4 , 33.7 ± 21.8 and 26.3 ± 19.4 in the group with true-positive results respectively, and 20.5 ± 16.3 , 19.5 ± 16.3 , 19.3 ± 15.9 and 7.2 ± 2.6 in the group with false-negative results respectively. The excess $\delta^{13}\text{CO}_2$ values in the false-negative group were significantly lower than that in the true-positive group of culture test (Figure 2; $P = 0.03$). In addition, there was also a trend toward decreased $\delta^{13}\text{CO}_2$ values in the false-negative group of histological examination and PCR assay (both $P = 0.07$).

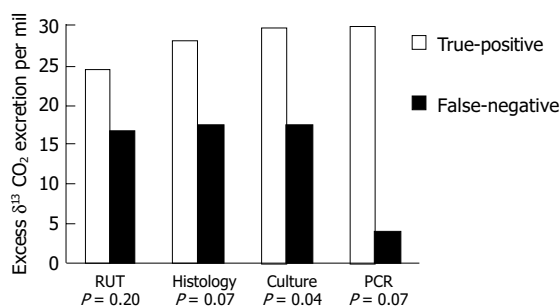


Figure 2 Comparison of the excess $\delta^{13}\text{CO}_2$ values of UBT between the true-positive and false-negative groups in the biopsy-based methods.

DISCUSSION

The *H pylori* status in a patient presenting with a bleeding ulcer must be documented to determine the method of further management. However, many studies have disclosed that biopsy-based tests including RUT, histology and culture have low sensitivities in detecting *H pylori* in bleeding peptic ulcers^[5,12,13]. Additionally, two recent reports^[26,27] also revealed a lack of accuracy in *H pylori* stool antigen (HpSA) tests in patients with ulcer bleeding. In this study, we also demonstrated that the sensitivities of RUT, histology and culture in bleeding peptic ulcer were only 66%, 43% and 37%, respectively. However, PCR could reach a diagnostic sensitivity of 91%, much higher than that of RUT, histology and culture. Additionally, the test had 100% specificity in diagnosing *H pylori* infection under bleeding conditions. This, therefore, is the most accurate biopsy-based method for determining *H pylori* status in bleeding peptic ulcers.

UBT is one of the non-invasive methods for diagnosing *H pylori* infection. Both its sensitivity and specificity are greater than 90% in patients with bleeding peptic ulcers. Its accuracy is comparable to that of PCR. Although the serological test has a high sensitivity in patients with bleeding peptic ulcers, it may not be a good choice for diagnosing *H pylori* infection in patients with a complicated ulcer because antibody tests lack a good specificity (only 65%). The presence of anti-*H pylori* IgG antibody implies prior exposure to the organisms, but does not imply the presence of a current infection. If a patient presenting with ulcer bleeding has a false-positive antibody test and is treated by eradication therapy, the physician may mistakenly believe that the cause of bleeding has been removed and will then not provide further preventive therapy to the patient. In such a case, the patient would have a high risk of recurrent bleeding^[6]. Therefore, establishing the *H pylori* status with certainty at the time of bleeding episode is quite important.

Following this work, we recommend that an endoscopist may initially perform a RUT to detect *H pylori* infection in a patient with bleeding peptic ulcer because of its simplicity, low cost, moderate sensitivity and excellent specificity. If the RUT is negative, either PCR or UBT can be used for the definite diagnosis of *H pylori* status. The choice of the final diagnostic modality may depend on the availability of tests in the hospital. Nonetheless, the aim of PCR is to detect specific DNA sequences rather than the whole viable bacterium. No special requirements pertain to the treatment, transport, or storage of the biopsy specimens for PCR^[28,29]. Several laboratories have reported the successful detection of *H pylori* by PCR from a biopsy specimen placed and transported by mail in the RUT^[16,30,31]. This capability is particularly useful for a gastroenterologist who does not have access to laboratory facilities and requires a confirmation of the RUT^[16].

In this study, the sensitivities of RUT, histology, culture and PCR were found to be 29%, 21%, 21% and 79% in patients with intragastric blood, and 90%, 57%, 48% and 100% in patients without intragastric blood. These data imply that blood may reduce the diagnostic yield of all endoscopic biopsy tests in patients with bleeding peptic ulcers. Additionally, we also demonstrated that the bacterial load in the false-negative group of culture was significantly lower

than that in the true-positive group. Furthermore, there was also a trend toward decreased bacterial load in the false-negative group of histological examination and PCR assay. The decreased bacterial density therefore, may be the major cause for decreased sensitivities of all biopsy-based assays. There are several possible reasons for the aforementioned findings. The decreased bacterial load in bleeding ulcer patients may be related to a direct suppression effect of intraluminal blood on *H pylori*, the administration of antisecretory drugs, or the removal of some *H pylori* from the gastric epithelium or mucus by gastric lavage before EGD^[32]. Recently, Leung *et al.*^[33], reported that a false-negative result of RUT in bleeding ulcer might be caused by the buffered effects of blood. An *in vitro* study^[34] also showed that sheep's blood inhibited the growth of *H pylori* in broth media. The exact reason concerning the association between bleeding ulcer and intragastric bacterial density merits further investigations.

In conclusion, PCR is the most accurate biopsy-based method for determining *H pylori* status in patients with bleeding peptic ulcers. RUT, histology and culture have a poor sensitivity under bleeding conditions. A decline in the intragastric bacterial density during bleeding ulcer may be a major cause of the reduced sensitivity of biopsy-based assays.

ACKNOWLEDGMENTS

The authors express their deep appreciation to Dr. Wei-Lun Tsai, Dr. Wen-Chi Chen, Dr. Lung-Chih Cheng, Dr. Hsien-Chung Yu, Dr. Chung-Jen Wu, Miss Min-Rong Huang and Miss Pei-Min Tsai for their assistance in the clinical follow up of the patients.

REFERENCES

- 1 Kurata JH, Corbo ED. Current peptic ulcer time trends: An epidemiological profile. *J Clin Gastroenterol* 1988; **10**: 259-268
- 2 Vaira D, Menegatti M, Miglioli M. What is the role of *Helicobacter pylori* in complicated ulcer disease? *Gastroenterology* 1997; **113**: S78-84
- 3 Hosking SW, Yung MY, Chung SC, Li AKC. Differing prevalence of *Helicobacter pylori* in bleeding and non-bleeding ulcers. *Gastroenterology* 1992; **102**: A85
- 4 Jensen DM, You S, Pelayo E, Jensen ME. The prevalence of *Helicobacter pylori* and NSAID use in patients with severe UGI hemorrhage and their potential role in recurrence of ulcer bleeding. *Gastroenterology* 1992; **102**: A85
- 5 Lee JM, Breslin NP, Fallon C, O'Morain CA. Rapid urease test lack sensitivity in *Helicobacter pylori* diagnosis when peptic ulcer disease presents with bleeding. *Am J Gastroenterol* 2000; **95**: 1166-1170
- 6 Laine L, Cohen H. *Helicobacter pylori*: drowning in a pool of blood? *Gastrointest Endosc* 1999; **49**: 398-402
- 7 Laine L. *Helicobacter pylori* and complicated ulcer diseases. *Am J Med* 1996; **100**: S52-59
- 8 Rokkas T, Karameris A, Mavrogeorgis A, Rallis E, Giannikos N. Eradication of *Helicobacter pylori* reduces the possibility of rebleeding in peptic ulcer disease. *Gastrointest Endosc* 1995; **41**: 1-4
- 9 Graham DY, Hepps KS, Ramirez FC, Lew GM, Saeed ZA. Treatment of *Helicobacter pylori* reduces the rate of rebleeding in peptic ulcer disease. *Scand J Gastroenterol* 1993; **28**: 939-942
- 10 Labenz J, Borsch G. Role of *Helicobacter pylori* eradication in the prevention of peptic ulcer bleeding relapse. *Digestion* 1994; **55**: 19-23
- 11 Cutler AF, Havstad S, Ma CK, Blaser MJ, Perez-Perez GI, Schubert TT. Accuracy of invasive and noninvasive testes to diagnose *Helicobacter pylori* infection. *Gastroenterology* 1995; **109**: 136-141
- 12 Tu TC, Lee CL, Wu CH, Chen TK, Chan CC, Huang SH, Lee MS. Comparison of invasive and noninvasive tests for detecting *Helicobacter pylori* infection in bleeding peptic ulcers. *Gastrointest Endosc* 1999; **49**: 302-306
- 13 Colin R, Czernichow P, Baty V, Touze I, Brazier F, Bretagne JF, Berkelmans I, Barthelemy P, Hemet J. Low sensitivity of invasive tests for the detection of *Helicobacter pylori* infection in patients with bleeding ulcer. *Gastroenterol Clin Biol* 2000; **24**: 31-35
- 14 Fabre R, Sobhani I, Laurent-Puig P, Hedef N, Yazigi N, Vissuzaine C, Rodde I, Potet F, Mignon M, Etienne JP. Polymerase chain reaction assay for the detection of *Helicobacter pylori* in gastric biopsy specimens: Comparison with culture, rapid urease test, and histopathological tests. *Gut* 1994; **35**: 905-908
- 15 Lin SY, Jeng YS, Wang CK, Ko FT, Lin KY, Wang CS, Lie JD, Chen PH, Chang JG. Polymerase chain reaction diagnosis of *Helicobacter pylori* in gastroduodenal diseases: comparison with culture and histopathological examinations. *J Gastroenterol Hepatol* 1996; **11**: 286-289
- 16 Ho GY, Windsor HM. Accurate diagnosis of *Helicobacter pylori*: polymerase chain reaction tests. *Gastroenterol Clin North Am* 2000; **29**: 903-915
- 17 Hsu PI, Lai KH, Tseng HH, Lin YC, Yen MY, Lin CK, Lo GH, Huang RL, Huang JS, Cheng JS, Huang WK, Ger LP, Chen W, Hsu PN. Correlation of serum immunoglobulin G *Helicobacter pylori* antibody titers with histological and endoscopic findings in patients with dyspepsia. *J Clin Gastroenterol* 1997; **25**: 587-591
- 18 Hsu PI, Lai KH, Chien EJ, Lin CK, Lo GH, Jou HS, Cheng JS, Chan HH, Hsu JH, Ger LP, Hsu PN, Tseng HH. Impact of bacterial eradication on the cell proliferation and p53 protein accumulation in *Helicobacter pylori*-associated gastritis. *Anti-cancer Res* 2000; **20**: 1221-1228
- 19 Dixon MF, Genta RM, Yardley JH, Correa P. Classification and grading of gastritis. The Updated Sydney System. *Am J Surg Pathol* 1996; **20**: 1161-1181
- 20 Hsu PI, Lai KH, Lo GH, Tseng HH, Lo CC, Chen HC, Tsai WL, Jou HS, Peng NJ, Chien CH, Chen JL, Hsu PN. Risk factors for ulcer development in patients with non-ulcer dyspepsia: Prospective two year follow up study of 209 patients. *Gut* 2002; **51**: 15-20
- 21 Peng NJ, Hsu PI, Lee SC, Tseng HH, Huang WK, Tsay DG, Ger LP, Lo GH, Lin CK, Tsai CC, Lai KH. A 15-minute [13C]-urea breath test for the diagnosis of *Helicobacter pylori* infection in patients with non-ulcer dyspepsia. *J Gastroenterol Hepatol* 2000; **15**: 284-289
- 22 Peng NJ, Lai KH, Liu RS, Lee SC, Tsay DG, Lo CC, Tseng HH, Huang WK, Lo GH, Hsu PI. Clinical significance of oral urease in diagnosis of *Helicobacter pylori* infection by [13C] urea breath test. *Dig Dis Sci* 2001; **46**: 1772-1778
- 23 Hsu PI, Hwang IR, Citty D, Lai KH, El-Zimaity HM, Gutierrez O, Kim JG, Osato MS, Graham DY, Yamaoka Y. Clinical presentation in relation to diversity within the *Helicobacter pylori* cag pathogenicity island. *Am J Gastroenterol* 2002; **97**: 2231-2238
- 24 Clayton CL, Kleanthous H, Coates PJ, Morgan DD, Tabaqchali S. Sensitive detection of *Helicobacter pylori* by using polymerase chain reaction. *J Clin Microbiol* 1992; **30**: 192-200
- 25 Peng NJ, Lai KH, Liu RS, Lee SC, Tsay DG, Lo CC, Tseng HH, Huang WK, Lo GH, Hsu PI. Endoscopic 13C-urea breath test for the diagnosis of *Helicobacter pylori* infection. *Dig Liver Dis* 2003; **35**: 73-77
- 26 van Leerdam ME, van der Ende A, ten Kate FJ, Rauws EA, Tytgat GN. Lack of accuracy of the noninvasive *Helicobacter pylori* stool antigen test in patients with gastroduodenal ulcer bleeding. *Am J Gastroenterol* 2003; **98**: 798-801

- 27 **Peitz U**, Leodolter A, Kahl S, Agha-Amiri K, Wex T, Wolle K, Gunther T, Steinbrink B, Malfertheiner P. Antigen stool test for assessment of *Helicobacter pylori* infection in patients with upper gastrointestinal bleeding. *Aliment Pharmacol Ther* 2003; **17**: 1075-1084
- 28 **Ho SA**, Hoyle JA, Lewis FA, Secker AD, Cross D, Mapstone NP, Dixon MF, Wyatt JI, Tompkins DS, Taylor GR. Direct polymerase chain reaction test for detection of *Helicobacter pylori* in humans and animals. *J Clin Microbiol* 1991; **29**: 2543-2549
- 29 **van Zwet AA**, Thijs JC, Kooistra-Smid AM, Schirm J, Snijder JA. Sensitivity of culture compared with that of polymerase chain reaction for detection of *Helicobacter pylori* from antral biopsy samples. *J Clin Microbiol* 1993; **31**: 1918-1920
- 30 **Hua J**, Roux D, de Mascarel A, Megraud F. PCR for *Helicobacter pylori* on biopsy samples in CLO test sent by mail [abstract]. *Gastroenterology* 1994; **106**: A97
- 31 **Lin TT**, Yeh CT, Yang E, Chen PC. Detection of *Helicobacter pylori* by polymerase chain reaction assay using gastric biopsy specimens taken for CLO test. *J Gastroenterol* 1996; **31**: 329-332
- 32 **Hsu PI**, Lai KH, Tseng HH, Lin CK, Lo GH, Cheng JS, Chan HH, Chen GC, Jou HS, Peng NJ, Ger LP, Chen W, Hsu PN. Risk factors for presentation with bleeding in patients with *Helicobacter pylori*-related peptic ulcer diseases. *J Clin Gastroenterol* 2000; **30**: 386-391
- 33 **Leung WK**, Sung JJ, Siu KL, Chan FK, Ling TK, Cheng AF. False-negative biopsy urease test in bleeding ulcers caused by the buffering effects of blood. *Am J Gastroenterol* 1998; **93**: 1914-1918
- 34 **Coudron PE**, Stratton CW. Factors affecting growth and susceptibility testing of *Helicobacter pylori* in liquid media. *J Clin Microbiol* 1995; **33**: 1028-1030

Science Editor Wang XL and Li WZ Language Editor Elsevier HK

Role of cytokines in promoting immune escape of FasL-expressing human colon cancer cells

Tong Xu, Bao-Cun Sun, Qiang Li, Xi-Shan Hao

Tong Xu, Qiang Li, Xi-Shan Hao, Department of Abdominal Surgery, Cancer Hospital Affiliated to Tianjin Medical University, Tianjin 300060, China

Bao-Cun Sun, Institute of Oncology, Tianjin Medical University, Tianjin 300060, China

Supported by the Science and Technology Commission Foundation of Tianjin, No. 003119711

Correspondence to: Dr. Tong Xu, Department of Abdominal Surgery, Cancer Hospital Affiliated to Tianjin Medical University, Tianjin 300060, China. tong_xu@126.com

Telephone: +86-22-23537796 Fax: +86-22-23359984

Received: 2004-08-18 Accepted: 2004-11-19

Abstract

AIM: To investigate the potential role of cytokines in promoting Fas ligand (FasL)-expressing colon cancer cells.

METHODS: Immunohistochemical SABC method was used to observe the expression of Fas receptor and ligand in SW620 colon cancer cell line and Jurkat T cells in order to provide the morphological evidence for the functions of Fas receptor and ligand. To examine the cytotoxicity of effector cells, CytoTox96[®] non-radioactive cytotoxicity assay was adopted to measure the lactate dehydrogenase-releasing value after SW620 cells were co-cultured with Jurkat T lymphocytes.

RESULTS: The FasL of colon cancer SW620 cells was positive. The positive substances were distributed in the cell membrane and cytoplasm. The Fas receptor of colon cancer SW620 cells was negative. The Fas receptor and ligand of Jurkat T lymphocytes turned out to be positive. The positive substances were distributed in the cell membrane. After phytohemagglutinin (PHA)-stimulated Jurkat T lymphocytes were co-cultured with phorbol 12-myristate 13-acetate (PMA)-plus-ionomycin-stimulated (for 48 h) SW620 cells or tumor necrosis factor-alpha (TNF- α)-stimulated (for 48 h) SW620 cells or unstimulated SW620 cells for 4 h, the cytotoxicity of SW620 cells to PHA-stimulated Jurkat cells at effector-to-target ratios of 10:1, 5:1, 2.5:1, and 1.25:1 was 74.6%, 40.8%, 32.4%, and 10.9% ($F = 8.19, P < 0.05$); or 54.9%, 35.3%, 22.0%, and 10.3% ($F = 11.12, P < 0.05$); or 14.9%, 10.5%, 6.9%, and 5.8% ($F = 3.45, P < 0.05$). After PHA-stimulated Jurkat T lymphocytes were co-cultured with unstimulated SW620 cells for 8 h, the cytotoxicity of SW620 cells to PHA-stimulated Jurkat cells at effector-to-target ratios of 5:1, 2.5:1, and 1.25:1 from the experiment was 83.9%, 74.1%, and 28.5% ($F = 137.04, P < 0.05$) respectively. Non-radioactive cytotoxicity assay showed that the apoptotic rate of Jurkat cells remarkably increased

with the increase of planting concentration of SW620 cells and co-culture time after the SW620 cells were co-cultured with the Jurkat T lymphocytes. The cytotoxicity was significantly enhanced by PMA+ionomycin or TNF- α .

CONCLUSION: The FasL expressed in human colon cancer cells may be regulated by endogenous factors in the microenvironment of the host and facilitate the escape of tumor cells from the host immune system.

© 2005 The WJG Press and Elsevier Inc. All rights reserved.

Key words: Cytokines; Fas/Fas ligand; Colon cancer; Apoptosis; Immune escape

Xu T, Sun BC, Li Q, Hao XS. Role of cytokines in promoting immune escape of FasL-expressing human colon cancer cells. *World J Gastroenterol* 2005; 11(25): 3915-3919

<http://www.wjgnet.com/1007-9327/11/3915.asp>

INTRODUCTION

The Fas/Fas ligand (FasL) system plays an important role in the transduction of apoptotic signal into cells. In recent years, numerous studies have demonstrated that Fas is expressed on the surface of cells, whereas FasL expression is restricted to a small number of cell types, such as lymphocytes, cells of the immune-privileged organs and many types of malignant tumor cells^[1]. Evidence has pointed to an abnormal increase in apoptosis among activated Fas-positive lymphocytes, mainly in the periphery of the FasL-expressing tumors^[2]. On the other hand, the occurrence of tumor is due to the fact that the converted cells cannot undergo a normal process of apoptosis. Resistance to apoptosis through the Fas receptor pathway coupled with expression of the FasL might enable many cancers to deliver a pre-emptive strike or counterattack against the immune system^[2-4]. This study aimed to observe the interaction *in vitro* between T cells expressing Fas and tumor cells expressing FasL, and to investigate the potential role of FasL-expressing colon cancer cells *in vitro* and the effect of endogenous cytokines on tumor cells counterattacking T lymphocytes.

MATERIALS AND METHODS

Reagents, antibodies, and apparatus

Ionomycin, PMA, and phytohemagglutinin (PHA) were purchased from Sigma Chemical Co., USA. Tumor necrosis factor-alpha (TNF- α) and CytoTox96[®] non-radioactive

cytotoxicity assay kits were purchased from Promega Co., USA. RPMI1640 and DMEM were obtained from Gibco Co. Fetal bovine serum (FBS) was purchased from Hyclone Co. Monoclonal mouse anti-human CD95/FAS and monoclonal mouse anti-human FasL were purchased from Zhongshan Co., Beijing, China. SABC detection kit was purchased from Bosden Co., Wuhan, China. A-5082 Sunrise automated ELISA reader was purchased from Tecan, Austria.

Cell lines and cell culture

The human colon cancer cell line SW620 from American Tissue Culture Collection (ATCC) was kindly donated by Dr. Joe O'Connell, Cork University Hospital, Ireland. The acute T cell leukemia cell line Jurkat (ATCC) was provided by Institute of Hematology, Chinese Academy of Medical Sciences. The human glioma cell line TJ905 was kindly donated by Dr. Zhang WZ, Tianjin Huanhu Hospital, China. SW620 and TJ905 cells were cultured in DMEM supplemented with 100 mL/L FBS. Jurkat T lymphocytes were cultured in RPMI1640 medium (with 100 mL/L FBS) and stimulated with 4 mg PHA/L^[3]. All cell lines were incubated at 37 °C in a humidified 50 mL/L CO₂ atmosphere.

Immunocytochemical procedures for detection of FasL and Fas protein

Jurkat, TJ905, and SW620 cells were cultured on glass chamber slides respectively. After fixation in 4% paraformaldehyde for 60 min respectively, slides were washed twice for 5 min in a wash buffer containing 50 mmol/L Tris-Cl, pH 7.6, 50 mmol/L NaCl, and 0.001% saponin. Endogenous peroxidase was quenched with 3% hydrogen peroxide in methanol for 5 min. Slides were washed as before except that the wash buffer contained 1% normal goat serum, and then blocked for 1 h in wash buffer containing 5% normal goat serum^[5]. Slides were washed and incubated overnight at a dilution of 1:200 with monoclonal mouse anti-human primary antibodies at 4 °C in a high-humidity chamber. Antibody binding was localized using biotinylated secondary antibody, avidin-conjugated horseradish peroxidase, and diaminobenzidine substrate. Slides were counterstained with hematoxylin, washed for 1 h with PBS, air-dried and covered with mounting medium. Negative control slides were processed with PBS in place of primary antibodies.

Fas-mediated cytotoxicity assay

To examine the cytotoxicity of effector cells, CytoTox96[®] non-radioactive cytotoxicity assay^[6] was adopted to measure lactate dehydrogenase (LDH)-releasing value after SW620 or TJ905 cells (control) were co-cultured with Jurkat T lymphocytes. Jurkat cells were incubated with PHA (4 mg/L)^[3] in RPMI1640 (50 mL/L FBS) for 24 h and counted with a hemocytometer before cytotoxicity assay. SW620 or TJ905 cells (control) were seeded on 96-well U-bottom tissue culture plates (Falcon) at a density of 2×10⁹/L, 1×10⁹/L, 5×10⁸/L, and 2.5×10⁸/L respectively, and kept under controlled conditions or stimulated with 10 µg/L PMA+500 µg/L ionomycin or with 20 µg/L TNF-α for 48 h. For a further 24 h of culture PHA-stimulated Jurkat cells (2×10⁴ in 100 µL) were added, keeping effector-to-target cell ratios at 10:1, 5:1, 2.5:1, and 1.25:1. PHA-stimulated Jurkat cells were co-

cultured with effector cells in 100 µL RPMI1640 medium (50 mL/L FBS) each well. Tissue culture plate was centrifuged at 250 r/min for 5 min at 4 °C to ensure cell-cell contact^[6]. In each experiment triplicate wells were analyzed. At the same time, the values of effector cell spontaneous LDH release, target cell spontaneous LDH release, target cell maximum LDH release, volume correction control, and culture medium background were measured. Then the following formula was applied in the calculation of percent cytotoxicity: cytotoxicity (%) = (experimental LDH release-effector cell spontaneous LDH release-target cell spontaneous LDH release)/(target cell maximum LDH release-target cell spontaneous LDH release)×100.

Statistical analysis

Results were compared by analysis of variance (ANOVA) using SPSS10.0 software. *P*<0.05 was considered statistically significant.

RESULTS

Immunocytochemical detection of FasL and Fas protein in SW620, Jurkat and TJ905 cells

FasL expression in colon cancer SW620 cells was strongly positive. The positive substances were distributed in the cell membrane and cytoplasm (Figure 1A), while Fas expression in SW620 cells was negative (Figure 1B). Fas and FasL expression in Jurkat T lymphocytes turned out to be positive. The positive substances were distributed in the cell membrane and cytoplasm, while the nuclei of the cells were negative (Figures 1C and D). Fas expression in TJ905 cells was positive. The positive substances were distributed in the cell membrane and cytoplasm (Figure 1E). FasL expression in TJ905 cells was weakly positive (Figure 1F).

Results of cytotoxicity assay

After the SW620 cells were co-cultured with the PHA-stimulated Jurkat T lymphocytes for 4 h, the cytotoxicity (Figure 2) of SW620 cells to PHA-stimulated Jurkat cells at different effector-to-target ratios had significant differences (*F* = 3.45, *P*<0.05). After stimulation with 10 µg/L PMA+500 µg/L ionomycin for 48 h, the SW620 cells were co-cultured with the PHA-stimulated Jurkat T lymphocytes for 4 h. The cytotoxicity (Figure 2) of SW620 cells to PHA-stimulated Jurkat cells at different effector-to-target ratios had significant differences (*F* = 8.19, *P*<0.05). After stimulation with 20 µg/L TNF-α for 48 h, the SW620 cells were co-cultured with the PHA-stimulated Jurkat T lymphocytes for 4 h. The cytotoxicity (Figure 2) of SW620 cells to PHA-stimulated Jurkat cells at different effector-to-target ratios had significant differences (*F* = 11.12, *P*<0.05). After the SW620 cells were co-cultured with the PHA-stimulated Jurkat T lymphocytes for 8 h, the cytotoxicity of SW620 cells to PHA-stimulated Jurkat cells at effector-to-target ratios of 5:1, 2.5:1, and 1.25:1 was 83.9%, 74.1%, and 28.5% respectively and had significant differences (*F* = 137.04, *P*<0.05). The cytotoxicity of Jurkat cells after co-culture with SW620 (different effector-to-target ratios) for 8 h was much higher than that after being co-cultured with SW620 (different effector-to-target ratios) for 4 h (*P*<0.05, Table 1).

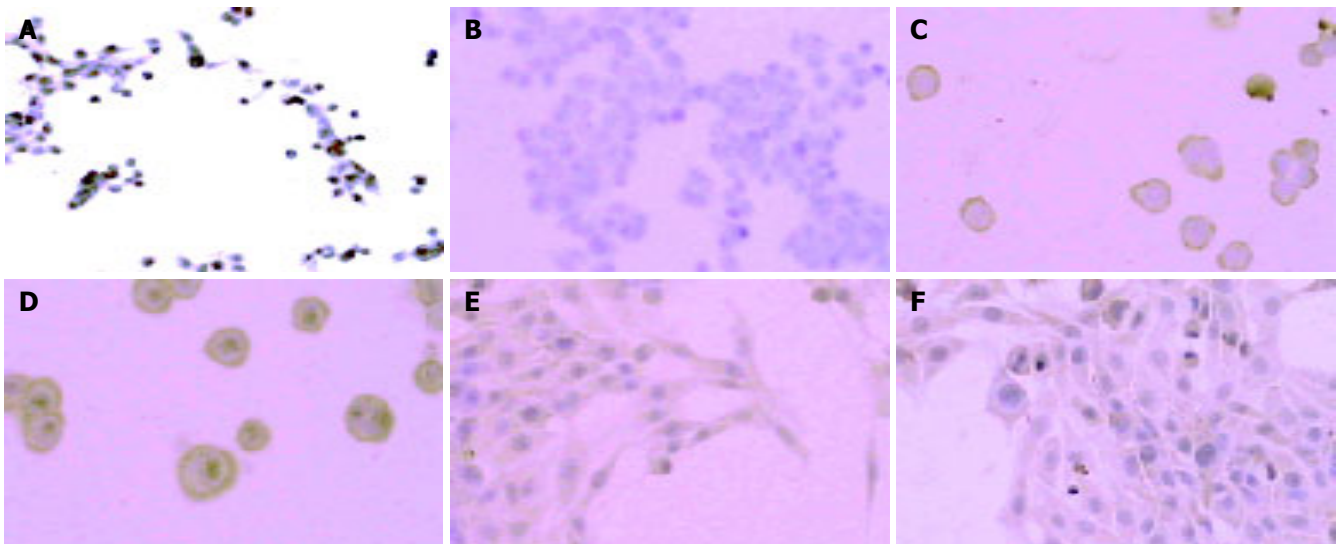


Figure 1 Expression of FasL and Fas in SW620 cells (A and B), Jurkat cells (C and D), and TJ905 cells (E and F).

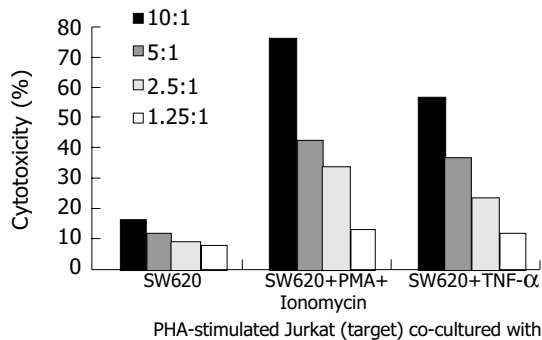


Figure 2 Comparison of cytotoxicity assay among three groups.

After PMA-plus-ionomycin-stimulated (for 48 h) SW620 cells or unstimulated SW620 cells were co-cultured with PHA-stimulated Jurkat T lymphocytes for 4 h, the cytotoxicity of PMA-plus-ionomycin-stimulated SW620 cells was much higher than that of control. The cytotoxicity had significant differences between the two groups ($P < 0.05$, Table 1). After TNF- α -stimulated (for 48 h) SW620 cells or unstimulated SW620 cells were co-cultured with PHA-stimulated Jurkat T lymphocytes for 4 h, the cytotoxicity of TNF- α -stimulated SW620 cells was much higher than that of control. The cytotoxicity had significant differences between the two groups ($P < 0.05$, Table 1).

After the TJ905 cells were co-cultured with the PHA-stimulated Jurkat T lymphocytes for 4 h, the cytotoxicity of TJ905 cells to PHA-stimulated Jurkat cells at different effector-to-target ratios had no differences ($F = 0.25$, $P > 0.05$).

TJ905 cells were not cytotoxic to Jurkat cells. After the TJ905 cells were co-cultured with the PHA-stimulated Jurkat T lymphocytes for 8 h, the cytotoxicity of TJ905 cells to PHA-stimulated Jurkat cells at different effector-to-target ratios had no differences ($F = 2.92$, $P > 0.05$). TJ905 cells were not cytotoxic to Jurkat cells. After the TJ905 cells were stimulated with 10 $\mu\text{g/L}$ PMA+500 $\mu\text{g/L}$ ionomycin for 48 h, the TJ905 cells were co-cultured with the PHA-stimulated Jurkat T lymphocytes for 4 h. The cytotoxicity of TJ905 cells to PHA-stimulated Jurkat cells at different effector-to-target ratios had no differences ($F = 0.04$, $P > 0.05$), TJ905 cells were not cytotoxic to Jurkat cells. After the TJ905 cells were stimulated with 20 $\mu\text{g/L}$ TNF- α for 48 h, the TJ905 cells were co-cultured with the PHA-stimulated Jurkat T lymphocytes for 4 h. The cytotoxicity of TJ905 cells to PHA-stimulated Jurkat cells at different effector-to-target ratios had no differences ($F = 0.97$, $P > 0.05$), TJ905 cells were not cytotoxic to Jurkat cells. Cytotoxicity assay showed that no cytotoxicity to human glioma TJ905 cells was observed in the PHA-stimulated Jurkat T lymphocytes.

DISCUSSION

Fas is constitutively expressed in lymphocytes of normal subjects. After lymphocytes are triggered by inflammatory cytokines or tumor antigen, Fas expression is significantly augmented. Since the expansion of tumor-specific CD4 and CD8 cells is the current goal of many promising immunotherapeutic strategies, it is important to understand the factors that may influence the fate of such specific cells. Moreover, uncloned CD4 cell line originally isolated from human tumor tissue^[7]

Table 1 Comparison of cytotoxicity assay after co-culturing PHA-stimulated Jurkat T lymphocytes with SW620 cells

Sources of deviations	F (8 h)	P	F (PMA-plus-ionomycin)	P	F (TNF- α)	P
Sample	475.99	<0.05	27.71	<0.05	57.87	<0.05
Column	77.62	<0.05	10.29	<0.05	129.92	<0.05
Intercept	51.09	<0.05	5.14	<0.05	15.75	<0.05

Two-way ANOVA.

as well as tumor-specific human cytotoxic T lymphocytes (CTLs) clones^[8] are also reported to express Fas *in vitro* and to be sensitive to its ligation. Recent evidence shows that tumor-infiltrating lymphocytes (TILs) exhibit significantly increased expression of Fas relative to peripheral blood lymphocytes^[9]. There is evidence that the lack of co-stimulatory signals such as B7.1, a feature of many tumors, promotes T-cell sensitivity to FasL in the tumor microenvironment^[10]. Since TILs are difficult to be isolated and expanded *in vitro*, we chose Jurkat T lymphocytes instead of TILs in our study.

Fas is expressed in each colonocyte of normal colon mucosa, and downregulated or lost in the majority of colon cancers. Immunohistology revealed that the majority of colon cancers express Fas at abnormally low levels or entirely lack Fas^[11]. Our results are compatible with these findings. Further more data have confirmed that colon cancer cell line is constitutively or at least relatively resistant to Fas-mediated apoptosis^[12,13]. Resistance to Fas-mediated apoptosis is a common feature of cancers, irrespective of cell surface expression of Fas^[14]. Thus, the downmodulation or abrogation of Fas on tumor cells and/or acquirement of relative resistance to Fas ligation might be a selection advantage, and constitute a mechanism of immune evasion to Fas-mediated killing by T cells^[15,16].

The FasL-expressing SW620 cell line is derived from a lymph node metastasis of primary colon cancer. The present study further confirmed that the expressed FasL was demonstrated to be functional, since co-culture experiments using FasL-expressing SW620 cells resulted in the apoptosis of Jurkat T leukemia cells that are sensitive to Fas-mediated apoptosis, which consequently may facilitate metastatic development. Our findings and other data suggest that tumor cells can evade immune attack by downregulating the Fas and inducing apoptosis in activated T lymphocytes through the expression of FasL. Furthermore, the constitutive expression of FasL in hepatic metastatic tumors suggests that FasL may also be important in their colonization in the liver through induction of apoptosis in the surrounding Fas-expressing hepatocytes^[17]. FasL expression in human colon cancers is associated with apoptotic depletion of TILs *in vivo*^[2]. In addition, upregulation of FasL expression probably induces killing of Fas-bearing tumor cells by promoting the selection of malignant tumor variants, because its Fas pathway has become insensitive to FasL binding. In the tumor microenvironment, IFN and other potentially relevant cytokines may be provided endogenously by immune system interaction, such as CD4⁺ T cells, following interaction with MHC class II⁺ antigen-presenting cells. Ag-specific CD8⁺ CTLs may then lyse cytokine-modified tumor cells through Fas-dependent and/or Fas-independent pathways, depending upon the intrinsic susceptibility of the tumor population to one or more immune effector mechanisms. Zeytun *et al.*^[18], reported a mutual killing model in which FasL⁺, Fas⁺ tumor cells, LSA and EL-4, kill Fas⁺ tumor-specific CTLs and are also killed by tumor-specific FasL⁺ CTLs. They concluded that the survival of the tumor or the host might depend on the cells which can accomplish FasL-based killing more efficiently. It is clear that the highly sophisticated and flexible adaptive immune response of higher vertebrates requires subtle regulation, particularly of receptors that can deliver

such a devastating outcome as cell death. Ding *et al.*^[19], reported that PMA+ionomycin and endogenous cytokines such as interleukin-18 (IL-18), TNF- α and IFN- γ upregulate the expression of FasL protein in human colon cancer cell lines DLD-1 and SW620. We further showed that the cytotoxicity was significantly enhanced by PMA+ionomycin and TNF- α . Since IFN- γ , TNF- α , and other potentially relevant cytokines are mainly secreted by activated T cells and macrophages, the upregulation of FasL in cancer cells in response to some cytokines may thus counterselect activated TILs and favor a microenvironment of T-cell anergy and the immune escape of cancer cells. Our data suggest that the FasL expressed in human colon cancer cells may be regulated by endogenous factors in the microenvironment of the host and facilitate the escape of tumor cells from the host immune system. Pages *et al.*^[20], observed that synthesis of IL-18 decreases or is abolished in colon adenocarcinomas compared to that in normal mucosa, thus resulting in decreasing IFN- γ production and impairing FasL-dependent cytotoxicity of immune cells. This feature is correlated with the existence of distant metastasis and an unfavorable outcome. Xu *et al.*^[21], reported that IFN- γ upregulates the expression of Fas and FasL in HT29 cells, a human colon adenocarcinoma cell line, and subsequently induces apoptosis of these cells in an autocrine and paracrine manner. However, it is important to note that many mechanisms of Fas-resistance can also occur, such as Fas-associated phosphatase-1, overexpression of bcl-2 and secretion of soluble Fas from tumor cells in a variety of human tumor cell lines that express Fas^[22,23]. TNF- α and IFN- γ are potent immunostimulatory cytokines with tumoricidal effects in a variety of cancers. But at the same time these cytokines might facilitate escape of tumor cells from the host immune system.

Taken together, we also considered a new mechanism of immune evasion, namely, the active destruction of T lymphocytes by tumor cells expressing CD95 ligand. It may provide insights into the processes of both tumor immunity and tumor escape for at least a potential subset or fraction of malignancies. Disarming the Fas counterattack is a conceptually appealing and exciting potential goal for tumor immunotherapy. Ongoing studies are aimed at further understanding the basis of Fas resistance and counterattack, thus determining how to restore tumor cell sensitivity to Fas or block expression or function of FasL in tumor cells.

ACKNOWLEDGMENTS

The authors thank Dr. Joe O'Connell (Cork University Hospital, Ireland) for generously providing the SW620 cell line. The authors also thank Dr. WZ Zhang for excellent technical assistance.

REFERENCES

- 1 Lamhamedi-Cherradi SE, Chen Y. Fas (CD95, Apo-1) ligand gene transfer. *J Clin Immunol* 2001; **21**: 24-29
- 2 Houston A, Bennett MW, O'Sullivan GC, Shanahan F, O'Connell J. Fas ligand mediates immune privilege and not inflammation in human colon cancer, irrespective of TGF-beta expression. *Br J Cancer* 2003; **89**: 1345-1351
- 3 Muschen M, Moers C, Warskulat U, Even J, Niederacher D, Beckmann MW. CD95 ligand expression as a mechanism of

- immune escape in breast cancer. *Immunology* 2000; **99**: 69-77
- 4 **Xu T**, Hao XS, Sun BC. Progress in the research of the relationship between Fas/FasL and tumor. *Zhongguo Zhongliu Linchuang Zazhi* 2003; **30**: 444-448
 - 5 **O'Connell J**, O'Sullivan GC, Collins JK, Shanahan F. The Fas counterattack: Fas-mediated T cell killing by colon cancer cells expressing Fas ligand. *J Exp Med* 1996; **184**: 1075-1082
 - 6 **Fischer U**, Ototake M, Nakanishi T. *In vitro* cell-mediated cytotoxicity against allogeneic erythrocytes in ginbuna crucian carp and goldfish using a non-radioactive assay. *Dev Comp Immunol* 1998; **22**: 195-206
 - 7 **Saff RR**, Spanjaard ES, Hohlbaum AM, Marshak-Rothstein A. Activation-induced cell death limits effector function of CD4 tumor-specific T cells. *J Immunol* 2004; **172**: 6598-6606
 - 8 **Zaks TZ**, Chappell DB, Rosenberg SA, Restifo NP. Fas-mediated suicide of tumor-reactive T cells following activation by specific tumor: selective rescue by caspase inhibition. *J Immunol* 1999; **162**: 3273-3279
 - 9 **Cardi G**, Heaney JA, Schned AR, Ernstoff MS. Expression of Fas (APO-1/CD95) in tumor-infiltrating and peripheral blood lymphocytes in patients with renal cell carcinoma. *Cancer Res* 1998; **58**: 2078-2080
 - 10 **Daniel PT**, Kroidl A, Cayeux S, Bargou R, Blankenstein T, Dorken B. Costimulatory signals through B7.1/CD28 prevent T cell apoptosis during target cell lysis. *J Immunol* 1997; **159**: 3808-3815
 - 11 **Zhu Q**, Deng C. The role of Fas/Fas ligand in tumorigenesis, immune escape, and counterattack in colonic cancer. *Zhonghua Neike Zazhi* 2002; **41**: 378-380
 - 12 **Owen-Schaub LB**, Radinsky R, Kruzel E, Berry K, Yonehara S. Anti-Fas on nonhematopoietic tumors: levels of Fas/APO-1 and bcl-2 are not predictive of biological responsiveness. *Cancer Res* 1994; **54**: 1580-1586
 - 13 **French LE**, Tschopp J. Defective death receptor signaling as a cause of tumor immune escape. *Semin Cancer Biol* 2002; **12**: 51-55
 - 14 **Houston A**, O'Connell J. The Fas signalling pathway and its role in the pathogenesis of cancer. *Curr Opin Pharmacol* 2004; **4**: 321-326
 - 15 **Kim R**, Emi M, Tanabe K, Uchida Y, Toge T. The role of Fas ligand and transforming growth factor beta in tumor progression: molecular mechanisms of immune privilege via Fas-mediated apoptosis and potential targets for cancer therapy. *Cancer* 2004; **100**: 2281-2291
 - 16 **Bennett MW**, O'Connell J, Houston A, Kelly J, O'Sullivan GC, Collins JK, Shanahan F. Fas ligand upregulation is an early event in colonic carcinogenesis. *J Clin Pathol* 2001; **54**: 598-604
 - 17 **Shiraki K**, Tsuji N, Shioda T, Isselbacher KJ, Takahashi H. Expression of Fas ligand in liver metastases of human colonic adenocarcinomas. *Proc Natl Acad Sci USA* 1997; **94**: 6420-6425
 - 18 **Zeytun A**, Hassuneh M, Nagarkatti M, Nagarkatti PS. Fas-Fas ligand-based interactions between tumor cells and tumor-specific cytotoxic T lymphocytes: a lethal two-way street. *Blood* 1997; **90**: 1952-1959
 - 19 **Ding EX**, Zhang W, Wang Q, Chen XY, Fu ZR. Cytokines upregulate Fas ligand protein expression in human colon cancer cells. *Aizheng* 2000; **19**: 966-968
 - 20 **Pages F**, Berger A, Henglein B, Piqueras B, Danel C, Zinzindohoue F, Thiounn N, Cugnenc PH, Fridman WH. Modulation of interleukin-18 expression in human colon carcinoma: consequences for tumor immune surveillance. *Int J Cancer* 1999; **84**: 326-330
 - 21 **Xu X**, Fu XY, Plate J, Chong AS. IFN-gamma induces cell growth inhibition by Fas-mediated apoptosis: requirement of STAT1 protein for up-regulation of Fas and FasL expression. *Cancer Res* 1998; **58**: 2832-2837
 - 22 **Yanagisawa J**, Takahashi M, Kanki H, Yano-Yanagisawa H, Tazunoki T, Sawa E, Nishitoba T, Kamishohara M, Kobayashi E, Kataoka S, Sato T. The molecular interaction of Fas and FAP-1. A tripeptide blocker of human Fas interaction with FAP-1 promotes Fas-induced apoptosis. *J Biol Chem* 1997; **272**: 8539-8545
 - 23 **Ivanov VN**, Lopez Bergami P, Maulit G, Sato TA, Sassooun D, Ronai Z. FAP-1 association with Fas (Apo-1) inhibits Fas expression on the cell surface. *Mol Cell Biol* 2003; **23**: 3623-3635

Science Editor Wang XL and Guo SY Language Editor Elsevier HK

Isoflurane preserves energy balance in isolated hepatocytes during *in vitro* anoxia/reoxygenation

Quan Li, Wei-Feng Yu, Mai-Tao Zhou, Xin Lu, Li-Qun Yang, Ming Zhu, Jian-Gang Song, Jun-Hua Lu

Quan Li, Wei-Feng Yu, Mai-Tao Zhou, Xin Lu, Li-Qun Yang, Ming Zhu, Jian-Gang Song, Department of Anesthesiology, Eastern Hepatobiliary Surgery Hospital, the Second Military Medical University, Shanghai 200438, China

Jun-Hua Lu, Department of Clinical Surgery, Eastern Hepatobiliary Surgery Hospital, the Second Military Medical University, Shanghai 200438, China

Supported by the National Natural Science Foundation of China, No. 39900140

Correspondence to: Dr. Wei-Feng Yu, Department of Anesthesiology, Eastern Hepatobiliary Surgery Hospital, the Second Military Medical University, Shanghai 200438, China. quanligene@sohu.com

Telephone: +86-21-55051447 Fax: +86-21-25070783

Received: 2004-09-23 Accepted: 2004-11-24

© 2005 The WJG Press and Elsevier Inc. All rights reserved.

Key words: Isoflurane; Hepatocytes; Anoxia; Energy balance

Li Q, Yu WF, Zhou MT, Lu X, Yang LQ, Zhu M, Song JG, Lu JH. Isoflurane preserves energy balance in isolated hepatocytes during *in vitro* anoxia/reoxygenation. *World J Gastroenterol* 2005; 11(25): 3920-3924

<http://www.wjgnet.com/1007-9327/11/3920.asp>

Abstract

AIM: To investigate the protective effect of isoflurane on energy balance in isolated hepatocytes during *in vitro* anoxia/reoxygenation, and to compare isoflurane with halothane.

METHODS: Hepatocytes freshly isolated from fed rats were suspended in Krebs-Henseleit buffer, and incubated in sealed flasks under O₂/CO₂ or N₂/CO₂ (95%/5%, V/V) for 30 or 60 min, followed by 5 or 10 min of reoxygenation, with an added volatile anesthetic or not. ATP, ADP, and adenosine monophosphate in hepatocytes were determined by high performance liquid chromatography, and energy charge was calculated.

RESULTS: During 30 min of anoxia, the energy charge and total adenine nucleotide steadily increased with the isoflurane dose from 0 to 2 minimum alveolar anesthetic concentration (MAC), then decreased from 2 to 3 MAC. In short incubations (30-35 min) at 1 MAC isoflurane, energy charge modestly decreased during anoxia, which was partially prevented by isoflurane and completely reversed by reoxygenation, and total adenine nucleotide did not decrease. In long incubations (60-70 min), both energy charge and total adenine nucleotide greatly decreased during anoxia, with partial and no reversal by reoxygenation, respectively. Isoflurane partly prevented decreases in both energy charge and total adenine nucleotide during anoxia and reoxygenation. In addition, 1 MAC isoflurane obviously increased ATP/ADP, which could not be changed by 1 MAC halothane.

CONCLUSION: Isoflurane partially protects isolated hepatocytes against decreases in both energy charge and total adenine nucleotide during short (reversible) or long (irreversible) anoxia.

INTRODUCTION

Hepatic anoxia, alone or as a component of ischemia, is an ever-present concern during abdominal surgery, because associated inhibition of energy supply threatens liver cell function and viability^[1,2]. Evidence is mounting that the inability of the liver to maintain or regain energy balance during and after surgery is one of the strongest predictors of liver damage and adverse outcome^[3,4]. Also, release from injured tissue of metabolites, such as adenosine, with cardiovascular effects may further compromise the anesthetic management of seriously ill or injured patients. Thus, surgeons and anesthesiologists need to be aware of, and to use, whatever measures are available to preserve energy balance in tissues.

The sum of ATP splitting by many concurrent energy-requiring reactions is called "ATP demand." ATP supply occurs mainly via mitochondrial oxidative phosphorylation, which is absolutely dependent on O₂. Under normal conditions, ATP supply easily keeps pace with ATP demand, and adenine nucleotide (high-energy phosphate) exists mainly in the form of ATP, along with relatively small amounts of ADP and adenosine monophosphate (AMP). However, when ATP supply is inhibited by lack of oxygen, ATP demand predominates, ADP and AMP then accumulate at the expense of ATP, and eventually adenosine and other non-nucleotide metabolites appear. Thus, shifts in the balance between ATP supply and demand can be assessed by measuring changes in the absolute and relative levels of ATP and its metabolites. A more complete and accurate expression is energy charge. Energy charge = (ATP+1/2ADP)/(ATP+ADP+AMP).

MATERIALS AND METHODS

Hepatocytes were isolated from adult male Sprague-Dawley rats (250-300 g) having free access to food and water^[5]. Livers were perfused *in situ* by using Ca²⁺-free Krebs-Henseleit buffer (pH 7.4) supplemented with 20 mmol/L

4-(2-hydroxyethyl)-1-piperazineethanesulfonic acid, maintained at 37 °C and equilibrated with O₂/CO₂ (95/5). Perfusion was continued for 10 min with buffer alone, then for another 12-14 min with added collagenase (Type I, Sigma Chemical Co., St. Louis, MO). The softened liver was transferred to a plastic weighing dish containing 25 mL Krebs+2% dissolved bovine serum albumin, teased apart with a spatula and chopped finely with sharp scissors. After further dilution to 100 mL with Krebs+2% dissolved bovine serum albumin, the cell slurry was washed into a 500-mL Erlenmeyer flask, gently swirled under a flowing O₂/CO₂ (95%/5% V/V) atmosphere at 37 °C for 15 min, then filtered through nylon mesh. Each 12 mL of crude cell suspension was mixed with 28 mL Percoll (Pharmacia, Sweden, obtained from Sigma) and centrifuged at 10 000 *g* for 10 min. The layer of intact, purified hepatocytes at the bottom of the gradient was rinsed free of Percoll by suspension in Krebs and centrifugation for 2 min at 50 r/min. The final pellet contained a total of 2-4×10⁸ cells that were 90-95% viable by dye exclusion. Cells were stored for 2 h on ice before use without loss of viability.

In 25-mL round-bottomed flasks, 12.5 million cells were suspended in a total volume of 2.5 mL Krebs+2% dissolved bovine serum albumin (pH 7.4). Flasks were sealed with rubber caps through which 14-gauge needles were inserted for in- and out-flow of gas mixture. After 10 min preincubation under O₂/CO₂, regassing and experimental incubations were carried out as follows: O₂/CO₂ for 35 or 70 min (= oxygenated), N₂/CO₂ for 30 or 60 min (= anoxic), or N₂/CO₂ for 30 or 60 min followed by O₂/CO₂ for 5 or 10 min, respectively (= reoxygenated). All incubations were performed by swirling the flasks in a water bath at 37 °C. When needed, anesthetics were added at the desired concentrations to the gas mixture used for gassing the flasks by means of a copper kettle vaporizer. Gas chromatography measurements established that anesthetic concentrations in liquid phase reached a constant value within 5-10 min. (The absolute concentrations in the liquid phase varied with anesthetic dose and cell concentration.) Incubations were terminated by injecting 0.5 mL 2 mol/L perchloric acid forcefully into the suspension to arrest enzyme-catalyzed reactions. After removal of precipitated membranes and protein by centrifugation, the clear supernatant containing extracted adenine nucleotides and other metabolites was neutralized with 2 mol/L potassium hydroxide and cooled on ice to precipitate excess potassium perchlorate. The supernatant was decanted and stored at -20 °C before metabolite measurements.

ATP, ADP, and AMP were analyzed by high performance liquid chromatography (LDC Analytical, Riviera Beach, FL, USA) using a CM4000 pump interfaced with a SM5000 detector. The separation was accomplished on a C18 reversed phase column. Elution with a binary gradient was carried out at a flow rate of 1.0 mL/min. Mobile phase A consisted of 30 mmol/L potassium phosphate as buffer (pH 6.0) and 8 mmol/L tetrabutylammonium hydrogen sulfate as ion-pairing reagent. Mobile phase B was identical except that it contained 500 mL/L methanol. Recovery of ATP, ADP, and AMP routinely exceeded 90-95%, as estimated from the concentration of caffeine added as an internal standard.

Statistical analysis

Data were presented as mean±SD. One- or two-way analysis of variance with replications and Scheffe's or paired *t*-tests were used for statistical analysis. *P*<0.05 was considered statistically significant.

RESULTS

Figure 1A shows the effect of isoflurane dose on adenine nucleotide levels in isolated hepatocytes after exposure to anoxia for 30 min. ATP levels increased and AMP levels decreased from their respective control values as isoflurane increased from 0 to 2 minimum alveolar anesthetic concentration (MAC, 0-3% concentration), with a slight reversal from 2 to 3 MAC (3-5% concentration). Total adenine nucleotide increased to a lesser degree with isoflurane dose and was significantly higher than baseline only at 2 MAC. Values of ADP did not change significantly from baseline at any dose of isoflurane. Values of energy charge (not shown) paralleled to those of ATP.

Figure 1B shows data obtained from incubations performed for 30-35 min. In cells incubated under O₂ for 35 min, amounts of ATP were maximal and balanced by relatively small amounts of ADP and AMP. Isoflurane slightly decreased ATP while increasing ADP and AMP. Although changes in individual nucleotide concentrations were not statistically significant, they combined to produce a significant decrease in energy charge.

In cells anoxic for 30 min (under N₂ rather than O₂), ATP substantially decreased and ADP and AMP increased compared to oxygenated cells. The associated decrease in energy charge confirmed that anoxia shifted energy balance toward a much lower degree of phosphorylation in the adenine nucleotide pool. When isoflurane was present during anoxia, ATP remained significantly higher and AMP lower than in anoxic cells without isoflurane. These two effects of isoflurane combined to maintain a proportionately higher value of energy charge.

Cells exposed to 30 min of anoxia followed by 5 min of reoxygenation showed values of all three adenine nucleotides and energy charge that were not significantly different from those of cells exposed to O₂ continuously for 30 min. Furthermore, no difference in any of these variables was seen for +isoflurane compared to -isoflurane.

Figure 1C shows results obtained from a second set of cell preparations subjected to incubations for 60-70 min. In cells incubated under O₂ alone for 70 min, absolute and relative amounts of ATP, ADP, and AMP were not significantly different from those incubated for 30 min. The changes produced by inclusion of isoflurane along with O₂ decreased ATP, increased ADP and AMP, and a statistically significant decrease in energy charge were only slightly (and not significantly) larger than in cells incubated for 35 min.

In cells that were anoxic (exposed to N₂) for 60 min, values of ATP, ADP, AMP, total adenine nucleotide, and energy charge were all significantly lower than in cells exposed anoxia for 30 min. The effects of including isoflurane during anoxia were also generally more pronounced in cells exposed to anoxia for 60 min: compared to values in the absence of isoflurane, ATP was more than double and energy charge almost double, ADP and total

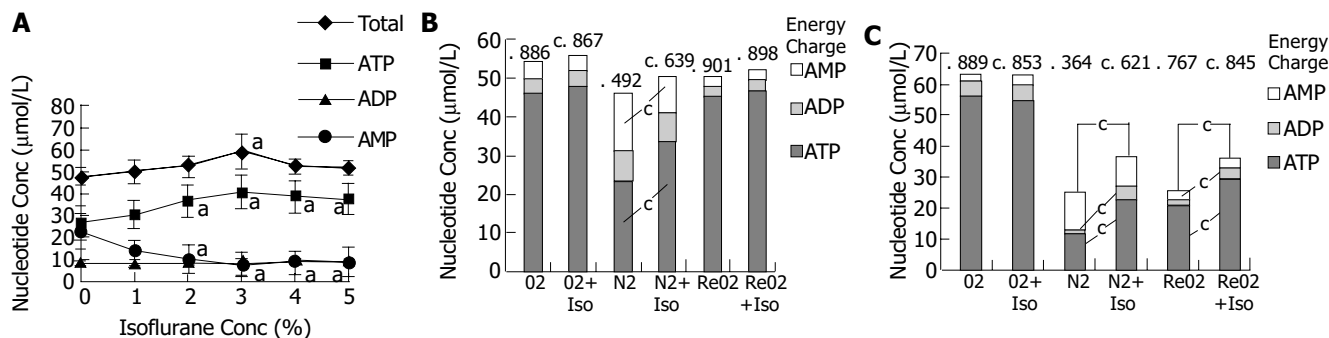


Figure 1 Dependence of ATP, ADP, AMP and total adenine nucleotide and energy charge in isolated hepatocytes on isoflurane during 30 min exposure to anoxia (A), anesthetic and oxygenation status during 30-35 min incubation (B) and during 60-70 min incubation (C). Iso, isoflurane; O₂, oxygenated; N₂,

anoxic; ReO₂, reoxygenated after anoxia. Values shown are means for $n = 8$ experiments. ^a $P < 0.05$ vs initial values at 0% isoflurane; ^c $P < 0.05$ vs control groups (isoflurane absent).

adenine nucleotide were significantly higher while AMP was not significantly lower.

Reoxygenated cells incubated for longer periods (N₂ for 60 min, O₂ for 10 min) differed greatly from cells subjected to shorter incubations (N₂ 30 min, O₂ 5 min), whereas values of ADP and AMP were not much different from those of oxygenated cells. Energy charge, ATP and total adenine nucleotide were drastically decreased. Another difference between longer and shorter incubations of reoxygenated cells was that in the longer ones, isoflurane-related differences in energy status persisted into the reoxygenation period; increases in ATP, ADP, and total adenine nucleotide during anoxia were maintained during reoxygenation.

Table 1 shows the data from a separate experiment carried out solely to compare isoflurane and halothane at approximately 1 MAC for their ability to alter energy status in isolated hepatocytes during 30-min exposure to anoxia. ATP/ADP was again higher with 1 MAC isoflurane present than in paired control incubation (isoflurane absent) using cells from the same preparation. With 1 MAC halothane, no difference at all in ATP/ADP during anoxia was seen, each incubated in the presence and absence of that agent.

Table 1 Different effects of isoflurane and halothane on energy status in hepatic cells during 30 min exposure to anoxia (mean±SE)

ATP/ADP	Isoflurane		Halothane	
	O ₂	N ₂	O ₂	N ₂
Non-anesthetics Group	5.3±0.6	0.7±0.1	7.4±1.1	1.1±0.3
Anesthetics Group	4.8±0.5	1.2±0.1 ^a	7.3±1.5	1.2±0.2

^a $P < 0.05$ vs non-anesthetics group, $n = 8$.

DISCUSSION

Intact isolated hepatocytes embody a physiologic balance of the reactions involved in ATP supply and demand in a form that permits uniform control and ready measurement of biochemical variables. We have studied these cells extensively under simulated intra-operative conditions to predict energetic responses at the tissue and organ level.

The data in Figure 1B show that the energy-protective

effect of isoflurane in anoxic hepatocytes varied in a systematic way with isoflurane dose. There was a graded dose-response relationship from 0 to 2 MAC, with a slight reversal of protection at 3 MAC. It seems that, at least in isolated cells, the energy-protective effect of isoflurane is optimal in the dose range used for clinical anesthesia. The basis for the response “ceiling” at 2 MAC awaits an understanding of the biochemical basis of the protective effect. An important question still to be addressed in this line of investigation is the extent to which the protective effect is associated with the anesthetic state. Is this effect limited to isoflurane or to other halogenated or volatile agents? Does ED₅₀ for the protective effect correlate with MAC?

In the shorter incubation (30-35 min) that examined varying oxygenation status, 1 MAC isoflurane tended to decrease ATP and increase ADP and AMP in cells exposed to oxygen, presumably because isoflurane inhibits mitochondrial recycling of ADP to ATP via oxidative phosphorylation^[6,7]. An opposite and larger effect of isoflurane on energy status was found in anoxic cells: superimposed on the great decrease in ATP and energy charge produced by anoxia, the effect of isoflurane was to enhance energy balance rather than to further impair it. In reoxygenated cells, there were neither protective nor detrimental effects of isoflurane on energy balance; and isoflurane produced no effect at all on any of the measured variables of energy status. The similarity between reoxygenated and continuously oxygenated cells indicates that exposure to 30-min anoxia with or without isoflurane has no irreversible effect on the energy status of hepatocytes.

The longer incubation (60-70 min) produced physiologically significant and/or irreversible effects of anoxia on cellular energy status. As in the 35-min incubation, data from cells oxygenated for 70 min showed that non-anoxic injury might have occurred during that period of incubation. The similarities in ATP, ADP, AMP, and total adenine nucleotide values suggest that the longer period of incubation is well tolerated, because damaged cells rapidly lose adenine nucleotides. The effects of anoxia on adenine nucleotide content and energy balance were considerably greater after 60-min exposure to anoxia than after 30-min exposure to anoxia. In anoxic cells after 60-min exposure to anoxia, there was a great decrease in total adenine nucleotide compared to oxygenated cells (*vs*

none at 30 min), the decrease in energy charge was also greater after 60-min exposure to anoxia than after 30-min exposure to anoxia. In reoxygenated cells, none of the effects of 60-min exposure to anoxia were reversed, in contrast to all of the effects of 30-min exposure to anoxia. The importance of total adenine nucleotide in limiting the levels of ATP, ADP, and AMP during brief recovery from anoxia was shown clearly by the almost identically lowered values of total adenine nucleotide in corresponding anoxic and reoxygenated cells after 70-min exposure to anoxia. Also, in contrast to the shorter incubation, in the longer incubation the protective effect of isoflurane was observed during anoxia-increased energy charge and total adenine nucleotide was persistent through the reoxygenation period.

As mentioned earlier, the measured values of ATP, ADP, and AMP concentrations and the calculated values of total adenine nucleotide and energy charge in isolated hepatocytes are sensitive indicators of changes in the dynamic balance of ATP supply and demand. The anesthetic effects reported here may well be due to the direct action of the drug on one or more of the intracellular reactions involved in producing or consuming ATP^[8-10]. The results of other studies suggested that the protective effect of isoflurane may be due to "decreased metabolism" and, more precisely, due to inhibition of ATP demand^[11-13]. The conclusion holds also for the findings of the present study. Previous studies showed that isoflurane causes a dose-related decrease in O₂ consumption in isolated hepatocytes^[14]. However, it would be erroneous to conclude that this decrease in O₂ consumption reflects primary inhibition of ATP demand (with secondary inhibition of mitochondrial oxidative phosphorylation via respiratory control), because volatile anesthetics are also able to inhibit oxidative phosphorylation directly^[15,16]. In fact, inhibition of ATP demand in intact cells can be ascertained only by direct measurement of ATP consumption.

Two possible mechanisms may be mentioned by which decreased AMP formation can maintain ATP levels. An anoxia-induced increase in AMP promotes its degradation to adenosine and other non-nucleotide metabolites^[17]. The latter step seems to be a physiologic "point of no return", because ATP is not easily resynthesized from its non-nucleotide metabolites when oxygen and ATP supply are restored^[17]. Thus, a decrease in AMP formation would decrease the rate of ensuing AMP degradation and loss of total adenine nucleotide. Also, a decrease in AMP formation from ADP via inhibition of adenylate kinase can preserve the availability of ADP for conversion back to ATP via glycolysis.

The present study demonstrates that 1 MAC isoflurane actually helps to preserve liver cell energy balance during anoxia (whereas 1 MAC halothane has no such effect). The demonstration of this protective effect might be crucially dependent on the specific experimental conditions used in this study. Relatively short periods of anoxic exposure may prevent enzymes that catalyze ATP-consuming reactions from being degraded to the extent that inhibition of their activity by isoflurane could not be detected. Also, the use of anoxia (0% O₂) rather than hypoxia may eliminate vestiges of mitochondrial ATP formation, anesthetic inhibition of which may decrease ATP/ADP and thus opposing or even

canceling ATP/ADP increases resulting from anesthetic inhibition of ATP consumption^[18,19].

For optimal anesthetic and surgical care, we need to know as much as possible about the effects and actions of the drugs we use, especially with regard to a process as essential as energy balance. The work described here has documented certain effects of isoflurane on ATP supply and demand at the cellular level and laid the groundwork for explaining them in terms of actions on specific biochemical reactions that produce and consume ATP. In addition to further elucidate such basic mechanisms, we also need to examine the consequence of these cellular effects in physiologic and clinical terms, by using more intact systems and measures of outcome.

REFERENCES

- 1 **Vagts DA**, Iber T, Puccini M, Szabo B, Haberstroh J, Villinger F, Geiger K, Noldge-Schomburg GF. The effects of thoracic epidural anesthesia on hepatic perfusion and oxygenation in healthy pigs during general anesthesia and surgical stress. *Anesth Analg* 2003; **97**: 1824-1832
- 2 **Ishida H**, Kadota Y, Sameshima T, Nishiyama A, Oda T, Kanmura Y. Comparison between sevoflurane and isoflurane anesthesia in pig hepatic ischemia-reperfusion injury. *J Anesth* 2002; **16**: 44-50
- 3 **Net M**, Valero R, Almenara R, Deulofeu R, Lopez-Boado MA, Capdevila L, Barros P, Bombi JA, Agusti M, Adalia R, Ruiz A, Arce Y, Manyalich M, Garcia-Valdecasas JC. Hepatic preconditioning after prolonged warm ischemia by means of S-adenosyl-L-methionine administration in pig liver transplantation from non-heart-beating donors. *Transplantation* 2003; **75**: 1970-1977
- 4 **Diskin MG**, Mackey DR, Roche JF, Sreenan JM. Effects of nutrition and metabolic status on circulating hormones and ovarian follicle development in cattle. *Anim Reprod Sci* 2003; **78**: 345-370
- 5 **Liu XL**, Li LJ, Chen Z. Isolation and primary culture of rat hepatocytes. *Hepatobiliary Pancreat Dis Int* 2002; **1**: 77-79
- 6 **Da-Silva WS**, Gomez-Puyou A, Gomez-Puyou MT, Moreno-Sanchez R, De Felice FG, De Meis L, Oliveira MF, Galina A. Mitochondrial bound hexokinase activity as a preventive antioxidant defense: Steady-state ADP formation as a regulatory mechanism of membrane potential and reactive oxygen species generation in mitochondria. *J Biol Chem* 2004; **279**: 39846-39855
- 7 **Ason B**, Handayani R, Williams CR, Bertram JG, Hingorani MM, O'Donnell M, Goodman MF, Bloom LB. Mechanism of loading the Escherichia coli DNA polymerase III beta sliding clamp on DNA. Bona fide primer/templates preferentially trigger the gamma complex to hydrolyze ATP and load the clamp. *J Biol Chem* 2003; **278**: 10033-10040
- 8 **Leal NA**, Olteanu H, Banerjee R, Bobik TA. Human ATP: Cob(I)alamin adenosyltransferase and its interaction with methionine synthase reductase. *J Biol Chem* 2004; **10**: 694-698
- 9 **Halestrap AP**. Mitochondrial permeability: dual role for the ADP/ATP translocator? *Nature* 2004; **430**: 1
- 10 **Kokoszka JE**, Waymire KG, Levy SE, Sligh JE, Cai J, Jones DP, MacGregor GR, Wallace DC. The ADP/ATP translocator is not essential for the mitochondrial permeability transition pore. *Nature* 2004; **427**: 461-465
- 11 **Korzeniewski B**. Influence of substrate activation (hydrolysis of ATP by first steps of glycolysis and beta-oxidation) on the effect of enzyme deficiencies, inhibitors, substrate shortage and energy demand on oxidative phosphorylation. *Biophys Chem* 2003; **104**: 107-119
- 12 **Koebmann BJ**, Westerhoff HV, Snoep JL, Solem C, Pedersen MB, Nilsson D, Michelsen O, Jensen PR. The extent to which ATP demand controls the glycolytic flux depends strongly on

- the organism and conditions for growth. *Mol Biol Rep* 2002; **29**: 41-45
- 13 **Korzeniewski B**. Parallel activation in the ATP supply-demand system lessens the impact of inborn enzyme deficiencies, inhibitors, poisons or substrate shortage on oxidative phosphorylation *in vivo*. *Biophys Chem* 2002; **96**: 21-31
- 14 **Pathak BL**, Becker GL, Reilly PJ, Hanson KA, Landers DF. Isoflurane partially preserves energy balance in isolated hepatocytes during *in vitro* anoxia. *Anesth Analg* 1991; **72**: 571-577
- 15 **Kayser EB**, Morgan PG, Sedensky MM. Mitochondrial complex I function affects halothane sensitivity in *Caenorhabditis elegans*. *Anesthesiology* 2004; **101**: 365-372
- 16 **Liu ZH**, He Y, Jin WQ, Chen XJ, Shen QX, Chi ZQ. Effect of chronic treatment of ohmefentanyl stereoisomers on cyclic AMP formation in Sf9 insect cells expressing human mu-opioid receptors. *Life Sc* 2004; **74**: 3001-3008
- 17 **Vincent MF**, Van den Berghe G, Hers HG. The pathway of adenine nucleotide catabolism and its control in isolated rat hepatocytes subjected to anoxia. *Biochem J* 1982; **202**: 117-123
- 18 **Becker GL**, Hensel P, Holland AD, Miletich DJ, Albrecht RF. Energy deficits in hepatocytes isolated from phenobarbital treated or fasted rats and briefly exposed to halothane and hypoxia *in vitro*. *Anesthesiology* 1986; **65**: 379-384
- 19 **Kenniston JA**, Baker TA, Fernandez JM, Sauer RT. Linkage between ATP consumption and mechanical unfolding during the protein processing reactions of an AAA+ degradation machine. *Cell* 2003; **114**: 511-520

Science Editor Wang XL and Guo SY Language Editor Elsevier HK

• BRIEF REPORTS •

Clinical evidence of growth hormone for patients undergoing abdominal surgery: Meta-analysis of randomized controlled trials

Yong Zhou, Xiao-Ting Wu, Gang Yang, Wen Zhuang, Mao-Ling Wei

Yong Zhou, Xiao-Ting Wu, Gang Yang, Wen Zhuang, Department of General Surgery, West China Hospital, Sichuan University, Chengdu 610041, Sichuan Province, China
Mao-Ling Wei, Chinese Evidence-Based Medicine/Cochrane Center, Chengdu 610041, Sichuan Province, China
Supported by the China Medical Board of New York No. 98-680
Correspondence to: Professor Xiao-Ting Wu, Department of General Surgery, West China Hospital, Sichuan University, 37 Guo Xue Road, Chengdu 610041, Sichuan Province, China. nutrition@163.com
Telephone: +86-28-85422480 Fax: +86-28-85422411
Received: 2004-05-27 Accepted: 2004-06-17

Key words: Perioperative growth hormone; Abdominal surgery

Zhou Y, Wu XT, Yang G, Zhuang W, Wei ML. Clinical evidence of growth hormone for patients undergoing abdominal surgery: Meta-analysis of randomized controlled trials. *World J Gastroenterol* 2005; 11(25): 3925-3930
<http://www.wjgnet.com/1007-9327/11/3925.asp>

Abstract

AIM: To assess the effectiveness and safety of perioperative growth hormone (GH) in patients undergoing abdominal surgery.

METHODS: We searched the following electronic databases: MEDLINE, EMBASE, the Cochrane Controlled Trials Register, Chinese Bio-medicine Database. The search was undertaken in February 2003. No language restrictions were applied. Randomized controlled trials (RCT) comparing GH with placebo in patients undergoing abdominal surgery were extracted and evaluated. Methodological quality was evaluated using the Jadad scale.

RESULTS: Eighteen trials involving 646 patients were included. The combined results showed that GH had a positive effect on improving postoperative nitrogen balance (standardized mean difference [SMD] = 3.37, 95%CI [2.46, 4.27], $P < 0.00001$), and decreasing the length of hospital stay (weighted mean difference [WMD] = -2.07, 95%CI [-3.03, -1.11], $P = 0.00002$), and reducing the duration of postoperative fatigue syndrome (SMD = -1.83, 95%CI [-2.37, -1.30], $P < 0.00001$), but it could increase blood glucose levels (WMD = 0.91, 95%CI [0.56, 1.25], $P < 0.00001$).

CONCLUSION: GH for patients undergoing abdominal surgery is effective and safe, if blood glucose can be controlled well. Further trials are required with a sufficient size to account for clinical heterogeneity and to measure other important outcomes such as infection, morbidity, mortality, fluid retention, immunomodulatory effects, and tumor recurrence.

INTRODUCTION

Catabolism and negative nitrogen balance is a part of the metabolic reaction to major abdominal surgical trauma. It is a concern to surgeons because the catabolic response is correlated with the overall surgical morbidity rate, causing prolonged convalescence. Growth hormone (GH) has been shown to have anabolic effects and to reduce or even prevent nitrogen catabolism in patients undergoing abdominal surgery. The effect of GH has recently been studied by many researchers. In 1974 Wilmore *et al.*^[1], suggested that adequate nutritional intake was necessary for GH to have nitrogen-saving effects. In 1986 the study by Phillips^[2] demonstrated that GH stimulated hepatic production of somatomedin (insulin-like growth factor-I, IGF-I) whose action could promote diverse anabolic processes, such as synthesis of RNA, DNA, proteins or proteoglycans. However, the effects of GH on nonmetabolic clinical outcome remain unclear.

Meta-analysis has been gradually used in medicine to improve the statistical efficiency, to evaluate the disadvantages of formulated researches and hypothesis, and to reach reliable conclusions from the mixed assortment of potentially relevant studies to determine the most promising directions for future researches. We performed a meta-analysis of available studies to assess the effectiveness and safety, in order to improve our understanding of the clinical effects of perioperative GH treatment of patients undergoing abdominal surgery; clinical outcomes including nitrogen balance, length of hospital stay, blood glucose, and postoperative fatigue syndrome were measured. Other important outcomes, such as infection, morbidity, mortality, fluid retention, immunomodulatory effects and tumor recurrence, were also measured.

MATERIALS AND METHODS

Identification of trials

Our aim was to identify all relevant randomized controlled trials (RCT) that compared GH with placebo in patients undergoing abdominal surgery. A RCT was defined as a

trial in which patients were assigned prospectively to one of two interventions by random allocation. We used a multimethod to identify relevant studies for the present review. A computerized literature search of MEDLINE from 1966 to October 2002 was conducted using the following search terms: operation OR surgery OR postoperative OR perioperative AND GH AND RCT (publication type) or controlled clinical trials or clinical trials, randomized. In addition, we searched Embase (1980-2002), Cochrane Controlled Trials Register (Issue 1, 2003), and Chinese Biomedicine Database (1979-2002), reviewed our personal files, and contacted experts in the field. Bibliographies of all selected articles and review articles that included information on GH were reviewed for other relevant articles. This search strategy was done iteratively, until no new potential, randomized, controlled trial citations were found on review of the reference lists of retrieved articles.

Study selection and data extraction

The following selection criteria were used to identify published studies for inclusion in this analysis: study design - randomized clinical trial, population - hospitalized adult patients undergoing abdominal surgery, intervention - GH *vs* placebo initiated at the same time and with the same nutrition support, and outcome variables - at least one of the following primary outcome variables: nitrogen balance, length of hospital stay, blood glucose, postoperative fatigue syndrome, incidence of infection, morbidity, mortality, fluid retention, immunomodulatory effects, and tumor recurrence. Study selection and data abstraction were conducted independently by the two investigators.

Data analysis

The incidences of infection, tumor recurrence, fluid retention, morbidity, and mortality were treated as binary variables. Nitrogen balance, length of hospital stay, blood glucose, postoperative fatigue syndrome, and immunomodulatory effects were treated as continuous variables. Data analysis was performed using the random effect model with meta-

analysis software (RevMan 4.2; Cochrane Collaboration, Oxford, UK). The continuous data outcomes were presented with 95% confidence intervals (CIs). When authors reported standard deviations, we used them directly. When standard deviations were not available, we computed them from the observed mean differences (either differences in changes or absolute readings) and the test statistics. When the test statistics were not available, given a *P* value, we computed the corresponding test statistics from tables for the normal distribution. We tested heterogeneity between trials with χ^2 tests, with *P*<0.05 indicating significant heterogeneity^[3]. Methodological quality was evaluated using the Jadad scale^[4].

RESULTS

From 460 articles screened, 38 were identified as RCT comparing GH with placebo and included for data extraction. Twenty studies were excluded, and the remaining 18 trials were included in the present meta-analysis^[5-22]. Only one study^[19] was in Chinese. Articles were excluded for the following reasons, namely the outcomes of interest were not recorded^[23-37] and some articles repeated^[38-42]. A total of 646 patients were enrolled in the included studies. The characteristics of studies included in meta-analysis comparing GH with placebo are presented in Table 1. Not all of the studies reported the outcome of interest, postoperative nitrogen balance was reported in 11 studies^[5-15], length of hospital stay in 3 studies^[17-19], postoperative fatigue syndrome in 3 studies^[20-22], blood glucose in 6 studies^[12-17].

The combined results showed that GH had a positive effect on improving the postoperative nitrogen balance (standardized mean difference [SMD] = 3.37, 95%CI [2.46, 4.27], *P*<0.00001) (Table 2A), and decreasing the length of hospital stay (weighted mean difference [WMD]=-2.07, 95%CI [-3.03, -1.11], *P* = 0.00002) (Table 2B), and reducing the duration of postoperative fatigue syndrome (SMD = -1.83, 95%CI [-2.37, -1.30], *P*<0.00001) (Table 2C), but it could increase blood glucose levels (WMD = 0.91, 95%CI [0.56, 1.25], *P*<0.00001) (Table 2D).

Table 1 Characteristics of studies included in meta-analysis comparing GH with placebo

Study	Year	Jadad score	Reference	Operation	GH
Lehner	1992	3	6	Major abdominal surgery	0.3 IU/kg/d for 5 d
López	1993	1	7	Major surgery of the digestive tract	0.2 IU/kg/d for 6 d
Wong	1995	2	8	Major abdominal surgery	0.2 IU/kg/d for 7 d
Tacke	1994	1	9	Major gastrointestinal surgery	0.3 IU/kg/d for 5 d
Saito	1992	3	10	Major abdominal operation	0.4 IU/kg/d for 6 d
Kolstad	2001	5	11	Laparoscopic cholecystectomy	13 IU/m ² /d for 3 d
Jensen	1998	5	12	Ileoanal anastomosis with a J pouch	12 IU/d for 6 d
Ponting	1988	2	13	Major gastrointestinal surgery	0.1 mg/kg/d for 7 d
Hammarqvist	1992	1	14	Elective cholecystectomy	0.3 IU/kg/d for 3 d
Jiang	1989	4	15	Gastrectomy or colectomy	0.15 IU/kg/d for 7 d
Mjaaland	1991	3	16	Gastrointestinal surgery	24 IU/d for 5 d
Barle	2001	1	17	Laparoscopic cholecystectomy	12 IU/d for 5 d
Vara-Thorbeck 1	1993	3	18	Cholecystectomy	8 IU/d for 7 d
Barry 2	1998	4	19	Abdominal aortic aneurysm repair	0.3 IU/kg/d for 6 d
Liu	2001	5	20	Abdominal surgery	0.3 IU/kg/d for 5 d
Barry 1	1999	3	21	Abdominal aortic aneurysm repair	0.3 IU/kg/d for 6 d
Kissmeyer-Nielsen	1999	5	22	Ileoanal J-pouch surgery	12 IU/d for 6 d
Vara-Thorbeck 2	1996	3	23	Cholecystectomy	8 IU/d for 7 d

Table 2 Random effect model of standardized mean difference (95%CI) in improving postoperative nitrogen balance (A) and in reducing the duration of postoperative fatigue syndrome (C) and weighted mean difference (95%CI) in decreasing the length of hospital stay (B) and in increasing blood glucose levels (D) with GH as compared with placebo

A

Study	Treatment <i>n</i>	Treatment Mean (SD)	Control <i>n</i>	Control Mean (SD)	Weight %	SMD (random) 95%CI
Ponting	6	1.80 (0.40)	5	-0.90 (0.70)	6.23	4.46 [1.85, 7.07]
Jiang	9	-7.10 (3.12)	9	-32.60 (4.20)	6.27	6.56 [3.97, 9.16]
Mjaaland	9	4.10 (1.10)	10	-3.10 (1.80)	8.36	4.55 [2.69, 6.41]
Hammarqvist	8	-2.32 (1.66)	9	-7.09 (0.71)	8.91	3.63 [1.94, 5.32]
Lehner	19	-4.30 (9.60)	21	-14.80 (3.30)	11.94	1.46 [0.76, 2.17]
Saito	18	-18.00 (3.30)	18	-185.00 (58.00)	10.60	3.98 [2.80, 5.15]
López	9	-7.30 (2.80)	9	-20.70 (4.10)	9.09	3.64 [2.00, 5.27]
Tacke	9	-10.00 (2.61)	10	-20.47 (3.86)	9.85	3.00 [1.60, 4.40]
Wong	8	3.00 (0.90)	7	-1.30 (0.75)	7.15	4.85 [2.59, 7.11]
Jenson	9	-47.00 (20.00)	10	-73.00 (20.00)	11.12	1.24 [0.24, 2.25]
Kolstad	11	-3.90 (0.40)	10	-5.70 (0.90)	10.49	2.53 [1.32, 3.73]
Total (95%CI)	115		118		100.00	3.37 [2.46, 4.27]

Test for heterogeneity: $\chi^2 = 44.48$, $df = 10$ ($P < 0.00001$), $I^2 = 77.5\%$. Test for overall effect: $Z = 7.27$ ($P < 0.00001$).

B

Study	Treatment <i>n</i>	Treatment Mean (SD)	Control <i>n</i>	Control Mean (SD)	Weight %	WMD (fixed) 95%CI
Barry 2	8	13.00 (2.00)	10	17.00 (3.00)	17.05	-4.00 [-6.32, -1.68]
Liu	10	9.70 (1.80)	10	10.50 (1.30)	48.41	-0.80 [-2.18, 0.58]
Vara-Thorbeck 1	87	9.60 (3.60)	93	12.50 (7.10)	34.54	-2.90 [-4.53, -1.27]
Total (95%CI)	105		113		100.00	-2.07 [-3.03, -1.11]

Test for heterogeneity: $\chi^2 = 6.93$, $df = 2$ ($P = 0.03$), $I^2 = 71.1\%$. Test for overall effect: $Z = 4.24$ ($P < 0.0001$).

C

Study	Treatment <i>n</i>	Treatment Mean (SD)	Control <i>n</i>	Control Mean (SD)	Weight %	SMD (fixed) 95%CI
Barry 1	7	1.60 (1.20)	10	4.90 (2.20)	21.23	-1.68 [-2.84, -0.52]
Kissmeyer-Nielsen	9	1.37 (0.55)	10	2.73 (2.00)	31.57	-0.86 [-1.82, 0.09]
Vara-Thorbeck 2	22	1.52 (0.43)	26	3.14 (0.75)	47.20	-2.55 [-3.33, -1.77]
Total (95%CI)	38		46		100.00	-1.83 [-2.37, -1.30]

Test for heterogeneity: $\chi^2 = 7.32$, $df = 2$ ($P = 0.03$), $I^2 = 72.7\%$. Test for overall effect: $Z = 6.72$ ($P < 0.00001$).

D

Study	Treatment <i>n</i>	Treatment Mean (SD)	Control <i>n</i>	Control Mean (SD)	Weight %	WMD (random) 95%CI
Barle	10	6.40 (1.00)	10	5.40 (0.50)	11.98	1.00 [0.31, 1.69]
Hammarqvist	8	5.60 (0.30)	9	4.80 (0.20)	20.69	0.80 [0.55, 1.05]
Jiang	9	6.17 (0.51)	9	6.06 (0.50)	16.26	0.11 [-0.36, 0.58]
Mjaaland	9	5.75 (0.43)	10	4.90 (0.30)	18.94	0.85 [0.51, 1.19]
Ponting	6	9.40 (0.70)	5	7.20 (0.50)	11.68	2.20 [1.49, 2.91]
Vara-Thorbeck 1	87	6.56 (1.02)	93	5.66 (0.71)	20.46	0.90 [0.64, 1.16]
Total (95%CI)	129		136		100.00	0.91 [0.56, 1.25]

Test for heterogeneity: $\chi^2 = 23.97$, $df = 5$ ($P = 0.0002$), $I^2 = 79.1\%$. Test for overall effect: $Z = 5.13$ ($P < 0.00001$).

DISCUSSION

The results must be interpreted with the difference in patients, dose or length of treatment, and unexplained heterogeneity. Clinical heterogeneity in the form of age, etiology and operation of patients points to the possibility of bias.

This meta-analysis did not show that GH had a positive effect on improving postoperative nitrogen balance. Eleven studies involving 233 patients were included. Although there was a heterogeneity (test for heterogeneity $\chi^2 = 44.48$, $df = 10$, $P < 0.00001$), the result was sure. Because all the 11 studies showed that GH had a positive effect on improving postoperative nitrogen balance with a statistical significance (minimum of SMD = 1.24, 95%CI [0.24, 2.25]). However,

it seems that different doses had different effects, subgroup was not used. What attention should be paid to is that some studies only reported the cumulated nitrogen balance or the daily nitrogen balance. Further research should be done to assess the possible best dose.

To date, only three studies involving 218 patients, have examined whether treatment with GH could influence the length of hospital stay. The combined results showed that administration of GH could decrease the length of hospital stay. The results must be interpreted with caution due to the small size. Two of three trials^[17,18] showed statistically and clinically significant differences in the length of hospital stay. So, further trials are required with a sufficient size to

account for clinical heterogeneity and length of hospital stay.

This meta-analysis showed that administration of GH could reduce the duration of postoperative fatigue syndrome after 1 mo. Three studies involving 84 patients were included. The evidence was not strong due to the small size and unexplained heterogeneity. It is also important to recognize that two^[20,21] of the RCTs included in this review were not designed specifically to reduce postoperative fatigue and provided few or no theoretical rationales as to why the intervention under study might be expected to attenuate it. Attempts to assess fatigue objectively by measuring, for example, physical activity, time taken to return to normal routine, or involuntary or voluntary muscle force were problematic because they could be confounded by numerous factors including pain and anxiety. Much effort has therefore been devoted to developing short and easy-to-use questionnaires that could provide some quantification of a patient's subjective feeling of fatigue. Future research should ensure that an adequate measure of subjective fatigue is employed, possibly in tandem with important objective measures, such as time taken to return to work.

This meta-analysis did not show that GH might increase blood glucose levels. Six studies involving 265 patients were included. Of the six, only the study of Jiang *et al.*^[14], did not reach a statistical significance (SMD = 0.11, 95%CI [-0.36, 0.58]). Low-dose GH and hypocaloric nutrition may be the reason. Confirmation of the diabetogenic properties of GH was made after it was administered in excess to experimental animals and men. Transgenic animals, which over-expressed GH, developed insulin resistance, marked hyperinsulinemia, hyperglycemia, and hypertriglyceridemia in association with a number of molecular abnormalities^[43,44]. Patients with acromegaly developed insulin resistance and hyperinsulinemia, while up to 40% became diabetic^[45,46]. There is evidence that insulin resistance caused by GH plays an important role in the rise of blood glucose. In addition, GH could stimulate lipolysis with the release of glycerol and non-esterified fatty acids (NEFA). This provides a further mechanism for the diabetogenic properties of GH through the effect of NEFA to increase hepatic glucose output and decrease peripheral glucose oxidation according to the glucose-fatty acid cycle^[47,48]. In fact, in the study of Berman *et al.*^[23], the GH group had significantly elevated urine glucose levels throughout the study period, consistent with the demonstrated hyperglycemia and only moderately elevated insulin levels. Treatment with GH did result in hyperglycemia, and two patients were removed from the study. Hyperglycemia associated with GH administration could be treated easily by insulin, especially in long-term GH administration.

Only one RCT^[36] conducted an analysis of a multicenter study with 104 patients undergoing major gastrointestinal surgery to assess the risk of long-term tumor recurrence after short-term (5 d) postoperative GH treatment. The study was a follow-up of a previous randomized study investigating the effect of three different doses of GH (0.075, 0.15, and 0.30 IU/kg/d) on the postoperative cumulative nitrogen balance in patients undergoing major surgery. Tumors recurred in 20 (35%) patients who were evaluated for and treated with GH ($n = 57$). This accounted for 4 of 17 (23%) patients given 0.075 IU/kg/d of GH, 9

of 20 (45%) given 0.15 IU/kg/d of GH, and 7 of 20 (35%) given 0.30 IU/kg/d. By comparison, tumors recurred in 8 of 18 (44%) of patients given placebo. The result of this study demonstrated that short-term treatment with GH for 5 d after major gastrointestinal surgery for adenocarcinoma did not increase the risk of tumor recurrence. But the group size was too small to further stratify the patients according to tumor type and tumor stage, so that no information was gained about the influence of GH dose in certain tumor stages.

Fluid retention is one of known side effects of GH administration. The sodium and fluid retaining impact of GH was demonstrated in humans almost 50 years ago by Ikkos *et al.*^[49]. Underlying mechanisms of GH-induced fluid retention are as follows. GH could increase glomerular filtration rate mediated by insulin-like growth factor (IGF-I)^[50-52], stimulate the renin-angiotensin-aldosterone system (RAAS)^[53-57], reduce atrial natriuretic factors^[58-61], and prostaglandins could play a role in GH-induced fluid retention^[62]. In the study of Berman *et al.*^[23], two GH patients were removed from the study for fluid retention. These patients were in the immediate postoperative period. However, whether the fluid retention was a result of surgery or GH administration could not be determined.

GH should not be given in acute inflammatory disease states. Findings by Takala *et al.*^[63], pointed to the immunomodulatory effects of GH. These authors described higher hospital mortality in a Finish and an European study on critically ill non-cancer patients. It was proposed that the higher mortality was due to the application of GH at a later stage during the inflammatory disease process, leading to uncontrolled systemic inflammation. However, infection was not measured in these trials except one^[17]. Only one RCT^[18] reported the morbidity and mortality, so we could not draw a conclusion due to the small size. But there are still four studies^[64-67] awaiting assessment in other languages or we cannot find the full text.

In conclusion, perioperative GH treatment of patients undergoing abdominal surgery can improve the postoperative nitrogen balance, and decrease the length of hospital stay, and reduce the duration of postoperative fatigue syndrome. But it might increase blood glucose levels. However, the evidence is not strong due to the difference in patients, dose or length of treatment, and unexplained heterogeneity. In order to examine the effectiveness and safety of perioperative GH treatment of patients undergoing abdominal surgery, further trials are required with a sufficient size to account for the clinical heterogeneity and to measure other important outcomes such as infection, morbidity, mortality, fluid retention, immunomodulatory effects, and tumor recurrence.

ACKNOWLEDGEMENTS

We are sincerely grateful to the principal investigators of all the trials who provided additional unpublished information. We also thank Susanne Ebrahim and Karla Bergerhoff for diligent working in Cochrane Metabolic and Endocrine Disorders Group and Ming Liu, He-Ming Huang, Bin Lv, Eewen, Jian-Kun Hu, Hua Jiang and Shu-Ai Xiao for providing additional references.

REFERENCES

- 1 **Wilmore DW**, Moylan JA Jr, Bristow BF, Mason AD Jr, Pruitt BA Jr. Anabolic effects of human growth hormone and high caloric feedings following thermal injury. *Surg Gynecol Obstet* 1974; **138**: 875-884
- 2 **Phillips LS**. Nutrition, somatomedins, and the brain. *Metabolism* 1986; **35**: 78-87
- 3 **Oxman AD**, Cook DJ, Guyatt GH. Users' guides to the medical literature. VI. How to use an overview. Evidence-Based Medicine Working Group. *JAMA* 1994; **272**: 1367-1371
- 4 **Jadad AR**, Moore RA, Carroll D, Jenkinson C, Reynolds DJ, Gavaghan DJ, McQuay HJ. Assessing the quality of reports of randomized clinical trials: is blinding necessary? *Control Clin Trials* 1996; **17**: 1-12
- 5 **Lehner JH**, Jauch KW, Berger G. A multicentre study of the dose response effect of human recombinant growth hormone (rhGH) on cumulative nitrogen balance (CNB) in patients after major abdominal surgery [abstract]. *Clin Nutr* 1992; **11** (Suppl): 75-76
- 6 **López J**, Fernández C, Carriedo D. Metabolic effects of recombinant growth hormone following major surgery of the digestive tract [abstract]. *Medicina Intensiva* 1993; **17**(Suppl): 82
- 7 **Wong WK**, Soo KC, Nambiar R, Tan YS, Yo SL, Tan IK. The effect of recombinant growth hormone on nitrogen balance in malnourished patients after major abdominal surgery. *Aust N Z J Surg* 1995; **65**: 109-113
- 8 **Tacke J**, Bolder U, Lohlein D. Improved cumulated nitrogen balance after administration of recombinant human growth hormone in patients undergoing gastrointestinal surgery. *Infusionsther Transfusionsmed* 1994; **21**: 24-29
- 9 **Saito H**, Taniwaka K, Muto T. Effects of growth hormone dose after major abdominal operation: a randomized, prospective, multicenter trial [abstract]. *Clin Nutr* 1992; **11**(Suppl): 9
- 10 **Kolstad O**, Jenssen TG, Ingebretsen OC, Vinnars E, Revhaug A. Combination of recombinant human growth hormone and glutamine-enriched total parenteral nutrition to surgical patients: effects on circulating amino acids. *Clin Nutr* 2001; **20**: 503-510
- 11 **Jensen MB**, Kissmeyer-Nielsen P, Laurberg S. Perioperative growth hormone treatment increases nitrogen and fluid balance and results in short-term and long-term conservation of lean tissue mass. *Am J Clin Nutr* 1998; **68**: 840-846
- 12 **Ponting GA**, Halliday D, Teale JD, Sim AJ. Postoperative positive nitrogen balance with intravenous hyponutrition and growth hormone. *Lancet* 1988; **1**: 438-440
- 13 **Hammarqvist F**, Stromberg C, von der Decken A, Vinnars E, Wernerman J. Biosynthetic human growth hormone preserves both muscle protein synthesis and the decrease in muscle-free glutamine, and improves whole-body nitrogen economy after operation. *Ann Surg* 1992; **216**: 184-191
- 14 **Jiang ZM**, He GZ, Zhang SY, Wang XR, Yang NF, Zhu Y, Wilmore DW. Low-dose growth hormone and hypocaloric nutrition attenuate the protein-catabolic response after major operation. *Ann Surg* 1989; **210**: 513-525
- 15 **Mjaaland M**, Unneberg K, Hotvedt R, Revhaug A. Nitrogen retention caused by growth hormone in patients undergoing gastrointestinal surgery with epidural analgesia and parenteral nutrition. *Eur J Surg* 1991; **157**: 21-27
- 16 **Barle H**, Rahlen L, Essen P, McNurlan MA, Garlick PJ, Holgersson J, Wernerman J. Stimulation of human albumin synthesis and gene expression by growth hormone treatment. *Clin Nutr* 2001; **20**: 59-67
- 17 **Vara-Thorbeck R**, Guerrero JA, Rosell J, Ruiz-Requena E, Capitan JM. Exogenous growth hormone: effects on the catabolic response to surgically produced acute stress and on postoperative immune function. *World J Surg* 1993; **17**: 530-538
- 18 **Barry MC**, Mealy K, Sheehan SJ, Burke PE, Cunningham AJ, Leahy A, Bouchier Hayes D. The effects of recombinant human growth hormone on cardiopulmonary function in elective abdominal aortic aneurysm repair. *Eur J Vasc Endovasc Surg* 1998; **16**: 311-319
- 19 **Liu W**. The impact of pretreatment with recombinant human growth hormone on intestinal barrier function and cell immune function. *Zhongguo Linchuang Yingyang Zazhi* 2001; **4**: 77-80
- 20 **Barry MC**, Mealy K, O'Neill S, Hughes A, McGee H, Sheehan SJ, Burke PE, Bouchier-Hayes D. Nutritional, respiratory, and psychological effects of recombinant human growth hormone in patients undergoing abdominal aortic aneurysm repair. *JPEN* 1999; **23**: 128-135
- 21 **Kissmeyer-Nielsen P**, Jensen MB, Laurberg S. Perioperative growth hormone treatment and functional outcome after major abdominal surgery: a randomized, double-blind, controlled study. *Ann Surg* 1999; **229**: 298-302
- 22 **Vara-Thorbeck R**, Guerrero JA, Ruiz-Requena E, Garcia-Carriazo M. Can the use of growth hormone reduce the postoperative fatigue syndrome? *World J Surg* 1996; **20**: 81-87
- 23 **Berman RS**, Harrison LE, Pearlstone DB, Burt M, Brennan MF. Growth hormone, alone and in combination with insulin, increases whole body and skeletal muscle protein kinetics in cancer patients after surgery. *Ann Surg* 1999; **229**: 1-10
- 24 **Carli F**, Webster JD, Halliday D. A nitrogen-free hypocaloric diet and recombinant human growth hormone stimulate postoperative protein synthesis: fasted and fed leucine kinetics in the surgical patient. *Metabolism* 1997; **46**: 796-800
- 25 **Carli F**, Webster JD, Halliday D. Growth hormone modulates amino acid oxidation in the surgical patient: leucine kinetics during the fasted and fed state using moderate nitrogenous and caloric diet and recombinant human growth hormone. *Metabolism* 1997; **46**: 23-28
- 26 **Hammarqvist F**, Sandgren A, Andersson K, Essen P, McNurlan MA, Garlick PJ, Wernerman J. Growth hormone together with glutamine-containing total parenteral nutrition maintains muscle glutamine levels and results in a less negative nitrogen balance after surgical trauma. *Surgery* 2001; **129**: 576-586
- 27 **Inoue Y**, Copeland EM, Souba WW. Growth hormone enhances amino acid uptake by the human small intestine. *Ann Surg* 1994; **219**: 715-724
- 28 **Kissmeyer P**, Moller J, Bach Jensen M, Laurberg S. Effect of growth hormone on the atabolic response to elective J-pouch surgery [abstract]. *Int J Colorectal Dis* 1997; **12**: 189
- 29 **Mjaaland M**. Growth hormone after gastrointestinal surgery: effect on skeletal muscle metabolism [abstract]. *Clin Nutr* 1990; **9**(Suppl): 13
- 30 **Mjaaland M**. The effect of growth hormone on postoperative nitrogen balance [abstract]. *Ann Chir Gynaecol* 1989; **78**: 14
- 31 **Mjaaland M**, Unneberg K, Larsson J, Nilsson L, Revhaug A. Growth hormone after abdominal surgery attenuated forearm glutamine, alanine, 3-methylhistidine, and total amino acid efflux in patients receiving total parenteral nutrition. *Ann Surg* 1993; **217**: 413-422
- 32 **Mjaaland M**, Unneberg K, Bjoro T, Revhaug A. Growth hormone treatment after abdominal surgery decreased carbohydrate oxidation and increased fat oxidation in patients with total parenteral nutrition. *Metabolism* 1993; **42**: 185-190
- 33 **Moller J**, Jensen MB, Frandsen E, Moller N, Kissmeyer P, Laurberg S. Growth hormone treatment improves body fluid distribution in patients undergoing elective abdominal surgery. *Clin Endocrinol* 1998; **49**: 597-602
- 34 **Plank LD**, Hill GL. Use of bioimpedance spectroscopy to assess effects of perioperative treatment with growth hormone on fluid changes in patients undergoing major surgery. *Ann N Y Acad Sci* 2000; **904**: 190-192
- 35 **Saito H**, Taniwaka K, Fukushima R, Sawada T, Muto T, Morioka Y. Growth hormone treatment stimulates immune responsiveness after abdominal surgery [abstract]. *Clin Nutr* 1990; **9**(Suppl): 16
- 36 **Tacke J**, Bolder U, Herrmann A, Berger G, Jauch KW. Long-term risk of gastrointestinal tumor recurrence after postoperative treatment with recombinant human growth hormone. *JPEN* 2000; **24**: 140-144
- 37 **Vara-Thorbeck R**, Guerrero JA, Ruiz-Requena ME, Capitan J, Rodriguez M, Rosell J, Mekinassi K, Maldonado M, Martin

- R. Effects of growth hormone in patients receiving total parenteral nutrition following major gastrointestinal surgery. *Hepatogastroenterology* 1992; **39**: 270-272
- 38 **Barle H**, Essen P, Nyberg B, Olivecrona H, Tally M, McNurlan MA, Wernerman J, Garlick PJ. Depression of liver protein synthesis during surgery is prevented by growth hormone. *Am J Physiol* 1999; **276**(4 Pt 1): E620-627
- 39 **He G**, Jiang Z, Yang N, Shu H, Wilmore DW. Effect of recombinant growth hormone on amino acids metabolism in blood and urine after major operation. *Zhongguo Yixue Kexueyuan Xuebao* 1997; **19**: 192-196
- 40 **Jiang Z**, He G, Wang X, Yang N, Wilmore DW. The effect of nutrition support and recombinant growth hormone on body composition and muscle function in postoperative patients. *Zhongguo Yixue Kexueyuan Xuebao* 1994; **16**: 443-447
- 41 **Mealy K**, Barry M, O'Mahony L, Sheehan S, Burke P, McCormack C, Whitehead AS, Bouchier-Hayes D. Effects of human recombinant growth hormone (rhGH) on inflammatory responses in patients undergoing abdominal aortic aneurysm repair. *Intensive Care Med* 1998; **24**: 128-131
- 42 **Vara-Thorbeck R**, Ruiz-Requena E, Guerrero-Fernandez JA. Effects of human growth hormone on the catabolic state after surgical trauma. *Horm Res* 1996; **45**: 55-60
- 43 **Valera A**, Rodriguez-Gil JE, Yun JS, McGrane MM, Hanson RW, Bosch F. Glucose metabolism in transgenic mice containing a chimeric P-enolpyruvate carboxykinase/bovine growth hormone gene. *FASEB J* 1993; **7**: 791-800
- 44 **Ikeda A**, Chang KT, Matsumoto Y, Furuhashi Y, Nishihara M, Sasaki F, Takahashi M. Obesity and insulin resistance in human growth hormone transgenic rats. *Endocrinology* 1998; **139**: 3057-3063
- 45 **Ezzat S**, Forster MJ, Berchtold P, Redelmeier DA, Boerlin V, Harris AG. Acromegaly. Clinical and biochemical features in 500 patients. *Medicine* 1994; **73**: 233-240
- 46 **Colao A**, Baldelli R, Marzullo P, Ferretti E, Ferone D, Gargiulo P, Petretta M, Tamburrano G, Lombardi G, Liuzzi A. Systemic hypertension and impaired glucose tolerance are independently correlated to the severity of the acromegalic cardiomyopathy. *J Clin Endocrinol Metab* 2000; **85**: 193-199
- 47 **Gerich JE**, Lorenzi M, Bier DM, Tsalikian E, Schneider V, Karam JH, Forsham PH. Effects of physiologic levels of glucagon and growth hormone on human carbohydrate and lipid metabolism. Studies involving administration of exogenous hormone during suppression of endogenous hormone secretion with somatostatin. *J Clin Invest* 1976; **57**: 875-884
- 48 **Ferrannini E**, Barrett EJ, Bevilacqua S, DeFronzo RA. Effect of fatty acids on glucose production and utilization in man. *J Clin Invest* 1983; **72**: 1737-1747
- 49 **Ikkos D**, Luft R, Sjogren B. Body water and sodium in patients with acromegaly. *J Clin Invest* 1954; **33**: 989-994
- 50 **Guler HP**, Schmid C, Zapf J, Froesch ER. Effects of recombinant insulin-like growth factor I on insulin secretion and renal function in normal human subjects. *Proc Natl Acad Sci USA* 1989; **86**: 2868-2872
- 51 **Hirschberg R**, Kopple JD. Evidence that insulin-like growth factor I increases renal plasma flow and glomerular filtration rate in fasted rats. *J Clin Invest* 1989; **83**: 326-330
- 52 **Hirschberg R**, Brunori G, Kopple JD, Guler HP. Effects of insulin-like growth factor I on renal function in normal men. *Kidney Int* 1993; **43**: 387-397
- 53 **Venning EH**, Lucis OJ. Effect of growth hormone on the biosynthesis of aldosterone in the rat. *Endocrinology* 1962; **70**: 486-491
- 54 **Ho KY**, Weissberger AJ. The antinatriuretic action of biosynthetic human growth hormone in man involves activation of the renin-angiotensin system. *Metabolism* 1990; **39**: 133-137
- 55 **Cuneo RC**, Salomon F, Wilmschurst P, Byrne C, Wiles CM, Hesp R, Sonksen PH. Cardiovascular effects of growth hormone treatment in growth-hormone-deficient adults: stimulation of the renin-aldosterone system. *Clin Sci* 1991; **81**: 587-592
- 56 **Herlitz H**, Jonsson O, Bengtsson BA. Effect of recombinant human growth hormone on cellular sodium metabolism. *Clin Sci* 1994; **86**: 233-237
- 57 **Ross EJ**, Vant Hoff W, Crabbe J, Thorn GW. Aldosterone excretion in hypopituitarism and after hypophysectomy in man. *Am J Med* 1960; **28**: 229-238
- 58 **Donath MY**, Zierhut W, Gosteli-Peter MA, Hauri C, Froesch ER, Zapf J. Effects of IGF-I on cardiac growth and expression of mRNAs coding for cardiac proteins after induction of heart hypertrophy in the rat. *Eur J Endocrinol* 1998; **139**: 109-117
- 59 **Donath MY**, Gosteli-Peter MA, Hauri C, Froesch ER, Zapf J. Insulin-like growth factor-I stimulates myofibrillar genes and modulates atrial natriuretic factor mRNA in rat heart. *Eur J Endocrinol* 1997; **137**: 309-315
- 60 **Tanaka N**, Ryoike T, Hongo M, Mao L, Rockman HA, Clark RG, Ross J Jr. Effects of growth hormone and IGF-I on cardiac hypertrophy and gene expression in mice. *Am J Physiol* 1998; **275**: H393-399
- 61 **Harder BA**, Schaub MC, Eppenberger HM, Eppenberger-Eberhardt M. Influence of fibroblast growth factor (bFGF) and insulin-like growth factor (IGF-I) on cytoskeletal and contractile structures and on atrial natriuretic factor (ANF) expression in adult rat ventricular cardiomyocytes in culture. *J Mol Cell Cardiol* 1996; **28**: 19-31
- 62 **Tonshoff B**, Nowack R, Kurilenko S, Blum WF, Seyberth HW, Mehls O, Ritz E. Growth hormone-induced glomerular hyperfiltration is dependent on vasodilating prostanoids. *Am J Kidney Dis* 1993; **21**: 145-151
- 63 **Takala J**, Ruokonen E, Webster NR, Nielsen MS, Zandstra DF, Vundelinckx G, Hinds CJ. Increased mortality associated with growth hormone treatment in critically ill adults. *N Engl J Med* 1999; **341**: 785-792
- 64 **Gottardis M**, Gruber E, Benzer A, Murr C, Schmoigl C, Hackl JM, Balogh D. Effects of short-term application of recombinant human growth hormone on urea production rate in patients in the early postoperative phase. *Infusionsther Transfusionsmed* 1993; **20**: 142-147
- 65 **Guerrero JA**, Capitan JM, Rosell J, Ruiz ME, Garcia E, Garcia-Carriazo M, Maldonado MJ, Vara Thorbeck R. Effect of growth hormone and parenteral nutrition on the catabolic phase following major digestive surgery. *Rev Esp Enferm Dig* 1992; **81**: 379-382
- 66 **Martin R**, Cano MD, Guerrero JA, Segovia E, Vara Thorbeck R. Growth hormone and its effects on cholesterol and lipoprotein metabolism following surgical intervention (hGH and cholesterol metabolism during surgery). *Nutr Hosp* 1998; **13**: 181-185
- 67 **Wennstrom I**, Wernerman J, Hammarqvist F. Postoperative effects of growth hormone and insulin-like growth factor-I on the nitrogen balance and muscle amino acid pattern [abstract]. *Clin Nutr* 1999; **18**(Suppl): 14

Autofluorescence excitation-emission matrices for diagnosis of colonic cancer

Bu-Hong Li, Shu-Sen Xie

Bu-Hong Li, Shu-Sen Xie, Biomedical Optics Laboratory, Institute of Laser and Optoelectronics Technology, Fujian Normal University, Fuzhou 350007, Fujian Province, China

Supported by the Natural Science Foundation of Fujian Province, No. A0310018 and No. 2002F008, and the Scientific Research Program of Fujian Province, No. JA03041

Correspondence to: Dr. Bu-Hong Li, Biomedical Optics Laboratory, Institute of Laser and Optoelectronics Technology, Fujian Normal University, Fuzhou 350007, Fujian Province, China. bhli@fjnu.edu.cn
Telephone: +86-591-83165373 Fax: +86-591-83465373

Received: 2004-09-22 Accepted: 2004-12-21

Abstract

AIM: To investigate the autofluorescence spectroscopic differences in normal and adenomatous colonic tissues and to determine the optimal excitation wavelengths for subsequent study and clinical application.

METHODS: Normal and adenomatous colonic tissues were obtained from patients during surgery. A FL/FS920 combined TCSPC spectrofluorimeter and a lifetime spectrometer system were used for fluorescence measurement. Fluorescence excitation wavelengths varying from 260 to 540 nm were used to induce the autofluorescence spectra, and the corresponding emission spectra were recorded from a range starting 20 nm above the excitation wavelength and extending to 800 nm. Emission spectra were assembled into a three-dimensional fluorescence spectroscopy and an excitation-emission matrix (EEM) to exploit endogenous fluorophores and diagnostic information. Then emission spectra of normal and adenomatous colonic tissues at certain excitation wavelengths were compared to determine the optimal excitation wavelengths for diagnosis of colonic cancer.

RESULTS: When compared to normal tissues, low NAD (P)H and FAD, but high amino acids and endogenous porphyrins of protoporphyrin IX characterized the high-grade malignant colonic tissues. The optimal excitation wavelengths for diagnosis of colonic cancer were about 340, 380, 460, and 540 nm.

CONCLUSION: Significant differences in autofluorescence peaks and its intensities can be observed in normal and adenomatous colonic tissues. Autofluorescence EEMs are able to identify colonic tissues.

© 2005 The WJG Press and Elsevier Inc. All rights reserved.

Key words: Autofluorescence spectroscopy; Excitation-emission matrix; Optical diagnosis; Colonic cancer

Li BH, Xie SS. Autofluorescence excitation-emission matrices for diagnosis of colonic cancer. *World J Gastroenterol* 2005; 11(25): 3931-3934

<http://www.wjgnet.com/1007-9327/11/3931.asp>

INTRODUCTION

Colonic cancer is an important public health concern in industrialized countries and around the world. Diagnosis and localization of early carcinoma play an important role in the prevention and curative treatment of colonic cancer. However, physical biopsies do not fully solve this problem because they are sampled at random locations, which is highly dependent on the skill and experience of the investigator. As a result, a significant number of lesions, especially the carcinoma *in situ* lesions, are not sampled and subsequently diagnosed^[1,2]. Laser-induced autofluorescence depends on endogenous fluorophores in the biological tissue, which undergoes a change related to malignant transformations. Therefore, it is possible for us to develop more sensitive techniques for the detection of early colonic tissue. During the past two decades, autofluorescence spectroscopy has been investigated as an effective and noninvasive method for detecting and imaging the abnormal tissues from the surrounding normal tissues.

Measurement of three-dimensional fluorescence spectroscopy or fluorescence excitation-emission matrices (EEMs) for tissue samples *in vitro* is a crucial step to exploit the endogenous fluorophores and determine which excitation wavelengths contain the most diagnostic information for clinical diagnostic analysis^[3-6]. However, an important limitation of most studies on the autofluorescence diagnosis of colonic cancer is that the selection of excitation wavelengths is based on the availability of a special light source, and few studies have been done to understand the real reasons responsible for the spectral differences^[6-9]. In this study, we conducted the measurement of autofluorescence EEMs in order to investigate the spectroscopic differences in normal and adenomatous colonic tissues, and to further determine the optimal excitation wavelengths. It is hoped that information from this investigation may be useful for subsequent studies and clinical diagnosis.

MATERIALS AND METHODS

Adenomatous colonic tissues ($n = 5$) were obtained from four patients during surgery for malignant tumors of the colon, and normal tissue sample ($n = 4$, matched controls) was also collected from the same patient. Each tissue sample was cut into two specimens. One specimen was sent to the

pathologist for standard histopathological evaluation, the other unstained and unfixed specimen was placed on a non-fluorescence quartz substrate for laser-induced autofluorescence within 2 h after surgical resection.

Autofluorescence EEM was performed using a FL/FS920 combined TCSPC spectrofluorimeter and a lifetime spectrometer system (Edinburgh Instruments Ltd, UK). The wavelength-selected excitation light onto the sample with a 60° incident angle and fluorescence emission was collected at 45° with respect to the normal quartz substrate in order to minimize the detection of the backscattered excitation light. The slit sizes of excitation and emission monochromator were 1.5 and 0.5 mm, respectively. The wavelength dependence of the excitation power and the detector response was corrected and calibrated for all emission spectra. Fluorescence EEMs were recorded by measuring the fluorescence emission spectra over a range of excitation wavelengths. The excitation wavelengths varied from 260 to 540 nm in 20-nm increments. At each excitation wavelength, the fluorescence emission spectra were recorded from a range starting 20 nm above the excitation wavelength and extending to 800 nm at 5-nm intervals. These wavelength ranges enabled characterization of all endogenous fluorophores, tryptophan, collagen, and elastin, NAD(P)H, FAD and endogenous porphyrins, present in tissues in the UV-Vis spectrum^[10,11]. This resulted in a total measurement time about 25 min for each EEM. After each measurement, a repeat fluorescence spectrum was measured at 260 nm excitation and compared to that measured at the beginning of the experiment to confirm that the measurement protocol used did not induce photobleaching. Fluorescence data from each single measurement were then combined to construct EEM containing fluorescence intensity as a function of both excitation and emission wavelengths.

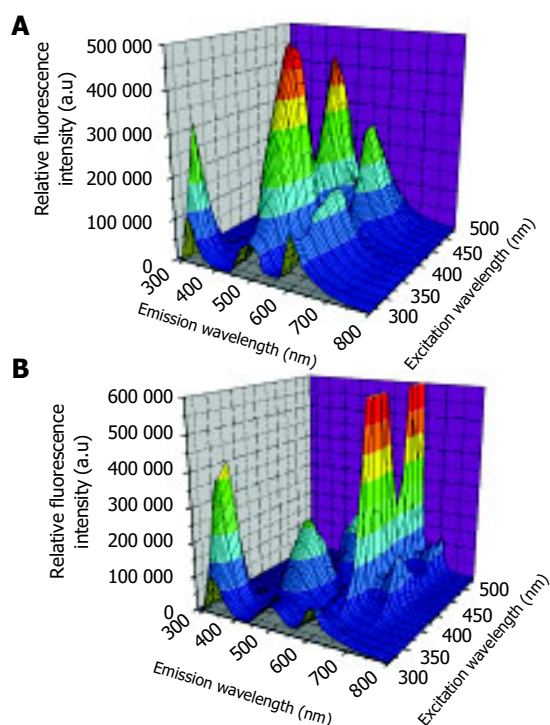


Figure 1 Three-dimensional autofluorescence spectra for normal colonic tissue (A) and adenomatous colonic tissue (B).

RESULTS

No significant differences were observed in the autofluorescence spectra of normal and cancerous tissues. However, remarkable differences in fluorescence peaks and intensities were detected between normal and adenomatous tissue from the same patient. The representative three-dimensional autofluorescence spectra for the normal colonic tissue and adenomatous colonic tissue are shown in Figures 1A and B, respectively. The relative fluorescence intensity was recorded as a function of both excitation and emission wavelengths. Although the fluorescence intensities were indicated in arbitrary units, the same experimental set-ups were maintained throughout our measurements for comparison.

The corresponding autofluorescence EEMs for normal and adenomatous colonic tissue are displayed in Figures 2A and B, respectively. The colorized scale represents different fluorescence intensities. The plots are shown on a log contour scale, where each contour connects points of equal fluorescence intensity.

In the case of autofluorescence EEM for normal colonic tissue in Figure 2A, the primary fluorescence peaks occurred at the excitation-emission wavelength pairs of 280-330, 350-480, 350/460-605, and 460-520 nm. According to the previous studies, these fluorescence peaks were attributed to the amino acids tryptophan and tyrosine, reduced nicotinamide adenine dinucleotide (NADH) or reduced nicotinamide adenine dinucleotide phosphate (NADPH), ceroid and flavin adenine dinucleotide (FAD), respectively^[10,12]. Adenomatous tissues exhibited emission peaks at 635 and 710 nm (Figure 2B) that were not observed in the emission spectra of normal colonic tissues. These remarkable peaks were the contribution of naturally occurring high endogenous porphyrins of protoporphyrin IX in cancerous tissues^[13-15]. Furthermore, the emission intensity from tryptophan and

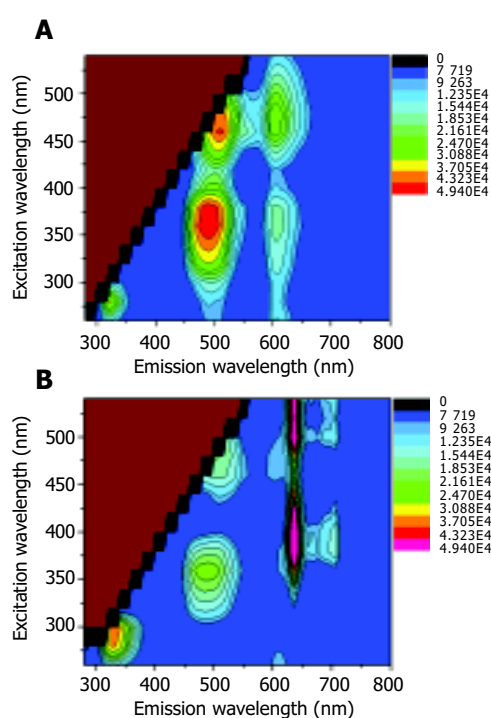


Figure 2 Autofluorescence EEMs for normal colonic tissue (A) and adenomatous colonic tissue (B).

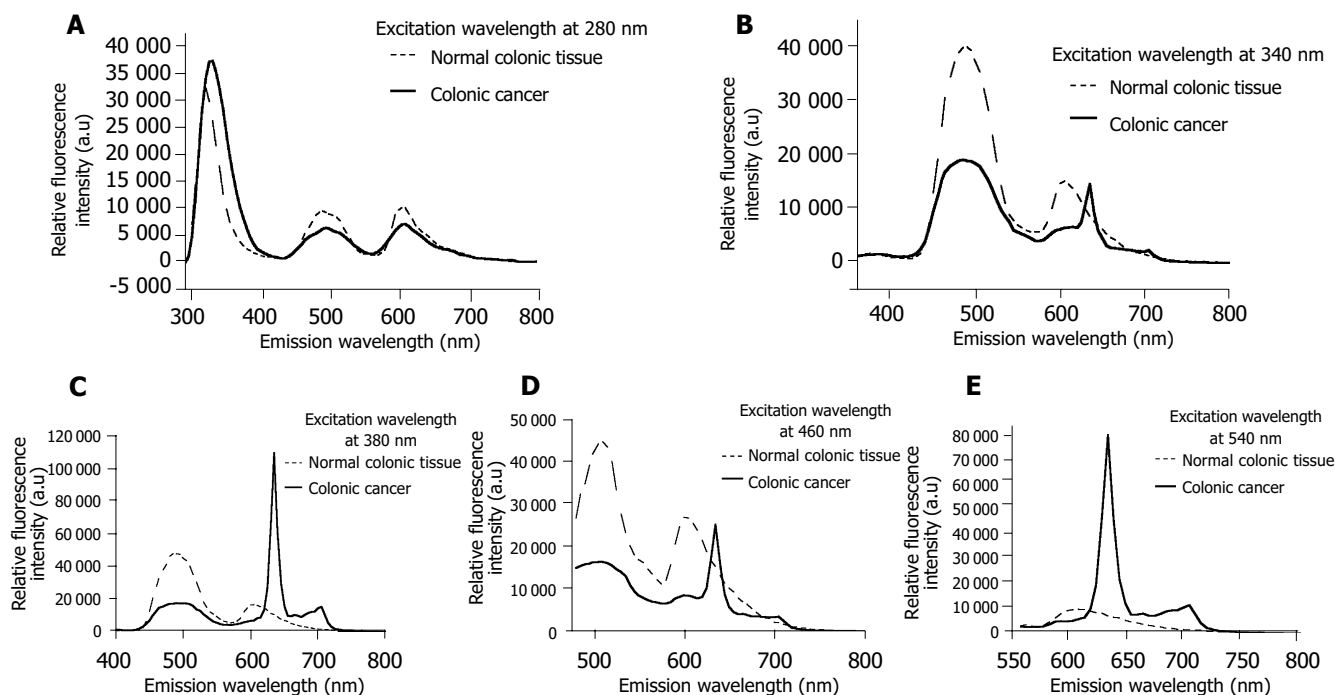


Figure 3 Fluorescence spectra of normal and cancerous tissues at excitation wavelengths of 280 (A), 340 (B), 380 (C), 460 (D), and 540 nm (E).

tyrosine was more intense in cancerous tissue than in normal tissue EEM. However, the endogenous fluorescence near 500 nm reduced in tumor tissues relative to normal colonic tissues. The differences might lie in the decrease of the oxidized forms of flavins and the relative amount of NAD(P)H in malignant tissues. As a result, low NAD(P)H and FAD but high amino acids and protoporphyrin IX accumulated in the human colonic malignancy. An evaluation of the average fluorescence spectrum at 260 nm excitation collected at the end of each EEM indicated that its peak fluorescence intensity was within 8% of that acquired at the beginning of each EEM. This means that minimal photobleaching occurred during the process of the 25-min EEM measurement.

In order to further determine the optimized excitation wavelengths for the diagnosis of colonic cancer, autofluorescence emission spectra at certain excitation wavelengths of 280, 340, 380, 460, and 540 nm for normal and adenomatous colonic tissues were compared in Figure 3, respectively. The greatest spectroscopic differences could be achieved for diagnosis of colonic cancer when the excitation wavelengths were 340, 380, 460, and 540 nm. In particular, the emission from endogenous porphyrins of protoporphyrin IX demonstrably characterized the autofluorescence spectroscopy of cancerous tissues when the excitation wavelength was higher than 380 nm.

DISCUSSION

In this study, autofluorescence EEMs were measured using a standard spectrofluorimeter to determine the location of the endogenous fluorescent peaks and their relative intensity in normal and adenomatous colonic tissues. We observed significant differences in the autofluorescence spectra of normal tissues and adenomatous colonic tissues, and these

differences could be attributed to the differences in fluorophores expression. The endogenous fluorophores that are speculated to cancerous transformations are the amino acids tryptophan and tyrosine, the structural proteins collagen and elastin, the coenzymes NAD(P)H and FAD, and porphyrins^[12].

Our results indicate that the fluorescence intensity of the amino acids tryptophan and tyrosine is dominant in both normal and cancerous colonic tissues at 280 nm excitation, which demonstrates the fact that amino acids are the basic structural units of protein and play an important role in biological tissues. These results also agree well with those of Pradhan *et al.*^[16], who suggested that there is an increase in tryptophan as cells progress from normal to cancerous state. Secondly, we observed that the intensity in the blue region of the autofluorescence spectra significantly reduced in adenomatous colonic tissues compared to normal tissues, which is in substantial agreement with the early work showing that the concentration of NADH and NADPH in adenomatous tissues is lower than that in normal tissues^[6,7]. Moreover, Anidjar *et al.*^[17], have demonstrated a decrease of FDA in cancerous tissues, which is proved in our research. However, Georgakoudi *et al.*^[18] and Drezek *et al.*^[19], suggested that low collagen and high NAD(P)H fluorescence characterize the high-grade dysplastic lesions when compared to nondysplastic cervix tissues. It is possible that the differences in NAD(P)H fluorescence may be due to different colonic and cervix tissues and the comparable measurements should be carried out for further confirmation. In addition, it should be noted that the emission specific peaks from collagen and elastin were not shown in our tissue EEMs except for one case, suggesting that the increments of excitation wavelength should be limited to 10 nm in order to exploit the emission fluorescence from structural proteins collagen and elastin. Bottiroli *et al.*^[7], have observed

a red fluorescence in some parts of tissue section from a cancerous colon. The red fluorescence has been reported by Moesta *et al.*^[13], and also demonstrated in this investigation, which can be definitely attributed to high endogenous porphyrins of protoporphyrin IX accumulating naturally in colonic cancer.

In summary, the presence or absence of fluorescence peaks in both normal and adenomatous colonic tissues can be explained by the different endogenous fluorophores to generate autofluorescence signals, and the ability of laser-induced autofluorescence EEMs to distinguish normal from cancerous colonic tissues. The present investigation offers evidence that low NAD(P)H and FAD but high amino acids and protoporphyrin IX characterize the high-grade malignant colonic tissues. Based on our results, the optimal excitation wavelengths for diagnosis of colonic cancer are 340, 380, 460, and 540 nm.

ACKNOWLEDGMENTS

We thank Professor Ming-Ren Li at the Department of Oncology of the First Affiliated Hospital of Fujian Medical University for providing the colonic tissue samples and the results of standard histopathological diagnosis.

REFERENCES

- 1 **Yova D**, Atlamazoglou V, Kavantzias N, Loukas S. Development of a fluorescence-based imaging system for colon cancer diagnosis using two novel rhodamine derivatives. *Lasers Med Sci* 2000; **15**: 140-147
- 2 **Prosst RL**, Gahlen J. Fluorescence diagnosis of colotrectal neoplasms: a review of clinical applications. *Int J Colorectal Dis* 2002; **17**: 1-10
- 3 **Heintzelman DL**, Utzinger U, Fuchs H, Zuluaga A, Gossage K, Gillenwater AM, Jacob R, Kemp B, Richards-Kortum RR. Optimal excitation wavelengths for *in vivo* detection of oral neoplasia using fluorescence spectroscopy. *Photochem Photobiol* 2000; **72**: 103-113
- 4 **Palmer GM**, Marshek CL, Vrotsos KM, Ramanujam N. Optimal methods for fluorescence and diffuse reflectance measurements of tissue biopsy samples. *Lasers Surg Med* 2002; **30**: 191-200
- 5 **Chang SK**, Follen M, Malpica A, Utzinger U, Staerckel G, Cox D, Atkinson EN, MacAulay C, Richards-Kortum R. Optimal excitation wavelengths for discrimination of cervical neoplasia. *IEEE Trans Biomed Eng* 2002; **49**: 1102-1111
- 6 **Richards-Kortum R**, Rava RP, Petras RE, Fitzmaurice M, Sivak M, Feld MS. Spectroscopic diagnosis of colonic dysplasia. *Photochem Photobiol* 1991; **53**: 777-786
- 7 **Bottiroli G**, Croce AC, Locatelli D, Marchesini R, Pignoli E, Tomatis S, Cuzzoni C, Di Palma S, Dalfante M, Spinelli P. Natural fluorescence of normal and neoplastic human colon: a comprehensive "ex vivo" study. *Lasers Surg Med* 1995; **16**: 48-60
- 8 **Banerjee B**, Miedema B, Chandrasekhar HR. Emission spectra of colonic tissue and endogenous fluorophores. *Am J Med Sci* 1998; **316**: 220-226
- 9 **Sheng JQ**, Li SR, Chen ZM, Gao G. Value of LIAF spectra for detection of colorectal carcinoma during colonoscopy. *Zhongguo Jiguang Yixue Zazhi* 2001; **10**: 145-147
- 10 **Richards-Kortum R**, Sevick-Muraca E. Quantitative optical spectroscopy for tissue diagnosis. *Annu Rev Phys Chem* 1996; **47**: 555-606
- 11 **Palmer GM**, Keely PJ, Breslin TM, Ramanujam N. Autofluorescence spectroscopy of normal and malignant human breast cell lines. *Photochem Photobiol* 2003; **78**: 462-469
- 12 **Ramanujam N**. Fluorescence spectroscopy *in vivo*, in Meyers RA ed. Encyclopedia of Analytical Chemistry. Chichester, John Wiley Sons Ltd 2000: 20-56
- 13 **Moesta KT**, Ebert B, Handke T, Nolte D, Nowak C, Haensch WE, Pandey RK, Dougherty TJ, Rinneberg H, Schlag PM. Protoporphyrin IX occurs naturally in colorectal cancers and their metastases. *Cancer Res* 2001; **61**: 991-999
- 14 **DaCosta RS**, Andersson H, Wilson BC. Molecular fluorescence excitation-emission matrices relevant to tissue spectroscopy. *Photochem Photobiol* 2003; **78**: 384-392
- 15 **Huang Z**, Zheng W, Xie S, Chen R, Zeng H, McLean DI, Lui H. Laser-induced autofluorescence microscopy of normal and tumor human colonic tissue. *Int J Oncol* 2004; **24**: 59-63
- 16 **Pradhan A**, Pal P, Durocher G, Villeneuve L, Balassy A, Babai F, Gaboury L, Blanchard L. Steady state and time-resolved fluorescence properties of metastatic and non-metastatic malignant cells from different species. *J Photochem Photobiol B* 1995; **31**: 101-112
- 17 **Anidjar M**, Cussenot O, Blais J, Bourdon O, Avrillier S, Etori D, Villette JM, Fiet J, Teillac P, Le Duc A. Argon laser induced autofluorescence may distinguish between normal and tumor human urothelial cells: a microspectrofluorimetric study. *J Urol* 1996; **155**: 1771-1774
- 18 **Georgakoudi I**, Jacobson BC, Muller MG, Sheets EE, Badizadegan K, Carr-Locke DL, Crum CP, Boone CW, Dasari RR, Van Dam J, Feld MS. NAD(P)H and collagen as *in vivo* quantitative fluorescent biomarkers of epithelial precancerous changes. *Cancer Res* 2002; **62**: 682-687
- 19 **Drezek R**, Sokolov K, Utzinger U, Boiko I, Malpica A, Follen M, Richards-Kortum R. Understanding the contributions of NADH and collagen to cervical tissue fluorescence spectra: modeling, measurements, and implications. *J Biomed Opt* 2001; **6**: 385-396

Science Editor Guo SY Language Editor Elsevier HK

Application of dietary fiber in clinical enteral nutrition: A meta-analysis of randomized controlled trials

Gang Yang, Xiao-Ting Wu, Yong Zhou, Ying-Li Wang

Gang Yang, Xiao-Ting Wu, Yong Zhou, Ying-Li Wang, Department of General Surgery, West China Hospital, Sichuan University, Chengdu 610041, Sichuan Province, China
Correspondence to: Professor Xiao-Ting Wu, Department of General Surgery, West China Hospital, Sichuan University, 37 Guo Xue Road, Chengdu 610041, Sichuan Province, China. yanggang2000@hotmail.com
Telephone: +86-28-88036679 Fax: +86-28-85422411
Received: 2004-05-29 Accepted: 2004-06-24

Abstract

AIM: To evaluate the effects of dietary fiber (DF) as a part of enteral nutrition (EN) formula on diarrhea, infection, and length of hospital stay.

METHODS: Following electronic databases were searched for randomized controlled trials about DF: Chinese Biomedicine Database (CBM), MEDLINE, EMBASE and Cochrane Controlled Trials Register. RevMan 4.1 was used for statistical analysis.

RESULTS: Seven randomized controlled trials with 400 patients were included. The supplement of DF in EN was compared with standard enteral formula in five trials. Combined analysis did not show a significant reduction in occurrence of diarrhea, but there were valuable results for non-critically ill patients. Combined analysis of two trials observing the infection also did not show any valid evidence that DF could decrease the infection rate, though the length of hospital stay was reduced significantly.

CONCLUSION: Based on the current eligible randomized controlled trials, there is no evidence that the value of DF in the diarrhea can be proved. Though length of hospital stay was shortened by the use of DF, there is no available evidence in preventing infection by DF. Further studies are needed for evaluating the value of DF in EN.

© 2005 The WJG Press and Elsevier Inc. All rights reserved.

Key words: Dietary fiber; Enteral nutrition; Meta-analysis

Yang G, Wu XT, Zhou Y, Wang YL. Application of dietary fiber in clinical enteral nutrition: A meta-analysis of randomized controlled trials. *World J Gastroenterol* 2005; 11(25): 3935-3938
<http://www.wjgnet.com/1007-9327/11/3935.asp>

INTRODUCTION

Dietary fiber (DF) is a category of carbohydrates that cannot be ingested by endogenic digestive enzymes in human body^[1].

Nevertheless, DF can be fermented into methane, hydrogen, CO₂, and short-chain fatty acid (SCFA) by bowel microflorae. SCFA, a primary important energy substance for colonic mucosal epithelium, is essential to maintain the metabolism and regeneration of epithelia, protect the structure and function, promote absorption of water and sodium, and regulate the function of bowel^[2-6]. Recent studies also suggest that SCFA can protect the intestinal barrier and prevent bacterial translocation^[7-9]. So DF has been widely recommended as an essential component of enteral nutrition (EN) in the last 20 years^[10-13]. It is believed that DF may play an important role in controlling diarrhea associated with EN, improving restoration of bowel function, reducing infection and improving prognosis of critically ill patients^[14-18]. But the conclusions of existing trials are controversial. The practical value of DF in clinical EN lacks evidence. This review is to evaluate the value of DF in clinical EN with the method of meta-analysis and to seek the best evidence for clinical EN.

MATERIALS AND METHODS

Data extraction and outcomes

We searched the following electronic databases for eligible trials: PubMed (from January 1980 to January 2003), EMBASE (from January 1989 to December 2002), Cochrane Controlled Trials Register and Chinese Biomedicine Database (from 1980 to 2002). The searching words were dietary fiber and enteral nutrition. Languages were restricted to English and Chinese.

The criteria were open or blind randomized studies. Patients were randomly allocated into receiving EN emended with DF or EN without DF, regardless of the type of DF.

Assessment of methodological quality

The assessment of methodological quality was undertaken by two of the authors independently, differences in assessment were solved by consensus. From each study, data were extracted on the type of patients, the method of administration of EN. Outcomes were the occurrence of diarrhea, infection of any type and length of hospital stay.

Jadad score and allocation concealment were adopted to evaluate the methodological quality of each trial: 0 for non-randomized controlled trials, 1-2 scores for poor-quality trials and 3-5 scores for high-quality trials. The concealment of allocation also was divided into three grades: A for adequate concealment, B for unclear concealment, C for inadequate concealment.

Analysis

RevMan 4.1 software supplied by Cochrane Collaboration

was used. The effect size of categorical variables was odds ratio (OR). For numerical variables, if the unit was identical, weighed mean difference (WMD) was used, and standardized mean difference was used when the unit was different. The homogeneity of adopted trials was tested before meta-analysis. If the heterogeneity had no statistical significant difference, a fixed effect model was used during meta-analysis. In contrast, we used a random effect model and subgroup analysis. Sensitivity analysis was also proceeded after the non-blinded, inadequate concealed trials were excluded.

RESULTS

Characteristics of trials and patients

Eight hundred and eleven papers were obtained by searching the databases, 587 in English, 224 in Chinese. Seventeen trials, all in English, were identified for further evaluation after the title and abstract were read. Seven measured up to the criteria and were included^[19-25]. There were no repetitive studies and meta-analysis. Seven of the 17 included trials, three were conducted in Germany^[19,20,24], one in USA^[22], one in Australia^[25], one in Belgium^[21] and Singapore^[23]. Two included critically ill patients^[22,25], three included postoperative patients^[19,20,23], one included sepsis^[21] and the other included a variety of diseases^[24]. The earliest study was published in 1990^[25], all were published in the past 14 years.

Methodological quality of trials

Of the seven trials, three were of a high quality (one had five scores according to Jadad, one had four scores, one had three scores), the other four were of a poor quality. Computerized random number was used in two trials, sealed envelopes in two, no randomization method in three. Four trials were double-blinded. The baselines of included subjects were compared in all studies, and no statistically significant differences existed. Table 1 gives the details of the seven trials.

Outcomes

Effect of DF on diarrhea in EN The occurrence of diarrhea in 276 patients receiving EN supplemented with or without DF was observed in five trials. There was no heterogeneity ($P = 0.087$) and fixed effect model was used. The combined OR was 0.61, 96% confidence interval was from 0.36 to 1.05 ($P = 0.07$) (Table 2). Subgroup analysis of two trials on uncritically ill patients showed that the combined OR was 0.33 (from 0.13 to 0.87, $P = 0.03$).

Effect of DF on infection The risk of infection was reported in two trials. The types of infection included pneumonia, sepsis, abdominal infection, urinary infection and incision infection. Two trials had homogeneity. Combined OR was 0.44 when the fixed effect model was used (0.20-1.00, $P = 0.05$).

Effect of DF on length of hospital stay Three trials reported the length of hospital stay of 124 postoperative patients. Among the three trials, one was excluded because it did not supply the standard deviation. Two adopted trials had homogeneity, combined WMD was -2.85 (from -3.76 to -1.93, $P < 0.00001$).

Sensitivity analysis

Three high-quality trials on diarrhea of 160 cases in EN were included. There was no heterogeneity among them ($P = 0.069$). Combined OR was 0.83 (0.43-1.60, $P = 0.6$). The result was identical with the previous analysis (Table 3). Sensitivity analysis was abandoned for the quality of trials about infection and length of hospital stay was poor.

DISCUSSION

Diarrhea is the most frequent complication in EN. Infusion speed, temperature, osmolality, bacterial contamination, hypoalbuminemia and antibiotics may play a part in diarrhea^[26]. Laboratory studies suggested that DF and SCFA, fermentation products of DF, were able to improve the rhythm of bowel peristalsis, promote absorption of water and sodium, and

Table 1 Characteristics of RCTs about EN supplemented with DF

	Number of patients (intervention/control)	Methodological quality	Patients	Diarrhea	Infection	Days of hospital stay (mean±SD)
Schultz 2000	44(22/22)	C: A:J: 5	Critically ill	6/7	NR	NR
Dobb 1990	91(45/46)	C: B:J: 4	Critically ill	16/13	NR	NR
Spapen 2001	25(13/12)	C: A:J: 3	Sepsis	6/11	NR	NR
Rayes 2002	64(32/32)	C: B:J: 2	Liver transplantation	NR	11/15	36±2.7/39±0.5
Rayes 2002(2)	60(30/30)	C: B:J: 2	Abdominal surgery	NR	3/9	15±7.4/16±5.5
Homann 1994	100(50/50)	C: B:J: 2	Inpatients	6/15	NR	NR
Khalil 1998	16(8/8)	C: B:J: 2	Postoperative	1/2	NR	NR

C = concealment of allocation; J = Jadad score; NR = not reported.

Table 2 Effect of EN with DF on diarrhea

Study	Favors DF- supplement n/N	Favors DF- free n/N	Weight %	OR (95%CI fixed)
Dobb 1990	16/45	13/46	24.0	1.40 [0.58,3.40]
Homann 1994	6/50	15/50	38.3	0.32 [0.11,0.91]
Khalil 1998	1/8	2/8	5.1	0.43 [0.03,5.99]
Schultz 2000	6/22	7/22	14.8	0.80 [0.22,2.94]
Spapen 2001	6/13	11/12	17.9	0.08 [0.01,0.79]
Total(95%CI)	35/138	48/138	100.0	0.61 [0.36,1.05]

Test for heterogeneity chi-square = 8.13, df = 4, $P = 0.087$; Test for overall effect $z = -1.79$, $P = 0.07$.

Table 3 Sensitivity-analysis of effects of EN with DF on diarrhea

Study	Favors DF-supplement n/N	Favors DF-free n/N	Weight %	OR (95%CI fixed)
Dobb 1990	16/45	13/46	24.0	1.40 [0.58,3.40]
Schultz 2000	6/22	7/22	14.8	0.80 [0.22,2.94]
Spapen 2001	6/13	11/12	17.9	0.08 [0.01,0.79]
Total(95%CI)	28/80	31/80	100.0	0.83 [0.43,1.60]

Test for heterogeneity $\chi^2 = 5.34$, $df = 2$, $P = 0.069$, Test for overall effect $z = -0.56$, $P = 0.6$.

regulate the inhibitor feedback mechanism^[27-31]. Accordingly, DF may have potentials beneficial to controlling diarrhea in EN^[32-35]. But the existing clinical trials did not show identical results, so strict evaluation is essential. The occurrence of diarrhea in trials adopted in this review was 30.01%, combined OR was 0.61, 95% confidence interval was from 0.36 to 1.05 ($Z = -1.79$, $P = 0.07$). The difference was not statistically significant. Subgroup analysis revealed that DF was beneficial to diarrhea in non-critically ill patients but uncertain in critically ill patients. Critically ill patients were apt to complicate severe hypoalbuminemia and superinfection, which could lead to refractory diarrhea^[34,35]. In the review, diarrhea occurred in 34.78% of critically ill patients, far higher than that in the non-critical patients (20.69%).

Diarrhea diagnosis is lack of objective criteria. Three trials in the review adopted Hatt and Dobb diarrhea score, which records defecation by volume and consistency. Diarrhea was defined as the scores more than 12. This score was convenient to compare different trials.

High attention has been paid to intestinal bacterial translocation leading to a considerable amount of infections. A series of animal experiments suggested that DF could effectively reduce the intestinal bacterial translocation in stress status^[36]. The mechanism remains unclear. DF is able to maintain the structure and function of epithelia, regulate immunological reactions, promote secretion of IgA and mucus, all these may play a role in diarrhea^[37-39]. Administration of DF can reduce the infection theoretically. However, analysis of the seven trials failed to show the anticipated results (combined OR 0.44, $P = 0.05$). The review suggests that DF could significantly shorten the length of hospital stay of patients who had undergone liver transplantation or abdominal surgery.

There is little evidence from these trials that DF is beneficial to diarrhea and infection of critically ill patients. It is necessary to design more large size and high-quality randomized controlled trials. The effect of DF on a variety of patients should also be further studied.

REFERENCES

- Englyst HN, Quigley ME, Hudson GJ. Definition and measurement of dietary fibre. *Eur J Clin Nutr* 1995; **49**(Suppl 3): S48-62
- Cummings JH, Macfarlane GT. Role of intestinal bacteria in nutrient metabolism. *JPEN J Parenter Enteral Nutr* 1997; **21**: 357-365
- Spaeth G, Gottwald T, Hirner A. Fibre is an essential ingredient of enteral diets to limit bacterial translocation in rats. *Eur J Surg* 1995; **161**: 513-518
- Kanauchi O, Suga T, Tochihiro M, Hibi T, Naganuma M, Homma T, Asakura H, Nakano H, Takahama K, Fujiyama Y, Andoh A, Shimoyama T, Hida N, Haruma K, Koga H, Mitsuyama K, Sata M, Fukuda M, Kojima A, Bamba T. Treatment of ulcerative colitis by feeding with germinated barley foodstuff: first report of a multicenter open control trial. *J Gastroenterol* 2002; **37**(Suppl 14): 67-72
- Wisker E, Daniel M, Rave G, Feldheim W. Fermentation of non-starch polysaccharides in mixed diets and single fibre sources: comparative studies in human subjects and *in vitro*. *Br J Nutr* 1998; **80**: 253-261
- Demetriades H, Botsios D, Kazantzidou D, Sakkas L, Tsalis K, Manos K, Dadoukis I. Effect of early postoperative enteral feeding on the healing of colonic anastomoses in rats. Comparison of three different enteral diets. *Eur Surg Res* 1999; **31**: 57-63
- Kripke SA, Fox AD, Berman JM, Settle RG, Rombeau JL. Stimulation of intestinal mucosal growth with intracolonic infusion of short-chain fatty acids. *J Parenter Enteral Nutr* 1989; **13**: 109-116
- Bowling TE, Raimundo AH, Grimble GK, Silk DB. Reversal by short-chain fatty acids of colonic fluid secretion induced by enteral feeding. *Lancet* 1993; **342**: 1266-1268
- Gomez Candela C, de Cos Blanco AI, Iglesias Rosado C. Fiber and enteral nutrition. *Nutr Hosp* 2002; **17**(Suppl 2): 30-40
- Nakao M, Ogura Y, Satake S, Ito I, Iguchi A, Takagi K, Nabeshima T. Usefulness of soluble dietary fiber for the treatment of diarrhea during enteral nutrition in elderly patients. *Nutrition* 2002; **18**: 35-39
- Wright J. Total parenteral nutrition and enteral nutrition in diabetes. *Curr Opin Clin Nutr Metab Care* 2000; **3**: 5-10
- Coulston AM. Clinical experience with modified enteral formulas for patients with diabetes. *Clin Nutr* 1998; **17**(Suppl 2): 46-56
- Sobotka L, Bratova M, Slemrova M, Manak J, Vizd' a J, Zadak Z. Inulin as the soluble fiber in liquid enteral nutrition. *Nutrition* 1997; **13**: 21-25
- Hebden JM, Blackshaw E, D'Amato M, Perkins AC, Spiller RC. Abnormalities of GI transit in bloated irritable bowel syndrome: effect of bran on transit and symptoms. *Am J Gastroenterol* 2002; **97**: 2315-2320
- Olah A, Belagyi T, Issekutz A, Gamal ME, Bengmark S. Randomized clinical trial of specific lactobacillus and fibre supplement to early enteral nutrition in patients with acute pancreatitis. *Br J Surg* 2002; **89**: 1103-1107
- Parisi GC, Zilli M, Miani MP, Carrara M, Bottona E, Verdianelli G, Battaglia G, Desideri S, Faedo A, Marzolino C, Tonon A, Ermani M, Leandro G. High-fiber diet supplementation in patients with irritable bowel syndrome (IBS): a multicenter, randomized, open trial comparison between wheat bran diet and partially hydrolyzed guar gum (PHGG). *Dig Dis Sci* 2002; **47**: 1697-1704
- Tonstad S, Smerud K, Hoie L. A comparison of the effects of 2 doses of soy protein or casein on serum lipids, serum lipoproteins, and plasma total homocysteine in hypercholesterolemic subjects. *Am J Clin Nutr* 2002; **76**: 78-84
- Jenkins DJ, Kendall CW, Vuksan V, Augustin LS, Li YM, Lee B, Mehling CC, Parker T, Faulkner D, Seyler H, Vidgen E, Fulgoni V. The effect of wheat bran particle size on laxation and colonic fermentation. *Am Coll Nutr* 1999; **18**: 339-345
- Rayes N, Seehofer D, Hansen S, Boucsein K, Muller AR, Serke S, Bengmark S, Neuhaus P. Early enteral supply of lactobacillus and fiber versus selective bowel decontamination: a controlled trial in liver transplant recipients. *Transplantation* 2002; **74**: 123-127
- Rayes N, Hansen S, Seehofer D, Muller AR, Serke S, Bengmark S, Neuhaus P. Early enteral supply of fiber and Lactobacilli versus conventional nutrition: a controlled trial in patients with major abdominal surgery. *Nutrition* 2002; **18**: 609-615
- Spapen H, Diltoer M, Van Malderen C, Opdenacker G, Suyts E, Huyghens L. Soluble fiber reduces the incidence of diarrhea in septic patients receiving total enteral nutrition: a prospective, double-blind, randomized, and controlled trial. *Clin Nutr* 2001; **20**: 301-305
- Schultz AA, Ashby-Hughes B, Taylor R, Gillis DE, Wilkins

- M. Effects of pectin on diarrhea in critically ill tube-fed patients receiving antibiotics. *Am J Crit Care* 2000; **9**: 403-411
- 23 **Khalil L**, Ho KH, Png D, Ong CL. The effect of enteral fibre-containing feeds on stool parameters in the post-surgical period. *Singapore Med J* 1998; **39**: 156-159
- 24 **Homann HH**, Kemen M, Fuessenich C, Senkal M, Zumtobel V. Reduction in diarrhea incidence by soluble fiber in patients receiving total or supplemental enteral nutrition. *J Parenter Enteral Nutr* 1994; **18**: 486-490
- 25 **Dobb GJ**, Towler SC. Diarrhoea during enteral feeding in the critically ill: a comparison of feeds with and without fibre. *Intensive Care Med* 1990; **16**: 252-255
- 26 **Burks AW**, Vanderhoof JA, Mehra S, Ostrom KM, Baggs G. Randomized clinical trial of soy formula with and without added fiber in antibiotic-induced diarrhea. *J Pediatr* 2001; **139**: 578-582
- 27 **Lin HC**, Zhao XT, Chu AW, Lin YP, Wang L. Fiber-supplemented enteral formula slows intestinal transit by intensifying inhibitory feedback from the distal gut. *Am J Clin Nutr* 1997; **65**: 1840-1844
- 28 **Bliss DZ**, Jung HJ, Savik K, Lowry A, LeMoine M, Jensen L, Werner C, Schaffer K. Supplementation with dietary fiber improves fecal incontinence. *Nurs Res* 2001; **50**: 203-213
- 29 **Bouin M**, Savoye G, Herve S, Hellot MF, Denis P, Ducrotte P. Does the supplementation of the formula with fibre increase the risk of gastro-oesophageal reflux during enteral nutrition? A human study. *Clin Nutr* 2001; **20**: 307-312
- 30 **Silk DB**, Walters ER, Duncan HD, Green CJ. The effect of a polymeric enteral formula supplemented with a mixture of six fibres on normal human bowel function and colonic motility. *Clin Nutr* 2001; **20**: 49-58
- 31 **Murray SM**, Patil AR, Fahey GC Jr, Merchen NR, Wolf BW, Lai CS, Garleb KA. Apparent digestibility and glycaemic responses to an experimental induced viscosity dietary fibre incorporated into an enteral formula fed to dogs cannulated in the ileum. *Food Chem Toxicol* 1999; **37**: 47-56
- 32 **Reese JL**, Means ME, Hanrahan K, Clearman B, Colwill M, Dawson C. Diarrhea associated with nasogastric feedings. *Oncol Nurs Forum* 1996; **23**: 59-66
- 33 **Kapadia SA**, Raimundo AH, Grimble GK, Aimer P, Silk DB. Influence of three different fiber-supplemented enteral diets on bowel function and short-chain fatty acid production. *J Parenter Enteral Nutr* 1995; **19**: 63-68
- 34 **Bass DJ**, Forman LP, Abrams SE, Hsueh AM. The effect of dietary fiber in tube-fed elderly patients. *J Gerontol Nurs* 1996; **22**: 37-44
- 35 **Lien KA**, McBurney MI, Beyde BI, Thomson AB, Sauer WC. Ileal recovery of nutrients and mucin in humans fed total enteral formulas supplemented with soy fiber. *Am J Clin Nutr* 1996; **63**: 584-595
- 36 **Nakamura T**, Hasebe M, Yamakawa M, Higo T, Suzuki H, Kobayashi K. Effect of dietary fiber on bowel mucosal integrity and bacterial translocation in burned rats. *J Nutr Sci Vitaminol* 1997; **43**: 445-454
- 37 **Caparros T**, Lopez J, Grau T. Early enteral nutrition in critically ill patients with a high-protein diet enriched with arginine, fiber, and antioxidants compared with a standard high-protein diet. The effect on nosocomial infections and outcome. *J Parenter Enteral Nutr* 2001; **25**: 299-308
- 38 **Tariq N**, Jenkins DJ, Vidgen E, Fleschner N, Kendall CW, Story JA, Singer W, D'Costa M, Struthers N. Effect of soluble and insoluble fiber diets on serum prostate specific antigen in men. *J Urol* 2000; **163**: 114-118
- 39 **Frankel W**, Zhang W, Singh A, Bain A, Satchithanandam S, Klurfeld D, Rombeau J. Fiber: effect on bacterial translocation and intestinal mucin content. *World J Surg* 1995; **19**: 144-148

• BRIEF REPORTS •

Personal experience with the procurement of 32 liver allografts

Guang-Wen Zhou, Cheng-Hong Peng, Hong-Wei Li

Guang-Wen Zhou, Cheng-Hong Peng, Hong-Wei Li, Department of Surgery, Ruijin Hospital, Shanghai Second Medical University, Shanghai 200025, China

Correspondence to: Guang-Wen Zhou, Department of Surgery, Ruijin Hospital, Shanghai Second Medical University, Shanghai 200025, China. gw_vrai@yahoo.com.cn

Telephone: +86-21-64370045-666705

Received: 2004-07-23 Accepted: 2004-09-19

Key words: Liver transplantation; Liver procurement; Donor; Arterial anomalies

Zhou GW, Peng CH, Li HW. Personal experience with the procurement of 32 liver allografts. *World J Gastroenterol* 2005; 11(25): 3939-3943

<http://www.wjgnet.com/1007-9327/11/3939.asp>

Abstract

AIM: To introduce the American Pittsburgh's method of rapid liver procurement under the condition of brain death and factors influencing the quality of donor liver.

METHODS: To analyze 32 cases of allograft liver procurement retrospectively and observe the clinical outcome of orthotopic liver transplantation.

RESULTS: Average age of donors was 38.24 ± 12.78 years, with a male:female ratio of 23:9. The causes of brain death included 21 cases of trauma (65.63%) and nine cases of cerebrovascular accident (28.13%). Fourteen grafts (43.75%) had hepatic arterial anomalies, seven cases only right hepatic arterial anomalies (21.88%), five cases only left hepatic arterial anomalies (15.63%) and two cases of both right and left hepatic arterial anomalies (6.25%) among them. Eight cases (57.14%) of hepatic arterial anomalies required arterial reconstruction prior to transplantation. Of the 32 grafts evaluated for early function, 27 (84.38%) functioned well, whereas three (9.38%) functioned poorly and two (6.25%) failed to function at all. Only one recipient died after transplantation and thirty-one recipients recovered. Four recipients needed retransplantation. The variables associated with less than optimal function of the graft consisted of donor age (35.6 ± 12.9 years vs 54.1 ± 4.3 years, $P < 0.05$), duration of donor's stay in the intensive care unit (ICU) (3.5 ± 2.4 d vs 7.4 ± 2.1 d, $P < 0.005$), abnormal graft appearance (19.0% vs 100%, $P < 0.05$), and such recipient problems as vascular thromboses during or immediately following transplantation (89.3% vs 50.0%, $P < 0.005$).

CONCLUSION: During liver procurement, complete heparization, perfusion *in situ* with localized low temperature and standard technique procedures are the basis ensuring the quality of the graft. The hepatic arterial anomalies should be taken care of to avoid injury. The donor age, duration of donor's staying in ICU, abnormal graft appearance and recipient problem are important factors influencing the quality of the liver graft.

INTRODUCTION

Enormous progress including surgical techniques has been achieved since the first orthotopic liver transplantation (OLT_x) was performed in humans in 1963 and OLT_x has established its role as a therapeutic option for patients with end-stage liver disease. Primary graft nonfunction (PGN) remains a dreadful complication of OLT_x, one that is associated with a high mortality and morbidity, and therefore liver allograft with good function is the most important point for ensuring the success of liver transplantation. A single donor surgeon's experience procuring the livers from 32 donors in Pittsburgh Transplant Center is analyzed in order to identify the role of a number of variables pertinent to the clinical outcome of OLT_x.

MATERIALS AND METHODS

Donor data

The author performed 32 allograft hepatectomies at the University of Pittsburgh Transplant Center. All donors were brain dead and the age of the donors varied from 12 to 63 years with the average of 38.24 ± 12.78 years. Among them, there were 23 male donors and 9 female donors. Table 1 lists the causes of death of the donors.

Table 1 Causes of brain death among 32 liver donors

Cause	n (%)
Trauma	21 (65.63)
Motor vehicle accident	16
Gunshot wound	1
Fall	2
Other	2
Cerebrovascular accident	9 (28.13)
Cerebral infarct	6
Subarachnoid hemorrhage	3
Others	2 (6.24)
Total	32 (100)

Donor selection criteria

In general, donors were selected who were less than 65 years

of age, had no history of liver disease such as hepatitis or alcoholism, and a total serum bilirubin less than 34 $\mu\text{mol/L}$, normal or near-normal alanine aminotransferase (ALT), aspartate aminotransferase (AST), alkaline phosphatase (AKP), γ -glutathione transferase (γ -GT) and prothrombin time (PT), and adequate arterial blood gas. Elevations of ALT, AST, AKP and γ -GT, with a tendency to decline, were not regarded as a contraindication for donation of the liver.

Donor maintenance

Donors were fluid-resuscitated once they had been pronounced brain dead in order to maintain a central venous pressure of 8-10 cm H₂O and urine output over 1 mL/(kg • h) as a guide. For donors receiving vasopressin for diabetes insipidus, the vasopressin was discontinued as soon as possible to avoid liver ischemia secondary to a decreased splanchnic blood flow. Urine output was replaced vigorously with intravenous fluids, usually one-half or quarter normal saline solution with potassium chloride. Electrolytes were checked frequently, especially to correct hypokalemia. Normothermia was maintained with a thermoblanquet. Blood was transfused to maintain the hematocrit above 30% in order to maintain adequate oxygen delivery to the tissues.

Operative technique

The technique of allograft hepatectomy involved both rapid perfusion and modified rapid perfusion^[1-3]. Rapid perfusion technique is as follows. Briefly, both the terminal aorta and the inferior mesenteric vein were dissected to insert aortic and portal perfusion cannulae. The supraceliac abdominal aorta was encircled and crossclamped. Following cardiectomy, dissection of liver hilum was performed in a bloodless field^[4,5]. Following identification of whether or not an aberrant right hepatic artery (HA) originating from superior mesenteric artery (SMA) in the retropancreatic portion, the right side of the SMA was dissected toward the aorta. A Carrel patch of aorta was excised, with care not to injure the origin of the renal arteries. This has been our preferred method of hepatectomy in unstable donors, or in cases of extreme urgency when the recipient is in fulminant liver failure due to fulminant hepatitis or graft nonfunction following OLTx. Modified rapid perfusion technique differs from the rapid perfusion technique in that dissection of the liver hilum occurs prior to crossclamping of the aorta and cannulation of the distal splenic vein with a larger caliber catheter for a quicker portal perfusion. This preliminary dissection allows more selective and rapid cooling of the liver than does the rapid perfusion technique. These additional preparatory steps required 30-45 min. This technique has been our choice for stable donors and for donors whose livers are of a questionable quality. During the preparatory dissection, changes in the color or consistency of the allograft were observed in response to diuresis, or better oxygenation.

Technique of vascular reconstruction for arterial anomalies

Arterial reconstruction of the liver graft is required prior to transplantation and is very pivotal if a common arterial channel is absent due to an anomaly. The most common arterial anomaly requiring reconstruction was the aberrant

right HA arising from the SMA, for which an end-to-end anastomosis was performed between the distal donor splenic artery and the proximal aberrant right HA. This was achieved with a Carrel patch of the SMA, obviating a small caliber anastomosis^[6]. Care was taken to avoid an inadvertent anastomosis with rotation. The continuous suture technique with 8-0 monofilament polypropylene (Prolene) was used for the reconstruction. Just before the sutures were tied, the reconstructed HA was allowed to distend by pulsatile infusion of cold solution. With the application of "growth factor" principle to the *ex vivo* condition, this method facilitated migration of Prolene sutures into the anastomosis and allowed secure anastomosis without leakage or stricture.

Classification of early graft function

Early graft function was divided into four grades as good, fair, poor and PGN. Good meant AST < 1 500 IU/L, ALT < 1 000 IU/L and fresh frozen plasma (FFP) was not necessary. Fair meant AST 1 500-3 500 IU/L, ALT 1 000-2 500 IU/L and FFP was not required. Poor meant AST > 3 500 IU/L, ALT > 2 500 IU/L and FFP was required. PGN was defined as the inability of graft to sustain the metabolic homeostasis of the recipient during the first postoperative week, presenting with the clinical manifestations of grade III or IV coma, coagulopathy with prothrombin time over 20 s, high ALT and AST values, renal failure, and progressive or persistent hyperbilirubinemia, resulting in retransplantation of the graft or death of the recipient.

Statistical analysis

Student's *t* and χ^2 tests were used for the statistical evaluation of the data.

RESULTS

Vascular anomalies

Table 2 lists the incidence of hepatic arterial anomalies and various methods of arterial reconstruction. Hepatic arterial anomalies were present in 14 grafts (43.75%): the aberrant right HA in seven (21.88%), the aberrant left HA in five (15.63%), and both aberrant right and left hepatic arteries in two grafts (6.25%). Of these, eight grafts (57.14%) required vascular reconstruction at the back table in order to construct a common arterial channel, and one of the anastomoses constructed at the back table required the revision due to rotation.

Table 2 Vascular reconstruction for hepatic arterial anomalies

Anomaly	n (%)	Method of reconstruction (n)
Aberrant RHA	7 (21.88)	
From SMA	6	Donor SpA to aberrant RHA (4)
From aorta	1	Donor SpA to aberrant RHA (1)
Aberrant LHA	5 (15.63)	
From CA	3	
From aorta	2	Donor SpA to PHA (1)
Aberrant RHA and LHA	2 (6.25)	
RHA from SMA	1	Donor SpA to RHA (1)
LHA from CA	1	CA to distal SMA (1)
Total	14 (43.75)	

RHA: right hepatic artery; SMA: superior mesenteric artery; SpA: splenic artery; LHA: left hepatic artery; CA: celiac axis, PHA: proper hepatic artery.

Injury of hepatic artery

A total of four complications (6.25%) occurred during or after allograft hepatectomy due to aberrant HA: inadvertent transection of the aberrant right HA, once originating directly from the aorta and once from the left side of the SMA. The transected aberrant right hepatic arteries were reconstructed using end-to-end anastomosis with the donor splenic artery with interrupted 8-0 Prolene sutures. Overall, none of the complications affected the outcome of the liver or other organ recipients.

Early graft function

Table 3 lists the early graft function of the 32 allografts after OLTx. Graft function was good or fair in 25 out of 28 (89.3%) of the grafts without recipient problems, whereas as many as two out of four (50%) of the grafts with recipient problems during or immediately following OLTx exhibited poor or nonfunction ($P < 0.005$; $\chi^2 = 12.96$). This was due to HA thrombosis and multi-organ failure and meanwhile HA thrombosis was caused not by HA anomaly during allograft procurement but by HA reconstruction. Table 4 shows the correlation between the donor or graft variables and the early graft function of the 28 grafts that survived the operation and did not develop the aforementioned recipient complications during or

immediately following OLTx. A statistically significant difference was noticed in the duration of patient's stay in ICU, requirement of cardiopulmonary resuscitation and the presence of abnormal graft appearance ($P < 0.05$). The donors of grafts with fair or poor function stayed in ICU longer than those with good function ($P < 0.005$), and the grafts with abnormal appearance were associated with a higher incidence of fair or poor graft function in recipients ($P < 0.05$; $\chi^2 = 6.21$). The donors of graft with poor or nonfunction were significantly older than those with good or fair function and there was no significant difference between good and fair groups. On the other hand, no definitive correlation with early graft function was observed in sex, results of liver function tests, infusion of high-dose vasopressors and cold ischemia time.

Recipient survival

Of the 32 patients who received liver allografts, 27 patients recovered and remained alive and well after first liver transplantation, four patients needed retransplantation and all were discharged. One patient died of multi-organ failure in one month after transplantation due to primary graft nonfunction.

DISCUSSION

Early graft function is very closely associated with donor age, duration of patient's stay in ICU and the presence of abnormal graft appearance. The effect of increased donor age on the outcome of OLTx remains controversial^[7,8]. Previously the upper limit of donor age was 50 years. As gradual accumulation of experience of clinical OLTx, now some transplant centers elevate the upper limit of donor age to 65 years. But we suggest that the donor age should be limited to below 60 years, or allograft dysfunction or non-function would easily appear and increase mortality^[9]. When the appearance of the liver has changes in color, blunt edge and anomalous nodulae, it is necessary for frozen pathological examination before transplantation. Steatosis is the most important cause of PGN. The comparatively simple differentiating method is that white four-by being put into the container will turn into pale yellowish after several minutes and this will suggest that the degree of fat infiltrating liver tissue will be over 30%, however, pathological examination to evaluate the degree of fatty infiltration is the most reliable method. As to the hemodynamic stability of the donor, hypotension or the requirement of high-dose dopamine has been associated with nonfunction or delayed function, respectively. Although no obvious harmful effects of cardiopulmonary resuscitation on the early function of the liver allograft were demonstrated in this study, suboptimal perfusion of the liver and warm ischemic injury were strongly suggested. As to the abnormal appearance of the graft, little is known about the correlation between gross appearance and quality of the graft. Livers from donors with diabetes insipidus, who have been on vasopressin for a prolonged period of time, are often firm and suggest the presence of ischemic injury and liver allograft will be harder to touch. Since the use of vasopressin has been associated with a marked reduction in the blood flow to the

Table 3 Early graft function after orthotopic liver transplantation

Early graft function	Number of recipient problems		Total (%)
	No (%)	Yes ¹ (%)	
Good	21 (75)	1 (25)	22 (68.75)
Fair	4 (14.29)	1 (25)	5 (14.29)
Poor	2 (7.14)	1 (25)	3 (9.38)
PGN	1 (3.57)	1 (25)	2 (6.25)
Total	28 (100)	4 (100)	32 (100)

¹Including hepatic artery thrombosis in one patient, intraoperative incidence from severe hemorrhage in two patients, and multi-organ failure in one patient.

Table 4 Correlation between donor or graft variables and early graft function

Variable	Good (n = 21)	Fair (n = 4)	Poor (n = 2)	PGN (n = 1)
Age (yr)	35.6±12.9	43.5±13.8	54.1±4.3	63
Sex (M:F)	15:6	2:2	2:0	1:0
AST(IU/L)	76.4±23.6	63.3±37.1	89.2±42.1	151
ALT(IU/L)	43.2±26.1	69.8±34.9	68.1±31.2	78.1
T. Bil (μmol/L)	12.5±3.4	14.5±7.4	11.8±7.9	20.5
PT(s)	15.2±1.4	14.8±1.2	14.2±1.6	15.5
CPR	4 (19.0%)	2 (50%)		
ICU stay (d)	3.5±2.4	6.2±3.3	7.4±2.1	12
High dose vasopressors	8 (38.1%)	2 (50%)	1 (50%)	0
Abnormal graft appearance	4 (19.0%)	1 (25%)	2 (100%)	1 (100%)
CIT (min)	379±128	421±183	389±214	402±103

CIT: cold ischemia time; T. Bil: total bilirubin; CPR: cardiopulmonary resuscitation.

liver, donors scheduled for liver procurement should stop vasopressin as soon as possible in order to minimize ischemic damage. Overhydration can distend the liver by an increase in central venous pressure and give a false impression as to the consistency of the liver. If the liver is distended from overhydration, the administration of intravenous diuretics can be used immediately.

As far as now, there have been two methods for procurement of liver allografts including aortic perfusion only (APO)^[10] and aortic and portal perfusion (APP). Due to shortage of donors, most American transplantation centers adopt multi-organ procurement, which means APO is the sole choice. The experience of Pittsburgh is that APO has no harm to allograft liver and its advantage is simple surgical procedure compared with APP^[11], meanwhile, superior mesenteric vein need not be exposed and therefore it reduces the separation and division of tissue. If RHA originates from superior mesenteric artery, the unexposure of superior mesenteric vein might avoid injuring aberrant right hepatic artery and ischemic injury of splenic organ due to arterial spasm by surgical procedure^[12-14].

The aberrant hepatic artery is very common; the aberrant rate was as high as 43.75% in our group. The right hepatic artery originating from SMA is the most common^[15]. In order to avoid injuring hepatic artery, it is very important to decide by touch whether or not there are pulses behind hepatoduodenal ligament before the abdominal aorta is clamped in the process of procurement of allograft liver. Even if there is no pulse, it could not exclude aberrant right hepatic artery. So routine division of the right side of SMA can often protect aberrant right hepatic artery before dissection of hepatoduodenal ligament. Once there exist the injuries of aberrant hepatic arteries, several aspects should be noticed in the process of the reconstruction of hepatic arteries as follows: (1) the inner membrane of hepatic artery should not be dragged; (2) it is achieved with Carrel patch of the SMA to obviate a small caliber anastomosis; (3) whether the continuous suture will be used depends on operator's mastering of the technique of vascular anastomosis; (4) just before the sutures were tied, the reconstructed HA was allowed to distend by pulsatile infusion of cold solution while the distal HA was occluded digitally and such method can identify whether the reconstructed anastomosis has leakage and stricture, or thrombosis of HA will occur which could cause biliary tract complication^[16-19].

Although division of third hepatic hilum caused severe bleeding for two recipients in our group, this would not affect the early function of allograft liver. Hepatic artery thrombosis and multi-organ failure in earlier stage after transplantation caused poor and non-function for another two patients. Pittsburgh Transplant Center adopts the anastomosis between hepatic artery at the level of gastroduodenal artery in recipient and hepatic artery in donor, hepatic artery thrombosis in earlier stage after transplantation is associated with the technique of anastomosis. The simple differentiating method is to observe the pulse of hepatic artery after anastomosis, Doppler for hepatic artery the first day after liver transplantation is the optimal for finding thrombosis as soon as possible. Multi-organ failure often

accompanies the instability of systemic hemodynamics and the liver is much easier to be affected by ischemic-reperfusion injury, while the injury of the liver also worsens the multi-organ failure and this pernicious recycle can cause patients to die.

For the assessment of allograft viability in clinical OLTx, there is, to date, no practical and simple technique available that is discriminately predictive of allograft function before the actual transplant procedure. Primary graft non-function remains a major cause of mortality, and although the shortage of donor organs remains a major limiting factor in clinical liver transplantation^[20], still we should have a careful attitude toward the choice of liver allograft and take into serious account several predictive factors. If so, better therapeutic effect will be achieved.

REFERENCES

- 1 **Starzl TE**, Miller C, Bronznick B, Makowka L. An improved technique for multiple organ harvesting. *Surg Gynecol Obstet* 1987; **165**: 343-348
- 2 **Boggi U**, Vistoli F, Del Chiaro M, Signori S, Pietrabissa A, Costa A, Bartolo TV, Catalano G, Marchetti P, Del Prato S, Rizzo G, Jovine E, Pinna AD, Filippini F, Mosca F. A simplified technique for the en bloc procurement of abdominal organs that is suitable for pancreas and small-bowel transplantation. *Surgery* 2004; **135**: 629-641
- 3 **Nunez A**, Goodpastor SE, Goss JA, Washburn WK, Halff GA. Enlargement of the cadaveric-liver donor pool using *in-situ* split-liver transplantation despite complex hepatic arterial anatomy. *Transplantation* 2003; **76**: 1134-1136
- 4 **Fukumori T**, Kato T, Levi D, Olson L, Nishida S, Ganz S, Nakamura N, Madariaga J, Ohkohchi N, Satomi S, Miller J, Tzakis A. Use of older controlled non-heart-beating donors for liver transplantation. *Transplantation* 2003; **75**: 1171-1174
- 5 **Pinna AD**, Dodson FS, Smith CV, Furukawa H, Sugitani A, Fung JJ, Corry RJ. Rapid en bloc technique for liver and pancreas procurement. *Transplant Proc* 1997; **29**: 647-648
- 6 **Jeon H**, Ortiz JA, Manzarbeitia CY, Alvarez SC, Sutherland DE, Reich DJ. Combined liver and pancreas procurement from a controlled non-heart-beating donor with aberrant hepatic arterial anatomy. *Transplantation* 2002; **74**: 1636-1639
- 7 **Marino IR**, Doria C, Doyle HR, Gayowski TJ. Matching donors and recipients. *Liver Transpl Surg* 1998; **4**(5 Suppl 1): S115-119
- 8 **Lopez-Navidad A**, Caballero F. For a rational approach to the critical points of the cadaveric donation process. *Transplant Proc* 2001; **33**: 795-805
- 9 **Oh CK**, Sanfey HA, Pelletier SJ, Sawyer RG, McCullough CS, Pruett TL. Implication of advanced donor age on the outcome of liver transplantation. *Clin Transplant* 2000; **14** (4 Pt 2): 386-390
- 10 **Chui AK**, Thompson JF, Lam D, Koutalistras N, Wang L, Verran DJ, Sheil AG. Cadaveric liver procurement using aortic perfusion only. *Aust NZ J Surg* 1998; **68**: 275-277
- 11 **de Ville de Goyet J**, Hausleithner V, Malaise J, Reding R, Lerut J, Jamart J, Barker A, Otte JB. Liver procurement without *in situ* portal perfusion. A safe procedure for more flexible multiple organ harvesting. *Transplantation* 1994; **57**: 1328-1332
- 12 **Wei WI**, Lam LK, Ng RW, Liu CL, Lo CM, Fan ST, Wong J. Microvascular reconstruction of the hepatic artery in live donor liver transplantation: experience across a decade. *Arch Surg* 2004; **139**: 304-307
- 13 **Soliman T**, Bodingbauer M, Langer F, Berlakovich GA, Wamser P, Rockenschaub S, Muehlbacher F, Steininger R. The role of complex hepatic artery reconstruction in orthotopic

- liver transplantation. *Liver Transpl* 2003; **9**: 970-975
- 14 **Turrion VS**, Alvira LG, Jimenez M, Lucena JL, Ardaiz J. Incidence and results of arterial complications in liver transplantation: experience in a series of 400 transplants. *Transplant Proc* 2002; **34**: 292-293
 - 15 **Hesse UJ**, Troisi R, Maene L, de Hemptinne B, Pattyn P, Lameire N. Arterial reconstruction in hepatic and pancreatic allograft transplantation following multi-organ procurement. *Transplant Proc* 2000; **32**: 109-110
 - 16 **Zhou GW**, Cai WY, Li HW, Zhu Y, Dodson F, Fung JJ. Transjugular intrahepatic portosystemic shunt for liver transplantation. *Hepatobiliary Pancreat Dis Int* 2002; **1**: 179-182
 - 17 **Thuluvath PJ**, Atassi T, Lee J. An endoscopic approach to biliary complications following orthotopic liver transplantation. *Liver Int* 2003; **23**: 156-162
 - 18 **Rerknimitr R**, Sherman S, Fogel EL, Kalayci C, Lumeng L, Chalasani N, Kwo P, Lehman GA. Biliary tract complications after orthotopic liver transplantation with choledochocholedochostomy anastomosis: endoscopic findings and results of therapy. *Gastrointest Endosc* 2002; **55**: 224-231
 - 19 **Nemec P**, Ondrasek J, Studenik P, Hokl J, Cerny J. Biliary complications in liver transplantation. *Ann Transplant* 2001; **6**: 24-28
 - 20 **First MR**. The organ shortage and allocation issues. *Transplant Proc* 2001; **33**: 806-810

Science Editor Zhu LH Language Editor Elsevier HK

5-Fluorouracil concentration in blood, liver and tumor tissues and apoptosis of tumor cells after preoperative oral 5'-deoxy-5-fluorouridine in patients with hepatocellular carcinoma

Jin-Fang Zheng, Hai-Dong Wang

Jin-Fang Zheng, Hai-Dong Wang, Department of Hepatobiliary Surgery, Hainan Provincial People's Hospital, Haikou 570311, Hainan Province, China

Correspondence to: Dr. Jin-Fang Zheng, Department of Hepatobiliary Surgery, Hainan Provincial People's Hospital, Haikou 570311, Hainan Province, China. zhengjf2000@hotmail.com

Telephone: +86-898-66771028 Fax: +86-898-68661664

Received: 2004-08-31 Accepted: 2004-12-21

Zheng JF, Wang HD. 5-Fluorouracil concentration in blood, liver and tumor tissues and apoptosis of tumor cells after preoperative oral 5'-deoxy-5-fluorouridine in patients with hepatocellular carcinoma. *World J Gastroenterol* 2005; 11 (25): 3944-3947

<http://www.wjgnet.com/1007-9327/11/3944.asp>

Abstract

AIM: To study the levels of 5-fluorouracil (5-FU) in plasma, liver and tumor in patients with hepatocellular carcinoma after oral administration of 5'-deoxy-5-fluorouridine (5'-DFUR).

METHODS: Thirty-nine patients with hepatocellular carcinoma were treated with oral 5'-DFUR for more than 4 d before operation. The contents of 5-FU in plasma, liver and tumor were measured by high performance liquid chromatography (HPLC) and apoptosis of tumor cells was evaluated by *in-situ* TUNEL after resection of tumor.

RESULTS: The concentrations of 5-FU were 1.1 $\mu\text{g/mL}$, 5.6, 5.9, and 10.5 $\mu\text{g/g}$ in plasma, the liver tissue, the center of tumor and the periphery of tumor, respectively. 5-FU concentration was significantly higher in the periphery of tumor than that in the liver tissue and the center of tumor (10.5 \pm 1.6 $\mu\text{g/g}$ vs 5.6 \pm 0.8 $\mu\text{g/g}$, $t = 21.38$, $P < 0.05$; 10.5 \pm 1.6 $\mu\text{g/g}$ vs 5.9 \pm 0.9 $\mu\text{g/g}$, $t = 20.07$, $P < 0.05$). 5-FU level was significantly lower in plasma than that in the liver and the tumor (1.1 \pm 0.3 $\mu\text{g/mL}$ vs 5.6 \pm 0.8 $\mu\text{g/g}$, $t = 19.63$, $P < 0.05$; 1.1 \pm 0.3 $\mu\text{g/mL}$ vs 10.5 \pm 1.6 $\mu\text{g/g}$, $t = 41.01$, $P < 0.05$). Apoptosis of tumor cells was significantly increased after oral 5'-DFUR compared to the control group without 5'-DFUR treatment.

CONCLUSION: There is a higher concentration of 5-FU distributed in the tumor compared with liver tissue and apoptosis of tumor cells is increased following oral 5'-DFUR compared with the control group. The results indicate that 5'-DFUR is hopeful as neo-adjuvant chemotherapy to prevent recurrence after resection of hepatocellular carcinoma.

© 2005 The WJG Press and Elsevier Inc. All rights reserved.

Key words: Hepatocellular carcinoma; 5'-Deoxy-5-fluorouridine; 5-Fluorouracil; Apoptosis

INTRODUCTION

Hepatocellular carcinoma (HCC) remains one of the most common neoplasms in the world^[1,2]. 5'-Deoxy-5-fluorouridine (5'-DFUR) is an oral fluoropyrimidine derivative and it is converted to 5-fluorouracil (5-FU) by Pyrimidine nucleoside phosphorylase (PyNPase) which is expressed with higher level in tumor tissues compared with normal tissues^[3,4]. Oral 5-FU derivatives have shown comparable antitumor activity and long-term oral administration of low-dose has been considered as postoperative adjuvant chemotherapy after curative resection of the cancer to reduce recurrence and improve survival rate^[5-9]. The selective antitumor activity of 5'-DFUR is correlated with PyNPase activity in tumor^[10]. Although the activity of 5-FU in tumor is well recognized, resistance to this agent is frequently observed and remains its major limitation. It was reported that doxifluridine still showed antitumor activity to tumor cells which were resistant to 5-FU^[11].

The purpose of the present study was to investigate the impact of preoperative oral 5'-DFUR on distribution of 5-FU in plasma, liver and tumor and apoptosis of tumor cells in patients with hepatocellular carcinoma.

MATERIALS AND METHODS

Chemicals and reagents

5'-DFUR capsule (Furtulon) was produced by Shanghai Roche Pharmaceuticals Co. (Shanghai, China), and standard 5-FU was provided by Sigma Chemicals Co. (USA). Methyl-tert butyl ether, acetonitrile, methanol (HPLC grade) and potassium hydrogen phosphate (AR grade) were purchased from Peking Chemical Plant (Beijing, China).

Chromatographic conditions

HPLC system consisted of LC-10AT HPLC pump and SPD-10A Detector (SHIMADZU Co. Japan). The analytical column was Kromasil C₁₈ (5 μm 200 mm \times 4.6 mm ID). The mobile phase consisted of acetonitrile, methanol, and 0.25 mol/L potassium hydrogen phosphate (1:4:5). The

flow rate was 1.0 mL/min and the wavelength was at 265 nm.

Collection of samples

Thirty-nine patients of 27 male and 12 female with hepatocellular carcinoma were included in this study. Their average age was 49.1 years and the diameters of tumors were from 5 to 7 cm. 5'-DFUR was administered orally and preoperatively (1 200 daily for more than 4 d before operation and 400 mg on the day of operation). The mean total dosage was 6.4 g. Blood sample and specimens of the normal liver tissue and the tumor tissue were collected 3-5 h after final administration. The liver and tumor tissues were cleaned by distilled water and blotted by filter paper. One gram tissue was weighed accurately and 4 mL distilled water was added to the container to crush the tissue. The blood samples and the crushed tissues were centrifuged, and 1 mL plasma or aqueous layer sample was then stored under -20 °C.

Extraction and determination of samples

Each 0.5 mL plasma or aqueous layer sample was added and mixed with 0.1 mL of potassium hydrogen phosphate (0.5 mol/L), followed by the addition of 5 mL methyl-tert butyl ether to each tube. The tube was then capped and shaken for 10 min on a shaker. The aqueous layer and the organic layer were separated by centrifugation at 3 000 r/min for 10 min. The aqueous layer was transferred to a clean test tube and evaporated to dryness under gentle stream of nitrogen at 50 °C. The residue was dissolved with 0.1 mL of mobile phase and vortexed. Then the sample was transferred into a micro-spin filter tube and was centrifuged at 3 000 r/min for 10 min. The filtrate was collected and the injection volume was 20 µL and the content of 5-FU was measured by high performance liquid chromatography (HPLC)^[12-14].

In vivo detection of apoptosis

TUNEL staining was used to detect DNA degradation *in situ* in the relatively late stage of apoptosis. Apoptotic cells were labeled by the TUNEL reaction using an *in situ* Cell Apoptosis Detection Kit. *In situ* Cell Apoptosis Detection Kits were purchased from Roche Diagnostics GmbH Co. in Germany. The detailed manipulation was conducted according to instructions for users. The procedure was performed following the instructions of the manufacturer and in reference of the previous observations^[15,16].

The positive cells were identified and analyzed based on morphological characteristics of apoptotic cells as previously described. Under the fluorescence microscopy, apoptotic cells manifested as brownish staining in the nuclei. Non-necrotic zone was selected in the tissue section and images were randomly selected. The positive cells were determined in at least five areas at ×400 magnification and divided into three categories as follows: (+) only sporadic positive cells were detected; (++) a cluster of apoptotic cells were observed; (+++) positive cells in a large scale or multi-cluster apoptotic cells were seen in representative tissue sections of each individual case. Twenty patients of HCC without oral 5'-DFUR treatment were included as the control group.

Statistical analysis

The data were expressed as mean±SD. Student's *t*-test was performed for statistical analysis. *P* value less than 0.05 was considered statistically significant.

RESULTS

Concentration of 5-FU in plasma, liver and tumor following oral administration of 5'-DFUR

The concentrations of 5-FU were 1.1 µg/mL, 5.6, 5.9, and 10.5 µg/g in plasma, the liver tissue, the center of tumor and the periphery of tumor, respectively. The 5-FU content was significantly higher in the periphery of tumor than that in the liver tissue and the center of tumor (*P*<0.05). Moreover, the 5-FU concentration was significantly lower in plasma than liver and tumor (*P*<0.05). However, the 5-FU level in the center of tumor was similar to that in the liver tissue (Table 1).

Table 1 5-FU concentrations in blood, liver and tumor after oral 5'-DFUR

Tissue	Level of 5-FU
Plasma (µg/mL)	1.1±0.3 ^a
Liver tissue (µg/g)	5.6±0.8
Central tissue of tumor (µg/g)	5.9±0.9
Periphery tissue of tumor (µg/g)	10.5±1.6 ^a

^a*P*<0.05 vs 5-FU concentration in liver tissue.

Apoptosis of the tumor cell demonstrated by TUNEL

Under the fluorescence microscope, apoptotic cells manifested as brownish staining in the nuclei. The degree of apoptosis was shown + in tissue sections of the control group in which sporadic positive cells were detected, and ++ in cases with oral 5'-DFUR in which clusters of apoptotic cells were seen (Figures 1A and B).

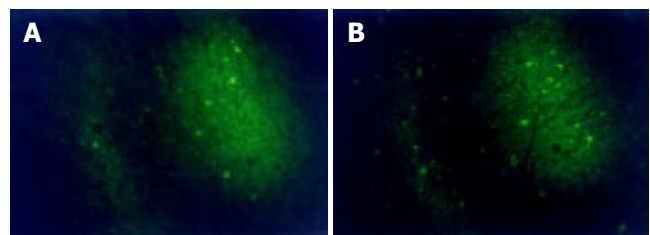


Figure 1 Apoptotic cancer cells detected by TUNEL method after oral administration of 5'-DFUR ×400. A: Sporadic apoptotic cells were detected; B: clusters of apoptotic cells were detected.

DISCUSSION

It is well known that hepatocellular carcinoma is one of the malignant tumors with poor chemosensitivity to anticancer agents^[17,18]. 5-FU is still the first choice for the chemotherapy of hepatocellular carcinoma^[19,20], because of its strong killing effects on the cancer cells. 5-FU can damage proliferating cells, reduce the tumor mass in size and prevent tumor

cells from spreading and metastasis. However, its usage is limited due to the rapid development of acquired resistance. The effects of 5-FU are not so satisfactory because 5-FU has a lower concentration in tumor tissue and relatively higher concentrations in blood after intravenous administration of 5-FU. Moreover, its side effects are serious and many patients are unable to tolerate.

5'-DFUR is a prodrug of 5-FU and it is converted to 5-FU by Pyrimidine nucleoside phosphorylase (PyNPase). PyNPase exists in all kinds of tumor tissues and its expression and activity in tumor tissue are higher than that in normal tissue^[3,4]. Nagata *et al.*^[21-24] reported that transfection of PyNPase gene into tumor cell can increase the sensitivity to 5'-DFUR, and thereby decreases the toxicity of the agent. In our study, it had been found that 5-FU level in tumor was 10 times higher than in plasma and 5-FU level was significantly higher in the periphery of tumor than in the liver tissue. The results suggested that more 5-FU was converted and accumulated within tumor tissue. This difference may be related to the higher PyNPase expression and activity in hepatocellular carcinoma. It had also been found that the 5-FU level was significantly higher in the periphery of tumor than the center of tumor. There was more 5-FU accumulated and converted in the periphery of tumor following oral 5'-DFUR administration. Oxygen, nutrition and growth factors were not equally distributed within the tumor tissue. Oxygen and nutrient of the central tumor tissue are supplied mainly by hepatic artery, and proliferation of the tumor in this region is slower and even partial necrosis appears. However, the periphery of tumor has effluent blood flow supplied by hepatic artery and portal vein, so the tumor cells can grow more rapidly. These results may indicate that large liver tumor is not sensitive to 5'-DFUR.

Oral 5'-DFUR is very convenient and its side effect is slight^[25]. The drug arrives in the liver firstly after being absorbed by the intestine. So most of 5'-DFUR can be converted to 5-FU in the liver or the liver tumor and accumulated in these tissues with higher concentration than that administered by iv approach. In this study, the 5-FU level in peripheral vein was only one-tenth of that in tumor tissue. 5-FU can be maintained at a certain level within the tumor tissue but not accumulated in the peripheral vein after regular oral administration of 5'-DFUR.

The expression and activity of PyNPase is higher in the tumor with vascular permeation and lymph node metastasis^[4,26,27]. Akao *et al.*^[28] reported that PyNPase activity was significantly higher in metastatic lymph node. Tazawa *et al.*^[29] found that 5'-DFUR could inhibit hepatic metastasis of tumor, which would be effective for the prophylactic treatment of metastatic disease. These indicate that PyNPase activity appears to be a new useful parameter for identifying both a poor prognosis and a highly malignant potential of tumor and 5'-DFUR is preferably sensitive in cancer patients with lymph node metastasis and vascular infiltration. 5'-DFUR is still effective to the tumor which is resistant to 5-FU therapy^[11]. Monden *et al.*^[30] found that vessel density and stage of tumor were correlated with expression of PyNPase which showed prognosis. 5'-DFUR not only is effective on primary tumor and metastatic lesion but also

suitable to postoperative prevention of tumor. Apoptosis of the tumor was enhanced after oral administration of 5'-DFUR. In this study, it was found that there were more apoptosis cells in the tumor after oral administration of 5'-DFUR.

In summary, our results showed that there was a higher concentration of 5-FU accumulated in the tumor tissue compared with liver tissue and apoptosis of the tumor cells was increased after oral administration of 5'-DFUR. 5'-DFUR is a hopeful agent for neo-adjuvant chemotherapy to prevent recurrence after resection of hepatocellular carcinoma.

REFERENCES

- 1 Yu MC, Yuan JM, Govindarajan S, Ross RK. Epidemiology of hepatocellular carcinoma. *Can J Gastroenterol* 2000; **14**: 703-709
- 2 El-Serag HB. Hepatocellular carcinoma: an epidemiologic view. *J Clin Gastroenterol* 2002; **35**(5 Suppl 2): S72-78
- 3 Kobayashi N, Kubota T, Watanabe M, Otani Y, Teramoto T, Kitajima M. Pyrimidine nucleoside phosphorylase and dihydropyrimidine dehydrogenase indicate chemosensitivity of human colon cancer specimens to doxifluridine and 5-fluorouracil, respectively. *J Infect Chemother* 1999; **5**: 144-148
- 4 Hiroyasu S, Shiraishi M, Samura H, Tokashiki H, Shimoji H, Isa T, Muto Y. Clinical relevance of the concentrations of both pyrimidine nucleoside phosphorylase (PyNPase) and dihydropyrimidine dehydrogenase (DPD) in colorectal cancer. *Jpn J Clin Oncol* 2001; **31**: 65-68
- 5 Ito K, Okushiba S, Morikawa T, Kondo S, Katoh H. Appropriate duration of postoperative oral adjuvant chemotherapy with HCFU for colorectal cancer. *Gan To Kagaku Ryoho* 2004; **31**: 55-59
- 6 Min JS, Kim NK, Park JK, Yun SH, Noh JK. A prospective randomized trial comparing intravenous 5-fluorouracil and oral doxifluridine as postoperative adjuvant treatment for advanced rectal cancer. *Ann Surg Oncol* 2000; **7**: 674-679
- 7 Andre T, Boni C, Mounedji-Boudiaf L, Navarro M, Taberero J, Hickish T, Topham C, Zaninelli M, Clingan P, Bridgewater J, Tabah-Fisch I, de Gramont A. Oxaliplatin, fluorouracil, and leucovorin as adjuvant treatment for colon cancer. *N Engl J Med* 2004; **350**: 2343-2351
- 8 Takiguchi N, Fujimoto S, Koda K, Oda K, Okui K, Nakajima N, Miyazaki M. Postoperative adjuvant chemotherapy is effective in gastric cancer with serosal invasion: significance in patients chosen for multivariate analysis. *Oncol Rep* 2002; **9**: 801-806
- 9 Zhou J, Tang ZY, Fan J, Wu ZQ, Ji Y, Xiao YS, Shi YH, Li XM, Sun QM, Liu YK, Ye SL. Capecitabine inhibits postoperative recurrence and metastasis after liver cancer resection in nude mice with relation to the expression of platelet-derived endothelial cell growth factor. *Clin Cancer Res* 2003; **9**(16 Pt 1): 6030-6037
- 10 Hata Y, Takahashi H, Sasaki F, Ogita M, Uchino J, Yoshimoto M, Akasaka Y, Nakanishi Y, Sawada Y. Intratumoral pyrimidine nucleoside phosphorylase (PyNPase) activity predicts a selective effect of adjuvant 5'-deoxy-5-fluorouridine (5'-DFUR) on breast cancer. *Breast Cancer* 2000; **7**: 37-41
- 11 Bajetta E, Di Bartolomeo M, Somma L, Del Vecchio M, Artale S, Zunino F, Bignami P, Magnani E, Buzzoni R. Doxifluridine in colorectal cancer patients resistant to 5-fluorouracil (5-FU) containing regimens. *Eur J Cancer* 1997; **33**: 687-690
- 12 Zuffia L, Aldaz A, Castellanos C, Giraldez J. Determination of 5-fluorouracil and its prodrug tegafur in plasma and tissue by high-performance liquid chromatography in a single injection: validation for application in clinical pharmacokinetic studies. *Ther Drug Monit* 2003; **25**: 221-228
- 13 Nassim MA, Shirazi FH, Cripps CM, Veerasinghan S, Molepo

- MJ, Obrocea M, Redmond D, Bates S, Fry D, Stewart DJ, Goel R. An HPLC method for the measurement of 5-fluorouracil in human plasma with a low detection limit and a high extraction yield. *Int J Mol Med* 2002; **10**: 513-516
- 14 **Ozawa S**, Hamada M, Murayama N, Nakajima Y, Kaniwa N, Matsumoto Y, Fukuoka M, Sawada J, Ohno Y. Cytosolic and microsomal activation of doxifluridine and tegafur to produce 5-fluorouracil in human liver. *Cancer Chemother Pharmacol* 2002; **50**: 454-458
- 15 **Xu Y**, Kajimoto S, Nakajo S, Nakaya K. Beta-hydroxyisovalerylshikonin and cisplatin act synergistically to inhibit growth and to induce apoptosis of human lung cancer DMS114 cells via a tyrosine kinase-dependent pathway. *Oncology* 2004; **66**: 67-75
- 16 **Barnett KT**, Fokum FD, Malafa MP. Vitamin E succinate inhibits colon cancer liver metastases. *J Surg Res* 2002; **106**: 292-298
- 17 **Huesker M**, Folmer Y, Schneider M, Fulda C, Blum HE, Hafkemeyer P. Reversal of drug resistance of hepatocellular carcinoma cells by adenoviral delivery of anti-MDR1 ribozymes. *Hepatology* 2002; **36**(4 Pt 1): 874-884
- 18 **Warmann S**, Gohring G, Teichmann B, Geerlings H, Pietsch T, Fuchs J. P-glycoprotein modulation improves *in vitro* chemosensitivity in malignant pediatric liver tumors. *Anti-cancer Res* 2003; **23**: 4607-4611
- 19 **Tono T**, Hasuike Y, Ohzato H, Takatsuka Y, Kikkawa N. Limited but definite efficacy of prophylactic hepatic arterial infusion chemotherapy after curative resection of colorectal liver metastases: A randomized study. *Cancer* 2000; **88**: 1549-1556
- 20 **Guo WJ**, Yu EX. Evaluation of combined therapy with chemoembolization and irradiation for large hepatocellular carcinoma. *Br J Radiol* 2000; **73**: 1091-1097
- 21 **Nagata T**, Nakamori M, Iwahashi M, Yamaue H. Overexpression of pyrimidine nucleoside phosphorylase enhances the sensitivity to 5'-deoxy-5-fluorouridine in tumour cells *in vitro* and *in vivo*. *Eur J Cancer* 2002; **38**: 712-717
- 22 **Evrard A**, Cuq P, Ciccolini J, Vian L, Cano JP. Increased cytotoxicity and bystander effect of 5-fluorouracil and 5-deoxy-5-fluorouridine in human colorectal cancer cells transfected with thymidine phosphorylase. *Br J Cancer* 1999; **80**: 1726-1733
- 23 **Kanyama H**, Tomita N, Yamano T, Miyoshi Y, Ohue M, Fujiwara Y, Sekimoto M, Sakita I, Tamaki Y, Monden M. Enhancement of the anti-tumor effect of 5'-deoxy-5-fluorouridine by transfection of thymidine phosphorylase gene into human colon cancer cells. *Jpn J Cancer Res* 1999; **90**: 454-459
- 24 **Evrard A**, Cuq P, Robert B, Vian L, Pelegrin A, Cano JP. Enhancement of 5-fluorouracil cytotoxicity by human thymidine-phosphorylase expression in cancer cells: *in vitro* and *in vivo* study. *Int J Cancer* 1999; **80**: 465-470
- 25 **Min JS**, Kim NK, Park JK, Yun SH, Noh JK. A prospective randomized trial comparing intravenous 5-fluorouracil and oral doxifluridine as postoperative adjuvant treatment for advanced rectal cancer. *Ann Surg Oncol* 2000; **7**: 674-679
- 26 **Yamagata M**, Mori M, Mimori K, Mafune KI, Tanaka Y, Ueo H, Akiyoshi T. Expression of pyrimidine nucleoside phosphorylase mRNA plays an important role in the prognosis of patients with oesophageal cancer. *Br J Cancer* 1999; **79**: 565-569
- 27 **Mimori K**, Ueo H, Shirasaka C, Shiraiishi T, Yamagata M, Haraguchi M, Mori M. Up-regulated pyrimidine nucleoside phosphorylase in breast carcinoma correlates with lymph node metastasis. *Ann Oncol* 1999; **10**: 111-113
- 28 **Akao S**, Inoue K. PyNPase and DPD expression potentially predict response to 5'-DFUR treatment for node-positive breast cancer patients. *Gan To Kagaku Ryoho* 2003; **30**: 1361-1364
- 29 **Tazawa K**, Sakamoto T, Kuroki Y, Yamashita I, Okamoto M, Katuyama S, Fujimaki M. Inhibitory effects of fluorinated pyrimidines, 5'-DFUR, UFT and T-506, in a model of hepatic metastasis of mouse colon 26 adenocarcinoma-assessment of inhibitory activity and adverse reactions at the maximum tolerated dose. *Clin Exp Metastasis* 1997; **15**: 266-271
- 30 **Monden T**, Haba A, Amano M, Kanoh T, Tsujie M, Ikeda K, Izawa H, Ohnishi T, Sekimoro M, Tomita N, Okamura J, Monden M. PyNPase expression and cancer progression in the colorectum. *Nippon Geka Gakkai Zasshi* 1998; **99**: 446-451

Prognostic value of KIT mutation in gastrointestinal stromal tumors

Xiao-Hong Liu, Chen-Guang Bai, Qiang Xie, Fei Feng, Zhi-Yun Xu, Da-Lie Ma

Xiao-Hong Liu, Zhi-Yun Xu, Institute of thoracic cardiac surgery, Changhai Hospital, Second Military Medical University, Shanghai 200433, China

Chen-Guang Bai, Qiang Xie, Fei Feng, Da-Lie Ma, Department of Pathology, Changhai Hospital, Second Military Medical University, Shanghai 200433, China

Co-first-authors: Qiang Xie

Co-correspondents: Zhi-Yun Xu

Correspondence to: Da-Lie Ma, Chief of Department of Pathology, Changhai Hospital, Second Military Medical University, Changhai Road, Shanghai 200433, China. madalie@yahoo.com.cn

Telephone: +21-25070660 Fax: +21-25072135

Received: 2004-07-12 Accepted: 2004-09-19

Abstract

AIM: To examine the prevalence and prognostic significance of C-kit gene mutation and analysis the correlation of C-kit gene mutation and the clinicalpathologic parameters of GISTs.

METHODS: Eighty-two GISTs were studied for the mutation of C-kit gene by PCR-SSCP, DNA sequence. Statistical comparison were used to analysis the correlation of C-kit gene mutation and clinicalpathology, clinical behavior, recurrence.

RESULTS: (1) Mutation-positive and mutation-negative GISTs were 34 and 48, respectively; (2) Among these patients with C-kit mutation remained a significantly poor prognosis associated with 59% 3-year survival compared to those whose tumors did not; (3) Tumor size, PCNA index, mitotic cell number, presence of necrosis, microscopic invasion to adjacent tissues, recurrence and distant metastasis among mutation-positive and mutation-negative GISTs were significantly different.

CONCLUSION: C-kit mutation is a undoubtedly pivotal event in GIST and may be associated with poor prognosis. Evaluation of C-kit gene mutation may have both prognosis and therapeutic significances.

© 2005 The WJG Press and Elsevier Inc. All rights reserved.

Key words: Gastrointestinal stromal tumor; Gene mutation; C-kit oncogene; Prognostic factor

Liu XH, Bai CG, Xie Q, Feng F, Xu ZY, Ma DL. Prognostic value of KIT mutation in gastrointestinal stromal tumors. *World J Gastroenterol* 2005; 11(25): 3948-3952
<http://www.wjgnet.com/1007-9327/11/3948.asp>

INTRODUCTION

Gastrointestinal stromal tumor (GIST) is designation for a major subset of mesenchymal tumors of the gastrointestinal tract. Their biological behavior is a persistent source of controversy. Concerning prognosis, various studies^[1-3] have endeavored in the establishment of clinicopathologic correlations, such as tumor size, location, mitotic cell count, proliferative activity, presence of necrosis, presence of hemorrhage, microscopic invasion to adjacent tissues, recurrence, distant metastasis, age, sex, cell type. Yet the criteria claimed to predict the biological behavior of GIST remains vague and do not even enable a confident discrimination between benign and malignant lesions. Discrimination of malignant GISTs based on an objectively defined factor would be of practical importance. In this study, we intend to contribute to this issue by examining the prevalence and prognostic significance of the above-mentioned parameters, C-kit expression and C-kit gene mutation, and analysis the correlation of C-kit gene mutation and the above-mentioned clinical parameters.

MATERIALS AND METHODS

Patients

During the period 1997-2001, 82 patients with primary mesenchymal tumors of the gastrointestinal tract underwent surgery at Changhai Hospital and were diagnosed as GISTs. Of these, 56 men and 26 women, the mean age of the GIST patients at the time of diagnosis was 53 years. The locations of the tumors were as follows: 3 in the esophagus, 42 in the stomach, 35 in the intestine, and 2 in the mesentery. According to the standard of Lewin's^[4], 82 cases were divided into 2 groups, 20 benign and 62 malignant GISTs. At the time of diagnosis, 16 were found microscopic invasion to mucous myometrium or placenta percreta, distant metastasis was found in 16 patients, 9 to the liver, 2 to bone, 1 to lung and 4 extensive metastasis; the remaining patients were free of distant metastasis. Thus, curative surgery was performed for 73 patients, and the patients with distant metastasis or peritoneal dissemination underwent only local resection. The mean follow-up period was 4.1 years, during the follow-up period, 18 patients suffered from recurrences, and 10 patients received reoperation for recurrences.

Immunohistochemistry

Paraffin sections (3 mm thick) of formalin-fixed tissues were used for conventional H&E staining and for immunohistochemistry. Rabbit polyclonal antibody against

human KIT and mouse monoclonal antibody against human PCNA were purchased from DAKO. Immunohistochemistry was performed using EnVision kit by two-step technique. PCNA index indicating the percentage of positive tumor nuclei was obtained by visual quantitative assessment of 100 tumor cells. Random fields were selected, excluding areas with excessive or scant immunostaining. Nuclear staining without cytoplasmic staining was considered a positive result. Negative result was set as “-”, PCNA index <10% +, PCNA index 10%-30% ++, >30% +++.

PCR-SSCP

DNA was extracted from formalin-fixed, paraffin-embedded tissues using standard methods with proteinase K digested and phenol/chloroform purified. Exon11 of the C-kit gene was amplified by PCR using the following oligonucleotide primer pairs: sense primer 5'-aactcagcctgttctctgg-3'-antisense primer: 5'-gatctattttccctttctc-3'. PCR products were subjected to 8% non-denaturation polyacrylamide gel electrophoresis (aer:bis = 49:1) with 5% glycerin and silver nitrate staining.

DNA sequencing

PCR products that showed abnormal gel shift by PCR-SSCP were selected for sequencing after cloned into PMD18-T vector. The sequencing procedures were performed by Songon Co., Shanghai.

Statistical analysis

Eighty-two GISTs were divided into mutation-positive and mutation-negative subtypes according to C-kit gene detection. χ^2 test was used to analyze the correlation of C-kit mutation and clinicopathological and prognostic factors. Two-sided $P < 0.05$ were considered to represent statistical significance. The relative importance of various prognostic factors for the postoperative was analyzed with Cox's proportional hazard model. Logistic regression analysis with the forward stepwise method was used to compare the difference of survival curves between the C-kit mutation-positive and mutation-negative subtypes. The possible prognostic factors included age, sex, location of tumors, tumor size, cell type, microscopic invasion to neighboring structures, mitotic cell number, PCNA index, distant metastasis at the time of diagnosis, peritoneal dissemination at the time of surgery, recurrences during the follow-up period, presence of necrosis, presence of hemorrhage, presence of C-kit mutation and expression.

RESULTS

Immunohistochemistry

Immunohistochemical analyses revealed strong and diffuse C-kit expression in 80 of 82 cases. PCNA staining intensity varied from very weak to intensely strong and from finely granular to uniformly dark red-brown (Table 1).

Evaluation of mutations in exon11 of C-kit gene

Two alleles were observed for the normal PCR segments, fast and slow fragments were designated as A and B alleles, respectively. Comparing to normal cases, 34 (41.5%) malignant

GISTs showed abnormal gel shifts while no mutant bands were observed in benign GISTs. Abnormal gel shifts included multiple shift bands, monomorphic fragment or band shifting. Sequencing of abnormal bands revealed point mutation, deletion mutation and insertion deletion. Mutation-positive and mutation-negative GISTs were 34 and 48, respectively.

Survival analysis

Three-year survival rate was 77%(63/82) of 82 cases. Among these patients with C-kit mutation remained a significantly poor prognosis associated with 59% 3-year survival compared to those whose tumors did not. ($\chi^2 = 11.6464$, $P < 0.05$, Figure 1).

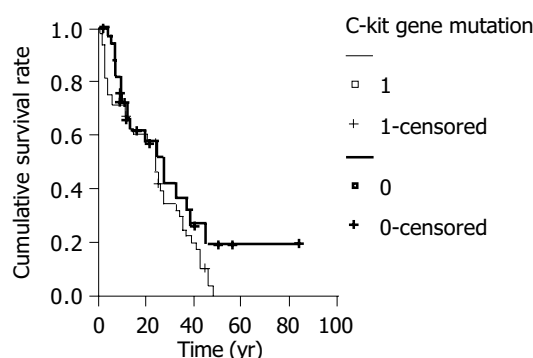


Figure 1 C-kit gene mutation and cumulative survival rate.

The relationship of C-kit mutation and clinicopathological marker

We examined whether the presence of C-kit mutation could be associated with clinicopathological features of GISTs (Table 1). Statistical analysis indicated that significant differences were detected with tumor size ($\chi^2 = 16.7950$, $P < 0.05$), PCNA index ($\chi^2 = 17.0990$, $P < 0.05$), mitotic cell number ($\chi^2 = 11.2327$, $P < 0.05$), presence of necrosis ($\chi^2 = 4.4036$, $P < 0.05$), microscopic invasion to adjacent tissues ($\chi^2 = 22.3912$, $P < 0.05$) between two terms. The age, sex, location of tumor, cell type, the presence of hemorrhage, and C-kit expression were independently related to the presence of C-kit mutation.

The correlation between C-kit mutation and prognostic factors

We also examined whether the presence of C-kit mutation was associated with the clinical outcome (Table 2). The mutation-positive GISTs showed more frequent recurrences ($\chi^2 = 16.333$, $P < 0.05$), distant metastasis ($\chi^2 = 12.9649$, $P < 0.05$) and higher mortality ($\chi^2 = 11.6464$, $P < 0.05$) than the mutation-negative GISTs. Of the patients with mutation-positive GIST, developed distant metastasis.

DISCUSSION

GISTs are the most common mesenchymal tumors of the human gastrointestinal tract which are enigmatic in terms of their line of differentiation or cell of origin and clinical behavior^[5]. Recently, many studies have shown that tumor size, location, mitotic cell count, cell type, proliferative

Table 1 Relationship of C-kit mutation and clinicopathological marker

Clinicalpathological	Total	C-kit		C-kit		χ^2	P
		Case	Percent	Case	Percent		
Total	82	34		48			
Age (yr)							
<40	12	5	15	7	15%	0.0002	0.9877
≥40	70	29	85	41	85%		
Sex							
Man	56	24	71	32	67%	0.1413	0.7069
Woman	26	10	29	16	33%		
Tumor size							
1-5.4	46	10	29	36	75%	16.7950	<0.0001
≥5.5	36	24	71	12	25%		
Location of tumors							
Esophagus	3	0	0	3	6%		
Stomach	42	14	41	28	58%	7.5243	0.0569
Intestine	35	18	53	17	36%		
Mesentery	2	2	6	0	0%		
Cell type							
Spindle	73	29	85	44	92%	0.8272	0.3631
Epithelioid	9	5	15	4	8%		
PCNA index							
0	19	7	21	12	25%		
+	49	15	44	34	71%	17.0990	0.0007
++	13	12	35	1	2%		
+++	1	0	0	1	2%		
Mitotic							
<5	67	22	65	45	94%	11.2327	0.00008
≥5/50	15	12	35	3	6%		
Hemorrhage							
Yes	25	12	35	13	27%	0.6331	0.4262
No	57	22	65	35	73%		
Necrosis							
Yes	37	20	59	17	35	4.4036	0.0359
No	45	14	41	31	65		
Microscopic							
Yes	16	15	44	1	2	22.3912	<0.0001
No	66	19	56	47	98		
C-kit expression							
Positive	80	33	97	47	98	0	1
Negative	2	1	3	1	2		

Table 2 Correlation between C-kit mutation and prognostic factors

Prognostic	Total	C-kit mutation-positive subtype		C-kit mutation-negative subtype		χ^2	P
		Case	Percent	Case	Percent		
Total	82	34	48				
Recurrence							
Yes	18	13	38	5	10	16.333	0.0001
No	64	21	62	43	90		
Metastasis	16	13	38	3	6	12.9649	0.0003
Live	10	9	26	1	2		
Abdominal cavity	3	2	6	1	2		
Distant	3	2	6	1	2		
Prognosis							
Survival	63	20	59	43	90	11.6464	0.0006
Death	19	14	41	5	10		

activity, presence of necrosis, presence of hemorrhage, microscopic invasion to adjacent tissues, recurrence, distant metastasis, as favorable factors of GIST. But histologic distinction of benign from malignant tumors is often difficult, and prediction of clinical outcome on the basis of histologic characteristics alone is not always reliable, many histologically malignant neoplasms were clinically benign. Moreover, some tumors had conflicting features of both benignancy and malignancy, and their malignant potential has been labeled uncertain or indeterminate. In recent years, C-kit protein expression and activated gene mutation have been found in GIST^[6-9], aggressive mastocytosis^[10], mast cell leukemia^[11], ANLL with/without mast cell involvement^[10], myeloproliferative disorders^[10], colon carcinoma^[12] and germ cell tumors^[13]. Dections of gene mutation have shown a good correlation with biologic behavior in such tumors and providing valuable adjunctive prognostic information. In this study, we examined whether the presence of mutation of C-kit gene is important as a prognostic factor of GIST and found it to indicate a significantly poorer prognosis.

First, we examined whether the presence of C-kit mutation could be associated with clinicopathological features of GISTs. Statistical analysis indicated that significant differences were detected with tumor size, PCNA index, mitotic cell number, presence of necrosis, microscopic invasion to adjacent tissues between mutation-positive and mutation-negative GISTs. While the age, sex, location of tumor, cell type, the presence of hemorrhage, and C-kit expression were independently related to the presence of C-kit mutation. This states that the mutation-positive GISTs were larger in size and showed more frequent invasion of adjacent tissues, the mutation-positive GISTs showed higher mitotic counts and PCNA index and more necrosis within the tumors histologically. Taken together, the mutation-positive GISTs had more malignant histological features than the mutation-negative GISTs. We also examined whether the presence of C-kit mutation was associated with the clinical outcome. The mutation-positive GISTs showed more frequent recurrences, distant metastasis and, higher mortality than the mutation-negative GISTs. There are at least possible two explanations for this : GIST may be classified into two subtypes, C-kit mutation-positive and mutation-negative GISTs mutation-positive GISTs showed more malignant features,; mutation-negative GISTs may acquire more malignant phenotype due to the addition of C-kit mutation.

Recently, gain-of-function mutations of the juxtramembrane domain of C-kit , including deletions or point mutations in exon11 were described in GIST^[14-18]. These mutations were shown to lead to spontaneous, ligand-independent tyrosine kinase activation. The stable transfection of murine lymphoid cells with the mutant C-kit complementary DNA was shown to induce malignant transformation, suggesting pathogenetic significance of such mutations. We have expanded these observations and found that the C-kit mutation in the exon11 predominantly occur in those GISTs that are histologically and clinically malignant while benign GISTs were not detected. This suggest that C-kit mutation in the exon11 may be an important pathogenetic mechanism of tumor malignant behavior. Moreover ,we found C-kit

mutations only in 60% of the malignant GISTs. This may suggest that additional pathogenetic mechanisms exist in other cases, or that mutations occur in alternative sites. Another study also showed correlation between the mutations and disease progression.

There is no effective therapy for unresectable or metastatic gastrointestinal stromal tumor, which is invariably fatal. STI571, a phenylaminopyrimidine derivative, is a small molecule that selectively inhibits the enzymatic activity of C-kit gene. Joensuu *et al.*^[19], found that inhibition by STI571 of the constitutively active mutant C-kit tyrosine kinase of gastrointestinal stromal tumors was an effective therapy for these tumors. There are two explanations for this: STI571 may be active in solid tumors that rely on the expression of C-kit, ABL, or platelet-derived growth factor receptor while GIST uniformly express C-kit; a tumor-specific C-kit mutation appears to be the chief cause of this neoplasm. Considering these findings, we conclude that C-kit mutation is a undoubtedly pivotal event in GIST and may be associated with poor prognosis. Evaluation of C-kit gene mutation may have both prognosis and therapeutic significances as the new tyrosine kinase inhibitor (STI571) treatments are available.

REFERENCES

- 1 **Wong NA**, Young R, Malcomson RD, Nayar AG, Jamieson LA, Save VE, Carey FA, Brewster DH, Han C, Al-Nafussi A. Prognostic indicators for gastrointestinal stromal tumours: a clinicopathological and immunohistochemical study of 108 resected cases of the stomach. *Histopathology* 2003; **43**: 118-126
- 2 **Nagasako Y**, Misawa K, Kohashi S, Hasegawa K, Okawa Y, Sano H, Takada A, Sato H. Evaluation of malignancy using Ki-67 labeling index for gastric stromal tumor. *Gastric Cancer* 2003; **6**: 168-172
- 3 **Kim MK**, Lee JK, Park ET, Lee SH, Seol SY, Chung JM, Kang MS, Yoon HK. Gastrointestinal stromal tumors: clinical, pathologic features and effectiveness of new diagnostic criteria. *Korean J Gastroenterol* 2004; **43**: 341-348
- 4 **Lewin KJ**, Riddle R, Weinstein W. Gastrointestinal Pathology and Its Clinical Implications. 2thnd. *New York: Igaku-Shoin Medical Pub* 1992: 284-341
- 5 **Ballarini C**, Intra M, Ceretti AP, Prestipino F, Bianchi FM, Sparacio F, Berti E, Perrone S, Silva F. Gastrointestinal stromal tumors: a "benign" tumor with hepatic metastasis after 11 years. *Tumori* 1998; **84**: 78-81
- 6 **Goldblum JR**. Gastrointestinal stromal tumors. A review of characteristics morphologic, immunohistochemical, and molecular genetic features. *Am J Clin Pathol* 2002; **117**(Suppl): S49-61
- 7 **Corless CL**, Fletcher JA, Heinrich MC. Biology of gastrointestinal stromal tumors. *J Clin Oncol* 2004; **22**: 3813-3825
- 8 **Ma DL**, Liu XH, Bai CG, Xie Q, Feng F. Effect of C-kit gene mutation on prognosis of gastrointestinal stromal tumor. *Zhonghua Waike Zazhi* 2004; **42**: 140-144
- 9 **Theou N**, Tabone S, Saffroy R, Le Cesne A, Julie C, Cortez A, Lavergne-Slove A, Debuire B, Lemoine A, Emile JF. High expression of both mutant and wild-type alleles of C-kit in gastrointestinal stromal tumors. *Biochim Biophys Acta* 2004; **1688**: 250-256
- 10 **Pardanani A**, Reeder TL, Kimlinger TK, Baek JY, Li CY, Butterfield JH, Tefferi A. Flt-3 and C-kit mutation studies in a spectrum of chronic myeloid disorders including systemic mast cell disease. *Leuk Res* 2003; **27**: 739-742
- 11 **Noack F**, Escribano L, Sotlar K, Nunez R, Schuetze K, Valent P, Horny HP. Evolution of urticaria pigmentosa into indolent

- systemic mastocytosis: abnormal immunophenotype of mast cells without evidence of C-kit mutation ASP-816-VAL. *Leuk Lymphoma* 2003; **44**: 313-319
- 12 **Sammarco I**, Capurso G, Coppola L, Bonifazi AP, Cassetta S, Delle Fave G, Carrara A, Grassi GB, Rossi P, Sette C, Geremia R. Expression of the proto-oncogene C-kit in normal and tumor tissues from colorectal carcinoma patients. *Int J Colorectal Dis* 2004; **19**: 545-553
- 13 **Looijenga LH**, de Leeuw H, van Oorschot M, van Gurp RJ, Stoop H, Gillis AJ, de Gouveia Brazao CA, Weber RF, Kirkels WJ, van Dijk T, von Lindern M, Valk P, Lajos G, Olah E, Nesland JM, Fossa SD, Oosterhuis JW. Stem cell factor receptor (C-kit) codon 816 mutations predict development of bilateral testicular germ-cell tumors. *Cancer Res* 2003; **63**: 7674-7678
- 14 **Beghini A**, Tibiletti MG, Roversi G, Chiaravalli AM, Serio G, Capella C, Larizza L. Germline mutation in the juxtamembrane domain of the kit gene in a family with gastrointestinal stromal tumors and urticaria pigmentosa. *Cancer* 2001; **92**: 657-662
- 15 **Lee JR**, Joshi V, Griffin JW Jr, Lasota J, Miettinen M. Gastrointestinal autonomic nerve tumor: immunohistochemical and molecular identity with gastrointestinal stromal tumor. *Am J Surg Pathol* 2001; **25**: 979-987
- 16 **Fukuda R**, Hamamoto N, Uchida Y, Furuta K, Katsube T, Kazumori H, Ishihara S, Amano K, Adachi K, Watanabe M, Kinoshita Y. Gastrointestinal stromal tumor with a novel mutation of KIT proto-oncogene. *Intern Med* 2001; **40**: 301-303
- 17 **Hirota S**, Nishida T, Isozaki K, Taniguchi M, Nakamura J, Okazaki T, Kitamura Y. Gain-of-function mutation at the extracellular domain of KIT in gastrointestinal stromal tumours. *J Pathol* 2001; **193**: 505-510
- 18 **Taniguchi M**, Nishida T, Hirota S, Isozaki K, Ito T, Nomura T, Matsuda H, Kitamura Y. Effect of C-kit mutation on prognosis of gastrointestinal stromal tumors. *Cancer Res* 1999; **59**: 4297-4300
- 19 **Joensuu H**, Roberts PJ, Sarlomo-Rikala M, Andersson LC, Tervahartiala P, Tuveson D, Silberman SL, Capdeville R, Dimitrijevic S, Druker B, Demetri GD. Effect of the tyrosine kinase inhibitor STI571 in a patient with a metastatic gastrointestinal stromal tumor. *N Engl J Med* 2001; **344**: 1052-1056

Science Editor Guo SY Language Editor Elsevier HK

Somatostatin receptor subtype 2-mediated scintigraphy and localization using ^{99m}Tc -HYNIC-Tyr³-octreotide in human hepatocellular carcinoma-bearing nude mice

Yong Li, Jian-Ming Si, Jun Zhang, Jin Du, Fan Wang, Bing Jia

Yong Li, Jian-Ming Si, Jun Zhang, Gastrointestinal Laboratory of Clinical Medical Institute of Sir Run Run Shaw Hospital, Zhejiang University, Hangzhou 310016, Zhejiang Province, China
Jin Du, Fan Wang, Bing Jia, the Medicine Isotope Research Center of Beijing University, Beijing 100083, China

Correspondence to: Jian-Ming Si, MD, Gastrointestinal Laboratory of Clinical Medical Institute of Sir Run Run Shaw Hospital, Zhejiang University, Hangzhou 310016, Zhejiang Province, China. sjm@163.net
Telephone: +86-571-87217002

Received: 2004-04-09 Accepted: 2004-05-24

Abstract

AIM: To investigate the uptake of ^{99m}Tc -HYNIC-Tyr³-octreotide (^{99m}Tc -HYNIC-TOC) in human hepatocellular carcinoma (HCC), which can provide the localizable diagnosis in hepatic carcinoma.

METHODS: The expression of somatostatin receptor 2 (SSTR2) messenger RNA (mRNA) in human HCC cell line HepG₂ was examined by reverse transcriptase-polymerase chain reaction (RT-PCR). Uptake of ^{99m}Tc -HYNIC-TOC was evaluated in the human HCC implanted into BALB/c nude mice. ANMIS2000 nuclear medicine analysis system was used to calculate the ratio of ^{99m}Tc uptake between tumor tissue and vital organs.

RESULTS: We demonstrated the expression of SSTR2 mRNA in human HCC cell line HepG₂ by RT-PCR. The size of the RT-PCR products was 364 bp detected by sequence analysis of the human SSTR2 mRNA. Scintigraphy proved that ^{99m}Tc -HYNIC-TOC was uptaken in the tumor tissue, liver and kidney of the tumor-bearing mice.

CONCLUSION: Based on expression of the SSTR2 mRNA in human HCC, ^{99m}Tc -HYNIC-TOC can markedly bind with and be uptaken by human HCC tissues as compared with normal liver tissue. The significant retention of radionuclide in kidney and bladder is probably related to non-specific peptide uptake in the tubulus cells of kidney and possibly due to excretion by kidney. Our results show that localizable diagnosis and targeting radiotherapy with radionuclide-labeled somatostatin analog for HCC are of great value to be further studied.

© 2005 The WJG Press and Elsevier Inc. All rights reserved.

Key words: Hepatocellular carcinoma; ^{99m}Tc -HYNIC-Tyr³-octreotide; Somatostatin receptor 2

Li Y, Si JM, Zhang J, Du J, Wang F, Jia B. Somatostatin receptor subtype 2-mediated scintigraphy and localization using ^{99m}Tc -HYNIC-Tyr³-octreotide in human hepatocellular carcinoma-bearing nude mice. *World J Gastroenterol* 2005; 11(25): 3953-3957

<http://www.wjgnet.com/1007-9327/11/3953.asp>

INTRODUCTION

The role of somatostatin (SS) analogs in the tumor diagnostic and therapeutic applications has attracted the concern of the people. It has been widely reported about the growth suppressing effects of SS and its analogs on many tumors^[1-4]. To date, it is known that their suppressing effect on tumor cell proliferation is mediated by the somatostatin receptors (SSTRs) presented in the tumor constitution^[5]. Like most neuroendocrine tumors, adenocarcinomas originating in the breast, colon, or pancreatic tumor, as well as meningiomas, express SSTRs, and the majority of these tumors express the somatostatin receptor subtype 2 (SSTR2)^[6,7]. However, all five receptor subtypes (SSTR1-5) bind native SS with a high affinity, while octreotide, an SS analog, binds with a very high affinity only to subtype 2 (SSTR2) and shows a moderately high affinity for SSTR5^[8]. Overexpression of the SSTR2 in some tumors has made it possible to use SS-receptor scintigraphy with indium111 or technetium 99m-labeled octreotide for the visualization of SS receptor-positive cancers^[9,10]. In addition to tumor scintigraphy, a new application of these radiolabeled peptides is peptide receptor radionuclide therapy^[11,12].

It has been known that hepatocellular carcinoma (HCC) is a leading cause of cancer-related death. At present, surgical resection of malignant liver lesions offers the best outcome and the only hope of cure. The 5-year survival rate for selected patients undergoing surgical resection of primary HCC was 30%, with a median survival of 30 mo. However, approximately 90% of patients presenting with primary HCC have inoperable disease^[13]. These patients must rely largely on various forms of chemotherapy and radiotherapy^[14,15]. These treatments have at times shown promising response rates, symptom palliation and have occasionally down-staged hepatic tumors to allow surgical resection, but these treatment modalities have not improved 5-year survival rates, which remain in the order of 1%^[16]. The persisting poor survival among the vast majority of patients presenting with liver cancer has led to renewed interest in developing targeted radiotherapy with radiolabeled SS analogs as a

possible treatment option for patients with non-resectable liver cancer. However, it has not been known that HCC can uptake radiolabeled SS analogs. The aim of this study was to scintigraphically identify the localization of HCC in order to reveal a possible role of radiolabeled SS analogs in the treatment of HCC, and determine the target cell of receptor subtype selective radiolabeled SS analogs for targeting radiotherapy of HCC.

MATERIALS AND METHODS

Materials

All reagents and solvents were obtained from commercial sources and were used without further purification except HYNIC-[Tyr³]-octreotide (HYNIC-TOC). We applied hydrazinonicotinic acid (HYNIC) as the ligand for ^{99m}Tc. Labeling with ^{99m}Tc was performed using a co-ligand required to stabilize ^{99m}Tc bound to the hydrazino residue of the peptide conjugate. HYNIC-TOC was synthesized at the Medicine Isotope Research Center of Peking University. Na^{99m}TcO₄ was obtained from commercial ⁹⁹Mo/^{99m}Tc generator. The methods of HYNIC-TOC synthesis and ^{99m}Tc labeling were employed as previously described^[17,18]. Reaction solutions were tested for radiochemical purity by the C18-SepPak column of high-performance liquid chromatography immediately and up to 24 h after preparation. ^{99m}Tc of radioactive purity > 95% was bound to HYNIC-TOC.

RT-PCR and sequencing of products

The human HCC cell line HepG2 was assessed for the presence of somatostatin receptor subtypes (SSTR1-5) messenger RNA (mRNA) to confirm the presence of the target receptor subtype for ^{99m}Tc-HYNIC-Tyr³-octreotide (^{99m}Tc-HYNIC-TOC), especially SSTR2. The following primer pairs (Boya Co., Shanghai, China) were applied: for human SSTR1, sense (1 543-1 652) 5'-TCATCCTCGGCT-ATGCCAAC-3' and antisense (1 789-1 898) 5'-GCAGGTG-CCATTACGGAAGA-3'; for SSTR2, sense (359-378) 5'-CTGTGGATGGCATCAATCAG-3' and antisense (723-741) 5'-TCGGATTCCAGAGGACTTCA-3'; for SSTR3, sense (1 193-1 212) 5'-GCCTCTGCTACCTGCTCATC-3' and antisense (1 618-1 637) 5'-CCATCCTCCTCCTCC-TCATC-3'; for SSTR4, sense (480-499) 5'-CAGCGTGGC-CAAGCTCATCA-3' and antisense (962-981) 5'-GATCGG-CGGAAGTTGTCGGA-3'; for SSTR5, sense (205-224) 5'-GCCAAGATGAAGACCGTAC-3' and antisense (668-887) 5'-AGCAGGTAGCACAGGCAGAT-3'; for β-actin, sense 5'-ACGTTATGGATGATGTATCGC-3' and antisense 5'-CTTAATGTCACGCACGATTTC-3'. RNA extraction and reverse transcription were performed according to the manufacturer's instructions. cDNA was amplified in a reaction mixture (total volume 20 μL) comprising cDNA (transcribed from 12 μg of total RNA), 2 μL of 10× PCR buffer, 0.4 μL of 10 mmol/L dNTP, and 1.5 μL of 25 mmol/L MgCl₂, 10 pmol/L of each of sense and antisense primers, and 2.5 U of Taq DNA polymerase. Following an initial denaturing step at 94 °C for 5 min, the amplification program of 30 cycles, each cycle consisting of denaturation at 94 °C for 30 s, annealing at 60 °C for 20 s, and extension at 72 °C for 30 s, was

carried out by a Gene Amplification PCR system 2 400 (PE Corp., USA). The amplification was terminated with the final extension step at 72 °C for 10 min. The amplified products, subsequently, were electrophoresed and photographed on 15 g/L agarose gel stained with ethidium bromide. The final products were verified by sequencing in Boya Co. (Shanghai, China). β-actin specific primers were used to amplify the cDNA fragment as an internal standard.

Tumor cell inoculation and tumor growth assessment

The human HCC cell line HepG2 was from Clinical Medical Institute of Sir Run Run Shaw Hospital. The cells were grown in RPMI1640 (Gibco Co., USA) supplemented with 100 mL/L fetal bovine serum (Hangzhou Sijiqing Co., China) at 37 °C in a humidified atmosphere containing 50 mL/L CO₂ and 950 mL/L O₂. Subculturing was executed every 2-3 d and the cells grew well along the walls of culture tube. Then, the cells (2×10⁶ cells/mouse) at logarithmic growth period were subcutaneously inoculated into right flank of BALB/c nude mice, aged 6-8 wk, weighing 18-20 g (purchased from Animal Center of Academy of Science, Shanghai, China). The total tumor load per mouse was approximately 1 cm³ at about 28 d post-injection. We took out the whole tumors, then, immediately put into saline containing 100 U/mL penicillin and streptomycin. Tumor pieces with a size 1-2 mm³ were made from the margins of the whole mass after winking the connective tissue around the mass. The mice were randomly divided into three groups in accordance with subcutaneous re-transplantation of tumor into right flanks (subcutaneous group) or *in situ* liver (intra-liver group), or without re-transplantation (control group). Each group consisted of three mice. The experiments were started at 21 d post re-implantation, when the size of tumor per mice was approximately 1 cm³.

In vivo imaging with ^{99m}Tc-HYNIC-TOC

Each mouse of tumor-bearing groups (subcutaneous group and intra-liver group) and control mice group received 100 μCi of ^{99m}Tc-HYNIC-TOC injected into the caudal vein under soluble pentobarbitone anesthesia. The mice were imaged at 2 and 4.5 h, respectively, after injection of ^{99m}Tc-HYNIC-TOC with mini-radioisotope gamma camera equipped with a pinhole collimator (Bingsong Corp., China). During imaging, the mice were maintained with a fixed band and positioned on dorsal recumbency with the legs extending from the body. The imaging analyses of ^{99m}Tc uptake in tumor tissue and vital organs were conducted using ANMIS 2000 nuclear medicine analysis system (Bingsong Corp.). Animals of the intra-liver group were killed after the second imaging session (4.5 h after injection of ^{99m}Tc-HYNIC-TOC) for examination of intra-liver tumor growth.

RESULTS

Expression and PCR products sequencing of SSTR2 mRNA in HCC cell line HepG2

PCR products of SSTRs were obtained for HepG2 cells. The size of the products corresponded to the predicted length of the synthesized cDNA fragment based on the position of the PCR primer. SSTR1-5 mRNAs were variably expressed in HepG2 cells. Expressions of SSTR1, SSTR2, and SSTR4 mRNA were found in HepG2 cells, respectively

(Figure 1), but those of SSTR3 and SSTR5 mRNAs were not observed. We identified that the product of SSTR2 mRNA was the specific fragment that we needed after performing sequencing and comparison with SSTRs mRNA rank of the GenBank^[19], it turned out to be a perfect coincidence with the fragment rank (Figure 2). The result showed that the amplification we executed was specific.

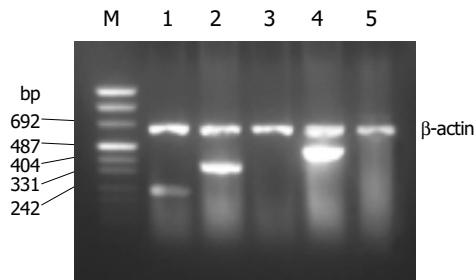


Figure 1 RT-PCR analysis for SSTR1-5 mRNA expression in HepG2. Lane m: marker; lane 1: SSTR1 (246 bp); lane 2: SSTR2 (384 bp); lane 3: SSTR3; lane 4: SSTR4 (502 bp); lane 5: SSTR5.

In vivo imaging with ^{99m}Tc-HYNIC-TOC

The gamma camera imagings of a representative mouse from the subcutaneous, intra-liver and control groups at 2 and 4.5 h after being injected with ^{99m}Tc- HYNIC-TOC are shown in Figure 3. These imagings showed visual accumulation of ^{99m}Tc-HYNIC-TOC detected in the tumor xenografts of mice (including subcutaneous group and intra-liver group). The retention of radioactivity in the kidney and excretion through the bladder were observed. The high-level uptake of radioactivity in the liver of tumor-bearing mice was also observed and compared with the control group. This tumor uptake was important to validate the dosing regimen that was used in therapy studies of liver cancer.

DISCUSSION

Radiolabeled SS analogs have brought new prospects to nuclear oncology for diagnosis and therapy of tumor. Due to their low molecular weight and high affinity to SSTRs, good tissue penetration properties, and being internalized

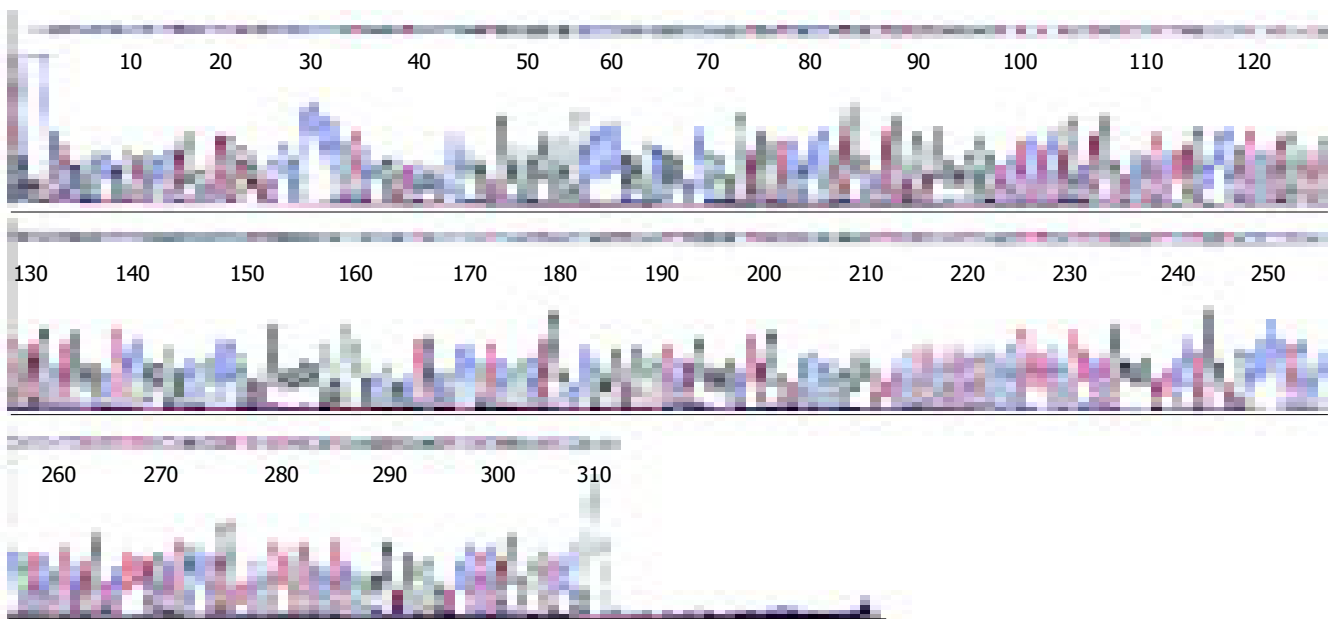


Figure 2 Sequencing of SSTR2 mRNA PCR products. The products were specifically amplified after the sequencing fragment was compared with human

SSTR2 of GenBank, and was a perfect coincidence with the fragment rank of human SSTR2 mRNA.

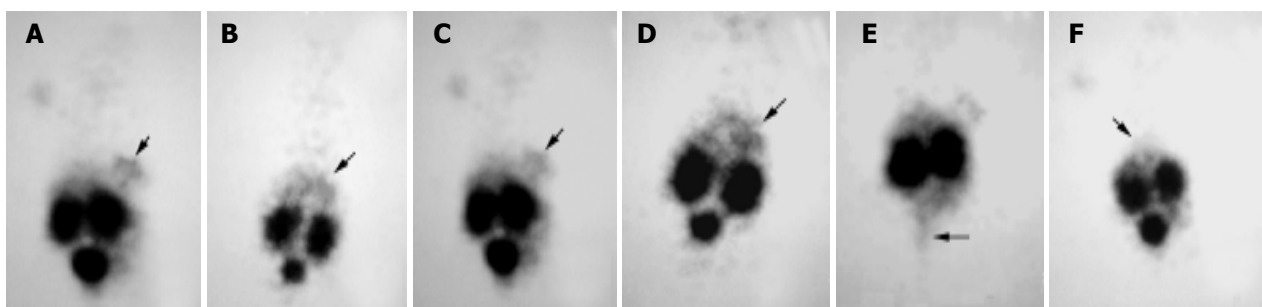


Figure 3 Scintigrams of mice at different times after injection of ^{99m}Tc-HYNIC-TOC. A and C: subcutaneous group at 2 and 3 h, respectively; B and D: intra-liver group at 2 and 4 h, respectively; E: subcutaneous group at 4.5 h, when the

bladder was emptied; F: control group at 2 h. The marked decrease in the liver (arrows) uptake was apparent in the control group mouse.

into the tumor cells after receptor binding^[20-22], they provide promising strategies for diagnosis and internal radionuclide therapy for various cancer types. Before radiolabeled, octreotide was employed in HCC, it has been studied with ¹²⁵I-[Tyr³]-octreotide for tumor diagnosis^[11]. However, some studies demonstrated that the SSTRs density in HCC was considerably lower than the receptor density found^[23,24], thus it has rarely been studied in the liver cancer. As radiotherapy of SS receptor-positive tumors with compounds such as ⁹⁰Y-labeled ones was applied, it is necessary to develop a new strategy for the treatment of liver cancer.

In this study, we evaluated the expression of SS receptor in human HCC cell line HepG2. The results showed that SSTR1, SSTR2 and SSTR4 were frequently expressed in human HCC, which was similar to previous reports^[25,26]. As the normal human liver does not express SSTR2 (predominant receptor subtype was SSTR1^[27]), the presence of SSTRs in HCC may be regarded as an overexpression of the receptors in this tumor. Like previous therapeutic experiments^[28], unlabeled octreotide was shown to bind with a high affinity to SSTR2, suggesting that the predominant receptor subtype was SSTR2. As to radiolabeled octreotide targeting therapy for HCC, the expression of SSTR2 in HCC is of high significance.

In scintigraphy experiment with ^{99m}Tc-HYNIC-TOC, the significant uptake of radionuclide by tumor xenografts in nude mice was found in both subcutaneous group and intra-liver group. And it was demonstrated that the hepatocarcinoma tissues had a fairly steady rate in uptaking ^{99m}Tc-HYNIC-TOC by the fact that there was still obvious radionuclide gathering at the tumor tissues at 4 h after administration. The results showed that the intensity of the signal was not as strong as for neuroendocrine tumor metastases. As a therapeutic tool, there are certainly potential clinical implications linked with the SS receptor expression in HCC.

The expression of some SS receptor subtypes was found in the liver and kidney as well^[24,29]. However, the physiological uptake of ^{99m}Tc-HYNIC-TOC in these organs was probably mainly due to some loss of technetium out of chelation (liver) and non-specific peptide uptake in the tubulus cells (kidney). Thus, in our receptor scintigram, the retention of radionuclide prominently in both kidney and bladder as well as the less uptake in liver, which was similar to previous reports^[30,31], was shown after injection of ^{99m}Tc-HYNIC-TOC. Because of the absence of SSTR2, the retention of technetium in the bladder, which was possibly due to the kidney excretion, almost vanished when bladder emptied (Figure 3E). Meanwhile, based on recent studies^[32-34], most of the radiolabeled octreotide, like our results, would accumulate in the kidney after glomerular filtration, followed by re-absorption into renal cells. It is necessary to take into consideration the induction of the kidney damage while performing targeting radiotherapy with radiolabeled octreotide.

In conclusion, HCC cell line HepG2 expresses SSTR2 mRNA. ^{99m}Tc-HYNIC-TOC, relying on the receptor mediation, can markedly bind with and be uptaken by human HCC tissues as compared to the normal liver tissue, which is probably mainly due to some loss of technetium

out of chelation. The significant retention of radionuclide in kidney and bladder is probably related to non-specific peptide uptake in the tubulus cells of kidney and possibly due to the excretion by kidney. This phenomenon has clued to potential radiation nephrotoxicity of the agents, which needs to be solved before a widespread application of targeting radiotherapy.

REFERENCES

- 1 **Lamberts SW**, de Herder WW, Hofland LJ. Somatostatin analogs in the diagnosis and treatment of cancer. *Trends Endocrinol Metab* 2002; **13**: 451-456
- 2 **Froidevaux S**, Eberle AN. Somatostatin analogs and radiopeptides in cancer therapy. *Biopolymers* 2002; **66**: 161-183
- 3 **Celinski SA**, Fisher WE, Amaya F, Wu YQ, Yao Q, Youker KA, Li M. Somatostatin receptor gene transfer inhibits established pancreatic cancer xenografts. *J Surg Res* 2003; **115**: 41-47
- 4 **Kumar M**, Liu ZR, Thapa L, Wang DY, Tian R, Qin RY. Mechanisms of inhibition of growth of human pancreatic carcinoma implanted in nude mice by somatostatin receptor subtype 2. *Pancreas* 2004; **29**: 141-151
- 5 **Pollak MN**, Schally AV. Mechanisms of antineoplastic action of somatostatin analogs. *Proc Soc Exp Biol Med* 1998; **217**: 143-152
- 6 **Reubi JC**, Kvols L, Krenning E, Lamberts SW. Distribution of somatostatin receptors in normal and tumor tissue. *Metabolism* 1990; **39**(9 Suppl 2): 78-81
- 7 **Lamberts SW**, Krenning EP, Reubi JC. The role of somatostatin and its analogs in the diagnosis and treatment of tumors. *Endocr Rev* 1991; **12**: 450-482
- 8 **Lamberts SW**, Van der Lely AJ, de Herder WW, Hofland LJ. Octreotide. *N Engl J Med* 1996; **334**: 246-254
- 9 **Weiner RE**, Thakur ML. Radiolabeled peptide in the diagnosis and therapy of oncological diseases. *Appl Radiat Isot* 2002; **57**: 749-763
- 10 **Decristoforo C**, Mather SJ. Technetium-99m somatostatin analogues: effect of labelling methods and peptide sequence. *Eur J Nucl Med* 1999; **26**: 869-876
- 11 **Towu E**, Boxer G, Begent R, Zweit J, Spitz L, Hobbs K, Winslet M. *In-vitro* uptake of radioactive lipiodol I-131 and I-125 by hepatoblastoma: implications for targeted radiotherapy. *Pediatr Surg Int* 2001; **17**: 609-613
- 12 **Heppler A**, Froidevaux S, Eberle AN, Maecke HR. Receptor targeting for tumor localisation and therapy with radiopeptides. *Curr Med Chem* 2000; **7**: 971-979
- 13 **Hussain SA**, Ferry DR, El-Gazzaz G, Mirza DF, James ND, McMaster P, Kerr DJ. Hepatocellular carcinoma. *Ann Oncol* 2001; **12**: 161-172
- 14 **Rougier P**, Mitry E, Clavero-Fabri MC. Chemotherapy and medical treatment of hepatocellular carcinoma (HCC). *Hepatogastroenterology* 1998; **45**(Suppl 3): 1264-1266
- 15 **Perez CA**, Brady LW. Principles and Practice of Radiation Oncology: Pancreatic and Hepatobiliary Cancer. *Lippincott Company* 1987: P810
- 16 **Liu CL**, Fan ST. Nonresectional therapies for hepatocellular carcinoma. *Am J Sur* 1997; **173**: 358-365
- 17 **Decristoforo C**, Mather SJ, Cholewinski W, Donnemiller E, Riccabona G, Moncayo R. ^{99m}Tc-EDDA/HYNIC-TOC: a new ^{99m}Tc-labelled radiopharmaceutical for imaging somatostatin receptor-positive tumours: first clinical results and intrapatient comparison with ¹¹¹In-labelled octreotide derivatives. *Eur J Nucl Med* 2000; **27**: 1318-1325
- 18 **von Guggenberg E**, Sarg B, Lindner H, Alafort LM, Mather SJ, Moncayo R, Decristoforo C. Preparation via coligand exchange and characterization of [^{99m}Tc-EDDA-HYNIC-D-Phe1, Tyr3] Octreotide (^{99m}Tc-EDDA/HYNIC-TOC). *J Label Compd Radiopharm* 2003; **46**: 307-318

- 19 <http://www.ncbi.nlm.nih.gov/blast>
- 20 **Krenning EP**, de Jong M, Kooij PP, Breeman WA, Bakker WH, de Herder WW, van Eijk CH, Kwekkeboom DJ, Jamar F, Pauwels S, Valkema R. Radiolabelled somatostatin analogue (s) for peptide receptor scintigraphy and radionuclide therapy. *Ann Oncol* 1999; **10**(Suppl 2): S23-29
- 21 **Weckbecker G**, Raule F, Stolz B, Bruns C. Somatostatin analogs for diagnosis and treatment of cancer. *Pharmacol Ther* 1993; **60**: 245-264
- 22 **Paganelli G**, Zoboli S, Cremonesi M, Bodei L, Ferrari M, Grana C, Bartolomei M, Orsi F, De Cicco C, Macke HR, Chinol M, de Braud F. Receptor-mediated radiotherapy with ⁹⁰Y-DOTA-D-Phe¹-Tyr³-octreotide. *Eur J Nucl Med* 2001; **28**: 426-434
- 23 **Reubi JC**, Zimmermann A, Jonas S, Waser B, Neuhaus P, Laderach U, Wiedenmann B. Regulatory peptide receptors in human hepatocellular carcinomas. *Gut* 1999; **45**: 766-774
- 24 **Deng-Guo YAN**, Qing-Jia OU. Somatostatin receptor subtype SSTR2 and SSTR3 mRNA expression in primary hepatic Carcinoma. *Aizheng* 2001; **20**: 152-155
- 25 **Hofland LJ**, Lamberts SW. Somatostatin receptor subtype expression in human tumors. *Ann Oncol* 2001; **12**(Suppl 2): S31-36
- 26 **Rohrer L**, Raulf F, Bruns C, Buettner R, Hofstaedter F, Schule R. Cloning and characterization of a fourth human somatostatin receptor. *Proc Natl Acad Sci USA* 1993; **90**: 4196-4200
- 27 **Kouroumalis E**, Skordilis P, Termos K, Vasilaki A, Moschandrea J, Manousos ON. Treatment of hepatocellular carcinoma with octreotide: a randomized controlled study. *Gut* 1998; **42**: 442-447
- 28 **Hofland LJ**, Lamberts SW. Somatostatin receptors and disease: Role of receptor subtypes. *Baillieres Clin Endocrinol Metab* 1996; **10**: 163-176
- 29 **Patel YC**. Somatostatin and its receptor family. *Front Neuroendocrinol* 1999; **20**: 157-198
- 30 **Reubi JC**, Horisberger U, Studer UE, Waser B, Laissue JA, Human kidney as target for somatostatin: high affinity receptors in tubules and vasa recta. *J Clin Endocrinol Metab* 1993; **77**: 1323-1328
- 31 **Bass LA**, Lanahan MV, Duncan JR, Erion JL, Srinivasan A, Schmidt MA, Anderson CJ. Identification of the soluble *in vivo* metabolites of indium-111-diethylenetriaminepentaacetic acid-DPhe¹-octreotide. *Bioconjug Chem* 1998; **9**: 192-200
- 32 **Duncan JR**, Stephenson MT, Wu HP, Anderson CJ. Indium-111-diethylenetriaminepentaacetic acid-octreotide is delivered *in vivo* to pancreatic, tumor cells, renal, and hepatocyte lysosomes. *Cancer Res* 1997; **57**: 659-671
- 33 **Akizawa H**, Arano Y, Uezono T, Ono M, Fujioka Y, Uehara T, Yokoyama A, Akaji K, Kiso Y, Koizumi M, Saji H. Renal metabolism of ¹¹¹In-DTPA-D-Phe¹-octreotide *in vivo*. *Bioconjug Chem* 1998; **9**: 662-670
- 34 **Akizawa H**, Arano Y, Mifune M, Iwado A, Saito Y, Mukai T, Uehara T, Ono M, Fujioka Y, Ogawa K, Kiso Y, Saji H. Effect of molecular charges on renal uptake of ¹¹¹In-DTPA- conjugated Peptides. *Nucl Med Biol* 2001; **28**: 761-768

Effects of He-Ne laser irradiation on chronic atrophic gastritis in rats

Xue-Hui Shao, Yue-Ping Yang, Jie Dai, Jing-Fang Wu, Ai-Hua Bo

Xue-Hui Shao, Yue-Ping Yang, Department of Medical Physics, Hebei North University, Zhangjiakou 075000, Hebei Province, China
Jie Dai, Ai-Hua Bo, Department of Pathology, Hebei North University, Zhangjiakou 075000, Hebei Province, China
Jing-Fang Wu, Department of Histology and Embryology, Hebei North University, Zhangjiakou 075000, Hebei Province, China
Supported by the Natural Science Foundation of Hebei Province, No. 301427

Co-correspondents: Jie Dai

Correspondence to: Xue-Hui Shao, Department of Medical Physics, Hebei North University, 14 Changqing Road, Zhangjiakou 075000, Hebei Province, China. sxhwby@sina.com
Telephone: +86-313-8041657

Received: 2004-08-26 Accepted: 2005-03-16

Abstract

AIM: To study the effects of He-Ne laser irradiation on experimental chronic atrophic gastritis (CAG) in rats.

METHODS: Sixty-three male adult Wistar rats were randomly divided into five groups including normal control group, model control group and three different dosages He-Ne laser groups. The chronic atrophic gastritis (CAG) model in rats was made by pouring medicine which was a kind of mixed liquor including 2% sodium salicylate and 30% alcohol down the throat for 8 wk to stimulate rat gastric mucosa, combining with irregular fasting and compulsive sporting as pathogenic factors; 3.36, 4.80, and 6.24 J/cm² doses of He-Ne laser were used, respectively for three different treatment groups, once a day for 20 d. The pH value of diluted gastric acid was determined by acidimeter, the histopathological changes such as the inflammatory degrees in gastric mucosa, the morphology and structure of parietal cells were observed, and the thickness of mucosa was measured by micrometer under optical microscope.

RESULTS: In model control group, the secretion of gastric acid was little, pathologic morphological changes in gastric mucosa such as thinner mucous, atrophic glands, notable inflammatory infiltration were found. After 3.36 J/cm² dose of He-Ne laser treatment for 20 d, the secretion of gastric acid was increased ($P < 0.05$), the thickness of gastric mucosa was significantly thicker than that in model control group ($P < 0.01$), the gastric mucosal inflammation cells were decreased ($P < 0.05$). Morphology, structure and volume of the parietal cells all recuperated or were closed to normal.

CONCLUSION: 3.36 J/cm² dose of He-Ne laser has a significant effect on CAG in rats.

Key words: Chronic atrophic gastritis; Laser; He-Ne; Rat

Shao XH, Yang YP, Dai J, Wu JF, Bo AH. Effects of He-Ne laser irradiation on chronic atrophic gastritis in rats. *World J Gastroenterol* 2005; 11(25): 3958-3961

<http://www.wjgnet.com/1007-9327/11/3958.asp>

INTRODUCTION

Chronic atrophic gastritis (CAG) is one of the most common digestive diseases worldwide^[1-4]. The patient's gastric mucosa atrophies, gastric sinus secret cells reduce, function is weakened, gastric acid secretion reduces, especially pathological changeable epithelium often contains intestine epithelium metaplasia and atypical hyperplasia, which are often seen as precancerous lesions of gastric carcinoma^[5-7]. To the author's knowledge, clinics still have no perfect and effective treatment projects^[8]. So we successfully established an animal model with CAG in rats^[9], used different radiation intensity of He-Ne laser to irradiate at the gastric projective area of rat with CAG, to study the therapeutic effects by examining changes of gastric acid and observing changes of pathologic histology in gastric mucosa.

MATERIALS AND METHODS

Animals

A total of 52 male adult Wistar rats weighing 180-230 g were purchased from Experimental Animal Center, Capital Medical University. They were housed in an air-conditioned room with 12 h dark/light cycle, and randomly divided into five groups: eight in normal control group, 11 in model control group, 11 in 3.36 J/cm² dose He-Ne laser group (small dose He-Ne laser group), 11 in 4.80 J/cm² dose He-Ne laser group (inside dose He-Ne laser group), 11 in 6.24 J/cm² dose He-Ne laser group (big dose He-Ne laser group). CAG model in rats were made by mixing 2% sodium salicylate and 30% alcohol and poured down their throats for 8 wk to stimulate their gastric mucosa, combined with irregular fasting and compulsive sporting.

He-Ne laser therapy

He-Ne laser therapy was carried out using the HJ-3DB He-Ne laser machine (wavelength 632.8 nm) which was made by Nanjing laser instrument factory, the He-Ne laser was amplified by convex lens, vertically radiated at the gastric projective area. The anterioposterior diameter of laser was 1 cm, its power density was 8 mW/cm². The following formed the course of treatment once a day for 20 d.

Small dose He-Ne laser treatment: irradiated 7 min each time, 3.36 J/cm² of dosage;

Inside dose He-Ne laser treatment: irradiated 10 min each time, 4.80 J/cm² of dosage;

Big dose He-Ne laser irradiation: irradiated 13 min each time, 6.24 J/cm² of dosage.

Process

The rats in each group were killed at the desired time-point. The animals were deprived of food but were offered enough water before being killed at 24 h. The rats were anesthetized with ether, the belly was opened immediately, cadre was ligature, the whole stomach was taken off, and the surface blood stains were washed by normal saline water, sucked dry with filter paper, then the gastric cavity was opened along greater curvature of stomach, flushed with distilled water, and the dilution gastric liquid (provided to measure the gastric acid pH value) was collected, then front and back gastric sinus and parts of stomach organized roughly into 3 mm×10 mm were taken in parallel with lesser curvature of stomach, fixed in neutral formalin, embedded in paraffin wax, 6 μm sections, stained with hematoxylin-eosin (HE) for pathological examination.

Determination of gastric acid

The rat's gastric acid (pH value) was determined five times for each example by acidimeter (PHS-3C) from Shanghai Instrument Factory, and took the average value as the pH value of this animal.

Pathology examinations

Take three sliced pieces for each example, and select three different visual fields for each slice such as the body of stomach, gastric sinus and the area of the body of stomach marked with gastric sinus. The whole gastric mucosa was observed under light microscope, which included the following aspects: (1) the immunity degree of the gastric mucosal ingluvititis cellular was divided into two grades such as negative (-) (no ingluvititis cells or some ingluvititis that jot spread at the gastric mucus) and positive (+) (more ingluvititis cell at the gastric mucosa or series of ingluvititis cells aggregated inside the mucus), counted the positive rate respectively by each visual field; (2) measured the thickness of the gastric mucosa with microscope, regarded μm as the unit, adopted the average of the mucosa thickness to show the reflection hyperplasia circumstance; (3) observed the parietal cell including the appearance, construction and arrangement.

Statistical analysis

Software SPSS 10.0 was used in the statistical analysis, parameters were expressed as mean±SD, and compared using One-way ANOVA analysis of variance, followed by χ^2 tests and differences were considered significant at $P<0.05$.

RESULTS

Gastric acid

The determination results of gastric acid showed that the secret function of gastric mucosa in model control rats was more decreased than that in both normal control group and small dose He-Ne laser group ($P<0.05$, Table 1).

Table 1 Detection of gastric results of pH value in Wistar rats

Group	n	pH value (mean±SD)
Normal control	6	3.72±1.02 ^a
Model control	7	5.86±1.45
Small dose He-Ne laser	7	4.43±1.18 ^a
Inside dose He-Ne laser	6	4.66±1.00
Big dose He-Ne laser	7	4.57±1.48

^a $P<0.05$ vs control group.

Pathological findings

The pathological histologies were observed under microscope. In normal control group, the gastric mucosa was thick, the epithelium was complete, only fell ingluvititis were spread, there was no obvious ingluvititis cellular immunity (Table 2). The parietal cells in normal control group were as follows: large volume, pyramid form, cell edge tactful, full, numerous, were arranged neatly and above 2/3 at a fundic gland (Figure 1A). In model control group, the gastric mucosa was thinner than that in normal control group ($P<0.01$), there were large quantities of immunity ingluvititis ($P<0.01$), most of the cells were lymphocytes and plasma cells. The parietal cells in model control group were as follows: volume sterigma, cell edge anomaly polygon, afterbirth syrup was wrinkled and arranged foul-up, intercellular space was enlarged, the ratio in syrup and nucleosidase increased the breadth of the gland antrum, and large quantity of cells were put through empty transformation (Figure 1B). In He-Ne laser groups, the gastric mucosa was thicker than that in model group ($P<0.01$), ingluvititis cells were less than that in model control group, particularly the small dose He-Ne laser group ($P<0.05$). The parietal cells in small dosage He-Ne laser

Table 2 Changes of gastric mucosa thickness and the observations of ingluvititis cellular immunity degree

Group	n	The thickness of gastric mucosa (μm) (mean±SD)	Ingluivititis cellular immunity degree			Ingluivititis edema	
			-	+	Positive rate (%)	Yes	No
Normal control	8	525.17±57.52 ^b	7	1	13 ^b		✓
Model control	11	387.21±51.60	1	10	91		✓
Small dose He-Ne laser	11	499.06±57.25 ^b	6	5	45 ^a		✓
Inside dose He-Ne laser	11	456.77±47.56 ^b	1	10	91	✓	
Big dose He-Ne laser	11	475.62±53.75 ^b	2	9	82	✓	

^a $P<0.05$, ^b $P<0.01$ vs model control group.

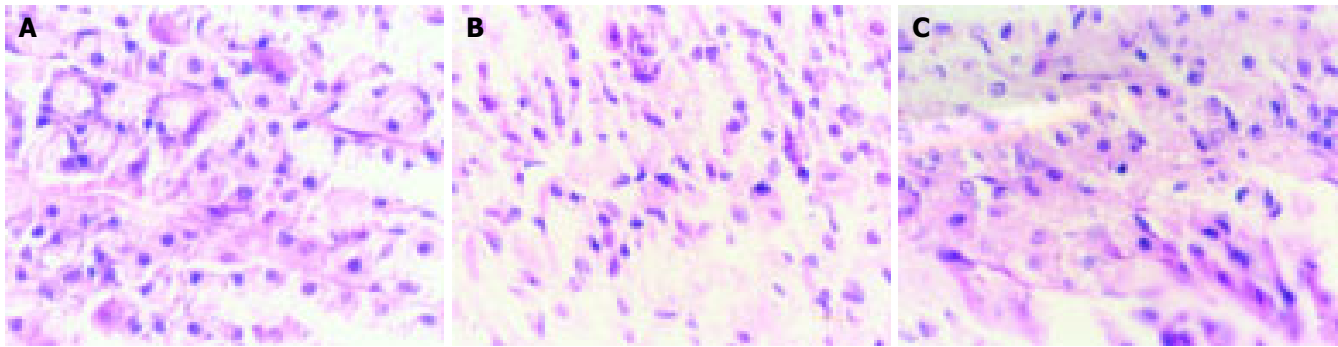


Figure 1 Pathology changes of parietal cells. **A:** parietal cells of gastric mucosa in normal control group (HE $\times 400$); **B:** parietal cells of gastric mucosa

in model control group (HE $\times 400$); **C:** parietal cells of gastric mucosa in small dose He-Ne laser group (HE $\times 400$).

group were as follows: cell appearance, volume and construction were all near to normal, and arranged neatly (Figure 1C). Besides, there was no obvious ingluvitis edema in normal control group, model control group and small dosage He-Ne laser group, but it was obvious in inside and large dose He-Ne laser groups, and the cells were transformed in the two groups.

DISCUSSION

The cause of disease and pathogenesis of chronic atrophic gastritis (CAG) are not yet completely clean, generally speaking, it is a synthesis factor with more effects and actions such as immunity, gall back streaming, pyloric infection, food, wine, smoke, and drugs^[2,8,9]. Research expressed that sodium salicylate could hurt gastric mucosa and enzyme could inhibit gastric cell growth^[10], alcohol could incite gastric mucosa. In our experiment, we poured a mixture of 2% sodium salicylate and 30% alcohol down the rat's throat for 8 wk, which could affect the natural cover and organize variety in gastric mucus, combined with fatigue from overwork, hunger and dissatisfaction in order to make the pathological changes of CAG appear on the gastric mucosa appear^[9]. Since the parietal cells reduced and degenerated, there was disorder both in gastric acid secretion and digestion enzyme weakness, the performance was a series of weak symptoms of the function of digestion and absorption such as the reduction of gastric acid secretion, diminishing of the gland and atrophy, and metaplasia of the intestinal epithelium^[9].

He-Ne laser, its characteristics such as 632.8 nm of wavelength, good directivity, high intensity, good monochromaticity, is a low-level laser^[11-14]. The low-level laser has some biology effects such as cell vitality^[15-18], phagocytosis^[19-21], immune responses^[22-25], but as far as its usage for the treatment of digestive disease, there were only few reports^[26-28]. On one hand, there was no difference between treating gastric ulcer through bark and by endoscope^[29]. On the other hand, external irradiation is easy, and patients can bear some pain with ease. We treated rats with CAG by external irradiation with He-Ne laser as amplified by a convex mirror, radiated at the gastric projective area. The results implied that the gastric acid secretion of the rats in CAG treated by He-Ne laser irradiation was increased, the best effect was on the animals treated by small dosage He-Ne laser. Some changes in gastric mucus such as thickness of gastric mucosa, alleviated

ingluvitis, and parietal cell hyperplasia were found in this experiment. We think the mechanism of He-Ne laser treated CAG in rats as follows: (1) partial microcirculation was ameliorated; (2) body immunity was enhanced; (3) the organized growth of gastric mucosa was promoted; (4) inflammation was eliminated. Moreover, in our experiment we found that three different dosages of He-Ne laser preceding the incitement to the rat in CAG, resulted in different effects. The best effect was the small dosage of He-Ne laser, the inside dose and the large dose were not as well as the small dose of He-Ne laser, which showed the dependence on dosage^[20,30,31]. Perhaps it is because the biology effect of He-Ne laser closely related to the action time, power density that organized He-Ne laser. Under the same power density (8 mW/cm²), different action time (small dose for 7 min, inside dose for 10 min, large dose for 13 min), produced different effects. These results showed that small dose He-Ne laser was a positive action, but large dose was an inhibitory action to incite lombricine organization^[32]. Besides, some damaged cells, individual swelling, afterbirth syrup degeneration and ingluvitis edema in the inside dose He-Ne laser group and the big dose He-Ne laser group were found in gastric mucus of rats under microscope. This may indicate the light dynamic damage of He-Ne laser. So we draw a further conclusion that big doses of He-Ne laser were deformative. In a word, the experiment showed that 3.36 J/cm² dose of He-Ne laser is a valid dose of external irradiation to incite life, it could promote the secretion of gastric acid and recover the function of gastric mucus to the CAG in rats.

In summary, 3.36 J/cm²/d dose of He-Ne laser irradiation is a well-tolerated, safe, and effective treatment in rats with CAG. The technique is easy, inexpensive, and of short duration^[25]. It is necessary to translate the outcome of this study into clinically relevant interventions by further studies which would develop a new way for the treatment of CAG.

REFERENCES

- 1 He WB, Gao GL, Hou S, Song G. Relationship between mucosal vascular lesion and gastric carcinoma in chronic atrophic gastritis of mice. *Shijie Huaren Xiaohua Zazhi* 1999; 7: 130-132
- 2 He RZ. Pathology (fourth edition). *Renmin Weisheng Chubanshe* 2003: 128-129
- 3 Asaka M, Sugiyama T, Nobuta A, Kato M, Takeda H, Graham DY. Atrophic gastritis and intestinal metaplasia in

- Japan: results of a large multicenter study. *Helicobacter* 2001; **6**: 294-299
- 4 **Wang RJ**, Du Q, Shao TY, Zhong TJ, Wu YL, Wang JH. Pathologic studies of Chinese drug Weiyanyao on experimental chronic atrophic gastritis in rats. *Shijie Huaren Xiaohua Zazhi* 2000; **4**: 382-285
 - 5 **Chen SY**, Wang JY, Ji Y, Zhang XD, Zhu CW. Effects of *Helicobacter pylori* and protein kinase C on gene mutation in gastric cancer and precancerous lesions. *Shijie Huaren Xiaohua Zazhi* 2001; **9**: 302-307
 - 6 **Wang XB**, Wang X, Zhang NZ. Inhibition of somatostatin analog Octreotide on human gastric cancer cell MKN45 growth *in vitro*. *Shijie Huaren Xiaohua Zazhi* 2002; **10**: 40-42
 - 7 **Yao XX**, Yin L, Zhang JY, Bai WY, Li YM, Sun ZC. hTERT expression and cellular immunity in gastric cancer and precancerosis. *Shijie Huaren Xiaohua Zazhi* 2001; **9**: 508-512
 - 8 **El-Zimaity HM**, Ota H, Graham DY, Akamatsu T, Katsuyama T. Patterns of gastric atrophy in intestinal type gastric carcinoma. *Cancer* 2002; **94**: 1428-1436
 - 9 **Shao XH**, Wang JG, Dai J. Establishment of chronic atrophic gastritis in a rat model. *Zhangjiakou Yixueyuan Xuebao* 2002; **2**: 11-13
 - 10 Nanjing pharmaceutical college. Medicament Chemistry. Beijing, *Renmin Weisheng Chubanshe* 1978: 172
 - 11 **Hu XM**. Medical physics (fifth edition). Beijing: *Renmin Weisheng Chubanshe* 2001: 351-352
 - 12 **Qin RJ**. Medical physics (third edition). Guilin: *Guangxi Shifan Daxue Chubanshe* 2002: 131-132
 - 13 **Stadler I**, Lanzafame RJ, Oskoui P, Zhang RY, Coleman J, Whittaker M. Alteration of skin temperature during low-level laser irradiation at 830 nm in a mouse model. *Photomed Laser Surg* 2004; **22**: 227-231
 - 14 **Rochkind S**, Ouaknine GE. New trend in neuroscience: low-power laser effect on peripheral and central nervous system (basic science preclinical and clinical studies). *Neurol Res* 1992; **14**: 2-11
 - 15 **Pogrel MH**, Chen JW, Zhang K. Effects of low-energy gallium-arsenide laser irradiation on cultured fibroblasts and keratinocytes. *Lasers Surg Med* 1997; **20**: 426-432
 - 16 **Ben-Dov N**, Shefer G, Irintchev A, Oron U, Halevy O, Irintchev A. Low energy laser irradiation affects satellite cell proliferation and differentiation *in vitro*. *Biochim Biophys Acta* 1999; **14**: 372-380
 - 17 **Grossman N**, Schneid N, Reuveni H, Halevy S, Lubart R. 780 nm low power diode laser irradiation stimulates proliferation of keratinocyte cultures: involvement of reactive oxygen species. *Lasers Surg Med* 1998; **22**: 212-218
 - 18 **Rochkind S**, Ouaknine GE. New trend in neuroscience: low-power laser effect on peripheral and central nervous system. *Neurol Res* 1992; **14**: 2-11
 - 19 **Pessoa ES**, Melhado RM, Theodoro LH, Garcia VG. A histologic assessment of the influence of low-intensity laser therapy on wound healing in steroid-treated animals. *Photomed Laser Surg* 2004; **22**: 199-204
 - 20 **Brosseau L**, Welch V, Wells G, DeBie R, Gam A, Harman K, Morin M, Shea B, Tugwell P. Low level laser therapy (Classes I, II and III) for treating osteoarthritis. *Cochrane Database Syst Rev* 2004; **3**: CD002046
 - 21 **Kans JS**, Hutschenreiter T, Haina D, Waidelich W. Effect of low-power density laser radiation on healing of open skin wounds in rats. *Arch Surg* 1981; **116**: 293-296
 - 22 **Hrnjak M**, Kulijic-Kapulica N, Budisin A, Giser A. Stimulatory effect of low-power density He-Ne laser radiation on human fibroblasts *in vitro*. *Vojnosanit Pregl* 1995; **52**: 539-546
 - 23 **Monteforte P**, Baratto L, Molfetta L, Rovetta G. Low-power laser in osteoarthritis of the cervical spine. *Int J Tissue React* 2003; **25**: 131-136
 - 24 **Ohta A**, Abergel RP, Uitto J. Laser modulation of human immune system, inhibition lymphocyte proliferation by a gallium-arsenide laser energy. *Lasers Surg Med* 1987; **7**: 199-201
 - 25 **Karu T**. Photobiology of low-power laser effects. *Health Phys* 1989; **6**: 691-704
 - 26 **Fukutomi H**, Kawakita I, Nakahara A. Endoscopic diagnosis and treatment of gastric cancer by laser beam. Laser Tokyo 81. Session 20. *Laser Endoscopy* 1981; **20**: 26
 - 27 **Overholt BF**, Danjehpour M, Haydek JM. Photodynamic therapy for Barrett's esophagus: follow-up in 100 patients. *Gastrointest Endosc* 1999; **49**: 1-7
 - 28 **Etienne J**, Dorme N, Bourg-Heckly G, Raimbert P, Flijou JF. Photodynamic therapy with green light and m-tetrahydroxyphenyl chlorin for intramucosal adenocarcinoma and high-grade dysplasia in Barrett's esophagus. *Gastrointest Endosc* 2004; **59**: 880-889
 - 29 **Wang KR**. The comparison of laser therapy on gastric ulcer through bark and by endoscopes. *Guowai Yixue* 1997; **4**: 188
 - 30 **Pinheiro AL**, do Nasclento SC, de Vieira AL, Rolim AB, da Silva PS, Brugnera A Jr. Does LLLT stimulate laryngeal carcinoma cells? An *in vitro* study. *Braz Dent J* 2002; **13**: 109-112
 - 31 **De Scheerder IK**, Wang K, Zhou XR, Verbeken E, Keelan MH Jr, Horn JB, Sahota H, Kipshidze N. Intravascular low power red laser light as an adjunct coronary stent implantation evaluated in a porcine C model. *J Invasive Cardiol* 1998; **10**: 263-268
 - 32 **Huang BX**, Wang HB, Liu HQ, Qu ZN, Liu XF, Cheng ZH, Gao L. Study on the Effects of He-Ne Laser Irradiation on the Activity of Humoral Immune Factors IL-2 in Mice. *Zhongguo Jiguang Zazhi* 2004; **2**: 249-252

• BRIEF REPORTS •

Expression of interferon-alpha/beta receptor protein in liver of patients with hepatitis C virus-related chronic liver disease

Xiang-Wei Meng, Bao-Rong Chi, Li-Gang Chen, Ling-Ling Zhang, Yan Zhuang, Hai-Yan Huang, Xun Sun

Xiang-Wei Meng, Bao-Rong Chi, Li-Gang Chen, Ling-Ling Zhang, Yan Zhuang, Hai-Yan Huang, Xun Sun, Department of Gastroenterology, the First Affiliated Hospital, Jilin University, Changchun 130021, Jilin Province, China
Correspondence to: Dr. Xiang-Wei Meng, Department of Gastroenterology, the First Affiliated Hospital, Jilin University, Changchun 130021, Jilin Province, China. xiangweimeng2003@yahoo.com.cn
Telephone: +86-431-5612437 Fax: +86-431-5612437
Received: 2004-07-09 Accepted: 2004-09-19

Abstract

AIM: To study the expression of interferon-alpha/beta (IFN- α/β) receptor protein in liver of patients with hepatitis C virus (HCV)-related chronic liver disease and its clinical significance.

METHODS: A total of 181 patients with HCV-related chronic liver disease included 56 with HCV-related liver cirrhosis (LC) and 125 with chronic hepatitis C (CHC). CHC patients were treated with five megaunits of interferon- α 1b six times weekly for the first 2 weeks and then every other day for 22 wk. The patients were divided into interferon (IFN) treatment-responsive and non-responsive groups, but 36 patients lost follow-up shortly after receiving the treatment. The expression of IFN- α/β receptor (IFN- α/β R) protein in liver of all patients was determined with immunofluorescence.

RESULTS: In liver of patients with HCV-related chronic liver disease, the expression of IFN- α/β R protein in liver cell membrane was stronger than that in cytoplasm and more obvious in the surroundings of portal vein than in the surroundings of central vein. Moreover, it was poorly distributed in hepatic lobules. The weak positive, positive and strong positive expression of IFN- α/β R were 40% (50/125), 28% (35/125), 32% (40/125), respectively in CHC group, and 91.1% (51/56), 5.35% (3/56), and 3.56% (2/56), respectively in LC group. The positive and strong positive rates were higher in CHC group than in LC group ($P < 0.01$). In IFN treatment responsive group, 27.8% (10/36) showed weak positive expression; 72.2% (26/36) showed positive or strong positive expression. In the non-responsive group, 71.7% (38/53) showed weak positive expression; 28.3% (15/53) showed positive or strong positive expression. The expression of IFN- α/β R protein in liver was more obvious in IFN treatment responsive group than in non-responsive group.

CONCLUSION: Expression of IFN- α/β R protein in liver of

patients with HCV-related chronic liver disease is likely involved in the response to IFN treatment.

© 2005 The WJG Press and Elsevier Inc. All rights reserved.

Key words: IFN- α/β receptor; Chronic hepatitis C; HCV-related liver cirrhosis

Meng XW, Chi BR, Chen LG, Zhang LL, Zhuang Y, Huang HY, Sun X. Expression of interferon-alpha/beta receptor protein in liver of patients with hepatitis C virus-related chronic liver disease. *World J Gastroenterol* 2005; 11(25): 3962-3965
<http://www.wjgnet.com/1007-9327/11/3962.asp>

INTRODUCTION

Interferon (IFN) is effective in the treatment of chronic hepatitis C. It results in viral eradication and normalization of liver function in about 35-40% of the patients^[1-4]. The anti-virus mechanism of IFN is to transmit the signal to nuclei and to activate 2'-5' adenylic acid synthase and protein kinase after IFN molecule combines with IFN receptor, which then blocks the translations of virus protein and RNA. IFN receptor (IFN-R) is the initial protein for the chain reaction of IFN^[5]. Human interferon receptors are divided into type I IFN-R which can combine with IFN- α/β , and type II IFN-R which has specific sensitivity to IFN- γ . Furthermore, it has been proved that type II IFN-R is also sensitive to IFN- α/β to some extent^[6], meanwhile IFN- β and subtypes of IFN- α have high sensitivity to IFN-R^[7].

In this study, we determined the expression of IFN-R protein in liver of patients with HCV-related chronic liver disease and its clinical significance.

MATERIALS AND METHODS

Patients

A total of 181 patients were enrolled in this study, including 125 patients with chronic hepatitis C and 56 patients with HCV-related liver cirrhosis. All the patients were seropositive for HCV-RNA and underwent liver biopsy. None of the patient was infected with other hepatitis viruses. All the patients with chronic hepatitis C received IFN treatment. However, only 89 patients were evaluated for treatment response since 36 patients lost follow-up shortly after receiving the treatment. According to the response to IFN treatment, we studied the expression of IFN- α/β R protein in liver of 89 patients with chronic hepatitis C at least six months after IFN treatment.

IFN treatment

IFN treatment was standardized as follows. Five megaunits of IFN- α 1b was administrated to 89 patients with chronic hepatitis C by intramuscular injection six times weekly for the first 2 weeks and then every other day for 22 wk. The total dosage of IFN was 470 MU^[8]. The study followed the ethical guidelines of the Declaration of Helsinki and was approved by the institutional ethics committee. Informed consent was obtained from all patients before IFN treatment.

Appraisal of IFN treatment

According to the response to IFN, 89 patients with chronic hepatitis C who were seropositive for HCV-RNA and received IFN treatment were divided into responder group (36) and non-responder group (53). Responders were defined as patients who were seronegative for HCV-RNA with their serum alanine aminotransferase (ALT) decreased to the normal range for at least 6 mo after IFN treatment. The other patients were non-responders.

Histopathological evaluation

Liver biopsy specimens were defined by Knodell's pathologic classification. The degree of liver fibrosis was determined according to the criteria for staging fibrosis (F₀ to F₄), including F₀ (no fibrosis), F₁ (portal area fibrosis), F₂ (bridging fibrosis), F₃ (bridging fibrosis with lobule deformation), F₄ (cirrhosis). Inflammation activities were scored as follows: 1-3 points (mild hepatitis), 4-8 points (moderate hepatitis), 9-12 points (severe hepatitis).

Determination of IFN- α/β in liver

Making specimens with immunofluorescence technique

IFN- α/β in the liver was immunostained with an indirect immunofluorescence technique. The liver biopsy specimens were sampled during laparoscopy, fixed with fixatives, and frozen to make histological sections. The sections were incubated with non-marked antibody for 45 min at 37 °C, washed thrice in 0.15 mol/L pH7.6 phosphate buffered saline (PBS) for 3 min and once in 0.01 mol/L pH 7.6 PBS for 1 min, then incubated with anti-idiotypic antibody (AId) for 30-45 min at 37 °C and washed with PBS. The sections were dehydrated at room temperature and mounted in glycerol. We cloned the gene coding for the outside-membrane of IFN- α/β in Daudi's cells and immunized white rabbits with protein produced by the gene-transfected *E.coli* to get the first antibody (Amersham, Buckinghamshire, UK). The AId (Amersham, Buckinghamshire, UK) was an anti-rabbit-IgG class antibody labeled with fluorochrome. Negative control was serum of rabbits.

Criteria of fluoroimmunoassay

Intensity of fluorescence was standardized as follows (Figure 1): weak positive (+), positive (++) and strong positive (+++). If a minority of hepatocytes in the portal area were stained, it was defined as weak positive (+). The strong positive (+++) means almost all hepatocytes in the hepatic lobule were stained, and hepatocytes between the two grades were defined as positive (++)

Statistical analysis

Statistical significance of difference was determined by χ^2 -test.

RESULTS

Expression of IFN- α/β protein in liver

IFN- α/β protein was expressed in all the samples of HCV-related chronic liver disease, however the degree of expression varied. Expression of IFN- α/β protein in cell membrane was stronger than that in cytoplasm (Figure 2A). The expression of protein in the surroundings of the portal vein was stronger than that in the surroundings of the central vein. The protein was poorly distributed in hepatic lobules (Figure 2B). Almost all the IFN- α/β proteins expressing cells were hepatic parenchymal cells. However, IFN- α/β proteins were also expressed in part of interlobular cholangioepithelia (Figure 2C).

Expression of IFN- α/β protein in patients with chronic hepatitis C and HCV-related liver cirrhosis

Among the 125 patients with chronic hepatitis C, 40% (50/125) showed weak positive (+), 28% (35/125) showed positive (++) , 32% (40/125) showed strong positive (+++) expression of IFN- α/β protein. Among the 56 patients with HCV-related liver cirrhosis, 91.1% (51/56) showed weak positive (+), 5.35% (3/56) showed positive (++) , 3.56% (2/56) showed strong positive (+++) expression of IFN- α/β protein. The total frequency of positive and strong positive expression in chronic hepatitis C patients was much higher than that in patients with HCV-related liver cirrhosis ($P < 0.01$ Table 1).

Table 1 Expression of IFN- α/β protein in liver of patients with HCV-related chronic liver disease

Group	n	Fluorescence intensity in cases, n (%)	
		+	++,+++
CHC	125	50 (40) ^b	75 (60) ^b
LC	56	51 (91.1)	5 (8.9)

^b $P < 0.01$ vs LC.

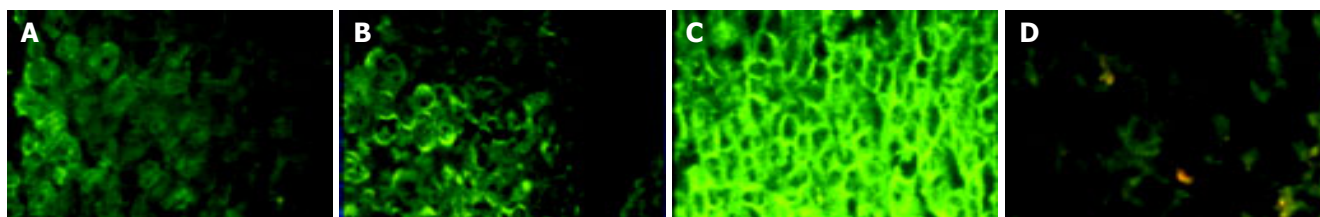


Figure 1 Weak positive (A), positive (B), strong positive (C) and negative (D)

expression of IFN- α/β ($\times 200$).

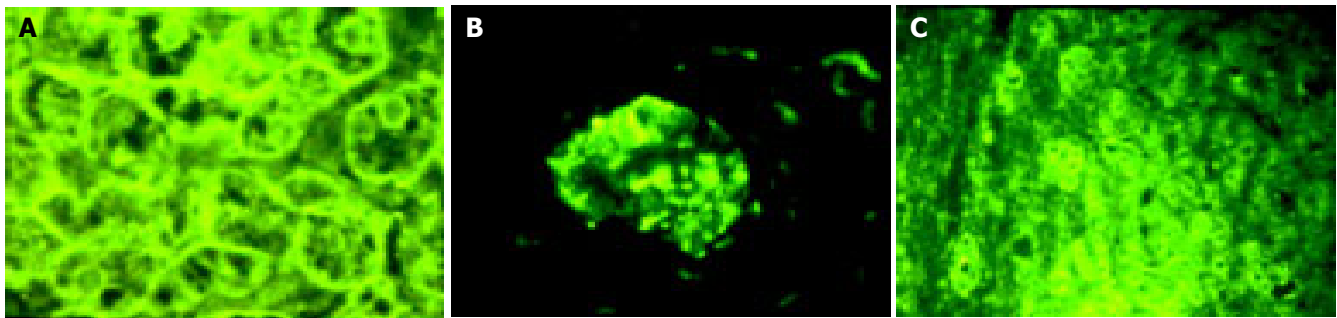


Figure 2 Expression of IFN- α / β R protein in cell membrane and cytoplasm (A), hepatic lobules (B), and hepatic parenchymal cells and part of interlobular

cholangioepithelia (C).

Expression of IFN α / β R protein in liver of patients with chronic hepatitis C after IFN treatment

Six months after IFN treatment, the responders and non-responders were 36 and 53 respectively, and 27.8% (10/36) of the responders showed weak positive (+), and 72.2% (26/36) showed positive (++) or strong positive (+++) expression of the IFN α / β R protein; 71.7% (38/53) of non-responders showed weak positive (+), and 28.3% (15/53) showed positive (++) or strong positive (+++) expression of the IFN- α / β R protein. After the treatment, the total frequency of positive (++) and strong positive (+++) expression of the IFN- α / β R protein in responder group was much higher ($P < 0.05$) than that in non-responder group (Table 2).

Table 2 Effect of IFN and expression of IFN- α / β R protein

IFN treatment effect	n	Fluorescence intensity in cases, n (%)	
		+	++, +++
Responders	36	10 (27.8) ^a	26 (72.2) ^a
Non-responders	53	38 (71.7)	15 (28.3)

^a $P < 0.05$ vs non-responders.

DISCUSSION

Isimura^[9] has proved that IFN R protein exists in liver by ELISA and reported that the expression degree of IFN- α R protein in cytoplasm is different. By immunohistochemical method and competitive polymerase chain reaction assay, Fujiwara *et al.*^[9], found that determination of the expression of IFN- α / β R protein is more useful than that of its mRNA. In this study, we found that expression of IFN- α / β R protein in cell membrane was stronger than that in cytoplasm by immunofluorescence assay. IFN- α / β R protein is a membrane receptor just like other cytoplasm receptors. Moreover, this study also found that the expression of IFN- α / β R protein in the surroundings of the portal vein was stronger than that in the central vein, and the protein was poorly distributed in hepatic lobules. This may be attributed to the following aspects. The blood stream in surrounding of the portal vein is more affluent, providing a good nutritional condition for virus infection which then induces the expression of IFN- α / β R. The expression intensity of IFN- α / β R protein varies in different chronic hepatic diseases. It is weaker in patients with HCV-related

liver cirrhosis than in patients with chronic C hepatitis. The reason may be that the bloodstream in patients with cirrhosis is not well-distributed and the blood supply becomes deficient due to various kinds of fibrosclerosis in hepatic lobules, and liver function and liver cell membrane are damaged because of hepatic cellular inflammation. Because of these factors, liver could not provide a good condition for the expression of IFN- α / β R protein in patients with cirrhosis. Defective expression of IFN- α / β R protein can reduce the intake of IFN, resulting in increased reproduction of virus and activity of hepatitis.

This study demonstrated that expression of IFN- α / β R protein had a close correlation with hepatic fibrosis. The majority of responders with chronic hepatitis C had a very strong expression of IFN- α / β R protein prior to the treatment, which coincides with other researches^[10-12]. The reasons are as follows. The infection of hepatitis virus C can induce expression of protein effectively^[13], since some patients with HCV-related chronic liver disease become very sensitive to IFN treatment. Expression of IFN- α / β R protein in liver in responsive cases is much stronger than that in non-responsive cases. That is to say, non-responsive reaction to the treatment may be caused by the defective expression of protein in patients with chronic hepatitis C. Although expression of IFN- α / β R protein in the responder group is stronger than that in non-responder group, the expression also exists in some non-responsive cases. On the contrary, expression of IFN- α / β R protein in some responsive cases is as weak as that in non-responsive cases. These inconsistencies are attributed to the following aspects. IFN- α / β R protein cannot represent all IFN R proteins involved in the anti-virus mechanism in chronic hepatitis C. The protein we studied is IFN- α / β R protein which could respond to IFN- α and IFN- β ^[7]. The protein plays a key role, in the anti-virus mechanism against HCV-related chronic disease. The combining activity of R protein maybe changed in the responsive cases when IFN- α / β R protein is expressed. Among the responsive and non-responsive cases, some patients with severe chronic hepatitis C and cirrhosis were not sensitive to IFN treatment, and defective expression of IFN- α / β R protein in these patients was a major cause. It coincides with other studies^[14,15]. In conclusion, expression of IFN- α / β R protein in liver of patients with HCV-related chronic disease is likely involved in response to IFN treatment, the expression of IFN- α / β R protein may be useful in

predicting IFN therapeutic effect, and defective expression of IFN- α/β R protein in liver may result in resistance to IFN treatment in patients with HCV-related chronic liver disease.

REFERENCES

- 1 **Hagiwara H**, Hayashi N, Mita E, Takehara T, Kasahara A, Fusamoto H, Kamada T. Quantitative analysis of hepatitis C virus RNA in serum during interferon alpha therapy. *Gastroenterology* 1993; **104**: 877-883
- 2 **Kanai K**, Kato M, Okamoto H. HCV genotypes in chronic hepatitis C and response to interferon. *Lancet* 1992; **339**: 1543
- 3 **Tsubota A**, Chayama K, Ikeda K, Yasuji A, Koida I, Saitoh S, Hashimoto M, Iwasaki S, Kobayashi M, Hiromitsu K. Factors predictive of response to interferon -alpha therapy in hepatitis C virus infection. *Hepatology* 1994; **19**: 1088-1094
- 4 **Poynard T**, Leroy V, Cohard M, Thevenot T, Mathurin P, Opolon P, Zarski JP. Meta-analysis of interferon randomized trials in the treatment of viral hepatitis C: Effects of dose and duration. *Hepatology* 1996; **24**: 778-789
- 5 **Muller U**, Steinhoff U, Reis LF, Hemmi S, Pavlovic J, Zinkernagel RM, Aguet M. Functional roles of type I and type II interferons in antiviral defense. *Science* 1994; **264**: 1918-1921
- 6 **Novick D**, Cohen B, Rubinstein M. The human interferon- α/β receptor Characterization and molecular cloning. *Cell* 1994; **77**: 391-400
- 7 **Colamonici OR**, Domanski P. Identification of a novel subunit of the Type I interferon receptor localized to human chromosome. *J Biol Chem* 1993; **268**: 10895-10899
- 8 Isimura. The significance of interferon in liver as an impact factor for hepatitis C therapy. *Hepatology* 1997; **38**: 292-299
- 9 **Fujiwara D**, Hino K, Yamaguchi Y, Ren F, Satoh Y, Korenaga M, Okuda M, Okita K. Hepatic expression of type I interferon receptor for predicting response to interferon therapy in chronic hepatitis C patients: a comparison of immunohistochemical method vs competitive polymerase chain reaction assay. *Hepatol Res* 2003; **25**: 377-384
- 10 **Morita K**, Tanaka K, Saito S, Kitamura T, Kondo M, Sakaguchi T, Morimoto M, Sekihara H. Expression of interferon receptor genes (IFNAR1 and IFNAR2 mRNA) in the liver may predict outcome after interferon therapy in patients with chronic genotype 2a or 2b hepatitis C virus infection. *Clin Gastroenterol* 1998; **26**: 135-140
- 11 **Mizukoshi E**, Kaneko S, Yanagi M, Ohno H, Kaji K, Terasaki S, Shimoda A, Matsushita E, Kobayashi K. Expression of interferon alpha/beta receptor in the liver of chronic hepatitis C patients. *J Med Virol* 1998; **56**: 217-223
- 12 **Fujiwara D**, Hino K, Yamaguchi Y, Kubo Y, Yamashita S, Uchida K, Konishi T, Nakamura H, Korenaga M, Okuda M, Okita K. Type I interferon receptor and response to interferon therapy in chronic hepatitis C patients: a prospective study. *J Viral Hepat* 2004; **11**: 136-140
- 13 **Yamaguchi Y**, Hino K, Fujiwara D, Ren F, Katoh Y, Satoh Y, Okita K. Expression of type I interferon receptor in liver and peripheral blood mononuclear cells in chronic hepatitis C patients. *Dig Dis Sci* 2002; **47**: 1611-1617
- 14 **Affabris E**, Romeo G, Belardelli F, Jemma C, Mechti N, Gresser I, Rossi GB. 2-5A synthetase activity does not increase in interferon-resistant Friend leukemia cell variants treated with alpha/beta interferon despite the presence of high-affinity interferon receptor sites. *Virology* 1983; **125**: 508-512
- 15 **Roffi L**, Colloredo G, Antonelli G, Belinati G, Panizzuti F, Piperno A, Pozzi M, Ravizza D, Angeli G, Diazani F, Mancina G. Breakthrough during recombinant interferon alpha therapy in patients with chronic hepatitis C virus infection: prevalence, etiology, and management. *Hepatology* 1995; **21**: 645-649

• BRIEF REPORTS •

Surgical treatment of hepatocellular carcinoma with bile duct tumor thrombi

Bao-Gang Peng, Li-Jian Liang, Shao-Qiang Li, Fan Zhou, Yun-Peng Hua, Shi-Min Luo

Bao-Gang Peng, Li-Jian Liang, Shao-Qiang Li, Fan Zhou, Yun-Peng Hua, Shi-Min Luo, Department of Hepatobiliary Surgery, the First Affiliated Hospital of Sun Yat-Sen University, Guangzhou 510080, Guangdong Province, China

Correspondence to: Dr. Bao-Gang Peng, Department of Hepatobiliary Surgery, the First Affiliated Hospital of Sun Yat-Sen University, Guangzhou 510080, Guangdong Province,

China. pengbaogang@163.net

Telephone: +86-20-87755766-8214 Fax: +86-20-87755766-8663

Received: 2004-06-28 Accepted: 2004-07-22

Abstract

AIM: To study the surgical treatment effect and outcome of hepatocellular carcinoma (HCC) with bile duct tumor thrombi (BDTT).

METHODS: Fifty-three consecutive HCC patients with BDTT admitted in our department from July 1984 to December 2002 were reviewed retrospectively. The clinical data, diagnostic methods, surgical procedures and outcome of these patients were collected and analyzed.

RESULTS: One patient rejected surgical treatment, 6 cases underwent percutaneous transhepatic cholangial drainage (PTCD) for unresectable primary disease, and the other 46 cases underwent surgical operation. The postoperative mortality was 17.6%, and the morbidity was 32.6%. Serum total bilirubin levels of these patients with obstructive jaundice decreased gradually after surgery. The survival time of six cases who underwent PTCD ranged from 2 to 7 mo (median survival of 3.7 mo). The survival time of the patients who received surgery was as follows: 2 mo for one patient who underwent laparotomy, 5-46 mo (median survival of 23.5 mo, which was the longest survival in comparison with patients who underwent other procedures, $P = 0.0024$) for 17 cases who underwent hepatectomy, 5-17 mo (median survival of 10.0 mo) for 5 cases who underwent HACE, 3-9 mo (median survival of 6.1 mo) for 11 cases who underwent simple thrombectomy and biliary drainage, and 3-8 mo (median survival of 4.3 mo) for four cases who underwent simple biliary drainage.

CONCLUSION: Jaundice caused by BDTT in HCC patients is not a contraindication for surgery. Only curative resection can result in long-term survival. Early diagnosis and surgical treatment are the key points to prolong the survival of patients.

© 2005 The WJG Press and Elsevier Inc. All rights reserved.

Key words: Hepatocellular carcinoma; Bile duct tumor thrombi

Peng BG, Liang LJ, Li SQ, Zhou F, Hua YP, Luo SM. Surgical treatment of hepatocellular carcinoma with bile duct tumor thrombi. *World J Gastroenterol* 2005; 11(25): 3966-3969
<http://www.wjgnet.com/1007-9327/11/3966.asp>

INTRODUCTION

Jaundice is present in 19-40% of patients with hepatocellular carcinoma (HCC) at the time of diagnosis and usually occurs in advanced stages of diseases. The etiology of jaundice is mainly due to diffuse tumor infiltration of liver parenchyma, progressive liver failure (advanced underlying cirrhosis) and hepatic hilar invasion^[1]. Obstructive jaundice caused by bile duct tumor thrombi (BDTT) arising from HCC is uncommon^[2,3]. Only 1-12% of HCC patients manifest obstructive jaundice as the initial manifestation^[4]. We have noticed this kind of obstructive jaundice caused by HCC with BDTT since 1980, and our initial report of HCC with BDTT was published in 1996^[5]. However, BDTT caused by HCC thrombus is often misdiagnosed as hilar cholangiocarcinoma, and has a particular mode of growth and clinical features. Herein, we report a total of 53 HCC patients with BDTT to make a better understanding of the nature of this disease.

MATERIALS AND METHODS

Patients

From July 1984 to December 2002, 53 consecutive HCC patients (47 males, 6 females, age range 20-69 years, mean age 48.2 ± 10.2 years) with BDTT were treated in our department. The common clinical manifestations included: jaundice, abdominal pain, poor appetite, abdominal distension, skin itch, clay-colored stools, *etc.* Eight cases had previous treatment in other hospitals before admission. Among them, four cases had recurrent HCC after hepatectomy, three received transcatheter arterial chemoembolization (TACE), and one underwent ³²P glass microspheres (³²P-GMS) internal radiotherapy thrice through hepatic artery cannulation and subcutaneous implantation of a drug pump.

Laboratory examination

The average level of serum total bilirubin was 311.9 ± 186.9 $\mu\text{mol/L}$ (range 20.3-776.6 $\mu\text{mol/L}$), ALT was 119 ± 82 IU/L (range 16-428 IU/L), ALP was 423 ± 241 IU/L (range 116-1 038 IU/L), γ -GT was 410 ± 346 IU/L (range 98-1 637 IU/L), ALB was 37 ± 6 g/L (range 24-46 g/L). The hepatitis B surface antigen was positive in 35 cases (35/53, 66.0%). The hepatitis C antibody assay was positive in one case. The concentration of α -fetoprotein (AFP) was higher than

400 µg/L in 29 cases (29/53, 54.7%). Cirrhosis was found in 28 cases (28/53, 52.8%), ascites in 10 cases (10/53, 18.9%).

Imaging findings

Primary tumors and total BDTT in the common hepatic duct or the common bile duct (CBD) were detected by image investigations including ultrasonography (US), computed tomography (CT), endoscopic retrograde cholangiopancreatography and magnetic resonance cholangiopancreatography (MRCP). Three patients were misdiagnosed as cholangiocarcinoma, among them two cases underwent laparotomy and T-tube drainage in other hospitals, one case was found to have lung metastasis at the initial diagnosis.

Location and size of HCC and BDTT

No obvious primary liver tumor was found in seven cases, among them three cases were misdiagnosed as hilar cholangiocarcinoma (Figure 1). The diameter of the primary tumors ranged from 0.9 to 12 cm (mean value 5.0 ± 2.6 cm) in the remaining 46 cases. Of these, the diameter of the major tumor was larger than 10 cm in 6 cases, between 5 and 10 cm in 15 cases, less than 5 cm in 25 cases. Seventeen cases had multiple nodules, 29 had a single nodule. The tumors were involved in the right lobe ($n = 19$), the left lobe ($n = 13$), and the caudate lobe of liver ($n = 3$), the whole liver ($n = 11$). The tumor thrombi of CBD occurred in all cases. Thrombi coexisted in intrahepatic bile duct ($n = 38$), the right hepatic duct ($n = 5$), the left hepatic duct ($n = 4$), and the left and right hepatic ducts ($n = 6$). In addition, the tumor thrombi presented in the right branch ($n = 1$), and the left branch of portal vein ($n = 1$), the right branch of portal vein and the right hepatic vein ($n = 1$).

Statistical analysis

A database was established by SPSS 10.0 software. Data were expressed as mean \pm SD. Kaplan-Meier method and log-rank test were used for survival statistics. $P < 0.05$ was considered statistically significant.

RESULTS

Treatments

One patient refused surgery for other reasons. Fifty-two cases received treatments. Among them, six cases received non-surgical procedures including percutaneous transhepatic cholangio-drainage (PTCD, $n = 4$), biliary stent placement ($n = 2$). Forty-six cases underwent surgical operations including hepatectomy with thrombectomy and biliary drainage ($n = 21$), hepatic artery chemoembolization (HACE) for unresectable primary diseases and biliary drainage ($n = 5$), simple thrombectomy with biliary drainage ($n = 14$), and simple biliary drainage ($n = 4$). Among the 21 cases who underwent hepatectomy for their primary liver tumors, 2 cases underwent right hemihepatectomy, 2 left hemihepatectomy, 11 partial right lobectomy, 4 partial left lobectomy, 1 left hemihepatectomy with caudate lobectomy, 1 left hemihepatectomy with caudate lobectomy and segmentectomy. Simultaneously, one case underwent thrombectomy for the right branch thrombi of portal vein and the right hepatic vein thrombi via the transaction surfaces. Of the 14 cases

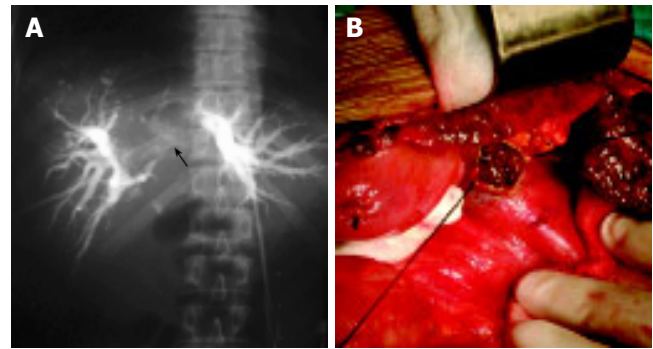


Figure 1 Location and size of HCC. **A:** Hilar obstruction indicating hilar cholangiocarcinoma (white arrow) shown by PTC. **B:** CBD tumor thrombi seen during intra-operation.

who underwent simple thrombectomy and biliary drainage, one underwent proper hepatic artery ligation (HAL), and the other right HAL at the same time.

Pathology

All the 53 cases were pathologically diagnosed as HCC by professional surgical pathologists. The BDTT consisted of tumor cells arranged like a nest of primary tumors, coexisting with red blood cells (RBC), leukocytes and necrotic tumor tissues.

Postoperative mortality and morbidity

Among the 46 patients who underwent operations, 8 died of hepatic failure postoperatively, the hospitalization mortality was 17.4% (8/46). One died 3 d after laparotomy, one died 26 d after simple thrombectomy with biliary drainage and right HAL, two died 7 and 45 d after simple thrombectomy with biliary drainage respectively, four died 7, 12, 15 and 38 d after hepatectomy with thrombectomy and biliary drainage respectively. Fifteen patients developed postoperative complications including liver function failure ($n = 8$), upper gastrointestinal hemorrhage ($n = 4$), pleural effusion ($n = 4$), serious coagulopathy ($n = 1$), intra-abdominal hemorrhage ($n = 1$), pleural hemorrhage ($n = 1$), biliary leakage ($n = 1$), subphrenic infection ($n = 1$), and lower limb venous thrombosis ($n = 1$). The postoperative morbidity was 32.6%. Of the six cases who received PTCD, one suffered from acute cholangitis, no death occurred.

Effect of treatment

The serum total bilirubin levels of these patients with obstructive jaundice decreased gradually. A total of 45 patients were followed up. One patient refused treatment and died 1 mo later. The survival time of six cases who underwent PTCD ranged from 2 to 7 mo (median survival of 3.7 mo). The survival time of the patients who received surgery was 2 mo for one patient who underwent laparotomy, 5-46 mo (median survival of 23.5 mo) for 17 cases who underwent hepatectomy, which was the longest survival compared to the patients who underwent other procedures (log-rank test, $P = 0.0024$), 5-17 mo (median survival of 10.0 mo) for 5 cases who underwent HACE, 3-9 mo (median survival of 6.1 mo) for 11 cases who underwent simple thrombectomy and biliary drainage, and 3-8 mo (median survival of 4.3 mo) for 4 cases who underwent simple biliary drainage.

DISCUSSION

BDTT derived from HCC is uncommon. However, bile duct invasion was commonly detected at necropsy in HCC patients with obstructive jaundice. In 1975, Lin *et al.*^[6], clinically classified such cases as “icteric type hepatoma”, which manifested as obstructive jaundice even at the early stage of tumors, and pointed out that its differential diagnosis was very difficult. In 1982, Kojiro *et al.*^[7], first described the clinical and pathological features of HCC invading the bile duct, and clarified that it was not equal to the portal vein thrombi (PVT), indicating the possibility of extensive dissemination in terms of severity of the disease. They considered that it was not necessarily a criterion of advanced disease. Actually, the rapid growth of the BDTT was rare and there was no report of BDTT extending to the duodenum. But BDTT could enlarge through blending with blood clotting and bile mucus, subsequently resulting in full obstruction of the biliary tract and obstructive jaundice.

The typical clinical features of BDTT were repeated episodes of cholangitis and fluctuating jaundice, which could be relieved by conservative treatment. For these manifestations, BDTT was often misdiagnosed as cholangiocarcinoma. Actually, in our series, three cases were misdiagnosed as hilar cholangiocarcinoma. In addition, it is essentially important to differ obstructive jaundice from hepatic jaundice caused by liver dysfunction due to extensive metastasis within the liver and underlying hepatitis and cirrhosis, because the later has no chance of surgery, but the former can gain a good outcome through operation and/or multi-modality treatment. We concluded that the following clues could help us differentiate BDTT from other types of jaundice. Patients had underlying hepatitis or liver cirrhosis, elevating serum AFP, and characteristic features of primary liver tumors presented in US and CT.

As to the imaging investigations, US is the most convenient and effective method to detect BDTT and intrahepatic primary tumors. Endoscopic sonography (EUS) can show a tumor thrombus with central echogenicity and a “nodule-in-nodule” pattern, which provides more accurate evidence for the diagnosis. Lee *et al.*^[8], reported a patient with a small HCC in caudate lobe and presence of obstructive jaundice. Preoperative EUS showed that it was tumor thrombi in CBD. In addition, intraoperative US could detect smaller or more deeply seated intrahepatic tumors. CT, MRI and MRCP could provide more information for us to know the extension of tumors and location of thrombi, and help us adopt proper treatment, in particular surgical procedure selection for patients. Intraoperative choledochoscopy and cholangiography can show the location of tumor thrombi and differentiate obstructions due to intraluminal mass, infiltrating ductal lesions or extrinsic mass compression. Jan and Chen^[9] reported 28 patients with obstructive jaundice as a result of floating tumor debris from ruptured tumors in CBD. Of these, 18 cases underwent choledochoscopy, and the tumor ruptured into right intrahepatic bile duct ($n = 9$), left intrahepatic bile duct ($n = 7$), and the confluence of the left and right hepatic ducts ($n = 2$). Hepatectomies were performed for four patients under the guide of choledochoscopy.

The size of primary tumors did not correlate with biliary metastasis^[10], and the primary liver tumors with obstructive

jaundice might be small and resectable. In our series, primary liver tumors were not detectable in seven cases. Twenty-five cases had tumors with a diameter of less than 5 cm, suggesting that obstructive jaundice is not a criterion of late-stage HCC and a contraindication for surgery necessarily^[11].

The managements of BDTT include hepatectomy, thrombectomy, biliary drainage, TACE, internal biliary stenting, radiotherapy, percutaneous transhepatic ethanol injection (PTEI), *etc.* Surgical resection has been the ideal treatment and the only way for patients to achieve a long-term survival^[12-14]. Most patients might have satisfactory palliation and opportunity for cure after surgery^[15]. The selection of surgical procedures was based on the nature and location of the main tumor and thrombi, severity of cirrhosis, associated biliary neoplastic strictures, the overall status of patients, and the experience of surgeons. If the condition of patients was good and the primary liver tumor was resectable, the primary tumor should be resected after thrombectomy. Even if it was only a palliative resection, it could increase the survival time. If no liver tumor was detected, biliary decompression and drainage should be performed through choledochotomy and thrombectomy. To the unresectable diseases, HAL and HACE might be beneficial to some selected cases^[16-19]. Shiomi *et al.*^[12], reviewed 132 patients with HCC who underwent hepatectomy between 1980 and 1999. Of these, 17 with BDTT underwent right hemihepatectomy, 1 caudate lobectomy, 11 right or left hemihepatectomy and 5 segmentectomy. Their 3- and 5-year survival rates were 47% and 28% respectively, and the median survival time was 2.3 years, similar to those achieved in 115 patients without BDTT. Fukuda *et al.*^[20], reported that after the patients with HCC and extrahepatic bile duct thrombi underwent tumor resection and HACE, the longest survival time of some patients reached 215 mo. In our 46 cases undergoing surgery, the postoperative mortality was 17.4%, and the morbidity was 32.6%. The survival time of the patients who underwent hepatectomy, thrombectomy and biliary drainage ranged from 5 to 46 mo with a median time of 23.5 mo. We concluded that the poor prognosis of these patients was due to the late diagnosis and obstructive jaundice that resulted in irreversible liver failure. In our study, one patient died 3 d after laparotomy, indicating that early diagnosis and surgical treatment are critically important to improve the prognosis of HCC patients.

BDTT is different from PVT. Complete removal of the later is sometimes difficult because portal vein provides the main blood supply for thrombi. However, it is easy to remove BDTT because most of thrombi do not adhere to the wall of bile duct tightly. Narita *et al.*^[21], reported one case of small HCC in the left lobe with bile duct thrombi, and they found that the thrombi just adhered to the mucosa of bile duct, rather than invaded submucosa. Primary tumor resection and thrombectomy may achieve satisfactory palliation and cure. However, active hemorrhage occurred during operation in some cases, this may be due to the continuity of BDTT with the main intrahepatic tumor or BDTT invading the bile duct wall. But bleeding could be easily controlled after primary tumor was removed. For patients with multiple and unresectable tumors or biliary hemorrhage, thrombectomy and T-tube drainage with HAL could control bleeding and

relieve jaundice, and subsequently improve liver function. The survival time of these patients may be prolonged.

PTCD and biliary stent placement could alleviate jaundice^[22,23]. TACE and PTEI could control the growth of tumors, improve the quality of life and survival rate after jaundice was relieved^[24-26]. Endoscopic biliary drainage (EBD) for unresectable HCC with obstructive jaundice remains controversial because of no benefit to survival. Matsueda *et al.*^[27], suggested that EBD was one of the effective treatments for patients with unresectable malignant biliary stenosis, and obstructive jaundice due to bile duct thrombi. However, EBD was often difficult in HCC patients with obstructive jaundice because of proximal biliary obstruction at the hilum, and multiple tumors diffusing in the whole liver. The decision to perform EBD should be based on the nature and location of thrombi, the condition of liver function, and the presence of PVT. In addition, endoscopic sphincterotomy could benefit the discharge of necrotic thrombi and further improvement of overall status, after endoscopic nasobiliary drainage resolved the obstruction^[28,29].

There is a considerable controversy over the role of transplantation in patients with HCC. Liver transplantation for HCC patients with BDTT is rare. Peng *et al.*^[30,31], have reported one patient who underwent piggyback orthotopic liver transplantation and survived for 27 mo. This suggests that selected HCC patients with BDTT may benefit from liver transplantation, but it needs to be studied further.

REFERENCES

- 1 **Becker FF.** Hepatoma-nature's model tumor. *Am J Pathol* 1974; **74**: 179-210
- 2 **Chen MF.** Icteric type hepatocellular carcinoma: clinical features, diagnosis and treatment. *Chang Gung Med J* 2002; **25**: 496-501
- 3 **Huang GT,** Sheu JC, Lee HS, Lai MY, Wang TH, Chen DS. Icteric type hepatocellular carcinoma: revisited 20 years later. *J Gastroenterol* 1998; **33**: 53-56
- 4 **Kew MC,** Paterson AC. Unusual clinical presentations of hepatocellular carcinoma. *Trop Gastroenterol* 1985; **6**: 10-22
- 5 **Peng BG,** Huang JF, Liang LJ, Lu MD. The surgical treatment of hepatocellular carcinoma involving the bile duct: 20 cases reported. *Chin J Practical Surg* 1996; **16**: 484-485
- 6 **Lin TY,** Chen KM, Chen YR, Lin WS, Wang TH, Sung JL. Icteric type hepatoma. *Med Chir Dig* 1975; **4**: 267-270
- 7 **Kojiro M,** Kawabata K, Kawano Y, Shirai F, Takemoto N, Nakashima T. Hepatocellular carcinoma presenting as intrabiliary duct tumor growth: a clinicopathologic study of 24 cases. *Cancer* 1982; **49**: 2144-2147
- 8 **Lee YC,** Wang HP, Huang SP, Chang YT, Wu CT, Yang CS, Wu MS, Lin JT. Obstructive jaundice caused by hepatocellular carcinoma: detection by endoscopic sonography. *J Clin Ultrasound* 2001; **29**: 363-366
- 9 **Jan YY,** Chen MF. Obstructive jaundice secondary to hepatocellular carcinoma rupture into the common bile duct: choledochoscopic findings. *Hepatogastroenterology* 1999; **46**: 157-161
- 10 **Tseng JH,** Hung CF, Ng KK, Wan YL, Yeh TS, Chiu CT. Icteric-type hepatoma: magnetic resonance imaging and magnetic resonance cholangiographic features. *Abdom Imaging* 2001; **26**: 171-177
- 11 **Hu J,** Pi Z, Yu MY, Li Y, Xiong S. Obstructive jaundice caused by tumor emboli from hepatocellular carcinoma. *Am Surg* 1999; **65**: 406-410
- 12 **Shiomi M,** Kamiya J, Nagino M, Uesaka K, Sano T, Hayakawa N, Kanai M, Yamamoto H, Nimura Y. Hepatocellular carcinoma with biliary tumor thrombi: aggressive operative approach after appropriate preoperative management. *Surgery* 2001; **129**: 692-698
- 13 **Nishio H,** Miyata K, Hanai M, Kato M, Yoneyama F, Kobayashi Y. Resection of an icteric type hepatoma with tumor thrombi filling the right posterior bile duct. *Hepatogastroenterology* 2002; **49**: 1682-1685
- 14 **Shimada M,** Takenaka K, Hasegawa H, Shirabe K, Gion T, Kano T, Sugimachi K. Hepatic resection for icteric type hepatocellular carcinoma. *Hepatogastroenterology* 1997; **44**: 1432-1437
- 15 **Murakami Y,** Yokoyama T, Kanehiro T, Uemura K, Sasaki M, Morifuji M, Sueda T. Successful diagnosis and resection of icteric type hepatocellular carcinoma. *Hepatogastroenterology* 2003; **50**: 1634-1636
- 16 **Jan YY,** Chen MF, Chen TJ. Long term survival after obstruction of the common bile duct by ductal hepatocellular carcinoma. *Eur J Surg* 1995; **161**: 771-774
- 17 **Tantawi B,** Cherqui D, Tran van Nhieu J, Kracht M, Fagniez PL. Surgery for biliary obstruction by tumour thrombus in primary liver cancer. *Br J Surg* 1996; **83**: 1522-1525
- 18 **Lau W,** Leung K, Leung TW, Liew CT, Chan MS, Yu SC, Li AK. A logical approach to hepatocellular carcinoma presenting with jaundice. *Ann Surg* 1997; **225**: 281-285
- 19 **Wang HJ,** Kim JH, Kim JH, Kim WH, Kim MW. Hepatocellular carcinoma with tumor thrombi in the bile duct. *Hepatogastroenterology* 1999; **46**: 2495-2499
- 20 **Fukuda S,** Okuda K, Imamura M, Imamura I, Eriguchi N, Aoyagi S. Surgical resection combined with chemotherapy for advanced hepatocellular carcinoma with tumor thrombus: report of 19 cases. *Surgery* 2002; **131**: 300-310
- 21 **Narita R,** Oto T, Mimura Y, Ono M, Abe S, Tabaru A, Yoshikawa I, Tanimoto A, Otsuki M. Biliary obstruction caused by intrabiliary transplantation from hepatocellular carcinoma. *J Gastroenterol* 2002; **37**: 55-58
- 22 **Lee JW,** Han JK, Kim TK, Choi BI, Park SH, Ko YH, Yoon CJ, Yeon KM. Obstructive jaundice in hepatocellular carcinoma: response after percutaneous transhepatic biliary drainage and prognostic factors. *Cardiovasc Intervent Radiol* 2002; **25**: 176-179
- 23 **Okazaki M,** Mizuta A, Hamada N, Kawamura N, Nakao K, Kikuchi T, Osada T. Hepatocellular carcinoma with obstructive jaundice successfully treated with a self-expandable metallic stent. *J Gastroenterol* 1998; **33**: 886-890
- 24 **Hu P,** Zhou DY, Gong B, Wang SZ, Yang GS, Wu MC. Endoscopic management of 1 215 malignant bile duct obstructions. *Chin J Surg* 2001; **39**: 195-198
- 25 **Tada K,** Kubota K, Sano K, Noie T, Kosuge T, Takayama T, Makuuchi M. Surgery of icteric-type hepatoma after biliary drainage and transcatheter arterial embolization. *Hepatogastroenterology* 1999; **46**: 843-848
- 26 **Huang JF,** Wang LY, Lin ZY, Chen SC, Hsieh MY, Chuang WL, Yu MY, Lu SN, Wang JH, Yeung KW, Chang WY. Incidence and clinical outcome of icteric type hepatocellular carcinoma. *J Gastroenterol Hepatol* 2002; **17**: 190-195
- 27 **Matsueda K,** Yamamoto H, Umeoka F, Ueki T, Matsumura T, Tezen T, Doi I. Effectiveness of endoscopic biliary drainage for unresectable hepatocellular carcinoma associated with obstructive jaundice. *J Gastroenterol* 2001; **36**: 173-180
- 28 **Naranjo Rodriguez A,** Puente Gutierrez J, Hervas Molina A, de Dios Vega JF, Monrobel Lancho A, Gonzalez Galilea A, Mino Fugarolas G. Endoscopic drainage with polyethylene endoprosthesis of malignant obstructive jaundice. *Gastroenterol Hepatol* 1999; **22**: 391-397
- 29 **Spahr L,** Frossard JL, Felley C, Brundler MA, Majno PE, Hadengue A. Biliary migration of hepatocellular carcinoma fragment after transcatheter arterial chemoembolization therapy. *Eur J Gastroenterol Hepatol* 2000; **12**: 243-244
- 30 **Peng SY,** Wang JW, Liu YB, Cai XJ, Deng GL, Xu B, Li HJ. Surgical intervention for obstructive jaundice due to biliary tumor thrombus in hepatocellular carcinoma. *World J Surg* 2004; **28**: 43-46
- 31 **Peng SY,** Wang JW, Liu YB, Cai XJ, Xu B, Deng GL, Li HJ. Hepatocellular carcinoma with bile duct thrombi: analysis of surgical treatment. *Hepatogastroenterology* 2004; **51**: 801-804

• ACKNOWLEDGEMENTS •

Acknowledgements to Reviewers of *World Journal of Gastroenterology*

Many reviewers have contributed their expertise and time to the peer review, a critical process to ensure the quality of *World Journal of Gastroenterology*. The editors and authors of the articles submitted to the journal are grateful to the following reviewers for evaluating the articles (including those were published and those were rejected in this issue) during the last editing period of time.

Satoshi Kondo, Professor and Chairman

Department of Surgical Oncology, Hokkaido University Graduate School of Medicine, N15 W7, Kita-ku, Sapporo 060-8638, Japan

Shoji Kubo, M.D.

Hepato-Biliary-Pancreatic Surgery, Osaka City University Graduate School of Medicine, 1-4-3 Asahimachi, Abeno-ku, Osaka 545-8585, Japan

Nicholas F LaRusso, M.D.

Department of Internal Medicine, Distinguished Investigator of the Mayo Foundation Mayo Medical School, 200 First Street, SW, Rochester MN 55905, United States

Frederick H Leibach, Professor

Department of Biochemistry and Molecular Biology, Medical College of Georgia, 1120 15th Street, Augusta 30912-2100, United States

Jie-Shou Li, M.D.

Academician of Chinese Academy of Engineering, Department of General Surgery, General Hospital of Nanjing Command Area, 305 East Zhongshan Road, Nanjing 210002, Jiangsu Province, China

Richard W McCallum, M.D.

Professor of Medicine, Director The Center for Gastrointestinal Nerve and Muscle Function & the Division of GI Motility, MS 1058, 901 Rainbow Boulevard, Kansas City, KS 66160, United States

Timothy H Moran, Professor

Department of Psychiatry, Johns Hopkins University School of Medicine, Ross 618, 720 Rutland Ave, Baltimore, Maryland 21205, United States

Hiroshi Nakagawa, Assistant Professor

Gastroenterology Division, University of Pennsylvania, 415 Curie Blvd. 638B CRB, Philadelphia 19104, United States

Josep M. Pique, M.D.

Department of Gastroenterology, Hospital Clínic of Barcelona, Villarroel, 170, Barcelona 08036, Spain

Gabriele Bianchi Porro, Professor

Gastroenterology Unit, "L. Sacco" University Hospital, Via G.B. Grassi 74, Milano 20157, Italy

Piero Portincasa, Professor

Internal Medicine - DIMIMP, University of Bari Medical School, Hospital Policlinico Piazza G. Cesare 11, Bari 70124, Italy

Lun-Xiu Qin, Professor

Liver Cancer Institute and Zhongshan Hospital, Fudan University, 180 Feng Lin Road, Shanghai 200032, China

Vasily Ivanovich Reshetnyak, Professor

Institute of General Reanimatology, 25-2, Petrovka Str., Moscow 107031, Russian Federation

Jose Sahel, Professor

Hepato-gastroenterology, Hospital sainti Marevenite, 1270 Boulevard AE Sainti Margrenise, Marseille 13009, France

Peng Shang, Professor

Department of Cell Biology, Faculty of Life Sciences, 127 Western Youyi Road, Northwestern Polytechnical University, Xi'an, 710072, Shaanxi Province, China

Ian David Wallace, M.D.

Gastroenterologist, President, New Zealand Society of Gastroenterology, School of Medicine Auckland University; Department Gastroenterology North Shore Hospital; Shakespeare Specialist Group, 181 Shakespeare Rd Milford, Auckland, New Zealand

Benjamin Wong, M.D.

Department of Medicine, University of Hong Kong, Pokfulam Road, Pokfulam, Hong Kong, China

George Y Wu, Professor

Department of Medicine, Division of Gastroenterology-Hepatology University of Connecticut Health Center, 263 Farmington Ave, Farmington, CT 06030, United States

Yuan Yuan, Professor

Cancer Institute of China Medical University, 155 North Nanjing Street, Heping District, Shenyang 110001, Liaoning Province, China

Man-Fung Yuen, Associate Professor

Department of Medicine, The University of Hong Kong, Queen Mary Hospital, Hong Kong, China

Jian-Zhong Zhang, Professor

Department of Pathology and Laboratory Medicine, Beijing 306 Hospital, 9 North Anxiang Road, PO Box 9720, Beijing 100101, China

Factors affecting recurrence after surgery for Crohn's disease

Takayuki Yamamoto

Takayuki Yamamoto, Inflammatory Bowel Disease Center and Department of Surgery, Yokkaichi Social Insurance Hospital, Yokkaichi, Mie 510-0016, Japan

Correspondence to: Takayuki Yamamoto, MD, Inflammatory Bowel Disease Center and Department of Surgery, Yokkaichi Social Insurance Hospital, 10-8 Hazuyamacho, Yokkaichi, Mie 510-0016, Japan. nao-taka@sannet.ne.jp

Telephone: +81-593-31-2000 Fax: +81-593-31-0354

Received: 2004-12-05 Accepted: 2005-01-05

Abstract

Although in Crohn's disease post-operative recurrence is common, the determinants of disease recurrence remain speculative. The aim of this study was to examine factors affecting post-operative recurrence of Crohn's disease. A Medline-based literature review was carried out. The following factors were investigated: age at onset of disease, sex, family history of Crohn's disease, smoking, duration of Crohn's disease before surgery, prophylactic medical treatment (corticosteroids, 5-amino salicylic acid [5-ASA] and immunosuppressants), anatomical site of involvement, indication for surgery (perforating or non-perforating disease), length of resected bowel, anastomotic technique, presence of granuloma in the specimen, involvement of disease at the resection margin, blood transfusions and post-operative complications. Smoking significantly increases the risk of recurrence (risk is approximately twice as high), especially in women and heavy smokers. Quitting smoking reduces the post-operative recurrence rate. A number of studies have shown a higher risk when the duration of the disease before surgery was short. There were, however, different definitions of 'short' among the studies. Prophylactic corticosteroids therapy is not effective in reducing the post-operative recurrence. A number of randomized controlled trials offered evidence of the efficacy of 5-ASA (mesalazine) in reducing post-operative recurrence. Recently, the therapeutic efficacy of immunosuppressive drugs (azathioprine and 6-mercaptopurine) in the prevention of post-operative recurrence has been investigated and several studies have reported that these drugs might help prevent the recurrence. Further clinical trials would be necessary to evaluate the prophylactic efficacy of immunosuppressants. Several studies showed a higher recurrence rate in patients with perforating disease than in those with non-perforating disease. However, evidence for differing recurrence rates in perforating and non-perforating diseases is inconclusive. A number of retrospective studies reported that a stapled functional end-to-end anastomosis was associated with a lower recurrence rate compared with other types of anastomosis. However, prospective randomized studies

would be necessary to draw a definite conclusion. Many studies found no difference in the recurrence rates between patients with radical resection and non-radical resection. Therefore, minimal surgery including stricturoplasty has been justified in the management of Crohn's disease. In this review, the following factors do not seem to be predictive of post-operative recurrence: age at onset of disease, sex, family history of Crohn's disease, anatomical site of disease, length of resected bowel, presence of granuloma in the specimen, blood transfusions and post-operative complications. The most significant factor affecting post-operative recurrence of Crohn's disease is smoking. Smoking significantly increases the risk of recurrence. A short disease duration before surgery seems, albeit to a very minor degree, to be associated with a higher recurrence rate. 5-ASA has been shown with some degree of confidence to lead to a lower recurrence rate. The prophylactic efficacy of immunosuppressive drugs should be assessed in future. A wider anastomotic technique after resection may reduce the post-operative recurrence rate, though this should be investigated with prospective randomized controlled trials.

© 2005 The WJG Press and Elsevier Inc. All rights reserved.

Key words: Crohn's disease; Post-operative recurrence; Predictive factors; Resection; Surgery

Yamamoto T. Factors affecting recurrence after surgery for Crohn's disease. *World J Gastroenterol* 2005; 11(26): 3971-3979

<http://www.wjgnet.com/1007-9327/11/3971.asp>

INTRODUCTION

Crohn's disease is a chronic inflammatory gastrointestinal disorder with an unpredictable clinical course characterized by the high incidence of recurrence. Nearly 80% of patients with Crohn's disease require surgery during their lifetime^[1]. Post-operative recurrence rates defined by clinical symptoms are 17-55% at 5 years, 32-76% at 10 years and 72-73% at 20 years^[2-14]. The rates of recurrence requiring re-operation are 11-32% at 5 years, 20-44% at 10 years and 46-55% at 20 years^[2-14]. Thus, the re-operation rate tends to steadily increase with time, reaching approximately 50% at 20 years after surgery. Although in Crohn's disease post-operative recurrence is common, the determinants of disease recurrence remain speculative. Several patients with Crohn's disease experience frequent recurrences while others have prolonged periods of remission after surgery.

Identifying risk factors for post-operative recurrence would be useful to spot patients at a high risk of future recurrence and to determine strategies for medical treatment after surgery. A number of factors have been evaluated as potentially influencing the recurrence rates after surgery for Crohn's disease^[14-39]: age at onset of disease, sex, family history of Crohn's disease, smoking, duration of Crohn's disease before surgery, prophylactic medical treatment (corticosteroids, 5-amino salicylic acid [5-ASA] and immunosuppressants), anatomical site of involvement, indication for surgery (perforating or non-perforating disease), length of resected bowel, anastomotic technique, presence of granuloma in the specimen, involvement of disease at the resection margin, blood transfusions and post-operative complications. A Medline-based literature review was carried out to examine factors affecting post-operative recurrence of Crohn's disease.

Age at onset of disease

Many studies examined the impact of age on the recurrence rate after surgery. Naturally, patients with early onset of disease seem to have a higher recurrence rate because of a longer follow-up duration. A younger age at onset of disease has been linked to a higher recurrence rate in several studies^[18,29,32-36] but not others^[17,20,21,26,28,30]. Thus, the reports about the importance of age have been conflicting and different studies have yielded contradictory results. In summary, age does not seem to be a definite predictive factor of post-operative recurrence.

Sex

A few studies have suggested that the sex of the patient influences the risk of recurrence after surgery, with slightly increased recurrence rates reported for both men^[37] and women^[32,38,39]. In many other studies, the recurrence rate was similar for both men and women^[15-17,20,21,26,27,29,30].

Family history of Crohn's disease

There have been only a few reports examining the relationship between family history of Crohn's disease and the recurrence rate after surgery^[17,35]. Chardavoine *et al.*^[17], found family history of Crohn's disease did not influence the recurrence rate. Our recent study found that patients with a family history had a higher recurrence rate^[35].

Smoking

There has been increasing speculation as to the role of cigarette smoking in the pathogenesis of inflammatory bowel diseases, since smokers are over-represented in groups of patients with Crohn's disease and under-represented in patients with ulcerative colitis^[40-43]. Not only is smoking associated with an increased risk of developing Crohn's disease, but several studies have demonstrated a significantly increased risk of recurrence after surgery^[35,46-52]. Sutherland *et al.*^[46], reported that the 5- and 10-year recurrence rates were significantly higher in smokers (36% and 70%) than in non-smokers (20% and 41%; odds ratio, 2.1; $P = 0.007$). When patients were stratified by sex, the increased risk was more apparent in women (odds ratio, 4.2; 95% confidence interval [CI], 2.0-4.2) than in men (odds ratio,

1.5; 95%CI, 0.8-6.0). Lindberg *et al.*^[47], found that heavy smokers (>10 cigarettes/day) had an increased risk of operation at least once; odds ratios for heavy smokers compared with non-smokers after 5 and 10 years were 1.14 and 1.24, respectively ($P = 0.03$ and $P = 0.017$). The risk of further operations was even higher and after 10 years the odds ratio was 1.79 ($P = 0.015$). Cottone *et al.*^[24], conducted multivariate analyses to examine predictive factors for three types of recurrence (clinical [symptomatic], endoscopic and surgical [reoperation] recurrences) after surgery for Crohn's disease. They found that smoking was an independent significant factor for clinical recurrence (odds ratio, 1.46; 95%CI, 1.1-1.8), endoscopic recurrence (odds ratio, 2.2; 95%CI, 1.2-3.8) and surgical recurrence (odds ratio, 2.0; 95%CI, 1.2-2.3). Breuer-Katschinski *et al.*^[48], studied 346 patients with Crohn's disease and found that 73% of smokers and 39% of non-smokers required one or more operations. The 5- and 10-year recurrence rates were 43% and 64% for smokers, which were significantly higher than 26% and 33% for non-smokers (odds ratio, 3.1; $P < 0.00$). For the 5- and 10-year recurrence rates the relative risk estimates for smokers versus non-smokers were 3.1 (95%CI, 1.7 - 5.8) and 6.7 (95%CI, 2.7-6.8). When stratified by sex, the increased risk for the recurrence was recognized in both sexes. For the number of cigarettes smoked a dose-response effect was obvious in women. Timmer *et al.*^[49], found that at 48 wk after surgery for Crohn's disease, the relapse rate [Crohn's disease activity index (CDAI) > 150 or an increase of CDAI of > 60] was 30% in non-smokers compared with 53% in smokers (odds ratio, 2.1; $P = 0.02$). Ex-smokers did not have an increased risk; the relapse rate was 35%, which was similar to 30% in non-smokers. In my research in the UK^[50], after resection for ileocecal Crohn's disease the 5- and 10-year recurrence rates were 35% and 55% for smokers compared with 19% and 36% for non-smokers (odds ratio, 2.3; $P = 0.007$). When smokers were further divided into two sub-groups according to the number of cigarettes smoked per day, the cumulative recurrence rate was higher in heavy smokers (15 or >15 cigarettes/d) compared with mild smokers (<15 cigarettes/d). In my another study,^[51] after resection (colectomy and ileorectal anastomosis) for Crohn's colitis the 5-, 10- and 15-year recurrence rates were 25%, 46%, and 52% for smokers and 11%, 15%, and 18% for non-smokers (odds ratio, 3.0; $P = 0.005$). In the multivariate analyses, only smoking was an independent significant factor for poor outcome after surgery for Crohn's colitis. Our recent study^[35] examined the impact of quitting smoking on re-operation for recurrence after surgery for Crohn's disease. We found that patients who quit smoking were less likely to have undergone one, two and three re-operations for recurrence (odds ratio, 0.25; 95%CI, 0.15-0.41; odds ratio, 0.30; 95%CI, 0.16-0.57 and odds ratio, 0.25; 95%CI, 0.10-0.71). These data indicate that patients with Crohn's disease who stop smoking reduce the risk of re-operation for recurrence after surgery.^[35] In contrast, two studies failed to find significant correlations between smoking and the recurrence rate after surgery for Crohn's disease, though in those studies the number of patients included was small and the detailed data concerning smoking were not presented^[53,54]. In summary, smoking significantly increases the risk of recurrence after

surgery for Crohn's disease (risk is approximately twice as high), especially in women and heavy smokers. Quitting smoking is associated with a lower recurrence rate compared with that in smokers. Because many patients with Crohn's disease are unaware of the risks that smoking has on their disease^[55,56], education and encouragement of patients to stop smoking are necessary in the management of Crohn's disease^[55-59]. The mechanism of the effect of smoking on Crohn's disease is as yet unclear. Potentially important mechanisms include immune modulation, gut vascularity, gut mucous composition, gut permeability and perturbation in eicosanoid production^[40-45].

Duration of disease before surgery

An association between duration of disease before the first operation and early recurrence has been suggested previously^[15,17,23,28,33,38,60]. A number of studies have shown a higher risk with a short history of disease^[15,23,28,33,38,60]. In one prospective study, Poggioli *et al.*^[28], found that duration of disease less than 6 years prior to surgery was associated with higher the recurrence rates compared to patients with an illness of longer than 6 years prior to surgery. Another study^[17] found that recurrent disease was more likely to occur in patients with a duration of disease of between 3 and 10 years before surgery. Sachar *et al.*^[15], found significantly higher recurrence rates in patients with disease duration less than 10 years. This has not been universal and other groups have failed to find a relationship between pre-surgical disease duration and recurrence^[16,18-21,26,30]. Differences in the definition of 'short duration' hamper comparison among the studies. In our previous study^[60], we selected the arbitrary intervals of 1 year between the onset of disease and surgery, 1 and 10 years and more than 10 years and found that recurrent disease was significantly associated with short duration of disease prior to primary surgery. It is not clear why a short duration of disease prior to surgery emerges as such a powerful association with recurrent disease in our study. It may be that a short interval between diagnosis and primary surgery is indicative of a more aggressive disease phenotype. However, it would seem unreasonable to defer surgery in a symptomatic patient with a short history of disease, merely because of the potential risk of early recurrence.

Prophylactic medical treatment (corticosteroids, 5-ASA and immunosuppressants)

Many studies report that corticosteroids therapy is ineffective in reducing recurrence of Crohn's disease^[61-66]. Several randomized controlled trials have demonstrated that 5-ASA (mesalazine) is effective in reducing the frequency of post-operative recurrence and in decreasing the severity of the lesions^[67-69]. Caprilli *et al.*^[67], studied 110 patients operated on for Crohn's disease by the first intestinal resection. Patients were randomly allocated to receive mesalazine (2.4 g/d) or no treatment at all. The cumulative proportion of recurrence at 6, 12, and 24 mo was significantly lower in the mesalazine group than in untreated group ($P = 0.002$). At 24 mo the cumulative proportions of endoscopic recurrence were 0.52 and 0.85, respectively. At the same time, the cumulative proportions of symptomatic recurrence

were 0.18 and 0.41 ($P = 0.006$). The cumulative proportions of the severe recurrence was also significantly lower in the mesalazine group (0.17 *vs* 0.38; $P = 0.021$). It was estimated that 5-ASA prevents 39% of all recurrences and 55% of the severe recurrences. In a double-blind, multicenter clinical trial^[68], 87 patients were treated with 3 g/d mesalamine (Pentasa) or with placebo within 1 mo after surgery. Seventeen clinical relapses (seven in the mesalamine group) were recorded. After 12 mo, the endoscopic lesions were less frequent and less severe in the mesalamine group than were those in the placebo group ($P < 0.008$). The overall rate of severe recurrence (on endoscopy or radiological documentation) was 24% in the mesalamine group and 56% in the placebo group ($P < 0.004$). In another randomized controlled trial^[69], 163 patients who underwent a surgical resection were randomized to a treatment group (1.5 g mesalamine twice a day) or a placebo control group within 8 wk of surgery. The follow-up period was a maximum of 72 mo. The symptomatic recurrence rate in the treatment group was 31% (27 of 87) compared with 41% (31 of 76) in the control group ($P = 0.031$). The relative risk of developing recurrent disease was 0.628 (90%CI, 0.40-0.97) for those in the treatment group ($P = 0.039$) using an intention-to-treat analysis and 0.532 (90%CI, 0.32-0.87) using an efficacy analysis. The endoscopic and radiological rate of recurrence was also significantly decreased with relative risks of 0.654 (90%CI, 0.47-0.91) in the effectiveness analysis and 0.635 (90%CI, 0.44-0.91) in the efficacy analysis. These results^[67-69] suggest that high-dose (2.4-3.0 g/d) 5-ASA therapy early in the post-operative period may be the most effective regimen. A meta-analysis^[70] was conducted to assess the effectiveness of 5-ASA in maintaining remission of quiescent Crohn's disease. Fifteen randomized, controlled trials of 5-ASA maintenance therapy involving a total of 2 097 patients were selected for the analysis. Therapy with 5-ASA significantly reduced the risk of symptomatic relapse (pooled risk difference, -6.3%; 95%CI, -10.4% to -2.1%). The pooled risk difference was significant in the post-surgical setting (-13.1%; 95%CI, -21.8% to -4.5%) but not in the medical setting (-4.7%; 95%CI, -9.6% to 2.8%). Multivariate model predicts that the probability of symptomatic relapse significantly decreases with 5-ASA treatment, by increasing proportion of patients with ileal disease, with prolonged disease duration, and with surgically induced remission.

Immunosuppressive drugs (azathioprine and 6-mercaptopurine [6-MP]) are effective in the setting of steroid dependence and steroid resistance, as well as for the treatment of perianal and fistulizing Crohn's disease unresponsive to antibiotics^[64-66,71]. Recently, therapeutic efficacy of azathioprine and 6-MP in the prevention of post-operative recurrence in patients with Crohn's disease has been investigated. In a prospective, open-label, randomized study^[72], 142 patients received azathioprine [2 mg/(kg·d)] or mesalamine (3 g/d) for 24 mo. The risk of clinical relapse was comparable in the azathioprine and mesalamine groups. No difference was observed with respect to surgical relapse between the two groups. In a sub-group analysis, azathioprine was more effective than mesalamine in preventing clinical relapse in patients with previous intestinal resections (odds ratio, 4.83; 95%CI, 1.47-15.8). The study concluded that while

no difference was observed in the efficacy of azathioprine and mesalamine in preventing clinical and surgical relapses after conservative surgery, azathioprine is more effective in those patients who have undergone previous intestinal resection. In another randomized trial^[73], 131 patients received 6-MP (50 mg), mesalamine (3 g) or placebo daily. The clinical recurrence rates (intent to treat) at 24 mo were 50% (95%CI, 34-68%), 58% (95%CI, 41-75%) and 77% (95%CI, 61-91%) in patients receiving 6-MP, mesalamine and placebo, respectively. The endoscopic recurrence rates were 43% (95%CI, 28-63%), 63% (95%CI, 47-79%) and 64% (95%CI, 46-81%) and the radiographic recurrence rates were 33% (95%CI, 19-54%), 46% (95%CI, 29-66%) and 49% (95%CI, 30-72%), respectively. 6-MP was more effective than placebo ($P < 0.05$) in preventing the clinical and endoscopic recurrence. The study concluded that 6-MP (50 mg/d) may be considered as a maintenance therapy after ileocolonic resection for Crohn's disease. Thus, azathioprine and 6-MP might help prevent post-operative recurrence of Crohn's disease. However, further clinical trials would be necessary to evaluate the efficacy of immunosuppressants in preventing clinical relapse after surgery for Crohn's disease.

Anatomical site of involvement

Three main sites (small bowel, large bowel and ileocolonic region) of gastrointestinal involvement have been discussed as clinical patterns in Crohn's disease. A number of studies examined the impact of anatomical site of disease on the recurrence and reported the different results^[15-17,19,27-30]. The risk of recurrence was highest in patients with small bowel disease^[29,31,74] and ileocolonic disease^[27,30]. In one study^[17], patients with predominantly large bowel disease ($n = 56$) were found to have a higher rate of re-resection (45%) when compared with 32% in patients with small bowel involvement ($n = 94$) and with 35% in patients with both small and large bowel involvement ($n = 37$) ($P = 0.04$)^[17]. Other studies failed to find any significant impact of the site of disease on the recurrence rate^[15,16,19,28]. Thus, the use of 'anatomical site of involvement' as a factor for post-operative recurrence is of limited value in clinical practice.

Indication for surgery

Crohn's disease has two different clinical forms, a relatively aggressive 'perforating' type and a more indolent 'non-perforating' type. Greenstein *et al.*^[75], defined a perforating disease as acute free perforation, sub-acute perforation with abscess or chronic perforation with internal or external fistula from findings at laparotomy. This definition has been widely used in clinical practice. Several studies examined the relationship between the type of disease and post-operative recurrence. Aeberhard *et al.*^[76], found that the median interval between the first and second operation was 1.7 years for patients with perforating disease, which was significantly shorter than 13 years for patients with non-perforating disease. Lautenbach *et al.*^[77], studied 88 patients who had undergone at least two resections for Crohn's disease to elucidate predictors of early post-operative recurrence. A perforating indication for initial surgery ($P < 0.001$) was found to be an independent predictor of early post-operative

recurrence after initial surgery. The indication for initial surgery was predictive of the indication at a subsequent surgery for the recurrence ($P = 0.001$). The other study found that patients with fistulizing type of symptoms were at a high risk of early recurrence after surgery^[78]. In contrast, the postoperative recurrence rates were similar for patients with perforating and non-perforating diseases in other studies^[26-28,30,60,79,80]. Evidence for differing the recurrence rates in perforating and non-perforating diseases is inconclusive. There may be concordance between patients initially presenting with perforating *vs* non-perforating disease and the pattern of disease recurrence^[12,28,75,79]. However, McDonald *et al.*^[80], reported that patients were no more likely to have the same indication for surgery at the time of the second resection or the third resection compared with the initial resection.

Length of resected bowel

Several studies have suggested that the recurrence is more common after resection of a long length of diseased bowel^[37,81,82]. Other studies found that the length of resected small and large bowel made no difference to the rates of recurrence^[4,5,16,33]. Thus, the length of resected bowel does not seem to be a definite predictive factor of post-operative recurrence.

Anastomotic technique

The type of anastomosis following resection is one of the important issues in the surgical management of Crohn's disease. The fecal stream is implicated in anastomotic recurrence in Crohn's disease following bowel resection^[26]. Relative obstruction with stasis and bacterial overgrowth is also recognized contributory factors to recurrent Crohn's disease^[14,83]. Therefore, the stapled functional end-to-end technique may reduce the risk of obstruction at the anastomosis because of a wider anastomotic lumen. One retrospective study^[84] examined 27 patients who underwent conventional sutured end-to-end anastomosis and 42 who underwent stapled functional end-to-end anastomosis following bowel resection for Crohn's disease. In the stapled group, only one patient (2%) required re-operation for recurrence. By contrast, 14 patients (43%) in the sutured group required 15 further resections for recurrence. The median follow-up duration was 23 mo for the stapled group compared with 52 mo in the sutured group. Our retrospective study^[85] studied 45 patients who underwent stapled functional end-to-end anastomosis and 78 underwent conventional sutured end-to-end anastomosis. In the stapled group only one patient required re-operation for ileocolonic anastomotic recurrence compared with 26 in the sutured group. The cumulative 1-, 2- and 5-year ileocolonic recurrence rates requiring surgery in the stapled group were 0%, 0% and 3%, which were significantly lower than 5%, 11% and 24% in the sutured group ($P = 0.007$ by log-rank test). The median duration of follow-up was 34 mo in the stapled group compared with 92 mo in the sutured group ($P < 0.01$). A case-control comparative analysis of patients with Crohn's disease from two major inflammatory bowel disease centers (Mayo clinic and Birmingham) treated with wide-lumen stapled anastomosis ($n = 69$) and a matched (age and gender) group treated with conventional sutured end-to-end anastomosis

($n = 69$) was conducted^[86]. A total of 55 patients developed recurrent symptoms, 39 (57%) in the conventional sutured end-to-end anastomosis and 16 (24%) in the wide-lumen stapled anastomosis group. The median follow-up was 70 mo for the sutured group and 46 mo for the stapled group. After conventional sutured end-to-end anastomosis 18 re-operations were required and after wide-lumen stapled anastomosis three re-operations were necessary. The cumulative re-operation rate for anastomotic recurrence was significantly lower ($P = 0.017$ by log-rank test) for the wide-lumen stapled anastomosis group. One prospective study comparing the long-term results of stapled and hand-sewn anastomoses reported a lower recurrence rate after the stapled anastomosis^[87]. Thus, the stapled functional end-to-end anastomosis was associated with a lower incidence of post-operative anastomotic recurrence than the conventional sutured end-to-end anastomosis in the surgical management of Crohn's disease. Caprilli *et al.*^[26], reporting on prognostic factors for the recurrence of Crohn's disease in a multicenter study, found a trend towards a higher rate of endoscopic recurrence after end-to-end anastomosis compared to side-to-side or end-to-side anastomosis. Recent retrospective study^[88] compared the post-operative recurrence rate after a hand-sewn end-to-side or side-to-side isoperistaltic anastomosis ($n = 30$) and stapled functional end-to-end anastomosis ($n = 76$) and found that there were 5 recurrences (16.7%) in the hand-sewn group and 2 recurrences (2.6%) in the stapled group. The other study^[74] compared the recurrence rate after stapled side-to-side ileocolonic anastomosis ($n = 12$) to those after stapled end-to-side ($n = 36$) or hand-sewn side-to-side anastomosis ($n = 36$). The stapled side-to-side anastomosis group obtained a better symptom-free survival than the stapled end-to-side group ($P = 0.04$). In the stapled and hand-sewn side-to-side groups the re-operation rates were significantly lower than in the stapled end-to-side group ($P = 0.01$ and $P = 0.05$, respectively). A longer follow-up showed a significantly lower incidence of re-operation for recurrence in the stapled and hand-sewn side-to-side anastomosis compared to the stapled end-to-side anastomosis group. Thus, a wider anastomosis may delay the onset of the symptomatic recurrence and be associated with a lower early recurrence rate after resection for Crohn's disease. Furthermore, the incidence of complications after the stapled anastomosis is low and the procedures are quick and easy^[84-88]. Therefore, the stapled functional end-to-end anastomosis may be the anastomotic configuration of choice following resection for Crohn's disease. However, most of the previous studies were non-randomized trials. The follow-up duration was inevitably shorter and the number of patients was smaller in the stapled anastomosis group because the stapled technique has been introduced recently. Multicenter prospective randomized study with a larger number of patients and a longer follow-up duration would be needed to find an absolute evidence of difference between the stapled functional end-to-end anastomosis and the other types of anastomosis.

Presence of granuloma in the specimen

There are contradictory reports in the literature regarding the impact of identifiable granuloma in the resection specimen on the recurrence^[5,16,17,30,60,89-91]. Anseline *et al.*^[30], found that

granuloma in the specimen was significantly associated with the recurrence. Other authors^[89,90] reported a decreased rate of the recurrence in patients who had granulomas in their specimen. Some groups have shown that microscopic disease in the specimen increases the rate of anastomotic recurrence of ileocolonic Crohn's disease^[5,16,17,91].

Disease involvement at the line of resection

Several reports have reported that the wide resection of normal bowel uninvolved microscopically (radical resection) was associated with a lower recurrence rate than non-radical resection^[6,18,92,93]. However, many studies have shown no difference in the recurrence rates between patients with radical resection and non-radical resection^[17,21,30,60,82,94-96]. Fazio *et al.*^[95], carried out a randomized controlled trial to investigate the impact of resection margins on the recurrence of Crohn's disease in the small bowel. Patients who underwent ileocolonic resection for Crohn's disease ($n = 152$) were randomly assigned to two groups in which the proximal line of resection was 2 cm (limited resection) or 12 cm (extended resection) from the macroscopically involved area. Patients also were classified by whether the margin of resection was microscopically normal (category 1), contained non-specific changes (category 2), were suggestive but not diagnostic for Crohn's disease (category 3) or were diagnostic for Crohn's disease (category 4). The median follow-up time was 55.7 mo. Disease recurred in 29 patients: 25% of patients in the limited resection group and 18% of patients in the extended resection group. In 90 patients in category 1 with normal tissue, the recurrence occurred in 16, whereas in the 41 patients with some degree of microscopic involvement, the recurrence occurred in 13. The recurrence rates were 36% in category 2, 39% in category 3 and 21% in category 4. No group differences were statistically significant. The recurrence of Crohn's disease is unaffected by the width of the margin of resection from macroscopically involved bowel. Thus, the recurrence rates also do not increase when microscopic Crohn's disease is present at the resection margins. Therefore, extensive resection margins are unnecessary.

As the recurrence was independent of microscopic involvement of the resection margins in many studies^[17,21,30,60,82,94-96], there has been an increasing tendency toward minimal surgery in the treatment of Crohn's disease. Strictureplasty conserves bowel and minimizes the risk of developing the short bowel syndrome. Nowadays, strictureplasty has become an established surgical option in the management of obstructive Crohn's disease. It is particularly suitable for patients at a risk of short bowel syndrome^[97-104]. After strictureplasty the segment of inflamed bowel is left *in situ*, because the sutures are placed through the diseased bowel. However, the most recurrences after strictureplasty occur at non-strictureplasty sites and the recurrence rate at the strictureplasty sites has been reported to be only 2.8-3.7%^[98,100].

Blood transfusions

The immunosuppressive effect of blood transfusions may modify the progression of Crohn's disease. The effect of peri-operative blood transfusions on the recurrence of Crohn's disease was investigated in several studies^[105-112]. Williams and Hughes^[105] examined 60 patients with Crohn's

disease who underwent small bowel resection. Twenty-eight patients received blood transfusions. The patients who received peri-operative blood transfusions had a significantly lower recurrence rate. Five years after the bowel resection, the cumulative recurrence rate in transfused patients was 19% compared with 59% in controls. Peters *et al.*^[106], studied 79 patients with Crohn's disease who underwent intestinal resection. In 45 patients who received multiple red blood cell transfusions, the recurrence developed in 22% by 36 mo and the median time to the recurrence was 35 mo. In 34 patients who did not receive multiple transfusions, the recurrence was found in 44% by 36 mo and the median time to the recurrence was 20 mo ($P < 0.04$). The recurrence in patients with disease limited to the small bowel or to the colon was not significantly affected by the transfusion status. However, the recurrence developed in only 10% of multiply transfused patients with ileocolonic disease by 36 mo, whereas the recurrence developed in 45% of the patients who were not multiply transfused ($P = 0.057$). Gooszen and Silvis^[107] studied 148 patients with Crohn's disease, 62 males and 86 females (49 non-parous and 37 parous females). Eighty-seven patients received peri-operative blood transfusions. Overall, blood transfusions showed no effect on the recurrence. Peri-operative transfusions seemed to protect against recurrent disease after colonic resection. Transfusions had a beneficial effect in parous females ($P = 0.068$) and after correction for the type of operation this beneficial effect was significant ($P = 0.026$). After peri-operative blood transfusions parous females had a similar prognosis regarding the recurrent Crohn's disease to that of non-parous females and males. In contrast, other studies^[108-111] failed to find any significant effect of peri-operative blood transfusions on the post-operative recurrence of Crohn's disease. A recent pooled analysis studied 622 patients with a primary and complete resection of macroscopic disease^[112]. Three hundred thirty-one patients (53%) received blood in the peri-operative period and the mean follow-up duration was 72.8 mo. For the overall sample, the 5-year recurrence rates were 26.9% for the transfused group and 25.2% for the non-transfused ($P = 0.456$). When the data were stratified by age, gender, disease location and length of resection, no difference in the 5-year recurrence rates between transfused and non-transfused patients could be detected. This pooled analysis found no protective effect of blood transfusions on the post-operative recurrence of Crohn's disease.

Post-operative complications

Crohn's disease is frequently associated with possible risk factors for post-operative complications; intestinal obstruction, pre-existing septic complications, impaired nutritional status, chronic corticosteroid medication and the need for multiple anastomoses^[9,113]. There have been only a few reports about the relationship between the postoperative complications and recurrence rate^[25,28,74]. Poggioli *et al.*^[28], found no relationship, but Holzheimer *et al.*^[25] and Scarpa *et al.*^[74] reported that the development of post-operative complications was associated with a high recurrence rate.

DISCUSSION

Smoking significantly increased the risk of recurrence after

surgery for Crohn's disease, especially in women. The effect of smoking was dose-dependent. Giving up smoking was associated with a lower probability of recurrence compared with smokers. A short disease duration before surgery seems, albeit to a very limited extent, to be associated with a higher recurrence rate, though the definition of short duration is different depending on the study. A number of randomized controlled trials offer encouraging evidence of the efficacy of 5-ASA in reducing post-operative recurrence. Recent studies have reported that immunosuppressive drugs were useful in the prevention of post-operative recurrence. However, further clinical trials would be necessary to evaluate the efficacy of immunosuppressants. Several authors found that perforating disease was associated with a higher recurrence rate compared with non-perforating disease, though evidence for differing the recurrence rates in perforating and non-perforating diseases is inconclusive. A number of retrospective studies found that a stapled functional end-to-end anastomosis was associated with a lower recurrence rate compared with other anastomotic techniques. However, prospective randomized trials would be necessary to find an absolute evidence of difference between the stapled functional end-to-end anastomosis and the other types of anastomosis. The following factors were not predictive of post-operative recurrence: age at onset of disease, sex, family history of Crohn's disease, anatomical site of disease, length of resected bowel, presence of granuloma in the specimen, peri-operative blood transfusions and post-operative complications.

REFERENCES

- 1 **Olaison G**, Sjodahl R, Tagesson C. Glucocorticoid treatment in ileal Crohn's disease: relief of symptoms but not of endoscopically viewed inflammation. *Gut* 1990; **31**: 325-328
- 2 **Hellberg R**, Hultén L, Rosengren C, Ahren C. The recurrence rate after primary excisional surgery for Crohn's disease. *Acta Chir Scand* 1980; **146**: 435-443
- 3 **Higgins CS**, Allan RN. Crohn's disease of the distal ileum. *Gut* 1980; **21**: 933-940
- 4 **Lock MR**, Farmer RG, Fazio VW, Jagelman DG, Lavery IC, Weakley FL. Recurrence and reoperation for Crohn's disease: the role of disease location in prognosis. *N Engl J Med* 1981; **304**: 1586-1588
- 5 **Trnka YM**, Glotzer DJ, Kasdon EJ, Goldman H, Steer ML, Goldman LD. The long-term outcome of restorative operation in Crohn's disease. Influence of location, prognostic factors and surgical guidelines. *Ann Surg* 1982; **196**: 345-355
- 6 **Lindhagen T**, Ekelund G, Leandoer L, Hildell J, Lindstrom C, Wenckert A. Recurrence rate after surgical treatment of Crohn's disease. *Scand J Gastroenterol* 1983; **18**: 1037-1044
- 7 **Heen LO**, Nygaard K, Bergan A. Crohn's disease. Results of excisional surgery in 133 patients. *Scand J Gastroenterol* 1984; **19**: 747-754
- 8 **Whelan G**, Farmer RG, Fazio VW, Goormastic M. Recurrence after surgery in Crohn's disease. Relationship to location of disease (clinical pattern) and surgical indication. *Gastroenterology* 1985; **88**: 1826-1833
- 9 **Hultén L**. Surgical treatment of Crohn's disease of the small bowel or ileocecum. *World J Surg* 1988; **12**: 180-185
- 10 **Williams JG**, Wong WD, Rothenberger DA, Goldberg SM. Recurrence of Crohn's disease after resection. *Br J Surg* 1991; **78**: 10-19
- 11 **Olaison G**, Smedh K, Sjodahl R. Recurrence of Crohn's disease in the neo-terminal ileum and colonic factors. *Lancet* 1991; **338**: 1401
- 12 **Pallone F**, Boirivant M, Stazi MA, Cosentino R, Prantera C,

- Torsoli A. Analysis of clinical course of postoperative recurrence in Crohn's disease of the distal ileum. *Dig Dis Sci* 1992; **37**: 215-219
- 13 Nordgren SR, Fash SB, Oresland TO, Hulten LA. Long-term follow-up in Crohn's disease. Mortality, Morbidity and functional status. *Scand J Gastroenterol* 1994; **29**: 1122-1128
 - 14 Borley NR, Motensen NJ, Jewell DP. Preventing postoperative recurrence of Crohn's disease. *Br J Surg* 1997; **84**: 1493-1502
 - 15 Sachar DB, Wolfson DM, Greenstein AJ, Goldberg J, Styczynski R, Janowitz HD. Risk factors for postoperative recurrence of Crohn's disease. *Gastroenterology* 1983; **85**: 917-921
 - 16 Ellis L, Calhoun P, Kaiser DL, Rudolf LE, Hanks JB. Postoperative recurrence in Crohn's disease: the effect of the initial length of bowel resection and operative procedure. *Ann Surg* 1984; **199**: 340-347
 - 17 Chardavoigne R, Flint GW, Pollack S, Wise L. Factors affecting recurrence following resection for Crohn's disease. *Dis Colon Rectum* 1986; **29**: 495-502
 - 18 Softley A, Myren J, Clamp SE, Bouchier IA, Watkinson G, de Dombal FT. Factors affecting recurrence after surgery for Crohn's disease. *Scand J Gastroenterol Suppl* 1988; **144**: 31-34
 - 19 Shivananda S, Hordijk ML, Pena AS, Mayberry JF. Crohn's disease: risk of recurrence and reoperation in a defined population. *Gut* 1989; **30**: 990-995
 - 20 Rutgeerts P, Geboes K, Vantrappen G, Beyls J, Kerremans R, Hiele M. Predictability of the postoperative course of Crohn's disease. *Gastroenterology* 1990; **99**: 956-963
 - 21 Wettergren A, Christiansen J. Risk of recurrence after resection for ileocolonic Crohn's disease. *Scand J Gastroenterol* 1991; **26**: 1319-1322
 - 22 Michelassi F, Balestracci T, Chappell R, Block GE. Primary and recurrent Crohn's disease. Experience with 1379 patients. *Ann Surg* 1991; **214**: 230-238
 - 23 Griffiths AM, Wesson DE, Shandling B, Sherman PM. Factors influencing postoperative recurrence of Crohn's disease in childhood. *Gut* 1991; **32**: 491-495
 - 24 Cottone M, Rosselli M, Orlando A, Oliva L, Puleo A, Cappello M, Traina M, Tonelli F, Pagliaro L. Smoking habits and recurrence in Crohn's disease. *Gastroenterology* 1994; **106**: 643-648
 - 25 Holzheimer RG, Molloy RG, Wittmann DH. Postoperative complications predict recurrence of Crohn's disease. *Eur J Surg* 1995; **161**: 129-135
 - 26 Caprilli R, Corrao G, Taddei G, Tonelli F, Torchio P, Visscido A. Gruppo Italiano per lo Studio del Colon e del Retto (GISC). Prognostic factors for postoperative recurrence of Crohn's disease. *Dis Colon Rectum* 1996; **39**: 335-341
 - 27 Raab Y, Bergstrom R, Ejerblad S, Graf W, Pahlman L. Factors influencing recurrence in Crohn's disease. An analysis of a consecutive series of 353 patients treated with primary surgery. *Dis Colon Rectum* 1996; **39**: 918-925
 - 28 Poggioli G, Laureti S, Sella S, Brignola C, Grazi GL, Stocchi L, Marra C, Magalotti C, Grigioni WF, Cavallari A. Factors affecting recurrence in Crohn's disease. Results of a prospective audit. *Int J Colorectal Dis* 1996; **11**: 294-298
 - 29 Post S, Herfarth C, Bohm E, Timmermanns G, Schumacher H, Schurmann G, Golling M. The impact of disease pattern, surgical management, and individual surgeons on the risk for relaparotomy for recurrent Crohn's disease. *Ann Surg* 1996; **223**: 253-260
 - 30 Anseline PF, Wlodarczyk J, Murugasu R. Presence of granulomas is associated with recurrence after surgery for Crohn's disease: experience of a surgical unit. *Br J Surg* 1997; **84**: 78-82
 - 31 Wolff BG. Factors determining recurrence following surgery for Crohn's disease. *World J Surg* 1998; **22**: 364-369
 - 32 Kyle J. Prognosis after ileal resection for Crohn's disease. *Br J Surg* 1971; **58**: 735-737
 - 33 de Dombal FT, Burton I, Goligher JC. Recurrence of Crohn's disease after primary excisional surgery. *Gut* 1971; **12**: 519-527
 - 34 Cooke WT, Mallas E, Prior P, Allan RN. Crohn's disease: course, treatment and long term prognosis. *Q J Med* 1980; **49**: 363-384
 - 35 Ryan WR, Allan RN, Yamamoto T, Keighley MR. Crohn's disease patients who quit smoking have a reduced risk of reoperation for recurrence. *Am J Surg* 2004; **187**: 219-225
 - 36 Scarpa M, Angriman I, Barollo M, Polese L, Ruffolo C, Bertin M, Pagano D, D'Amico DF. Risk factors for recurrence of stenosis in Crohn's disease. *Acta Biomed Ateneo Parmense* 2003; **74**(Suppl 2): 80-83
 - 37 Atwell JD, Duthie HL, Goligher JC. The outcome of Crohn's disease. *Br J Surg* 1965; **52**: 966-972
 - 38 Lennard Jones JE, Stalder GA. Prognosis after resection of chronic regional ileitis. *Gut* 1971; **8**: 332-336
 - 39 Bernell O, Lapidus A, Hellers G. Risk factors for surgery and postoperative recurrence in Crohn's disease. *Ann Surg* 2000; **231**: 38-45
 - 40 Tobin MV, Logan RF, Langman MJ, McConnell RB, Gilmore IT. Cigarette smoking and inflammatory bowel disease. *Gastroenterology* 1987; **93**: 316-321
 - 41 Cosnes J, Carbonnel F, Beaugerie L, Le Quintrec Y, Gendre JP. Effects of cigarette smoking on the long-term course of Crohn's disease. *Gastroenterology* 1996; **110**: 424-431
 - 42 Lindberg E, Tysk C, Andersson K, Jarnerot G. Smoking and inflammatory bowel disease. A case control study. *Gut* 1988; **29**: 352-357
 - 43 Person PG, Ahlbom A, Hellers G. Inflammatory bowel disease and tobacco smoke-a case control study. *Gut* 1990; **31**: 1377-1381
 - 44 Cosnes J, Nion-Larmurier I, Afchain P, Beaugerie L, Gendre JP. Gender differences in the response of colitis to smoking. *Clin Gastroenterol Hepatol* 2004; **2**: 41-48
 - 45 Loftus EV Jr. Clinical epidemiology of inflammatory bowel disease: Incidence, prevalence, and environmental influences. *Gastroenterology* 2004; **126**: 1504-1517
 - 46 Sutherland LR, Ramcharan S, Bryant H, Fick G. Effects of cigarette smoking on recurrence of Crohn's disease. *Gastroenterology* 1990; **98**: 1123-1128
 - 47 Lindberg E, Jarnerot G, Huitfeldt B. Smoking in Crohn's disease: effect on location and clinical course. *Gut* 1992; **33**: 779-782
 - 48 Breuer-Katschinski BD, Hollander N, Goebell H. Effect of cigarette smoking on the course of Crohn's disease. *Eur J Gastroenterol Hepatol* 1996; **8**: 225-228
 - 49 Timmer A, Sutherland LR, Martin F. The Canadian Mesalamine for Remission of Crohn's Disease Study Group. Oral contraceptive use and smoking are risk factors for relapse in Crohn's disease. *Gastroenterology* 1998; **114**: 1143-1150
 - 50 Yamamoto T, Keighley MR. The association of cigarette smoking with a high risk of recurrence after ileocolonic resection for ileocecal Crohn's disease. *Surg Today* 1999; **29**: 579-580
 - 51 Yamamoto T, Allan RN, Keighley MR. Smoking is a predictive factor for outcome after colectomy and ileorectal anastomosis in patients with Crohn's colitis. *Br J Surg* 1999; **86**: 1069-1070
 - 52 Girodengo L, Barthet M, Desjeux A, Berdah S, Berthezene P, Bellon P, Salducci J, Grimaud JC. Risk factors for Crohn's disease relapse after treatment of intestinal stenosis. *Ann Chir* 2001; **126**: 296-301
 - 53 Martin G, Heyen F, Dube S. Factors of recurrence in Crohn disease. *Ann Chir* 1994; **48**: 685-690
 - 54 Medina C, Vergara M, Casellas F, Lara F, Naval J, Malagelada JR. Influence of the smoking habit in the surgery of inflammatory bowel disease. *Rev Esp Enferm Dig* 1998; **90**: 771-778
 - 55 Ryan WR, Ley C, Allan RN, Keighley MR. Patients with Crohn's disease are unaware of the risks that smoking has on their disease. *J Gastrointest Surg* 2003; **7**: 706-711
 - 56 Shields PL, Low-Beer TS. Patients' awareness of adverse relation between Crohn's disease and their smoking: questionnaire survey. *BMJ* 1996; **313**: 265-266
 - 57 Yamamoto T, Keighley MR. Smoking and disease recurrence after operation for Crohn's disease. *Br J Surg* 2000; **87**: 398-404
 - 58 Cosnes J. Tobacco and IBD: relevance in the understanding

- of disease mechanisms and clinical practice. *Best Pract Res Clin Gastroenterol* 2004; **18**: 481-496
- 59 **Hauser W**, Grandt D. Tobacco associated gastrointestinal disorders: smoking cessation therapy-a task for gastroenterologists. *Z Gastroenterol* 2002; **40**: 815-821
- 60 **Yamamoto T**, Bain IM, Allan RN, Keighley MR. Risk factors for anastomotic recurrence after ileocolonic resection for Crohn's disease: the importance of smoking. *Gastroenterology* 1998; **114**(Suppl): A1118-1119
- 61 **Summers RW**, Switz DM, Sessions JT Jr, Bechtel JM, Best WR, Kern F Jr, Singleton JW. National Co-operative Crohn's Disease Study: results of drug treatment. *Gastroenterology* 1979; **77**: 847-869
- 62 **Malchow H**, Ewe K, Brandes JW, Goebell H, Ehms H, Sommer H, Jesdinsky H. European Co-operative Crohn's Disease Study (ECCDS): results of drug treatment. *Gastroenterology* 1984; **86**: 249-266
- 63 **Brignola C**, Campieri M, Farruggia P, Tragnone A, Pasquali S, Iannone P, Lanfranchi GA, Barbara L. The possible utility of steroids in the prevention of relapses of Crohn's disease in remission. A preliminary study. *J Clin Gastroenterol* 1988; **10**: 631-634
- 64 **Cottone M**, Orlando A, Viscido A, Calabrese E, Camma C, Casa A. Review article: prevention of postsurgical relapse and recurrence in Crohn's disease. *Aliment Pharmacol Ther* 2003; **17**(Suppl 2): 38-42
- 65 **Rutgeerts P**. Strategies in the prevention of post-operative recurrence in Crohn's disease. *Best Pract Res Clin Gastroenterol* 2003; **17**: 63-73
- 66 **Stein RB**, Hanauer SB. Medical management of Crohn's disease. *Drugs Today* 1998; **34**: 541-548
- 67 **Caprilli R**, Andreoli A, Capurso L, Corrao G, D'Albasio G, Gioieni A, Assuero Lanfranchi G, Paladini I, Pallone F, Ponti V, Rigo GP, Rossini FP, Sturniolo GC, Tonelli F, Ronti V. Gruppo Italiano Per Lo Studio Del Colon E Del Retto. Oral mesalazine (5-aminosalicylic acid; Asacol) for the prevention of post-operative recurrence of Crohn's disease. *Aliment Pharmacol Ther* 1994; **8**: 35-43
- 68 **Brignola C**, Cottone M, Pera A, Ardizzone S, Scribano ML, De Franchis R, D'Arienzo A, D'Albasio G, Pennestri D. Mesalamine in the prevention of endoscopic recurrence after intestinal resection for Crohn's disease. Italian Cooperative Study Group. *Gastroenterology* 1995; **108**: 345-349
- 69 **McLeod RS**, Wolff BG, Steinhart AH, Carryer PW, O'Rourke K, Andrews DF, Blair JE, Cangemi JR, Cohen Z, Cullen JB, Chaytor RG, Greenberg GR, Jaffer NM, Jeejeebhoy KN, MacCarty RL, Ready RL, Weiland LH. Prophylactic mesalamine treatment decreases postoperative recurrence of Crohn's disease. *Gastroenterology* 1995; **109**: 404-413
- 70 **Cammà C**, Giunta M, Rosselli M, Cottone M. Mesalamine in the maintenance treatment of Crohn's disease: a meta-analysis adjusted for confounding variables. *Gastroenterology* 1997; **113**: 1465-1473
- 71 **Markowitz JF**. Therapeutic efficacy and safety of 6-mercaptopurine and azathioprine in patients with Crohn's disease. *Rev Gastroenterol Disord* 2003; **3**(Suppl 1): S23-29
- 72 **Ardizzone S**, Maconi G, Sampietro GM, Russo A, Radice E, Colombo E, Imbesi V, Molteni M, Danelli PG, Taschieri AM, Bianchi Porro G. Azathioprine and mesalamine for prevention of relapse after conservative surgery for Crohn's disease. *Gastroenterology* 2004; **127**: 730-740
- 73 **Hanauer SB**, Korelitz BI, Rutgeerts P, Peppercorn MA, Thisted RA, Cohen RD, Present DH. Postoperative maintenance of Crohn's disease remission with 6-mercaptopurine, mesalamine, or placebo: a 2-year trial. *Gastroenterology* 2004; **127**: 723-729
- 74 **Scarpa M**, Angriman I, Barollo M, Polese L, Ruffolo C, Bertin M, D'Amico DF. Role of stapled and hand-sewn anastomoses in recurrence of Crohn's disease. *Hepatogastroenterology* 2004; **51**: 1053-1057
- 75 **Greenstein AJ**, Lachman P, Sachar DB, Springhorn J, Heimann T, Janowitz HD, Aufses AH Jr. Perforating and non-perforating indications for repeated operations in Crohn's disease: evidence for two clinical forms. *Gut* 1988; **29**: 588-589
- 76 **Aeberhard P**, Berchtold W, Riedtmann HJ, Stadelmann G. Surgical recurrence of perforating and nonperforating Crohn's disease: a study of 101 surgically treated patients. *Dis Colon Rectum* 1996; **39**: 80-87
- 77 **Lautenbach E**, Berlin JA, Lichtenstein GR. Risk factors for early postoperative recurrence of Crohn's disease. *Gastroenterology* 1998; **115**: 259-267
- 78 **Hofer B**, Bottger T, Hernandez-Richter T, Seifert JK, Junginger T. The impact of clinical types of disease manifestation on the risk of early postoperative recurrence in Crohn's disease. *Hepatogastroenterology* 2001; **48**: 152-155
- 79 **Yamamoto T**, Allan RN, Keighley MR. Perforating ileocecal Crohn's disease does not carry a high risk of recurrence but usually re-presents as perforating disease. *Dis Colon Rectum* 1999; **42**: 519-524
- 80 **McDonald PJ**, Fazio VW, Farmer RG, Jagelman DG, Lavery IC, Ruderman WB, Easley KA, Harper PH. Perforating and nonperforating Crohn's disease. An unpredictable guide to recurrence after surgery. *Dis Colon Rectum* 1989; **32**: 117-120
- 81 **Schofield PF**. The natural history and treatment of Crohn's disease. *Ann R Coll Surg Engl* 1965; **36**: 258-279
- 82 **Hamilton SR**, Boitnott JK, Morson BC. Relationships of disease extent and margin lengths to recurrence of Crohn's disease after ileocolonic anastomosis. *Gastroenterology* 1981; **80**: 1166
- 83 **Alexander-Williams J**. Small bowel Crohn's disease. In: Inflammatory Bowel Disease. 2nd ed. Allan RN, Keighley MR, Alexander-Williams J, Hawkins C, eds. *Edinburgh: Churchill Livingstone* 1990: 459-472
- 84 **Hashemi M**, Novell JR, Lewis AA. Side-to-side stapled anastomosis may delay recurrence in Crohn's disease. *Dis Colon Rectum* 1998; **41**: 1293-1296
- 85 **Yamamoto T**, Bain IM, Mylonakis E, Allan RN, Keighley MR. Stapled functional end-to-end anastomosis versus sutured end-to-end anastomosis after ileocolonic resection in Crohn disease. *Scand J Gastroenterol* 1999; **34**: 708-713
- 86 **Munoz-Juarez M**, Yamamoto T, Wolff BG, Keighley MR. Wide-lumen stapled anastomosis vs. conventional end-to-end anastomosis in the treatment of Crohn's disease. *Dis Colon Rectum* 2001; **44**: 20-25
- 87 **Ikeuchi H**, Kusunoki M, Yamamura T. Long-term results of stapled and hand-sewn anastomoses in patients with Crohn's disease. *Dig Surg* 2000; **17**: 493-496
- 88 **Tersigni R**, Alessandrini L, Barreca M, Piovanello P, Prantera C. Does stapled functional end-to-end anastomosis affect recurrence of Crohn's disease after ileocolonic resection? *Hepatogastroenterology* 2003; **50**: 1422-1425
- 89 **Glass RE**, Baker WN. Role of the granuloma in recurrent Crohn's disease. *Gut* 1976; **17**: 233-242
- 90 **Chambers TJ**, Morson BC. The granuloma in Crohn's disease. *Gut* 1979; **20**: 269-274
- 91 **Van Patter WN**, Barga JA, Dockerty MB, Feldman WH, Mayo CW, Waugh JM. Regional enteritis. *Gastroenterology* 1954; **26**: 347-450
- 92 **Karesen R**, Serch-Hanssen A, Thoresen BD, Hertzberg J. Crohn's disease: long-term results of surgical treatment. *Scand J Gastroenterol* 1981; **16**: 57-64
- 93 **Wolff BG**, Beart RW Jr, Frydenberg HB, Weiland LH, Agrez MV, Ilstrup DM. The importance of disease-free margins in resections for Crohn's disease. *Dis Colon Rectum* 1983; **26**: 239-243
- 94 **Kotanagi H**, Kramer K, Fazio VW, Petras R. Do microscopic abnormalities at resection margins correlate with increased anastomotic recurrence in Crohn's disease? retrospective analysis of 100 cases. *Dis Colon Rectum* 1991; **34**: 909-916
- 95 **Fazio VW**, Marchetti F, Church M, Goldblum JR, Lavery C, Hull TL, Milsom JW, Strong SA, Oakley JR, Secic M. Effect of resection margins on the recurrence of Crohn's disease in the small bowel: a randomized controlled trial. *Ann Surg* 1996; **224**: 563-571
- 96 **Botti F**, Carrara A, Antonelli B, Quadri F, Maino M, Cesana

- B, Contessini-Avesani E. The minimal bowel resection in Crohn's disease: analysis of prognostic factors on the surgical recurrence. *Ann Ital Chir* 2003; **74**: 627-633
- 97 **Dehn TC**, Kettlewell MG, Mortensen NJ, Lee EC, Jewell DP. Ten-year experience of stricturoplasty for obstructive Crohn's disease. *Br J Surg* 1989; **76**: 339-341
- 98 **Fazio VW**, Tjandra JJ, Lavery IC, Church JM, Milsom JW, Oakley JR. Long-term follow-up of stricturoplasty in Crohn's disease. *Dis Colon Rectum* 1993; **36**: 355-361
- 99 **Spencer MP**, Nelson H, Wolff BG, Dozois RR. Stricturoplasty for obstructive Crohn's disease: the Mayo experience. *Mayo Clin Proc* 1994; **69**: 33-36
- 100 **Stebbing JF**, Jewell DP, Kettlewell MG, Mortensen NJ. Long-term results of recurrence and reoperation after stricturoplasty for obstructing Crohn's disease. *Br J Surg* 1995; **82**: 1471-1474
- 101 **Hurst RD**, Michelassi F. Stricturoplasty for Crohn's disease: techniques and long-term results. *World J Surg* 1998; **22**: 359-363
- 102 **Yamamoto T**, Bain IM, Allan RN, Keighley MR. An audit of stricturoplasty for small-bowel Crohn's disease. *Dis Colon Rectum* 1999; **42**: 797-803
- 103 **Dietz DW**, Laureti S, Strong SA, Hull TL, Church J, Remzi FH, Lavery IC, Fazio VW. Safety and longterm efficacy of stricturoplasty in 314 patients with obstructing small bowel Crohn's disease. *J Am Coll Surg* 2001; **192**: 330-338
- 104 **Yamamoto T**, Allan RN, Keighley MR. Long-term outcome of surgical management for diffuse jejunoileal Crohn's disease. *Surgery* 2001; **129**: 96-102
- 105 **Williams JG**, Hughes LE. Effect of perioperative blood transfusion on recurrence of Crohn's disease. *Lancet* 1989; **2**: 131-133
- 106 **Peters WR**, Fry RD, Fleshman JW, Kodner IJ. Multiple blood transfusions reduce the recurrence rate of Crohn's disease. *Dis Colon Rectum* 1989; **32**: 749-753
- 107 **Gooszen HG**, Silvis R. Protective effect of blood transfusions on postoperative recurrence of Crohn's disease in parous women. *Neth J Med* 1994; **45**: 65-71
- 108 **Makowiec F**, Loble M, Jenss H, Starlinger M. Do perioperative blood transfusions affect the postoperative recurrence rate in Crohn disease? *Z Gastroenterol* 1992; **30**: 20-23
- 109 **Post S**, Kunhardt M, Sido B, Schurmann G, Herfarth C. Effect of blood transfusions on rate of recurrence of Crohn disease. *Chirurg* **63**: 35-38
- 110 **Scott AD**, Ritchie JK, Phillips RK. Blood transfusion and recurrent Crohn's disease. *Br J Surg* 1991; **78**: 455-458
- 111 **Steup WH**, Brand A, Weterman IT, Zwinderman KH, Lamers CB, Gooszen HG. The effect of perioperative blood transfusion on recurrence after primary operation for Crohn's disease. *Scand J Gastroenterol* 1991; **188**(Suppl): 81-86
- 112 **Hollaar GL**, Gooszen HG, Post S, Williams JG, Sutherland LR. Perioperative blood transfusion does not prevent recurrence in Crohn's disease. A pooled analysis. *J Clin Gastroenterol* 1995; **21**: 134-138
- 113 **Yamamoto T**, Allan RN, Keighley MR. Risk factors for intra-abdominal sepsis after surgery in Crohn's disease. *Dis Colon Rectum* 2000; **43**: 1141-1145

Science Editor Guo SY Language Editor Elsevier HK

Antitumor efficacy of lidamycin on hepatoma and active moiety of its molecule

Yun-Hong Huang, Bo-Yang Shang, Yong-Su Zhen

Yun-Hong Huang, Bo-Yang Shang, Yong-Su Zhen, Institute of Medicinal Biotechnology, Chinese Academy of Medical Sciences and Peking Union Medical College, Beijing 100050, China
Supported by the National High Technology Research and Development Program of China (863 program), No. 2002AA2Z3107
Correspondence to: Professor Yong-Su Zhen, Institute of Medicinal Biotechnology, Chinese Academy of Medical Sciences and Peking Union Medical College, 1 Tiantan Xili, Beijing 100050, China. zhenys@public.bta.net.cn
Telephone: +86-10-63010985 Fax: +86-10-63017302
Received: 2004-07-23 Accepted: 2004-08-30

Abstract

AIM: To study the *in vitro* and *in vivo* antitumor effect of lidamycin (LDM) on hepatoma and the active moiety of its molecule.

METHODS: MTT assay was used to determine the growth inhibition of human hepatoma BEL-7402 cells, SMMC-7721 cells and mouse hepatoma H22 cells. The *in vivo* therapeutic effects of lidamycin and mitomycin C were determined by transplantable hepatoma 22 (H22) in mice and human hepatoma BEL-7402 xenografts in athymic mice.

RESULTS: In terms of IC_{50} values, the cytotoxicity of LDM was 10 000-fold more potent than that of mitomycin C (MMC) and adriamycin (ADM) in human hepatoma BEL-7402 cells and SMMC-7721 cells. LDM molecule consists of two moieties, an apoprotein (LDP) and an enediyne chromophore (LDC). In terms of IC_{50} values, the potency of LDC was similar to LDM. However, LDP was 10^5 -fold less potent than LDM and LDC to hepatoma cells. For mouse hepatoma H22 cells, the IC_{50} value of LDM was 0.025 nmol/L. Given by single intravenous injection at doses of 0.1, 0.05 and 0.025 mg/kg, LDM markedly suppressed the growth of hepatoma 22 in mice by 84.7%, 71.6% and 61.8%, respectively. The therapeutic indexes (TI) of LDM and MMC were 15 and 2.5, respectively. By 2 *iv.* injections in two experiments, the growth inhibition rates by LDM at doses of 0.1, 0.05, 0.025, 0.00625 and 0.0125 mg/kg were 88.8-89.5%, 81.1-82.5%, 71.2-74.9%, 52.3-59.575%, and 33.3-48.3%, respectively. In comparison, MMC at doses of 5, 2.5, and 1.25 mg/kg inhibited tumor growth by 69.7-73.6%, 54.0-56.5%, and 31.5-52.2%, respectively. Moreover, in human hepatoma BEL-7402 xenografts, the growth inhibition rates by LDM at doses of 0.05 mg/kg $\times 2$ and 0.025 mg/kg $\times 2$ were 68.7% and 27.2%, respectively. However, MMC at the dose of 1.25 mg/kg $\times 2$ showed an inhibition rate of 34.5%. The

inhibition rate of tumor growth by LDM was higher than that by MMC at the tolerated dose.

CONCLUSION: Both LDM and its chromophore LDC display extremely potent cytotoxicity to hepatoma cells. LDM shows a remarkable therapeutic efficacy against murine and human hepatomas *in vivo*.

© 2005 The WJG Press and Elsevier Inc. All rights reserved.

Key words: Lidamycin; Hepatoma; Mitomycin

Huang YH, Shang BY, Zhen YS. Antitumor efficacy of lidamycin on hepatoma and active moiety of its molecule. *World J Gastroenterol* 2005; 11(26): 3980-3984

<http://www.wjgnet.com/1007-9327/11/3980.asp>

INTRODUCTION

Lidamycin (LDM, also called C-1027), a macromolecular antitumor antibiotic produced by *Streptomyces globisporus* C-1027, can markedly inhibit the growth of transplantable tumors in mice including leukemia L1210, P388, sarcoma 180 and melanoma Harding-Passey^[1-4]. LDM consists of an apoprotein (LDP) of 10.5 ku and an enediyne chromophore (LDC) of 843 ku. These two parts of the molecule, connecting each other through non-covalent binding, can be dissociated^[5]. LDM can induce DNA damages including double-strand breaks, single-strand breaks and formation of abasic sites which is proved to be the major mechanism of the cytotoxicity of LDM. It is also reported that LDC can interact in DNA minor grooves and cleave double-helical DNA with a remarkable sequence-selectivity. The double-strand cleavage sites occurring predominantly at CTTT/AAAAG, ATAAT/ATTAT, CTTTA/TAAAG, CTCTT/AAGAG, and especially GTTAT/ATAAC, consist of nucleotide sequences with a two-nucleotide 3'-stagger of the cleaved residues^[6].

Recently, LDM has entered phase I clinical trials. In this study, we report the growth inhibition of various carcinoma cell lines by LDM, and the therapeutic efficacy of LDM against hepatoma in mice and human hepatoma xenografts in athymic mice.

MATERIALS AND METHODS

Materials

Highly purified LDM and LDP were prepared in our institute. MTT was obtained from Sigma Chemical Co. (St.

Louis, MO, USA). Mitomycin C (MMC) was purchased from Kyowa Hakkō Kogyo Co. Ltd. Adriamycin (ADM) was purchased from Zhejiang Hisun Pharmaceutical Co. Ltd., China.

Cell culture

Human hepatoma BEL-7402 cells, SMMC-7721 cells and murine hepatoma 22 cells were cultured at 37 °C with 50 ml/L CO₂ in RPMI-1640 medium supplemented with 10% heat-inactivated fetal bovine serum, penicillin G (100 U/mL) and streptomycin (100 µg/mL). All cell lines were passaged every 3 d and maintained in exponential growth to approximately 80% confluence for experiments.

Dissociation of LDM molecule

After 10 mg LDM was mixed with 5 mL methanol for 5 min at 4 °C, the mixture was placed at -20 °C and tossed for one time. LDC in the supernatant of reaction mixture was obtained by centrifugation of 16 000 *g* for 20 min at 4 °C. In order to extract LDC entirely, the operation was repeated three times.

MTT assay

Cells were detached by trypsinization, seeded at 3 000 cells/well in a 96-well plate (Costar, Cambridge, MA) over night. Then different concentrations of LDM were added and incubated for an additional 48 h. The effect on cell growth was examined by MTT assay. Briefly, 20 µL of MTT solution (5 mg/mL) was added to each well and incubated at 37 °C for 4 h. The supernatant was removed, and the MTT formazan formed by metabolically viable cells was dissolved in 150 µL of DMSO, and then monitored with a microplate reader (Bio-Rad) at a wavelength of 560 nm. Survival ratio was calculated according to the following formula:

$$\text{Survival ratio} = (A_{\text{test}} - A_{\text{blank}}) / (A_{\text{control}} - A_{\text{blank}}) \times 100\%$$

Animals and in vivo studies

Female Kunming mice weighting 20 ± 2 g and BALB/c (nu/nu) athymic mice were obtained from the Institute of Experimental Animals, Chinese Academy of Medical Sciences (CAMS) and Peking Union Medical College (PUMC).

Therapeutic effects of LDM and MMC were assessed using murine hepatoma 22 models. Groups of 10 Kunming female mice were subcutaneously implanted with 1.5 × 10⁶ tumor cells. For experiment I, the drugs were administrated 24 h after tumor transplantation with single intravenous injection. For experiments I and II, the drugs were *iv* administrated 24 h and 7 d after tumor transplantation. PBS was used as control in each experiment. Animals were sacrificed on day 11 and tumor weights (*W*) were measured. Inhibition rate of tumor growth and therapeutic index were calculated respectively as follows:

$$\text{Inhibition (\%)} = ((W_{\text{control}} - W_{\text{treated}}) / W_{\text{control}}) \times 100$$

$$\text{Therapeutic index (TI)} = LD_{50} / ID_{50}$$

Therapeutic effect of LDM on human hepatoma BEL-7402 xenografts in athymic mice was assessed. Groups of six athymic female mice were subcutaneously implanted with hepatoma BEL-7402 tumor tissue fragments, 2 mm

in diameter, one for each mouse. LDM and MMC in PBS were administrated *iv* on d 3 and 10 after tumor implantation. PBS was used as control. Tumor volume (*V*) was measured twice a week using a caliper and calculated using the formula: $V \text{ (mm}^3\text{)} = 1/2ab^2$, where *a* and *b* represent the long diameter and perpendicular short diameter (mm) of the tumor, respectively.

Statistical analysis

Significant difference between two values was determined with Student's *t*-test. *P* < 0.05 was considered statistically significant.

RESULTS

Cytotoxicity of LDM, MMC and ADM to hepatoma cells

As shown in Figures 1A and B, LDM displayed extremely potent cytotoxicity to hepatoma BEL-7402 and SMMC-7721 cells. In comparison, the cytotoxicity of LDM was much more potent than that of MMC and ADM. The IC₅₀ value of LDM, MMC and ADM was 0.0030, 152, and 51.7 nmol/L for BEL-7402 cells respectively, and 0.064, 1136.6, and 378 nmol/L for SMMC-7721 cells respectively. In terms of IC₅₀ values, the cytotoxicity of LDM to hepatoma cells was 10 000-fold more potent than that of MMC and ADM (Table 1). In addition, the growth inhibitory IC₅₀ value of LDM for mouse hepatoma 22 was 0.025 nmol/L by MTT assay (curve not shown).

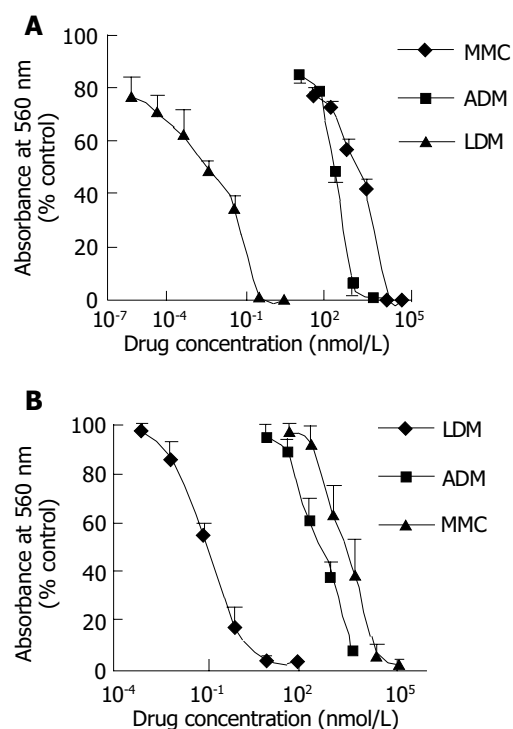


Figure 1 Growth inhibition of hepatoma BEL-7402 cells (A) and SMMC-7721 cells (B) by LDM, MMC and ADM.

Cytotoxicity of LDM and its constituents (LDC and LDP) to hepatoma cells

The inhibitory effects of LDM and its constituents, LDC

administration at the doses of 0.1, 0.05, 0.025, 0.0125, and 0.00625 mg/kg inhibited tumor growth by 84.7%, 71.6% and 61.8%, 60.6% and 40.8% ($P < 0.01$), respectively. Whereas, the inhibition rate of MMC at the doses of 5, 2.5, and 1.25 mg/kg was 58.9%, 49.9%, and 44.2%, respectively. The therapeutic index (TI) of LDM and MMC was 15 and 2.5, respectively. The therapeutic index of LDM was much higher than that of MMC. In experiments II and III, the drugs were administered on d 3 and 7. The growth inhibition rate by LDM was also higher than that of MMC. At doses used in these experiments, no body weight loss and other severe side-effects were observed, implying that LDM at tolerated doses displayed remarkable therapeutic efficacy.

Inhibition effect of LDM and MMC on the growth of human hepatoma BEL-7402 in athymic mice

For further *in vivo* evaluation, the athymic mice bearing BEL-7402 hepatoma xenografts were treated by injection of LDM and MMC into the tail vein for the first time 3 d after subcutaneous tumor inoculation. At that time the tumor diameters ranged from 2 to 4 mm. Then the drugs were administered for the second time on d 10. As shown in Figure 3, LDM significantly inhibited the growth of BEL-7402 tumors. According to the tumor volume on d 24 (Table 3), the inhibition rate by LDM at the doses of 0.05 and 0.025 mg/kg was 68.7% ($P < 0.05$) and 27.2%, respectively. MMC at the dose of 1.25 mg/kg inhibited tumor growth by 34.5%. LDM showed much higher efficacy against the growth of hepatoma xenografts.

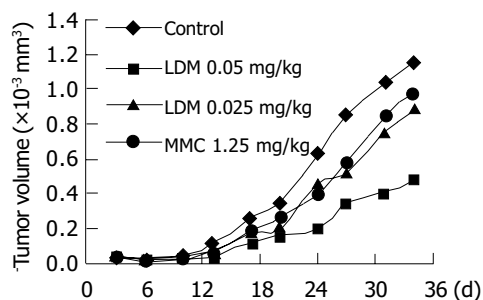


Figure 3 Inhibitory effect of LDM and MMC on the growth of human hepatoma BEL-7402 xenografts in athymic mice.

Table 3 Inhibition of the growth of human hepatoma BEL-7402 xenografts by LDM and MMC in athymic mice

Groups	Dose (mg/kg)	Number of mice (begin/end)	BWC (g)	Tumor volume (mm ³)	Inhibition rate (%)
Control		6/6	-0.1	624.7±360.1	-
LDM	0.05	6/6	+0.3	195.6±94.1	68.7 ^a
	0.025	6/6	-0.1	454.9±302.3	27.2
MMC	1.25	6/6	-1.5	409.1±225.9	34.5

^a $P < 0.05$ vs control.

DISCUSSION

Hepatoma progresses rapidly and has a poor prognosis.

Although the cause is not fully understood, there are several known risk factors, including over 40 years of age, male sex, cirrhosis, and exposure to hepatitis viruses (hepatitis B, C, D and G), *etc.* Although surgical operation could cure some patients with hepatoma, many patients with carcinomas are not good surgical candidates because of large tumor size, diminished liver function, or cirrhosis. Therefore, it is urgent to develop new drugs for the treatment of carcinoma.

It was reported that LDM strongly inhibits DNA synthesis in hepatoma BEL-7402 cells. In terms of effective concentration, LDM is over 1 000-fold potent than MMC or ADM. LDM also inhibits RNA synthesis in hepatoma BEL-7402 cells without affecting protein synthesis, blocks BEL-7402 cells at G₂/M phase^[7] and induces mitotic cell death of human hepatoma BEL-7402 cells^[8]. In the present study, LDM showed extreme cytotoxicity to hepatoma cells, including BEL-7402 SMMC-7721 and H22 cells *in vitro*. In our study, LDM displayed obvious tumor inhibition effect *in vivo*. The therapeutic efficacy of LDM was 6-fold higher than that of MMC. In addition, LDM showed potent anti-tumor effect on human hepatoma BEL-7402 xenografts in athymic mice in a dose dependent manner.

LDM has drawn much attention of researchers because of its potent anti-tumor effect, unique structure and action mechanism. Its apoprotein gene has been successfully cloned and nucleotide sequencing was determined^[9]. Recently, as an example of enediyne anti-tumor antibiotics, the biosynthetic genes of LDM have become a hot spot^[10]. In our studies on targeted anti-tumor drugs, LDM could act as a novel "effector moiety" to construct molecule-downsized and highly potent monoclonal antibody drugs. The downsized Fab'-LDM immunoconjugate is generated by chemical methods^[11], which shows potent anti-tumor effect both *in vitro* and *in vivo*. We have demonstrated in this study that LDC has a similar potency as intact LDM molecule. In contrast, its apoprotein LDP displays weak effect on tumor cells. Recently, an energized fusion protein, Fv-LDP-AE, has been prepared. The highly potent fusion protein is composed of Fv fragment of antibody, protein moiety of LDM molecule, and the active enediyne (AE) of lidamycin^[12]. The molecular weight of enediyne-energized fusion protein Fv-LDP-AE is only 38.7 ku, much smaller than the reported immunotoxin Fv-PE (67 ku). The method of preparing energized fusion protein Fv-LDP-AE may also provide a useful technical platform to construct scFv-based engineering and enediyne-energized fusion proteins specifically targeted to various cancers expressing different molecular markers.

In summary, both lidamycin and lidamycin chromophore have extremely potent cytotoxicity to liver cancer cells, and lidamycin shows remarkable therapeutic efficacy against murine transplantable hepatoma and human hepatoma xenografts.

REFERENCES

- 1 Hu J, Xue YC, Xie MY, Zhang R, Otani T, Minami Y, Yamada Y, Marunaka T. A new macromolecular antitumor antibiotics, C-1027 I. Discovery, Taxonomy of producing organism fermentation and biological activity. *J Antibiot* 1988; **41**:

- 1575-1579
- 2 **Otani T**, Minami Y, Marunaka T, Zhang R, Xie MY. A new macromolecular antitumor antibiotic, C-1027 II. Isolation and physico-chemical properties. *J Antibiot* 1988; **41**: 1580-1585
 - 3 **Zhen YS**, Ming XY, Yu B, Otani T, Saito H, Yamada Y. A new macromolecular antitumor antibiotic, C-1027. III. Antitumor activity. *J Antibiot* 1989; **42**: 1294-1298
 - 4 **Zhen YS**, Xue YC, Shao RG. Antitumor activity of the enediyne antibiotic C1027. *Zhongguo Kangshengsu Zazhi* 1994; **19**: 164-168
 - 5 **Shao RG**, Zhen YS. Relationship between the molecular composition of C-1027, a new macromolecular antibiotic with enediyne chromophore, and its antitumor activity. *Yaoxue Xuebao* 1995; **30**: 336-342
 - 6 **Xu YJ**, Zhen YS, Goldberg IH. C-1027 chromophore, a potent new enediyne antitumor antibiotic, induces sequence-specific double-strand DNA cleavage. *Biochemistry* 1994; **33**: 5947-5954
 - 7 **Xu YJ**, Li DD, Zhen YS. Mode of action of C-1027, a new macromolecular antitumor antibiotic with highly potent cytotoxicity, on human hepatoma BEL-7402 cells. *Cancer Chemother Pharmacol* 1990; **27**: 41-46
 - 8 **He QY**, Liang YY, Wang DS, Li DD. Characteristics of mototic cell death induced by enediyne antibiotic lidamycin in human epithelial tumor cells. *Inter J Oncol* 2002; **20**: 261-266
 - 9 **Sakata N**, Ikeno S, Hori M, Hamada M, Otani T. Cloning and nucleotide sequencing of the antitumor antibiotic C-1027 apoprotein gene. *Biosci Biotechnol Biochem* 1992; **56**: 1592-1595
 - 10 **Liu W**, Christenson SD, Standage S, Shen B. Biosynthesis of the enediyne antitumor antibiotic C-1027. *Science* 2002; **297**: 1170-1173
 - 11 **Liu XY**, Zhen YS. Antitumor effect of lidamycin-containing monoclonal antibody immunoconjugate with downsized-molecule. *Zhongguo Yixue Kexueyuan Xuebao* 2001; **23**: 563-567
 - 12 **Li L**, Huang YH, Miao QF, Shang BY, Liu XJ, Zhen YS. Fv-LDP-AE, an engineered and enediyne-energized fusion protein, shows highly potent antitumor efficacy and antiangiogenic activity. *Proc Am Assoc Cancer Res* 2004; **45**: 2884

Science Editor Wang XL and Guo SY Language Editor Elsevier HK

Human scFv antibody fragments specific for hepatocellular carcinoma selected from a phage display library

Bing Yu, Ming Ni, Wen-Han Li, Ping Lei, Wei Xing, Dai-Wen Xiao, Yu Huang, Zhen-Jie Tang, Hui-Fen Zhu, Guan-Xin Shen

Bing Yu, Wen-Han Li, Ping Lei, Wei Xing, Dai-Wen Xiao, Yu Huang, Zhen-Jie Tang, Hui-Fen Zhu, Guan-Xin Shen, Department of Immunology, Tongji Medical College, Huazhong University of Science and Technology, Wuhan 430030, Hubei Province, China
Ming Ni, Department of Infectious Diseases, Tongji Hospital, Tongji Medical College, Huazhong University of Science and Technology, Wuhan 430030, Hubei Province, China

Supported by the Major State Basic Research Development Program of China, 973 Program, No. 2002CB513100

Correspondence to: Guan-Xin Shen, Department of Immunology, Tongji Medical College, Huazhong University of Science and Technology, Wuhan 430030, Hubei Province, China. guanxin_shen608@hotmail.com

Telephone: +86-27-83692611 Fax: +86-27-83693500

Received: 2004-10-23 Accepted: 2004-11-19

carcinoma and affords experiment evidence for its immunotherapy study.

© 2005 The WJG Press and Elsevier Inc. All rights reserved.

Key words: ScFv; Biopanning; HCC; IMAC; Phage display

Yu B, Ni M, Li WH, Lei P, Xing W, Xiao DW, Huang Y, Tang ZJ, Zhu HF, Shen GX. Human scFv antibody fragments specific for hepatocellular carcinoma selected from a phage display library. *World J Gastroenterol* 2005; 11(26): 3985-3989
<http://www.wjgnet.com/1007-9327/11/3985.asp>

Abstract

AIM: To identify the scFv antibody fragments specific for hepatocellular carcinoma by biopanning from a large human naive scFv phage display library.

METHODS: A large human naive scFv phage library was used to search for the specific targets by biopanning with the hepatocellular carcinoma cell line HepG2 for the positive-selecting and the normal liver cell line L02 for the counter-selecting. After three rounds of biopanning, individual scFv phages binding selectively to HepG2 cells were picked out. PCR was carried out for identification of the clones containing scFv gene sequence. The specific scFv phages were selected by ELISA and flow cytometry. DNA sequences of positive clones were analyzed by using Applied Biosystem Automated DNA sequencers 3730. The expression proteins of the specific scFv antibody fragments in *E.coli* HB2151 were purified by the affinity chromatography and detected by SDS-PAGE, Western blot and ELISA. The biological effect of the soluble antibody fragments on the HepG2 cells was investigated by observing the cell proliferation.

RESULTS: Two different positive clones were obtained and the functional variable sequences were identified. Their DNA sequences of the scFv antibody fragments were submitted to GenBank (accession nos: AY686498 and AY686499). The soluble scFv antibody fragments were successfully expressed in *E.coli* HB2151. The relative molecular mass of the expression products was about 36 ku, according to its predicted M_r value. The two soluble scFv antibody fragments also had specific binding activity and obvious growth inhibition properties to HepG2 cells.

CONCLUSION: The phage library biopanning permits identification of specific antibody fragments for hepatocellular

INTRODUCTION

Hepatocellular carcinoma is the third leading cause of cancer deaths in the world and the prognosis of patients remains poor. Immunotherapeutic strategies against cancer have been developed during the last 20 years. In this respect, mouse monoclonal antibodies against tumor marks have been used for tumor targeting and imaging^[1]. The use of murine monoclonal antibodies for therapy in humans has limitations because of the human anti-mouse antibody response. Moreover, whole antibodies are large molecules and have poor tumor penetration. Several advances made during the past years will probably facilitate the development of therapeutic antibodies^[2]. Indeed, a chimeric anti-CD20^[3] antibody and a humanized anti-HER2^[4] antibody have been approved by FDA for the treatment of non-Hodgkins lymphoma and metastatic breast cancer respectively. These successes indicate that immunotherapeutic modalities are effective^[5]. On the other hand, the antibody-mediated tumor immunotherapy has become critical parts of biotherapy and is used for the diagnosis of cancer and metastasis, fine staging, and decisions regarding therapeutic approaches^[6]. So, it is urgent to obtain new humanized antibody specific for tumor targeting, and it is the same state in the therapy of hepatocellular carcinoma^[7]. Phage libraries displaying antibody fragments provide the fastest route to obtain human antibody fragments^[8]. The advent of antibody fragment display on phage and the development of large ($>6 \times 10^9$ clones) phage display libraries^[9,10] offer a potential way of detecting new targets by biopanning using tumor cells and counter-selecting using non-tumor cells^[11-13]. Significant progress has been made using this method to screen the antibodies against cell surface antigens^[14-17]. Targeting with scFv antibody fragments may overcome some of the limitations of murine monoclonal antibodies, and provide greater targeting specificity^[18-20]. Here, we report the selection of scFv antibodies binding specifically to HepG2 cells by

using L02 as counter-selecting cells biopanning from a large human naive scFv phage library (Griffin. 1 library)^[21].

MATERIALS AND METHODS

Materials

The human naive scFv library (Griffin. 1 library) used in this study was a generous gift from Professor Winter, University of Cambridge, UK. *E. coli* TG1 (suppressor strain for propagation of phage particles), *E. coli* HB2151 (non-suppressor strain for expression of antibody fragments) and helper phage M13K07 were purchased from Pharmacia-Biotech. Mouse anti-M13 antibody was from Amersham. Goat anti-mouse IgG conjugated HRP was provided by Kirkegaard Perry Laboratories. Goat anti-mouse IgG conjugated with FITC was obtained from Zhongsheng, Beijing. 9E10 antibody, Ni-NTA, FACS were purchased from Santa Cruz Biotechnology, Qiagen, and BD, respectively.

Methods

Cell culture The hepatocellular carcinoma cell line HepG2 and liver cell line L02 were incubated in RPMI 1640 supplemented with 100 mL/L FBS at 37 °C with 50 mL/L CO₂.

Screening of scFv phages from phage library using whole cells An aliquot containing 1×10^{12} cfu from a large human scFv phage library was added to 1×10^6 L02 cells and mixed gently for 30 min at room temperature (RT). The phage-containing supernatant was used to resuspend a fresh pellet of 1×10^6 L02 cells and incubated for 30 min at RT, followed by pelleting the cells. Then, the resultant subtracted phage supernatant was incubated with 5×10^6 HepG2 cells for 1 h at RT with gentle mixing. The cell-bound phages were eluted with 0.5 mL of PBS containing 100 mmol/L citric acid (pH 2.2) for 10 min and neutralized with 0.5 mL of 1.0 mol/L Tris-HCl (pH 7.5). *E. coli* TG1 was infected with the eluted phages and plated on 2×TY agar containing 1% glucose and 100 µg/mL ampicillin. The resultant colonies were propagated and used to prepare phages. Biopanning was performed in triplicate using 1×10^{12} cfu.

FCM for polyclonal scFv phages The polyclonal scFv phages were blocked with 6% BSA in PBS. The blocked scFv-phage supernatants were added to parallel plates containing 1×10^5 HepG2 cells (1 h, 4 °C, gentle agitation). The cells were washed twice and centrifuged. Pellets were then resuspended in 100 µL of mouse anti-M13 antibody and incubated for 20 min at 4 °C. After being washed twice, the cells were resuspended in 100 µL of goat anti-mouse IgG conjugated with FITC and incubated for 20 min at 4 °C. After being washed thrice, the cells were analyzed by flow cytometry.

ELISA and FCM for monoclonal scFv phages *E. coli* TG1 was infected with the third round scFv phages and plated on 2×TY agar to obtain the monoclonal bacteria. PCR was carried out for identifying clones containing the scFv gene sequence. The clones containing scFv gene sequence were infected with helper phage to prepare monoclonal scFv phages. The ELISA for monoclonal scFv phages was performed as the FCM for polyclonal scFv phages described above.

After being washed the cells were resuspended in 100 µL of goat anti-mouse IgG conjugated with HRP instead of goat anti-mouse IgG conjugated with FITC, then incubated for 20 min at 4 °C. Cell pellets were resuspended in 100 µL of TMB reagents. The ELISA plates were read ($A_{405}-A_{630}$) and data were analyzed using a spreadsheet program (Microsoft Excel). Monoclonal scFv phages binding to HepG2 cells specifically were prepared for FCM.

Sequencing and analyzing of scFv DNA The positive monoclonal bacteria were isolated and sent to BoYa Shanghai Company for sequencing of DNA. The results of sequencing were Blast in GenBank and analyzed using IMG/Quest software.

IMAC purification of soluble scFv antibody fragments Bacterial clones were cultured in 1 L of 2×TY, 100 µg/mL ampicillin, 0.1% glucose and induced with 1 mmol/L final concentration of IPTG for 20 h at 30 °C. The scFv antibody fragments were harvested from the periplasm and purified by IMAC of pentahistidine tag fused to the scFv fragments. The samples were dialyzed in PBS, filtered, concentrated and stored at 4 °C in about 1 mg/mL PBS.

Western blot Five micrograms of purified scFv antibody fragments was run on a 10% SDS-PAGE gel and transferred onto nitro-cellulose. Filters were blocked for 1 h at RT in 10% Marvel/PBS. The scFv antibody fragments were detected with the murine monoclonal antibody 9E10 followed by anti-mouse IgG horseradish peroxidase conjugate. Horseradish peroxidase was visualized with diaminobenzidine tablets in the presence of cobalt ions.

Cell ELISA for purified soluble scFv antibody fragments L02, HepG2, Hela, MCF-7 and K562 cell lines were selected for cell ELISA to identify the specificity of the purified soluble scFv antibody fragments binding to HepG2. The method of cell ELISA was the same as the monoclonal scFv-phage ELISA described above. The purified SLH04 or SLH10 was used as the first antibody, and antibody 9E10 was used as the second antibody.

Test of HepG2 cell proliferation A total of 10^4 HepG2 cells were cultured in a 24-well cell culture plate. Two wells were incubated with 500 µL of purified soluble scFv antibody fragments, SLH04 or SLH10. One well was incubated with 500 µL unrelated antibody, the other well was not treated with any antibody. Cells were cultured for a week and counted everyday.

RESULTS

Recovery rate of scFv-phage biopanning

An aliquot containing 1×10^{12} cfu scFv phage was selected on the HepG2 and L02 cell lines. The recovery rate of the third round biopanning was close to that of the second round indicating that positive clones were fully enriched (Table 1).

Table 1 Recovery rate of phage in each round of biopanning

Round	Input phage (cfu)	Eluted phage (cfu)	Recall rate (%)
1	1×10^{12}	1.9×10^8	1.9×10^{-6}
2	1×10^{12}	1.2×10^7	1.2×10^{-5}
3	1×10^{12}	1.5×10^7	1.5×10^{-5}

The recovery rate = eluted phage titer / input phage titer.

Selection of scFv phages

The selected and amplified polyclonal scFv phages were tested by FCM (Figure 1). The result also showed that positive clones were enriched well.

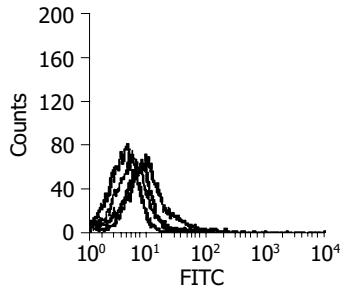


Figure 1 Result of polyclonal scFv phages by FCM (from left to right: purple -negative; green-1st round; red-2nd round; blue-3rd round).

After *E.coli* TG1 was infected with scFv phages of the third round and plated on 2×TY agar, 31 clones were isolated. PCR was carried out for identification of the clones combined with scFv gene sequence. Twelve positive clones were isolated to prepare monoclonal scFv phages. By ELISA, three scFv phages showed obviously higher binding activity in HepG2 cells according to the data of $A_{405}-A_{630}$ (Figure2). By FCM, clones 4, 10 and 25 showed more extensive activity in HepG2 cells (Figure 3).

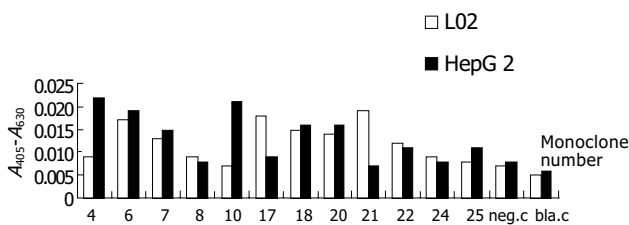


Figure 2 ELISA for monoclonal scFv phages.

Sequence of scFv DNA

The results of sequencing and Blast showed that clones 4 and 10 had homologous sequence of human immunoglobulin

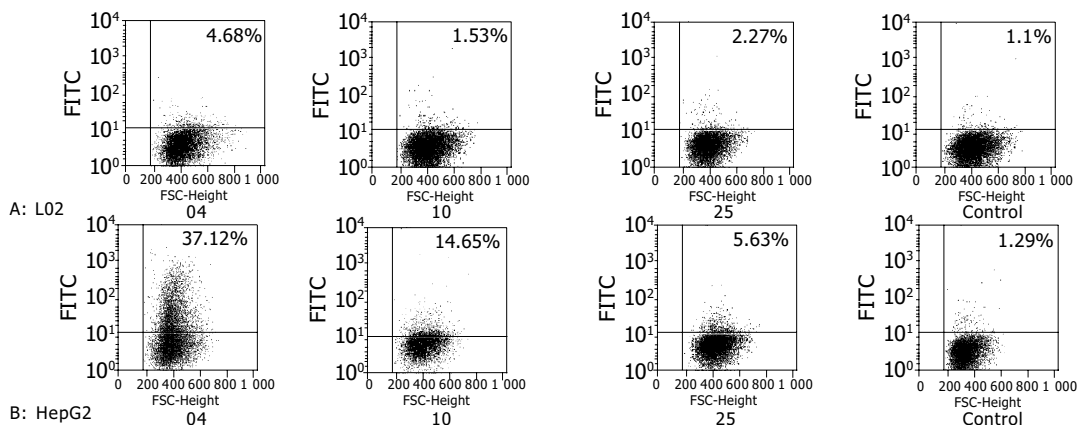


Figure 3 FCM for monoclonal scFv phages.

in GenBank. The scFv DNA sequences were analyzed by IMGT/V-Quest software and submitted to GenBank (accession nos: AY686498 and AY686499). The region of CDR3 of VH was absent in clone 25 and the terminator codon was found in its open reading frame.

Result of IMAC purification

The scFv antibody fragments were harvested from the periplasm of 1 L *E.coli* HB2151 infected with positive phage SLH04 or SLH10 and the scFv antibody eluted effectively in PBS with 40 or 60 mmol/L imidazole by IMAC purification (Figure 4). SLH10 had the same result as SLH04 (data not shown).

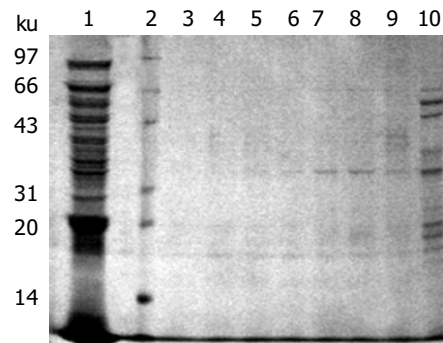


Figure 4 SLH04 scFv antibody fragments eluted with different concentrations of imidazole. Lane 1: periplasm before eluting; lane 2: protein marker; lane 3, 4, 5, 6, 7, 8, 9, 10: elution washings at different imidazole concentrations, 200, 150, 100, 80, 60, 40, 20, 10 mmol/L, respectively.

Results of Western blot

Five micrograms of purified scFv antibody fragments was run on a 10% SDS-PAGE gel and transferred to nitro-cellulose and detected with the antibody 9E10 (Figure 5).

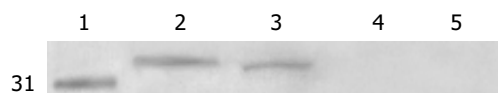


Figure 5 Western blot of purified scFv antibodies SLH10 and SLH04. Lane 1: protein marker; lane 2: purified scFv antibody SLH10; lane 3: purified scFv antibody SLH04; lane 4: the induced bacterial periplasmic of HB2151; lane 5: induced bacterial periplasm of HB2151 with pHEN2 vector.

Results of cell ELISA of purified soluble scFv antibody fragments

The two positive soluble scFv antibody fragments showed higher ability to bind to HepG2 cells than to other cell lines (Figure 6).

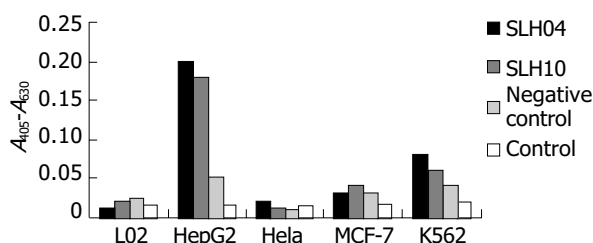


Figure 6 Two purified soluble scFv antibody fragments cells ELISA.

Proliferation of HepG2 cell inhibited by purified antibody fragments

The soluble scFv antibody fragments SLH04 and SLH10 showed growth inhibitory effects (Figure 7).

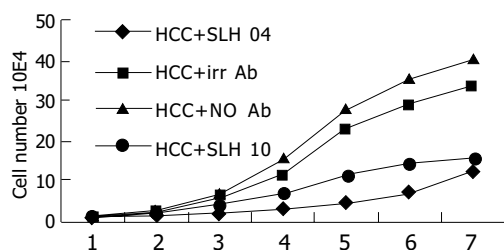


Figure 7 Proliferation of HepG2 cell inhibited by purified antibody fragments.

DISCUSSION

Antibodies displayed on phages are powerful tools for the identification of ligand specificity to targets of interest^[22]. Binding ligands from this library are usually selected by repetitive biopanning rounds usually performed on pure antigens on a solid phase^[23]. The isolation of antibodies for cellular receptors using whole cells as affinity matrix has a number of advantages. The receptors are likely to be in their native conformation compared to their purified one. Furthermore, a large number of known and novel surface antigens can be screened at the same time^[24,25]. In this respect, some investigators have selected a number of phage antibodies that bind to known and novel surface antigens using whole cells^[26,27].

In this study, two scFv antibody fragments were identified which could bind more extensively to HepG2 than to L02 cell line by biopanning of liver cells from a large naive antibody phage library. After three rounds of biopanning, the result indicated that positive clones were fully enriched. Then 12 monoclonal TG1 were picked out from the clones combined with scFv gene sequence. By

ELISA, seven of them showed no diversity binding to the two kinds of cells, two of them bound more extensively to L02 cells, three of them showed more extensive binding to HepG2 cells. The three clones were identified as the final positive clones at the end of biopanning. By sequencing and analyzing these three scFv DNA sequences, two clones were discovered having the right full open reading frame; the terminator codon was found in the open reading frame of clone 25 and its region of CDR3 of VH was absent and mutated. Probably this is why the affinity of binding to HepG2 showed no more specificity than the two other positive scFv antibody fragments. Blast in GenBank indicates that heavy chain of the scFv-04 belongs to IGHV2 family and its light chain belongs to Vk2 family, while the heavy chain of the scFv-10 belongs to IGHV1 family and its light chain belongs to Vλ3 family. Our data indicate that most soluble scFv antibody fragments are expressed in periplasm of the positive *E.coli* HB2151, few of them can be detected in bacterial supernatant. Therefore, we cannot obtain more soluble scFv antibodies purified from bacterial supernatant by IMAC as described previously^[28]. By cell ELISA the two soluble scFv antibody fragments showed higher ability to bind to HepG2 cells than to other cell lines, suggesting that scFv antibodies can bind to living HepG2 cells specifically. Furthermore, our data demonstrate that the two soluble scFv antibody fragments have growth inhibitory effects when cultured with HepG2 cells. Some antibodies have such biological effects on target cells because they are able to mimic the receptor-ligand interaction by triggering specific intracellular cascades of reactions, which eventually lead to biological signals such as inhibition of cell growth. In this regard, anti-transferrin receptor monoclonal antibody has the above characteristics^[29,30]. However, the fact that the transferrin receptor is expressed in most cell types makes these antibodies less interesting for cancer therapy. According to our results, the two scFv antibody fragments binding specifically to HepG2 cells can be used as target molecules in the treatment of hepatocellular carcinoma. Antibody phage biopanning method offers a potential application in the identification of human antibodies suitable for antitumor therapy^[31]. In summary, large human naive scFv antibody phage library is a useful tool for the selection of antibodies against antigens. The ability of the human scFv antibody fragments to bind to HepG2 cell surfaces will allow them to become a diagnostic and therapeutic reagent of HCC.

REFERENCES

- 1 **Robinson MK**, Weiner LM, Adams GP. Improving monoclonal antibodies for cancer therapy. *Drug Development Res* 2004; **61**: 172-187
- 2 **Romanov VI**. Phage display selection and evaluation of cancer drug targets. *Curr Cancer Drug Targets* 2003; **3**: 119-129
- 3 **Reff ME**, Carner K, Chambers KS, Chinn PC, Leonard JE, Raab R, Newman RA, Hanna N, Anderson DR. Depletion of B cells *in vivo* by a chimeric mouse human monoclonal antibody to CD20. *Blood* 1994; **83**: 435-445
- 4 **Carter P**, Presta L, Gorman CM, Ridgway JB, Henner D, Wong WL, Rowland AM, Kotts C, Carver ME, Shepard HM. Humanization of an anti-p185HER2 antibody for human cancer therapy. *Proc Natl Acad Sci USA* 1992; **89**: 4285-4289
- 5 **Kim ES**, Khuri FR, Herbst RS. Epidermal growth factor receptor biology (IMC-C225). *Curr Opin Oncol* 2001; **13**: 506-513

- 6 **Schneebaum S**, Troitsa A, Avital S, Haddad R, Kashtan H, Gitstein G, Baratz M, Brazovsky E, Papo J, Skornick Y. Identification of lymph node metastases in recurrent colorectal cancer. *Recent Results Cancer Res* 2000; **157**: 281-292
- 7 **Butterfield LH**. Immunotherapeutic strategies for Hepatocellular Carcinoma. *Gastroenterology* 2004; **127**: 232-241
- 8 **Clackson T**, Hoogenboom HR, Griffiths AD, Winter G. Making antibody fragments using phage display libraries. *Nature* 1991; **352**: 624-628
- 9 **Waterhouse P**, Griffiths AD, Johnson KS, Winter G. Combinatorial infection and *in vivo* recombination: a strategy for making large phage antibody repertoires. *Nucleic Acids Res* 1993; **21**: 2265-2266
- 10 **Sheets MD**, Amersdorfer P, Finnern R, Sargent P, Lindquist E, Schier R, Hemingsen G, Wong C, Gerhart JC, Marks JD, Lindqvist E. Efficient construction of a large nonimmune phage antibody library: the production of high-affinity human single-chain antibodies to protein antigens. *Proc Natl Acad Sci USA* 1998; **95**: 6157-6162
- 11 **Marks JD**, Ouwehand WH, Bye JM, Finnern R, Gorick BD, Voak D, Thorpe SJ, Hughes-Jones NC, Winter G. Human antibody fragments specific for human blood group antigens from a phage display library. *Biotechnology* 1993; **11**: 1145-1149
- 12 **Portolano S**, McLachlan SM, Rapoport B. High affinity, thyroid-specific human autoantibodies displayed on the surface of filamentous phage use V genes similar to other autoantibodies. *J Immunol* 1993; **151**: 2839-2851
- 13 **de Kruif J**, Terstappen L, Boel E, Logtenberg T. Rapid selection of cell subpopulation-specific human monoclonal antibodies from a synthetic phage antibody library. *Proc Natl Acad Sci USA* 1995; **92**: 3938-3942
- 14 **Van Ewijk W**, de Kruif J, Germeraad WT, Berendes P, Ropke C, Platenburg PP, Logtenberg T. Subtractive isolation of phage-displayed single-chain antibodies to thymic stromal cells by using intact thymic fragments. *Proc Natl Acad Sci USA* 1997; **94**: 3903-3908
- 15 **Cai X**, Garen A. Anti-melanoma antibodies from melanoma patients immunized with genetically modified autologous tumor cells: selection of specific antibodies from single-chain Fv fusion phage libraries. *Proc Natl Acad Sci USA* 1995; **92**: 6537-6541
- 16 **Cai X**, Garen A. A melanoma-specific VH antibody cloned from a fusion phage library of a vaccinated melanoma patient. *Proc Natl Acad Sci USA* 1996; **93**: 6280-6285
- 17 **Cai X**, Garen A. Comparison of fusion phage libraries displaying VH or single-chain Fv antibody fragments derived from the antibody repertoire of a vaccinated melanoma patient as a source of melanoma-specific targeting molecules. *Proc Natl Acad Sci USA* 1997; **94**: 9261-9266
- 18 **Bird RE**, Hardman KD, Jacobson JW, Johnson S, Kaufman BM, Lee SM, Lee T, Pope SH, Riordan GS, Whitlow M. Single-chain antigen-binding proteins. *Science* 1988; **242**: 423-426
- 19 **Yokota T**, Milenic DE, Whitlow M, Schlom J. Rapid tumor penetration of a single-chain Fv and comparison with other immunoglobulin forms. *Cancer Res* 1992; **52**: 3402-3408
- 20 **Mayer A**, Chester KA, Flynn AA, Begent RH. Taking engineered anti-CEA antibodies to the clinic. *J Immunol Methods* 1999; **231**: 261-273
- 21 **Winter G**, Griffiths AD, Hawkins RE, Hoogenboom HR. Making antibodies by phage display technology. *Annu Rev Immunol* 1994; **12**: 433-455
- 22 **Hoogenboom HR**. Overview of antibody phage-display technology and its applications. *Methods Mol Biol* 2002; **178**: 1-37
- 23 **Griffiths AD**, Williams SC, Hartley O, Tomlinson IM, Waterhouse P, Crosby WL, Kontermann RE, Jones PT, Low NM, Allison TJ. Isolation of high affinity human antibodies directly from large synthetic repertoires. *EMBO J* 1994; **13**: 3245-3260
- 24 **Kristensen P**, Ravn P, Jensen KB, Jensen KH. Applying phage display technology in aging research. *Biogerontology* 2000; **1**: 67-78
- 25 **Sawyer C**, Embleton J, Dean C. Methodology for selection of human antibodies to membrane proteins from a phage-display library. *J Immunol Methods* 1997; **204**: 193-203
- 26 **Pereira S**, Maruyama H, Siegel D, Van Belle P, Elder D, Curtis P, Herlyn D. A model system for detection and isolation of a tumor cell surface antigen using antibody phage display. *J Immunol Methods* 1997; **203**: 11-24
- 27 **Figini M**, Obici L, Mezzanzanica D, Griffiths A, Colnaghi MI, Winter G, Canevari S. Panning phage antibody libraries on cells: isolation of human Fab fragments against ovarian carcinoma using guided selection. *Cancer Res* 1998; **58**: 991-996
- 28 **Casey JL**, Keep PA, Chester KA, Robson L, Hawkins RE, Begent RH. Purification of bacterially expressed single chain Fv antibodies for clinical applications using metal chelate chromatography. *J Immunol Methods* 1995; **179**: 105-116
- 29 **Kovar J**, Naumann PW, Stewart BC, Kemp JD. Differing sensitivity of non-hematopoietic human tumors to synergistic anti-transferrin receptor monoclonal antibodies and deferoxamine *in vitro*. *Pathobiology* 1995; **63**: 65-70
- 30 **Valentini M**, Gregorini A, Bartolucci M, Porcellini A, Papa S. The blockage of the human transferrin receptor by a monoclonal antibody, EA.3, induces growth inhibition in leukemia cell lines. *Eur J Histochem* 1994; **38**(Suppl): 61-68
- 31 **Cooke SP**, Boxer GM, Lawrence L, Pedley RB, Spencer DIR, Begent RHJ, Chester KA. A strategy for antitumor vascular therapy by targeting the vascular endothelial growth factor: Receptor complex. *Cancer Res* 2001; **61**: 3653-3659

Hydrogen sulfide protects colon cancer cells from chemopreventative agent β -phenylethyl isothiocyanate induced apoptosis

Peter Rose, Philip K Moore, Shen Han Ming, Ong Choon Nam, Jeffrey S Armstrong, Matt Whiteman

Peter Rose, Jeffrey S Armstrong, Matt Whiteman, Department of Biochemistry, National University of Singapore, 8 Medical Drive, 117597, Singapore

Philip K Moore, Department of Pharmacology, National University of Singapore, 18 Medical Drive, 117597 Singapore

Shen Han Ming, Ong Choon Nam, Department of Community, Occupational and Family Medicine, National University of Singapore, 16 Medical Drive, 117597, Singapore

Correspondence to: Dr. Peter Rose, Department of Biochemistry, National University of Singapore, 8 Medical Drive, 117597, Singapore. bchpccr@nus.edu.sg

Telephone: +65-6874-4996

Received: 2004-08-25 Accepted: 2004-09-15

Abstract

AIM: Hydrogen sulfide (H_2S) is a prominent gaseous constituent of the gastrointestinal (GI) tract with known cytotoxic properties. Endogenous concentrations of H_2S are reported to range between 0.2-3.4 mmol/L in the GI tract of mice and humans. Considering such high levels we speculate that, at non-toxic concentrations, H_2S may interact with chemical agents and alter the response of colonic epithelium cells to such compounds. The GI tract is a major site for the absorption of phytochemical constituents such as isothiocyanates, flavonoids, and carotenoids, with each group having a role in the prevention of human diseases such as colon cancer. The chemopreventative properties of the phytochemical agent β -phenylethyl isothiocyanate (PEITC) are well recognized. However, little is currently known about the physiological or biochemical factors present in the GI tract that may influence the biological properties of ITCs. The current study was undertaken to determine the effects of H_2S on PEITC mediated apoptosis in colon cancer cells.

METHODS: Induction of apoptosis by PEITC in human colon cancer HCT116 cells was assessed using classic apoptotic markers namely SubG1 population analysis, caspase-3 like activity and nuclear fragmentation and condensation coupled with the MTT (3-(4,5-dimethylthiazol-2-yl)-2,5-diphenyl tetrasodium bromide) viability assay and LDH leakage.

RESULTS: PEITC significantly induced apoptosis in HCT116 cells as assessed by SubG1 population formation, nuclear condensation, LDH leakage and caspase-3 activity after 24 h, these data being significant from control groups ($P < 0.01$). In contrast, co-treatment of cells with physiological concentrations of H_2S (0.1-1 mmol/L) prevented PEITC mediated apoptosis as assessed using the parameters

described.

CONCLUSION: PEITC effectively induced cell death in the human adenocarcinoma cell line HCT116 *in vitro* through classic apoptotic mechanisms. However, in the presence of H_2S , apoptosis was abolished. These data suggest that H_2S may play a significant role in the response of colonic epithelial cells to beneficial as well as toxic agents present within the GI tract.

© 2005 The WJG Press and Elsevier Inc. All rights reserved.

Key words: Apoptosis; Colon cancer; Hydrogen sulfide; β -phenylethyl isothiocyanate

Rose P, Moore PK, Ming SH, Nam OC, Armstrong JS, Whiteman M. Hydrogen sulfide protects colon cancer cells from chemopreventative agent β -phenylethyl isothiocyanate induced apoptosis. *World J Gastroenterol* 2005; 11(26): 3990-3997

<http://www.wjgnet.com/1007-9327/11/3990.asp>

INTRODUCTION

Cruciferous vegetables such as broccoli, watercress and Brussels sprouts are an important food source of phytochemicals known as glucosinolates (GSLs). Following tissue disruption GSLs can be converted by plant and/or enteric gut bacterial myrosinase to the organosulfur compounds isothiocyanates (ITCs)^[1,2]. Exposure to ITCs can reduce carcinogen induced tumor formation in a diverse range of organs such as lung, mammary gland, esophagus, liver and intestine^[3,4]. Supporting these findings are recent epidemiological studies showing that consumption of cruciferous vegetables, the primary source of ITCs in the human diet, can reduce cancer incidence in humans^[5,6]. Due to the promising chemopreventative properties of crucifers and ITCs, numerous reports have attempted to determine the mechanism(s) of action of ITC. ITCs can inhibit phase I enzymes^[7] and induce phase II detoxification enzymes^[8-12]. Moreover, the induction of apoptosis in target tissues and cancer cells has also been demonstrated. Previous investigations have shown that β -phenylethyl isothiocyanate (PEITC), benzyl isothiocyanate (BITC), allyl isothiocyanate (AITC) and sulforaphane (MSB) can induce apoptosis in both *in vitro* and *in vivo* situations^[13-19].

Considering the beneficial effects of ITC exposure in the diet, surprisingly few studies have placed much emphasis on endogenous or exogenous factors that may alter the beneficial properties of these phytochemical agents. To date, storage and cooking regimes, plant and bacterial myrosinase

activity and altered conversion of GSLs to non-bioactive nitriles have been shown to influence the response of host tissues and cells to ITCs^[20-24]. As ITCs are predominately absorbed along the gastrointestinal tract (GI) it is conceivable that the colonic environment may also contribute to the host's response to ITCs.

Hydrogen sulfide (H₂S) is a well known pungent gas and a prominent constituent present in the GI lumen. Exogenous sources show high toxicity towards the nervous, cardiovascular and respiratory systems in humans^[25]. The toxic effect of H₂S exposure are associated with its ability to bind reversibly to the heme site of cytochrome c aa3 site of cytochrome c oxidase thus inhibiting oxidative phosphorylation, although other mechanism(s) may also be involved. In addition, endogenous sites of H₂S production also exist in mammals^[26]. Catabolism of the amino acids L-cysteine and homocysteine by cystathionine- β -synthetase (CBS) generates appreciable levels of H₂S in the brain. CBS is highly expressed in the hippocampus and cerebellum and CBS knockout mice have no detectable amounts of H₂S in brain tissues. In contrast, H₂S is also formed from the same precursors by cystathionine- β -lyase (CSE) which is the predominant enzyme in the vasculature. In addition, mammalian cells may also be exposed to high levels of H₂S through the actions of enteric sulfate reducing bacteria in the GI tract^[27]. Recent studies have shown that H₂S concentrations in the large intestine of mice ranges between 0.2-1 mmol/L and are comparable to the concentration of H₂S in human feces (0.3-3.4 mmol/L)^[28,29]. Considering the high *in vivo* levels of H₂S it is plausible that such concentrations may directly affect the GI environment. Indeed, several clinical trials have shown a correlation between H₂S levels and the development of colorectal cancer and ulcerative colitis, such studies highlighting a potential deleterious effect of H₂S exposure^[30]. However, it is not currently known whether H₂S is the causative factor or a consequence of such diseases. In a more recent study Deplanck and Gaskins^[31] demonstrated that H₂S promotes cell cycle entry, MAPkinase activation, and cell proliferation in non-transformed intestinal IEC-18 cell *in vitro*. This data suggests a link between H₂S exposure and cell cycle dysregulation which perhaps contributes to colon cancer and ulcerative colitis development. However, considering the potential toxic effects of H₂S the GI tract has developed mechanism(s) to reduce the adverse effects of H₂S such as increased rhodanese expression and activity, detoxification via oxidation to thiosulfate and bicarbonate secretion^[32-34]. Therefore, H₂S production in health subjects may not lead to disease formation due to adequate protective mechanisms. Recent studies have shown that H₂S prevents glutamate induced oxidative stress in human neurons by stimulating glutathione biosynthesis^[35]. H₂S has also been shown to inhibit peroxynitrite, hydrogen peroxide and superoxide mediated cellular damage and death in neurons and myocytes by acting as an antioxidant^[36,37]. Likewise, organisms like *Saccharomyces cerevisiae* and deep sea hydrothermal vent *Archaea* use H₂S for the detoxification of methylmercury and heavy metal ion (Cu, Zn and Co) induced toxicity^[38,39], thus physiological concentrations in the human GI tract may protect colon cancer cells from undergoing apoptosis.

In view of the large quantities of H₂S in the GI tract we have systematically evaluated whether H₂S can alter the biological response of human colon cancer HCT116 cells to the chemopreventative agent PEITC. Such data may provide a novel insight as to how H₂S, at non-toxic concentrations, may act indirectly on colonic cells apoptosis.

MATERIALS AND METHODS

Cells and chemicals

Human colon cancer HCT116, HT29, SW480 and LS174T cell lines were purchased from the American Culture Collection (Rockville, MD). HCA-7 cells were kindly supplied by Susan. C. Kirkland, Royal Postgraduate Medical School, UK. β -Phenylethyl isothiocyanate, DMSO, ATP, SDS, penicillin and streptomycin were purchased from Sigma-Aldrich (St. Louis, MO, USA); MEM, trypsin and FBS from GIBCO BRL (Gaithersburg, MD, USA).

Cell culture

HCT116, HT29, HCA-7 and LS174T cells were cultured in complete DMEM (containing 100 mL/L FBS, 100 000 U/L penicillin, 100 mg/L streptomycin, pH 7.4) in 75-cm culture flasks at 37 °C in 50 mL/L CO₂. Similarly, SW480 cells were grown in RPMI 1640 medium under the above cell culture conditions.

Cell culture treatment

NaSH was used to generate readily controlled amounts of H₂S as it dissociates to Na⁺ and HS⁻ in solution, then HS⁻ associates with H⁺ to produce H₂S. We herein use the term H₂S to reflect the sum of the species H₂S, HS⁻ or S₂⁻ present at physiological pH. PEITC was dissolved in DMSO to a final concentration of 100 mmol/L and adjusted to the required concentration by dilution in cell culture medium. All reagents were prepared fresh for each individual experiment.

Cell viability testing

Cell viability was determined using the MTT (3-(4, 5-dimethylthiazol-2-yl)-2, 5-diphenyl tetrasodium bromide) viability assay as previously described^[40]. Activity of lactate dehydrogenase (LDH) in the medium was measured using an Abbott VP Biochemical Analyser with the test kit (Abbott Laboratories, Irving, TX, USA). The total LDH activity was determined by ultrasonication and assessed by expressing as percentage LDH leakage (LDH in medium/total LDH activity \times 100).

Detection of nuclear morphological changes and apoptosis

To assess apoptotic cell death morphologic changes in chromatin structure were detected by DAPI staining. Briefly, attached cells were harvested washed with PBS, and re-suspended in PBS prior to fixing with 700 mL/L ethanol for 15 min at room temperature. Cells were centrifuged, re-suspended in PBS and stained with 2 g/L DAPI in the dark for 5 min. Cell suspensions were mounted on glass slides and subjected to fluorescence microscopic examination using a Nikon photomicroscope (Thornwood, NY, USA). Apoptotic cells were identified by their morphology and by

the condensation and fragmentation of their nuclei.

DNA fragmentation in HCT116 cells was measured using propidium iodide staining followed by flow cytometry analysis as described^[41]. From each treatment 10 000 cells were analyzed using flow cytometry (Coulter Epics Elite ESP, Miami, FL, USA). Data was analyzed using WinMDI 2.7 software (Scripps Institute, La Jolla, CA, USA).

Measurement of caspase activity

Caspase-3 activity was determined spectrofluorometrically using the synthetic substrate Ac-DEVD-AFC respectively (BIOMOL Research Labs, Plymouth, PA, USA) as previously described^[42,43]. Cell homogenates were incubated with synthetic substrate 0.2 mmol/L at 37 °C/2 h. The fluorescence intensity of liberated AFC was monitored using a Tecan spectrofluor plus plate reader (USA) using an excitation wavelength of 400 nm and an emission wavelength of 505 nm.

Statistical analysis

All data are represented by three separate experiments. All experimental data consists of mean±SD unless otherwise stated and were analyzed by one-way ANOVA.

RESULTS

Evaluation of PEITC mediated reduction of colon cancer cell viability

Accumulating evidence has shown that cancer cells treated with PEITC undergo apoptosis by inducing mitochondrial dysfunction, sequential caspase activation, and MAPKinase mediated apoptotic signaling^[14,16]. To evaluate the cytotoxic effects of PEITC on the viability of colon cancer cells, we preferentially screened several commonly available cell lines namely colorectal carcinoma HCT116, and colorectal adenocarcinoma cell lines HT29, SW480, HCA-7 and LS174T cells, following 24h treatments with increased concentrations of PEITC. Cell viability was determined by MTT assay. All cells lines were responsive to PEITC treatment with viability decreasing in a concentration dependent manner (Figure 1).

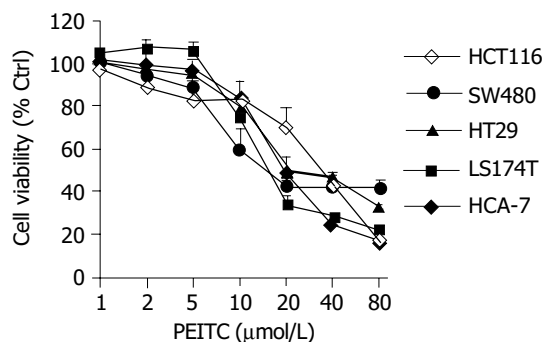


Figure 1 (A) Concentration dependant loss of cell viability induced by PEITC in colon cancer cells as determined at 24 h using the MTT viability assay. Data are representative of three or more separate experiments (mean±SD).

Induction of apoptosis by PEITC

We next selected two cell lines for further study these being

the HCT116 and HT29 cell lines. Several key parameters that are known to be involved in PEITC induced apoptosis in HCT116 cells and HT29 cells were evaluated. Previous investigations have shown both HCT116 and HT29 cells are responsive to PEITC treatment, which we needed to reconfirm under our laboratory conditions^[14,44]. As represented in Figure 2, PEITC mediated a time and concentration dependant induction of caspase-3 like activity in HCT116 and HT29 cells. Caspase activity was determined by measurement of AFC fluorescence intensity derived from the catalytic cleavage of the substrate Ac-DEVD-AFC by endogenous caspase. The fluorescence intensity of treated over control cells, was used to determine the fold increase in caspase activity. Supporting a role of caspases in PEITC induced apoptosis was the inhibitory effects of the pharmacological caspase inhibitors Z-VAD-FMK (pan-caspase inhibitor), Ac-LEHD-CHO (caspase 9 inhibitor), and Ac-DEVD-CHO (caspase 3 inhibitor) on PEITC induced apoptosis. In both cell types tested all inhibitors reduced DNA fragmentation as determined by measurement of SubG1 populations by propidium iodide staining and LDH leakage (Figure 2).

Inhibition of PEITC mediated apoptosis by low molecular weight sulfur compounds

Because PEITC is absorbed along the GI tract we next evaluated whether hydrogen sulfide and other low molecular weight sulfur compounds could protect HCT116 cells from PEITC mediated apoptosis. Incubation of HCT116 cells with up to 1 mmol/L concentrations of hydrogen sulfide (H₂S) and its metabolic by-products sulfate (SO₄), sulfite (SO₃) and thiosulfate (S₂O₃²⁻) had no appreciable effects on cell viability as determined using the MTT assay and LDH leakage at 24 h (Figure 3). Co-treatment of individual sulfur compounds (SO₃, SO₄, S₂O₃²⁻) at 1 mmol/L concentrations failed to prevent the apoptotic effects of PEITC (40 μmol/L). In contrast, H₂S co-treatment but not pre-treatment inhibited PEITC induced apoptosis in a concentration dependant manner that was comparable to the low molecular weight thiol *N*-acetylcysteine (Figure 3). Associated with the inhibitory effects of both H₂S and NAC was a significant reduction in caspase activity (Figure 3D).

H₂S and NAC protect against BSO mediated sensitization of HCT116 cells to PEITC induced apoptosis

Intracellular depletion of glutathione (GSH) can be achieved using buthionine-S-sulfoximine (BSO), an inhibitor of the rate limiting enzyme required for GSH biosynthesis. BSO treatment sensitizes cells to apoptotic agents by reducing intracellular GSH levels. The sensitizing effects of combined treatment of PEITC and BSO in HCT116 cells were next investigated in the presence of H₂S and NAC. BSO at the concentration used had no appreciable effects on cell viability. Pre-treatment with 0.5 mmol/L BSO/24 h increased the apoptotic response of HCT116 cells to PEITC (40 μmol/L) as determined by the MTT assay and LDH leakage (Figure 4A). Indeed, BSO pre-treatment decreased cell viability by 83% and increased LDH leakage to 84.9% (*P*<0.01) in PEITC treated cells. Cellular protection was afforded by co-treatment with either H₂S or NAC (1 mmol/L). Moreover, evaluation of morphological

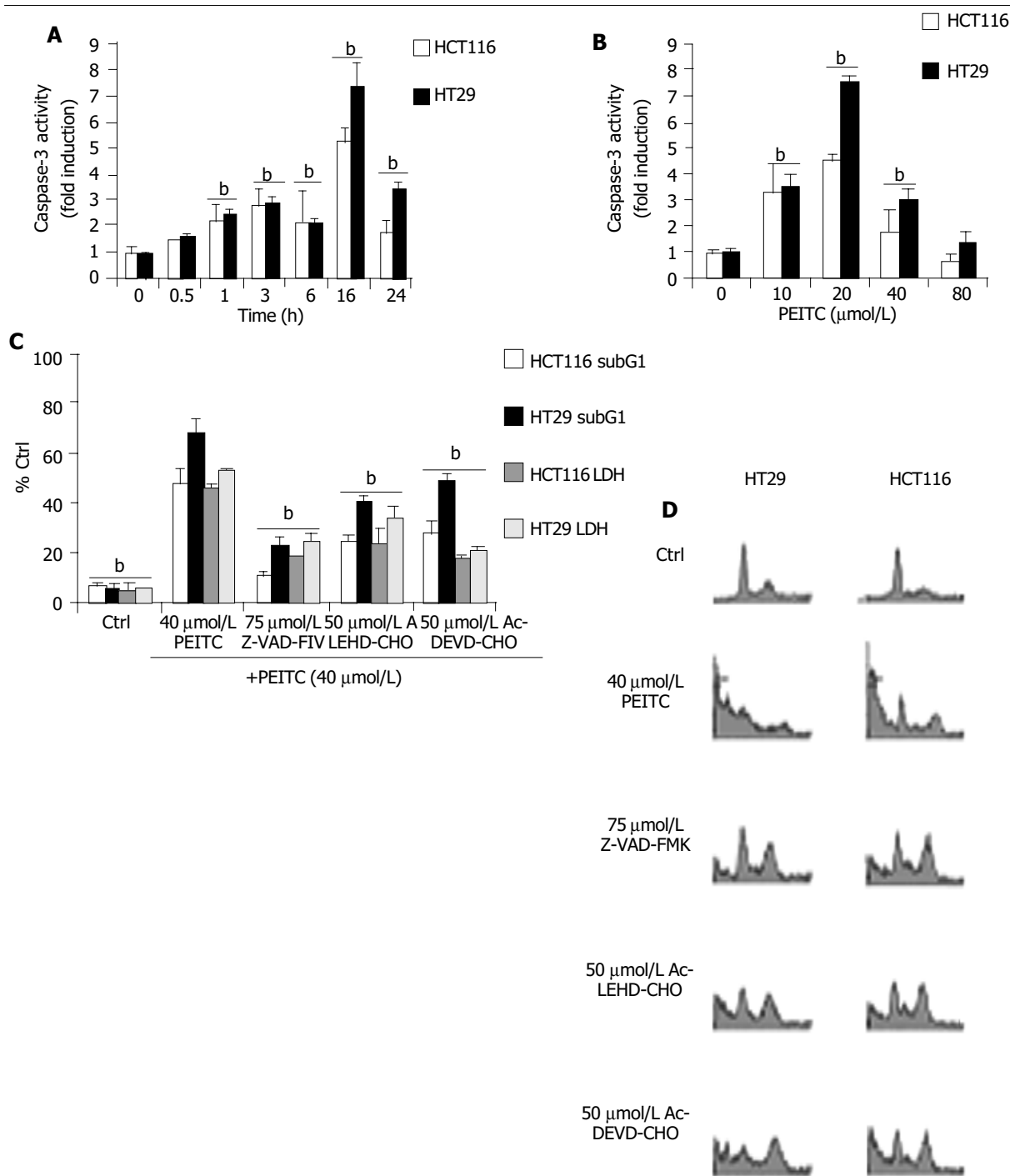


Figure 2 A: Time dependant Induction of caspase -3 activities in HCT116 and HT29 cells treated with 40 μmol/L PEITC as determined at 0.5, 1, 3, 6, 16 and 24 h. B: Concentration dependant activation of caspase-3 as determined at 24 h after incubation with PEITC (10-80 μmol/L). C: Z-VAD-FMK, Ac-LEHD-CHO and Ac-DEVD-CHO inhibition on PEITC mediated apoptosis as determined at 24 h. ^bP<0.01, significant difference compared to control groups. Cells were treated with individual caspase inhibitors for 1 h prior to the addition of 40 μmol/L PEITC. SubG1 populations were determined by propidium iodide staining followed by

flow cytometry analysis as described in the materials and methods. ^bP<0.01, comparing PEITC (alone) with control groups. D: Representative flow cytometry analysis of HCT116 and HT29 cells was used to determine the extent of DNA fragmentation in cells treated with PEITC (40 μmol/L) in the presence of caspase inhibitors. Data were determined by PI staining at 24 h. Figure shows representative example of at least 3 experiments. In each analysis, 10 000 events were recorded. ^bP<0.01, PEITC (alone) vs control and caspase inhibitor treated groups.

and nuclear condensation also demonstrated that both H₂S and NAC prevent BSO mediated sensitization of HCT116 cells to PEITC.

DISCUSSION

In the present investigation we sought to examine whether

exogenous sources of the reductant H₂S could alter the response of human colon cancer cells to β-phenylethyl isothiocyanate induced apoptosis. PEITC is known to possess potent chemopreventative properties against carcinogen induced colon cancer in rodent models, perhaps mediated largely by the induction of carcinogen detoxification pathways, anti-inflammatory affects, and apoptosis^[8,11,18,19,45]. It is

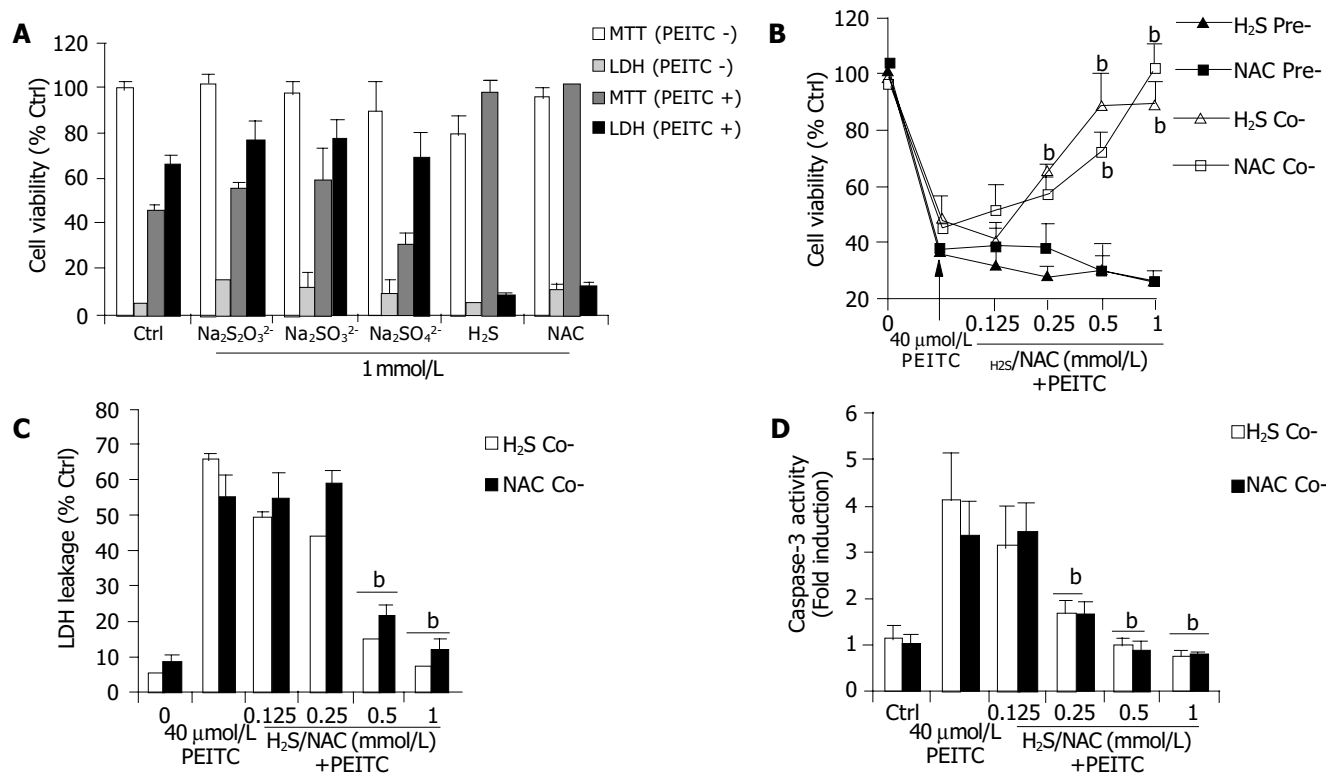


Figure 3 A: Effects of low molecular weight sulfur compounds on PEITC mediated loss of cell viability; B and C: Inhibition of PEITC mediated loss of cell viability in HCT116 cells following either co-treatment or pre-treatment (24 h) with H₂S or NAC (125 μmol-1 mmol/L) as determined by MTT or LDH leakage. Data are expressed as mean±SD, (n = 8); D: Co-treatment with either H₂S or

NAC (125 μmol-1 mmol/L) inhibits PEITC induced caspase-3 activity as determined at 16 h and Data are representative of 3 or more separate experiments conducted on separate occasions. mean±SD, ^bP<0.01 vs PEITC treated groups.

interesting to note, that previous investigations have shown that colon cancer cells are more sensitive to ITC mediated cytotoxicity than their detransformed counterparts. This property has been proposed to protect against the development of colorectal cancer by inhibiting the growth of transformed cell clones within the gastrointestinal mucosa^[46,47]. However, factors that may limit these beneficial effects have been largely unexplored.

The biological properties of ITCs, including PEITC, are predominantly mediated by the electrophilic central carbon atom of the isothiocyanate groups (R-N = C = S)^[48]. The NCS residue readily reacts with nucleophilic centers of deprotonated thiols such as those present on glutathione (GSH) and N-acetylcysteine (NAC) leading to the formation of N-substituted mono-dithiocarbamate conjugates. Such interactions alter the intracellular redox state and activate phase II detoxification enzymes or apoptotic signaling pathways.

Considering that sulfur metabolizing bacteria generate appreciable levels of the thiol H₂S in the GI tract, via metabolism of inorganic and organic sulfur compounds, we investigated whether H₂S could act in a similar manner to GSH or NAC in the detoxification of PEITC. Early work conducted by Zuman and Zahradnik^[49] demonstrated that organic ITCs can reversibly react with the hydrosulfide ion of H₂S forming N-mono-substituted dithiocarbamates, such findings supporting our hypothesis. However, whether these interactions could change the biological properties of PEITC, as well as other ITCs were not explored. H₂S

concentrations in the GI tract range between 0.2-1 mmol/L in mice and up to 3.4 mmol/L in human feces, therefore chemical interaction between H₂S and PEITC are highly plausible. On the basis of the chemical nature of H₂S and its similar biological characteristics to that of both GSH and NAC e.g. antioxidant properties and a deprotonated thiol group in aqueous solution, perhaps H₂S at physiological concentrations may impair the biological properties of electrophilic chemopreventive agents against colon cancer cells.

In our study, PEITC reduced colon cancer cell viability in a concentration manner in all cell lines studied (Figure 1). In addition, we also confirmed that the loss of cell viability in HT29 and HCT116 cells was due to the induction of apoptosis as assessed by nuclear fragmentation and condensation, LDH leakage, caspase-3 like activation and an increase in the SubG1 population (Figure 2). We next addressed using the HCT116 cell line whether H₂S could impair PEITC induced apoptosis. In each assay examined H₂S significantly reduced the apoptotic response of HCT116 cells to PEITC at concentrations well within the physiological reported levels (up to 3.4 mmol/L). Indeed, H₂S was almost as effective on a molar basis at inhibiting PEITC induced apoptosis as the antioxidant thiol N-acetylcysteine, a known inhibitor of PEITC intracellular up-take^[12]. We assume that the mechanism of inhibition by H₂S is similar to NAC, although this requires further study.

Understanding the mechanisms by which PEITC mediates apoptosis and factors that may influence its *in vivo* efficacy is of considerable importance as PEITC mediated

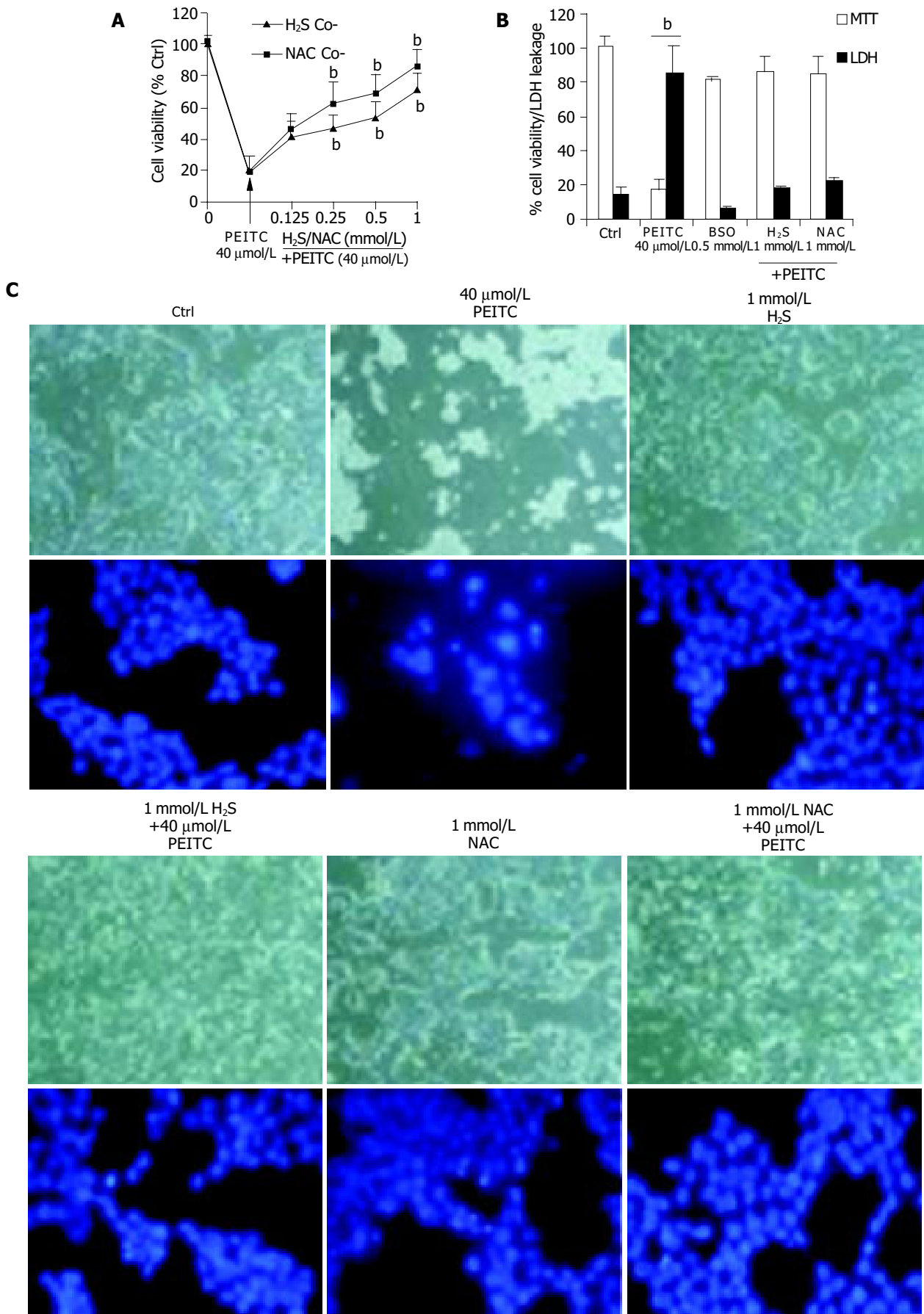


Figure 4 Inhibition of PEITC mediated loss in cell viability in GSH depleted cells following pre-treatment with 0.5 mmol/L BSO for 24 h. Both H₂S and NAC inhibited PEITC induced loss of cell viability in concentration dependant manner as determined using the MTT assay (A) and (B) LDH leakage. (C) Respective

photographs and DAPI stained cells showing cell morphological changes and nuclear condensation. Data are representative of 3 or more separate experiments conducted on separate occasions. mean±SD, ^bP<0.01 vs PEITC treated to control groups.

apoptosis is thought to contribute to its chemopreventative effects. In particular, extensive induction in apoptosis by PEITC has been observed in cell culture studies and rodent models of colon cancer. Similarly, an inverse correlation between ITC exposure and a reduction in colon cancer prevalence has been demonstrated in some epidemiological studies. Whether elevated levels of H₂S observed in colon cancer and ulcerative colitis impair chemopreventative or chemotherapeutic drug induced anti-inflammatory and apoptotic effects of has yet to be demonstrated.

In summary, our data reports for the first time that physiological concentrations of H₂S can inhibit the apoptotic effects of the chemopreventative agent PEITC. It is possible based on our data that changes in H₂S levels along the GI tract may influence the extent of PEITC mediated apoptosis *in vivo*. The potential interaction of H₂S with other dietary constituents as well as chemotherapeutic drugs requires further study.

REFERENCES

- 1 **Fahey JW**, Zalcman AT, Talalay P. The chemical diversity and distribution of glucosinolates and isothiocyanates among plants. *Phytochemistry* 2001; **56**: 5-51
- 2 **Rask L**, Andreasson E, Ekblom B, Eriksson S, Pontoppidan B, Meijer J. Myrosinase: gene family evolution and herbivore defence in Brassicaceae. *Plant Mol Biol* 2000; **42**: 93-113
- 3 **Zhang Y**, Talalay P. Anticarcinogenic activities of organic isothiocyanates: chemistry and mechanisms. *Cancer Res* 1994; **54**: 1976S-1981
- 4 **Verhoeven DT**, Verhagen H, Goldbohm RA, Van Poppel G. A review of mechanisms underlying anticarcinogenicity by brassica vegetables. *Chem Biol Interact* 1997; **103**: 79-126
- 5 **London SJ**, Yuan JM, Chung FL, Gao JT, Coetzee GA, Ross RK, Yu MC. Isothiocyanates, glutathione S-transferase M1 and T1 polymorphisms, and lung-cancer risk: a prospective study of men in Shanghai, China. *Lancet* 2000; **356**: 724-729
- 6 **Zhao B**, Seow A, Lee EI, Poh WT, The M, Eng P, Wang YT, Tan WC, Yu MC, Lee HP. Dietary isothiocyanates, glutathione S-transferase -M1, -T1 polymorphisms and lung cancer risk among Chinese women in Singapore. *Cancer Epidemiol Biomarkers Prev* 2001; **10**: 1063-1067
- 7 **Conaway CC**, Jiao D, Chung FL. Inhibition of rat liver cytochrome P450 isozymes by isothiocyanates and their conjugates: a structure-activity relationship study. *Carcinogenesis* 1996; **17**: 2423-2427
- 8 **Rose P**, Faulkner K, Williamson G, Mithen R. 7-Methylsulfinylheptyl and 8-methylsulfinyloctyl isothiocyanates from watercress are potent inducers of phase II enzymes. *Carcinogenesis* 2000; **21**: 1983-1988
- 9 **Mithen R**, Faulkner K, Magrath R, Rose P, Williamson G, Marquez J. Development of isothiocyanate-enriched broccoli, and its enhanced ability to induce phase 2 detoxification enzymes in mammalian cells. *Theor Appl Genet* 2003; **106**: 727-734
- 10 **Zhang DD**, Hannink M. Distinct cysteine residues in Keap1 are required for Keap1-dependent ubiquitination of Nrf2 and for stabilization of Nrf2 by chemopreventive agents and oxidative stress. *Mol Cell Biol* 2003; **23**: 8137-8151
- 11 **Zhang Y**, Talalay P. Mechanism of differential potencies of isothiocyanates as inducers of anticarcinogenic Phase 2 enzymes. *Cancer Res* 1998; **58**: 4632-4639
- 12 **Zhang Y**. Molecular mechanism of rapid cellular accumulation of anticarcinogenic isothiocyanates. *Carcinogenesis* 2001; **22**: 425-431
- 13 **Gamet-Payrastrre L**, Li P, Lumeau S, Cassar G, Dupont MA, Chevolleau S, Gasc N, Tulliez J, Terce F. Sulforaphane, a naturally occurring isothiocyanate, induces cell cycle arrest and apoptosis in HT29 human colon cancer cells. *Cancer Res* 2000; **60**: 1426-1433
- 14 **Hu R**, Kim BR, Chen C, Hebbar V, Kong AN. The roles of JNK and apoptotic signaling pathways in PEITC-mediated responses in human HT-29 colon adenocarcinoma cells. *Carcinogenesis* 2003; **24**: 1361-1367
- 15 **Rose P**, Whiteman M, Huang SH, Halliwell B, Ong CN. beta-Phenylethyl isothiocyanate-mediated apoptosis in hepatoma HepG2 cells. *Cell Mol Life Sci* 2003; **60**: 1489-1503
- 16 **Rose P**, Armstrong JS, Chua YL, Ong CN, Whiteman M. beta-Phenylethyl isothiocyanate mediated apoptosis; contribution of Bax and the mitochondrial death pathway. *Int J Biochem Cell Biol* 2005; **37**: 100-119
- 17 **Xu K**, Thornalley P. Studies on the mechanism of the inhibition of human leukaemia cell growth by dietary isothiocyanates and their cysteine adducts *in vitro*. *Biochem Pharmacol* 2000; **60**: 221-231
- 18 **Chung FL**, Conaway CC, Rao CV, Reddy BS. Chemoprevention of colonic aberrant crypt foci in Fischer rats by sulforaphane and phenethyl isothiocyanate. *Carcinogenesis* 2000; **21**: 2287-2291
- 19 **Smith TK**, Mithen R, Johnson IT. Effects of Brassica vegetable juice on the induction of apoptosis and aberrant crypt foci in rat colonic mucosal crypts *in vivo*. *Carcinogenesis* 2003; **24**: 491-495
- 20 **Matusheski NV**, Juvik JA, Jeffery EH. Heating decreases epithiospecifier protein activity and increases sulforaphane formation in broccoli. *Phytochemistry* 2004; **65**: 1273-1281
- 21 **Hwang ES**, Jeffery EH. Effects of different processing methods on induction of quinone reductase by dietary broccoli in rats. *J Med Food* 2004; **7**: 95-99
- 22 **Keck AS**, Qiao Q, Jeffery EH. Food matrix effects on bioactivity of broccoli-derived sulforaphane in liver and colon of F344 rats. *J Agric Food Chem* 2003; **51**: 3320-3327
- 23 **Rouzaud G**, Young SA, Duncan AJ. Hydrolysis of glucosinolates to isothiocyanates after ingestion of raw or microwaved cabbage by human volunteers. *Cancer Epidemiol Biomarkers Prev* 2004; **13**: 125-131
- 24 **Rouzaud G**, Rabot S, Ratcliffe B, Duncan AJ. Influence of plant and bacterial myrosinase activity on the metabolic fate of glucosinolates in gnotobiotic rats. *Br J Nutr* 2003; **90**: 395-404
- 25 Integrated Risk Information System (2003) Toxicological review of hydrogen sulphide. U.S. Environmental Protection Agency EPA/635/R-03/005 [www document]. URL <http://www.epa.gov/iris> [accessed 1 November 2003]
- 26 **Kamoun P**. Endogenous production of hydrogen sulfide in mammals. *Amino Acids* 2004; **26**: 243-254
- 27 **Deplancke B**, Finster K, Graham WV, Collier CT, Thurmond JE, Gaskins HR. Gastrointestinal and microbial responses to sulfate-supplemented drinking water in mice. *Exp Biol Med* 2003; **228**: 424-433
- 28 **Florin T**, Neale G, Gibson GR, Christl SU, Cummings JH. Metabolism of dietary sulphate: absorption and excretion in humans. *Gut* 1991; **32**: 766-773
- 29 **Maghee EA**, Richardson CJ, Hughes R, Cummings JH. Contribution of dietary protein to sulfide production in the large intestine: an *in vitro* and a controlled feeding study in humans. *Am J Clin Nutr* 2000; **72**: 1488-1494
- 30 **Huycke MM**, Gaskins HR. Commensal bacteria, redox stress, and colorectal cancer: mechanisms and models. *Exp Biol Med* 2004; **229**: 586-597
- 31 **Deplancke B**, Gaskins HR. Hydrogen sulfide induces serum-independent cell cycle entry in non-transformed rat intestinal epithelial cells. *FASEB J* 2003; **17**: 1310-1312
- 32 **Picton R**, Eggo MC, Merrill GA, Langman MJ, Singh S. Mucosal protection against sulphide: importance of the enzyme rhodanese. *Gut* 2002; **50**: 201-205
- 33 **Furne J**, Springfield J, Koenig T, DeMaster E, Levitt MD. Oxidation of hydrogen sulfide and methanethiol to thiosulfate by rat tissues: a specialized function of the colonic mucosa.

- Biochem Pharmacol* 2001; **62**: 255-259
- 34 **Roediger WE**, Lawson MJ, Kwok V, Grant AK, Pannall PR. Colonic bicarbonate output as a test of disease activity in ulcerative colitis. *J Clin Pathol* 1984; **37**: 704-707
- 35 **Kimura Y**, Kimura H. Hydrogen sulfide protects neurons from oxidative stress. *FASEB J* 2004; **18**: 1165-1167
- 36 **Whiteman M**, Armstrong JS, Chu SH, Jia-Ling S, Wong BS, Cheung NS, Halliwell B, Moore PK. The novel neuromodulator hydrogen sulfide: an endogenous peroxynitrite 'scavenger'? *J Neurochem* 2004; **90**: 765-768
- 37 **Geng B**, Chang L, Pan C, Qi Y, Zhao J, Pang Y, Du J, Tang C. Endogenous hydrogen sulfide regulation of myocardial injury induced by isoproterenol. *Biochem Biophys Res Commun* 2004; **318**: 756-763
- 38 **Ono B**, Ishii N, Fujino S, Aoyama I. Role of hydrosulfide ions (HS⁻) in methylmercury resistance in *Saccharomyces cerevisiae*. *Appl Environ Microbiol* 1991; **57**: 3183-3186
- 39 **Edgcomb VP**, Molyneaux SJ, Saito MA, Lloyd K, Boer S, Wirsén CO, Atkins MS, Teske A. Sulfide ameliorates metal toxicity for deep-sea hydrothermal vent archaea. *Appl Environ Microbiol* 2004; **70**: 2551-2555
- 40 **Hansen MB**, Nielsen SE, Berg K. Re-examination and further development of a precise and rapid dye method for measuring cell growth/cell kill. *J Immunol Methods* 1989; **119**: 203-210
- 41 **Nicoletti I**, Migliorati G, Pagliacci MC, Grignani F, Riccardi C. A rapid and simple method for measuring thymocyte apoptosis by propidium iodide staining and flow cytometry. *J Immunol Methods* 1991; **139**: 271-279
- 42 **Thornberry NA**, Rano TA, Peterson EP, Rasper DM, Timkey T, Garcia-Calvo M, Houtzager VM, Nordstrom PA, Roy S, Vaillancourt JP, Chapman KT, Nicholson DW. A combinatorial approach defines specificities of members of the caspase family and granzyme B. Functional relationships established for key mediators of apoptosis. *J Biol Chem* 1997; **272**: 17907-17911
- 43 **Garcia-Calvo M**, Peterson EP, Leiting B, Ruel R, Nicholson DW, Thornberry NA. Inhibition of human caspases by peptide-based and macromolecular inhibitors. *J Biol Chem* 1998; **273**: 32608-32613
- 44 **Powolny A**, Takahashi K, Hopkins RG, Loo G. Induction of GADD gene expression by β -phenethyl isothiocyanate in human colon adenocarcinoma cells. *J Cell Biochem* 2003; **90**: 1128-1139
- 45 **Jeong WS**, Kim IW, Hu R, Kong AN. Modulatory properties of various natural chemopreventive agents on the activation of NF-kappaB signaling pathway. *Pharm Res* 2004; **21**: 661-670
- 46 **Musk SR**, Johnson IT. Allyl isothiocyanate is selectively toxic to transformed cells of the human colorectal tumour line HT29. *Carcinogenesis* 1993; **14**: 2079-2083
- 47 **Musk SR**, Stephenson P, Smith TK, Stening P, Fyfe D, Johnson IT. Selective toxicity of compounds naturally present in food toward the transformed phenotype of human colorectal cell line HT29. *Nutr Cancer* 1995; **24**: 289-298
- 48 **Podhradsky D**, Drobnica L, Kristian P. Reactions of cysteine, its derivatives, glutathione coenzyme A, and dihydrolipoic acid with isothiocyanates. *Experientia* 1979; **35**: 154-155
- 49 **Zahradnik R**, Zuman P. Kinetics and decomposition mechanism of dithiocarbamic acids solutions. Polarographic study. *Z Phys Chem* 1957; **208**: 135-140

Science Editor Li WZ Language Editor Elsevier HK

• COLORECTAL CANCER •

Microsatellite instable double primary cancers of the colorectum and stomach exhibit less favorable outcome

Young Ho Kim, Sang Yong Song, Young Dae Kwon, Dae Shick Kim, Ho Kyung Chun, Jong Chul Rhee

Young Ho Kim, Jong Chul Rhee, Department of Medicine, Samsung Medical Center, Sungkyunkwan University School of Medicine, Seoul 135-710, Republic of Korea
Sang Yong Song, Dae Shick Kim, Department of Pathology, Samsung Medical Center, Sungkyunkwan University School of Medicine, Seoul 135-710, Republic of Korea
Young Dae Kwon, Department of Preventive Medicine, Samsung Medical Center, Sungkyunkwan University School of Medicine, Seoul 135-710, Republic of Korea
Ho Kyung Chun, Department of Surgery, Samsung Medical Center, Sungkyunkwan University School of Medicine, Seoul 135-710, Republic of Korea
Correspondence to: Dr. Sang Yong Song, Department of Pathology, Samsung Medical Center, 50 Irwon-dong, Gangnam-gu, Seoul 135-710, Republic of Korea. yodasong@smc.samsung.co.kr
Telephone: +82-2-3410-2800 Fax: +82-2-3410-0025
Received: 2004-08-26 Accepted: 2004-10-07

Abstract

AIM: To ascertain the adequacy of the microsatellite instability (MSI) as a prognostic indicator by assessing MSI status of patients with double primary gastric and colorectal cancer (DPGCC).

METHODS: Sixteen patients were studied, all of whom exhibited sporadic DPGCC, and had no family history of hereditary non-polyposis colorectal cancer, according to the Amsterdam criteria. A total of 32 cancers from 16 DPGCC patients, and 216 single primary CRC, were assessed for MSI in 5 microsatellite loci, BAT25, BAT26, D2S123, D5S346, and D17S250.

RESULTS: MSI was observed in 6 (37.5%) of 16 GC and 4 (25.0%) of 16 CRC. Thirty tumors (13.9%) out of 216 single primary CRC and one tumor (16.7%) out of 6 double primary CRC were found to be microsatellite unstable. Of the 6 GC with MSI in DPGCC, 5 (31.3%) were MSI-high and one (6.3%) was MSI-low. In 5 of 16 DPGCC patients, the cancer recurred in or adjacent to the anastomosis or metastasized to the kidney or lung. The MSI-high DPGCC cases were associated with a younger age of onset (47.5 years vs 62.5 years), higher frequency of lymph node metastasis (100% vs 25%), and advanced Dukes stage (C, 100% vs 41.7%), as well as a higher frequency of recurrence or metastasis (100% vs 8.3%). Only recurrence or metastasis showed statistical significance by Fisher's exact test.

CONCLUSION: Our data suggest that MSI may play an important role in the development of DPGCC, and that it may be used clinically as a molecular predictive marker

for recurrence or late metastasis of DPGCC.

© 2005 The WJG Press and Elsevier Inc. All rights reserved.

Key words: Stomach neoplasms; Colorectal neoplasms; Microsatellite instability; Double primary

Kim YH, Song SY, Kwon YD, Kim DS, Chun HK, Rhee JC. Microsatellite instable double primary cancers of the colorectum and stomach exhibit less favorable outcome. *World J Gastroenterol* 2005; 11(26): 3998-4002
<http://www.wjgnet.com/1007-9327/11/3998.asp>

INTRODUCTION

Gastric cancers (GC) and colorectal cancers (CRC) are common neoplasms in Korea and Japan. Almost 5% of GC and CRC patients develop other primary gastrointestinal (GI) cancers, either synchronously or metachronously^[1]. GC is the most prevalent extra CRC among multiple primary GI cancers involving CRC in Korea and Japan^[2,3]. The determination of high-risk groups of patients with multiple primary cancers involving the GI tract is important for clinical management, especially with regard to the prediction of patient's prognoses^[4]. The most well-known example of multiple primary cancers is hereditary non-polyposis colorectal cancer (HNPCC), an autosomally dominant hereditary syndrome which is caused by germline mutations in mismatch repair genes, including hMSH2, hMLH1, hPMS1, hPMS2, and hMSH6. Ninety percent of HNPCCs exhibit microsatellite instability (MSI)^[5]. MSI has also been observed in approximately 15-30% of single sporadic GC^[6,7] and in 10-15% of single sporadic CRC^[8,9]. Germline mutations of MLH1 and MSH2 occur at approximately equal frequencies in HNPCC, whereas virtually all sporadic MSI-high cancers develop due to epigenetic silencing of the MLH1 promoter through somatic hypermethylation^[10-13]. MSI may impart a favorable prognosis in colorectal, gastric, pancreatic, and probably esophageal cancers, but a poor prognosis in non-small cell lung cancer^[14].

Some reports have suggested the contribution of MSI in double primary cancers involving both the colorectum and stomach in the same patient^[4,15-17]. According to these reports, MSI is an indicator of increased cancer susceptibility in these double primary gastric and colorectal cancer (DPGCC) patients and genetic instability may play an important role in the development of these cancers. However, little remains known regarding the prognostic role of MSI in DPGCC, although a number of previous studies

have focused on the etiology or carcinogenic mechanisms of DPGCC. Therefore, we examined MSI status in patients with DPGCC in order to ascertain the adequacy of MSI as a prognostic indicator.

MATERIALS AND METHODS

Patients

Sixteen patients with sporadic DPGCC were studied. None of these cases had any family history of the HNPCC, according to the Amsterdam criteria for HNPCC. All patients underwent curative resections of both stomach and large bowel with tumor-free resection margins at the Department of Surgery, Samsung Medical Center, between January, 1994 and December, 2002, with the exception of one (case 12). Clinicopathological features are summarized in Table 1. Ages ranged from 35 to 76 (58.8 ± 10.1) years. Patients with synchronous DPGCC were defined as cases diagnosed with a secondary cancer that was detected within 6 mo of the detection of primary cancer, and those with metachronous DPGCC were defined as cases diagnosed with a secondary cancer detected more than 6 mo later, as previously described^[15,18]. Our study included 12 cases of synchronous (75.0%) and 4 cases of metachronous (25.0%) DPGCC. In one out of the 4 metachronous cases, the initial cancer was GC; in the remaining 3, it was CRC. The average ages of patients with synchronous and metachronous DPGCC were the same as the mean, 58.8 years. In cases of GC, 10 were found to be intestinal type (62.5%), and 6 cases were diffuse type (37.5%). Four cases were early type (25.0%), and 12 cases were advanced type (75.0%). No lymph node metastasis was detected in any of the cases of GC, and all cases were at stage I. In cases of CRC, six (37.5%) were located at the left-side of the colon or in the rectum. Four cases exhibited mucinous differentiation (25.0%) and 12 cases evidenced moderate tubular differentiation (75.0%). Nine cases (56.3%) of CRC exhibited lymph node metastasis, and 14 (87.5%) were at an advanced

stage (Dukes B or C).

Two hundred and sixteen single primary CRC, and 6 double primary CRC, were analyzed for MSI for the comparison in the current study for DPGCC.

We followed the recurrence and survival of 16 patients with DPGCC for at least 18 mo.

DNA extraction and MSI analysis

Microdissection was performed by an expert pathologist in this field using 10- μ m-thick hematoxylin-stained tissue sections in order to reduce contamination from other cellular DNA components. DNA was extracted from formalin-fixed, paraffin-embedded archival specimens of tumors and matched normal tissues, using the DNeasy Tissue kit (Qiagen, Hilden, Germany).

Five primers from independent genomic sites, including two mononucleotide repeat microsatellites (BAT25 and BAT26) and three dinucleotide repeat microsatellites (D2S123, D5S346 and D17S250), all of which were recommended by the National Cancer Institute workshop, were used in this study. Forward primers were synthesized with a fluorescent tag (FAM and NED) on the 5' end, and were purified by standard high-performance liquid chromatography. One hundred nanograms of DNA was amplified in a 20 μ L reaction solution, which containing 2 μ L of 10 \times buffer (Roche, Mannheim, Germany), 1.75-3 mmol/L MgCl₂, 0.4 μ mol/L primer pairs, 250 μ mol/L deoxynucleoside triphosphate, and 2.5 units of DNA polymerase (Roche, Mannheim, Germany). Amplifications were performed using a 2 min initial denaturation at 94 $^{\circ}$ C, followed by 30 cycles of 45 s at 94 $^{\circ}$ C, 45 s at 55 $^{\circ}$ C, and 45 s at 72 $^{\circ}$ C, and 5 min final extension at 72 $^{\circ}$ C. The fluorescence-labeled PCR products were electrophoresed on an Applied Biosystems 3100 automated DNA sequencer (Applied Biosystems, Foster, USA), and the fluorescent signals from the differently-sized alleles were recorded and analyzed using Genescan software (version 2.7; Applied Biosystems).

Table 1 Clinicopathologic features of double primary gastric and colorectal cancers

Case	Sex	Age (yr)	Onset	Gastric cancer			Site	Colorectal cancer				
				Differentiation	T	N		Stage	Differentiation	T	N	Stage
1	Male	49	Synchronous	Diffuse	1	0	1	TC	Moderate	4	1	3/C
2	Male	35	Synchronous	Intestinal	2	0	1	AC	Mucinous	3	2	3/C
3	Male	50	Metachronous	Intestinal	2	0	1	DC	Moderate	3	1	3/C
4	Male	56	Synchronous	Intestinal	1	0	1	C	Moderate	3	1	3/C
5	Male	68	Synchronous	Intestinal	1	0	1	SC	Mucinous	3	0	2/B
6	Male	57	Synchronous	Diffuse	1	0	1	R	Moderate	3	2	3/C
7	Male	54	Synchronous	Intestinal	2	0	1	SC	Moderate	2	0	1/A
8	Male	61	Synchronous	Intestinal	1	0	1	AC	Moderate	2	0	1/A
9	Female	76	Metachronous	Intestinal	1	0	1	TC	Moderate	3	0	2/B
10	Male	65	Synchronous	Intestinal	1	0	1	AC	Moderate	3	0	2/B
11	Female	65	Synchronous	Diffuse	1	0	1	AC	Mucinous	3	1	3/C
12	Male	48	Metachronous	Diffuse	?	?	?	AC	Moderate	3	2	3/C
13	Male	71	Synchronous	Intestinal	1	0	1	AC	Well	3	1	3/C
14	Male	65	Synchronous	Diffuse	1	0	1	SC	Moderate	3	0	2/B
15	Male	59	Synchronous	Intestinal	1	0	1	AC	Mucinous	3	0	2/B
16	Male	61	Metachronous	Diffuse	2	0	1	SC	Moderate	3	1	3/C

C, cecum; AC, ascending colon; TC, transverse colon; DC, descending colon; SC, sigmoid colon; R, rectum.

Statistical analysis

Either Fisher's exact tests or Mann-Whitney tests were used to analyze variations in MSI status between various parameters. *P* values of less than 0.05 were considered statistically significant. Specialized statistical assistance was warranted by the small number of samples.

RESULTS

A total of 32 cancers from 16 Korean DPGCC patients and 216 single primary CRC cases were assessed for MSI, for 5 microsatellite loci. MSI results are summarized in Table 2. MSI was observed in six (37.5%) of 16 GC and 4 (25.0%) of 16 CRC in DPGCC patients (Figure 1). Thirty (13.9%) tumors of 216 single primary CRCs and one (16.7%) tumor of 6 double primary CRCs were found to be microsatellite unstable. Of the 6 GC with MSI in DPGCC, 5 (31.3%) were MSI-high and one (6.3%) was MSI-low. All CRC with MSI were MSI-high. There was an increasing tendency of MSI detected, with the lowest probability in single primary CRC, followed by double primary CRC, CRC of DPGCC, and GC of DPGCC. Two of six patients with MSI (33.3%) exhibited heterogeneity in terms of microsatellite alterations. For example, one lesion exhibited the MSI phenotype, but the other lesion in the same patient proved uninformative. One MSI in double primary CRC showed homogeneity with regard to MSI-high status.

Five patients of 16 DPGCC exhibited recurrence, either in or adjacent to the anastomosis or metastasis to different organs, such as the kidney or lung (Table 2). Case 1 exhibited recurrence of GC, 21 mo after the initial diagnosis, and recurrence of CRC 22 mo, after the initial diagnosis, both occurring at the anastomosis site. Case 2 exhibited metastatic GC in the right kidney, 88 mo after initial diagnosis. Case 3 exhibited an ampulla of Vater cancer at the time of initial diagnosis. Case 4 exhibited a recurrent CRC in another colonic segment (initial, cecum; recurred, transverse colon)

10 mo after the initial diagnosis. Case 16 exhibited metastatic CRC in the left lung 67 mo after the initial diagnosis.

The MSI-high DPGCC was associated with a younger age of onset (47.5 years *vs* 62.5 years), a higher frequency of lymph node metastasis (100% *vs* 25%), advanced Dukes stage (C, 100% *vs* 41.7%), and higher frequency of recurrence or metastasis (100% *vs* 8.3%) (Table 3). Only recurrence or metastasis showed statistical significance, with *P* values of less than 0.005, by Fisher's exact test.

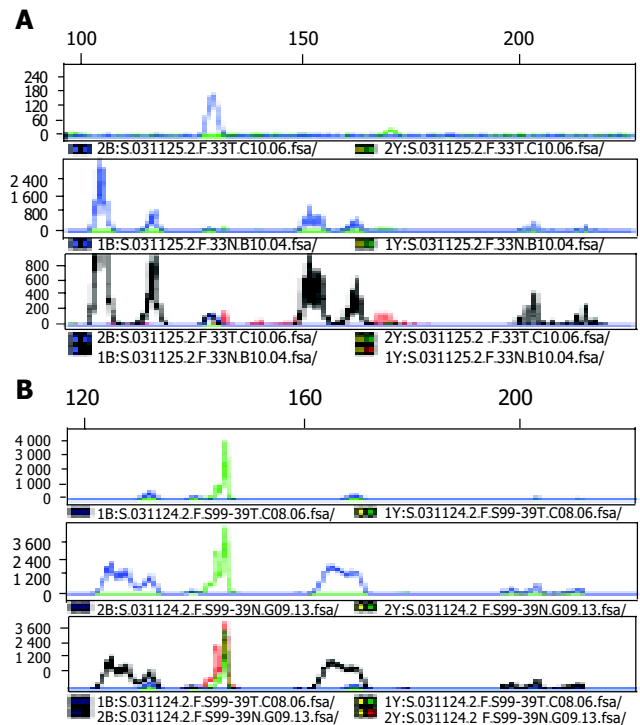


Figure 1 Typical results of microsatellite instability (MSI) of tumors. **A:** Abnormal MSI peaks (arrows) of gastric cancer from case 4; **B:** Abnormal MSI peaks (arrows) of colonic cancer from case 2(upper row: normal tissue, middle row: cancer tissue, low row: upper row + middle row).

Table 2 Microsatellite instability (MSI) and follow-up results of double primary gastric and colorectal cancers

Case	Gastric cancer (GC)						Colorectal cancer (CRC)						Follow-up (mo)
	bat26	D5S346	bat25	D17S250	D2S123	MSI	bat26	D5S346	bat25	D17S250	D2S123	MSI	
1	●	●	○	○	●	H	●	○	●	○	○	H	21, alive, RGC 22, alive, RCRC
2	●	●	●	○	●	H	●	●	○	○	○	H	88, alive, MGC, kidney
3	●	●	●	○	●	H	●	○	●	○	●	H	58, alive, +AOV cancer
4	●	○	●	○	○	H	●	○	●	○	○	H	10, alive, RCRC
5	●	●	●	●	●	H	○	○	○	○	○	I	18, alive, NED
6	○	○	●	○	○	L	○	○	○	○	○	I	38, alive, NED
7	○	○	○	○	○	S	○	○	○	○	○	S	29, alive, NED
8	○	○	○	○	○	S	○	○	○	○	○	S	18, alive, NED
9	○	○	○	○	○	S	○	○	○	○	○	S	114, alive, NED
10	○	○	○	○	○	S	○	○	○	○	○	S	85, alive, NED
11	○	○	○	○	○	S	○	○	○	○	○	S	61, alive, NED
12	○	○	○	○	○	S	○	○	○	○	○	S	82, alive, NED
13	○	○	○	○	○	I	○	○	○	○	○	S	19, alive, NED
14	○	○	○	○	○	S	○	○	○	○	○	I	17, alive, NED
15	○	○	○	○	○	I	○	○	○	○	○	S	29, alive, NED
16	○	○	○	○	○	I	○	○	○	○	○	S	67, alive, MCRC, lung

H, MSI-high; L, MSI-low; I, inconclusive; NED, no evidence of disease; RGC, recurrent gastric cancer; RCRC, recurrent colorectal cancer; MGC, metastatic gastric cancer; MCRC, metastatic colorectal cancer; AOV, ampulla of Vater.

Table 3 Differences of double primary gastric and colorectal cancers according to microsatellite instability (MSI)

	Both MSI-high (n = 4)	Others (n = 12)	P
Male : Female	4 : 0	10 : 2	NS
Age (yr)	47.5±8.9 (35-56)	62.5 ±7.6 (48-76)	NS
Gastric cancer			
- intestinal : diffuse	3 : 1	7 : 5	NS
- size (cm)	2.8	3.1	NS
Colorectal cancer			
- tubular : mucinous	3 : 1	9 : 3	NS
- size (cm)	4.7	4.2	NS
- node metastasis	100%	25%	NS
- Dukes A : B : C	0 : 0 : 4	2 : 5 : 5	NS
Recurrence, metastasis, or other organ malignancy	100%	8.3%	<0.005

NS: not significant.

DISCUSSION

MSI has been suggested to play an important role in the development of multiple primary cancers of the gastrointestinal tract. Thus, MSI appears to be useful in screening for the detection of a high-risk group for secondary primary cancer in some patients with sporadic single gastric and colorectal cancers, because it is rapid and inexpensive.

MSI has been observed in approximately 15-30% of single sporadic gastric cancers^[6,7] and 10-15% of single sporadic colorectal cancers^[8,9]. Our results regarding MSI rate in double primary CRC and single sporadic CRC, were not radically different from the results of other investigators. In our study, MSI was observed in 31.3%, 25.0%, 16.7%, and 13.9% of GC in patients with DPGCC, CRC of patients with DPGCC, double primary CRC, and single primary CRC, respectively. This indicates that genetic instability may play an important role in the development of multiple primary cancers of the GI tract. MSI has been observed more frequently in multiple GI cancer patients than in those with single primary gastric or colorectal cancers, as demonstrated in previous reports^[3,4]. Concordant MSI rate, and MSI-high status in both cancers, has been reported 17.7-25.0% of DPGCC^[3,15]. Our result is very similar to these. Yamashita *et al.*^[4], reported that MSI-high status was seen more frequently in the same organ group, especially in multiple GC patients, than in different organ groups, and lesions from different organ groups tended to show MSI-low or stable phenotype. Thus, MSI in multiple GI cancers containing GC appears to be relatively common, and may play an important role in multi-organ carcinogenesis.

The relationship between MSI of DPGCC and patient prognosis or clinicopathological features remains unclear. Kim *et al.*^[3], reported that MSI-positive CRC was characterized by fungating tumor gross, poor or mucinous differentiation, and rare nodal metastasis. MSI-positive GC was characterized by intestinal type, smaller size, and rare nodal spread. They were unable to explain discrepancies in size and differentiation between CRC and GC. According to our result, the clinicopathological features of GC were basically the same concordantly MSI-positive GC as was observed in other cases of DPGCC. Studied cases were usually intestinal type,

and at a relatively early stage. Differences, in general, were seen in the age and the clinicopathological features of CRC. Concordantly MSI-positive CRC was associated with younger age, larger tumor size, more frequent nodal metastasis, higher stage, and more frequent recurrence and distant metastasis. Our results were also different from others. Ohtani *et al.*^[15], reported that concordantly MSI-positive CRC was usually associated with better prognosis. There were no dead patients found, among 5 concordantly MSI-positive DPGCC, and 4 dead patients (26.7%) among the 15 remaining cases. However, no explanation was given in their report regarding about the causes of death. In our results, we found no cancer-related or natural deaths in the studied cases. Ikeda *et al.*^[19], compared the prognosis of patients with DPGCC with patients with single cancer, and reported that the former was better than the latter. One explanation for this difference in prognosis may be that DPGCC is often discovered at an early stage. According to our results, the stage of DPGCC was more advanced in concordantly MSI-positive DPGCC. Thus, we suggested that the prognosis of patients with DPGCC appears to be dependent on stage.

Interestingly, there have been no reports regarding the recurrence or late metastasis in patients with DPGCC. We followed the hospital course of all studied cases. Case 1 was a unique example of cancer recurrence in patients with concordantly MSI-positive DPGCC. This patient had mucosa-confined early gastric cancer and Dukes C CRC in the transverse colon synchronously, and underwent curative resection for both organs with ample resection margins. However, both tumors recurred at the anastomosis sites, 21 and 22 mo after the initial diagnosis. Case 2 was also very unique. He had submucosa-confined early gastric cancer and Dukes C CRC in the ascending colon synchronously, and underwent curative resection for both organs with ample resection margins. The patient then had an uneventful history for 7 years. However, renal metastasis of previous early gastric cancer was found 88 mo after the initial diagnosis. Cases 4 and 16 were examples of recurrence and late distant metastasis of advanced-stage CRC. Recent studies have revealed the significance of MSI in gastric carcinogenesis. Kashiwagi *et al.*^[20], reported that MSI in the gastric biopsy specimens of chronic gastritis patients may predict the risk of progression to adenoma and well-differentiated adenocarcinoma. Kim *et al.*^[21], reported that gastric carcinomas arising from adenomas are frequently associated with MSI. These data, and ours, suggest that MSI might play an important role in the early phase of carcinogenesis, and is, therefore, related to the delayed development of recurrent disease. Less clear is the role of and mechanisms underlying MSI-low status. In our study, only one MSI-low was found.

Due to its rarity, the meaning of MSI in DPGCC, whether concordantly-positive or not, is still a topic which warrants future investigation. Our data suggest that MSI may play an important role in the development of DPGCC, and that it may be used clinically as a molecular marker for the prediction of recurrence or late metastasis of DPGCC.

REFERENCES

- 1 Tomoda H, Taketomi A, Baba H, Kohnoe S, Seo Y, Saito T.

- Multiple primary colorectal and gastric carcinoma in Japan. *Oncol Rep* 1998; **5**: 147-149
- 2 **Akagi Y**, Araki Y, Ogata Y, Morodomi T, Shirouzu K, Isomoto H, Kakegawa T. Clinicopathological studies of multiple cancers in the large bowel and other organs. *Kuume Med J* 1993; **40**: 81-88
 - 3 **Kim HC**, Kim CN, Jung CS, Yu CS, Kim JC. Multiple primary malignant neoplasm with colorectal cancer. *J Korean Cancer Assoc* 1998; **30**: 668-674
 - 4 **Yamashita K**, Arimura Y, Kurokawa S, Itoh F, Endo T, Hirata K, Imamura A, Kondo M, Sato T, Imai K. Microsatellite instability in patients with multiple primary cancers of the gastrointestinal tract. *Gut* 2000; **46**: 790-794
 - 5 **Liu B**, Parsons R, Papadopoulos N, Nicolaides NC, Lynch HT, Watson P, Jass JR, Dunlop M, Wyllie A, Peltomaki P, de la Chapelle A, Hamilton SR, Vogelstein B, Kinzler KW. Analysis of mismatch repair genes in hereditary non-polyposis colorectal cancer patients. *Nat Med* 1996; **2**: 169-174
 - 6 **Strickler JG**, Zheng J, Shu Q, Burgart LJ, Alberts SR, Shibata D. p53 mutations and microsatellite instability in sporadic gastric cancer: when guardians fail. *Cancer Res* 1994; **54**: 4750-4755
 - 7 **Chong JM**, Fukayama M, Hayashi Y, Takizawa T, Koike M, Konishi M, Kikuchi-Yanoshita R, Miyaki M. Microsatellite instability in the progression of gastric carcinoma. *Cancer Res* 1994; **54**: 4595-4597
 - 8 **Brown SR**, Finan PJ, Hall NR, Bishop DT. Incidence of DNA replication errors in patients with multiple primary cancers. *Dis Colon Rectum* 1998; **41**: 765-769
 - 9 **Aaltonen LA**, Peltomaki P, Mecklin JP, Jarvinen H, Jass JR, Green JS, Lynch HT, Watson P, Tallqvist G, Juhola M. Replication errors in benign and malignant tumors from hereditary nonpolyposis colorectal cancer patients. *Cancer Res* 1994; **54**: 1645-1648
 - 10 **Thibodeau SN**, French AJ, Cunningham JM, Tester D, Burgart LJ, Roche PC, McDonnell SK, Schaid DJ, Vockley CW, Michels VV, Farr GH Jr, O'Connell MJ. Microsatellite instability in colorectal cancer: Different mutator phenotypes and the principal involvement of hMLH1. *Cancer Res* 1998; **58**: 1713-1718
 - 11 **Esteller M**, Levine R, Baylin SB, Ellenson LH, Herman JG. MLH1 promoter hypermethylation is associated with the microsatellite instability phenotype in sporadic endometrial carcinomas. *Oncogene* 1998; **17**: 2413-2417
 - 12 **Kane MF**, Loda M, Gaida GM, Lipman J, Mishra R, Goldman H, Jessup JM, Kolodner R. Methylation of the hMLH1 promoter correlates with lack of expression of hMLH1 in sporadic colon tumors and mismatch repair-defective human tumor cell lines. *Cancer Res* 1997; **57**: 808-811
 - 13 **Young J**, Simms LA, Biden KG, Wynter C, Whitehall V, Karamatic R, George J, Goldblatt J, Walpole I, Robin SA, Borten MM, Stitz R, Searle J, McKeone D, Fraser L, Purdie DR, Podger K, Price R, Buttenshaw R, Walsh MD, Barker M, Leggett BA, Jass JR. Features of colorectal cancers with high-level microsatellite instability occurring in familial and sporadic settings: Parallel pathways of tumorigenesis. *Am J Pathol* 2001; **159**: 2107-2116
 - 14 **Lawes DA**, SenGupta S, Boulos PB. The clinical importance and prognostic implications of microsatellite instability in sporadic cancer. *Eur J Surg Oncol* 2003; **29**: 201-212
 - 15 **Ohtani H**, Yashiro M, Onoda N, Nishioka N, Kato Y, Yamamoto S, Fukushima S, Hirakawa-Ys Chung K. Synchronous multiple primary gastrointestinal cancer exhibits frequent microsatellite instability. *Int J Cancer* 2000; **86**: 678-683
 - 16 **Kim HS**, Cho NB, Yoo JH, Shin KH, Park JG, Kim YI, Kim WH. Microsatellite instability in double primary cancers of the colorectum and stomach. *Mod Pathol* 2001; **14**: 543-548
 - 17 **Ericson K**, Halvarsson B, Nagel J, Rambech E, Planck M, Piotrowska Z, Olsson H, Nilbert M. Defective mismatch-repair in patients with multiple primary tumours including colorectal cancer. *Eur J Cancer* 2003; **39**: 240-248
 - 18 **Lyons MF**, Redmond J 3rd, Covelli H. Multiple primary neoplasia of the head and neck and lung. *Cancer* 1986; **57**: 2193-2197
 - 19 **Ikeda Y**, Mori M, Kajiyama K, Haraguchi Y, Sugimachi K. Multiple primary gastric and colorectal cancer in Japan. *Int Surg* 1995; **80**: 37-40
 - 20 **Kashiwagi K**, Watanabe M, Ezaki T, Kanai T, Ishii H, Mukai M, Hibi T. Clinical usefulness of microsatellite instability for the prediction of gastric adenoma or adenocarcinoma in patients with chronic gastritis. *B J Cancer* 2000; **82**: 1814-1818
 - 21 **Kim HS**, Woo DK, Bae SI, Kim YI, Kim WH. Microsatellite instability in the adenoma-carcinoma sequence of the stomach. *Lab Invest* 2000; **80**: 57-64

Radiosensitivity of human colon cancer cell enhanced by immunoliposomal docetaxel

Qing-Wei Wang, Hui-Lan Lü, Chang-Cheng Song, Hong Liu, Cong-Gao Xu

Qing-Wei Wang, Hui-Lan Lü, Hong Liu, Cong-Gao Xu, Cancer Research Center, Qilu Hospital of Shandong University, Jinan 250012, Shandong Province, China

Chang-Cheng Song, Basic Research Program, Laboratory of Cancer Prevention, SAIC-Frederick, Inc., National Cancer Institute at Frederick, MD 21702, United States

Supported by the Department of Science and Technology of Shandong Province

Correspondence to: Dr. Qing-Wei Wang, Cancer Research Center, Qilu Hospital of Shandong University, Jinan 250012, Shandong Province, China. wangqingwei@cscsco.org.cn

Telephone: +86-531-2169831

Received: 2004-07-09 Accepted: 2004-08-25

Abstract

AIM: To enhance the radiosensitivity of human colon cancer cells by docetaxel.

METHODS: Immunoliposomal docetaxel was prepared by coupling monoclonal antibody against carcinoembryonic antigen to cyanuric chloride at the PEG terminus of liposome. LoVo adenocarcinoma cell line was treated with immunoliposomal docetaxel or/and irradiation. MTT colorimetric assay was used to estimate cytotoxicity of immunoliposomal docetaxel and radiotoxicity. Cell cycle redistribution and apoptosis were determined with flow cytometry. Survivin expression in LoVo cells was verified by immunohistochemistry. D801 morphologic analysis system was used to semi-quantify immunohistochemical staining of survivin.

RESULTS: Cytotoxicity was induced by immunoliposomal docetaxel alone in a dose-dependent manner. Immunoliposomal docetaxel yielded a cytotoxicity effect at a low dose of 2 nmol/L. With a single dose irradiation, the relative surviving fraction of LoVo cells showed a dose-dependent response, but there were no significant changes as radiation delivered from 4 to 8 Gy. Compared with liposomal docetaxel or single dose irradiation, strongly radiopotentiating effects of immunoliposomal docetaxel on LoVo cells were observed. A low dose of immunoliposomal docetaxel could yield sufficient radiosensitivity. Immunoliposomal docetaxel were achieved both specificity of the conjugated antibody and drug radiosensitization. Combined with radiation, immunoliposomal docetaxel significantly increased the percentage of G₂/M cells and induced apoptosis, but significantly decreased the percentage of cells in G₂/G₁ and S phase by comparison with liposomal docetaxel. Immunohistochemical analysis showed that the brown

stained survivin was mainly in cytoplasm of LoVo cells. Semi-quantitative analysis of the survivin immunostaining showed that the expression of survivin in LoVo cells under irradiation with immunoliposomal docetaxel was significantly decreased.

CONCLUSION: Immunoliposomal docetaxel is strongly effective for target radiosensitization in LoVo colon carcinoma cells, and may offer the potential to improve local radiotherapy.

© 2005 The WJG Press and Elsevier Inc. All rights reserved.

Key words: Radiosensitivity; Human colon cancer cell; Docetaxel; Immunoliposomes

Wang QW, Lü HL, Song CC, Liu H, Xu CG. Radiosensitivity of human colon cancer cell enhanced by immunoliposomal docetaxel. *World J Gastroenterol* 2005; 11(26): 4003-4007 <http://www.wjgnet.com/1007-9327/11/4003.asp>

INTRODUCTION

Colorectal cancer is one of the most common malignant diseases in the world^[1-3]. In the treatment of colorectal cancer, local recurrence is a major problem. To improve the overall survival and reduce the local recurrence rate after surgery, additional radiotherapy is given either preoperatively or postoperatively^[4-7]. Docetaxel has substantial radiosensitizing properties for malignant tumors. It inhibits microtubule disassembly and interferes with mitotic spindle function to block cells at G₂/M, the most radiosensitive phase of cell cycle^[8,9].

Conventional radiosensitizers alone are limited by side effects due to their poor selectivity for tumors. Monoclonal antibody specific tumor antigen makes them possible to enhance the selectivity by a targeted delivery approach^[10,11]. Radiation induces apoptosis of neoplastic cells. The extent of radiation-induced apoptosis correlates closely with radiosensitivity^[12,13]. Apoptosis is regulated by activators and inhibitors in signal transduction pathways. In this study, we attempted to investigate the radiosensitization of colon carcinomas targeting with docetaxel liposome conjugated antibody specific for carcinoembryonic antigen (CEA). The aim of this study was to selectively deliver of docetaxel and to enhance the radiation sensitivity of human colon cancer cells. In order to increase radiotherapy effects on local tumors and to improve the quality of life and overall survival, radiosensitizers should be delivered into the tumor.

This workshop considered a new approach by use of targeted radiosensitizers to improve radiotherapy.

MATERIALS AND METHODS

Chemical and biological materials

Cholesterol, and soy phosphatidylcholine were purchased from Shanghai Chemical Agent company. 3-(4,5-Dimethylthiazol-2-yl)-2,5-diphenyltetrazolium bromide (MTT), cyanuric chloride, O-(2-aminoethyl) polyethylene glycol 3000, N,N-diisopropylethylamine, dimethyl sulfoxide (DMSO), 1,2-dipalmitoyl-sn-glycero-3-phosphoethanolamine (DPPE) were purchased from Sigma. Docetaxel was kindly supplied by Jiangsu Hengrui Medicine Co. Monoclonal antibody specific for CEA was purchased from Beijing Zhongshan Biotechnology Co. Immunocytochemical detection kit was from Wuhan Boster Biological Technology Co.

Preparation of immunoliposomal docetaxel

Immunoliposomal docetaxel was prepared according to the method described by Bendas^[14-17] with minor modifications. Briefly, a 2-fold molar of N, N-diisopropylethylamine and a 3-fold molar cyanuric chloride were added to chloroform solution of DPPE, mixed for 12 h, then DPPE-cyanuric chloride was isolated. DPPE-PEG-OH was prepared by adding a 1-fold molar aminopolyethylene glycol 3000 and a 2-fold molar of N,N-diisopropylethylamine to DPPE-cyanuric chloride. PEG terminus was activated by reaction with 1-fold molar of cyanuric chloride in addition to a 2-fold molar of N,N-diisopropylethylamine. DPPE-cyanuric chloride (cyanur-PEG-PE) was synthesized.

Liposomal docetaxel was prepared with soy phosphatidylcholine cholesterol 2:1 (molar ratio), cyanur-PEG-PE (0.5 mmol/L), docetaxel (1 μ mol/L). Multilamellar vesicles were extruded through a 200 nm polycarbonate membrane. Antibody conjugated with docetaxel liposomes: anti-CEA-antibody molar ratio of 1 000:1 was prepared in 0.15 mol/L NaCl (pH 8.8). Unbound antibodies were separated by gel permeation chromatography using Sepharose 4B.

Cell culture

LoVo cells, the CEA-expressing human colon adenocarcinoma cell line, were maintained in Dulbecco's modified Eagle's medium supplemented with 10% heat-inactivated fetal calf serum, 100 μ g/mL streptomycin, 100 units/mL penicillin. The population doubling time was approximately 30 h. LoVo cells were grown at 37 °C in a humidified atmosphere of 50 mL/L CO₂.

Treatment with immunoliposomal docetaxel and irradiation

LoVo cells (5 \times 10³) were plated onto 96-well plates or 6-well plates. Before the administration of appropriate doses of immunoliposomal docetaxel or radiation, cells were plated for 24 h to allow attachment. LoVo cells were incubated with different concentrations of immunoliposomal docetaxel or liposomal docetaxel as equivalent docetaxel doses of 1 nmol/L, 2 nmol/L, 10 nmol/L, 100 nmol/L and 1 000 nmol/L for 2 h at 37 °C. After washing thrice with culture medium, the cells with or without radiation were

incubated for 24 h or 48 h at 37 °C. Cells were X-irradiated at 0, 2, 4, 6 and 8 Gy respectively. Irradiation was performed with 6-MV photons generated by a Philips SL-75 linear accelerator at a dose rate of 1.3 Gy/min. In the combined treatment modality studies, the treated cells were incubated for 24 h before radiation treatment. All doses were delivered without interruption and with the same focus-target distance.

MTT assay

LoVo cells were treated with various concentrations of immunoliposomal docetaxel, and some were exposed to radiation. To measure cell proliferation, the colorimetric method based on MTT assay was used^[18,19]. Cells were stained with MTT (50 mg/mL) and incubated for 4 h at 37 °C in a humidified atmosphere of 50 mL/L CO₂. Then the cells were lysed in DMSO, and the solutions were read in a Bio-Tek spectrophotometer at 570 nm. The production of formazan crystals, and the intensity of color after their dissolution, were proportional to the number of viable cells.

Flow cytometric analysis

At the end of each treatment, LoVo cells were harvested with 0.5 g/L trypsin and 0.2 g/L EDTA. Cells were fixed in 2 mL of 70% cold ethanol at 4 °C for 2 h, centrifuged, washed twice with phosphate buffered saline (PBS), and resuspended in 0.5 mL propidium iodide (PI)/RNase A solution. The mixed cells were incubated in the dark at room temperature for 10 min. The fluorescence emission of stained cells was measured with a Becton Dickinson flow cytometer. The number of cells and DNA content were detected by flow cytometry, the fraction of cells in each phase of cell cycle was analyzed. Apoptotic cells were determined by the hypodiploid peak.

Immunohistochemistry

Streptavidin-biotin peroxidase complex technique was used for staining cells. The treated LoVo cells were harvested and plated on slides. The cells were fixed in 95% aqueous alcohol. The endogenous peroxidase activity was blocked by a 3% solution of hydrogen peroxide in methanol for 30 min. Cells were immunostained using monoclonal antibody against human survivin for 1 h at 37 °C. After three further washes with PBS, a second biotinylated rabbit anti-mouse antibody was applied for 1 h at room temperature. Following extensive washes with PBS, color development was demonstrated with diaminobenzidine tetrahydrochloride chromagen. The slides were lightly counterstained with hematoxylin. Stained cells were examined using light microscopy and photographed. JD801 morphologic analysis system for color-image measurement was used to semi-quantify immunohistochemical staining of survivin.

RESULTS

Determination of the cytotoxicity of immunoliposomal docetaxel to LoVo cells

To determine the cytotoxicity of immunoliposomal docetaxel to human colon cancer cells, LoVo cells were treated with various concentrations of immunoliposomal docetaxel for 24 or 48 h. Relative survival data for LoVo

cells are shown in Figure 1. Under the treatment with 2 nmol/(L · d) immunoliposomal docetaxel for 24 h, survival was decreased 12% as compared with 1 nmol/L a immunoliposomal docetaxel. The results for Figure 1 also indicate that LoVo cells were more sensitive to immunoliposomal docetaxel treatment in 24 h than for 48 h. The cytotoxicity was induced by immunoliposomal docetaxel alone in a dose-dependent manner. The immunoliposomal docetaxel yielded a cytotoxicity effect at a low dose of 2 nmol/L.

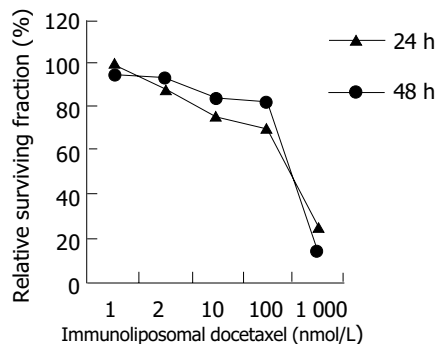


Figure 1 Cytotoxicity of immunoliposomal docetaxel to LoVo cells.

Radiotoxicity to LoVo cells

LoVo cells received a series of test doses of radiation, ranging from 2 to 8 Gy. The radiotoxicity generated is shown in Figure 2. At the doses of 4 to 8 Gy, the reaction to irradiation appeared less pronounced.

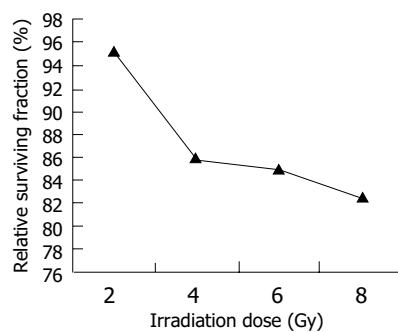


Figure 2 Radiotoxicity to LoVo cells irradiated with single doses.

Target radiopotentiating effect of immunoliposomal docetaxel

To examine whether immunoliposomal docetaxel could target LoVo cells and reveal radiopotentiating effect, these cells were treated with immunoliposomal docetaxel and liposomal docetaxel, respectively, then irradiated at the dose of 2 Gy radiation doses. The control cells were irradiated alone. Using MTT assay, the relative surviving fractions were obtained. The results in Figure 3 showed that immunoliposomal docetaxel was strongly radiopotentiated in LoVo cells, compared with the effects of liposomal docetaxel or single irradiation ($P < 0.05$). No significant

radiopotentiating effects were found after treatment with liposomal docetaxel.

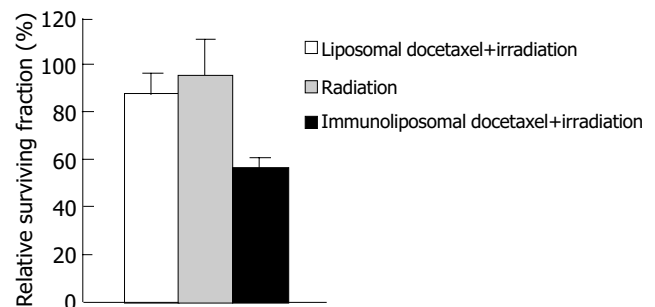


Figure 3 Target radiopotentiating effects of docetaxel immunoliposomes on LoVo cells.

Cell cycle effects

To determine whether immunoliposomal docetaxel in combination with radiation could increase cellular sensitivity to radiation through cell cycle redistribution, we analyzed the LoVo cells by flow cytometry. After treatment with immunoliposomal docetaxel or liposomal docetaxel, all cells were irradiated at 2 Gy. The response of LoVo cell cycle to radiation is shown in Figure 4. Compared to treatment with liposomal docetaxel, the percentage of G_2/M cells treated with immunoliposomal docetaxel was significantly increased ($P < 0.01$), but the percentages of cells both in G_2/G_1 phase and in S phase were decreased significantly ($P < 0.05$). Apoptosis was also monitored by flow cytometry (Figure 4). Apoptosis was significantly increased in LoVo cells due to the combined effects of immunoliposomal docetaxel and radiation.

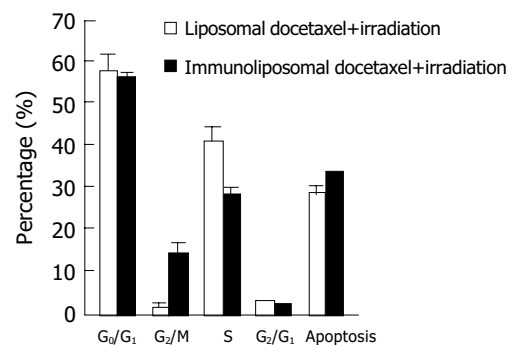


Figure 4 Combined effect of immunoliposomal docetaxel and radiation on cell cycle distribution and apoptosis.

Immunohistochemical analysis of survivin

Survivin expression in LoVo cells after irradiation and treatment with immunoliposomal docetaxel was verified by immunocytochemistry. Survivin was positively stained with anti-survivin monoclonal antibody. Representative results are shown in Figure 5.

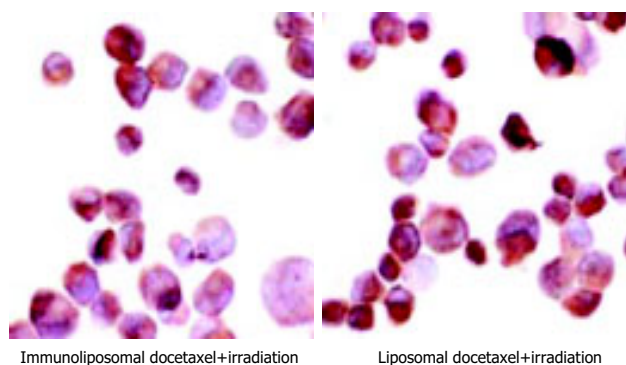


Figure 5 Expression of survivin in LoVo cells.

Semiquantitative assessment of survivin staining

Positive staining of survivin was mainly present as diffuse cytoplasmic staining with variable intensity. Integral optical density of survivin was detected semiquantitatively by immunohistochemical staining combined with image analysis. For density measurement, color-images were directly analyzed using D801 morphologic analysis system. The semiquantitative data reported here were directly comparable to image analysis data. Survivin expression in LoVo cells after irradiation and treatment with immunoliposomal docetaxel was significantly decreased in comparison to treatment with liposomal docetaxel ($P < 0.001$, Figure 6).

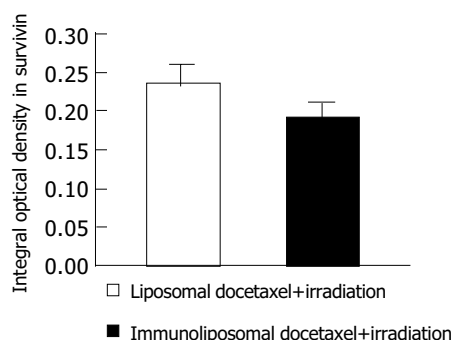


Figure 6 Survivin expression in LoVo cells were determined by quantitative image analysis.

DISCUSSION

Docetaxel plays an important role in the treatment of human malignancies, particularly ovarian and breast cancer^[17,18]. It inhibits mitotic progression and induces programmed cell death^[19]. For systemic toxicity of docetaxel, the optimal usage is the targeted delivery.

Liposome is used as a potential vector for targeted delivery of radiosensitizers^[20]. Liposome is a phospholipid bilayer membrane-bound vesicle capable of encapsulating a wide variety of substances either within their lipid membrane or their central aqueous core. Liposome incorporates polyethylene glycol components and has a prolonged circulation half-life. Liposomal doxorubicin is understanding clinical phase II pilot study in patients with inoperable squamous cell cancer of the head and neck^[21].

Maruyama *et al.*^[22], introduced a PEG-PE derived lipid with a terminal maleimide group for the reaction with thiolated antibodies. Allen *et al.*^[23], synthesized a thiol-reactive PEG anchor for reaction with maleimide-containing antibodies. The terminal coupled antibody shows an increased target binding ability compared with conventional immunoliposomes^[24]. A drawback of these coupling procedures is the need of derivation for the attachment of antibody. Two reagents are needed to activate PEG-derivatives with carboxy groups. In this study, a new liposomal membrane anchor was introduced for the covalent attachment of antibody to liposomes. Anti-CEA-antibody is simply and rapidly coupled to cyanuric chloride at the PEG terminus of liposome without previous derivatization.

Immunoliposomal docetaxel may be an attractive strategy for target radiopotential because it can radiosensitize LoVo cells. Docetaxel is targeted by specific anti-CEA-antibody. Our study demonstrate that docetaxel conjugated to a monoclonal antibody specific for CEA tumor-associated antigen could exert efficient and specific cytotoxicity to CEA-expressing LoVo cells. Immunoliposomal docetaxel alone showed dose-dependent cytotoxicity to LoVo cells. Furthermore, anti-CEA-antibody enhanced the target effects of docetaxel and led to radiosensitization.

Immunoliposomal docetaxel achieved both specificity of the conjugated antibody and drug radiosensitization. Using a low dose of immunoliposomal docetaxel could yield sufficient radiosensitization. Radiation combined with immunoliposomal docetaxel caused a significant increase in the population of G₂/M cells. One of the mechanisms may correlate to the effects of docetaxel such as interfering with normal microtubule function, blocking cells in G₂/M, and enhancing the sensitivity to apoptosis^[25,26]. The presence of arrest in G₂/M did not seem to be a sufficient condition to enhance radiation sensitivity. Redistribution of cell cycle due to radiosensitization induced by immunoliposomal docetaxel was observed. Increased apoptosis may have a potential correlation to increased radiosensitivity.

Furthermore, apoptosis may be regulated by a complex balance in signal transduction pathways between apoptosis-activating factors, such as p53 and bax, and antiapoptotic factors, such as the bcl-2 family and inhibitor of apoptosis protein (IAP) family^[27]. Survivin, a newly identified member in IAP family, is a strong apoptosis inhibitor. It can be found during fetal development and in colorectal cancer^[28]. Expression of survivin may confer a certain degree of radioresistance to rectal cancer cells^[29-31]. In the present study, we attempted to find a relationship between the expression of survivin and radiation-induced apoptosis.

Immunohistochemistry examination showed that survivin was mainly in cytoplasm of LoVo cells. Moreover, semiquantitative analysis of the immunohistochemical staining of survivin indicated that a low survivin expression was associated with a significantly higher radiosensitivity after treatment with immunoliposomal docetaxel combined with irradiation. LoVo cells were radiosensitized significantly by decreased expression of survivin. The alteration of survivin expression in LoVo cells may partially explain the enhanced apoptosis and radiation sensitivity.

In conclusion, immunoliposomal docetaxel is strongly

effective for target radiosensitizing in LoVo colon carcinoma cells, and may offer the potential to improve local radiotherapy.

REFERENCES

- 1 **Shunyakov L**, Ryan CK, Sahasrabudhe DM, Khorana AA. The influence of host response on colorectal cancer prognosis. *Clin Colorectal Cancer* 2004; **4**: 38-45
- 2 **Sarid D**, Wigler N, Gutkin Z, Merimsky O, Leider-Trejo L, Ron IG. Cutaneous and subcutaneous metastases of rectal cancer. *Int J Clin Oncol* 2004; **9**: 202-205
- 3 **Munro AJ**, Bentley AH. Deprivation, comorbidity and survival in a cohort of patients with colorectal cancer. *Eur J Cancer Care* 2004; **13**: 254-262
- 4 **Hahnloser D**, Haddock MG, Nelson H. Intraoperative radiotherapy in the multimodality approach to colorectal cancer. *Surg Oncol Clin N Am* 2003; **12**: 993-1013
- 5 **Hocht S**, Hammad R, Thiel HJ, Wiegel T, Siegmann A, Willner J, Wust P, Herrmann T, Eble M, Flentje M, Carstens D, Bottke D, Neumann P, Hinkelbein W. Recurrent rectal cancer within the pelvis. A multicenter analysis of 123 patients and recommendations for adjuvant radiotherapy. *Strahlenther Onkol* 2004; **180**: 15-20
- 6 **Souglakos J**, Androulakis N, Mavroudis D, Kourousis C, Kakolyris S, Vardakis N, Kalbakis K, Pallis A, Ardavanis A, Varveris C, Georgoulas V. Multicenter dose-finding study of concurrent capecitabine and radiotherapy as adjuvant treatment for operable rectal cancer. *Int J Radiat Oncol Biol Phys* 2003; **56**: 1284-1287
- 7 **Horgan AF**, Finlay IG. Preoperative staging of rectal cancer allows selection of patients for preoperative radiotherapy. *Br J Surg* 2000; **87**: 575-579
- 8 **Onishi H**, Kuriyama K, Yamaguchi M, Komiyama T, Tanaka S, Araki T, Nishikawa K, Ishihara H. Concurrent two-dimensional radiotherapy and weekly docetaxel in the treatment of stage III non-small cell lung cancer: a good local response but no good survival due to radiation pneumonitis. *Lung Cancer* 2003; **40**: 79-84
- 9 **Mason KA**, Hunter NR, Milas M, Abbruzzese JL, Milas L. Docetaxel enhances tumor radioresponse *in vivo*. *Clin Cancer Res* 1997; **3**: 2431-2438
- 10 **Fernando NH**, Hurwitz HI. Targeted therapy of colorectal cancer: clinical experience with bevacizumab. *Oncologist* 2004; **9**(Suppl 1): 11-18
- 11 **Veronese ML**, O'Dwyer PJ. Monoclonal antibodies in the treatment of colorectal cancer. *Eur J Cancer* 2004; **40**: 1292-1301
- 12 **Vavrova J**, Rezacova M, Vokurkova D, Psutka J. Cell cycle alteration, apoptosis and response of leukemic cell lines to gamma radiation with high- and low-dose rate. *Physiol Res* 2004; **53**: 335-342
- 13 **Belka C**, Jendrosseck V, Pruschy M, Vink S, Verheij M, Budach W. Apoptosis-modulating agents in combination with radiotherapy-current status and outlook. *Int J Radiat Oncol Biol Phys* 2004; **58**: 542-554
- 14 **Bendas G**, Krause A, Bakowsky U, Vogel J, Rothe U. Targetability of novel immunoliposomes prepared by a new antibody conjugation technique. *Int J Pharm* 1999; **181**: 79-93
- 15 **Rossi L**, Corvo R. Retinoic acid modulates the radiosensitivity of head-and-neck squamous carcinoma cells grown in collagen gel. *Int J Radiat Oncol Biol Phys* 2002; **53**: 1319-1327
- 16 **Raju U**, Nakata E, Yang P, Newman RA, Ang KK, Milas L. *In vitro* enhancement of tumor cell radiosensitivity by a selective inhibitor of cyclooxygenase-2 enzyme: mechanistic considerations. *Int J Radiat Oncol Biol Phys* 2002; **54**: 886-894
- 17 **Ray-Coquard I**. Docetaxel and ovarian cancer. *Bull Cancer* 2004; **91**: 159-165
- 18 **Yardley DA**. Gemcitabine and docetaxel in metastatic and neoadjuvant treatment of breast cancer. *Semin Oncol* 2004; **31** (2 Suppl 5): 37-44
- 19 **Mani S**, Macapinlac M Jr, Goel S, Verdier-Pinard D, Fojo T, Rothenberg M, Colevas D. The clinical development of new mitotic inhibitors that stabilize the microtubule. *Anticancer Drugs* 2004; **15**: 553-558
- 20 **Harrington KJ**, Rowlinson-Busza G, Syrigos KN, Vile RG, Uster PS, Peters AM, Stewart JS. Pegylated liposome-encapsulated doxorubicin and cisplatin enhance the effect of radiotherapy in a tumor xenograft model. *Clin Cancer Res* 2000; **6**: 4939-4949
- 21 **Koukourakis MI**, Koukouraki S, Giatromanolaki A, Archimandritis SC, Skarlatos J, Beroukas K, Bizakis JG, Retalis G, Karkavitsas N, Helidonis ES. Liposomal doxorubicin and conventionally fractionated radiotherapy in the treatment of locally advanced non-small-cell lung cancer and head and neck cancer. *J Clin Oncol* 1999; **17**: 3512-3521
- 22 **Maruyama K**, Takizawa T, Yuda T, Kennel SJ, Huang L, Iwatsuru M. Targetability of novel immunoliposomes modified with amphipathic poly(ethylene glycol)s conjugated at their distal terminals to monoclonal antibodies. *Biochim Biophys Acta* 1995; **1234**: 74-80
- 23 **Allen TM**, Brandeis E, Hansen CB, Kao GY, Zalipsky S. A new strategy for attachment of antibodies to sterically stabilized liposomes resulting in efficient targeting to cancer cells. *Biochim Biophys Acta* 1995; **1237**: 99-108
- 24 **Bendas G**. Immunoliposomes: a promising approach to targeting cancer therapy. *BioDrugs* 2001; **15**: 215-224
- 25 **Berchem GJ**, Bosseler M, Mine N, Avalosse B. Nanomolar range docetaxel treatment sensitizes MCF-7 cells to chemotherapy induced apoptosis, induces G2M arrest and phosphorylates bcl-2. *Anticancer Res* 1999; **19**: 535-540
- 26 **Strunz AM**, Peschke P, Waldeck W, Ehemann V, Kissel M, Debus J. Preferential radiosensitization in p53-mutated human tumour cell lines by pentoxifylline-mediated disruption of the G2/M checkpoint control. *Int J Radiat Biol* 2002; **78**: 721-732
- 27 **Yang Y**, Yu X. Regulation of apoptosis: the ubiquitous way. *FASEB J* 2003; **17**: 790-799
- 28 **Kim PJ**, Plescia J, Clevers H, Fearon ER, Altieri DC. Survivin and molecular pathogenesis of colorectal cancer. *Lancet* 2003; **362**: 205-209
- 29 **Asanuma K**, Moriai R, Yajima T, Yagihashi A, Yamada M, Kobayashi D, Watanabe N. Survivin as a radioresistance factor in pancreatic cancer. *Jpn J Cancer Res* 2000; **91**: 1204-1209
- 30 **Rodel C**, Haas J, Groth A, Grabenbauer GG, Sauer R, Rodel F. Spontaneous and radiation-induced apoptosis in colorectal carcinoma cells with different intrinsic radiosensitivities: survivin as a radioresistance factor. *Int J Radiat Oncol Biol Phys* 2003; **55**: 1341-1347
- 31 **Lu B**, Mu Y, Cao C, Zeng F, Schneider S, Tan J, Price J, Chen J, Freeman M, Hallahan DE. Survivin as a therapeutic target for radiation sensitization in lung cancer. *Cancer Res* 2004; **64**: 2840-2845

• COLORECTAL CANCER •

Effect of caffeic acid phenethyl ester on proliferation and apoptosis of colorectal cancer cells *in vitro*

Dong Wang, De-Bing Xiang, Yu-Jun He, Zeng-Peng Li, Xiao-Hua Wu, Jiang-Hong Mou, Hua-Liang Xiao, Qing-Hong Zhang

Dong Wang, De-Bing Xiang, Zeng-Peng Li, Xiao-Hua Wu, Jiang-Hong Mou, Hua-Liang Xiao, Qing-Hong Zhang, Cancer Center, Daping Hospital and Research Institute of Surgery, Third Military Medical University, Chongqing 400042, China
Yu-Jun He, Department of General Surgery, Daping Hospital and Research Institute of Surgery, Third Military Medical University, Chongqing 400042, China
Supported by the National Natural Science Foundation of China, No. 30100228, and the Applied Basic Research Programs of Science and Technology Commission Foundation of Chongqing, No. 6824
Correspondence to: De-Bing Xiang, Cancer Center, Daping Hospital and Research Institute of Surgery, Third Military Medical University, Chongqing 400042, China. xdb86@hotmail.com
Telephone: +86-23-68757706 Fax: +86-23-68757706
Received: 2004-05-30 Accepted: 2004-06-24

Abstract

AIM: To study the effect of caffeic acid phenethyl ester (CAPE) on proliferation, cell cycle, apoptosis and expression of β -catenin in cultured human colorectal cancer (CRC) cell line HCT116.

METHODS: HCT116 cells were treated with CAPE at serial concentrations of 80, 40, 20, 10, 5, 2.5 mg/L. The proliferative status of HCT116 cells was measured by using methabenzthiazuron (MTT) assay. Cell cycle was analyzed by using flow cytometry (FCM) with propidium iodide (PI) labeling method. The rate of apoptosis was detected by using FCM with annexin V-FITC and PI double labeling method. β -catenin levels were determined by Western blotting. β -catenin localization in HCT116 was determined by indirect immunofluorescence.

RESULTS: After HCT116 cells were exposed to CAPE (80, 40, 20, 10, 5, and 2.5 mg/L) for 24, 48, 72, 96 h, CAPE displayed a strong growth inhibitory effect in a dose- and time-dependent manner against HCT116 cells. FCM analysis showed that the ratio of G_0/G_1 phase cells increased, S phase ratio decreased and apoptosis rate increased after HCT116 cells were exposed to CAPE (10, 5, and 2.5 mg/L) for 24 h. CAPE treatment was associated with decreased cytoplasmic β -catenin, nuclear β -catenin and a concurrent increase in β -catenin protein expression at cell-cell junctions.

CONCLUSION: CAPE could inhibit HCT116 cell proliferation and induce cell cycle arrest and apoptosis. Decreased β -catenin protein expression may mediate the anti-proliferative effects of CAPE.

Key words: Caffeic acid phenethyl ester; Proliferation; Colorectal cancer

Wang D, Xiang DB, He YJ, Li ZP, Wu XH, Mou JH, Xiao HL, Zhang QH. Effect of caffeic acid phenethyl ester on proliferation and apoptosis of colorectal cancer cells *in vitro*. *World J Gastroenterol* 2005; 11(26): 4008-4012

<http://www.wjgnet.com/1007-9327/11/4008.asp>

INTRODUCTION

Colorectal cancer (CRC) is one of the most common human malignancies, and is the fourth leading cause of cancer deaths. The incidence tends to increase in China. Aberrant WNT pathway signaling is an early progression event in 90% of colorectal cancers. It occurs through mutations mainly of APC and less often of CTNNB1 (encoding β -catenin) or AXIN2 (encoding axin-2, also known as conductin). Activation of WNT signaling leads to inhibition of GSK-3 β activity, resulting in accumulation of cytoplasmic (signaling) β -catenin, which becomes available to bind the TCF/LEF family of transcription factors and to induce target gene expression^[1]. Dysregulation of WNT signaling and hence β -catenin expression is believed to be central to the early stages of sporadic colorectal carcinogenesis in human beings^[2]. Therefore, control of β -catenin and/or control of downstream TCF target gene expression represents an ideal target for CRC chemoprevention. Caffeic acid phenethyl ester (CAPE), an active component of propolis, has many biological and pharmacological activities including antioxidant, anti-inflammation, antiviral action, anticancer effect, *etc.*^[3-7]. It also inhibited the development of azoxymethane-induced aberrant crypts in the colon of rats^[8]. Thus, we investigated the effects of CAPE on proliferation, cell cycle, apoptosis and expression of β -catenin in the cultured human colorectal cancer (CRC) cell line HCT116.

MATERIALS AND METHODS

Drugs and reagents

CAPE, dimethyl sulphoxide (DMSO), PI and MTT were purchased from Sigma-Aldrich (USA). RPMI-1640 medium was purchased from Hyclone. Mouse monoclonal anti-human β -catenin antibody was obtained from Sigma-Aldrich (USA). FITC and horseradish peroxidase-conjugated secondary antibody were obtained from Pierce Biotechnology (USA). Annexin-V and PI double staining kit was purchased from Roche (USA). CAPE was prepared as 80 g/L stock solutions in DMSO. Control flasks or plates contained DMSO at an equivalent dilution to that in cultures containing CAPE.

Cell culture

The human CRC cell line HCT116 was purchased from the American Type Culture Collection (ATCC). The cells were cultured in RPMI1640 medium (pH 7.2-7.4) supplemented with penicillin G (100 U/mL), streptomycin (100 U/mL) and 10% fetal calf serum (FCS) at 37 °C in a 50 mL/L CO₂ humidified atmosphere. Cells were routinely sub-cultured using 2.5 g/L trypsin/ethylenedinitrile tetraacetic acid (EDTA) solution (obtained from Sigma).

MTT assay for determination of cell growth

The logarithmically growing HCT116 cells were plated at a density of 4×10³ cells/well into a 96-well plate. After 24 h, cells were treated with CAPE at various concentrations (80, 40, 20, 10, 5, and 2.5 mg/L) for 24, 48, 72, and 96 h. Control wells were treated with 0.1% DMSO alone. Then, 20 µL MTT (5 g/L) was added to each well and incubated for an additional 4 h, and then culture media were discarded followed by addition of 0.15 mL DMSO and vibrated for 10 min. The absorbance was measured at 490 nm using a model 550 microplate reader. The inhibitory rates (IR) were calculated as follows: IR (%) = (1-absorbance of the treated wells)/(absorbance of the control wells) ×100%. The 50% inhibitory concentration (IC₅₀) value was determined using a CalcuSyn software.

Analysis of cellular DNA content by flow cytometry

The cells were grown at 50–60% confluence in T75 flasks, serum-starved for 24 h and then treated with a range of CAPE (10, 5, and 2.5 mg/L) for 24 h. At the end of the treatment, the floating cells were collected by centrifugation, whereas adherent cells were harvested by trypsin-EDTA solution to produce a single cell suspension. The cells were then pelleted by centrifugation and washed twice with PBS. Then, the cell pellets were suspended in 0.5 mL PBS and fixed in 5 mL ice-cold 70% ethanol at 4 °C. The fixed cells were spun by centrifugation and the pellets were washed with PBS. After resuspension with 1 mL PBS, the cells were incubated with RNase A (20 mg/L) and PI (50 mg/L) and shaken for 1 h at 37 °C in the dark. The stained cells were analyzed using a FACScan flow cytometer in combination with BD lysis II software (Becton Dickinson).

Assessment of apoptosis by annexin-V and PI double-staining flow cytometry

The cells were treated and harvested as above. Annexin-V and PI double staining kit (Roche) was used to assess apoptosis, then cells were immediately analyzed by flow cytometry. Early apoptotic cells were localized in the lower right quadrant of a dot-plot graph using annexin-V-fluorescein *vs* PI.

TUNEL assay for determination of apoptotic cells

Cells grown on glass coverslips were treated for 24 h with CAPE (10, 5, and 2.5 mg/L) or an equivalent dilution of DMSO, under standard culture conditions as described above. Cells were fixed immediately in 4% formaldehydum polymerisatum at 20 °C for 60 min and washed twice in PBS. Apoptosis of HCT-116 cells was evaluated by using an *in situ* cell death detection kit (Roche Co. Ltd, Germany). Monolayers were treated with proteinase K and then 0.3%

H₂O₂, labeled with fluorescein dUTP in a humidified box for 1 h at 37 °C. The cells were then combined with POD-horseradish peroxidase, colorized with diaminobenzidine tetrahydrochloride (DAB). Controls consisted of omission of fluorescein dUTP. Cells were visualized under a light microscope.

Western blot analysis

Cells were seeded into flasks and grown to 50-60% confluence for 24 h. The cells were then placed in serum-free medium with or without CAPE (10, 5, and 2.5 mg/L) for a period of 24 and 48 h. In the end, the attached cells and floating cells were extracted in lysis buffer using standard methods. Western blot was carried out using standard techniques. Briefly, equal amounts of proteins in each sample were resolved in 10% sodium dodecyl sulfate polyacrylamide gel electrophoresis (SDS-PAGE) and the proteins transferred onto PVDF membranes. After blocking with non-fat dried milk, the membranes were incubated with the appropriate dilution of primary antibody (mouse monoclonal anti-human β-catenin antibody). The membranes were then incubated with a horseradish peroxidase-conjugated secondary antibody. The proteins were detected by an enhanced chemiluminescence detection system, and light emission was captured on Kodak X-ray films.

Indirect immunofluorescence

Cells grown on glass coverslips were treated for 24 and 48 h with CAPE (10, 5, and 2.5 mg/L) or an equivalent dilution of DMSO, under standard culture conditions as described above. Cells were fixed in 100% methanol at -20 °C for 10 min and washed twice in PBS. Monolayers were incubated with primary antibody (mouse monoclonal anti-human β-catenin antibody) in PBS plus 10 g/L dried skimmed milk powder overnight at 4 °C. Omission of the respective primary antibody was used as a negative control. Monolayers were incubated with FITC-conjugated secondary antibody in 1% dried skimmed milk in PBS for 30 min at 37 °C. Confocal microscopy was performed using a Leica TCS SP laser scanning confocal microscope.

Statistical analysis

Data were expressed as mean±SD. Analysis of data was performed using one-way ANOVA. *P*<0.05 was considered statistically significant.

RESULTS

Effect of CAPE on cell proliferation

HCT116 cells were treated with CAPE at various concentrations for 1-4 d, and the cell viability was determined as described above by MTT assay. As shown in Figure 1, CAPE inhibited the growth of HCT116 cells in a dose- and time-dependent manner. The IC₅₀ value for CAPE at 24, 48, 72, 96 h after treatment was 22.45, 12.07, 6.47, 5.36 mg/L, respectively.

Effect of CAPE on apoptosis

After HCT116 cells were exposed to CAPE (10, 5, and 2.5 mg/L) for 24 h, annexin-V and PI double-staining FCM analysis showed that the apoptosis rates were 25.5±3.3%,

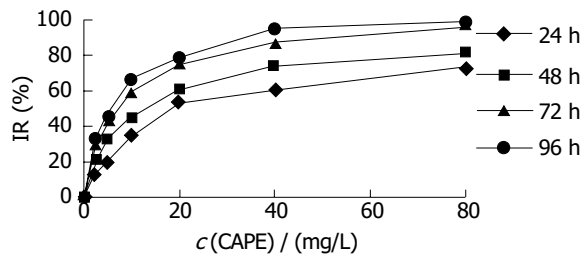


Figure 1 Effect of CAPE on HCT116 cell proliferation.

16.6±0.6%, 10.2±0.7%, respectively, which were significantly higher than control (5.5±0.9%) ($P<0.01$). CAPE induced apoptosis in a concentration-dependent manner in HCT116 cells (Figures 2 and 3). TUNEL assay showed that the apoptosis cells were significantly increased in a concentration-dependent manner in HCT116 cells (Figure 4).

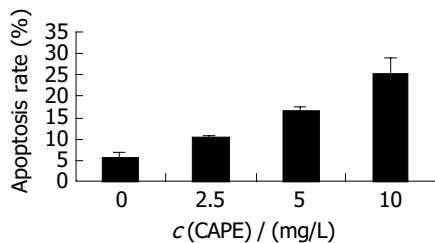


Figure 2 Effect of CAPE on HCT116 cell apoptosis rates.

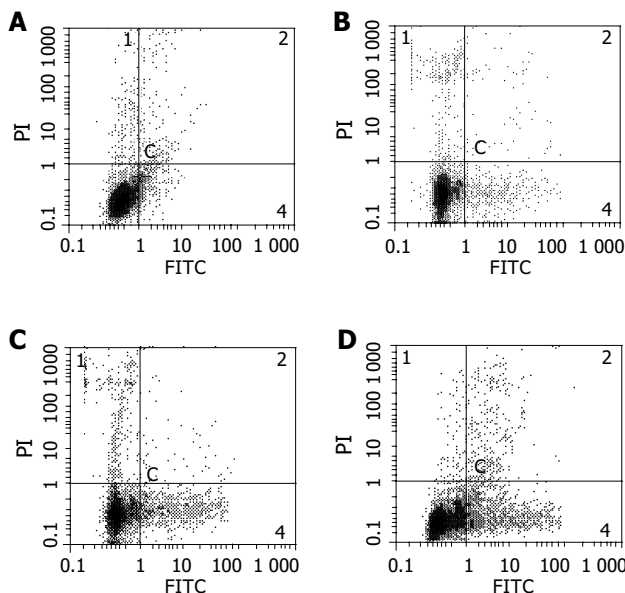


Figure 3 Annexin-V and PI double-staining FCM of HCT116 cells following 24 h incubation with (A) control, (B) 2.5 mg/L CAPE, (C) 5.0 mg/L CAPE, (D) 10 mg/L CAPE.

Effect of CAPE on cell cycle parameters

After HCT116 cells were exposed to CAPE (10, 5, and 2.5 mg/L) for 24 h, FCM analysis showed that the

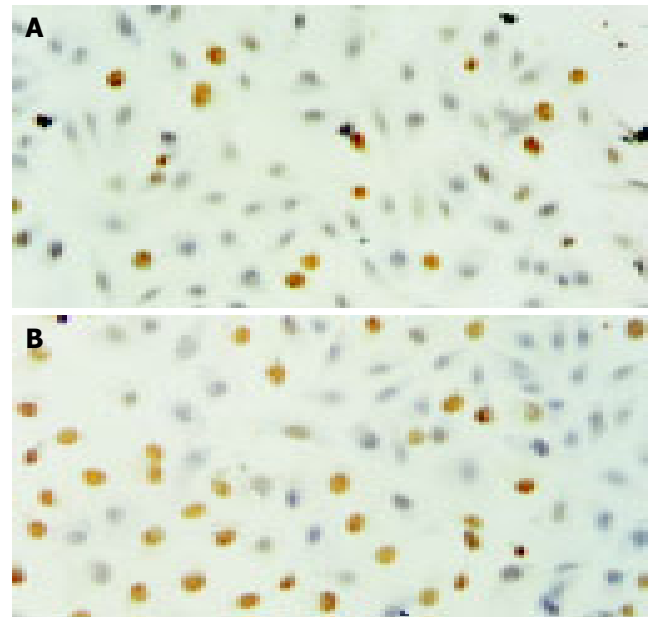


Figure 4 TUNEL assay of HCT116 cells following 24 h incubation with (A) 2.5 mg/L CAPE, (B) 10 mg/L CAPE.

proportion of cells in G_0/G_1 phase increased, the proportion of cells in S phase decreased in a concentration-dependent manner (Table 1, Figure 5).

β -Catenin expression during CAPE treatment

After HCT116 cells were exposed to CAPE (10, 5, and 2.5 mg/L) for 24 and 48 h, Western blot analysis showed that CAPE treatment was associated with a concentration-dependent decrease in β -catenin protein expression in HCT116 cells (Figure 6).

Indirect immunofluorescence studies of β -catenin localization in HCT116 cells revealed that CAPE treatment was associated with decreased cytoplasmic β -catenin, nuclear β -catenin and a concurrent increase in β -catenin protein expression at cell-cell junctions (Figure 7) compared with cells treated with DMSO alone.

Table 1 Effect of CAPE on HCT116 cell cycle parameters

CAPE (mg/L)	G_0/G_1	G_2/M	S
0	0.40±0.04	0.15±0.04	0.45±0.08
2.5	0.52±0.06	0.16±0.05	0.32±0.02
5	0.56±0.01 ^b	0.15±0.01	0.29±0.01 ^a
10	0.60±0.01 ^b	0.15±0.05	0.25±0.04 ^a

^a $P<0.05$, ^b $P<0.01$ vs control.

DISCUSSION

Polyphenolic compounds derived from natural products are well known to have various beneficial effects namely anti-tumor^[9,10], anti-inflammatory and antioxidant properties^[11,12]. CAPE is also a phenolic compound and an active component of honeybee propolis^[13,14]. Several investigators have demonstrated that CAPE has anti-proliferative effect, apoptosis-inducing effect against various tumor cell lines^[3-7,15] and an

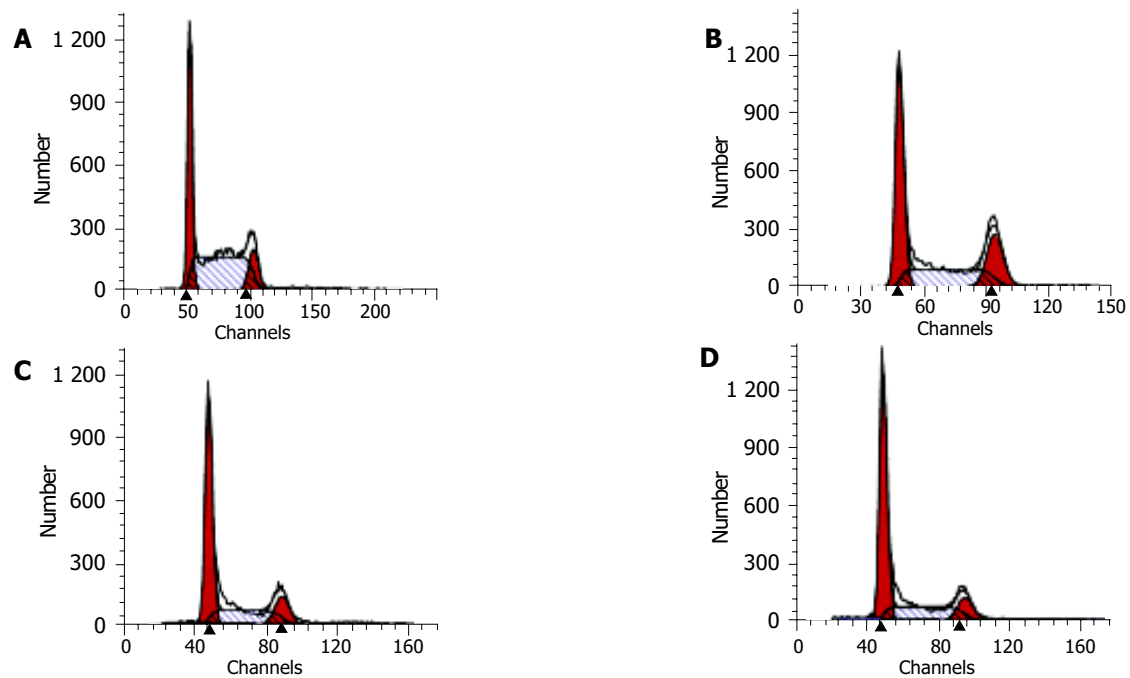


Figure 5 Flow cytometry of HCT116 cells following 24 h incubation with (A) control, (B) 2.5 mg/L CAPE, (C) 5.0 mg/L CAPE, (D) 10 mg/L CAPE.

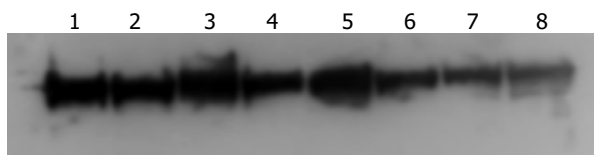


Figure 6 Western blot analysis of β -catenin protein expression in HCT116 cells following 24 h (Lanes 1-4) and 48 h (Lanes 5-8) incubation with different concentrations of CAPE. Lanes 1-4: control, 2.5 mg/L CAPE, 5.0 mg/L CAPE, 10 mg/L CAPE; Lanes 5-8: control, 2.5 mg/L CAPE, 5.0 mg/L CAPE, 10 mg/L CAPE.

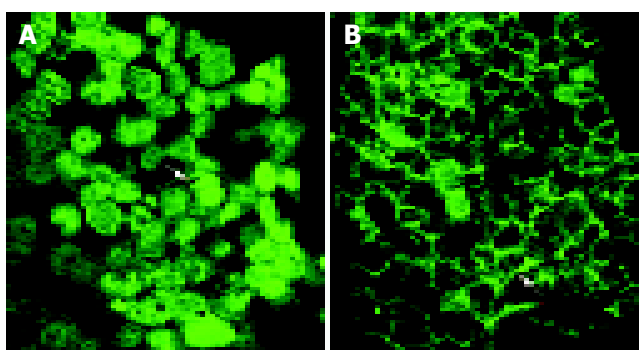


Figure 7 Indirect immunofluorescence analysis of β -catenin protein expression in HCT116 cells following 48 h incubation with (A) control, (B) 10 mg/L CAPE.

antioxidant effect by lipoxygenase inhibition^[16]. Also, dietary intake of CAPE decreased tumor formation and expression of the oncoprotein catenin in the enterocytes of the Min/+ mouse^[17]. In the present study, we investigated the effect of CAPE on the proliferation, cell cycle and apoptosis of CRC HCT116 cells. Our data demonstrated that CAPE treatment was associated with a strong inhibition of proliferation in a dose- and time-dependent manner, along with induction

of G₀/G₁ arrest and apoptosis in HCT116 cells. Similar to our findings, CAPE entered HL-60 cells very quickly and then inhibited their survival in a concentration- and time-dependent manner. CAPE induced characteristic DNA fragmentation and morphological changes typical of apoptosis in these cells^[4].

To investigate the mechanism of the anti-proliferative effects of CAPE on HCT116 cells, we studied the effect of CAPE on the expression of β -catenin, a multifunctional protein, responsible for the transduction of WNT mediated signals as well as for cell-cell adhesion^[18,19]. The signaling function of β -catenin is particularly important in colon cancer in which activation of β -catenin, as a result of mutations in APC or stabilizing mutations in the N-terminal region of β -catenin, is common^[20]. Activating mutations of β -catenin are also common in many other cancers^[21]. β -catenin signaling promotes the G₁ to S-phase transition, inhibits anoikis and allows cells to progress into S-phase after radiation damage^[22]. WNT-1 signaling also inhibits apoptosis by activation of β -catenin/TCF-mediated transcription^[23] and β -catenin signaling plays an important role in the growth of colon cancer cells^[24].

In our study, Western blot analysis showed that CAPE treatment was associated with a concentration-dependent decrease in β -catenin protein expression in HCT116 cells. The immunofluorescence data suggest that downregulation of β -catenin protein measured by Western blot analysis following CAPE treatment was associated with decreased cytoplasmic β -catenin, nuclear β -catenin and a concurrent increase in β -catenin protein expression at cell-cell junctions. Multiple molecular mechanisms seem to be involved in the tumor suppressive effects of CAPE. Recently, it is reported that CAPE induced apoptosis via Fas signal activation in human breast cancer MCF-7 cells^[25]. Moreover, tumor suppressor protein p53 and p38 MAPK play a prominent role in the

CAPE-induced apoptotic cell death which might contribute to the antitumor effects of CAPE in C6 glioma cells^[26].

In summary, we have identified that CAPE could inhibit HCT116 cell proliferation and induce cell cycle arrest and apoptosis. Decreased β -catenin protein expression may mediate the anti-proliferative effects of CAPE. The present findings may help to explain some features of CAPE-mediated chemoprevention. Future experiments will tell which β -catenin-related downstream genes may be affected by CAPE and whether CAPE may play a role in chemoprevention strategies.

REFERENCES

- 1 **Cadigan KM**, Nusse R. Wnt signaling: a common theme in animal development. *Genes Dev* 1997; **11**: 3286-3305
- 2 **Behrens J**. Control of beta-catenin signaling in tumor development. *Ann N Y Acad Sci* 2000; **910**: 21-35
- 3 **Chen YJ**, Shiao MS, Wang SY. The antioxidant caffeic acid phenethyl ester induces apoptosis associated with selective scavenging of hydrogen peroxide in human leukemic HL-60 cells. *Anticancer Drugs* 2001; **12**: 143-149
- 4 **Chen YJ**, Shiao MS, Hsu ML, Tsai TH, Wang SY. Effect of caffeic acid phenethyl ester, an antioxidant from propolis, on inducing apoptosis in human leukemic HL-60 cells. *J Agric Food Chem* 2001; **49**: 5615-5619
- 5 **Lee YJ**, Liao PH, Chen WK, Yang CY. Preferential cytotoxicity of caffeic acid phenethyl ester analogues on oral cancer cells. *Cancer Lett* 2000; **153**: 51-56
- 6 **Usia T**, Banskota AH, Tezuka Y, Midorikawa K, Matsushige K, Kadota S. Constituents of Chinese propolis and their antiproliferative activities. *J Nat Prod* 2002; **65**: 673-676
- 7 **Nomura M**, Kaji A, Ma W, Miyamoto K, Dong Z. Suppression of cell transformation and induction of apoptosis by caffeic acid phenethyl ester. *Mol Carcinog* 2001; **31**: 83-89
- 8 **Borrelli F**, Izzo AA, Di Carlo G, Maffia P, Russo A, Maiello FM, Capasso F, Mascolo N. Effect of a propolis extract and caffeic acid phenethyl ester on formation of aberrant crypt foci and tumors in the rat colon. *Fitoterapia* 2002; **73**(Suppl): S38-43
- 9 **Suganuma M**, Okabe S, Sueoka N, Sueoka E, Matsuyama S, Imai K, Nakachi K, Fujiki H. Green tea and cancer chemoprevention. *Mutat Res* 1999; **428**: 339-344
- 10 **Kuroda Y**, Hara Y. Antimutagenic and anticarcinogenic activity of tea polyphenols. *Mutat Res* 1999; **436**: 69-97
- 11 **Martinez J**, Moreno JJ. Effect of resveratrol, a natural polyphenolic compound, on reactive oxygen species and prostaglandin production. *Biochem Pharmacol* 2000; **59**: 865-870
- 12 **Chan MM**, Mattiacci JA, Hwang HS, Shah A, Fong D. Synergy between ethanol and grape polyphenols quercetin, and resveratrol, in the inhibition of the inducible nitric oxide synthase pathway. *Biochem Pharmacol* 2000; **60**: 1539-1548
- 13 **Banskota AH**, Tezuka Y, Kadota S. Recent progress in pharmacological research of propolis. *Phytother Res* 2001; **15**: 561-571
- 14 **Murad JM**, Calvi SA, Soares AM, Bankova V, Sforcin JM. Effects of propolis from Brazil and Bulgaria on fungicidal activity of macrophages against *Paracoccidioides brasiliensis*. *J Ethnopharmacol* 2002; **79**: 331-334
- 15 **Nagaoka T**, Banskota AH, Tezuka Y, Saiki I, Kadota S. Selective antiproliferative activity of caffeic acid phenethyl ester analogues on highly liver-metastatic murine colon 26-L5 carcinoma cell line. *Bioorg Med Chem* 2002; **10**: 3351-3359
- 16 **Ozyurt H**, Irmak MK, Akyol O, Sogut S. Caffeic acid phenethyl ester changes the indices of oxidative stress in serum of rats with renal ischaemia-reperfusion injury. *Cell Biochem Funct* 2001; **19**: 259-263
- 17 **Mahmoud NN**, Carothers AM, Grunberger D, Bilinski RT, Churchill MR, Martucci C, Newmark HL, Bertagnolli MM. Plant phenolics decrease intestinal tumors in an animal model of familial adenomatous polyposis. *Carcinogenesis* 2000; **21**: 921-927
- 18 **Moon RT**, Bowerman B, Boutros M, Perrimon N. The promise and perils of Wnt signaling through beta-catenin. *Science* 2002; **296**: 1644-1646
- 19 **Gottardi CJ**, Gumbiner BM. Adhesion signaling: how beta-catenin interacts with its partners. *Curr Biol* 2001; **11**: R792-794
- 20 **Bright-Thomas RM**, Hargest R. APC, beta-Catenin and hTCF-4; an unholy trinity in the genesis of colorectal cancer. *Eur J Surg Oncol* 2003; **29**: 107-117
- 21 **Hajra KM**, Fearon ER. Cadherin and catenin alterations in human cancer. *Genes Chromosomes Cancer* 2002; **34**: 255-268
- 22 **Orford K**, Orford CC, Byers SW. Exogenous expression of beta-catenin regulates contact inhibition, anchorage-independent growth, anoikis, and radiation-induced cell cycle arrest. *J Cell Biol* 1999; **146**: 855-868
- 23 **Chen S**, Guttridge DC, You Z, Zhang Z, Fribley A, Mayo MW, Kitajewski J, Wang CY. Wnt-1 signaling inhibits apoptosis by activating beta-catenin/T cell factor-mediated transcription. *J Cell Biol* 2001; **152**: 87-96
- 24 **Gottardi CJ**, Wong E, Gumbiner BM. E-cadherin suppresses cellular transformation by inhibiting beta-catenin signaling in an adhesion-independent manner. *J Cell Biol* 2001; **153**: 1049-1060
- 25 **Watabe M**, Hishikawa K, Takayanagi A, Shimizu N, Nakaki T. Caffeic acid phenethyl ester induces apoptosis by inhibition of NF-B and activation of Fas in human breast cancer MCF-7 cells. *J Biol Chem* 2004; **279**: 6017-6026
- 26 **Lee YJ**, Kuo HC, Chu CY, Wang CJ, Lin WC, Tseng TH. Involvement of tumor suppressor protein p53 and p38 MAPK in caffeic acid phenethyl ester-induced apoptosis of C6 glioma cells. *Biochem Pharmacol* 2003; **66**: 2281-2289

Science Editor Zhu LH Language Editor Elsevier HK

• VIRAL HEPATITIS •

Herbal medicine Ninjinyoeito ameliorates ribavirin-induced anemia in chronic hepatitis C: A randomized controlled trial

Yoshiharu Motoo, Hisatsugu Mouri, Koushiro Ohtsubo, Yasushi Yamaguchi, Hiroyuki Watanabe, Norio Sawabu

Yoshiharu Motoo, Hisatsugu Mouri, Koushiro Ohtsubo, Yasushi Yamaguchi, Hiroyuki Watanabe, Norio Sawabu, Department of Internal Medicine and Medical Oncology, Cancer Research Institute, Kanazawa University, Kanazawa, Japan
Supported by the research grant from the Institute of Kampo Medicine, Japan

Correspondence to: Yoshiharu Motoo, MD, Department of Medical Oncology, Kanazawa Medical University, 1-1 Daigaku, Uchinada, Ishikawa 920-0293, Japan. motoo@kanazawa-med.ac.jp
Telephone: +81-76-218-8284 Fax: +81-76-218-8283
Received: 2004-10-27 Accepted: 2004-12-20

Abstract

AIM: Ribavirin (RBV) shows a strong antiviral effect on hepatitis C virus when used in combination with interferon. However, RBV-induced anemia is a major problem in this therapy. It would be of great clinical importance to ameliorate the anemia without reducing the RBV dose. We report here that, Ninjinyoeito (NYT), a herbal medicine can reduce the RBV-induced anemia.

METHODS: Twenty-three patients with chronic hepatitis C were treated with interferon alpha 2b plus RBV with (NYT group) or without (control group) NYT by a randomized selection. Eighteen patients completed the treatment schedule, and hemato-biochemical and virological effects were evaluated.

RESULTS: There was no significant difference in biochemical and virological responses between the two groups. However, anemia was significantly reduced in the NYT group compared with the control group. The maximal decrease of Hb in the NYT group (2.59 ± 1.10 g/dL) was significantly ($P = 0.026$) smaller than that in the control group (3.71 ± 0.97 g/dL). There was no significant difference in serum glutathione peroxidase activity, serum RBV concentration, and Th1/Th2 balance between the two groups. There was no specific adverse effect in NYT administration.

CONCLUSION: These results suggest that NYT could be used as a supportive remedy to reduce the RBV-induced anemia in the treatment of chronic hepatitis C.

© 2005 The WJG Press and Elsevier Inc. All rights reserved.

Key words: Chronic hepatitis C; Ribavirin; Interferon; Herbal medicine; Anemia

Motoo Y, Mouri H, Ohtsubo K, Yamaguchi Y, Watanabe H,

Sawabu N. Herbal medicine Ninjinyoeito ameliorates ribavirin-induced anemia in chronic hepatitis C: A randomized controlled trial. *World J Gastroenterol* 2005; 11(26): 4013-4017
<http://www.wjgnet.com/1007-9327/11/4013.asp>

INTRODUCTION

Chronic hepatitis C often gradually progresses to cirrhosis, and hepatocellular carcinoma develops especially in advanced hepatic fibrosis^[1]. Recently, ribavirin (RBV) has been used in combination with pegylated interferon (IFN) as the most effective antiviral therapy^[2]. However, RBV-induced anemia is the major dose-limiting factor in the combined therapy of RBV and IFN products^[3]. The pathogenesis of RBV-induced anemia is reported to be the destruction of erythrocytes due to the retention of RBV inside the erythrocytes because there is no RBV dephosphorylase in erythrocytes^[4], possibly leading to the oxidative damage to the erythrocytic membrane. When anemia is progressive, the dose of RBV is usually reduced, and even the IFN-RBV therapy itself might be stopped in case of severe anemia. If we could prevent or at least reduce RBV-induced anemia to some extent, patients would receive a sufficient amount of RBV and could show a favorable virological response. There have been only a few reports on the attempt to ameliorate the RBV-induced anemia^[5,6].

Ninjinyoeito (NYT), a herbal medicinal formula, shows antiviral action on hepatitis C virus (HCV)^[7], as well as antioxidant^[8], immunomodulatory^[9], and hematopoietic^[10-12] effects. We speculated that the antioxidant effect of NYT could protect the erythrocytic membrane from the RBV-induced hemolysis and that NYT would promote erythropoiesis in response to the RBV-induced anemia.

In this report, we aimed to elucidate a beneficial effect of NYT on the RBV-induced anemia by conducting a randomized controlled trial.

MATERIALS AND METHODS

Patients

Patients with chronic hepatitis C were selected for the treatment protocol with the following criteria: serum levels of HCV-RNA more than 100 kIU/mL by RT-PCR (or more than 1 Meq/mL by a branched DNA probe assay) in naive patients, or ineffective or recurrent after the interferon monotherapy. Patients were excluded due to the following criteria: pregnant women, allergic to interferon, administration of a herbal medicine "Shosaikoto", severe heart failure, chronic renal failure, and past history of depression. Twenty-

three patients with chronic hepatitis C were enrolled into this study. Seventeen were male and six were female. The mean age of the patients was 51.1 (range 26-74). The diagnosis was confirmed histologically with liver biopsy in 13 patients. The other patients were diagnosed by hematological, biochemical, and virological findings.

Treatment protocol

Interferon-alpha 2b (Intron A[®], Schering-Plough, Kenilworth, NJ, USA) and RBV (Rebetol[®], Schering-Plough) were used as antiviral agents as previously described^[6,7]. In principle, interferon-alpha 2b (IFN) was administered intramuscularly 6 d a week for 2 wk at a dose of 10 MU, then thrice a week for 22 wk at the same dose. RBV was administered orally for 24 wk at a dose of 800 mg per day when the patient had a body weight over 60 kg, and at a dose of 600 mg when under 60 kg. Ninjinyoeito extract granules (NYT, Chinese name: Renshen-yangrong-tang, TJ-108, Tsumura & Co., Tokyo, Japan), including 6.0 g of NYT extract, was administered orally for 24 wk at a dose of 9 g per day. The patients were assigned into two groups in a random selection (Figure 1). The NYT group was treated with the three agents (IFN, RBV, and NYT), and the control group was treated with the two agents (IFN and RBV). No specific drugs were administered after the 24-wk treatment. A written informed consent was obtained from all the patients enrolled. Criteria for dose-down or stopping of the IFN and RBV were as follows: criteria by hemoglobin (Hb): dose-down of RBV from 800 to 600 mg or from 600 to 400 mg/d without the change of IFN dose when Hb less than 10 g/dL; administration of both IFN and RBV were stopped when Hb less than 8.5 g/dL; criteria by WBC and platelet counts: dose down of IFN without the change of RBV dose when WBC counts were less than 1 500/ μ L or platelet counts were 50 000/ μ L; administration of both IFN and RBV were stopped when WBC counts were less than 1 000/ μ L or platelet counts were 25 000/ μ L. Other criteria for dose-down or discontinuation of treatment included subjective symptoms such as anorexia, general malaise, or depressive tendency.

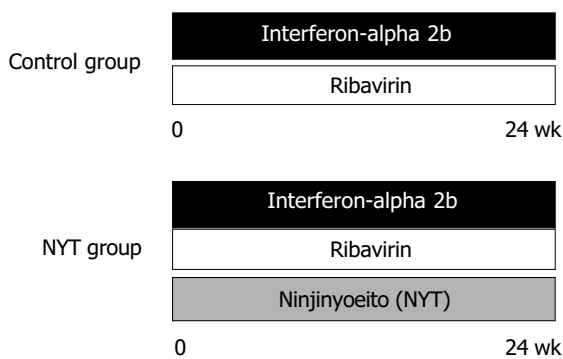


Figure 1 Study design.

Blood sampling and laboratory tests

Approximately 20 mL of blood was taken from the patients before treatment and again at 2, 4, 8, 12, and 24 wk after the start of treatment, and 24 wk after the end of treatment.

Hematological, biochemical, and virological tests were performed.

HCV-RNA assay and HCV serotypes

Serum HCV-RNA was detected with an Amplicor HCV test (Roche Diagnostics, Tokyo, Japan), and was quantified using an Amplicor HCV Monitor test, version 2.0, Roche Diagnostics). Serotypes of HCV were determined using an enzyme immunoassay (Genotyping EIA, International Reagents, Kobe, Japan). Sustained virological response (SVR) was considered to be obtained when the serum HCV-RNA was negative and serum ALT was within normal limits at 24 wk from the end of the IFN/RBV treatment.

Determination of ribavirin concentration

RBV concentration was determined in 18 patients, using high performance liquid chromatography (HPLC, SRL, Tokyo, Japan). Two-hundred microliters of serum was applied to HPLC after deproteination. The range of this assay system was from 50 to 20 000 ng/mL.

Determination of serum erythropoietin concentration

Serum levels of erythropoietin concentration were determined in eight male patients at wk 0 and 4 (four patients from each group), using radioimmunoassay (SRL, Inc., Tokyo, Japan). The eight patients were selected because their sera were available and it was considered to be adequate to compare the male patients only instead of mixing a few female patients.

Measurement of Th1/Th2 balance

The Th1/Th2 balance as a marker for cellular immunological response was assayed using the flow cytometry-based "Fastimmune Cytokine System" (Beckton Dickinson Biosciences, San Jose, CA, USA). Briefly, the blood was collected in sodium heparin, and was activated with ionomycin (IM), Brefeldin-A (BFA), and phorbol 12-myristate 13 acetate (PMA). After lysing and permeabilization, intracellular staining with fluorescent-conjugated monoclonal antibodies against cytokines was done. The two-color interferon- γ /interleukin-4 staining (Fastimmune system, Beckton Dickinson Biosciences) was utilized. Laser flow cytometer (FACS Caliber, Beckton Dickinson Biosciences) was used for analysis.

Glutathione peroxidase assay

Glutathione peroxidase activity as an antioxidant activity was determined using the Glutathione Peroxidase Assay kit (Cayman Chemical Company, Ann Arbor, MI, USA).

Statistical analysis

The software package Statmate III (Atms, Tokyo, Japan) was used for statistical analysis. The two-tailed Mann-Whitney *U* test was used to assess the significance of difference between the various laboratory test items such as Hb. The Fisher's exact test was used for the comparison of antiviral effects between the two groups. Multiple regression analysis was performed for the analysis on the factors influencing the anemia. All data were expressed as the mean \pm SD. A *P* value less than 0.05 was considered to be statistically significant.

RESULTS

Enrollment and follow-up of the registered patients

Patients were treated with IFN plus RBV either with ($n = 13$) or without ($n = 10$) NYT. Eighteen patients (nine patients in each group) completed the 24-wk treatment. There were five patients who dropped out due to anorexia and general malaise in three cases (all in the control group) and due to social problems in two cases (one case in each group). There was no significant difference between the NYT and control groups in age, gender, body weight, serum ALT levels, Hb levels, HCV-RNA levels before treatment, and HCV serotypes (Table 1). During the course of treatment, the dose of RBV was stopped in 1 patient, but not reduced in any of the remaining 9 patients in the NYT group, whereas it was reduced due to anemia in 2 of 13 patients, resulting in stopping of RBV in 4 patients in the control group ($P = 0.45$).

Table 1 Patients' characteristics before therapy

	NYT	Control	<i>P</i>
Age (yr)	46.3±14.3	54.9±10.3	0.113
Gender (M/F)	9/1	8/5	0.123
Body weight (kg)	65.2±9.8	60.6±9.1	0.291
ALT (U/L)	74.9±38.2	58.1±25.1	0.457
Hb (g/dL)	14.3±1.4	14.0±1.6	0.709
HCV RNA (kIU/mL)	553.5±315.0	637.6± 314.0	0.673
HCV serotype (1/2)	8/2	9/4	0.377

Biochemical and virological responses

There was no significant difference in RBV concentrations at wk 4 between the two groups. In the intention-to-treat analysis as in Table 2, serum ALT levels were within normal limits in 7 of 10 (70.0%) patients in the NYT group whereas they were normal in 6 of 13 (46.2%) patients in the control group at the end of the IFN/RBV treatment ($P = 0.253$). At the same time point, HCV-RNA turned negative in 8 of 10 (80.0%) patients in the NYT group whereas it was negative in 7 of 13 (53.8%) patients in the control group ($P = 0.192$). At 6 mo after the NYT/RBV treatment, serum ALT levels were within normal limits in 8 of 10 (80.0%) patients in the NYT group while they were within normal limits in 4 of 13 (30.8%) patients in the control group ($P = 0.489$). Sustained virological response (SVR) was obtained in 4 of 10 (40.0%) patients in the NYT group whereas it was seen in 4 of 13 (30.8%) in the control group ($P = 0.645$). In patients with serotype 1, SVR was obtained in 3 of 8 (37.5%) patients in the NYT group and 1 of 9 (11.1%) patients in the control group ($P = 0.311$), whereas in patients with serotype 2, SVR was recognized in 2 of 2 (100%) in the NYT group and 3 of 4 (75%) in the control group ($P = 0.316$).

Table 2 Virological and biochemical results

	NYT (%)	Control (%)	<i>P</i>
Enrolled cases	10	13	
Normal ALT at the end of therapy	7 (70.0)	6 (46.2)	0.253
Negative HCV RNA at the end of therapy	8 (80.0)	7 (53.8)	0.192
Normal ALT 6 mo after therapy	8 (80.0)	4 (30.8)	0.489
Negative HCV RNA 6 mo after therapy	4 (40.0)	4 (30.8)	0.645

Hematological changes

We analyzed the hematological changes in the 18 patients who received the IFN/RBV treatment for more than 4 wk. As shown in Table 3 and Figure 2, the maximal decrease of Hb in the NYT group (2.59 ± 1.10 g/dL) was significantly ($P = 0.026$) smaller than that in the control group (3.71 ± 0.97 g/dL). The minimal Hb during the treatment in the NYT group (11.66 ± 1.78 g/dL) tended to be higher than that in the control group (10.10 ± 1.08 g/dL, $P = 0.079$). Maximal decrease of erythrocytes in the NYT group ($868\ 000 \pm 474\ 000/\mu\text{L}$) tended to be smaller than that ($1\ 244\ 000 \pm 419\ 000/\mu\text{L}$) in the control group ($P = 0.178$). As shown in Table 1, there were some differences, although not significant, in age, gender, and body weight, which might influence the grade of anemia. We performed a multivariate analysis using the multiple regression method. Backward stepwise regression was performed, and a *P* value greater than 0.20 was used for a variable removal, and the NYT administration and serum creatinine were picked up. The final linear regression model selected only the NYT administration as a significant variable ($P = 0.0042$) influencing maximal hemoglobin decrease (Table 4). There were no significant differences in the WBC or platelet (Plts) counts between the two groups.

Table 3 Hematological and immunological results

	NYT	Control	<i>P</i>
max Δ RBC ($\times 10^9$)	868±474	1.244±419	0.178
max Δ Hb (g/dL)	2.59±1.10	3.71±0.97	0.026
min Hb (g/dL)	11.66±1.78	10.10±1.08	0.079
WBC (wk 24)	3 444±1731	3 204±1143	0.894
Plts (wk 24, $\times 10^9$)	14.69±5.52	12.77±4.22	0.709
Th1 (wk 4, %)	27.29±11.6	30.20±8.66	0.480
Th2 (wk 4, %)	2.77±1.06	2.30±1.09	0.232
Th1/Th2 (wk 4)	10.89±5.68	15.48±6.87	0.130
GPx[wk 4, nmol/(min · mL)]	76.41±31.79	78.96±31.96	0.522

GPx: glutathione peroxidase.

Table 4 Multiple regression analysis

Variable	Parameter estimate	Standard error	<i>P</i>
Intercept	-1.61742	1.12391	0.1707
NYT administration	1.47645	0.43746	0.0042
Serum creatinine (wk 0)	-3.05400	1.57891	0.0722

Maximal hemoglobin decrease = $1.477 \times [\text{NYT administration}] - 3.054 \times [\text{serum creatinine at wk 0}] - 1.617$ (NYT administration: the NYT group, 1; the control group, 2) Adjusted R square: 0.3923.

Changes in serum erythropoietin concentrations

Serum levels of erythropoietin were determined in eight male patients at wk 0 and 4 (four patients from each group), and there was no significant difference in the increase of erythropoietin from wk 0 to wk 4 between the two groups (38.4 ± 21.6 ng/mL in the NYT group *vs* 45.2 ± 30.3 ng/mL in the control group, $P = 0.885$).

Changes in the Th1/Th2 balance

There were no significant changes in Th1, Th2, or the Th1/Th2 ratio in either group during the observation period in

Table 5 Comparison of NYT and other drugs which were reported to be effective for RBV-induced anemia

	Action	Mechanisms	Indication for anemia in health insurance system of Japan	Form	Adverse reactions	Daily cost (yen)
NYT	Promotion of erythropoiesis, protection of erythrocytic membrane, improvement of erythrocytic deformability	Activation of immature erythroid cells, antioxidant effect	Anemia in general,	Granule	Abdominal discomfort (frequency unknown)	227.7
EPA	Increase in erythrocyte deformability	Increase in EPA content in erythrocytic membrane phospholipids	None	Capsule	Jaundice, gynecomastia (frequency unknown), hemorrhagic tendency, liver injury (<0.1%)	353.4
EPO	Increase in erythropoiesis	Stimulation of stem cell differentiation to erythroid cells	Renal anemia	Vial for injection	Thromboembolism, cerebral hemorrhage, shock (frequency unknown), high blood pressure, liver injury (0.1-5%)	1 643 (750 IU)

each group, and there were no significant differences in these cellular immunological markers between the two groups at any time point. Table 3 shows the results at wk 4.

Changes in glutathione peroxidase activity

There were no significant changes in glutathione peroxidase activity during the observation period, and there was no significant difference in this activity between the two groups at any time point. Table 3 shows the results at wk 4.

DISCUSSION

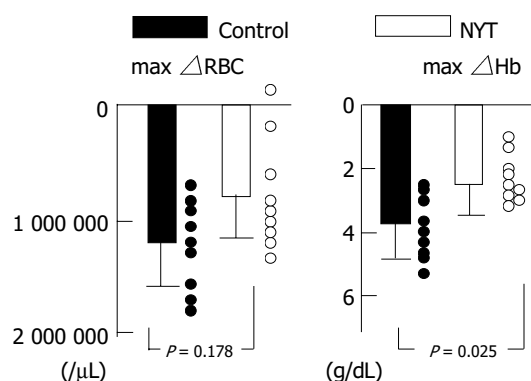
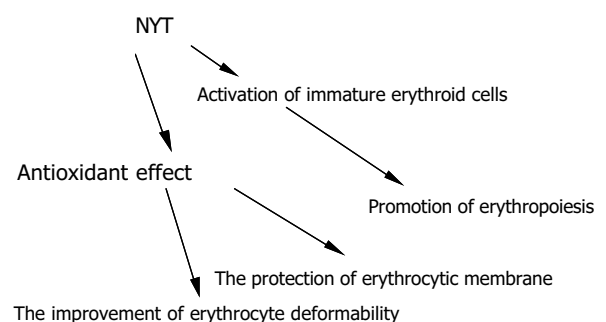
In this study, we elucidated, for the first time, the anemia-ameliorating effect of NYT in the IFN/RBV treatment for chronic hepatitis C in a randomized controlled trial. Although NYT possesses a hematopoietic action^[10-12], we speculate that anemia-reducing effect of NYT was derived from its anti-oxidant^[8] and stabilizing actions on the erythrocytic membrane, ameliorating the hemolytic anemia. NYT is reported to show an anti-HCV action^[7], but NYT did not affect the anti-viral effect of IFN/RBV therapy in this study. If we can reduce the grade of anemia and discontinuation of therapy, it would lead to the increase in number of patients with SVR.

As mentioned above, NYT is reported to have the following effects: hematopoietic^[10-12], antioxidant^[8], hepatocyte-protective^[13], Th1/Th2 balancing^[9], and direct anti-HCV^[7]. NYT has been used in the treatment of asthenic or fatigued patients, especially after operation or severe infectious diseases^[14]. NYT is effective for various signs

and symptoms, including anemia, general malaise, anorexia, night sweating, sensation of cold in the extremities, cough, and insomnia^[14]. These effects have been analyzed and verified in the theory of Traditional Chinese Medicine. From the viewpoint of hepatitis treatment, these effects of NYT are suitable for ameliorating the adverse effects of IFN (general malaise, anorexia, and psychiatric problems) and that of RBV (anemia). The dose of NYT was 9.0 g/d in this study, which is a normal dose in Japan.

The precise mechanisms of RBV-induced anemia are unknown, but several reports^[3,4] suggest that the accumulation of phosphorylated RBV in erythrocytes due to the lack of dephosphorylase in erythrocytes impairs the deformability of erythrocytes. The accumulated RBV may affect the antioxidant defense mechanisms of the erythrocytic membrane. These changes in erythrocytes would lead to the extravascular destruction of erythrocytes (hemolysis). Since NYT has an antioxidant action, it may show a beneficial effect on the erythrocytic membrane. Although NYT would not affect the accumulated RBV inside the erythrocyte, NYT might improve erythrocytic deformability in a different manner, like other herbal medicines with common components. Therefore, the reasons why NYT ameliorates RBV-induced anemia might include the protection of erythrocytic membrane, the improvement of erythrocytic deformability, and erythropoiesis (Figure 3).

Previous reports showed that erythropoietin^[5] and eicosapentaenoic acid^[6] can be effective against RBV-induced anemia. In the prospective, double-blind, randomized controlled study by Afdhal *et al.*, in 185 patients^[5], erythropoietin (EPO) was administered after anemia

**Figure 2** Effect of Ninjinyoeito on the RBV-induced anemia.**Figure 3** Speculated mechanisms of Ninjinyoeito's beneficial effect on RBV-induced anemia.

developed, and the mean Hb increase was 2.2 ± 1.3 g/dL, which was significantly greater than 0.1 ± 1.0 g/dL in the placebo group. However, the use of EPO would be expensive and would not address the solution of hemolysis. In the uncontrolled, pilot study by Ide *et al.*, in six patients^[6], eicosapentaenoic acid (EPA) was also administered after the development of anemia, and the mean Hb significantly increased from 10.8 to 11.4 g/dL in 1 mo. The effect of EPA seems to be marginal, and it was tested in a pilot study and would need a randomized trial. EPA improves erythrocyte deformability and increases EPA content in erythrocytic membrane phospholipids^[6]. Table 5 summarizes the comparison among NYT, EPO, and EPA from the viewpoints of effectiveness, adverse reactions, and cost-benefits. EPO is expensive, with more adverse effects, but most effective. NYT is economical, with little adverse reaction. EPA seems to be intermediate between the above two drugs.

In our study, NYT was administered from the beginning of IFN/RBV treatment, and we cannot simply compare the results between the above-mentioned studies and ours. We would like to test whether NYT improves the RBV-induced anemia after it occurs, or whether pretreatment with NYT prevents the anemia.

Erythropoietin response is reported to be subnormal in the IFN/RBV treatment. Although NYT has a bone marrow-stimulatory action via enhancing colony stimulating factors^[11], there was no significant difference in the endogenous erythropoietin response between the NYT and control groups in our study. Therefore, NYT might ameliorate RBV-induced anemia, not by stimulating hematopoiesis, but by reducing hemolysis. We measured serum glutathione peroxidase activity before and after the IFN/RBV therapy with or without NYT. There was no significant change both in time course and between the NYT and control groups. But, according to the previous reports^[8,13] it is likely that NYT may exert its protective effect on the erythrocytic membrane by antioxidative action and membrane stabilization. Serum antioxidant markers other than glutathione peroxidase might reveal the effect of NYT.

Regarding the combination therapy of IFN and herbal medicines, Shosaikoto (SST, Shao-chaihu-tang) is prohibited for use in combination with IFN because this combination is reported to increase the risk of interstitial pneumonia. The herbal component *Scutellariae radix* alone does not cause interstitial pneumonia, but when used in combination with other herbal components, some unknown factors causing interstitial pneumonia are considered to be expressed. NYT does not contain five of the seven medicinal herbs used in SST, including *Scutellariae radix*. Interstitial pneumonia or any other adverse reactions in relation to NYT use were not found in this study. Since NYT was used safely in the IFN/RBV therapy, NYT could be used in combination with PEG-IFN+RBV for 48 wk, which is considered as the most effective anti-HCV therapy^[2]. This current worldwide standard was not available during the period of this study in Japan.

In conclusion, NYT ameliorated the RBV-induced anemia in RCT. NYT did not show any stronger antiviral effect on HCV, but it was used safely without any adverse reaction in the combination treatment with IFN/RBV. These results

provide good evidence for the effect of the herbal medicine NYT. It is suggested that NYT can be used as a supportive drug for IFN/RBV therapy for chronic hepatitis C. Active mechanisms are to be elucidated and these results would be verified in additional studies with more patients.

REFERENCES

- 1 **Gish RG.** Treating hepatitis C: the state of the art. *Gastroenterol Clin North Am* 2004; **33**: S1-S9
- 2 **Hadziyannis SJ,** Sette H Jr, Morgan TR, Balan V, Diago M, Marcellin P, Ramadori G, Bodenheimer H Jr, Bernstein D, Rizzetto M, Zeuzem S, Pockros PJ, Lin A, Ackrill AM. PEGASYS International Study Group. Peginterferon-alpha2a and ribavirin combination therapy in chronic hepatitis C: a randomized study of treatment duration and ribavirin dose. *Ann Intern Med* 2004; **140**: 346-355
- 3 **De Franceschi L,** Fattovich G, Turrini F, Ayi K, Brugnara C, Manzato F, Noventa F, Stanzial AM, Solero P, Corrocher R. Hemolytic anemia induced by ribavirin therapy in patients with chronic hepatitis C virus infection: role of membrane oxidative damage. *Hepatology* 2000; **31**: 997-1004
- 4 **Page T,** Connor JD. The metabolism of ribavirin in erythrocytes and nucleated cells. *Int J Biochem* 1990; **22**: 379-383
- 5 **Pockros PJ,** Shiffman ML, Schiff ER, Sulkowski MS, Younossi Z, Dieterich DT, Wright TL, Mody SH, Tang KL, Goon BL, Bowers PJ, Leitz G, Afdhal NH. PROACTIVE Study Group. Epoetin alfa maintains ribavirin dose in HCV-infected patients: a prospective, double-blind, randomized controlled study. *Gastroenterology* 2004; **126**: 1302-1311
- 6 **Ide T,** Okamura T, Kumashiro R, Koga Y, Hino T, Hisamochi A, Ogata K, Tanaka K, Kuwahara R, Seki R, Sata M. A pilot study of eicosapentaenoic acid therapy for ribavirin-related anemia in patients with chronic hepatitis C. *Int J Mol Med* 2003; **11**: 729-732
- 7 **Cyong JC,** Ki SM, Iijima K, Kobayashi T, Furuya M. Clinical and pharmacological studies on liver diseases treated with Kampo herbal medicine. *Am J Chin Med* 2000; **28**: 351-360
- 8 **Egashira T,** Takayama F, Komatsu Y. Changes of materials that scavenge 1,1-diphenyl-2-picrylhydrazyl radicals in plasma by per-oral administration of Kampo medicine, Ninjin-yoei-to in rats. *J Pharm Pharmacol* 2003; **55**: 367-371
- 9 **Nakada T,** Watanabe K, Jin GB, Toriizuka K, Hanawa T. Effect of Ninjin-yoei-to on Th1/Th2 type cytokine production in different mouse strains. *Am J Chin Med* 2002; **30**: 215-223
- 10 **Miura S,** Kawamura I, Yamada A. Effect of a traditional Chinese herbal medicine ren-shen-yang-rong-tang (Japanese name: ninjin-yoei-to) on hematopoietic stem cells in mice. *Int J Immunopharmacol* 1989; **11**: 771-780
- 11 **Okamura S,** Shimoda K, Yu LX, Omori F, Niho Y. A traditional Chinese herbal medicine, ren-shen-yang-rong-tang (Japanese name: ninjin-yoei-to) augments the production of granulocyte-macrophage colony-stimulating factor from human peripheral blood mononuclear cells *in vitro*. *Int J Immunopharmacol* 1991; **13**: 595-598
- 12 **Fujii Y,** Imamura M, Han M, Hashino S, Zhu X, Kobayashi H, Imai K, Kasai M, Sakurada K, Miyazaki T. Recipient-mediated effect of a traditional Chinese herbal medicine, ren-shen-yang-rong-tang (Japanese name: ninjin-yoei-to), on hematopoietic recovery following lethal irradiation and syngeneic bone marrow transplantation. *Int J Immunopharmacol* 1994; **16**: 615-622
- 13 **Takayama F,** Egashira T, Yamanaka Y. Protective effect of Ninjin-yoei-to on damage to isolated hepatocytes following transient exposure to tert-butyl hydroperoxide. *Jpn J Pharmacol* 2001; **85**: 227-233
- 14 **Terasawa K.** Ninjin-yoei-to. In: Terasawa K. *Kampo: Japanese-Oriental Medicine: Insights from clinical cases*. 1st ed. Tokyo: K.K. Standard McIntyre, 1993: 242

Screening for PreS specific binding ligands with a phage displayed peptides library

Qiang Deng, Ming Zhuang, Yu-Ying Kong, You-Hua Xie, Yuan Wang

Qiang Deng, Ming Zhuang, Yu-Ying Kong, You-Hua Xie, Yuan Wang, State Key Laboratory of Molecular Biology, Institute of Biochemistry and Cell Biology, Shanghai Institutes of Life Science, Chinese Academy of Sciences, Shanghai 200031, China
Qiang Deng, You-Hua Xie, Yuan Wang, Sino-France Center for Life Science and Genome Research

Supported by Basic Research Program from Ministry of Science and Technology of China, No. G1999054105, and special funds for Sino-France Center for Life Science and Genome Research from Chinese Academy of Sciences and Pasteur Institute in France

Co-correspondent: You-Hua Xie

Correspondence to: Yuan Wang, Institute of Biochemistry and Cell Biology, 320 Yue-Yang Road, Shanghai 200031, China. wangy@sibs.ac.cn

Telephone: +86-21-54921103 Fax: +86-21-54921011

Received: 2004-05-29 Accepted: 2004-07-11

Abstract

AIM: To construct a random peptide phage display library and search for peptides that specifically bind to the PreS region of hepatitis B virus (HBV).

METHODS: A phage display vector, pFuse8, based on the gene 8 product (pVIII) of M13 phage was made and used to construct a random peptide library. *E. coli* derived thioredoxin-PreS was purified with Thio-bond beads, and exploited as the bait protein for library screening. Five rounds of bio-panning were performed. The PreS-binding specificities of enriched phages were characterized with phage ELISA assay.

RESULTS: A phage display vector was successfully constructed as demonstrated to present a pVIII fused HBV PreS1 epitope on the phage surface with a high efficiency. A cysteine confined random peptide library was constructed containing independent clones exceeding 5×10^8 clone forming unit (CFU). A pool of phages showing a PreS-binding specificity was obtained after the screening against thio-PreS with an enrichment of approximately 400 times. Five phages with high PreS-binding specificities were selected and characterized. Sequences of the peptides displayed on these phages were determined.

CONCLUSION: A phage library has been constructed, with random peptides displaying as pVIII-fusion proteins. Specific PreS-binding peptides have been obtained, which may be useful for developing antivirals against HBV infection.

Key words: Hepatitis B virus; Phage; Peptide

Deng Q, Zhuang M, Kong YY, Xie YH, Wang Y. Screening for PreS specific binding ligands with a phage displayed peptides library. *World J Gastroenterol* 2005; 11(26): 4018-4023
<http://www.wjgnet.com/1007-9327/11/4018.asp>

INTRODUCTION

The attachment to hepatocytes by hepatitis B virus (HBV) during infection has long been proposed to be a potential target for antiviral intervention. It is thought that molecules specifically binding to HBV particles may interfere with viral attachment and hence reduce or block subsequent infection^[1-3]. Ideally, these molecules should mimic the structural elements of a cell surface HBV receptor. Unfortunately, although a few host proteins have been demonstrated to interact with HBV particles or viral surface antigens, such a cell surface HBV receptor remains elusive^[4-8]. Consequently, our knowledge on the molecular events leading to HBV attachment to hepatocytes is very limited. One longstanding notion is the role of HBV PreS region in mediating HBV attachment to the putative receptor on hepatocytes^[8-11]. Specifically, the aa 21-47 segment within the PreS1 domain is believed to be essential for this process^[11]. It is noteworthy that other important functions of the PreS region have also been reported, for example, in the assembly and budding of HBV virion^[12-14]. Therefore, the PreS region has become a potential target for screening antivirals against HBV infection.

Strategies for ligands discovery are usually based on procedures for assembling a large number of compounds to produce a diverse array of molecules, followed by a screening process against targets of interest. Among various technologies for ligand discovery, phage display has evolved into one of the main approaches for obtaining lead molecules^[15,16]. Filamentous phage M13 has a rather simple architecture composed of five different structure proteins. The product of gene 8 (pVIII) is a major capsid protein. There are approximately 2 700 pVIII molecules all over a phage particle, while other structural proteins are located at the tail of the phage particle with only a few copies of each^[17]. Thus, by fusing with pVIII, hundreds or thousands of ligands can theoretically be displayed on the surface of the phage particle, which should help strengthen its interaction with a target^[15,16]. Thus, pVIII fusion protein based phage display will offer a greater chance to find mildly binding ligands.

In this study, we have constructed a structurally constrained phage display library in which random peptides are displayed

as N-terminal fusions to pVIII and confined in a loop by a pair of flanking cysteine residues^[15,18,19]. Recombinant thio-PreS protein was used as target in screening for the PreS-binding peptides. A pool of phages showing PreS-binding specificity was obtained with an enrichment factor of approximately 400. Phages with high PreS-binding specificities were selected and characterized. Sequences of the peptides displayed on five of PreS-binding phages were determined.

MATERIALS AND METHODS

Materials

The pCANTAB5E vector, T7 DNA sequencing kit, and HRP-conjugated M13 specific monoclonal antibody (anti-M13 mAb) are products of Amersham Pharmacia Biotech (Piscataway, USA). XL1-blue F['] *E. coli* strain and helper phage VCSM13 were purchased from Stratagene (La Jolla, USA). PreS1 specific mAb 125E11 has been previously described^[20,21]. Maxisorp F16 module (Nunc, Denmark) was used for protein coating. Thiobond™ affinity resin and the thioredoxin specific mAb (anti-thio) were from Invitrogen (Carlsbad, USA). Recombinant enterokinase (rEK) was purchased from Novagen (Madison, USA).

Construction of random peptide phage display library

pCANTAB5E was utilized as the parental vector for constructing a pVIII fusion protein display vector. The coding sequence for M13 pVIII was amplified with specific primers (pVIII-forward: 5'-TAAGGATCCGGTGGTGCTGAGGGTGACGATCCCGC-3', pVIII-reverse: 5'-AGGAATTCATGTACCGTAACACTG-3') using the VCSM13 genome as template. PCR product was digested with *Bam*HI and *Eco*RI, and inserted into the same sites in pCANTAB5E, replacing the original gene 3. The resulted vector was named pFuse8 (Figure 1A). To construct pFuse8-E that encodes a PreS1 epitope fused with pVIII (Figure 1A), annealed oligonucleotides (sense: 5'-CAGCAATGGCAGGC AGCCTGAACCCTAGCTGGGATGGTGGCGGAGGATCCG-3', antisense: 5'-AATTCGGATCCTCCGCCACC ATCCAGCTAGGGTTCAGGCTGCCTGCCATTGCTGGCT-3', the epitope coding sequence is underlined) were ligated to pFuse8 digested with *Sfi*I and *Bam*HI.

For the construction of peptide library, antisense oligonucleotides containing random nucleotides (5'-ATTGCGGATCCACACC(MNN)₃GCA(MNN)₇ACA(MNN)₃GCCTGCTGCCATTGCTGC-3', N = A, T, C or G; M = A or C) was synthesized (Invitrogen). A complementary primer (5'-CAGCAA TGGCAGCAGGC-3') was annealed to the 3' end of the long oligonucleotides, followed by the fill-in reaction with the Klenow polymerase to generate the double-stranded DNA. The DNA duplex was then digested with *Bam*HI and ligated into pFuse8 cut with *Sfi*I and *Bam*HI. The ligation mixture was used to transform XL1-blue F['] competent cells by electroporation. The phage library was established by co-infection of helper phage VCSM13 (MOI, 10:1) to the transformed cells as previously described^[22]. Complexity of the library was estimated according to the number of independent transformed clones.

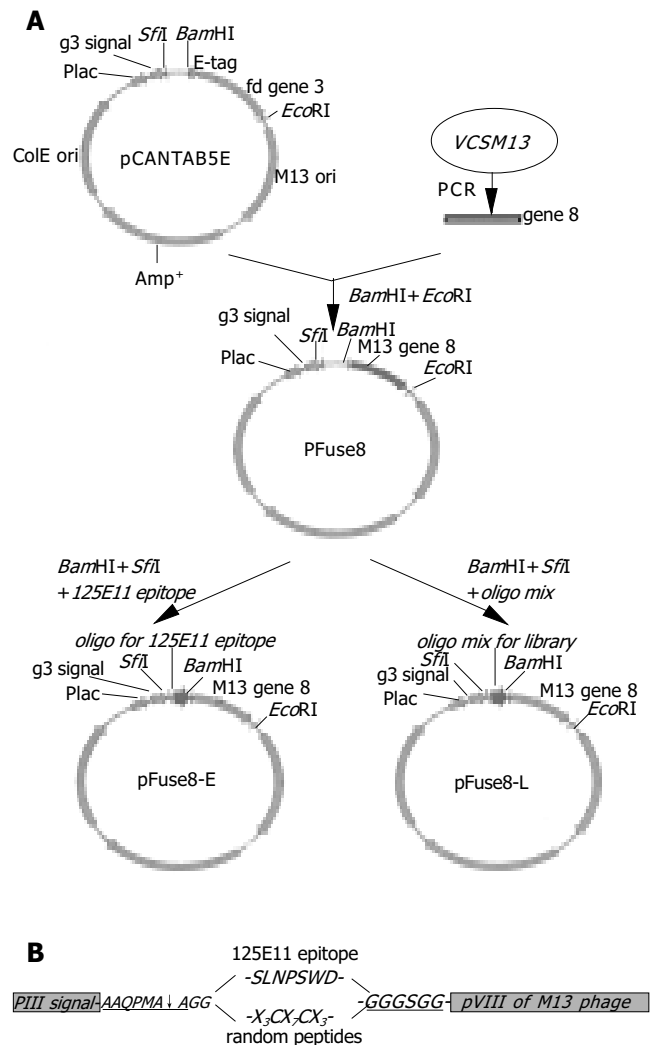


Figure 1 Diagram of library construction. **A:** a schematic representation of the steps in the construction of the phagemid encoding the pVIII fusion protein. pCANTAB5E, a pIII displaying vector; pFuse8, the vector harboring gene 8 coding sequence in replace of gene 3; pFuse8-E, the coding sequence for a specific epitope recognized by the 125E11 mAb is inserted into pFuse8; pFuse8-L, the coding sequences for random peptides are inserted into pFuse8; **B:** Inserted sequences in pFuse8-E and pFuse8-L after translation. SLNPSWD is the specific epitope recognized by the 125E11 mAb. In pFuse8-L, the epitope is replaced with X3CX7CX3.

DNA sequencing

Phagemid pool of randomly picked-up clones from the library was prepared with SV minipreps kit (Promega). DNA sequencing was performed with T7 DNA sequencing kit according to the manufacturer's instruction.

Preparation of PreS fusion protein

Prokaryotic expression plasmid pThioHisA-PreS was constructed for the synthesis of thioredoxin fused PreS (thio-PreS) in *E. coli*^[23]. An affinity purification for the expression product was performed with Thiobond™ beads according to the manufacturer's instruction.

Library screening

Totally 10¹¹ phages were mixed with 30 μL of the thio-PreS bound Thiobond™ beads and incubated on a rotating wheel for 10 min. After washing with PBS containing 0.05% Tween

20 for four times, the beads were treated with 1 unit of rEK at 30 °C for 6 h. Phages binding specifically to the PreS region were supposed to detach off the beads. Eluted phages in the collected supernatant were subject to propagation in XL1-blue F' cells, followed by VCSM13 co-infection to produce a phage pool for next round of panning^[22]. A total of five rounds of selection were performed.

Western blot

Western blot of thio-PreS was performed according to a standard method^[24]. Thio-PreS coupled on resins with or without rEK treatment were boiled and separated on SDS-PAGE, and transferred to nitrocellulose filters. Anti-thio mAb (1:1 000) was used as the primary antibody for the detection. Blots were developed using the ECL method with HRP-labeled rabbit anti-mouse Ig (1:2 000, DaKo, USA).

Phage ELISA

Phage ELISA was carried out as described previously^[22]. Purified thio-PreS proteins (1 µg/well) were immobilized on the microwells in PBS buffer overnight. Phages propagated from infected XL1-blue F' cells were precipitated by 0.1 volume of PEG8000/NaCl (20% PEG8000, 3 mol/L NaCl), resuspended in PBS buffer and applied to thio-PreS coated wells, followed by an incubation at room temperature for 1 hour. An HRP-labeled anti-M13 mAb (1:1 000) was used for the detection of bound phages.

Virus capture assay

For capturing HBV virions, each microwell was coated with 10¹¹ phages in carbonate buffer (pH 9.5) at 4 °C overnight. After blocking with 1% BSA at 37 °C for 2 h, cultured medium of HepG2.2.15^[25] that contains HBV particles was added and incubated for 1 h at 37 °C, followed by a washing process with PBS buffer containing 0.05% Tween 20. An HRP-conjugated anti-HBs antibody was used to detect the captured HBV particles according to the manufacturer's protocol (Sino-American Biotech, Shanghai).

RESULTS

Construction of pVIII based phage display vector

To construct the vector pFuse8, M13 gene 8 was amplified using the genomic DNA of VCSM13 phage as template. The PCR product was inserted into pCANTAB5E to replace the coding sequence of gene 3 and the E-tag (Figure 1A). The inserted gene 8 is located downstream to a leader signal sequence of gene 3, which is used to direct the pVIII fusion protein to the surface of the phage particle. In the phagemid pFuse8-E as shown in Figure 1B, a spacer between the leader signal and gene 8 encodes an in-frame peptide AAQPMAAG-SLNPSWD-GGSGG. The first part of the peptide (AAQPMAAG) is a recognition sequence of the *peI*B signal peptidase^[26]. The 7-amino acids in the middle of this peptide represents an epitope within the HBV PreS1 domain that is recognized by the 125E11 mAb (unpublished data), providing a molecular marker for detection of phage display. The ensuing glycine tether is used to link the peptide to pVIII, increasing the flexibility of the peptide.

Phages were generated by co-infection of the pFuse8-E transformed XL1-blue F' cells with helper phage VCSM13.

The displayed 125E11 epitope was readily detected by phage ELISA in a dose dependent manner with the immobilized 125E11 mAb but not with an irrelevant mAb (anti-HBs) (Figure 2). As shown in Figure 2, the *lac* promoter employed in the vector was somewhat leaky so that pVIII-fused epitope could be easily detected even without IPTG induction^[27].

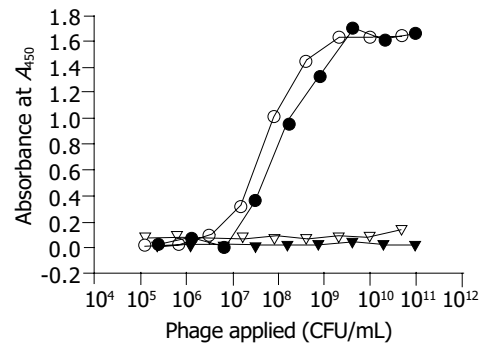


Figure 2 Surface display of the epitope recognized by 125E11. The SLNPSWD epitope displayed on the surface of the phage particle was detected by phage ELISA. The circles indicate the phages that bind 125E11 coated wells. Triangles represent phages captured by an irrelevant mAb (anti-HBs). The synthesis of pVIII fusion proteins with or without IPTG induction is denoted as white or black, respectively.

Construction of structure-confined random peptide phage display library

Structure-confined random peptide library has the advantage to present peptides in a fixed loop so that their conformations are relatively rigid^[18,19]. In this study, random peptides fused with pVIII assume a form of X₃CX₇CX₃, where X stands for any amino acids. Two cysteine residues flank the 7 random amino acids in the middle. Under a non-reducing environment in the periplasm of *E. coli*, these cysteine residues may spontaneously form a disulfide bond that constrains the conformation of the displayed peptide^[18,19]. The oligonucleotides mixture coding for the random peptides was inserted into the pFuse8 vector (pFuse8-L, Figure 1A). The resulting library had the size of about 5.0×10⁸ independent clones that represented a great complexity. The random property of the library was verified by DNA sequence analysis. As shown in Figure 3, in the region coding for the random peptides, all four kinds of nucleotides are equally distributed at the first two positions of the triplet codons, while T or G varies at the third position, indicating a sufficient diversity of the library.

Screening for PreS-binding peptides

The PreS region of HBV, when synthesized alone in *E. coli*, is vulnerable to degradation and largely insoluble. To overcome these problems, the PreS region was fused with the C-terminus of thioredoxin (Figure 4A), which has dramatically enhanced both the stability and the solubility of the PreS region (Figure 4B). An enterokinase site located at the junction between the PreS region and the thioredoxin tag (Figure 4A) facilitates the release of the PreS region by digestion with rEK, leaving the thioredoxin tag on the affinity matrix (Figure 4C). Thus, the PreS-binding phages could be

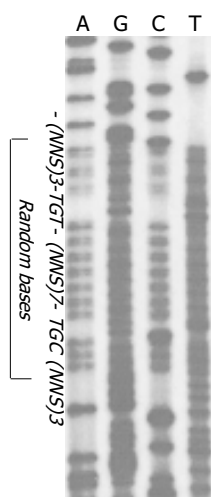


Figure 3 Diversity of the constructed library. In the region coding for the random peptides, four kinds of nucleotides are equally distributed at the first two loci of the triplet codons, while T or G varies at the last. Oligonucleotides for cysteine confined random peptides (5'-GCAGCAGGC-(NNS)3-TGT(NNS)7-TGC(NNS)3-3-GGTGGTGA-3', N = A, T, C or G; S = A or C) are shown.

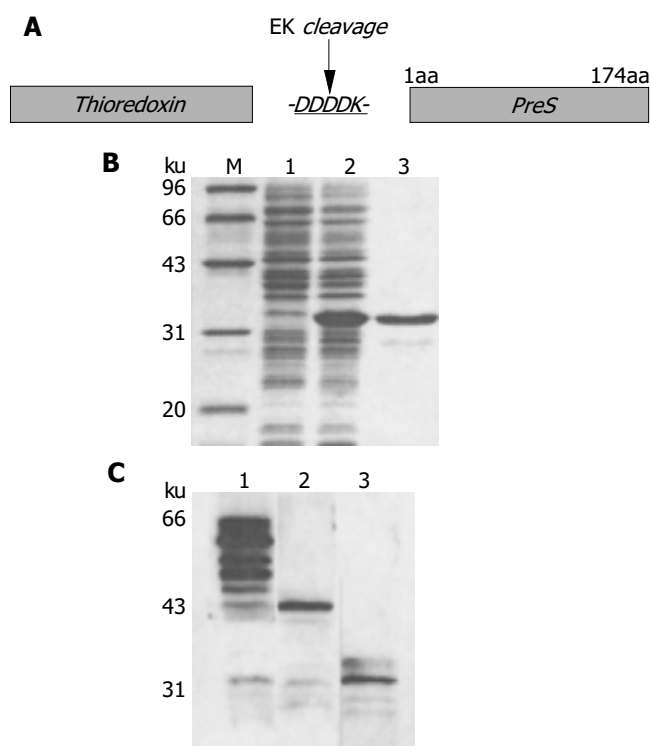


Figure 4 Synthesis of thio-PreS. **A:** a schematic representation of the thio-PreS fusion protein. DDDDK is a cleavage site of rEK; **B:** SDS-PAGE analysis. Lane 1, the *E. coli* lysate without IPTG induction; lane 2, the soluble lysate after IPTG induction, thio-PreS of 33 ku is indicated with a triangle; lane 3, the purified thio-PreS; **C:** Western blot with the anti-thio mAb. Lane 1, thio-PreS coupled to the Thiobond™ beads; lane 2, thio-PreS coupled beads treated in the absence of rEK; lane 3, thio-PreS coupled beads treated in the presence of rEK.

dissociated from the resin and enriched. It was expected that cleavage by rEK might decrease a nonspecific enrichment of phages binding to the thioredoxin tag. It is noteworthy that the degradation of the free PreS region should not influence the recovery of the PreS-binding phages.

A total of five rounds of screening were performed.

As shown in Table 1, the PreS-binding phages were greatly enriched as evidenced by a steadily rising enrichment factor (EF, phage eluted/phage applied). An approximately 400-fold of enrichment (EF_{5th}/EF_{1st}) was achieved as estimated by the titer of the phages after the screening. The pool of phages from the final round of selection bound to the thio-PreS immobilized wells specifically in a dose-dependent manner, in sharp contrast to the original pool of phages before selection (Figure 5). A much weaker noise was noticed with the thioredoxin immobilized wells serving as a control, indicating that the thioredoxin-binding phages were also selected, though they might only be a small minority.

Characterization of the PreS-binding phages

The specificity of the phages with regard to PreS-binding was further characterized by virus capture assay. When coated on microplate wells, the pool of phages from each round of selection was tested for their abilities to capture HBV virions from the cultured medium of HepG2.2.15. The binding capacity to HBV virions increased greatly after the final round of selection (Figure 6), suggesting that the PreS-binding phages were truly selected. Phages from the final round of selection were picked for a further analysis. The specificities of these phages with regard to PreS-binding were analyzed with phage ELISA assay. Phages with a strong binding capacity to thioredoxin were considered nonspecific and discarded (data not shown). The corresponding phagemids of five of the PreS-binding phages were subjected to DNA sequencing. Amino acid sequences of the potential PreS-binding peptides were deduced (Figure 7).

DISCUSSION

The filamentous phage display system, whereby the expressed peptides are displayed as fusions to phage coat proteins, has been effective in the discovery of ligands^[15,16]. Commonly exploited strategy is the surface display of N-terminus fusions to the minor coat protein pIII (product of phage gene 3). It represents a low-valent surface display, as only three to five copies of pIII are present at the tail of the phage particle, providing a selection platform for an interaction with a high affinity^[15]. In our work, a pVIII fusion protein based vector was successfully constructed, and proved to work well in peptide displaying. Since pVIII is a major coat protein with thousands of molecules on a single phage, thus pVIII fusion protein based phage display will offer a greater chance to find mildly or weakly binding ligands. As PreS-binding peptides are concerned, the pVIII fusion protein based system may be a better choice than the pIII fusion protein based system. It is supposed that the affinity of the HBV virion to its putative receptor on hepatocytes may not be strong, because an ensuing intracellular event of dissociation may occur closely after the penetration of the viral particle during the infection.

Linear oligopeptides likely present various solution conformations that may be quite different from the structure in the native or bound forms of a protein. It has been demonstrated that the structurally active region in native protein may be mimicked by cyclic amino acid sequences of constrained peptides displayed on the phage surface^[15,18,19]. A pair of flanked cysteine residues was adopted to confine the random peptides in the middle by presumably forming

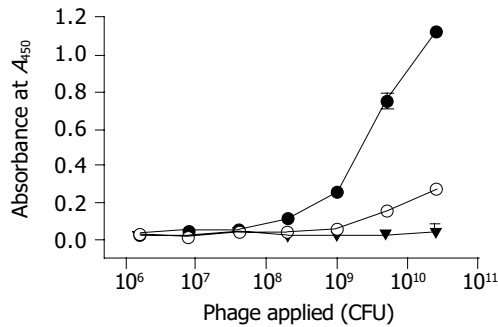


Figure 5 Phage ELISA of the enriched phages after the final round of screening. Black dots, the enriched phages bind to thio-PreS; Empty dots, the enriched phages bind to thioredoxin as a control; Black triangles, phages in the original library do not bind to thio-PreS.

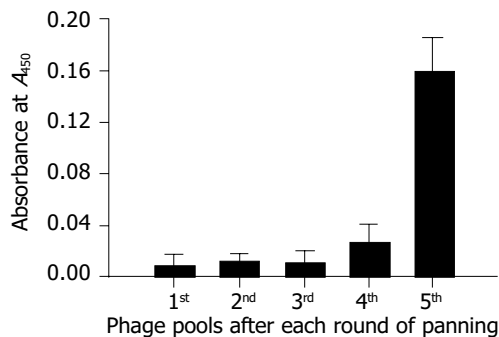


Figure 6 Virus capture assay. The phage pool (10^{11} CFU) after each round of screening shows an increasing binding capacity to HBV virions in the culture medium of HepG2.2.15.

FTG C SRLLYGW C SLN
 AWT C LFSTGGI C QSS
 TLI C MVKIQVK C PMQ
 PTW C LEFMITA C IRG
 SAV C VSFENFM C IGP

Figure 7 Amino acid sequences of PreS specific oligopeptides. The amino acid sequences of the peptides encoded by the phagemids derived from five of the PreS-binding phages were deduced from DNA sequencing analysis. The C in bold indicates the invariable residues of cysteines.

an intra-molecular disulfide bond that provides a more defined scaffold when folded in the periplasmic environment of *E. coli*. In this study, we have constructed a conformation

constrained random peptide phage display library and performed the screening with this library, in the hope that potential peptides with more defined conformations may better fulfill the structural features required for PreS-binding. On the other hand, such a conformation-constrained library has its weaknesses. It is likely that during the interaction process between PreS and a potential peptide, both partners may exert their influences on each other so that the conformation of the potential peptide adjusts to better bind PreS. In such a situation, the peptide with a constrained conformation may be too rigid to accommodate itself upon binding PreS, which will probably result in a reduced binding affinity.

During the life cycle of HBV, the PreS region of the large surface antigen (LHBs) plays a crucial role in virion assembly and budding as well as in viral attachment to hepatocytes^[8-12,28,29]. Given the pivotal role of the PreS region in HBV life cycle, the specific PreS-binding ligands are expected to be useful as inhibitors to block viral entry to hepatocytes, or to interfere with the process of virion assembly in HBV infected cells. Similar ideas have been pursued widely in the field of HIV research and proved to be a potential way for antiviral drug development^[30,31]. Moreover, studies on the PreS-binding peptides will likely provide helpful information about the interaction between HBV virion and hepatocytes that may aid the identification of a yet-to-be-found receptor of HBV.

The binding capacity of the pool of phages to HBV virions increased greatly after the final round of selection. Thus, the thio-PreS fusion protein was proved to be an 10 effective bait protein that might mimic the conformation adopted by the PreS region in the native virions. In addition, the affinity screening for the PreS-binding phages represents a promising approach for discovering HBV binding ligands. Several peptides encoded by the phagemids of five of the PreS-binding phages were determined. No consensus sequence or conserved amino acids were found in these five peptides. Therefore, these peptides likely bind to different fragments of the PreS region. On the other hand, sequences of more PreS-binding peptides need to be determined and the binding properties of the PreS-binding peptides await further investigations, which are currently on the way.

ACKNOWLEDGMENTS

125E11 is a kind gift from Professor Zhu-Chuan Zhang.

REFERENCES

- Urban S, Gripon P. Inhibition of duck hepatitis B virus infection by a myristoylated pre-S peptide of the large viral surface protein. *J Virol* 2002; **76**: 1986-1990

Table 1 Enrichment of phages binding to thio-PreS coupled beads

Round of panning	Thio-PreS coupled beads			Thioredoxin coupled beads		
	Phage applied	Phage eluted	EF ¹	Phage applied	Phage eluted	EF
1 st	2.0 ± 10^{11}	2.6 ± 10^4	1.3 ± 10^{-7}	2.0 ± 10^{11}	3.4 ± 10^4	1.7 ± 10^{-7}
2 nd	1.0 ± 10^{11}	1.2 ± 10^4	1.2 ± 10^{-7}	1.0 ± 10^{11}	9.5 ± 10^3	9.5 ± 10^{-8}
3 rd	1.0 ± 10^{11}	9.3 ± 10^4	9.3 ± 10^{-7}	1.0 ± 10^{11}	3.9 ± 10^4	1.2 ± 10^{-7}
4 th	5.0 ± 10^{10}	3.5 ± 10^5	7.0 ± 10^{-6}	5.0 ± 10^{10}	3.6 ± 10^4	7.2 ± 10^{-7}
5 th	5.0 ± 10^{10}	2.6 ± 10^6	5.1 ± 10^{-5}	5.0 ± 10^{10}	8.8 ± 10^4	1.8 ± 10^{-6}

¹Enrichment factor (EF) = phage eluted/phage applied.

- 2 **Hong HJ**, Ryu CJ, Hur H, Kim S, Oh HK, Oh MS, Park SY. *In vivo* neutralization of hepatitis B virus infection by an anti-preS1 humanized antibody in chimpanzees. *Virology* 2004; **318**: 134-141
- 3 **Park SS**, Ryu CJ, Gripon P, Guguen-Guillouzo C, Hong HJ. Generation and characterization of a humanized antibody with specificity for preS2 surface antigen of hepatitis B virus. *Hybridoma* 1996; **15**: 435-441
- 4 **Stefas I**, Rucheton M, D'Angeac AD, Morel-Baccard C, Seigneurin JM, Zarski JP, Martin M, Cerutti M, Bossy JP, Misse D, Graafland H, Veas F. Hepatitis B virus Dane particles bind to human plasma apolipoprotein H. *Hepatology* 2001; **33**: 207-217
- 5 **Ryu CJ**, Cho DY, Gripon P, Kim HS, Guguen-Guillouzo C, Hong HJ. An 80-kilodalton protein that binds to the pre-S1 domain of hepatitis B virus. *J Virol* 2000; **74**: 110-116
- 6 **De Falco S**, Ruvoletto MG, Verdoliva A, Ruvo M, Raucci A, Marino M, Senatore S, Cassani G, Alberti A, Pontisso P, Fassina G. Cloning and expression of a novel hepatitis B virus-binding protein from HepG2 cells. *J Biol Chem* 2001; **276**: 36613-36623
- 7 **Gong ZJ**, De Meyer S, van Pelt J, Hertogs K, Depla E, Soumillion A, Fevery J, Yap SH. Transfection of a rat hepatoma cell line with a construct expressing human liver annexin V confers susceptibility to hepatitis B virus infection. *Hepatology* 1999; **29**: 576-584
- 8 **De Meyer S**, Gong ZJ, Suwandhi W, van Pelt J, Soumillion A, Yap SH. Organ and species specificity of hepatitis B virus (HBV) infection: a review of literature with a special reference to preferential attachment of HBV to human hepatocytes. *J Viral Hepat* 1997; **4**: 145-153
- 9 **Le Seyec J**, Chouteau P, Cannie I, Guguen-Guillouzo C, Gripon P. Infection process of the hepatitis B virus depends on the presence of a defined sequence in the pre-S1 domain. *J Virol* 1999; **73**: 2052-2057
- 10 **Pontisso P**, Alberti A. The role of preS1 in the interaction of hepatitis B virus with human hepatocytes. *Hepatology* 1991; **14**: 405-406
- 11 **Neurath AR**, Kent SB, Strick N, Parker K. Identification and chemical synthesis of a host cell receptor binding site on hepatitis B virus. *Cell* 1986; **46**: 429-436
- 12 **Bruss V**. A short linear sequence in the pre-S domain of the large hepatitis B virus envelope protein required for virion formation. *J Virol* 1997; **71**: 9350-9357
- 13 **Ponsel D**, Bruss V. Mapping of amino acid side chains on the surface of hepatitis B virus capsids required for envelopment and virion formation. *J Virol* 2003; **77**: 416-422
- 14 **Poisson F**, Severac A, Hourieux C, Goudeau A, Roingeard P. Both pre-S1 and S domains of hepatitis B virus envelope proteins interact with the core particle. *Virology* 1997; **228**: 115-120
- 15 **Burritt JB**, Bond CW, Doss KW, Jesaitis AJ. Filamentous phage display of oligopeptide libraries. *Anal Biochem* 1996; **238**: 1-13
- 16 **Sidhu SS**. Phage display in pharmaceutical biotechnology. *Curr Opin Biotechnol* 2000; **11**: 610-616
- 17 **Cabilly S**. The basic structure of filamentous phage and its use in the display of combinatorial peptide libraries. *Mol Biochem* 1999; **12**: 143-148
- 18 **Hoess RH**, Mack AJ, Walton H, Reilly TM. Identification of a structural epitope by using a peptide library displayed on filamentous bacteriophage. *J Immunol* 1994; **153**: 724-729
- 19 **Luzzago A**, Felici F, Tramontano A, Pessi A, Cortese R. Mimicking of discontinuous epitopes by phage-displayed peptides. I. Epitope mapping of human H ferritin using a phage library of constrained peptides. *Gene* 1993; **128**: 51-57
- 20 **Yang HL**, Jin Y, Cao HT, Xu X, Li GD, Wang Y, Zhang ZC. Affinity purification of hepatitis B virus surface antigen containing preS1 region. *Shengwu Huaxue Yu Shengwu Wuli Xuebao* 1996; **28**: 412-417
- 21 **Hui J**, Li G, Kong Y, Wang Y. Expression and characterization of chimeric hepatitis B surface antigen particles carrying preS epitopes. *J Biotechnol* 1999; **72**: 49-59
- 22 **Zhang XX**, Deng Q, Zhang SY, Liu J, Cai Q, Lu ZM, Wang Y. Broadly cross-reactive mimotope of hypervariable region 1 of hepatitis C virus derived from DNA shuffling and screened by phage display library. *J Med Virol* 2003; **71**: 511-517
- 23 **Deng Q**, Kong YY, Xie YH, Wang Y. Expression and purification of the complete PreS region of hepatitis B Virus. *World J Gastroenterol* 2005; **11**: 3060-3064
- 24 **Sambrook J**, Fritsch EF, Maniatis T. Molecular cloning: A laboratory manual. 2nd ed. *Cold Spring Harbor Laboratory Press* 1989:
- 25 **Sells MA**, Zelent AZ, Shvartsman M, Acs G. Replicative intermediates of hepatitis B virus in HepG2 cells that produce infectious virions. *J Virol* 1988; **62**: 2836-2844
- 26 **Eerola R**, Saviranta P, Lilja H, Pettersson K, Lovgren T, Karp M. Expression of prostate specific antigen on the surface of a filamentous phage. *Biochem Biophys Res Commun* 1994; **200**: 1346-1352
- 27 **Cramer R**, Jaussi R, Menz G, Blaser K. Display of expression products of cDNA libraries on phage surfaces. A versatile screening system for selective isolation of genes by specific gene-product/ligand interaction. *Eur J Biochem* 1994; **226**: 53-58
- 28 **Bruss V**, Ganem D. The role of envelope proteins in hepatitis B virus assembly. *Proc Natl Acad Sci USA* 1991; **88**: 1059-1063
- 29 **Ponsel D**, Bruss V. Mapping of amino acid side chains on the surface of hepatitis B virus capsids required for envelopment and virion formation. *J Virol* 2003; **77**: 416-422
- 30 **Zhang X**, Gaubin M, Briant L, Srikanth V, Murali R, Saragovi U, Weiner D, Devaux C, Autiero M, Piatier-Tonneau D, Greene MI. Synthetic CD4 exocyclics inhibit binding of human immunodeficiency virus type 1 envelope to CD4 and virus replication in T lymphocytes. *Nat Biotechnol* 1997; **15**: 150-154
- 31 **Choi YH**, Rho WS, Kim ND, Park SJ, Shin DH, Kim JW, Im SH, Won HS, Lee CW, Chae CB, Sung YC. Short peptides with induced beta-turn inhibit the interaction between HIV-1 gp120 and CD4. *J Med Chem* 2001; **44**: 1356-1363

Ephrin-B2 is differentially expressed in the intestinal epithelium in Crohn's disease and contributes to accelerated epithelial wound healing *in vitro*

Christian Hafner, Stefanie Meyer, Thomas Langmann, Gerd Schmitz, Frauke Bataille, Ilja Hagen, Bernd Becker, Alexander Roesch, Gerhard Rogler, Michael Landthaler, Thomas Vogt

Christian Hafner, Stefanie Meyer, Ilja Hagen, Bernd Becker, Alexander Roesch, Michael Landthaler, Thomas Vogt, Department of Dermatology, University Hospital of Regensburg, D-93042 Regensburg, Germany

Thomas Langmann, Gerd Schmitz, Department of Clinical Chemistry, University Hospital of Regensburg, D-93042 Regensburg, Germany

Frauke Bataille, Institute of Pathology, University Hospital of Regensburg, D-93042 Regensburg, Germany

Gerhard Rogler, Department of Internal Medicine, University Hospital of Regensburg, D-93042 Regensburg, Germany

Supported by the German Research Society (DFG-SFB 585/A8) and the Dr. Heinz Maurer Grant KFB 1.7

Co-first-authors: Stefanie Meyer

Correspondence to: Professor Dr. Thomas Vogt, Department of Dermatology, University of Regensburg, D-93042 Regensburg, Germany. thomas.vogt@klinik.uniregensburg.de

Telephone: +49-941-944-9606 Fax: +49-941-944-9608

Received: 2004-08-26 Accepted: 2004-10-07

Abstract

AIM: Eph receptor tyrosine kinases and their membrane bound receptor-like ligands, the ephrins, represent a bi-directional cell-cell contact signaling system that directs epithelial movements in development. The meaning of this system in the adult human gut is unknown. We investigated the Eph/ephrin mRNA expression in the intestinal epithelium of healthy controls and patients with inflammatory bowel disease (IBD).

METHODS: mRNA expression profiles of all Eph/ephrin family members in normal small intestine and colon were established by real-time RT-PCR. In addition, differential expression in IBD was investigated by cDNA array technology, and validated by both real-time RT-PCR and immunohistochemistry. Potential effects of enhanced EphB/ephrin-B signaling were analyzed in an *in vitro* IEC-6 cell scratch wound model.

RESULTS: Human adult intestinal mucosa exhibits a complex pattern of Eph receptors and ephrins. Beside the known prominent co-expression of EphA2 and ephrinA1, we found abundantly co-expressed EphB2 and ephrin-B1/2. Interestingly, cDNA array data, validated by real-time PCR and immunohistochemistry, showed upregulation of ephrin-B2 in both perilesional and lesional intestinal epithelial cells of IBD patients, suggesting a role in epithelial homeostasis. Stimulation of ephrin-B signaling in ephrin-

B1/2 expressing rat IEC-6-cells with recombinant EphB1-Fc resulted in a significant dose-dependent acceleration of wound closure. Furthermore, fluorescence microscopy showed that EphB1-Fc induced coordinated migration of wound edge cells is associated with enhanced formation of lamellipodial protrusions into the wound, increased actin stress fiber assembly and production of laminin at the wound edge.

CONCLUSION: EphB/ephrin-B signaling might represent a novel protective mechanism that promotes intestinal epithelial wound healing, with potential impact on epithelial restitution in IBD.

© 2005 The WJG Press and Elsevier Inc. All rights reserved.

Key words: Ephrin-B2; Crohn's disease; IBD; IEC-6; Wound healing; Epithelial restitution

Hafner C, Meyer S, Langmann T, Schmitz G, Bataille F, Hagen I, Becker B, Roesch A, Rogler G, Landthaler M, Vogt T. Ephrin-B2 is differentially expressed in the intestinal epithelium in Crohn's disease and contributes to accelerated epithelial wound healing *in vitro*. *World J Gastroenterol* 2005; 11(26): 4024-4031

<http://www.wjgnet.com/1007-9327/11/4024.asp>

INTRODUCTION

The rapid resealing of the intestinal surface partly relies on the highly adaptive ability of epithelial wound-edge cells to rapidly form pseudopodial protrusions, reorganize the cytoskeleton, and migrate into a wound defect in a coordinated manner^[1-3]. In the intestine, the fast epithelial healing is particularly important considering the necessity to protect the host with a one-cell-layer epithelium against a considerable microbial threat and exposure to a multitude of immunogenic and toxic factors^[1]. Since epithelial integrity is critically linked to the prevention and healing of inflammatory bowel disease (IBD), the investigation of wound closure modifying factors has attracted a lot of attention in this field. Growth factors (EGF, TGF- β , HGF, KGF, IGF), trefoil peptides, cytokines (IL-1 β , IL2), nutrients (SCFA, polyamines), and matrix components (laminin) are among the best studied contributors to epithelial restitution^[1,4].

In contrast to those established soluble co-factors, the Eph receptor tyrosine kinases (RTKs), and their membrane-

bound receptor-like ligands, the ephrins, specifically direct collaborative cell movements by direct cell-cell signaling^[5,6]. Based on their sequence homology, structure, and binding affinity, the Eph-RTKs and ephrins are divided into two subclasses, A and B. With few exceptions, the two classes (A and B) of Eph-RTKs exhibit a differential affinity for the distinct A- and B-subsets of ephrins. In contrast to humoral signaling systems, the ligands in this system are membrane-bound. A-ephrins are tethered to the outer leaflet of the plasma membrane by virtue of a glycosylphosphatidylinositol (GPI) anchor, whereas, B-ephrins are transmembrane proteins^[7,8]. With the discovery that ephrins can by themselves induce a “reverse” cellular signaling response by exhibiting receptor-like functions, it is apparent that the Eph-RTK/ephrin interactions represent a cell-cell signaling system that is capable of mediating a bidirectional response in both the ligand and the receptor-bearing cell^[9]. The generated juxtacrine signals organize the coordinated movement of cells during development, e.g. in axonal guidance, remodelling of blood vessels, and formation of epithelial surfaces^[10-13]. It has also been demonstrated that the differential expression of ephrin ligands and Eph-RTKs along the crypt-villus axis determines the correct positioning and allocation of the proliferating versus differentiating compartment during development of crypts in the small intestine^[14]. Disruption of those genes leads to intermingling between both of these compartments.

While the meaning of Eph-RTKs/ephrins in embryonic morphogenesis has been well established, their physiologic role in adult tissues is unknown. However, recent data indicate a possible role in tissue repair and maintenance^[15]. EphA2/ephrin-A1 signaling, previously termed epithelial cell kinase (Eck) and protein B61, has already been suggested to be involved in the homeostasis of the intestinal barrier in adults^[16]. Since cytokines such as IL-1 β , IL-2 and TGF- β can modulate the steady-state levels of the expression of EphA2/ephrin-A1 *in vitro*, a role in inflammatory bowel disease (IBD) is possible^[16]. Therefore, we investigated the full repertoire of Eph-RTKs and ephrins in the gut epithelium and possible differential expression in IBDs. Furthermore, possible consequences of the observed changes for the intestinal wound closure capacity were evaluated.

MATERIALS AND METHODS

Tissue specimens and RNA isolation

The corresponding protocols for the study have been accepted by the local ethics committee and biopsies were taken after informed consent of the patients. For establishing of an Eph-RTK/ephrin mRNA expression profile of the normal human gut, total mucosa biopsies were obtained from normal colon ($n = 5$, ages ranged from 28 to 75 years). Normal small intestine mRNAs ($n = 5$, ages ranged from 20 to 61 years) were purchased from Clontech (BD Biosciences, Palo Alto, USA). For each tissue, the RNAs were pooled to avoid bias due to potential interindividual differences.

Affymetrix[®] HGU133A and HGU133B GeneChip array data, recently published by our collaborators, indicated possible differential expression of some Eph-RTK/ephrin family members^[17]. In that array analysis, samples had been

collected from resected terminal ileum and colon of control subjects ($n = 4$, ages ranged from 52 to 60 years), Morbus Crohn (MC) patients ($n = 4$, ages ranged from 23 to 43 years), and Colitis ulcerosa (CU) patients ($n = 4$, ages ranged from 20 to 57 years). The material was obtained from non-inflamed regions at least 10 cm distant from visibly inflamed areas to avoid bias due to inflammatory cells. From the same cohort of patients, individual (not pooled) RNAs were available for real-time RT-PCR based validation of selected genes in this study.

For low density array analysis, biopsies were used provided by the core facility “primary cells and tissues” of the Regensburg-SFB585 (German interdisciplinary research initiative on “immune functions in the gut”; <http://www.uniregensburg.de/Einrichtungen/Klinikum/SFB>). To control the sampling process, sets of six biopsies were taken from each patient or control subjects from identical sites. One of those biopsies was archived and paraffin-embedded for histopathological analysis by an expert pathologist (F.B.). The remaining biopsies were used for research purposes in this set of experiments. Bias due to stromal and inflammatory cells was avoided by preparation of intestinal epithelial cells (IECs). In brief, five needle-head sized biopsies were sampled in 10 mL HBSS/2 mmol/L EDTA buffer. Epithelial cells and crypts were detached by vigorous shaking at 37 °C for 15 min at 225 r/min. After vortexing for a few seconds, the remaining parts of the biopsies were manually removed. Crypts and cells were then spun down by short centrifugation and resolved directly into 350 μ L RLT buffer (RNeasy, Qiagen, Hildesheim, Germany). Due to this IEC preparation, IBD biopsies could be investigated from actively inflamed sites in this series. Four control samples (ages ranged from 22 to 66 years), seven MC samples (ages ranged from 33 to 48 years) and four CU samples (ages ranged from 28 to 62 years) were included.

For all samples, RNA extraction was performed according to the manufacturer’s protocol (RNeasy Mini Kit, Qiagen, Hilden, Germany). RNA quality was assessed with the 6000 Nano LabChip[®] using an Agilent 2100 bioanalyzer (Agilent Technologies, Palo Alto, USA) and quantified spectrophotometrically following standard protocols.

Real-time fluorescence RT-PCR

Real-time TaqMan[®] RT-PCR (PE Applied Biosystems, Darmstadt, Germany) was performed on a ABI Prism 7900 HT Sequence Detection System as previously published^[15,18]. Briefly, cDNA was synthesized using the Reverse Transcription Kit from Promega (Madison, USA) according to the manufacturer’s protocol. Probes and primers for TaqMan[®] analysis were designed on the basis of gene-specific nonhomologous DNA sequence of the corresponding members^[15]. The standard curve method was used for the quantification of the relative amounts of gene expression products. This method provides unitless normalized expression values that can be used for direct comparison of the relative amounts of target mRNA in different samples. All reactions were performed as triplicates.

Low density arrays

Due to limited representation of the Eph-RTK/ephrin

family on the Affymetrix® HGU 133 A/B chips, we established a custom low density array comprising 91 important RTKs, including the complete family of Eph-RTKs/ephrins and a selection of other receptor and non-receptor tyrosine kinases. The selection of non-Eph-RTKs was based on a current review on kinase signaling^[19]. The detailed list of genes can be requested from the authors.

The low density arrays were prepared as follows. 50-mer amino modified oligonucleotide probes were arrayed onto CodeLink™ Slides (Amersham Biosciences) using a conventional Pin-and-Ring™ spotter (Affymetrix) in a controlled environment (20 °C and 65-75% humidity). Optimal sequences of the 50mer probes (two for each gene) were determined by a MWG Biotech proprietary software (MWG Biotech, Ebersberg, Germany). The 2×91 oligonucleotides were spotted together with 9 reference oligos (mwghuman10K #11000-#11008) in linear pattern with 4 replicates each, resulting in a total number of 955 spots per slide. Labeled cRNA was synthesized from total RNA using Cy3-UTP (Amersham Biosciences) in accordance with the linear RNA amplification procedures described in the MWG Array-Application Guide. The cRNA was applied onto the microarray surface using 120 µL Gene Frames® (ABgene) and hybridized for 16 h at 42 °C. For data analysis, the microarrays were scanned at 10 micron resolution and analyzed using the program ScanAlyze (M. Eisen; available at <http://rana.lbl.gov/EisenSoftware.htm>). Areas of the array with obvious bad signals were manually flagged and excluded from subsequent analyses. A linear normalization method was used, assuming that most of the genes represented on an array show the same expression profile. Expression ratios were then calculated and further evaluated using the Significance Analysis of Microarrays (SAM) algorithm^[20]. The SAM calculates the false discovery rate (FDR) as an estimate of the percentage of false positive genes, i.e. genes identified as differentially expressed by chance. Two-class unpaired analysis was applied to compare MC and CU samples to the control samples, separately. Identical FDRs were used to compare the significance of the regulated genes in MC *vs* control and CU *vs* control expression patterns.

Immunohistochemistry

For immunohistochemical staining of ephrin-B2 the anti-ephrin-B2 antibody (Santa Cruz, CA, USA) was used in a dilution of 1:75. Sections of intestinal tissue were boiled (10 min) in citrate buffer for antigen retrieval. Isotype matched antibody controls were run in parallel. The remaining staining procedure according to the ABC-technique followed standard protocols. Ten control sections of healthy individuals (ages ranged from 43 to 78 years), 10 cases of CU (ages ranged from 26 to 80 years), and 10 cases of MC (ages ranged from 21 to 49 years) were analyzed.

IEC-6 in vitro scratch wound assays

To evaluate possible consequences of enhanced ephrin-B dependent signaling effects on wound closure of intestinal cells, not transformed rat IEC-6 cells were chosen as a model. IEC-6 cells are able to close monolayer scratch

wounds within a timeframe assuring that closure is a function of migration competence of the cells at the wound margin rather than proliferation^[21]. In our hands, both HT29 cells and CaCo2 cells failed to fulfil this criterion. Briefly, the IEC-6 cells were seeded into six-wells and grown to confluence in Dulbecco's MEM (Biochrom AG, Berlin, Germany) supplemented with 5% fetal calf serum (FCS) (PAN Biotech, Aldenbach, Germany). After reaching confluence, the cells were fed with starving medium (0.1% FCS) and small scratch-wounds (-1 mm width) were produced with a cell scraper drawn over the surface of the monolayer along a ruler. The cells were stimulated with varying concentrations of recombinant rat EphB1-Fc Chimera (R&D Systems, Minneapolis, USA). The used doses ranged from 0.05 µg/mL (~0.33 nmol/L) to 5 µg/mL (~33 nmol/L). For control experiments, recombinant human IgG-Fc (R&D Systems) was used. Wound closure was monitored at 0, 6, and 24 h after wounding. Images of the wounds were taken by a digital camera on top of the cell culture microscope from exactly the same position at various time points (100× magnification). The closure of the wounds was assessed by calculating the difference between the initial wound area and the remaining wound area at a certain time point. Wound area calculations were performed using the publicly available J-Image software of the NCBI (Bethesda, MA, USA). For each condition, four wounded areas were analyzed in parallel, and all experiments were repeated twice.

Immunofluorescence microscopy of wound margins

Cells were plated on fibronectin coated glass cover slips and grown for 16 h in Dulbecco's MEM plus 5% FCS. Cells were starved for one night with 0.1% FCS medium, then the monolayer was wounded by a cell scraper and stimulated with recombinant EphB1-Fc (5 µg/mL) or IgG-Fc (5 µg/mL) as control for 6 h. For actin staining, cells were fixed with 4% paraformaldehyde for 5 min at room temperature and permeabilized with 0.1% Triton-X 100 for 5 min. The cells were then incubated for 30 min with rhodamine-conjugated phalloidine (1:100) (Chemicon, Temecula, CA, USA) as recommended by the supplier. Each experimental condition was performed on eight replicate cover slips. For detection of wound edge deposits of laminin an affinity purified laminin specific antibody L9393 from Sigma (St. Louis, MS, USA) and FITC labeled secondary goat anti-rabbit antibody (Vector, Burlingame, USA) were used. Images were taken on a Leitz microscope equipped with a fluorescence lamp and appropriate filters. Cells were photographed at 400× magnification.

Immunoblotting

To demonstrate the ability of the recombinant rat EphB1-Fc (R&D Systems) used to bind and potentially activate ephrin-B2 in IEC-6 cells, immunoprecipitation of ephrin-B2 was performed using the Seize™ Classic Mammalian Immunoprecipitation Kit (Pierce, Rockford, USA). Ephrin-B2 protein was precipitated using this recombinant rat EphB1-Fc. Precipitates were analyzed by SDS-PAGE and blotted according to standard protocols. For detection of ephrin-B2, a polyclonal anti-ephrin-B2 antibody (Santa Cruz) was used.

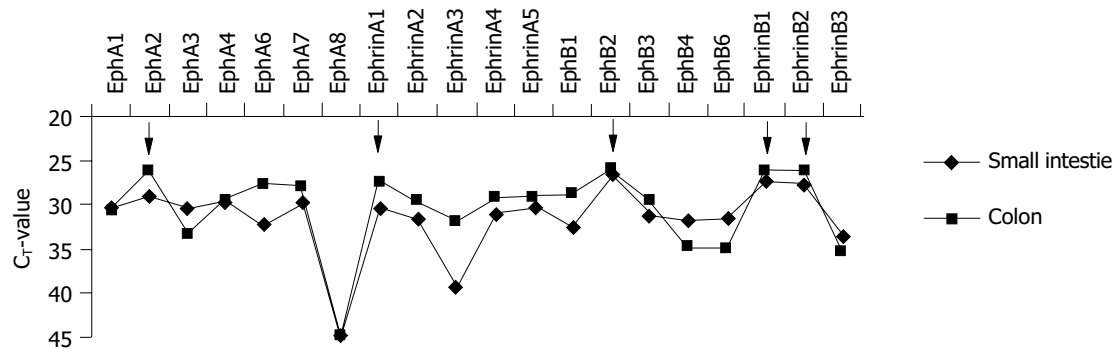


Figure 1 Expression profile of Eph-RTKs and ephrins in normal human mucosa of the small intestine ($n = 5$) and colon ($n = 5$) assessed by real time TaqMan[®] RT-PCR. The CT-values allow a relative quantification of the mRNA expression

of the single members. Low CT-values indicate a high expression level and vice versa. The arrows indicate marked expression of the family members EphA2, ephrin-A1, EphB2, and ephrin-B1/2.

Statistical analysis

Non-parametric testing was performed (Mann-Whitney test) for comparing the mean values in the wound closure experiments. Significance was indicated by a $P < 0.05$.

RESULTS

Intestinal mucosa expresses a broad gut-specific spectrum of Eph-RTKs and ephrins

The role of Eph-RTKs and ephrins is well defined in developmental biology. However, the expression and function in adult tissues is only marginally known, yet. Therefore, we established a profile of the expression of the members of this family in the small intestine and colon from normal control individuals. For this purpose, a library of real time TaqMan[®] RT-PCR probes and primers was employed that was recently established in our lab^[15]. The results are shown in Figure 1. Small intestine and colon mucosa exhibit the presence of a broad spectrum of A- and B-class Eph receptors and ephrins with some organotypic differences of the expression profiles. Ephrin-A1 (formerly protein B61) and ephrin-B1/2 are the most abundantly expressed ligands. On the receptor site, EphA2 (formerly epithelial cell kinase, Eck) and EphB2 are the most abundantly expressed receptors.

Ephrin-B2 is upregulated in mucosa samples from IBD patients

A recently published gene array analysis (Affymetrix[®] platform) of pooled IBD samples and control patients produced detectable signals only for a minor fraction of Eph-RTKs and ephrins (EphA2, ephrin-A1, EphB2, EphB4 and ephrin-B1/2)^[17]. Interestingly, these were almost exactly the most abundantly expressed genes of this family in our real-time RT-PCR profile (Figure 1).

That array analysis had further revealed an up-regulation of ephrin-B2 (2.4-fold in the small intestine and 1.5-fold in the colon) in perilesional, not inflamed mucosa of MC patients^[17]. In this study, we validated those observations in the same cohort of patients. For this purpose, we used our established TaqMan[®] probe and primer set for ephrin-B2. In these experiments, the individual (not pooled) samples of all 4 well characterized cases of MC, CU and controls were analyzed (Figure 2). A significant up-regulation of ephrin-B2 could be confirmed in the individual MC patients

both in the small intestine and in the colon samples. The individual probes of the CU patients also showed a significant up-regulation in the colon samples. In contrast, a 0.5-fold downregulation of EphB4 in the colon of CU patients, as indicated by previous Affymetrix[®] array analysis^[17], did not reach significance in the real-time RT-PCR validation.

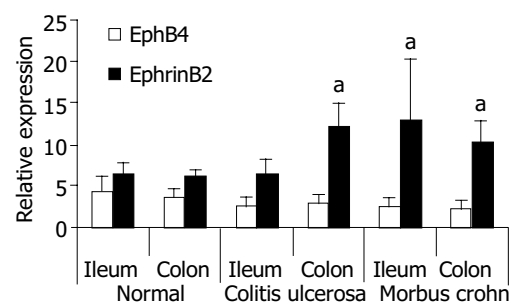


Figure 2 Differential gene expression of Eph-RTKs and ephrins in the mucosa of IBD patients (TaqMan[®] RT-PCR validation of Affymetrix[®] cDNA array results^[17]). Individual RNAs from perilesional total mucosa biopsies (ileum terminale and colon) of 4 control subjects, 4 MC patients and 4 CU patients were analyzed. Real-time RT-PCR confirmed significant up-regulation of ephrin-B2 in MC patients (ileum and colon) and CU (colon). Differential expression of EphB4, as suggested by the Affymetrix[®] array data, was not significant. The relative expression values were calculated according to the standard curve method of the TaqMan[®] protocol (Applied Biosystems, Darmstadt, Germany) by normalization with a housekeeper gene (18S rRNA) and are therefore unitless (for details, see^[15]). ^a $P < 0.05$ vs normal.

Low density arrays confirm the up-regulation of ephrin-B2 in intestinal epithelial cells (IECs) prepared from lesional IBD biopsies

Since RT-PCR suggested a much more diversified presence of Eph-RTKs and ephrins in gut mucosa than it was detectable by the HGU 133 A/B chip generation, we employed low density 50 mer oligonucleotide technology based on protocols developed by MWG (MWG Biotech, Ebersberg, Germany). To further substantiate the specificity of the results for the epithelial compartment, in this series of experiments the IECs were isolated from sets of biopsies of controls and lesional inflamed mucosa biopsies of MC patients and CU patients, respectively.

SAM (significance analysis of microarray data) analysis revealed that ephrin-B2 reached the highest significance score

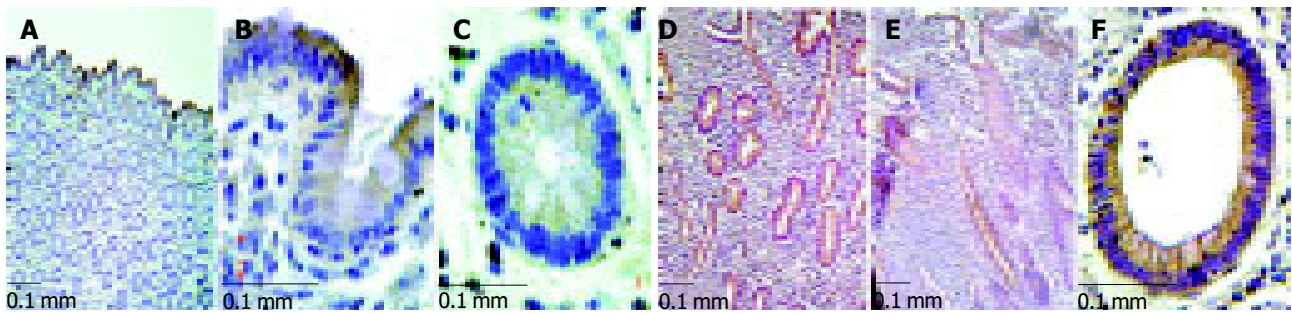


Figure 3 Immunohistochemistry of ephrin-B2 from biopsies of normal colon and lesional colon in IBD. (A-C: normal colon; D, F: MC; E: CU). A-C: ephrin-B2 expression shows a physiologic gradient along the crypt-axis in normal epithelium of the colon, i.e. the maximum staining is found in the luminal,

terminally differentiated epithelium of normal colon mucosa. D-F: In MC and CU this gradient is disturbed, i.e. strong ectopic expression in the deep parts of the crypts can be observed. C and F represent cross sections of the deep part of a crypt.

in MC patients among 16 further genes with significant scores at an estimated false positive rate of 5%. This is consistent with the previous Affymetrix[®] array analysis^[17] and our real time RT-PCR data (Figure 2). Interestingly, with this 50 mer low density chip further Eph-RTKs and ephrins produced measurable signals and were identified as potentially regulated in the (lesional) intestinal epithelium of MC patients (ephrin-A5, EphB1, EphB4). Moreover, FGFR-3, INSR, NGFR, PDGFR- β were among the candidate genes, growth factor receptors that have already been linked to epithelial healing, proliferation and many other aspects of IBD-physiology^[22]. In contrast, no significantly regulated genes were observed in the CU group.

Immunohistochemistry confirms up-regulation and ectopic epithelial expression of ephrin-B2 in lesional IBD biopsies

Immunohistochemistry revealed that ephrin-B2 is expressed most prominently in the upper parts of the crypts in normal mucosa of the human colon, i.e. the most intense expression is found in the terminally differentiated epithelium at the luminal surface. Apparently, there is a gradient along the crypt-axis with decreasing expression in the deeper parts of the crypts. In contrast, in inflamed MC samples a strong staining of the entire epithelium was observed from the basis to the top of the crypts with an obvious loss of this gradient (Figure 3). In CU samples, this distortion of ephrin-B2 expression was also seen in some samples, but not as consistent as in MC.

IEC-6 in vitro scratch wound assays indicate an enhanced wound closure upon stimulating the ephrin-B reverse signaling pathway

Since both array analysis and quantitative RT-PCR data suggested up-regulation of ephrin-B2 in lesional and perilesional intestinal epithelium of MC patients, we investigated possible functional consequences of intensified reverse ephrin-B signaling in an intestinal epithelial model cell line. Not transformed rat intestinal IEC-6 cells were chosen for two reasons: (1) Constitutive expression of the ligand ephrin-B2 and the receptor EphB2 in this cell line could be confirmed by quantitative RT-PCR, immunocytochemistry (data not shown) and immunoblotting (Figure 4); (2) IEC-6 cells exhibit a basal wound closure competence *in vitro*, which exceeded the competence of human intestinal cancer cell lines (HT-29, CaCo-2, SW-480) tested in our lab.

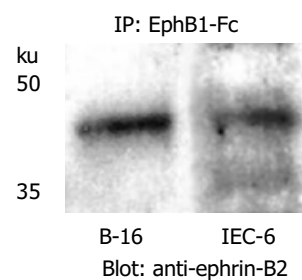


Figure 4 Immunoprecipitation of ephrin-B2 with EphB1-Fc demonstrates that the recombinant rat EphB1-Fc binds to ephrin-B2 (42 ku), and ephrin-B2 is constitutively expressed by rat IEC-6 cells. Ephrin-B2 transfected B16 melanoma cells served as positive control.

Wounded monolayers of IEC-6 cells were treated with recombinant rat EphB1-Fc for stimulation of ephrin-B dependent pathways. As shown in Figure 5, a dose-dependent acceleration of wound closure by stimulation with EphB1 could be observed after 6 and 24 h ($P < 0.05$). Interestingly, maximal effects were already obtained with 0.05 $\mu\text{g/mL}$ (~ 0.33 nmol/L) concentration of EphB1-Fc. Higher concentrations slightly decreased the wound closure activity. Control experiments were performed with equal amounts of IgG-Fc.

Stimulating the ephrin-B reverse signaling pathways in IEC-6 cells induces cellular responses indicating enhanced wound closure capacity

As shown in Figure 6, starved unstimulated IEC-6 cells exhibit only a limited wound closure activity 6 h after wounding (Figure 6A). In contrast, the EphB1-Fc stimulated cells already show signs of organized motile activity forming multiple archipelago-like sheets of cells stretching into the denuded area (Figure 6B). Notably, asymmetric lamellipodial protrusions are formed by those wound-edge cells. Further cytoskeletal correlations of inducible wound-edge activities can be demonstrated by actin staining with phalloidin. The unstimulated cells show a rounded morphology with less polymerized actin bundles (Figure 6C). The EphB1-Fc exposed cells show a stretched-out, bizarre morphology and apparent assembly of stress fibers. The spike-structures may reflect increased focal adhesion assembly (Figure 6D). Furthermore, the enhanced wound closure of the stimulated cells is also accompanied by

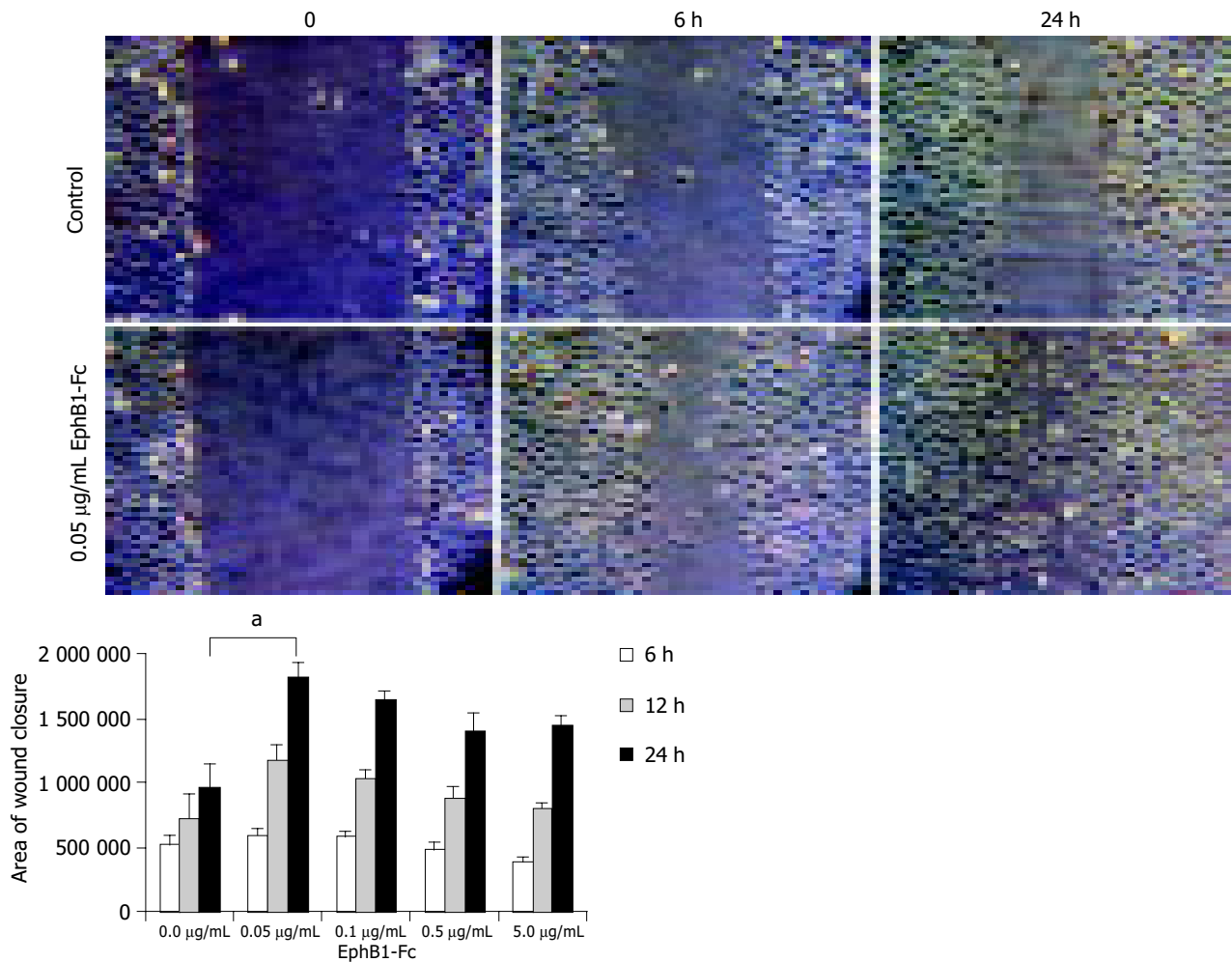


Figure 5 IEC-6 *in vitro* scratch wound assays indicate an enhanced wound closure activity upon stimulation with EphB1-Fc. IEC-6 cell monolayers were wounded in a standardized manner using a cell scraper, and relative wound

closure was monitored after 6 h and 24 h. Subnanomolar doses of EphB1-Fc (0.05 µg/mL–0.33 nmol/L) significantly enhanced the wound closure ($^*P < 0.05$). Higher doses did not further increase this effect.

increased deposition of laminin as a provisional basal membrane at the wound edge (Figure 6E, F).

DISCUSSION

This study demonstrates a complex spectrum of Eph-RTK and ephrin expression in the normal human adult intestinal mucosa. This suggests that Eph-RTKs and ephrins may contribute to tissue maintenance throughout life, in addition to their well-established roles in development^[23]. Consistent with a previous study by Podolsky and co-workers^[16], we found EphA2 and ephrin-A1 among the most prominently expressed family members both in the small intestine and colon. To the best of our knowledge, this is the first study showing a concurrent prominent co-expression of EphB2 and ephrin-B1/2 in normal human intestine. Other family members revealed a less abundant expression. This gut ‘signature’ is unique among other normal tissues in humans^[15]. In addition, this study reports a differential regulation of ephrin-B2 in the intestinal epithelium of MC patients. In the light of recent insights into the function of ephrin-B2, its upregulation suggests a possible ephrin-B2-dependent modulation of cytoskeletal dynamics and migration competence of epithelial cells in IBD. The multi-modal

interaction of ephrin-B2 with downstream effectors of the cytoskeleton such as focal adhesion kinase (FAK) and cdc42 has been recently demonstrated^[24].

Therefore, we addressed possible functional effects of an enhanced EphB/ephrin-B-dependent exchange of intercellular signals on epithelial repair processes. The stimulation of rat IEC-6 cells with recombinant ephrin-B2-binding EphB1-Fc receptors effectively enhanced their wound closure competence at doses below 1 nmol/L. Consistent with this ‘repair phenotype’, EphB1-Fc stimulation induced a concerted migratory response of wound-edge cells. This was documented by early archipelagolike movements at the wound-edge associated with increased stress-fiber polymerization and adoption of a stretched-out morphology with multiple wound-oriented lamellipodia. Furthermore, the increased deposition of laminin provides a new basement for integrin-dependent anchorage and survival of the cells^[25]. Although the IEC-6 model suggests mechanisms in favor of enhanced wound healing, any conclusions regarding the *in vivo* situation have to be drawn with caution. As shown by immunohistochemistry of MC lesions, the physiologic expression gradients extending from the basis of the intestinal crypts to the apical epithelium are apparently lost in MC epithelia. This graded expression

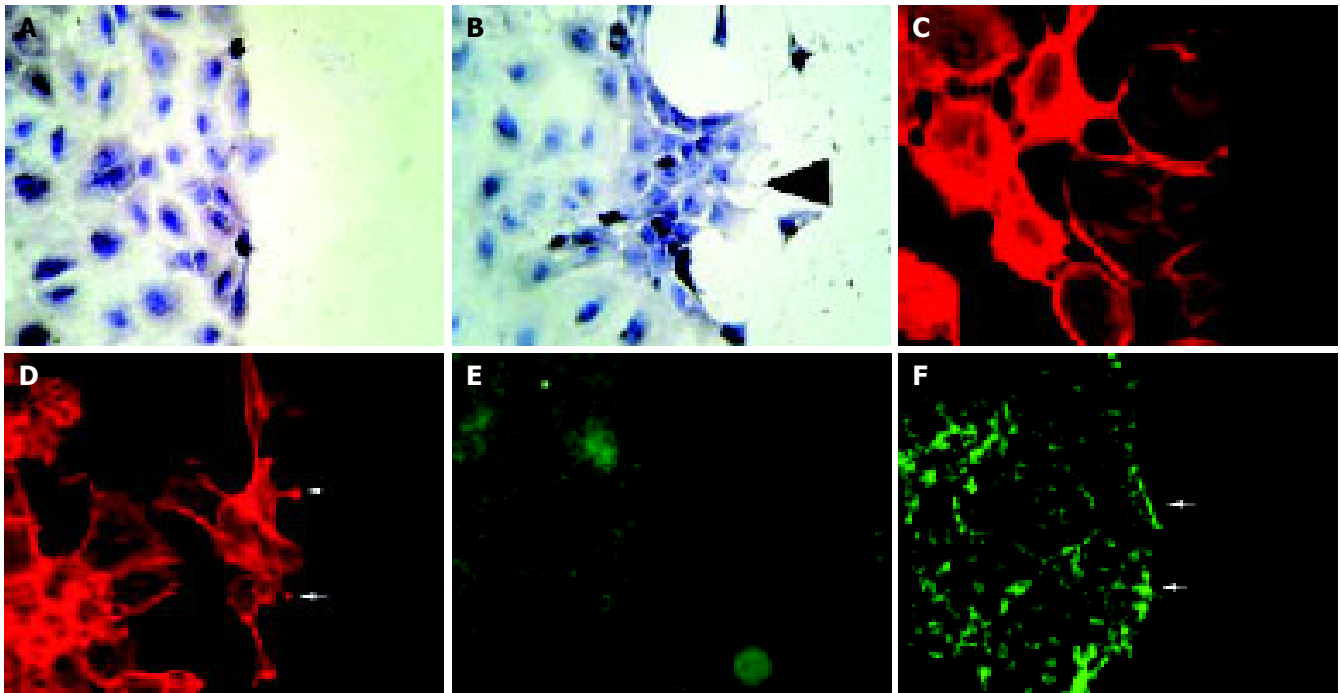


Figure 6 Stimulation of IEC-6 cells with EphB1-Fc induces subcellular responses compatible with enhanced wound closure capacity. Compared to the non-stimulated control (A), recombinant EphB1-Fc stimulated cells produce an organized migratory activity forming multiple archipelago-like sheets of cells stretching into the denuded area already 6 h after stimulation. In addition, asymmetric lamellipodia are seen (arrow). (B). Staining of actin with phalloidin

shows a rounded morphology with less polymerized actin bundles in unstimulated cells (C), whereas EphB1-Fc stimulated cells display a stretched-out, bizarre morphology and apparent assembly of abundant stress fibers. Spike-like protrusions may correspond to focal adhesion assembly (arrows) (D). EphB1-Fc also induces an increased deposition of laminin as a provisional basal membrane at the wound edge (F) (arrows) compared to control cells (E).

is tightly regulated by β -catenin and TCF, and has been shown to be responsible for the spatial separation of the proliferative and differentiated epithelial compartment along the crypt-villus axis during development^[14]. Since the expression gradient may be the driving principle of organized cell replacement, from the base to the top along the crypt-villus axis, this ectopic expression in MC could also be deleterious. Finally, the upregulation of ephrin-B2 does not necessarily mean enhanced ephrin-B2-dependent signaling in the epithelium, since counteracting mechanisms (e.g. phosphatases such as FAP-1 and PTP-BL) may be up-regulated as well^[26].

Extrapolations on *in vivo* effects of single family members are also hampered by the complexity involved. Members of this largest class of Eph-RTKs in humans can evolve seemingly disparate effects depending on the cellular system and the relative balance of A vs B receptors and ligands. For instance, Lawrenson *et al.*, have reported that ephrin-A5, also in our list of upregulated candidate genes in MC epithelium, can induce de-adhesion of EphA3 expressing 293T and melanoma cells^[27]. The contrary has been reported for CaCo2 cells^[16]. With PC-3 prostate cancer cells transfected with EphA2, stimulation with ephrin-A1 resulted in an inhibition of cell adhesion and spreading on laminin and fibronectin^[28]. EphA2 is also linked with the p53 tumor-suppressor protein family and can induce apoptosis^[29]. In contrast, ephrin-B/EphB-interaction can promote integrin-mediated cell attachment in embryonic kidney cells^[30], endothelial cells^[31], platelets^[23] and P19 cells^[32]. Obviously, the composition and fine-tuned balance of expressed individual members of this large family is a critical

point and might contribute to the movement of intestinal cells along the crypt-villus axis^[14], or from the wound margin to the center of epithelial defects.

Nevertheless, therapeutically it could be very interesting to strengthen the effects of the protective members and to weaken the effects of the counteracting members in this system, since our study demonstrates that nM doses can provoke significant effects on wound healing in the IEC-6 cell model. With the discovery of defined peptides that activate or specifically block selected molecules of this family^[33], a differentiated biological targeting of this delicately balanced system is possible in the near future. Since T-cell homing and interferon- γ production are also dependent on their Eph-RTK/ephrin environment, strategies could evolve that both regain the epithelial homeostasis and attenuate immunologic responses in IBD patients.

We conclude that the EphB/ephrin-B induced pathways should be placed on the list of targets for future molecular therapies trying to intervene with neomorphogenic pathways in IBD epithelia. However, the specifics of such interventions like potential interactions with the immune system, and the function of numerous partly counteracting family members, have to be better understood first.

ACKNOWLEDGMENTS

The skillful technical assistance and support of Mrs. Nadine Wandtke and Lydia Künzel is gratefully acknowledged.

REFERENCES

- 1 Wilson AJ, Gibson PR. Epithelial migration in the colon: fill-

- ing in the gaps. *Clin Sci* 1997; **93**: 97-108
- 2 **Podolsky DK.** Healing the epithelium: solving the problem from two sides. *J Gastroenterol* 1997; **32**: 122-126
 - 3 **Jacinto A, Martinez-Arias A, Martin P.** Mechanisms of epithelial fusion and repair. *Nat Cell Biol* 2001; **3**: E117-123
 - 4 **Dignass AU.** Mechanisms and modulation of intestinal epithelial repair. *Inflamm Bowel Dis* 2001; **7**: 68-77
 - 5 **Drescher U.** Eph family functions from an evolutionary perspective. *Curr Opin Genet Dev* 2002; **12**: 397-402
 - 6 **Cowan CA, Henkemeyer M.** Ephrins in reverse, park and drive. *Trends Cell Biol* 2002; **12**: 339-346
 - 7 **Pasquale EB.** The Eph family of receptors. *Curr Opin Cell Biol* 1997; **9**: 608-615
 - 8 **Murai KK, Pasquale EB.** 'Eph'ective signaling: forward, reverse and crosstalk. *J Cell Sci* 2003; **116**: 2823-2832
 - 9 **Holland SJ, Gale NW, Mbamalu G, Yancopoulos GD, Henkemeyer M, Pawson T.** Bidirectional signalling through the EPH-family receptor Nuk and its transmembrane ligands. *Nature* 1996; **383**: 722-725
 - 10 **Flanagan JG, Vanderhaeghen P.** The ephrins and Eph receptors in neural development. *Annu Rev Neurosci* 1998; **21**: 309-345
 - 11 **Holder N, Klein R.** Eph receptors and ephrins: effectors of morphogenesis. *Development* 1999; **126**: 2033-2044
 - 12 **Gale NW, Yancopoulos GD.** Growth factors acting via endothelial cell-specific receptor tyrosine kinases: VEGFs, angiopoietins, and ephrins in vascular development. *Genes Dev* 1999; **13**: 1055-1066
 - 13 **Gale NW, Baluk P, Pan L, Kwan M, Holash J, DeChiara TM, McDonald DM, Yancopoulos GD.** Ephrin-B2 selectively marks arterial vessels and neovascularization sites in the adult, with expression in both endothelial and smooth-muscle cells. *Dev Biol* 2001; **230**: 151-160
 - 14 **Battle E, Henderson JT, Beghtel H, van den Born MM, Sancho E, Huls G, Meeldijk J, Robertson J, van de Wetering M, Pawson T, Clevers H.** Beta-catenin and TCF mediate cell positioning in the intestinal epithelium by controlling the expression of EphB/ephrinB. *Cell* 2002; **111**: 251-263
 - 15 **Hafner C, Schmitz G, Meyer S, Bataille F, Hau P, Langmann T, Dietmaier W, Landthaler M, Vogt T.** Differential gene expression of Eph receptors and ephrins in benign human tissues and cancers. *Clin Chem* 2004; **50**: 490-499
 - 16 **Rosenberg IM, Goke M, Kanai M, Reinecker HC, Podolsky DK.** Epithelial cell kinase-B61: an autocrine loop modulating intestinal epithelial migration and barrier function. *Am J Physiol* 1997; **273**: G824-832
 - 17 **Langmann T, Moehle C, Mauerer R, Scharl M, Liebisch G, Zahn A, Stremmel W, Schmitz G.** Loss of detoxification in inflammatory bowel disease: Dysregulation of pregnane X receptor target genes. *Gastroenterology* 2004; **127**: 26-40
 - 18 **Langmann T, Mauerer R, Zahn A, Moehle C, Probst M, Stremmel W, Schmitz G.** Real-time reverse transcription-PCR expression profiling of the complete human ATP-binding cassette transporter superfamily in various tissues. *Clin Chem* 2003; **49**: 230-238
 - 19 **Blume-Jensen P, Hunter T.** Oncogenic kinase signalling. *Nature* 2001; **411**: 355-365
 - 20 **Tusher VG, Tibshirani R, Chu G.** Significance analysis of microarrays applied to the ionizing radiation response. *Proc Natl Acad Sci USA* 2001; **98**: 5116-5121
 - 21 **Sturm A, Sudermann T, Schulte KM, Goebell H, Dignass AU.** Modulation of intestinal epithelial wound healing *in vitro* and *in vivo* by lysophosphatidic acid. *Gastroenterology* 1999; **117**: 368-377
 - 22 **Beck PL, Podolsky DK.** Growth factors in inflammatory bowel disease. *Inflamm Bowel Dis* 1999; **5**: 44-60
 - 23 **Prevost N, Woulfe DS, Tognolini M, Tanaka T, Jian W, Fortna RR, Jiang H, Brass LF.** Signaling by ephrinB1 and Eph kinases in platelets promotes Rap1 activation, platelet adhesion, and aggregation via effector pathways that do not require phosphorylation of ephrinB1. *Blood* 2004; **103**: 1348-1355
 - 24 **Cowan CA, Henkemeyer M.** The SH2/SH3 adaptor Grb4 transduces B-ephrin reverse signals. *Nature* 2001; **413**: 174-179
 - 25 **Lotz MM, Nusrat A, Madara JL, Ezzell R, Wewer UM, Mercurio AM.** Intestinal epithelial restitution. Involvement of specific laminin isoforms and integrin laminin receptors in wound closure of a transformed model epithelium. *Am J Pathol* 1997; **150**: 747-760
 - 26 **Palmer A, Zimmer M, Erdmann KS, Eulenburg V, Porthin A, Heumann R, Deutsch U, Klein R.** EphrinB phosphorylation and reverse signaling: regulation by Src kinases and PTP-BL phosphatase. *Mol Cell* 2002; **9**: 725-737
 - 27 **Lawrenson ID, Wimmer-Kleikamp SH, Lock P, Schoenwaelder SM, Down M, Boyd AW, Alewood PF, Lackmann M.** Ephrin-A5 induces rounding, blebbing and de-adhesion of EphA3-expressing 293T and melanoma cells by CrkII and Rho-mediated signalling. *J Cell Sci* 2002; **115**: 1059-1072
 - 28 **Miao H, Burnett E, Kinch M, Simon E, Wang B.** Activation of EphA2 kinase suppresses integrin function and causes focal-adhesion-kinase dephosphorylation. *Nat Cell Biol* 2000; **2**: 62-69
 - 29 **Dohn M, Jiang J, Chen X.** Receptor tyrosine kinase EphA2 is regulated by p53-family proteins and induces apoptosis. *Oncogene* 2001; **20**: 6503-6515
 - 30 **Huynh-Do U, Stein E, Lane AA, Liu H, Cerretti DP, Daniel TO.** Surface densities of ephrin-B1 determine EphB1-coupled activation of cell attachment through alphavbeta3 and alpha5beta1 integrins. *Embo J* 1999; **18**: 2165-2173
 - 31 **Huynh-Do U, Vindis C, Liu H, Cerretti DP, McGrew JT, Enriquez M, Chen J, Daniel TO.** Ephrin-B1 transduces signals to activate integrin-mediated migration, attachment and angiogenesis. *J Cell Sci* 2002; **115**: 3073-3081
 - 32 **Stein E, Lane AA, Cerretti DP, Schoecklmann HO, Schroff AD, Van Etten RL, Daniel TO.** Eph receptors discriminate specific ligand oligomers to determine alternative signaling complexes, attachment, and assembly responses. *Genes Dev* 1998; **12**: 667-678
 - 33 **Koolpe M, Dail M, Pasquale EB.** An ephrin mimetic peptide that selectively targets the EphA2 receptor. *J Biol Chem* 2002; **277**: 46974-46979

Effect of the ulcerogenic agents ethanol, acetylsalicylic acid and taurocholate on actin cytoskeleton and cell motility in cultured rat gastric mucosal cells

Siamak Bidel, Harri Mustonen, Giti Khalighi-Sikaroudi, Eero Lehtonen, Pauli Puolakkainen, Tuula Kiviluoto, Eero Kivilaakso

Siamak Bidel, Harri Mustonen, Giti Khalighi-Sikaroudi, Eero Lehtonen, Pauli Puolakkainen, Tuula Kiviluoto, Eero Kivilaakso, Department of Surgery, Helsinki University Central Hospital, Haartmaninkatu 8, Helsinki, Finland

Supported by the Grants from Antti and Jenny Wihuri Foundation and Research Foundation of Helsinki University Central Hospital, TYH4228

Co-first-authors: Harri Mustonen

Correspondence to: Harri Mustonen DSc, Helsinki University Central Hospital, Department of Surgery, Biomedicum Helsinki, Haartmaninkatu 8, Helsinki 00290,

Finland. harri.mustonen@helsinki.fi

Telephone: +358-9-471-71829 Fax: +358-9-471-74675

Received: 2004-09-01 Accepted: 2004-10-07

In addition, ethanol and ASA caused degradation of actin cytoskeleton. Oxidative stress seems to underlie ethanol, but not ASA or taurocholate, induced cytoskeletal damage.

© 2005 The WJG Press and Elsevier Inc. All rights reserved.

Key words: Gastric mucosa; Ethyl alcohol; Taurocholate; Aspirin; Actin

Bidel S, Mustonen H, Khalighi-Sikaroudi G, Lehtonen E, Puolakkainen P, Kiviluoto T, Kivilaakso E. Effect of the ulcerogenic agents ethanol, acetylsalicylic acid and taurocholate on actin cytoskeleton and cell motility in cultured rat gastric mucosal cells. *World J Gastroenterol* 2005; 11(26): 4032-4039

<http://www.wjgnet.com/1007-9327/11/4032.asp>

Abstract

AIM: To assess the effects of ulcerogenic agents on actin cytoskeleton and cell motility and the contribution of oxidative stress.

METHODS: Rat gastric mucosal cell monolayers were cultured on coverslips. The cells were exposed, with or without allopurinol (2 mmol/L), for 15 min to ethanol (10-150 mL/L), ASA (1-20 mmol/L) or taurocholate (1-20 mmol/L), then the cells were processed for actin and vinculin staining. Cell migration after wounding was also measured.

RESULTS: Exposure to 10 mL/L ethanol caused divergence of zonula adherens-associated actin bundles of adjacent cells and decreased rate of migration. These actions were opposed by xanthine oxidase inhibitor allopurinol. Exposure to 50 mL/L ethanol induced degradation and divergence of zonula adherens-associated vinculin from adjacent cells, which was, again, partially reverted by allopurinol. With 1 mmol/L ASA actin filaments became shorter and thicker. However, higher concentrations (10, 20 mmol/L) of ASA returned microfilaments thinner and longer, and decreased rate of migration. Zonula adherens-associated actin bundles were moderately distorted with 10 mmol/L ASA and with 10 mmol/L taurocholate. Exposure to taurocholate provoked changes resembling those of ASA. Taurocholate 5-20 mmol/L decreased the rate of migration dose dependently. The effects of ASA and taurocholate were not prevented by allopurinol.

CONCLUSION: All ulcerogenic agents decreased the rate of migration dose dependently and induced divergence of zonula adherens-associated actin bundles of adjacent cells.

INTRODUCTION

The gastric mucosa is frequently exposed to different exogenous and endogenous ulcerative agents, such as ethanol, aspirin and taurocholate. These agents have been extensively investigated with methods, including biochemistry, morphology, electrophysiology, tissue permeability, *etc.*, but the cellular mechanisms of injury are still poorly defined.

In digestive epithelia actin cytoskeleton is involved, for example, in organization of cytoplasm, maintenance of cell shape, generation and maintenance of epithelial polarity and in migration. The cytoplasm of epithelial cell is spatially and temporally organized by microfilaments, microtubules and intermediate filaments, which form a lattice-like intracellular meshwork^[1,2].

The actin cytoskeleton is highly conserved in eukaryotic cells, including more than 70 categorized types of actin-binding proteins^[3]. The human actin family includes α -, β -, and γ -actin, which share most of their amino acid sequences. The actin filaments are formed by polymerization of actin monomers. The polymeric actins are assembled into a filamentous network, which is regulated by actin-binding proteins. These proteins regulate, for example, polymerization, cross linking, nucleation and branching, anchoring, capping, membrane interaction, cell-extracellular matrix interaction, cell-cell interaction and contractility of actin filaments^[4]. The actin filaments are bundled together by various actin cross-linking proteins to form complex three-dimensional structures. The filaments are extensively branched near the plasma membrane, focal adhesions, and adherens and tight junctions.

Arp2/3 complex is involved in this branching^[5].

Different components of the cytoskeleton are tightly involved in cell motility^[6]. Actin based cell motility has several important tasks in epithelial cell functions, such as in secretory vesicle movement and cell migration during wound healing^[7]. The cell migration starts with lamellipodia extension and formation of new focal adhesions, followed by the contraction of the cell body and detachment of the tail. Rho guanosine triphosphatases have a key role in regulating different phases of migration. Rac1 seems to be involved in initiation of migration^[8] and in stimulation of lamellipodium extension^[9], while Rho seems to contribute mainly to cell body contraction^[6].

Epithelial cells have specialized mechanisms to enable cell-cell and cell-extracellular matrix adhesions. These connections are formed by transmembrane proteins, which bind to extracellular matrix or adjacent cells with their extracellular domains, while the intracellular domains bind to intracellular cytoskeleton via cytoplasmic adaptor proteins, many of which interact with the actin cytoskeleton^[10]. Integrins mediate cellular adhesion to the extracellular matrix. They are linked to the actin cytoskeleton in focal adhesion complexes, which include a multitude of proteins, such as vinculin, talin, paxillin and calpain. These focal adhesions are involved in regulation of the cell migration and proliferation. The classical E-cadherins mediate Ca²⁺ dependent cell-cell adhesion through their extracellular Ca²⁺ binding repeats, while their cytoplasmic part binds to the actin cytoskeleton via β - and α -catenin. This complex is associated with a variety of other proteins, including vinculin, α -actinin, and paxillin. Zonula adherens is an E-cadherin based belt-like adherent junction just below the tight junctions encircling the epithelial cells adhered to each other. Along the cytoplasmic side of the zonula adherens runs a contractile bundle of actin filaments, which are associated to zonula adherens with a set of intracellular proteins, such as a-catenin, vinculin, -actinin and plakoglobin. Vinculin is a large protein with multiple binding sites to different adhesion related proteins, including actin, a-actinin, talin, paxillin, VASP, ponsin, vinexin and PKC^[11,12]. Vinculin is thought to mediate the linkage between actin cytoskeleton and cadherins or integrins in cell-cell or cell-extracellular matrix adhesions. Recently vinculin has been shown to transiently associate with arp2/3 complex in the nascent focal complexes in the leading edge^[13], possibly linking cellular protrusion and adhesion to extracellular matrix. Ethanol is known to cause oxidative stress in rat hepatocytes and in gastric mucosal cells^[14,15]. Oxidative stress can cause various effects in the cell, such as oxidation and fragmentation of cellular proteins, peroxidations of membrane lipids, fragmentation of DNA and mitochondrial damage. Among the very early effects of oxidative stress might be disruption of the cytoskeleton^[16].

The aim of the present study was to characterize the effects of different ulcerogenic agents on actin cytoskeleton, cell adhesion molecules and cell migration, and to investigate the possible role of oxidative stress in the cellular injury induced by them. This was accomplished by confocal and normal fluorescence imaging of actin and vinculin during exposure of the epithelial cells to the ulcerogenic agents. We also measured the rate of cell migration during exposure to the ulcerogenic agents to assess the functional state of

the cytoskeleton. We further studied the possible role of reactive oxygen species in epithelial injury by inhibiting endogenous intracellular generation of superoxide radicals from purines with a xanthine oxidase inhibitor, allopurinol.

MATERIALS AND METHODS

Immortal rat gastric mucosal cells (RGM-1, Riken Cell Bank, Riken, Japan)^[17] were cultured on coverslips to confluent monolayers at 37 °C in humidified atmosphere containing 50 mL/L CO₂ in air. The medium used was an equal mixture of Ham's F12 and Dulbeccos's MEM supplemented with inactivated 200 mL/L fetal bovine serum, 100 U/mL penicillin, 100 µg/mL streptomycin and 0.125 µg/mL amphotericin.

The cells were exposed for 15 min to the following ulcerogenic agents: ethanol (10-150 mL/L), acetylsalicylic acid (ASA, 1-20 mmol/L) and taurocholate (1-20 mmol/L) at 37 °C. In allopurinol experiments the samples were treated with 2 mmol/L allopurinol 24 h before and during the exposure of the ulcerogenic agent. Thereafter the cells were fixed with 35 mL/L paraformaldehyde in PBS for 15-20 min at room temperature and stained as described below.

Actin filaments and focal adhesion plaques were stained with phallotoxins conjugated to Alexa 488 fluorophore (Molecular Probes, A-12379). After fixation the cells were washed three times for 5-10 min with PBS at room temperature, permeabilized with 1 mL/L Triton-X, 1 mL/L bovine serum albumin in PBS and washed again three times for 5-10 min in PBS. Thereafter, the samples were incubated for 30-60 min in PBS with 80 mL/L bovine serum albumin and washed three times for 5-10 min with PBS and incubated overnight with the mouse monoclonal anti-vinculin (10 µg/mL, with 10 mL/L bovine serum albumin). The samples were washed three times for 5-10 min with PBS and were incubated with secondary antibody goat anti-mouse Alexa 568 (10 µg/mL) and Alexa 488 phalloidin (1:1 000) with 1 mL/L bovine serum albumin in PBS for 30 min at room temperature. Thereafter, the samples were washed three times for 5-10 min with PBS and mounted with DABCO containing mounting media. Confocal fluorescence microscopy was performed with a Leica TCS SP2 confocal microscope and normal fluorescence microscopy with an Olympus IX50 microscope.

Cell migration assay

RGM cells were cultured to confluency on plastic culture dishes as described above. In allopurinol series the confluent monolayers were treated with allopurinol after and 24 h before wounding. Artificial round-shaped wounds were created in the cell monolayer with a silicon tip, where after control (water) or ulcerogenic agents were added. The migration distance of the cells at the wound edge was measured during the next 6 h at 2 h intervals by measuring the change in cell free area. The rate of migration was calculated from the change of cell free area measured at 0 and 6 h, as described previously^[18].

Statistical analysis

The results are expressed as mean±95% confidence intervals.

Student's unpaired *t*-test was used for statistical analysis of the raw data. *P* values less than 0.05 were considered as statistically significant.

RESULTS

Ethanol

In control cells, actin filaments were thin, showing branched actin networks and zonula adherens-associated actin bundles near the cell-cell contact sites (Figures 1 and 2). Exposure to 10 mL/L (vol/vol) ethanol for 15 min (Figure 1) did not cause any apparent changes in actin cytoskeleton. Increasing the ethanol concentration to 50 mL/L caused moderate degradation and irregularity in the actin filament organization. These changes became more prominent with 100 mL/L ethanol, displaying almost complete degradation of the actin filaments. Exposure to 150 mL/L ethanol for 15 min provoked detachment of the cells from each other (Figure 1). The damage of the actin filaments was severe, and in some microscopic fields only shadows of cells and nuclei remained visible.

In control cultures, the zonula adherens-associated actin bundles were normally seen as continuous belt-like accumulations between the cells, and the actin belts of adjacent

cells could not be distinguished from each other. Exposure to 10 mL/L ethanol caused actin belts of adjacent cells to diverge from each other and the gap between them was widened with increasing ethanol concentrations (20-50 mL/L, Figure 2). Treatment with allopurinol (2 mmol/L), which acts as an inhibitor of xanthine oxidase and inhibits production of intracellular reactive oxidative species, prevented completely the divergence of actin belts in cells exposed to 10 mL/L ethanol and partially in cells exposed to 20 mL/L ethanol, but not in cells exposed to 50 mL/L ethanol.

In control cultures, vinculin was visible at the focal adhesions as well as in the zonula adherens between the adjacent cells. The zonula adherens-associated vinculin of adjacent cells could not be distinguished. Exposure to 10-20 mL/L ethanol did not change the distribution of vinculin, but 50 mL/L ethanol exposure caused degradation and divergence of zonula adherens-associated vinculin staining. Allopurinol treatment moderately attenuated this change (Figure 3).

Exposure to 10 mL/L ethanol decreased the rate of migration during the first six hours after wounding (27 ± 3 and 17 ± 2 $\mu\text{m}/\text{h}$ for control and ethanol experiments, respectively; $P < 0.001$, $n = 20$, Figure 4). This decrease in

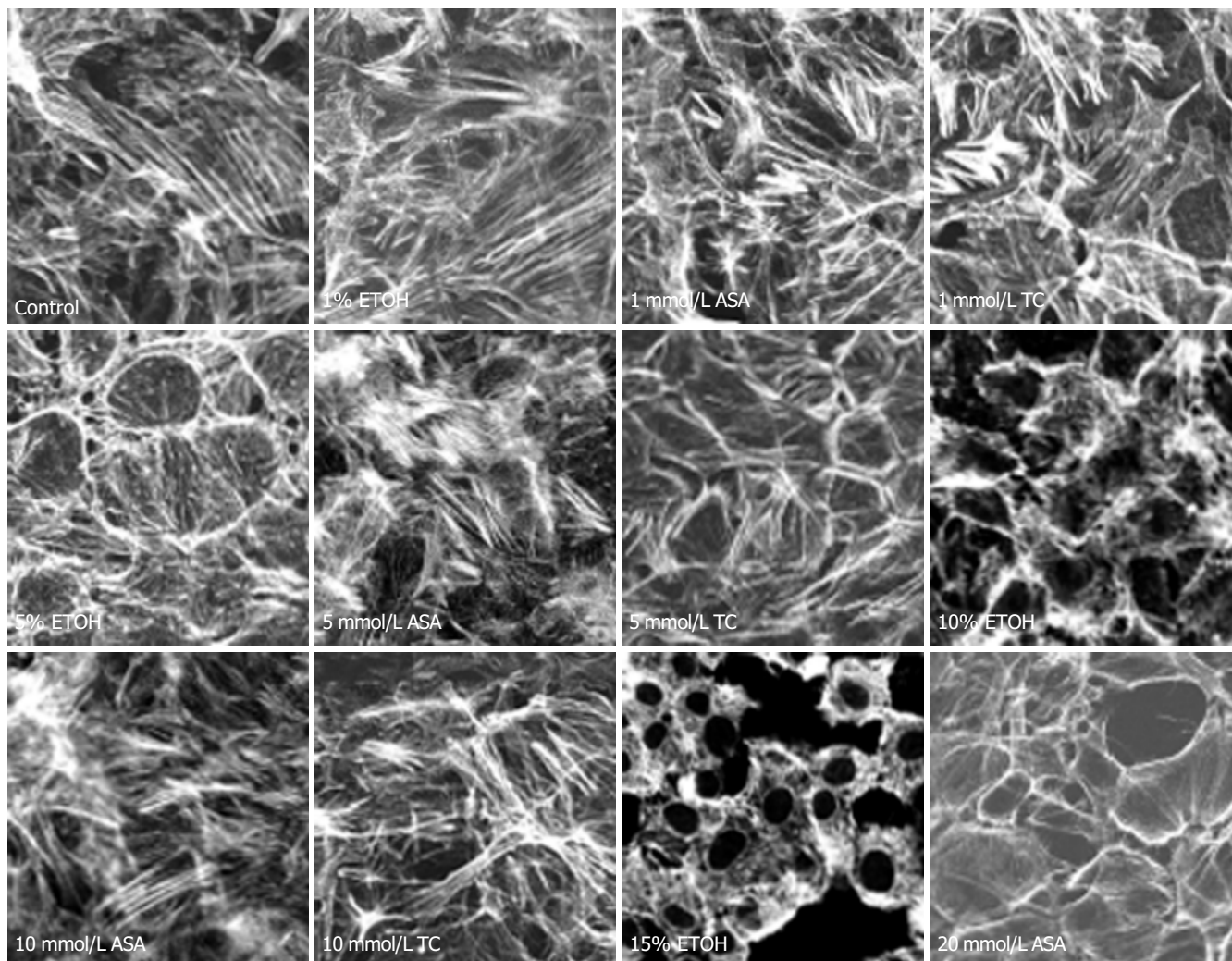


Figure 1 Effects of different doses of ethanol (ETOH), acetylsalicylic acid (ASA)

and taurocholate (TC) on actin filaments of RGM rat gastric surface epithelial cells.

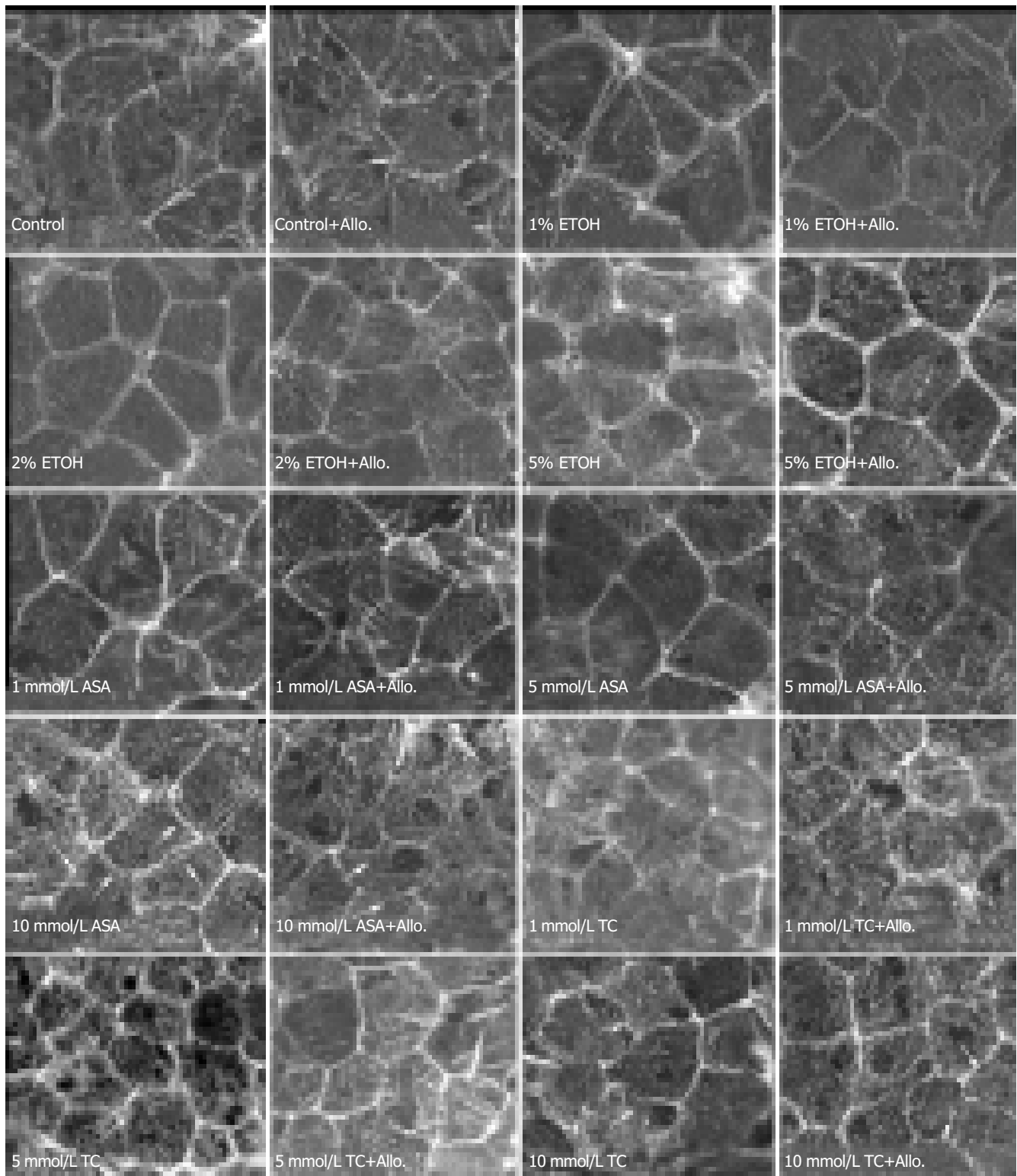


Figure 2 Effects of different doses of ethanol (ETOH), acetylsalicylic acid (ASA) and taurocholate (TC) on the zonula adherens-associated belt-like actin bundles

in RGM cells and their modulation by allopurinol (2 mmol/L) treatment. Arrows indicate perturbations in the actin belt organization.

migration was partially abolished by allopurinol pretreatment (17 ± 2 and 23 ± 2 $\mu\text{m}/\text{h}$ for ethanol and ethanol+allopurinol experiments, respectively; $P = 0.025$, $n = 20$). Allopurinol treatment alone had no effect on the rate of migration (27 ± 3 and 27 ± 2 $\mu\text{m}/\text{h}$ for control and allopurinol experiments, respectively). The migration distances are shown in Figure 4. With higher ethanol concentrations the rate of migration

was further decreased (to 7 ± 3 $\mu\text{m}/\text{h}$ with 30 mL/L ethanol) and even numerically reversed (to -17 ± 13 $\mu\text{m}/\text{h}$ with 50 mL/L ethanol), indicating enlarging of the wound, possibly due to a direct toxic effect of ethanol and/or to overall cell shrinkage in the monolayer caused by ethanol. At these higher concentrations of ethanol (30-50 mL/L) allopurinol did not prevent the ethanol promoted decrease in migration.

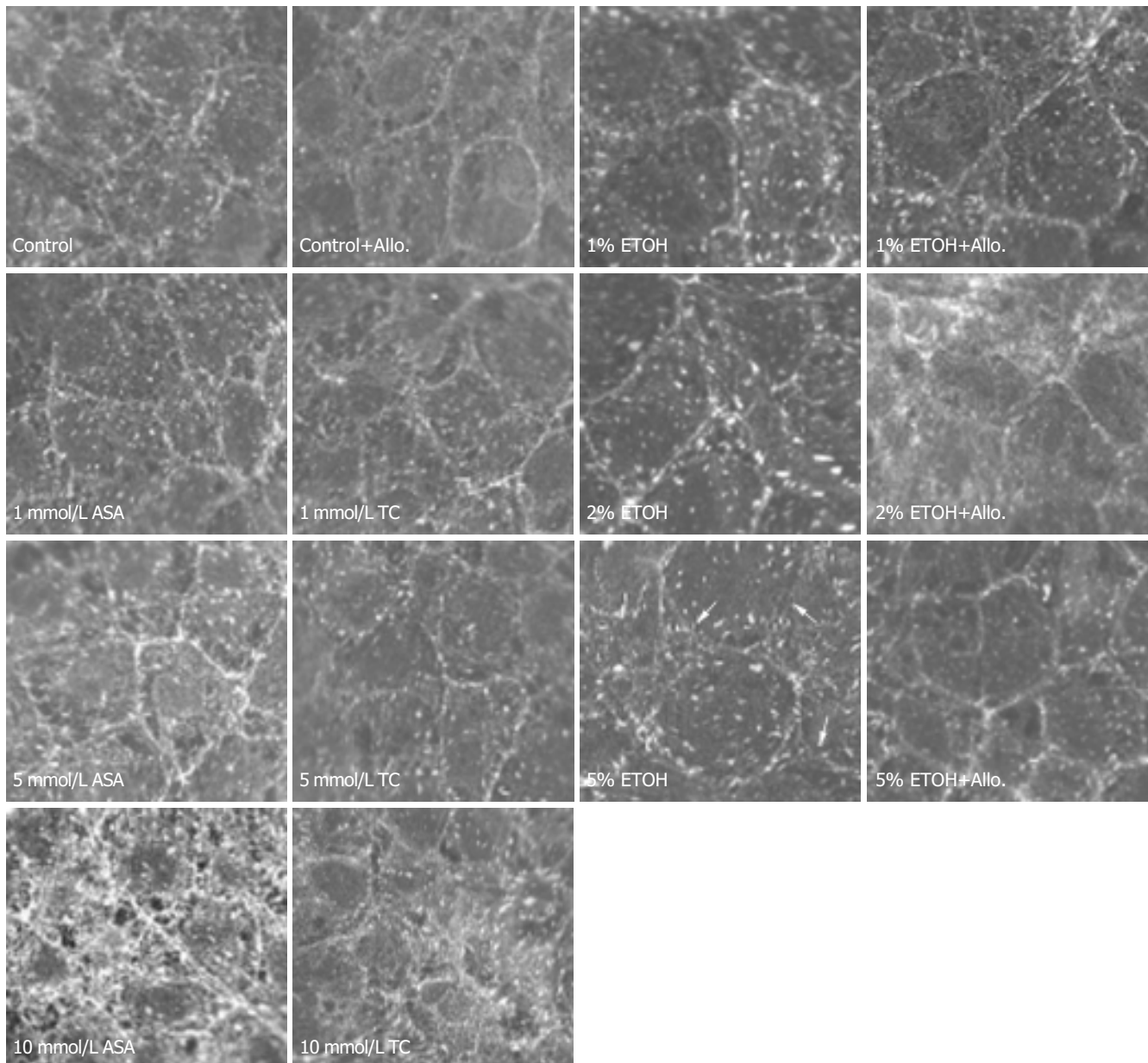


Figure 3 Effects of different doses of ethanol (ETOH), acetylsalicylic acid (ASA) and taurocholate (TC) on vinculin distribution in RGM cells and their modulation

by allopurinol (2 mmol/L) treatment. Arrows indicate perturbations in vinculin organization.

Acetylsalicylic acid (ASA)

After 15 min exposure to 1 mmol/L ASA, the actin filaments were contracted and became shorter and thicker, but no signs of cell detachment from each other were visible. However, with higher concentrations of ASA (10 and 20 mmol/L) the microfilaments became thinner and longer again, but failed to resume their original size and shape. Increasing ASA concentration to 20 mmol/L detached the cells partially from each other, which was manifested also as a divergence of the zonula adherens-associated actin bundles of adjacent cells (Figure 1). Also degradation of the actin filaments was visible.

Exposure to 1-5 mmol/L ASA had no effect on the zonula adherens-associated belt-like actin bundles. Exposure to 10 mmol/L ASA moderately distorted these actin belts and this was not prevented with allopurinol treatment (Figure 2).

Exposure to 1-10 mmol/L ASA had no effect on vinculin distribution (Figure 3). Likewise, exposure to 1-5 mmol/L ASA had no effect on the rate of migration, but exposure to 10 mmol/L ASA retarded migration after wounding from 16.8 ± 0.5 to 13.7 ± 1.2 $\mu\text{m}/\text{h}$ ($P = 0.008$, $n = 6$).

Taurocholate

Following exposure to low concentrations of taurocholate (1 and 5 mmol/L) the actin filaments were contracted, becoming shorter and thicker than in controls. These effects became more conspicuous with increasing concentrations of taurocholate (Figure 1). In fact, taurocholate caused similar changes as was seen with low concentrations of ASA, but the alterations were of lesser degree. Exposure to 1-5 mmol/L taurocholate did not cause any change in the zonula adherens-associated actin bundles, but 10 mmol/L

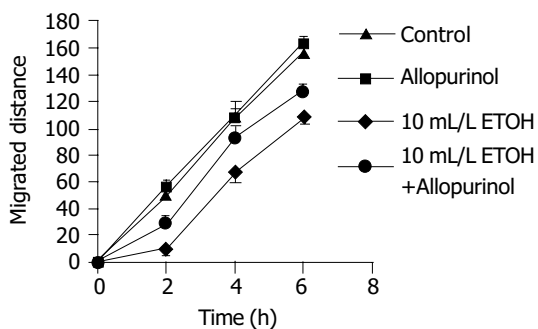


Figure 4 Effect of ethanol on cellular migration distance, with and without allopurinol treatment. Ethanol significantly reduced the migrated distance. Allopurinol partially abolished the ethanol promoted inhibition of cell migration.

taurocholate showed a moderate perturbation of these belts, which was not prevented by allopurinol treatment (Figure 2). Exposure to taurocholate (1-10 mmol/L) had no effect on vinculin distribution (Figure 3).

Exposure to 1 mmol/L taurocholate had no effect on the rate of migration after wounding, but 5-20 mmol/L taurocholate retarded migration dose dependently (migration speed 16.8 ± 0.6 , 14.5 ± 0.8 ($P = 0.01$), 12.7 ± 0.4 ($P < 0.001$) and 1.6 ± 0.8 ($P < 0.001$) $\mu\text{m}/\text{h}$ for 0 mmol/L (control), 5, 10 and 20 mmol/L taurocholate, respectively; P values are given in comparison with control, $n = 6$).

DISCUSSION

The gastric mucosa is normally exposed to a large number of ulcerogenic compounds, including ethanol, ASA (aspirin) and bile salts. The effects of these agents on cell cytoskeleton have not been thoroughly studied. In the healing of superficial gastric mucosal lesions, intact actin cytoskeleton is essential for cell migration and survival. The normal wound healing process in gastric mucosa is initiated by epithelial restitution whereby the surviving epithelial cells around wound edge migrate over the injured area to cover it with a flattened neo-epithelium. The migrating cells form lamellipodia and vinculin, RhoA and Rac are strongly expressed along the wound edge^[19]. Ulcerogenic agents can profoundly modulate this healing process.

Ethanol promotes narrowing of lamellipodia as well as retards cell migration and inhibits cellular proliferation after wounding in rabbit gastric mucosa^[20,21]. Exposure to 50-100 mL/L ethanol causes extensive disorganization and fragmentation of the actin cytoskeleton leading to its complete collapse in an intestinal epithelial cell line^[22,23]. We have previously shown that 50 mL/L luminal ethanol causes the opening of basolateral potassium channels leading to cell volume shrinkage^[24]. In the present work we demonstrated that the same concentration of ethanol affects also various components of the cytoskeleton. The changes in the structure and arrangement of the cytoskeleton are in line with cell shrinkage and the consequent increase in the gaps between the cells. Since an intact cytoskeleton is of utmost importance for the epithelial integrity and function, these minor changes may be the first manifestations of the ethanol-induced damage to the epithelial cells. At 100 mL/L ethanol concentration,

there was an extensive distortion of the actin cytoskeletal network, and even stronger ethanol (150 mL/L) caused severe damage to the cells with complete degradation of all actin filaments.

The zonula adherens-associated belt-like actin bundles of adjacent cells were diverged from each other already during exposure to a rather low (10 mL/L) concentration of ethanol. This divergence was prevented with 2 mmol/L allopurinol treatment. Allopurinol is a cell membrane permeable xanthine oxidase inhibitor, which blocks endogenous intracellular enzymatic generation of superoxide radicals from purines. This suggests that superoxide radicals are involved in ethanol induced divergence of the actin belts. Ethanol also perturbed the distribution of the zonula adherens junction-associated protein, vinculin, but only after exposure to 50 mL/L ethanol. Further, this change was moderately opposed by allopurinol treatment. The damage in zonula adherens-associated vinculin became apparent only with higher ethanol concentrations than was needed for changes in zonula adherens-associated actin bundles, which suggests that the changes in the actin belts might precede the zonula adherens junction damage. Allopurinol also opposed the ethanol provoked decrease in cell migration after artificial monolayer wounding, a further indication of the involvement of superoxide radicals in ethanol induced cytoskeletal damage.

The above findings suggest that oxidative stress might underlie the observed ethanol induced changes in actin cytoskeleton. Epithelial cells exposed to ethanol increase superoxide production^[25] and superoxide dismutase activity is decreased in rat stomach exposed to pure ethanol^[26]. Also, oxidative stress and mitochondrial damage precede death in gastric mucosal cells exposed to ethanol^[15]. The number of propidium iodide positive cells, indicating loss of cell viability, was increased following exposure to 50 mL/L ethanol and ethanol caused mitochondrial cell membrane depolarization and mitochondrial permeability transition, indicating mitochondrial dysfunction^[15].

It has been suggested, that NSAIDs, including ASA, damage gastrointestinal tract both by direct local effects and by systemic inhibition of prostaglandin synthesis. Davenport first demonstrated that ASA diffuses into the gastric mucosa as an undissociated molecule leading to disruption of the gastric mucosal barrier and backdiffusion of luminal acid into the mucosa, which, in turn, leads, presumably via generation of an inflammatory cascade, to break-down of the mucosal tissue^[27]. Although prostaglandins contribute to cell migration in several cell types^[28,29], addition of exogenous prostaglandins or inhibition of endogenous prostaglandin synthesis had no effect on gastric epithelial cell migration^[18]. On the other hand, NSAIDs may directly retard cell migration and decrease actin staining in gastric epithelial cell (RGM1) monolayer^[30].

The present results with ASA are well in accordance with our earlier finding that ASA causes major cell shape deformations in *Necturus* gastric antrum (unpublished results). The shrinkage of actin cytoskeleton probably contributes to cell-cell detachment, which was shown to occur at higher ASA concentrations. ASA decreased migration at 10 mmol/L concentration and degradation of actin filaments was visible

at 20 mmol/L ASA concentration. Zonula adherens-associated actin bundles were moderately damaged with 10 mmol/L ASA and this was not affected by allopurinol treatment, suggesting a mechanism different from ethanol-induced divergence of these actin bundles.

To our knowledge there is very little information about the actions of ASA on cellular actin cytoskeleton in the gastric epithelium. Electrophysiological measurements have shown that there is a slight initial increase in transepithelial resistance following exposure to 10 mmol/L ASA (at pH 3), which is, however, due to increase in apical cell membrane resistance. However, during more prolonged exposure to ASA the transepithelial resistance decreased, which might be a consequence of tight junction disruption, widening of intercellular space and/or loosening of cell-cell adhesions^[31]. The changes in the zonula adherens-associated actin bundles observed in the present study might contribute to the previously observed decrease in transepithelial resistance.

In earlier studies bile salts have been shown to retard wound restitution and repair in cultured rabbit gastric epithelial cells^[32]. In the present study, taurocholate caused similar effects in cell migration reducing it dose dependently in concentrations of 5 mmol/L and higher. The mechanism of taurocholate induced decrease in migration speed is still unclear, but bile salts are known to increase intracellular calcium levels^[33,34] and this might have an effect on cellular migration.

Taurocholate is known to interact with cell membranes and as a lipophilic compound it may diffuse into the cell membranes increasing its permeability to extracellular agents^[35]. Taurocholate may also act as a detergent dissolving cell membrane phospholipids eventually breaking up the cell membrane^[36]. Apical cell membrane resistance was decreased significantly with 10 mmol/L taurocholate in *Necturus antrum*^[31], suggesting that cell membranes may be the main target in taurocholate induced cellular damage. Zonula adherens associated actin bundles were moderately damaged with 10 mmol/L taurocholate, but this was not affected by allopurinol treatment suggesting, again, a mechanism different from ethanol induced damage. Previously, it has been shown that bile salts induce depolarization of mitochondrial membrane potential, which might be due to disturbed oxidative phosphorylation in mitochondria^[37]. In the present study, the possible oxidative damage was not prevented with allopurinol exposure, suggesting that xanthine oxidase is not involved in taurocholate-induced cellular injury.

In conclusion, our results show that deformations of the actin cytoskeleton are involved in the epithelial cell damage caused by the three ulcerogenic agents tested. Reactive oxidative species seems to underlie ethanol, but not ASA or taurocholate, induced cytoskeletal damage.

ACKNOWLEDGMENTS

The authors thank Ms. Paula Kokko for excellent technical assistance.

REFERENCES

- 1 **Luby-Phelps K.** Physical properties of cytoplasm. *Curr Opin Cell Biol* 1994; **6**: 3-9
- 2 **Seksek O, Biwersi J, Verkman AS.** Translational diffusion of macromolecule-sized solutes in cytoplasm and nucleus. *J Cell Biol* 1997; **138**: 131-142
- 3 **Alberts B, Johnson A, Lewis J, Raff M, Roberts K, Walter P.** Molecular Biology of the Cell. 4th ed. *New York: Garland Science* 2002
- 4 **Ayscough KR.** *In vivo* functions of actin-binding proteins. *Curr Opin Cell Biol* 1998; **10**: 102-111
- 5 **Ku NO, Zhou X, Toivola DM, Omary MB.** The cytoskeleton of digestive epithelia in health and disease. *Am J Physiol* 1999; **277**: G1108-G1137
- 6 **Mitchison TJ, Cramer LP.** Actin-based cell motility and cell locomotion. *Cell* 1996; **84**: 371-379
- 7 **Weber I, Gerisch G, Heizer C, Murphy J, Badelt K, Stock A, Schwartz JM, Faix J.** Cytokinesis mediated through the recruitment of cortexillins into the cleavage furrow. *EMBO J* 1999; **18**: 586-594
- 8 **Ridley AJ.** Rho GTPases and cell migration. *J Cell Sci* 2001; **114**: 2713-2722
- 9 **Pollard TD, Blanchoin L, Mullins RD.** Molecular mechanisms controlling actin filament dynamics in nonmuscle cells. *Annu Rev Biophys Biomol Struct* 2000; **29**: 545-576
- 10 **Furuse M, Hirase T, Itoh M, Nagafuchi A, Yonemura S, Tsukita S, Tsukita S.** Occludin: a novel integral membrane protein localizing at tight junctions. *J Cell Biol* 1993; **123**: 1777-1788
- 11 **Critchley DR.** Focal adhesions-the cytoskeletal connection. *Curr Opin Cell Biol* 2000; **12**: 133-139
- 12 **Pokutta S, Weis WI.** The cytoplasmic face of cell contact sites. *Curr Opin Struct Biol* 2002; **12**: 255-262
- 13 **DeMali KA, Barlow CA, Burridge K.** Recruitment of the Arp2/3 complex to vinculin: coupling membrane protrusion to matrix adhesion. *J Cell Biol* 2002; **159**: 881-891
- 14 **Higuchi H, Adachi M, Miura S, Gores GJ, Ishii H.** The mitochondrial permeability transition contributes to acute ethanol-induced apoptosis in rat hepatocytes. *Hepatology* 2001; **34**: 320-328
- 15 **Hirokawa M, Miura S, Yoshida H, Kurose I, Shigematsu T, Hokari R, Higuchi H, Watanabe N, Yokoyama Y, Kimura H, Kato S, Ishii H.** Oxidative stress and mitochondrial damage precedes gastric mucosal cell death induced by ethanol administration. *Alcohol Clin Exp Res* 1998; **22**: 111S-114S
- 16 **Bellomo G, Mirabelli F.** Oxidative stress and cytoskeletal alterations. *Ann N Y Acad Sci* 1992; **663**: 97-109
- 17 **Kobayashi I, Kawano S, Tsuji S, Matsui H, Nakama A, Sawaoka H, Masuda E, Takei Y, Nagano K, Fusamoto H, Ohno T, Fukutomi H, Kamada T.** RGM1, a cell line derived from normal gastric mucosa of rat. *In Vitro Cell Dev Biol Anim* 1996; **32**: 259-261
- 18 **Ranta-Knuutila T, Kiviluoto T, Mustonen H, Puolakkainen P, Watanabe S, Sato N, Kivilaakso E.** Migration of primary cultured rabbit gastric epithelial cells requires intact protein kinase C and Ca²⁺/calmodulin activity. *Dig Dis Sci* 2002; **47**: 1008-1014
- 19 **Watanabe S, Hirose M, Yasuda T, Miyazaki A, Sato N.** Role of actin and calmodulin in migration and proliferation of rabbit gastric mucosal cells in culture. *J Gastroenterol Hepatol* 1994; **9**: 325-333
- 20 **Murai T, Watanabe S, Hirose M, Miwa H, Miyazaki A, Sato N.** Ethanol retards gastric epithelial restoration in monolayer cultures. *Dig Dis Sci* 1996; **41**: 2062-2069
- 21 **Murai T, Watanabe S, Hirose M, Kobayashi O, Maehiro K, Ohkura R, Miwa H, Kitamura T, Ogihara T, Oide H, Miyazaki A, Sato N.** Evaluation of ethanol on gastric epithelial restoration *in vitro*. *Alcohol Clin Exp Res* 1996; **20**: 45A-46A
- 22 **Banan A, Smith GS, Kokoska ER, Miller TA.** Role of actin cytoskeleton in prostaglandin-induced protection against ethanol in an intestinal epithelial cell line. *J Surg Res* 2000; **88**: 104-113
- 23 **Miller TA, Smith GS, Banan A, Kokoska ER.** Cytoskeleton as a target for injury in damaged intestinal epithelium. *Microsc Res Tech* 2000; **51**: 149-155

- 24 **Mustonen H**, Kivilaakso E. Effect of luminal ethanol on epithelial resistances and cell volume in isolated Necturus gastric mucosa. *Dig Dis Sci* 2003; **48**: 2037-2044
- 25 **Hiraishi H**, Shimada T, Ivey KJ, Terano A. Role of antioxidant defenses against ethanol-induced damage in cultured rat gastric epithelial cells. *J Pharmacol Exp Ther* 1999; **289**: 103-109
- 26 **Kwiecien S**, Brzozowski T, Konturek SJ. Effects of reactive oxygen species action on gastric mucosa in various models of mucosal injury. *J Physiol Pharmacol* 2002; **53**: 39-50
- 27 **Davenport HW**. Gastric mucosal injury by fatty and acetylsalicylic acids. *Gastroenterology* 1964; **46**: 245-253
- 28 **Joyce NC**, Mekler B. PGE₂: a mediator of corneal endothelial wound repair *in vitro*. *Am J Physiol* 1994; **266**: C269-C275
- 29 **Gotlieb AI**. Prostaglandin induced shape changes in fibroblasts grown in cell culture. *Prostaglandins* 1980; **19**: 865-871
- 30 **Pai R**, Szabo IL, Giap AQ, Kawanaka H, Tarnawski AS. Nonsteroidal antiinflammatory drugs inhibit re-epithelialization of wounded gastric monolayers by interfering with actin, Src, FAK, and tensin signaling. *Life Sci* 2001; **69**: 3055-3071
- 31 **Kiviluoto T**, Mustonen H, Kivilaakso E. Effect of barrier-breaking agents on intracellular pH and epithelial membrane resistances: studies in isolated Necturus antral mucosa exposed to luminal acid. *Gastroenterology* 1989; **96**: 1410-1418
- 32 **Watanabe S**, Wang XE, Hirose M, Yoshizawa T, Iwazaki R, Oide H, Kitamura T, Miwa H, Miyazaki A, Sato N. Effects of rebamipide on bile acid-induced inhibition of gastric epithelial repair in a rabbit cell culture model. *Aliment Pharmacol Ther* 1996; **10**: 927-932
- 33 **Dziki AJ**, Batzri S, Harmon JW, Molloy M. Cellular hypercalcemia is an early event in deoxycholate injury of rabbit gastric mucosal cells. *Am J Physiol* 1995; **269**: G287-G296
- 34 **Molloy M**, Batzri S, Dziki AJ, Goldberg WJ, Hale DA, Harmon JW. Reversibility of deoxycholate-induced cellular hypercalcemia in rabbit gastric mucosal cells. *Surgery* 1996; **119**: 89-97
- 35 **Duane WC**, Wiegand DM, Sievert CE. Bile acid and bile salt disrupt gastric mucosal barrier in the dog by different mechanisms. *Am J Physiol* 1982; **242**: G95-G99
- 36 **Thomas AJ**, Nahrwold DL, Rose RC. Detergent action of sodium taurocholate on rat gastric mucosa. *Biochim Biophys Acta* 1972; **282**: 210-213
- 37 **Miura S**, Fukumura D, Shiozaki H, Suzuki M, Kurose I, Suematsu M, Tsuchiya M, Ishii H. Bile acid-induced depolarization of mitochondrial membrane potential preceding cell injury in cultured gastric mucosal cells. *J Gastroenterol Hepatol* 1995; **10**: 621-626

Science Editor Li WZ Language Editor Elsevier HK

Acupuncture for irritable bowel syndrome: A blinded placebo-controlled trial

Alastair Forbes, Sue Jackson, Clare Walter, Shafi Quraishi, Meron Jacyna, Max Pitcher

Alastair Forbes, Sue Jackson, Clare Walter, Shafi Quraishi, Meron Jacyna, Max Pitcher, St Mark's Hospital, Watford Road, Harrow HA1 3UJ, United Kingdom

Supported by the a donation gratefully received from the T-R Golden Charitable Trust

Correspondence to: Dr. Alastair Forbes, St Mark's Hospital, Watford Road, Harrow HA1 3UJ, United Kingdom. alastair.forbes@ic.ac.uk
Telephone: +44-20-8235-4046 Fax: +44-20-8235-4039

Received: 2002-12-22 Accepted: 2003-11-12

Abstract

AIM: Irritable bowel syndrome (IBS) is a common disorder and many patients fail to find adequate relief from conventional therapies for their symptoms. This study tests the claim that acupuncture is effective for a majority of these patients.

METHODS: A prospective, blinded, sham acupuncture-controlled trial of traditional Chinese acupuncture was performed at a single postgraduate teaching hospital in Europe. Sixty patients with well-established IBS were recruited. The blinded comparator was sham acupuncture administered by the second of two acupuncturists who alone was aware of the randomization, and who otherwise followed the prescription of the first. The primary end-point was a defined fall in the symptom score at 13 wk (by intention to treat). The prior expectation was a 30% placebo response, and a response rate of 70% from acupuncture, for which the study was adequately powered.

RESULTS: Patients in treated and sham groups improved significantly during the study-mean improvement in scores being equal (minus 1.9) and significant for both ($P < 0.05$; one-tailed t test). There was a small numeric but non-significant difference between the response rate in patients receiving acupuncture (40.7%) and sham treatment (31.2%). Several secondary end-points marginally favored active treatment, but an improved symptom score of any degree of magnitude occurred more often with sham therapy (65.6% vs 59.2%). For no criterion was statistical significance approached.

CONCLUSION: Traditional Chinese acupuncture is relatively ineffective in IBS in the European hospital setting, and the magnitude of any effect appears insufficient to warrant investment in acupuncture services.

© 2005 The WJG Press and Elsevier Inc. All rights reserved.

Key words: Acupuncture; Complementary therapy; Irritable bowel syndrome; Traditional medicine

Forbes A, Jackson S, Walter C, Quraishi S, Jacyna M, Pitcher M. Acupuncture for irritable bowel syndrome: A blinded placebo-controlled trial. *World J Gastroenterol* 2005; 11 (26): 4040-4044

<http://www.wjgnet.com/1007-9327/11/4040.asp>

INTRODUCTION

Acupuncture has been utilized for a variety of conditions, by up to 19% of the European population, and with as many as 12 million treatments per year in the USA^[1]. Gastrointestinal problems are addressed^[2], and in addition to publications in the traditional Chinese medicine (TCM) literature there has been support in more mainstream journals^[3,4]. Not all reviewers have been so positive however^[5]. Irritable bowel syndrome (IBS) is common, and many patients fail to find adequate relief from conventional therapies. It is claimed that acupuncture is effective for a majority of patients with IBS, but there are few data to support this. Case reports do not adequately address the large placebo response in this condition, the often substantial inter-subject variability in response, nor the differing systems of nomenclature in acupuncture. The US NIH consensus did not include IBS amongst 12 conditions for which it found evidence favoring acupuncture^[4]. The only paper specific to acupuncture in IBS that we have found is a pilot study of seven patients, which recorded improvements in bloating and general well-being^[6]. A complex Austrian study in which acupuncture or sham acupuncture (inter alia) was used for irritable colon demonstrated benefit at 1 mo (43.7% vs 26.7% relief; $P < 0.01$)^[7]. However, the definition of response, the nature of the randomization, and the mechanism of blinding are unclear. Evidence in favor of acupuncture for IBS cannot be considered definite.

Previous attempts to assess the placebo response in acupuncture therapy have been criticized. Orthodox clinician-scientists object to poor blinding, while acupuncturists argue that attempts to blind therapy negate the diagnostic and therapeutic process, and confound the individualization of the chosen regime necessary for the TCM paradigm. The present study addresses a single hypothesis and tackles the issues of methodology in a novel and creative fashion.

MATERIALS AND METHODS

Patients and consent

Patients were selected by personal approach in the St Mark's Hospital clinics. Eligibility required a confident clinical diagnosis of IBS and age of over 16 years. Patients were to

satisfy the Rome criteria^[8] and the Manning criteria^[9]. The Rome II criteria^[10] became available during the study; their fulfillment was noted but not required. Patients were to have had symptoms for at least 3 mo and to have failed to respond to standard therapies including: increased dietary fiber, reduction of lactose-containing foods, antispasmodics, simple laxatives (in those with predominant constipation), and opioids (in those with predominant diarrhea). Other physical disease was required to be absent or inactive. Formal psychiatric disease was an exclusion criterion. Patients were not permitted to use psychotropic drugs during the study period unless these had been commenced at least 3 mo before recruitment and were maintained at static dose throughout. Potentially fertile women were required to use effective contraception.

Normality of routine hematology, renal, hepatic and thyroid biochemistry, and of inflammatory markers was required. All subjects had a normal sigmoidoscopic examination within 3 mo of entry. Those over 40 years of age were required to have had colonoscopy, or flexible sigmoidoscopy and barium enema within 2 years of entry. All were given an information leaflet and were required to provide written informed consent.

Study methodology

The study was a double blind, sham-controlled trial of TCM acupuncture therapy. Two acupuncturists, fully trained in traditional Chinese acupuncture and accredited to the British Acupuncture Council, were responsible for the active and sham interventions. Recruited patients were allocated according to computer-generated random numbers concealed in sealed envelopes. Ten treatments were administered, at approximately 1-wk intervals.

Technical aspects of active and sham acupuncture

The first acupuncturist was the “diagnosing acupuncturist” (DA), whom the patient saw for the initial consultation, and before and after each treatment. A full case history was taken by the DA, together with tongue and pulse examination, to arrive at an individual diagnosis in accordance with the principles of TCM, with an additional lesser emphasis on Five Element Acupuncture^[11-14]. Although all patients in the study had IBS, this corresponded to a wide range of TCM patterns, making individual diagnosis essential. Dietary and lifestyle advice (important in treatment according to TCM principles) was given to all patients by the DA, who then selected acupuncture points.

The second “treating acupuncturist” (TA) opened the randomization envelope, and for the duration of the study remained the only individual aware of treatment allocation. The TA carried out the treatment—either according to instructions issued by the DA or using sham points, depending on the randomization.

In TCM meridian-based acupuncture the aim is to manipulate or remove blocking of the “Qi”. A variety of needling techniques is necessary, both to achieve requisite ‘deqi’ or ‘needling sensation’, and, subsequently, a range of therapeutic effects. Eight to sixteen needles were inserted at 4-8 specified acupuncture sites, bilaterally, in each session. Needles were left in place momentarily, or for up to 25 min,

depending on the desired effect. For active patients the TA implemented the instructions of the DA, including the needle technique, and the length of time of their retention.

‘Sham’ acupuncture points were chosen from three different areas on the body (the anterior thigh distally, the posterior thigh, and the lateral aspect of the lower back), which do not correspond to recognized acupuncture points and are deemed to have no therapeutic value. These were varied to some degree each week as in genuine treatment, including variation in needle technique and length of time of retention. No deqi needling sensation was sought or obtained at sham points.

Sterile single-use ‘Carbo’ brand needles were used (mostly 0.22 mm×25 mm, some 0.25 mm×40 mm). Insertion may be uncomfortable but is not normally painful (less discomfort than venepuncture). Needles were generally well tolerated, and were gently stimulated, as required, by the acupuncturist during treatment.

Moxibustion (therapeutic burning of the herb *Artemisia vulgaris*) is integral to the practice of traditional Chinese acupuncture, but was not used during the study, although there were a number of patients for whom it was considered indicated. This reflected hospital fire regulations and added difficulties with blinding.

The DA re-examined the patients’ pulses at the end of every session, as pulse changes during treatment are considered important indicators of efficacy. On the basis of these, and the verbal, pulse and tongue feedback at the start of the next session, the DA varied the emphasis on different treatment principles and the choice of acupuncture points prescribed for the next treatment.

Outcome measures and data analysis

Patients completed weekly symptom diaries, supplemented by psychological and quality of life scales at entry and at 12th wk (or prior exit). Therapeutic effects were judged from the diaries and questionnaires, and by physician assessment. The symptom diary is based on the Bristol scale^[15] and has been previously validated^[16]. It employs eight Likert scales relating to abdominal symptomatology and their interference with activities (Appendix), and permits the compilation of a numerical (non-linear) global “symptom score” between 0 and 30. Patients also completed the Hospital Anxiety and Depression (HAD) scale^[17], and the EuroQol^[18] quality of life questionnaire.

The principal outcome measure was a change in the symptom score. A reduction of four is considered indicative of a clinically useful response, and was expected from sham or placebo therapy in approximately 30% of eligible patients. Acupuncturists expect to obtain a useful response in around 70% of patients with IBS (informal enquiries of several practitioners), with the proviso that limitations imposed by the experimental protocol might reduce this a little.

Secondary outcome measures included assessment by one of the blinded investigators at the end of the study period, which made a simple categorization of patient status as “improved”, “unchanged” or “worse”. Secondary outcomes also included changes on the HAD and EuroQol instruments. As the principal objective is to reduce symptomatology and to improve quality of life, the patients’ perceptions of

these are the outcomes of critical interest to them. The end-points recorded are comparable to those utilized in respected studies of this condition.

Statistical calculations for 60 subjects provided for a study with 60% power to demonstrate a 30% numerical (not relative) difference between the two groups, if a placebo response of 30% is assumed. Results were analyzed by intention to treat.

Apart from the hospital notes all data were retained anonymously. The study complied with the requirements of the Declaration of Helsinki (1996 modification), the British Data Protection Act (1984), the International Conference on Harmonization Tripartite Guideline for Good Clinical Practice, and had approval from the Harrow Research Ethics Committee.

Patients

Sixty patients (40 female) were recruited; one female withdrew after recruitment but before randomization. Results are therefore recorded for 59 individuals (Table 1). Twenty-eight patients were allocated to acupuncturist A as the DA and to acupuncturist B as the TA, with the converse in the other 31. There was a good balancing of the two groups: for no parameter was there a statistically significant difference at study entry (Table 1).

Role of sponsors: None in either design of the study or in the writing of the report.

Table 1 Patient characteristics at study entry

	Acupuncture group	Sham group
Number	27	32
Number female	16	23
Mean age (yr)	43.0	44.4
Age range (yr)	19-67	17-79
Predominant symptom		
Pain	11	10
Bloating	7	11
Diarrhea	7	9
Constipation	2	2
Mean symptom score	13.5	13.1
Mean anxiety score (HAD)	10.2	11.2
Mean depression score (HAD)	5.8	6.8
Mean EuroQol LAS score (%)	59	64

HAD = hospital anxiety and depression scale. LAS = linear analog scale.

RESULTS

The mean global symptom score in the acupuncture-treated patients fell from 13.5 ± 4.51 to 11.6 ± 5.13 , and in the sham group from 13.1 ± 4.30 to 11.2 ± 4.17 ($P < 0.05$ for one-tailed t test for the improvements in both study groups) (Figure 1). A reduction in symptom score was observed in 16 acupuncture subjects (59.2%), and by at least four points in 11 (40.7%). The equivalent figures for the sham group were 21 (65.6%) and 10 (31.2%). The differences between sham and actively treated groups did not approach statistical significance.

The blinded clinician considered 13 of the acupuncture group (48.1%) improved, compared to 10 of the sham group (31.2%) (NS). These were predominantly the same patients who considered themselves improved (reduction in symptom score of four or more). Similar proportions in the two groups were considered to have deteriorated or had withdrawn (18.5% *vs* 21.9%; NS).

For those with pain predominance at enrollment the median score of 13 remained at 13 in the actively treated group, and fell from 15 to 10 in the sham group; for bloating the equivalent figures were 14 to 9, and 14 to 11; for diarrhea 11 to 8 compared to 11 to 10.5; and for constipation 16 to 15 *vs* 11 to 8.

There were no significant differences between the HAD scores for the sham and active groups, but a slightly higher proportion of the sham-treated group had anxiety scores in the "probable" (≥ 12) range (47% *vs* 41%). The response rate (drop of ≥ 4 symptom points) was 27% in the subset of anxious patients receiving sham treatment and 54% in those on active therapy (NS).

The EuroQol score rose slightly (improvement) in the actively treated (59.4-64.6%) and the sham treated (64.6-65.6%); neither change was significant. There was no correlation between initial EuroQol score and the likelihood of a response.

Acupuncturist A (as TA) treated 31 patients, of whom 19 were allocated to sham therapy. Their mean score of 13.6 ± 4.84 fell to 12.3 ± 4.56 ; the score fell by ≥ 4 in 7 (36.8%). In the 12 patients who received active acupuncture the mean score fell from 14.3 ± 4.68 to 11.6 ± 6.69 , with a fall of ≥ 4 in 6 (50%). Acupuncturist B (as TA) treated 28 patients of whom 13 were allocated to sham; the score fell by ≥ 4 in 3 (23.1%) of these. In the 15 patients randomized

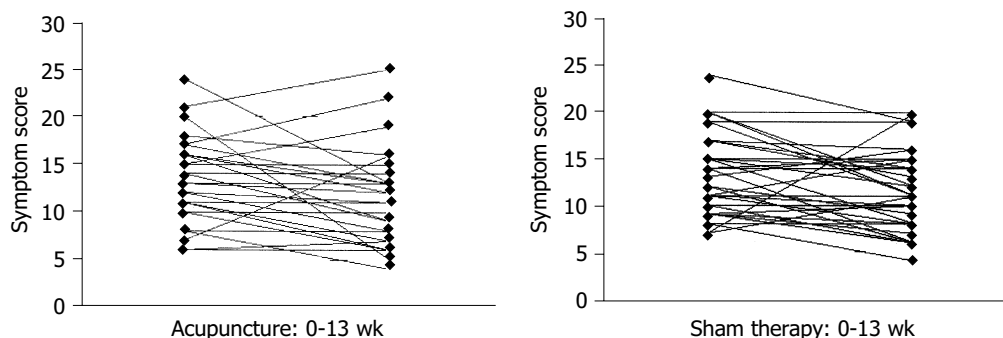


Figure 1 Change in the global symptom score from entry to 13 wk. The upper panel shows the individual values for the actively treated patients and the lower

panel those for sham-treated patients.

to active acupuncture a “qualifying” fall in score occurred in 5 (33.3%). Overall 41.9% of patients “diagnosed” by acupuncturist B and “treated” by acupuncturist A responded with a qualifying fall in score, compared to 28.6% of those with the acupuncturists filling the alternative roles (NS).

Adverse events and non-completing patients

No direct adverse events were elicited. One patient was commenced on antidepressants after psychiatric consultation, and another on beta-blockers for anxiety. Six other patients failed to complete the study period. Of these eight withdrawals, five belonged to the acupuncture group and three to sham. These patients have been included in the above analyses by intention to treat. If the principal outcome measure is applied only to those completing the intended therapy the results are unchanged: the mean symptom score at completion of the acupuncture course was 11.4 compared to 10.9 in the sham group (NS).

DISCUSSION

As expected there was a response to TCM acupuncture and to sham treatment. The number of responding patients in the sham group and the magnitude of the responses were in line with our prior expectations (31.2% good responders compared to an anticipated 30% placebo response). The study group is therefore likely to be generally representative. Formal acupuncture failed to elicit significant advantage (40.7% responders). There were several areas in which numeric advantage lay with acupuncture, including the clinician’s assessment and the proportion achieving at least a four point reduction in symptom score, but sham therapy had the numeric advantage if responses of any degree of magnitude are included (65.6% *vs* 59.2%). There was no obvious trend according to predominant symptom at study entry, but initial anxiety possibly predicts a better response.

The inference that TCM acupuncture is of very limited value in IBS is supported by the absence of positive data in the literature, its absence from the conclusions of the NIH consensus^[4], and from a small study which showed no effect on colonic motility in constipation^[19]. We are confident that our sham technique was performed with retention of complete blinding of the DA, the gastroenterologist and the patient. This necessarily unblinded nature of the treating acupuncturist clearly had important effects on the two practitioners concerned, who felt uncomfortable “deliberately denying” the patient, a therapy in which they had confidence. It is possible that this proved a confounding factor. The close similarity of the outcome from sham therapy to that expected from placebo suggests that neither positive nor negative effects predominate. In consequence, it is not clear that anything would have been gained by the use of sham needles, as has been advocated^[20], since while this strategy has the potential to conceal sham administration from the TA it may unblind the patient. It is acknowledged that the use of sham needling probably elicits important physiological effects (such as increased endorphin activation), but the absence of an obvious difference in response rate in our sham group from that anticipated from “other” placebos indicates that the effect is not one of lasting clinical consequence.

The combination of acupuncturist B as diagnostician with acupuncturist A as acupuncturist appeared “better” than the converse. This was probably a direct consequence of the individualization of therapy (by the TA as well as that planned by the DA), but represents a post hoc and non-significant observation. We deliberately chose to permit both acupuncturists to engage in therapy so as to increase the generalizability of the study, hence avoiding results dependent on the consequences of a unique pairing of practitioners.

The outcome may have included systematic bias against acupuncture. The specific dietary and lifestyle advice considered important to TCM was given to all patients regardless of randomization. It is unlikely that this was a major influence as the sham response was closely similar to that expected for placebo. The proscription of moxibustion would be expected to have placed the actively treated group at a disadvantage compared to those treated outside the study context. However, this technique cannot easily be a practical proposition in health service premises in which fire regulations and the presence of smoke detectors are ubiquitous. The third factor potentially disadvantageous to acupuncture therapy was the impossibility of completely individualized therapy in a formal trial, and perhaps adverse influences from other constraints of the hospital environment. This drawback was considered carefully during the devising of the study and felt to be an acceptable compromise between Western scientific method and traditional Chinese practice. The possibility that simplified acupuncture as delivered by Western-medicine-trained acupuncturists might have given a different result is intriguing and may warrant further study.

The study was underpowered to demonstrate a small benefit, but it was of sufficient size to confirm the large difference that was anticipated. If such an effect has been missed by the present study it is our opinion that it is of insufficient clinical relevance to justify *de novo* investment in provision of acupuncture services to hospital patients with IBS.

ACKNOWLEDGMENTS

We are also grateful for the support of our research nurses, to the clinicians who referred patients to us, and to the patients themselves. We greatly appreciate the very useful comments of Dr. Andrew Thillainayagam, MD, FRCP (medically trained acupuncturist), on an earlier draft of the manuscript.

REFERENCES

- 1 **Fisher P**, Ward A. Complementary medicine in Europe. *Br Med J* 1994; **309**: 107-111
- 2 **Eskinazi DP**, Jobst KA. National institutes of health office of alternative medicine—food and drug administration workshop on acupuncture. *J Altern Complement Med* 1996; **2**: 3-6
- 3 **Li Y**, Tougas G, Chiverton SG, Hunt RH. The effect of acupuncture on gastrointestinal function and disorders. *Am J Gastroenterol* 1992; **87**: 1372-1381
- 4 Anon. NIH Consensus Conference. Acupuncture. *JAMA* 1998; **280**: 1518-1524
- 5 **Mayer DJ**. Acupuncture: an evidence-based review of the clinical literature. *Annu Rev Med* 2000; **51**: 49-63

- 6 **Chan J**, Carr I, Mayberry JF. The role of acupuncture in the treatment of irritable bowel syndrome: a pilot study. *Hepatology* 1997; **44**: 1328-1330
- 7 **Kunze M**, Seidel HJ, Stübe G. Comparative studies of the effectiveness of brief psychotherapy, acupuncture and papaverin therapy in with irritable bowel syndrome. *Z Gesamte Inn Med Grenz* 1990; **45**: 625-627
- 8 **Thompson WG**, Dotevall G, Drossman DA, Heaton KW, Kruis W. Irritable bowel syndrome: guidelines for the diagnosis. *Gastroenterol Int* 1989; **2**: 92-95
- 9 **Manning AP**, Thompson WG, Heaton KW, Morris AF. Towards positive diagnosis of the irritable bowel. *Br Med J* 1978; **2**: 653-654
- 10 **Drossman DA**, Corazziari E, Talley NJ, Thompson WG, Whitehead WE, Rome II. The functional gastrointestinal disorders. 2nd Ed. McLean VA: *Degnon Association* 2000; **355**: 360
- 11 **Deadman P**. A Manual of Acupuncture. *J Chinese Med Publications* 1998
- 12 **Maciocia G**. The Foundations of Chinese Medicine. *Churchill Livingstone* 1989
- 13 **Maciocia G**. The Practice of Chinese Medicine. *Churchill Livingstone* 1994
- 14 **Mole P**. Energy Balancing for Body, Mind & Spirit
- 15 **Heaton KW**, Ghosh S, Braddon FE. How bad are the symptoms and bowel dysfunction of patients with the irritable bowel syndrome? A prospective, controlled study with emphasis on stool form. *Gut* 1991; **32**: 73-79
- 16 **Forbes A**, MacAuley S, Chiotakakou-Faliakou E. Hypnototherapy and therapeutic audiotape: effective in previously unsuccessfully treated irritable bowel syndrome? *Int J Colorectal Dis* 2000; **15**: 328-334
- 17 **Zigmond AS**, Snaith RP. The hospital anxiety and depression scale. *Acta Psych Scand* 1983; **67**: 361-370
- 18 **Johnson JA**, Coons SJ. Comparison of the EQ-5D and SF-12 in an adult US sample. *Qual Life Res* 1998; **7**: 155-166
- 19 **Klauser AG**, Rubach A, Bertsche O, Muller-Lissner SA. Body acupuncture: effect on colonic function in chronic constipation. *Z Gastroenterol* 1993; **31**: 605-608
- 20 **Streitberger K**, Kleinhenz J. Introducing a placebo needle into acupuncture research. *Lancet* 1998; **352**: 364-365

Science Editor Wang XL and Guo SY Language Editor Elsevier HK

Adeno-associated virus mediated interferon-gamma inhibits the progression of hepatic fibrosis *in vitro* and *in vivo*

Miao Chen, Guang-Ji Wang, Yong Diao, Rui-An Xu, Hai-Tang Xie, Xin-Yan Li, Jian-Guo Sun

Miao Chen, Guang-Ji Wang, Yong Diao, Hai-Tang Xie, Xin-Yan Li, Jian-Guo Sun, Jiangsu Key Lab of Drug Metabolism and Pharmacokinetics, China Pharmaceutical University, No.24 Tongjiaxiang, Nanjing 210009, Jiangsu Province, China
Rui-An Xu, Gene Therapy Laboratory, Genome Research Center, The University of Hong Kong, 8S-01, Kadoorie BioScience Bldg, Pokfulam Road, Hong Kong, China
Supported by the National High Technology Research and Development Program of China, 863 Program, No. 2003AA2Z347A
Correspondence to: Professor Guang-Ji Wang, Jiangsu Key Lab of Drug Metabolism and Pharmacokinetics, China Pharmaceutical University, No. 24 Tongjiaxiang, Nanjing 210009, Jiangsu Province, China. gjwang@cpu.edu.cn
Telephone: +86-25-83271544 Fax: +86-25-83302827
Received: 2004-10-18 Accepted: 2004-11-26

© 2005 The WJG Press and Elsevier Inc. All rights reserved.

Key words: Adeno-associated virus; Interferon- γ ; Hepatic stellate cells; Hepatic fibrosis

Chen M, Wang GJ, Diao Y, Xu RA, Xie HT, Li XY, Sun JG. Adeno-associated virus mediated interferon-gamma inhibits the progression of hepatic fibrosis *in vitro* and *in vivo*. *World J Gastroenterol* 2005; 11(26): 4045-4051
<http://www.wjgnet.com/1007-9327/11/4045.asp>

Abstract

AIM: To investigate the effects of adeno-associated virus (AAV) mediated expression of human interferon- γ for gene therapy in experimental hepatic fibrosis *in vitro* and *in vivo*.

METHODS: We constructed the recombinant AAV encoding human INF- γ (rAAV- INF- γ) and took the primary rat hepatic stellate cells and carbon tetrachloride induced rats as the experimental hepatic fibrosis model *in vitro* and *in vivo*. Immunocytochemistry analysis was used to reveal the expression of α -SMA, the marker protein expressed in hepatic stellate cells. The mRNA expression of TGF- β , TIMP-1, and MMP-13 were analyzed by RT-PCR method. *In vivo* study, the hydroxyproline content in liver and serum AST, ALT were also detected.

RESULTS: *In vitro* study, AAV vector could mediated efficient expression of human INF- γ , which inhibit the activation of hepatic stellate cells, decrease the expression of α -SMA and mRNA of TIMP-1, TGF- β , with the MMP-13 unchanged. *In vivo* study, the histological examination revealed that rAAV- INF- γ could inhibit the progression of the hepatic fibrosis. In the rAAV-INF- γ induced group, the hydroxyproline content and serum AST, ALT level were decreased to 177 ± 28 μ g/g wet liver, 668.5 ± 140.0 , 458.4 ± 123.5 U/L, compare with the fibrosis control group 236 ± 31 μ g/g wet liver, $1\ 019.1 \pm 276.3$, 770.5 ± 154.3 U/L, respectively ($P < 0.01$). mRNA expression of TIMP-1 in the rAAV-INF- γ induced rat liver was decreased while no significant change was observed in TGF- β and MMP-13.

CONCLUSION: All these results indicated that rAAV-INF- γ has potential effects for gene therapy of hepatic fibrosis, which could inhibit the progression of hepatic fibrosis.

INTRODUCTION

Liver fibrosis is a very common disease in China and other countries, it is a wound-healing response to chronic liver injury, results from viral hepatitis, ethanol and drug abuse, which if persistent can lead to cirrhosis or liver failure. The main feature of the fibrosis is the increased deposition of extracellular matrix (ECM) caused by activated hepatic stellate cells (HSCs, Ito cells or fat-storing cells)^[1,2].

In normal liver, HSCs undergo the quiescent state, contain retinoid lipid droplets and synthesize low levels of matrix proteins. But, as a result of liver injury, HSCs are in the process of activation, proliferate and transform to myofibroblast like cells. Activated HSCs are characterized by loss of retinoid, appearance of α -smooth muscle actin (α -SMA) and procollagen I, III, which are known to be the primary source of excess ECM deposited in liver fibrosis^[3-5]. Meanwhile, the balance between generation and degradation of ECM is broken, cytokines and proteases secreted by hepatocytes, Kupffer cells and leukocytes make up a complicated pathways enhance the activation of HSCs^[6,7]. Some growth factors such as transforming growth factor- β (TGF- β) is enhanced in both availability and activity, stimulate the transcription of procollagen, fibronectin and other ECM genes. Also effect of the matrix metalloproteinase (MMP-13), the key enzyme in the degradation of ECM, is decreased by over expression of its inhibitor, the tissue inhibitors of matrix metalloproteinase (TIMP-1). Furthermore, the accumulation of ECM in turn increase not only the number of HSCs but also their capacity to synthesize the matrix proteins, which ultimately results in cirrhosis^[1,3,5].

The interferons (INFs) are a family of cytokines with several crucial biological functions, such as antiviral and immunomodulatory activities, which have first been used in the treatment of chronic hepatitis. Among the INFs, INF- α and INF- β (INF type I) are widely used to treat hepatitis C virus (HCV) infection in clinics, whereas INF- γ (INF type II) has a 10-100 fold lower specific antiviral activity than

INF type I, but 100-10 000 times more immunomodulatory activities^[8,9]. Recently, more and more studies have shown that INF- γ could inhibit the proliferation and activation of HSCs, thus prevent the production of ECM and decrease the expression of procollagen and other cytokines^[10-12]. However the serum elimination half-life of INF- γ is only 2-3 h^[12]. To make the therapeutic concentration in target organ, administration of INF- γ through a subcutaneous route may results in a much higher level of INF- γ in the serum, which could cause the adverse effects of flu-like symptoms, leucopenia and mental depression^[13].

Therefore, vector mediated local INF- γ expression in the liver could expand the clinical use of INF- γ in hepatic fibrosis. In this study, the AAV was introduced as the delivery vector for gene therapy. AAV is a number of small single stranded DNA viruses of the genus *Dependovirus* in the Parvoviridae family. Not only is AAV non-pathogenic and of minimal immune responses, but it could also infect both dividing and terminally-differentiated cells with high efficiency, expressing the transgene for at least 6 mo. Moreover it has a broad range of host cells and tissues^[14-18]. We constructed the recombinant AAV coding human INF- γ and examined its potential effects for gene therapy of hepatic fibrosis *in vitro* and *in vivo*.

MATERIALS AND METHODS

Generation of recombinant AAV virion

The plasmid of AAV vector, rAAV-eGFP and packaging helper plasmids pAd, pAAD are kindly provided by Prof Rui-An Xu (University of Hong Kong, Genome Research Center). The recombinant plasmid rAAV-INF- γ contains a hybrid of the cytomegalovirus immediate-early enhancer and the chicken β -actin/rabbit β -globin promoter (CAG), inserted with the reporter gene, a 511bp *EcoRI/XhoI* fragment of complementary DNA (cDNA) encoding full-length human INF- γ . Also the woodchuck hepatitis B virus post-transcriptional regulatory element is inserted to boost expression levels (Figure 1).

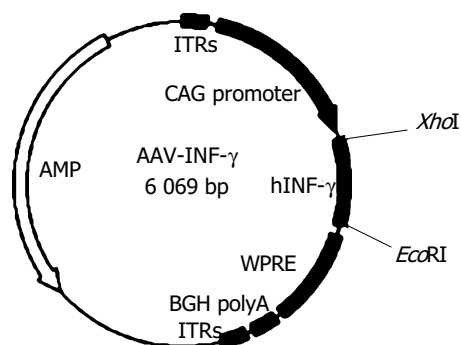


Figure 1 Structure of recombinant plasmid AAV-INF- γ . Human INF- γ cDNA obtained from RT-PCR was cloned into AAV plasmid, which contains a CAG promoter, WPRE enhancer and BGH polyA.

To generate the rAAV virions, we cotransfect the recombinant plasmid AAV-INF- γ or AAV-eGFP and two packaging helper plasmids into HEK 293 cells (ATCC CRL 1573) by

calcium phosphate precipitate. The cells were harvested 60 h after transfection and lysed by incubating with 5 g/L deoxycholate in the presence of 50 U/mL benzonase (Sigma, St. Louis, MO, USA), then isolated the recombinant AAV particles by using heparin affinity column chromatography (Amersham, HiTrap). The titles of the rAAV-INF- γ and rAAV-eGFP preparations were determined by AAV Titration ELISA kit (Progen). The virions were stored at -80 °C before experimental use.

Primary cell culture of rat HSCs

Primary rat HSCs were extracted from Sprague-Dawley rat (450-550 g, Animal Center of China Pharmaceutical University, Nanjing, China) liver by sequential *in situ* perfusion with collagenase and pronase followed by density gradient centrifugation and then cultured in 20% FBS DMEM, maintained in a humidified 50 mL/L CO₂ incubator at 37 °C^[19,20]. Experiments described in this study were performed on HSCs between the second and ninth serial passages with highly activated cells as tested. HSCs were cultured in 10 cm culture plates at a density of 2×10⁴ cells/cm². After changing the medium, HSCs were maintained in presence or absence of rAAV-INF- γ and rAAV-eGFP at 5×10⁴ v.g./cell for 72 h, meanwhile collect the medium every 12 h to analysis the expression of human INF- γ by ELISA. Then HSCs were in preparation for RNA isolation and immunocytochemistry analysis.

ELISA assay of INF- γ

We used the ELISA kit (R&D systems) to quantitative determine the expression of human INF- γ in the cell culture supernatant. The antibody specific for human INF- γ has been pre-coated onto a microplate. Pipette the samples into the wells, any present INF- γ was bound by the immobilized antibody. Then washed away the unbound substances, an enzyme-linked antibody was added to the wells. After washing any unbound antibody-enzyme reagent, a substrate solution was added to the wells and color developed in proportion to the amount of INF- γ bound in the initial step. Finally, stop the reaction and determined the optical density of each well at 540 or 570 nm within 30 min.

Immunocytochemistry

HSCs were washed with PBS and fixed in the slides with 40 g/L phosphate buffered paraformaldehyde (PFA) at 4 °C for 20 min. Then eliminated endogenous peroxidase activity by adding 30 mL/L H₂O₂ in PBS at room temperature for 30 min to permeabilized and blocked with goat serum blocking solution at room temperature for 1 h. After blocking, cells were incubated with primary antibody, anti- α -SMA (diluted 1:200 in PBS, Sigma) at 4 °C overnight. Washed the slides thrice in PBS, incubated the cells with secondary antibody biotinylated anti-mouse IgG from goat for 30 min, washed five times and added the solution of avidin-biotin peroxidase. Incubating for 30 min, the cells were then stained with DAB (3,3'-diaminobenzidine tetrahydrochloride, Sigma) peroxidase substrate solution-brown and counterstained with hematoxylin (Sigma). Finally, dehydrate the slides, clear in xylene and coverslip with permanent mounting medium.

RNA extraction and RT-PCR

Total RNA was extracted from HSCs and snap-frozen liver tissue using TRIzol Reagent (Gibco BRL) according to the method of Chomczynski and Sacchi^[21]. Then 4 μ g RNA of each sample was used for cDNA synthesis using a RevertAid First Strand cDNA Synthesis Kit (Fermentas). The amplification was carried out with 1 μ L of synthesized cDNA in a 50 μ L PCR mixture containing 20 pmol of a primer pair, 1.5 mmol/L MgCl₂, 0.2 mmol/L dNTPs and 1 U of recombinant Taq DNA polymerase. In total, 30 cycles of the reaction were carried out at 95 °C for 1 min, 57 °C for 1 min and 72 °C for 2 min. The PCR products were electrophoresed on a 20 g/L agarose gel and stained with ethidium bromide. The primers used in this study are listed in Table 1. The density of the band was analyzed using a BIO-RAD Gel Doc 2 000 densitometer.

Animal model of hepatic fibrosis

Hepatic fibrosis was induced in male Sprague-Dawley rats (140-150 g) by carbon tetrachloride (CCl₄) administration^[22]. Animals were maintained on standard chow and water. A total of 48 rats administered 500 mL/L CCl₄ dissolved in olive oil at a dose of 1 mL CCl₄/kg body weight twice weekly (every Monday and Thursday) via gastrogavage for 8 wk. One group of six rats received olive oil as control. This method reproducibly results in early fibrosis within 3-4 wk, and advanced fibrosis by 6-8 wk^[23]. After 3 wk, six rats of CCl₄ treated and untreated group were killed for examination of hepatic fibrosis development. After 6 wk, the remaining model rats were injected via the hepatic portal vein with a single infusion of 500 μ L of either saline ($n = 8$), 3×10^{11} v.g./mL rAAV-INF- γ ($n = 8$), and 3×10^{11} v.g./mL rAAV-eGFP ($n = 8$). After 8 wk, all the rats were killed and the liver were fixed in 40 g/L PFA for histological examination or snap-frozen in liquid nitrogen in preparation for measurement of hydroxyproline and RNA isolation. Also the blood samples were taken immediately before the rats were sacrificed for biochemical analysis.

Histological examination

For light-microscopic examination, the fixed liver specimens were embedded in paraffin. Sections were cut at a thickness of 4 μ m and stained with hematoxylin-eosin for routine examination.

Measurement of hydroxyproline content

The liver tissue was finely minced and then homogenized in nine volumes of ice-cold PBS, hydrolyzed in HCl and the hydroxyproline content was determined by the method of Sakaida *et al.*^[24], with minor modifications.

Measurement of AST and ALT

Blood was collected from femoral artery, allow the samples to clot for 30 min before centrifugation for 10 min at 1 000 r/min. Remove serum for aspartate aminotransferase (AST) and alanine aminotransferase (ALT) determination.

Statistical analysis

The data presented are the mean \pm SD of each group. A statistical analysis was performed using the Student's *t* test, $P < 0.05$ was considered to be statistically significant.

RESULTS

Effect of recombinant AAV-INF- γ on the primary cultured HSCs

Freshly isolated HSCs could emit blue-green fluorescence, which is easily quenched, stimulated by radiation of 328 nm laser source. Five days after isolation, HSCs exhibited expanded cytoplasmic processes and enlarged nuclei corresponding to the intermediate stage of the activation process. After 10 d culture, HSCs could undergo a totally activated process.

To confirm that AAV-INF- γ was transcriptional active, total RNA of infected HSCs was isolated and examined by RT-PCR analysis. Human INF- γ mRNA transcripts were detected in HSCs infected with rAAV-INF- γ , but undetectable in sham-infected or rAAV-eGFP infected HSCs (Figure 2A). Also the expression and secretion of human INF- γ was next evaluated by ELISA. In the group of rAAV-eGFP infected HSCs, 24 h after infection, human INF- γ expression was 265 ± 67 pg/mL in the supernatant and its level reaches the peak value, $1\ 211 \pm 178$ pg/mL at 60 h after infection (Figure 2B).

Because α -SMA is the marker protein of activated HSCs, the immunocytochemistry examination was introduced to evaluate the effects of rAAV-INF- γ on activated HSCs. The results revealed that the expression of α -SMA was suppressed by supplementation with rAAV-INF- γ (Figure 3A-D).

Additionally, INF- γ has a notable feature of immunomodulatory activity, which could affect the cytokines and proteases expression in HSCs. The mRNA expression of TGF- β , MMP-13 and TIMP-1 between the activated HSCs and HSCs infected with rAAV-eGFP and rAAV-INF- γ were examined by RT-PCR method (Figure 4A). There was no significant difference in the mRNA expression between the untreated and rAAV-eGFP infected HSCs. But the levels of TGF- β and TIMP-1 mRNA were decreased in the rAAV-INF- γ infected HSCs, with an unchanged expression in MMP-13 in contrast to those two groups of HSCs (Figure 4 B).

Histology of CCl₄ induced hepatic fibrosis and AAV-INF- γ treatment

Histological analysis confirmed that CCl₄ could cause the

Table 1 Primer pairs for RT-PCR used in this study

Gene	Forward primer	Reverse primer
INF- γ	5'-CCGCTCGAGATGAAATATACAAGTTATATC-3'	5'-CGGAATTCTTACTGGGATGCTCTTCGACC-3'
TGF- β	5'-CTTCAGCTCCACAGAGAAGAACTGC-3'	5'-CACGATCATGTGGACAAGCTGCTCC-3'
TIMP-1	5'-CCGCAGACGGCGTTCTGCAA-3'	5'-TCGAGACCCAAGGGATTGCC-3'
MMP-13	5'-TGACTATGCGTGGCTGGAA-3'	5'-AAGCTGAAATCTTGCCCTTGA-3'
GAPDH	5'-GTCAACGGATTGGTCTGATT-3'	5'-AGTCTTCTGGGTGGCAGTGAT-3'

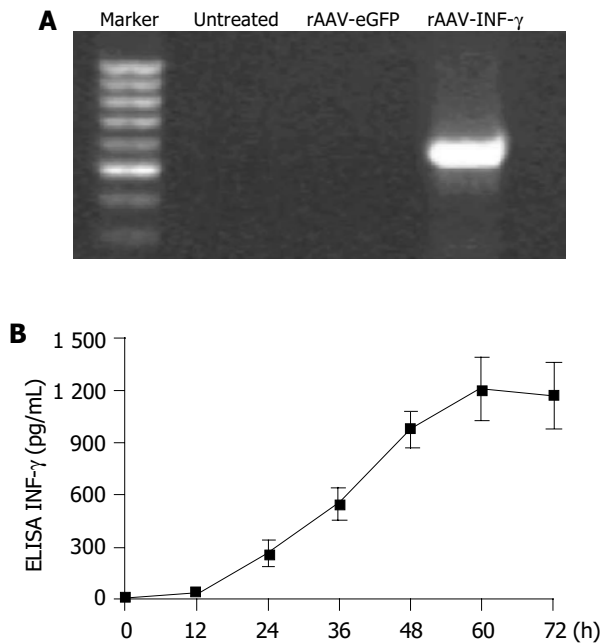


Figure 2 The expression of INF- γ in rAAV-INF- γ infected HSCs. **A:** RT-PCR analysis of INF- γ expression in rAAV-INF- γ infected HSCs. The untreated and rAAV-eGFP infected HSCs did not show any PCR band; **B:** Time course of the INF- γ expression in the HSC supernatants after rAAV-INF- γ infection. (Data are mean \pm SD, $n = 6$).

hepatic fibrosis. After 3 wk, the mature collagen fibrils bridging vascular structures were obviously presented in the CCl₄ treated group, showing a early stage of hepatic fibrosis (Figures 5 A and B). At the end of 8 wk, the saline and rAAV-eGFP treated model group revealed cirrhotic-like structural patterns: fibrous connective tissue components

in Glisson's sheath, pseudolobule formations and formation of fibrotic septa and thickened reticulin fibers joining central areas. In contrast, the rat liver that received rAAV-INF- γ showed only light bridging fibrosis and diminished fibrosis in both the periportal and centrilobular liver (Figures 5C-E).

Hydroxyproline content in liver

In collagen, 13.4% of total amino acid is hydroxyproline, whereas little content in elastin and inexistence in other proteins. So hydroxyproline content could reflect the collagen content in connective tissue. Determination of hydroxyproline content in different groups of rat liver confirmed the histological studies that hydroxyproline content in the rAAV-INF- γ treated group was significantly reduced to 177 ± 28 $\mu\text{g/g}$ wet liver, compare with the fibrosis control group 236 ± 31 $\mu\text{g/g}$ wet liver (Table 2).

Measurement of AST and ALT

The serum AST and ALT levels in the group of rats treated with CCl₄/saline and CCl₄/rAAV-eGFP were $1\ 019.1\pm 276.3$, 770.5 ± 154.3 U/L and 985.4 ± 241.6 , 727.2 ± 175.0 U/L, respectively. No significant difference was observed between those two groups. In contrast to the CCl₄/saline control group, the serum AST and ALT level of CCl₄/rAAV-INF- γ treated rats were reduced to 668.5 ± 140.0 , 458.4 ± 123.5 U/L, suggesting that the INF- γ gene expression inhibited the hepatic toxicity caused by CCl₄ (Table 2).

mRNA expression of TGF- β , TIMP-1, and MMP-13 in the liver

The mRNA expression of TGF- β , MMP-13 and TIMP-1 between the control group and the group induced with rAAV-INF- γ were analyzed by RT-PCR method (Figure 6A). There was a similar result between the *in vivo* and *in vitro*

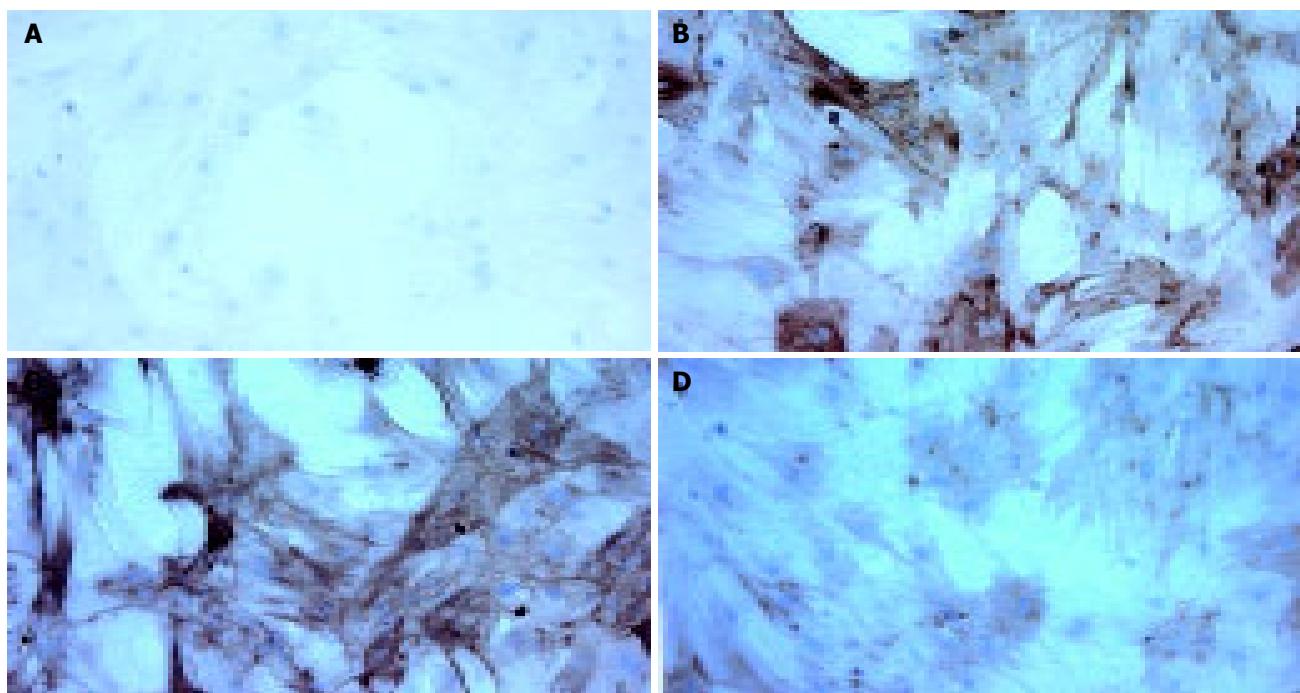


Figure 3 The expression of α -SMA in different group of primary cultured HSCs. Expressions of α -SMA were determined by immunocytochemical method. **A:** Immunocytochemistry of untreated HSCs without primary antibody as the negative

control; **B:** Immunocytochemistry of untreated HSCs; **C:** Immunocytochemistry of rAAV-eGFP infected HSCs; **D:** Immunocytochemistry of rAAV-INF- γ infected HSCs.

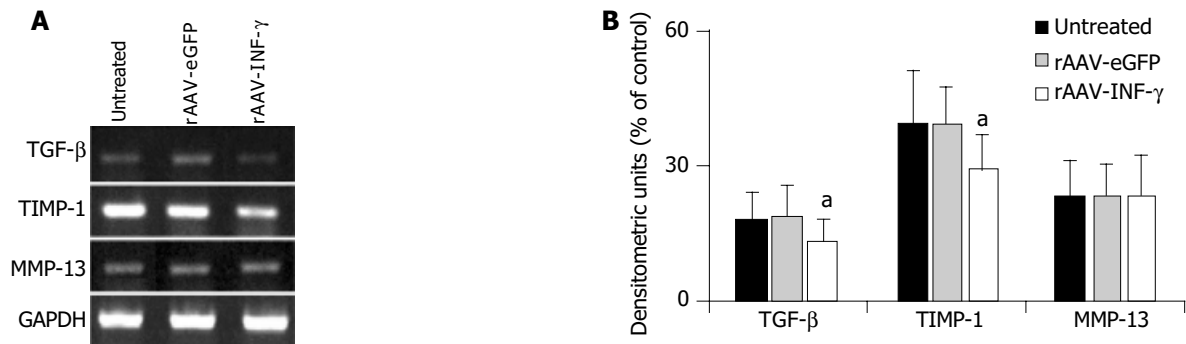


Figure 4 The mRNA expression of fibrosis related cytokines and proteases in different group of primary cultured HSCs. **A:** mRNA expression of TGF- β , MMP-13 and TIMP-1 in HSCs were examined by RT-PCR method; **B:** Densitometric

units were calculated by dividing the density of individual bands by that of GAPDH. Closed column, untreated. Lined column, rAAV-eGFP induced. Dotted column, rAAV-INF- γ induced. (Data are mean \pm SD, $n = 8$, ^a $P < 0.05$).

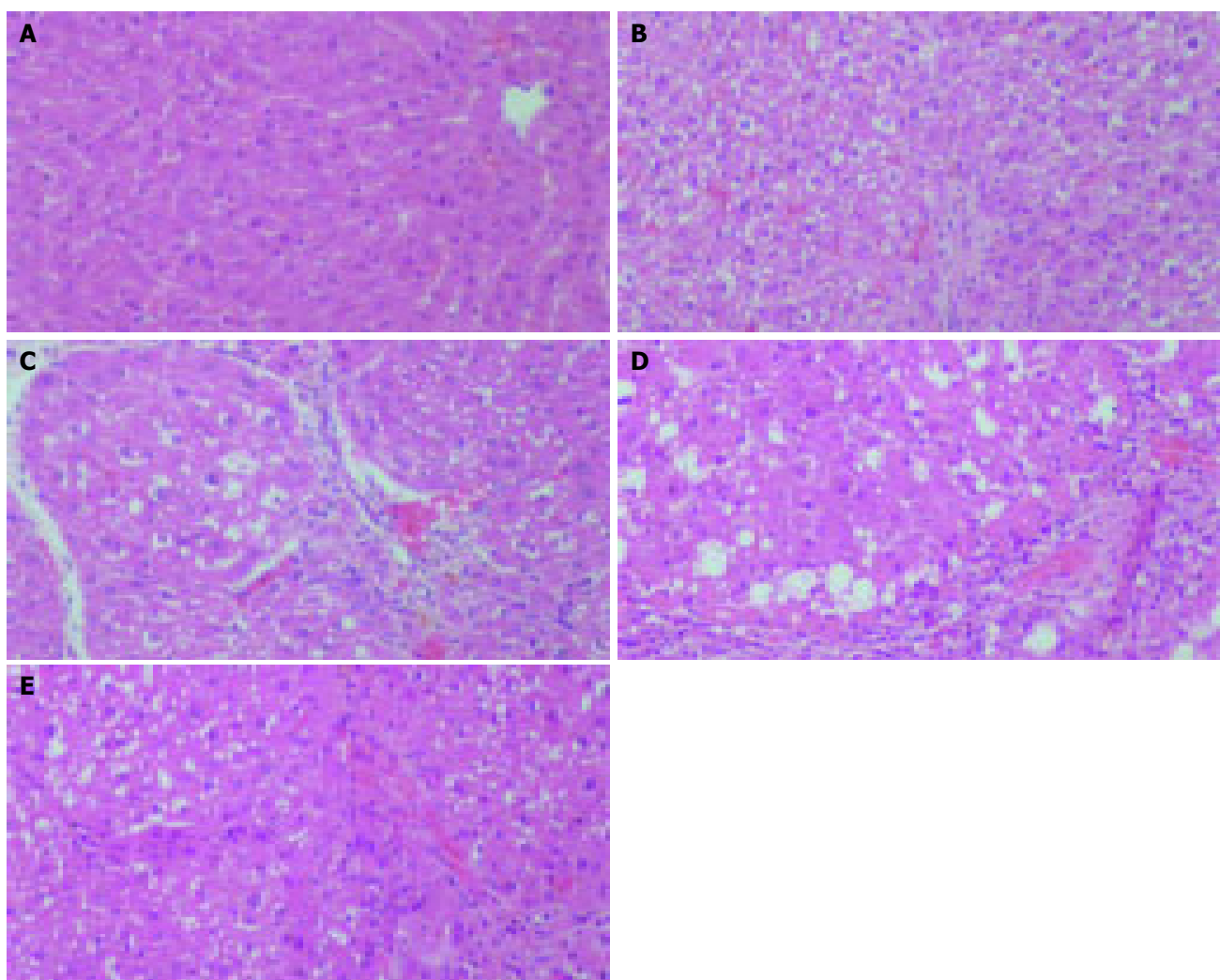


Figure 5 Improvement of CCl₄ induced experimental hepatic fibrosis by rAAV-INF- γ treatment in histology analysis. Rat liver section in each group stained

with Hematoxylin Eosin: **A:** No treatment; **B:** CCl₄ (3 wk); **C:** CCl₄/saline; **D:** CCl₄/rAAV-eGFP; **E:** CCl₄/rAAV-INF- γ . (Magnification 200 \times).

study, with one difference that mRNA expression of TGF- β were unchanged in three groups of rat liver (Figure 6B).

DISCUSSION

Liver fibrosis is reversible, whereas cirrhosis, the end stage consequence of fibrosis, is generally irreversible. Thus, efforts

to understand fibrosis may focus primarily on events that lead to the early accumulation of ECM in hopes of identifying therapeutic targets to slow its progression^[25,26]. Endogenous INF- γ is a lymphokine produced by natural killer cells and T lymphocytes, which plays a central role in the control of the immune response. It is also known for its regulatory effects on collagen synthesis. Tissue repair is characterized

Table 2 Serum markers of hepatic fibrosis and damage

	Number	Hydroxyproline ($\mu\text{g/g}$ wet liver)	AST (U/L)	ALT (U/L)
No treatment	6	96 \pm 11	76.3 \pm 6.3	53.0 \pm 6.9
CCl ₄ (3 wk)	6	162 \pm 14	561.2 \pm 81.4	358.0 \pm 85.4
CCl ₄ /Saline	8	236 \pm 31	1 019.1 \pm 276.3	770.5 \pm 154.3
CCl ₄ /rAAV-eGFP	8	249 \pm 37	985.4 \pm 241.6	727.2 \pm 175.0
CCl ₄ /rAAV-INF- γ	8	177 \pm 28 ¹	668.5 \pm 140.0 ²	458.4 \pm 123.5 ³

Hydroxyproline content and serum AST, ALT are shown with mean \pm SD for each group. There are no significant differences between group of CCl₄/saline and CCl₄/rAAV-eGFP in all three markers. The group of CCl₄/rAAV-INF- γ vs CCl₄/saline: ¹ $P = 0.0015$; ² $P = 0.0064$; ³ $P = 0.0032$.

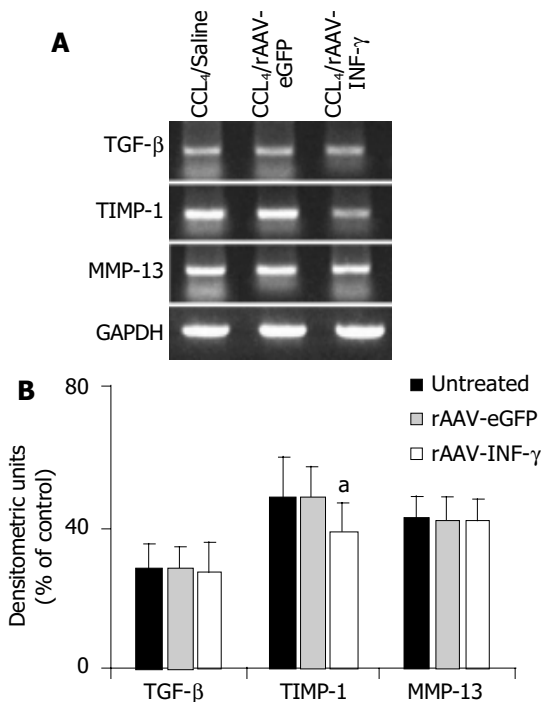


Figure 6 The mRNA expression of fibrosis related cytokines and proteases in different group of rat liver. **A:** mRNA expressions of TGF- β , MMP-13 and TIMP-1 in the rat liver were examined by RT-PCR method; **B:** Densitometric units were calculated by dividing the density of individual bands by that of GAPDH. Closed column, untreated. Lined column, rAAV-eGFP induced. Dotted column, rAAV-INF- γ induced. (Data are mean \pm SD, $n = 8$, ^a $P < 0.05$).

by infiltration of inflammatory, immune and mesenchymal cells in injured areas accompanied by release of cytokines, followed proliferation of mesenchymal cells involved in synthesis and deposition of collagen. The effects of INF- γ on collagen production have been the objects of a number of studies suggest that INF- γ acts as an endogenous mediator reducing collagen synthesis^[27,28].

In this study, rAAV-INF- γ could infect the primary cultured HSCs effectively. The expression of INF- γ reached the peak level, 1 211 \pm 178 pg/ml, at 60 h after infection with 5 \times 10⁴ v.g./cell rAAV-INF- γ . α -SMA expression and mRNA of TGF- β , TIMP-1 were down regulated with the expression of INF- γ , attenuated the HSCs activation and proliferation *in vitro*. Also, rAAV-INF- γ could inhibit the development of experimental hepatic fibrosis induced by CCl₄ administration *in vivo*, though it seemed hard to reverse it. The histology results revealed that hepatic fibrosis rats treated with rAAV-INF- γ showed light fibrosis compared with the control groups. In the rAAV-INF- γ induced group,

the hydroxyproline content and serum AST, ALT level were decreased to 177 \pm 28 $\mu\text{g/g}$ wet liver, 668.5 \pm 140.0, 458.4 \pm 123.5 U/L, compare with the fibrosis control group 236 \pm 31 $\mu\text{g/g}$ wet liver, 1 019.1 \pm 276.3, 770.5 \pm 154.3 U/L, respectively ($P < 0.01$). mRNA expression of TIMP-1 in the rAAV-INF- γ induced rat liver was decreased while no significant change was observed in TGF- β and MMP-13.

There is a difference between *in vitro* and *in vivo* study, expression of TGF- β mRNA was inhibited in HSCs infected with rAAV-INF- γ , but keeps unchanged in AAV-INF- γ treated rat liver compare with the control group. TGF- β is the important mediator involved in the transdifferentiation of HSCs from quiescent to activated phenotypes and biosynthesis of collagens type I, resulting in production of ECM^[29]. In liver, Kupffer cells are another main source of TGF- β besides HSCs. Since INF- γ could also activate macrophages including Kupffer cells, the total effect of INF- γ in liver does not change the mRNA expression of TGF- β ^[30]. Thus the protein production and receptor expression of TGF- β should be investigated to make a more elaborate description of the change about TGF- β modulated by INF- γ .

The majority of clinical use of INF- γ up to date has been conducted with subcutaneous route of purified recombinant INF- γ protein. The cost of standard INF- γ regimen is very expensive that limits its access to the patients. So gene therapy appears to be the more powerful strategy than other forms in gene therapy of hepatic fibrosis. Potential advantages of gene therapy are sustained expression of transgene and highly localized delivery within a single injection. The advantages of localized vector delivery are obvious because it can induce a high level of transgenic proteins *in situ* to achieve potential efficient activity and reduce adverse effects compared with systemic delivery. In recent studies, several gene delivery systems were reported for gene therapy targeting the liver disease. Adenoviruses are the vectors used most commonly for gene therapy, but its effective host immune response and the toxic/anaphylactic reaction limits its clinical use^[31-32]. Protzer *et al.*^[33], demonstrated that INF gene transfer by the hepatitis B virus vector efficiently suppressed wild-type virus infection, however the gene transfer efficiency in the liver is comparatively low. Compare with those two vectors, AAV vectors have little immunogenicity and far higher transfer efficiency. Furthermore, AAV vectors can mediate the long-term *in vivo* expression in host cells, with persistent expression up to 6 mo^[18,34,35]. Actually, the human clinical trials for cystic fibrosis and for hemophilia B have been enrolling patients

since 1996 and 1999, respectively, via recombinant AAV vectors. While comprehensive reviews exist of the current scope of clinical conditions for AAV vectors are being developed, it is likely that clinical trials involving delivery to the liver will commence in the near future^[15].

Taking all these results together, rAAV-INF- γ has potential effects for gene therapy of hepatic fibrosis. We believe that this system could now be applied in clinical trials, though we must continue to explore critical pre-clinical evaluation of risks in the age of clinical trials.

REFERENCES

- 1 Hui AY, Friedman SL. Molecular basis of hepatic fibrosis. *Expert Rev Mol Med* 2003; **2003**: 1-23
- 2 Alcolado R, Arthur MJ, Iredale JP. Pathogenesis of liver fibrosis. *Clin Sci* 1997; **92**: 103-112
- 3 Safadi R, Friedman SL. Hepatic fibrosis-role of hepatic stellate cell activation. *Med Gen Med* 2002; **4**: 27
- 4 Gressner AM. Cytokines and cellular crosstalk involved in the activation of fat-storing cells. *J Hepatol* 1995; **22**: 28-36
- 5 Friedman SL. Molecular mechanisms of hepatic fibrosis and principles of therapy. *J Gastroenterol* 1997; **32**: 424-430
- 6 McGuire RF, Bissell DM, Boyles J, Roll FJ. Role of extracellular matrix in regulating fenestrations of sinusoidal endothelial cells isolated from normal rat liver. *Hepatology* 1992; **15**: 989-997
- 7 Schuppan D, Ruehl M, Somasundaram R, Hahn EG. Matrix as modulator of stellate cell and hepatic fibrogenesis. *Semin Liver Dis* 2001; **21**: 351-372
- 8 Farrar MA, Schreiber RD. The molecular cell biology of interferon-gamma and its receptor. *Annu Rev Immunol* 1993; **11**: 571-611
- 9 Shen H, Zhang M, Minuk GY, Gong Y. Different effects of rat interferon alpha, beta and gamma on rat hepatic stellate cell proliferation and activation. *BMC Cell Biol* 2002; **3**: 9
- 10 Sakaida I, Uchida K, Matsumura Y, Okita K. Interferon gamma treatment prevents procollagen gene expression without affecting transforming growth factor-beta1 expression in pig serum-induced rat liver fibrosis *in vivo*. *J Hepatol* 1998; **28**: 471-479
- 11 Mallat A, Preaux AM, Blazejewski S, Rosenbaum J, Dhumeaux D, Mavier P. Interferon alfa and gamma inhibit proliferation and collagen synthesis of human Ito cells in culture. *Hepatology* 1995; **21**: 1003-1010
- 12 Thompson JA, Cox WW, Lindgren CG, Collins C, Neraas KA, Bonnem EM, Fefer A. Subcutaneous recombinant gamma interferon in cancer patients: toxicity, pharmacokinetics, and immunomodulatory effects. *Cancer Immunol Mmunother* 1987; **25**: 47-53
- 13 Baroni GS, D'Ambrosio L, Curto P, Casini A, Mancini R, Jezequel AM, Benedetti A. Interferon gamma decreases hepatic stellate cell activation and extracellular matrix deposition in rat liver fibrosis. *Hepatology* 1996; **23**: 1189-1199
- 14 Monahan PE, Samulski RJ. Adeno-associated virus vectors for gene therapy: more pros than cons? *Mol Med Today* 2000; **6**: 433-440
- 15 Monahan PE, Samulski RJ. AAV vectors: is clinical success on the horizon? *Gene Ther* 2000; **7**: 24-30
- 16 During MJ, Symes CW, Lawlor PA, Lin J, Dunning J, Fitzsimons HL, Poulsen D, Leone P, Xu R, Dicker BL, Lipski J, Young D. An oral vaccine against NMDAR1 with efficacy in experimental stroke and epilepsy. *Science* 2000; **287**: 1453-1460
- 17 Cao L, Liu Y, During MJ, Xiao W. High-titer, wild-type free recombinant adeno-associated virus vector production using intron-containing helper plasmids. *J Virol* 2000; **74**: 11456-11463
- 18 Xu R, Sun X, Tse LY, Li H, Chan PC, Xu S, Xiao W, Kung HF, Krissansen GW, Fan ST. Long-term expression of angiostatin suppresses metastatic liver cancer in mice. *Hepatology* 2003; **37**: 1451-1460
- 19 Riccalton-Banks L, Bhandari R, Fry J, Shakesheff KM. A simple method for the simultaneous isolation of stellate cells and hepatocytes from rat liver tissue. *Mol Cell Biochem* 2003; **248**: 97-102
- 20 Friedman SL, Rockey DC, McGuire RF, Maher JJ, Boyles JK, Yamasaki G. Isolated hepatic lipocytes and Kupffer cells from normal human liver: morphological and functional characteristics in primary culture. *Hepatology* 1992; **15**: 234-243
- 21 Chomczynski P, Sacchi N. Single-step method of RNA isolation by acid guanidinium thiocyanate-phenol-chloroform extraction. *Anal Biochem* 1987; **162**: 156-159
- 22 Proctor E, Chatamra K. High yield micronodular cirrhosis in the rat. *Gastroenterology* 1982; **83**: 1183-1190
- 23 Rockey DC, Boyles JK, Gabbiani G, Friedman SL. Rat hepatic lipocytes express smooth muscle actin upon activation *in vivo* and in culture. *J Submicrosc Cytol Pahol* 1992; **24**: 193-203
- 24 Sakaida I, Hironaka K, Uchida K, Suzuki C, Kayano K, Okita K. Fibrosis accelerates the development of enzyme-altered lesions in the rat liver. *Hepatology* 1998; **28**: 1247-1252
- 25 Benyon RC, Iredale JP. Is liver fibrosis reversible? *Gut* 2000; **46**: 443-446
- 26 Friedman SL. The Cellular Basis of Hepatic Fibrosis. Mechanisms and Treatment Strategies. *N Engl J Med* 1993; **328**: 1828-1835
- 27 Czaja MJ, Weiner FR, Eghbali M, Giambone MA, Zern MA. Differential effects of gamma-interferon on collagen and fibronectin gene expression. *J Biol Chem* 1987; **262**: 13348-13351
- 28 Rockey DC, Maher JJ, Jarnagin WR, Gabbiani G, Friedman SL. Inhibition of rat hepatic lipocytes activation in culture by interferon-gamma. *Hepatology* 1992; **16**: 776-784
- 29 Friedman SL. Cytokines and fibrogenesis. *Semin Liver Dis* 1999; **19**: 129-140
- 30 Tiggelman AM, Boers W, Linthorst C, Sala M, Chamuleau RA. Collagen synthesis by human liver (myo)fibroblasts in culture: evidence for a regulatory role of IL-1 beta, IL-4, TGF beta and IFN gamma. *J Hepatol* 1995; **23**: 307-317
- 31 Suzuki K, Aoki K, Ohnami S, Yoshida K, Kazui T, Kato N, Inoue K, Kohara M, Yoshida T. Adenovirus-mediated gene transfer of interferon alpha improves dimethylnitrosamine-induced liver cirrhosis in rat model. *Gene Ther* 2003; **10**: 765-773
- 32 Abriss B, Hollweg G, Gressner AM, Weiskirchen R. Adenoviral-mediated transfer of p53 or retinoblastoma protein blocks cell proliferation and induces apoptosis in culture-activated hepatic stellate cells. *J Hepatol* 2003; **38**: 169-178
- 33 Protzer U, Nassal M, Chiang PW, Kirschfink M, Schaller H. Interferon gene transfer by a hepatitis B virus vector efficiently suppresses wild-type virus infection. *Proc Natl Acad Sci USA* 1999; **96**: 10818-10823
- 34 Ferry N, Heard JM. Liver-directed gene transfer vectors. *Hum Gene Ther* 1998; **9**: 1975-1981
- 35 de Roos WK, Fallaux FJ, Marinelli AW, Lazaris-Karatzas A, von Geusau AB, van der Eb MM, Cramer SJ, Terpstra OT, Hoeben RC. Isolated-organ perfusion for local gene delivery: efficient adenovirus-mediated gene transfer into the liver. *Gene Ther* 1997; **4**: 55-62

• CLINICAL RESEARCH •

Lansoprazole prevents experimental gastric injury induced by non-steroidal anti-inflammatory drugs through a reduction of mucosal oxidative damage

Corrado Blandizzi, Matteo Fornai, Rocchina Colucci, Gianfranco Natale, Valter Lubrano, Cristina Vassalle, Luca Antonioli, Gloria Lazzeri, Mario Del Tacca

Corrado Blandizzi, Matteo Fornai, Rocchina Colucci, Mario Del Tacca, Division of Pharmacology and Chemotherapy, Department of Oncology, Transplants and Advanced Technologies in Medicine, University of Pisa, Pisa, Italy

Gianfranco Natale, Gloria Lazzeri, Department of Human Morphology and Applied Biology University of Pisa, Pisa, Italy
Valter Lubrano, Cristina Vassalle, Luca Antonioli, Institute of Clinical Physiology, National Research Council, Pisa, Italy

Correspondence to: Professor Mario Del Tacca, MD, Division of Pharmacology and Chemotherapy, Department of Oncology, Transplants and Advanced Technologies in Medicine University of Pisa, Via Roma, 55- I-56126 Pisa, Italy. m.deltacca@med.unipi.it
Telephone: +39-50-830148 Fax: +39-50-562020

Received: 2004-07-17 Accepted: 2004-11-04

Abstract

AIM: This study investigated the mechanisms of protection afforded by the proton pump inhibitor lansoprazole against gastric injury induced by different non-steroidal anti-inflammatory drugs (NSAIDs) in rats.

METHODS: Male Sprague-Dawley rats were orally treated with indomethacin (100 µmol/kg), diclofenac (60 µmol/kg), piroxicam (150 µmol/kg) or ketoprofen (150 µmol/kg). Thirty minutes before NSAIDs, animals were orally treated with lansoprazole 18 or 90 µmol/kg. Four hours after the end of treatments, the following parameters were assessed: gastric mucosal PGE₂, malondialdehyde (MDA), myeloperoxidase (MPO) or non-proteinic sulfhydryl compounds (GSH) levels; reverse transcription-polymerase chain reaction (RT-PCR) of mucosal COX-2 mRNA; gastric acid secretion in pylorus-ligated animals; *in vitro* effects of lansoprazole (1-300 µmol/L) on the oxidation of low density lipoproteins (LDLs) induced by copper sulphate.

RESULTS: All NSAIDs elicited mucosal necrotic lesions which were associated with neutrophil infiltration and reduction of PGE₂ levels. Increments of MPO and MDA contents, as well as a decrease in GSH levels were detected in the gastric mucosa of indomethacin- or piroxicam-treated animals. Indomethacin enhanced mucosal cyclooxygenase-2 expression, while not affecting cyclooxygenase-1. At the oral dose of 18 µmol/kg lansoprazole partly counteracted diclofenac-induced mucosal damage, whereas at 90 µmol/kg it markedly prevented injuries evoked by all test NSAIDs. Lansoprazole at 90 µmol/kg reversed also the effects of NSAIDs on

MPO, MDA and GSH mucosal contents, without interfering with the decrease in PGE₂ levels or indomethacin-induced cyclooxygenase-2 expression. However, both lansoprazole doses markedly inhibited acid secretion in pylorus-ligated rats. Lansoprazole concentration-dependently reduced the oxidation of LDLs *in vitro*.

CONCLUSION: These results suggest that, besides the inhibition of acid secretion, lansoprazole protection against NSAID-induced gastric damage depends on a reduction in mucosal oxidative injury, which is also responsible for an increment of sulfhydryl radical bioavailability. It is also suggested that lansoprazole does not influence the down-regulation of gastric prostaglandin production associated with NSAID treatment.

© 2005 The WJG Press and Elsevier Inc. All rights reserved.

Key words: Lansoprazole; Gastric injury; Non-steroidal anti-inflammatory drugs

Blandizzi C, Fornai M, Colucci R, Natale G, Lubrano V, Vassalle C, Antonioli L, Lazzeri G, Tacca MD. Lansoprazole prevents experimental gastric injury induced by non-steroidal anti-inflammatory drugs through a reduction of mucosal oxidative damage. *World J Gastroenterol* 2005; 11(26): 4052-4060
<http://www.wjgnet.com/1007-9327/11/4052.asp>

INTRODUCTION

Non-steroidal anti-inflammatory drugs (NSAIDs) are among the most commonly prescribed drugs due to their high efficacy in the treatment of pain, fever and inflammation. However, the use of these drugs is associated with the occurrence of adverse digestive effects, consisting most notably of gastric erosions, ulceration, bleeding and perforation^[1]. It is widely accepted that both the beneficial and detrimental effects of NSAIDs are attributable to their ability to inhibit prostaglandin synthesis through a direct blockade of cyclooxygenase (COX)^[2]. In particular, the sequelae of suppressed prostaglandin production, which may contribute to the pathogenesis of gastroduodenal ulceration, include a decrease in mucus synthesis and secretion of mucus, an inhibition of bicarbonate secretion, a reduction of mucosal blood flow, an alteration of microvascular structure and an increase in acid and pepsinogen secretion^[1,3].

The pathogenesis of NSAID-induced gastrointestinal

damage may also depend on prostaglandin-independent mechanisms, such as uncoupling of oxidative phosphorylation, alterations of mucosal cell turnover as well as neutrophil activation followed by enhanced endothelial adhesion^{1,4}. These mechanisms, in combination with those related to prostaglandin suppression, lead to microvessel occlusion and subsequent hyperproduction of reactive oxygen metabolites. Such substances are then able to induce oxidative tissue injury which seems to play a prominent role in the development of mucosal ulceration caused by NSAIDs^{3,5}.

The impairment of mucosal defence allows gastric acid to cause injury. Therefore, gastric acid is regarded as a pivotal step in the pathogenesis of gastroduodenal ulceration, and acid suppression is viewed as a main option in the treatment of NSAID-induced mucosal damage⁶. For these reasons, proton pump inhibitors (PPIs), including lansoprazole and other related compounds, have been investigated in clinical studies in patients under treatment with NSAIDs, and proven to be effective in both prevention and healing of NSAID-induced gastric lesions⁷. Indeed, PPIs can markedly reduce gastric acidity through the blockade of H⁺, K⁺-ATPase, the enzyme responsible for the final step in the secretion of hydrochloric acid by parietal cells⁸. However, there is also evidence to suggest that these drugs can activate gastric protective mechanisms independent of acid reduction^{9,10}. For instance, in previous studies omeprazole and lansoprazole prevented gastric injury elicited by acidified ethanol or hemorrhagic shock through an enhancement of mucosal defence⁹.

At present, a large variety of endogenous factors, including prostaglandins, growth factors, digestive hormones, sensory peptides, nitric oxide, and sulfhydryl compounds, has been implicated in the mechanisms through which gastric mucosa counteracts ulcerative stimuli¹¹, and some of these factors have been proposed to account for the gastroprotective effects of PPIs^{9,10}. Nevertheless, the possible contribution of acid-independent mechanisms to the protective effects of these drugs against NSAID-induced gastric injury remains to be clarified. Overall, the present study was designed to: (1) examine the influence of lansoprazole on gastric mucosal damage induced by different NSAIDs; (2) evaluate to what extent factors and mechanisms related to gastric mucosal defence are involved in the protective actions of lansoprazole; (3) assess whether lansoprazole is endowed with direct antioxidant properties.

MATERIALS AND METHODS

Animals and experimental design

Albino male Wistar rats, with 200–220 g body weight, were used throughout the study. They were fed standard laboratory chow and tap water *ad libitum* and were not used for at least one week after their delivery to the laboratory. The animals were housed, four in a cage, in temperature-controlled rooms on a 12-h light cycle at 22–24 °C and 50–60% relative humidity. They were deprived of food 24 h before the experiment. However, free access to water *ad libitum* was allowed until 1 h before the beginning of experiments. Experiments were performed in accordance with the provisions of the European Community (EC)

Council Directive 86-609, recognized and adopted by the Italian Government.

In experiments on gastroprotection, lansoprazole (18 or 90 µmol/kg) or its vehicle was administered by intragastric gavage. The following NSAIDs, which are associated with moderate to high levels of risk for gastric injury in clinical settings⁴, were then administered by intragastric gavage at doses known to induce gastric lesions in rats: indomethacin (100 µmol/kg¹²), diclofenac (60 µmol/kg¹³), piroxicam (150 µmol/kg¹⁴), and ketoprofen (150 µmol/kg¹⁵). In all cases, a 30 min interval was allowed between lansoprazole and NSAID administration. Four hours after treatment with NSAIDs, the animals were sacrificed by cervical dislocation, their stomachs were rapidly removed and processed for the evaluation of the following parameters: (1) histomorphometric analysis of gastric mucosal damage; (2) quantitative estimation of mucosal inflammatory activity; (3) assay of malondialdehyde (MDA), non-proteinic sulfhydryl compounds and prostaglandin E₂ (PGE₂) in the mucosal layer; (4) assessment of mucosal expression of COX isoforms (COX-1, COX-2).

In an additional set of experiments, the effects of lansoprazole (18 or 90 µmol/kg) or its vehicle were assayed on gastric acid secretion in rats subjected to pylorus ligation. Dose levels of lansoprazole were selected on the basis of previous studies in rat models of gastric injury, showing that this PPI exerted maximal protective actions at 90 µmol/kg⁹.

Animals subjected to NSAID-induced gastric mucosal damage

Histomorphometric evaluation of gastric mucosal damage The histomorphometric estimation of gastric mucosal damage was carried out as previously described¹⁶. Briefly, the stomach was opened along the greater curvature, gently washed with saline (154 mmol/L NaCl), pinned upon a cork plate with the mucosal surface turned upwards, and fixed in 10% formalin buffered with phosphate for 24 h at 4 °C. Each stomach was dissected in parallel strips perpendicular to the lesser curvature at a distance of 2 mm. The strips from each stomach were sequentially placed on a glass slide and oriented with the side of each strip distal to the pylorus upwards. A solution of melted 3% agar was gently poured on the strips and quickly cooled at 4 °C to induce solidification. The agar block was then removed from the glass slide, dehydrated, and embedded in paraffin wax. Three micrometers thick paraffin sections were cut using a microtome and stained with hematoxylin and eosin. Sections were examined by light microscopy and the length of both total and damaged mucosa was evaluated by means of a micrometric scale. The lesion index was estimated as the length fraction of damaged mucosa over the total length of mucosa, and expressed in percentage values.

Determination of mucosal myeloperoxidase content

Myeloperoxidase (MPO) was assayed as previously reported by Pacheco *et al.*¹⁷, and assumed as a quantitative index to estimate the degree of mucosal infiltration by polymorphonuclear cells elicited by treatment with test NSAIDs. Briefly, specimens of mucosa were rapidly scraped from the underlying tissue layers of gastric wall using two glass slides kept cold on ice. Mucosal samples (300 mg) were homogenized 3 times (30 s each) at 4 °C with a polytron homogenizer (Cole Parmer Homogenizer, Vernon Hills,

IL, USA) in 1 mL of ice-cold 50 mmol/L phosphate buffer (pH 6.0) containing 0.5% of hexadecyltrimethylammonium bromide to prevent the pseudoperoxidase activity of hemoglobin as well as to solubilize membrane-bound MPO. The homogenate was sonicated for 10 s, frozen-thawed 3 times and spun by centrifugation for 20 min at 18 000 *g*. The supernatant was then recovered and used for determination of MPO concentration by means of enzyme-linked immunosorbent assay (ELISA) (Bioxytech, Oxis International Inc., Portland, OR, USA). All samples were assayed within 2 d after collection. The results were expressed as ng of MPO per 100 mg of gastric mucosa.

Quantitative evaluation of mucosal oxidative damage
MDA concentrations in samples of gastric mucosa were determined to obtain quantitative estimations of membrane lipid peroxidation evoked by test NSAIDs. For this purpose, specimens of mucosa were scraped from the underlying tissue layers of gastric wall using two glass slides kept cold on ice. The mucosa was weighed, minced by forceps, homogenized in 2 mL of cold buffer (Tris-HCl 20 mmol/L, pH 7.4) using a polytron homogenizer (Cole Parmer Homogenizer), and spun by centrifugation at 1 500 *g* for 10 min at 4 °C. Aliquots of supernatants were then used for subsequent assay procedures. Mucosal MDA concentrations were estimated by colorimetric assay (Calbiochem-Novabiochem Corporation, San Diego, CA, USA), and the results were expressed as nmol of MDA per milligram of gastric mucosa.

Assay of sulfhydryl compounds in gastric mucosa The concentrations of reduced glutathione (GSH) in specimens of gastric mucosa were determined to estimate the tissue content of non-proteic sulfhydryl compounds^[18]. For this purpose, samples of mucosa were scraped from the underlying layers of gastric wall using two glass slides kept cold on ice. The scraped mucosa was weighed, minced by forceps, homogenized in 2 mL of cold buffer [0.4 mol/L 2-(*N*-morpholino)-ethanesulfonic acid, 0.1 mol/L phosphate, and 2 mmol/L ethylenediaminetetraacetic acid (EDTA), pH 6] using a polytron homogenizer (Cole Parmer Homogenizer), and spun by centrifugation at 10 000 *r/min* for 15 min at 4 °C. Aliquots of supernatants were deproteinated by a solution containing 1.25 mol/L metaphosphoric acid and 4 mol/L triethanolamine, to avoid interferences due to particulate components or proteic sulfhydryl groups, and then used for the subsequent assay procedures. Gastric mucosal levels of GSH were determined by enzyme colorimetric assay (Cayman Chemicals, Ann Arbor, MI, USA), and the results were expressed as nmol of GSH per milligram of gastric mucosa.

Assay of PGE2 in gastric mucosa

Enzyme immunoassay of PGE2 in gastric mucosa was performed by means of a commercial kit (Cayman Chemical Company, Ann Arbor, MI, USA). Briefly, specimens of mucosa were rapidly scraped from the underlying tissue layers of gastric wall using two glass slides kept cold on ice. The mucosa was weighed, minced by forceps, and homogenized in 1 mL of cold phosphate buffer (PBS 0.1 mol/L, pH 7.4, containing 1 mmol/L EDTA and 10 µmol/L indomethacin) per gram of tissue using a polytron

homogenizer (Cole Parmer Homogenizer, Vernon Hills, IL, USA). The resulting homogenate was added with an equal volume of absolute ethanol, and stirred with vortex. After 5-min incubation at room temperature, the homogenate was spun by centrifugation at 1 500 *r/min* for 10 min at 4 °C. The supernatant was added with 1 mol/L HCl until pH 4. Before the assay, samples were subjected to purification by means of superclean LC-18 SPE columns (Sigma Co., St. Louis, MO, USA). For this purpose, 0.5 mL of sample was added to 2 mL of ethanol and vortexed. After incubation at room temperature for 5 min, the sample was spun by centrifugation at 3 000 *r/min* for 10 min. The supernatant was then removed and applied to the LC-18 SPE column which was previously activated with 5 mL of methanol and then with 5 mL of ultrapure water. The column was subsequently washed with 5 mL of ultrapure water and 5 mL of hexane. PGE2 was then eluted with 5 mL of ethyl acetate containing 1% methanol. The eluted ethyl acetate fractions were collected and evaporated to dryness with nitrogen. Aliquots were then used for subsequent enzyme immunoassay. PGE2 concentration was expressed as nanogram per gram of mucosal tissue.

Western blot assay of COX-1 and COX-2 in gastric mucosa

Specimens of mucosa were scraped from the underlying tissue layers of gastric wall using two glass slides kept cold on ice. Mucosal samples were weighed and homogenized in lysis buffer containing: HEPES 10 mmol/L, NaCl 30 mmol/L, EDTA 0.2 mmol/L, phenylmethylsulphonyl fluoride 2 mmol/L, leupeptin 10 µg/mL, aprotinin 10 µg/mL, sodium fluoride 1 mmol/L, sodium orthovanadate 1 mmol/L, glycerol 2%, MgCl₂ 0.3 mmol/L, and Triton-X 100 1%, using the polytron homogenizer. Mucosal homogenates were spun by centrifugation at 20 000 *g* for 15 min at 4 °C, and the resulting supernatants were then separated from pellets and stored at -80 °C. Protein concentration was determined in each sample by the Bradford method (Protein Assay kit, Bio-Rad, Hercules, CA, USA). To perform Western blot analysis of COX-1 and COX-2, equivalent amounts of protein lysates (50 µg) were separated by electrophoresis on sodium dodecylsulfate polyacrylamide gel (8%) and transferred onto a nitrocellulose membrane. The blots were then blocked overnight with 5% non-fat dried milk in phosphate buffered saline, and incubated overnight at room temperature with goat polyclonal antiserum raised against rat COX-1 or COX-2 (dilution 1:1 000). After repeated washings with 0.1% Tween-20 in Tris-buffered saline, a peroxidase-conjugated rabbit anti-goat antibody (dilution 1:10 000) was added for 1 h at room temperature. After repeated washings with 0.1% Tween-20 in Tris-buffered saline, the immunoreactive bands were visualized by enhanced chemiluminescence (ECL, Amersham Biosciences Europe GmbH, Cologno Monzese, Italy). The relative expression of COX-1 or COX-2 was quantified by densitometric analysis with NIH Image computer program (Scion Corporation, USA).

Animals subjected to pylorus ligation

Pylorus ligation was carried out as previously described^[19]. Briefly, during a short anesthesia with diethyl ether, the

abdomen was opened by a midline laparotomy and the duodenum was exteriorized. Then, lansoprazole (18 or 90 $\mu\text{mol/kg}$) or its vehicle was directly injected into the distal portion of duodenum by means of a 25-gauge needle, the pylorus was ligated, the abdominal incision was closed with clips, and the animals were allowed to recover from anesthesia for 10 min. Two hours after pylorus ligation, the esophageal-gastric junction was ligated, and the whole stomach was excised. The gastric content was emptied, carefully collected in graduated centrifuge tubes, and spun by centrifugation at 3 000 r/min for 10 min. Samples with more than 0.5 mL of sediment were discarded. The level of acidity was measured by automatic potentiometric titration to pH 7.0 with 0.01 mol/L NaOH, using an Autotitrator pH Meter PHM82 (Radiometer, Copenhagen, Denmark), and evaluated as H^+ output. The effect of lansoprazole was expressed as $\mu\text{EqH}^+ / 2 \text{ h}$.

In vitro assay of antioxidant activity of lansoprazole

To evaluate whether lansoprazole is endowed with direct antioxidant properties, the drug was incubated in a reaction mixture where human native low density lipoproteins (LDLs) were subjected to oxidation upon exposure to CuSO_4 at 37 °C for 120 min, in accordance with a standardized method^[20]. Lansoprazole was assayed at concentrations ranging from 1 to 300 $\mu\text{mol/L}$. The reaction mixture consisted of 2 mL of a phosphate buffer (10 mmol/L $\text{KH}_2\text{PO}_4/\text{K}_2\text{HPO}_4$, pH 5.3) containing LDLs 150 $\mu\text{g/mL}$ and CuSO_4 1 $\mu\text{mol/L}$. At the end of incubation, the oxidative reaction was stopped by addition of butyldihydroxytoluene 0.5 mol/L in acetonitrile, and the extent of LDL oxidation was estimated by measurement of 8-iso-prostaglandin $\text{F}_2\alpha$ (8-iso-PGF 2α) concentrations. For this purpose, 100- μL aliquots of the reaction mixture were used to assay 8-iso-PGF 2α by means of a commercial kit for competitive enzyme-linked immunoassay (Cayman Chemicals, Ann Arbor, MI, USA). The results were expressed as pg of 8-iso-PGF 2α per mL.

Statistical analysis

The results are given as mean \pm SE. The statistical significance of data was evaluated by one-way analysis of variance (ANOVA) followed by *post hoc* analysis by Student-Newman-Keuls test, and *P* values lower than 0.05 were considered significant; "n" indicates the number of experiments. All statistical procedures were performed by personal computer programs. **Drugs** The following drugs and reagents were used: indomethacin, ketoprofen, diclofenac, piroxicam, human native low density lipoproteins, butyldihydroxytoluene, HEPES, EDTA, phenylmethylsulphonyl fluoride, leupeptin, aprotinin, sodium orthovanadate, glycerol, Triton-X, Tween-20, sodium dodecylsulfate, hexadecyltrimethylammonium bromide (Sigma Chemicals Co., St. Louis, MO, USA); lansoprazole (kindly provided by Takeda Italia Farmaceutici, Rome, Italy); diethyl ether (Mallinckrodt Baker BV, Deventer, The Netherlands); polyacrylamide (Bio-Rad, Hercules, CA, USA); goat anti-rat COX-1 and COX-2 antibodies, peroxidase-conjugated rabbit anti-goat antibody (Santa Cruz Biotechnology Inc., Santa Cruz, CA, USA). Other reagents were of analytical grade. Lansoprazole and

test NSAIDs were suspended in 1% methocel and administered in a volume of 0.5 mL.

RESULTS

Animals subjected to NSAID-induced gastric mucosal damage

Effects of lansoprazole on gastric mucosal damage induced by NSAIDs Intra-gastric administration of test NSAIDs caused various degrees of macroscopically evident mucosal damage (not shown). Histological examination of gastric sections showed that treatment with test NSAIDs elicited necrotic mucosal lesions associated with widespread areas of infiltration by polymorphonuclear cells in the upper part of the submucosal layer and the lower part of mucosa (Figure 1). Histomorphometric analysis of gastric tissue revealed negligible lesions of surface epithelium in control animals, as well as those receiving lansoprazole alone, with a total damage accounting for (0.27 \pm 0.12)% (control), (0.18 \pm 0.11)% (lansoprazole 18 $\mu\text{mol/kg}$) and (0.09 \pm 0.03)% (lansoprazole 90 $\mu\text{mol/kg}$). By contrast, in animals treated with indomethacin, diclofenac, piroxicam or ketoprofen, histomorphometry displayed a necrotic damage affecting (6.38 \pm 0.32)%, (4.48 \pm 0.26)%, (6.43 \pm 0.54)%, and (5.62 \pm 0.39)% of gastric mucosa, respectively (Figure 2). Under these conditions, pretreatment with lansoprazole (90 $\mu\text{mol/kg}$) caused marked reductions of NSAID-induced gastric mucosal injury (Figure 2), which was associated with a concomitant decrease in the degree of infiltration by polymorphonuclear cells (Figure 1). When assayed at the dose of 18 $\mu\text{mol/kg}$, lansoprazole exerted a slight influence on NSAID-induced mucosal damage, achieving a level of statistical significance only in animals exposed to diclofenac (Figure 2).

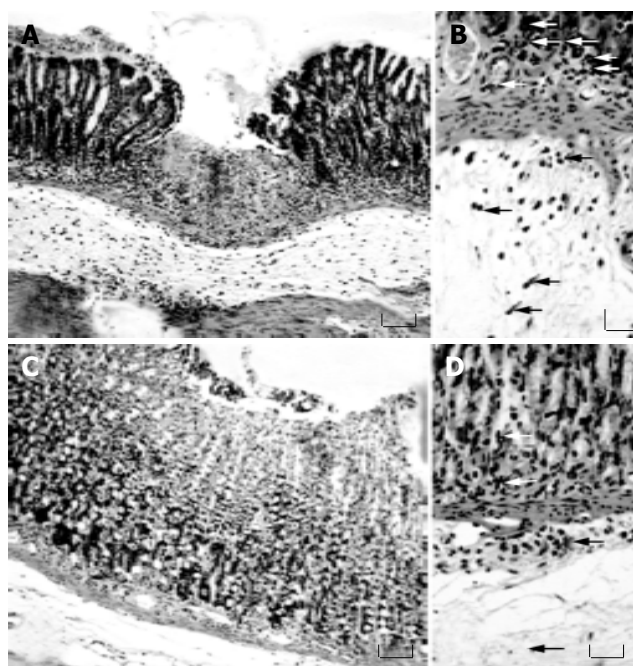


Figure 1 H&E-stained sections of rat gastric mucosa. A, treatment with indomethacin 100 $\mu\text{mol/kg}$; A: severe lesion with necrosis of gastric mucosa; B: several polymorphonuclear cells can be detected (arrows); C and D: Rats treated with lansoprazole 90 $\mu\text{mol/kg}$ plus indomethacin 100 $\mu\text{mol/kg}$; C: less severe lesion with lysis of mucosal cells; D: few polymorphonuclear cells can be evidenced (arrows). A and C: original magnification 100; bar = 150 μm . B and D: original magnification 170 x; bar = 60 μm .

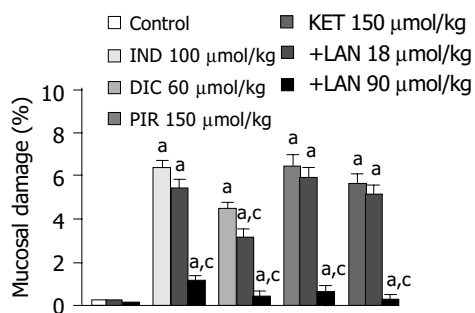


Figure 2 Histomorphometric evaluation of gastric mucosal damage in rats subjected to intragastric administration of indomethacin (IND, 100 $\mu\text{mol/kg}$), diclofenac (DIC, 60 $\mu\text{mol/kg}$), piroxicam (PIR, 150 $\mu\text{mol/kg}$) or ketoprofen (KET, 150 $\mu\text{mol/kg}$) either alone or in the presence of lansoprazole (LAN, 18 and 90 $\mu\text{mol/kg}$). Each column indicates the mean value obtained from 6-8 animals \pm SE (vertical lines). ^a $P < 0.05$ vs control values; ^c $P < 0.05$ between the respective values obtained in animals treated with a test NSAID alone.

Assay of MPO, MDA, and GSH in gastric mucosa

MPO levels in the gastric mucosa of control animals were 3.57 ± 0.78 ng/100 mg, and this value was not significantly affected by treatment with lansoprazole alone (90 $\mu\text{mol/kg}$). In this set of experiments, indomethacin, and piroxicam induced marked increments of mucosal MPO concentrations (+116.8% and +131.1%, respectively), which no longer occurred after pretreatment of animals with lansoprazole (Figure 3A).

MDA levels in the gastric mucosa of control rats were 5.6 ± 1.4 nmol/mg tissue. Lansoprazole alone (90 $\mu\text{mol/kg}$) did not influence basal MDA concentrations. Treatment with indomethacin or piroxicam caused a significant increase in mucosal MDA concentrations (+148.2% and +112.5%, respectively), and pretreatment with lansoprazole significantly prevented the tissue accumulation of MDA promoted by test NSAIDs (Figure 3B).

In control animals, mucosal GSH levels reached 0.064 ± 0.006 nmol/mg. Under these conditions, lansoprazole alone (90 $\mu\text{mol/kg}$) did not significantly affect the mucosal concentration of endogenous sulfhydryl compounds. Treatment with indomethacin or piroxicam elicited a significant reduction of mucosal GSH levels (-70.3% and -79.7%, respectively). However, the decrease in gastric GSH concentration caused

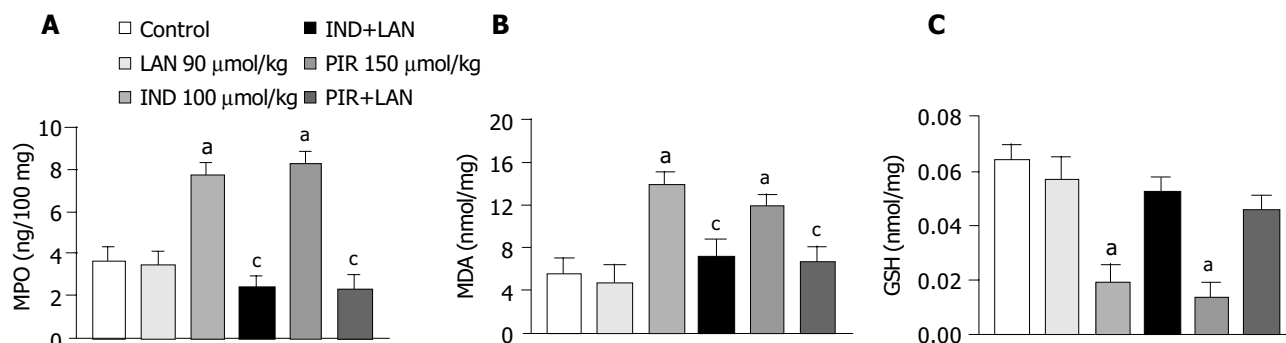


Figure 3 MPO (A), MDA (B) and GSH (C) levels in the gastric mucosa of rats treated with indomethacin (IND, 100 $\mu\text{mol/kg}$) or piroxicam (PIR, 150 $\mu\text{mol/kg}$), either alone or in the presence of lansoprazole (LAN, 90 $\mu\text{mol/kg}$). Each column

by test NSAIDs no longer occurred upon pretreatment of animals with lansoprazole (Figure 3C).

Assay of PGE₂ in gastric mucosa

Basal PGE₂ levels in the gastric mucosa of control animals accounted for 151.9 ± 13.3 ng/g, this value being not significantly affected by administration of lansoprazole alone (90 $\mu\text{mol/kg}$). All test NSAIDs caused a significant reduction in mucosal PGE₂ levels. Marked inhibitory effects were observed in animals treated with indomethacin, piroxicam and ketoprofen (-74.8%, -79% and -86.6%, respectively), whereas a moderate inhibitory action could be detected in diclofenac-treated rats (-48.4%). Pretreatment with lansoprazole did not significantly interfere with the inhibitory actions of test NSAIDs on mucosal PGE₂ production (Figure 4).

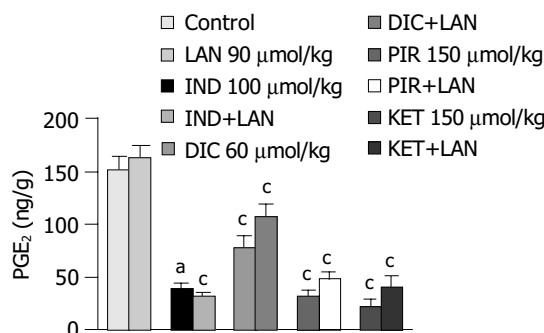


Figure 4 PGE₂ levels in the gastric mucosa of rats treated with indomethacin (IND, 100 $\mu\text{mol/kg}$), diclofenac (DIC, 60 $\mu\text{mol/kg}$), piroxicam (PIR, 150 $\mu\text{mol/kg}$) or ketoprofen (KET, 150 $\mu\text{mol/kg}$), either alone or in the presence of lansoprazole (LAN, 90 $\mu\text{mol/kg}$). Each column represents the mean value obtained from 6 to 8 animals \pm SE (vertical lines). ^a $P < 0.05$ vs control values; ^c $P < 0.05$ between the respective values obtained in animals treated with a test NSAID alone.

Western blot assay of COX-1 and COX-2 in gastric mucosa

The protein expression of COX isoforms was evaluated by Western blot analysis of gastric mucosal samples obtained from animals subjected to vehicle, indomethacin, lansoprazole or lansoprazole plus indomethacin administration. Western blot assay revealed the expression of both COX-1 and COX-2 in the gastric mucosa of control animals as well as in

represents the mean value obtained from 7 to 10 animals \pm SE. ^a $P < 0.05$ vs control values; ^c $P < 0.05$ between the respective values obtained in animals treated with indomethacin or piroxicam alone.

rats treated with lansoprazole alone (90 $\mu\text{mol/kg}$) (Figure 5). The densitometric analysis of immunoreactive bands showed that the relative expression of COX-1 or COX-2, in the presence of lansoprazole, did not differ significantly from that estimated in control animals. Treatment with indomethacin was followed by a marked enhancement of COX-2, but not COX-1, expression in the gastric mucosa. A similar effect was exerted by indomethacin upon pretreatment of animals with lansoprazole (Figure 5).

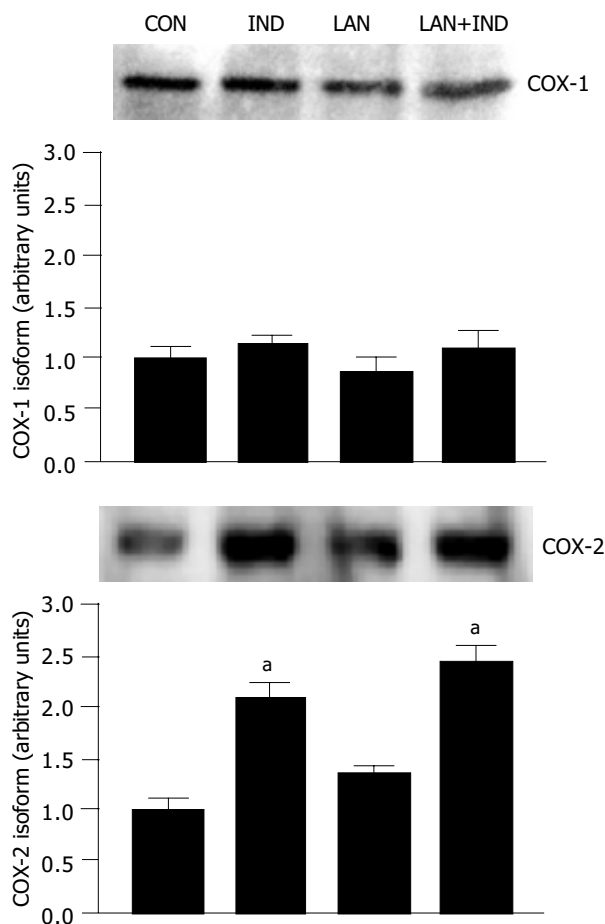


Figure 5 Western blot analysis of COX-1 and COX-2 protein expression in gastric mucosal lysates obtained from animals treated with indomethacin (IND), lansoprazole (LAN, 90 $\mu\text{mol/kg}$) or lansoprazole plus indomethacin (LAN+IND). ^a $P < 0.05$ vs the control values (CON).

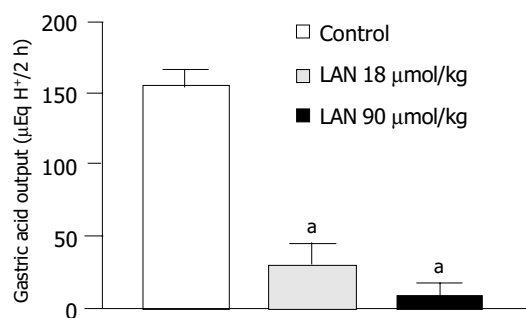


Figure 6 Rats subjected to pylorus ligation. Effect of lansoprazole (LAN, 18 and 90 $\mu\text{mol/kg}$) on gastric acid secretion. Each column represents the mean value obtained from six experiments \pm SE (vertical lines). ^a $P < 0.05$ vs the control values.

Animals subjected to pylorus ligation

In control animals subjected to pylorus ligation for 2 h and pretreated with lansoprazole vehicle the gastric acid output accounted for $153.7 \pm 5.8 \mu\text{EqH}^+ / 2 \text{ h}$ ($n = 6$). The administration of lansoprazole (18 or 90 $\mu\text{mol/kg}$) at the time of pylorus ligation caused a significant decrease in acidity (-81.4% and -93.1%, respectively; Figure 6).

In vitro assay of antioxidant activity of lansoprazole

In control experiments, 8-iso-PGF₂ α generation promoted by CuSO₄-induced oxidation of LDLs accounted for $1261.3 \pm 113.7 \text{ pg/mL}$. When the oxidative reaction was carried out in the presence of increasing concentrations of lansoprazole (1-300 $\mu\text{mol/L}$), the production of 8-iso-PGF₂ α underwent a progressive decrease. Under these conditions, the antioxidant activity of lansoprazole achieved a significant level at 3 $\mu\text{mol/L}$ (-17%), and a maximal effect could be detected at the concentration of 100 $\mu\text{mol/L}$ (-85.9%, Figure 7).

DISCUSSION

It is currently acknowledged that the ability of PPIs to prevent NSAID-associated gastric ulcers in clinical settings results from their inhibition of acid secretion^[1]. However, several lines of evidence indicate that acid-independent mechanisms may contribute to the antiulcer actions of PPIs^[9,10]. In the present study, the protective properties of lansoprazole were examined in a rat model of mucosal injury evoked by NSAIDs associated with high risk of adverse digestive events in clinical practice^[4]. The histomorphometric analysis of gastric sections showed that the damaging effects of test NSAIDs were prevented by lansoprazole, and evidence was also obtained that the ability to interfere with the oxidative and inflammatory injuries evoked by NSAID treatment plays a relevant role in the gastroprotective action of this benzimidazole derivative.

NSAIDs assayed in the present investigation elicited areas of mucosal necrosis which were associated with destruction of glandular architecture, submucosal edema, and extensive infiltration by polymorphonuclear cells. This pattern of gastric damage was also characterized by a marked

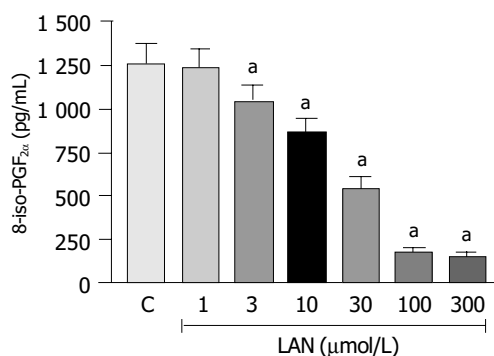


Figure 7 8-Iso-PGF₂ α levels generated *in vitro* upon oxidation of native LDLs by CuSO₄, either in the absence (C, control) or in the presence of increasing concentrations of lansoprazole (LAN). Each column represents the mean value obtained from 5-6 experiments \pm SE (vertical lines). ^a $P < 0.05$ vs the control values.

increase in mucosal MPO levels, regarded as a reliable marker of tissue neutrophil infiltration, which occurred together with an increment of mucosal MDA content and a decrease in GSH concentration. MDA is an end product resulting from peroxidation of polyunsaturated fatty acids and related esters within cell membranes, and the measurement of this substance represents a suitable index of oxidative tissue injury^[21]. On the other hand, sulfhydryl compounds are involved in the maintenance of gastric integrity, particularly when reactive oxygen species are implicated in the pathophysiology of tissue damage^[22,23]. Indeed, GSH participates in many aspects of oxidative metabolism, including the neutralization of hydroperoxides and the maintenance of the physiological sulfhydryl status of proteins^[23,24]. Overall, the present findings are consistent with previous evidence indicating that NSAIDs, acting through both local and systemic mechanisms, promote ischemic and inflammatory alterations which result in gastric neutrophil infiltration, release of oxygen metabolites, and cell membrane peroxidation^[1,3]. In particular, focal ischemia, characterized by neutrophil adherence to vascular endothelium, capillary congestion and intravascular fibrin deposition, has been recognized as an early event in the pathogenesis of NSAID-induced gastric oxidative injury, and these alterations are further amplified by subsequent tissue infiltration with polymorphonuclear cells, the activation of which causes a massive release of reactive oxygen radicals and other inflammatory mediators responsible for epithelial damage^[1,25]. In these respects, rat models, as that adopted in the present study, can be regarded as predictive of NSAID-induced gastric alterations occurring in clinical settings, since gastric erosions elicited by aspirin in healthy volunteers were accompanied by marked increments of mucosal MPO activity and lipid peroxidation^[5].

It is recognized that acid secretion can facilitate or exacerbate the damage to gastric mucosa evoked by exogenous agents, including NSAIDs, and acid suppression is then regarded as the main target of most pharmacological treatments designed to prevent or heal gastric ulcers^[26]. However, NSAID-induced ulcers result mainly from alterations of protective mechanisms, and some arguments suggest that acid secretion may not represent a pivotal step in the pathophysiology of NSAID gastropathy^[1,3]. For instance, achlorhydria does not protect patients against upper digestive ulcers during NSAID use^[27], and H₂ receptor antagonists appear to be scarcely effective in preventing NSAID-associated gastric ulcers under both experimental and clinical conditions^[28]. In the present study, NSAID-induced gastric lesions were extensively prevented by lansoprazole 90 µmol/kg, whereas rather weak effects were detected with 18 µmol/kg, a dose shown to ensure a marked blockade of acid secretion in pylorus-ligated rats. On these bases, it can be proposed that acid-independent mechanisms concur with inhibition of acid secretion for gastric protection afforded by lansoprazole against NSAIDs. In particular, since in our experiments lansoprazole prevented mucosal MDA generation elicited by test NSAIDs, it is conceivable that this drug is endowed with antioxidant properties accounting for its gastroprotective actions.

At least two mechanisms can be advocated to explain

the defence exerted by lansoprazole against gastric oxidative damage associated with NSAID treatment, as this drug might directly scavenge reactive oxygen species or interfere with the oxidative metabolism arising from the activation of polymorphonuclear cells. To address this issue, we carried out a series of experiments on an *in vitro* model, and evidence was obtained that lansoprazole directly protects native LDLs from copper-induced oxidation. These results agree with the experiments performed by Lapenna *et al.*^[29], where omeprazole was shown to significantly scavenge hypochlorous acid as well as to inhibit iron- and copper-driven oxidative reactions in appropriate *in vitro* systems. When taking into account indirect antioxidant mechanisms, it is important to consider that the increased output of free oxygen radicals, arising from activated polymorphonuclear cells, requires the acidification of phagolysosomes, and that such a process is accomplished by a proton pump which is fully susceptible to blockade by benzimidazole derivatives^[30,31]. Indeed, omeprazole blocked the oxidative burst of isolated polymorphonuclear cells^[30,32]. In addition, lansoprazole inhibited the output of free oxygen radicals from neutrophils activated by *Helicobacter pylori*^[33], and counteracted the increase in plasma levels of peroxidated lipids in patients with duodenal ulcer^[34]. Overall, it can be proposed that lansoprazole, acting via both direct and indirect antioxidant mechanisms, protects the gastric mucosa against oxidative injury caused by NSAID-induced focal ischemia and neutrophil activation.

Sulfhydryl radicals take a significant part in mechanisms deputed to the defence of tissues against oxidative injury, and there is evidence to suggest that sulfhydryl donor drugs can afford protection against gastric mucosal injuries elicited by various necrotizing agents, stress or ischemia^[22]. Adequate levels of sulfhydryl compounds appear also to be an important requirement for prevention of NSAID-induced gastropathy, since previous reports showed that a mucosal depletion of endogenous sulfhydryl radicals contributed to the pathogenesis of gastric lesions evoked by different NSAIDs^[14,15], and GSH concentrations were significantly decreased in mucosal bioptic specimens obtained from patients with NSAID-induced gastric bleeding^[35]. Consistent with these observations, in the present study animals treated with indomethacin or piroxicam displayed a marked reduction in mucosal GSH levels, and in both cases the decreasing action could be reversed by pretreatment with lansoprazole. The latter finding can be interpreted in light of the antioxidant properties of lansoprazole, through which this drug is expected to preserve mucosal sulfhydryl compounds from the excess of gastric scavenging activity required to counteract NSAID-induced oxidation, and therefore it is likely that an increased bioavailability of endogenous sulfhydryls plays a significant role in the prevention afforded by lansoprazole against gastropathy associated with NSAID therapy. In keeping with this view, lansoprazole was previously shown to interfere with the decrease in mucosal GSH concentrations in a rat model of gastric necrosis and oxidative injury caused by intraluminal application of acidified ethanol^[36].

The implication of prostaglandins in the antiulcer effects of PPIs is currently debated. In previous studies in rat

models, single-dose administration of lansoprazole did not influence gastric prostaglandin production^[36,37]. Furthermore, omeprazole failed to affect the release of prostaglandins from cultured gastric mucosal cells^[38]. More recently, Tsuji *et al.*^[10], observed that, after a treatment course of 14 d, lansoprazole promoted a gastrin-dependent increment of both gastric COX-2 expression and PGE2 concentration in rats. In the present study, a series of experiments was designed to evaluate PGE2 levels and the expression of COX isoforms in the gastric mucosa. PGE2 mucosal concentrations were consistently decreased after administration of test-NSAID, as expected, but such inhibitory effects were not influenced by pretreatment with lansoprazole. Moreover, indomethacin enhanced the mucosal expression of COX-2, but not COX-1, in line with previous findings^[39], whereas the expression of both isoforms was not modulated by lansoprazole neither in the absence nor in the presence of indomethacin. Therefore, lansoprazole does not appear to exert positive influences on gastric PGE2 levels, at least upon blockade of COX isoforms by NSAID treatment. In agreement with these observations, omeprazole prevented indomethacin-induced gastric ulcers in rabbits, without interfering with the concomitant decrease in mucosal PGE2 formation^[40].

In conclusion, the present results support the view that, besides the inhibition of acid secretion, the protective effects exerted by lansoprazole against NSAID-induced gastric damage can be ascribed to a reduction of gastric oxidative injury, which is also responsible for an increased bioavailability of mucosal sulfhydryl compounds. It is also suggested that lansoprazole does not exert any modulator influence on the down-regulation of gastric prostaglandin formation associated with NSAID treatment.

REFERENCES

- Wallace JL. Pathogenesis of NSAID-induced gastroduodenal mucosal injury. *Best Pract Res Clin Gastroenterol* 2001; **15**: 691-703
- Vane JR, Botting RM. Mechanism of action of anti-inflammatory drugs. *Int J Tissue React* 1998; **20**: 3-15
- Whittle BJ. Gastrointestinal effects of nonsteroidal anti-inflammatory drugs. *Fundam Clin Pharmacol* 2003; **17**: 301-313
- Hawkey CJ. Nonsteroidal anti-inflammatory drug gastropathy. *Gastroenterology* 2000; **119**: 521-535
- Pohle T, Brzozowski T, Becker JC, Van Der Voort IR, Markman A, Konturek SJ, Moniczewski A, Domschke W, Konturek JW. Role of reactive oxygen metabolites in aspirin-induced gastric damage in humans: gastroprotection by vitamin C. *Aliment Pharmacol Ther* 2001; **15**: 677-687
- McCarthy DM. Prevention and treatment of gastrointestinal symptoms and complications due to NSAIDs. *Best Pract Res Clin Gastroenterol* 2001; **15**: 755-773
- Matheson AJ, Jarvis B. Lansoprazole: An update of its place in the management of acid-related disorders. *Drugs* 2001; **61**: 1801-1833
- Welage LS. Pharmacologic properties of proton pump inhibitors. *Pharmacotherapy* 2003; **23**(10 Pt 2): 74S-80S
- Blandizzi C, Natale G, Gherardi G, Lazzeri G, Marveggio MC, Colucci R, Carignani D, Del Tacca M. Acid-independent gastroprotective effects of lansoprazole in experimental mucosal injury. *Dig Dis Sci* 1999; **44**: 2039-2050
- Tsuji S, Sun WH, Tsuji M, Kawai N, Kimura A, Kakiuchi Y, Yasumaru S, Komori M, Murata H, Sasaki Y, Kawano S, Hori M. Lansoprazole induces mucosal protection through gastrin receptor-dependent up-regulation of cyclooxygenase-2 in rats. *J Pharmacol Exp Ther* 2002; **303**: 1301-1308
- Wallace JL, Granger DN. The cellular and molecular basis of gastric mucosal defence. *FASEB J* 1996; **10**: 731-740
- Takeuchi K, Mizoguchi H, Araki H, Komoike Y, Suzuki K. Lack of gastric toxicity of nitric oxide-releasing indomethacin, NCX-530, in experimental animals. *Dig Dis Sci* 2001; **46**: 1805-1818
- Wallace JL, Reuter B, Cicala C, McKnight W, Grisham M, Cirino G. A diclofenac derivative without ulcerogenic properties. *Eur J Pharmacol* 1994; **257**: 249-255
- Avila JR, De la Lastra CA, Martin MJ, Motilva V, Luque I, Delgado I, Esteban J, Herrerias J. Role of endogenous sulphhydryls and neutrophil infiltration in the pathogenesis of gastric mucosal injury induced by piroxicam in rats. *Inflamm Res* 1996; **45**: 83-88
- De la Lastra CA, Nieto A, Martin MJ, Cabre F, Herrerias JM, Motilva V. Gastric toxicity of racemic ketoprofen and its enantiomers in rat: Oxygen radical generation and COX expression. *Inflamm Res* 2002; **51**: 51-57
- Natale G, Lazzeri G, Blandizzi G, Gherardi G, Lenzi P, Pellegrini A, Del Tacca M. Seriate histomorphometry of whole rat stomach: An accurate and reliable method for quantitative analysis of mucosal damage. *Toxicol Appl Pharmacol* 2001; **174**: 17-26
- Pacheco I, Michiro O, Jin M, Sasahara H, Iwabuchi A, Odashima M, Konishi N, Wada I, Masamune O, Watanabe S. Corticosteroid pretreatment prevents small intestinal lesions induced by acetic acid-perfusion model in rats. *Dig Dis Sci* 2000; **45**: 2337-2346
- Tashima K, Fujita A, Takeuchi K. Aggravation of ischemia/reperfusion-induced gastric lesions in streptozotocin-diabetic rats. *Life Sci* 2000; **67**: 1707-1718
- Blandizzi C, Gherardi G, Marveggio C, Natale G, Carignani D, Del Tacca M. Mechanisms of protection by omeprazole against experimental gastric mucosal damage in rats. *Digestion* 1995; **56**: 220-229
- Lubrano V, Vassalle C, Blandizzi C, Del Tacca M, Palombo C, L'Abbate A, Boldi S, Natali A. The effects of lipoproteins on endothelial nitric oxide synthase is modulated by lipoperoxides. *Eur J Clin Invest* 2003; **33**: 117-125
- Kwicien S, Brzozowski T, Konturek SJ. Effects of reactive oxygen species action on gastric mucosa in various models of mucosal injury. *J Physiol* 2002; **53**: 39-50
- Szabo S. Mechanisms of gastric mucosal injury and protection. *J Clin Gastroenterol* 1991; **13**(Suppl 2): S21-S34
- Loguercio C, Di Pierro M. The role of glutathione in the gastrointestinal tract: A review. *Ital J Gastroenterol Hepatol* 1999; **31**: 401-407
- Hayes JD, McLellan LI. Glutathione and glutathione-dependent enzymes represent a coordinately regulated defence against oxidative stress. *Free Radical Res* 1999; **31**: 273-300
- Anthony A, Sim R, Dhillon AP, Pounder RE, Wakefield AJ. Gastric mucosal contraction and vascular injury induced by indomethacin precede neutrophil infiltration in the rat. *Gut* 1996; **39**: 363-368
- Lehmann F, Hildebrand P, Beglinger C. New molecular targets for treatment of peptic ulcer disease. *Drugs* 2003; **63**: 1785-1797
- Janssen M, Dijkmans BA, Vandenbroucke JP, Biemond I, Lamers CB. Achlorhydria does not protect against benign upper gastrointestinal ulcers during NSAID use. *Dig Dis Sci* 1994; **39**: 362-365
- Scarpignato C, Pelosini I. Prevention and treatment of non-steroidal anti-inflammatory drug-induced gastro-duodenal damage: rationale for the use of antisecretory compounds. *Ital J Gastroenterol Hepatol* 1999; **31**(Suppl 1): S63-S72
- Lapenna D, De Gioia S, Ciofani G, Festi D, Cuccurullo F. Antioxidant properties of omeprazole. *FEBS Lett* 1996; **382**: 189-192
- Suzuki M, Mori M, Miura S, Suematsu M, Fukumura D, Kimura H, Ishii H. Omeprazole attenuates oxygen-derived free radical production from human neutrophils. *Free Radical*

- Biol Med* 1996; **21**: 727-731
- 31 **Agastya G**, West BC, Callahan JM. Omeprazole inhibits phagocytosis and acidification of phagolysosomes of normal human neutrophils *in vitro*. *Immunopharmacol Immunotoxicol* 2000; **22**: 357-372
- 32 **Wandall JH**. Effects of omeprazole on neutrophil chemotaxis, super oxide production, degranulation, and translocation of cytochrome b245. *Gut* 1992; **33**: 617-621
- 33 **Suzuki M**, Nakamura M, Mori M, Miura S, Tsuchiya M, Ishii H. Lansoprazole inhibits oxygen-derived free radical production from neutrophils activated by *Helicobacter pylori*. *J Clin Gastroenterol* 1995; **20**(Suppl 2): S93-S96
- 34 **Manjari V**, Das UN. Oxidant stress, anti-oxidants, nitric oxide and essential fatty acids in peptic ulcer disease. *Prostagl Leukotr Essent Fatty Acids* 1998; **59**: 401-406
- 35 **Savoie G**, Miralles-Barrachina O, Dechelotte P, Belmonte-Zalar L, Brung-Lefebvre M, Zalar A, Hochain P, Herve S, Colin R, Lerebours E, Ducrotte P. Low levels of gastric mucosal glutathione during upper gastric bleeding associated with the use of nonsteroidal anti-inflammatory drugs. *Eur J Gastroenterol Hepatol* 2001; **13**: 1309-1313
- 36 **Natale G**, Lazzeri G, Lubrano V, Colucci R, Vassalle C, Fornai M, Blandizzi C, Del Tacca M. Mechanisms of gastroprotection by lansoprazole pretreatment against experimentally induced injury in rats: Role of mucosal oxidative damage and sulfhydryl compounds. *Toxicol Appl Pharmacol* 2004; **195**: 62-72
- 37 **Fukuda T**, Arakawa T, Shimizu Y, Ohtani K, Higuchi K, Kobayashi K. Effects of lansoprazole on ethanol-induced injury and PG synthetic activity in rat gastric mucosa. *J Clin Gastroenterol* 1995; **20**(Suppl 2): S5-S7
- 38 **Ota S**, Takahashi M, Yoshiura K, Hata Y, Kawabe T, Terano A, Omata M. Antiulcer drugs and gastric prostaglandin E2: An *in vitro* study. *J Clin Gastroenterol* 1993; **17**(Suppl 1): S15-S21
- 39 **Tanaka A**, Hase S, Miyazawa T, Takeuchi K. Up-regulation of cyclooxygenase-2 by inhibition of cyclooxygenase-1: A key to nonsteroidal anti-inflammatory drug-induced intestinal damage. *J Exp Pharmacol Ther* 2002; **300**: 754-761
- 40 **Lee M**, Kallal SM, Feldman M. Omeprazole prevents indomethacin-induced gastric ulcers in rabbits. *Aliment Pharmacol Ther* 1996; **10**: 571-576

Science Editor Zhu LH Language Editor Elsevier HK

Ultrasonography of splenic abnormalities

Ming-Jen Chen, Ming-Jer Huang, Wen-Hsiung Chang, Tsang-En Wang, Horng-Yuan Wang, Cheng-Hsin Chu, Shee-Chan Lin, Shou-Chuan Shih

Ming-Jen Chen, Wen-Hsiung Chang, Tsang-En Wang, Horng-Yuan Wang, Cheng-Hsin Chu, Shee-Chan Lin, Shou-Chuan Shih, Division of Gastroenterology, Department of Internal Medicine, Mackay Memorial Hospital, Mackay Medicine, Nursing and Management College, Taipei, Taiwan, China

Ming-Jer Huang, Division of Hematology and Oncology, Department of Internal Medicine, Mackay Memorial Hospital, Taipei, Taiwan, China

Correspondence to: Dr. Shou-Chuan Shih, Division of Gastroenterology, Department of Internal Medicine, Mackay Memorial Hospital, No. 92, Sec. 2, Chungshan North Road, Taipei, Taiwan, China. jessierc@ms28.hinet.net

Telephone: +886-2-25433535-2260 Fax: +886-2-25433642

Received: 2004-10-12 Accepted: 2004-11-19

Abstract

AIM: This report gives a comprehensive overview of ultrasonography of splenic abnormalities. Certain ultrasonic features are also discussed with pathologic correlation.

METHODS: We review the typical ultrasonic characteristics of a wide range of splenic lesions, illustrating them with images obtained in our institution from 2000 to 2003. One hundred and three patients (47 men, 56 women), with a mean age of 54 years (range 9-92 years), were found to have an abnormal ultrasonic pattern of spleen.

RESULTS: We describe the ultrasonic features of various splenic lesions such as accessory spleen, splenomegaly, cysts, cavernous hemangiomas, lymphomas, abscesses, metastatic tumors, splenic infarctions, hematomas, and rupture, based on traditional gray-scale and color Doppler sonography.

CONCLUSION: Ultrasound is a widely available, noninvasive, and useful means of diagnosing splenic abnormalities. A combination of ultrasonic characteristics and clinical data may provide an accurate diagnosis. If the US appearance alone is not enough, US may also be used to guide biopsy of suspicious lesions.

© 2005 The WJG Press and Elsevier Inc. All rights reserved.

Key words: Ultrasonography; Ultrasound; Splenic abnormalities; Spleen

Chen MJ, Huang MJ, Chang WH, Wang TE, Wang HY, Chu CH, Lin SC, Shih SC. Ultrasonography of splenic abnormalities. *World J Gastroenterol* 2005; 11(26): 4061-4066
<http://www.wjgnet.com/1007-9327/11/4061.asp>

INTRODUCTION

By structure and function, the spleen resembles two separate organs combined in one. On the one hand, it is an organ of the immune system, with the white pulp involved in the maturation of lymphocytes and plasma cells and in the generation of antibodies. On the other hand, it has a phagocytic role, with the red pulp removing particulate matter from the blood and participating in the destruction of senescent red blood cells. In early life the red pulp also plays a role in hematopoiesis and the storage and sequestration of blood. The length of the spleen is variable, averaging 11 cm^[1]. The weight varies from 50 to 300 g, with an average of 150 g. The normal adult spleen decreases in size with age^[2]. The normal appearance of the parenchyma on ultrasound (US) is very homogeneous and uniform, with an echogenicity slightly greater than that of normal hepatic parenchyma. In comparison with other solid abdominal organs, the spleen is relatively rarely the primary site affected by disease. By contrast to the widely studied lesions of the liver, the US appearance of disease in the spleen is rather nonspecific. An understanding of the history and associated symptoms may help narrow the differential diagnosis. The ability of US to detect focal or diffuse splenic lesions depends on numerous factors: spleen size; size, number, and echogenicity of focal lesions; and ancillary adjacent findings.

MATERIALS AND METHODS

Ultrasonographic data of abdominal imaging with a diagnosis of splenic abnormalities from 2000 to 2003 at Mackay Memorial Hospital were reviewed retrospectively. In this period, 103 patients (47 men, 56 women), with a mean age of 54 years (range 9-92 years), were found to have an abnormal US pattern of spleen (exclusion of splenomegaly in patients with cirrhosis and thalassemia) from about 100 000 US evaluations. The indications for patient to undergo abdominal US were abdominal pain referred from emergency room in 13% of evaluations, abdominal relating symptoms referred from ordinary wards or intensive care units in 11% of evaluations, screening of viral hepatitis, abnormal liver function, liver cirrhosis, hepatoma or other malignancy referred from out-patient departments in 76% of evaluations. The spleen was scanned by a real time ultrasound using a 3.5 to 6 MHz transducer and color Doppler imaging was applied in some cases. The final diagnosis of each lesion in our patients was determined by pathologic, bacteriology examination or clinical history and serial imaging study.

RESULTS

These 103 splenic abnormalities were accessory spleen in 5

patients, true cysts in 22 and pseudocysts in 9 patients, splenic calcification and Gamna-Gandy bodies in 10 patients, cavernous hemangiomas in 15 patients, abscesses in 8 patients, lymphomas in 8 patients, metastatic tumors in 5 patients, splenic infarctions in 10 patients, hematomas and rupture in 11 patients.

Diseases of the spleen

Congenital abnormalities Some congenital anomalies of the spleen are common, such as splenic lobulation and accessory spleen, while other conditions are rare, such as wandering spleen^[3] and polysplenia^[4]. Failure of fusion of splenic tissue results in the formation of an accessory spleen. US appearances usually present as a homogenous, less than 4 cm round contour near the hilum and an echogenicity identical to that of adjacent spleen. Pathologic processes affecting the spleen also affect the accessory spleen, indicating that they have the same developmental origin (Figure 1). An intrapancreatic or intrahepatic accessory spleen is a homogenous mass in the parenchyma of the pancreas or liver that may mimic a neoplastic lesion^[5,6]. As it poses no danger, accurate diagnosis is necessary to avoid unnecessary treatment. The diagnosis of ectopic splenic tissue is best made by technetium-99m colloid scintigraphy^[7].



Figure 1 There is a homogenous, round contour near the hilum, identified as an accessory spleen (AS) in a 62-year-old female. One anechoic cyst is noted within the accessory spleen. The pathologic process affecting the spleen (small cyst) also affects the accessory spleen (large cyst).

Splenomegaly and portal hypertension As the spleen is an irregularly shaped organ, no completely satisfactory technique has been developed to measure the volume accurately. Estimating the volume with the formula $0.524 \times W \times T \times (ML + CCL) / 2$ (where ML = maximum length, W = width, T = thickness, and CCL = craniocaudal length) provides better overall accuracy^[8]. The differential diagnosis for splenomegaly includes infection, portal hypertension, storage disorders, blood dyscrasias, and neoplasm. Mild splenomegaly can be seen in infections and portal hypertension. Moderate splenomegaly suggests leukemia, lymphoma, or infectious mononucleosis. Massive splenomegaly is seen in myelofibrosis or chronic myeloid leukemia. The presence of portosystemic collateral vessels, ascites, and cirrhosis of the liver indicates portal hypertension^[9]. The presence of space-occupying lesions within an enlarged

spleen suggests lymphoma, metastases, or abscesses.

Splenic calcification and Gamna-Gandy bodies Foci of hemosiderin and calcium deposits in the splenic parenchyma secondary to intraparenchymal hemorrhage are called Gamna-Gandy bodies (Figure 2). They are commonly seen in patients with liver cirrhosis and portal hypertension and are also found in patients with splenic vein thrombosis, hemolytic anemia, hemochromatosis, or trauma^[10]. Echogenic foci with acoustic shadowing indicating calcification are found in chronic granulomatous infections such as tuberculosis, hamartomas, sickle cell disease^[11] and trauma.

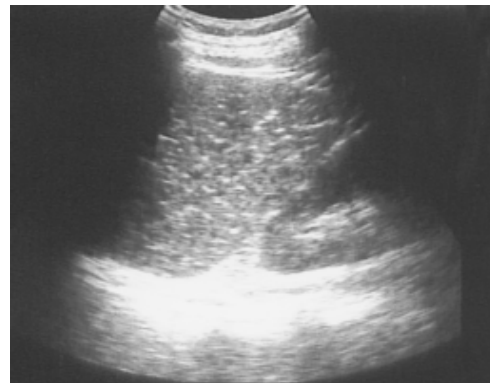


Figure 2 Multiple tiny calcified spots involving almost the entire spleen are found in a 58-year-old female with liver cirrhosis, called Gamna-Gandy bodies.

Splenic cysts Splenic cysts are rarely seen, but they are still probably the commonest splenic lesions. They are much less common than those arising in the kidney, liver, or ovary. They can be true cysts, pseudocysts, or hydatid cysts. The true cyst, also known as an epidermoid cyst, is defined by the presence of an inner endothelial lining. Pseudocysts that lack such a lining are usually secondary to old trauma, a resolved infection, or infarction. Hydatid cysts are formed by the larval stage of the dog tapeworm *Echinococcus granulosus*. Simple cysts pose less diagnostic problems if they have the classic ultrasonic features of being anechoic and thin-walled with posterior echo enhancement. Splenic cysts usually are located completely within the spleen, thus differing from hepatic or renal cysts which may have an exophytic component. Infection or hemorrhage may cause debris and echogenic contents within thick-walled pseudocysts (Figure 3). Brightly foci with acoustic shadow due to calcification within the wall is also a correlative US feature to pseudocysts. A rare complication of pancreatic pseudocyst may be erosion into the adjacent spleen, where it mimics a huge simple splenic cyst (Figure 4). Rupture of an intrasplenic pancreatic pseudocyst can result in massive hemoperitoneum. Miele stated that internal septa are more frequent in true cysts while parietal calcifications are typical of pseudocysts^[12]. However, the final diagnosis is made histologically.

Splenic abscess A splenic abscess is a collection of pus, most commonly caused by hematogenous spread of infection from elsewhere. Intravenous drug abusers are predominantly affected. Other causes include penetrating wounds or

complications of a hematoma resulting from infarction or trauma. A pyogenic abscess is typically hypoechoic and often has thick, irregular walls. Other findings include gas, progressive enlargement of the lesion, subcapsular extension and collections of extracapsular fluid^[13]. If gas has formed within the abscess, hyperechogenicity with distal dirty shadowing can be seen. Through transmission indicates the cystic nature of an abscess even when it contains echogenic material. Color Doppler examination may reveal hypervascularity in the thick wall. The clinical triad suggestive of splenic abscess consists of fever, left upper quadrant pain, and leukocytosis. The typical triad was seen in 44% of patients in one series of 34 cases^[14]. Although splenic abscess is rare, there is a high mortality if diagnosis and treatment are delayed. Percutaneous drainage of a single abscess and splenectomy for multiple abscesses are recommended. Fine-needle aspiration is useful when an abscess is suspected, as this may confirm the diagnosis as well allowing culture of the pathogen. In the series noted above, multiple or gas-containing abscesses had a poor prognosis^[14].



Figure 3 A pseudocyst cyst of the spleen after trauma reveals debris or echogenic contents within the thick wall (arrows) in a 60-year-old female.

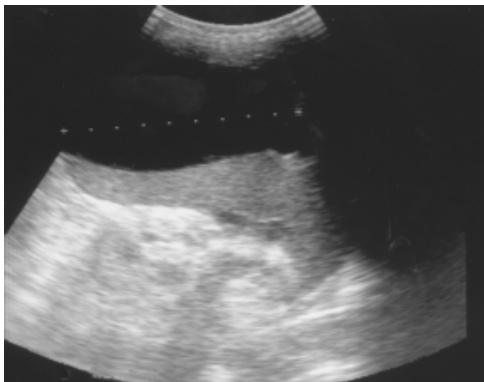


Figure 4 Pancreatic pseudocyst eroding into the adjacent spleen and mimicking a huge splenic simple cyst was noted after an episode of acute alcoholic pancreatitis in a 32-year-old male patient.

Hemangioma A hemangioma is characterized by a proliferation of blood-filled spaces lined and separated by endothelium. Cavernous hemangiomas are the most common solid benign lesion seen in the spleen and are found

incidentally. The US appearance varies widely from a predominately solid to mixed to a pure cystic lesion. Hemangiomas usually have a periphery and a hypoechoic center with a through transmission character similar to cavernous hemangioma of the liver. Color Doppler may show blood flow within the solid portions. Atypical features are commoner in larger lesions and include heterogeneous echogenicity with hypoechoic areas due to necrosis, hemorrhage, and thrombosis (Figure 5). Rarely, hemangiomas may be large or multiple and can involve the whole spleen (Figure 6). The most frequent complications are rupture and bleeding. Although up to 14% of patients in autopsy series have been reported to have splenic hemangiomas^[2], but they are less frequently identified on imaging.



Figure 5 An atypical hemangioma can have mixed echogenicity with a dominant cystic portion. Mild through transmission points to the cystic nature of the hemangioma.



Figure 6 Large and multiple hemangiomas occupy the entire spleen. The hypoechoic areas shown in Figure 5 are filled with blood clots and thrombosis. The 48-year-old male received splenectomy due to LUQ pain caused by venous thrombosis in spleen.

Lymphoma Primary malignant tumors of the spleen are uncommon, with primary lymphoma and angiosarcoma being the most frequently reported. Splenomegaly is a frequent finding in lymphoma, but a normal sized spleen does not exclude the diagnosis^[15]. The US patterns correspond to the three macroscopic morphologies: (1) infiltrative and diffuse, (2) miliary and nodular, and (3) focal

and cyst-like (Figure 7)^[16]. In cyst-like lymphoma, the appearance of a distinct boundary is an important clue in distinguishing lymphoma from cyst^[17]. Indistinct boundary echo pattern indicated splenic lymphomas. Hodgkin and non-Hodgkin lymphoma can not be distinguished by the US appearance.

Metastatic tumor Metastatic involvement of the spleen is very uncommon, usually seen in patients with widespread, terminal malignant disease. The most frequent metastases arise from lymphoma and melanoma, followed by carcinoma of the ovary, breast, lung, and stomach in decreasing order of frequency^[2]. Target lesions with a hypoechoic halo suggest metastasis (Figure 8). This appearance is said to be a sign of aggressive behavior, but other authors have postulated that it is due to necrosis or hemorrhage. Miliary tuberculosis, atypical mycobacteria, and *pneumocystis carinii*, especially in immunocompromised patients, can also result in multiple hypoechoic focal lesions^[18]. These should be differentiated from splenic metastases.

Splenic infarction Infarction can result from either occlusion of the splenic artery or venous thrombosis in the splenic sinusoids. Splenic infarction is typically seen in patients prone to embolic phenomena or, more recently, as a complication of transcatheter arterial embolization of a hepatoma. In splenic vein thrombosis, the entire spleen may be involved, resulting in massive splenomegaly. US typically show a peripheral, wedge-shaped region of hypoechoogenicity

(Figure 9). Color Doppler imaging may show a lack of perfusion; however, the presence of flow within a lesion does not exclude the diagnosis because the embolus may subsequently lyse. Splenic infarcts may initially be large and then become small and echogenic as fibrosis occurs.

Hematoma and rupture The spleen, liver, and kidney are the three intraperitoneal organs most commonly injured by blunt trauma. If the capsule of the injured spleen remains intact, an intraparenchymal or subcapsular hematoma (Figure 10) may result. Echogenicity of a hematoma depends on the stage at which the scan was performed. Fresh blood is liquid and initially echo-free but over the course of several days becomes more echogenic and thus more difficult to identify. Free fluid in the left upper quadrant is strongly suggestive of splenic injury, which must be excluded in such a case^[19]. Less frequently, a splenic laceration or rupture is identified as a blood-filled cleft with capsular rupture. (Figures 11 and 12).

Biopsy procedures In many cases, pathologic confirmation is necessary to provide a definitive diagnosis. The traditional dry cytologic aspiration is relatively safe but provides only a small sample. Siniluoto *et al.* reported false-negative results for malignancy is about 31% of biopsies using a 22-gauge fine needle aspiration technique^[20]. Core-needle biopsies with and 18 or 20-gauge cutting-biopsy needle may increase the diagnostic accuracy by obtaining a sufficiently large

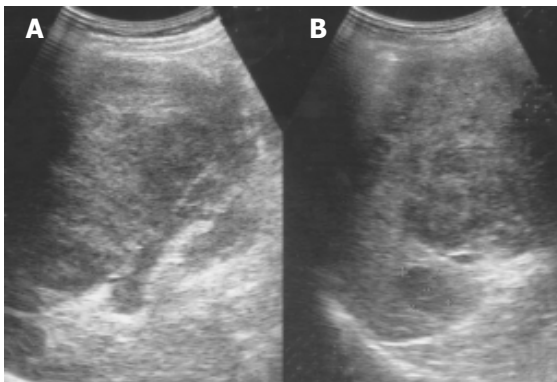


Figure 7 An enlarged spleen (A) demonstrates a diffusely coarse echotexture with several mixed echoic lesions (B) in a 58-year-old male patient.

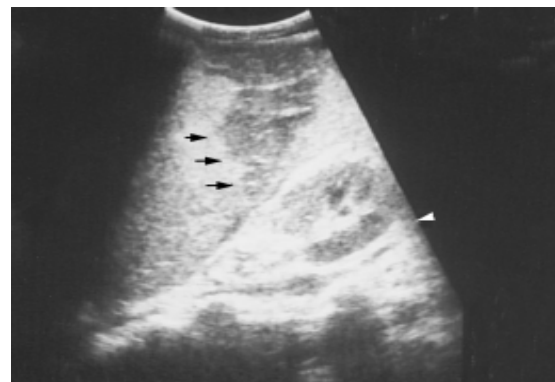


Figure 9 A peripheral wedge-shaped hypoechoic region (arrows) was noted at the upper pole of spleen from an infarction after transcatheter arterial embolization in a 45-year-old male with hepatoma.



Figure 8 Splenic metastasis from a lung carcinoma in a 68-year-old male is seen as a hypoechoic mass with a target sign.



Figure 10 A subcapsular crescent-shaped hypoechoic lesion is noted at the upper pole of spleen.

specimen. And Katsumi *et al.*^[21], reported the safety of this procedure in four cases. All procedures should be carefully planned in advance to avoid hitting the intestine, pancreas, kidneys or pleura as the needle is advanced. Color Doppler imaging helps avoid passing the needle through a large vessel. Endoscopic ultrasound-guided fine needle aspiration may be used in if the lesion is adjacent to the hilum or too small for a CT- or US-guided biopsy. A linear echo endoscope and 22-gauge needles are used to obtain specimens for cytology^[22]. To avoid unnecessary morbidity and mortality, laparotomy and splenectomy for pathologic confirmation should be used only when absolutely required.



Figure 11 Several linear hypoechoic foci and a subcapsular fluid accumulation are noted in a spleen. Loss of the normal architecture was seen after a traffic accident in a 38-year-old male.



Figure 12 A splenic laceration and rupture (in Figure 11) is identified as a blood-filled cleft (lower arrow) and capsular rupture (upper arrow) on contrast CT.

DISCUSSION

Because splenic abnormalities are relatively rare, the clinician is unlikely to be as familiar with them as with those of the liver. Although some of the experience gained with hepatic US is useful in examining the spleen, there are some differences that must be noted. The classic US finding of posterior echo enhancement suggesting a cyst in the liver or kidney is noted in only 25% of splenic cysts according to Ishida^[17] and in our experience (6/22) as well. While the reason for this discrepancy is not known for sure, Ishida suggested it might relate to differences in the acoustic patterns of the parenchyma of the two organs^[17]. Splenic

cysts are reportedly located completely within the spleen, and we have never found one of 28 cases that extends outside the capsule. Because the spleen is closely surrounded by other organs, it might be difficult for an exophytic cyst to develop. Another difference is that cystic portions occur more commonly and prominently in splenic hemangiomas compared with liver hemangiomas, which are more likely to be solid, in contrast with the variable appearance of hemangiomas in the spleen.

While there have been to differentiate benign from malignant focal lesions in the spleen based on US appearance, the results have been disappointing. There is too much overlap between the echo patterns^[23]. Therefore, US should be supplemented with other diagnostic techniques in such cases. However, certain criteria have been proposed that are at least suggestive. For example, malignant lesions are more likely to be multifocal, as with metastatic lesions, or to be diffuse and ill defined because of rapid growth. A soft tissue lesion associated with calcification usually indicates a long term process. Gas in the parenchyma usually originates from bacterial infection and indicates benign disease. Wan *et al.* said that solitary lesions with an anechoic pattern or echogenic foci with gas or calcification are more likely benign, while multifocal or diffuse solid lesions associated with a target sign or extrasplenic abdominal masses are suggestive of malignancy^[24].

Over the past decade, great efforts have been made to improve both tissue harmonic imaging and contrast sonography. The former is a gray-scale imaging technique that uses information from harmonic signals generated by non-linear propagation. This minimizes artifacts from the body, side lobe, and scatter and thus improves the signal-to-noise ratio. Contrast imaging uses gas microbubbles^[25], which has dramatically extended the ability of liver US to assess blood flow in a tumor^[26]. Preliminary experience with this modality has produced spleen-specific enhancement^[27]. Thorelius *et al.* suggested that contrast enhanced sonography might be useful in the detection of lesions in which blood flow is reduced such as infarctions, hematomas, necrotic tissue, and non-vascular cysts in the spleen^[28].

In conclusion, US is a widely available, noninvasive, and useful means of diagnosing splenic abnormalities. A combination of ultrasonic characteristics and clinical data may provide an accurate diagnosis, particularly for such disorders as hemangiomas, splenomegaly secondary to portal hypertension, simple cysts, malignant lesions with a target sign, or lesions associated with other obvious intra-abdominal pathology. In many cases, pathologic confirmation is necessary to make a definitive diagnosis. Fine needle aspiration, core-needle cutting biopsy, and endoscopic ultrasound-guided fine needle aspiration have been developed to assist diagnosis.

REFERENCES

- 1 O'Donohue J, Ng C, Catnach S, Farrant P, Williams R. Diagnostic value of Doppler assessment of the hepatic and portal vessels and ultrasound of the spleen in liver disease. *Eur J Gastroenterol Hepatol* 2004; **16**: 147-155
- 2 Andrews MW. Ultrasound of the spleen. *World J Sug* 2000; **24**: 183-187
- 3 Berkenblit RG, Mohan S, Bhatt GM, Rosenzweig M, Blitz A.

- Wandering spleen with torsion: appearance on CT and ultrasound. *Abdom Imaging* 1994; **19**: 459-460
- 4 **Harper L**, Michel JL, Hameury F, De Napoli-Cocci S, Udomkaewkanjana P, Gruau M, De Clermont H, Bechonnet G. Interest of laparoscopy in polysplenia syndrome. *Eur J Pediatr Surg* 2003; **13**: 417-420
 - 5 **Ota T**, Ono S. Intrapaneatic accessory spleen: diagnosis using contrast enhanced ultrasound. *Br J Radiol* 2004; **77**: 148-149
 - 6 **Izzo L**, Caputo M, Galati G. Intrahepatic accessory spleen: imaging features. *Liver Int* 2004; **24**: 216-217
 - 7 **Ota T**, Kusaka S, Mizuno M. A splenic pseudotumor: an accessory spleen. *Ann Nucl Med* 2003; **17**: 159-160
 - 8 **Yetter EM**, Acosta KB, Olson MC, Blundell K. Estimating splenic volume: sonographic measurements correlated with helical CT determination. *Am J Roentgenol* 2003; **181**: 1615-1620
 - 9 **La Seta F**, Patti R, Sciarrino E, Valenza F, Costanzo GS, Tese L, Lagalla R. Ultrasound, spleen and portal hypertension. *Radiol Med* 2004; **107**: 332-343
 - 10 **Dufour JF**, Dinkel HP, Zimmermann A. Image of the month. Gamma-Gandy bodies. *Gastroenterology* 2003; **125**: 1010
 - 11 **Senol U**, Luleci E, Keser I, Guzeloglu-Kayisli O, Toraman AD, Luleci G, Canatan D. Sickle-beta-thalassemia and splenic calcification. *Abdom Imaging* 2001; **26**: 557
 - 12 **Miele V**, Galluzzo M, Cortese A, Bellussi A, Valenti M. Diagnostic imaging of splenic cysts in children. *Radiol Med* 1998; **95**: 62-65
 - 13 **Ng KK**, Lee TY, Wan YL, Tan CF, Lui KW, Cheung YC, Cheng YF. Splenic abscess: diagnosis and management. *Hepatogastroenteology* 2002; **49**: 567-571
 - 14 **Changchien CS**, Tsai TL, Hu TH, Chiou SS, Kuo CH. Sonographic patterns of splenic abscess: an analysis of 34 proven cases. *Abdom Imaging* 2002; **27**: 739-745
 - 15 **Goerg C**, Schwerek WB, Goerg K, Havemann K. Sonographic patterns of the affected spleen in malignant lymphoma. *J Clin Ultrasound* 1990; **18**: 569-574
 - 16 **Urrutia M**, Mergo PJ, Ros LH, Torres GM, Ros PR. Cystic masses of the spleen: radiologic-pathologic correlation. *Radiographics* 1996; **16**: 107-129
 - 17 **Ishida H**, Konno K, Ishida J, Naganuma H, Komatsuda T, Sato M, Watanabe S. Splenic lymphoma: differentiation from splenic cyst with ultrasonography. *Abdom Imaging* 2001; **26**: 529-532
 - 18 **Schinina V**, Rizzi EB, Mazzuoli G, David V, Bibbolino C. US and CT findings in splenic focal lesions in AIDS. *Acta Radiol* 2000; **41**: 616-620
 - 19 **Richards JR**, McGahan PJ, Jewell MG, Fukushima LC, McGahan JP. Sonographic patterns of intraperitoneal hemorrhage associated with blunt splenic injury. *J Ultrasound Med* 2004; **23**: 387-394
 - 20 **Siniluoto T**, Paivansalo M, Tikkakoski T, Apaja-Sarkkinen M. Ultrasound-guided aspiration cytology of the spleen. *Acta Radiol* 1992; **33**: 137-139
 - 21 **Morita K**, Numata K, Tanaka K, Mitsui K, Matsumoto S, Kitamura T, Saito S, Kiba T, Sekihara H. Sonographically guided core-needle biopsy of focal splenic lesions: report of four cases. *J Clin Ultrasound* 2000; **28**: 417-424
 - 22 **Fritscher-Ravens A**, Mylonaki M, Pantas A, Topalidis T, Thonke F, Swain P. Endoscopic ultrasound-guided biopsy for the diagnosis of focal lesions of the spleen. *Am J Gastroenterol* 2003; **98**: 1022-1027
 - 23 **Goerg C**, Schwerek WB, Goerg K. Splenic lesions: sonographic patterns, follow-up, differential diagnosis. *Eur J Radiol* 1991; **13**: 59-66
 - 24 **Wan YL**, Cheung YC, Lui KW, Tseng JH, Lee TY. Ultrasonographic findings and differentiation of benign and malignant focal splenic lesions. *Postgrad Med J* 2000; **76**: 488-493
 - 25 **Calliada F**, Campani R, Bottinelli O, Bozzini A, Sommaruga MG. Ultrasound contrast agents: basic principles. *Eur J Radiol* 1998; **27**: S157-160
 - 26 **Wilson SR**, Burns PN, Muradali D, Wilson JA, Lai X. Harmonic hepatic US with microbubble contrast agent: initial experience showing improved characterization of hemangioma, hepatocellular carcinoma, and metastasis. *Radiology* 2000; **215**: 153-161
 - 27 **Lim AK**, Patel N, Eckersley RJ, Taylor-Robinson SD, Cosgrove DO, Blomley MJ. Evidence for spleen-specific uptake of a microbubble contrast agent: a quantitative study in healthy volunteers. *Radiology* 2004; **231**: 785-788
 - 28 **Thorelius L**. Contrast-enhanced ultrasound for extrahepatic lesions : preliminary experience. *Eur J Radiol* 2004; **51**: S31-38

• CLINICAL RESEARCH •

Head-to-head comparison of H₂-receptor antagonists and proton pump inhibitors in the treatment of erosive esophagitis: A meta-analysis

Wei-Hong Wang, Jia-Qing Huang, Ge-Fan Zheng, Harry Hua-Xiang Xia, Wai-Man Wong, Shiu-Kum Lam, Benjamin Chun-Yu Wong

Wei-Hong Wang, Department of Gastroenterology, Peking University First Hospital, Beijing, China

Wei-Hong Wang, Jia-Qing Huang, Ge-Fan Zheng, Harry Hua-Xiang Xia, Wai-Man Wong, Shiu-Kum Lam, Benjamin Chun-Yu Wong, Department of Medicine, Faculty of Medicine, University of Hong Kong, Hong Kong, China

Jia-Qing Huang, Clinical Trials Centre, Faculty of Medicine, University of Hong Kong, Hong Kong, China

Wei-Hong Wang, Jia-Qing Huang, Contributed Equally to This Work

Supported by the Gastroenterological Research Fund, University of Hong Kong, Hong Kong, China

Correspondence to: Benjamin Chun-Yu Wong, Department of Medicine, University of Hong Kong, Queen Mary Hospital, Hong Kong, China. bcywong@hku.hk

Telephone: +852-2855-4541 Fax: +852-2872-5828

Received: 2004-07-28 Accepted: 2004-09-24

the recommended dose are equally effective for healing esophagitis.

© 2005 The WJG Press and Elsevier Inc. All rights reserved.

Key words: Erosive esophagitis; H₂-receptor antagonists; Proton pump inhibitors; Meta-analysis

Wang WH, Huang JQ, Zheng GF, Xia HHX, Wong WM, Lam SK, Wong BCY. Head-to-head comparison of H₂-receptor antagonists and proton pump inhibitors in the treatment of erosive esophagitis: A meta-analysis. *World J Gastroenterol* 2005; 11(26): 4067-4077

<http://www.wjgnet.com/1007-9327/11/4067.asp>

Abstract

AIM: To systematically evaluate the efficacy of H₂-receptor antagonists (H₂RAs) and proton pump inhibitors in healing erosive esophagitis (EE).

METHODS: A meta-analysis was performed. A literature search was conducted in PubMed, Medline, Embase, and Cochrane databases to include randomized controlled head-to-head comparative trials evaluating the efficacy of H₂RAs or proton pump inhibitors in healing EE. Relative risk (RR) and 95% confidence interval (CI) were calculated under a random-effects model.

RESULTS: RRs of cumulative healing rates for each comparison at 8 wk were: high dose vs standard dose H₂RAs, 1.17 (95%CI, 1.02-1.33); standard dose proton pump inhibitors vs standard dose H₂RAs, 1.59 (95%CI, 1.44-1.75); standard dose other proton pump inhibitors vs standard dose omeprazole, 1.06 (95%CI, 0.98-1.06). Proton pump inhibitors produced consistently greater healing rates than H₂RAs of all doses across all grades of esophagitis, including patients refractory to H₂RAs. Healing rates achieved with standard dose omeprazole were similar to those with other proton pump inhibitors in all grades of esophagitis.

CONCLUSION: H₂RAs are less effective for treating patients with erosive esophagitis, especially in those with severe forms of esophagitis. Standard dose proton pump inhibitors are significantly more effective than H₂RAs in healing esophagitis of all grades. Proton pump inhibitors given at

INTRODUCTION

Gastro-esophageal reflux disease (GERD) is one of the most common chronic conditions affecting 20-40% of adult populations and has a major adverse impact on the quality of life^[1-3]. About 40-60% of patients with symptoms of GERD may have substantial injury of esophageal mucosa ranging from mild inflammation and erythema to various grades of erosions. The major complications of GERD are esophageal ulcer and bleeding, esophageal stricture, and Barrett's esophagus^[1-4].

Reflux esophagitis is generally considered to be the result of prolonged and repeated exposure of the distal esophageal mucosa to acidic gastric contents^[5,6]. It is increasingly clear that the key to reducing symptoms and to healing erosive esophagitis is to decrease the duration of exposure to the acidic refluxate. Acid-suppressing drugs that have been used to treat GERD include H₂-receptor antagonist (H₂RAs) and proton pump inhibitors. The efficacy of medical treatment depends on the ability to increase and maintain the intragastric and intra-esophageal pH above 4.0 over the 24-h period^[7,8]. H₂RAs are limited in their ability to inhibit postprandial gastric acid secretion and are ineffective in controlling reflux symptoms and healing esophagitis^[9,10]. In contrast to H₂RA, proton pump inhibitors block the final step of acid secretion, resulting in a profound and long-lasting acid suppression regardless of the stimulus^[11,12]. Results from 33 randomized clinical trials with over 3 000 patients showed that symptomatic relief could be anticipated in 83% of proton pump inhibitors-treated patients compared with 60% of patients receiving H₂RAs. Similarly, esophagitis was healed in 78% and 50%

of patients treated with proton pump inhibitors and H₂RAs, respectively^[13]. Previously there have been several systematic reviews and meta-analyses of clinical trials assessing the effects of medical treatments for erosive esophagitis^[14-17]. Chiba and colleagues^[14], and Caro and colleagues^[15] compared the effectiveness of proton pump inhibitors and H₂RAs in the healing of esophagitis, whereas the comparative efficacy among proton pump inhibitors was analyzed by Sharma *et al.*^[16], and Edwards *et al.*^[17]. However, comparison of the effects between treatments with proton pump inhibitors and H₂RAs in patients with esophagitis has been difficult because of the difference in the study design. For example, studies included in the previous meta-analyses were not all head-to-head comparative trials^[14,15]. The overall estimates of healing rate calculated by one-step pooling from different pairs of comparatives, may produce bias due to the ignorance of study differences such as sample size and differential difference in effect sizes. In addition, healing of esophagitis is significantly influenced by the initial grade of esophagitis, with healing rate being lower for the severe form of esophagitis than for the mild form of esophagitis^[18,20]. However, no meta-analysis has been published to systematically evaluate the impact of the initial grading of esophagitis on esophagitis healing rates in head-to-head comparative trials. Therefore, the objectives of the current study were firstly to evaluate any difference in healing erosive esophagitis between proton pump inhibitors and H₂RAs in head-to-head comparative trials, and secondly to estimate the impact of baseline grade of esophagitis on esophagitis healing rates.

MATERIALS AND METHODS

Literature search

A computerized literature search was performed in the PubMed, Medline, Embase and Cochrane databases for clinical trials published in English up to May 2004 with the following MeSH terms and/or text words in various combinations: gastroesophageal reflux, GERD, GORD, esophagitis, and healing, as well as the name of each respective drug (H₂-receptor antagonists: cimetidine, ranitidine, famotidine, nizatidine, roxatidine; proton pump inhibitors: omeprazole, lansoprazole, pantoprazole, rabeprazole, esomeprazole). The title and abstract of all potentially relevant studies were screened for their relevance before retrieval of full articles. Full articles were also scrutinized for relevance if the title and abstract were ambiguous. Fully recursive searches were performed from the reference list of all retrieved articles to ensure a complete and comprehensive search of the published literature. All searches were conducted independently by at least two reviewers.

Study selection

The inclusion criteria were as follows: (1) Randomized, controlled clinical trials in adults with an endoscopically confirmed diagnosis of GERD. (2) Two or more treatment arms: high dose *vs* standard dose H₂RA, or an H₂RA *vs* a proton pump inhibitor, or a proton pump inhibitor *vs* a proton pump inhibitor. (3) Healing of esophagitis was documented by endoscopy. (4) Studies with explicit information about the number of patients treated in each group, drug

dosage and schedule, and healing rate of esophagitis.

We excluded studies that only assessed symptom relief without endoscopic documentation of esophagitis healing. Also excluded were studies dealing only with relapsed or recurrent esophagitis, studies of pediatric patients, duplicate publications or studies published only in abstract form, or those focusing on pharmacokinetics and pharmacodynamics. Combination treatments such as an anti-secretory agent and a prokinetic drug were also excluded.

Data extraction

Data was extracted from each study independently and entered into a computerized database. Differences were resolved by discussion to reach consensus between the reviewers. The information retrieved covered country of study, study design, characteristics of population, grading of esophagitis, treatment regimen, number of patients treated, evaluated and healed, and confounding variables such as alcohol use, cigarette smoking, and caffeine use, where applicable. Healing data, up to 12 wk were extracted for both intention-to-treat (ITT) and per-protocol (PP) analyses. Data on healing based on the initial grade of esophagitis were also extracted, if applicable. In studies where only per-protocol healing rates were reported, we calculated the ITT healing rates based on the initial randomized number of patients. Articles that did not specify the type of analysis were assumed to report per-protocol data.

Quality assessment

Study quality was assessed by a series of validity criteria, including study design, level of blinding, method of randomization, patient selection, baseline characteristics, severity of esophagitis, definition of healing, compliance, and analysis by intention to treat criteria. Discrepancies in quality assessment were resolved by consensus among the authors. No quality score was assigned to any study to avoid possible introduction of subjectivity by the authors.

Statistical analysis

The data were grouped as follows: high dose *vs* standard dose H₂RAs; proton pump inhibitors *vs* H₂RAs, or one proton pump inhibitor *vs* another proton pump inhibitor. We defined standard dose of each drug as: ranitidine 300 mg/d, famotidine 40 mg/d, nizatidine 300 mg/d, cimetidine 800 mg/d, omeprazole 20 mg/d, lansoprazole 30 mg/d, pantoprazole 40 mg/d, rabeprazole 20 mg/d, esomeprazole 40 mg/d. The newer proton pump inhibitors include lansoprazole, pantoprazole, rabeprazole and esomeprazole.

The outcomes considered were healing rates of esophagitis for each group at different time points (2, 4, 6, 8, and 12 wk), based on initial grade of esophagitis, if applicable. Healing rate was calculated by pooling raw data from qualified studies within each group. These data were then expressed as a healing-time curve that plotted the cumulative percentage of patients healed *vs* the end point in weeks.

Relative risk (RR) and 95% confidence interval (CI), under a random-effects model^[21], were calculated using raw data of the selected studies at specified time points (2, 4, 6, 8, and 12 wk). The potential effect of publication bias was assessed using a funnel plot suggested by Egger *et al.*^[22].

Statistical heterogeneity between studies was assessed using the Q value calculated from the Mantel-Haenszel method. In the presence of statistical heterogeneity, we searched for the sources of any possible clinically important heterogeneity, i.e., methodological or biological heterogeneity. We did not simply exclude outliers on the basis of statistical test of heterogeneity. Furthermore, to test the robustness of the analysis, we performed sensitivity analyses to evaluate whether exclusion of a single study substantially altered the result of the summary estimate.

All analyses were carried out using EasyMa software for meta-analysis written by M Cucherat, Lyon, France (EasyMa, 2001).

RESULTS

Study characteristics

We identified a total of 485 citations with the computerized search. Screening of the title and abstract of the citations identified 72 potentially relevant studies for full article retrieval. Of these, 52 studies met the inclusion criteria^[19,20,23-72], and 20 studies were subsequently excluded for the following reasons: 17 were not head-to-head comparative studies^[73-89], 1 duplicate publication^[90], 1 without raw data^[91], and 1 with a confusing treatment allocation^[92]. The manual search of the reference list of the retrieved articles did not yield any additional studies. Of the 52 studies, the majority were double blind studies (51/52, 98.1%). Ten (19.2%) compared high dose H₂RA with standard dose H₂RA^[23-32], 26 (50.0%) compared a proton pump inhibitor with an H₂RA^[33-57,71], and 16 (30.8%) compared a proton pump inhibitor with another proton pump inhibitor^[19,20,58-70,72]. Only 25 (48.1%) reported raw healing data by the initial grade of esophagitis^[19,20,23,24,30,32,35,38,43-47,49,52,53,55-58,60,61,69-71].

The proportion of patients with a smoking history was reported in 61.5% of studies, alcohol consumption was reported in 48.1% of studies. The initial grade of esophagitis was reported in 58% studies. However, only 48.1% studies provided raw data on healing by the initial grade of esophagitis.

Healing of esophagitis

High dose H₂RAs vs standard dose H₂RAs Ten studies involving 27 treatment arms compared high dose ($n = 2041$ patients) with standard dose H₂RAs ($n = 1967$ patients)^[23-32]. Table 1 summarizes the pooled healing rates of esophagitis in patients treated with high dose H₂RAs *vs* standard dose H₂RAs. Statistical significance was achieved at 4, 8 and 12 wk,

indicating that high dose H₂RAs healed significantly more esophagitis than did standard dose H₂RAs (Table 1).

No comparative study reported data on the healing of esophagitis at 2 wk. Only one study^[29] reported healing rates at 3 wk, of 17.2% (29/169) for high dose H₂RAs and 19.6% (33/168) for standard dose H₂RAs (RR 0.87, 95%CI 0.56-1.37) (Table 1).

Proton pump inhibitors vs H₂RAs There were 14 studies with 28 treatment arms comparing standard dose proton pump inhibitors ($n = 861$ patients) with standard dose H₂RAs ($n = 752$ patients)^[33-45,71]. The pooled healing rates achieved with the standard dose proton pump inhibitors were superior to that of H₂RAs at all given time points (Table 2). Similar findings were observed when the comparison was made between high dose H₂RAs ($n = 234$ patients) and the standard dose proton pump inhibitors ($n = 237$ patients)^[50,51] (Table 2).

Three studies compared low dose proton pump inhibitors ($n = 279$ patients) with standard dose H₂RAs ($n = 276$ patients) for healing esophagitis^[52,53,71]. The pooled healing rates of the low dose proton pump inhibitors were higher than that of the standard dose H₂RAs at both 4 and 8 wk (Table 2).

Omeprazole 20 mg daily vs other proton pump inhibitors Eleven studies with 23 treatment arms reported comparative results on the healing of esophagitis between omeprazole 20 mg daily ($n = 3137$ patients) and other proton pump inhibitors at standard doses ($n = 3397$ patients)^[20,59-68]. No significant difference in the healing rate was observed between omeprazole 20 mg daily and other proton pump inhibitors at 2-8 wk (Table 3).

The esophagitis healing time curves are depicted in Figures 1-3. As shown in Figure 1, high dose H₂RA achieved higher healing rates than standard dose H₂RA. However, the healing rate achieved with standard dose proton pump inhibitors at 2 wk was even higher than that of H₂RAs at wk 8 (63.4% *vs* 52.0%), suggesting that proton pump inhibitors healed esophagitis significantly faster than did H₂RAs (Figure 2). Similar healing rates were also observed when the newer proton pump inhibitors were compared with omeprazole 20 mg daily (Figure 3).

Refractory esophagitis

Refractory esophagitis was defined as treatment failure with a standard dose of H₂RAs given for at least 12 wk^[55-57]. Three studies compared the effectiveness of proton pump inhibitors with ranitidine for the treatment of refractory esophagitis^[55-57] (Table 4). Two of them reported that lansoprazole 30 mg daily achieved significantly higher healing

Table 1 Healing rate of esophagitis by ITT with standard dose vs high dose of H₂RA at 3, 4, 6, 8, 12 wk

		3-wk	4-wk	6-wk	8-wk	12-wk
Number of comparisons		1	5	9	5	12
High dose	Pooled data	29/169	297/669	607/1294	413/669	1142/1729
	Pooled healing rate (%)	17.2	44.4	46.9	61.7	66.0
Standard dose	Pooled data	33/168	198/573	584/1361	309/573	920/1520
	Pooled healing rate (%)	19.6	34.6	42.9	53.9	60.5
Summary RR		0.874	1.281	1.096	1.165	1.084
95% CI		0.557-1.371	1.036-1.583	0.930-1.293	1.020-1.329	1.019-1.152

ITT, intention-to-treat analysis; No, number; RR, relative risk; 95%CI.

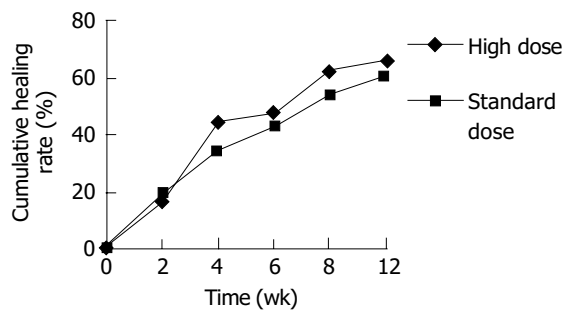


Figure 1 Healing-time curve of esophagitis in patients treated with H₂RA. Statistical significance was achieved at 4, 8, and 12 wk, indicating that high dose H₂RAs achieved significantly better healing rates for erosive esophagitis than standard dose H₂RAs.

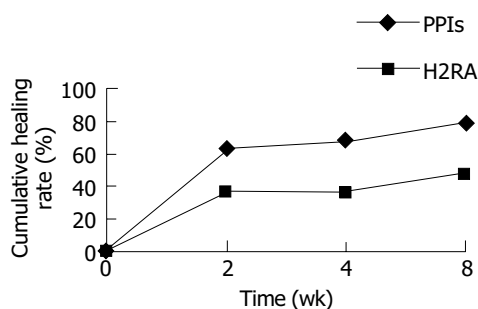


Figure 2 Healing-time curve of esophagitis in patients treated with standard doses of proton pump inhibitors vs H₂RAs. At wk 2, 4, 8, proton pump inhibitors significantly healed more patients than did H₂RAs.

rates than ranitidine 300 mg, daily at 4 wk (RR 1.38; 95%CI 1.31-1.83) and 8 wk (RR 2.54; 95%CI 1.86-3.46)^[55,56]. The

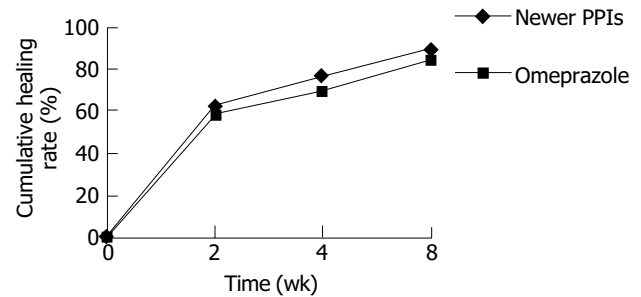


Figure 3 Healing-time curve of esophagitis in patients treated with standard dose of the newer proton pump inhibitors vs omeprazole. No significant difference in the pooled healing rates between the newer proton pump inhibitors and omeprazole was observed.

other study indicated that treatment with high dose omeprazole (40 mg/d) in patients refractory to H₂RAs therapy significantly improved esophagitis healing when compared to high dose ranitidine (600 mg/d) (RR 3.69, 95%CI 2.30-5.90 at 4 wk; and RR2.03, 95%CI 1.54-2.67 at 8 wk)^[57].

Healing by initial grade of esophagitis

Twenty-five studies^[19,20,23,24,30,32,35,38,43-47,49,52,53,55-58,60,61,69-71] with 54 treatment arms provided raw data on healing by the initial grade of esophagitis (Tables 5-7). Because data by intention-to-treat analysis were not available from the majority of trials, the healing rate by per-protocol analysis was therefore used.

When the healing rate was adjusted according to the initial severity of esophagitis, no significant differences in the healing rates was observed when patients with the severe

Table 2 Healing rate of esophagitis by ITT at 2, 3, 4, 8, 12 wk comparing proton pump inhibitors (PPIs) with H₂RA

	PPIs				H ₂ RA			
	2-wk	4-wk	8-wk	12-wk	2-wk	4-wk	8-wk	12-wk
sd PPIs vs sd H ₂ RA								
Number of arms	2	13	12		2	13	12	
Pooled data	116/183	577/824	640/783		60/163	271/713	350/673	
Pooled healing rate (%)	63.4	70.0	81.7		36.8	38.0	52.0	
Summary RR	1.759	1.832	1.586					
95%CI	1.398-2.213	1.622-2.070	1.438-1.749					
hd PPIs vs sd H ₂ RA								
Number of arms		4	4	1		4	4	1
Pooled data		150/204	175/201	72/80		79/211	106/207	49/81
Pooled healing rate (%)		73.5	87.1	90.0		37.4	51.2	60.5
Summary RR		1.722	1.623	1.488				
95%CI		1.464-2.027	1.417-1.859	1.230-1.800				
sd PPIs vs hd H ₂ RA								
Number of arms		2	2		2	2		
Pooled data		152/235	208/235		87/234	155/234		
Pooled healing rate (%)		64.7	88.5		37.2	66.2		
Summary RR		1.744	1.336					
95%CI		1.442-2.110	1.206-1.481					
ld PPIs vs sd H ₂ RA								
Number of arms		3	3		3	3		
Pooled data		187/279	219/279		120/276	161/276		
Pooled healing rate (%)		67.0	78.5		43.5	58.3		
Summary RR		1.605	1.374					
95%CI		1.156-2.229	1.081-1.744					

hd: high dose; sd: standard dose; ld: low dose; ITT, intention-to-treat analysis; No., number; RR, relative risk; 95% CI, 95% CIs.

Table 3 Healing rate (ITT) of esophagitis at 2, 4, 8 wk comparing PPIs with omeprazole

	Other PPIs			Omeprazole		
	2-wk	4-wk	8-wk	2-wk	4-wk	8-wk
sd PPIs vs sd Omeprazole						
Number of arms	1	12	12	1	12	12
Pooled data	264/421	2 615/3 412	3 050/3 411	257/431	2 229/3 217	2 719/3 216
Pooled healing rate (%)	62.7	76.6	89.4	59.6	69.3	84.5
Summary RR				1.052	1.044	1.061
95%CI				0.945-1.171	0.983-1.109	0.979-1.055
ld PPIs vs sd Omeprazole						
Number of arms		2	2		2	2
Pooled data		590/822	724/822		551/811	707/811
Pooled healing rate (%)		71.8	88.1		67.9	87.2
Summary RR					1.026	0.981
95%CI					0.904-1.164	0.870-1.105
sd PPIs vs hd Omeprazole						
Number of arms		2	1		2	1
Pooled data		310/440	284/337		302/434	282/332
Pooled healing rate (%)		70.5	84.3		69.6	84.9
Summary RR					1.031	0.985
95%CI					0.937-1.015	0.883-1.099

hd: high dose; sd: standard dose; ld: low dose; ITT, intention-to-treat analysis; No., number; RR, relative risk; 95% CI, 95% CIs.

Table 4 Healing rate of refractory esophagitis at 2, 4, 6, 8, 12 wk comparing PPIs with H₂RA

Author	PPIs						H ₂ RAs					
	Number of			Healing rate (ITT)			Number of			Healing rate (ITT)		
	Drug	Dose	Patient	4 wk	8 wk	12 wk	Drug	Dose	Patient	4 wk	8 wk	12 wk
sd PPIs vs sd H₂RA												
Feldman ⁽⁵⁵⁾	Lan	30 o.d.	61		54/61		Ran	150 b.d.	32		12/32	
Sontag ⁽⁵⁶⁾	Lan	30 o.d.	105	75/105	84/105		Ran	150 b.d.	54	28/54	16/54 ¹	
Pooled data			166	75/105	138/166				86	28/54	28/86	
Pooled rate (%)				71.4	83.1					51.9	32.6	
hd PPIs vs hd H₂RA												
Lundell ⁽⁵⁷⁾	Ome	40 o.d.	51	32/51	35/51	46/51	Ran	300 b.d.	47	8/47	18/47	22/47

Ome: omeprazole; Lan: lansoprazole; Ran: ranitidine; o.d.: once daily in the morning; b.d.: twice daily; h.d.: high dose; sd: standard dose. ¹This study did not report cumulative healing rate at 8 wk. All patients' endpoint was at 8 wk. The decreased healing rate at 8 wk for ranitidine group may be due to subsequent relapse of esophagitis.

form of esophagitis (\geq grade III) were treated with either high dose or standard dose H₂RAs. However, a significant difference was observed for patients with grade II esophagitis at 4 wk (Table 5). No patients with grade IV esophagitis were included in any of the studies comparing high dose with standard dose H₂RAs.

Proton pump inhibitors achieved consistently and significantly higher healing rates than H₂RAs across all grades

of esophagitis, irrespective of the dose and duration of treatment (Table 6). With a wide range of CI, the superiority of proton pump inhibitors over H₂RAs was even greater when the initial grade of esophagitis was considered in studies of patients with refractory esophagitis (Table 6) despite that one study reported the same effects on grade I esophagitis at 12 wk, when omeprazole 40 mg daily was compared with ranitidine 300 mg daily^[47]. The healing rates

Table 5 Healing by grade with standard dose vs high dose of H₂RA at 4, 6, 8, 12 wk (PP rate)

		4-wk		6-wk			8-wk		12-wk		
		II	III	I	II	III	II	III	I	II	III
Number of arms		3	3	4	4	4	3	3	4	6	6
Standard dose	Pooled data	84/190	22/105	86/137	102/266	42/180	126/187	37/105	107/129	264/383	119/256
	Pooled rate (%)	44.2	21.0	62.8	38.3	23.3	67.4	35.2	82.9	69.0	46.5
High dose	Pooled data	177/325	60/198	112/157	120/272	60/214	226/323	92/198	122/153	400/532	190/376
	Pooled rate (%)	54.4	30.3	71.3	44.1	28.0	70.0	46.5	79.7	75.2	50.5
Summary RR											
95% CI		1.231	1.430	1.136	1.150	1.200	1.039	1.316	0.962	1.032	1.059
		1.020-1.486	0.941-2.202	0.966-1.337	0.939-1.408	0.854-1.686	0.919-1.174	0.977-1.774	0.860-1.076	0.961-1.108	0.913-1.229

PP, per-protocol analysis; No., number; RR, relative risk; 95%CI.

Table 6 Healing by grade at 4, 8, 12 wk comparing PPIs with H₂RAs (PP rate)

		4 wk				8 wk				12 wk	
		I	II	III	IV	I	II	III	IV	I	II
Number of arms		2	4	3		2	5	3	1		
sd PPIs	Pooled data	53/60	128/162	20/54		23/23	166/178	28/47	2/3		
	Pooled rate (%)	88.3	79.0	37.0		100.0	93.3	59.6	66.7		
sd H ₂ RAs	Pooled data	27/54	65/172	2/41		16/25	101/182	6/34	0/2		
	Pooled rate (%)	50.0	37.8	4.9		64.0	55.5	17.6	0		
Summary RR		1.760	2.037	5.588		1.502	1.648	2.766	2.525		
95%CI		1.329-2.332	1.631-2.545	1.701-18.363		1.107-2.038	1.440-1.885	1.284-5.916	1.046-6.093		
No. of arms		2	4	2		2	4	2		1	1
hd PPIs	Pooled data	40/46	88/123	21/30		46/46	104/120	24/30		29/29	42/46
	Pooled rate (%)	87.0	71.5	70.0		100.0	86.7	80.0		100.0	91.3
sd H ₂ RAs	Pooled data	26/50	49/126	3/28		37/49	62/121	6/28		28/32	19/35
	Pooled rate (%)	52.0	38.9	10.7		75.5	51.2	21.4		87.5	54.3
Summary RR		1.665	1.835	6.110		1.300	1.689	3.626		1.111	1.676
95%CI		1.248-2.222	1.436-2.345	2.138-17.459		1.102-1.534	1.400-2.036	1.772-7.418		0.957-1.291	1.222-2.298
Number of arms		2	1	1		2	1	1			
ld PPIs	Pooled data	144/175	34/42	9/28		162/175	42/44	15/28			
	Pooled rate (%)	82.3	81.0	32.1		92.6	95.5	53.6			
sd H ₂ RAs	Pooled data	104/175	15/50	1/22		132/175	27/49	2/21			
	Pooled rate (%)	59.4	30.0	4.5		75.4	55.1	9.5			
Summary RR		1.384	2.698	7.071		1.227	1.732	5.625			
95%CI		1.202-1.592	1.724-4.224	0.967-51.707		1.116-1.349	1.335-2.249	1.440-21.980			
Refractory esophagitis											
Number of arms			1		1		2	1		2	
sd PPIs	Pooled data		62/77		11/22		105/116	13/15		18/29	
	Pooled rate (%)		80.5		50.0		90.5	86.7		62.1	
sd H ₂ RAs	Pooled data		20/40		1/11		26/61	2/8		0/14	
	Pooled rate (%)		50.0		9.1		42.6	25.0		0	
Summary RR			1.606		5.500		2.117	3.229		35.881	
95%CI			1.158-2.228		0.835-25.337		1.575-2.845	1.034-10.091		0.728-1767.6	

sd: standard dose; ld: low dose.

were similar between omeprazole and the newer proton pump inhibitors across all grades of esophagitis (Table 7).

Testing for between-study heterogeneity and sensitivity analyses

In the comparison of the healing rates achieved with omeprazole and the newer proton pump inhibitors, a significant heterogeneity was found at 4 and 8 wk ($P < 0.001$). However, no further heterogeneity ($P = 0.43$ at 4 wk, and $P = 0.92$ at 8 wk) was found after exclusion of the studies from Kahrilas *et al.*^[67], and Richter *et al.*^[68], suggesting that the heterogeneity was caused by these two studies. Further scrutiny of these two studies revealed that *Helicobacter pylori* (*H. pylori*) positive patients were excluded in both studies, whereas other studies

did not use *H. pylori* status as an exclusion criterion. No additional confounding factors such as the study design, level of blinding and compliance of patients were identified. Sensitivity analysis showed no difference in the healing rates of erosive esophagitis between omeprazole and the newer proton pump inhibitors (RR 1.00, 95% CI 0.96-1.04 at 4 wk; and RR 0.99, 95% CI 0.97-1.02) when the data from the two studies were excluded. There was no evidence of heterogeneity in any other comparisons.

Publication bias

Tests for publication bias were assessed with funnel plots using RRs against the sample size of each study. Due to the inadequacy of the number of studies in each comparison,

Table 7 Healing by grade at 4, 8 wk comparing standard dose of other PPIs vs omeprazole

		4-wk				8-wk			
		I	II	III	IV	I	II	III	IV
Number of arms		3	3	3	1	3	3	3	1
sd PPIs	Pooled data	195/239	302/362	148/210	3/7	214/235	329/360	175/209	2/4
	Pooled rate (%)	81.6	83.4	70.5	42.9	91.1	91.4	83.7	50.0
sd omeprazole	Pooled data	190/238	315/393	132/195	3/5	214/233	345/390	159/188	1/2
	Pooled rate (%)	79.8	80.2	67.8	60.0	91.8	88.5	84.6	50.0
Summary RR		1.022	1.041	1.041	0.733	0.992	1.033	0.990	1.000
95%CI		0.936-1.116	0.973-1.113	0.914-1.186	0.250-2.147	0.938-1.048	0.985-1.084	0.927-1.057	0.213-4.694

sd: standard dose.

funnel plots did not demonstrate strong patterns. Therefore, figures are not shown.

DISCUSSION

There have been a few systematic reviews and meta-analyses summarizing the effect of medical treatments for reflux esophagitis^[14-17]. However, most of them suffered from methodological flaws. The current study was the first attempt to systematically evaluate the effects of antisecretory agents in healing esophagitis based on head-to-head comparative trials. We believe that analysis of comparative trials provides more robust results than that obtained from simple pooling of results from non-comparative trials because no stratification was used in the latter form of analysis. We found that high dose H₂RAs was superior to standard dose H₂RAs in healing erosive esophagitis at wk 4, 8, and 12, and proton pump inhibitors achieved significantly higher healing rates of esophagitis than did H₂RAs, irrespective of dose and treatment duration. However, no statistically significant difference in healing rates was observed between standard dose omeprazole and the newer proton pump inhibitors after 4 and 8 wk of treatment.

The difference in the rate of healing esophagitis between proton pump inhibitors and H₂RAs can also be expressed as a healing-time curve for the ease of comparison^[14]. Using this method, we have shown that proton pump inhibitors healed esophagitis at a rate approximately twice that of H₂RAs at all time points and the healing rate achieved at 2 wk with proton pump inhibitors was greater than that obtained with H₂RAs at 8 wk. This is consistent with the findings from previous meta-analyses using a different study design^[14-17].

H₂RAs are less effective for healing esophagitis because they cannot effectively inhibit meal-stimulated acid secretion^[9,10]. Moreover, tolerance may occur to H₂RAs, resulting in a significant decrease in their anti-secretory effect^[93,94]. Therefore, patients with reflux esophagitis often require high dose H₂RAs to maintain an intragastric pH above the critical threshold of 4.0 to achieve satisfactory symptom relief and remission of esophagitis^[7,8]. Proton pump inhibitors have been proved to be effective in suppressing gastric acid secretion throughout the 24-h period, including meal-stimulated acid production^[95,96]. So far, tolerance to proton pump inhibitors has not been reported in the literature even after long-term treatment.

The severity of esophagitis is a good predictor of a successful treatment^[97]. In this analysis, we have shown that high dose H₂RAs achieved a significantly better healing rate of esophagitis than standard dose H₂RAs. However, this difference disappeared when the results were adjusted by the initial grade of esophagitis except for the comparison at 4 wk when high dose H₂RAs healed 10% more esophagitis (Table 5). A possible explanation for the rapid loss of superiority of anti-secretory effect of high dose H₂RAs over standard dose H₂RAs after 4 wk could be due to the subsequent development of tolerance to the continuous use of H₂RAs^[93,94].

Our study has confirmed that proton pump inhibitors were significantly more effective than H₂RAs in healing erosive esophagitis across all grades. In patients with mild

forms of esophagitis (grades I and II), the healing rate achieved with proton pump inhibitors was significantly higher than that with H₂RAs (100.0% *vs* 64.0% for grade I, and 93.3% *vs* 55.5% for grade II) at 8 wk (Table 6). This suggested that, even in patients with the mild form of esophagitis, H₂RAs is a less effective treatment compared to proton pump inhibitors. The difference was even greater in patients with grade III/IV esophagitis. The healing rate achieved with proton pump inhibitors at 8 wk was 59.6%, but only 17.6% with H₂RAs (Table 6). In patients refractory to H₂RAs, proton pump inhibitors healed 50.0% and 62.1% of grade IV esophagitis after 4 and 8 wk of treatment, respectively (Table 4). Thus, proton pump inhibitors are significantly more effective than H₂RAs for treating all grades of esophagitis, including patients refractory to H₂RAs.

It is known that individual proton pump inhibitors differ with respect to the onset of action and duration of effect because of the variability in their bioavailability. Although omeprazole has a relative lower bioavailability than other proton pump inhibitors^[98-100], which may contribute to the late onset of symptom relief, this has not been translated into a disadvantage in healing rate of esophagitis of all grades when compared with the newer proton pump inhibitors according to the results of this analysis.

A statistically significant heterogeneity was found in the overall analysis comparing the efficacy of healing esophagitis among different proton pump inhibitors. Two studies identified to have contributed to the heterogeneity, compared esomeprazole to omeprazole and excluded patients with *H pylori* infection in their analyses^[67,68]. Although a higher healing rate of reflux esophagitis has been observed in patients with *H pylori* infection compared to uninfected patients when treated with proton pump inhibitors^[101,102], there is no evidence that esomeprazole would work better on *H pylori* negative patients. Therefore, there might in fact be real difference in efficacy between esomeprazole and omeprazole, because esomeprazole is the enantiomer of omeprazole and the active compound is the achiral cyclic sulfenamide. Comparing 40 mg of esomeprazole with 20 mg of omeprazole would be more or less the same, as comparing double dose of omeprazole^[103]. More data are needed to further confirm the presumption.

There are several limitations in this meta-analysis. Firstly, the quality of a meta-analysis, in general is dependent on the quality of original studies, particularly the study design and reporting. To correct reporting bias from original studies is difficult and requires collaboration of investigators involved. Because of the practical difficulties, such as lapse in time between the time of publication and the time of this analysis, we did not contact investigators for raw data or clarification of unclear presentation. Secondly, three different esophagitis grading systems were used in the individual studies, which might have confounded the results of analyses. Huang *et al.*, previously reported that there is a systematic difference in healing rates between studies using Hetzel-Dent scoring system and those using Savary-Miller system^[104]. Therefore, we considered that the impact of different esophagitis scoring systems on the analysis of esophagitis healing rates deserves a systematic evaluation in its own right. This warrants an immediate consensus of using a

standard esophagitis scoring system among investigators so that a truly meaningful comparison of the efficacy of different drugs can be made. Thirdly, the stratified analysis by the initial grade of esophagitis may also be biased because per-protocol data were used in the analysis. Fourthly, we excluded meeting abstracts and non-English publications for technical reasons such as inadequate reporting of outcomes in meeting abstracts and no resources for translation of non-English articles. This might have introduced selection bias. To estimate the magnitude of possible impact, we searched the literature and identified six articles published in non-English literature, but with an English abstract^[18,105-109]. Four studies compared a standard dose proton pump inhibitor with an H₂RA, one between two H₂RAs and one between two different doses of cimetidine. The conclusions of these trials are consistent with those of this meta-analysis. Therefore, we believe that the inclusion of non-English studies would not change the conclusions of this analysis. Fifthly, relief of reflux symptoms is another important aspect in the management of patients with GERD. However, the large variability in measuring and reporting symptom data in the literature prohibited us from conducting a reliable meta-analysis of the effects of antisecretory agents on relieving reflux symptoms. This requires an urgent attention to establishing a standard instrument for the assessment of symptom response in patients with GERD.

In conclusion, this meta-analysis of comparative trials clearly identifies that H₂RAs are not effective treatment for patients with esophagitis of all grades irrespective of dose. Proton pump inhibitors are significantly more effective than H₂RAs for healing esophagitis of all grades including those refractory to H₂RAs. No significant differences in healing esophagitis exist among standard dose of different proton pump inhibitors. Therefore, proton pump inhibitors should be used for patients with esophagitis of all grades.

ACKNOWLEDGMENT

Dr. WH Wang is the recipient of Visiting Professorship under the Croucher Foundation Chinese Visitorship Scheme of the University of Hong Kong, Hong Kong.

REFERENCES

- 1 **Spechler SJ**. Epidemiology and natural history of gastroesophageal reflux disease. *Digestion* 1992; **51**: 24-29
- 2 **Castell DO**, Johnston BT. Gastro-esophageal reflux disease. Current strategies for patient management. *Arch Fam Med* 1996; **5**: 221-227
- 3 **Wong WM**, Lai KC, Lam KF, Hui WM, Hu WH, Lam CL, Xia HH, Huang JQ, Chan CK, Lam SK, Wong BC. Prevalence, clinical spectrum and health care utilization of gastro-oesophageal reflux disease in a Chinese population: a population-based study. *Aliment Pharmacol Ther* 2003; **18**: 595-604
- 4 **Johnston BT**, Collins JS, McMarland RJ. Are esophageal symptoms reflux-related? A study of different scoring systems in a cohort of patients with heartburn. *Am J Gastroenterol* 1994; **89**: 497-502
- 5 **Orlando RC**. The pathogenesis of gastroesophageal reflux disease: The relationship between epithelial defense, dysmotility, and acid exposure. *Am J Gastroenterol* 1997; **92**: 3S-5
- 6 **Holloway RH**, Dent J, Narielvala F. Relation between oesophageal acid exposure and healing of esophagitis with omeprazole in patients with severe reflux esophagitis. *Gut* 1996; **38**: 649-654
- 7 **Bell NJV**, Burget D, Howden CW, Wilkinson J, Hunt RH. Appropriate acid suppression for management of gastro-oesophageal reflux disease. *Digestion* 1992; **51**(Suppl 1): 59-67
- 8 **Hunt RH**. Importance of pH control in the management of GERD. *Arch Intern Med* 1999; **159**: 649-657
- 9 **Johnston DA**, Wormsley KG. Time of administration influences gastric inhibitory effects of ranitidine. *Scand J Gastroenterol* 1988; **23**(Suppl 9): 1137-1140
- 10 **Merki HS**, Halter F, Wilder-Smith CH, Allemann P, Witzel L, Kempf M, Roehmel J, Walt RP. Effect of food on H₂-receptor blockade in normal subjects and duodenal ulcer patients. *Gut* 1990; **31**(Suppl 2): 148-150
- 11 **Simon B**, Muller P, Marinis E, Luhmann R, Huber R, Hartmann R, Wurst W. Effect of repeated oral administration of BY 1023/SK&F 96022-A new substituted benzimidazole derivative-On pentagastrin-stimulated gastric acid secretion and pharmacokinetics in man. *Aliment Pharmacol Ther* 1990; **4**: 373-379
- 12 **Teyssen S**, Pfuertzer R, Stephan F, Singer MV. Comparison of the effect of a 28-d long term therapy with the proton pump inhibitor pantoprazole with the H₂-receptor antagonist ranitidine on intragastric pH in healthy human subjects. *Gastroenterology* 1995; **108**(Suppl 4): A240
- 13 **DeVault KR**, Castell DO. The practice parameters committee of the american college of gastroenterology. Updated guidelines for the diagnosis and treatment of gastroesophageal reflux disease. *Am J Gastroenterol* 1999; **94**: 1434-1442
- 14 **Chiba N**, de Gara CJ, Wilkinson JM, Hunt RH. Speed of Healing and symptom relief in grade II to IV gastroesophageal reflux disease: a meta-analysis. *Gastroenterology* 1997; **112**: 1798-1810
- 15 **Caro JJ**, Salas M, Ward A. Healing and relapse rates in gastroesophageal reflux disease treated with the newer proton-pump inhibitors lansoprazole, rabeprazole, and pantoprazole compared with omeprazole, ranitidine, and placebo: evidence from randomized clinical trials. *Clinical Therapeutics* 2001; **23**: 998-1017
- 16 **Sharma VK**, Leontiadis GI, Howden CW. Meta-analysis of randomized controlled trials comparing standard clinical doses of omeprazole and lansoprazole in erosive oesophagitis. *Aliment Pharmacol Ther* 2001; **15**: 227-231
- 17 **Edwards SJ**, Lind T, Lundell L. Systematic review of proton pump inhibitors for the acute treatment of reflux oesophagitis. *Aliment Pharmacol Ther* 2001; **15**: 1729-1736
- 18 **Gallo S**, Dibildox M, Moguel A, Di Silvio M, Rodriguez F, Almaguer I, Garcia C. Clinical superiority of pantoprazole over ranitidine in the treatment of reflux esophagitis grade II and III. A prospective, double-blind, double-placebo study. Mexican clinical experience. Mexican Pantoprazole Study Group. *Rev Gastroenterol Mex* 1998; **63**: 11-16
- 19 **Mulder CJ**, Dekker W, Gerretsen M. Lansoprazole 30 mg versus omeprazole 40 mg in the treatment of reflux esophagitis grade II, III and IV. A Dutch multicentre trial. Dutch Study Group. *Eur J Gastroenterol Hepatol* 1996; **8**: 1101-1106
- 20 **Castell DO**, Kahrilas PJ, Richter JE, Vakil NB, Johnson DA, Zuckerman S, Skammer W, Levine JG. Esomeprazole (40 mg) compared with lansoprazole (30 mg) in the treatment of erosive esophagitis. *Am J Gastroenterol* 2002; **97**: 575-583
- 21 **DerSimonian R**, Laird N. Meta-analysis in clinical trials. *Controlled Clin Trials* 1986; **7**: 177-188
- 22 **Egger M**, Davey Smith G, Schneider M, Minder C. Bias in meta-analysis detected by a simple, graphical test. *BMJ* 1997; **315**: 629-634
- 23 **Johnson NJ**, Boyd EJ, Mills JG, Wood JR. Acute treatment of reflux oesophagitis: a multicentre trial to compare 150 mg ranitidine b.d. with 300 mg ranitidine q.d.s. *Aliment Pharmacol Ther* 1989; **3**: 259-266
- 24 **McCarty-Dawson D**, Sue SO, Morrill B, Murdock RH Jr. Ranitidine versus cimetidine in the healing of erosive esophagitis. *Clin Ther* 1996; **18**: 1150-1160
- 25 **Johnson NJ**, Laws S, Mills JG, Wood JR. Effect of 3 ranitidine

- dosage regimens in the treatment of reflux esophagitis - results of a multicenter trial. *European J Gastroenterol Hepatol* 1991; **3**: 769-774
- 26 **Wesdorp IC**, Dekker W, Festen HP. Efficacy of famotidine 20 mg twice a day versus 40 mg twice a day in the treatment of erosive or ulcerative reflux esophagitis. *Dig Dis Sci* 1993; **38**: 2287-2293
- 27 **Simon TJ**, Berlin RG, Tipping R, Gilde L. Efficacy of twice daily doses of 40 or 20 milligrams famotidine or 150 milligrams ranitidine for treatment of patients with moderate to severe erosive esophagitis. Famotidine Erosive Esophagitis Study Group. *Scand J Gastroenterol* 1993; **28**: 375-380
- 28 **Pace F**, Sangaletti O, Bianchi Porro G. Short and long-term effect of two different dosages of ranitidine in the therapy of reflux oesophagitis. *Ital J Gastroenterol* 1990; **22**: 28-32
- 29 **Cloud ML**, Offen WW. Nizatidine versus placebo in gastroesophageal reflux disease. A six-week, multicenter, randomized, double-blind comparison. Nizatidine Gastroesophageal Reflux Disease Study Group. *Dig Dis Sci* 1992; **37**: 865-874
- 30 **Quik RF**, Cooper MJ, Gleeson M, Hentschel E, Schuetze K, Kingston RD, Mitchell M. A comparison of two doses of nizatidine versus placebo in the treatment of reflux oesophagitis. *Aliment Pharmacol Ther* 1990; **4**: 201-211
- 31 **Simon TJ**, Berenson MM, Berlin RG, Snapinn S, Cagliola A. Randomized, placebo-controlled comparison of famotidine 20 mg b.d. or 40 mg b.d. in patients with erosive oesophagitis. *Aliment Pharmacol Ther* 1994; **8**: 71-79
- 32 **Tytgat GN**, Nicolai JJ, Reman FC. Efficacy of different doses of cimetidine in the treatment of reflux esophagitis. A review of three large, double-blind, controlled trials. *Gastroenterology* 1990; **99**: 629-634
- 33 **Ruth M**, Enbom H, Lundell L, Lonroth H, Sandberg N, Sandmark S. The effect of omeprazole or ranitidine treatment on 24-h esophageal acidity in patients with reflux esophagitis. *Scand J Gastroenterol* 1988; **23**: 1141-1146
- 34 **Bianchi Porro G**, Parente F. Topically active drugs in the treatment of peptic ulcers. Focus on colloidal bismuth subcitrate and sucralfate. *J Clin Gastroenterol* 1992; **14**: 192-198
- 35 **Sandmark S**, Carlsson R, Fausa O, Lundell L. Omeprazole or ranitidine in the treatment of reflux esophagitis. Results of a double-blind, randomized, Scandinavian multicenter study. *Scand J Gastroenterol* 1988; **23**: 625-632
- 36 **Zeitoun P**, Desjars De Keranroue N, Isal JP. Omeprazole versus ranitidine in erosive oesophagitis. *Lancet* 1987; **2**: 621-622
- 37 **Porro GB**, Pace F, Peracchia A, Bonavina L, Vigneri S, Scialabba A, Franceschi M. Short-term treatment of refractory reflux esophagitis with different doses of omeprazole or ranitidine. *J Clin Gastroenterol* 1992; **15**: 192-198
- 38 **Bardhan KD**, Hawkey CJ, Long RG, Morgan AG, Wormsley KG, Moules IK, Brocklebank D. Lansoprazole versus ranitidine for the treatment of reflux oesophagitis. UK Lansoprazole Clinical Research Group. *Aliment Pharmacol Ther* 1995; **9**: 145-151
- 39 **Sontag SJ**, Schnell TG, Chejfec G, Kurucar C, Karpf J, Levine G. Lansoprazole heals erosive reflux oesophagitis in patients with Barrett's oesophagus. *Aliment Pharmacol Ther* 1997; **11**: 147-156
- 40 **Robinson M**, Sahba B, Avner D, Jhala N, Greskirose PA, Jennings DE. A Comparison of Lansoprazole and Ranitidine in the Treatment of Erosive Esophagitis. *Aliment Pharmacol Ther* 1995; **9**: 25-31
- 41 **Koop H**, Schepp W, Dammann HG, Schneider A, Luhmann R, Classen M. Comparative trial of pantoprazole and ranitidine in the treatment of reflux esophagitis. Results of a German multicenter study. *J Clin Gastroenterol* 1995; **20**: 192-195
- 42 **Armbrecht U**, Abucar A, Hameeteman W, Schneider A, Stockbrugger RW. Treatment of reflux oesophagitis of moderate and severe grade with ranitidine or pantoprazole-comparison of 24-h intragastric and oesophageal pH. *Aliment Pharmacol Ther* 1997; **11**: 959-965
- 43 **Soga T**, Matsuura M, Kodama Y, Fujita T, Sekimoto I, Nishimura K, Yoshida S, Kutsumi H, Fujimoto S. Is a proton pump inhibitor necessary for the treatment of lower-grade reflux esophagitis? *J Gastroenterol* 1999; **34**: 435-440
- 44 **Kawano S**, Murata H, Tsuji S, Kubo M, Tatsuta M, Iishi H, Kanda T, Sato T, Yoshihara H, Masuda E, Noguchi M, Kashio S, Ikeda M, Kaneko A. Randomized comparative study of omeprazole and famotidine in reflux esophagitis. *J Gastroenterol Hepatol* 2002; **17**: 955-959
- 45 **Armstrong D**, Pare P, Pericak D, Pyzyk M. Symptom relief in gastroesophageal reflux disease: a randomized, controlled comparison of pantoprazole and nizatidine in a mixed patient population with erosive esophagitis or endoscopy-negative reflux disease. *Am J Gastroenterol* 2001; **96**: 2849-2857
- 46 **Vantrappen G**, Rutgeerts L, Schurmans P, Coenegrachts JL. Omeprazole (40 mg) is superior to ranitidine in short-term treatment of ulcerative reflux esophagitis. *Dig Dis Sci* 1988; **33**: 523-529
- 47 **Havelund T**, Laursen LS, Skoubo-Kristensen E, Andersen BN, Pedersen SA, Jensen KB, Fenger C, Hanberg-Sorensen F, Lauritsen K. Omeprazole and ranitidine in treatment of reflux oesophagitis: double blind comparative trial. *Br Med J* 1988; **296**: 89-92
- 48 **Blum AL**, Riecken EO, Dammann HG, Schiessel R, Lux G, Wienbeck M, Rehner M, Witzel L. Comparison of omeprazole and ranitidine in the treatment of reflux esophagitis. *N Engl J Med* 1986; **314**: 716
- 49 **Klinkenberg-Knol EC**, Jansen JM, Festen HP, Meuwissen SG, Lamers CB. Double-blind multicentre comparison of omeprazole and ranitidine in the treatment of reflux oesophagitis. *Lancet* 1987; **1**: 349-351
- 50 **Jansen JB**, Van Oene JC. Standard-dose lansoprazole is more effective than high-dose ranitidine in achieving endoscopic healing and symptom relief in patients with moderately severe reflux oesophagitis. The Dutch Lansoprazole Study Group. *Aliment Pharmacol Ther* 1999; **13**: 1611-1620
- 51 **Farley A**, Wruble LD, Humphries TJ. Rabeprazole versus ranitidine for the treatment of erosive gastroesophageal reflux disease: a double-blind, randomized clinical trial. Rabeprazole Study Group. *Am J Gastroenterol* 2000; **95**: 1894-1899
- 52 **Dettmer A**, Vogt R, Sielaff F, Luhmann R, Schneider A, Fischer R. Pantoprazole 20 mg is effective for relief of symptoms and healing of lesions in mild reflux oesophagitis. *Aliment Pharmacol Ther* 1998; **12**: 865-872
- 53 **van Zyl JH**, de K Grundling H, van Rensburg CJ, Retief FJ, O'Keefe SJ, Theron I, Fischer R, Bethke T. Efficacy and tolerability of 20 mg pantoprazole versus 300 mg ranitidine in patients with mild reflux-oesophagitis: a randomized, double-blind, parallel, and multicentre study. *Eur J Gastroenterol Hepatol* 2000; **12**: 197-202
- 54 **Dehn TC**, Shepherd HA, Colin-Jones D, Kettlewell MG, Carroll NJ. Double blind comparison of omeprazole (40 mg od) versus cimetidine (400 mg qd) in the treatment of symptomatic erosive reflux oesophagitis, assessed endoscopically, histologically and by 24 h pH monitoring. *Gut* 1990; **31**: 509-513
- 55 **Feldman M**, Harford WV, Fisher RS, Sampliner RE, Murray SB, Greski-Rose PA, Jennings DE. Treatment of reflux esophagitis resistant to H₂-receptor antagonists with lansoprazole, a new H⁺/K⁺-ATPase inhibitor: a controlled, double-blind study. Lansoprazole Study Group. *Am J Gastroenterol* 1993; **88**: 1212-1217
- 56 **Sontag SJ**, Kogut DG, Fleischmann R, Campbell DR, Richter J, Robinson M, McFarland M, Sabesin S, Lehman GA, Castell D. Lansoprazole heals erosive reflux esophagitis resistant to histamine H₂-receptor antagonist therapy. *Am J Gastroenterol* 1997; **92**: 429-437
- 57 **Lundell L**, Backman L, Ekstrom P, Enander LH, Fausa O, Lind T, Lonroth H, Sandmark S, Sandzen B, Unge P. Omeprazole or high-dose ranitidine in the treatment of patients with reflux oesophagitis not responding to 'standard doses' of H₂-receptor antagonists. *Aliment Pharmacol Ther* 1990; **4**: 145-155

- 58 **Vcev A**, Stimac D, Vceva A, Rubinic M, Ivandic A, Ivanis N, Horvat D, Volaric M, Karner I. Lansoprazole versus omeprazole in the treatment of reflux esophagitis. *Acta Med Croatica* 1997; **51**: 171-174
- 59 **Hatlebakk JG**, Berstad A, Carling L, Svedberg LE, Unge P, Ekstrom P, Halvorsen L, Stallemo A, Hovdenak N, Trondstad R. Lansoprazole versus omeprazole in short-term treatment of reflux oesophagitis. Results of a Scandinavian multicentre trial. *Scand J Gastroenterol* 1993; **28**: 224-228
- 60 **Castell DO**, Richter JE, Robinson M, Sontag SJ, Haber MM. Efficacy and safety of lansoprazole in the treatment of erosive reflux esophagitis. The Lansoprazole Group. *Am J Gastroenterol* 1996; **91**: 1749-1757
- 61 **Mee AS**, Rowley JL. Rapid symptom relief in reflux oesophagitis: a comparison of lansoprazole and omeprazole. *Aliment Pharmacol Ther* 1996; **10**: 757-763
- 62 **Mossner J**, Holscher AH, Herz R, Schneider A. A double-blind study of pantoprazole and omeprazole in the treatment of reflux oesophagitis: a multicentre trial. *Aliment Pharmacol Ther* 1995; **9**: 321-326
- 63 **Corinaldesi R**, Valentini M, Belaiche J, Colin R, Geldof H, Maier C. Pantoprazole and omeprazole in the treatment of reflux oesophagitis: a European multicentre study. *Aliment Pharmacol Ther* 1995; **9**: 667-671
- 64 **Vcev A**, Stimac D, Vceva A, Takac B, Ivandic A, Pezerovic D, Horvat D, Nedic P, Kotromanovic Z, Maksimovic Z, Vranjes Z, Males J, Jurisic-Orzen D, Vladika I, Stimac T, Mandic B. Pantoprazole versus omeprazole in the treatment of reflux esophagitis. *Acta Med Croatica* 1999; **53**: 79-82
- 65 **Dekkers CP**, Beker JA, Thjodleifsson B, Gabryelewicz A, Bell NE, Humphries TJ. Double-blind comparison [correction of Double-blind, placebo-controlled comparison] of rabeprazole 20 mg vs omeprazole 20 mg in the treatment of erosive or ulcerative gastro-oesophageal reflux disease. The European Rabeprazole Study Group. *Aliment Pharmacol Ther* 1999; **13**: 49-57
- 66 **Delchier JC**, Cohen G, Humphries TJ. Rabeprazole, 20 mg once daily or 10 mg twice daily, is equivalent to omeprazole, 20 mg once daily, in the healing of erosive gastroesophageal reflux disease. *Scand J Gastroenterol* 2000; **35**: 1245-1250
- 67 **Kahrilas PJ**, Falk GW, Johnson DA, Schmitt C, Collins DW, Whipple J, D'Amico D, Hamelin B, Joelsson B. Esomeprazole improves healing and symptom resolution as compared with omeprazole in reflux oesophagitis patients: a randomized controlled trial. The Esomeprazole Study Investigators. *Aliment Pharmacol Ther* 2000; **14**: 1249-1258
- 68 **Richter JE**, Kahrilas PJ, Johanson J, Maton P, Breiter JR, Hwang C, Marino V, Hamelin B, Levine JG. Esomeprazole Study Investigators. Efficacy and safety of esomeprazole compared with omeprazole in GERD patients with erosive esophagitis: a randomized controlled trial. *Am J Gastroenterol* 2001; **96**: 656-665
- 69 **Bardhan KD**, Van Rensburg C. Comparable clinical efficacy and tolerability of 20 mg pantoprazole and 20 mg omeprazole in patients with grade I reflux oesophagitis. *Aliment Pharmacol Ther* 2001; **15**: 1585-1591
- 70 **Holtmann G**, Bytzer P, Metz M, Loeffler V, Blum AL. A randomized, double-blind, comparative study of standard-dose rabeprazole and high-dose omeprazole in gastro-oesophageal reflux disease. *Aliment Pharmacol Ther* 2002; **16**: 479-485
- 71 **Kovacs TO**, Wilcox CM, DeVault K, Miska D, Bochenek W. Pantoprazole US Gerd Study Group B. Comparison of the efficacy of pantoprazole vs. nizatidine in the treatment of erosive oesophagitis: a randomized, active-controlled, double-blind study. *Aliment Pharmacol Ther* 2002; **16**: 2043-2052
- 72 **Korner T**, Schutze K, van Leendert RJ, Fumagalli I, Costa Neves B, Bohuschke M, Gatz G. Comparable efficacy of pantoprazole and omeprazole in patients with moderate to severe reflux esophagitis. Results of a multinational study. *Digestion* 2003; **67**: 6-13
- 73 **Roufail W**, Belsito A, Robinson M, Barish C, Rubin A. Ranitidine for erosive oesophagitis: a double-blind, placebo-controlled study. Glaxo Erosive Esophagitis Study Group. *Aliment Pharmacol Ther* 1992; **6**: 597-607
- 74 **Euler AR**, Murdock RH Jr, Wilson TH, Silver MT, Parker SE, Powers L. Ranitidine is effective therapy for erosive esophagitis. *Am J Gastroenterol* 1993; **88**: 520-524
- 75 **Silver MT**, Murdock RH Jr, Morrill BB, Sue SO. Ranitidine 300 mg twice daily and 150 mg four-times daily are effective in healing erosive oesophagitis. *Aliment Pharmacol Ther* 1996; **10**: 373-380
- 76 Comparison of roxatidine acetate and ranitidine in the treatment of reflux esophagitis. The Roxatidine Esophagitis Study Group. *Clin Ther* 1993; **15**: 283-293
- 77 **Bate CM**, Booth SN, Crowe JP, Hepworth-Jones B, Taylor MD, Richardson PD. Does 40 mg omeprazole daily offer additional benefit over 20 mg daily in patients requiring more than 4 wk of treatment for symptomatic reflux oesophagitis? *Aliment Pharmacol Ther* 1993; **7**: 501-507
- 78 **Carlsson R**, Dent J, Watts R, Riley S, Sheikh R, Hatlebakk J, Haug K, de Groot G, van Oudvorst A, Dalvag A, Junghard O, Wiklund I. Gastro-oesophageal reflux disease in primary care: an international study of different treatment strategies with omeprazole. International GORD Study Group. *Eur J Gastroenterol Hepatol* 1998; **10**: 119-124
- 79 **Cloud ML**, Offen WW, Robinson M. Nizatidine versus placebo in gastroesophageal reflux disease: a 12-week, multicenter, randomized, double-blind study. *Am J Gastroenterol* 1991; **86**: 1735-1742
- 80 **Cloud ML**, Enas N, Humphries TJ, Bassion S. Rabeprazole in treatment of acid peptic diseases: results of three placebo-controlled dose-response clinical trials in duodenal ulcer, gastric ulcer, and gastroesophageal reflux disease (GERD). The Rabeprazole Study Group. *Dig Dis Sci* 1998; **43**: 993-1000
- 81 **Earnest DL**, Dorsch E, Jones J, Jennings DE, Greski-Rose PA. A placebo-controlled dose-ranging study of lansoprazole in the management of reflux esophagitis. *Am J Gastroenterol* 1998; **93**: 238-243
- 82 **Hetzel DJ**, Dent J, Reed WD, Narielvala FM, Mackinnon M, McCarthy JH, Mitchell B, Beveridge BR, Laurence BH, Gibson GG. Healing and relapse of severe peptic esophagitis after treatment with omeprazole. *Gastroenterology* 1988; **95**: 903-912
- 83 **Laursen LS**, Havelund T, Bondesen S, Hansen J, Sanchez G, Sebelin E, Fenger C, Lauritsen K. Omeprazole in the long-term treatment of gastro-oesophageal reflux disease. A double-blind randomized dose-finding study. *Scand J Gastroenterol* 1995; **30**: 839-846
- 84 **Palmer RH**, Miller DM, Hedrich DA, Karlstadt RG. Cimetidine QID and BID in rapid heartburn relief and healing of lesions in gastroesophageal reflux disease. *Clin Ther* 1993; **15**: 994-1001
- 85 **Richter JE**, Bochenek W. Oral pantoprazole for erosive esophagitis: a placebo-controlled, randomized clinical trial. Pantoprazole US GERD Study Group. *Am J Gastroenterol* 2000; **95**: 3071-3080
- 86 **Robinson M**, Campbell DR, Sontag S, Sabesin SM. Treatment of erosive reflux esophagitis resistant to H2-receptor antagonist therapy. Lansoprazole, a new proton pump inhibitor. *Dig Dis Sci* 1995; **40**: 590-597
- 87 **Sabesin SM**, Berlin RG, Humphries TJ, Bradstreet DC, Walton-Bowen KL, Zaidi S. Famotidine relieves symptoms of gastroesophageal reflux disease and heals erosions and ulcerations. Results of a multicenter, placebo-controlled, dose-ranging study. USA Merck Gastroesophageal Reflux Disease Study Group. *Arch Intern Med* 1991; **151**: 2394-2400
- 88 **Sontag SJ**, Hirschowitz BI, Holt S, Robinson MG, Behar J, Berenson MM, McCullough A, Ippoliti AF, Richter JE, Ahtaridis G. Two doses of omeprazole versus placebo in symptomatic erosive esophagitis: the U.S. Multicenter Study. *Gastroenterology* 1992; **102**: 109-118
- 89 **van Rensburg CJ**, Honiball PJ, Grundling HD, van Zyl JH, Spies SK, Eloff FP, Simjee AE, Segal I, Botha JF, Cariem AK,

- Marks IN, Theron I, Bethke TD. Efficacy and tolerability of pantoprazole 40 mg versus 80 mg in patients with reflux oesophagitis. *Aliment Pharmacol Ther* 1996; **10**: 397-401
- 90 **Lundell L.** Prevention of relapse of reflux oesophagitis after endoscopic healing: the efficacy and safety of omeprazole compared with ranitidine. *Digestion* 1990; **47**(Suppl 1): 72-75
- 91 **James OF, Parry-Billings KS.** Comparison of omeprazole and histamine H₂-receptor antagonists in the treatment of elderly and young patients with reflux oesophagitis. *Age Ageing* 1994; **23**: 121-126
- 92 **Umeda N, Miki K, Hoshino E.** Lansoprazole Versus Famotidine in Symptomatic Reflux Esophagitis-A Randomized, Multicenter Study. *J Clinical Gastroenterol* 1995; **20**: S17-23
- 93 **Wilder-Smith CH, Halter F, Ernst T, Gennoni M, Zeyen B, Halter F, Merki HS.** Loss of acid suppression during dosing with H₂-receptor antagonists. *Aliment Pharmacol Ther* 1990; **4** (Suppl 1): 15-27
- 94 **Wilder-Smith CH, Merki HS.** Tolerance during dosing with H₂-receptor antagonists. An overview. *Scand J Gastroenterol Suppl* 1992; **193**: 14-19
- 95 **Houben GM, Hooi J, Hameeteman W, Stockbrugger RW.** Twenty-four hour intragastric acidity: 300 mg ranitidine b.d, 20 mg omeprazole o.m, 40 mg omeprazole o.m. vs placebo. *Aliment Pharmacol Ther* 1995; **9**: 649-654
- 96 **Blum RA, Shi H, Karol M, Greski-Rose P, Hunt RH.** The comparative effects of lansoprazole, omeprazole, and ranitidine in suppressing gastric acid secretion. *Clin Ther* 1997; **19**: 1013-1023
- 97 **Bell NJ, Hunt RH.** Role of gastric acid suppression in the treatment of gastro-oesophageal reflux disease. *Gut* 1992; **33**: 118-124
- 98 **Landes BD, Petite JP, Flouvat B.** Clinical pharmacokinetics of lansoprazole. *Clin Pharmacokinet* 1995; **28**: 458-470
- 99 **Pue MA, Laroche J, Meineke I, de Mey C.** Pharmacokinetics of pantoprazole following single intravenous and oral administration to healthy male subjects. *Eur J Clin Pharmacol* 1993; **44**: 575-578
- 100 **Lind T, Rydberg L, Kyleback A, Jonsson A, Andersson T, Hasselgren G, Holmberg J, Rohss K.** Esomeprazole provides improved acid control versus omeprazole in patients with symptoms of gastro-oesophageal reflux disease. *Aliment Pharmacol Ther* 2000; **14**: 861-867
- 101 **Holtmann G, Cain C, Malfertheiner P.** Gastric *Helicobacter pylori* infection accelerates healing of reflux esophagitis during treatment with the proton pump inhibitor pantoprazole. *Gastroenterology* 1999; **117**: 11-16
- 102 **Meneghelli UG, Boaventura S, Moraes-Filho JP, Leitao O, Ferrari AP, Almeida JR, Magalhaes AF, Castro LP, Haddad MT, Tolentino M, Jorge JL, Silva E, Maguilnik I, Fischer R.** Efficacy and tolerability of pantoprazole versus ranitidine in the treatment of reflux esophagitis and the influence of *Helicobacter pylori* infection on healing rate. *Dis Esophagus* 2002; **15**: 50-56
- 103 **Kromer W.** Relative efficacies of gastric proton-pump inhibitors on a milligram basis. Desired and undesired SH reactions. Impact of chirality. *Scand J Gastroenterol Suppl* 2001; **36**: 3-9
- 104 **Huang JQ, Sumanac K, Hunt RH.** Impact of scoring systems on the evaluation of erosive esophagitis (EE) healing? A meta-analysis. *Gastroenterology* 2002; **122**(Suppl): W1169
- 105 **Zeitoun P, Rampal P, Barbier P, Isal JP, Eriksson S, Carlsson R.** Omeprazole (20 mg daily) compared to ranitidine (150 mg twice daily) in the treatment of esophagitis caused by reflux. Results of a double-blind randomized multicenter trial in France and Belgium. *Gastroenterol Clin Biol* 1989; **13**: 457-462
- 106 **Kimmig JM.** Cimetidine and ranitidine in the treatment of reflux esophagitis. *Z Gastroenterol* 1984; **22**: 373-378
- 107 **Barbier JP, Haccoun P, Bergmann JF, Arnould B, Hamelin B.** Prognostic factors influencing healing of reflux esophagitis. A controlled trial of omeprazole versus ranitidine. Study group Omega. *Ann Gastroenterol Hepatol* 1993; **29**: 213-218
- 108 **Siewert JR, Ottenjann R, Heilmann K, Neiss A, Dopfer H.** Therapy and prevention of reflux esophagitis. Results of a multicenter study with cimetidine. I: Epidemiology and results of acute therapy. *Z Gastroenterol* 1986; **24**: 381-395
- 109 **Dammann HG, Blum AL, Lux G, Rehner M, Riecken EO, Schiessel R, Wienbeck M, Witzel L, Berger J.** Different healing tendencies of reflux esophagitis following omeprazole and ranitidine. Results of a German-Austrian-Swiss multicenter study. *Dtsch Med Wochenschr* 1986; **111**: 123-128

• CLINICAL RESEARCH •

Development of a semi-quantitative food frequency questionnaire for middle-aged inhabitants in the Chaoshan area, China

Feng-Yan Song, Takezaki Toshiro, Ke Li, Ping Yu, Xu-Kai Lin, He-Lin Yang, Xiao-Ling Deng, Yu-Qi Zhang, Lai-Wen Lv, Xin-En Huang, Tajima Kazuo

Feng-Yan Song, Ke Li, Ping Yu, Xiao-Ling Deng, Yu-Qi Zhang, Lai-Wen Lv, Department of Preventive Medicine, Shantou Medical University, Shantou 515041, Guangdong Province, China
Takezaki Toshiro, Department of International Island and Community Medicine, Kagoshima University Graduate School of Medical and Dental Sciences, 8-35-1 Sakuragaoka, Kagoshima 890-8544, Japan
Xu-Kai Lin, Shantou Disease Preventive and Control Center, Shantou 515031, Guangdong Province, China
He-Lin Yang, the Board of Health Nan'ao County, Shantou 515000, Guangdong Province, China
Xin-En Huang, Jiangsu Province Cancer Hospital, Nanjing 210009, Jiangsu Province, China
Tajima Kazuo, Division of Epidemiology and Prevention, Aichi Cancer Center Research Institute, Aichi 464-8681, Nagoya, Japan
Supported by the Science and Technology Project Foundation of Guangdong Province, No. 2003C33706, and Grant-in-Aid for Scientific Research on Priority Areas (C) from the Ministry of Education, Science, Sports, Culture and Technology, Japan
Correspondence to: Dr. Ke Li, Department of Preventive Medicine, Shantou Medical University, Shantou 515041, Guangdong Province, China. kli@stu.edu.cn
Telephone: +86-754-8900445 Fax: +86-754-8557562
Received: 2004-07-23 Accepted: 2005-01-05

Abstract

AIM: This paper aims to develop a data-based semi-quantitative food frequency questionnaire (SQFFQ) covering both urban and rural areas in the Chaoshan region of Guangdong Province, China, for the investigation of relationships between food intake and lifestyle-related diseases among middle-aged Chinese.

METHODS: We recruited 417 subjects from the general population and performed an assessment of the diet, using a 3-d weighed dietary record survey. We employed contribution analysis (CA) and multiple regression analysis (MRA) to select food items covering up to a 90% contribution and a 0.90 R^2 , respectively. The total number of food items consumed was 523 (443 in the urban and 417 in the rural population) and the intake of 29 nutrients was calculated according to the actual consumption by foods/recipes.

RESULTS: The CA selected 233, 194, and 183 foods/recipes for the combined, the urban and the rural areas, respectively, and then 196, 157, and 160 were chosen by the MRA. Finally, 125 foods/recipes were selected for the final questionnaire. The frequencies were classified into eight categories and standard portion sizes were also calculated.

CONCLUSION: For adoption of the area-specific SQFFQ, validity and reproducibility tests are now planned to determine how the combined SQFFQ performs in actual assessment of disease risk and benefit.

© 2005 The WJG Press and Elsevier Inc. All rights reserved.

Key words: Nutrients; Weighed diet records; Contribution analysis; Multiple regression analysis

Song FY, Toshiro T, Li K, Yu P, Lin XK, Yang HL, Deng XL, Zhang YQ, Lv LW, Huang XE, Kazuo T. Development of a semi-quantitative food frequency questionnaire for middle-aged inhabitants in the Chaoshan area, China. *World J Gastroenterol* 2005; 11(26): 4078-4084
<http://www.wjgnet.com/1007-9327/11/4078.asp>

INTRODUCTION

Lifestyle is the most important environmental factor related to chronic diseases such as cardiovascular diseases, diabetes and cancer^[1-5], now the major causes of death in the developed countries and also increasing their impact in the developing world^[6]. While genetic factors are also of interest in terms of etiology, from the viewpoint of disease prevention, environmental factors are more important, because they are controllable and thus targetable for health promotion. Unlike smoking, which only does harm to health^[7], the diet has two profiles: appropriate intake is necessary for life, but excessive intake or imbalance may be deleterious. The investigation of reliable internal associations between food intake and health/diseases requires sufficient and accurate information on diet intake.

Increasing interest in relationships between long-term dietary intake and the occurrence of chronic disease has thus stimulated the development of evaluation methods to assess dietary factors among large groups of individuals. As a relatively new but efficient method, the semi-quantitative food frequency questionnaire (SQFFQ) has become widely used worldwide, especially in the US and European countries^[8,9]. Compared with other approaches, the SQFFQ has the following advantages: (1) it is simple and convenient to implement; (2) it has the ability to provide food information over a relatively long time period; (3) it can be applied with focuses on specific age groups^[10]. At present, the SQFFQ is therefore the best tool to obtain information for investigation of the relationship between the diet and health or disease.

Recently, the economic status in China has greatly

improved, but a nationwide survey of food and nutrient intake in the country has revealed that geographical variations between urban and rural areas still exist in most regions. This variation demands the development of an appropriate SQFFQ covering both urban and rural populations to investigate the association between dietary factors and cancer risk, cases naturally being recruited from both areas. To develop a feasible combined SQFFQ, we here conducted a survey of food and nutrient intake using a 3-d weighed dietary record method (WDR) in urban and rural areas of Chaoshan.

MATERIALS AND METHODS

The Chaoshan region, including Shantou, Chaozhou and Jieyang cities, is located in the east of Guangdong Province of China, with a population of approximately 10 million. People here still retain their own language and traditional culture. We have demonstrated that Nan'ao county in Chaoshan has the highest incidence and mortality rates of esophageal cancer in all China^[11]. We here selected Chaozhou and Jieyang areas, including Nan'ao county, as representative of the countryside, and Shantou as representative of the new city.

Study subjects

We initially recruited 520 healthy residents aged 30-55 years for participation in our investigation, but only 417 (200 males and 217 females) completed the 3-d WDR survey (70 in Chaozhou, 247 in Shantou and 100 in Nan'ao). The remainder dropped out because of their busy schedules or difficulties in recording. The fraction of sampling for the whole region was 41 per million.

Part juniors in the Chaozhou Normal College, staff of the Shantou Disease Preventive and Control Center, the Director General of the Nan'ao Board of Health and some doctors of Nan'ao Hospitals joined in our research team and were responsible for making contact with the subjects. Supervisors examined the completeness and accuracy of the information from the survey.

Dietary assessment

A 3-d WDR (2 weekdays and 1 weekend day) was performed from December 2002 to August 2003, with a 24-h recall method also used as a supplement. Foods/recipes were individually weighed and recorded for their raw weights before cooking, except with cooked foods bought from markets. The completeness and accuracy of information were also reviewed by the research nutritionists.

Nutrients of interest

The nutrients of interest comprised 29 items: energy, protein, fat, carbohydrates, crude fiber, retinol, carotene, vitamin C, vitamin E, folic acid, sodium, potassium, magnesium, calcium, iron, zinc, copper, selenium, phosphorus, saturated fatty acids (SFA), mono-unsaturated fatty acids (MUFA), poly-unsaturated fatty acids (PUFA), oleic acid, linoleic acid, arachidonic acid, linolenic acid, eicosapentaenoic acid (EPA), docosahexaenoic acid (DHA) and cholesterol.

Selection of foods/recipes

Nutrient intake was calculated by multiplying the food intake

(grams) by the nutrient content per gram of food listed in the China Food Composition 2002, compiled by the Institute of Nutrition and Food Safety, China CDC^[12]. Where necessary we also used data from the Japanese Standard Tables of Food Composition, 5th revised edition^[13] for the nutrient content of foods which were not listed in the China Food Composition.

The selection of food items for developing the SQFFQ was performed using the same procedure as adopted by Tokudome and his colleagues^[14]. At first, contribution analysis (CA) was performed for all nutrients of interest^[14-16], and each food item was listed according to the intake amount of nutrient. We selected food/recipe items with up to a 90% cumulative contribution. Then, multiple regression analysis (MRA) was carried out by adopting the total intake of specific nutrient as the dependent variable and overall amounts of this nutrient from the selected food/recipe items by CA as the independent variables for 417 individuals and secondly choosing foods/recipes with up to a 0.90 cumulative square of the multiple correlation coefficient^[14,16]. Finally, we determined food items for the SQFFQ both by CA and MRA. Some food items with up to 0.90 R^2 but very small % contribution were excluded, because they may be marginal for total nutrient intake. The foods contributing less than three nutrients, with relatively small % contributions, were also excluded. The statistical package SPSS for Windows 10.0 (SPSS Inc., Chicago, IL, USA) was employed for the data analysis.

Intake frequency

The food intake frequencies in SQFFQ were classified into seven categories: almost never; 1-3 times per month; 1-2 times per week; 3-4 times per week; 5-6 times per week; 1-2 times per day; and 3 times per day or more.

Portion size

The standard portion size of each food item per meal was determined using the mean amount, typical/standard value or the natural unit. Portion size in SQFFQ was divided into six categories: none, 0.5, 0.75, 1.0, 1.5, 2.0 or more. As estimation of condiment and oil consumption per meal was difficult, four categories were employed: none, less than normal, normal and more than normal. The normal intake was determined as the mean amount in the 3-d WDR, and allocation to less or more than normal was estimated with reference to the standard deviation. We also took pictures of the most representative foods with a standard portion size and made a food model booklet for standardization of the intake amount.

RESULTS

Characteristics of the subjects studied

Table 1 shows the characteristics of the investigated subjects. The mean age was slightly older for the rural than the urban subjects in both genders. Although the mean height was not different, the mean weight and BMI in urban males were larger than those in their rural counterparts, with statistical significance. This was not the case for females.

Intake of energy and selected nutrients

Table 2 shows mean intake and standard deviations for energy,

Table 1 Characteristics of the investigated subjects

	Males		P	Females		P
	Rural n = 115	Urban n = 102		Rural n = 102	Urban n = 98	
Age (yr)	43.1±6.9	42.4±7.1	0.803	42.9±6.8	41.3±7.7	0.245
Height (cm)	169.7±6.0	170.3±3.7	0.496	158.6±4.2	158.6±4.4	0.417
Weight (kg)	62.0±6.4	65.9±6.8	0.004	53.5±6.3	53.8±6.9	0.175
BMI	21.8±2.2	22.6±2.3	0.003	20.9±2.4	21.5±2.4	0.072

Table 2 Intake of nutrients by the urban and rural subjects

	Males		P	Females		P
	Rural n = 115	Urban n = 102		Rural n = 102	Urban n = 98	
Energy (kcal)	2 268±539	2 237±520	0.447	2 560±661	2 449±635	0.084
Protein (g)	83.5±26.7	85.5±23.8	0.375	85.0±27.4	91.8±27.3	0.244
Fat (g)	84.7±28.2	90.8±41.8	0.196	103.9±26.9	104.3±40.5	0.121
Carbohydrate (g)	295.1±106.8	271.9±101.1	0.320	327.2±129.8	301.3±111.8	0.758
Crude fiber (g)	10.2±4.7	10.0±3.7	0.707	9.5±3.6	12.0±9.8	0.017
Cholesterol (mg)	389.1±221.0	352.7±165.2	0.174	344.7±249.8	441.3±217.7	0.004
Carotene (μg)	2 576.7±2 105.7	2 693.8±2 009.1	0.675	2566.5±2132.6	3 487.0±1 872.2	0.001
Retinol (μg)	118.0±84.0	116.6±118.8	0.92	90.4±78.6	137.1±86.5	0.000
Folic acid (mg)	395.6±219.9	357.6±129.9	0.128	375.5±155.0	452.6±172.3	0.001
Vitamin C (mg)	88.4±52.3	80.4±39.6	0.205	96.2±61.0	102.2±38.8	0.416
Vitamin E (mg)	22.7±10.8	27.0±11.7	0.005	24.2±10.9	28.9±11.1	0.003
Calcium (mg)	525.6±191.7	446.8±190.2	0.412	406.9±187.4	505.0±155.1	0.000
Phosphorus (mg)	963.9±311.0	937.2±216.8	0.468	1 042.0±390.2	1 099.8±222.0	0.202
Potassium (mg)	1 718.0±575.5	1 745.0±459.3	0.705	1 808.9±666.6	2 006.6±453.2	0.015
Sodium (mg)	4 584.7±1 856.1	4 460.9±2 297.6	0.66	6 091.1±2 436.2	4 733.4±1 590.2	0.000
Magnesium (mg)	298.8±93.4	280.2±63.2	0.09	311.4±104.2	326.7±64.4	0.215
Iron (mg)	23.3± 8.8	22.9± 7.3	0.744	22.7±8.2	25.5±6.8	0.009
Zinc (mg)	12.73± 4.78	11.53±2.80	0.028	13.25±5.42	13.99±3.54	0.256
Selenium (μg)	64.92± 29.60	69.40±37.20	0.322	77.81±42.63	72.55±38.14	0.36
Copper (mg)	2.46±1.53	2.24±1.02	0.227	2.30±1.19	2.38±0.68	0.589
SFA (g)	21.14±7.51	22.83±7.92	0.107	24.12±10.56	25.84±8.78	0.215
MUFA (g)	32.05±10.68	35.83±10.47	0.009	36.53±15.36	42.34±10.26	0.002
PUFA (g)	18.62±8.27	23.01±9.70	0.000	21.90±15.58	26.41±8.92	0.013
Oleic acid (g)	29.40±9.79	33.12±9.76	0.005	33.50±13.74	38.46±9.39	0.003
Linoleic acid (g)	16.76±7.41	20.89±8.76	0.000	18.93±8.63	23.92±8.12	0.000
Linolenic acid (g)	1.64±1.30	1.67±1.46	0.895	1.74±1.62	2.76±2.06	0.000
Arachidonic acid (g)	0.088±0.041	0.087±0.041	0.951	0.092±0.056	0.096±0.047	0.626
EPA (g)	0.038±0.046	0.039±0.036	0.900	0.050±0.041	0.034±0.032	0.004
DHA (g)	0.079±0.100	0.069±0.063	0.385	0.118±0.095	0.072±0.073	0.000

SFA: saturated fatty acid; MUFA: mono-unsaturated fatty acid; PUFA: poly-unsaturated fatty acid; EPA: eicosapentaenoic acid; DHA: docosahexaenoic acid.

protein, fat, carbohydrate and other nutrients. Geographical variation of energy and major nutrient intake was not apparent in either sex, except for greater intake of crude fiber in urban males. Urban males and females consumed more vitamin E, MUFA, PUFA, oleic acid, and linoleic acid than rural subjects. In males, urban subjects consumed more cholesterol, carotene, retinol, folic acid, calcium, potassium and linolenic acid, whereas rural subjects had greater intakes of sodium, DHA and EPA. In females, rural subjects took more zinc and manganese.

We compared the consumption of each nutrient with the Recommended Nutrient Intake (RNI) for the first and second degree of work in China^[17]. The energy consumption in our urban and rural males was similar to RNI, but with females the values were high. The consumption of protein and fat in both genders of urban and rural areas was higher than the RNI, especially for fat, but that for carbohydrate was relatively low.

Selection of food items

The total number of food/recipe items consumed by all subjects over 3 d was 523 (443 and 417 in the urban and rural cases, respectively). The numbers of food items with up to 90% cumulative contribution for 29 nutrients were 233, 194, and 183 in the combined, urban and rural areas, and those for up to 0.9 cumulative R^2 were 196, 157, and 160, respectively. Then, we combined several food items with similar nutrient contents. Finally, we selected 125 food items for a combined SQFFQ. Alcohol beverages were not included in them, because the number of regular drinkers was very small. However, liquor and beer were intentionally added in this SQFFQ, because they are important dietary factors involved in the risk of diabetes and cancer^[4,5].

The number of food items selected for each nutrient by CA and MRA are listed in Table 3. The mean numbers by CA were 58, 46, and 48 for the combined, the urban and

Table 3 Numbers of foods contributing to 29 nutrients with up to 90 cumulative % and 0.9 cumulative r^2

	Cumulative %			Cumulative r^2		
	Rural	Urban	Combined	Rural	Urban	Combined
Energy	49	51	60	33	22	37
Protein	79	85	94	51	26	55
Fat	23	23	25	150	11	17
Carbohydrate	26	29	33	3	8	77
Crude fiber	65	61	74	74	13	21
Cholesterol	31	36	37	47	10	12
Carotene	23	21	38	47	12	8
Retinol	25	30	33	28	7	55
Folic acid	53	49	59	40	13	19
Vitamin C	38	27	44	52	17	70
Vitamin E	48	45	54	116	5	16
Calcium	94	93	104	70	19	30
Phosphorus	85	91	102	41	28	51
Potassium	114	99	120	63	36	1
Sodium	13	16	16	145	4	3
Magnesium	86	98	109	41	31	58
Iron	84	94	104	45	22	35
Zinc	72	78	86	41	15	44
Selenium	73	88	96	82	8	22
Copper	76	75	88	91	9	31
SFA	22	22	36	100	10	14
MUFA	16	17	21	70	9	8
PUFA	18	16	23	138	5	113
Oleic acid	15	15	17	142	6	8
Linoleic acid	17	15	18	143	5	8
Linolenic acid	31	28	56	136	1	2
Arachidonic acid (g)	24	32	53	53	17	17
EPA	22	32	51	30	17	23
DHA	14	29	36	24	13	12
Mean	46	48	58	72	14	30

SFA: saturated fatty acid; MUFA: mono-unsaturated fatty acid; PUFA: poly-unsaturated fatty acid; EPA: eicosapentaenoic acid; DHA: docosahexaenoic acid.

the rural cases, respectively, as compared with 30, 14, and 72 with the MRA.

List of food items

The percentage contributions of the top five foods/recipes for energy, protein, fat and carbohydrate for rural, urban

and combined areas are listed in Tables 4 and 5. Rice was the most important food source for energy, protein and carbohydrate intake, accounting for more than one-third of the energy, followed by peanut oil, pork, mixed oil, and lard, this being similar in both urban and rural areas. One-fourth of protein and more than two-thirds of carbohydrates

Table 4 Percentage contributions of the top five foods for energy and protein

Energy						Protein					
Rural		Urban		Combined		Rural		Urban		Combined	
Rice	45.8	Rice	38.2	Rice	41.9	Rice	28.6	Rice	23.6	Rice	25.7
Pork	7.7	Peanut oil	8.9	Peanut oil	7.8	Pork	7.5	Pork	6.6	Pork	6.8
Peanut oil	6.9	Pork	6.9	Pork	7.1	Grass carp	3.4	Beef	4.0	Grass carp	3.6
Mixed oil	4.2	Mixed oil	6.4	Mixed oil	5.3	Egg	3.2	Grass carp	3.8	Egg	3.5
Lard	4.1	Lard	3.2	Lard	3.7	Fish	2.9	Egg	3.8	Beef	2.9

Table 5 Percentage contribution of the top five foods for fat and carbohydrate

Fat						Carbohydrate					
Rural		Urban		Combined		Rural		Urban		Combined	
Peanut oil	21.7	Peanut oil	24.2	Peanut oil	22.9	Rice	70.4	Rice	67.5	Rice	70.4
Pork	20.2	Mixed oil	17.6	Pork	17.4	Noodle	3.2	Noodle	3.3	Noodle	3.2
Mixed oil	13.3	Pork	15.7	Mixed oil	15.6	Bread	2.3	Bread	3.0	Bread	2.3
Lard	13.1	Lard	11.0	Lard	11.0	Rice noodles	1.7	Rice noodles	2.1	Rice noodles	1.7
Pork chops	3.7	Pork chops	3.6	Pork chops	3.6	White sugar	1.6	White sugar	1.9	White sugar	1.6

were also contributed by rice. Peanut oil supplied more than one-fifth of fats, followed by pork, mixed oil, lard, pig chops and rice according to the CA. As for energy, the combined, urban and rural data also demonstrated almost have the same ranking for protein, fat and carbohydrate.

According to the category of the China Food Composition 2002, the 125 foods/recipes listed in the SQFFQ comprised: cereals (11 items), legumes (6), fresh legumes (3), vegetables (13), melons and nightshade (5), cauliflower (1), roots (7), fruits (11), meats (11), poultry (5), milk (2), eggs (3), pickles (4), marine products (16), mushrooms (5), nuts (2), cakes (3), condiments (6), oils (3) and beverages (8).

Nutrition coverage in the SQFFQ

Table 6 shows the percentage coverage of 29 nutrients by the SQFFQ. The selected food items covered 17, 19, and 16 nutrients with up to 90% of the total intake for the rural, urban and combined SQFFQ, and the lowest coverage percentage of the combined SQFFQ was still 82.7%, for linolenic acid.

DISCUSSION

The present study showed that variation in nutrient consumption between urban and rural subjects in the Chaoshan area was small, and the selected food items for the rural and urban SQFFQs were similar, covered all 29 nutrients with acceptable

percentage values. The present results thus revealed that development of a combined SQFFQ for rural and urban populations is feasible.

The nationwide survey of China held in 1992 showed the national average energy intake to be higher in urban than in rural areas, especially in those with middle and high incomes^[18]. Recent economic improvement may have reduced the variation in diet between rural and urban populations, and increased the amount of nutrient intake in both, but especially in rural individuals. The total energy intake in males was 2.4% higher in the present urban area and 21.0% higher in the rural area than those in the representative urban and rural areas of the same province by nationwide survey. The mean intakes of major nutrients in the present study were 6.4% higher in the urban area and 25.9% higher in the rural area for protein; 15.6% higher and 70.6% higher for fat; 2.1% lower and 1.0% higher for carbohydrate; and 31.9% higher and 15.9% higher for crude fiber, compared with the respective figures from the nationwide survey. The present urban population took more unsaturated fatty acid from vegetables, and the rural population took more animal fat, although geographical variation in total fat intake was not apparent.

Here we chose the 3-d WDR method as the “gold standard” rather than others to develop a SQFFQ for Chaoshan area, because it is the most efficient method for collecting dietary information at present. To decrease the

Table 6 Percentage coverage of nutrients by the SQFFQ

	% coverage		
	Rural	Urban	Combined
Energy	94.3	94.2	93.7
Protein	91.7	90.1	88.4
Fat	95.0	93.5	93.8
Carbohydrate	94.3	95.4	94.6
Crude fiber	86.5	87.3	87.5
Cholesterol	93.3	88.9	86.3
Carotene	88.7	93.9	90.3
Retinol	91.8	81.7	89.1
Folic acid	91.5	92.8	92.5
Vitamin C	86.3	94.6	91.2
Vitamin E	89.7	88.3	89.4
Calcium	87.3	87.3	88.6
Phosphorus	92.4	90.5	86.4
Potassium	86.8	90.5	88.2
Sodium	97.7	96.1	95.1
Magnesium	89.7	90.9	90.1
Iron	83.5	90.3	89.6
Zinc	90.9	91.9	91.6
Selenium	86.6	83.7	85.8
Copper	87.9	86.8	87.4
SFA	94.7	90.5	92.6
MUFA	96.2	95.6	88.4
PUFA	91.1	91.7	97.6
Oleic acid	96.5	95.7	90.2
Linoleic acid	94.2	92.1	97.6
Linolenic acid	91.2	92.2	82.7
Arachidonic acid (g)	90.3	88.5	92.7
EPA	82.4	80.2	87.6
DHA	88.4	81.9	82.9
Mean	90.7	90.2	90.0

SFA: saturated fatty acid; MUFA: mono-unsaturated fatty acid; PUFA: poly-unsaturated fatty acid; EPA: eicosapentaenoic acid; DHA: docosahexaenoic acid.

influence of seasonal variation on food survey, we conducted the survey in three seasons of winter, spring and summer, because there is no major climatic difference between the fall and winter. Although the sample size was relatively small, the number of subjects appeared sufficient from previous studies to develop SQFFQs, including the ones conducted in China^[14,19,20].

We used the two contrasting methods of CA and MRA to select representative food items for stable food intake. Each method has its own particular advantages and disadvantages^[13,14]. The former approach is based on the absolute food and nutrient intake and is especially suitable for investigation of the associations between absolute nutrient intake and disease risk. The latter, in contrast, is based on variance of nutrient intake, and is efficient for categorizing individuals. Therefore, the combination of the two methods for food selection should provide a more suitable SQFFQ for the assessment of food and nutrient intake.

We selected 125 food items, including alcoholic beverages, for the combined SQFFQ. Most were frequently consumed by the local inhabitants. Although the coverage rates of all 29 nutrients were over 80%, the potential for overestimation or underestimation does exist, because of

the incompleteness of the composition table, and the exclusion of food items, such as some marine products, in the selection for the SQFFQ.

We have already developed data-based SQFFQs in Jiangsu, in the central coastal region of China, and Chongqing, more than 1 000 km west inland from Jiangsu, using a standardized method developed in Japan^[14]. We compared the top three food items of three SQFFQs developed in Jiangsu^[19], Chongqing^[20] and the present study area, Chaoshan, more than 1 000 km south of Jiangsu, according to the percentage contribution for energy, protein, fat and carbohydrate by the urban and rural area (Table 7). Most items were shared in common, except for fat. These comparisons suggest the possibility to developing a common SQFFQ to assess and compare dietary factors impacting on cancer by the standardized method^[21].

In summary, in the present investigation we clarified common intake of foods and 29 nutrients in urban and rural areas of Chaoshan, Guangdong Province, China, for adoption in an area-specific SQFFQ. Validity and reproducibility tests^[22-24] are now planned to determine how the combined SQFFQ performs in the actual assessment of disease risk and benefit.

Table 7 Comparison of percentage contributions of the top three foods for energy, protein, fat, and carbohydrates in urban and rural areas of Jiangsu, Chongqing and Chaoshan in China

		Percentage contribution					
Energy							
Urban							
	Jiangsu	Rice	36.9	Salad oil	6.9	Flour	5.9
	Chongqing	Rice	30.1	Rape oil	10.2	Pork	6.2
	Chaoshan	Rice	45.8	Pork	7.7	Peanut oil	6.9
Rural							
	Jiangsu	Rice	39.5	Lard	14.2	Pork	5.3
	Chongqing	Rice	32.1	Rape oil	12.2	Flour	7.7
	Chaoshan	Rice	38.2	Peanut oil	8.9	Pork	6.9
Protein							
Urban							
	Jiangsu	Rice	23.1	Pork	7.2	Egg	5.0
	Chongqing	Rice	17.5	Horse bean	8.0	Pork	6.5
	Chaoshan	Rice	28.6	Pork	7.5	Grass card	3.4
Rural							
	Jiangsu	Rice	34.4	Pork	6.5	Egg	4.3
	Chongqing	Rice	20.4	Pork	7.4	Flour	7.0
	Chaoshan	Rice	23.6	Pork	6.6	Beef	4.0
Fat							
Urban							
	Jiangsu	Salad oil	22.1	Soybean oil	17.1	Pork	9.5
	Chongqing	Rape oil	30.0	Pork	15.3	Salad oil	1.5
	Chaoshan	Peanut oil	21.7	Pork	20.2	Salad oil	13.3
Rural							
	Jiangsu	Lard	45.8	Pork	16.4	Rape oil	11.7
	Chongqing	Rape oil	32.3	Lard	13.5	Pork	12.2
	Chaoshan	Peanut oil	24.2	Salad oil	17.6	Pork	15.7
Carbohydrate							
Urban							
	Jiangsu	Rice	57.1	Flour	8.7	Noodle	2.9
	Chongqing	Rice	55.1	Flour	10.3	Noodle	7.9
	Chaoshan	Rice	73.7	Noodle	2.8	Bread	1.7
Rural							
	Jiangsu	Rice	59.6	Noodle	5.8	Corn	5.7
	Chongqing	Rice	60.1	Flour	16.6	Peas	2.8
	Chaoshan	Rice	67.5	Noodle	3.3	Bread	3.0

ACKNOWLEDGMENT

The authors thank Dr. Malcolm A. Moore for his language assistance in preparing this manuscript.

REFERENCES

- 1 **Chen H**, Zhang S, Hernan M, Willett WC, Ascherio A. Dietary intakes of fat and risk of Parkinson's disease. *Am J Epidemiol* 2003; **157**: 1007-1014
- 2 **Blumenfeld A**, Fleshner N, Casselman B, Trachtenberg J. Nutritional aspects of prostate cancer: a review. *Can J Urol* 2000; **7**: 927-935
- 3 **Swinburn B**. Sustaining dietary changes for preventing obesity and diabetes: lessons learned from the successes of other epidemic control programs. *Asia Pac J Clin Nutr* 2002; **11** (Suppl 3): S598-606
- 4 **Wannamethee S**, Camargo C Jr, Manson J. Alcohol drinking patterns and risk of type 2 diabetes mellitus among younger women. *Arch Intern Med* 2003; **163**: 1329-1336
- 5 **Willett W**. Diet and cancer. *Oncologist* 2000; **5**: 393-404
- 6 **Kopczynski J**, Wojtyniak B, Gorynski P, Lewandowski Z. The future of chronic diseases. *Cent Eur J Public Health* 2001; **9**: 3-13
- 7 **Pride N**, Soriano J. Chronic obstructive pulmonary disease in the United Kingdom: trends in mortality, morbidity, and smoking. *Curr Opin Pulm Med* 2002; **8**: 95-101
- 8 **Bergmann M**, Bussas U, Boeing H. Follow-up procedures in EPIC-Germany-data quality aspects. European prospective investigation into cancer and nutrition. *Ann Nutr Metab* 1999; **43**: 225-234
- 9 **Key TJ**, Appleby PN, Davey GK, Allen NE, Spencer EA, Travis RC. Mortality in British vegetarians: review and preliminary results from EPIC-Oxford. *Am J Clin Nutr* 2003; **78** (3 Suppl): 533S-538
- 10 **Willett W**, Colditz G. Approaches for conducting large cohort studies. *Epidemiol Rev* 1998; **20**: 91-99
- 11 **Li K**. Mortality and incidence trends from esophagus cancer in selected geographic areas of China circa 1970-90. *Int J Cancer* 2002; **102**: 271-274
- 12 **Yang YX**, Wang GY, Pan XC. China Food Composition 2002. Beijing: *Peking University Medical Press* 2002: 21-338
- 13 Resources Council, Science and Technology Agency, Japan. Standard Tables of Food Composition in Japan, 5th revised ed. Tokyo: *Resource Council Science and Technology Agency* 2000: 29-303
- 14 **Tokudome S**, Ikeda M, Tocudome Y, Imaeda N, Kitagawa I, Fujiwara N. Development of a data-based semi-quantitative food Frequency questionnaire for dietary studies in middle-aged Japanese. *Jpn J Clin Oncol* 1998; **28**: 679-687
- 15 **Stiggelbout AM**, van der Giezen AM, Blauw YH, Blok E, van Staveren WA, West CE. Development and relative validity of a food frequency questionnaire for the estimation of intake of retinol and beta-carotene. *Nutr Cancer* 1989; **12**: 289-299
- 16 **Overvad K**, Tjonneland A, Haraldsdottir J, Ewertz M, Jensen OM. Development of a semiquantitative food frequency questionnaire to assess food, energy and nutrient intake in Denmark. *Int J Epidemiol* 1991; **20**: 900-905
- 17 Chinese Nutrition Society. Chinese Dietary Reference Intakes, DRIs. *Yingyang Xuebao* 2001; **3**: 193-196
- 18 **Ge KY**, Zhai FY, Yan HC, Cheng L, Wang Q, Jia FM. The dietary and nutritional status of chinese population in 1990s. *Yingyang Xuebao* 1995; **2**: 123-134
- 19 **Wang YM**, Mo BQ, Takezaki T, Imaeda N, Kimura M, Wang XR, Tajima K. Geographical variation in nutrient intake between urban and rural areas of Jiangsu province, China and development of a semi-quantitative food frequency questionnaire for middle-aged inhabitants. *J Epidemiol* 2003; **13**: 80-89
- 20 **Zhou Z**, Takezaki T, Mo B, Sun H, Wang W, Sun L, Liu S, Ao L, Cheng G, Wang Y, Cao J, Tajima K. Geographical variation in nutrient intake between urban and rural areas of Chongqing, China and development of a data-based semi-quantitative food frequency questionnaire for both populations. *Asia Pac J Clin Nutr* 2004; **13**: 273-283
- 21 **Aydemir G**. Research on nutrition and cancer: The importance of the standardized dietary assessments. *Asian Pac J Cancer Prev* 2002; **3**: 177-180
- 22 **Tokudome S**, Imaeda N, Tocudome Y, Fujiwara N, Nagaya T, Sato J, Kuriki K, Ikeda M, Maki S. Relative validity of a semi-quantitative food frequency questionnaire versus 28 d weighed diet records in Japanese female dietitians. *Eur J Nutr* 2001; **55**: 735-742
- 23 **Imaeda N**, Fujiwara N, Tokudome Y, Ikeda M, Kuriki K, Nagaya T, Sato J, Goto C, Maki S, Tokudome S. Reproducibility of a semi-quantitative food frequency questionnaire in Japanese female dietitians. *J Epidemiol* 2003; **12**: 45-53
- 24 **Kim J**, Kim DH, Ahn YO, Tokudome Y, Hamajima N, Inoue M, Tajima K. Reproducibility of a food frequency questionnaire in Koreans. *Asian Pac J Cancer Prev* 2003; **4**: 253-257

Science Editor Guo SY Language Editor Elsevier HK

• BRIEF REPORTS •

Prevalence of hepatitis C virus infection and its related risk factors in drug abuser prisoners in Hamedan - Iran

Amir Houshang Mohammad Alizadeh, Seyed Moayed Alavian, Khalil Jafari, Nastaran Yazdi

Amir Houshang Mohammad Alizadeh, Research Center for Gastroenterology and Liver Disease, Shaheed Beheshti University of Medical Sciences, Tehran, Iran

Seyed Moayed Alavian, Baghiatallah University of Medical Sciences, Tehran, Iran

Khalil Jafari, Nastaran Yazdi, Hamedan University of Medical Sciences, Hamedan, Iran

Correspondence to: Amir Houshang Mohammad Alizadeh, Research Center for Gastroenterology and Liver Disease, Shaheed Beheshti University of Medical Sciences, 7th Floor, Taleghani Hospital, Yaman Str., Evin, Tehran 19857, Iran. article@rcgld.org
Telephone: +98-21-2418871 Fax: +98-21-2402639

Received: 2004-10-12 Accepted: 2004-10-26

2005; 11(26): 4085-4089

<http://www.wjgnet.com/1007-9327/11/4085.asp>

Abstract

AIM: Recent studies in Iran has shown that prevalence of hepatitis C virus (HCV) infection among Iranian prisoners is high, in spite of low HCV seroprevalence in general population.

METHODS: This study was carried out in the central prison of Hamedan - Iran, in year 2002. Inmates were interviewed using a standard questionnaire including demographic, imprisonment history and HCV-related risk behaviors items. Thereafter, the sera drawn from the participants were tested for anti-HIV and anti-HCV antibodies.

RESULTS: A total number of 427 drug abuser inmates participated in our study. Three hundred and ninety-seven (93%) were men and 30 (7%) were women. Total number of IV drug abusers (IDA) and non-IV drug abusers (NIDA) was 149 (34.9%) and 278 (65.1%), respectively. The overall rate of antibody positivity among inmates was 0.9% for HIV and 30% for HCV. Of all IDAs, 31.5% and of NIDAs, 29.1% had serological evidence of HCV infection.

CONCLUSION: The seroprevalence of HCV infection among drug abuser prisoners in comparison with the general population in Iran, is very high (30% *vs* in italics 0.2%). Our results indicate the importance of policies to prevent transmission of HCV infection during and following incarceration.

© 2005 The WJG Press and Elsevier Inc. All rights reserved.

Key words: Hepatitis C virus; Prisoners; Drug abusers; Iran

Alizadeh AHM, Alavian SM, Jafari K, Yazdi N. Prevalence of hepatitis C virus infection and its related risk factors in drug abuser prisoners in Hamedan - Iran. *World J Gastroenterol*

INTRODUCTION

Hepatitis C virus (HCV) infection is increasingly recognized as a major health care problem throughout the world. Approximately 85% of individuals infected with HCV will develop chronic HCV infection^[1,2]. Identified risk factors for HCV infection include intravenous drug use, exposure to infected blood/blood products, and intranasal drug use^[3]. Surveys of HCV infection among IDU have reported prevalence rates as high as 70-90%^[4-6] among habitual injectors. High risk sexual activity (multiple sexual partners), history of sexually transmitted disease, tattooing, and skin piercing have also been suggested to be associated with increased risk for HCV; however, study results have been contradictory^[7].

Whereas the overall seroprevalence of HCV among Iranian blood donors has been estimated to be 0.12%^[8] the prevalence of HCV has been shown to be as high as 45% in populations of incarcerated IV drug users^[9]. HCV seroprevalence among prison inmates varies markedly from country to country^[10,11]. Worldwide hepatitis C data similarly report significant prevalence figures in high risk populations ranging from 30% to 50%, with intravenous drug use being the predominant risk factor^[12-15]. High risk populations are individuals most at risk for hepatitis C, including those medically underserved, have a history of IV drug injection and high-risk behaviors. A dramatic growth in the number of prisoners associated with high-risk behaviors and high rates of community re-entry emphasizes the need for detection and treatment of hepatitis C virus infection in this unique group.

This study could be of particular interest, as in comparison with worldwide hepatitis C data, the seroprevalence of hepatitis C infection among Iranian general population is low. However, recent studies in Iran has shown that the level of hepatitis C infection among Iranian prisoners is as high as HCV seroprevalence in incarcerated population of countries with high prevalence of HCV infection in their general population.

MATERIALS AND METHODS

This study was carried out in the central prison of Hamedan (one of the largest penal institutions in Iran), from mid-June to mid-September 2002. The study protocol conforms to the ethical guideline of the 1975 Declaration of Helsinki, as revised in 1983. The sample was selected by drawing the numbered individual prison files, available to investigators,

in intervals determined by a random number generator. There were 427 drug abuser inmates in our study. Participation in this study was voluntary and confidentiality was guaranteed. All inmates were counseled about the study and they were required to provide signed informed consent. Thereafter, inmates were interviewed using a standard questionnaire including demographic items, specific questions relative to their imprisonment history and HCV-related risk behaviors such as intravenous drugs abuse, having received blood and/or blood products, tattoos, body piercing, sexual activity, and history of sexually transmitted diseases.

Physical examination was performed on all participants and afterward 8 mL of blood was taken. The sera were tested for anti-HIV and anti-HCV antibodies by using an enzyme-linked immunosorbant assay (ELISA) 3rd generation (for anti-HCV antibodies we used HCV 3.0 ELISA Test System with Enhanced SAvE; ORTHO®, Raritan, NJ, USA). All anti-HCV Ab positive sera were retested, using recombinant immunoblot assay (RIBA) 2nd generation (HCV Blot 3.0; Genelabs® Diagnostics, Singapore) as a complementary test. Patients with both ELISA and RIBA positive reports were considered to be infected with HCV.

Microsoft Access 2000 database software was used (Microsoft Corp., Redmond, WA, USA). Basic descriptive statistics were performed using SPSS for Windows (version 11.0; SPSS Inc., Chicago, IL, USA) software. Risk factors prevalences were generated using data from all consented study participants. Standard χ^2 and χ^2 trend tests were performed to assess the univariate relationship of demographic and behavioral variables and HCV seroprevalence. Univariate ORs were computed with 95% confidence intervals (CIs) for each risk factor.

RESULTS

A total number of 427 drug abuser inmates participated in

our study. Three hundred and ninety-seven (93%) were men and 30 (7%) were women. Total number of IV drug abusers (IDA) was 149 (34.9%). The remaining 278 individuals (65.1%) were non-IV drug abusers (NIDA). Demographic characteristics of drug abuser inmates are depicted in Table 1.

The overall rate of antibody positivity among inmates for HIV was 0.9% (4/427) and for HCV was 30% (128/427). Of all IDAs, 31.5% (47/149) had serological evidence of HCV infection and in NIDAs seropositivity for HCV was 29.1% (81/278). There were no significant statistical differences for HCV seropositivity between the two groups.

About HIV infection in the two groups, only one inmate (out of 149, 0.67%) was seropositive for HIV in IDA group and in NIDA we found three inmates with anti-HIV antibodies (3/278, 1.07%). Because the number of HIV infected participants was small, no statistical comparisons were conducted. Among three HIV positive individuals, all were male and their ages were between 30 and 49 (mean 37.5), one was IV drug abuser for 36 mo, one reported history of tattoos and one had received blood transfusion, they spent 2-26 mo in prison.

As shown in Table 1, the pattern of HCV antibody prevalence differed within each demographic characteristic.

The mean \pm SD of participants was 37.9 \pm 9.7 (range 15-77 years old). Most participants belonged to 30-39 years old age group (34.7%) and HCV seropositivity in \leq 20 years and 40-49 years old age group was highest (40% and 31.6%, respectively; $P = 0.70$).

None of the inmates had high risk job (health-care related) be infected by HCV or HIV. 42.6% of HCV seropositive participants were labourers and 41% had private business, 8.2% were farmers, 6.6% housekeepers, and 1.6% were unemployed (no significant difference, $P = 0.4$).

As depicted in Table 2, we studied the association between some behavioral characteristics and HCV seropositivity. The

Table 1 Demographic characteristics and their association with HCV seropositivity among drug abuser inmates, Hamedan, Iran

Variable	Total (n = 427)		HCV positive ¹ (n = 128) ²	
	n	%	n	%
Sex				
Male	397	93	119	93
Female	30	7	9	7
Age group (yr)				
<20	5	1.2	2	1.6
20-29	83	19.6	26	20.4
30-39	148	34.9	45	35.1
40-49	136	32.1	43	33.5
50-59	41	9.7	11	8.6
60 or more	11	2.6	1	0.8
Marital status				
Single	136	31.9	48	37.5
Married	291	68.1	80	62.5
Education level				
Uneducated	141	33	32	25
Primary school	191	44.8	60	46.9
High school	89	20.8	33	25.8
University	6	1.4	3	2.3
Total	427	100	128	30

¹We found no significant statistical difference. ²Basis of numbers and %s may be slightly smaller due to missing values.

Table 2 Behavioral characteristics and their association with HCV seropositivity among drug Abuser prisoners in Hamedan, Iran

Variable	Total (n = 427) n (%)	HCV positive ¹ (n = 128) ²		
		n (%)	P	(OR, 95%CI) ³
Months of imprisonment			0.02	
<12	49 (12.5)	11 (22.4)		
12-23	75 (19.1)	26 (34.7)		
24-35	70 (17.9)	19 (27.1)		
36-47	57 (14.5)	14 (24.6)		
48-59	42 (10.7)	13 (31)		
60-71	21 (5.4)	7 (33.3)		
72-83	25 (6.4)	10 (40)		
84-95	9 (2.3)	1 (11.1)		
96-107	6 (1.5)	5 (83.3)		
108-119	2 (0.5)	2 (100)		
>120	36 (9.2)	8 (22.2)		
History of blood transfusion			0.1	(1.5, 0.8-2.8)
No	300 (89)	110 (28.9)		
Yes	47 (11)	18 (38.3)		
History of phlebotomy			0.7	(1.1, 0.5-2.2)
No	387 (90.6)	115 (29.7)		
Yes	40 (9.4)	13 (32.5)		
History of getting wounded			0.4	(0.8, 0.5-1.2)
No	238 (55.7)	75 (31.5)		
Yes	189 (44.3)	53 (28)		
History of STD ⁴			0.5	(1.4, 0.4-3.9)
No	378 (95.9)	113 (29.9)		
Yes	16 (4.1)	6 (37.5)		
History of tattooing			0.8	(1.05, 0.7-1.6)
No	184 (43.1)	54 (29.3)		
Yes	243 (56.9)	74 (30.5)		
History of surgery			0.2	(1.3, 0.8-2.01)
No	285 (66.7)	80 (28.1)		
Yes	142 (33.3)	48 (33.8)		
History of dental procedure			0.9	(0.9, 0.4-2.2)
No	26 (6.1)	8 (30.8)		
Yes	401 (93.9)	120 (29.9)		
Months of IV drug abuse			0.1	(1.7, 0.9-3)
<12	104 (69.8)	29 (27.9)		
≥12	45 (30.2)	18 (40)		
Sharing needles			0.6	(0.8, 0.4-1.7)
No	77 (18.3)	26 (33.8)		
Yes	72 (16.8)	22 (30.6)		

¹Hepatitis C Virus. ²Basis of numbers and %s may be slightly smaller due to missing values. ³Odds ratio, 95% confidence interval. ⁴Sexually transmitted disease.

seroprevalence of HCV was associated with duration of imprisonment ($P = 0.02$). Remarkably, 100% of the individuals who reported 108-119 mo of imprisonment were infected with HCV.

DISCUSSION

High risk populations are individuals most at risk of contracting hepatitis C, including those who come from medically underserved and minority communities and /or have a history of IV drug injection, alcohol abuse, and multiple sex partners^[16]. IV drug abusing remains the predominant mode of HCV transmission risk in prison systems^[17].

In this study we evaluated the seroprevalence of HCV and HIV among drug abuser inmates (IV drug abusers (IDA) and non-IV drug abusers (NIDA)). Prevalence of HCV antibody positivity among all participants was 30%. HCV seroprevalence in IDA and NIDA groups was 31.5% and 29.1%, respectively, and confirms the high prevalence of

blood borne disease in those with imprisonment history^[18-20]. Different studies have estimated the seroprevalence of HCV antibody among the general population (blood donors, mostly) to be about 0.16-6% world-wide^[8,21-24]. In high risk population in comparison to the general population, IV drug abusing, sharing needles and tattooing may increase risk status.

We found only one published similar investigation on Iranian prisoners. In Zali *et al.* study^[9], the seroprevalence of HCV among IDAs was 45%. In the studies on prisoners of Australia, Brazil, France, India, Ireland, UK and United States the HCV seroprevalence were about 38%, 6.3%, 30%, 16%, 37%, 30%, and 41%, respectively^[25-28,10,12,13]. According to other investigations worldwide, hepatitis C antibody positivity prevalence in high risk ranges from 31% to 50%, while intravenous drug abuse is the predominant risk factor^[11,29-33].

Limited available data indicate the majority of HCV infections are acquired before incarceration^[16]. Blood serum evaluations among 265 male prison inmates in Maryland

(USA) revealed a hepatitis C prevalence of 38% at intake^[34].

In our study, the overall rate of HIV antibody among prisoners was 0.9% (4/427). In IDA and NIDA groups, we found 0.67% and 1.07% positive HIV antibodies. The HCV prevalence rate in our study was higher than HIV prevalence. However, the findings are in accordance with those in many countries - including Germany, Nederland, Switzerland and Australia^[35,36]. In Iran we have no similar investigation on HIV seroprevalence of prisoners in comparison with our results.

Prevalence of antibodies of HIV in Irish and Brazilian prisoners was 2% and 3.2%, respectively^[13,26]. The HIV prevalence reported in prison studies from other developed countries is similar^[37-40].

Some limitations of our study should be considered. As with any convenience sample, this study had the limitation of being a self-selected group and may not be a representative of all Iranian prisoners. In addition, because of religious beliefs and security problems of prisons, many individuals could not respond properly to the questions containing sex behavior characteristics. Therefore we excluded the sex behavior related risk factors from statistical analysis. Because of financial problems we couldn't perform PCR on our samples.

In our investigation we studied some risk factors related to HCV and HIV infection. Participants who had spent more time in prison, however, and those who had history of hospitalization were significantly more likely to be positive for antibodies to HCV. Being in prison in Iran may be an independent risk factor for hepatitis C infection. We found no statistical association between HCV and other risk factors and there was no significant difference in HCV seropositivity prevalence between IV drug abusers and non IV drug abusers recommending the possibility of some other unknown etiologic factors. The high percentage of HCV positive cases with no apparent risk factor further emphasizes the need for further investigation on the routes of transmission and other factors, which have not yet been concerned. It should be noted that in some investigations, there were considerable numbers of HCV infected cases with no apparent risk factors, depicting the complex nature of HCV transmission^[41-45].

Although the inmates participating in this study cannot be considered representative of all prisoners in Iran, the results obtained have important implications for penal and public health administrators, indicating the importance of policies to prevent transmission of these infections during and following incarceration. These policies must include primary concern on not only identification of those most at risk but also on provision of appropriate treatment^[8,12,16,26]. Specific harm-reduction strategies directed toward preventative education and counselling are also crucial. In addition, testing programs in prisons, which should be seen as an opportunity to improve the health outcome of those infected and prevent further transmission of infectious agents^[46-48].

There are few studies involving large multicentre sampling that provided epidemiological aspects of HCV infection among prison inmates in Iran. In conclusion, prospective studies with meticulous assessment of confounding risk factors are required to assess the potential risk factors of HCV and HIV infections in prisons of Iran, effectively.

REFERENCES

- 1 **Conry-Cantilena C**, VanRaden M, Gibble J, Melpolder J, Shakil AO, Viladomiu L, Cheung L, DiBisceglie A, Hoofnagle J, Shih JW, Kaslow R, Ness P, Alter HJ. Routes of infection, viremia, and liver disease in blood donors found to have hepatitis C virus infection. *N Engl J Med* 1996; **334**: 1691-1696
- 2 **Alter MJ**, Margolis HS, Krawczynski K, Judson FN, Mares A, Alexander WJ, Hu PY, Miller JK, Gerber MA, Sampliner RE. The natural history of community-acquired hepatitis C in the United States. The Sentinel Counties Chronic non-A, non-B Hepatitis Study Team. *N Engl J Med* 1992; **327**: 1899-1905
- 3 **Alter HJ**, Conry-Cantilena C, Melpolder J, Tan D, Van Raden M, Herion D, Lau D, Hoofnagle JH. Hepatitis C in asymptomatic blood donors. *Hepatology* 1997; **26**(Suppl 1): 29-33
- 4 **Crofts N**, Hopper JL, Milner R, Breschkin AM, Bowden DS, Locarnini SA. Blood-borne virus infections among Australian injecting drug users: implications for spread of HIV. *Eur J Epidemiol* 1994; **10**: 687-694
- 5 **Goldberg D**, Cameron S, McMenamin J. Hepatitis C virus antibody prevalence among injecting drug users in Glasgow has fallen but remains high. *Commun Dis Public Health* 1998; **1**: 95-97
- 6 **Samuel MC**, Doherty PM, Bulterys M, Jenison SA. Association between heroin use, needle sharing and tattoos received in prison with hepatitis B and C positivity among street-recruited injecting drug users in New Mexico, USA. *Epidemiol Infect* 2001; **127**: 475-484
- 7 **Alter MJ**. Hepatitis C virus infection in the United States. *J Hepatol* 1999; **31**: 88-91
- 8 **Alavian SM**, Gholami B, Masarrat S. Hepatitis C risk factors in Iranian volunteer blood donors: a case-control study. *J Gastroenterol Hepatol* 2002; **17**: 1092-1097
- 9 **Zali MR**, Noroozi A, Amirrasooli H, Darvishi M. Prevalence of Anti-HCV antibody and routes of hematological transmission in addicts of Ghasr prison[in persian]. *Pajouhesh* 1998; **22**: 26-32
- 10 **Skipper C**, Guy JM, Parkes J, Roderick P, Rosenberg WM. Evaluation of a prison outreach clinic for the diagnosis and prevention of hepatitis C: implications for the national strategy. *Gut* 2003; **52**: 1500-1504
- 11 **Crofts N**, Stewart T, Hearne P, Ping XY, Breshkin AM, Locarnini SA. Spread of bloodborne viruses among Australian prison entrants. *BMJ* 1995; **310**: 285-288
- 12 **Spaulding A**, Greene C, Davidson K, Schneidermann M, Rich J. Hepatitis C in state correctional facilities. *Prev Med* 1999; **28**: 92-100
- 13 **Allwright S**, Bradley F, Long J, Barry J, Thornton L, Parry JV. Prevalence of antibodies to hepatitis B, hepatitis C, and HIV and risk factors in Irish prisoners: results of a national cross sectional survey. *BMJ* 2000; **321**: 78-82
- 14 **Weild AR**, Gill ON, Bennett D, Livingstone SJ, Parry JV, Curran L. Prevalence of HIV, hepatitis B, and hepatitis C antibodies in prisoners in England and Wales: a national survey. *Commun Dis Public Health* 2000; **3**: 121-126
- 15 **Burattini M**, Massad E, Rozman M, Azevedo R, Carvalho H. Correlation between HIV and HCV in Brazilian prisoners: evidence for parenteral transmission inside prison. *Rev Saude Publica* 2000; **34**: 431-436
- 16 **Reindollar RW**. Hepatitis C and the correctional population. *Am J Med* 1999; **107**: 100-103
- 17 **Alter MJ**. Epidemiology of hepatitis C. *Hepatology* 1997; **26** (3 Suppl 1): 62-65
- 18 **Capoccia A**, Ranieri R, Busnelli M, Passaretti B, Milella AM, Vecchi L. Serologic study on the prevalence of HIV, HBV infection and on the false positive reaction of VDRL at a prison. *Minerva Med* 1991; **82**: 125-130
- 19 **Glaser JB**, Greifinger RB. Correctional health care: a public health opportunity. *Ann Intern Med* 1993; **118**: 139-145
- 20 **Hoxie NJ**, Chen MH, Prieve A, Haase B, Pfister J, Vergeront JM. HIV seroprevalence among male prison inmates in the Wisconsin Correctional System. *WJG* 1998; **97**: 28-31
- 21 **Merino-Conde E**, Orozco JA, Rojo-Medina J, Tovar A.

- Prevalence of hepatitis C virus among candidates for blood donation at the Hospital General de Mexico. *In Vivo* 1994; **8**: 621-623
- 22 **Ito S**, Yao DF, Nii C, Hibino S, Kamamura M, Nisikado T, Honda H, Shimizu I, Meng XY. Epidemiological characteristics of the incidence of hepatitis C virus (C100-3) antibodies in patients with liver diseases in the inshore area of the Yangtze River. *J Gastroenterol Hepatol* 1993; **8**: 232-237
- 23 **Soni PN**, Tait DR, Kenoyer DG, Fernandes-Costa F, Naicker S, Gopaul W, Simjee AE. Hepatitis C virus antibodies among risk groups in a South African area endemic for hepatitis B virus. *J Med Virol* 1993; **40**: 65-68
- 24 **Allen SA**, Spaulding AC, Osei AM, Taylor LE, Cabral AM, Rich JD. Treatment of chronic hepatitis C in a state correctional facility. *Ann Intern Med* 2003; **138**: 187-190
- 25 **Butler TG**, Dolan KA, Ferson MJ, McGuinness LM, Brown PR, Robertson PW. Hepatitis B and C in New South Wales prisons: prevalence and risk factors. *Med J Aust* 1997; **166**: 127-130
- 26 **Catalan-Soares BC**, Almeida RT, Carneiro-Proietti AB. Prevalence of HIV-1/2, HTLV-I/II, hepatitis B virus (HBV), hepatitis C virus (HCV), *Treponema pallidum* and *Trypanosoma cruzi* among prison inmates at Manhuacu, Minas Gerais State, Brazil. *Rev Soc Bras Med Trop* 2000; **33**: 27-30
- 27 **Claudon-Charpentier A**, Hoibian M, Glasser P, Lalanne H, Pasquali JL. Drug-addicted prisoners: seroprevalence of human immunodeficiency virus and hepatitis B and C virus soon after the marketing of buprenorphine. *Rev Med Interne* 2000; **21**: 505-509
- 28 **Kar P**, Gangwal P, Budhiraja B, Singhal R, Jain A, Madan K, Gupta RK, Barua SP, Nath MC. Analysis of serological evidence of different hepatitis viruses in acute viral hepatitis in prisoners in relation to risk factors. *Indian J Med Res* 2000; **112**: 128-132
- 29 **Ford PM**, White C, Kaufmann H, MacTavish J, Pearson M, Ford S, Sankar-Mistry P, Connop P. Voluntary anonymous linked study of the prevalence of HIV infection and hepatitis C among inmates in a Canadian federal penitentiary for women. *CMAJ* 1995; **153**: 1605-1609
- 30 **Pinducciu G**, Arnone M, Piu G, Usai M, Melis A, Pintus L, Pitzus F. Prevalence of hepatitis virus (HBV and HCV) and HIV-1 infections in a prison community. *Ann Ig* 1990; **2**: 359-363
- 31 **Nara K**, Kawano M, Igarashi M. Prevalence of hepatitis C virus and human immunodeficiency virus infection among female prison inmates in Japan [In Japanese]. *Nippon Koshu Eisei Zasshi* 1997; **44**: 55-60
- 32 **Holsen DS**, Harthug S, Myrmed H. Prevalence of antibodies to hepatitis C virus and association with intravenous drug abuse and tattooing in a national prison in Norway. *Eur J Clin Microbiol Infect Dis* 1993; **12**: 673-676
- 33 [No authors listed]. Seroprevalence of hepatitis C virus infection at the time of entry to prison in the prison population in the north-east of Spain [In Spanish]. *Rev Esp Salud Publica* 1998; **72**: 43-51
- 34 **Vlahov D**, Nelson KE, Quinn TC, Kendig N. Prevalence and incidence of hepatitis C virus infection among male prison inmates in Maryland. *Eur J Epidemiol* 1993; **9**: 566-569
- 35 **van den Hoek JA**, van Haastrecht HJ, Goudsmit J, de Wolf F, Coutinho RA. Prevalence, incidence, and risk factors of hepatitis C virus infection among drug users in Amsterdam. *J Infect Dis* 1990; **162**: 823-826
- 36 **Chamot E**, de Saussure P, Hirschel B, Deglon JJ, Perrin LH. Incidence of hepatitis C, hepatitis B and HIV infections among drug users in a methadone-maintenance programme. *AIDS* 1992; **6**: 430-431
- 37 **Bird AG**, Gore SM, Burns SM, Duggie JG. Study of infection with HIV and related risk factors in young offenders' institution. *BMJ* 1993; **307**: 228-231
- 38 **Gore SM**, Bird AG, Burns SM, Goldberg DJ, Ross AJ, Macgregor J. Drug injection and HIV prevalence in inmates of Glenochil prison. *BMJ* 1995; **310**: 293-296
- 39 **Bellis MA**, Weild AR, Beeching NJ, Mutton KJ, Syed Q. Prevalence of HIV and injecting drug use in men entering Liverpool prison. *BMJ* 1997; **315**: 30-31
- 40 **Gaughwin MD**, Douglas RM, Liew C, Davies L, Mylvaganam A, Treffke H, Edwards J, Ali R. HIV prevalence and risk behaviours for HIV transmission in South Australian prisons. *AIDS* 1991; **5**: 845-851
- 41 **Stratton E**, Sweet L, Latorraca-Walsh A, Gully PR. Hepatitis C in Prince Edward Island: a descriptive review of reported cases, 1990-1995. *Can J Public Health* 1997; **88**: 91-94
- 42 **Garcia-Bengochea M**, Emparanza JI, Sarriugarte A, Cortes A, Vega JL, Gonzalez F, Arenas JI. Antibodies to hepatitis C virus: a cross-sectional study in patients attending a trauma unit or admitted to hospital for elective surgery. *Eur J Gastroenterol Hepatol* 1995; **7**: 237-241
- 43 **Crawford RJ**, Gillon J, Yap PL, Brookes E, McOmish F, Simmonds P, Dow BC, Follett EA. Prevalence and epidemiological characteristics of hepatitis C in Scottish blood donors. *Transfus Med* 1994; **4**: 121-124
- 44 **Chetwynd J**, Brunton C, Blank M, Plumridge E, Baldwin D. Hepatitis C seroprevalence amongst injecting drug users attending a methadone programme. *N Z Med J* 1995; **108**: 364-366
- 45 **Tsega E**, Nordenfelt E, Hansson BG. Hepatitis C virus infection and chronic liver disease in Ethiopia where hepatitis B infection is hyperendemic. *Trans R Soc Trop Med Hyg* 1995; **89**: 171-174
- 46 **Cohen D**, Scribner R, Clark J, Cory D. The potential role of custody facilities in controlling sexually transmitted diseases. *Am J Public Health* 1992; **82**: 552-556
- 47 **Heimberger TS**, Chang HG, Birkhead GS, DiFerdinando GD, Greenberg AJ, Gunn R, Morse DL. High prevalence of syphilis detected through a jail screening program. A potential public health measure to address the syphilis epidemic. *Arch Intern Med* 1993; **153**: 1799-1804
- 48 **Polonsky S**, Kerr S, Harris B, Gaiter J, Fichtner RR, Kennedy MG. HIV prevention in prisons and jails: obstacles and opportunities. *Public Health Rep* 1994; **109**: 615-625

Association between TRAIL expression on peripheral blood lymphocytes and liver damage in chronic hepatitis B

Gong-Ying Chen, Jian-Qin He, Guo-Cai Lu, Ming-Wei Li, Chen-Huai Xu, Wei-Wei Fan, Chen Zhou, Zhi Chen

Gong-Ying Chen, Institute of Liver Disease, Hangzhou Sixth People's Hospital, Hangzhou 310014, Zhejiang Province, China
Jian-Qin He, Guo-Cai Lu, Ming-Wei Li, Chen-Huai Xu, Wei-Wei Fan, Chen Zhou, Zhi Chen, Institute of Infectious Disease, The First Affiliated Hospital of Medical College, Zhejiang University, Hangzhou 310003, Zhejiang Province, China
Supported by a liver disease research foundation for the young and middle aged scientists, Chinese Medical Association
Co-first-author: Zhi Chen

Correspondence to: Dr. Gong-Ying Chen, Institute of Liver Disease, Hangzhou Sixth People's Hospital, Hangzhou 310014, Zhejiang Province, China. chengongying@hotmail.com
Telephone: +86-571-85463969 Fax: +86-571-85463908
Received: 2004-08-30 Accepted: 2004-12-16

Abstract

AIM: To explore a novel mechanism for tumor necrosis factor-related apoptosis-inducing ligand (TRAIL), upregulation of CD4⁺ and CD8⁺ T lymphocytes participating in the pathophysiological process of chronic hepatitis B (CHB).

METHODS: The levels of serum soluble TRAIL (sTRAIL), serum IFN- γ and membrane-bound TRAIL expression on peripheral leucocytes from 58 CHB patients were examined by ELISA and flow cytometry respectively. The levels of TRAIL were compared with the baseline levels of 17 healthy controls, and correlation analysis was performed between ALT, TBIL, PT, morphological change in hepatic tissues, and serum IFN- γ .

RESULTS: The results showed that TRAIL levels on membranes of CD4⁺, CD8⁺ T cells in CHB patients were much higher than those in healthy controls ($P < 0.001$), and were correlated with serum TBIL ($r = 0.354$, $P = 0.008$ for CD4⁺ and $r = 0.522$, $P = 0.000$ for CD8⁺, respectively), ALT ($r = 0.393$, $P = 0.003$ for CD8⁺), PT ($r = 0.385$, $P = 0.004$ for CD8⁺) and serum IFN- γ level ($r = 0.302$, $P = 0.011$ for CD4⁺ and $r = 0.307$, $P = 0.009$ for CD8⁺). On the contrary to membrane-bound TRAIL expression, serum level of sTRAIL was not correlated with that of TBIL and PT, though it was higher than that of the normal population and was positively correlated with serum HBeAg expression ($r = 0.695$, $P = 0.001$).

CONCLUSION: The expression level of TRAIL on the membrane of lymphocytes was upregulated and associated with the liver injury in CHB patients. These findings suggest that upregulation of TRAIL expression may be induced by virus antigen and inflammatory cytokine IFN- γ .

Key words: HBV; CD8⁺ lymphocyte; CD4⁺ lymphocyte; TRAIL; Liver function

Chen GY, He JQ, Lu GC, Li MW, Xu CH, Fan WW, Zhou C, Chen Z. Association between TRAIL expression on peripheral blood lymphocytes and liver damage in chronic hepatitis B. *World J Gastroenterol* 2005; 11(26): 4090-4093
<http://www.wjgnet.com/1007-9327/11/4090.asp>

INTRODUCTION

The TNF- α and Fas systems as well as the perforin/granzyme system have been implicated in hepatocyte apoptotic processes in viral hepatitis. Tumor necrosis factor-related apoptosis-inducing ligand (TRAIL), a type II transmembrane protein^[1], is a recently identified member of the TNF family and is capable of inducing apoptosis in virus-infected cells. This suggests that TRAIL may play an important role in HBV immunopathology. Human CD4⁺ T cell clones exhibit TRAIL-mediated cytotoxicity against certain target cells^[2], indicating that TRAIL constitutes an additional pathway of T cell-mediated cytotoxicity. The aim of this study was to study a possible novel mechanism for TRAIL upregulation of CD4⁺ and CD8⁺ T lymphocytes participating in the pathophysiological process of chronic hepatitis B (CHB).

MATERIALS AND METHODS

Patients

Fifty-eight patients seropositive for HBV marker (HBsAg) for more than 6 mo were the subjects of this study. Thirty were seropositive for HBV DNA, and all were negative for other hepatitis virus and HIV markers in sera. None had received any antiviral therapy or immunotherapy in the preceding 6 mo. They were classified into four groups^[3]: 13 cases with mild chronic hepatitis (CH1), 14 cases with moderate chronic hepatitis (CH2-3), 15 with liver cirrhosis (LC) and 16 with chronic severe hepatitis (CSH). Seventeen healthy laboratory workers negative for HBsAg and normal in liver functions were assessed at the same time and served as controls. The demographic data of all participants are summarized in Table 1. Serum specimens for antibody to HAV, HCV, HDV, HEV, as well as antibody to HIV were tested by enzyme immunoassay. Immunoassay for the *in vitro* qualitative determination of serum HBsAg and HBeAg was tested on Roche Elecsys immunoassay analyzers, HBV DNA was assayed by quantitative PCR.

Leukocyte and flow cytometry

Citrated blood samples were obtained. Aliquots of 100 μ L

were incubated for 15 min with 20 μ L antibody against TRAIL-PE (eBioscience, Clone number RIK-2), CD4-FITC, CD8-FITC, or isotype control (CALTAG, USA) at room temperature. After labeling with the antibody, leukocyte suspensions were washed and erythrocytes were lysed using FACS brand lysing solution (Becton Dickinson, USA). Washed cells were resuspended in 300 μ L of PBS and analyzed. FACS scan flow cytometer (Becton Dickinson, USA) and cell quest software were used for acquisition and analysis of the data. Populations of lymphocytes were identified from forward and side scatter characteristics on dot plot profiles and were analyzed for fluorescence intensity using fixed defined gate. At least 10 000 cells per sample were acquired.

ELISA

Serum specimens collected were stored at -80°C , and IFN- γ and soluble TRAIL (sTRAIL) protein levels were determined using immunoassay kit according to manufacturer's specifications.

Statistical analysis

Statistically significant differences among groups of patients were determined by ANOVA, correlation coefficients were determined by Pearson (two-tailed) using SPSS10.0 software, and P values ≤ 0.05 were considered as significant.

RESULTS

Changes of serum soluble TRAIL and modulation of membrane-bound TRAIL expression on peripheral T lymphocytes in chronic hepatitis

The results showed that TRAIL levels in membranes of

CD4⁺ and CD8⁺ T lymphocytes and the serum levels of sTRAIL in CHB patients were much higher than those in healthy controls ($P < 0.001$). Membrane-bound TRAIL expression was shown to correlate with the activity of viral hepatitis, that of CD4⁺ and CD8⁺ T lymphocytes correlated with serum TBIL ($r = 0.354$, $P = 0.008$ for TRAIL of CD4⁺ *vs* TBIL and $r = 0.522$, $P = 0.000$ for TRAIL of CD8⁺ *vs* TBIL) and that of CD8⁺ T lymphocytes was correlated with serum ALT ($r = 0.393$, $P = 0.003$), and PT ($r = 0.385$, $P = 0.004$). A positive relationship between serum IFN- γ level and the degree of TRAIL antigen expressions of CD4⁺ and CD8⁺ T lymphocytes ($r = 0.302$, $P = 0.011$ for TRAIL of CD4⁺ *vs* IFN- γ ; $r = 0.307$, $P = 0.009$ for TRAIL of CD8⁺ *vs* IFN- γ) was shown. Serum level of sTRAIL was not correlated with TBIL and PT, though it was higher than that in normal population. The related results are shown in Table 2.

Positive correlation between liver histological findings and membrane-bound TRAIL expression

In 30 samples from 58 HBV patients, with the aggravation of liver inflammation grade, membrane-bound TRAIL expression in peripheral T lymphocytes in chronic hepatitis was upregulated. There was a positive correlation between the inflammation grade and level of TRAIL antigen expression ($r = 0.677$, $P < 0.01$). Statistical analysis is shown in Table 3.

Positive correlation between serum IFN- γ level and membrane-bound TRAIL expression

The serum level of IFN- γ in patients with CHB was 24.04 ± 19.03 pg/mL for CH1, 76.02 ± 84.35 pg/mL for

Table 1 Demographic data, HBV marker and histological findings of the liver in the study population

Characteristics	Normal control	Chronic HBV infection			
		CH1	CH2-3	CSH	LC
Number	17	13	14	16	15
Male:female	12:5	9:4	10:4	11:5	11:4
Median age (range)	33.5 (26-50)	34 (24-58)	36 (23-64)	33 (24-56)	44 (21-68)
ALT (U/L)	33 \pm 12	57.8 \pm 73.6	190.3 \pm 207.8	238.3 \pm 381.2	85.5 \pm 60.4
TBIL (mmol/L)	15 \pm 5.2	22.4 \pm 20.1	70.0 \pm 46.7	405.8 \pm 132.9	64.4 \pm 47.4
Alb (g/L)		40.78 \pm 5.3	35.4 \pm 6.8	31.8 \pm 3.6	34.9 \pm 4.5
PT (s)		13.7 \pm 3.4	17.4 \pm 5.2	32.1 \pm 10.9	21.8 \pm 6.4
HBV DNA (positive cases)	0	9	10	4	7
Liver histological findings					
Not done	(n) 17		8	11	9
G ₀₋₁	(n)	11			
G ₂₋₃	(n)	2	6		
G ₄	(n)			5	6

Table 2 Changes of serum sTRAIL and modulations of membrane-bound TRAIL expression on peripheral T lymphocytes in chronic hepatitis

Group	n	CD4 ⁺ T lymphocyte TRAIL expression (%)	CD8 ⁺ T lymphocyte TRAIL expression (%)	sTRAIL (pg/mL)
CH1	13	2.82 \pm 1.00 ^b	5.10 \pm 2.01 ^b	1 001.93 \pm 474.23
CH2-3	14	4.64 \pm 2.08 ^b	6.56 \pm 3.56 ^b	1 358.38 \pm 391.66 ^b
CSH	16	5.33 \pm 2.38 ^b	8.31 \pm 3.62 ^b	969.56 \pm 377.41
Cirrhosis	13	4.20 \pm 1.92 ^b	5.09 \pm 2.50 ^b	
Normal	17	1.21 \pm 0.57	3.04 \pm 1.72	800.24 \pm 322.9

^b $P < 0.001$ vs normal controls.

Table 3 Positive correlation between liver histological findings and membrane-bound TRAIL expression

Inflammation grade	n	CD4 ⁺ T lymphocyte TRAIL expression (%)	CD8 ⁺ T lymphocyte TRAIL expression (%)
G ₀₋₁	11	2.51±0.96	5.22±2.25
G ₂₋₃	8	4.66±2.30 ^a	6.43±3.00 ^a
G ₄	11	4.74±2.00 ^a	7.92±3.58 ^a

^aP<0.05 vs G₀₋₁.

CH2-3, 81.81±63.11 pg/mL for CSH. There was a positive relationship between serum levels of IFN- γ and TRAIL antigen expression in CD4⁺T ($r = 0.302$, $P = 0.011$) and CD8⁺T ($r = 0.307$, $P = 0.009$). No relationship between serum levels of IFN- γ and sTRAIL was found.

DISCUSSION

In this paper, a possible novel mechanism for TRAIL upregulation of CD4⁺, CD8⁺ T lymphocytes participating in the pathophysiological process of CHB was studied in patients with CHB. HBV is the main etiologic agent for viral hepatitis. Cytotoxic T lymphocytes (CTLs) recognize viral peptides, which have been intracellularly processed and expressed on cell surface of hepatocytes in conjunction with MHC class I molecules. CTL-induced immunological tissue destruction is one of the hallmarks of liver injury in viral hepatitis. Apoptosis is now recognized to play a significant role in the pathogenesis. Different pathways, which include the Fas and TNF- α system as well as the perforin/granzyme system, have been implicated in hepatocyte apoptotic processes^[4]. Fas has been shown to be correlated with the activity of viral hepatitis^[5], and Fas expression can be induced either by virus-specific protein expression or by inflammatory cytokines such as interleukin-1. Activated CTLs express FasL and induce hepatocyte apoptosis via Fas signaling cascades. TNF-R1 expression has also been shown to be enhanced in HBV, and the increased production of TNF- α has been demonstrated in peripheral blood mononuclear cells in hepatitis B. Additionally, HBx has been shown to sensitize cultured and transfected hepatocytes to TNF- α -induced apoptosis^[6]. In contrast to Fas and TNF- α signaling, the potential hepatotoxicity of TRAIL is still controversial, especially its ability to induce hepatocyte apoptosis. A recombinant soluble version of TRAIL ligand fused to a trimerizing leucine zipper failed to induce hepatotoxicity in mice^[7], whereas a polyhistidine-tagged recombinant soluble form of TRAIL was reported to induce apoptosis in cultured human hepatocytes^[8]. Because of the rapid dedifferentiation of cultured hepatocytes, it is difficult to extrapolate these experiments to *in vivo* condition. Furthermore, these discrepancies may be attributed to the different TRAIL agonists. Although there is expression of TRAIL receptors 1 and 2 mRNA in human liver, a more recent report^[9] demonstrated that TRAIL-R2 protein was minimally expressed in human hepatocytes and a specific TRAIL-R2 agonist did not induce apoptosis in cultured human hepatocytes. Therefore, TRAIL signaling seems to play a less important role in pathophysiological process of hepatocyte apoptosis than Fas or TNF- α . In this paper we

found that even serum sTRAIL in healthy individuals is very high, which also supports this theory. However, since TRAIL-R expression can be induced, for example, by DNA damage or by bile acid^[10,11], it is also possible that hepatocyte sensitivity to TRAIL may increase in disease states. Viral infection triggering sensitivity to TRAIL-mediated apoptosis has been reported. Yoon *et al.*^[4], have recently observed that in HBV-transfected HepG2 cells, TRAIL-R1 expression level was higher than in their parent cell line, HepG2 cells. Moreover, the HBV-transfected cells were more sensitive to TRAIL-induced apoptosis than the untransfected ones, and this sensitization was reduced by anti-viral treatment. Our group also demonstrated that in HBV-transfected HepG2 cells, TRAIL expression level was higher than in their parent cell line (unpublished data). Mundt *et al.*^[12], also reported that HBV-mediated acute liver failure resulted in upregulation of protein expression of TRAIL and TRAIL receptors, thereby activating the TRAIL-specific death pathway in HBV-infected hepatocytes. Our study is the first report that membrane-bound TRAIL expression on peripheral T lymphocytes in CHB was upregulated and was correlated with the activity of viral hepatitis. Serum level of sTRAIL was not correlated with TBIL and PT, and same results were also reported by Janssen *et al.*^[13]. It suggested that serum level of sTRAIL was unable to accurately reflect the severity of disease.

Recently it was reported that the expression level of sTRAIL was positively correlated with the level of HBeAg. Furthermore, we found that there existed a positive correlation between the degree of TRAIL antigen expression and serum levels of IFN- γ . The IFN-induced gene family is now known to comprise the death ligand TRAIL, the dsRNA-dependent protein kinase, interferon regulatory factors and the promyelocytic leukemia gene, all of which have been reported to be the mediators of cell death^[14]. Our study suggests that interaction of TRAIL signaling and IFN- γ participates in the pathophysiological process in CHB patients.

TRAIL expression in liver tissues, especially in lymphocytes needs to be analyzed further.

REFERENCES

- 1 Wiley SR, Schooley K, Smolak PJ, Din WS, Huang CP, Nicholl JK, Sutherland GR, Smith TD, Rauch C, Smith CA. Identification and characterization of a new member of the TNF family that induces apoptosis. *Immunity* 1995; **3**: 673-682
- 2 Kayagaki N, Yamaguchi N, Nakayama M, Kawasaki A, Akiba H, Okumura K, Yagita H. Involvement of TNF-related apoptosis-inducing ligand in human CD4⁺ T cell-mediated cytotoxicity. *J Immunol* 1999; **162**: 2639-2647
- 3 Chinese Society of Infectious Disease and Parasitology, Chinese Society of Hepatology, Chinese Medical Association. The programme of prevention and treatment for viral hepatitis. *Zhonghua Ganzangbing Zazhi* 2000; **8**: 324-329
- 4 Yoon JH, Gores GJ. Death receptor-mediated apoptosis and the liver. *J Hepatol* 2002; **37**: 400-410
- 5 Mochizuki K, Hayashi N, Hiramatsu N, Katayama K, Kawanishi Y, Kasahara A, Fusamoto H, Kamada T. Fas antigen expression in liver tissues of patients with chronic hepatitis B. *J Hepatol* 1996; **24**: 1-7
- 6 Marinos G, Naoumov NV, Rossol S, Torre F, Wong PY, Gallati H, Portmann B, Williams R. Tumor necrosis factor receptors in patients with chronic hepatitis B virus infection. *Gastroenterol* 1995; **108**: 1453-1463

- 7 **Walczak H**, Miller RE, Arian K, Gliniak B, Griffith TS, Kubin M, Chin W, Jones J, Woodward A, Le T, Smith C, Smolak P, Goodwin RG, Rauch CT, Schuh JC, Lynch DH. Tumoricidal activity of tumor necrosis factor-related apoptosis-inducing ligand *in vivo*. *Nat Med* 1999; **5**: 157-163
- 8 **Jo M**, Kim TH, Seol DW, Esplen JE, Dorko K, Billiar TR, Strom SC. Apoptosis induced in normal human hepatocytes by tumor necrosis factor-related apoptosis-inducing ligand. *Nat Med* 2000; **6**: 564-567
- 9 **Ichikawa K**, Liu W, Zhao L, Wang Z, Liu D, Ohtsuka T, Zhang H, Mountz JD, Koopman WJ, Kimberly RP, Zhou T. Tumoricidal activity of a novel anti-human DR5 monoclonal antibody without hepatocyte cytotoxicity. *Nat Med* 2001; **7**: 954-960
- 10 **Wu GS**, Burns TF, McDonald ER 3rd, Jiang W, Meng R, Krantz ID, Kao G, Gan DD, Zhou JY, Muschel R, Hamilton SR, Spinner NB, Markowitz S, Wu G, el-Deiry WS. KILLER/DR5 is a DNA damage-inducible p53-regulated death receptor gene. *Nat Genet* 1997; **17**: 141-143
- 11 **Higuchi H**, Yoon JH, Grambihler A, Werneburg N, Bronk SF, Gores GJ. Bile acids stimulate cFLIP phosphorylation enhancing TRAIL-mediated apoptosis. *J Biol Chem* 2003; **278**: 454-461
- 12 **Mundt B**, Kuhnle F, Zender L, Paul Y, Tillmann H, Trautwein C, Manns MP, Kubicka S. Involvement of TRAIL and its receptors in viral hepatitis. *FASEB J* 2003; **17**: 94-96
- 13 **Janssen HL**, Higuchi H, Abdulkarim A, Gores GJ. Hepatitis B virus enhances tumor necrosis factor-related apoptosis-inducing ligand (TRAIL) cytotoxicity by increasing TRAIL-R1/death receptor 4 expression. *J Hepatol* 2003; **39**: 414-420
- 14 **Barber GN**. Host defense, viruses and apoptosis. *Cell Death Differ* 2001; **8**: 113-126

Science Editor Zhu LH and Guo SY Language Editor Elsevier HK

Preparation of anti-mouse caspase-12 mRNA hammerhead ribozyme and identification of its activity *in vitro*

Shan Jiang, Qing Xie, Wei Zhang, Xia-Qiu Zhou, You-Xin Jin

Shan Jiang, Qing Xie, Wei Zhang, Xia-Qiu Zhou, Department of infectious disease, Ruijin Hospital, Shanghai Second Medical University, Shanghai 200025, China

You-Xin Jin, State Key Laboratory of Molecular Biology, Shanghai Institute of Biochemistry, Chinese Academy of Sciences, Shanghai 200031, China

Supported by the National Natural Science Foundation of China, No. 30170850 and Shanghai Education Foundation

Co-first-authors: Dr. You-Xin Jin

Correspondence to: Dr. Qing Xie, Department of infectious disease, Ruijin Hospital, Shanghai Second Medical University, Shanghai 200025, China. xieqing@sh163.net

Telephone: +86-21-64311242

Received: 2004-08-31 Accepted: 2004-10-20

cleave mouse caspase-12 mRNA with an excellent efficiency. It shows a potential to suppress the expression of caspase-12 *in vivo*, thus provided a new way to protect cells from ER stress induced apoptosis.

© 2005 The WJG Press and Elsevier Inc. All rights reserved.

Key words: ER stress; Apoptosis; Caspase-12; Ribozyme

Jiang S, Xie Q, Zhang W, Zhou XQ, Jin YX. Preparation of anti-mouse caspase-12 mRNA hammerhead ribozyme and identification of its activity *in vitro*. *World J Gastroenterol* 2005; 11(26): 4094-4097

<http://www.wjgnet.com/1007-9327/11/4094.asp>

Abstract

AIM: To prepare and identify specific anti-mouse caspase-12 hammerhead ribozymes *in vitro*, in order to select a more effective ribozyme against mouse caspase-12 as a potential tool to rescue cells from endoplasmic reticulum stress induced apoptosis.

METHODS: Two hammerhead ribozymes directed separately against 138 and 218 site of nucleotide of mouse caspase-12 mRNA were designed by computer software, and their DNA sequences were synthesized. The synthesized ribozymes were cloned into an eukaryotic expression vector-neo^rpBSKU6 and embedded in U6 SnRNA context for further study. Mouse caspase-12 gene segment was cloned into PGEM-T vector under the control of T7 RNA polymerase promoter (containing gene sequence from positions nt 41 to nt 894) as target. *In vitro* transcription both the ribozymes and target utilize T7 promoter. The target was labeled with [α -³²P]UTP, while ribozymes were not labeled. After gel purification the RNAs were dissolved in RNase free water. Ribozyme and target were incubated for 90 min at 37 °C in reaction buffer (40 mmol/L Tris-HCL, pH 7.5, 10 mmol/L Mg²⁺). Molar ratio of ribozyme vs target was 30:1. Samples were analyzed on 6% PAGE (containing 8 mol/L urea).

RESULTS: Both caspase-12 and ribozyme gene sequences were successfully cloned into expression vector confirmed by sequencing. Ribozymes and caspase-12 mRNA were obtained by *in vitro* transcription. Cleavage experiment showed that in a physiological similar condition (37 °C, pH 7.5), Rz138 and Rz218 both cleaved targets at predicted sites, for Rz138 the cleavage efficiency was about 100%, for Rz218 the value was 36.66%.

CONCLUSION: Rz138 prepared *in vitro* can site specific

INTRODUCTION

Apoptosis plays an important role in the pathogenesis of liver diseases^[1]. Activation of death receptors and mitochondrial damage are well-described common apoptotic pathways. Recently, a novel pathway via endoplasmic reticulum (ER) stress was reported^[2]. Following studies have demonstrated that many liver diseases are associated with ER stress, including nonalcoholic steatohepatitis, cholestasis, alcohol induced liver diseases, and viral hepatitis^[3-5].

Among the death-specific enzymes in apoptosis is a family of cysteine-dependent aspartate-specific proteases known as caspases^[6]. Activation of caspases is a central mechanism in the apoptotic cell death process^[7].

Caspase-12 resides in the endoplasmic reticulum and is specifically involved in the apoptosis that results from ER stress, Apoptosis triggered through pathways that do not involve the ER, such as serum deprivation or Fas-activation, do not result in activation of caspase-12. Cells isolated from transgenic mice that lack intact caspase-12 protein were more resistant to ER stress-induced apoptosis than wild type cells^[2].

Caspases are central to both normal programmed cell death and injury-dependent apoptosis, so any therapy that manipulates caspase activity must take into account the possible effects on tissue homeostasis. In this regard, caspase-12 seems to have a strong advantage as a target over other caspases. In contrast to other caspase knockouts, caspase-12 deficient mice have no noticeable developmental or behavioral defects, and have a normal incidence of tumors^[2]. So caspase-12 may be a promising target for treating ER stress associated diseases with few side effect.

Until now, no specific caspase-12 inhibitors are available. Ribozymes (Rz) are RNA molecules with enzymatic activity

that can associate with a larger target RNA by base-pairing to cleave a specific phosphodiester bond^[2,8]. In the past years, ribozyme-mediated gene inhibition has been demonstrated for many examples in cell lines. Selective downregulation of a particular caspase by ribozyme provides an alternative approach to rescue cells from apoptosis^[9-11].

Catalytic cleavage of caspase-12 mRNA by ribozyme may block ER stress induced apoptotic pathway, thus protect liver cells from apoptosis. In the present study, ribozymes were designed and synthesized against the sequences of caspase-12 mRNA which cleave at nucleotide positions 138 and 218 respectively. Also mutant ribozymes were synthesized for future study. Transcription and cleavage reaction were performed *in vitro* to determine the activity of ribozymes designed and assess the potential value of them against caspase-12 mediated apoptosis.

MATERIALS AND METHODS

Material

PGEM-T vector kit, transcription kit, TRIzol kit, and T4 DNA ligase were purchased from Promega Company. RT-PCR kit, Restriction endonucleases were purchased from TaKaRa Company. [α -³²P]UTP was the product of Amersham Biosciences UK. E coli DH5 α and eukaryotic expression vector-neo^rpBSKU6 for ribozyme were kind gifts from Dr. YouXin Jin. The PCR primers and ribozyme gene sequences were synthesized in the Beckman Oligo-1000 DNA synthesizer.

Methods

Cloning of Caspase-12 cDNA Mouse caspase-12 mRNA gene sequence was obtained from online Genbank of NCBI (GI: 2094805). Total RNA of fresh mouse liver tissue was extracted using Trizol kit. The up stream primer for RT-PCR amplification of caspase-12 gene segment was F: 5'-TCT AGA CCA GGA GGA CAC ATG AAA GA-3' (41-60 bp), the 5' extension underlined is *Xba*I site, the downstream primer was R: 5'-GGA TCC TCT CAG ACT CCG ACA GTT AG-3' (894-875 bp), the 5' extension underlined is *Bam*HI site. PCR product contained gene sequence from position nt 41 to nt 894 with *Xba*I site ahead and *Bam*HI site behind. Purified PCR product were inserted into pGEM-T vector through A-T pairing under the control of T7 RNA polymerase promoter. The recombinants were transfected into competent JM109 E Coli cells for blue/white screening on LB plate. The selected clone containing Caspase-12 cDNA was confirmed by sequencing and named pCaspase-12.

Ribozyme Construction The hammerhead ribozymes were designed according to the computer software compiled by Professor Chen Nong-An (Shanghai Institute of Biochemistry of the Chinese Academy of Science). The specificity of ribozymes designed for mouse caspase-12 mRNA were determined by sequence analysis with other RNA sequences of mouse cells in NCBI GenBank using blastn. The sequences of the two ribozymes are shown in Table 1. G in the catalytic core for active ribozyme, A for inactive ribozyme. The inactive ribozymes allow binding to the target RNA, but lack cleavage ability^[12]. Oligonucleotides

encoding Rz138 and Rz218 were designed to generate *Xba*I/*Bam*HI ends upon annealing and were ligated with the *Bam*HI and *Xba*I digested neo^rpBSKU6 plasmid embedded in U6 SnRNA context containing U6 SnRNA promoter/enhancer and terminator. The reconstructed plasmids were named pRz138, pRz138m(mutant), pRz218, pRz218m respectively according to the confirmation of DNA sequencing, and the reconstructed Rz plasmids were prepared for further *in vivo* study.

Table 1 Ribozyme sequence

	5' binding arm	Catalytic core	3' binding arm
Rz138	5' TCCATTTAA	CT(G/A)ATGAGTCCGT GAGGACGAA	ACATTCTT 3'
Rz218	5' TCTCTAAG	CT(G/A)ATGAGTCCGT GAGGACGAA	AGTTCTC 3'

In vitro transcription of ribozymes and target RNA

In vitro transcription were prepared according to the supplier (Promega). Both the ribozymes and substrate were transcribed with T7 RNA polymerase. Transcription of target RNA started with an additional 46 nt derived from the vector and terminated just at the end of *Bam*HI linearized pCaspase-12. The total length was 910 nt. Substrate transcription was performed in 20 μ L volume in the presence of 1 μ L [α -³²P]UTP (10 uci/ μ L), while ribozymes were not labeled with isotope. Ribozyme templates were produced by PCR, primers were complementary to the flanking U6 sequence adjacent to the embedded ribozyme, T7 promoter was pulsed to the F primer 5'-TCT AGA GTA ATA CGA CTC ACT ATA GGG C CTT CGG CAG CAC ATA TAC-3', the underlined sequence represents T7 promoter. Primer R was 5'-TAT GGA ACG CTT CAG GAT-3'. PCR products were purified by 12 g/L agarose gel electrophoresis as templates for transcription. The products of transcription were purified with 6% denaturing polyacrylamide gels (PAGE), the bands were cut off from the gel and soaked in NES (0.5 mol/L NH₄Ac, 1 mmol/L EDTA, 0.1% SDS) at 45 °C overnight. After centrifuge, the supernatant were precipitated by ethanol and 3 mol/L sodium acetate, washed twice by 75% ethanol, then dissolved in RNase free water. The [α -³²P]UTP labeled substrate was counted in a Beckman-LS 6500 counter^[13]. As many studies show that inactive mutant ribozymes have no cleavage activity^[12,14,15], we preferred to use the normal Rz *in vitro* study.

Identification of ribozyme activity by cleavage reaction

The molar quantity of target RNA was estimated according to the cpm value combined with the UTP number in the RNA. Rz molar concentration was estimated according to the spectrophotometric A_{260} value. Ribozyme and substrate were incubated for 90 min at 37 °C in reaction buffer (40 mmol/L Tris-HCl, pH 7.5, 10 mmol/L Mg²⁺). Molar ratio of ribozyme versus substrate was 30:1. Samples were analyzed on 6% PAGE (containing 8 mol/L urea). The cleavage efficiency [CE] was calculated from cpm values of the bands of undigested substrate (S) and product (P) separated from denaturing PAGE. CE = [P/(P+S)]•100%.

RESULTS

Transcription of caspase-12 cDNA fragment

RT-PCR amplified caspase-12 cDNA segment was separated by 1.2% agarose gel and stained with ethidium bromide. The length of product containing restriction endonuclease site was 866bp. (Figure 1).

Purified caspase-12 PCR product was inserted into pGEM-T vector by A-T base pairing. After blue/white screening on LB plate and DNA sequencing, pCaspase-12 was confirmed. Then, *Bam*HI linearized pCaspase-12 was used as transcription template. The length of transcribed target RNA as shown in Figure 2 was 910 nt.

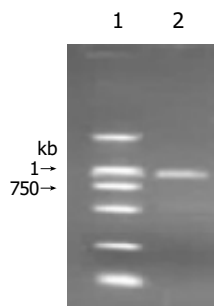


Figure 1 Agarose gel electrophoresis of caspase-12 RT-PCR product. Lane 1: DL 2000 DNA Marker; lane 2: The 866 bp caspase-12 gene segment produced by RT-PCR.

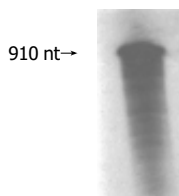


Figure 2 *In vitro* transcription product of caspase-12 segment, separated by 6% PAGE, the transcript was 910 nt.

Transcription of ribozymes

The length of Rz templates for transcription produced by PCR were about 100 bp (Figure 3). Transcription products were also purified through 6% PAGE, using upper ultraviolet to determine the position of the bands. The bands were excised and dissolved in RNase free water and reserved under -20 °C.

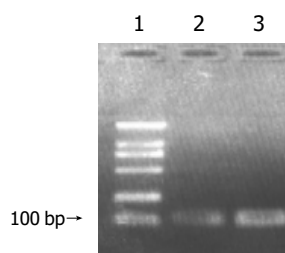


Figure 3 Agarose gel electrophoresis of PCR amplified ribozyme templates. Lane 1: DL 2000 DNA Marker; lane 2: Rz138 template produced by PCR; lane 3: Rz218 template produced by PCR.

Cleavage *in vitro*

As shown in Figure 4A, The length of target RNA transcribed from *Bam*HI linearized pCaspase-12, which contains the mouse caspase-12 cDNA segment, should be 910 nt, and the expected fragments cleaved by Rz138 *in vitro* should be 150 nt and 760 nt. Rz218 cleavage would generate 230 nt and 680 nt. The cleavage result showed that at a 30:1 ribozyme-to-target ratio, both Rz138 and Rz218 cleaved target at the predicted sites which were consistent with our design and proved to be correct (Figure 4B). The cleavage efficiency of Rz138 was about 100%, while 36.66% for Rz218.

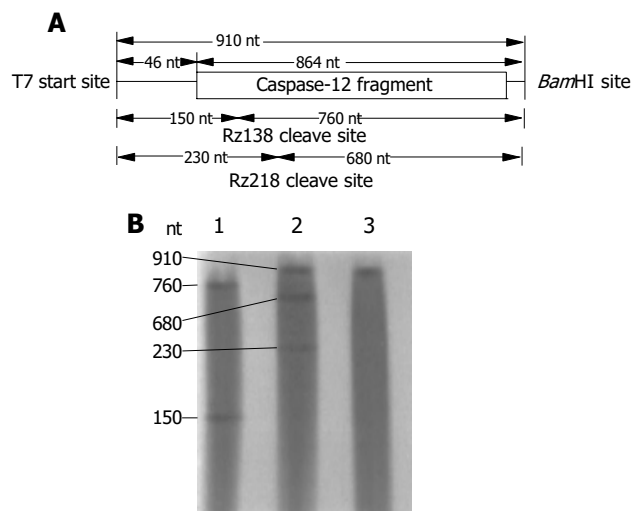


Figure 4 *In vitro* Cleavage of mouse caspase-12 mRNA by ribozymes. **A:** The length of caspase-12 segment transcribed from *Bam*HI linearized pCaspase-12 which contains the mouse caspase-12 gene segment, and its anticipated cleavage products. **B:** The results of cleavage reaction by PAGE electrophoresis. Lane 1: Rz138 cleavage result; lane 2: Rz218 cleavage result; lane 3: control (control contains all other components except ribozyme.).

DISCUSSION

Apoptosis is essential to development of multicellular organisms as well as to physiologic cell turn over. Excessive apoptosis may contribute to organ injury^[16]. A novel apoptotic pathway via ER stress was recently testified in mouse. Prolonged ER stress leads to cell death and is linked to the pathogenesis of some neurodegenerative disorders. ER stress also plays an important role in several liver diseases^[3-5,17]. Activation of caspase-12 from procaspase-12 is specifically induced by insult to the ER, ER stress triggers a specific cascade involving caspase-12,-9,-3. Although it was reported that human caspase-12 may have no significant effect on apoptotic sensitivity^[18,19], many evidences show that functional caspase-12 exists in many human cell types and is associated with ER stress induced apoptosis.^[20-22] It was knowing that cells lack of intact caspase-12 protein were more resistant to ER stress-induced apoptosis than wild type cells. Inhibition of caspase-12 expression by ribozyme may block ER stress induced apoptotic pathway, thus protect liver cells from apoptosis.

The ribozymes are divided into two groups: small ribozymes and large ribozymes. Small ribozymes, approximately those less than 100 nucleotides, include the

hammerhead ribozyme, hairpin ribozyme, and hepatitis delta virus ribozyme. Large ribozymes contain ribonuclease P RNA and group I and group II introns. Hammerhead ribozyme is simple in structure with high turnover in cleavage reaction. The activity of the hammerhead ribozyme is significant higher than that of all other ribozymes *in vitro*. It's being widely used to inhibit endogenous gene expression of basic biochemical pathways such as angiogenesis and apoptosis. It's the first to be approved to use in clinical trial^[23]. It contains a tripartite structure consisting of a central catalytic core that is flanked on both sides by two antisense side arms that can form base pairs with the RNA substrate, thus providing the sequence specificity of the endonuclease action. Sequences 5' to the catalytic domain form helix I and sequences 3' to it form helix III when complexed with the target RNA^[24].

Ribozyme used as molecular tool for specific inhibition of gene translation is affected by many factors including the mRNA secondary structures and target accessibility. Our studies show that computer aided energy minimization algorithms predicted regions in mouse caspase-12 mRNA are accessible to ribozyme cleavage. The cleavage reaction revealed that Rz138 and Rz218 prepared *in vitro* possessed perfect specific catalytic cleavage activity. Rz138 has an excellent cleavage efficiency. The results were consistent with our designed. This finding made it worthy to do further study on the cleavage activity of these ribozymes *in vivo* and to develop them as a therapeutic nucleic acid drug in the future. Considering that the *in vitro* activity does not represent exactly the efficiency of a ribozyme in degrading the target mRNA in intact cells, we've cloned the two ribozymes in eukaryotic expression vector for further study *in vivo*.

REFERENCES

- Ockner RK. Apoptosis and liver disease: recent concepts of mechanism and significance. *J Gastroenterol Hepatol* 2001; **16**: 248-260
- Nakagawa T, Zhu H, Morishima N, Li E, Xu J, Yankner BA, Yuan J. Caspase-12 mediates endoplasmic-reticulum-specific apoptosis and cytotoxicity by amyloid- β . *Nature* 2000; **403**: 98-103
- Ji C, Kaplowitz N. Betaine decreases hyperhomocysteinemia, endoplasmic reticulum stress, and liver injury in alcohol-fed mice. *Gastroenterology* 2003; **124**: 1488-1499
- Xu Z, Jensen G, Yen TS. Activation of hepatitis B virus S promoter by the viral large surface protein via induction of stress in the endoplasmic reticulum. *J Virol* 1997; **71**: 7387-7392
- Foo NC, Ahn BY, Ma X, Hyun W, Yen TS. Cellular vacuolization and apoptosis induced by hepatitis B virus large surface protein. *Hepatology* 2002; **36**: 1400-1407
- Wolf B B, Green D R. Suicidal tendencies: apoptotic cell death by caspase family proteinase. *J Bio Chem* 1999; **274**: 20049-20052
- Cryns V, Yuan J. Proteases to die for. *Genes Dev* 1998; **12**: 1551-1570
- Kato Y, Kuwabara T, Toda H, Warashina M, Taira K. Suppression of BCR-ABL mRNA by various ribozymes in HeLa cells. *Nucleic Acids Symp Ser* 2000; **44**: 283-284
- Eldadah BA, Ren RF, Faden AI. Ribozyme-mediated inhibition of caspase-3 protects cerebellar granule cells from apoptosis induced by serum-potassium deprivation. *J Neurosci* 2000; **20**: 179-186
- Xu R, Liu J, Chen X, Xu F, Xie Q, Yu H, Guo Q, Zhou X, Jin Y. Ribozyme-mediated inhibition of caspase-3 activity reduces apoptosis induced by 6-hydroxydopamine in PC12 cells. *Brain Res* 2001; **899**: 10-19
- Yaghootfam A, Gieselmann V. Specific hammerhead ribozymes reduce synthesis of cation-independent mannose 6-phosphate receptor mRNA and protein. *Gene Ther* 2003; **10**: 1567-1574
- Mendoza-Maldonado R, Zentilin L, Fanin R, Giacca M. Purging of chronic myelogenous leukemia cells by retrovirally expressed anti-bcr-abl ribozymes with specific cellular compartmentalization. *Cancer Gene Ther* 2002; **9**: 71-86
- Grassi G, Forlino A, Marini JC. Cleavage of collagen RNA transcripts by hammerhead ribozymes *in vitro* is mutation-specific and shows competitive effects. *Nucleic Acids Res* 1997; **25**: 3451-3458
- Pennati M, Colella G, Folini M, Citti L, Daidone MG, Zaffaroni N. Ribozyme-mediated attenuation of surviving expression sensitizes human melanoma cells to cisplatin-induced apoptosis. *J Clin Invest* 2002; **109**: 285-286
- Sriram B, Thakral D, Panda SK. Target cleavage of hepatitis E virus 3' end RNA mediated by hammerhead ribozymes inhibits viral RNA replication. *Virology* 2003; **312**: 350-358
- Thompson CB. Apoptosis in the pathogenesis and treatment of disease. *Science* 1995; **267**: 1456-1462
- Schuchmann M, Galle PR. Apoptosis in liver disease. *Eur J Gastroenterol Hepatol* 2001; **13**: 785-790
- Fischer H, Koenig U, Eckhart L, Tschachler E. Human caspase-12 has acquired deleterious mutations. *Biochem Biophys Res Commun* 2002; **293**: 722-726
- Saleh M, Vaillancourt JP, Graham RK, Huyck M, Srinivasula SM, Alnemri ES, Steinberg MH, Nolan V, Baldwin CT, Hotchkiss RS, Buchman TG, Zehnbauser BA, Hayden MR, Farrer LA, Roy S, Nicholson DW. Differential modulation of endotoxin responsiveness by human caspase-12 polymorphisms. *Nature* 2004; **429**: 75-79
- Morishima N, Nakanishi K, Takenouchi H, Shibata T, Yasuhiko Y. An endoplasmic reticulum stress-specific caspase cascade in apoptosis. *J Biol Chem* 2002; **277**: 34287-34294
- Rao RV, Hermel E, Castro-Obregon S, del Rio G, Ellerby LM, Ellerby HM, Bredesen DE. Coupling endoplasmic reticulum stress to the cell death program. *J Biol Chem* 2001; **276**: 33869-33874
- Xie Q, Khaoustov VI, Chung CC, Sohn J, Krishnan B, Lewis DE, Yoffe B. Effect of tauroursodeoxycholic acid on endoplasmic reticulum stress -induced caspase-12 activation. *Hepatology* 2002; **36**: 592-601
- Wong-Staal F, Poeschla EM, Looney DJ. A controlled, Phase 1 clinical trial to evaluate the safety and effects in HIV-1 infected humans of autologous lymphocytes transduced with a ribozyme that cleaves HIV-1 RNA. *Hum Gene Ther* 1998; **9**: 2407-2425
- Chen S, Song CS, Lavrovsky Y, Bi B, Vellanoweth R, Chatterjee B, Roy AK. Catalytic cleavage of the androgen receptor messenger RNA and functional inhibition of androgen receptor activity by a hammerhead ribozyme. *Mol Endocrinol* 1998; **12**: 1558-1566

Comparative study on radiosensitivity of various tumor cells and human normal liver cells

Jian-She Yang, Wen-Jian Li, Guang-Ming Zhou, Xiao-Dong Jin, Jing-Guang Xia, Ju-Fang Wang, Zhuan-Zi Wang, Chuan-Ling Guo, Qing-Xiang Gao

Jian-She Yang, Wen-Jian Li, Guang-Ming Zhou, Xiao-Dong Jin, Jing-Guang Xia, Ju-Fang Wang, Zhuan-Zi Wang, Chuan-Ling Guo, Institute of Modern Physics, Chinese Academy of Sciences, Lanzhou 730000, Gansu Province, China

Qing-Xiang Gao, Life Science School of Lanzhou University, Lanzhou 730000, Gansu Province, China

Supported by the National Natural Science Foundation of China, No. 10335050; Ministry of Science and Technology of the People's Republic of China, No. 2003CCB00200

Correspondence to: Dr. Jian-She Yang, Radiobiology Laboratory, Institute of Modern Physics, Chinese Academy of Sciences, Lanzhou 730000, Gansu Province, China. tuyangjs@impcas.ac.cn

Telephone: +86-931-4969338 Fax: +86-931-4969201

Received: 2004-11-03 Accepted: 2004-11-19

Abstract

AIM: To investigate the radiation response of various human tumor cells and normal liver cells.

METHODS: Cell lines of human hepatoma cells (SMMC-7721), liver cells (L02), melanoma cells (A375) and cervical tumor (HeLa) were irradiated with ^{60}Co γ -rays. Cell survive was documented by a colony assay. Chromatid breaks were measured by counting the number of chromatid breaks and isochromatid breaks immediately after prematurely chromosome condensed by Calyculin-A.

RESULTS: Linear quadratic survival curve was observed in all of four cell lines, and dose-dependent increase in radiation-induced chromatid and isochromatid breaks were observed in G₂B phase. Among these four cell lines, A375 was most sensitive to radiation, while, L02 had the lowest radiosensitivity. For normal liver cells, chromatid breaks were easy to be repaired, isochromatid breaks were difficult to be repaired.

CONCLUSION: The results suggest that the γ -rays induced chromatid breaks can be possibly used as a good predictor of radiosensitivity, also, unrejoined isochromatid breaks probably tightly related with cell cancerization.

© 2005 The WJG Press and Elsevier Inc. All rights reserved.

Key words: Radiosensitivity; Tumor cells; Normal; Liver cells

Yang JS, Li WJ, Zhou GM, Jin XD, Xia JG, Wang JF, Wang ZZ, Guo CL, Gao QX. Comparative study on radiosensitivity of various tumor cells and human normal liver cells. *World J Gastroenterol* 2005; 11(26): 4098-4101

<http://www.wjgnet.com/1007-9327/11/4098.asp>

INTRODUCTION

Liver cancer is one kind of malignancy tumor with the highest incidence and clinical risk, especially popular in China. As till now, radiotherapy is the most acceptable and effective method. Low LET (Linear energy transfer) rays, such as X-ray, γ -ray, were often used. Radiobiologists aim to develop an assay or a combinative assay to predict the radiation response of human cancers. Precise prediction of response to radiation could provide the basis for selecting and designing clinical treatment project.

Colony assay or growth assay has the good correlation with the radiation response^[1-5]. But as a routine predictive assay, it will take at least 2 or 3 weeks to form the clone, is unlikely to be used for clinical diagnosis and treatment.

The PCC (premature chromosome condensation) technique is very useful for measuring the radiation-induced chromatin breaks in all of the cell cycles^[6-9], especially in G₂ phase. In the present study, we investigated the G₂ phase radiosensitivity of human hepatoma cells and normal liver cells, compared with other two type of human malignancy tumors. The results showed that the radiosensitivity of normal liver cells is lowest among these four cell lines, suggest that in the course of liver cancer radiotherapy, liver cells will less injured than hepatoma cells and other two tumor cell lines when absorbed same dose of radiation.

MATERIALS AND METHODS

Cell culture and irradiation

Four cell lines (From CCTCC) were grown in RPMI-1640 medium supplemented with 10% fetal calf serum at 37 °C in 50 mL/L CO₂, additional 0.25 U/mL insulin was added into the L02 culture medium.

Exponentially growing cells were irradiated with γ -rays generated by ^{60}Co source with a dose rate 0.2 Gy/min at Lanzhou medicine college, dose range was from 0 to 8 Gy.

Chromosome preparation

Calyculin-A (BIOMOL America) was used as the PCC inducer, which was dissolved in 100% ethanol as 1 mmol/L stock solution; 50 nmol/L of Calyculin-A was added to the cell cultures before irradiation to score the initial chromatid breaks. Then, cells were incubated for a further 30 min at 37 °C in 50 mL/L CO₂. Chromosome spreads were then harvested by swelling cells in 75 mmol/L KCl for 20 min at 37 °C and fixed with Carnoy's fixation. A final wash and fixation in the same fixative was completed before dropping

cells onto a glass slide and hot humidity drying.

Chromosome was stained with 5% Giemsa for 20 min. More than 40 G₂ phase cells were scored for each dose point according to the standard criteria^[10]. Briefly, chromatid discontinuing, misalignment of the distal to the lesion, or a non-stained region longer than the chromatid width was classified as a break. Isochromatid breaks were scored two breaks. The total chromatid breaks were calculated by summing the production of chromatid and isochromatid breaks. The process of kinetic repair of damaged chromosome by PCC technique was same as initial ones.

RESULTS

G₂ PCC chromosome spreads

Calyculin A is a phosphatase inhibitor, can effectively induce the cells into G₂ phase by very little time. It is easy to detect the chromosome damage using PCC technique. Figure 1 shows the G₂ PCC chromosome spreads of L02 cell lines exposed to 8 Gy of γ -rays and SMMC-7721 cell lines of 0.5 Gy.

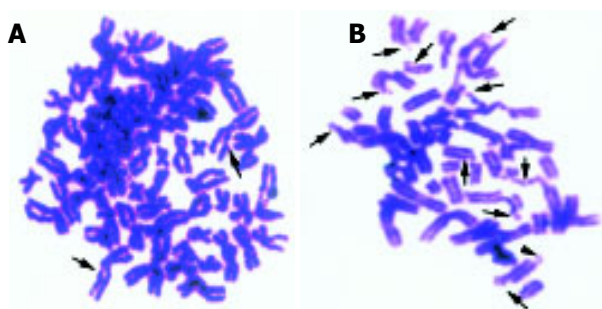


Figure 1 G₂ phase prematurely condensed chromosome spreads. **A:** SMMC-7721 cells after exposed to the γ -rays of 0.5 Gy; **B:** L02 cells after exposed to the γ -rays of 8 Gy. Arrows show the chromatid breaks, arrowheads show the isochromatid breaks.

Survival curves

Colony assay is a routine method for analyzing the cell survival fraction. Classical model of cell survival curve after exposed to low LET rays, such as X-ray, γ -ray, was linear quadratic. In present study, four cell lines' fitted survival curve were well agreement with the linear quadratic model. Figure 2 shows the detail of it.

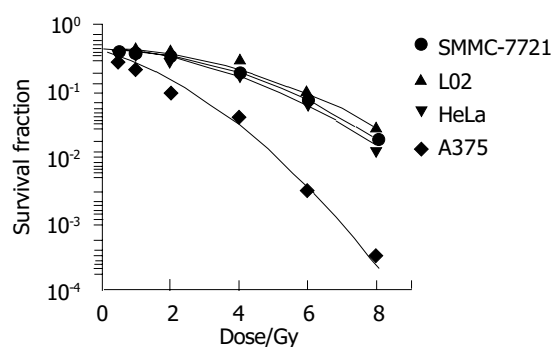


Figure 2 Cell survival curve after exposed to γ -rays. All of four cell lines have a linear quadratic survival curve, which were good agreement with classical model.

Initial chromatid and isochromatid breaks after irradiated with γ -rays in G₂ phase

Figures 3A and B express the chromatid and isochromatid breaks of four cell lines after irradiated with various absorbed dose. Though some inter-exchanges or inner-exchanges exist in chromosome spreads, its number was rare. We only observed the main chromosome break type, i.e., chromatid and isochromatid breaks. Chromatid and isochromatid breaks linearly increased with the dose increase of these four cell lines, the number of chromatid breaks was much more than that of isochromatid breaks at each dose point.

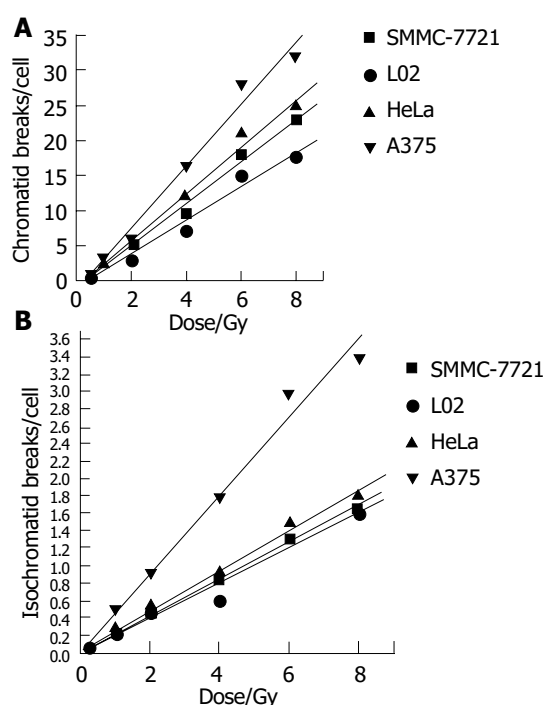


Figure 3 G₂ chromosome breaks at various absorbed dose. **A:** chromatid breaks; **B:** isochromatid breaks.

Kinetic repair of chromosome breaks of L02 cells in 48 h of post-irradiation time

Figures 4 and 5 show the unrejoined chromatid breaks/cell/Gy at 0, 24, and 48 h. In this kinetic process, almost

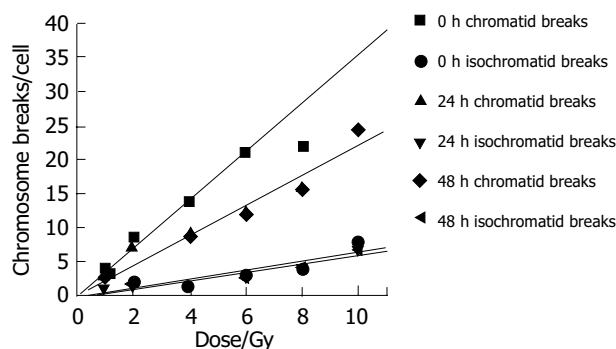


Figure 4 Correlation between chromatid breaks and absorbed dose at 0, 24, and 48 h after exposed to radiation.

50% chromatid breaks got repaired, for isochromatid ones, just 15% got repaired at most. Also we can see, during 24-48 h, both of these two type breaks were nearly the same level, i.e., from 2.16 to 1.93 breaks/cell/Gy for chromatid breaks, from 0.476 to 0.48 breaks/cell/Gy for isochromatid ones. However, from 0 to 24 h these values were 2.95-2.16 breaks/cell/Gy, 0.502-0.476 breaks/cell/Gy, respectively. Compared with chromatid breaks, isochromatid breaks nearly keep the original state within 48 h after exposed to radiation. This is to say, at the early 24 h after exposure, chromosome repair process finished.

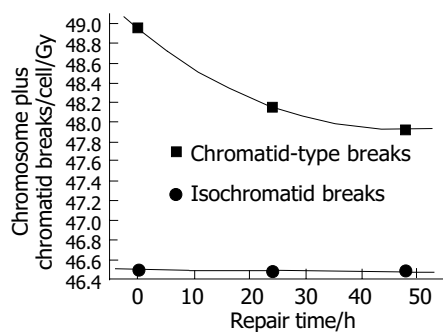


Figure 5 Kinetic repair of chromosome breakages within 48 h after L02 cell line was exposed to γ -rays. The chromatid breaks plus 46 (number of normal human chromosomes) make this change remarkably.

DISCUSSION

Liver cancer is of high risk and mortality. Besides the surgical excision, radiotherapy is the main method after the discovery of X-rays. Before radiotherapy, prompt and exact detection of radiosensitivity of target cells is of great importance.

Many researchers have reported a linear-quadratic cell survival curve in various cell lines irradiated by X-rays, γ -rays, also, linear relationship between chromosome breaks and absorbed dose was discovered^[5,8,9,11-15]. With the introduction of the premature chromosome condensation technique^[16-18], it is easy to study initial radiation-induced chromosome damage (Figure 1).

In the present study, fitted cell survival curve of four cell lines were linear quadratic (Figure 2), which were consistent with previous studies^[8-9]. Among these four cell lines, survival fraction of L02 was highest, A375 was lowest after absorbed same dose of radiation, suggested that human normal liver cells was of much higher resistance to γ -rays than human hepatoma cells, melanoma cells and cervical tumor cells. Radiation injury mainly resulted from oxidative free radicals, reductive glycogens synthesized in liver cells which interact with free radicals reduce the radiation injury.

Linear relationship was found between dose and the chromatid breaks after the cells were exposed to ^{60}Co γ -rays in this study (Figure 3). This relationship has proved by previous studies^[5,8,14,19,20]. An increased production of chromatid breaks induced by X-ray irradiation has been reported by Durante^[21-23], an increased production of isochromatid breaks produced by exposure to X-ray was also reported by Kawata^[8,9]. It suggested that with the higher

dose, the electrons which hit the target-chromosome increased, so, the production increased. While, the absolutely production increase of isochromatid breaks was smaller than that of chromatid breaks. Kawata *et al.*^[8], has reported that after low LET irradiation, the chromatid breaks dominated, while for high LET rays, such as heavy ions, isochromatid breaks dominated, suggesting that most isochromatid breaks resulted from two separate breaks on sister chromatids induced by independent electron tracks. For low LET rays, it can not deposit enough energy during unit range to penetrate sister chromatids meantime, so, most breaks were chromatid ones.

Since normal liver cells were more radioresistant to γ -rays than other three kind of cancer cells, study the kinetic repair of chromosome damage of L02 cells has the essentiality. Data^[4,9,15,16] showed that these irradiation could induce the chromosome damage, the damage will probably result in cancerization. Correct and effective repair of injured chromosome is very important to stop cancerization course. Figures 4 and 5 show the correlation between chromatid breaks and dose at 0, 24 and 48 h after radiation. In the present study, at each time point, chromatid breaks and isochromatid breaks were increased linearly with the dose, and the absolute number of chromatid breaks was much more than that of isochromatid ones, this phenomenon was described by Kawata *et al.*^[8]; Suzuki *et al.*^[15], reported that this repairing process occurred during the early 10 h after irradiation. This means in the early 24 h, most of any kind of cells end their spontaneous repair process if they are injured. After 24 h, without any artificial factors, injured and normal cells will be stable and continue synthesizing, mitosing, and so on.

Though the radiotherapy by using common irradiation such as γ -ray is very effective, we could not neglect the side-effect which largely reduce the curative effect due to the injury of normal tissue. Heavy ions have the good biophysics characteristics such as Bragg peak of dose distribution which result in the lowest side scatter, higher RBE (relative biological effect) and lower OER (oxygen enhancement ratio). Present study will enrich the essential data for the Heavy-Ion-Radiotherapy project in the Institute of Modern Physics, Chinese academy of Sciences when the national great engineering HIRFL-CSR (heavy ion research facility of Lanzhou-cooling restore cycle) complete at 2005.

REFERENCES

- 1 **Girinsky T**, Bernheim A, Lubin R, Tavakolirazavi T, Baker F, Janot F, Wibault P, Cosset JM, Duvillard P, Duverger A, Fertil B. *In vitro* parameters and treatment outcome in head and neck cancers treated with surgery and /or radiation: cell characterization and correlation with local control and overall survival. *Int J Radiat Oncol Biol Phys* 1994; **30**: 789-794
- 2 **West CM**, Davidson SE, Burt PA, Hunter RD. The intrinsic radiosensitivity of cervical carcinoma: correlations with clinical data. *Int J Radiat Oncol Biol Phys* 1995; **31**: 841-846
- 3 **West CM**, Davidson SE, Roberts SA, Hunter RD. The independence of intrinsic radiosensitivity as a prognostic factor for patient response to radiotherapy of carcinoma of cervix. *Br J Cancer* 1997; **76**: 1184-1190
- 4 **Coco Martin JM**, Mooren E, Ottenheim C, Burrill W, Nunez MI, Sprong D, Bartelink H, Begg AC. Potential of radiation-

- induced chromosome aberrations to predict radiosensitivity in human tumor cells. *Int J Radiat Biol* 1999; **75**: 1161-1168
- 5 **Kawata T**, Ito H, George K, Wu H, Uno T, Isobe K, Cucinotta FA. Radiation-induced chromosome aberrations in ataxia telangiectasia cells: high frequency of deletions and misrejoining detected by fluorescence *in situ* hybridization. *Radiat Res* 2003; **159**: 597-603
- 6 **Gotoh E**, Kawata T, Durante M. Chromatid break rejoining and exchange aberration formation following γ -ray exposure: analysis in GB2B human fibroblasts by chemical-induced premature chromosome condensation. *Int J Radiat Biol* 1999; **75**: 1129-1135
- 7 **Durante M**, Frusawa Y, George K, Gialanella G, Greco O, Grossi G, Matsufuji N, Pugliese M, Yang TC. Rejoining and misrejoining of radiation-induced chromatin breaks. IV. Charged particle. *Radiat Res* 1998; **149**: 446-454
- 8 **Kawata T**, Gotoh E, Durante M, Wu H, George K, Frusawa Y, Cucinotta FA. High-LET radiation-induced aberrations in prematurely condensed G2 chromosome of human fibroblasts. *Int J Radiat Biol* 2000; **76**: 929-937
- 9 **Kawata T**, Durante M, Frusawa Y, George K, Takai N, Wu H, Cucinotta FA. Dose-response of initial G2-chromatid breaks induced in normal human fibroblasts by heavy ions. *Int J Radiat Biol* 2001; **77**: 165-174
- 10 **Savage JR**. Classification and relationships of induced chromosomal structural changes. *J Med Genet* 1976; **13**: 103-122
- 11 **Pantelias GE**, Maillie HD. Direct analysis of radiation-induced chromosome fragments and rings in unstimulated human peripheral blood lymphocytes by means of the premature chromosome condensation technique. *Mutat Res* 1985; **149**: 67-72
- 12 **Bedford JS**, Goodhead DT. Breakage of human interphase chromosomes by alpha particles and X-rays. *Int J Radiat Biol* 1989; **55**: 211-216
- 13 **Goodwin EH**, Blakely EA, Tobias CA. Chromosomal damage and repair in G1-phase Chinese hamster ovary cells exposed to charged-particle beams. *Radiat Res* 1994; **138**: 343-351
- 14 **Cornforth MN**, Goodwin EH. The dose-dependent fragmentation of chromatin in human fibroblast by 3.5-MeV α particles from ²³⁸Pu: Experimental and theoretical consideration pertaining to single-track effects. *Radiat Res* 1991; **127**: 64-74
- 15 **Suzuki M**, Watanabe M, Suzuki K, Nakano K, Matsui K. Heavy-ion induced chromosome breakage studied by premature chromosome condensation (PCC) in Syrian hamster embryo cells. *Int J Radiat Biol* 1992; **62**: 581-586
- 16 **Suzuki M**, Watanabe M, Kanai T, Kase Y, Yatagai F, Kato T, Matsubara S. LET dependence of cell death, mutation induction and chromatin damage in human cells irradiated with accelerated carbon ions. *Adv Space Res* 1996; **18**: 127-136
- 17 **Suzuki M**, Kase Y, Kanai T, Yatagai F, Watanabe M. LET dependence of cell death and chromatin-break induction in normal human cells irradiated by neon-ion beams. *Int J Radiat Biol* 1997; **72**: 497-503
- 18 **Johnson RT**, Rao PN. Mammalian cell fusion: induction of premature chromosome condensation in interphase nuclei. *Nature* 1970; **226**: 717-722
- 19 **Hittelman WN**, Rao PN. Premature chromosome condensation. I. Visualization of x-ray-induced chromosome damage in interphase cells. *Mutat Res* 1974; **23**: 251-258
- 20 **Cornforth MN**, Bedford JS. X-ray-induced breakage and rejoining of human interphase chromosomes. *Science* 1983; **222**: 1141-1143
- 21 **Pandita TK**, Hittelman WN. The contribution of DNA and chromosome repair deficiencies to the radiosensitivity to ataxia-telangiectasia. *Radiat Res* 1992; **131**: 214-223
- 22 **Sasai K**, Evans JW, Kovacs MS, Brown JM. Prediction of human cell radiosensitivity: comparison of colongenic assay with chromosome aberrations scored using premature chromosome condensation with fluorescence *in situ* hybridization. *Int J Radiat Oncol Biol Phys* 1994; **30**: 1127-1132
- 23 **Durante M**, Gialanella G, Grossi GF, Nappo M, Pugliese M, Bettega D, Calzolari P, Chiorda GN, Ottolenghi A, Tallone-Lombardi L. Radiation-induced chromosomal aberrations in mouse 10T1/2 cells: dependence on the cell-cycle stage at the time of irradiation. *Int J Radiat Biol* 1994; **65**: 437-447

Genetic alterations of hepatocellular carcinoma by random amplified polymorphic DNA analysis and cloning sequencing of tumor differential DNA fragment

Zhi-Hong Xian, Wen-Ming Cong, Shu-Hui Zhang, Meng-Chao Wu

Zhi-Hong Xian, Wen-Ming Cong, Shu-Hui Zhang, Meng-Chao Wu, Department of Pathology, Eastern Hepatobiliary Surgery Hospital, Second Military Medical University, Shanghai 200438, China

Supported by the National Natural Science Foundation of China, No. 30370645 and the Hundred Leading Scientists Program of the Public Health Sector of Shanghai, No. 98BR007

Correspondence to: Wen-Ming Cong, Department of Pathology, Eastern Hepatobiliary Surgery Hospital, Second Military Medical University, Shanghai 200438, China. xianzh7210@163.com

Telephone: +86-21-25070860 Fax: +86-21-25070854

Received: 2004-06-16 Accepted: 2004-07-22

mechanism of hepatocarcinogenesis.

© 2005 The WJG Press and Elsevier Inc. All rights reserved.

Key words: Genetic alterations; Hepatocellular carcinoma; DNA fragment

Xian ZH, Cong WM, Zhang SH, Wu MC. Genetic alterations of hepatocellular carcinoma by random amplified polymorphic DNA analysis and cloning sequencing of tumor differential DNA fragment. *World J Gastroenterol* 2005; 11(26): 4102-4107 <http://www.wjgnet.com/1007-9327/11/4102.asp>

Abstract

AIM: To study the genetic alterations and their association with clinicopathological characteristics of hepatocellular carcinoma (HCC), and to find the tumor related DNA fragments.

METHODS: DNA isolated from tumors and corresponding noncancerous liver tissues of 56 HCC patients was amplified by random amplified polymorphic DNA (RAPD) with 10 random 10-mer arbitrary primers. The RAPD bands showing obvious differences in tumor tissue DNA corresponding to that of normal tissue were separated, purified, cloned and sequenced. DNA sequences were analyzed and compared with GenBank data.

RESULTS: A total of 56 cases of HCC were demonstrated to have genetic alterations, which were detected by at least one primer. The detectability of genetic alterations ranged from 20% to 70% in each case, and 17.9% to 50% in each primer. Serum HBV infection, tumor size, histological grade, tumor capsule, as well as tumor intrahepatic metastasis, might be correlated with genetic alterations on certain primers. A band with a higher intensity of 480 bp or so amplified fragments in tumor DNA relative to normal DNA could be seen in 27 of 56 tumor samples using primer 4. Sequence analysis of these fragments showed 91% homology with *Homo sapiens* double homeobox protein DUX10 gene.

CONCLUSION: Genetic alterations are a frequent event in HCC, and tumor related DNA fragments have been found in this study, which may be associated with hepatocarcinogenesis. RAPD is an effective method for the identification and analysis of genetic alterations in HCC, and may provide new information for further evaluating the molecular

INTRODUCTION

Hepatocellular carcinoma (HCC) is one of the most common cancers worldwide and a leading cause of death in many countries, mainly in Asia and Africa^[1]. It is commonly associated with chronic hepatitis B virus (HBV) and hepatitis C virus (HCV) infections, with chronic exposure to mycotoxin, aflatoxin B1 (AFB1), and is a complication of alcoholic cirrhosis^[2]. The development of HCC is a multistep process associated with multiple genetic alterations, including the genetic alteration of cancer cells^[3,4]. In the past several years, many molecular genetic studies have been extensively performed to clarify the molecular events related with initiation, development and progression of human cancers^[4-7]. Like other cancers, a variety of genetic changes have frequently been found in HCC^[8-13], including p53 mutations^[1,14], loss of heterozygosity (LOH) on chromosome arms 1p, 4q, 5q, 6q, 8p, 10q, 11p, 16p, 16q, 22q^[7-12]. Microsatellite instability has also been recognized in some HCCs^[12,15-17]. However, no information on genetic alterations in the entire genome of HCC is available.

The random amplified polymorphic DNA (RAPD) method is a DNA fingerprinting technique based on polymerase chain reaction (PCR) amplification of random fragments of genomic DNA with single short primers of arbitrary nucleotide sequences^[18]. Unlike the microsatellite instability analysis which can only detect specific microsatellite loci, the RAPD method can simply and rapidly detect genetic alterations in the entire genome without knowledge of specific DNA sequence information^[19]. The RAPD method is a powerful tool for population and pedigree analysis, phylogenetic studies, and bacterial strain identification^[20]. Recently, the RAPD method was used as a means for identifying the genetic alterations in human tumors and revealed that genetic

alterations occurred frequently in lung cancer^[21], squamous cell carcinoma of the head and neck^[22], brain tumor^[23], ovarian cancer^[24], breast cancer^[25], or human aberrant crypt foci and colon cancer^[26]. In the present study, genetic alterations in HCC were investigated using RAPD in order to determine the relationship between the frequency of genetic alterations and the clinicopathological characteristics of HCC, and to find the tumor related DNA fragments.

MATERIALS AND METHODS

Patients and samples

Fifty-six liver cancer tissues were obtained from surgically resected samples in Eastern Hepatobiliary Surgery Hospital, Second Military Medical University. All patients did not receive any prior treatment. All specimens were confirmed with histopathological examination. This study included 43 men and 13 women. The age ranged from 29 years to 78 years. Thirty-five of fifty-six patients had serum AFP ≥ 20 $\mu\text{g/L}$. There were 39 cases with positive HBsAg. Twelve cases had small (≤ 3 cm) and 44 were advanced (>3 cm) HCCs. Tumor differentiation was graded according to WHO criteria (2000). Twenty HCCs were well differentiated, 28 were moderately differentiated and 8 were poorly differentiated. Of the 56 patients, 45 had evidence of intrahepatic metastasis (portal vein invasion and/or intrahepatic dissemination). Forty-seven HCCs were detected accompanied with liver cirrhosis.

DNA extraction

Fresh samples were obtained, immediately frozen in liquid nitrogen and stored at -70 $^{\circ}\text{C}$ until analysis. A microdissection technique with a cryostat was used to separate tumor cells from corresponding noncancerous liver tissues. Genomic DNA was extracted from carcinoma tissues and corresponding noncancerous liver tissues using the standard phenol/chloroform extraction and ethanol precipitation method^[24]. The concentration of DNA was determined with both spectrophotometric and fluorometric methods.

RAPD analysis

For RAPD analysis, 10 arbitrary 10-mer primers were used. These primers were designed, referred to sequences reported previously^[19-25] and synthesized commercially. The sequences of these primers were:

- P1, 5'-CCGGCTACGG-3';
- P2, 5'-CAGGCCCTTC-3';
- P3, 5'-TACGGACACG-3';
- P4, 5'-AGCTTCAGGG-3';
- P5, 5'-AGGCATTCCC-3';
- P6, 5'-GGTCTGAACC-3';
- P7, 5'-TAGGCTCACG-3';
- P8, 5'-ACGGTACACT-3';
- P9, 5'-GTCCTCAACG-3';
- P10, 5'-CTTCACCCGA-3'

In a total volume of 25 μL , 50 ng of genomic DNA extracted from carcinoma tissues or corresponding noncancerous liver tissues was amplified in 10 mmol/L Tris-HCl (pH 8.3), 1.5 mmol/L MgCl_2 , 200 $\mu\text{mol/L}$ each of dNTP, 0.4 $\mu\text{mol/L}$ of each arbitrary primer, and 1.0 units of

AmpliTaq Gold DNA polymerase (Perkin-Elmer, Norwalk, CT). Forty cycles of denaturation (at 94 $^{\circ}\text{C}$ for 30 s), annealing (at 36 - 40 $^{\circ}\text{C}$ for 1 min), and extension (at 72 $^{\circ}\text{C}$ for 2 min) were carried out in a DNA thermocycler (Biomet). Five microliters of the PCR products mixed with loading buffer was loaded in 1.5% agarose gels and electrophoresed with 100 V for 1 h. The gels were stained with ethidium bromide (0.5 mg/mL) and visualized under UV light.

Loss or gain of band(s) and clearly detectable changes in intensity were scored. Scoring was done by two independent observers. A change of band intensities was defined as an increase or decrease of the signal intensity by 50% in the tumor DNA compared to normal DNA by gray scanning with an EDAS290 digital camera system (Kodak) and image analysis with the PDQuest 6.2 software (Bio-Rad).

Cloning and sequencing of RAPD-PCR amplified products

The amplified 480 bp or so fragments from HCC DNA using the primer P4 were excised from the agarose gel and purified. The purified DNAs were reamplified with the primer P4 using the same concentration of reaction mixture constituents and the PCR cycle conditions as described above. The PCR products were analyzed on agarose gels to confirm their size and purity. The reamplified 480 bp DNA fragments were cloned using the TA cloning kit (Invitrogen, Carlsbad, CA, USA) following the protocol provided by the manufacturer. Restriction analysis of the recombinant plasmid DNA prepared by the alkaline lysis purification method was carried out to determine the appropriate insert size^[27-29]. The pure clone amplified DNA insert was sequenced with an automated DNA sequencer through the MegaBACE-500 capillary array electrophoresis instrument in our department. Sequences obtained from our clones were compared with the known sequences in the GenBank database using the BLASTn and BLASTx programs.

Statistical analysis

The relationship between the frequency of genetic alterations and clinicopathological features was assessed by using the χ^2 test, $P < 0.05$ was considered statistically significant.

RESULTS

Genetic alterations in HCC

We examined 56 HCC tissues and corresponding noncancerous liver tissues using the RAPD method to detect the genetic alterations in HCC. Our results indicated that RAPD-PCR was an effective tool for identifying genetic alterations in cancer tissues. All the cases of HCC were demonstrated to have genetic alterations in at least one of ten primers. The incidence of genetic alterations ranged from 20% to 70% in each case, and 17.9% (15/56) to 50% (28/56) in each primer. The primer with the highest frequency of genetic alteration was P4. Genetic alterations were identified as band loss, gain, intensity change and shift in the tumor DNA lane as compared to the paired normal DNA lane (Figure 1A).

Correlation with clinicopathological characteristics

The correlation between the frequency of genetic alterations and clinicopathological features in HCC is shown in Table 1.

Table 1 Correlation between clinicopathological features and genetic alterations in hepatocellular carcinoma

Clinicopathological features		No.	P1	P2	P3	P4	P5	P6	P7	P8	P9	P10
Sex	M	43	14	14	7	20	19	9	18	10	10	22
	F	13	3	5	3	7	3	6	5	4	3	7
Age (yr)	<50	24	6	12	6	11	8	7	9	8	5	14
	≥50	32	11	7	4	16	14	8	14	6	8	15
Serum AFP level (μg/L)	<20	21	3	6	5	9	5	7	9	9	6	8
	≥20	35	14	13	5	18	17	8	14	5	7	21
HBsAg	Positive	39	17	12	8	24	16	10	13	13	8	27
	Negative	17	0 ^b	7	2	3 ^a	6	5	10	1 ^a	5	2 ^b
Tumor size (cm)	≤3	12	3	3	7	4	5	2	6	3	3	7
	>3	44	14	16	3 ^a	23	17	13	17	11	10	22
Histological grade	Well	20	0	4	7	5	8	5	10	7	3	13
	Moderately	28	12 ^b	12	2	17 ^a	12	8	10	5	8	13
	Poorly	8	5 ^b	3	1	5 ^a	2	2	3	2	2	3
Liver cirrhosis	Absent	9	2	3	3	3	4	3	5	1	3	4
	present	47	15	16	7	24	18	12	18	13	10	25
Tumor capsule	Absent	11	5	3	0	6	5	2	5	1	2	4
	Not intact	31	9	13	4 ^a	16	10	11	13	10	7	17
	Intact	14	3	3	6 ^a	5	7	2	5	3	4	8
Intrahepatic metastasis	Not observed	11	3	5	7	2	5	2	5	3	5	7
	Observed	45	14	14	3 ^b	25 ^a	17	13	18	11	8	22
Total [n (%)]		56	17 (30.4)	19 (33.9)	10 (17.9)	27 (48.2)	22 (39.3)	15 (26.8)	23 (41.1)	14 (25)	13 (23.2)	28 (50)

^a $P < 0.05$, ^b $P < 0.01$, χ^2 test.

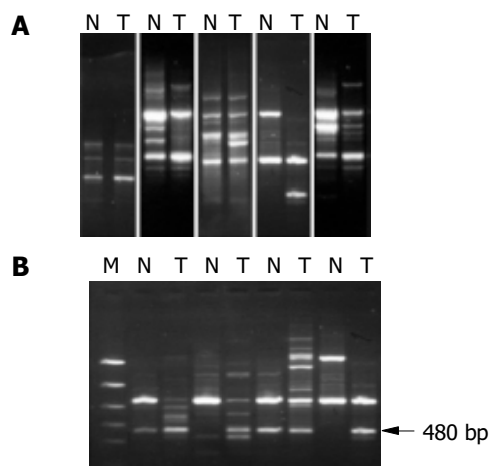


Figure 1 RAPD-PCR analysis of hepatocellular carcinoma. Corresponding noncancerous liver tissue DNA (N), and tumor DNA (T) were amplified by PCR with obvious primers and electrophoresed in agarose gels. **A:** Genetic alterations identified as band loss, gain, shift and intensity change in the tumor DNA lane as compared to the paired normal DNA lane; **B:** Amplified 480 bp fragments from HCC DNA using the primer P4, the 1.5 kb ladder was used as a marker (M).

No significant correlation was observed between the genetic alterations and serum AFP concentration, HBV infection, tumor size, cirrhosis, histological grade, tumor capsule, as well as tumor intrahepatic metastasis. As to the primers, the frequencies of genetic alterations on primer P1, P4, P8 and P10 were significantly higher in patients with positive HBsAg than in those with negative HBsAg ($P < 0.01$). Genetic alterations on P3 were more frequent in tumors less than 3 cm in size ($P < 0.05$ or $P < 0.01$). Genetic alterations on P1 and P4 were more frequent in poorly or moderately differentiated tumors than in well-differentiated tumors ($P < 0.01$ and $P < 0.05$), but genetic alterations on P3 were

more frequent in well-differentiated tumors than in poorly or moderately differentiated tumors ($P < 0.05$). Genetic alterations on P3 were significantly higher in patients without intact tumor capsules than in those with intact capsules ($P < 0.01$). Genetic alterations on P4 were more frequently detected in tumors with intrahepatic metastasis than in those without. Similarly, genetic alterations on P3 were significantly lower in patients with intrahepatic metastasis than in those without ($P < 0.01$).

Cloning and sequencing of amplified differential fragments from P4, sequence homology search

The amplified 480 bp fragments from HCC DNA using the primer P4 were separated on the agarose gels, excised, eluted, and reamplified with the same primer (Figure 1B). After analysis of the PCR products on an agarose gel to confirm their size and purity, these amplified DNA products were cloned using the TA cloning kit. After confirmation of positively cloned DNA by hybridization with the purified RAPD-amplified fragments, sequences were obtained from several clones and compared with known sequences in GenBank. Figure 2 shows the electropherograms from sequencing with amplified 476 bp fragments using P4 primer. The followings were the nucleotide sequences of the fragments: TCCCCGCGATGGCCCTCCTGACAGCT-TCGGACAGCACCCACCCTGCAGAAGCACATTAAC-AGGAATGACGAAGGAGACTCCTTTGGAACC-CGAGCCAAAGCGAGGCCCTGAGAGCCTGCT-TTGAGCAAACCCATAGCCGGGTATCGCCACAAGAG-AATGGCTGGCCAGGCCATCGGCATTCCAG-AACCCAGGGTCCAGATTTGGTTTCAGAAATGAGA-GGTCACGGCAGCTGAGGCAGCACCCGGCGGGA-ATCTCGCCCTGGCCTGGGAGACGCGGCCAGCAA-GAAGGCAGGTGAAAGTGGACCGCCGTCACCAGATCC-CAGACCGCCCTGCTCCTCCGAGCCTTTGAGAA-

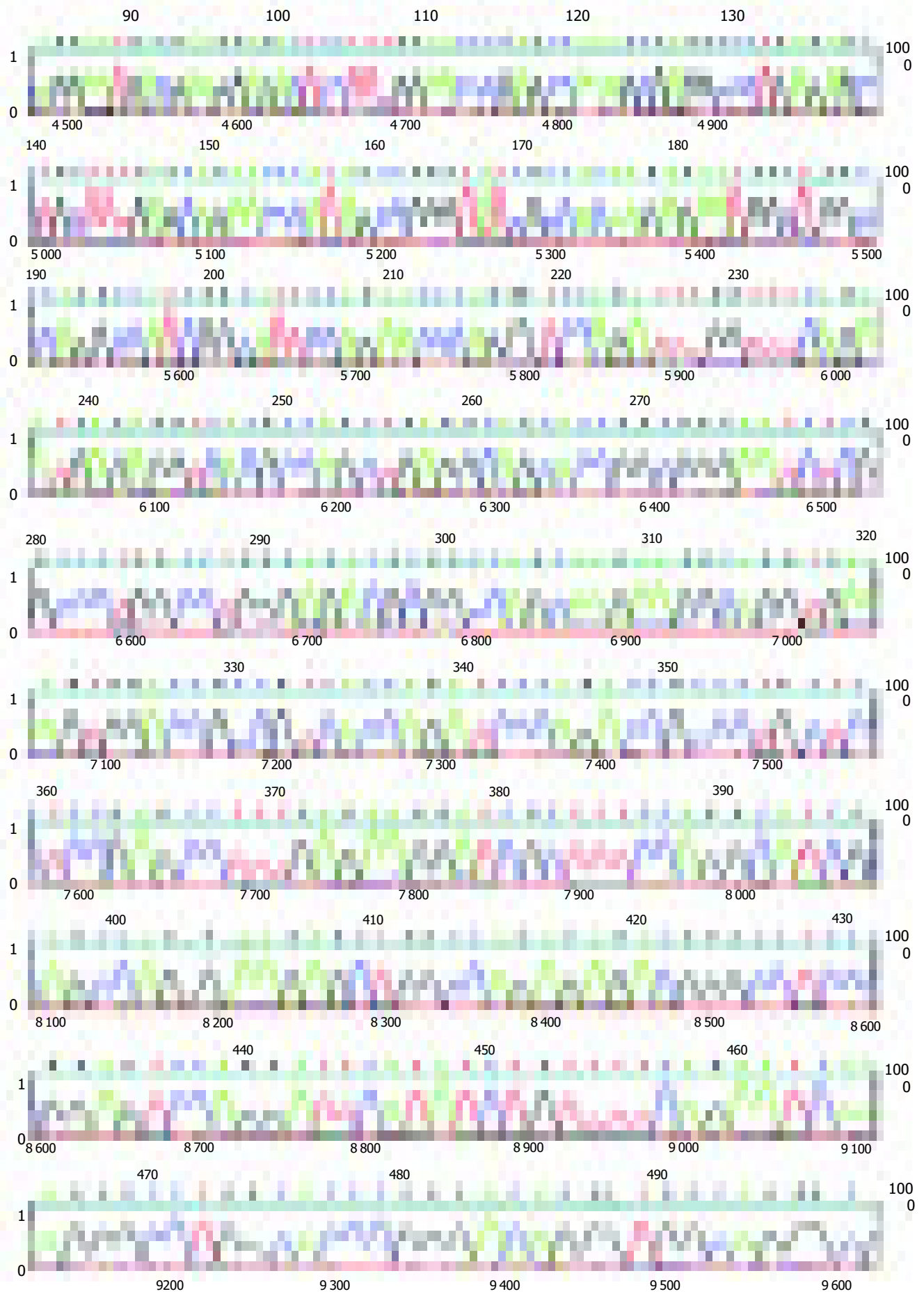


Figure 2 Electropherogram from sequencing with an amplified 476-bp fragment using P4 primer.

GGATCGCTTCCAGGCATCGCAGCCAGGA-
AGGCTGGCCAGAGAGACGGGCTCCCG-
GAGTCCAGGATTCATATCTGTTTTC-
GAATCAAAGGGCCTGGCACCCGGGAC-
AGGGTGGCAGGGCGAACACGCA.

BLAST analysis revealed that there were significant matches of the 480 bp or so RAPD fragments with any known gene in this database either at the DNA level or its corresponding amino acid sequence. The tumor-specific P4 amplified 476-bp fragment sequences showed 92% homology with homo sapiens 3 BAC RP11-413E6 (Roswell Park Cancer Institute Human BAC Library, accession number AC108724.4) from nt 84 643 to nt 84 168, and with human DNA sequence clones RP11-298A19 on chromosome 22 (accession number AL592170.21) from nt 84717 to nt 842981, and 91% homology with homo sapiens double homeobox protein DUX10 gene from nt 316 to nt 788 (accession number Ay044051.1), and with homo sapien putative proteins and FSHD region gene 2 protein (HSA10-FRG2) genes (accession number AY028079.1) from nt 118 939 to nt 119 411.

DISCUSSION

The RAPD method, a PCR-based method for nucleic acid fingerprinting, was originally reported by Williams *et al.*^[18], and it is thought to be suitable for investigation of genetic alterations. RAPD-PCR multiple bands amplified with arbitrary primers could generate a complex DNA fingerprint that can detect qualitative (structural) and quantitative (aneuploid) genetic differences between normal and tumor cell genomes. Mutations can affect the fingerprint by altering the distance between the two primers, the ability of the primer to anneal, and the relative amounts of target amplification^[19]. In the present study, we identified genetic alterations in HCC at the level of ethidium bromide stained agarose gels. Genetic alterations indicating distance band shift or band loss/gain were observed. Mutations occurred at the primer-template interaction sites resulted in the loss or gain of a band, and mutations occurred between the primer-template interaction sites, such as deletions or insertions, resulted in a mobility shift of bands. However, single base situations between two primers could not be detected by this method. In addition to these qualitative alterations, we also observed decrease or increase in the relative intensities of the bands in tumor DNA compared to those in normal tissue DNA. Allelic losses due to their linkage to suppressor genes, might result in decrease of band intensities, and gene amplification or chromosomal aneuploidy might result in increase of band intensities. Furthermore, we found a significant correlation between the instability of certain primers and HBV infection, tumor size, cirrhosis, histological grade, tumor capsule, as well as tumor intrahepatic metastasis at some primers. These results suggest that the high frequency of genetic alterations identified by the RAPD method may be involved in the malignant potential of HCC.

Since this method permits the direct cloning and characterization of amplified DNA bands which represent genetic alterations specific in HCC genome during tumor progression, further research in this direction will find out new genes contributing to progression in liver cancer. The

most important finding in the present study is that a band with a higher intensity of 480 bp or so amplified fragments in tumor DNA relative to normal DNA could be seen in 27 and 56 tumor samples using primer 4. An enhancement of the signal intensity of amplified DNA fragments may be related to localized overamplification of that gene locus in the genome, or could result from changes at the chromosome level, such as trisomy or tetrasomy. These events could play an important role in the development of HCC or they could occur during the clonal expansion of genetically unstable tumor cells. Sequence analysis of the fragments showed 92% homology with homo sapiens 3 BAC RP11-413E6 (Roswell Park Cancer Institute Human BAC Library) complete sequence, and with human DNA sequences from clone RP11-298A19 on chromosome 22, complete sequence. Also the fragment sequences showed 91% homology with homo sapiens double homeobox protein DUX10 gene, and with homo sapiens putative protein and FSHD region gene 2 protein (HSA10-FRG2) genes. Homeobox protein genes comprise a large and essential family of developmental regulators that are vital for all aspects of growth and differentiation. Although many studies have reported their deregulated expression in cancer, few studies have established direct functional roles for homeobox genes in carcinogenesis^[30]. Our data suggest that homeobox protein gene family members are activated as an important pathway in hepatocarcinogenesis.

In summary, genetic alterations are a frequent event in HCC. Furthermore, serum AFP concentration, HBV infection, tumor size, histological grade, tumor capsule, as well as tumor intrahepatic metastasis, may be correlated with allelic losses with certain primers. A band with a higher intensity of 480 bp or so amplified fragments in tumor DNA relative to normal DNA can be seen tumor samples and sequence analysis of the fragments can show 91% homology with homo sapiens double homeobox protein DUX10 gene. The RAPD method is an effective tool for the identification and analysis of genetic alterations in HCC tissues and it may provide some new information about the molecular mechanism of hepatocarcinogenesis.

REFERENCES

- 1 **Buendia MA.** Genetics of hepatocellular carcinoma. *Semin Cancer Biol* 2000; **10**: 185-200
- 2 **Feitelson MA,** Sun B, Satiroglu Tufan NL, Liu J, Pan J, Lian Z. Genetic mechanisms of hepatocarcinogenesis. *Oncogene* 2002; **21**: 2593-2604
- 3 **Thorgeirsson SS,** Grisham JW. Molecular pathogenesis of human hepatocellular carcinoma. *Nat Genet* 2002; **31**: 339-346
- 4 **McGlynn KA,** Edmonson MN, Michielli RA, London WT, Lin WY, Chen GC, Shen FM, Buetow KH. A phylogenetic analysis identifies heterogeneity among hepatocellular carcinomas. *Hepatology* 2002; **36**: 1341-1348
- 5 **Tsopanomichalou M,** Kouroumalis E, Ergazaki M, Spandidos DA. Loss of heterozygosity and microsatellite instability human non-neoplastic hepatic lesions. *Liver* 1999; **19**: 305-311
- 6 **Loeb KR,** Loeb LA. Significance of multiple mutations in cancer. *Carcinogenesis* 2000; **21**: 379-385
- 7 **Suriawinata A,** Xu R. An update on the molecular genetics of hepatocellular carcinoma. *Semin Liver Dis* 2004; **24**: 77-88
- 8 **Maggioni M,** Coggi G, Cassani B, Bianchi P, Romagnoli S, Mandelli A, Borzio M, Colombo P, Roncalli M. Molecular changes in hepatocellular dysplastic nodules on microdissected

- liver biopsies. *Hepatology* 2000; **32**: 942-946
- 9 **Okabe H**, Ikai I, Matsuo K, Satoh S, Momoi H, Kamikawa T, Katsura N, Nishitai R, Takeyama O, Fakumoto M, Yamaoka Y. Comprehensive allelotyping study of hepatocellular carcinoma: potential differences in pathways to hepatocellular carcinoma between hepatitis B virus-positive and -negative tumors. *Hepatology* 2000; **31**: 1073-1079
 - 10 **Liao C**, Zhao M, Song H, Uchida K, Yokoyama KK, Li T. Identification of the gene for a novel liver-related putative tumor suppressor at a high-frequency loss of heterozygosity region of chromosome 8p23 in human hepatocellular carcinoma. *Hepatology* 2000; **32** (4 Pt1): 721-727
 - 11 **Tamura S**, Nakamori S, Kuroki T, Sasaki Y, Furukawa H, Ishikawa O, Imaola S, Nakamura Y. Association of cumulative allelic losses with tumor aggressiveness in hepatocellular carcinoma. *J Hepatol* 1997; **27**: 669-676
 - 12 **Kondo Y**, Kanai Y, Sakamoto M, Mizokami M, Ueda R, Hirohashi S. Microsatellite instability associated with hepatocarcinogenesis. *J Hepatol* 1999; **31**: 529-536
 - 13 **Li SP**, Wang HY, Li JQ, Zhang CQ, Feng QS, Huang P, Yu XJ, Huang LX, Liang QW, Zeng YX. Genome-wide analyses on loss of heterozygosity in hepatocellular carcinoma in Southern China. *J Hepatol* 2001; **34**: 840-849
 - 14 **Grisham JW**. Interspecies comparison of liver carcinogenesis: implications for cancer risk assessment. *Carcinogenesis* 1997; **18**: 59-81
 - 15 **Salvucci M**, Lemoine A, Saffroy R, Azoulay D, Lepere B, Gaillard S, Bismuth H, Reynes M, Debuire B. Microsatellite instability in European hepatocellular carcinoma. *Oncogene* 1999; **18**: 181-187
 - 16 **Kondo Y**, Kanai Y, Sakamoto M, Mizokami M, Ueda R, Hirohashi S. Genetic instability and aberrant DNA methylation in chronic hepatitis and cirrhosis-A comprehensive study of loss of heterozygosity and microsatellite instability at 39 loci and DNA hypermethylation on 8 CpG islands in microdissected specimens from patients with hepatocellular carcinoma. *Hepatology* 2000; **32**: 970-979
 - 17 **Macdonald GA**, Greenon JK, Saito K, Cherian SP, Appelman HD, Boland CR. Microsatellite instability and loss of heterozygosity at DNA mismatch repair gene loci occurs during hepatic carcinogenesis. *Hepatology* 1998; **28**: 90-97
 - 18 **Williams JG**, Kubelik AR, Livak KJ, Rafalski JA, Tingey SV. DNA polymorphisms amplified by arbitrary primers are useful as genetic markers. *Nucleic Acids Res* 1990; **18**: 6531-6535
 - 19 **Papadopoulos S**, Benter T, Anastassiou G, Pape M, Gerhard S, Bornfeld N, Ludwig WD, Dorken B. Assessment of genomic instability in breast cancer and uveal melanoma by random amplified polymorphic DNA analysis. *Int J Cancer* 2002; **99**: 193-200
 - 20 **Hering O**, Nirenberg HI. Differentiation of *Fusarium sambucinum* Fuckel sensu lato and related species by RAPD PCR. *Mycopathologia* 1995; **129**: 159-164
 - 21 **Ong TM**, Song B, Qian HW, Wu ZL, Whong WZ. Detection of genomic instability in lung cancer tissues by random amplified polymorphic DNA analysis. *Carcinogenesis* 1998; **19**: 233-235
 - 22 **Maeda T**, Jikko A, Hiranuma H, Fuchihata H. Analysis of genomic instability in squamous cell carcinoma of the head and neck using the random amplified polymorphic DNA method. *Cancer Lett* 1999; **138**: 183-188
 - 23 **Dil-Afroze**, Misra A, Sulaiman IM, Sinha S, Sarkar C, Mahapatra AK, Hasnain SE. Genetic alterations in brain tumors identified by RAPD analysis. *Gene* 1998; **206**: 45-48
 - 24 **Sood AK**, Buller RE. Genomic instability in ovarian cancer: a reassessment using an arbitrarily primed polymerase chain reaction. *Oncogene* 1996; **13**: 2499-2504
 - 25 **Singh KP**, Roy D. Identification of novel breast tumor-specific mutation(s) in the q11.2 region of chromosome 17 by RAPD/AP-PCR fingerprinting. *Gene* 2001; **269**: 33-43
 - 26 **Luo L**, Li B, Pretlow TP. DNA alterations in human aberrant crypt foci and colon cancers by random primed polymerase chain reaction. *Cancer Res* 2003; **63**: 6166-6169
 - 27 **Navarro JM**, Jorcano JL. The use of arbitrarily primed polymerase chain reaction in cancer research. *Electrophoresis* 1999; **20**: 283-290
 - 28 **Misra A**, Chosdol K, Sarkar C, Mahapatra AK, Sinha S. Alteration of a sequence with homology to human endogenous retrovirus (HERV-K) in primary human glioma: implications for viral repeat mediated rearrangement. *Mutat Res* 2001; **484**: 53-59
 - 29 **Comes AM**, Humbert JF, Laurent F. Rapid cloning of PCR-derived RAPD probes. *Biotechniques* 1997; **23**: 210-212
 - 30 **Monica K**, Galili N, Nourse J, Saltman D, Cleary ML. PBX2 and PBX3, new homeobox genes with extensive homology to the human proto-oncogene PBX1. *Mol Cell Biol* 1991; **11**: 6149-6157

• BRIEF REPORTS •

Correlation of *Chlamydia pneumoniae* infection with primary biliary cirrhosis

Hai-Ying Liu, An-Mei Deng, Jian Zhang, Ye Zhou, Ding-Kang Yao, Xiao-Qing Tu, Lie-Ying Fan, Ren-Qian Zhong

Hai-Ying Liu, Clinical Laboratory, General Hospital of Guangzhou Military Command of PLA, Guangzhou 510010, Guangdong Province, China

An-Mei Deng, Jian Zhang, Ye Zhou, Xiao-Qing Tu, Lie-Ying Fan, Ren-Qian Zhong, Laboratory Diagnostics, Changzheng Hospital, Second Military Medical University, and Clinical Immunology Center of PLA, Shanghai 200003, China

Ding-Kang Yao, Department of Gastroenterology, Changzheng Hospital, Second Military Medical University, Shanghai 200003, China

Supported by the National Natural Science Foundation of China, No. 30300157

Correspondence to: Dr. Hai-Ying Liu, Clinical Laboratory, General Hospital of Guangzhou Military Command of PLA, Guangzhou 510010, Guangdong Province, China. xiangliu haiying@21cn.com
Telephone: +86-20-61653458 Fax: +86-20-36225361

Received: 2004-09-30 Accepted: 2004-11-26

Abstract

AIM: To evaluate the association between *Chlamydia pneumoniae* (*Cpn*) infection and primary biliary cirrhosis (PBC).

METHODS: *Cpn* IgG and IgM were determined by enzyme-linked immunosorbent assay (ELISA) in 41 well-established PBC patients and two race-matched control groups (post-hepatitis cirrhosis, $n = 70$; healthy controls, $n = 57$).

RESULTS: The mean level and seroprevalence of *Cpn* IgG in PBC group and post-hepatitis cirrhosis (PHC) group were significantly higher than those in healthy controls (46.8 ± 43.4 RU/mL, 49.5 ± 45.2 RU/mL vs 28.3 ± 32.7 RU/mL; 68.3%, 71.4%, 42.1%, respectively; $P < 0.05$). There was a remarkably elevated seroprevalence of *Cpn* IgM in patients with PBC (22.0%) compared to the PHC and healthy control (HC) groups. For the PBC patients versus the HCs, the odds ratios (ORs) of the presence of *Cpn* IgG and IgM were 2.7 (95% CI 0.9-6.1) and 5.1 (95% CI 1.4-18.5), respectively. Though there was no correlation in the level of *Cpn* IgG with total IgG in sera of patients with PBC ($r = -0.857$, $P = 0.344 > 0.05$), *Cpn* IgM was related with the abnormally high concentrations of total IgM in PBC group.

CONCLUSION: The results of this study do not support the hypothesis that infection with *Chlamydia pneumoniae* may be a triggering agent or even a causative agent in PBC, but suggest that *Chlamydia pneumoniae* infection probably contributes to the high level of IgM present in most patients with PBC.

© 2005 The WJG Press and Elsevier Inc. All rights reserved.

Key words: Primary biliary cirrhosis; *Chlamydia pneumoniae*; Antibodies; ELISA

Liu HY, Deng AM, Zhang J, Zhou Y, Yao DK, Tu XQ, Fan LY, Zhong RQ. Correlation of *Chlamydia pneumoniae* infection with primary biliary cirrhosis. *World J Gastroenterol* 2005; 11(26): 4108-4110

<http://www.wjgnet.com/1007-9327/11/4108.asp>

INTRODUCTION

PBC is a chronic inflammatory process that mainly affects the medium-sized intrahepatic bile ducts, leads to chronic cholestasis, and often develops to cirrhosis and liver failure that requires liver transplantation. This disease is characterized by the presence of anti-mitochondrial autoantibodies and is considered as an autoimmune disease. However, its exact mechanism of pathogenesis and etiology remains elusive. Several studies have demonstrated cross-reactivity at both B-cell and T-cell levels between autoantigen-pyruvate dehydrogenase complex (PDC) and polypeptides derived from the sequences of potential pathogens^[1,2]. It is suggested that molecular mimicry between pathogen and self-antigen might result in tolerance breakdown. A good deal of evidence suggests an infectious component in the development of PBC, and to date, some bacteria and viruses have been found to be linked to with the disease^[3-5]. Nevertheless, so far no microbiological agent has been confirmed in PBC, though the possibility of a pathophysiological role for some viral or bacterial micro-organisms has not been excluded. It was reported that infection with the respiratory bacterium *Cpn* might be a triggering agent or even a causative agent in PBC^[6]. If that is the case, antibiotic treatment could be effective. We attempted to confirm these findings serologically by designing a case-control study, to assess whether PBC patients had any serologic evidence of *Cpn*, and to evaluate the correlation of *Cpn* infection with PBC by testing the levels of serum antibodies IgG and IgM against *Cpn* in Chinese patients with PBC.

MATERIALS AND METHODS

Patients

A total of 211 subjects, recruited in 2002 and 2003, were divided into three groups. Patient groups involved 41 Chinese patients with well-established PBC from Eastern China including Zhejiang, Jiangsu and Shanghai, who met

the following diagnostic criteria for PBC recommended by the American Association for the Study of Liver Diseases (AASLD)^[7]: (1) presence of cholestatic liver disease manifestations including jaundice, fatigue and pruritus with abnormally high levels of cholestatic parameters such as ALP, serum bilirubin and γ -GT; (2) absence of biliary obstruction as confirmed by ultrasonography, computed tomography, or endoscopic cholangiography; (3) serum positive AMA titre $\geq 1:40$. Information of each patient was obtained at the first visit. The ratio of male to female in the study was about 1:6 (6/35). The average age of the patients was 52.5 years (range: 29-87 years). All patients showed AMA positive and anti-M2 was detectable in 35 PBC patients (85.4%). Two groups of race-matched control individuals with no known cardiac disease were selected on the basis of similar age and sex. A control group consisted of 70 Chinese patients with PHC. The third control group included 57 healthy subjects for estimating the prevalence of *Cpn* antibodies in the general population.

Testing of *Cpn* antibodies

The sera were tested at dilution of 1:101 for *Cpn* specific IgG and IgM antibodies with ELISA kits (Euroimmun, Luebeck, Germany), according to the manufacturer's instructions. The coated antigens in the wells contained all relevant antigens localized in the outer membrane of HEp-2 cells infected with the "CDC/CWL-029" strain of *Cpn*. The outer membrane is composed of lipopolysaccharide (LPS) and numerous proteins (outer membrane proteins, OMPs). IgG antibodies against *Cpn* were quantitated with three calibration sera at concentrations of 2, 20, and 200 RU/mL. IgM antibodies were quantified by calculating a certain ratio against the calibration serum. If the ratio ≥ 1 , the serum was defined as positive; if the ratios < 1.0 , the serum was defined as negative.

Clinical laboratory tests

Quantitative measurements of IgG and IgM were analyzed on sera of all PBC patients with a Dade-Behring nephelometer. Anti-mitochondrial autoantibodies (AMA) were tested by indirect immunofluorescence (Euroimmun, Luebeck, Germany). Anti-M2 antibody was tested by immunoblotting assay using a humanized M2 trimer as antigen source.

Statistical analysis

All statistical analyses were performed with SPSS for Windows 10.0. The frequencies of antibodies were processed by χ^2 test or Fisher's exact test. The *t*-test was used for the comparison of group means. $P < 0.05$ was considered statistically significant. Odds ratios (ORs) were calculated with exact 95% confidence intervals (CIs).

RESULTS

The mean level of *Cpn* IgG in PBC and PHC groups (46.8 ± 43.4 , 49.5 ± 45.2 RU/mL, respectively) was much higher than that in the HC group (28.3 ± 32.7 RU/mL), and there was no statistical difference between the two groups ($P < 0.05$). According to the cut-off value of 20 RU/mL recommended by the kits, the frequency of *Cpn* IgG in PBC,

PHC, and HC groups was 28/41 (68.3%), 50/70 (71.4%) and 24/57 (42.1%), respectively. The positive rate of *Cpn* IgG in PBC and PHC groups was different from that in HC group ($P = 0.02$ and 0.001 respectively as shown in Figure 1). In contrast, the proportion of IgM positive samples in the PBC group (22.0%, 9/41) was much higher than that in the control groups (PHC, 7.1%; HC, 5.3%), and this difference was statistically significant ($P = 0.023$ for PBC vs PHC and 0.013 for PBC vs HC). Compared to the healthy controls, the ORs of the presence of *Cpn* IgG and IgM antibodies in the PBC patients were 2.7 (95%CI: 0.9-6.1) and 5.1 (95%CI: 1.4-18.5) respectively.

Twenty-eight of the forty-one (68.3%) patients had high total IgG and IgM levels and 22 of the 28 PBC patients were *Cpn* IgG positive (78.6%), but there was no difference in total IgG level between *Cpn* IgG positive and negative patients ($P = 0.275$). However, the correlation between *Cpn* IgG level and sera total IgG was statistically insignificant ($r = -0.857$, $P = 0.344$). Nine of the twenty-eight (32.1%) patients with increased IgM level were *Cpn* IgM positive. *Cpn* IgM was related to abnormally high level of total IgM. Anti-mitochondrial antibodies were found in all the 41 PBC patients, 35 cases (85.4%) of them were M2 autoantibodies positive. Between *Cpn* IgM positive and negative PBC patients, no significant differences were found in age, age at onset, disease duration and other laboratory parameters including ALP, γ GT, serum bilirubin and bile acids.

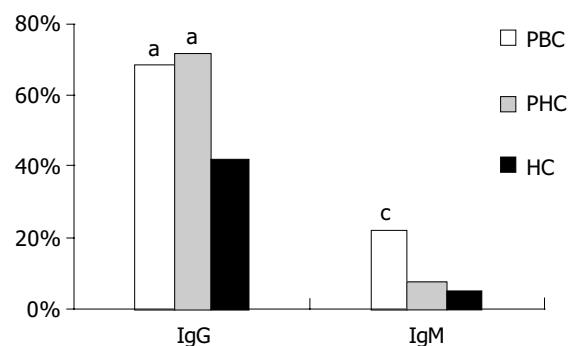


Figure 1 Proportion of patients positive for *Cpn* IgG and IgM. ^a $P < 0.05$ vs HC group ^b $P < 0.05$ vs PHC and HC group.

DISCUSSION

Cpn is a common cause of community acquired acute respiratory infection with a seroprevalence rate of over 50% adults in many countries. It has been shown that *Cpn* may play a potential role in autoimmune diseases such as atherosclerosis^[8], multiple sclerosis^[9] and even primary sclerosing cholangitis^[10] that is also an autoimmune cholangitis. The presence of *Cpn* antigen and RNA in biopsies from patients with autoimmune diseases suggests that *Cpn* antigen may trigger an immune response through molecular mimicry^[11,12]. The role of *Cpn* in the etiology of autoimmunity is however controversial.

It was found that in periportal and lobular hepatocytes of liver tissues from patients with PBC, *Cpn* antigens are present instead of *C. trachomatis* by immunohistochemical

staining^[6], suggesting that *Cpn* infection is closely related with PBC. High level of *Cpn* IgG is an important marker for previous infection whereas IgM reactivity represents acute infection. In this study, up to 68.3% PBC patients were infected with *Cpn*. Though their prevalence and mean level of *Cpn* IgG were higher than healthy controls, no difference was seen compared to PHC patients. Therefore, it is difficult to conclude that *Cpn* infection is the cause of PBC or the result of chronic liver diseases.

Abnormally high level of serum IgM is one of the serological characteristics of PBC. However, the reasons for high level of IgM and the nature of IgM remain unclear. In our study, 70% PBC patients had a high level of IgM and about one third of them were *Cpn* IgM positive, indicating that increased serum IgM in PBC patients is closely related to *Cpn* IgM and *Cpn* infection may be one of the factors for abnormally high level of IgM in PBC patients.

Recently, studies with animal model of experimental allergic encephalitis (EAE) indicate that *Cpn* infection increases the severity of EAE that can be attenuated with anti-infective therapy, and that infection of the central nervous system with *Cpn* can amplify the autoreactive pool of lymphocytes and regulate the expression of autoimmune diseases^[13,14]. Though we did not find any difference between patients with or without acute *Cpn* infection in clinical features and biochemical parameters, including ALP, AST and GGT, *Cpn* may secrete high immunogenic substrates or provide an inflammatory microenvironment to enhance the self-reactivity of pathogenic T lymphocytes. How *Cpn* infection acts on the process of PBC remains to be clarified in future studies.

In conclusion, the results of this study do not support the hypothesis that infection with *Cpn* may be a triggering agent or even a causative agent at least in Chinese patients with PBC, but suggest that *Cpn* infection may contribute to the high level of IgM present in most PBC patients.

REFERENCES

- 1 **Bogdanos DP**, Baum H, Grasso A, Okamoto M, Butler P, Ma Y, Rigopoulou E, Montalto P, Davies ET, Burroughs AK, Vergani D. Microbial mimics are major targets of crossreactivity with human pyruvate dehydrogenase in primary biliary cirrhosis. *J Hepatol* 2004; **40**: 31-39
- 2 **Vilagut L**, Vila J, Vias O, Pares A, Gines A, Jimenez deAnta MT, Rodes J. Cross-reactivity of anti-Mycobacterium gordonae antibodies with the major mitochondrial autoantigens in primary biliary cirrhosis. *J Hepatol* 1994; **21**: 673-677
- 3 **Butler P**, Valle F, Hamilton-Miller JM, Brumfitt W, Baum H, Burroughs AK. M2 mitochondrial antibodies and urinary rough mutant bacteris in patients with primary biliary cirrhosis and in patients with recurrent bacteriuria. *J Hepatol* 1993; **17**: 408-414
- 4 **Mayo I**, Arizti P, Pares A, Oliva J, Doforno RA, De Sagarra MR, Rodes J, Castano JG. Antibodies against the COOH-terminal region of E. coli ClpP protease in patients with primary biliary cirrhosis. *J Hepatol* 2000; **33**: 528-536
- 5 **Xu L**, Shen Z, Guo L, Fodera B, Keogh A, Joplin R, O'Donnell B, Aithen J, Carman W, Neuberger J, Mason A. Does a betaretrovirus infection trigger primary biliary cirrhosis? *Proc Natl Acad Sci USA* 2003; **100**: 8454-8459
- 6 **Abdulkarim AS**, Petrovic LM, Kim WR, Angulo P, Lloyd RV, Lindor KD. Primary biliary cirrhosis: an infectious disease caused by Chlamydia pneumonia? *J Hepatol* 2004; **40**: 380-384
- 7 **Heathcote EJ**. Management of primary biliary cirrhosis. The American association for the study of liver diseases practice guidelines. *Hepatology* 2000; **31**: 1005-1013
- 8 **Shoenfeld Y**, Sherer Y, Harats D. Atherosclerosis as an infectious, inflammatory and autoimmune disease. *Trends Immunol* 2001; **22**: 293-296
- 9 **Layh-Schmitt G**, Bendl C, Hildt U, Dong-Si T, Juttler E, Schnitzler P, Grond-Ginstach C, Grau AJ. Evidence for infection with Chlamydia pneumoniae in a subgroup of patients with multiple sclerosis. *Ann Neurol* 2000; **47**: 652-655
- 10 **Ponsioen CY**, Defoer J, Ten Kate FJ, Weverling GJ, Tytgat GN, Pannekoek Y, Wertheim-Dillen PM. A survey of infectious agents as risk factors for primary sclerosing cholangitis: are Chlamydia species involved? *Eur J Gastroenterol* 2002; **14**: 641-648
- 11 **Bachmaier K**, Neu N, de la Maza LM, Pal S, Hessel A, Penninger JM. Chlamydia infections and heart disease linked through antigenic mimicry. *Science* 1999; **283**: 1335-1339
- 12 **Conant SB**, Swanborg RH. MHC class II peptide flanking residues of exogenous antigens influence recognition by autoreactive T cells. *Autoimmun Rev* 2003; **2**: 8-12
- 13 **Lenz DC**, Lu L, Conant SB, Wolf NA, Gerard HC, Whittum-Hudson JA, Hudson AP, Swanborg RH. A *Chlamydia pneumoniae*-specific peptide induces experimental autoimmune encephalomyelitis in rats. *J Immunol* 2001; **167**: 1803-1808
- 14 **Du C**, Yao SY, Ljunggren-Rose A, Sriram S. Chlamydia pneumoniae infection of the central nervous system worsens experimental allergic encephalitis. *J Exp Med* 2002; **196**: 1639-1644

Splenic hemangiopericytoma and serosal cavernous hemangiomas of the adjacent colon

Tuncay Yilmazlar, Turkey Kirdak, Omer Yerci, Saduman B. Adim, Ozkan Kanat, Osman Manavoglu

Tuncay Yilmazlar, Turkey Kirdak, Department of General Surgery, Uludag University School of Medicine, Gorukle, Bursa 16059, Turkey
Omer Yerci, Saduman B. Adim, Department of Pathology, Uludag University School of Medicine, Gorukle, Bursa 16059, Turkey
Ozkan Kanat, Osman Manavoglu, Department of Medical Oncology, Uludag University School of Medicine, Gorukle, Bursa 16059, Turkey

Correspondence to: Professor Tuncay Yilmazlar, Department of General Surgery, Uludag University School of Medicine, 16059, Gorukle, Bursa 16059, Turkey. tunyi@uludag.edu.tr
Telephone: +90-224-4428400 Fax: +90-224-4428398
Received: 2004-11-08 Accepted: 2004-12-20

Abstract

A healthy 31-years-old man presented with a three-year history of abdominal discomfort. Radiological examinations revealed multifocal tumoral lesions in the spleen. The patient underwent splenectomy for differential diagnosis and treatment. During the operation, in addition to the splenic masses, there were also multiple millimetric purpuric-like lesions on the colonic serosal surfaces adjacent to the splenic hilum. One of them was excised. Histologic examination showed hemangiopericytoma of the spleen and cavernous hemangioma of the adjacent colon. This is the first report showing the close association of these two distinct lesions with vascular origin in the literature. Despite not having any apparent evidence, there may be a sequential relationship between the hemangiopericytoma of the spleen and cavernous hemangiomas.

© 2005 The WJG Press and Elsevier Inc. All rights reserved.

Key words: Hemangiopericytoma of the spleen; Cavernous hemangiomas

Yilmazlar T, Kirdak T, Yerci O, Adim SB, Kanat O, Manavoglu O. Splenic hemangiopericytoma and serosal cavernous hemangiomas of the adjacent colon. *World J Gastroenterol* 2005; 11(26): 4111-4113

<http://www.wjgnet.com/1007-9327/11/4111.asp>

INTRODUCTION

Hemangiopericytoma is a perivascular tumor originating from pericytes located along capillaries and venules^[1]. Tumor may be benign or malign in behavior. It is most common in the lower extremity, also occurs in the pelvic retroperitoneum or other sites^[2]. Hemangiopericytoma of the spleen is a rare tumor and so far only eight patients have been reported in the

literature. It tends to occur at adult ages, but can be diagnosed in childhood^[3]. There is not any specific symptom or sign of the disease. There may be single^[3-6] or multifocal^[3,7-9] tumors in the spleen. On the other hand, cavernous hemangioma is a benign vascular tumor consisting of dilated blood vessels. In the present case, interestingly, in addition to the splenic hemangiopericytoma there were multiple cavernous hemangiomas on the adjacent colonic serosal surfaces. There may be a sequential, rather than co-incidental, relationship between the two distinct pathologies. We report a case of multifocal hemangiopericytoma of the spleen and cavernous hemangiomas of the adjacent colonic serosa.

CASE REPORT

A healthy 31-years-old man presented with a three-year history of early satiety and abdominal discomfort. He had no history of weight loss. Physical and laboratory examinations were normal. Gastroendoscopy showed no pathologic finding. Abdominal ultrasonography revealed suspicious nodular lesions in the spleen. Computed tomography and magnetic resonance imaging showed hypervascular and hypodense masses located in the splenic hilum (Figure 1). Maximum size of the masses was 4 cm in diameter.

The patient underwent splenectomy for suspicion of primary or secondary splenic malignancy. During the operation, there were three exophytic nodular lesions in the splenic hilum. In addition, there were also multiple small lesions dark-red in color and 4-5 mm in diameter, resembling to the purpuric lesions macroscopically, on the serosal surface of the splenic flexura of the colon and descending colon. One of them was excised.

Histopathological findings

Spleen was 10 cm×8 cm×7 cm in diameter and weighted 200 g and there were three masses located in the splenic hilum. The gross appearance of the masses showed colour exchange into grayish-brown with a maximum diameter of 3 cm. Tumors were unencapsulated and their borders were irregular. On microscopical examination, there was a tumoral tissue consisting of slightly pleomorphic, atypical cells which were ovoid or spindle in shape. Tumor cells were widespread around the capillary vessels and had fusiform nuclei with prominent nucleolus and eosinophilic cytoplasm (Figures 2 A and B). Mitotic activity was not observed. Tumoral cells were stained positively with CD34 and Vimentin, but negatively with lysozyme, cytokeratin, smooth muscle actin, S-100, factor 8-related antigen, desmin, HMB-45, CD117 and epithelial membrane antigen immunohistochemically. This lesion was reported as hemangiopericytoma.

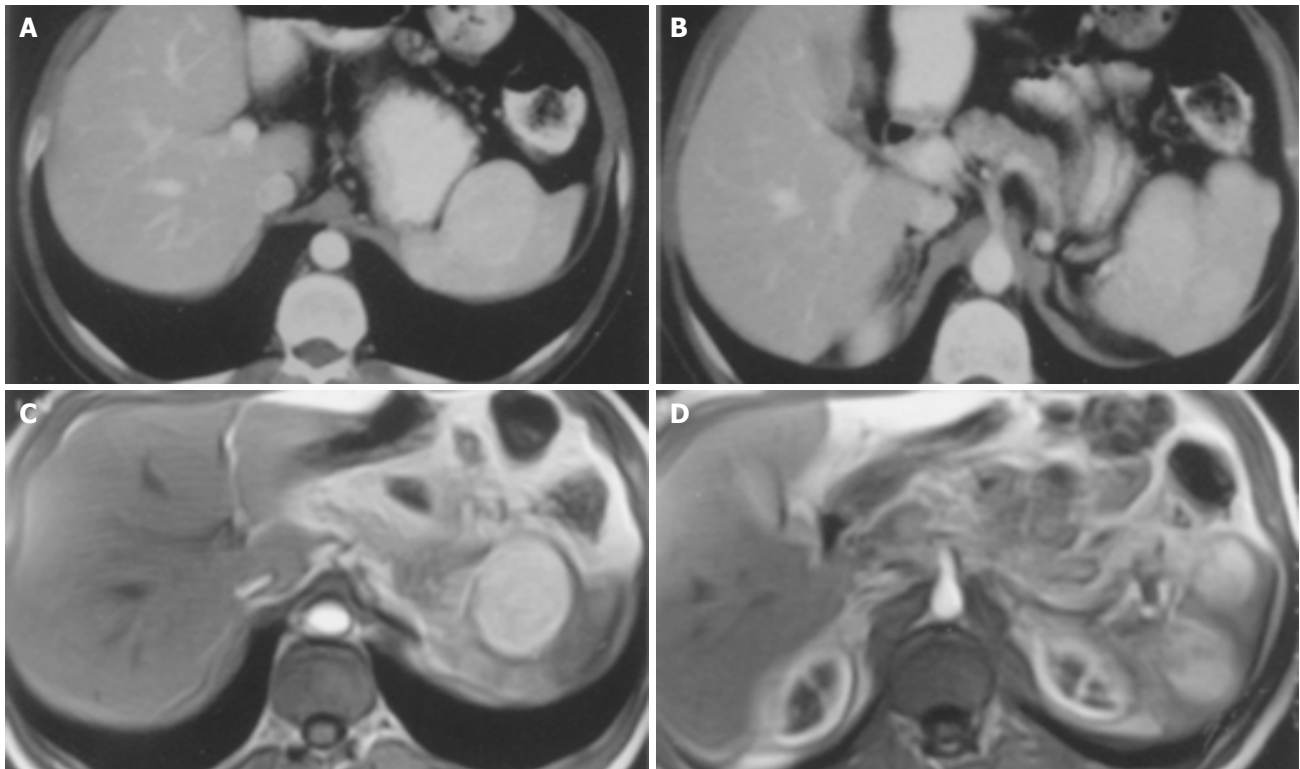


Figure 1 CT and MR images of splenic hemangiopericytoma. **A** and **B**: Enhanced computed tomography scan showing high-density masses located

in the spleen. **C** and **D**: T1-weighted abdominal magnetic resonance images showing multifocal hypervascular lesions in the spleen.

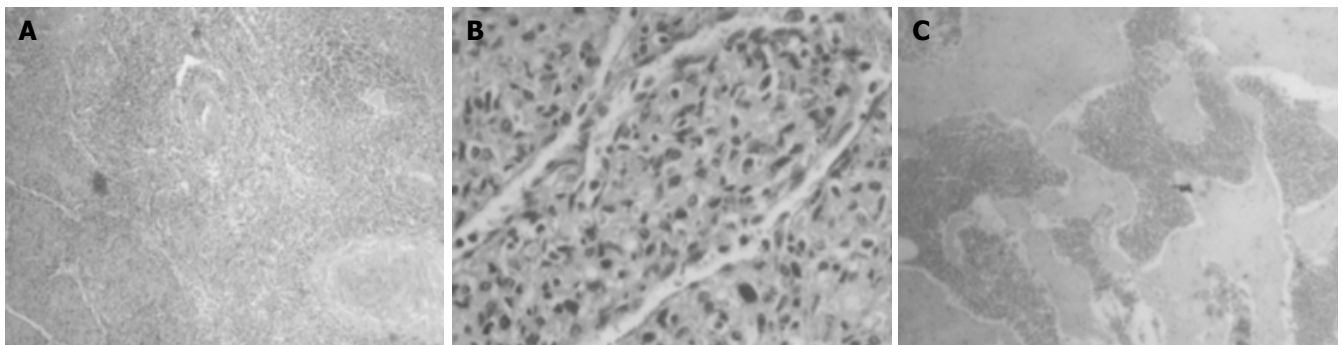


Figure 2 **A**: Spindle-shaped cells of hemangiopericytoma with eosinophilic cytoplasm around the capillary vessels in the spleen (HE $\times 40$); **B**: (HE $\times 200$);

C: Dilated vessels of the cavernous hemangioma of the colonic serosa (HE $\times 40$).

On histologic examination of the lesion excised from the serosal surface of the splenic colon flexura, there was a tumoral tissue consisting of dilated blood vessels with flattened endothelium and their lumens were containing erythrocytes (Figure 2C). This lesion was reported as cavernous hemangioma.

Immunohistochemistry of the both specimens (hemangiopericytoma and cavernous hemangioma) did not display vascular endothelial growth factor (VEGF) expression.

The patient had an uneventful recovery and discharged on postoperative d 5. He did not take any additional therapy and has been disease free for 36 mo of follow-up.

DISCUSSION

Despite the advances in imaging techniques, differential

diagnosis and management of the splenic hemangiopericytoma may be problematic because of the rarity of the disease. In the present case, ultrasonography, computed tomography, magnetic resonance imaging techniques were inconclusive. In most of the cases, splenectomy seems to be necessary for establishing prompt histologic diagnosis and providing initial treatment of the disease.

Multiple millimetric cavernous hemangiomas of the serosal surfaces of the colon is a rare condition and also splenic hemangiopericytoma is rare. These two distinct tumoral lesions were in the same region, multiple and all three masses in the splenic hilum were growing as exophytic tumors. We hypothesized that there may be triggering substances, which were secreted locally from the tumoral cells, leading paracrine stimulation of the some inducible receptor positive cells in the adjacent tissue. These inducible

potential cells had proliferated and developed vascular neoplasia by the effect of these substances. Similarly it has been reported that VEGF may play a role in the pathogenesis of vascular lesions such as cerebral cavernous malformations^[10] or cerebral hemangiopericytomas^[11]. However VEGF reactivity was negative in both of cavernous hemangioma and splenic hemangiopericytoma in the present case. On the other hand, another substance or mechanism that are not yet clear may play a role in the genesis of this association. We believe that presence of two distinct lesions in the same region was not a co-existence. It may be sequential rather than co-incidental.

Hallen^[6] reported that it was difficult to decide whether the splenic hemangiopericytoma was benign or malignant. They also reported that presence of multifocal tumors and mitoses may be an indicator of poor prognosis. In the present case, there were multifocal tumors but mitotic activity was not observed on the histologic examination. Despite multicentric lesions, recurrence has not been described for 36 mo follow-up. Therefore, we think that microscopic features, especially presence of mitosis, may be more important than the presence of multifocal tumors in predicting malign tumor behavior.

In conclusion, splenic hemangiopericytoma and cavernous hemangiomas can be found in the same region and there may be a sequential relationship between these tumoral lesions.

REFERENCES

- 1 **Stout AP, Murray MR.** Hemangiopericytoma. a vascular tumor featuring zimmerman's pericytes. *Ann Surg* 1942; **116**: 26-33
- 2 **Enzinger FH, Smith BH.** Hemangiopericytoma. an analysis of 106 cases. *Hum Pathol* 1976; **7**: 61-82
- 3 **Ciftci AO, Gedikoglu G, Firat PA, Senocak ME, Buyukpamukcu N.** Childhood splenic hemangiopericytoma: a previously unreported entity. *J Pediatr Surg* 1999; **34**: 1884-1886
- 4 **Neil JSA, Park HK.** Hemangiopericytoma of the spleen. *Am J Clin Pathol* 1991; **95**: 680-683
- 5 **Ferozzi F, Catanase C, Campani R.** Emangiopericytoma splenico: aspetti con tomografia computerizzata in due casi. *Radiol Med* 1998; **95**: 122-124
- 6 **Hallen M, Parada LA, Gorunova L, Palsson B, Dictor M, Johansson B.** Cytogenetic abnormalities in a hemangiopericytoma of the spleen. *Cancer Genet Cytogenet* 2002; **136**: 62-65
- 7 **Jurado JG, Fuentes FT, Menendez CG, Jimenez AL, de la Riva ML.** Hemangiopericytoma of the spleen. *Surgery* 1989; **106**: 575-577
- 8 **Hosotoni R, Momoi H, Uchida H, Okabe Y, Kudo M, Todo A, Ishikava T.** Multiple hemangiopericytomas of the spleen. *Am J Gastroenterol* 1992; **87**: 1863-1865
- 9 **Gilsanz C, Garcia-Castano J, Villalba MV, Vaquenizo MJ, Lopez de la Riva M.** Hémangiopéricytoma splénique. *Presse Med* 1995; **24**: 1316
- 10 **Jung KH, Chu K, Jeong SW, Park HK, Bae HJ, Yoon BW.** Cerebral cavernous malformations with dynamic and progressive course: correlation study with vascular endothelial growth factor. *Arch Neurol* 2003; **60**: 1613-1618
- 11 **Hatva E, Bohling T, Jaaskelainen J, Persico MG, Haltia M, Alitalo K.** Vascular growth factors and receptors in capillary hemangioblastomas and hemangiopericytomas. *Am J Pathol* 1996; **148**: 763-775

Science Editor Guo SY Language Editor Elsevier HK

• CASE REPORT •

Acute exacerbation of autoimmune hepatitis induced by Twinrix

Antal Csepregi, Gerhard Treiber, Christoph Röcken, Peter Malfertheiner

Antal Csepregi, Gerhard Treiber, Christoph Röcken, Peter Malfertheiner, Department of Gastroenterology, Hepatology, and Infectious Diseases, Department of Pathology, Otto-von-Guericke University, Leipziger Str. 44, Magdeburg 39120, Germany

Correspondence to: Antal Csepregi, MD, PhD, Department of Gastroenterology, Hepatology, and Infectious Diseases, Otto-von-Guericke University, Leipziger Str. 44, Magdeburg D-39120, Germany. csepregi.antal@medizin.uni-magdeburg.de
Telephone: +49-391-67-13-100 Fax: +49-391-67-13-105
Received: 2004-11-09 Accepted: 2004-11-29

Abstract

We report on a 26-year-old man who presented with severe jaundice and elevated serum liver enzyme activities after having received a dose of Twinrix®. In his past medical history, jaundice or abnormal liver function tests were never recorded. Following admission, an elevated immunoglobulin G level and antinuclear antibodies at a titer of 320 with a homogenous pattern were found. Histology of a liver biopsy showed marked bridging liver fibrosis and a chronic inflammation, compatible with autoimmune hepatitis. Treatment was started with budesonide and ursodeoxycholic acid, and led to complete normalization of the pathological liver function tests. We believe that Twinrix® led to an acute exacerbation of an unrecognized autoimmune hepatitis in our patient. The pathogenesis remains to be clarified. It is tempting to speculate that inactivated hepatitis A virus and/or recombinant surface antigen of the hepatitis B virus -as seen in patients with chronic hepatitis C and unrecognized autoimmune hepatitis who were treated with interferon alpha-might have been responsible for disease exacerbation.

© 2005 The WJG Press and Elsevier Inc. All rights reserved.

Key words: Twinrix®; Autoimmune hepatitis; Budesonide

Csepregi A, Treiber G, Röcken C, Malfertheiner P. Acute exacerbation of autoimmune hepatitis induced by Twinrix. *World J Gastroenterol* 2005; 11(26): 4114-4116
<http://www.wjgnet.com/1007-9327/11/4114.asp>

INTRODUCTION

Autoimmune hepatitis (AIH) is a chronic immunity-mediated inflammatory liver disease and is characterized by a marked female preponderance, hypergammaglobulinemia, non-tissue specific autoantibodies and a characteristic good response to immunosuppressive treatment. Without treatment AIH progresses to liver cirrhosis, and in 50% of patients advanced liver fibrosis or complete cirrhosis is already present at the

time of diagnosis. Patients usually present with variable unspecific symptoms. In a significant number of patients, the presentation of AIH may be acute or fulminant mimicking acute viral hepatitis^[1]. We wish to report on a young male patient, who presented with severe acute exacerbation of a previously unrecognized AIH after the third dose of Twinrix®.

CASE REPORT

A 26-year-old Caucasian man presented in August 2003 with severe jaundice associated with elevated serum liver enzyme activities after having received the third dose of Twinrix®. The first dose was given five months ago, in March 2003, and the second in April 2003. The past medical history of the patient was unremarkable and jaundice or abnormal liver function tests were previously unknown. He denied any alcohol intake or drug (ab)use, and had not been exposed to any blood products. No family history of liver diseases was given. The physical examination showed a moderately enlarged liver without stigmata of chronic liver disease. Blood tests showed elevated alanine aminotransferase (ALT) with 50.4 $\mu\text{mol/s.L}$ (reference interval 0.17-0.60 $\mu\text{mol/s.L}$), aspartate aminotransferase (AST) with 33.2 $\mu\text{mol/s.L}$ (reference interval <0.17-0.60 $\mu\text{mol/s.L}$), and serum bilirubin with 17.2 mg/dL (reference interval <1.1 mg/dL), while the γ -globulin fraction was with 23.3% only slightly elevated. Full blood count, creatinine, urea and electrolytes were within the normal limits. Serological tests for viral hepatitis, including hepatitis A, B, and C viruses, and human herpes viruses were all negative. There was no evidence of a metabolic liver disease or biliary obstruction. Because serum liver function tests did not improve on follow-up (Figure 1), a percutaneous liver biopsy was taken in November 2003 (see below). A month later the patient was referred to our University Hospital for further evaluation. On admission, serum ALT was raising again (16.40 $\mu\text{mol/s.L}$). Additionally, we found elevated immunoglobulin G fraction with 22.70 g/L (reference interval 9-16 g/L) and antinuclear antibodies at a titer of 320 with homogenous immunofluorescence pattern suggestive of AIH. The liver biopsy was re-examined using paraffin sections stained with hematoxylin and eosin (H&E), periodic-acid Schiff (PAS) reagent with and without diastase pretreatment, Masson's trichrome stain, reticulin stain, and iron stain. Histologically, marked bridging fibrosis was noted (Figure 2A). A moderate chronic inflammatory infiltrate with few scattered eosinophils was found in the septa, an interface hepatitis was noted and small, partly confluent necroinflammatory foci were present in the parenchyma (Figures 2B and C). A pathological iron deposition or diastase-resistant PAS-positive globuli indicating α 1-antitrypsin deficiency, were not found. The histopathological

findings were compatible with advanced AIH. The patients were then treated with budesonide (Budenofalk®), 3 mg tiw and ursodeoxycholic acid (Ursofalk®), 250 mg tiw, which resulted in complete normalization of the liver function tests (Figure 1). The excellent response to immunosuppressive therapy further supports the diagnosis of AIH.

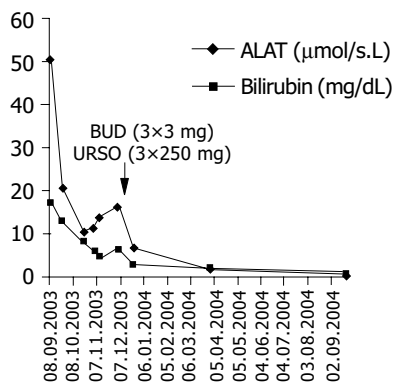


Figure 1 Changes of alanine aminotransferase activity and serum bilirubin level on follow-up and during the therapy with budesonide and ursodeoxycholic acid.

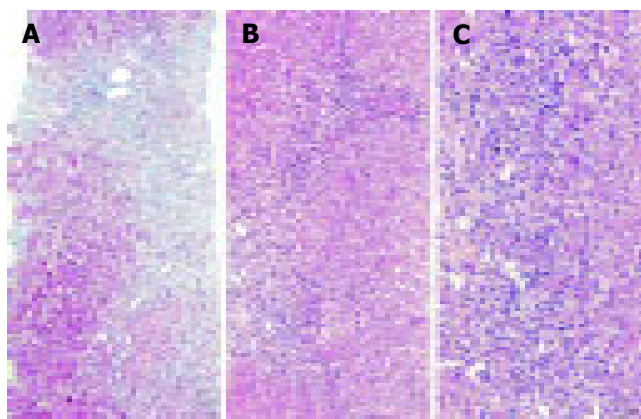


Figure 2 A liver biopsy obtained 3 mo after the first clinical presentation of the patient showed marked bridging fibrosis (A). A moderate chronic inflammatory infiltrate with few scattered eosinophils was found in the septa (B), and an interface hepatitis was also noted (C). The histopathological findings were compatible with AIH. Masson trichrome stain (A) and H&E-stain (B and C). Original magnifications 100x (A and B) and 200x (C).

DISCUSSION

Hepatitis A and B viruses (HAV and HBV) are responsible for considerable morbidity and mortality^[2]. Twinrix® is a sterile suspension of inactivated HAV and recombinant surface antigen of the HBV (rHBsAg) and used for active immunization^[3]. Vaccination with rHBsAg has been reported to be associated with the development of autoimmune diseases, especially with rheumatoid arthritis^[4]. Some patients with vaccination-induced rheumatoid arthritis share the common HLA DR3 and DR4 haplotypes (DRB*0301, *0401)^[4]. Evidence exists that AIH has also a specific genetic background including HLA A1, B8 and DR3 or DR4 alleles. The majority of patients with AIH was reported to be either

DRB3*0101 or DRB4*0401 positive^[1,5].

AIH was reported repeatedly to manifest after viral infections. Some reports suggested that HAV might induce AIH in genetically susceptible persons^[6,7], and protracted HAV infection was strongly associated with HLA-DRB*1301, which is a marker for AIH in pediatric patients^[8]. The activation of an anti-HBsAg response was, however, not sufficient to induce AIH in an HBV envelope transgenic mouse model^[9]. In our patient, who had a previously unrecognized, clinically silent AIH with advanced liver fibrosis, the exposure to Twinrix® led to the development of severe jaundice and an acute, clinically overt exacerbation of chronic liver disease. No other case of AIH after vaccination has been reported yet. Postmarketing studies occasionally described on jaundice and acute hepatitis after the use of Havrix® and abnormal liver function tests using Engerix-B®^[3]. Moreover, vaccination was never reported to lead to chronic liver disease. The pathogenesis of acute exacerbation of this previously clinically silent AIH remains to be clarified. Inactivated HAV and/or rHBsAg are not known to be hepatotoxins, therefore, an intrinsic hepatotoxic effect is highly unlikely. Rather, Twinrix® probably caused an idiosyncratic reaction, i.e. hypersensitivity. Several drugs can cause chronic hepatitis, biochemically, serologically, and histologically almost indistinguishable from AIH and have been named drug-induced AIH^[10].

In view of the advanced liver fibrosis in our patient, and the relatively recent immunization with Twinrix®, we believe that our patient already suffered from AIH. Drug-induced AIH usually have a long and variable latency period until clinical presentation and was not observed in our patient. Similarly, patients with chronic hepatitis C receiving interferon alpha^[11] may also experience an acute exacerbation of AIH. This further supports our assumption that in our patient Twinrix® caused an acute exacerbation rather than an induction of AIH in a previously healthy liver. The therapy with the local active corticosteroid, budesonide, resulted in complete remission of the disease which-based also on our clinical experiences-represents an effective treatment of AIH^[12].

REFERENCES

- 1 **Manns MP**, Strassburg CP. Autoimmune hepatitis: clinical challenges. *Gastroenterology* 2001; **120**: 1502-1517
- 2 Disease burden from viral hepatitis A, B, and C in the United States. Atlanta: Centers for Disease Control and Prevention, 2002
- 3 Prescribing Information. GlaxoSmithKline, Rixensart, Belgium, 2003, US License No 1617
- 4 **Csepregi A**, Nemesánszky E, Rojkovich B, Poór G. Rheumatoid arthritis and hepatitis B virus: Evaluating the pathogenic link. *J Rheumatol* 2001; **28**: 474-477
- 5 **Doherty DG**, Donaldson PT, Underhill JA, Farrant JM, Duthie A, Mieli-Vergani G, McFarlane IG, Johnson PJ, Eddleston AL, Mowat AP. Allelic sequence variation in the HLA class II genes and proteins on patients with autoimmune hepatitis. *Hepatology* 1994; **19**: 609-615
- 6 **Vento S**, Garofano T, Di Perri G, Dolci L, Concia E, Bassetti D. Identification of hepatitis A virus as a trigger for autoimmune chronic hepatitis type 1 in susceptible individuals. *Lancet* 1991; **337**: 1183-1187
- 7 **Huppertz HI**, Treichel U, Gassel AM, Jeschke R, Meyer zum

- Buschenfelde KH. Autoimmune hepatitis following hepatitis A virus infection. *J Hepatol* 1995; **23**: 204-208
- 8 **Fainboim L**, Canero Velasco MC, Marcos CY, Ciocca M, Roy A, Theiler G, Capucchio M, Nuncifora S, Sala L, Zelazko M. Protracted, but not acute, hepatitis A virus infection is strongly associated with HLA-DRB*1301, marker for pediatric autoimmune hepatitis. *Hepatology* 2001; **33**: 1512-1517
- 9 **Wirth S**, Guidotti LG, Ando K, Schlicht HJ, Chisari FV. Breaking tolerance leads to autoantibody production but not autoimmune liver disease in hepatitis B virus envelope transgenic mice. *J Immunol* 1995; **154**: 2504-2515
- 10 **Liu ZX**, Kaplowitz N. Immune-mediated drug-induced liver disease. *Clin Liver Dis* 2002; **6**: 467-486
- 11 **Garcia-Buey L**, Garcia-Monzon C, Rodriguez S, Borque MJ, Garcia-Sanchez A, Iglesias R, DeCastro M, Mateos FG, Vicarion JL, Balas A. Latent autoimmune hepatitis triggered during interferon therapy in patients with chronic hepatitis C. *Gastroenterology* 1995; **108**: 1770-1777
- 12 **Csepregi A**, Treiber G, Klauck S, Malfertheiner P. Budesonid bei Autoimmunhepatitis and Überlappungssyndromen. *Z Gastroenterol* 2004; **42**: 908

Science Editor Guo SY Language Editor Elsevier HK

Solid-pseudopapillary tumor of the pancreatic tail

Frank Eder, Hans-Ulrich Schulz, Christoph Röcken, Hans Lippert

Frank Eder, Hans-Ulrich Schulz, Hans Lippert, Department of General Surgery, Department of General Surgery, Otto-von-Guericke-University, Medical Faculty, Leipziger Straße 44, Magdeburg D-39120, Germany

Christoph Röcken, Institute of Pathology, Otto-von-Guericke-University, Medical Faculty, Leipziger Str. 44, Magdeburg D-39120, Germany

Correspondence to: Dr. Frank Eder, Department of General Surgery, Otto-von-Guericke-University, Medical Faculty, Leipziger Straße 44, Magdeburg D-39120, Germany. frank.eder@medizin.uni-magdeburg.de
Telephone: +391-6715500 Fax: +391-6715570
Received: 2004-12-02 Accepted: 2005-01-05

Abstract

We report a case of the rare solid-pseudopapillary tumor of the pancreas. In contrast to other pancreatic tumors, the solid-pseudopapillary tumor has a favorable prognosis. The 60-year-old female patient we report on here was treated by left pancreatic resection combined with splenectomy for a non-metastasizing tumor of the pancreas. A solid-pseudopapillary tumor was found on histology. The patient had no signs of metastases at present. Since a microscopically invasive tumor growth is assumed, oncologically curative resection should be preferred vs the less radical enucleation. The rare solid-pseudopapillary tumor of the pancreas has a good prognosis after successful oncological resection.

© 2005 The WJG Press and Elsevier Inc. All rights reserved.

Key words: Pancreas; Solid-pseudopapillary tumor

Eder F, Schulz HU, Röcken C, Lippert H. Solid-pseudopapillary tumor of the pancreatic tail. *World J Gastroenterol* 2005; 11(26): 4117-4119

<http://www.wjgnet.com/1007-9327/11/4117.asp>

INTRODUCTION

Solid-pseudopapillary tumor of the pancreas is a rare condition. In the literature, about 300 cases have been reported. This tumor was first described in 1959^[1]. It is also known under the term FRANTZ tumor, named after the author who first described this tumor, which has also been referred to as solid cystic tumor; papillary epithelial neoplasia; solid and papillary epithelial neoplasia; or papillary epithelial tumor. In 1996, this tumor was included in the WHO classification of pancreatic tumors^[2]. The origin of the solid-pseudopapillary tumor has not yet been clarified. It is discussed to originate either from ductal epithelium^[3-6], acinar cells^[7-11], or from endocrine cells^[12,13]. Another hypothesis is that this tumor arises

from pluripotent embryonic cells of the pancreas^[12,14,15] or from ridges/ovarian anlage related cells, which were attached to the pancreatic tissue during early embryogenesis^[16,17].

Solid-pseudopapillary tumor of the pancreas has a tendency to predominantly affect young women aged between 25 and 35 years^[4,8,14,18-22]. Age is reported to range from 8^[15] to 70 years^[3]. However, a relationship to oral contraception has not been proven^[8]. This tumor rarely affects men^[23-26] and is characterized by a long asymptomatic course and unspecific symptoms. Therefore, it is not uncommon that solid-pseudopapillary tumor is detected only when it has reached a remarkable size (8-10 cm)^[4,10]. Even a tumor size of 20 cm in diameter has been reported^[27].

One feature of this tumor is its low malignant potential. Although the liver is found to be the site mostly affected by metastases, these are only rarely seen^[15,23,27,28]. Furthermore, there are only few reports about invasive growth^[3,4]. Survival time has been reported to reach up to 21 years^[1].

Here, we report on a 60-year-old woman, who was found to suffer from a non-metastasizing solid-pseudopapillary tumor of the pancreatic tail. Curative resection was performed.

CASE REPORT

A 60-year-old Caucasian woman attended her GP for recurring headache. An X-ray of the spine showed calcifications projecting onto the left upper kidney. Ultrasound and CT-scan of the abdomen showed a polycystic tumor in the tail of the pancreas, which measured approximately 14 cm in maximum diameter.

After the patient was referred to a general hospital a biopsy for cytology was obtained using endoscopic ultrasonography and provided suspicion of a malignant tumor. MRT of the abdomen showed a lesion, which was incompatible with a benign tumor or pseudocyst, and raised suspicion of a cystadenocarcinoma of the pancreas. Finally the patient was referred to our University. The past medical history of the patient included uncomplicated deliveries of four children, no abortions or miscarriages. No history was given suggestive of chronic pancreatitis. The family and social history gave no evidence of a familial cancer syndrome. On admission the patient was mobile, orientated in time, place and person, afebrile and normotonic. Palpation of the abdomen revealed a mild dull pain in the left upper abdomen.

Blood tests showed mild hypercholesterolemia and normal LFT, U&E, and FBC. The tumormarkers CEA, CA19-9 and CA125 were normal. X-ray of the chest and ECG were normal.

A laparotomy was performed and the a tumor of the pancreatic tail explored. No metastases were found. The preparation of the tumor showed a brown colored and good separated growth. A distal pancreatectomy combined

with splenectomy was indicated and deperformed. The pancreatic resection margin was free of cancer as demonstrated by frozen section.

Ten days later the patient was discharged from our University hospital without any postoperative complications. The patient is followed up in our tumor dispensaire.

The pancreatic tumor measured 14 cm in greatest diameter and was located in the pancreatic tail. The cut surface was yellow in color with hemorrhages (Figure 1A).

Histologically, the tumor was encapsulated by a fibrous pseudocapsule and characterized by extensive old necroses, large hyalin scars, cholesterol crystals surrounded by foreign body giant cells and calcifications. After extensive sampling small areas of preserved tumor were found under the fibrous capsule. The tumor tissue exhibits a solid monomorphic pattern with small polyhedral cells lining fibrovascular stalks (Figure 1C). A pseudopapillary pattern was noted in areas with regressive changes (Figure 1B). Perineural invasion, angioinvasion, or deep invasion were not found. Immunohistochemistry with antibodies directed against alpha-1-antitrypsin (Figure 1D), neuron-specific enolase, and CEA showed immunostaining of tumor cells. Immunostaining was not observed with antibodies directed against pancytokeratin (AE1/AE3), CK 8, CK18, chromogranin A, synaptophysin, S-100, and alpha-fetoprotein.

The histological and immunohistochemical findings were in keeping with the diagnosis of a solid-pseudopapillary tumor of the pancreas.

DISCUSSION

Although the vast majority of patients with a solid pseudopapillary tumor of the pancreas are young women, our patient, affected by this lesion, was already 60 years old. In 85-90% of the patients the prognosis of the tumor is excellent^[16]. Some authors^[15,21] described an aggressive growth of the tumor in older patients. Our observations are not in accordance with them. A 53-year-old woman with a solid-pseudopapillary tumor of the pancreatic head treated by radical partial pancreaticoduodenectomy in 1998 is still tumor free at present.

Owing to the slow growth of solid-pseudopapillary tumors, typical early symptoms are lacking. These are only found in conjunction with a higher number of local displacements. In our case, the patient consulted her doctor because of recurrent headache. She never had suffered from epigastric or abdominal pain. In order to investigate putative causes for recurrent headache, X-rays were taken from the spine and calcifications were noted projecting onto the left upper kidney. A tumor of the pancreatic tail was found on ultrasound and CT-scan of the abdomen. In general, owing to the lack of symptoms, a diagnosis of these tumors is possible only when their diameter is in the range of 12-14 cm. There seems to be no correlation between tumor size and behavior^[23]. Venous invasion, degree of nuclear atypia, mitotic count and large necrotic clusters are considered histological markers of an increased potential of malignancy^[23]. A further criterion is the nuclear DNA-ploidy grade. Kamei and

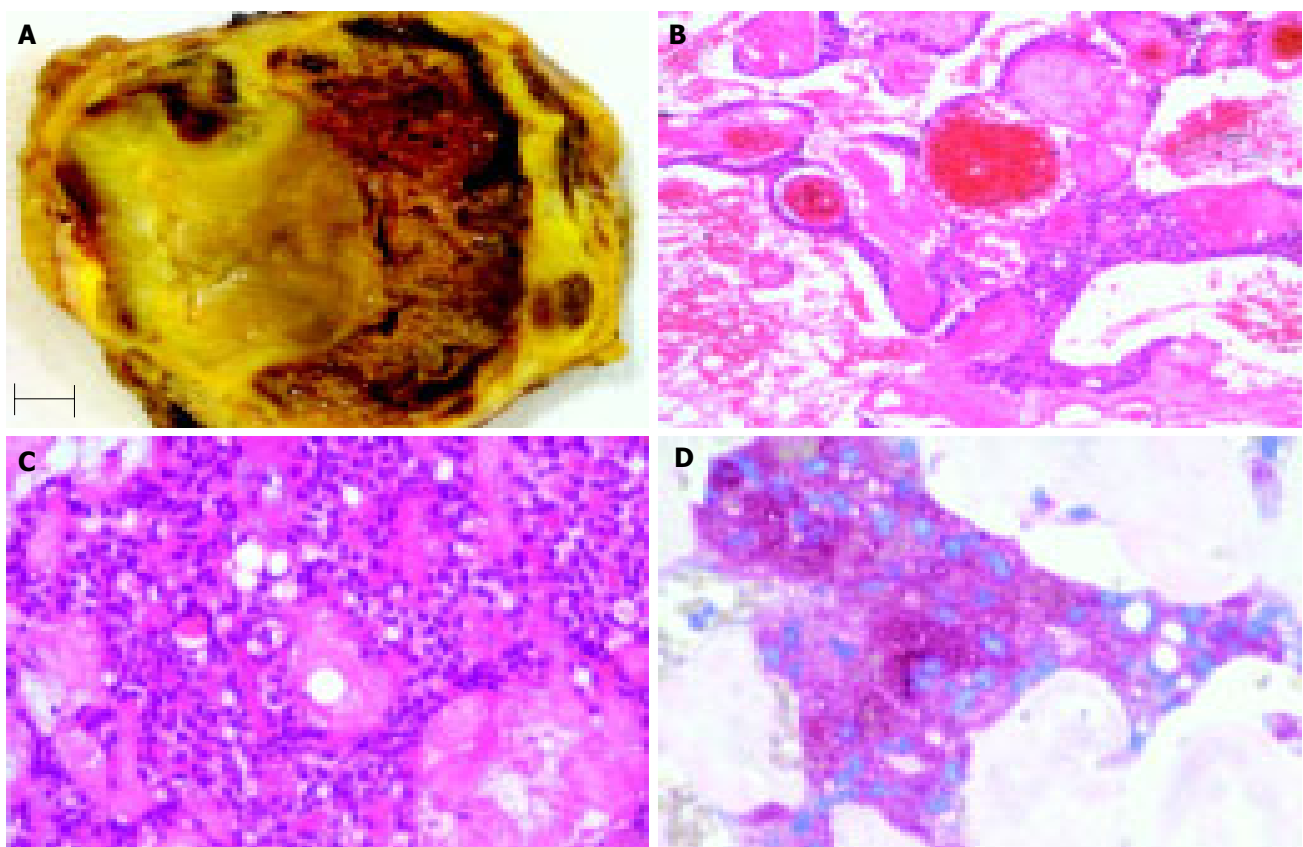


Figure 1 cross section of the pancreatic tumor showed a yellow tumor with hemorrhages (A); bar indicates 1 cm. The tumor tissue exhibits a solid monomorphic pattern with a pseudopapillary pattern in areas with regressive changes (B) and

small polyhedral cells lining fibrovascular stalks (C). The tumor cells were immunoreactive for alpha-1-antitrypsin (D). Hematoxylin and eosin (B and C), anti-alpha-1-antitrypsin (D); Original magnification: x100 (B), x200 (C), x400 (D).

Nishihara^[23] demonstrated aneuploidy in patients with metastases, whereas patients without any sign of malignancy showed diploidy. However, this issue is controversially discussed in the literature. In any case, patients exhibiting these markers should be subject to particularly critical surveillance. Opposite to our patient, a complete fibrous capsule always be found in these tumors^[23]. Capsular invasions have been described^[3] and typically the preserved tumor tissue is found in the periphery, as shown here. Furthermore, tumors may infiltrate into both the sane pancreatic parenchyma and peripancreatic adipose tissue^[19]. Therefore, resection according to oncological criteria should be preferred over “radical enucleation”^[11] and/or local excision^[20]. In addition, since the tumor is confined to the organ or develops metastases only at later time points, radical surgery of a solid-pseudopapillary tumor of the pancreas could be curative.

In conclusion, the patient bearing a solid-pseudopapillary tumor of the pancreas has a good prognosis if the tumor is resected completely, shows no histological evidence of malignancy and demonstrates a diploid population of tumor cells in DNA analysis.

REFERENCES

- 1 **Frantz VK.** Tumor of the pancreas. In: Blumberg CW (ed) Atlas of Tumor Pathology. Series 1, Fascicles 27 and 28. Washington, DC 1959: 32-33
- 2 **Klöppl G,** Solcia E, Longnecker DS, Capella C, Sobin LH. Histological typing of tumours of the exocrine pancreas. In: WHO International Classification of Tumours. Berlin Heidelberg New York, Springer 1996: 8452/1
- 3 **Compagno J,** Oertel JE, Krezmar M. Solid and papillary neoplasm of the pancreas, probably of small duct origin: A clinicopathologic study of 52 cases. *Lab Invest* 1979; **40**: 248-249
- 4 **Cubilla AL,** Fitzgerald PJ. Tumors of the exocrine pancreas. In: Hartmann WH, Sobin LH (eds.) Atlas of Tumor Pathology; Series 2, Fascicle 19. Washington, DC 1984: 201-207
- 5 **Kaufman SL,** Reddick RL, Stiegel MD, Wild RE, Thomas CG. Papillary cystic neoplasm of the pancreas: A curable pancreatic tumor. *World J Surg* 1986; **10**: 851-859
- 6 **Sanfey H,** Mendelson G, Cameron JL. Solid and papillary neoplasm of the pancreas. A potentially curable surgical lesion. *Ann Surg* 1983; **197**: 272-275
- 7 **Höfler H.** Prognosefaktoren beim Pankreascarcinom. *Chirurg* 1994; **65**: 253-257
- 8 **Klöppl G,** Morohoshi T, John HD, Oehmichen W, Opitz K, Angelkort A, Lietz H, Ruckert K. Solid and cystic acinar cell tumor of the pancreas: a tumor in young women with favourable prognosis. *Virchows Arch A Pathol Anat Histol* 1981; **392**: 171-183
- 9 **Learmonth GM,** Price SK, Visser AE, Emms M. Papillary and cystic neoplasm of the pancreas. An acinar cell tumor? *Histopathology* 1985; **9**: 63-79
- 10 **Morohoshi T,** Held G, Klöppl G. Exocrine pancreatic tumours and their histological classification. A study based on 167 autopsy and 97 surgical cases. *Histopathology* 1983; **7**: 645-661
- 11 **Rückert K,** Klöppl G, Treu HA, Altmeier A, Hempel D, Lingg G. Solid-zystischer Acinuszelltumor des Pankreas. *Dtsch Med Wochenschr* 1982; **107**: 1015-1020
- 12 **Schlosnagle DC,** Campbell WG. The papillary and solid neoplasm of the pancreas. *Cancer* 1981; **47**: 2603-2610
- 13 **Yagihashi S,** Sato I, Kaimori M, Matsumoto J, Nagai K. Papillary and cystic tumor of the pancreas. Two cases indistinguishable from islet cell tumor. *Cancer* 1988; **61**: 1241-1247
- 14 **Mao C,** Guvendi M, Domenico DR, Kim K, Thomford NR, Howard JM. Papillary cystic and solid tumors of the pancreas: a pancreatic embryonic tumor? Studies of three cases and cumulative review of the world's literature. *Surgery* 1995; **118**: 821-828
- 15 **Matsunou H,** Konishi F. Papillary-cystic neoplasm of the pancreas. A clinicopathologic study concerning the tumor aging and malignancy of nine cases. *Cancer* 1990; **65**: 283-291
- 16 **Klöppl G,** Kosmahl M. Cystic lesions and neoplasms of the pancreas. The Features are becoming clearer. *Pancreatology* 2001; **1**: 648-655
- 17 **Rebhandl W,** Felberbauer FX, Puig S, Kurosh P, Hochschorner S, Barlan M, Horcher E. Solid-pseudopapillary tumor of the pancreas (Frantz tumor) in children: report of four cases and review of the literature. *J Surg Oncol* 2001; **76**: 289-296
- 18 **Rustin RB,** Broughan TA, Hermann RE, Grundfest-Broniatowski SF, Petras RE, Hart WR. Papillary cystic epithelial neoplasms of the pancreas. A clinical study of four cases. *Arch Surg* 1986; **121**: 1073-1076
- 19 **Siech M,** Merkle E, Mattfeldt T, Widmaier U, Brambs HJ, Beger HG. Solid-pseudopapilläre tumoren des pankreas. *Chirurg* 1996; **67**: 1012-1015
- 20 **Tarpila E,** Borch K, Franzen L, Andersson R, Evander A, Lasson A, Lindström CG, Ihse I. Cystic neoplasms of the pancreas: A clinicopathological study of 38 cases. *Dig Surg* 1989; **6**: 138-141
- 21 **Warshaw AL,** Compton CC, Lewandrowski K, Cardenosa G, Müller PR. Cystic tumors of the pancreas. New clinical, radiologic and pathologic observations in 67 patients. *Ann Surg* 1990; **212**: 432-443
- 22 **Yamaguchi K,** Hirakata R, Kitamura K. Papillary cystic neoplasm of the pancreas: radiological and pathological characteristics in 11 cases. *Br J Surg* 1990; **77**: 1000-1003
- 23 **Nishihara K,** Nagoshi M, Tsuneyoshi M, Yamaguchi K, Hayashi I. Papillary cystic tumors of the pancreas. Assessment of their malignant potential. *Cancer* 1993; **71**: 82-92
- 24 **Ohashi K,** Nakajima Y, Hisanaga M, Nakano H, Tsutsumi M, Kondoh S, Konishi Y. A solid and papillary [solid-cystic] tumor of the pancreas occurring in a 36-year-old man: report of case. *Surg Today* 1993; **23**: 551-555
- 25 **Ohiwa K,** Igarashi M, Nagasue N, Nagasaki M, Harada T. Solid and cystic tumor [SCT] of the pancreas in an adult man. *HPB Surg* 1997; **10**: 315-321
- 26 **Wilson MB,** Adams DB, Garen PD, Gansler TS. Aspiration cytologic, ultrastructural, and DNA cytometric findings of solid and papillary tumor of the pancreas. *Cancer* 1992; **69**: 2235-2243
- 27 **Cappellari JO,** Geisinger KR, Albertson KR, Wolfman NT, Kute TE. Malignant papillary cystic tumor of the pancreas. *Cancer* 1990; **66**: 193-198
- 28 **Horisawa M,** Niinomi N, Sato T, Yokoi S, Oda K, Ichikawa M, Hayakawa S. Frantz's tumor [solid and cystic tumor of the pancreas] with liver metastasis: successful treatment and long-term follow-up. *J Pediatr Surg* 1995; **30**: 724-726

• CASE REPORT •

Diagnostic laparoscopy and laparoscopic ultrasonography with local anesthesia in hepatocellular carcinoma

Mariano Gómez-Rubio, Mercedes Moya-Valdés, Jesús García

Mariano Gómez-Rubio, Mercedes Moya-Valdés, Jesús García, Department of Digestive Diseases, Getafe University Hospital, Getafe, Madrid, Spain

Correspondence to: Dr. Mariano Gómez-Rubio, Servicio de A. Digestivo, Hospital Universitario de Getafe, Carretera de Toledo Km 12.500, 28905 Getafe, Madrid, Spain. mgomezr.hugf@salud.madrid.org
Telephone: +34-916834501 Fax: +34-916834501

Received: 2004-09-08 Accepted: 2004-10-06

Abstract

Diagnosis of hepatocellular carcinoma (HCC), a common digestive malignancy, remains a challenge. The aim of this study was to evaluate the feasibility of performing laparoscopy and laparoscopic ultrasound with local anesthesia as a diagnostic procedure in HCC. Laparoscopy and laparoscopic ultrasound with local anesthesia was performed in the gastrointestinal endoscopy unit in three patients diagnosed of HCC. Endoscopy staged diffuse liver disease. Laparoscopic ultrasonography identified all liver tumors not visible during endoscopy and guided needle biopsy in one case. No complications happened. In conclusion, laparoscopy and laparoscopic ultrasound, performed as a minimally invasive diagnostic procedure can be a safe and very promising tool in planning therapy of HCC.

© 2005 The WJG Press and Elsevier Inc. All rights reserved.

Key words: Laparoscopy; Laparoscopic ultrasonography; Hepatocellular carcinoma

Gómez-Rubio M, Moya-Valdés M, García J. Diagnostic laparoscopy and laparoscopic ultrasonography with local anesthesia in hepatocellular carcinoma. *World J Gastroenterol* 2005; 11(26): 4120-4123

<http://www.wjgnet.com/1007-9327/11/4120.asp>

INTRODUCTION

Hepatocellular carcinoma (HCC) is the most common primary liver cancer^[1]. Nevertheless, less than a third of patients are candidate to radical treatments^[2]. Besides the low hepatic reserve of usual underlying cirrhosis, one of the explanations of these poor results are the limited accuracy and discrepancies between the imaging techniques in the discovering and staging of neoplasm^[3,4]. There is a common agreement that the most accurate diagnostic method is operative assessment with ultrasound^[5,6]. But this approach

bears an unacceptable morbidity and mortality precluding its general use.

Laparoscopy, initially introduced in gastroenterology, affords an excellent view of the intra-abdominal organs, although the inner part is not accessible to inspection^[7]. In the mid-1980's pilot studies described laparoscopic ultrasound that combined the advantages of a visual assessment of peritoneal cavity and all the organs, specifically the liver, with the high resolution of intraoperative ultrasound examination^[8-10]. More recently, with the incorporation of laparoscopic surgery into the practice of general surgery, it has been shown that this procedure optimizes staging in hepatic malignancy^[11-14]. However, surgical laparoscopic ultrasound typically performed under general anesthesia exposes patients to certain risks and increases costs. So, laparoscopy with ultrasound scanning, performed under local anesthesia could be a safer procedure providing meaningful information.

Our initial experience using diagnostic laparoscopy and laparoscopic ultrasound with local anesthesia is shown.

CASE REPORT

Laparoscopy with laparoscopic ultrasound procedures was performed in three consecutive patients diagnosed of HCC. The procedures were performed with local anesthesia in the gastrointestinal endoscopy unit. Oxygen saturation and heart rate were automatically monitored. After puncturing in the left upper quadrant of the abdomen, near the umbilicus, with a multihole 21-gauge needle, pneumoperitoneum with oxygen insufflation was established. Then, two 11-mm laparoscopic trocars were inserted. The first one was inserted through the pneumoperitoneum puncture site. Then, a frontal high-resolution video laparoscope (*Olympus GTV-S6*, Olympus Optical Co., Ltd, Japan) was introduced into the cannula, performing an initial endoscopic exploration of the peritoneal cavity. Another trocar was positioned to introduce the ultrasonic probe making a choice between the right paraumbilical region and the right inferior quadrant in accordance with abdominal characteristics. The laparoscopic ultrasonography was performed using ultrasonographic equipment (*Olympus IU-E1*, Olympus Optical Co., Ltd, Japan) that included a linear 7.5 MHz, 9.9 mm in diameter, orientable-tip probe (*Olympus MH-300*, Olympus Optical Co., Ltd, Japan) placed in contact with liver capsule. All probe manipulations during ultrasound scanning were guided by direct eye vision. The liver was systematically scanned at its front, upper (diaphragmatic), and lateral surfaces by moving the probe. For the left lobe

exploration of the liver, the probe was transferred to the epigastric port. The parenchyma, hepatic and portal veins were then carefully scanned, by using advancement-withdrawal maneuvers, lateral movements, sweeping and rotating the probe over the liver surface, in an attempt to identify the segmental anatomy. Duration of procedure ranged between 60 and 90 min. Recovery monitoring was performed for 15 min in gastrointestinal suite. Patients were then admitted for 22-h observation and later discharged.

Case 1

A 69-year-old male patient with previous chronic C hepatitis was diagnosed after abdominal ultrasonography and biopsy of HCC. Ultrasonography and abdominal computed tomography showed one tumor, 36 mm in diameter, located in the right lobe (segment V) (Figure 1). Laparoscopic examination demonstrated liver cirrhosis without tumor in surface (Figure 2A). Laparoscopic sonogram described the neoplastic deposit that was impossible to endoscopically visualize (Figure 2B). No other tumors were discovered inside the liver. Two grams of magnesium metazolone were intravenously administered at the end of procedure. Some days later, laparotomy with intraoperative ultrasonography was carried out with no additional findings, and then a surgical atypical hepatectomy was performed. Postoperatory was unremarkable and patient has remained without recurrence for 21 mo.

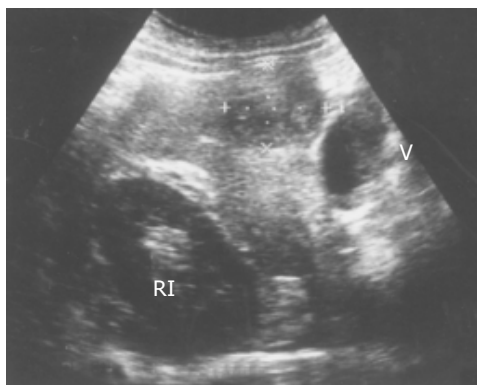


Figure 1 Oblique sonogram of right lobe of the liver showing a predominantly hypoechoic mass. V: gallbladder. RI: right kidney.



Figure 2 A: Endoscopic liver image of cirrhosis. Ultrasonic probe is placed in contact to a fibrotic depressed whitish area near the gallbladder; B: Laparoscopic sonogram revealing a tumor under liver surface.

Case 2

A 51-year-old male diagnosed of alcoholic and viral C liver cirrhosis with portal hypertension developed ascites. He had a history of a hemangioma in both liver lobes. Former abdominal ultrasonography and computed tomography discovered a new 16-mm nodule whose biopsy diagnosed a HCC (Figure 3). Laparoscopy showed liver cirrhosis with portal hypertension and ascites (Figure 4A), whereas laparoscopic ultrasonography confirmed previous conventional radiological findings (Figure 4B). No analgesic drugs were required. Although the patient was selected for resection at that moment, during laparotomy unresectability was determined after discovering malignant diaphragm implant, and then radio-frequency treatment was carried out. The patient, in Child-Pugh B functional stage, refused liver transplantation and no antitumoral therapy was given.



Figure 3 Sonogram showing a 16-mm hypoechoic hepatic nodule in segment IV, histologically diagnosed of HCC.

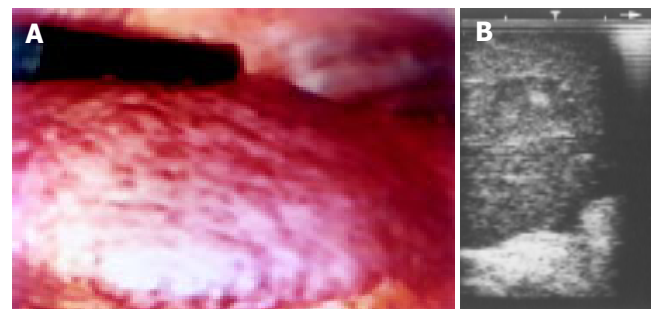


Figure 4 A: Laparoscopy displaying the left lobe of the liver with medium-sized nodules and without evidences of neoplasm; B: The endoscopic sonogram confirming the intrahepatic presence of uninodular HCC.

Case 3

A 59-year-old male with prior history of 140 g/d of ethanol intake started with right hypocondrium pain. After abdominal sonogram, computed tomography scans and abnormal serum α -fetoprotein (2 440 ng/mL) a diagnosis of HCC was made (Figure 5). There were 4 tumors in right lobe, ranging from 1 to 7 cm in diameter. On laparoscopy chronic non-cirrhotic liver disease without neoplasm on surface was discovered (Figure 6A). Laparoscopic ultrasonography showed all the lesions. Sonographically guided biopsy gave a confirmatory result of HCC (Figure 6B). Non-neoplastic tissue obtained at

laparoscopy revealed an alcoholic hepatitis with fibrosis but without cirrhosis. Magnesium metamizole (2 g) combined with atropine (1 mg) were intravenously given during the procedure. Twenty months later the patient is alive in a consumptive state.



Figure 5 Sonogram revealing a hypo-isoechoic tumor in the center of the right lobe of the liver.

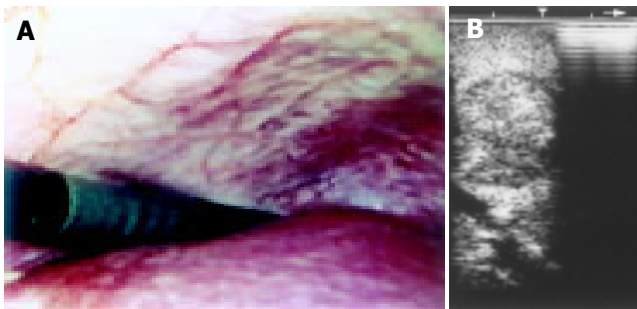


Figure 6 A: Upper aspect of right lobe of the liver. The surface is not perfectly smooth owing to the presence of alternately reddish areas slightly elevated with respect to lighter colored ones; B: Laparoscopic sonogram showing a very well defined tumor near a vascular structure.

DISCUSSION

Staging surgical laparoscopy with laparoscopic ultrasound, has been reported in the last several years as an important tool in the diagnostic approach to hepatobiliary and pancreatic malignancy, avoiding unnecessary laparotomy in up to 46% of patients^[11-14]. In HCC, surgical laparoscopy with laparoscopic ultrasound also optimizes patient selection for curative hepatic resection, discovering unresectable disease in as much as 63% of cases^[15-17].

Some years ago, Ido *et al.*, reported in Japan^[18] that laparoscopic ultrasound performed with local anesthesia diagnosed new nodular lesions in 64 out of 186 patients (34%). Twenty-eight nodules in 23 of the 186 patients (12%) were identified as HCC after biopsy. During the follow-up other 10 lesions, which had initially described as noncarcinomatous nodules, were diagnosed as HCC. So, laparoscopic ultrasonography discovered new HCC nodules in 17% of patients, defining multicentric neoplasm and avoiding unnecessary open surgery.

In our patients, laparoscopy with laparoscopic ultrasound was successfully performed in the gastrointestinal endoscopy

unit. There were no complications related to procedure that was done just under local anesthesia with non-narcotic analgesic drugs. So, this type of diagnostic laparoscopy seems as safe as standard laparoscopy^[7]. Endoscopic findings were liver cirrhosis in two cases (one with portal hypertension and ascites) and chronic liver disease without cirrhosis in the other one. There were no tumors on the liver surface. Extrahepatic, including peritoneal, spread was not detected.

Laparoscopic ultrasonography confirmed location and number of lesions diagnosed by conventional imaging. In particular, ultrasonographic pictures had similar characteristics to those of transparietal sonography, but with higher quality and definition. In the patient lacking previous histologic diagnosis, the tumor was biopsied with laparoscopic ultrasound guidance, achieving a definitive confirmation of hepatocellular carcinoma.

In conclusion, our preliminary experience suggests that laparoscopy with laparoscopic ultrasonography carried out with local anesthesia in a nearly ambulatory setting could be a safe, effective and relatively simple procedure in staging of HCC and optimizing patient selection for liver resection or transplantation. The procedure, that is well tolerated and carried out with minimal drug therapy, may be cost-effective for HCC diagnostic assessment. Ultrasonography, providing the image of interior of the liver and guiding puncture, increased sensitivity to laparoscopic procedure. On the other hand, endoscopic examination diagnosed in one case a non-cirrhotic liver, later confirmed after biopsy, finding that is associated with a better chance of hepatectomy and survival. Staging was correct in all cases except one wherein diaphragm infiltration was not detected at endoscopic study. The visual assessment of some areas, as dorsal surface of the right lobe, is still difficult and led to this false negative result. This problem could probably be overcome employing an orientable-tip device. Besides, this technique could be also useful in detection and ultrasonography-guided biopsy of lesions not accessible to conventional diagnostic approach. Consequently, this procedure, which may be a powerful tool in the management of HCC, must be extensively evaluated.

ACKNOWLEDGMENT

The authors thank Olympus España (Medical Europa) for the ultrasonographic equipment used in this study.

REFERENCES

- 1 **Bosch FX**, Ribes J, Borràs J. Epidemiology of primary liver cancer. *Semin Liver Dis* 1999; **19**: 271-285
- 2 **Llovet JM**, Burroughs A, Bruix J. Hepatocellular carcinoma. *Lancet* 2003; **362**: 1907-1917
- 3 **Wernecke K**, Rummeny E, Bongartz G, Vassallo P, Kivelitz D, Wiesmann W, Peters PE, Reers B, Reiser M, Pircher W. Detection of hepatic masses in patients with carcinoma: comparative sensitivities of sonography, CT, and MR imaging. *Am J Roentgenol* 1991; **157**: 731-739
- 4 **Murakami T**, Mochizuki K, Nakamura H. Imaging evaluation of the cirrhotic liver. *Semin Liver Dis* 2001; **21**: 213-224
- 5 **Makuuchi M**, Takayama T, Kosuge T, Yamazaki S, Yamamoto J, Hasegawa H, Takayasu K. The value of ultrasonography for hepatic surgery. *Hepatogastroenterology* 1991; **38**: 64-70
- 6 **Luck AJ**, Maddern GJ. Intraoperative abdominal ultrasono-

- graphy. *Br J Surg* 1999; **86**: 5-16
- 7 **Schneider ARJ**, Eickoff A, Arnold JC, Riemann JF. Diagnostic laparoscopy. *Endoscopy* 2001; **33**: 55-59
 - 8 **Fukuda M**, Mima S, Tanabe T, Haniu T, Suzuki Y, Hirata K, Terada S. Endoscopic sonography of the liver- diagnostic application of echolaparoscope to localize intrahepatic lesions. *Scand J Gastroenterol Suppl* 1984; **102**: 24-38
 - 9 **Okita K**, Kodama T, Oda M, Takemoto T. Laparoscopic ultrasonography: diagnosis of liver and pancreatic cancer. *Scand J Gastroenterol Suppl* 1984; **94**: 91-100
 - 10 **Frank K**, Bliesze H, Bonhof JA, Beck K, Hammes P, Linhart P. Laparoscopic sonography: a new approach to intraabdominal disease. *J Clin Ultrasound* 1985; **13**: 60-65
 - 11 **John TG**, Greig JD, Crosbie JL, Miles WF, Garden OJ. Superior staging of liver tumors with laparoscopy and laparoscopic ultrasound. *Ann Surg* 1994; **220**: 711-719
 - 12 **Callery MP**, Strasberg SM, Doherty GM, Soper NJ, Norton JA. Staging laparoscopy with laparoscopic ultrasonography: optimizing resectability in hepatobiliary and pancreatic malignancy. *J Am Coll Surg* 1997; **185**: 33-39
 - 13 **de Castro SM**, Tilleman EH, Busch OR, van Delden OM, Lameris JS, van Gulik TM, Obertop H, Gouma DJ. Diagnostic laparoscopy for primary and secondary liver malignancies: impact of improved imaging and change criteria for resection. *Ann Surg Oncol* 2004; **11**: 522-529
 - 14 **Berber E**, Garland AM, Engle KL, Rogers SJ, Siperstein AE. Laparoscopic ultrasonography and biopsy of hepatic tumors in 310 patients. *Am J Surg* 2004; **187**: 213-218
 - 15 **Lo CM**, Lai EC, Liu CL, Fan ST, Wong J. Laparoscopy and laparoscopic ultrasonography avoid exploratory laparotomy in patients with hepatocellular carcinoma. *Ann Surg* 1998; **227**: 527-532
 - 16 **Montorsi M**, Santambrogio R, Bianchi P, Opocher E, Cornalba GP, Dapri G, Bonavina L, Zuin M, Podda M. Laparoscopy with laparoscopic ultrasound for pretreatment staging of hepatocellular carcinoma: a prospective study. *J Gastrointestinal Surg* 2001; **5**: 312-315
 - 17 **Awad SS**, Fagan S, Abudayyeh S, Karim N, Berger DH, Ayub K. Preoperative evaluation of hepatic lesions for the staging of hepatocellular and metastatic liver carcinoma using endoscopic ultrasonography. *Am J Surg* 2002; **184**: 601-604
 - 18 **Ido K**, Nakazawa Y, Isoda N, Kawamoto C, Nagamine N, Ono K, Hozumi M, Sato Y, Kimura K, Sugano K. The role of laparoscopic ultrasound and laparoscopic ultrasound-guided aspiration biopsy in the diagnosis of multicentric hepatocellular carcinoma. *Gastrointest Endosc* 1999; **50**: 523-526

Science Editor Li WZ Language Editor Elsevier HK

• LETTERS TO THE EDITOR •

Familial gastric cancers with Li-Fraumeni Syndrome: A case repast

Il-Jin Kim, Hio Chung Kang, Yong Shin, Byong Chul Yoo, Han-Kwang Yang, Jae-Gahb Park

Il-Jin Kim, Hio Chung Kang, Yong Shin, Byong Chul Yoo, Han-Kwang Yang, Jae-Gahb Park, Korean Hereditary Tumor Registry, Cancer Research Institute and Cancer Research Center, Seoul National University, Seoul, South Korea; Research Institute and Hospital, National Cancer Center, Goyang, Gyeonggi, South Korea
Correspondence to: Jae-Gahb Park, MD, President of Research Institute and Hospital, National Cancer Center, 809 Madu-dong, Ilsan-gu, Goyang, Gyeonggi 411-764, South Korea. park@ncc.re.kr
Telephone: +82-31-920-1501 Fax: +82-31-920-1511
Received: 2004-12-27 Accepted: 2005-03-31

© 2005 The WJG Press and Elsevier Inc. All rights reserved.

Key words: Familial gastric cancers; Li-Fraumeni syndrome; *TP53* mutation

Kim IJ, Kang HC, Shin Y, Yoo BC, Yang HK, Park JG. Familial gastric cancers with Li-Fraumeni Syndrome: A case repast. *World J Gastroenterol* 2005; 11(26): 4124-4126
<http://www.wjgnet.com/1007-9327/11/4124.asp>

TO THE EDITOR

Although the incidence of gastric cancer has declined somewhat in recent years, it remains one of the most common cancers worldwide^[1], and is the most common cancer in East Asian countries such as Korea and Japan^[2]. In terms of the genetics of gastric cancer, mutations in *CDH1* (*E-cadherin*) have been associated with hereditary diffuse gastric cancer (HDGC). The first germline mutation in *CDH1* was reported in a large Maori HDGC family^[1], with subsequent corroborations in Western and Asian HDGC families^[3-5]. *CDH1* mutations are believed to be associated with up to 50% of HDGC families^[5], but have not been linked with sporadic or intestinal types of gastric cancer^[5]. Interestingly, the observed *CDH1* germline mutations differ between Western and Asian countries; the mutation frequencies are higher in Western countries, with predominately truncating germline mutations observed, whereas only a few different missense mutations have been reported in Asian countries^[6]. This ethnic difference and the low frequencies of *CDH1* germline mutation in Asian populations prompted researchers to seek other susceptibility gene for Asian familial gastric cancer (FGC)^[2,7]. We found a *MET* germline mutation in a FGC patient suffering from a diffuse type of gastric cancer^[2], and another group reported a *MET* germline mutation in a gastric cancer patient without detailed family history information^[7]. These *MET* germline mutations were also found in Korean gastric cancer patients, but the overall *MET* mutation frequencies seem to be low

(1%^[7] and 5%^[2]), suggesting that while *MET* germline mutations may be causative in Korean or Asian gastric cancer patients, they likely do not play a major role in the development of FGC. Thus, no major FGC-related susceptibility gene has been identified in Asian countries to date.

The *TP53* tumor suppressor gene is known to cause Li-Fraumeni Syndrome (LFS), a rare hereditary clustering of malignancies including sarcoma, breast cancer, brain tumor, leukemia and adrenocortical carcinoma (Table 1)^[8]. Along with these five major cancers, LFS has also been associated with a wider range of tumors, such as melanoma, Wilms' tumor, lung, gastric, and pancreatic carcinoma^[8]. The definition of LFS includes a proband diagnosed with sarcoma before 45 years of age, a first-degree relative with cancer before this same age, and another first- or second-degree relative in the lineage with any cancer before this age or sarcoma at any age^[9]. *TP53* germline mutations have been reported in around 80% of LFS and 40% of Li-Fraumeni-like (LFL) syndrome patients^[8].

Recently, Keller *et al.*, reported a *TP53* germline mutation in one German FGC patient^[10]. They further performed mutational screening of *CDH1* and *TP53* in 35 FGC patients, which led to identification of two *CDH1* (one frameshift and one missense) and one *TP53* (missense) germline mutation (1 out of 34, for a 3% mutation frequency in *TP53*; only the proband was available for analysis). This novel report of a *TP53* germline mutation in one FGC patient suggested that *TP53* might play a role in the development of FGC. Based on this, Keller *et al.*, recommended that the *TP53* gene should be included in genetic screening of FGC patients with a suspected genetic predisposition for the disease.

Very recently, Oliveira *et al.*, reported a *TP53* germline mutation in 1 out of 10 screened FGC families from Portugal, which also has a high incidence of gastric cancer^[11]. Interestingly, the Portuguese family with the *TP53* germline mutation had a family history of both FGC (three gastric cancer members) and atypical LFS (one pancreatic cancer patient and one colon cancer patient). This family had previously been described as a Li-Fraumeni kindred^[12]. Based on these results, Oliveira *et al.*, reiterated the suggestion of Keller *et al.*, that families with an excess of gastric cancer should be considered for *TP53* mutation screening. These two reports differ from two previous studies of Japanese FGC families, in which no *TP53* germline mutations were identified^[13,14].

In our lab, we screened the entire coding region of *TP53* in probands from 23 Korean FGC families. We identified a nonsense (E287X) *TP53* germline mutation in 1 (SNU-G2)

Table 1 Definition of Li-Fraumeni syndrome and familial gastric cancer subtypes (familial gastric cancer, hereditary diffuse gastric cancer, and familial intestinal gastric cancer)

	Hereditary cancer	Definition	Reference
1	Li-Fraumeni syndrome (LFS)	A proband with a sarcoma under 45 yr Plus 1st degree relative under 45 yr with any cancer Plus an additional 1 st or 2 nd degree relative in the same lineage with any cancer aged under 45 yr or sarcoma at any age	8
2	Familial gastric cancer (FGC)	At least two gastric cancer patients within 1 st degree relatives and one patient diagnosed before the age of 50	6
2-(1)	Hereditary diffuse gastric cancer (HDGC)	(1) Two or more diffuse gastric cancer patients in 1 st or 2 nd degree relatives, with at least one diagnosed before the age of 50 (2) Three or more diffuse gastric cancer patients in 1 st or 2 nd degree relatives, independently of age of onset	15
2-(2)	Familial intestinal gastric cancer (FIGC)	At least three relatives should have intestinal gastric cancer and one of them should be a 1 st degree relative of the other two Plus at least two successive generations should be affected plus in one of the relatives, gastric cancer should be diagnosed before the age of 50	15

Criteria for countries with high incidence of gastric cancer.

out of the 23 screened individuals^[6]. The E287X *TP53* mutation segregated with the cancer phenotype in family members from whom DNA samples were available. As there were seven individuals in this family affected with gastric cancer, we initially believed that *TP53* might be a new candidate gene for FGC. However, a thorough clinical investigation revealed that two members of this family were afflicted with brain tumors, seven with gastric cancers, two with sarcomas and one with both gastric cancer and a sarcoma. This family history is compatible with both FGC and LFS. Thus, it is highly probable that the identified *TP53* germline mutation in our family (and perhaps those investigated in the other papers) is associated with LFS regardless of FGC history.

Based on this observation, we examined the pedigree in which Keller *et al.*^[10], identified their *TP53* germline mutation. This family included three gastric cancer patients, 1 individual who died of leukemia at age 17, one individual who died of liver carcinoma at age 34, and two individuals (younger brothers of the proband) for whom the causes of death were not listed. Although this family history satisfies the criteria for FGC, the family cannot be excluded from meeting the LFS criteria^[8,9]. Indeed, if this family was listed as including one sarcoma patient, the family history could satisfy the classical LFS criteria^[8,9].

Thus, the three recent papers^[6,10,11] appear to indicate that germline mutations in *TP53* likely do not contribute significantly to the development of FGC, but are instead associated with LFS, which may be accompanied by FGC in countries with high gastric cancer incidences. As there is presently insufficient clinical data to assess the incidence and prevalence of LFS in countries with high gastric cancer incidence rates, these results are very important for directing the genetic screening and counseling of FGC families. As suggested by Keller *et al.*^[10], and Oliveira *et al.*^[11], *TP53* mutation screening should be performed in FGC families with LFS-related cancers, whether or not the mutation is causative of FGC or only LFS. In addition, further work

will be warranted to determine more clearly whether or not *TP53* contributes to the development of FGC with LFS-related clinical symptoms.

REFERENCES

- 1 **Guilford P**, Hopkins J, Harraway J, McLeod M, McLeod N, Harawira P, Taite H, Scouler R, Miller A, Reeve AE. E-cadherin germline mutations in familial gastric cancer. *Nature* 1998; **392**: 402-405
- 2 **Kim IJ**, Park JH, Kang HC, Shin Y, Lim SB, Ku JL, Yang HK, Lee KU, Park JG. A novel germline mutation in the MET extracellular domain in a Korean patient with the diffuse type of familial gastric cancer. *J Med Genet* 2003; **40**: e97
- 3 **Gayther SA**, Goringe KL, Ramus SJ, Huntsman D, Roviello F, Grehan N, Machado JC, Pinto E, Seruca R, Halling K, MacLeod P, Powell SM, Jackson CE, Ponder BA, Caldas C. Identification of germ-line E-cadherin mutations in gastric cancer families of European origin. *Cancer Res* 1998; **58**: 4086-4089
- 4 **Oliveira C**, Bordin MC, Grehan N, Huntsman D, Suriano G, Machado JC, Kiviluoto T, Aaltonen L, Jackson CE, Seruca R, Caldas C. Screening E-cadherin in gastric cancer families reveals germline mutations only in hereditary diffuse gastric cancer kindred. *Hum Mutat* 2002; **19**: 510-517
- 5 **Brooks-Wilson AR**, Kaurah P, Suriano G, Leach S, Senz J, Grehan N, Butterfield YS, Jeyes J, Schinas J, Bacani J, Kelsey M, Ferreira P, MacGillivray B, MacLeod P, Micek M, Ford J, Foulkes W, Australie K, Greenberg C, LaPointe M, Gilpin C, Nikkel S, Gilchrist D, Hughes R, Jackson CE, Monaghan KG, Oliveira MJ, Seruca R, Gallinger S, Caldas C, Huntsman D. Germline E-cadherin mutations in hereditary diffuse gastric cancer: assessment of 42 new families and review of genetic screening criteria. *J Med Genet* 2004; **41**: 508-517
- 6 **Kim IJ**, Kang HC, Shin Y, Park HW, Jang SG, Han SY, Lim SK, Lee MR, Chang HJ, Ku JL, Yang HK, Park JG. A *TP53* truncating germline mutation (E287X) in a family with characteristics of both hereditary diffuse gastric cancer and li-fraumeni syndrome. *J Hum Genet* 2004; **49**: 591-595
- 7 **Lee JH**, Han SU, Cho H, Jennings B, Gerrard B, Dean M, Schmidt L, Zbar B, Vande Woude GF. Related A novel germ line juxtamembrane Met mutation in human gastric cancer. *Oncogene* 2000; **19**: 4947-4953
- 8 **Varley JM**. Germline TP53 mutations and Li-Fraumeni syndrome. *Hum Mutat* 2003; **21**: 313-320
- 9 **Chompret A**. The Li-Fraumeni syndrome. *Biochimie* 2002;

- 84:** 75-82
- 10 **Keller G**, Vogelsang H, Becker I, Plaschke S, Ott K, Suriano G, Mateus AR, Seruca R, Biedermann K, Huntsman D, Doring C, Holinski-Feder E, Neutzling A, Siewert JR, Hofler H. Germline mutations of the E-cadherin(CDH1) and TP53 genes, rather than of RUNX3 and HPP1, contribute to genetic predisposition in German gastric cancer patients. *J Med Genet* 2004; **41**: e89
- 11 **Oliveira C**, Ferreira P, Nabais S, Campos L, Ferreira A, Cirnes L, Castro Alves C, Veiga I, Fragoso M, Regateiro F, Moreira Dias L, Moreira H, Suriano G, Carlos Machado J, Lopes C, Castedo S, Carneiro F, Seruca R. E-Cadherin (CDH1) and p53 rather than SMAD4 and Caspase-10 germline mutations contribute to genetic predisposition in Portuguese gastric cancer patients. *Eur J Cancer* 2004; **40**: 1897-1903
- 12 **Chompret A**, Brugieres L, Ronsin M, Gardes M, Dessarps-Freichy F, Abel A, Hua D, Ligot L, Dondon MG, Bressac-de Paillerets B, Frebourg T, Lemerle J, Bonaiti-Pellie C, Feunteun J. P53 germline mutations in childhood cancers and cancer risk for carrier individuals. *Br J Cancer* 2000; **82**: 1932-1937
- 13 **Kusano M**, Kakiuchi H, Mihara M, Itoh F, Adachi Y, Ohara M, Hosokawa M, Imai K. Absence of microsatellite instability and germline mutations of E-cadherin, APC and p53 genes in Japanese familial gastric cancer. *Tumour Biol* 2001; **22**: 262-268
- 14 **Shinmura K**, Kohno T, Takahashi M, Sasaki A, Ochiai A, Guilford P, Hunter A, Reeve AE, Sugimura H, Yamaguchi N, Yokota J. Familial gastric cancer: clinicopathological characteristics, RER phenotype and germline p53 and E-cadherin mutations. *Carcinogenesis* 1999; **20**: 1127-1131
- 15 **Caldas C**, Carneiro F, Lynch HT, Yokota J, Wiesner GL, Powell SM, Lewis FR, Huntsman DG, Pharoah PD, Jankowski JA, MacLeod P, Vogelsang H, Keller G, Park KG, Richards FM, Maher ER, Gayther SA, Oliveira C, Grehan N, Wight D, Seruca R, Roviello F, Ponder BA, Jackson CE. Familial gastric cancer: overview and guidelines for management. *J Med Genet* 1999; **36**: 873-880

Science Editor Guo SY Language Editor Elsevier HK

Inflammatory bowel diseases: From the mystical to the cellular and now the molecular

Joseph B. Kirsner

Joseph B. Kirsner, The Louis Block Distinguished Service Professor of Medicine, Department of Medicine - Section of Gastroenterology, The University of Chicago, IL 60637, United States
Received: 2005-04-10 Accepted: 2005-05-23

© 2005 The WJG Press and Elsevier Inc. All rights reserved.

Kirsner JB. Inflammatory bowel diseases: From the mystical to the cellular and now the molecular. *World J Gastroenterol* 2005; 11(26): 4127-4128
<http://www.wjgnet.com/1007-9327/11/4127.asp>



Joseph B. Kirsner, *Evolution of our understanding of inflammatory bowel diseases: From the mystical to the cellular and now the molecular.*

'Science (IBD) is moving but slowly, slowly creeping on from point to point'.
Alfred Lord Tennyson (1809-1892)

It is of interest in an era of increasing biomedical sophistication to recall that a relatively short time ago, early in the 20th century, 'simple' ulcerative colitis was an obscure 'medical curiosity' emerging slowly from an unknown past. Crohn's disease was yet unidentified as a separate entity although careful review of the IBD literature documented its early presence, masquerading as 'intestinal tuberculosis'. Into the 1930s, the etiology and pathogenesis of ulcerative colitis and Crohn's disease were unknown, and investigative hypotheses were scarce. Therapeutic resources were limited and treatment was primitive. At a time of limited biomedical knowledge and minimal clinical awareness, unsubstantiated views prevailed, including 'vague reactions to foods' (sugar, margarine, corn flakes), deficiency of a 'protective factor' in pig intestine, and psychiatric disease.

The position of inflammatory bowel diseases in the medical world today is vastly different. Ulcerative colitis and Crohn's disease are now recognized worldwide, are frequent subjects at medical meetings and increasingly provide the focus of important clinical and laboratory research. Indeed, few diseases in gastroenterology present as varied an array of investigative opportunities. This dramatic change began in the mid-20th century with the increasing support of biomedical research and the

subsequent growth of the basic sciences, highlighted by the adiscoveries of sulfonamides in the 1930s, antibiotics in the 1940s, and ACTH and adrenocorticosteroids in the 1950s. The entry of young physicians into gastroenterology during the 1930s and 1940s, trained in the rigors of basic research and controlled clinical study, contributed to this advance. Progress accelerated following the establishment of the General Medicine Study Section of the National Institutes of Health in 1956, which subsequently provided a major source for support of research in gastroenterology, the growth of academic medicine, and the establishment of the Crohn's and Colitis Foundation of America. By the 1970s, sufficient new clinical and scientific information on IBD had been accumulated to justify a comprehensive publication on ulcerative colitis and Crohn's disease, the 1975 1st Edition of *Inflammatory Bowel Diseases*, a volume of approximately 400 pages, with contributions from 25 authors. Subsequent editions of *Inflammatory Bowel Diseases*, appearing approximately every five years, documented the increasing depth and sophistication of clinical and scientific knowledge of ulcerative colitis and Crohn's disease. The 3rd Edition of *Inflammatory Bowel Diseases* in 1985, involving 44 authorities, had doubled in size and included chapters on the nature of intestinal defenses, the M cell, early information on immunologic and genetic aspects of ulcerative colitis and Crohn's disease, as well as advances in the pathology, radiology and endoscopy of IBD, and its improving medical and surgical treatment. Psychiatric and other early 20th century hypotheses had been replaced by concepts based in the disciplines of epidemiology, microbiology, immunology and genetics.

Into the 1990s, with more investigators involved, knowledge of the inflammatory bowel diseases increased exponentially. Etiologic possibilities, as outlined by R Balfour Sartor, now were more definitive, including persistent pathogenic microbial infection, enhanced intestinal mucosal permeability, 'dysbiosis' or the altered balance of protective bacteria *vs* aggressive commensals, and 'dysregulated' immune responses, leading to loss of oral tolerance to commensal bacteria and aggressive cellular activation. Academically based IBD centers generated more focused research and controlled therapeutic trials. IBD research in the laboratory had advanced from the study of tissues and epithelial cells to cellular biology and cellular constituents. Chapters now included the biologic nature of the IBD tissue reactions, the gut mucosal immune system and more advanced immunological and genetic mechanisms. Ulcerative colitis and Crohn's disease had become features of national and international medical meetings attracting large audiences.

The 1999 5th Edition included more than 70 authorities

submitting increasingly diverse chapters on epithelial cell function in health and disease (including heat shock proteins, and trefoil peptides), cytokines, chemokines, growth factors, eicosanoids and other bioactive molecules in clinical IBD and experimental intestinal inflammation, leukocyte-endothelial interactions, altered intestinal neuromuscular function, and the nature of oral tolerance. Genetic studies had identified susceptibility loci for ulcerative colitis and, most importantly, a locus (now identified as NOD-2) on chromosome 16 for Crohn's disease, particularly involving the ileum, the first gene linked with susceptibility to Crohn's disease. Transgenic and recombinatorial science now facilitated the creation of a variety of experimental animal models seeking to approximate human IBD, thereby enabling the more comprehensive study of intestinal tissue injury. The molecular nature of inflammation now became a prime area of investigation, with therapeutic dividends. After one hundred years of intermittent immunologic research led to the identification of tumor necrosis factor (TNF), an antibody to TNF proved to be a highly effective treatment, though not a cure, for Crohn's disease. Newly recognized bioactive molecules, IL-1, IL-2R, CAMS, addressins, defensins, flagellins, granulysins, selectins, claudins, annexins, guanylyns, laminins, intimins, aquaporins, and microsins now filled the IBD literature. Into the 21st century, additional bioactive molecules relevant to intestinal inflammation were identified at a rapid pace: adaptins, fibrillarins, syndecan-1, stromelysin, integrins, galanin-1, tropomyosin, fibroblast growth factor, epidermal growth factor, permeability-enhancing factor, neurotrophins, survivins, ubiquitins and zonulins.

The many pro-inflammatory and immunoregulation molecules, countless cytokines, and other biological substances, generated a series of novel biologic therapeutic agents (CP571, IDEC-131, OPC 6535, LDP02, CDP870 J695), creating a formidable, if not intimidating, array of terms and pathways for the IBD physician and investigator alike. How do these molecules relate to IBD and to each other? Where are the signaling mechanisms and pathways determining their coordinated action? Are they different in ulcerative colitis and Crohn's disease? Does NF κ B have both pro-inflammatory and anti-inflammatory actions, also involving trace elements (boron, selenium, vanadium, zinc)? Are there other dominant pro-inflammatory molecules analogous to TNF which can be successfully blocked? What is the possible role of the Peyer's patch microenvironment in the regulation of T cell function? Since the intestinal bacterial flora play a critical role in the pathogenesis of IBD, what might be the abnormalities in the commensal mucosal flora or the defects in the intestinal epithelium barrier leading to chronic intestinal inflammation? The role of human regulatory T cells? The 5q31 cytokine gene cluster? The role of the M cell in the entry of protective or detrimental antigens? The pivotal regulatory role of AP₂₀ in intestinal inflammation? The role of the intestinal epithelial barrier in the development of intestinal immunity? The possibility of increasing the production of local secretory IgA antibodies as a protection against bacterial infection and inflammation? The possible involvement of nitric oxide in the inflammatory responses and immune reaction of

IBD? The possible role of maternal immunologic memory in predisposing children to IBD and the genetic regulation of the intestinal epithelium? Important clinical issues similarly await resolution: the nature of the environment associated with urban industrialization and its relationship to IBD; and the role of today's 'hygienic home environment' in the vulnerability to IBD among children? Jewell and his colleagues recently have pointed out 'the importance of NOD-2/CARD 15 and the HLA region in determining clinical subgroups of Crohn's disease, which may provide the initial basis for the construction of a molecular classification of Crohn's disease.'

The discovery of new therapeutic approaches, in addition to currently available methotrexate, cyclosporine, antimicrobial compounds, thalidomide, and the adhesion molecule inhibitor heparin, including: growth factors, anti NF κ B transcriptional agents, the prostaglandin receptor EP4, anti-A4 integrin antibody, inhibitors of stress-activated MAP kinases, antisense oligonucleotides vasoactive intestinal polypeptide and heterologous hemopoietic stem-cell transplantation. Sartor has raised the possibility of more effective local treatment of IBD via 'targeted delivery of biologically active immunosuppressive molecules by recombinant bacteria colonizing mucosal surfaces.' More immediately available microenvironmental approaches include the resurrection of 'old' treatment probiotics, live microbial food ingredients (lactobacilli, bifidobacteria species) and prebiotics (germinated barley and nonabsorbed carbohydrates) and their newly recognized actions: production of antimicrobials and short chain fatty acids, inhibition of microbial adherence to the intestinal epithelium and restoration of normal intestinal permeability. In classic Karl Popper fashion, the expanding IBD research has generated many new important IBD questions and new research opportunities, necessitating a new IBD 'road map.' Despite the extraordinary progress in scientific information, more fundamental knowledge awaits discovery as the pace and the dimensions of IBD research continue to increase.

The impressive scientific advances in IBD, illuminating fundamental biologic and physiologic aspects of intestinal function, accentuate the importance of the 6th Edition of *Kirsner's Inflammatory Bowel Diseases*, and also defines its purpose: to clarify the new intestinal biology, its relevance to the clinical situation, and provide a launching pad for the remarkable advances towards etiology and the cure of IBD yet to come. *Kirsner's Inflammatory Bowel Diseases*-6th Edition, provides the currently indispensable 'road map' guiding IBD physicians and scientists through the multi-complex IBD labyrinth. Co-editors, Dr. R Balfour Sartor, Professor of Medicine, Microbiology and Immunology at the University of North Carolina, and Dr. William J Sandborn, Professor of Medicine at the Mayo Clinic, have assembled a superb panel of national and international authorities and a 'cutting edge' array of IBD scientific and clinical topics. This book, *Kirsner's Inflammatory Bowel Diseases*, since 1975, has played a vital part in assembling and expertly analyzing for the medical world the increasing 'basic' science and the expanding clinical information and will continue this important role, befitting the status of *Kirsner's Inflammatory Bowel Diseases* as 'the best book in the IBD field.'

Kirsner's inflammatory bowel disease

R Balfour Sarto, William J Sandborn

R Balfour Sarto, Professor of Medicine, Microbiology and Immunology, Division of Gastroenterology and Hepatology, Director, Multidisciplinary Center for IBD Research and Treatment, University of North Carolina School of Medicine, Chapel Hill, NC, United States

William J Sandborn, Professor of Medicine, Mayo Medical School, Head of the IBD Interest Group, Director of the IBD Clinical Research Unit, Mayo Clinic, Rochester, MN, United States

Received: 2005-04-10 Accepted: 2005-05-23

© 2005 The WJG Press and Elsevier Inc. All rights reserved.

Sarto RB, Sandborn WJ. Kirsner's inflammatory bowel disease. *World J Gastroenterol* 2005; 11(26): 4129
<http://www.wjgnet.com/1007-9327/11/4129.asp>

Very few medical textbooks have so thoroughly dominated, and even defined a field, as has *Inflammatory Bowel Diseases* by Joe Kirsner. Originally co-edited with Roy Shorter of Mayo Clinic, this book, beginning with its first edition in 1975, encapsulated the science and art of caring for patients with Crohn's disease and ulcerative colitis. Thus it is with considerable respect, and indeed some awe and trepidation, that we eagerly embraced the opportunity to assume the editorship of this preeminent textbook and the obligation to transition it to reflect the changing, increasingly complex pathophysiology and treatment of these diseases.

Our editorial principle has been 'evolution, not revolution', in an effort to maintain the unique character of the original book while advancing its format and scope to encompass the important recent developments in basic and clinical investigation and to emphasize translational areas. We added multiple new chapters, including clinical pharmacology, epithelial/immune and epithelial/bacterial interactions, T lymphocyte dysregulation, T lymphocyte trafficking, fibrogenesis, serology and laboratory markers of disease activity, assessment of disease activity and clinical trial design, pouchitis, and pharmacoeconomics, and split genetics and colon cancer into basic and clinical components. In the process of changing the character of the contents, 30 new primary authors have contributed chapters. These authors are a blend of established thought leaders and younger investigators who have brought new concepts to the field, but all authors share the common characteristics of having

a global perspective and being the premier investigator in their respective field. We thank the individual authors for their considerable efforts to create concise yet authoritative chapters and for their good humor in our exhortations to meet deadlines and to make suggested alterations. This adherence to deadlines and the timely production schedule by Elsevier have resulted in the most current textbook on IBD, with a lapse of only 7 mo from final submission to publication. Thus, recent trends in treatment and the latest concepts in pathogenesis are reflected in this book.

The cover encapsulates the evolving concepts of applying new insights into the pathogenesis of ulcerative colitis and Crohn's disease to their diagnosis and treatment. This book discusses the interactions between mucosal innate and acquired immune responses and between enteric commensal microflora and environmental triggers that lead to disease in genetically susceptible hosts. Novel mechanisms of diagnosis provide earlier and more precise diagnosis of disease, and novel biologic treatments bring new opportunities to induce a remission, and hopefully maintain disease quiescence. The individual chapters collectively develop the theme of genetic and molecular heterogeneity that results in distinct phenotypes of disease. The sub-classification of both Crohn's disease and ulcerative colitis should define clinically relevant populations of patients that selectively and predictably respond to individual therapeutic agents, resulting in highly effective and minimal cost treatment. Ultimately, preclinical diagnosis will lead to a way to prevent onset of clinical disease and associated complications in genetically susceptible individuals.

Finally, we must thank our family members, especially Em and Kenna, who have encouraged and supported this undertaking and in the process have endured many lonely weekends and holidays as the task was completed. We dedicate this book to these family members; to Joe Kirsner, for his guidance and confidence in our ability to continue his superb tradition, to our colleagues, fellows and students who provide continued stimulation and important questions; to the authors for their eloquent and comprehensive contributions; to the publishers for their strong support and professional production; and to the patients who have entered the clinical studies which have advanced our knowledge of the pathogenesis, epidemiology, diagnosis, and treatment of these disease. We hope that our readers will profit by this collective experience and make suggestions to improve future editions.

• ACKNOWLEDGMENTS •

Acknowledgments to Reviewers of *World Journal of Gastroenterology*

Many reviewers have contributed their expertise and time to the peer review, a critical process to ensure the quality of *World Journal of Gastroenterology*. The editors and authors of the articles submitted to the journal are grateful to the following reviewers for evaluating the articles (including those were published and those were rejected in this issue) during the last editing period of time.

Jacques Belghiti, Professor

Department of HepatoPancreatoBiliary Surgery Beaujon Hospital, 100 Bd Gal Leclerc, Clichy 92110, France

Chiung-Yu Chen, Associate Professor

College of Medicine, National Cheng Kung University, 138 Sheng Li Road, Tainan 704, Taiwan, China

Da-Jun Deng, Professor

Department of Cancer Etiology, Peking University School of Oncology, 1 Da-Hong-Luo-Chang Street, Western District, Beijing 100034, China

Er-Dan Dong, Professor

Department of Life Science, Division of Basic Research in Clinic Medicine, National Natural Science Foundation of China, 83 Shuanqing Road, Haidian District, Beijing 100085, China

Gan-Sheng Feng, M.D.

Huazhong University of Science and Technology, Tongji Medical College, Union Hospital, Wuhan 430032, Hubei Province, China

Kazuhiro Hanazaki, M.D.

Department of Surgery, Shinonoi General Hospital, 666-1 Ai, Shinonoi, Nagano 388-8004, Japan

Naohiko Harada, PhD

Department of Gastroenterology, Fukuoka Higashi Medical Center, Chidori 1-1-1, Koga, Fukuoka 811-3195, Japan

Bow Ho, Professor

Department of Microbiology, National University of Singapore, 5 Science Drive 2, Block MD4a, Room 03-12, Kent Ridge 117597, Singapore

Yik-Hong Ho, Professor

Department of Surgery, School of Medicine, James Cook University, Townsville 4811, Australia

Michael Horowitz, Professor

Department of Medicine, University of Adelaide and Director, Endocrine and Metabolic Unit, Royal Adelaide Hospital, Level 6, Eleanor Harrald Building, North Terrace, Adelaide 5000, Australia

Toru Ishikawa, M.D.

Department of Gastroenterology, Saiseikai Niigata Second Hospital, Teraji 280-7, Niigata, Niigata 950-1104, Japan

Joseph B Kirsner, M.D.

Department of Medicine/GI, Univ. of Chicago Hospitals & Clinics, University of Chicago Hosp. & Clinics, 5841 S. Maryland Ave., Mail Code 2100. Chicago IL 60637-1470, United States

Burton I Korelitz, M.D.

Department of Gastroenterology, Lenox Hill Hospital, 100 East 77th Street, 3 Achelis, New York, N.Y 10032, United States

Richard A Kozarek, M.D.

Department of Gastroenterology, Virginia Mason Medical Center, 1100 Ninth Avenue, PO Box 900, Seattle 98111-0900, United States

Hiromitsu Saisho, Professor

Department of Medicine and Clinical Oncology, Graduate School of Medicine, Chiba University, 1-8-1, Inohana, Chuo-ku, Chiba 260-0856, Japan

Hidetsugu Saito, Assistant Professor

Department of Internal Medicine, Keio University, 35 Shinanomachi, Shinjuku-ku, Tokyo 1608582, Japan

Chifumi Sato, Professor

Department of Analytical Health Science, Tokyo Medical and Dental University, Graduate School of Health Sciences, 1-5-45 Yushima, Bunkyo-ku, Tokyo 113-8519, Japan

Manfred Stolte, Professor

Institute of Pathology, Klinikum Bayreuth, Preuschwitzer Str. 101, Bayreuth 95445, Germany

Qin Su, Professor

Department of Pathology, Cancer Hospital and Cancer Institute, Chinese Academy of Medical Sciences and Peking Medical College, PO Box 2258, Beijing 100021, China

Peng Shang, Professor

Department of Cell Biology, Faculty of Life Sciences, 127 Western Youyi Road, Northwestern Polytechnical University, Xi'an 710072, Shaanxi Province, China

George Y Wu, Professor

Department of Medicine, Division of Gastroenterology-Hepatology, University of Connecticut Health Center, 263 Farmington Ave, Farmington, CT 06030, United States

Jia-Yu Xu, Professor

Shanghai Second Medical University, Rui Jin Hospital, 197 Rui Jin Er Road, Shanghai 200025, China

• REVIEW •

Multidisciplinary approach to understand the pathogenesis of gastric cancer

Juan Shang, AS Peña

Juan Shang, Hospital of Guangdong University of Technology, Guangzhou 510090, Guangdong Province, China
AS Peña, Laboratory of Immunogenetics and Department of Gastroenterology, VU University Medical Centre, PO Box 7057, 1007 MB Amsterdam, the Netherlands
Supported by the Foundation of Immunogenetics and Cluster I of VU University Medical Center, Amsterdam
Correspondence to: Juan Shang, Hospital of Guangdong University of Technology, Guangzhou 510090, Guangdong Province, China. juanshang@yahoo.com
Telephone: +86-20-38459380 Fax: +86-20-38458695
Received: 2004-10-01 Accepted: 2004-12-09

Abstract

Gastric carcinoma remains a common disease worldwide with a dismal prognosis. Therefore, it represents a very important health problem. It occurs with a high incidence in Asia and is one of the leading causes of cancer death in the world. Although the incidence and mortality of gastric carcinoma are decreasing in many countries, gastric cancer still represents the second most frequent malignancies in the world and the fourth in Europe. The 5-year survival rate of gastric carcinoma is low. The etiology and pathogenesis are not yet fully known. The study of gastric cancer is important in clinical medicine as well as in public health. Over the past 15 years, integrated research in molecular pathology has clarified the details of genetic and epigenetic abnormalities of cancer-related genes in the course of the development and progression of gastric cancer. Gastric cancer, as all cancers, is the end result of the interplay of many risk factors as well as protective factors. Although epidemiological evidence indicates that environmental factors play a major role in gastric carcinogenesis, the role of immunological, genetic, and immunogenetic factors are thought to contribute to the pathogenesis of gastric carcinoma. Among the environmental factors, diet and *Helicobacter pylori* are more amenable to intervention aimed at the prevention of gastric cancer. The aim of the present paper is to review and include the most recent published evidence to demonstrate that only a multidisciplinary approach will lead to the advancement of the pathogenesis and prevention of gastric cancer. On the immunogenetic research it is clear that evidence is accumulating to suggest that a genetic profile favoring the proinflammatory response increases the risk of gastric carcinoma.

Key words: Gastric cancer; *H pylori*; Immunogenetics; IL-1; Diet; Trefoil regulation; gp130

Shang J, Peña AS. Multidisciplinary approach to understand the pathogenesis of gastric cancer. *World J Gastroenterol* 2005; 11(27): 4131-4139
<http://www.wjgnet.com/1007-9327/11/4131.asp>

DISEASE DEFINITION AND CLASSIFICATION

The stomach wall is divided into three major areas: fundus, corpus, or body, and antrum and it has five layers: the inner lining (the mucosa) contains glands. Underneath is the submucosa; then is the layer of muscle; next is the subserosa. The outer layer is the serosa. Gastric cancers are malignancies arising in any part of stomach. Most gastric cancers arise in the antrum, the distal third of the stomach. The predominant site of gastric cancer occurrence has changed over the last 30 years^[1-6]. A large number of tumors involving the proximal stomach and gastro-esophageal junction have been found. The lesser curvature of the stomach is more frequently involved than the greater curvature.

Several different types of cancer can occur in the stomach. Adenocarcinoma, which starts in the glandular cells, is the most common cancer of the digestive tract and histology accounts for 90-95% of all gastric malignancies. It can spread to nearby lymph nodes (LN) and other areas of the body, such as the liver, pancreas, colon, lung, and ovaries. Other types of malignancy in the stomach are sarcoma arising from the cells of the muscle layer, and more common, lymphoma arising in the B and T cells of the lamina propria. The latter two types of malignancies have different prognosis and require different management than adenocarcinoma.

In this review we will concentrate in adenocarcinoma of the stomach mainly because other types have rarely been reported^[7,8].

Several classification systems are used for gastric cancer. Borrmann types, developed by Borrmann in 1923, identify five different types. This tissue classification of gastric cancer is characterized by the shape of the tumor on gastric mucosa and its pervading style in gastric wall.

Lauren developed the DIO system of the histomorphological classification, which assumes two main biological groups: diffuse gastric cancer (D) and intestinal gastric cancer (I), and other (O)^[9,10]. The former two groups account for 90% of all stomach cancers. The intestinal type is well differentiated and characterized by polypoid or fungating

lesions that may ulcerate centrally. Many evidences show that this type is strongly associated with *Helicobacter pylori* (*H. pylori*), and usually arises on a backdrop of chronic gastritis, gastric atrophy, and intestinal metaplasia^[11]. Clinically, the latter is present with diffuse thickening of the stomach wall, rather than a discernible mass. A genetic predisposition is presumed in young patients with a diffuse type of gastric cancer, in contrast to the intestinal type associated with older age^[12,13]. The intestinal type of adenocarcinoma has a better prognosis than the diffuse variant, most of which have spread beyond the confines of the stomach at the time of diagnosis. As with other cancers, stage is the most important determinant of outcome^[14].

According to the standard of WHO, the cellular classification in gastric carcinoma has these subtypes: papillary adenocarcinoma, tubular adenocarcinoma, mucinous adenocarcinoma, signet-ring cell carcinoma, squamous cell carcinoma, adenoacanthoma, undifferentiated carcinoma, unclassified carcinoma and carcinoid tumor.

The Fifth International Union Against Cancer tumor node metastasis (UICC TNM) classification, which was published in 1997, based on the number of metastatic LN, has proved to be a reliable and objective method as the principal assessing the extent and severity of disease and determining the prognosis of cancer patients^[15]. The new TNM classification not only is an objective, simple and reproducible system, but also a significant prognostic index for gastric cancer superior to the old classification. The new TNM classification represents a prognostic factor equally powerful to the old classification. Especially, the new N-classification is superior to the old N-classification in terms of the homogeneity of each N group^[16,17].

X-ray examination after taking barium meal may eventually contribute to detecting delayed gastric emptying quantitatively and indicates the degree of tumor infiltration. Similarly and more accurately, spiral CT is of help in the identification of the gross type, invasion to serous layer and adjacent organs of gastric cancer in its stage of progression. The CT scan is also valuable in detecting metastatic as hepatic, splenic, and abdominal apart from the involvement of LN near the lesion. Enhanced dynamic CT scan plays a significant role in the diagnosis of gastric carcinoma; early enhancing phase scanning is the technique of choice nowadays for demonstrating tumor lesions. Sophisticated scanning technique is mandatory in improving the diagnostic accuracy of gastric carcinoma^[18,19].

The ultrasound examination of stomach so far has been still a difficult technique that requires expertise. It can be used to observe the infiltration of the tumor into the lower layer of the mucous membrane. Endoscopic ultrasonography is very accurate in assessing the depth of tumor infiltration and the lymph node metastasis. It also can be used to determine the progress and prognosis of gastric carcinoma^[20].

DISEASE CHARACTERISTICS

Precancerous lesions of stomach

Six different pathological disorders have been described as increasing the risk for malignancy in the stomach. The following processes have been implicated as precancerous lesions.

Chronic atrophic gastritis There is evidence from animal model that nitrosamine plays a role in developing malignancy. Achlorhydria in atrophic gastritis allows bacterial colonization of the stomach, most extremely in places where overgrowth may cause nitrate reduction and transform the nitrate, which exist in many foods to potentially develop carcinogenic N-nitroso compounds^[21]. This occurs more often in antrum gastritis with intestinal metaplasia and non-typical proliferation. The course of gastritis is rather long and gastric cancer is believed to develop slowly over many years. Some patients present dyspepsia, vague abdominal fullness (after meal), irregular pain, belching, nausea, and vomiting, but not specific. Severe cardiac gastritis may produce glossitis and anemia.

Gastric polyps Familial adenomatous polyps are associated with upper gastrointestinal adenomas and adenocarcinoma. Based on Nakamura's classification^[22,23], hyperplastic polyps were further classified into the following subtypes: the foveolar epithelial type, fundic glandular hyperplastic type, and pyloric glandular hyperplastic type. It was found that atypical hyperplastic foci usually appear in the foveolar epithelial subtype, indicating a close relationship to cancer. This finding suggests that the subclassification of hyperplastic gastric polyp has a higher practical value in clinical application^[24].

Gastric ulcer Some gastric cancers are considered to transform from gastric ulcers, but with a low rate, 1-5% in China. Cancerous degeneration of ulcer was small and the epithelial regeneration at the ulcer's edge and benign fusion of the muscularis mucosa with the muscularis propria were very common. The cancerous tissue extending to node metastasis was rare. Therefore, the cancerous tissue down to the submucosa was found at the margin but not at the base of the ulcer. These patients should be thought seriously, specially if they are more than 45 years old, the symptoms of gastric ulcer are persistent 1 mo after treatment. These findings that conform well to Hauser's criteria blood test are positive. These results suggest that multiple biopsies should be taken from the edge of chronic ulcers. The most distinct feature of malignant ulcer was the lack of cancerous infiltration and muscular residue in the scar tissue of ulcer base. The existence of this type of ulcer clinically and pathomorphologically supports the viewpoint that gastric cancer ulcer can undergo malignant change^[25].

Cancer of gastric remnant Patients after gastrectomy have more opportunity to get vicious tumor than normal people, and the course from remnant stomach to gastric cancer is nearly 15-30 years. Refluxing of intragastric and bile after gastrectomy became the base of gastritis. Furthermore the pH is increased and is beneficial to the abnormal proliferation of cell, carcinogen such as nitrite transfer to nitrosamine. Bile salt, a carcinogen, sometimes can lead to cancer.

Cholecystitis It was found that both the content of various kinds of biliary acid salt and pH value of gastric juice were much higher in patients with gastric cancer, gastric ulcer, and chronic atrophic gastritis than in normal controls. Bile acid salt is known to be harmful to gastric mucosa and the damage becomes more severe with the increase of bile acid salt concentration and prolongation of exposure. Therefore,

our results suggest that the bile acid salt in the gastric juice is one of the carcinogenic factors^[26].

Pernicious anemia Pernicious anemia can lead to atrophic gastritis and is well known to be associated with gastric cancer. Pernicious anemia and autoimmune disease in general is rare in Chinese patients. There are few reports of pernicious anemia in Chinese patients and does not play a significant role as a predisposing cause of gastric cancer in China^[27,28].

Gastric schistosomiasis Gastric carcinoma has been found arising from schistosomiasis in the epidemic area of south China and this chronic inflammation has been linked to development of gastric cancer in this area of China^[29].

Early gastric cancer

The designation early gastric cancer (EGC) refers to a gastric carcinoma, which does not infiltrate beyond the submucosa. This definition is not influenced by absence or presence of metastases or by the diameter of the tumor. The 5-year survival of EGC is 90% or more. The diagnosis can regularly be made if, in the case of persistent vague upper abdominal complaints, an optimal radiological examination of the stomach is done. At even the slightest radiological suspicion, or if complaints persist in spite of negative radiological findings, gastroscopic examination and multiple-aimed biopsies should follow. Attention should be focused on the gastric angular incisure, antrum and lesser curvature to perform site-directed biopsy. Final diagnosis depended on the pathological diagnosis of the biopsy material. Pathologic diagnosis would be correct, provided the biopsy material was taken from the proper site^[30,31].

An investigation from Liaoning Province reported pathological characteristics of EGC in Chinese patients. The peak age of the patients was between 50 and 59 years. The incidence in female before 50 years was higher than that in male but reverse after this age. The most common site was in lower part of the stomach. Highly differentiated carcinomas were more frequently found in those cancer foci of no larger than 0.5 cm in diameter. More signet ring cell carcinomas were found. Lymphatic metastasis was more in type IIc+III and the least in type I. Comparing with the Japanese cases, it was found that the peak age of EGC patients in Japanese was 10 years older than that in Chinese patients and most of the tumor occurred in middle part of the stomach. Type III and mucinous adenocarcinoma was hardly found^[32].

The recurrence rate was higher in submucosal tumors than in mucosal tumors, in lymphatic and vascular vessel invasion-positive cases than in negative cases, in synchronous multiple gastric cancer than in solitary tumors, in tumors of 1.5 cm or more in diameter than in tumors of less than 1.5 cm. The rate of hematogenic metastasis to the liver or lung was 45.5%, and the recurrence in the residual stomach was 27.3% and in lymph node was 27.3%^[33].

Advanced gastric cancer

Because of the elusive nature of gastric disorders, gastric cancer usually is advanced when symptoms first appear. There are several characteristic routes by which gastric carcinoma will progress and metastasize: (1) by extension

and infiltration along the mucosal surface and stomach wall or lymphatic vessels, (2) via lymphatic or vascular embolism, probably to regional LN, (3) by direct extension into adjacent structures such as the pancreas, liver, or esophagus, and (4) by blood-borne spread. The pattern of metastatic spread of gastric cancer correlates with the size and the location of tumor. Lesions of the distal portion of the stomach usually metastasize to infra-pyloric, inferior gastric, and celiac LN. Tumors in the proximal portion often metastasize to pancreatic, pericardial, and gastric LN. With advanced gastric cancer, involvement of the left supraclavicular nodes may occur. Distant metastatic sites are the lung, adrenal glands, bone, liver, pancreas, and peritoneal cavity^[34].

Clinical syndromes

In the early stage, GC seldom showed significant symptoms, some of which are common to other, less serious gastrointestinal disorders (bloating, gas, and a sense of fullness). Some degrees of dysplasia occur, appetite loss, heartburn, vague abdominal fullness, flatus, excessive belching, and breath odor, mild or severe, were similar as in the presentation of chronic gastritis or gastric ulcer previously reported. Soon afterwards the difficulty in swallowing, particularly difficulty that increases over time, nausea and vomiting, abdominal pain and weight loss were on the rise. In the late stage some patients might vomit blood; have blood in the stools or black stools, tiredness due to anemia, abdominal pain and weight loss are aggravated, a decline in general health.

As other malignancies, early detection, early diagnosis, and early treatment remain the key to improve the survival of patients with resected cancer of the gastric cardia. Why residual tumor left at the resection edge and the presence of tumor thrombi do not influence survival needs to be further studied.

EPIDEMIOLOGY

The epidemiology of gastric cancer involves many features, since there are significant geographical, ethnical, and cultural factors influencing the prevalence of GC. It is more frequent in the developing world than in the developed world, more common in Asia than in Europe, and more in Latin America than in North America and Africa^[35]. Stomach cancer in China has distinct geographically different distribution. The morbidity in urban areas is higher than in rural areas, giving a difference of 1.9 times^[36]. According to an investigation between 1989 and 1999, in Linqu County of China, no reduction in GC mortality was observed in the highest risk population worldwide^[37].

The most recent estimates indicate that gastric cancer is the second most common cancer in the world after lung cancer. It represents 11% of all cancers in men and 7% of all cancers in women. In developing countries, lung cancer ranks first, representing 13% of all cancers and gastric cancer second (12%). In developed countries gastric cancer ranks fifth, representing 7% of all cancers, three-fourth of which occur in Asia. About 80% of the cases diagnosed in Asia occur in China and Japan. Steady decline in the rates of gastric cancer has been observed everywhere in the last few decades. However, the total number of new cases

diagnosed worldwide is increasing mainly because of increasing and aging of the population. It was estimated that there were 700 000 new cases in 1980, 755 000 in 1985, 900 000 in 1990, 1 013 000 in 1995, and 1 000 000 in 2000. This indicates that the impact of gastric cancer in public health is not decreasing^[4].

ETIOLOGY

Gastric cancer, of all cancers, is the end result of the interplay of many risk factors as well as protective factors. Genetic and environmental factors are likely to play a role in the etiology of the disease. Several factors are suspected to play a role in gastric carcinogenesis, including the effects of diet, exogenous chemicals, intragastric synthesis of carcinogens, genetic factors, infectious agents, and pathological conditions in the stomach (such as gastritis). According to Correa, there is evidence from pathology and epidemiology studies that gastric carcinogenesis develops with the following sequential stages: chronic gastritis; atrophy; intestinal metaplasia; and dysplasia. The initial stages of gastritis and atrophy have been linked to excessive salt intake and infection with *H pylori*^[38].

Environmental factors and gene polymorphisms involved in the susceptibility of gastric cancer

Several epidemiological evidences indicate that environmental factors play an important role in gastric carcinogenesis. The fact that immigrants exhibit incidence rates similar to those of their country of origin has led researchers to accept exogenous influences such as environment and diet. The investigation from China showed that the risk factors of gastric cancer were living in high incidence area for a long period, low economic income, low consumption of fresh vegetables and fruits and animal protein, high intake of sweet potato and ink fish and salted meat, eating and drinking too much at one meal and mental injury, and a family history of gastric cancer. High intake of grains and low intake of animal fat and proteins appear to be associated with a decreased risk. Diets rich in vitamins A and C are associated with low risk for gastric cancer. Controversy exists over the role of nitrates found in soil-grown foods, drinking water, and prepared foods. Because refrigeration and a high intake of ascorbic acid inhibit the formation of nitrates, it is postulated that the presence of these factors may account for decreasing gastric cancer. Neither smoking tobacco nor drinking alcohol has been demonstrated to increase the risk of gastric carcinoma^[32,39-44].

H pylori

Gastric carcinogenesis is a multistep and multifactorial process beginning with *H pylori*-associated gastritis in most cases. *H pylori* infection, together with other environmental factors and individual susceptibility, determine the final risk for the development of gastric cancer. The discovery of *H pylori* in the early 1980s has proved a turning point in understanding the pathogenicity of this malignancy. *H pylori* infection is common worldwide and about half of the human population believed to be infected. But only a small fraction of infected individuals develop gastric cancer.

Additional factors must be involved in the progression toward cancer^[45,46,50].

H pylori are highly host-adapted bacterial pathogens that establish a chronic infection in the human stomach and have no known animal or environmental reservoirs. It shows a high degree of genetic heterogeneity due to mutations and frequent recombination. In the past, specific genes have been identified which are associated with bacterial virulence. These genes (e.g., *vacA*, cytotoxin associated gene A (*cagA*), and *iceA*) have been studied individually, and distinct genotypes have been defined. There is accumulating evidence that the different genotypes of *H pylori* show a particular geographic distribution^[51]. *H pylori* strains containing the *cagA* protein are associated with more severe disease and harbor a 40-kb pathogenicity island (PAI) induce NF- κ B activation and interleukin (IL)-8 secretion in gastric epithelial cells. *H pylori* changes the expression of genes encoding growth factors and cytokine/chemokines and their receptors, apoptosis proteins, transcription factors, and metalloprotease-disintegrin proteins, and tissue inhibitors of metalloproteinases^[47].

H pylori stimulate endothelial cells to upregulate adhesion molecule expression and to increase the production of neutrophil-recruiting chemokines. The PAI encodes a bacterial type IV secretory system that secretes and translocates the *cagA* protein into host cells, where it is phosphorylated by a host-cell kinase and causes morphological changes. Innocenti *et al.*, found that several, but not all, *H pylori* strains are able to activate endothelial cells to express the adhesion molecules VCAM-1, ICAM-1, and E-selectin and to secrete neutrophil-recruiting chemokines, and therefore contribute to tissue damage and ulcer formation^[48,49]. Among people infected with *H pylori*, the virulence of the infecting strain is a major determinant which develops disease. Strains producing vacuolating cytotoxin activity are more commonly isolated from people with peptic ulcers than without. The gene encoding the toxin, *vacA*, varies between strains, especially in its signal sequence and mid regions. *vacA* genotype influence cytotoxin activity, and signal sequence type correlates closely with peptic ulceration. Infection with strains possessing *cagA* is more common among people with peptic ulceration or gastric adenocarcinoma than without. *CagA*+ *H pylori* infection is more closely associated with gastric cancers and peptic ulcers than *cagA*-infection. Because *cagA*+ infection may be associated with the development of atrophic gastritis, *cagA* infection is believed to be a risk factor for intestinal-type gastric cancer. But Deguchi *et al.*, reported that *cagA* infection is also associated with diffuse-type gastric cancer in Japan. They also found that all p53 alteration were in *H pylori*-positive gastric cancer and their mutations were more frequent in the *cagA* group, although the correlation between p53 mutation and *H pylori* infection did not reach statistical significance. p53 abnormality was clinically correlated with prognostic factors (e.g., tumor size, depth, lymph node metastasis) of gastric cancer. These findings indicated that *cagA*+ *H pylori* infection might have an important role in the development of gastric cancer with p53 mutation^[52].

The p53 tumor suppressor gene, located on chromosome

17p13, is one of the most commonly mutated genes in all types of human cancer. p53 codon 72, which produces variant proteins with an arginine (Arg) or proline (Pro), has been reported to be associated with cancers of the lung, esophagus, and cervix. Recently, studies in Japan suggested that the Pro/Pro genotype at p53 codon 72 contributes to susceptibility of diffuse-type gastric cancer patient with *H pylori*-CG^[53]. The mutation of p53 and inactivation of p21WAF1 and p16 play an important role in carcinogenesis of stomach. However, *H pylori* infection was not associated with the abnormal expression of these three genes in China^[54].

Human Chk1 and Chk2 are DNA damage-activated protein kinases that function as downstream mediators of ataxia-telangiectasia mutated, which are involved in G₂/M cell-cycle arrest. A study from Japan found a significant correlation between the levels of expression of Chk1 and p53 proteins in gastric carcinomas. Chk2 might be important in the checkpoint function in human gastric carcinomas with p53 mutation^[56]. Mutations of an oncogene, K-ras, may be involved in the early stage of carcinogenesis of the intestinal types. The incidence of K-ras mutations in gastric cancer is only 10%. However, by histological classifications, the incidence of K-ras mutation was more frequent in intestinal types than in diffuse types of gastric adenocarcinoma. In addition, K-ras mutations in *H pylori*-associated chronic gastritis were significantly more frequent in gastric cancer patients than in cancer-free patients (50% *vs* 3.7%, $P = 0.037$)^[57].

No evidence for the involvement of antigastric antibodies in the stimulation of apoptosis was found. Therefore, host factors may be at least as important as bacterial factors in determining gastric mucosal responses to *H pylori*^[55].

Interleukin gene polymorphisms and gastric cancer

The presence of *H pylori* in gastric antrum is, in most cases, associated with mucosal inflammatory changes consisting of infiltration of a large number of polymorphonuclear and mononuclear phagocytes. *H pylori* reside in the mucus layer overlying the epithelium and do not invade epithelial cells. However, accumulating evidence indicates that gastric infection with *H pylori* induces the expression of several proinflammatory cytokines, including IL-1 β , IL-6, IL-8, IL-18 and TNF- α in gastric mucosa.

IL-1 β is a potent proinflammatory cytokine and powerful inhibitor of gastric acid secretion that is upregulated in the presence of *H pylori* and is important in initiating and amplifying the inflammatory response to this infection. El-Omar *et al.*, reported that gene polymorphisms in the interleukin gene family of cytokines (IL-1 β -31C, IL-1 β -511T, and IL-1RN*2 alleles) are associated with an increased risk of both hypochlorhydria, in *H pylori* negative infected first-degree relatives of gastric carcinoma^[58,59]. A study from Portugal supported the hypothesis that host genetic factors that affect IL-1 gene determine why some individuals infected with *H pylori* develop gastric cancer while others do not^[60,61]. The polymorphism of promoter region -31C/T of IL-1 β gene and the polymorphism of IL-1RN genes 1/2 and 2/2 are associated with the susceptibility of gastric cancer in Chinese. Carrying -31T

allele increases the risk of gastric cancer. Polymorphism of IL-1RN and IL-1 β gene may be used as indicators of susceptibility of gastric carcinogenesis^[62]. A study from Japan investigated the polymorphism of -511 T-to-C located in the IL-1 β gene. According to these authors in view of the results for the IM or CAG without *H pylori* group, the presence of the C allele may also indicate a risk of mucosal atrophy of the stomach in the Japanese population^[63].

Serum levels of IL-8 and nitrogen monoxide (NO) are correlated with CagA+*H pylori* strain infection. Combined detection of serum level of IL-8, NO, and HP-CagA will contribute to the early diagnosis of precancerous lesion in the stomach^[64]. Secretion of IL-8 by gastric epithelial cell upon *H pylori* infection is dependent on activation of NF- κ B^[65].

IL-18 is a recently identified cytokine (originally termed interferon γ -inducing factor) and is related to the IL-1 family both structurally and functionally. Recently research has showed that IL-18 was increased in a variety of human inflammatory conditions, including Crohn's disease, rheumatoid arthritis, and tuberculoid leprosy with pleiotropic immunomodulatory functions. It has been found that IL-18 mRNA expression was greater in *H pylori*-positive than in *H pylori*-negative patients with normal mucosa. But mature IL-18 protein and active caspase-1 p20 are present in mucosa of both *H pylori*-infected and -uninfected subjects. The presence of the mature form of IL-18 in both normal and gastric mucosa suggests that gastric IL-18 has an important role in promoting local production of interferon-N and cell-mediated responses in the gastric mucosa^[47].

H pylori induces the production of tumor necrosis factor- α (TNF- α), which is closely related to epithelial injury. TNF- α plays a crucial role in host defense against infection, but a high concentration of TNF- α may cause severe pathology. The gene for TNF- α is located within the class III region of the major histocompatibility complex, which is a highly polymorphic region. The most common exchanges are G to A transitions in the TNF- α promoter at positions -308 (-308A) and -238 (-238A), and these genetic changes have been reported to influence TNF- α concentrations. It is possible that increased TNF- α concentrations, as a result of -308A polymorphism, alter the immune response, which confers susceptibility to gastric disease with *H pylori*-cagA subtype infection^[66]. In a study in Spain, these results suggest that TNF and LTA gene polymorphisms are related to the development of gastric and duodenal ulcer and may determine disease outcome in *H pylori* infection^[67].

Wu *et al.*, have reported that no association was noted between gastric cancer and the distribution of IL-1 and TNF- α genotypes in Taiwanese Chinese. Logistic regression analysis revealed that *H pylori* infection, cigarette smoking, and IL-10 genotype are independent risks for gastric cancer in the Taiwanese. Similar studies should be carried out in different populations and as Wu *et al.*, have correctly performed the risk of genotypes should be adjusted with confounding environmental risks^[68].

Genetic polymorphisms of some metabolizing enzymes

Environmental genotoxic chemical agents arising from the

diet, smoking, and air pollution are responsible for carcinogenesis in humans. It is generally accepted that the majority of carcinogenic chemical do not produce their biological effects *per se*, but require metabolic activation by host enzymes: phase I enzymes including cytochrome P450 enzyme and phase II enzymes including epoxide hydroxylase, *N*-acetyltransferase 2 (NAT2), and glutathione *S*-transferase (GSTs). Genetic polymorphisms have been recently shown in many of these enzymes, indicating that there are genetic differences among individuals in the ability to metabolize chemicals. Such genetic polymorphisms may affect the individual susceptibility to chemical carcinogenesis. From this point of view, the relationship between the genetic polymorphisms and carcinogenicity has been extensively examined to determine which polymorphic enzymes are highly associated with the susceptibility to cancers. Japanese researchers suggested that a combination of GSTM1 and NAT2 decreases the risk of gastric cancer in Japanese patients^[69]. A population-based case-control study in China suggested that the GSTP1 genotype seems not to be associated with the risk of gastric cancer and chronic gastritis in a high-risk Chinese population^[70]. The polymorphic genes of cytochrome P450, CYP2A6, and CYP2E1 have been implicated in increased susceptibility to certain malignancies. The CYP2A6 deletion was associated with gastric adenocarcinoma among Japanese population^[72].

KILLER/death receptor DR5

The KILLER/death receptor DR5 has been identified as a potent inducer of apoptosis, and mapped to chromosome 8p21-22, showing frequent allelic loss in gastric cancer. As stated before, the p53-induced apoptosis is an important biological process to prevent the development of cancer, and is mediated in part by expression of KILLER/DR5 only in cells with wild-type p53 protein, but not in those lacking p53 function. A report from Japan suspected that inactivation of KILLER/DR5 caused by mutations of KILLER/DR5 may be one of the possible escaping mechanisms against KILLER/DR5-mediated apoptosis and that inactivating mutation of KILLER/DR5 may contribute to the promotion or progression of a subset of gastric cancers^[71]. In Japan, another cancer registry-based study found that the incidence of gastric cancer was increased up to 5-fold in male relatives of early-onset prostate cancer patients. Currently unknown genes might contribute to the observed link between prostate and gastric cancer^[73].

E-cadherin

E-cadherin is a member of the cadherin family of calcium-dependent cell adhesion molecules. These molecules are localized in lateral cell-cell contacts of the epithelial cells and regulate the process of homophilic/homotypic adhesion between epithelial cells and play a role as a tumor suppressor gene. E-cadherin associates with α -catenin, β -catenin, and γ -catenin to form a complex that is essential for cell-cell communication and cell adhesion. Indeed, abnormal E-cadherin expression (characterized by loss, reduced, and/or cytoplasmic expression) has been observed in several types of carcinoma, and is frequently associated with poor differentiated/undifferentiated carcinomas and/or invasive

tumors. A co-operative study among Portugal, Germany, and Belgium reported that E-cadherin inactivation is significantly related with the diffuse histotype in gastric carcinoma, not only in "pure" diffuse carcinomas but also in the diffuse component of mixed tumors, β -catenin mRNA levels are increased in the vast majority of intestinal-type gastric cancers and this overexpression is independent of *H pylori* infection^[74,75].

Trefoil regulation, gp130, and gastric cancer

For a long time it was believed that the stomach and the intestine respond differently to inflammation. The immunological system of the stomach appears less fully developed than the intestine. This in part is due to the fact that nature has given the stomach a mechanism to protect itself with the production of hydrochloric acid and therefore an environment where only special bacteria, such as *H pylori* can survive. The intestine on the contrary is full of bacteria; however, seemingly ends in unrelated diseases. Inflammatory bowel disease and gastric cancer share in common an origin in chronic inflammation. An important and interesting finding that has arisen from research in mice with a "knock-in" mutation abrogating the Src-homology tyrosine phosphatase 2 (SHP2)-Ras-ERK signaling that developed gastric adenomas by 3 mo of age. Mice with a mutation eliminating the STAT1/3 signaling gp130 (Delta STAT)) showed impaired colonic mucosal wound healing^[76]. As stated in an editorial in Nature Medicine^[77], given the close interplay between the immune response and epithelial cells, it is not surprising that perturbations in signaling of immune system mediators play a key role in disease of the gut. It is the gp130 receptor, which binds the IL-6 family (IL-6 and IL-11) of cytokines that serve as an inflammation intersection between the stomach and the intestine. The homodimers of gp130, a transmembrane receptor β -chain, contain two discrete functional modules which signal through SHP-2/Erk and STAT1/3 that are responsible for the different behavior exhibited by the stomach and the intestine in response to inflammation. To understand the pathogenesis, it is necessary to understand the function of other family of genes called the trefoil factor (TFF) family that intimately appear to work with the gp130 molecule. Suemori *et al.*^[78], discovered in 1991 a group of small proteins designated intestinal trefoil factor. These authors demonstrated that it is primarily expressed and secreted onto the intestinal surface by goblet cells, suggesting that it may be an important component of intrinsic mechanisms for defending mucosal integrity. They are upregulated around areas of epithelial damage, ulceration, and neoplasia^[79].

IL-1 and IL-6 overexpression in chronic gastritis may lead to mucosal damage and gastric carcinogenesis through transcriptional repression of TFF1 and TFF2^[80]. TFF1 knockout mice developed multiple gastric adenomas and carcinomas, suggesting that TFF1 is a gastric-specific tumor-suppressor gene^[81]. The gp130 directly regulates the TFF genes. The trefoils are key downstream targets of the SHP2/Erk and STAT signaling pathways. The data also add to TFF1's credibility as a gastric-specific tumor-suppressor gene and TFF3's as a mediator of intestinal homeostasis. The hyperproliferative lesions was observed in the stomachs

of gp130 arise as a result of enhanced STAT3 activity in the absence of a counter-acting signal from the SHP2-Ras-Erk pathway rather than from the complete absence of (IL-6 and IL-11-mediated) gp130 signaling. IL-6 is likely to have an important role in the initial phase of intestinal wound healing. Furthermore, endogenous IL-11, unlike pharmacologically administered IL-11, seemed to have negligible effects on the intestinal epithelium.

In conclusion, although the incidence of gastric cancer is decreasing in some parts of the world, it still takes a significant toll among the inhabitants of Japan, China, Chile, Finland, Poland, Austria, Yugoslavia, and Costa Rica. The key to prevention of cancer of stomach lies in dietary intake. It is important to consume a balanced diet high in fresh fruits and vegetables and moderate amount of animal protein and fats. Salted, smoked, and pickled foods should be consumed in low quantities.

Screening and early detection programs are very useful. If detected at an early stage and treated aggressively, gastric cancer can be cured. As with all other forms of gastrointestinal cancers, gastric cancer is insidious in its onset and development. It usually infiltrates rapidly and can be disseminated throughout the body before overt signs of cancer are manifested. Overall 5-year survival rates are reported to range from about 8% to 16%. Gastric cancer mimics several other gastrointestinal maladies and diseases such as polyps, ulcers, dyspepsia, and gastritis. Some of the most difficult aspects of prevention and early detection are informing and motivating people at risk for the development of gastric cancer to seek medical attention for chronic "stomach problems". Inappropriate use of home remedies, self-medication, and misdiagnosis are major hurdles to overcome.

REFERENCES

- Gonzalez CA, Sala N, Capella G. Genetic susceptibility and gastric cancer risk. *Int J Cancer* 2002; **100**: 249-260
- Ladero JM, Agundez JA, Olivera M, Lozano L, Rodriguez-Lescure A, Diaz-Rubio M, Benitez J. N-acetyltransferase 2 single-nucleotide polymorphisms and risk of gastric carcinoma. *Eur J Clin Pharmacol* 2002; **58**: 115-118
- Yasui W, Oue N, Kuniyasu H, Ito R, Tahara E, Yokozaki H. Molecular diagnosis of gastric cancer: present and future. *Gastric Cancer* 2001; **4**: 113-121
- Yamashita S, Wakazono K, Sugimura T, Ushijima T. Profiling and selection of genes differentially expressed in the pylorus of rat strains with different proliferative responses and stomach cancer susceptibility. *Carcinogenesis* 2002; **23**: 923-928
- Alexander HR, Grem JL, Pass HI, Hamilton M, McAtee N, Fraker DL, Allegra CJ. Neoadjuvant chemotherapy for locally advanced gastric adenocarcinoma. *Oncology* 1993; **7**: 37-42
- Powell J, McConkey CC. Increasing incidence of adenocarcinoma of the gastric cardia and adjacent sites. *Br J Cancer* 1990; **62**: 440-443
- Xue ZQ. Primary gastric malignant lymphoma-analysis of 32 cases. *Zhonghua Zhongliu Zazhi* 1989; **11**: 133-135
- Liu XF, Huang YR. Primary gastric malignant lymphoma-analysis of 40 patients. *Zhonghua Zhongliu Zazhi* 1987; **9**: 298-301
- Lauren P. Histogenesis of intestinal and diffuse types of gastric carcinoma. *Scand J Gastroenterol Suppl* 1991; **180**: 160-164
- Lauren PA, Nevalainen TJ. Epidemiology of intestinal and diffuse types of gastric carcinoma. A time-trend study in Finland with comparison between studies from high- and low-risk areas. *Cancer* 1993; **71**: 2926-2933
- Lawrence W Jr, Menck HR, Steele GD Jr, Winchester DP. The National Cancer Data Base report on gastric cancer. *Cancer* 1995; **75**: 1734-1744
- Taal BG, van Loon HJ, Kahn N, de Jong D, Vasen HF, van 't Veer LJ. The role of genetic factors in the development of gastric cancer. *Ned Tijdschr Geneesk* 1999; **143**: 342-346
- Heiss MM, Babic R, Allgayer H, Gruetzner KU, Jauch KW, Loehrs U, Schildberg FW. The prognostic impact of the urokinase-type plasminogen activator system is associated with tumour differentiation in gastric cancer. *Eur J Surg Oncol* 1996; **22**: 74-77
- Wang MX. Pathological characteristics of early gastric cancer in 1477 Chinese patients. *Zhonghua Zhongliu Zazhi* 1993; **15**: 368-371
- Hyung WJ, Noh SH, Yoo CH, Huh JH, Shin DW, Lah KH, Lee JH, Choi SH, Min JS. Prognostic significance of metastatic lymphnode ratio in T3 gastric cancer. *World J Surg* 2002; **26**: 323-329
- Wang Z, Xu H, Wang S, Chen J. Relationship between new TNM classification and the prognosis and biological behavior of gastric cancer. *Zhonghua Waike Zazhi* 2000; **38**: 493-495
- Katai H, Yoshimura K, Maruyama K, Sasako M, Sano T. Evaluation of the New International Union Against Cancer TNM staging for gastric carcinoma. *Cancer* 2000; **88**: 1796-1800
- Lu C, Xu H, Zhang X. Judgement of gross type and local invasion of advanced gastric carcinoma by spiral computed tomography. *Zhonghua Zhongliu Zazhi* 2000; **22**: 235-237
- Jiang L, Shi M, Hao Y. Two-phase dynamic CT findings of gastric carcinoma and its value for tumor detection and gross classification. *Zhonghua Zhongliu Zazhi* 1998; **20**: 374-376
- Yang A, Lu X, Chen Y. The role of endoscopic ultrasonography and epidermal growth factor receptor assay in preoperative staging for gastric carcinoma. *Zhonghua Neike Zazhi* 1995; **34**: 743-746
- Stockbruegger RW. Bacterial overgrowth as a consequence of reduced gastric acidity. *Scand J Gastroenterol Suppl* 1985; **111**: 7-16
- Nakamura T, Nakano G. Histopathological classification and malignant change in gastric polyps. *J Clin Pathol* 1985; **38**: 754-764
- Muratani M, Nakamura T, Nakano GI, Mukawa K. Ultrastructural study of two subtypes of gastric adenoma. *J Clin Pathol* 1989; **42**: 352-359
- Zhao GH. Histopathological analysis of gastric polyps: classification and relationship to cancer. *Zhonghua Binglixue Zazhi* 1993; **22**: 279-281
- Zhao JS. Comparative pathologic study on the peri-ulcer mucosal lesion around benign and malignant gastric ulcer. *Zhonghua Zhongliu Zazhi* 1992; **14**: 357-359
- Xu MR. The relationship between bile acid and factors relative to gastric cancer. *Zhonghua Waike Zazhi* 1992; **30**: 719-721
- Au WY, Hui CH, Chan LC, Liang RH, Kwong YL. Clinicopathological features of megaloblastic anaemia in Hong Kong: a study of 84 Chinese patients. *Clin Lab Haematol* 1998; **20**: 217-219
- Zuidema PJ. A Chinese patient with pernicious anemia; a medical experience from the Indonesian period. *Ned Tijdschr Geneesk* 1996; **140**: 561-563
- Zhou XX. Relationship between gastric schistosomiasis and gastric cancer, chronic gastric ulcer and chronic gastritis: pathological analysis of 79 cases. *Zhonghua Binglixue Zazhi* 1986; **15**: 62-64
- Dekker W, Op Den Orth JO. Early gastric cancer. *Radiol Clin* 1977; **46**: 115-129
- Zhang B, Cai J, Chen G. Diagnosis and treatment of early gastric cancer: an experience from 61 cases. *Zhonghua Zhongliu Zazhi* 1999; **21**: 383-385
- Wang R. The epidemiological study of subtype risk factors of gastric cancer. *Zhonghua Liuxingbingxue Zazhi* 1993; **14**: 295-299

- 33 **Shan J**, Chen J, Wang S. Recurrence of early gastric cancer. *Zhonghua Yixue Zazhi* 1996; **76**: 750-752
- 34 **Macdonald JS**. Gastric cancer: chemotherapy of advanced Disease. *Hematol Oncol* 1992; **10**: 37-42
- 35 **Neugut AI**, Hayek M, Howe G. Epidemiology of gastric cancer. *Semin Oncol* 1996; **23**: 281-291
- 36 **Sun X**, Mu R, Zhou Y, Dai X, Qiao Y, Zhang S, Huangfu X, Sun J, Li L, Lu F. 1990-1992 mortality of stomach cancer in China. *Zhonghua Zhongliu Zazhi* 2002; **24**: 4-8
- 37 **Riecken B**, Pfeiffer R, Ma JL, Jin ML, Li JY, Liu WD, Zhang L, Chang YS, Gail MH, You WC. No impact of repeated endoscopic screens on gastric cancer mortality in a prospectively followed Chinese population at high risk. *Prev Med* 2002; **34**: 22-28
- 38 **Correa P**. Human gastric carcinogenesis: a multistep and multifactorial process-First American Cancer Society Award Lecture on Cancer Epidemiology and Prevention. *Cancer Res* 1992; **52**: 6735-6740
- 39 **Huang JQ**, Hunt RH. The evolving epidemiology of *Helicobacter pylori* infection and gastric cancer. *Can J Gastroenterol* 2003; **17** (Suppl): 18B-20
- 40 **Gill S**, Shah A, Le N, Cook EF, Yoshida EM. Asian ethnicity-related differences in gastric cancer presentation and outcome among patients treated at a canadian cancer center. *J Clin Oncol* 2003; **21**: 2070-2076
- 41 **Lee SA**, Kang D, Shim KN, Choe JW, Hong WS, Choi H. Effect of diet and *Helicobacter pylori* infection to the risk of early gastric cancer. *J Epidemiol* 2003; **13**: 162-168
- 42 **Kelley JR**, Duggan JM. Gastric cancer epidemiology and risk factors. *J Clin Epidemiol* 2003; **56**: 1-9
- 43 **La Vecchia C**, Franceschi S, Levi F. Epidemiological research on cancer with a focus on Europe. *Eur J Cancer Prev* 2003; **12**: 5-14
- 44 **El-Omar EM**, Chow WH, Rabkin CS. Gastric cancer and *H pylori*: Host genetics open the way. *Gastroenterology* 2001; **121**: 1002-1004
- 45 **Magnusson PKE**, Enroth H, Eriksson I, Held M, Nyren O, Engstrand L, Hansson LE, Gyllensten UB. Gastric cancer and human leukocyte antigen: distinct DQ and DR alleles are associated with development of gastric cancer and infection by *Helicobacter pylori*. *Cancer Res* 2001; **61**: 2684-2689
- 46 **Cox JM**, Clayton CL, Tomita T, Wallace DM, Robinson PA, Crabtree JE. cDNA array analysis of cag pathogenicity island-associated *Helicobacter pylori* epithelial cell response genes. *Infect Immun* 2001; **69**: 6970-6980
- 47 **Salama N**, Guillemin K, McDaniel TK, Sherlock G, Tompkins L, Falkow S. A whole-genome microarray reveals genetic diversity among *Helicobacter pylori* strains. *Proc Natl Acad Sci USA* 2000; **97**: 14668-14673
- 48 **Innocenti M**, Thoreson AC, Ferrero RL, Stromberg E, Bolin I, Eriksson L, Svennerholm AM, Quiding-Jarbrink M. *Helicobacter pylori*-induced activation of human endothelial cells. *Infect Immun* 2002; **70**: 4581-4590
- 49 **Huang JQ**, Hunt RH. Review article: *Helicobacter pylori* and gastric cancer-the clinicians' point of view. *Aliment Pharmacol Ther* 2000; **14**(Suppl 3): 48-54
- 50 **Achtman M**, Azuma T, Berg DE, Ito Y, Morelli G, Pan ZJ, Suerbaum S, Thompson SA, van der Ende A, van Doorn LJ. Recombination and clonal groupings within *Helicobacter pylori* from different geographical regions. *Mol Microbiol* 1999; **32**: 459-470
- 51 **Van Doorn LJ**, Figueiredo C, Megraud F, Pena S, Midolo P, Queiroz DM, Carneiro F, Pegado MD, Sanna R, De Boer W, Schneeberger PM, Correa P, Ng EK, Atherton J, Blaser MJ, Quint WG. Geographic distribution of vacA allelic types of *Helicobacter pylori*. *Gastroenterology* 1999; **116**: 823-830
- 52 **Deguchi R**, Takagi A, Kawata H, Inoko H, Miwa T. Association between CagA+ *Helicobacter pylori* infection and p53, bax and transforming growth factor-beta-RII gene mutations in gastric cancer patients. *Int J Cancer* 2001; **91**: 481-485
- 53 **Hiyama T**, Tanaka S, Kitadai Y, Ito M, Sumii M, Yoshihara M, Shimamoto F, Haruma K, Chayama K. p53 Codon 72 polymorphism in gastric cancer susceptibility in patients with *Helicobacter pylori*-associated chronic gastritis. *Int J Cancer* 2002; **100**: 304-308
- 54 **Tian SF**, Xiong YY, Yu SP, Lan J. Relationship between *Helicobacter pylori* infection and expressions of tumor suppressor genes in gastric carcinoma and related lesions. *Aizheng* 2002; **21**: 970-973
- 55 **Moss SF**, Sordillo EM, Abdalla AM, Makarov V, Hanzely Z, Perez-Perez GI, Blaser MJ, Holt PR. Increased gastric epithelial cell apoptosis associated with colonization with cagA + *Helicobacter pylori* strains. *Cancer Res* 2001; **61**: 1406-1411
- 56 **Shigeishi H**, Yokozaki H, Oue N, Kuniyasu H, Kondo T, Ishikawa T, Yasui W. Increased expression of CHK2 in human gastric carcinomas harboring p53 mutations. *Int J Cancer* 2002; **99**: 58-62
- 57 **Hiyama T**, Haruma K, Kitadai Y, Masuda H, Miyamoto M, Tanaka S, Yoshihara M, Shimamoto F, Chayama K. K-ras mutation in *Helicobacter pylori*-associated chronic gastritis in patients with and without gastric cancer. *Int J Cancer* 2002; **97**: 562-566
- 58 **El-Omar EM**, Carrington M, Chow WH, McColl KE, Bream JH, Young HA, Herrera J, Lissowska J, Yuan CC, Rothman N, Lanyon G, Martin M, Fraumeni JF Jr, Rabkin CS. The role of interleukin-1 polymorphisms in the pathogenesis of gastric cancer. *Nature* 2001; **412**: 99
- 59 **El-Omar EM**, Carrington M, Chow WH, McColl KE, Bream JH, Young HA, Herrera J, Lissowska J, Yuan CC, Rothman N, Lanyon G, Martin M, Fraumeni JF Jr, Rabkin CS. Interleukin-1 polymorphisms associated with increased risk of gastric cancer. *Nature* 2000; **404**: 398-402
- 60 **Machado JC**, Pharoah P, Sousa S, Carvalho R, Oliveira C, Figueiredo C, Amorim A, Seruca R, Caldas C, Carneiro F, Sobrinho-Simoes M. Interleukin 1B and interleukin 1RN polymorphisms are associated with increased risk of gastric carcinoma. *Gastroenterology* 2001; **121**: 823-829
- 61 **Figueiredo C**, Machado JC, Pharoah P, Seruca R, Sousa S, Carvalho R, Capelinha AF, Quint W, Caldas C, van Doorn LJ, Carneiro F, Sobrinho-Simoes M. *Helicobacter pylori* and interleukin 1 genotyping: an opportunity to identify high-risk individuals for gastric carcinoma. *J Natl Cancer Inst* 2002; **94**: 1680-1687
- 62 **He X**, Jiang L, Fu B, Zhang X. Relationship between interleukin-1B and interleukin-1 receptor antagonist gene polymorphisms and susceptibility to gastric cancer. *Zhonghua Yixue Zazhi* 2002; **82**: 685-688
- 63 **Kato S**, Onda M, Yamada S, Matsuda N, Tokunaga A, Matsukura N. Association of the interleukin-1 beta genetic polymorphism and gastric cancer risk in Japanese. *J Gastroenterol* 2001; **36**: 696-699
- 64 **Song CF**, Sun LP, Dai WY, Yuan Y. Significance of serum level of NO and IL-8 in *Helicobacter pylori* associated gastric diseases. *Zhonghua Zhongliu Zazhi* 2003; **25**: 258-260
- 65 **Shi T**, Liu WZ, Gao F, Xiao SD. The role of nuclear factor kappa B in secretion of interleukin-8 by gastric cancer cell line SGC 7901 induced by *Helicobacter pylori*. *Zhonghua Yixue Zazhi* 2003; **83**: 133-136
- 66 **Yea SS**, Yang YI, Jang WH, Lee YJ, Bae HS, Paik KH. Association between TNF-alpha promoter polymorphism and *Helicobacter pylori* cagA subtype infection. *J Clin Pathol* 2001; **54**: 703-706
- 67 **Lanas A**, Garcia-Gonzalez MA, Santolaria S, Crusius JB, Serrano MT, Benito R, Pena AS. TNF and LTA gene polymorphisms reveal different risk in gastric and duodenal ulcer patients. *Genes Immun* 2001; **2**: 415-421
- 68 **Wu MS**, Wu CY, Chen CJ, Lin MT, Shun CT, Lin JT. Interleukin-10 genotypes associate with the risk of gastric carcinoma in Taiwanese Chinese. *Int J Cancer* 2003; **104**: 617-623
- 69 **Oda Y**, Kobayashi M, Ooi A, Muroishi Y, Nakanishi I. Genotypes of glutathione S-transferase M1 and N-acetyltransferase 2 in Japanese patients with gastric cancer. *Gastric Cancer* 1999; **2**: 158-164
- 70 **Setiawan VW**, Zhang ZF, Yu GP, Lu QY, Li YL, Lu ML, Wang MR, Guo CH, Yu SZ, Kurtz RC, Hsieh CC. GSTP1

- polymorphisms and gastric cancer in a high-risk Chinese population. *Cancer Causes Control* 2001; **12**: 673-681
- 71 **Park WS**, Lee JH, Shin MS, Park JY, Kim HS, Kim YS, Park CH, Lee SK, Lee SH, Lee SN, Kim H, Yoo NJ, Lee JY. Inactivating mutations of KILLER/DR5 gene in gastric cancers. *Gastroenterology* 2001; **121**: 1219-1225
- 72 **Tsukino H**, Kuroda Y, Qiu D, Nakao H, Imai H, Katoh T. Effects of cytochrome P450 (CYP) 2A6 gene deletion and CYP2E1 genotypes on gastric adenocarcinoma. *Int J Cancer* 2002; **100**: 425-428
- 73 **Ikonen T**, Matikainen M, Mononen N, Hyytinen ER, Helin HJ, Tammola S, Tammela TL, Pukkala E, Schleutker J, Kallionzemi OP, Koivisto PA. Association of E- polymorphism cadherin germ-line alterations with prostate cancer. *Clin Cancer Res* 2001; **7**: 3465-3471
- 74 **Machado JC**, Soares P, Carneiro F, Rocha A, Beck S, Blin N, Berx G, Sobrinho-Simoes M. E-cadherin gene mutations provide a genetic basis for the phenotypic divergence of mixed gastric carcinomas. *Lab Invest* 1999; **79**: 459-465
- 75 **Ebert MP**, Fei G, Kahmann S, Muller O, Yu J, Sung JJ, Malfertheiner P. Increased beta-catenin mRNA levels and mutational alterations of the APC and beta-catenin gene are present in intestinal-type gastric cancer. *Carcinogenesis* 2002; **23**: 87-91
- 76 **Tebbutt NC**, Giraud AS, Inglese M, Jenkins B, Waring P, Clay FJ, Malki S, Alderman BM, Grail D, Hollande F, Heath JK, Ernst M. Reciprocal regulation of gastrointestinal homeostasis by SHP2 and STAT-mediated trefoil gene activation in gp130 mutant mice. *Nat Med* 2002; **8**: 1089-1097
- 77 **Wang TC**, Goldenring JR. Inflammation intersection: gp130 balances gut irritation and stomach cancer. *Nat Med* 2002; **8**: 1080-1082
- 78 **Suemori S**, Lynch-Devaney K, Podolsky DK. Identification and characterization of rat intestinal trefoil factor: tissue- and cell-specific member of the trefoil protein family. *Proc Natl Acad Sci USA* 1991; **88**: 11017-11021
- 79 **Beck S**, Sommer P, Blin N, Gott P. 5'-flanking motifs control cell-specific expression of trefoil factor genes (TFF). *Int J Mol Med* 1998; **2**: 353-361
- 80 **Dossinger V**, Kayademir T, Blin N, Gott P. Down-regulation of TFF expression in gastrointestinal cell lines by cytokines and nuclear factors. *Cell Physiol Biochem* 2002; **12**: 197-206
- 81 **Park WS**, Oh RR, Park JY, Lee JH, Shin MS, Kim HS, Lee HK, Kim YS, Kim SY, Lee SH, Yoo NJ, Lee JY. Somatic mutations of the trefoil factor family 1 gene in gastric cancer. *Gastroenterology* 2000; **119**: 691-698

Science Editor Guo SY Language Editor Elsevier HK

• *Helicobacter pylori* •

Gastrin and antral G cells in course of *Helicobacter pylori* eradication: Six months follow up study

Aleksandra Sokic-Milutinovic, Vera Todorovic, Tomica Milosavljevic, Marjan Micev, Neda Drndarevic, Olivera Mitrovic

Aleksandra Sokic-Milutinovic, Tomica Milosavljevic, Clinic for Gastroenterology and Hepatology, Institute for Digestive Diseases, Clinical Center of Serbia, Serbia and Montenegro
Vera Todorovic, Neda Drndarevic, Olivera Mitrovic, Department of Immunohistochemistry and Electron Microscopy, Institute for Medical Research, Belgrade, Serbia and Montenegro
Marjan Micev, Pathology Department, Institute for Digestive Diseases, Clinical Center of Serbia, Serbia and Montenegro
Supported by a Grant From Serbian Ministry for Science, Technology and Development, No. 1752
Correspondence to: Aleksandra Sokic-Milutinovic, MD, MSc, Clinical Center of Serbia, Clinic for Gastroenterology and Hepatology, Koste Todorovica 6, Belgrade 11000, Serbia and Montenegro. asokic2002@yahoo.com
Telephone: +381-11-3617777-3734 Fax: +381-11-361-5432
Received: 2004-10-13 Accepted: 2004-11-23

(416±40 and 0.48±0.09). No significant change of the G cell/total endocrine cell ratio was observed during the 6 mo of follow up in any of the groups. A reversible increase in G cell secretory function was seen in all infected individuals, demonstrated by a more prominent secretory apparatus. However, differences between DU and gastritis group were identified.

CONCLUSION: *H pylori* infection induces antral G cell hyperfunction resulting in increased gastrin synthesis and secretion. After eradication therapy complete morphological and functional recovery is observed in patients with gastritis. In the DU patients some other factors unrelated to the *H pylori* infection influence antral G cell morphology and function.

© 2005 The WJG Press and Elsevier Inc. All rights reserved.

Abstract

AIM: To assess long-term effects of *Helicobacter pylori* (*H pylori*) eradication on antral G cell morphology and function in patients with and without duodenal ulcer (DU).

METHODS: Consecutive dyspeptic patients referred to the endoscopy entered the study. Out of 39 *H pylori* positive patients, 8 had DU (*H pylori* +DU) and 31 gastritis (*H pylori* +G). Control groups consisted of 11 uninfected dyspeptic patients (CG1) and 7 healthy volunteers (CG2). Basal plasma gastrin (PGL), antral tissue gastrin concentrations (ATGC), immunohistochemical and electron microscopic characteristics of G cells were determined, prior to and 6 mo after therapy.

RESULTS: We demonstrated elevated PGL in infected patients compared to uninfected controls prior to therapy. Elevated PGL were registered in all *H pylori*+patients (*H pylori* +DU: 106.78±22.72 pg/mL, *H pylori* +G: 74.95±15.63, CG1: 68.59±17.97, CG2: 39.24±5.59 pg/mL, $P<0.01$). Successful eradication (e) therapy in *H pylori*+patients lead to significant decrease in PGL (*H pylori*+DU: 59.93±9.40 and *H pylori* +Ge: 42.36±10.28 pg/mL, $P<0.001$). ATGC at the beginning of the study were similar in infected and uninfected patients and eradication therapy lead to significant decrease in ATGC in *H pylori* +gastritis, but not in DU patients. In the *H pylori* +DU patients, the mean number of antral G cells was significantly lower in comparison with all other groups ($P<0.01$), but after successful eradication was close to normal values found in controls. By contrast, G cell number and volume density were significantly decreased ($P<0.01$) in *H pylori* +Ge group after successful eradication therapy (294±32 and 0.31±0.02, respectively), in comparison to values before eradication

Key words: Gastrin; G cell; Duodenal ulcer; Gastritis; *Helicobacter pylori*

Sokic-Milutinovic A, Todorovic V, Milosavljevic T, Micev M, Drndarevic N, Mitrovic O. Gastrin and antral G cells in course of *Helicobacter pylori* eradication: Six months follow up study. *World J Gastroenterol* 2005; 11(27): 4140-4147
<http://www.wjgnet.com/1007-9327/11/4140.asp>

INTRODUCTION

Helicobacter pylori (*H pylori*) causes chronic active type B gastritis and is involved in the pathogenesis of peptic ulcer disease (PUD) and gastric cancer^[1]. PUD symptoms were almost immediately attributed to the presence of *H pylori* infection, however a positive correlation between the infection and non-ulcer dyspepsia (NUD) was acknowledged only after the results of meta-analysis^[2]. NUD should be considered in dyspeptic patients when symptoms persist for at least a month and endoscopy reveals neither peptic ulcer nor signs of gastric cancer^[3].

Gastrin is a secretory product of antral and duodenal G cells. Two main forms of gastrin (gastrin-17 and -34) are present in the circulation. About 95% of antral gastrin is gastrin-17^[3,4]. Stimuli for gastrin secretion are well identified and include food intake, presence of digested amino acids in the lumen, cholinergic stimuli, and antral alkalization^[3,4].

Although elevated serum gastrin levels are frequently observed in individuals with chronic *H pylori* infection^[5-7], its pathophysiological significance in gastric mucosal inflammation remains unclear. Gastrin is capable of

up-regulating CXC chemokines in gastric epithelial cells and therefore may contribute to the progression of the inflammatory process in the stomach⁸. Chronic hypergastrinemia is also associated with gastric argiophil cell hyperplasia in rats and humans and carcinoid tumor in Mongolian gerbils⁹. In the antrum of *H pylori* infected gerbils and humans enhanced apoptosis is an early and transient cell cycle event whilst epithelial cell proliferation peaks later and is related to increased gastrin levels. Based on these findings it was suggested that gastrin-dependent mechanism might be responsible for epithelial cell growth in *H pylori* colonized gastric mucosa^{10,11}. It can be assumed that restored antral G cell function after *H pylori* eradication resulting in lower basal and meal-stimulated gastrin release would be a desirable event in both chronic gastritis and PUD. Most studies conducted so far focused on the effects of *H pylori* infection on gastric endocrine cells in patients with duodenal ulcer and came to different conclusions^{5,6}. There have been few reports concerning G cell morphology¹²⁻¹⁴ and/or gastrin secretion⁷ in patients with gastritis.

The aim of our study was to investigate changes in antral G cell morphology and function in dyspeptic patients with *H pylori* infection and its possible restoration in course of eradication therapy.

MATERIALS AND METHODS

Patients

We conducted an outpatient based prospective study in the Clinic for Gastroenterology and Hepatology, Clinical Center of Serbia, lasting for 6 mo after patients completed eradication therapy. Fifty consecutive dyspeptic patients referred to the endoscopy and seven healthy asymptomatic volunteers entered the study. Out of 39 *H pylori* positive patients had 31 histological signs of gastritis- *H pylori* +G and 8 DU- *H pylori* +DU. Control group 1 (CG1) consisted of 11 *H pylori* negative dyspeptic patients while 7 healthy asymptomatic volunteers were assigned to the control group 2 (CG2). All patients gave informed consent and the study protocol was approved by the local Ethics Committee. Mean age was 48±15 years (28 males and 22 females), 21 were smokers and 21 had personal history of PUD. Exclusion criteria were in concordance with the recommendations from European *H pylori* Study Group¹⁵. *H pylori* infection was diagnosed by rapid urease test (RUT), histology and serology. A patient was defined as *H pylori* positive if histology and at least one of the other applied diagnostic methods were positive.

Diagnostic methods

Routine endoscopy and biopsy samples Upper endoscopy was performed before therapy in all dyspeptic patients and repeated 6 mo after appropriate therapy. In healthy volunteers (CG2) endoscopy was performed only once. During endoscopy antral biopsy specimens, intended for routine histology, RUT test, determination of tissue gastrin levels, immunohistochemistry and electron microscopy were taken.

***H pylori* serology** Blood samples were taken from the patients after endoscopic examination and sera were

separated by centrifugation and stored at -20 °C until analyzed. The concentration of anti- *H pylori* IgG antibodies was analyzed using the Pyloriset EIA-G IIITM (Orion Diagnostica, Finland), according to the manufacturers' instructions.

Therapy A triple eradication therapy consisting of omeprazole 20 mg twice a day (bid), amoxicillin 1 000 mg b.i.d. and metronidazole 500 mg b.i.d. was administered for 7 d in patients with *H pylori* infection. In uninfected patients, symptomatic therapy consisting of antacids, H₂ antagonists or proton pump inhibitors (PPIs) was prescribed for 2 wks. In the course of *H pylori* eradication, the disappearance of spiral bacteria from antral and corpus gastric mucosa, according to a negative RUT and histological examination, were observed.

Histological assessment Biopsies from antral and corpus mucosa were stained using hematoxylin- eosin and modified Giemsa staining procedure. Biopsy specimens were assessed according to the Sydney System^{16,17} by a single, experienced pathologist who was blinded to the clinical presentation, endoscopic data and RUT results of the patient.

Assessment of plasma and tissue gastrin levels

Plasma preparation Full blood samples for estimating fasting plasma gastrin levels were placed in ice/chilled tubes (5 mL) containing EDTA (2 mg) and proteinase inhibitor (Trasyol, 2 500 KIU). Plasma was extracted using standard procedure and stored below -70 °C until further analysis.

Tissue extract preparation Each antral mucosa biopsy was washed with saline solution, measured and placed in to the tube together with 1 mL of distilled water. Gastrin extraction was performed in water bath on 95 °C for 10 min, supernatant collected and after cooling stored below -70 °C until further analysis.

Radioimmunoassay procedure (RIA) Plasma and tissue gastrin was determined under basal conditions using RIA protocol provided by Affiniti (UK) with rabbit antihuman gastrin-17 antiserum. Final dilutions were for plasma 1:100 000 and for the tissue 1:500 000. Intra-assay and inter-assay coefficients were 9.0 and 8.4 respectively. Sensitivity of the method was 1 pmol/L.

Evaluation of antral G cells

Immunohistochemistry Two antral biopsies from each patient were used for immunohistochemistry and light microscopic morphometry. These were fixed with 10% buffered formalin and embedded in paraffin in the usual manner. Only well-oriented antral mucosa biopsies that allowed assessment of the full mucosal thickness were studied. The sections were stained with different immunohistochemical methods in order to identify antral gastrin-producing cells and evaluate the ratio of antral G cells/all antral endocrine cells. Immunohistochemical staining for G cells was performed using rabbit anti human gastrin-17 (1:300 dilution, Code No A0568, DAKO A/S, Denmark) and peroxidase-labeled streptavidin biotin method (DAKO LSAB+/HRP, DAKO A/S, Denmark). In addition, sections were double immunostained with both polyclonal antibody to gastrin mentioned above and mAb to synaptophysin (1:50 dilution, Code No. A0010,

DAKO A/S, Denmark), using DAKO EnVision[®] double stain system (Code No. K1395). For double immunostaining, antisynaptophysin antibody was applied first with DAB as a chromogen, followed by antigastrin-17 antibody as the second antibody, with AEC as a chromogen. Negative controls were conjugated with normal horse serum^[18].

Routine electron microscopy The biopsy specimens of antral mucosa were immediately placed in a mixture of 2% glutaraldehyde in 0.2 mol/L sodium cacodylate buffer, pH 7.4, and fixed in the same fixative for 20 h at 4 °C. After postfixation for 1 h in 1% osmium tetroxide in cacodylate buffer, the specimens were dehydrated in graded ethanol and embedded in Epon 812[®], with mucosa surface perpendicular to the cutting surface. The blocks were sectioned with an LKB ultratome II. Ultra thin sections were double-stained with uranyl acetate and lead-citrate before examination in an Opton 109 electron microscope.

Morphometric analysis of G cells detected by immunohistochemistry Three 5-µm thick immunostained sections of antral mucosa at intervals of 50 µm were analyzed. Weibel multipurpose test system containing 42 points and 21 lines was used for evaluation of volume density and number of G cells^[19,20]. The total number of G cells per mm² of antral mucosa, as well as, ratio of antral G/total antral endocrine cells was calculated by examination of single or double immunostained sections. All sections were examined randomly by two histologists.

Morphometric analysis of G cells detected by electron microscopy G cells were identified as described previously^[21]. Morphometric analysis was performed using the methods described previously^[19,20]. Cell profile areas were estimated by drawings of G-cells using Camera Lucida attached to a Reichert microscope and analyzed with an image analyzing system (MOP 3 Video plan; Carl Zeiss)^[19,20].

Statistical analysis

Each time mean and SD was calculated for results presentation. A two sample paired or unpaired Student's *t*-test and Wilcoxon rank sum test and ANOVA were used. A *P* value less than 0.05 was considered significant.

RESULTS

Clinical data

Clinical and demographic characteristics of the patients are shown in Table 1. Out of 39 *H pylori*-positive patients

eradication therapy was successful in 32 (82.1%). In all DU patients the infection was successfully treated, together with 24 patients with gastritis (*H pylori* +Ge). In seven patients with gastritis eradication therapy failed (*H pylori* +Gne). No significant difference in demographic and clinical data between *H pylori*+Gne and *H pylori*+Ge patients was observed.

Basal plasma gastrin levels (PGL)

Basal plasma gastrin-17 levels were compared between groups of patients at the beginning of the study. These findings are shown in Figure 1. PGL in *H pylori*+DU patients were significantly higher at the beginning of the study than in any other group of patients irrespective of the presence of infection (*H pylori* +DU: 106.78±22.72 pg/mL vs *H pylori* +Ge: 74.95±15.63, *H pylori*+Gne: 74.21±10.99, CG1: 68.59±17.97 and CG2: 39.24±5.59 pg/mL, *P*<0.001). Healthy asymptomatic controls (CG2) had significantly lower plasma gastrin levels than all other dyspeptic patients (*P*<0.01). After 6 mo, statistically significant decrease of PGL were observed in all successfully eradicated patients (*H pylori*+DU: 59.93±9.40 and *H pylori*+Ge: 42.36±10.28 pg/mL, *P*<0.001). However, no significant change was seen in other groups (*H pylori*+Gne: 76.81±19.54 and CG1: 58.29±17.97 pg/mL, *P*>0.05).

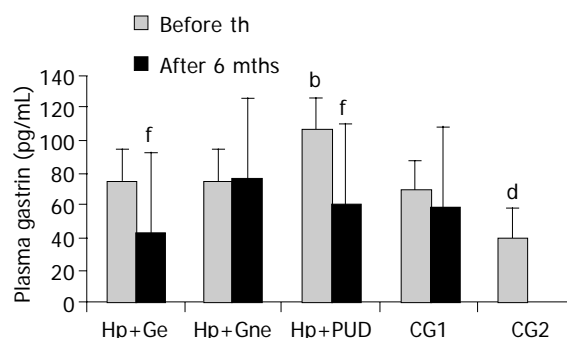


Figure 1 Basal plasma gastrin levels in patients with and without duodenal ulcer before and after eradication of *H pylori* infection. *H pylori*+Ge-*H pylori*+eradicated patients with gastritis; *H pylori*+Gne-*H pylori*+non eradicated patients with gastritis; *H pylori*+DU- patients with *H pylori*+duodenal ulcer; CG1- *H pylori* negative dyspeptic patients; CG2- asymptomatic volunteers; th-therapy; mths-months; ^b*P*<0.001 in *H pylori*+DU vs all other groups, ^d*P*<0.01 in CG2 vs all other groups, ^f*P*<0.001 before vs after eradication therapy.

Table 1 Clinic and demographic data in *H pylori* positive patients with DU and gastritis and in the control groups at the beginning of the study

	<i>H pylori</i> +Ge (n = 24)	<i>H pylori</i> + Gne (n = 7)	<i>H pylori</i> +DU (n = 8)	CG1 (n = 11)	CG2 (n = 7)	<i>P</i>
Age (yr)	47±13	48±9	47±23	47±19	33±11	NS
Sex (males)	13	1	2	5	2	NS
Smokers	8	3	2	4	4	NS
Alcohol intake	12	3	1	1	1	NS
PH of PUD	8	0	6	7	0	NS
FH of PUD	11	3	5	6	3	NS

H pylori +Ge-*H pylori*+eradicated patients with gastritis; *H pylori*+Gne-*H pylori*+non eradicated patients with gastritis; *H pylori* +DU- patients with *H pylori*+duodenal ulcer; CG1-*H pylori* negative dyspeptic patients; CG2- asymptomatic volunteers; PUD -peptic ulcer disease; PH-personal history; FH- family history; NS-not statistically significant.

Basal tissue gastrin concentrations

At the beginning of the study there was no significant difference ($P>0.05$) in antral tissue gastrin concentrations (ATGC) between groups of infected (*H pylori*+Ge: 0.23 ± 0.05 , *H pylori*+Gne: 0.23 ± 0.05 , *H pylori*+DU: 0.24 ± 0.03 pg/g wet weight) and uninfected patients (CG1: 0.22 ± 0.04 and CG2: 0.24 ± 0.03 pg/g wet weight). After successful eradication therapy significant decrease in ATGC was observed only in *H pylori*+Ge group (0.20 ± 0.05 pg/g wet weight, $P<0.05$), while in *H pylori*+DU group no significant change was observed (0.22 ± 0.04 pg/wet weight, $P>0.05$). ATGC in the *H pylori*+Gne and CG1 did not change significantly (0.26 ± 0.07 and 0.26 ± 0.06 pg/g wet weight, respectively, $P>0.05$). These findings are seen in Figure 2.

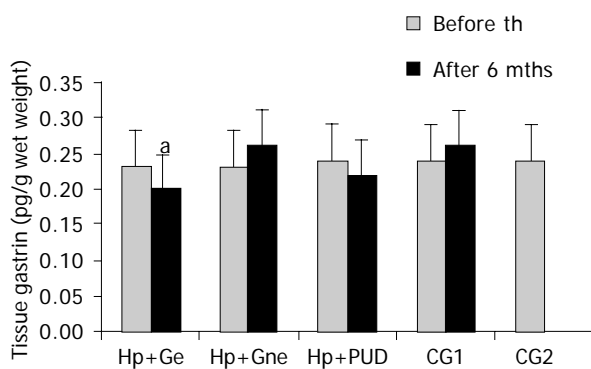


Figure 2 Antral tissue gastrin levels in patients with and without duodenal ulcer before and after eradication of *H pylori* infection. *H pylori* +Ge-*H pylori*+eradicated patients with gastritis; *H pylori*+Gne-*H pylori*+non eradicated patients with gastritis; *H pylori* +DU-patients with *H pylori*+duodenal ulcer; CG1- *H pylori* negative dyspeptic patients; CG2- asymptomatic volunteers; th-therapy; mths-months.

Antral G cell number

Antral G cell number was expressed as number of identified G cells per mm² of antral mucosa, G cell volume density (%) and a ratio of antral G/total antral endocrine cell count (Table 2). Antral G cell number remained unchanged after

6 mo of follow-up in *H pylori*+Gne (405 ± 32 vs 432 ± 18), CG1 (413 ± 61 vs 428 ± 80) and CG2 (426 ± 57) patients. In the *H pylori*+DU patients mean number of antral G cells per mm² of mucosa was lower at the beginning of the study (292 ± 20) than in any other group analyzed ($P<0.01$). At the end of the follow-up and after successful eradication of *H pylori* infection number of antral G cells identified in DU patients was increased (400 ± 32) and comparable to both control groups (CG1 and CG2). By contrast, in patients with gastritis successful treatment lead to a decrease in both antral G cell number (416 ± 40 vs 294 ± 32 , $P<0.01$) and volume density (0.48 ± 0.09 vs 0.31 ± 0.02 , $P<0.01$), as seen in Figure 3. However, no significant change of the G cell/ total endocrine cell ratio was observed during the 6 mo of follow up in any of the groups, including *H pylori* +Ge group (Figure 4).

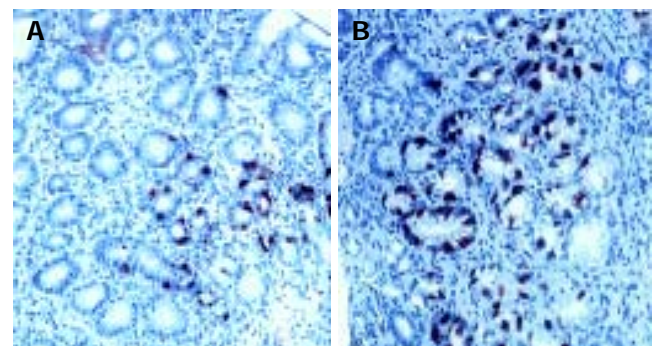


Figure 3 Pyloric gland area of *H pylori* associated gastritis before (A) and after eradication (B) therapy. DAKO LSAB+ immunohistochemical staining and diaminobezidine (DAB) as chromogen; x20 (A) and x10 (B). There is evident lower gastrin cell number after successful eradication therapy.

Ultrastructural morphometric analysis of gastric antral G cell

Ultrastructural characteristics of antral G cells in healthy controls (Figure 5) and dyspeptic patients (Figure 6) before and after therapy were assessed using electron microscopy morphometric study (Table 3). Electron microscopy revealed

Table 2 Antral G cell in dyspeptic patients before and after eradication therapy-morphometric analysis on light microscopy

	<i>H pylori</i> +Ge (n = 24)	<i>H pylori</i> +Gne (n = 7)	<i>H pylori</i> +DU (n = 8)	CG1 (n = 11)	CG2 (n = 7)	P
G cell number (per mm² of antral mucosa)						
Before therapy	416±40	405±32	292±20 ^a	413±61	426±57	0.05 ^a
After therapy	294±32 ^a	432±18	400±32 ^b	428±80	/	NS
P	0.05 ^a	NS	0.01 ^b	NS	/	
G cell volume density (%)						
Before therapy	0.48±0.09	0.43±0.11	0.42±0.02	0.48±0.03	0.44±0.02	NS
After therapy	0.31±0.02 ^a	0.40±0.04	0.43±0.01	0.50±0.03	/	NS
P	0.05	NS	NS	NS	/	
Antral G/ total antral endocrine cells ratio						
Before therapy	0.44±0.04	0.40±0.03	0.37±0.05	0.44±0.29	0.45±0.07	NS
After therapy	0.44±0.02	0.47±0.07	0.41±0.07	0.44±0.37	/	NS
P	NS	NS	NS	NS	/	

H pylori +Ge- *H pylori*+eradicated patients with gastritis; *H pylori*+Gne-*H pylori*+non eradicated patients with gastritis; *H pylori*+DU-patients with *H pylori*+duodenal ulcer; CG1-*H pylori* negative dyspeptic patients; CG2- asymptomatic volunteers; NS- $P>0.05$; ^a $P<0.05$; ^b $P<0.01$.

Table 3 Ultrastructural characteristics of antral G cell in dyspeptic patients before and after therapy assessed by electron microscopy morphometric study

Antral G cell	<i>H pylori</i> +Ge (n = 24)	<i>H pylori</i> +Gne (n = 7)	<i>H pylori</i> +DU (n = 8)	CG1 (n = 11)	CG2 (n = 7)	P
Number of cells analyzed						
Before therapy	93	30	33	55	37	
After therapy	113	31	30	47		
Cell profile surface (μm^2)						
Before therapy	142 \pm 14	138 \pm 20	188 \pm 14 ^a	130 \pm 10	136 \pm 10	0.05 ^a
After therapy	140 \pm 15	133 \pm 12	138 \pm 10 ^d	133 \pm 12	/	NS
P	NS	NS	0.001 ^d	NS	/	
Endoplasmatic reticulum (μm^2) (profile surface)						
Before therapy	6.9 \pm 2.3 ^a	6.2 \pm 2.3	17.9 \pm 2.3 ^b	5.3 \pm 0.9	5.5 \pm 0.9	^a 0.05; ^b 0.01
After therapy	5.0 \pm 2.3	6.0 \pm 1.0	5.7 \pm 1.3 ^d	5.5 \pm 0.7		NS
P	NS	NS	0.001 ^d	NS		
Volumen density of cytoplasmic granules						
Before therapy	17.3 \pm 1.9 ^a	13.1 \pm 3.2	47.0 \pm 4.9 ^b	14.6 \pm 2.7	13.6 \pm 2.7	^a 0.05; ^b 0.01
After therapy	9.7 \pm 1.1 ^b	14.2 \pm 3.1	17.3 \pm 1.9	13.2 \pm 2.0	/	NS
P	0.01 ^b	NS	NS	NS	/	
Number of cytoplasmic granules/cell profile						
Before therapy	232 \pm 18 ^a	199 \pm 34	330 \pm 13 ^b	190 \pm 37	196 \pm 21	^a 0.05; ^b 0.01
After therapy	180 \pm 13	202 \pm 45	220 \pm 31	196 \pm 20	/	NS
P	NS	NS	NS	NS	/	
Mean diameter of cytoplasmic granules (nm)						
Before therapy	220 \pm 23	245 \pm 11	327 \pm 23 ^a	237 \pm 4	227 \pm 7	0.01 ^a
After therapy	223 \pm 23	229 \pm 22	257 \pm 21 ^b	223 \pm 9	/	NS
P	NS	NS	0.01 ^b	NS	/	
Golgi apparatus (μm^2) (profile surface)						
Before therapy	2.9 \pm 0.10 ^b	2.10 \pm 0.3	3.33 \pm 0.10 ^a	2.11 \pm 0.33	2.05 \pm 0.23	0.01 ^a
After therapy	2.15 \pm 0.10	2.23 \pm 0.2	2.20 \pm 0.11 ^b	2.20 \pm 0.22	/	NS
P	0.01 ^b	NS	0.01 ^b	NS	/	

^aP<0.05, ^bP<0.01, ^dP<0.001 vs others.

changes in antral G cell morphology in all *H pylori*+patients. Namely, more prominent endoplasmatic reticulum (Figure 6B) and Golgi apparatus together with an increase in number and volume density of cytoplasmic granules (Figure 6A) were identified in all *H pylori* infected individuals. Antral G cells of *H pylori*+DU patients, however, exhibited some specific features, such as increased cell profile surface and increased mean diameter of cytoplasmic granules. It was

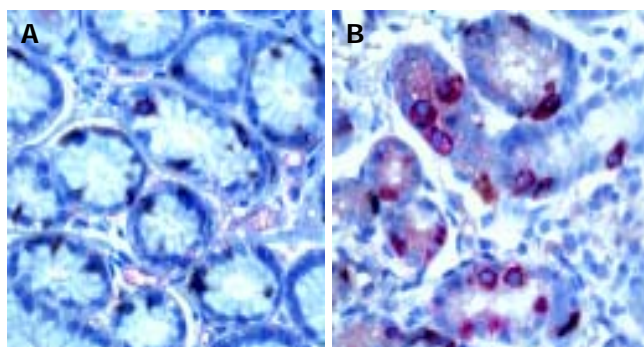


Figure 4 Synaptophysin and gastrin double immunostaining in pyloric gland of *H pylori*-associated gastritis before (A) and after (B) eradication therapy. DAKO EnVision double stain method; DAB is chromogen for G cells and aminoethylcarbazole (AEC) is chromogen for synaptophysin containing endocrine cells. x20 (A) and x10 (B). G cells (red)/ other endocrine cells (brown) ratio is equal before (A) and after (B) succesful eradication of *H pylori* infection.

also found that G cells in DU patients, in comparison with healthy controls, have an increased proportion of dense core granules. In *H pylori*+Ge patients more granules per profile and higher volumen density, but similar diameter of secretory granules was identified when compared to the CG1 patients.

After successful eradication all those alterations were normalized and G cell ultrastructurally resembled to those found in CG2 group, with the exception of the diameter and volume density of cytoplasmic granules that remained higher in the *H pylori* +DU patients.

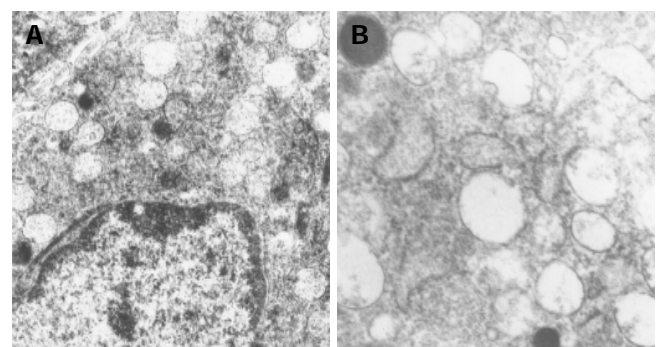


Figure 5 Electron micrographs of gastrin producing cells from healthy persons antral mucosa. Normal ultrastructure is characterized by the presence of numerous secretory granules of different electron density. Uranyl acetate, lead citrate; x8 400 (A) and x12 680 (B).

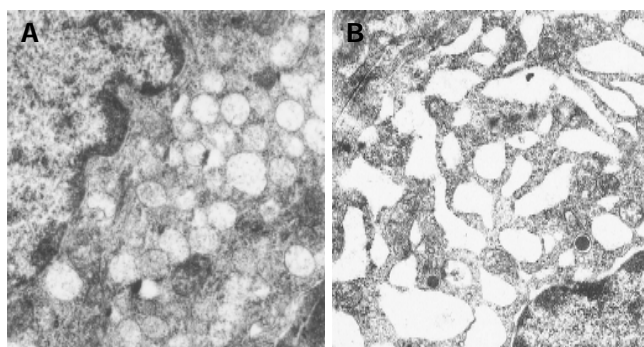


Figure 6 Electron micrographs of gastrin producing cells from *H pylori* infected individuals with gastritis (A) and duodenal ulcer (B) before eradication therapy. Uranyl acetate, lead citrate; x8 400 (both A and B). Note that total number of granules is higher than in controls and that dense core granules are more numerous in *H pylori*+patient with gastritis (A). Endoplasmic reticulum is very prominent in *H pylori*+patient with duodenal ulcer.

DISCUSSION

In our study, eradication therapy was successful in 82% (32/39) of all *H pylori* infected patients, all DU (100%, 8/8), and 77% of patients (24/31) with gastritis that accords with previously proposed acceptable eradication rate of approximately 80%^[2,22]. Eradication rate in our study is in line with results obtained with this eradication protocol that is, according to the literature, ranging from 53–81%^[23,24].

It is well known that *H pylori* leads to chronic gastritis and affects gastric acid secretion in virtually all infected individuals. The underlying mechanism responsible for changes in gastric acid secretion in *H pylori* infected individuals is not completely explained, however it is probably a result of impaired gastrin and somatostatin secretion and elevated proinflammatory cytokines in the infected gastric mucosa^[8,22,25]. Gastrin secretion and morphofunctional features of antral G cells in patients with *H pylori* infection and gastritis or DU was scarcely studied using a comparative study, before and after eradication of the infection.

In the present study, healthy asymptomatic individuals (CG2) had significantly lower plasma gastrin levels than all dyspeptic patients. Higher gastrin concentrations were registered in the plasma of *H pylori* infected individuals, both with gastritis and especially when duodenal ulcer was found on endoscopy. After 6 mo, significant decrease in plasma gastrin levels was registered in all successfully eradicated patients. However, no significant change was seen in other groups, including noneradicated patients with gastritis (*H pylori*+Gne) and dyspeptic patients without *H pylori* infection (CG1).

Higher basal plasma gastrin levels in *H pylori* infected patients and animals compared to the uninfected controls were previously reported by different authors^[3–6,10,25]. Our results showed that in infected patients with DU have significantly higher plasma levels of gastrin-17 when compared to *H pylori*+patients with gastritis, as was previously demonstrated both in adults by Kamada *et al.*^[26], and in children by Kato *et al.*^[27], but opposed to the results of other studies^[14]. After successful eradication of *H pylori* infection, plasma gastrin levels decreased markedly in both DU and gastritis patients, as demonstrated previously in adults^[1,26,28–30] and pediatric patients^[27,31] by other authors.

This change was not observed in non-eradicated patients and uninfected dyspeptic controls, implicating that decrease in plasma gastrin is directly related to the eradication of the bacterium from the stomach.

Antral tissue gastrin concentrations at the beginning of our study were similar in both infected (DU and gastritis group) and uninfected patients, as in other studies^[31,32]. Successful eradication therapy lead to a significant decrease in antral tissue gastrin concentrations in patients with gastritis, as seen in other studies^[33], but not in DU patients.

Immunohistochemical and ultrastructural examination of G cell morphology at the beginning of the study revealed significantly lower antral G cell number in *H pylori*+DU patients compared to all the other groups. However, after successful eradication antral G cell number was close to values observed in controls (both CG1 and CG2). By contrast, successful eradication therapy lead to a decrease in G cell number in the antrum of infected patients with gastritis. On the other hand no significant change in gastrin/total endocrine cell ratio was observed during the 6 mo of follow up, neither in infected nor uninfected patients.

Majority of authors agree that there is no significant difference in antral G cell number in infected and uninfected patients before therapy^[11,26,28,31,32]. Yacoub *et al.*, in a similar study, did not find differences in antral G, D, and EC cell densities and G/D, G/EC and D/EC cell ratios in DU patients^[13] compared to controls. On the other hand, a study by Chamouard *et al.*^[34], showed significantly lower number of antral G cells in DU patients, that is in agreement with the results of our study. The decrease in antral G cell number in subjects with DU (that can also correspond to the degranulation of very active gastrin-producing cells resulting in profound hypergastrinemia) could be related to the fact that the number of bacteria and/or severity of antral gastritis is greater in DU patients. Other possible explanation could be related to differences in *H pylori* strains that colonize the antrum of patients with DU. Namely, we previously reported that in Serbia and Montenegro there is high seroprevalence of *cagA*-positive *H pylori* strains in dyspeptic patients with and without peptic ulcer, while *VacA*-positive strains are more closely related to peptic ulcer disease^[35]. However, Gaider *et al.*, found *CagA*+ strains in 78% patients with *H pylori* infection and DU and described the absence of *CagA*+strains in individuals with antral G-cell hyperplasia^[36].

Based on the ultrastructural findings, we propose that in the *H pylori* +DU patients strongly stimulated remaining antral G cells, as a result of a compensatory mechanism, develop a strong synthetic and secretory phenotype before eradication therapy. In addition, after successful eradication all ultrastructural alterations registered in *H pylori*+DU patients were normalized to appearance expected in control group, excluding cytoplasmic granules volume density and their diameter which retained some higher values, but the observed difference was not statistically significant in comparison to values in healthy subjects. These findings suggest that remaining alterations in G cell morphology in DU should be attributed to an unknown host factor.

After successful *H pylori* eradication in dyspeptic patients with gastritis both unchanged^[35] and decreased^[31] antral G cell number was reported, that is consistent with

our results where eradication therapy lead to a decrease in antral G cell number.

Ultrastructural examinations in *H pylori*+ patients with gastritis at the beginning of the study revealed similar, but less prominent subcellular alterations of G cell morphology detected the DU patients. We confirmed in our study, previously reported, increased cytoplasmic cell granule index in patients with *H pylori*-related gastritis using electron microscopy and immunohistochemical examination of antral G cells^[12]. After successful eradication, all detected alterations were reversed and antral G cells had morphological features similar to those in healthy controls. This is consistent with the findings of Sugamata *et al.*^[14], demonstrating the reversibility of antral G cell morphology changes after elimination of the infection.

We identified total antral endocrine cell population and calculated number of G cells using double immunostaining for both synaptophysin and gastrin. Synaptophysin was considered an adequate pan-neuroendocrine marker based on the distribution background in the human antrum, while its importance in the other parts of gastrointestinal tract remains limited. The co-localization study revealed that synaptophysin immunoreactivity occurred in virtually all antral gastrin, somatostatin and serotonin-producing cells^[38]. In the antrum, proportion G cells accounts for 40% of all endocrine cells^[9], as described in all of our examined groups of patients and healthy controls. The fact that the antral G cells/total endocrine cell ratio remained unchanged after eradication of *H pylori* implicates that other gastric endocrine cell types disturbances are related with the presence of the infection. This finding is important for the understanding of the potential important role of other endocrine cell types and their interactive, functional relationship in gastric regulatory physiology in gastritis and peptic ulcer disease associated with *H pylori* infection. Namely, previous studies reported the increase in basal and gastrin-stimulated somatostatin-containing (D) cell activity in the early phase (4-8 wks) after *H pylori* eradication in gastric ulcers^[22] and gastritis^[39], suggesting that both antral G and D cell morphology and function should be considered in the gastric mucosal response to the presence of *H pylori* infection. Decreased antral D cell number in patients with *H pylori*-related chronic gastritis might be one of the reasons for the existing hypergastrinemia^[12].

Possible mechanisms responsible for hypergastrinemia in *H pylori* associated gastritis or duodenal ulcer could be different. Some recent studies indicated that ypergastrinemia related to *H pylori* infection is associated with enhanced activity of platelet activating factor (PAF) produced locally, in the affected gastric mucosa and higher expression of nuclear factor kappaB (NF-kappaB)^[40,41]. PAF may contribute to the hypergastrinemia of *H pylori* infection by stimulating gastrin release from G cells involving influx of extracellular calcium via L-type channels and activation of protein kinase C^[40]. NF-kappaB activation is considered crucial event in the production of proinflammatory molecules in *H pylori*-associated gastritis. In the uninflamed stomach, NF-kappaB was highly expressed and active in a subset of epithelial cells, which were identified as predominantly G cells. In accordance with this activity, antral

mucosa of infected individuals expressed high levels of the NF-kappaB target cytokine TNF-alpha, a well-documented stimulator of gastrin production. In patients with *H pylori*-associated gastritis, NF-kappaB activity was markedly enhanced and activation occurred preferentially in the epithelial cells^[41]. In addition, treatment of cultured canine antral G-cells with *H pylori* constituents enhances subsequent basal and bombesin-stimulated gastrin release suggesting that direct contact between *H pylori* and G-cells in the gastric antrum may be responsible for the hypergastrinemia seen in the infected individuals^[42].

In conclusion, it may be concluded that in *H pylori* infected patients with chronic gastritis, changes in morphology and function of antral G cell are completely reversible and attributable exclusively to the presence of the bacterium in the gastric mucosa. However, duodenal ulcer formation in infected individuals is partly attributable to the presence of the infection, but host factors are of importance as well, since more profound alterations are observed and a certain extent of antral G cell hyperfunction, resulting in prolonged hypergastrinemia, is detected. Further investigations are needed in order to identify relevant host characteristics leading to the ulcer formation including gene polymorphisms of proinflammatory cytokines involved in the control of gastric acid secretion.

REFERENCES

- 1 **Bobrzynski A.** Hormonal, secretory and morphological alterations in gastric mucosa in the course of *Helicobacter pylori* eradication in patients with duodenal ulcer and non-ulcer dyspepsia. *J Physiol Pharmacol* 1997; **48**: S4-S16
- 2 **Hunt RH, Huang JQ.** The case for treatment of dyspeptic patient infected with *H pylori*. *Eur J Surg Suppl* 1998; **582**: 6-10
- 3 **Dockray GJ.** Gastrin and gastric epithelial physiology. *J Physiol* 1999; **518**: 315-324
- 4 **Kaneko H, Konagaya T, Kusugami K.** *Helicobacter pylori* and gut hormones. *J Gastroenterol* 2002; **37**: 77-86
- 5 **Gisbert JP, Boixeda D, Vila T, De Rafael L, Redondo C, De Argila CM.** Basal and stimulated gastrin levels and gastric acid output five months after therapy for *Helicobacter pylori* eradication in duodenal ulcer patients. *J Clin Gastroenterol* 1996; **22**: 90-95
- 6 **Haruma K, Sumii K, Okamoto S, Yoshihara M, Kajiyama G, Wagner S.** *Helicobacter pylori* infection associated with low antral somatostatin content in young adults: implications for the pathogenesis of hypergastrinemia. *Scand J Gastroenterol* 1995; **30**(6 Pt 1): 550-553
- 7 **Feldman M, Cryer B, Lee E.** Effects of *Helicobacter pylori* gastritis on gastric secretion in healthy human beings. *Am J Physiol Gastrointest Liver Physiol* 1998; **274**(6 Pt 1): G1011-G1017
- 8 **Hiraoka S, Miyayaki Y, Kitamura S, Toyota M, Kiyohara T, Shinomura Y, Mukaida N, Matsuzawa Y.** Gastrin induces CXC chemokine expression in gastric epithelial cells through activation of NF-kB. *Am J Physiol Gastrointest Liver Physiol* 2001; **281**: G735-742
- 9 **Sugiyama A, Ikeno T, Maruta F, Kawasaki S, Hayama M, Ota H, Yoshiyawa A, Nakajuma K, Fukushima M, Honda T.** Long-term *Helicobacter* colonization produces G cell hyperplasia and carcinoid tumor in Mongolian gerbils. *J Cell Mol Med* 2000; **4**: 308-309
- 10 **Peek RM Jr, Wirth HP, Moss SF, Yang M, Abdalla AM, Tham KT, Zhang T, Tang LH, Modlin IM, Blaser MJ.** *Helicobacter pylori* alters gastric epithelial cell cycle events and gastric acid secretion in Mongolian gerbils. *Gastroenterology* 2000; **118**: 48-59
- 11 **Drndarevic N, Todorovic V, Micev M, Sokic-Milutinovic A,**

- Milosavljevic T, Spuran M. Assessment of epithelial cell proliferation in gastric mucosal biopsies of patients with *Helicobacter pylori* infection. *Gut* 2003; **52**: A151
- 12 **Tzaneva M.** Light and microscopic immunohistochemical investigation on G and D cells in antral mucosa in *Helicobacter pylori* related gastritis. *Exp Toxicol Pathol* 2001; **52**: 523-528
- 13 **Yacoub WR,** Thomson ABR, Hooper P, Jewell LD. Immunocytochemical and morphometric studies of gastrin-, somatostatin- and serotonin- producing cells in the stomach and duodenum of patients with acid peptic disorders. *Can J Gastroenterol* 1996; **10**: 395-400
- 14 **Sugamata M,** Ihara T, Todate A, Sugamata M, Hirakawa R, Yoshida Y, Yamanaka T, Miyata M, Miura M. Ultrastructural study of antral G cells in patients with duodenal ulcer: effect of *Helicobacter pylori* eradication. *Helicobacter* 1997; **2**: 118-122
- 15 **Malfertheiner P,** Megraud F, O' Morain CO, Bell D, Bianchi Porro G, Deltenre M, Forman D, Gasbarrini G, Jaup B, Misiewicz JJ, Pajares J, Quina M, Rauws E. Current European concepts in the management of *Helicobacter pylori* infection – the Maastricht consensus report. *Eur J Gastroenterol Hepatol* 1997; **9**: 91-92
- 16 **Goodwin CS.** The Sydney system – microbial gastritis. *J Gastroenterol Hepatol* 1991; **6**: 223-235
- 17 **Dixon MF,** Genta RM, Yardley JH, Correa P. Classification and grading of gastritis. The updated Sydney System. *Am J Surg Pathol* 1996; **20**: 1161-1181
- 18 **Sternberg LA.** Immunohistochemistry. *New York: Zwiley and Sons* 1986
- 19 **Koko V,** Todorovic V, Varagic J, Micev M, Korac A, Bajcetic M, Cakic-Milosevic M, Nedeljkovic M, Drndarevic N. Gastrin producing G-cells after chronic ethanol and low protein nutrition. *Ind J Exp Biol* 1998; **36**: 1093-1101
- 20 **Todorovic V,** Koko V, Varagic J, Lackovic V, Vuzevski V, Milin J. Effects of chronic ethanol administration on the serotonin-producing cells in rat antral and duodenal mucosa. *Histol Histopathol* 1993; **8**: 285-296
- 21 **Bordi C,** D' Adda T, Azzoni C, Ferraro G. Classification of gastric endocrine cells at light and electron microscopical levels. *Microsc Res Techn* 2000; **48**: 258-271
- 22 **Hayakawa T,** Kaneko H, Konagaya T, Shinoyaki K, Kasahara A, Funaki Y, Mori S, Yokoi T, Hirooka Y, Kusugami K, Kakunu S. Enhanced somatostatin secretion into the gastric juice with recovery of basal acid output after *Helicobacter pylori* eradication in gastric ulcers. *Gastroenterol Hepatol* 2003; **18**: 505-511
- 23 **Lind T,** Van Zanten SV, Unge P, Spiller R, Bayerdorffer E, O'Morain C, Bardhan K, Bradette M, Chiba N, Wrangstadh M. Eradication of Hp using one week triple therapies combining omeprazole with two antimicrobials: the MACH I study. *Helicobacter* 1996; **1**: 138-144
- 24 **Bayerdorffer E,** Lind T, Dite P, Dev Bardhan K, O'Morain C, Delchier JC, Spiller R, Van Zanten SV, Sipponen P, Megraud F, Zeijlon L. Omeprazole, amoxicillin and metronidazole for the cure of Hp infection. *Eur J Gastroenterol Hepatol* 1999; **11**: S19-S22
- 25 **Zhao CM,** Wang X, Friis-Hansen L, Waldum HL, Halgunset J, Waldstrom T, Chen D. Chronic *Helicobacter pylori* infection results in gastric hypoacidity and hypergastrinemia in wild-type mice but vagally induced hypersecretion in gastrindeficient mice. *Regul Pept* 2003; **15**: 161-170
- 26 **Kamada T,** Haruma K, Kawaguchi H, Yoshihara M, Sumii K, Kajiyama G. The association between antral G and D cells and mucosal inflammation, atrophy, and *Helicobacter pylori* infection in subjects with normal mucosa, chronic gastritis and duodenal ulcer. *Am J Gastroenterol* 1998; **93**: 748-752
- 27 **Kato S,** Oyawa K, Koike T, Sekine H, Ohara S, Minoura T, Iinuma K. Effect of *Helicobacter pylori* infection on gastric acid secretion and meal-stimulated serum gastrin in children. *Helicobacter* 2004; **9**: 100-105
- 28 **Park SM,** Lee HR, Kim JG, Park JW, Jung G, Han SH, Cho JH, Kim MK. Effect of *Helicobacter pylori* infection on antral gastrin and somatostatin cells and on serum gastrin concentrations. *Korean J Int Med* 1999; **14**: 15-20
- 29 **Kim JH,** Park HJ, Cho JS, Lee KS, Lee SI, Park IS, Kim CK. Relationship of cagA to serum gastrin concentrations and antral G, D cell densities in *Helicobacter pylori* infection. *Yonsei Med J* 1999; **40**: 301-306
- 30 **Williams MP,** Usselman B, Chilton A, Sercombe J, Nwokolo CU, Pounder RE. Eradication of *Helicobacter pylori* increases nocturnal intragastric acidity during dosing with rabeprazole, omeprazole, lansoprazole and placebo. *Aliment Pharmacol Ther* 2003; **17**: 775-783
- 31 **Queiroz DM,** Mendes EN, Rocha GA, Moura SB, Resende LM, Barbosa AJ, Coehlo LG, Passos MC, Castro LP, Oliveira CA. Effect of *Helicobacter pylori* eradication on antral gastrin- and somatostatin-immunoreactive cell density and gastrin and somatostatin concentrations. *Scand J Gastroenterol* 1993; **28**: 858-864
- 32 **Odum L,** Petersen HD, Andersen IB, Hansen BF, Rehfeld JF. Gastrin and somatostatin in *Helicobacter pylori* infected antral mucosa. *Gut* 1994; **35**: 615-618
- 33 **Kwan CP,** Tytgat GN. Antral G cell hyperplasia: a vanishing disease? *Eur J Gastroenterol Hepatol* 1995; **7**: 1099-1103
- 34 **Chamouard P,** Walter P, Wittersheim C, Demuyneck P, Meunier O, Baumann R. Antral and fundic D-cell numbers in *Helicobacter pylori* infection. *Eur J Gastroenterol Hepatol* 1997; **9**: 361-365
- 35 **Sokic Milutinovic A,** Wex T, Todorovic V, Milosavljevic T, Malfertheiner P. Anti- CagA and anti-VacA antibodies in *Helicobacter pylori* infected patients with and without peptic ulcer disease in Serbia and Montenegro. *Scand J Gastroenterol* 2004; **30**: 222-226
- 36 **Gaidar IuA,** Stepanova EV, Mosiichuk LN, Demeshkina LV, Shekhetova GA, Bepalova EV, Kudriavtseva VE, Vcherashiaia NN. Particular features of the relationship of *Helicobacter pylori* and G cells in patients with duodenal ulcer, with special reference to the *Helicobacter pylori* strain. *Lik Sprava* 2001; **4**: 176-177
- 37 **Graham DY,** Lew GM, Lechago J. Antral G-cell and D-cell numbers in *Helicobacter pylori* infection: effect of *H pylori* eradication. *Gastroenterology* 1993; **104**: 1655-1660
- 38 **Portela-Gomes GM,** Stridsberg M, Johansson H, Grimelius L. Co-localization of synaptophysin with different neuroendocrine hormones in the human gastrointestinal tract. *Histochem Cell Biol* 1999; **111**: 49-54
- 39 **Milutinovic AS,** Todorovic V, Milosavljevic T, Micev M, Spuran M, Drndarevic N. Somatostatin and D cells in patients with gastritis in the course of *Helicobacter pylori* eradication: a six-month, follow-up study. *Eur J Gastroenterol Hepatol* 2003; **15**: 755-766
- 40 **Beales IL.** Effect of platelet-activating factor on gastrin-release from cultured rabbit G-cells. *Dig Dis Sci* 2001; **46**: 301-306
- 41 **Van Den Brink GR,** Ten Kate EJ, Ponsioen CY, Rive MM, Tytgat GN, van Deventer SJ, Peppelenbosch MP. Expression and activation of NF/kappa B in the antrum of the human stomach. *J Immunol* 2000; **164**: 3353-3359
- 42 **Beales IL,** Calam J. *Helicobacter pylori* increases gastrin release from cultured canine antral- G-cells. *Eur J Gastroenterol Hepatol* 2000; **12**: 641-644

• *Helicobacter pylori* •

Enhanced plasma ghrelin levels in *Helicobacter pylori*-colonized, interleukin-1-receptor type 1-homozygous knockout (IL-1R1^{-/-}) mice

Yuka Abiko, Hidekazu Suzuki, Tatsuhiro Masaoka, Sachiko Nomura, Kumiko Kurabayashi, Hiroshi Hosoda, Kenji Kangawa, Toshifumi Hibi

Yuka Abiko, Hidekazu Suzuki, Tatsuhiro Masaoka, Sachiko Nomura, Kumiko Kurabayashi, Toshifumi Hibi, Department of Internal Medicine and Center for Integrated Medical Research, Keio University School of Medicine, Shinjuku-ku, Tokyo 160-8582, Japan
Hiroshi Hosoda, Kenji Kangawa, Department of Biochemistry, National Cardiovascular Center Research Institute, Suita, Osaka 565-8565, Japan

Supported by a Grant-in-Aid for Scientific Research C (2) from the Japan Society for the Promotion of Science (JSPS) (15590686, to H.S.), and a grant from the Keio University School of Medicine
Correspondence to: Hidekazu Suzuki, MD, PhD, Assistant Professor, Department of Internal Medicine, School of Medicine, Keio University, 35 Shinanomachi, Shinjuku-ku, Tokyo 160-8582, Japan. hsuzuki@sc.itc.keio.ac.jp
Telephone: +81-3-5363-3914 Fax: +81-3-5363-3967
Received: 2004-10-14 Accepted: 2004-11-29

which is also induced by the infection, resulting in the body weight loss of mice with *H pylori* infection.

© 2005 The WJG Press and Elsevier Inc. All rights reserved.

Key words: Ghrelin; *H pylori*; IL-1; Body weight; Myeloperoxidase

Abiko Y, Suzuki H, Masaoka T, Nomura S, Kurabayashi K, Hosoda H, Kangawa K, Hibi T. Enhanced plasma ghrelin levels in *Helicobacter pylori*-colonized, interleukin-1-receptor type 1-homozygous knockout (IL-1R1^{-/-}) mice. *World J Gastroenterol* 2005; 11(27): 4148-4153

<http://www.wjgnet.com/1007-9327/11/4148.asp>

Abstract

AIM: Ghrelin is an endogenous ligand for the growth hormone secretagogue receptor, and it plays a role in stimulating the growth hormone secretion, food intake, body weight gain and gastric motility. Eradication of *Helicobacter pylori* (*H pylori*) was shown to be associated with increase of the body weight. On the other hand, *H pylori* infection evokes the release of gastric IL-1 β . The present study was designed to investigate the involvement of the gastric IL-1 signal in the ghrelin dynamics in *H pylori*-colonized mice.

METHODS: Twelve-week-old female IL-1-receptor type 1-homozygous-knockout mice (IL-1R1^{-/-}) and their wild-type littermates (WT) were orally inoculated with *H pylori* (Hp group), while other cohorts received oral inoculation of culture medium (Cont group). Thirteen weeks after the inoculation, the mice were examined. The plasma and stomach ghrelin levels and the gastric preproghrelin mRNA were measured.

RESULTS: Although the WT mice with *H pylori* infection showed a significantly decreased body weight as compared with that of the animals without *H pylori* infection, *H pylori* infection did not influence the body weight of the IL-1R1-knockout (IL-1R1^{-/-}) mice. In the *H pylori*-infected IL-1R1^{-/-} mice, the total and active ghrelin levels in the plasma were significantly increased, and the gastric ghrelin level was decreased. No significant differences were noted in the gastric preproghrelin mRNA expression.

CONCLUSION: Ghrelin secretion triggered by *H pylori* infection might be suppressed by IL-1 β , the release of

INTRODUCTION

Ghrelin, an endogenous ligand for the growth hormone secretagogue receptor (GHS-R), stimulates growth hormone (GH) release from cultured pituitary cells in a dose-dependent manner^[1], and is produced and secreted from the A-like cells found mainly in the oxyntic glands of the gastric fundus^[2]. Ghrelin is now known to play a role in not only GH release, but also in controlling the appetite and body weight. Since both parenterally and intracerebroventricularly administered ghrelin have been shown to stimulate food intake and increase the body weight of mice and rats with free access to food, even those animals with GH deficiency^[3,4], the control of appetite and body weight may be independent of GH release. Ghrelin, a 28-amino-acid peptide, is activated when its third serine residue is acylated by n-octanoic acid, and GHS-R is responsive to the first four or five residues including the octanoylated serine residue of the whole ghrelin peptide^[5]. GHS-R has been shown to be present in the pituitary, hypothalamus, adrenal glands, thyroid, pancreas, myocardium, spleen and testes^[1,6-8]. Ghrelin stimulates the expression of both NPY and AGRP mRNA in the hypothalamus. The central orexigenic effect of ghrelin is mediated by the NPY/AGRP-expressing neurons in the hypothalamus^[3,9-11]. On the other hand, ghrelin has also been reported to suppress vagal afferent activity^[2]. The peripheral orexigenic effect of ghrelin may be mediated, at least in part, by its suppressive effect on the vagal afferent activity.

IL-1 β is a pro-inflammatory cytokine that mediates the cachectic process by stimulating the expression and release of leptin,^[12] and/or by mimicking the effect on the hypothalamus of excessive negative-feedback signaling from

leptin^[13]. Cachexia is a condition characterized by wasting, emaciation, feebleness and inanition. It was recently reported that the levels of both ghrelin peptide and ghrelin mRNA in the stomach were up-regulated in a mouse model of cancer cachexia^[14]. In cachectic mice with increased plasma levels of IL-1 β , the plasma concentrations of ghrelin also increased with the progression of cachexia^[15]. This result suggests that a close relationship might exist between the ghrelin dynamics and the cachectic process mediated by IL-1. IL-1 β is an anorexigenic substance, just like CCK, leptin, gastrin-related protein and bombesin, and antagonizes the actions of ghrelin. Asakawa *et al.*, reported that parenterally administered IL-1 β decreased NPY mRNA expression in the hypothalamus and preproghrelin mRNA expression in the stomach, and that intraperitoneally administered ghrelin inhibited the severity of IL-1 β -induced anorexia.

Helicobacter pylori (*H pylori*) infection is known to be a major pathogenetic factor in the development of gastritis, peptic ulcer disease and gastric malignancy^[16,17]. Attachment of *H pylori* to the gastric mucosa induces inflammation, which is associated with the release of various cytokines, including IL-1 β ^[18]. Although the importance of the anorexigenic effect of IL-1 β in cases with *H pylori* infection has not yet been clarified, it has been observed clinically that *H pylori* eradication is often followed by improvement of some nutritional parameters, such as the body weight and the serum levels of total cholesterol, total protein and albumin^[19]. We recently reported that *H pylori* infection could modify the plasma and gastric ghrelin dynamics in Mongolian gerbils^[20]. In humans, however, *H pylori* infection has been reported not to be associated with any changes of the plasma ghrelin levels^[21,22], although eradication of *H pylori* has been shown by some to be associated with increases of the plasma ghrelin levels^[23]. Therefore, regulation of the ghrelin dynamics and its influence on the body weight control in cases with *H pylori* infection still remains to be clarified.

We designed the present study to investigate the role of the gastric IL-1 signal in the regulation of the ghrelin dynamics and its influence on the body weight control under in cases with *H pylori* infection.

MATERIALS AND METHODS

Animal procedures

All experiments and procedures carried out on the animals were approved by the Keio University Animal Research Committee (No. 023009). Twelve-week-old, specific-pathogen-free female interleukin-1 (IL-1)-receptor type 1-homozygous-knockout mice (IL-1R1^{-/-}) on a C57BL/6 background (The Jackson Lab., Bar Harbor, ME, USA) and their wild-type cohorts as controls (WT) were used for the study. The Sydney Strain of *H pylori* (SS1) was grown from frozen stocks at 37 °C under microaerobic conditions for 24–36 h in lysed horse-blood agar supplemented with antibiotics, harvested in Brucella broth, and administered to the mice immediately after being harvested. Six IL-1R1^{-/-} mice and five WT mice were orally inoculated with *H pylori* (1.5 \times 10⁸ CFU/mL, 0.5 mL), while another six IL-1R1^{-/-} mice and five WT mice were orally inoculated with the culture medium alone as control. A week later, each animal

was inoculated again with the aforementioned bacterial strain. Thirteen weeks after the first inoculation, all the mice were examined under ether anesthesia. The mice were then deprived of food for 17 h before being killed. The body weight of each mouse was measured just before the examination.

Confirmation of Infection

H pylori infection was diagnosed by determining the number of CFUs in a microaerobic bacterial culture. Briefly, the diluted homogenates of the stomachs were plated on to Brucella agar plates containing 10% horse blood, 2.5 μ g/mL amphotericin B, 9 μ g/mL vancomycin, 0.32 μ g/mL polymyxin B, 5 μ g/mL trimethoprim, and 50 μ g/mL 2, 3, 5-triphenyl-tetrazolium chloride. The plates were then incubated at 37 °C in a microaerobic atmosphere for 7 d^[24]. All of the *H pylori* inoculated animals were confirmed as *H pylori* positive by this procedure in the present study.

Measurement of plasma ghrelin levels

Whole-blood samples were obtained from the right ventricle in tubes containing EDTA-2Na (1 mg/mL blood) and aprotinin (500 kIU/mL blood). The tubes were centrifuged and the plasma samples were stored at -80 °C.

Plasma total ghrelin was measured using the Desacyl-Ghrelin ELISA Kit (Mitsubishi Kagaku Medical, Inc., Ibaraki, Japan), and plasma active ghrelin was measured using the Active Ghrelin ELISA Kit (Mitsubishi Kagaku Medical, Inc., Ibaraki, Japan). Total ghrelin, i.e., active plus inactive ghrelin, was measured using an antibody directed against the C-terminal end (residues 1 to 11) of ghrelin, while an antibody directed against the N-terminal end of ghrelin (residues 13 to 28) was used for the measurement of active ghrelin. The plasma samples were placed in testing wells coated with the ghrelin antibodies. Then, the plate with the wells was incubated for 2 h at room temperature. After incubation, the samples were washed and diluted HRP was added to the wells. The plate was then incubated again for 1 h at room temperature. The samples were washed and substrate solution was added to the wells. The plate was incubated for a further 30 min at room temperature under shade conditions. After the reaction, a reagent was added to stop the reaction, and the absorbance of each well was measured at 450 nm.

Measurement of myeloperoxidase activity

Immediately after the mice were sacrificed, the stomachs of the animals were removed and opened along the greater curvature. Tissue samples of the gastric mucosa were collected in tubes containing PBS and protease inhibitors (100 μ mol/L phenylmethylsulfonyl fluoride, 10 μ g/mL aprotinin) and sonicated over ice in 30 consecutive 0.5 s bursts at 0.5 s intervals, at a power setting of 150 W (VCX 50; Sonics and Materials, Inc., Newton, CT, USA). The total protein content in the homogenates was measured by modified Lowry's method^[25], as described by Smith *et al.*^[26].

Myeloperoxidase (MPO) activity, as an index of tissue-associated neutrophil accumulation, was determined by a modification of Grisham *et al.*'s method^[27]. Aliquots containing 100 μ L of the mucosal homogenates were

centrifuged at 8 000 r/min for 15 min at 4 °C to separate the pellets of insoluble cellular debris. The pellets were rehomogenized in an equal volume of 0.05 mol/L potassium phosphate buffer (pH 5.4) containing 0.5%-hexadecyltrimethylammonium bromide. The samples were then centrifuged at 8 000 r/min for 15 min at 4 °C and the supernatants were reserved. The MPO activity in the supernatants was assessed by measuring the H₂O₂-dependent oxidation of 3, 3', 5, 5'-tetramethylbenzidine. One unit of enzyme activity was defined as the amount of MPO that caused a change in the absorbance of 1.0/min at 655 nm, at 25 °C.

Measurement of the gastric ghrelin levels

Fresh whole-anterior-wall specimens of the glandular stomach were frozen immediately after collection in liquid nitrogen and stored at -80 °C. Each sample was boiled for five min in a 10-fold volume of water to inactivate the intrinsic proteases. The solution was adjusted to 1N acetic acid by addition of 180 microliter acetic acid after cooling, and the tissue was homogenized. The supernatant was lyophilized and subjected to RIA to measure the ghrelin level. The extraction efficiency of tissue ghrelin was more than 95%.

Two RIA techniques were used for measuring ghrelin, as described previously^[28]. Briefly, ghrelin levels were measured using two polyclonal rabbit antibodies raised against an N terminal (1-11) (Gly1-Lys11) or C terminal (13-28) (Gln13-Arg28) fragment of rat ghrelin. Two tracer ligands were synthesized: [Tyr29]-rat ghrelin for antirat ghrelin (1-11) antiserum and [Tyr12]-rat ghrelin [13-28] for antirat ghrelin [13-28] antiserum. The RIA incubation mixtures containing 100 µL of either standard ghrelin or unknown samples containing 200 µL of antiserum diluted in RIA buffer containing 0.5% normal rabbit serum, were initially incubated for 12 h. Then, the mixture was incubated for 36 h after the addition of 100 µL of ¹²⁵I labeled tracer (15 000 cpm). Antirabbit IgG goat serum (100 µL) was added followed by incubation for an additional 24 h. Free and bound tracers were then separated by centrifugation at 3 000 r/min for 30 min. Following aspiration of the supernatant, the radioactivity in the pellet was quantified using a gamma counter (ARC-600; Aloka, Tokyo, Japan). All assays were performed at 4 °C. The antirat ghrelin (1-11) antiserum specifically recognized the n-octanoylated form of rat ghrelin, but not the des-acyl form. The antirat ghrelin (13-28) antiserum recognized both the acylated and des-acyl forms of rat ghrelin equally efficiently. Both antisera were equally cross-reactive with human and gerbil ghrelin, and did not recognize the other enteric peptides. The respective intra- and interassay coefficients of variation for the N terminal RIA were 3% and 6%, and for the C terminal RIA were 6% and 9%.

Measurement of the preproghrelin mRNA expression level in the stomach

Total RNA was extracted from the stomach of the mice using the RNeasy Mini Kit (Qiagen). A TaqMan quantitative real-time RT-PCR was performed to detect preproghrelin mRNA and GAPDH mRNA using the ABI PRISM 7700 sequence detection system (PE Applied Biosystems)^[29].

The following primers were used to amplify preproghrelin mRNA: forward-ghrelin (5'-GGA ATC CAA GAA GCC ACC AGC-3'), reverse-ghrelin (5'-GCT CCT GAC AGC TTG ATG CCA-3'), and Taqman-ghrelin (5'-FAM-AAC TGC AGC CAC GAG CTC TGG AAG GC-TAMRA-3'). The following primers were used to amplify GAPDH mRNA as the internal control: forward primer (5'-TTC AAC GGC ACA GTC AAG GC-3'), reverse primer (5'-GCC TTC TCC ATG GTG GTG AAG-3'), and Taqman probe (5'-FAM-CCC ATC ACC ATC TTC CAG GAG CGA GA-TAMRA-3').

The preproghrelin mRNA expression levels were normalized using the GAPDH mRNA expression levels.

Statistical analysis

All the data were expressed as the mean±SE. The data were analyzed using one-way analysis of variance, followed by Scheffe's multiple comparison tests. A value of *P*<0.05 was considered to denote statistical significance.

RESULTS

Among the WT mice, the *H pylori*-infected mice showed a significantly reduced body weight as compared to the uninfected and control mice (*P*<0.001). Although the basic body weight of the IL-1R1^{-/-} mice was lower than that of the WT mice, no further reduction of the body weight of these mice was observed after *H pylori* infection (Table 1).

H pylori infection increased the MPO activity in the gastric mucosa in both the WT (*P*<0.01) and IL-1R1^{-/-} (*P*<0.01) mice, although in the IL-1R1^{-/-} mice, the increase was significantly less marked (*P*<0.05) (Figure 1).

Table 1 Body weight of the mice at the time of the examination

Wild type mice (g)		IL-1R1 ^{-/-} mice (g)	
Not-infected	Infected	Not-infected	Infected
26.0±0.71	22.1±0.54 ^b	23.4±0.51	23.1±0.34

Among the wild-type mice, the body weight of *H pylori*-infected mice (*n* = 4) was lower than that of the uninfected mice (*n* = 5); on the other hand, among the IL-1R1^{-/-} mice, no significant difference in the body weight was noted between the infected (*n* = 6) and uninfected (*n* = 6) mice. ^b*P*<0.001 vs the uninfected mice.

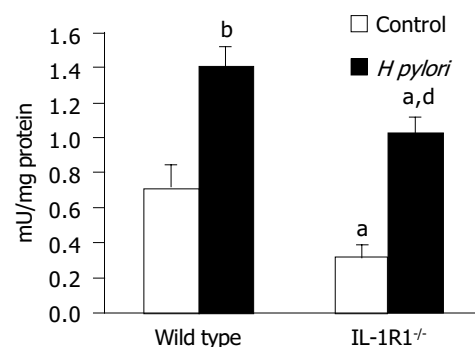


Figure 1 Myeloperoxidase (MPO) activity in the stomach. Both wild-type (filled column: *n* = 4) and IL-1R1^{-/-} (spotted filled column: *n* = 6) mice with *H pylori* infection showed increased MPO activity as compared with the uninfected wild-type (clear column: *n* = 5) and IL-1R1^{-/-} (spotted clear column: *n* = 5). ^a*P*<0.05 vs the wild-type mice, ^b*P*<0.001, ^d*P*<0.01 vs the uninfected mice.

Among the WT mice, the *H pylori*-infected animals showed no significant increase of the plasma total ghrelin levels as compared to the uninfected and control mice. In the case of the IL-1R1^{-/-} mice, although simple lack of the IL-1 signal did not affect the plasma total ghrelin dynamics, *H pylori* infection of these mice was associated with a marked increase of the plasma total ghrelin levels ($P < 0.05$; compared with the uninfected mice, $P < 0.001$; compared with the wild-type mice) (Figure 2).

The same tendency was shown for the plasma active ghrelin dynamics. Among the WT mice, the *H pylori*-infected mice showed a tendency towards increase in the plasma active ghrelin levels as compared to the uninfected and control mice, but the increase was not statistically significant. On the other hand, in the IL-1R1^{-/-} mice, while a simple lack of the IL-1 signal did not affect the plasma active ghrelin dynamics, *H pylori* infection of these animals was associated with a marked increase of the plasma active ghrelin levels ($P < 0.01$; compared with the uninfected mice, $P < 0.05$; compared with the wild-type mice) (Figure 3).

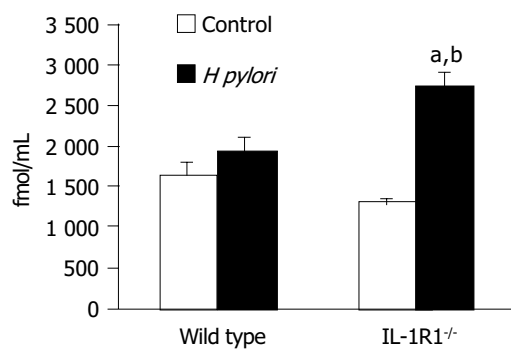


Figure 2 The total ghrelin levels in the plasma. Although neither simple lack of the IL-1 signal (spotted clear column: $n = 4$) nor *H pylori* infection alone (filled column: $n = 4$) was associated with any changes in the total plasma ghrelin levels as compared with the levels in the uninfected wild-type mice (clear column: $n = 5$), *H pylori* infection induced a marked increase of the total plasma ghrelin levels in the IL-1R1^{-/-} mice (spotted filled column: $n = 6$). ^a $P < 0.05$ vs the uninfected mice. ^b $P < 0.001$ vs the wild-type mice.

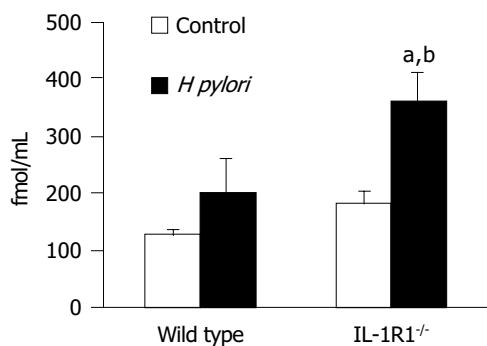


Figure 3 The active ghrelin levels in the plasma. Neither simple lack of the IL-1 signal (spotted clear column: $n = 6$) nor *H pylori* infection alone (filled column: $n = 3$) was associated with any changes in the total plasma ghrelin levels as compared with the levels in the uninfected wild-type mice (clear column: $n = 5$). *H pylori* infection induced a marked increase of the plasma active ghrelin levels in the IL-1R1^{-/-} mice (spotted filled column: $n = 6$). ^a $P < 0.05$ vs the wild-type mice; ^b $P < 0.01$ vs the uninfected mice.

In contrast to the effects of *H pylori* on the plasma ghrelin dynamics, the ghrelin levels in the stomach, both total and active, were significantly decreased in the *H pylori*-infected IL-1R1^{-/-} mice ($P < 0.05$) (Figure 4A and B), indicating that ghrelin is secreted into the blood from its stores in the stomach.

Preproghrelin mRNA expression, evaluated in comparison with the expression of GAPDH mRNA, was not modified by either *H pylori* infection or lack of the IL-1 signal, or both (Figure 5). These results suggest that the stomach ghrelin stores were not replenished after ghrelin secretion into the blood.

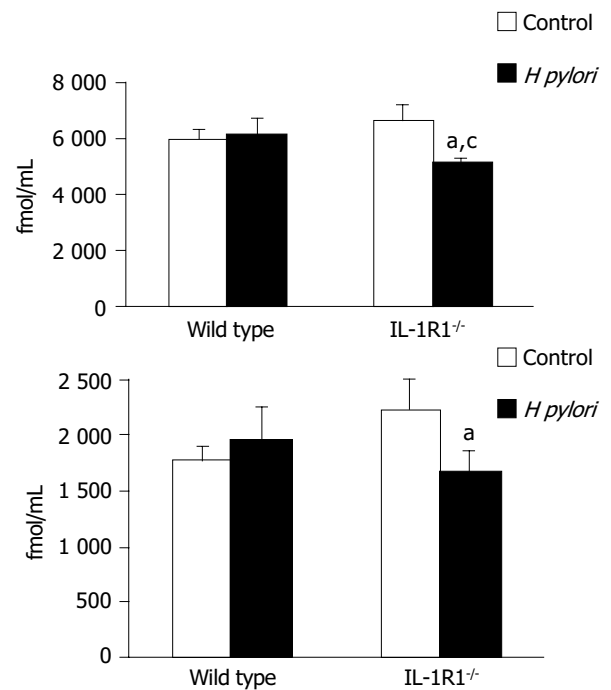


Figure 4 The gastric (A: total, B: active) ghrelin levels. Although neither a simple lack of the IL-1 signal (spotted clear column: (A) $n = 5$, (B) $n = 5$) nor *H pylori* infection alone (filled column: (A) $n = 5$, (B) $n = 5$) was associated with any changes in the gastric ghrelin levels as compared with the levels in the uninfected wild-type mice (clear column: (A) $n = 5$, (B) $n = 5$), *H pylori* infection induced a marked decrease of the a) total and b) active gastric ghrelin levels in the IL-1R1^{-/-} mice (spotted filled column: (A) $n = 6$, (B) $n = 5$). ^a $P < 0.05$ vs the uninfected mice; ^c $P < 0.05$ vs the wild-type mice.

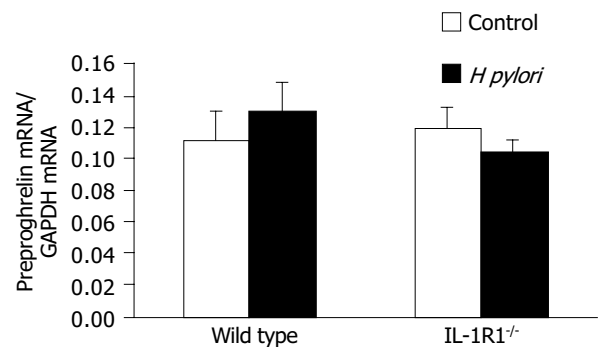


Figure 5 Preproghrelin mRNA levels in the gastric mucosa. No significant differences were observed among the uninfected wild-type mice (clear column: $n = 5$), uninfected IL-1R1^{-/-} mice (spotted clear column: $n = 6$), *H pylori*-infected wild-type mice (filled column: $n = 5$) and *H pylori*-infected IL-1R1^{-/-} mice (spotted filled column: $n = 6$).

DISCUSSION

It is widely known that *H pylori* infection is associated with loss of body weight. In the present study, although *H pylori*-infected wild-type (WT) mice showed body weight loss, no such weight loss was observed in IL-1R1^{-/-} mice with *H pylori* infection (Table 1). On the other hand, although an increase in the level of gastric mucosal neutrophil accumulation was noted in both WT and IL-1R1^{-/-} mice with *H pylori* infection, the neutrophil accumulation was significantly less marked in *H pylori*-infected IL-1R1^{-/-} mice than in *H pylori*-infected WT mice (Figure 1), indicating that the lack of the IL-1 signal could affect the regulatory mechanisms of both body weight and gastric mucosal inflammation.

It has previously been reported that the administration of lipopolysaccharide (LPS) is associated with a reduction in the plasma levels of ghrelin^[30, 31] and increase in the plasma levels of IL-1β^[31]. According to the study by Burgess *et al.*^[32], while intracerebroventricular administration of LPS greatly reduced the food intake in WT mice, no such effect was observed in mice deficient in the IL-1 β-converting enzyme. In addition, as mentioned above, it has been reported that injection of IL-1β was followed by a decrease in the gastric preproghrelin mRNA expression^[9]. These results suggest that the anorexigenic effect of LPS may be mediated by IL-1β and ghrelin, a downstream molecule in the cascade. The production of IL-1β might be enhanced by LPS and the release of ghrelin might be suppressed by IL-1 β.

We recently reported from a study in Mongolian gerbils, that the plasma levels of ghrelin are enhanced for a restricted period after *H pylori* inoculation^[20]. In the present study, while the plasma levels of ghrelin showed no significant increase in the WT mice with *H pylori* infection, the levels were significantly elevated in IL-1R1^{-/-} mice with *H pylori* infection (Figure 2, 3), indicating that IL-1 may suppress ghrelin secretion, as mentioned above. As in Mongolian gerbils, *H pylori* infection also stimulates ghrelin secretion in mice, but the secretion is suppressed by IL-1 β, a mediator whose production is also enhanced by *H pylori* infection. Therefore, in IL-1-signal-deficient mice with *H pylori* infection, ghrelin production and release into the blood occurs unopposed by the inhibitory action of IL-1 on these processes.

Contrary to the observations on the ghrelin dynamics, the gastric expression of leptin mRNA, one of the important anorexigenic peptides produced by adipocytes, is significantly increased by *H pylori* infection^[33]; expression of this mRNA is also significantly enhanced by IL-1 administration^[12]. The central pathway of appetite control by ghrelin is reported to be mediated by neuropeptide Y (NPY)-expressing neurons in the hypothalamus. Ghrelin increases the activity of NPY-expressing neurons, and hence food intake^[9, 10]. The same NPY-expressing neurons in the hypothalamus have also been reported to be involved in the suppression of appetite by leptin. Leptin decreases the mRNA expression of NPY in the neurons of the hypothalamus^[11], thereby suppressing food intake and causing loss of body weight^[3, 11]. The effects of ghrelin and leptin are considered to be competitively regulated by the hypothalamic NPY-expressing neurons.

Thus, in the WT mice, *H pylori* infection stimulates both

ghrelin secretion and IL-1β release, but excessive ghrelin secretion is suppressed by IL-1β, whereas leptin secretion, also stimulated by *H pylori*, is promoted by IL-1β. The competitive actions of ghrelin and leptin in the hypothalamic NPY-expressing neurons result in a decrease of the appetite and body weight of WT mice with *H pylori* infection. On the other hand, in the *H pylori*-infected IL-1R1^{-/-} mice, the inhibitory effect of the IL-1 signal on ghrelin secretion is absent, and the enhanced ghrelin secretion combined with the enhanced leptin secretion might result in a dominant effect of ghrelin on the appetite control, and body weight loss does not become manifest in these animals.

While the secretion of stored gastric ghrelin is affected by *H pylori*, the gastric preproghrelin mRNA expression was not significantly enhanced by *H pylori* infection in the present study (Figure 5). While in Mongolian gerbils, *H pylori* infection was associated with increased plasma ghrelin levels and decreased gastric ghrelin and preproghrelin mRNA expression^[20], the infection in mice had no significant effect on any of the above three parameters. According to Asakawa *et al.*^[9], IL-1 administration reduced gastric preproghrelin mRNA expression; this may be the reason why the IL-1-receptor-knockout mice in the present study did not show any changes of the gastric preproghrelin mRNA expression. Thus, there may be species differences in the hormone dynamics and their reactivity to stimulation, such as in the event of *H pylori* infection.

In conclusion, ghrelin secretion triggered by *H pylori* infection might be suppressed by IL-1β, resulting in body weight loss of the infected mice.

ACKNOWLEDGMENTS

A part of the present data was presented in the Topic Forum of Digestive Disease Week on May, 17th, 2004, in New Orleans, USA.

REFERENCES

- 1 **Kojima M**, Hosoda H, Date Y, Nakazato M, Matsuo H, Kangawa K. Ghrelin is a growth-hormone-releasing acylated peptide from stomach. *Nature* 1999; **402**: 656-660
- 2 **Date Y**, Murakami N, Toshinai K, Matsukura S, Nijima A, Matsuo H, Kangawa K, Nakazato M. The role of the gastric afferent vagal nerve in ghrelin-induced feeding and growth hormone secretion in rats. *Gastroenterology* 2002; **123**: 1120-1128
- 3 **Nakazato M**, Murakami N, Date Y, Kojima M, Matsuo H, Kangawa K, Matsukura S. A role for ghrelin in the central regulation of feeding. *Nature* 2001; **409**: 194-198
- 4 **Wren AM**, Small CJ, Ward HL, Murphy KG, Dakin CL, Taheri S, Kennedy AR, Roberts GH, Morgan DG, Ghatei MA, Bloom SR. The novel hypothalamic peptide ghrelin stimulates food intake and growth hormone secretion. *Endocrinology* 2000; **141**: 4325-4328
- 5 **Bednarek MA**, Feighner SD, Pong SS, McKee KK, Hreniuk DL, Silva MV, Warren VA, Howard AD, Van Der Ploeg LH, Heck JV. Structure-function studies on the new growth hormone-releasing peptide, ghrelin: minimal sequence of ghrelin necessary for activation of growth hormone secretagogue receptor 1a. *J Med Chem* 2000; **43**: 4370-4376
- 6 **Gaytan F**, Barreiro ML, Caminos JE, Chopin LK, Herington AC, Morales C, Pinilla L, Paniagua R, Nistal M, Casanueva FF, Aguilar E, Dieguez C, Tena-Sempere M. Expression of ghrelin and its functional receptor, the type 1a growth hor-

- mone secretagogue receptor, in normal human testis and testicular tumors. *J Clin Endocrinol Metab* 2004; **89**: 400-409
- 7 **Guan XM**, Yu H, Palyha OC, McKee KK, Feighner SD, Sirinathsingji DJ, Smith RG, Van der Ploeg LH, Howard AD. Distribution of mRNA encoding the growth hormone secretagogue receptor in brain and peripheral tissues. *Brain Res Mol Brain Res* 1997; **48**: 23-29
- 8 **Gnanapavan S**, Kola B, Bustin SA, Morris DG, McGee P, Fairclough P, Bhattacharya S, Carpenter R, Grossman AB, Korbonits M. The tissue distribution of the mRNA of ghrelin and subtypes of its receptor, GHS-R, in humans. *J Clin Endocrinol Metab* 2002; **87**: 2988
- 9 **Asakawa A**, Inui A, Kaga T, Yuzuriha H, Nagata T, Ueno N, Makino S, Fujimiya M, Niijima A, Fujino MA, Kasuga M. Ghrelin is an appetite-stimulatory signal from stomach with structural resemblance to motilin. *Gastroenterology* 2001; **120**: 337-345
- 10 **Kamegai J**, Tamura H, Shimizu T, Ishii S, Sugihara H, Wakabayashi I. Central effect of ghrelin, an endogenous growth hormone secretagogue, on hypothalamic peptide gene expression. *Endocrinology* 2000; **141**: 4797-4800
- 11 **Shintani M**, Ogawa Y, Ebihara K, Aizawa-Abe M, Miyanaga F, Takaya K, Hayashi T, Inoue G, Hosoda K, Kojima M, Kangawa K, Nakao K. Ghrelin, an endogenous growth hormone secretagogue, is a novel orexigenic peptide that antagonizes leptin action through the activation of hypothalamic neuropeptide Y/Y1 receptor pathway. *Diabetes* 2001; **50**: 227-232
- 12 **Sarraf P**, Frederich RC, Turner EM, Ma G, Jaskowiak NT, Rivet DJ 3rd, Flier JS, Lowell BB, Fraker DL, Alexander HR. Multiple cytokines and acute inflammation raise mouse leptin levels: potential role in inflammatory anorexia. *J Exp Med* 1997; **185**: 171-175
- 13 **Inui A**. Cancer anorexia-cachexia syndrome: are neuropeptides the key? *Cancer Res* 1999; **59**: 4493-4501
- 14 **Hanada T**, Toshinai K, Kajimura N, Nara-Ashizawa N, Tsukada T, Hayashi Y, Osuye K, Kangawa K, Matsukura S, Nakazato M. Anti-cachectic effect of ghrelin in nude mice bearing human melanoma cells. *Biochem Biophys Res Commun* 2003; **301**: 275-279
- 15 **Hanada T**, Toshinai K, Date Y, Kajimura N, Tsukada T, Hayashi Y, Kangawa K, Nakazato M. Upregulation of ghrelin expression in cachectic nude mice bearing human melanoma cells. *Metabolism* 2004; **53**: 84-88
- 16 **Marshall BJ**, Warren JR. Unidentified curved bacilli in the stomach of patients with gastritis and peptic ulceration. *Lancet* 1984; **1**: 1311-1315
- 17 **Uemura N**, Okamoto S, Yamamoto S, Matsumura N, Yamaguchi S, Yamakido M, Taniyama K, Sasaki N, Schlemper RJ. *Helicobacter pylori* infection and the development of gastric cancer. *N Engl J Med* 2001; **345**: 784-789
- 18 **Yamaoka Y**, Kita M, Kodama T, Sawai N, Kashima K, Imanishi J. Induction of various cytokines and development of severe mucosal inflammation by cagA gene positive *Helicobacter pylori* strains. *Gut* 1997; **41**: 442-451
- 19 **Furuta T**, Shirai N, Xiao F, Takashima M, Hanai H. Effect of *Helicobacter pylori* infection and its eradication on nutrition. *Aliment Pharmacol Ther* 2002; **16**: 799-806
- 20 **Suzuki H**, Masaoka T, Hosoda H, Ota T, Minegishi Y, Nomura S, Kangawa K, Ishii H. *Helicobacter pylori* infection modifies gastric and plasma ghrelin dynamics in Mongolian gerbils. *Gut* 2004; **53**: 187-194
- 21 **Gokcel A**, Gumurdulu Y, Kayaselcuk F, Serin E, Ozer B, Ozsahin AK, Guvener N. *Helicobacter pylori* has no effect on plasma ghrelin levels. *Eur J Endocrinol* 2003; **148**: 423-426
- 22 **Suzuki H**, Masaoka T, Hosoda H, Nomura S, Ohara T, Kangawa K, Ishii H, Hibi T. Plasma ghrelin concentration correlates with the levels of serum pepsinogen I and pepsinogen I/II ratio-a possible novel and non-invasive marker for gastric atrophy. *Hepatogastroenterology* 2004; **51**: 1249-1254
- 23 **Nwokolo CU**, Freshwater DA, O'Hare P, Randeve HS. Plasma ghrelin following cure of *Helicobacter pylori*. *Gut* 2003; **52**: 637-640
- 24 **Takahashi S**, Keto Y, Fujita H, Muramatsu H, Nishino T, Okabe S. Pathological changes in the formation of *Helicobacter pylori*-induced gastric lesions in Mongolian gerbils. *Dig Dis Sci* 1998; **43**: 754-765
- 25 **Lowry OH**, Rosebrough NJ, Farr AL, Randall RJ. Protein measurement with the Folin phenol reagent. *J Biol Chem* 1951; **193**: 265-275
- 26 **Smith PK**, Krohn RI, Hermanson GT, Mallia AK, Gartner FH, Provenzano MD, Fujimoto EK, Goeke NM, Olson BJ, Klenk DC. Measurement of protein using bicinchoninic acid. *Anal Biochem* 1985; **150**: 76-85
- 27 **Grisham MB**, Hernandez LA, Granger DN. Xanthine oxidase and neutrophil infiltration in intestinal ischemia. *Am J Physiol* 1986; **251**: G567-574
- 28 **Hosoda H**, Kojima M, Matsuo H, Kangawa K. Ghrelin and des-acyl ghrelin: two major forms of rat ghrelin peptide in gastrointestinal tissue. *Biochem Biophys Res Commun* 2000; **279**: 909-913
- 29 **Masaoka T**, Suzuki H, Hosoda H, Ota T, Minegishi Y, Nagata H, Kangawa K, Ishii H. Enhanced plasma ghrelin levels in rats with streptozotocin-induced diabetes. *FEBS Lett* 2003; **541**: 64-68
- 30 **Basa NR**, Wang L, Arteaga JR, Heber D, Livingston EH, Tache Y. Bacterial lipopolysaccharide shifts fasted plasma ghrelin to postprandial levels in rats. *Neurosci Lett* 2003; **343**: 25-28
- 31 **Zuckerman SH**, Shellhaas J, Butler LD. Differential regulation of lipopolysaccharide-induced interleukin 1 and tumor necrosis factor synthesis: effects of endogenous and exogenous glucocorticoids and the role of the pituitary-adrenal axis. *Eur J Immunol* 1989; **19**: 301-305
- 32 **Burgess W**, Gheusi G, Yao J, Johnson RW, Dantzer R, Kelley KW. Interleukin-1 β -converting enzyme-deficient mice resist central but not systemic endotoxin-induced anorexia. *Am J Physiol* 1998; **274**: R1829-1833
- 33 **Azuma T**, Suto H, Ito Y, Ohtani M, Dojo M, Kuriyama M, Kato T. Gastric leptin and *Helicobacter pylori* infection. *Gut* 2001; **49**: 324-329

Mechanisms of action of leptin in preventing gastric ulcer

Edward O. Adeyemi, Salim A. Bastaki, Irwin S. Chandranath, Mohammed Y. Hasan, Mohammed Fahim, Abdu Adem

Edward O. Adeyemi, Department of Internal Medicine, Faculty of Medicine and Health Sciences, UAE University, Al Ain, United Arab Emirates

Salim A. Bastaki, Irwin S. Chandranath, Mohammed Y. Hasan, Abdu Adem, Department of Pharmacology, Faculty of Medicine and Health Sciences, UAE University, Al Ain, United Arab Emirates
Mohammed Fahim, Department of Physiology, Faculty of Medicine and Health Sciences, UAE University, Al Ain, United Arab Emirates
Supported by the Faculty of Medicine and Health Sciences Research Grant, UAE University, United Arab Emirates

Correspondence to: Professor Abdu Adem, Department of Pharmacology, FMHS, UAE University, PO Box 17666, Al Ain, United Arab Emirates. abdu.adem@uaeu.ac.ae

Telephone: +971-3-7137522 Fax: +971-3-7672033

Received: 2004-10-23 Accepted: 2005-01-13

also suggest that leptin prevents ulcer formation by increasing the activities of the cyclo-oxygenase and/or nitric oxide pathways and by increasing mucus secretion.

© 2005 The WJG Press and Elsevier Inc. All rights reserved.

Key words: Indomethacin; Acidified ethanol; Gastric ulcer; Prostaglandin; Ranitidine; Omeprazole; Lansoprazole; *N*⁶-nitro L-arginine methyl ester; Wistar rats

Adeyemi EO, Bastaki SA, Chandranath IS, Hasan MY, Fahim M, Adem A. Mechanisms of action of leptin in preventing gastric ulcer. *World J Gastroenterol* 2005; 11(27): 4154-4160

<http://www.wjgnet.com/1007-9327/11/4154.asp>

Abstract

AIM: To investigate the effects of leptin (1-20 µg/kg) on acidified ethanol (AE)- and indomethacin (Indo)-induced gastric lesions in rats and compare it with ranitidine, lansoprazole, and omeprazole and to determine its mechanisms of actions.

METHODS: Gastric ulcers, which were approximately 1 mm in width, formed in the glandular portion of the gastric mucosa produced by oral administration of either AE or Indo were taken as ulcer index. The inhibitory effect of subcutaneous administration of leptin, two proton pump inhibitors (PPIs) lansoprazole and omeprazole, or H₂-receptor antagonist ranitidine 30 min before AE or Indo was evaluated. A radioimmunoassay was used to determine the PGE₂ concentration in the homogenate of the glandular portion of the stomach. We performed histological study of the glandular stomach for the evaluation of total, acidic, and sulfated mucus content.

RESULTS: Subcutaneous administration of leptin, two PPIs lansoprazole and omeprazole or H₂-receptor antagonist ranitidine 30 min before AE or Indo produced a dose-dependent and reproducible inhibition of gastric ulcers (GUs). This inhibition was found to be more potent than other antagonists used. In *N*⁶-nitro L-arginine methyl ester (L-NAME)-pretreated animals, the ulcer prevention ability of leptin in AE-induced ulcer was significantly reduced, compared to rats without L-NAME pretreatment. However, the ulcer prevention ability of leptin was not altered by L-NAME treatment in Indo-induced ulcers. Leptin produced a dose-dependent increase in PGE₂ level in the gastric glandular tissues. Leptin also increased mucus secretion.

CONCLUSION: The results of the present study show that leptin inhibits GU formation by AE or Indo in a dose-dependent and reproducible manner in rats. The results

INTRODUCTION

Peptic ulcer is caused by a break in the mucosal integrity, close to the acid-secreting areas of the gastrointestinal tract. It is a disease that was characterized by remissions and exacerbations before the era of gastric acid secretion modifying drugs or *Helicobacter pylori* (*H. pylori*). It is often located in the stomach (gastric ulcer, GU), in the proximal duodenum (duodenal ulcer), rarely in the esophagus, jejunum (distal to a gastrojejunal anastomosis) or the Meckel's diverticulum, containing ectopic gastric mucosa. Development of a peptic ulcer depends on the balance between the known aggressive factors and mucosal defense mechanisms. Some of the aggressive factors are gastric acid^[1,2], bile salts, abnormal motility^[3], pepsin, use of nonsteroidal anti-inflammatory drugs (NSAID)^[4], infection with micro-organisms (*H. pylori*, herpes simplex and others). Mucus secretion, gastroduodenal bicarbonate production^[5], prostaglandin synthesis^[6], cholecystokinin and somatostatin^[7], cellular regeneration, and normal tissue microcirculation protect against ulcer formation.

Leptin, a 167-amino acid peptide hormone, is secreted by the adipocytes into the circulation, lowers the body weight by decreasing appetite and increasing energy expenditure^[8-10]. It has also been found to be present in the gastric mucosa^[11], and this has been thought to control food intake in man. Another way of interpreting the presence of leptin in the gastric mucosa is to invoke its ability to function as a mucosal defense factor in the stomach. Indeed, a Polish group of workers showed recently that leptin has a gastro-protective effect in rats^[12]. Much more recently, a Turkish group of workers showed that leptin has a gastro-protective effect on mucosal injury induced by ischemia reperfusion^[13]. To date, there is a dearth of information in the literature about the mechanism by which leptin prevents ulcer formation in the stomach. Thus, the primary aim of this project was to investigate the effect of leptin on PGE₂ synthesis on ulcer formation by

indomethacin (Indo), a NSAID, or acidified ethanol (AE) in rats. The second aim was to study the role of leptin in relation to other established anti-ulcer agents, such as ranitidine^[14] and PPIs^[15] on peptic ulcer prevention in rats.

MATERIALS AND METHODS

The following drugs and chemicals were used for the experiments: absolute alcohol (BDH, Poole, UK), hydrochloric acid (BDH), lansoprazole (Sigma, St. Louis, MO, USA), omeprazole (Astra, Uppsala, Sweden), Indo (Sigma, UK), L-NAME (Sigma, UK) and high sensitivity prostaglandin E₂ Chemiluminescence Enzyme Immunoassay Kit (Assay Designs Inc., MI, USA). Leptin was a generous gift from Amgen Inc., USA. All solutions were freshly prepared and diluted in normal saline.

Experimental protocols

Wistar rats weighing 200–250 g were fasted for 18 h in wire mesh cages to avoid coprophagy. The animals were deprived of food but had free access to water *ad libitum*. The temperature of the animal room was maintained at 22±2 °C and a 12–12 h dark-light cycle was maintained. All animals used for the study had an ethical clearance from the Animal Users' Committee of the Faculty of Medicine, United Arab Emirates University.

Indomethacin-induced ulceration and effect of leptin treatment

Indo (30 mg/kg) was administered orally to induce GUs in 18-h fasted Wistar rats. Gastric lesions were formed 6 h after Indo administration. The rats were divided into different groups of six animals each and Indo was given to each animal 30 min after administering leptin (1–50 µg/kg, subcutaneously) or normal saline (1 mL/kg, subcutaneously), and the animals were killed 6 h later by cervical dislocation and exsanguinations. The abdomen was incised, the stomach removed and cut open along the greater curvature and rinsed with water to remove any adherent food particles and mucus. The opened stomach was spread on a sheet of cork so as to have a clear macroscopic view of the gastric mucosa. The total lengths of the hemorrhagic lesions, which were approximately 1 mm in width formed in the glandular portion of the gastric mucosa, were taken as ulcer index. An observer unaware of the drug treatments confirmed the ulcer index. The percentage reduction of the ulcer index in the drug-treated groups was calculated from the saline-treated groups.

Indomethacin-induced ulceration: comparison of leptin with ranitidine

The ability of different doses of leptin (1–50 µg/kg) and a fixed dose of ranitidine (50 mg/kg), all administered subcutaneously, to prevent the formation of Indo-induced GU was studied. The rats were killed 6 h after administering Indo by cervical dislocation and exsanguinations. The abdomen was incised and the stomach removed and the ulcer index was determined as described above. The reduction of the ulcer in the drug-treated groups was calculated as a percentage of the ulcer index in the saline-treated group.

Indomethacin-induced ulceration: comparison of leptin with two proton pump inhibitors

In another experiment, 10 mg/kg each of lansoprazole and

omeprazole, or 10 µg/kg of leptin was administered 30 min before the animals received Indo orally. The rest of the experiment and determination of the ulcer index were performed as described earlier.

Acidified ethanol-induced ulceration and effect of leptin treatment

AE was administered orally to induce GUs in rats. We used 60% ethanol in 150 mmol/L HCl as an ulcerogenic agent, based on earlier observation that ethanol 50% and above caused a reproducible model of gastric damage^[16,17]. Gastric lesions were formed 1 h after administering AE. The rats were divided into different groups of six animals each and each group received either saline (1 mL/kg) or leptin (1–20 µg/kg), subcutaneously. Thirty minutes later, AE was given orally to each animal at a dose of 1 mL per rat and the animals were killed 1 h later by cervical dislocation and exsanguinations. The ulcer index was determined as described above.

Leptin ulcer prevention ability in indomethacin pre-treated rats

In order to study the influence of prostaglandin on the cytoprotective activity of leptin, Indo was administered at a dose of 10 mg/kg subcutaneously (a dose, which inhibits prostaglandin synthesis, but does not induce gastric ulceration) to one group of animals followed by subcutaneous administration of leptin (10 µg/kg), 30 min later. AE was given to each animal 30 min after drug administration and the animals were killed 1 h later. The stomachs were subsequently removed to measure the ulcer index as described earlier.

Leptin ulcer prevention ability in L-NAME pre-treated rats

In another group of animals, N^G-nitro L-arginine methyl ester (L-NAME, 25 mg/kg), an inhibitor of nitric oxide synthase activity, was administered subcutaneously 15 min before giving leptin (10 µg/kg, subcutaneously). AE was given orally 30 min later and the animals were killed 1 h after ethanol administration to determine the ulcer index. In another group of L-NAME-pretreated animals, Indo was given orally instead of AE to induce ulcers, and the animals were killed 6 h later to determine the ulcer index.

Effect of leptin on prostaglandin E₂ (PGE₂) levels in the gastric mucosa

The glandular portion of the control and leptin-treated rat stomachs were homogenized in 1.5 mL of Tris buffer (50 mmol/L; pH 7.5) containing 10 µg/mL Indo to prevent further cyclo-oxygenase activity at 0 °C. The tissue homogenate was acidified by addition of 2 mmol/L HCl to a pH of 3.5, and allowed to settle at 4 °C for 15 min before centrifuging the samples in a microcentrifuge at 1 000 r/min for 5 min to remove the tissue debris. The supernatant was harvested and stored at -20 °C until assayed, usually within 24 h. A radioimmunoassay was used to determine the PGE₂ concentration in the supernatant according to the instructions of the manufacturer (Assay Designs Inc., MI, USA). The assay is based on the competitive binding technique by which PGE₂ present in a sample competes with a fixed amount of alkaline phosphatase-labeled PGE₂ for sites on a mouse mAb. During incubation, the mouse mAb is bound to the

goat anti-mouse antibody coated onto the microtiter well plate. Following a wash to remove excess conjugate and unbound sample, a substrate solution is added to the wells to determine the bound enzyme activity. Immediately following the color development, the luminescence is read in a luminometer. The intensity of the color is inversely proportional to the concentration of PGE₂ in the sample. A standard curve was constructed from a series of known concentrations of PGE₂ solution provided by the kit manufacturer, and the PGE₂ concentrations of the unknown samples were determined by interpolation.

Determination of mucus in glandular mucosa

We performed histological study of the glandular stomach for the evaluation of total, acidic, and sulfated mucus content. Cross-sectional areas of the portion of the gland stained red by periodic acid Schiff (PAS) were measured to give the total glycoprotein present in the gastric pits. The Alcian Blue (AB) method at pH 1 was used to measure the sulfated macromolecular content in the gastric pits, whereas at pH 2.5 were used to measure the total acidic mucus content.

The glandular portion of the stomach was fixed in Zamboni fixative overnight. Smaller pieces cut from the glandular portion was dehydrated with ethanol and embedded in paraffin. Two series of sections (6 μmol/L thick) were made by cutting the block in a plane perpendicular to the mucosal surface. Sections, after being deparaffinized

and hydrated to distilled water and placed in acetic acid solution, were stained with PAS and/or AB (pH 2.5 and 1). They were serially dehydrated in 95% ethyl alcohol, absolute alcohol, and xylene and mounted in resinous medium. The sections were evaluated in a randomized blinded fashion by a histologist who was unaware of the experimental protocol.

Statistical analysis

All results were expressed as mean±SE. Ulcer index obtained for test drugs and saline controls were compared using one-way ANOVA. A two-tailed *P* value <0.05 was considered significant.

RESULTS

Indo caused a marked ulceration of the stomach in those rats given normal saline (Figures 1A-D). Figure shows hemorrhagic lesions on the glandular area of the rat stomach caused by AE (A) and Indo (C) in the absence (A and C) and presence (B and D) of 10 μg/kg leptin. A significant inhibition of the hemorrhagic lesions due to the leptin treatment was evident. When the animals were treated with leptin (1-50 μg/kg), there was a dose-dependent increase of the ulcer prevention ability of leptin, against Indo and formed a plateau at a dose of 20 μg/kg leptin. The ulcer index at each of the leptin concentrations from 5-50 μg/kg was significantly less (*P*<0.05) than the ulcer index in normal saline-treated rats (Figure 2A).

Figure 2B reveals the degree of preventing Indo-induced

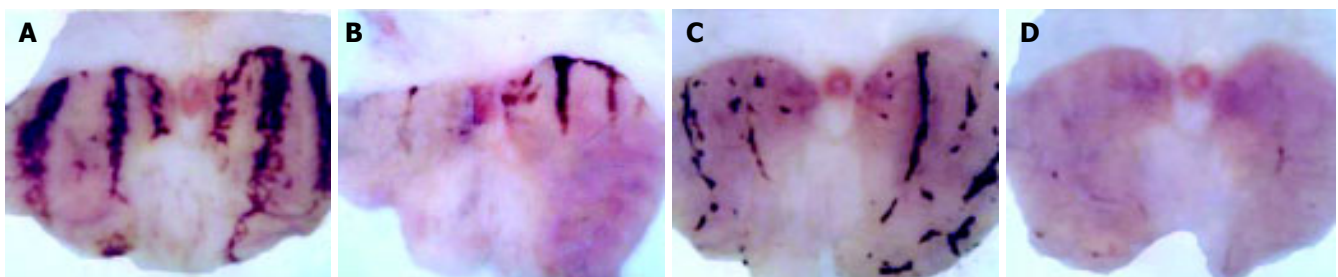


Figure 1 Photomicrograph of macroscopic appearance of the glandular mucosa, showing the effect of AE (A) and Indo (C) in the absence (A and C) and presence

of 10 μg/kg dose of leptin (B and D). These photographs are typical of six such tissues.

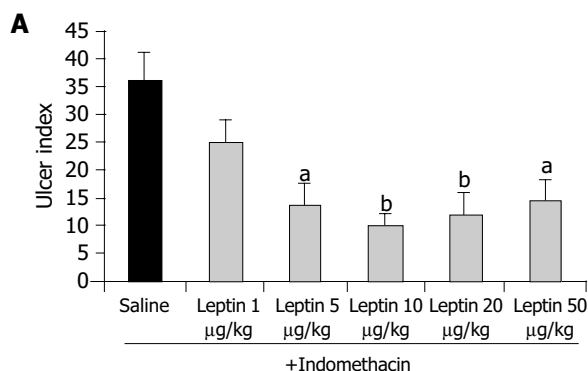
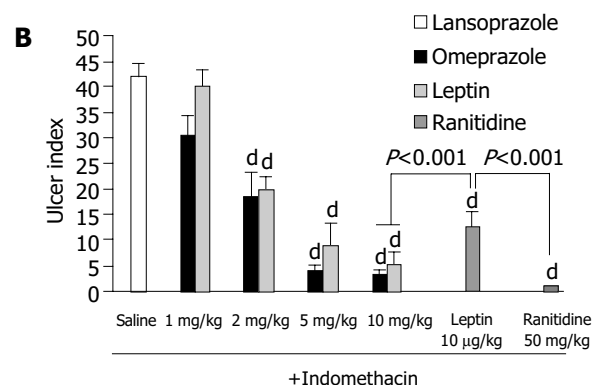


Figure 2 A: The ulcer indices of saline and different concentrations of leptin (1-50 μg/kg) against Indo. Each value is a mean±SE. Asterisks indicate significant difference when compared to saline control (^a*P*<0.05, ^b*P*<0.01); **B:** The degree of prevention of Indo-induced ulcerations after treatment with different doses of



lansoprazole and omeprazole (each used at 1-10 mg/kg), leptin (10 μg/kg) and ranitidine (50 mg/kg). Each value is a mean±SE. Asterisks indicate significant difference (^d*P*<0.001) when compared to saline control.

ulcerations when the animals were treated with lansoprazole and omeprazole, each used at a dose of 1, 2, 5, and 10 mg/kg. There was a profound inhibition of ulcer formation at 10 mg/kg of both lansoprazole and omeprazole. The difference between the drug-treated group (lansoprazole or omeprazole at 2-10 mg/kg) and the saline-treated group was significant ($P<0.001$); with lansoprazole showing a slightly more powerful inhibition than omeprazole but the difference between them was not statistically significant. The leptin ulcer inhibition at 10 $\mu\text{g}/\text{kg}$ dosage was significantly less ($P<0.001$) than that achieved with lansoprazole or omeprazole, each administered at 10 mg/kg (1 000 times the dose of leptin used; Figure 2B). When the rats were treated with 50 mg/kg of ranitidine (5 000 times the dose of leptin), the ulcer prevention activity was significantly higher ($P<0.001$) than that achieved with 10 $\mu\text{g}/\text{kg}$ leptin (Figure 2B).

When the animals were treated with increasing doses of leptin (1-10 $\mu\text{g}/\text{kg}$), lansoprazole (1-20 mg/kg) and omeprazole (0.5-10 mg/kg) 30 min before they received AE, there was a dose-dependent inhibition of ulcer formation by leptin and each of the PPIs (Figure 3).

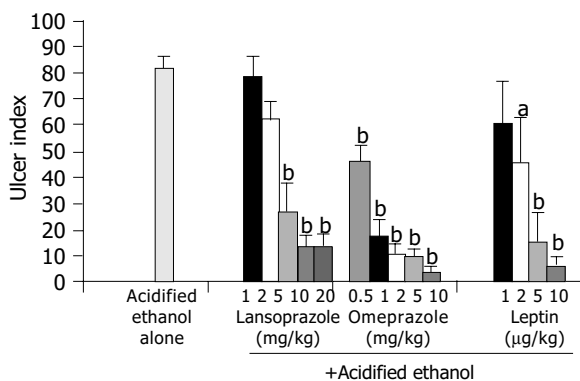


Figure 3 The effect of increasing doses of leptin (1-10 $\mu\text{g}/\text{kg}$), lansoprazole (1-10 mg/kg), and omeprazole (0.5-10 mg/kg) on AE-induced ulceration in rats. Each value is a mean \pm SE. Asterisks indicate significant difference, $^*P<0.05$, $^bP<0.001$ vs controls.

Leptin (10 $\mu\text{g}/\text{kg}$) produced a significant ($P<0.001$) inhibition of Indo-induced ulcers in L-NAME-pretreated animals, which was not statistically significantly different from the ulcer index for leptin in animals without L-NAME pretreatment (Figure 4).

Leptin caused a profound ulcer inhibition, which was significantly greater ($P<0.001$) for 10 $\mu\text{g}/\text{kg}$ of leptin than saline-treated controls when AE was used to induce gastric ulceration in Indo-pretreated animals (Figure 5). When ulcer induction was performed with AE in L-NAME-pretreated rats, there was a significantly greater degree ($P<0.001$) of GU inhibition by leptin than saline-treated controls (Figure 5). However, the inhibition by leptin of AE-induced ulcer formation was significantly less ($P<0.001$) in the presence of L-NAME than in its absence (Figure 5). Injection of increasing doses of leptin to the animals before AE led to increasing degrees of peptic ulcer prevention and higher tissue concentrations of PGE₂ (Figure 6). Leptin increased

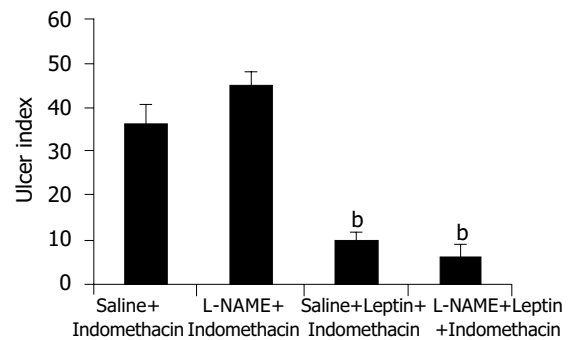


Figure 4 The ulcer prevention ability of leptin (10 $\mu\text{g}/\text{kg}$), when Indo was used to induce ulcer in L-NAME-pretreated animals. Each value is a mean \pm SE. Asterisks indicate significant difference, $^bP<0.001$ vs controls.

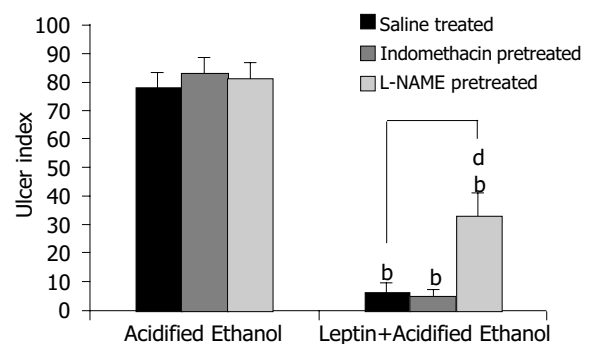


Figure 5 The ulcer prevention ability of leptin (10 $\mu\text{g}/\text{kg}$), in AE-induced ulcer after Indo or L-NAME pretreatment. Each value is a mean \pm SE. Asterisks indicate significant difference, $^bP<0.001$ vs controls. $^dP<0.001$ shows the significant difference in the effect of leptin on saline-treated and L-NAME-pretreated rats.

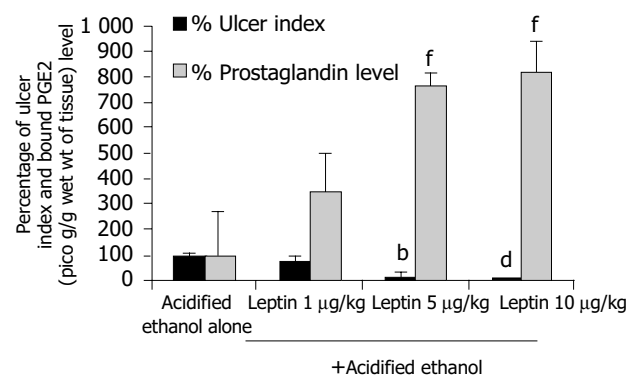


Figure 6 The effect of increasing doses of leptin (1-10 $\mu\text{g}/\text{kg}$) on AE-induced ulcer and prostaglandin E₂ levels in the gastric glandular mucosa in rats. Each value is a mean \pm SE. $^bP<0.01$, $^dP<0.001$ indicate significant difference in percentage ulcer index compared to AE-treated rats taken as 100%. $^fP<0.01$ shows the significant difference in the level of prostaglandin E₂ compared to AE-treated rats taken as 100%.

mucus secretion (Figures 7D, F) and prevented injury to the epithelial layer (Figures 7A-C) thus showing the involvement of mucus as the mechanism of gastroprotection.

DISCUSSION

Leptin is a peptide that is produced by the adipocytes and it

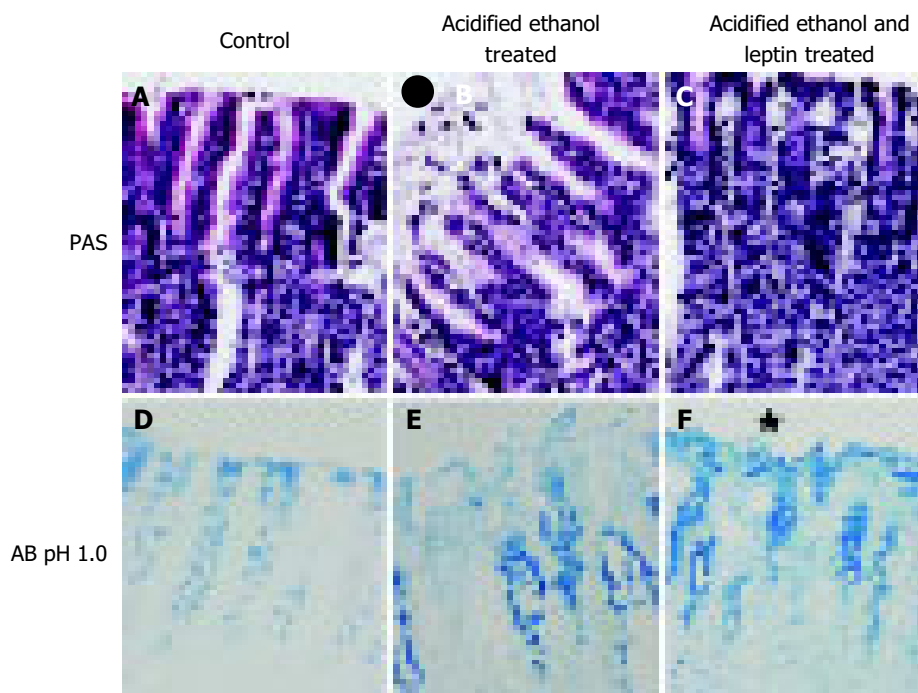


Figure 7 Gastric mucosal layer of rats stained with PAS showing (A) normal epithelium from control rats; (B) damaged epithelium (●) and (C) repaired epithelium after leptin treatment. Lower panel shows the AB (pH 1.0) staining

showing mucus in (D) normal epithelium; (E) loss of epithelial mucus due to AE (★) and (F) presence of epithelial mucus after leptin treatment (bar = 6 μ m; magnification 40 \times).

regulates the function of the satiety center in the hypothalamus^[8]. Although it has also been found in the stomach^[11] its function in the stomach is not clear. In this study, we investigated the property of leptin as an ulcer-preventing agent in an experimental animal model. Our results showed that exogenous leptin demonstrated profound ulcer prevention ability in rats when their gastric mucosa was exposed to ulcer-inducing agents, such as Indo and AE. Exogenous administration of leptin increased the leptin levels in the blood plasma, fundus, and antrum of the stomach^[18,19]. The basal leptin concentration did not prevent by itself the ulcerogenic effect of Indo or AE. However, exogenously administered leptin prevented this effect indicating a pharmacological action of leptin.

Indo is a well-known ulcerogenic agent. In this study, Indo produced hemorrhagic lesions in the gastric mucosa 6 h after its ingestion, which is in accord with previous reports^[20-23]. In Indo-induced ulceration, the ulcer prevention ability of leptin was dose-dependent, reaching a maximum at 10 μ g/kg. No further increase was observed when the leptin dose was doubled. Indeed, its ulcer prevention ability was reduced at a higher leptin dose of 50 μ g/kg. This phenomenon may be explained by an increase in gastric acid secretion that was observed in this study (unpublished data). At this dosage, the leptin ulcer prevention ability was significantly less ($P < 0.05$) than that achieved with ranitidine, which was used at 50 mg/kg, 5 000 times the dose of leptin. However, the ulcer prevention ability of leptin at 10 μ g/kg compares well with that of omeprazole or lansoprazole, each used at 10 mg/kg, 1 000 times the dose at which leptin was employed.

AE, a well-known ulcerogenic agent, was used in the study to produce gastric mucosal damage by causing areas

of focal hyperemia and hemorrhage^[22,24,25]. Moreover, intragastric ethanol increases vascular permeability and vascular damage in capillaries near the luminal surface and not in the deeper muscularis mucosa that might indicate a role for impaired blood flow in the production of AE-induced gastric lesions. Leptin demonstrated a profound ulcer prevention ability, which compared well with that of each of the PPIs, lansoprazole and omeprazole, when AE was employed as an ulcerogenic agent. This is in line with previous reports^[12] that leptin has gastro-protective effect on the gastric mucosal injury induced by topical application of 75% ethanol.

It was interesting to note that the leptin ulcer prevention ability was slightly greater in AE- than in Indo-induced ulceration, although it did not reach statistical level of significance. This may be due to the fact that the AE-induced ulcers are formed superficially at the epithelial layer unlike that induced by Indo, which affects the deeper layer, the submucosa. This profound effect of inhibiting AE-induced ulcer formation by leptin was maintained, even when the animals were pretreated with low dose of Indo. However, a competition in the production of gastric mucosal PGE₂ between Indo (inhibition) and leptin (stimulation) cannot be ruled out. In AE-induced ulceration, evaluation of the effect of leptin on gastric tissue prostaglandin synthesis revealed a dose-dependent increase of gastric mucosal PGE₂ concentration^[26]. This finding suggests that leptin might act in part via the cyclo-oxygenase pathway in preventing ulcer formation. Furthermore our findings that leptin stimulated mucus secretion support the notion that this peptide acted by stimulating PGE₂ production. It has been reported previously that PGE₂ stimulates mucus secretion^[26-28]. In contrast to our results Brzozowski *et al.*^[12], reported that

prostaglandins are not involved in the gastro-protective effect of leptin. The contradictory finding observed in our present results could be due to methodological differences in inducing ulcer.

The influence of leptin-induced histamine release, which has a protective effect on the gastric mucosa, was reported by several workers^[13,29]. Morimoto *et al.*^[29], have reported that histamine release in the hypothalamus was significantly increased by leptin administration. Erkasap *et al.*^[13], have reported that leptin exerts a cytoprotective effect by increasing gastric tissue histamine content which in turn maintain the gastric mucosal blood flow, thereby suggesting that histamine is involved in the prevention of ischemia reperfusion-induced gastric mucosal injury. Goiot *et al.*^[30], reported that the co-existence of leptin and STAT-3 proteins in antral cells provide evidence for the involvement of leptin in the control of gastric secretions. Konturek *et al.*^[31], have investigated the effect of leptin on gastric acid secretion using *H. pylori*-positive and -negative patients and reported that gastric meal- and CCK-induced leptin is capable of inhibiting basal and meal stimulated gastric H⁺ secretion in *H. pylori*-positive patients. But in *H. pylori*-negative patients the release of leptin was reduced in response to CCK and meal. We have shown that subcutaneous administration of low doses of leptin (1-50 µg/kg) potentiates the gastric acid stimulating effect of dimaprit, an H₂ receptor agonist, and pentagastrin, a gastrin receptor agonist, in anaesthetized rats (results not shown). The variation in our results and those of others may be due to the methodological approach towards the evaluation of leptin effect. Taken together our data and those of Azuma *et al.*^[32], Morimoto *et al.*^[29], Erkasap *et al.*^[13], and Konturek *et al.*^[19], suggested that, in addition to the local effect of leptin, a generalized effect of leptin could not be ruled out.

Pretreatment of the animals with L-NAME (25 mg/kg, subcutaneously), an inhibitor of the nitric oxide synthase, before AE-induced gastric ulcerations, reduced the peptic ulcer prevention ability of leptin (10 µg/kg) significantly. However, it did not blot it out completely. This finding suggests that the peptic ulcer prevention ability of leptin does not depend solely on the nitric oxide pathway. This again is in line with the observation of Brzozowski *et al.*^[12], that L-NAME reduced the ulcer-preventing ability of leptin against AE. Brzozowski *et al.*^[33], have also investigated the effect of centrally and intraperitoneally administered leptin and reported that its gastro-protective action, accompanied by increased gastric blood flow and increased plasma gastrin levels, depends on vagal activity and involves hyperemia mediated by NO.

Our results may have consequences for the clinical practice. Based on our data, one would want to recommend the use of leptin subcutaneously in a pilot study in humans, in order to assess its efficacy as an ulcer prevention drug in patients in the intensive care unit, who are prone to develop stress ulcers^[34] during the course of their treatment. Another potential area for its use is among patients with active rheumatoid arthritis^[35] who need to use NSAID for their inflammatory joint disease. This is mainly because the existing epidemiological data support a causal relationship between NSAID use and the development of clinically

important ulcer disease or its complications, including upper GI bleeding.

In conclusion, we have shown that leptin, at low doses (1-10 µg/kg), has ulcer prevention ability, which is comparable to that of ranitidine, an H₂-receptor antagonist or omeprazole and lansoprazole. The ulcer prevention ability of leptin varies according to the ulcerogenic agent used. It is more effective in inhibiting AE-induced than Indo-induced ulcers. The ulcer prevention ability of leptin in AE-induced ulcer involves the cyclooxygenase and the nitric oxide pathways, whereas it acts only via the cyclooxygenase pathway in preventing Indo-induced ulcers.

ACKNOWLEDGMENTS

We would like to thank Amgen Inc., USA, for kindly donating the leptin, which was used in this study. We would also like to thank Dr. Eric Mensah-Brown for his help in studying the photomicrographs and Mr. Naseer Omar for assisting in animal experiments and Dr. Edward Adeyemi who passed away at the end of the year 2004.

REFERENCES

- 1 **Magalhaes AF**, Macedo C, Hauck JR, Carvalhaes A, De Nucci G, Magna LA, Pedrazzoli J Jr. Acid suppression with ranitidine plus oral triple therapy improves ulcer healing but not *Helicobacter pylori* eradication. *Hepatogastroenterology* 1998; **45**: 2161-2164
- 2 **Brown LF**, Wilson DE. Gastroduodenal ulcers: causes, diagnosis, prevention and treatment. *Compr Ther* 1999; **25**: 30-38
- 3 **Azuma T**, Dodge M, Ito S, Yamazaki Y, Miyaji H, Ito Y, Sutte H, Kuriyama M, Kato T, Kohli Y. Bile reflux due to disturbed gastric movement is a cause of spontaneous gastric ulcer in W/W^v mice. *Dig Dis Sci* 1999; **44**: 1177-1183
- 4 **Gaw AJ**, Williams LV, Spraggs CF, Jordan CC. Role of pepsin in the development of indomethacin-induced antral ulceration in the rat. *Aliment Pharmacol Ther* 1995; **9**: 167-172
- 5 **Hogan DL**, Ainsworth NA, Isenberg J. Review article: Gastroduodenal bicarbonate secretion. *Aliment Pharmacol Ther* 1994; **8**: 475-478
- 6 **Peskar BM**, Maricic N. Role of prostaglandins in gastro protection. *Dig Dis Sci* 1998; **43**(Suppl 9): 23S-29
- 7 **Brzozowski T**, Konturek PC, Konturek SJ, Kwiecien S, Pajdo R, Brzozowska I, Hahn EG. Involvement of endogenous cholecystokinin and somatostatin in gastroprotection induced by intraduodenal fat. *J Clin Gastroenterol* 1998; **27**(Suppl 1): S125-137
- 8 **Zhang Y**, Proenca R, Maffei M, Barone M, Leopold L, Friedman JM. Positional cloning of the mouse obese gene and its human homologue. *Nature* 1994; **372**: 425-432
- 9 **Halaas JL**, Gajiwala KS, Maffei M. Weight reducing effects of the plasma protein encoded by the obese gene. *Science* 1995; **269**: 543-546
- 10 **Pelleymounter MA**, Cullen MJ, Baker MB, Hecht R, Winters D, Boone T. Effects of the obese gene product on body weight regulation in ob/ob mice. *Science* 1995; **269**: 540-543
- 11 **Bado A**, Lévassieur S, Attoub S, Kermorgant S, Laigneau JP, Bortoluzzi MN, Moizo L, Lehy T, Guerre-Millo M, Le Marchand-Brustel Y, Lewin MJ. The stomach is a source of leptin. *Nature* 1998; **394**: 790-793
- 12 **Brzozowski T**, Konturek PC, Konturek SJ, Pajdo R, Duda A, Pierzchalski P, Bielanski W, Hahn EG. Leptin in gastro protection induced by cholecystokinin or by a meal. Role of vagal and sensory nerves and nitric oxide. *Eur J Pharmacol* 1999; **374**: 263-266
- 13 **Erkasap N**, Uzuner K, Serteser M. Gastroprotective effect of

- leptin on gastric mucosal injury induced by ischaemia-reperfusion is related to gastric histamine content in rats. *Peptides* 2003; **24**: 1181-1187
- 14 **Lazzaroni M**, Bianchi Porro G. Prophylaxis and treatment of non-steroidal anti-inflammatory drug-induced upper gastrointestinal side effects. *Dig Liver Dis* 2001; **33**(Suppl 2): S44-48
- 15 **Warzecha Z**, Dembinski A, Brzozowski T. Histamine in stress ulcer prophylaxis in rats. *J Physiol Pharmacol* 2001; **52**: 407-421
- 16 **Nishida A**, Takinami Y, Yuki H. YM022{®}-1-[2,3-dihydro-1-(2'-methylphenacyl)-2-oxo-5-phenyl-1H-1,4benzodiazepin-3-yl]-3 (methylphenyl)urea, a potent and selective gastrin/cholecystokinin-B receptor antagonist, prevents gastric and duodenal lesions in rats. *J Pharmacol Exp Ther* 1994; **270**: 1256-1261
- 17 **Mercer DW**, Cross JM, Barreto JC. Cholecystokinin is a potent protective agent against alcohol-induced gastric injury in the rat. *Dig Dis Sci* 1995; **40**: 651-660
- 18 **Sobhani I**, Bado A, Vissuzaine C, Buysse M, Kermogrant S, Laigneau JP, Attoub S, Lehy T, Henin D, Mignon M, Lewin MJ. Leptin secretion and leptin receptor in the human stomach. *Gut* 2000; **47**: 178-183
- 19 **Konturek PC**, Brzozowski T, Sulekova Z, Meixner H, Hahn EG, Konturek SJ. Enhanced expression of leptin following acute gastric injury in rat. *J Physiol Pharmacol* 1999; **50**: 587-595
- 20 **Kasuya Y**, Urushidani T, Okabe S. Effects of various drugs and vagotomy on indomethacin-induced gastric ulcers in the rat. *Jap J Pharmacol* 1979; **29**: 670-673
- 21 **Ueki S**, Takeuchi K, Okabe S. Gastric motility is an important factor in the pathogenesis of indomethacin-induced gastric mucosal lesions in rats. *Dig Dis Sci* 1988; **33**: 209-216
- 22 **Bastaki SMA**, Chandranath SI, Singh J. Comparison of the antisecretory and antiulcer activity of epidermal growth factor, urogastrone and transforming growth factor alpha and its derivative in rodents *in vivo*. *Mol Cell Biochem* 2002; **236**: 83-94
- 23 **Chandranath SI**, Bastaki SMA, Singh J. Comparative study on the activity of lansoprazole, omeprazole and PD-136450 on acidified ethanol- and indomethacin-induced gastric lesions in the rat. *Clin Exp Pharmacol Physiol* 2002; **29**: 173-180
- 24 **Lacy ER**, Ito S. Microscopic analysis of ethanol damage to rat gastric mucosa after treatment with a prostaglandin. *Gastroenterology* 1982; **83**: 619-625
- 25 **Szabo S**, Trier J, Brown A. Early vascular injury and increased vascular permeability in gastric mucosal injury caused by ethanol in the rat. *Gastroenterology* 1985; **88**: 228-236
- 26 **Bastaki SMA**, Chandranath SI, Adem A. The role of prostaglandin E₂ in the ulcer preventing ability of leptin. *Gut* 2004; **53** (Suppl 3): A77
- 27 **Wallace JL**, Tigley AW. New insights into prostaglandins and mucosal defense. *Aliment Pharmacol Ther* 1995; **9**: 227-235
- 28 **Bastaki SMA**, Wallace JL. Pathogenesis of nonsteroidal anti-inflammatory drug gastropathy: clues to preventive therapy. *Can J Gastroenterol* 1999; **13**: 123-127
- 29 **Morimoto T**, Yamamoto Y, Yamatodani A. Leptin facilitates histamine release from the hypothalamus in rats. *Brain Res* 2000; **868**: 367-369
- 30 **Goiot H**, Attoub S, Kermogrant S, Laigneau JP, Lardeux B, Lehy T, Lewin MJ, Bado A. Antral mucosa expresses functional leptin receptors coupled to STAT-3 signaling, which is involved in the control of gastric secretions in the rat. *Gastroenterology* 2001; **121**: 1417-1427
- 31 **Konturek JW**, Konturek SJ, Kwiecien N, Bielanski W, Pawlik T, Rembiasz K, Domschke W. Leptin in the control of gastric secretion and gut hormones in humans infected with *Helicobacter pylori*. *Scand J Gastroenterol* 2001; **36**: 1148-1154
- 32 **Azuma T**, Suto H, Ito Y, Ohtani M, Dojo M, Kuriyama M, Kato T. Gastric leptin and *Helicobacter pylori* infection. *Gut* 2001; **49**: 324-329
- 33 **Brzozowski T**, Konturek PC, Pajdo R, Kwiecien S, Ptak A, Sliwowski Z, Drozdowicz D, Pawlik M, Konturek SJ, Hahn EG. Brain-gut axis in gastroprotection by leptin and cholecystokinin against ischemia-reperfusion induced gastric lesions. *J Physiol Pharmacol* 2001; **52**: 583-602
- 34 **Overmier JB**, Murison R. Anxiety and helplessness in the face of stress predisposes, precipitates and sustains gastric ulceration. *Behav Brain Res* 2000; **110**: 161-164
- 35 **Hochberg MC**. Association of nonsteroidal anti-inflammatory drugs with upper gastrointestinal disease: epidemiological and economic considerations. *J Rheumatol* 1992; **19** (Suppl 36): 63-67

Differentiation of embryonic stem cells into insulin-producing cells promoted by Nkx2.2 gene transfer

Akira Shiroy, Shigehiko Ueda, Yukiteru Ouji, Ko Saito, Kei Moriya, Yuko Sugie, Hiroshi Fukui, Shigeaki Ishizaka, Masahide Yoshikawa

Akira Shiroy, Yukiteru Ouji, Kei Moriya, Yuko Sugie, Shigeaki Ishizaka, Masahide Yoshikawa, Division of Developmental Biology, Department of Parasitology, Nara Medical University, Kashihara, Nara 634-8521, Japan
Shigehiko Ueda, Ko Saito, Hiroshi Fukui, Department of Gastroenterology and Hepatology, Nara Medical University, Kashihara, Nara 634-8521, Japan
Correspondence to: Masahide Yoshikawa, Division of Developmental Biology, Department of Parasitology, Nara Medical University, 840 Shijo-cho, Kashihara, Nara 634-8521, Japan. myoshika@naramed-u.ac.jp
Telephone: +81-744-29-8857 Fax: +81-744-24-7122
Received: 2004-11-29 Accepted: 2005-01-05

ability to differentiate into insulin-producing cells.

© 2005 The WJG Press and Elsevier Inc. All rights reserved.

Key words: Embryonic stem cells; Insulin; Nkx2.2; Dithizone

Shiroy A, Ueda S, Ouji Y, Saito K, Moriya K, Sugie Y, Fukui H, Ishizaka S, Yoshikawa M. Differentiation of embryonic stem cells into insulin-producing cells promoted by Nkx2.2 gene transfer. *World J Gastroenterol* 2005; 11(27): 4161-4166
<http://www.wjgnet.com/1007-9327/11/4161.asp>

Abstract

AIM: To investigate the ability of a genetically altered embryonic stem (ES) cell line to generate insulin-producing cells *in vitro* following transfer of the Nkx2.2 gene.

METHODS: Hamster Nkx2.2 genes were transferred into mouse ES cells. Parental and Nkx2.2-transfected ES cells were initiated toward differentiation in embryoid body (EB) culture for 5 d and the resulting EBs were transferred to an attached culture system. Dithizone (DTZ), a zinc-chelating agent known to selectively stain pancreatic beta cells, was used to detect insulin-producing cells. The outgrowths were incubated in DTZ solution (final concentration, 100 µg/mL) for 15 min before being examined microscopically. Gene expression of the endocrine pancreatic markers was also analyzed by RT-PCR. In addition, insulin production was determined immunohistochemically and its secretion was examined using an ELISA.

RESULTS: DTZ-stained cellular clusters appeared after approximately 14 d in the culture of Nkx2.2-transfected ES cells (Nkx-ES cells), which was as much as 2 wk earlier, than those in the culture of parental ES cells (wt-ES). The frequency of DTZ-positive cells among total cultured cells on day 28 accounted for approximately 1.0% and 0.1% of the Nkx-ES- and wt-ES-derived EB outgrowths, respectively. The DTZ-positive cellular clusters were found to be immunoreactive to insulin, while the gene expressions of pancreatic-duodenal homeobox 1 (PDX1), proinsulin 1 and proinsulin 2 were observed in the cultures that contained DTZ-positive cellular clusters. Insulin secretion was also confirmed by ELISA, whereas glucose-dependent secretion was not demonstrated.

CONCLUSION: Nkx2.2-transfected ES cells showed an

INTRODUCTION

It has been proposed that approximately 150 million people worldwide have diabetes mellitus, which may double by 2025, and 5-10% of those suffer from type 1 diabetes, for which injections of insulin are unavoidable. Transplantation of pancreatic islets for type 1 diabetes is a promising therapeutic strategy^[1], however, an inadequate supply of donor islets is a major obstacle. Thus, embryonic stem (ES) cells are being considered as a potential source for generating insulin-producing cells. ES cells come from clonal cell lines derived from the inner cell mass of developing blastocysts^[2,3], and are able to proliferate *in vitro* and have shown a capacity to differentiate into a broad spectrum of derivatives of all three embryonic germ layers including hematopoietic cells, cardiomyocytes, smooth muscle cells, neurons, hepatocytes, and insulin-producing cells^[4-10]. We recently reported the appearance of the islet-like cellular clusters containing insulin-producing cells in embryoid body (EB) outgrowth cultures with the use of a zinc-chelating substance, dithizone (DTZ)^[11]. However, the development of islet-like cellular clusters was found in only a small portion of the EB outgrowths and required long-term cultures of more than 3 wk.

Nkx2.2 and Nkx6.1 are NK-homeodomain genes expressed in early pancreatic progenitor cells as well as neurogenin-3 (Ngn3)-expressing islet precursor cells, and are considered to be β-cell competence factors^[12-14]. Nkx2.2 mutants completely lack insulin expression^[14], while Nkx6.1 mutants show a less dramatic impaired differentiation of β-cells^[15]. Further, Nkx2.2 expression lasts for a longer period of time in differentiated islet cells. These findings suggest that Nkx2.2 is a critical transcription factor in early pancreatic endocrine development and the following differentiation into pancreatic β-cells.

In the present study, we generated Nkx2.2-expressing

cell lines by transfection of the Nkx2.2 gene into undifferentiated ES cells, and investigated their ability to differentiate into insulin-producing cells in EB outgrowth cultures. We found that insulin-producing cells appeared as much as 2 wk earlier in the EB outgrowths derived from Nkx2.2-transfected ES (Nkx-ES) cells than in those from parental ES (wt-ES) cells. Further, the frequency of insulin-producing cells on culture d 28 was approximately 1% in the Nkx-ES-derived EB outgrowths, a 10-fold greater efficiency as compared to that on the wt-ES-derived EB outgrowths. These results suggest that Nkx2.2 acts to promote the differentiation of ES cells into insulin-producing cells.

MATERIALS AND METHODS

Murine ES cell lines

We utilized a mouse ES cell line, EB3 (129/SvJ mouse ES cells, a kind gift from Dr. Hitoshi Niwa, RIKEN Center for Developmental Biology, Kobe, Japan)^[15], which was a subline derived from E14tg2a ES cells^[16] and carried the blasticidin S-resistant selection marker gene driven by the Oct-3/4 promoter (active under undifferentiated status)^[17]. Undifferentiated EB3 cells were maintained on gelatin-coated dishes without feeder cells in the maintenance medium, which was knockout-DMEM medium (Gibco-BRL) supplemented with 10% fetal bovine serum (FBS; GIBCO/BRL), 0.1 mmol/L of 2-mercaptoethanol (Sigma), 10 mmol/L of non-essential amino acids (GIBCO/BRL), L-glutamine, and 1 000 U/mL of leukemia inhibitory factor (LIF; GIBCO/BRL).

Generation of Nkx2.2-expressing ES (Nkx-ES) cells

The hamster Nkx2.2 gene was obtained from the plasmid pBAT12.shNkx2.2 (kindly provided by Dr. M. German, University of California, San Francisco). The cDNA was inserted into the BstXI-stuffer site of the expression vector pPyCAGIRESzeocinpA^[18]. The constructed plasmid pPyCAGIRESzeocinpA-Nkx2.2 contained the zeocin resistance gene driven by the chicken β -actin promoter. The Nkx2.2 vector (20 μ g) was transfected using a lipofection method with lipofectAmine (GIBCO/BRL). Transfected ES cells were selected by growth in the presence of 20 μ g/mL of zeocin, and three clones expressing Nkx2.2 (Nkx-ES) were established. Undifferentiated Nkx-ES cells were maintained in the same manner as undifferentiated wt-ES cells.

EB outgrowths with non-selective differentiation

The method used for the EB outgrowths has been previously described^[11]. Briefly, undifferentiated ES cells were dissociated into single-cell suspensions and then cultured in hanging drops to induce embryoid body (EB) formation at an initial cell density of 500 cells per drop (20 μ L) of ES cell-medium in the absence of LIF. After 5 d in a hanging drop culture, the resulting EBs were plated in plastic 30-mm gelatin-coated dishes (five EBs per dish), and then allowed to attach and form outgrowth cultures. A half amount of culture medium was replenished with new medium every 2 d. The culture medium used was the maintenance medium lacking LIF and known differentiation-inducing factors.

Throughout the whole culture, no growth factors or cytokines including insulin were added to the culture medium.

Dithizone (DTZ)-staining

A DTZ (Merck, Whitehouse Station, NJ, USA) stock solution was prepared with 50 mg of DTZ in 5 mL of dimethylsulfoxide (DMSO) and stored briefly at -15 °C. The staining solution was filtered through a 0.2 μ m nylon filter and then used as a DTZ working solution. *In vitro* DTZ staining was performed by adding 10 μ L of the stock solution to 1 mL of culture medium, then the culture dishes were incubated at 37 °C for 15 min in the DTZ solution. After the dishes were rinsed thrice with HBSS, clusters stained crimson red were examined using a stereomicroscope. After examination, the dishes were refilled with DMEM containing 10% FBS. Although the stain completely disappeared from the cells after 5 h, the cultures that had not been treated with DTZ were used for RT-PCR and insulin secretion studies to avoid the influence of the treatment. In some experiments, the number of DTZ-stained cells in the cultures was determined by counting crimson red cells after trypsinization following DTZ stain.

RT-PCR

Total RNA was extracted from the cells using TRIzol (GIBCO/BRL). DNase-treated total RNA was used for the first-strand cDNA. This reaction was performed using M-MLV Reverse Transcriptase (Promega) and Random Primer (Takara Bio Inc.), following the protocols of the manufacturers. cDNA samples were subjected to PCR amplification with specific primers under linear conditions in order to reflect the original amount of the specific transcript. The cycling parameters were as follows: denaturation at 94 °C for 1 min, annealing at 52-60 °C for 1 min (depending on the primer), elongation at 72 °C for 1 min (35 cycles), and a final extension for 20 min at 72 °C. The PCR primers and the lengths of the amplified products were as follows: β -actin (TGAAGTGGCTGACTGCTGTG and CATCCTTGGCCTCAGCATAG, 174 bp); pro-insulin 1 (GTTGGTGCCTTCCCTACCCCTG and GTAGAGGGAGCAGATGCTGGTG, 300 bp); pro-insulin 2 (GTGGATGCGCTTCCCTGCCCTG and GTAGAGGGAGCAGATGCTGGTG, 300 bp); PDX1 (GGCCACACAGCTCTACAAGG and TTCCACTTCATGCGACGGTT, 582 bp); and mouse-nkx2.2 (TGACCAACACAAAGACGGGGT and GCACGTTTCATCTTGTAGCGA, 650 bp). A set of mouse-nkx2.2 primers was used for the detection of hamster Nkx2.2.

Immunocytochemistry

Cells in culture dishes were fixed with 4% paraformaldehyde in phosphate-buffered solution and immunocytochemistry was carried out using a standard protocol. As the primary antibody for Nkx2.2, mouse anti-chick Nkx2.2 mAb (Hybridoma Bank, University of Iowa) was used at a dilution of 1:40. For detection of the primary antibody, a biotinylated anti-mouse antibody, ABC kit (VECTASTAIN Elite ABC KIT), and DAB (Dojindo; Kumamoto, Japan) were utilized according to the manufacturers' instructions.

For detection of the primary antibody, a fluorescent labeled secondary antibody, goat anti-guinea pig IgG conjugated with fluorescein-5-isothiocyanate (Cappel 57000, ICN Pharmaceuticals, Inc., OH, USA), was utilized according to the manufacturer's instructions. All nuclei were stained with DAPI (Dojindo; Kumamoto, Japan).

Insulin detection assay

Cells in the culture dishes were washed thrice with PBS and pre-incubated in Krebs Ringer bicarbonate buffer (KRBB) containing 2.8 mmol/L of glucose for 1 h, then placed in 1 000 μ L of KRBB with 2.8 mmol/L of glucose for 2 h. Next, the supernatant was collected and the dishes were rinsed thrice with PBS, after which the cells were re-incubated with KRBB containing 25.5 mmol/L of glucose for 2 h. Subsequently, conditioned medium samples were collected, and insulin levels were measured using an enzyme immunoassay (Mouse Insulin ELISA TMB Kit AKRIN-011T, Shibayagi Co., Ltd. Gunma, Japan) that detects mouse insulin in a range between 156 and 10 000 pg/mL with no cross-reactivity to C-peptide.

RESULTS

Establishment of Nkx2.2-expressing ES cell lines

ES cells were transfected with the Nkx2.2 expression vector and selected with zeocin. Three stable clones at a time were obtained and screened for Nkx2.2 expression by RT-PCR and three clones with a high expression of Nkx2.2 were finally selected (Figure 1A). Subsequently, immunocytochemistry showed that all three clones expressed Nkx2.2 protein (Figure 1B). Each Nkx-ES clone demonstrated similar results in the following experiments, thus representative results from only clone 3 are shown.

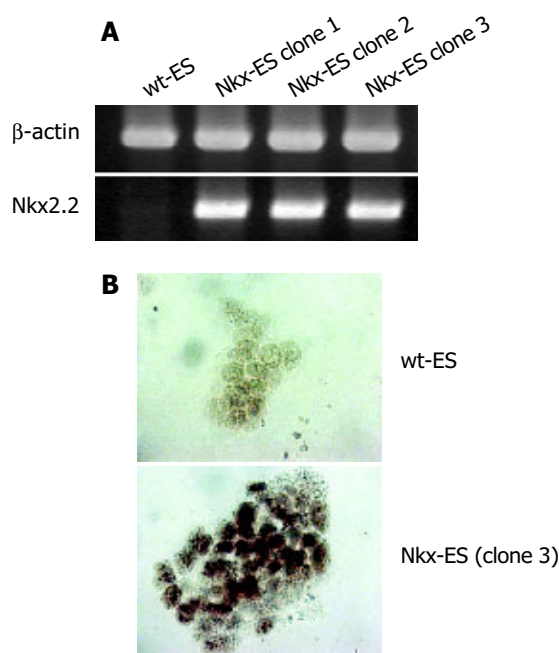


Figure 1 Expression of Nkx2.2 in parental (wt-ES cells) and Nkx2.2-transfected ES cells (Nkx-ES cells). **A:** Nkx-ES cells, but not wt-ES cells, expressed Nkx2.2 mRNA; **B:** Nkx2.2 protein was mainly observed in the nuclei of Nkx-ES cells. Original magnification, $\times 200$.

Early appearance of DTZ-stained cells in EB outgrowths

DTZ, a zinc-chelating agent, is known to selectively stain pancreatic β -cells crimson red^[19-21] and we previously demonstrated that DTZ stain could also be applied for the detection of ES-derived insulin-producing cells. Figure 2 shows the outline of the EB outgrowth culture and results of DTZ-staining. DTZ-positive cellular clusters appeared as much as 2 wk earlier in the EB outgrowths derived from Nkx-ES cells. On d 14, DTZ-positive cells were already present in the EB outgrowths derived from Nkx-ES cells (Figure 2D), whereas they were absent in those from wt-ES cells (Figure 2A). On d 21, distinct DTZ-positive cellular clusters were observed in the Nkx-ES-derived EB outgrowths (Figure 2E), while they were obscure in the differentiating wt-ES cultures (Figure 2B). In the wt-ES-derived EB outgrowths, DTZ-positive cellular clusters became distinct on d 28 (Figure 2C). The appearance of DTZ-positive clusters on d 28 in Nkx-ES-derived EB outgrowths was quite similar to that seen on d 21 (Figures 2E and F).

DTZ-stained clusters that appeared in Nkx-ES-derived EB outgrowths were frequently larger than those in wt-ES-derived EB outgrowths. To estimate the frequency of the emerged DTZ-stained cells in the cultures, the number of DTZ-stained red cells was directly counted under a microscope after trypsinization following the treatment with DTZ. The percentages of DTZ-stained cells among total cells on day 28 were $1.0 \pm 0.2\%$ of the Nkx-ES-derivatives and less than 0.1% of the wt-ES-derivatives.

Gene expression and immunohistochemistry of differentiating EB outgrowths

Pdx 1, a key transcriptional factor of pancreatic differentiation, was faintly detected in Nkx-ES cells and completely absent in wt-ES cells on d 0. Thereafter, Pdx 1 was expressed in all EB outgrowths on d 14, 21, and 28 as well as in isolated mouse islets. In contrast, Nkx2.2 was not detected on d 14, faintly detected on d 21, and clearly detected on d 28 in the differentiating wt-ES cells. In addition, pro-insulin 1 and 2 were detected on d 14 in the Nkx-ES-derived EB outgrowths, though not until d 28 in the wt-ES-derived EB outgrowths. To confirm the expression of insulin protein, we performed an immunohistochemistry examination in parallel with the DTZ-stain examination (Figure 3B). Immunoreactivity against insulin was found to coincide with the DTZ-stained culture areas within the EB outgrowths. In Nkx-ES-derived EB outgrowths, insulin-immunoreactivity was detected as early as on d 14, whereas it did not become positive until d 28 in the wt-ES-derived EB outgrowths. No immunoreactivity was found on d 14 or 21 in the wt-ES-derived EB outgrowths.

Insulin secretion

EB outgrowths on d 28 were used for the detection of released insulin. Insulin concentrations in culture media of wt-ES-derived EB outgrowths incubated with 2.8 and 25 mmol/L of glucose were 163 ± 38 and 191 ± 31 pg/mL, respectively, while those in media of Nkx-ES-derived EB outgrowths were 525 ± 132 and 660 ± 171 pg/mL with 25.5 mmol/L of glucose, respectively. Glucose-dependent insulin secretion was not observed in wt-ES- or Nkx-ES-

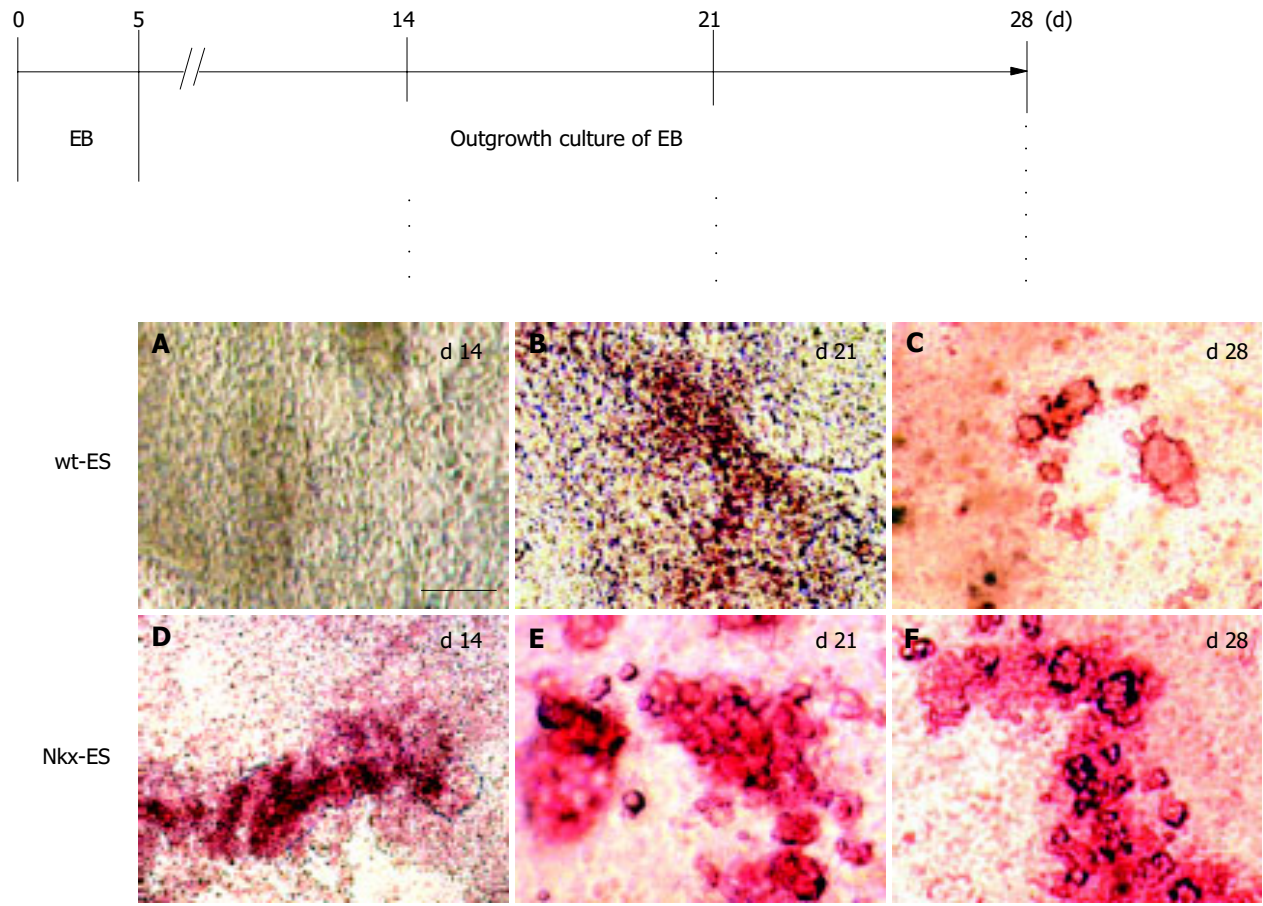


Figure 2 A-F: Early appearance of insulin-producing cells in EB outgrowths. An outline of the culture processes and results of DTZ-staining are shown. Scale

bar represents 100 μ m in length.

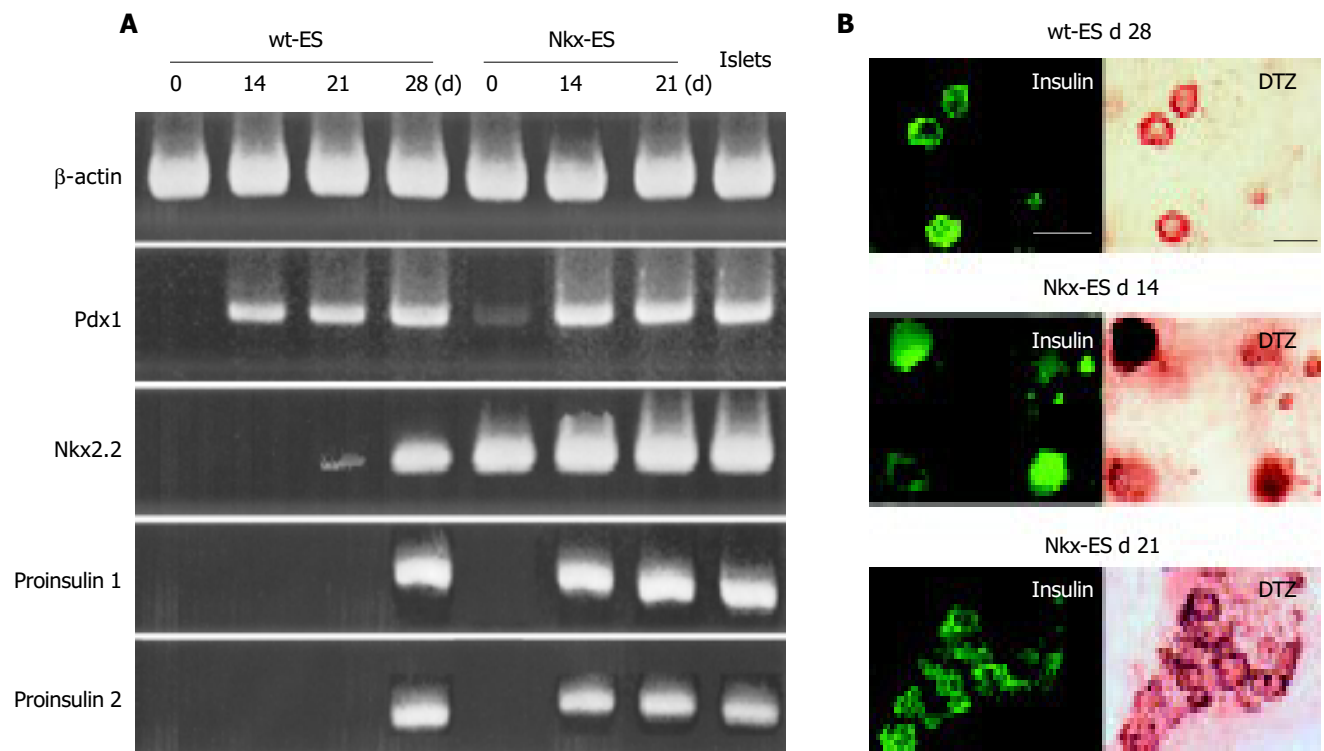


Figure 3 Gene expression and immunohistochemistry findings for differentiating EB outgrowths. **A:** The expression of Pdx 1, Nkx2.2, pro-insulin 1 and pro-insulin 2 was examined in differentiating wt-ES cells and Nkx-ES cells; **B:**

Insulin-immunoreactivity was examined in the EB outgrowths with DTZ-staining. Scale bars represent 100 μ m in length.

derived EB outgrowth cultures, whereas secreted insulin was detected in the Nkx-ES-derived EB outgrowth cultures, in amounts several times greater than in the wt-ES-derived EB outgrowth cultures.

DISCUSSION

The homeodomain transcription factor Nkx2.2 is one of the key transcription factors in pancreatic β -cell differentiation and expressed throughout all development periods, as well as broadly in the initial pancreatic precursor population, and in Ngn3-expressing islet progenitor cells and differentiated islet cells^[12,13,22]. Mice homozygous for a null mutation of Nkx2.2 develop severe hyperglycemia leading to death shortly after birth, because of the lack of insulin-producing β -cells^[14], and show a variety of functional defects in the islet cells that produce endocrine hormones other than insulin. In the present study, we examined genetically altered ES cells after transfection of the Nkx2.2 gene to determine their ability to differentiate into insulin-producing cells *in vitro*.

To assess the effect of the exogenous Nkx2.2 transgene on generation of insulin-producing ES-derived cells, we considered that an EB-based 1-step culture protocol^[11,15,23] that supported natural differentiation of ES cells would be better than an EB-based multi-step protocol^[24] that directed an oriented differentiation of ES cells toward pancreatic cell lineages using serum-free culture followed by a combination of growth factors. Since a promoted induction of insulin-producing cells was expected, a less efficient differentiation protocol was better suited to demonstrate the promoted action than a more sophisticated and efficient protocol. In addition, some investigators have speculated that the insulin-immuno-positive nature of cultured cells derived in an EB-based multi-step method is due to the incorporation of insulin from the culture medium^[25,26], while it is also suspected that such insulin-incorporated cells are apoptotic. Therefore, in the present study, EBs are simply allowed to attach and grow in gelatin-coated dishes in media containing FCS without growth factors, including insulin.

Since the emergence of insulin-producing cells among the simple EB outgrowths was expected to be rare, we used DTZ to locate those that produced insulin. DTZ is a zinc-binding substance, and known to stain crimson red the pancreatic islets from such animals, as mice, dogs and pigs, as well as those from human beings^[19-21]. We previously reported that DTZ-stained cellular clusters appeared in EB outgrowths and that the clusters demonstrated characteristics similar to pancreatic islets^[11]. In the present study, DTZ-stained cellular clusters appeared 2 wk earlier in the Nkx-ES-derived EB outgrowths, as compared to the wt-ES-derived EB outgrowths. Those cellular clusters were immunopositive for insulin and the presence of secreted insulin was confirmed by ELISA. Further, in addition to an early emergence, an increased frequency of DTZ-stained cells was also observed in the Nkx-ES-derived EB outgrowths. These results suggest that the fate of differentiating cells was favorably affected toward the generation of insulin-producing cells.

In spite of our success, the DTZ-positive cellular fraction still accounted for only 1% of the differentiated Nkx-ES cells. To achieve a more efficient generation of insulin-

producing cells from ES cells *in vitro*, controlled regulation of other transcriptional factors that are involved in pancreatic β -cell differentiation might be necessary. Indeed, a highly efficient production of insulin-producing cells from ES cells has been reported by the expression of exogenously transfected *pdx-1*, *pax 4*, or *Nkx6.1*^[27-29].

The precise mechanisms by which Nkx-ES cells promote the induction of insulin-producing cells is unknown, thus sequential analyses of a number of transcription factors that are involved in pancreatic β -cell differentiation must be examined in differentiating Nkx-ES cells. Although we have not performed such an analysis, an important finding to investigate is the early expression of insulin seen in the present differentiating Nkx-ES cells. Nkx2.2 expression preceded insulin expression in differentiating wt-ES cells (Figure 3A), which has also been seen in the pancreatic β -cell development^[30]. Therefore, Nkx-ES cells may directly skip to that process following Nkx2.2 expression. Glucose-dependent insulin secretion was not observed in the cultures of ES-derived insulin-secreting cells, which we considered may have been due to the high concentration of glucose present in the culture media, in which the ES cells were allowed to differentiate until the insulin detection assay.

In summary, we generated gene-engineered Nkx2.2-expressing ES cells and demonstrated their ability to induce insulin-producing cells *in vitro*. Our results show that gene-engineered ES may be a useful source of insulin-producing cells.

REFERENCES

- 1 **Shapiro AM**, Lakey JR, Ryan EA, Korbutt GS, Toth E, Warnock GL, Kneteman NM, Rajotte RV. Islet transplantation in seven patients with type 1 diabetes mellitus using a glucocorticoid-free immunosuppressive regimen. *N Engl J Med* 2000; **343**: 230-238
- 2 **Evans MJ**, Kaufman MH. Establishment in culture of pluripotent cells from mouse embryos. *Nature* 1981; **292**: 154-156
- 3 **Martin GR**. Isolation of a pluripotent cell line from early mouse embryos cultured in medium conditioned by teratocarcinoma stem cells. *Proc Natl Acad Sci USA* 1981; **78**: 7634-7638
- 4 **Assady S**, Maor G, Amit M, Itskovitz-Eldor J, Skorecki KL, Tzukerman M. Insulin production by human embryonic stem cells. *Diabetes* 2001; **50**: 1691-1697
- 5 **Hori Y**, Rulifson IC, Tsai BC, Heit JJ, Cahoy JD, Kim SK. Growth inhibitors promote differentiation of insulin-producing tissue from embryonic stem cells. *Proc Natl Acad Sci USA* 2002; **99**: 16105-16110
- 6 **Kahan BW**, Jacobson LM, Hullett DA, Ochoada JM, Oberley TD, Lang KM, Odorico JS. Pancreatic precursors and differentiated islet cell types from murine embryonic stem cells: an *in vitro* model to study islet differentiation. *Diabetes* 2003; **52**: 2016-2024
- 7 **Moritoh Y**, Yamato E, Yasui Y, Miyazaki S, Miyazaki J. Analysis of insulin-producing cells during *in vitro* differentiation from feeder-free embryonic stem cells. *Diabetes* 2003; **52**: 1163-1168
- 8 **Segev H**, Fishman B, Ziskind A, Shulman M, Itskovitz-Eldor J. Differentiation of human embryonic stem cells into insulin-producing clusters. *Stem Cells* 2004; **22**: 265-274
- 9 **Blyszczuk P**, Wobus AM. Stem cells and pancreatic differentiation *in vitro*. *J Biotechnol* 2004; **113**: 3-13
- 10 **Lester LB**, Kuo HC, Andrews L, Nauert B, Wolf DP. Directed differentiation of rhesus monkey ES cells into pancreatic cell phenotypes. *Reprod Biol Endocrinol* 2004; **2**: 42
- 11 **Shiroi A**, Yoshikawa M, Yokota H, Fukui H, Ishizaka S,

- Tatsumi K, Takahashi Y. Identification of insulin-producing cells derived from embryonic stem cells by zinc-chelating dithizone. *Stem Cells* 2002; **20**: 284-292
- 12 **Schwitzgebel VM**, Scheel DW, Conners JR, Kalamaras J, Lee JE, Anderson DJ, Sussel L, Johnson JD, German MS. Expression of neurogenin 3 reveals an islet cell precursor population in the pancreas. *Development* 2000; **127**: 3533-3542
- 13 **Sander M**, Sussel L, Conners J, Scheel D, Kalamaras J, Dela Cruz F, Schwitzgebel V, Hayes-Jordan A, German M. Homeobox gene Nkx6.1 lies downstream of Nkx2.2 in the major pathway of beta-cell formation in the pancreas. *Development* 2000; **127**: 5533-5540
- 14 **Sussel L**, Kalamaras J, Hartigan-O'Connor DJ, Meneses JJ, Pedersen RA, Rubenstein JL, German MS. Mice lacking the homeodomain transcription factor Nkx2.2 have diabetes due to arrested differentiation of pancreatic beta cells. *Development* 1998; **125**: 2213-2221
- 15 **Yamada T**, Yoshikawa M, Takaki M, Torihashi S, Kato Y, Nakajima Y, Ishizaka S, Tsunoda Y. *In vitro* functional gut-like organ formation from mouse embryonic stem cells. *Stem Cells* 2002; **20**: 41-49
- 16 **Hooper M**, Hardy K, Handyside A, Hunter S, Monk M. HPRT-deficient (Lesch-Nyhan) mouse embryos derived from germline colonization by cultured cells. *Nature* 1987; **326**: 292-295
- 17 **Niwa H**, Miyazaki J, Smith AG. Quantitative expression of Oct-3/4 defines differentiation, dedifferentiation or self-renewal of ES cells. *Nat Genet* 2000; **24**: 372-376
- 18 **Niwa H**, Burdon T, Chambers I, Smith A. Self-renewal of pluripotent embryonic stem cells is mediated via activation of STAT3. *Genes Dev* 1998; **12**: 2048-2060
- 19 **Latif ZA**, Noel J, Alejandro R. A simple method of staining fresh and cultured islets. *Transplantation* 1988; **45**: 827-830
- 20 **Clark SA**, Borland KM, Sherman SD, Rusack TC, Chick WL. Staining and *in vitro* toxicity of dithizone with canine, porcine, and bovine islets. *Cell Transplant* 1994; **3**: 299-306
- 21 **Shewade YM**, Umrani M, Bhonde RR. Large-scale isolation of islets by tissue culture of adult mouse pancreas. *Transplant Proc* 1999; **31**: 1721-1723
- 22 **Watada H**, Scheel DW, Leung J, German MS. Distinct gene expression programs function in progenitor and mature islet cells. *J Biol Chem* 2003; **278**: 17130-17140
- 23 **Yamada T**, Yoshikawa M, Kanda S, Kato Y, Nakajima Y, Ishizaka S, Tsunoda Y. *In vitro* differentiation of embryonic stem cells into hepatocyte-like cells identified by cellular uptake of indocyanine green. *Stem Cells* 2002; **20**: 146-154
- 24 **Lumelsky N**, Blondel O, Laeng P, Velasco I, Ravin R, McKay R. Differentiation of embryonic stem cells to insulin-secreting structures similar to pancreatic islets. *Science* 2001; **292**: 1389-1394
- 25 **Rajagopal J**, Anderson WJ, Kume S, Martinez OI, Melton DA. Insulin staining of ES cell progeny from insulin uptake. *Science* 2003; **299**: 363
- 26 **Sipione S**, Eshpeter A, Lyon JG, Korbitt GS, Bleackley RC. Insulin expressing cells from differentiated embryonic stem cells are not beta cells. *Diabetologia* 2004; **47**: 499-508
- 27 **Miyazaki S**, Yamato E, Miyazaki J. Regulated expression of pdx-1 promotes *in vitro* differentiation of insulin-producing cells from embryonic stem cells. *Diabetes* 2004; **53**: 1030-1037
- 28 **Blyszczuk P**, Czyz J, Kania G, Wagner M, Roll U, St-Onge L, Wobus AM. Expression of Pax4 in embryonic stem cells promotes differentiation of nestin-positive progenitor and insulin-producing cells. *Proc Natl Acad Sci USA* 2003; **100**: 998-1003
- 29 **Leon-Quinto T**, Jones J, Skoudy A, Burcin M, Soria B. *In vitro* directed differentiation of mouse embryonic stem cells into insulin-producing cells. *Diabetologia* 2004; **47**: 1442-1451
- 30 **Soria B**. *In-vitro* differentiation of pancreatic beta-cells. *Differentiation* 2001; **68**: 205-219

Science Editor Guo SY Language Editor Elsevier HK

Comparison of murine cirrhosis models induced by hepatotoxin administration and common bile duct ligation

Ming-Ling Chang, Chau-Ting Yeh, Pei-Yeh Chang, Jeng-Chang Chen

Ming-Ling Chang, Chau-Ting Yeh, Liver Research Unit, Department of Hepatogastroenterology, Chang Gung Memorial Hospital, Taoyuan, Taiwan, China

Pei-Yeh Chang, Jeng-Chang Chen, Department of Surgery, Chang Gung Children's Hospital, Taoyuan, Taiwan, China

Supported by the Chang Gung Memorial Hospital, Taoyuan, Taiwan, China, CMRPG 33014, CMRPG 33063 and CMRP 800

Correspondence to: Jeng-Chang Chen, Department of Surgery, Chang Gung Children's Hospital, 5 Fu-Shin Street, Kweishan, 333, Taoyuan, Taiwan, China. jengchang@so-net.net.tw

Telephone: +886-3-3281200-8227 Fax: +886-3-3287261

Received: 2004-10-20 Accepted: 2004-12-23

Key words: Common bile duct ligation; Fibrosis; Hepatotoxin; Liver; Mice

Chang ML, Yeh CT, Chang PY, Chen JC. Comparison of murine cirrhosis models induced by hepatotoxin administration and common bile duct ligation. *World J Gastroenterol* 2005; 11(27): 4167-4172

<http://www.wjgnet.com/1007-9327/11/4167.asp>

Abstract

AIM: To build up the research models of hepatic fibrosis in mice.

METHODS: Inbred wild-type FVB/N mice were either treated with alpha-naphthyl-isothiocyanate (ANIT), allyl alcohol (AA), carbon tetrachloride (CCl₄), 3,5-diethoxycarbonyl-1,4-dihydrocollidine (DDC), and silica, or subjected to common bile duct ligation (CBDL) to induce hepatic injury. Liver biopsies were performed every 4 wk to evaluate hepatic fibrosis over a period of 6 mo. Cumulative cirrhosis and survival curves were constructed by life table method and compared with Wilcoxon test.

RESULTS: Under the dosages used, there was neither mortality nor cirrhosis in AA and silica-treated groups. DDC and ANIT caused cirrhosis within 4-12 and 12-24 wk, respectively. Both showed significantly faster cirrhosis induction at high dosages without significant alteration of survival. The duration for cirrhosis induction by CCl₄ ranged from 4 to 20 wk, mainly dependent upon the dosage. However, the increase in CCl₄ dosage significantly worsened survival. Intraperitoneal CCl₄ administration resulted in better survival in comparison with gavage administration at high dosage, but not at medium and low dosages. After CBDL, all the mice developed liver cirrhosis within 4-8 wk and then died by the end of 16 wk.

CONCLUSION: CBDL and administrations of ANIT, CCl₄, and DDC ensured liver cirrhosis. CBDL required the least amount of time in cirrhosis induction, but caused shortened lives of mice. It was followed by DDC and ANIT administration with favorable survival. As for CCl₄, the speed of cirrhosis induction and the mouse survival depended upon the dosages and the administration route.

INTRODUCTION

Being the final outcome of chronic liver damage regardless of the underlying etiologies, hepatic fibrosis demands thorough study. The studies of hepatic fibrosis rely upon the availability of animal models. Although no experimental model exactly reproduces human liver fibrosis by etiologies, animal models serve to improve our understanding of pathogenetic mechanisms of liver fibrosis. In view of the cost-effectiveness in inducing hepatic injuries, hepatotoxin administration and common bile duct ligation (CBDL) were considered as useful methods^[1].

In recent years, advances in molecular biology have helped to generate a transgenic mouse model of liver fibrosis^[2]. This represents a new form of perturbation analysis whereby selective expression of novel or altered genes are used to perturb a complex system so that the information about the changes during development, functioning and malfunctioning can be deduced^[3]. This approach potentially allows development of animal models with liver fibrosis that are inducible and genetically similar to that of man. A reliable and reproducible model of hepatic fibrosis in wild-type control mice will aid to unveil the pathologic mechanisms deduced from genetic and molecular approaches. However, informative data of mouse hepatic fibrosis generated in the laboratory remained lacking in the literature because rats had long been the most common animal model for studying hepatic fibrosis induced by various chemical or surgical hepatic injuries^[1]. Since different animal models display distinct characteristics in the nature of pathogenesis of fibrosis or cirrhosis, the data acquired from rats could not apply to mice without bias^[4-8]. This urged us to set up a mouse model of hepatic fibrosis using CBDL or the administration of various hepatotoxins including alpha-naphthyl-isothiocyanate (ANIT)^[9,10], silica^[11], carbon tetrachloride (CCl₄)^[12-14], 3,5-diethoxycarbonyl-1,4-dihydrocollidine (DDC)^[15,16], and allyl alcohol (AA)^[17-19]. This study mainly focused on the strain of FVB/N inbred mice, which have been widely used to generate a variety of transgenic lines owing to their high reproduction rate and easy access in microinjection^[20,21].

MATERIALS AND METHODS

Mice

Inbred FVB/N mice (8-10 wk old) were obtained from the National Laboratory Animal Center (Taipei, Taiwan). All animals received care as outlined in the "Guides for the Care and Use of Laboratory Animals" prepared by the Committee of Animal Research, Chang Gung Memorial Hospital. Mice were supplied with food and water and exposed to a 12-h light-dark cycle. Ten mice (five males and five females) composed a group to which surgical CBDL or a hepatotoxin via intraperitoneal (IP) or oral gavage (OG) administration at the same dosage was given during a period of 6 mo.

Methods to induce hepatic injuries

ANIT (Sigma Chemical Co., St. Louis, MO, USA) ANIT was dissolved in corn oil and administered via IP or OG route, respectively. For each route of administration, there were three subgroups according to the maintenance dose as follows: 25 mg/kg (low dosage), 50 mg/kg (medium dosage) and 125 mg/kg (high dosage). After a single loading dose of 100 mg/kg, the maintenance doses were given twice a week. Additionally, there was a modified method of OG administration with a single loading dose of 100 mg/kg and subsequent maintenance doses of 50 mg/kg for the 1st and 2nd mo, 75 mg/kg for the 3rd and 4th mo, and 100 mg/kg for the 5th and 6th mo.

AA (Sigma Chemical Co.) AA was prepared in double distilled water and administered via OG route for five subgroups according to the dosages as follows: 0.2, 0.4, 0.6, 0.8, and 1.0 mmol/kg twice a week.

CCl₄ (Sigma Chemical Co.) The mice were fed via OG or IP route with CCl₄ (density = 1.594 g/L) diluted in double distilled water. As for each route of administration, they were further subgrouped into three according to the maintenance doses as follows: 0.8 g/kg (low dosage), 1.6 g/kg (medium dosage) and 2.0 g/kg (high dosage). After a single loading dose of 2.4 g/kg, the maintenance doses were then administered twice a week.

DDC (Sigma Chemical Co.) The mice were fed via OG with DDC in corn oil twice a week. They were subgrouped by four different dosages as follows: 0.25, 0.5, 2.5, and 5 mg. In addition, 0.1% DDC contained diet (Purina Mills TestDiet, St. Louis, MO, USA) was used as the 5th subgroup.

Silica (US Silica Company, Berkeley Springs, WV, USA) Silica was dissolved in Dulbecco's modified eagle media and given subcutaneously at the dose of 3.5 g/kg, or intraperitoneally at the dose of 1.6 g/kg twice a week.

CBDL The surgical procedure was performed under sterile conditions. The mice were anesthetized with isoflurane. Midline laparotomy was performed for exploring the hepatic hilum and identifying CBD. Under the dissecting microscope, CBD was then isolated, doubly ligated and transected between two ligatures.

Liver biopsy

Liver biopsy demanded survival procedures and sterile techniques. After anesthesia with isoflurane, midline laparotomy was performed to expose the mouse liver. A liver block sized 0.5 cm in diameter was taken and then the cut surface was sutured for hemostasis. Serial biopsy was

performed monthly (per 4 wk) for each mouse till cirrhosis was well documented by histopathology. At the first liver biopsy, ascites, and intra-abdominal adhesion were examined and recorded.

Histopathology

Mouse livers from biopsies were fixed in 10% neutral buffered formaldehyde solution and embedded in paraffin. Sections, 4 μ m in thickness, were stained with hematoxylin and eosin. Fatty change of hepatocytes was recorded when hepatocytes showed fat accumulation, balloon-like swelling or formation of fat cysts. For liver necrosis, there were the disorganization of liver cell cords, homogeneous cytoplasm, pyknotic nuclei and periportal infiltration of inflammatory cells. Fibrosis was defined as the presence of fibrous scarring band in the liver parenchyma by Mason's trichrome collagen stain. Once the irregular zones of fibrosis developed and surrounded the remaining parenchymal tissues to display a pattern of nodularity under microscope, cirrhosis was diagnosed.

Statistical analysis

For survival and cirrhosis rate analyses, life table method was used. The length of time intervals used in this study was 4 wk. Any mouse which died, or whose liver was pathologically documented to be cirrhotic was considered to have experienced an event. When a mouse died before cirrhosis was confirmed at cirrhosis rate analysis, it was counted as a withdrawal and treated the same way as cases lost to follow-up. Plots were constructed with weeks after inducing liver injury vs survival or cirrhosis rate. The Wilcoxon test was employed to compare the curves. Differences were regarded as significant if a *P* value was less than 0.05.

RESULTS

Mouse survival

During the period of 6 mo, none of the 260 mice enrolled in this study died of the procedures for CBDL, liver biopsy or administration of hepatotoxins. There was no mortality case in the AA and silica groups. As for the other groups, 71 mice died in the course of this study. Among the 71 deaths, 20 occurred before cirrhosis could be histopathologically confirmed (pre-cirrhotic) and the remaining 51 after cirrhosis was found (post-cirrhotic). Nineteen of the 20 pre-cirrhotic deaths occurred in the CCl₄ group. As for the post-cirrhotic deaths, there were 4 in the ANIT group, 26 in the CCl₄ group, 11 in the DDC group and 10 in the CBDL group. The case numbers of mortality in each subgroup were listed in Table 1. Mortality had been found in all the CCl₄ subgroups, ranging from 40% to 100%. In the DDC group, mortality was mainly post-cirrhotic, and seen in 2.5 and 5 mg and 0.1% diet subgroup. All the mice in CBDL group had post-cirrhotic death by the end of 16 wk. The overall comparison for the survival curves in the ANIT and DDC groups could not reach any statistical significance (*P* = 0.0823 and 0.1227, respectively), whereas there was a significant difference in the CCl₄ subgroup (*P* < 0.0001). Pairwise comparisons for survival curves of the six CCl₄ subgroups showed that the

low dosage (IP0.8 and OG0.8) was significantly better than the medium dosage (IP1.6 and OG1.6, Figure 1, $P = 0.0010-0.0317$), and the medium dosage was also superior to the high dosage (IP2.0 and OG2.0, Figure 1, $P = 0.0002-0.0044$). Considering the administration routes, IP route compared favorably in survival with OG route at the high dosage ($P = 0.0221$), but not at the medium and low dosages ($P = 0.7899$ and 0.5902 , respectively).

Table 1 Case number of pre-cirrhotic and post-cirrhotic deaths

	Pre-cirrhotic death	Post-cirrhotic death
ANIT OG 25 mg/kg	0	0
ANIT OG 50 mg/kg	0	0
ANIT OG 125 mg/kg	0	3
ANIT IP 25 mg/kg	0	0
ANIT IP 50 mg/kg	0	0
ANIT IP 125 mg/kg	1	0
ANIT modified	0	1
AA OG from 0.2 to 1.0 mmol/kg	0	0
CCl ₄ OG 0.8 g/kg	0	5
CCl ₄ OG 1.6 g/kg	2	7
CCl ₄ OG 2.0 g/kg	5	5
CCl ₄ IP 0.8 g/kg	4	0
CCl ₄ IP 1.6 g/kg	6	1
CCl ₄ IP 2.0 g/kg	2	8
DDC OG 0.25 mg	0	0
DDC OG 0.5 mg	0	1
DDC OG 2.5 mg	0	3
DDC OG 5 mg	0	4
DDC 0.1% diet	0	3
Silica (SC 3.5 g/kg or IP 1.6 g/kg)	0/0	0/0
CBDL	0	10

OG: Oral gavage; IP: intraperitoneal; SC: subcutaneous.

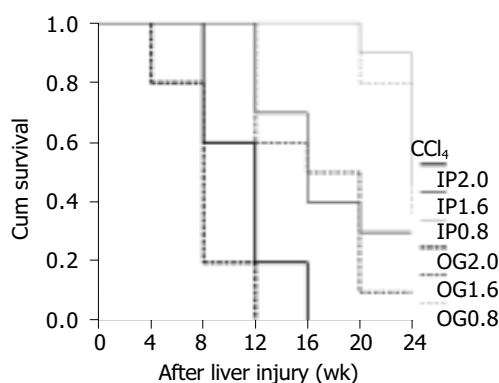


Figure 1 Survival curves of six CCl₄ subgroups are shown. The number immediately behind the IP or OG indicates the dosage of CCl₄ used in g/kg.

Ascites and intraabdominal adhesion

Ascites was universally found at laparotomy when the hepatotoxins were administered via IP route. In the CBDL group, there were only three mice presenting with ascites at the subsequent laparotomy. Intraabdominal adhesion existed in over 50% of cases (ranging from 50% to 100%) when IP route or CBDL was used. Additionally, granuloma-like masses were intraperitoneally identified in all the cases of silica IP subgroup and in nine cases of ANIT IP subgroups

(two for 25 mg/kg, one for 50 mg/kg and six for 125 mg/kg).

Histopathology

The case numbers of histopathological findings in each subgroup were listed in Table 2. Fatty change was seen mainly in the ANIT and CCl₄ groups, and sporadically in the AA group (1 for 0.8 mmol/kg and 2 for 1.0 mmol/kg). Bile lakes were the common findings in the DDC and CBDL groups. Liver necrosis and fibrosis were demonstrated almost in all the cases of the ANIT, CCl₄, DDC, and CBDL groups, two cases of the AA group (one for 0.8 mmol/kg and the other for 1.0 mmol/kg), but none of the silica group. The necrosis and fibrosis were detected at the first or second liver biopsy (4-8 wk after liver injury). Liver fibrosis in the two mice from the AA group did not progress to cirrhosis by the end of this study. Cirrhotic nodules could be identified in 30 mice (42.9%) of ANIT group ($n = 70$), 32 mice (53.3%) of CCl₄ group ($n = 60$), 39 mice (78.0%) of DDC group ($n = 50$) and all the mice (100%) of CBDL group ($n = 10$). DDC subgroup with higher dosages (2.5 and 5 mg) and 0.1% diet could substantially reach 100% successful rate of cirrhosis induction as seen in the CBDL group.

Durations required for cirrhosis induction

Results from life table analysis for the durations were presented in the curves with weeks after inducing liver injury *vs* cirrhosis rate. CBDL represented a rapid method to induce liver cirrhosis with 70-100% of successful rate within 4-8 wk (Figure 2A). DDC caused liver cirrhosis within 4-12 wk (Figure 2B). Statistical analysis revealed that the lower the DDC dosage, the longer the time spent by DDC in inducing cirrhosis among 0.5, 2.5 and 5 mg subgroups (DDC0.5 *vs* DDC2.5, $P = 0.0387$ and DDC2.5 *vs* DDC5, $P = 0.0004$). There was no significant difference between 0.25 and 0.5 mg DDC subgroups ($P = 0.1311$). DDC 0.1% diet required significantly less time to induce cirrhosis than DDC 0.25 mg ($P = 0.0001$), 0.5 mg ($P = 0.0008$) and 2.5 mg ($P = 0.0032$), but was not significantly different from 5 mg subgroups ($P = 0.3415$). As for CCl₄, the duration for inducing cirrhosis was quite variable, ranging from 4 to 20 wk (Figure 3A). The IP and OG high dosages (2.0 g/kg) of CCl₄ spent significantly less time in cirrhosis induction than IP and OG low dosages (0.8 g/kg) of CCl₄ ($P = 0.0005-0.0209$). There was no difference of the cirrhosis curves between IP and OG administrations at the high ($P = 0.1760$) and low ($P = 0.1661$) dosages, whereas OG administration compared favorably in cirrhosis induction than IP administration at the medium dosage (1.6 g/kg) of CCl₄ ($P = 0.0060$). The OG medium dosage (OG1.6) had no significant difference from the high dosage ($P = 0.1852$ for OG2.0 and $P = 0.7241$ for IP2.0), and the IP medium dosage (IP1.6) had no significant difference from the low dosage ($P = 0.8822$ for OG0.8 and $P = 0.1514$ for IP0.8). Cirrhosis caused by ANIT did not show up until 12-24 wk (Figure 3B). The high dosage of ANIT significantly spent less time in cirrhosis induction than the medium ($P = 0.0002-0.0263$) and low dosages ($P = 0.0002-0.0027$), whereas the medium dosage could not be significantly superior to the low dosage ($P = 0.0904-1.0000$). At the same ANIT dosage used, there was no significant difference of cirrhosis curves between OG and

Table 2 Histopathological changes after inducing liver injuries

	Fatty change	Necrosis/fibrosis	Cirrhosis	Bile lake
ANIT OG 25 mg/kg	0	10	2	0
ANIT OG 50 mg/kg	4	10	4	0
ANIT OG 125 mg/kg	5	10	8	0
ANIT IP 25 mg/kg	0	9	1	0
ANIT IP 50 mg/kg	1	10	1	0
ANIT IP 125 mg/kg	4	10	9	0
ANIT modified	4	10	5	0
AA OG from 0.2 to 1.0 mmol/kg	3 ¹	2 ²	0	0
CCl ₄ OG 0.8 g/kg	4	10	5	0
CCl ₄ OG 1.6 g/kg	5	10	8	0
CCl ₄ OG 2.0 g/kg	8	10	5	0
CCl ₄ IP 0.8 g/kg	3	10	2	0
CCl ₄ IP 1.6 g/kg	5	10	4	0
CCl ₄ IP 2.0 g/kg	6	10	8	0
DDC OG 0.25 mg	0	10	3	6
DDC OG 0.5 mg	0	10	6	9
DDC OG 2.5 mg	0	10	10	10
DDC OG 5 mg	0	10	10	10
DDC 0.1% diet	0	10	10	9
Silica (SC 3.5 g/kg or IP 1.6 g/kg)	0/0	0/0	0/0	0/0
CBDL	0	10	10	10

OG: oral gavage; IP: intraperitoneal; SC: subcutaneous. ¹1 for 0.8 mmol/kg and 2 for 1.0 mmol/kg; ²1 for 0.8 mmol/kg and 1 for 1.0 mmol/kg.

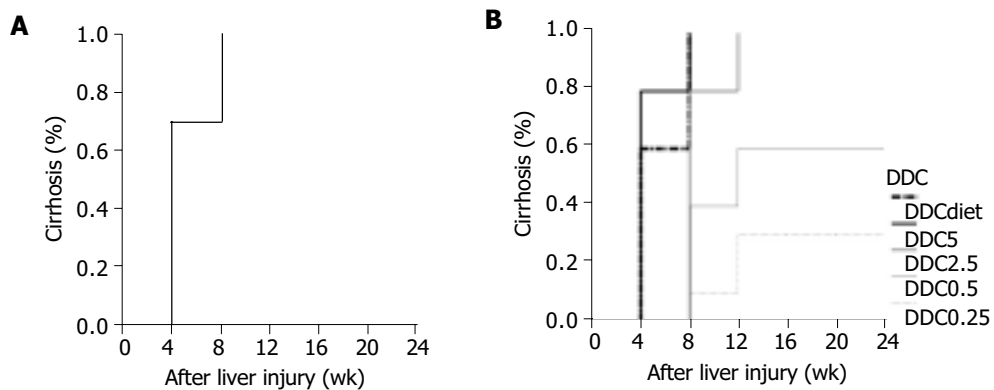


Figure 2 Cirrhosis rates of CBDL and DDC groups. **A:** The cirrhosis curve for CBDL group is shown; **B:** The cirrhosis curves for 5 DDC subgroups are

shown. The number immediately behind DDC indicates its dosage used in mg per mouse. DDC diet represents 0.1% DDC contained diet.

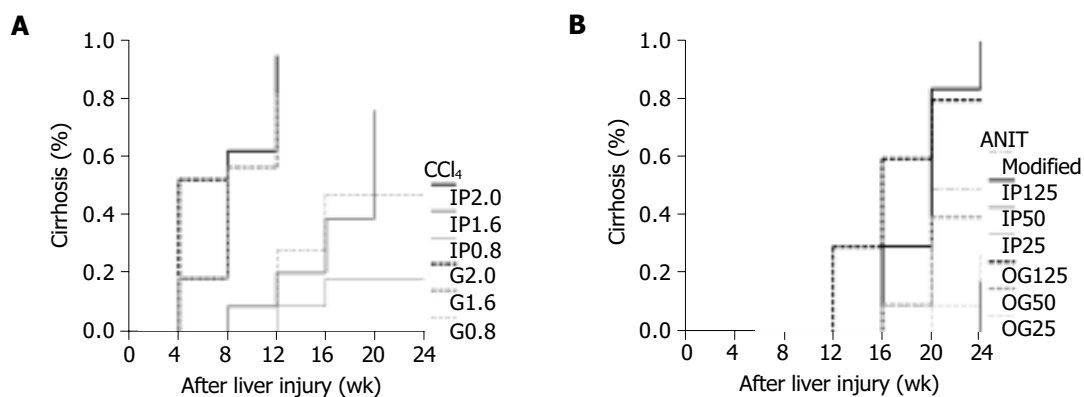


Figure 3 Cirrhosis rates of CCl₄ and ANIT groups. **A:** The cirrhosis curves for six CCl₄ subgroups are shown. The number immediately behind the IP or OG indicates the dosage of CCl₄ used in g/kg; **B:** The cirrhosis curves for seven

ANIT subgroups are shown. The number immediately behind the IP or OG indicates the dosage of ANIT used in mg/kg.

IP administrations ($P = 0.2444$ for high dosage, $P = 0.0904$ for medium dosage, and $P = 0.5032$ for low dosage). The modified method for ANIT administration compared

favorably in cirrhosis induction P only with IP low dosage and IP medium dosage ($P = 0.0349$, for both), but poorly with OG high dosage ($P = 0.0303$).

DISCUSSION

In this 6-mo study of experimental cirrhosis induction, AA and silica were ineffective in inducing liver fibrosis let alone cirrhosis. AA administration in the drinking water (50 ppm equivalent to 0.08-0.11 mmol/kg per d) for 15 wk has no effect on the histopathological examination of rat livers^[19]. Moreover, IP injection of AA in rats only produced variable periportal liver necrosis predominantly at 6-12 h, followed by restitutive proliferation of periportal necrosis to repopulate the necrotic zone. Eventually, the liver architecture was essentially restored by 1 wk^[18]. It indicated that AA merely induced short-term toxicity in rats. Although we had observed liver necrosis and fibrosis in two mice with OG administration of 0.8 and 1.0 mmol/kg AA, this liver damage was transient and insufficient to result in cirrhosis. It suggested that rats and FVB/N mice had similar hepatotoxic resistance to AA. As for silica, subcutaneous or IP administration was reported to cause liver fibrosis and cirrhosis in nude mice at 12 mo and in (C57BL/6×BALB/c) F₁ mice at 18 mo^[22]. Thus, a 6-mo duration might not be long enough for silica to cause hepatic injury with subsequent fibrosis and cirrhosis in FVB/N mice. As a result, a longer-term administration of silica might be required for inducing liver cirrhosis in FVB/N mice. A major drawback with silica administration was the granuloma formation at the injection site. This might be of concern to subsequent laparotomy for liver biopsy when the IP route is used.

The IP or OG administration of ANIT, CCl₄ or DDC could effectively lead to liver fibrosis within 4-8 wk. All the liver fibrosis in mice did not always progress to microscopic cirrhotic nodules by the end of 24 wk. It suggested that restitutive response of mice to the injuries by those hepatotoxins sometimes restore liver architecture. ANIT has been used for years to study cholangiolitic hepatotoxicity in laboratory animals^[9,10]. This study showed that ANIT usually led to mouse cirrhosis within 12-24 wk after administration. Mortality was only seen in the subgroups with high dosage and modified administration. However, there was no significant difference among the survival curves of all the ANIT subgroups. The high dosage of ANIT could more rapidly induce liver cirrhosis than the medium or low dosage. At the same dosage of ANIT, it made no significant difference between IP and OG administrations in cirrhosis induction. The modified method by gradual increase of ANIT dosage could not substantially provide any benefit in cirrhosis induction in this study. Overall, ANIT model required a longer period for the formation of cirrhosis. This might provide more time for researchers to investigate the progression of liver fibrosis.

CCl₄ has been used extensively for decades to induce liver injury in various experimental models to elucidate the mechanisms behind hepatotoxicity^[23]. Also, it was commonly used as a hepatotoxic agent in transgenic mice to evaluate liver fibrosis and cirrhosis on the basis of the selective expression of some novel or altered genes^[13,14,24]. We experienced that the major problem in association with the use of CCl₄ to induce liver fibrosis or cirrhosis had been the high mortality rates of mice, accounting for 40-100 % in those subgroups. Animals might die before or after cirrhosis was found. The higher CCl₄ dosage was associated with the worse survival

curve. The duration required for cirrhosis induction by CCl₄ was quite variable, ranging from 4 to 20 wk, mainly depending upon the dosage. The high dosage (2.0 g/kg) of CCl₄ could rapidly cause liver cirrhosis within 4-12 wk, but led to poor survival. Under the circumstances, IP administration will be suggested since IP route posed better survival than OG route only at the high dosage of CCl₄. The low dosage (0.8 g/kg) of CCl₄ required 12-24 wk to successfully induce cirrhosis. At the low dosage, it was shown that the administration routes had no influence on the survival and the cirrhosis induction. At the medium dosage (1.6 g/kg) of CCl₄, OG administration was more rapid to induce cirrhosis than IP administration, but did not significantly differ in survival curves from IP administration. Nevertheless, the high mortality rate along with the use of CCl₄ must be taken into consideration since it will prematurely terminate the sequential studies or observations of liver fibrosis or cirrhosis. Furthermore, CCl₄ might not be an ideal solvent for investigating hepatocarcinoma since liver carcinogenesis might be due to the genotoxic chemical carcinogen effect of CCl₄ itself as well as CCl₄-induced liver cirrhosis^[25,26].

DDC did not result in pre-cirrhotic death, but tended to lead to post-cirrhotic death at higher dosage (2.5 and 5 mg) and 0.1% DDC diet. The overall comparison for all survival curves of those DDC subgroups led to the insignificant difference. It took about 4-12 wk for DDC to successfully induce cirrhosis. Except 0.25 mg DDC subgroup, the successful rate of cirrhosis induction was quite satisfactory. The higher the dosage of DDC we used, the lesser the time we needed to induce cirrhosis. DDC 0.1% diet could not be superior to 5 mg DDC subgroup in cirrhosis induction. A major concern of DDC use was the high proportion of bile lake formation. This might cause some biases in observing the relationship between cirrhosis and its sequelae.

CBDL represented a rapid and consistent method to induce liver fibrosis and cirrhosis. Hepatocellular injuries were caused by cholestasis, leading to liver dysfunction, promoting fibrogenesis and ultimately resulting in liver failure and death. All the mice with CBDL rapidly progressed to cirrhosis within 4-8 wk after operation, and died by the end of 16 wk. The rapid progression to cirrhosis and death by CBDL might limit its application in chronic fibrosis studies and make it difficult to carry out a long-term investigation of liver cirrhosis. A major technical problem was the reversibility of histological changes due to recanalization of bile ducts^[1]. In our tested animals, the bile ducts remained totally obstructed till their death in view of bile lakes at final pathology and the coloration of peritoneum and auricle. The successful obstruction by CBDL might be due to the fact that CBDL was doubly ligated and transected between two ligatures^[27]. Besides, intraabdominal adhesion could be an obstacle for subsequent survival laparotomy to study CBDL livers.

In summary, CBDL and hepatotoxins of ANIT, CCl₄ and DDC could be effective in causing liver fibrosis of mice. CBDL rapidly and irreversibly led to liver fibrosis and subsequently to cirrhosis within 4-8 wk, but inevitably caused mortality by the end of 16 wk. As a result, CBDL was suitable for creating a mouse model for the short-term study of liver fibrogenesis. Although CCl₄ had been commonly used for inducing liver fibrosis and cirrhosis, the duration

required for cirrhosis induction varied (4-20 wk) and mainly depended upon the dosage. It could be used in mice for studying both acute and chronic liver fibrogenesis. A major drawback in association with CCL₄ use was a relatively high mortality. DDC could effectively induce cirrhosis within 4-12 wk. The time required for cirrhosis induction by DDC was quite similar to that of CBDL, but the survival experience was better in the DDC group. ANIT slowly induced liver cirrhosis in mice. The duration from initial liver inflammatory damage to cirrhosis formation by ANIT was more than 12 wk after administration. Thus, ANIT was quite a good toxin for a long-term study of fibrosis progression into cirrhosis.

ACKNOWLEDGMENTS

We thank Dr. Yun-Fan Liaw for his suggestions, helpful discussions and support.

REFERENCES

- 1 **Wu J**, Norton PA. Animal models of liver fibrosis. *Scand J Gastroenterol* 1996; **31**: 1137-1143
- 2 **Sanderson N**, Factor V, Nagy P, Kopp J, Kondaiah P, Wakefield L, Roberts AB, Sporn MB, Thorgeirsson SS. Hepatic expression of mature transforming growth factor beta 1 in transgenic mice results in multiple tissue lesions. *Proc Natl Acad Sci USA* 1995; **92**: 2572-2576
- 3 **Hanahan D**. Transgenic mice as probes into complex systems. *Science* 1989; **246**: 1265-1275
- 4 **Quick DJ**, Shuler ML. Use of in vitro data for construction of a physiologically based pharmacokinetic model for naphthalene in rats and mice to probe species differences. *Biotechnol Prog* 1999; **15**: 540-555
- 5 **Lindstrom AB**, Yeowell-O'Connell K, Waidyanatha S, McDonald TA, Golding BT, Rappaport SM. Formation of hemoglobin and albumin adducts of benzene oxide in mouse, rat, and human blood. *Chem Res Toxicol* 1998; **11**: 302-310
- 6 **Cunningham ML**, Bucher JR. Pharmacodynamic responses of F344 rats to the mouse hepatocarcinogen oxazepam in a 90-d feed study. *Toxicol Appl Pharmacol* 1998; **149**: 41-48
- 7 **Watt KC**, Buckpitt AR. Species differences in the regio- and stereoselectivity of 1-nitronaphthalene metabolism. *Drug Metab Dispos* 2000; **28**: 376-378
- 8 **Dill JA**, Lee KM, Bates DJ, Anderson DJ, Johnson RE, Chou BJ, Burka LT, Roycroft JH. Toxicokinetics of inhaled 2-butoxyethanol and its major metabolite, 2-butoxyacetic acid, in F344 rats and B6C3F1 mice. *Toxicol Appl Pharmacol* 1998; **153**: 227-242
- 9 **Palmeira CM**, Ferreira FM, Rolo AP, Oliveira PJ, Santos MS, Moreno AJ, Cipriano MA, Martins MI, Seica R. Histological changes and impairment of liver mitochondrial bioenergetics after long-term treatment with alpha-naphthyl-isothiocyanate (ANIT). *Toxicology* 2003; **190**: 185-196
- 10 **Ohta Y**, Kongo M, Sasaki E, Harada N. Change in hepatic antioxidant defense system with liver injury development in rats with a single alpha-naphthylisothiocyanate intoxication. *Toxicology* 1999; **139**: 265-275
- 11 **Williams AO**, Knapton AD. Hepatic silicosis, cirrhosis, and liver tumors in mice and hamsters: studies of transforming growth factor beta expression. *Hepatology* 1996; **23**: 1268-1275
- 12 **Natsume M**, Tsuji H, Harada A, Akiyama M, Yano T, Ishikura H, Nakanishi I, Matsushima K, Kaneko S, Mukaida N. Attenuated liver fibrosis and depressed serum albumin levels in carbon tetrachloride-treated IL-6-deficient mice. *J Leukoc Biol* 1999; **66**: 601-608
- 13 **Brenner DA**, Veloz L, Jaenisch R, Alcorn JM. Stimulation of the collagen alpha 1 (I) endogenous gene and transgene in carbon tetrachloride-induced hepatic fibrosis. *Hepatology* 1993; **17**: 287-292
- 14 **Inagaki Y**, Truter S, Bou-Gharios G, Garrett LA, de Crombrughe B, Nemoto T, Greenwel P. Activation of Proalpha2(I) collagen promoter during hepatic fibrogenesis in transgenic mice. *Biochem Biophys Res Commun* 1998; **250**: 606-611
- 15 **Preisegger KH**, Factor VM, Fuchsbichler A, Stumptner C, Denk H, Thorgeirsson SS. Atypical ductular proliferation and its inhibition by transforming growth factor beta1 in the 3,5-diethoxycarbonyl-1,4-dihydrocollidine mouse model for chronic alcoholic liver disease. *Lab Invest* 1999; **79**: 103-109
- 16 **Fickert P**, Trauner M, Fuchsbichler A, Stumptner C, Zatloukal K, Denk H. Bile acid-induced Mallory body formation in drug-primed mouse liver. *Am J Pathol* 2002; **161**: 2019-2026
- 17 **Alam K**, Nagi MN, Al-Shabanah OA, Al-Bekairi AM. Beneficial effect of nitric oxide synthase inhibitor on hepatotoxicity induced by allyl alcohol. *J Biochem Mol Toxicol* 2001; **15**: 317-321
- 18 **Yavorkovsky L**, Lai E, Ilic Z, Sell S. Participation of small intraportal stem cells in the restitutive response of the liver to periportal necrosis induced by allyl alcohol. *Hepatology* 1995; **21**: 1702-1712
- 19 **Carpanini FM**, Gaunt IF, Hardy J, Gangolli SD, Butterworth KR, Lloyd AG. Short-term toxicity of allyl alcohol in rats. *Toxicology* 1978; **9**: 29-45
- 20 **Taketo M**, Schroeder AC, Mobraaten LE, Gunning KB, Hanten G, Fox RR, Roderick TH, Stewart CL, Lilly F, Hansen CT. FVB/N: an inbred mouse strain preferable for transgenic analyses. *Proc Natl Acad Sci USA* 1991; **88**: 2065-2069
- 21 **Perret-Gentil MI**, Murray L, Bird DJ, Ladiges WC. Evaluation of FVB/N mice as recipients for transgenic embryos. *Lab Anim Sci* 1999; **49**: 427-428
- 22 **Ebbesen P**. Chirality of quartz. Fibrosis and tumour development in dust inoculated mice. *Eur J Cancer Prev* 1991; **1**: 39-41
- 23 **Plaa GL**. Chlorinated methanes and liver injury: highlights of the past 50 years. *Annu Rev Pharmacol Toxicol* 2000; **40**: 42-65
- 24 **Schnur J**, Olah J, Szepesi A, Nagy P, Thorgeirsson SS. Thioacetamide-induced hepatic fibrosis in transforming growth factor beta-1 transgenic mice. *Eur J Gastroenterol Hepatol* 2004; **16**: 127-133
- 25 **Zalatnai A**, Lapis K. Simultaneous induction of liver cirrhosis and hepatocellular carcinomas in F-344 rats: establishment of a short hepatocarcinogenesis model. *Exp Toxicol Pathol* 1994; **46**: 215-222
- 26 **Beddowes EJ**, Faux SP, Chipman JK. Chloroform, carbon tetrachloride and glutathione depletion induce secondary genotoxicity in liver cells via oxidative stress. *Toxicology* 2003; **187**: 101-115
- 27 **Prado IB**, dos Santos MH, Lopasso FP, Iriya K, Laudanna AA. Cholestasis in a murine experimental model: lesions include hepatocyte ischemic necrosis. *Rev Hosp Clin Fac Med Sao Paulo* 2003; **58**: 27-32

Tetramethylpyrazine stimulates cystic fibrosis transmembrane conductance regulator-mediated anion secretion in distal colon of rodents

Qiong He, Jin-Xia Zhu, Ying Xing, Lai-Ling Tsang, Ning Yang, Dewi Kenneth Rowlands, Yiu-Wa Chung, Hsiao-Chang Chan

Qiong He, Jin-Xia Zhu, Ying Xing, Ning Yang, Department of Physiology, Medical School, Zhengzhou University, Zhengzhou 450052, Henan Province, China

Qiong He, Jin-Xia Zhu, Lai-Ling Tsang, Ning Yang, Dewi Kenneth Rowlands, Yiu-Wa Chung, Hsiao-Chang Chan, Epithelial Cell Biology Research Center, Department of Physiology, Faculty of Medicine, The Chinese University of Hong Kong, Shatin, Hong Kong, China

Supported by the Innovation and Technology Fund of Hong Kong, China

Correspondence to: Dr. Hsiao-Chang Chan, Epithelial Cell Biology Research Center, Department of Physiology, Faculty of Medicine, The Chinese University of Hong Kong, Shatin, NT, Hong Kong, China. hsiaoChan@cuhk.edu.hk

Telephone: +852-2609-6839 Fax: +852-2603-5022

Received: 2004-08-19 Accepted: 2004-10-05

Abstract

AIM: To investigate the effect of tetramethylpyrazine (TMP), an active compound from *Ligustium Wollichii Franchet*, on electrolyte transport across the distal colon of rodents and the mechanism involved.

METHODS: The short-circuit current (I_{sc}) technique in conjunction with pharmacological agents and specific inhibitors were used in analyzing the electrolyte transport across the distal colon of rodents. The underlying cellular signaling mechanism was investigated by radioimmunoassay analysis (RIA) and a special mouse model of cystic fibrosis.

RESULTS: TMP stimulated a concentration-dependent rise in I_{sc} , which was dependent on both Cl^- and HCO_3^- , and inhibited by apical application of diphenylamine-2,2'-dicarboxylic acid (DPC) and glibenclamide, but resistant to 4,4'-diisothiocyanatostilbene-2,2'-disulfonic acid disodium salt hydrate (DIDS). Removal of Na^+ from basolateral solution almost completely abolished the I_{sc} response to TMP, but it was insensitive to apical Na^+ replacement or apical Na^+ channel blocker, amiloride. Pretreatment of colonic mucosa with BAPTA-AM, a membrane-permeable selective Ca^{2+} chelator, did not significantly alter the TMP-induced I_{sc} . No additive effect of forskolin and 3-isobutyl-1-methylxanthine (IBMX) was observed on the TMP-induced I_{sc} , but it was significantly reduced by a protein kinase A inhibitor, H_{89} . RIA results showed that TMP (1 mmol/L) elicited a significant increase in cellular cAMP production, which was similar to that elicited by the adenylate cyclase activator, forskolin (10 μ mol/L). The TMP-elicited I_{sc} as well as forskolin- or IBMX-induced I_{sc} were abolished in

mice with homozygous mutation of the cystic fibrosis transmembrane conductance regulator (CFTR) presenting defective CFTR functions and secretions.

CONCLUSION: TMP may stimulate cAMP-dependent and CFTR-mediated Cl^- and HCO_3^- secretion. This may have implications in the future development of alternative treatment for constipation.

© 2005 The WJG Press and Elsevier Inc. All rights reserved.

Key words: Tetramethylpyrazine; Ligustrazine; Colonic mucosa; Cl^- ; HCO_3^- ; cAMP; CF mice

He Q, Zhu JX, Xing Y, Tsang LL, Yang N, Rowlands DK, Chung YW, Chan HC. Tetramethylpyrazine stimulates cystic fibrosis transmembrane conductance regulator-mediated anion secretion in distal colon of rodents. *World J Gastroenterol* 2005; 11(27): 4173-4179

<http://www.wjgnet.com/1007-9327/11/4173.asp>

INTRODUCTION

Constipation presents a massive impact on health services, and the epidemiology investigation has demonstrated that the prevalence of constipation in many areas around the world is significantly high^[1,2]. Studies have shown that constipation results primarily from changes in gastrointestinal motility^[3]. In addition, alterations in regulating fluid and electrolyte transport across gut epithelia may represent another contributing factor in the pathophysiology of constipation^[4].

The mammalian colon is the final station of the gastrointestinal tract, where the organism has the last opportunity to modify the electrolyte contents in the feces with balanced absorptive and secretory activities. The epithelial layer covering the inner surface of colon is a typical electrolyte-transporting epithelium, which under physiological conditions absorbs water, sodium and chloride while secreting NaCl as well as potassium and bicarbonate through a number of ion channels, carriers, and pumps, located either on the luminal or on the basolateral membrane. Epithelial Na^+ channels populated in the apical membranes of the absorptive cells in the colon, which are amiloride-sensitive and well-known targets for mineralocorticoids, are responsible for Na^+ absorption^[5]. Cystic fibrosis transmembrane conductance regulator (CFTR), a cAMP-dependent Cl^- channel, is predominantly expressed in colonic

crypts^[6,7] and known to mediate both Cl^- ^[8,9] and HCO_3^- secretion^[10,11]. Disturbance of ion transport, like cholera toxin and cystic fibrosis (CF) may result in diarrhea^[12] or constipation^[13] with severe pathological consequences^[9].

The traditional therapeutic proposals, such as the employment of cathartic medications, stool softeners, lubricant grease, and enemas have some effects on constipation, but their side effects have restricted their use^[14].

In our previous study, we have observed that Bak Foong Pill, consisting of more than 20 herbal ingredients, a well known Chinese remedy widely used for treating gynecological disorders, exerts a stimulatory effect on anion secretion by the human colonic epithelia cell line T₈₄ primarily via the cAMP pathway with minor contribution from the Ca^{2+} pathway^[15]. This result highlights the potential for exploring an active component of Bak Foong Pills for treatment of constipation or other obstructive bowel syndromes in patients.

Tetramethylpyrazine (TMP, $\text{C}_8\text{H}_{12}\text{N}_2$, molecular weight 136.20), also known as ligustrazine, is the active compound extracted from one of the component herbs of Bak Foong Pill, *Ligustium Wollichii*. TMP is used in clinic to treat cardiovascular disorders because of its multitude of biological effects such as improving blood circulation and metabolism of cardiac muscle, increasing coronary flow, decreasing oxygen consumption, lowering blood pressure and inhibiting thrombosis^[16-18]. TMP may act as an inhibitor of phosphodiesterase (PDE) to increase intracellular cAMP thereby exerting its antiplatelet and vasodilatation effects^[19]. On the other hand, the effect of TMP on the release of calcium from internal stores has also been reported^[17]. Therefore, it is possible that TMP may be the active compound responsible for mediating the effect of Bak Foong Pills. The focus of this study was to investigate the effect of TMP on water and electrolyte transport properties of native mammalian colon with the hope of exploring new alternative treatment for constipation or obstructive bowel syndromes.

MATERIALS AND METHODS

Materials

TMP was purchased from the Fourth Pharmaceutical Factory of Beijing (Beijing, China). 3-Isobutyl-1-methylxanthine (IBMX), amiloride, DIDS, BAPTA-AM, POP and POPOP were obtained from Sigma Chemical Company (St. Louis, MO, USA). Calbiochem (San Diego, CA, USA) was the source for bumetanide, forskolin, TTX, H₈₉, and glibenclamide. Diphenylamine-2,2'-dicarboxylic acid (DPC) was purchased from Riedel de Haen Chemicals (Hannover, Germany). cAMP measurement kit was purchased from the Institute of Atomic Energy Science (Beijing, China). Stock solutions of all the chemicals were dissolved in DMSO. Final DMSO concentrations never exceeded 1 mL/L. Preliminary experiments indicated that the vehicle did not alter any baseline electrophysiological parameters.

Krebs-Henseleit (KH) solution contained (in mmol/L): 117, NaCl; 4.7, KCl; 1.2, MgCl_2 ; 1.2, KH_2PO_4 ; 24.8, NaHCO_3 ; 2.5, CaCl_2 ; 11.1, glucose. The solution was continuously bubbled with 95% O_2 and 50 mL/L CO_2 to

maintain the pH at 7.4. In Cl^- free solution, NaCl, KCl, and CaCl_2 were replaced by sodium gluconate, potassium gluconate, and calcium gluconate, respectively^[20]. When HCO_3^- free solution was used, NaHCO_3 was replaced by NaCl, and the solution was buffered with 10 mmol/L Hepes with a pH of 7.4 when gassed with 100% O_2 . In the Cl^- and HCO_3^- free solutions, NaCl and NaHCO_3 were replaced by sodium gluconate, KCl by potassium gluconate, and CaCl_2 by calcium gluconate. The solution was buffered with 10 mmol/L Hepes with a pH of 7.4 when gassed with 100% O_2 . In all solutions, the osmolarity was adjusted to 290 mOsm/L with D-mannitol if necessary.

Methods

Tissue preparation Adult male Sprague-Dawley rats (Laboratory Animal Services Center at The Chinese University of Hong Kong) ranging in age from 8 to 12 wk had free access to standard rodent laboratory food and water until the day of the experiments. The animals were killed by CO_2 asphyxiation in accordance with a protocol approved by Animal Research Ethics Committee of the Chinese University of Hong Kong. Segments of distal colon about 5 cm proximal to the anus were quickly removed, cut along the mesenteric border into a flat sheet and flushed with ice-cold KH solution. The tissues were pinned flat with the mucosal side down in a Sylgard-lined petri dish containing ice-cold oxygenated solution. The serosa, submucosa, and muscular layer were stripped away with fine forceps to obtain a mucosa preparation. Two to three of these stripped mucosal preparations were obtained from one animal. TTX was used to exclude possible involvement of neuronal circuitry.

CFTR mice CFTR mice, B6.129P2-*Cftr*^{tm1UncJ}, were purchased from Jackson's Laboratory (Bar Harbor, ME 04609, USA) and then bred in Laboratory Animal Services Center at The Chinese University of Hong Kong by mating heterozygous pairs genotyped by PCR amplification of genomic DNA isolated from the animals' tails, as described previously^[21]. Homozygous CFTR mutation (-/-) mice and their littermate wild-type CFTR (+/+) controls were utilized in the study. Preparation of mouse colonic mucosa was similar to that described for the rat. Mice were cared for in accordance with the Laboratory Animal Services Center of the Chinese University of Hong Kong guidelines.

Short circuit current measurement The short-circuit current (I_{sc}) was measured *in vitro* in Ussing chambers^[22]. Flat sheets of distal colon with intact mucosa were mounted between two halves of modified Ussing chambers, in which the total cross-sectional area was 0.45 cm^2 . The mucosal and serosal surfaces of tissues were bathed with 10 mL of KH solution by recirculation from a reservoir maintained at 37 °C during the experiment. The solution was gassed with 95% O_2 and 50 mL/L CO_2 to maintain the pH at 7.4. An equilibration period of 30 min was given before the experiments. The tissues were continuously short-circuited, and the transepithelial potential difference (PD) was measured through Ag/AgCl reference electrodes (World Precision Instruments, Sarasota, Boca Raton, FL, USA) connected to a preamplifier that was connected in turn to a voltage clamp amplifier (DVC 1000; World Precision

Instruments). Voltage offset of two voltage electrodes and fluid resistance were adjusted and compensated prior to the onset of each measurement. At 0.5 intervals, a transepithelial PD of 0.1 mV (U) was applied to the tissue and the change in current (*I*) was measured. The tissue conductance (*G_t*) and the open-circuit PD could be calculated from these values according to Ohm's law ($G_t = I/U$ and $PD = I/G_t$). Drugs could be added directly to the apical or basolateral side of epithelium. Responses were continuously recorded on a chart recorder. The change in *I_{SC}* was calculated on the basis of the value before and after stimulation and normalized as current per unit area of epithelium ($\mu\text{A}/\text{cm}^2$), according to which, the total transmembrane charges ($\mu\text{C}/\text{cm}^2$) for 30 min could be calculated. The methodology for tissue preparation and measurement of electrical parameters across the mucosal sheets was described earlier^[23,24].

Measurement of cAMP Cytosolic cAMP concentrations were measured by radioimmunoassay analysis (RIA). After a 20-min period of equilibration in normal KH solution at 37 °C, the isolated mucosal sheet was treated with TMP, forskolin, TMP with IBMX, TMP with IBMX and forskolin. The mucosal sheet without treatment could act as control. The mucosal sheets were further incubated for 2 min and then rapidly frozen in liquid nitrogen and weighed 50.0 mg frozen tissue precisely. The tissues were homogenized in 2 mL of 1 N perchloric acid using a glass homogenizer. The homogenate was centrifuged at 1 000 r/min, 600 μL of the supernatant was extracted and neutralized with 300 μL of 20% KOH. The sediment was discarded after centrifugation. Six hundred microliters of the supernatant was extracted and evaporated in an electrothermal blast drier at 80 °C and the residue was dissolved in 200 μL TE buffer for further measurement. The amount of cAMP was determined by RIA with a ³H-labeled cAMP kit (Institute of Atomic Energy Science). Procedures were performed according to the manufacturer's instructions.

Statistical analysis

Results were expressed as mean \pm SE. The number of experiments represented independent measurements on separate stripped mucosal preparation (two to three of these tissue preparations were obtained from one animal).

Comparisons between groups of data were made by either the Student's *t*-test (two-group comparison) or one-way ANOVA with Newman-Keuls post hoc test (three or more-group comparison). $P < 0.05$ was considered statistically significant. EC₅₀ values were determined by nonlinear regression using GraphPad Prism software.

RESULTS

TMP-induced *I_{SC}* response in rat distal colon

Addition of TMP to either the apical or basolateral membrane could elicit *I_{SC}* responses with a greater response obtained with basolateral challenge. The present study only focused on the responses elicited by basolateral addition of TMP. As shown in Figure 1, the TMP response was concentration-dependent with an apparent EC₅₀ of 0.994 mmol/L. At a concentration greater than 3 mmol/L, TMP induced a biphasic response with a fast transient peak followed by a sustained plateau.

To exclude possible involvement of enteric nervous system, 1 $\mu\text{mol/L}$ TTX was added to the basolateral side before the administration of TMP and no significant change in the TMP-evoked increase in *I_{SC}* was observed.

Ion basis of TMP-evoked *I_{SC}*

The increase in *I_{SC}* could be attributed to either enhanced movement of positive charges from the luminal to the serosal side (i.e., Na⁺) or movement of negative charges into the lumen (i.e., Cl⁻ and/or HCO₃⁻). Ion substitution experiments were conducted to determine the ionic basis for the increases in *I_{SC}* induced by TMP (Figure 2). When extracellular Cl⁻ or HCO₃⁻ was removed, the TMP-induced response measured by total charge transfer per unit area over a 30-min period was reduced by 58.4% ($n = 5$, $P < 0.01$) and 70.8% ($n = 4$, $P < 0.01$), respectively. When both Cl⁻ and HCO₃⁻ were replaced, 98.1% ($n = 6$, $P < 0.001$) of the response was abolished, indicating substantial contribution of Cl⁻ and HCO₃⁻ to the TMP-induced response (Figure 2A).

To test whether the TMP-induced *I_{SC}* responses were due to electrogenic Na⁺ absorption, apical Na⁺ was replaced but it did not reduce the TMP response ($n = 6$), excluding electrogenic Na⁺ absorption across the colonic mucosa.

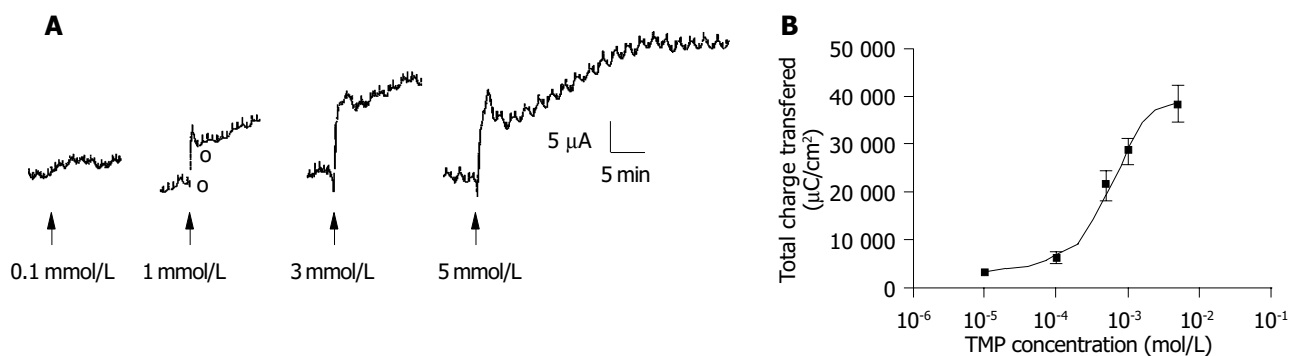


Figure 1 Effect of TMP on ion transport across rat colonic mucosa. **A:** Representative recordings of *I_{SC}* response to TMP (0.1, 1.0, 3.0, and 5.0 mmol/L) added to basolateral side. Arrowheads indicate the time of addition of TMP; **B:** Concentration-response curve of TMP with response indicated by the total

charge transfer per unit area over a 30-min period. Each data point was obtained from at least four individual experiments. Values are mean \pm SE of maximal increase in *I_{SC}*.

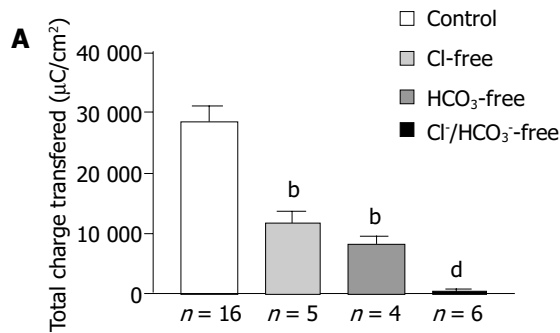
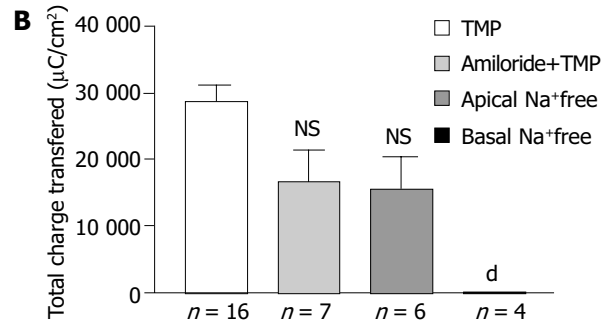


Figure 2 Ionic basis of TMP-induced I_{SC} . **A**: One millimole per liter of TMP-induced I_{SC} response (total charge transfer per unit area over 30-min period) obtained in various solutions was plotted with normal KH solution as the control; **B**: Summarized data showing the effect of 1 mmol/L of TMP-evoked



I_{SC} response in the apical presence of amiloride (0.1 mmol/L), apical Na⁺ removal, and basolateral Na⁺ removal from the bath solution. Values are mean±SE; ^b $P < 0.001$, ^d $P < 0.01$ vs control. NS, not significant.

However, removing Na⁺ from basolateral or bilateral bathing solution abolished TMP-induced I_{SC} response by 99.5% ($n = 4$, $P < 0.001$, Figure 2B), suggesting that both Cl⁻ and HCO₃⁻ secretion might involve transport mechanisms that depend on basolateral Na⁺.

Effect of ion channel blockers

To investigate whether the TMP-induced I_{SC} response was mediated by activation of the apical anion channel, different anion channel blockers were used. As shown in Figure 3, the TMP-induced I_{SC} was completely inhibited by apical application of glibenclamide (1 mmol/L, $n = 9$), which has previously been shown to block CFTR^[25] or DPC (2 mmol/L, $n = 10$, data not shown). However, the TMP-induced I_{SC} response was not sensitive to apical addition of DIDS (100, 500 μmol/L, and 1 mmol/L, $n = 5$), known to block the Ca²⁺-activated Cl⁻ channel.

Amiloride, an inhibitor of the epithelial Na⁺ channel, was also used to assess the involvement of Na⁺ absorption. In our preparation of rat colonic mucosa, a small amount of amiloride-sensitive current was observed under basal conditions. However, we did not detect any decrement of TMP-induced I_{SC} response following apical amiloride (0.1 mmol/L) pretreatment ($n = 7$, Figure 2B).

Involvement of the second messengers

To address whether [Ca²⁺]_i was involved in mediating TMP-evoked anion secretion, BAPTA-AM (100 μmol/L), a membrane-permeable selective Ca²⁺ chelator, was

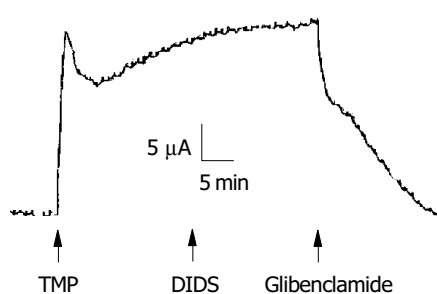


Figure 3 Effect of Cl⁻ channel blockers. Representative I_{SC} recording with arrows indicating the response to TMP (5 mmol/L, basolateral) and apical addition of channel blockers DIDS (100 mmol/L) and glibenclamide (1 mmol/L).

added bilaterally to the colonic mucosa for 45 min prior to the addition of TMP. The subsequent TMP-evoked I_{SC} was slightly reduced but not significant ($n = 6$, $P > 0.05$, Figure 4).

To test whether TMP exploited the cAMP pathway, the additive effect of forskolin (10 μmol/L, $n = 7$) or IBMX (100 μmol/L, $n = 6$) was examined. As shown in Figure 5A, no further increase in I_{SC} by TMP was observed when the I_{SC} was first elicited by the adenylate cyclase (AC) activator, forskolin, or PDE inhibitor, IBMX. Similarly, little or reduced forskolin or IBMX-induced I_{SC} response was observed if the I_{SC} was first activated by TMP (data not shown), indicating significant overlapping of the TMP signaling pathway with the cAMP-dependent one. This possibility was further tested by examining the effect of the protein kinase A (PKA) inhibitor, H₈₉. The I_{SC} response to TMP could be blocked by 91.7% upon bilateral pretreatment with 5 μmol/L H₈₉ ($n = 7$, Figure 5B).

It is also possible that TMP may alter arachidonic acid metabolism affecting production of prostaglandins (PG), which are also known to be a mediator of other secretagogues of intestinal secretion^[26]. Therefore, the effect of PG synthesis inhibitor, indomethacin, on TMP-induced I_{SC} increase was also determined. In the presence of basolateral indomethacin (10 μmol/L), the TMP-induced I_{SC} response reduced but substantial response remained with concentration-dependent characteristics (Figure 6). The indomethacin-insensitive TMP response could be inhibited by H₈₉ (data not shown), consistent with the involvement of the cAMP pathway.

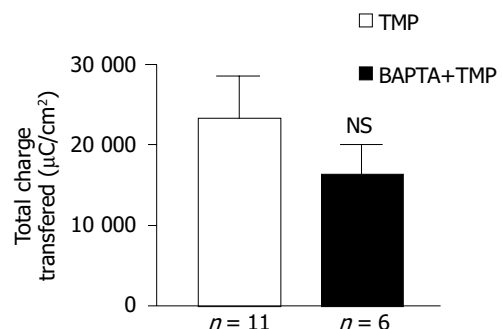


Figure 4 Effect of BAPTA-AM on TMP-evoked I_{SC} . Values are mean±SE; NS, not significant.

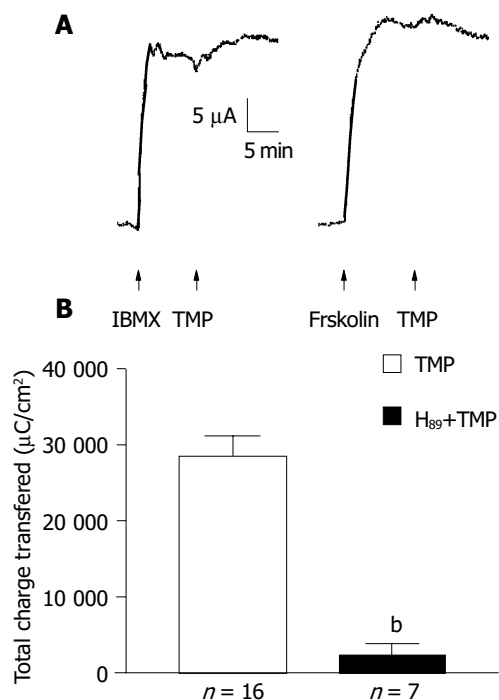


Figure 5 Involvement of cAMP in TMP-induced I_{sc} response. **A**: Representative recordings of I_{sc} response to IBMX (100 $\mu\text{mol/L}$), forskolin (10 $\mu\text{mol/L}$) without additive effect observed upon subsequent challenge of TMP (1 mmol/L); **B**: Effect of H₈₉ (5 $\mu\text{mol/L}$) on TMP (1 mmol/L)-induced I_{sc} response. Values are mean \pm SE; ^b P <0.001 vs control.

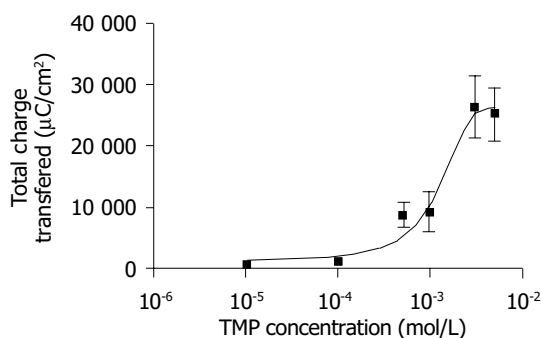


Figure 6 Concentration-response curve for TMP-induced transmembrane charges (30 min) in the presence of indomethacin (10 $\mu\text{mol/L}$). Each data point was obtained from at least four individual experiments. Values are mean \pm SE of maximal increase in charge.

Intracellular cAMP measurement

RIA was performed to study the effect of TMP on colonic epithelial intracellular cAMP levels and the results are shown in Figure 7. The intracellular cAMP content could be stimulated from a basal level of 20.0 \pm 5.8 nmol/L (n = 9) to 45.8 \pm 5.0 nmol/L (n = 6, P <0.005) in response to AC activator forskolin (10 $\mu\text{mol/L}$), or to 48.8 \pm 9.9 nmol/L (n = 10, P <0.05) in response to TMP (1 mmol/L).

Effect of TMP on CF mouse colonic mucosa

Since CFTR is a cAMP-dependent Cl⁻ channel, the involvement of the cAMP-dependent pathway as shown above suggests that the secretory response elicited by TMP may be mediated by CFTR. To test this hypothesis, mutant CF mice with homozygous mutation of CFTR (-/-) were

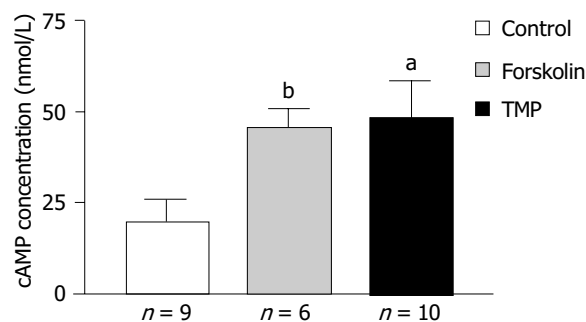


Figure 7 Effect of TMP on intracellular cAMP level. Each column represents mean \pm SE; ^a P <0.05, ^b P <0.01 vs control (KHS).

used and the effect of TMP on colonic mucosa was compared to that obtained from the wild type, CFTR (+/+). TMP (5 mmol/L) added to the basolateral side of the wild type colonic mucosa produced a sustained increase in I_{sc} response (n = 3, Figure 8A), which mimicked the forskolin-induced I_{sc} response (n = 3, Figure 8B). The same concentration of TMP was used to challenge colonic mucosa from CF mice and no TMP response was observed (n = 5, Figure 8C), neither with addition of forskolin (10 $\mu\text{mol/L}$, n = 3) or IBMX (100 $\mu\text{mol/L}$, n = 3), indicating that both TMP-induced Cl⁻ and HCO₃⁻ secretion was mediated by CFTR.

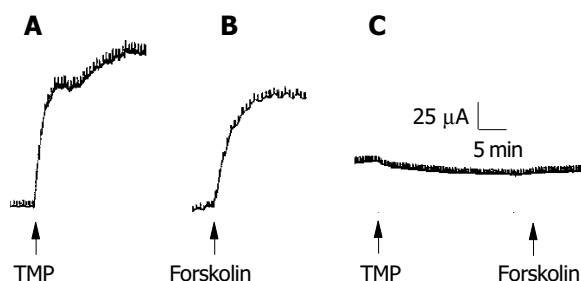


Figure 8 A-C: TMP-induced I_{sc} response in colonic mucosa of mice with CFTR wild-type and homozygous mutation.

DISCUSSION

The present study has demonstrated a stimulatory effect of TMP on colonic anion secretion but not Na⁺ absorption. The TMP-induced increase in I_{sc} is not considered to be mediated by electrogenic Na⁺ absorption because it was not inhibited by apical addition of amiloride, the epithelial sodium channel blocker, or by Na⁺ removal from apical side. Previous studies have also shown that isolated rat distal colon is largely devoid of electrogenic Na⁺ transport^[27]. However, replacement of extracellular Cl⁻ and HCO₃⁻ ions, or addition of Cl⁻ channel blockers, greatly attenuated the TMP-induced I_{sc} , suggesting that TMP has a primary effect on the anion secretion by the colon of rodents. It is interesting to note that both Cl⁻ and HCO₃⁻ secretions seem to be Na⁺-dependent since Na⁺ removal from basolateral solution almost completely abolished the TMP-induced I_{sc} , suggesting involvement of basolateral

Na⁺-dependent transporting mechanisms, i.e., both Na⁺-HCO₃⁻ cotransporter^[28] and Na⁺-K⁺-2Cl⁻ cotransporter^[29] are implicated in secondary active Cl⁻ and HCO₃⁻ secretion in many epithelia including the intestine.

The results of the present study suggest that CFTR is the likely candidate pathway for apical Cl⁻ and HCO₃⁻ exit since the TMP-evoked anion secretion was completely inhibited by glibenclamide and DPC, which are known to block CFTR^[25,30], but not by DIDS which has no effect on the activity and conductance of CFTR^[31]. The strong evidence indicating the involvement of CFTR came from the studies on CF mice with CFTR homozygous mutation. The complete abolition of the TMP-induced response in CFTR mutated colonic mucosa suggests that both TMP-stimulated Cl⁻ and HCO₃⁻ secretions are mediated by CFTR, which is consistent with an important role of CFTR in HCO₃⁻ as well as Cl⁻ secretion in many epithelial tissues^[32]. It is interesting to note that removing Cl⁻ or HCO₃⁻ alone from the bathing solution resulted in 58.4% and 70.8% attenuation in TMP-induced *I*_{SC}, respectively. The summated inhibition is more than 100%, suggesting interaction between the two ions, possibly during their transport by CFTR. The phenomena that the presence of one ion interferes with the transport of another ion have been previously reported to be associated with CFTR^[33]. In native guinea pig pancreatic duct cells, CFTR is between 3-5 times more selective for Cl⁻ over HCO₃⁻; however, extracellular HCO₃⁻ significantly inhibits CFTR current carried by Cl⁻. The interaction between Cl⁻ and HCO₃⁻ secretion may also have physiological bearing in the colon, the details of which, especially the role of CFTR, remain to be elucidated.

The involvement of CFTR also suggests that the effect of TMP is mediated primarily by the cAMP-dependent pathway since CFTR is a cAMP-activated Cl⁻ channel^[34] and mainly responsible for cAMP-dependent anion secretion^[35]. The amount of cAMP available to activate PKA to phosphorylate CFTR is determined by the balance between cAMP production by AC and cAMP hydrolysis by PDE^[36]. cAMP can be stimulated either by activation of AC or inhibition of PDE. The observation that TMP failed to further increase the *I*_{SC}, or lack of additive effect after a maximal stimulation with forskolin (AC activator) or IBMX (PDE inhibitor) suggests that the signaling pathway mediating the effect of TMP may overlap with the cAMP pathway. These indicate that TMP, forskolin and IBMX share a common intracellular pathway (i.e., a rise in [cAMP]_i). This notion is further supported by the inhibition of the TMP responses by H₈₉, an inhibitor of PKA, which is the primary target for intracellular cAMP. The present results obtained from RIA studies demonstrate an enhancement of intracellular cAMP by TMP in the rat colon.

While there is no question about the involvement of cAMP in mediating the TMP effect, how TMP activates intracellular cAMP remains to be elucidated. Previous studies reported that the antiplatelet activity of TMP is due to the enhancement of intracellular cAMP by acting as a PDE inhibitor^[19]. Although we do not have any substantial evidence to support this, the asymmetrical *I*_{SC} response to apical and basolateral challenge of TMP suggests differential distribution of the component(s) of the signaling pathway

involved. In this regard, it is interesting to note that PDE subtypes are differently localized in the apical and basolateral membrane domains of T₈₄ colonic epithelial cells^[8]. Therefore, the more potent effect of TMP observed when applied to the basolateral membrane can be explained by the presence of greater amount of a certain PDE subtype in the basolateral domain of the colonic mucosa, if TMP is indeed acting as a PDE inhibitor. Further studies along this line are necessary in order to understand the detail mechanism of cAMP activation by TMP.

It should be mentioned that while the TMP effect does not appear to involve the enteric nervous system, portion of the TMP effect could be blocked by indomethacin, an inhibitor of PG synthesis, indicating the involvement of PG which is well known for its function as the mediator of other secretagogues and acts by stimulating AC in the intestinal epithelium^[37]. The present studies also demonstrate that both the indomethacin-sensitive and indomethacin-insensitive TMP response could be blocked by H₈₉ indicating the involvement of cAMP in both cases. Therefore, TMP may indirectly activate cAMP via PG, apart from its possible direct action as a PDE inhibitor.

Although previous studies demonstrating effects of TMP on cardiac vascular function^[17] have suggested its action on the Ca²⁺ pathway, the present results suggest that TMP acts primarily on the cAMP but not on the Ca²⁺ pathway, at least for the concentration range used in the present study. However, it should be noted that the treatment with BAPTA-AM in the present study did appear to reduce the TMP response although the effect was not significant. Therefore, TMP might have a minor action on the Ca²⁺-dependent pathway, which may also be TMP concentration dependent. We have preliminary data indicating increased Ca²⁺ involvement with increased TMP concentrations. Further studies using direct Ca²⁺ measurement may be required to clarify this.

The effect of TMP on colonic anion secretion by a primary action on the cAMP pathway is consistent with our previous studies with Bak Foong Pills, indicating that TMP may be an active compound responsible for mediating the stimulatory effect of Bak Foong Pills on colonic anion secretion previously observed^[15]. Since Cl⁻ secretion is the main driving force for fluid secretion across the colon^[9], and HCO₃⁻ secretion at the luminal surface is considered to have a decisive influence on a constant pH microclimate sustenance^[38], the ability of TMP to enhance the secretion of these anions secretion may have implications in future development of alternative treatment for constipation. Most importantly, as an active compound of many popular traditional Chinese medicines, TMP has been in clinical use with trivial side effects and few clinically relevant drug interactions reported. Taken together, TMP may have therapeutic potential for treatment of constipation caused by disturbance of electrolyte and fluid transport in the GI tract.

REFERENCES

- 1 Pan G, Lu S, Ke M, Han S, Guo H, Fang X. Epidemiologic study of the irritable bowel syndrome in Beijing: stratified randomized study by cluster sampling. *Chin Med J* 2000; **113**: 35-39

- 2 **Bommelaer G**, Dorval E, Denis P, Czernichow P, Frexinos J, Pelc A, Slama A, El Hasnaoui A. Prevalence of irritable bowel syndrome in the French population according to the Rome I criteria. *Gastroenterol Clin Biol* 2002; **26**: 1118-1123
- 3 **Belai A**, Wheeler H, Burnstock G. Innervation of the rat gastrointestinal sphincters: Changes during development and aging. *Int J Dev Neurosci* 1995; **13**: 81-95
- 4 **Burleigh DE**. Evidence for a functional cholinergic deficit in human colonic tissue resected for constipation. *J Pharm Pharmacol* 1988; **40**: 55-57
- 5 **Dawson DC**. Ion channels and colonic salt transport. *Annu Rev Physiol* 1991; **53**: 321-339
- 6 **Sood R**, Bear C, Auerbach W, Reyes E, Jensen T, Kartner N, Riordan JR, Buchwald M. Regulation of CFTR expression and function during differentiation of intestinal epithelial cells. *EMBO J* 1992; **11**: 2487-2494
- 7 **Strong TV**, Boehm K, Collins FS. Localization of cystic fibrosis transmembrane conductance regulator mRNA in the human gastrointestinal tract by *in situ* hybridization. *J Clin Invest* 1994; **93**: 347-354
- 8 **O'Grady SM**, Jiang X, Maniak PJ, Birmachou W, Scribner LR, Bulbulian B, Gullikson GW. Cyclic AMP-dependent Cl secretion is regulated by multiple phosphodiesterase subtypes in human colonic epithelial cells. *J Membr Biol* 2002; **185**: 137-144
- 9 **Kunzelmann K**, Mall M. Electrolyte transport in the mammalian colon: mechanisms and implications for disease. *Physiol Rev* 2002; **82**: 245-289
- 10 **Clarke LL**, Harline MC. Dual role of CFTR in cAMP-stimulated HCO₃⁻ secretion across murine duodenum. *Am J Physiol* 1998; **274**(4 Pt 1): G718-726
- 11 **Seidler U**, Blumenstein I, Kretz A, Viellard-Baron D, Rossmann H, Colledge WH, Evans M, Ratcliff R, Gregor M. A functional CFTR protein is required for mouse intestinal cAMP-, cGMP- and Ca²⁺-dependent HCO₃⁻ secretion. *J Physiol* 1997; **505**: 411-423
- 12 **Lencer WI**, Delp C, Neutra MR, Madara JL. Mechanism of cholera toxin action on a polarized human intestinal epithelial cell line: role of vesicular traffic. *J Cell Biol* 1992; **117**: 1197-1209
- 13 **Ewe K**. Intestinal transport in constipation and diarrhoea. *Pharmacology* 1988; **36**: 73-84
- 14 **Campillos Paez MT**, Valles Ugarte ML, San Laureano Palomero T, Perez Hernansaiz M. Constipation and laxative consumption in the elderly. *Aten Primaria* 2000; **26**: 430-432
- 15 **Zhu JX**, Chan YM, Tsang LL, Chan LN, Zhou Q, Zhou CX, Chan HC. Cellular signaling mechanisms underlying pharmacological action of Bak Foong Pills on gastrointestinal secretion. *Jpn J Physiol* 2002; **52**: 129-134
- 16 **Xu J**, Li YK, Liang ZJ. Effects of tetramethylpyrazine and ferulic acid alone or combined on vascular smooth muscle, blood viscosity and toxicity. *Zhongguo Zhongyao Zazhi* 1992; **17**: 680-682
- 17 **Liu SY**, Sylvester DM. Antiplatelet activity of tetramethylpyrazine. *Thromb Res* 1994; **75**: 51-62
- 18 **Lin LN**, Wang WT, Xu ZJ. Clinical study on ligustrazine in treating myocardial ischemia and reperfusion injury. *Zhongguo Zhongxiyijiehe Zazhi* 1997; **17**: 261-263
- 19 **Lin CI**, Wu SL, Tao PL, Chen HM, Wei J. The role of cyclic AMP and phosphodiesterase activity in the mechanism of action of tetramethylpyrazine on human and dog cardiac and dog coronary arterial tissues. *J Pharm Pharmacol* 1993; **45**: 963-966
- 20 **Kenyon JL**, Gibbons WR. Effects of low-chloride solutions on action potentials of sheep cardiac Purkinje fibers. *J Gen Physiol* 1977; **70**: 635-660
- 21 **Snouwaert JN**, Brigman KK, Latour AM, Malouf NN, Boucher RC, Smithies O, Koller BH. An animal model for cystic fibrosis made by gene targeting. *Science* 1992; **257**: 1083-1088
- 22 **Ussing HH**, Zerahn K. Active transport of sodium as the source of electric current in the short-circuited isolated frog skin. *Acta Physiol Scand* 1951; **23**: 110-127
- 23 **Strabel D**, Diener M. Evidence against direct activation of chloride secretion by carbachol in the rat distal colon. *Eur J Pharmacol* 1995; **274**: 181-191
- 24 **Andres H**, Rock R, Bridges RJ, Rummel W, Schreiner J. Submucosal plexus and electrolyte transport across rat colonic mucosa. *J Physiol* 1985; **364**: 301-312
- 25 **Schultz BD**, DeRoos AD, Venglarik CJ, Singh AK, Frizzell RA, Frizzell RA, Bridges RJ. Glibenclamide blockade of CFTR chloride channels. *Am J Physiol* 1996; **271**(2 Pt 1): L192-200
- 26 **Mall M**, Bleich M, Schürlein M, Kuhr J, Seydewitz HH, Brandis M, Greger R, Kunzelmann K. Cholinergic ion secretion in human colon requires coactivation by cAMP. *Am J Physiol Gastrointest Liver Physiol* 1998; **275**(6 Pt 1): G1274-1281
- 27 **Foster ES**, Zimmerman TW, Hayslett JP, Binder HJ. Corticosteroid alteration of active electrolyte transport in rat distal colon. *Am J Physiol* 1983; **245**(5 Pt 1): G668-675
- 28 **Bachmann O**, Rossmann H, Berger UV, Colledge WH, Ratcliff R, Evans MJ, Gregor M, Seidler U. cAMP-mediated regulation of murine intestinal/pancreatic Na⁺/HCO₃⁻ cotransporter subtype pNBC1. *Am J Physiol Gastrointest Liver Physiol* 2003; **284**: 37-45
- 29 **Haas M**, Forbush B. The Na⁺-K⁺-Cl⁻ cotransporter of secretory epithelia. *Annu Rev Physiol* 2000; **62**: 515-534
- 30 **Ito Y**, Mizuno Y, Aoyama M, Kume H, Yamaki K. CFTR-Mediated anion conductance regulates Na⁺-K⁺-pump activity in Calu-3 human airway cells. *Biochem Biophys Res Commun* 2000; **274**: 230-235
- 31 **Greger R**. Role of CFTR in the colon. *Annu Rev Physiol* 2000; **62**: 467-491
- 32 **Geibel JP**, Singh S, Rajendran VM, Binder HJ. HCO₃⁻ secretion in the rat colonic crypt is closely linked to Cl⁻ secretion. *Gastroenterology* 2000; **118**: 101-107
- 33 **Gray MA**, O'Reilly C, Winpenny J, Argent B. Functional interactions of HCO₃⁻ with cystic fibrosis transmembrane conductance regulator. *JOP* 2001; **2**: 207-211
- 34 **Dalemans W**, Barbry P, Champigny G, Jallat S, Dott K, Dreyer D, Crystal RG, Pavirani A, Lecocq JP, Lazdunski M. Altered chloride ion channel kinetics associated with the F508 cystic fibrosis mutation. *Nature* 1991; **354**: 526-528
- 35 **Barrett KE**, Keely SJ. Chloride secretion by the intestinal epithelium: molecular basis and regulatory aspects. *Annu Rev Physiol* 2000; **62**: 535-572
- 36 **Kopito RR**. Biosynthesis and degradation of CFTR. *Physiol Rev* 1999; **79**(1 Suppl): S167-173
- 37 **Craven PA**, DeRubertis FR. Stimulation of rat colonic mucosal prostaglandin synthesis by calcium and carbamylcholine: relationship to alterations in cyclic nucleotide metabolism. *Prostaglandins* 1981; **21**: 65-81
- 38 **Genz AK**, v Engelhardt W, Busche R. Maintenance and regulation of the pH microclimate at the luminal surface of the distal colon of guinea-pig. *J Physiol* 1999; **517**: 507-519

• BASIC RESEARCH •

Procedure for preparing peptide-major histocompatibility complex tetramers for direct quantification of antigen-specific cytotoxic T lymphocytes

Xian-Hui He, Li-Hui Xu, Yi Liu

Xian-Hui He, Key Laboratory of Ministry of Education of China for Tissue Transplantation and Immunology, Jinan University, Guangzhou 510632, Guangdong Province, China

Li-Hui Xu, Institute of Bioengineering, Jinan University, Guangzhou 510632, Guangdong Province, China

Yi Liu, Department of Dermatology, First Affiliated Hospital, Zhengzhou University, Zhengzhou 450052, Henan Province, China

Supported by the National Natural Science Foundation of China, No. 30230350 and No. 30371651, and Major State Basic Research Development Program of China, 973 Program, No. G2000057006
Correspondence to: Dr. Xian-Hui He, Key Laboratory of Ministry of Education of China for Tissue Transplantation and Immunology, Jinan University, 601 Huangpu Road West, Guangzhou 510632, Guangdong Province, China. thehx@jnu.edu.cn

Telephone: +86-20-85220679 Fax: +86-20-85221337

Received: 2004-08-18 Accepted: 2004-11-19

Abstract

AIM: To establish a simplified method for generating peptide-major histocompatibility complex (MHC) class I tetramers.

METHODS: cDNAs encoding the extracellular domain of human lymphocyte antigen (HLA)-A*0201 heavy chain (A2) and β_2 -microglobulin (β_2m) from total RNA extracted from leukocytes of HLA-A2⁺ donors were cloned into separate expression vectors by reverse transcription-polymerase chain reaction. The recombinant A2 and β_2m proteins were expressed in *Escherichia coli* strain BL21(DE3) and recovered from the inclusion body fraction. Soluble A2 proteins loaded with specific antigen peptides were refolded by dilution from the heavy chain in the presence of light chain β_2m and HLA-A2-restricted peptide antigens. The refolded A2 monomers were biotinylated with a commercial biotinylation enzyme (BirA) and purified by low pressure anion exchange chromatography on a Q-Sepharose (fast flow) column. The tetramers were then formed by mixing A2 monomers with streptavidin-PE in a molar ratio of 4:1. Flow cytometry was used to confirm the expected tetramer staining of CD8⁺ T cells.

RESULTS: Recombinant genes for HLA-A*0201 heavy chain (A2) fused to a BirA substrate peptide (A2-BSP) and mature β_2m from HLA-A2⁺ donor leukocytes were successfully cloned and highly expressed in *E. coli*. Two soluble monomeric A2-peptide complexes were reconstituted from A2-BSP in the presence of β_2m and peptides loaded with either human cytomegalovirus pp65₄₉₅₋₅₀₃ peptide (NLVPMVATV, NLV; designated as A2-NLV) or influenza virus matrix

protein Mp58-66 peptide (GILGFVFTL, GIL; designated as A2-GIL). Refolded A2-NLV or A2-GIL monomers were biotinylated and highly purified by single step anion exchange column chromatography. The tetramers were then formed by mixing the biotinylated A2-NLV or A2-GIL monomers with streptavidin-PE, leading to more than 80% multiplication as revealed by SDS-PAGE under non-reducing, unboiled conditions. Flow cytometry revealed that these tetramers could specifically bind to CD8⁺ T cells from a HLA-A2⁺ donor, but failed to bind to those from a HLA-A2⁻ donor.

CONCLUSION: The procedure is simple and efficient for generating peptide-MHC tetramers.

© 2005 The WJG Press and Elsevier Inc. All rights reserved.

Key words: Major histocompatibility complex; HLA-A2; Tetramers; Cytomegalovirus; Immune responses; Cytotoxic T lymphocytes

He XH, Xu LH, Liu Y. Procedure for preparing peptide-major histocompatibility complex tetramers for direct quantification of antigen-specific cytotoxic T lymphocytes. *World J Gastroenterol* 2005; 11(27): 4180-4187

<http://www.wjgnet.com/1007-9327/11/4180.asp>

INTRODUCTION

Cytotoxic T lymphocytes (CTLs), or CD8⁺ T cells, play a critical role in the clearance of viral infections and the eradication of tumors^[1]. A better understanding of cellular immunity against viruses and/or tumor cells requires careful analysis of the responding CD8⁺ T cells, particularly in terms of their numbers and effector functions^[2]. Because specific CD8⁺ T cells are often vastly outnumbered by irrelevant T cells, quantification of antigen-specific T cells often requires *in vitro* culture and re-stimulation, which may introduce bias in the results^[2]. The standard method for deriving specific CTL frequency information is limiting dilution analysis (LDA)^[2]. However, accumulating evidence indicates that this technique may significantly underestimate the number of specific CTLs, because it does not detect cells that lack proliferative potential^[2,3]. This limitation has been overcome by the introduction of peptide-major histocompatibility complex (MHC) class I tetrameric complex technology^[3-6], which initiates a profound revolution in the field of cellular immunology^[7-10]. Peptide-MHC tetramer-based assays have enabled direct flow cytometric quantification^[3-6], phenoty-

ping^[3,8-11] and even functional analysis^[8,11] of antigen-specific CD8⁺ T cells. Thus, peptide-MHC tetramer technology is a powerful tool for evaluating the fundamental aspects of T-cell immunity.

Though tetramer technology for direct quantification of the frequency and/or function of antigen-specific CTLs has been generally accepted, wide application of tetramer strategies is limited by the complex procedures necessary for tetramer production^[3]. Moreover, the expression level of recombinant human MHC class I heavy chain in *Escherichia coli* is usually minimal due to the low translation frequency of human proteins in *E. coli*^[12]. To address these problems, we sought to develop a simplified and efficient method for production of peptide-MHC class I tetramers. We constructed prokaryotic expression vectors for recombinant human lymphocyte antigen (HLA)-A2 heavy chain and β_2m -microglobulin (β_2m) proteins, in which nucleotide residues in the translation initiation region (TIR) were substituted to the preferred codons for *E. coli*^[13] and decreased the G/C content in this region^[14]. The recombinant A2 and β_2m proteins were overexpressed in *E. coli* in the form of inclusion bodies, thus facilitating their high purity isolation by simple washing and centrifugation. Further simple procedures allowed us to establish an efficient, streamlined procedure for the preparation of HLA-A2 tetramers. This improved procedure should facilitate the general application of tetramer technology in both basic research and clinical applications.

MATERIALS AND METHODS

Materials

E. coli strain DH5 α was stored in our laboratory. *E. coli* strain BL21(DE3) and plasmid pET-3c were purchased from Novagen (Madison, WI, USA). *Nde*I, *Bam*HI, T4 DNA ligase and high fidelity DeepVent Taq polymerase were purchased from New England Biolabs (Beverly, MA, USA). The TRIzol reagent and ThermoScript reverse transcription-polymerase chain reaction (RT-PCR) system were obtained from Invitrogen (Carlsbad, CA, USA). Q-Sepharose (fast flow) was obtained from Amersham (Uppsala, Sweden). Mouse anti-human monoclonal antibodies CD3-FITC, CD8-CyChrome and HLA-A2-FITC were purchased from PharMingen (San Diego, CA, USA). Streptavidin R-phycoerythrin (PE) conjugate (streptavidin-PE) was purchased from Molecular Probes (Eugene, OR, USA). Protein molecular mass markers were obtained from Sigma (St. Louis, MO, USA). The biotinylation enzyme, BirA, was purchased from Avidity (www.avidity.com). The NLVPMVATV (NLV) peptide derived from pp65 (pp65₄₉₅₋₅₀₃) of HCMV^[11], and the GILGFVFTL (GIL) peptide derived from the matrix protein (Mp₅₈₋₆₆) of the influenza A virus^[15], were synthesized by BioAsia (Shanghai, China) and purified to >98%. All other chemicals were from Sigma and were analytically pure.

Cloning of HLA-A*0201 heavy chain and β_2m cDNAs

Heparinized human peripheral blood was collected from three HLA-A2 positive (identified by anti-human HLA-A2-FITC staining and flow cytometric analysis) donors by venipuncture. Total RNA was extracted from freshly isolated

PBMCs using the TRIzol reagent. cDNAs were synthesized from the isolated RNA using the ThermoScript RT-PCR system according to the recommended procedure. PCR amplification of the resultant cDNA was performed in a total volume of 50 μ L containing high fidelity DeepVent Taq polymerase. For amplification of β_2m , PCR was performed with an initial denaturation for 2 min at 94 °C, followed by 35 cycles of 94 °C for 30 s, 55 °C for 30 s and 72 °C for 1 min, and a final extension for 10 min at 72 °C. The primers (5'-ATA TCC ATA TGT CTC GCT CCG TGG CCT TAG-3' and 5'-AAC TAG GGA TCC TTA CAT GTC TCG ATC CCA C-3') were designed to amplify the entire coding sequence of human β_2m cDNA. For amplification of the mature HLA-A*0201 heavy chain, PCR was performed as above except that the extension time at 72 °C was 1.5 min and the primers (5'-TAT ACA TAT GGG CTC TCA CTC CAT GAG GTA TTT C-3' and 5'-AAC CAG GGA TCC TAC ACT TTA CAA GCT GTG AGA G-3') were designed to amplify the entire coding sequence of mature A2. The resultant PCR products were cloned into the *Nde*I-*Bam*HI sites of the pET-3c vector. Randomly selected clones were *Nde*I/*Bam*HI digested and screened for the presence of a correctly sized insert. Several independent clones were submitted for DNA sequencing of the HLA-A*0201 heavy chain cDNA using the dye-labeled deoxy-terminator protocol on a 377 automated DNA sequencer (Applied Biosystems). The cloned β_2m cDNA was also confirmed by DNA sequencing analysis.

Construction of expression vector for mature β_2m

To create a β_2m expression construction with optimized codon usage and G/C content, the DNA fragment for mature β_2m was PCR amplified from the cloned β_2m cDNA using specific primers (5'-AT ATC CAT ATG ATT CAA CGT ACT CCA AAA ATT CAA GTT TAC TCA CGT CAT CC-3' and 5'-CGA CTG GAT CCT TAC ATG TCT CGA TCC CAC TTA AC-3'). The underlined codons were optimized for expression in *E. coli*^[13] by synonymous substitutions from ATC, CAG, AAG, CAG to ATT, CAA, AAA and CAA, respectively. These alterations also reduced the G/C content in the TIR. The resulting PCR product was inserted into the *Nde*I-*Bam*HI sites of the pET-3c vector, and a positive clone with a correct sized insert was confirmed by DNA sequencing. This recombinant plasmid was designated as pET- β_2m .

Construction of expression vector for extracellular domain of HLA-A2 heavy chain fused with BirA substrate peptide (BSP)

To construct an expression vector in which the HLA-A2 heavy chain was fused with BSP, the DNA fragment encoding a Gly-Ser linker and a BSP (LHHILDAQKMVWNHR) was fused to the 3' end of the cDNA encoding the extracellular domain of the HLA-A2 heavy chain (1-275) by PCR amplification from cloned HLA-A2 heavy chain cDNA with specific primers (5'-ATA CAT ATG GGT TCT CAT TCT ATG CGT TAT TTT TTT ACA TCT GTT TCC CGG CCC GGC CGC-3' and the 3' primer 5'-GCG CGG ATC CTT AAC GAT GAT TCC ACA CCA TTT TCT GTG CAT CCA GAA TAT GAT GCA GAG AGC CCG GCT CCC ATC TCA GGG T-3'). The underlined codons were

optimized for expression in *E. coli*^[13], and reduced the G/C content without any changes in amino acid sequence. These codons were changed from GGC, CAC, TCC, AGG, TTC, TTC, TCC and GTG, respectively. The resultant PCR product was *NdeI/BamHI* digested and subcloned into plasmid pET-3c. Clones with correct sized inserts were verified by direct sequencing, and the recombinant plasmid was designated as pET-A2-BSP.

Expression and isolation of recombinant A2-BSP and β_2m proteins

BL21(DE3) competent cells were transformed with either pET- β_2m or pET-A2-BSP, single colonies were used to inoculate 100 mL of LB medium, and cultures were incubated at 37 °C overnight until cells reached the stationary phase. Each stationary culture was diluted 10-fold with fresh LB medium (to 1 L) and incubated at 37 °C for a further 2 h, 0.4 mmol/L isopropyl β -D-thiogalactopyranoside (IPTG) was added, and cells were incubated for an additional 4 h. Cells were collected by centrifugation, and insoluble protein aggregates (inclusion bodies) were purified essentially as described^[16]. In brief, each cell pellet was re-suspended in 50 mmol/L Tris-HCl buffer (pH 8.0) containing 1 mmol/L EDTA, 0.1 mmol/L phenylmethylsulfonyl fluoride (PMSF) and 10 mmol/L dithiothreitol (DTT), and then sonicated on ice. The insoluble pellet was collected by centrifugation and washed with washing buffer (50 mmol/L Tris-HCl pH 8.0, 100 mmol/L NaCl, 1 mmol/L EDTA, 1 mmol/L DTT and 5 g/L Triton X-100), followed by three more rounds of sonication, centrifugation and collection. The pellet was washed three more times with washing buffer without Triton X-100 and the isolated inclusion body pellet was dissolved in 20 mmol/L 2-(*N*-morpholino)ethanesulfonic acid (pH 6.0, containing 8 mol/L urea, 10 mmol/L EDTA, and 0.1 mmol/L DTT). The insoluble material was pelleted by centrifugation and removed. The protein concentration of the remaining solution was determined by measuring $A_{280\text{ nm}}$ and $A_{260\text{ nm}}$, and calculated according to the empirical formula ($1.45 \times A_{280\text{ nm}} - 0.74 \times A_{260\text{ nm}} = \text{protein concentration in mg/mL}$). The protein solution was immediately frozen at -70 °C.

Refolding of monomeric HLA-A2

The HLA-A2 monomers were refolded essentially as described by Garboczi and Wiley^[17], with slight modifications. Briefly, 2 mg of peptide (NLV or GIL peptide) dissolved in DMSO was added in drops to 200 mL of pre-chilled refolding buffer (100 mmol/L Tris-HCl pH 8.0, containing 400 mmol/L L-arginine, 2 mmol/L EDTA, 5 mmol/L reduced glutathione, 0.5 mmol/L oxidized glutathione and 0.2 mmol/L PMSF). Then, 6 mg A2-BSP in 1 mL injection buffer containing 3 mol/L guanidine-HCl pH 4.2, 10 mmol/L sodium acetate and 10 mmol/L EDTA was forcefully injected to the stirring reaction through a 26-gauge needle as close to the stir bar as possible. Five micrograms of β_2m was injected similarly, and the refolding mixture was incubated at 10 °C for 3 d. At the end of the incubation, 200 mL of the refolding mixture was concentrated to 5 mL with an ultrafiltration apparatus (Amicon, Millipore, Bedford, MA, USA) containing a 10 ku molecular mass cut-off membrane,

and dialyzed against 10 mmol/L Tris-HCl buffer (pH 8.0, containing 0.2 mmol/L PMSF). The refolded monomeric HLA-A2 was centrifuged to eliminate precipitates, and then biotinylated.

Biotinylation and purification of monomeric HLA-A2

The refolded HLA-A2 was enzymatically biotinylated by incubation with BirA according to the procedure provided by the supplier (Avidity Co.). The biotinylated HLA-A2 was dialyzed against 10 mmol/L Tris-HCl buffer (pH 8.0, containing 0.2 mmol/L PMSF) and loaded onto an anion-exchanger Q-Sepharose column (2 cm \times 8 cm) equilibrated with the same buffer. The column was eluted with a 0-300 mmol/L NaCl linear gradient, and 1.5 mL fraction was collected. Fractions exhibiting both HLA-A2 heavy chain and β_2m bands upon SDS-PAGE analysis were pooled and concentrated to 300 μ L. The buffer of the biotinylated HLA-A2 was changed to 0.01 mol/L phosphate-buffered saline (PBS, pH 7.4) containing 0.2 mmol/L PMSF and 2 mmol/L EDTA through ultrafiltration.

Tetramerization of soluble HLA-A2 monomers

HLA-A2 tetramers were formed by mixing the biotinylated proteins with streptavidin-PE at a molar ratio of 4:1. Tetramers were analyzed by SDS-PAGE of samples prepared without boiling, in a loading buffer that contained no reducing reagent^[10].

Tetramer staining and flow cytometry

Peripheral blood mononuclear cells (PBMCs) were separated from 3 mL whole blood of two volunteers (over 40 years) by centrifugation over a Ficoll-Hypaque density gradient (Lymphoprep; NYCOMED, Norway). For staining, 1×10^6 cells suspended in 50 μ L PBS containing 20 mL/L fetal calf serum and 1 g/L sodium azide were incubated on ice for 1 h with 10 μ L of CD3-FITC, 10 μ L of CD8-CyChrome and 1 μ g of HLA-A2 tetramer. After being washed, the cells were fixed in 300 μ L of 10 g/L paraformaldehyde and detected on a FACSCalibur flow cytometer (Becton Dickinson, San Jose, CA, USA). For each sample, 50 000 events were collected and analyzed with the CELLQuest software (Becton Dickinson). The results were expressed as the percentages of tetramer-binding cells in the total T cell population.

RESULTS

Cloning of cDNA for HLA-A*0201 heavy chain and β_2m

The cDNA encoding the mature HLA-A2 heavy chain was RT-PCR amplified from total RNA of three HLA-A2 positive donors (identified as such by flow cytometry after anti-HLA-A2-FITC staining). The DNA fragments with the expected length (1 100 bp) were inserted into pET-3c, and eight independently transformed DH5a clones were identified to have the correct insert (Figure 1). DNA sequencing of these clones showed that six clones from donors 1 and 2 contained the cDNA for HLA-A*0201 heavy chain (designated pET-A2), while those from donor 3 contained the cDNA for HLA-A*0207 heavy chain. The cDNA sequence for HLA-A*0201 was submitted to GenBank (accession number AY191309).

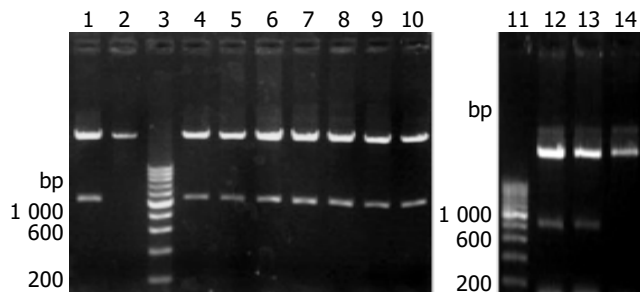


Figure 1 Identification of clones with correct sized inserts, using *NdeI/BamHI* double digestion. Lanes 1 and 4-8: pET-A2 clones from donors 1 and 2; lanes 2 and 14: pET-3c; lanes 3 and 11: 200-bp DNA ladder; lanes 9 and 10: pET-A2 clones from donor 3; lanes 12 and 13: pET-A2-BSP.

Similarly, the cDNA encoding β_2m was cloned from the total RNA of one donor and inserted into pET-3c (data not shown). The sequence was verified by DNA sequencing and found to be identical to the published one (submitted to GenBank, accession number AY187687).

Construction of expression vectors for recombinant A2-BSP and β_2m proteins

According to Altman's strategy^[3], the DNA fragment encoding a Gly-Ser linker and a BSP (LHHILDAQKMVWNHR) was fused to the 3' end of the DNA fragment encoding the extracellular domain of HLA-A*0201 heavy chain (residues from 1 to 275) by PCR amplification of plasmid pET-A2. In order to increase the expression level in *E. coli*, our primers introduced synonymous substitutions at the 5' region, intended to reduce the G/C content of the TIR and to optimize codons for the bias usage of *E. coli*^[13,14]. The amplified DNA fragment (900 bp) was inserted into pET-3c. Two clones with the correct insert were confirmed by DNA sequencing, and the generated expression vector was designated as pET-A2-BSP (Figure 1).

The expression vector for mature β_2m was similarly constructed by PCR amplification using cloned β_2m cDNA as template. The codons at the 5' region were optimized for better expression of β_2m in *E. coli*. The sequence of the insert was verified by DNA sequencing, and the vector was designated as pET- β_2m .

Refolding and biotinylation of monomeric HLA-A2

The expression vectors pET-A2-BSP and pET- β_2m were transformed into *E. coli* BL21(DE3). The cells showed leaky expression of the two proteins, and the expression levels increased dramatically after induction with IPTG (Figure 2). The molecular mass of the recombinant β_2m was approximately 12 ku, which was consistent with that of native human β_2m , while the engineered A2 heavy chain-BSP fusion protein (A2-BSP) had the expected molecular mass of 33 ku. The expression levels of these two recombinant proteins accounted for more than 20% of the total cellular proteins (Figure 2). The yields were approximately 32 and 50 mg/L for A2-BSP and β_2m , respectively. Western blotting showed that the recombinant β_2m could react with antibodies against human native β_2m (data not shown). HLA-A2 heavy chain expression was not analyzed by Western blotting, because

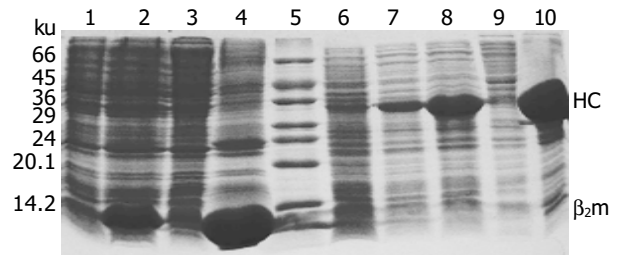


Figure 2 SDS-PAGE (150 g/L) analyses of recombinant A2-BSP and β_2m proteins expressed in *E. coli* strain BL21(DE3). Lane 1: BL21 (pET- β_2m) before IPTG induction; lane 2: BL21 (pET- β_2m)+IPTG; lane 3: supernatant of BL21 (pET- β_2m) lysate; lane 4: washed inclusion body of β_2m ; lane 5: MW marker; lane 6: BL21 (pET-3c)+IPTG; lane 7: BL21 (pET-A2-BSP) before IPTG induction; lane 8: BL21 (pET-A2-BSP)+IPTG; lane 9: supernatant of BL21 (pET-A2-BSP) lysate; lane 10: washed inclusion body of A2-BSP. HC: heavy chain.

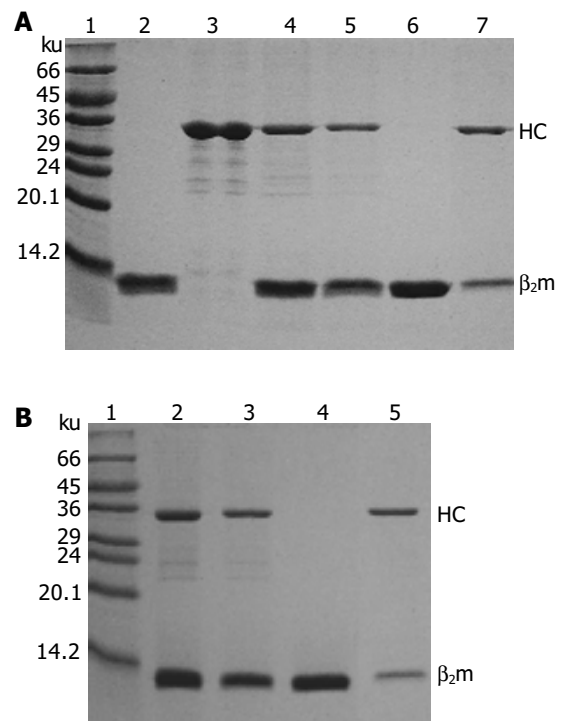


Figure 3 Analyses of refolded A2-GIL (A) and A2-NLV (B) monomers after purification and biotinylation with SDS-PAGE (150 g/L). In (A) lane 1: protein MW marker; lane 2: solubilized β_2m ; lane 3: solubilized A2-BSP; lane 4: refolded A2-GIL monomer; lane 5: biotinylated A2-GIL monomer; lane 6: peak I (β_2m) (Figure 4); lane 7: peak II (purified A2-GIL). In (B) lane 1: protein MW marker; lane 2: refolded A2-NLV monomer; lane 3: biotinylated A2-NLV monomer; lane 4: peak I (β_2m); lane 5: peak II (purified A2-NLV). HC: heavy chain.

no suitable antibody was available. Both A2-BSP and β_2m were largely expressed in the insoluble fraction (inclusion bodies), which facilitated purification through simple washing and centrifugation (Figure 3, lanes 2 and 3).

Monomeric HLA-A2 was refolded by dilution of A2-BSP and β_2m with refolding buffer in the presence of HLA-A*0201-restricted antigenic peptides. Two peptides were used to reconstitute the HLA-A2 complex. One was the immunodominant NLVPMVATV (NLV) peptide, which was derived from pp65 (pp65₄₉₅₋₅₀₃) of HCMV^[11] and used to

reconstitute the HLA-A2-NLV (hereafter referred to as A2-NLV) complex. The other was the predominant CTL epitope GILGFVFTL (GIL) peptide derived from the matrix protein (Mp₅₈₋₆₆) of influenza A virus^[15], which was used to reconstitute the HLA-A2-GIL (referred to as A2-GIL) complex. The yield of refolding was about 10-15%. The refolded A2-NLV and A2-GIL complexes appeared as two bands (A2-BSP and β_2m) on SDS-PAGE (Figure 3). After biotinylation, each complex was purified by single Q-Sepharose column chromatography. Typically, three peaks eluted from the column, as shown by monitoring of absorbance at 280 nm (Figure 4). Soluble β_2m eluted as the first peak. The second peak comprised the desired soluble HLA-A2 complex (A2-NLV or A2-GIL) consisting of a heavy chain and β_2m (Figure 3), which was of 95% purity as analyzed with the PhotoCapt Ver11.01 software (Vilber Lourmat, France). The fractions in this peak were pooled and concentrated by ultrafiltration. The third peak contained non-protein materials with a much higher absorbance at 260 nm than at 280 nm. Refolding without peptide (negative control) yielded no stable HLA-A2 complex.

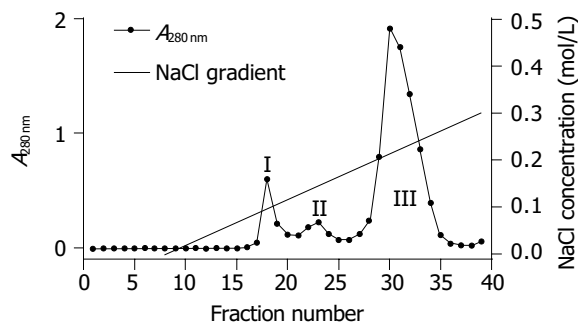


Figure 4 A typical elution profile of biotinylated HLA-A2 monomer from Q-Sepharose (fast flow) column (2 cm x 8 cm).

Formation of HLA-A2 tetramers

HLA-A2 tetramers were formed by mixing the biotinylated A2-NLV or A2-GIL monomers with streptavidin-PE at a 4:1 molar ratio. SDS-PAGE analysis of the HLA-A2 tetramers could be used to estimate the extent of tetramer formation, because the complex formed between streptavidin and biotin was stable in the absence of boiling treatment and DTT^[10]. As shown in Figure 5, the single main band observed in the lanes of monomeric A2-NLV or A2-GIL corresponded to the 33 ku heavy chain, as β_2m quickly migrated to the bottom of the gel. Software analysis (PhotoCapt Ver11.01) showed that the amount of heavy chain in the A2-NLV tetramer lane was about 10-20% of that in the lane containing monomeric HLA-A2, indicating that about 80% of the A2-NLV monomer formed multimers with streptavidin-PE. The A2-GIL tetramer showed a similar extent of multimer formation.

Staining of CTLs with HLA-A2 tetramers

Finally, the A2-NLV and A2-GIL tetramers were tested by flow cytometry for their abilities to identify HCMV- or influenza-specific CD8⁺ T cells in freshly isolated PBMCs

from HLA-A2 positive and negative donors. PBMCs were analyzed by three-color flow cytometry after A2-NLV and A2-GIL tetramer staining. Background staining was performed with streptavidin-PE instead of the tetramers.

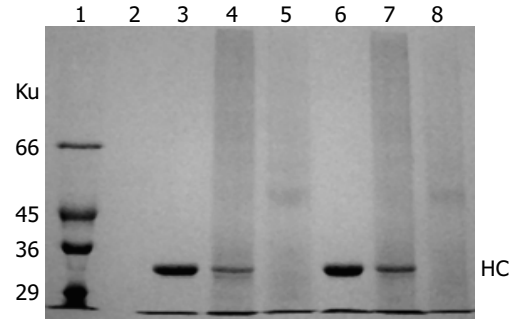


Figure 5 SDS-PAGE (75 g/L) analyses of A2-NLV and A2-GIL tetramers under non-reducing conditions without boiling. Lane 1: protein MW marker; lane 2: empty; lane 3: A2-NLV monomer (5 μ g); lane 4: A2-NLV tetramer (5 μ g A2-NLV monomer+8 μ g streptavidin-PE); lanes 5 and 8: streptavidin-PE (8 μ g); lane 6: A2-GIL monomer (5 μ g); lane 7: A2-GIL tetramer (5 μ g A2-GIL monomer+8 μ g streptavidin-PE). HC: heavy chain.

Subpopulations of CD8⁺ T cells specific for either pp65₄₉₅₋₅₀₃ or Mp₅₈₋₆₆ epitopes were found in HLA-A2 positive donors by A2-NLV or A2-GIL tetramer staining. Of the total T cells, 0.19% were stained by the A2-NLV tetramer, while 0.17% bound to the A2-GIL tetramer (Figure 6). However, only 0.07% and 0.12% of T cells from the HLA-A2 negative donor were nonspecifically stained by the A2-NLV or A2-GIL tetramers, respectively, which was comparable to the control staining with streptavidin-PE (0.06%). This result suggests that these tetramers are quite specific for MHC-restricted T cells.

DISCUSSION

As the current method of limiting dilution assay (LDA) tends to underestimate CTL frequency^[2,3], other methods have been sought for the quantification of antigen-specific CD8⁺ T cells in immune responses. T cell antigen receptors (TCR) expressed on CD8⁺ T cells can recognize peptide-MHC complexes, the specific ligands on the antigen-presenting cells (APCs). Therefore, direct staining of CD8⁺ T cells with their soluble cognate ligands should be an ideal approach. However, the strategy initially failed because soluble monomeric peptide-MHC complexes have low affinities for the T-cell receptor (TCR)^[1-3]. This obstacle has been overcome by Altman *et al.*^[3]. Tetramer reagents have been shown to bind specifically to cognate T cells in numerous systems, allowing fast and direct quantification of antigen-specific T cells by flow cytometry^[3,4,8,9,18-20]. Thus, tetramer-based assays have become a powerful new technology for detecting antigen-specific T cells^[4,8,21]. However, the general application of this strategy is limited by the complex, labor intensive protocols required for preparing specific peptide-MHC tetramers.

It is difficult to prepare a large amount of MHC class I heavy chain, because the translation efficiency in *E. coli* is very

low. However, optimization of codons in the TIR has been shown to increase translation efficiency^[14]. Sato *et al.*^[12], found that the expression of wild type HLA-A*2402 heavy chain in *E. coli* is undetectable, whereas a synonymous mutant in which the TIR mammalian usage codons are replaced by those of *E. coli*, can be expressed at high levels. Lakey *et al.*^[22], showed that the production of recombinant mycobacterial proteins increases 54-fold following selective replacement of low-usage *E. coli* codons in mycobacterial proteins with high-usage *E. coli* codons. In addition, the high G/C content in the TIR can block the expression of human proteins in *E. coli*^[14]. The previous paper did not include a detailed description of the expression vector or *E. coli* system, instead of referring readers to the system used by Garboczi^[17], in which no codon or G/C content changes were described. In the present study, recombinant proteins were expressed largely in the form of inclusion bodies, which greatly facilitated isolation and purification of the refolded peptide-MHC complexes, thus simplifying the tetramer preparation procedure. In addition to the difficulty in obtaining a large amount of MHC heavy chain, the practical application of tetramers is also limited by the complexity of the necessary

preparation procedures. In this study, we reconstituted the monomeric HLA-A2 complexes based on the dilution strategy described by Garboczi^[17]. After biotinylation, the HLA-A2 monomer could be highly purified by single step ion-exchange chromatography. It should be noted that the purification in the present study was carried out in a low pressure chromatography system requiring no HPLC facilities, whereas the previous protocol included three purification steps with high performance column chromatography^[3].

The results of this study indicate that the generated reagents can be used for the detection of antigen-specific T cells. Our novel procedure for generating tetramers should be applicable for preparing other HLA-A2 tetramers or for generating tetramers of other human MHC class I alleles.

Tetramer technology is primarily used to determine the frequency of antigen-specific T cells^[3-5], and has been extensively used in evaluating the dynamics of cytomegalovirus (CMV)-specific CTL responses in humans^[5-7,9,11]. It is generally believed that adults over 40 years in developing countries are almost 100% CMV positive^[9], and that the pp65₄₉₅₋₅₀₃ NLV peptide (NLVPMVATV) is the predominant CMV epitope presented by HLA-A2 molecules^[11,23]. Quantification

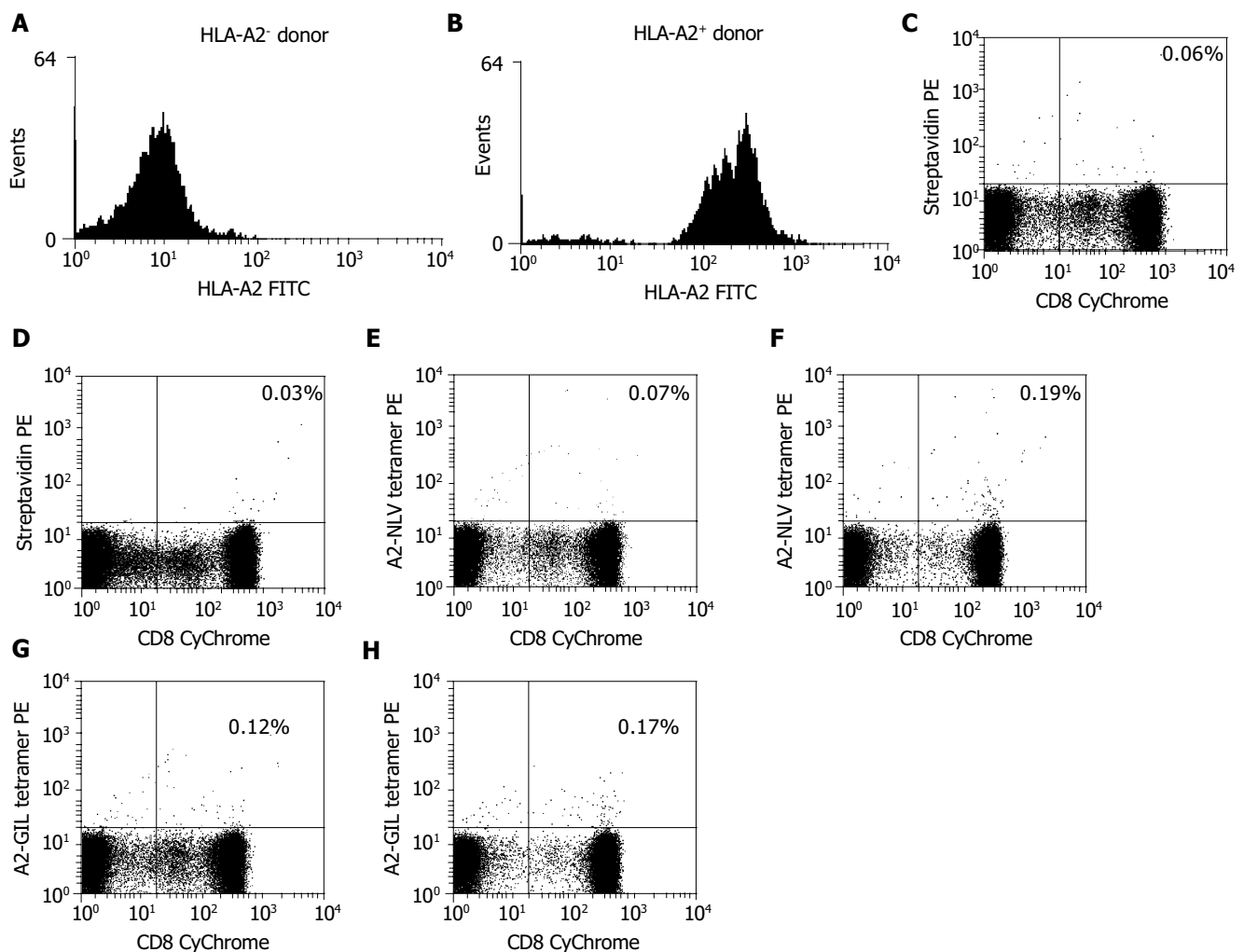


Figure 6 Flow cytometry of antigen-specific CD8⁺ T cells stained with A2-NLV tetramer (panels E and F) and A2-GIL tetramer (panels G and H) from both HLA-

A2 positive (B) and negative (A) donors. Background staining was performed with streptavidin-PE instead of the tetramers (C and D).

of specific T cells in the peripheral blood of healthy CMV carriers using an A2-NLV tetramer demonstrated that the percentage of NLV-specific CTLs in CMV carriers is about 0.02-6.19% within the CD8⁺ T cell population^[24]. In our study, tetramer staining showed that there were 0.19% NLV-specific CTLs among total T cells from the peripheral blood of a randomly selected HLA-A2-positive volunteer over 40 years, confirming again that NLV dominates the HLA-A2-restricted cellular immune response against CMV^[23]. There is substantial evidence that quantification of NLV-specific CTLs by tetramers is of clinical significance^[5-7,9,11,24,25]. Despite antiviral therapy, CMV remains an important cause of morbidity and mortality after allogeneic stem cell transplantation (SCT)^[26]. Through direct quantification of CMV-specific CD8⁺ T cells using A2-NLV tetramers, several studies demonstrated that recovery of CMV-specific CD8⁺ T cells after SCT is critical for protection against CMV disease^[6,7,25]. Accordingly, enumeration of HLA-restricted, CMV-specific CD8⁺ T cells by tetramer technology in grafts, and monitoring of these cells after SCT may constitute a rapid and sensitive tool for identifying SCT recipients at risk for developing CMV disease. Hence, tetramer technology is of value both in the development of novel transplant protocols and in clinical management of individual cases^[5-7,9,25].

It is also possible to combine tetramer staining with other flow cytometry-based assays to gain more phenotypic or even functional information on antigen-specific CTLs^[3,8,10,12]. For example, tetramer staining can be combined with intracellular detection of cytokines (e.g. interferon- γ), chemokines (e.g. macrophage inflammatory protein 1 α), and cytotoxins (e.g. perforin/granzymes) following *in vitro* antigen/mitogen stimulation to assess the functional status of tetramer-positive T cells^[27,28]. Moreover, tetramers can be used in the isolation of antigen-specific cells for characterization and even expansion of immunotherapeutic use^[11,25,29]. Conjugation of a specific tetramer with antibodies against a tumor-associated antigen has been used to redirect CMV-specific CTLs to kill tumor cells by binding to the surface of tumor cells and sensitizing them to lysis by tetramer-specific CTLs, suggesting the potential therapeutic application of tetramers^[30]. Thus, tetramer technology has opened new routes for further study of T-cell responses and tumor immunotherapy.

In summary, we have established a simplified and efficient procedure for generating peptide-MHC tetramers, a highly specific and very useful reagent with a number of important applications in cellular immune response studies. The present method may provide an alternative method for the preparation of MHC class I tetramers, and promote the use of this exciting technology.

REFERENCES

- Harty JT, Tivnnerheim AR, White DW. CD8⁺ T cell effector mechanisms in resistance to infection. *Annu Rev Immunol* 2000; **18**: 275-308
- Doherty PC, Christensen JP. Accessing complexity: the dynamics of virus-specific T cell responses. *Annu Rev Immunol* 2000; **18**: 561-592
- Altman JD, Moss PA, Goulder PJ, Barouch DH, McHeyzer-Williams MG, Bell JI, McMichael AJ, Davis MM. Phenotypic analysis of antigen-specific T lymphocytes. *Science* 1996; **274**: 94-96
- Meidenbauer N, Hoffmann TK, Donnenberg AD. Direct visualization of antigen-specific T cells using peptide-MHC-class I tetrameric complexes. *Methods* 2003; **31**: 160-171
- Gratama JW, Cornelissen JJ. Diagnostic potential of tetramer-based monitoring of cytomegalovirus-specific CD8⁺ T lymphocytes in allogeneic stem cell transplantation. *Clin Immunol* 2003; **106**: 29-35
- Gratama JW, van Esser JW, Lamers CH, Tournay C, Lowenberg B, Bolhuis RL, Cornelissen JJ. Tetramer-based quantification of cytomegalovirus (CMV)-specific CD8⁺ T lymphocytes in T-cell-depleted stem cell grafts and after transplantation may identify patients at risk for progressive CMV infection. *Blood* 2001; **98**: 1358-1364
- Cwynarski K, Ainsworth J, Cobbold M, Wagner S, Mahendra P, Apperley J, Goldman J, Craddock C, Moss PA. Direct visualization of cytomegalovirus-specific T-cell reconstitution after allogeneic stem cell transplantation. *Blood* 2001; **97**: 1232-1240
- Xu XN, Screaton GR. MHC/peptide tetramer-based studies of T cell function. *J Immunol Methods* 2002; **268**: 21-28
- Lacey SF, Diamond DJ, Zaia JA. Assessment of cellular immunity to human cytomegalovirus in recipients of allogeneic stem cell transplants. *Biol Blood Marrow Transplant* 2004; **10**: 433-447
- Bouso P. Generation of MHC-peptide tetramers: a new opportunity for dissecting T-cell immune responses. *Microbes Infect* 2000; **2**: 425-429
- Bodinier M, Peyrat MA, Tournay C, Davodeau F, Romagne F, Bonneville M, Lang F. Efficient detection and immunomagnetic sorting of specific T cells using multimers of MHC class I and peptide with reduced CD8 binding. *Nat Med* 2000; **6**: 707-710
- Sato Y, Sahara H, Tsukahara T, Kondo M, Hirohashi Y, Nabeta Y, Kawaguchi S, Ikeda H, Torigoe T, Ichimiya S, Tamura Y, Wada T, Yamashita T, Goto M, Takasu H, Sato N. Improved generation of HLA class I/peptide tetramers. *J Immunol Methods* 2002; **271**: 177-184
- Andersson SG, Kurland CG. Codon preferences in free-living microorganisms. *Microbiol Rev* 1990; **54**: 198-210
- Song ZL, Pan QH, Wang J, Yang Y, Zhu DM, Chen XI, Liu CL, Hong A. Cloning and high expression of hbFGF with a new strategy. *Yichuan Xuebao* 2002; **29**: 84-89
- Brosterhus H, Brings S, Leyendeckers H, Manz RA, Miltenyi S, Radbruch A, Assenmacher M, Schmitz J. Enrichment and detection of live antigen-specific CD4⁺ and CD8⁺ T cells based on cytokine secretion. *Eur J Immunol* 1999; **29**: 4053-4059
- He XH, Xu LH, Liu Y, Zeng YY. Cloning of human β_2 -microglobulin gene and its high expression in *Escherichia coli*. *Shengwu Gongcheng Xuebao* 2004; **20**: 99-103
- Garboczi DN, Hung DT, Wiley DC. HLA-A2-peptide complexes: refolding and crystallization of molecules expressed in *Escherichia coli* and complexed with single antigenic peptides. *Proc Natl Acad Sci USA* 1992; **89**: 3429-3433
- Trudeau JD, Kelly-Smith C, Verchere CB, Elliott JF, Dutz JP, Finegood DT, Santamaria P, Tan R. Prediction of spontaneous autoimmune diabetes in NOD mice by quantification of autoreactive T cells in peripheral blood. *J Clin Invest* 2003; **111**: 217-223
- Skinner PJ, Haase AT. In situ tetramer staining. *J Immunol Methods* 2002; **268**: 29-34
- Ferrari G, Neal W, Ottinger J, Jones AM, Edwards BH, Goepfert P, Betts MR, Koup RA, Buchbinder S, McElrath MJ, Tartaglia J, Weinhold KJ. Absence of immunodominant anti-Gag p17 (SL9) responses among Gag CTL-positive, HIV-uninfected vaccine recipients expressing the HLA-A*0201 allele. *J Immunol* 2004; **173**: 2126-2133
- Gratama JW, Kern F. Flow cytometric enumeration of antigen-specific T lymphocytes. *Cytometry* 2004; **58**: 79-86
- Lahey DL, Voladri RK, Edwards KM, Hager C, Samten B, Wallis RS, Barnes PF, Kernodle DS. Enhanced production of recombinant *Mycobacterium tuberculosis* antigens in *Escherichia coli* by replacement of low-usage codons. *Infect Immun* 2000; **68**: 233-238
- Wills MR, Carmichael AJ, Mynard K, Jin X, Weekes MP,

- Plachter B, Sissons JG. The human cytotoxic T-lymphocyte (CTL) response to cytomegalovirus is dominated by structural protein pp65: frequency, specificity, and T-cell receptor usage of pp65-specific CTL. *J Virol* 1996; **70**: 7569-7579
- 24 **Hassan-Walker AF**, Vargas Cuero AL, Mattes FM, Klenerman P, Lechner F, Burroughs AK, Griffiths PD, Phillips RE, Emery VC. CD8⁺ cytotoxic lymphocyte responses against cytomegalovirus after liver transplantation: correlation with time from transplant to receipt of tacrolimus. *J Infect Dis* 2001; **183**: 835-843
- 25 **Einsele H**, Roosnek E, Rufer N, Sinzger C, Riegler S, Loffler J, Grigoleit U, Moris A, Rammensee HG, Kanz L, Kleihauer A, Frank F, Jahn G, Hebart H. Infusion of cytomegalovirus (CMV)-specific T cells for the treatment of CMV infection not responding to antiviral chemotherapy. *Blood* 2002; **99**: 3916-3922
- 26 **Broers AE**, van Der Holt R, van Esser JW, Gratama JW, Henzen-Logmans S, Kuenen-Boumeester V, Lowenberg B, Cornelissen JJ. Increased transplant-related morbidity and mortality in CMV-seropositive patients despite highly effective prevention of CMV disease after allogeneic T-cell-depleted stem cell transplantation. *Blood* 2000; **95**: 2240-2245
- 27 **Appay V**, Nixon DF, Donahoe SM, Gillespie GM, Dong T, King A, Ogg GS, Spiegel HM, Conlon C, Spina CA, Havlir DV, Richman DD, Waters A, Easterbrook P, McMichael AJ, Rowland-Jones SL. HIV-specific CD8⁺ T cells produce antiviral cytokines but are impaired in cytolytic function. *J Exp Med* 2000; **192**: 63-75
- 28 **Lichterfeld M**, Yu XG, Waring MT, Mui SK, Johnston MN, Cohen D, Addo MM, Zaunders J, Alter G, Pae E, Strick D, Allen TM, Rosenberg ES, Walker BD, Altfeld M. HIV-1-specific cytotoxicity is preferentially mediated by a subset of CD8⁺ T cells producing both interferon-gamma and tumor necrosis factor-alpha. *Blood* 2004; **104**: 487-494
- 29 **Keenan RD**, Ainsworth J, Khan N, Bruton R, Cobbold M, Assenmacher M, Milligan DW, Moss PA. Purification of cytomegalovirus-specific CD8 T cells from peripheral blood using HLA-peptide tetramers. *Br J Haematol* 2001; **115**: 428-434
- 30 **Robert B**, Guillaume P, Luescher I, Romero P, Mach JP. Antibody-conjugated MHC class I tetramers can target tumor cells for specific lysis by T lymphocytes. *Eur J Immunol* 2000; **30**: 3165-3170

Science Editor Wang XL and Guo SY Language Editor Elsevier HK

• CLINICAL RESEARCH •

Association of polymorphic alleles of *CTLA4* with inflammatory bowel disease in the Japanese

Haruhisa Machida, Kazuhiro Tsukamoto, Chun-Yang Wen, Yukiko Narumi, Saburo Shikuwa, Hajime Isomoto, Fuminao Takeshima, Yohei Mizuta, Norio Niikawa, Ikuo Murata, Shigeru Kohno

Haruhisa Machida, Hajime Isomoto, Yohei Mizuta, Fuminao Takeshima, Shigeru Kohno, Second Department of Internal Medicine, Nagasaki University School of Medicine, 1-7-1 Sakamoto, Nagasaki 852-8501, Japan

Kazuhiro Tsukamoto, Yukiko Narumi, Ikuo Murata, Department of Pharmacotherapeutics, Nagasaki University Graduate School of Biomedical Sciences, 1-14 Bunkyo-machi, Nagasaki 852-8521, Japan

Chun-Yang Wen, Department of Molecular Pathology, Atomic Bomb Disease Institute, Nagasaki University Graduate School of Biomedical Sciences, 1-12-4 Sakamoto, Nagasaki 852-8523, Japan

Saburo Shikuwa, Department of Gastroenterology, National Hospital Organization Nagasaki Medical Center, 2-1001-1 Kubara, Omura 856-8562, Japan

Norio Niikawa, Department of Human Genetics, Nagasaki University Graduate School of Biomedical Sciences, 1-12-4 Sakamoto, Nagasaki 852-8523, Japan

Correspondence to: Kazuhiro Tsukamoto, MD, PhD, Department of Pharmacotherapeutics, Nagasaki University Graduate School of Biomedical Sciences, 1-14 Bunkyo-machi, Nagasaki 852-8521, Japan. ktsuka@net.nagasaki-u.ac.jp

Telephone: +81-95-819-2448 Fax: +81-95-819-2895

Received: 2004-11-04 Accepted: 2004-11-23

Abstract

AIM: To examine an association between the cytotoxic T-lymphocyte antigen 4 (*CTLA4*) gene that plays a role in downregulation of T-cell activation and inflammatory bowel disease consisting of ulcerative colitis (UC) and Crohn's disease (CD) in the Japanese.

METHODS: We studied 108 patients with UC, 79 patients with CD, and 200 sex-matched healthy controls, with respect to three single nucleotide polymorphisms (SNPs) in *CTLA4*, such as C-318T in the promoter region, A+49G in exon 1 and G+6230A in the 3' untranslated region (3'-UTR) by a PCR-restriction fragment length polymorphism method, and to an (AT)_n repeat polymorphism in 3'-UTR by fragment analysis with fluorescence-labeling on denaturing sequence gels. Frequency of alleles and genotypes and their distribution were compared statistically between patients and controls and among subgroups of patients, using χ^2 and Fisher exact tests.

RESULTS: The frequency of "A/A" genotype at the G+6230A SNP site was statistically lower in UC patients than in controls (3.7% vs 11.0%, $P = 0.047$, odds ratio (OR) = 0.311). Moreover, the frequency of "G/G" genotype at the A+49G SNP site was significantly higher in CD

patients with fistula (48.6%) than those without it (26.2%) ($P = 0.0388$, OR=2.67).

CONCLUSION: The results suggest that *CTLA4* located at 2q33 is a determinant of UC and responsible for fistula formation in CD in the Japanese.

© 2005 The WJG Press and Elsevier Inc. All rights reserved.

Key words: Ulcerative colitis; *CTLA4* gene; Disease-susceptible gene; Crohn's disease; Fistula formation

Machida H, Tsukamoto K, Wen CY, Narumi Y, Shikuwa S, Isomoto H, Takeshima F, Mizuta Y, Niikawa N, Murata I, Kohno S. Association of polymorphic alleles of *CTLA4* with inflammatory bowel disease in the Japanese. *World J Gastroenterol* 2005; 11(27): 4188-4193

<http://www.wjgnet.com/1007-9327/11/4188.asp>

INTRODUCTION

Chronic inflammatory bowel disease (IBD) is a multifactorial disorder characterized by non-specific inflammation of the gastrointestinal tract, resulting in intestinal malabsorption and immune defense abnormalities, especially an exaggerated T-cell response^[1,2]. Ulcerative colitis (UC) and Crohn's disease (CD) are common major forms of IBD. Although the etiology of IBD remains unknown, both environmental and genetic factors may contribute to the occurrence of this disorder^[3,4]. Genome-wide linkage analyses and candidate gene-based association studies have shown possible IBD-susceptibility loci at 16q12 (IBD1), 12p13 (IBD2), 6p21 (IBD3), 14q11 (IBD4), 5q31-q33 (IBD5), 19p13 (IBD6), 1p36 (IBD7), and 16p (IBD8)^[5-7]. The caspase activating recruitment domain 15/nucleotide oligomerization domain 2 gene (*CARD15/NOD2*) located at 16q12 is one of them, and its mutations were associated with CD in the Caucasians, but not in the Japanese^[8-11]. This may be due to different genetic background between the races.

As a candidate gene susceptible to IBD, we focused on the cytotoxic T-lymphocyte antigen 4 (*CTLA4*) gene located at 2q33, because *CTLA4* is a T-cell receptor that binds to B7-1 (CD80) and B7-2 (CD86) during antigenic stimulation of T cells, and plays a role in downregulation of T-cell activation against another competitive receptor, CD28, which operates on upregulation of T-cell activation^[12-14]. Since *CTLA4*-deficient mice developed a lethal lymphoproliferative

disease characterized by massive T-lymphocytic infiltration in all tissues^[15,16], diminution of downregulation of T-cell activation through CTLA4 may result in an exaggerated T-cell response and subsequent continuous inflammation in the gastrointestinal mucosae, probably leading to the development of IBD. Three single nucleotide polymorphisms (SNPs) in the human *CTLA4*, i.e., a C-318T SNP in the promoter region^[17], an A+49G SNP in exon 1^[12], and a G+6230A SNP in the 3' untranslated region (3'-UTR)^[18], and an (AT)_n repeat polymorphism in 3'-UTR^[19] have been reported. Current studies showed an association of *CTLA4* polymorphic alleles with inhibitory function of CTLA4 at the mRNA and protein levels in peripheral blood mononuclear cells^[20,21], and also with various autoimmune diseases, such as Graves' disease^[18,22], rheumatoid arthritis^[23], multiple sclerosis^[24], type I diabetes mellitus^[18,25], Hashimoto's disease^[18,26], and others^[27-29], of which pathoetiology is probably similar to IBD. However, there was no association of two *CTLA4* SNPs, C-318T and A+49G, with IBD in both the Dutch and Chinese populations^[30].

In this study, we examined on whether three *CTLA4* SNPs, C-318T, A+49G, and G+6230A, and an (AT)_n repeat polymorphism in 3'-UTR are associated with IBD in the Japanese.

MATERIALS AND METHODS

Subjects

The subjects studied comprised 108 patients with UC, 79 patients with CD, and 200 gender-matched unrelated healthy volunteers as controls (Table 1). All participants were Japanese who were randomly recruited from eight general health clinics in the Nagasaki district, Japan. The study protocol was approved by the Committee for the Ethical Issue on Human Genome and Gene Analysis in Nagasaki University, and written informed consent was obtained from each participant. Diagnosis of IBD was made according to endoscopic, radiological, histological, and clinical criteria provided by both the Council for International Organizations of Medical Sciences in WHO and the International Organization for the Study of Inflammatory Bowel Disease^[31-33]. Patients with indeterminate colitis, multiple sclerosis, systemic lupus erythematosus, or other recognized autoimmune diseases were excluded from the subjects studied.

Table 1 Clinical characteristics of study subjects

Characteristics	Patients with		Controls
	UC	CD	
Number of subjects	108	79	200
Age range (yr)	14-83	17-75	20-60
Age (mean±SD)	44.0±16.9 ^b	34.5±12.7	32.5±11.1
Male/female (%)	57 (52.8)/51 (47.2)	47 (59.5)/32 (40.5)	125 (62.5)/75 (37.5)

^bP<0.01 vs controls.

Patients with UC were classified into three subgroups according to age at onset (<40 or ≥40 years), localization and extension of disease (pancolitis, left-sided colitis, or proctitis), and presence or absence of colectomy as an

indicator of severity. Likewise, patients with CD were divided into subgroups according to age at onset (<40 or ≥40 years), localization and extension of lesions (ileum, ileocolon, or colon), presence or absence of fistula, and performance of operation such as partial resection of intestine, and stricture plasty.

Determination of three SNPs and (AT)_n repeat polymorphism

Genomic DNA was extracted from whole blood of each subject using the DNA Extractor WB-rapid Kit (Wako, Osaka, Japan) according to the manufacturer's protocol. Presence or absence of polymorphic alleles at three SNP sites in the human *CTLA4*, a C/T SNP at nt -318 (C-318T) in the promoter region^[17], an A/G SNP at nt +49 in exon 1 (A-49G)^[12], and a G/A SNP at nt +6 230 (G+6230A) in 3'-UTR^[18], were determined with the PCR-restriction fragment length polymorphism methods. Polymorphic region was amplified by PCR with a GeneAmp PCR System 9700 thermal cycler (Applied Biosystems, Foster City, CA, USA) using 150 µg of genomic DNA in a 25-µL reaction solution containing 10 mmol/L Tris-HCl (pH 8.3), 50 mmol/L KCl, 1.5 mmol/L MgCl₂, 0.2 mmol/L each dNTPs, 15 pmol of forward primer: 5'-AATGAATTGGACTGGATGG-3' and reverse primer: 5'-TTACGAGAAAGGAAGCCGTG-3' for C-318T SNP^[17]; forward primer: 5'-CTGAACACCGCTC-CCATAAA-3' and reverse primer: 5'-CCTCCTCCATCTT-CATGCTC-3' for A+49G SNP; or forward primer: 5'-TGATTCATTCAGTATCTGGTGGAG-3' and reverse primer: 5'-AGGGGAGGTGAAGAACCCTGT-3' for G+6230A SNP, and 1 U Taq DNA polymerase. The amplification protocol comprised initial denaturation at 94 °C for 5 min, 35 cycles of denaturation at 94 °C for 30 s, annealing at 60 °C (C-318T), at 65 °C (A+49G), and at 62 °C (G+6230A) for 30 s, and extension at 72 °C for 30 s, and final extension at 72 °C for 5 min. The PCR products were digested with *Mse*I (New England BioLabs Inc., Beverly, MA, USA), *Bbv*I (New England BioLabs Inc.), and *Taq*I (MBI Fermentas Inc., Hanover, MD, USA), to detect C-318T, A+49G, and G+6230A, respectively. All these products were subjected to electrophoresis on a 6% polyacrylamide gels and visualized with UV transilluminator (Alpha Innotech Co., San Leandro, CA, USA).

A (AT)_n repeat polymorphism in 3'-UTR of *CTLA4*^[19] was investigated by fragment analysis with fluorescence-labeling on denaturing sequence gels. Polymorphic region was amplified by PCR using 150 µg of genomic DNA in a 25-µL reaction solution containing 10 mmol/L Tris-HCl (pH 8.3), 50 mmol/L KCl, 1.5 mmol/L MgCl₂, 0.2 mmol/L each dNTPs, 15 pmol of forward primer labeled with 6-carboxyfluorescein dye (Applied Biosystems): 5'-GCCAG-TGATGCTAAAGGTTG-3' and reverse primer: 5'-AACATACGTGGCTCTATGCA-3', and 1 U Taq DNA polymerase. The amplification protocol comprised initial denaturation at 94 °C for 5 min, 35 cycles of denaturation at 94 °C for 30 s, annealing at 64 °C for 30 s, and extension at 72 °C for 30 s, and final extension at 72 °C for 5 min. The PCR products were analyzed on a 6% denaturing sequence gel with an internal size marker, GeneScan 500XL ROX (Applied Biosystems), by ABI Prism 377 genetic analyzer and ABI Prism 3100 genetic analyzer (Applied Biosystems).

Statistical analysis

Gender and age values between UC or CD patients and controls were evaluated by χ^2 -test and unpaired Student's *t*-test, respectively. Allele frequencies were estimated by the gene-counting method, and χ^2 -test was used to identify significant departures from the Hardy–Weinberg equilibrium. SNP and genotype frequencies and their distributions were compared between UC or CD patients and controls, between individuals with and without a genotype, and among subgroups of UC or CD patients, using χ^2 and Fisher exact tests. Odds ratio (OR) with 95% confidence interval was calculated by multiple logistic regression analysis using the JMP program package (version 5, SAS Institute Inc., Cary, NC, USA) and the StatView program package (version 5, SAS Institute Inc.). A *P* value of 0.05 or less was considered statistically significant.

RESULTS

Frequencies and distributions of CTLA4 polymorphic alleles

We identified frequencies and distributions of alleles at the

three SNP sites and seven alleles of the (AT)_{*n*} repeat polymorphism of *CTLA4* among the subjects examined (Table 2). Distributions of *CTLA4* polymorphic alleles in our study population well corresponded to the Hardy–Weinberg equilibrium (Table 2). The results imply that the population we studied has a homogeneous genetic background. The alleles, “C” at nt -384, “A” at nt +49, “G” at nt +6 230, and “(AT)₇” in 3'-UTR, are wild types, while other alleles are variants. Since the frequencies of two alleles, (AT)₂₀ and (AT)₂₂, were very low (<2%), they were not considered for subsequent multiple logistic regression analysis. There were no significant differences in frequency of any alleles between IBD and controls.

Frequencies and distributions of CTLA4 genotypes

Of a total of 108 UC patients, 4 (3.7%) had “A/A” genotype at the G+6230A SNP site, the incidence being significantly lower than that (22/200, 11.0%) in the controls (*P* = 0.047, OR = 0.311) (Tables 3 and 4). There were no significant

Table 2 Distribution of *CTLA4* polymorphic alleles among study subjects

Polymorphic site	Allele	Number (%) of alleles in		Controls
		UC	CD	
nt -318	C	192 (88.9)	140 (88.6)	362 (90.5)
	T	24 (11.1)	18 (11.4)	38 (9.5)
nt +49	A	84 (38.9)	59 (37.3)	159 (39.8)
	G	132 (61.1)	99 (62.7)	241 (60.2)
nt +6 230	G	158 (73.1)	115 (72.8)	278 (69.5)
	A	58 (26.9)	43 (27.2)	122 (30.5)
(AT) _{<i>n</i>} in 3'-UTR	(AT) ₇	107 (49.5)	83 (52.5)	205 (51.3)
	(AT) ₁₅	45 (20.8)	22 (13.9)	82 (20.5)
	(AT) ₁₆	50 (23.1)	35 (22.2)	87 (21.8)
	(AT) ₁₇	3 (1.4)	15 (9.5)	16 (4.0)
	(AT) ₁₈	11 (5.1)	1 (0.6)	8 (2.0)
	(AT) ₂₀	0	2 (1.3)	0
	(AT) ₂₂	0	0	2 (0.5)
Total number of alleles		216	158	400

Table 3 Distribution of *CTLA4* genotypes among study subjects

Polymorphic site	Genotype	Number (%) of subjects with genotype		
		UC (<i>n</i> = 108)	CD (<i>n</i> = 79)	Controls (<i>n</i> = 200)
nt -318	C/C	84 (77.8)	63 (79.8)	163 (81.5)
	C/T	24 (22.2)	14 (17.7)	36 (18.0)
	T/T	0	2 (2.5)	1 (0.5)
nt +49	A/A	14 (13.0)	9 (11.4)	33 (16.5)
	A/G	56 (51.8)	41 (51.9)	93 (46.5)
	G/G	38 (35.2)	29 (36.7)	74 (37.0)
nt +6 230	G/G	54 (50.0)	39 (49.4)	100 (50.0)
	G/A	50 (46.3)	37 (46.8)	78 (39.0)
	A/A	4 (3.7)	3 (3.8)	22 (11.0)
(AT) _{<i>n</i>} in 3'-UTR	(AT) ₇ /(AT) ₇	52 (48.1)	41 (51.9)	101 (50.5)
	(AT) ₇ /(AT) ₁₅	2 (1.9)	1 (1.3)	1 (0.5)
	(AT) ₇ /(AT) ₁₆	1 (0.9)	0	2 (1.0)
	(AT) ₁₅ /(AT) ₁₅	16 (14.8)	5 (6.3)	31 (15.5)
	(AT) ₁₅ /(AT) ₁₆	11 (10.2)	9 (11.4)	18 (9.0)
	(AT) ₁₅ /(AT) ₁₇	0	2 (2.5)	1 (0.5)
	(AT) ₁₆ /(AT) ₁₆	18 (16.7)	13 (16.4)	30 (15.0)
	(AT) ₁₆ /(AT) ₁₇	2 (1.9)	0	6 (3.0)
	(AT) ₁₆ /(AT) ₁₈	0	0	1 (0.5)
	(AT) ₁₇ /(AT) ₁₇	0	6 (7.6)	3 (1.5)
	(AT) ₁₇ /(AT) ₁₈	1 (0.9)	1 (1.3)	3 (1.5)
	(AT) ₁₈ /(AT) ₁₈	5 (4.6)	0	2 (1.0)
	(AT) ₂₀ /(AT) ₂₀	0	1 (1.3)	0
(AT) ₂₂ /(AT) ₂₂	0	0	1 (0.5)	

Table 4 Number of subjects with or without "G" allele at the G+6230A SNP site of *CTLA4*

Genotype	Number (%) of subjects with genotype		
	UC (n = 108)	CD (n = 79)	Control (n = 200)
G/G+G/A	104 (96.3)	76 (96.2)	178 (89.0)
A/A	4 (3.7) ^a	3 (3.8)	22 (11.0)

^aP<0.05 vs controls (P = 0.047, OR = 0.311).

differences in frequency of genotypes at three other polymorphic sites between patients with IBD and the controls.

Frequencies and distributions of genotypes among UC and CD subgroups classified according to clinical features were shown in Tables 5 and 6, respectively. With respect to A+49G SNP, the frequency of "G/G" genotype was significantly higher in CD patients with fistula (48.6%) than

Table 5 Number of UC patients classified by clinical features

Polymorphic site	Genotype	Number of patients (n = 108, %)	Age at onset (yr)	
			<40	≥40
C-318T	C/C	84 (77.8)	55	29
	C/T	24 (22.2)	18	6
	T/T	0	0	0
A+49G	A/A	14 (13.0)	8	6
	A/G	56 (51.8)	40	16
	G/G	38 (35.2)	25	13
G+6230A	G/G	54 (50.0)	39	15
	G/A	50 (46.3)	31	19
	A/A	4 (3.7)	3	1
(AT) _n in 3'-UTR	(AT) ₇ /(AT) ₇	52 (48.1)	33	19
	(AT) ₇ /(AT) _n , or others	56 (51.9)	40	16

(Continued)

Pancolitis	Location		Colectomy	
	Left-sided colitis	Proctitis	Yes	No
42	29	13	7	77
10	13	1	1	23
0	0	0	0	0
9	4	1	0	14
28	20	8	3	53
15	18	5	5	33
20	27	7	6	48
28	15	7	2	48
4	0	0	0	4
31	14	7	1	51
23	26	7	7	49

Table 6 Number of CD patients classified by clinical features

Polymorphic site	Genotype	Number of patients (n = 79, %)	Age at onset (yr)	
			<40	≥40
C-318T	C/C	63 (79.8)	54	9
	C/T	14 (17.7)	12	2
	T/T	2 (2.5)	2	0
A+49G	A/A	9 (11.4)	8	1
	A/G	41 (51.9)	35	6
	G/G	29 (36.7)	25	4
G+6230A	G/G	39 (49.4)	35	4
	G/A	37 (46.8)	30	7
	A/A	3 (3.8)	3	0
(AT) _n in 3'-UTR	(AT) ₇ /(AT) ₇	41 (51.9)	34	7
	(AT) ₇ /(AT) _n , or others	38 (48.1)	34	4

(Continued)

Ileocolon	Location of lesion		Operation		Fistula	
	Ileum	Colon	Yes	No	Presence	Absence
40	14	9	33	30	27	36
11	1	2	9	5	8	6
2	0	0	2	0	2	0
7	2	0	5	4	5	4
25	11	5	20	21	14	27
21	2	6	19	10	18	11
25	5	7	21	18	19	20
25	8	4	22	15	18	19
1	2	0	1	2	0	3
27	10	4	24	17	19	22
26	9	3	20	18	17	21

those without it (26.2%) ($P = 0.0388$, OR = 2.67; Table 7). There were no significant differences in frequency of other genotypes among any other subgroups of IBD patients.

Table 7 Relationship between genotype at the A+49G SNP site and presence/absence of fistula in CD patients

Genotype	No. (%) of patients	
	With fistula (n = 37)	Without fistula (n = 42)
A/A+A/G	19 (51.4)	31 (73.8)
G/G	18 (48.6) ^a	11 (26.2)

^a $P < 0.05$ vs without fistula ($P = 0.0388$, OR = 2.67).

DISCUSSION

We have shown that "A/A" genotype at the G+6230A SNP site of *CTLA4* is associated with insusceptibility to UC. This suggests that individuals with "A/A" genotype at nt +6 230 may have some resistance to UC, or reversely, those with "G/G" or "G/A" genotypes are susceptible to UC. Moreover, "G/G" genotype at the A+49G SNP site was more frequently observed in CD patients with fistula than those without it. These findings suggest that *CTLA4* is one of genetic factors for the predisposition to the onset and/or development of UC and CD. However, since the number of UC patients with "A/A" genotype at the G+6230A SNP site in our study population is small (Table 5), it remains to be confirmed whether the association is reproducible in larger Japanese samples as well as in other populations. Although a previous study in the Dutch and Chinese populations did not find an association between *CTLA4* and IBD, it never dealt with the G+6230A SNP site^[30]. Therefore, the present study is the first report on an association of *CTLA4* polymorphisms with IBD.

CTLA4 consists of four exons that encode leader peptide, ligand-binding domain, transmembrane domain, and cytoplasmic tail, respectively. In humans, there are two isoforms of *CTLA4*, which are a full-length isoform (*f*/*CTLA4* transcript) and a soluble isoform (*s*/*CTLA4* transcript) which lacks exon 3 by alternative splicing. Especially, *s*CTLA4 is secreted and circulating in human sera^[34,35]. It binds CD80/86 molecules and subsequently inhibits T-cell proliferation *in vitro*^[35]. Expression of the human *CTLA4* mRNA isoforms by alternative splicing correlates genotype, G+6230A SNP^[18]. The ratio of *s*CTLA4 to *f*CTLA4 at mRNA level in unstimulated T cells was 50% lower in individuals with "G/G" genotype at nt +6 230 than in those with "A/A" genotype^[18]. Although expression of *CTLA4* isoforms at protein level and activities of T-cell signal pathway were not examined, individuals with "G/G" genotype at nt +6 230 may reduce the production of *s*CTLA4 transcript, and subsequently diminish the inhibition of T-cell activation, probably leading to an increase in T-cell proliferation and chronic inflammation in epithelial cells of the colon. Moreover, the A+6230G SNP was associated with the susceptibility to autoimmune diseases, i.e., Grave's disease, autoimmune hypothyroidism, and type 1 diabetes mellitus^[18]. As well as these autoimmune diseases, autoantibodies against

colonic epithelial cells, such as anticolon antibodies, antitropomyosin antibodies, and antineutrophil cytoplasmic antibodies, are frequently found in sera of patients with UC^[36-38]. Thus, it is plausible that UC is also an autoimmune disease and some genetic factors are common between UC and autoimmune diseases.

Fistula formation in CD patients is one of the indicators of severity. Our results indicated that CD patients with "G/G" genotype at nt +49 more frequently had fistula. Since intracellular distribution of CTLA4 in individuals with "G/G" genotype at nt +49 was qualitatively different from that with "A/A", and downregulation of T-cell activation in individuals with "G/G" genotype was reduced^[39], CD patients with "G/G" genotype may show progressive and severe clinical course. It remains to be investigated why the A+49G SNP is associated with fistula formation in Japanese CD patients.

In conclusion, our study showed that *CTLA4* is one of the determinants of UC and responsible for fistula formation in CD in the Japanese.

ACKNOWLEDGMENTS

We are grateful to physicians, patients, and volunteers for participating in this study. We thank Miss Naoko Sakemi and Dr. Hiroshi Soda for their support.

REFERENCES

- 1 **Fiocchi C**. Inflammatory bowel disease: etiology and pathogenesis. *Gastroenterology* 1998; **115**: 182-205
- 2 **Farrell RJ**, Peppercorn MA. Ulcerative colitis. *Lancet* 2002; **359**: 331-340
- 3 **Yang H**, Taylor KD, Rotter JI. Inflammatory bowel disease. I. Genetic epidemiology. *Mol Genet Metab* 2001; **74**: 1-21
- 4 **Watts DA**, Satsangi J. The genetic jigsaw of inflammatory bowel disease. *Gut* 2002; **50** (Suppl 3): 31-36
- 5 **Taylor KD**, Yang H, Rotter JI. Inflammatory bowel disease. II. Gene mapping. *Mol Genet Metab* 2001; **74**: 22-44
- 6 **Cho JH**, Nicolae DL, Ramos R, Fields CT, Rabenau K, Corradino S, Brant SR, Espinosa R, LeBeau M, Hanauer SB, Bodzin J, Bonen DK. Linkage and linkage disequilibrium in chromosome band 1p36 in American Chaldeans with inflammatory bowel disease. *Hum Mol Genet* 2000; **9**: 1425-1432
- 7 **Hampe J**, Frenzel H, Mirza MM, Croucher PJ, Cuthbert A, Mascheretti S, Huse K, Platzer M, Bridger S, Meyer B, Nurnberg P, Stokkers P, Krawczak M, Mathew CG, Curran M, Schreiber S. Evidence for a NOD2-independent susceptibility locus for inflammatory bowel disease on chromosome 16p. *Proc Natl Acad Sci USA* 2002; **99**: 321-326
- 8 **Hugot JP**, Chamaillard M, Zouali H, Lesage S, Cezard JP, Belaiche J, Almer S, Tysk C, O'Morain CA, Gassull M, Binder V, Finkel Y, Cortot A, Modigliani R, Laurent-Puig P, Gower-Rousseau C, Macry J, Colombel JF, Sahbatou M, Thomas G. Association of NOD2 leucine-rich repeat variants with susceptibility to Crohn's disease. *Nature* 2001; **411**: 599-603
- 9 **Ogura Y**, Bonen DK, Inohara M, Nicolae DL, Chen FF, Ramos R, Britton H, Moran T, Karaliuskas R, Duerr RH, Achkar JP, Brant SR, Bayless TM, Kirschner BS, Hanauer SB, Nunez G, Cho JH. A frameshift mutation in NOD2 associated with susceptibility to Crohn's disease. *Nature* 2001; **411**: 603-606
- 10 **Inoue N**, Tamura K, Kinouchi Y, Fukuda Y, Takahashi S, Ogura Y, Inohara N, Nunez G, Kishi Y, Koike Y, Shimosegawa T, Shimoyama T, Hibi T. Lack of common NOD2 variants in Japanese patients with Crohn's disease. *Gastroenterology* 2002; **123**: 86-91
- 11 **Yamazaki K**, Takazoe M, Tanaka T, Kazumori T, Nakamura

- U. Absence of mutation in the NOD2/CARD15 gene among 483 Japanese patients with Crohn's disease. *J Hum Genet* 2002; **47**: 469-472
- 12 **Harper K**, Balzano C, Rouvier E, Mattei MG, Luciani MF, Golstein P. CTLA-4 and CD28 activated lymphocyte molecules are closely related in both mouse and human as to sequence, message expression, gene structure, and chromosomal location. *J Immunol* 1991; **147**: 1037-1044
- 13 **Karandikar NJ**, Vanderlugt CL, Walunas TL, Miller SD, Bluestone JA. CTLA-4: a negative regulator of autoimmune disease. *J Exp Med* 1996; **184**: 783-788
- 14 **Salomon B**, Bluestone JA. Complexities of CD28/B7: CTLA-4 costimulatory pathways in autoimmunity and transplantation. *Annu Rev Immunol* 2001; **19**: 225-252
- 15 **Waterhouse P**, Penninger JM, Timms E, Wakeham A, Shahinian A, Lee KP, Thompson CB, Griesser H, Mak TW. Lymphoproliferative disorders with early lethality in mice deficient in CTLA-4. *Science* 1995; **270**: 985-988
- 16 **Liu Z**, Geboes K, Hellings P, Maerten P, Heremans H, Vandenberghe P, Boon L, van Kooten P, Rutgeerts P, Ceuppens JL. B7 interactions with CD28 and in chronic experimental colitis. *J Immunol* 2001; **167**: 1830-1838
- 17 **Deichmann K**, Heinzmann A, Brüggelnohe E, Forster J, Kuehr J. An Mse I RFLP in the human CTLA4 promoter. *Biochem Biophys Res Commun* 1996; **225**: 817-818
- 18 **Ueda H**, Howson JM, Esposito L, Heward J, Snook H, Chamberlain G, Rainbow DB, Hunter KM, Smith AN, Di Genova G, Herr MH, Dahlman I, Payne F, Smyth D, Lowe C, Twells RC, Howlett S, Healy B, Nutland S, Rance HE, Everett V, Smink LJ, Lam AC, Cordell HJ, Walker NM, Bordin C, Hulme J, Motzo C, Cucca F, Hess JF, Metzker ML, Rogers J, Gregory S, Allahabadia A, Nithiyananthan R, Tuomilehto-Wolf E, Tuomilehto J, Bingley P, Gillespie KM, Undlien DE, Ronningen KS, Guja C, Ionescu-Tirgoviste C, Savage DA, Maxwell AP, Carson DJ, Patterson CC, Franklyn JA, Clayton DG, Peterson LB, Wicker LS, Todd JA, Gough SC. Association of the T-cell regulatory gene CTLA4 with susceptibility to autoimmune disease. *Nature* 2003; **423**: 506-511
- 19 **Polymeropoulos MH**, Rath DS, Xiao H, Merrill CR. Dinucleotide repeat polymorphisms at the human CTLA4 gene. *Nucleic Acids Res* 1991; **19**: 4018
- 20 **Kouki T**, Sawai Y, Gardine CA, Fisfalen ME, Alegre ML, DeGroot LJ. CTLA-4 gene polymorphism at position 49 in exon 1 reduces the inhibitory function of CTLA-4 and contributes to the pathogenesis of Grave's disease. *J Immunol* 2000; **165**: 6606-6611
- 21 **Ligers A**, Teleshova N, Masterman T, Huang WX, Hillert J. CTLA-4 gene expression is influenced by promoter and exon 1 polymorphisms. *Genes Immunol* 2001; **2**: 145-152
- 22 **Kosta K**, Watson PF, Weetman AP. A CTLA-4 gene polymorphism is associated with both Grave's disease and autoimmune hypothyroidism. *Clin Endocrinol* 1997; **46**: 551-554
- 23 **Rodríguez MR**, Núñez-Roldán A, Aguilar F, Valenzuela A, García A, Gonzalez-Escribano MF. Association of the CTLA4 3' untranslated region polymorphism with the susceptibility to rheumatoid arthritis. *Hum Immunol* 2002; **63**: 76-81
- 24 **Harbo HF**, Celius EG, Vardal F, Spurkland A. CTLA4 promoter and exon 1 dimorphisms in multiple sclerosis. *Tissue Antigens* 1999; **53**: 106-110
- 25 **Marrohn MP**, Raffel LJ, Garchon HJ, Jacob CO, Serrano-Rios M, Martinez Larrad MT, Teng WP, Park Y, Zhang ZX, Goldstein DR, Tao YW, Beaurain G, Bach JF, Huang HS, Luo DF, Zeidler A, Rotter JI, Yang MC, Modilevsky T, Maclaren NK, She JX. Insulin-dependent diabetes mellitus (IDDM) is associated with CTLA4 polymorphisms in multiple ethnic groups. *Hum Mol Genet* 1997; **6**: 1275-1282
- 26 **Donner H**, Braun J, Seidl C, Rau H, Finke R, Ventz M, Walfish PG, Usadel KH, Badenhop K. Codon 17 polymorphism of the cytotoxic T lymphocyte antigen 4 gene in Hashimoto's thyroiditis and Addison's disease. *J Clin Endocrinol Metab* 1997; **82**: 4130-4132
- 27 **Ahmed S**, Ihara K, Kanemitsu S, Nakashima H, Otsuka T, Tsuzaka K, Takeuchi T, Hara T. Association of CTLA-4 but not CD28 gene polymorphisms with systemic lupus erythematosus in the Japanese population. *Rheumatology* 2001; **40**: 662-667
- 28 **Ligers A**, Xu C, Saarinen S, Hillert J, Olerup O. The CTLA-4 gene is associated with multiple sclerosis. *J Neuroimmunol* 1999; **97**: 182-190
- 29 **Agarwal K**, Jones DEJ, Daly AK, James OFW, Vaidya B, Pearce S, Bassemidine MF. CTLA-4 gene polymorphism confers susceptibility to primary biliary cirrhosis. *J Hepatol* 2000; **32**: 538-541
- 30 **Xia B**, Crusius JBA, Wu J, Zwiers A, Zwiers A, van Bodegraven AA, Peña AS. CTLA4 gene polymorphisms in Dutch and Chinese patients with inflammatory bowel disease. *Scand J Gastroenterol* 2002; **37**: 1296-1300
- 31 **Podolsky DK**. Inflammatory bowel disease (1). *N Eng J Med* 1991; **325**: 928-937
- 32 **Podolsky DK**. Inflammatory bowel disease (2). *N Eng J Med* 1991; **325**: 1008-1016
- 33 **Lennard-Jones JE**. Classification of inflammatory bowel disease. *Scand J Gastroenterol Suppl* 1989; **170**: 2-6
- 34 **Magistrelli G**, Jeannin P, Herbault N, Benoit De Coignac A, Gauchat JF, Bonnefoy JY, Delneste Y. A soluble form of CTLA-4 generated by alternative splicing is expressed by nonstimulated human T cells. *Eur J Immunol* 1999; **29**: 3596-3602
- 35 **Oaks MK**, Hallett KM, Penwell RT, Stauber EC, Warren SJ, Tector AJ. A native soluble form of CTLA-4. *Cell Immunol* 2000; **201**: 144-153
- 36 **Fiocchi C**, Roche JK, Michener WM. High prevalence of antibodies to intestinal epithelial antigens in patients with inflammatory bowel disease and their relatives. *Ann Intern Med* 1989; **110**: 786-794
- 37 **Geng X**, Biancone L, Dai HH, Lin JJ, Yoshizaki N, Dasgupta A, Pallone F, Das KM. Tropomyosin isoforms in intestinal mucosa: production of autoantibodies to tropomyosin isoforms in ulcerative colitis. *Gastroenterology* 1998; **114**: 912-922
- 38 **Duerr RH**, Targan SR, Landers CJ, Sutherland LR, Shanahan F. Antineutrophil cytoplasmic antibodies in ulcerative colitis: comparison with other colitis/diarrheal illness. *Gastroenterology* 1991; **100**: 1590-1596
- 39 **Maurer M**, Loserth S, Kolb-Maurer A, Ponath A, Wiese S, Kruse N, Rieckmann P. A polymorphism in the human cytotoxic T-lymphocyte antigen 4 (*CTLA4*) gene (exon 1 +49) alters T-cell activation. *Immunogenetics* 2002; **54**: 1-8

• CLINICAL RESEARCH •

Patients with primary biliary cirrhosis have increased serum total antioxidant capacity measured with the crocin bleaching assay

George Notas, Niki Miliaraki, Marilena Kampa, Fillipos Dimoulios, Erminia Matrella, Adam Hatzidakis, Elias Castanas, Elias Kouroumalis

George Notas, Fillipos Dimoulios, Erminia Matrella, Elias Kouroumalis, Laboratory of Gastroenterology and Hepatology, University of Crete, Faculty of Medicine, Heraklion 71003, Greece

Niki Miliaraki, Laboratory of Clinical Chemistry, University of Crete, Faculty of Medicine, Heraklion 71003, Greece

Marilena Kampa, Elias Castanas, Laboratory of Experimental Endocrinology, University of Crete, Faculty of Medicine, Heraklion 71003, Greece

Adam Hatzidakis, Department of Radiology, University of Crete, Faculty of Medicine, Heraklion 71003, Greece

Co-first-author: Niki Miliaraki
Correspondence to: Dr. George Notas, Laboratory of Gastroenterology and Hepatology, University of Crete, School of Medicine, PO Box 2208, Heraklion 71003, Greece. gnotas@med.uoc.gr

Telephone: +30-810-394634 Fax: +30-810-394634
Received: 2004-09-11 Accepted: 2004-10-18

and this maybe related to the pathophysiology of the disease. UDCA treatment restores the levels of CTAC to control levels.

© 2005 The WJG Press and Elsevier Inc. All rights reserved.

Key words: Antioxidants; Serum total antioxidant capacity; Primary biliary cirrhosis; Chronic hepatitis C; Viral HCV cirrhosis; Ursodeoxycholic acid

Notas G, Miliaraki N, Kampa M, Dimoulios F, Matrella E, Hatzidakis A, Castanas E, Kouroumalis E. Patients with primary biliary cirrhosis have increased serum total antioxidant capacity measured with the crocin bleaching assay. *World J Gastroenterol* 2005; 11(27): 4194-4198
<http://www.wjgnet.com/1007-9327/11/4194.asp>

Abstract

AIM: The balance between oxidants and antioxidants can play an important role in the initiation and development of liver diseases. Recently, we have described a new automated method for the determination of total antioxidant capacity (TAC) in human serum and plasma.

METHODS: We measured TAC and corrected TAC (CTAC -abstraction of interactions due to endogenous uric acid, bilirubin and albumin) in 52 patients with chronic liver diseases (41 patients with primary biliary cirrhosis (PBC), 10 patients with chronic hepatitis C and 13 patients with viral HCV cirrhosis) as well as in 10 healthy controls. In 23 PBC patients measurement were also done 6 mo after treatment with ursodeoxycholic acid (UDCA). The TAC assay was based on a modification of the crocin bleaching assay. The results were correlated with routine laboratory measurements and the histological stage of PBC.

RESULTS: There were no significant differences in TAC between the various groups. However, CTAC was considerably increased in the PBC group compared to controls and cirrhotics. Analysis of these patients according to disease stages showed that this increase was an early phenomenon observed only in stages I and II compared to controls, cirrhotics and patients with chronic hepatitis C). After 6 mo of treatment with UDCA, levels of CTAC decreased to those similar to that of controls.

CONCLUSION: Patients in the early stages of PBC present with high levels of corrected total antioxidant capacity

INTRODUCTION

Evidence of enhanced production of free radicals or significant decrease of antioxidant defense have been reported in all types of liver damage. A large number of studies have focused on the pathogenetic significance of oxidative stress in liver injury as well as on therapeutic interventions with antioxidant and metabolic scavengers^[1-4]. Primary biliary cirrhosis (PBC) is a chronic granulomatous cholestatic disorder characterized by a possible immunological attack on bile ducts leading to fibrosis, cirrhosis, liver failure, and death. Several studies suggest that oxidant stress plays a key role in the progression of this disease^[5-7].

Circulation of oxidative molecules has been incriminated in lipoprotein oxidation and the generation of increased arterial deposits, ultimately leading to atherosclerosis^[8-11]. However marked hypercholesterolemia, typical of severe longstanding cholestasis in PBC patients, is not associated with an excess risk of cardiovascular disease^[12]. Since the antioxidant status in PBC has been reported to be compromised, with several important components of the antioxidant defense mechanism being significantly decreased^[5] there is a disagreement between these data.

Recently, we have introduced a new automated method for the estimation of the plasma total antioxidant capacity^[13]. In the present study we assayed and evaluated the levels of antioxidant capacity in patients with chronic liver diseases, by this method. In addition, we have also corrected these results per a number of analytes, directly affecting redox potential, thus introducing the concept of "corrected antioxidant capacity". Our results indicate that, although the total

antioxidant capacity of patients with chronic liver diseases do not differ significantly from normal subjects, the corrected antioxidant capacity is increased in PBC patients, indicating that a counterbalancing mechanism might be present.

MATERIALS AND METHODS

Patient population

The study included 41 Greek patients with PBC (35 women and 6 men, median age 62 years, range 31-85 years) followed up at the Department of Gastroenterology of the University Hospital of Heraklion, Crete. Thirty-seven of them were positive for antimitochondrial antibody (AMA)-M2 testing by immunofluorescence and by ELISA. All patients had typical biochemical pattern. Liver histology consistent with PBC was available in 38 patients. Three patients with clinical evidence of portal hypertension (esophageal varices) and positive AMA-M2 were not submitted to liver biopsy. At the time of diagnosis 25 patients (median age 58 years, range 31-71) were in histological stage I or II and 16 patients (median age 67 years, range 54-85) were in histological stage III or IV, according to Ludwig *et al.*, criteria^[14]. Laboratory data and clinical details at the time of diagnosis and prior to initiation of UDCA therapy are shown in Table 1. All patients were negative for markers of hepatitis B and C.

UDCA at a dose of 15 mg/(kg • d) was administered to all patients. Serum levels of TAC were measured in all patients prior to initiation of UDCA therapy. In 23 patients (14 in stages I-II and 9 in stages III-IV) TAC was also measured after 6 mo of UDCA therapy. No patients were withdrawn from treatment during this 6-mo period.

A group of 13 patients (8 men and 5 women, median age 53 years, range 41-64 years) with biopsy-proven postviral HCV liver cirrhosis was also enrolled. Another group of 10 patients (5 men and 5 women, median age 36 years, range 22-49 years), with biopsy-proven chronic hepatitis C was also included in the study as disease controls. No patient used alcohol. Finally, 10 healthy volunteers, matched to the PBC population for age and sex, served as a reference group.

In another group of 10 cirrhotic PBC patients and in all 13 control cirrhotics TAC levels estimations were also made in blood taken from the hepatic vein during catheterization for the measurement of wedged hepatic pressure done for assessment of portal hypertension. The group of PBC patients catheterized had been receiving UDCA treatment for at least 1 year.

Blood was collected from all patients and controls and was immediately centrifuged at 4 °C. All serum samples were stored at -70 °C until assayed. The study was approved by the local hospital Ethics committee, and written informed consent was obtained from all patients.

Determination of TAC

Plasma total antioxidant capacity (TAC) was measured on an Olympus AU-600 analyzer using the TAC kit (Medikon SA, Gerakas, Greece) as described previously^[13]. Briefly, antioxidants in the sample inhibit the bleaching of crocin from ABAP [2,2-azobis-(2-amidinopropane) dihydrochloride] to a degree that is proportional to their concentration. The assay was performed at 37 °C in the following steps: 2 µL

of sample, calibrator or control were mixed with 250 µL of crocin reagent (R1) and incubated for 160 s. Subsequently, 250 µL of ABAP (R2) were added and the decrease in absorbance at 450 nm was measured 26 s later. Values of TAC were expressed as mmol/L.

Routine clinical chemistry

Plasma uric acid, albumin, total bilirubin, alkaline phosphatase, aminotransferases, and γ-glutamyl transpeptidase were determined on an Olympus AU-600 analyzer using Olympus reagents provided by Medicon Hellas (Gerakas, Greece).

Statistical analysis

Statistical analysis of data was performed by the use of the SyStat v 10.0 program (SPSS Inc, Chicago, IL, USA), and the Origin v 5.0 program (MicroCal, Northampton, MA, USA). Paired and unpaired *t*-test were used where applicable. A *P* value less than 0.05 was considered statistically significant.

RESULTS

Total and corrected plasma antioxidant capacity in chronic liver diseases (Table 1)

Figure 1 presents levels of TAC in the several groups tested. It appears that TAC values are slightly elevated in PBC patients, but this was not of statistical significance. No statistically significant differences between any of the groups could be identified. Since all patients did not have decompensated disease, our results show that the total antioxidant capacity is unaltered in non-hospitalized patients.

Table 1 TAC and CTAC in patients and controls

Group	TAC (mmol/L)	CTAC (mmol/L)
Control	1.493±0.059	0.797±0.057
Cirrhotics	1.532±0.095	0.723±0.069
PBC	1.664±0.062	1.012±0.068
PBC I-II	1.691±0.080	1.096±0.077
PBC III-IV	1.593±0.086	0.789±0.117
CAH	1.477±0.080	0.875±0.072

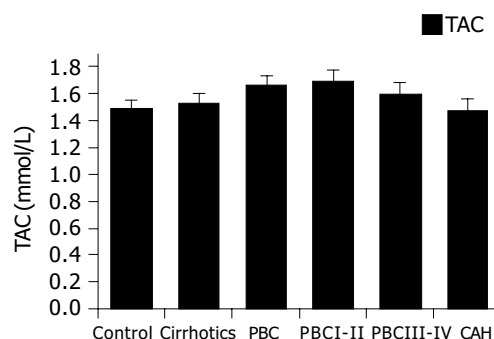


Figure 1 Total plasma antioxidant capacity in chronic liver diseases. Slightly elevated TAC levels were found in PBC patients.

As TAC is a complex measurement, that is affected by a number of serum constituents, including bilirubin, we also calculated the corrected TAC. Corrected TAC (CTAC) is depicted in Figure 2. As stated in our previous work^[13], this

calculated parameter represents the fraction of circulating antioxidants, after elimination of interference by endogenous metabolites. Our previous work has shown that uric acid and bilirubin, and in a lesser degree albumin, are the major endogenous substances linearly interfering with coefficients of 0.11, 0.11, and 0.01 mmol/L of TAC per mg/dL respectively. We have therefore assayed these analytes and subtracted their interferences from the obtained values of TAC to estimate possible modifications of the antioxidant activity, without those interferences. Increased levels of CTAC in patients with PBC compared to controls ($P<0.05$) and cirrhotics ($P<0.01$) were found (Figure 2). Further analysis shows that this increase is mainly attributed to early PBC patients (stages I and II $P<0.01$, compared to controls, cirrhotics and patients with chronic hepatitis C), while late PBC patients (stages III and IV) had CTAC levels similar to controls.

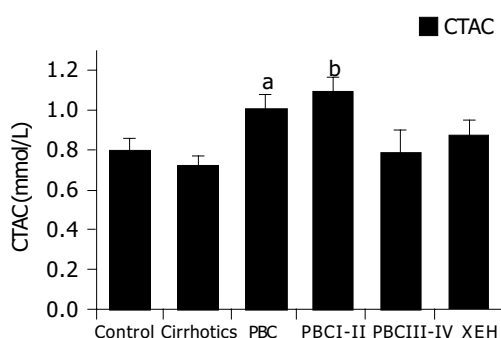


Figure 2 Corrected plasma antioxidant capacity in chronic liver diseases. Increased levels of CTAC were found in PBC patients. Only early PBC patients (stages I and II) had high CTAC levels. ^a $P<0.05$, ^b $P<0.01$ vs controls.

UDCA treatment reduces TAC and CTAC values to control levels (Table 2)

In 23 patients that received 6 mo of UDCA therapy a reduction of both TAC and CTAC was noticed as shown in Figure 3. Reduction was significant in the early stages of PBC. In late stages, a reduction of CTAC was also noted but this was at the limit of statistical significance.

Table 2 TAC and CTAC in PBC patients before and after UDCA treatment

Group		Before UDCA	After UDCA	Significance
PBC Total	TAC	1.697±0.077	1.289±0.093	<0.001
	CTAC	1.068±0.071	0.601±0.093	<0.001
PBC I-II	TAC	1.762±0.082	1.243±0.124	<0.001
	CTAC	1.169±0.076	0.660±0.115	<0.001
PBC III-IV	TAC	1.527±0.184	1.410±0.049	NS
	CTAC	0.789±0.153	0.448±0.091	NS

CTAC values are higher in peripheral blood samples compared to hepatic vein samples (Table 3)

Hepatic vein samples, taken during catheterization for estimation of portal hypertension had lower values of both TAC and CTAC as shown in Figure 4 compared to peripheral

vein samples. This was significant only for the cirrhotic patients. In the treated PBC patients a similar trend was observed but it did not reach statistical significance.

Table 3 TAC and CTAC in serum samples collected from hepatic and peripheral vein in cirrhotic and PBC patients

Group		Hepatic	Peripheral	Significance
Cirrhotics	TAC	1.357±0.052	1.532±0.095	<0.05
	CTAC	0.563±0.031	0.757±0.073	<0.05
PBC	TAC	1.494±0.074	1.587±0.071	NS
	CTAC	0.821±0.032	0.913±0.042	NS

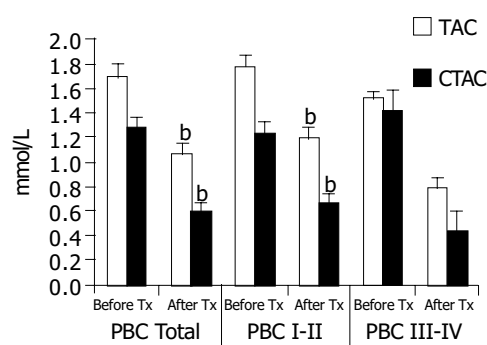


Figure 3 UDCA treatment reduces TAC and CTAC values. A significant reduction of CTAC was observed in the early stages of PBC. In late stages, a reduction of CTAC was also noted but this was at the limit of statistical significance. ^b $P<0.001$ vs TAC.

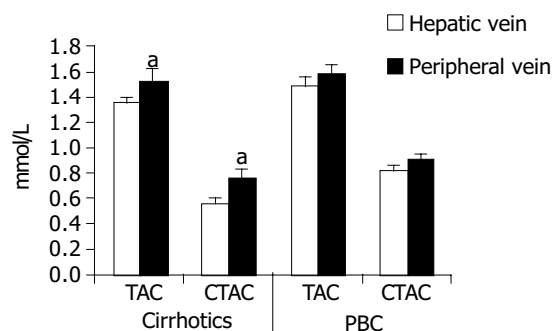


Figure 4 CTAC values are higher in peripheral blood samples compared to hepatic vein samples. Hepatic vein samples had lower values of both TAC and CTAC compared to peripheral vein samples. This was significant only for the cirrhotic patients. In the treated PBC patients a similar trend was observed but it did not reach statistical significance. ^a $P<0.05$ vs others.

DISCUSSION

Production of reactive species, including free radicals, is an integral part of human metabolism. Because of the high potential to damage vital biological systems, reactive species have now been incriminated in aging and in more than 100 disease states^[15,16]. A complex system of neutralizing antioxidants exists in plasma and intra- and extracellular fluids, but an imbalance (oxidant stress) between free radical production and use can cause damage to DNA, lipids, proteins, and other biomolecules^[5]. Nevertheless, most markers of oxidative

damage have not been fully validated^[17]. Endogenous antioxidant defenses (superoxide dismutases, H₂O₂-removing enzymes, metal binding proteins) are inadequate to prevent damage completely, so diet-derived antioxidants are important in maintaining health^[16,18,19]. The sum of endogenous plus food-derived antioxidants represents the total antioxidant capacity of extracellular fluid. The overall antioxidant capacity may give more relevant biological information compared to that obtained by the measurement of individual parameters, as it considers the cumulative effect of all antioxidants present in plasma and body fluids^[20].

A great variety of methods have been proposed for the assay of total antioxidant activity or capacity of serum or plasma^[20,21]. Many researchers have stressed the distinction between antioxidant *activity* and antioxidant *capacity*: *Antioxidant activity* corresponds to the rate constant of a single antioxidant against a given free radical; *antioxidant capacity*, on the other hand, is the number of moles of a given free radical scavenged by a test solution, independently of the capacity of any one antioxidant present in the mixture. In the case of plasma being a heterogeneous solution of diverse antioxidants the antioxidant status is better reflected by antioxidant capacity rather than activity. This capacity is a combination of all redox chain antioxidants, including several analytes such as thiol bearing proteins, and uric acid. An increase of antioxidant capacity of plasma indicates absorption of antioxidants and improved *in vivo* antioxidant status^[22], or the result of the activation of an adaptation mechanism to oxidative stress. It should be noted that, due to the participation of diverse metabolites to the antioxidant capacity of human plasma, its increase may not be necessarily a desirable condition. Indeed, in some cases, such as renal failure (uric acid), icteric status (bilirubin), hepatic damage (hypoalbuminemia) the variation of several metabolites modify plasma antioxidant capacity in a deleterious direction, a situation returning to normal values after correction of the underlying disease^[23]. Recently, we have introduced a new automated method for the assay of the plasma antioxidant activity, based on crocin bleaching. This method (the TAC assay) gives an estimation of the integrated plasma antioxidant capacity. Furthermore, we also determine the interference of a number of endogenous analytes, such as uric acid, and bilirubin, which have been found to produce a major interference of TAC, while albumin results in a smaller interference^[13].

In the present work, we have simultaneously assayed TAC and the concentrations of these analytes in patients with chronic liver diseases. As reported in the results no differences between TAC levels of the study groups were noted but patients in early stages of PBC had higher levels of CTAC. Other researchers have reported low total antioxidant capacity in PBC patients. Aboutwerat *et al.*, reported that oxidant stress, as reflected in a spectrum of lipid peroxidation and antioxidant markers, is a significant feature of early-stage PBC. They also reported that the total antioxidant capacity in whole serum (measured with an enhanced chemiluminescent technique) was significantly reduced in PBC patients but was normal in protein-free serum, suggesting that protein-bound components make an important contribution^[5]. Floreani *et al.*, measured a number

of antioxidant substances in both primary biliary cirrhosis and primary sclerosing cholangitis patients and reported significantly lower levels of retinol, alpha-tocopherol, total carotenoids, lutein, zeaxanthin, lycopene, alpha- and beta-carotene in these patients compared to healthy controls^[24]. Discrepancies among these studies and our results could be attributed to different factors:

1. The different methods of assay of TAC, measuring a number of discrete molecules. The TAC assay, used in the present study is an integrator of the totality of antioxidants circulating at a given time point in the blood.

2. The distinction of activity and capacity discussed previously. Indeed, through chain oxidative-reduction reactions, a number of antioxidants measured at a given time point may not act as antioxidants *per se*^[25].

Calculation of the corrected TAC (in which the interference of a number of endogenous metabolites has been subtracted) appears to provide a better estimate of the real antioxidant activity of the organism. However, the interpretation of the changes in plasma or serum antioxidant capacity depends upon not only the method used in detecting these changes, but also the conditions under which the plasma or serum antioxidant capacity is determined, because the determined antioxidant capacity reflects changes in a dynamic system. Furthermore an increased antioxidant capacity in plasma or serum is not necessarily a desirable condition if it is due to an adaptive response to increased oxidative stress at an early stage^[21]. Our finding of increased CTAC in the early stages of PBC may reflect such an early response.

Ursodeoxycholic acid has been reported of having a marginal therapeutic effect for primary biliary cirrhosis^[26]. Ursodeoxycholic acid treatment reduces intracellular hydrophobic bile acid levels and thereby may have a cytoprotective effect on cell membranes^[27]. It has also been reported that UDCA reduced the deoxycholic acid-associated loss of the mitochondrial membrane potential and decreased the production of reactive oxygen species^[28-30]. Our finding of TAC and CTAC reduction after UDCA treatment especially in the early stages of PBC maybe an indication that UDCA contributes to the normalization of the oxidative status in PBC patients.

Finally this is the first report that presents evidence of increased total antioxidant capacity originating from the periphery compared to the hepatic veins in patients with viral cirrhosis. Although the group of PBC patients used in this study had received UDCA treatment a similar trend can be noticed. Whether this is a feature of cirrhosis or a universal phenomenon cannot be concluded from our data. Although similar measurements cannot be performed in normal subjects, it would be interesting to further validate this result with studies on a bigger PBC population.

In conclusion, CTAC is considerably increased in the serum of PBC patients of stages I and II, but not in patients with viral cirrhosis or chronic hepatitis C. This increased antioxidant capacity in serum maybe due to an adaptive response to increased oxidative stress. Treatment with UDCA decreased the levels of CTAC to values similar to those of controls indicating a possible normalizing effect of UDCA on the oxidative status in PBC patients. Further study is needed for the finding of higher levels of CTAC in blood

samples drawn from peripheral veins compared to samples from hepatic veins in cirrhotic patients.

ACKNOWLEDGMENTS

G. Notas is a recipient of the Manasaki scholarship (University of Crete).

REFERENCES

- 1 **Jones BE**, Czaja MJ. III. Intracellular signaling in response to toxic liver injury. *Am J Physiol* 1998; **275**(5 Pt 1): G874-G878
- 2 **Kaplowitz N**. Mechanisms of liver cell injury. *J Hepatol* 2000; **32**: 39-47
- 3 **Loguercio C**, Federico A. Oxidative stress in viral and alcoholic hepatitis. *Free Radic Biol Med* 2003; **34**: 1-10
- 4 **Mori N**, Hirayama K. Long-term consumption of a methionine-supplemented diet increases iron and lipid peroxide levels in rat liver. *J Nutr* 2000; **130**: 2349-2355
- 5 **Aboutwerat A**, Pemberton PW, Smith A, Burrows PC, McMahon RF, Jain SK, Warnes TW. Oxidant stress is a significant feature of primary biliary cirrhosis. *Biochim Biophys Acta* 2003; **1637**: 142-150
- 6 **Paradis V**, Kollinger M, Fabre M, Holstege A, Poynard T, Bedossa P. *In situ* detection of lipid peroxidation by-products in chronic liver diseases. *Hepatology* 1997; **26**: 135-142
- 7 **Ono M**, Sekiya C, Ohhira M, Ohhira M, Namiki M, Endo Y, Suzuki K, Matsuda Y, Taniguchi N. Elevated level of serum Mn-superoxide dismutase in patients with primary biliary cirrhosis: possible involvement of free radicals in the pathogenesis in primary biliary cirrhosis. *J Lab Clin Med* 1991; **118**: 476-483
- 8 **Sigal E**, Laughton CW, Mulkins MA. Oxidation, lipoxygenase, and atherogenesis. *Ann NY Acad Sci* 1994; **714**: 211-224
- 9 **Stam H**, Hulsmann WC, Jongkind JF, van der Kraaij AM, Koster JF. Endothelial lesions, dietary composition and lipid peroxidation. *Eicosanoids* 1989; **2**: 1-14
- 10 **Lyons TJ**. Glycation and oxidation: a role in the pathogenesis of atherosclerosis. *Am J Cardiol* 1993; **71**: 26B-31B
- 11 **Offermann MK**, Medford RM. Antioxidants and atherosclerosis: a molecular perspective. *Heart Dis Stroke* 1994; **3**: 52-57
- 12 **Longo M**, Crosignani A, Battezzati PM, Squarcia GC, Invernizzi P, Zuin M, Podda M. Hyperlipidaemic state and cardiovascular risk in primary biliary cirrhosis. *Gut* 2002; **51**: 265-269
- 13 **Kampa M**, Nistikaki A, Tsaousis V, Maliaraki N, Notas G, Castanas E. A new automated method for the determination of the Total Antioxidant Capacity (TAC) of human plasma, based on the crocin bleaching assay. *BMC Clin Pathol* 2002; **2**: 3
- 14 **Ludwig J**, Dickson ER, McDonald GS. Staging of chronic nonsuppurative destructive cholangitis (syndrome of primary biliary cirrhosis). *Virchows Arch A Pathol Anat Histol* 1978; **379**: 103-112
- 15 **Ames BN**, Shigenaga MK, Hagen TM. Oxidants, antioxidants, and the degenerative diseases of aging. *Proc Natl Acad Sci USA* 1993; **90**: 7915-7922
- 16 **Halliwell B**, Gutteridge JM, Cross CE. Free radicals, antioxidants, and human disease: where are we now? *J Lab Clin Med* 1992; **119**: 598-620
- 17 **McCall MR**, Frei B. Can antioxidant vitamins materially reduce oxidative damage in humans? *Free Radic Biol Med* 1999; **26**: 1034-1053
- 18 **Halliwell B**. Free radicals, antioxidants, and human disease: curiosity, cause, or consequence? *Lancet* 1994; **344**: 721-724
- 19 **Halliwell B**. Antioxidants in human health and disease. *Annu Rev Nutr* 1996; **16**: 33-50
- 20 **Ghiselli A**, Serafini M, Natella F, Scaccini C. Total antioxidant capacity as a tool to assess redox status: critical view and experimental data. *Free Radic Biol Med* 2000; **29**: 1106-1114
- 21 **Prior RL**, Cao G. *In vivo* total antioxidant capacity: comparison of different analytical methods. *Free Radic Biol Med* 1999; **27**: 1173-1181
- 22 **Cao G**, Booth SL, Sadowski JA, Prior RL. Increases in human plasma antioxidant capacity after consumption of controlled diets high in fruit and vegetables. *Am J Clin Nutr* 1998; **68**: 1081-1087
- 23 **Jackson P**, Loughrey CM, Lightbody JH, McNamee PT, Young IS. Effect of hemodialysis on total antioxidant capacity and serum antioxidants in patients with chronic renal failure. *Clin Chem* 1995; **41**: 1135-1138
- 24 **Floreani A**, Baragiotta A, Martines D, Naccarato R, D'odorico A. Plasma antioxidant levels in chronic cholestatic liver diseases. *Aliment Pharmacol Ther* 2000; **14**: 353-358
- 25 **Barbaste M**, Berke B, Dumas M, Soulet S, Delaunay JC, Castagnino C, Arnaudinaud V, Cheze C, Vercauteren J. Dietary antioxidants, peroxidation and cardiovascular risks. *J Nutr Health Aging* 2002; **6**: 209-223
- 26 **Glud C**, Christensen E. Ursodeoxycholic acid for primary biliary cirrhosis. *Cochrane Database Syst Rev* 2002; **1**: CD000551
- 27 **Szalay F**. Treatment of primary biliary cirrhosis. *J Physiol Paris* 2001; **95**: 407-412
- 28 **Rodrigues CM**, Fan G, Wong PY, Kren BT, Steer CJ. Ursodeoxycholic acid may inhibit deoxycholic acid-induced apoptosis by modulating mitochondrial transmembrane potential and reactive oxygen species production. *Mol Med* 1998; **4**: 165-178
- 29 **Rodrigues CM**, Fan G, Ma X, Kren BT, Steer CJ. A novel role for ursodeoxycholic acid in inhibiting apoptosis by modulating mitochondrial membrane perturbation. *J Clin Invest* 1998; **101**: 2790-2799
- 30 **Rodrigues CM**, Ma X, Linehan-Stieers C, Fan G, Kren BT, Steer CJ. Ursodeoxycholic acid prevents cytochrome c release in apoptosis by inhibiting mitochondrial membrane depolarization and channel formation. *Cell Death Differ* 1999; **6**: 842-854

Science Editor Guo SY Language Editor Elsevier HK

• CLINICAL RESEARCH •

Sclerosing cholangitis following severe trauma: Description of a remarkable disease entity with emphasis on possible pathophysiologic mechanisms

Johannes Benninger, Rainer Grobholz, Yurdaguel Oeztuerk, Christoph H. Antoni, Eckhart G. Hahn, Manfred V. Singer, Richard Strauss

Johannes Benninger, Yurdaguel Oeztuerk, Eckhart G. Hahn, Richard Strauss, Department of Medicine I, Friedrich-Alexander-University Erlangen-Nuremberg, Ulmenweg 18, Erlangen D-91054, Germany

Christoph H. Antoni, Manfred V. Singer, Department of Medicine II, Ruprecht-Karls-University Heidelberg, University Hospital Mannheim, Theodor-Kutzer-Ufer 1-3, Mannheim D-68135, Germany

Rainer Grobholz, Department of Pathology, Ruprecht-Karls-University Heidelberg, University Hospital Mannheim, Theodor-Kutzer-Ufer 1-3, Mannheim D-68135, Germany

Correspondence to: Johannes Benninger, Department of Medicine I, Friedrich-Alexander-University Erlangen-Nuremberg, Ulmenweg 18, Erlangen D-91054,

Germany. johannes.benninger@med1.imed.uni-erlangen.de

Telephone: +49-9131-85-35204 Fax: +49-9131-85-209

Received: 2004-08-26 Accepted: 2004-09-06

cholestasis after severe trauma.

© 2005 The WJG Press and Elsevier Inc. All rights reserved.

Key words: Life-threatening trauma; Arterial hypotension; Cholestasis; Ischemia of intrahepatic bile ducts; Secondary sclerosing cholangitis; Posttraumatic sclerosing cholangitis

Benninger J, Grobholz R, Oeztuerk Y, Antoni CH, Hahn EG, Singer MV, Strauss R. Sclerosing cholangitis following severe trauma: Description of a remarkable disease entity with emphasis on possible pathophysiologic mechanisms. *World J Gastroenterol* 2005; 11(27): 4199-4205

<http://www.wjgnet.com/1007-9327/11/4199.asp>

Abstract

AIM: Persistent cholestasis is a rare complication of severe trauma or infections. Little is known about the possible pathomechanisms and the clinical course.

METHODS: Secondary sclerosing cholangitis was diagnosed in five patients with persistent jaundice after severe trauma (one burn injury, three accidents, one power current injury). Medical charts were retrospectively reviewed with regard to possible trigger mechanisms for cholestasis, and the clinical course was recorded.

RESULTS: Diagnosis of secondary sclerosing cholangitis was based in all patients on the primary sclerosing cholangitis (PSC)-like destruction of the intrahepatic bile ducts at cholangiography after exclusion of PSC. In four patients, arterial hypotension with subsequent ischemia may have caused the bile duct damage, whereas in the case of power current injury direct thermal damage was assumed to be the trigger mechanism. The course of secondary liver fibrosis was rapidly progressive and proceeded to liver cirrhosis in all four patients with a follow-up >2 years. Therapeutic possibilities were limited.

CONCLUSION: Posttraumatic sclerosing cholangitis is a rare but rapidly progressive disease, probably caused by ischemia of the intrahepatic bile ducts via the peribiliary capillary plexus due to arterial hypotension. Gastroenterologists should be aware of this disease in patients with persistent

INTRODUCTION

For a long time it is known that after severe trauma marked cholestasis can occur^[1-3]. Different reasons were held responsible for this including hepatic hypoxia, inflammation, and mass transfusions^[1,4]. Unfortunately, cholangiographic studies to detect changes of the bile ducts to exclude obstructive jaundice were not done, primarily as most of these studies were performed in the pre-ERCP era.

On the other side, gastroenterologists are occasionally confronted with patients with a history of persistent cholestasis who have survived life-threatening events with long-term stays in intensive care units. In the diagnostic work-up ERC in some of these patients shows a PSC-like picture with strictures and dilatations of the intrahepatic bile ducts.

Except one recent report by Engler *et al.*^[5], these patients are characterized badly in the literature. Therefore, we report on five patients with secondary sclerosing cholangitis after life-threatening injuries in order to demonstrate the clinical course, evaluate measures for diagnosis, and discuss possible trigger mechanisms for posttraumatic sclerosing cholangitis.

MATERIALS AND METHODS

All five patients (one woman and four men; age 18-71 years) presented with acute or persistent cholestasis. Three of them were seen as outpatients between January 2001 and June 2003, 4 to 22 mo after occurrence of cholestasis (Table 1). Patient 5 was seen as consultant during the initial stay of the patient on the intensive care unit of a burn clinic after

occurrence of jaundice, patient 1 is a former case of one of the hospitals that has already been published and who was re-evaluated^[6].

Time between the occurrence of cholestasis and definitive diagnosis ranged between 2 and 27 mo.

All patients experienced life-threatening injuries and needed long-term treatment on intensive care units (ICU) (from 23 to 88 d, Table 1). Mechanical ventilation was necessary in all patients (from 13 to 62 d). Temporary acute renal failure occurred in patients 3 and 4 (maximum creatinine 3.6 mg/dL [-1.0] on d 5 and 1.6 mg/dL on d 4, respectively). In all patients several surgeries had to be performed (without abdominal surgery), in three of them pleural drainages were necessary.

The charts of these patients at their initial hospital stay were intensely reviewed, especially concerning periods of hypotension, therapy with vasopressors and RBC units, septic fever, antibiotics, mechanical ventilation, and liver function tests to find triggers for subsequent bile duct damage. Pre-injury liver function tests were documented if available. Diagnostic work-up included ERC, liver biopsy, imaging studies of the liver and vessels of the liver hilus (ultrasound, doppler ultrasound, CT, and/or MRI), and the exclusion of other liver diseases (e.g. viral hepatitis, hereditary, and autoimmune liver diseases). Liver biopsies (also from hospitals outside) were re-evaluated by one pathologist. The further course was observed and recorded.

For the purpose of the study an increase in liver function tests more than twice above the upper limit of normal was defined abnormal.

RESULTS

Before the trauma no patient had known liver disease. No comorbidities were present with the exception of patient 3 (arterial hypertension, cardiac arrhythmias). No patient reported about alcohol abuse. On hospital admission patient 5 (power current injury) had increased values of ALT (alanine aminotransferase) and AST (aspartate aminotransferase) due to direct thermal cell damage. In all other patients liver function tests were normal on admission. No other liver diseases or thrombosis of hepatic artery and veins were found.

Early course

In all patients as the first sign of bile duct damage a permanent increase of GGT (gamma glutamyl transferase) twice above the upper limit of normal was first documented between d 4 and 11 (Table 2). Alkaline phosphatase (AP) and bilirubin rose during the next 2 weeks in all but patient 1 in whom bilirubin increased after four weeks and patient 2 whose bilirubin levels according to a milder course of cholestasis reached twice the upper limit of normal only once. Aminotransferases always increased secondary to signs of cholestasis (Table 2). As an example the early course (first month) of AST, ALT, GGT, AP, and bilirubin in patient 3 is shown in Figure 1A.

Possible reasons for bile duct damage

Details of different parameters during intensive care of the patients are shown in Table 2.

Table 1 Summary of patients' characteristics

	Patient 1	Patient 2	Patient 3	Patient 4	Patient 5
Sex	Female	Male	Male	Male	Male
Age (yr)	56	41	56	71	18
Initial event	Room fire	Motorbike accident	Tractor accident	Fall from a raised hide	Power current accident and fall
Injuries	Burn injury: 34 % of body surface (hands, head, neck, back)	Polytrauma with avulsions (left subclavian artery, forearm, anterior tibial artery) and fractures (left humeral shaft, pelvis, both lower legs)	Polytrauma with serial rib fracture, hemothorax, pleural effusion, fracture of right joint ankle	Polytrauma with burst fractures of lumbar spine, paraplegia, rib fractures, pneumothorax	Burn injury (36 % of body surface), multiple rib fractures, hemothorax, fractures of the thoracic vertebrae 5 to 9
Intensive care (d)	58	23	34	26	88
Time from occurrence of cholestasis until diagnosis (mo)	4	27	4	13	2
Treatment start with UDCA	mo 4	mo 22	mo 4	mo 13	mo 1
Follow-up(mo)	55 (death)	48	41	33	12
Complications	Liver cirrhosis (Child-Pugh C), variceal bleeding, death due to liver insufficiency	Small intrahepatic gallstones after 6 mo (endoscopically extracted), liver cirrhosis (Child-Pugh A)	unbearable pruritus during first year, liver cirrhosis (Child-Pugh A)	liver cirrhosis (Child-Pugh B), recurrent stomal bleeding	-

UDCA: urso deoxycholic acid.

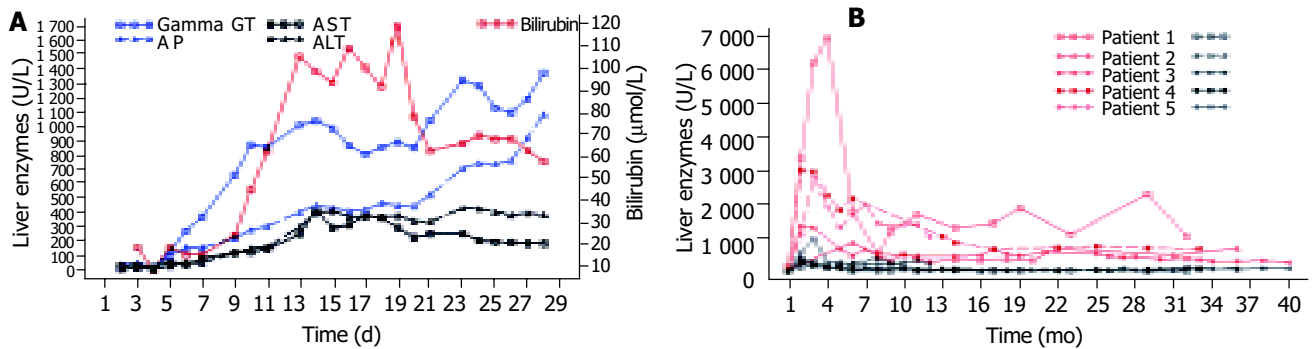


Figure 1 A: Liver function tests of patient 3 in the first month showing the strong increase of cholestasis followed by a milder rise of aminotransferases; B: Long-time course of AP (red) and ALT (black) of all patients showing the initial strong

increase of AP with a subsequent slow decrease and only a mild initial rise of ALT with nearly normal values in the long term.

Severe arterial hypotension with a systolic blood pressure of ≤ 70 mmHg as a possible cause of bile duct ischemia occurred in four patients. Only patient 5 experienced no hemodynamic instability throughout the whole course. In contrast to all other patients aminotransferases were already increased at clinic admission and nearly normalized during the following days. According to the pattern of his burns current flow through the body was diagnosed. Therefore, a direct thermal damage of the intrahepatic bile ducts can be suspected.

Two patients (patients 2 and 3) suffered of sudden strong blood loss requiring mass transfusions in patient 2 (30 RBC units, 11 fresh frozen plasma units, and four platelet concentrates during the first four hours after hospital admission), whereas a moderate decrease of the hemoglobin occurred in the other patients. After ICU admission all patients received parenteral nutrition via central venous lines, and additional enteral feeding via a nasogastric tube was

started in all cases between d 2 and 5.

Imaging findings

Imaging findings are shown in Table 3.

Ultrasound Ultrasound was repeatedly performed in all patients. Depending on the time since occurrence of cholestasis different findings were recorded (Table 3).

In the early phase (first 2 mo) the liver was described as normal or enlarged with homogeneous or hyperechoic parenchyma, bile ducts were normal in all patients, gallbladder sludge was seen in four patients. Later on liver parenchyma got more and more inhomogeneous and signs of liver cirrhosis (nodularity/irregularity of liver surface, inhomogeneous parenchyma, splenomegaly) occurred. Intrahepatic bile ducts showed segmental dilatation in two patients after 12 to 24 mo, whereas the common bile duct remained normal in all patients.

Table 2 Patients' data and important findings during the early course at the intensive care unit

	Patient 1	Patient 2	Patient 3	Patient 4	Patient 5
Time of increase of liver function tests $> 2 \times$ ULN (d)					
GGT	10 ¹	6	5	4	11
AP	18	18	9	12	15
Bilirubin	36	6 ²	10	8	13
AST	18	52	9	12	16
ALT	18	23	9	7	19
Mechanical ventilation (d)	36;	13;	25;	16;	62;
	PEEPmax. 6 mmHg; FiO ₂ not documented	PEEPmax. 10 mmHg; FiO ₂ max. 0.6	PEEPmax. 8 mmHg; FiO ₂ max. 0.6	PEEPmax. 15 mmHg; FiO ₂ max. 0.7	PEEPmax. 20 mmHg; FiO ₂ max. 0.6
Severe hypotension (systolic blood pressure < 70 mm Hg) ³	d 1 (2 h)	d 1 (45 min)	d 2 (30 min) and d 3 (60 min)	d 1 (30 min)	None
Vasopressor therapy	Dobutamine d 1-8 dopamine d 1-18 norepinephrine d 1-7	None	Norepinephrine d 3-5 and d 9-17	Norepinephrine d 2-4	None
Minimum hemoglobin ³	7.3 g/dL (d 3)	2.4 g/dL (d 1)	7.2 g/dL (d 3)	8.6 g/dL (d 1)	7.9 g/dL (d 4)
Transfusions (RBC units) ³	30	34	10	10	24
Fever (> 38.0 °C)	d 7-16	d 6-13	d 2-25	d 5-17	d 2- >20
Antibiotics ³	Cefotaxim, imipenem, sulbactam, mezlocillin	None	Piperacillin/sulbactam	None	Piperacillin/tazobactam, ciprofloxacin, meropenem, levofloxacin, fluconazol

ALT: alanine aminotransferase; AP: alkaline phosphatase; AST: aspartate aminotransferase; FiO₂max.: maximum fraction of inspired oxygen; GGT: gamma glutamyl transferase; PEEPmax.: maximum positive end-expiratory pressure; ULN: upper limit of normal ¹No control of liver function tests between d 4 and 10; ²A bilirubin value $2 \times$ ULN was noted only once at d 6; ³Until increase of GGT $\geq 2 \times$ ULN.

Table 3 Diagnostic findings in posttraumatic sclerosing cholangitis during the course of the disease (ultrasound, MRT/MRCP, ERCP, and liver histology)

	Patient 1	Patient 2	Patient 3	Patient 4	Patient 5
1 - 2 mo					
Ultrasound	L normal, BD normal, GB sludge	L normal, BD normal, GB sludge	L normal, BD normal, GB sludge	L normal, BD normal, GB sludge	L enlarged, hyperechoic, BD normal, GB contracted, splenomegaly
ERC	Stenoses and loss of IHBD, CBD normal, GB normal	-	IHBD irregular, CBD normal, GB normal	-	-
MRT/MRCP	-	-	-	L normal, BD normal, GB normal	-
4 - 6 mo					
Ultrasound	L cirrhosis, BD normal, GB stones	L inhomogeneous, BD normal	L inhomogeneous with hyperechoic areas alongside the IHBD, BD normal, GB normal,	-	L enlarged, BD normal, BD normal, splenomegaly
ERC	-	-	IHBD: multifocal short strictures and dilatations, CBD normal, GB normal (Figure 2)	-	IHBD irregular, beaded appearance, CBD normal, GB normal
Liver histology	Substantial cholestasis; inflammation of the portal tracts, liver lobules, and sporadically the bile ducts; feathery degeneration of hepatocytes; fibrosis around bile ducts; regenerative bile duct proliferations	Portal tract inflammation, occasionally lymphocytes in bile duct epithelium; several necrotic foci with foamy macrophages in the liver acini; bridging fibrosis; regenerative bile duct proliferations	Canalicular bile thrombi; edematously swollen portal tracts; inflammatory infiltrates, esp. around bile ducts; occasionally feathery degeneration of hepatocytes; minimal fibrosis	-	-
12 - 24 mo					
Ultrasound	L inhomogeneous cirrhosis BD normal, GB stones and sludge, splenomegaly, distinct ascites	L enlarged, inhomogeneous, hyperechoic areas segment 7/8, IHBD slightly dilated, CBD normal, GB stones, splenomegaly	L cirrhosis, BD normal, GB normal, splenomegaly	L cirrhosis, IHBD slightly dilated, CBD normal, GB normal, splenomegaly	-
ERC	stenoses and loss of IHBD, CBD normal, GB normal	IHBD: loss and stenoses of right-sided bile ducts, a long, stretched running left bile duct (suitable to liver hypertrophy), CBD normal, GB stones	-	IHBD: multifocal high-grade strictures and dilatations on the left side, bile ducts on the right side not presentable, CBD normal	-
MRT/MRCP	-	L atrophy of right liver, hypertrophy of left liver; reduced signal intensity of segments 2 and 3 and partly 7 and 8; IHBD segmentally dilated, CBD pseudoobstruction, GB stones, splenomegaly	L macronodular cirrhosis, CBD pseudoobstruction, splenomegaly	-	-
Liver histology	No cholestasis; complete liver cirrhosis	-	Occasionally canalicular cholestasis; mild portal inflammation (predominantly lymphocytes); some regenerative bile duct proliferations; mild fibrosis; (sampling error ?)	Substantial cholestasis (bile thrombi in dilated canaliculi); occasionally lymphocytes in the epithelium of bile ducts; numerous regenerative bile duct proliferations in the periphery of portal tracts; cirrhosis (Figure 4)	

BD: bile ducts; CBD: common bile duct; GB: gallbladder; IHBD: intrahepatic bile ducts; L: liver.

Computed tomography CT scans performed in patient 1 18 mo and in patient 3 10 d and 4 mo after the onset of cholestasis confirmed sonographic findings.

MRT/MRCP MRT/MRCP in patient 3 in the early phase showed normal abdominal findings. In two patients MRT/MRCP was performed after 2 years. In patient 2 MRT/MRCP disclosed atrophy of the right liver, hypertrophy of the left liver, a reduced signal intensity in segments 2 and 3 and partly 7 and 8, and peripheral segmental dilatation of intrahepatic bile ducts rather unusual findings (Figure 2). In patient 3 signs of liver cirrhosis with large nodules and inhomogeneous liver parenchyma were present.

ERC Diagnostic ERC was performed in all patients. Together with the history it led to diagnosis in all patients. Already three weeks after first signs of cholestasis slight changes of the intrahepatic bile ducts were noticed (patient 3). After four to six months multifocal strictures and dilatations of the intrahepatic bile ducts (comparable to lesions in primary sclerosing cholangitis) occurred (Figure 3), that were also present after 12-24 mo. The common bile duct and the cystic duct were normal in all patients at all times.

Liver histology

Liver biopsy was performed in four patients (in no one in the acute phase), at least once in three patients and three times in one patient (patient 3) (Table 3). After 4-6 mo

portal inflammation (predominantly lymphocytes) with involvement of the bile ducts, necrosis of periportal hepatocytes, fibrosis of different degree, and depending on the biochemical extent of cholestasis bile thrombi were present. After 12-24 mo complete liver cirrhosis was diagnosed in patients 1 and 4, whereas in patient 3 only mild fibrosis was diagnosed, possibly due to a sampling error (clinically cirrhosis). Inflammation of the portal tracts with involvement of bile ducts was still present. Regenerative bile duct proliferations were a prominent feature. As an example liver histology of patient 4 is shown in Figure 4.

Follow-up, treatment, and complications

The patients were followed between 12 and 55 mo after trauma (Table 1).

The long-time courses of AP and ALT of all patients are shown in Figure 1B.

All patients were treated with ursodeoxycholic acid after different periods of time (Table 1).

Liver cirrhosis was diagnosed clinically and/or histologically in all four patients with a follow-up of >2 years. It occurred already at mo 5 in patient 4. In this case it was diagnosed macroscopically during colostomy which was performed due to fecal incontinence following paraplegia. Decompensation of liver cirrhosis with large amounts of ascites occurred in patient 1 already after 18 mo. This patient died after 55 mo due to hepatic insufficiency.

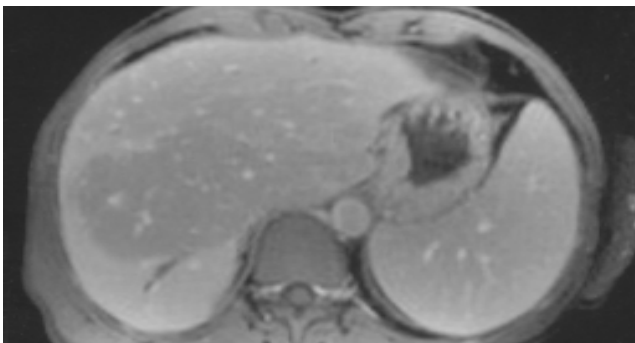


Figure 2 MRT of patient 2 (T1-weighted after contrast medium) showing an area centrally in the liver with reduced signal intensity, a dilatation of the bile duct in segment 6, and splenomegaly.



Figure 3 ERCP of patient 3 showing a normal cystic and common bile duct, but multifocal short strictures and dilatations of the intrahepatic bile ducts (4 mo after occurrence of cholestasis).

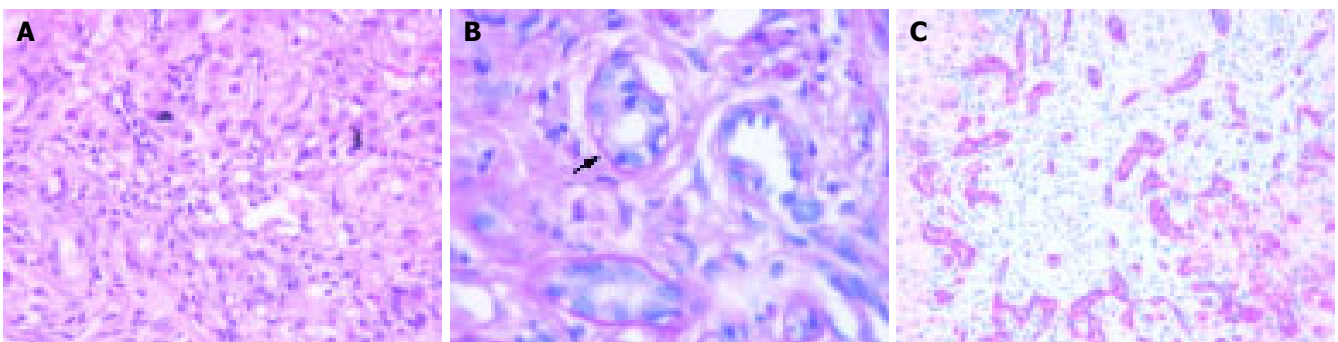


Figure 4 Liver histology of patient 4 (13 mo after occurrence of cholestasis). **A:** Portal inflammation, severe cholestasis with bile thrombi, HE (20x); **B:** Lymphocytic infiltration of a small bile duct (arrow). Periodic acid Schiff's reaction

after treatment with diastase (100x); **C:** Immunostaining for cytokeratin 7. Regenerative bile duct proliferations show a strong expression of cytokeratin 7 (25x).

Liver transplantation was planned for patient 3 after 4 mo, but due to improvement of liver function tests and clinical symptoms transplantation was cancelled. Patient 5 is designated for liver transplantation.

DISCUSSION

Cholestasis is common in long-term ICU patients. However, in most cases it is mild and resolves within weeks after clinical improvement of the patient.

Secondary sclerosing cholangitis after trauma ("posttraumatic SC") is a rare and probably underdiagnosed complication of severe trauma with to our knowledge only two publications in the literature^[5,6]. Our patients shared the following findings, thus leading to the diagnosis: (1) a severe, life-threatening trauma; (2) slowly increasing signs of cholestasis with a secondary moderate rise of aminotransferases; (3) the typical PSC-like appearance of the intrahepatic bile ducts with multifocal strictures and dilatations; and (4) the exclusion of other liver diseases. All patients except patient 5 had normal liver function tests at hospital admission. After a few days a slow, but constant increase of signs of cholestasis was noted with a subsequent rise of aminotransferases that never exceeded 15 times of ULN. This differs from "shock liver" where an acute elevation of the aminotransferases to at least 20 times ULN is required for diagnosis^[7]. According to our results ERC is of essential importance for the diagnosis. Probably earlier than MRC, ERC best shows the PSC-like bile duct changes (multifocal strictures and dilatations, beaded appearance) that occur only intrahepatically in posttraumatic SC. The possibility to aspirate bile for microbiological examination is another advantage of ERC compared to all non-invasive imaging procedures as to our experience and some case reports in the literature in some intensive care patients with severe, long-lasting infections requiring mechanical ventilation jaundice may be caused by secondary bacterial or fungal cholangitis without preexisting biliary obstruction^[8,9]. The value of ultrasound, CT, and MRT in the early course is to exclude obvious biliary obstruction, later they may help to diagnose secondary development of liver cirrhosis.

Posttraumatic SC seems to be rapidly progressive. Liver cirrhosis was diagnosed clinically or by liver biopsy in all patients with a follow-up of more than 2 years, in one patient already after 5 mo, in the others after 18-24 mo. After decompensation of liver cirrhosis at mo 18 and esophageal variceal bleeding at mo 22, one patient died after 55 mo due to hepatic insufficiency. This rapidly progressive course compares well with the experience of Engler *et al.*^[5]. In their series all four patients with a follow-up of more than 2 years developed liver cirrhosis, three of them during the second year.

All patients were treated with UDCA after 1-22 mo. As this was an uncontrolled retrospective study clear conclusions concerning the therapeutic value of UDCA are not possible, but the efficacy seems to be rather limited. In patients with posttraumatic SC and end-stage liver disease liver transplantation may be the only therapeutic option. In contrast to Engler *et al.* we are not convinced that endoscopic interventions for treatment of strictures (dilatation or

stenting) are beneficial as bile duct strictures were multifocal and localized intrahepatically in all of our patients. This is comparable to PSC where only patients with a dominant extrahepatic stricture appear to have some potential benefit from endoscopic treatment^[10]. Even in the patients of Engler *et al.*^[5], endoscopic therapy (with the additional risk of secondary bacterial cholangitis) did not stop disease progression. However, for diagnostic reasons early ERC appears necessary.

Interestingly, bilirubin levels of all patients decreased without intervention after 2-6 mo. Proliferation of bile ducts in the portal tracts with metaplasia of hepatocytes may have improved bile flow. This phenomenon was also described in drug-induced prolonged cholestasis with ductopenia^[11]. However, posttraumatic SC progresses in spite of decreasing bilirubin levels.

What are the possible mechanisms for posttraumatic sclerosing cholangitis? As shown in Table 2 we examined several factors that are discussed in the literature, which could have contributed to bile duct damage^[5,6,12]. In our opinion the dominant cause is arterial hypotension with subsequent ischemia of the intrahepatic bile ducts which occurred in four of the five patients in the early course after the accident (in patient 5 according to the pattern of burns current flow through the body was diagnosed suggesting a direct thermal damage of the intrahepatic bile ducts). It can be assumed that through temporary hypoperfusion, possibly aggravated by vasopressor therapy, an ischemic damage of the intrahepatic bile duct epithelium occurred which led to secondary scarring of the bile ducts and subsequent cholestasis. In contrast to shock liver the initial damage is not characterized by rapidly increasing aminotransferases as the liver via the portal vein - seems to be perfused sufficiently. After the acute ischemic phase, parallel to bile duct changes, increasing signs of cholestasis occur. Later, aminotransferases raise secondary to bile duct obstruction as in other obstructive bile duct diseases. Possibly due to the non-reversible scarring of the bile ducts with persistence of cholestasis and comparable to experimental bile duct ligation liver fibrosis and cirrhosis develop rather quickly^[13].

In all of our patients only the intrahepatic bile ducts were affected. The reason may be the blood supply of the bile ducts^[14-16]. Whereas the extrahepatic biliary system seems to be well supplied, mainly by two parallel to the common bile duct running arteries which are fed by branches of eight arteries on the average (retroduodenal artery, gastroduodenal artery, left and right hepatic artery, *etc.*), the intrahepatic ducts are supplied by a nonaxial network of small arteries deriving only from the right and left hepatic artery. They form a plexus of arterioles, venules, and capillaries within the peribiliary adventitia with a second plexus within the biliary wall primarily composed of capillaries ("peribiliary capillary plexus"). This structure, possibly especially the blood supply via the left and right hepatic artery as functional end arteries, may cause the vulnerability of the intrahepatic bile ducts to ischemic events. Except in the periphery of the liver portal-venous blood plays no role in the supply of the bile ducts.

Other factors like systemic inflammation or transfusions

may contribute to progressing cholestasis in some patients, but may be of minor importance.

In conclusion, after severe, life-threatening injuries a small number of patients develop jaundice that is caused by multiple intrahepatic bile duct strictures. The main trigger may be ischemia and subsequent damage of the bile ducts due to transient arterial hypotension. Slowly progressive cholestasis after severe injury in patients without prior liver disease is the hallmark of posttraumatic sclerosing cholangitis. The diagnosis is confirmed by ERC. The major characteristics of posttraumatic SC are summarized in Table 4. The course of this form of secondary sclerosing cholangitis appears to be rather progressive without promising therapeutic options (except probably liver transplantation). Gastroenterologists should be aware of this disease in patients with cholestasis after severe trauma.

Table 4 Characteristics of posttraumatic sclerosing cholangitis

1	No former liver disease
2	Severe life-threatening injury with temporary severe arterial hypotension
3	Slowly increasing signs of cholestasis
4	Secondary moderate rise of aminotransferases
5	PSC-like appearance of intrahepatic bile ducts (multifocal strictures and dilatations)
6	Exclusion of other liver diseases (esp. hepatic artery thrombosis)

ACKNOWLEDGMENTS

The authors thank the surgical hospitals, the Berufsgenossenschaftliche Unfallklinik Ludwigshafen and the Clinic Nuremberg, both Germany, for the permission to analyze the medical files and therefore enabling this paper.

REFERENCES

- Nunes G, Blaisdell FW, Margaretten W. Mechanism of hepatic dysfunction following shock and trauma. *Arch Surg* 1970; **100**: 546-556
- Champion HR, Jones RT, Trump BF, Decker R, Wilson S, Stega M, Nolan J, Crowley RA, Gill W. Post-traumatic hepatic dysfunction as a major etiology in post-traumatic jaundice. *J Trauma* 1976; **16**: 650-657
- Hartley S, Scott AJ, Spence M. Benign postoperative jaundice complicating severe trauma. *N Z Med J* 1977; **86**: 174-178
- Te Boekhorst T, Urlus M, Doesburg W, Yap SH, Goris RJA. Etiologic factors of jaundice in severely ill patients. *J Hepatol* 1988; **7**: 111-117
- Engler S, Elsing C, Flechtenmacher C, Theilmann L, Stremmel W, Stiehl A. Progressive sclerosing cholangitis after septic shock: a new variant of vanishing bile duct disorders. *Gut* 2003; **52**: 688-693
- Schmitt M, Koelbl CB, Mueller MK, Verbeke CS, Singer MV. Sclerosing cholangitis after burn injury. *Z Gastroenterol* 1997; **35**: 929-934
- Seeto RK, Fenn B, Rockey DC. Ischemic hepatitis: Clinical presentation and pathogenesis. *Am J Med* 2000; **109**: 109-113
- Scheppach W, Druge G, Wittenberg G, Mueller JG, Gassel AM, Gassel HJ, Richter F. Sclerosing cholangitis and liver cirrhosis after extrabiliary infections: Report on three cases. *Crit Care Med* 2001; **29**: 438-441
- Domagk D, Bisping G, Poremba C, Fegeler W, Domschke W, Menzel J. Common bile duct obstruction due to candidiasis. *Scand J Gastroenterol* 2001; **36**: 444-446
- Lee YM, Kaplan MM. Practice guideline committee of the ACG. American college of gastroenterology. Management of primary sclerosing cholangitis. *Am J Gastroenterol* 2002; **97**: 528-534
- Degott C, Feldmann G, Larrey D, Durand-Schneider AM, Grange D, Machayekhi JP, Moreau A, Potet F, Benhamou JP. Drug-induced prolonged cholestasis in adults: a histological semiquantitative study demonstrating progressive ductopenia. *Hepatology* 1992; **15**: 244-251
- Labori KJ, Bjornbeth BA, Raeder MG. Aetology and prognostic implication of severe jaundice in surgical trauma patients. *Scand J Gastroenterol* 2003; **38**: 102-108
- Johnstone JM, Lee EG. A quantitative assessment of the structural changes the rat's liver following obstruction of the common bile duct. *Br J Exp Pathol* 1976; **57**: 85-94
- Batts KP. Ischemic cholangitis. *Mayo Clin Proc* 1998; **73**: 380-385
- Northover JM, Terblanche J. A new look at the arterial supply of the bile duct in man and its surgical implications. *Br J Surg* 1979; **66**: 379-384
- Cho KJ, Lunderquist A. The peribiliary vascular plexus: The microvascular architecture of the bile duct in the rabbit and in clinical cases. *Radiology* 1983; **147**: 357-364

• CLINICAL RESEARCH •

Thermo-chemo-radiotherapy for advanced bile duct carcinoma

Terumi Kamisawa, Yuyang Tu, Naoto Egawa, Katsuyuki Karasawa, Tadayoshi Matsuda, Kouji Tsuruta, Atsutake Okamoto

Terumi Kamisawa, Yuyang Tu, Naoto Egawa, Department of Internal Medicine, Tokyo Metropolitan Komagome Hospital, 3-18-22 Honkomagome, Bunkyo-ku, Tokyo, Japan
Katsuyuki Karasawa, Tadayoshi Matsuda, Department of Radiology, Tokyo Metropolitan Komagome Hospital, 3-18-22 Honkomagome, Bunkyo-ku, Tokyo, Japan
Kouji Tsuruta, Atsutake Okamoto, Department of Surgery, Tokyo Metropolitan Komagome Hospital, 3-18-22 Honkomagome, Bunkyo-ku, Tokyo, Japan
Correspondence to: Dr. Terumi Kamisawa, Department of Internal Medicine, Tokyo Metropolitan Komagome Hospital, 3-18-22 Honkomagome, Bunkyo-ku, Tokyo, Japan. kamisawa@cick.jp
Telephone: +81-3-3823-2101 Fax: +81-3-3824-1552
Received: 2004-12-28 Accepted: 2005-01-13

Abstract

AIM: Complete resection of the bile duct carcinoma is sometimes difficult by subepithelial spread in the duct wall or direct invasion of adjacent blood vessels. Nonresected extrahepatic bile duct carcinoma has a dismal prognosis, with a life expectancy of about 6 mo to 1 year. To improve the treatment results of locally advanced bile duct carcinoma, we have been conducting a clinical trial using regional hyperthermia in combination with chemoradiation therapy.

METHODS: Eight patients complaining of obstructive jaundice with advanced extrahepatic bile duct underwent thermo-chemo-radiotherapy (TCRT). All tumors were located in the upper bile duct and involved hepatic bifurcation, and obstructed the bile duct completely. Radiofrequency capacitive hyperthermia was administered simultaneously with chemotherapeutic agents once weekly immediately following radiotherapy at 2 Gy. We administered heat to the patient for 40 min after the tumor temperature had risen to 42 °C. The chemotherapeutic agents employed were cis-platinum (CDDP, 50 mg/m²) in combination with 5-fluorouracil (5-FU, 800 mg/m²) or methotrexate (MTX, 30 mg/m²) in combination with 5-FU (800 mg/m²). Number of heat treatments ranged from 2 to 8 sessions. The bile duct at autopsy was histologically examined in three patients treated with TCRT.

RESULTS: In respect to resolution of the bile duct, there were three complete regression (CR), two partial regression (PR), and three no change (NC). Mean survival was 13.2±10.8 mo (mean±SD). Four patients survived for more than 20 mo. Percutaneous transhepatic biliary drainage (PTBD) tube could be removed in placement of self-expandable metallic stent into the patency-restored bile duct after TCRT. No major side effects occurred. At

autopsy, marked hyalinization or fibrosis with necrosis replaced extensively bile duct tumor and wall, in which suppressed cohesiveness of carcinoma cells and degenerative cells were sparsely observed.

CONCLUSION: Although the number of cases is rather small, TCRT in the treatment of locally advanced bile duct carcinoma is promising in raising local control and thus, long-term survival.

© 2005 The WJG Press and Elsevier Inc. All rights reserved.

Key words: Hyperthermia; Chemotherapy; Radiotherapy; Bile duct carcinoma

Kamisawa T, Tu Y, Egawa N, Karasawa K, Matsuda T, Tsuruta K, Okamoto A. Thermo-chemo-radiotherapy for advanced bile duct carcinoma. *World J Gastroenterol* 2005; 11(27): 4206-4209
<http://www.wjgnet.com/1007-9327/11/4206.asp>

INTRODUCTION

Extrahepatic bile duct carcinomas are typically slow-growing and locally invasive tumors, which spread along nerves and invade adjacent vascular structures^[1]. Optimal treatment of these tumors includes complete surgical resection with negative histologic margins^[2]. However, complete resection is sometimes difficult by local extension, which occur perineurally, via lymphatic channels, by subepithelial spread in the duct wall, and by direct invasion of adjacent blood vessels^[3]. Nonresected extrahepatic bile duct carcinoma has a dismal prognosis, with a life expectancy of about 6 mo to 1 year^[4].

Hyperthermia has been used in combination with radiation therapy and chemotherapy, and is considered to be effective for certain type of tumors^[5]. We have been conducting a clinical trial of regional hyperthermia in combination with chemoradiotherapy for advanced extrahepatic bile duct carcinoma. In this study, clinical effectiveness of thermo-chemo-radiotherapy (TCRT) for locally advanced extrahepatic bile duct carcinoma was evaluated.

MATERIALS AND METHODS

Study patients

Eight patients complaining of obstructive jaundice with advanced extrahepatic bile duct underwent TCRT. All tumors were located in the upper bile duct and involved hepatic bifurcation. Bile duct was completely obstructed on

percutaneous transhepatic or endoscopic retrograde cholangiography. Six patients underwent percutaneous transhepatic biliary drainage (PTBD). Unresectable reasons were involvement of the portal vein ($n = 5$) and extensive involvement of hepatic hilus ($n = 3$, Table 1). None of them showed distant metastasis.

Table 1 Cases with bile duct carcinoma treated with thermo-chemo-radiotherapy

Case	Age (yr)	Sex	Unresectable reasons
1	70	m	Extensive involvement of hepatic hilus
2	57	m	Involvement of the portal vein
3	73	m	Extensive involvement of hepatic hilus
4	70	m	Involvement of the portal vein
5	70	f	Involvement of the portal vein
6	78	m	Involvement of the portal vein
7	65	m	Involvement of the portal vein
8	71	m	Extensive involvement of hepatic hilus

Thermo-chemo-radiotherapy (TCRT) techniques

The heating equipment was radiofrequency (RF) capacitive heating device, Thermotron RF-8 (Yamamoto Vinita Company, Osaka, Japan)^[6]. The patient lay in the prone position. The target was sandwiched with upper and lower electrodes, and 8 MHz RF wave was applied. We administered heat to the patient for 40 min after the tumor temperature had risen to 42 °C. Tumor temperature was measured continuously using a needle thermosensor on each heating. The thermosensor was inserted beside the tumor from the skin surface through 18-G angiocatheter under the aid of ultrasonography. The chemotherapeutic agents employed were cis-platinum (CDDP, 50 mg/m²) in combination with 5-fluorouracil (5-FU, 800 mg/m²) or methotrexate (MTX, 30 mg/m²) in combination with 5-FU (800 mg/m²). The hyperthermia and chemotherapeutic agents were administered simultaneously once weekly immediately following radiotherapy at 2 Gy. Usually it started within 15 min after the irradiation (Figure 1). Number of heat treatments ranged from 2 to 8 sessions (mean±SD, 4.5±2.5). Two cases were retreated (Table 2).

Table 2 Thermo-chemo-radiotherapy in each case

Case	Heat session	Chemotherapy	Dose of radiation (Gy)
1	×4, ×4	MTX + 5Fu	50+40
2	×2, ×6	CDDP + 5Fu	46
3	×6	MTX + 5Fu	56
4	×4	MTX + 5Fu	56
5	×4	CDDP + 5Fu	50
6	×2	CDDP + 5Fu	46
7	×2	MTX + 5Fu	50
8	×2	MTX + 5Fu	16

MTX: Methotrexate, 5Fu: 5-fluorouracil, CDDP: cis-platinum.

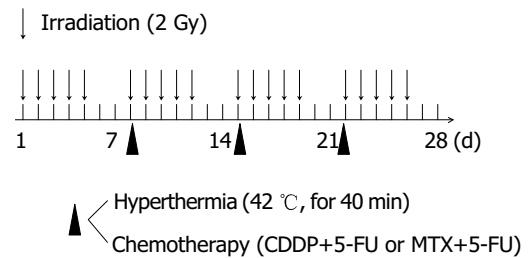


Figure 1 Schedule of TCRT.

Response and toxicity criteria

The effectiveness of TCRT on the advanced bile duct carcinoma was evaluated about resolution of biliary obstruction by cholangiography. Response of obstructed bile duct was graded as complete regression (CR: more than 80% resolution), partial regression (PR: more than 50% and less than 80% resolution), and no change (NC).

We examined histologically the state of the bile duct at autopsy in three patients with advanced bile duct carcinoma treated with TCRT.

Side effects were evaluated and graded according to the National Cancer Institute Common Toxicity Criteria^[7].

RESULTS

Effectiveness of TCRT

In respect to resolution of the bile duct, there were 3 CR, 2 PR, and 3 NC. CR rate and CR+PR rate was 38% and 63%. Mean survival was 13.2±10.8 mo. Four patients survived for more than 20 mo (Table 3). We placed self-expandable metallic stent into the patency-restored bile duct for prevention of restenosis ($n = 1$) and partially resolved bile duct ($n = 2$) after TCRT for improvement of patients' quality of life (Figures 2A and B). In these three patients, PTBD tube could be withdrawn.

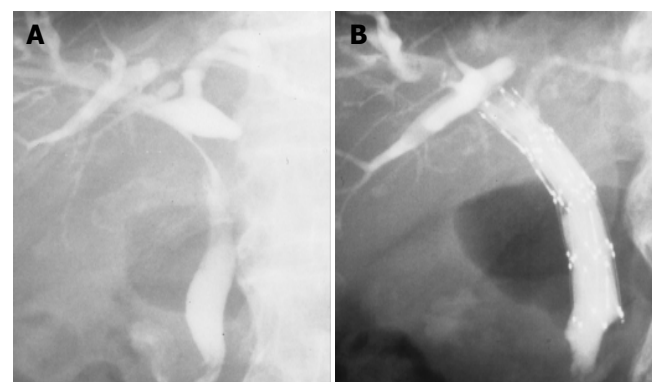


Figure 2 A: Completely obstructed upper bile duct was partially resolved after TCRT; B: self-expandable metallic stent was placed into the patency-restored bile duct, and PTBD tube could be removed.

Histological findings at autopsy in patients treated with TCRT

Marked hyalinization or fibrosis with necrosis replaced extensively bile duct tumor and wall, in which suppressed

Table 3 Effectiveness of thermo-chemo-radiotherapy and survival months

Case	Resolution of the bile duct	Survival months
1	Complete response	33
2	Complete response	22
3	Complete response	22
4	Partial response	21.5
5	Partial response	6
6	No change	13.5
7	No change	4
8	No change	2.5

cohesiveness of carcinoma cells and degenerative cells were sparsely observed. Carcinoma cells were also detected peripherally. Common bile duct of two cases was not completely obstructed, though it was partly obstructed with debris or necrotic mass.

Complication of TCRT

Treatment complications by TCRT were nausea and vomiting (grades 1 and 2, five cases), gastritis (grade 2, three cases), leukocytopenia (grade 2, three cases), and thrombocytopenia (grade 1, one case). These complications were successfully treated conservatively.

DISCUSSION

Optimal treatment of bile duct carcinoma is complete surgical resection with negative histologic margins^[2]. However, complete resection is sometimes difficult by local extension, especially when the tumor located near the hepatic bifurcation. Deeply invaded tumors are apt to spread to the intrahepatic bile duct or the connective tissues in the hepatoduodenal ligament, with encasement of major vessels. Moreover, tumor cells that spread to the ligament often cannot be cleared away completely, even when dissection of the tissue is performed. In nonresected cases, tumor involving the hepatic hilus frequently induces the development of obstructive jaundice which cannot be under control, resulting in early death from cholangitis. One of the desirable strategies for advanced bile duct carcinoma appears to control over involvement of the hepatic hilar bile duct and the hepatoduodenal ligament.

We have treated advanced gallbladder carcinoma with TCRT and reported the effectiveness^[8]. Then, we undertook a preliminary study involving TCRT for unresectable bile duct carcinomas. In respect to resolution of the bile duct, there were three CR and two PR of eight treated cases. Four patients survived for more than 20 mo. PTBD tube could be removed in three patients, in whom self-expandable metallic stent was placed into the patency-restored bile duct after TCRT.

Hyperthermia involves two biological interactions with radiation, a radiosensitizing effect^[9,10] and a direct cytotoxic effect on tumor cells^[11]. When the target lesion is heated up to around 42 °C, the cancer-killing effect of radiation or anticancer drug is enhanced^[12]. Experimental studies strongly

suggest that the extracellular pH of the tumor and a hypoxic environment sensitize tumor cells to direct heat killing^[13]. Hyperthermia in combination with radiotherapy for superficial malignancies has contributed to a better rate of complete response and reduction in the rate of recurrence compared with radiotherapy alone^[14]. Data on hyperthermia for deep-seated tumors were still preliminary, because the heating and thermal measurement techniques were not yet established. However, the effectiveness of TCRT for deep-seated tumors has been recently revealed by prospective randomized studies^[15,16]. The treatment protocol of TCRT was established and its effectiveness was evidenced by Sugimachi and his colleagues^[17]. They treated esophageal carcinoma with TCRT and demonstrated significant improvement in the clinical effectiveness and 5-year survival ratio. Anatomically, the bile duct is located near the abdominal wall, which is advantageous to heating and thermal measurement. Thus, it seems that TCRT may be a favorable treatment strategy for advanced bile duct carcinoma.

In conclusion, although our clinical trial was preliminary and the number of patients was small, the results were better than we expected. We prefer HCRT in place of aggressive surgical approach for patients with locally advanced bile duct carcinoma.

REFERENCES

- 1 Suzuki M, Takashima T, Ouchi K, Matsuno S. The development and extension of hepatohilar bile duct carcinoma. A three-dimensional tumor mapping in the intrahepatic biliary tree visualized with the aid of a graphics computer system. *Cancer* 1989; **64**: 658-666
- 2 Klempnauer J, Ridder GJ, Werner M, Weimann A, Picklmayr R. What constitutes long-term survival after surgery for hilar cholangiocarcinoma? *Cancer* 1997; **79**: 26-34
- 3 Sakamoto E, Nimura Y, Hayakawa N, Kamiya J, Kondo S, Nagino M, Kanai M, Miyachi M, Uesaka K. The pattern of infiltration at the proximal border of hilar bile duct carcinoma: a histologic analysis of 62 resected cases. *Ann Surg* 1998; **227**: 405-411
- 4 D'Angelica MI, Jarnagin WR, Blumgart LH. Resectable hilar cholangiocarcinoma: surgical treatment and long-term outcome. *Surg Today* 2004; **34**: 885-890
- 5 Arcangeli G, Cividalli A, Nervi C, Creton G, Lovisolo G, Mauro F. Tumor control and therapeutic gain with different schedules of combined radiotherapy and local external hyperthermia in human cancer. *Int J Radiat Oncol Biol Phys* 1983; **9**: 1125-1134
- 6 Hiraoka M, Jo S, Akuta K, Nishimura Y, Takahashi M, Abe M. Radiofrequency capacitive hyperthermia for deep-seated tumors. II. Effects of thermoradiotherapy. *Cancer* 1987; **60**: 128-135
- 7 Appendix A Grading of toxicity. Manual of oncologic therapeutics. *Philadelphia: J.B. Lippincott* 1989
- 8 Okamoto A, Tsuruta K, Ishiwata J, Isawa T, Kamisawa T, Tanaka Y. Treatment of T3 and T4 carcinomas of the gallbladder. *Int Surg* 1996; **81**: 130-135
- 9 Arcangeli G, Casale C, Colistro F, Benassi M, Lovisolo G, Begnozzi L. One versus four heat treatments in combination with radiotherapy in metastatic mammary carcinoma. *Int J Radiat Oncol Biol Phys* 1991; **21**: 1569-1574
- 10 Kim JH, Hahn EW, Ahmed SA. Combination hyperthermia and radiation therapy for malignant melanoma. *Cancer* 1982; **50**: 478-482
- 11 Overgaard J. Effect of hyperthermia on malignant cells *in vivo*. A review and hypothesis. *Cancer* 1977; **37**: 2637-2648

- 12 **Song CW.** Effect of local hyperthermia and blood flow and microenvironment: a review. *Cancer Res* 1984; **44**(10 Suppl): 4721S-4730
- 13 **Lin JC, Levitt SH, Song CW.** Relationship between vascular thermotolerance and intratumor pH. *Int J Radiat Oncol Biol Phys* 1992; **22**: 123-129
- 14 **Perez CA, Gillespie B, Pajak T, Hornback NB, Emani B, Rubin P.** Quality assurance problems in clinical hyperthermia and their impact on therapeutic outcome: a report by the radiation therapy oncology group. *Int J Radiat Oncol Biol Phys* 1989; **16**: 551-558
- 15 **Harima Y, Nagata K, Harima K, Oka A, Ostapenko VV, Shikata N, Ohnishi T, Tanaka Y.** Bax and Bcl-2 protein expression following radiationtherapy versus radiation plus thermoradiotherapy in stage IIIB cervical carcinoma. *Cancer* 2000; **88**: 132-138
- 16 **Van der Zee J, Gonzalez Gonzalez D, van Rhoon GC, van Dijk JD, van Putten WL, Hart AA.** Comparison of radiotherapy plus hyperthermia in locally advanced pelvic tumors: a prospective randomized multicenter trial. Dutch Deep Hyperthermia Group. *Lancet* 2000; **335**: 1119-1125
- 17 **Sugimachi K, Matsuda H, Ohno S, Fukuda A, Matsuoka H, Mori M, Kuwano H.** Long term effects of hyperthermia combined with chemotherapy and irradiation of the treatment of patients with carcinoma of the esophagus. *Surg Gynecol Obstet* 1988; **167**: 319-323

Science Editor Guo SY Language Editor Elsevier HK

• CLINICAL RESEARCH •

Effect of itopride, a new prokinetic, in patients with mild GERD: A pilot study

Yong Sung Kim, Tae Hyeon Kim, Chang Soo Choi, Young Woo Shon, Sang Wook Kim, Geom Seog Seo, Yong Ho Nah, Myung Gyu Choi, Suck Chei Choi

Yong Sung Kim, Tae Hyeon Kim, Chang Soo Choi, Young Woo Shon, Geom Seog Seo, Yong Ho Nah, Suck Chei Choi, Department of Internal Medicine, School of Medicine, Wonkwang University and Digestive Disease Research Institute, Iksan, South Korea

Sang Wook Kim, Department of Internal Medicine, School of Medicine, Chonbuk National University, Jeonju, South Korea

Myung Gyu Choi, Department of Internal Medicine, School of Medicine, Catholic University, Seoul, South Korea

Supported by the 2004 Research Fund of Wonkwang University
Correspondence to: Dr. Suck Chei Choi, Department of Internal Medicine, School of Medicine, Wonkwang University, Iksan, South Korea. medcsc@wmc.wonkwang.ac.kr

Telephone: +82-63-850-1075 Fax: +82-63-854-7675

Received: 2004-09-29 Accepted: 2004-10-18

Abstract

AIM: Itopride is a newly developed prokinetic agent, which enhances gastric motility through both antidopaminergic and anti-acetylcholinesterasic actions. The importance of esophageal motor dysfunction in the pathogenesis of gastro-esophageal reflux disease (GERD) makes it interesting to examine the effect of itopride on esophageal acid exposure.

METHODS: The effect of itopride on esophageal acid reflux variables for 24 h was studied in 26 patients with GERD symptoms, pre-entry total acid exposure time (pH<4) of more than 5% and mild esophagitis (Savary-Miller grades I, II) proven by endoscopy. Ambulatory 24-h pH-metry and symptom assessment were performed after treatments with 150 or 300 mg itopride thrice a day (t.i.d.) for 30 d in random order, using an open label method. For evaluating the safety of itopride, blood biochemical laboratory test was performed and the serum prolactin level was also examined before and after treatment.

RESULTS: Total symptom score was significantly decreased after treatment in 150- or 300-mg group. Itopride 300 mg was significantly effective than 150 mg on decreasing the total per cent time with pH<4, total time with pH<4 and DeMeester score. No serious adverse effects were observed with administration of itopride in both groups.

CONCLUSION: Itopride 100 mg t.i.d. is effective on decreasing pathologic reflux in patient with GERD and therefore it has the potential to be effective in the treatment of this disease.

Key words: Gastro-esophageal reflux disease; Itopride

Kim YS, Kim TH, Choi CS, Shon YW, Kim SW, Seo GS, Nah YH, Choi MG, Choi SC. Effect of itopride, a new prokinetic, in patients with mild GERD: A pilot study. *World J Gastroenterol* 2005; 11(27): 4210-4214

<http://www.wjgnet.com/1007-9327/11/4210.asp>

INTRODUCTION

Gastro-esophageal reflux disease (GERD) is characterized by the reflux of gastric content into esophagus with or without histological changes. However, the excessive reflux of gastric acid induces some complications such as esophagitis, esophageal stenosis, cancer, or Barrett's esophagus. Pathogenesis of GERD are lower esophageal sphincter (LES) dysfunction, abnormal clearing capacity of refluxed materials, delayed gastric emptying and abnormal resistance of esophageal mucosa to gastric acid, but the primary motor dysfunction is regarded as the most important factor in general^[1,2]. Therefore, prokinetic agent that restores gastric motility with increasing of LES and esophageal motility has been developed and used frequently in the treatment of GERD^[3]. There are several prokinetic agents such as bethanechol, metoclopramide, domperidone, and cisapride that potentiate acetylcholine effects on smooth muscle of gastrointestinal tract or antagonize the activity of dopamine.

However, these prokinetic agents have some limitations for prescribing to GERD patients, because they show uncertain efficacies on GERD except for cisapride and have some problems in safety^[4,5]. Especially, cisapride accelerates the esophageal acid clearance by an enhancement of esophageal propulsive motility, which strengthens LES and stimulates the gastric emptying. So it is regarded that cisapride has the same efficacy as an inhibitor of gastric acid secretion for GERD. In spite of these predominant effects, cisapride is restricted to use because of a safety problem that it provokes arrhythmia.

Itopride, a new type of the prokinetic agent, acts both as a dopamine D₂ receptor antagonist and as an acetylcholine esterase inhibitor. It accelerates gastric emptying, improves gastric tension and sensitivity, and has an anti-emetic action. And also, itopride was identified to have equivalent efficacy with cisapride in functional dyspepsia. These mechanisms of itopride may be useful to GERD patients, but no clinical data are available from them as yet.

The aim of this pilot study is to evaluate the efficacy of

itopride for the treatment of GERD by evaluating the improvement of the clinical symptom and esophageal pH change.

MATERIALS AND METHODS

Study design

This study was performed prospectively to evaluate the efficacy and dose-response of itopride for the treatment of GERD by estimating ambulatory 24-h pH-metry and clinical symptoms before and after treatment. Patients satisfying the entry criteria were assigned to two groups by the randomization allocation schedule and received either 150 or 300 mg of itopride per day.

Inclusion/exclusion criteria

Twenty-six patients (range 18-65 years) who visited the Department of Internal Medicine in Wonkwang University and agreed to participate in this study were recruited based on the following entry criteria:

Inclusion criteria were (1) more than moderate heartburn symptom; (2) more than one upper dyspeptic symptoms such as regurgitation, epigastric pain, nausea, vomiting, dysphagia, chest pain lasting for more than 4 wk; (3) less than grade II esophagitis by Savary-Miller classification by endoscopic examination; (4) abnormal acid exposure on 24-h pH-metry (fraction of time of >5% with pH below 4).

For each symptom, the severity scores are as follows: 0 (none) = absent; 1 (mild) = symptom was not spontaneously reported but elicited upon specific questions; 2 (moderate) = symptom needs to be treated but not interfered with normal activities; 3 (severe) = symptom interfered with normal activities; 4 (very severe) = impossible to do normal activities due to symptom.

Exclusion criteria were the following: (1) acute esophagitis related to strong stimuli; (2) corrosive esophagitis by a toxicant; (3) esophagitis or some symptoms by inflammatory infection or radiotherapy; (4) regular use of H₂ blockers, prokinetic or anticholinergic agents for previous 4 wk; (5) previous gastrointestinal surgery; (6) inflammatory bowel disease; (7) cardiological, respiratory, gastrointestinal disease, endocrine metabolic disease and neuro-psychological disease; (8) clinically significant hepatic or renal dysfunction; (9) pregnancy or lack of adequate contraception in the case of women at child-bearing age; (10) patients who are inappropriate to this study by investigator's opinion.

Study procedures

This study was approved by the institutional review board of Wonkwang University Hospital and informed consent was obtained from patients for inclusion in this study. The patients were asked about basic information and previous treatment history. And they were screened as physical examination, vital sign and lab examination. Any drugs that could influence the study were postponed for at least 1 wk before that examination.

The baseline symptom of GERD was evaluated by questionnaire. Endoscopic examination was performed to check the organic lesion like cancer or ulcer, and to evaluate the severity of esophagitis. After examination, ambulatory

24-h pH-metry was carried out.

Patients who met the entry criteria were allocated randomly to 150- or 300-mg group of itopride. Fifty or 100 mg of itopride was administered thrice per day for 4 wk. After treatment of itopride for 4 wk, physical examination, vital sign, laboratory test, and symptoms of GERD were evaluated and ambulatory 24-h pH-metry was performed.

Efficacy parameters were (1) changes in acid reflux episodes measured by ambulatory pH-metry such as number of reflux episodes, number of reflux episodes lasting for more than 5 min, duration of longest episodes, % time with pH <4, and DeMeester score; (2) changes in subjective symptom of patient with GERD.

Safety parameters were (1) results of laboratory test (biochemistry, complete blood count, urinalysis and prolactin level); (2) occurrences of adverse events after the treatment. If adverse events occurred, the time of onset, duration, severity, relationship to itopride and the requirement of treatment were evaluated.

Statistical analysis

Two sample *t*-test and paired *t*-test were used for continuous variables presented as a normal distribution; Wilcoxon signed rank test and Wilcoxon rank sum test were used for those not presented as a normal distribution. And χ^2 test or Fisher's exact test was used for categorical variables. All data were statistically analyzed with SAS package (version 8.0) and differences with a value of $P < 0.05$ were considered significant.

RESULTS

Patients' characteristics

The mean age and body weight of patients in 150-mg group were 44±9 years and 64±11 kg, those of patients in 300-mg group were 45±12 years and 61±12 kg. Seven were men, six were women in 150-mg group and five were men, eight were women in 300-mg group.

Baseline characteristics of patients in two groups are detailed in Table 1 and no statistical differences were noted

Table 1 Clinical characteristics of patients

	150 mg	300 mg	P
Age (yr)	44±9	45±12	0.814 ¹
Sex	Male	7	0.734
	Female	6	
Weight	64±11	61±12	0.428 ¹
Duration of reflux disease	<6 mo	5	0.412
	6 mo-2 yr	6	
	>2 yr	2	
Pre-medication	Yes	2	0.828
	No	11	
Endoscopy (Savary-Miller grade)	0	5	0.717
	I	7	
	II	1	
Drinking	Yes	2	0.884
	No	11	
Smoking	Yes	3	1
	No	10	

¹P value by χ^2 test except for two sample *t*-test.

in the past history, smoking and drinking history and endoscopic results.

Efficacy of itopride on GERD symptoms

A significant improvement of all symptoms including heartburn, a main symptom of GERD, was identified after the 150 and 300 mg of itopride treatment compared with the pre-treatment (Figure 1A). No statistically significant differences were found between two groups in the symptom improvement (Figure 2B).

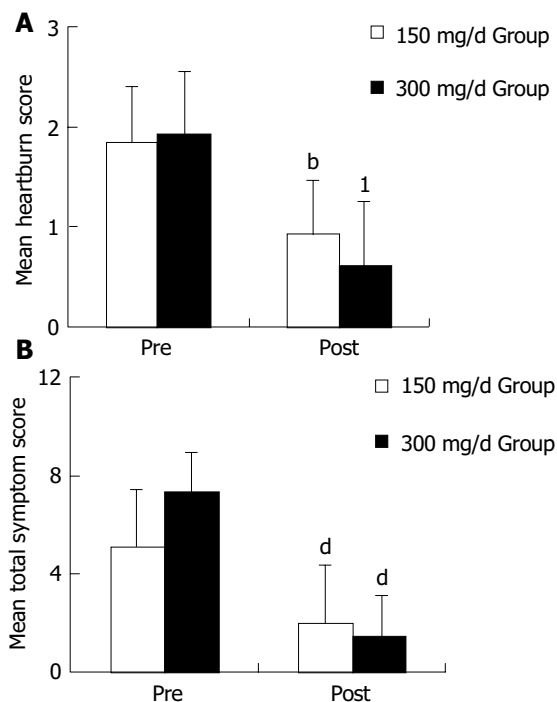


Figure 1 A: Change in mean heartburn score after treatment of itopride. The heartburn score of patients with GERD was improved in both groups of itopride significantly. ^b $P < 0.0001$, ¹ $P = 0.0006$ vs pretreatment by paired *t*-test; B: Change in mean total symptom score after treatment of itopride. The mean total symptom score of patients with GERD was improved in both groups of itopride significantly. ^d $P < 0.0001$ vs pretreatment by paired *t*-test.

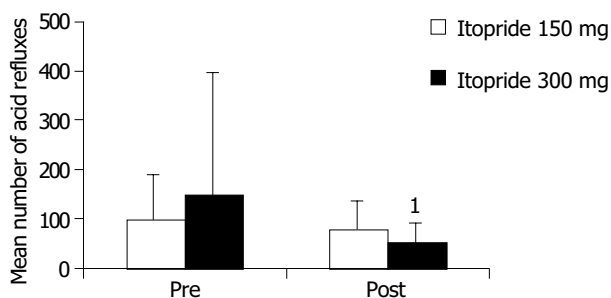


Figure 2 Change in mean number of acid refluxes after itopride treatment. Mean number of acid refluxes was significantly improved in 300-mg group. ¹ $P = 0.057$ vs pretreatment by Wilcoxon's signed rank test.

Efficacy of itopride on esophageal acid reflux variables

Among the acid reflux variables recorded, total time of

pH<4, per cent time with pH<4 and DeMeester score were significantly improved in 300-mg group compared with the pre-treatment (Figure 2). In 150-mg group, itopride significantly reduced the duration of longest episode compared with the pre-treatment. The individual values of acid reflux variable before and after treatment with 150 or 300 mg of itopride are given in Table 2.

Safety of itopride

Itopride was well tolerated and only minor adverse events were reported. There were no significant changes in the mean level of prolactin with the 4-wk treatment of 150- or 300-mg itopride (Figure 3). In two patients of the 300-mg group, prolactin level was increased over 15 ng/mL, but there were no adverse events like lacteal secretion.

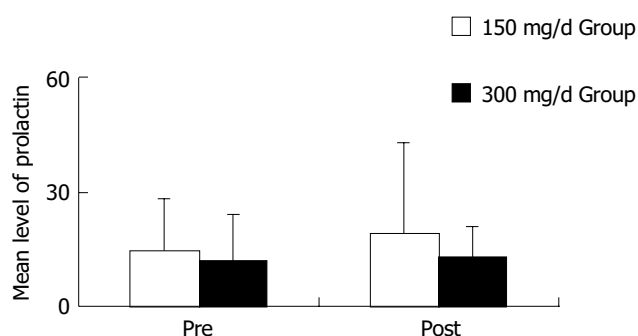


Figure 3 Change in mean level of prolactin after itopride treatment. The level of prolactin was not changed after treatment of itopride in GERD.

DISCUSSION

The result of this pilot study demonstrates that itopride decreases esophageal acid reflux and relieved symptoms without any significant adverse event in patients with GERD. These results show that itopride can improve the pathologic conditions of GERD.

The aims of treatment for GERD are relief of symptoms and healing of damaged lesion if endoscopic or pathologic examinations revealed mucosal damage of esophagus. Currently, it is being considered that long-term treatment is required because GERD has been regarded as chronic-relapsing disease like hypertension and diabetes mellitus^[12,13].

Among several therapeutic drugs, a prokinetic agent has been used for the treatment and improvement of pathogenic mechanism of GERD such as gastrointestinal motility disorder, incompetent LES relaxation, impaired esophageal acid clearance, and prolonged gastric emptying. Among the kinds of prokinetic drugs, many studies have focused on the effect of cisapride on GERD. In one of them, cisapride increased tones of esophageal peristalsis and LES dose-dependency in healthy subjects^[14,15]. On the contrary, in the other study, cisapride did not have any influence on the postprandial esophageal peristalsis, gastric acid^[16] and LES pressure^[17] in healthy subjects.

Even though this study does not confirm the efficacy of itopride on the esophageal peristalsis and LES, considering that itopride improves symptoms of the patients with GERD and decreases acid reflux effectively, we can speculate that

Table 2 Changes of acid reflux variables and DeMeester score in 26 patients with GERD after treatment with 150 or 300 mg of itopride

Variable	Group (mg/d)	Itopride Tx.	n	Mean	SD	P	
Number of acid refluxes	150	Pre	12	99.25	88.57	0.97	
		Post	12	76.92	60.53		
	300	Pre	13	150.77	246.15		0.057
		Post	13	52.23	39.79		
Number of acid refluxes longer than 5 min	150	Pre	12	6.08	5.32	0.287	
		Post	12	3.83	5.32		
	300	Pre	13	6.23	5.12		0.054
		Post	13	2.69	2.5		
Longest time acid refluxes (min)	150	Pre	12	30.55	33.37	0.018	
		Post	12	14.09	11.03		
	300	Pre	13	30.25	56.4		0.289
		Post	13	20.78	33.64		
Total time below pH 4 (min)	150	Pre	12	138.42	98.56	0.16	
		Post	12	92.09	78.07		
	300	Pre	13	145.08	86.1		0.011
		Post	13	71.77	51.43		
Fraction time below pH 4 (%)	150	Pre	12	11.13	9.26	0.211	
		Post	12	10.12	12.69		
	300	Pre	13	11.2	6.69		0.005
		Post	13	5.27	3.57		
DeMeester score	150	Pre	12	32.5	16.96	0.16	
		Post	12	22.89	18.75		
	300	Pre	13	44.48	37.5		0.007
		Post	13	19.56	14.72		

itopride exerts some effects on improving esophageal motor dysfunction. Further studies will be required for making out the effect of itopride on the esophageal motor dysfunction of GERD.

From the viewpoint of improving symptom and healing mucosa, it was observed that administration of cisapride 10 mg four times a day (q.i.d.) and 20 mg twice a day (b.i.d.) improved the esophageal reflux compared with placebo, and cisapride had the same effect as H₂ blocker on treatment of patients with mild esophagitis^[6,7]. Additionally, it was reported that a combination therapy with cisapride and H₂ blocker was more effective than monotherapy in patients with severe reflux esophagitis^[18].

Although a few studies on functional dyspepsia show that the efficacy of itopride was equivalent to that of cisapride^[11], this is the first study reporting that administration of itopride for 4 wk improves symptoms of GERD including heartburn (the main symptom of GERD) in both 150- and 300-mg group. So hereafter, additional studies will be required for evaluating the effect of itopride monotherapy or combination therapy with H₂ receptor inhibitors on the esophagitis with mucosal damage as the initial and maintenance treatment.

The most standard method to measure the variation of esophageal acid is ambulatory 24-h pH-metry. In other studies using a similar method, cisapride 10 mg q.i.d. for 8 wk was more effective than placebo in terms of decreasing the number of reflux episodes, duration of longest episode, and percent time with pH<4. These results suggest that cisapride is useful for acid reflux in patients with GERD^[19].

In the study of mosapride 40 mg every day (q.d.) for 2 d, it reduced the number of reflux episodes, the number of reflux episodes >5 min, and percent time with pH<4 and improved acid clearance time^[20]. In this study, itopride

100 mg t.i.d. for 4 wk was effective in decreasing percent time with pH <4 and DeMeester score. In this regard, it can be considered that itopride has a similar effect on decreasing acid reflux as cisapride or mosapride, although it is different in the action mechanism or duration of treatment from cisapride or mosapride^[9,10].

The action mechanism of itopride on the reflux variables is unclear so far. But, dual mechanism of itopride, acetylcholine esterase inhibitory action and antagonistic activity on dopamine D₂ receptor, which is known to inhibit activities of acetylcholine^[21], seems to make this drug effective on promoting the esophageal and gastrointestinal movement and on improving acid clearance. It has been known that the threshold of itopride to promote gastrointestinal motility is higher than that of cisapride, metoclopramide and domperidone^[8].

Prokinetic drugs that inhibit dopamine D₂ receptor may elicit some adverse events such as fatigue, confusion, extrapyramidal symptom, and hyperprolactinemia that cause lacteal secretion or breast enlargement. Although there was no extensive study concerned about safety of itopride, the development of extrapyramidal symptom or hyperprolactinemia was uncommon with the administration of usual dosage of itopride (150 mg/d). In this study, there was no hyperprolactinemia and extrapyramidal symptoms in 150-mg group of itopride and there were two cases showing over 15 ng/mL of prolactin level in 300-mg group of itopride without adverse events like lacteal secretion^[22].

Taken together, these results demonstrate that the administration of 150 or 300 mg of itopride for 4 wk improves symptoms of GERD and that the administration of 300 mg of itopride for 4 wk improves mild esophagitis and pathologic acid reflux. Therefore, itopride can be useful for treatment of the patients with GERD.

REFERENCES

- 1 **Lundell L**, Myers JC, Jamieson GG. Is motility impaired in the entire upper gastrointestinal tract in patients with gastro-oesophageal reflux disease? *Scand J Gastroenterol* 1996; **31**: 131-135
- 2 **Rydberg L**, Ruth M, Lundell L. Does oesophageal motor function improve with time after successful antireflux surgery? Results of a prospective, randomized clinical study. *Gut* 1997; **41**: 82-86
- 3 **Achem SR**, Robinson M. A prokinetic approach to treatment of gastroesophageal reflux disease. *Dig Dis* 1998; **16**: 38-46
- 4 **Ramirez B**, Richter JE. Review article: promotility drugs in the treatment of gastro-oesophageal reflux disease. *Aliment Pharmacol Ther* 1993; **7**: 5-20
- 5 **Kim YB**, Song CW, Kim HR, Lee SW, Bak YT, Hyun JH, Moon JS, Park HC. The incidence of gastroesophageal reflux disease and the effect of cisapride in patients with epigastric soreness. *Korean J Gastrointestinal Motility* 2000; **6**: 168-195
- 6 **Richter JE**, Long JF. Cisapride for gastroesophageal reflux disease: a placebo-controlled, double-blind study. *Am J Gastroenterol* 1995; **90**: 423-430
- 7 **Castell DO**, Sigmund C Jr, Patterson D, Lambert R, Hasner D, Clyde C, Zeldis JB. Cisapride 20 mg b.i.d. provides symptomatic relief of heartburn and related symptoms of chronic mild to moderate gastroesophageal reflux disease. CIS-USA-52 Investigator Group. *Am J Gastroenterol* 1998; **93**: 547-552
- 8 **Iwanaga Y**, Miyashita N, Morikawa K, Mizumoto A, Kondo Y, Itoh Z. A novel water-soluble dopamine-2 antagonist with anticholinesterase activity in gastrointestinal motor activity. Comparison with domperidone and neostigmine. *Gastroenterology* 1990; **99**: 401-408
- 9 **Iwanaga Y**, Miyashita N, Mizutani F, Morikawa K, Kato H, Ito Y, Itoh Z. Stimulatory effect of N-[4-[2-(dimethylamino)ethoxy] benzyl]-3,4-dimethoxybenzamide hydrochloride (HSR-803) on normal and delayed gastrointestinal propulsion. *Jpn J Pharmacol* 1991; **56**: 261-269
- 10 **Choi MG**, Choo KY, Kim BW, Choi H, Park SH, Oh JH, Han SW, Kim JK, Chung IS, Chung KW, Sun HS. The effect of itopride on proximal gastric tone and visceral perception in healthy human. *Kor J Gastroenterol* 2000; **36**: 293-301
- 11 **Kim JK**, Moon SB, Choi H, Kim SW, Chung KW, Sun HS, Lee HY, Hong SS. An effectiveness and safety of Itopride versus Cisapride in functional dyspepsia. *Kor J Gastroenterol* 1999; **33**: 749-756
- 12 **DeVault KR**. Overview of medical therapy for gastroesophageal reflux disease. *Gastroenterol Clin North Am* 1999; **28**: 831-845
- 13 **DeVault KR**, Castell DO. Updated guidelines for the diagnosis and treatment of gastroesophageal reflux disease. The Practice Parameters Committee of the American College of Gastroenterology. *Am J Gastroenterol* 1999; **94**: 1434-1442
- 14 **Gilbert RJ**, Dodds WJ, Kahrilas PJ, Hogan WJ, Lipman S. Effect of cisapride, a new prokinetic agent, on esophageal motor function. *Dig Dis Sci* 1987; **32**: 1331-1336
- 15 **Ceccatelli P**, Janssens J, Vantrappen G, Cucchiara S. Cisapride restores the decreased lower oesophageal sphincter pressure in reflux patients. *Gut* 1988; **29**: 631-635
- 16 **Wallin L**, Kruse-Andersen S, Madsen T, Boesby S. Effect of cisapride on the gastro-oesophageal function in normal human subjects. *Digestion* 1987; **37**: 160-165
- 17 **Holloway RH**, Downton J, Mitchell B, Dent J. Effect of cisapride on postprandial gastro-oesophageal reflux. *Gut* 1989; **30**: 1187-1193
- 18 **Galmiche JP**, Brandstatter G, Evreux M, Hentschel E, Kerstan E, Kratochvil P, Reichel W, Schutze K, Soule JC, Vitaux J. Combined therapy with cisapride and cimetidine in severe reflux oesophagitis: a double blind controlled trial. *Gut* 1988; **29**: 675-681
- 19 **Nah YH**, Song JH. Effect of Cisapride on ambulatory 24 - hour esophageal pH profile in gastroesophageal reflux disease. *Kor J Gastroenterol* 1990; **22**: 515-521
- 20 **Ruth M**, Hamelin B, Rohss K, Lundell L. The effect of mosapride, a novel prokinetic, on acid reflux variables in patients with gastro-oesophageal reflux disease. *Aliment Pharmacol Ther* 1998; **12**: 35-40
- 21 **Glavin GB**, Szabo S. Dopamine in gastrointestinal disease. *Dig Dis Sci* 1990; **35**: 1153-1161
- 22 **Perkel MS**, Hersh T, Moore C, Davidson ED. Metoclopramide therapy in fifty-five patients with delayed gastric emptying. *Am J Gastroenterol* 1980; **74**: 231-236

Science Editor Guo SY Language Editor Elsevier HK

• CLINICAL RESEARCH •

Clinical analysis of multiple primary malignancies in the digestive system: A hospital-based study

Hui-Yun Cheng, Cheng-Hsin Chu, Wen-Hsiung Chang, Tzu-Chi Hsu, Shee-Chan Lin, Chuan-Chuan Liu, An-Ming Yang, Shou-Chuan Shih

Hui-Yun Cheng, Chuan-Chuan Liu, An-Ming Yang, Shou-Chuan Shih, Health Evaluation Center, Mackay Memorial Hospital, Taipei, Taiwan, China

Hui-Yun Cheng, Cheng-Hsin Chu, Wen-Hsiung Chang, Shee-Chan Lin, An-Ming Yang, Shou-Chuan Shih, Department of Internal Medicine, Mackay Memorial Hospital, Taipei, Taiwan, China
Tzu-Chi Hsu, Department of Surgery, Mackay Memorial Hospital, Taipei, Taiwan, China

Cheng-Hsin Chu, Shou-Chuan Shih, Mackay Medicine, Nursing and Management College, Taipei, Taiwan, China

Correspondence to: Dr. Shou-Chuan Shih, Department of Internal Medicine, Mackay Memorial Hospital, No. 92, Section 2, Chung Shan North Road, Taipei, Taiwan, China. hychey@msl.mmh.org.tw
Telephone: +886-2-25433535-2860

Received: 2004-11-05 Accepted: 2004-12-08

lesions, based on an awareness of the possibility of second and third cancers, and multidisciplinary treatment strategies will substantially increase the survival of these patients.

© 2005 The WJG Press and Elsevier Inc. All rights reserved.

Key words: Multiple primary malignancies; Digestive system

Cheng HY, Chu CH, Chang WH, Hsu TC, Lin SC, Liu CC, Yang AM, Shih SC. Clinical analysis of multiple primary malignancies in the digestive system: A hospital-based study. *World J Gastroenterol* 2005; 11(27): 4215-4219
<http://www.wjgnet.com/1007-9327/11/4215.asp>

Abstract

AIM: To analyze the characteristics of multiple primary malignancies (MPMs) of digestive system; including incidence, types of tumor combinations, time intervals between development of multiple tumors, clinical course, and prognostic factors affecting survival and mortality.

METHODS: Data from a total of 129 patients treated from January 1991 to December 2000 for pathologically proved MPMs, including at least one originating from the digestive system, were reviewed retrospectively.

RESULTS: Among 129 patients, 120 (93.02%) had two primary cancers and 9 (6.98%) had three primary cancers. The major sites of MPMs of the digestive system were large intestine, stomach, and liver. Associated non-digestive cancers included 40 cases of gynecological cancers, of which 31 were carcinoma of cervix and 10 cases of genitourinary cancers, of which 5 were bladder cancers. Other cancers originated from the lung, breast, nasopharynx, larynx, thyroid, brain, muscle, and skin. Reproductive tract cancers, especially cervical, ovarian, bladder, and prostate cancers were the most commonly associated non-GI cancers, followed by cancer of the lung and breasts. Forty-three cases were synchronous, while the rest (86 cases) were metachronous cancers. Staging of MPMs and treatment regimes correlated with the prognosis between survival and non-survival groups.

CONCLUSION: As advances in cancer therapy bring about a progressively larger percentage of long-term survivors, the proportion of patients with subsequent primary lesions will increase. Early diagnosis of these

INTRODUCTION

Many types of cancer, when treated early and aggressively, can be cured. The potential, however, for cancer to occur independently a second time, or more often, in the same patients remains an ever present risk. Interest in multiple primary malignancies (MPMs) is long-standing since Warren and Gates in 1932. He proposed that each suspected primary tumor (1) must be clearly malignant as determined by histological evaluation; (2) must be geographically separate and distinct. The lesion should be separated by normal appearing mucosa. If a secondary neoplasm is contiguous to the initial primary tumor or is separated by mucosa with intraepithelial neoplastic changes, the two should be considered as confluent growth rather than multi-centric carcinomas; and (3) the possibility that the second neoplasm represents a metastasis should be excluded. The observation that the invasive carcinoma arises from an overlying epithelium, which demonstrates a transition from carcinoma *in situ* to invasive carcinoma, is helpful, and when the separate foci have significant differences in histology, the diagnosis of separate primary cancers is appropriate^[1,2].

Multiple primary cancers may be synchronous or metachronous depending on the interval between their diagnosis. Synchronous cancers are diagnosed simultaneously or within an interval of about 6 mo, and metachronous cancers are secondary cancers that developed more than 6 mo after the diagnosis of primary cancers usually after treatment of primary lesions^[2].

MPMs were classified into four types: (1) multicentric, if the two distinct carcinomata arise in the same organ or tissue; (2) systemic, if they arise on anatomically or

functionally allied organs of the same system (colon and rectum cancers), (3) paired organs, as in the breasts, and (4) random, if they occur as a co-incident or accidental association in unrelated sites^[3].

The development of more sophisticated invasive and non-invasive diagnostic tools has made it possible to detect cancer at an early stage. Furthermore, it has contributed to the detection of synchronous occult tumors, which were formerly overlooked.

An individual developing more than one primary tumor in anatomically and functionally unrelated organs may be considered as cancer-prone. People with a family history of cancer will inherit genetic cancer susceptibility as a risk factor for cancer. Gene mutations influence cancer susceptibility through changes of metabolism and catabolism of carcinogens. Tumor suppressor genes, such as *p53* and *FHIT*, may be candidates for target genes of these risk factors^[4]. Genetic instability is also considered as a driving force behind carcinogenesis and the alterations of the length of single repetitive genomic sequences or microsatellite instability, implicating impaired DNA repair mechanism^[5]. People with newly diagnosed cancers and survivors of earlier cancers who have genetic cancer susceptibility, therefore, have an increased risk of MPMs.

This study has analyzed the incidence of MPMs in digestive system, as well as the different tumor combinations, time interval between occurrence of tumors, staging, clinical course, and prognostic features of survival and non-survival groups.

The purpose of this study is to determine whether certain organs or systems are particularly susceptible to second or third primary cancers and, by clarifying this tendency, to aid in the early diagnosis of these lesions.

MATERIALS AND METHODS

Retrospective data from a total of 9 807 patients treated at the Mackay Memorial Hospital from January 1991 to December 2000 for pathologically proven cancer were reviewed from the Cancer Registry. Of these, 246 patients had multiple primary cancers, among which 129 (58 males and 71 females) had MPMs in the digestive system and were included in this study.

The histological criteria described by Warren and Gates^[1] and Moertel *et al.*^[3], were used for diagnosing multiple separate primary malignancies.

Clinical histories, diagnostic methods, histology, staging, and clinical course of each tumor were reviewed in all patients. The age at the onset of the primary cancer and the time intervals between two or more cancers were recorded. The distribution of the digestive and associated non-digestive cancers in these 129 patients was also investigated. Fifty-two patients had received previous radiotherapy or chemotherapy for their first cancers, and interval between the first and second cancers were recorded. All tumors had been staged according to the American Joint Committee on Cancer TNM staging system^[6]. The prognostic factors between survival and non-survival groups were analyzed for double primary cancers.

The differences between groups were analyzed by Student's *t*-test for continuous variables and the χ^2 test for

categorical data. A *P* value of <0.05 was considered as statistical significance.

RESULTS

Among the 9 807 pathologically proven cancer patients, 246 had MPMs, with an incidence of 2.5%. Among these, 129 (52.43%), including 58 males (44.96%) and 71 females (55.04%), had MPMs of the digestive system. One hundred and twenty patients (93.02%) had two primary malignancies, and nine (6.98%) had three primary malignancies. The age at onset of the primary cancers ranged from 29 to 89 years (mean 60.3 ± 13.05 years) in double cancers, and 43 to 68 years (mean 50.22 ± 7.9 years) in triple cancers. Forty-three patients (35.8%) were over 65 years of age. Fifty-two patients (40.3%) had received previous radiotherapy or chemotherapy for their first cancer. The interval between the first and second cancers was 0.5-28 years (mean 8.1 ± 2.5 years) and 0.5-5 years (mean 3.2 ± 3.7 years) in the 32 patients receiving radiotherapy and the 17 patients receiving chemotherapy respectively.

The distribution and incidence of MPMs of the digestive system are shown in Table 1. The major site for MPMs of the digestive system was the large intestine (colon, 23.17%; rectum, 25.82%), followed by the stomach (23.17%) and liver (15.23%).

Distributions of associated non-digestive cancers in patients with MPMs are shown in Table 2. There were

Table 1 Distribution of MPMs in digestive tract

Site	Number of MPMs	Total number	Incidence (%)	% in GI MPMs
Esophagus	8	374	2.14	5.29
Stomach	35	1 770	1.98	23.17
Small bowel	3	76	3.95	1.98
Ampulla Vater	3	76	3.95	1.98
Liver	23	2 081	1.11	15.23
Gall bladder	2	58	3.45	1.32
Pancreas	3	303	0.99	1.98
Colon	35	1 010	3.47	23.17
Rectum	39	1 059	3.68	25.82

From January 1991 to December 2000.

Table 2 Distribution of associated non-GI cancers in patients with MPMs in digestive system

Site	<i>n</i> (%)	%
Gynecological cancers	40	45.97
Cervix	31/40 (77.50)	
Endometrium	2/40 (5)	
Ovary	7/40 (17.50)	
Genitourinary cancers	10	11.49
Bladder	5/10 (50)	
Kidney	2/10 (20)	
Prostate	3/10 (30)	
Lung	10	11.49
NPC	5	5.74
Breast	10	11.49
Skin	4	4.59
Thyroid gland	2	2.29
Neuromuscular tumor	2	2.29
Tongue	2	2.29
Gum	1	1.14
Brain	1	1.14

40 cases (45.97%) with gynecological cancers, of which 31 cases (77.5%) were carcinoma of uterine cervix; 10 cases (11.49%) with genitourinary cancer, among which 5 (50%) had bladder cancers and 3 (30%) had prostate cancers.

The most common tumor combination in double primary malignancies (both cancers originating from the digestive tract) was colon and rectum (10 cases), as shown in Tables 5-8.

The most common tumor combination in double primary malignancies (at least one originating from the digestive system) was rectum and cervical cancer (14 cases) and shown in Table 4.

Nine patients had triple cancers (Table 9). Mean time interval between diagnosis of the first and second primary cancer was 7.2 ± 3.86 years and for the second and third cancer was 5.24 ± 3.85 years. Two out of these nine patients had initial squamous cell cancers of cervix and nasopharynx

Table 3 Distribution of synchronous and metachronous MPMs in digestive system

Site	Synchronous (n)	Metachronous (n)	
		(1)	(2)
Colon ¹	13	10	19
Stomach ¹	8	3	11
Liver ¹	6	1	7
Esophagus ¹	0	1	1
Others ¹	0	2	1
Double GI	16	30	0
Total	43	47	39

¹Exclude double GI cases. (1): Primary GI tract cancer, secondary cancers of other sites. (2): Primary cancers of other sites, secondary GI tract cancers.

Table 4 Distribution of MPMs in large intestine: 42 cases¹

Subgroup	Large intestine	n	Non-GI cancers	n
(1)	Colon	5	Cervix	1
			Larynx	1
			Lung	1
			Uterus	1
			Left breast	1
	Rectum	5	Ovary	1
			Cervix	2
			Right breast	1
			Bladder	1
			Bladder	1
(2)	Colon	7	Cervix	2
			Ovary	1
			Thyroid	1
			Right thigh	1
			Bladder	1
	Rectum	12	Nose	1
			Cervix	9
			Right breast	1
			Thyroid	1
			Brain	1
(3)	Colon	7	Cervix	3
			Ovary	4
			Cervix	3
	Rectum	6	Left breast	1
			Lung	2
			Lung	2

¹Excluding double primary GI tract cancers (22 cases). (1): Primary GI tract cancer, secondary cancers of other sites. (2): Primary cancers of other sites, secondary GI tract cancers. (3): Synchronous.

and developed synchronous adenocarcinoma of rectum and colon, with disease intervals of 9.4 and 5.9 years respectively.

Most of the tumors in double or triple primary malignancies were diagnosed at stages 3 or 4. Synchronous cancers were found in 43 cases, while 86 cases had metachronous cancers, among which 13 cases developed secondary cancers more than 10 years after diagnosis of primary malignancies (Tables 3 and 10).

There were no significant differences between the survival and non-survival groups in terms of age, gender, and time interval between first and second primary cancers. However, stage of tumor, especially stages 1-3 and radical treatment regimes correlated with prognosis in these two groups.

Table 5 Distribution of MPMs in stomach: 22 cases¹

Subgroup	Stomach	n	Non-GI cancers	n
(1)	Adenocarcinoma	3	Right breast	2
			NPC	1
(2)	Adenocarcinoma	11	Cervix	4
			Prostate	2
			Bladder	1
			Left kidney	1
			Tongue	1
			Larynx	1
			NPC	1
(3)	Adenocarcinoma	8	NPC	2
			Lung	3
			Prostate	1
			Bladder	1
			Skull	1

¹Exclude double GI cases (12 cases). (1): Primary GI tract cancer, secondary cancers of other sites. (2): Primary cancers of other sites, secondary GI tract cancers. (3): Synchronous.

Table 6 Distribution of MPMs in liver: 14 cases¹

Subgroup	Liver	n	Non-GI cancers	n
(1)	Hepatoma	1	Bladder	1
(2)	Hepatoma	7	Cervix	4
			Right breast	2
			Right leg	1
(3)	Hepatoma	6	Gum	1
			Skull	1
			Right kidney	1
			Lung	3

¹Exclude double GI cases (10 cases). (1): Primary GI cancer, secondary cancers of other sites. (2): Primary cancers of other sites, secondary GI cancers. (3): Synchronous.

Table 7 Distribution of synchronous double GI MPMs: 16 cases

Site	n	Site	n
Esophagus	2	Stomach	1
		Gall bladder	1
Stomach	3	Rectum	1
		Gall bladder	1
		Sigmoid colon	1
Duodenum	1	Sigmoid colon	1
Sigmoid colon	3	Appendix	1
		Rectum	2
		Ascending colon	3
Rectum	3	Hepatic flexure	1
		Stomach	3
Liver	4	Hepatic flexure	1
		Stomach	3

Table 8 Distribution of metachronous double GI MPMs: 30 cases

1 st cancer	n	2 nd cancer	n
Esophagus	3	Stomach	1
		Liver	2
Stomach	4	Rectum	1
		Esophagus	1
		Liver	1
		Pancreatic head	1
		Liver	1
GIST of ileum	1	Liver	1
Ampulla Vater	2	Liver	2
Appendix	2	Rectum	2
Cecum	2	Stomach	2
Colon	6	Liver	2
		Stomach	1
Rectum	10	Pancreatic head	3
		Stomach	1
		Liver	1
		Transverse colon	5
		Esophagus	3

Table 9 Sites and dates of diagnosis of triple primary cancers (nine cases)

Age (yr)/sex	First primary	Second primary	Third primary
68/Female	3/84 Cervix	6/93 Rectum	6/93 Sigmoid colon
46/Female	9/85 Cervix	8/88 Rectum	8/95 Ascending colon
49/Female	8/84 Ovary	10/86 Cervix	3/90 Rectum
47/Female	8/79 Breast	9/89 Cervix	10/97 Liver
50/Male	6/82 Stomach	5/85 Skin	4/91 Ascending colon
45/Male	8/84 Stomach	3/86 Prostate	1/92 Ascending colon
43/Male	3/89 Nasopharynx	2/95 Sigmoid colon	2/95 Rectum
46/Female	1/84 Larynx	4/88 Sigmoid colon	3/91 Esophagus
58/Female	3/71 Right breast	6/82 Sigmoid colon	6/92 Ascending colon

The age listed is that at the time of diagnosis of the first primary.

Table 10 Demographic and clinical data in survival and non-survival groups¹

	Survival n = 40	Non-survival n = 80	P
Median age (yr)	61.50±13.60 (29-84)	60.00±14.78 (30-89)	0.46
Gender			
Male	16	39	0.18
Female	24	41	0.18
Time interval (mo)	32.78±27.07	32.98±18.58	0.49
Staging			
Stage 1	14	2	<0.01 ^b
Stage 2	19	2	<0.01 ^b
Stage 3	6	41	0.04 ^a
Stage 4	1	35	0.16
Treatment regimes ²			
Radical	36	16	<0.01 ^b
Palliative	2	36	0.08
Supportive	2	28	0.08

¹Excluding triple primary cancers nine cases. ²Radical treatment includes radical surgery±radiotherapy±chemotherapy. Palliative treatment includes palliative surgery±radiotherapy±chemotherapy. ^aP<0.05, ^bP<0.01 vs others.

DISCUSSION

The presence of a single tumor does not offer immunity against the development of second, third, or additional

primary malignant lesions in the same patient. Multiple primary malignant tumors in the same individual are experienced more frequently as advances in cancer treatment prolong life. Improved survival rates for patients with neoplastic disease, largely due to early diagnosis, allow more patients to survive long enough to develop subsequent primary tumors.

The incidence of MPMs has been carried out by the review of cancer registries in several countries, and ranged from 0.7 to 11%^[7-10]. In our study, the incidence of MPMs was 2.21%, which was similar to the 2.6% as reported by Okamoto *et al.*^[11].

In our study, the major site of MPMs in the digestive system was the large intestine, followed by stomach and liver. Cancers of the large intestine, particularly hereditary nonpolyposis colorectal cancers, were associated with increased frequencies of endometrial and ovarian cancers^[12]. However, MPMs of large intestine in our study were most commonly associated with carcinoma of cervix (17 cases) and stomach (8 cases), while only two were associated with carcinoma of endometrium and six were with ovarian cancers. The significance of these differences may be due to the fact that carcinoma of cervix is much more common than endometrial cancer in our country. Unfortunately, no genetic evaluation was performed in our patients.

The predilection of MPMs for the large intestine is noted in numerous reports in the literatures^[13-15]. In our series, 49 of 129 patients (37.98%) had colorectal malignancy as the first primary lesion. Of these, seven (14.28%) had a second primary cancer in the colon or rectum and four (8.16%) had a second primary cancer in the stomach. The interval between the diagnosis of the first primary colorectal cancer and the development of the second colorectal carcinoma averaged 7 years, and ranged from 1½ to 14 years. This suggests that patients without evidence of disease for 5 years after operation of colorectal cancers still require careful follow-up studies of gastrointestinal tract.

Genitourinary cancers, especially cervical and ovarian cancers, bladder and prostate cancers were the common associated non-GI cancers, followed by cancers of lung and breast. Thus, attention should be paid to these sites during the period of post-operative follow-up of the first primary cancer.

The majority of MPMs may occur as a result of random chance^[16]. Nonetheless, different mechanisms have been considered to be involved in MPMs, such as intense exposure to carcinogens, the effects of chemo- and/or radiotherapy and the influence of genetic predisposition.

Both the chemo- and radiotherapy have been shown to be carcinogenic in several reports^[17,18]. In our study, 52 patients (40.3%) had received previous radiotherapy or chemotherapy for their first cancer, and the interval between the first and second cancers was 0.5-28 years (mean 8.1 years) and 0.5-5 years (mean 3.2 years) in the 32 patients receiving radiotherapy and the 20 patients receiving chemotherapy respectively. This suggests that radiotherapy and/or chemotherapy may play an important role in the development of MPMs.

The main problem in proving a correlation between antineoplastic therapies and secondary cancer may be

attributable to detection bias rather than to carcinogenic therapy^[19]. Beyond an increased zeal in searching, diagnostic agents and methods have improved such that the detection of cancer today is enhanced by improvements in technology, cytogenetics, and surveillance.

Based on a pooled analysis involving 316 relatives of 12 families, Lynch *et al.*^[20], have demonstrated a 21.5% incidence of MPMs, a consistent 3% risk for a second primary cancer in each year of survival following the first onset, and a significantly higher 6.9% risk per year for the development of a third primary cancer following the second neoplasm.

In our study, there were no significant differences between the survival and non-survival groups in terms of age, gender, and time intervals between first and second primary cancers. Only stage of tumors, especially stages 1-3, and radical treatment regimes correlated with prognosis in these two groups.

Two important inferences can be obtained from our analysis: (1) the early diagnosis of a second primary lesion may alter survival rate. Hence more intensive surveillance and appropriate cytogenetic and molecular studies should be developed in order to improve strategies to detect MPMs, and (2) multidisciplinary treatment strategies are important to ameliorate quality of life and survival rates in patients with MPMs.

It is fundamental that patients who have been treated for cancers require careful follow-up studies. When symptoms and signs of tumor develop in a patient who has been treated for an initial cancer, they should not be assumed to represent metastases. The possibility of a localized and curable second primary cancer should be considered and evaluated. As advances in cancer therapy bring about a progressively large percentage of long-term survivors, the proportion of patients with subsequent primary lesions will increase. Early diagnosis of these lesions, based on an awareness of the possibility of second and third cancers, and multidisciplinary treatment will substantially increase the survival of these patients.

REFERENCES

- 1 Warren S, Gates O. Multiple primary malignant tumors: A survey of the literature and statistical study. *Am J Cancer* 1932; **16**: 1358-1414
- 2 Kapsinow R. Multiple primary cancer. A classification with report of cases. *J La State Med Soc* 1962; **114**: 194-200
- 3 Moertel CG, Dockerty MB, Baggenstoss AH. Multiple primary malignant neoplasms. II. Tumors of different tissues or organs. *Cancer* 1961; **14**: 231-237
- 4 Morita M, Saeki H, Mori M, Kuwano H, Sugimachi K. Risk factors for esophageal cancer and the multiple occurrence of carcinoma in the upper aerodigestive tract. *Surgery* 2002; **131** (1 Suppl): S1-6
- 5 Sardi I, Franchi A, Bocciolini C, Mechi C, Frittelli A, Bruschini L, Gallo O. Microsatellite instability as biomarker for risk of multiple primary malignancies of the upper aerodigestive tract. *Oncol Rep* 2001; **8**: 393-399
- 6 American Joint Committee on Cancer. Manual for staging cancer. 4th ed. Philadelphia: *JB Lippincott* 1992: 75-82
- 7 Coleman MP. Multiple primary malignant neoplasms in England and Wales, 1971-1981. *Yale J Biol Med* 1986; **59**: 517-531
- 8 Levi F, Randimbson L, Te VC, Rolland-Portal I, Franceschi S, La Vecchia C. Multiple primary cancers in the Vaud Cancer Registry, Switzerland, 1974-89. *Br J Cancer* 1993; **67**: 391-395
- 9 Tsukuma H, Fujimoto I, Hanai A, Hiyama T, Kitagawa T, Kinoshita N. Incidence of second primary cancers in Osaka residents, Japan, with special reference to cumulative and relative risks. *Jpn J Cancer Res* 1994; **85**: 339-345
- 10 Frodin JE, Ericsson J, Barlow L. Multiple primary malignant tumors in a national cancer registry-reliability of reporting. *Acta Oncol* 1997; **36**: 465-469
- 11 Okamoto N, Morio S, Inoue R, Akiyama K. The risk of a second primary cancer occurring in five-year-survivors of an initial cancer. *Jpn J Clin Oncol* 1987; **17**: 205-213
- 12 Watson P, Lynch HT. Extracolonic cancer in hereditary nonpolyposis colorectal cancer. *Cancer* 1993; **71**: 677-685
- 13 Rosenthal I, Baronofsky ID. Prognostic and therapeutic implications of polyps in metachronous colic carcinoma. *JAMA* 1960; **172**: 37-41
- 14 Polk HC Jr, Spratt JS Jr, Butcher HR Jr. Frequency of multiple primary malignant neoplasms associated with colorectal carcinoma. *Am J Surg* 1965; **109**: 71-75
- 15 Bachulis BL, Williams RD. Multiple primary malignancies. *Arch Surg* 1966; **92**: 537-540
- 16 Robinson E, Neugut AI. Clinical aspects of multiple primary neoplasms. *Cancer Detect Prev* 1989; **13**: 287-292
- 17 Brumback RA, Gerber JE, Hicks DG, Strauchen JA. Adenocarcinoma of stomach following irradiation and chemotherapy for lymphoma in young patients. *Cancer* 1984; **54**: 994-998
- 18 Sandler RS, Sandler DP. Radiation-induced cancers of the colon and rectum: assessing the risk. *Gastroenterology* 1983; **84**: 51-57
- 19 Craig SL, Feinstein AR. Antecedent therapy versus detection bias as causes of neoplastic multimorbidity. *Am J Clin Oncol* 1999; **22**: 51-56
- 20 Lynch HT, Harris RE, Lynch PM, Guirgis HA, Lynch JF, Bardawil WA. Role of heredity in multiple primary cancer. *Cancer* 1977; **40**(4 Suppl): 1849-1854

• CLINICAL RESEARCH •

Surgical experience in splitting donor liver into left lateral and right extended lobes

Ji-Qi Yan, Thomas Becker, Michael Neipp, Cheng-Hong Peng, Rainer Lueck, Frank Lehner, Hong-Wei Li, Juergen Klempnauer

Ji-Qi Yan, Cheng-Hong Peng, Hong-Wei Li, Department of Surgery, Ruijin Hospital Affiliated to Shanghai Second Medical University, Shanghai 200025, China

Ji-Qi Yan, Thomas Becker, Michael Neipp, Rainer Lueck, Frank Lehner, Juergen Klempnauer, Department of Abdominal and Transplant Surgery, Medical School of Hannover, Carl-Neuberg-Str. 1, Hannover 30625, Germany

Supported by the DAAD Foundation

Correspondence to: Ji-Qi Yan, MD, Department of Surgery, Ruijin Hospital Affiliated to Shanghai Second Medical University, Shanghai 200025, China. jiqiyan@yahoo.com

Telephone: +86-21-64370045 Fax: +86-21-64333548

Received: 2004-10-09 Accepted: 2004-11-19

Yan JQ, Becker T, Neipp M, Peng CH, Lueck R, Lehner F, Li HW, Klempnauer J. Surgical experience in splitting donor liver into left lateral and right extended lobes. *World J Gastroenterol* 2005; 11(27): 4220-4224

<http://www.wjgnet.com/1007-9327/11/4220.asp>

Abstract

AIM: To outline the surgical experience with donor liver splitting in split liver transplantation.

METHODS: From March 1 to September 1 in 2004, 10 donor livers were split *ex situ* into a left lateral lobe (segments II and III) and a right extended lobe (segments I, IV-VIII) in Medical School of Hannover, and thereafter split liver transplantation was performed successfully in 19 cases. The average age, weight and ICU staying period of the donors were 32.7 years (15-51 years), 64.5 kg (45-75 kg) and 2.4 d (1-8 d) respectively.

RESULTS: The average weight of the whole graft and the left lateral lobe was 1 322.6 g (956-1 665 g) and 281.8 g (198-373 g) respectively, and the average ratio of left lateral lobe to the whole graft was 0.215 (0.178-0.274). The average graft to recipient weight ratio (GRWR) of the left lateral lobe and the right extended lobe reached 2.44% (1.22-5.41%) and 1.73% (1.31-2.30%) respectively. On average it took approximately 105 min (85-135 min) to split the donor liver. Five donor organs showed anatomic variation including the left hepatic vein variation in two cases, the left hepatic artery variation in two cases and the bile duct variation in one case.

CONCLUSION: Split liver transplantation has become a mature surgical technique to expand the donor pool with promising results. In the process of graft splitting, close attention needs to be paid to potential anatomic variations, especially to variations of the left hepatic vein, the left hepatic artery, and the bile duct.

© 2005 The WJG Press and Elsevier Inc. All rights reserved.

Key words: Split; Donor liver; Anatomic variation

INTRODUCTION

Orthotopic liver transplantation (OLT) has been widely accepted as an effective treatment for end-stage liver diseases. The advent of new immunosuppressive agents and refinement of the surgical techniques have accounted for remarkable progress in the years since the first OLT was performed in 1963. Thousands of patients who would have died otherwise have been saved by the improved results of organ transplantation. However, the past two decades have also witnessed an exceptional increase in the number of patients awaiting liver transplantation, and the ever-growing great disparity between demand and supply of donor organs has become the major limiting factor for further expansion of liver transplantation. Hence, a death rate on the waiting of 10-15% would even be underestimated^[1]. Historically, the situation has been worse for children because of the difficulty of finding size-matched donor organs^[2]. However, the development of a reduced-size liver transplant technique has provided a first step to alleviate this problem^[3-5]. Although such technique does not increase the number of grafts available, it shifts available organs from adult to pediatric recipient. Obviously, split liver transplantation, first successfully performed in the Medical School of Hannover^[6], is becoming an efficient approach to expand the donor pool for both adults and children.

MATERIALS AND METHODS

From March 1 to September 1 in 2004, a total of 10 donor livers were split *ex situ* in Medical School of Hannover. All these donor livers were divided into a left lateral lobe (segments II and III) and a right extended lobe (segments I, IV-VIII), and thus making available split liver transplantation to 19 patients (in 6 cases the right extended lobe was sent to another transplantation center). The average age and weight of those 10 brain death donors were 32.7 years (15-51 years) and 64.5 kg (45-75 kg) respectively. Before the organ procurement, the average ICU stay of the donors was 2.4 d (1-8 d), and the average serum level of AST, creatinine, sodium and total bilirubin was 53.0 IU/L (14-122 IU/L), 0.91 mg/dL (0.40-1.25 mg/dL), 148.5 mmol/L (137-158 mmol/L), and 0.70 mg/dL (0.09-1.60 mg/dL) respectively.

Ten pediatric patients, three boys and seven girls, received left lateral lobe liver transplantation. The average age and weight of the pediatric recipients were 48.1 mo (5-82 mo) and 14.3 kg (6.9-23.8 kg) respectively. Indications included seven cases of congenital biliary atresia (one child receiving liver re-transplantation due to chronic rejection after the first transplant), two cases of progressive familial intrahepatic cholestasis and one case of acute liver failure. Nine adult or adolescent patients, five males and four females, received right extended lobe liver transplantation. The average age and weight of the adult recipients were 30.7 years (10-49 years) and 64.1 kg (39.9-88.5 kg) respectively. Indications included four cases of postnecrotic cirrhosis, two cases of primary sclerosing cholangitis, one case of Wilson's disease, one case of autosomal recessive polycystic kidney deficiency combined with liver fibrosis, and one case of acute liver necrosis caused by ligation of the hepatic artery due to rupture of the hepatic arterial aneurysm. Two patients were emergency cases, one due to postnecrotic cirrhosis and the other due to acute liver necrosis (Tables 1 and 2).

The key to successful liver division is to share vascular and biliary structures between the two sides but without handicapping either, and preferably to provide either graft with single first order arterial and biliary elements. Normally, the inferior vena cava, the common bile duct, and the main trunk of the portal vein as well as the hepatic artery are preserved for the right extended graft. We emphasize on performing dissection of the hepatic hilum only from the left side and always keeping the right side untouched, the steps of *ex situ* splitting the donor liver into a left lateral lobe and a right extended lobe were described briefly as

follows: (1) completing the conventional bench hepatic graft preparation and resecting the gallbladder, briefly checking the portal vein, the hepatic artery, the bile duct, and the hepatic vein; (2) exposing the left hepatic artery and identifying the segment IV artery, and then transecting the left hepatic artery distally to the origin of segment IV artery; (3) isolating and transecting the left portal vein, and ligating the branches supplying segment IV originating from left portal vein; (4) splitting the liver parenchyma step by step along with umbilical scissure from downward to upward, and the various tiny vessels and bile ducts handled with ligation or metal clips; (5) exposing the left hepatic vein when dividing close to suprahepatic inferior vena cava, and then transecting the left hepatic vein leaving a suitable stump; (6) finally transecting the bile duct connecting the two parts of donor liver; and (7) injecting cold preservation solution via portal vein, hepatic artery as well as bile duct to check for leaks. None of these 10 cases of donor livers was applied cholangiography or angiography in the process of splitting.

RESULTS

All the 10 donor livers were split successfully into a left lateral lobe (segments II and III) and a right extended lobe (segments I, IV-VIII), and subsequently split liver transplantation was performed in 19 cases. The average weight of the whole graft before splitting was 1 322.6 g (956-1 665 g), and the average weight of the left lateral lobe and the right extended lobe after splitting was 281.8 g (198-373 g) and 1 075.8 g (726-1 299 g) respectively. The average ratio of left lateral lobe to total graft was 0.215

Table 1 Basic data of donors

	Age/Sex	Height (cm)/weight (kg)	ICU (d)	AST (IU/L)	Crea (mg/dL)	Na (mmol/L)	BIL (mg/dL)	Whole graft weight (g)
1	15/M	168/70	1	22	1.20	152	1.60	1 290
2	35/M	185/50	3	14	1.10	152	0.63	1 580
3	46/F	176/70	2	16	0.80	153	0.09	1 296
4	43/F	175/70	2	122	1.25	158	0.48	1 435
5	37/F	170/75	8	77	1.22	137	0.28	1 665
6	51/F	160/45	2	28	0.40	146	0.70	1 000
7	40/F	170/65	2	23	0.59	138	0.10	1 209
8	15/F	175/65	1	94	1.01	153	1.56	1 225
9	27/F	175/75	2	30	0.70	155	0.88	956
10	18/F	165/60	1	105	0.80	144	0.71	1 570

Table 2 Basic data of recipients receiving left lateral lobe and right extended lobe liver transplantation

	Patients receiving left lateral lobe				Patients receiving right extended lobe			
	Age (m) /sex	Weight (kg)	Graft weight (g)	GRWR (%)	Age (yr) /sex	Weight (kg)	Graft weight (g)	GRWR (%)
1	74/F	18.6	242	1.30	46/M	80.0	1 048	1.31
2	50/F	15.0	281	1.87	42/F	88.5	1 299	1.47
3	72/F	15.7	318	2.03	49/M	70.5	978	1.39
4	78/F	21.9	275	1.26	17/M	60.5	1 160	1.92
5	5/M	6.9	373	5.41	49/F	63.0	1 292	2.05
6	20/F	10.0	274	2.74	-	-	-	-
7	11/F	7.1	268	3.72	14/F	64.6	941	1.46
8	8/M	7.8	270	3.46	26/M	55.0	955	1.73
9	82/M	16.2	198	1.22	10/M	39.9	758	1.90
10	81/F	23.8	319	1.34	23/F	54.5	1 251	2.30

The right extended lobe from case 6 was sent to the other center.

(0.178-0.274). The average GRWR of the left lateral lobe and the right extended lobe reached 2.44% (1.22-5.41%) and 1.73% (1.31-2.30%) respectively. The average weight ratio of donor to pediatric recipient was 5.47 (2.52-10.87). The average time required to split the donor liver was 105 min (85-135 min).

A total number of five anatomic variations occurred in the process of graft splitting. The left hepatic vein variation occurred in two cases, where the segment II hepatic vein, the segment III hepatic vein and the middle hepatic vein draining separately into inferior vena cava appeared to be a trifurcation at the junction. In order to obtain a sufficiently long left hepatic vein, some part of the lateral wall of the middle hepatic vein and suprahepatic inferior vena cava was sacrificed, the defect was repaired with part of donor common iliac vein (Figures 1 and 2). Two donor organs had anatomical variations of the left hepatic artery. In one case with the segment IV artery arising very distal from the left hepatic artery, only 3 mm of the common trunk of segments II and III arteries could be obtained after painstakingly dissecting the liver parenchyma of the left lateral lobe. There was one case where the replaced left hepatic artery originated from the left gastric artery (Figure 3). Although partial blood supply of the segment II liver from the segment IV artery could be identified, the diameter of this branch was less than 2 mm with quite good backflow under perfusion, consequently no reconstruction was required. Finally there was the anatomical bile duct variation. In this case the union of segments II and III bile ducts was right to the umbilical fissure resulting in two separate

openings of bile duct on the cutting surface of left lateral lobe. Fortunately in this case the distance between the two bile duct openings was quite close and in the shape of a figure '8'; therefore, one opening could be achieved by plastic reconstruction (Figure 4).

DISCUSSION

Pichlmayr *et al.*^[6], reported the first clinical attempt of split liver transplantation in 1988, and 1 year later Bismuth *et al.*^[7], described two patients with fulminant hepatic failure, each receiving a split graft. In 1990, Broelsch *et al.*^[8], presented the first series of 30 split liver transplantations in 21 children and 5 adults. In this early experience, patient survival was inferior to that reported in series of cadaveric whole-size orthotopic liver transplants. Despite skepticism as to the lasting role of split liver transplantation, several European centers, faced with an increasing waiting list of death rate due to the scarcity of donor organs, pursued the split liver options. In 1995, the results of a collective experience of 50 donor livers, providing 100 grafts during a 5-year period from the European Split Liver Registry^[9] demonstrated no significant difference when compared to conventional whole-sized OLT during the same period.

With the present improved surgical techniques, it is commonly acceptable to split the donor liver into two transplantable grafts, one for a pediatric and the other for an adult recipient. A series comprising 110 consecutive split liver transplantations in 55 adults and 55 pediatric recipients showed that patient survival of split liver transplantation

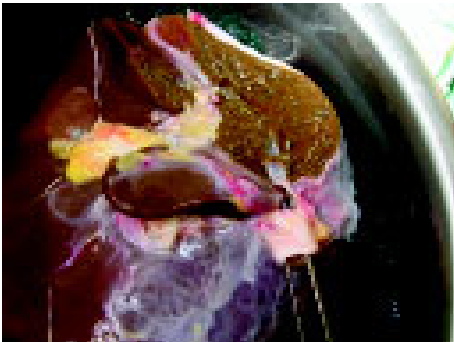


Figure 1 Partial defect of MHV and IVC after splitting.



Figure 2 Repair of defect of MHV and IVC by part of common iliac vein.



Figure 3 Left replaced hepatic artery originating from the left gastric artery, with segment II blood supply partially from a small branch of segment IV artery.



Figure 4 Appearance after plastic reconstruction of separate openings of segments II and III bile ducts nearby.

was not significantly different from whole-organ OLT^[10]. Similar results are also reported by Broering *et al.*^[11]. Such view is strongly evidenced by more and more current clinical data^[12-15]. Our experience with more than 150 cases of split liver transplantation since 1988 has confirmed these results. Between 1993 and 1999, split liver transplantation activities increased in central Europe from 1.2% to 10.4%^[16]. Currently split liver transplantations make up more than 20% of all liver transplantations performed at the Medical School of Hannover. With the refinement of surgical skill, split liver transplantation could even be applied in the cases of retransplantation and emergency.

What kind of donor liver is suitable for splitting calls for thorough consideration and evaluation whenever an organ donor is available. Besides meeting the basic prerequisites regarding the donor livers, the following factors are worth to be considered based on our experience and opinions from other authors^[10,11,17]: (1) a donor age below 50 years and above 10 years; (2) hemodynamic stability, if in use of vasopressor, maintaining good blood pressure at least; (3) the preferable donor ICU stay less than 5 d; and (4) no status of hypernatremia, a serum sodium concentration of <170 mmol/L or even better <150 mmol/L. Although donor parameters are critical when selecting livers for a splitting procedure, the experience accumulated over the years clearly indicates that the most reliable basis for the decision on splitting is the judgment of an experienced transplant surgeon. Microscopic examination should become a kind of supplement to macroscopic observation. It is pivotal to scrutinize whether the donor liver has a soft consistency, a sharp edge and is well perfused. One has to appreciate the frank remark of Busuttill on criteria for splittable donor livers^[10]: "I think that the ultimate exclusion criterion is when you go and look at the liver, if the liver does not look good, you do not split it."

With the current technique, it is quite reliable to split a donor liver into a left lateral lobe (segments II and III) and a right extended lobe (segments I, IV-VIII) for one child recipient and one adult recipient. Our results confirmed that the right extended liver lobe would account for about 80% of the standard volume in humans, and can be allocated like a full-size liver if careful consideration is given to recipient selection^[18]. Actually in our group the maximum weight of recipients was up to 88.5 kg with satisfactory outcome of transplantation. In this study, the average GRWR of the right extended lobe was 1.73%. For the right extended lobe graft 1% GRWR is sufficient for the low risk recipient in stable condition and good nutritional status. However, GRWR should be not less than 1.5% for the high risk recipient with decompensatory liver function and severe portal hypertension^[19,20]. For the left lateral lobe graft the ideal weight ratio of donor to child should be 3-10 times.

Compared to splitting liver into a full left lobe and a full right lobe^[21,22], fewer anatomical variations might occur when splitting liver into a left lateral lobe and a right extended lobe. Nevertheless, it is crucial for the success of the subsequent liver transplantation how the various potential variations are handled in the process of splitting. Considering that the left liver lobe is more constant regarding anatomical variations,

it can be said that the more one stays on the left, the fewer anatomical variants one is confronted with.

In most of cases, the left hepatic vein joins the middle hepatic vein, thus forming the common trunk entering the antero-left surface of the inferior vena cava^[23]. Instead of joining the segment II hepatic vein to form the left hepatic vein, the segment III hepatic vein seldom joins the middle hepatic vein individually with the probability for about 5-10%. The diameter of the extrahepatic portion of the left hepatic vein is around 10 mm, and the smaller diameter less than 7 mm is sufficient to suspect such circumstance. In the present study, left hepatic vein variation occurred in two cases, the segments II and III draining of hepatic veins appeared with the middle hepatic vein as a trifurcation. Under certain circumstances, the dividing line needs to be moved slightly to the right slightly in order to guarantee one venous drainage from the graft of left lateral lobe. The defect of middle hepatic vein and inferior vena cava could be repaired by the common iliac vein from the donor.

Intrahepatic portal venous variations can be seen in approximately 20% of the population^[24]. However, unless the rare absence of a portal vein bifurcation with only 0.9% possibility, will it become the contradiction of graft splitting. In the majority of cases the portal vein inflow to segment IV is accomplished by the left umbilical section of the left portal vein. However, those branches originating from umbilical section will inevitably be transected. Fortunately, in most cases the additional portal vein branches to segment IV arising from the portal vein bifurcation and the right portal vein could be expected. By preserving these veins and moving the transection line to the left, partial portal vein supply to segment IV can be achieved.

Variations of the hepatic artery are comparatively frequent^[25]. Only 50-70% of livers present with "normal" anatomy^[26,27]. If the left main hepatic artery originates from the left gastric artery (10-15%) both the length and the diameter of this artery would be adequate for the anastomosis in the recipient. Such a situation occurred in one case. Although one branch from the segment IV artery supplying segment II could be identified, no reconstruction was required with small diameter and good backflow under perfusion. Since in most cases the portal vein supply to segment IV has to be sacrificed in the process of splitting, arterial supply will largely determine survival of this segment, and therefore, every effort should be made to preserve the segment IV artery. In most cases the segment IV artery originates from the left hepatic artery, and its origin should have some distance to the union of segments II and III arteries. The segment IV artery rarely arises far distal from the left hepatic artery, and the three arteries of segments II, III, and IV might form a trifurcation at their origins. A similar situation occurred in one of our cases when with painstaking efforts only a length of 3 mm of the common trunk of segments II and III arteries could be obtained at last. In case the segment IV artery has to be cut down, it is suggested to anastomose it with the stump of the left hepatic artery on the backtable.

Close attention should also be paid to variations of bile ducts. During the initial period of left lateral split liver transplantation, many groups isolated the main left hepatic

duct next to the main bile duct bifurcation when harvesting the left lateral lobe, in order to create a nice bile duct stump for anastomosis. However, this technique seems to be associated with a high rate of biliary complications on both grafts for the following reasons. First, leaving the long stump of bile duct with the left lateral graft might result in ischemic necrosis due to damaging the parabiliary vascular plexus in the isolation of the left hepatic duct^[8]. Second, a high incidence of damage to the segments I and IV bile duct of the right extended graft might occur with such a method^[28]. Therefore, we kept the connective tissue surrounding bile ducts untouched, and only used a metal probe or Arrow[®] catheter to identify the trend of bile duct, and transected bile duct as the last step of the whole splitting procedure. Although in 15% of donor livers the union of segments II and III bile ducts is located right to the umbilical fissure, which means two separate openings of bile duct appear on the cutting surface of the left lateral graft, we would still rather keep the transecting line curving a little to the left in order to retain an undamaged segment IV bile duct. If the distance between two separate bile duct openings is quite close, they might be merged into one through plastic reconstruction.

Undoubtedly, split liver transplantation has become a well-established approach to extend the donor pool for both pediatric and adult patients. Careful donor and recipient selection, good knowledge of the liver anatomy, excellent surgical skills and meticulous postoperative management all contribute to the success of each case of split liver transplantation.

REFERENCES

- 1 **Abouljoud M**, Yoshida A, Dagher F, Moonka D, Brown K. Living donor and split-liver transplantation: an overview. *Transplant Proc* 2003; **35**: 2772-2774
- 2 **Emond JC**, Whittington PF, Thistlethwaite JR, Alonso EM, Broelsch CE. Reduced-size orthotopic liver transplantation: use in the management of children with chronic liver disease. *Hepatology* 1989; **10**: 867-872
- 3 **Bismuth H**, Houssin D. Reduced-sized orthotopic liver graft in hepatic transplantation in children. *Surgery* 1984; **95**: 367-372
- 4 **Broelsch CE**, Emond JC, Thistlethwaite JR, Whittington PF, Zucker AR, Baker AL, Aran PF, Rouch DA, Lichtor JL. Liver transplantation including the concept of reduced-size liver transplants in children. *Ann Surg* 1988; **208**: 410-420
- 5 **Otte JB**, de Ville de Goyet J, Solak E, Alberti D, Moulin D, de Hemptinne B, Veyckemans F, van Obbergh L, Carlier M, Clapuyt P. Size reduction of the donor liver is a safe way to alleviate the shortage of size-matched organs in pediatric liver transplantation. *Ann Surg* 1990; **211**: 146-157
- 6 **Pichlmayr R**, Ringe B, Gubernatis G, Hauss J, Bunzendahl H. Transplantation of a donor liver to 2 recipients (splitting transplantation)-a new method in the further development of segmental liver transplantation. *Langenbecks Arch Chir* 1988; **373**: 127-130
- 7 **Bismuth H**, Morino M, Castaing D, Gillon MC, Descorps Declere A, Saliba F, Samuel D. Emergency orthotopic liver transplantation in two patients using one donor. *Br J Surg* 1989; **76**: 722-724
- 8 **Broelsch CE**, Emond JC, Whittington PF, Thistlethwaite JR, Baker AL, Lichtor JL. Application of reduced size liver transplants as split grafts, auxiliary orthotopic grafts and living related segmental transplants. *Ann Surg* 1990; **212**: 368-377
- 9 **de Ville de Goyet J**. Split liver transplantation in Europe-1988 to 1993. *Transplantation* 1995; **59**: 1371-1376
- 10 **Ghobrial RM**, Yersiz H, Farmer D, Amersi F, Goss J, Chen P, Dawson S, Lerner S, Nissen N, Imagawa D, Colquhoun S, Arnout W, McDiarmid SV, Busuttil RW. Predictors of survival after *in vivo* split liver transplantation: analysis of 110 consecutive patients. *Ann Surg* 2000; **232**: 312-323
- 11 **Broering DC**, Topp S, Schaefer U, Fisher L, Gundlach M, Sterneck M, Schoder V, Pothmann W, Rogiers X. Split liver transplantation and risk to the adult recipient: analysis using matched pairs. *J Am Coll Surg* 2002; **195**: 648-657
- 12 **Renz JF**, Yersiz H, Reichert PR, Hisatake GM, Farmer DG, Emond JC, Busuttil RW. Split-liver transplantation: a review. *Am J Transplant* 2003; **3**: 1323-1335
- 13 **Moreno A**, Meneu JC, Moreno E, Garcia I, Loinaz C, Jimenez C, Gomez R, Abradelo M, Calvo J, Fundora Y, Ortiz C. Results in split liver transplantation. *Transplant Proc* 2003; **35**: 1810-1811
- 14 **Gridelli B**, Spada M, Petz W, Bertani A, Lucianetti A, Colledan M, Altobelli M, Alberti D, Guizzetti M, Riva S, Melzi ML, Stroppa P, Torre G. Split-liver transplantation eliminates the need for living-donor liver transplantation in children with end-stage cholestatic liver disease. *Transplantation* 2003; **75**: 1197-1203
- 15 **Deshpande RR**, Bowles MJ, Vilca-Melendez H, Srinivasan P, Girlanda R, Dhawan A, Mieli-Vergani G, Muiesan P, Heaton ND, Rela M. Results of split liver transplantation in children. *Ann Surg* 2002; **236**: 248-253
- 16 **Klempnauer J**, Schrem H, Becker T, Nashan B, Luck R. Liver transplantation today. *Transplant Proc* 2002; **33**: 3433-3435
- 17 **Emond JC**, Freeman RB Jr, Renz JF, Yersiz H, Rogiers X, Busuttil RW. Optimizing the use of donated cadaver livers: analysis and policy development increase the application of split-liver transplantation. *Liver Transpl* 2002; **8**: 863-872
- 18 **Renz JF**, Emond JC, Yersiz H, Ascher NL, Busuttil RW. Split-liver transplantation in the United States: outcomes of a national survey. *Ann Surg* 2004; **239**: 172-181
- 19 **Heaton N**. Small-for-size liver syndrome after auxiliary and split liver transplantation: donor selection. *Liver Transpl* 2003; **9**: S26-S28
- 20 **Macros A**. Split-liver transplantation for adult recipients. *Liver Transpl* 2000; **6**: 707-709
- 21 **Yersiz H**, Renz JF, Hisatake G, Reicher PR, Feduska NJ, Lerner S, Farmer DG, Ghobrial RM, Geevarghese S, Baquerizo A, Chen P, Busuttil RW. Technical and logistical consideration of in situ split liver transplantation for two adults: Part I. Creation of left segment II, III, IV and right segment I, V-VIII grafts. *Liver Transpl* 2001; **7**: 1077-1080
- 22 **Yersiz H**, Renz JF, Hisatake G, Reicher PR, Feduska NJ, Lerner S, Farmer DG, Ghobrial RM, Geevarghese S, Baquerizo A, Chen P, Busuttil RW. Technical and logistical consideration of in situ split liver transplantation for two adults: Part II. Creation of left segment I-IV and right segment V-VIII grafts. *Liver Transpl* 2002; **8**: 78-81
- 23 **Noujaim HM**, Mirza DF, Mayer DA, De Ville De Goyet J. Hepatic vein reconstruction in ex situ split-liver transplantation. *Transplantation* 2002; **74**: 1018-1021
- 24 **Atri M**, Bret PM, Fraser-Hill MA. Intrahepatic portal venous variations: prevalence with US. *Radiology* 1992; **184**: 157-158
- 25 **Hiatt JR**, Gabbay J, Busuttil RW. Surgical anatomy of the hepatic arteries in 1000 cases. *Ann Surg* 1994; **220**: 50-52
- 26 **Kawarada Y**, Das BC, Taoka H. Anatomy of the hepatic hilar area: the plate system. *J Hepatobiliary Pancreat Surg* 2000; **7**: 580-586
- 27 **Hardy KJ**, Jones RM. Hepatic artery anatomy in relation to reconstruction in liver transplantation: some unusual variations. *Aust N Z J Surg* 1994; **64**: 437-440
- 28 **Stapleton GN**, Hickman R, Terblanche J. Blood supply of the right and left hepatic ducts. *Br J Surg* 1998; **85**: 202-207

• BRIEF REPORTS •

Evaluation of serum cathepsin B and D in relation to clinicopathological staging of colorectal cancer

Elzbieta Skrzydlewska, Mariola Sulkowska, Andrzej Wincewicz, Mariusz Koda, Stanislaw Sulkowski

Elzbieta Skrzydlewska, Department of Analytical Chemistry, Medical University of Bialystok, Poland

Mariola Sulkowska, Andrzej Wincewicz, Mariusz Koda, Stanislaw Sulkowski, Department of Pathology, Medical University of Bialystok, Poland

Supported by the Polish State Committee for Scientific Research, No. 3 PO5B 07922

Correspondence to: Professor Elzbieta Skrzydlewska MD, PhD, Department of Analytical Chemistry, Medical University of Bialystok, Mickiewicza 2, 15-230 Bialystok, Poland. skrzydle@amb.edu.pl

Telephone: +48-85-7485707 Fax: +48-85-7485707

Received: 2004-10-19 Accepted: 2005-01-05

© 2005 The WJG Press and Elsevier Inc. All rights reserved.

Key words: Proteases; Cathepsin D; Cathepsin B; Colorectal cancer

Skrzydlewska E, Sulkowska M, Wincewicz A, Koda M, Sulkowski S. Evaluation of serum cathepsin B and D in relation to clinicopathological staging of colorectal cancer. *World J Gastroenterol* 2005; 11(27): 4225-4229

<http://www.wjgnet.com/1007-9327/11/4225.asp>

Abstract

AIM: Proteolytic degradation of the extracellular matrix facilitates cancer invasion and promotes metastasis. The study aims at evaluation of preoperative and postoperative serum cathepsins B and D levels in correlation with selected anatomoclinical features of colorectal cancer.

METHODS: Blood samples were collected from 63 colorectal cancer patients before curative operation of the tumor 10 d later. Blood that was obtained from 20 healthy volunteers, served as a control. The activity of cathepsin B was measured with Bz-DL-arginine-pNA as a substrate at pH 6.0, while cathepsin D activity was determined with urea-denatured hemoglobin (pH 4.0).

RESULTS: The preoperative and postoperative activities of cathepsin B were significantly ($P < 0.00001$) lower in serum of colorectal cancer patients than in control group. However, postoperative values of this protease were significantly increased in comparison with preoperative ones ($P = 0.031$). Activity of cathepsin D appeared to be significantly higher in colorectal cancer sera ($P < 0.00001$) compared with controls. No statistically significant differences between preoperative and postoperative activity of cathepsin D were noted ($P = 0.09$). We revealed a strong linkage of cathepsins' levels with lymph node status and pT stage of colorectal cancer.

CONCLUSION: Blood serum activities of cathepsin B and D depend on the time of sampling, tumor size and lymph node involvement. Significantly, increased activity of cathepsin D could indicate a malignant condition of the large intestine. In our work, the serum postoperative decrease of cathepsin B activity appears as an obvious concomitant of local lymph node metastasis—the well-known clinicopathological feature of poor prognosis.

INTRODUCTION

Normal cells undergo several changes to converse into invasive malignant clones with metastatic capability. Progress of these alternations is manifested in distinguishable histological and temporal stages—for instance: normal tissue, hyperplasia with a high incidence of proliferating cells, dysplasia with the induction of angiogenesis that precedes following metamorphosis of observed cell clusters into tumors with metastasis. Analysis of the subsequent stages of tumor progression has provided a multistage theory of carcinogenesis on the basis of genetic changes that include activation of oncogenes, inactivation of tumor suppressor genes, and altered expression of tumor-associated molecules.

Cellular transformation provokes tissue remodeling inside neoplastic lesions and in the periphery of the tumor. Disorders in stroma or extracellular matrix (ECM) play an essential role in cancer progression. It is suggested that perturbation of the tissue microenvironment may be sufficient to induce tumor formation. Moreover, local carcinomatous invasion and metastasis also require the destruction of the EMC during local dissemination of malignant cells, angiogenesis, intravasation and extravasation. These processes are enabled by multiple degradation of stromal structure which is achieved due to cooperation of various specific intra- and extracellular proteases. Lysosomal aspartyl and cysteine enzymes—cathepsin D and B are the most important of intracellular proteases that participate in stromal destruction, which facilitates tumor invasion of deeper tissue layers^[1]. These enzymes can act directly by proteolysis of EMC components or indirectly by costimulation of a cascade of other proteases such as metalloproteases or elastase, which then decompose protein elements of the EMC and basal membranes. This stromal disarrangement allows migration of malignant cells to different regions and compartments of the human body, what accelerates tumor growth and favors metastasis. Not only does overexpression of cathepsin B and D in cancer cells reflect intensity of

neoplasm development, but also increased serum activity of mentioned proteases does the same as well. Apart from mentioned functions, independently of its catalytic activity human cathepsin D stimulates tumor growth as a direct or indirect mitogenic factor for cancer cells^[1]. Cathepsin D affects tumor angiogenesis in a mysterious way. It was suggested that cathepsin D might favor angiogenesis by releasing ECM-bound bFGF^[2]. Suggestions of its proangiogenic function contrast with the fact that pro-cathepsin D is responsible for the generation of specific inhibitor of angiogenesis-angiostatin^[3]. Now it is presumed that cathepsin D may stimulate endothelial cell growth via a paracrine loop, acting as a protein ligand, by directly or indirectly triggering a yet unidentified cell surface receptor^[4].

Increased expression, enhanced secretion and cell surface association of cathepsin B were found in different types of tumor cells especially in their more malignant variants^[5]. Last studies have revealed that augmented production and release of cathepsin B in tumor cells lead to tumor cell growth, invasion and metastasis^[6]. This cathepsin may act at the contact regions of tumor cells and basement membrane or interstitial stroma. Low pH is necessary for activation of secreted precursors to active forms, which degrade the protein components of basement membranes and interstitial connective matrix including laminin, fibronectin, elastin, and various types of collagen^[7]. Cathepsin B split fibronectin into smaller parts and change conformation of this protein components. In such a way the CS-1 sequence and alternatively spliced type III connecting segment (IIICS) are uncovered, exposed and recognized by the integrin $\alpha_4\beta_1$ -receptor^[8]. Thereby, cathepsin B may be involved in cellular signal transduction beside extracellular protein degradation.

Therefore, the aim of this work was to investigate the activity of lysosomal proteases-cathepsin B and D in blood serum and their potential impact on cancer progression and metastasis in cases of colorectal cancer.

MATERIALS AND METHODS

The study included 63 patients (42 men and 21 women) with a mean age of 64 years that were required to undergo a colorectal cancer operation. Thirty tumors were located in the rectum and 33 were found in the colon. The patients had no preoperative chemo- or radiotherapy. All the patients were monitored after the operation. Two independent pathologists assessed conventional histopathological parameters (including AJCC/UICC TNM stage, tumor type and grade of differentiation). Differentiation and histological type of the tumors was determined following the World Health Organization guidelines. Fifty-eight colorectal cancers were classified histopathologically as adenocarcinoma and 5 as mucinous adenocarcinoma: 43 cases with G2 grade and 15 cases with G3 grade. Because of too small a number of tumors that were classified as pT1, pT2 and pT4 patients were divided into two groups: five tumors comprised pT1+pT2 group and 53 cancer cases belonged to pT3+pT4 group. Forty-six percent patients had involved lymph nodes at the time of diagnosis.

Biochemical analysis

The blood samples were collected from colorectal cancer

patients twice: before and 10 d after the curative operation. The blood was centrifuged at 4 °C and the serum samples were stored at -80 °C until examination. The control group included of 20 healthy volunteers (12 men and 8 women) with a mean age of 59 years. The control blood samples were collected only once. Serum was gained from collected blood and the activity of cathepsin B was determined with Bz-DL-arginine-pNA as a substrate at pH 6.0^[9], while the cathepsin D activity was measured with urea-denatured hemoglobin (pH 4.0)^[10].

RESULTS

The preoperative and postoperative activities of cathepsin B were significantly ($P < 0.00001$) smaller than in control group. However, postoperative values of this protease were significantly increased in comparison with preoperative ones ($P = 0.031$). On the other hand the activity of aspartyl protease-cathepsin D appeared to be significantly higher ($P < 0.00001$) in comparison with the control group data. In addition, no statistically significant differences between preoperative and postoperative activity were noted ($P = 0.09$, Table 1).

Table 1 Activity of cathepsin B and D in serum of patients with colorectal carcinoma

	Healthy people (n = 20)	Control serum	66.9±2.8
Cathepsin B nmolPNA/mL	Colorectal patients (n = 63)	Before operation1 (serum sample a)	7.9±8.5 ^{1b}
		After operation (serum sample b)	21.0±8.7 ^f
	Healthy people (n = 20)	Control serum	30.2±2.2
Cathepsin D nmol Tyr/mL	Colorectal patients (n = 63)	Before operation (serum sample a)	58.7±24.2 ^{2d}
		After operation (serum sample b)	49.9±16.9 ^h

Statistical differences: ¹ $P = 0.031$ -comparison between cathepsin B serum samples a and b. ² $P = 0.09$ -comparison between cathepsin D serum samples a and b. ^b $P < 0.00001$, ^d $P < 0.00001$, ^h $P < 0.00001$, ^f $P < 0.00001$ vs control serum.

We revealed a strong linkage of cathepsins' levels with lymph node status and pT stage of colorectal cancer. As referred to TNM classification, patient group of pT1 and pT2 tumors showed significantly higher preoperative serum activity of cathepsin B than it was detected in preoperative serum of patients with tumors classified to pT3 and pT4 group ($P = 0.0057$). This trend of differences was not apparent enough to reach a level of statistical significance in case of postoperative serum values of cathepsin B. We assume that statistical significance could not be achieved in analysis of homologous postoperative data because of wide variation of postoperative cathepsin B values in set of patients with pT1 and pT2. Similarly values of cathepsin D before operations (serum sample A) were more increased with nearly statistical significance in pT1 and pT2 vs pT3 and pT4 groups respectively ($P = 0.053$).

As shown in Table 2, node-negative (N-) colorectal cancer patients displayed significantly higher postoperative

serum levels of cathepsin B in opposition to patients with lymph node involvement (N+) ($P = 0.0054$). These groups of patients did not significantly differ in cathepsin B levels before operation. We drew out a similar comparison between activities of cathepsin D in node negative and node positive sets of colorectal cancer-but inversely to cathepsin B-remarkable distinction of cathepsin D serum levels appeared before surgery. Namely, the preoperative serum activity of cathepsin D was increased in node negative (N-) *vs* node positive (N+) colorectal cancer patients with statistical significance ($P = 0.019$).

DISCUSSION

Cancer development is characterized by severe disarrangement of the intra- and extracellular metabolism and structural alterations. Cancer cells overexpress and secrete a large proportion of lysosomal proteases-cathepsins. The activity increase of cathepsin B and D was discovered to be statistically significant in both the neoplastic tissue cytosol and homogenate, compared to the cytosol and homogenate of adjacent healthy tissue^[11]. Marked tissue immunoreactivity of cathepsin B and D takes place in carcinoma of uterus, ovary, lung, intestines and many other organs^[12-15]. Moreover, it was reported that tumor cell lines secrete cathepsin B and D^[16]. On the other hand it was reported that serum cathepsin B level did not differ significantly both in benign and malignant neoplasms of ovaries^[17]. In cancers there was elevated serum value of cystatin C in comparison with benign ovarian tumors and controls, which negatively affected the amount of cathepsin B. However, ovarian cancer cells are strongly positive for cathepsin B in immunohistochemical analysis, while benign ovarian tumors lacked any positive reaction of this kind^[17].

It is suggested that colorectal cancer development is enhanced by oxidative stress. Oxidative stress is maintained as the effect of excessive concentration of lipid hydroperoxides in the vascular net and their participation in the oxidant generation. The other possible explanation might be overproduction of oxidants by inflammatory and/or cancer cells and suppression of antioxidant system in cancer cells. In these conditions free radicals may enhance lipid peroxidation.

Products of this process are responsible for membrane alteration. Reactive oxygen species cause protein damage and as a result changes in biological function of active proteins and membrane permeability for intracellular compounds may appear due to increased susceptibility for drugs that induce apoptosis of neoplastic cells^[1,18]. It may explain translocation of cathepsins from lysosomes via cytosol and cellular membrane into body fluids.

As we have demonstrated in our previous works, generation of free radicals accompanies the development of cancer^[18]. Reactive oxygen species cause an oxidative damage of cell membranes which results in an increase of membrane permeability. That implies influx of cathepsin D to extracellular fluid. Therefore, elevated activity of cathepsin D is observed in the serum as an evidence for impairment of general cellular functions like maintenance of the barrier between intracellular and extracellular environment. Advancement of tumor growth and neoplastic spreading across the whole organism seem to reflect the severity of cellular damage. Cathepsin B -cysteine protease is so sensitive to free radicals, that the latter probably inactivate cathepsin B. Thereby it would explain why serum activity of cathepsin B is lower in serum of patients with colorectal cancer in comparison to serum values of this protease in healthy volunteers. Production of free radicals is upregulated and activity of cathepsin B falls down along with the enlargement of tumors and neoplastic extent into lymph nodes. This statement is supported by our present study in which we detected lower levels of cathepsin B in group pT3 and pT4 *vs* pT1 and pT2 as well as in node positive (N+) *vs* node negative (N-) patients after surgery. Total resection of cancer could contribute to limit ROS generation and by means of the inactivation of cathepsin B, ROS generation was reduced enough which is shown in the results obtained.

The concentrations of cathepsin B and D were increased also in the blood serum of patients with other carcinomas^[19-21]. Additionally, the increase of cathepsin B correlated with the advancement of cancer assessed with Duke's scale. Moreover patients with both elevated levels of cathepsin B and CEA were classified as the group of poor prognosis^[20]. Nevertheless, in our present investigations, we discovered

Table 2 Correlation of serum cathepsin B and D activity and clinicopathological findings

Variable		n = 63	Cathepsin B (nmol/L pNA/mL)				Cathepsin D (nmol Tyr/mL)			
			Before operation	P	After operation	P	Before operation	P	After operation	P
Sex	M	42	19.1±8.9	NS	21.7±9.1	NS	59.4±26.3	NS	49.5±16.3	NS
	F	21	15.3±6.6		19.6±7.9		57.0±19.2		50.9±18.4	
Age (yr)	≤60	16	20.4±12.3	NS	17.4±8.0	P = 0.064	54.2±17.0	NS	51.7±22.0	NS
	>60	47	17.02±6.6		22.4±8.7		60.2±26.1		49.3±14.7	
Tumor site	Rectum	30	16.5±7.4	NS	18.4±7.6	NS	59.8±21.6	NS	51.2±19.9	NS
	Colon	33	19.1±9.2		23.5±9.1		57.7±26.3		48.8±13.6	
HPtype	Adc.	58	18.1±8.4	NS	21.02±8.9	NS	58.7±24.4	NS	50.7±17.0	NS
	Adc. m.	5	10.1±9.3		20.9±7.0		56.0±21.2		43.2±14.2	
pT	pT 1+2	5	25.3±0.7	P = 0.0057	30.3±18.7	NS	76.8±23.0	P = 0.053	48.8± 16.5	NS
	pT 3+4	53	17.1±8.5		20.3±7.3		56.7±23.6		50.1± 17.0	
G	2	43	18.8±8.8	NS	21.5±9.2	NS	62.5±25.5	NS	50.4±17.3	NS
	3	15	15.8±7.3		19.9±7.7		50.3±18.8		49.2±16.2	
N	(-)	34	18.5±8.5	NS	23.9±8.9	P = 0.0054	65.9±26.5	P = 0.019	49.7±17.2	NS
	(+)	29	17.03±8.4		17.3±7.1		49.1±16.7		50.3±16.6	

Statistical differences: see Table 1.

only the increase of cathepsin D while levels of cathepsin B were decreased in sera of colorectal cancer patients.

Overexpression of cathepsins may prelude the loss of integrity of ECM protein components. It is known that cathepsin D as endopeptidase degrades ECM proteins and proteins of the basal epithelium as well as many intracellular and endocytosed proteins. It occurs mainly in phagosome-like acid vesicles with acidic pH where EMC components are trapped^[22]. Cathepsin D may cooperate with cathepsin B in the process of proteolysis and cancer progression. Cathepsin D probably activates cysteine procathepsins B and L^[23]. Cathepsin B activates the urokinase-type plasminogen which can subsequently activate the plasmin-metalloproteinases proteolytic pathway^[24,25]. Moreover, cathepsin B may change the balance of metalloproteinases and their inhibitors and directly cleave and inactivate some of MMPs inhibitors -TIMP-1 and TIMP-2^[26]. In such a way cathepsin B assists tumor cells in their detachment from ECMs and metastasis. Furthermore during proteolysis of interstitial extracellular structure some ECMs-bound growth factors, e.g. bFGF, EGF, TGF- β , IGF-I and VEGF, may get free from their chains of connections to the matrix and thanks to the fact that they can escape to join suitable receptors of stromal and tumor cells which indicates their bioavailability for growth modulation^[27].

Cathepsin B can multiply the effect of protein digestion and disarrangement by triggering trypsinogen activation^[28]. Lysosomal cathepsin B activates trypsinogen *in vitro* and the intensity of trypsinogen activation improves with acidic pH^[15,29]. Human trypsinogen is produced on a wide scale by human colorectal cells^[30]. Anyway further findings in colon cancer cell lines suggest that this production is limited only to such trypsin levels that are enough to activate PAR-2 receptor on the same cancer cells in possible autocrine/paracrine manner^[31]. It is worth mentioning that trypsin triggers matrilysin (matrix metalloproteinase-7) activity. So it is an important factor of colorectal cancer progression as immunohistochemical labeling of trypsin correlated with the depth of carcinomatous infiltration, lymphatic and venous involvement, metastasis, recurrence and shorter overall survival of patients^[32]. In our study the activity of cathepsin B could be insufficient to recruit trypsinogen activation in volume that would significantly affect tumor invasion as we detected lower cathepsin B activities in colorectal cancer compared with healthy volunteers.

The role of cathepsin B is supposed to be diverse. Namely, it can promote neoplastic invasion by lysis of EMC protein nets. Furthermore, by paracrine loop, it could cause death of neighboring cancer cells directly by proteolytic damage of cell membranes and changes in structure superficial cell receptors. Indirectly cathepsin B might act as TNF- α -induced apoptotic second messenger that mediates damage of mitochondria and release cytochrome c from these organelles^[33]. Thus, the components of cellular producer cathepsin B can be responsible for harmful suicidal injury. It can explain why higher serum levels of cathepsin B were associated with smaller size of tumor.

Cathepsin comes from two kinds of cells: carcinomatous ones and inflammatory cells that constitute immunologic response to neoplasm. According to our present results, we

suspect that along with progression of colorectal cancer, inflammatory cells might become significant producers of cathepsins. We observed lower activity of cathepsins in cases of larger tumors (pT3 and pT4 group) in comparison with smaller ones (pT1 and pT2 group) in measurements before surgery. The cause of it, can be a more escalated immunologic reaction in the onset and early stages of cancer than in advanced and late phases of neoplastic disease. Simultaneously, the outflow of cathepsins into extracellular environment destroys stromal protein structure, which is suspected to facilitate neoplastic spreading, but on the other hand, it can influence the vitality of cancer cells. So cathepsins particularly cathepsin B (probably in lower concentrations that do not induce trypsinogen activity) may disable neoplastic cells in such a way that they cannot forcibly invade surroundings despite promoting invasion by proteolysis of the interstitium. This action of cathepsin B is presumably responsible for relatively higher postoperative levels of serum cathepsin B in case of node negative patients *vs* node positive ones.

Blood serum activity of cathepsin B and D depends on the time of sampling, tumor size and lymph node involvement. Significantly increased activity of cathepsin D could indicate malignant colorectal condition. However, decreased activity of cathepsin B indicates that also different mechanisms besides proteolytic ones, participate in cancer invasion and metastasis. In comparison with analogous higher activity in node negative colorectal cancers, the significant downfall of postoperative cathepsin B activity coexisted with cancerous node involvement. Therefore, in our work, the decrease of this serum protease levels appears as an obvious concomitant of local lymph node metastasis the well-known clinicopathological feature of poor prognosis.

REFERENCES

- 1 **Berchem G**, Glondu M, Gleizes M, Brouillet JP, Vignon F, Garcia M, Liaudet-Coopman E. Cathepsin-D affects multiple tumor progression steps *in vivo*: proliferation, angiogenesis and apoptosis. *Oncogene* 2002; **21**: 5951-5955
- 2 **Briozzo P**, Badet J, Capony F, Pieri I, Montcourrier P, Barritault D, Rochefort H. MCF7 mammary cancer cells respond to bFGF and internalize it following its release from extracellular matrix: a permissive role of cathepsin D. *Exp Cell Res* 1991; **194**: 252-259
- 3 **Morikawa W**, Yamamoto K, Ishikawa S, Takemoto S, Ono M, Fukushi J, Naito S, Nozaki C, Iwanaga S, Kuwano M. Angiostatin generation by cathepsin D secreted by human prostate carcinoma cells. *J Biol Chem* 2000; **275**: 8912-8920
- 4 **Glondu M**, Coopman P, Laurent-Matha V, Garcia M, Rochefort H, Liaudet-Coopman E. A mutated cathepsin-D devoid of its catalytic activity stimulates the growth of cancer cells. *Oncogene* 2001; **20**: 6920-6929
- 5 **Campo E**, Munoz J, Miquel R, Palacin A, Cardesa A, Sloane BF, Emmert-Buck MR. Cathepsin B expression in colorectal carcinomas correlates with tumor progression and shortened patient survival. *Am J Pathol* 1994; **145**: 301-309
- 6 **Talieri M**, Papadopoulou S, Scorilas A, Xynopoulos D, Arnogianaki N, Plataniotis G, Yotis J, Agnanti N. Cathepsin B and cathepsin D expression in the progression of colorectal adenoma to carcinoma. *Cancer Lett* 2004; **205**: 97-106
- 7 **Buck MR**, Karustis DG, Day NA, Honn KV, Solane BF. Degradation of extracellular-matrix proteins by human cathepsins B from normal and tumor tissues. *Biochem J* 1992; **282**: 273-277
- 8 **Ugarova TP**, Ljubimov AV, Deng L, Plow EF. Proteolysis regulates exposure of the IIICS-1 adhesive sequence in plasma

- fibronectin. *Biochemistry* 1996; **35**: 10913-10921
- 9 **Tawatari T**, Kawabata Y, Katunuma M. Crystallization and properties of cathepsin B from rat liver. *Eur J Biochem* 1979; **102**: 279-289
- 10 **Barrett AJ**. Cathepsin D and other carboxyl proteinases In: Proteinases in mammalian cells and tissues. *North Holland Publishing Company* 1977: 240-243
- 11 **Lah TT**, Kalman E, Najjar D, Gorodetsky E, Brennan P, Somers R, Daskal I. Cells producing cathepsins D, B, and L in human breast carcinoma and their association with prognosis. *Hum Pathol* 2000; **31**: 149-160
- 12 **Ioachim EE**, Goussia AC, Macher M, Tsianos EV, Kappas AM, Agnantis NJ. Immunohistochemical evaluation of cathepsin D expression in colorectal tumors: a correlation with extracellular matrix components, p53, pRb, bcl-2, c-erbB-2, EGFR and proliferation indices. *Anticancer Res* 1999; **19**: 2147-2155
- 13 **Matsuo K**, Kobayashi I, Tsukuba T, Kiyoshima T, Ishibashi Y, Miyoshi A, Yamamoto K, Sakai H. Immunohistochemical localization of cathepsins D and E in human gastric cancer: a possible correlation with local invasive and metastatic activities of carcinoma cells. *Hum Pathol* 1996; **27**: 184-190
- 14 **Chabowski A**, Sulkowska M, Sulkowski S, Famulski W, Skrzydłewska E, Kisielewski W. Immunohistochemical evaluation of cathepsin D expression in colorectal cancer. *Folia Histochem Cytobiol* 2001; **39**: 153-154
- 15 **Brouillet JP**, Dufour F, Lemamy G, Garcia M, Schlup N, Grenier J, Mani JC, Rochefort H. Increased cathepsin D level in the serum of patients with metastatic breast carcinoma detected with a specific pro-cathepsin D immunoassay. *Cancer* 1997; **79**: 2132-2136
- 16 **van der Stappen JW**, Williams AC, Maciewicz RA, Paraskeva C. Activation of cathepsin B, secreted by a colorectal cancer cell line requires low pH and is mediated by cathepsin D. *Int J Cancer* 1996; **67**: 547-554
- 17 **Nishikawa H**, Ozaki Y, Nakanishi T, Blomgren K, Tada T, Arakawa A, Suzumori K. The role of cathepsin B and cystatin C in the mechanisms of invasion by ovarian cancer. *Gynecol Oncol* 2004; **92**: 881-886
- 18 **Skrzydłewska E**, Kozusko B, Sulkowska M, Bogdan Z, Kozłowski M, Snarska J, Puchalski Z, Sulkowski S, Skrzydłowski Z. Antioxidant potential in esophageal, stomach and colorectal cancers. *Hepatogastroenterology* 2003; **50**: 126-131
- 19 **Amiguet JA**, Jimenez J, Monreal JJ, Hernandez MJ, Lopez-Vivanco G, Vidan JR, Conchillo F, Liso P. Serum proteolytic activities and antiproteases in human colorectal carcinoma. *J Physiol Biochem* 1998; **54**: 9-13
- 20 **Kos J**, Nielsen HJ, Krasovec M, Christensen IJ, Cimerman N, Stephens RW, Brunner N. Prognostic values of cathepsin B and carcinoembryonic antigen in sera of patients with colorectal cancer. *Clin Cancer Res* 1998; **4**: 1511-1516
- 21 **Strojan P**, Budihna M, Smid L, Vrhovec I, Skrk J. Cathepsin D in tissue and serum of patients with squamous cell carcinoma of the head and neck. *Cancer Lett* 1998; **130**: 49-56
- 22 **Sis B**, Sagol O, Kupelioglu A, Sokmen S, Terzi C, Fuzun M, Ozer E, Bishop P. Prognostic significance of matrix metalloproteinase-2, cathepsin D, and tenascin-C expression in colorectal carcinoma. *Pathol Res Pract* 2004; **200**: 379-387
- 23 **Nishimura Y**, Kawabata T, Kato K. Identification of latent procathepsins B and L in microsomal lumen: characterization of enzymatic activation and proteolytic processing *in vitro*. *Arch Biochem Biophys* 1988; **261**: 64-71
- 24 **Ikeda Y**, Ikata T, Mishiro T, Nakano S, Ikebe M, Yasuoka S. Cathepsins B and L in synovial fluids from patients with rheumatoid arthritis and the effect of cathepsin B on the activation of pro-urokinase. *J Med Invest* 2000; **47**: 61-75
- 25 **Levicar N**, Kos J, Blejec A, Golouh R, Vrhovec I, Frkovic-Grazio S, Lah TT. Comparison of potential biological markers cathepsin B, cathepsin L, stefin A and stefin B with urokinase and plasminogen activator inhibitor-1 and clinicopathological data of breast carcinoma patients. *Cancer Detect Prev* 2002; **26**: 42-49
- 26 **Kostoulas G**, Lang A, Nagase H, Baici A. Stimulation of angiogenesis through cathepsin B inactivation of the tissue inhibitors of matrix metalloproteinases. *FEBS Lett* 1999; **455**: 286-290
- 27 **Hirtenlehner K**, Pec M, Kubista E, Singer CF. Influences of stroma-derived growth factors on the cytokine expression pattern of human breast cancer cell lines. *Arch Gynecol Obstet* 2002; **266**: 108-113
- 28 **Halangk W**, Lerch MM, Brandt-Nedelev B, Roth W, Ruthenbuenger M, Reinheckel T, Domschke W, Lippert H, Peters C, Deussing J. Role of cathepsin B in intracellular trypsinogen activation and the onset of acute pancreatitis. *J Clin Invest* 2000; **106**: 773-781
- 29 **Teich N**, Bodeker H, Keim V. Cathepsin B cleavage of the trypsinogen activation peptide. *BMC Gastroenterol* 2002; **2**: 16
- 30 **Williams SJ**, Gotley DC, Antalis TM. Human trypsinogen in colorectal cancer. *Int J Cancer* 2001; **93**: 67-73
- 31 **Ducroc R**, Bontemps C, Marazova K, Devaud H, Darmoul D, Laburthe M. Trypsin is produced by and activates protease-activated receptor-2 in human cancer colon cells: evidence for a new autocrine loop. *Life Sci* 2002; **70**: 1359-1367
- 32 **Yamamoto H**, Iku S, Adachi Y, Imsumran A, Taniguchi H, Nosho K, Min Y, Horiuchi S, Yoshida M, Itoh F, Imai K. Association of trypsin expression with tumor progression and matrilysin expression in human colorectal cancer. *J Pathol* 2003; **199**: 176-184
- 33 **Foghsgaard L**, Wissing D, Mauch D, Lademann U, Bastholm L, Boes M, Elling F, Leist M, Jaattela M. Cathepsin B acts as a dominant execution protease in tumor cell apoptosis induced by tumor necrosis factor. *J Cell Biol* 2001; **153**: 999-1010

Fecal loading in the cecum as a new radiological sign of acute appendicitis

Andy Petroianu, Luiz Ronaldo Alberti, Renata Indelicato Zac

Andy Petroianu, Luiz Ronaldo Alberti, Renata Indelicato Zac, Alfa Institute of Gastroenterology of the Hospital of Clinics of the Federal University of Minas Gerais, Avenida Alfredo, Balena, 110-2 andar, Belo Horizonte, MG, Brazil
Correspondence to: Professor Andy Petroianu, Avenida Afonso Pena, 1626 apto. 1901, Belo Horizonte, MG 30130-005, Brazil. petroian@medicina.ufmg.br
Telephone: +55-31-3274-7744 Fax: +55-31-3274-7744
Received: 2004-10-13 Accepted: 2004-12-08

Abstract

AIM: Although the radiological features of acute appendicitis have been well documented, the value of plain radiography has not been fully appreciated. The aim of this study was to determine the frequency of the association of acute appendicitis with images of fecal loading in the cecum.

METHODS: Plain abdominal radiographs of 400 patients operated upon for acute appendicitis ($n = 100$), acute cholecystitis ($n = 100$), right acute pelvic inflammatory disease ($n = 100$) and right nephrolithiasis ($n = 100$) were assessed. The presence of fecal loading was recorded and the sensitivity and specificity of this sign for acute appendicitis were calculated.

RESULTS: The presence of fecal loading in the cecum occurred in 97 patients with acute appendicitis, 13 patients with acute cholecystitis, 12 patients with acute inflammatory pelvic disease and 19 patients with nephrolithiasis. The sensitivity of this sign for appendicitis was 97% and its specificity to this disease was 85.3%. Its positive predictive value for appendicitis was 68.7%; however, its negative predictive value for appendicitis was 98.8%.

CONCLUSION: The present study suggests that the presence of radiological images of fecal loading in the cecum may be a useful sign of acute appendicitis, and the absence of this sign probably excludes this disease. This is the first description of fecal loading as a radiological sign for acute appendicitis.

© 2005 The WJG Press and Elsevier Inc. All rights reserved.

Key words: Appendicitis; Radiography; Cecum; Fecal loading; Diagnosis

Petroianu A, Alberti LR, Zac RI. Fecal loading in the cecum as a new radiological sign of acute appendicitis. *World J Gastroenterol* 2005; 11(27): 4230-4232
<http://www.wjgnet.com/1007-9327/11/4230.asp>

INTRODUCTION

Abdominal pain in the right lower quadrant is probably one of the most challenging problems in Medicine^[1-4]. In most patients, acute appendicitis is diagnosed on the basis of clinical examination, white blood cell count, abdominal radiographic studies, and abdominal ultrasound^[1-5]. However, the less than perfect accuracy of these exams leads to a high rate of misdiagnosis leading to a rate of negative appendectomies of about 15%^[1,2,6,7]. In order to avoid the unnecessary removal of the appendix, other investigation methods, such as computed tomography and abdominal scintigraphy have been proposed, without real advantages^[2-5].

In the presence of acute abdominal pain, abdominal radiographs are relevant and helpful, but little significance is attached to this exam in appendicitis although associated radiological features have been documented, such as localized adynamic ileum (51-81% of cases), increase in soft-tissue density in the right lower quadrant (12-33%), appendicoliths (7-14%) and deformity of cecum (4-5%)^[1,5,8-10]. The aim of this prospective study was to evaluate an apparently new sign present in the plain abdominal radiography of patients with acute appendicitis, i.e., images of fecal loading in the cecum. This sign was studied comparatively with other patients presenting acute right abdominal pain due to other diseases. This is the first description of fecal loading as a radiological sign for acute appendicitis.

MATERIALS AND METHODS

Four hundred consecutive patients with acute right abdominal pain were prospectively studied at the Alfa Institute of Gastroenterology of the Hospital of Clinics and Hospital Julia Kubitshek between 2002 and 2004. No patient was discarded from this investigation.

Plain abdominal radiographies were obtained for all patients before treatment in order to verify the presence of fecal images in the cecum. These patients were divided into the following four groups, with 100 patients each, according to their disease.

Acute appendicitis

Patients of both sexes (62 men and 38 women) ranging in age from 10 to 73 (28.3 ± 12.2) years. All patients were operated for acute appendicitis and the diagnosis was confirmed in all cases by histologic examination of the removed appendix. Fifty of the patients with positive fecal loading in the cecum during the appendicitis period were submitted to a new plain abdominal radiography on the

second postoperative day, to verify the presence of this sign after the appendicectomy.

Acute cholecystitis

Patients of both sexes (30 men and 70 women) ranging in age from 17 to 75 (mean 49.4±16.3 years). All patients were operated for acute cholecystitis and the diagnosis was confirmed in all cases by histologic examination of the removed gallbladder. Eight of these cases presented acute cholangitis as well.

Right pelvic inflammatory disease

Women of the age from 20 to 45 (mean 32.3±8.1 years). The complaint of these cases was due to right hydrosalpingitis (69 cases), right Fallopian pregnancy (14 cases), rupture of a right ovarian cyst (12 cases) and torsion of the right ovary (5 cases). The diagnoses were confirmed in all cases by clinical follow-up, pelvic ultrasound, laparoscopy, and surgical procedures.

Right nephrolithiasis

Patients of both sexes (42 men and 58 women) ranging in age from 10 to 73 (43.5±14.3) years. The diagnosis was confirmed in all these cases by plain abdominal radiography, urography, ultrasound and CT scan.

The radiological image studied was cecal intraluminal mass consisting of a mixture of soft tissue and internal gas bubble like feces, suggesting fecal impaction, or residual feces. The amount of fecal material and consequent cecal dilatation were considered.

The sensitivity and specificity of this radiological sign, as well as its positive and negative predictive values for acute appendicitis were calculated.

The present study followed the Ethics Principles of Research in Humans, according to World Medical Association Helsinki Declaration, adopted in 1964 and amended in 1996, and was approved by the Ethical Committee of the Department of Surgery of the Medical School of the Federal University of Minas Gerais, Belo Horizonte, Brazil. All exams performed on these patients are routinely employed in the presence of acute abdominal pain in the hospitals where this investigation was carried out.

RESULTS

Table 1 describes the presence of fecal loading in the cecum of the patients of the four groups (Figure 1A). Some of these radiographs showed cecal dilatation by the large amount of fecal mass (Figure 1B).

The sensitivity of this sign was 97% for acute appendicitis, 13% for acute cholecystitis, 12% for right acute pelvic inflammatory disease and 19% for right nephrolithiasis. The specificity of fecal loading in the cecum for acute appendicitis was 85.3%. The positive predictive value of this sign for acute appendicitis was 68.7%; however, its negative predictive value for appendicitis was 98.8%.

On the second postoperative day, only two of the 50 patients with previous positive radiological sign preserved the fecal loading in the cecum. In the other 48 patients, this sign disappeared from the cecum.

Table 1 Presence of fecal loading in plain abdominal radiographs of 400 patients with right acute abdominal pain divided into four groups (n = 100 each)

Disease	Fecal loading			
	Present		Absent	
	n	(%)	n	(%)
Acute appendicitis	97	97	3	3
Acute cholecystitis	13	13	87	87
Right pelvic inflammatory disease	12	12	88	88
Right nephrolithiasis	19	19	81	81

DISCUSSION

Although a few studies have suggested that plain abdominal radiography is not helpful anymore in patients with acute abdominal pain, its indiscriminate use remains the rule in most emergency units^[6,8,9-11]. However, the radiological signs described in the literature are not constant or characteristic of appendicitis. Recent investigations have called into question the value of routine use of plain abdominal radiography in patients with suspected appendicitis^[1,3,4,9]. Many physicians consider ultrasound studies as standard in acute abdominal pain, believing the impact of radiograph is not of value.

In this prospective study, the association of acute

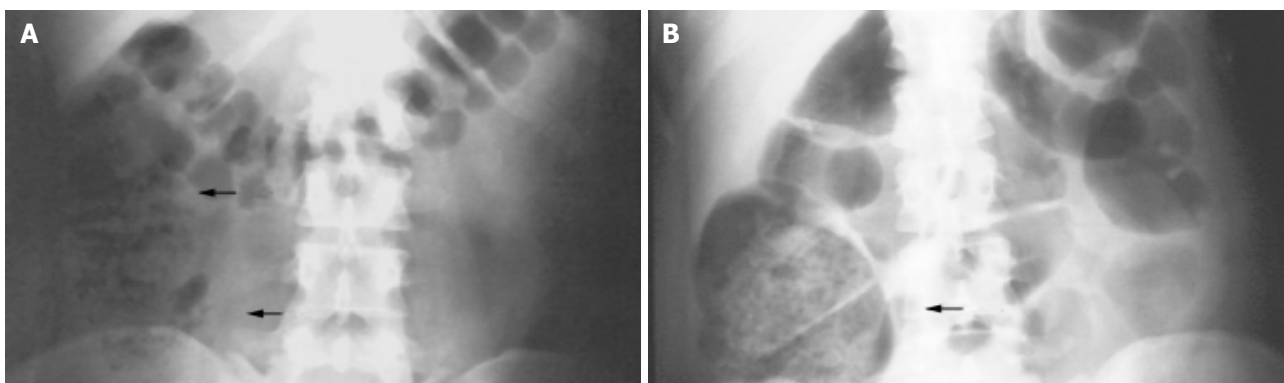


Figure 1 Plain radiographs of the abdomen in the presence of acute appendicitis, showing the fecal loading (cecal intraluminal mass consisting of a mixture of soft tissue and internal gas bubble like feces). **A:** The image of fecal loading in the

cecum (arrow) and right colon (arrow); **B:** The film of another patient with acute appendicitis. Observe residual gross fecal loading with consequent dilatation of the cecum (arrow).

appendicitis with images of fecal loading in the cecum had a sensitivity of 97% and a specificity of 85.3% when compared with other common causes of acute right abdominal pain. This rate is higher than the frequency of other clinical, laboratory, or radiological signs associated with acute appendicitis.

Another important result of the present study is based on the predictive value. According to these data, the possibility of appendicitis in the presence of fecal loading in the cecum is 68.7%. However, the absence of this sign practically excludes the diagnosis of appendicitis, which may occur in only 1.2% of cases.

We could not understand the pathophysiology to answer why appendicitis could lead to fecal loading in the cecum. However, we believe it is worth supposing that this sign may be related to a local ileum of the cecum with stool, which occurred in the presence of an acute inflammatory condition. This is the first description of fecal loading as a radiological sign for acute appendicitis.

In conclusion, the results of the present work suggest that the presence of images of fecal loading in the cecum on plain abdominal radiographs may be a useful sign associated with acute appendicitis. This association should be emphasized, mainly considering that this sign is rare in the presence of other acute inflammatory abdominal

diseases and disappears when the inflamed appendix is removed.

REFERENCES

- 1 **Boleslawski E**, Panis Y, Benoist S, Denet C, Mariani P, Valleur P. Plain abdominal radiography as a routine procedure for acute abdominal pain of the right lower quadrant. *World J Surg* 1999; **23**: 262-264
- 2 **Birnbaum BA**, Wilson SR. Appendicitis at the millenium. *Radiology* 2000; **215**: 337-348
- 3 **Sivit CJ**. Imaging the child with right lower quadrant pain and suspected appendicitis. *Pediatr Radiol* 2004; **34**: 447-453
- 4 **Hayes R**. Abdominal pain. *Eur Radiol* 2004; **14**: L123-L137
- 5 **Rao PM**, Rhea JT, Rao JA, Conn AKT. Plain abdominal radiography in clinically suspected appendicitis. *Am J Emerg Med* 1999; **17**: 325-328
- 6 **Thorpe JA**. The plain abdominal radiograph in acute appendicitis. *Ann Roy Coll Surg Engl* 1979; **61**: 45-47
- 7 **Petroianu A**, Oliveira Neto JE. Prevalence of acute appendicitis in a mixed population. *Dig Surg* 1997; **14**: 195-197
- 8 **Shimkin PM**. Radiology of acute appendicitis. *Am J Roentgenol* 1978; **130**: 1001-1004
- 9 **Shorvon PJ**. Imaging of appendicitis. *Br J Radiol* 2002; **75**: 717-720
- 10 **Shelton T**, McKinlay R, Schwartz RW. Acute appendicitis. *Curr Surg* 2003; **60**: 502-505
- 11 **Petroianu A**, Oliveira Neto JE, Alberti LR. Incidência comparativa da apendicite aguda em população miscigenada, de acordo com a cor da pele. *Arq Gastroenterol* 2004; **41**: 24-26

Science Editor Guo SY Language Editor Elsevier HK

• BRIEF REPORTS •

Effect of autologous blood donation on the central venous pressure, blood loss and blood transfusion during living donor left hepatectomy

Bruno Jawan, Yu-Fan Cheng, Chia-Chi Tseng, Yaw-Sen Chen, Chih-Chi Wang, Tung-Liang Huang, Hock-Liew Eng, Po-Ping Liu, King-Wah Chiu, Shih-Hor Wang, Chih-Che Lin, Tsan-Shiun Lin, Yueh-Wei Liu, Chao-Long Chen

Bruno Jawan, Chia-Chi Tseng, Department of Anesthesiology, Chang Gung Memorial Hospital, Kaohsiung Medical Center, Taiwan, China

Yu-Fan Cheng, Yaw-Sen Chen, Chih-Chi Wang, Tung-Liang Huang, Hock-Liew Eng, Po-Ping Liu, King-Wah Chiu, Shih-Hor Wang, Chih-Che Lin, Yueh-Wei Liu, Tsan-Shiun Lin, Chao-Long Chen, Liver Transplantation Program, Chang Gung Memorial Hospital, Kaohsiung Medical Center, Taiwan, China

Correspondence to: Chao-Long Chen, MD, Superintendent, Chang Gung Memorial Hospital, Ta-pei Road 123, Niao Shung Hsiang, Kaohsiung, Taiwan, China. clchen@adm.cgmh.org.tw
Telephone: +886-7-7317123 Fax: +886-7-7320142

Received: 2004-11-18 Accepted: 2005-01-05

Key words: Patient; Living donor; Surgery; Hepatectomy; Blood; Autologous; Monitoring; Central venous pressure; Blood loss

Jawan B, Cheng YF, Tseng CC, Chen YS, Wang CC, Huang TL, Eng HL, Liu PP, Chiu KW, Wang SH, Lin CC, Lin TS, Liu YW, Chen CL. Effect of autologous blood donation on the central venous pressure, blood loss and blood transfusion during living donor left hepatectomy. *World J Gastroenterol* 2005; 11(27): 4233-4236

<http://www.wjgnet.com/1007-9327/11/4233.asp>

Abstract

AIM: Autologous blood donation (ABD) is mainly used to reduce the use of banked blood. In fact, ABD can be regarded as acute blood loss. Would ABD 2-3 d before operation affect the CVP level and subsequently result in less blood loss during liver resection was to be determined.

METHODS: Eighty-four patients undergoing living donor left hepatectomy were retrospectively divided as group I (GI) and group II (GII) according to have donated 250-300 mL blood 2-3 d before living donor hepatectomy or not. The changes of the intraoperative CVP, surgical blood loss, blood products used and the changes of perioperative hemoglobin (Hb) between groups were analyzed and compared by using Mann-Whitney *U* test.

RESULTS: The results show that the intraoperative CVP changes between GI ($n = 35$) and GII ($n = 49$) up to graft procurement were the same, subsequently the blood loss, but ABD resulted in significantly lower perioperative Hb levels in GI.

CONCLUSION: Since none of the patients required any blood products perioperatively, all the predonated bloods were discarded after the patients were discharged from the hospital. It indicates that ABD in current series had no any beneficial effects, in term of cost, lowering the CVP, blood loss and reduce the use of banked blood products, but resulted in significant lower Hb in perioperative period.

INTRODUCTION

Donor hepatectomy with maximal safety while preserving graft viability and adequacy, in terms of size and function for both recipient and donor, is of principal concern in living donor liver transplantation (LDLT). There are compelling reasons for avoiding surgical blood loss with subsequent blood transfusion^[1]. Allogenic blood transfusion cannot only transmit the infectious diseases, but also induce variety of immunologic responses, such as alloimmunization, transfusion-associated graft vs host diseases, and immunosuppression, which would result in malignant tumor recurrence and increased postoperative infection rate^[2]. Preoperative autologous blood donation (ABD) has been successfully applied in reducing the use of allogenic blood transfusion in liver resection^[3,4]. It is recommended that the last blood donation should not be collected later than 72 h before surgery, to allow for restoration of intravascular volume^[5]. Indeed, ABD can be regarded as acute blood loss. On the other side, low intraoperative central venous pressure (CVP) is associated with less surgical blood loss in hepatectomy surgery^[4,6,7]. Would preoperative ABD 2-3 d before living donor hepatectomy, without intravenous (IV) crystalloid replacement of the loss, affect the intraoperative CVP levels, subsequently reduce the blood loss and blood transfusion during living donor hepatectomy is to be determined. Aims of this retrospective study were to compare the intraoperative CVP levels, blood loss, and the requirement of blood transfusion in patients with and without preoperative ABD during living donor hepatectomy.

MATERIALS AND METHODS

Only consanguineous relatives up to the fifth degree and

lawfully wedded spouses are considered legal live donors in Taiwan. Donor volunteers underwent anthropometric measurements, thorough laboratory analysis, psychosocial evaluation, and detailed imaging studies including Doppler ultrasonography to check the quality of liver parenchyma and patency of blood vessels, and magnetic resonance, venography, arteriography, and cholangiography to check hepatic and portal venous anatomy and hepatic artery and biliary tree branching patterns as previously reported^[8]. Donors should be free of the active liver disease and the donor-recipient pair must be blood group identical or compatible.

After obtaining approval from the Ethics Committee of the Department of Health, Taiwan and written informed consent for surgery and anesthesia from the patients, the patients came into operation room without premedication and IV line. After establishment of the IV line, the anesthesia was induced with thiopental and fentanyl. Succinylcholine was used for facilitating the tracheal intubation. The anesthesia was maintained with isoflurane in oxygen-air mixture and atracurium was used as muscle relaxant. All patients were monitored with electrocardiography, arterial line for continuous blood pressure monitoring, CVP, pulse oximetry, end tidal CO₂, body temperature and urine output.

IV fluids restriction combined with the use of furosemide were applied to lower the intraoperative CVP levels. The deficit of the insensible fluids loss from no per os intake of the patients was not replaced before graft procurement; the intraoperative fluids were maintained to 2-4 mL/(kg · h) before the liver graft is dissected. If the CVP was higher than 10 cm H₂O, furosemide was given; second dose of furosemide was also given if the urine output was lower than 0.5 mL/(kg · h). After the liver graft was procured, IV fluid was increased to approximately 10 mL/(kg · h) until the end of the surgery to replace the cumulative deficits from the procedure. Concerning the surgical procedure and liver parenchymal transection with strict adherence to a meticulous surgical technique without vascular inflow, occlusion to either side of the liver has been previously published^[1].

The anesthesia records were retrospectively reviewed. Patients who had donated 250-300 mL blood 2-3 d before operation was grouped in group I (GI), while no blood donation in group II (GII). The grouping was not at random or blinded; ABD was performed without normovolemic replacement of the loss by IV infusion of the crystalloid in the first 37 cases. Since none of those patients required blood transfusion after successful LDLT, the protocol of ABD was stopped. Data such as anesthesia time, CVP levels (hourly), blood loss, blood transfusion, crystalloids, doses of furosemide and urine output were collected, compared and analyzed between groups by using Mann-Whitney *U* test. All the data were given in mean±SD. Statistical calculations were performed using the SPSS advanced statistics module (SPSS Inc., Chicago, IL, USA). *P* value <0.05 was regarded as significant.

RESULTS

From June 1994 to October 2002, 123 LDLT were performed. Only patients with healthy liver (Table 1) and

undergoing left hepatectomy were enrolled in this study. Right hepatectomy (2/37 in GI and 37/86 in GII) was excluded due to most of the patients of ABD received left hepatectomy. Thirty-five patients were included in ABD group (GI) and 49 in non-ABD group (GII). Table 1 shows the characteristics of the patients of GI and GII. The age, weight, liver functions, anesthesia time, blood loss, and mean dose of furosemide used was not significantly different. Likewise, the crystalloids infusion before and after graft procurement was not significantly different either, but the preoperative hemoglobin (Hb) as well as postoperative d 1-4 of GI was significantly lower in GI in comparison to GII. Figure 1 shows the changes of the CVP levels of both groups, the initial CVP of both groups were higher than 10 cm H₂O, it decreased gradually, under the influence of fluids restriction and diuresis effect of furosemide, and reached a level of 7.9±2.5, 7.7±2.2 and 7.8±1.7, 8.3±1.8 cm H₂O at 6th-7th h after anesthesia begin for GI and GII respectively. It was at that time that the parenchymal transection was performed. After procurement of the liver graft, the IV infusion rate was increased from 3.0±2.3 and 3.4±0.9 to 9.4±6.3 and 10±3.7 mL/(kg · h) for GI and GII respectively. The recovery of the CVP of GI was significantly slower after graft procurement in comparison to GII.

Table 1 Characteristics of patients of GI and GII

	GI (n = 35)	GII (n = 49)
Age (yr)	31.1±5.9	33.9±8.7
Weight (kg)	59.1±9.1	56±8.8
Gender (female/male)	24/11	31/18
SGOT (U/L)	17±6.5	46.3±4.7
SGPT (U/L)	15±11.2	20.9±4.4
ALP (U/L)	53.9±21	56.4±15.7
Total bilirubin (mg, %)	0.58±0.22	0.67±0.2
BUN (mg, %)	12.8±3.3	15.8±13.9
Creatinine (mg, %)	0.79±0.7	0.75±0.1
Anesthesia time (h)	10.4±1.5	10±1.1
Blood loss (mL)	63.8±56	67±63
Fluid 1 [mL/(kg · h)]	3.0±2.3	3.4±0.9
Fluid 2 [mL/(kg · h)]	9.4±6.3	10±3.7
Urine 1 [mL/(kg · h)]	1.6±0.7	1.6±0.7
Urine 2 [mL/(kg · h)]	2.0±1.8	1.7±1.3
Preoperative Hb (g/dL)	11.9±1.8 ^a	12.3±1.5
Postoperative d 1 Hb (g/dL)	11.4±1.83 ^a	12.4±1.6
Postoperative d 2 Hb (g/dL)	11.2±2.0 ^a	12.3±1.5
Postoperative d 3 Hb (g/dL)	10.5±1.6 ^a	11.7±1.4
Postoperative d 4 Hb (g/dL)	9.8±0.9 ^a	11.7±1.69
Furosemide (mg)	11.6±5.0	12.2±1.5

1: Before graft procurement, 2: after graft procurement. ^a*P*<0.05 vs others. SGOT: serum glutamic oxaloacetic transaminase; SGPT: serum glutamic pyruvic transaminase; ALP: alkaline phosphatase.

DISCUSSION

LDLT is a new form of therapy for pediatric and adult patients with end-stage liver diseases to overcome the problem of organ donor shortage. However, the major medical and ethical concern of this technique is the risk to the healthy donor. This concern is legitimate, since

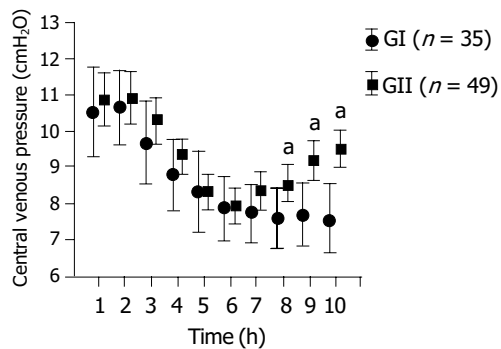


Figure 1 The CVP changes were not significantly different between GI and GII from the first measurement up to the graft procurement, but the recovery of the CVP of GI was slower in comparison to GII after increasing the infusion rate from T8 till the end of the operation ^a $P < 0.05$ vs GI.

hepatectomy is a major upper abdominal surgery with potential risk of massive blood loss and subsequent requirement for blood transfusion, which is correlated significantly with postoperative morbidity and mortality^[9]. It is known that low CVP resulted in significant less blood loss during liver resection. Therefore, maintaining a low CVP has been regarded as a simple and effective way to reduce blood loss during parenchymal transaction^[3,4,6]. A low CVP is accompanied by low pressure in the hepatic veins and sinusoids, theoretically favoring less blood loss during parenchymal transection and allows easier control of inadvertent venous injury^[1]. Low CVP indicates less intravascular volume and ABD is in fact a kind of acute blood loss. If the volume loss is not replaced, theoretically would result in lowering of the intravascular volume, subsequently the CVP and blood loss of liver resection. Our results show that donation of 250-300 mL of blood 2-3 d before donor hepatectomy without IV fluids replacement seemed not to affect the changes of the CVP levels during the surgical procedure in comparison to the group without ABD (Figure 1). The mechanism is probably due to the fact that the volume loss of the donated blood has been fully compensated by the oral intake of the healthy donors within 2-3 d. Figure 1 shows that, under the same anesthesia, same regime in lowering the CVP by fluids restriction and forced diuresis with furosemide, the changes of the CVP, from the first measurement to graft procurement, were not significantly different between GI and GII. The CVP of both groups decreased gradually from 10.5 ± 3.6 and 10.8 ± 2.8 to 7.9 ± 2.5 , 7.7 ± 2.2 and 7.8 ± 1.7 , 8.3 ± 1.8 cm H₂O at the time of parenchymal transection (around T6-7) for GI and GII respectively. The recovery of the CVP level after procurement of the liver graft to the end of the operation was slower in GI after increasing the infusion rate aimed to replace the cumulative fluid deficit to expand intravascular volume and to preserve renal function. Table 1 shows that the blood loss was not significantly different between groups. Both had only minimal blood loss with a mean loss of 63.8 ± 56 and 67 ± 63 mL for GI and GII respectively.

Current results indicated that ABD itself did not have favorable effect in lowering the intraoperative CVP levels and likewise the blood loss in comparison to non-ABD

group. In contrary, it significantly lowered the preoperative Hb level as well as its levels at postoperative d 1-4 (Table 1). It indicated that GI patients would reach earlier low Hb and transfusion threshold. Heiss *et al.*, reported that the blood transfusion rate was indeed higher in the autologous blood group than in the homologous group in patients undergoing colorectal cancer surgery, mainly because these patients had lower preoperative Hb concentrations owing to the blood donation^[10].

Allogenic blood transfusion is often life saving and crucial in the treatment of major blood loss^[11]. Although the safety of the banked blood supply has been improved recently but it can still have adverse effects^[2,12]. The risks of autologous transfusion are less than those of allogenic RBC transfusions^[12,13], but it is still not risk free^[13-16]. Complications such as bacterial contamination, hemolysis due to administrative error, volume overload were reported^[14]. Furthermore, studies have unexpectedly shown similar postoperative infectious complications and immunosuppression in patients receiving autologous blood donated before surgery, as with those receiving homologous blood^[13,17]. Factors such as histamine, plasminogen activator, superoxide and eosinophil cation protein, released into the plasma during storage may be of major importance in enhancing overall immunosuppression^[18]. The best policy in avoiding blood transfusion is to improve the surgical and anesthetic technique to minimize blood loss. Anyway, ABD is still an acceptable alternative measurement to reduce the use of allogenic blood if the amount of expected surgical blood loss is large enough requiring blood transfusion^[3,4]. Since none of our patients required any blood products perioperatively, the predonated autologous bloods of GI were discarded after the patients being discharged from the hospital. In contrary to previous reports^[3,4], ABD in current series had no any beneficial effect, in terms of cost, lowering the CVP, blood loss and reducing the use of banked blood products, but resulted in significant lower Hb in perioperative period, subsequently increasing the chance of getting autologous blood transfusion from their anemia.

In conclusion. Autologous donation of 250-300 mL blood 2-3 d before liver hepatectomy in LDLT seemed not to affect the intraoperative CVP level and subsequently no favorable effect in reducing the blood loss during liver resection. In contrary, it resulted in significant lower Hb in perioperative period, subsequent increasing the chance of getting autologous blood transfusion from their anemia. ABD in living donor left hepatectomy is not recommended if minimal surgical bleeding can be maintained.

REFERENCES

- 1 **Chen CL**, Chen YS, de Villa VH, Wang CC, Lin CL, Goto S, Wang SH, Cheng YF, Huang TL, Jawan B, Cheung HK. Minimal blood loss living donor hepatectomy. *Transplantation* 2000; **69**: 2580-2586
- 2 **Klein HG**. Immunomodulatory aspects of transfusion: a once and future risk? *Anesthesiology* 1999; **91**: 861-865
- 3 **Chan AC**, Blumgart LH, Wuest DL, Melendez JA, Fong Y. Use of preoperative autologous blood donation in liver resections for colorectal metastases. *Am J Surg* 1998; **175**: 461-465
- 4 **Itamoto T**, Katayama K, Nakahara H, Tashiro H, Asahara T. Autologous blood storage before hepatectomy for hepato-

- cellular carcinoma with underlying liver disease. *Br J Surg* 2003; **90**: 23-28
- 5 **Vanderlinde ES**, Heal JM, Blumberg N. Autologous transfusion. *Bmj* 2002; **324**: 772-775
- 6 **Jones RM**, Moulton CE, Hardy KJ. Central venous pressure and its effect on blood loss during liver resection. *Br J Surg* 1998; **85**: 1058-1060
- 7 **Melendez JA**, Arslan V, Fischer ME, Wuest D, Jarnagin WR, Fong Y, Blumgart LH. Perioperative outcomes of major hepatic resections under low central venous pressure anesthesia: blood loss, blood transfusion, and the risk of postoperative renal dysfunction. *J Am Coll Surg* 1998; **187**: 620-625
- 8 **Chen YS**, Cheng YF, De Villa VH, Wang CC, Lin CC, Huang TL, Jawan B, Chen CL. Evaluation of living liver donors. *Transplantation* 2003; **75**: S16-19
- 9 **Gozzetti G**, Mazziotti A, Grazi GL, Jovine E, Gallucci A, Gruttadauria S, Frena A, Morganti M, Ercolani G, Masetti M. Liver resection without blood transfusion. *Br J Surg* 1995; **82**: 1105-1110
- 10 **Heiss MM**, Mempel W, Jauch KW, Delanoff C, Mayer G, Mempel M, Eissner HJ, Schildberg FW. Beneficial effect of autologous blood transfusion on infectious complications after colorectal cancer surgery. *Lancet* 1993; **342**: 1328-1333
- 11 **Greenburg AG**. Benefits and risks of blood transfusion in surgical patients. *World J Surg* 1996; **20**: 1189-1193
- 12 **Goodnough LT**, Brecher ME, Kanter MH, AuBuchon JP. Transfusion medicine. First of two parts-blood transfusion. *N Engl J Med* 1999; **340**: 438-447
- 13 **Goodnough LT**, Brecher ME, Kanter MH, AuBuchon JP. Transfusion medicine. Second of two parts-blood conservation. *N Engl J Med* 1999; **340**: 525-533
- 14 **Linden JV**, Kruskall MS. Autologous blood: always safer? *Transfusion* 1997; **37**: 455-456
- 15 **Domen RE**. Adverse reactions associated with autologous blood transfusion: evaluation and incidence at a large academic hospital. *Transfusion* 1998; **38**: 296-300
- 16 **Goldman M**, Remy-Prince S, Trepanier A, Decary F. Autologous donation error rates in Canada. *Transfusion* 1997; **37**: 523-527
- 17 **Nielsen HJ**. Influence on the immune system of homologous blood transfusion and autologous blood donation: impact on the routine clinical practice/differences in oncological and non-tumour surgery? *Anesthesiol Intensivmed Notfallmed Schmerzther* 2000; **35**: 642-645
- 18 **Nielsen HJ**. Detrimental effects of perioperative blood transfusion. *Br J Surg* 1995; **82**: 582-587

Science Editor Guo SY Language Editor Elsevier HK

• BRIEF REPORTS •

Colchicine sensitizes human hepatocellular carcinoma cells to damages caused by radiation

Chia-Yuan Liu, Hui-Fen Liao, Shou-Chuan Shih, Shee-Chan Lin, Wen-Hsiung Chang, Cheng-Hsin Chu, Tsang-En Wang, Yu-Jen Chen

Chia-Yuan Liu, Shou-Chuan Shih, Shee-Chan Lin, Wen-Hsiung Chang, Cheng-Hsin Chu, Tsang-En Wang, Division of Gastroenterology, Department of Internal Medicine, Mackay Memorial Hospital, Taipei, Taiwan, China
Chia-Yuan Liu, Hui-Fen Liao, Yu-Jen Chen, Department of Medical Research, Mackay Memorial Hospital, Taipei, Taiwan, China
Shou-Chuan Shih, Mackay Medicine, Nursing and Management College, Taipei, Taiwan, China
Hui-Fen Liao, Yu-Jen Chen, Graduate Institute of Sports Coaching Science, Chinese Culture University, Taipei, Taiwan, China
Yu-Jen Chen, Department of Radiation Oncology, Mackay Memorial Hospital, Taipei, Taiwan, China
Hui-Fen Liao, Department of Molecular Biology and Biochemistry, National Chiayi University, Chiayi, 300 Taiwan, China
Supported by the MMH grant from Mackay Memorial Hospital, No. 9252

Correspondence to: Dr. Yu-Jen Chen, Department of Radiation Oncology, Mackay Memorial Hospital, 92, Section 2, Chung San North Road, Taipei 104, Taiwan, China. chenmdphd@yahoo.com
Telephone: +886-2-28094661 Fax: +886-2-28096180
Received: 2004-11-24 Accepted: 2004-12-20

Abstract

AIM: We studied the effect of colchicine combined with radiation on the survival of human hepatocellular carcinoma (HCC) HA22T/VGH cells.

METHODS: Twenty-four hours after treatment with 0-8 ng/mL colchicine, HA22T/VGH cells were irradiated at various doses (0, 1, 2, 4, and 8 Gy). Colony assay was performed to assess the surviving cell fraction. Survival curves were fitted by using a linear-quadratic model to estimate the sensitizer enhancement ratio (SER). Flow cytometry was used for cell cycle analysis.

RESULTS: Colchicine at lower concentrations (1 and 2 ng/mL) had obvious synergy with radiation to inhibit HCC cell growth, whereas higher concentrations (4 and 8 ng/mL) had only additive effect to radiation. Pretreatment with 1 and 2 ng/mL colchicine for 24-h enhanced cell killing by radiation with SERs of 1.21 and 1.53, respectively. G₂/M arrest was only observed with higher colchicine doses (8 and 16 ng/mL) after 24-h treatment; this effect was neither seen with lower doses (1, 2, and 4 ng/mL) nor with any dose after only 1 h of treatment.

CONCLUSION: Our results suggest that colchicine has potential as an adjunct to radiotherapy for HCC treatment. Lower doses of colchicine possess radiosensitizing effects via some mechanism other than G₂/M arrest. Further study is necessary to elucidate the mechanism.

© 2005 The WJG Press and Elsevier Inc. All rights reserved.

Key words: Colchicine; Radiation sensitizer; Hepatocellular carcinoma

Liu CY, Liao HF, Shih SC, Lin SC, Chang WH, Chu CH, Wang TE, Chen YJ. Colchicine sensitizes human hepatocellular carcinoma cells to damages caused by radiation. *World J Gastroenterol* 2005; 11(27): 4237-4240
<http://www.wjgnet.com/1007-9327/11/4237.asp>

INTRODUCTION

Colchicine interferes with microtubule formation, thereby affecting mitosis and other microtubule-dependent functions^[1]. It has been used in clinical practice for a long time, including for the treatment of acute gout^[2], prophylaxis of recurrent gout^[3], Behcet's disease^[4], chronic hepatitis B^[5], and primary biliary cirrhosis^[6]. It is a relatively safe and an effective drug when used with appropriate dosage^[7].

Hepatocellular carcinoma (HCC) is a highly malignant tumor with poor prognosis and high mortality. It is a common malignancy in Asian countries. In China, the incidence has been increasing over the past two decades. The age-adjusted rate of death per 100 000/year was 20.37 in the 1990s. In the USA, the incidence of HCC has approximately doubled over the past three decades^[8]. Aggressive treatment with a variety of modalities, including surgery, transarterial chemoembolization, percutaneous ethanol injection, radiofrequency ablation, microwave coagulation therapy, and laser-induced thermotherapy have all been used in an attempt to control this disease. However, the overall 5-year survival is still around 5%. Few tumors are resectable because of advanced stage or the presence of associated liver disease^[9,10].

Radiation therapy (RT) has not played an important role in HCC treatment in the past because normal liver tissue has low tolerance to radiation. Radiation hepatitis usually develops with whole liver irradiation at or above 35 Gy, yet this dose level may not be sufficient to eradicate the tumor. However, small portions of the liver can be irradiated with 50-60 Gy without significant long-term morbidity. Recent advances in RT including three-dimensional conformal radiation therapy (3DRT) limits the exposure of normal liver tissue and allows delivery of higher RT doses (40-80 Gy)^[11]. 3DRT has improved treatment outcome and reduced normal liver damage in unresectable HCC^[12]. There is a dose-response relationship with 3-DRT for primary HCC, with only the

radiation dose being a significant factor for predicting treatment response^[13]. It is important to develop novel ways to improve the efficacy of RT, not only by physical technique but also by pharmacological agents. The development of radiosensitizers in order to reduce the required cytotoxic RT dose for HCC is especially important for this disease that arises in the midst of radiosensitive normal tissue.

Other studies have demonstrated that cells are most radiosensitive in the G₂/M phase, whereas the most resistant are in late S phase^[14]. Because colchicine arrests the cell cycle at the G₂/M phase, we designed this study to assess its effect in combination with radiation on HA22T/VGH, a poorly differentiated HCC cell line^[15,16].

MATERIALS AND METHODS

Preparation of colchicine

Colchicine (C₂₂H₂₅NO₆, molecular weight 399.4, purity 95%) was purchased from Sigma Co. (St. Louis, MO, USA). The powder was dissolved in distilled water to form an aqueous stock solution and diluted with PBS before use.

Cell culture

The human poorly differentiated HCC cell line HA22T/VGH^[15,16] was cultured in DMEM (GIBCO, Grand Island, NY, USA) supplemented with 10% heat-inactivated fetal calf serum (FCS, Hyclone, Logan, UT, USA), NaHCO₃ (10 mmol/L) and HEPES (20 mmol/L) at 37 °C in a humidified 50 mL/L CO₂ incubator. For routine subculturing, the cells were grown to near confluence, collected by 0.25% trypsin, counted using the trypan blue exclusion test, and adjusted to an initial density of approximately 10⁴ cells/mL.

Colchicine treatment and radiation delivery

In preliminary work, we determined the cytotoxic effect of different colchicine concentrations on HA22T/VGH HCC cells by using a 3-(4,5-dimethylthiazol-2-yl)-2,5-diphenyl-tetrazolium bromide (MTT) assay and found that concentrations up to 2 ng/mL were non-toxic. Based on these preliminary results, we used colchicine concentrations of 0-8 ng/mL to test for radiosensitization. HA22T/VGH HCC cells were treated with 0, 1, 2, 4, and 8 ng/mL colchicine for 24 h, and the colchicine was washed out before RT. RT with 6 MeV electron beam energy was delivered by a linear accelerator (Clinac[®] 1800, Varian Associates, Inc., CA, USA; dose rate 2.4 Gy/min) at various doses (0, 1, 2, 4, and 8 Gy) in a single fraction. Full electron equilibrium was ensured for each fraction by a parallel plate PR-60C ionization chamber (CAPINTEL, Inc., Ramsey, NJ, USA). One hundred and fifty viable tumor cells were plated onto 35-mm six-well culture dishes and were allowed to grow in DMEM medium containing 10% heat-inactivated FCS and the various concentrations of colchicine at 37 °C in a humidified 50 mL/L CO₂ incubator for 24 h. Then the cells were treated with various radiation doses. Following radiation, a colony assay was performed.

Colony assay

After 10-14 d, the culture dishes were stained with 3%

crystal violet and colonies (≥ 50 cells) were counted. The surviving fraction was calculated as mean colonies/cells inoculated. The mean plating efficiency for untreated HA22T/VGH HCC cells was 43%. Survival curves were fitted by using a linear-quadratic model^[17]. The sensitizer enhancement ratio (SER) was calculated as the radiation dose needed for radiation alone divided by the dose needed for colchicine plus radiation at a surviving fraction of 37% (D₀ in radiobiology).

Cell cycle analysis by flow cytometry

Cells were treated with various doses of colchicine (0, 1, 2, 4, 8, and 16 ng/mL) for 1 or 24 h, then harvested and fixed at 4 °C for 1 h with 70% ethanol. The cells were stained for 30 min with propidium iodide (PI) solution (PI, 0.5 mg/mL; RNase, 0.1 mg/mL; Sigma Co.) from a CycleTEST plus DNA reagent kit (Becton Dickinson, Lincoln Park, NJ, USA). Analysis of DNA content was performed using a FACScalibur flow cytometer (Becton Dickinson). The data from 10⁴ cells were collected and analyzed using ModFit software (Becton Dickinson).

Statistical analysis

Data were expressed as percentage and mean \pm SE.

We used Sigma Plot software (version 8.0, SPSS Inc., Chicago, IL, USA) to fit survival curves with a linear-quadratic model. One-way analysis of variance was used to compare the colony formation between different groups (SPSS, version 10.0, Chicago, IL, USA).

RESULTS

Cell survival and SER

The results of colony assays of various doses colchicine combined with radiation are shown in Table 1. There was an obvious synergistic effect of low-dose colchicine (1 and 2 ng/mL) plus radiation. When the dose was increased to 4 and 8 ng/mL, only mild additive effects were noted.

As the survival curves in Figure 1 demonstrate, low-dose colchicine sensitized HA22T/VGH HCC cells to radiation in a dose-dependent manner. The RT doses required for a surviving fraction of 37% (D₀ in radiobiology) after pretreatment with 0, 1, and 2 ng/mL colchicine were 9.45, 7.80, and 6.16 Gy respectively. The calculated SERs of colchicine were 1.21 for 1 ng/mL and 1.53 for 2 ng/mL.

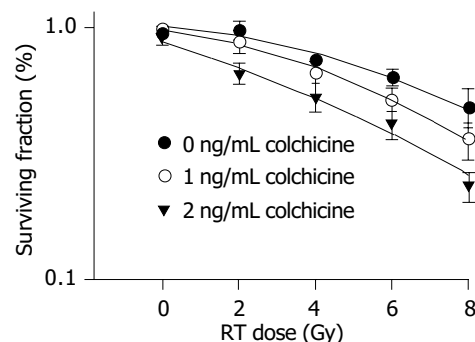


Figure 1 Radiation survival curves for human HA22T/VGH hepatocellular carcinoma cells. Cells were treated with vehicle (●), colchicine 1 ng/mL (○) and 2 ng/mL (▼) for 1 h before radiation.

Table 1 Colony assay of human HA22T/VGH hepatocellular carcinoma cells. Data are expressed as mean±SE

Colchicine (ng/mL)	0	1	2	4	8
RT 0 Gy	81.0±4.0	78.7±1.0	72.8±3.3	57.5±4.0	29.2±2.7
1	78.3±4.1	70.5±5.1	52.7±4.5	43.3±4.3	22.3±3.0
2	59.8±3.5	53.5±4.2	42.3±3.6	33.2±2.5	12.8±3.0
4	51.2±3.0	41.5±3.2	32.8±3.2	27.0±3.3	11.5±2.7
8	38.2±5.6	27.3±3.5	18.5±1.8	15.3±2.4	6.7±1.8

Cell cycle analysis after varying doses of colchicine

Although colchicine is reported to arrest mitosis, no HA22T/VGH HCC cells were clearly seen in the G₂/M phase 1-h treatment (data not shown). After 24 h of colchicine treatment, significant G₂/M arrest was induced by higher doses (8 and 16 ng/mL) but not by doses, which were less than 8 ng/mL (Table 2). The DNA histograms after 24 h of treatment with varying doses of colchicine are shown in Figure 2.

Table 2 Cell cycle analysis of human HA22T/VGH hepatocellular carcinoma cells. Cell were treated with various doses of colchicine for 24 h and analyzed by flow cytometry

Colchicine (ng/mL)	Cell cycle distribution (%)		
	G ₀ /G ₁	S	G ₂ +M
0	49.0±1.4	24.6±1.1	26.4±1.0
1	51.4±1.1	21.7±1.4	26.9±1.0
2	52.2±1.5	21.5±1.4	26.3±0.9
4	51.6±1.9	22.0±1.5	26.5±0.9
8	43.0±2.1 ^a	21.7±1.7	35.4±1.2 ^b
16	17.6±1.3 ^b	23.5±1.3	58.9±2.2 ^b

^aP<0.05, ^bP<0.01 vs colchicine treatment with 0 ng/mL.

DISCUSSION

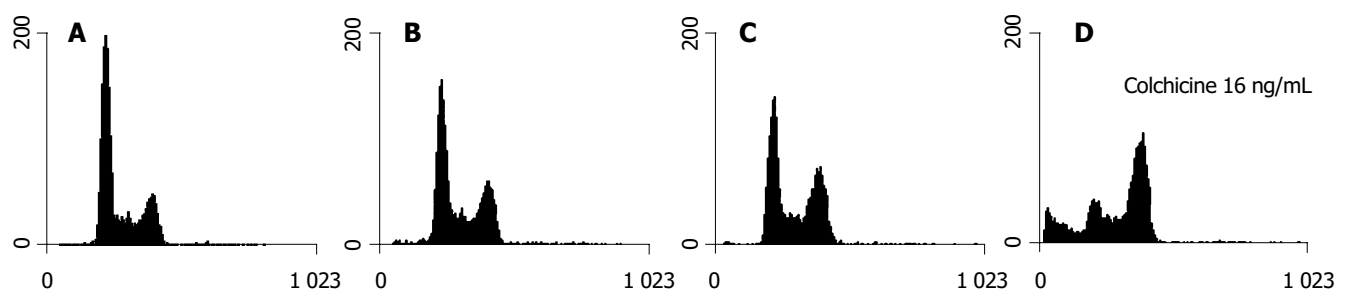
The present study demonstrates that pretreatment with colchicine is capable of reducing the survival of irradiated human HCC HA22T/VGH cells. The combined effect varies with the dose of colchicine. Pretreatment with colchicine at lower doses (1-2 ng/mL) 1 h prior to RT yielded a synergistic effect on radiation-induced cytotoxicity. Higher doses gave only a mild additive effect. However,

the G₂/M arrest phenomenon was not found with low doses or short-term (1 h) colchicine treatment. Evident G₂/M arrest was observed after treatment with higher doses (8 and 16 ng/mL) of colchicine for 24 h. Alteration of cell cycle distribution therefore may not play a major role in the radiosensitizing effect of colchicine in this combined therapy.

RT plays an important role in combined treatment for several malignant tumors^[18,19]. However, the risk of radiation-induced toxicity limits its use in liver tumors^[20]. While 3DRT is increasingly used for HCC, limiting the volume of irradiated normal liver and allowing adjustment of the radiation dose to improve the therapeutic index, it still has many limitations. Advanced liver cirrhosis or poor liver reserve is a common problem in patients with HCC^[21]. The risk of hepatic failure after cytotoxic doses of RT therefore remains as a great problem. Radiosensitizers may give patients with poor liver reserve a better chance of controlling their tumor. Pentoxifylline and ganglioside GD3 have been shown to act as radiosensitizers in the human HCC cell line HepG2. Pentoxifylline may do so by causing cell cycle arrest in the G₂/M phase. Ganglioside GD3 may have a dual action in producing radiosensitization by interacting with mitochondria and by inactivating NF-κB^[22,23].

The safety and therapeutic range of colchicine are well established. The doses of colchicine (0-8 ng/mL) we used before RT are much lower than those in previous reports for other *in vitro* disease models^[7]. Our results demonstrate that colchicine enhances the radiation effect *in vitro*, thus reducing the radiation dose needed to inhibit tumor growth. Most RT-related complications develop not early in the course of RT but rather after a high cumulative dose. Using colchicine at low doses yielded an SER of 1.21 at 1 ng/mL and 1.53 at 2 ng/mL. This means that if the original planned RT dose was 50 Gy, the same cytotoxic effect would be achieved by only 32.68 Gy after pretreatment with 2 ng/mL of colchicine. This reduced RT dose is close to 30 Gy, the threshold for whole liver irradiation, which may result in lethal liver damage with a 5% probability in 5 years (TD 5/5)^[20].

Our results suggest that lower doses of colchicine sensitize HA22T/VGH HCC cells to radiation. At lower doses (1 and 2 ng/mL), 24 h of treatment with colchicine did not change the G₂/M phase distribution significantly. At higher doses (8 and 16 ng/mL), the drug arrested that cell cycle at the G₂/M phase. There was an accompanying evident sub-G₁ peak noted on the DNA histogram (Figure 2). This implies that the synergistic effect of colchicine and RT may involve multiple mechanisms,

**Figure 2** DNA histograms in cell cycle analyses of HA22T/VGH cells by flow cytometry. A: Control; B: Colchicine 2 ng/mL; C: Colchicine 8 ng/mL;

D: Colchicine 16 ng/mL.

perhaps including cell cycle regulation, induction of apoptosis, and others.

In conclusion, colchicine at optimal doses sensitizes human HA22T/VGH HCC cells to radiation by a mechanism other than cell cycle arrest at the G₂/M phase.

ACKNOWLEDGMENTS

The authors wish to thank Dr. Mary Jeanne Buttrey for critical reading and correction of the manuscript.

REFERENCES

- 1 **Ben-Chetrit E**, Levy M. Colchicine: 1998 update. *Semin Arthritis Rheum* 1998; **28**: 48-59
- 2 **Emmerson BT**. The management of gout. *N Engl J Med* 1996; **334**: 445-451
- 3 **Yu TF**, Gutman AB. Efficacy of colchicine prophylaxis in gout. Prevention of recurrent gouty arthritis over a mean period of five years in 208 gouty subjects. *Ann Intern Med* 1961; **55**: 179-192
- 4 **Masuda K**, Nakajima A, Urayama A, Nakae K, Kogure M, Inaba G. Double-masked trial of cyclosporin versus colchicine and long-term open study of cyclosporin in Behcet's disease. *Lancet* 1989; **1**: 1093-1096
- 5 **Floreani A**, Lobello S, Brunetto M, Aneloni V, Chiaramonte M. Colchicine in chronic hepatitis B: a pilot study. *Aliment Pharmacol Ther* 1998; **12**: 653-656
- 6 **Lee YM**, Kaplan MM. Efficacy of colchicine in patients with primary biliary cirrhosis poorly responsive to ursodiol and methotrexate. *Am J Gastroenterol* 2003; **98**: 205-208
- 7 **Wallace SL**, Singer JZ. Review: systemic toxicity associated with the intravenous administration of colchicine-guidelines for use. *J Rheumatol* 1988; **15**: 495-499
- 8 **El-Serag HB**. Hepatocellular carcinoma: an epidemiologic view. *J Clin Gastroenterol* 2002; **35**(5 Suppl 2): S72-S78
- 9 **Faivre J**, Forman D, Esteve J, Obradovic M, Sant M. Survival of patients with primary liver cancer, pancreatic cancer and biliary tract cancer in Europe. *Eur J Cancer* 1998; **34**: 2184-2190
- 10 **El-Serag HB**, Mason AC, Key C. Trends in survival of patients with hepatocellular carcinoma between 1977 and 1996 in the United States. *Hepatology* 2001; **33**: 62-65
- 11 **Nguyen MH**, Keeffe EB. Treatment of Hepatocellular cancer. In: Rustgi AK, Crawford JM. *Gastrointestinal Cancers*. London: Saunders 2003: 615
- 12 **Cheng SH**, Lin YM, Chuang VP, Yang PS, Cheng JC, Huang AT, Sung JL. A pilot study of three-dimensional conformal radiotherapy in unresectable hepatocellular carcinoma. *J Gastroenterol Hepatol* 1999; **14**: 1025-1033
- 13 **Park HC**, Seong J, Han KH, Chon CY, Moon YM, Suh CO. Dose-response relationship in local radiotherapy for hepatocellular carcinoma. *Int J Radiat Oncol Biol Phys* 2002; **54**: 150-155
- 14 **Sinclair WK**, Morton RA. X-ray sensitivity during the cell generation cycle of cultured Chinese hamster cells. *Radiat Res* 1966; **29**: 450-474
- 15 **Lin YM**, Hu CP, Chou CK, Lee TW, Wu KT, Chen TY, Peng FK, Lin TJ, Ko JL, Chang CM. A new human hepatoma cell line: establishment and characterization. *Zhonghua Minguo Weisheng Wujia Mianyixue Zazhi* 1982; **15**: 193-201
- 16 **Chang C**, Lin Y, Lee TW, Chou CK, Lee TS, Lin TJ, Peng FK, Chen TY, Hu CP. Induction of plasma protein secretion in a newly established human hepatoma cell line. *Mol Cell Biol* 1983; **3**: 1133-1137
- 17 **Hall EJ**. Cell survival curves. In: *Radiobiology for the radiologist*. 5th ed. Philadelphia: Lippincott Williams & Wilkins 2000: 32-37
- 18 **Kuban DA**, Dong L. High-dose intensity modulated radiation therapy for prostate cancer. *Curr Urol Rep* 2004; **5**: 197-202
- 19 **Olmi P**, Fallai C, Cerrotta AM, Lozza L, Badii D. Breast cancer in the elderly: the role of adjuvant radiation therapy. *Crit Rev Oncol Hematol* 2003; **48**: 165-178
- 20 **Emami B**, Lyman J, Brown A, Coia L, Goitein M, Munzenrider JE, Shank B, Solin LJ, Wesson M. Tolerance of normal tissue to therapeutic irradiation. *Int J Radiat Oncol Biol Phys* 1991; **21**: 109-122
- 21 **Alsowmely AM**, Hodgson HJ. Non-surgical treatment of hepatocellular carcinoma. *Aliment Pharmacol Ther* 2002; **16**: 1-15
- 22 **Wu DH**, Liu L, Chen LH. Radiosensitization by pentoxifylline in human hepatoma cell line HepG2 and its mechanism. *Diyi Junyi Daxue Xuebao* 2004; **24**: 382-385
- 23 **Paris R**, Morales A, Coll O, Sanchez-Reyes A, Garcia-Ruiz C, Fernandez-Checa JC. Ganglioside GD3 sensitizes human hepatoma cells to cancer therapy. *J Biol Chem* 2002; **277**: 49870-49876

Science Editor Guo SY Language Editor Elsevier HK

• BRIEF REPORTS •

Co-infection of SENV-D among chronic hepatitis C patients treated with combination therapy with high-dose interferon-alfa and ribavirin

Chia-Yen Dai, Wan-Long Chuang, Wen-Yu Chang, Shinn-Cherng Chen, Li-Po Lee, Ming-Yen Hsieh, Nei-Jen Hou, Zu-Yau Lin, Ming-Yuh Hsieh, Liang-Yen Wang, Ming-Lung Yu

Chia-Yen Dai, Wan-Long Chuang, Wen-Yu Chang, Shinn-Cherng Chen, Li-Po Lee, Ming-Yen Hsieh, Nei-Jen Hou, Zu-Yau Lin, Ming-Yuh Hsieh, Liang-Yen Wang, Ming-Lung Yu, Hepatobiliary Division, Department of Internal Medicine, Kaohsiung Medical University Hospital, Kaohsiung, Taiwan, China
Chia-Yen Dai, Nei-Jen Hou, Department of Internal Medicine, Kaohsiung Municipal Hsiao-Kang Hospital, Kaohsiung, Taiwan, China
Chia-Yen Dai, Department of Occupational Medicine, Kaohsiung Municipal Hsiao-Kang Hospital, Kaohsiung, Taiwan, China
Supported by the National Science Council Grant, No. NSC-91-2314-B037-344

Correspondence to: Ming-Lung Yu, MD, PhD, Hepatobiliary Division, Department of Internal Medicine, Kaohsiung Medical University Hospital, No. 100, Shih-Chuan 1st Road, Kaohsiung 807, Taiwan, China. d780178@kmu.edu.tw
Telephone: +886-7-3121101-7475 Fax: +886-7-3123955
Received: 2004-11-08 Accepted: 2004-12-20

Abstract

AIM: The clinical significance of co-infection of SENV-D among patients with chronic hepatitis C (CHC) and response of both viruses to combination therapy with high-dose interferon-alfa (IFN) plus ribavirin remain uncertain and are being investigated.

METHODS: Total 164 (97 males and 67 females, the mean age 48.1 ± 11.4 years, range: 20-73 years, 128 histologically proved) naive CHC patients were enrolled in this study. SENV-D DNA was tested by PCR method. Detection of serum HCV RNA was performed using a standardized automated qualitative RT-PCR assay (COBAS AMPLICOR HCV Test, version 2.0). HCV genotypes 1a, 1b, 2a, 2b, and 3a were determined by using genotype-specific primers. Pretreatment HCV RNA levels were determined by using the branched DNA assay (Quantiplex HCV RNA 3.0). There are 156 patients receiving combination therapy with IFN 6 MU plus ribavirin for 24 wk and the response to therapy is determined.

RESULTS: Sixty-one (37.2%) patients were positive for SENV-D DNA and had higher mean age than those who were negative (50.7 ± 10.6 years vs 46.6 ± 11.6 years, $P = 0.026$). The rate of sustained viral response (SVR) for HCV and SENV-D were 67.3% (105/156) and 56.3% (27/48), respectively. By univariate analysis, the higher rate of SVR was significantly related to HCV genotype non-1b ($P < 0.001$), younger ages ($P = 0.014$), lower

pretreatment levels of HCV RNA ($P = 0.019$) and higher histological activity index (HAI) score for intralobular regeneration and focal necrosis ($P = 0.037$). By multivariate analyses, HCV genotype non-1b, younger age and lower pretreatment HCV RNA levels were significantly associated with HCV SVR (odds ratio (OR)/95% confidence interval (CI): 12.098/0.02-0.19, 0.936/0.890-0.998, and 3.131/1.080-9.077, respectively). The SVR of SENV-D was higher among patients clearing SENV-D than those who had viremia at the end of therapy ($P = 0.04$).

CONCLUSION: Coexistent SENV-D infection, apparently associated with higher ages, is found in more than one-third Taiwanese CHC patients. Both HCV and SENV-D are highly susceptible to combination therapy with high-dose IFN and ribavirin and SENV-D co-infection does not affect the HCV response. HCV genotype, pretreatment HCV RNA levels and age are predictive factors for HCV SVR.

© 2005 The WJG Press and Elsevier Inc. All rights reserved.

Key words: Chronic hepatitis C; Combination therapy; Interferon; Ribavirin; SENV-D

Dai CY, Chuang WL, Chang WY, Chen SC, Lee LP, Hsieh MY, Hou NJ, Lin ZY, Hsieh MY, Wang LY, Yu ML. Co-infection of SENV-D among chronic hepatitis C patients treated with combination therapy with high-dose interferon-alfa and ribavirin. *World J Gastroenterol* 2005; 11(27): 4241-4245
<http://www.wjgnet.com/1007-9327/11/4241.asp>

INTRODUCTION

A new family of DNA viruses was recently isolated and designated as SEN virus (SENV)^[1,2]. SENV is a single-stranded circular DNA virus distantly related to the large TT virus family with eight different variants (A-H) shown by phylogenetic analysis^[3]. Two strains of SENV (SENV-D and SENV-H) are more prevalent among patients with transfusion-associated non-AE hepatitis than in healthy blood donors that suggested the significant associations between SENV-D/H and transfusion-associated hepatitis^[2,4]. Nevertheless, the clinical implication and etiological importance in association with liver diseases of SENV infection still remain undetermined.

HCV is the major etiologic agent of post-transfusion hepatitis and leads to chronic liver disease and primary

hepatocellular carcinoma^[5,6]. With the prevalence rate of chronic hepatitis C (CHC) ranging from 0.95% to 2.6% among the general population^[7,8], we had previously reported a positive rate of anti-HCV up to 57.9% in some communities in southern Taiwan^[9]. For CHC, the combination therapy with interferon- α (IFN) and ribavirin has been considered as first-line therapy. Previous reports have demonstrated the increased rate of sustained viral response (SVR) to 31-43% after combination therapy for 24 or 48 wk than 6-19% of IFN monotherapy^[10,11]. Lai *et al.*, reported a SVR rate of 43% after combination therapy with standard IFN dose in Taiwan^[12]. In our previous study, the rate of HCV SVR with a high-dose IFN monotherapy achieved 41.2% among Taiwanese CHC patients^[13] and the tailored-dose IFN monotherapy according to the virological characteristics of CHC patients yielded a better efficacy^[14]. The benefits of high-dose IFN may be gained in the combination therapy for CHC.

The clinical significance of SENV infection in combination with HCV infection remains controversial. For patients with CHC, Rigas *et al.*, reported that co-infection with SENV might adversely affect the outcome of treatment with combination therapy^[15]. Another study, however, did not support their findings^[16]. The aims of the present study are to survey the prevalence and clinical implications of SENV-D co-infection on biochemical, pathological, and virological profiles among CHC patients. The response of HCV and SENV-D to combination therapy with high-dose IFN and ribavirin are also investigated. Furthermore, we elucidate the predictive factors for HCV SVR and the influence of concurrent SENV-D infection on HCV response to combination therapy.

MATERIALS AND METHODS

Patients

Between May 1998 and May 2001, a total of 164 Taiwanese CHC patients in the clinics of hepatological division of the Kaohsiung Medical University Hospital, 97 men and 67 women, aged between 20 and 73 years (mean 48.1 ± 11.4 years) were enrolled in the study. All patients were diagnosed with chronic HCV infection based on continuous positivity for second-generation antibody to HCV (anti-HCV) in serum for more than 6 mo and positive for HCV RNA. Liver biopsies were carried out in 128 patients and the disease activity grade and fibrosis stage were quantitatively scored according to the histological activity index (HAI) scoring system^[17]. Patients who were positive for hepatitis B surface antigen (HBsAg) had human immunodeficiency virus type I infection, autoimmune liver disease, metabolic liver diseases including α -1 anti-trypsin deficiency hemochromatosis or Wilson's disease, alcoholic liver disease or intravenous drug abuse were excluded. All the serum samples, when collected from patients at the time of their evaluation, were stored at -70°C before testing. The study had been approved by the Ethics Committee of Kaohsiung Medical University Hospital and all patients had given their informed consent.

Methods

Laboratory tests Serum HBsAg was assayed using

commercially available kits (General Biological HBsAg radio-immunoassay; General Biological Cooperation, Taiwan) and second-generation HCV antibody (anti-HCV) was detected with commercially available ELISA kits (Abbott, North Chicago, IL, USA). Alanine aminotransferase (ALT, normal upper limit of serum ALT = 34 IU/L) was measured on a multichannel autoanalyzer.

Detection of SENV-D DNA and detection/quantification/genotyping of serum HCV RNA The presence of SENV-D DNA was determined by PCR as described previously^[18]. Detection of serum HCV RNA was performed using a standardized automated qualitative RT-PCR assay (COBAS AMPLICOR HCV Test, version 2.0; Roche, Branchburg, NJ, USA). The detection limit was 50 IU/mL. HCV genotypes 1a, 1b, 2a, 2b, and 3a were determined by amplification of the core region using genotype-specific primers described by Okamoto *et al.*^[19]. Pretreatment HCV RNA levels were determined by using the branched DNA assay (Quantiplex HCV RNA 3.0, Bayer, Emeryville, CA, USA), performed strictly in accordance with the manufacturer's instructions. The quantification limit was 615 IU of HCV RNA per milliliter.

Combination therapy with high-dose IFN and ribavirin Total 156 CHC-naïve patients (92 males, 64 females, mean age: 48.0 ± 11.5 years, 122 patients with liver biopsies) received combination therapy for 24 wk using IFN subcutaneously at a dosage of 6 MU thrice a week and ribavirin by mouth at a dosage of 1 000-1 200 mg daily. After the cessation of therapy, all of them received 24 wk of follow up for evaluation of the response. A SVR for HCV was defined as clearance of serum HCV RNA at the end of the therapy and 24 wk after the cessation of combination therapy. All other patients were defined as non-responders (NR). To evaluate the response of SENV-D, the presence of SENV-D DNA was determined at wk 24 and 48. An end-of-treatment viral response (ETVR) and a SVR for SENV-D were indicated by negative PCR results at wk 24 and 48, respectively.

Statistical analysis

Serum HCV RNA levels were expressed as the mean \pm SD after logarithmic transformation of original values. Frequency was compared between groups using the χ^2 test or Fisher's exact test, and group means were compared using the *t*-test. For all tests a *P* value lesser than 0.05 was considered to be significant. Stepwise logistic regression was used to analyze factors associated with response to combination therapy in CHC patients. Odds ratios (ORs) and their associated 95% confidence intervals (CIs) were used to quantify the magnitude of their associations.

RESULTS

Study population

The mean pretreatment ALT and HCV RNA levels of the 164 CHC patients was 136.9 ± 168.9 IU/L and 5.79 ± 0.67 log IU/mL, respectively. There were 140 (85.4%) patients with abnormal ALT levels. The HCV genotype distribution was as follows: 1b in 80 (48.8%) patients, 2a in 48 (29.3%) patients, 2b in 18 (11.0%) patients, mixed in 13 (7.9%)

patients and unclassified in 5 (3.0%) patients. Of 128 patients undergoing liver biopsies, the mean scores for peri-portal necrosis, intralobular necrosis, portal inflammation (grading) and fibrosis were 1.11 ± 1.34 , 0.52 ± 0.88 , 1.91 ± 1.24 , 3.51 ± 2.55 , and 1.25 ± 1.36 , respectively.

SENV-D viremia in chronic hepatitis C patients

Of 164 CHC patients, 61 patients were positive for SENV-D DNA showing a prevalence of 37.2%. The comparison of clinical characteristics between patients with and without SENV-D co-infection was shown in Table 1. The mean age was higher among patients with positive SENV-D DNA than those who were negative for SENV-D DNA (50.7 ± 10.6 years *vs* 46.6 ± 11.6 years, $P = 0.026$). No other clinical and virological factor was related to positive SENV-D DNA. Among 128 patients that underwent liver biopsies, all the mean scores were similar between SENV-D DNA-positive and -negative patients.

Table 1 Comparison of clinical characteristics between individuals with and without SENV-D viremia in 164 CHC patients

	SENV-D viremia		P
	Positive (n = 61)	Negative (n = 103)	
Sex (male) (%)	36 (59.0)	61 (59.2)	NS
Age (yr)	50.7 ± 10.6	46.6 ± 11.6	0.026
Serum ALT (IU/L)	144.0 ± 164.3	125.8 ± 164.2	NS
Normal (≤ 34 IU/L) (%)	8 (33.3)	16 (66.7)	NS
Abnormal (> 34 IU/L) (%)	53 (37.9)	87 (62.1)	
HCV RNA levels (log IU/mL)	5.72 ± 0.70	5.85 ± 0.63	NS
HCV genotype 1b (%)	26 (42.6)	54 (52.4)	NS
Histology (HAI scores)	46	82	
Peri-portal necrosis	1.11 ± 1.34	1.11 ± 1.35	NS
Intralobular necrosis	0.70 ± 1.00	0.41 ± 0.78	NS
Portal inflammation	1.80 ± 1.31	1.98 ± 1.21	NS
Total score (grading)	3.54 ± 2.65	3.49 ± 2.52	NS
Fibrosis	1.39 ± 1.50	1.16 ± 1.28	NS

Results are expressed as mean \pm SD. HAI: histological activity index, NS: no significance.

HCV virological response to combination therapy

Of all 156 naive CHC patients receiving combination therapy, the HCV genotype distribution was as follows: 1b in 76 (48.7%) patients, 2a in 47 (30.1%) patients, 2b in 16 (10.3%) patients, mixed in 12 (7.7%) patients, and unclassified in 5 (3.2%) patients. The mean pretreatment ALT and HCV RNA levels were 134.8 ± 166.8 IU/L and 5.79 ± 0.66 log IU/mL, respectively with 133 (85.3%) and

99 (63.5%) patients having abnormal ALT levels and high serum HCV levels ($\geq 200\ 000$ IU/mL). Of 122 patients undergoing liver biopsies, the mean scores for peri-portal necrosis, intralobular necrosis, portal inflammation (grading), and fibrosis were 1.09 ± 1.31 , 0.52 ± 0.89 , 1.93 ± 1.22 , 3.52 ± 2.48 , and 1.23 ± 1.33 , respectively. After combination therapy with high dose IFN and ribavirin for 24 wk, 105 (67.3%) of 156 patients achieved SVR. The clinical and virological features between CHC patients with HCV SVR and those with NR are shown in Table 2. In comparison between these two groups by univariate analysis, the higher rate of SVR was significantly related to younger ages ($P = 0.014$), lower pretreatment levels of HCV RNA ($< 200\ 000$ IU/mL, $P = 0.019$), HCV genotype non-1b ($P < 0.001$) and higher HAI score for intralobular regeneration and focal necrosis ($P = 0.037$). No significant association between other clinical and virological factors and HCV response of combination therapy was observed. Based on multivariate regression analyses, the significant factors associated with HCV SVR after combination therapy were HCV genotype non-1b, younger age and pretreatment HCV RNA levels less than $200\ 000$ IU/mL with the OR and 95%CI of these factors summarized in Table 3.

Table 2 Comparison of clinical and virological features between sustained viral responders (SVR) and non-responders (NR) of CHC patients after combination therapy

	HCV response		P
	NR (n = 51)	SVR (n = 105)	
Sex (male) (%)	31 (60.8)	61 (58.1)	NS
Age (yr)	51.24 ± 11.3	46.4 ± 11.3	0.014
Serum ALT (IU/L)	122.2 ± 105.0	140.9 ± 189.9	NS
Normal (≤ 34 IU/L) (%)	4 (18.2)	18 (81.8)	NS
Abnormal (> 34 IU/L) (%)	47 (34.6)	87 (65.4)	
HCV RNA levels (log IU/mL)	5.90 ± 0.62	5.73 ± 0.68	NS
High level ($\geq 200\ 000$ IU/mL) (%)	39 (39.4)	60 (60.6)	0.019
Low level ($< 200\ 000$ IU/mL) (%)	12 (21.1)	45 (78.9)	
HCV genotype 1b (%)	44 (86.3)	32 (30.5)	<0.0001
Positive SENV-D DNA (%)	16 (31.4)	41 (39.0)	NS
Histology (HAI scores)			
Patients no.	37	85	
Peri-portal necrosis	1.08 ± 1.30	1.091 ± 1.323	NS
Intralobular necrosis	0.278 ± 0.61	0.64 ± 0.97	0.037
Portal inflammation	2.03 ± 1.17	1.89 ± 1.25	NS
Total score (grading)	3.32 ± 2.22	3.60 ± 2.59	NS
Fibrosis	1.41 ± 1.38	1.157 ± 1.31	NS

Results are expressed as mean \pm SD. HAI: histological activity index, NS: no significance.

Table 3 Stepwise logistic regression analysis of factors significantly associated with HCV sustained virologic response (SVR) after combination therapy in 156 CHC patients

Dependent variable	Independent variable	Comparison	OR (95%CI)	P
HCV SVR	HCV genotypes	1b = 0	12.098 (0.02–0.19)	<0.001
		Non-1b = 1		
	Age	Per year increased	0.936 (0.890–0.998)	0.011
	HCV RNA level	High ($\geq 200\ 000$ IU/mL) = 0	3.131 (1.080–9.077)	0.036
	Low ($< 200\ 000$ IU/mL) = 1			

¹CI: Confidence interval.

Clearance of SENV-D DNA after combination therapy

SENV-D DNA was followed in 48 CHC patients (28 males, 20 females, mean age: 50.2±10.5 years) concomitant with SENV-D viremia before combination therapy. Their mean ALT level was 154.6±179.8 IU/L (range: 16-112 years) and 41 patients were abnormal. The HCV genotype distribution is as follows: 1b in 19 patients, 2a in 19 patients, 2b in 4 patients, mixed in 5 patients, and unclassified in 1 patient. The clinical characteristics and virological features between individuals with and without SENV-D DNA after combination therapy were analyzed and shown in Table 4. At the end of treatment, SENV-D DNA was negative in 37 patients (77.1%). Thirteen of thirty-seven patients (35.1%) had reappearance of serum SENV-D DNA when followed 24 wk after the cessation of therapy. Three of eleven patients (27.3%) with positive SENV-D DNA at the end of treatment were cleared of SENV-D DNA 24 wk after the cessation of therapy. The rate of SVR of SENV-D DNA after combination therapy was 56.3% (27/48). As shown in Table 4, the SVR of SENV-D was higher among patients with ETVR than those who were SENV-D viremia at the end of treatment (88.9% vs 61.9%, $P = 0.04$). No other clinical and virological factor was related to SVR for SENV-D.

Table 4 Comparison of clinical characteristics and virological features between 48 CHC patients with and without sustained clearance of SENV-D after combination therapy

	SENV-D response		P
	NR (n = 21)	SVR (n = 27)	
Sex (male) (%)	15 (71.4)	13 (48.2)	NS
Age (yr)	48.3±10.6	51.7±10.3	NS
Serum ALT (IU/L)	157.6±122.9	152.4±216.3	NS
High HCV RNA level (≥200 000 IU/mL) (%)	9 (42.9)	18 (66.7)	NS
HCV genotype 1b (%)	7 (33.3)	12 (44.4)	NS
SENV-D ETVR (%)	13 (61.9)	24 (88.9)	0.04
HCV SVR (%)	17 (81.0)	18 (66.7)	NS

Results are expressed as mean±SD. ETVR: end-of-treatment viral response, SVR: sustained viral responder, NR: non-responders, NS: no significance.

DISCUSSION

The geographic distribution of different SENV variants has been noted. In Japan, SENV-D is more prevalent than SENV-H^[20-23], but the predominant strain of SENV-H has been reported in the USA^[4]. Kao *et al.*, reported that the prevalence of SENV-H was 2-7 times higher than that of SENV-D in different northern Taiwanese individuals^[16,24]. The findings of the present study revealed that 37.1% of Taiwanese patients with CHC were co-infected with SENV-D which is higher by 28% than reports by Kao *et al.*^[16]. Our previous studies have shown that the prevalence of SENV-D was also higher than SENV-H not only among southern Taiwan blood donors (19.7% and 5.8%)^[18] but also among patients on maintenance hemodialysis (46.5% and 27.3%)^[25]. Furthermore, we found the prevalence of SENV-H was 19.2% among Taiwanese CHC patients (unpublished data) which is lower than that of SENV-D. It is interesting that a

marked difference of genotypic distribution of SENV between southern and northern Taiwan exists.

There was a higher mean age among CHC patients who were SENV-D viremic than non-viremic. We found similar results among blood donors too^[18]. However, we did not observe significant correlation between age and the prevalence of SENV-H among blood donors^[18] and CHC patients (unpublished data). The cause of discrepancy between trends of change in the prevalence of SENV-D and -H was not clear. Whether the possible assumptions such as the different exposure rate or routes of infection or different rates of spontaneous clearance between these two strains can clarify the issues needs further large-scale and longitudinal studies.

The clinical significance of SENV infection in combination with HCV infection remains unclear^[15,16]. Kao *et al.*, reported the relevance between HCV genotype 2a and SENV co-infection^[16]. The present study revealed that the pretreatment mean ALT levels and HCV RNA levels, and the histological scores between CHC patients with and without SENV-D co-infection were compatible and failed to show association between SENV-H and HCV genotype. Nevertheless, we have found a correlation between SENV-H co-infection and HCV genotype 1b among CHC patients (unpublished data). The discrepancy needs further studies. The biochemical and histological characteristics of CHC patients were not influenced by SENV-D co-infection that indicated the irrelevance between severity of liver disease and SENV-D co-infection.

As previous reports from researchers in Taiwan, the SVR rate of CHC patients was high (40-43%) after combination therapy with IFN 3 MU and ribavirin for 24 wk^[12,16]. In the present study, the HCV SVR rate was 67.3% after combination therapy with 6 MU IFN and ribavirin for 24 wk, which may further indicate the favorable results of combination therapy for Taiwanese CHC patients. The positive predictors of SVR to combination therapy with high-dose IFN were elucidated as HCV genotype non-1b, lower pretreatment HCV RNA levels and younger age. HCV genotype non-1b, having 12 times of SVR rate than genotype 1b in the present study, is the most important factor predicting SVR. Previous reports have demonstrated that HCV with SENV co-infection affected HCV response to combination therapy with IFN plus ribavirin adversely^[15] but the other report denied the relevance between HCV response and SENV co-infection^[16,22]. Our data here indicates that SENV-D co-infection does not affect the HCV response in the combination therapy with high dose IFN and ribavirin. In addition to co-infection with GB virus C/hepatitis G virus or TT virus that had no impact on the response to IFN monotherapy in CHC patients in our previous studies^[13,26,27], it seems unnecessary to determine whether CHC patients coinfect these viruses or not before they received combination therapy.

After combination therapy with 6 MU IFN and ribavirin for 24 wk among 48 CHC patients concomitant with SENV-D viremia, the rates of viral clearance at the end of follow-up achieved 56.3%. In an earlier study on the response of SENV-D among CHC patients, the sustained response rate of SENV-D has recently been reported by Umemura

et al., (73.3%) after high-dose IFN monotherapy^[22] and by Kao *et al.*, (87.5%) after combination therapy with 3 MU IFN and ribavirin for 24 wk^[16]. The lower SVR rate of SENV-D than SENV-H (78.3%, unpublished data) in our study from southern Taiwan was different from results from northern Taiwan that showed higher SENV-D SVR rate (87.5%) than SENV-H (26.8%)^[16]. The causes of different response to combination therapy, in addition to the different prevalence, of these two strains in southern and northern Taiwan need further research.

In conclusion, we find that more than one-third Taiwanese patients with CHC are coinfecting with SENV-D and coexistent SENV-D infection is apparently associated with higher ages but does not have an influence on the clinico-pathological characteristics of HCV infection. SENV-D is highly susceptible and does not affect the HCV response to combination therapy. After combination therapy with high dose IFN and ribavirin, two-thirds of Taiwanese CHC patients achieve SVR and HCV genotype non-1b, lower pretreatment HCV RNA levels and younger age are predictive factors for SVR.

REFERENCES

- Mushahwar IK. Recently discovered blood-borne viruses: are they hepatitis viruses or merely endosymbionts? *J Med Virol* 2000; **62**: 399-404
- Bowden S. New hepatitis viruses: contenders and pretenders. *J Gastroenterol Hepatol* 2001; **16**: 124-131
- Tanaka Y, Tanaka Y, Primi D, Wang RY, Umemura T, Yeo AE, Mizokami M, Alter HJ, Shih JW. Genomic and molecular evolutionary analysis of a newly identified infectious agent (SEN virus) and its relationship to the TT virus family. *J Infect Dis* 2001; **183**: 359-367
- Umemura T, Yeo AE, Sottini A, Moratto D, Tanaka Y, Wang RY, Shih JW, Donahue P, Primi D, Alter HJ. SEN virus infection and its relationship to transfusion-associated hepatitis. *Hepatology* 2001; **33**: 1303-1311
- Alter MJ, Margolis HS, Krawczynski K, Judson FN, Mares A, Alexander WJ, Hu PY, Miller JK, Gerber MA, Sampliner RE. The natural history of community-acquired hepatitis C in the United States. *New Engl J Med* 1992; **327**: 1899-1905
- Lauer GM, Walker BD. Hepatitis C virus infection. *N Engl J Med* 2001; **345**: 41-52
- Chuang WL, Chang WY, Lu SN, Lin ZY, Chen SC, Hsieh MY, Wang LY, You SL, Chen CJ. The role of hepatitis C virus in chronic hepatitis B virus infection. *Gastroenterol Jpn* 1993; **28** (Suppl 5): 23-27
- Chen DS, Chen DS, Wang JT, Chen PJ, Wang TH, Sung JL. Hepatitis C virus infection in Taiwan. *Gastroenterol Jpn* 1991; **26**(Suppl 3): 164-166
- Wang JH, Lu SN, Wu JC, Huang JF, Yu ML, Chen SC, Chuang WL. A hyperendemic community of hepatitis B virus and hepatitis C virus infection in Taiwan. *Trans R Soc Trop Med Hyg* 1999; **93**: 253-254
- McHutchison JG, Gordon SC, Schiff ER, Shiffman ML, Lee WM, Rustgi VK, Goodman ZD, Ling MH, Cort S, Albrecht JK. Interferon alpha-2b alone or in combination with ribavirin as initial treatment for chronic hepatitis C. *N Engl J Med* 1998; **339**: 1485-1492
- Poynard T, Marcellin P, Lee SS, Niederau C, Minuk GS, Ideo G, Bain V, Heathcote J, Zeuzem S, Trepo C, Albrecht J. Randomised trial of interferon alpha2b plus ribavirin for 48 wk or for 24 wk versus interferon alpha2b plus placebo for 48 wk for treatment of chronic infection with hepatitis C virus. *Lancet* 1998; **352**: 1426-1432
- Lai MY, Kao JH, Yang PM, Wang JT, Chen PJ, Chan KW, Chu JS, Chen DS. Long-term efficacy of ribavirin plus interferon alfa in the treatment of chronic hepatitis C. *Gastroenterology* 1996; **111**: 1307-1312
- Dai CY, Yu ML, Lin ZY, Chen SC, Hsieh MY, Lee LP, Hou NJ, Hsieh MY, Wang LY, Tsai JF, Chuang WL, Chang WY. Clinical significance of TT Virus (TTV) infection in chronic hepatitis C patients with high dose interferon-alpha therapy in Taiwan: re-evaluated by using new set of TTV primers. *Hepatol Res Hepatol Res* 2003; **27**: 95-100
- Yu ML, Dai CY, Chen SC, Lee LP, Huang JF, Lin ZY, Hsieh MY, Wang LY, Chuang WL, Chang WY. A prospective study on treatment of chronic hepatitis C with tailored and extended interferon-alpha regimens according to pretreatment virological factors. *Antiviral Res Antiviral Res* 2004; **63**: 25-32
- Rigas B, Hasan I, Rehman R, Donahue P, Wittkowski KM, Lebovics E. Effect on treatment outcome of coinfection with SEN viruses in patients with hepatitis C. *Lancet* 2001; **358**: 1961-1962
- Kao JH, Chen W, Chen PJ, Lai MY, Chen DS. SEN virus infection in patients with chronic hepatitis C: preferential coinfection with hepatitis C genotype 2a and no effect on response to therapy with interferon plus ribavirin. *J Infect Dis* 2003; **187**: 307-310
- Knodel RG, Ishak KG, Black WC, Chen TS, Craig R, Kaplowitz N, Kiernan TW, Wollman J. Formulation and application of a numerical scoring system for assessing histological activity in asymptomatic chronic active hepatitis. *Hepatology* 1981; **1**: 431-435
- Dai CY, Yu ML, Lin ZY, Chen SC, Hsieh MY, Wang LY, Tsai JF, Chuang WL, Chan WY. Prevalence and clinical significance of SEN virus infection among volunteer blood donors in southern Taiwan. *Dig Dis Sci* 2004; **49**: 1181-1185
- Okamoto H, Tokita H, Sakamoto M, Horikita M, Kojima M, Iizuka H, Mishiro S. Characterization of the genomic sequence of type V (or 3a) hepatitis C virus isolates and PCR primers for specific detection. *J Gen Virol* 1993; **74**(Pt 11): 2385-2390
- Kobayashi N, Tanaka E, Umemura T, Matsumoto A, Iijima T, Higuchi M, Hora K, Kiyosawa K. Clinical significance of SEN virus infection in patients on maintenance haemodialysis. *Nephrol Dial Transplant* 2003; **18**: 348-352
- Umemura T, Alter HJ, Tanaka E, Yeo AE, Shih JW, Orii K, Matsumoto A, Yoshizawa K, Kiyosawa K. Association between SEN Virus Infection and Hepatitis C in Japan. *J Infect Dis* 2001; **184**: 1246-1251
- Umemura T, Alter HJ, Tanaka E, Orii K, Yeo AE, Shih JW, Matsumoto A, Yoshizawa K, Kiyosawa K. SEN virus: response to interferon alpha and influence on the severity and treatment response of coexistent hepatitis C. *Hepatology* 2002; **35**: 953-959
- Shibata M, Wang RY, Yoshida M, Shih JW, Alter HJ, Mitamura K. The presence of a newly identified infectious agent (SEN virus) in patients with liver diseases and in blood donors in Japan. *J Infect Dis* 2001; **184**: 400-404
- Kao JH, Chen W, Chen PJ, Lai MY, Chen DS. Prevalence and Implication of a Newly Identified Infectious Agent (SEN Virus) in Taiwan. *J Infect Dis* 2002; **185**: 389-392
- Dai CY, Chuang WL, Chang WY, Chen SC, Sung MH, Hsieh MY, Lin ZY, Hsieh MY, Wang LY, Tsai JF, Yu ML. SEN virus infection among patients on maintenance hemodialysis in southern Taiwan. *J Infection* 2005: (in press)
- Yu ML, Chuang WL, Dai CY, Chen SC, Lin ZY, Hsieh MY, Tsai JF, Wang LY, Chang WY. GB virus C/hepatitis G virus infection in chronic hepatitis C patients with and without interferon-alpha therapy. *Antiviral Res* 2001; **52**: 241-249
- Dai CY, Yu ML, Chuang WL, Hou NJ, Hou C, Chen SC, Lin ZY, Hsieh MY, Wang LY, Chang WY. The response of hepatitis C virus and TT virus to high dose and long duration interferon-alpha therapy in naive chronic hepatitis C patients. *Antiviral Res* 2002; **53**: 9-18

Composition of common bile duct stones in Chinese patients during and after endoscopic sphincterotomy

Wei-Lun Tsai, Kwok-Hung Lai, Chiun-Ku Lin, Hoi-Hung Chan, Ching-Chu Lo, Ping-I Hsu, Wen-Chi Chen, Jin-Shiung Cheng, Gin-Ho Lo

Wei-Lun Tsai, Kwok-Hung Lai, Chiun-Ku Lin, Hoi-Hung Chan, Ching-Chu Lo, Ping-I Hsu, Wen-Chi Chen, Jin-Shiung Cheng, Gin-Ho Lo, Division of Gastroenterology, Department of Internal Medicine, Kaohsiung Veterans General Hospital, School of Medicine, National Yang Ming University, Taiwan, China

Supported by the Grants From National Science Council, No. NSC 89-2314-B-075B-007, No. NSC 89-2315-13-075B-003, and No. NSC 90-2314-B-075B-001

Correspondence to: Kwok-Hung Lai, Division of Gastroenterology, Department of Internal Medicine, Kaohsiung Veterans General Hospital, 386 Ta-Chung 1st Road, Kaohsiung 813, Taiwan, China. khilai@isca.vghks.gov.tw

Telephone: +886-7-3468366 Fax: +886-7-3456888

Received: 2004-12-10 Accepted: 2005-01-05

CONCLUSION: Bilirubinate stone is the predominant composition of initial or recurrent CBD stone in Chinese patients. The composition of CBD stones may be different from initial stones after ES.

© 2005 The WJG Press and Elsevier Inc. All rights reserved.

Key words: Endoscopic sphincterotomy; Common bile duct stone; Bilirubinate stone; Cholesterol stone

Tsai WL, Lai KH, Lin CK, Chan HH, Lo CC, Hsu PI, Chen WC, Cheng JS, Lo GH. Composition of common bile duct stones in Chinese patients during and after endoscopic sphincterotomy. *World J Gastroenterol* 2005; 11(27): 4246-4249
<http://www.wjgnet.com/1007-9327/11/4246.asp>

Abstract

AIM: Endoscopic sphincterotomy (ES) is a well-established therapeutic modality for the removal of common bile duct (CBD) stones. After ES there are still around 10% of patients that experience recurrent CBD stones. The aim of this study is to investigate the composition of CBD stones before and after ES and its clinical significance in Chinese patients.

METHODS: From January 1996 to December 2003, 735 patients with CBD stones received ES at Kaohsiung Veterans General Hospital and stone specimens from 266 patients were sent for analysis. Seventy-five patients had recurrent CBD stones and stone specimens from 44 patients were sent for analysis. The composition of the stones was analyzed by infrared (IR) spectrometry and they were classified as cholesterol or bilirubinate stones according to the predominant composition. Clinical data were analyzed.

RESULTS: In the initial 266 stone samples, 217 (82%) were bilirubinate stones, 42 (16%) were cholesterol stones, 3 were calcium carbonate stones, 4 were mixed cholesterol and bilirubinate stones. Patients with bilirubinate stones were significantly older than patients with cholesterol stones (66 ± 13 years vs 56 ± 17 years, $P = 0.001$). In the 44 recurrent stone samples, 38 (86%) were bilirubinate stones, 3 (7%) were cholesterol stones, and 3 were mixed cholesterol and bilirubinate stones. In 27 patients, both initial and recurrent stone specimens can be obtained, 23 patients had bilirubinate stones initially and 2 became cholesterol stones in the recurrent attack. In the four patients with initial cholesterol stones, three patients had bilirubinate stones and one patient had a cholesterol stone in the recurrent attack.

INTRODUCTION

The prevalence of gallstone diseases varied from 10% to 30% in the normal population and increased with age^[1-3]. Most gallstones are asymptomatic, but symptomatic gallstones may occur due to either cystic duct obstruction or common bile duct (CBD) stone formation. Endoscopic sphincterotomy (ES) is a well-established therapeutic modality for the removal of CBD stones. In follow-up studies after ES, 3-21% of patients developed recurrent CBD stones^[4-6] and most of them can be treated successfully by endoscopy^[4,7].

The main composition of gallstones is cholesterol and bile pigments^[8]. The major composition of GB stones obtained from Western patients is cholesterol (consisting of more than 50% cholesterol)^[8]. However, in the Asian patients, most gallstones are pigmented stones^[9]. Pigmented stones can be classified as black stones, associated with hemolysis or brown stones, associated with infection or bile stasis^[10-13]. Stones in the CBD are often brown, pigmented stones^[14-16]. After ablation of sphincter, bactobilia may happen and the pathogenesis of CBD stone formation may be different from the patients with intact sphincters^[17,18]. There have been few studies reporting the composition of recurrent CBD stones in patients after ES.

The aim of this study is to determine the composition of initial and recurrent CBD stones by infrared (IR) spectrometry and investigate the relationship of clinical characteristics and the change of the composition of recurrent stones after ES.

MATERIALS AND METHODS

Since January 1996 to December 2003, total 735 patients

with CBD stones received successful ES with clearance of CBD stones in Kaohsiung Veterans General Hospital and 266 stone specimens were collected and sent for stone analysis. During clinical follow-up, 75 patients had recurrent stones and 44 stone specimens were collected for stone analysis. Clinical data such as age, sex, diameter of CBD, size, number and color of stones, presence of juxtapapillary diverticulum (JPD), gallbladder (GB) status, and GB stones were recorded. GB stone was detected by sonogram or computed tomography of abdomen. Diameter of CBD and size and number of stones were measured during endoscopic retrograde cholangiopancreatography.

The stone sample was retrieved by Dormia basket (FG-22Q-1, Olympus) or snarenet (Roth snarenet, U.S.E.) from the bile duct. The stone specimen was pulverized into a homogenous powder, mixed with KBr and ground into fine particles. The mixed powder was pressed with a hydraulic pressure of 400 psi for 1 min to form a disc. Sample disc was analyzed with IR spectrometer. The stones were classified as cholesterol or bilirubinate stone according to the predominant composition. The characteristic band features and key band locations were in accordance with those reported in the literature^[9,19]. Bilirubinate stones had characteristic IR absorption bands at 970, 1 186, 1 250, 1 568, 1 627, and 1 650/cm with a key band at 1 250/cm; cholesterol stones had characteristic IR absorption bands at 728, 836, 952, 1 050, 1 375, 1 470, and 2 950/cm with key bands at 1 050 and 1 470/cm.

This protocol was approved by the Department of Medical Research and Education of Kaohsiung Veterans General Hospital. The values are expressed as mean±SD. Categorical variables were analyzed with χ^2 -test or Fisher's exact test and continuous variables were analyzed by Student's *t*-test. A *P* value <0.05 was regarded as significant.

RESULTS

Among the 735 patients with CBD stones and receiving successful ES, there were no significant differences in age, sex, presence of JPD, or cholecystectomy between the patients whose stones were collected for analysis or not (Table 1). In the group of patients with stone collection, their CBD diameter and stone size were larger.

Table 1 Patients' characteristics between stone collected and uncollected groups

	Collected (n = 266)	Uncollected (n = 469)	<i>P</i>
Age (yr)	64±14	65±14	0.454
Sex (M/F)	156/110	297/172	0.210
JPD ¹ (%)	105 (39) ²	158 (34)	0.116
Cholecystectomy (%)	65 (24) ²	108 (23)	0.665
CBD size (cm)	1.7±0.6	1.5±0.6	<0.001
CBD stone size (cm)	1.2±0.6	0.6±0.7	<0.001

¹JPD: Juxtapapillary diverticulum; CBD: common bile duct. ²Number of cases; the number inside the parenthesis shows the percentage.

In the 266 stone samples, 217 (82%) were bilirubinate stones, 42 (16%) were cholesterol stones, 3 were calcium carbonate stones, 4 were mixed cholesterol and bilirubinate

stones. Patients with bilirubinate stones were significantly older than patients with cholesterol stones (66±13 years *vs* 56±17 years, *P* = 0.001). There were no significant differences in sex, CBD diameter, size or number of CBD stones, presence of JPD, GB status, or presence of gallstones between patients with bilirubinate or cholesterol stones (Table 2).

Table 2 Patients' characteristics and initial stone compositions

	Bilirubinate (n = 217)	Cholesterol (n = 42)	<i>P</i>
Age (yr)	66±13	56±17	0.001
Sex (M/F)	130/87	22/20	0.365
CBD diameter (cm)	1.7±0.5	1.6±0.6	0.119
Stone size (cm)	1.2±0.6	1.2±0.7	0.410
Stone number (S/M)	111/106	16/26	0.121
JPD			0.084
Present	93 (43) ¹	12 (29)	
Absent	124 (57) ¹	30 (71)	
GB status			0.323
Cholecystectomy	57 (26) ¹	8 (19)	
Intact GB	160 (74)	34 (81)	
With stone	111 (51)	20 (48)	

Seven patients were excluded (three were calcium carbonate stones, four were mixed cholesterol and bilirubinate stones). CBD: Common bile duct; S/M: single/multiple; JPD: juxtapapillary diverticulum; GB: gallbladder. ¹Number of cases; the number inside the parenthesis shows the percentage.

A total 75 patients had recurrent CBD stones and received another endoscopic treatment. Stone specimens were collected from 44 patients for stone analysis. In the 44 recurrent stone samples, 38 (86%) were bilirubinate stones, 3 (7%) were cholesterol stones, and 3 were mixed cholesterol and bilirubinate stones. Among the three patients with recurrent cholesterol stones, two patients had intact GBs with stones and one had received a cholecystectomy 6 mo prior to recurrence. There were no significant differences in age, sex, CBD diameter, size or number of CBD stones, GB status, or presence of gallstones between patients with recurrent bilirubinate or cholesterol stones (Table 3).

Table 3 Patients' characteristics and compositions of recurrent CBD stones

	Bilirubinate (n = 38)	Cholesterol (n = 3)	<i>P</i>
Age (yr)	66±10	65±6	0.836
Sex (M/F)	21/17	3/0	0.254
CBD diameter (cm)	1.9±0.6	1.4±0.2	0.159
Stone number (S/M)	16/22	1/2	1.000
Stone size (cm)	1.4±0.8	0.8±0.4	0.096
JPD			0.543
Present	13 (34) ¹	2 (67)	
Absent	25 (66)	1 (33)	
GB status			1.000
Cholecystectomy	18 (47) ¹	1 (33)	
Intact GB	20 (53)	2 (67)	
With stone	15 (39)	2 (67)	

Three patients with mixed cholesterol and bilirubinate stones were excluded. CBD: Common bile duct; S/M: single/multiple; JPD: juxtapapillary diverticulum; GB: gallbladder. ¹Number of cases; the number inside the parenthesis shows the percentage.

In 27 patients, both initial and recurrent stone specimens can be obtained and sent for analysis, 23 patients had bilirubinate stones at initial treatment, 21 of them still had bilirubinate stones and 2 patients had cholesterol stones after recurrence. Both the patients with recurrent cholesterol stones also had GB stones. Four patients had cholesterol stones in the initial attack, three of them had bilirubinate stones, one patient still had cholesterol stones with recurrence and this patient had received cholecystectomy 6 mo prior to recurrence (Table 4).

Table 4 Change of stone compositions between initial and recurrent stone

Recurrent	Initial	
	Bilirubinate (n = 23)	Cholesterol (n = 4)
Bilirubinate (n = 24)	21	3
Cholesterol (n = 3)	2	1

Among the initial 266 stone samples, colors of stones were recorded. In the 217 patients with bilirubinate stones, 55 were yellowish, 93 were blackish, 64 were brownish and 5 were greenish. In the 42 patients with cholesterol stones, 15 were yellowish, 12 were blackish, 15 were brownish. In patients with mixed bilirubinate and cholesterol stones, two were yellowish and two were blackish. In patients with calcium carbonate stones, two were yellowish and one was blackish (Table 5).

Table 5 Compositions and color of stones

	Bilirubinate stone (n = 217)	Cholesterol stone (n = 42)	Mixed bilirubinate and cholesterol stone (n = 4)	Calcium carbonate stone (n = 3)
Yellow	55	15	2	2
Black	93	12	2	1
Brown	64	15	0	0
Green	5	0	0	0

DISCUSSION

We found that 82% of our patients had bilirubinate stones in the first attack, so the mechanism of CBD stone formation is different from the Western countries, but it is similar to some Asian studies^[9,20,21]. After ablation of sphincter of Oddi by ES, bactobilia may happen from direct extension of duodenal organisms into the CBD and β -glucuronidase released by the bacteria can promote the formation of bilirubinate stones^[17,18,22-24]. This explains why bilirubinate stone is the predominant composition of recurrent CBD stones (86%) after ES. Unlike the cholesterol stones, bilirubinate stones are often soft and easily broken^[16], so complete clearance of bilirubinate stones even after ES may be inadequate; some radiologically undetectable small fragments of bilirubinate stones may be left in the CBD; in addition to impaired biliary emptying, it may lead to bilirubinate stone formation at a later time.

Among the initial 42 patients with cholesterol stones, 8

patients received cholecystectomy at least 3 mo (median: 60 mo, range: 3-120 mo) before ES and 14 patients had intact GB but no GB stones. Besides spontaneous pass-out of stones, *de novo* formation of cholesterol stones from CBD may also be possible in these patients^[14,16].

In previous reports, JPD may facilitate primary CBD stone, but not GB stones formation^[16,25]. In our study, patients with initial bilirubinate stones had higher incidence of JPD than patients with initial cholesterol stones (43% *vs* 29%), but the difference did not reach statistical significance ($P = 0.084$).

In the 23 patients with initial bilirubinate stones, 21 had bilirubinate stones at recurrence, 2 had cholesterol stones when recurrence and these 2 patients also had GB stones at the time of recurrence, so stone pass-out from the GB may possibly explain the cholesterol composition of their CBD stones. In the four patients with initial cholesterol stones, three patients had bilirubinate stones and one had cholesterol stones at recurrence. The patient, who had recurrent cholesterol stones, had received cholecystectomy 6 mo before. It is difficult to determine whether the cholesterol stone is formed in the bile duct or GB. Our results indicated that different mechanism of CBD stone formation might occur in the same patient after ablation of sphincter leading to the formation of a different composition of stones.

In this study, we found that patients with bilirubinate stones are older than patients with cholesterol stones. Similar data have been found in Western patients with cholesterol *vs* pigment GB stones^[26]. It is well known that the duodenum is usually sterile in young healthy patients, but immunological and motor function of the alimentary tract may deteriorate gradually with age^[27]. The bacterial colonization of the CBD is an age-dependent phenomenon^[23] and this may explain the higher incidence of bilirubinate stones in older patients.

Cholesterol stones were usually yellowish or brownish^[15,28], but 12 out of 42 (29%) cholesterol stones in our patients were black in color, whereas 93 out of 217 (43%) bilirubinate stones were black in color. The nature of CBD stones cannot be completely determined by gross appearance alone^[28,29] and the IR spectroscopy is an important tool to determine the exact composition of stones.

For most patients, endoscopic retrieval of stones for analysis is more difficult than surgical procedure. In our study, only 266 out of 735 patients had received the analysis of stones. It could be speculated that different stone composition may influence the collection of stone for analysis during extraction procedure. Cholesterol stones are often smoother and harder while bilirubinate stones, on the other hand, are softer and tend to be broken down into small fragments when retrieved by basket or even a snarenet. This infers that the real percentage of bilirubinate stones in our patients may be actually higher. However, our analysis does not show significant difference in age, sex, presence of JPD, or cholecystectomy between patients whose stones were collected for analysis or not. Even though the CBD diameter and stone size are larger in the patients with stone analysis, there is no difference in CBD size or stone size between bilirubinate or cholesterol stones. We believe that little selection bias has taken place in our patients, despite only about 36% of patients' stones were collected for analysis.

In conclusion, bilirubinate stones are the predominant composition of initial and recurrent CBD stone after ES in Chinese patients. Patients with bilirubinate stones are older than those with cholesterol stones. The composition of stones may change after ES.

ACKNOWLEDGMENTS

The authors thank Mr. E-Ming Wang, Miss. Min-Ching Wei, and Ming-Ti Fu for their assistance in follow-up visits and data management and Dr. Ying-Huei Lee for stone analysis.

REFERENCES

- 1 **Bates T**, Harrison M, Lawson C, Padley N. Longitudinal study of gall stone prevalence at necropsy. *Gut* 1992; **33**: 103-107
- 2 **Heaton KW**, Braddon FEM, Mountford RA, Hughes AO, Emmett PM. Symptomatic and silent gall stones in the community. *Gut* 1991; **32**: 316-320
- 3 **Su CH**, Lui WY, P'eng FK. Relative prevalence of gallstone diseases in Taiwan: A nationwide cooperative study. *Dig Dis Sci* 1992; **37**: 764-768
- 4 **Lai KH**, Peng NJ, Lo GH, Cheng JS, Huang RL, Lin CK, Huang JS, Chiang HT, Ger LP. Prediction of recurrent cholelithiasis by quantitative chlescintigraphy in patients after endoscopic sphincterotomy. *Gut* 1997; **41**: 399-403
- 5 **Hawes RH**, Cotton PB, Vallon AG. Follow-up 6-11 years after duodenoscopic sphincterotomy for stones in patients with prior cholecystectomy. *Gastroenterology* 1990; **98**: 1008-1012
- 6 **Seifert E**. Long-term follow-up after endoscopic sphincterotomy (EST). *Endoscopy* 1988; **20**: 232-235
- 7 **Lai KH**, Lo GH, Lin CK, Hsu PI, Chan HH, Cheng JS, Wang EM. Do patients with recurrent choledocholithiasis after endoscopic sphincterotomy benefit from regular follow-up. *Gastrointest Endosc* 2002; **55**: 523-526
- 8 **Carey MC**. Pathogenesis of gallstones. *Am J Surg* 1993; **165**: 410-419
- 9 **Huang SM**, Su CH, Wu LH, Chang TJ, Wu CW, Lee CH, Lui WY. Polarising microscopy versus infrared absorption spectroscopy in gallstone analysis- a preliminary report. *Asian J Surg* 1989; **12**: 172-177
- 10 **Cahalane MJ**, Neubrand MW, Carey MC. Physical-chemical pathogenesis of pigment gallstones. *Semin Liver Dis* 1988; **8**: 317-328
- 11 **Crowther RS**, Soloway RD. Pigment gallstone pathogenesis: from man to molecules. *Semin Liver Dis* 1990; **10**: 171-180
- 12 **Trotman BW**. Pigments gallstone disease. *Gastroenterol Clin N Am* 1991; **20**: 111-126
- 13 **Leuschner U**, Guldutuna S, Hellstern A. Pathogenesis of pigment stones and medical treatment. *J Gastroenterol Hepatol* 1994; **9**: 87-98
- 14 **Malet PF**, Dabezies MA, Huang G, Long WB, Gadacz TR, Soloway RD. Quantitative infrared spectroscopy of common bile duct gallstones. *Gastroenterology* 1988; **94**: 1217-1221
- 15 **Bernhoft RA**, Pellegrini CA, Motson RW, Way LW. Composition and morphologic and clinical features of common duct stones. *Am J Surg* 1984; **148**: 77-85
- 16 **Sandstd O**, Osnes T, Skar V, Urdal P, Osnes M. Common bile duct stones are mainly brown and associated with duodenal diverticula. *Gut* 1994; **35**: 1464-1467
- 17 **Gregg JA**, Girolami PD, Carr-Locke DL. Effects of sphincteroplasty and endoscopic sphincterotomy on the bacteriologic characteristics of the common bile duct. *Am J Surg* 1985; **149**: 668-671
- 18 **Skar V**, Skar AG, Midtvedt T, Osnes M. Bacterial growth in the duodenum and in the bile of patients with gallstone disease treated with endoscopic papillotomy (EPT). *Endoscopy* 1986; **18**: 10-13
- 19 **Lee YH**, Chen MT, Huang JK, Chang LS. Analysis of urinary calculi by infrared spectroscopy. *Chin Med J* 1990; **45**: 157-165
- 20 **Tanaka M**, Takahata S, Konomi H, Matsunaga H, Yokohata K, Takeda T, Utsunomiya N, Ikeda S. Long-term consequence of endoscopic sphincterotomy for bile duct stones. *Gastrointest Endosc* 1998; **48**: 465-469
- 21 **Kim DI**, Kim MH, Lee SK, Seo DW, Chol WB, Lee SS, Park SJ, Joo YH, Yoo KS, Kim HJ. Risk factors for recurrence of primary bile duct stones after endoscopic biliary sphincterotomy. *Gastrointest Endosc* 2001; **54**: 42-48
- 22 **Cetta F**. Do surgical and endoscopic sphincterotomy prevent or facilitate recurrent common duct stone formation? *Arch Surg* 1993; **128**: 329-336
- 23 **Cetta F**. The possible role of sphincteroplasty and surgical sphincterotomy in the pathogenesis of recurrent common duct brown stones. *HPB Surg* 1991; **4**: 261-270
- 24 **Ho KJ**, Lin XZ, Yu SC, Chen JS, Wu CZ. Cholelithiasis in Taiwan: Gallstone characteristics, surgical incidence, bile lipid composition and role of B-glucuronidase. *Dig Dis Sci* 1995; **40**: 1963-1973
- 25 **Lotveit T**. The composition of biliary calculi in patients with juxtapapillary duodenal diverticula. *Scand J Gastroenterol* 1982; **17**: 653-656
- 26 **Trotman BW**, Ostrow JD, Soloway RD. Pigment vs cholesterol cholelithiasis: comparison of stone and bile composition. *Am J Dig Dis* 1974; **19**: 585-590
- 27 **Cetta F**. The route of infection in patients with bactibilia. *World J Surg* 1983; **7**: 562
- 28 **Wei TC**. Quantitative determination of chemical composition of gallstones by infrared absorption spectrophotometry. *J Formos Med Assoc* 1982; **81**: 145-157
- 29 **Chen YJ**, Liu MH, Chen PH, Lo HW, Wang CS, Yuan J, Wen KL. Composition analysis of gallstones by fourier transformed infrared spectroscopy. *Chin J Gastroenterol* 1992; **9**: 1-8

Clinical evaluation of serum concentrations of intercellular adhesion molecule-1 in patients with colorectal cancer

Xu Kang, Fang Wang, Jin-Dong Xie, Jun Cao, Pei-Zhong Xian

Xu Kang, Jin-Dong Xie, Pei-Zhong Xian, Department of Gastro-intestinal Surgery, Affiliated Hospital, Guangdong Medical College, Zhanjiang 524001, Guangdong Province, China

Fang Wang, South China Sea Institute of Oceanology, Chinese Academy of Sciences, Guangzhou 510301, Guangdong Province, China

Jun Cao, Department of Pathology, Affiliated Hospital, Guangdong Medical College, Zhanjiang 524001, Guangdong Province, China

Supported by the Youth Science Foundation of Guangdong Medical College, No. 2002110

Co-first-author: Fang Wang

Correspondence to: Dr. Xu Kang, Department of Gastro-intestinal Surgery, Affiliated Hospital, Guangdong Medical College, Zhanjiang 524001, Guangdong Province, China. kangxuwf@163.com

Telephone: +86-759-2387416 Fax: +86-759-2231754

Received: 2004-12-25 Accepted: 2005-01-12

Abstract

AIM: To investigate the correlation between the serum soluble intercellular adhesion molecule-1 (sICAM-1) and the clinicopathologic features and to evaluate the possible prognostic significance of sICAM-1 concentration in colorectal cancer.

METHODS: A total of 56 patients (mean age 57.3 years) having transitional cell carcinoma of the colorectal and 25 control patients (mean age 42.6 years) were enrolled in the study. The serum samples of the patients were obtained on the day before surgery. Sera were obtained by centrifugation, and stored at -80 °C until assay. Serum concentrations of ICAM-1 were measured with enzyme-linked immunoassay. Differences between the two groups were analyzed by Student's *t*-test.

RESULTS: No significant increase of serum sICAM-1 could be demonstrated in the Dukes A₁ patients (352.63±61.82 µg/L) compared to the control group (345.72±49.81 µg/L, *P*>0.05), Dukes A₁ patients (352.63±61.82 µg/L) compared to Dukes A_{2,3} patients (491.17±86.36 µg/L, *P*<0.05). Furthermore, the patients with Dukes B had significantly higher serum concentrations of sICAM-1 than those of the control group (496.82±93.04 µg/L vs 345.72±49.81 µg/L, *P*<0.01). Compared with Dukes A_{2,3}, B colorectal cancer patients, patients with more advanced clinical stage (Dukes C and D) had higher levels of sICAM-1 (743.68±113.74 µg/L vs 491.17±86.36 µg/L and 496.82±93.04 µg/L, *P*<0.001). The difference was statistically significant in sICAM-1 levels between patients with positive lymph node status and those without lymph node involvement (756.25±125.57 µg/L vs 445.62±69.18 µg/L, *P*<0.001). Patients with poorly differentiated colorectal cancer had

a higher level of sICAM-1 than those with differentiated and highly differentiated cancer (736.49±121.97 µg/L vs 410.23±67.47 µg/L, *P*<0.001).

CONCLUSION: In this study, serum ICAM-1 levels were found to be related to tumor presence, clinical stages, and grade. Increased ICAM-1 in patients with colorectal cancer which should be considered when the diagnostic and/or prognostic usefulness of soluble ICAM-1 is to be evaluated. sICAM-1 should prove useful for monitoring malignant disease stage and for evaluating the effectiveness of various therapeutic approaches for colorectal carcinomas.

© 2005 The WJG Press and Elsevier Inc. All rights reserved.

Key words: sICAM-1; Colorectal cancer; Tumor metastasis; Clinicopathological factors

Kang X, Wang F, Xie JD, Cao J, Xian PZ. Clinical evaluation of serum concentrations of intercellular adhesion molecule-1 in patients with colorectal cancer. *World J Gastroenterol* 2005; 11(27): 4250-4253

<http://www.wjgnet.com/1007-9327/11/4250.asp>

INTRODUCTION

Colorectal cancer is the third most common malignant neoplasm worldwide^[1] and has a higher incidence rate in Guangdong, Shanghai, Jiangsu, and Zhejiang Province. Moreover, with the development of economy, diets are high in total fat, protein, calories, alcohol, and meat (both red and white) and low in calcium and folate, which incline to increased incidence of colorectal cancer. The prevalence of colorectal cancer increased gradually in recent years. Efforts to identify causes and to develop effective preventive measures have led scientists pay much attention to it.

Intercellular adhesion molecule-1 (ICAM-1) is a monomeric, transmembrane molecule of the immunoglobulin superfamily with a molecular weight of 95-110 ku. Two ligands, the lymphocyte function-associated antigen-1 and the membrane adhesion complex-1, mediate adhesion and transvascular migration^[2]. This protein mediates adhesion and transmigration of leukocytes through the endothelium. Surface expressed ICAM-1 is apparently shed from the cells and then circulates as soluble ICAM-1 (sICAM-1). Although the source of sICAM-1 has not been fully elucidated, it can be released by cancer cells and also by mononuclear blood, endothelial, and fibroblastic cells^[3]. It has been reported that

the upregulated expression of ICAM-1 on cell surfaces occurred in a variety of diseases, including autoimmune diseases, endocrine diseases, and some cancers^[4,5]. A soluble form of ICAM-1 (sICAM-1) lacking cytoplasmic tail and transmembrane region has also been found^[5]. sICAM-1 can compete with membranous ICAM-1 to bind LFA-1, so that it can block leukocyte LFA-1 and prevent effective recognition and lysis of target cells by effector leukocyte. This phenomenon represents an important mechanism for tumor escape from immune surveillance^[6,7]. Shedding of ICAM-1 by circulating tumor cells may allow their escape from surveillance by cytotoxic T cell and natural killer cells and thus promote metastasis^[8]. In our research, we have found that some anticancer gene and proto-oncogene have different expression in colorectal cancer^[9,10]. In this study, we investigate the clinical significance of serum adhesion molecule levels at the time of diagnosis in patients with colorectal carcinoma and to evaluate the usefulness of these assays in terms of prognosis and survival.

MATERIALS AND METHODS

Patients and specimens

Serum samples were taken from 56 patients (32 men, 24 women, average age 57.3 years) with colorectal cancer admitted to the Affiliated Hospital of Guangdong Medical College from 2001 to 2002. In all patients the diagnosis was proven by histology. Staging was performed according to the criteria of Dukes system (Table 1). The reference group consisted of 25 others with non-malignant diseases (9 women and 16 men, average age 42.6 years). Blood samples were obtained from patients before the initial treatment. All blood samples were processed immediately for centrifugation. All sera were stored at -80 °C until assayed and determined not taking clinical information into account.

Table 1 Colorectal cancer patients and disease characteristics

Stage	n	%
Dukes A ₁	3	5.36
Dukes A _{2,3}	6	10.71
Dukes B	21	37.50
Dukes C and D	26	46.43
Histologic differentiation		
Highly	22	39.29
Moderate	24	42.86
Poorly	10	17.85
Localization		
Right colon	17	30.36
Left colon	21	37.50
Rectum	18	32.14

Measurement of sICAM-1

The serum levels of soluble receptors were determined quantitatively by specific enzyme-linked immunosorbent assay (ELISA). The serum samples were diluted 10 times according to the manufacturer's instructions (R&D Systems), and as described previously^[11]. Soluble receptor concentrations were calculated from standard curves generated by standard dilutions of known concentrations. The mean intra-assay CV, determined by assaying the sICAM-1 concentration in three serum samples in replicates of 10, is reported to be

4.4%. The mean inter-assay CV, determined by assaying three serum samples in duplicate in 18 separate assays by four operators, has been determined to be 7.4%. The cut-off values were calculated as the mean±SD were 860 ng/mL for sICAM-1. The reported sensitivity of the ELISA is less than 0.35 ng/mL.

Statistical analysis

The Student's *t*-test was used for statistical significance of differences between groups. *P*<0.05 was considered to be significant.

RESULTS

We studied the correlation between the sICAM-1 levels and clinicopathological factors, Table 1 shows the relationships between the concentration of sICAM-1 antigen in the sera and various clinicopathologic features of the patients. No significant increase of serum sICAM-1 could be demonstrated in the Dukes A₁ patients (352.63±61.82 µg/L) compared to a control group (345.72±49.81 µg/L, *P*>0.05). There is a significant statistic difference when Dukes A₁ patients (352.63±61.82 µg/L) compared to Dukes A_{2,3} patients (491.17±86.36 µg/L, *P*<0.05). Furthermore, serum sICAM-1 levels were significantly higher in patients with Dukes B when compared to the control group (496.82±93.04 µg/L *vs* 345.72±49.81 µg/L, *P*<0.01). Among patient groups, while there was no significant difference between Dukes A_{2,3} and Dukes B, a significant difference was found between Dukes B and Dukes C and D. Compared with Dukes A_{2,3}, B colorectal cancer patients, the patients with more advanced clinical stage Dukes C and D, had higher levels of sICAM-1 (743.68±113.74 µg/L *vs* 491.17±86.36 µg/L and 496.82±93.04 µg/L, *P*<0.001). Difference was statistically significant in sICAM-1 levels between patients with positive lymph node status and those without lymph node involvement (756.25±125.57 µg/L *vs* 445.62±69.18 µg/L, *P*<0.001). Poor differentiation was observed to have a higher level of sICAM-1 than moderated and highly differentiated patients *P*<0.001. The positive rates of each group were calculated with mean±SD of normal control sICAM-1 as a limit. The results are shown in Table 2.

Table 2 Correlation between soluble ICAM-1 concentrations and clinicopathologic factors in colorectal cancer

Factors	n	ICAM-1 (mean±SD, µg/L)	χ ²	P
Clinical staging				
Dukes A ₁	3	352.63±61.82 ^a		
Dukes A _{2,3}	6	491.17±86.36	2.88	<0.05
Dukes B	21	496.82±93.04 ^d	0.18	>0.05
Dukes C and D	26	743.68±113.74	12.38	<0.001
Grade of differentiation				
Highly differentiated	22	410.23±67.47 ^b		
Differentiated	24	486.53±103.64 ^d	4.08	<0.01
Poorly differentiated	10	736.49±121.967	10.48	<0.001
Metastasis				
Liver	3	769.19±127.32		
Lymph node positive	23	756.25±125.57 ^d	0.32	>0.05
Lymph node negative	30	445.62±69.18	16.98	<0.001

^a*P*<0.05, Dukes A₁ *vs* Dukes A_{2,3}; ^b*P*<0.01, highly differentiated *vs* differentiated; ^d*P*<0.001, Dukes B *vs* Dukes C and D; Differentiated *vs* poorly differentiated; lymph node positive *vs* lymph node negative.

DISCUSSION

Soluble forms of cell adhesion molecules have been identified in the circulation and may be monitored as markers of inflammation and endothelial dysfunction^[4]. Neoplastic transformation and the evolution to metastatic disease are characterized by a dramatic aberration in cellular cohesive interactions. The adhesion molecules have also been shown to facilitate tumor cell motility, adhesion of tumor cells to endothelium, neovascularization at the metastatic sites, and host inflammatory response to cancer. Evaluation of sICAM-1 has shown important clinical implications in many types of cancer. In particular, the measurement of serum concentrations of ICAM-1 might provide important prognostic values independent of conventional pathologic factors in cancer patients^[12-14].

In the present study of colorectal cancer, revealed that serum sICAM-1 levels were elevated in patients with colorectal cancer. These parameters were elevated in both local and metastatic disease and significant correlations between the parameters and stage of disease were seen. The data of the present study are in agreement with those previously reported which described an increase in the sICAM-1 content of serum in colorectal carcinoma^[15,16]. We have also demonstrated that concentrations of sICAM-1 are increased in colorectal cancer, particularly in patients with distant metastasis. Our study also showed that sICAM-1 levels were correlated with both clinical staging and lymph node during liver metastasis involvement. Basoglu^[17] reported that the concentrations of sICAM-1 and TSA were significantly higher in patients with Dukes C and D, and they presume that sICAM-1 and TSA are the best of the tested markers. These markers should prove useful for monitoring malignant disease stage and for evaluating the effectiveness of various therapeutic approaches for colorectal carcinomas. In contrast to our study, it was demonstrated that the expression of sICAM-1 was inversely correlated with lymph node metastasis^[18].

With regard to prognosis, Liu reported in gastric cancer that serum sICAM-1 concentration may be a valuable parameter for predicting the prognosis and degree of the gastric cancer. Liu^[19] measured the circulating ICAM-1 in the sera of nasopharyngeal, oral, and laryngeal cancer cases and indicated that the circulating ICAM-1 was not elevated in the sera of oral and laryngeal cancer patients, but increased in nasopharyngeal cancer patients. They speculated that the discrepancy in the level of ICAM-1 among these three groups of patients with head and neck carcinoma might be attributed to either the different immunological reaction profiles or a cell-specific response. The cellular source and the mechanisms for releasing the soluble components of these endothelial adhesion molecules, although not well known, could involve either shedding or enzymatic cleavage from endothelial cells, leukocyte surfaces or tumor cells^[20]. Some mechanisms have been proposed concerning the elevation of sICAM-1 in serum, such as enzymatic cleavage of cell surface adhesion molecules or secretion of alternatively spliced forms lacking the transmembrane domain. Additionally, that sICAM-1 has been described on malignant epithelial tissue may be the source of at least some of the sICAM-1 present in sera of cancer patients^[21]. It is widely accepted

that histological stage is a powerful prognostic factor in colorectal cancer. In this study, it was revealed that ICAM-1 status has prognostic value coincide with histological stage. Therefore, these results suggested that it may be possible to add ICAM-1 status to conventional clinicopathological factors to predict recurrence.

In conclusion, our study demonstrates that ICAM-1 expression may be a useful indicator of prognosis in patients with colorectal cancer. Patients with lymph node, liver invasion, and advanced clinical stage of tumors had significantly higher serum concentrations of sICAM-1. Invasion status and clinical stage are significant prognostic indicators. Though serum level of sICAM-1 cannot be served as a specific parameter for colorectal cancer, it is no doubt that the measurement of the ICAM-1 level may provide a convenient means to obtain a general indication of colorectal cancer. Therefore, sICAM-1 may be a valuable predictor for colorectal cancer clinically.

REFERENCES

- 1 **Shike M**, Winawer SJ, Greenwald PH, Bloch A, Hill MJ, Swaroop SV. Primary prevention of colorectal cancer: the WHO collaborating centre for the prevention of colorectal cancer. *Bull World Health Organ* 1990; **68**: 377-385
- 2 **Wollenberg B**, Jan N, Sutier W, Hofmann K, Schmitt UM, Stieber P. Serum levels of intercellular adhesion molecule-1 squamous cell carcinoma of the head and neck. *Tumour Biol* 1997; **18**: 88-94
- 3 **Nakata B**, Hori T, Sunami T, Ogawa Y, Yashiro M, Maeda K, Sawada T, Kato Y, Ishikawa T, Hirakawa K. Clinical significance of serum soluble intercellular adhesion molecule 1 in gastric cancer. *Clin Cancer Res* 2000; **6**: 1175-1179
- 4 **Springer TA**. Adhesion receptors of the immune system. *Nature* 1990; **346**: 425-434
- 5 **Rothlein R**, Mainolfi EA, Czajkowski M, Marlin SD. A form of circulating ICAM-1 in human serum. *J Immunol* 1991; **147**: 3788-3793
- 6 **Becker JC**, Dummer R, Hartmann AA, Burg G, Schmidt RE. Shedding of ICAM-1 from human melanoma cell lines induced by IFN- γ and tumor necrosis factor- α : functional consequences on cell-mediated cytotoxicity. *J Immunol* 1991; **147**: 4398-4401
- 7 **Becker JC**, Christian T, Schmidt RE, Brocker EB. Soluble intercellular adhesion molecule-1 inhibits MHC-restricted specific T cell/tumor interaction. *J Immunol* 1993; **151**: 7224-7232
- 8 **Banks RE**, Gearing AJH, Hemingway IK, Norfolk DR, Perren TJ, Selby PJ. Circulating intercellular adhesion molecule-1 (ICAM-1), E-selectin and vascular cell adhesion molecule-1 (vcam-1) in human malignancies. *Br J Cancer* 1993; **68**: 122-124
- 9 **Kang X**, Xie PZ, Cao J. Relationship between expression p53 protein, c-erbB2, PCNA, and bcl-2 in colorectal cancer and clinical pathological features. *Hainan Med J* 2004; **15**: 14-16
- 10 **Kang X**, Xie PZ, Xu FP. Study of p16/MTS1 gene inactivation in Colorectal Carcinoma. *Chinese New Med* 2004; **5**: 1345-1346
- 11 **Koundouros E**, Odell E, Coward PY, Wilson RF, Palmer RM. Soluble adhesion molecules in serum of smokers and nonsmokers, with and without periodontitis. *J Periodontol Res* 1996; **31**: 596-599
- 12 **Benekli M**, Gullu IH, Tekuzman G, Savas MC, Hayran M, Hascelik G, Firat D. Circulating intercellular adhesion molecule-1 and E-selectin levels in gastric cancer. *Br J Cancer* 1998; **78**: 267-271
- 13 **Dwivedi C**, Dixit M, Hardy RE. Plasma lipid-bound sialic acid alterations in neoplastic diseases. *Experientia* 1990; **46**: 91-97
- 14 **Tsujisaki M**, Imai K, Hirata H, Hanzawa Y, Masuya J, Nakano T, Sugiyama T, Matsui M, Hinoda Y, Yachi A. Detection of

- circulating intercellular adhesion molecule-1 antigen in malignant diseases. *Clin Exp Immunol* 1991; **85**: 3-8
- 15 **Velikova G**, Banks RE, Gearing A, Hemingway I, Forbes MA, Preston SR, Hall NR, Jones M, Wyatt J, Miller K, Ward U, Al-Maskatti J, Singh SM, Finan PJ, Ambrose NS, Primrose JN, Selby PJ. Serum concentrations of soluble adhesion molecules in patients with colorectal cancer. *Br J Cancer* 1998; **77**: 1857-1863
- 16 **Reinhardt KM**, Steiner M, Zillig D, Nagel HR, Blann AD, Brinckmann W. Soluble intercellular adhesion molecule-1 in colorectal cancer and its relationship to acute phase proteins. *Neoplasma* 1996; **43**: 65-67
- 17 **Basoglu M**, Yildirgan MI, Taysi S, Yilmaz I, Kiziltunc A, Balik AA, Celebi F, Atamanalp SS. Levels of soluble intercellular adhesion molecule-1 and total sialic acid in serum of patients with colorectal cancer. *J Surg Oncol* 2003; **83**: 180-184
- 18 **Maeda K**, Kang SM, Sawada T, Nishiguchi Y, Yashiro M, Ogawa Y, Ohira M, Ishikawa T, Hirakawa YS, Chung K. Expression of intercellular adhesion molecule-1 and prognosis in colorectal cancer. *Oncol Rep* 2002; **9**: 511-516
- 19 **Liu CM**, Sheen TS, Ko JY, Shun CT. Circulating intercellular adhesion molecule-1 (ICAM-1), E-selectin and vascular cell adhesion molecule-1 (VCAM-1) in head and neck cancer. *Br J Cancer* 1999; **79**: 360-362
- 20 **Ferdeghini M**, Gadducci A, Prontera C, Annicchiarico C, Gagetti O, Bianchi M, Facchini V, Genazzani AR. Preoperative serum intercellular adhesion molecule-1 (ICAM-1) and E-selectin (Endothelial cell leukocyte adhesion molecule, ELAM-1) in patients with epithelial ovarian cancer. *Anticancer Res* 1995; **15**: 2255-2260
- 21 **Ros-Bullon MR**, Sanchez-Pedreno P, Martinez-Liarte JH. Serum sialic acid in malignant melanoma patients: an ROC curve analysis. *Anticancer Res* 1999; **19**: 3619-3622

Science Editor Guo SY Language Editor Elsevier HK

• BRIEF REPORTS •

Immunization of mice with concentrated liquor from male zoid of *Antheraea pernyi*

Sheng Li, Bo Zhang, Wei-Dong Zhang, Ting-Hang Ma, Yong Huang, Long-Hai Yi, Jin-Ming Yu

Sheng Li, Bo Zhang, Ting-Hang Ma, Yong Huang, Long-Hai Yi, Jin-Ming Yu, Shandong Tumor Hospital, Jinan 250117, Shandong Province, China
Wei-Dong Zhang, Basic Medical Institute of Shandong Academy of Medical Sciences, Jinan 250062, Shandong Province, China
Supported by the National Natural Science Foundation of China, No. 30472260
Co-correspondence: Jin-Ming Yu
Correspondence to: Sheng Li, Shandong Tumor Hospital, Jinan 250117, Shandong Province, China. drlisheng@sohu.com
Fax: +86-531-8550649
Received: 2004-11-02 Accepted: 2004-12-21

Abstract

AIM: To study the effects of concentrated liquor from male zoid of *Antheraea pernyi* on immunological mice.

METHODS: For each experiment, 40 mice were randomly divided into normal saline group (control group) and three tested groups that were administered different dosages of concentrated liquor from male zoid of *A. pernyi* and food for 15 d. The typical FSR and HC₅₀ value, monocyte-phagocytic exponent *K* and emended monocyte-phagocytic exponent α were determined and calculated respectively.

RESULTS: After 24 and 48 h, the FSR values of the three tested groups improved significantly in comparison to the control group by variance analysis. The HC₅₀ values showed a significant difference between the high dosage group and the control group, as well as between the high dosage group and other two tested groups. The monocyte-phagocytic exponent *K* and emended exponent α showed rising tendencies, but no significant differences were found by variance analysis.

CONCLUSION: The concentrated liquor from male zoid of *A. pernyi* can significantly enhance cellular and humoral immune function in mice, but has no distinct influence on the monocyte-phagocytic system in mice.

© 2005 The WJG Press and Elsevier Inc. All rights reserved.

Key words: *Antheraea pernyi*; Male zoid; Concentrated liquor; Mice; Immune function

Li S, Zhang B, Zhang WD, Ma TH, Huang Y, Yi LH, Yu JM. Immunization of mice with concentrated liquor from male zoid of *Antheraea pernyi*. *World J Gastroenterol* 2005; 11 (27): 4254-4257
<http://www.wjgnet.com/1007-9327/11/4254.asp>

INTRODUCTION

The concentrated liquor from male zoid of *Antheraea pernyi* is a pure preparation of traditional Chinese medicine, which possesses many health-care functions. According to The Great Dictionary of Traditional Chinese Medicine, *A. pernyi* is the matured insect of silkworm. The major components of male zoid are proteins and more than 20 kinds of free amino acids, cytochrome C^[1], with the actions of tonifying the liver and invigorating the kidney, strengthening Yang Qi and astringing essence^[2]. So male zoid is mainly employed to treat impotence, seminal emission, and stranguria with hematuria. This agent is made from unmated male zoid of *A. pernyi*. The effective components are extracted from its combined lixivium of edible level, then isolated, purified, and concentrated with advanced cryogenic techniques. The qualitative and quantitative analyses are tested by thin-layer chromatography. We undertook this animal experiment to study the effects of the concentrated liquor on cellular, humoral, and monocyte-phagocytic immune functions in mice.

MATERIALS AND METHODS

Experimental materials

Raw materials from male zoid of *A. pernyi* were provided by the Silkworm Research Institute of Shandong Agriculture Science Academy, purified and concentrated in our laboratory^[3].

The whole blood of Guinea pig was sampled and centrifuged. The concentrated RBCs of mice were added to 5 mL of extracted Guinea pig serum and stored at 4 °C for 30 min before use, then centrifuged at 1 500 r/min for 15 min. Preclusion of unspecific hemolysis caused by complement was eliminated by extraction of supernatant. The processed serum diluted in normal saline at 1:10 served as the experimental complement.

Effects of concentrated liquor from male zoid of *Antheraea pernyi* on cellular immune function of mice

Forty Kunming mice (6-8 wk) weighing 18-20 g were randomized into three tested groups (high-, medium-, and low-dosage group), and treated with 16.53, 2.62, and 0.564 mg/kg of concentrated liquor from male zoid of *A. pernyi* respectively. During the 15-d process of continuous oral filling, a dosage of 2% 0.2 mL (1×10⁶/mL) (V/V) SRBC was injected into the abdominal cavity of each mouse on the 10th d. Four days later, sizes of the left plantars of the immunized mice were measured with slide gaud, then another dosage of 20 μL (1×10⁶/mL) 20 mol/L (V/V)

SRBC was injected subcutaneously at the measured site of each mouse. Twenty-four and forty-eight hours after injection, thickness of the left plantar of each treated mouse was measured respectively. Each site was measured thrice, and the average value was used to calculate the FSR. $FSR = \text{thickness of the left plantar before injection} - \text{thickness of the left plantar after injection (mm)}$.

Effects of concentrated liquor from male zoid of *Antheraea pernyi* on humoral immune function of mice

Kunming mice (6–8 wk) weighing 18–22 g were randomized into three testing groups and fed with concentrated liquor from male zoid of *A. pernyi* at the dosages of 16.53, 2.62, and 0.564 mg/kg, respectively. During the 15-d process of continuous oral filling, a dosage of 0.2 mL (1×10^6 /mL) 20 mol/L (V/V) SRBC was injected into the abdominal cavity of each mouse on the 10th d. Five days later, whole blood was sampled from each mouse by eye extraction, and then the serum was prepared. Hemolysin in serum was determined as follows: the prepared serum from each mouse was diluted at 1:50, 1 mL of the diluted serum was added into a 10-mL test tube, and then 0.5 and 1 mL complement of 10% SRBC was added into the tube. A control tube was added with normal saline instead of serum. After incubation at 37 °C for 30 min, the reaction was stopped in ice bath, centrifuged at 2 000 r/min for 10 min, the supernatant was extracted and 3 mL of Du's reagent was added. At the same time, 0.25 mL 10% SRBC was added into Du's reagent to a final volume of 4 mL and placed at room temperature. The optical densities of all preparations were tested by type-722 spectrophotometer in 1-cm color matching cups, the optical density of the control test tube was defined as zero value. The semi-hemolytic value (HC_{50}) was calculated as: $HC_{50} = \frac{\text{optical density value of each sample tube}}{\text{optical density value of SRBC at semi-hemolysis} \times \text{dilution multiples}}$.

Effects of concentrated liquor from male zoid of *Antheraea pernyi* on monocyte-phagocytic function of mice

Kunming mice (6–8 wk) weighing 18–22 g were randomized into three tested groups and fed with concentrated liquor from male zoid of *A. pernyi* for 15 d at the same dosages as the above. After the last dosage was given, charcoal particle clearance test was performed. The detailed procedure was as follows: Each mouse was injected with diluted Chinese ink through its tail vein, 20 μ L whole blood was sampled from the medial canthus of each mouse at the 2nd and 10th min respectively, distilled water was added to a final volume of 2 mL, and the A value at 600 nm was determined. Then, the mice were killed by dearticulation, the liver, and spleen were removed and weighed. The monocyte-phagocytic exponent K was calculated as $K = \frac{\lg A_2 - \lg A_{10}}{(t_2 - t_1)}$, and the emended monocyte-phagocytic exponent α as $\alpha = \frac{\text{body weight}}{(\text{liver weight} + \text{spleen weight})} \times K^{1/3}$. The A_2 and A_{10} were the values at the 2nd and 10th min respectively, t_1 and t_2 represented the sampling time (both representing the ability of monocyte-phagocytic system to clear colloid charcoal particles in mice).

Statistical analysis

Variance analysis was performed with the statistical software

SPSS (version 10.0). The data were expressed as mean \pm SD, $P < 0.05$ was considered statistically significant.

RESULTS

Effects of concentrated liquor from male zoid of *Antheraea pernyi* on cellular immune function of mice

Twenty-four and forty-eight hours after immunization with SRBC, the FSR values of the three tested groups improved significantly compared to the control group by variance analysis (Table 1), indicating that the cellular immune function of mice could be improved obviously by concentrated liquor from male zoid of *A. pernyi*.

Table 1 Effects of concentrated liquor from male zoid of *A. pernyi* on cellular immune function of mice (mean \pm SD)

Group	Dosage (mg/kg)	Animal (n)	FSR (mm)	
			24 h	48 h
Control	dH ₂ O	10	0.66 \pm 0.25 ^b	0.20 \pm 0.16 ^d
Low-dosage	0.564	10	1.22 \pm 0.28	0.61 \pm 0.26
			<0.01	<0.01
Medium-dosage	2.62	10	1.24 \pm 0.23	0.61 \pm 0.19
			<0.01	<0.01
High-dosage	16.53	9	1.45 \pm 0.25	0.66 \pm 0.26
			<0.01	<0.01

^b $P < 0.01$, FSR (mm) of control group vs that of high-, medium- and low-dosage groups at 24 h respectively. ^d $P < 0.01$, FSR (mm) of control group vs that of high-, medium- and low-dosage groups at 48 h respectively.

Effects of concentrated liquor from male zoid of *Antheraea pernyi* on humoral immune function of mice

As shown in Table 2, the HC_{50} values representing the humoral immune function of mice showed a significant difference between the high dosage group and the control group by variance analysis ($F = 7.965$, $P < 0.01$). The same results were also observed between the high-dosage group and the other two tested groups ($P < 0.01$). The concentrated liquor from male zoid of *A. pernyi* had certain positive effect on the humoral immune function of mice.

Table 2 Effects of concentrated liquor from male zoid of *A. pernyi* on humoral immune function of mice (mean \pm SD)

Group	Dosage (mg/kg)	Animal (n)	HC_{50}
Control	dH ₂ O	7	42.2 \pm 18.2 ^b
Low-dosage	0.564	8	46.4 \pm 23.01 ^b
Medium-dosage	2.62	8	40.13 \pm 15.16 ^b
High-dosage	16.53	8	91.16 \pm 37.6
			<0.01 ^{b,d}

^b $P < 0.01$, high-dosage group vs control group. ^d $P < 0.01$, high-dosage group vs low- and medium-dosage groups respectively.

Effects of concentrated liquor from male zoid of *Antheraea pernyi* on monocyte-phagocytic function of mice

The monocyte-phagocytic exponent K and emended

Table 3 Effects of concentrated liquor from male zooid of *A. pernyi* on monocyte-phagocytic function of mice (mean±SD)

Group	Dosage (mg/kg)	Animal (n)	K	α
Control	dH ₂ O	10	0.0514±0.0122 ^a	6.249±0.772 ^c
Low-dosage	0.56	10	0.0527±0.0157 P>0.05	6.304±0.967 P>0.05
Medium-dosage	2.62	10	0.0517±0.0104 P>0.05	6.354±0.761 P>0.05
High-dosage	16.53	10	0.0570±0.0111 P>0.05	6.438±0.690 P>0.05

^aP>0.05, K value, high-, medium-, and low-dosage groups vs control group respectively. ^cP>0.05, α value, high-, medium-, and low-dosage groups vs control group respectively.

monocyte-phagocytic exponent α (both representing the ability of monocyte-phagocytic system to clear colloid charcoal particles in mice) are shown in Table 3. Both exponent K and emendated exponent α displayed a rising tendency, but no significant differences were observed among the groups by variance analysis (P>0.05).

DISCUSSION

The male zooid is an animal material medicine in China, whose functions are well documented in Compendium of Materia Medica as follows^[4]: invigorating essential Qi, strengthening vagina, untiring of sexual intercourse, and arresting essence. In Ri Hua Zi Ben Cao (Ri Hua Zi Materia Medica), it is documented to have the following actions: strengthening sexual function, checking spermatorrhea and stranguria with hematuria, warming kidney, extinguishing sore and scar, indications: wound from metal instrument injury, acute catarrhal and allergic conjunctivitis, and frostbite, heat-induced sore. Thus, male zooid can tonify the liver and invigorate the kidney, consolidate essence and strengthen Yang, check bleeding and promote muscle growth. The male zooid of *A. pernyi* contains many active substances, such as brain hormone, pro-thymosin, hormone of *A. pernyi*, diuretics, which can adjust metabolism and restore immune functions^[5-10].

Hu *et al.*^[11], using the fruit fly (*Drosophila melanogaster*) as a longevity model, examined the effect of hu-bao (HB) and seng-bao (SB), two marketed health products made from a mixture of natural ingredients, and found that the effect of HB and SB are specific for the male fly. The life-span of the male significantly increased when HB or SB was added to the culture medium. When the male silkworm moth ingredient was removed from HB or SB, the life-span prolongation effect of HB and SB drastically diminished, suggesting that the male silkworm moth is a key ingredient in combination with other components for specific prolongation of the life-span of male flies. The immune system in the Chinese oak silk moth, *A. pernyi*, originated from a single ancestral gene with that of the Cecropia moth whose antibacterial activity has been tested against nine different bacterial species^[12]. Zhang *et al.*^[13], reported that the cecropins from Chinese oak silkworm *A. pernyi* possess effective anti-tumor activity with no cytotoxicity against normal eukaryotic cells, and impede the neoplastic process in murine large intestines.

T cells play a role in immune response, killing tumor cells and suppressing tumor growth. Due to the actions of

estrogen, paracrine of tumor, negative nitrogen balance, the immune functions of patients can be suppressed and lead to immune escape, proliferation, and metastasis of tumor cells^[14]. Th1 and Th2 are two subgroups of CD4+Th cells. Most tumor tissues can secrete functional cytokine of Th2, causing the shift from Th1 to Th2 and immune suppression. Thus, promoting shift from Th2 to Th1 may be a method of tumor immunotherapy. The androgen-like action of male zooid can antagonize the immuno-suppression of high-level E2, promote high-expression of IL-18, induce production of IFN- γ , IL-2, IL-12, IL-18, and GM-CSF by monocytes, enhance cytotoxicity of NK and Th1 cells, accelerate proliferation of T cells and induce differentiation of Th1 cells^[15]. Amino acids in male zooid can adjust negative nitrogen balance and restore immune functions. Peptides in male zooid can also improve immune functions, enhance T cell activity by killing tumor cells^[16].

In general, the concentrated liquor from male zooid of *A. pernyi* can enhance non-specific immunity and CTL-mediated specific immunity, and has therapeutic functions in tumor therapy and adjuvant therapy.

Our study showed that the concentrated liquor from male zooid of *A. pernyi* could suppress tumor growth and improve immune function in mice. For immune modulation, it was observed in animal experiments that it could enhance cellular immunity significantly in all the three tested groups. In the high dosage group, the humoral immunity also obviously improved. A rising tendency was shown without significant difference.

In conclusion, the concentrated liquor from male zooid of *A. pernyi* is a potential anti-tumor agent by strengthening anti-pathogenic Qi. Further researches should be performed on its immuno-modulating effects on pancreatic and liver cancer.

REFERENCES

- 1 Piao HS, Ju Y, Zheng YH, Li YI, Zheng CJ, Shen GH. Extraction separation and identification of amino acid components in the semen of male silk moths. *Yanbian Daxue Yixue Xuebao* 1997; **20**: 147-148
- 2 Li QY, Hu PL. The study of antheraea pernyi and boxbyxmoril. *Shanghai Zhongyiyao Zazhi* 1996; **11**: 45-47
- 3 Xu SY, Bian RL, Chen X. Experimental methodology of pharmacology. Beijing: the People's Health Press 1991: 1233-1238
- 4 Ming D, Li SZ. Compendium of materia medica. 4TH edition. Beijing: the People's Health Press 1981: 2247-2255
- 5 Tang JH. The effect of antheraea pernyi. *Huaxia Yixue* 1999; **12**: 341

- 6 **Liu TY**, Li DJ. Chinese medicine: *Antheraea Pernyi*. *Beijing Zhongyiyao Daxue Xuebao* 1994; **17**: 22-23
- 7 **Mao G**, Cui DJ, Xu QM. The effect of *Antheraea Pernyi*. *Liaoning Zhongyi Zazhi* 1994; **21**: 231-232
- 8 **Liu XM**, Zhou LS. The anti-fatigue function of the capsule Wei Li Kang. *Guangdong Yiyao* 2003; **24**: 248-249
- 9 **Mo ZQ**, Zhou SY, Sang T, Wen SK. The pharmacological investigation and application of *Antheraea Pernyi*. *Zhongyiyao* 1995; **18**: 101-103
- 10 **Cao Cai**, Wei HY. Pharmacological study of *Antheraea Pernyi*. *Zhongguo Zhongyi Zazhi* 1991; **16**: 368-370
- 11 **Hu K**, Wang Q, Hu PQ. The male silkworm moth (*Antheraea pernyi*) is a key ingredient in hu-bao and sheng-bao for specific prolongation of the life-span of the male fruit fly (*Drosophila melanogaster*). *Am J Chin Med* 2002; **30**: 263-270
- 12 **Qu Z**, Steiner H, Engstrom A, Bennich H, Boman HG. Insect immunity: isolation and structure of cecropins B and D from pupae of the Chinese oak silk moth, *Antheraea pernyi*. *Eur J Biochem* 1982; **127**: 219-224
- 13 **Zhang WM**, Lai ZS, He MR, Xu G, Huang W, Zhou DY. Effects of the antibacterial peptide cecropins from Chinese oak silkworm, *Antheraea pernyi* on 1, 2-dimethylhydrazine-induced colon carcinogenesis in rats. *Diyi Junyi Daxue Xuebao* 2003; **23**: 1066-1068
- 14 **Vermeiren J**, Ceuppens JL, Van Ghelue M, Witters P, Bullens D, Mages HW, Kroczeck RA, Van Gool SW. Human T cell activation by costimulatory signal-deficient allogeneic cells induces inducible costimulator-expressing anergic T cells with regulatory cell activity. *J Immunol* 2004; **172**: 5371-5378
- 15 **Makar KW**, Wilson CB. DNA methylation is a nonredundant repressor of the Th2 effector program. *J Immunol* 2004; **173**: 4402-4406
- 16 **Xie ZW**. The effects of Chinese traditional medicine on the Th1/Th2 balance. *Guowai Yixue* 2002; **24**: 335-337

Science Editor Wang XL and Guo SY Language Editor Elsevier HK

Surgical treatment of giant esophageal leiomyoma

Bang-Chang Cheng, Sheng Chang, Zhi-Fu Mao, Mao-Jin Li, Jie Huang, Zhi-Wei Wang, Tu-Sheng Wang

Bang-Chang Cheng, Sheng Chang, Zhi-Fu Mao, Jie Huang, Zhi-Wei Wang, Tu-Sheng Wang, Department of Thoracic Cardiovascular Surgery, Renmin Hospital of Wuhan University, Wuhan 430060, Hubei Province, China
Mao-Jin Li, Department of Radiology, Renmin Hospital of Wuhan University, Wuhan 430060, Hubei Province, China
Supported by the Science and Technology Foundation of Hubei Province, No. 992P1203
Co-first-author: Sheng Chang
Correspondence to: Professor Bang-Chang Cheng, Department of Thoracic Cardiovascular Surgery, Renmin Hospital of Wuhan University, Wuhan 430060, Hubei Province, China. dr_cheng@126.com
Telephone: +86-27-88041919-2240
Received: 2004-12-25 Accepted: 2005-01-12

Abstract

AIM: To summarize the operative experiences for giant leiomyoma of esophagus.

METHODS: Eight cases of giant esophageal leiomyoma (GEL) whose tumors were bigger than 10 cm were treated surgically in our department from June 1980 to March 2004. All of these cases received barium swallow roentgenography and esophagoscopy. Leiomyoma located in upper thirds of the esophagus in one case, middle thirds of the esophagus in five cases, lower thirds of the esophagus in two cases. Resection of tumors was performed successfully in all of these cases. Operative methods included transthoracic extramucosal enucleation and buttressing the muscular defect with pedicled great omental flap (one case), esophagectomy and esophago-gastrostomy above the arch of aorta (three cases), total esophagectomy and esophageal replacement with colon (four cases). Histological examination confirmed that all of these cases were leiomyoma.

RESULTS: All of the eight patients recovered approvingly with no mortality and resumed normal diet after operation. Vomiting during meals occurred in one patient with esophagogastrostomy, and remained 1 mo. Reflux esophagitis occurred in one patient with esophago-gastrostomy and was alleviated with medication. Thoracic colon syndrome (TCS) occurred in one patient with colon replacement at 15 mo postoperatively. No recurrence occurred in follow-up from 6 mo to 8 years.

CONCLUSION: Surgical treatment for GEL is both safe and effective. The choices of operative methods mainly depend on the location and range of lesions. We prefer to treat GEL via esophagectomy combined with esophago-gastrostomy or esophagus replacement with colon. The long-time quality of life is better in the latter.

© 2005 The WJG Press and Elsevier Inc. All rights reserved.

Key words: Giant esophageal leiomyoma; Esophagus; Greater omentum; Esophageal replacement with colon

Cheng BC, Chang S, Mao ZF, Li MJ, Huang J, Wang ZW, Wang TS. Surgical treatment of giant esophageal leiomyoma. *World J Gastroenterol* 2005; 11(27): 4258-4260
<http://www.wjgnet.com/1007-9327/11/4258.asp>

INTRODUCTION

Leiomyoma is the most common benign tumor found in the esophagus but it is, however, a rare neoplasm. It is found mainly in the lower and middle thirds of the esophagus and, in most cases are single lesions^[1]. Leiomyoma can occur at any age but 90% of cases occur in patients between the ages of 20 and 69 years, with peak incidence in the third to fifth decades^[2]. The male-to-female ratio is approximately 2:1. About half the patients with leiomyoma are asymptomatic and malignant change is rare. Transthoracic extramucosal enucleation is a safe and effective procedure for about 96% of esophageal leiomyoma^[3]. However, few of esophageal leiomyoma becomes giant-sized gradually (diameter of tumor larger than 10 cm) and show the symptoms caused by compression of tumor, obstruction of esophagus or dysfunction of cardia. The surgical treatment strategy of such GEL is not the same of common esophageal leiomyoma, especially when mucosa is damaged by leiomyoma or lesions have potential sarcomatous change. This report summarized the operative experience of GEL in our department.

MATERIALS AND METHODS

Materials

Between June 1980 and March 2004, there were 8 cases of GEL whose tumors were larger than 10 cm that underwent surgical treatment in our department. These patients comprised five males and three females, whose age ranged from 25 to 58 years (mean age, 42.5 years). Duration of symptoms was from 5 to 12 years. All of the eight patients had dysphagia and complained of retrosternal pain and backache in five cases, superior belly distention in five cases, weight loss in four cases, heartburn in three cases, cough in two cases, took normal diet in two cases, semi-liquid diet in four cases, liquid diet in two cases. All of the eight patients received barium swallow roentgenography and esophagoscopy. CT scan was performed in five cases, MRI in three cases, endoscopic ultrasonography (EUS) in one case. Leiomyoma located in upper thirds of the esophagus

in one case, middle thirds of the esophagus in five cases, lower thirds of the esophagus in two cases. The shapes of tumors were multinode-like in four cases, spiral-like in three cases, horseshoe-like in one case.

Methods

All patients received operation under general anesthesia. One patient underwent extramucosal enucleation of tumor and buttressing of the muscular defect with pedicled greater omental flap. In this case, the tumor located in lower thirds of the esophagus (Figure 1). Left posterolateral thoracotomy was performed through the sixth intercostal space. After removing the tumor, the muscular defect was found too large to allow a tension-free suture. Through a radial incision near esophageal hiatus, we made the great omentum into a pedicle flap (26 cm×9 cm) and pulled it up into thoracic cavity to cover the muscular defect. Three patients accepted esophagectomy and esophagogastrostomy above the arch of aorta through left posterolateral thoracotomy. Nasogastric tube and plasmatic canal were placed to aid in drainage and nutrition. Another four patients underwent total esophagectomy and esophageal replacement with colon. In these cases, patients were laid in supine position at the beginning. Esophageal interposition was performed with left colon (isoperistaltic, retrosternal) through left cervical abdominal incision. Then the patient's position was changed to full left lateral decubitus. Tumor and total esophagus were resected through right posterolateral thoracotomy. A feeding jejunostomy was used in these four patients, and enteral feeding was begun after 24 h with 5% dextrose in water and continued with an elemental diet after 48 h. The minimum size of tumor was 10 cm×10 cm×6 cm, the maximum was 20 cm×15 cm×15 cm. Histological examination confirmed that all of these were leiomyoma.

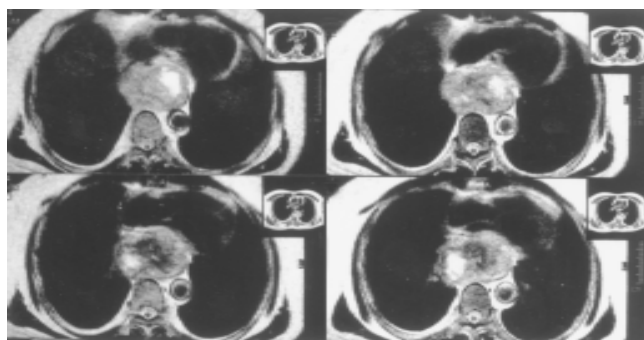


Figure 1 A 42-year-old male with giant esophageal leiomyoma. MRI image shows the tumor located in lower thirds of the esophagus. The size of tumor is 10 cm×10 cm×6 cm.

RESULTS

All of the eight patients recovered approvingly with no mortality and resumed normal diet after operation. Postoperative complications included leakage of cervical esophageal stoma (one case), pulmonary atelectasis (one case), thoracic infection (one case), chylothorax (one case). They all healed with conservative interventions and drainage. Patients were followed up from 6 mo to 8 years. Vomiting

after meals occurred in one patient with esophagogastrostomy, and remained for 1 mo. Vomiting after meals was not seen in patients with colonic interposition. Reflux esophagitis occurred in one patient with esophagogastrostomy and was alleviated with medication. Thoracic colon syndrome (TCS) occurred in one patient with colon replacement at 15 mo postoperatively, and recovered with re-operation. No recurrence occurred.

DISCUSSION

Leiomyoma is the most common benign tumor found in the esophagus but is nonetheless rare. Of all esophageal tumors, benign tumors account for fewer than 10%, of which 4% are leiomyomas^[4]. These tumors are usually found in middle age and are almost twice as common in men. They are located mainly in the lower and middle thirds of the esophagus. Leiomyoma may undergo cystic degeneration, calcification occurs infrequently and malignant change is rare^[5]. Leiomyoma is a slow growing tumor and the size of the lesion may not change for many years. Approximately one-half of all tumors are smaller than 5 cm, but 5% may be larger than 10 cm. Giant leiomyoma involving the entire esophagus and weighing up to 5 kg have been reported^[6]. Giant leiomyoma of esophagus should be removed when diagnosed, but its operative method is not the same of common leiomyoma.

Since most leiomyomas are intramural, eccentric, and well encapsulated, they can be easily shelled out (enucleated) without resorting to esophageal resection. One concern after enucleation of a large leiomyoma is that the myotomy may result functionally in achalasia. It is generally accepted that tumors up to 8 cm can be safely enucleated without significant postoperative dysphagia as long as the mucosa is intact and the myotomy is reapproximated^[3,7]. Larger lesions can be removed via enucleation but often result in the muscular defects too large to allow a tension-free suture, requiring a tissue flap to prevent mucosal bulging. We resected a 10 cm×10 cm×6 cm esophageal leiomyoma successfully with extramucosal enucleation and buttressing the muscular defect with pedicled greater omental flap. No postoperative dysphagia occurred during follow-up.

The greater omentum (GO) square is large and allows the covering of various tissue defects. The pedicled GO flap has the advantages of its own blood supply and anti-inflammatory effect^[14]. Using the GO to fill or buttress tissular defect is not novel in thoracic surgery^[14]. Angiography shows many types of vascular supply for the GO. Therefore, the GO flap exsection technique is very important. The flap transposition through the diaphragm is not difficult. The opening should not be very wide for good great omentum tissue adhesion and too narrow to prevent compression of the vessels.

Majority of GEL may require esophageal resection. The choices of this method depend on several factors: (1) The esophageal leiomyoma is too large to allow a resection without damaging the mucosa; (2) Adhesion between leiomyoma and the esophageal mucosa is tight and extensive; (3) Unrepairable mucosal defect caused by resection of tumor; (4) Large leiomyomas locate in the distal esophagus and extend downward across the cardia; (5) Leiomyosarcoma

is suspected. Resection for GEL is typically performed with esophagectomy and gastric pull-up through left posterolateral thoracotomy. In our experience, blood supply of the GEL was abundant, especially at the region posterior to the arch of aorta and upper part of the diaphragm. Careful dissection and hemostasia was necessary. Be cautious not to damage thoracic duct. For this purpose, transfixing the trunk of thoracic duct above the diaphragm between descending aorta and azygos vein was helpful. Gastric pull-up has some postoperative morbidity including reflux esophagitis, stricture formation, dumping, diarrhea, reduced meal capacity, and weight loss^[8]. Many of these complications are thought to be caused by division of the vagal nerves and the subsequent loss of parasympathetic innervation to the foregut^[9].

The rationale for use of the colon is that there will be fewer complications related to acid reflux than when the stomach is used for esophageal replacement. If the GEL is located in the upper thirds of the esophagus and the mucosa is damaged by GEL, esophageal replacement with colon (ERC) might be the best choice in this situation. Our techniques of ERC are different to others. The retrosternal colon replacement is performed through left cervical abdominal approaches in supine position at first, and then resects tumor and total esophagus through right posterolateral thoracotomy in full left lateral decubitus. We prefer this approach to synchronous abdominothoracic incision, for the former has allowed better exposure.

Several factors are important to decrease the mortality and postoperative complications of ERC: (1) Choosing suitable colonic segment and ensuring an adequate arterial supply. Before cutting the mesocolon, we usually clamp the communicating branches for 3~5 min in order to ensure that blood supply is enough; (2) Adopting isoperistaltic interposition. Studies show that isoperistaltic interposition is superior to antiperistaltic interposition and the long-time quality of life is better in the former^[10,13]; (3) Single-layer esophagocolonic anastomosis. Our studies show that single-layer anastomosis can reduce the morbidity of fistula and stricture^[11]; (4) Choosing colonic pull-up approach properly. The upward approach of colonic segment is decided by the condition of individual patient and the experience of the surgeon; (5) Avoiding redundancy of the colonic segment. Colon redundancy can be due to technical error at the time of operation (i.e., leaving redundancy in the interposition graft), intrathoracic herniation of colon, or differential colon growth. Proper attention to the length of the colon segment is important to prevent intrathoracic redundancy^[16]. Yildirim *et al.*^[17] suggest that the colon is one of the best substitutes for the esophagus, and there is no need to perform a routine pyloroplasty or antireflux procedure as an adjunct to the primary surgery. Our patients

healed satisfactorily and the long-time quality of life was good during follow-up and it was coincident with the literature^[12,13,15].

REFERENCES

- 1 **Hatch GF 3rd**, Wertheimer-Hatch L, Hatch KF, Davis GB, Blanchard DK, Foster RS Jr, Skandalakis JE. Tumors of the esophagus. *World J Surg* 2000; **24**: 401-411
- 2 **Lawrence SL**, Sunil S, Clayton JB, Blair M, Michael LK, Larry RK, John CK. Current management of esophageal leiomyoma. *J Am Coll Surg* 2004; **198**: 136-146
- 3 **Bonavina L**, Segalin A, Rosati R, Pavanello M, Peracchia A. Surgical therapy of esophageal leiomyoma. *J Am Coll Surg* 1995; **181**: 257-262
- 4 **Jesic R**, Randjelovic T, Gerzic Z, Zdravkovic DJ, Krstic M, Milinic N, Pavlovic A, Svecic T, Bulajic M. Leiomyoma of the esophagus. Case report. *Srp Arh Celok Lek* 1997; **125**: 113-115
- 5 **Nagashima R**, Takeda H, Motoyama T, Tsukamoto O, Takahashi T. Coexistence of superficial esophageal carcinoma and leiomyoma: case report of an endoscopic resection. *Endoscopy* 1997; **29**: 683-684
- 6 **Aurea P**, Grazia M, Petrella F, Bazzocchi R. Giant leiomyoma of the esophagus. *Euro J Cardiothorac Surg* 2002; **22**: 1008-1010
- 7 **Roviaro GC**, Maciocco M, Varoli F, Rebuffat C, Vergani C, Scarduelli A. Videothoracoscopic treatment of oesophageal leiomyoma. *Thorax* 1998; **53**: 190-192
- 8 **Watson TJ**, Peters JH, DeMeester TR. Esophageal replacement for end-stage benign esophageal disease. *Surg Clin North Am* 1997; **77**: 1099-1113
- 9 **Banki F**, Mason RJ, DeMeester SR, Hagen JA, Balaji NS, Crookes PF, Bremner CG, Peters JH, DeMeester TR. Vagal-sparing esophagectomy: a more physiologic alternative. *Ann Surg* 2002; **236**: 324-335
- 10 **Cheng BC**, Lu SQ, Gao SZ, Tu ZF, Lin DM, Wang TS. Colon replacement for esophagus: clinical experience from 240 cases. *Chin Med J* 1994; **107**: 216-218
- 11 **Gao SZ**, Wang TS, Yao Z, Cheng BC, Tu ZF, Ling DM, Peng SY. Experimental study and clinical application of a single-row suturing esophagogastronomy. *J Surg Oncol* 1990; **43**: 167-171
- 12 **Cheng BC**, Gao SZ, Tu ZF, Lu DT, Zhou SG, Cai XT, Huang ZR, Wang CX. The clinical study on the route of colon segment for replacement of the esophagus. *Chin J Thorac Cardiovasc Surg* 2000; **16**: 283-285
- 13 **Cheng BC**, Shao K. Evaluation of the quality of life after esophageal replacement with colon. *Chin J Clin Rehabilitation* 2002; **6**: 2676-2677
- 14 **Levashev YN**, Akopov AL, Mosin IV. The possibilities of greater omentum usage in thoracic surgery. *Eur J Cardiothorac Surg* 1999; **15**: 465-468
- 15 **Thomas P**, Fuentes P, Giudicelli R, Reboud E. Colon interposition for esophageal replacement: current indications and long-term function. *Ann Thorac Surg* 1997; **64**: 757-764
- 16 **Domreis JS**, Jobe BA, Aye RW, Deveney KE, Sheppard BC, Deveney CW. Management of long-term failure after colon interposition for benign disease. *Am J Surg* 2002; **183**: 544-546
- 17 **Yildirim S**, Koksall H, Celayir F, Erdem L, Oner M, Baykan A. Colonic Interposition vs Gastric Pull-Up After Total Esophagectomy. *J Gastrointest Surg* 2004; **8**: 675-678

Mutations outside the YMDD motif in the P protein can also cause DHBV resistant to Lamivudine

Jin-Yang He, Yu-Tong Zhu, Rui-Yi Yang, Li-Ling Feng, Xing-Bo Guo, Feng-Xue Zhang, Hong-Shan Chen

Jin-Yang He, Yu-Tong Zhu, Rui-Yi Yang, Li-Ling Feng, Xing-Bo Guo, Feng-Xue Zhang, Tropical Medicine Institute of Guangzhou University of Traditional Chinese Medicine, Guangzhou 510405, Guangdong Province, China
Hong-Shan Chen, Institute of Medical Biotechnology of CAMS and PUMC, Beijing 100050, China

Correspondence to: Jin-Yang He, MD, Tropical Medicine Institute of Guangzhou University of Traditional Chinese Medicine, Guangzhou 510405, Guangdong Province, China. sunny12345678_89@yahoo.com.cn

Telephone: +86-20-31774402

Received: 2004-12-22 Accepted: 2005-01-12

Abstract

AIM: To observe the Lamivudine resistance character of a DHBV strain *in vitro* and *in vivo*, and to analyze if the Lamivudine resistance character is caused by gene mutation or by abnormality of the Lamivudine metabolism.

METHODS: Congenitally DHBV-negative Guangdong brown ducks and duck embryo liver cells were respectively taken as animal and cell model. The Lamivudine-susceptible DHBV and Lamivudine-resistant DHBV (LRDHBV) were infected and Lamivudine was administered according to the divided groups. The changes of DHBV quantity in the animal and cell model were tested. Three Lamivudine-resistant and two Lamivudine-susceptible DHBV complete genomes were successfully amplified, sequenced and then submitted to GenBank. All the DHBV complete sequences in the GenBank at present were taken to align with the three LRDHBV to analyze the mutational points related to the Lamivudine-resistant mutation.

RESULTS: Both the animal and cell model showed that the large and the small dosage Lamivudine have no significant inhibitory effect on the LRDHBV. Five sequences of DHBV complete genomes were successfully cloned. The GenBank accession numbers of the three sequences of LRDHBV are AY521226, AY521227, and AY433937. The two strains of Lamivudine-susceptible DHBV are AY392760 and AY536371. The correlated mutational points are KorR86Q and AorE591T in the P protein.

CONCLUSION: The Lamivudine resistance character of this DHBV strain is caused by genome mutation; the related mutational points are KorR86Q and AorE591T and have no relations with the YMDD motif mutation.

© 2005 The WJG Press and Elsevier Inc. All rights reserved.

Key words: DHBV; Lamivudine resistance; Mutational points

He JY, Zhu YT, Yang RY, Feng LL, Guo XB, Zhang FX, Chen HS. Mutations outside the YMDD motif in the P protein can also cause DHBV resistant to Lamivudine. *World J Gastroenterol* 2005; 11(27): 4261-4267

<http://www.wjgnet.com/1007-9327/11/4261.asp>

INTRODUCTION

More than 400 million people worldwide are chronically infected by HBV^[1]. HBV infections, the 10th leading cause of death worldwide, result in 500 000 to 1.2 million deaths per year caused by chronic hepatitis, cirrhosis, and hepatocellular carcinoma^[2]. Lamivudine had been considered to be a great progress in the area of anti-virus drug. It can make the blood HBV DNA of more than 90% of patients changed to negative when administered for 1 year by 100 mg/d^[3,4]. But it can also lead to YMDD mutant and cause Lamivudine resistance. YMDD mutations developed in 12.1%, 49.7% and 70.5% of the patients respectively at year 1, 2, and 3^[5]. So the searching of Lamivudine-resistant problem is very important. It is believed consistently that the cause of Lamivudine resistance is HBV gene mutation. The main mutant motif is the YMDD in the P protein of HBV^[6-8]. But there are no animal and cell models of Lamivudine-resistant HBV which can be conveniently used, which cause very little progress that has been the problem of Lamivudine-resistant HBV.

After the finding of the DHBV by Summers *et al.*^[9,10], the process of replication and genome sequence of DHBV had been discovered rapidly. These facilitated the understanding of the related aspects of HBV. Because of the similarity of the DHBV and HBV in the replicating manner and pathogenesis, the duck hepatitis B model had been used as animal model of anti-HBV drug screening and HBV pathogenesis searching. When we persistently used the congenitally infected duck as animal model to screen anti-HBV drug, one congenitally infected duck had been found to have the character of Lamivudine resistance. We named it Lamivudine-resistant duck (LRD). The LRD-infected virus was named as Lamivudine-resistant DHBV (LRDHBV). We proved the character of Lamivudine resistance of LRDHBV in embryo duck liver cell model and postnatally infected duck model. Then the complete genome of LRDHBV and Lamivudine-susceptible DHBV were cloned and sequenced. The LRDHBV-related mutant points were analyzed.

MATERIALS AND METHODS

Animals

One-day-old Guangdong brown ducks were obtained from

a duck factory on the Shi-Jing town of Guangzhou city. Congenitally DHBV-negative ducks were chosen by dot blot assay to be experimental animals. The ducks were fed a standard duck diet and water according to the guidelines approved by the China Association of Laboratory Animal Care.

Primary hepatocytes

Guangdong brown duck eggs were purchased from a commercial supplier. The eggs were incubated for 20 d in the environment of 37.6 °C and 50-60% humidity. The eggs were opened and were proved to be congenitally DHBV negative using PCR method. The duck embryo liver was plucked out and digested with 0.2% collagenase (type II, Gibco) in 3 mL of serum-free William E medium (Sigma) supplemented with 2 mol/L L-glutamine, 15 mol/L HEPES (N-2-hydroxyethylpiperazine-N'-2-ethane-sulfonic acid [pH 7.2]), 100 U of penicillin per mL, 100 µg of streptomycin, 10⁻⁵ mol/L hydrocortisone, 1 µg of insulin per mL, and 1.5% dimethyl sulfoxide (all from Sigma, Germany) for 30 min at 37 °C. After washing twice with 5 mL of medium, the cells from one liver were suspended in 20-24 mL of medium, seeded onto 10-12 tissue culture dishes (60-mm diameter; 2 mL per dish, the density is 5×10⁵ cells per well), and cultivated at 37 °C and 50 mL/L CO₂. The medium was first changed 30 min after seeding, and further medium changes were done daily. Cellular toxicity was tested daily by light microscope examination and MTT assay of Mosmann^[11] as described by Alley *et al.*^[12].

Serum and DHBV infection

Lamivudine-susceptible DHBV serum was from congenitally infected ducks that had been proved to be DHBV positive by dot blot method. LRDHBV serum was from LRD at the time point of 10-d Lamivudine administration. In the animal model, 0.2 mL of Lamivudine-susceptible DHBV or LRDHBV was injected to the shank vein of every duck that were 2 d old. The primary hepatocytes were infected between 24 and 48 h after seeding by adding 50 µL Lamivudine-susceptible DHBV or LRDHBV per dish directly to the medium. After 3-h incubation at 37 °C, the inoculum was removed, and 2 mL of fresh medium was added.

Groups and dot blot assay

Twelve ducks infected with Lamivudine-susceptible DHBV and 18 ducks infected with LRDHBV were chosen and randomly divided into five groups. Group A were infected with Lamivudine-susceptible DHBV; group B were infected with LRDHBV; group C were infected with LRDHBV and fed with large dosage Lamivudine (100 mg/kg, b.i.d.); group D were infected with LRDHBV and fed with small dosage Lamivudine (20 mg/kg, b.i.d.); group E were infected with Lamivudine-susceptible DHBV and fed with small dosage Lamivudine (20 mg/kg, b.i.d.). The serum samples were collected at time points of 1 d before drug administration (D0), 5th d of drug administration (D5), 10th d of drug administration (D10) and 3rd d post stopping of drug administration (P3). The primary hepatocytes were also divided into five groups similar to the animal experiment. The hepatocytes were also

treated with two concentrations of Lamivudine (100 and 1 000 µmol/L) starting from 3 d after virus inoculation. The hepatocytes were collected and DNA was extracted at the time points of 3, 6, 9, and 12 d after virus inoculation respectively. Forty microliters of serum or twenty-five microliters of hepatocytes DHBVDNA extraction dissolution was spotted, and DHBVDNA was detected with a full-length DHBV genomic DNA probe labeled with [α -³²P] dCTP as described previously^[13]. A quantity analysis was carried out using enzyme photometer. The limit of detection of serum viral DNA by this assay is 100 pg/mL.

Amplification of the DHBV complete genome

Three samples of LRDHBV DNA were extracted from the serum of LRD which was the same as the LRDHBV serum used to infect the congenitally DHBV-negative ducks and duck embryo liver cells. Two samples of Lamivudine-susceptible DHBVDNA were extracted from serum of two ducks that were susceptible to Lamivudine. One pair of primers was used to test if there was DHBVDNA in the extraction solutions. The primer sequences^[14] are: P1 -5'-GCG CTT TCC AAG ATA CTG GAG CCC AA-3' (sense) and P2-5'-CTG GAT GGG CCG TCA GCA GGA TTA TA-3' (anti-sense). The PCR condition is: 94 °C 30 s, 55 °C 30 s, 72 °C 1 min, 30 cycles. One pair of primers was designed to amplify the complete genome of DHBV. The primer sequences are Q1-5'-ACC CCT CTC TCG AAA GCA ATA-3' (sense) and Q2-5'-GTG TAT GTA AGA GCC GTC CAA TC-3' (anti-sense). The LAPCR condition is: 94 °C 30 s; 52 °C 1 min; 72 °C 3.5 min, after 30 cycles, another 72 °C 5 min was supplemented. One percent agarose gel was used to analyze the LAPCR product.

Cloning and sequencing of DHBV complete genome

The 3.0-kb PCR product was inserted into the pMD18-T vector using the TAKARA Ligation kit. JM109 competent cells were made with the method of CaCl₂ which was found by Mandel *et al.*^[15,16]. Three LRDHBV DNA recombinants and two Lamivudine-susceptible DHBV DNA recombinants were transformed into the JM109 competent cells. The five kinds of *E coli* containing the five kinds of recombinants were conserved and sent to TAKARA to do bidirectional sequencing. The sequencing results were analyzed with related software.

Statistical analysis

Results were expressed as mean±SD. Statistical comparisons between the groups were done using Nemenyi method. *P* values less than 0.05 were considered statistically significant.

RESULTS

Lamivudine could not inhibit LRDHBV in duck animal model

We first examined if the LRDHBV could be inhibited in body of the other duck. We injected the LRDHBV-positive serum to the congenitally DHBV-negative ducks. These ducks were infected with LRDHBV and treated with Lamivudine. Lamivudine were used in large and small dosage groups. The feeding was maintained for 10 d. Serum samples were collected at four time points from 1 d before administration to 3rd d post stopping of administration. The DHBV in the

serum samples were quantified by dot blot assay. After 10 d of Lamivudine administration, the quantity of Lamivudine-susceptible DHBV in the duck blood markedly got down. But 3 d after stopping of administration, the quantity of susceptible DHBV rose up to former level. No significant effect was observed when the large and small dosage of Lamivudine was fed to the LRDHBV-infected ducks (Table 1 and Figure 1). So it can be concluded that the LRDHBV can also show the character of Lamivudine resistance in the ducks postnatally infected with the LRDHBV.

Table 1 and Figure 1 showed that no significant effect was observed when the large and small dosage of Lamivudine was fed to the LRDHBV-infected ducks. While the 10-d Lamivudine administration could make the Lamivudine-susceptible DHBV markedly get down in the duck model.

The dynamic change of the DHBV quantity in the blood before and after lamivudine administration

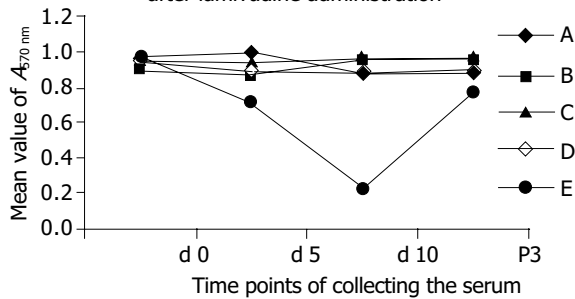


Figure 1 A: Lamivudine-susceptible DHBV control group; B: LRDHBV control group; C: LRDHBV-infected group administrated by large dose Lamivudine group; D: LRDHBV-infected group administrated by small dose Lamivudine group; E: Lamivudine-susceptible DHBV-infected group administrated by small dose Lamivudine group.

Lamivudine could not inhibit LRDHBV in the duck embryo liver cells

We inoculated the LRDHBV to the primary duck embryo liver cells and administrated Lamivudine according to the divided groups to observe if the LRDHBV have the Lamivudine-resistant character in the liver cells. Lamivudine administration was started from 3rd d post DHBV inoculation and maintained for 9 d. The liver cells were collected at four time points from 3 to 12 d post DHBV inoculation. The total DHBV in the cells was extracted immediately after cell collection. The DHBV quantity was tested by dot blot assay. The results showed that the Lamivudine-susceptible DHBV got down markedly at the time points of 6th, 9th, and 12th d post DHBV inoculation, while both the small and large dosage Lamivudine have no significant effect on the LRDHBV in the duck embryo liver cells (Figure 3). So

the LRDHBV showed Lamivudine-resistant character in the duck embryo liver cells too. We also tested the cytotoxicity of Lamivudine to the embryo liver cells. However, no significant cytotoxicity was detected in liver cells cultured with different concentrations of Lamivudine for 9 d by daily microscope examination (Figure 2) and by MTT method.

Lamivudine-susceptible DHBV was inhibited markedly at the time points of 6th, 9th, and 12th d post DHBV inoculation, while both the small and large dosage Lamivudine have no significant effect on the LRDHBV in the duck embryo liver cells.

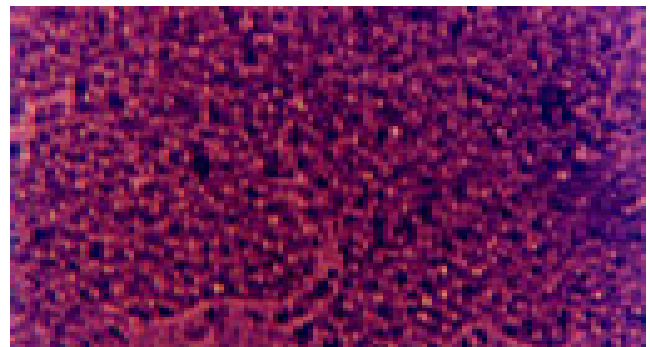


Figure 2 Duck embryo liver cells (5 d after DHBV inoculation, optic microscope ×40). They have no significant effect of Duck embryo liver cells infected with DHBV or LRDHBV.

Effects of lamivudine to the lamivudine susceptible and resistant DHBV in duck embryo liver cell culture

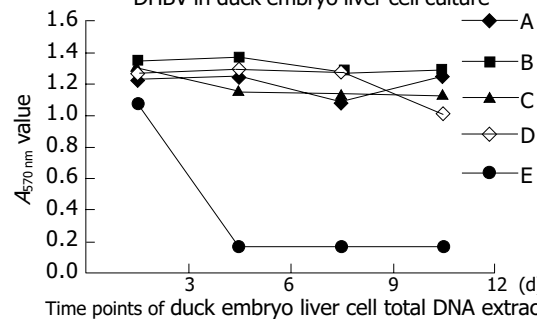


Figure 3 A: Lamivudine-susceptible DHBV control; B: LRDHBV control; C: LRDHBV-infected cells administrated by large dosage Lamivudine; D: LRDHBV-infected cells administrated by small dosage Lamivudine; E: Lamivudine-susceptible DHBV-infected cells administrated by small dosage Lamivudine.

DHBV complete genomes were successfully amplified and cloned

We designed two pairs of primer to amplify the DHBV complete genome. One was designed according to the method

Table 1 DHBV quantity in the duck blood of various groups expressed by A_{570 nm} value (mean±SD)

Groups	D0	D5	D10	P3
Lamivudine-susceptible DHBV control	0.96±0.31	1.00±0.06	0.87±0.05	0.87±0.02
LRDHBV control	0.91±0.03	0.86±0.01	0.95±0.01	0.95±0.04
LRDHBV-infected group administrated by large dose Lamivudine	0.96±0.03	0.94±0.02	0.97±0.05	0.97±0.03
LRDHBV-infected group administrated by small dose Lamivudine	0.96±0.02	0.88±0.02	0.87±0.01	0.90±0.05
Lamivudine-susceptible DHBV-infected group administrated by small dose Lamivudine	0.96±0.05	0.73±0.05 ^b	0.22±0.03 ^b	0.69±0.02 ^b

^bP<0.01 group A vs group E.

of Gunther to amplify the HBV complete genome^[17]. It covered the DR1 of DHBV genome. Another pair of primer covered the DR2 of DHBV genome and LAPCR was used to amplify. We found that the primer covering the DR1 could not amplify the DHBV genome after optimizing the LAPCR condition. However, when we used the primer covering the DR2, the complete genome of DHBV was easily amplified (Figure 4). So we amplified three strains of LRDHBV and two strains of Lamivudine-susceptible DHBV complete genome. Then we inserted these DHBV complete genomes into the pMD18-T vector and transformed them to the JM 109 competent cells (Figure 4). Then the *E. coli* that included the five DHBV complete genomes were sent to the TAKARA to sequencing. The five complete sequences of DHBV complete genomes were submitted to the GenBank. Three strains of LRDHBV are AY521226, AY521227, and AY433937. Two strains of Lamivudine-susceptible DHBV are AY392760 and AY536371.

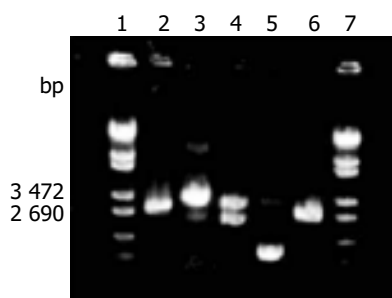


Figure 4 Electrophoresis graph of the amplification of DHBV complete genome and enzyme cutting of the recombinant. Lanes 1 and 7: λ -EcoT14I digest marker; lane 2: the LAPCR product of DHBV complete genome; lane 3: the cloning product of DHBV complete genome; lane 4: *EcoRI* enzyme cutting product of DHBV complete genome recombinants; lane 5: loop product of pMD18-T vector; lane 6: *EcoRI* enzyme cutting product of loop product of pMD18-T vector.

Analyze the related mutant points in the LRDHBV genome

Firstly, we compared the complete nucleotide sequences of the AY521226, AY521227, and AY433937, and the identity is the same 98%. The identity of the AY392760 and the AY536371 is also 98%. But comparing the nucleotide sequences of the LRDHBV (AY521226, AY521227, and AY433937) with the Lamivudine-susceptible DHBV (AY392760 and AY536371), the identity in the nucleotide level is the same 92%. So it seems that there are marked differences between LRDHBV and the Lamivudine-susceptible DHBV in nucleotide level. As the HBV or DHBV P protein is the target of Lamivudine, we turned to the P protein sequences of these DHBV. We initially aligned the P protein sequences of AY521226, AY521227, AY433937 with AY392760, AY536371. There were too many mutant points to analyze which points were related to the Lamivudine-resistant character. As the identities of AY392760 and AY433937 is only 88%, alignment should be done in a wider range. We downloaded all the DHBV protein sequences and aligned with the three Lamivudine-resistant sequences AY521226, AY521227, and AY433937. We found that there were two mutational points in the P protein. The two mutational points are KorR86Q and AorE591T (Figures 5A and B). We have not found any

significant mutational points in S or C protein sequences. The KorR86Q is located in the TP (terminal protein) domain, and the AorE591T is located in the RT (reverse transcriptase) domain. So we guessed that these two mutational points were related to the character of Lamivudine resistance.

DISCUSSION

We referred to Gunther's method^[17] when we designed the primers of amplifying the DHBV complete genome. This method noted that only the primers cover the DR1 sequence of HBV, the HBV genome can be wholly amplified. We first used one pair of primers that cover the DR1 of DHBV to amplify DHBV complete genome. Though all kinds of methods of optimizing the PCR condition were tested, the DHBV complete genome could not be amplified. So we guessed that the DR2 of DHBV sequence is also an important obstacle of amplifying the DHBV complete genome. In our experience, it is very hard to get the target products when the primers are located at both sides of the DR2. Additionally, the DR2 is located at the terminal of DHBV-positive strand. There is nick part followed by DR2 in the positive strand of DHBV. So we designed one pair of primers to cover the DR2 to amplify the whole DHBV genome. To our surprise, the complete genomes of DHBV were easily amplified. This phenomenon may be because the genome structure of DHBV is different to the HBV.

If Lamivudine-resistant character of LRDHBV was caused by unusual metabolism of Lamivudine in the duck body and did not correlate with virus genome mutation, it should not have the Lamivudine-resistant character in duck embryo liver cells and other ducks infected with the LRDHBV. Our results showed that the LRDHBV resistant to the Lamivudine appeared both in duck embryo liver cells and in duck body. So we concluded that the Lamivudine-resistant character is caused by DHBV mutation.

To our present knowledge, most of the Lamivudine-resistant phenomena of HBV are related to the YMDD motif mutation^[6-8,18]. Similar to HBV, mutagenesis *in vitro* in the YMDD motif of DHBV can also cause Lamivudine resistance^[19]. So we speculate that the mutational points were also located in the YMDD motif of LRDHBV. But the sequencing results denied this speculation.

After we obtained the five DHBV complete sequences, we found that there are no YMDD motif mutations in the P protein sequences of the three LRDHBV sequences. Then we aligned the P protein sequences of three LRDHBV with the two Lamivudine-susceptible DHBV P protein sequences. There were too many different points to analyze the mutational points related to the character of Lamivudine resistance. So we planned to align these three LRDHBV P protein sequences with more DHBV P protein sequences. There should be a prerequisite that the DHBV P protein sequences aligned with the three LRDHBV P protein sequences come from the DHBV which are susceptible to Lamivudine. Because it was never reported that there was a naturally occurred LRDHBV and we found only one strain of DHBV that have the Lamivudine-resistant character in so many years of laboratory work, we believed that the LRDHBV that occurred naturally is very few. So we

A		B	
AF493986	61 VRAPLSHVRAATIDLPRLGKGLPA	538	ELGIRINFDKTTSPVNEIRFLGYQID
AY294656	RHHLGKLSGLYQMGCTFNPEWKVPDISDTHFNLD		ENFMKIEESRWKELRTVIKKIKVGEWYDWKCIQ
AF047045	VRAPLSHVRAATIDLPRLGKGLPA		ELGIRINFDKTTSPVNEIRFLGYQID
AF505512	RHHLGKLSGLYQMGCTFNPEWKVPDISDTHFNLD		ENFMKIEESRWKELRTVIKKIKVGEWYDWKCIQ
AY294029	VRAPLSHVRAATIDLPRLGKGLPA		ELGIRINFDKTTSPVNEIRFLGYQID
K01834	RHHLGKLSGLYQMGCTFNPEWKVPDISDTHFNLD		ENFMKIEESRWKELRTVIKKIKVGEWYDWKCIQ
AY250901	VRAPLSHVRAATIDLPRLGKGLPA		ELGIRINFDKTTSPVNEIRFLGYQID
AY250902	RHHLGKLSGLYQMGCTFNPEWKVPDISDTHFNLD		ENFMKIEESRWKELRTVIKKIKVGEWYDWKCIQ
AY250903	VRAPLSHVRAATIDLPRLGKGLPA		ELGIRINFDKTTSPVNEIRFLGYQID
AY250904	RHHLGKLSGLYQMGCTFNPEWKVPDISDTHFNLD		ENFMKIEESRWKELRTVIKKIKVGEWYDWKCIQ
AY294028	VRAPLSHVRAATIDLPRLGKGLPA		ELGIRINFDKTTSPVNEIRFLGYQID
M60677	RHHLGKLSGLYQMGCTFNPEWKVPDISDTHFNLD		ENFMKIEESRWKELRTVIKKIKVGEWYDWKCIQ
X74623	VRAPLSHVRAATIDLPRLGKGLPA		ELGIRINFDKTTSPVNEIRFLGYQID
X12798	RHHLGKLSGLYQMGCTFNPEWKVPDISDTHFNLD		ENFMKIEESRWKELRTVIKKIKVGEWYDWKCIQ
X58567	VRAPLSHVRAATIDLPRLGKGLPA		ELGIRINFDKTTSPVTEIRFLGYQID
AY494850	RHHLGKLSGLYQMGCTFNPEWKVPDISDTHFDLE	539	EQFMKIEESRWKELRTVIKKIKIGEWYDWKCIQ
AY494851	VRAPLSHVRAATIDLPRLGKGLPA	539	ELGVRINFDKTTSPVNEIRFLGYQID
AY521226	RHHLGKLSGLYQMGCTFNPEWKVPDISDTHFKSE	540	QRYMKIEESRWKELRTVIKKIKIGEWYDWKCIQ
AY521227	VRAPLSHVRAATIDLPRLGKGLPA		ELGIRINFDKTTSPVTDIRFLGNQID
AY433937	RHHLGKLSGLYQMGCSFNPEWKVPDISDTHFDLQ		EKYMKIEESRWKELRTVIKKIKVGTWYDWKCIQ
NC_001344	VRAPLSHVRAATIDLPRLGKGLPA		ELGIRINFDKTTSPVNDIRFLGYQID
X60213	RHHLGKLSGLYQMGCSFNPEWKVPDISDTHFDLQ		ELGIRINFDKTTSPVNDIRFLGYQID
M32990	VRAPLSHVRAATIDLPRLGKGLPA		QKFMKIEESRWIELRTVIKKIKIGAWYDWKCIQ
M32991	RHHLGKLSGLYQMGCTFNPEWKVPDISDTHFDLQ		ELGIRINFDKTTSPVNDIRFLGYQID
AJ006350	VRAPLSHVRAATIDLPRLGKGLPA		QKFMKIEESRWKELRTVIKKIKIGAWYDWKCIQ
AF404406	RHHLGKLSGLYQMGCTFNPEWKVPDISDTHFNLD	539	ELGIRINFDKTTSPVTEIRFLGYQID
M21953	VRAPLSHVRAATIDLPRLGKGLPA	539	QKFMKIEESRWKELRTVIKKIKIGAWYDWKCIQ
AY392760	RHHLGKLSGLYQMGCTFNPEWKVPDISDTHFDLQ	540	ELGIRINFDKTTSPVNEIRFLGYQID
AY536371	VRAPLSHVRAATVDLPRLGKGLPA	540	QKYMKIEESRWSELRTVIKKIKVGEWYDWKCIQ
X58568	RHHLGKLSGLYQMGCTFNPEWKVPDISDTHFDLQ	539	ELGIRINFDKTTSPVNEIRFLGYQID
X58569	VRAPLSRVRAATEDLPRLGKGLPA	539	HRFMKIEESRWKELRTVIKKIKIGEWYDWKCIQ
	RHHLGKLSGLYQMGCTFNPEWKVPDISDTHFDLQ		ELGIRINFDKTTSPVNEIRFLGYQID
			QRFMKIEESRWKELRTVIKKIKIGEWYDWKCIQ

Figure 5 A: KorR86Q mutant point in the P protein of the LRDHBV; B: AorE591T mutant point in the P protein of the LRDHBV.

presumed that the DHBV sequences in the GenBank up to now come from DHBV that are susceptible to Lamivudine. So we downloaded all the DHBV sequences in the GenBank and aligned the P protein sequences of these DHBV. The results showed that there were two mutational points that occurred in the P protein sequences of LRDHBV. It is KorR86Q in the TP domain and AorE591T in the RT domain. The TP domain of DHBV P protein mainly acts as a primer to originate the synthesis of DHBV-negative strand^[20]. But it is the tyrosine residue in 96aa of TP domain that primed the reverse transcription of negative strand^[21,22]. AorE591T is located in the lower reaches of YMDD motif. So the roles of KorR86Q and AorE591T in the Lamivudine-resistant phenomenon need deeper research.

For both hepadnaviruses and HIV, the mechanism of action of Lamivudine requires phosphorylation to 3TC-5'-triphosphate (3TC-TP), which in turn specifically inhibits the viral polymerase^[23-26]. The specificity is conferred by the much lower affinity of 3TC-TP for the cellular α - and β -polymerase^[25,27]. The mechanism of inhibition of hepadnavirus involves inhibition of the viral polymerase^[26,28,29]. Acting as a chain terminator for the DNA polymerase activities, the Lamivudine inhibit the reverse transcriptase in a manner that resemble competitive inhibition with respect to dCTP^[30]. The side groups of isoleucine and valine of the YMDD mutants sterically prevent Lamivudine from appropriately configuring into the nucleotide binding site of the reverse transcriptase^[31]. This can cause Lamivudine resistance. Can the KorR86Q and AorE591T mutants also prevent Lamivudine from appropriately configuring into the nucleotides binding site of the reverse transcriptase? It needs more research.

A 4-year clinical research showed that YMDD mutants only could explain the 75% of Lamivudine resistances. Polymerase gene mutations were observed in 82.5% of virological breakthroughs but also in 75% of the non-responders^[32]. So the mutations outside the YMDD motif in the P protein can independently cause DHBV resistant to Lamivudine is not very strange.

REFERENCES

- 1 **Lin KW**, Kirchner JT. Hepatitis B. *Am Fam Physician* 2004; **69**: 75-82
- 2 **Lavanchy D**. Hepatitis B virus epidemiology, disease burden, treatment, and current and emerging prevention and control measures. *J Viral Hepat* 2004; **11**: 97-107
- 3 **Nevens F**, Main J, Honkoop P, Tyrrell DL, Barber J, Sullivan MT, Fevery J, De Man RA, Thomas HC. Lamivudine therapy for chronic hepatitis B: α six month randomized dose-ranging study. *Gastroenterology* 1997; **113**: 1258-1263
- 4 **Yao G**, Wang B, Cui Z. Long-term effect of Lamivudine treatment in chronic hepatitis B virus infection. *Chin J Hepatol* 1999; **7**: 80-83
- 5 **Yao GB**, Wang BE, Cui ZY, Yao JL, Zeng MD. The long-term efficacy of Lamivudine in chronic hepatitis B: interim analysis of 3-year's clinical course. *Chin J Intern Med* 2003; **42**: 382-387
- 6 **Allen MI**, Deslauriers M, Andrews CW, Tipples GA, Walters KA, Tyrrell DL, Brown N, Condreay LD. Identification and characterization of mutations in hepatitis B virus resistant to Lamivudine. Lamivudine Clinical Investigation Group. *Hepatology* 1998; **27**: 1670-1677
- 7 **Honkoop P**, Niesters HG, de Man RA, Osterhaus AD, Schalm SW. Lamivudine resistance in immunocompetent chronic hepatitis B. Incidence and patterns. *J Hepatol* 1997; **26**: 1393-1395
- 8 **Fu L**, Cheng YC. Role of additional mutations outside the YMDD motif of hepatitis B virus polymerase in L-SddC(3TC) resistance. *Biochem Pharmacol* 1998; **55**: 1567-1572
- 9 **Summers J**, Mason WS. Replication of the genome of a hepatitis B-like virus by reverse transcription of an RNA intermediate. *Cell* 1982; **20**:403-415
- 10 **Mason WS**, Seal G, Summers J. Virus of Pekin ducks with structural and biological relatedness to human hepatitis B virus. *J Virol* 1980; **36**: 829-836
- 11 **Mosmann T**. Rapid colorimetric assay for cellular growth and survival: application to proliferation and cytotoxicity assays. *J Immunol Methods* 1983; **65**: 55-63
- 12 **Alley MC**, Scudireo DA, Monks A, Hursey ML, Czerwinski MJ, Fine DL, Abbott BJ, Mayo JG, Shoemaker RH, Boyd MR. Feasibility of drug screening with panels of human tumor cell lines using a microculture tetrazolium assay. *Cancer Res* 1988; **48**: 589-601
- 13 **Lambert V**, Fernhols D, Sprengel R, Fourel I, Deleage G, Wildner G, Peyret C, Trepo C, Cova L, Will H. Virus-neutralizing monoclonal antibody to a conserved epitope on the duck hepatitis B virus pre-S protein. *J Virol* 1990; **64**: 1290-1297
- 14 **Kock J**, Schlicht HJ. Analysis of the earliest steps of hepadnaviral replication: genome repair after infectious entry into hepatocytes does not depend on viral polymerase activity. *J Virol* 1993; **67**: 4876-4874
- 15 **Mandel M**, Higa A. Calcium-dependent bacteriophage DNA infection. *J Mol Biol* 1970; **53**: 154
- 16 **Cohen SN**, Chang AC, Hsu L. Nonchromosomal antibiotic resistance in bacteria: Genetic transformation of *Escherichia coli* by R-factor DNA. *Proc Natl Acad Sci USA* 1972; **69**: 2110
- 17 **Gunther S**, Li BC, Miska S, Kruger DH, Meisel H, Will H. A novel method for efficient amplification of whole hepatitis B virus genomes permits rapid functional analysis and reveals deletion mutants in immunosuppressed patients. *J Virol* 1995; **69**: 5437-5444
- 18 **Niesters HG**, Honkoop P, Haagsma EB, de Man RA, Schalm SW, Osterhaus AD. Identification of more than one mutation in the hepatitis B virus polymerase gene arising during prolonged Lamivudine treatment. *J Infect Dis* 1998; **177**: 1382-1385
- 19 **Seigner B**, Aguesse-Germon S, Pichoud C, Vuillermoz I, Jarnard C, Trepo C, Zoulim F. Duck hepatitis B virus polymerase gene mutants associated with resistance to Lamivudine have a decreased replication capacity *in vitro* and *in vivo*. *J Hepatol* 2001; **34**: 114-122
- 20 **Wang GH**, Seeger C. The reverse transcriptase of hepatitis B virus acts as a protein primer for viral DNA synthesis. *Cell* 1992; **71**: 663-670
- 21 **Weber M**, Bronsema V, Bartors H, Bosserhoff A, Bartenschlager R, Schaller H. Hepadnavirus P protein utilizes a tyrosine residue in the TP domain to primer reverse transcription. *J Virol* 1994; **68**: 2994-2999
- 22 **Zoulim F**, Seeger C. Reverse transcription in hepatitis B viruses is primed by a tyrosine residue of the polymerase. *J Virol* 1994; **68**: 6-13
- 23 **Cammack N**, Rouse P, Marr CL, Reid PJ, Boehme RE, Coates JA, Penn CR, Cameron JM. Cellular metabolism of (-)-enantiomeric 2'-deoxy-3'-thiacytidine. *Biochem Pharmacol* 1992; **43**: 2509-2604
- 24 **Chang CN**, Skalski V, Zhou JH, Cheng YC. Biochemical pharmacology of (+)- and (-)-2'-deoxy-3'-thiacytidine as anti-hepatitis B virus agents. *J Biol Chem* 1992; **267**: 22414-22420
- 25 **Hao ZD**, Cooney DA, Hartman NR, Perno CF, Fridland A, DeVico AL, Sarngadharan MG, Broder S, Johns DG. Factors determining the activity of 2'-deoxy-3'-dideoxynucleosides in suppressing human immunodeficiency virus *in vitro*. *Mol Pharmacol* 1988; **34**: 431-435
- 26 **Coates JA**, Cammack N, Jenkinson HJ, Mutton IM, Pearson BA, Storer R, Cameron JM, Penn CR. The separated enanti-

- omers of 2'-deoxy-3'-thiacytidine(BCH189)both inhibit human immunodeficiency virus replication *in vitro*. *Antimicrob Agents Chemocher* 1992; **36**: 202-205
- 27 **Hart GJ**, Orr DC, Penn CR, Figueiredo HT, Gray NM, Boehme RE, Cameron JM. Effects of (-) 2',3'-dideoxy-3'-thiacytidine (3TC) 5'-triphosphate on human immunodeficiency virus reverse transcriptase and mammalian DNA polymerase alpha, beta and gamma. *Antimicrob Agents Chemocher* 1992; **36**: 1688-1694
- 28 **Chang CN**, Doong SL, Zhou JH, Beach JW, Jeong LS, Chu CK, Tsai CH, Cheng YC, Liotta D, Schinazi R. Deoxycytidine deaminase-resistant stereoisomer is the active form of (\pm)-2', 3'-dideoxy-3'-thiacytidine in the inhibition of hepatitis B virus replication. *J Biol Chem* 1992; **267**: 13938-13942
- 29 **Coates JA**, Cammack N, Jenkinson HJ, Jowett AJ, Jowett MI, Pearson BA, Penn CR, Rouse PL, Viner KC, Cameron JM. (-)-2'-dideoxy-3'-thiacytidine is a potent ,highly selective inhibitor of human immunodeficiency virus type 1 and type 2 replication *in vitro*. *Antimicrob Agents Chemother* 1992; **36**: 733-739
- 30 **Severini A**, Liu XY, Wilson JS, Tyrrell DL. Mechanism of inhibition of duck hepatitis B virus polymerase by (-)- α -L-2', 3'-dideoxy-3'-thiacytidine. *Antimicrob Agents Chemother* 1995; **39**: 1430-1435
- 31 **Doo E**, Liang TJ. Molecular anatomy and pathophysiologic implications of drug resistance in hepatitis B virus infection. *Gastroenterology* 2001; **120**: 1000-1008
- 32 **Gaia S**, Marzano A, Smedile A, Barbon V, Abate ML, Olivero A, Lagget M, Paganin S, Fadda M, Niro G, Rizzetto M. Four years of treatment with Lamivudine: clinical and virological evaluations in HBe antigen-negative chronic hepatitis B. *Aliment Pharmacol Ther* 2004; **20**: 281-287

Science Editor Guo SY Language Editor Elsevier HK

Genetic polymorphisms of *N*-acetyltransferase 2 and colorectal cancer risk

Lu-Jun He, Yue-Ming Yu, Fang Qiao, Jing-Shan Liu, Xiao-Feng Sun, Ling-Ling Jiang

Lu-Jun He, Ling-Ling Jiang, Department of Biochemistry, Hebei Medical University, Shijiazhuang 050017, Hebei Province, China
Fang Qiao, Jing-Shan Liu, Laboratory of HLA, Hebei Province Blood Center, Shijiazhuang 050071, Hebei Province, China
Yue-Ming Yu, Department of Surgery, No. 4 Hospital of Hebei Medical University, Shijiazhuang 050011, Hebei Province, China
Xiao-Feng Sun, Department of Oncology, Institute of Biomedicine and Surgery, University of Linköping, S-581 85 Linköping, Sweden
Correspondence to: Dr. Ling-Ling Jiang, Department of Biochemistry, Hebei Medical University, Shijiazhuang 050017, Hebei Province, China. guiyang1959@yahoo.com
Telephone: +86-311-6265639 Fax: +86-311-7061014
Received: 2004-10-19 Accepted: 2004-11-26

Abstract

AIM: To identify the distribution of *N*-acetyltransferase 2 (NAT2) polymorphism in Hebei Han Chinese and the effects of the polymorphism on the development of colorectal cancer.

METHODS: We performed a hospital-based case-control study of 237 healthy individuals and 83 colorectal cancer patients of Hebei Han Chinese. DNA was extracted from peripheral blood and cancer tissues. The genotypes of the polymorphisms were assessed by PCR-restriction fragment length polymorphism (RFLP).

RESULTS: There were four NAT2 alleles of WT, M1, M2, and M3 both in the healthy subjects and in the patients, and 10 genotypes of WT/WT, WT/M1, WT/M2, WT/M3, M1/M1, M1/M2, M1/M3, M2/M2, M2/M3, M3/M3. M2 allele was present in 15.61% of healthy subjects and 29.52% of patients ($\chi^2 = 15.31$, $P < 0.0001$), and M3 allele was present in 30.59% of healthy subjects and 16.87% of patients ($\chi^2 = 25.33$, $P < 0.0001$). There were more WT/M2 ($\chi^2 = 34.42$, $P < 0.0001$, odd ratio = 4.99, 95%CI = 2.27-9.38) and less WT/M3 ($\chi^2 = 3.80$, $P = 0.03$) in the patients than in the healthy subjects. In 70.3% of the patients, there was a difference in NAT2 genotype between their tumors and blood cells. Patients had more WT/M2 ($\chi^2 = 5.11$, $P = 0.02$) and less M2/M3 ($\chi^2 = 4.27$, $P = 0.039$) in their blood cells than in the tumors. Furthermore, 53.8% (7/13) of M2/M3 in tumors were from WT/M2 of blood cells.

CONCLUSION: There is a possible relationship between the NAT2 polymorphisms and colorectal cancer in Hebei Han Chinese. The genotype WT/M2 may be a risk factor for colorectal cancer.

Key words: NAT2 gene; Colorectal cancer; RFLP

He LJ, Yu YM, Qiao F, Liu JS, Sun XF, Jiang LL. Genetic polymorphisms of *N*-acetyltransferase 2 and colorectal cancer risk. *World J Gastroenterol* 2005; 11(27): 4268-4271
<http://www.wjgnet.com/1007-9327/11/4268.asp>

INTRODUCTION

Colorectal cancer is one of the common tumors in Hebei Province of China. *N*-acetyltransferase 2 (NAT2) is polymorphic and catalyzes both *N*-acetylation (usually deactivation) and *O*-acetylation (usually activation) of a variety of heterocyclic amine drugs and carcinogens^[1]. Heterocyclic amines which are found mainly in well-cooked meat, require metabolic activation to function as mutagens and animal carcinogens. Enzymes such as cytochrome P4501A2 (CYP1A2) and NAT2 perform this task. Genetic studies in humans have shown that individuals may be classified as rapid or slow acetylators according to the rates at which drugs are acetylated by NAT2^[2]. NAT2 polymorphism is a representative genetic trait of individual's susceptibility to several cancers^[3]. Epidemiological studies suggest that the NAT2 acetylation polymorphisms modify the risk of developing carcinoma of urinary bladder, colorectal and breast cancer, head and neck cancer, pulmonary and prostatic cancer. Associations between slow NAT2 acetylator genotypes and urinary bladder cancer as well as between rapid NAT2 acetylator genotypes and colorectal cancer are the most consistently reported^[3]. However, whether there is a true association between colorectal cancer and NAT2 polymorphism is controversial. Human epidemiological studies suggest that rapid acetylator phenotypes may be associated with higher incidences of colorectal cancer in American populations^[4]. Researchers in UK^[5] found that no significant differences in NAT2 allelic frequencies (WT, M1, M2, M3 alleles) or genotypes are observed between colorectal cancer patients and the healthy population. Ethnic differences exist in NAT2 genotype frequencies that may be a factor in cancer incidence, emphasizing the need to investigate the distribution frequency of NAT2 genotypes and the association of their polymorphism with colorectal cancer in Hebei Han Chinese population.

We identified the distribution of NAT2 polymorphisms in Chinese healthy individuals and colorectal cancer patients from Hebei Province. We also performed a case-control study to investigate whether the NAT2 genetic polymorphism was a risk factor for colorectal cancer in these Chinese population.

MATERIALS AND METHODS

Subjects

We conducted a case-control study of colorectal cancer patients between April 2001 and April 2003. Both patients and controls were Hebei Han Chinese. Eighty-three patients (46 males, 37 females) with histopathologically confirmed diagnosis of colorectal cancer, were recruited from the Department of Surgery at Hebei No. 4 Hospital. Their mean age was 47.5 years (ranging 25-77 years). The control group consisted of 237 (124 males, 113 females) healthy individuals selected from the blood donors in Hebei Province Blood Center. Their average age was 42.6 years (ranging 20-80 years).

DNA extraction

The peripheral blood was treated with EDTA. Tumor samples were obtained from colorectal cancer patients and immediately frozen in liquid nitrogen and stored at -80°C until used. Genomic DNA was isolated from peripheral leukocytes by PEL-FREEZE reagent protocol or from the tumor samples by the standard procedure of proteinase K/RNase digestion and phenol/chloroform extraction.

Typing NAT2 polymorphism

PCR-RFLP was performed to investigate the NAT2 allele. PCR was performed in 40 μL reaction mixture containing 50-200 ng DNA, 20 mmol/L of each primer, 1.25 mmol/L of dNTPs, 25 mmol/L of MgCl_2 , 1 PCR buffer, 5U of thermostable Taq DNA polymerase using a programmable thermocycler. The primer sequences were 5'-GGA ACA AAT TGG ACT TGG-3' and 5'-TCT AGC ATG AAT CAC TCT GC-3'. PCR conditions were 5 min at 95°C ; 35 cycles of 1 min at 95°C , 1 min at 57°C and 1.5 min at 72°C ; followed by a final extension for 5 min at 72°C . After amplification, the 1 093 bp PCR-products were digested with *KpnI* (M1 allele), *BamHI* (M3 allele), *MspI/AfuI* (M4 allele) for 16-18 h at 37°C and *TaqI* (M2 allele) for 16-18 h at 65°C separately in a 25 μL final volume. Digested fragments were then separated by electrophoresis on 20 g/L agarose gel (M1, M3) or 40 g/L agarose gel (M2, M4) and visualized by ethidium bromide staining. All the experiments included positive and negative controls for each studied polymorphism.

Statistical analysis

Statistical analysis was performed with SAS 6.0 for Windows. Hardy-Weinberg equilibrium test was carried out using statistical software for linkage analysis. χ^2 and Fisher's exact test were used for comparisons of frequencies. Associations were expressed as odd ratios (OR) with 95% confidence interval (95%CI). $P < 0.05$ was considered statistically significant.

RESULTS

Polymorphism of NAT2 gene in Hebei Han Chinese

The results of genotype analysis are shown in Figure 1. In 237 healthy and 83 colorectal cancer patients of Hebei Han Chinese, there were four kinds of NAT2 alleles including wild-type gene WT allele and polymorphisms of M1, M2, and M3 alleles (Table 1). No M4 polymorphism was found. Ten genotypes including WT/WT, WT/M1, WT/M2, WT/M3, M1/M1, M1/M2, M1/M3, M2/M2, M2/M3, M3/M3 and their frequencies in both groups are shown in Table 2. M3 (59.67%) was the major polymorphism in healthy group. The distribution of NAT2 genotypes in healthy group was consistent with Hardy-Weinberg equilibrium ($\chi^2 = 7.2533$, $g = 8$, $P > 0.5$). In healthy group, 71.3% and 28.7% were classified as rapid-acetylator genotypes (WT/WT, WT/Mx, $x = 1, 2, 3$) and slow-acetylator genotypes (Mx/Mx), respectively. The frequency of WT/M3 (29.1%) in the rapid-acetylator genotypes was the highest.

The frequency of allele M2 (29.5%) was the highest in the 83 patients, 18 (21.7%) were slow-acetylator genotypes (Mx/Mx), and 65 (78.3%) were rapid-acetylator genotypes (WT/WT, WT/Mx), 35 (53.8%) of them being WT/M2 (Table 2).

Association of NAT2 polymorphism with susceptibility to colorectal cancer in Hebei Han Chinese

M3 allele was present in 30.59% (154/474) of the healthy subjects and in 16.87% (28/166) of the patients ($\chi^2 = 25.33$, $P < 0.0001$). The M2 allele frequency was significantly different between healthy (15.61%) and patient groups (29.52%) ($\chi^2 = 15.31$, $P < 0.0001$). There was no difference in rapid-acetylator or slow-acetylator frequency between healthy and patient groups. However, there was a significant

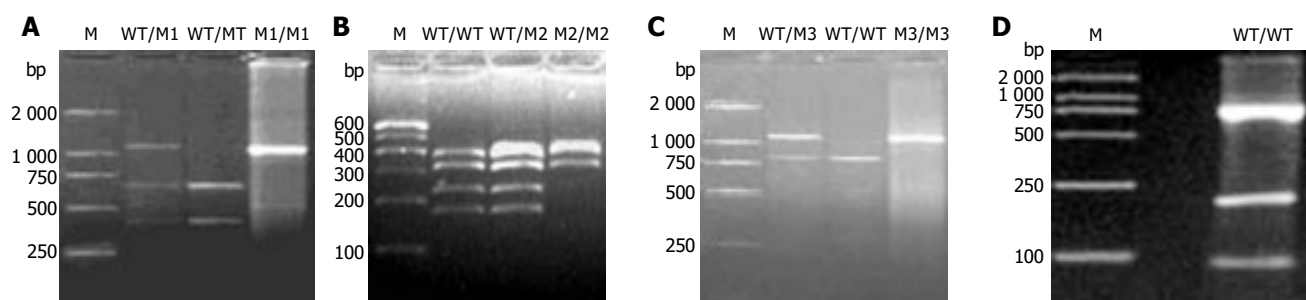


Figure 1 NAT2 genotype analysis by PCR-RFLP. M: DNA Marker (100, 250, 500, 750, 1 000, 2 000 bp); **A**: digest with *KpnI* (M1 allele) shows wildtype genotype (lane 2: 660 and 433 bp, WT/WT), variant genotype (lane 3: 1 093 bp, M1/M1) and heterozygote genotype (lane 1: 1 093, 660 and 433 bp, WT/M1); **B**: digest with *TaqI* (M2 allele) shows wildtype genotype (lane 1: 380, 317, 226 and 170 bp, WT/WT), variant genotype (lane 3: 396, 380 and

317 bp, M2/M2) and heterozygote genotype (lane 2: 396, 380, 317, 226 and 170 bp, WT/M2); **C**: digest with *BamHI* (M3 allele) shows wildtype genotype (lane 2: 811 and 282 bp, WT/WT), variant genotype (lane 3: 1 093 bp, M3/M3) and heterozygote genotype (lane 1: 1 093, 811 and 282 bp, WT/M3); **D**: digest with *MspI/AfuI* (M4 allele) shows wildtype genotype (lane 1: 759, 189, 91 and 53 bp, WT/WT).

Table 1

Alleles	Healthy controls		Patients	
	Number	Frequency	Number	Frequency
WT	231	0.4874	80	0.4819
M1	24	0.0506	9	0.0542
M2	74	0.1561 ^{1b}	49	0.2952
M3	145	0.3059 ^{2d}	28	0.1687
M4	0	0	0	0
SUM	474	1.0000	166	1.0000

¹ $\chi^2=15.31$, ^b $P<0.0001$ and ² $\chi^2=25.33$, ^d $P<0.0001$ vs patients.

Table 2

	Rapid-acetylator genotype					Slow-acetylator genotype						
	WT/WT	WT/M1	WT/M2	WT/M3	Sum	M1/M1	M1/M2	M1/M3	M2/M2	M2/M3	M3/M3	Sum
Controls <i>n</i>	62	9	29	69	169	1	4	9	5	31	18	68
%	26.2	3.8	12.2	29.1	71.3	0.4	1.7	3.8	2.1	13.1	7.6	28.7
Patients <i>n</i>	15	1	35	14	65	1	2	4	3	6	2	18
%	18.1	1.2	42.2	16.9	78.3	1.2	2.4	4.8	3.6	7.2	2.4	21.7
χ^2	2.20	0.64	34.42	3.80	1.54	0.00	0.00	0.007	0.12	2.06	2.01	1.54
<i>P</i>	0.14	0.42	<0.0001	0.03	0.22	1.00	1.00	0.94	0.73	0.15	0.16	0.22

difference between WT/M2 ($\chi^2 = 34.42$, $P < 0.0001$) and WT/M3 ($\chi^2 = 3.80$, $P < 0.05$) compared to the healthy controls. The risk associated with combinations of NAT2 genotypes is shown in Table 3. The genotype WT/M2 might be a risk factor for colorectal cancer (OR = 4.99, 95%CI = 2.27-9.38).

Comparable analysis of WT/M2 and M2/M3 genotypes in blood cells and cancer tissues of colorectal cancer patients

In 70.4% of patients, there was a difference in NAT2 genotype between tumor tissues and blood cells. The frequency of NAT2 genotypes, especially WT/M2 and M2/M3, was significantly different between tumor tissues and blood cells ($\chi^2 = 5.11$, $P < 0.05$; $\chi^2 = 4.27$, $P < 0.05$, Table 4). The frequency of genotype M2/M3 was 9.3% in

peripheral blood cells and 24.1% in cancer tissue. Furthermore, 53.8% (7/13) of the tumors had M2/M3 while the corresponding blood cells had WT/M2.

DISCUSSION

Human NAT2 is a genetic polymorphism. Different genotypes (WT/WT, WT/Mx, Mx/Mx, x = 1, 2, 3, 4) are composed of different NAT2 alleles (wild type allele WT, mutation allele Mx). According to the intensity of acetyl action, a different genotype shows a different phenotype (rapid-acetylator genotype and slow-acetylator genotype). Genotypes composed of any two mutation alleles (Mx/Mx) show slow-acetylator genotypes, while those consisted of WT/WT or WT/Mx show rapid-acetylator genotypes. Bell

Table 3

Genotypes	Control		Patients		OR (95%CI)
	<i>n</i>	%	<i>n</i>	%	
WT/WT	62	26.2	15	18.1	1.00
WT/M2	29	12.2	35	42.2	4.99 (2.27-9.38)
WT/M1	9	3.8	1	1.2	0.46 (0.05-3.92)
WT/M3	69	29.1	14	16.9	0.84 (0.38-1.88)
WT/WT and WT/Mx	169	71.3	65	78.3	1.59 (0.85-2.99)
Mx/Mx	68	28.7	18	21.7	1.09 (0.51-2.35)

x = 1, 2, 3, 4, OR: odds ratio; CI: confidence interval.

Table 4

	WT/M2		M2/M3		Others	
	<i>n</i>	%	<i>n</i>	%	<i>n</i>	%
Blood cells	23	42.6	5	9.3	26	48.2
Cancer tissues	12	22.2 ¹	13	24.1 ²	29	53.7

¹ $\chi^2 = 5.11$, $P = 0.020$ and ² $\chi^2 = 4.27$, $P = 0.039$ vs blood cells.

et al.^[6], reported that there are significant differences in the frequency of WT, M1, and M4 alleles between Caucasian and African-Americans, while the frequency of M2 and M3 alleles is similar. The M4 allele is not detectable in Caucasian-Americans, while 18% African-Americans carry at least one M4 allele. The frequencies of NAT2 WT, M1, M2, M3, and M4 alleles in Singapore Chinese are 0.51, 0.07, 0.32, 0.10, and 0.00, respectively^[7]. The proportions of rapid and slow acetylators do also vary remarkably between ethnic groups as well as between populations of different geographical origins^[8]. For example, the percentage of slow acetylators is 5% in Canadian Eskimos, over 80% in Egyptians and 90% in Moroccans^[9,10]. Singapore Chinese have 72% of rapid-acetylator genotypes. In our study, four NAT2 alleles (WT, M1, M2, M3) and ten NAT2 genotypes (WT/WT, WT/M1, WT/M2, WT/M3, M1/M1, M1/M2, M1/M3, M2/M2, M2/M3, M3/M3) were found in Hebei Han Chinese. M4 was not present in Hebei Han Chinese, while 29.1% of healthy controls carried at least one M3 allele. Hebei Han Chinese had 71.3% of rapid-acetylator genotypes. The frequencies of the NAT2 M4 allele and rapid-acetylator genotypes are similar in both Hebei Han Chinese and Singapore Chinese, but there are significant differences in the frequencies of WT, M1, M2, and M3 between the two populations.

NAT2 is an important enzyme for the detoxification and/or bioactivation of several carcinogenic arylamines, its activity directly affects metabolic response of carcinogen *in vivo* and intensity of toxic reaction^[11]. It was reported that the polymorphism of NAT2 gene is associated with the occurrence of colorectal cancer^[12]. Genetic epidemiological studies suggest that rapid acetylator phenotype may be associated with the higher incidence of colorectal cancer in the UK populations^[12]. Lee *et al.*^[7], also showed that the rapid acetylator genotype is associated with cancer occurring in Singapore Chinese. However, our results suggest that rapid-acetylator genotype or slow-acetylator genotype does not appear to be associated with colorectal cancer development, but there is an association between the WT/M2 genotype and colorectal cancer. The M2 allele was more frequent in the patients than in the healthy subjects ($\chi^2 = 15.31$, $P < 0.0001$). Odds ratio (OR) for genotype WT/M2 was 4.99 (95%CI = 2.27-9.38). The data suggest that genotype WT/M2 may be a risk factor for colorectal cancer in Hebei Han Chinese.

Schnakenberg *et al.*^[13], detected the loss of heterozygosity in slow and rapid acetylator genotypes in bladder cancer patients. They observed allelic loss at the NAT2 locus in 11 of 60 tumor samples (18.3%), but not in controls. The

present study also demonstrated changes of NAT2 genotypes in 70.4% of the tumor specimens. The rising M2/M3 in tumors seems to be transformed from genotype WT/M2 of blood cells, and also suggests that WT/M2 may be a risk factor for colorectal cancer. Our findings may contribute to the early diagnosis of colorectal cancer.

REFERENCES

- 1 Pande JN, Pande A, Singh SP. Acetylator status, drug metabolism and disease. *Natl Med J India* 2003; **16**: 24-26
- 2 Hein DW. Molecular genetics and function of NAT1 and NAT2: role in aromatic amine metabolism and carcinogenesis. *Mutant Res* 2002; **30**: 65-77
- 3 Hein DW, Doll MA, Fretland AJ, Leff MA, Webb SJ, Xiao GH, Devanaboyina US, Nangju NA, Feng Y. Molecular genetics and epidemiology of the NAT1 and NAT2 acetylation polymorphisms. *Cancer Epidemiol Biomarkers Prev* 2000; **9**: 29-42
- 4 Rodriguez JW, Kirilin WG, Ferguson RJ, Doll MA, Gray K, Rustan TD, Lee ME, Kemp K, Urso P, Hein DW. Human acetylator genotype: relationship to colorectal cancer incidence and arylamine N-acetyltransferase expression in colon cytosol. *Arch Toxicol* 1993; **67**: 445-452
- 5 Sachse C, Smith G, Wilkie MJ, Barrett JH, Waxman R, Sullivan F, Forman D, Bishop DT, Wolf CR. A pharmacogenetic study to investigate the role of dietary carcinogens in the etiology of colorectal cancer. *Carcinogenesis* 2002; **23**: 1839-1849
- 6 Bell DA, Taylor JA, Butler MA, Stephens EA, Wiest J, Brubaker LH, Kadlubar FF, Lucier GW. Genotype/phenotype discordance for human arylamine N-acetyltransferase (NAT2) reveals a new slow-acetylator allele common in African-Americans. *Carcinogenesis* 1993; **14**: 1689-1692
- 7 Lee EJ, Zhao B, Seow-Choen F. Relationship between polymorphism of N-acetyltransferase gene and susceptibility to colorectal carcinoma in a Chinese population. *Pharmacogenetics* 1998; **8**: 513-517
- 8 Fretland AJ, Leff MA, Doll MA, Hein DW. Functional characterization of human N-acetyltransferase 2 (NAT2) single nucleotide polymorphisms. *Pharmacogenetics* 2001; **11**: 207-215
- 9 Weber WW, Hein DW. N-acetylation pharmacogenetics. *Pharmacol Rev* 1985; **37**: 25-79
- 10 Evans DA. N-acetyltransferase. *Pharmacol Ther* 1989; **42**: 157-234
- 11 Zhao B, Seow A, Lee EJ, Lee HP. Correlation between acetylation phenotype and genotype in Chinese women. *Eur J Clin Pharmacol* 2000; **56**: 689-692
- 12 Barrett JH, Smith G, Waxman R, Gooderham N, Lightfoot T, Garner RC, Augustsson K, Wolf CR, Bishop DT, Forman D. Colorectal Cancer Study Group. Investigation of interaction between N-acetyltransferase 2 and heterocyclic amines as potential risk factors for colorectal cancer. *Carcinogenesis* 2003; **24**: 275-282
- 13 Schnakenberg E, Ehlers C, Feyerabend W, Werdin R, Hubotter R, Dreikorn K, Schloot W. Genotyping of the polymorphic N-acetyltransferase (NAT2) and loss of heterozygosity in bladder cancer patients. *Clin Genet* 1998; **53**: 396-402

• BRIEF REPORTS •

Expression of albumin, IGF-1, IGFBP-3 in tumor tissues and adjacent non-tumor tissues of hepatocellular carcinoma patients with cirrhosis

Shi-Min Luo, Wei-Min Tan, Wei-Xiong Deng, Si-Min Zhuang, Jian-Wei Luo

Shi-Min Luo, Wei-Min Tan, Wei-Xiong Deng, Si-Min Zhuang, Jian-Wei Luo, Department of Cadre Surgery, The First Municipal People's Hospital of Guangzhou, Guangzhou 510180, Guangdong Province, China

Correspondence to: Wei-Min Tan, Department of Cadre Surgery, The First Municipal People's Hospital of Guangzhou, 1 Panfu Lu, Guangzhou 510180, Guangdong Province, China. lsmin@gzsums.edu.cn
Telephone: +86-20-81048285 Fax: +86-20-81048285
Received: 2004-11-12 Accepted: 2005-01-05

Abstract

AIM: To explore the expression of albumin (ALB), insulin-like growth factor (IGF)-1, and insulin-like growth factor binding protein (IGFBP)-3 in tumor tissues and adjacent non-tumor tissues of hepatocellular carcinoma (HCC) patients with cirrhosis.

METHODS: Twenty-four HCC patients with cirrhosis who underwent hepatectomy were studied. ALB mRNA, IGF-1 mRNA, and IGFBP-3 mRNA in liver tissues (including tumor tissues and adjacent non-tumor tissues) were detected by reverse transcriptase-polymerase chain reaction (RT-PCR). Liver Ki67 immunohistochemistry staining was studied. At the same time, 12 patients with cholelithiasis or liver angioma who underwent operation were segregated as normal control.

RESULTS: In HCC patients with cirrhosis, hepatic ALB mRNA, IGF-1 mRNA, and IGFBP-3 mRNA of tumor tissues or adjacent non-tumor tissues were lower than the normal liver tissues, while in tumor tissues, hepatic ALB mRNA and IGFBP-3 mRNA were lower, hepatic IGF-1 mRNA was higher than in adjacent non-tumor tissues. Liver Ki67 labeling index (Ki67 LI) in tumor tissues or adjacent non-tumor tissues were higher than that in the normal liver tissues, while in tumor tissues it was higher than that in adjacent non-tumor tissues.

CONCLUSION: Imbalance of IGF-1 and IGFBP-3 may play a role in hepatocarcinogenesis and tumor development of liver cirrhosis patients.

© 2005 The WJG Press and Elsevier Inc. All rights reserved.

Key words: Hepatocellular carcinoma; Insulin growth factor-1; Insulin-like growth factor binding protein-3

Luo SM, Tan WM, Deng WX, Zhuang SM, Luo JW. Expression

of albumin, IGF-1, IGFBP-3 in tumor tissues and adjacent non-tumor tissues of hepatocellular carcinoma patients with cirrhosis. *World J Gastroenterol* 2005; 11(27): 4272-4276
<http://www.wjgnet.com/1007-9327/11/4272.asp>

INTRODUCTION

Extensive research on insulin-like growth factors (IGFs) during the last decade has greatly advanced our understanding of these peptides that are not only the endocrine mediators of growth hormone (GH)-induced metabolic and anabolic actions but also polypeptides that act in a paracrine and autocrine manner to regulate cell growth, differentiation, apoptosis, and transformation^[1]. In biological fluids, IGFs are complexed with specific binding proteins (IGFBPs)^[2-4]. The functions of IGFBPs are to modulate the biologic activity of IGFs. Imbalance of these diverse processes may preferentially favor uncontrolled cell proliferation leading to malignant transformation. Recent evidence from epidemiologic studies has confirmed an association between serum levels of IGFs and several malignancies at the population level and has resulted in a resurgence of scientific interest in this field.

IGF-1 and IGF-2 are single chain polypeptides, which have 62% homology with proinsulin. Serum concentrations of IGF-2 are higher than IGF-1 (400-600 ng/mL *vs* 100-200 ng/mL) in humans of all ages, are relatively stable after puberty and are not regulated by GH. IGF-2 has proliferative and antiapoptotic actions similar to IGF-1 since its effects are exerted by the IGF-1R^[5]. However, IGF-2 plays a fundamental role in embryonic and fetal growth, whereas its role in the postnatal period is less important as it is substituted by IGF-1.

The liver is the central organ of the endocrine GH/IGF-1 axis. GH is secreted by the somatotrophic cells of the anterior pituitary, transported in the circulation by the high affinity growth hormone binding protein and acts through the hepatic GH receptor to regulate the production of the potent mitogenic growth factor IGF-1. The availability of IGF-1 to its tissue receptors is further regulated by the high affinity IGFBPs (IGFBP-1 to -6) of which the liver is also a significant source, with IGFBP-3 being most abundant^[6]. Epidemiologic studies have found high circulating IGF-1 and low IGFBP-3 levels to be associated with an increased risk of developing breast, endometrial, lung, colorectal, and prostate cancer. IGFBP-3 was reported to be a growth suppressor in variable pathways^[7,8].

Hepatocellular carcinoma (HCC) is the fifth most common cancer worldwide, with estimated 467 000 new cases per year^[9]. HCC is one of the most common malignant tumors in the world. Since the 1990s HCC has become the second killer in various cancers in China. Most HCC cases arise in HBV and liver cirrhosis. In carcinogenesis induced by viral infection, the frequency of gene mutation is considered to increase as the mitotic activity of cells gets greater. Under conditions that increase the proliferative activity of hepatocytes such as chronic hepatitis and liver cirrhosis, the probability of mutation increases, resulting in increased occurrence of HCC.

Albumin (ALB) is the major protein produced in the liver, and its primary functions include transportation of a variety of substances in the blood and maintenance of osmotic pressure. In normal adults, ALB constitutes more than 65% of the total plasma protein content. The plasma concentration of ALB reflects its synthesis, degradation, and distribution. Thus, the expression of hepatic ALB mRNA was more useful in reflecting the degree of liver injury or liver functional reserve than serum ALB.

In this study, we used the reverse transcriptase-polymerase chain reaction (RT-PCR) technique to detect ALB mRNA, IGF-1 mRNA, IGFBP-3 mRNA in tumor tissues and adjacent non-tumor tissues of HCC patients with cirrhosis. At the same time, we have immunochemically detected Ki67 antigen which appears in all phases of the cell cycle of proliferating cells but is negative in G₀^[10] on paraffinized section by microwave antigen retrieval method and compared the proliferative activity between adjacent non-tumor tissue as well as tumor tissues. We explored the roles of IGF-1 and IGFBP-3 in hepatocarcinogenesis and tumor development of liver cirrhosis patients.

MATERIALS AND METHODS

Patients and tissue samples

Of the patients at our department who underwent curative resection for HCC with liver cirrhosis between September 2002 and June 2003. Curative resection was defined as complete resection of all macroscopically detectable tumor with histological tumor clearance (the entire tumor mass was included in the surgical specimen without exposure of tumor cells on the cut edge). At the time of study entry, the inclusion criteria had no evidence of endocrine disease. Twenty-four HCC patients with liver cirrhosis who underwent hepatectomy were studied. At the same time, 12 patients with cholelithiasis or liver angioma who underwent operation were segregated as normal control and these patients had no liver cirrhosis and endocrine disease.

Liver samples (including HCCs and adjacent non-tumor tissues) were excised at the operation, immediately freeze clamped with liquid nitrogen, and stored at -70 °C for analysis of ALB mRNA, IGF-1 mRNA, and IGFBP-3 mRNA. For histological examination, some liver samples were fixed in 10% neutral-buffered formalin, embedded in paraffin.

Reverse transcriptase polymerase chain reaction (RT-PCR)

RT-PCR was performed to measure the expression levels

of ALB mRNA, IGF-1 mRNA, and IGFBP-3 mRNA in liver tissues. The primers used were deduced from the cDNA sequence. The sequences of the primers for ALB sense and antisense were 5'-CCCAAGTGTCAACTCCAAC-3' (sense) and 5'-GCAGGTCTCCTTATCGTCAG-3' (antisense), a 456 bp long fragment was amplified. The sequences of the primers for IGF-1 sense and antisense were 5'-AGCAGTCTTCCAACCCAATTA-3' (sense) and 5'-CACGGACAGAGCGAGCTG-3' (antisense), a 355 bp long fragment was amplified. The sequences of the primers for IGFBP-3 sense and antisense were 5'-ATATGGTCCCTGCCGTAGA-3' (sense) and 5'-AAATCGAGGCTGTAGCCAG-3' (antisense), a 345 bp long fragment was amplified. The sequences of the primers for β -actin sense and antisense were 5'-ACTCTTCCAGCCTTCCTTCC-3' (sense) and 5'-TCACCTTACCAGTTCAGTTT-3' (antisense), a 513 bp long fragment was amplified.

Total RNA was extracted from frozen liver specimens by the guanidinium isothiocyanate method. The RNA was quantified and checked for purity by spectrophotometry at 260 and 280 nm. Aliquots of total RNA were reverse transcribed using SperSriptII Reverse Transcriptase (Invitrogen Corp.) and subsequently amplified by PCR using the Taq DNA polymerase (Promega Corp.).

The PCR was carried out in 25 μ L of reaction mixture containing 0.5 μ L cDNA template, 2.5 μ L 10 \times PCR-Buffer, 1.5 μ L 25 mmol/L MgCl₂, 0.5 μ L 10 mmol/L dNTPs, 0.5 μ L 10 μ mol/L ALB or IGF-1 or IGFBP-3 primers, 0.15 μ L 10 μ mol/L β -actin primers, 0.5 μ L 5 IU/ μ L Taq DNA polymerase. The mixture was heated for 5 min at 94 °C for initial DNA denaturation, followed by 30 cycles of denaturation (at 94 °C for 45 s), annealing (ALB at 50 °C for 45 s, IGF-1 at 48 °C for 45 s, IGFBP-3 at 55 °C for 45 s), polymerization (at 72 °C for 1 min) and then a final extension of 10 min at 72 °C. PCR reactions were stored frozen until analysis by agarose gel electrophoresis.

PCR reactions were electrophoresed on 1.5% agarose gel, stained with ethidium bromide and quantitated using the interactive build analysis system. The band intensity of the ALB or IGF-1 or IGFBP-3 was compared with the band intensity of the β -actin, and the amount of ALB mRNA, IGF-1 mRNA, and IGFBP-3 mRNA was estimated.

Immunohistochemistry

Two-step immunohistochemical staining technique was used. Main reagent included rabbit polyclonal antibody Ki67 Ab-4 (Neomarkers Corp.) and PV-6000 PicTure™ Kits. Briefly, sections were deparaffinized, rehydrated, and then immersed in 0.1 mol/L citric acid buffer (pH 6.0) and boiled for 5-10 min in a microwave oven. The slides were then rinsed gently with PBS at pH 7.2-7.4, and treated with 0.3% hydrogen peroxide in absolute methanol for 1 h at room temperature to remove endogenous peroxidase. The sections were then incubated with the primary antibody Ki67 Ab-4 (1:200 dilution) for 30 min at 37 °C. After rinsing thrice with PBS, each for 2 min, the sections were incubated with PV-6000 for 30 min at 37 °C. They were then rinsed thrice with PBS for 2 min, and visualized with DAB. Finally, the sections were then counterstained with hematoxylin.

On each slide, Ki67-positive nuclei were evaluated by

means of light microscopy at 400 magnification. A minimum of 1 000 cells, evaluated through a minimum of 200 cells per field in five different fields. The Ki67 labeling index (Ki67 LI) is the number (%) of positive cells.

Statistical analysis

Data are expressed as mean±SE. The statistical software SPSS 10.0 was used. Statistical significance was set at $P<0.05$.

RESULTS

In HCC patients with cirrhosis, hepatic ALB mRNA, IGF-1 mRNA, IGFBP-3 mRNA of tumor tissues or adjacent non-tumor tissues were lower than the normal liver tissues, while in tumor tissues, hepatic ALB mRNA and IGFBP-3 mRNA were lower, hepatic IGF-1 mRNA was higher than in adjacent non-tumor tissues. Liver Ki67 LI in tumor tissues was higher than that in adjacent non-tumor tissues, while in adjacent non-tumor tissues it was higher than that in the normal liver tissues (Table 1).

Table 1 Comparison of hepatic ALB mRNA, IGF-1 mRNA, IGFBP-3 mRNA and liver Ki67 LI

	<i>n</i>	ALB mRNA	IGF-1 mRNA	IGFBP-3 mRNA	Liver Ki67 LI (%)
Normal liver tissues	12	0.69±0.05	0.95±0.02	2.02±0.04	0±0
Tumor tissues	24	0.38±0.01 ^a	0.76±0.03 ^a	0.45±0.13 ^a	17.3±5.9 ^a
Adjacent non-tumor tissues	24	0.50±0.05 ^{ac}	0.43±0.06 ^{ac}	0.72±0.17 ^{ac}	0.2±0.1 ^{ac}

^a $P<0.05$, tumor tissues or adjacent non-tumor tissues vs normal liver tissues;

^c $P<0.05$, adjacent non-tumor tissues vs tumor tissues.

DISCUSSION

The liver is probably the major source of circulating IGF-1 with GH confirmed as the dominant regulator of IGF-1 gene expression and serum levels in human disease^[11-13]. IGF-1 is an important anabolic polypeptide with various effects. IGF-1 synthesis is disturbed in liver cirrhosis and reflects the severity of the clinical stage. It represents a good marker of hepatic function. The etiology of cirrhosis does not seem to influence its levels^[14]. Serum IGFBP-3 proves to be a better marker for the hepatic synthetic capacity than serum ALB or cholinesterase^[15]. Serum IGF-1, IGF-2, and IGFBP-3 may provide a new dimension in the assessment of liver dysfunction. Combined detection of serum IGF-1, IGF-2, and IGFBP-3 with Child-Pugh score is more effective in predicting prognosis than Child-Pugh score alone.

Giovannucci presented a model integrating nutrition, insulin and IGF-1 physiology ("bioactive" IGF-1), and carcinogenesis based on the following: (1) insulin and the IGF-1 axis function in an integrated fashion to promote cell growth and survival; (2) chronic exposure to these growth properties enhances carcinogenesis; and (3) factors that influence bioactive IGF-1 will affect cancer risk. The model presented here summarizes the data that chronic exposure to high levels of insulin and IGF-1 may mediate many of the risk factors for some cancers that are high in

Western populations. This hypothesis may help explain some of the epidemiologic patterns observed for these cancers, both from a cross-national perspective and within populations^[16]. In HCC, HBV stimulates IGF-1R expression^[17] and enhances IGF-2 gene expression^[18]. Hepatitis C virus has also been related to increased IGF-2 transcription in HCC^[19]. HCC is associated with a higher IGF-1:IGFBP-3 ratio than that found in patients with liver cirrhosis and a similar degree of liver failure^[20].

IGF-1 and IGFBP-3 play a crucial role in the regulation of growth, cellular proliferation and transformation, and apoptosis. The local tissue expression of IGF-1 and IGFBP-3 has been associated with tumor grade, pathologic stage, and disease progression for patients with various malignancies. Epidemiologic studies have found high circulating IGF-1 and low IGFBP-3 levels to be associated with an increased risk of developing breast, endometrial, lung, colorectal, and prostate cancer. IGFBP-3 was reported to be a growth suppressor in variable pathways^[7,8]. In the IGF receptor dependent pathway, IGFBP-3 binds to IGF-1 and 2 and suppresses its growth signal. In the IGF receptor independent pathways, the IGFBP-3 mediates wide varieties of growth suppression signal.

This study showed hepatic IGF-1 mRNA, IGFBP-3 mRNA of tumor tissues or adjacent non-tumor tissues were lower than the normal liver tissues, while in tumor tissues, hepatic IGFBP-3 mRNA was lower but hepatic IGF-1 mRNA was higher than in adjacent non-tumor tissues. Thus, imbalance of IGF-1 and IGFBP-3 are thought to be important in hepatocarcinogenesis and tumor development of liver cirrhosis patients. IGFBP-3 mRNA which decreased in local tissues may take part in important roles in carcinogenesis. As the IGFBP-3 is produced mainly in the liver, IGFBP-3 may play an important role in the carcinogenesis of HCC. IGFBP-3 functions as a general mediator of growth inhibitory and apoptosis-inducing pathways.

IGFBP-3 is the most abundant IGFBP in human serum and has been shown to be a growth inhibitory, apoptosis-inducing molecule, capable of acting via IGF-dependent and IGF-independent mechanisms. Over the last decade, several clinical studies have proposed that individuals with IGFBP-3 levels in the upper normal range may have a decreased risk for certain common cancers. This includes evidence of a protective effect against breast, prostate, colorectal, and lung cancer. In addition, a series of *in vitro* studies and animal experiments point towards an important role for IGFBP-3 in the regulation of cell growth and apoptosis. Epidemiologic and experimental evidence suggesting a role for IGFBP-3 as an anti-cancer molecule^[21]. At the intracellular level this may either involve modulation of the bcl-2/bax ratio^[22] or the p53 protein^[23]. Kuemmerle *et al.*, reported that endogenous IGFBP-3 directly inhibits proliferation of human intestinal smooth muscle cells by activation of TGF-betaRI and Smad 2, an effect which is independent of its effect on IGF-1 stimulated growth^[24]. Interestingly, IGFBP-3 has been localized in the nucleus, implying a more direct transcriptional regulatory role, but it remains largely unknown how extracellular IGFBP-3 enters the cell^[25].

The liver has the unique capacity to regulate its growth

and mass both in humans and in animals. This property is particularly remarkable because hepatocytes are cells which in their normal state rarely divide. However, their proliferative capacity and the ability of the liver to adapt to variable metabolic demands are not lost. To assess the proliferating cells, we have immunochemically detected Ki-67 nuclear antigen. Characterization of the Ki-67 antibody revealed an interesting staining pattern. The antibody was reactive with a nuclear structure present exclusively in proliferating cells. A detailed cell cycle analysis revealed that the antigen was present in the nuclei of cells in the G₁, S, and G₂ phases of the cell division cycle as well as in mitosis. Quiescent or resting cells in the G₀ phase did not express the Ki-67 antigen. Because the Ki-67 antigen was present in all proliferating cells (normal and tumor cells), it soon became evident that the presence of this structure is an excellent operational marker to determine the growth fraction of a given cell population. For this reason, antibodies against the Ki-67 protein were increasingly used as diagnostic tools in cell proliferation.

ALB is a ubiquitous protein that is synthesized only by hepatocytes. ALB is a polypeptide chain of 580 amino acids that is produced by hepatocytes^[26]. The number of ALB molecules produced by a single hepatocyte has been estimated to be ~40 000^[27]. The expression of ALB gene is reduced in various liver diseases and the degree of reduction in the hepatic ALB mRNA level is generally correlated with the severity of the disease^[28]. This study showed that liver Ki67 LI in tumor tissues was higher than that in adjacent non-tumor tissues, which was higher than that in normal liver tissues, but hepatic ALB mRNA in tumor tissues was lower than that in adjacent non-tumor tissues, which was higher than that in normal liver tissues. It represented that proliferating hepatocytes or tumor tissues had less function.

The IGF system performs a fundamental role in the regulation of cellular proliferation, differentiation, and apoptosis. Disruptions in the balance of IGF system components leading to excessive proliferation and survival signals have been implicated in the development of different tumor types. This study represented the imbalance of IGF-1 and IGFBP-3 which are thought to be important in hepatocarcinogenesis and tumor development of liver cirrhosis patients. Epidemiologic evidence indicates that increased levels of IGF-I, reduced levels of IGFBP-3 or an increased ratio of IGF-1 to IGFBP-3 in the circulation are associated with an increased risk for the development of several common cancers, including those of the breast, prostate, lung, and colon. The results of preclinical studies indicate that a diversity of interventions which antagonize IGF-1R signaling or augment IGFBP-3 function inhibit tumor cell growth in models of human cancers. A more comprehensive understanding of the interplay between cellular targets of the IGF system and antineoplastic agents will facilitate the development of novel strategies for the prevention and treatment of cancer^[29]. Thus, the GH/IGF-I axis may be a target for cancer prevention and treatment.

REFERENCES

- Holly JM, Wass JA. Insulin-like growth factors: autocrine, paracrine or endocrine? New perspectives of the somatome-
- Zapf J, Waldvogel M, Froesch ER. Binding of nonsuppressible insulinlike activity to human serum. Evidence for a carrier protein. *Arch Biochem Biophys* 1975; **168**: 638-645
- Martin JL, Baxter RC. Insulin-like growth factor-binding protein from human plasma. Purification and characterization. *J Biol Chem* 1986; **261**: 8754-8760
- D'Ercole AJ, Stiles AD, Underwood LE. Tissue concentrations of somatomedin C: further evidence for multiple sites of synthesis and paracrine or autocrine mechanisms of action. *Proc Natl Acad Sci USA* 1984; **81**: 935-939
- O'Dell SD, Day IN. Insulin-like growth factor II (IGF-II). *Int J Biochem Cell Biol* 1998; **30**: 767-771
- Rajaram S, Baylink DJ, Mohan S. Insulin-like growth factor-binding proteins in serum and other biological fluids: regulation and functions. *Endocr Rev* 1997; **18**: 801-831
- De Mellow JS, Baxter RC. Growth hormone-dependent insulin-like growth factor (IGF) binding protein both inhibits and potentiates IGF-I-stimulated DNA synthesis in human skin fibroblasts. *Biochem Biophys Res Commun* 1988; **156**: 199-204
- Valentinis B, Bhala A, DeAngelis T, Baserga R, Cohen P. The human insulin-like growth factor (IGF) binding protein-3 inhibits the growth of fibroblasts with a targeted disruption of the IGF-I receptor gene. *Mol Endocrinol* 1995; **9**: 361-367
- Murray CJ, Lopez AD. Mortality by cause for eight regions of the world: Global Burden of Disease Study. *Lancet* 1997; **349**: 1269-1276
- Gerdes J, Schwab U, Lemke H, Stein H. Production of a mouse monoclonal antibody reactive with a human nuclear antigen associated with cell proliferation. *Int J Cancer* 1983; **31**: 13-20
- Mathews LS, Norstedt G, Palmiter RD. Regulation of insulin-like growth factor I gene expression by growth hormone. *Proc Natl Acad Sci USA* 1986; **83**: 9343-9347
- Kratzsch J, Blum WF, Schenker E, Keller E, Jahreis G, Hausteil B, Vantz M, Rotzsch W. Measurement of insulin-like growth factor I (IGF-I) in normal adults, patients with liver cirrhosis and acromegaly: experience with a new competitive enzyme immunoassay. *Exp Clin Endocrinol* 1993; **101**: 144-149
- Schoenle EJ, Zapf J, Prader A, Torresani T, Werder EA, Zachmann M. Replacement of growth hormone (GH) in normally growing GH-deficient patients operated for craniopharyngioma. *J Clin Endocrinol Metab* 1995; **80**: 374-378
- Vyzantiadis T, Theodoridou S, Giouleme O, Harsoulis P, Evgenidis N, Vyzantiadis A. Serum concentrations of insulin-like growth factor-I (IGF-I) in patients with liver cirrhosis. *Hepatogastroenterology* 2003; **50**: 814-816
- Sidlova K, Pechova M, AKotaska K, Prusa R. Insulin-like growth factor binding protein-3 in patients with liver cirrhosis. *Physiol Res* 2002; **51**: 587-590
- Giovannucci E. Nutrition, insulin, insulin-like growth factors and cancer. *Horm Metab Res* 2003; **35**: 694-704
- Kim SO, Park JG, Lee YI. Increased expression of the insulin-like growth factor I (IGF-I) receptor gene in hepatocellular carcinoma cell lines: implications of IGF-I receptor gene activation by hepatitis B virus X gene product. *Cancer Res* 1996; **56**: 3831-3836
- Kang-Park S, Lee JH, Shin JH, Lee YI. Activation of the IGF-II gene by HBV-X protein requires PKC and p44/p42 map kinase signalings. *Biochem Biophys Res Commun* 2001; **283**: 303-307
- Tanaka S, Takenaka K, Matsumata T, Mori R, Sugimachi K. Hepatitis C virus replication is associated with expression of transforming growth factor-alpha and insulin-like growth factor-II in cirrhotic livers. *Dig Dis Sci* 1996; **41**: 208-215
- Mattera D, Capuano G, Colao A, Pivonello R, Manguso F, Puzziello A, D'Agostino L. Increased IGF-I: IGFBP-3 ratio in patients with hepatocellular carcinoma. *Clin Endocrinol* 2003; **59**: 699-706
- Ali O, Cohen P, Lee KW. Epidemiology and biology of insulin-like growth factor binding protein-3 (IGFBP-3) as an anti-

- cancer molecule. *Horm Metab Res* 2003; **35**: 726-733
- 22 **Butt AJ**, Firth SM, King MA, Baxter RC. Insulin-like growth factor-binding protein-3 modulates expression of Bax and Bcl-2 and potentiates p53-independent radiation-induced apoptosis in human breast cancer cells. *J Biol Chem* 2000; **275**: 39174-39181
- 23 **Williams AC**, Collard TJ, Perks CM, Newcomb P, Moorghen M, Holly JM, Paraskeva C. Increased p53-dependent apoptosis by the insulin-like growth factor binding protein IGFBP-3 in human colonic adenoma-derived cells. *Cancer Res* 2000; **60**: 22-27
- 24 **Kuemmerle JF**, Murthy KS, Bowers JG. IGFBP-3 activates TGF-beta receptors and directly inhibits growth in human intestinal smooth muscle cells. *Am J Physiol Gastrointest Liver Physiol* 2004; **287**: G795-802
- 25 **Moschos SJ**, Mantzoros CS. The role of the IGF system in cancer: from basic to clinical studies and clinical applications. *Oncology* 2002; **63**: 317-332
- 26 **Yamaguchi K**, Nalesnik MA, Carr BI. *In situ* hybridization of albumin mRNA in normal liver and liver tumors: identification of hepatocellular origin. *Virchows Arch B Cell Pathol Incl Mol Pathol* 1993; **64**: 361-365
- 27 **Sell S**, Thomas K, Michalson M, Salatrepat J, Bonner J. Control of albumin and alpha-fetoprotein expression in rat liver and in some transplantable hepatocellular carcinomas. *Biochim Biophys Acta* 1979; **564**: 173-178
- 28 **Ozaki I**, Motomura M, Setoguchi Y, Fujio N, Yamamoto K, Kariya T, Sakai T. Albumin mRNA expression in human liver diseases and its correlation to serum albumin concentration. *Gastroenterol Jpn* 1991; **26**: 472-476
- 29 **Jerome L**, Shiry L, Leyland-Jones B. Deregulation of the IGF axis in cancer: epidemiological evidence and potential therapeutic interventions. *Endocr Relat Cancer* 2003; **10**: 561-578

Science Editor Guo SY Language Editor Elsevier HK

Nuclear factor-kappaB activation on the reactive oxygen species in acute necrotizing pancreatic rats

Jin Long, Na Song, Xi-Ping Liu, Ke-Jian Guo, Ren-Xuan Guo

Jin Long, Na Song, Xi-Ping Liu, Ke-Jian Guo, Ren-Xuan Guo, Department of Surgery, The First Affiliated Hospital, China Medical University, Shenyang 110001, Liaoning Province, China
Correspondence to: Jin Long, MD, Department of Surgery, The First Affiliated Hospital, China Medical University, Shenyang 110001, Liaoning Province, China. ljcmu@sina.com
Telephone: +86-24-23256666-6237 Fax: +86-24-22717355
Received: 2004-12-30 Accepted: 2005-01-12

Abstract

AIM: To investigate the potential role of nuclear factor kappa-B (NF- κ B) activation on the reactive oxygen species in rat acute necrotizing pancreatitis (ANP) and to assess the effect of pyrrolidine dithiocarbamate (PDTC, an inhibitor of NF- κ B).

METHODS: Rat ANP model was established by retrograde injection of 5% sodium taurocholate into biliopancreatic duct. Rats were randomly assigned to three groups (10 rats each): Control group, ANP group and PDTC group. At the 6th h of the model, the changes of the serum amylase, nitric oxide (NO), malondialdehyde (MDA), superoxide dismutase (SOD) and pancreatic morphological damage were observed. The expressions of inducible nitric oxide (iNOS) were observed by SP immunohistochemistry. And the expressions of NF- κ B p65 subunit mRNA were observed by hybridization *in situ*.

RESULTS: Serum amylase and NO level decreased significantly in ANP group as compared with PDTC administrated group [(7 170.40 \pm 1 308.63) U/L vs (4 074.10 \pm 1 719.78) U/L, P <0.05], [(76.95 \pm 9.04) μ mol/L vs (65.18 \pm 9.02) μ mol/L, P <0.05] respectively. MDA in both ANP and PDTC group rose significantly over that in control group [(9.88 \pm 1.52) nmol/L, (8.60 \pm 1.41) nmol/L, vs (6.04 \pm 1.78) nmol/L, P <0.05], while there was no significant difference between them. SOD levels in both ANP and PDTC group underwent a significant decrease as compared with that in control [(3 214.59 \pm 297.74) NU/mL, (3 260.62 \pm 229.44) NU/mL, vs (3 977.80 \pm 309.09) NU/mL, P <0.05], but there was no significant difference between them. Though they were still higher than those in Control group, pancreas destruction was slighter in PDTC group, iNOS expression and NF- κ B p65 subunit mRNA expression were lower in PDTC group as compared with ANP group.

CONCLUSION: We conclude that correlation among NF- κ B activation, serum amylase, reactive oxygen species level and tissue damage suggests a key role of NF- κ B in the pathogenesis of ANP. Inhibition of NF- κ B activation

may reverse the pancreatic damage of rat ANP and the production of reactive oxygen species.

© 2005 The WJG Press and Elsevier Inc. All rights reserved.

Key words: Pancreatitis; Acute necrotizing; Nuclear factor-kappaB; Reactive oxygen species

Long J, Song N, Liu XP, Guo KJ, Guo RX. Nuclear factor-kappaB activation on the reactive oxygen species in acute necrotizing pancreatic rats. *World J Gastroenterol* 2005; 11(27): 4277-4280

<http://www.wjgnet.com/1007-9327/11/4277.asp>

INTRODUCTION

Acute pancreatitis is clinically classified into mild and severe forms. Mild or edematous acute pancreatitis is a self-limiting disease with a low complication and mortality rate. However, ANP has an unacceptably high morbidity and mortality rate. Multiple therapeutic modalities have been suggested for acute pancreatitis, but none has been unambiguously proven to be effective yet. The major problem is that the pathophysiology of the disease is not fully understood^[1,2].

Oxygen free radicals are molecules produced continuously in cells by several mechanisms. The generation of oxygen free radicals is physiologic. In most circumstances, oxygen free radicals are neutralized immediately by enzymatic scavengers. But when formation of oxygen free radicals overwhelms radical neutralization in cells, oxidative stress occurs. As they are very reactive, they react well with all biological substances such as proteins, polysaccharides, and nucleic acids, resulting in tissue injury. It has been suggested that oxygen free radicals are responsible for a wide variety of diseases or conditions, for they play an important role in the pathogenesis of pancreatitis in some experimental models, and they are involved in the initiation of pancreatitis. Also, it was reported that oxygen free radicals acted as important mediators of tissue damage in experimental acute pancreatitis^[3,4].

Nuclear factor kappa-B (NF- κ B) is a sequence-specific transcription factor known to be involved in inflammatory and immune responses. It plays an important role in physiologic and pathologic conditions as an inducible nuclear factor. NF- κ B is able to mediate a variety of inflammatory mediators involved in acute pancreatitis, including cytokines and adhesion molecules, as well as specific inducible isoform of nitric oxide synthase enzymes. Recent experimental studies appeared to have shed some light on the intracellular signaling

pathway in the inflammatory cascade in acute pancreatitis^[5-7]. Hence, the role of NF- κ B in acute pancreatitis has attracted more and more attention.

Therefore, this study was conducted to evaluate the role of NF- κ B in experimental model of rat ANP and to analyze the role of NF- κ B activation on nitric oxide (NO) and other reactive oxygen species in the pathogenesis of ANP.

MATERIALS AND METHODS

Experimental groups and models

We randomized 30 male Wistar rats (weighing 250-300 g) to three groups, Control group, ANP group, and PDTC group. After having fasted for 24 h before the experiment, and allowed only drinking water freely, all rats were intraperitoneally infused with 2.5% pentobarbital sodium. When the abdominal cavity was opened through the median incision, the common bile duct and the pancreatic duct were found. After intubation from the end of pancreatic duct, the pancreatic duct was shut both at the duodenal ampulla and near the hepatic hilum transiently to prevent regurgitation of the infusion into the liver or duodenum. The ANP and PDTC group were induced by slow and even infusion of 5% sodium taurocholate (Sigma, St. Louis, MO, USA) into the pancreatic duct. The Control group received infusion of saline of the same amount instead of sodium taurocholate. In addition to sodium taurocholate, PDTC group received intravenous infusion of PDTC (Sigma, St. Louis, MO, USA) 10 mg/kg, while Control and ANP group received the same amount of saline instead.

Tested parameters

At the 6th h of the model, blood was collected from the abdominal aorta of rats, and the pancreas was removed according to the following measurement: (1) Serum amylase detected by HITACHI 7170 automatic biochemical analyzer; (2) Ratio of NO₂⁻ to NO₃⁻ determined by copper-zinc-cadmium reductive chromatometry, which reflects NO level; (3) Malondialdehyde (MDA) detected by TBA chromatometry; (4) Superoxide dismutase (SOD) detected by hydroxylamine chromatometry; (5) Morphological damage to pancreas observed microscopically after fixation in 10% neutral formaldehyde solution and HE stain, morphological alterations were graded using a scale of the degree of inflammation, necrosis and edema; (6) Expressions of iNOS in pancreatic tissue detected by iNOS immunohistochemical kits (Beijing Zhongshan Biotechnology Co., Ltd. Beijing, China) iNOS antibody was diluted 50 fold, tested with SP method, and cells stained with brown-yellow granules were considered to be positive; (7) Expressions of NF- κ B p65 subunit mRNA in pancreatic tissue: After fixation in 4%

citromint and 1% DEPC, expression of NF- κ B p65 subunit mRNA *in situ* kits (Wuhan Boster Bioengineering Co., Ltd. Wuhan, Hubei, China) Plasma and nucleus of pancreatic acinar stained with brown-yellow granules were considered to be positive. All immunohistochemistry or *in situ* images were analyzed and processed using MetaMorph v4.6 software (Universal Imaging Corp.). The intensity of expression was represented by average gray value, and the difference of average gray value reflected the difference of expression. Two pathologists assessed all of histopathologic sections in 20 fields/organ, and they were not aware as to which groups the sections belonged.

Statistical analysis

SASS 6.12 statistical analytic software was applied to process the data collected, and $P < 0.05$ was considered statistically significant.

RESULTS

Change of serum amylase, NO, MDA, and SOD (Table 1)

After the above treatment, serum amylase in ANP group rose rapidly. Although it was significantly higher than that in control group ($P < 0.05$), serum amylase of PDTC group was still significantly lower than that in ANP group ($P < 0.05$). NO levels in both ANP and PDTC group increased. The former, however, was significantly higher than the latter ($P < 0.05$). MDA in both ANP and PDTC group rose significantly over that in control group ($P < 0.05$), while there was no significant difference between the two results themselves. SOD levels in both ANP and PDTC group underwent a significant decrease as compared with that in control group ($P < 0.05$), but there was no significant difference between either of them.

Morphological change of the pancreatic tissue (Figure 1)

The only gross change in the abdominal cavity in control group was the mildly edematous pancreas. No structural damage was found microscopically in the pancreatic tissue, except for some local interstitial edema. In ANP group, bloody ascites, necrotic foci in pancreas, and fat necrosis in mesentery and omentum were found grossly. Interstitial lobular inflammatory infiltrations were observed in pancreas microscopically, as well as diffusive bleeding and piecemeal necrosis. In PDTC group, ascites and fat necrosis diminished notably compared with those in ANP group. Microscopically, slight bleeding, mild acinar degeneration and mild structure damage to lobules were observed together with declining inflammatory infiltration. The damage of ANP group is obviously grave than PDTC group [Histopathologic score: (5.76 ± 1.12) vs (4.00 ± 1.50) , $P < 0.05$].

Table 1 Changes of serum amylase, NO, MDA, SOD

Group	Amylase (U/L)	NO (umol/L)	MDA (nmol/L)	SOD (NU/mL)
Control	990.20±189.32	56.97±13.31	6.04±1.78	3977.80±309.09
ANP	7170.40±1308.63 ^c	76.95±9.04 ^c	9.88±1.52 ^c	3214.59±297.74 ^c
PDTC	4074.10±1719.78 ^{a,c}	65.18±9.02 ^a	8.60±1.41 ^c	3260.62±229.44 ^c

^a $P < 0.05$ vs ANP group; ^c $P < 0.05$ vs control group.

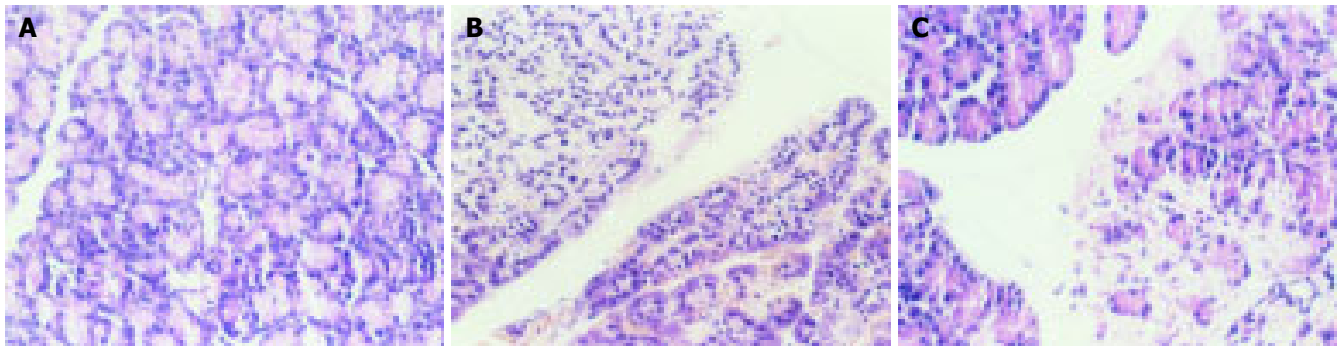


Figure 1 Morphological change of the pancreatic tissue (original magnification, $\times 400$). A: Control group; B: ANP group; C: PDTC group.

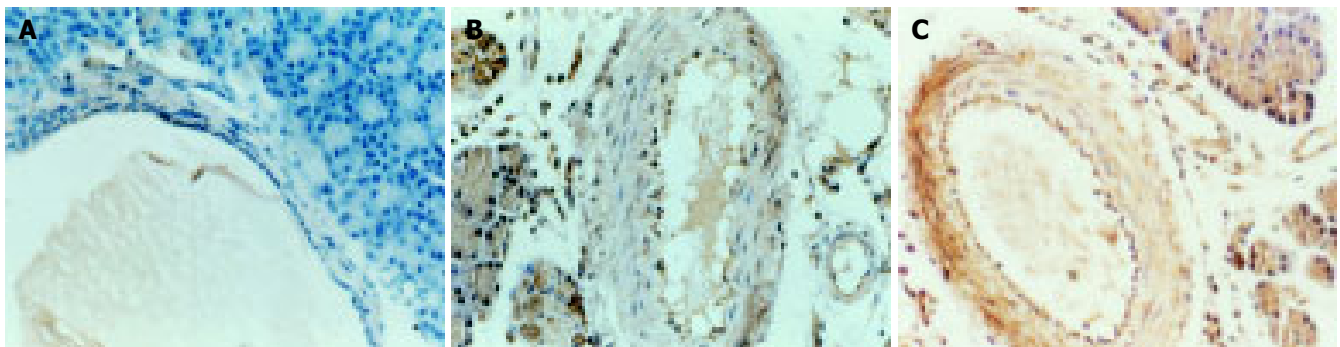


Figure 2 Expression of NOS in pancreatic tissue (DAB, original magnification, $\times 400$). A: Control group; B: ANP group; C: PDTC group.

Expressions of iNOS in pancreatic tissue (Figure 2)

Expression of iNOS was negative in control group while positive in both ANP and PDTC group, mainly found in endotheliums and smooth muscle cells. The iNOS expression is significantly lower with PDTC group than ANP group [Average gray value: (80.43 ± 10.48) *vs* (64.26 ± 9.18) , $P < 0.05$].

Expressions of NF- κ B p65 subunit mRNA in pancreatic tissue (Figure 3)

In control group, expression of NF- κ B was negative in all acinar nuclei, and positive only in some plasma. In ANP group, however, the expression was positive in both nucleus and plasma of pancreatic acinar. And the expression in nucleus and plasma decreased significantly in PDTC group [Average gray value: (104.25 ± 19.08) *vs* (67.28 ± 8.95) , $P < 0.05$].

DISCUSSION

One of the most severe complications of ANP is multiple system organ failure (MSOF) in early stage. The early systemic complication is the major cause of death in ANP, which leads to a mortality rate of 20%. Although it has been indicated that trypsin activation, auto-digestion of pancreas, cytokines, endotoxin, reactive oxygen species, and arachidnate^[8-11] play an important role in the progression of MSOF in ANP, the mechanisms of the development of this disease remain obscure.

Like what happens in other inflammatory diseases, reactive oxygen species are generated in the early stage of

ANP, and they play quite a vital role in the onset and development of ANP^[11]. During ANP, activated neutrophils are attached to endothelial cells, infiltrate into tissues, and produce large amount of reactive oxygen species and a kind of cytokines, which may cause severe damage to the pancreatic tissue. NO, in addition to potent function of vasodilation, can also inhibit the adherence, infiltration, and activation of white blood cells, and affect the production of reactive oxygen species^[11,12]. NO is generated by two classes of nitric oxide synthase (NOS): One that is constitutive, Ca²⁺-dependent and physiologically activated (cNOS) and the other is inducible (iNOS). cNOS produces temperate amount of NO relieving ANP, whereas iNOS produces excess NO exacerbating the damage of ANP to the body^[12].

Excessive production of NO causes vasodilatation and hypotension leading to organ hypoperfusion, edema, and organ dysfunction. Moreover, the reaction of NO with superoxide causes the formation of peroxynitrite, which is a powerful oxidant and cytotoxic agent and may play an important role in the cellular damage associated with the overproduction of NO. The spontaneous reaction of peroxynitrite with proteins makes the nitration of tyrosine residues to form nitrotyrosine, which is a specific nitration product of peroxynitrite and a marker for peroxynitrite-induced oxidative tissue damage. In this study, we found the concentration of SOD as an antioxidant decreased and that of MDA as the lipid peroxide increased, indicating the role of NO on the free radical reaction and oxidation response could intensify ANP.

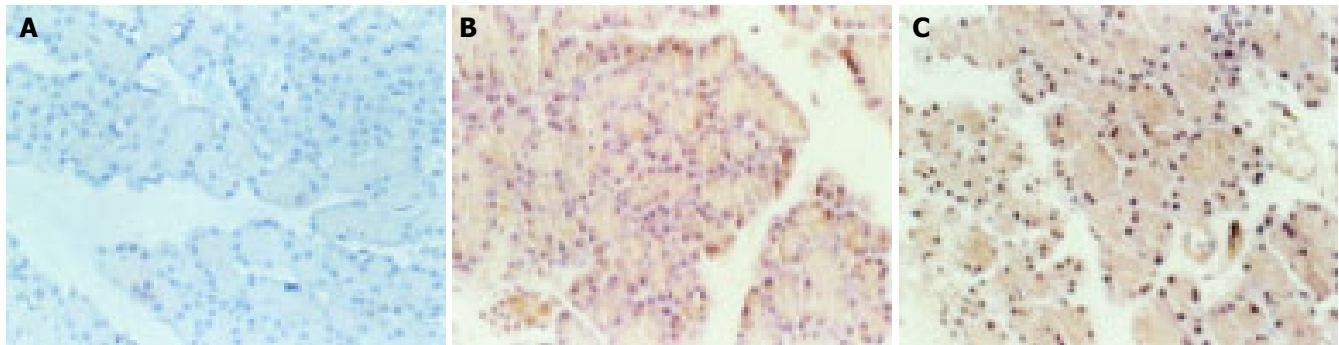


Figure 3 Expression of NF- κ B p65 mRNA in pancreatic tissue (DAB, original

magnification, $\times 400$). **A:** Control group; **B:** ANP group; **C:** PDTC group.

NF- κ B is a kind of pleiotropic regulative protein of transcription. Its activation takes part in the pathogenesis of ANP. Inhibition of the action can ameliorate the rat ANP^[13,14]. NF- κ B is also capable of regulating the expression of multiple inflammatory genes, such as tumor necrosis factor α (TNF- α), interleukin-6,8 (IL-6,8), and iNOS^[15]. Over-expressions of these discussed genes, however, can cause damage to the pancreatic and extra-pancreatic tissues in ANP. NF- κ B activation does relate to the reactive oxygen species in ANP.

Our study provides evidence that the injection of sodium taurocholate can cause ANP, with manifestation of the rise of serum amylase and NO, MDA level, damage to pancreas, inflammatory infiltration, and the decrease of SOD. Hybridization *in situ* and immunohistochemical results suggest that NF- κ B is activated immediately at the onset of ANP, accompanied by high expression of iNOS. And there is otherwise no expression of NF- κ B and iNOS under physiological conditions. The lower expression of NF- κ B p65 subunit mRNA in PDTC group indicates that the administration of PDTC may inhibit the NF- κ B activation. PDTC also leads to lower increase in serum amylase and slighter histological damage to pancreas. All these results are consistent with previous studies, substantiating that NF- κ B activation is involved in the pathogenesis of ANP, and inhibition of the activation may reverse rat ANP^[13,14]. Compared with those in ANP group, the NO and MDA level decreases, SOD level increases, and iNOS expression decreases. It is the increase of iNOS expression that aggravates ANP. Expression of iNOS is regulated by NF- κ B activation and inhibition of the activation may reduce iNOS expression, thus relieve ANP. Correlation among NF- κ B activation, NO, MDA, SOD level, tissue damage, and iNOS expression suggests a key role of NF- κ B activation in the pathogenesis of ANP model. By inhibiting iNOS expression, NF- κ B activation sets back over-production of reactive oxygen species like NO, therefore it reverses the damage of ANP to rats.

We may finally draw the conclusion from the above study that NF- κ B activation in rat ANP may reduce over-production of reactive oxygen species, thus ameliorate the

severity of ANP, all of which is achieved by inhibiting iNOS expression. The drug that can inhibit the activation of NF- κ B may become a way of the therapy of ANP.

REFERENCES

- 1 **Yousaf M**, McCallion K, Diamond T. Management of severe acute pancreatitis. *Br J Surg* 2003; **90**: 407-420
- 2 **Banks PA**. Practice guidelines in acute pancreatitis. *Am J Gastroenterol* 1997; **92**: 377-386
- 3 **Schoenberg MH**, Birk D, Beger HG. Oxidative stress in acute and chronic pancreatitis. *Am J Clin Nutr* 1995; **62** (6 Suppl): 1306S-1314S
- 4 **Sweiry JH**, Mann GE. Role of oxidative stress in the pathogenesis of acute pancreatitis. *Scand J Gastroenterol Suppl* 1996; **219**: 10-15
- 5 **Jaffray C**, Yang J, Carter G, Mendez C, Norman J. Pancreatic elastase activates pulmonary nuclear factor kappa B and inhibitory kappa B, mimicking pancreatitis-associated adult respiratory distress syndrome. *Surgery* 2000; **128**: 225-231
- 6 **Frossard JL**, Pastor CM, Hadengue A. Effect of hyperthermia on NF-kappaB binding activity in cerulein-induced acute pancreatitis. *Am J Physiol Gastrointest Liver Physiol* 2001; **280**: G1157-1162
- 7 **Algul H**, Tando Y, Schneider G, Weidenbach H, Adler G, Schmid RM. Acute Experimental Pancreatitis and NF-kappaB/Rel Activation. *Pancreatology* 2002; **2**: 503-509
- 8 **Karne S**, Gorelick FS. Etiopathogenesis of acute pancreatitis. *Surg Clin North Am* 1999; **79**: 699-710
- 9 **Denham W**, Norman J. The potential role of therapeutic cytokine manipulation in acute pancreatitis. *Surg Clin North Am* 1999; **79**: 767-781
- 10 **Norman J**. The role of cytokines in the pathogenesis of acute pancreatitis. *Am J Surg* 1998; **175**: 76-83
- 11 **Schulz HU**, Niederau C, Klonowski-Stumpe H, Halangk W, Luthen R, Lippert H. Oxidative stress in acute pancreatitis. *Hepatogastroenterology* 1999; **46**: 2736-2750
- 12 **Jaworek J**, Jachimczak B, Tomaszewska R, Konturek PC, Pawlik WW, Sendur R, Hahn EG, Stachura J, Konturek SJ. Protective action of lipopolysaccharides in rat caerulein-induced pancreatitis: role of nitric oxide. *Digestion* 2000; **62**: 1-13
- 13 **Gukovsky I**, Gukovskaya AS, Blinman TA, Zaninovic V, Pandolfi SJ. Early NF-kappaB activation is associated with hormone-induced pancreatitis. *Am J Physiol* 1998; **275**(6 Pt 1): G1402-1414
- 14 **Dunn JA**, Li C, Ha T, Kao RL, Browder W. Therapeutic modification of nuclear factor kappa B binding activity and tumor necrosis factor-alpha gene expression during acute biliary pancreatitis. *Am Surg* 1997; **63**: 1036-1043
- 15 **Abraham E**. NF-kappaB activation. *Crit Care Med* 2000; **28**: N100-104

Metastatic liver cancer: A rare case

Bong-Wan Kim, Hee-Jung Wang, In-Ho Jeong, Sang-Ick Ahn, Myoung-Wook Kim

Bong-Wan Kim, Hee-Jung Wang, In-Ho Jeong, Sang-Ick Ahn, Myoung-Wook Kim, Department of Surgery, Ajou University School of Medicine, Suwon, South Korea

Correspondence to: Hee-Jung Wang, MD, PhD, Department of Surgery, Ajou University School of Medicine, San-5 Youngtong ku, Wonchon dong, Suwon 442-749, South Korea. wanghj@ajou.ac.kr
Telephone: +82-31-219-5011 Fax: +82-31-219-5755

Received: 2004-11-29 Accepted: 2005-01-05

Abstract

Hemangiopericytoma is a rare tumor especially when it rises in the peritoneal cavity. We present a case of a 60-year-old woman with an isolated recurrent hemangiopericytoma of the liver. The patient presented with a palpable right upper quadrant abdominal mass, which occurred 7 years after undergoing resection of a malignant hemangiopericytoma arising from the greater omentum. She had not followed up 6 mo after surgery. Various imaging studies showed a single large, well-capsulated liver tumor with central necrosis, accompanied by hypervascularity typical of a vascular tumor. Preoperative laboratory HBsAg and anti-HCV workup were both negative. Under the impression of recurrent malignant hemangiopericytoma, right trisegmentectomy was performed to completely resect the tumor. Pathological examination confirmed the diagnosis of recurrent hemangiopericytoma. Even though the incidence of the hemangiopericytoma is relatively low, malignant hemangiopericytoma has a tendency to recur frequently after a long-term disease-free interval. Also, the recurrent hemangiopericytoma is not easily detected early during follow-up until it becomes symptomatic because there are no specific tumor markers, and because of the diversity with regard to site of recurrence. The authors suggest that Positron Emission Tomogram (PET) may be a useful tool for the detection of recurrent hemangiopericytoma. We describe herein some characteristics and behaviors of malignant hemangiopericytoma, particularly after surgical resection.

© 2005 The WJG Press and Elsevier Inc. All rights reserved.

Key words: Hemangiopericytoma; Greater omentum; Hepatic metastasis; Follow-up; Positron emission tomography

Kim BW, Wang HJ, Jeong IH, Ahn SI, Kim MW. Metastatic liver cancer: A rare case. *World J Gastroenterol* 2005; 11 (27): 4281-4284

<http://www.wjgnet.com/1007-9327/11/4281.asp>

INTRODUCTION

Hemangiopericytoma was first described in 1942 by Stout

and Murray, and approximately 1 000 cases have been reported to date in the literature. Hemangiopericytomas arise from the pericyte of Zimmermann, and although it may occur in any part of the human body, the frequency of occurrence has been reported to be the lower extremities, pelvic cavity, retro-peritoneum, thoracic cavity, and upper extremities, in descending order. Most tumors have been reported to occur in the deep portions of the body, and those arising within the peritoneum are rare^[1]. Generally, although hemangiopericytomas arising in the peritoneal cavity show better prognosis compared to adenocarcinomas that occur in the gastrointestinal tract, surgery seems to be the only effective mode of therapy.

Histologically benign hemangiopericytomas are known to be curable by complete surgical resection, while the malignant type, albeit characterized by slow growth, has been known to recur frequently after curative surgical resection. Another reported characteristic of hemangiopericytomas is the development of non-islet-cell-tumor hypoglycemia in the latter phase of the natural course^[1], and this has been related to the production of the insulin-like growth factor II by the tumor^[2,3]. Malignant hemangiopericytomas are characterized by an indolent rate of growth, but recurrence has been demonstrated in more than half of the cases which had been followed up. In addition, the diversity of the sites of recurrence via hematological and lymphatic routes and lack of specific tumor markers has contributed to the difficulty in detecting recurrent disease. The lungs have been shown to be the most common distal site of recurrence, while other sites include the brain, scalp, chest wall, liver, subcutaneous lymph node, gastrointestinal tract, and ovaries^[4,5].

The authors report a surgically treated case of hemangiopericytoma of the greater omentum, and which recurred as a metachronous solitary liver metastasis 7 years after complete resection. We also suggest the employment of the positron emission tomography (PET) method as a useful tool in the post-operative follow-up of patients with a history of hemangiopericytomas, as there is no other definite established mode of follow-up.

CASE REPORT

A gravida 6, para 5, at present 60-years old, female patient had presented with a palpable lower abdominal mass referred initially from a private gynecologic clinic in March 1997, under the impression of a myoma of the uterus. Her past gynecologic history showed that she had entered menopause at 49 years of age. Physical examination showed a mobile, solid mass in the lower abdomen. Transvaginal ultrasonography demonstrated that the mass did not originate from the uterus. A magnetic resonance imaging was performed to determine if the mass was of ovarian origin, and which

showed that an 8 cm sized, solitary mass of unknown origin was present in the pelvic cavity. There was no evidence of lymph node enlargement. The tumor markers β -HCG, CA19-9, CA-125, CEA were all within the normal range. The patient subsequently underwent exploratory laparotomy under the impression of a possible ovarian malignancy, upon which a 10 cm \times 8 cm \times 7 cm mass originating from the greater omentum was observed. There was no gross evidence of other pathology such as surrounding adhesions or lymph node pathology, and the patient consequently underwent tumor excision including a portion of the omentum. Pathologic examination revealed necrosis in the central portion of the tumor, atypical hyperplasia of spindle-shaped tumor cells, and five mitoses per 10 HPF, suggestive of a malignant hemangiopericytoma. The patient was discharged 7 d after surgery and no further adjuvant anti-cancer therapy was administered. She had not followed up 6 mo after surgery.

The patient was asymptomatic until October 2004, when she began to complain of a palpable right upper quadrant mass, and she visited our department for evaluation. Initial abdominal computerized tomography (CT) demonstrated a large mass in the right hepatic lobe. To ascertain whether this lesion was a possible hepatocellular carcinoma, a common cause of liver tumors in Korea, viral marker studies were conducted, and which showed HBsAg (-), anti-HBs (+), anti-HBc (+), and anti-HCV (-). Also, the tumor markers

AFP, CEA, CA19-9, and CA125 were all within normal limits. Plain chest X-ray was also normal.

Abdominal CT scan showed that the tumor was of a hypervascular nature, with active contrasting from the periphery of the tumor in the arterial phase, and remaining contrast in the delayed phase suggesting a tumor of vascular origin. The hepatic artery angiogram confirmed that the tumor was hypervascular, with vessels from major arteries providing branches surrounding and entering into the deep portions of the tumor (Figure 1). These findings were highly suggestive of a recurrent malignant hemangiopericytoma. To determine the presence of any distant metastatic lesion, a head and neck CT (normal) was performed, while the ^{18}F -FDG PET scan showed a standardized uptake value (SUV) of 4.8 in the right hepatic lobe indicative of ^{18}F -FDG uptake. There were no other suspicious sites other than the liver (Figure 2). The patient therefore underwent laparotomy and right trisegmentectomy of the liver under the impression of recurrent malignant hemangiopericytoma. Gross findings showed a 15 cm, large solitary sarcomatous lesion with central necrosis. Microscopic examination of the tumor confirmed the presence of malignant hemangiopericytoma identical to that of the lesion of 1997, with free resection margins (Figures 3 and 4). The patient was discharged on the 20th postoperative day without complications.

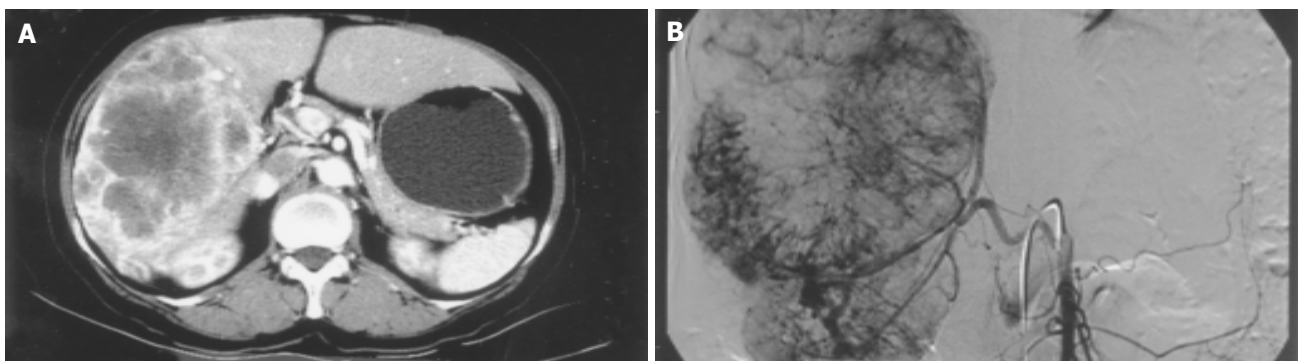


Figure 1 A: Liver CT scan showed a huge tumor in the right lobe of the liver with enhancement from the periphery in the arterial phase; B: The hepatic arteriogram

demonstrated numerous feeding vessels surrounding and entering into the tumor. The patient had variation of the right hepatic artery from the superior mesenteric artery.

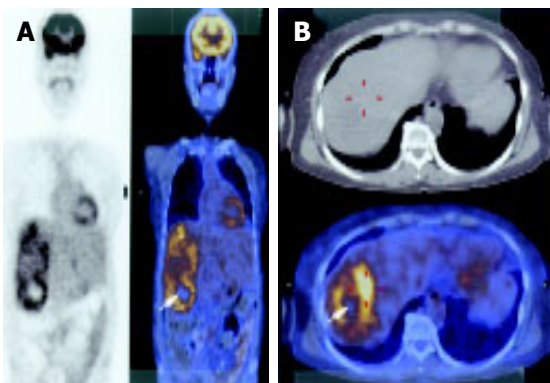


Figure 2 A: ^{18}F -FDG PET showed high uptake at the tumor without any distant lesions. The silent area in the center of the tumor suggests central necrosis (arrow); B: The highest uptake area measured 4.8 SUV (red line mark).



Figure 3 Resected specimen showed a huge single tumor with sarcomatous consistency. The margin was irregular because of the constrictive envelopment of feeding vessels. The central necrosis is indicated (arrow).

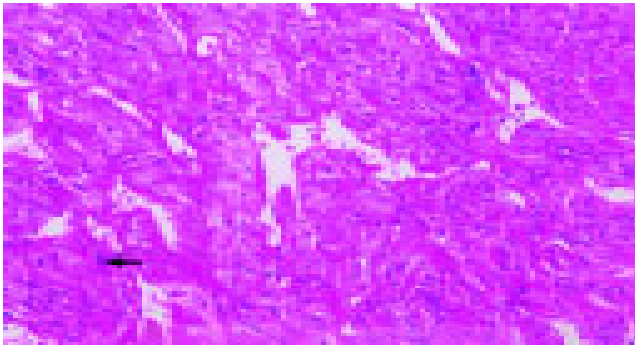


Figure 4 Microscopic examination demonstrated numerous atypical vessels (stag-horn appearance) in the high population of spindle-shaped tumor cells. A mitotic figure is seen (arrow), H&E, $\times 200$.

DISCUSSION

Hemangiopericytomas primarily occurring in the abdominal cavity are very rare, and only 12 cases in the world-wide literature have reported those occurring in the greater omentum. It is thought that surgical removal of the tumor is the most effective mode of therapy for hemangiopericytomas, but as yet there is no established range of surgical resection for malignant types that occur in the abdomen. As demonstrated in our case, in light of the fact that secondary surgery confirmed recurrent metastatic liver tumor 7 years after initial simple excision, and that there was no local recurrence in the omentum and the peritoneal cavity, we do not feel that complete anatomical removal of the total greater omentum would lead to superior prognosis compared to simple excision only. This finding is similar to previously reported cases of greater omental hemangiopericytomas^[6].

Grossly, malignant hemangiopericytomas have been reported usually as a solitary lesion, but in some series, several hundred, multiple nodules have also been observed^[7]. In most cases, the tumor is observed as smoothly encapsulated, while the areas where the vessels enter into the tumor surface are characterized as irregular due to local tumor retraction. As hemangiopericytomas are hypervascular tumors, angiography demonstrates a feature of numerous feeding vessels surrounding and entering into the tumor, sometimes being observed as multiple cork-screw type feeding vessels. These findings, however, are not common findings, and are not highly regarded as a distinctive diagnostic feature^[8,9]. Moreover, it is difficult to ascertain both a diagnosis of hemangiopericytoma and malignant characteristic with these radiological and gross findings alone.

Microscopic observation of H&E staining demonstrates numerous neovascularized vessels within a highly concentrated area of tumor cells, and which also frequently show a stag-horn feature. The tumor cells are mostly spindle-shaped, but may be spherical or other shapes, the nuclear to cytoplasm ratio is increased, while the cytoplasm is pale staining. Differential diagnosis includes glomus tumor, fibrous histiocytoma, synovial sarcoma, and mesenchymal sarcoma, and advances in immunohistochemical techniques usually allows differentiation from a malignant hemangiopericytoma. It has been reported in the previous literature that malignant

hemangiopericytomas comprise about half of all cases, and that after local excision and long-term follow-up, approximately 60% of patients experience local or distant recurrence^[4]. The disease-free interval has been reported to vary markedly between 2 mo and 26 years^[10]. Specific features that qualify a hemangiopericytoma as a malignant lesion are more than four mitoses per 10 HPF, pleomorphic cells with abnormal chromatin pattern, and accompanied by either central tumor necrosis or intra-tumoral hemorrhage.

Observations of previous data regarding hemangiopericytomas arising in the greater omentum have shown that the presence of more than four mitoses per 10 HPF is closely related to recurrence of disease. Also, the number of increased mitoses has also been suggested to be related with increased tumor size, and that tumors of more than 20 cm in diameter imply poor prognosis^[6].

Other modes of therapy for malignant hemangiopericytoma may consist of anticancer chemotherapy and radiotherapy for residual or metastatic tumors^[11,12], and these are usually the preferred mode of adjuvant therapy after surgery because of limited efficacy.

From the clinical perspective, compared to other common malignant tumors of the gastrointestinal tract, malignant hemangiopericytomas have a comparatively longer disease-free interval after surgical resection and an indolent natural history^[13]. However, it should be mentioned that in many cases of recurrent disease after a long disease-free interval, it is common that either the qualified gastrointestinal surgeon concludes that the disease has been completely cured after a certain length of follow-up, or that the patient refuses further follow-up. This is also reflected in our case, whereby the patient presented with a recurred large intra-abdominal mass, or with related cancer symptoms such as hypoglycemia.

Another difficulty involving postoperative management of hemangiopericytoma is that since there is no established follow-up protocol after surgery, the length of follow-up and the diagnostic methods employed varies from surgeon to surgeon. Moreover, the absence of specific tumor markers makes it all the more difficult to detect recurrent disease. The authors of this study suggest that the PET scan is a valid, non-invasive diagnostic procedure in the ascertainment of recurrent malignant hemangiopericytoma. This may be particularly true in patients where if the preoperative PET demonstrates a hemangiopericytoma, the presence of a recurrent tumor of a similar character will be detected by PET in the follow-up. However, it should be noted that there may be differences in the degree of uptake between histologically identical hemangiopericytomas. In our case ¹⁸F-FDG uptake was increased within the tumor, but other series have shown that ¹¹C-methionine and ¹⁵O-H₂O uptake was increased rather than ¹⁸F-FDG^[14]. That report is different from ours, so we think further evaluations about useful radio-isotope of PET for malignant hemangiopericytoma are needed. Another study suggested the correlation between the high uptake of ¹⁸F-FDG in hemangiopericytomas and poor prognosis^[15]. Consequently, it is the opinion of the authors that such variable uptakes by malignant hemangiopericytoma as seen in PET scans contribute more to the detection of recurrent disease after surgical removal, rather than to the

establishment of preoperative differential diagnosis. Also, the PET scans the whole body, and therefore allows detection of recurrent hemangiopericytoma, which has a wide pattern of recurrence.

In conclusion, although the pattern of recurrent malignant hemangiopericytoma is diverse, surgical intervention after early detection may allow another long disease-free period. For this to be accomplished, long-term follow-up is imperative, and we suggest that yearly PET scans are useful in attaining this goal.

REFERENCES

- 1 **Enzinger FM**, Smith BH. Hemangiopericytoma. An analysis of 106 cases. *Hum Pathol* 1976; **7**: 61-82
- 2 **Sohda T**, Yun K. Insulin-like growth factor II expression in primary meningeal hemangiopericytoma and its metastasis to the liver accompanied by hypoglycemia. *Hum Pathol* 1996; **27**: 858-861
- 3 **Grunenberger F**, Bachellier P, Chenard MP, Massard G, Caraman PL, Perrin E, Zapf J, Jaeck D, Schlienger JL. Hepatic and pulmonary metastases from a meningeal hemangiopericytoma and severe hypoglycemia due to abnormal secretion of insulin-like growth factor: a case report. *Cancer* 1999; **85**: 2245-2248
- 4 **McMaster MJ**, Soule EH, Ivins JC. Hemangiopericytoma. A clinicopathologic study and long-term follow up of 60 patients. *Cancer* 1975; **36**: 2232-2244
- 5 **Begum M**, Katabuchi H, Tashiro H, Suenaga Y, Okamura H. A case of metastatic malignant hemangiopericytoma of the ovary: recurrence after a period of 17 years from intracranial tumor. *Int J Gynecol Cancer* 2002; **12**: 510-514
- 6 **Kaneko K**, Shirai Y, Wakai T, Hasegawa G, Kaneko I, Hatakeyama K. Hemangiopericytoma arising in the greater omentum: report of a case. *Surg Today* 2003; **33**: 722-724
- 7 **Matsuda S**, Usui M, Sakurai H, Suzuki H, Ogura Y, Shiraiishi T. Insulin-like growth factor II-producing intra-abdominal hemangiopericytoma associated with hypoglycemia. *J Gastroenterol* 2001; **36**: 851-855
- 8 **Marc JA**, Takei Y, Schechter MM, Hoffman JC. Intracranial hemangiopericytomas. Angiography, pathology and differential diagnosis. *Am J Roentgenol Radium Ther Nucl Med* 1975; **125**: 823-832
- 9 **Guthrie BL**, Ebersold MJ, Scheithauer BW, Shaw EG. Meningeal hemangiopericytoma: histopathological features, treatment, and long-term follow-up of 44 cases. *Neurosurgery* 1989; **25**: 514-522
- 10 **Schirger A**, Uihlein A, Parker HL, Kernohan JW. Hemangiopericytoma recurring after 26 years; report of a case. *Mayo Clin Proc* 1958; **33**: 347-352
- 11 **Wong PP**, Yagoda A. Chemotherapy of malignant hemangiopericytoma. *Cancer* 1978; **41**: 1256-1260
- 12 **Staples JJ**, Robinson RA, Wen BC, Hussey DH. Hemangiopericytoma-the role of radiotherapy. *Int J Radiat Oncol Biol Phys* 1990; **19**: 445-451
- 13 **Spitz FR**, Bouvet M, Pisters PW, Pollock RE, Feig BW. Hemangiopericytoma: a 20-year single-institution experience. *Ann Surg Oncol* 1998; **5**: 350-355
- 14 **Kracht LW**, Bauer A, Herholz K, Terstegge K, Friese M, Schroder R, Heiss WD. Positron emission tomography in a case of intracranial hemangiopericytoma. *J Comput Assist Tomogr* 1999; **23**: 365-368
- 15 **Reisser C**, Haberkorn U, Strauss LG. Diagnosis of energy metabolism in ENT tumors-a PET study. *Hno* 1992; **40**: 225-231

Science Editor Guo SY Language Editor Elsevier HK

• CASE REPORT •

Successful endoscopic hemostasis for gastric arterial bleeding due to invasion of malignant lymphoma

Kenichi Nomura, Shinya Yamada, Daisuke Shimizu, Takashi Okuda, Yuri Kamitsuji, Naohisa Yoshida, Yosuke Matsumoto, Naoki Wakabayashi, Kazuya Mikami, Shigeo Horiike, Takeshi Okanoue, Masafumi Taniwaki

Kenichi Nomura, Shinya Yamada, Daisuke Shimizu, Yuri Kamitsuji, Yosuke Matsumoto, Shigeo Horiike, Masafumi Taniwaki, Molecular Hematology and Oncology, Kyoto Prefectural University of Medicine Graduate School of Medical Science, Kyoto, Japan
Yuri Kamitsuji, Inflammation and Immunology, Kyoto Prefectural University of Medicine Graduate School of Medical Science, Kyoto, Japan

Takashi Okuda, Naohisa Yoshida, Naoki Wakabayashi, Takeshi Okanoue, Molecular Gastroenterology and Hepatology, Kyoto Prefectural University of Medicine Graduate School of Medical Science, Kyoto, Japan

Kazuya Mikami, Department of Urology, Kyoto Prefectural University of Medicine Graduate School of Medical Science, Kyoto, Japan

Daisuke Shimizu, Masafumi Taniwaki, Clinical Molecular Genetics and Laboratory Medicine, Kyoto Prefectural University of Medicine Graduate School of Medical Science, Kyoto, Japan

Correspondence to: Kenichi Nomura, MD, PhD, Molecular Hematology and Oncology, Kyoto Prefectural University of Medicine Graduate School of Medical Science, Kawaramachi-Hirokoji, Kamigyo-ku, Kyoto, 602-0841, Japan. nomuken@sun.kpu-m.ac.jp
Telephone: +81-75-251-5521 Fax: +81-75-251-0710

Received: 2004-09-23 Accepted: 2004-10-13

Abstract

A 75-year-old male with malignant lymphoma (ML) accompanied with gastric lesion was treated with combination chemotherapy. The patient produced tarry stool on the 4th d, and emergency gastroscopy showed arterial bleeding from the lesion. Hemostasis was achieved by injecting pure ethanol and using hemostatic clips. There is only one previous report on endoscopic hemostasis being effective for bleeding due to lymphoma. Since gastric bleeding causes significant mortality, endoscopic hemostasis should be considered as first-line treatment for ML patients who were treated with chemotherapy.

© 2005 The WJG Press and Elsevier Inc. All rights reserved.

Key words: Malignant lymphoma; Endoscopic hemostasis; Pure ethanol injection; Hemostatic clips

Nomura K, Yamada S, Shimizu D, Okuda T, Kamitsuji Y, Yoshida N, Matsumoto Y, Wakabayashi N, Mikami K, Horiike S, Okanoue T, Taniwaki M. Successful endoscopic hemostasis for gastric arterial bleeding due to invasion of malignant lymphoma. *World J Gastroenterol* 2005; 11(27): 4285-4286
<http://www.wjgnet.com/1007-9327/11/4285.asp>

INTRODUCTION

Patients with stage I-II primary gastric lymphoma are

commonly treated with chemotherapy alone or in combination with radiation therapy to avoid long-term sequelae after gastric resection^[1,2]. Although gastrointestinal bleeding during chemotherapy has been observed in only 3% of cases^[2], it is a definite cause of mortality. However, only emergency gastrectomy may be able to rescue patients with neutropenia and thrombocytopenia after chemotherapy^[3].

Endoscopic hemostasis has been established as a first-line treatment for acute bleeding in all patients with peptic ulcer. Among various methods employed, injection with pure ethanol or the use of hemostatic clips is one of the most effective treatments for achieving definitive hemostasis^[4-8]. However, there has been only one report describing a case of successful endoscopic hemostasis for bleeding from lymphoma in the stomach. However, this case underwent hemostatic treatment before chemotherapy^[9].

Our report concerns an elderly patient with gastric bleeding due to invasion of lymphoma after standard chemotherapy. Although this patient was considered inoperable before chemotherapy, we managed to achieve hemostasis by injecting pure ethanol and using hemostatic clips.

CASE REPORT

A 75-year-old man was admitted to our hospital in January 2004 because of lumbar pain. Computed tomography detected a huge mass at the kidney and swelling of the paraaortic lymph nodes. He was diagnosed as having renal cell carcinoma with lymph node invasion and underwent surgical treatment in March. However, the swelling of the lymph nodes was histologically diagnosed as diffuse large B-cell lymphoma (DLBCL), and because ⁶⁷Ga-citrate scintigraphy showed uptake at the stomach, we performed upper gastrointestinal endoscopy. An ulcerative lesion was detected in the upper body (Figure 1), which, although suspected of being invasion of lymphoma, a biopsy sample showed to be a benign ulcer. Because there were no other signs of lymphoma, the patient was treated with interferon therapy for renal cell carcinoma as adjuvant therapy. Omeprazole and cimetidine were administered for the gastric lesion. After 2 mo, multiple superficial lymph node swelling was observed. Biopsy of the cervical lymph node indicated recurrence of DLBCL, but because our patient was considered inoperable, we started CHOP therapy (cyclophosphamide, adriamycin, vincristine, and prednisolone) on 6th July. However, the patient produced massive tarry stool on d 4, resulting in a drop in the hemoglobin level to 44 g/L. Emergency endoscopy was performed that detected arterial bleeding from the ulcerative lesion in the upper body (Figure 2).

The condition had not changed since the previous examination in spite of the treatment with anti-peptic agents. Ethanol injections (0.1 mL at a time) into the surrounding tissue close to the bleeding vessels, at a few injecting sites 2 mm from the bleeding vessels, suppressed the pulsatile bleeding, and definitive hemostasis was achieved with the concomitant use of hemostatic clips. During the following 2 weeks, the ulcerative lesions became smaller and no further bleeding was detected (Figure 3).

The second biopsy samples were histologically compatible with lymphoma.



Figure 1 Giant ulcer at cardia of stomach.



Figure 2 Emergency gastroscopy showed pulsatile arterial bleeding.



Figure 3 No bleeding was observed in the ulcer injected with ethanol.

DISCUSSION

This report concerns a patient with arterial bleeding from the stomach due to lymphoma invasion. We had considered surgical resection of the stomach before chemotherapy to avoid bleeding, but we performed chemotherapy as first treatment instead, because surgery was considered to carry serious risks. The reasons for these were that (1) the patient had previously undergone laparotomy for renal cell carcinoma and adhesion of viscera was suspected to be severe, (2) paraaortic lymph nodes were swollen making it difficult to create anastomoses for a gastroduodenostomy, and (3) lymphoma was expected to progress rapidly during recovery from the operation.

Because the mechanism of hemostasis is thought to consist of solidification caused by vascular shrinking resulting from the direct action of ethanol and degeneration of the vascular endothelial cells, there is good reason for attempting endoscopic hemostasis for bleeding due to lymphoma. We successfully achieved hemostasis with ethanol injection and clips, although the fundus of the ulcer remained fragile due to necrosis of the lymphoma after chemotherapy. Because lymphoma is curable with chemotherapy alone, endoscopic hemostasis should be considered as a first-line treatment for bleeding due to lymphoma.

ACKNOWLEDGMENT

The authors are grateful to Ms. Yuko Kanbayashi for her pharmacological advice.

REFERENCES

- 1 **Maor MH**, Velasquez WS, Fuller LM, Silvermintz KB. Stomach conservation in stages IE and IIE gastric non-Hodgkin's lymphoma. *J Clin Oncol* 1990; **8**: 266-271
- 2 **Ferreri AJ**, Cordio S, Ponzoni M, Villa E. Non-surgical treatment with primary chemotherapy, with or without radiation therapy, of stage I-II high-grade gastric lymphoma. *Leuk Lymphoma* 1999; **33**: 531-541
- 3 **Sakakura C**, Hagiwara A, Nakanishi M, Yasuoka R, Shirasu M, Togawa T, Taniwaki M, Yamagishi H. Bowel perforation during chemotherapy for non-hodgkin's lymphoma. *Hepatogastroenterology* 1999; **46**: 3175-3177
- 4 **Exon DJ**, Sydney Chung SC. Endoscopic therapy for upper gastrointestinal bleeding. *Best Pract Res Clin Gastroenterol* 2004; **18**: 77-98
- 5 **Asaki S**. Tissue solidification in coping with digestive tract bleeding: hemostatic effect of local injection of 99.5% ethanol. *Tohoku J Exp Med* 1981; **134**: 223-227
- 6 **Hepworth CC**, Swain CP. Mechanical endoscopic methods of haemostasis for bleeding peptic ulcers: a review. *Baillieres Best Pract Res Clin Gastroenterol* 2000; **14**: 467-476
- 7 **Raju GS**, Gajula L. Endoclips for GI endoscopy. *Gastrointest Endosc* 2004; **59**: 267-279
- 8 **Shimoda R**, Iwakiri R, Sakata H, Ogata S, Kikkawa A, Ootani H, Oda K, Ootani A, Tsunada S, Fujimoto K. Evaluation of endoscopic hemostasis with metallic hemoclips for bleeding gastric ulcer: comparison with endoscopic injection of absolute ethanol in a prospective, randomized study. *Am J Gastroenterol* 2003; **98**: 2198-2202
- 9 **Nishimura H**, Saito M, Shibata K, Ueno K, Maeura Y, Murata A. A case of malignant lymphoma accompanied with arterial bleeding from the gastric lesion. *Jpn J Med* 1989; **28**: 604-607

Imaging features of ciliated hepatic foregut cyst

Song-Hua Fang, Dan-Jun Dong, Shi-Zheng Zhang

Song-Hua Fang, Dan-Jun Dong, Shi-Zheng Zhang, Department of Radiology, Sir Run Run Shaw Hospital, Zhejiang University, Hangzhou 310016, Zhejiang Province, China

Correspondence to: Song-Hua Fang, Department of Radiology, Sir Run Run Shaw Hospital, Zhejiang University, Hangzhou 310016, Zhejiang Province, China. fangsonghua@163.com
Telephone: +86-571-86090073-4609

Received: 2004-10-09 Accepted: 2004-11-26

Abstract

Ciliated hepatic foregut cyst (CHFC) is a very rare cystic lesion of the liver that is histologically similar to bronchogenic cyst. We report one case of CHFC that was hard to distinguish from solid-cystic neoplasm in imaging features. Magnetic resonance imaging was helpful in differentiating these cysts from other lesions.

© 2005 The WJG Press and Elsevier Inc. All rights reserved.

Key words: Ciliated foregut cyst; Liver; Magnetic resonance imaging; X-ray computed tomography

Fang SH, Dong DJ, Zhang SZ. Imaging features of ciliated hepatic foregut cyst. *World J Gastroenterol* 2005; 11(27): 4287-4289

<http://www.wjgnet.com/1007-9327/11/4287.asp>

INTRODUCTION

Ciliated hepatic foregut cyst (CHFC) is a very rare, benign and solitary cyst^[1,2]. It is most often unilocular^[2]. To our knowledge, 5 cases of CHFC were reported in the 19th century, 53 cases in the 20th century and 5 cases in the 21st and its medical imaging findings are seldom reported^[1,3]. It is difficult to differentiate the CHFC from malignant tumor^[1,4,5]. Herein, we present the radiologic features from one CHFC that was not similar to other nonparasitic cysts, but rather mimicked cystic-solid mass of the liver on the images obtained.

CASE REPORT

A 30-year-old man presented with a 5-mo history of left upper abdominal discomfort and mild fatigue. Physical examination and laboratory studies had no positive findings including hepatitis.

A plain radiograph of the abdomen was normal. Sonographic examination revealed a well-delineated hypoechoic mass, 3 cm×4 cm in size, in the liver. It was located in the medial segment of the left lobe (segment IV),

just adjacent to the surface of the liver. Unenhanced computed tomographic (CT) scan was obtained, and the lesion appeared slightly hypoattenuating relative to surrounding liver parenchyma (Figure 1A). The attenuation value of the lesion was 47 HU. At contrast material-enhanced CT, this lesion was not enhanced and appeared slightly hypoattenuating with well-defined margin (Figure 1B). On delayed CT scan, it had still no enhancement. Magnetic resonance (MR) imaging at 1.5 T was performed for more detailed examination. The lesion appeared isointense relative to surrounding liver parenchyma on T1-weighted imaging (Figure 1C) and markedly homogeneously hyperintense on T2-weighted imaging (Figure 1D). It was also not enhanced after Gd-DTPA administration (Figure 1E).

The lesion was resected surgically because the possibility of hypovascular neoplasm could not be excluded completely according to the imaging. The resected specimen revealed an unilocular cystic lesion containing a mucinous fluid.

On pathologic examination, the cyst had a fibrous wall lined by ciliated pseudostratified columnar epithelial cells, which was consistent with a CHFC (Figure 1F).

DISCUSSION

The histogenesis of CHFC is still unclear, but most authors consider that it arises from the embryonic foregut in the liver^[1,2,5]. CHFC is usually a benign, solitary cyst consisting of a ciliated pseudostratified columnar epithelium, a subepithelial connective tissue layer, a smooth muscle layer and an outer fibrous capsule^[2,6]. It is often smaller than 3 cm in diameter and found most commonly in the medial segment of the left hepatic lobe, just beneath the hepatic surface^[5,7]. CHFC is not actually a neoplasm and usually found incidentally on radiologic imaging during surgical exploration or autopsy. It is mostly asymptomatic and surgical resection should be avoided^[5]. However, on the other hand, it was reported recently that one case causes portal vein compression and the other shows malignant transformation through squamous metaplasia (it is not surprising to find squamous mucosa because tracheobronchial tree derives from the embryologic foregut), which warns to examine CHFC cautiously^[8,9], and suggests that a large-sized symptomatic CHFC should be excised, especially when radiologic studies yield equivocal results^[10].

Generally CHFC is a well-delineated anechoic or slightly hypoechoic small mass on ultrasonography. Because CHFC can contain various elements ranging from clear serous material to milky white to brown mucoid material, and these have variable viscosities, and the different CT attenuation numbers can be shown^[5]. The lesion can be hypoattenuating as our case or isoattenuating relative to surrounding liver parenchyma at unenhanced CT. Even it has very high

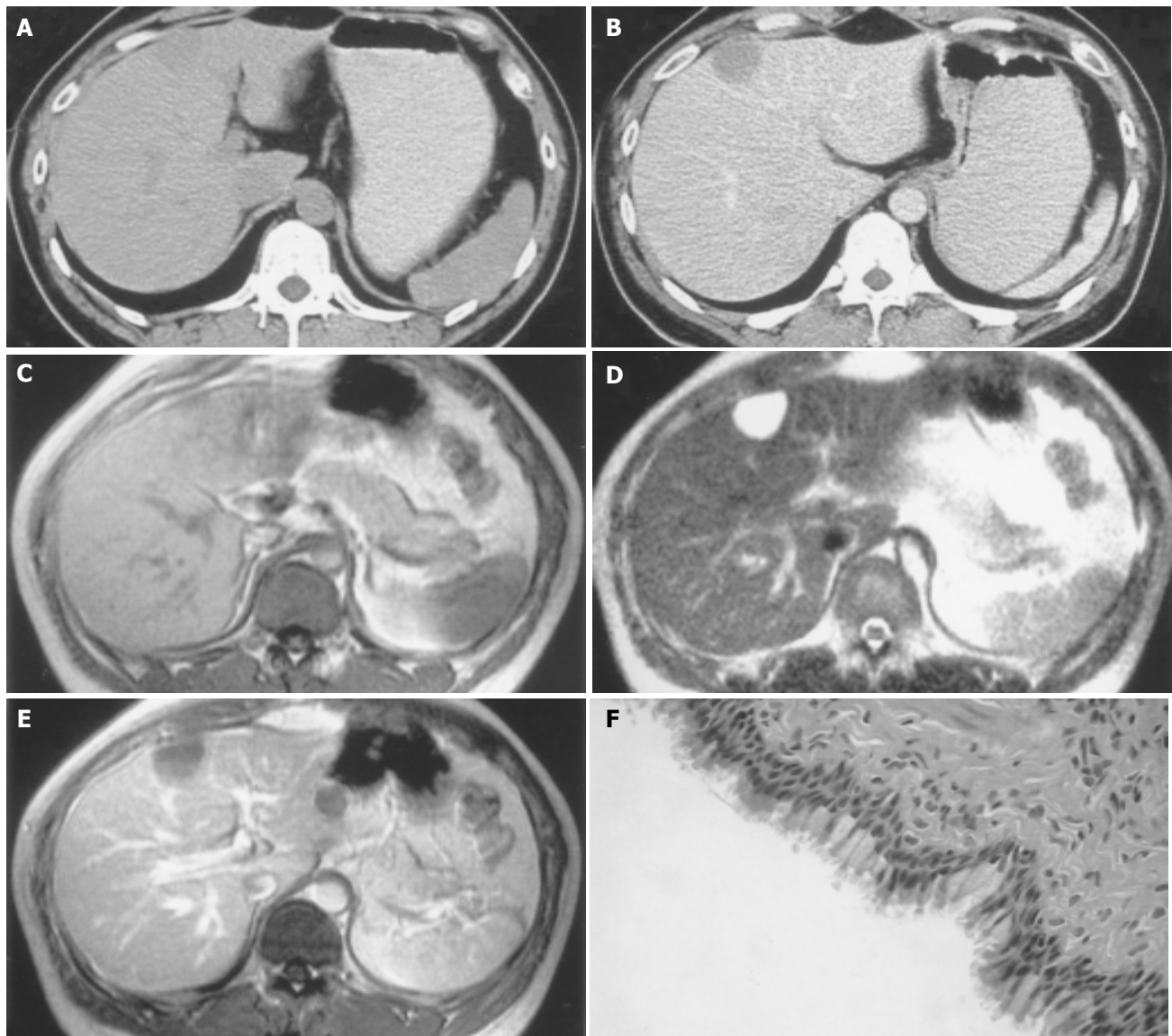


Figure 1 CHFC in a 30-year-old man. **A:** Unenhanced CT scan shows a slightly hypoattenuating (47 HU) mass in the medial segment beneath the hepatic surface; **B:** On enhanced CT scan, a well-defined hypoattenuating mass is revealed with no enhancement; **C:** On axial T1-weighted imaging, the lesion appears isointense relative to surrounding liver parenchyma; **D:** Axial

T2-weighted imaging shows markedly homogeneously hyperintense mass in the left liver; **E:** Enhanced T1-weighted imaging delineates slightly hypointense mass just beneath the hepatic surface; **F:** Photomicrograph reveals a cyst lined by ciliated pseudostratified columnar epithelial cells (HE $\times 400$).

attenuation numbers because the lesion contains calcium^[5]. All the CHFCs have no enhancement after injection of contrast materials, which is one of the characteristics of CHFC and has significance in the differential diagnosis. On MR imaging, all lesions are hyperintense on T2-weighted sequences. However, on T1-weighted images, they may be hypointense, isointense, or hyperintense according to the various elements the lesions contain, including clear serous material or milky white or brown mucous with abundant protein and lipid sometimes^[5,11,12].

When a CHFC appears hypoechoic at US and the attenuation at CT ranges from that of soft tissue to very high attenuation, it is hard to differentiate the CHFC from a solid lesion. However, MR imaging is found to be useful in differential diagnosis, especially on T2-weighted imaging. When a CHFC is demonstrated as anechoic lesion at US,

cystadenoma may be included in the differential diagnosis because the lesion may be malignant. Differential points are that cystadenomas are usually multilocular and sometimes reveal mural nodules, and these features are well revealed on radiologic imaging^[5].

CHFC occurs more frequently in men and is found most commonly in the medial segment of the left hepatic lobe just beneath the hepatic surface, unlike most other solitary cysts that show a female predominance and greater occurrence in the right hepatic lobe^[7]. Therefore, this location is also one of the characteristics of CHFC and probably an important diagnostic consideration. Meanwhile, MRI is helpful to differentiate CHFC from other solitary cysts that usually show markedly homogeneously hypointense on T1-weighted imaging.

In conclusion, when a well-demarcated subcapsular

lesion of the left hepatic lobe with the varied internal appearance as we described above is demonstrated, CHFC should be considered.

REFERENCES

- 1 **Horii T**, Ohta M, Mori T, Sakai M, Hori N, Yamaguchi K, Fujino H, Oishi T, Inada Y, Nakamura K, Okanoue T, Kashima K. Ciliated hepatic foregut cyst. A report of one case and a review of the literature. *Hepatol Res* 2003; **26**: 243-248
- 2 **Bogner B**, Hegedus G. Ciliated hepatic foregut cyst. *Pathol Oncol Res* 2002; **8**: 278-279
- 3 **Hirata M**, Ishida H, Konno K, Nishiura S. Ciliated hepatic foregut cyst: case report with an emphasis on US findings. *Abdom Imaging* 2001; **26**: 594-596
- 4 **Wu ML**, Abecassis MM, Rao MS. Ciliated hepatic foregut cyst mimicking neoplasm. *Am J Gastroenterol* 1998; **93**: 2212-2214
- 5 **Kadoya M**, Matsui O, Nakanuma Y, Yoshikawa J, Arai K, Takashima T, Amano M, Kimura M. Ciliated hepatic foregut cyst: radiologic features. *Radiology* 1990; **175**: 475-477
- 6 **Rosai J**. Liver. In: Rosai J, ed. *Ackerman's surgical pathology*. 8th ed. St Louis: *Mosby* 1996: 898-899
- 7 **Vick DJ**, Goodman ZD, Deavers MT, Cain J, Ishak KG. Ciliated hepatic foregut cyst: a study of six cases and review of the literature. *Am J Surg Pathol* 1999; **23**: 671-677
- 8 **Harty MP**, Hebra A, Ruchelli ED, Schnauffer L. Ciliated hepatic foregut cyst causing portal hypertension in an adolescent. *Am J Roentgenol* 1998; **170**: 688-690
- 9 **Furlanetto A**, Dei Tos AP. Squamous cell carcinoma arising in a ciliated hepatic foregut cyst. *Virchows Arch* 2002; **441**: 296-298
- 10 **de Lajarte-Thirouard AS**, Rioux-Leclercq N, Boudjema K, Gandon Y, Ramee MP, Turlin B. Squamous cell carcinoma arising in a hepatic foregut cyst. *Pathol Res Pract* 2002; **198**: 697-700
- 11 **Murakami T**, Imai A, Nakamura H, Tsuda K, Kanai T, Wakasa K. Ciliated foregut cyst in cirrhotic liver. *J Gastroenterol* 1996; **31**: 446-449
- 12 **Shoenut JP**, Semelka RC, Levi C, Greenberg H. Ciliated hepatic foregut cysts: US, CT, and contrast-enhanced MR imaging. *Abdom Imaging* 1994; **19**: 150-152

Science Editor Wang XL and Guo SY Language Editor Elsevier HK

• ACKNOWLEDGMENTS •

Acknowledgments to Reviewers of *World Journal of Gastroenterology*

Many reviewers have contributed their expertise and time to the peer review, a critical process to ensure the quality of *World Journal of Gastroenterology*. The editors and authors of the articles submitted to the journal are grateful to the following reviewers for evaluating the articles (including those were published and those were rejected in this issue) during the last editing period of time.

Yasuji Arase, M.D.

Department of Gastroenterology, Toranomon Hospital, 2-2-2 Toranomon minato-ku, Tokyo 105-8470, Japan

Takeshi Azuma, Associate Professor

Second Department of Internal Medicine, University of Fukui, Faculty of Medical Sciences, Matsuoka-cho, YoshIDA-gun, Fukui 910-1193, Japan

Xian-Ming Chen, M.D.

Mayo Medical School, Clinic and Foundation, 200 First Street, SW, Rochester, MN 55905, United States

Jaime Guardia, Professor

Internal Medicine and Liver Unit, Hospital Universitari 'Vall d'Hebron'. Universitat Autònoma de Barcelona, Hospital Universitari Vall d'Hebron, Pg Vall d'Hebron, 119, Barcelona 08035, Spain

Hajime Isomoto,

Basic Research Center for Digestive Diseases, Division of Gastroenterology and Hepatology, Mayo Clinic, 200 First Street, Rochester 55905, United States

Seigo Kitano, Professor

Department of Surgery I, Oita University Faculty of Medicine, 1-1 Idaigaoka Hasama-machi, Oita 879-5593, Japan

Zahariy Krastev, Professor

Department of Gastroneterology, Universiti Hospital "St. Ivan Rilski", #15, blvd "Acad. Ivan Geshov", Sofia 1431, Bulgaria

Ai-Ping Lu, Professor

China Academy of Traditional Chinese Medicine, Dongzhimen Nei, 18 Beixincang, Beijing 100700, China

Reza Malekzadeh, Professor

Director, Digestive Disease Research Center, Tehran University of Medical Sciences, Shariati Hospital, Kargar Shomali Avenue, 19119 Tehran, Iran

Timothy H Moran, Professor

Department of Psychiatry, Johns Hopkins University School of Medicine, Ross 618, 720 Rutland Ave, Baltimore, Maryland

21205, United States

Yoshiharu Motoo, Associate Professor

Cancer Research Institute, Kanazawa University, 13-1 Takaramachi, Kanazawa 920-0934, Japan

Hiroshi Nakagawa, Assistant Professor

Gastroenterology Division, University of Pennsylvania, 415 Curie Blvd. 638B CRB, Philadelphia 19104, United States

Pankaj Jay Pasricha, M.D.

Department of Internal Medicine, The University of Texas Medical Branch, 301 University Boulevard, Rt. 0764, Galveston, TX 77555-0764, United States

Michiie Sakamoto, Professor

Department of Pathology, Keio University School of Medicine, 35 Shinanomachi, Shinjuku-ku, Tokyo 160-8582, Japan

Qin Su, Professor

Department of Pathology, Cancer Hospital and Cancer Institute, Chinese Academy of Medical Sciences and Peking Medical College, PO Box 2258, Beijing 100021, China

Kiichi Tamada, M.D.

Department of Gastroenterology, Jichi Medical School, 3311-1 Yakushiji, Minamikawachi, Kawachigun, Tochigi 329-0498, Japan

Hans Ludger Tillmann, Professor

Medizinische Klinik und Poliklinik II, University Leipzig, Philipp Rosenthal Str. 27, Leipzig 04103, Germany

Karel van Erpecum, M.D.

Department of Gastroenterology and Hepatology, University Hospital Utrecht, Utrecht 3508GA, The Netherlands

Yuan Wang, Professor

Institute of Biochemistry and Cell Biology, Shanghai Institutes for Biological Sciences, Chinese Academy of Sciences, Shanghai 200031, China

Hiroyuki Watanabe, Assistant Professor

Department of Internal Medicine, Cancer Research Institute, Kanazawa University, 13-1 Takaramachi, Kanazawa University, Kanazawa 920-8641, Japan

Harry H-X Xia, M.D.

Department of Medicine, The University of Hong Kong, Pokfulam Road, Hong Kong, China

Hiroshi Yoshida, M.D.

First Department of Surgery, Nippon Medical School, 1-1-5 Sendagi, Bunkyo-ku, Tokyo 113-8603, Japan

Treatment of uncomplicated reflux disease

Joachim Labenz, Peter Malfertheiner

Joachim Labenz, Department of Medicine, Jung-Stilling Hospital Siegen, Germany

Peter Malfertheiner, Department of Gastroenterology, Hepatology and Infectious Diseases, University of Magdeburg, Germany

Correspondence to: Joachim Labenz, MD, Jung-Stilling Hospital, Wichern str. 40, D-57074 Siegen, Germany. j.labenz@t-online.de
Telephone: +49-271-333-4569 Fax: +49-271-333-4242

Received: 2004-12-24 Accepted: 2005-01-13

Abstract

Uncomplicated reflux disease comprises the non-erosive reflux disease (NERD) and erosive reflux disease (ERD). The objectives of treatment are the adequate control of symptoms with restoration of quality of life, healing of lesions and prevention of relapse. Treatment of NERD consists in the administration of proton pump inhibitors (PPI) for 2-4 wk, although patients with NERD show an overall poorer response to PPI treatment than patients with ERD owing to the fact that patients with NERD do not form a pathophysiologically homogenous group. For long-term management on-demand treatment with a PPI is probably the best option. In patients with ERD, therapy with a standard dose PPI for 4-8 wk is always recommended. Long-term treatment of ERD is applied either intermittently or as continuous maintenance treatment with an attempt to reduce the daily dosage of the PPI (step-down principle). In selected patients requiring long-term PPI treatment, antireflux surgery is an alternative option. In patients with troublesome reflux symptoms and without alarming features empirical PPI therapy is another option for initial management. Therapy should be withdrawn after initial success. In the case of relapse, the long-term care depends on a careful risk assessment and the response to PPI therapy.

© 2005 The WJG Press and Elsevier Inc. All rights reserved.

Key words: Erosive reflux disease; Non-erosive reflux disease; Proton pump inhibitor; Uninvestigated reflux disease

Labenz J, Malfertheiner P. Treatment of uncomplicated reflux disease. *World J Gastroenterol* 2005; 11(28): 4291-4299
<http://www.wjgnet.com/1007-9327/11/4291.asp>

INTRODUCTION

Gastroesophageal reflux disease (GERD) is a common condition affecting approximately 10-20% of the adult population of industrialized countries^[1]. In the great majority

of patients with GERD, the disease does not lead to complications, instead presents with often severe symptoms. Some 60% of patients in primary care with troublesome reflux symptoms have no endoscopically recognizable lesions of the esophageal mucosa, 35% have erosive esophagitis (75% of which are mild, corresponding to Los Angeles A/B, and 25% severe, corresponding to Los Angeles C/D). In about 5% of the patients, complications, such as stricture, ulcer and in particular Barrett's esophagus or even adenocarcinoma, must be expected (Figure 1)^[2]. Epidemiological data support the hypothesis that GERD is not a spectrum disease with occasional reflux symptoms but no lesions at the one end, and severe complications at the other, but can instead be classified into three distinct categories—nonerosive reflux disease (NERD)—erosive reflux disease (ERD), and Barrett's esophagus—in each of which the respective patient remains, that is, progression of the disease over time is, overall, very rare^[3]. This category model of GERD is supported by the latest data from a large prospective European study (ProGERD) involving more than 6 000 patients with NERD and ERD: the rate of progression (to severe esophagitis or Barretts') for patients with NERD and mild erosive esophagitis (Los Angeles A/B) was less than 1% per year (Labenz *et al.*, unpublished data).

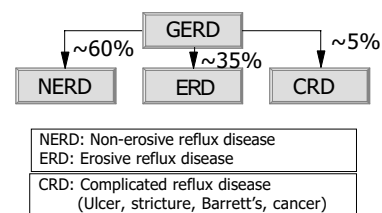


Figure 1 GERD—a categorical disease with three distinct entities^[after 2,3].

INITIAL MANAGEMENT OF GERD

Uncomplicated reflux disease comprises the non-erosive form, that is, symptoms that impact negatively on the patient's quality of life, but which are not associated with endoscopic evidence of mucosal breaks in the esophagus, and erosive reflux esophagitis of varying degrees of severity, e.g. grades A-D in the Los Angeles classification^[4].

Contrary to commonly held beliefs, symptom evaluation is the most important assessment for the initial phase of GERD management^[5], although an evidence-based analysis of symptoms is hardly possible^[6]. Characteristic symptoms are heartburn and acid regurgitation^[6]. However, these symptoms are predictive of GERD in only 70% of the patients, even in cases with an unequivocal history^[7]. It must

be emphasized that there is no diagnostic gold standard for GERD: endoscopy has a sensitivity of only 30-40%, microscopic features such as dilated intracellular spaces and regenerative changes in the absence of endoscopically visible mucosal breaks of the squamous epithelium in the distal esophagus are currently not sufficiently validated, and pH-monitoring is far from being a diagnostic gold standard, since 30-60% of patients with NERD, as well as 10-20% of those with ERD, have normal results of 24-h pH-monitoring, and intra-individual comparisons have also shown that pH-metry is subject to appreciable fluctuations^[4,8]. Moreover, there is consistent observation that there is virtually no correlation between the severity of endoscopic findings and symptom severity (Figure 2)^[9]. All these aspects have an important impact on the clinical management of GERD which is distinct in the initial phase and long-term care.

Basic goals of treatment are:

- to provide complete, or at least sufficient, control of symptoms,
- to maintain symptomatic remission,
- to heal underlying esophagitis and maintain endoscopic remission, and
- to treat or, ideally, prevent complications.

Adequate control of symptoms is considered to have been achieved when mild reflux symptoms occur at most once a week-more frequent or more pronounced complaints are not accepted as satisfactory by the patient^[10]. Initially, a symptom-based diagnosis is established, and an individual risk assessment made (Figure 3). If such alarming symptoms such as dysphagia, unintended weight loss and/or signs of bleeding are present, an endoscopic examination is mandatory, with further management dictated by the endoscopic findings. Other indications for endoscopy at this point in time may include, for example, a family history of upper gastrointestinal tract malignancies, a long prior history of severe complaints, age over 50 years, use of NSAIDs, and a positive *Helicobacter pylori* status^[11]. Otherwise, empirical therapy can be offered (Figure 3). Withholding endoscopy in the initial phase is, of course, associated with the theoretical risk that serious complications of GERD or other significant pathologies in the upper gastrointestinal tract mimicking the symptoms of reflux disease may be overlooked or recognized too late. On the other hand, given the facts that GERD is extremely common, and complications are generally rare, endoscopic evaluation of all patients with GERD is hardly justifiable, especially since an endoscopy-based management strategy has not been subjected to appropriate evaluation. In a cross-sectional study from Finland the detection rate of serious complications of GERD did not differ between regions with low and those with high referral to endoscopy^[12]. Considering that most patients have mild GERD and that the disease is not progressive over time, restricted use of endoscopy does not appear to put the patients at risk. However, the economic impact of different diagnostic strategies on expense remains to be established, at least in countries with low endoscopy costs^[13]. A recent study in 742 patients with uncomplicated GERD showed no correlation between endoscopic findings and subsequent therapeutic decisions^[14]. Further arguments

for a primarily symptom-driven strategy are that the ultimate benchmark for the clinical efficacy of treatment of GERD is patient satisfaction and that accurate determination of esophagitis requires the withholding of therapy before endoscopy, which in many cases is not possible^[15].

For the sake of simplicity, the following sections first discuss the initial and long-term treatment of patients with NERD and ERD (endoscopy-based approach), and then consider the management of uninvestigated GERD, which is doubtless the more common treatment that is applied in the clinical setting.

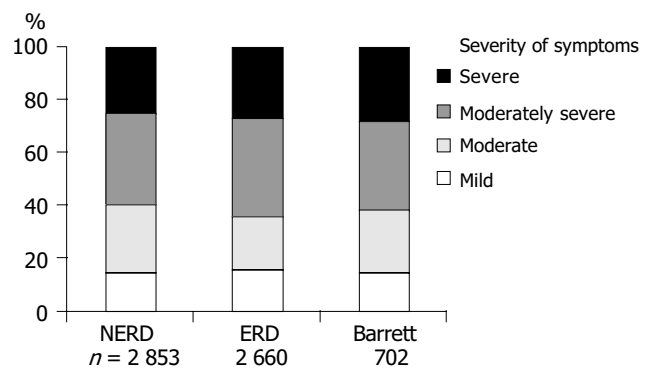


Figure 2 No correlation between endoscopic findings and symptom severity in patients with GERD^[9].

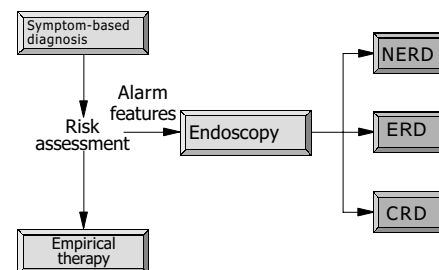


Figure 3 Initial management of patients with symptoms suggestive of GERD.

TREATMENT OF NERD

While NERD is the most common manifestation of reflux disease, patients with this entity do not form a pathophysiologically homogeneous group. A differentiation can be made between patients with unequivocally pathological acid reflux, patients with an acid-sensitive (hypersensitive) esophagus, which means that more than 50% of the symptomatic episodes were associated with acid reflux (positive symptom index), and those with symptoms that are independent of acid-reflux events (functional heartburn)^[8,16]. This latter category explains the observation that patients with NERD did not respond as well to acid suppressants as patients with erosive esophagitis do^[17,18]. Possible pathophysiological causes of functional heartburn include non-acid reflux (liquid, gas, mixed), minute changes in the esophageal acidity above a pH of 4, motility disorders such as sustained contractions of the longitudinal musculature, visceral hypersensitivity, and emotional and psychological abnormalities^[19].

Initial therapy of NERD

Initially, patients should receive a proton pump inhibitor (PPI) for 2-4 wk (Figure 4). The effect of other substances such as H₂ blockers or prokinetic drugs is hardly better than that of placebo^[20]. In a large, placebo-controlled study, a dose-response relationship was established for omeprazole: omeprazole 20 mg proved to be more effective than omeprazole 10 mg^[21]. In a further controlled study, lansoprazole 30 mg was no more effective than lansoprazole 15 mg^[22]. The S-isomer of omeprazole, esomeprazole, was investigated in two large, double-blind, multicenter studies involving patients with NERD^[23]. Esomeprazole at a dose of 20 and 40 mg per day proved more effective than placebo, but a dose-response effect could not be shown. Three further randomized, double-blind, multicenter studies involving a total of more than 2 600 patients with NERD treated for 4 wk with omeprazole 20 mg, and esomeprazole 20 or 40 mg revealed comparable success rates (resolution of symptoms in 60-70% of the patients)^[24]. Assessment of the response to treatment in studies like these are greatly influenced by the target criterion (e.g. complete elimination of symptoms, satisfactory symptom control), so that the studies can hardly be compared. From the above remarks it may be concluded that appropriately dosed PPI treatment can achieve a satisfactory initial response in some two-thirds of the patients. If initial treatment with 4 wk of PPI fails to elicit adequate symptom control (Figure 4), increasing the PPI dose (e.g. standard dose PPI twice daily) is recommended, since studies have shown that patients with acid-sensitive esophagus respond better to a high PPI dose^[25-27]. In non-responders to appropriate PPI treatment, it is recommended that esophageal pH-monitoring be performed during PPI therapy and, if symptomatic acid reflux can be excluded, to discontinue PPI therapy and initiate a trial with a low-dose tricyclic antidepressant at bedtime^[28]. Potential therapeutic options for the future might be serotonin reuptake inhibitors, kappa agonists and substances with an impact on transient sphincter relaxation such as baclofen.

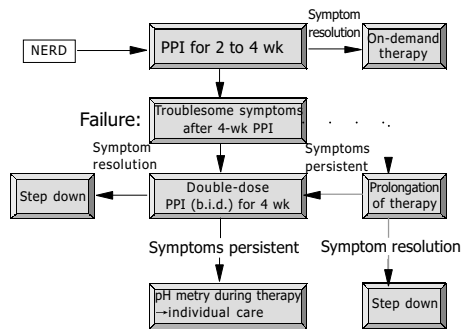


Figure 4 Initial therapy and long-term care of patients with NERD.

Long-term care of patients with NERD

If initial treatment is successful, medication should be discontinued, since 25% (or more) of the patients may remain in remission over prolonged periods of time^[29], and this clinical entity does not appear to necessitate measures aimed at preventing complications. In the event of a relapse, indicating the need for long-term management, a number

of different options are available: continuous maintenance therapy starting with a PPI and subsequent attempts to step down to lower dosages of the PPI or even less potent drugs (Figure 5)^[5], intermittent courses of treatment for 2-4 wk with initially successful PPI^[30], and patient-controlled on-demand therapy with a PPI^[11]. On-demand therapy means that the patient himself determines both the start and the end of treatment. Medication should be discontinued when the symptoms have been eliminated. This last option in particular, has met with great interest in recent years on account of its potential economic advantages^[31,32]. In a first large randomized, controlled study lasting 6 mo, Lind *et al.*, were able to show that more than 80% of the patients were satisfactorily treated with an on-demand strategy employing omeprazole 20 mg^[33]. In this study, omeprazole 20 mg proved more effective than omeprazole 10 mg. The convincing efficacy of this new treatment option was then confirmed with esomeprazole 20 mg^[34,35]. All these studies also showed that roughly one-half of these patients were satisfactorily treatable with placebo medication and the use of antacids as required. In a recently presented randomized, open international multicenter study involving 598 patients, on-demand treatment with esomeprazole 20 mg was compared with continuous treatment with esomeprazole 20 mg o.d. in patients with NERD^[36]. The vast majority of patients in both treatment groups were satisfied with the regimen, and medication consumption was considerably lower in the on-demand therapy arm (average consumption: 0.41 *vs* 0.91 tablets per day). However, the final endoscopic examination revealed mild erosive esophagitis (Los Angeles A: *n* = 14; Los Angeles B: *n* = 1) in 5% of the patients receiving on-demand treatment, while none of the patients on continuous treatment had this finding. From the viewpoint of a clinician, this observation

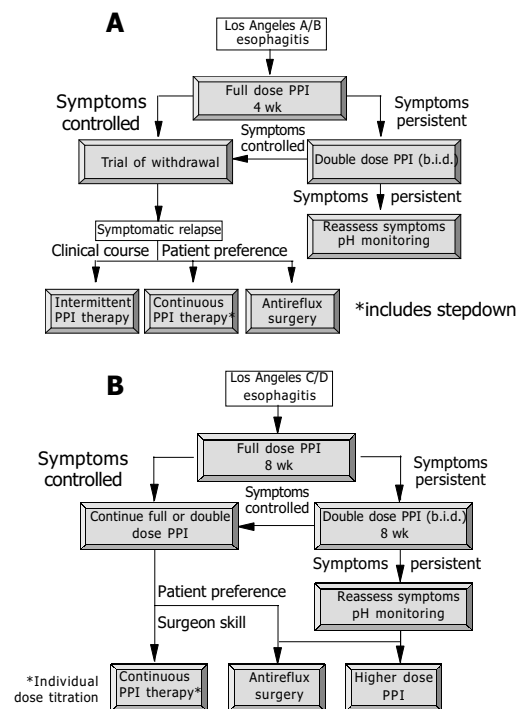


Figure 5 Management of patients with mild to moderate erosive esophagitis (A) and moderate to severe esophagitis (B)^[after 4,5].

occasions no major concern, since alternation between the categories NERD and mild ERD (corresponding to Los Angeles A and B) often occurs during the spontaneous course of the disease. In another large scale study, 622 patients with NERD were randomized to esomeprazole 20 mg on demand or lansoprazole 15 mg o.d. for 6 mo after an initial successful treatment with esomeprazole^[37]. Based on the target criterion "willingness to continue" on-demand treatment was superior to continuous treatment (93% vs 88%; $P = 0.02$). Patients on continuous treatment complained more often about heartburn and adverse events, the main reasons for "unwillingness to continue". Other PPIs (lansoprazole, pantoprazole, rabeprazole) have also proven their superiority to placebo in on-demand treatment in individual studies^[11]. Head-to-head comparisons between various PPIs are, however, lacking, so that a comparative assessment is not possible.

TREATMENT OF ERD

Erosive reflux esophagitis can be found in about 30-40% of GERD patients^[2]. Endoscopically, reflux esophagitis is categorized into various degrees of severity. In recent years, and especially in therapeutic studies, the Los Angeles classification in particular has been applied^[38,39]. This distinguishes the four degrees of severity A-D (A: mucosal breaks of less than 5 mm on the top of folds; B: mucosal breaks >5 mm in extent on mucosal folds; C: circumferential spreading of mucosal breaks involving less than 75% of the circumference; D: mucosal breaks involving more than 75% of the circumference). The gradings A and B correspond to mild to moderate esophagitis and C and D to moderate to severe esophagitis. One fourth of patients with erosive esophagitis are categorized in grade C or D^[40-42].

Numerous controlled studies have investigated the efficacy of a variety of medications in the healing of esophagitis and the elimination of symptoms. In a meta-analysis, Chiba *et al.*^[43], showed that PPIs (omeprazole, lansoprazole, pantoprazole) heal the esophagitis within 8 wk in 83.6% of the patients, with a symptom-resolution rate of 77.4%. All other medications (H_2 -receptor antagonists, cisapride, sucralfate) were appreciably less effective. A placebo-related healing rate of 28.2% documents the fluctuating nature of the course of reflux disease in some patients, with spontaneous remissions and exacerbations. When using highly potent PPIs, elimination of symptoms after 8 wk is predictive for healing of the esophagitis^[41,42].

Initial therapy of ERD

In patients with erosive reflux esophagitis, treatment with a standard dose of a PPI is always recommended (Figure 5)^[4]. Mild cases (Los Angeles grade A/B) usually heal within 4 wk, while severe cases (Los Angeles C/D) often require longer treatment-eight or, in some cases, more weeks. Resolution of symptoms in those responding to therapy is achieved appreciably more quickly (median time to sustained symptom resolution 5-10 d). The major predictive factor for the healing rate is the severity of the erosive esophagitis, but also of significance are concomitant Barrett's metaplasia in the lower esophagus, which reduces the healing rate,

and infection with *H pylori*, which enhances the efficacy of the PPI^[44,45].

Is there any clinically relevant difference between the PPIs available in the market? Racemic PPIs (omeprazole, lansoprazole, pantoprazole, rabeprazole) differ in such pharmacokinetic characteristics as bioavailability and the rapidity with which an effect occurs. This, however, is irrelevant for the healing of esophagitis at 4 and 8 wk^[46,47], although the substances do differ in terms of the time required to eliminate symptoms. In a large randomized, controlled study involving more than 3 500 patients with erosive esophagitis, lansoprazole 30 mg o.d. relieved heartburn significantly faster than did omeprazole 20 mg o.d.^[48]. There is a linear relationship between the degree of acid suppression measured by the time per day that gastric pH is higher than 4, and the healing kinetics of esophagitis^[49]. With regard to the healing rates of reflux esophagitis after 4 and 8 wk, no differences are to be seen between the standard doses of the racemic PPIs (omeprazole 20 mg, lansoprazole 30 mg, pantoprazole 40 mg, rabeprazole 20 mg)^[46,47], nor did doubling the individual dose (e.g. lansoprazole 60 mg, pantoprazole 80 mg) increase efficacy. Of significance for the healing rates and symptom elimination, however, is cytochrome 2C19 polymorphism. Thus, it has been recently shown that the response to treatment with lansoprazole 30 mg o.d. is poorer in extensive metabolizers than in intermediate and poor metabolisers^[50].

Cross-over pH-monitoring studies in healthy volunteers and patients with GERD have shown that esomeprazole is more effective than corresponding doses of the racemic PPIs omeprazole, lansoprazole, pantoprazole and rabeprazole^[51,52]. In large controlled studies, significantly higher healing rates were achieved with esomeprazole at a dose of 40 mg o.d. than with omeprazole 20 mg o.d., lansoprazole 30 mg o.d., and pantoprazole 40 mg o.d.^[40-42,53,54]. The therapeutic advantage of esomeprazole over the other PPIs increased with increasing severity of the esophagitis as defined by the Los Angeles classification^[55]. These studies also showed a significant superiority of esomeprazole in terms of the time to sustained symptom (heartburn) resolution. Small non-inferiority studies claiming equivalence between different PPIs did not have the statistical power to detect a difference of the magnitude that has been consistently established by the large scale studies mentioned above^[56-58].

In the event of inadequate efficacy (insufficient control of symptoms or healing of the esophagitis), doubling the individual dose of PPI does not reliably improve clinical efficacy, but switching to another PPI, or shortening the interval between doses (e.g. twice daily) might increase the response to treatment^[59]. In recent years there has been intense discussion on the clinical relevance of nocturnal acid breakthrough (NABT) in difficult-to-treat cases^[60,61]. NABT is defined as a decrease in gastric pH to <4 for more than 1 h during the course of the night. The clinical relevance of this phenomenon has not yet been established. H_2 -receptor antagonists given at bedtime can prevent this acid breakthrough, but when administered over a longer period of time, they rapidly lose this effect^[62]. Treatment with combinations of PPI and prokinetic drugs is of unproven value.

Long-term care of patients with ERD

After responding well to initial treatment, ERD shows a tendency to relapse. Up to 90% of the patients will relapse already within the next 6 mo^[29]. Patients with mild esophagitis (Los Angeles A/B) often have a longer relapse-free interval than patients with severe esophagitis (Los Angeles C/D), who frequently suffer a relapse within days of discontinuing successfully the initial treatment^[63,64]. In the light of these observations, it is recommended that, in patients with mild esophagitis, therapy should first be discontinued and the further course of the disease kept under surveillance, while in severe esophagitis, initial successful therapy should be followed, *a priori*, by maintenance treatment (Figure 5). Established options for long-term management are intermittent treatment for some weeks and continuous maintenance treatment with an attempt to reduce the daily dosage of the PPI (step-down principle)^[4,30]. On-demand therapy has, to date, been investigated in only two studies in patients with erosive esophagitis^[65,66]. Satisfactory control of symptoms was achieved in the vast majority of patients, but continuous therapy proved to be superior with respect to maintenance of remission of erosive esophagitis, so that an evidenced-based recommendation is currently not possible. However, since GERD is usually not progressive, attempts to realize on-demand treatment does not appear to harm the patients^[3].

For the prevention of relapse in patients with healed esophagitis, PPIs are clearly superior to H₂-receptor antagonists, prokinetic drugs and combinations of these medications^[67-69]. The yield between a standard dose of a PPI and one-half of this dose is, in individual studies, often small, although significant, and even probably clinically relevant differences have occasionally been observed^[67]. On the basis of a cost effectiveness analysis using a Markov model designed to simulate the economic and clinical outcomes of GERD in relation to the cost per symptom-free patient years gained and the cost per QALY gained treatment with a standard dose of a PPI appears to be superior despite the higher drug costs^[69]. Nevertheless, in view of the overall high response rates, an initial attempt with half the standard dose of a PPI is recommended in patients with mild erosive esophagitis, while patients with more severe disease should be kept on the dose of PPI required to induce remission (Figure 5). If this approach proves successful, a dose reduction, or a changeover to a less potent drug can be attempted^[70,71]. If the reduced dose proves unsuccessful, the dose must be increased appropriately. Occasionally, a higher-than-standard dose may be necessary to maintain remission^[72].

With long-term therapy also, differences are found between the isomeric PPI esomeprazole, and the racemic PPIs lansoprazole or pantoprazole. In large double-blind randomized studies in patients with healed esophagitis, esomeprazole 20 mg o.d. applied over 6 mo was significantly more effective than lansoprazole 15 mg o.d. (therapeutic gain 8-9%), or pantoprazole 20 mg o.d. (therapeutic gain 12%)^[73-75]. As in the case of acute treatment, this superiority was more pronounced with increasing disease severity. Apart from the severity of the baseline esophagitis, concomitant Barrett's esophagus (poorer results) and *H pylori* infections

(better results) also have a role as predictors of treatment outcome^[76].

Eradication of *Helicobacter pylori* in patients with GERD

Whether a concomitant *H pylori* infection in patients with GERD should be treated or not is still under discussion^[77,78]. Since *H pylori* is probably not involved in the pathogenesis of GERD, it cannot be expected that its eradication can heal this condition^[79] nor, according to the data of Moayyedi *et al.*, is an aggravation of the spontaneous course of GERD to be expected. *H pylori* does, however, have an impact on the pH-elevating effect of PPIs, which leads to higher healing rates and faster elimination of symptoms in patients with reflux esophagitis^[45]. PPI treatment in *H pylori*-infected patients leads to an aggravation of corpus gastritis, possibly also accompanied by an accelerated development of atrophy, while at the same time, antral gastritis is improved. The resulting gastritis type (corpus dominant) is found more frequently in patients with gastric cancer, and is therefore termed as "risk gastritis" or "gastritis of the cancer phenotype". Whether long-term PPI treatment in patients with *H pylori* gastritis actually does increase the gastric cancer risk is unclear. It does, however, appear certain that PPI treatment for over more than 10 years is also safe in patients infected with *H pylori*^[72]. Whether this also applies to treatment for over 20, 30 or more years is not known at present. On the basis of these considerations, some authors advocate the eradication of *H pylori* before initiating long-term PPI treatment^[80].

Antireflux surgery

In selected patients requiring long-term PPI treatment, a possible alternative option is antireflux surgery, which, however, is no more effective than tailored PPI therapy, and also carries a significant complication risk^[81-83]. To date, no advantages of surgery in terms of economics have been unequivocally demonstrated^[83,84]. The best candidates for fundoplication are probably those with esophagitis documented by endoscopy, a need for continuous PPI therapy, abnormal pH monitoring studies, normal esophageal motility studies, and at least partial symptom relief with PPI therapy^[85]. Further arguments for surgery are high-volume reflux and young age. Relevant concomitant diseases, in contrast, tend to militate in favor of sticking with a conservative approach. A "treatment-refractory" GERD patient should certainly not be automatically referred for antireflux surgery.

Endoscopic antireflux procedures

In recent years, a number of different methods for endoscopic endoluminal treatment of GERD have been investigated (endoscopic gastroplication with differing suturing techniques, application of radiofrequency energy to the lower esophageal sphincter, endoscopic submucosal or intramuscular injection of inert materials). To date, the efficacy of endoluminal therapy for GERD is not supported by a high level of evidence^[86]. Only a single fully published controlled study (radio-frequency energy delivery *vs* sham procedure) that documented a benefit in terms of symptom relief, but no effect on acid reflux, has been reported^[87].

Overall, too few data are currently available on efficacy and safety, so that the use of these methods outside of controlled studies cannot be recommended. In particular, controlled studies comparing endoscopic antireflux procedures with the established options of treatment would be desirable.

UNINVESTIGATED GERD

In patients with troublesome reflux symptoms but no alarm symptoms (e.g. dysphagia, unintended loss of weight, signs of bleeding), empirical PPI therapy is another option for initial management.

The goals of empirical therapy are: (1) to succeed with initial therapy; (2) to determine need for ongoing therapy; (3) to maintain satisfactory symptom control; (4) to minimize risks from esophagitis and other consequences of abnormal reflux.

These aims should be achieved at the lowest possible cost and with minimal risks^[88]. Initial therapy should via rapid relief of symptoms confirm the symptom based diagnosis, reassure the patient as to the benign and treatable nature of the reflux disease, and if present cure the esophagitis. For many years, patients with GERD received step-up therapy beginning with weakly effective substances, such as antacids and H₂-receptor antagonists, and increasing the intensity of the treatment if the effect was inadequate. With this strategy, the above-mentioned aims of empirical treatment cannot be achieved. For this reason, initiation of treatment with a PPI at a standard dose applied for 4 wk is favored (step-in approach) (Figure 6). However, few scientific data are available on this approach. In a four-arm controlled double-blind study involving 593 patients and conducted over 20 wk, the patients initially received lansoprazole 30 mg o.d. or ranitidine 150 mg b.i.d. over a period of 8 wk, followed by either continuation of this medication, or a step-down from lansoprazole to ranitidine or a step-up from ranitidine to lansoprazole^[89]. The most effective strategy was step-in with a PPI and continuation with this medication. These results were confirmed in another study comparing omeprazole with ranitidine^[90].

Therapy should be withdrawn after initial success. In the case of a relapse, the long-term care depends on a careful assessment of the risk and the response to PPI therapy. Potential strategies are on-demand therapy or intermittent treatment. In a controlled three-arm study involving 1 357 patients with uninvestigated GERD, Meineche-Schmidt *et al.*^[91], compared on-demand therapy with esomeprazole 20 mg and GP-controlled intermittent strategy with esomeprazole 40 mg o.d. for 2 or 4 wk applied over 6 mo. The direct medical costs were similar in all three arms, but the total costs were substantially higher in patients treated with a GP-controlled intermittent strategy. If continuous maintenance therapy is needed to preserve remission, or if an initial positive response is rapidly followed by relapse, an endoscopic evaluation to exclude/detect severe erosive esophagitis or complicated reflux disease is recommended. If initial treatment is not successful, and if the clinical data militate against a severe form of GERD, the PPI dose can be increased (standard dose twice daily) or a changeover to a more potent substance implemented^[59]; otherwise, in this clinical situation, too, endoscopy should

be performed^[88]. It is not clear whether patients who respond to initial treatment with a PPI and are then well controlled with on-demand therapy need to be submitted to endoscopy at all. Earlier calls for “once in a life-time” endoscopy for every patient with reflux disease are no longer considered mandatory. Moreover, the timing of endoscopy is critical: endoscopy off therapy is required to correctly assess the severity of esophagitis, which is important for the choice of further management, and endoscopy on therapy is needed to assess Barrett’s esophagus which is important with regard to cancer risk and the planning of surveillance.

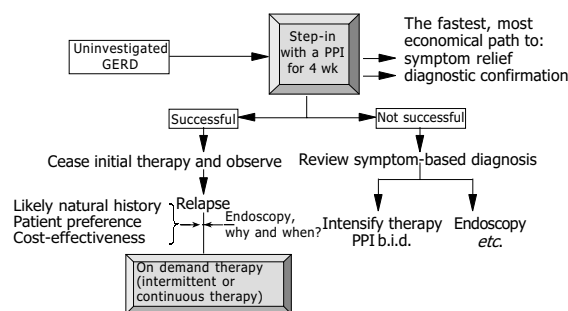


Figure 6 Proposal for the empirical management of patients with uninvestigated GERD^[88].

REFERENCES

- 1 Locke GR, Talley J, Fett SL, Zinsmeister AR, Melton LJ. Prevalence and clinical spectrum of gastroesophageal reflux: a population-based study in Olmsted County, Minnesota. *Gastroenterology* 1997; **112**: 1448-1456
- 2 Quigley EM. Non-erosive reflux disease (NERD); part of the spectrum of gastro-oesophageal reflux, a component of functional dyspepsia, or both? *Eur J Gastroenterol Hepatol* 2001; **13** (Suppl 1): S13-18
- 3 Fass R, Ofman JJ. Gastroesophageal reflux disease – should we adopt a new conceptual framework? *Am J Gastroenterol* 2002; **97**: 1901-1907
- 4 Dent J, Brun J, Fendrick AM, Fennerty MB, Janssens J, Kahrilas PJ, Lauritsen K, Reynolds JC, Shaw N, Talley NJ. An evidence-based appraisal of reflux disease management – the Genval Workshop Report. *Gut* 1999; **44**(Suppl 2): S1-S16
- 5 Dent J. Management of reflux disease. *Gut* 2002; **50**(Suppl 4): iv67-71
- 6 Dent J, Armstrong D, Delaney B, Moayyedi P, Talley NJ, Vakil N. Symptom evaluation in reflux disease: workshop background, processes, terminology, recommendations, and discussion outputs. *Gut* 2004; **53**(Suppl 4): iv1-24
- 7 Klauser AG, Schindlbeck NE, Müller-Lissner SA. Symptoms in gastro-oesophageal reflux disease. *Lancet* 1990; **335**: 205-208
- 8 Martinez SD, Malagon IB, Garewal HS, Cui H, Fass R. Non-erosive reflux disease (NERD) – acid reflux and symptom patterns. *Aliment Pharmacol Ther* 2003; **17**: 537-545
- 9 Kulig M, Nocon M, Vieth M, Leodolter A, Jaspersen D, Labenz J, Meyer-Sabellek W, Stolte M, Lind T, Malfertheiner P, Willich SN. Risk factors of gastroesophageal reflux disease: methodology and first epidemiological results of the ProGERD study. *J Clin Epidemiol* 2004; **57**: 580-589
- 10 Junghard O, Carlsson R, Lind T. Sufficient control of heartburn in endoscopy-negative gastro-oesophageal reflux disease trials. *Scand J Gastroenterol* 2003; **38**: 1197-1199
- 11 Bytzer P, Blum AL. Personal view: rationale and proposed algorithms for symptom-based proton pump inhibitor therapy

- for gastro-oesophageal reflux disease. *Aliment Pharmacol Ther* 2004; **20**: 389-398
- 12 **Mäntynen T**, Färkkilä M, Kunnamo I, Mecklin JP, Voutilainen M. The impact of upper GI endoscopy referral volume on the diagnosis of gastroesophageal reflux disease and its complications: 1-year cross sectional study in a referral area with 260 000 inhabitants. *Am J Gastroenterol* 2002; **97**: 2524-2529
 - 13 **Koop H**. Gastroesophageal reflux disease and Barrett's esophagus. *Endoscopy* 2004; **36**: 103-109
 - 14 **Blustein PK**, Beck PL, Meddings JB, Van Rosendaal GM, Bailey RJ, Lalor E, Thomson AB, Verhoef MJ, Sutheland LR. The utility of endoscopy in the management of patients with gastroesophageal reflux symptoms. *Am J Gastroenterol* 1998; **93**: 2508-2512
 - 15 **Jones MP**. Acid suppression in gastro-oesophageal reflux disease: Why? How? How much and when? *Postgrad Med J* 2002; **78**: 465-468
 - 16 **Fass R**, Tougas G. Functional heartburn: the stimulus, the pain, and the brain. *Gut* 2002; **51**: 885-892
 - 17 **Dean BB**, Gano AD Jr, Knight K, Ofman JJ, Fass R. Effectiveness of proton pump inhibitors in nonerosive reflux disease. *Clin Gastroenterol Hepatol* 2004; **2**: 656-664
 - 18 **Venables TL**, Newland RD, Patel AC, Hole J, Wilcock C, Turbitt ML. Omeprazole 10 milligrams once daily, omeprazole 20 mg once daily, or ranitidine 150 milligrams twice daily, evaluated as initial therapy for the relief of symptoms in general practice. *Scand J Gastroenterol* 1997; **32**: 965-973
 - 19 **Tack J**, Fass R. Review article: approaches to endoscopic-negative reflux disease: part of the GERD spectrum or a unique acid-related disorder? *Aliment Pharmacol Ther* 2004; **19**(Suppl 1): 28-34
 - 20 **Lauritsen K**. Management of endoscopy-negative reflux disease: progress with short-term treatment. *Aliment Pharmacol Ther* 1997; **11**(Suppl 2): 87-92
 - 21 **Lind T**, Havelund T, Carlsson R, Anker-Hansen O, Glise H, Hernqvist H, Junghard O, Lauritsen K, Lundell L, Pedersen SA, Stubberöd A. Heartburn without oesophagitis: efficacy of omeprazole therapy and features determining therapeutic response. *Scand J Gastroenterol* 1997; **32**: 974-979
 - 22 **Richter JE**, Kovacs TOG, Greski-Rose PA, Huang B, Fisher R. Lansoprazole in the treatment of heartburn in patients without erosive oesophagitis. *Aliment Pharmacol Ther* 1999; **13**: 795-804
 - 23 **Katz PO**, Castell DO, Levine D. Esomeprazole resolves chronic heartburn in patients without erosive oesophagitis. *Aliment Pharmacol Ther* 2003; **18**: 875-883
 - 24 **Armstrong D**, Talley NJ, Lauritsen K, Moum B, Lind T, Tunturi-Hihnala H, Venables T, Green J, Bigard MA, Mössner J, Junghard O. The role of acid suppression in patients with endoscopy-negative reflux disease: the effect of treatment with esomeprazole or omeprazole. *Aliment Pharmacol Ther* 2004; **20**: 413-421
 - 25 **Bate CM**, Riley SA, Chapman RW, Durnin AT, Taylor MD. Evaluation of omeprazole as a cost-effective diagnostic test for gastro-oesophageal reflux disease. *Aliment Pharmacol Ther* 1999; **13**: 59-66
 - 26 **Fass R**, Ofman JJ, Grainek IM, Johnson C, Camargo E, Sampliner RE, Fennerty MB. Clinical and economic assessment of the omeprazole test in patients with symptoms suggestive of gastroesophageal reflux disease. *Arch Intern Med* 1999; **159**: 2161-2168
 - 27 **Watson RG**, Tham TC, Johnston BT, McDougall NI. Double blind cross-over study of omeprazole in the treatment of patients with reflux symptoms and physiological levels of acid reflux - the "sensitive oesophagus". *Gut* 1997; **40**: 587-590
 - 28 **Kahrilas PJ**. Refractory heartburn. *Gastroenterology* 2003; **124**: 1941-1945
 - 29 **Carlsson R**, Dent J, Watts R, Riley S, Sheikh R, Hatlebakk J, Haug K, de Groot G, van Oudvorst A, Dalvag A, Junghard O, Wiklund I. Gastro-oesophageal reflux disease (GORD) in primary care - an international study of different treatment strategies with omeprazole. *Eur J Gastroenterol Hepatol* 1998; **10**: 119-124
 - 30 **Bardhan KD**, Müller-Lissner S, Bigard MS, Bianchi Porro G, Ponce J, Hosie J, Scott M, Wein DG, Gillon KRW, Peacock RA, Fulton C. Symptomatic gastro-oesophageal reflux disease: double-blinded controlled study of intermittent treatment with omeprazole or ranitidine. *BMJ* 1999; **318**: 502-507
 - 31 **Gerson LB**, Robbins AS, Garber A, Hornberger J, Triadafilopoulos G. A cost-effectiveness analysis of prescribing strategies in the management of gastroesophageal reflux disease. *Am J Gastroenterol* 2000; **95**: 395-407
 - 32 **Wahlqvist P**, Junghard O, Higgins A, Green J. Cost effectiveness of proton pump inhibitors in gastro-oesophageal reflux disease without oesophagitis: comparison of on-demand esomeprazole with continuous omeprazole strategies. *Pharmacoeconomics* 2002; **20**: 267-277
 - 33 **Lind T**, Havelund T, Lundell L, Glise H, Lauritsen K, Pedersen SA, Anker-Hansen O, Stubberöd A, Eriksson G, Carlsson R, Junghard O. On demand therapy with omeprazole for the long-term management of patients with heartburn without oesophagitis - a placebo-controlled randomized trial. *Aliment Pharmacol Ther* 1999; **13**: 907-914
 - 34 **Talley NJ**, Lauritsen K, Tunturi-Hihnala H, Lind T, Moum B, Bang C, Schulz T, Omland TM, Delle M, Junghard O. Esomeprazole 20 mg maintains symptom control in endoscopy-negative gastro-oesophageal reflux disease: a controlled trial of on-demand therapy for 6 mo. *Aliment Pharmacol Ther* 2001; **15**: 347-354
 - 35 **Talley NJ**, Venables TL, Green JR, Armstrong D, O'Kane KP, Gaffer M, Bardhan KD, Carlsson RG, Chen S, Hasselgren GS. Esomeprazole 40 mg and 20 mg is efficacious in the long-term management of patients with endoscopy-negative gastro-oesophageal reflux disease: a placebo-controlled trial of on-demand therapy for 6 mo. *Eur J Gastroenterol Hepatol* 2002; **14**: 857-863
 - 36 **Bayerdörffer E**, Sipponen P, Bigard M, Weiss W, Mearin F, Rodrigo L, Dominguez-Munoz J, Grundling H, Naucler E, Svedberg L, Keeling N, Eklund S. Esomeprazole 20 mg continuous versus on demand treatment of patients with endoscopy-negative reflux disease (ENRD). *Gut* 2004; **53** (Suppl 4): A106
 - 37 **Tsai HH**, Chapman R, Shepherd A, McKeith D, Anderson M, Vearey D, Duggan S, Rosen JP. Esomeprazole 20 mg on-demand is more acceptable to patients than continuous lansoprazole 15 mg in the long-term maintenance of endoscopy-negative gastro-oesophageal reflux patients: the COMMAND study. *Aliment Pharmacol Ther* 2004; **20**: 657-665
 - 38 **Armstrong D**, Bennett JR, Blum AL, Dent J, De Dombal FT, Galmiche JP, Lundell L, Margulies M, Richter JE, Spechler SJ, Tytgat GN, Wallin L. The endoscopic assessment of esophagitis: a progress report on observer agreement. *Gastroenterology* 1996; **111**: 85-92
 - 39 **Lundell LR**, Dent J, Bennett JR, Blum AL, Armstrong D, Galmiche P, Johnson F, Hongo M, Richter JE, Spechler SJ, Tytgat GN, Wallin L. Endoscopic assessment of oesophagitis: clinical and functional correlates and further validation of the Los Angeles classification. *Gut* 1999; **45**: 172-180
 - 40 **Richter JE**, Kahrilas PJ, Johanson J, Maton P, Breiter JR, Hwang C, Marino V, Hamelin B, Levine JG. Efficacy and safety of esomeprazole compared with omeprazole in GERD patients with erosive esophagitis: a randomized controlled trial. *Am J Gastroenterol* 2001; **96**: 656-665
 - 41 **Castell DO**, Kahrilas PJ, Richter JE, Vakil NB, Johnson DA, Zuckerman S, Skammer W, Levine JG. Esomeprazole (40 mg) compared with lansoprazole (30 mg) in the treatment of erosive esophagitis. *Am J Gastroenterol* 2002; **97**: 575-583
 - 42 **Labenz J**, Armstrong D, Lauritsen K, Katelaris P, Schmidt S, Schütze K, Wallner G, Juergens H, Preiksaitis H, Keeling N, Naucler E, Eklund S. A randomized comparative study of esomeprazole 40 mg versus pantoprazole 40 mg for healing erosive oesophagitis: the EXPO study. *Aliment Pharmacol Ther* 2005; **21**: 739-746
 - 43 **Chiba N**, De Gara CJ, Wilkinson JM, Hunt RH. Speed of

- healing and symptom relief in grade II to IV gastroesophageal reflux disease: a meta-analysis. *Gastroenterology* 1997; **112**: 1798-1810
- 44 **Malfertheiner P**, Lind T, Willich S, Vieth M, Jaspersen D, Labenz J, Meyer-Sabellek W, Junghard O, Stolte M. Prognostic influence of Barrett's oesophagus and of *H pylori* infection on healing of erosive GORD and symptom resolution in non-erosive GORD: Report from the ProGORD study. *Gut* 2005; **54**: 746-751
- 45 **Holtmann G**, Cain C, Malfertheiner P. Gastric *Helicobacter pylori* infection accelerates healing of reflux esophagitis during treatment with the proton pump inhibitor pantoprazole. *Gastroenterology* 1999; **117**: 11-16
- 46 **Edwards SJ**, Lind T, Lundell L. Systematic review of proton pump inhibitors for the acute treatment of reflux oesophagitis. *Aliment Pharmacol Ther* 2001; **15**: 1729-1736
- 47 **Vakil N**, Fennerty MB. Systematic review: direct comparative trials of the efficacy of proton pump inhibitors in the management of gastro-oesophageal reflux disease and peptic ulcer. *Aliment Pharmacol Ther* 2003; **18**: 559-568
- 48 **Richter JE**, Kahrilas PJ, Sontag SJ, Kovacs TO, Huang B, Pencyl JL. Comparing lansoprazole and omeprazole in onset of heartburn relief: results of a randomized, controlled trial in erosive esophagitis patients. *Am J Gastroenterol* 2001; **96**: 3089-3098
- 49 **Bell NJ**, Burget D, Howden CW, Wilkinson J, Hunt RH. Appropriate acid suppression for the management of gastroesophageal reflux disease. *Digestion* 1992; **51**(Suppl 1): 59-67
- 50 **Kawamura M**, Ohara S, Koike T, Iijima K, Suzuki J, Kayaba S, Noguchi K, Hamada S, Noguchi M, Shimosegawa T. The effects of lansoprazole on erosive reflux oesophagitis are influenced by CYP2C19 polymorphism. *Aliment Pharmacol Ther* 2003; **17**: 965-973
- 51 **Miner P Jr**, Katz PO, Chen Y, Sostek M. Gastric acid control with esomeprazole, lansoprazole, omeprazole, pantoprazole, and rabeprazole: a five-way crossover study. *Am J Gastroenterol* 2003; **98**: 2616-2620
- 52 **Röhss K**, Wilder-Smith C, Nauclér E, Jansson L. Esomeprazole 20 mg provides more effective intragastric acid control than maintenance-dose rabeprazole, lansoprazole or pantoprazole in healthy volunteers. *Clin Drug Invest* 2004; **24**: 1-7
- 53 **Kahrilas PJ**, Falk GW, Johnson DA, Schmitt C, Collins DW, Whipple J, D'Amico D, Hamelin B, Joelsson B. Esomeprazole improves healing and symptom resolution as compared with omeprazole in reflux esophagitis patients: a randomized controlled trial. *Aliment Pharmacol Ther* 2000; **14**: 1249-1258
- 54 **Fennerty MB**, Johanson J, Hwang C, Hoyle P, Sostek M. Esomeprazole 40 mg versus lansoprazole 30 mg in healing and symptom relief in patients with moderate to severe erosive esophagitis (Los Angeles C & D). *Gut* 2004; **53**(Suppl 4): A111-112
- 55 **Labenz J**, Armstrong D, Katelaris P, Schmidt S, Nauclér E, Eklund S. Analysis of healing associated with 4 weeks' esomeprazole 40 mg treatment relative to lansoprazole 30 mg and pantoprazole 40 mg in patients with all grades of erosive esophagitis. *Gut* 2004; **53**(Suppl 4): A105
- 56 **Gillessen A**, Beil W, Modlin IM, Gatz G, Hole U. 40 mg pantoprazole and 40 mg esomeprazole are equivalent in the healing of esophageal lesions and relief from gastroesophageal reflux disease-related symptoms. *J Clin Gastroenterol* 2004; **38**: 332-340
- 57 **Scholten T**, Gatz G, Hole U. Once-daily pantoprazole 40 mg and esomeprazole 40 mg have equivalent overall efficacy in relieving GERD-related symptoms. *Aliment Pharmacol Ther* 2003; **18**: 587-594
- 58 **Tinmouth JM**, Steele LS, Tomlinson G, Glazier RH. Are claims of equivalency in digestive disease trials supported by the evidence? *Gastroenterology* 2004; **126**: 1700-1710
- 59 **Fass R**, Thomas S, Traxler B, Sostek M. Patient reported outcome of heartburn improvement: doubling the proton pump inhibitor (PPI) dose in patients who failed standard dose PPI versus switching to a different PPI. *Gastroenterology* 2004; **126**: A37
- 60 **Hatlebakk JG**, Katz PO, Kuo B, Castell DO. Nocturnal gastric acidity and acid breakthrough on different regimens of omeprazole 40 mg daily. *Aliment Pharmacol Ther* 1998; **12**: 1235-1240
- 61 **Ours TM**, Fackler WK, Richter JE, Vaezi MF. Nocturnal acid breakthrough: clinical significance and correlation with esophageal acid exposure. *Am J Gastroenterol* 2003; **98**: 545-550
- 62 **Fackler WK**, Ours TM, Vaezi MF, Richter JE. Long-term effect of H2RA therapy on nocturnal gastric acid breakthrough. *Gastroenterology* 2002; **122**: 625-632
- 63 **Vakil NB**, Shaker R, Johnson DA, Kovacs T, Baerg RD, Hwang C, D'Amico D, Hamelin B. The new proton pump inhibitor esomeprazole is effective as a maintenance therapy in GERD patients with healed erosive esophagitis: a 6-mo, randomized, double-blind, placebo-controlled study of efficacy and safety. *Aliment Pharmacol Ther* 2001; **15**: 927-935
- 64 **Johnson DA**, Benjamin SB, Vakil NB, Goldstein JL, Lamet M, Whipple J, D'Amico D, Hamelin B. Esomeprazole once daily for 6 mo is effective therapy for maintaining healed erosive esophagitis and for controlling gastroesophageal reflux disease symptoms: a randomized, double-blind, placebo-controlled study of efficacy and safety. *Am J Gastroenterol* 2001; **96**: 27-34
- 65 **Johnsson F**, Moum B, Vilien M, Grove O, Simren M, Thoring M. On-demand treatment in patients with esophagitis and reflux symptoms: comparison of lansoprazole and omeprazole. *Scand J Gastroenterol* 2002; **37**: 642-647
- 66 **Sjöstedt S**, Befrits R, Sylvan A, Carling L, Harthorn C, Modin S, Stubberöd A, Toth E, Lind T. On demand versus continuous treatment with esomeprazole (ESO) 20 mg once daily in subjects with healed erosive esophagitis (EE) after initial healing with ESO 40 mg once daily. An open, randomised, Swedish multicenter study. *Gut* 2004; **53**(Suppl 4): A68
- 67 **Richter JE**, Fraga P, Mack M, Sabesin SM, Bochenek W. The Pantoprazole US GERD Study Group. Prevention of erosive esophagitis relapse with pantoprazole. *Aliment Pharmacol Ther* 2004; **20**: 1-9
- 68 **Vigneri S**, Termini R, Leandro G, Badalamenti S, Pantalena M, Savarino V, Di Mario F, Battaglia G, Sandro Mela G, Pilotto A, Blebani M, Davi G. A comparison of five maintenance therapies for reflux esophagitis. *N Engl J Med* 1995; **333**: 1106-1110
- 69 **You JH**, Lee AC, Wong SC, Chan FK. Low-dose or standard dose proton pump inhibitors for maintenance therapy of gastro-oesophageal reflux disease: a cost-effectiveness analysis. *Aliment Pharmacol Ther* 2003; **17**: 785-792
- 70 **Inadomi JM**, Jamal R, Murata GH, Hoffman RM, Lavezo LA, Vigil JM, Swanson KM, Sonnenberg A. Step-down management of gastroesophageal reflux disease. *Gastroenterology* 2001; **121**: 1095-1100
- 71 **Inadomi JM**, McIntyre L, Bernard L, Fendrick AM. Step-down from multiple- to single-dose proton pump inhibitors (PPIs): a prospective study of patients with heartburn or acid regurgitation completely relieved with PPIs. *Am J Gastroenterol* 2003; **98**: 1940-1944
- 72 **Klinkenberg-Knol EC**, Nelis F, Dent J, Snel P, Mitchell B, Prichard P, Lloyd D, Havu N, Frame MH, Roman J, Walan A. Long-term omeprazole treatment in resistant gastroesophageal reflux disease: efficacy, safety, and influence on gastric mucosa. *Gastroenterology* 2000; **118**: 661-669
- 73 **Lauritsen K**, Devière J, Bigard MA, Bayerdörffer E, Mózsik G, Murray F, Kristjánsdóttir S, Savarino V, Vetvik K, De Freitas D, Orive V, Rodrigo L, Fried M, Morris J, Schneider H, Eklund S, Larkö A. Esomeprazole 20 mg and lansoprazole 15 mg in maintaining healed reflux esophagitis: Metropole study results. *Aliment Pharmacol Ther* 2003; **17**: 333-341
- 74 **DeVault KR**, Liu S, Hoyle P, Sostek M. Esomeprazole 20 mg versus lansoprazole 15 mg for maintenance of healing of erosive esophagitis. *Am J Gastroenterol* 2004; **99**(Suppl): S6-S7
- 75 **Labenz J**, Armstrong D, Katelaris P, Schmidt S, Adler J,

- Eklund S. A comparison of esomeprazole and pantoprazole for maintenance treatment of healed erosive esophagitis. *Gut* 2004; **53**(Suppl 4): A108
- 76 **Labenz J**, Armstrong D, Katelaris P, Schmidt S, Eklund S. The effect of *Helicobacter pylori* status on maintenance therapy for healed erosive esophagitis with esomeprazole 20 mg or pantoprazole 20 mg. *Helicobacter* 2004; **9**: 544
- 77 **Labenz J**. Protagonist: Should we eradicate *Helicobacter pylori* before long term antireflux therapy? *Gut* 2001; **49**: 614-616
- 78 **Freston JW**. Antagonist: Should we eradicate *Helicobacter pylori* before long term antireflux therapy? *Gut* 2001; **49**: 616-617
- 79 **Moayyedi P**, Bardhan C, Young L, Dixon MF, Brown L, Axon AT. *Helicobacter pylori* eradication does not exacerbate reflux symptoms in gastroesophageal reflux disease. *Gastroenterology* 2001; **121**: 1120-1126
- 80 **Malfertheiner P**, Megraud F, O'Morain C, Hungin AP, Jones R, Axon A, Graham DY, Tytgat G. Current concepts in the management of *Helicobacter pylori* infection - the Maastricht 2-2000 Consensus Report. *Aliment Pharmacol Ther* 2002; **16**: 167-180
- 81 **Lundell L**, Miettinen P, Myrvold HE, Pedersen SA, Liedman B, Hatlebakk JG, Julkonen R, Levander K, Carlsson J, Lamm M, Wiklund I. Continued (5-year) follow-up of a randomized clinical study comparing antireflux surgery and omeprazole in gastroesophageal reflux disease. *J Am Coll Surg* 2001; **192**: 172-179
- 82 **Lundell L**, Miettinen P, Myrvold HE, Pedersen SA, Thor K, Lamm M, Blomqvist A, Hatlebakk JG, Janatuinen E, Levander K, Nyström P, Wiklund I. Long-term management of gastroesophageal reflux disease with omeprazole or open antireflux surgery: results of a prospective, randomized clinical trial. *Eur J Gastroenterol Hepatol* 2000; **12**: 879-887
- 83 **Arguedas MR**, Heudebert GR, Klapow JC, Centor RM, Eloubeidi MA, Wilcox CM, Spechler SJ. Re-examination of the cost-effectiveness of surgical versus medical therapy in patients with gastroesophageal reflux disease: the value of long-term data collection. *Am J Gastroenterol* 2004; **99**: 1023-1028
- 84 **Myrvold HE**, Lundell L, Miettinen P, Pedersen SA, Liedman B, Hatlebakk J, Julkonen R, Levander K, Lamm M, Mattson C, Carlsson J, Stalhammar NO. The cost of long term therapy for gastro-oesophageal reflux disease: a randomised trial comparing omeprazole and open antireflux surgery. *Gut* 2001; **49**: 488-494
- 85 **Freston JW**, Triadafilopoulos G. Review article: approaches to the long-term management of adults with GERD - proton pump inhibitor therapy, laparoscopic fundoplication or endoscopic therapy? *Aliment Pharmacol Ther* 2004; **19**(Suppl 1): 35-42
- 86 **Arts J**, Tack J, Galmiche JP. Endoscopic antireflux procedures. *Gut* 2004; **53**: 1207-1214
- 87 **Corley DA**, Katz P, Wo J, Stefan A, Patti M, Rothstein R, Edmundowicz S, Kline M, Mason R, Wolfe MM. Improvement of gastroesophageal reflux symptoms after radiofrequency energy: a randomized, sham-controlled trial. *Gastroenterology* 2003; **125**: 668-676
- 88 **Dent J**, Talley NJ. Overview: initial and long-term management of gastro-oesophageal reflux disease. *Aliment Pharmacol Ther* 2003; **17**(Suppl 1): 53-57
- 89 **Howden CW**, Henning JM, Huang B, Lukasik N, Freston JW. Management of heartburn in a large, randomized, community-based study: comparison of four therapeutic strategies. *Am J Gastroenterol* 2001; **96**: 1704-1710
- 90 **Armstrong D**, Barkun AN, Chiba N, Veldhuyzen van Zanten S, Thomson ABR, Smyth S, Chakraborty B, Sinclair P. 'Start high' - A better acid suppression strategy for heartburn-dominant uninvestigated dyspepsia (DU) in primary care practice (PCP) - the CADET-HR study. *Gastroenterology* 2002; **122**: A472
- 91 **Meineche-Schmidt V**, Hauschildt Juhl H, Ostergaard JE, Luckow A, Hvenegaard A. Costs and efficacy of three different esomeprazole treatment strategies for long-term management of gastro-oesophageal reflux symptoms in primary care. *Aliment Pharmacol Ther* 2004; **19**: 907-915

• GASTRIC CANCER •

Oral Xeloda plus bi-platinu two-way combined chemotherapy in treatment of advanced gastrointestinal malignancies

Li Fan, Wen-Chao Liu, Yan-Jun Zhang, Jun Ren, Bo-Rong Pan, Du-Hu Liu, Yan Chen, Zhao-Cai Yu

Li Fan, Wen-Chao Liu, Yan-Jun Zhang, Jun Ren, Bo-Rong Pan, Du-Hu Liu, Yan Chen, Zhao-Cai Yu, Department of Oncology, Xijing Hospital, Fourth Military Medical University, Xi'an 710032, Shaanxi Province, China

Supported by the Funds of Clinical New Technology from Xijing Hospital, Fourth Military Medical University, No. XJGXO4018M13

Correspondence to: Li Fan, Department of Oncology, Xijing Hospital, Fourth Military Medical University, Xi'an 710032, Shaanxi Province, China. fanli@medmail.com.cn
Telephone: +86-29-83375680

Received: 2004-11-20 Accepted: 2005-01-26

Abstract

AIM: To compare the effect, adverse events, cost-effectiveness and dose intensity (DI) of oral Xeloda vs calcium folinate (CF)/5-FU combination chemotherapy in patients with advanced gastrointestinal malignancies, both combined with bi-platinu two-way chemotherapy.

METHODS: A total of 131 patients were enrolled and randomly selected to receive either oral Xeloda (X group) or CF/5-FU (control group). Oral Xeloda 1 000 mg/m² was administered twice daily from d 1 to 14 in X group, while CF 200 mg/m² was taken as a 2-h intravenous infusion followed by 5-FU 600 mg/m² intravenously for 4-6 h on d 1-5 in control group. Cisplatin and oxaliplatin were administered in the same way to both the groups: cisplatin 60-80 mg/m² by hyperthermic intraperitoneal administration, and oxaliplatin 130 mg/m² intravenously for 2 h on d 1. All the drugs were recycled every 21 d, with at least two cycles. Pyridoxine 50 mg was given t.i.d. orally for prophylaxis of the hand-foot syndrome (HFS). Then the effect, adverse events, cost-effectiveness and DI of the two groups were evaluated.

RESULTS: Hundred and fourteen cases (87.0%) finished more than two chemotherapy cycles. The overall response rate of them was 52.5% (X group) and 42.4% (control group) respectively. Tumor progression time (TTP) was 7.35 mo vs 5.95 mo, and 1-year survival rate was 53.1% vs 44.5%. There was a remarkable statistical significance of TTP and 1-year survival between the two groups. The main Xeloda-related adverse events were myelosuppression, gastrointestinal toxicity, neurotoxicity and HFS, which were mild and well tolerable. Therefore, no patients withdrew from the study due to side effects before two chemotherapy cycles were finished. Both groups finished pre-arranged DI and the relative DI was nearly 1.0. The average cost for 1 patient in one cycle was ¥9 137.35 (X group) and ¥8 961.72 (control group), or US \$1 100.89

in X group and \$1 079.73 in control group. To add 1% to the response rate costs ¥161.44 vs ¥210.37 respectively (US \$19.45 vs \$25.35). One-month prolongation of TTP costs ¥1 243.18 vs ¥1 506.17 (US \$149.78 vs \$181.47). Escalation of 1% of 1-year survival costs ¥172.74 vs ¥201.64 (US \$20.75 vs \$24.29).

CONCLUSION: Oral Xeloda combined with bi-platinu two-way combination chemotherapy is efficient and tolerable for patients with advanced gastrointestinal malignancies; meanwhile the expenditure is similar to that of CF/5-FU combined with bi-platinu chemotherapy, and will be cheaper if we are concerned about the increase of the response rate, TTP or 1-year-survival rate pharmaco-economically.

© 2005 The WJG Press and Elsevier Inc. All rights reserved.

Key words: Pharmaco-economic; Xeloda; Advanced gastrointestinal malignancy; Hyperthermic intraperitoneal chemotherapy; Dose intensity

Fan L, Liu WC, Zhang YJ, Ren J, Pan BR, Liu DH, Chen Y, Yu ZC. Oral Xeloda plus bi-platinu two-way combined chemotherapy in treatment of advanced gastrointestinal malignancies. *World J Gastroenterol* 2005; 11(28): 4300-4304
<http://www.wjgnet.com/1007-9327/11/4300.asp>

INTRODUCTION

Pharmaco-economics is a method to study the various economic costs associated with prescribing a given drug or a treatment regimen. This field of health services research and technology assessment developed in the 1960s, and it is only in the last decade that scholars have been trying to develop strong standards for its use^[1]. There are four main kinds of cost analysis involved. First, the analysis of cost minimization is to find the most inexpensive treatment. Second, the cost-effectiveness analysis takes a single outcome into account, such as years of life saved, and attempts to determine the cost for each year of those additional years. The third analysis is cost utility. It is a subtype of cost-effectiveness and incorporates quality-of-life measures that focus on a patient's Quality Adjusted Life Year. The fourth is cost-benefit analysis. This analysis puts a dollar amount on additional years of life. Among the four analyses, the cost-effectiveness analysis is widely and more often used to compare the costs and clinical outcomes of competing treatment options^[2]. This analysis provides an estimate of

the costs incurred to achieve a particular outcome. It is measured by dividing a therapy's total cost by its therapeutic effectiveness, which might be cure rate, remission rate, or some other end point depending on the drug and disease involved^[3-5]. Oncology pharmacoeconomics differs slightly from pharmacoeconomics for drugs for other diseases. Pharmacoeconomics of anticancer drugs is to offer an effective, safe and economic regimen for patients with end-stage cancer under the precondition of limited medical cost.

Gastrointestinal cancer ranks the top of the morbidity and mortality of the cancer in China. The general chemotherapy usually has little effect on the end-stage patients with little opportunity to resect because of implantation in cavity, local recurrence after operation, or metastasis of lymph node or viscera. From December 2001 to April 2004, 131 end-stage cases of carcinoma of stomach and colorectum in our department were admitted for the new combination chemotherapy. Among them, 51 cases received the regimen of oral Xeloda with bi-platinu (oxaliplatin and cisplatin) in two ways (intravenous and intraperitoneal administration), the other cases received the regimen of calcium folinate (CF)/5-FU with bi-platinu in the same two ways as the former. The cost-effectiveness and quality-of-life index effect of this new chemotherapy regimen were compared with another chemotherapy. The dosage intensity of these two chemotherapy regimens were also compared.

MATERIALS AND METHODS

Patients

A total of 131 cases of advanced gastrointestinal cancer with 80 men and 51 women, mean age being 57.6 years ranging from 33 to 83 years were included. There were 61 cases of gastric carcinoma and 70 cases of colorectal cancer. All the patients were in stage IV by clinical assessment, which was confirmed by biopsy. About 83.7% of patients had received one combination chemotherapy at least, but no chemotherapy was administered to them within a month. Karnofsky performance status of all these patients measured at baseline was ≥ 60 , and the anticipative survival time was ≥ 3 mo with observable objective index of the focus. They were randomly divided into two groups, Xeloda and control group (abbreviated as X group and C group, respectively). The main clinical characteristics of the two groups are listed in Table 1.

Table 1 Clinical characteristics of stage IV gastrointestinal cancer

Clinical characteristics	Gastric cancer		Colorectal cancer	
	X group	C group	X group	C group
Male/female	21/11	17/12	19/16	23/12
Age: mean (range/yr)	63.6 (36-83)	61.0 (33-80)	62.9 (45-75)	60.8 (34-74)
Recurrence (%)	14 (43.8)	14 (48.3)	8 (22.9)	9 (25.7)
Metastasis				
Liver (%)	17 (53.1)	16 (55.2)	21 (60.0)	22 (62.9)
Lung (%)	8 (25.0)	7 (24.1)	11 (31.4)	10 (28.6)
Celiac lymph node (%)	21 (65.6)	21 (72.4)	14 (40.0)	15 (42.9)
Others (%)	8 (25.0)	9 (31.0)	12 (34.3)	10 (28.6)
Previous chemotherapy	23 (71.9)	22 (75.9)	17 (48.6)	19 (54.3)

Drugs

Xeloda® was supplied as white film-coated tablets containing 500 mg capecitabine manufactured by Roche Pharmaceutical Ltd. CF and oxaliplatin were purchased from Jiangshu Henrui Pharmaceutical Co. Ltd, packed in 100 or 50 mg per vial and 20 mg of cisplatin in a vial was supplied by Shandong Qilu Pharmaceutical Factory. 5-FU was packed in 250 mg per ampule and manufactured by Shanghai Pharmaceutical Factory.

Treatment regimen

Oral Xeloda 1 000 mg/m² was administered twice daily from d 1 to 14 in X group, while CF 200 mg/m² was taken as a 2-h intravenous infusion followed by 5-FU 600 mg/m² intravenous infusion for 4-6 h on d 1-5 in C group. Cisplatin and oxaliplatin were given in the same way to both the groups: cisplatin 60-80 mg/m² hyperthermic intraperitoneal administration, and oxaliplatin 130 mg/m² intravenous infusion for 2 h on d 1. All the drugs were recycled every 21 d, with at least two cycles. Granisetron 40 µg/kg was given by intravenous before intravenous or intraperitoneal chemotherapy. Pyridoxine (vitamin B6) 50 mg was given t.i.d. orally for prophylaxis of the hand-foot syndrome (HFS).

Effectiveness and side effects

The short-term effect is classified into four grades as complete remission (CR), part remission (PR), no-change (NC) and progress of disease (PD) by the evaluation standard of short-term effect introduced by WHO^[6]. The responsible effective rate (RR) is prescribed to CR+PR (%). There are two other indexes, TTP (time of tumor progress) and 1-year survival rate, which have been adopted to evaluate the mid-term effect. Side effects were added up by standard grade, also introduced by WHO^[7] in both the groups regardless of the kind of disease. The classification HFS was graded according to the criteria of WHO^[8]: I-dysesthesia/paresthesia, tingling in the hands and feet; II- discomfort in holding objects and upon walking, painless swelling or erythema; III-painful erythema and swelling of palms and soles, periungual erythema and swelling; IV- desquamation, ulceration, blistering, severe pain.

Dose intensity estimation

Two indexes of dose intensity (DI) were calculated by the following formula: DI = total dosage (mg/m²)/duration of treatment (weeks), relative DI = actual DI/standard DI^[9].

Costs estimation

The costs evaluated consisted of two parts, the direct medical cost and the indirect one^[5]. The cost of drugs (chemical drug, GM-CSF or G-CSF, the drug to ameliorate gastrointestinal side effect, and so on), hospital stays, the required medical staff, laboratory and diagnostic tests were included in the direct medical cost. The part indirect cost contained the material loss because of the absence of the patients and their relatives from work. Two periods of treatment were added up, then the average cost per patient in one cycle was obtained. The cost of therapy was expressed in Chinese currency (Ren-Min-Bi, ¥) and in US dollars

Table 2 Different chemotherapeutic effect of gastrointestinal cancers

Therapeutic effect	Gastric cancer		Colorectal cancer		Total	
	X group	C group	X group	C group	X group	C group
<i>n</i>	24	25	31	34	55	59
CR (<i>n</i>)	1	1	1	0	2	1
PR (<i>n</i>)	13	10	14	14	27	24
NC (<i>n</i>)	5	10	12	14	17	24
PD (<i>n</i>)	5	4	4	6	9	10
CR+PR (<i>n</i>)	14	11	17	14	29	25
(%)	58.3	44.0	54.8	41.2	52.7	42.4
TTP (mo)	7.0±1.3 ^a	5.4±0.9	7.8±1.9 ^a	6.7±2.0	7.4±1.7 ^a	6.0±1.5
1-yr survival (%)	41.7 ^a	36.0	64.5 ^a	52.9	53.1 ^a	44.5

^a*P*<0.05 vs C group.

Table 3 Chemotherapeutic side effects of gastrointestinal cancers (*n*)

Side effects	X group (<i>n</i> = 55)				C group (<i>n</i> = 59)			
	I	II	III	IV	I	II	III	IV
Leukopenia	21	8	5	0	20	8	4	0
Thrombocytopenia	10	5	1	0	13	4	2	0
Nausea	15	19	10	2	16	20	11	2
Vomiting	11	11	4	1	14	12	3	2
Diarrhea	7	9	3	0	5	6	2	0
HFS	32	2	1	0	8	2	0	0
Neurotoxicity	12	11	0	0	14	12	1	0

(US \$). The rate of exchange between them was 1:8.3.

Cost-effectiveness analysis

Based on the total costs, the expenses that add to 1% of the response rate (costs/total efficient rate), one-month prolongation of TTP (costs/TTP) and the escalation of 1% of 1 year (costs/1-year survival rate) were calculated, respectively.

Statistical analysis

All data are expressed as mean±SD, except as otherwise stated. Parameters were compared by using *t* test, or χ^2 test.

RESULTS

Effect

In 131 cases, 17 patients (13.0%) terminated treatment after one cycle because of disease progression, refusal to continue chemotherapy or other reasons. Fifty-eight cases (44.3%) finished two or three cycles of chemotherapy, 33 patients (25.2%) finished four or five cycles of chemotherapy, the other 23 cases (17.6%) finished six or more cycles of chemotherapy. The average number of completed chemotherapy cycles was 2.6. These 114 who finished more than two chemotherapy cycles were analyzed. For both the short-term and mid-term effect, the X group was better than C group. But there was no statistical difference in the short-term effect. Short-term effect of gastric cancer group was superior to that of colorectal cancer group, whereas mid-term effect of the former was inferior to that of the latter (Table 2).

Side effects

To 114 patients who finished more than two chemotherapy cycles, the side effects were observed and summed up when

the second cycle ended (Table 3). In X group, the rates of leukopenia, thrombocytopenia, nausea, vomiting, diarrhea and neurotoxicity above grade II were 23.6%, 10.9%, 56.4%, 29.1%, 21.8%, and 20.0%, respectively. In C group, the rates were 20.3%, 10.2%, 55.9%, 28.8%, 13.6%, and 22.0%, respectively. No statistical difference was revealed between the two groups.

The occurrence of HFS that appeared in X group was higher than that of C group (63.6% vs 16.9%, *P*<0.05), but 97.1% of HFS episodes were grade 1 or 2. No patient withdrew from the study, and none required dose modification due to side effects before two chemotherapy cycles were finished.

Dose intensity

Relative DI mg/(m²×week) cannot be achieved due to the delay in the treatment (including side effect and noncompliance), which means that the actual DI is lower than standard DI. There was no statistical difference in relative DI between the two groups (Table 4).

Table 4 Chemotherapeutic DI of gastrointestinal cancers, mg/(m²-wk)

DI	X group			C group			
	Oxal ¹	DDP ¹	Xeloda	Oxal ¹	DDP ¹	CF	5-FU
Standard	43.3	40.0	9 333.3	43.3	40.0	333.3	1 000.0
Actual	40.7	38.3	8 662.7	41.3	38.7	322.7	966.7
Relative	0.94	0.96	0.93	0.95	0.97	0.97	0.97

¹Oxal - oxaliplatin; DDP - cisplatin.

Costs and cost-effectiveness

There was a statistical difference in the average hospitalization

Table 5 The average cost per patient of two groups (mean±SD, ¥, US \$)

Group	Hospitalization(d)	Cost of drug		Other cost		Total cost	
		¥	US \$	¥	US \$	¥	US \$
X	5.94±3.11 ^a	7 887.33±140.92 ^a	950.28±16.98 ^a	1 250.02±101.43 ^a	150.60±12.22 ^a	9 137.35±121.18	1 100.89±14.60
C	9.37±2.73	6 108.97±205.44	736.02±24.75	2 852.75±217.73	343.70±26.23	8 961.72±211.59	1 079.73±25.50

^a*P*<0.05 vs C group.**Table 6** Comparison of cost-effectiveness of two groups

Group	Costs/efficient		Costs/TTP		Costs/1-year survival	
	¥	US \$	¥	US \$	¥	US \$
X	161.44±2.14 ^a	19.45±0.26 ^a	1 243.18±16.49 ^a	149.78±1.99 ^a	172.24±2.28 ^a	20.75±0.27 ^a
C	210.37±4.97	25.35±0.60	1 506.17±35.56	181.47±4.28	201.61±4.76	24.29±0.57

^a*P*<0.05 vs C group.

time between the two groups (*P*<0.05, Table 5). The drug costs of X group was higher than that of C group, but other costs (the costs of hospitalization, cancer clinic care and others) were adverse, so there was no difference in the total costs between the two groups. The cost-effectiveness ratio obtained from X group was more satisfactory than that of C group no matter what the cost of percentage response rate, per TTP and per life-year survival (Table 6).

DISCUSSION

The morbidity caused by gastric and colorectal carcinoma are respectively the first and the fourth in China^[10,11]. It is difficult to cure the patients at the end stage without a chance for operation or with recurrence and metastasis. 5-FU is a basic drug for gastrointestinal cancer, but its effective rate is only 10-20%. Increasing the dosage, intravenous injection continually or in combination with intensifier can enhance the effect of 5-FU, whereas its side effects and medical costs will increase too. For example, increasing the dosage can result in higher incidence of stomatitis and extremity syndrome, and intravenous injection continually or in combination with intensifier leads to more severe phlebitis, and all of which raise the cost. The regimen of 5-FU combined with CF and levamisole has stood the dominant status in treating tumor of the digestive system for more than 20 years^[12,13]. Recently, oxaliplatin combined with 5-FU and CF has become the most frequent and effective chemical therapy for patients with colorectal cancer, and also has been used to treat gastric cancer^[14-17].

Xeloda (capecitabine) is a novel, oral, selectively tumor-activated fluoropyrimidine carbamate and absorbed by small intestine in antetype term. It can be activated and transformed to 5-FU by thymidine phosphorylase that has high competence in tumor. So the concentration of 5-FU in tumor tissue is much higher than that in normal tissue and its systemic side effect is lower^[18-21]. Xeloda has already been used to treat advanced gastrointestinal cancer with much better result. If combined with oxaliplatin, there will be good results.

The heat-chemical therapy of abdominal cavity includes heat and chemical drug treatments. This therapy has many advantages. It can increase the concentration, the contact surface and the time of the drug in abdominal cavity by

perfusing heat drug into abdominal cavity, which is in favor of prolonging action time and killing of cancer cell. A part of the drug can be absorbed by the peritoneum and come into the liver *via* portal vein, which can prevent and eliminate metastatic focus in liver. Its heat effect (40-45 °C) can reduce the pH value in and around the tumor, which will result not only in metabolic disturbance of the tumor, but also the amelioration of the function of the cellular immunity. Furthermore, the heat can kill the tumor cell directly by cytotoxic effect^[22-24]. Considering those advantages, the oral Xeloda combined with bi-platinu two-way heat-chemical therapeutic regimen was adopted to treat 55 patients with advanced gastrointestinal cancer and this regimen was compared with another regimen, 5-FU/CF combined with bi-platinu two-way heat-chemical therapeutic regimen simultaneously. Our results revealed that the effect, 1 year survival and TTP of the former were much better than the latter, and that there was little difference in primary side effect, such as the reaction of the alimentary system and nervous system, bone marrow depression and extremity syndrome between the two groups.

There is a relationship between the dose and effect for cancer chemotherapy. Following the increasing dosage, the effect will be improved, but the side effect and expenses will be increased. So a balance between effect, side effect and expense is needed. Pharmacoeconomics and the study of DI are the new hot points in cancer chemotherapy. To choose the optimal regimen and distribute the limited medical cost, the cost-effectiveness and quality-of-life index effect of oral Xeloda were investigated and compared with CF/5-FU combination chemotherapy in patients with advanced gastrointestinal malignancies, both combined with bi-platinu two-way chemotherapy. Generally, the expenses of the treatment include the direct medical and non-medical fees and indirect medical fee. The average cost for a patient in one cycle was ¥9 137.35 in X group. This cost was a little higher than that in control group (¥8961.72). But the cost-effectiveness analysis is more important, because the elongation of survival time and increasing the survival rate should be emphasized in addition to the effective rate^[25]. The costs of Xeloda group and the cost of unit effect were fewer than C group. Because Xeloda was administered in

lower dosage (1 000 mg/m² twice daily) in our study, not 1 250 mg/m² twice daily as recommended, the incidence of grade 3 or 4 of HFS was reduced. Pyridoxine being given at a high dose from the beginning may be useful for the prophylaxis of the occurrence of HFS^[7,26]. For other minor side effects of the two regimens, all patients having accomplished the treatment on time, would mean the relative DI of two groups is close to one. However, the shorter intermission of Xeloda group (about 7 d) leads to the stronger of the actual DI [8 662.7 mg/(m²·wk)] which probably is another reason for the better effect of Xeloda group than control group. The DI is an index to evaluate the drug or regimen. The analysis of relation between DI and effect will help to improve the effect of the chemical therapy by increasing the dosage of unit time or decreasing intermission of chemical therapy^[27-29].

In summary, oral capecitabine can mimic continuous infusion of 5-FU and avoid the inconvenience, complications, and additional costs associated with intravenous chemotherapy. The regimen of oral Xeloda with bi-platinum in two ways (intravenous and intraperitoneal administration) to treat the advanced gastrointestinal cancer has better short-term and long-term effect. It is an effective, safe and economic regimen for patients, even for the old. For ideal pharmacoeconomics, satisfying DI and good compliance, this regimen has a good prospect in the future.

ACKNOWLEDGMENTS

The authors thank Xiao-Yan Zhang, Ai-Le Zhang and other medical representatives of Xi'an Branch Office of Shanghai Roche Pharmaceuticals Ltd, for their valuable discussion and comments.

REFERENCES

- 1 **Amber D.** Pharmacoeconomic analyses make way into oncology. *J Natl Cancer Inst* 2000; **92**: 1204-1205
- 2 **Walt JG, Lee JT.** A cost-effectiveness comparison of bimatoprost versus latanoprost in patients with glaucoma or ocular hypertension. *Surv Ophthalmol* 2004; **49**(Suppl 1): S36-44
- 3 **Collazo Herrera M, Cardenas Rodriguez J, Gonzalez Lopez R, Miyar Abreu R, Galvez Gonzalez AM, Cosme Casulo J.** Health economics: should it concern the health sector? *Rev Panam Salud Publica* 2002; **12**: 359-365
- 4 **Cohen BJ.** Discounting in cost-utility analysis of healthcare interventions: reassessing current practice. *Pharmacoeconomics* 2003; **21**: 75-87
- 5 **Clegg A, Scott DA, Sidhu M, Hewitson P, Waugh N.** A rapid and systematic review of the clinical effectiveness and cost-effectiveness of paclitaxel, docetaxel, gemcitabine and vinorelbine in non-small-cell lung cancer. *Health Technol Assess* 2001; **5**: 1-195
- 6 **Omori H, Nio Y, Yano S, Itakura M, Koike M, Toga T, Matsuura S.** A fractal dimension analysis: a new method for evaluating the response of anticancer therapy. *Anticancer Res* 2002; **22**: 2347-2354
- 7 **Cassidy J, Twelves C, Van Cutsem E, Hoff P, Bajetta E, Boyer M, Bugat R, Burger U, Garin A, Graeven U, McKendrick J, Maroun J, Marshall J, Osterwalder B, Perez-Manga G, Rosso R, Rougier P, Schilsky RL.** First-line oral capecitabine therapy in metastatic colorectal cancer: a favorable safety profile compared with intravenous 5-fluorouracil/leucovorin. *Ann Oncol* 2002; **13**: 566-575
- 8 **Abushullaih S, Saad ED, Munsell M, Hoff PM.** Incidence and severity of hand-foot syndrome in colorectal cancer patients treated with capecitabine: a single-institution experience. *Cancer Invest* 2002; **20**: 3-10
- 9 **Feng FY, Zhou AP.** Dose intensity and high dose chemotherapy used in breast neoplasm cancer. *Chin J Oncol* 2002; **24**: 200-202
- 10 **Jin ML.** Gastric cancer. In: Sun Yan: *Medical Oncology*. 1sted. *Peopl's health Press, Beijing* 2001: 549-572
- 11 **Shao YF, Zhou ZX, Liu SM, Wang LH, Qian TN, Xu BH.** Colorectal cancer. In: Sun Yan: *Medical oncology*. 1sted. *Peopl's health Press, Beijing* 2001: 593-629
- 12 **Christopoulou A.** Chemotherapy in metastatic colorectal cancer. *Tech Coloproctol* 2004; **8**(Suppl 1): S43-46
- 13 **Sobrero A, Caprioni F, Fornarini G, Mammoliti S, Comandini D, Baldo S, Decian F.** Pemetrexed in gastric cancer. *Oncology* 2004; **18**(13 Suppl 8): 51-55
- 14 **Macdonald JS.** Clinical overview: adjuvant therapy of gastrointestinal cancer. *Cancer Chemother Pharmacol* 2004; **54**(Suppl 1): S4-11
- 15 **Gowda A, Goel R, Berdzik J, Leichman CG, Javle M.** Hypersensitivity Reactions to oxaliplatin: incidence and management. *Oncology* 2004; **18**: 1671-16755
- 16 **Grothey A, Goldberg RM.** A review of oxaliplatin and its clinical use in colorectal cancer. *Expert Opinion Pharmacother* 2004; **5**: 2159-2170
- 17 **Rustum YM.** Thymidylate synthase: a critical target in cancer therapy? *Front Biosci* 2004; **9**: 2467-2473
- 18 **Diaz-Rubio E.** New chemotherapeutic advances in pancreatic, colorectal, and gastric cancers. *Oncologist* 2004; **9**: 282-294
- 19 **Hong YS, Song SY, Lee SI, Chung HC, Choi SH, Noh SH, Park JN, Han JY, Kang JH, Lee KS, Cho JY.** A phase II trial of capecitabine in previously untreated patients with advanced and/or metastatic gastric cancer. *Ann Oncol* 2004; **15**: 1344-1347
- 20 **Diaz-Rubio E, Evans TR, Tabemero J, Cassidy J, Sastre J, Eatock M, Bisset D, Regueiro P, Baselga J.** Capecitabine (Xeloda) in combination with oxaliplatin: a phase I, dose-escalation study in patients with advanced or metastatic solid tumors. *Ann Oncol* 2002; **13**: 558-565
- 21 **Scheithauer W, Kornek GV, Raderer M, Schull B, Schmid K, Kovats E, Schneeweiss B, Lang F, Lenauer A, Depisch D.** Randomized multicenter phase II trial of two different schedules of capecitabine plus oxaliplatin as first-line treatment in advanced colorectal cancer. *J Clin Oncol* 2003; **21**: 1307-1312
- 22 **Takahashi I, Emi Y, Hasuda S, Kakeji Y, Maehara Y, Sugimachi K.** Clinical application of hyperthermia combined with anticancer drugs for the treatment of solid tumors. *Surgery* 2002; **131**(1 Suppl): S78-84
- 23 **Rossi CR, Mocellin S, Pilati P, Foletto M, Quintieri L, Palatini P, Lise M.** Pharmacokinetics of intraperitoneal cisplatin and doxorubicin. *Surg Oncol Clin N Am* 2003; **12**: 781-794
- 24 **Rossi CR, Foletto M, Mocellin S, Pilati P, De SM, Deraco M, Cavaliere F, Palatini P, Guasti F, Scalera R, Lise M.** Hyperthermic intraoperative intraperitoneal chemotherapy with cisplatin and doxorubicin in patients who undergo cytoreductive surgery for peritoneal carcinomatosis and sarcomatosis: phase I study. *Cancer* 2002; **94**: 492-499
- 25 **Wisloff F, Gulbrandsen N, Nord E.** Therapeutic options in the treatment of multiple myeloma: pharmacoeconomic and quality-of-life considerations. *Pharmacoeconomics* 1999; **16**: 329-341
- 26 **Lassere Y, Hoff P.** Management of hand-foot syndrome in patients treated with capecitabine (Xeloda). *Eur J Oncol Nurs* 2004; **8**(Suppl 1): S31-40
- 27 **Piccatt MJ, Biganzoli L, Di Leo A.** The impact of chemotherapy dose density and dose intensity on breast cancer outcome: what have we learned? *Eur J Cancer* 2000; **36**(Suppl): S4-10
- 28 **Duthoy W, De Gerssem W, Vergote K, Boterberg T, Derie C, Smeets P, De Wagter C, De Neve W.** Clinical implementation of intensity-modulated arc therapy (IMAT) for rectal cancer. *Int J Radiat Oncol Biol Phys* 2004; **60**: 794-806
- 29 **Sanz Rubiales A, del Valle Rivero ML, Garavis Vicente M, Rey Castro P, Lopez-Lara Martin F.** Dose intensity of chemotherapy in small-cell lung carcinoma. Review of comparative studies. *An Med Interna* 2000; **17**: 378-385

Effect of superoxide dismutase and malondialdehyde metabolic changes on carcinogenesis of gastric carcinoma

Shao-Hong Wang, Yi-Zhong Wang, Ke-Yi Zhang, Jin-Hui Shen, Hou-Qiang Zhou, Xiao-Yang Qiu

Shao-Hong Wang, Jin-Hui Shen, Hou-Qiang Zhou, Xiao-Yang Qiu, Department of Pathology, Central Hospital of Shantou City, Shantou 515031, Guangdong Province, China
Yi-Zhong Wang, Department of Laboratory, Central Hospital of Shantou City, Shantou 515031, Guangdong Province, China
Ke-Yi Zhang, Department of Surgical Oncology, Central Hospital of Shantou City, Shantou 515031, Guangdong Province, China
Supported by the Youth Science Fund of Guangdong Province Medicine and Hygiene, No. B19960095
Correspondence to: Dr. Shao-Hong Wang, Department of Pathology, Central Hospital of Shantou City, Shantou 515031, Guangdong Province, China. wsh196303@tom.com
Telephone: +86-754-8550450
Received: 2004-07-05 Accepted: 2005-03-10

Abstract

AIM: To investigate the relationship between the superoxide dismutase (SOD), malondialdehyde (MDA) metabolic changes and the gastric carcinogenesis.

METHODS: The SOD activity and MDA content were measured in the gastric tissues from the focus center, peripheral and far-end areas of gastric carcinoma ($n = 52$) and gastric ulcer ($n = 10$). All the tissues were subjected to routine histological examinations and classifications.

RESULTS: The SOD activity was greatly reduced but the MDA content was markedly increased in the center areas of the non-mucous gastric carcinoma (non-MGC); and the poorly differentiated gastric carcinoma varied. The SOD activity was gradually decreased and the MDA content was gradually increased in the tissues from the focus far-end, peripheral to center areas of non-MGC. Both of the SOD activity and the MDA content were significantly declined and were respectively at same low level in the tissues from the focus center, peripheral, and far-end area with the mucous gastric carcinoma (MGC). In contrast to the gastric ulcer and grade I or II of non-MGC, the same level of the SOD activity and the MDA content were found in the focus center areas. Between non-MGC (groups A-D) and gastric ulcer (group F), the differences of SOD activity and MDA content were very noticeable in the gastric tissues from the focus peripheral and far-end areas, in which the SOD activity showed noticeable increase and the MDA content showed noticeable decrease in the gastric ulcer.

CONCLUSION: The active free radical reaction in the gastric tissues can induce the carcinogenesis of non-MGC. The utmost low ability of antioxidation in the gastric tissues can induce the carcinogenesis of MGC. The metabolic

change of the free radicals centralized mostly in the center of ulcerated lesions only, which suggested the ability of antioxidation was declined only in these lesions. However, the metabolism of free radicals varied significantly and the ability of antioxidation declined not only in the local focus area but also in the abroad gastric tissues with gastric carcinoma.

© 2005 The WJG Press and Elsevier Inc. All rights reserved.

Key words: Gastric carcinoma; Free radical; Superoxide dismutase

Wang SH, Wang YZ, Zhang KY, Shen JH, Zhou HQ, Qiu XY. Effect of superoxide dismutase and malondialdehyde metabolic changes on carcinogenesis of gastric carcinoma. *World J Gastroenterol* 2005; 11(28):4305-4310
<http://www.wjgnet.com/1007-9327/11/4305.asp>

INTRODUCTION

Free radical is the middle product during the phase of the biochemical metabolism in the body^[1], and it is the intense toxicant because of being very active in the biochemical nature and oxidizing ability^[2-5]. Although recent work has shown that free radical is related to the causing and development of many digestive system diseases^[6-8], it did not distinct the relationship between the free radical and the gastric carcinogenesis^[9,10]. In the investigation, it was researched that metabolic changes of the free radical play a role in the gastric carcinogenesis, development of gastric carcinoma by investigating the metabolism condition and regularity of the free radicals in the fresh samples of the gastric carcinoma tissues.

MATERIALS AND METHODS

Patients and tissues

From 1998 to 2002, 52 cases of gastric carcinoma and 10 cases of gastric ulcer were obtained from the Central Hospital of Shantou City. All fresh stomach samples were surgically removed from these patients and regular routine histological examination and classification were made. The patients with gastric carcinoma were 11 women and 41 men. The mean age was 59.83 years, ranging from 34 to 76 years. The patients with gastric ulcer were 1 woman and 9 men and the mean age was 53.30 years, ranging from 19 to 69 years.

Measurement of SOD activity and MDA content

Stomach samples were obtained, the tissues at the center,

peripheral (2 cm away from focus lesion) and far-end areas (8-10 cm away from focus lesion) sampled respectively. The fresh tissues were made into 10% tissue homogenate for measurement of the superoxide dismutase (SOD) activity and malondialdehyde (MDA) content. The SOD activity was examined with xanthine oxidase method and the MDA content was examined with sulfur barbituric acid method^[11]. SOD and MDA detection kits were purchased from Nanjing Jiancheng Bioengineering Institute.

Statistical analysis

All data were disposed by SPSS9.0 statistical software. Statistical comparisons between interior groups were analyzed with ANOVA followed by Student's *t*-test. Statistical comparisons between different groups were analyzed with one-way ANOVA followed by *q*-test. Experimental results were finally expressed as mean±SD. *P* value less than 0.05 was considered statistically significant.

RESULTS

Histological examination

Fifty-two patients with gastric carcinoma were confirmed by histological examination. Among the 52 cases, 44 were non-mucous gastric carcinoma (non-MGC) including papillary, tubular, poorly differentiated, undifferentiated carcinoma, and were graded into four groups: grade I, 12 cases (group A, Figure 1A); grade II, 15 cases (group B, Figure 1B); grade III, 11 cases (group C, Figure 1C); grade IV, 6 cases (group D, Figure 1D). Eight cases were mucous gastric carcinoma (MGC) including mucinous adenocarcinoma and signet-ring cell carcinoma (group E, Figure 1E). Another 10 patients who were confirmed had gastric ulcer (group F, Figure 1F).

Detection of SOD activity (Table 1 and Figure 2)

The SOD activity was declined gradually in the tissues from the focus far-end, peripheral, to center areas in non-MGC (groups A-D). The SOD activity in the focus center areas was the lowest in the measured gastric tissue. SOD activity reduction was correlated with the grade and differentiation of gastric carcinoma in the focus center areas, in which the level of the SOD activity in groups A and B (grades I and II) was higher than that in groups C and D (grades III and IV). There was no significant difference of the SOD activity in the tissues from the focus far-end areas between groups A-D.

The level of SOD activity was extremely low in the focus center areas in MGC (group E). The level of SOD activity was noticeably low in the focus peripheral and far-end areas. Although reduction tendency was minimized, there were no significant differences of the SOD activity in the tissues from the focus far-end, peripheral to center areas; suggesting that the SOD activity in these areas was at the same low level.

The level of SOD activity was low in the focus center area with gastric ulcer (group F). Notable reduction tendency about SOD activity was shown in the tissues from the focus far-end, peripheral to center areas. The common metabolic characteristics were found in gastric ulcer (group F) and non-MGC (groups A-D). The SOD activity was gradually declined from the focus far-end, peripheral to center areas. The SOD activity was at the same level in the tissues from the focus center areas between gastric ulcer (group F) and non-MGC (grades I and II, groups A and B). Importantly, the SOD activity was noticeably higher in the tissues from the focus peripheral and far-end areas in the gastric ulcer (group F) than non-MGC (groups A-D). To compare the gastric ulcer (group F) and the MGC (group E), the level

Table 1 SOD activity detection in the gastric tissue with gastric carcinoma and gastric ulcer (mean±SD) NU/mg Pr

Group	<i>n</i>	Focus center area (1)	Focus peripheral area (2)	Focus far-end area (3)
Non-MGC				
I (A)	12	85.88±8.97	122.79±12.08	135.33±14.74
II (B)	15	81.26±8.68	104.73±11.24	123.13±14.46
III (C)	11	49.01±4.97	93.35±8.32	109.59±11.45
IV (D)	6	52.05±5.13	70.71±6.01	102.25±10.34
MGC (E)	8	23.64±2.31	31.34±3.79	33.47±4.78
Gastric ulcer (F)	10	95.63±8.01	162.88±12.26	186.22±11.74

P: (Statistical comparisons interior group)

①A ₁ :A ₂ <0.05	A ₁ :A ₃ <0.01	A ₂ :A ₃ >0.05	②B ₁ :B ₂ >0.05	B ₁ :B ₃ <0.05	B ₂ :B ₃ >0.05
③C ₁ :C ₂ <0.01	C ₁ :C ₃ <0.01	C ₂ :C ₃ >0.05	④D ₁ :D ₂ <0.05	D ₁ :D ₃ <0.01	D ₂ :D ₃ <0.05
⑤E ₁ :E ₂ >0.05	E ₁ :E ₃ >0.05	E ₂ :E ₃ >0.05	⑥F ₁ :F ₂ <0.01	F ₁ :F ₃ <0.01	F ₂ :F ₃ >0.05

P: (Statistical comparisons between different groups)

①A ₁ :B ₁ >0.05	A ₁ :C ₁ <0.01	A ₁ :D ₁ <0.05	A ₁ :E ₁ <0.01	A ₁ :F ₁ >0.05	B ₁ :C ₁ <0.01
B ₁ :D ₁ <0.05	B ₁ :E ₁ <0.05	B ₁ :F ₁ >0.05	C ₁ :D ₁ >0.05	C ₁ :E ₁ <0.05	C ₁ :F ₁ <0.01
D ₁ :E ₁ <0.05	D ₁ :F ₁ <0.01	E ₁ :F ₁ <0.01			
②A ₂ :B ₂ >0.05	A ₂ :C ₂ <0.05	A ₂ :D ₂ <0.01	A ₂ :E ₂ <0.01	A ₂ :F ₂ <0.05	B ₂ :C ₂ <0.05
B ₂ :D ₂ <0.05	B ₂ :E ₂ <0.01	B ₂ :F ₂ <0.01	C ₂ :D ₂ <0.05	C ₂ :E ₂ <0.01	C ₂ :F ₂ <0.01
D ₂ :E ₂ <0.05	D ₂ :F ₂ <0.01	E ₂ :F ₂ <0.01			
③A ₃ :B ₃ >0.05	A ₃ :C ₃ >0.05	A ₃ :D ₃ >0.05	A ₃ :E ₃ <0.01	A ₃ :F ₃ <0.01	B ₃ :C ₃ >0.05
B ₃ :D ₃ >0.05	B ₃ :E ₃ <0.01	B ₃ :F ₃ <0.01	C ₃ :D ₃ >0.05	C ₃ :E ₃ <0.01	C ₃ :F ₃ <0.01
D ₃ :E ₃ <0.01	D ₃ :F ₃ <0.01	E ₃ :F ₃ <0.01			

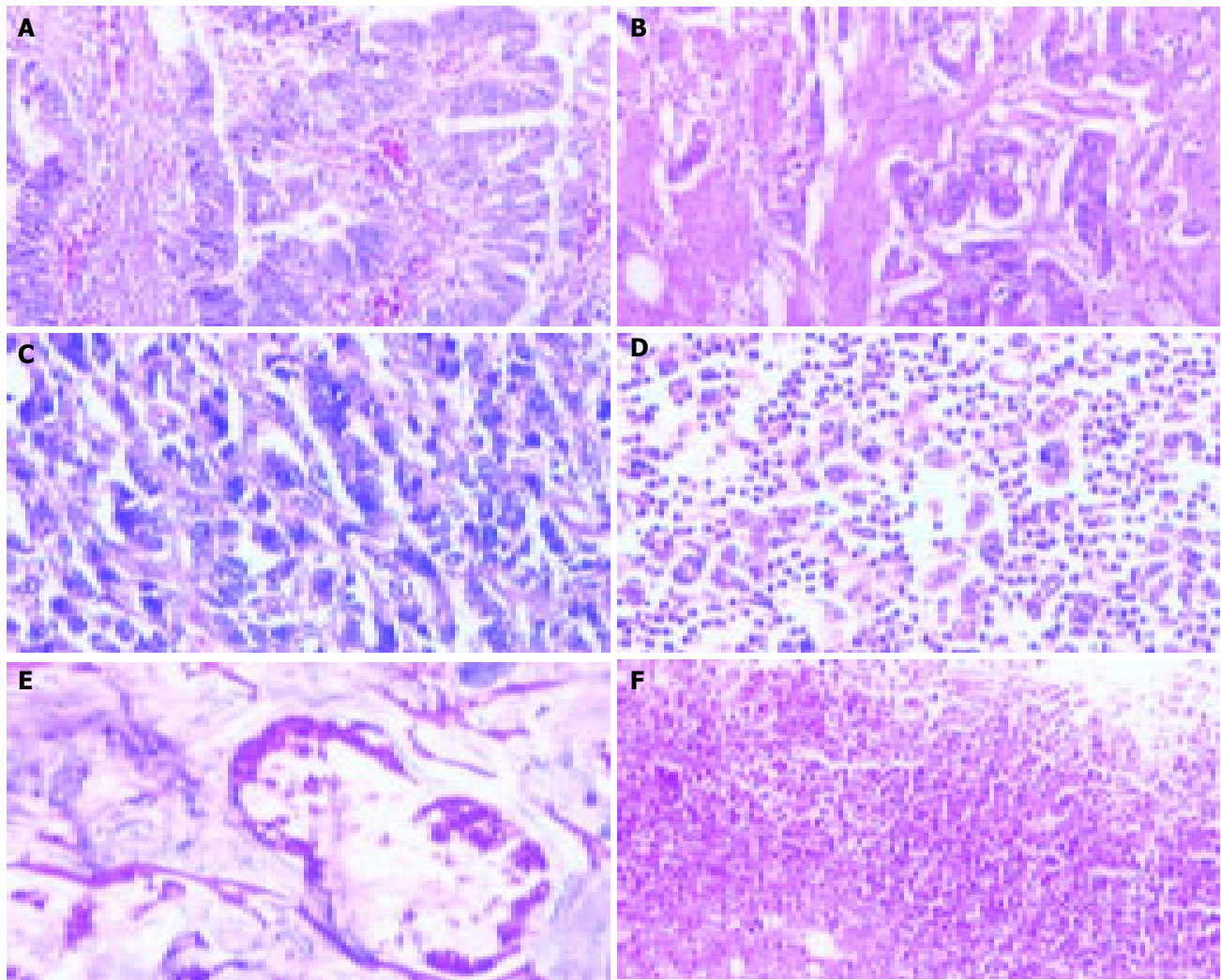


Figure 1 Non-mucous gastric carcinoma. **A:** non-mucous gastric carcinoma, grade I HE $\times 100$; **B:** non-mucous gastric carcinoma, grade II HE $\times 100$; **C:** non-

mucous gastric carcinoma, grade III HE $\times 200$; **D:** non-mucous gastric carcinoma, grade IV HE $\times 200$; **E:** mucous gastric carcinoma HE $\times 100$; **F:** gastric ulcer HE $\times 100$.

of SOD activity was noticeably higher in all the tissues in the former than the later, and the SOD activity showed a gradual reduction tendency in the former, same low level in the later from the focus far-end, peripheral to center areas.

Detection of MDA content (Table 2 and Figure 3)

The MDA content increased gradually in the tissues from the focus far-end, peripheral to center areas in non-MGC

(groups A-D). The MDA content in the focus center areas was the highest in the measured gastric tissue. The level of MDA content correlated with the grade and differentiation of gastric carcinoma in the tissues from the center areas. The study showed that the level of the MDA content in the groups A and B (grades I and II) was lower than groups C and D (grades III and IV). There were significant differences of the MDA content in the tissues from far-end areas, in which the level of MDA content was noticeably lower in

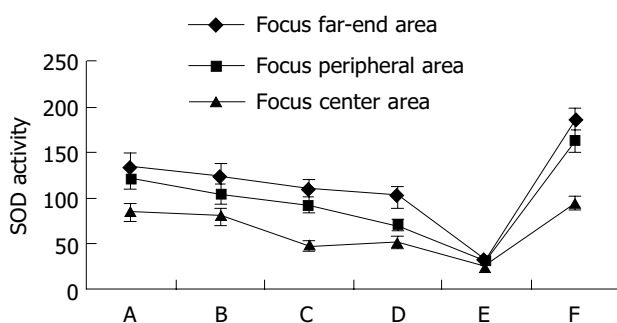


Figure 2 SOD activity detection in the gastric tissue with gastric carcinoma and gastric ulcer.

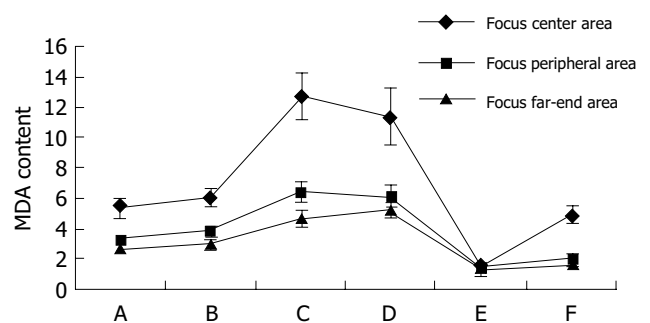


Figure 3 MDA content detection in the gastric tissue with gastric carcinoma and gastric ulcer.

Table 2 MDA content detection in the gastric tissue with gastric carcinoma and gastric ulcer (mean±SD) nmol/mg Pr

Group	n	Focus center area (1)	Focus peripheral area (2)	Focus far-end area (3)	
Non-MGC					
I (A)	12	5.37±0.61	3.28±0.23	2.56±0.18	
II (B)	15	6.07±0.62	3.85±0.31	2.96±0.25	
III (C)	11	12.75±1.52	6.46±0.65	4.65±0.52	
IV (D)	6	11.41±1.91	6.10±0.71	5.20±0.45	
MGC (E)	8	1.55±0.23	1.43±0.18	1.12±0.12	
Gastric ulcer (F)	10	4.89±0.56	2.06±0.22	1.68±0.16	
P: (Statistical comparisons interior group)					
①A ₁ :A ₂ <0.01	A ₁ :A ₃ <0.01	A ₂ :A ₃ <0.05	②B ₁ :B ₂ <0.01	B ₁ :B ₃ <0.01	B ₂ :B ₃ <0.01
③C ₁ :C ₂ <0.01	C ₁ :C ₃ <0.01	C ₂ :C ₃ <0.05	④D ₁ :D ₂ <0.05	D ₁ :D ₃ <0.05	D ₂ :D ₃ >0.05
⑤E ₁ :E ₂ >0.05	E ₁ :E ₃ >0.05	E ₂ :E ₃ >0.05	⑥F ₁ :F ₂ <0.01	F ₁ :F ₃ <0.01	F ₂ :F ₃ >0.05
P: (Statistical comparisons between different groups)					
①A ₁ :B ₁ >0.05	A ₁ :C ₁ <0.01	A ₁ :D ₁ <0.01	A ₁ :E ₁ <0.01	A ₁ :F ₁ >0.05	B ₁ :C ₁ <0.01
B ₁ :D ₁ <0.05	B ₁ :E ₁ <0.01	B ₁ :F ₁ <0.05	C ₁ :D ₁ >0.05	C ₁ :E ₁ <0.01	C ₁ :F ₁ <0.01
D ₁ :E ₁ <0.01	D ₁ :F ₁ <0.01	E ₁ :F ₁ <0.05			
②A ₂ :B ₂ >0.05	A ₂ :C ₂ <0.01	A ₂ :D ₂ <0.01	A ₂ :E ₂ <0.01	A ₂ :F ₂ <0.05	B ₂ :C ₂ <0.01
B ₂ :D ₂ <0.01	B ₂ :E ₂ <0.01	B ₂ :F ₂ <0.01	C ₂ :D ₂ >0.05	C ₂ :E ₂ <0.01	C ₂ :F ₂ <0.01
D ₂ :E ₂ <0.01	D ₂ :F ₂ <0.01	E ₂ :F ₂ >0.05			
③A ₃ :B ₃ >0.05	A ₃ :C ₃ <0.01	A ₃ :D ₃ <0.01	A ₃ :E ₃ <0.01	A ₃ :F ₃ <0.05	B ₃ :C ₃ <0.01
B ₃ :D ₃ >0.01	B ₃ :E ₃ <0.01	B ₃ :F ₃ <0.01	C ₃ :D ₃ >0.05	C ₃ :E ₃ <0.01	C ₃ :F ₃ <0.01
D ₃ :E ₃ <0.01	D ₃ :F ₃ <0.01	E ₃ :F ₃ >0.05			

the groups A and B than the groups C and D.

The level of MDA content was extremely low in the center, peripheral, and far-end areas in MGC (group E). There was no significant difference of the MDA content; it was at the same low level, although a minimum gradual increase tendency was found in the tissues from the focus far-end, peripheral to center areas.

The level of MDA content was noticeably high in the tissues from the focus center areas in the gastric ulcer (group F). The gradual increase tendency also showed in the tissues from the focus far-end, peripheral to center areas. The common metabolic characteristics were that the MDA content showed a gradual increase tendency in the tissues from the focus far-end, peripheral to center areas between gastric ulcer (group F) and non-MGC (groups A-D). And both in the group F and groups A and B, the MDA content was at the same level in the tissues from the focus center areas. However, when the gastric ulcer (group F) compared to the non-MGC (groups A-D), there was a significant difference: the MDA content declined markedly and varied in the tissues from the focus peripheral and far-end areas. The MDA content was noticeably higher in the tissues from the focus center areas in the gastric ulcer (group F) than the MGC (group E). But, the MDA content was at the same level in the tissues from the peripheral and focus far-end. And in the gastric ulcer (group F) compared to the MGC (group E), it showed a gradual increase tendency in the former, the later was at same low level in the tissues from the focus far-end, peripheral to center areas.

DISCUSSION

SOD is the most important substance that eliminated free radical system in the cell; it makes superoxide anion free radical (O₂⁻), dismutates into H₂O₂ and protects the cells from the focus damage by cleaning up O₂⁻. The level of

SOD activity represents the intracellular antioxidation ability^[8,10,12]. MDA is the main metabolite in the lipid peroxidation reaction. The free radicals affect on the membrane structures of the cells, including the membranes of the cell, mitochondrion, lysosome, endoplasmic reticulum, *etc.*, then injury of the cells. The level of MDA content represents the extent of the intracellular lipid peroxidation reaction^[13-15]. The SOD activity and the MDA content are the main index of the metabolic condition of the free radicals. We acquired the new knowledge that the free radicals play a key role in the mechanism of the gastric carcinogenesis from our experimental data.

Active free radical reaction in gastric tissue advances the arising of non-MGC

The gastric mucosa from the focus far-end, peripheral to center area in non-MGC showed a pathological change from normal, atypical hyperplasia to carcinoma, by morphological observation. The SOD activity also showed a gradual reduction and the MDA content a gradual increase in gastric tissues from the focus far-end, peripheral to center areas. These results showed that the intracellular antioxidation ability in the gastric tissue was gradually reduced and the free radical reaction was gradually active, resulting in the injury of cells by the lipid peroxidation reaction, which stimulated the pathological changes from normal gastric mucous membrane to carcinoma^[16-18].

The results further showed that the lower the differentiation degree of the gastric carcinoma, the more prominent the change of the free radicals metabolism. The SOD activity was lower and the MDA content higher in the groups C and D (gastric carcinoma grades III and IV) than the groups A and B (gastric carcinoma grades I and II). These results suggest two possible mechanisms: the first one was that the active free radical reaction severely damages the gastric mucous membrane cells, resulting in malignant

change in the gastric mucous membrane from the normal cell to poorly differentiated and undifferentiated carcinomas. The second was that the carcinoma cells with poorly differentiated, undifferentiated need to produce an amount of the active free radicals for cells blooming division and breeding for themselves^[15,19].

Interestingly, our results showed that there was no significant difference of the SOD activity in the far-end area between groups A, B, C, and D. However, the differences of the MDA content were very noticeable, i.e., the MDA content of the groups C and D (gastric carcinoma grades III and IV) were very much higher than groups A and B (gastric carcinoma grades I and II), indicated that abnormal lipid peroxidation reaction of the gastric tissue in far-end areas in groups C and D was not regulated by the SOD activity, and the reduction of the ability of the antioxidation was correlated with the widespread infiltration of the gastric carcinoma tissue (gastric carcinoma grades III and IV).

The tendency changes of the SOD activity and the MDA content of gastric tissues in non-MGC (groups A-D) were consistent with that in gastric ulcer (group F) from the focus center, peripheral to far-end areas. Between groups A, B and group F, the same level of the SOD activity and the MDA content were found in the gastric tissues from the focus center areas. Importantly, between the non-MGC (groups A-D) and the gastric ulcer (group F), the differences of the SOD activity and the MDA content were highly noticeable in the gastric tissues from the focus peripheral and far-end areas, which the SOD activity showed noticeable increase and the MDA content showed noticeable decrease in the gastric ulcer. It was suggested that there was high ability of the antioxidation for protecting itself against damage by the free radicals and could balance free radical metabolism in the gastric tissue from the focus peripheral and far-end areas in the gastric ulcer (group F). Meantime, it was suggested that the changes of the free radicals metabolism centralized mostly in the center area of gastric ulcer, where the ability of the antioxidation was reduced only in the local focus. Compared to the gastric ulcer (group F), the variation of the SOD activity and the MDA content were very small in the peripheral area and far-end area in the non-MGC (groups A-D), suggested that the ability of the antioxidation was reduced not only in the local focus area but also in the abroad gastric tissues. This imbalance of the free radical metabolism occurs in whole gastric tissue, resulting in the reduction of the protection itself of the gastric tissue and inducing the gastric carcinogenesis, i.e., the arising of non-MGC^[20,21].

Extreme reduction of the antioxidation ability in the gastric tissue contributes to the arising of MGC

The mucinous adenocarcinoma and the signet-ring cell carcinoma arising from the gastric mucosa possess large quantity of mucus, inside or/and around the cancer cells. And because of that characteristic nature, the cancer cells have strong ability of infiltration and widespread distribution in the gastric tissue. There were obvious differences of the SOD activity and the MDA content in gastric mucinous adenocarcinoma and signet-ring cell carcinoma, and classified

as a special group (group E), compared to other type gastric carcinoma. The obvious reduction and the same low level of the SOD activity and the MDA content were found in the tissues of the focus center, peripheral and far-end areas in the MGC, where the free radical metabolism changed obviously. The data in previous experiments showed an inverse relationship between the SOD activity and the MDA content in the tissues^[13,15]. The low SOD activity induced the reduction of the antioxidation ability and the increase of the lipid peroxidation reaction, the metabolic product, MDA, in the tissues. On the contrary, the increase of the SOD activity inhibited the reaction of the lipid peroxidation, resulting in the reduction of the metabolic product, MDA, in the tissues. But in this study, the SOD activity decreased greatly in the gastric tissue in the MGC, and the MDA content as well. Interestingly, the SOD activity and the MDA content decreased markedly to the same low level in the tissues wherever focus center, peripheral and far-end areas in the MGC. This condition of the free radicals metabolism maybe related with the special pathological changes, where there was an abundance of mucus in the tissues. The SOD is the most important substance to eliminate free radical system in cells and tissues and the level of SOD activity represents the intracellular antioxidation ability^[12,22]. The utmost low level of the SOD activity represents the utmost low level of the intracellular antioxidation ability in gastric tissue with the MGC. It was considered accordingly that the antioxidation ability was the base and precondition in maintaining the normal physiological function, differentiation, division, multiplication of the cells^[20,23]. The loss of the antioxidation ability may contribute to make the normal cells become carcinoma cells^[9,24-26] and the gastric tissues cannot resist the infiltration of the cancer cells, resulting in cancer cells spreading extensively in stomach wall.

Compared to gastric ulcer, there was a very low level of the SOD activity in gastric tissues of center, peripheral and far-end areas with the MGC and the low antioxidation ability and the low defense function by themselves. The MDA content, in the tissues from the focus peripheral and far-end areas with the MGC and the ulcer, both were at the same low level. But the SOD activity was increased greatly in the tissues from the focus peripheral and far-end area with gastric ulcer (group F). It suggested that there was still a very strong antioxidation and protecting ability in the gastric tissues from the peripheral and far-end areas with the gastric ulcer (group F). It also confirmed that the extreme low antioxidation ability and the low SOD activity in the gastric tissues in the MGC (group E) were related to the causing and development of the MGC, and can induce the formation of the MGC. On the other hand, the very low level of the MDA suggests the lipid peroxidation reaction was inactive, which indicated that the arising of the MGC was not related with the lipid peroxidation reaction to damage of the tissues.

REFERENCES

- 1 **Khantzode SS, Khantzode SD, Dakhale GN.** Serum and plasma concentration of oxidant and antioxidants in patients of *Helicobacter pylori* gastritis and its correlation with gastric cancer. *Cancer Lett* 2003; **195**: 27-31

- 2 **Janssen AM**, Bosman CB, van Duijn W, Oostendorp-van de Ruit MM, Kubben FJ, Griffioen G, Lamers CB, van Krieken JH, van de Velde CJ, Verspaget HW. Superoxide dismutases in gastric and esophageal cancer and the prognostic impact in gastric cancer. *Clin Cancer Res* 2000; **6**: 3183-3192
- 3 **Fujisawa S**, Atsumi T, Ishihara M, Kadoma Y. Cytotoxicity, ROS-generation activity and radical-scavenging activity of curcumin and related compounds. *Anticancer Res* 2004; **24**: 563-569
- 4 **Sander CS**, Chang H, Hamm F, Elsner P, Thiele JJ. Role of oxidative stress and the antioxidant network in cutaneous carcinogenesis. *Int J Dermatol* 2004; **43**: 326-335
- 5 **Sanders PM**, Tisdale MJ. Role of lipid-mobilising factor (LMF) in protecting tumour cells from oxidative damage. *Br J Cancer* 2004; **90**: 1274-1278
- 6 **Kim JJ**, Chae SW, Hur GC, Cho SJ, Kim MK, Choi J, Nam SY, Kim WH, Yang HK, Lee BL. Manganese superoxide dismutase expression correlates with a poor prognosis in gastric cancer. *Pathobiology* 2002-2003; **70**: 353-360
- 7 **Korenaga D**, Yasuda M, Honda M, Nozoe T, Inutsuka S. MnSOD expression within tumor cells is closely related to mode of invasion in human gastric cancer. *Oncol Rep* 2003; **10**: 27-30
- 8 **Yasuda M**, Takesue F, Inutsuka S, Honda M, Nozoe T, Korenaga D. Prognostic significance of serum superoxide dismutase activity in patients with gastric cancer. *Gastric Cancer* 2002; **9**: 148-153
- 9 **Toh Y**, Kuninaka S, Oshiro T, Ikeda Y, Nakashima H, Baba H, Kohnoe S, Okamura T, Mori M, Sugimachi K. Overexpression of manganese superoxide dismutase mRNA may correlate with aggressiveness in gastric and colorectal adenocarcinomas. *Int J Oncol* 2000; **17**: 107-112
- 10 **Izutani R**, Asano S, Imano M, Kuroda D, Kato M, Ohyanagi H. Expression of manganese superoxide dismutase in esophageal and gastric cancers. *J Gastroenterol* 1998; **33**: 816-822
- 11 **Pang ZJ**, Zhou M, Chen Y. The research method of free radicals medical science. 1st. Beijing: *PEOPLE HYGIENE Pub* 2000: 64-66
- 12 **Inoue M**, Sato EF, Nishikawa M, Park AM, Kira Y, Imada I, Utsumi K. Mitochondrial generation of reactive oxygen species and its role in aerobic life. *Curr Med Chem* 2003; **10**: 2495-2505
- 13 **Arivazhagan S**, Kavitha K, Nagini S. Erythrocyte lipid peroxidation and antioxidants in gastric cancer patients. *Cell Biochem Funct* 1997; **15**: 15-18
- 14 **Lee IS**, Nishikawa A. Polyozellus multiplex, a Korean wild mushroom, as a potent chemopreventive agent against stomach cancer. *Life Sci* 2003; **73**: 3225-3234
- 15 **Skrzydewska E**, Kozusko B, Sulkowska M, Bogdan Z, Kozlowski M, Snarska J, Puchalski Z, Sulkowski S, Skrzydlewski Z. Antioxidant potential in esophageal, stomach and colorectal cancers. *Hepatogastroenterology* 2003; **50**: 126-131
- 16 **Vukobrat-Bijedic Z**. Carcinoma of the stomach. *Med Arh* 2003; **57**(1 Suppl 2): 81-83
- 17 **Tahara E**. Genetic pathways of two types of gastric cancer. *IARC Sci Publ* 2004; **157**: 327-349
- 18 **Correa P**. The biological model of gastric carcinogenesis. *IARC Sci Publ* 2004; **157**: 301-310
- 19 **Policastro L**, Molinari B, Larcher F, Blanco P, Podhajcer OL, Costa CS, Rojas P, Duran H. Imbalance of antioxidant enzymes in tumor cells and inhibition of proliferation and malignant features by scavenging hydrogen peroxide. *Mol Carcinog* 2004; **39**: 103-113
- 20 **Eapen CE**, Madesh M, Balasubramanian KA, Pulimood A, Mathan M, Ramakrishna BS. Mucosal mitochondrial function and antioxidant defences in patients with gastric carcinoma. *Scand J Gastroenterol* 1998; **33**: 975-981
- 21 **Zavros Y**, Kao JY, Merchant JL. Inflammation and cancer III. Somatostatin and the innate immune system. *Am J Physiol Gastrointest Liver Physiol* 2004; **286**: G698-701
- 22 **Izutani R**, Kato M, Asano S, Imano M, Ohyanagi H. Expression of manganese superoxide dismutase influences chemosensitivity in esophageal and gastric cancers. *Cancer Detect Prev* 2002; **26**: 213-221
- 23 **Zheng QS**, Sun XL, Wang CH. Redifferentiation of human gastric cancer cells induced by ascorbic acid and sodium selenite. *Biomed Environ Sci* 2002; **15**: 223-232
- 24 **Magalova T**, Bella V, Brtkova A, Beno I, Kudlackova M, Volkovova K. Copper, zinc and superoxide dismutase in precancerous, benign diseases and gastric, colorectal and breast cancer. *Neoplasma* 1999; **46**: 100-104
- 25 **Shimoyama S**, Aoki F, Kawahara M, Yahagi N, Motoi T, Kuramoto S, Kaminishi M. Early gastric cancer development in a familial adenomatous polyposis patient. *Dig Dis Sci* 2004; **49**: 260-265
- 26 **Macarthur M**, Hold GL, El-Omar EM. Inflammation and Cancer II. Role of chronic inflammation and cytokine gene polymorphisms in the pathogenesis of gastrointestinal malignancy. *Am J Physiol Gastrointest Liver Physiol* 2004; **286**: G515-520

Nutritional factors and gastric cancer in Zhoushan Islands, China

Jiong-Liang Qiu, Kun Chen, Jian-Ning Zheng, Jian-Yue Wang, Li-Jun Zhang, Li-Ming Sui

Jiong-Liang Qiu, Jian-Ning Zheng, Department of Health and Quarantine, Ningbo Entry-Exit Inspection and Quarantine Bureau, Ningbo 315012, Zhejiang Province, China

Kun Chen, Department of Epidemiology, Zhejiang University School of Public Health, Hangzhou 310006, Zhejiang Province, China

Jian-Yue Wang, Zhoushan Center for Disease Prevention and Control, Zhoushan 316000, Zhejiang Province, China

Li-Jun Zhang, Li-Ming Sui, Jiangdong Center for Disease Prevention and Control, Ningbo 315000, Zhejiang Province, China

Supported by the Foundation of Ministry of Public Health of China, No. WKZ-2001-1-17

Correspondence to: Dr. Jiong-Liang Qiu, Department of Health and Quarantine, Ningbo Entry-Exit Inspection and Quarantine Bureau, 9 Ma-yuan Road, Ningbo 315012, Zhejiang Province, China. qiujunliang@163.com

Telephone: +86-574-87022519 Fax: +86-574-87146206

Received: 2004-10-26 Accepted: 2004-12-21

increased risk of gastric cancer is associated with high intakes of protein, saturated fat, cholesterol and sodium, while consumption of polyunsaturated fat, vitamin A and ascorbic acid may have a protective effect against gastric cancer.

© 2005 The WJG Press and Elsevier Inc. All rights reserved.

Key words: Gastric cancer; Nutrient intake; Case-control; Risk factor; Protective effect; Antioxidants

Qiu JL, Chen K, Zheng JN, Wang JY, Zhang LJ, Sui LM. Nutritional factors and gastric cancer in Zhoushan Islands, China. *World J Gastroenterol* 2005; 11(28): 4311-4316
<http://www.wjgnet.com/1007-9327/11/4311.asp>

Abstract

AIM: To investigate the association between nutrient intakes and high incidence rate of gastric cancer among residents in Zhoushan Islands.

METHODS: A frequency-matched design of case-control study was used during the survey on dietary factors and gastric cancer in Zhoushan Islands, China. A total of 103 cases of gastric cancer diagnosed in 2001 were included in the study and 133 controls were randomly selected from the residents in Zhoushan Islands. A food frequency questionnaire was specifically designed for the Chinese dietary pattern to collect information on dietary intake. A computerized database of the dietary and other relative information of each participant was completed. Total calories and 15 nutrients were calculated according to the food composition table and their adjusted odds ratios (ORs) and 95% confidence intervals (CIs) were estimated by gender using unconditional logistic regression models.

RESULTS: High intakes of protein, saturated fat, and cholesterol were observed with the increased risk of gastric cancer particularly among males (OR_{Q4 vs Q1} were 10.3, 3.24, 2.76 respectively). While carbohydrate was a significant high-risk nutrient (OR_{Q4 vs Q1} = 14.8; *P* for linear trend = 0.024) among females. Regardless of their gender, the cases reported significantly higher daily intake of sodium mainly from salts. As to the nutrients of vitamins A and C, an inversed association with the risk of GC was found. Baseline characteristics of participants were briefly described.

CONCLUSION: The findings from this study confirm the role of diet-related exposure in the etiology of gastric cancer from the point of view of epidemiology. An

INTRODUCTION

Though a decreasing trend is observed in nearly all countries, gastric cancer is one of the most common cancers in the world and the second leading cause of cancer death^[1]. Although many risk factors have been suggested, the causative and protective agents for gastric cancer remain to be clarified. Nutritional factors are thought to be paramount, with *N*-nitroso and other dietary compounds acting as carcinogens, while anti-oxidants and other protective substances in foods inhibit the carcinogenic process^[2].

In China, parts of high-risk areas for gastric cancer are located in the eastern coastlands including Zhoushan Islands, the fourth archipelago and also the largest fishing ground in China. As the first leading cancer in Zhoushan, the age-standardized annual incidence rate of gastric cancer varied from 35 to 40 per 100 000 in 1980-1985, which is higher than the national level (about 25.0 per 100 000). To investigate the risk factors for this common cancer in the coastal areas, we conducted a population-based case-control study in Zhoushan to obtain information on the frequency of consumption and portion size of common foods, and found that intake of certain nutrients in these foods influences the risk of gastric cancer.

MATERIALS AND METHODS

The data-collection period for the study spanned through the whole year of 2001 and comprised all the islands in Zhoushan, Zhejiang Province. The study population included 138 newly diagnosed patients with gastric cancer between December 1, 2000 and November 30, 2001 and 140 controls as a representative sample of residents in the same area.

All the cases were identified at the five largest hospitals in Zhoushan Islands. Of the 138 eligible patients, 10 (7.3%) died before interview, 18 (10.2%) could not be contacted as they were from distant islands, 7 (5.1%) refused to participate. Of the 103 (81 men and 22 women) patients included in the analysis, 56.3% were confirmed by histology according to the Lauren classification^[3] and 43.7% by other diagnostic methods including surgery, endoscopy, X-ray and ultrasound. Controls were selected from permanent residents in Zhoushan Islands, frequency matched to the expected distribution of cases by gender, age (10-year groups), and residents of the islands. Of the 140 eligible controls randomly selected from the Zhoushan resident files, 133 (95 men and 38 women) were interviewed, yielding a response rate of 95.0%. Each subject was interviewed face-to-face by trained interviewers.

Dietary information

A questionnaire was designed to collect information on demographic and socio-economic conditions, diet, cigarette smoking, alcohol drinking, history of selected diseases, family history of cancer, occupation, and other factors. Frequency of intake and portion size in a 12-mo period 1 year before the interview were assessed for more than 60 food and beverage items, which included information on dairy products, fruits, meat, processed meat, fish, vegetables and candies, *etc.* These items accounted for over 85% of food intake in Zhoushan residents. For each food, amount consumed was estimated according to models of the more frequently consumed foods. Consumption of seasonal vegetables and fruits was assessed on the basis of average intake during the relevant period of the year.

Nutrient intake

Fifteen priority nutrients and total calories were selected beforehand as previously described^[4-6]. Quantitative estimate of cumulative nutrient intake per day in each food was based on food tables derived from the Chinese Food Composition Tables. Total intake of each nutrient was summed over all foods consumed. The Matlab5.0 software was used for processing these procedures by the method of multiplication of matrix^[7].

Data analysis and control of confounding

Descriptive analysis of nutrient intake for cases and controls was carried out by computing medians and percentages because of biased distributions of the data, which could not be transformed into normal with logarithmic transformations. The medians were compared by the nonparametric median test.

Then continuous variables of nutrient intake were divided into quartiles based on the distribution in controls, with an approximately equal number of controls in each intake stratum. The amount of intake varied substantially between the sexes, hence sex-specific cutpoints were used for amount of nutrient intake. Risk of gastric cancer associated with dietary factors was estimated by odds ratios (ORs) and its 95% confidence intervals (CIs), using unconditional logistic regression models. Each classified nutrient was introduced into the model as a dummy variable.

The lowest level of consumption was used as the reference category in the estimation. All ORs were adjusted for age, economic status (based on monthly family *per capita* income), present residence, educational level and total calories. In addition, ORs for men were further adjusted for cigarette smoking and alcohol drinking, confounding factors common in Chinese men but not in Chinese women (only 5% of women smoke, and 6.7% drink alcohol regularly).

For testing of linear trends, the ordinal nutrient intake variables were treated as continuous variables. In this step, $P \leq 0.05$ was considered as evidence for a dose-response relationship. All analyses were carried out by the SPSS version 10.0 software.

RESULTS

Selected characteristics of the study population are shown in Table 1. Due to the frequency-matching procedure by age, gender and present residence, the characteristics of these three variables were similar. Compared to controls, only the age of patients was slightly older (median age 63 years for cases and 60 years for controls). Among

Table 1 Distribution of 103 cases of gastric cancer and 133 controls according to age, gender, address and selected variables

Characteristics	Cases (n = 103)	Controls (n = 133)	χ^2	P
Age (yr)				
Average	3 (30-85)	60 (28-82)		
≤45	6	20		
46-55	27	32		
56-65	32	38		
66-75	30	38		
76-85	8	5	6.40	0.172
Gender				
Males	81	95		
Females	22	38	1.59	0.210
Present residence ¹				
Large islands	70	76		
Medium islands	17	33		
Small islands	16	24	3.20	0.202
Education (yr)				
<7	43	45		
7-12	58	76		
≥13	2	12	5.89	0.053
Economic status				
Low	46	30		
Medium	32	44		
High	25	51	12.15	0.002
Cigarette smoking				
Ever-smokers	62	70		
Non-smokers	41	63	1.35	0.246
Alcohol drinking				
Ever-drinkers	58	63		
Non-drinkers	45	70	1.86	0.173

¹Three categories of islands were classified according to the number of permanent residents on islands: Dinghai, Putuo, and Daishan Islands, which are the three main islands in Zhoushan, predefined as the large islands; the islands on which the number of permanent residents is over 25 000, defined as the medium islands; the residual defined as the small islands.

Table 2 Medians of daily intake of nutrients in gastric cancer cases and controls, Zhoushan, China

Nutrient/d	Males		Females		All	
	Cases (n = 81)	Controls (n = 95)	Cases (n = 22)	Controls (n = 38)	Cases (n = 103)	Controls (n = 133)
Total calories (kJ)	2 963.25	3 073.16	3 002.32 ^b	2 420.08 ^b	2 984.54	2 937.73
Macronutrients						
Protein (g)	94.21	88.33	98.34 ^a	76.92 ^a	95.17 ^a	85.21 ^a
Fat (g)	61.04	65.04	56.23 ^a	42.65 ^a	60.60	57.48
Saturated fat (g)	8.90	9.44	6.33 ^a	4.64 ^a	8.70	8.44
Mono-unsaturated fat (g)	22.42	24.47	18.29	14.92	22.38	20.82
Polyunsaturated fat (g)	16.74	16.69	14.43	14.46	16.11	16.23
Fiber (g)	10.11	10.40	9.78	9.39	10.10	10.33
Carbohydrates (g)	403.36	404.93	411.34	287.31	404.19	359.27
Cholesterol (mg)	170.75	136.44	144.57 ^a	62.56 ^a	160.43 ^a	115.02 ^a
Micronutrients						
Carotene (µg)	443.54 ^b	521.48 ^b	455.38	827.38	443.62 ^a	555.30 ^a
Vitamin A (µg)	135.35 ^a	181.01 ^a	164.59	175.70	142.13 ^a	179.96 ^a
Vitamin C (mg)	42.49	38.94	49.29	61.36	43.64	41.04
Vitamin E (mg)	26.12	25.64	21.54	21.46	24.82	24.95
Mineral salts						
Na (mg)	6 700.32	5 074.32	7 000.52 ^a	4 960.27 ^a	6 734.41 ^a	4 963.28 ^a
Ca (mg)	464.08	448.26	560.28	460.57	478.91	448.26
Se (µg)	57.35	49.78	53.60	56.02	53.96	52.13

^aP<0.05; ^bP<0.10 vs others.

non-dietary variables considered, the major determinants of gastric cancer risk were indicators of socio-economic status. For instance, 41.8% of the cases and 33.8% of the controls reported less than 7 years of education, 58.2% of the cases and 66.2% of the controls reported 7 years or more of education. As for the economic status, patients tended to have lower monthly income (44.7% of cases and 22.6% of controls with an average *per capita* income of 36 Chinese Yuan/month or less). No material difference in smoking/drinking habits was observed between cases and controls.

Table 2 shows the medians of daily nutrient intakes in the gastric-cancer cases and the controls according to gender.

Overall, the cases reported significantly higher consumption of protein, cholesterol and Na (sodium) than controls, but these differences were significant only in the females. For controls, consumption of carotene and vitamin E was much higher, and on the contrary, the differences were significant in the males.

The multivariate-adjusted ORs for the quartile distributions of the macronutrients (Table 3) showed a significant positive linear trend for the risk of gastric cancer with increasing consumption of protein and cholesterol in males, whereas total fat and carbohydrates in females. The ORs for the highest quartile compared to the lowest quartile of consumption frequency significantly elevated for protein

Table 3 Odds ratios¹ (ORs) and 95% confidence intervals (CIs) of gastric cancer in relation to quartiles of macronutrients by sex, Zhoushan, China

Nutrient/d ²	Males				P for trend	Females				P for trend
	Q ₁	Q ₂	Q ₃	Q ₄		Q ₁	Q ₂	Q ₃	Q ₄	
Total calories	1.0	1.20 (0.50–2.87)	1.02 (0.39–2.64)	1.26 (0.51–3.11)	>0.10	1.0	1.45 (0.27–7.89)	1.41 (0.26–7.74)	2.75 (0.45–16.84)	>0.10
Protein	1.0	3.00 (1.02–8.85)	5.11 (1.26–20.76)	10.30 (1.83–58.12)	0.010	1.0	4.28 (0.50–36.77)	1.71 (0.13–22.37)	6.10 (0.39–94.66)	>0.10
Fat	1.0	1.29 (0.52–3.2)	1.21 (0.46–3.17)	1.01 (0.35–2.92)	>0.10	1.0	1.38 (0.21–8.9)	1.85 (0.23–14.74)	8.26 (1.03–66.51)	0.023
Saturated fat	1.0	2.51 (0.90–6.97)	2.34 (0.81–6.8)	3.24 (1.11–9.49)	0.060	1.0	0.24 (0.02–3.11)	3.34 (0.52–21.44)	3.42 (0.48–24.49)	0.094
Monounsaturated fat	1.0	1.62 (0.67–3.94)	1.24 (0.49–3.17)	1.17 (0.43–3.22)	>0.10	1.0	0.30 (0.03–2.59)	1.83 (0.31–10.76)	1.32 (0.17–10.4)	>0.10
Polyunsaturated fat	1.0	1.21 (0.46–3.17)	1.72 (0.66–4.46)	0.96 (0.33–2.78)	>0.10	1.0	0.21 (0.03–1.37)	0.47 (0.09–2.57)	0.10 (0.01–0.80)	0.068
Fiber	1.0	1.69 (0.58–4.92)	0.69 (0.20–2.37)	2.41 (0.51–11.52)	>0.10	1.0	1.82 (0.30–10.9)	1.9 (0.27–13.44)	0.72 (0.06–8.97)	>0.10
Carbohydrates	1.0	1.39 (0.47–4.11)	1.6 (0.41–6.27)	2.14 (0.35–13.04)	>0.10	1.0	0.94 (0.1–8.57)	3.27 (0.37–28.84)	14.78 (1.11–197.32)	0.024
Cholesterol	1.0	1.08 (0.40–2.87)	2.53 (0.99–6.44)	2.76 (1.01–7.53)	0.050	1.0	6.05 (0.53–69.17)	5.31 (0.44–63.44)	11.9 (0.97–146.53)	0.062

¹Adjusted for age, present residence, education, economic status, smoking (males only), alcoholics (males only) and total calories intake; ²Data are ORs, with 95% CIs in parentheses.

Table 4 Odds ratios (ORs)¹ and 95% confidence intervals (CIs) of gastric cancer in relation to quartiles of micronutrients and mineral salts by sex, Zhoushan, China

Nutrient/d ²	Males				P for trend	Females				P for trend
	Q ₁	Q ₂	Q ₃	Q ₄		Q ₁	Q ₂	Q ₃	Q ₄	
Carotene	1.0	1.82 (0.81-4.08)	0.40 (0.12-1.35)	0.81 (0.23-2.85)	>0.10	1.0	0.37 (0.08-1.70)	0.37 (0.08-1.78)	³	0.025
Vitamin A	1.0	0.59 (0.24-1.45)	0.91 (0.39-2.15)	0.43 (0.16-1.21)	>0.10	1.0	0.32 (0.05-2.21)	0.55 (0.10-3.14)	0.10 (0.01-0.89)	0.091
Vitamin C	1.0	1.15 (0.42-3.18)	1.40 (0.53-3.67)	0.88 (0.31-2.53)	>0.10	1.0	0.48 (0.09-2.5)	0.73 (0.15-3.6)	0.07 (0.01-0.95)	>0.10
Vitamin E	1.0	0.79 (0.29-2.11)	0.88 (0.34-2.29)	0.77 (0.26-2.26)	>0.10	1.0	0.93 (0.17-5.03)	1.32 (0.24-7.26)	0.95 (0.15-6.16)	>0.10
Na	1.0	1.36 (0.50-3.7)	0.91 (0.33-2.5)	3.22 (1.25-8.26)	0.070	1.0	3.70 (0.43-31.75)	0.75 (0.09-6.62)	8.40 (1.09-64.77)	>0.10
Ca	1.0	1.65 (0.64-4.20)	1.30 (0.46-3.62)	2.37 (0.81-6.91)	>0.10	1.0	2.30 (0.32-16.54)	3.78 (0.44-32.28)	4.79 (0.58-39.17)	>0.10
Se	1.0	0.48 (0.17-1.37)	0.78 (0.26-2.39)	1.23 (0.37-4.09)	>0.10	1.0	1.18 (0.20-6.87)	0.68 (0.11-4.23)	0.75 (0.12-4.68)	>0.10

¹Adjusted for age, present residence, education, economic status, smoking (males only), alcoholics (males only) and total calories intake; ²Data are ORs, with 95% CIs in parentheses; ³OR_{Q₄ vs Q₁} and 95%CI_{Q₄ vs Q₁} could not be calculated because of the null value of cases in the 4th group among females.

(OR, 10.30; 95%CI, 1.83-58.12), saturated fat (OR, 3.24; 95%CI, 1.11-9.49) and cholesterol (OR, 2.76; 95%CI, 1.01-7.53) in males. In females the risks remained elevated with increasing consumption of total fat (OR_{Q₄ vs Q₁}, 8.26; 95%CI, 1.03-66.51) and carbohydrates (OR_{Q₄ vs Q₁}, 14.78; 95%CI, 1.11-197.32). A marginally significant inverse linear trend was also observed for frequent consumption of polyunsaturated fat (OR_{Q₄ vs Q₁}, 0.10; 95%CI, 0.01-0.80) with the test for trend ($P = 0.068$).

The results of the micronutrient-intake (Table 4) uncovered a protective effect of vitamin A, with a marginally significant linear trend that held only for females (OR_{Q₄ vs Q₁}, 0.10; 95%CI, 0.01-0.89). Similarly, a protective effect was seen for the highest category of vitamin C consumption in female cases of gastric cancer (OR, 0.07; 95%CI, 0.01-0.95), but no linear trend was found ($P > 0.10$). In this data set, we found no significant relationship of gastric cancer with intake of vitamin E and carotene, although most OR values suggested a protective effect of them. Results from the analysis of mineral salt intake suggested a significant high-risk effect of sodium, regardless of their gender (OR_{Q₄ vs Q₁}, 3.22; 95%CI, 1.25-8.26 in males; OR_{Q₄ vs Q₁}, 8.4; 95%CI, 1.09-64.77 in females).

Further adjustment for other potential confounding factors, such as green tea drinking, occupation and family history of cancer, did not affect the associations with nutrient intakes. While 44% of the cases were diagnosed by methods other than histological confirmation, exclusion of these cases also did not alter our main findings.

DISCUSSION

The findings of this study confirm that several dietary factors identified elsewhere can also explain the incidence of gastric cancer in Zhoushan, Zhejiang Province, though gastric cancer did not decline in Zhoushan during the last 20 years. We also found that the incidence of gastric cancer in males and females is differently related to the intake of specific nutrients.

The results pertaining to an increased risk of gastric cancer due to the consumption of protein, fat and cholesterol are similar to those reported by Palli *et al.*, in Italy^[4]. In our study, the relationship between protein, saturated fat and cholesterol intake and gastric cancer was stronger in males after adjustment for other confounding

factors. Nitrites and salt in processed and smoked meats, commonly in the Zhoushan diet, are thought to play a role in the etiology of gastric cancer^[9]. In this regard, it is possible that saturated fat, cholesterol and protein consumption should be considered as proxy indicators for processed-meat consumption. We also found a protective effect of polyunsaturated fat against gastric cancer particularly in females, which is supported by other studies^[10,11].

A positive association with dietary carbohydrates has been reported in several studies of gastric cancer^[5,12,13]. In our study, the excess risk associated with carbohydrates contained in rice, noodles, and biscuits in the Chinese diet, could not be explained by education, present residence and economic status, although residual confounding by these or other unmeasured variables remains possible. Furthermore, the risk effect was stronger in females. The mechanism by which high consumption of carbohydrates may increase the risk of gastric cancer is unclear, but several possibilities have been suggested, including physical irritation (especially from rough whole-grain cereals), reduction in gastric mucin, and lowering of gastric pH with promotion of acid-catalyzed nitrosation^[14].

The most consistent finding in the relation between diet and gastric cancer is the protective effect of vegetables and fruits^[15-17]. A large number of potentially anti-carcinogenic agents are found in these food sources, such as carotenoids, vitamin C, vitamin A, fiber, and vitamin E, *etc.* In our study, we found a strong protective effect of vitamin A and vitamin C consumption against gastric cancer, particularly in females. Although the protective effect of vitamin C against gastric cancer has been mostly ascribed to its ability to inhibit formation of *N*-nitroso compounds from secondary amines and nitrite in the stomach, the role of vitamin C as a free-radical scavenger may be equally important^[18,19]. Vitamin A is also a well-known antioxidant, but its protective effect against gastric cancer is only occasionally reported^[12,20]. The decrease of gastric cancer risk in association with consumption of dietary fiber has also been observed^[21]. However, the mechanism of this protective effect has not yet been identified^[9]. Because vegetables and fruits not only are sources of fiber, but are the main contributions of vitamins A and C. Fiber may simply be a good indicator of consumption of plant food. As for the protective effect of vitamin E against gastric cancer, the epidemiologic results

are also inconsistent^[6,13,22-24]. In view of the anti-oxidant properties of vitamin E, it has the same mechanism as ascorbic acid. Our results are more inclined to support the hypothesis that vitamin E might reduce the risk of gastric cancer.

The analysis of mineral salts suggested that only sodium mainly from salts had an increased risk for gastric cancer, regardless of the gender. Foods that are high in salt or preserved with salt in some form (dried or pickled food) are associated with an increased risk for gastric cancer^[1,23,25]. Although the exact mechanism by which salt predisposes to gastric cancer is not known, salt can irritate the gastric cancer mucosa, making it more susceptible to carcinogenic change. Salt may also lead to atrophic gastritis, which is associated with increased risk for gastric cancer^[26-29]. Atrophic gastritis can lead to colonization by bacteria that can catalyze the conversion of nitrites to carcinogenic N-nitroso compounds^[30,31].

Although our findings are consistent with most previous studies of gastric cancer conducted in other countries, several potential limitations of our study should be noted. While the participation rate of the controls was relatively high (95%), only 75% of the eligible cases participated. Since there was generally a 3-mo delay between diagnosis and interview with cases, a few (10%) could not be connected for living in distant islands. Another main reason for non-participation was the death that occurred among cases (7.3%), thus raising the possibility of survival bias. If the identified risk factors could also affect the survival of gastric cancer patients, then exclusion of deceased cases may underestimate the true risks associated with these factors. On the other hand, selection bias, which tends to shift the risk estimates away from unity, should also be minimal since a small percentage of subjects refused to participate. As for the recall bias commonly existed in the dietary survey, efforts have been made to minimize it in various ways, including extensive training of interviewers, use of a standardized questionnaire and models of the more frequently consumed foods. But there were still many other potential recall biases not considered.

An additional limitation is that many nutrients are contained in the same food, and there is some correlation between the intake of certain nutrients, making it difficult to differentiate individual effects. Associations may also appear merely by chance because of the associations analyzed.

In summary, our results from the coastal areas confirm again that the diet plays an important role in the etiology of gastric cancer, and interventions against bad dietary structures may be important for the prevention of gastric cancer.

ACKNOWLEDGMENTS

The authors thank Dr. Yong-Nian Zhou *et al.*, and interns Jing Zhen *et al.*, for their participation in the dietary survey, and Zhoushan No. 1 Hospital, Zhoushan No. 3 Hospital, Zhoushan Traditional Chinese Medicine Hospital, People's Hospital of Putuo Islands, People's Hospital of Daishan Islands for their participation in this study.

REFERENCES

- 1 Geng GY, Liu RZ, Wang PS. EPIDEMIOLOGY (Volume Three). *Beijing, People's Medical Publishing House* 1996: 210-238
- 2 Palli D. Epidemiology of gastric cancer: an evaluation of available evidence. *J Gastroenterol* 2000; **35**(Suppl): 1284-1289
- 3 Laur'En P. The two histological main types of gastric carcinoma: diffuse and so called intestinal-type carcinoma. An attempt at a histo-clinical classification. *Acta Pathol Microbiol Scand* 1965; **64**: 31-49
- 4 Palli D, Russo A, Decarli A. Dietary patterns, nutrient intake and gastric cancer in a high-risk area of Italy. *Cancer Causes Control* 2001; **12**: 163-172
- 5 Chen H, Tucker KL, Graubard BI, Heineman EF, Markin RS, Potischman NA, Russell RM, Weisenburger DD, Ward MH. Nutrient intakes and adenocarcinoma of the esophagus and distal stomach. *Nutr Cancer* 2002; **42**: 33-40
- 6 Lopez-Carrillo L, Lopez-Cervantes M, Ward MH, Bravo-Alvarado J, Ramirez-Espitia A. Nutrient intake and gastric cancer in Mexico. *Int J Cancer* 1999; **83**: 601-605
- 7 Xiao JS, Wang MR. Matlab5.X and Scientific Calculation. *Beijing, Tsinghua Publishing House* 2000: 28-36
- 8 Ngoan LT, Mizoue T, Fujino Y, Tokui N, Yoshimura T. Dietary factors and stomach cancer mortality. *Br J Cancer* 2002; **87**: 37-42
- 9 van den Brandt PA, Botterweck AA, Goldbohm RA. Salt intake, cured meat consumption, refrigerator use and stomach cancer incidence: a prospective cohort study (Netherlands). *Cancer Causes Control* 2003; **14**: 427-438
- 10 Kim DY, Cho MH, Yang HK, Hemminki K, Kim JP, Jang JJ, Kumar R. Detection of methylation damage in DNA of gastric cancer tissues using 32P postlabelling assay. *Jpn J Cancer Res* 1999; **90**: 1104-1108
- 11 Chung S, Park S, Yang CH. Unsaturated fatty acids bind Myc-Max transcription factor and inhibit Myc-Max-DNA complex formation. *Cancer Lett* 2002; **188**: 153-162
- 12 Azevedo LF, Salgueiro LF, Claro R, Teixeira-Pinto A, Costa-Pereira A. Diet and gastric cancer in Portugal-a multivariate model. *Eur J Cancer Prev* 1999; **8**: 41-48
- 13 Jedrychowski W, Popiela T, Steindorf K, Tobiasz-Adamczyk B, Kulig J, Penar A, Wahrendorf J. Nutrient intake patterns in gastric and colorectal cancers. *Int J Occup Med Environ Health* 2001; **14**: 391-395
- 14 Munoz N, Plummer M, Vivas J, Moreno V, De Sanjose S, Lopez G, Oliver W. A case-control study of gastric cancer in Venezuela. *Int J Cancer* 2001; **93**: 417-423
- 15 De Stefani E, Correa P, Boffetta P, Ronco A, Brennan P, Deneo-Pellegrini H, Mendilaharsu M. Plant foods and risk of gastric cancer: a case-control study in Uruguay. *Eur J Cancer Prev* 2001; **10**: 357-364
- 16 Engel LS, Chow WH, Vaughan TL, Gammon MD, Risch HA, Stanford JL, Schoenberg JB, Mayne ST, Dubrow R, Rotterdam H, West AB, Blaser M, Blot WJ, Gail MH, Fraumeni JF Jr. Population attributable risks of esophageal and gastric cancers. *J Natl Cancer Inst* 2003; **95**: 1404-1413
- 17 Palli D, Russo A, Ottini L, Masala G, Saieva C, Amorosi A, Cama A, D'Amico C, Falchetti M, Palmirotta R, Decarli A, Costantini RM, Fraumeni JF Jr. Red meat, family history, and increased risk of gastric cancer with microsatellite instability. *Cancer Res* 2001; **61**: 5415-5419
- 18 Steinmetz KA, Potter JD. Vegetables, fruit, and cancer. II. Mechanisms. *Cancer Causes Control* 1991; **2**: 427-442
- 19 Bartsch H, Ohshima H, Pignatelli B. Inhibitors of endogenous nitrosation. Mechanisms and implications in human cancer prevention. *Mutat Res* 1988; **202**: 307-324
- 20 Abneth CC, Qiao YL, Dawsey SM, Buckman DW, Yang CS, Blot WJ, Dong ZW, Taylor PR, Mark SD. Prospective study of serum retinol, beta-carotene, beta-cryptoxanthin, and lutein/zeaxanthin and esophageal and gastric cancers in China. *Cancer Causes Control* 2003; **14**: 645-655
- 21 Roth J, Mobarhan S. Preventive role of dietary fiber in gastric cardia cancers. *Nutr Rev* 2001; **59**: 372-374
- 22 Taylor PR, Qiao YL, Abneth CC, Dawsey SM, Yang CS, Gunter

- EW, Wang W, Blot WJ, Dong ZW, Mark SD. Prospective study of serum vitamin E levels and esophageal and gastric cancers. *J Natl Cancer Ins* 2003; **95**: 1414-1416
- 23 **Ekstrom AM**, Serafini M, Nyren O, Hansson LE, Ye W, Wolk A. Dietary antioxidant intake and the risk of cardia cancer and noncardia cancer of the intestinal and diffuse types: a population-based case-control study in Sweden. *Int J Cancer* 2000; **87**: 133-140
- 24 **Kono S**, Hirohata T. Nutrition and stomach cancer. *Cancer Causes Control* 1996; **7**: 41-55
- 25 **Tsugane S**, Sasazuki S, Kobayashi M, Sasaki S. Salt and salted food intake and subsequent risk of gastric cancer among middle-aged Japanese men and women. Salt and salted food intake and subsequent risk of gastric cancer among middle-aged Japanese men and women. *Br J Cancer* 2004; **90**: 128-134
- 26 **Wang M**, Guo C, Li M. A case-control study on the dietary risk factors of upper digestive tract cancer. *Zhonghua Liuxingbingxue Zazhi* 1999; **20**: 95-97
- 27 **Fox JG**, Dangler CA, Taylor NS, King A, Koh TJ, Wang TC. High-salt diet induces gastric epithelial hyperplasia and parietal cell loss, and enhances *Helicobacter pylori* colonization in C57BL/6 mice. *Cancer Res* 1999; **59**: 4823-4828
- 28 **Tuyns AJ**. Salt and gastrointestinal cancer. *Nutr Cancer* 1988; **11**: 229-232
- 29 **Kuipers EJ**. Review article: Relationship between *Helicobacter pylori*, atrophic gastritis and gastric cancer. *Aliment Pharmacol Ther* 1998; **12**(Suppl 1): 25-36
- 30 **Hill MJ**. Bacterial N-nitrosation and gastric carcinogenesis in humans. *Ital J Gastroenterol* 1991; **23**: 17-23
- 31 **Walters CL**, Smith PL, Reed PI, Haines K, House FR. N-nitroso compounds in gastric juice and their relationship to gastroduodenal disease. *IARC Sci Publ* 1982: 345-355

Science Editor Wang XL and Guo SY Language Editor Elsevier HK

Growth inhibition of high-intensity focused ultrasound on hepatic cancer *in vivo*

Xiu-Jie Wang, Shu-Lan Yuan, Yan-Rong Lu, Jie Zhang, Bo-Tao Liu, Wen-Fu Zeng, Yue-Ming He, Yu-Rui Fu

Xiu-Jie Wang, Shu-Lan Yuan, Yan-Rong Lu, Jie Zhang, Division of Experimental Oncology, Key Laboratory of Biotherapy of Human Diseases of Ministry of Education, PR China; West China Hospital, Sichuan University, Chengdu 610041, Sichuan Province, China
Bo-Tao Liu, Wen-Fu Zeng, Yue-Ming He, Yu-Rui Fu, Mianyang Electronic Equipment Factory, Mianyang 621000, Sichuan Province, China

Supported by the Grant from National Economic Trade Committee, No. 2000-312-2

Correspondence to: Xiu-Jie Wang, Division of Experimental Oncology, Key Laboratory of Biotherapy of Human Diseases of Ministry of Education, PR China; West China Hospital, Sichuan University, Chengdu 610041, Sichuan Province, China. xiujiawang@sina.com

Telephone: +86-28-5423039 Fax: +86-28-85171476

Received: 2004-09-25 Accepted: 2004-10-26

Abstract

AIM: To investigate the damaging effect of high-intensity focused ultrasound (HIFU) on cancer cells and the inhibitory effect on tumor growth.

METHODS: Murine H₂₂ hepatic cancer cells were treated with HIFU at the same intensity for different lengths of time and at different intensities for the same length of time *in vitro*, the dead cancer cells were determined by trypan blue staining. Two groups of cancer cells treated with HIFU at the lowest and highest intensity were inoculated into mice. Tumor masses were removed and weighed after 2 wk, tumor growth in each group was confirmed pathologically.

RESULTS: The death rate of cancer cells treated with HIFU at 1 000 W/cm² for 0.5, 1, 2, 4, 8, and 12 s was 3.11±1.21%, 13.37±2.56%, 38.84±3.68%, 47.22±5.76%, 87.55±7.32%, and 94.33±8.11%, respectively. A positive relationship between the death rates of cancer cells and the length of HIFU treatment time was found ($r = 0.96$, $P < 0.01$). The death rate of cancer cells treated with HIFU at the intensity of 100, 200, 400, 600, 800, and 1 000 W/cm² for 8 s was 26.31±3.26%, 31.00±3.87%, 41.97±5.86%, 72.23±8.12%, 94.90±8.67%, and 99.30±9.18%, respectively. A positive relationship between the death rates of cancer cells and the intensities of HIFU treatment was confirmed ($r = 0.98$, $P < 0.01$). The cancer cells treated with HIFU at 1 000 W/cm² for 8 s were inoculated into mice *ex vivo*. The tumor inhibitory rate was 90.35% compared to the control ($P < 0.01$). In the experimental group inoculated with the cancer cells treated with HIFU at 1 000 W/cm² for 0.5 s, the tumor inhibitory rate was 22.9% ($P < 0.01$). By pathological examination, tumor

growth was confirmed in 8 out of 14 mice (57.14%, 8/14) inoculated with the cancer cells treated with HIFU at 1 000 W/cm² for 8 s, which was significantly lower than that in the control (100%, 15/15, $P < 0.05$).

CONCLUSION: HIFU is effective on killing or damage of H₂₂ hepatic cancer cells *in vitro* and on inhibiting tumor growth in mice *ex vivo*.

© 2005 The WJG Press and Elsevier Inc. All rights reserved.

Key words: HIFU; Liver cancer; Growth inhibition

Wang XJ, Yuan SL, Lu YR, Zhang J, Liu BT, Zeng WF, He YM, Fu YR. Growth inhibition of high-intensity focused ultrasound on hepatic cancer *in vivo*. *World J Gastroenterol* 2005; 11(28): 4317-4320

<http://www.wjgnet.com/1007-9327/11/4317.asp>

INTRODUCTION

High-intensity focused ultrasound (HIFU) consists of focused ultrasound (ULS) waves emitted from a transducer and is capable of inducing tissue damage. By means of this thermal effect and other mechanisms, HIFU-treated tumor tissues result in direct thermal cytotoxic necrosis and fibrosis, thus leading to inhibition of tumor growth. Therefore, HIFU is a new-sophisticated high-technology based minimally invasive treatment option for some cancers, which allows radiation-free treatment. Until now there are many kinds of tumors, such as tumors of prostate, liver, kidney, bladder, breast, and brain, that were treated with HIFU clinically and experimentally, some cancers were effectively controlled after HIFU treatment. As one of the minimally invasive surgical techniques for cancer treatment, HIFU is of great interest today^[1,2].

Malignant cells are sensitive to therapeutic ULS treatment, which leads to a transient decrease in cell proliferation^[3] through inducing a complex signaling cascade with upregulation of proapoptotic genes and downregulation of cellular survival genes^[4]. In *in vitro* study, it was confirmed that CZ901 HIFU inhibits proliferation and induces apoptosis of cancer cells^[5]. This study aimed to investigate the effects of HIFU on cancer cell damage *in vitro* and tumor growth inhibition *ex vivo*.

MATERIALS AND METHODS

Experimental materials

Cancer cell line in mouse Murine hepatoma H₂₂ cell line

was kept in liquid nitrogen for regular use in our laboratory^[6].

Experimental animals Female Balb/C mice, weighing 18–22 g, were purchased from Beijing Biological Products Research Institute under Ministry of Public Health (approval number: 013072). The procedures involving animals and their care were conducted in accordance with institutional guidelines for Laboratory Animal Care of Experimental Animal Center, Sichuan University.

Experimental device CZ901 HIFU device for cancer treatment was designed and supplied by Mianyang Electronic Equipment Factory.

Experimental methods

Experiment *in vitro* Ascites taken from H₂₂ hepatic cancer bearing mouse on d 8 or 9 was diluted with normal saline at 1:5 (2.5×10^7 cells/mL) and distributed into 14 PVC tubes, 7 tubes in each test, each containing 1.8 mL. Twelve tubes were treated with HIFU, and two were used as controls. H₂₂ hepatic cancer cells were treated with HIFU at the frequency of 1.048 MHz and at the intensity of 1 000 W/cm² for 0.5, 1, 2, 4, 8, and 12 s, respectively, and for 8 s at intensity of 100, 200, 400, 600, 800, and 1 000 W/cm², respectively. After HIFU treatment, the cells were incubated in a humidified atmosphere of 50 µg/mL CO₂ at 37 °C for 6 h, and then the viability of cancer cells was determined by exclusion of trypan blue staining. The viable cells were not stained, the dead cells were stained blue. The viable cells and dead cells were counted with an erythrocytometer under microscope, respectively (total cell number counted >1 000). The death rate was determined by $\frac{\text{dead cell number}}{\text{dead cell number} + \text{viable cell number}} \times 100\%$. Each experiment was performed in triplicate.

Inoculation of HIFU-treated cancer cells *ex vivo* Cancer

cells including viable and dead cells treated with HIFU at 1 000 W/cm² for 8 s were inoculated into 14 mice, 2×10^6 cells/0.2 mL per mouse. The same number of untreated cancer cells was inoculated into 20 mice as control. In addition, cancer cells treated with HIFU at 1 000 W/cm² for 0.5 s were inoculated into 18 mice, 2×10^6 cells/0.2 mL per mouse. The same number of untreated cancer cells was inoculated into 20 mice as control.

Examining the tumor growth *ex vivo* The animals inoculated with cancer cells were raised routinely, with free access to food and water and weighed every 2 d. After 2 wk of inoculation, the animals were killed, the tumor masses were removed and weighed, and the tumor inhibitory rate was calculated^[6].

Histopathological examination Tumor masses were fixed with 4% paraformaldehyde, embedded with paraffin, sectioned and stained with HE. The tumor growth inhibition was confirmed by microscopy.

Statistical analysis

The experimental data were expressed as mean ± SD and analyzed with χ^2 test. $P < 0.05$ was considered statistically significant.

RESULTS

Cell damage effect of HIFU *in vitro*

The death rate of cancer cells in controls was 3–5% (Figure 1A), and increased significantly after HIFU treatment (Figure 1B). The death rate of cancer cells treated with HIFU at 1 000 W/cm² for 0.5, 1, 2, 4, 8, and 12 s were $3.11 \pm 1.21\%$, $13.37 \pm 2.56\%$, $38.84 \pm 3.68\%$, $47.22 \pm 5.76\%$, $87.55 \pm 7.32\%$, and $94.33 \pm 8.11\%$, respectively (Figure 1C). A positive

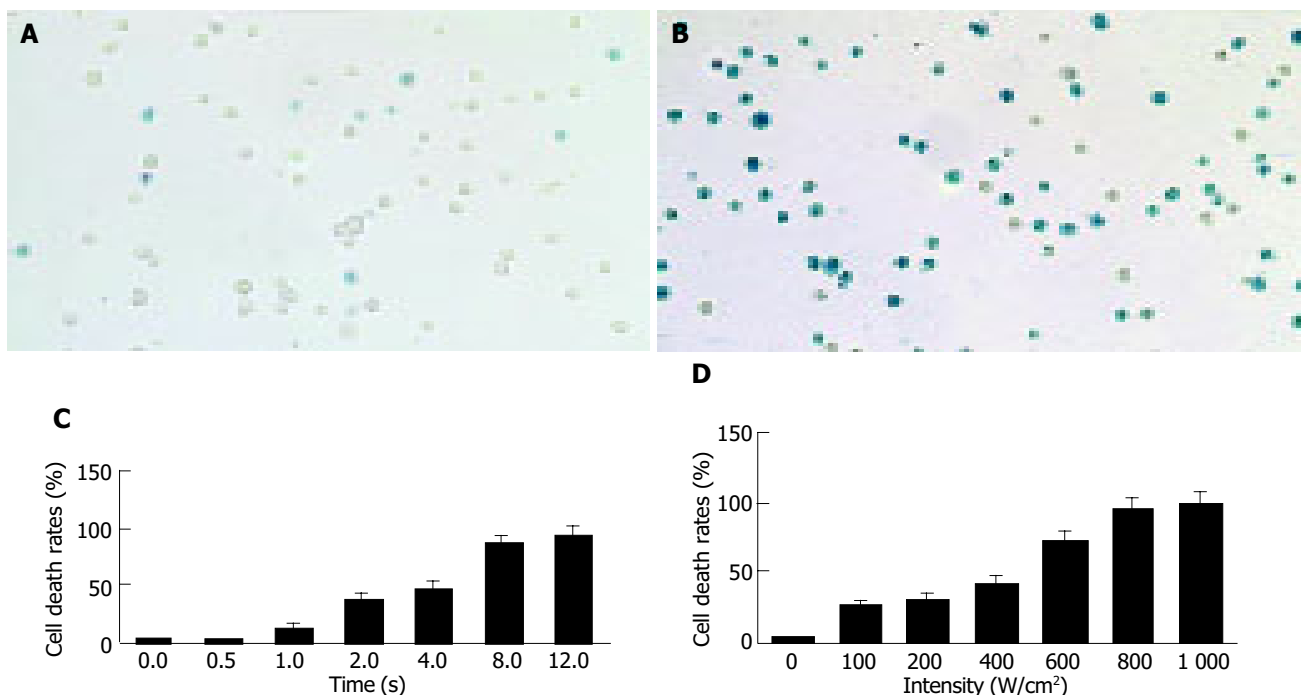


Figure 1 Cell damage effect of HIFI *in vitro*. **A:** Murine hepatic cancer cells before HIFU treatment; **B:** murine hepatic cancer cells treated with HIFU at 1 000 W/cm² for 8 s; **C:** significant difference between cell death rate and time of HIFU

treatment; **D:** significant difference between the cell death rate and intensity of HIFU treatment.

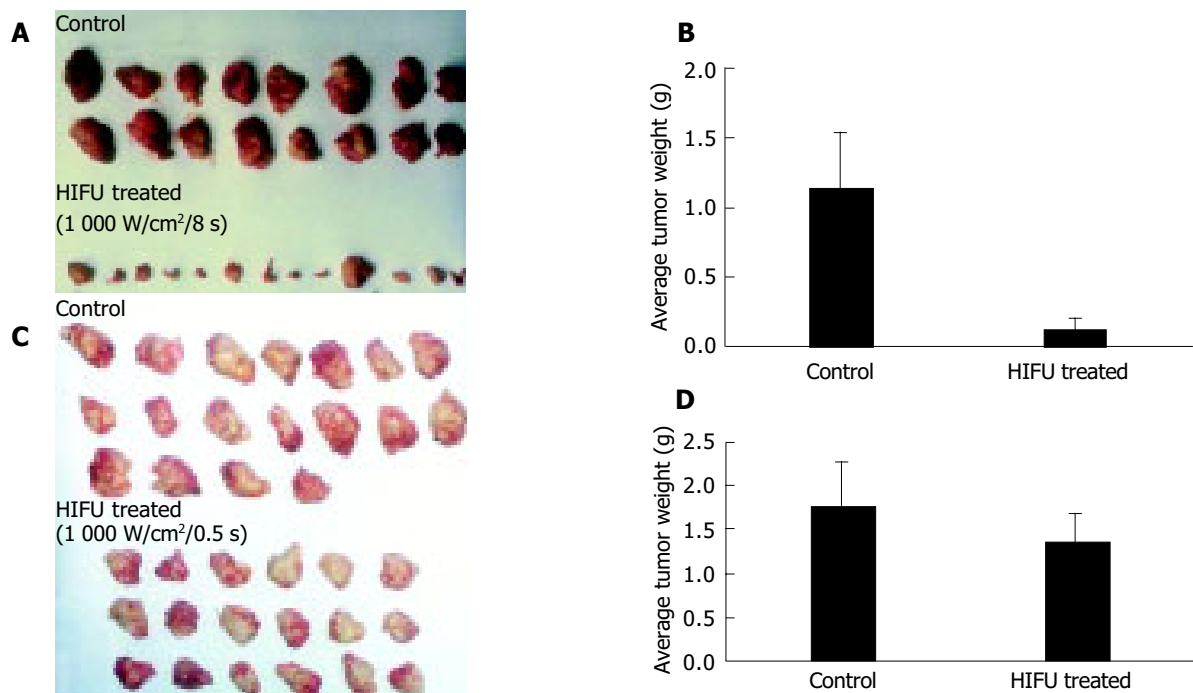


Figure 2 Tumor growth inhibition of HIFU *ex vivo*. **A:** Tumor growth inhibition of HIFU at 1 000 W/cm² for 8 s; **B:** significant difference in average tumor weight between the control and HIFU-treated mice; **C:** tumor growth inhibition of HIFU

at 1 000 W/cm² for 0.5 s; **D:** significant difference in average tumor weight between the control and HIFU-treated mice.

relationship was found between the death rate of cancer cells and the time of HIFU treatment ($r = 0.96, P < 0.01$).

The death rate of cancer cells treated with HIFU at the intensity of 100, 200, 400, 600, 800, and 1 000 W/cm² for 8 s was 26.31±3.26%, 31.00±3.87%, 41.97±5.86%, 72.23±8.12%, 94.90±8.67%, and 99.30±9.18%, respectively (Figure 1D). A positive relationship was confirmed between the death rates of cancer cells and the intensities of HIFU treatment ($r = 0.98, P < 0.01$).

Tumor growth inhibition of HIFU *ex vivo*

Tumor growth inhibition of cancer cells treated with HIFU *ex vivo* is listed in Table 1. In experiment 1, six mice in the control group died of tumor burden spontaneously, none died in the HIFU-treated group. There was no significant difference in body weight increase between two groups of animals. In the group of animals inoculated with cancer cells treated with HIFU at 1 000 W/cm² for 8 s, the average tumor weight was 0.11±0.16 g, and the average tumor weight in control group was 1.14±0.4 g (Figures 2A and B), the tumor inhibition rate was 90.35% compared to the control ($P < 0.01$). In experiment 2, cancer cells treated with HIFU

at 1 000 W/cm² for 0.5 s were inoculated. The average tumor weight in HIFU-treated group and control was 1.36±0.33 and 1.75±0.53 g, respectively (Figures 2C and D), the tumor inhibitory rate was 22.90% ($P < 0.01$).

By pathological examination, tumor growth was confirmed in 8 out of 14 mice (57.14%, 8/14) inoculated with cancer cells treated with HIFU at 1 000 W/cm² for 8 s, which was significantly lower than that of the control (100%, 15/15, $P < 0.05$).

DISCUSSION

HIFU consists of focused ULS waves emitted from a transducer and is capable of inducing tissue damage. By means of this thermal effect and other mechanisms, HIFU-treated tumor tissues resulted in direct thermal cytotoxic necrosis and fibrosis, thus leading to inhibition of tumor growth. Therefore, HIFU is a new-sophisticated high-technology based, minimally invasive treatment option for some cancers^[1,4,5]. But, there are many factors affecting its therapeutic effect, such as, intensity of the transmitted pulse, the exposure time, the signal frequency, the time interval

Table 1 Inhibitory effect of HIFU on growth of hepatic cancer *ex vivo* (mean±SD)

Experiment group	HIFU treatment (1 000 W/cm ²)	Animals (n)		Average BW (g)		Tumor wt (g)	TIR (%)	
		d _i	d ₁₄	d _i	d ₁₄			
1	Control	0	20	15	19.05±2.03	19.62±2.13	1.14±0.40	90.35
	HIFU	8	14	14	19.69±1.34	21.45±0.99	0.11±0.16 ^b	
2	Control	0	20	19	21.03±2.14	28.39±3.83	1.75±0.53	22.29
	HIFU	0.5	18	18	22.68±2.73	27.46±4.03	1.36±0.33 ^b	

BW: Body weight; wt: weight; TIR: tumor inhibitory rate. ^b $P < 0.01$ vs control.

between two firing bursts, and biological medium, *etc.*^[1,7-9].

The HIFU device used in this experimental study was designed and manufactured in Mianyang Electronic Equipment Factory. Its signal frequency emitted is 1.048 MHz, the intensity of the transmitted pulse and exposure time can be manipulated^[5]. In this experimental study, H₂₂ hepatic cancer cells were treated with HIFU at the same intensity for different lengths of time and for the same length of time at different intensities *in vitro*. It showed a intensity and time-dependent damaging effect on cancer cells (Figures 1B-D), suggesting that HIFU has a damaging or killing effect on cancer cells *in vitro*. The effective parameters are: an intensity of 1 000 W/cm² and an exposure time of 8 s.

There are many experimental and clinical studies on treatment of tumors with HIFU^[1,10-14], especially hepatic cancers^[15-19]. The results of these studies *in vitro* and *in vivo* indicate that HIFU has damaging or killing effect on cancer cells *in vitro* and inhibitory effect on tumor growth *in vivo*. However, to our best knowledge, there is no study on the growth potential of cancer cells after HIFU treatment. The findings in this study indicate that most cancer cells treated with HIFU at 1 000 W/cm² would die and lose the proliferating potential, but few cells may survive and form tumors.

Although minimally invasive methods for the treatment of cancer, such as HIFU, and high-energy shock waves, have been proposed recently, their feasibility for treatment of human cancers needs to be confirmed^[1,20]. This experimental study has confirmed that HIFU has effects on killing or damage of H₂₂ hepatic cancer cells *in vitro* and on the inhibiting tumor growth in mice *ex vivo*. Its inhibitory and therapeutic effects on other cancers, and mechanisms of action need to be studied and confirmed further.

REFERENCES

- 1 **Chaussy CG**, Thuroff S. High-intensive focused ultrasound in localized prostate cancer. *J Endourol* 2000; **14**: 293-299
- 2 **Beerlage HP**, Thuroff S, Madersbacher S, Zlotta AR, Aus G, de Reijke TM, de la Rosette JJ. Current status of minimally invasive treatment options for localized prostate carcinoma. *Eur Urol* 2000; **37**: 2-13
- 3 **Ashush H**, Rozenszajn LA, Blass M, Barda-Saad M, Azimov D, Radnay J, Zipori D, Rosenschein U. Apoptosis induction of human myeloid leukemic cells by ultrasound exposure. *Cancer Res* 2000; **60**: 1014-1020
- 4 **Abdollahi A**, Domhan S, Jenne JW, Hallaj M, Aqua GD, Mueckenthaler M, Richter A, Martin H, Debus J, Ansoerge W, Hynynen K, Huber PE. Apoptosis signals in lymphoblasts induced by focused ultrasound. *FASEB J* 2004; **18**: 1413-1414
- 5 **Wang XJ**, Yuan SL, Zhang J, Lu YR, Wang YP, Chen XH, Ning QZ, Fu YR, Liu BT, Zeng WF, He YM. A study of the proliferation inhibition effect of HIFU and its mechanism of action on human breast cancer cells. *Sichuan Daxue Xuebao Yixueban* 2004; **35**: 60-63
- 6 **Wang X**, Yuan S, Wang C. A preliminary study of the anti-cancer effect of tanshinone on hepatic carcinoma and its mechanism of action in mice. *Zhonghua Zhongliu Zazhi* 1996; **18**: 412-414
- 7 **Beerlage HP**, Thuroff S, Debruyne FM, Chaussy C, de la Rosette JJ. Transrectal high-intensity focused ultrasound using the Ablatherm device in the treatment of localized prostate carcinoma. *Urology* 1999; **54**: 273-277
- 8 **Chapelon JY**, Ribault M, Vernier F, Souchon R, Gelet A. Treatment of localised prostate cancer with transrectal high intensity focused ultrasound. *Eur J Ultrasound* 1999; **9**: 31-38
- 9 **Wang Z**, Bai J, Li F, Du Y, Wen S, Hu K, Xu G, Ma P, Yin N, Chen W, Wu F, Feng R. Study of a "biological focal region" of high-intensity focused ultrasound. *Ultrasound Med Biol* 2003; **29**: 749-754
- 10 **Yang R**, Reilly CR, Rescorla FJ, Faught PR, Sanghvi NT, Fry FJ, Franklin TD Jr, Lumeng L, Grosfeld JL. High-intensity focused ultrasound in the treatment of experimental liver cancer. *Arch Surg* 1991; **126**: 1002-1009
- 11 **Cheng SQ**, Zhou XD, Tang ZY, Yu Y, Bao SS, Qian DC. Iodized oil enhance the thermal effect of high-intensity focused ultrasound on ablating experimental liver cancer. *J Cancer Res Clin Oncol* 1997; **123**: 639-744
- 12 **Adams JB**, Moore RG, Anderson JH, Strandberg JD, Marshall FF, Davoussi LR. High-intensity focused ultrasound ablation of rabbit kidney tumors. *J Endourol* 1996; **10**: 71-75
- 13 **Madersbacher S**, Kratzik C, Susani M, Pedevilla M, Marberger M. Transcutaneous high-intensity focused ultrasound and irradiation: an organ-preserving treatment of cancer in a solitary testis. *Eur Urol* 1998; **33**: 195-201
- 14 **Van Leenders GJ**, Beerlage HP, Ruijter ET, de la Rosette JJ, van de Kaa CA. Histopathological changes associated with high intensity focused ultrasound (HIFU) treatment for localised adenocarcinoma of the prostate. *J Clin Pathol* 2000; **53**: 391-394
- 15 **Prat F**, Centarti M, Sibille A, Abou el Fadil F, Henry L, Chapelon JY, Cathignol D. Extracorporeal high-intensity focused ultrasound for VX2 liver tumors in the rabbit. *Hepatology* 1995; **22**: 832-836
- 16 **Sibille A**, Prat F, Chapelon JY, Abou el Fadil F, Henry L, Theillere Y, Ponchon T, Cathignol D. Extracorporeal ablation of liver tissue by high-intensity focused ultrasound. *Oncology* 1993; **50**: 375-379
- 17 **Yang R**, Sanghvi NT, Rescorla FJ, Kopecky KK, Grosfeld JL. Liver cancer ablation with extracorporeal high-intensity focused ultrasound. *Eur Urol* 1993; **23**(Suppl 1): 17-22
- 18 **Sibille A**, Prat F, Chapelon JY, Abou el F, Henry L, Theillere Y, Ponchon T, Cathignol D. Characterization of Extracorporeal ablation of normal and tumor-bearing liver tissue by high-intensity focused ultrasound. *Ultrasound Med Biol* 1993; **19**: 803-813
- 19 **Arefiev A**, Prat F, Chapelon JY, Tavakkoli J, Cathignol D. Ultrasound-induced tissue ablation: studies on isolated perfused porcine liver. *Ultrasound Med Biol* 1998; **24**: 1033-1043
- 20 **Thuroff S**, Chaussy C. High-intensity focused ultrasound: complications and adverse events. *Mol Urol* 2000; **4**: 183-187

Classification of right hepatectomy for special localized malignant tumor in right liver lobe

Ning Fan, Guang-Shun Yang, Jun-Hua Lu, Ning Yang

Ning Fan, Guang-Shun Yang, Jun-Hua Lu, Ning Yang, Department of Laparoscopy, Affiliated Eastern Hospital of Hepatobiliary Surgery, Second Military Medical University, Shanghai 200438, China

Co-first-authors: Guang-Shun Yang and Ning Fan

Correspondence to: Professor Guang-Shun Yang, Department of Laparoscopy, Affiliated Eastern Hospital of Hepatobiliary Surgery, Second Military Medical University, Shanghai 200438, China. guangshun@smmu.edu.cn

Telephone: +86-21-25070803 Fax: +86-21-25070803

Received: 2004-12-06 Accepted: 2005-01-05

Abstract

AIM: To describe a new classification method of right hepatectomy according to the different special positions of tumors.

METHODS: According to positions, 91 patients with malignant hepatic tumor in the right liver lobe were divided into six groups: tumors in the right posterior lobe and (or) the right caudate lobe compressing the right portal hilum ($n = 14$, 15.4%), tumors in the right liver lobe compressing the inferior vena cava and (or) hepatic veins ($n = 11$, 12.9%), tumors infiltrating diaphragmatic muscle ($n = 7$, 7.7%), tumors in the hepatorenal recess (infiltrating the right fatty renal capsule, transverse colon and right adrenal gland, $n = 8$, 8.8%), tumors deeply located near the vertebral body ($n = 3$, 3.3%), tumors at other sites in the right liver lobe (the control group, $n = 48$, 52.75%). The values of intraoperative blood loss (IBL), tumor's maxim cross-section area (TMCSA), and time of hepatic hilum clamping (THHC) and incidence of postoperative complications were compared between five groups of tumor and control group, respectively.

RESULTS: The THHC in groups 1-4 was significantly longer than that in the control group, the IBL in groups 1-4 was significantly higher than that in the control group, the TMCSA in groups 2-4 was significantly larger than that in the control group, and the ratio of IBL/TMCSA in group 1 was significantly higher than that in the control group. There was no significant difference in the indexes between group 5 and the control group.

CONCLUSION: The site of tumor is the key factor that determines IBL.

© 2005 The WJG Press and Elsevier Inc. All rights reserved.

Key words: Hepatectomy; Tumor; Position; Complication;

Blood Loss; Clamping time

Fan N, Yang GS, Lu JH, Yang N. Classification of right hepatectomy for special localized malignant tumor in right liver lobe. *World J Gastroenterol* 2005; 11(28): 4321-4325 <http://www.wjgnet.com/1007-9327/11/4321.asp>

INTRODUCTION

Clinically, 60% of malignant tumors occur in the right liver which has a great physical volume and complicated anatomic structure, with a large number of vessels inside and important organs around, such as diaphragmatic muscle, right kidney, right adrenal gland, colon, and inferior vena cava. Therefore, tumors in the right liver lobe with different sizes and diversified positions may induce a widely different series of problems in the process of resection of these tumors. Generally, the easily removed tumor has a diameter less than 5 cm and is located on the surface of liver without infiltrating the surrounding important organs, or does not compress the main blood vessels in the liver. The features of tumors which are different to resect are as follows. (1) The diameter of tumor is larger than 5 cm and the tumor is close to or even infiltrates the major vessels of liver; (2) Although the diameter of tumor is less than 5 cm, it protrudes from the liver surface infiltrating surrounding organs. The tumor is deeply located and hard to be exposed during surgery. The tumor which meets one or more of the above standards is defined as the malignant tumor within the right liver with special position (MTRLSP). For the much more intraoperative blood loss (IBL), the longer the time of hepatic hilum clamping (THHC), the more the postoperative complications. MTRLSP has been a difficulty in right hepatectomy. Little information is available on the classification of right hepatectomy for MTRLSP. This paper presents a prospective observation on the surgical features of 91 cases of right hepatectomies, and the classification according to the standards mentioned above.

MATERIALS AND METHODS

Study population

Ninety-one patients with malignant tumor within the right liver underwent right hepatectomy from 2002-05 to 2003-09 at Eastern Hepatobiliary Surgery Hospital of Second Military Medical University. There were 73 male and 18 female patients, ranging 25-78 years of age, including 87 cases of primary liver cancer, 2 cases of colon metastatic cancer, 1 case of rectum metastatic cancer, and 1 case of

liver lymphoma. There were four cases of tumor thrombosis in portal vein and two cases in the bile duct. No death occurred in hospital.

Grouping

Forty-three cases of MTRLSPs were divided into five groups in light of tumor positions, and 48 cases of tumors at other sites within right liver lobe in the corresponding period served as the control (Table 1).

Table 1 Grouping of 91 cases of right hepatectomies

Tumor position		Cases (%)	Total (%)
MTR			
LSP	Group 1 Tumors within right posterior lobe and (or) right caudate lobe compressing right portal hilum	14/91 (15.4)	43/91 (47.25)
	Group 2 Massive tumors within right liver lobe compressing the inferior vena cava and (or) hepatic veins	11/91 (12.09)	
	Hepato-renal infiltrating transverse colon	7/91 (7.7)	
	Recess infiltrating right adrenal gland	4/91 (4.4)	
	Group 3 Tumors infiltrating diaphragmatic muscle	3/91 (3.3)	
	Group 4 Tumors in the infiltrating right fatty renal capsule	1/91 (1.1)	
	Group 5 Tumors deeply located near vertebral body control	3/91 (3.3)	
	Group 6 Tumors in other places	48/91 (52.75)	

Methods

The Pringle's maneuver was routinely adopted in tumor resection to control bleeding. The THHC was recorded during surgery, and the IBL and the TMCSA were measured after surgery. The postoperative complication of each patient was also recorded. The IBL, THHC (used for evaluating tumor size), TMCSA and postoperative complications in each group were compared to those in the control group respectively.

Statistical analysis

The data were expressed as mean±SE. SPSS for Windows, version 11.0 was used with Dunnett-*t* or Wilcoxon signed rank test.

RESULTS

The values of THHC in each group are shown in Table 2. The time in groups 1-4 was much longer than that in group 6 ($P<0.05$), but not in group 5 ($P>0.05$). For *F*-test = 0.078>0.05, bilateral Dunnett-*t* was used.

The values of IBL in each group are shown in Table 3. The value of IBL in groups 1-4 was much greater than that in group 6 ($P<0.05$), but not in group 5 ($P>0.05$). For *F*-test = 0.007<0.05, bilateral Wilcoxon signed rank test was used.

The values of TMCSA in each group are shown in Table 4. The value of TMCSA in groups 2-4 was much larger than that in group 6 ($P<0.05$), but not in groups 1 and 5 ($P>0.05$). For *F*-test = 0.000<0.05, bilateral Wilcoxon signed rank test was used.

The ratios of IBL/TMCSA in each group are shown in Table 5. The value of IBL in groups 2-5 was not significantly higher than that in group 6 ($P>0.05$), but not in group 1 ($P<0.05$). For *F*-test = 0.114>0.05, bilateral Dunnett-*t* was used.

The rate of blood transfusion during surgery and the

Table 2 THHC in groups 1-6 (mean±SE)

Group	1	2	3	4	5	6
THHC (min)	31.00±3.53	36.72±2.41	31.42±4.56	29.75±2.53	17±2.51	19.148±1.27
<i>P</i> values	0.001 ^a	0.000 ^a	0.013 ^a	0.028 ^a	0.998	-

^a $P<0.05$ vs control.

Table 3 IBL in groups 1-6 (mean±SE)

Group	1	2	3	4	5	6
IBL (mL)	642.85±132.89	1 054.54±200.16	1 085.71±310.47	850.00±185.16	483.33±60.09	257.40±29.44
<i>P</i> values	0.033 ^a	0.005 ^a	0.046 ^a	0.011 ^a	0.285	-

^a $P<0.05$ vs control.

Table 4 TMCSA in groups 1-6 (mean±SE)

Group	1	2	3	4	5	6
TMCSA (cm ²)	20.61±4.67	84.95±11.76	56.38±12.50	46.87±5.59	51.88±40.2	22.77±3.67
<i>P</i> values	0.683	0.003 ^a	0.028 ^a	0.012 ^a	0.593	-

^a $P<0.05$ vs control.

Table 5 IBL/TMCSA in groups 1-6 (mean±SE)

Group	1	2	3	4	5	6
IBL/TMCSA (mL/cm ²)	38.14±9.91	14.81±2.79	22.85±6.76	17.13±2.61	34.33±20.98	13.42±2.24
P values	0.003 ^a	1.000	0.788	0.994	0.387	

^aP<0.05 vs control.

Table 6 Blood transfusion and incidence of postoperative complications in groups 1-6 (%)

Group	1	2	3	4	5	6
Blood transfusion	35.71	45.45	42.86	37.5	0	0
Incidence of postoperative complications	14.29	36.36	71.43	37.5	0	0

incidence of postoperative complications in each group are shown in Table 6, the above two values were all zero in groups 5 and 6. The main postoperative complication in groups 1, 2, and 4 was right pleural effusion. The main postoperative complications in group 3 were right pleural effusion and rupture of diaphragm.

DISCUSSION

According to the definition of MTRLSP, the proportion of MTRLSP is 47.25% (Table 1), which shows that nearly half of right hepatectomies for malignant tumors are the high-risk resections for MTRLSPs. The IBL, THHC, and postoperative complications are the three risk factors for the resection for MTRLSP; tumor size and site determine these factors. In this study, taking the influence of tumor size as the index of IBL/TMCSA, we divided the MTRLSPs into five groups according to their positions to analyze and identify the main reason for high-risk resections of tumors in each group.

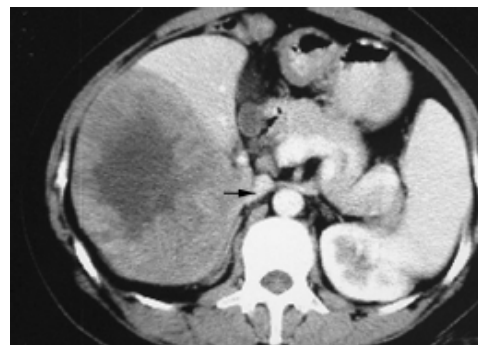
Tumors in the group 1 ($n = 14$, 15.4%) within the right posterior lobe and (or) right caudate lobe usually compressed or even infiltrated the right posterior portal vein (RPPV, Figure 1), occasionally with the tumor thrombus in vessels. Tumor thrombi almost all occurred in this (in portal branch, $n = 3$, 3/4 = 75%; in bile duct, $n = 2$, 2/2 = 100%). The tumor was usually located between the first and third hepatic hilum with some main blood vessels around, such as the RPPV, inferior vena cava (IVC). It was difficult to control bleeding in an extremely dangerous state once these main vessels rupture when the tumor was exposed, and to injure

the first hepatic hilum if blind suture was used to stop bleeding. Therefore, the IBL (642.85 ± 132.89 mL) was much greater than that in the control group (257.40 ± 29.44 mL, $P = 0.033$), and the THHC (31.00 ± 3.53 min) was also significantly longer than that in the control group (19.148 ± 1.27 , $P = 0.001$), though there was no statistical difference ($P = 0.683$) in TMCSA between this group (20.61 ± 4.67 cm²) and control group (22.77 ± 3.67 cm²). The main reason for high-risk resection of tumors of this group is the site but not the size of tumors, which is further proved by the fact that the index of IBL/TMCSA (38.14 ± 9.91) was significantly higher than that in the control group (13.42 ± 2.24 , $P = 0.003$).

For example, an operation of 1 patient with the tumor in the right caudate going down to left caudate ran into trouble. After the tumor was ablated from the wall of the compressed IVC and RPPV, it was impossible to suture the wound because the nude right portal branch was just on the surface of the incision wedge. A drainage tube was placed instead of suture of the wound. A bile leakage was found 3 d after surgery which was closed after drainage.

Generally, to handle the tumor at this site, we should remove it as soon as possible, and suture the liver wound by any possible way, and observe the characteristics of drainage carefully in case the severe bile leakage occurs after surgery^[1].

Tumors ($n = 11$, 12.9%) in group 2 compressing part or completely at the inferior vena cava ($n = 6$, Figure 2) and (or) hepatic veins ($n = 4$, Figure 3) had the largest size in groups 1-6, with TMCSA being 84.95 ± 11.76 cm², larger than that in the control group 22.77 ± 3.67 cm², $P = 0.003$. They were so large that they almost occupy the whole right

**Figure 1** Tumor infiltrating right posterior portal vein (→).**Figure 2** Tumor compressing IVC (→).

liver lobe.

The IBL ($1\ 054.54 \pm 200.16$ mL) and THHC (36.72 ± 2.41 min) were much greater and longer than those in the control group (IBL: 257.40 ± 29.44 mL, $P = 0.005$; THHC: 19.148 ± 1.27 min, $P = 0.000$), suggesting a higher risk for surgery in this group. But there was no statistical difference in the index of IBL/TMCSA (14.81 ± 2.79) between this group and control group (13.42 ± 2.24 , $P = 1.000$), suggesting that IBL is not much greater than that in the control group when the influence of tumor size is excluded. Apparently, the biggest tumor size is the main reason for the top 36 min THHC and 1 054 mL IBL in this group.

Some troubles caused by the compression of the IVC from tumors are as follows. When the tumor is removed from normal liver, severe bleeding may occur due to lacerated breakage on the IVC wall or crevasse of the hepatic short vein (HSV) with ligation falling off. After the tumor is removed, the remnant liver with full-length IVC uncovered on a wide surface of the incision wedge may be hard to be sutured for the fear of IVC obstruction due to compression from suture of wound. The obstruction can induce liver swelling and severe cirrhosis. The treatment strategies may be summarized as follows. (1) If the image of a tumor shows preoperatively that the tumor compresses or infiltrates the IVC, the blocking string should be preplaced around the superior and inferior IVC to the effect that severe bleeding can be easily controlled. The breakage is better sutured with 3-0 prolene, but not clamped. In addition, the HSV and the right adrenal gland vein should be abscised and ligated carefully; (2) To avoid compression of the IVC, an incision wedge should be shaped 'arc' so that both sides can be sutured with the IVC untouched at the bottom of the wound, and the remnant liver can be suspended to the abdomen wall. If the above measures do not work, the sutures of liver wound should be taken out, and then after careful hemostasis, the epiploon can be sutured to the incision wedge. Recently, some studies reported^[2,3] that fibrin sealant can be ejected to the surface of liver wound to hemostasis, and results are quick and good.

The other sort of troubles comes from compression and infiltration of right hepatic veins (RHV) by a tumor under which there is usually a part of normal liver (Figure 3). Whether this part of normal liver should be excised with the tumor depends on the following two situations: (1) If a patient has severe liver cirrhosis and small left liver lobe,

the normal liver in right posterior should be retained, and so does the RHV or dilated HSV to ensure blood flowing back^[4]; (2) If a patient has mild liver cirrhosis and thick left liver lobe, the remnant liver and RHV can be excised with the tumor.

Tumors in group 3 ($n = 7$, 7.7%) had the highest value of IBL among all groups ($1\ 085.71 \pm 310.47$ mL *vs* the control 257.40 ± 29.44 mL, $P = 0.046$). One reason is that tumors usually grow out of liver surface and adhere to diaphragm with abundant bypass blood vessels. The other reason is the large TMCSA (56.38 ± 12.50 cm² *vs* the control 22.77 ± 3.67 cm², $P = 0.028$). The larger the tumor and the wider the interface between tumor and diaphragm, the more the bleeding during surgery. But there was no statistical difference in the index of IBL/TMCSA (22.85 ± 6.76) between this group and control group (13.42 ± 2.24 , $P = 0.788$), suggesting that IBL is not much greater than that in the control group when the influence of tumor size is excluded. The higher IBL and bigger TMCSA induce longer THHC (31.42 ± 4.56 min *vs* the control 19.148 ± 1.27 min, $P = 0.013$) and higher incidence of postoperative complications ($n = 5/7 = 71.43\%$, Table 6) such as right pleural effusion ($n = 3$) and diaphragm rupture ($n = 2$).

Tumors which infiltrate the diaphragm growing in an expansible fashion are usually too big to control during surgery, and should be excised integrally without the diaphragm being broken. But because of limited operational space for removal of surrounding ligaments around the liver, it is inevitable that tumors are occasionally oppressed. Once tumor ruptures, a large quantity of low osmosis water should be used to wash the peritoneal cavity to prevent tumor planting. In addition, a part of the diaphragm approaching the liver is also flimsy and frangible^[5] (Figure 4).

Thoracoabdominal approach for resection of this sort of tumors has been adopted by Xia *et al.*^[6]. They found that the IBL is less and better exposed to hemostasia than abdominal approach, without an increasing incidence of postoperative complications, but with increased trauma and more complicated operative procedure. Our study also found a higher volume of the IBL and a higher incidence of postoperative complications. Therefore, along with the development of surgical technique and perioperative intensive care, thoracoabdominal approach may be reasonable for the resection of this sort of tumors.

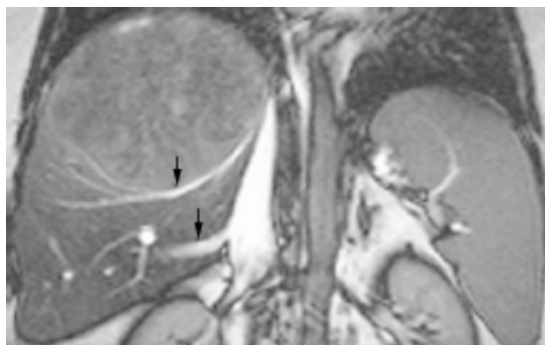


Figure 3 Tumor compressing RHV (→).

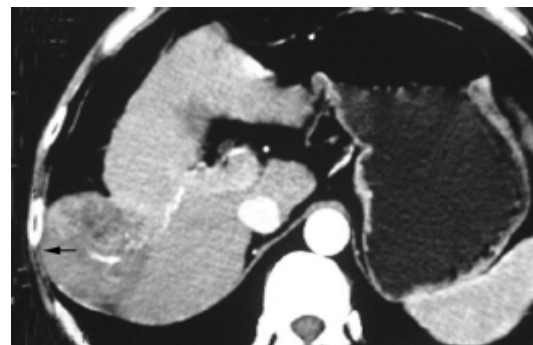


Figure 4 Tumor infiltrating diaphragm muscle (→).

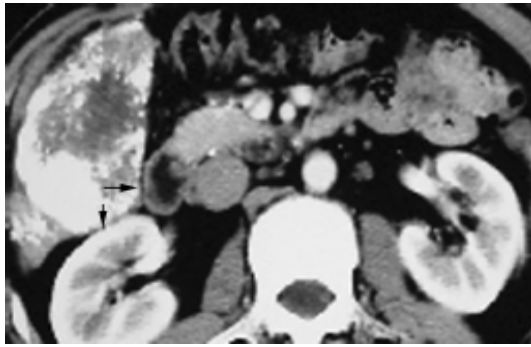


Figure 5 Tumor infiltrating colon (→) and right fatty renal capsule (←).

Tumors in group 4 ($n = 8$, 8.8%; infiltrating right fatty renal capsule $n = 4$, transverse colon $n = 3$, right adrenal gland, $n = 1$) protruding to hepatorenal recess were prone to infiltrate the right fatty renal capsule, transverse colon (Figure 5) or right adrenal gland and induce wide conglutination which caused the following difficulties. (1) Abundant bypass vessels between tumor and its surroundings were likely to bleed in the course of exploration and liberation. The IBL of this group (850.00 ± 185.16 mL) was significantly greater than that in the control group (257.40 ± 29.44 mL, $P = 0.011$); (2) Because of larger size (TMCSA 46.87 ± 5.59 cm² *vs* the control 22.77 ± 3.67 cm², $P = 0.012$) and severe infiltration and conglutination with surrounding tissues, tumor became a mass which did not leave enough space for hands to move the liver lobe for liberating right ligaments. But there was no statistical difference in the index of IBL/TMCSA (14.81 ± 2.79) between this group and the control group (13.42 ± 2.24 , $P = 1.000$). The retrograde hepatectomy can be used to deal with this situation, and this method has been used for difficult hepatectomy for years^[7-9].

Tumors in group 5 were located within the right posterior-inferior segment (Figure 6), and difficult to be exposed during surgery, and had to be padded with absorbent gauze on the surface of post-parietal peritoneum to lift liver and tumors up for a good exposure after liberation of ligaments. As long as there was good exposure, it was not very difficult to remove the tumor in this group.

In conclusion, this study isolated the MTRLSP from malignant tumors in the right liver and classified them into

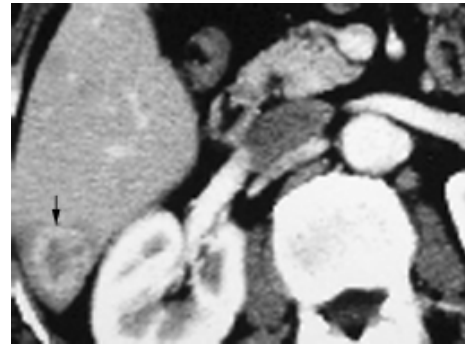


Figure 6 Tumor (→) deeply located at the level of posterior margin of vertebral body.

five sorts in terms of their position. The surgical features of each sort are described, which may improve the resection rate of malignant tumors within the right liver lobe and reduce the complications after surgery.

REFERENCES

- 1 **Tanaka S**, Hirohashi K, Tanaka H, Shuto T, Lee SH, Kubo S, Takemura S, Yamamoto T, Uenishi T, Kinoshita H. Incidence and management of bile leakage after hepatic resection for malignant hepatic tumors. *J Am Coll Surg* 2002; **195**: 484-489
- 2 **Davidson BR**, Burnett S, Javed MS, Seifalian A, Moore D, Doctor N. Study of a novel fibrin sealant for achieving haemostasis following partial hepatectomy. *Br J Surg* 2000; **87**: 790-795
- 3 **Liu M**, Lui WY. The use of fibrin adhesive for hemostasis after liver resection. *Zhonghua Yixue Zazhi* 1993; **51**: 19-22
- 4 **Smyrniotis V**, Arkadopoulos N, Kehagias D, Kostopanagiotou G, Scondras C, Kotsis T, Tsantoulas D. Liver resection with repair of major hepatic veins. *Am J Surg* 2002; **183**: 58-61
- 5 **Luo YQ**, Wang Y, Chen H, Wu MC. Influence of preoperative transcatheter arterial chemoembolization on liver resection in patients with respectable hepatocellular carcinoma. *Zhonghua Putong Waikē Zazhi* 2002; **17**: 149-151
- 6 **Xia F**, Poon RT, Fan ST, Wong J. Thoracoabdominal Approach for Right-Sided Hepatic Resection for Hepatocellular Carcinoma. *J Am Coll Surg* 2003; **196**: 418-427
- 7 **Lin TY**, Sridharan M, Ho ST. Retrograde resection of hepatic lobe for extensive carcinoma of liver. *Med Chir Dig* 1977; **6**: 87
- 8 **Lai EC**, Fan ST, Lo CM, Chu KM, Liu CL. Anterior approach for difficult major right hepatectomy. *World J Surg* 1996; **20**: 314-317
- 9 **Wu ZQ**, Fan J, Zhou J, Qiu SJ, Ma CZ, Zhou XD, Tang ZY. Retrograde hepatectomy and research on its procedure. *Zhonghua Gandan Waikē Zazhi* 1999; **5**: 301-303

Apoptosis and its pathway in X gene-transfected HepG₂ cells

Na Lin, Hong-Ying Chen, Dan Li, Sheng-Jun Zhang, Zhi-Xin Cheng, Xiao-Zhong Wang

Na Lin, Hong-Ying Chen, Dan Li, Sheng-Jun Zhang, Zhi-Xin Cheng, Xiao-Zhong Wang, Department of Gastroenterology, Affiliated Union Hospital, Fujian Medical University, Fuzhou 350001, Fujian Province, China

Correspondence to: Dr. Xiao-Zhong Wang, Department of Gastroenterology, Affiliated Union Hospital, Fujian Medical University, Fuzhou 350001, Fujian Province, China. drwangxz@pub6.fz.fj.cn
Telephone: +86-591-83357896-8482

Received: 2004-11-02 Accepted: 2004-11-24

Abstract

AIM: To investigate the effect of hepatitis B virus (HBV) X gene on apoptosis and expressions of apoptosis factors in X gene-transfected HepG₂ cells.

METHODS: The HBV X gene eukaryon expression vector *pcDNA₃-X* was transiently transfected into HepG₂ cells by lipid-media transfection. Untransfected HepG₂ and HepG₂ transfected with *pcDNA₃* were used as controls. Expression of HBx in HepG₂ was identified by RT-PCR. MTT and TUNEL were employed to measure proliferation and apoptosis of cells in three groups. Semi-quantified RT-PCR was used to evaluate the expression levels of Fas/FasL, Bax/Bcl-xL, and c-myc in each group.

RESULTS: HBV X gene was transfected into HepG₂ cells successfully. RT-PCR showed that HBx was only expressed in HepG₂/*pcDNA₃-X* cells, but not expressed in HepG₂ and HepG₂/*pcDNA₃* cells. Analyzed by MTT, cell proliferation capacity was obviously lower in HepG₂/*pcDNA₃-X* cells (0.08910 ± 0.003164) than in HepG₂ (0.14410 ± 0.004927) and HepG₂/*pcDNA₃* cells (0.12150 ± 0.007159) ($P < 0.05$ and $P < 0.01$). Analyzed by TUNEL, cell apoptosis was much more in HepG₂/*pcDNA₃-X* cells (980/2 000) than HepG₂ (420/2 000), HepG₂/*pcDNA₃* cells (520/2 000) ($P < 0.05$ and $P < 0.01$). Evaluated by semi-quantified RT-PCR, the expression level of Fas/FasL was significantly higher in HepG₂ cells transfected with HBx than in HepG₂ and HepG₂/*pcDNA₃* cells ($P < 0.05$ and $P < 0.01$). Bax/Bcl-xL expression level was also elevated in HepG₂/*pcDNA₃-X* cells ($P < 0.05$ and $P < 0.01$). Expression of c-myc was markedly higher in HepG₂/*pcDNA₃-X* cells than in HepG₂ and HepG₂/*pcDNA₃* cells ($P < 0.05$ and $P < 0.01$).

CONCLUSION: HBV X gene can impair cell proliferation capacity, improve cell apoptosis, and upregulate expression of apoptosis factors. The intervention of HBV X gene on the expression of apoptosis factors may be a possible mechanism responsible for the change in cell apoptosis and proliferation.

Key words: HBx; Transfect; HepG₂; Apoptosis; Fas; FasL; Bax; Bcl-xL; c-myc

Lin N, Chen HY, Li D, Zhang SJ, Cheng ZX, Wang XZ. Apoptosis and its pathway in X gene-transfected HepG₂ cells. *World J Gastroenterol* 2005; 11(28): 4326-4331
<http://www.wjgnet.com/1007-9327/11/4326.asp>

INTRODUCTION

Hepatitis B virus (HBV) is a small DNA virus with partial double-stranded DNA genome. HBV contains four opening reading frames (ORF) namely preS₁/preS₂/S, preC/C, P, and X. X gene is a unique ORF which is well conserved in different mammalian hepadnaviruses, its product consists of 154 amino acids with a molecular weight of 16.7 ku. Based on epidemical data, HBx is thought to be associated with HBV-related primary hepatocellular carcinoma (HCC), but the molecular basis for the oncogenic activity of HBx remains elusive. HBx is a multiple-functional protein and plays an essential role in viral pathogenesis. HBx can deregulate cell cycle check points, transactivate cells and viral genes, which involve in transcription regulation, single transduction pathway, cell cycle regulation, *etc.*^[1] It has been shown that HBx can co-ordinate balance between proliferation and programmed cell death, and it is able to induce or block apoptosis. The deregulation of apoptosis is involved in a wide range of pathological processes, including development of HCC.

In the present study, we investigated the effect of HBx expression on apoptosis in human hepatoma cell line HepG₂, and its effect on the expression level of apoptosis factors.

MATERIALS AND METHODS

Materials

PcDNA₃ expression vector and HBV X gene eukaryon expression vector *pcDNA₃-X* were previously constructed. Human hepatoma cell line HepG₂ was provided by Cell Bank of Chinese Academy of Sciences. Modified Eagle's medium (MEM) was bought from Hyclone Company, USA. Reverse transcription system, DNA purification system, and Transfast™ transfection reagent were obtained from Promega Biotech (USA). Total RNA isolation kit was purchased from Jingmei Biotech Company (Shanghai, China). PCR primers were synthesized by Shanghai Biotechnology Company. In-site cell apoptosis detection kit was provided by Roche Company.

Methods

Cell culture and DNA transfection HepG₂ cells were cultured in MEM supplemented with 10% heat-inactivated

fetal bovine serum, 100 IU/mL penicillin and 100 mg/mL streptomycin in a humidified incubator with 50 mL/L CO₂. A total of 1.5×10⁶ cells/mL were seeded into a 25 cm² cell plate before the experiment. When cells were grown to 80% confluence, *pcDNA₃* or *pcDNA₃-X* plasmid was transfected into HepG₂ cells by lipofection technique, which were named as HepG₂/*pcDNA₃* cells and HepG₂/*pcDNA₃-X* cells. A mixture containing 2 mL serum-free MEM (prewarmed to 37 °C), 5 µg plasmid DNA, 15 µL transfect reagent was added to a cell plate. After incubation for 24 h, 4 mL complete medium was added into cell plate and then incubated for another 48 h. HepG₂ cells, untransfected with any plasmid DNA, were used as controls.

Detection of X gene expression by RT-PCR Total RNA was extracted from HepG₂, HepG₂/*pcDNA₃*, and HepG₂/*pcDNA₃-X* cells respectively, and reverse transcribed into cDNA. One microliter of RT product was used as template, PCR was carried out. The sequences of X gene primers were: 5'-ATGCAAGCTTATGGCTGCTAGGC-TGTACTG-3' and 5'-TGCGAATTCTTAGGCAGAGG-TGAAAAAGTTG-3'. The expected amplification fragment was 467 bp. PCR conditions were as follows: pre-denaturation at 95 °C for 5 min, 32 amplification cycles (denaturation at 94 °C for 35 s, annealing at 65 °C for 35 s, and extension at 72 °C for 1 min), and a final extension at 72 °C for 7 min. The PCR products were separated by electrophoresis on 1.5% agarose gel, and detected by ultraviolet radiography.

Cell viability assay Cell viability was assayed by MTT. HepG₂, HepG₂/*pcDNA₃*, and HepG₂/*pcDNA₃-X* cells were planted into 96-well plates. Cells in logarithmic growth were used in experiments. One day before the experiment, complete medium was replaced by serum-free medium. During experiment, 75 µL MTT (5 mg/mL, containing in 0.01 mol/L PBS) was added into each well and incubated for 4 h. Then, the medium was replaced by DMSO (75 µL each well) and shaken gently until all crystals were dissolved. A₄₉₂ was detected to measure the proliferative capacity of each group.

Cell apoptosis assay Cell apoptosis was estimated by TUNEL staining. HepG₂, HepG₂/*pcDNA₃*, and HepG₂/*pcDNA₃-X* cells were planted into 96-well plates. Cells at 80% confluence were fixed with 4% paraformaldehyde, and chilled in ice

bath for 2 min with permeabilization solution (0.1% Triton X-100 in 0.1% sodium nitrate). Then, 50 µL TUNEL mixture was added, incubated in a humidified chamber at 37 °C for 1 h. TUNEL mixture was removed, 50 µL Converter-AP was added and incubated for another 30 min. The cells were rinsed with PBS, counterstained with NBT/BCIP, and detected by optic microscopy.

Effect of HBx transient transfection on apoptosis factor mRNA expression Expressions of Fas/FasL, Bax/Bcl-xL, and c-myc gene were assayed by semi-quantitative RT-PCR. β-Actin was used as internal control. Total RNA was extracted respectively with RNA isolation kit, and reverse transcribed into cDNA. PCR was performed in a 50 µL reaction volume containing 5 µL 10× PCR buffer, 5 µL 2 mmol/L MgCl₂, 1 µL 10 mmol/L dNTP, 1 µL 20 pmol/µL target gene sense and anti-sense primers, 0.5 µL 12.5 pmol/µL β-actin primer pair, 2 µL RT product, 1.5 U Taq DNA polymerase. The sequences of gene primers and amplification conditions are listed in Table 1. The initial denaturation was at 94 °C for 5 min. An additional extension step at 72 °C for 10 min was done finally. About 10 µL PCR products was separated by electrophoresis on 1.5% agarose gel, and detected by ultraviolet radiography. The densities of bands were analyzed by Bio imaging system, the ratio of target gene density to β-actin density was representative of the relative expression level of mRNA. The semi-quantitative detection was analyzed five times.

Statistical analysis

All data were expressed as mean±SE. The significance for the difference between groups was assessed with SPSS 10.0 by one-way ANOVA. *P*<0.05 was considered statistically significant.

RESULTS

Expression of HBV X mRNA in HepG₂ cells

Expressions of HBx mRNA were detected by RT-PCR. The expected band between 400 and 500 bp was found in HepG₂/*pcDNA₃-X* cells, but not in HepG₂ and HepG₂/*pcDNA₃* cells (Figure 1).

Table 1 Sequences of gene primers and amplification conditions

Target gene	Primer sequences	Amplification conditions	Product (base)
Fas	5'-TCA GTA CCG AGT TGG GGA AG-3' 5'-CAG GCC TTC CAA GTT CTG AG-3'	Denaturation at 94 °C for 45 s, annealing at 64 °C for 30 s, extension at 72 °C for 1 min, 35 cycles	207 bp
FasL	5'-GAT GAT GGA GGG GAA GAT GA-3' 5'-TGG AAA GAA TCC CAA AGT GC-3'	Denaturation at 94 °C for 45 s, annealing at 58 °C for 30 s, extension at 72 °C for 1 min, 38 cycles	203 bp
Bax	5'-TTT GCT TCA GGG TTT CAT CC-3' 5'-CAG TTG AAG TTG CCG TCA GA-3'	Denaturation at 94 °C for 45 s, annealing at 58 °C for 30 s, extension at 72 °C for 1 min, 30 cycles	246 bp
Bcl-xL	5'-GGC TGG GAT ACT TTT GTG GA-3' 5'-ATG TGG TGG AGC AGA GAA GG-3'	Denaturation at 94 °C for 45 s, annealing at 64 °C for 30 s, extension at 72 °C for 45 s, 25 cycles	198 bp
c-myc	5'-TTC GGG TAG TGG AAA ACC AG-3' 5'-CAG CAG CTC GAA TTT CTT CC-3'	Denaturation at 94 °C for 45 s, annealing at 58 °C for 30 s, extension at 72 °C for 1 min, 30 cycles	203 bp
β-actin	5'-GGC ATC GTG ATG GAC TCC G-3' 5'-GCT GGA AGG TGG ACA GCG A-3'	Changed according to different target genes	607 bp

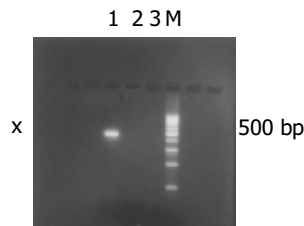


Figure 1 Expression of HBV X mRNA in HepG₂ cells. M: 100-bp DNA ladder; lane 1: HepG₂/pcDNA₃-X cells; lane 2: HepG₂/pcDNA₃ cells; lane 3: HepG₂ cells.

Cell viability assay

Cell viability was assessed by MTT. All data are shown in Table 2. A_{492} of HepG₂/pcDNA₃-X cells obviously decreased compared to that in other groups ($P < 0.05$ and $P < 0.01$), indicating that transient expression of HBx impaired the proliferative capacity of HepG₂ cells (Figure 2).

Table 2 A_{492} of HepG₂, HepG₂/pcDNA₃ and HepG₂/pcDNA₃-X cells (mean±SE)

Group	n	A_{492}
HepG ₂	10	0.14410±0.004927
HepG ₂ /pcDNA ₃	10	0.12150±0.007159
HepG ₂ /pcDNA ₃ -X	10	0.08910±0.003164

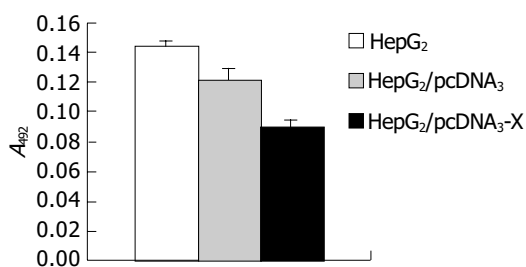


Figure 2 Effect of HBx on cell viability in HepG₂ cells.

Cell apoptosis assay

Apoptosis in the three groups was assessed with in-site cell death detecting kit (TUNEL). A total of 2 000 cells of each group were calculated. The number of apoptosis cells was 980 in HepG₂/pcDNA₃-X, 520 in HepG₂/pcDNA₃ and 420 in HepG₂. Cell apoptosis markedly increased in HepG₂/pcDNA₃-X (Table 3 and Figure 3), indicating that transient expression of HBx could promote apoptosis of HepG₂ cells (Figure 4).

Table 3 Effect of HBx on cell apoptosis of HepG₂ cells (mean±SE)

Group	n	Apoptosis
HepG ₂	5	0.2200±0.1000
HepG ₂ /pcDNA ₃	5	0.2800±0.1000
HepG ₂ /pcDNA ₃ -X	5	0.4750±0.015

Effects of HBx transient transfection on apoptosis factors' mRNA expression

Fas/FasL mRNA mRNA level of Fas and FasL was

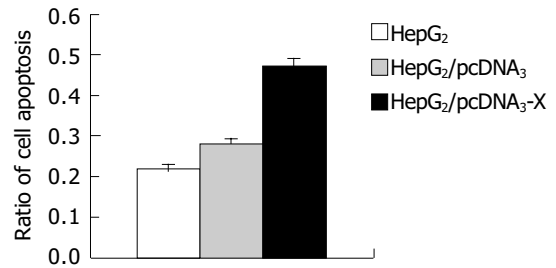


Figure 3 Effect of HBx on apoptosis of HepG₂ cells.

elevated in HepG₂/pcDNA₃-X cells (Figures 5A and B, 6A and B), indicating that transient expression of HBx induced expression of Fas and FasL in HepG₂ cells.

Bcl-xL/Bax mRNA mRNA level of Bcl-xL and Bax was enhanced in HepG₂/pcDNA₃-X cells (Figures 5C and D, 6C and D), indicating that transient expression of HBx induced expression of Bcl-xL or Bax in HepG₂ cells.

C-myc mRNA mRNA level of c-myc in HepG₂/pcDNA₃-X cells was the highest (Figures 5E and 6E), indicating that transient expression of HBx induced expression of c-myc in HepG₂ cells.

DISCUSSION

In previous studies, it was found that HBx inhibits cell apoptosis in different ways. For example, HBx antagonizes TNF- α -induced apoptosis through activating PI3-kinase signaling pathway^[2], and inhibits apoptosis in p53-independent manner^[3]. There is evidence that HBx activates NF- κ B and induce it to translocate into nuclei, NF- κ B acts as an inhibitor of cell apoptosis; HBx also downmodulates expression of Bid and blocks Bid-mediated cell apoptosis^[4], inactivates caspase-3 through inhibition of CCP32 enzyme, and blocks caspase pathway^[5]. It is thought that anti-apoptosis function of HBx is an important mechanism in the development of HCC.

HBx can either inhibit or promote cell apoptosis in a dose-dependent manner. When HBx expresses at high level, it displays pro-apoptosis effect; whereas it inhibits apoptosis when expressing at physiological level. It was reported that moderate expression level of HBx can inhibit liver regeneration in HBx-expressing transgenic mice after partial hepatectomy^[6]. HBx stimulates expression of FasL, which plays an important role in cell's escaping from immune surveillance by inducing apoptosis of T cell bearing Fas^[7,8]. HBx boosts cell survival by abrogating Bcl-2-mediated cell protection^[9,10]. It can also induce expression of myc protein in certain settings, myc sensitizes cells to be killed plus TNF- α ^[11]. HBx acts through the way that involves DDB2-independent nuclear function of DDB1^[12]. Some researchers found that HBx can also localize in mitochondria, bind to voltage-dependent anion channel, which results in alteration of the mitochondrial transmembrane potential, promotes cytochrome C and apoptosis-inducing factors to release into cytosol and induces cell apoptosis^[13]. In short, HBx has bi-directional function on cell apoptosis regulation. HBx expression levels, availability of survival *vs* apoptogenic factors, and stage of infection may profoundly influence

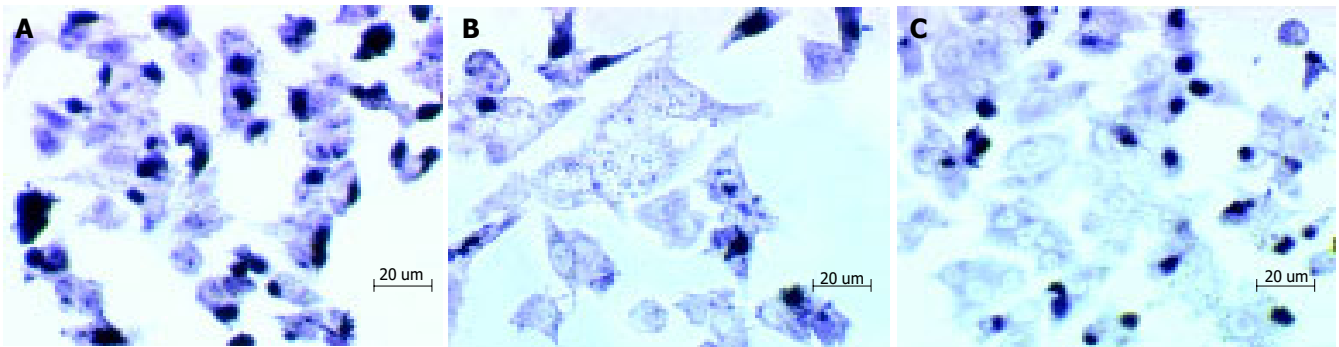


Figure 4 Apoptosis in HepG₂/pcDNA₃-X (A), HepG₂/pcDNA₃ (B), and HepG₂ (C) cells.

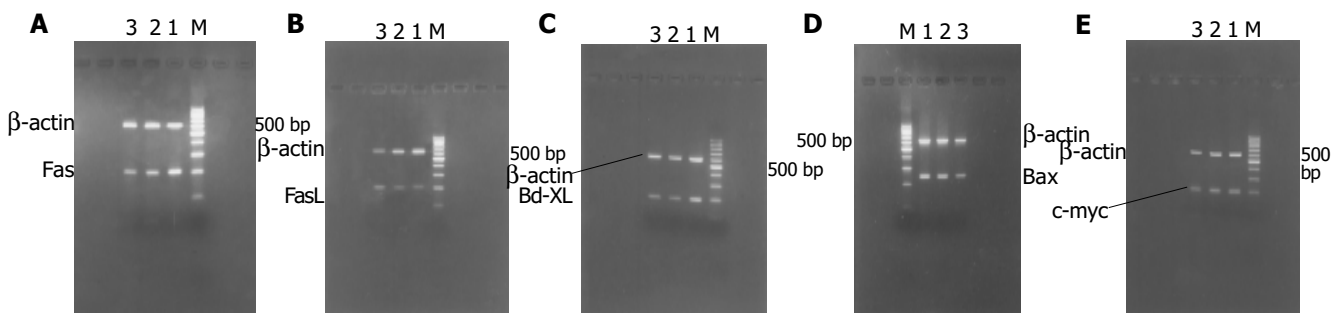


Figure 5 RT-PCR results of mRNA expression of Fas (A), FasL (B), Bcl-XI (C), Bax (D), and c-myc (E) in HepG₂. M: 100-bp DNA ladder; lane 1: HepG₂

cells; lane 2: HepG₂/pcDNA₃ cells; lane 3: HepG₂/pcDNA₃-X cells.

the fate of cells.

Higher organisms have several mechanisms to eliminate cells by apoptosis. One important role is the signaling pathway mediated by “death factors” including TNFR1, Fas, TNFR2, and their cognate ligand (TNF- α , FasL, and TRAIL) Fas (CD₉₅). The first identified member of “death factors”, is a type I glycoprotein which expresses on cell surface. Crosslinking Fas by binding to the ligand FasL leads to conformational changes of Fas, which results in formation of death induced signal complex (DISC) followed by activation of caspase-8. Activated caspase-8 activates itself and other caspases that switch on apoptosis signal cascade^[14,15]. It has been found that Fas and FasL express in hepatocytes and hepatoma cells. Since hepatocytes are highly sensitive to Fas/FasL-mediated apoptosis, Fas/FasL pathway plays an essential role in liver lesion and eliminating virus. In our research, HBx elevated expression of Fas and FasL in HepG₂ cells. Although the precise mechanism remains unclear, HBx can activate FasL promoter through binding site for Egr and enhance Egr binding to the co-activator cAMP-response element-binding protein, and induce pro-inflammatory cytokines at transcriptional level such as IL-18 which can amplify the expression of FasL^[16]. c-FLIP, a key regulator of the DISC, inhibits the Fas/FasL-mediated death pathway in tumors. HBx abrogates the apoptosis-inhibiting function of c-FLIP and renders cells hypersensitive towards the TNF- α apoptotic signal even below the threshold concentration^[17,18].

Members of Bcl-2 family are also involved in apoptosis regulation. Members of this family are divided into three subgroups. One group is composed of anti-apoptosis proteins

such as Bcl-2, Bcl-xL, with four Bcl-2 homology domains (BH1, BH2, BH3, and BH4). Another group consists of pro-apoptosis proteins such as Bax, Bak, with BH1, BH2, BH3 domains. The last group includes pro-proteins such as Bid, Bik, with only BH3 domain^[4,19]. As Bcl-2 family members reside in upstream of irreversible cell damage, they play a pivotal role in deciding whether cells die or live. Indeed, the ratio between pro- and anti-apoptosis molecules determines, in part, the susceptibility of cells to death signal^[20]. It was reported recently that the anti-apoptosis members lose their ability to inhibit release of pro-apoptosis factors (such as cytochrome C) and trigger apoptosis if they interact with activated pro-apoptosis members^[21]. Our data demonstrate that HBx upregulates either pro-apoptosis subset Bax or anti-apoptosis subset Bcl-xL. MTT and TUNEL displayed that apoptosis of HepG₂ cells transfected with HBx was enhanced while cell viability was impaired. We postulated that though HBx can upregulate expression of Bax and Bcl-xL, it may promote expression of Bax ever more than Bcl-xL, thus resulting in the predominance of pro-apoptosis protein in the ratio between pro- and anti-apoptosis subsets, then cell apoptosis. On the other hand, interacting with activated Bax, Bcl-xL may lose its anti-apoptosis function and trigger cell death.

C-myc belongs to cell oncogene. HBx accelerates development of primary liver tumors by co-operating with c-myc^[22-25]. It was reported that myc can sensitize cells to apoptosis by about two folds in certain conditions such as exposure to TNF- α or other apoptosis factors. In our study, HBx promoted expression of c-myc. Overexpression of c-myc is essential for acute sensitization of cells to be killed

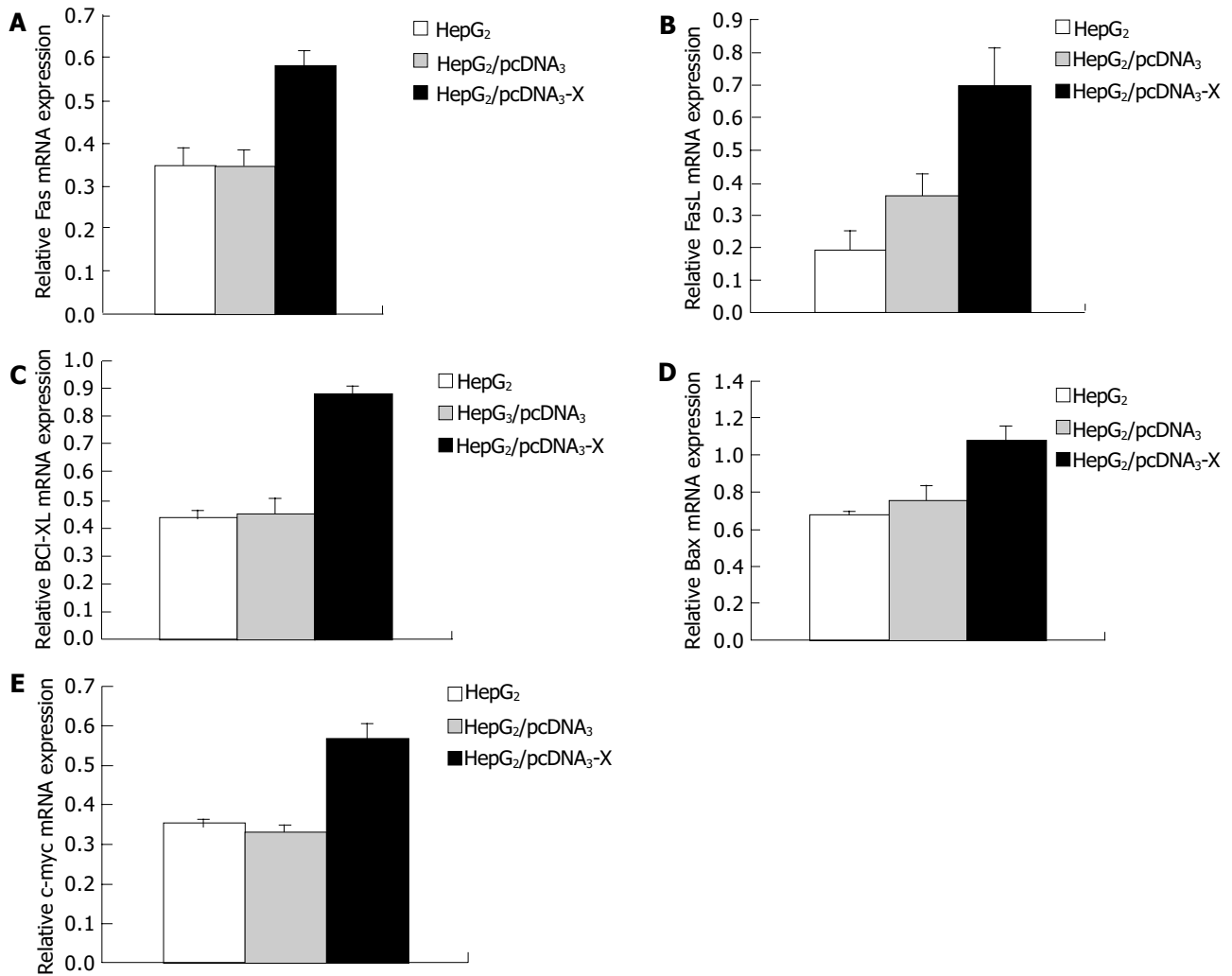


Figure 6 Relative mRNA expression levels of Fas (A), FasL (B), Bcl-XI (C),

Bax (D), and c-myc (E) in HepG₂ cells.

by HBx plus TNF- α ^[11,26-28], and may enhance cell apoptosis. This result agrees with the data of MTT and TUNEL in our study.

In hepatocarcinogenesis, preneoplastic, and neoplastic cells display an increased ratio of apoptosis as well as enhanced cell proliferation^[30]. It is believed that the anti-apoptosis function of HBx is the major determinant factor for development of HCC. The pro-apoptosis function of HBx, however, is also thought to contribute to hepatocarcinogenesis. Firstly, HBx-induced cell apoptosis results in releasing of hepatocyte growth factor that enhances regeneration of liver cells and accumulation of genetic mutation, thus paving the way for cell malignant transformation^[29-31]. Secondly, increased apoptosis increase the opportunity of mutation, leading cells to grow out of control and develop to HCC^[28,32]. Thirdly, HBx induces expression of FasL in liver cells which can attack T cell bearing Fas and lead to impair of immune defense, which is beneficial for cell bearing HBx to escape from immune detection^[33]. Finally, although the accurate mechanism of apoptosis induced by HBx has not been elucidated completely, it may facilitate propagation of viral infection by permitting efficient particle release from cells while minimizing the antiviral inflammation response^[14].

Further study should be focused on protein level. Besides, apoptosis mechanic on stably transfected HBx gene in HepG₂ cells is another pivot.

REFERENCES

- Madden CR**, Slagle BL. Stimulation of cellular proliferation by hepatitis B virus X protein. *Dis Markers* 2001; **17**: 153-157
- Shih WL**, Kuo ML, Chuang SE, Cheng AL, Doong SL. Hepatitis B virus X protein inhibits transforming growth factor-beta-induced apoptosis through the activation of phosphatidylinositol 3-Kinase pathway. *J Biol Chem* 2000; **275**: 25858-25864
- Shintani Y**, Yotsuyanagi H, Moriya K, Fujie H, Tsutsumi T, Kanegae Y, Kimura S, Saito I, Koike K. Induction of apoptosis after switch-on of the hepatitis B virus X gene mediated by the Cre/loxP recombination system. *J Gen Virol* 1999; **80** (Pt 12): 3257-3265
- Chen GG**, Lai PB, Chan PK, Chak EC, Yip JH, Ho RL, Leung BC, Lau WY. Decreased expression of Bid in human hepatocellular carcinoma is related to hepatitis B virus X protein. *Eur J Cancer* 2001; **37**: 1695-1702
- Gottlob K**, Fuko M, Levrero M, Graessmann A. The hepatitis B virus HBx protein inhibits caspase 3 activity. *J Biol Chem* 1998; **273**: 33347-33353
- Guilherme Tralhao J**, Roudier J, Morosan S, Giannini C, Tu H, Goulenok C, Carnot F, Zavala F, Joulin V, Kremsdorf D,

- Brechot C. Paracrine *in vivo* inhibitory effects of hepatitis B virus X protein (HBx) on liver cell proliferation: An alternative mechanism of HBx-related pathogenesis. *Proc Natl Acad Sci USA* 2002; **99**: 6991-6996
- 7 **Yoo YG**, Lee MO. Hepatitis B virus X protein induces expression of fas ligand gene through enhancing transcriptional activity of early growth response factor. *J Biol Chem* 2004; **279**: 36242-36249
- 8 **Shin EC**, Shin JS, Park JH, Kim H, Kim SJ. Expression of fas ligand in human hepatoma cell lines: role of hepatitis-B virus X (HBx) in induction of Fas ligand. *Int J Cancer* 1999; **82**: 587-591
- 9 **Schuster R**, Gerlich WH, Schaefer S. Induction of apoptosis by the transactivating domains of the hepatitis B virus X gene leads to suppression of oncogenic transformation of primary rat embryo fibroblasts. *Oncogene* 2000; **19**: 1173-1180
- 10 **Terradillos O**, de La Coste A, Pollicino T, Neuveut C, Sitterlin D, Lecoeur H, Gougeon ML, Kahn A, Buendia MA. The hepatitis B virus X protein abrogates Bcl-2-mediated protection against Fas apoptosis in the liver. *Oncogene* 2002; **21**: 377-386
- 11 **Su F**, Theodosis CN, Schneider RJ. Role of NF-kappaB and myc proteins in apoptosis induced by hepatitis B virus HBx protein. *J Virol* 2001; **75**: 215-225
- 12 **Bontron S**, Lin-Marq N, Strubin M. Hepatitis B virus X protein associated with UV-DDB1 induces cell death in the nucleus and is functionally antagonized by UV-DDB2. *J Biol Chem* 2002; **277**: 38847-38854
- 13 **Waris G**, Huh KW, Siddiqui A. Mitochondrially associated hepatitis B virus X protein constitutively activates transcription factors STAT-3 and NF-kappa B via oxidative stress. *Mol Cell Biol* 2001; **21**: 7721-7730
- 14 **Nagata S**. Apoptosis by death factor. *Cell* 1997; **88**: 355-365
- 15 **Chang YC**, Xu YH. Expression of Bcl-2 inhibited Fas-mediated apoptosis in human hepatocellular carcinoma BEL-7404 cells. *Cell Res* 2000; **10**: 233-242
- 16 **Lee MO**, Choi YH, Shin EC, Kang HJ, Kim YM, Jeong SY, Seong JK, Yu DY, Cho H, Park JH, Kim SJ. Hepatitis B virus X protein induced expression of interleukin 18 (IL-18): a potential mechanism for liver injury caused by hepatitis B virus (HBV) infection. *J Hepatol* 2002; **37**: 380-386
- 17 **Korkolopoulou P**, Goudopoulou A, Voutsinas G, Thomas-Tsagli E, Kapralos P, Patsouris E, Saetta AA. c-FLIP expression in bladder urothelial carcinomas: its role in resistance to Fas-mediated apoptosis and clinicopathologic correlations. *Urology* 2004; **63**: 1198-1204
- 18 **Kim KH**, Seong BL. Pro-apoptotic function of HBV X protein is mediated by interaction with c-FLIP and enhancement of death-inducing signal. *EMBO J* 2003; **22**: 2104-2116
- 19 **Reed JC**. Bcl-2 family proteins. *Oncogene* 1998; **17**: 3225-3236
- 20 **Gross A**, McDonnell JM, Korsmeyer SJ. BCL-2 family members and the mitochondria in apoptosis. *Genes Dev* 1999; **13**: 1899-1911
- 21 **Fu YF**, Fan TJ. Bcl-2 family proteins and apoptosis. *Shengwu Huaxue Yu Shengwu Wuli Xuebao* 2002; **34**: 389-394
- 22 **Lakhtakia R**, Kumar V, Reddi H, Mathur M, Dattagupta S, Panda SK. Hepatocellular carcinoma in a hepatitis B 'x' transgenic mouse model: A sequential pathological evaluation. *J Gastroenterol Hepatol* 2003; **18**: 80-91
- 23 **Terradillos O**, Pollicino T, Lecoeur H, Tripodi M, Gougeon ML, Tiollais P, Buendia MA. p53-independent apoptotic effects of the hepatitis B virus HBx protein *in vivo* and *in vitro*. *Oncogene* 1998; **17**: 2115-2123
- 24 **Hung L**, Kumar V. Specific inhibition of gene expression and transactivation functions of hepatitis B virus X protein and c-myc by small interfering RNAs. *FEBS Lett* 2004; **560**: 210-214
- 25 **Rabe C**, Cheng B, Caselmann WH. Molecular mechanisms of hepatitis B virus-associated liver cancer. *Dig Dis* 2001; **19**: 279-287
- 26 **Kleefstrom J**, Arighi E, Littlewood T, Jaattela M, Saksela E, Evan GI, Alitalo K. Induction of TNF-sensitive cellular phenotype by c-Myc involves p53 and impaired NF-kappaB activation. *EMBO J* 1997; **16**: 7382-7392
- 27 **Foo SY**, Nolan GP. NF-kappa B to the rescue: RELs, apoptosis and cellular transformation. *Trends Genet* 1999; **15**: 229-235
- 28 **Su F**, Schneider RJ. Hepatitis B virus HBx protein sensitizes cells to apoptotic killing by TNF- α . *Proc Natl Acad Sci USA* 1997; **94**: 8744-8749
- 29 **Kim H**, Lee H, Yun Y. X-gene Product of hepatitis B virus induces apoptosis in liver cells. *J Biol Chem* 1998; **273**: 381-385
- 30 **Jin YM**, Yun C, Park C, Wang HJ, Cho H. Expression of hepatitis B Virus X protein is closely correlated with the high periportal inflammatory activity of liver diseases. *J Viral Hepatitis* 2001; **8**: 322-330
- 31 **Pollicino T**, Terradillos O, Lecoeur H, Gougeon ML, Buendia MA. Pro-apoptotic effect of the hepatitis B virus X gene. *Biomed Pharmacother* 1998; **52**: 363-368
- 32 **Sirma H**, Giannini C, Poussin K, Paterlini P, Kremsdorf D, Brechot C. Hepatitis B virus X mutants, present in hepatocellular carcinoma tissue abrogate both the antiproliferative and transactivation effects of HBx. *Oncogene* 1999; **18**: 4848-4859
- 33 **Milich DR**. Influence of T-helper cell subsets and cross-regulation in hepatitis B virus infection. *J Viral Hepatol* 1997; **4**: 48-59

• COLORECTAL CANCER •

Treatment of metastatic colorectal carcinomas by systemic inhibition of vascular endothelial growth factor signaling in mice

Volker Schmitz, Mirosław Kornek, Tobias Hilbert, Christian Dzienisowicz, Esther Raskopf, Christian Rabe, Tilman Sauerbruch, Cheng Qian, Wolfgang H Caselmann

Volker Schmitz, Mirosław Kornek, Tobias Hilbert, Christian Dzienisowicz, Esther Raskopf, Christian Rabe, Tilman Sauerbruch, Medizinische Klinik und Poliklinik I, Universitätsklinikum Bonn, Germany
Cheng Qian, Universidad de Navarra, Clínica Universitaria, Pamplona, Spain
Wolfgang H Caselmann, Bavarian State Ministry of the Environment, Public Health and Consumer Protection, Munich 81901, Germany
Supported by the Deutsche Krebshilfe, No. 70-3065-SchmI
Correspondence to: Dr. Volker Schmitz, Medizinische Klinik I, Sigmund-Freud-Str. 25, Bonn 53105, Germany. volker.schmitz@ukb.uni-bonn.de
Telephone: +49-228-2876469 Fax: +49-228-2874698
Received: 2004-07-31 Accepted: 2004-11-04

aminotransferase determination.

CONCLUSION: In this study we confirmed the value of a systemic administration of AdsFlt1-3 to block VEGF signaling as antitumor therapy in an experimental metastatic colorectal carcinoma model in mice.

© 2005 The WJG Press and Elsevier Inc. All rights reserved.

Key words: Colorectal carcinomas; Vascular endothelial growth factor; Systemic inhibition

Schmitz V, Kornek M, Hilbert T, Dzienisowicz C, Raskopf E, Rabe C, Sauerbruch T, Qian C, Caselmann WH. Treatment of metastatic colorectal carcinomas by systemic inhibition of vascular endothelial growth factor signaling in mice. *World J Gastroenterol* 2005; 11(28): 4332-4336
<http://www.wjgnet.com/1007-9327/11/4332.asp>

Abstract

AIM: Tumor angiogenesis has been shown to be promoted by vascular endothelial growth factor (VEGF) via stimulating endothelial cell proliferation, migration, and survival. Blockade of VEGF signaling by different means has been demonstrated to result in reduced tumor growth and suppression of tumor angiogenesis in distinct tumor entities. Here, we tested a recombinant adenovirus, AdsFlt1-3, that encodes an antagonistically acting fragment of the VEGF receptor 1 (Flt-1), for systemic antitumor effects in pre-established subcutaneous CRC tumors in mice.

METHODS: Murine colorectal carcinoma cells (CT26) were inoculated subcutaneously into Balb/c mice for *in vivo* studies. Tumor size and survival were determined. 293 cell line was used for propagation of the adenoviral vectors. Human lung cancer line A₅₄₉ and human umbilical vein endothelial cells were transfected for *in vitro* experiments.

RESULTS: Infection of tumor cells with AdsFlt1-3 resulted in protein secretion into cell supernatant, demonstrating correct vector function. As expected, the secreted sFlt1-3 protein had no direct effect on CT26 tumor cell proliferation *in vitro*, but endothelial cell function was inhibited by about 46% as compared to the AdLacZ control in a tube formation assay. When AdsFlt1-3 (5×10⁹ PFU/animal) was applied to tumor bearing mice, we found a tumor inhibition by 72% at d 12 after treatment initiation. In spite of these antitumoral effects, the survival time was not improved. According to reduced intratumoral microvessel density in AdsFlt1-3-treated mice, the antitumor mechanism can be attributed to angiostatic vector effects. We did not detect increased systemic VEGF levels after AdsFlt1-3 treatment and liver toxicity was low as judged by serum alanine

INTRODUCTION

Colorectal carcinoma (CRC) is one of the most common malignant diseases in the Western countries. Even after successful resection of the primary tumor, about one-third of the patients develop tumor recurrence. The most common place of distant CRC metastases are liver and lung^[1]. In particular, metastatic CRC disease is associated with limited life expectancy and progressive tumor disease in CRC is associated with increased VEGF levels^[2]. Considering clinical studies successfully employing tyrosine kinase inhibitors for systemic tumor therapy^[3] and experimental studies showing the antitumor efficacy of VEGF-antagonism in a pancreatic adenocarcinoma animal model^[4] and follicular thyroid carcinoma animal model^[5], including successful local treatment of subcutaneous CRC^[6], we evaluated and confirmed the antitumoral efficacy and mechanism of a systemic gene delivery of a Flt-1 fragment (sFlt1-3) in subcutaneous metastatic CRC in mice.

Vascular endothelial growth factor (VEGF) expression correlates with tumor vascularization in most tumor types, also in CRC^[2,7,8]. VEGF binds with different affinity to its cell surface receptors, VEGF receptor 1 (Flt-1), VEGF receptor 2 (Flk-1) and VEGF receptor 3 (Flt-4). All three VEGF receptors are members of the class III receptor-type tyrosine kinase receptor family^[9]. Several findings suggest that binding of VEGF to Flt-1 regulates angiogenesis by controlling inter-cellular endothelial interactions^[10].

Since angiostatic therapies do not attack the malignant tumor cell itself, but address tumor vascularization, a systemic

treatment is of particular interest. Therefore, we investigated the effect of interruption of the VEGF cascade by systemic gene delivery on pre-established tumors.

MATERIALS AND METHODS

Animals, cell lines and culture conditions

Balb/c mice, 6 wk old, were purchased from Charles River (Sulzfeld, Germany) and kept in the local central animal facility. The mice were housed under standard conditions and had free access to water and food. Animal procedures were performed in accordance to approved protocols and followed recommendations for proper care and use of laboratory animals.

For propagation of adenoviral vectors, 293 cells (embryonic E1 transformed kidney cell line) were obtained from American Type Culture Collection (ATCC, Manassas, VA, USA). Cells were maintained in Dulbecco's modified Eagle medium (DMEM) with 10% heat-inactivated fetal bovine serum (FBS).

To demonstrate vector function and gene expression standard techniques using the human lung cancer cell line *A*₅₄₉ (ATCC, Manassas, VA, USA) were employed for *in vitro* transfection experiments. Cells were cultured in DMEM supplemented with 10% heat-inactivated FBS. Human umbilical vein endothelial (HUVE) cells were obtained from Cascade Biologics (Portland, OR, USA) and were cultured according to the supplier's instructions.

Murine CRC CT26 cells have originally been described by Brattain^[11]. Cells were cultured in DMEM supplemented with 10% heat-inactivated FCS and 1% penicillin/streptomycin.

Construction of recombinant adenoviruses encoding a soluble form of Flt1-3 and vector propagation

The recombinant adenoviruses encoding the LacZ-gene was constructed as described previously^[12]. The AdsFlt1-3 construct was generously provided by R. Mulligan, Boston, MA, USA, it consists of the extracellular immunoglobulin-like domains 1-3 of the VEGF-receptor 1 (Flt-1) and has a His-tag; its construction has been described elsewhere^[13]. Recombinant adenoviruses were expanded, and purified by double cesium-chloride ultra-centrifugation. Purified viruses were dialyzed against 10 mmol/L Tris/1 mmol/L MgCl₂ and stored in glycerol aliquots at -80 °C. Virus concentrations were determined by measuring virus particles (opu/mL) and by cytotoxic plaque assay (pfu/mL) in 293 cells. Virus productions were tested for wild-type adenovirus contamination by cytotoxic plaque assay in *A*₅₄₉ cells.

Analysis of protein expression in vitro

*A*₅₄₉ tumor cells were transfected with 250 multiplicity of infection (MOI) of AdLacZ or AdsFlt1-3. Forty-eight hours later, cells and culture medium (CM) were harvested. RNA was isolated from the using the GenElute Total Mammalian RNA Kit (Sigma, Taufkirchen, Germany) according to the manufacturer's protocol. RNA was then digested with RQ1 DNase (Promega, Mannheim, Germany). RNA concentrations were determined and 1 µg RNA was used in the RT reaction with random primers (Promega, Mannheim, Germany) and MMLV reverse transcriptase (Promega, Mannheim,

Germany). PCR for sFlt1-3 was performed with the forward primer 5'-CGTTCAGTCTTTCAACACC-3' and reverse primer 5'-CCAAGGAAACGTGAAAGC-3'. As positive control, primers for human β-actin were used. The size of the amplified product was about 250 bp. Analysis of the PCR products occurred by electrophoresis on a 1% agarose gel.

For detection of sFlt1-3 100 µL of the harvested CM was dispensed in a 96-well ELISA plate and incubated at 4 °C overnight. After washing thrice with PBS, the ELISA plate was incubated for 2 h with anti mouse VEGF-R1 (Flt-1) antibody (1:200, R&D Systems, Wiesbaden-Nordenstadt, Germany). After antibody incubation, the plate was washed with PBS and incubated with secondary antibody (1:25 000, monoclonal anti-sheep/goat peroxidase conjugate, Sigma, St. Louis, MO, USA) 2 h. After washing with PBS the plate was incubated for 15 min with TMB substrate (Biozol, Eching, Germany). Color intensity was measured in an ELISA reader (Dynatech Laboratories, Frankfurt, Germany).

BrdU proliferation assay

Five thousand CT26 cells were resuspended in 40 µL of culture medium and dispensed in each well of a 96-culture plate and pre-incubated with 50 µL of CM. After 30 min of pre-incubation time, 150 µL of RPMI 1640 containing 10% FCS was added. Cell culture was continued for 18 h and then cells were labeled with BrdU for further 24 h. The BrdU assay was performed according to the manufacturer's protocol (BrdU proliferation assay, Roche Diagnostics, Mannheim, Germany).

In vitro testing of antiangiogenic effects (tube formation assay)

A 24-well plate was coated with 300 µL Matrigel (BD Biosciences, Bedford, MA, USA). Twenty-four hours later, HUVE cells (passage number <10) in 75 µL Medium200 (2.5×10⁴ cells) were seeded on the Matrigel and pre-incubated for 30 min with 75 µL of CM (derived from Huh7 cells). One hundred and fifty microliters of Medium200 was added and the cells were additionally incubated for 4-6 h. Tube-like formations were counted under the light microscope in high power fields.

Tumor induction

In vivo antitumoral efficacies were studied in a subcutaneous CRC mouse model in C3H mice. 10⁶ CT26 cells were resuspended in 100 µL FCS-free culture medium and injected subcutaneously via a 28-G syringe.

In vivo antitumor treatment

When reaching a tumor volume of 40 mm³, tumor treatment was initiated by intravenous injection of 5×10⁹ pfu/animal AdLacZ (*n* = 11) and AdsFlt1-3 (*n* = 10) in 150 µL NaCl. Tumor volumes were calculated by the formula: $v = \text{length} \times \text{width}^2 \times 0.52$. From a subgroup of animals treated intravenously with AdLacZ (*n* = 2), or AdsFlt1-3 (*n* = 3) serum and tumor samples were taken at different time points (at d 3, 6, 9, 14, 19, and 25) for VEGF-ELISA and histology, respectively.

Immunohistochemistry

Tumor samples were embedded in tissue tech (DAKO), snap

frozen in liquid nitrogen and stored at -80°C for anti-von Willebrand staining. Five millimeters of cryostat sections were gently warmed up at RT. Then fixed in acetone for 10 min and dried on air. Sections were stained with dilution of primary antibody (polyclonal rabbit antihuman von Willebrand factor, 1:1 600). After washing with PBS, sections were incubated with secondary antibody dilution of biotinylated pig antirabbit immunoglobulin G (1:300) and streptavidin conjugated to horseradish peroxidase (DAKO). Sections were visualized by using the Dako ChemMate™ detection kit and counterstained with hematoxylin (DAKO).

Statistical analysis

All measured data are given with mean \pm SE. Differences between values of different experimental groups were analyzed for statistical significance by a non-parametric, two-tailed test (Mann-Whitney test) for unpaired samples and in case of histology by unpaired Student's *t*-test. Survival rates are presented as Kaplan-Maier curves. An error level $P < 0.05$ was supposed to indicate significance.

RESULTS

Propagation of adenoviral vectors

Wild-type contamination of the adenoviral stock solutions was analyzed in A_{549} cells in a cytotoxic plaque assay. Virus concentrations were determined as optical particle units and ranged from 2.13×10^{12} opu/mL for AdLacZ to 7.04×10^{12} opu/mL for AdsFlt1-3, respectively. Virus titration in 293 cell plaque assays showed corresponding concentrations of 8.0×10^{12} pfu/mL for AdLacZ and 1.027×10^{12} pfu/mL for AdsFlt1-3.

Protein expression and secretion of sFlt1-3

CM of infected A_{549} cells was harvested to demonstrate sFlt1-3 gene expression and protein secretion into cell supernatant. The analysis of the RT-PCR showed similar bands for β -actin (500 bp) in all samples and only AdsFlt1-3 infected cells showed an extra band at about 250 bp representing the encoded transgene sFlt1-3 (Figure 1). Protein expression was confirmed by ELISA in AdsFlt1-3 infected cells (106 ng/mL). This data demonstrate correct vector function and protein secretion.

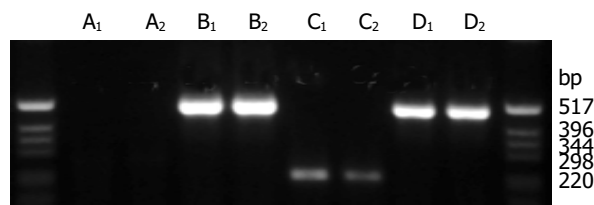


Figure 1 Gene expression of sFlt1-3 *in vitro*. RT-PCR was performed with A_{549} cells infected with AdsFlt1-3 or AdLacZ. Specific primer pairs for sFlt1-3 resulted in bands of about 250 bp (C_1 and C_2), whereas no bands were detectable in the negative control AdLacZ (A_1 and A_2). Expression of the house keeping gene β -actin (514 bp) was similar for AdLacZ (B_1 and B_2) and AdsFlt1-3 (D_1 and D_2).

BrdU proliferation assay

To check for direct effects of sFlt1-3 on CRC tumor cells,

conditioned CM was tested for antitumor effects on CT26 tumor cells. As expected, we did not observe any direct anti-proliferative effects (data not shown). We concluded that potential antitumor effects were mediated by indirect (angiostatic) mechanism and not by cytotoxic effects.

In vitro testing of antiangiogenic effects (tube formation assay)

The tube formation assay tests the capability of HUVE cells to form tube-like structures comprising endothelial cell function like migration and tube formation. The results showed that sFlt1-3 inhibited these cell functions by about 46% (Figure 2) compared to the AdLacZ control. This indicates biological activity of sFlt1-3 *in vitro*.

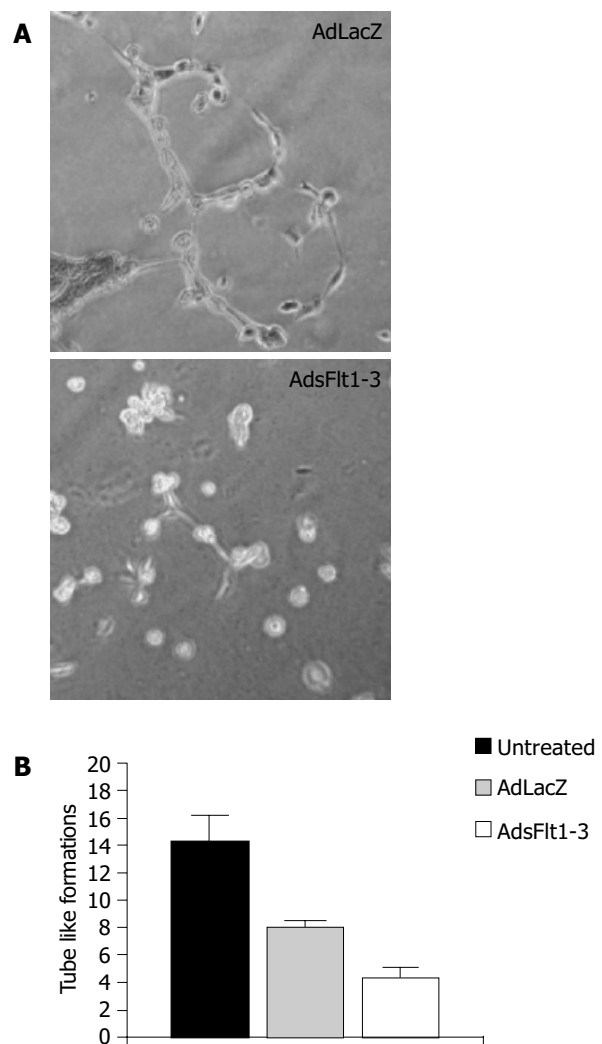


Figure 2 Tube formation assay *in vitro*. HUVE cells were incubated on Matrigel with CM from AdsFlt1-3- or AdLacZ-infected tumor cells. **A:** Exemplary light microscope image (40 \times magnifications) of HUVE cells incubated with CM of AdLacZ-infected cells and with CM of AdsFlt1-3-infected cells; **B:** So called tube-like formations were quantified per high power field. Data are shown as mean and SE ($P = 0.10$ compared to the control).

Systemic treatment

Since CT26 tumor cells express and secrete VEGF (68 pg/mL) into cell supernatant, the CT26 tumor model is suitable to study antitumor effects of an anti-VEGF therapy. The systemic injection of 5×10^9 pfu/mL AdsFlt1-3 significantly

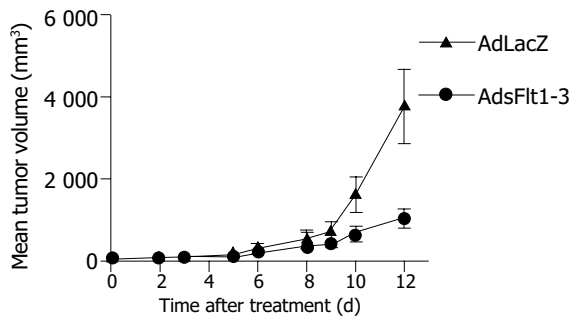


Figure 3 Tumor treatment of pre-established CT-26 CRC. Vectors were administered systemically (5×10^9 pfu, AdsFlt1-3, $n = 10$; AdLacZ, $n = 11$). Data are given as mean tumor volume and SE ($P = 0.006$ compared to the control).

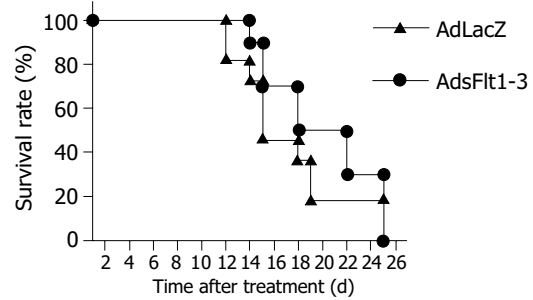


Figure 4 No effect of AdLacZ and AdsFlt1-3 on the survival rate of tumor bearing mice. Tumor treatment of pre-established CT-26 CRC. Vectors were administered systemically (5×10^9 pfu, AdsFlt1-3, $n = 10$; AdLacZ, $n = 11$).

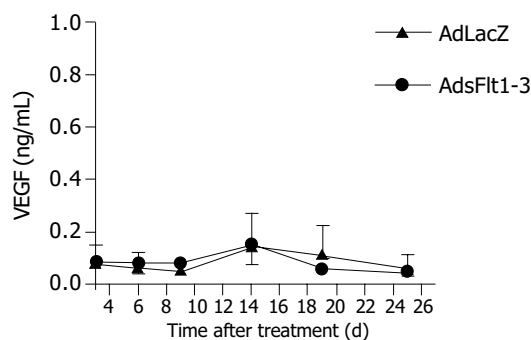


Figure 5 Time course of *in vivo* VEGF serum levels of tumor bearing mice that had been treated with AdLacZ or AdsFlt1-3 (mean \pm SE).

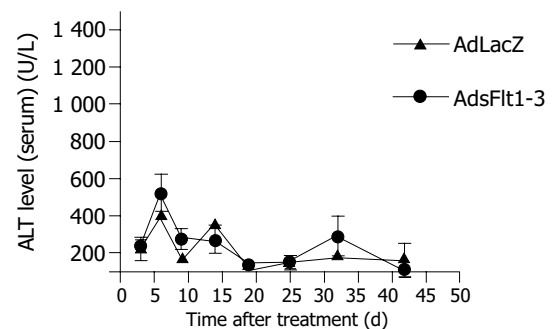


Figure 6 Time course of ALT serum levels as marker of liver toxicity at d 3, 6, 9, 14, 19, 25, 32, and 42 after AdLacZ and AdsFlt1-3 treatment initiation (mean \pm SE).

reduced tumor growth by 72% compared to the AdLacZ control 12 d after treatment initiation (Figure 3), but did not improve the survival rate (Figure 4). VEGF serum levels were similar in both groups, AdLacZ and AdsFlt1-3, (Figure 5) and we did not observe any compensatory upregulation of VEGF levels in serum. Liver toxicity was tolerable according to alanine aminotransferase levels in serum (Figure 6).

Inhibition of tumor angiogenesis by AdsFlt1-3 *in vivo*

Intratumoral microvessels density was determined by immunohistochemistry for von Willebrand factor. Tumors

were removed 9 d after treatment and as shown in Figure 7, tumors of animals that had received AdLacZ showed intense staining for von Willebrand factor, indicating effective tumor vascularization, and tumor sections of AdsFlt1-3-treated animals showed a marked reduction by 42% in microvessel density (Figure 7).

DISCUSSION

VEGF has been acknowledged as one of the most important pro-angiogenic factors that are known to be involved in

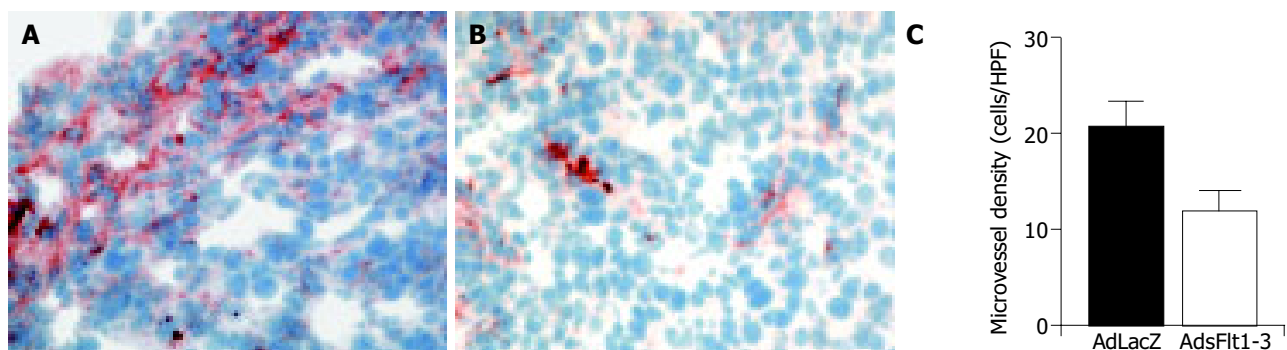


Figure 7 Effective inhibition of tumor angiogenesis *in vivo* by treatment with AdsFlt1-3. Pre-established CRC tumors were treated with AdLacZ or AdsFlt1-3. Animals were killed on d 9 after treatment and tumor tissue was removed. Microvessel density was determined by anti-von Willebrand factor staining. **A** and **B**: Representative

photomicrographs show microvessel staining in tumors of AdLacZ- or AdsFlt1-3-treated mice; **C**: quantitative analysis of microvessel density was made by counting the positively stained cells per high-power fields (200 \times magnification). Data are given as mean of cell number/HPF and SE ($P = 0.02$ compared to the control).

tumor angiogenesis^[7,14-16]. In particular, VEGF expression has been shown to be elevated in metastatic CRC disease^[2]. In the case of metastatic CRC, therapeutic options are still limited and innovative approaches are warranted. Therefore, we intended to confirm the antitumor efficacy of blocking VEGF signaling by systemic administration of an adenovirus delivering the VEGF receptor 1 fragment sFlt1-3 in a subcutaneous metastatic murine CRC tumor model. Our data show that the systemic vector application of AdsFlt1-3 induced significant antitumor effects in CRC.

Recently, several angiostatic antitumor approaches have been used to inhibit experimental CRC. In a previous publication, we were able to show that the local gene delivery of angiostatin-like molecule (K1-3) inhibited tumor growth in the same CRC model by 41% at d 8 after treatment initiation. Another group had used a similar approach employing an adenoviral construct encoding a distinct Flt-1 fragment to treat subcutaneous tumors, but then only the local treatment was effective^[6]. But principally, angiostatic antitumor strategies do not intend to directly control growth of the malignant tumor cell but rather to curb tumor vascularization. Therefore, systemic gene delivery of angiostatic proteins might even be more effective than local applications. The vector construct we used in this study had been shown to inhibit e.g. tumor growth of fibrosarcoma and lung cancer in experimental studies after systemic vector administration^[13]. Here, we were able to confirm the antitumoral efficacy of the AdsFlt1-3 construct in a metastatic subcutaneous CRC model. But, according to other angiostatic gene therapy studies and own findings, the survival rate was not improved.

Since we could not observe any direct antiproliferative effects of sFlt1-3 on CT26 CRC cells, antitumoral effects most probably were mediated by indirect angiostatic effects. This was supported by immune staining for von Willebrand factor revealing decreased microvessel density in the AdsFlt1-3 treatment group. Taken together, these results correspond well to other publications reporting anti-angiogenic effects of similar constructs in corneal or ocular neovascularization assays^[13].

Recently, potential side effects of adenoviruses have provoked severe concerns of systemic vector applications regarding particularly liver toxicity. Indeed, we observed some ALT elevations, but at the dosage applied toxicity was well tolerated.

In summary our data demonstrate that the systemic gene transfer of sFlt1-3 induced significant antitumor effects on pre-established subcutaneous metastatic CRC and antitumor mechanism based on angiostatic effects. Thus, these data further confirmed the value of blocking VEGF signaling as an effective approach to treat CRC disease.

ACKNOWLEDGMENTS

AdsFlt1-3 construct was generously provided by R. Mulligan,

Boston, MA, USA. We thank I. Höschler for her expert assistance.

REFERENCES

- 1 **Ohlsson B, Palsson B.** Follow-up after colorectal cancer surgery. *Acta Oncol* 2003; **42**: 816-826
- 2 **Hanrahan V, Currie MJ, Gunningham SP, Morrin HR, Scott PA, Robinson BA, Fox SB.** The angiogenic switch for vascular endothelial growth factor (VEGF)-A, VEGF-B, VEGF-C, and VEGF-D in the adenoma-carcinoma sequence during colorectal cancer progression. *J Pathol* 2003; **200**: 183-194
- 3 **Fernando NH, Hurwitz HI.** Inhibition of vascular endothelial growth factor in the treatment of colorectal cancer. *Semin Oncol* 2003; **30** (3 Suppl 6): 39-50
- 4 **Tseng JF, Mulligan RC.** Gene therapy for pancreatic cancer. *Surg Oncol Clin N Am* 2002; **11**: 537-569
- 5 **Ye C, Feng C, Wang S, Wang KZ, Huang N, Liu X, Lin Y, Li M.** sFlt-1 gene therapy of follicular thyroid carcinoma. *Endocrinology* 2004; **145**: 817-822
- 6 **Kong HL, Hecht D, Song W, Kovesdi I, Hackett NR, Yayon A, Crystal RG.** Regional suppression of tumor growth by *in vivo* transfer of a cDNA encoding a secreted form of the extracellular domain of the flt-1 vascular endothelial growth factor receptor. *Hum Gene Ther* 1998; **9**: 823-833
- 7 **Robinson CJ, Stringer SE.** The splice variants of vascular endothelial growth factor (VEGF) and their receptors. *J Cell Sci* 2001; **114**: 853-865
- 8 **Fong GH, Rossant J, Gertsenstein M, Breitman ML.** Role of the Flt-1 receptor tyrosine kinase in regulating the assembly of vascular endothelium. *Nature* 1995; **376**: 66-70
- 9 **Brattain MG, Strobel-Stevens J, Fine D, Webb M, Sarrif AM.** Establishment of mouse colonic carcinoma cell lines with different metastatic properties. *Cancer Res* 1980; **40**: 2142-2146
- 10 **Qian C, Bilbao R, Bruna O, Prieto J.** Induction of sensitivity to ganciclovir in human hepatocellular carcinoma cells by adenovirus-mediated gene transfer of herpes simplex virus thymidine kinase. *Hepatology* 1995; **22**: 118-123
- 11 **Kuo CJ, Farnebo F, Yu EY, Christofferson R, Swearingen RA, Carter R, von Recum HA, Yuan J, Kamihara J, Flynn E, D'Amato R, Folkman J, Mulligan RC.** Comparative evaluation of the antitumor activity of antiangiogenic proteins delivered by gene transfer. *Proc Natl Acad Sci USA* 2001; **98**: 4605-4610
- 12 **Kim KJ, Li B, Winer J, Armanini M, Gillett N, Phillips HS, Ferrara N.** Inhibition of vascular endothelial growth factor-induced angiogenesis suppresses tumour growth *in vivo*. *Nature* 1993; **362**: 841-844
- 13 **Shibuya M.** Role of VEGF-flt receptor system in normal and tumor angiogenesis. *Adv Cancer Res* 1995; **67**: 281-316
- 14 **Ferrara N, Houck K, Jakeman L, Leung DW.** Molecular and biological properties of the vascular endothelial growth factor family of proteins. *Endocr Rev* 1992; **13**: 18-32
- 15 **Schmitz V, Wang L, Barajas M, Gomar C, Prieto J, Qian C.** Treatment of colorectal and hepatocellular carcinomas by adenoviral mediated gene transfer of endostatin and angiostatin-like molecule in mice. *Gut* 2004; **53**: 561-567
- 16 **Gehlbach P, Demetriades AM, Yamamoto S, Deering T, Xiao WH, Duh EJ, Yang HS, Lai H, Kovesdi I, Carrion M, Wei L, Campochiaro PA.** Periocular gene transfer of sFlt-1 suppresses ocular neovascularization and vascular endothelial growth factor-induced breakdown of the blood-retinal barrier. *Hum Gene Ther* 2003; **14**: 129-141

Effect of NS398 on metastasis-associated gene expression in a human colon cancer cell line

Xue-Qin Gao, Jin-Xiang Han, Hai-Yan Huang, Bao Song, Bo Zhu, Chang-Zheng Song

Xue-Qin Gao, Jin-Xiang Han, Hai-Yan Huang, Bao Song, Bo Zhu, Chang-Zheng Song, Key Laboratory of Ministry of Public Health for Biotech-Drug, Shandong Medicinal and Biotechnology Center, Shandong Academy of Medical Sciences, Jinan 250062, Shandong Province, China

Xue-Qin Gao, Jin-Xiang Han, Shandong University School of Medicine, Jinan 250062, Shandong Province, China

Supported by the Key Technology Research and Development Program of Shandong Province, No. 011100105

Correspondence to: Professor Jin-Xiang Han, Shandong Medicinal and Biological Center, Shandong Academy of Medical Sciences, 89 Jingshi Road, Jinan 250062, Shandong Province, China. han9888@sina.com

Telephone: +86-531-82919888 Fax: +86-531-82951586

Received: 2004-09-08 Accepted: 2004-12-03

Gao XQ, Han JX, Huang HY, Song B, Zhu B, Song CZ. Effect of NS398 on metastasis-associated gene expression in a human colon cancer cell line. *World J Gastroenterol* 2005; 11(28): 4337-4343

<http://www.wjgnet.com/1007-9327/11/4337.asp>

INTRODUCTION

N-[2-(cyclohexyloxy)-4-nitrophenyl] methanesulfonamide (NS398) is a highly selective cyclooxygenase-2 (COX-2) inhibitor. Its mechanism in anticancer effects involves many signal pathways. One is induction of apoptosis of different tumor cells. NS398 inhibits the viability of colon cancer cell lines by apoptosis by the release of cytochrome C from mitochondria and by the activation of caspase-9 and caspase-3 and cleavage of poly (ADP-ribose) polymerase. Cytochrome C pathway plays an important role in NS398-induced apoptosis in colon cancer cell lines^[1]. NS398 may also suppress the growth of tumor cells by inhibiting the cell cycle progression. It can increase the inhibitor of cell cycles p27Kip1 by inhibiting protein degradation to suppress the proliferation of human lung cancer cells, and this in turn is caused by modulating p27Kip1 proteolysis. Non-steroid anti-inflammatory drugs (NSAIDs) suppress the expression of chymotrypsin-like catalytic subunits (LMP5, LMP7, and LMP2), but do not directly block enzymatic activity and inhibit proteasome activity. Reverse transcriptase-competitive PCR and promoter activity assays showed that this inhibition occurred at the transcriptional level^[2]. NS398 can exert its anti-angiogenesis and anti-metastasis effects by inhibiting the expression of vascular endothelial growth factor (VEGF)^[3]. Its inhibitory effects on the metastasis *in vitro* and *in vivo* are mainly mediated by regulating the matrix metalloproteinase (MMP) family components. NS398 can inhibit the invasiveness of prostate cancer by reducing the release of MMP-2 and MMP-9 and increase of TIMP-2 but not TIMP-1^[4]. NS398 inhibits MMP-2 mRNA expression and also decreases the amount of MMP-2 in human lung cancer cells. Additionally, this COX-2 inhibitor attenuates the degrading activity of MMP-2. The synthesis and processing of MMP-2 was significantly suppressed by NS398. NS398 directly inhibits MMP-2 promoter activity. However, the inhibitory effect of NS398 is not fully dependent on inhibition of COX-2 because a high concentration of NS398 is needed to suppress MMP-2 expression and addition of prostaglandin E2 only partially reverses the action of NS398^[5].

NS398 and aspirin also upregulate RECK mRNA level in CL-1 human lung cancer cells. Additionally, NSAIDs increase

Abstract

AIM: To investigate the effect of NS398 on the metastasis-associated gene expression in LoVo colorectal cancer cells.

METHODS: LoVo cells were treated with NS398 at the concentration of 100 $\mu\text{mol/L}$ for 24 and 48 h respectively. Total RNA was extracted with TRIZOL reagents and reverse transcribed with Superscript II and hybridized with cDNA microarray (containing oncogenes, tumor suppressor genes, signal transduction molecules, adhesive molecules, growth factors, and ESTs) fabricated in our laboratory. After normalization, the ratio of gene expression of NS398 treated to untreated LoVo cells was either 2-fold up or 0.5-fold down was defined as the differentially expressed genes. Semi-quantitative RT-PCR was used to validate the microarray results.

RESULTS: Among the 447 metastasis-associated genes, 9 genes were upregulated and 8 genes were downregulated in LoVo cells treated with NS398 for 24 h compared to untreated cells. While 31 genes were upregulated and 14 genes were downregulated in LoVo cells treated with NS398 for 48 h. IGFBP-5, PAI-2, JUN, REL, BRCA1, and BRCA2 might be the new targets of NS398 in treatment of colorectal cancer.

CONCLUSION: NS398 might exert its anti-metastasis effect on colorectal cancer by affecting several metastasis-associated gene expression.

© 2005 The WJG Press and Elsevier Inc. All rights reserved.

Key words: NS398; Colorectal cancer gene expression; Metastasis; cDNA microarray

RECK protein level which was associated with reduction of MMP-2 activity. NSAID-activated RECK expression may not be mediated via inhibition of COXs because addition of prostaglandin E₂ (PGE₂) cannot counteract the effect of NSAIDs and overexpression of COX-2 cannot downregulate RECK^[6]. To promote the application of NS398 in the treatment and chemoprevention of colorectal cancer, and observe whether it has other target genes, we detected the effect of NS398 on the expression of metastasis-associated genes in colorectal cancer cell lines by cDNA microarray.

MATERIALS AND METHODS

Microarray fabrication

A total of 447 cDNA clones were obtained from Research Genetics (Invitrogen, Life Technologies, USA). *E. coli* with inserted metastasis-associated genes were cultured with Luria-Bertain culture medium supplemented with ampicillin (50 mg/L in final concentration) or chloromycin (170 mg/L) in Innova™4330 refrigerated incubator shaker (New Brunswick Scientific, USA) at the speed of 250 r/min overnight at 37 °C. Clone plasmids were extracted with Edge BioSystems (Gaithersburg, MD, Germany). Clone inserts were PCR-amplified from the plasmids with M13 vector-specific universal primer (M13F: 5'-GGT GTA AAA CGA CGG CCA GTG-3'; M13R: 5'-CAC ACA GGA AAC AGC TAT G-3') in 96-well PCR microtiter. The PCR products were purified with protocols published^[7], and resuspended in Arrayit spot solution. The purified PCR products were printed on silanated slides (CEL Associates, Houston, TX, USA) with Cartesian PixSys 5500 robot (Cartesian Technologies, Irvine, CA, USA) and cDNA microarrays were UV-cross-linked at 3 500 mJ using Cl-1000 ultraviolet cross-linker (Stratagene). Microarrays were post-processed according to protocol online^[8].

Cell culture and drug treatment

LoVo cells were grown in the culture incubator at 37 °C with 50 mL/L CO₂ in RPMI 1640 (Life Technologies, USA) supplemented with 10% neonatal bovine serum. After the cells were cultured to 60-70% confluence, 12 μL of NS398 dissolved in dimethyl sulfoxide (Me₂SO) was added to make the final concentration 100 μmol/L and further cultured for 24 and 48 h respectively. The same amount of Me₂SO was added to the control.

RNA extraction

LoVo cells treated with NS398 or Me₂SO were lysed with TRIzol (Life Technologies Inc., Rockville, MD, USA) according to the manufacturer's protocol and total RNA was extracted and stored at -80 °C. The concentration of total RNA were measured with a biophotometer (Eppendorf AG22331, Hamberg, Germany) and the 260/280 ratio of RNA was 1.8-2.0.

Probe preparation

Probes were prepared as described previously^[9,10] with some modifications. First strand cDNA was synthesized by priming 10 μg total RNA with 6 μg random hexamers (Life Technologies Inc., Rockville, MD, USA) by heating at

70 °C for 10 min, snap-cooling on ice for 30 s and placed at room temperature for additional 5-10 min. Reverse transcription was performed in the presence of 500 μmol/L each of dATP, dCTP and dGTP, 200 μmol/L aminoallyl-dUTP (Sigma Chemical Co., St. Louis, MO, USA), 300 μmol/L dTTP, 1× first strand buffer, 10 mmol/L dithiothreitol, and 400 U superscript II (Life Technologies) in 30 μL reaction at 42 °C overnight. Reactions were quenched with 0.5 mol/L EDTA and RNA template was hydrolyzed by addition of 10 μL NaOH of 1 mol/L followed by heating at 70 °C for 10 min. Reactions were neutralized with 10 μL 1 mol/L HCl and cDNA was purified with Amicon Microcon YM100 (Millipore Corporation, Bedford, MA, USA) according to the manufacturer's protocol. cDNA was dried in speed vacuum concentrator 5301 (Eppendorf, Germany) and resuspended in 4.5 μL 0.1 mol/L (pH 9.0) sodium carbonate buffer. Aliquot of Cy3 NHS ester dye (Amersham Pharmacia Biotech, UK) was dissolved in 4.5 μL Me₂SO (1 mg dye from one tube was dissolved in 73 μL of Me₂SO and aliquot in 16 tubes, dried in speed vacuum and stored at 4 °C) and added to the resuspended cDNA and reactions were incubated at room temperature in the dark for 1 h. Coupling reactions were quenched by addition of 41 μL 0.1 mol/L sodium acetate (pH 5.2), and unincorporated dye was removed using QIAquick PCR purification kit (Qiagen, Germany) following manufacturer's instructions.

Hybridization and image processing

Each slide was printed with duplicate microarrays. Slides were pre-hybridized in 1% BSA, 5× SSC, 0.1% SDS for 45 min, washed twice in de-ionized double distilled H₂O and 2-propanol and air-dried and used in 1 h. Fluorescent cDNA probes were dried in speed vacuum and resuspended in 10 μL hybridization buffer p5 μL formamide, 2.5 μL 20× SSC, 1.0 μL reagent grade double distilled water (RGDD H₂O), 0.5 μL 2% SDS and 1 μL human cot-1DNA]. Probes were denatured at 100 °C water bath for 2 min and cooled at room temperature for 5 min. Room temperature probes of NS398 treated and untreated group were applied to the duplicate microarrays on the same pre-hybridized microarrays, covered with hybridized coverslip (Sigma) and placed in the hybridization chamber (Corning). Hybridizations was carried out at 42 °C water bath for 20-22 h followed by washing in 2× SSC and 0.1% SDS for 3 min, 1× SSC for 2 min and 0.2× SSC for 1 min and 0.05× SSC for 10 s, and dried by spin at horizontal plate centrifuge at 90 r/min for 4 min. Microarrays were scanned using a ScanArray 4000 (Packard Bioscience, PE, USA) dual color confocal laser scanner. Data were saved as paired TIFF images.

Data analysis

Spots were identified and local background subtracted in the QuantArray 3.0. In the first step, a grid consisting of square cells was drawn around each array element. Spot segmentation was then performed using a fixed segmentation method that uses the distribution of pixel intensity to separate probable signal from background and a binary threshold approach to identify spots, followed by a procedure to exclude disconnected features. Raw intensity for each

element was obtained by first excluding saturated pixels, then summing all remaining pixel intensities inside the spot contours. The area outside the spot contour but inside the cell was used to calculate local background. Background per pixel was estimated as a median of the pixels in this area and multiplied by the spot area to give an estimated spot background value. In the final step, this integrated background value was subtracted from the raw integrated spot intensity to produce the background-subtracted integrated intensities used for further analysis. Furthermore, a quality control filter was used to remove questionable array features. Two criteria for spot rejection were the spot shape deviating greatly from a circle and a low signal to noise ratio. Spots for which the ratio of area to circumference deviated by more than 20% from the value for an ideal circle and spots containing less than 50% of pixels above the median background values were flagged and eliminated from further consideration. The spot intensity above blank plus 2SD was used for the final analysis. Then the data were normalized to total with software supplied by the manufacturer. The two fold up- or down-regulated genes were shown in red or green respectively.

Semi-quantitative RT-PCR validation of microarray results

The upregulated gene IGFBP-5 was measured by RT-PCR to verify the microarray results. RT-PCR was performed on MJ-PTC200 DNA engine using TaKaRa two-step reaction with protocols supplied by the manufacturer. The primers for IGFBP-5 were forward: 5'-TTG CCT CAA CGA AAA GAG C-3', reverse: 5'-AGA ATC CTT TGC GGT CAC A3'^[11]. The primers for β -actin were forward: 5'-AAG TAC TCC GTG TGG ATC GG -3', reverse: 5'-TCA AGT TGG GGG ACA AAA AG -3'^[12]. PCR was performed at 94 °C for 2 min, and 30 cycles at 94 °C for 30 s, at 50 °C for 30 s and at 72 °C for 60 s and a final extension at 72 °C for 5 min. PCR products were electrophoresed on 1% agarose gel. Images were captured with Alpha Image™ 2000. The band density was measured with the software supplied by the same system.

RESULTS

Plasmid extraction

The plasmids were extracted by Edge biosystems plasmids extraction kit (Gaithersburg, MD, Germany). The extracted plasmids were run on 1% agarose gel. The results shown in Figure 1 are representative of the 447 clones. PCR amplification of the 447 clones for the inserts is shown in Figure 2. The single band amplification rate was 93%.

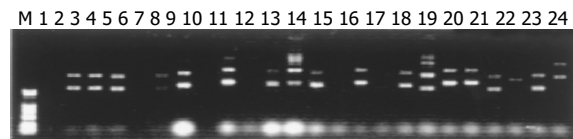


Figure 1 Electrophoresis of clone 73-95 plasmids on 0.7% agarose. M: DL2000, lanes 1-24 represent plasmids of clone 73-95.

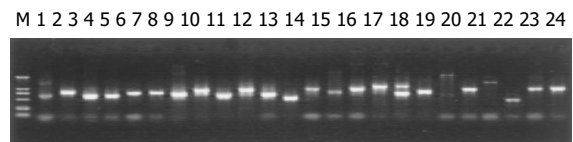


Figure 2 Electrophoresis of PCR products in 1% agarose. M: DL2000, lanes 1-24: the PCR amplification of clone 73-95.

To identify metastasis-associated genes affected by NS398, LoVo cells were treated with 100 μ mol/L NS398 for 24 and 48 h respectively. The representative image is shown in Figure 3. Image A represents the hybridized results of untreated cells. Image B represents the hybridization results of the NS398-treated LoVo cells and image C is the overlay image of NS398-treated to control LoVo cells.

After treatment with NS398 for 24 h, 9 genes were upregulated and 8 genes downregulated (Table 1). The

Table 1 Up- and down-regulated genes in NS398-treated LoVo cells for 24 h (mean \pm SD)

Accession number	Gene descriptions	Ratio
Not found	Hs.23723, "ESTs" (346390)	2.67 \pm 1.66
Not found	Hs.106513, "EST" (348242)	2.31 \pm 0.67
BC040844	Hs.198253, NS1-associated protein 1 (435598)	1.96 \pm 0.25
BC011714	Hs.9605, heterogeneous nuclear ribonucleoprotein D-like (190165)	2.08 \pm 0.46
Not found	Hs.277401, ESTs (35363)	2.04 \pm 0.13
NT_024524	Hs.277704, PIBF1 gene product (124966)	2.29 \pm 0.81
BC007674	Hs.180414, CD24 antigen (small cell lung carcinoma cluster 4 antigen) (115306)	1.98 \pm 0.22
NM_003127	Hs.87497, spectrin, alpha, non-erythrocytic 1 (alpha-fodrin, 3021698)	2.27 \pm 0.53
Not found	Hs.272073, ESTs (1296662)	1.95 \pm 0.24
BT007404	Hs.8037, CD24 antigen (small cell lung carcinoma cluster 4 antigen, 124098)	0.49 \pm 0.04
K01500	Hs.18443, alpha-1-antichymotrypsin (117439)	0.51 \pm 0.05
Not found	Hs.45209, EST(2118886)	0.49 \pm 0.04
NM_005564	LCN2 (oncogene 24p3, 595821)	0.47 \pm 0.17
NM_001022	Hs.43913, ribosomal protein S19 (453963)	0.53 \pm 0.06
NM_003259	Intercellular adhesion molecule 5, telencephalin (ICAM5, 180864)	0.36 \pm 0.14
NM_002228	v-jun avian sarcoma virus 17 oncogene homolog (JUN, 823612)	0.51 \pm 0.07
NM_002908	v-rel avian reticuloendotheliosis viral oncogene homolog (REL, 2723459)	0.45 \pm 0.06

Table 2 Up- and down-regulated genes in NS398-treated LoVo cells for 48 h (mean±SD)

Accession number	Gene description	Ratio
Not found	Hs.23723, "ESTs" (346390)	3.41±1.76
Not found	Hs.106513, "EST" (348242)	3.05±1.88
BC040844	Hs.198253, NS1-associated protein 1 (435598)	2.51±0.53
AF257505	Hs.23317, butyrophilin, subfamily 3, member A2 (219410)	2.12±0.56
NT_033899	Hs.28043, KIAA0712 gene product (219914)	2.13±0.40
BC011714	Hs.9605, heterogeneous nuclear ribonucleoprotein D-like (190165)	2.34±0.51
M62782	Hs.22907, human insulin-like growth factor binding protein 5 (IGFBP5) mRNA (31397)	2.15±0.43
NM_003127	Hs.87497, spectrin, alpha, non-erythrocytic 1 (alpha-fodrin, 3021698)	2.14±0.13
BC008005	Hs.116459, nucleotide binding protein 2 (<i>E coli</i> MinD like, 2498589)	2.01±0.29
Not found	Hs.43913, ESTs (2498857)	2.20±0.28
Not found	Hs.272073, ESTs (1296662)	2.33±0.43
BM508995	Hs.106513, ESTs, highly similar to proteasome (<i>H sapiens</i> , 1302647)	2.47±0.76
NM_000624	Hs.150580, alpha-1-antichymotrypsin (1322220)	2.14±0.35
AF248734	Hs.87497, apoptotic protease activating factor (963055)	2.28±0.45
BC002965	Lysosomal-associated membrane protein 2 (LAMP2), transcript variant LAMP2A (134418)	2.34±0.69
NM_006536	Chloride channel, calcium activated, family member 2 (CLCA2, 781187)	2.39±0.42
M90657	Tumor-associated antigen L6 (1964132)	2.85±1.58
Not found	Spliceosome associated protein 145 (1964680)	2.28±0.34
AW674474	Putative insulin-like growth factor ii associated (229316)	2.32±0.50
AF041835	Laminin, gamma 3 (LAMC3, 2497685)	2.16±0.48
AB019987	Chromosome-associated polypeptide-c (2597847)	2.06±0.09
AW277011	Putative vacuolar protein sorting-associated protein c (2744695)	2.20±0.64
BC032547	Homeo box A1 (HOXA1, 3923611)	2.27±1.18
NM_003391	Wingless-type MMTV integration site family member 2 (WNT2, 149373)	2.27±0.28
BC027948	c-fos induced growth factor (VEGF D, FIGF, 160946)	2.15±0.27
NM_001792	Cadherin 2, N-cadherin (neuronal, CDH2, 3617894)	2.03±0.10
NM_001964	Early growth response 1 (EGR1, 182411)	2.61±0.47
AF071400	Plasminogen activator inhibitor, type II (arginine-serpin, PAI2, 323255)	2.41±0.39
NM_002447	Macrophage stimulating 1 receptor (c-met-related tyrosine kinase, MST1R, 586698)	2.45±0.62
NM_003254	Tissue inhibitor of metalloproteinase 1 (erythroid potentiating activity, collagenase inhibitor, TIMP1, 771755)	2.02±0.18
NM_003182	Tachykinin, precursor 1 (substance P, neurokinin 1, neurokinin 2, neuromedin L, neurokinin alpha, neuropeptide K, neuropeptide gamma, TAC1), transcript variant beta (784179)	2.22±0.30
BC004986	Hs.77202, ribosomal protein S25 (178052)	0.49±0.06
BC035128	Hs.23317, Max-interacting protein (130696)	0.45±0.05
Not found	Hs.23954, ESTs (132543)	0.51±0.06
AJ001810	Hs.106513, pre-mRNA cleavage factor Im (25 ku)	0.48±0.01
BC053521	66834, Hs.76847, spectrin, alpha, non-erythrocytic 1 (alpha-fodrin, 31230)	0.47±0.15
M64716	Hs.234726, ribosomal protein S25 (4932742)	0.46±0.05
BC032589	No, beta-2-microglobulin (1907327)	0.48±0.11
Not found	Hs.45209, EST (2118886)	0.47±0.11
NT_024524	Hs.15058, PIBF1 gene product (1596167)	0.50±0.05
NM_001779	CD58 antigen (lymphocyte function-associated antigen 3, CD58, 490368)	0.50±0.15
NM_002228	v-jun avian sarcoma virus 17 oncogene homolog (JUN, 823612)	0.41±0.11
NM_020979	Adaptor protein with pleckstrin homology and src homology 2 domains (APS, 3056093)	0.49±0.17
NM_000059	Breast cancer 2, early onset (BRCA2, 3850805)	0.30±0.10
NM_001223	Caspase 1, apoptosis-related cysteine protease (interleukin 1, beta, convertase, CASP1, 3858119)	0.48±0.09

The number in parenthesis represents the IMAGE clone number.

downregulated genes included lipocalin 2 (oncogene 24p3) (LCN2), intercellular adhesion molecule 5, telencephalin (ICAM5), v-jun avian sarcoma virus 17 oncogene homolog (JUN), v-rel avian reticuloendotheliosis viral oncogene homolog (REL). Five genes after being treated for 24 h were still highly expressed until 48 h and one gene was still inhibited until 48 h.

After 48 h of treatment more genes were regulated by NS398. Of the 447 genes analyzed, 31 genes were upregulated and 14 genes downregulated (Table 2). IGFBP-5,

APAF, LAMP2, CLCA2, laminin gamma3, HOXA1, WNT2, N-cadherin, PAI-2, TIMP could inhibit the metastasis of tumor.

Validation of microarray results by semi-quantitative RT-PCR
IGFBP-5 gene expression was validated with TAKARA version 2.1 RT-PCR kit. The expression level was measured with alpha InnoTech™ 2000 spot density method. The NS398-treated LoVo cells expressed more IGFBP-5 mRNA (Figure 4). The relative expression ratio to β -actin was 0.21,

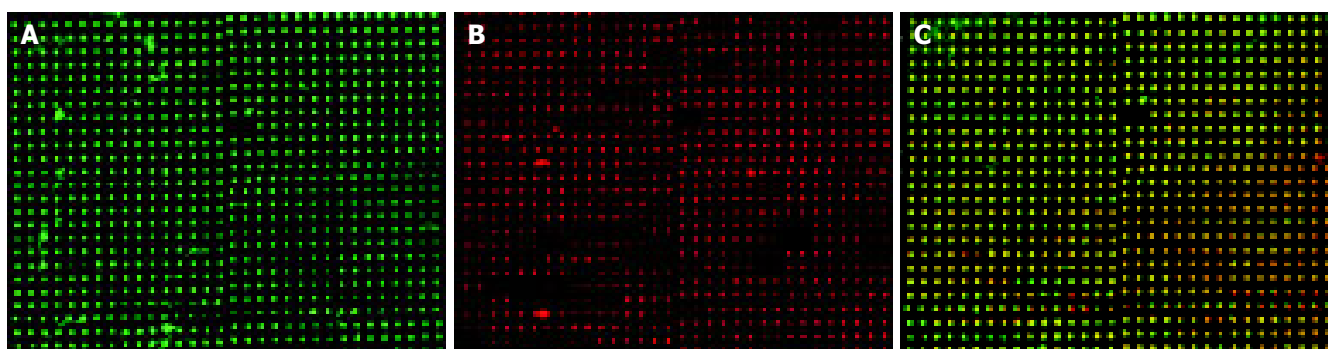


Figure 3 Representative image of cDNA microarray. **A:** Image of the DMSO treated control, **B:** image of NS398-treated LoVo cell, **C:** overlay image of NS398-treated LoVo cell to control.

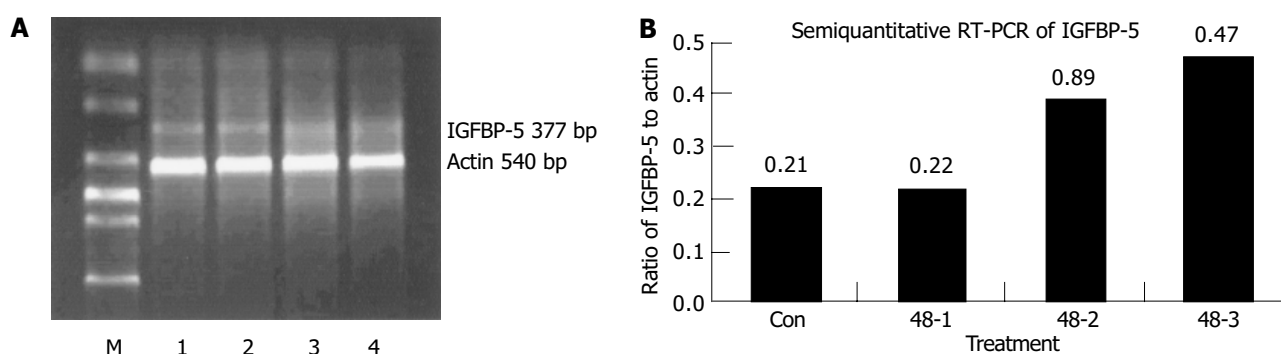


Figure 4 IGFBP-5 mRNA expression in NS398-treated LoVo cell. **A:** mRNA level measured with semi-quantitative RT-PCR. M: DL2000, lanes 1-4 control

and 3 replicates of NS398 treated loVo cell; **B:** Relative ratios of the IGFBP-5 to actin.

0.22, 0.39, and 0.47 for the control and the three NS398-treated replicate experiments. The IGFBP-5 mRNA level in NS398-treated LoVo cells to untreated LoVo cells was 1.05, 1.85, and 2.23 respectively for the three replicate experiments. It was in accord with the microarray results.

DISCUSSION

NS398 is a highly selective COX-2 inhibitor. Its anticancer effects have been linked to cell apoptosis and inhibition of MMP and anti-angiogenesis. NS398 also exerts its synergistic effect with radiotherapy for the treatment of head and neck squamous cell cancer (HNSCC) by inhibiting radiation-induced expression of COX-2^[12] and increases the sensitivity of chemotherapy by enhancing the expression of cyclin-dependent kinase inhibitors p21 (Waf1) and p27 (Kip1), promoting apoptosis of tumor cells, therefore makes the cells stay in G₁ arrest^[13].

cDNA microarray has been widely used in the screening of drug targets. To identify whether NS398 had other target genes in the treatment of colorectal cancer, we treated LoVo cells with NS398 and the expression of metastasis-associated genes were measured with microarray. The results showed that NS398 influenced the expression of some metastasis genes. After being treated for 24 h, NS398 increased the production of NS1-associated protein 1, PIBF1 gene, CD24 antigen, and some ESTS. Simultaneously NS398 can inhibit the expression of some oncogenes such as alpha-1-antichymotrypsin, LCN2 (oncogene 24p3), ICAM5, JUN

and REL. It was reported that NS398 downregulates the expression of COX-2, nuclear factor-kappaB, p50 and Rel A p65, and its anti-tumor effect is associated with COX-2 transcription inhibition^[14].

After being treated for 48 h with NS398, the metastasis-associated genes expressed by LoVo cells changed more profoundly. Thirty-one genes were upregulated, including NS1-associated protein 1, IGFBP5, spectrin, nucleotide binding protein 2, alpha-1-antichymotrypsin, apoptotic protease activating factor, LAMP2, CLCA2, tumor-associated antigen L6, putative insulin-like growth factor, chromosome-associated polypeptide-c, HOXA1, WNT2, FIGF, N-cadherin, PAI2, macrophage-stimulating 1 receptor (MST1R), TIMP1, tachykinin, and precursor.

E-cadherin and N-cadherin are members of the cadherin family of calcium-dependent cell adhesion molecules that play an important role in the embryonic development and maintenance of normal tissues. N-cadherin present in the most invasive and dedifferentiated breast cancer cell lines, and its exogenous expression in tumor cells induces a scattered morphology and high motility, invasion, and metastasis. N-cadherin co-operates with the fibroblast growth factor receptor, resulting in signals that lead to the upmodulation of MMP-9 and cellular invasion. N-cadherin probably also supports the systemic dissemination of tumor cells by enabling the circulation of tumor cells to associate with the stroma and the endothelium at distant sites^[15]. Ectopically expressed N-cadherin fails to assemble cadherin/catenin adhesion complexes and to inhibit invasion. The

association of N-cadherin with long P120 (ctn) and tyrosine may explain why N-cadherin cannot replace E-cadherin in pancreatic carcinoma cells^[16]. But there are conflicting results of the expression of N-cadherin with the invasion of tumor. P-cadherin is detectable in 40%, N-cadherin in 30%, and E-cadherin in 81% invasive carcinomas. P-cadherin but not E/N-cadherin expression in breast carcinomas shows a strong correlation with higher grade (poorer differentiation), lack of ERs, and presence of EGFR, and its expression may aid in the further subdivision of high grade carcinomas^[17]. In the upregulated genes, IGFBP-5 is of great importance. Until now the role of IGFBP-5 in the tumor development is different in different tumors. Expression of IGFBP-5, both by stable transfection and adenoviral-mediated infection, can inhibit the growth of MDA-MB-231 and Hs578T human breast cancer cells over a 13-d period. IGFBP-5 is a potent growth inhibitor and proapoptotic agent in human breast cancer cells via modulation of cell cycle and apoptotic mediators^[18].

IGFBP5 is also overexpressed in thyroid tumors. IGFBP-5 and gene 44 are significantly overexpressed in papillary carcinoma^[19]. IGFBP-5 mRNA levels are the highest in the benign group without edema of meningiomas, whereas IGFBP-6 mRNA levels are the highest in the group with brain invasion^[20]. The presence of IGFBP-5 significantly inhibits cell death induced by C2 or RGD. IGFBP-5 promotes the attachment and survival of Hs578T cells by modulating the balance between ceramide and opposing survival signals^[21]. IGFBP-5 has no effect on the proliferation, migration and invasiveness of RSVT2/C cells *in vitro*^[22].

Insulin-like growth factor (IGF)-I and -II are potent mitogens, and can exert autocrine and paracrine effects on growth regulation in human gastric cancer. Their mitogenic effects are regulated by the IGFBPs. The expression pattern of IGFBPs was heterogeneous in the gastric cancer cell lines. IGFBP-2 is expressed in all gastric cancer cell lines, whereas IGFBP-1 is not detectable in any cell line. IGFBP-4 is expressed in most cell lines. IGFBP-3, IGFBP-5, and IGFBP-6 are expressed in approximately 50% of cell lines. In addition, exogenous IGF-I and -II stimulate the proliferation of gastric cancer cells, suggesting the existence of a functional IGF system in gastric cancer. Our data suggest that the IGF-IGFBP system may play an important role in the initiation, progression, and metastasis of gastric cancer^[23].

Osteosarcoma cells transfected with IGFBP-5 reduce proliferation under both anchorage-dependent and -independent manner. The increase of proliferation observed in IGFBP-5-secreting clones after addition of exogenous IGF is significantly less than that observed in mock-transfected cells or parental cells. A similar result has been obtained with long [R3] IGF-I which has a low affinity for all IGFBPs, suggesting that the inhibitory effect of IGFBP-5 is only partially IGF-dependent and this effect may be due to an induction of differentiation in these cells because IGFBP-5 increases the normal component secretion of osteosarcoma cells^[24].

Upregulation of PAI-2 in LoVo cells may be another mechanism of NS398 underlying the inhibitory effects of

tumor cells. PAI-2 is downregulated in esophageal adenocarcinoma compared to normal esophageal tissues^[25].

Plasminogen activator inhibitor-2 (PAI-2), a gene whose expression has been linked to cell invasion, has been identified in head and neck tumor cell line. In addition, immunohistochemical evaluation of biopsy samples reveals a high expression of PAI-2 in both normal and dysplastic epithelia with a marked decrease of expression in areas of the biopsies containing HNSCC^[26].

The downregulated genes include Max-interacting protein, spectrin, beta-2-microglobulin, CD58 antigen, JUN, APS, BRCA2, CASP1, and some ESTS. BRCA1 and BRCA2 staining increases in the apical cell pole of epithelial malignant cells and in colorectal tumor specimens. Increased BRCA1 and BRCA2 expression may be explained by the fact that colorectal tissue is subjected to very active proliferation and differentiation^[27]. High BRCA2 mRNA level is associated with poor outcome and correlates positively and strongly with cell proliferation in breast cancer^[28]. NS398 may inhibit the growth of colorectal cancer by downregulating the expression of BRCA2.

In conclusion, the upregulated and downregulated genes identified by cDNA microarray may be the new target genes of NS398.

REFERENCES

- 1 **Li M, Wu X, Xu XC.** Induction of apoptosis in colon cancer cells by cyclooxygenase-2 inhibitor NS398 through a cytochrome c-dependent pathway. *Clini Cancer Res* 2001; **7**: 1010-1016
- 2 **Hung WC, Chang HC, Pan MR, Lee TH, Chuang LY.** Induction of p27(KIP1) as a mechanisms underlying NS398-induced growth inhibition in lung cancer cells. *Mol Pharmacol* 2000; **58**: 1398-1403
- 3 **Liu XH, Kirschenbaum A, Yao S, Stearns ME, Holland JF, Claffey K, Levine AC.** Upregulation of vascular endothelial growth factor by cobalt chloride-simulated hypoxia is mediated by persistent induction of cyclooxygenase-2 in a metastatic human prostate cancer cell line. *Clin Exp Metastasis* 1999; **17**: 687-694
- 4 **Attiga FA, Fernandez PM, Weeraratna AT, Manyak Michael MJ, Patierno SR.** Inhibitors of prostaglandin synthesis inhibit human prostate tumor cell invasiveness and reduce the release of matrix metalloproteinases. *Cancer Res* 2000; **60**: 4629-4637
- 5 **Pan MR, Chuang LY, Hung WC.** Non-steroidal anti-inflammatory drugs inhibit matrix metalloproteinase-2 expression via repression of transcription in lung cancer cells. *FEBS Lett* 2001; **508**: 365-368
- 6 **Liu LT, Chang HC, Chiang LC, Hung WC.** Induction of RECK by nonsteroidal anti-inflammatory drugs in lung cancer cells. *Oncogene* 2002; **21**: 8347-8350
- 7 **DNA precipitations/Preparation of DNA samples.** [Last Update, December1999] [Bioinformatics Manual]. Available from: http://cmgm.stanford.edu/pbrown/protocols/2_DNA.html
- 8 **Post-processing of arrays/Experimental Protocols** [updated September 1999] [BioinformaticsManual]http://www.cmgm.stanford.edu/pbrown/protocols/3_post_process.html
- 9 **Hasseman JP.** Aminoallyl labeling of RNA for microarray. Revision Level:2 (http://pga.tigr.org/sop/Moo4_1a.pdf)
- 10 **Yang IV, Chen E, Hasseman JP, Liang W, Frank BC, Wang SB, Sharov V, Saeed AI, White J, Li J, Lee NH, Yeatman TJ, Quackenbush J.** Within the fold: assessing differential expression measures and reproductivity in microarray assays. *Genome Biol* 2002; **3**: 1-12

- 11 **Bushman TL**, Kuemmerle JF. IGFBP-3 and IGFBP-5 production by human intestinal muscle: reciprocal regulation by endogenous TGF- β 1. *Am J Physiol* 1998; **275**(6 Pt 1): G1282-G1290
- 12 **Amirghahari N**, Harrison L, Smith M, Rong X, Naumann I, Ampil F, Shi R, Glass J, Nathan CA. NS 398 radiosensitizes an HNSCC cell line by possibly inhibiting radiation-induced expression of COX-2. *Int J Radiat Oncol Biol Phys* 2003; **57**: 1405-1412
- 13 **Peng JP**, Liu LT, Chang HC, Hung WC. Enhancement of chemotherapeutic drug-induced apoptosis by a cyclooxygenase-2 inhibitor in hypopharyngeal carcinoma cells. *Cancer Lett* 2003; **201**: 157-163
- 14 **Wen B**, Deutsch E, Eschwege P, De Crevoisier R, Nasr E, Eschwege F, Bourhis J. Cyclooxygenase-2 inhibitor NS398 enhances anti-tumor effect of irradiation on hormone refractory human prostate carcinoma cells. *J Urol* 2003; **170**: 2036-2039
- 15 **Hazan RB**, Qiao R, Keren R, Badano I, Suyama K. Cadherin switch in tumor progression. *Ann N Y Acad Sci* 2004; **1014**: 155-163
- 16 **Seidel B**, Braeg S, Adler G, Wedlich D, Menke A. E- and N-cadherin differ with respect to their associated p120(ctn) isoforms and their ability to suppress invasive growth in pancreatic cancer cells. *Oncogene* 2004; **23**: 5532-5542
- 17 **Kovacs A**, Dhillon J, Walker RA. Expression of P-cadherin, but not E-cadherin or N-cadherin, relates to pathological and functional differentiation of breast carcinomas. *Mol Pathol* 2003; **56**: 318-322
- 18 **Butt AJ**, Dickson KA, McDougall F, Baxter RC. Insulin-like growth factor-binding protein-5 inhibits the growth of human breast cancer cells *in vitro* and *in vivo*. *J Biol Chem* 2003; **278**: 29676-29685
- 19 **Stolf BS**, Carvalho AF, Martins WK, Runza FB, Brun M, Hirata R Jr, Jordao Neves E, Soares FA, Postigo-Dias J, Kowalski LP, Reis LF. Differential expression of IGFBP-5 and two human ESTs in thyroid glands with goiter, adenoma and papillary or follicular carcinomas. *Cancer Lett* 2003; **191**: 193-202
- 20 **Nordqvist AC**, Mathiesen T. Expression of IGF-II, IGFBP-2, -5, and -6 in meningiomas with different brain invasiveness. *J Neurooncol* 2002; **57**: 19-26
- 21 **McCaig C**, Perks CM, Holly JM. Signaling pathways involved in the direct effects of IGFBP-5 on breast epithelial cell attachment and survival. *J Cell Biochem* 2002; **84**: 784-794
- 22 **Lee BP**, Rushlow WJ, Chakraborty C, Lala PK. Differential gene expression in premalignant human trophoblast: role of IGFBP-5. *Int J Cancer* 2001; **94**: 674-684
- 23 **Yi HK**, Hwang PH, Yang DH, Kang CW, Lee DY. Expression of the insulin-like growth factors (IGFs) and the IGF-binding proteins (IGFBPs) in human gastric cancer cells. *Eur J Cancer* 2001; **37**: 2257-2263
- 24 **Schneider MR**, Zhou R, Hoeflich A, Krebs O, Schmidt J, Mohan S, Wolf E, Lahm H. Insulin-like growth factor-binding protein-5 inhibits growth and induces differentiation of mouse osteosarcoma cells. *Biochem Biophys Res Commun* 2001; **288**: 435-442
- 25 **Hourihan RN**, O'Sullivan GC, Morgan JG. Transcriptional gene expression profiles of oesophageal adenocarcinoma and normal oesophageal tissues. *Anticancer Res* 2003; **23**: 161-165
- 26 **Hasina R**, Hulett K, Biccato S, Di Bello C, Petruzzelli GJ, Lingen MW. Plasminogen activator inhibitor-2: a molecular biomarker for head and neck cancer progression. *Cancer Res* 2003; **63**: 555-559
- 27 **Bernard-Gallon DJ**, Peffault de Latour M, Hizel C, Vissac C, Cure H, Pezet D, Dechelotte PJ, Chipponi J, Chassagne J, Bignon YJ. Localization of human BRCA1 and BRCA2 in non-inherited colorectal carcinomas and matched normal mucosas. *Anticancer Res* 2001; **21**: 2011-2020
- 28 **Bieche I**, Tozlu S, Girault I, Lidereau R. Identification of a three-gene expression signature of poor-prognosis breast carcinoma. *Mol Cancer* 2004; **3**: 37

Outcome of lamivudine-resistant hepatitis B virus is generally benign except in cirrhotics

Yock-Young Dan, Chun-Tao Wai, Yin-Mei Lee, Dede Selamat Sutedja, Bee-Leng Seet, Seng-Gee Lim

Yock-Young Dan, Chun-Tao Wai, Yin-Mei Lee, Dede Selamat Sutedja, Bee-Leng Seet, Seng-Gee Lim, Division of Gastroenterology, National University Hospital, Singapore Supported by the National University of Singapore Grant, No. R-182-000-0001-731

Correspondence to: Dr. Seng-Gee Lim, Division of Gastroenterology, Department of Medicine, National University Hospital, 5 Lower Kent Ridge Road, 119074 Singapore. mdclimsg@nus.edu.sg
Telephone: +65-67724353 Fax: +65-67794112
Received: 2004-12-07 Accepted: 2005-01-13

Abstract

AIM: We set to determine factors that determine clinical severity after the development of resistance.

METHODS: Thirty-five Asian patients with genotypic lamivudine resistance were analyzed in three groups: 13/35 (37%) were non-cirrhotics with normal pre-treatment ALT (Group IA), 12/35 (34%) were non-cirrhotics with elevated pre-treatment ALT (Group IB), and 10/35 (29%) were cirrhotics (Group II). Patients were followed for a median of 98 wk (range 26-220) after the emergence of genotypic resistance.

RESULTS: Group IA patients tended to retain normal ALT. Group IB patients showed initial improvement of ALT with lamivudine but 9/12 patients (75%) developed abnormal ALT subsequently. On follow-up however, this persisted in only 33%. Group II patients also showed improvement while on treatment, but they deteriorated with the emergence of resistance with 30% death from decompensated liver disease. Pretreatment ALT levels and CPT score (in the cirrhotic group) were predictive of clinical resistance and correlated with peak ALT levels and CPT score.

CONCLUSION: The phenotype of lamivudine-resistant HBV correlated with the pretreatment phenotype. The clinical course was generally benign in non-cirrhotics. However, cirrhotics had a high risk of progression and death (30%) with the development of lamivudine resistance.

© 2005 The WJG Press and Elsevier Inc. All rights reserved.

Key words: Lamivudine resistance; YMDD mutants; Hepatitis B treatment; Nucleoside analog

Dan YY, Wai CT, Lee YM, Sutedja DS, Seet BL, Lim SG. Outcome of lamivudine-resistant hepatitis B virus is generally benign except in cirrhotics. *World J Gastroenterol* 2005; 11(28): 4344-4350
<http://www.wjgnet.com/1007-9327/11/4344.asp>

INTRODUCTION

Treatment of CHB was revolutionized by the introduction of orally administered antiviral agents. Lamivudine, a nucleoside analog and the first orally available antiviral agent for CHB, had demonstrated significant results in clinical trials, with universal suppression of HBV DNA level by 3 logs, 55% improvement in histological necroinflammatory score, normalization of ALT in the majority of patients after 1 year of treatment^[1,2]. Even among patients with decompensated hepatitis B cirrhosis, there was clinical improvement^[3], thus enabling some of them to be taken off liver transplant waiting lists.

However, drug resistance with lamivudine occurs with prolonged usage, rising from 14-24% at the end of first year, to 57% by the end of year 3^[4,5]. Resistance occurred primarily as a result of mutations in the YMDD motif of the polymerase gene although subsequently, mutations at other sites have been reported^[6]. Initial reports suggested that lamivudine-resistant HBV virus may be less virulent and replication-defective, as the ALT and HBV DNA levels caused by these mutant viruses were lower than the pretreatment values^[7]. However, subsequent reports of decompensation, acute exacerbations, and deaths from such mutant viruses suggested otherwise^[8,9]. This has given rise to the suggestion of limiting lamivudine therapy to 12 mo duration in order to avoid the development of these mutants^[10].

Lamivudine resistance can be divided into genotypic and clinical phenotypic resistance. Genotypic resistance refers to the presence of a lamivudine-resistant strain such as the YMDD mutants, which in itself may not lead to any clinical sequela, since such strains have been detected in patients who have not had prior exposure to lamivudine^[11]. Clinical phenotypic resistance refers to the presence of genotypic resistance with the subsequent development of clinical deterioration, defined as elevation of transaminases and/or deterioration of liver histology and liver function. Factors that predict the development of genotypic resistance^[5,12] had been evaluated in many studies, which included pretreatment HBV DNA level, ALT level, body mass index, adw serotype, and core promoter mutations^[13-15]. However, these studies did not address the more important question of which factor(s) actually lead to clinical resistance.

Hence, we set to examine variables that determined the clinical phenotypes after the development of genotypic lamivudine resistance.

MATERIALS AND METHODS

Patients

From January 1996 to April 2003, we prospectively followed

all patients started on lamivudine 100 or 150 mg daily monotherapy for clinical indications, or who had completed trials of lamivudine monotherapy, at 3 monthly intervals. These included patients who were recruited from the Asian Multicentre Lamivudine Trial and its subsequent rollover follow-up study NUCB3018^[1,4,16], which also included patients with normal pre-treatment ALT levels. Patients were also given lamivudine if it was clinically indicated, such as persistently abnormal ALT levels (greater than twice upper limit of normal for at least 3 mo duration), decompensated liver disease (development of variceal hemorrhage, ascites, and hepatic encephalopathy), or were on the liver transplant waiting list. All patients had detectable HBV DNA by a non-PCR based assay prior to initiation of therapy. Lamivudine was prescribed for at least a year and was continued even when genotypic resistance developed. During the duration of the study, none of the patients were given adefovir dipivoxil as a rescue therapy as it was not yet available in Singapore. This study was approved by the Institutional Review Board of the National University Hospital, Singapore.

Exclusion criteria

Patients who tested positive for anti-HCV, anti-HDV, and HIV, had significant history of alcohol intake (defined as more than seven drinks per week), or were non-compliant with lamivudine were excluded from the study. Patients who developed resistance after liver transplants were also excluded.

Measurement of HBV DNA

Prior to March 2000, the Abbott HBV DNA assay (Abbott Laboratories, North Chicago, IL, USA) was used for HBV DNA viral load quantification. After March 2000, this assay was substituted to a branched-chain assay (Chiron QuantiplexTM, Chiron Corp). Results of the Abbott HBV DNA assay were converted using the Multimeasurement Method^[17].

Phenotypes

Eligible patients were classified into three distinct phenotypes according to their baseline characteristics. The presence of cirrhosis was determined by liver biopsy or by ultrasonographic features in those with clinical decompensated disease.

- | | |
|----------|---|
| Group IA | Non-cirrhotic patients with normal baseline ALT level |
| Group IB | Non-cirrhotic patients with abnormal baseline ALT level |
| Group II | Cirrhotic patients |

Genotypic lamivudine resistance

Genotypic resistance was defined as reappearance of at least two consecutive detectable HBV DNA levels after a period of undetectable level whilst on continuous lamivudine therapy for more than 6 mo.

Characterization of lamivudine resistance by sequencing

Confirmation of genotypic resistance was performed by comparison of results from direct sequencing of the HBV polymerase of the HBV DNA samples before starting lamivudine, and after development of resistance. DNA was extracted and direct sequencing was performed at a 750 bp region between nt 253 and 1 006 of the HBV genome

using the two primers:

Forward primer: 5'-GAC TCG TGG TGG ACT TCT CTC AA- 3'.

Reverse primer: 5'-CCC ACA ATT CTT TGA CAT ACT TTC C-3'. The forward and reverse sequences were aligned using the Seqman program (DNASTar). This segment has been known to contain all the mutations known to confer lamivudine resistance. New mutations emerging after treatment of lamivudine were determined for their resistance conferring properties from previously published data and categorized using the new nomenclature^[6,18].

Clinical resistance

All patients were followed for a minimum of 6 mo after the emergence of genotypic resistance and for as long as the patients were continued on lamivudine. Serial analysis of ALT, bilirubin, prothrombin time, HBeAg, anti HBe and HBV DNA level by Chiron QuantiplexTM, at 3 monthly intervals were done. Serial Child-Pugh Turcot (CPT) scores were also calculated. No serial liver biopsy was performed in our patients.

In the non-cirrhotic group, clinical resistance was defined as abnormal rise in ALT greater than twice upper limit of normal. In the cirrhotic group, clinical resistance was defined as abnormal rise in ALT greater than twice the normal upper limit, or an increase of CPT Score by two points or more.

Clinical severity was assessed at four time points: timepoint 1 (baseline or pretreatment), timepoint 2 (6 mo after the commencement of lamivudine therapy), timepoint 3 (peak ALT or CPT levels after the development of genotypic resistance), and timepoint 4 (last ALT or CPT on follow-up).

HBV genotyping

HBV genotyping was performed using restriction fragment length polymorphism created by Ava2 and Dpn2 action on an amplified segment of the pre-S region as previously described^[19].

Statistical analysis

Changes in ALT level and CPT Score were compared at four timepoints within each group of patients. Statistical analysis was performed by Wilcoxon Matched-Pairs Signed Rank Test to avoid the effect of pooling results from different patients. The relationship of two continuous variables was tested by Spearman ρ Correlation test. *P* values of less than 0.05 were considered statistically significant.

The following parameters: age, sex, baseline ALT, ALT at the point of emergence of resistance, baseline HBV DNA level, peak HBV DNA post genotypic resistance, duration of lamivudine treatment, type of mutation, genotype and HBeAg seroconversion were analyzed by univariate analysis to determine factors associated with phenotypic resistance. Categorical variables and continuous variables were compared by Fisher's exact test and Student's *t*-test, as appropriate. Significant factors from univariate analysis were then analyzed by multivariate analysis by forward logistic regression to determine independent factors associated with phenotypic resistance.

All statistical analysis was performed using computer software, SPSS 10.0 for Windows (SPSS Inc., Chicago, IL, USA).

RESULTS

Patients

A total of 78 patients were prescribed lamivudine for hepatitis B related indications or had completed a clinical trial of lamivudine therapy at our institution for a minimum of 1 year during the study period. Of these, 35 patients (45%) developed genotypic resistance to lamivudine while on treatment after a median of 143 wk (range 35-212 wk) and were included in this study. Twenty-one (60%) were part of the Asian Lamivudine Trial (NUCB 3009/NUCB3018)^[1], of which 11 received uninterrupted lamivudine treatment while 10 were restarted on open label lamivudine after viral breakthrough when they were on placebo. The remainder of the patients was given lamivudine for clinical indications of chronic hepatitis ($n = 4$, 11%) and cirrhotic liver disease ($n = 10$, 29%), respectively. One patient was eligible to enter a trial of adefovir/lamivudine (NUCB 20904) treatment for persistent abnormal transaminases at 56 wk after emergence of resistance. Data up to the point of trial entry was used for analysis but data thereafter was censored. No patient received liver transplant after the emergence of resistance. Thus in total, 35 patients were eligible for analysis. There were no missing patients or dropouts from the cohort.

All 35 patients were stratified into three groups (Table 1): 13 patients (37%) were in Group IA (non-cirrhotic patients with normal baseline ALT), 12 (34%) of patients were in Group IB (non-cirrhotic patients with abnormal baseline ALT), and the remainder of the patients

($n = 10$, 29%) were in Group II (cirrhotic patients). Group IA and B patients were predominantly from the Asian Lamivudine trial and had a median age of 35 years (range: 21-48 years) and 34 years (range 20-45 years), respectively. Patients in Group II were expectedly older with median age of 52 years (range 42-68). There was a preponderance of male patients (M:F = 30:5). With the exception of one Malay patient, all remaining patients were Chinese (97%). Of these 35 patients, genotypic resistance developed at a median of 143 wk after being on lamivudine (range 35-212). Median patients follow-up after genotypic resistance was 102 wk (range 26-220).

HBV genotypes

Majority of the patients had either genotypes B or C. Eighteen (51%) were of HBV genotype B while 13 patients (37%) had genotype C. Four (12%) had other genotypes: one was Genotype A, one had a mixture of B/C genotypes, and two were untypable (Table 2).

Mutations involved in lamivudine resistance

Sixteen of thirty-five patients (46%) were found to have the rtM204I (YIDD) mutation at the YMDD motif, whilst 12/35 (34%) demonstrated the rtM204V (YVDD) mutation and the remainder had at least one acquired mutation that was not present at the baseline and was known to confer resistance against lamivudine. (Figure 1). These included various combinations of mutations at rtA181T, rtL80V/I and rtL187I.

Table 1 Baseline characteristics of all patients

	Group IA $n = 13$ (37%)	Group IB $n = 12$ (34%)	Group II $n = 10$ (29%)	All patients $n = 35$ (100%)
Median age (range)	35 (21-48)	34 (20-45)	52 (42-68)	38 (20-68)
Male (%)	9 (69)	11 (92)	10 (100)	30 (86)
Chinese ethnicity (%)	13 (100)	11 (92)	10 (100)	34 (97)
Median (range) baseline ALT, U/L	28 (16-58)	136 (78-1 124)	87 (33-761)	74(16-1 124)
Median (range) baseline HBV DNA, Meg/mL	294 (120-1 680)	253 (38-616)	291 (20-786)	280 (20-1 680)
Median baseline CPT score	NA	NA	7.0 (5-13)	NA
Median (range) duration of lamivudine at emergence of genotypic resistance, wk	160 (35-198)	110 (42-212)	62 (36-120)	143 (35-212)
Follow-up after genotypic resistance, wk	96 (48-220)	124 (26-208)	64 (34-102)	102 (26-220)
Number (%) with phenotypic resistance	3 (23)	9 (75)	6 (60)	18 (51)

Table 2 Comparison between patients with and without phenotypic resistance in univariate analysis

	Patients with phenotypic resistance $n = 18$	Patients without phenotypic resistance $n = 17$	<i>P</i>
Median (range) age (yr)	34 (21-60)	37(20-68)	0.95
Male (%)	17 (94)	13 (76)	0.16
Chinese (%)	17/18 (94)	17/17 (100)	0.28
Genotype (B:C:others)	7B/ 7C/ 2 others	11B /6C/ 2 others	0.56
Type of mutation (rtM204I:rtM204V:others)	12:2:4	4:10:3	0.074
Median (range) baseline ALT level, U/L	96 (42-1 124)	40 (16-143)	0.018
ALT level at emergence of genotypic resistance, U/L	48 (22-82)	36 (24-68)	0.36
Successful HBeAg seroconversion (%)	12	17.7	0.43
Median (range) baseline HBV DNA, Meq/mL	249 (20-788)	336 (20-1 680)	0.17
Median (range) peak HBV DNA after emergence of resistance, pg/mL	186 (8.8-1 064)	314 (9-3 920)	0.33
Median (range) duration of lamivudine at onset of resistance, wk	88 (35-212)	124 (36-202)	0.16
Median (range) duration of follow up after resistance, wk	124 (52-204)	102 (26-220)	0.29
Median (range) baseline CPT Score for cirrhotic patients, $n = 10$	($n = 6$) 8 (5-13)	($n = 4$) 7 (5-9)	0.038

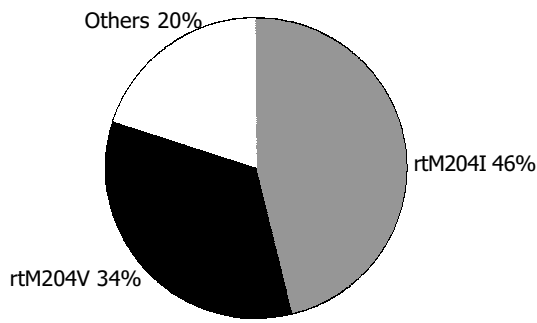


Figure 1 Distribution of the type HBV DNA mutations in the polymerase gene.

Clinical resistance

(1) Group IA (non-cirrhotic with normal baseline ALT), *n* = 13 (Figure 2A).

Only three patients (23%) developed abnormal ALT after the emergence of genotypic resistance at median follow-up of 96 (range: 48-220 wk). The changes in ALT in the group between the four timepoints were non-significant. All three patients normalized their ALT after a median duration of 6 (range: 4-12 wk), one of whom achieved HBeAg seroconversion; (2) Group IB (non-cirrhotic with abnormal

baseline ALT), *n* = 12 (Figure 2B).

Normalization of ALT levels 6 mo after starting lamivudine was seen in all patients (Wilcoxon signed Rank *P* = 0.012). However, with the emergence of genotypic resistance, 9 out of 12 patients (75%) developed abnormal ALT (Wilcoxon signed Rank *P* = 0.017) after median follow-up of 124 (range: 26-208) wk. Two patients registered peak ALT elevations of more than 10 times upper limit of normal, one of whom had the highest ALT (>17 X ULN) at the baseline. ALT level at timepoints 3 and 4 were similar to the baseline level at timepoint 1 (*P*>0.05). Five of the nine (56%) patients normalized their ALT after a median duration of 8 (range: 4-14) wk, two of whom achieved HBeAg seroconversion.

(3) Group II (patients with cirrhosis), *n* = 10 (Figure 3).

Six patients (60%) had abnormal ALT at the baseline (Figure 3A). All patients showed ALT improvement after treatment with lamivudine (Wilcoxon signed Rank Test, *P* = 0.015). With the emergence of genotypic resistance, abnormal ALT elevations occurred in five patients (50%) after a median follow-up of 64 (range: 34-102) wk. The development of abnormal ALT at timepoint 3 compared to timepoint 2 was statistically significant (*P* = 0.017). When ALT levels among timepoints 1, 3, and 4 were compared, no significant difference was found. All the five patients with flares of ALT normalized their ALT level after a median duration

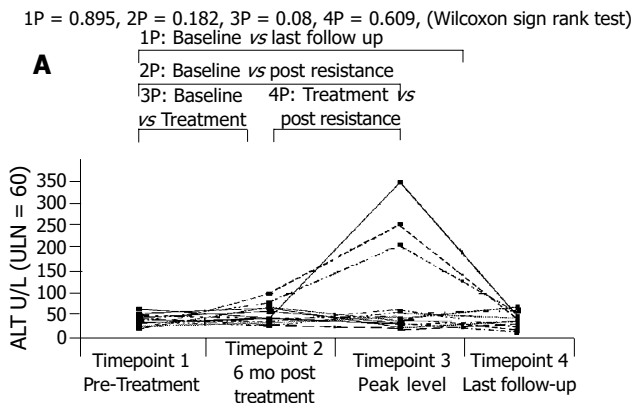
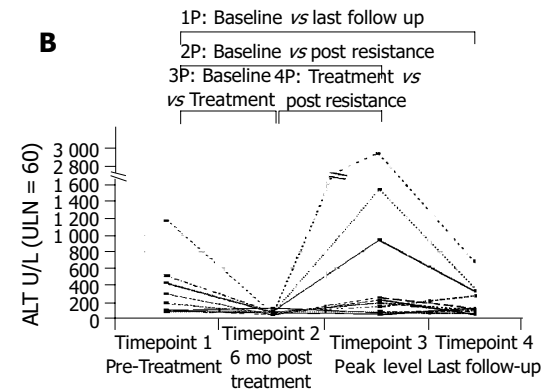


Figure 2 ALT of Group IA and IB. A: ALT of Group IA: non cirrhotic patients with normal pre-treatment ALT (*n* = 13); B: ALT of Group IB: non-cirrhotic patients with

1P = 0.38, 2P = 0.30, 3P = 0.012, 4P = 0.017, (Wilcoxon sign rank test)



elevated pre-treatment ALT (*n* = 12).

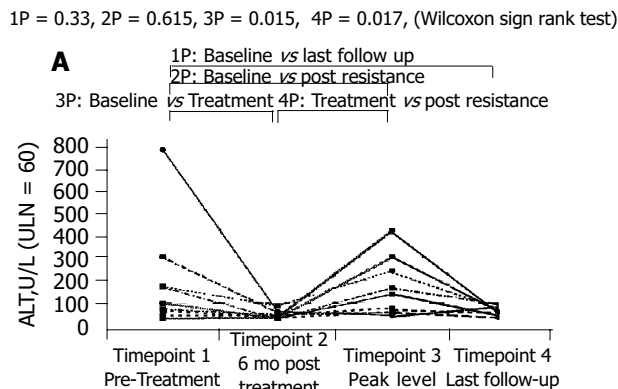
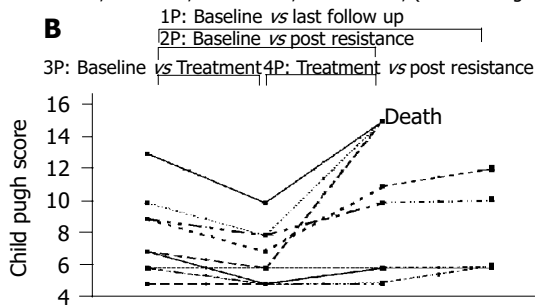


Figure 3 ALT and CPT of Cirrhotic patients. A: ALT of Cirrhotic patients; B: CPT

1P = 0.77, 2P = 0.32, 3P = 0.002, 4P = 0.004, (Wilcoxon sign rank test)



of Cirrhotic patients.

of 4 (range: 4-8 wk).

CPT score analysis showed a similar trend in this group (Figure 3B). The CPT score at timepoint 2 showed significant improvement compared to timepoint 1 (Wilcoxon Signed Rank, $P = 0.016$) but deteriorated with the emergence of resistance at timepoint 3 (Wilcoxon Signed Rank, $P = 0.041$). No statistical significance was detected between CPT Score at timepoint 1 and timepoint 3 as well as between timepoints 1 and 4, with follow-up median duration of 64 wk after resistance (range 34-102). Three patients died from liver decompensation at 42, 78, and 96 wk, respectively after resistance developed, two of whom had the poorest pretreatment CPT score. None of the patients achieved HBeAg seroconversion although 40% (4 out of 10) were eAg negative Hepatitis B cirrhotics to begin with.

Factors that determine clinical severity of lamivudine-resistant mutants

At univariate analysis, only the baseline ALT in non-cirrhotics and the baseline CPT score in cirrhotics were predictive of phenotypic resistance ($P = 0.018$ and $P = 0.038$, respectively, Table 2).

Multivariate analysis was then performed with these two parameters. Using logistic regression analysis, the baseline ALT was shown to be significantly predictive of phenotypic resistance (OR 9.6, 95%CI 1.2-4.0, $P = 0.03$). The peak ALT level post resistance also correlated with the baseline ALT. (Spearman's $\rho = 0.441$, $P = 0.027$).

Similarly for CPT score, regression analysis showed baseline CPT score to be predictive of phenotypic resistance in terms of deterioration in CPT score after resistance ($P = 0.022$). Every additional CPT score at baseline predicts an additional 1.19 CPT score after resistance ($B = 1.19$, 95% CI: 0.235-2.15). Expectedly, peak CPT score after resistance showed strong correlation with baseline CPT score (Spearman's $\rho = 0.785$, $P = 0.007$).

Interestingly, neither the pretreatment nor the peak HBV DNA post-resistance were shown to be predictive of phenotypic resistance although the peak HBV DNA level post-resistance was noted to correlate with the pretreatment HBV DNA level (Spearman's $\rho = 0.414$, $P = 0.013$).

DISCUSSION

The most important finding of our study was that the course of lamivudine-resistant hepatitis B was generally benign except in cirrhotics. In Group IA (patients with normal baseline ALT), despite the emergence of lamivudine resistance, most (10 of 13, 77%) of the patients maintained normal ALT up to median follow-up of 96 wk. In addition, all three patients in Group IA who developed elevated ALT subsequently normalized their ALT level on follow-up. In Group IB (patients with persistently elevated baseline ALT), lamivudine normalized ALT during therapy, but upon development of resistance, ALT increased in 75% of patients. However, only 4/12 (33%) of patients continued to have persistently elevated ALT on follow-up. Finally, in Group II (patients with decompensated cirrhosis), there was normalization of ALT levels and reduction in CPT scores during lamivudine therapy, but both parameters increased

to baseline levels once lamivudine resistance occurred.

Thus the clinical picture of lamivudine-resistant hepatitis B virus demonstrates a spectrum of disease from normal ALT to hepatitis B flares and liver decompensation. Our findings suggest that at the peak of abnormality, the clinical picture correlates most closely with baseline clinical characteristics of the patient. On subsequent follow-up however, the course was relatively benign except for cirrhotics.

The inclusion of patients with normal baseline ALT (Group 1A) provided an invaluable group of patients for studying the pathogenic effects of lamivudine-resistant Hepatitis B virus. This group of patients were treated with lamivudine only because they were part of the Asian Lamivudine Multicenter Trial. Yet on developing lamivudine resistance, most of them retained normal ALT in their follow up. Even in the few who had transient abnormal ALT, these universally resolved in contrast to those with abnormal baseline ALT or liver function. This suggests that lamivudine-resistant virus may not be more pathogenic than the wildtype virus. Although further study with larger number of patients is needed to confirm this, such study would be difficult to perform as clinical guidelines from America, Europe and Asia did not recommend lamivudine treatment for patients with normal baseline ALT levels^[20-22].

Our findings also fit the known biology of HBV. Clinical disease in chronic Hepatitis B is a complex interplay between the virus and the immune system. Mutations in the YMDD motif confer resistance to lamivudine and allow high viral replication to resume. On the other hand, it is the mutations in the core region that have been most closely associated with increased immune responses to the virus^[23].

Our study complements that of Yuen, who concluded that the majority of patients with lamivudine-resistant hepatitis B flares recovered except some with cirrhosis^[24]. In our patients with abnormal baseline ALT, although 75% had elevation of ALT at any time, only 33% had persistently elevated ALT on prolonged follow-up suggesting that the final clinical outcome in those without cirrhosis generally shows a benign course. Similarly, Lok^[25] also concluded that lamivudine-resistance led to good outcomes in non-cirrhotics, but this cannot be extrapolated to cirrhotics. Cirrhotic patients, having poorer liver reserve, are less able to tolerate the further necroinflammation that may resume with the return of viral replication in those phenotypically susceptible. Our cohort of cirrhotic patients (Group II) developed decompensation following lamivudine resistance, resulting in death in 30% of patients. These findings concur with the results of NUCB 4006 (CALM study)^[26]. In this landmark study, lamivudine therapy in cirrhotic patients proved to provide significant benefit in terms of reduced progression of liver disease and reduction in hepatocellular carcinoma. Patients who developed lamivudine-resistant mutations showed a reduction in this endpoint efficacy, as we have shown, developing progression of their liver disease. Nevertheless, they still had less clinical endpoints than patients on placebo. Unlike the CALM study which enrolled patients with early and non-decompensated cirrhosis, most of the cirrhotic patients in our study had decompensated liver disease and had poor outcomes when lamivudine resistance developed.

We acknowledge the following limitations of our study. Firstly, we did not have histological confirmation of progression of liver disease. However, abnormal ALT has been accepted as a good surrogate marker for necroinflammation of the liver^[27]. In addition, an increase in CPT score clearly signifies progressive liver damage and deterioration. Consequently, we feel that the lack of histological data does not detract from the findings of this study. Although our sample size was relatively small, the spectrum of patients included in our study is typical of those seen in a normal hepatology practice or hospital, rather than the pre-selected patients included in clinical trials. In addition, the findings in general are also observed in larger clinical studies. Our study also includes patients with normal ALT and decompensated cirrhosis, which have not been previously described. The duration of follow-up in our series was 102 wk, longer than in most other published studies^[8,12,24].

We believe the results of our study could have two therapeutic implications. Firstly, the clinical severity of lamivudine-resistant HBV resembled the baseline phenotype, although on follow-up, the vast majority of the increased ALT normalized. Recent updated American guidelines for Hepatitis B recommends options of continuing or stopping lamivudine or converting to other antiviral drug when lamivudine resistance develops, depending on the patient's clinical state, ALT and HBV DNA levels^[20]. Our study suggests that baseline activity can be used as predictive factor in identifying patients who are likely to resume active disease and who thus, should be monitored more closely. Secondly, in patients with poor liver reserve at baseline who developed lamivudine resistance, additional rescue therapy such as adefovir dipivoxil should be instituted early, before clinical deterioration occurred.

In conclusion, the clinical phenotype of patients with genotype resistance to lamivudine resembled the baseline clinical phenotype, suggesting loss of virus suppression and return to the pre-treatment state. Patients with high baseline ALT level or CPT score tended to return to a high ALT level or CPT score once lamivudine resistance occurred. With time, there was normalization of raised ALT levels in those with non-cirrhotic lamivudine resistance. Consequently, in treatment of hepatitis B, lamivudine therapy need not be stopped prematurely for fear of developing more pathogenic lamivudine-resistant strains. However, patients with cirrhosis, particularly decompensated cirrhosis, need to be monitored closely and adefovir dipivoxil started expediently when resistance occurs.

ACKNOWLEDGMENTS

We would like to thank GlaxoSmithkline (Singapore) Private Limited for permission and access to the data for patients in the Asian Multicentre Lamivudine Trial, and Ms. Shen Liang from the Clinical Trials and Epidemiology Research Unit, Singapore Ministry of Health, for statistical support.

REFERENCES

- Lai CL, Chien RN, Leung NW, Chang TT, Guan R, Tai DI, Ng KY, Wu PC, Dent JC, Barber J, Stephenson SL, Gray DF. A one-year trial of lamivudine for chronic hepatitis B. Asia Hepatitis Lamivudine Study Group. *N Engl J Med* 1998; **339**: 61-68
- Dienstag JL, Schiff ER, Wright TL, Perrillo RP, Hann HW, Goodman Z, Crowther L, Condreay LD, Woessner M, Rubin M, Brown NA. Lamivudine as initial treatment for chronic hepatitis B in the United States. *N Engl J Med* 1999; **341**: 1256-1263
- Villeneuve JP, Condreay LD, Willems B, Pomier-Layrargues G, Fenyves D, Bilodeau M, Leduc R, Peltekian K, Wong F, Margulies M, Heathcote EJ. Lamivudine treatment for decompensated cirrhosis resulting from chronic hepatitis B. *Hepatology* 2000; **31**: 207-210
- Leung NW, Lai CL, Chang TT, Guan R, Lee CM, Ng KY, Lim SG, Wu PC, Dent JC, Edmundson S, Condreay LD, Chien RN. Extended lamivudine treatment in patients with chronic hepatitis B enhances hepatitis B e antigen seroconversion rates: results after 3 years of therapy. *Hepatology* 2001; **33**: 1527-1532
- Lai CL, Dienstag J, Schiff E, Leung NW, Atkins M, Hunt C, Brown N, Woessner M, Boehme R, Condreay L. Prevalence and clinical correlates of YMDD variants during lamivudine therapy for patients with chronic hepatitis B. *Clin Infect Dis* 2003; **36**: 687-696
- Fu L, Cheng YC. Role of additional mutations outside the YMDD motif of hepatitis B virus polymerase in L(-)SddC (3TC) resistance. *Biochem Pharmacol* 1998; **55**: 1567-1572
- Melegari M, Scaglioni PP, Wands JR. Hepatitis B virus mutants associated with 3TC and famciclovir administration are replication defective. *Hepatology* 1998; **27**: 628-633
- Liaw YF, Chien RN, Yeh CT, Tsai SL, Chu CM. Acute exacerbation and hepatitis B virus clearance after emergence of YMDD motif mutation during lamivudine therapy. *Hepatology* 1999; **30**: 567-572
- Kim JW, Lee HS, Woo GH, Yoon JH, Jang JJ, Chi JG, Kim CY. Fatal submassive hepatic necrosis associated with tyrosine-methionine-aspartate-aspartate-motif mutation of hepatitis B virus after long-term lamivudine therapy. *Clin Infect Dis* 2001; **33**: 403-405
- Leung NW, Chan HL, Sung JJ. How good is 1 year lamivudine treatment in HBeAg positive chronic hepatitis B patients with elevated ALT levels? Experience from a regional hospital. [ABSTRACT]. *J Gastroenterol Hepatol* 2001; **16** (Suppl): 212
- Kobayashi S, Ide T, Sata M. Detection of YMDD motif mutations in some lamivudine-untreated asymptomatic hepatitis B virus carriers. *J Hepatol* 2001; **34**: 584-586
- Yuen MF, Sablon E, Hui CK, Yuan HJ, Decraemer H, Lai CL. Factors associated with hepatitis B virus DNA breakthrough in patients receiving prolonged lamivudine therapy. *Hepatology* 2001; **34** (4 Pt 1): 785-791
- Mutimer D, Pillay D, Dragon E, Tang H, Ahmed M, O'Donnell K, Shaw J, Burroughs N, Rand D, Cane P, Martin B, Buchan S, Boxall E, Barmat S, Gutekunst K, McMaster P, Elias E. High pre-treatment serum hepatitis B virus titre predicts failure of lamivudine prophylaxis and graft re-infection after liver transplantation. *J Hepatol* 1999; **30**: 715-721
- Zollner B, Petersen J, Schroter M, Laufs R, Schoder V, Feucht HH. 20-fold increase in risk of lamivudine resistance in hepatitis B virus subtype adw. *Lancet* 2001; **357**: 934-935
- Lok AS, Hussain M, Cursano C, Margotti M, Gramenzi A, Grazi GL, Jovine E, Benardi M, Andreone P. Evolution of hepatitis B virus polymerase gene mutations in hepatitis B e antigen-negative patients receiving lamivudine therapy. *Hepatology* 2000; **32**: 1145-1153
- Liaw YF, Leung NW, Chang TT, Guan R, Tai DI, Ng KY, Chien RN, Dent J, Roman L, Edmundson S, Lai CL. Effects of extended lamivudine therapy in Asian patients with chronic hepatitis B. Asia Hepatitis Lamivudine Study Group. *Gastroenterology* 2000; **119**: 172-180
- Krajden M, Minor J, Cork L, Comanor L. Multi-measurement method comparison of three commercial hepatitis B virus DNA quantification assays. *J Viral Hepat* 1998; **5**: 415-422
- Stuyver LJ, Locarnini SA, Lok A, Richman DD, Carman WF,

- Dienstag JL, Schinazi RF. Nomenclature for antiviral-resistant human hepatitis B virus mutations in the polymerase region. *Hepatology* 2001; **33**: 751-757
- 19 **Lindh M**, Gonzalez JE, Norkrans G, Horal P. Genotyping of hepatitis B virus by restriction pattern analysis of a pre-S amplicon. *J Virol Methods* 1998; **72**: 163-174
- 20 **Lok AS**, McMahon BJ. Chronic hepatitis B: update of recommendations. *Hepatology* 2004; **39**: 857-861
- 21 **de Franchis R**, Hadengue A, Lau G, Lavanchy D, Lok A, McIntyre N, Mele A, Paumgartner G, Pietrangelo A, Rodes J, Rosenberg W, Valla D. EASL International Consensus Conference on Hepatitis B. 13-14 September, 2002 Geneva, Switzerland. Consensus statement (long version). *J Hepatol* 2003; **39** (Suppl 1): S3-25
- 22 **Liaw YF**, Leung N, Guan R, Lau GK, Merican I. Asian-Pacific consensus statement on the management of chronic hepatitis B: an update. *J Gastroenterol Hepatol* 2003; **18**: 239-245
- 23 **Koziel MJ**. The immunopathogenesis of HBV infection. *Antivir Ther* 1998; **3** (Suppl 3): 13-24
- 24 **Yuen MF**, Kato T, Mizokami M, Chan AO, Yuen JC, Yuan HJ, Wong DK, Sum SM, Ng IO, Fan ST, Lai CL. Clinical outcome and virologic profiles of severe hepatitis B exacerbation due to YMDD mutations. *J Hepatol* 2003; **39**: 850-855
- 25 **Lok AS**, Lai CL, Leung N, Yao GB, Cui ZY, Schiff ER, Dienstag JL, Heathcote EJ, Little NR, Griffiths DA, Gardner SD, Castiglia M. Long-term safety of lamivudine treatment in patients with chronic hepatitis B. *Gastroenterology* 2003; **125**: 1714-1722
- 26 **Liaw YF**, Sung JJ, Chow WC, Farrell G, Lee CZ, Yuen H, Tanwandee T, Tao QM, Shue K, Keene ON, Dixon JS, Gray DF, Sabbat J. Lamivudine for patients with chronic hepatitis B and advanced liver disease. *N Engl J Med* 2004; **351**: 1521-1531
- 27 **Cahen DL**, van Leeuwen DJ, ten Kate FJ, Blok AP, Oosting J, Chamuleau RA. Do serum ALAT values reflect the inflammatory activity in the liver of patients with chronic viral hepatitis? *Liver* 1996; **16**: 105-109

Science Editor Guo SY Language Editor Elsevier HK

Possible mechanism for hepatitis B virus X gene to induce apoptosis of hepatocytes

Sheng-Jun Zhang, Hong-Ying Chen, Zhi-Xin Chen, Xiao-Zhong Wang

Sheng-Jun Zhang, Hong-Ying Chen, Zhi-Xin Chen, Xiao-Zhong Wang, Department of Gastroenterology, Union Hospital of Fujian Medical University, Fuzhou 350001, Fujian Province, China
Supported by the Science and Technology Fund of Fujian Province, No. 99-Z-162

Correspondence to: Xiao-Zhong Wang, Department of Gastroenterology, Union Hospital of Fujian Medical University, Fuzhou 350001, Fujian Province, China. drwangxz@pub6.fz.fj.cn
Telephone: +86-591-83357896-8482

Received: 2004-11-23 Accepted: 2004-11-26

Abstract

AIM: To investigate the possible mechanism for HBV X gene to induce apoptosis of hepatocyte HL-7702 cells.

METHODS: HBV X gene eukaryon expression vector pcDNA3-X was established and transfected into HL-7702 cells by lipid-mediated transfection, including transient and stable transfection. Positive clones were screened by incubating in the selective medium with 600 µg/mL G418 and named HL-7702/HBV-encoded X protein (HBx) cells. The expressions of Fas/FasL, Bax/Bcl-2, and c-myc mRNA were measured by semi-quantitative RT-PCR in HL-7702/HBx and control group, respectively.

RESULTS: RT-PCR analysis confirmed that HBV X gene was transfected into HL-7702 cells successfully. By semi-quantitative RT-PCR analysis, Bax and c-myc mRNA levels in HL-7702/HBx cells of transient transfection were significantly higher than those in control, FasL and c-myc mRNA levels in HL-7702/HBx cells of stable transfection were significantly higher than those in control, whereas the Bcl-2 mRNA levels in HL-7702/HBx cells of transient and stable transfection were significantly lower than those in control.

CONCLUSION: HBV X gene may promote the apoptosis of hepatocytes by regulating the expressions of Fas/FasL, Bax/Bcl-2, and c-myc gene in a dose-dependent manner.

© 2005 The WJG Press and Elsevier Inc. All rights reserved.

Key words: Hepatitis B virus; X gene; Apoptosis; Gene expression

Zhang SJ, Chen HY, Chen ZX, Wang XZ. Possible mechanism for hepatitis B virus X gene to induce apoptosis of hepatocytes. *World J Gastroenterol* 2005; 11(28): 4351-4356
<http://www.wjgnet.com/1007-9327/11/4351.asp>

INTRODUCTION

HBV X gene is the smallest open reading frame of HBV, codes for a 16.5-ku protein (X protein, HBx) consisted of 154 amino acids. Previous studies showed that HBV X gene and HBx modulate apoptosis of hepatocytes and play an important role in HBV-associated liver disease^[1]. HBV X gene could inhibit apoptosis of hepatocytes in several ways and contribute to the generation of hepatocellular carcinoma (HCC). It was reported that HBx displays a pro-apoptotic function and induces apoptosis of liver cells^[2-5]. But the relationship between this function of HBx and HBV-associated liver disease remains obscure. So far no molecular mechanism or target for HBx-mediated apoptosis has been clearly elucidated. In this study, we transfected X gene into hepatocyte line HL-7702 by transient and stable transfection. Thus, cell lines that expressed different levels of HBx were established. To explore the possible mechanism for HBx to modulate apoptosis, we investigated the effect of HBx on expressions of apoptosis-associated genes in hepatocytes. The expressions of Fas/FasL, Bax/Bcl-2, and c-myc mRNA were measured by semi-quantitative RT-PCR in HL-7702/HBx and control group, respectively.

MATERIALS AND METHODS

Materials

PcDNA3 expression vector and HBV X gene eukaryon expression vector pcDNA3-X were previously constructed and stored^[6]. The normal hepatic cell line HL-7702 was provided by Cell Bank of Chinese Academy of Sciences. Reverse transcription system, DNA purification system, G418, and TransFast™ transfection reagent were obtained from Promega Biotech. Total RNA isolation kit was purchased from Jingmei Biotech Company. PCR primers were synthesized by Shanghai Biotechnology Company. RPMI-1640 was bought from Gibco BRL Company.

Transfection and expression of HBV X gene in HL-7702

Cell culture and DNA transfection HL-7702 cells were cultured in RPMI-1640 supplemented with 20% FBS. The cells in logarithmic growth were separately transfected with pcDNA3-X and pcDNA3 plasmids using lipid-mediated transfection technique according to the protocol for transient or stable transfection of adherent cells. About 2 mL transfection mixture containing 5 µg plasmid DNA, 15 µL TransFast™ reagent and RPMI-1640 was added to a 25-mm² culture plate. At 48 h post-transfection, all cells were trypsinized. Cells for transient transfection were

transferred to a 25-mm² culture plate and cultured in RPMI-1640 supplemented with 20% FBS for 72 h. Cells used for stable transfection were cultured in the selective medium with 600 µg/mL G418 for 2 wk. Then, drug-resistant individual clones were isolated and transferred to a 96-well plate for further amplification in the presence of selective medium. Cells that transiently transfected with pcDNA3-X and pcDNA3 were named as HL-7702/HBx^T and HL-7702/pcDNA3^T, respectively. Cells that stably transfected with pcDNA3-X and pcDNA3 were named as HL-7702/HBx^S and HL-7702/pcDNA3^S, respectively. HL-7702 was used as control.

Determination of X gene expression by RT-PCR analysis Total RNA was extracted separately from the cells of each group with a RNA isolation kit, and RT-PCR was carried out. β-Actin served as an internal control, 2 µL of RT product was used as template, X gene and β-actin were amplified together. The sequence of β-actin primers was 5'-GGCATCGTGATGGACTCCG-3' and 5'-GCTGGAAGGTGGACAGCGA-3'. The sequence of X gene primers was: 5'-ATGCAAGCTTATGGCTGCT-AGGCTGTACTG-3' and 5'-TGCGAATTCTTAGGCA-GAGGTGAAAAAGTTG-3'. The expected amplification fragment length of β-actin and X gene was 607 and 467 bp, respectively. PCR was carried out as follows: pre-denaturation at 95 °C for 5 min, 32 amplification cycles (denaturation at 94 °C for 35 s, annealing at 65 °C for 35 s, and extension at 72 °C for 1 min), and a final extension at 72 °C for 7 min.

Effect of HBV X gene on apoptosis-associated gene mRNA expression in hepatocytes by transient and stable transfection RT-PCR for Fas/FasL, Bax/Bcl-2, and c-myc Total RNA was extracted from HL-7702/HBx, HL-7702/pcDNA3, and HL-7702 according to the RNA isolation kit instructions. The content and purity of total RNA were determined by spectrophotography. RNA (260/280 was between 1.8 and 2.0) was further used for reverse transcription reaction, which was carried out according to the reverse transcription kit instructions. Two microgrammes of total RNA was used

in each reverse transcription reaction and the final volume was 20 µL. Glyceraldehyde-3-phosphate dehydrogenase (GAPDH) was used as an internal control and amplified together with target genes. PCR was performed in 50 µL reaction volume containing 5 µL 10×PCR buffer, 5 µL 2 mmol/L MgCl₂, 1 µL 10 mmol/L dNTP, 1 µL 20 pmol/µL target gene sense and anti-sense primers, 0.4 µL 12.5 pmol/µL GAPDH primer pair, 2 µL RT product, 1.5 U *Taq* DNA polymerase. The specific sets of primers and the target gene amplification conditions are shown in Table 1. All initial denaturations were at 94 °C for 5 min. Finally an additional extension step at 72 °C for 7 min was done.

Result determination The PCR products were electrophoresed on 2% agarose gel and visualized by ethidium bromide staining. Bioimaging system was used to detect the densities of bands of the PCR products. The ratio of target gene density to GAPDH density was respectively used to represent the relative expression level of Fas/FasL, Bax/Bcl-2, and c-myc mRNA. The semi-quantitative detection was analyzed five times.

Statistical analysis

All data were expressed as mean±SE. The significance for the difference between the groups was assessed with SPSS 10.0 by one-way ANOVA. *P*<0.05 was considered statistically significant.

RESULTS

Expression of HBV X gene mRNA in HL-7702 cells

HBV X gene mRNA was detected in HL-7702/HBx^T and HL-7702/HBx^S cells by RT-PCR. The expected band was found between 400 and 500 bp in both kinds of transfected cells (Figure 1). The relative level of HBV X gene mRNA in HL-7702/HBx^T was higher than that in HL-7702/HBx^S by about 2.5-folds (0.815±0.013 vs 0.308±0.021), indicating that HBV X gene mRNA could be expressed in HL-7702 after transient or stable transfection, and cell lines that expressed different levels of HBx were established.

Table 1 Primer sequences for PCR and amplification conditions for each target gene

Primer	Sequence	Amplification conditions	Product (base)
Fas	5'-TCAGTACGGAGTTGGGAAG-3' 5'-CAGGCCTCCAAGTCTGAG-3'	Denaturation at 94 °C for 45 s, annealing at 63 °C for 30 s and synthesizing at 72 °C for 1 min for 35 cycles	207
FasL	5'-GATGATGGAGGGGAAGATGA-3' 5'-TGGAAGAATCCCAAAGTGC-3'	Denaturation at 94 °C for 45 s, annealing at 58 °C for 30 s and synthesizing at 72 °C for 1 min for 30 cycles	203
Bax	5'-TTTGCTTCAGGTTTCATCC-3' 5'-CAGTTGAAGTTGCCGTCAGA-3'	Denaturation at 94 °C for 45 s, annealing at 58 °C for 30 s and synthesizing at 72 °C for 1 min for 30 cycles	246
Bcl-2	5'-CGACGACTTCTCCCGCCGCTACCGC-3' 5'-CCGCATGCTGGGGCCGTACAGTTC-3'	Denaturation at 94 °C for 45 s, annealing at 67 °C for 30 s and synthesizing at 72 °C for 1 min for 30 cycles	318
c-myc	5'-TTCGGGTAGTGAAAACCAG-3' 5'-CAGCAGCTCGAATTTCTCC-3'	Denaturation at 94 °C for 45 s, annealing at 58 °C for 30 s and synthesizing at 72 °C for 1 min for 28 cycles	203
GAPDH	5'-ACCACAGTCCATGCCATCAC-3' 5'-TCCACCACCTGTGCTGTA-3'	Changed according to different target genes	452

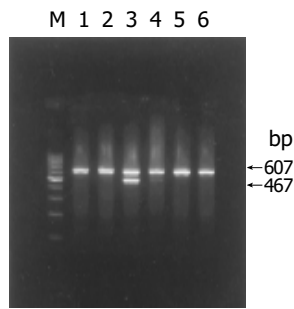


Figure 1 RT-PCR analysis of HBV X gene mRNA expression in HL-7702. M: 100-bp DNA ladder; lane 1: HL-7702^T; lane 2: HL-7702/pcDNA3^T; lane 3: HL-7702/HBx^T; lane 4: HL-7702/HBx^S; lane 5: HL-7702/pcDNA3^S; lane 6: HL-7702^S.

Effects of HBV X gene on apoptosis-associated genes mRNA expression in HL-7702 by transient transfection

Fas/FasL mRNA As shown in Figures 2A, B, and 3A, both Fas mRNA and FasL mRNA were expressed in HL-7702 of each group. Both of their expression levels had no significant differences among the three groups, indicating that HBx had no effect on Fas and FasL expression in normal hepatocytes though it was expressed at a relatively high level after transient transfection.

Bcl-2/Bax mRNA Both Bax and Bcl-2 mRNA were expressed in HL-7702 after transient transfection (Figures 2C, D, and 3B). As it could be seen from Figures 2C, 3B, and C, the expression level of Bax mRNA in HL-7702/HBx^T was higher than that in HL-7702 or in HL-7702/pcDNA3^T (0.614 ± 0.014 vs 0.536 ± 0.009 or 0.494 ± 0.015 , $P < 0.01$). The expression level of Bcl-2 mRNA in HL-7702/HBx^T was lower than that in HL-7702 or in HL-7702/pcDNA3^T (0.811 ± 0.010 vs 1.243 ± 0.033 , $P < 0.01$) (0.811 ± 0.010 vs

0.901 ± 0.014 , $P < 0.05$). There was also a significant difference in Bcl-2 mRNA expression level between the two control groups (0.901 ± 0.014 vs 1.243 ± 0.033 , $P < 0.01$; Figures 2D, 3B, and D). The data indicated that HBx could induce the pro-apoptotic factor Bax expression in normal hepatocytes and inhibit the anti-apoptotic factor Bcl-2 expression.

c-myc mRNA c-myc mRNA was expressed in both HL-7702 and HL-7702/pcDNA3, and there was no significant difference between them. The expression level of c-myc mRNA was significantly higher in HL-7702/HBx^T, suggesting that HBx was able to promote the c-myc expression in normal hepatocytes (0.719 ± 0.020 vs 0.569 ± 0.026 , $P < 0.01$, 0.719 ± 0.020 vs 0.630 ± 0.012 , $P < 0.05$; Figures 2E and 3C).

Effects of HBV X gene on apoptosis-associated gene mRNA expression in HL-7702 by stable transfection

Fas/FasL mRNA The expression levels of Fas mRNA had no significant difference among the three groups (Figures 4A and 5A). There was no significant difference in FasL mRNA expression between HL-7702 and HBV X gene expressing stable cell line HL-7702/HBx^S. The expression of FasL in HL-7702/HBx^S was significantly higher than that in HL-7702/pcDNA3^S (0.261 ± 0.043 vs 0.217 ± 0.012 , $P < 0.01$), suggesting that HBx at a low level could improve the FasL expression, which was different from the effect of HBx at a relatively higher level as shown in the former part (Figures 4B, 5A, and B).

Bax/Bcl-2 mRNA HBV X gene stably expressed in HL-7702/HBx^S seemed to have no effect on Bax mRNA expression (Figures 4C, 5B, and C). The expression level of Bcl-2 mRNA had no significant difference between the

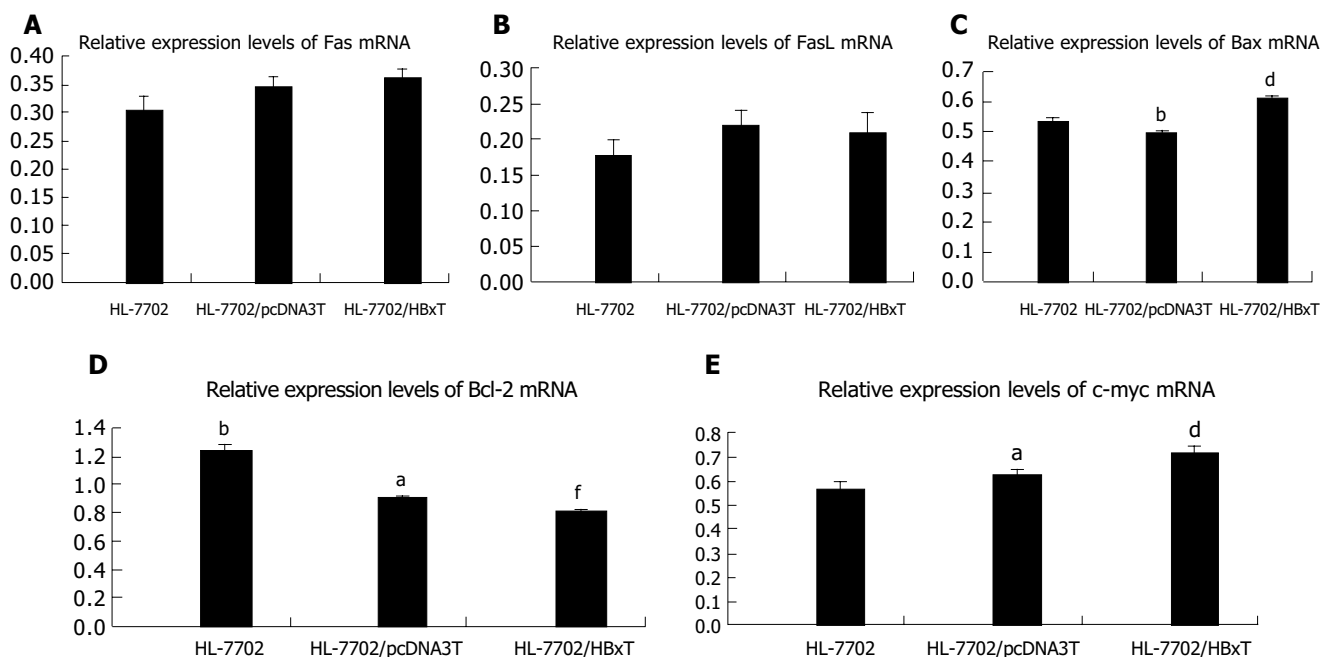


Figure 2 Relative expression levels of apoptosis-associated gene mRNA in HL-7702 of different transiently transfected groups assessed by RT-PCR. **A**: Relative Fas mRNA expression levels; **B**: relative FasL mRNA expression levels; **C**: relative Bax mRNA expression levels; **D**: relative Bcl-2 mRNA

expression levels; **E**: relative c-myc mRNA expression levels. ^a $P < 0.05$ vs HL-7702/HBx^T, ^b $P < 0.01$ vs HL-7702/HBx^T, ^d $P < 0.01$ vs HL-7702, ^f $P < 0.01$ vs HL-7702/pcDNA3^T, $P > 0.05$ between random two groups.

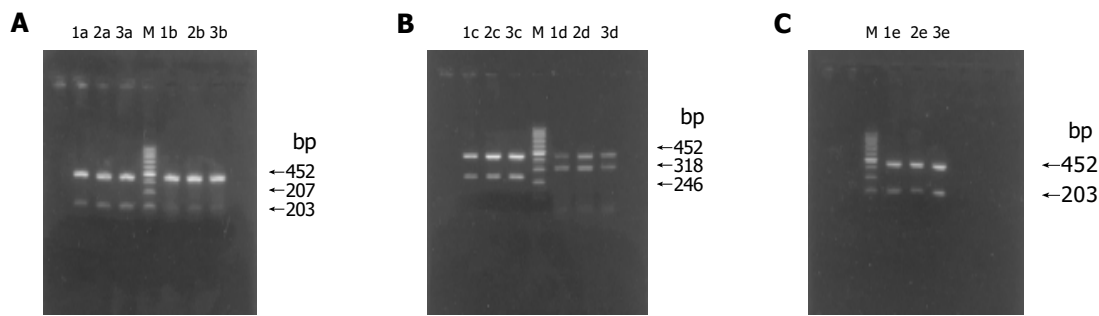


Figure 3 RT-PCR results of apoptosis-associated gene mRNA expression in HL-7702 of different transiently transfected groups. **A:** RT-PCR results of Fas/FasL mRNA expression; **B:** RT-PCR results of Bax/Bcl-2 mRNA expression;

C: RT-PCR results of c-myc mRNA expression; M: 100-bp DNA ladder; lane 1: HL-7702; lane 2: HL-7702/pcDNA3^T; lane 3: HL-7702/HBx^T; a: Fas; b: FasL; c: Bax; d: Bcl-2; e: c-myc.

two control groups, HL-7702 and HL-7702/pcDNA3^S, but it was lower in HL-7702/HBx^S (0.300 ± 0.028 vs 0.498 ± 0.035 , $P < 0.01$; 0.300 ± 0.028 vs 0.420 ± 0.032 , $P < 0.05$; Figures 4D, 5B, and D), suggesting that HBx could downregulate Bcl-2 expression in normal hepatocytes.

c-myc mRNA Similar to the effect of HBV X gene transient transfection, c-myc was expressed in both HL-7702 and HL-7702/pcDNA3^S, and there was no significant difference between them. The expression level of c-myc mRNA was significantly higher in HL-7702/HBx^S, suggesting that even a low level of HBx was able to upregulate the c-myc expression in normal hepatocytes (0.603 ± 0.035 vs 0.449 ± 0.023 or 0.461 ± 0.022 , $P < 0.01$; Figures 4E and 5C).

DISCUSSION

HBV infection is a major cause of chronic hepatitis, cirrhosis, and hepatocellular carcinoma and accounts for one million

deaths annually. HBx is a multifunctional protein that is implicated in the pathogenesis of HBV-associated liver disease by regulating gene transcription, causing cell proliferation, suppressing DNA repair and inducing cell death^[7]. The role of HBx in carcinogenesis and its transactivation function have been well documented^[8]. The role of HBx in liver cell proliferation and apoptosis is still controversial. A number of studies have revealed that HBx exert dual activity on cell apoptosis^[9,10].

On the one hand, HBx has an anti-apoptosis function in different ways and plays an important role in the development of HCC. HBx can activate and upregulate transcription factor NF- κ B^[11]. It induces Fas-ligand in human hepatoma cells, which contributed to the apoptosis of T cells, thus the hepatoma cells might escape from immune surveillance^[12]. There is evidence that HBx blocks apoptosis via downregulating expression of Bid in human hepatocellular carcinoma^[13]. The distal C-terminal domain of HBx, independent of its

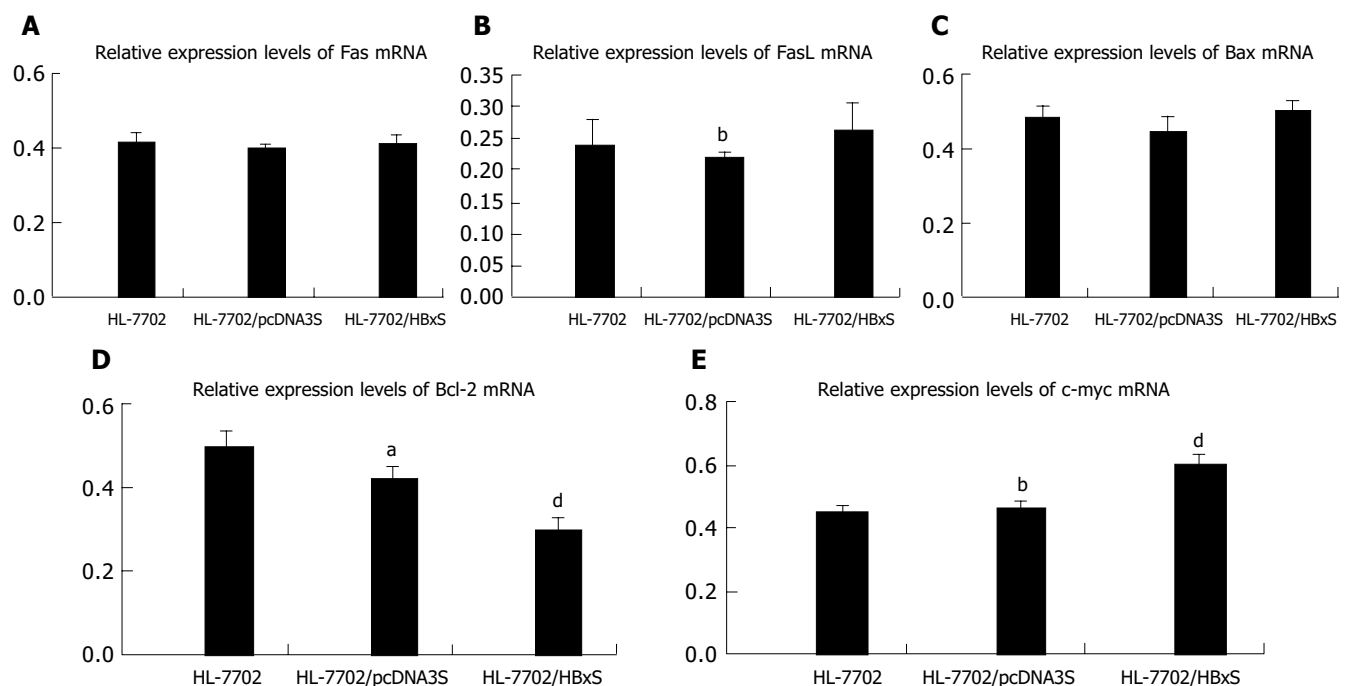


Figure 4 Relative expression levels of apoptosis-associated gene mRNA in HL-7702 of different stably transfected groups assessed by RT-PCR. **A:** Relative Fas mRNA expression levels; **B:** relative FasL mRNA expression levels; **C:** relative Bax mRNA expression levels; **D:** relative Bcl-2 mRNA

expression levels; **E:** relative c-myc mRNA expression levels. ^a $P < 0.05$ vs HL-7702/HBx^S; ^b $P < 0.01$ vs HL-7702/HBx^S; ^d $P < 0.01$ vs HL-7702, $P > 0.05$ between random two groups.

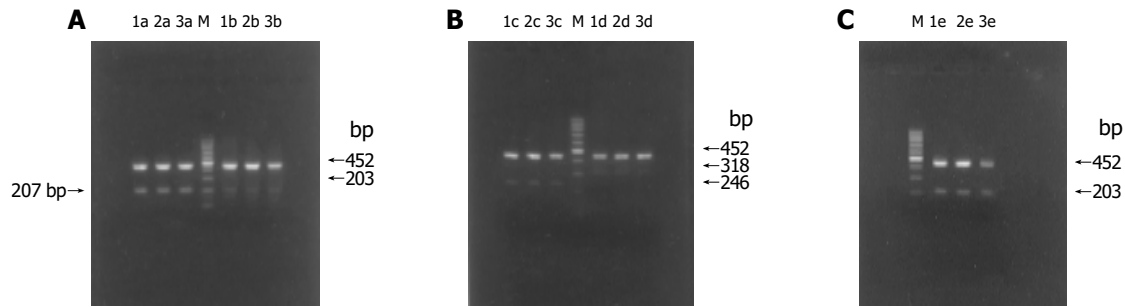


Figure 5 RT-PCR results of apoptosis-associated gene mRNA expression in HL-7702 of different stably transfected groups. **A:** RT-PCR results of Fas/FasL mRNA expression; **B:** RT-PCR results of Bax/Bcl-2 mRNA expression; **C:**

RT-PCR results of c-myc mRNA expression; M: 100-bp DNA ladder; lane 1: HL-7702; lane 2: HL-7702/pcDNA3^S; lane 3: HL-7702/HBx^S; a: Fas; b: FasL; c: Bax; d: Bcl-2; e: c-myc.

transactivation activity, is complexed with p53 in the cytoplasm and partially prevents its nuclear entry and ability to induce apoptosis^[14]. On the other hand, HBx induces or sensitizes cells to apoptotic killing by pro-apoptotic stimuli^[2-5]. The possible mechanisms may include upregulating the expression of Fas and Fas-ligand in hepatocytes^[15,16], inducing cell death by causing loss of mitochondrial membrane potential and mitochondrial aggregation at the nuclear periphery^[17,18], antagonizing the anti-apoptosis function of the normal level of p53^[19], abrogating the apoptosis-inhibitory function of c-FLIP and enhancing the death-inducing signal^[20], inducing TNF- α expression and sensitizing liver cells to TNF- α -mediated apoptosis even below the threshold concentration^[20-22], affecting the apoptosis control function of Bcl-2 family members by interaction with mitochondria^[23]. The above data suggest that the possible mechanism for HBx to regulate cell apoptosis is a “network” implicated with multiple factors and various pathways, and the exact mechanism remains obscure.

Fas and FasL are regarded as the most important factors that switch on the Fas/FasL-mediated apoptosis. The Bcl-2 family proteins play an important role in modulating cell survival and apoptosis. Bcl-2 and Bax act as an anti-apoptotic factor and a pro-apoptotic factor respectively. The proportion of apoptosis-inducing forces and apoptosis-inhibiting forces determines the cells' response to death-inducing signals and their final fate^[24-26]. C-myc, usually acting as a proto-oncogene and exerting a dual activity on cell proliferation and apoptosis, is also involved in apoptosis regulation. We have previously demonstrated that the apoptosis rate in HBx-expressing cells by transient or stable transfection is much higher than that in control groups, suggesting that there is a quantity-effect relationship between HBx expression and apoptosis rate, and that HBx can induce apoptosis in normal hepatocytes, during which the expression level of HBV X gene may play a vital role. This study aimed to investigate the possible mechanism for HBV X gene to induce apoptosis of hepatocytes. Thereby, we established cell models that expressed different levels of HBV X gene by transfecting HBV X gene into HL-7702 through transient and stable transfection, and studied the effect of HBx on the mRNA expression of apoptosis-associated genes.

We found that HBx at a relatively higher level could induce the pro-apoptotic factor Bax expression in normal

hepatocytes and inhibit the anti-apoptotic factor Bcl-2 expression, though it had no effect on Fas and FasL expression. However, HBx at a low level could improve FasL expression, while it had no effect on Bax. The data show that HBx may induce the apoptosis of HL-7702 by reinforcing the death signal of Fas-FasL pathway and increasing the proportion of pro-apoptotic forces and anti-apoptotic forces in Bcl-2 family members. The dose of HBx may decide which is the chief pathway. The c-myc expression in HL-7702 significantly increased after transient or stable transfection with X gene expression vector, which is consistent with previous reports^[9,27]. C-myc protein could sensitize cells to apoptotic killing in certain conditions, such as during exposure to TNF- α or other factors^[28-30]. Thus, c-myc may also act as an important medium in HBx-mediated apoptosis. Su *et al.*^[30], found that the combination of HBx and c-myc increases the sensitivity of WT 3T3 cells to TNF- α killing by about 10-fold. They also demonstrated that cell killing by HBx plus TNF- α is suppressed by activation of NF- κ B, but can be overridden by a high level of c-myc protein.

Our results show that different levels of HBV X gene expression have different effects on apoptosis-associated gene expression. Wang *et al.*^[31], studied the effects of regulatory endoplasmic HBx expression on hepatic cell apoptosis and found that low HBx expression cannot induce apoptosis. Thereby, the effect of HBx on apoptosis may be dose dependent. We hypothesize that there may be a threshold concentration for HBx to induce apoptosis, only that beyond the threshold can exert a pro-apoptosis function. Further studies are needed to confirm it.

In conclusion, HBx may induce apoptosis in part via regulating the expression of apoptosis-associated genes. HBV X gene expression may play a vital role, although the underlying mechanism may be complicated and crisscrossing.

REFERENCES

- 1 **Birrer RB**, Birrer D, Klavins JV. Hepatocellular carcinoma and hepatitis virus. *Ann Clin Lab Sci* 2003; **33**: 39-54
- 2 **Terradillos O**, Pollicino T, Lecoecur H, Tripodi M, Gougeon ML, Tiollais P, Buendia MA. p53-independent apoptotic effects of the hepatitis B virus HBx protein *in vivo* and *in vitro*. *Oncogene* 1998; **17**: 2115-2123
- 3 **Pollicino T**, Terradillos O, Lecoecur H, Gougeon ML, Buendia MA. Pro-apoptotic effect of the hepatitis B virus X gene. *Biomed Pharmacother* 1998; **52**: 363-368

- 4 **Chirillo P**, Pagano S, Natoli G, Puri PL, Burgio VL, Balsano C, Levrero M. The hepatitis B virus X gene induces p53-mediated programmed cell death. *Proc Natl Acad Sci USA* 1997; **94**: 8162-8167
- 5 **Shintani Y**, Yotsuyanagi H, Moriya K, Fujie H, Tsutsumi T, Kanegae Y, Kimura S, Saito I, Koike K. Induction of apoptosis after switch-on of the hepatitis B virus X gene mediated by the Cre/loxP recombination system. *J Gen Virol* 1999; **80**(Pt 12): 3257-3265
- 6 **Chen HY**, Tang NH, Zhang SJ, Chen ZX, Wang XZ. Construction of hepatitis B virus X gene expression vector in eucaryotic cells and its transfection in HL-7702 cells. *Shijie Huaren Xiaohua Zazhi* 2004; **12**: 614-617
- 7 **Murakami S**. Hepatitis B virus X protein: a multifunctional viral regulator. *J Gastroenterol* 2001; **36**: 651-660
- 8 **Yoo YG**, Oh SH, Park ES, Cho H, Lee N, Park H, Kim DK, Yu DY, Seong JK, Lee MO. Hepatitis B virus X protein enhances transcriptional activity of hypoxia-inducible factor-1alpha through activation of mitogen-activated protein kinase pathway. *J Biol Chem* 2003; **278**: 39076-39084
- 9 **Su F**, Schneider RJ. Hepatitis B virus HBx protein sensitizes cells to apoptotic killing by tumor necrosis factor. *Proc Natl Acad Sci USA* 1997; **94**: 8744-8749
- 10 **Lee S**, Tam C, Wang WH, Chen S, Hullinger RL, Andrisani OM. Hepatitis B virus X protein differentially regulates cell cycle progression in X-transforming versus nontransforming hepatocyte (AML12) cell lines. *J Biol Chem* 2002; **277**: 8730-8740
- 11 **Su F**, Schneider RJ. Hepatitis B virus HBx protein activates transcription factor NF-kappaB by acting on multiple cytoplasmic inhibitors of I-kappaB-related proteins. *Virology* 1996; **70**: 4558-4566
- 12 **Shin EC**, Shin JS, Park JH, Kim H, Kim SJ. Express of fas ligand in human hepatoma cell lines: role of hepatitis-B virus X (HBX) in induction of Fas ligand. *Cancer* 1999; **82**: 587-591
- 13 **Chen GG**, Lai PB, Chan PK, Chak EC, Yip JH, Ho RL, Leung BC, Lau WY. Decreased expression of Bid in human hepatocellular carcinoma is related to hepatitis B virus X protein. *Eur J Cancer* 2001; **37**: 1695-1702
- 14 **Elmore LW**, Hancock AR, Chang SF, Wang XW, Chang S, Callahan CP, Geller DA, Will H, Harris CC. Hepatitis B virus X protein and p53 tumor suppressor interactions in the modulation of apoptosis. *Proc Natl Acad Sci USA* 1997; **94**: 14707-14712
- 15 **Yoo YG**, Lee MO. Hepatitis B virus X protein induces expression of Fas ligand gene through enhancing transcriptional activity of early growth response factor. *J Biol Chem* 2004; **279**: 36242-36249
- 16 **Sejima T**, Miyagawa I. The evaluation of Fas/Fas ligand system in renal cell carcinoma-the effect of preoperative interferon-alpha therapy. *Nippon Hinyokika Gakkai Zasshi* 1999; **90**: 826-832
- 17 **Shirakata Y**, Koike K. Hepatitis B virus X protein induces cell death by causing loss of mitochondrial membrane potential. *J Biol Chem* 2003; **278**: 22071-22078
- 18 **Takada S**, Shirakata Y, Kaneniwa N, Koike K. Association of hepatitis B virus X protein with mitochondria causes mitochondrial aggregation at the nuclear periphery, leading to cell death. *Oncogene* 1999; **18**: 6965-6973
- 19 **Kim H**, Lee H, Yun Y. X-gene product of hepatitis B virus induces apoptosis in liver cells. *J Biol Chem* 1998; **273**: 381-385
- 20 **Kim KH**, Seong BL. Pro-apoptotic function of HBV X protein is mediated by interaction with c-FLIP and enhancement of death-inducing signal. *EMBO J* 2003; **22**: 2104-2116
- 21 **Lara-Pezzi E**, Majano PL, Gomez-Gonzalo M, Garcia-Monzon C, Moreno-Otero R, Levrero M, Lopez-Cabrera M. The hepatitis B virus X protein up-regulates tumor necrosis factor alpha gene expression in hepatocyte. *Hepatology* 1998; **28**: 1013-1021
- 22 **Yi YS**, Park SG, Byeon SM, Kwon YG, Jung G. Hepatitis B virus X protein induces TNF-alpha expression via down-regulation of selenoprotein P in human hepatoma cell line, HepG2. *Biochim Biophys Acta* 2003; **1638**: 249-256
- 23 **Terradillos O**, de La Coste A, Pollicino T, Neuveut C, Sitterlin D, Lecoeur H, Gougeon ML, Kahn A, Buendia MA. The hepatitis B virus X protein abrogates Bcl-2-mediated protection against Fas apoptosis in the liver. *Oncogene* 2002; **21**: 377-386
- 24 **Cory S**, Adams JM. The Bcl2 family: regulators of the cellular life-or-death switch. *Nat Rev Cancer* 2002; **2**: 647-656
- 25 **Gross A**, McDonnell JM, Korsmeyer SJ. BCL-2 family members and the mitochondria in apoptosis. *Genes Dev* 1999; **13**: 1899-1911
- 26 **Bouillet P**, Strasser A. BH3-only proteins-evolutionarily conserved proapoptotic Bcl-2 family members essential for initiating programmed cell death. *J Cell Sci* 2002; **115**: 1567-1574
- 27 **Balsano C**, Avantiaggiati ML, Natoli G, De Marzio E, Will H, Perricaudet M, Levrero M. Full-length and truncated versions of the hepatitis B virus (HBV) X protein (pX) transactivate the cmyc protooncogene at the transcriptional level. *Biochem Biophys Res Commun* 1991; **176**: 985-992
- 28 **Juin P**, Hueber AO, Littlewood T, Evan G. c-Myc-induced sensitization to apoptosis is mediated through cytochrome c apoptosis release. *Genes Dev* 1999; **13**: 1367-1381
- 29 **Juin P**, Hunt A, Littlewood T, Griffiths B, Swigart LB, Korsmeyer S, Evan G. c-Myc functionally cooperates with Bax to induce apoptosis. *Mol Cell Biol* 2002; **22**: 6158-6169
- 30 **Su F**, Theodosis CN, Schneider RJ. Role of NF-kappaB and myc proteins in apoptosis induced by hepatitis B virus HBx protein. *J Virol* 2001; **75**: 215-225
- 31 **Wang HP**, Chen XP, He SQ, Ding L. Effects of regulatory endoplasmic HBX expression on hepatic cell apoptosis. *Zhonghua Ganzangbing Zazhi* 2003; **11**: 440

• *Helicobacter pylori* •

Expression of CD86 and increased infiltration of NK cells are associated with *Helicobacter pylori*-dependent state of early stage high-grade gastric MALT lymphoma

Sung-Hsin Kuo, Li-Tzong Chen, Chi-Long Chen, Shin-Lian Doong, Kun-Huei Yeh, Ming-Shiang Wu, Tsui-Lien Mao, Hui-Chen Hsu, Hsiu-Po Wang, Jaw-Town Lin, Ann-Lii Cheng

Sung-Hsin Kuo, Departments of Oncology, National Taiwan University Hospital, Taipei; Cancer Research Center, and Graduate Institute of Clinical Medicine, National Taiwan University College of Medicine, Taipei, Taiwan, China

Li-Tzong Chen, Division of Cancer Research, National Health Research Institutes, Taipei; Department of Internal Medicine, Kaohsiung Medical University Hospital, Kaohsiung, Taipei, Taiwan, China

Chi-Long Chen, Department of Pathology, Taipei Medical University, Taipei, Taiwan, China

Shin-Lian Doong, Graduate Institute of Microbiology, National Taiwan University College of Medicine, Taipei, Taiwan, China

Kun-Huei Yeh, Hui-Chen Hsu, Departments of Oncology, National Taiwan University Hospital, Taipei; Cancer Research Center, National Taiwan University College of Medicine, Taipei, Taiwan, China

Ming-Shiang Wu, Jaw-Town Lin, Department of Internal Medicine, National Taiwan University Hospital, Taipei, Taiwan, China

Tsui-Lien Mao, Department of Pathology, National Taiwan University Hospital, Taipei, Taiwan, China

Hsiu-Po Wang, Department of Emergency Medicine, National Taiwan University Hospital, Taipei, Taiwan, China

Ann-Lii Cheng, Department of Internal Medicine and Department of Oncology, National Taiwan University Hospital, Taipei; Cancer Research Center, National Taiwan University College of Medicine, Taipei; Division of Cancer Research, National Health Research Institutes, Taipei, Taiwan, China

Supported by the Research Grants, No. NSC91-3112-B-002-009, No. NSC92-3112-B-002-027, and No. NSC93-3112-B-002-007 from the National Science Council, No. NHRI-CN-CA9201S (92A084, and 93A059) from the National Health Research Institutes, and No. NTUH 93-N012, No. NTUH 94S155 from National Taiwan University Hospital, Taiwan, China

Correspondence to: Ann-Lii Cheng, MD, PhD, Department of Internal Medicine and Department of Oncology, National Taiwan University Hospital, No. 7, Chung-Shan South Road, Taipei, Taiwan, China. andrew@ha.mc.ntu.edu.tw

Telephone: +886-2-2312-3456-7251 Fax: +886-2-2371-1174

Received: 2004-11-04 Accepted: 2004-12-08

Abstract

AIM: A high percentage of early-stage high-grade gastric mucosa-associated lymphoid tissue (MALT) lymphomas remain *Helicobacter pylori* (*H pylori*)-dependent. However, unlike their low-grade counterparts, high-grade gastric MALT lymphomas may progress rapidly if unresponsive to *H pylori* eradication. It is mandatory to identify markers that may predict the *H pylori*-dependent status of these tumors. Proliferation of MALT lymphoma cells depends on cognate help and cell-to-cell contact of *H pylori*-specific intratumoral T-cells. To examine whether the expression

of co-stimulatory marker CD86 (B7.2) and the infiltration of CD56 (+) natural killer (NK) cells can be useful markers to predict *H pylori*-dependent status of high-grade gastric MALT lymphoma.

METHODS: Lymphoma biopsies from 26 patients who had participated in a prospective study of *H pylori*-eradication for stage I_E high-grade gastric MALT lymphomas were evaluated. Tumors that resolved to Wotherspoon grade II or less after *H pylori* eradication were classified as *H pylori*-dependent; others were classified as *H pylori*-independent. The infiltration of NK cells and the expression of CD86 in pre-treatment paraffin-embedded lymphoma tissues were determined by immunohistochemistry.

RESULTS: There were 16 *H pylori*-dependent and 10 *H pylori*-independent cases. CD86 expression was detected in 11 (68.8%) of 16 *H pylori*-dependent cases but in none of 10 *H pylori*-independent cases ($P = 0.001$). *H pylori*-dependent high-grade gastric MALT lymphomas contained significantly higher numbers of CD56 (+) NK cells than *H pylori*-independent cases ($2.8 \pm 1.4\%$ vs $1.1 \pm 0.8\%$; $P = 0.003$). CD86 positive MALT lymphomas also showed significantly increased infiltration of CD56 (+) NK cells compared to CD86-negative cases ($2.9 \pm 1.1\%$ vs $1.4 \pm 1.3\%$; $P = 0.005$).

CONCLUSION: These results suggest that the expression of co-stimulatory marker CD86 and the increased infiltration of NK cells are associated with *H pylori*-dependent state of early-stage high-grade gastric MALT lymphomas.

© 2005 The WJG Press and Elsevier Inc. All rights reserved.

Key words: MALT lymphoma; *H pylori*; CD86; CD56

Kuo SH, Chen LT, Chen CL, Doong SL, Yeh KH, Wu MS, Mao TL, Hsu HC, Wang HP, Lin JT, Cheng AL. Expression of CD86 and increased infiltration of NK cells are associated with *Helicobacter pylori*-dependent state of early stage high-grade gastric MALT lymphoma. *World J Gastroenterol* 2005; 11(28): 4357-4362

<http://www.wjgnet.com/1007-9327/11/4357.asp>

INTRODUCTION

Extranodal marginal zone B-cell lymphoma of mucosa-

associated lymphoid tissue (MALT) of the stomach is the most common extranodal lymphoma of humans. Although not completely acknowledged by all experts, gastric MALT lymphoma is often classified into high-grade and low-grade subtypes by histological criteria^[1-3]. Low-grade gastric MALT lymphoma is characterized by its close association with *Helicobacter pylori* (*H pylori*) infection; and eradication of *H pylori* by antibiotics, cures 70% of these tumors^[4-6]. However, high-grade gastric MALT lymphomas, in contrast to their low-grade counterparts, are believed to consist of highly-transformed cells, the growth of which is independent of *H pylori*^[7-9].

Recently, several groups of investigators have demonstrated that a substantial portion of early-stage high-grade gastric MALT lymphomas remains *H pylori*-dependent, and can be cured by *H pylori* eradication^[10-12]. However, high-grade gastric MALT lymphoma, unlike its low-grade counterpart, may progress rapidly if unresponsive to *H pylori* eradication therapy. Molecular markers such as chromosomal aberration t(11;18), which is highly predictive of *H pylori*-independent status of low-grade gastric MALT lymphoma, are rarely found in the high-grade counterpart^[13]. It is mandatory to identify cellular or molecular markers which can help predict the *H pylori*-dependent status of newly diagnosed patients.

In the early process of MALT lymphomagenesis, the proliferation response depends at least partly on the stimulation of *H pylori*-specific intratumoral T-cells^[14]. *In vitro* experiments have demonstrated that the growth and differentiation of MALT lymphoma cells requires CD40-mediated signaling and T helper-2 (Th-2)-type cytokines^[15,16]. The dependence on T-cells for the growth of malignant B-cell clones may explain the tendency of early-stage low-grade MALT lymphomas to remain localized and to regress after *H pylori* eradication. Expression of co-stimulatory molecules, including CD80 (B7.1), CD86 (B7.2), and their ligands, has been demonstrated in gastric MALT lymphoma cells^[17]. The presence of the co-stimulatory marker CD86 (B7.2) on lymphoma cells may promote T-cell-mediated neoplastic B cell proliferation. We hypothesized that a loss of co-stimulatory markers might preclude tumor cell/reactive T-cell interaction and thereby contribute to the transition from a *H pylori*-dependent to a *H pylori*-independent state in high-grade gastric MALT lymphoma.

CD56 (+) natural killer (NK) cells are important components of the innate immune system, and have the ability to modulate both humoral- and cell-mediated immune responses^[18,19]. *H pylori* can stimulate T-cells and thereby enhance the production of Th-2 cytokines, which can promote the proliferation of CD56 (+) NK cells in gastric MALT lymphomas^[20,21]. Although low-grade gastric MALT lymphomas contain significantly higher numbers of CD56 (+) NK cells than high-grade gastric MALT lymphomas^[21], the presence of CD56 (+) NK cells in high-grade gastric MALT lymphomas indicate that the promotion of these lymphoma cells triggered by *H pylori*-specific intratumoral T-cells and Th-2 type cytokines may still be present *in vivo*. Therefore, these CD56 (+) NK cells may limit the autonomous growth of MALT lymphoma cells, and may contribute to the remission of high-grade MALT lymphomas after the eradication of *H pylori*.

This study, was conducted to examine the expression of CD86 and the infiltration of CD56 (+) NK cells in 16

H pylori-dependent and 10 *H pylori*-independent high-grade gastric MALT lymphomas.

MATERIALS AND METHODS

Patients, treatment, and evaluation of the tumors

Twenty-six patients who had participated in a prospective study of *H pylori* eradication for stage I_E high-grade gastric MALT lymphomas at our institutions from June 1995 to June 2003 were included in this study. The clinicopathologic features of the 22 patients have been previously reported^[13]. Although high-grade MALT lymphomas are classified as diffuse large B-cell lymphomas (with areas of marginal zone/MALT-type lymphoma) in the REAL/WHO classification^[2], and a consensus on the use of the term "high-grade MALT lymphoma" has not been achieved, many experts consider it as a useful and reasonable clinicopathologic entity^[1,3,10,21]. In this study, the diagnosis of high-grade gastric MALT lymphoma was made using the histologic criteria as described by Chan *et al.*^[1], and de Jong *et al.*^[3], based on the presence of a diffuse increase of large cells resembling centroblasts or lymphoblasts to between 1% and 10% of the total tumor cells within predominantly low-grade centrocyte-like cell infiltrate, or the predominance of a high-grade lymphoma with only a small residue, low-grade foci and/or the presence of lymphoepithelial lesions. Specimens with occasional clusters of transformed blast cells or sheets of transformed blast cells (upto 20 cells not forming larger sheets) confined within the colonized follicles were found within a low-grade lymphoma, they were considered as an immune response to *H pylori* stimulation rather than high-grade MALT lymphoma. Patients with primary pure large cell lymphoma, without evidence of a low-grade component of the stomach were excluded from this study. All specimens were immunohistochemically stained by CD20, CD79a, CD3, and CD45RO for routine diagnostic purposes and to highlight lymphoepithelial lesions. Moreover, to exclude misinterpretation of reactive, benign germinal centers as transformed foci, CD21 (follicular dendritic cells markers) and BCL-2 (highly suggestive of a neoplastic origin of the blast cells) were included in all cases. The histopathologic characteristics of all tumor specimens were independently reviewed by two expert hematopathologists. Staging was based on Musshoff's modification of the Ann Arbor staging system^[22]. Staging procedures included physical examination, routine laboratory tests, inspection of Waldeyer's ring, chest radiography, chest and abdominal CT scan, bone marrow aspiration, and trephine biopsy. Diagnosis of *H pylori* infection was based on histologic examination, biopsy urease test, or bacterial culture. When at least one test was positive, the cases were considered as *H pylori* infected. All patients consented to a brief trial of *H pylori* eradication therapy.

At the beginning of the study period in June 1995, the eradication regimen consisted of amoxicillin 500 mg and metronidazole 250 mg q.i.d., with either bismuth subcitrate 120 mg q.i.d. or omeprazole 20 mg b.i.d., for 4 wk. The regimen was changed to amoxicillin 500 mg q.i.d., clarithromycin 500 mg b.i.d., plus omeprazole 20 mg b.i.d. for 2 wk beginning in March 1996. Patients were scheduled to undergo a first follow-up upper gastrointestinal endoscopic examination 4-6 wk after completion of antimicrobial

therapy, and follow-up was then repeated every 6-12 wk until histologic evidence of remission was found. At each follow-up examination, four to six biopsy specimens were taken from the antrum and body of the stomach for a *H pylori* infection evaluation, and a minimum of six biopsy specimens were taken from each of the tumors and suspicious areas for histologic evaluation. Tumors that resolved to Wotherspoon grade II or less were considered as histological complete remission^[4]. Tumors showing both histological and endoscopic complete remission were considered *H pylori*-dependent. Tumors showing stable or progressive disease on follow-up endoscopic examination and persistent or increasing proportion of large cells on microscopic examination were considered *H pylori*-independent.

Immunohistochemistry

Formalin-fixed paraffin embedded sections cut at a thickness of 4 μ m were deparaffinized and rehydrated through xylene and a graded descending series of alcohol. After antigen retrieval by heat treatment in 0.1 mol/L citrate buffer at pH 6.0, endogenous peroxidase activity was blocked by 3% H₂O₂. Briefly, slides were incubated for 30 min in 2.5% normal donkey serum or goat serum. The slides were then incubated overnight at 4 °C either with goat polyclonal anti-CD86 antibody (1:50; AF-141-NA; R&D Systems, Abingdon, UK) or mouse monoclonal anti-CD56 antibody (1:100; NCL-CD56-1B6, Novacastra), and incubated with secondary antibodies (CD86, donkey antigoat immunoglobulin; CD56, goat antimouse immunoglobulin; Santa Cruz Biotechnology, Santa Cruz, CA, USA), following the manufacturer's instructions. Finally, antibody binding was detected with the avidin-biotin-peroxidase method. Reaction

products were developed using 3',5'-diaminobenzidine (Dako) as a substrate for peroxidase. Sections were counterstained with Mayer's hematoxylin. All the washes were performed in PBS (pH 7.4). Staining was considered as positive for CD86 when the protein was detected in more than 10% of tumor cells. A minimum of 1 000 cells (normal and neoplastic) were counted for each single determination and reported as the percentage of CD56 (+) NK cells in total mononuclear cells.

Statistical analysis

The primary aims of this study were to investigate the correlation between the *H pylori*-dependent status of MALT lymphomas, the expression of CD86 and the infiltration of CD56 (+) NK cells. Fisher's exact test and χ^2 test were used to analyze the correlation between the *H pylori*-dependent status of MALT lymphomas with CD86 expression patterns. The results for the CD56 (+) NK cells are expressed as mean \pm SD of percentages of positive cells in the total cell count for a given marker. Nonparametric Mann-Whitney *U* test was used to evaluate the difference in the distribution of positive CD56 (+) NK cell count between *H pylori*-dependent and *H pylori*-independent high-grade MALT lymphomas and the difference in the distribution of positive CD56 (+) NK cell count between CD86 positive and CD86 negative high-grade MALT lymphomas.

RESULTS

Patients and tumor response

There were 16 patients with *H pylori*-dependent and 10 patients with *H pylori*-independent tumors. The clinicopathologic features of these patients are summarized in Table 1. The

Table 1 Clinicopathologic features of the patients and tumor expression of CD86

Patient number	Sex	Age (yr)	Depth of tumor invasion	Tumor response to <i>H pylori</i> eradication	Current status	Immunohistochemistry CD86
1	F	48	Muscularis propria	CR		-
2	M	21	Muscularis propria	PD	Chemotherapy	-
3	F	63		SD	Chemotherapy	-
4	F	68		CR		+
5	F	52	Submucosa	PD	Chemotherapy	-
6	F	42	Serosa	CR		+
7	F	66	Serosa	CR		-
8	F	71	Muscularis propria	CR		+
9	F	54		CR		+
10	M	83	Muscularis propria	PD	Chemotherapy	-
11	F	52	Submucosa	CR		+
12	F	73	Muscularis propria	CR		+
13	M	46	Submucosa	CR		-
14	F	38		CR		-
15	M	73	Serosa	PD	Chemotherapy	-
16	F	45	Muscularis propria	PD	Chemotherapy	-
17	F	56	Submucosa	CR		+
18	F	59	Serosa	PD	C/T+gastrectomy	-
19	F	65		CR		+
20	M	35	Submucosa	CR		+
21	F	73		CR		-
22	M	45	Serosa	SD	Chemotherapy	-
23	F	53	Submucosa	SD	Chemotherapy	-
24	F	80	Muscularis propria	PD	Chemotherapy	-
25	M	70	Submucosa	CR		+
26	F	84	Submucosa	CR		+

Evaluated by EUS (19 cases) and histologic examination of surgical specimens (1 case). +: Positive; -: negative; CR, complete remission; SD, stable disease; PD, progressive disease.

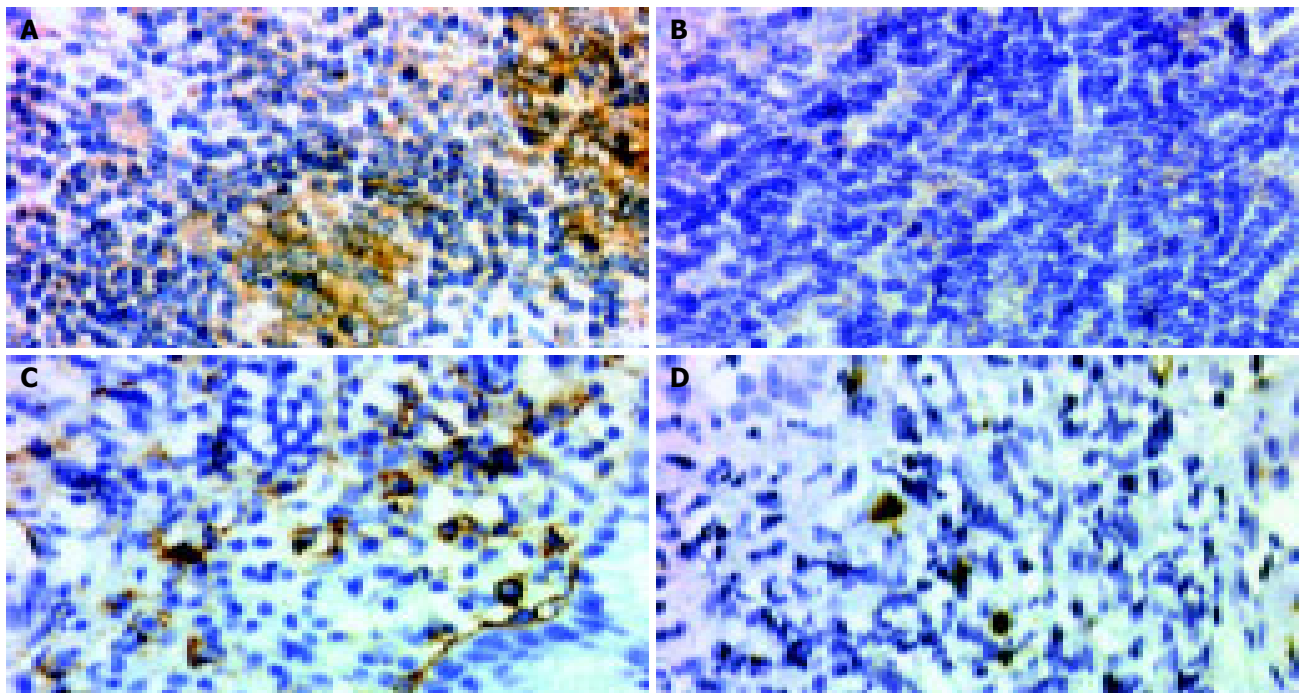


Figure 1 Examples of immunohistochemical analysis of CD86 and CD56 (+) NK on B-cells of high-grade gastric MALT lymphoma. **A:** *H pylori*-dependent case (case 4) shows positive staining for CD86; **B:** *H pylori*-independent case (case 18) shows

negative staining for CD86; **C:** *H pylori*-dependent case (case 8) carries a larger proportion of CD56 (+) NK cells; **D:** *H pylori*-independent case (case 5) contains a lower proportion of CD56 (+) NK cells. Original magnification, $\times 400$.

median duration between *H pylori* eradication and complete histologic remission was 5.0 mo (range, 1.5-17.7 mo). At a median follow-up of 56 mo (range, 8.0-90 mo), all 16 patients who had achieved complete histologic remission after eradication of *H pylori* were alive and free of lymphoma. Seven patients whose tumors grossly increased in size or had microscopic findings of an increased large-cell fraction and three patients whose tumor remained grossly stable at the first follow-up endoscopic examination, were immediately referred for systemic chemotherapy.

Correlation of expression of CD86 and infiltration of CD56 (+) NK cells with tumor response to *H pylori* eradication

The expression of CD86 was detected in 11 (68.8%) of 16 *H pylori*-dependent high-grade gastric MALT lymphomas, but in none of 10 *H pylori*-independent MALT lymphomas ($P = 0.001$, Figure 1 and Table 1). Therefore, the expression of CD86 had a sensitivity of 68.8% and a specificity of 100% in predicting the *H pylori*-dependence of high-grade gastric MALT lymphomas.

As shown in Figure 2, the infiltration of CD56 (+) NK cells differed between *H pylori*-dependent and *H pylori*-independent high-grade gastric MALT lymphomas. *H pylori*-dependent high-grade gastric MALT lymphomas contained significantly higher numbers of CD56 (+) NK cells than *H pylori*-independent MALT lymphomas ($2.8 \pm 1.4\%$ vs $1.1 \pm 0.8\%$; $P = 0.003$). Meanwhile, CD86 positive MALT lymphomas also showed significantly increased infiltration of CD56 (+) NK cells compared to CD86-negative cases ($2.9 \pm 1.1\%$ vs $1.4 \pm 1.3\%$; $P = 0.005$).

DISCUSSION

In this study, we found that expression of CD86 on tumor

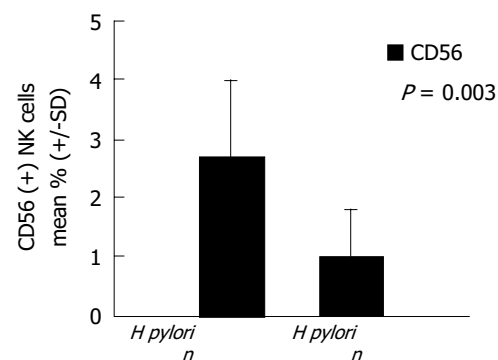


Figure 2 Histograms showing the mean percentage (\pm SD) of cells staining CD56 (+) NK in *H pylori*-dependent and *H pylori*-independent high-grade gastric MALT lymphomas ($2.8 \pm 1.4\%$ vs $1.1 \pm 0.8\%$; $P = 0.003$).

cells and increased infiltration of NK cells in tumor tissues were associated with the *H pylori*-dependent status of early-stage high-grade gastric MALT lymphomas. These findings suggest that the interaction of B- and T-cells may play a pivotal role in the determination of antigen-dependence, as well as in the subsequent response to *H pylori* eradication therapy in a substantial portion of early-stage high-grade gastric MALT lymphomas. Since high-grade gastric MALT lymphomas may progress rapidly if unresponsive to *H pylori* eradication therapy, this information is invaluable for the physician who must select a first-line treatment.

It has been demonstrated that the growth of MALT lymphomas requires the help of *H pylori*-reactive tumor-infiltrating T-cells. For effective communication between T-cells and neoplastic B-cells, two subsets of co-stimulatory molecules, CD80 (B7.1) and CD86 (B7.2), of the neoplastic B-cells should interact with CD28 or CTLA-4 of the

T-cells^[23]. However, the precise role of CD80 and CD86 molecules in the signaling of B-cells remains unclear. In earlier studies, the CD28-CTLA4/B7-signaling pathway was found to be involved in the proliferation and differentiation of B-cells^[24,25]. There is also evidence that CD86 may promote proliferation and immunoglobulin synthesis of normal B-cells and malignant B cells^[26]. Compared with CD86, CD80 delivered a down-regulator signal for B-cell response^[26]. In a recent study of low-grade gastric MALT lymphomas, the expression of CD86 was significantly associated with *H pylori*-dependence, while CD80 and CD40 and their ligands were not^[27]. These results are in line with our observation that the co-stimulatory molecule CD86 is present in high-grade gastric MALT lymphomas, and is also significantly associated with *H pylori*-dependence. Our findings support the notion that the growth of a substantial portion of early-stage high-grade gastric MALT lymphomas, as well as their low-grade counterparts, remains dependent on functional B-cell/T-cell interaction.

In addition to promoting the proliferation and differentiation of malignant B-cell clones, tumor-infiltrating T-cells in low-grade gastric MALT lymphomas are found to be defective in both perforin-mediated cytotoxicity and Fas-Fas ligand mediated apoptosis^[28]. On the other hand, the tumor tissues of high-grade MALT lymphomas appear to contain a much higher number of apoptotic lymphoma cells and CD8+ cytotoxic T lymphocytes (CTLs)^[21]. Study using a murine model demonstrated that Th-1 response and CD8+ CTLs activity were strongly inhibited in the presence of persistent gastric *H pylori* infection^[29]. Moreover, activated CD8+ CTLs may compete with CD56 (+) NK cells and downregulate the function of the latter^[17]. Besides regulating the differentiation of CD8+ CTLs, CD56 (+) NK cells may have an equally important role in immune regulation, where they limit the host response to foreign antigens and prevent autoimmunity^[18]. Recently, it has been demonstrated that CD56 (+) NK cells can be functionally activated by co-stimulatory molecules through the interaction of their activation receptor and CD86 on target cells, and thereby limit the extent of *H pylori*-related auto-reactive and neoplastic B lymphoid cells in the stomach^[30]. In the current study, we found that *H pylori*-dependent high-grade MALT lymphomas showed significantly increased infiltration of CD56 (+) NK cells compared to *H pylori*-independent lymphomas. Interestingly, we also found that CD86 positive MALT lymphomas showed significantly increased infiltration of CD56 (+) NK cells compared to CD86-negative cases. These findings suggest that the loss of *H pylori*-dependence may be associated with a change in the immunological microenvironment, including a shift towards a Th-1 response that enhances the activity of CD8+ CTLs, and decreases the activity of CD56 (+) NK cells.

In conclusion, the expression of co-stimulatory marker CD86 on lymphoma cells and the increased infiltration of CD56 (+) NK cells in tumor tissues are useful markers in the identification of *H pylori*-dependent tumors and in the selection of patients for first-line *H pylori* eradication therapy.

REFERENCES

- 1 Chan JK, Ng CS, Isaacson PG. Relationship between high-grade lymphoma and low-grade B-cell lymphoma of mucosa-associated lymphoid tissue (MALToma) of the stomach. *Am J Pathol* 1990; **136**: 1153-1164
- 2 Harris NL, Jaffe ES, Stein H, Banks PM, Chan JK, Cleary ML, Delsol G, De Wolf-Peeters C, Falini B, Gatter KC. A revised European-American classification of lymphoid neoplasms: A proposal from the International Lymphoma Study Group. *Blood* 1994; **84**: 1361-1392
- 3 de Jong D, Boot H, van Heerde P, Hart GA, Taal BG. Histological grading in gastric lymphoma: Pretreatment criteria and clinical relevance. *Gastroenterology* 1997; **112**: 1466-1474
- 4 Wotherspoon AC, Dogliani C, Diss TC, Pan L, Moschini A, de Boni M, Isaacson PG. Regression of primary low-grade B-cell gastric lymphoma of mucosa-associated lymphoid tissue type after eradication of *Helicobacter pylori*. *Lancet* 1993; **342**: 575-577
- 5 Du MQ, Isaacson PG. Gastric MALT lymphoma: from aetiology to treatment. *Lancet Oncol* 2002; **3**: 97-104
- 6 Boot H, De Jonge D. Gastric lymphoma: the revolution of the past decade. *Scand J Gastroenterol* 2002; **236** (Suppl): 27-36
- 7 Bayerdorffer E, Neubauer A, Rudolph B, Thiede C, Lehn N, Eidt S, Stolte M. Regression of primary low-grade B-cell gastric lymphoma of mucosa-associated lymphoid tissue type after cure of *Helicobacter pylori* infection. *Lancet* 1995; **345**: 1591-1594
- 8 Neubauer A, Thiede C, Morgner A, Alpen B, Ritter M, Neubauer B, Wundisch T, Ehninger G, Stolte M, Bayerdorffer E. Cure of *Helicobacter pylori* infection and duration of remission of low-grade gastric mucosa associated lymphoid tissue lymphoma. *J Natl Cancer Inst* 1997; **89**: 1350-1355
- 9 Zucca E, Roggero E, Pileri S. B-cell lymphoma of MALT type: A review with special emphasis on diagnostic and management problems of low-grade gastric tumors. *Br J Haematol* 1998; **100**: 3-14
- 10 Morgner A, Miehle S, Fischbach W, Schmitt W, Muller-Hermelink H, Greiner A, Thiede C, Schetelig J, Neubauer A, Stolte M, Ehninger G, Bayerdorffer E. Complete remission of primary high-grade B cell gastric lymphoma after cure of *Helicobacter pylori* infection. *J Clin Oncol* 2001; **19**: 2041-2048
- 11 Nakamura S, Matsumoto T, Suekane H, Takeshita M, Hizawa K, Kawasaki M, Yao T, Tsuneyoshi M, Iida M, Fujishima M. Predictive value of endoscopic ultrasonography for regression of gastric low grade and high-grade MALT lymphomas after eradication of *Helicobacter pylori*. *Gut* 2001; **48**: 454-460
- 12 Chen LT, Lin JT, Shyu RY, Jan CM, Chen CL, Chiang IP, Liu SM, Su JJ, Cheng AL. Prospective study of *Helicobacter pylori* eradication therapy in stage I_E high-grade mucosa-associated lymphoid tissue lymphoma of the stomach. *J Clin Oncol* 2001; **19**: 4245-4251
- 13 Kuo SH, Chen LT, Yeh KH, Wu MS, Hsu HC, Yeh PY, Mao TL, Chen CL, Doong SL, Lin JT, Cheng AL. Nuclear expression of BCL10 or nuclear factor kappa B predicts *Helicobacter pylori*-independent status of early-stage, high-grade gastric mucosa-associated lymphoid tissue lymphomas. *J Clin Oncol* 2004; **22**: 3491-3497
- 14 Hussell T, Isaacson PG, Crabtree JE, Spencer J. *Helicobacter pylori* specific tumor infiltrating T-cells provide contact dependent help for the growth of malignant B-cells in low-grade gastric lymphoma of mucosa-associated lymphoid tissue. *J Pathol* 1996; **178**: 122-127
- 15 Hauer AC, Finn TM, MacDonald TT, Spencer J, Isaacson PG. Analysis of TH1 and TH2 cytokine production in low-grade B-cell gastric MALT-type lymphomas stimulated in vitro with *Helicobacter pylori*. *J Clin Pathol* 1997; **50**: 957-959
- 16 Greiner A, Knorr C, Qin Y, Sebald W, Schimpl A, Banchereau J, Muller-Hermelink HK. Low-grade B-cell lymphomas of mucosa-associated lymphoid tissue (MALT-type) require CD40-mediated signalling and Th2-type cytokines for *in vitro* growth and differentiation. *Am J Pathol* 1997; **150**: 1583-1593
- 17 Vyth-Dreese FA, Boot H, Dellemijn TA, Majoor DM, Oomen LC, Laman JD, Van Meurs M, De Weger RA, De Jong D. Localization *in situ* of costimulatory molecules and cytokines in B-cell non-Hodgkin's lymphoma. *Immunology* 1998; **94**:

580-586

- 18 **Kos FJ**, Engleman EG. Immune regulation: a critical link between NK cells and CTLs. *Immunol Today* 1996; **17**: 174-176
- 19 **Horwitz DA**, Gray JD, Ohtsuka K, Hirokawa M, Takahashi T. The immunoregulatory effects of NK cells: the role of TGF-beta and implication for autoimmunity. *Immunol Today* 1997; **18**: 538-542
- 20 **Biron CA**, Nguyen KB, Pien GC, Cousens LP, Salazar-Mather TP. Natural killer cells in antiviral defense function and regulation by innate cytokines. *Annu Rev Immunol* 1999; **17**: 189-220
- 21 **Guidoboni M**, Doglioni C, Laurino L, Boiocchi M, Dolcetti R. Activation of infiltrating cytotoxic T lymphocytes and lymphoma cell apoptotic rates in gastric MALT lymphomas: Differences between high-grade and low-grade cases. *Am J Pathol* 1999; **155**: 823-829
- 22 **Musshoff K**. Klinische Stadieneinteilung der nicht-Lymphome. *Strahlentherapie Onkol* 1977; **153**: 218-221
- 23 **Guindi M**. Role of activated host T cells in the promotion of MALT lymphoma growth. *Semin Cancer Biol* 2000; **10**: 341-344
- 24 **Boussiotis VA**, Freeman GJ, Gribben JG, Nadler LM. The role of B7-1/B7-2: CD28/CTLA4 pathways in the prevention of anergy, induction of productive immunity and down-regulation of the immune response. *Immunol Rev* 1996; **153**: 5-26
- 25 **Ikemizu S**, Gilbert RJ, Fennelly JA, Collins AV, Harlos K, Jones EY, Stuart DI, Davis SJ. Structure and dimerization of a soluble form of B7-1. *Immunity* 2000; **12**: 51-60
- 26 **Suvas S**, Singh V, Sahdev S, Vohra H, Agrewala JN. Distinct Role of CD80 and CD86 in the Regulation of the Activation of B Cell and B Cell Lymphoma. *J Biol Chem* 2002; **277**: 7766-7775
- 27 **de Jong D**, Vyth-Dresse F, DelleMijn T, Verra N, Ruskone-Fourmestreaux A, Lavergne-Slove A, Hart G, Boot H. Histological and immunological parameters to predict treatment outcome of *Helicobacter pylori* eradication in low-grade gastric MALT lymphoma. *J Pathol* 2001; **193**: 318-324
- 28 **D'Elia MM**, Amedei A, Manghetti M, Costa F, Baldari CT, Quazi AS, Telford JL, Romagnani S, Del Prete G. Impaired T-cell regulation of B-cell growth in *Helicobacter pylori*-related gastric low-grade MALT lymphoma. *Gastroenterology* 1999; **117**: 1105-1112
- 29 **Shirai M**, Arichi T, Nakazawa T, Berzofsky JA. Persistent infection by *Helicobacter pylori* down-modulates virus-specific CD8+ cytotoxic T cells response and prolongs viral infection. *J Infect Dis* 1998; **177**: 72-80
- 30 **Wilson JL**, Charo J, Martin-Fontecha A, Dellabona P, Casorati G, Chambers BJ, Kiessling R, Bejarano MT, Ljunggren HG. NK cells triggering by the human costimulatory molecules CD80 and CD86. *J Immunol* 1999; **163**: 4207-4212

Science Editor Guo SY Language Editor Elsevier HK

• *Helicobacter pylori* •

Effect of *Helicobacter pylori* infection on *p53* expression of gastric mucosa and adenocarcinoma with microsatellite instability

Jian-Hua Li, Xian-Zhe Shi, Shen Lv, Min Liu, Guo-Wang Xu

Jian-Hua Li, Shen Lv, Min Liu, Laboratory of Molecular Biology, the Second Hospital of Dalian Medical University, Dalian 116027, Liaoning Province, China

Xian-Zhe Shi, Guo-Wang Xu, National Chromatographic Research and Application Center, Dalian Institute of Chemical Physics, The Chinese Academy of Sciences, Dalian 116011, Liaoning Province, China

Correspondence to: Professor Shen Lv, PhD, Laboratory Center of Molecular Biology, the Second Hospital of Dalian Medical University, Dalian 116027, Liaoning Province, China. lijianhua_ljh@126.com
Telephone: +86-411-84687554

Received: 2004-10-26 Accepted: 2004-12-03

Abstract

AIM: To investigate the relationship between *Helicobacter pylori* (*H pylori*) infection, microsatellite instability and the expressions of the *p53* in gastritis, intestinal metaplasia and gastric adenocarcinoma and to elucidate the mechanism of gastric carcinogenesis relating to *H pylori* infection.

METHODS: One hundred and eight endoscopic biopsies and gastric adenocarcinoma were available for the study including 33 cases of normal, 45 cases of gastritis, 30 cases of intestinal metaplasia, and 46 cases of gastric adenocarcinoma. Peripheral blood samples of these patients were also collected. *H pylori* infection and *p53* expressions were detected by means of streptavidin-peroxidase (SP) immunohistochemical method. Microsatellite loci were studied by PCR-SSCP-CE using the markers BAT-26, D17S261, D3S1283, D2S123, and D3S1611. MSI was defined as the peak shift in the DNA of the gastric tissue compared with that of the peripheral blood samples. Based on the number of mutated MSI markers, specimens were characterized as high MSI (MSI-H) if they manifested instability at two or more markers, low MSI (MSI-L) if unstable at only one marker, and microsatellite stable (MSS) if they showed no instability at any marker.

RESULTS: *H pylori* infection was detected in the samples of gastritis, intestinal metaplasia, and gastric adenocarcinoma and the infection frequencies were 84.4%, 76.7%, and 65.2%, respectively, whereas no *H pylori* infection was detected in the samples of normal control. There was a significant difference in the infection rates between gastritis and carcinoma samples ($P = 0.035$). No MSI was detected in gastritis samples, one MSI-H and two MSI-L were detected among the 30 intestinal metaplasia samples, and 12 MSI-H and 3 MSI-L were detected in the 46 gastric carcinomas. In those gastric carcinomas, the MSI-H frequency in *H pylori*-positive group was significantly higher than that in *H pylori*-

negative group. No *p53* expression was detected in the normal and gastritis samples from dyspeptic patients. *p53*-positive immunohistochemical staining was detected in 13.3% of intestinal metaplasia samples and in 43.5% of gastric carcinoma samples. The levels of *p53* in *H pylori*-positive samples were higher than those in the negative group when the carcinoma samples were subdivided into *H pylori*-positive and -negative groups ($P = 0.013$). Eight samples were detected with positive *p53* expression out of the 11 MSI-H carcinomas with *H pylori* infection and no *p53* expression could be seen in the *H pylori*-negative samples.

CONCLUSION: *H pylori* affect the *p53* pattern in gastric mucosa when MMR system fails to work. Mutations of the *p53* gene seem to be an early event in gastric carcinogenesis.

© 2005 The WJG Press and Elsevier Inc. All rights reserved.

Key words: Dyspepsia; *H pylori*; Gastric cancer; MSI; *p53*

Li JH, Shi XZ, Lv S, Liu M, Xu GW. Effect of *Helicobacter pylori* infection on *p53* expression of gastric mucosa and adenocarcinoma with microsatellite instability. *World J Gastroenterol* 2005; 11(28): 4363-4366

<http://www.wjgnet.com/1007-9327/11/4363.asp>

INTRODUCTION

Gastric cancer is one of the most common forms of malignant tumors in adults and is the leading cause of death from carcinomas in China. A close association between *Helicobacter pylori* (*H pylori*) and gastric cancer has been found^[1,2], mainly on the basis of epidemiological data. Although *H pylori* has been classified as a type I carcinogen for gastric cancer by the International Agency for Research on Cancer (IARC), the exact pathway has remained indistinct^[3,4]. It has been known that some gastric carcinomas are characterized by microsatellite instability resulting from defect of mismatch repair. Mismatch repair genes, as house keeping genes, have a central role in maintaining genomic stability by repairing DNA replication errors and inhibiting recombination between non-identical sequences. Loss of MMR genes causes destabilization of the genome and results in high mutation rates, which predisposes human to diverse cancers including gastric carcinoma^[5-7]. The *p53* protein is a transcriptional factor that arrests the cell cycle in the G1 phase when DNA is damaged by inducing the expression of the p21 protein, an inhibitor of Cdk kinase and PCNA^[8,9]. Thus, damaged

DNA cannot replicate, allowing time for the repair system to act^[8]. If this system fails, *p53* induces apoptosis by transactivation of the *bax* gene^[10]. Both mismatch repair and suppressor are two main pathways involved in the tumorigenesis of gastric carcinoma. In this study, we examine microsatellite instability and *p53* protein accumulation in patients with *H pylori*-infected gastric mucosa and in patients with gastric adenocarcinoma to elucidate whether any relationship exists between these genetic alterations and *H pylori* infection.

MATERIALS AND METHODS

Patients

One hundred and eight dyspeptic patients (65 men and 43 women; median age, 46 years; range, 20-73 years) undergoing upper endoscopy, and 46 consecutive patients (29 men and 17 women; median age, 56 years; range, 32-69 years) who underwent surgical excision for gastric adenocarcinoma at the hospitals of Dalian area entered the study. Peripheral blood samples of these patients were also collected. The ethical approval for this study was granted by the Local Research Ethics Committee. Endoscopic biopsies were removed with standard gastric biopsy forceps and then cut in half with sterile scalpel blades. Half the biopsy sample was fixed in 10% buffered neutral formalin and embedded in paraffin and serial sections (4- μ m thick), while the other half was stored at -80 °C. Hematoxylin-eosin (HE) staining was used for the histopathological diagnosis. Among the 108 endoscopic biopsies, 33 samples were normal, 45 samples were gastritis and 30 samples were intestinal metaplasia.

DNA extraction

DNA was extracted from the frozen gastric tissues and peripheral leukocytes using a regular phenol-chloroform method and stored at -20 °C until use.

Microsatellite analysis

Microsatellite instability was studied using five markers (Table 1), PCR was performed in 12.5 μ L of reaction mixture containing 1.5 mmol/L MgCl₂, 200 μ mol/L each dNTP, 0.5 Unit ampli Taq polymerase (TaKaRa Biotech., Dalian, China), 0.5 μ mol/L of each primer, and 50 ng genomic DNA. The reaction was carried out in a thermal cycler (Perkin-Elmer Model 2700, CA, USA) at 94 °C for 30 s, 58-60 °C for 30 s, and 72 °C for 30 s, for 35 cycles with an initial denaturation step of 94 °C for 5 min and a final extension step of 72 °C for 5 min. 0.5 μ L each PCR product was mixed with 1 μ L GeneScan 500 size standard and 12 μ L water, and heated at 95 °C for 10 min, then immediately put into ice water and kept for 5 min. Microsatellite was analyzed by an ABI PRISM 310 (Perkin-Elmer, ABI Prism) with 6% SLP and 8 mol/L urea as sieving medium under constant voltage 15 kV at 60 °C. Single-stranded microsatellite fragments were detected by LIF and the data were collected and analyzed by GeneScan. MSI was defined as the peak shift in the DNA of the gastric tissue compared with that of the peripheral blood samples. Based on the number of mutated MSI markers, specimens were characterized as high MSI (MSI-H) if they manifested instability at two or more markers, low MSI (MSI-L) if unstable at only one

marker, and microsatellite stable (MSS) if they showed no instability at any marker.

Table 1 Primers of microsatellite markers

Markers	Primers	T _m (°C)
BAT-26	5'-FAM-TGACTACTTTTGACTTCAGCC 5'-AACCATTCAACATTTTAAACCC	58
D17S261	5'-HEX-AGGGATACTATTCAGCCCGAGGTG 5'-ACTGCCACTCCTTGCCCATTC	60
D3S1283	5'-TET-GGCAGTACCACCTGTAGAAATG 5'-GAGTAACAGAGGCATCGTGTATTTC	60
D2S123	5'-FAM-AAACAGGATGCCTGCCTTTA 5'-GGACTTCCACCTATGGGAC	60
D3S1611	5'-HEX-CCCCAAGGCTGCACTT 5'-AGCTGAGACTACAGGCATTTG	60

Immunohistochemical staining

Immunostaining was performed using the streptavidin-peroxidase (SP) method as previously described by Lan *et al.* Negative control sections were processed in the same manner, replacing the primary antibody with buffered saline. A total of 300 cells were counted in random fields from representative areas and the immunoreactive cells were assessed and expressed as percentages. Samples with *p53* staining in more than 10% were considered positive (the nuclei, staining brown-yellow). However, the *H pylori* immunostaining was assessed positive as long as the brown-black dotish were stained on the surface of mucosa.

Statistical analysis

The χ^2 test and the Fisher's exact probability test were used to compute the frequencies by SPSS 12.0 for Windows. $P < 0.05$ was considered to be statistically significant.

RESULTS

H pylori status

Sixty-one of the 108 (56.5%) dyspeptic patients and 30 of the 46 (65.2%) gastric cancer patients showed *H pylori* infection. None of the normal gastric mucosa was infected with *H pylori*. The infection rates of gastritis, intestinal metaplasia and tumor samples were largely more than the normal. χ^2 tests also revealed a significant difference in the infection rates between gastritis and carcinoma samples ($P = 0.035$, Table 2).

Table 2 *H pylori* infection in the normal, gastritis, intestinal metaplasia, and tumor samples

Tissue type	Number of samples	Infection number of <i>H pylori</i>	Infection rates (%)
Normal	33	0	0
Gastritis	45	38	84.4
Intestinal metaplasia	30	23	76.7
Carcinoma	46	30	65.2

Microsatellite analysis

In the 33 normal and 45 gastritis samples, no microsatellite status shift was detected. One MSI-H and two MSI-L were

Table 3 MSI frequency according to *H pylori* status

MSI frequency	<i>H pylori</i> positive (30)	<i>H pylori</i> negative (16)	P ¹
MSI-H (12)	36.7% (11/30)	6.3% (1/16)	0.035
MSI-L (3)	6.7% (2/30)	6.25 % (1/16)	1.000

¹*H pylori* positive vs *H pylori* negative.

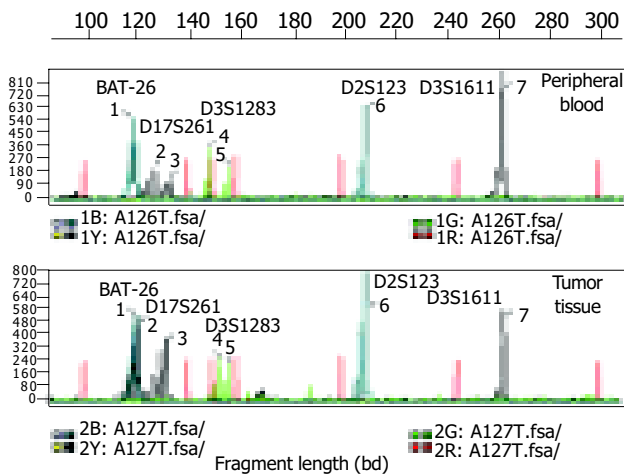


Figure 1 Electropherograms of five microsatellite loci in the peripheral blood sample and tumor tissue of one gastric cancer patient. Red peaks: interval standard peaks.

detected among the 30 samples of intestinal metaplasia, whereas in the 46 gastric carcinomas, 12 MSI-H and 3 MSI-L were detected. The MSI status was significantly higher in *H pylori* positive samples of carcinomas than that in *H pylori* negative samples of carcinomas (Table 3 and Figure 1).

p53 overexpression

No *p53* expression was detected in the normal and gastritis

Table 4 P53 expression with regard to *H pylori* status in carcinomas

<i>H pylori</i> status	P53 positive (20)	P
<i>H pylori</i> positive (30)	17	0.013 ¹
<i>H pylori</i> negative (16)	3	

¹*H pylori* positive vs *H pylori* negative.

samples from dyspeptic patients. Four of the 30 intestinal metaplasia samples showed *p53*-positive immunohistochemical staining, and in the 46 patients with gastric cancer, 20 (43%) *p53*-positive samples were identified. Eight manifested *p53* positivity out of the 11 MSI-H carcinomas with *H pylori* infection and no *p53* expression could be seen in the *H pylori*-negative group. When the carcinoma samples were subdivided into *H pylori*-positive and -negative groups, immunohistochemical staining revealed that the levels of *p53* in *H pylori*-positive samples were higher than those in the negative samples ($P = 0.013$, Tables 4 and 5, Figures 2A and B).

DISCUSSION

Both genetic and environmental factors are crucial in gastric cancer development and progression. *H pylori* infection has been documented as an important risk factor for gastric cancer^[12]. It is fully agreed that the bacterium is effectively able to induce chronic mucosal injury with increased mucosal proliferation that could facilitate malignant transformation^[13-15]. In this study, we detected a high infection rate of *H pylori* in both dyspeptic samples and gastric adenocarcinoma samples, which is consistent with the documents^[16,17]. The reason why infection rate was significantly higher in gastritis samples than that in carcinoma samples is probable that *H pylori* density is lower in atrophic gastritis mucosa and very low in the intestinal metaplasia and in patients with gastric cancer, the degree of atrophic gastritis and intestinal metaplasia is

Table 5 Length of representative fragments of five microsatellite loci in the normal tissue and peripheral blood sample of the gastric cancer patient

Peak no.	BAT-26 1 [†] (bp)	D17S261		D3S1283		D2S123 6 [†] (bp)	D3S1611 7 [†] (bp)
		2 [†] (bp)	3 [†] (bp)	4 [†] (bp)	5 [†] (bp)		
Normal	119.15	127.52	133.78	149.12	147.25	209.42	262.76
Tumor	120.30	121.63	131.45	143.23	147.36	209.30	262.85

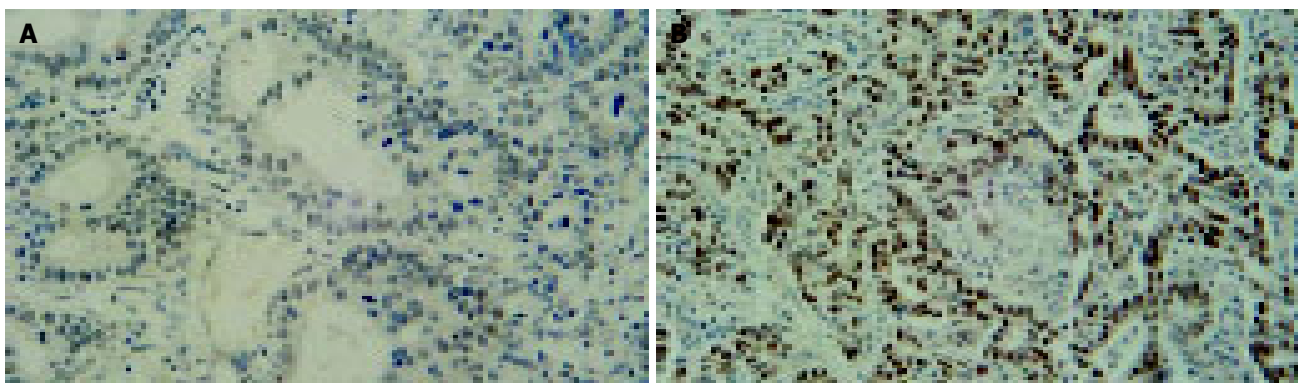


Figure 2 p53 in the normal and gastric carcinoma samples. **A:** p53-Negative staining in normal gastric glands from a dyspeptic patient, **B:** gastric carcinoma

showing nuclear p53 immunoreactivity.

higher than in patients without cancer. Another reason may be that different strains contribute differently to the occurrence of gastritis or gastric carcinoma, and it is not adequate to compare *H pylori* infection only by histology.

Epithelial cell proliferation is not carcinogenic in itself. It is likely that *H pylori* promote neoplastic transformation in combination with additional factors. In this study, we detected microsatellite instability and p53 protein expression in accordance with the development from gastric gastritis, intestinal metaplasia to gastric cancer with regard to *H pylori* infection status.

Microsatellites are short sequences of tandem repeats dispersed throughout the mammalian genome. Repeat units range from 1 to 4 bp in length, and the entire sequence of a typical repeat tract is less than 100 bp long^[18,19]. Microsatellite instability is characterized by the insertion or deletion of one or more repeat units, which is caused by a failure of the DNA-MMR system to repair errors that occur during the replication of DNA^[20]. MSI has been regarded as one of the most important indication of MMR defect. In this study, we detected five microsatellite loci sensitive to gastric cancer and found MSI-H in 26% carcinoma samples. The frequency of MSI-H in *H pylori*-positive group was significantly higher than that in *H pylori*-negative group. Among gastritis and intestinal metaplasia samples, the MSI-H frequency was 0% and 3% respectively although with higher *H pylori* infection. MSI existed in intestinal metaplasia samples although the frequency was much lower than that in carcinoma samples. That is to say, MMR defect happened before the malignant transformation of gastric mucous membrane cells. These results together indicated that *H pylori* infection induce tumorigenesis of gastric carcinoma when MMR system of gastric mucosa fails to work functionally.

It has been proved that wild type p53 protein can induce cell apoptosis but the intracellular accumulation of mutant p53 protein can inhibit cell apoptosis and promote cell transformation and proliferation, resulting in carcinogenesis. The overexpression of p53 protein is generally mutant forms, for the half-life of wild-type p53 is very short and p53 protein expression is usually negative in normal tissues. In our present study, p53 expressions were found in 0% of the control, 0% of gastritis samples, 13.3% of intestinal metaplasia samples and 43% gastric carcinomas samples. The detection of p53 expression in intestinal metaplasia indicates that p53 mutation can be an early event in the pathogenesis of gastric cancer. When the carcinomas samples were subdivided into *H pylori*-positive and -negative, and the positive rates of their p53 expression compared, we found a higher expression rate in *H pylori*-positive group than that in *H pylori*-negative group. The carcinoma samples from MSI study were also analyzed to determine whether there was any relationship with p53 protein accumulation. No significant difference was shown to exist between samples in terms of their MSI status and p53 expression. Nevertheless, MSI was found in 11 with *H pylori* infection, 8 manifested p53 positive, this suggests that *H pylori* infection may play a role by inducing p53 gene mutations in those MSI or MMR defect gastric mucosa, but only in certain individuals.

In conclusion, the association between *H pylori* infection, MSI and p53 mutations observed in intestinal metaplasia and gastric carcinoma samples leads us to hypothesize that *H pylori* affect p53 pattern in gastric mucosa when MMR system fails to work. Mutations of the p53 gene seem to be an early event in gastric carcinogenesis.

REFERENCES

- 1 Xia HH, Talley NJ. Apoptosis in gastric epithelium induced by *Helicobacter pylori* infection: implications in gastric carcinogenesis. *Am J Gastroenterol* 2001; **96**: 16-26
- 2 Meining A, Bayerdorffer E, Stolte M. Extent, topography and symptoms of *Helicobacter pylori* gastritis. Phenotyping for accurate diagnosis and therapy? *Pathologie* 2001; **22**: 13-18
- 3 Fujioka T, Honda S, Tokieda M. *Helicobacter pylori* infection and gastric carcinoma in animal models. *J Gastroenterol Hepatol* 2000; **15**(Suppl): D55-59
- 4 International Agency for research on Cancer. Schistosomes, Liver flukes and *Helicobacter pylori*. Evaluation of carcinogenic risks to humans. *IARC Monograph Evaluating Carcinogenic Risks to Humans* 1994; **61**: 1-241
- 5 Jacob S, Praz F. DNA mismatch repair defects: role in colorectal carcinogenesis. *J Biochimie* 2002; **84**: 27-47
- 6 Coleman WB, Tsongalis GJ. The role of genomic instability in human carcinogenesis. *Anticancer Res* 1999; **19**: 4645-4664
- 7 Duval A, Hamelin R. Genetic instability in human mismatch repair deficient cancers. *Ann Genet* 2002; **45**: 71-75
- 8 Kastan MB, Onyekwere O, Sidransky D, Vogelstein B, Craig RW. Participation of p53 protein in the cellular response to DNA damage. *Cancer Res* 1991; **51**: 6304-6311
- 9 Chen J, Jackson PK, Kirschner MW, Dutta A. Separate domains of p21 involved in the inhibition of Cdk kinase and PCNA. *Nature* 1995; **374**: 386-388
- 10 Waga S, Hannon GJ, Beach D, Stillman B. The p21 inhibitor of cyclin-dependent kinases controls DNA replication by interaction with PCNA. *Nature* 1994; **369**: 574-578
- 11 Miyashita T, Reed JC. Tumor suppressor p53 is a direct transcriptional activator of the human bax gene. *Cell* 1995; **80**: 293-299
- 12 Fuchs CS, Mayer RJ. Gastric carcinoma. *N Engl J Med* 1995; **333**: 32-41
- 13 Parente F, Caselli M, Bianchi Porro G. Gastric apoptosis and *Helicobacter pylori* infection: an intricate matter. *Scand J Gastroenterol* 2001; **2**: 113-115
- 14 Parsonnet J, Friedman GD, Vandersteen DP, Chang Y, Vogelman JH, Orentreich N, Sibley RK. *Helicobacter pylori* infection and the risk of gastric carcinoma. *N Engl J Med* 1991; **325**: 1127-1131
- 15 Blaser MJ, Chyou PH, Nomura A. Age at establishment of *Helicobacter pylori* infection and gastric carcinoma, gastric ulcer, and duodenal ulcer risk. *Cancer Res* 1995; **55**: 562-565
- 16 Berloco P, Russo F, Cariola F, Gentile M, Giorgio P, Caruso ML, Valentini AM, Di Matteo G, Di Leo A. Low presence of p53 abnormalities in *H pylori*-infected gastric mucosa and in gastric adenocarcinoma. *J Gastroenterol* 2003; **38**: 28-36
- 17 Wang XW, Tseng A, Ellis NA, Spillare EA, Linke SP, Robles AI, Seker H, Yang Q, Hu P, Beresten S, Bemmels NA, Garfield S, Harris CC. Functional interaction of p53 and BLM DNA helicase in apoptosis. *J Biol Chem* 2001; **276**: 32948-32955
- 18 Aaltonen LA, Peltomaki P, Leach FS, Sistonen P, Pylkkanen L, Mecklin JP, Jarvinen H, Powell SM, Jen J, Hamilton SR, Leach FS. Clues to the pathogenesis of familial colorectal cancer. *Science* 1993; **260**: 812-816
- 19 Bowcock A, Osborne-Lawrence S, Barnes R, Chakravarti A, Washington S, Dunn C. Microsatellite polymorphism linkage map of human chromosome 13q. *Genomics* 1993; **15**: 376-386
- 20 Harfe BD, Robintson SJ. DNA mismatch repair and genetic instability. *Annu Rev Genet* 2000; **34**: 359-399

• CLINICAL RESEARCH •

Sensory-motor responses to mechanical stimulation of the esophagus after sensitization with acid

Asbjørn Mohr Drewes, Hariprasad Reddy, Camilla Staahl, Jan Pedersen, Peter Funch-Jensen, Lars Arendt-Nielsen, Hans Gregersen

Asbjørn Mohr Drewes, Hariprasad Reddy, Camilla Staahl, Jan Pedersen, Hans Gregersen, Center for Biomechanics and Pain, Department of Gastroenterology, Aalborg Hospital, Aarhus University Hospital, Aalborg, Denmark

Lars Arendt-Nielsen, Center for Sensory-Motor Interactions (SMI), Department of Health Science and Technology, Aalborg University, Aalborg, Denmark

Peter Funch-Jensen, Department of Surgical Gastroenterology L, Aarhus University Hospital, Aarhus, Denmark

Supported by the "Det Obelske Familiefond", "Spar Nord Fonden" and the Danish Technical Research Council

Correspondence to: Professor Asbjørn Mohr Drewes, MD, PhD, DMSc, Center for Biomechanics and Pain, Department of Medical Gastroenterology, Aalborg Hospital, DK-9000 Aalborg, Denmark. drewes@smi.auc.dk

Telephone: +45-99322505 Fax: +45-99322503

Received: 2004-11-09 Accepted: 2004-12-23

the sensory pathways and facilitates secondary contractions. The new model can be used to study abnormal sensory-motor mechanisms in visceral organs.

© 2005 The WJG Press and Elsevier Inc. All rights reserved.

Key words: Esophagus; Mechanical; Sensitization; Motility; Reflux; Pain

Drewes AM, Reddy H, Staahl C, Pedersen J, Funch-Jensen P, Arendt-Nielsen L, Gregersen H. Sensory-motor responses to mechanical stimulation of the esophagus after sensitization with acid. *World J Gastroenterol* 2005; 11(28): 4367-4374 <http://www.wjgnet.com/1007-9327/11/4367.asp>

Abstract

AIM: Sensitization most likely plays an important role in chronic pain disorders, and such sensitization can be mimicked by experimental acid perfusion of the esophagus. The current study systematically investigated the sensory and motor responses of the esophagus to controlled mechanical stimuli before and after sensitization.

METHODS: Thirty healthy subjects were included. Distension of the distal esophagus with a balloon was performed before and after perfusion with 0.1 mol/L hydrochloric acid for 30 min. An impedance planimetry system was used to measure cross-sectional area, volume, pressure, and tension during the distensions. A new model allowed evaluation of the phasic contractions by the tension during contractions as a function of the initial muscle length before the contraction (comparable to the Frank-Starling law for the heart). Length-tension diagrams were used to evaluate the muscle tone before and after relaxation of the smooth muscle with butylscopolamine.

RESULTS: The sensitization resulted in allodynia and hyperalgesia to the distension volumes, and the degree of sensitization was related to the infused volume of acid. Furthermore, a nearly 50% increase in the evoked referred pain was seen after sensitization. The mechanical analysis demonstrated hyper-reactivity of the esophagus following acid perfusion, with an increased number and force of the phasic contractions, but the muscle tone did not change.

CONCLUSION: Acid perfusion of the esophagus sensitizes

INTRODUCTION

Pain arising from the esophagus is very common clinically and in the normal population, but the mechanisms involved are poorly understood^[1]. Due to the difficulties in characterizing clinical pain, human experimental models have been developed to investigate the pain pathways in a standardized way in volunteers and patients. These models provide the possibility to control the stimulus parameters and to assess the response quantitatively^[2,3]. Furthermore, the nociceptive system can be sensitized in the laboratory, resulting in allodynia (painful sensations to stimuli that are not normally painful), hyperalgesia (increased sensation to stimuli that are normally painful) and increase in the evoked referred pain area^[4]. The sensitization most likely plays an important role in chronic visceral pain disorders^[3,5]. Experimental chemical stimulation with acid has been used to sensitize the esophagus^[6-8]. However, the literature has not been consistent with respect to the evoked mechanical hyperalgesia, probably due to methodological problems related to the stimulus modalities used^[9].

Distension of the gut is a physiologic stimulus, and consequently most researchers have used experimental balloon distension models to investigate basic pain mechanisms in the gastrointestinal (GI) tract^[10]. Most previous studies have used volume and pressure as proxies of the mechanical deformation and force applied to the gut wall^[10]. However, the mechanical parameters tension, stress and strain are of more value than pressure and volume when studying the esophagus, as these parameters provide more valid information about the mechanical forces and deformation (elastic properties) during distension^[11-15]. Furthermore, the muscle function is better evaluated when

the forces and tensions can be quantitated, rather than measuring the luminal pressure^[16-18]. However, the sensory-motor responses of the organ during a mechanical stimulus cannot be evaluated independently of the mechanical forces and deformation. Thus, phasic contractions and changes in muscle tone can influence the sensory response themselves^[18], and in diseases of the esophagus hyper-reactivity may give major contribution to the symptoms^[19,20]. Methods to estimate and control the mechanical response will thus allow better explanations of the effects on the sensory-motor response during the mechanical stimulations with and without sensitization of the pain system.

Systematic investigation of both the sensory and motor responses to controlled mechanical stimuli following experimental sensitization of the esophagus has to the best of our knowledge never been investigated. The aims of the current study were to (1) investigate the effect on sensitization of the esophagus with acid on the sensory response to controlled mechanical stimulation; (2) calculate the evoked referred pain areas to the mechanical stimulation before and after sensitization as a proxy for the central neuronal changes; and (3) evaluate the motor response to the sensitization by a new *in vivo* method evaluating the change in tension during contraction (the afterload tension) as function of the initial muscle length before the contraction (the preload radius).

MATERIALS AND METHODS

Thirty healthy subjects, 14 males and 16 females, mean age 36.5 ± 12.9 years, were included. The subjects did not suffer from any kind of chronic pain, GI symptoms or disturbances in personality. All subjects gave informed written and verbal consent prior to the study. The protocol was approved by the local ethics committee and performed in accordance with the Helsinki Declaration.

Mechanical stimulations

The impedance planimetry system including the principle for measurement of the cross-sectional area (CSA) has been described in detail previously^[18,21,22]. The 70-cm long probe with a diameter of 4.5 mm had a cylindrical large-sized bag near the tip. The bag was 40 mm in length and was made of 35- μ m thick, non-conducting polyester urethane. A side-hole for acid perfusion was placed 2 cm above the bag. The probe had a four-electrode impedance planimetry system with four sets of ring electrodes inside the bag (GMC Aps, Hornslet, Denmark). The bag could be inflated with electrically conducting fluid (0.09% saline) through a pair of infusion channels. The change in impedance of the fluid during distension of the bag reflects the change in the CSA^[18]. The infusion channels were connected to an infusion pump (Type 111, Ole Dich Instrument Makers, Hvidovre, Denmark) that was able to fill or empty the bag continuously. The bag could be inflated to a CSA of approximately 2 000 mm² (diameter equal to 50 mm) without stretching the wall of the bag. The fluid in the connecting tube between the pump and the probe was heated to 37 °C. A safety valve was connected with the pump allowing the subjects to stop the infusion at any time. The system was calibrated before

the probe was inserted into the esophagus. Non-linearity of the CSA was corrected for in the whole measurement range by means of a software feature. The pressure was measured by means of a low-compliance perfusion system connected to external transducers.

Sensory ratings

The sensory intensity was assessed continuously during the experiment using an electronic visual analog scale (VAS, GMC, Hornslet, Denmark). The volunteers were trained in assessment of sensation to deep pressure at the muscles on the right forearm several times before the visceral stimuli were given. A scale for both non-painful and painful sensations was used^[3]. The intensities of the *non-painful* sensations were scored with the following descriptors added to facilitate the scoring: 1 = vague perception of mild sensation; 2 = definite perception of mild sensation; 3 = vague perception of moderate sensation; 4 = definite perception of moderate perception; 5 = the pain threshold. For the *painful* sensations the patients used the scale from 5 to 10 anchored at 5 = pain threshold to 10 = unbearable pain, with the following anchor words: 6 = slight pain; 7 = moderate pain; 8 = medium pain intensity; 9 = intense pain; and 10 = unbearable pain. This part of the scale was red to clearly separate the non-painful and painful range of sensations. The first three distensions were used to practice the sensory ratings^[3]. The subjects were carefully instructed to score the evoked chest pain and to differentiate this from the unpleasantness in the throat caused by traction due to the distension-evoked esophageal contractions. The scale has previously been shown to be robust, and to discriminate sensations in the esophagus^[8,11,12], and the small and large intestine^[13,14,23,24].

After the last distension before butylscopolamine injection (see below) the volunteers were asked about referred pain to the chest or other remote areas evoked by the distensions at moderate pain (VAS = 7). If present the referred pain area was marked with a pen and transferred to a transparent paper. Later the area was digitized (ACECAD D900+ Digitizer, Taiwan) and the size calculated (Sigma-Scan, Jandel Scientific, Canada).

Protocol

The subjects fasted for at least 4 h prior to the experiment. Intubation was performed through the mouth. The bag was inserted into the stomach and then retracted to identify the location of the lower esophageal sphincter as a zone of high resting pressure that decreased with swallowing. Then the bag was placed 7 cm proximal to the sphincter and the probe was taped to the cheek. The subjects were asked to lie down with the head tilted by 30° after the placement of the bag. The experiment was performed in that position after 30 min of rest.

Three bag distension stimuli with a constant infusion rate of 25 mL/min were done to precondition the tissue and to obtain repeatable sensory data^[3,13,15,23,24]. The inter-stimulus interval was 60 s for all experiments. When the subjects reported slight pain (6 on the VAS), the bag was deflated using the same flow rate as during the inflation until it was empty. After these stimuli, two more distensions

were done at the same infusion rate. When moderate pain intensity (7 on the VAS) was reached, the pump was reversed and the bag deflated. Then 20 mg butylscopolamine was given intravenously and after abolishment of the contractile activity the two last distensions were repeated.

After the first series of mechanical stimuli, the participants underwent a modified acid perfusion test^[25]. Hence, during a perfusion channel in the catheter 0.1 mol/L hydrochloric acid was infused at a rate of 7 mL/min for 30 min. If the evoked sensations due to the acid stimulation were reported unpleasant (rated ≥ 5 on the VAS), the perfusion was stopped for 30 s and the subjects were allowed to swallow 10 mL water. In case the perfusion was too unpleasant for the subjects, it was stopped and the amount of infused acid was measured.

After the acid perfusion, bag distensions before and after butylscopolamine were given using the same protocol as described above, before acid perfusion.

During all stimuli autonomic reactions were monitored and displayed on-screen using a Biopac MP100 system (Biopac Systems Inc., Santa Barbara, CA, USA) including sensors and recording system for electrocardiogram, pulse rate and respiration.

Data analysis

The circumferential wall tension was calculated according to the law of Laplace for cylindrical structures as

$$T = \Delta P r$$

where T is the circumferential wall tension, r is the balloon radius, and ΔP is the transmural pressure. The geometry of the esophagus during distension can be considered circular except at very low pressure levels^[18]. Therefore, the radius was determined as

$$r = \sqrt{\frac{CSA}{\pi}}$$

All subjects stated that they more reliably rated the sensory intensity at the second distension compared to the first. Therefore, only data from the second distension were used in the analysis. After butylscopolamine the first distension was used as the maximal decrease in contractile activity was seen at the first few minutes after the injection.

As criteria for valid contractions before and after acid perfusion a pressure amplitude above 2.5 kPa was used.

In a representative sample of 10 subjects (5 males and 5 females, mean age 36.1 ± 14.3 years) the change in tension during individual distension-induced contractions (afterload tension) was computed and expressed as function of the radius immediately before the contractions (preload radius). The diagrams were made before and after perfusion of the distal esophagus with a mean of 123 mL hydrochloric acid. An example from an individual subject is shown in Figure 1. The data were fitted with a third order polynomial. These diagrams correspond to the well-known heart ventricular function curves in terms of the ventricular stroke working as function of the mean atrial length. Such curves demonstrate the Frank-Starling mechanism of the heart now adapted to the esophagus-see appendix.

The pressure and CSA data obtained between the evoked contractions (without infusion of butylscopolamine) were

used to compute the total tonic tension, whereas the tracings during butylscopolamine infusion were used for calculation of the passive tension. The active tonic tension was obtained by subtracting the passive tension from the total tonic tension^[14,18].

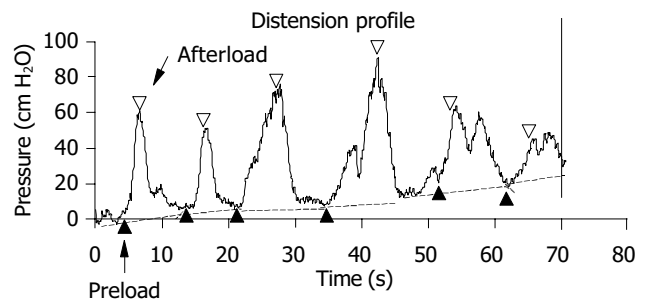


Figure 1 Raw data in a typical subject showing the change in pressure during bag-distension-induced contractions. The change in tension during maximal distension-induced contractions (afterload tension) was computed at the open triangles and expressed as function of the radius immediately before the contractions marked with solid triangles (preload radius). The radius was calculated on the basis of the CSA measured simultaneously. For details regarding the calculations see Methods section.

Statistical analysis

The results are expressed as mean \pm SD unless otherwise indicated. Continuous data were analyzed using t -tests. For multiple comparisons, two-way analysis of variance (ANOVA) was used with the factors: (1) before and after acid and (2) the different VAS levels. $P < 0.05$ was considered significant. The software package SPSS v. 10.0 was used for the statistical analysis.

RESULTS

Mechanical stimuli before and after acid

All subjects completed the experiment. After the preconditioning stimuli, the curve characteristics and sensory ratings were reproducible in all subjects. The stimulus-response curves after preconditioning the tissue are shown in Figure 2 for the infused volume, CSA, pressure, and tension. The sensation intensity was approximately linear as functions of all four stimulation variables. The sensory rating increased after acid, when expressed as a function of the volume ($F = 4.75$, $P = 0.03$), whereas no differences were found for the CSA ($F = 1.0$, $P = 0.3$), pressure ($F = 0.7$, $P = 0.4$) and tension ($F = 1.2$, $P = 0.3$). The curves during butylscopolamine infusion showed the same pattern as described above, before and after acid perfusion (data not shown).

The acid infusion resulted in a more hyper-reactive esophagus as the number of contractions with pressure amplitudes above 2.5 kPa during the distensions increased from 2.9 ± 1.5 to 3.5 ± 1.5 after acid perfusion ($P = 0.03$).

The change in tension during bag-distension-induced contractions (the afterload tension) was plotted as a function of the preload radius for 10 representative subjects (Figure 3). No contractions were observed at radii below 5 mm. Before acid infusion the afterload tension increased until a plateau was reached. This corresponds to the ‘Frank-Starling mechanism’ relating to the less interdigitation of

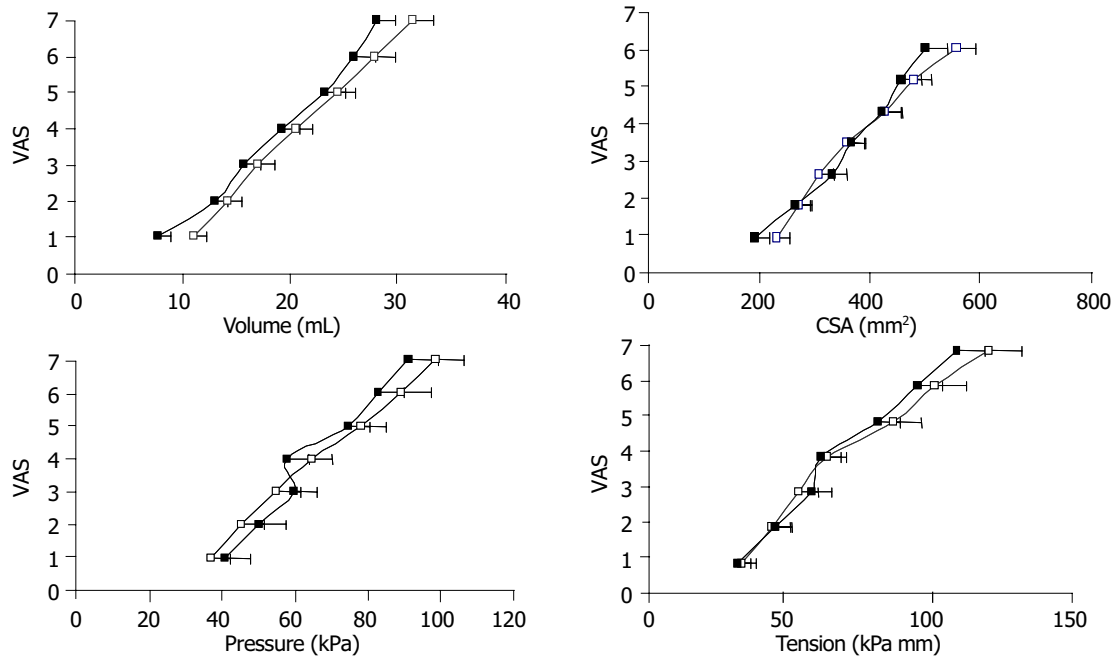


Figure 2 Sensory response to bag distension of the distal esophagus expressed as functions of the volume, CSA, pressure and tension. The curves were drawn before (□) and after (■) perfusion of the distal esophagus with acid. The

sensory response increased after acid perfusion when expressed as a function of the volume.

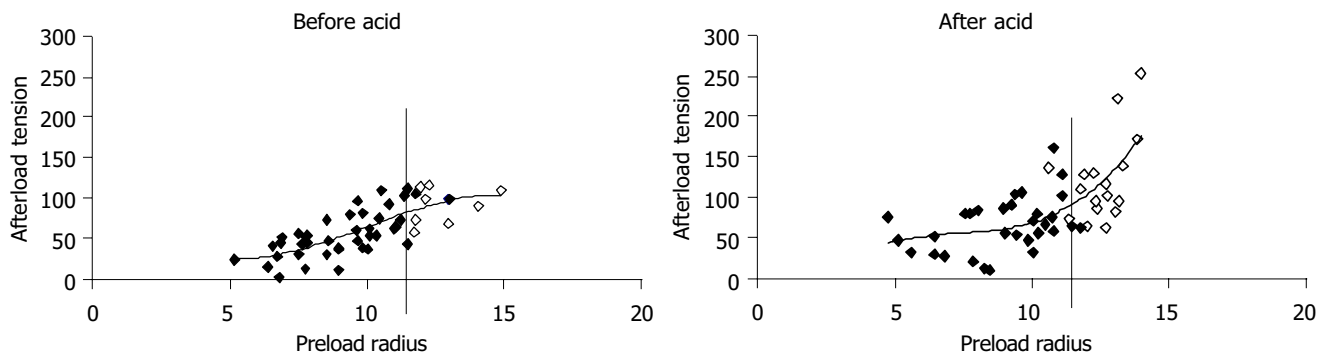


Figure 3 Tension during bag-distension-induced contractions (the afterload tension) plotted as functions of the radius immediately before the contractions (the preload radius) as shown in Figure 1. Five to eight datasets were computed

during the distension for 10 representative subjects. Data calculated at painful sensations were all above preload radii of 11.5 mm and are shown as open markings.

muscle filaments when the muscles are overstretched. Painful sensations ($VAS \geq 5$) were experienced at preload radii higher than 11.5 mm. After the acid infusion higher afterload tensions were observed at both low and high radii as compared to baseline, and there was a tendency to more spreading of the data as some individuals obtained very high afterload tensions. The painful sensations were also only evoked at radii higher than 11.5 mm.

The total, passive and active tonic tensions before and after acid infusion are shown in Figure 4. There was no difference in curve shape between before and after acid, indicating that acid infusion does not change esophageal muscle tone.

High and low acid responders

The subjects tolerated a mean of 101 ± 53 mL of acid. To see if the sensory response was related to the amount of acid infused, the subjects were divided into two groups. One group could accept 100-200 mL of acid ($n = 17$) and

the other group, less than 100 mL of acid ($n = 13$). There was a relation between the evoked sensitization and the acid load as those who accepted more than 100 mL were sensitized to volume ($F = 5.3$, $P = 0.02$), pressure ($F = 5.5$, $P = 0.02$) and tension ($F = 6.0$, $P = 0.01$), but not to CSA ($F = 0.9$, $P = 0.3$). The group tolerating less than 100 mL were not sensitized to neither volume ($F = 0.3$, $P = 0.6$), pressure ($F = 0.6$, $P = 0.4$), tension ($F = 0.8$, $P = 0.4$) nor CSA ($F < 0.01$, $P = 0.99$).

Referred pain areas

All subjects reported referred pain to the stimulations. The referred pain areas to mechanical stimuli at moderate pain are shown in Figure 5. Additionally one male and two females had referred pain in the back. The referred pain areas increased from 27.9 ± 29.3 cm² before acid to 41.4 ± 39.0 cm² after acid ($P = 0.047$), although the volume was smaller at the distensions after acid.

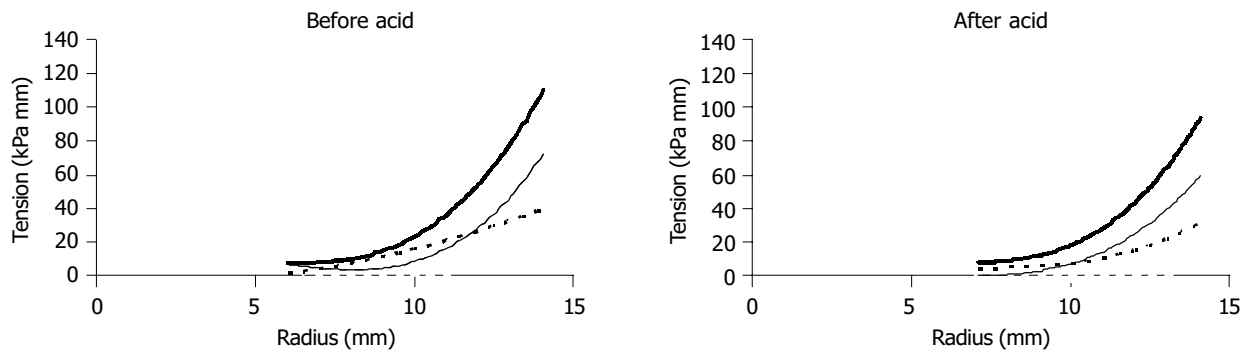


Figure 4 Plots of the total tonic (top), the passive (dotted) and the active (thin) tonic tensions as functions of radius before and after acid infusion. For explanations

see text. Acid did not change the curve shapes. Hence, esophageal muscle tone was not affected by the acid infusion.

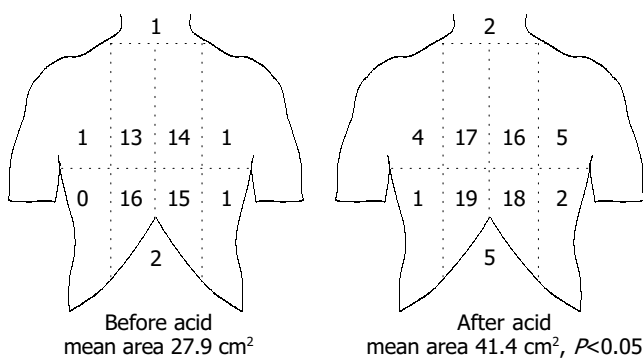


Figure 5 A schematic illustration of the referred pain areas drawn by the subjects following mechanical stimuli of the esophagus before and after perfusion with acid. The stimuli were given with an intensity corresponding to moderate pain. The chest was divided into eight areas by a horizontal line 5 cm above the xiphoid process, a vertical midline and two vertical lines 5 cm lateral to the midline. The numbers on the figure refer to the number of subjects reporting referred pain to that particular region of the chest. The referred pain area increased following the sensitization with acid.

DISCUSSION

The current experiment used controlled ramp distensions and preconditioning to evoke experimental pain in the esophagus in 30 subjects. The sensory response was assessed before and after sensitization of the lower esophagus by acid perfusion. The sensory rating increased after acid when expressed as a function of the volume, and the degree of sensitization was related to the infused volume of acid. Furthermore, an increase in referred pain to a standardized distension was seen reflecting activation of central facilitatory pain mechanisms. The mechanical analysis demonstrated hyper-reactivity of the esophagus following acid perfusion, with an increased number and force of the phasic contractions, but the muscle tone did not change. This illustrates that acid perfusion not only sensitizes the sensory pathways, but also facilitates motor reflexes.

Sensory response to sensitization with acid

Chronic pain is associated with modifications of the central nervous system such as central sensitization^[4]. Animal experiments have demonstrated neuronal changes such as increased spontaneous activity, decreased firing threshold, and expansion of the receptive fields of spinal neurons subjected to activation and/or experimental sensitization

of their peripheral afferents^[5,26,27]. Sensitization of the human esophagus with acid is a valuable experimental pain model, as the evoked allodynia, hyperalgesia and referred pain patterns reflect sensitization of the nervous system and can be studied systematically^[3]. Hence, decreased thresholds to physiologic stimuli seem to contribute to many of the symptoms reported by patients with inflammatory and functional diseases in the gut^[28,29]. Thus, a combination of mechanical stimulation and sensitization of the esophagus may mimic the widespread pain and other sensations reported by patients with reflux disease and unexplained chest pain^[16,30,31].

Acid-sensitive fibers have been demonstrated in animal studies, and mucosal afferents are often sensitive to different chemical stimuli^[32,33]. Increased responses to mechanical, electrical and thermal stimuli after acid perfusion of the esophagus have also been demonstrated in human beings^[6-9,34], although previous studies using latex balloons were not consistent. This can be due to methodological problems using latex balloons, where the distension data must be corrected for the intrinsic mechanical properties of the balloons and for the uncontrollable deformation in longitudinal direction^[9,16]. Non-compliant polyester urethane bags overcome these problems. The effect of preconditioning the tissue by several distensions until the stress-strain relationship becomes reproducible has also not been considered in most previous studies^[3,18]. Different modifications of the acid perfusion test have been used as a chemogenic stimulus by several authors^[6,7,9,35,36]. When the current material was divided into those who tolerated below and above 100 mL of acid, significant increased sensation to the mechanical stimulus was only seen in the high acid group. Hence, it is recommended to use volumes higher than 100 mL in future studies.

The present study demonstrated increased sensation to the infused bag volume, but not to pressure and tension. The intraluminal pressure and tension are highly dependent of the contractile force state of the esophageal muscles, and hence not as reliable parameters as the deformation^[18]. Despite the decrease in volume after acid infusion, the CSA did not decrease significantly. Thus it seems that the bag conforms to a shape where it is shorter after acid infusion. Such a shape change is likely caused by changes in the contractile activity in the acid exposed area and even in regions affected by nerve-mediated reflex responses.

Secondary contractions and muscle hyper-responsiveness can be evoked by acid in the distal esophagus due to reflex loops between mucosal afferents and the motor system^[37-40]. After acid perfusion increased force of the secondary contractions was evoked by the distension in the non-painful and painful range. Animal studies have shown that in contrast to the somatic system-afferents encoding both non-painful and painful sensations can sensitize in the viscera^[41]. The current observations in the human esophagus are in line with these studies, as the sensitization of afferents encoding conscious sensations to distension seems to change the contractile activity in the muscle via local and/or central reflexes^[42,43]. However, the curve form changed mostly in the pain range (to the right of the vertical line in Figure 3) and hence there seems to be a higher effect of sensitization on the painful sensations. The Frank-Starling mechanism predicts a decrease in contractile activity when the muscle is overstretched corresponding to less optimal interdigitation of actin and myosin filaments. In the current experiment the baseline curve form showed no decrease in afterload tension at maximal distension. The fact that the afterload tensions were higher after acid infusion indicates that bag distension itself does not activate the muscle maximally.

Another manifestation of the acid perfusion was the increased referred pain area to the mechanical stimulation, although the bag volume was lower after the perfusion. Enlarged referred pain areas is also a characteristic in clinical gut disorders^[44-46], and are very similar to what is observed in patients suffering from chronic musculoskeletal pain^[47]. Previously, we have shown that sensitization of the esophagus results in increased referred pain areas^[8], a finding which was confirmed in the current study. The mechanism is of central origin^[4], which was also shown in previous papers using neurophysiological assessment of the spinal and supraspinal pain response after acid perfusion of the esophagus^[8,48].

Mechanical and motor responses to sensitization with acid

The sensitization resulted not only in allodynia and hyperalgesia to the distension volumes, but the esophagus also exhibited hyper-reactivity as illustrated by the increased number of contractions after the acid perfusion. Such hyper-reactivity has also been seen in animal studies^[37,38]. The contractions were also stronger to a given preload radius. However, the acid infusion did not change the total tonic tension, the passive tension and the active tonic tensions (Figure 4). Hence, the hyper-reactivity only accounts for phasic contractions, not for tone in the esophageal body. Previously, Sifrim *et al.*^[49], showed that acid reflux into the esophagus stimulated tone in the esophageal body. However, simultaneous distension seemed to inhibit the acid induced tone. These issues obviously need further investigations.

The preload radius where contractions were evoked by the painful stimuli (VAS = 5 and higher) did not change after acid (vertical line in Figure 2). This corresponds with the "strain theory", *i.e.*, that the mechanoreceptors are activated by circumferential stretch independent of the contractile state of the muscles^[12,13,15,50]. The receptors encoding distension of the gut are mainly believed to be localized in the muscle and nerve layers, where they are not

exposed to acid^[33,43]. Hence, the contractions are probably initiated by reflex loops between strain-sensitive mechanosensitive afferents localized in the muscle layers and the smooth muscle cells. Whether such reflexes are local or mediated via central (vagal and/or spinal) afferents cannot be concluded from the current data^[40,42,43]. We believe, however, that a central component is important as the contractions were more powerful after perfusion with acid. The acid perfusion may thus result in sensitization of mucosal afferents as well as central hyperexcitability^[8,43,48]. As the enteric nervous system is partly under inhibitory central control^[51], the sensitization may result in dampening of the central control. This mechanism is expedient as such reflexes will tend to move acid from reflux towards the stomach where it is harmless.

Modeling diseases of the esophagus

Sensation and pain detection thresholds to distension, electrical and acid stimuli of the esophagus were found to be lower in patients with non-cardiac chest pain compared to healthy subjects^[6,7,52,53]. Such hypersensitivity can be mimicked in the current model. Furthermore, the muscles of the esophagus are hyper-reactive in patients with unexplained chest pain^[19,54-56]. In the present model the acid perfusion evoked an increased number of contractions, which were characterized by a higher force. Thus diseases characterized by primary and secondary motor disorders can also be mimicked experimentally, and in patients the preload-afterload plots will be valuable for description of the aberrant motor function. The model can therefore be used to study abnormal sensory-motor mechanisms in visceral organs, and may also prove useful in pharmacological studies with drugs targeted to treat patients with unexplained chest pain and motor disorders of the esophagus.

Appendix

The preload is considered in this study to be initial muscle length (radius) preceding the contraction during the distension, whereas the afterload is evaluated as the active tension during the contraction. In cardiac physiology the preload is usually considered to be the end-diastolic pressure or radius and the afterload is considered to be the arterial pressure during the systole. The explanation of the Frank-Starling mechanism is that when an extra amount of blood flows into the ventricles, the cardiac muscle itself is stretched to greater length. This in turn causes the muscle to contract with increased force because the actin and myosin filaments then are brought to a more nearly optimal degree of interdigitation for force generation. In cardiac physiology the importance of the concept of preload and afterload is that in many abnormal functional states of the heart and circulation, the pressure during filling of the ventricle or the arterial pressure against which the ventricle must contract, or both, are severely altered from the normal. The Frank-Starling mechanism has been important in the understanding of drugs with effect on the myocardial function, and transferring this concept to esophageal physiology, the development in the current model will have interest for evaluation of normal esophageal physiology and in the pathophysiology of esophageal disorders.

REFERENCES

- 1 **Bochus HL.** Abdominal Pain. In: Berk JE, ed. *Gastroenterology. Philadelphia: WB Saunders* 1985: 22-47
- 2 **Arendt-Nielsen L.** Induction and assessment of experimental pain from human skin, muscle, and viscera. In: Jensen TS, Turner JA, and Wiesenfeld-Hallin Z, eds. *Proceedings of the 8th World Congress of Pain, Progress in Pain Research and Management. Seattle: ISAP Press* 1997: 393-425
- 3 **Drewes AM, Gregersen H, Arendt-Nielsen L.** Experimental pain in gastroenterology: A reappraisal of human studies. *Scand J Gastroenterol* 2003; **38**: 1115-1130
- 4 **Arendt-Nielsen L, Laursen RJ, Drewes AM.** Referred pain as an indicator for neural plasticity. *Prog Brain Res* 2000; **129**: 343-356
- 5 **Garrison DW, Chandler MJ, Foreman RD.** Viscerosomatic Convergence Onto Feline Spinal Neurons from Esophagus, Heart and Somatic Fields - Effects of Inflammation. *Pain* 1992; **49**: 373-382
- 6 **Mehta AJ, De Caestecker JS, Camm AJ, Northfield TC.** Sensitization to painful distention and abnormal sensory perception in the esophagus. *Gastroenterology* 1995; **108**: 311-319
- 7 **Sarkar S, Aziz Q, Woolf CJ, Hobson AR, Thompson DG.** Contribution of central sensitisation to the development of non-cardiac chest pain. *Lancet* 2000; **356**: 1154-1159
- 8 **Drewes AM, Schipper KP, Dimcevski G, Petersen P, Andersen OK, Gregersen H, Arendt-Nielsen L.** Multi-modal induction and assessment of allodynia and hyperalgesia in the human oesophagus. *Eur J Pain* 2003; **7**: 539-549
- 9 **Hu WH, Martin CJ, Talley NJ.** Intraesophageal acid perfusion sensitizes the esophagus to mechanical distension: a Barostat study. *Am J Gastroenterol* 2000; **95**: 2189-2194
- 10 **Whitehead WE, Delvaux M.** Standardization of barostat procedures for testing smooth muscle tone and sensory thresholds in the gastrointestinal tract. *Dig Dis Sci* 1997; **42**: 223-224
- 11 **Drewes AM, Schipper KP, Dimcevski G, Petersen P, Andersen OK, Gregersen H, Arendt-Nielsen L.** Multimodal assessment of pain in the esophagus: a new experimental model. *Am J Physiol Gastrointest Liver Physiol* 2002; **283**: G95-103
- 12 **Drewes AM, Pedersen J, Liu W, Arendt-Nielsen L, Gregersen H.** Controlled mechanical distension of the human oesophagus: Sensory and biomechanical findings. *Scand J Gastroenterol* 2003; **38**: 27-35
- 13 **Gao C, Arendt-Nielsen L, Liu W, Petersen P, Drewes AM, Gregersen G.** Sensory and biomechanical responses to ramp-controlled distension of the human duodenum. *Am J Physiol Gastrointest Liver Physiol* 2003; **284**: G461-471
- 14 **Pedersen J, Gao C, Egekvist H, Bjerring P, Arendt-Nielsen L, Gregersen H, Drewes AM.** Pain and biomechanical responses to distension of the duodenum in patients with systemic sclerosis. *Gastroenterol* 2003; **124**: 1230-1239
- 15 **Petersen P, Gao C, Arendt-Nielsen L, Gregersen H, Drewes AM.** Pain intensity and biomechanical responses during ramp-controlled distension of the human rectum. *Dig Dis Sci* 2003; **48**: 1310-1316
- 16 **Gregersen H, Kassab G.** Biomechanics of the gastrointestinal tract. *Neurogastroenterol Motil* 1996; **8**: 277-297
- 17 **Gregersen H, Christensen J.** Gastrointestinal tone. *Neurogastroenterol Mot* 2000; **12**: 501-508
- 18 **Gregersen H.** Biomechanics of the Gastrointestinal Tract. *London: Springer Verlag* 2002
- 19 **Rao SS, Gregersen H, Hayek B, Summers RW, Christensen J.** Unexplained chest pain: the hypersensitive, hyperreactive, and poorly compliant esophagus. *Ann Intern Med* 1996; **124**: 950-958
- 20 **Richter JE.** Oesophageal motility disorders. *Lancet* 2001; **358**: 823-828
- 21 **Gregersen H, Andersen MB.** Impedance measuring system for cross-sectional area in the gastrointestinal tract. *Med Biol Eng Comput* 1991; **29**: 108-110
- 22 **Gregersen H, Giversen IM, Rasmussen LM, Tottrup A.** Biomechanical wall properties and collagen content in the partially obstructed opossum esophagus. *Gastroenterology* 1992; **103**: 1547-1551
- 23 **Drewes AM, Schipper KP, Dimcevski G, Petersen P, Gregersen H, Funch-Jensen P, Arendt-Nielsen L.** Gut pain and hyperalgesia induced by capsaicin: A human experimental model. *Pain* 2003; **104**: 333-341
- 24 **Drewes AM, Babenko L, Birket-Smith L, Funch-Jensen P, Arendt-Nielsen L.** Induction of non-painful and painful intestinal sensations by hypertonic saline: A new human experimental model. *Eur J Pain* 2003; **7**: 81-91
- 25 **Bernstein LM, Baker LA.** A clinical test for esophagitis. *Gastroenterology* 1958; **34**: 760-781
- 26 **Coderre TJ, Katz J, Vaccarino AL, Melzack R.** Contribution of central neuroplasticity to pathological pain: review of clinical and experimental evidence. *Pain* 1993; **52**: 259-285
- 27 **Laird JMA, de la Rubia PG, Cervero F.** Excitability changes of somatic and viscerosomatic nociceptive reflexes in the decerebrate-spinal rabbit: role of NMDA receptors. *J Physiol* 1995; **489**: 545-555
- 28 **Mayer EA, Munakata J, Mertz H, Lembo T, Bernstein CN.** Visceral hyperalgesia and irritable bowel syndrome. In: Gebhart GF, ed. *Visceral pain, Progress in Pain Research and Management. Volume 5. Seattle: IASP Press* 1995: 429-468
- 29 **Yaksh TL.** Spinal systems and pain processing: development of novel analgesic drugs with mechanistically defined methods. *Trends Pharmacol Sci* 1999; **20**: 329-337
- 30 **Eslick GD, Fass R.** Noncardiac chest pain: evaluation and treatment. *Gastroenterol Clin N Am* 2003; **32**: 531-552
- 31 **Clouse RE, Richter JE, Heading RC, Janssens J, Wilson JA.** Functional esophageal disorders. *Gut* 1999; **45**: 31-36
- 32 **Ness TJ, Gebhart GF.** Visceral pain: a review of experimental studies. *Pain* 1990; **41**: 167-234
- 33 **Sengupta JN, Gebhart GF.** Gastrointestinal afferent fibers and sensation. In: Johnson L, ed. *Physiology of the Gastrointestinal Tract. Third ed. New York: Raven Press* 1994: 484-519
- 34 **Sarkar S, Hobson AR, Hughes A, Growcott J, Woolf CJ, Thompson DG, Aziz Q.** The prostaglandin E2 receptor-1 (EP-1) mediates acid-induced visceral pain hypersensitivity in humans. *Gastroenterology* 2003; **124**: 18-25
- 35 **DeVault KR.** Acid infusion does not affect intraesophageal balloon distention-induced sensory and pain thresholds. *Am J Gastroenterol* 1997; **92**: 947-949
- 36 **Fass R, Naliboff B, Higa L, Johnson C, Kodner A, Munakata J, Ngo J, Mayer EA.** Differential effect of long-term esophageal acid exposure on mechanosensitivity and chemosensitivity in humans. *Gastroenterology* 1998; **115**: 1363-1373
- 37 **Shirazi S, Schulzedelrieu K, Custerhagen T, Brown CK, Ren J.** Motility changes in opossum esophagus from experimental esophagitis. *Dig Dis Sci* 1989; **34**: 1668-1676
- 38 **White RJ, Zhang Y, Morris GP, Paterson WG.** Esophagitis-related esophageal shortening in opossum is associated with longitudinal muscle hyperresponsiveness. *Am J Physiol Gastrointest Liver Physiol* 2001; **280**: G463-469
- 39 **Schoeman MN, Holloway RH.** Integrity and Characteristics of Secondary Esophageal Peristalsis in Patients with Gastroesophageal Reflux Disease. *Gut* 1995; **36**: 499-504
- 40 **Lang IM, Medda BK, Shaker R.** Mechanisms of reflexes induced by esophageal distension. *Am J Physiol Gastrointest Liver Physiol* 2001; **281**: G1246-1263
- 41 **Gebhart GF.** Pathobiology of visceral pain: molecular mechanisms and therapeutic implications IV. Visceral afferent contributions to the pathobiology of visceral pain. *Am J Physiol Gastrointest Liver Physiol* 2000; **278**: G834-838
- 42 **Grundy D.** Neuroanatomy of visceral nociception: vagal and splanchnic afferent. *Gut* 2002; **51**: 12-15
- 43 **Szurszewski JH, Ermilov LG, Miller SM.** Prevertebral ganglia and intestinofugal afferent neurones. *Gut* 2002; **51**: 16-110
- 44 **Mayer EA, Gebhart GF.** Basic and clinical aspects of visceral hyperalgesia. *Gastroenterology* 1994; **107**: 271-293
- 45 **Sanger GJ.** Hypersensitivity and hyperreactivity in the irritable bowel syndrome: An opportunity for drug discovery. *Dig Dis* 1999; **17**: 90-99

- 46 **Mertz H**, Fullerton S, Naliboff B, Mayer EA. Symptoms and visceral perception in severe functional and organic dyspepsia. *Gut* 1998; **42**: 814-822
- 47 **Johansen MK**, Graven-Nielsen T, Olesen AS, Arendt-Nielsen L. Generalised muscular hyperalgesia in chronic whiplash syndrome. *Pain* 2001; **89**: 293-295
- 48 **Sarkar S**, Hobson AR, Furlong PL, Woolf CJ, Thompson DG, Aziz Q. Central neural mechanisms mediating human visceral hypersensitivity. *Am J Physiol Gastrointest Liver Physiol* 2001; **281**: G1196-1202
- 49 **Sifrim D**, Tack J, Lerut T, Janssens J. Transient lower esophageal sphincter relaxations and esophageal body muscular contractile response in reflux esophagitis. *Dig Dis Sci* 2000; **45**: 1293-1300
- 50 **Barlow JD**, Gregersen H, Thompson DG. Identification of biomechanical factors associated with the perception of distension in the human esophagus. *Am J Physiol Gastrointest Liver Physiol* 2002; **282**: G683-689
- 51 **Christensen J**. Motor functions of the pharynx and esophagus. In: Johnson LR, Christensen J, Jackson MJ, Jacobsen ED, Walsh JH, eds. *Physiology of the gastrointestinal tract*. Second ed. New York: Raven press 1987: 595-612
- 52 **Frobert O**, Arendt-Nielsen L, Bak P, Funch-Jensen P, Peder BJ. Pain perception and brain evoked potentials in patients with angina despite normal coronary angiograms. *Heart* 1996; **75**: 436-441
- 53 **Smout AJ**, Devore MS, Dalton CB, Castell DO. Cerebral Potentials-evoked by esophageal distension in patients with noncardiac chest pain. *Gut* 1992; **33**: 298-302
- 54 **Rao SS**. Visceral hyperalgesia: the key for unrevealing functional gastrointestinal disorders. *Dig Dis* 1996; **14**: 271-275
- 55 **Balaban DH**, Yamamoto Y, Liu JM, Pehlivanov N, Wisniewski R, DeSilvey D, Mittal RK. Sustained esophageal contraction: A marker of esophageal chest pain identified by intraluminal ultrasonography. *Gastroenterology* 1999; **116**: 29-37
- 56 **Pehlivanov N**, Liu JM, Mittal RK. Sustained esophageal correlate of heartburn contraction: a motor symptom. *Am J Physiol Gastrointest Liver Physiol* 2001; **281**: G743-751

Science Editor Guo SY Language Editor Elsevier HK

• CLINICAL RESEARCH •

Relationship between gastrointestinal and extra-gastrointestinal symptoms and delayed gastric emptying in functional dyspeptic patients

N Pallotta, P Pezzotti, E Calabrese, F Baccini, E Corazziari

N Pallotta, P Pezzotti, E Calabrese, F Baccini, E Corazziari, Dpt Scienze Cliniche, Università degli Studi di Roma "La Sapienza"; Reparto AIDS e Malattie Sessualmente Trasmesse, Istituto Superiore di Sanità; Rome, Italy

Correspondence to: Professor E Corazziari, Dpt di Scienze Cliniche, Università "La Sapienza", Policlinico "Umberto I", V.le del Policlinico, Rome 00161, Italy. enrico.corazziari@uniroma1.it
Telephone: +39-6-49978384 Fax: +39-6-49978385

Received: 2004-07-17 Accepted: 2005-01-05

Abstract

AIM: Delayed gastric emptying and an enlarged fasting gastric antrum are common findings in functional dyspepsia but their relationship with gastrointestinal (GI), and the frequently associated extra-GI symptoms remains unclear. This study evaluated the relationship between GI and extra-GI symptoms, fasting antral volume and delayed gastric emptying in functional dyspepsia.

METHODS: In 108 functional dyspeptic patients antral volume and gastric emptying were assessed with ultrasonography (US). Symptoms were assessed with standardized questionnaire. The association of symptoms and fasting antral volume with delayed gastric emptying was estimated with logistic regression analysis.

RESULTS: Delayed gastric emptying was detected in 39.8% of the patients. Postprandial drowsiness (AOR 11.25; 95%CI 2.75-45.93), nausea (AOR 3.51; 95%CI 1.19-10.32), fasting antral volume (AOR 1.93; 95%CI 1.22-3.05), were significantly associated with delayed gastric emptying. Symptoms, mainly the extra-GI ones as postprandial drowsiness and nausea, combined with fasting antral volume predicted the modality of gastric emptying with a sensitivity and specificity of 78%.

CONCLUSION: In functional dyspeptic patients, (1) an analysis of fasting antral volume and of symptoms can offer valuable indication on the modality of gastric emptying, and (2) it seems appropriate to inquire on postprandial drowsiness that showed the best correlation with delayed gastric emptying.

© 2005 The WJG Press and Elsevier Inc. All rights reserved.

Key words: Functional dyspepsia; Gastric emptying; Ultrasonography

Pallotta N, Pezzotti P, Calabrese E, Baccini F, Corazziari E.

Relationship between gastrointestinal and extra-gastrointestinal symptoms and delayed gastric emptying in functional dyspeptic patients. *World J Gastroenterol* 2005; 11(28): 4375-4381
<http://www.wjgnet.com/1007-9327/11/4375.asp>

INTRODUCTION

The term dyspepsia is widely used in clinical practice to describe symptoms arising from the upper abdomen and, depending on the definition, its prevalence has been reported to vary from 20% to 40%^[1-3] in the adult population. Although dyspeptic symptoms may arise from several pathological conditions, more than 70%^[4-8] of patients, do not have definite structural or biochemical alterations^[9-11] and, based on the Rome Diagnostic Criteria functional dyspepsia (FD) is made^[12,13]. In the assumption that symptoms may predict specific underlying pathophysiology of FD it has been suggested that patients be subdivided in accordance with symptom clusters^[12] such as ulcer-like and dysmotility-like dyspepsia or, more recently, with the predominant symptom^[13]. Several studies have looked for possible correlation between symptoms and pathophysiological abnormalities such as *Helicobacter pylori* infection, visceral hypersensitivity and abnormal motor function of the stomach. Up to 40% of patients with FD evaluated in referral centers have delayed gastric emptying^[14] and 40% impaired postprandial relaxation of the proximal stomach^[15]. So far however, there is little evidence^[16] that gastric motor abnormalities correlate unequivocally with different symptom clusters^[17-19] and not even in those patients with dysmotility-like dyspepsia, referring symptoms suggestive of an abnormal motor function of the stomach such as postprandial fullness, nausea, early satiety and vomiting. Female gender, and, severe and predominant, postprandial fullness and vomiting have been reported to be associated with delayed gastric emptying^[20], a finding not confirmed in a subsequent study^[21] performed in a large cohort of patients with dysmotility-functional and organic (i.e., diabetic) dyspepsia. Drowsiness is a subjective experience often reported after food ingestion and it has been shown that solid meal results in a decreased sleep onset latency in healthy volunteers^[22].

Patients with functional dyspepsia complain of several gastrointestinal (GI) and extra-GI symptoms^[23], some of the latter like drowsiness^[24,25] and headache^[24] are related to meal ingestion. It is not known, however, whether postprandial drowsiness and other extra-GI symptoms have any relationship with gastric functions.

An enlarged fasting antral volume assessed by ultrasonography (US)^[26,27] is an additional finding in patients with FD but its relationship, if any, with delayed gastric emptying is not known.

We, therefore aimed to evaluate in functional dyspeptic patients whether and which symptoms either GI or extra-GI are related to, and might predict, delayed gastric emptying of a regular meal. Additional aim was to assess whether the US measurement of basal antral volume may predict the modality of gastric emptying.

MATERIALS AND METHODS

Two hundred and ten consecutive patients referring symptoms of dyspepsia (140 F; age 42.8 ± 12.5 years, mean \pm SD) referred to the gastroenterology outpatient clinic were assessed. Functional dyspepsia was defined as persistent or recurrent pain or discomfort centered in the upper abdomen for at least 3 mo in the preceding 12 mo, in the absence of any known organic disease that is likely to explain the symptoms^[12,13] and no evidence that dyspeptic symptoms were exclusively relieved by defecation or associated with the onset of a change in stool frequency or stool form^[13].

Organic abnormalities, psychiatric illnesses, history of alcohol abuse, use of NSAIDs, steroids or drugs affecting gastric functions, previous surgery of the GI tract (except appendectomy and cholecystectomy) and systemic disorders were ruled out by history, clinical examination, biochemical investigations, upper GI endoscopy, and transabdominal US. Dyspeptic patients with Rome diagnostic criteria of irritable bowel syndrome (IBS) and/or referring heartburn and/or regurgitation as predominant or frequent symptoms, were excluded from the study.

Epigastric pain and upper abdominal discomfort were graded 0-4 according to its influence on patient's daily activities: 0, absent; 1, mild (present but easily bearable if distracted by usual activities); 2, moderate (bearable but not influencing usual activities); 3, relevant (influencing usual activities); 4, severe (interruption of usual activities).

Patients were enrolled into the study if symptomatic at the time of evaluation with a symptom score value of ≥ 2 for epigastric pain or discomfort.

Overall 102 patients (67 F, age 46 ± 13.2 years, mean \pm SD) were excluded from the study because of the following diagnosis: gastroesophageal reflux disease, 52; IBS, 15; peptic ulcer, 14; migraine, 16; psychiatric disorders, 3; celiac disease, 2.

One hundred and eight patients with functional dyspepsia entered the study (73 F, age 42 ± 12.5 years, mean \pm SD). Twenty-eight healthy asymptomatic volunteers (10 F, mean age 31 ± 5.5 years, mean \pm SD) were also investigated. None of them had GI disorders or symptoms or were taking medications of any kind. None had been previously submitted to surgery of the GI tract.

Informed consent was obtained from each subject and the study protocol was approved by the local ethics committee.

Analysis of symptoms

Consecutive patients were interviewed with a standardized questionnaire^[28] made of 50 items, inquiring on demography (5 items), daily habits (10 items) that included meal timing

and composition, alcohol consumption, smoking and sleep, past medical history (3 items), GI symptoms (15 items), gastroesophageal symptoms (4 items), bowel pattern (7 items), and somatic extra-GI symptoms that included 5 items as indicated in a previously published study^[23]. Postprandial drowsiness, defined as a state of impaired awareness associated with a desire or inclination to sleep^[29] was also included in the questionnaire since this meal-related symptom has been reported^[2] and confirmed by personal observations, to be bothersome in dyspeptic patients. Dyspeptic symptoms were defined according to Rome criteria^[12,13].

Frequency and time relationship with meal assumption was assessed for each investigated symptom and, relationship of drowsiness with sleep disturbances was specifically looked for.

In addition patients were requested to refer any other symptom they considered to be bothersome and relating to meal ingestion.

Assessment of gastric emptying

Gastric emptying was evaluated with US according to previously validated and standardized methods^[30-34]. Gastric antral volume was evaluated by US according to previously published methods^[33,34] with a 4 MHz linear probe and 3.5 MHz convex probe (Toshiba SAL 38B, Tosbee, Toshiba, Japan).

All drugs affecting the GI tract were discontinued at least 3 d before the gastric emptying studies. Subjects refrained from smoking for a 12-h period preceding, and during, the examination. After an overnight fast the subjects ate an ordinary standard solid 1 050 kcal meal containing 140 g bread, 70 g cheese, 80 g ham, (50% carbohydrates, 25% lipids, 25% proteins), 3.5 g alimentary fibers, 250 mL of water. The time of meal ingestion did not exceed 30 min (range 15-30 min). Gastric antral US measurements were performed by the same operator with the subjects standing in the upright position, in fasting condition, immediately, and at 30 and 60 min after the end of the meal ingestion, and at 60-min intervals thereafter over a total period of 300 min. In the intervals between measurements subjects could move freely.

Delayed gastric emptying was defined as the final antral volume (i.e., gastric antral volume at 300 min after meal ingestion) exceeding the mean value plus 2SDs of the 28 healthy volunteers (31 mL).

Statistical analysis

Descriptive statistics as median values and interquartile ranges were calculated. Box-plots^[35] were used for inter-group comparison of antral volume distributions. The Mann-Whitney test^[35] was used to compare the median values of antral volume between healthy controls, FD patients with delayed and those with normal gastric emptying.

Sensitivity and specificity of each symptom for three different threshold levels of fasting antral volume were calculated. Odds ratios (OR) were also calculated as a synthetic measure of both sensitivity and specificity^[35].

Logistic regression analysis^[36] was then applied to estimate crude and adjusted odds-ratios (AOR) and 95% confidence intervals (95%CI) of having delayed gastric emptying for

each symptom, fasting antral volume, gender, age, and body mass index (BMI). In addition, we reported results from two multivariate logistic regression analyses, respectively, without and with fasting antral volume, obtained through a backward selection strategy having excluded factors with a log-likelihood *P*-value >0.20^[35]. Two-sided *P* values were defined statistically significant when *P*<0.05, and marginally significant when 0.05<*P*<0.2.

Estimated coefficients from multivariate logistic regression were used to calculate the probability of having (or not having) delayed gastric emptying. Through these probabilities, it is possible to calculate sensitivity, specificity, and the percentage of patients correctly classified^[36]. All the analyses were performed using STATA release 5.0^[37].

RESULTS

Figure 1 shows antral volume values before, immediately, and in the 300 min after meal ingestion in normal controls and in functional dyspeptic patients with normal and delayed gastric emptying.

In healthy volunteers, the mean gastric antral volume was 13±5 mL in the fasting state and reached its maximal value at the end of meal ingestion (67±24 mL), then decreased almost linearly to reach 18±6.5 mL at the end of the study. In FD patients, the mean fasting antral volume was 14±8 mL (ns *vs* controls) and reached its maximal value at the end of the meal (53±21 mL) (ns *vs* controls), then decreased to reach the final value of 30±16 mL (*P*<0.0001 *vs* controls).

Gastric emptying was delayed in 43 (39.8%) patients (28 F; mean age 41.4 years; range 23-64 years) and their final AV was 46±11 mL (Figure 1). The mean fasting AV (17±10 mL) was larger in patients with delayed gastric emptying than in those with normal gastric emptying (12±5 mL, *P* = 0.005, Figure 1). The mean delta variation between fasting and final antral volume was 29±14 mL in

dyspeptic patients with delayed gastric emptying and 7±8 mL in those with normal gastric emptying (*P*<0.0001).

Frequency, as well as sensitivity, specificity, and crude OR in predicting delayed gastric emptying of each of the GI and extra-GI symptoms reported by at least eight patients as well as fasting antral volume are reported in Table 1. Delayed gastric emptying was not related to age (OR = 1.03; *P* = 0.84), gender (OR = 0.7; *P* = 0.4), while there was a marginally significant inverse association, with BMI (OR = 0.89 per 1 kg/m² increase; *P* = 0.06, data not shown in Table 1).

None of the patients with post-prandial drowsiness complained of sleeplessness.

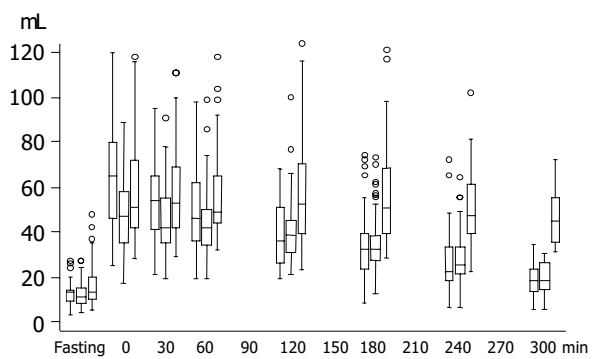


Figure 1 Box-and-whiskers plots of gastric antral volume before (fasting), immediately (0) at 30- and 60-min intervals, after the end of the ingestion of a standard meal, in controls (left) and in dyspeptic patients with normal (middle) and delayed (right) gastric emptying. The boxes at each time unit extend from the 25th percentile ($X_{[25]}$) to the 75th percentile [$X_{[75]}$], i.e., the interquartile range (IQ); the lines inside the boxes represent the median values. The line emerging from the boxes (i.e., the "whiskers") extend to the upper and lower adjacent values. The upper adjacent value is defined as the largest data point $\leq X_{[75]} + 1.5 \times IQ$, and the lower adjacent value is defined as the smallest data point $\geq X_{[25]} - 1.5 \times IQ$. Observed values more extreme than the adjacent values, if any, are individually plotted (circles). The widths of the boxes are proportional to the number of observations available at each time unit.

Table 1 Prevalence, sensitivity and specificity and crude OR for delayed gastric emptying of symptoms and of fasting antral volume at three cut-off levels

	Prevalence %	Sensitivity %	Specificity %	OR
Pain centered in the upper abdomen	45.4	58.1	63.1	2.37
Discomfort centered in the upper abdomen	79.6	81.4	21.5	1.20
Upper abdominal bloating	84.3	88.4	18.5	1.72
Fullness	68.5	62.8	27.7	0.64
Early satiety	45.4	48.8	56.9	1.26
Nausea	42.6	53.5	64.6	2.10
Heartburn	26.9	34.9	78.5	1.95
Epigastric burning	11.1	9.3	87.7	0.73
Belching	74	74.4	26.1	1.03
Vomiting	27.8	20.9	67.7	0.55
Acid regurgitation	19.4	23.3	83	1.48
Drowsiness	16.7	32.6	93.9	7.36
Headache	41.7	46.5	61.5	1.39
Palpitation	7.4	6.9	92.3	0.90
Fasting antral volume (mL)				
<10 mL (reference group)	33.3	18.6	43	1.09
10-14 mL	34.3	39.5	30.8	2.97
>15 mL	32.4	41.9	26.2	3.71

Table 2 AOR with 95%CI of having delayed gastric emptying on the basis of symptoms and fasting antral volume (FAV)

	Without FAV and BMI		With FAV and BMI	
	AOR	95%CI	AOR	95%CI
Pain centered in the upper abdomen	3.74	1.34-10.41	2.78	0.92-8.41
Nausea	2.92	1.15-7.44	3.51	1.19-10.32
Postprandial fullness	0.41	0.14-1.14	0.27	0.08-0.84
Discomfort centered in the upper abdomen	3.42	0.88-13.25	4.59	0.99-21.20
Vomiting	0.44	0.15-1.31	0.32	0.09-1.11
Heartburn	-	-	2.31	0.80-6.71
Drowsiness	9.37	2.47-35.45	11.25	2.75-45.93
BMI	-	-	0.89	0.77-1.02
Fasting antral volume ¹	-	-	1.93	1.22-3.05

FAV: Fasting antral volume; AOR: adjusted odds-ratio. ¹AOR estimated per 5 mL increase (e.g., a FAV of 20 mL vs 15 mL).

The AOR for symptoms with or without fasting antral volume and BMI included in the multivariate analyses are shown in Table 2. Not taking into consideration fasting antral volume and BMI in the multivariate analyses, upper abdominal pain, nausea, and drowsiness showed a statistically significant association, whereas upper discomfort showed only a marginally significant association with delayed gastric emptying. Post-prandial fullness or vomiting showed a marginally significant association with normal gastric emptying. Including fasting antral volume and BMI in the multivariate analyses, nausea and drowsiness were highly significantly associated with delayed gastric emptying, while upper abdominal pain, upper abdominal discomfort, and heartburn were only marginally significantly associated with delayed gastric emptying. Post-prandial fullness showed a highly significant, and vomiting a marginally significant, association with normal gastric emptying. Fasting antral volume was significantly associated with delayed gastric emptying increasing the OR of 93% for any additional volume increase of 5 mL. BMI showed a marginally

significant inverse association with delayed gastric emptying with an OR decrease of 11% for any 1 kg/m² increase.

Using other two different cut-points (29 and 33 mL), instead of 31 mL, as discriminant final antral volume for normal and delayed gastric emptying, all the results of univariate and multivariate analyses did not vary.

Furthermore probabilities of having delayed gastric emptying were assessed with the selected symptoms, fasting antral volume, and BMI as reported from the second model (Table 2 and Figure 2). Sensitivity and specificity of the applied model are plotted for different values of estimated prevalence of delayed gastric emptying ranging from 0 to 1. At the cut-off value of 0.398, i.e., the estimated prevalence of delayed gastric emptying in this sample, sensitivity and specificity were about 78% with a correct classification of 73.3% of the patients. Applying a model based on selected symptoms only, the estimated sensitivity and specificity were negligibly lower, than those obtained with the model including fasting antral volume and BMI, with a correct classification of 68.1% of the patients at the cut-off value of 0.398 (data not shown).

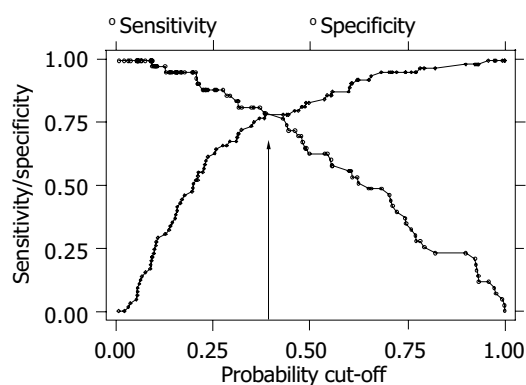


Figure 2 Proportion of patients with delayed and normal gastric emptying who were correctly classified on the basis of their predicted probabilities obtained from the estimated coefficients of the second model reported in Table 2 (i.e., sensitivity and specificity, respectively). These proportions are plotted with cut-off levels varying between 0 and 1 (see "lsens" function in Ref. [37]). As expected, when the cut-off value is close to zero all individuals with an actual delayed gastric emptying will be correctly classified and thus having a very high sensitivity. In contrast, with very low cut-off values also those having a normal gastric emptying will be classified as "delayed" by the model and thus having a very low specificity. As the cut-off value used for classification increases, the model will provide the worst performances for the sensitivity and the best performances for the specificity. Circles identify sensitivity and squares specificity. Arrow indicates the probability cut-off value of 0.398, i.e., the estimated prevalence of delayed gastric emptying in this sample.

DISCUSSION

In the attempt to clarify the pathophysiology of symptoms in functional dyspepsia it has been proposed to classify patients with functional dyspepsia into clinically distinct subgroups on the basis of symptom clusters^[12]. Thus the presence of the variable combination of upper abdominal bloating, upper abdominal fullness, early satiety, nausea, belching, retching, and vomiting have been regarded as suggestive of impaired gastric motor activity^[38-40]. However several studies^[16-19] have so far failed to demonstrate in this subgroup of patients a close correlation between symptoms and disturbances of motor function. More recently^[13] it has been proposed to classify dyspeptic subgroup on the basis of the predominant symptom. Nevertheless two studies^[15,20] in the attempt to assess the relationship between predominant symptoms and gastric dysfunction reported non-univocal results in populations that did not exclude patients with IBS and gastroesophageal reflux disease (GERD). Delayed gastric emptying was independently associated with severe post-prandial fullness and severe vomiting in the first study^[20] and with severe nausea in the second one^[15] that also reported early satiety as specifically

associated with impaired gastric accommodation to a meal. In both studies, however, the association between the mentioned symptoms and the altered gastric function was not a universal finding but limited to a subgroup of patients. The uncertainty of the matter is further illustrated by a third study^[21] that failed to find an association between any of the dyspeptic symptoms, as well as their severity, and delayed gastric emptying.

Although reported in previous studies^[23-25] and frequently referred by dyspeptic patients little attention has been paid to other symptoms not referable to the GI tract. The present study aimed to assess whether single GI or extra-GI symptoms and the simple non-invasive US measure of the gastric antral volume in fasting condition could predict the presence of delayed gastric emptying, in a group of dyspeptic patients in whom symptoms of IBS and GERD were excluded.

The present study differs from the previous ones also for other aspects. A meal having the same composition of a normal everyday lunch was used in the present study whereas unusual experimental and/or low caloric meals (≤ 700 kcal)^[17-19] used previously might have not sufficiently challenged the upper GI function. Most of the previously published studies evaluated gastric emptying with the scintigraphic technique that, differently from the US technique, assesses the emptying of the radiolabeled component of the meal rather than of the entire postcibal gastric contents. In addition previous scintigraphic studies have assessed the gastric emptying rate or $t^{1/2}$ gastric emptying time extrapolated from a limited observation period after meal ingestion, two variables that had been shown to be unable to express final gastric emptying time in functional dyspeptic patients^[41]. The serial US measurements of the antral volume enables to assess two relevant aspects of the gastric function, i.e., the antral volume, which is the expression of antral distension and the final gastric emptying time. The former cannot be assessed with scintigraphy and the latter has been shown to be the variable that best correlates with the scintigraphic method and to discriminate patients with delayed gastric emptying from controls^[30-32,42]. In the present study extra-GI symptoms were reported by 53.7% of the patients. Of relevance is that of all investigated symptoms, including GI symptoms usually regarded characteristic of dyspepsia, post-prandial drowsiness is the one that most correlates with, and is the best predictor of, delayed gastric emptying. Also nausea and pain centered in the upper abdomen, albeit to a lesser degree than post-prandial drowsiness, showed a statistical correlation with delayed gastric emptying. Differently from typical abdominal dyspeptic symptoms, drowsiness showed a high specificity in predicting delayed gastric emptying. The other most frequently referred extra-GI symptoms such as headache and palpitation were not statistically related with delayed gastric emptying. Drowsiness can occur in several neurological conditions, including autonomic failure and truncal vagotomy. In none of the investigated patients drowsiness could be explained with any detectable disorders. In healthy subjects it has been shown that in comparison with an equal volume of water and equicaloric liquid meal, solid meal results in a decreased sleep onset latencies^[22].

Furthermore it has been reported a transient decrease in sleep latency after consuming a meal compared to sham feeding^[43]. These results together with the observation of a increased feeling of drowsiness after intravenous injection of CCK administration^[44], support the hypothesis of a GI effect on postprandial sleepiness. It is conceivable that meal ingestion may release CCK and other neuroendocrine substances, such as serotonin, or activate nervous afferences, that affect the state of consciousness and delay gastric emptying. Alternatively prolonged postprandial antral distension may participate via vagal afferences in the activation of central nervous network regulating the state of consciousness. The sensation of drowsiness may vary from slight to severe and be related to sleep disturbances. Postprandial drowsiness reported in the present investigation refers to a sensation regarded to be bothersome enough to interfere with the daily activities and it was not related to sleeplessness.

In addition this study shows that the fasting antral volume of 15 mL is the cut-off value that may be used to predict delayed gastric emptying. Adjusting data for fasting antral volume and BMI, the following symptoms: nausea and drowsiness appear to be significant independent predictors of delayed gastric emptying.

None of the symptoms conventionally considered to be manifestation of dyspepsia was of value to discriminate between patients with normal and delayed gastric emptying.

The different results of the present study from previously mentioned scintigraphy-based studies, may be due to the use of a different technique and/or the different selection of the patients and/or the different assessment of patient's symptoms^[20].

Alternatively, the different results may express a different underlying dysfunction for some of the dyspeptic symptoms. So it may be hypothesized that in patients with functional dyspepsia early satiety^[15] is mainly related to impaired relaxation of the proximal stomach; postprandial fullness and vomiting to a reduced rate of gastric emptying^[20]; post-prandial drowsiness, nausea, to a delayed final gastric emptying.

This study confirms^[26,27] the frequent occurrence in patients with FD of an abnormally distended antral volume during fasting. Whether increased antral volumes may reflect hypotonia of the antral muscular wall or intraluminal distension secondary to gastric retention could not be addressed in the present study.

An increased final antral volume does not necessarily indicate delayed gastric emptying as it may coexist with a normal gastric emptying rate if the fasting antral volume is increased. In the present study, however, the mean final antral volume of dyspeptic patients with delayed gastric emptying exceeded the fasting antral volume of 28 mL indicating the presence of a genuine slowing of the gastric emptying rate.

To identify the cut-off level of 31 mL to discriminate normal and delayed gastric emptying we used data from a control group of healthy people. Similar results were obtained with additional assessments based on other cut-off levels chosen below and above 31 mL. Compared to our patients the control group had a lower percentage of women

and a younger age. However, these differences did not affect the results because these two factors (age and gender) did not have, in the multivariate analysis, any relationship with the gastric emptying. This study confirms previous observations of a statistical correlation between BMI and delayed gastric emptying^[20]. This relationship may be interpreted as an effect of gastric dysfunction often associated with symptoms, such as nausea or pain that limit food ingestion. Patients with eating disorders may be underweight and show abnormal gastric function. In the present study patients with such disorders were excluded and the finding of equally delayed gastric emptying in both genders would support that eating disorders were not present. We did not routinely test for *H pylori* in this study, but there is no evidence that Hp infection has any relationship with symptoms and delayed gastric emptying in functional dyspepsia^[45-49]. Thus, it seems unlikely that knowledge of the Hp status would have altered the conclusions of the present study.

In conclusion, the presence or, alternatively, the absence of nausea and post-prandial drowsiness, appear to be indicative of delayed or, respectively, normal gastric emptying in functional dyspeptic patients.

Interestingly, despite that the symptom of post-prandial drowsiness is often reported by dyspeptic patients and in some of them it may be the predominant disturbance, it has not been considered part of the definition of dyspepsia. This study shows that post-prandial drowsiness is the symptom that most correlates with delayed gastric emptying and would suggest including it in the clinical definition of functional dyspepsia.

Although it would appear that in FD patients an analysis of dyspeptic symptoms and fasting antral volume can offer valuable indication on the modality of gastric emptying, their ability, either alone or in combination, of correctly classifying individuals with or without delayed gastric emptying was not greater than 73%.

REFERENCES

- 1 **Johnsen R**, Straume B, Forde OH. Peptic ulcer and non-ulcer dyspepsia a disease and a disorder. *Scand J Prim Health Care* 1988; **6**: 239-243
- 2 **Jones RH**, Lydeard SE, Hobbs FD, Kenkre JE, Williams EI, Jones SJ, Repper JA, Caldwell JL, Dunwoodie WM, Bottomley JM. Dyspepsia in England and Scotland. *Gut* 1990; **31**: 401-405
- 3 **Talley NJ**, Zinsmeister AR, Schleck CD, Melton LI 3rd. Dyspepsia and dyspepsia subgroups: a population-based study. *Gastroenterology* 1992; **102**: 1259-1268
- 4 **Barnes RJ**, Gear MW, Nicol A, Dew AB. Study of dyspepsia in a general practice as assessed by endoscopy and radiology. *Br Med J* 1974; **26**: 214-216
- 5 **Mollmann KM**, Bonnevie O, Gudbrand-Hoyer E, Wulff HR. A diagnostic study of patients with upper abdominal pain. *Scand J Gastroenterol* 1975; **10**: 805-809
- 6 **Horrocks JC**, De Dombal FT. Clinical presentation of patients with "dyspepsia". Detailed systematic study of 360 patients. *Gut* 1978; **19**: 19-26
- 7 **Holdstock G**, Harman M, Machin D, Patel C, Lloyd RS. Prospective testing of a scoring system designed to improve case selection for upper gastrointestinal investigation. *Gastroenterology* 1986; **90**: 1164-1169
- 8 **Capurso L**, Koch M, Dezi A. Towards a quantitative diagnosis of dyspepsia: the value of clinical symptoms. The dyspepsia project report. *Ital J Gastroenterol* 1988; **20**: 191-202
- 9 **Richter JE**. Dyspepsia: organic causes and differential characteristics from functional dyspepsia. *Scand J Gastroenterol Suppl* 1991; **182**: 11-16
- 10 **Heikkinen M**, Pikkarainen P, Takala J, Rasanen H, Julkunen R. Etiology of dyspepsia: four hundred unselected consecutive patients in general practice. *Scand J Gastroenterol* 1995; **30**: 519-523
- 11 **Klauser AG**, Voderholzer WA, Knesewitsch PA, Schindlbeck NE, Muller-Lissner SA. What is behind dyspepsia? *Dig Dis Sci* 1993; **38**: 147-154
- 12 **Talley NJ**, Colin-Jones D, Koch KL. Functional dyspepsia: a classification with guidelines for diagnosis and management. *Gastroenterol Int* 1991; **4**: 145-160
- 13 **Talley NJ**, Stanghellini V, Heading RC, Koch KL, Malagelada JR, Tytgat GN. Functional gastroduodenal disorder. *Gut* 1999; **45**(Suppl 2): II37-42
- 14 **Bytzer P**, Talley NJ. Dyspepsia. *Ann Int Med* 2001; **134**: 815-822
- 15 **Tack J**, Piessevaux H, Coulie B, Caenepeel P, Janssens J. Role of impaired gastric accommodation to a meal in functional dyspepsia. *Gastroenterology* 1998; **115**: 1346-1352
- 16 **Barbara L**, Camilleri M, Corinaldesi R, Crean GP, Heading RC, Johnson AG, Malagelada JR, Stanghellini V, Wienbeck M. Definition and investigation of dyspepsia. Consensus of an International ad hoc working party. *Dig Dis Sci* 1989; **34**: 1272-1276
- 17 **Wegener M**, Borsch G, Schaffstein J, Reuter C, Leverkus F. Frequency of idiopathic gastric stasis and intestinal transit disorders in essential dyspepsia. *J Clin Gastroenterol* 1989; **11**: 163-168
- 18 **Waldron B**, Cullen PT, Kumar R, Smith D, Jankowski J, Hopwood D, Sutton D, Kennedy N, Campbell FC. Evidence for hypomotility in non-ulcer dyspepsia: a prospective multifactorial study. *Gut* 1991; **32**: 246-251
- 19 **Talley NJ**, Shuter B, McCrudden G, Jones M, Hoschl R, Piper DW. Lack of association between gastric emptying of solids and symptoms in non-ulcer dyspepsia. *J Clin Gastroenterol* 1989; **11**: 625-630
- 20 **Stanghellini V**, Tosetti C, Paternico A, Barbara G, Morselli-Labate AM, Monetti N, Marengo M, Corinaldesi R. Risk indicators of delayed gastric emptying of solids in patients with functional dyspepsia. *Gastroenterology* 1996; **110**: 1036-1042
- 21 **Talley NJ**, Verlinden M, Jones M. Can symptoms discriminate among those with delayed or normal gastric emptying in dysmotility-like dyspepsia? *Am J Gastroenterol* 2001; **96**: 1422-1428
- 22 **Orr WC**, Shadid G, Harnish MJ, Elsenbruch S. Meal composition and its effect on postprandial sleepiness. *Physiol Behav* 1997; **62**: 709-712
- 23 **Talley NJ**, Phillips SF, Bruce B, Zinsmeister AR, Wiltgen C, Melton LJ. Multisystem complaints in patients with irritable bowel syndrome and functional dyspepsia. *Eur J Gastroenterol Hepatol* 1991; **3**: 71-77
- 24 **Corinaldesi R**, Stanghellini V, Raiti C, Rea E, Salgemini R, Barbara L. Effect of chronic administration of cisapride on gastric emptying of solid meal and on dyspeptic symptoms in patients with idiopathic gastroparesis. *Gut* 1987; **28**: 300-305
- 25 **Distrutti E**, Fiorucci S, Hauer SK, Pensi MO, Vanasia M, Morelli A. Effect of acute and chronic levosulpiride administration on gastric tone and perception in functional dyspepsia. *Aliment Pharmacol Ther* 2002; **16**: 613-622
- 26 **Ricci R**, Bontempo I, La Bella A, De Tschudy A, Corazzieri E. Dyspeptic symptoms and gastric antrum distribution. An ultrasonographic study. *Ital J Gastroenterol* 1987; **19**: 215-217
- 27 **Hausken T**, Berstad A. Wide gastric antrum in patients with non-ulcer dyspepsia. Effect of cisapride. *Scand J Gastroenterol* 1992; **27**: 427-432
- 28 **Talley NJ**. Optimal design of treatment trials. In DA Drossman, JE Richter, NJ Talley, WG Thompson, E Corazzieri, WE Whitehead (eds). *Functional Gastrointestinal Disorders*:

- Diagnosis, Pathophysiology and Treatment.* Boston, Little Brown and Company 1994: 265-310
- 29 **Aldrich MS.** Narcolepsy. *Neurology* 1992; **42**(Suppl 6): 34-43
- 30 **Hveem K,** Jones KL, Chatterton BE, Horowitz M. Scintigraphic measurements of gastric emptying and ultrasonographic assessment of antral area: relation to appetite. *Gut* 1996; **38**: 816-821
- 31 **Benini L,** Sembenini C, Heading RC, Giorgetti PG, Montemezzi S, Zamboni M, Di Benedetto P, Brighenti F, Vantini I. Simultaneous measurement of gastric emptying of a solid meal by ultrasound and by scintigraphy. *Am J Gastroenterol* 1999; **94**: 2861-2865
- 32 **Benini L,** Sembenini C, Castellani G, Caliani S, Fioretta A, Vantini I. Gastric emptying and dyspeptic symptoms in patients with gastroesophageal reflux. *Am J Gastroenterol* 1996; **91**: 1351-1354
- 33 **Bolondi L,** Bortolotti M, Santi V, Calletti T, Gaiani S, Labò G. Measurement of gastric emptying time by real-time ultrasonography. *Gastroenterology* 1985; **89**: 752-759
- 34 **Ricci R,** Bontempo I, Corazziari E, La Bella A, Torsoli A. Real-time ultrasonography of the gastric antrum. *Gut* 1993; **34**: 173-176
- 35 **Altman DG.** Practical statistics for medical research. Chapman and Hall; 1991
- 36 **Hosmer DW,** Lemeshow S. Applied logistic regression. New York John Wiley and sons, Inc.; 1989
- 37 StataCorp. Stata Statistical Software: Release 5.0. Stata Corporation, College Station, TX, USA, 1997
- 38 **Malagelada JR,** Stanghellini V. Manometric evaluation of functional upper gut symptoms. *Gastroenterology* 1985; **88**: 1223-1231
- 39 **Rees WD,** Miller LJ, Malagelada JR. Dyspepsia, antral motor dysfunction, and gastric stasis of solids. *Gastroenterology* 1980; **78**: 360-365
- 40 **Metcalf R,** Youngs GR. Prevalence of symptoms of dyspepsia. *BMJ* 1989; **298**: 526-527
- 41 **Guo JP,** Maurer AH, Fisher RS, Parkman HP. Extending gastric emptying scintigraphy from two to four hours detects more patients with gastroparesis. *Dig Dis Sci* 2001; **46**: 24-29
- 42 **Bortolotti M,** Bolondi L, Santi V, Sarti P, Brunelli F, Barbara L. Patterns of gastric emptying in dysmotility-like dyspepsia. *Scand J Gastroenterol* 1995; **30**: 408-410
- 43 **Harnish MJ,** Greenleaf SR, Orr WC. A comparison of feeding to cephalic stimulation on postprandial sleepiness. *Physiol Behav* 1998; **64**: 93-96
- 44 **Stacher G,** Bauer H, Steinringer H. Cholecystokinin decreases appetite and activation evoked by stimuli arising from the preparation of a meal in man. *Physiol Behav* 1979; **23**: 325-331
- 45 **McColl K,** Murray L, El-Omar E, Dickson A, El-Nujumi A, Wirz A, Kelman A, Penny C, Knill-Jones R, Hilditch T. Symptomatic benefit from eradicating *Helicobacter pylori* infection in patients with nonlcer dyspepsia. *N Engl J Med* 1998; **339**: 1869-1874
- 46 **Blum AL,** Talley NJ, O'Morain C, Veldhuyzen van Zanted S, Labenz J, Stolte M, Louw JA, Stubberod A, Theodors A, Sundin M, Bolling-Sternevald E, Junghard O. OCAY study Group. Lack of effect of treating *Helicobacter pylori* infection in patients with non-ulcer dyspepsia. *N Engl J Med* 1998; **339**: 1875-1881
- 47 **Talley NJ,** Vakil N, Ballard ED, Fennerty MB. Absence of benefit of eradicating *Helicobacter pylori* in patients with non-ulcer dyspepsia. *N Engl J Med* 1999; **341**: 1106-1111
- 48 **Tucci A,** Corinaldesi R, Stanghellini V, Tosetti C, Di Febo G, Paparo GF, Varoli O, Paganelli GM, Morselli AM, Masci C, Zoccoli G, Monetti N, Barbara L. *Helicobacter pylori* infection and gastric function in patients with chronic idiopathic dyspepsia. *Gastroenterology* 1992; **103**: 768-774
- 49 **Rhee PL,** Kim YH, Son HJ, Kim JJ, Koh KC, Paik SW, Rhee JC, Choi KW. Lack of association of *Helicobacter pylori* infection with gastric hypersensitivity. *Am J Gastroenterol* 1999; **94**: 3165-3169

Science Editor Guo SY Language Editor Elsevier HK

• CLINICAL RESEARCH •

Expression of adhesion molecules on mature cholangiocytes in canal of Hering and bile ductules in wedge biopsy samples of primary biliary cirrhosis

Hiroaki Yokomori, Masaya Oda, Mariko Ogi, Go Wakabayashi, Shigeyuki Kawachi, Kazunori Yoshimura, Toshihiro Nagai, Masaki Kitajima, Masahiko Nomura, Toshifumi Hibi

Hiroaki Yokomori, Department of Internal Medicine, Kitasato Institute Medical Center Hospital, Saitama 364-8501, Japan
Masaya Oda, Organized Center of Clinical Medicine, International University of Health and Welfare, Tokyo 107-0052, Japan
Mariko Ogi, Laboratory of Pathology, Kitasato Institute Medical Center Hospital, Saitama 364-8501, Japan
Go Wakabayashi, Shigeyuki Kawachi, Masaki Kitajima, Department of Surgery, School of Medicine, Keio University, Tokyo 160-0016, Japan
Kazunori Yoshimura, Masahiko Nomura, Physiology, Saitama Medical School, Saitama 350-0495, Japan
Toshihiro Nagai, Electron Microscopy Laboratory, School of Medicine, Keio University, Tokyo 160-0016, Japan
Toshifumi Hibi, Department of Internal Medicine, School of Medicine, Keio University, Tokyo 160-0016, Japan
Correspondence to: Hiroaki Yokomori, MD, Kitasato Institute Medical Center Hospital, 121-1 Arai, Kitamotoshi, Saitama 364-8501, Japan. yokomori-hr@kitasato.or.jp
Telephone: +81-485-93-1212 Fax: +81-485-93-1239
Received: 2004-07-28 Accepted: 2004-08-31

Abstract

AIM: To examine the expression of intercellular adhesion molecule-1 (ICAM-1) and lymphocyte function-associated antigen-1 (LFA-1) expression on canals of Hering (CoH) and bile ductules associated with the autoimmune process of bile duct destruction in primary biliary cirrhosis (PBC).

METHODS: Ten wedged liver biopsies of PBC (five cases each of stages 2 and 3) were studied. The liver specimens were processed for transmission electron microscopy. Immunohistochemistry was performed using anti-ICAM-1 and anti-LFA-1 mouse mAbs. *In situ* hybridization was done to examine the messenger RNA expression of ICAM-1 in formalin-fixed, paraffin-embedded sections using peptide nucleic acid probes and the catalyzed signal amplification (CSA) technique. Immunogold-silver staining for electron microscopy was performed using anti-ICAM and anti-LFA-1 mouse mAbs. The immunogold particles on epithelial cells of bile ductules and cholangiocytes of CoH cells were counted and analyzed semi-quantitatively. Western blotting was performed to confirm ICAM-1 protein expression.

RESULTS: In liver tissues of PBC patients, immunohistochemistry showed aberrant ICAM-1 expression on the plasma membrane of epithelial cells lining bile ductules, and also on mature cholangiocytes but not on hepatocytes in CoH. LFA-1-positive lymphocytes were closely associated

with epithelial cells in bile ductules. ICAM-1 expression at protein level was confirmed by Western blot. *In situ* hybridization demonstrated ICAM-1 mRNA expression in bile ductules and LFA-1 mRNA in lymphocytes infiltrating the bile ductules. By immunoelectron microscopy, ICAM-1 was demonstrated on the basal surface of epithelial cells in bile ductules and on the luminal surfaces of cholangiocytes in damaged CoH. Cells with intermediate morphology resembling progenitor cells in CoH were not labeled with ICAM-1 and LFA-1.

CONCLUSION: *De novo* expression of ICAM-1 both on mature cholangiocytes in CoH and epithelial cells in bile ductules in PBC implies that lymphocyte-induced destruction through adhesion by ICAM-1 and binding of LFA-1-expressing activated lymphocytes takes place not only in bile ductules but also in the CoH.

© 2005 The WJG Press and Elsevier Inc. All rights reserved.

Key words: Primary biliary cirrhosis; Canal of Hering; Small bile ductule; ICAM-1; LFA-1; Immunohistochemistry; Western blot; Immunogold electron microscopy

Yokomori H, Oda M, Ogi M, Wakabayashi G, Kawachi S, Yoshimura K, Nagai T, Kitajima M, Nomura M, Hibi T. Expression of adhesion molecules on mature cholangiocytes in canal of Hering and bile ductules in wedge biopsy samples of primary biliary cirrhosis. *World J Gastroenterol* 2005; 11(28): 4382-4389
<http://www.wjgnet.com/1007-9327/11/4382.asp>

INTRODUCTION

The canal of Hering (CoH) is named after Hering who in 1855 described the structure as a link between the hepatocyte canalicular system and biliary tree^[1]. Under the electron microscope, the small cells of CoH have a basement membrane like the more distal portions of the biliary tree but an apical surface that appears similar to hepatic canalicular membrane^[2]. Functionally, bile canalicular contraction is involved in the canalicular bile flow as demonstrated by an inverted microscope linked to a SIT camera, and disturbance of canalicular contraction would lead to intrahepatic cholestasis^[3]. Moreover, contraction of the CoH has been demonstrated, and the interval between contractions was approximately five times longer than that seen in canaliculi^[4]. Hepatic cholestasis and hepatic injury are accompanied with

striking morphologic changes. Examination of periportal changes in the liver of graft-*vs*-host disease mice shows that hepatocytes in close contact with lymphocytes had minor degenerative changes, whereas periportal bile ductules and CoH are constantly injured by inflammatory cells^[5]. Study of the three-dimensional structure of ductular reactions in massive necrosis suggests that cytokeratin 19-positive reactions are in fact proliferations of the cells lining the CoH^[6].

Primary biliary cirrhosis (PBC) is a chronic, progressive cholestatic liver disease characterized by inflammatory obliteration of the intrahepatic bile ducts, leading to fibrosis and ultimately to cirrhosis complicated by liver failure or hypertension^[7,8]. Although the pathogenesis of bile duct destruction in PBC remains unknown, increasing evidence has suggested that it is related to autoimmune abnormalities^[8-10]. Immunohistochemical analysis of the lymphocytes infiltrating the portal tracts including the bile duct lesions indicates that activated T lymphocyte subsets may play an important role in bile duct destruction^[11]. Therefore bile ducts (centrally located, accompanied by a hepatic arterial branch) are the prime targets for immune-mediated damages in PBC and are reduced in number as the disease progresses. Bile ductules (peripherally located, usually without a conspicuous lumen) increase in number in response to bile duct damage (ductular reaction). Bile ductules are frequently associated with a mixed population of inflammatory cells. However, there is no clear evidence that these inflammatory cells are associated with bile ductular destruction^[12]. Recent studies have demonstrated increased expression of intercellular adhesion molecule (ICAM)-1 on the bile duct epithelium in PBC^[13,14], suggesting that the activated T lymphocytes may specifically react with the bile duct epithelial cells through these adhesion molecules. Expression of intracellular adhesion molecules and their specific ligands are essential for cell-to-cell interactions in autoimmune mechanism^[15]. In PBC, ICAM-1 is expressed on plasma membrane of epithelial cell in bile ducts characterized by chronic non-suppurative destructive cholangitis (CNSDC) and on the sinusoidal endothelial cells^[16,17]. While immunohistochemical findings of ICAM-1 and lymphocyte function-associated antigen (LFA)-1 expression in PBC tissue have been reported^[17], no studies have correlated protein expression of the antigens on CoH by examining serial sections using immunoelectron microscopy. The aim of the present study was to clarify the roles of ICAM-1 and LFA-1 expression on the bile ductule and CoH in PBC. The aim of the present study was to clarify ICAM-1 and LFA-1 expression on the bile ductule and CoH in PBC. We conducted immunohistochemistry, *in situ* hybridization and immunoelectron microscopy on liver biopsy specimens from PBC patients.

MATERIALS AND METHODS

Materials

Surgical liver biopsy specimens were obtained from 10 patients (all female, mean age 55.9 years, range 48-65 years) with PBC (five cases each of Scheuer's stages 2 and 3). PBC was diagnosed clinically and histologically according to the criteria proposed by the Japanese Joint Research Group for Autoimmune Hepatitis^[18]. As controls, wedge biopsy specimens from normal portions of the liver were obtained

from five patients (four male and one female; aged from 54 to 71 years with a mean of 62.6 years) who underwent surgical resection for metastatic liver carcinoma (four colonic carcinomas).

Electron microscopy

The liver specimens were cut into small blocks (approximately 1 mm×1 mm×1 mm). The blocks were fixed in fresh 2.5% glutaraldehyde solution for 1 h at 4 °C, followed by post-fixation in 2% osmium tetroxide with 0.1 mol/L cacodylate buffer (pH 7.4), and then dehydrated in a graded series of ethanol solutions. For transmission electron microscopy, the liver tissue blocks were embedded in Epon after dehydration. Ultrathin sections were cut with a diamond knife on a LKB ultramicrotome (Bromma), stained with uranyl acetate and lead citrate and observed under a transmission electron microscope (JEM-1200 EX, JEOL, Tokyo, Japan) with a 80-kV acceleration voltage.

Immunohistochemical staining

Liver tissues (approximately 5 mm×5 mm×5 mm) were fixed in periodate-lysine-paraformaldehyde^[19], rinsed in 0.01 mol/L phosphate buffer (pH 7.4) containing 15-30% sucrose, embedded in Tissue-Tek OCT-compound (Miles Inc., Elkhart, Inc., Germany) and frozen at -80 °C until use. The tissue was incubated overnight at 4 °C with anti-ICAM-1 mouse mAb (CD54; DAKO, Glostrup, Denmark) diluted at 1:50 or anti-LFA-1 mouse mAb (CD11a; DAKO, Glostrup, Denmark) diluted at 1:20, and then incubated with horseradish peroxidase-conjugated anti-mouse IgG goat antibody (Cosmo Bio Inc., Tokyo, Japan) diluted 1:100. After repeated washes with PBS, the sections were reacted with diaminobenzidine solution containing 0.01% H₂O₂, and counterstained with hematoxylin for light-microscopic study.

In situ hybridization technique

Messenger RNA of ICAM-1 was detected in formalin-fixed, paraffin-embedded sections by *in situ* hybridization using peptide nucleic acid (PNA) probes^[20] and the catalyzed signal amplification (CSA) technique. Liver tissues were cut into 4 µm-thick sections and adhered to silanated RNase-free glass slides (prepared by heating in an oven at 60 °C for 30 min). The sections were dewaxed in xylene (for 15 min, each twice), treated with a graded ethanol series, rehydrated in RNase-free distilled water, and incubated for 30 min in target retrieval buffer (DAKO Japan, Kyoto, Japan) preheated and maintained at 95 °C. The slides were allowed to cool at room temperature for 20 min and then digested with 20 µg/mL proteinase K (DAKO) at room temperature for 30 min. The slides were rinsed in distilled water and rapidly air dried. The air-dried sections were covered with approximately 15 mL of hybridization solution containing 100 g/L dextran sulfate, 10 mmol/L NaCl, 300 mL/L formamide, 1 g/L sodium pyrophosphate, 2 g/L polyvinylpyrrolidone, 2 g/L Ficoll, 5 mmol/L Na₂EDTA, 50 mmol/L Tris-HCl, pH 7.5, and 1 µg/mL PNA probe. Probes were constructed according to the sequence information of ICAM-1 and LFA-1^[21,22]. The following probes were used: ICAM-1 antisense (FITC-ATTATGACTGCGGCTGC), ICAM-1 sense (FITC-GCAGCCGCAGTCATAAT),

LFA-1 antisense (FITC-CATCCAGCTGCAGAGTGT), and LFA-1 sense (FITC-ACACTCTGCAGCTGGATG). The slides were evenly covered with the hybridization solution and incubated in a moist chamber at 43 °C for 90 min. Following hybridization, the cover slips were removed, and the slides were transferred to pre-warmed TBS in a water bath at 49 °C and washed for 30 min with gentle shaking (PNA Hybridization Kit; DAKO, Tokyo, Japan). A non-isotopic, colorimetric signal amplification system (GenPoint kit, DAKO Japan) was used to visualize specific hybridization signals. Briefly, tissue sections were incubated with a FITC-horseradish peroxidase reagent for 15 min, washed thrice with TBST (150 mmol/L NaCl, 10 mmol/L Tris; pH 7.5, 11 mL/L Tween 20), incubated with a solution containing H₂O₂ and biotinyl tyramide for 15 min, and washed thrice with TBST^[23]. This step resulted in CSA by additional deposition of biotin at the site of probe hybridization. The sections were then incubated in streptavidin-horseradish peroxidase for 15 min, and washed thrice in TBST. Colorimetric signals were developed by incubation in diaminobenzidine solution containing 0.01% H₂O₂, and counterstained with hematoxylin for light microscopic examination.

Immunogold-silver staining method for electron microscopy

For light microscopy, the sections were immersed in three changes of 0.01% PBS (pH 7.4) for 15 min, and then incubated overnight in a moist chamber at 4 °C with anti-ICAM-1 mouse mAb at 1:50 dilution and anti-LFA-1 mouse mAb at 1:20 dilution. After washing thrice with PBS for 15 min, the sections were incubated for 40 min with 10-nm colloidal gold-conjugated anti-mouse IgG antibody (Cosmo Bio Co., Tokyo, Japan) diluted at 1:100. The slides were developed with a developing solution described below for 50 min at 20 °C in a dark room. After having washed in running water, the sections were briefly counterstained with 0.1% nuclear fast red in 5% aluminum sulfate aqueous solution, dehydrated, cleared and mounted on Biolet. The developing solution had two components. Solution A contained 45 mL of 20% gum arabic aqueous solution (Kanto Chemical Co., Tokyo, Japan) and 1 mL of 10% silver nitrate solution. The gum arabic solution was prepared by centrifuging a 20% suspension at 18 000 g for 30 min at 0 °C and separating the supernatant for use. Solution B contained 200 mg of hydroquinone (Kanto Chemical Co., Tokyo, Japan) and 300 mg of citric acid monohydrate (Kanto Chemical Co., Tokyo, Japan) in 10 mL of distilled water. The working developing solution was prepared by mixing solutions A and B in a dark room under illumination of a photographic safety lamp^[24].

For electron microscopy, the tissue specimens processed for light microscopy as above were treated thrice, with PBS for 15 min, and fixed for 1 h at 4 °C in 1.2% glutaraldehyde buffered with 0.01% phosphate buffer (pH 7.4), followed by a graded series of ethanol solutions. After postfixation with 1% osmium tetroxide in 0.01% phosphate buffer (pH 7.4), the liver tissues were embedded in Epon. Ultrathin sections cut with a diamond knife on a LKB ultramicrotome were stained with uranyl acetate and observed under a transmission electron microscope (JEM-1200 EX, Tokyo, Japan) operated at an acceleration voltage of 80 kV.

Western blotting

Western blotting was conducted using fresh control and PBC liver tissues. Briefly, liver tissues were homogenized in 10 volumes of homogenization buffer (20 mmol/L Tris-HCl; pH 7.5, 5 mmol/L MgCl₂, 0.1 mmol/L PMSF, 20 μmol/L pepstatin A, and 20 μmol/L leupeptin) using a polytron homogenizer at setting 7 for 90 s. The homogenates were centrifuged at 100 000 g for 45 min. The membranes were washed thrice, resuspended in 10 volumes of homogenization buffer, homogenized using a Teflon/glass homogenizer, and centrifuged. The membrane proteins thus obtained were used for immunoblotting. Proteins were separated on SDS/PAGE (4-20% gel, Daiichi-Ikagaku, Tokyo, Japan) and transferred onto polyvinylidene difluoride (PVDF) membranes (Millipore, Bedford, MA). The blots were blocked with 50 g/L dried milk in PBS for 30 min, incubated with 20 μg/mL anti-ICAM-1 (G-5; Santa Cruz Bio., Santa Cruz, CA, USA), washed in 0.1% Tween 20 in PBS, and transferred onto PVDF membranes (NTN Life Science Products). The blots were blocked with 50 g/L dried milk in PBS for 30 min, incubated with anti-mouse goat IgG conjugated with horseradish peroxidase (Amershampharmacia) in 0.1% Tween 20 in PBS, and then processed by the Vectastain ABC system (Vector laboratories, Inc., Burlingame, CA, USA). The immunoreactive bands were visualized with diaminobenzidine solution containing 0.01% H₂O₂.

Semi-quantitative analysis

The immunogold particles on epithelial cells of bile ductules and cholangiocytes of CoH cells were counted. Photographs from 10 fields between the bile ductules and canal of Hering were investigated. The magnification was ×2 000.

RESULTS

Electron microscopic finding

Electron microscopic observation of the PBC liver specimens revealed lymphocytes associated with the bile ductular membrane in bile ductules (Figure 1A). Lymphocytes frequently migrated into the epithelial layer of CoH through their basement membrane (Figure 1B).

Immunohistochemical finding

We examined the immunohistochemical reactions of both ICAM-1 and LFA-1 in serial sections. In control liver specimens, ICAM-1 protein was expressed on sinusoidal lining cells but no specific immunoreactivity was observed on bile duct epithelial cells (Figure 2A). Immunostaining for LFA-1 appears to be present in portal lymphoid cells. Interlobular bile ducts appear to be negative for LFA-1, although there was sparse expression in bile duct epithelial cells (Figure 2B). In PBC liver tissue, *de novo* expression of ICAM-1 was found on the plasma membrane on the luminal side of epithelial cells in bile ductules and on some lymphocytes infiltrating small bile ductules or possibly small blood vessels. ICAM-1 immunoreactivity was also seen on the sinusoidal endothelial cells (Figure 2C). LFA-1 protein was expressed mainly in lymphocytes around and among the proliferated bile ductules (Figure 2D). Immunostaining of ICAM-1 and LFA-1 in CoH was less clearly depicted by immunostaining examined under a light microscope.

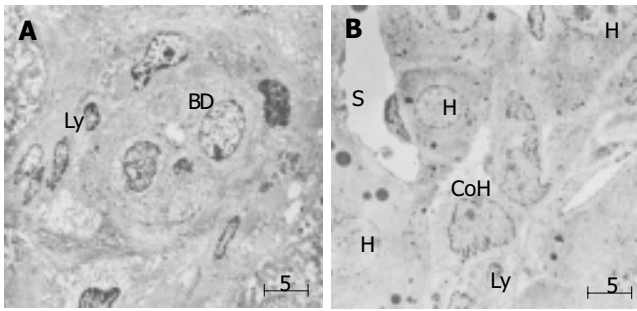


Figure 1 Electron microscopic finding in small bile ductule and CoH in liver specimen of PHC. **A:** Interaction of lymphocytes appear to interact with the bile ductule. Lymphocytes frequently migrate into the epithelial layer of small bile duct through the basement membrane. BD: bile ductule, ly: lymphocyte; **B:** Association of lymphocytes with the cholangiocytes of the CoH. CoH: canal of Hering. S: sinusoid, H: hepatocytes, Ly: lymphocytes, Bar: 5 µm.

Western blot

To confirm the immunohistochemical results, we investigated ICAM-1 protein expression by Western blotting. Samples containing 20 µg of protein were subjected to SDS/PAGE (4-20% gel) and analyzed by blotting with anti-ICAM-1 antibody. A band around 110 ku indicating ICAM-1 was found in abundance in PBC liver tissue (Figure 3).

In situ hybridization

Next, we investigated the expression of ICAM-1 and LFA-1 at mRNA level in PBC liver samples using *in situ* hybridization with PNA probes (Figure 4). Signals showing ICAM-1 mRNA were typically localized in bile ductular

epithelial cells surrounding the CNSDC lesions (Figures 4A and B). Interestingly, signals showing LFA-1 were localized in lymphocytes inside the bile ductules of CNSDC lesions (Figures 4C and D).

Immunoelectron microscopy

Light microscopic examination of PBC liver samples depicted the localization of ICAM-1 and LFA-1 in bile ductules, but the localization in the CoH was less clear. We therefore conducted immunoelectron microscopic examination. By immunogold electron microscopy, gold-labeled ICAM-1 particles were observed on cholangiocytes, distributing on the luminal surfaces of small bile ductules. ICAM-1 immunoreactivity was also observed on small portal or peripheral blood vessels and sinusoidal endothelial cells (Figure 5A). In the canal of Hering, gold-labeled ICAM-1 particles were observed on the luminal surfaces of cholangiocytes and hepatocytes (Figure 5C). LFA-1 labeling was concentrated on lymphocytes that were found around bile ductules (Figure 5B) and also around cholangiocytes of CoH (Figure 5D). Immature cells resembling progenitor cells were observed in CoH, and these cells did not show ICAM-1 immunoreactivity (Figure 5E). Around these cells, infiltration of lymphocytes was also absent (Figure 5F).

In the semi-quantitative analysis, immunogold–silver complex particles on epithelial cells of bile ductules and cholangiocytes of CoH were enumerated on immunoelectron micrographs (Figure 6). ICAM-1 immunoreactivity was found in CoH in 4 of the 10 PBC cases and in bile ductules

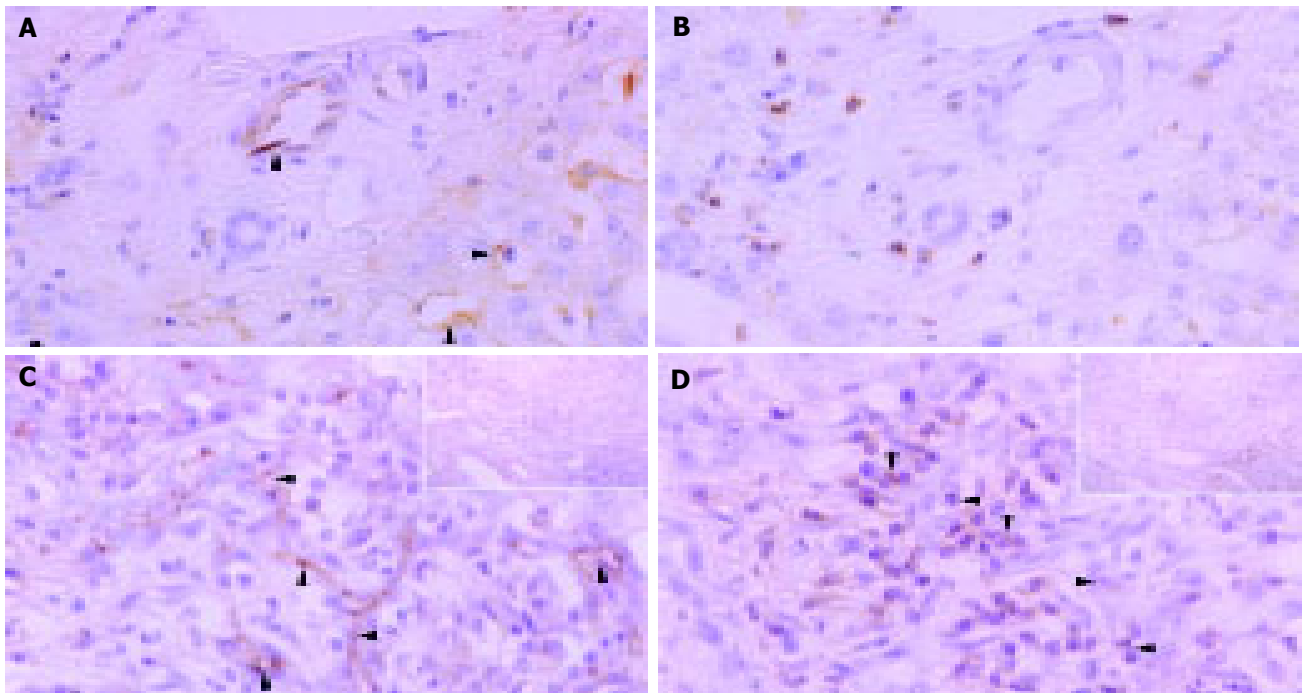


Figure 2 Immunohistochemical distributions of ICAM-1 (A and C) and LFA-1 (B and D) in control liver tissue (A and D) and liver tissue of PHC (C and D). **A:** ICAM-1 protein expression on sinusoidal lining cells but no specific immunoreactivity on bile duct epithelial cells in control liver specimens; **B:** LFA-1 immunoreactivity in portal lymphoid cells, negative in interlobular bile ducts and sparse expression in bile duct epithelial cells; **C:** Marked ICAM-1 immunoreactivity on the plasma

membrane on the luminal side of bile ductules or possibly small blood vessels. Some lymphocytes around the bile ducts were also positive for ICAM-1. Arrowheads denote localization of ICAM-1 (arrows); **D:** LFA-1 immunoreactivity in lymphocytes around and among damaged bile ducts (arrowheads). Original magnification; ×400, hematoxylin counterstained.

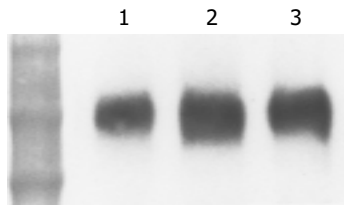


Figure 3 Western blot analysis of expression of ICAM-1 protein in human control and PBC liver tissue. Samples containing 20 μ g protein were subjected to SDS/PAGE (4-20% gel) and analyzed by blotting. ICAM-1 was found in abundance in PBC liver tissues. Lanes 2 and 3: PBC liver tissue, lane 1: control liver tissue. Positions of molecular mass markers are shown (ku).

in 8 of the 10 cases. LFA-1 immunoreactivity was found in CoH in 4 of the 10 PBC cases and in bile ductules in 7 of the 10 cases. The extent of immunoreactivity (number of immunogold particles per unit CoH or bile ductule) was also stronger in bile ductules than in CoH. No immunogold-silver complex particles for ICAM-1 and LFA-1 were found in bile ductules and CoH of control liver tissues.

DISCUSSION

Bile duct inflammation and destruction are the fundamental lesions of PBC^[25]. Interlobular bile ducts with external diameters of 30-100 μ m are selectively affected, displaying variable necrotic and proliferative changes of biliary epithelial cells, as well as periductal lymphoplasmacytic infiltration. These findings are also frequently noted around damaged bile ducts, especially in the early histologic stages of the disease^[25]. In our immunohistochemical study, ICAM-1 was strongly expressed on damaged bile ducts and infiltrating inflammatory cells, while LFA-1 was expressed on infiltrating lymphocytes. The presence of ICAM-1/LFA-1 linkage has been reported in CNSDC in PBC^[16,17].

In our previous study, we correlated protein and mRNA expression of ICAM-1 and LFA-1 by conducting immunohistochemical and *in situ* hybridization studies on serial sections of CNSDC lesions^[26]. We demonstrated abundant protein and mRNA expression of ICAM-1 on damaged biliary epithelial cells and LFA-1 on lymphocytes in CNSDC lesions, strongly suggesting the ICAM-1/LFA-1 linkage^[26].

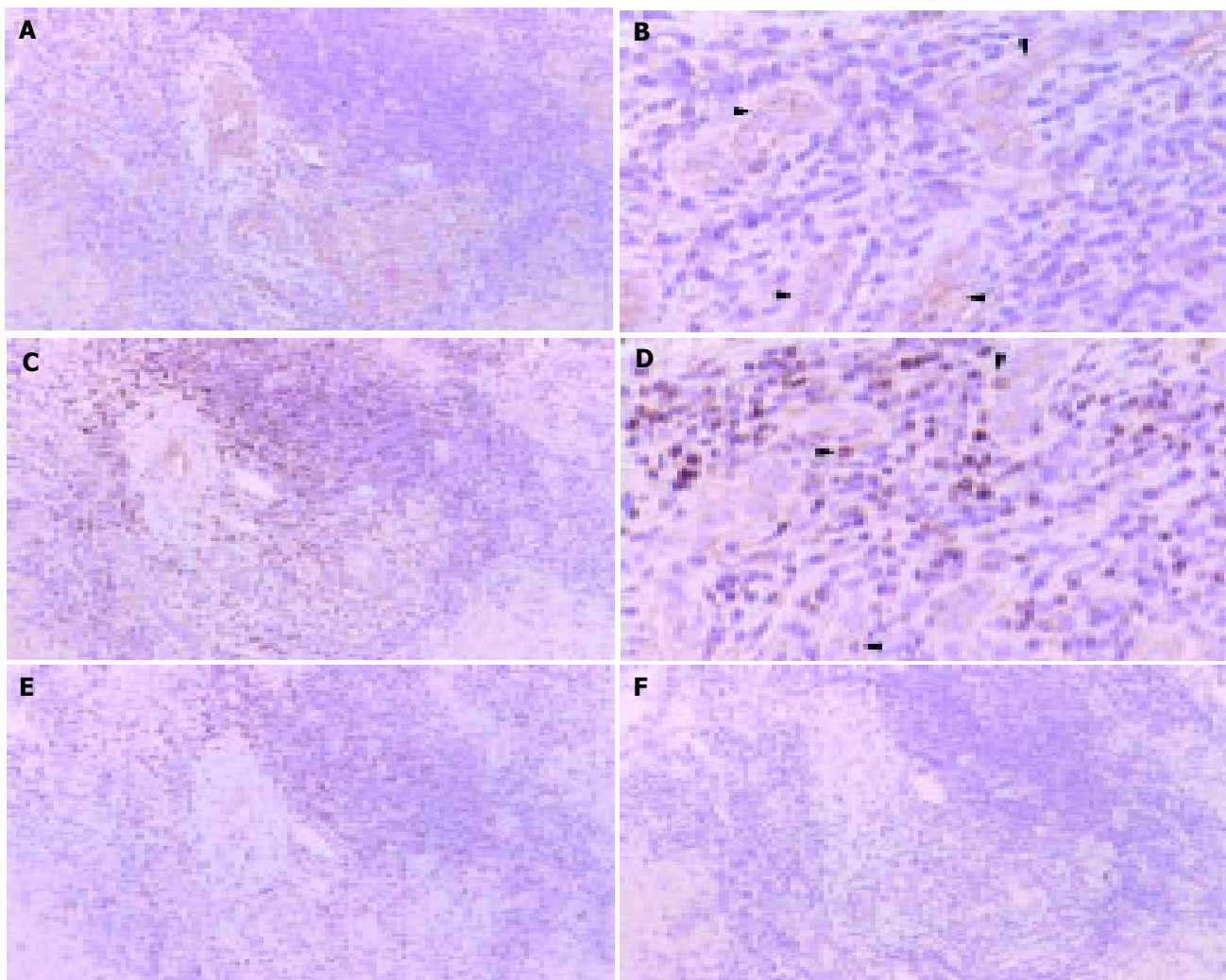


Figure 4 Localization of ICAM-1 (A and B) and LFA-1 (C and D) mRNA at bile ductules in PBC liver tissue by *in situ* hybridization with CSA. A: ICAM-1 mRNA was expressed in a cytoplasmic pattern on epithelial cells of bile ductule. (A: $\times 100$ and B: $\times 300$) Arrowhead denotes reaction product; C: LFA-1 mRNA is

expressed in a cytoplasmic pattern in lymphocytes around bile ductule. (C: $\times 100$ and D: $\times 300$). Negative controls: E: ICAM-1 sense probe, F: LFA-1 sense probe. All panels: color was developed by DAB chromogen and hematoxylin counterstained. Arrowhead denotes reaction product.

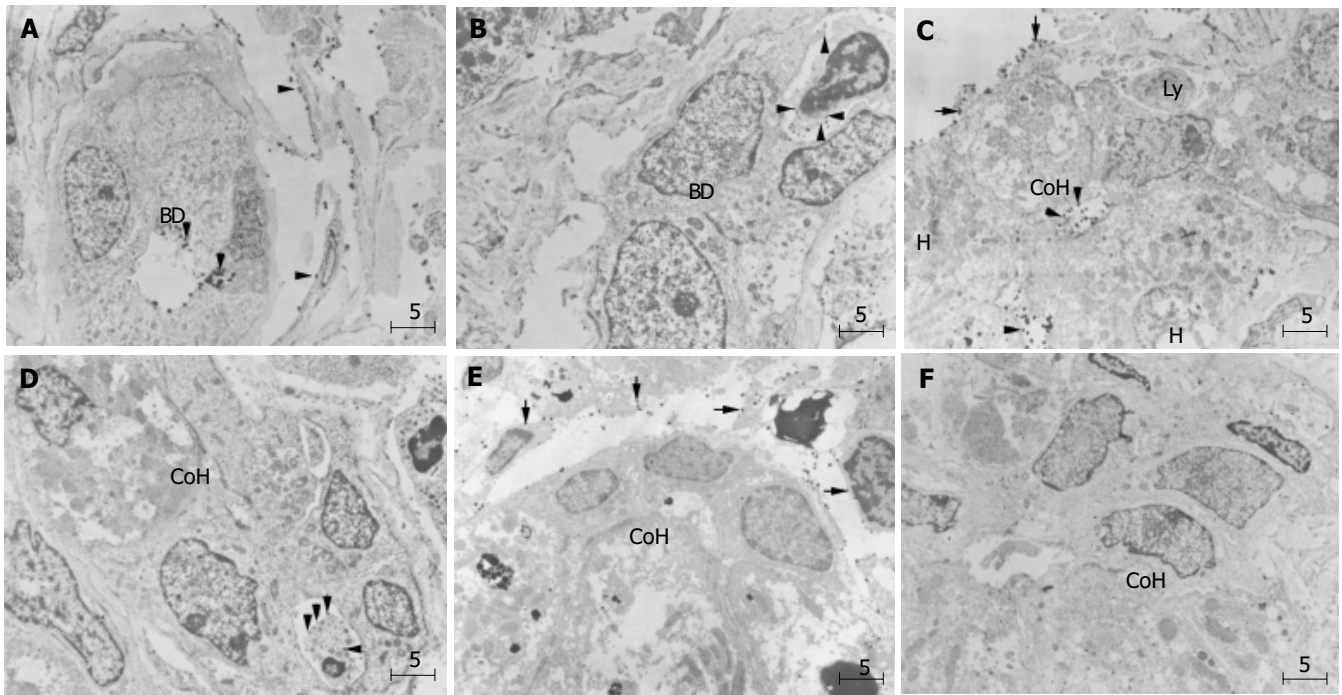


Figure 5 Immunoelectron microscopic findings of ICAM-1 (A, C, and E) and LFA-1 (B, D, and F) in periportal small bile ductule and canal of Hering in PBC liver. **A:** Gold-labeled ICAM-1 particles on the surface of cholangiocytes (arrowhead) facing the lumen of small bile ductule, a small portal or peripheral blood vessel, and also on sinusoidal endothelial cells (arrowheads). BD denotes bile ductule; **B:** Lymphocytes with dense labeling of LFA-1 (arrowhead) around small ductule; **C:** Gold-labeled ICAM-1 particles on the luminal surfaces of

hepatocytes and cholangiocytes of CoH, on bile canaliculus and also on sinusoidal endothelial cells (arrows); **D:** Lymphocytes densely labeled with LFA-1 (arrows) on the basolateral membrane of cholangiocytes of the CoH; **E:** No ICAM-1 immunoreactivity show immature cells resembling progenitor cells (asterisk) in CoH, and these cells; **F:** No infiltration of lymphocytes is observed around the progenitor-like cells (asterisk). Bar, 5 μ m; BD, bile ductule; Ly, lymphocyte; CoH, canal of Hering; H, hepatocyte. Uranyl acetate stain.

Frequent and variable infiltration of lymphocytes, mainly T cells, and other inflammatory cells of the biliary epithelium has been reported in PBC^[27]. Some lymphocytes infiltrate

by crossing the basement membrane of bile ducts. These changes appear as necro-inflammatory lesions inside the basement membrane of bile ducts and ductules.

Our immunoelectron microscopic study has confirmed for the first time the ultrastructural localization of ICAM-1 on cholangiocytes and LFA-1 on infiltrating inflammatory cell in damaged CoH. The lymphocytes and other inflammatory cells then penetrated the peribiliary vascular plexus and portal venules, and migrated into perivenular tissue toward the bile ducts^[12]. When early stage PBC specimens were immunostained for cytokeratin 19 and HLA-DR, the CoH were found mostly around portal tracts in stages 2 and 3 PBC, but they were destroyed in concert with the destruction of bile ductules^[28]. Therefore, CoH in PBC specimens are difficult to be depicted by immunohistochemistry using light microscopy. Our immunoelectron microscopic study successfully demonstrated the ultrastructural localization of ICAM-1 and LFA-1 on CoH.

Previous studies of cell adhesion molecules, especially ICAM, in PBC have reported conflicting results. Adams *et al.*^[14], reported a series of 13 patients with PBC studied at liver transplantation and found that ICAM was expressed on interlobular bile ducts and proliferating bile ductules. In contrast, Broome *et al.*^[29], found ICAM in 3 of 10 patients with PBC while almost all patients expressed HLA-DR on biliary epithelium. Bloom *et al.*^[30] found ICAM-1 expression on bile ducts in two of seven cases of early disease and in only one of five patients with stage three or four disease. According to these reports, ICAM-1 expression in PBC is not very common and not clearly associated with a particular

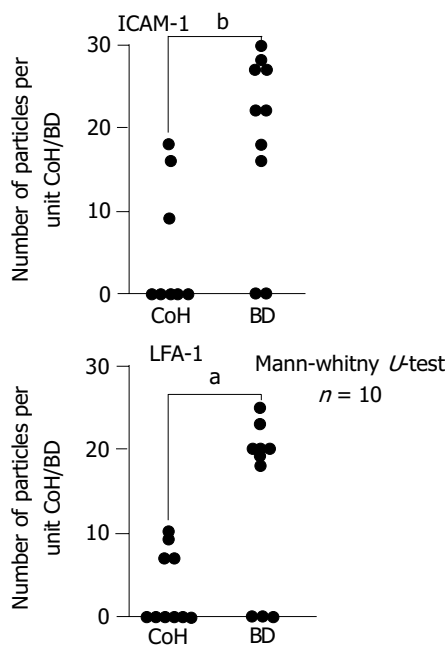


Figure 6 Semi-quantitative analysis of immunogold-silver complex particles on epithelial cells of bile ductules and cholangiocytes of CoH enumerated on immunoelectron micrographs (expressed in number of particles per unit CoH or small bile ductule). Immunoreactivity was significantly greater on bile ductules (Mann-Whitney test). BD, bile ductule; CoH, canal of Hering. ^a $P < 0.05$, ^b $P < 0.01$ vs CoH.

disorder. Using immunoelectron microscopy, we found that 8 of 10 PBC patients expressed ICAM-1 and 7 of 10 patients expressed IFA-1 on bile ductules. The higher rate probably reflects the higher sensitivity of our method.

In this study, we observed membranous staining of hepatocytes and bile ductules with different intensity with ICAM-1 antibodies (Figure 1C) in PBC. However, ICAM-1 expression on hepatocytes is indefinite or only faint in normal livers. These findings may suggest the involvement of immune-mediated hepatocytolysis related to expression and presentation of target antigens^[12].

Bile duct loss can be evaluated semi-quantitatively by calculating the ratio of portal tracts devoid of interlobular bile ducts and also the proportion of hepatic arterial branches without parallel running interlobular bile ducts^[12]. Regrowth of bile ducts has been reported, and a ductular reaction precedes the reappearance of neo-bile ducts. In this process, hepatic stem cells or progenitor cells migrate from the periportal area into the biliary tree^[31]. On the other hand, in rat liver injury, the role of ICAM-1 is to adhere to neutrophils, and excessive parenchymal apoptosis may be a signal for this neutrophil-induced inflammatory and necrotic reaction^[32]. Apoptosis of bile ductules could be one of the processes that explain the reduced proliferation of bile ductules^[33]. Therefore, strong expression of ICAM-1 on bile ductules may be a cause of the reduction in proliferation of bile ductules^[25,33].

Our semi-quantitative study of immunogold-silver complex in bile ductile epithelium and cholangiocytes in CoH of PBC liver revealed that the rate and intensity of ICAM-1 and IFA-1 expression were higher in the bile ductules than in the upstream CoH. The reason is that there are less mature cholangiocytes in the CoH. We observed cells with intermediate morphology in CoH, which may be progenitor cells labeled with ICAM-1 and LFA-1. Since the adhesion molecules appear to be expressed only on the mature cholangiocytes, this implies that the mature cholangiocytes are targeted for autoimmune destruction in PBC. Destruction in the CoH upstream of bile ductules also occurs because of the presence of mature cholangiocytes. Recently, a human bipotent liver progenitor cell line has been established, which shows comparable immunophenotype restricted to bile neoductules^[34]. The mechanisms of how progenitor cells are protected from destruction by the host immune system should be studied.

REFERENCES

- Hering E. Über den bau der Wirbeltiereber, Sitzber. *Akad wiss Wien Math Naturic Kl* 1865; **54**: 496-515
- Steiner JW, Carruthers JS. Studies on the fine structure of the terminal branches of the biliary tree. *Am J Pathol* 1961; **38**: 639-661
- Watanabe N, Tsukada N, Smith CR, Phillips MJ. Motility of bile canaliculi in the living animal- implications for bile flow. *J Cell Biol* 1991; **113**: 1069-10802
- Ishii K, Phillips MJ. *In vivo* contractions of the duct of Hering. *Hepatology* 1995; **22** (4 Pt 2): 159
- Nonomura A, Kono N, Mizukami Y, Nakanuma Y, Matsubara F. Histological changes in the liver in experimental graft-versus-host disease across minor histocompatibility barriers. IV. A light and electron microscopic study of the periportal changes. *Liver* 1991; **11**: 278-286
- Theise ND, Saxena R, Portmann B, Thung SN, Yee H, Chiriboga L, Kumar A, Crawford JM. The canals of Hering and hepatic stem cells in humans. *Hepatology* 1999; **30**: 1425-1433
- Kaplan MM. Primary biliary cirrhosis. *N Engl J Med* 1987; **316**: 512-528
- James SP, Hoofnagle JH, Strober W. Primary biliary cirrhosis: a model autoimmune disease. *Ann Intern Med* 1983; **99**: 500-512
- Thomas HC, Potter BJ, Sherlock S. Is primary biliary cirrhosis an immunocomplex disease? *Lancet* 1977; **2**: 1216-1263
- Wands JR, Dienstag JL, Bhan AK, Feller ER, Isselbacher KJ. Circulating immune complexes and complement activation in primary biliary cirrhosis. *N Engl J Med* 1978; **298**: 233-237
- Cancellieri V, Scaroni C, Vernace SJ, Schaffner F, Paronetto F. Subpopulation of T lymphocyte in primary biliary cirrhosis. *Clin Immunol Immunopathol* 1981; **20**: 255-260
- Nakanuma Y, Yasoshimura M, Tsuneyama K, Harada K. Histopathology of primary biliary cirrhosis with emphasis on expression of adhesion molecules. *Semi Liver Dis* 1997; **17**: 35-47
- Volpes R, Van Den Oord JJ, Desmet VJ. Immunohistochemical study of adhesion molecules in liver inflammation. *Hepatology* 1990; **12**: 59-65
- Adams DH, Hubscher SG, Shaw J, Johnson GD, Babbs C, Rothlein R, Neuberger JM. Increased expression of ICAM-1 on bile ducts in primary biliary cirrhosis and primary sclerosing cholangitis. *Hepatology* 1991; **14**: 426-443
- Altmann DM, Hogg N, Trowsdale J, Wilkinson D. Co-transfection of ICAM-1 and HLA-DR reconstitutes human antigen presenting cell function in mouse L lines. *Nature* 1990; **338**: 512-514
- Kaneko H, Oda M, Yokomori H, Kazemoto S, Kamegaya Y, Komatsu H, Tsuchiya M. Immunohistochemical microscopic analysis of bile duct destruction in primary biliary cirrhosis: Involvement of intercellular adhesion molecules. *Int Hepatol Commu* 1994; **2**: 271-276
- Yasoshima M, Nakanuma Y, Tsuneyama K, van de Water J, Gershwin ME. Immunohistochemical analysis of adhesion molecules in the micro-environment of portal tracts in relation to aberrant expression of PDC-E2 and HLA-DR on the bile ducts in primary biliary cirrhosis. *J Pathol* 1995; **175**: 319-325
- Ohta Y. Diagnostic criteria for primary biliary cirrhosis. *Acta Hepatol Jpn* 1992; **33**: 657
- McLean IW, Nakane PK. Periodate-lysine-paraformaldehyde fixative: a new fixative for immunoelectron microscopy. *J Histochem Cytochem* 1974; **22**: 1077-1083
- Thisted M, Just T, Pluzek KJ, Petersen KH, Hyldig-Nielsen JJ, Godtfredsen SE. Detection of immunoglobulin kappa light chain mRNA in paraffin sections by *in situ* hybridization using peptide nucleic acid probes. *Cell Vision* 1996; **3**: 358-363
- Simmons D, Makgoba MW, Seed B. ICAM, an adhesion ligand of LFA-1, is homologous to the neural cell adhesion molecule NCAM. *Nature* 1988; **331**: 624-627
- Larson RS, Corbi AL, Berman L, Springer T. Primary structure of the leukocyte function-associated molecule-1 alpha subunit: an integrin with an embedded domain defining a protein superfamily. *J Cell Biol* 1989; **108**: 703-712
- Kerstens HM, Poddighe PJ, Hanselaar AG. A novel *in situ* hybridization signal amplification method based on the deposition of biotinylated tyramine. *J Histochem Cytochem* 1995; **43**: 347-352
- Fujimori O, Nakamura M. Protein A gold-silver staining methods for light microscopic immunohistochemistry. *Arch Histol Jap* 1985; **48**: 449-452
- Nakanuma Y, Ohta G. Quantitation of hepatic granulomas and epitheloid cells in primary biliary cirrhosis. *Hepatology* 1983; **3**: 423-427
- Yokomori H, Oda M, Yoshimura K, Nomura M, Ogi M, Wakabayashi G, Kitajima M, Ishii H. Expression of intercel-

- lular adhesion molecule-1 and lymphocyte function-associated antigen protein and messenger RNA in primary biliary cirrhosis. *Internal Med* 2003; **42**: 947-954
- 27 **Yamada G**, Hyodo I, Tobe K, Mizuno M, Nishihara T, Kobayashi T, Nagashima H. Ultrastructural immunocytochemical analysis of lymphocytes infiltrating bile duct epithelium in primary biliary cirrhosis. *Hepatology* 1986; **6**: 385-391
- 28 **Saxena R**, Hytiroglou P, Thung SN, Theise ND. Destruction of canals of Hering in primary biliary cirrhosis. *Hum Pathol* 2002; **33**: 983-988
- 29 **Broome U**, Hultcrantz R, Forsum U. Lack of concomitant expression of ICAM-1 and HLA-DR on bile duct cells from patients with primary sclerosing cholangitis and primary biliary cirrhosis. *Scand J Gastroenterol* 1993; **28**: 126-130
- 30 **Bloom S**, Fleming K, Chapman R. Adhesion molecule expression in primary sclerosing cholangitis and primary biliary cirrhosis. *Gut* 1995; **36**: 604-609
- 31 **Gerber MA**, Thung SN. Liver stem cells and development. *Lab Invest* 1993; **68**: 261-263
- 32 **Kobayashi A**, Imamura H, Isobe M, Matsuyama Y, Sorda J, Matsunaga K, Kawasaki S. Mac-1(CD11b/CD18) and intercellular adhesion molecule-1 in ischemia-reperfusion injury of rat liver. *Am J Physiol* 2001; **281**: G577-585
- 33 **Bhathal PS**, Gall JA. Deletion of hyperplastic biliary epithelial cells by apoptosis following removal of the proliferative stimuli. *Liver* 1985; **5**: 311-325
- 34 **Parent R**, Marion MJ, Furio L, Trépo C, Petit MA. Origin and characterization of a human bipotent liver progenitor cell line. *Gastroenterology* 2004; **126**: 1147-1156

Science Editor Wang XL Language Editor Elsevier HK

• CLINICAL RESEARCH •

Excretion and detection of SARS coronavirus and its nucleic acid from digestive system

Xin-Wei Wang, Jin-Song Li, Ting-Kai Guo, Bei Zhen, Qing-Xin Kong, Bin Yi, Zhong Li, Nong Song, Min Jin, Xiao-Ming Wu, Wen-Jun Xiao, Xiu-Mei Zhu, Chang-Qing Gu, Jing Yin, Wei Wei, Wei Yao, Chao Liu, Jian-Feng Li, Guo-Rong Ou, Min-Nian Wang, Tong-Yu Fang, Gui-Jie Wang, Yao-Hui Qiu, Huai-Huan Wu, Fu-Huan Chao, Jun-Wen Li

Xin-Wei Wang, Qing-Xin Kong, Zhong Li, Nong Song, Min Jin, Chang-Qing Gu, Jing Yin, Guo-Rong Ou, Fu-Huan Chao, Jun-Wen Li, Tianjin Institute of Environment and Health, Tianjin 300050, China
Jin-Song Li, Bei Zhen, Xiao-Ming Wu, Wen-Jun Xiao, Wei Wei, Min-Nian Wang, Gui-Jie Wang, Institute of Microbiology and Epidemiology, Beijing 100072, China

Ting-Kai Guo, Xiu-Mei Zhu, Wei Yao, Jian-Feng Li, Yao-Hui Qiu, Huai-Huan Wu, Xiao Tang Shan Hospital, Beijing 102211, China
Bin Yi, 309 Hospital of PLA, Beijing 100091, China

Chao Liu, Beijing Institute of Pharmacology and Toxicology, Beijing 100850, China

Tong-Yu Fang, Beijing Institute of Basic Medicine, Beijing 100850, China
Supported by the National High Technology Research and Development Program of China, 863 Program, No. 2004AA649100, and the National Natural Science Foundation of China, No. 30471436

Correspondence to: Dr. Jun-Wen Li, Tianjin Institute of Environment and Health, Tianjin 300050, China. junwenli@eyou.com

Telephone: +86-22-84655345 Fax: +86-22-23328809

Received: 2004-04-22 Accepted: 2004-05-24

Abstract

AIM: To study whether severe acute respiratory syndrome coronavirus (SARS-CoV) could be excreted from digestive system.

METHODS: Cell culture and semi-nested RT-PCR were used to detect SARS-CoV and its RNA from 21 stool and urine samples, and a kind of electropositive filter media particles was used to concentrate the virus in 10 sewage samples from two hospitals receiving SARS patients in Beijing in China.

RESULTS: It was demonstrated that there was no live SARS-CoV in all samples collected, but the RNA of SARS-CoV could be detected in seven stool samples from SARS patients with any one of the symptoms of fever, malaise, cough, or dyspnea, in 10 sewage samples before disinfection and 3 samples after disinfection from the two hospitals. The RNA could not be detected in urine and stool samples from patients recovered from SARS.

CONCLUSION: Nucleic acid of SARS-CoV can be excreted through the stool of patients into sewage system, and the possibility of SARS-CoV transmitting through digestive system cannot be excluded.

© 2005 The WJG Press and Elsevier Inc. All rights reserved.

Key words: Severe acute respiratory syndrome; Nucleic acid; Digestive system

Wang XW, Li JS, Guo TK, Zhen B, Kong QX, Yi B, Li Z, Song N, Jin M, Wu XM, Xiao WJ, Zhu XM, Gu CQ, Yin J, Wei W, Yao W, Liu C, Li JF, Ou GR, Wang MN, Fang TY, Wang GJ, Qiu YH, Wu HH, Chao FH, Li JW. Excretion and detection of SARS coronavirus and its nucleic acid from digestive system. *World J Gastroenterol* 2005; 11(28): 4390-4395

<http://www.wjgnet.com/1007-9327/11/4390.asp>

INTRODUCTION

By the end of 2002, there were reports from Guangdong Province in southern China of cases of severe acute respiratory syndrome (SARS). Over 8 439 SARS cases and 812 SARS-related deaths were reported to WHO from 32 countries around the world till 5th July, 2003^[1,2]. In response to this outbreak, WHO coordinated an international collaboration that included clinical, epidemiological, laboratory investigations, and initiated efforts to control the spread of SARS. Attempts to identify the etiology of SARS outbreak were successful during the 3rd wk of March 2003, when laboratories in the USA, Canada, Germany, Hong Kong, and China isolated a novel coronavirus from SARS patients^[3-6]. Unlike other human coronaviruses, it was possible to isolate the novel coronavirus in Vero cells. Evidence of the coronavirus infection was documented in SARS patients throughout the world. The coronavirus RNA was frequently detected in respiratory specimens, and convalescent-phase serum specimens from SARS patients containing antibodies that reacted with the coronavirus. There was a strong evidence that this new virus was etiologically linked to the outbreak of SARS^[5-8].

Investigations of the global outbreak of SARS have shown that the major mode of transmission of SARS virus was through close personal contact, in particular exposure to droplets of respiratory secretions from an infected person^[1,9-14]. While in a cluster of SARS cases in an apartment block in Hong Kong, sewage was believed to have played a role through droplets containing coronavirus from the sewage system^[11,12]. However, there is no direct evidence to prove that the coronavirus exists in sewage system and is contagious.

In order to confirm whether the digestive system was a possible major transmission way of SARS-CoV, cell culture and the semi-nested RT-PCR were used to directly detect SARS-CoV and its RNA. A kind of electropositive filter media particle^[15] was used to concentrate the SARS-CoV from the sewage of hospitals receiving SARS patients in Beijing of China, and then the virus and its RNA were detected.

MATERIALS AND METHODS

Viruses and culture methods

To identify viruses that existed in stools, urine samples, and sewage system, we inoculated a variety of specimens onto Vero E6. Because of the toxicity of sewage concentrates, all cell cultures were inoculated in the presence of growth medium for 1 h at 37 °C. This procedure virtually eliminated problems with the toxicity of sewage concentrates. Medium was replaced after 1-2 d of incubation. Culture was terminated 7 d after inoculation, and the culture was observed daily for cytopathic effects. Cultures exhibiting identifiable cytopathic effects were subjected to several procedures to identify the cause of the effect^[16-18]. If there was no cytopathic effect on the cell culture, the supernate was harvested and added into additional flasks to isolate viruses. The cultures were then used until three generations without cytopathic effects.

Stools and urine samples of SARS patients

Twenty-one stool and urine samples were collected from the Xiao Tang Shan Hospital and 309 Hospital of PLA, which were specially assigned to receive SARS patients in Beijing in 2003, among which 11 samples were collected from the SARS patients with any one of the symptoms of fever, malaise, cough, or dyspnea, and 10 samples were from recovered patients.

Sewage and disinfection

Ten sewage samples were collected at 7 o'clock in the morning from Xiao Tang Shan Hospital and 309 Hospital of PLA for 7 d. Two thousand and five hundred milliliters of sewage before disinfection or 25 000-50 000 mL after disinfection by chlorine was collected.

Electropositive filter media particle

The positively charged filter media particles, which were used to concentrate SARS-CoV from sewage, were prepared as previously described^[15].

Detection of residual chlorine

The residual chlorine in sewage was determined by the *N*, *N*, diethyl-*p*-phenyldiamine colorimetric method^[19].

Concentration of SARS-CoV from sewage

Two thousand and five hundred milliliters and 25 000 mL sewage from the hospitals before or after disinfection by chlorine were placed in a 25-L capacity plastic bucket, and 10 mL Na₂S₂O₃ (100 g/L) was added to neutralize the residual chlorine. Five hundred or 820 g filter media was packed in a polymethyl methacrylate column (89 or 130 mm i.d.). The filter media bed height was 14 cm. The flow rate was kept at 10 mL/min per cm² of the filter surface area. The adsorbed viruses were eluted from filter media with 700 or 900 mL 6× nutrient broth (pH 7.2). The collected eluates were re-concentrated by PEG precipitation and centrifugation. The pellets were resuspended in 40 mL PBS and assayed.

RNA extraction

Virus RNA extracting kit (TRIzol Reagent) made by Invitrogen™ Life Technologies for extraction of exceedingly pure viral RNA was utilized in our experiment to extract

virus RNA, and all procedures were strictly implemented in accordance with the reagent instruction manual.

Primer design for assay of SARS-CoV nucleic acid

Three sets of primers from WHO Network Laboratories^[20] were used to detect the SARS-CoV RNA: Cor-p-F2 (+) 5'-CTAACATGCTTAGGATAATGG-3', Cor-p-F3 (+) 5'-GCCTCTCTTGTTCCTTGCTCGC-3', and Cor-p-R1 (-) 5'-CAGGTAAGCGTAAAACATC-3'. Cor-p-F2/Cor-p-R1 gave a 368-bp product, and Cor-p-F3/Cor-p-R1 yielded a 348-bp segment.

Primer design for assay of enterovirus nucleic acid

A pair of consensus primers of enteroviruses was from the 5' non-coding region because of their presence in many enterovirus serotypes. The sequences of primers were as follows: E1 5'-ATTGTCACCATAAGCAGCCA-3', E2 5'-CCAGCACTTCTGTTTCCCCGG-3', and the product size was 440 bp^[21].

Detection of SARS-CoV by semi-nested RT-PCR

Two microliters of RNA solution was analyzed with RT-PCR assay. The KaTaRa one step RNA PCR kit (KaTaRa Biotechnology, Dalian) was used for the reaction (20 µL total volume). Positive and negative RT-PCR controls were included in each run. Reactions contained 10 µL of buffer concentrate, 2 mmol/L of magnesium sulfate, 0.8 µL of enzyme mixture, and 1.9 µmol/L of each of Cor-p-F2 and Cor-p-R1 primers. Thermal cycling comprised 42 °C for 30 min, 95 °C for 3 min; 10 cycles of 95 °C for 10 s, 55 °C for 15 s (decreasing by 1 °C per cycle), 72 °C for 40 s; 40 cycles of 95 °C for 10 s, 56 °C for 10 s, and 72 °C for 40 s. To confirm the PCR products, a semi-nested PCR was developed. The template was the first PCR product, and the primers were Cor-p-F3 and Cor-p-R1, and yielded a 348-bp product. The amplification efficiency of the primers was confirmed by SARS-CoV of BJ-01 isolated from a SARS patient in Guangzhou city, China (Figure 2).

Detection of enteroviruses by RT-PCR

As most of enteroviruses can also grow on the Vero cells, and yield cytopathic effects, enteroviruses should be detected by the specific primers^[21]. The RT-PCR method was similar to that for SARS-CoV.

Detection of PCR products

PCR products were analyzed by electrophoresis with 15 g/L agarose gels containing 0.5 µg of ethidium bromide per mL, and visualized with UV illumination and photographed. DNA molecular size standards (100-bp ladder, Gibco/BRL) were included in each run of agarose gel electrophoresis.

In view of the serious nature of SARS and the person-to-person transmission, all clinical specimens were treated in a biosafety level 3 environment. All divisions into aliquots, pipetting, concentration for small sewage and culture attempts were performed in laminar-flow safety cabinets. A similar environment was used when specimens from which nucleic acid was to be extracted and placed in a buffer solution.

Nucleotide sequence analysis

The PCR products from four different samples were purified

with the QIAquick PCR purification kit (QIANEN, Inc.) and sequenced with the ABI PRISM dye terminator cycle sequencing ready reaction kit with AmpliTaq DNA polymerase FS (Perkin-Elmer, Applied Biosystem) following the manufacturer's instructions. The sequences were compared with the genome of SARS-CoV in the GenBank and EMBL databases by using the FASTA program of the GCG.

RESULTS

Detection of SARS-CoV by the semi-nested RT-PCR

The detection specificity and sensitivity of semi-nested RT-PCR were confirmed by the isolated SARS-CoV (BJ-01) from Institute of Microbiology and Epidemiology, Academy of Military Medical Sciences, Beijing, China. It was shown that two amplicons were yielded, which were in agreement with the information on the designed primers (Figure 1). The minimum amount of SARS-CoV RNA detected by semi-nested PCR was equivalent to 10^6 TCID₅₀ (Figure 2).

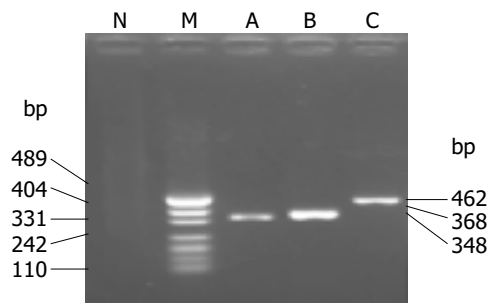


Figure 1 Amplification of SARS-CoV RNA BJ-01 by semi-nested RT-PCR. M: DNA marker (pUC19 DNA/MSP I marker); lane A: 348 bp; lane B: 368 bp; lane C: positive RT-PCR control, 462 bp; lane N: negative RT-PCR control.

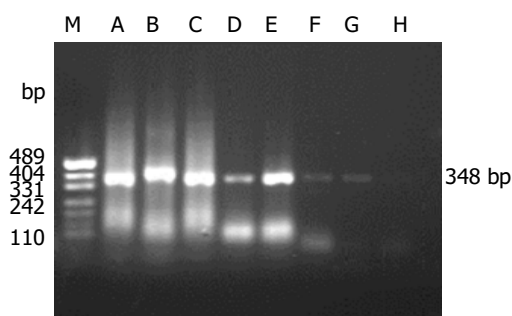


Figure 2 Sensitivity of semi-nested RT-PCR for SARS-CoV. M: DNA marker (pUC19 DNA/MSP I marker); lane A-G: virus concentration was 10^6 - 10^{10} TCID₅₀, lane H: negative control.

Isolation of SARS-CoV and detection of SARS-CoV RNA from stool samples of patients

All the 21 stool samples tested for the presence of infectious SARS-CoV in cell culture were negative. SARS-CoV RNA could be detected in 7 of 11 stool samples from patients with symptoms by semi-nested RT-PCR (Figure 3). However, SARS-CoV RNA could not be detected from the samples of patients who recovered.

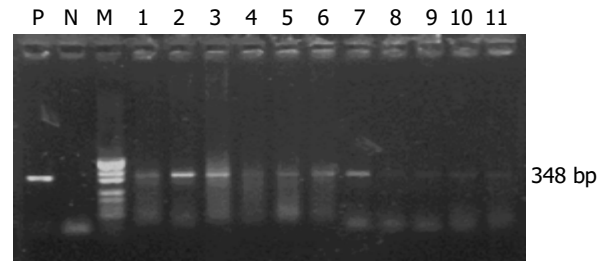


Figure 3 Amplification of SARS-CoV RNA from stool samples. M: DNA marker (pUC19 DNA/MSP I marker); lanes 1-11: samples from different SARS patients; N: negative control; P was the positive RT-PCR control from the RNA of SARS-CoV BJ-01.

Isolation of SARS-CoV and detection of SARS-CoV RNA from urine samples of patients

All the 21 urine samples tested for the presence of infectious SARS-CoV in cell culture were also negative. SARS-CoV RNA could not be detected from the samples or the supernate of cell cultures by semi-nested RT-PCR.

Concentration and detection of SARS-CoV from sewage before disinfection

All sewage samples tested for the presence of infectious SARS-CoV in cell culture were negative. SARS-CoV RNA could be found in the concentrates of sewage from the two hospitals by semi-nested PCR, and in the inoculated cells of the sewage concentrates from 309 Hospital but not from Xiao Tang Shan Hospital. However, SARS-CoV RNA copies in the samples were too low to be detected by the first amplification reaction, the semi-nested RT-PCR in which the products of first amplification reaction were the template of the second PCR, gave the positive amplification results (Tables 1 and 2).

Table 1 Concentration and detection of SARS-CoV in 2 500-mL sewage before disinfection in Xiao Tang Shan Hospital¹

Date	Cell cult ²	Concentrate +PCR ³	Inoculated cells+PCR ⁴	Entero. ⁵ PCR
10 June	-	+	-	-
11 June	-	+	-	-
12 June	-	+	-	-
13 June	-	+	-	-
14 June	-	+	-	-
15 June	-	+	-	-

¹Glass column diameter: 19 mm, bed height: 14 cm, eluate volume: 500 mL; ²Cell culture was maintained for 14 d to observe the cytopathic effect; ³PCR template was from the concentrates; ⁴PCR template was from the cultured cells; ⁵Enteroviruses were detected by general primer RT-PCR for enteroviruses.

Table 2 Concentration and detection of SARS-CoV in 2 500-mL sewage before disinfection in 309 Hospital of PLA¹

Date	Cell cult	Concentrate +PCR	Inoculated cells+PCR	Entero. PCR
11 June	-	+	-	-
12 June	-	+	-	-
13 June	-	+	-	-
14 June	-	+	-	-
15 June	-	+	-	-
16 June	-	+	-	-

¹All explanatory notes are same as in Table 1.

Concentration and detection of SARS-CoV from sewage after disinfection

The samples (25 000 or 50 000 mL) from the two hospitals were all negative by the infectivity methods. SARS-CoV RNA was detected from the concentrates and inoculated cells in three samples (June 11, 13, and 15) from 309 Hospital by semi-nested RT-PCR, while the other samples were negative (Tables 3 and 4).

Table 3 Concentration and detection of SARS-CoV in 25 000- or 50 000-mL sewage after disinfection in Xiao Tang Shan Hospital¹

Date	Cell culture	Concentrate +PCR	Inoculated cells+PCR	Enterovirus PCR
11 June	-	-	-	-
12 June	-	-	-	-
13 June	-	-	-	-
14 June	-	-	-	-
15 June	-	-	-	-

¹All explanatory notes are same as in Table 1.

Table 4 Concentration and detection of SARS-CoV in 25 000-mL sewage after disinfection in 309 Hospital of PLA¹

Date	Cell culture	Concentrate +PCR	Inoculated cells+PCR	Enterovirus PCR
11 June	-	+	+	-
12 June	-	-	-	-
13 June	-	+	+	-
14 June	-	-	-	-
15 June	-	+-	+	-

¹All explanatory notes are same as in Table 1.

Result of nucleotide sequence analysis

The PCR products from the sewage samples of the two hospitals were sequenced, and submitted to GenBank. The accession numbers are bankit579728 and bankit579738, respectively. Comparison of the nucleotide sequences of PCR products with data from GenBank revealed that the sequences of the PCR products were close to those of SARS-COV genomes, showing about 99% nucleotide homolog.

DISCUSSION

Most SARS cases to date have occurred in young adults. The health care workers in hospitals, patient family members and international travelers were the commonly infected people^[22,23].

The isolation of a novel coronavirus was obtained from the respiratory secretions of patients with SARS, and points to the etiologic association with SARS^[3-6,8,24-26].

The mechanism of transmission of SARS-CoV is not yet understood completely. However, the fact that transmission has been limited to close contacts with patients, such as household members, health care workers, or other patients who were not protected with contact or respiratory precautions, suggests that either droplet secretions or direct or indirect contact probably has a role^[1,10-14,27].

On 15th April, 2003, health authorities reported a total

of 321 individuals infected with SARS virus who were residents in Amoy Gardens. A large proportion of cases were concentrated in vertically linked flats in a single building, Block E. On April 17, the Hong Kong Government announced that not one single factor could account for the outbreak in Block E of Amoy Gardens, and attention was focused on possible transmission via the sewage system because laboratory studies showed that patients with the disease excreted coronaviruses in their stools and these viruses were able to survive much longer in feces than on ordinary surfaces, and noted a swab sample taken from the toilet of an infected resident showed a positive test for the coronavirus' genetic material, and about 60% of patients in Amoy Gardens had diarrhea during their illness, and probably would have discharged a large amount of viruses into the soil stacks. Finally, the virus would spread with water droplets through the U-traps of the floor drains, which were dried up in many cases^[11,24,28,29].

The elevated levels of aspartate aminotransferase and lactate dehydrogenase indeed suggest that SARS-CoV was also replicating outside the respiratory tract^[1]. Electron microscopic examination showed that virus-like particles with 100-150 nm in diameter were found in cytoplasm and dilated reticular endoplasm of the infected alveolar epithelial cells and endothelial cells^[6,26,30,31]. Shedding of the virus in feces might be an additional source of spreading, provided the virus was stable in this environment^[8].

Tsang *et al.*, reported that there were three nurses who worked at Hospital B, where a patient was admitted and remained for 6 d for treatment of pneumonia before he was transferred to Hospital C. During this period, the nurses spent five 8-h shifts stationed on the general ward where the patient was hospitalized. The three nurses recalled close encounter with the patient during which they cleaned him when he had fecal incontinence after an episode of diarrhea on March 3, 2003. The nurses did not wear masks or gowns during their routine nursing care of any patients on the ward and finally were all infected^[1].

The detection of SARS-CoV in fecal and serum samples from patients, as well as in respiratory specimens, suggested that this virus, like many animal coronaviruses, might spread both by fecal contamination and by respiratory droplets^[4].

Zhang reviewed the data of SARS transmission and believed that, as previously described, most coronaviruses could cause either a respiratory or an enteric disease, which is also transmitted by the fecal-oral route. During this outbreak of SARS, symptoms of the gastrointestinal tract in patients were noticed. Many investigators^[1,10,32] found that gastrointestinal symptoms, including diarrhea (19-50%), nausea and vomiting (19.6%), and abdominal pain (13%) were common in SARS patients.

All the above reports suggested that stools of SARS patients or sewage containing stools of SARS patients would transmit the coronavirus. However, except that the positive PCR results were obtained in some patient stools, there were no reports that live viruses were present in patient stool or sewage.

In this study, we isolated and detected the SARS-CoV in stools, urine samples, and sewage from hospitals which were assigned specially to receive SARS patients in Beijing of China. Just as expected, SARS-CoV RNA was detected from

stools of patients, but no live viruses were isolated from stool samples, and no SARS-CoV RNA was found in all stools from patients who recovered. It is suggested that the nucleic acid of SARS-CoV could be really excreted from stools of patients, but infectious SARS-CoV could not be confirmed to excrete through the digestive system. No live virus and its RNA were isolated from the urine samples of patients. It is suggested that SARS-CoV and its RNA could not be excreted from the urinary system.

In order to explore the growth and decline of SARS-CoV and its RNA in environment, SARS-CoV and its RNA were isolated from sewage of hospitals. Although the concentration method of SARS-CoV from sewage has not been reported yet, the concentration of enteroviruses from water using different methods was reported, and the electropositive filters have been considered as the most promising method^[34,35].

We developed a simple method for concentration of enteroviruses from water with electropositive particles, the adsorption of bacteriophage ϕ_2 was reliable and efficient, not affected by the pH value, temperature, turbidity, and organic materials in water, and gave a recovery of 88.7% for poliovirus I and a comparable recovery of HAV, CoxB₃, and Echo 7 from 100 L of tap water^[15].

We attempted to concentrate SARS-CoV in sewage from Xiao Tang Shan Hospital and 309 Hospital in Beijing by the electropositive particle adsorption method. The sewage systems in these two hospitals were similar, i.e. the sewage was collected from each isolation ward and converged into the reaction sedimentation basin, and disinfectant (chlorine) was added to inactivate SARS-CoV and other pathogenic microorganisms; finally, the sewage was discharged from the reaction sedimentation basin after a 60-min reaction.

Results of testing for the presence of SARS-CoV in the sewage indicated that no infectious SARS-CoV or live virus could be recovered in these two hospitals. The nucleic acid of SARS-CoV was found in the sewage before disinfection from both hospitals by semi-nested RT-PCR, while after disinfection of sewage by chlorine, SARS-CoV RNA could only be detected in the samples taken on 11th, 13th, and 15th June, 2003 from 309 Hospital.

Cell culture is a very demanding test. However, negative cell culture results or RT-PCR results could not exclude the presence of SARS-CoV. The detection of SARS-CoV from SARS patients could be negative for the following reasons^[17]. Patients were not infected with SARS coronavirus, the illness was due to another infectious agent (virus, bacterium, fungus) or a non-infectious cause. The test results were incorrect. Current tests need to be further developed to improve their sensitivity. SARS-CoV was so susceptible to environments that it was inactivated quickly out of the body. SARS-CoV might have been inactivated or eliminated by immunoglobulins (antibody) from the recovered patients before excretion, or in the sewage. Palmer *et al.*^[35], reported that human immunoglobulins were used to eliminate the enteroviruses in concentrated sewage when they evaluated the immunodeficiency virus (HIV) in sewage effluent by infectivity assay and RT-PCR.

Hong Kong Government explained the reasons of a cluster of SARS cases in Amoy Gardens and believed that there was a combination of factors, including the presence

of an index patient who caused the first batch of infections, person-to-person spread, transmission via the sewage system, and environmental contamination^[11,29]. This study demonstrated that SARS-CoV RNA could be excreted through the feces or/and urine samples of patients into sewage system.

In conclusion, this study demonstrated that there was SARS-CoV RNA in stool samples of patients with symptoms and in sewage of hospitals though there was no live SARS-CoV isolated from all samples. It provides evidence that the nucleic acid of SARS-CoV can be excreted through the stools of patients into sewage system, but cannot exclude the possibility of SARS-CoV transmitting through the digestive system. Much attention should be paid to the treatment of stools of patients and the sewage of hospitals receiving SARS patients.

ACKNOWLEDGEMENTS

The authors thank Dr. Da-Sheng Zhao, De-Xue Li, Jian-Zhong Sun, Zhong-Hou Huo and Yun-Bo Li from the P3 Laboratory Center for Microorganism Detection, China for supporting of this project; Dr. Fu-Yu Wang, Ying-Kai Li, Meng-Fu Zhu, Jian-Yong Su, Cheng-Yuan Gong, Wu-Chun Chao, Tai-Thi Gong, Bing-Yin Si and Bao-Zhong Guo for providing many reagents, helpful guidance and discussion; Drs. Hong-Wei Zhao, Xin-An Du, Zong-Ze Wang, Ling-Jia Qian, Qing-Yu Zhu, Xiao-Jun Zhang, Tao-Xing Shi, Fei Yu, Jian-Zhong Man, Fan-Rong Zeng, Bang-Rong Han, Yue Jiang, Zhu-Ge Xi, Zhi-Peng Ju and Hua-Shan Zhang for advice and organizing the experiments; the Center for Logistics, Xiao-Tang Shan Hospital for technical support and cooperation. We are also indebted to Professor Su-Qi Cheng for English revision.

REFERENCES

- 1 **Tsang KW**, Ho PL, Ooi GC, Yee WK, Wang T, Chan-Yeung M, Lam WK, Seto WH, Yam LY, Cheung TM, Wong PC, Lam B, Ip MS, Chan J, Yuen KY, Lai KN. A cluster of cases of Severe acute respiratory syndrome in Hong Kong. *N Engl J Med* 2003; **348**: 1977-1985
- 2 World Health Organization. SARS: breaking the chains of transmission. Available from: URL: <http://www.who.int/features/2003/07/en>
- 3 **Rota PA**, Oberste MS, Monroe SS, Nix WA, Campagnoli R, Icenogle JP, Penaranda S, Bankamp B, Maher K, Chen MH, Tong S, Tamin A, Lowe L, Frace M, DeRisi JL, Chen Q, Wang D, Erdman DD, Peret TC, Burns C, Ksiazek TG, Rollin PE, Sanchez A, Liffick S, Holloway B, Limor J, McCaustland K, Olsen-Rasmussen M, Fouchier R, Gunther S, Osterhaus AD, Drosten C, Pallansch MA, Anderson LJ, Bellini WJ. Characterization of a novel coronavirus associated with severe acute respiratory syndrome. *Science* 2003; **300**: 1394-1399
- 4 **Holmes KV**. SARS-associated coronavirus. *N Engl J Med* 2003; **348**: 1948-1951
- 5 **Fouchier RA**, Kuiken T, Schutten M, Van Amerongen G, Van Doornum GJ, Van Den Hoogen BG, Peiris M, Lim W, Stohr K, Osterhaus AD. Aetiology: Koch's postulates fulfilled for SARS virus. *Nature* 2003; **423**: 240
- 6 **Ksiazek TG**, Erdman D, Goldsmith CS, Zaki SR, Peret T, Emery S, Tong S, Urbani C, Comer JA, Lim W, Rollin PE, Dowell SF, Ling AE, Humphrey CD, Shieh WJ, Guarner J, Padlock CD, Rota P, Fields B, DeRisi J, Yang JY, Cox N, Hughes JM, LeDuc JW, Bellini WJ, Anderson LJ. A Novel coronavirus associated with severe acute respiratory syndrome. *N Engl J Med* 2003; **348**: 1953-1966

- 7 **Marra MA**, Jones SJ, Astell CR, Holt RA, Brooks-Wilson A, Butterfield YS, Khattra J, Asano JK, Barber SA, Chan SY, Cloutier A, Coughlin SM, Freeman D, Girn N, Griffith OL, Leach SR, Mayo M, McDonald H, Montgomery SB, Pandoh PK, Petrescu AS, Robertson AG, Schein JE, Siddiqui A, Smailus DE, Stott JM, Yang GS, Plummer F, Andonov A, Artsob H, Bastien N, Bernard K, Booth TF, Bowness D, Czub M, Drebot M, Fernando L, Flick R, Garbutt M, Gray M, Grolla A, Jones S, Feldmann H, Meyers A, Kabani A, Li Y, Normand S, Stroher U, Tipples GA, Tyler S, Vogrig R, Ward D, Watson B, Brunham RC, Krajden M, Petric M, Skowronski DM, Upton C, Roper RL. The Genome sequence of the SARS-associated coronavirus. *Science* 2003; **300**: 1399-1404
- 8 **Qin ED**, Zhu QY, Peng WM, Jiang T, Fan BC, Chang GH, Yu M, Si BY, Liu BH, Deng YQ, Liu H, Zhang Y. Determination of the partial polymerase gene sequence of novel coronavirus isolated from lung tissue of SARS patients. *Junshi Yixue Kexueyuan Yuankan* 2003; **27**: 81-83
- 9 **Enserink M**, Vogel G. Infectious diseases. Hungry for details, scientists zoom in on SARS genomes. *Science* 2003; **300**: 715-716
- 10 **Lee N**, Hui D, Wu A, Chan P, Cameron P, Joynt GM, Ahuja A, Yung MY, Leung CB, To KF, Lui SF, Szeto CC, Chung S, Sung JJ. A major outbreak of severe acute respiratory syndrome in Hong Kong. *N Engl J Med* 2003; **348**: 1986-1994
- 11 World Health Organization. Amoy Gardens investigation findings make public. Available from: URL: <http://www.who.int/csr/sars/en> (17 April, 2003)
- 12 **Cyranoski D**, Abbott A. Apartment complex holds clues to pandemic potential of SARS. *Nature* 2003; **423**: 3-4
- 13 **Poutanen SM**, Low DE, Henry B, Finkelstein S, Rose D, Gree K, Tellier R, Draker R, Adachi D, Ayers M, Chan AK, Skowronski DM, Salit I, Simor AE, Slutsky AS, Doyle PW, Krajden M, Petric M, Brunham RC, McGeer AJ. Identification of severe acute respiratory syndrome in Canada. *N Engl J Med* 2003; **348**: 1995-2005
- 14 **Donnelly CA**, Ghani AC, Leung GM, Hedley AJ, Fraser C, Riley S, Abu-Raddad LJ, Hob LM, Thach TQ, Chau P, Chan KP, Lam TH, Tse LY, Tsang T, Liu SH, Kong JH, Lau EM, Ferguson NM, Anderson RM. Epidemiological determinants of spread of causal agent of severe acute respiratory syndrome in Hong Kong. *Lancet* 2003; **361**: 1761-1766
- 15 **Li JW**, Wang XW, Rui QY, Song N, Zhang FG, Ou YC, Chao FH. A new and simple method for concentration of enteric viruses from water. *J Virol Methods* 1998; **74**: 99-108
- 16 World Health Organization. Recommendations for laboratories testing by PCR for presence of SARS coronavirus-RNA. Available from: URL: <http://www.who.int/csr/sars/coronarecommendation/en>
- 17 World Health Organization. Severe Acute Respiratory Syndrome (SARS): Laboratory diagnostic tests. Available from: URL: <http://www.who.int/csr/sars/diagnostictests/en>
- 18 World Health Organization. Use of laboratory methods for SARS diagnosis. Available from: URL: <http://www.who.int/csr/sars/labmethods/en>
- 19 **Olivieri VP**, Snead MC, Kruse CW, Kawata K. Stability and effectiveness of chlorine disinfectants in water distribution systems. *Environ Health Perspect* 1986; **69**: 15-29
- 20 World Health Organization. PCR primers for SARS developed by WHO Network Laboratories. Available from: URL: <http://www.who.int/csr/sars/primers/en>
- 21 **Zoll GJ**, Melchers WJ, Kopecka H, Jambroes G, van der Poel HJ, Galama JM. General primer-mediated polymerase chain reaction for detection of enteroviruses: application for diagnostic routine and persistent infections. *J Clin Microbiol* 1992; **30**: 160-165
- 22 World Health Organization. Update 58 - First global consultation on SARS epidemiology, travel recommendations for Hebei Province (China), situation in Singapore. Available from: URL: http://www.who.int/csr/sars/archive/2003_05_17/en/
- 23 World Health Organization. SARS epidemiology to date. Available from: URL: http://www.who.int/csr/sars/epi2003_04_11/en/
- 24 **Peiris JS**, Lai ST, Poon LL, Guan Y, Yam LY, Lim W, Nicholls J, Yee WK, Yan WW, Cheung MT, Cheng VC, Chan KH, Tsang DN, Yung RW, Ng TK, Yuen KY. Coronavirus as a possible cause of severe acute respiratory syndrome. *Lancet* 2003; **361**: 1319-1325
- 25 World Health Organization. Update 31 - Coronavirus never before seen in humans is the cause of SARS. Available from: URL: http://www.who.int/csr/sars/archive/2003_04_16/en/
- 26 **Drosten C**, Gunther S, Preiser W, van der Werf S, Brodt HR, Becker S, Rabenau H, Panning M, Kolesnikova L, Fouchier RAM, Berger A, Burguiere AM, Cinatl J, Eickmann M, Escriou N, Grywna K, Kramme S, Manuguerra JC, Müller S, Rickerts V, Stürmer M, Vieth S, Klenk HD, Osterhaus AD, Schmitz H, Doerr HW. Identification of a novel coronavirus in patients with severe acute respiratory syndrome. *N Engl J Med* 2003; **348**: 1967-1976
- 27 **Seto WH**, Tsang D, Yung RW, Ching TY, Ng TK, Ho M, Ho LM, Peiris JS. Effectiveness of precautions against droplets and contact in prevention of nosocomial transmission of severe acute respiratory syndrome (SARS). *Lancet* 2003; **361**: 1519-1520
- 28 World Health Organization. Update 32-Situation in China and Hong Kong, status of diagnostic tests. Available from: URL: http://www.who.int/csr/sarsarchive/2003_04_17/en
- 29 Amoy Gardens investigation findings make public. Available from: URL: <http://www.info.gov/csr/sars/labmethods/en>
- 30 **Wang CE**, Qin ED, Gan YH, Li YC, Wu XH, Cao JT, Yu M, Si BY, Yan G, Li JF, Zhu QY. Pathological observation on sucking mice and Vero E6 cells inoculated with SARS samples. *Jiefangjun Yixue Zazhi* 2003; **28**: 383-384
- 31 **Hong T**, Wang JW, Sun YL, Duan SM, Chen LB, Qu JG, Ni AP, Liang GD, Ren LL, Yang RQ, Guo L, Zhou WM, Chen J, Li DX, Wen XB, Xu H, Guo YJ, Dai SL, Bi SL, Dong XP, Ruan L. Chlamydia-like and coronavirus-like agents found in dead cases of atypical pneumonia by electron microscopy. *Zhonghua Yixue Zazhi* 2003; **83**: 632-636
- 32 **Riley S**, Fraser C, Donnelly CA, Ghani AC, Abu-Raddad LJ, Hedley AJ, Leung GM, Ho LM, Lam TH, Thach TQ, Chau P, Chan KP, Lo SV, Leung PY, Tsang T, Ho W, Lee KH, Lau EM, Ferguson NM, Anderson RM. Transmission dynamics of the etiological agent of SARS in Hong Kong: impact of public health interventions. *Science* 2003; **300**: 1961-1966
- 33 **Sobsey MD**, Jones BL. Concentration of Poliovirus from tap water using positively charged microporous filters. *Appl Environ Microbiol* 1979; **37**: 588-595
- 34 **Sobsey MD**, Glass JS. Poliovirus concentration from tap water with electropositive adsorbent filters. *Appl Environ Microbiol* 1980; **40**: 201-210
- 35 **Palmer CJ**, Lee MH, Bonilla GF, Javier BJ, Siwak EB, Tsai YL. Analysis of sewage effluent for human immunodeficiency virus (HIV) using infectivity assay and reverse transcriptase polymerase chain reaction. *Can J Microbiol* 1995; **41**: 809-815

Effects of iron manipulation on trace elements level in a model of colitis in rats

M Barollo, R D'Inca, M Scarpa, V Medici, R Cardin, M Bortolami, C Ruffolo, I Angriman, GC Sturniolo

M Barollo, R D'Inca, M Scarpa, V Medici, R Cardin, M Bortolami, C Ruffolo, I Angriman, GC Sturniolo, Department of Surgical and Gastroenterological Sciences, University of Padua, Italy
Supported by the MIUR 60% 2000
Correspondence to: GC Sturniolo, Divisione di Gastroenterologia, Via Giustiniani 2, Padova 35128, Italy. gc.sturniolo@unipd.it
Telephone: +39-49-821-8726 Fax: +39-49-876-0820
Received: 2004-05-25 Accepted: 2004-08-22

Abstract

AIM: Trace elements (TE) metabolism is altered in inflammatory bowel diseases. TE (zinc and copper) are constituents of antioxidant enzymes. Iron is involved in the pathogenesis of chronic inflammation. The aim was to evaluate zinc and copper status and the effects of iron manipulation in experimental colitis.

METHODS: Twenty-four male Sprague-Dawley rats were divided into four groups: standard diet, iron-deprived diet, iron-supplemented diet, and sham-treated controls. Macroscopic damage was scored. DNA adducts were measured in the colon. Liver and colonic concentration of TE were measured.

RESULTS: Macroscopic damage was reduced in iron-deprived groups and increased in iron-supplemented rats. Damage to the DNA was reduced in iron-deprived groups and increased in iron-supplemented groups. Liver and colonic iron concentrations were reduced in iron-deprived and increased in iron-supplemented rats. Liver zinc concentration was reduced after supplementation whereas colonic levels were similar in controls and treated rats. Liver copper concentration was reduced in all the colitic groups except in the iron-supplemented group whereas colonic concentration was increased in iron-deprived rats.

CONCLUSION: Iron deprivation diminishes the severity of DNBS colitis while supplementation worsens colitis. Zinc and copper status are modified by iron manipulation.

© 2005 The WJG Press and Elsevier Inc. All rights reserved.

Key words: Trace elements; Colitis

Barollo M, D'Inca R, Scarpa M, Medici V, Cardin R, Bortolami M, Ruffolo C, Angriman I, Sturniolo GC. Effects of iron manipulation on trace elements level in a model of colitis in rats. *World J Gastroenterol* 2005; 11(28): 4396-4399
<http://www.wjgnet.com/1007-9327/11/4396.asp>

INTRODUCTION

Trace elements such as zinc and copper are essential for human health^[1]. Zinc is required for cell membrane integrity, cell proliferation, and immune function. Several zinc-dependent antioxidant enzyme such as superoxide dismutase and metallothionein can neutralize free radicals production. Copper is necessary for the function of many enzymes involved in cell respiration and in cellular iron metabolism. Copper and zinc are both components of antioxidant enzymes such as superoxide dismutase. On the other hand, copper excess increases free radical levels thus enhancing the biological damage free radicals mediated^[2].

In inflammatory conditions large amounts of reactive oxygen species are produced and this contributes with different mechanisms to damage tissue proteins, DNA chains and lipids^[3]. Iron is a major peroxidative agent and animal studies demonstrated increased oxidative stress and intestinal inflammation after iron supplementation^[4]. As previously reported by Kato *et al.*, in Long Evans Cinammon rats, a model of copper liver toxicity, increased iron level is associated to copper excess and iron-deprived diet reduced mortality and fulminant hepatitis^[5]. Trace elements homeostasis is altered both in human and animal models of inflammatory bowel diseases with possible implication for disease activity and carcinogenesis^[6-8].

We previously demonstrated that dietary iron deprivation is effective in reducing DNA damage and improves the outcome of colitis. The aim of this study was to evaluate the effects of iron supplementation compared to deprivation on disease activity, on trace elements status and on colonic DNA oxidative damage in a model of experimental colitis.

MATERIALS AND METHODS

Experimental protocol

Twenty-four male Sprague-Dawley rats weighing 200 g were divided into four groups; one group was fed with standard diet containing 200 mg/kg of iron and given drinking water ad libitum. The second group was fed with an iron-controlled diet (50 mg/kg) and allowed to drink iron-free water for 5 wk and the third with an iron-supplemented diet (1 700 mg/kg) for 5 wk. The fourth group was fed with a standard diet (200 mg/kg of iron) and at the time of colitis induction was sham treated with saline.

Colitis was induced by the intrarectal instillation of 58 mg dinitro-benzene-sulfonic acid (DNBS) dissolved in 50% ethanol. The rats were anesthetized with ether and a silicone catheter was introduced intrarectally to 5 cm. Animals were kept in the Trendelenburg position for 10 min

to avoid the rapid evacuation of the enema. On d 8, 1 wk after colitis induction, the animals were weighed and anesthetized with intraperitoneal chloral hydrate (400 mg/kg) after which the abdomen was opened with a midline incision and exsanguination was performed. The colon was removed, opened along the antimesenteric border, rinsed with iron-free water and weighed.

The damage was assessed by scoring the number and extension of ulcers, adhesions, and thickness of the colonic wall according to Morris *et al.*^[9].

Operators were unaware of the treatment of each group. Colonic tissue samples were obtained and processed for myeloperoxidase and 8-hydroxydeoxyguanosine (8-OHdG) determination and for measuring iron, zinc, and copper concentrations. Similarly liver samples were obtained for the determination of iron, zinc, and copper concentrations.

Iron, zinc, and copper determination

Trace elements concentrations were measured using atomic absorption spectrophotometry. Intestinal and liver tissues, obtained from rats, were dried at 42 °C for 24 h. The dried samples were weighed on an analytical balance, transferred into element-free tubes and then dissolved using 4.5 mL of 300 mL/L nitric acid solution. The tubes were incubated at 42 °C for 24 h. Iron, copper, and zinc standard solutions (0.05, 0.10, 0.20, 0.50, and 1 µg/mL) were prepared by dilution of concentrated stock solution (Titrisol, Merck Darmstadt, Germany) in deionized water. A Perkin Elmer 3100 atomic absorption spectrophotometer operated with an acetylene air mixture. A lean blue (oxidizing) flame was used with a cathode lamp current of 15 mA, a monochromator wavelength of 248.3 nm, and a slit width of 0.2 nm for Fe; lamp current of 25 mA, a wavelength of 213.9, and a slit width of 0.7 nm for Zn; lamp current of 15 mA, a wavelength of 324.8 nm, and a slit width of 0.7 mm for Cu.

Samples were aspirated directly and the concentration of the element of interest was determined from appropriate standard curves. Standard controls (Bovine liver, Trimital, Magenta, Milan, Italy) were prepared using the same extraction procedure used for sample preparation.

Results were expressed taking into account the dry weight and the dilution factor of the samples.

Myeloperoxidase

MPO activity was assessed following previously described methods^[10]. Briefly colonic tissue samples were minced in 1 mL of 50 mmol/L potassium phosphate buffer (pH 6.0) containing 14 mmol/L hexadecyltrimethylammonium bromide (Fluka), homogenized and sonicated. The lysates have to be frozen and thawed thrice, then centrifuged for 2 min in cold at 15 000 *g*. Aliquots of the supernatants

were mixed with potassium phosphate buffer containing *o*-dianisidine-HCl (Sigma-Aldrich, St. Louis, MO, USA) and 0.0005% H₂O₂. MPO activity was expressed as units/g of wet tissue. The enzyme unit was defined as the conversion of 1 mol of H₂O₂ per minute at 25 °C.

8-OHdG

Oxidative DNA damage was assessed following previously described methods^[11]. Briefly colonic biopsy specimens were thawed, homogenized in a separation buffer and approximately 20 µg of purified DNA per sample was injected in the HPLC (Shimadzu, Kyoto, Japan). The 8-OHdG was detected using an electrochemical detector (ESA Coulochem II 5200A, Bedford, MA, USA). The levels of 8-OHdG were expressed as the number of 8-OHdG adducts per 10⁵ dG bases. The coefficient of variation was <10%; 100 µg of DNA were required for the determination.

Statistical analysis

Data are expressed as mean +/- standard error. Statistical data were analyzed with Mann-Whitney *U* test for comparison of the four groups and Spearman's rank correlation test to evidence any relation between the evaluated parameters. *P* values less than 0.05 were considered significant.

RESULTS

Before colitis was induced body weight was similar in all groups of animals. The colon weight, a rough measure of edema and inflammation, was significantly increased in colitic animals with respect to controls (*P*<0.05), while iron-deprived rats had colonic weights similar to controls. The macroscopic damage score was significantly lower in the group receiving iron-deprived diet than in the colitis groups. MPO activity was significantly increased in iron-supplemented rats. Iron deprivation was associated with significantly higher MPO levels than controls.

Clinical and biochemical aspects of colitis in all rat groups are summarized in Table 1.

Dietary iron deprivation significantly decreased hepatic and colonic iron concentrations. Iron supplementation increases the iron concentration in liver and colon compared to healthy controls. Iron concentration was increased in the liver and colon of rats with colitis (Fe, 200 mg/kg) whereas supplementation did not affect hepatic iron concentration (Figure 1). There was a significant correlation between hepatic and colonic iron concentrations (*R* = 0.567, *P*<0.002).

Inflammation significantly increased hepatic zinc concentration but neither iron deprivation or supplementation modified zinc concentration in the liver. Although no

Table 1 Clinical and biochemical aspects of colitis

	Controls	Standard diet (Fe, 200 mg/kg)	Iron-supplemented diet (1 700 mg/kg)	Iron-deprived diet (45 mg/kg)
Colon wet weight (g)	2.2±0.2	4.0±0.9 ^a	3.8±0.8	2.1±0.4 ^f
Macroscopic damage score	0±0	8.75±2.5	7.4±1.4	3.6±1.1 ^e
Myeloperoxidase U/mg	3.5±0.6	19.4±5.2	61.4±7.9 ^b	24.5±7.1

^a*P*<0.05 vs controls; ^b*P*<0.01 vs standard diet; ^c*P*<0.05 vs standard diet.

significant change was revealed in any of the treatments the more the colon was damaged the lower was the colonic zinc concentration ($R = -0.460$, $P = 0.02$).

Hepatic copper concentration was reduced in all colitic groups with respect to controls except in the iron-supplemented group. On the other hand, copper colonic concentration was increased in the iron-deprived diet group irrespective of treatment and inflammatory status (Table 2). Hepatic copper concentration correlated with colonic copper ($R = 0.39$, $P < 0.04$).

Colonic DNA adducts were significantly reduced in rats fed with an iron-deprived diet for 5 wk (Figure 2). Colonic DNA adducts significantly correlated with iron colonic concentration ($R = 0.44$, $P < 0.02$).

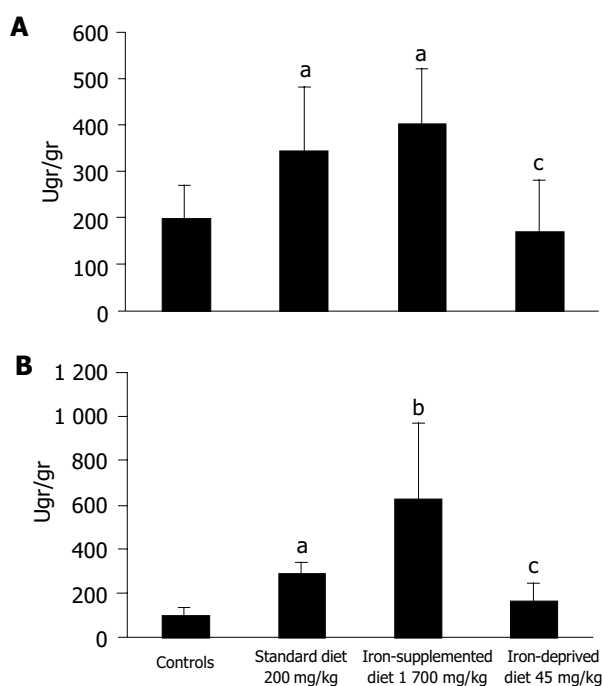


Figure 1 Liver (A) and colonic (B) iron concentrations. ^a $P < 0.05$, ^b $P < 0.01$ vs controls; ^c $P < 0.05$ vs standard diet.

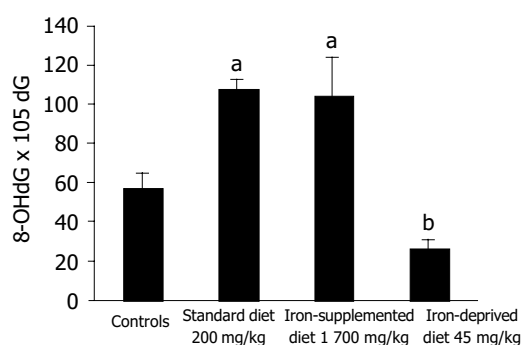


Figure 2 Colonic DNA adducts. ^a $P < 0.05$ vs controls; ^b $P < 0.01$ vs standard diet.

DISCUSSION

Iron has a major role in chronic inflammatory diseases. Lin *et al.*, demonstrated *in vitro* that iron chelation effectively

Table 2 Hepatic and colonic zinc and copper concentrations in controls and colitis

	Zinc $\mu\text{g/g}$		Copper $\mu\text{g/g}$	
	Hepatic	Colonic	Hepatic	Colonic
Controls	99.8 \pm 2.1	133.4 \pm 6.1	54.4 \pm 1.6	18.6 \pm 0.9
Standard diet	140.2 \pm 6.2 ^a	113.9 \pm 5.8	20.8 \pm 0.7 ^d	18.6 \pm 0.9
Iron-supplemented diet	92.6 \pm 5 ^b	132.2 \pm 10.2	44.2 \pm 3.9	21 \pm 2.1
Iron-deprived diet	117.2 \pm 4.4	101.6 \pm 5.1	19.7 \pm 0.8 ^d	36.2 \pm 5.9 ^c

^a $P < 0.05$ vs controls; ^b $P < 0.01$ vs standard diet; ^c $P < 0.05$ vs controls and standard diet; ^d $P < 0.001$ vs controls.

blocks NF-kappa B activation and upregulates TNF- α and IL-6 genes in a model of cholestatic liver injury, suggesting a basic role for iron in the activation of the inflammatory process^[12]. In patients with Crohn's disease and anemia, treatment with oral ferrous fumarate decreased cysteine and glutathione peroxidase with consequent altered plasma antioxidant status^[13]. Moreover, oxidative stress is increased *in vitro* cell lines from patients with ulcerative colitis treated with iron^[14].

Recent evidence showed that iron dietary deprivation is a reasonable approach to many diseases with a free radical component^[15]. It is known that Deferoxamine, an iron chelating agent, effectively reduces mucosal oxidant activity by decreasing the luminol-amplified chemiluminescence *in vitro* by 44% in active ulcerative colitis biopsies^[16]. This effect was attributed more to iron chelation than to a direct antioxidant activity.

We observed that iron deprivation was associated with less macroscopic colonic mucosal damage while iron supplementation worsened colitis. Iron and inflammation seem to have a synergic action since MPO levels were greatly increased in the iron-supplemented group. Our observations suggest that iron manipulation may modulate inflammatory damage.

The results of this study confirm that dietary iron deprivation reduces inflammation and oxidative DNA damage in the rat model of DNBS-induced colitis while iron supplementation worsens colitis as we previously reported (in press)^[17]. These results further reinforce our previous findings on the role of iron deprivation in DNBS colitis. Carrier *et al.*, recently reported that oral iron supplementation may aggravate inflammation and oxidative stress in dextran sulfate sodium-induced colitis^[18]. Oxidative damage, expressed by DNA adducts level, was decreased in iron-deprived rats. According to Seril *et al.*, reactive oxygen species, produced in abundance in the presence of iron during inflammation, can directly mediate DNA damage thus leading to alterations, which cause loss of suppressor genes and gain of oncogenes function^[19].

Trace elements are altered during inflammation and their status is critical for normal cell and enzymes function. Many enzymes, involved in DNA repair mechanisms, are zinc-dependent thus trace elements alteration could contribute to DNA damage^[20]. Several human and animal studies have demonstrated altered trace elements status during inflammation. Al Awadi *et al.*, reported a significant reduction of colonic zinc level in experimental colitis while copper and manganese remained unaltered^[8]. Zinc and copper serum levels were altered in well-nourished patients

with ulcerative colitis and correlated with hematological parameters of disease activity suggesting their role in inflammation^[21]. We previously demonstrated that zinc supplementation regulates tight junction permeability in experimental colitis with possible implication on mucosal healing^[22]. Several studies have pointed out that zinc, copper, and iron may affect the progression of colonic tumors in experimental model of preneoplastic lesions^[23]. Moreover, Ames has recently reported that zinc and other micronutrient deficiencies mimic the effect of radiation on DNA chain with strong implication for carcinogenesis^[24].

Hepatic zinc concentration is significantly reduced during iron dietary deprivation. Colonic zinc concentration is similar to controls in all treated groups and it is independent from iron metabolism. The inverse correlation with macroscopic score and colonic weight may suggest the relevant effect of zinc on mucosa healing. In fact as recently reported by Kruidenier superoxide dismutase Zn/Cu dependent is decreased in colonic mucosa of IBD patients with active inflammation^[25].

Colonic copper is increased during iron dietary deprivation. Iron supplementation does not seem to affect copper absorption as recently demonstrated in ileostomy subjects^[26]. Colonic copper alterations seem therefore a consequence of local inflammation. On the other hand our data showed that inflammation decreased copper concentration in the liver except in the presence of iron supplementation. This is in agreement with the results reported in Long Evans Cinammon rats, in which an iron deprived diet reduced mortality and fulminant hepatitis^[5].

In conclusion, we pointed out that iron manipulation affects the severity of experimental colitis. Iron manipulation results in changes of zinc and copper status which may, after a chemical insult, alter the natural course of intestinal inflammation and may have important implications for the development of antioxidant treatment of IBD patients.

REFERENCES

- Bogden JD**, Klevay LM. Clinical nutrition of the essential trace elements and minerals. The guide for health professionals. 2000 Humana Press Inc.
- Olivares M**, Uauy R. Copper as an essential nutrient. *Am J Clin Nutr* 1996; **63**: 791S-796S
- Emerit J**, Beaumont C, Trivin F. Iron metabolism, free radicals, and oxidative injury. *Biomed Pharmacother* 2001; **55**: 333-339
- Reifen R**, Matas Z, Zeidel L, Berkovitch Z, Bujanover Y. Iron supplementation may aggravate inflammatory status of colitis in a rat model. *Dig Dis Sci* 2000; **45**: 394-397
- Kato J**, Kobune M, Kohgo Y, Sugawara N, Hisai H, Nakamura T, Sakamaki S, Sawada N, Niitsu Y. Hepatic iron deprivation prevents spontaneous development of fulminant hepatitis and liver cancer in Long-Evans Cinnamon rats. *J Clin Invest* 1996; **98**: 923-929
- Ringstad J**, Kildebo S, Thomassen Y. Serum selenium, copper, and zinc concentrations in Crohn's disease and ulcerative colitis. *Scand J Gastroenterol* 1993; **28**: 605-608
- Brignola C**, Belloli C, De Simone G, Evangelisti A, Parente R, Mancini R, Iannone P, Mochecciani E, Fabris N, Morini MC. Zinc supplementation restores plasma concentrations and thymulin in patients with Crohn's disease. *Aliment Pharmacol Ther* 1993; **7**: 275-280
- Al-Awadi FM**, Khan I, Dashti HM, Srikumar TS. Colitis-induced changes in the level of trace elements in rat colon and other tissues. *Ann Nutr Metab* 1998; **42**: 304-310
- Morris GP**, Beck PL, Herridge MS, Depew WT, Szewczuk MR, Wallace JL. Hapten-induced model of chronic inflammation and ulceration in the rat colon. *Gastroenterology* 1989; **98**: 795-803
- Krawisz JE**, Sharon P, Stenson WF. Quantitative assay for acute intestinal inflammation based on myeloperoxidase activity. Assessment of inflammation in rat and hamster models. *Gastroenterology* 1984; **87**: 1344-1350
- Helbock HJ**, Beckman KB, Shigenaga MK, Walter PB, Woodall AA, Yeo HC, Ames BN. DNA oxidation matters: the HPLC-electrochemical detection assay of 8-oxo-deoxyguanosine and 8-oxo-guanosine. *Proc Natl Acad Sci USA* 1998; **95**: 288-293
- Lin M**, Rippe RA, Niemela O, Brittenham G, Tsukamoto H. Role of iron in NF-kappa B activation and cytokine gene expression by rat hepatic macrophages. *Am J Physiol* 1997; **272**: G1355-1364
- Erichsen K**, Hausken T, Ulvik RJ, Svoldal A, Berstad A, Berge RK. Ferrous fumarate deteriorated plasma antioxidant status in patients with Crohn disease. *Scand J Gastroenterol* 2003; **38**: 543-548
- Millar AD**, Rampton DS, Blake DR. Effects of iron and iron chelation *in vitro* on mucosal oxidant activity in ulcerative colitis. *Aliment Pharmacol Ther* 2000; **14**: 1163-1168
- Polla BS**. Therapy by taking away: the case of iron. *Biochem Pharmacol* 1999; **57**: 1345-1349
- Carotenuto P**, Pontesilli O, Cambier JC, Hayward AR. Desferoxamine blocks IL 2 receptor expression on human T lymphocytes. *J Immunol* 1986; **136**: 2342-2347
- Barollo M**, D'Inca R, Scarpa M, Medici V, Cardin R, Fries W, Angriman I, Sturniolo GC. Effects of iron deprivation or chelation on DNA damage in experimental colitis. *Int J Colorectal Dis* 2004; **19**: 461-466
- Carrier J**, Aghdassi E, Platt I, Mullen J, Allard JP. Effect of oral iron supplementation on oxidative stress and colonic inflammation in rats with induced colitis. *Aliment Pharmacol Ther* 2001; **15**: 1989-1999
- Seril DN**, Liao J, Yang GY, Yang CS. Oxidative stress and ulcerative colitis -associated carcinogenesis: studies in humans and animal models. *Carcinogenesis* 2003; **24**: 353-362
- Leon O**, Roth M. Zinc fingers: DNA binding and protein-protein interactions. *Biol Res* 2000; **33**: 21-30
- Dalekos GN**, Ringstad J, Savaidis I, Seferiadis KI, Tsianos EV. Zinc, copper and immunological markers in the circulation of well nourished patients with ulcerative colitis. *Eur J Gastroenterol Hepatol* 1998; **10**: 331-337
- Sturniolo GC**, Fries W, Mazzon E, Di Leo V, Barollo M, D'Inca R. Effect of zinc supplementation on intestinal permeability in experimental colitis. *J Lab Clin Med* 2002; **39**: 311-315
- Davis CD**, Feng Y. Dietary copper, manganese and iron affect the formation of aberrant crypts in colon of rats administered 3,2-dimethyl-4-aminobiphenyl. *J Nutr* 1999; **129**: 1060-1067
- Ames BN**. DNA damage from micronutrient deficiencies is likely to be a major cause of cancer. *Mutation Research* 2001; **475**: 7-20
- Kruidenier L**, Kuiper I, van Duijn W, Marklund SL, van Hogezaand RA, Lamers CB, Verspaget HW. Differential mucosal expression of three superoxide dismutase isoforms in inflammatory bowel disease. *J Pathol* 2003; **201**: 7-16
- Troost FJ**, Brummer RJ, Dainty JR, Hoogewerff JA, Bull VJ, Saris WH. Iron supplements inhibit zinc but not copper absorption *in vivo* in ileostomy subjects. *Am J Clin Nutr* 2003; **78**: 1018-1023

• BRIEF REPORTS •

Relationship between β -catenin expression and epithelial cell proliferation in gastric mucosa with intestinal metaplasia

Adriana Romiti, Angelo Zullo, Francesco Borrini, Ida Sarcina, Cesare Hassan, Simon Winn, Silverio Tomao, Aldo Vecchione, Sergio Morini, Pietro Mingazzini

Adriana Romiti, Ida Sarcina, Aldo Vecchione, Medical Oncology, "Sant' Andrea" Hospital, Rome, Italy
Angelo Zullo, Cesare Hassan, Simon Winn, Sergio Morini, Gastroenterology and Digestive Endoscopy, "Nuovo Regina Margherita" Hospital, Rome, Italy
Francesco Borrini, Pietro Mingazzini, Department of Experimental Medicine and Pathology, "La Sapienza" University, Rome, Italy
Silverio Tomao, Oncology, IRCCS "Regina Elena", Rome, Italy
Co-first-authors: Adriana Romiti and Angelo Zullo
Co-correspondence: Aldo Vecchione
Correspondence to: Dr. Adriana Romiti, Ospedale "S. Andrea", Oncologia Medica, Via di Grottarossa 1035, Rome 00189, Italy. sanoncol@libero.it
Telephone: +39-6-80345338 Fax: +39-6-80345001
Received: 2004-03-23 Accepted: 2005-01-05

increases cell proliferation. *H pylori* infection does not seem to play a direct role in β -catenin alterations, whilst it significantly increases cell proliferation.

© 2005 The WJG Press and Elsevier Inc. All rights reserved.

Key words: β -Catenin; Intestinal metaplasia; Proliferation; *Helicobacter pylori*

Romiti A, Zullo A, Borrini F, Sarcina I, Hassan C, Winn S, Tomao S, Vecchione A, Morini S, Mingazzini P. Relationship between β -catenin expression and epithelial cell proliferation in gastric mucosa with intestinal metaplasia. *World J Gastroenterol* 2005; 11(28): 4400-4403
<http://www.wjgnet.com/1007-9327/11/4400.asp>

Abstract

AIM: To investigate β -catenin expression in patients with intestinal metaplasia, and to look for a possible relationship between β -catenin expression and either epithelial proliferation values or *Helicobacter pylori* (*H pylori*) infection.

METHODS: Twenty patients with complete type intestinal metaplasia were studied. β -Catenin expression and epithelial cell proliferation in antral mucosa were assessed using an immunohistochemical analysis. *H pylori* infection was detected by histology and a rapid urease test.

RESULTS: Reduced β -catenin expression on the surface of metaplastic cells was detected in 13 (65%) out of 20 patients. Moreover, in eight (40%) patients intranuclear expression of β -catenin was found. When patients were analyzed according to *H pylori* infection, the prevalence of both β -catenin reduction at the cell surface and its intranuclear localization did not significantly differ between infected and uninfected patients. Cell proliferation was higher in patients with intranuclear β -catenin expression as compared to the remaining patients, although the difference failed to reach the statistical significance (36 ± 8.9 vs 27.2 ± 11.4 , $P = 0.06$). On the contrary, a similar cell proliferation value was observed between patients with reduced expression of β -catenin on cell surface and those with a normal expression (28.1 ± 11.8 vs 26.1 ± 8.8 , $P = 0.7$). *H pylori* infection significantly increased cell proliferation ($33.3 \pm 10.2\%$ vs $24.6 \pm 7.4\%$, respectively, $P = 0.04$).

CONCLUSION: Both cell surface reduction and intranuclear accumulation of β -catenin were detected in intestinal metaplasia. The intranuclear localization of β -catenin

INTRODUCTION

Catenins are a family of transmembrane proteins, which play a pivotal role in epithelial intercellular adhesion^[1]. Moreover, β -catenin participates in the regulation of cell proliferation, being a critical component of the surface-to-nucleus WNT signal transduction pathways^[2,3]. Alterations of β -catenin expression have been shown to be involved in cancer development^[4]. Indeed, such alterations have been detected in gastric cancer, showing a correlation with tumor type, degree of differentiation, and poor survival of patients^[5-9]. On the other hand, scanty data are available regarding β -catenin expression in precancerous conditions. Although alterations of some adhesion molecules have been detected in patients with intestinal metaplasia^[10], no significant remarks emerged from the studies regarding β -catenin expression in these patients^[10,11]. However, such studies were based on gastrectomy specimens of patients with gastric cancer and, therefore, only an advanced step of the carcinogenic process was evaluated.

Gastric carcinogenesis is a multistep process consisting of a cascade of alterations starting with chronic active gastritis and progressing to atrophy, metaplasia, and dysplasia^[12]. In particular, intestinal metaplasia is widely recognized as being the most prevalent precursor of intestinal type gastric carcinoma^[13]. Among environmental factors involved in carcinogenesis of the stomach, *Helicobacter pylori* (*H pylori*) infection appears to play an important role. Indeed, epidemiological studies have clearly demonstrated a significant association between this infection and gastric cancer development. Moreover, several changes involved in gastric carcinogenesis such as epithelial cell hyperproliferation,

free oxygen radical formation, ascorbic acid reduction, genetic alterations have been described in the gastric mucosa of infected patients^[14-16].

The present study was designed in order to assess β -catenin expression in patients with intestinal metaplasia but with neither dysplasia nor gastric cancer, and to look for a possible relationship between β -catenin expression and either epithelial proliferation index of gastric mucosa or *H pylori* infection status.

MATERIALS AND METHODS

Patients

Patients with dyspeptic symptoms consecutively referred for upper endoscopy with presence of histology of intestinal metaplasia in the antrum and without concomitant evidence of either dysplasia in the stomach or neoplastic lesions in the upper gastrointestinal tract were selected. Patients were enrolled irrespectively of *H pylori* status. Patients who received proton pump inhibitors, H₂-receptor antagonists, antibiotics or NSAIDs in the 4 wk preceding the study as well as those previously treated for *H pylori* infection were excluded from the study. Patients with either liver impairment or kidney failure were also excluded.

Endoscopic procedure

After overnight fasting, all patients underwent upper endoscopy and three biopsies were taken from the antrum and three from the gastric body. Two biopsies from the antrum and two from the gastric body were used for histological assessment. Biopsy specimens of the antrum were also used for immunohistochemical analysis. The remaining two biopsies (one each from the antrum and gastric body) were used to carry out a rapid urease test (CP-test, Yamanouchi, Milan, Italy). *H pylori* infection was considered to be present when both the histological assessment on Giemsa staining revealed the presence of bacteria and rapid urease test was positive, as suggested in current guidelines^[17].

Immunohistochemical analysis

For β -catenin and proliferation assessment, immunohistochemistry was carried out by the avidin-biotin-peroxidase method. Briefly the sections were deparaffinized in xylene and rehydrated through a graded alcohol series to distilled water. Antigen retrieval was performed by immersing the slides in 10 mol/L citrate buffer (pH 6.0) and heating them in a microwave for 3 cycles, 5 min each, at 750 W. Endogenous peroxidase activity and non-specific bindings were blocked by incubation with 3% hydrogen peroxide and nonimmune serum, respectively. Sections were then incubated with mAbs against β -catenin (Clone 14, 1:500 dilution; Transduction Laboratories, Lexington, KY, USA) and mAbs against Ki-67 (Clone MIB-1, 1:100 dilution YLEM, Italy) for 1 h at room temperature. Immunoreactivity was revealed with the chromogen DAB test and the sections were counterstained with Mayer hematoxylin solution for 7 min. Negative control sections were prepared by substituting primary antibody with buffered saline.

A semiquantitative approach was used for scoring the

β -catenin expression according to the method previously described by Mingchao^[10]. Briefly, the staining pattern of the intestinal metaplastic areas was compared with that of the adjacent normal gastric mucosa. Expression of β -catenin in metaplastic areas was considered 'normal' when both the intensity and the frequency of the cell membrane stains were equivalent to those found on the bordering nonmetaplastic gastric mucosa, 'reduced' when the staining was less than the adjacent mucosa, and 'negative' in the absence of staining. In addition, when β -catenin stained clearly in the nuclei of more than 10% of gastric epithelial cells, expression was judged to be positive for nuclear staining.

A quantitative approach was used instead for scoring the Ki67 expression. The number of cells was determined by counting the positively-stained nuclei on 10-20 randomly selected fields at 400 \times .

All immunostaining evaluations were performed blindly and by two independent observers. All sections for which the two observers disagreed were re-evaluated and, after opportune discussion, a final agreement was achieved.

Statistical analysis

Data between patient subgroups were compared using the Student's *t*-test for unpaired data, and the Fisher's exact test with Yate's correction for small numbers. A *P* value less than 0.05 was considered statistically significant.

RESULTS

Overall, 20 consecutive patients (9 male and 11 female; mean age: 60.8 \pm 8.4 years) were enrolled. At endoscopy, no macroscopic alterations of the gastric mucosa were detected, whilst two patients showed erosions in the duodenal bulb. *H pylori* infection was present in 13 (65%) patients and absent at both rapid urease test and histology in the seven remaining patients. Intestinal metaplasia was graded as complete type in all cases.

β -catenin expression in gastric mucosa

No case of completely negative β -catenin immunostaining was observed. A reduced expression of β -catenin on the surface of metaplastic cells as compared to adjacent normal glands was detected in 13 (65%) out of 20 patients. Moreover, in eight (40%) patients an intranuclear expression of β -catenin was detected. Among this group, six (75%) patients also showed reduced β -catenin expression. When patients were analyzed according to *H pylori* infection, β -catenin expression was decreased in 8 out of 13 infected patients as well as in 5 out of 7 uninfected cases (*P* = 0.5). Similarly, the prevalence of intranuclear localization of β -catenin expression did not significantly differ between infected and uninfected patients (4/13 *vs* 4/7, respectively; *P* = 0.2).

Cell proliferation in gastric mucosa

The mean value of Ki67 labeling index proved to be distinctly higher in eight patients with intranuclear β -catenin expression as compared to the remaining 13 patients, although the difference failed to reach statistical significance (36 \pm 8.9 *vs* 27.2 \pm 11.4, *P* = 0.06). On the contrary, by

excluding those patients with intranuclear localization of β -catenin, a similar cell proliferation value was observed between the seven patients with reduced membranous expression of β -catenin and the five patients with normal expression (28.1 ± 11.8 vs 26.1 ± 8.8 , $P = 0.7$). As far the role of *H. pylori* infection is concerned, data found that patients with infection had a significantly increased cell proliferation value than that of uninfected patients ($33.3 \pm 10.2\%$ vs $24.6 \pm 7.4\%$, respectively, $P = 0.04$).

DISCUSSION

The integrity of the function of adhesion molecules, such as E-cadherin and α , β , γ -catenins, allows the maintenance of normal interactions between cells necessary during embryogenesis, cell growth, and differentiation^[1-3,18]. Loss of intercellular adhesiveness plays a role in the early steps of neoplastic transformation, and it is implicated in invasive growth and metastasization^[5-9,19]. β -catenin participates in the adhesion process by binding the cytoplasmic domain of E-cadherin and it has been involved in the surface-to-nucleus WNT signal transduction pathways. Its translocation into the nucleus may contribute to accelerated cell proliferation^[3]. β -catenin mutations in exon 3, interfering with the GSK-3 β phosphorylation domain and leading to intranuclear accumulation of the protein, have been reported in intestinal gastric carcinoma as well as in colorectal cancer^[20-23]. Moreover reduced β -catenin expression was recorded both in intestinal type of gastric cancer^[5,6,24] and in intestinal metaplasia surrounding cancer lesions^[25], although data are controversial^[10,11,24]. In order to determine whether β -catenin alterations could be detected early in gastric carcinogenesis, the present study focused on β -catenin expression in intestinal metaplasia not associated with gastric cancer. Unlike previous study^[26], in our series a reduction of β -catenin on the epithelial surface was observed in more than half of the patients. Intriguingly, a nuclear accumulation of β -catenin expression in 40% of patients with intestinal metaplasia was also found, and it was associated with reduced immunostaining at the intercellular boundaries in 75% of these cases. A previous study reported a nuclear accumulation of β -catenin in about 10% of 401 gastric carcinomas, all but one exhibiting reduced membranous staining^[24]. Similarly, an inverse correlation between decreased membranous and increased nuclear staining of β -catenin was also observed in colorectal cancer^[27,28]. Interestingly, we observed that patients with intranuclear β -catenin expression showed higher values of cell proliferation in the gastric mucosa as compared to those without it. This is a noteworthy remark in keeping with previously reported studies focused on the role of nuclear localization of β -catenin^[3]. Indeed, in an experimental model, colonocyte hyperproliferation was associated with immunohistochemical alterations in subcellular distribution of β -catenin and with accumulation of the protein in the nuclear compartment^[29]. This finding, however, has been not observed in gastric cancer^[23,24]. Therefore, it could be hypothesized that the nuclear β -catenin expression may be linked to the early stage of carcinogenesis, as seen in colorectal polyps^[30]. Conversely, loss of membranous expression could allow regenerating cells to dedifferentiate

and lose cell-cell cohesiveness, properties that would facilitate the process of epithelial regeneration, as reported for E-cadherin expression during the reparative process of peptic ulcer^[31]. Similarly, in endometrial glandular cells in the mid-to-late proliferative phase, nuclear accumulation of β -catenin was described, suggesting that it could play a physiological role in the rapid turnover of the cell cycle without gene mutation^[32].

As far the role of *H. pylori* infection is concerned, we failed to observe a significant difference in β -catenin expression between infected and uninfected patients, suggesting that this infection is not directly implicated in this phenomenon. On the contrary, in agreement with the results of several studies^[14,16], a significant increase in the epithelial cell proliferation index was detected in *H. pylori*-positive patients as compared to uninfected patients.

In conclusion, in the present immunohistochemical study, we described alterations in β -catenin expression in the gastric mucosa with intestinal metaplasia not associated to other more advanced histological lesions. β -catenin alterations consisted of both a weakness of membrane staining and in an intranuclear accumulation of the protein. Moreover, we observed a distinct increase in cell proliferation in those patients with intranuclear localization of β -catenin expression. *H. pylori* infection does not seem to play a role in β -catenin alterations, whilst it significantly increases cell proliferation in gastric mucosa with intestinal metaplasia.

REFERENCES

- 1 Gumbiner BM. Cell adhesion: the molecular basis of tissue architecture and morphogenesis. *Cell* 1996; **84**: 345-357
- 2 Behrens J, von Kries JP, Kuhl M, Bruhn L, Wedlich D, Grosschedl R, Birchmeier W. Functional interaction of beta-catenin with the transcription factor. *Nature* 1996; **382**: 638-642
- 3 Barker N, Clevers H. Beta-catenins WNT signaling and cancer. *Bioessays* 2000; **22**: 961-965
- 4 Hugh TJ, Dillon SA, O'Dowd G, Getty B, Pignatelli M, Poston GJ, Kinsella AR. Beta-catenin expression in primary and metastatic colorectal carcinoma. *Int J Cancer* 1999; **82**: 504-511
- 5 Shun CT, Wu MS, Lin MT, Chang MC, Lin JT, Chuang SM. Immunohistochemical evaluation of cadherin and catenin expression in early gastric carcinomas: correlation with clinicopathologic characteristics and *Helicobacter pylori* infection. *Oncology* 2001; **60**: 339-345
- 6 Joo YE, Rew JS, Choi SK, Bom HS, Park CS, Kim SJ. Expression of E-cadherin and catenins in early gastric cancer. *J Clin Gastroenterol* 2002; **35**: 35-42
- 7 Ougolkov A, Yamashita K, Bilim V, Takahashi Y, Mai M, Minamoto T. Abnormal expression of E-cadherin, β -catenin, and c-erbB-2 in advanced gastric cancer: its association with liver metastasis. *Int J Colorectal Dis* 2003; **18**: 160-166
- 8 Utsunomiya T, Doki Y, Takemoto H, Shiozaki H, Yano M, Inoue M, Yasuda T, Fuhwara Y, Monden M. Clinical significance of disordered beta-catenin expression pattern in human gastric cancers. *Gastric Cancer* 2000; **3**: 193-201
- 9 Karatzas G, Karayiannakis AJ, Syrigos KN, Chatzigianni E, Papanikolaou S, Simatos G, Papanikolaou D, Bogris S. Expression pattern of the E-cadherin-catenin cell-cell adhesion complex in gastric cancer. *Hepatogastroenterology* 2000; **47**: 1465-1469
- 10 Ma MC, Devereux TR, Stockton P, Sun K, Sills RC, Clayton N, Portier M, Flake G. Loss of E-cadherin expression in gastric intestinal metaplasia and later stage p53 altered expression in gastric carcinogenesis. *Exp Toxic Pathol* 2001; **53**: 237-246
- 11 Jawhari A, Jordan S, Poole S, Browne P, Pignatelli M, Far-

- thing JG. Abnormal immunoreactivity of the E-cadherin-catenin complex in gastric carcinoma: relationship with patient survival. *Gastroenterology* 1997; **112**: 48-54
- 12 **Correa P.** Human gastric carcinogenesis: a multistep and multifactorial process - First American cancer society award lecture on cancer epidemiology and prevention. *Cancer Res* 1992; **52**: 6735-6740
- 13 **Leung WK, Sung JJ.** Review article: intestinal metaplasia and gastric carcinogenesis. *Aliment Pharmacol Ther* 2002; **16**: 1209-1216
- 14 **Ierardi E, Francavilla A, Balzano T, Traversa A, Principi M, Monno RA, Amoroso A, Ingrosso M, Pisani A, Panella C.** Effect of *Helicobacter pylori* eradication on gastric epithelial proliferation. Relationship with ras oncogene p21 expression. *Ital J Gastroenterol Hepatol* 1997; **29**: 214-219
- 15 **Zullo A, Rinaldi V, Hassan C, Diana F, Winn S, Castagna G, Attili AF.** Ascorbic acid and intestinal metaplasia in the stomach: a prospective, randomised study. *Aliment Pharmacol Ther* 2000; **14**: 1303-1309
- 16 **Zullo A, Romiti A, Rinaldi V, Vecchione A, Hassan C, Winn S, Tomao S, Attili AF.** Gastric epithelial cell proliferation in patients with liver cirrhosis. *Dig Dis Sci* 2001; **46**: 550-554
- 17 **Caselli M, Parente F, Palli D, Covacci A, Alvisi V, Gasbarrini G, Bianchi Porro G.** Cervia Working Group Report: guidelines on the diagnosis and treatment of *Helicobacter pylori* infection. *Digest Liver Dis* 2001; **33**: 7-80
- 18 **Frenette PS, Wagner DD.** Adhesion molecules. *N Engl J Med* 1996; **334**: 1526-1529
- 19 **Guilford P.** E-cadherin downregulation in cancer: fuel on the fire? *Mol Med Today* 1999; **5**: 172-177
- 20 **Park WS, Oh RR, Park JY, Lee SH, Shin MS, Kim YS, Kim SY, Lee HK, Kim PJ, Oh ST, Yoo NJ, Lee JY.** Frequent somatic mutations of the beta-catenin gene in intestinal-type gastric cancer. *Cancer Res* 1999; **59**: 4257-4260
- 21 **Iwao K, Nakamori S, Kameyama M, Imoaka S, Kinoshita M, Fukui T, Ishiguro S, Nakamura Y, Miyoshi Y.** Activation of the β -catenin gene by interstitial deletions involving exon 3 in primary colorectal carcinomas without adenomatous polyposis coli mutations. *Cancer Res* 1998; **58**: 1021-1026
- 22 **Miyaki M, Iijima T, Kimura J, Yasuno M, Mori T, Hayashi Y, Koike M, Shitara N, Iwama T, Kuroki T.** Frequent mutation of beta-catenin and APC genes in primary colorectal tumors from patients with hereditary nonpolyposis colorectal cancer. *Cancer Res* 1999; **59**: 4506-4509
- 23 **Miyazawa K, Iwaya K, Kuroda M, Harada M, Serizawa H, Koyanagi Y, Sato Y, Mizokami Y, Matsuoka T, Mukai K.** Nuclear accumulation of beta-catenin in intestinal-type gastric carcinoma: correlation with early tumor invasion. *Virchows Arch* 2000; **437**: 508-513
- 24 **Grabsch H, Takeno S, Nogushi T, Hommel G, Gabbert HE, Mueller W.** Different patterns of β -catenin expression in gastric carcinomas: relationship with clinicopathological parameters and prognostic outcome. *Histopathology* 2001; **39**: 141-149
- 25 **Chan AO, Wong BC, Lan HY, Loke SL, Chan WK, Hui WM, Yuen Ng I, Hou I, Wong WM, Yuen MF, Luk JM, Lam SK.** Deregulation of E-cadherin-catenin complex in precancerous lesions of gastric adenocarcinoma. *J Gastroenterol Hepatol* 2003; **18**: 534-539
- 26 **Gulmann C, Grace A, Leader M, Butler D, Patchett S, Kay E.** Adenomatous polyposis coli gene, beta-catenin, and E-cadherin expression in proximal and distal gastric cancers precursor lesions: an immunohistochemical study using tissue microarray. *Appl Immunohistochem Mol Morphol* 2003; **11**: 230-237
- 27 **Inomata M, Ochiai A, Akimoto S, Hirobashi S.** Alteration of β -catenin expression in colonic epithelial cells of familial adenomatous polyposis patients. *Cancer Res* 1996; **56**: 2213-2217
- 28 **Hao X, Tomlinson I, Ilyas M, Palazzo JP, Talbot IC.** Reciprocity between membranous and nuclear expression of β -catenin in colorectal tumors. *Virchows Arch* 1997; **431**: 167-172
- 29 **Sellin JH, Umar S, Xiao J, Morris AP.** Increased b-catenin expression and nuclear translocation accompany cellular hyperproliferation *in vitro*. *Cancer Res* 2001; **61**: 2899-2906
- 30 **Barker N, Huls G, Korinek V, Clevers H.** Restricted high level expression of Tcf-4 protein in intestinal and mammary gland epithelium. *Am J Pathol* 1999; **154**: 29-35
- 31 **Hanby AM, Chinery R, Poulosom R, Playford RJ, Pignatelli M.** Downregulation of E-cadherin in the reparative epithelium of the human gastrointestinal tract. *Am J Pathol* 1996; **148**: 723-729
- 32 **Nei H, Saito T, Yamasaki H, Mizumoto H, Ito E, Kudo R.** Nuclear localization of beta-catenin in normal and carcinogenic endometrium. *Mol Carcinog* 1999; **25**: 207-218

• BRIEF REPORTS •

Expression of c-erbB-2 and glutathione S-transferase-pi in hepatocellular carcinoma and its adjacent tissue

Zhao-Shan Niu, Mei Wang

Zhao-Shan Niu, Department of Pathology, Medical College of Qingdao University, Qingdao 266021, Shandong Province, China

Mei Wang, Institute of Education, the University of Reading, Britain RG6 1HY, Reading, United Kingdom

Supported by the Scientific Research Foundation of Shandong Provincial Education Committee (J94, K26)

Correspondence to: Zhao-Shan Niu, Department of Pathology, Medical College of Qingdao University, 38 Dengzhou Road, Qingdao 266021, Shandong Province, China. niu miao1993@hotmail.com

Telephone: +86-532-3812410

Received: 2004-09-22 Accepted: 2004-11-19

Abstract

AIM: To investigate the possible role of c-erbB-2 and glutathione S-transferase (GST-Pi) in primary hepatocellular carcinogenesis and the relationship between liver hyperplastic nodule (LHN), liver cirrhosis (LC), and hepatocellular carcinoma (HCC).

METHODS: The expression of c-erbB-2 and GST-Pi was detected immunohistochemically in 41 tissue specimens of HCC and 77 specimens of its adjacent tissue.

RESULTS: The positive expression of c-erbB-2 in LHN (28.6%) was significantly higher than that in LC (0%) ($P = 0.032 < 0.05$), but no significant difference was seen between HCC and LHN or LC ($P > 0.05$, $\chi^2 = 0.002$, 3.447). The positive expression of GST-Pi in HCC (89.6%) or LHN (71.1%) was significantly higher than that in LC (22.9%, $P < 0.001$, $\chi^2 = 49.91$, 16.96). There was a significant difference between HCC and LHN ($P < 0.05$, $\chi^2 = 6.353$).

CONCLUSION: The c-erbB-2 expression is an early event in the pathogenesis of HCC. GST-Pi may be a marker enzyme for immunohistochemical detection of human HCC and its preneoplastic lesions. LHN seems to be a preneoplastic lesion related to hepatocarcinogenesis.

© 2005 The WJG Press and Elsevier Inc. All rights reserved.

Key words: Liver neoplasm; Hyperplastic nodule; C-erbB-2 gene; GST-pi gene; Immunohistochemistry

Niu ZS, Wang M. Expression of c-erbB-2 and glutathione S-transferase-pi in hepatocellular carcinoma and its adjacent tissue. *World J Gastroenterol* 2005; 11(28): 4404-4408
<http://www.wjgnet.com/1007-9327/11/4404.asp>

INTRODUCTION

Primary hepatocellular carcinoma (HCC) is one of the most common malignant tumors in Asia, and the incidence and mortality of HCC show a tendency to rise year by year. Therefore, the detection of preneoplastic lesions of HCC is crucial for the analysis of carcinogenic processes and developing strategies for prevention and treatment. For many years, liver hyperplastic nodule (LHN) has been considered as a preneoplastic lesion. Our previous studies have also confirmed that LHN is closely related to human HCC.

In the present study, the immunohistochemical LSAB method was used to detect the expression of c-erbB-2 oncogene and glutathione S-transferase-pi (GST-pi) in HCC and pericarcinomatous tissues, in order to investigate the possible roles of these genes in the HCC carcinogenesis, and to find out the relationship between LHN, liver cirrhosis (LC), and HCC.

MATERIALS AND METHODS

Materials

HCC specimens from 100 patients were selected during surgical resections or biopsies performed at the Affiliated Hospital of Medical College of Qingdao University, China. Of these patients, 76 were males and 24 females with an average age of 50.4 years. None of the patients received chemo- or radiotherapy before resection. We randomly selected 41 and 77 cases of HCC to detect the expression of c-erbB-2 and GST-pi, respectively. The same specimens from 16 cases were detected for both c-erbB-2 and GST-pi, which were too few to be analyzed in terms of the correlation between them in the present study. Forty-one specimens for detecting c-erbB-2 oncogene contained 18 pericarcinomatous tissues, including 14 LHN, 17 LC. Seventy-seven specimens for detecting GST-pi contained 40 pericarcinomatous tissues, including 38 LHN, and 35 LC.

Methods

All specimens were routinely processed, alcohol-fixed and paraffin-embedded. Serial paraffin sections of 4 μ m thickness were cut and used for hematoxylin and eosin and immunohistochemical staining. Immunohistochemical LSAB method was used to detect c-erbB-2 and GST-pi. Anti-c-erbB-2 multiple clonal antibody, anti-GST-pi multiple clonal antibody and LSAB kits were purchased from Dako Co. Before staining, the sections were microwave heated in 0.05 mol citric acid solution for antigen retrieval. In each staining run, a known c-erbB-2 or GST-pi positive section was added as positive control, PBS was used as substitutes

of the first antibodies for negative control.

Analysis of immunohistochemical staining

When brown granules were found on cell membrane of liver cells and cancer cells, c-erbB-2 was identified positive. When only cytoplasm was stained brown, c-erbB-2 was identified negative. The c-erbB-2 expression was graded semi-quantitatively according to the intensity and the percentage of positivity into negative (-): no positive cells or a weak staining of c-erbB-2 with positive cells <5%; positive (+): c-erbB-2 expression was relatively stronger with the positive cells >5%. For GST-pi, cells with brown granules in cytoplasm were regarded as positive. The criteria of the evaluation of GST-pi expression in this study were as follows. The positive number was semi-quantitatively evaluated by counting that in 5-10 randomly chosen medium power ($\times 100$ magnification), and the three grades for GST-pi were considered as negative (-): no positive cells; positive (+): the positive reaction being brown and the positive cells <30%; strong positive (++) : the positive reaction being brown and the positive cells >30% according to the intensity and extent of GST-pi staining.

Statistical analysis

Results were analyzed by χ^2 -test and direct probability calculation. $P < 0.05$ was considered statistically significant.

RESULTS

Expression of c-erbB-2 oncogene in HCC and its adjacent tissue

The positive staining for c-erbB-2 in cancer cells was exclusively located in cell membrane stained brown, the expression of c-erbB-2 was observed in both cell membrane and cytoplasm in one of four cases of LHN expressing c-

erbB-2 (Figure 1A). The c-erbB-2 positive rate was significantly higher in LHN (28.6%) than that in LC (0%, P value 0.032, direct probability calculation, $P < 0.05$), but no significant difference was seen between HCC (Figure 1B) and LHN or LC (χ^2 values 0.002, 3.447, $P > 0.05$, Table 1).

Table 1 Expression of c-erbB-2 oncogene in HCC and its adjacent tissue

Histological type	Case	Expression of c-erbB-2 oncogene		Positive rate (%)
		-	+	
HCC	41	31	10	24.4 ^a
LHN	14	10	4	28.6 ^a
LC	17	17	0	0

^a $P < 0.05$ vs LC.

Expression of GST-pi in HCC and its adjacent tissue

The positive staining for GST-pi appeared as brown granules, which was predominantly located in the cytoplasm, and the staining of the nuclei was seen in part of the cancer cells. There was strong staining of GST-pi in bile duct epithelial cells. A weak staining of GST-pi was observed in LC with a positive rate of 22.9% (8/35). GST-pi expression was markedly stronger in HCC or LHN (Figure 1C). The rates of positivity were 89.6% (69/77) and 71.1% (27/38), respectively, and significantly higher than that in LC (χ^2 values 49.91, 16.96, $P < 0.001$). There was also a significant difference between HCC (Figure 1D) and LHN (χ^2 value 6.353, $P < 0.05$, Table 2).

DISCUSSION

The c-erbB-2/neu is a transforming proto-oncogene encoding

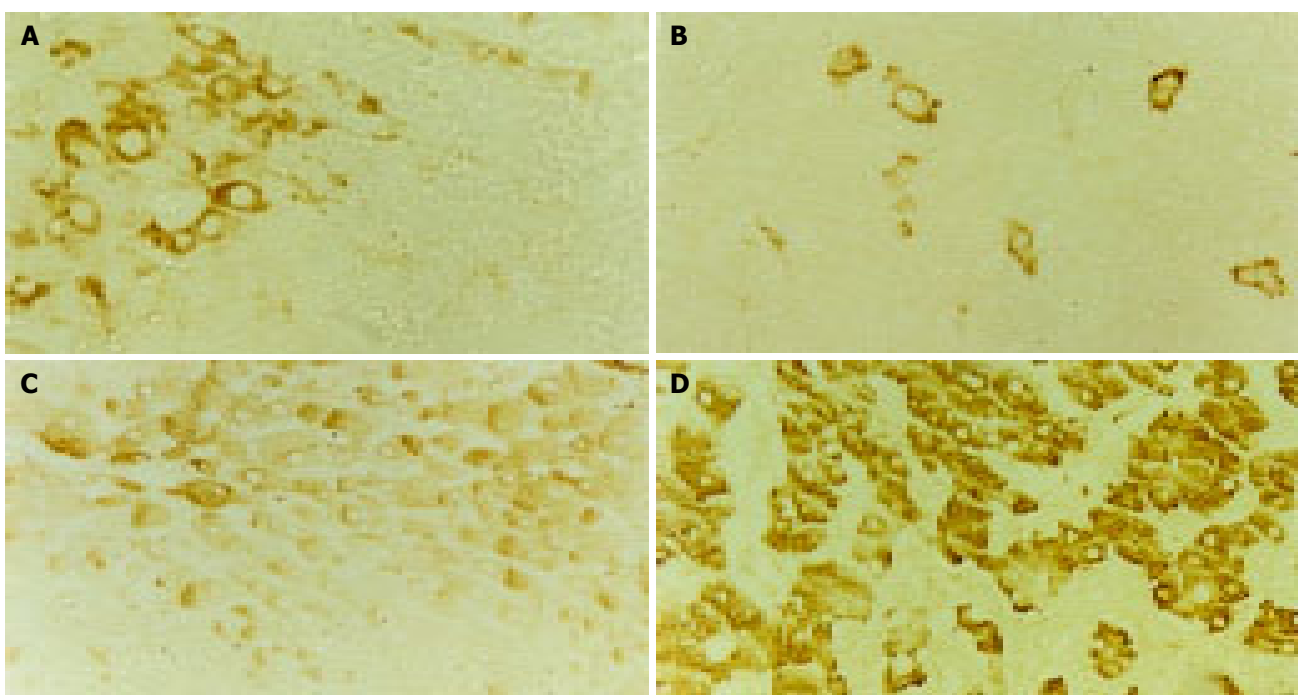


Figure 1 Positive expression of c-erbB-2 and GST-pi in LHN (A,C) and HCC

(B,D), LSAB $\times 200$.

Table 2 Expression of GST-pi in HCC and its adjacent tissue

Histological type	Case	Expression of GST-pi			Positive rate (%)
		- (%)	+ (%)	++ (%)	
HCC	77	8 (10.4)	55 (71.4)	14 (18.2)	89.6
LHN	38	11 (28.9)	25 (65.8)	2 (5.3)	71.1 ^a
LC	35	27 (77.1)	8 (22.9)	0	22.9 ^b

^a $P < 0.05$, $\chi^2 = 6.353$ vs HCC; ^b $P < 0.001$, $\chi^2 = 16.96, 49.91$ vs LHN and HCC.

a transmembrane glycoprotein of 185 ku (P185) with tyrosine kinase activity and extensive sequence homology to epidermal growth factor receptor. The c-erbB-2 is in a state of inactivation under normal condition, and is involved in regulating cell growth and proliferation^[1]. Having been affected by some endogenous or extraneous carcinogens, its structure or expression is dysregulated, thus being activated, and c-erbB-2 becomes oncogene with tumor transformation activity. In human malignancies, the activation of c-erbB-2 is most frequently caused by gene amplification, there is extremely high concordance between copy number of gene amplification and protein overexpression^[2,3]. The c-erbB-2 is frequently overexpressed in different tumors in humans, and the activation of c-erbB-2 appears to be an early event in tumorigenesis for some cancers^[4-7]. However, there seems to be conflicting reports concerning the role of c-erbB-2 oncogene in carcinogenesis of HCC. Some studies reported that c-erbB-2 does not play a role in tumorigenesis of HCC^[7], whereas others reported that the overexpression of c-erbB-2 is found in the middle stage of hepatocarcinogenesis, and might only have promoting effects during the development of this lesion^[8]. In the present study, c-erbB-2 overexpression was observed in 24.4% ($n = 41$) of HCC tissue specimens and 22.2% ($n = 18$) of its adjacent tissue specimens, suggesting that the overexpression of c-erbB-2 oncogene plays an initial role in hepatocarcinogenesis, and is an early molecule change in the carcinogenesis of HCC. In addition, the expression of c-erbB-2 did not decrease in the transition from pericarcinomatous tissues into HCC in the present study, indicating that c-erbB-2 expression also occurs later in the process of hepatocarcinogenesis and maintains the transformed hepatocyte phenotype. Apparently, c-erbB-2 expression can contribute to the initiation and progression of HCC.

Many studies have demonstrated that c-erbB-2 gene product not only contributes to the development and maintenance of malignant phenotype, but also plays a pivotal role in transformation and tumorigenesis^[4,5,9], because 3T3 cells or immortalized cells transfected with c-erbB-2 oncogene show a highly transformed and tumorigenic phenotype^[10,11]. It can be inferred from these studies that those cells overexpressing c-erbB-2 oncogene are either cancerous or have malignant phenotype. In the present study, all four cases overexpressing c-erbB-2 oncogene in pericarcinomatous tissues were LHN, thus, the positive expression rate of c-erbB-2 in LHN was 28.6% ($n = 14$), and similar to that of HCC, suggesting that those cells overexpressing c-erbB-2 oncogene in LHN have at least acquired the malignant phenotype, which may reflect the alterations in different biologic state of LHN. Some studies

reported that the increased oncogene expression brings cells into a state of active proliferation that results in an increased frequency of mutation^[12]. Therefore, it is reasonable to postulate that the overexpression of c-erbB-2 oncogene may make LHN transform malignantly, and parts of LHN are actually in the preneoplastic state or might be cancerous. In contrast to LHN, the expression of c-erbB-2 oncogene is negative in LC, implying that there is no activation of c-erbB-2 in LC, i.e., it is impossible in this situation for malignant transformation. There is also no mutation of p53 in LC, consequently, LC does not necessarily link with hepatocarcinogenesis. Our findings further confirm the notion that it is not LC but LHN, is a preneoplastic lesion for the occurrence of HCC in humans.

GSTs play an important role in protecting cells against cytotoxic and carcinogenic agents. GST-pi is an acid GST, isolated and purified from human term placenta, which possesses catalytic and ligand-binding properties, and is regarded as a new marker enzyme for tumors. Some studies reported that GST-pi or GST-pi mRNA is hardly detectable in normal liver, but markedly increases in preneoplastic hepatic lesions such as hyperplastic nodules and in HCC by immunohistochemical staining or *in situ* hybridization^[13-16], suggesting that GST-pi is a sensitive marker enzyme for preneoplastic lesions and neoplastic cells, not only at the protein level but also at the mRNA level, throughout the hepatocarcinogenesis in rat liver. In addition, other studies reported that single cells immunohistochemically positive for GST-pi induced in the rat liver carcinogenesis by chemical carcinogens are precursor-initiated cells of preneoplastic foci, GST-pi content in the single cells is higher than that in preneoplastic foci, and GST-pi is a more sensitive marker for detection of HCC than γ -GT or AFP^[17-20]. Therefore, it has been generally considered that GST-pi is the most accurate marker enzyme for detection of the very early "initiated cells" in chemically induced hepatocarcinogenesis in rats. It is known that human GST-pi has highly immunological cross-reaction with rat GST-pi, and the alteration of GST-pi precedes that of cell morphology. Studies in human HCC are not as advanced as in rats but have revealed close similarities. To investigate the relationship between GST-pi and HCC and its preneoplastic lesions, accordingly, may offer an important enzyme for the early diagnosis of HCC.

The expression of GST-pi might increase abnormally in the course of the carcinogenesis of many tumors, and it has been associated with preneoplastic and neoplastic changes^[21,22]. Recently, many researches demonstrated that loss of transcription activity of GST-pi gene promoter in human malignancies appears to be the result of CpG island DNA methylation, and this phenomenon is most frequent in breast and renal carcinomas, and might contribute to the carcinogenic process in these two carcinomas, while other tumor types show GST-pi promoter methylation only rarely or not at all^[21-23]. However, some studies reported that GST-pi promoter hypermethylation changes occur frequently in human HCC, suggesting that somatic GST-pi inactivation via CpG island hypermethylation might contribute to the pathogenesis of HCC^[24-27]. When cells display complete GST-pi hypermethylation in the CpG island, and they fail to express GST-pi mRNA and the corresponding protein

product, which is different from our findings. GST-pi expression was present in 89.6% of HCC and in 71.1% of LHN in the present study. There are several possibilities for this (1) There is rare or no GST-pi promoter hypermethylation in pathogenesis of HCC. (2) There is GST-pi promoter hypermethylation, but loss of GST-pi promoter hypermethylation in HCC may be due to the emergence of tumor subclones unmethylated at the GST-pi promoter during HCC transformation. Such subclones may gain additional genetic lesions that rendered GST-pi inactivation no longer necessary for neoplastic cell survival. (3) There is GST-pi promoter hypermethylation, but it is not responsible for GST-pi expression, it is the p53 gene mutation existing in LHN and HCC that activates GST-pi. p53 mutation is frequently observed in Asian HCC, but it is not a common event in Western HCC, thus, it is not difficult to interpret the reason why GST-pi is overexpressed in some studies whereas GST-pi is absent in other studies though GST-pi promoter hypermethylation may exist in pathogenesis of HCC. (4) GST-pi promoter hypermethylation is not a frequent event in pathogenesis of HCC, it may relate to the different etiologies of HCC in different geographical areas.

Markedly increased GST-pi content has been found in HCC investigated, indicating that HCC cells have characteristics of some fetal cells, as GST-pi content in fetal cells is noticeably higher than that in adult cells. It can be preliminarily inferred that GST-pi has relevance to detoxification of liver in pathogenesis of HCC. Meanwhile, the high expression of GST-pi in HCC might be associated with the resistance to anticancer drugs and might protect the tumor cells themselves against the cytotoxic effects of free radicals, as described in other tumors^[28-31]. It is well-known that GST-pi can detoxify not only electrophiles derived from xenobiotics, but also endogenous electrophiles usually with the consequence of free radical damage. These data indicate that the overexpression of GST-pi may impart a proliferative advantage in HCC cells due to induction of resistance to several different cytotoxic mechanisms. In the present study, the positive rate of GST-pi in HCC was higher than that in pericarcinomatous tissues, and was significantly higher in LHN than in LC, showing that GST-pi is activated during initiation stage or much earlier stage of cell transformation induced by chemical carcinogens, and may be acquired in increased amounts during malignant progression. Therefore, the data obtained in the present study suggest that GST-pi may be an effective marker enzyme for HCC and its preneoplastic lesions.

As an important enzyme of detoxification, GST-pi protects cells against the influence of carcinogenic materials. However, GST-pi is taken as a double-edged sword in tumorigenesis, namely, GST-pi protects all cells expressing it, including normal cells, cells with malignant phenotype, and tumor cells as well. Many cells in LHN are in a state of active proliferation, and have acquired the malignant phenotype, thus GST-pi evolves specifically to protect these proliferating cells, and these cells inevitably proliferate rapidly, presenting a clonal expansion. Our findings suggest that cells overexpressing GST-pi in LHN may relate to the carcinogenesis of LHN, and some cells in LHN are altered hepatocytes, which should be treated as preneoplastic cells

of HCC. In contrast to LHN, the cells in LC appear to represent quiescent phenotypes unlikely to progress into HCC.

REFERENCES

- 1 **Zhou BP**, Hung MC. Dysregulation of cellular signaling by HER2/neu in breast cancer. *Semin Oncol* 2003; **30** (5 Suppl 16): 38-48
- 2 **Bankfalvi A**. HER-2 diagnostics. *Magy Onkol* 2002; **46**: 11-15
- 3 **Nathanson DR**, Culliford AT 4th, Shia J, Chen B, D' Alessio M, Zeng ZS, Nash GM, Gerald W, Barany F, Paty PB. HER 2/neu expression and gene amplification in colon cancer. *Int J Cancer* 2003; **105**: 796-802
- 4 **Lazar H**, Baltzer A, Gimmi C, Marti A, Jaggi R. Over-expression of erbB-2/neu is paralleled by inhibition of mouse-mammary-epithelial-cell differentiation and developmental apoptosis. *Int J Cancer* 2000; **85**: 578-583
- 5 **Kumar R**, Yarmand-Baagheri R. The role of HER2 in angiogenesis. *Semin Oncol* 2001; **28** (5 Suppl 16): 27-32
- 6 **Zhang L**, bewick M, Lafrenie RM. EGFR and ErbB2 differentially regulate Raf-1 translocation and activation. *Lab Invest* 2002; **82**: 71-78
- 7 **Vlasoff DM**, Baschinsky DY, De Young BR, Morrison CD, Nuovo GJ, Frankel WL. C-erbB2 (Her2/neu) is neither overexpressed nor amplified in hepatic neoplasms. *Appl Immunohistochem Mol Morphol* 2002; **10**: 237-241
- 8 **Shi G**, Sun C, Han X, Meng X, Wang M, Gu M. Expression of rasp21, C-myc, C-erbB-2, and AFP in 2-FAA induced experimental hepatocarcinogenesis. *Zhonghua Ganzangbing Zazhi* 2001; **9**: 98-99
- 9 **Neve RM**, Lane HA, Hynes NE. The role of overexpressed HER2 in transformation. *Ann Oncol* 2001; **12**(Suppl 1): S9-13
- 10 **Yu D**, Hamada J, Zhang H, Nicolson GL, Hung MC. Mechanisms of c-erbB-2/neu oncogene-induced metastasis and repression of metastatic properties by adenovirus 5 E1A gene products. *Oncogene* 1992; **7**: 2263-2270
- 11 **Kusakari T**, Kariya M, Mandai M, Tsuruta Y, Hamid AA, Fukuhara K, Nanbu K, Takakura K, Fujii S. C-erbB-2 or mutant Ha-ras induced malignant transformation of immortalized human ovarian surface epithelial cells *in vitro*. *Br J Cancer* 2003; **89**: 2293-2298
- 12 **Lian ZR**. HBV status and expression of ets-2, IGF-II, C-myc and N-ras in human hepatocellular carcinoma and adjacent nontumorous tissues-a comparative study. *Zhonghua Zhongliu Zazhi* 1991; **13**: 5-8
- 13 **Sawaki M**, Hattori A, Tsuzuki N, Sugawara N, Enomoto K, Sawada N, Mori M. Chronic liver injury promotes hepatocarcinogenesis of the LEC rat. *Carcinogenesis* 1998; **19**: 331-335
- 14 **Nishikawa T**, Wanibuchi H, Ogawa M, Kinoshita A, Morimura A, Hiroi T, Funae Y, Kishida H, Nakae D, Fukushima S. Promoting effects of monomethylarsonic acid, dimethylarsinic acid and trimethylarsine oxide on induction of rat liver preneoplastic glutathione S-transferase placental form positive foci: a possible reactive oxygen species mechanism. *Int J Cancer* 2002; **100**: 136-139
- 15 **Shukla Y**, Arora A. Enhancing effects of mustard oil on preneoplastic hepatic foci development in Wistar rats. *Hum Exp Toxicol* 2003; **22**: 51-55
- 16 **Imai T**, Masui T, Ichinose M, Nakanishi H, Yanai T, Masegi T, Muramatsu M, Tatematsu M. Reduction of glutathione S-transferase P-form mRNA expression in remodeling nodules in rat liver revealed by in situ hybridization. *Carcinogenesis* 1997; **18**: 545-551
- 17 **Satoh K**, Itoh K, Yamamoto M, Tanaka M, Hayakari M, Ookawa K, Yamazaki T, Sato T, Tsuchida S, Hatayama I. Nrf2 transactivator-independent GSTP1-1 expression in "GSTP1-1 positive" single cells inducible in female mouse liver by DEN: a preneoplastic character of possible initiated cells. *Carcinogenesis* 2002; **23**: 457-462
- 18 **Satoh K**, Hatayama I. Anomalous elevation of glutathione

- S-transferase P-form (GST-P) in the elementary process of epigenetic initiation of chemical hepatocarcinogenesis in rats. *Carcinogenesis* 2002; **23**: 1193-1198
- 19 **Tatematsu M**, Mera Y, Inoue T, Satoh K, Sato K, Ito N. Stable phenotypic expression of glutathione S-transferase placental type and unstable phenotypic expression of gamma-glutamyltransferase in rat liver preneoplastic and neoplastic lesions. *Carcinogenesis* 1988; **9**: 215-220
- 20 **Yusof YA**, Yan KL, Hussain SN. Immunohistochemical expression of pi class glutathione S-transferase and alpha-feto-protein in hepatocellular carcinoma and chronic liver disease. *Anal Quant Cytol Histol* 2003; **25**: 332-328
- 21 **Esteller M**, Corn PG, Urena JM, Gabrielson E, Baylin SB, Herman JG. Inactivation of glutathione S-transferase P1 gene by promoter hypermethylation in human neoplasia. *Cancer Res* 1998; **58**: 4515-4518
- 22 **Miyaniishi K**, Takayama T, Ohi M, Hayashi T, Nobuoka A, Nakajima T, Takimoto R, Kogawa K, Kato J, Sakamaki S, Niitsu Y. Glutathione S-transferase-pi overexpression is closely associated with K-ras mutation during human colon carcinogenesis. *Gastroenterology* 2001; **121**: 865-874
- 23 **Esteller M**. CpG island hypermethylation and tumor suppressor gene: a booming present, a brighter future. *Oncogene* 2002; **21**: 5427-5440
- 24 **Zhong S**, Tang MW, Yeo W, Liu C, Lo YM, Johnson PJ. Silencing of GSTP1 gene by CpG island DNA hypermethylation in HBV-associated hepatocellular carcinomas. *Clin Cancer Res* 2002; **8**: 1087-1092
- 25 **Bakker J**, Lin X, Nelson WG. Methyl-CpG binding domain protein 2 represses transcription from hypermethylated pi-class glutathione S-transferase gene promoters in hepatocellular carcinoma cells. *J Biol Chem* 2002; **277**: 22573-22580
- 26 **Yang B**, Guo M, Herman JG, Clark DP. Aberrant promoter methylation profiles of suppressor genes in hepatocellular carcinoma. *Am J Pathol* 2003; **163**: 1101-1107
- 27 **Lee S**, Lee HJ, Kim JH, Lee HS, Jang JJ, Kang GH. Aberrant CpG island hypermethylation along multistep hepatocarcinogenesis. *Am J Pathol* 2003; **163**: 1371-1378
- 28 **Ruscoe JE**, Rosario LA, Wang T, Gate L, Arifoglu P, Wolf CR, Henderson CJ, Ronai Z, Tew KD. Pharmacologic or genetic manipulation of glutathione S-transferase P1-1(GSTpi) influences cell proliferation pathways. *J Pharmacol Exp Ther* 2001; **298**: 339-345
- 29 **Goto S**, Kamada K, Soh Y, Ihara Y, Kondo T. Significance of nuclear glutathione S-transferase pi in resistance to anti-cancer drugs. *Jpn J Cancer Res* 2002; **93**: 1047-1056
- 30 **Hara T**, Ishii T, Fujishiro M, Masuda M, Ito T, Nakajima J, Inoue T, Matsuse T. Glutathione S-transferase P1 has protective effects on cell viability against camptothecin. *Cancer Lett* 2004; **203**: 199-207
- 31 **Chandra RK**, Bentz BG, Haines GK 3rd, Robinson AM, Radosevich JA. Expression of glutathione S-transferase pi in benign mucosa, Barrett's metaplasia, and adenocarcinoma of the esophagus. *Head Neck* 2002; **24**: 575-581

Science Editor Wang XL and Guo SY Language Editor Elsevier HK

Association of polymorphisms of IL and CD14 genes with acute severe pancreatitis and septic shock

Dian-Liang Zhang, Hong-Mei Zheng, Bao-Jun Yu, Zhi-Wei Jiang, Jie-Shou Li

Dian-Liang Zhang, Hong-Mei Zheng, Department of General Surgery, Affiliated Hospital, Qingdao University Medical College, Qingdao 266003, Shandong Province, China

Bao-Jun Yu, Zhi-Wei Jiang, Jie-Shou Li, Research Institute of General Surgery, Jinling Hospital, Nanjing 210093, Jiangsu Province, China

Supported by the Affiliated Hospital of Qindao University Medical College Doctoral Foundation, No. 2003-6

Correspondence to: Dian-Liang Zhang, Department of General Surgery, Affiliated Hospital, Qingdao University Medical College, Qingdao 266003, Shandong Province, China. phd zd l@ yahoo. com
Telephone: +86-532-2911324 Fax: +86-532-2911111

Received: 2004-08-26 Accepted: 2005-01-05

Abstract

AIM: To investigate IL-1 β +3 594 in the 5th intron, IL-10-1 082 and CD14-159 polymorphisms in patients with acute pancreatitis (AP) and septic shock.

METHODS: The study included 215 patients (109 with acute severe pancreatitis (SAP), 106 with acute mild pancreatitis (MAP)) and 116 healthy volunteers. Genomic DNA was prepared from peripheral blood leukocytes. Genotypes and allele frequencies were determined in patients and healthy controls using restriction fragment length polymorphism analysis of PCR products.

RESULTS: The frequencies of IL-1 β +3 594T, IL-10-1082G and CD14-159T allele were similar in patients with mild or severe pancreatitis and in controls. Within SAP patients, no significant differences were found in the allele distribution examined when etiology was studied again. Patients with septic shock showed a significantly higher prevalence of IL-10-1082G allele than those without shock ($\chi^2 = 5.921$, $P = 0.015$).

CONCLUSION: IL-10-1082G plays an important role in the susceptibility of SAP patients to septic shock. Genetic factors are not important in determination of disease severity or susceptibility to AP.

© 2005 The WJG Press and Elsevier Inc. All rights reserved.

Key words: Gene polymorphism; Septic shock; Pancreatitis; Genes

Zhang DL, Zheng HM, Yu BJ, Jiang ZW, Li JS. Association of polymorphisms of IL and CD14 genes with acute severe pancreatitis and septic shock. *World J Gastroenterol* 2005; 11(28): 4409-4413

<http://www.wjgnet.com/1007-9327/11/4409.asp>

INTRODUCTION

Acute pancreatitis (AP) is a common disease that normally runs a benign course in the majority of patients. However, in up to 20% of individuals the disease is severe and may have a mortality close to 20%^[1]. Two weeks after the onset of acute severe pancreatitis (SAP), sepsis-related complications resulting from systemic inflammatory response syndrome (SIRS) or infection of pancreatic necrosis or bacteria translocation often occur. There is evidence that the production of tumor necrosis factor- α , interleukin (IL)-1 β , IL-6, and IL-8 may play a vital role in AP. In addition, anti-inflammatory response, especially IL-10, plays an important role in determining prognosis of AP^[2]. Several methods for estimating the complications are widely used in clinic, such as Atlanta classification, Acute Physiology and Chronic Health Evaluation II, Imrie and Ranson scores, Balthazar computed tomographic scoring system, and C-reactive protein. However, these methods have little value in predicting which patients will develop pancreatic infection and SAP-associated septic shock.

It has been hypothesized that there is a correlation between polymorphisms in TNF- α , IL-1 β , and IL-10 genes and differential production of respective cytokines^[3]. Some of these polymorphisms affect clinical outcome in inflammatory diseases including AP^[3-5]. IL-10 is an anti-inflammatory cytokine and plays an important role in downregulating cell-mediated inflammatory responses. Human IL-10 gene is located on chromosome 1 and has been mapped to the junction between 1q31 and 1q32. Three single base pair (bp) substitutions in IL-10 gene promoter at positions -1 082G-A, -819T-C, and -592A-C from the transcriptional start site have been identified. At position -1 082 bp from the transcriptional start site, the presence of G is associated with higher and A with lower production of IL-10 by PBMC cultures^[6]. In contrast, IL-1 β is a potent proinflammatory cytokine released by macrophages in systemic inflammatory responses. It not only has important biologic effect but also regulates inflammatory reaction and immune response by promoting expression of other cytokines, such as IL-6 and IL-12. IL-1 β gene located on chromosome 2 is 7 kb, and has seven exons and six introns. A polymorphism is found at position +3 954 located in the 5th intron of IL-1 β gene with a T substitution of C. *In vitro* study demonstrated that IL-1 β +3 594 at the 5th exon significantly influences the production of IL-1 β ^[7]. Their polymorphisms may have some association with the development of severe AP and septic shock.

CD14, a 55 ku membrane-anchored protein, is a pattern-recognition receptor for several microbial products,

such as lipopolysaccharide (LPS). It can be expressed on neutrophils, monocytes/macrophages, and fibroblasts, all of which can produce cytokines such as IL-1 and TNF- α in response to LPS stimulation^[9]. Recently, a-159 G/A polymorphism in the promoter region of CD14 gene involves a C>T substitution at bp -159 of the 5' flanking region of CD14 gene. Genotypes include CC, CT, and TT alleles. Subjects carrying the T allele have been shown to have significantly higher sCD14 levels than those carrying the C allele^[8,9]. Therefore, CD14 polymorphism could be a genetic factor responsible for interindividual differences in the susceptibility to bacterial infection. However, to the best of our knowledge, there were no reports on the linkage of CD14 and pancreatitis.

Our previous studies have shown that some polymorphisms in TNF gene correlate with severe sepsis or SAP-associated septic shock, although no association has been found between TNF gene polymorphisms and SAP^[4,5,10]. The purpose of this study was to test the hypothesis that IL and CD14 gene polymorphisms have some correlation with the development of SAP and septic shock.

MATERIALS AND METHODS

Subjects

Patients with a first attack of unequivocal AP from July 2001 to December 2003 were prospectively considered. The diagnosis of AP was based on an increased-amylase activity (enzymatic colorimetric test) in serum and CT verification of pancreatitis. Etiology of AP was gallstones found in radiological and endoscopic retrograde cholangiopancreatography findings, alcoholic if patients were heavy consumers of alcohol (more than 80 g of alcohol per day for over 6 mo)^[11], and idiopathic if no other identifiable cause could be discovered. Pancreatitis was classified as severe when APACHE II score ≥ 8 ^[12] and CT severity index ≥ 4 ^[13]. Septic shock was defined according to ACCP/SCCM consensus conference criteria^[14]. The control group consisted of 116 healthy volunteers. All subjects gave written informed consent, and the protocol was approved by the local ethics committee.

In order to be eligible for the enrollment, all the subjects from the two groups were yellow Chinese Han. The exclusion criteria were defined as follows: age > 75 years, cardiac failure (class > III), liver insufficiency (Child C), patients with evidence suggestive of a diagnosis of chronic pancreatitis and consanguineous mating.

DNA extraction

Genomic DNA was purified from 5 mL of peripheral blood samples using Wizard genomic DNA purification kit (Promega) according to the manufacturer's instructions.

IL-10-1082 G to A substitution

PCR was used to amplify a 377-bp fragment of the IL-10 genomic sequence using primers: upstream, 5'-CCAAGACA-ACACTACTAAGGCTCCTTT-3'; downstream, 5'-GCTTCTTATATGCTAGTCAGGTA-3'^[15] (Nanjing Bio Eng Co.). The PCR conditions were at 95 °C for 2 min, 35 cycles of 95 °C for 40 s, 56 °C for 40 s, 72 °C for 40 s, 72 °C

for 7 min using reagents purchased from Promega on a gene cycler (BIO-RAD, Japan). The PCR products were digested directly with 2 U *Xba*I restriction enzyme (Promega) at 37 °C for 6 h. Digested DNA was analyzed on 5% polyacrylamide gels. Ethidium bromide staining of the gel demonstrated three fragments of 253, 97, and 27 bp for G/G, four fragments of 280, 253, 97, and 27 bp for G/A, two fragments of 280 and 97 bp for A/A.

IL-1 β polymorphism

A 249-bp fragment of the IL-1 β genomic sequence including the polymorphic *Taq*I site was amplified using PCR. The following nucleotide sequences were used for PCR amplification: 5'-GTTGTCATCAGACTTTGACC-3', 5'-TTCAGTTCATATGGACCAGA-3'^[16] (Nanjing Bio Eng Co.). The PCR conditions were at 97 °C for 2 min, 35 cycles of 95 °C for 40 s, 55 °C for 40 s, 74 °C for 30 s, 72 °C for 7 min using reagents purchased from Promega on a gene cycler (BIO-RAD, Japan). The PCR products were digested directly with 2 U *Taq*I restriction enzyme (Promega) at 37 °C for 4 h. Digested DNA was analyzed on 5% polyacrylamide gels. Ethidium bromide staining of the gel demonstrated the original 249 bp fragment for T/T, two fragments of 135 and 114 bp for C/C, three fragments of 249, 135, and 114 bp for C/T.

CD14-159 C/T polymorphism

PCR was used to amplify a 166-bp fragment of the CD14 genomic sequence using primers: upstream, 5'-TGCCAG-GAGACACAGAACCC-3'; downstream, 5'-TGTCATTCA-GTTCCCTCCTG-3'^[9] (Nanjing Bio Eng Co.). The PCR conditions were at 96 °C for 2 min, 35 cycles of 96 °C for 40 s, 54 °C for 40 s, 72 °C for 30 s, and 72 °C for 7 min using reagents purchased from Promega on a gene cycler (BIO-RAD, Japan). The PCR products were digested directly with 2 U *Hae*III restriction enzyme (Promega) at 37 °C for 4 h. Digested DNA was analyzed on 5% polyacrylamide gels. Ethidium bromide staining of the gel demonstrated the original 166-bp fragment for T/T, two fragments of 86 and 80 bp for C/C, three fragments of 86, 80, and 166 bp for C/T.

In addition, 30% of samples were randomly selected to be genotyped a second time to ensure reproducibility. Genotyping for all subjects was performed with no knowledge of clinical status.

Statistical analysis

Allelic frequencies were determined for statistical significance by χ^2 test. Analysis was made by SPSS 11.0, and $P < 0.05$ was considered statistically significant.

RESULTS

Characteristics of the patients

On the basis of the selection criteria, 109 patients (59 females and 50 males) with SAP were studied. Thirty-three developed septic shock (septic shock group), and 76 did not develop septic shock (nonseptic shock group). The APACHE II and CT scores at the time of admission were similar in both septic shock group and nonseptic group.

This study was undertaken in selected patients with acute mild pancreatitis (MAP) ($n = 106$) as defined by CT severity index and APACHE II score, and matched with SAP for age, sex, and cause of pancreatitis. Patients with MAP had an uneventful recovery. The control group included 116 healthy volunteers (65 females and 51 males).

Polymorphisms of two IL genes

The distribution of IL-10-1 082 and IL-1 β polymorphisms in different groups is shown in Tables 1 and 2. The overall IL-10-1 082G and IL-1 β +3 594T allele frequencies were similar in patients with mild or severe pancreatitis. Further, no significant difference in allele frequencies studied was noted between patients with AP and control subjects.

Table 1 Comparison of allele frequency between MAP group and SAP group

	MAP ($n = 106$)	SAP ($n = 109$)	<i>P</i>
IL-1 β +3 594			
CC	94	95	
CT	12	14	
TT	0	0	
T allele	12 (5.7)	14 (6.4)	0.740
GG	0	0	
IL-10 -1 082			
AA	75	81	
GA	31	28	
G allele	31 (14.6)	28 (12.8)	0.592
CC	62	66	
CD-14 -159			
TT	14	14	
CT	30	29	
T allele	58 (27.4)	57 (26.1)	0.777

Table 2 Comparison of allele frequency between AP and controls

	AP ($n = 215$)	Controls ($n = 116$)	<i>P</i>
IL-1 β +3 594			
CC	189	98	
CT	26	18	
TT	0	0	
T allele	26 (6.0)	18 (7.8)	0.399
GG	0	0	
IL-10 -1 082			
AA	156	79	
GA	59	37	
G allele	59 (13.7)	37 (15.9)	0.437
CC	128	71	
CD-14 -159			
TT	28	13	
CT	59	32	
T allele	115 (26.7)	58 (25.0)	0.626

The distribution of IL-10-1082G and IL-1 β allele frequencies between septic shock group and nonseptic shock group is shown in Table 3. Patients with septic shock showed a significantly higher prevalence of the IL-10-1082G than those without septic shock ($\chi^2 = 5.921$, $P = 0.015$). No significant difference in IL-1 β +3594T allele frequency was found between septic shock patients and nonseptic shock patients.

CD14-159 C/T polymorphism

The distribution of CD14-159 polymorphism in different groups is shown in Tables 1 and 2. The CD14-159T allele frequency was similar in patients with mild or severe

pancreatitis. No significant difference in CD14-159T allele frequency was noted between patients with AP and control subjects.

Comparison of CD14-159 allele frequency between septic shock group and nonseptic shock group is shown in Table 3. No significant difference was found in the allele frequency between septic shock patients and nonseptic shock patients.

Comparisons of polymorphisms in different etiologies of SAP

No significant differences were found in the distribution of allele frequency between any two groups (Table 4).

Table 3 Comparison of allele frequency between septic shock and nonseptic shock groups

	Septic shock ($n = 33$)	Nonseptic shock ($n = 76$)	<i>P</i>
IL-1 β +3 594			
CC	27	68	
CT	6	8	
TT	0	0	
T allele	6 (9.1)	8 (5.3)	0.289
GG	0	0	
IL-10 -1 082			
AA	19	62	
GA	14	14	
G allele	14 (21.2)	14 (9.2)	0.015
CC	19	47	
CD-14 -159			
TT	5	9	
CT	9	20	
T allele	19 (28.8)	38 (25.0)	0.559

Table 4 Comparison of allele frequency based on different etiologies of SAP (n)%

Allele	Alcoholic SAP ($n = 23$)	Gallstone SAP ($n = 49$)	Idiopathic SAP ($n = 34$)	<i>P</i>
IL-1 β +3 594 T	3 (6.5)	6 (6.1)	5 (7.4)	0.952
IL-10-1 082 G	7 (15.2)	12 (12.2)	9 (13.2)	0.886
CD-14-159 T	11 (23.9)	25 (25.5)	21 (30.9)	0.653

DISCUSSION

In humans, there is increasing evidence that the host's cytokine response is genetically determined^[17]. Polymorphic gene sequences of certain cytokines may be potential markers of susceptibility and clinical outcome in different human infectious diseases. In our study, the frequency of well-described variants in IL-1 β +3 594 at the 5th exon, IL-10-1 082, and CD14-159 was examined. Our results demonstrated that IL-1 β +3594T, IL-10-1082G, and CD14-159T had no correlation with the occurrence or severity of AP. However, the distribution of IL-10-1082G in SAP patients varied, and IL-10-1082G allele was found to be more frequent in septic shock patients than in nonseptic shock patients ($P < 0.05$). The association between septic shock patients and IL-10 polymorphism was restricted to the IL-10-1082G, no such a correlation was seen to either IL-1 β +3 594 at the 5th exon or CD14-159 variant.

Before evaluating the role of a cytokine polymorphism played in any disease, three questions need to be answered^[18,19]. First, are the subjects homogeneous? To avoid artifact in

population admixture, we selected only Chinese Han people in China. In addition, the consanguineous mating subjects were precluded from our study. Second, does the product of the studied gene play an important role in the pathogenesis of the disease? The central role of IL-1 β , IL-10, and CD14 in the occurrence or severity of AP and septic shock has been clearly demonstrated by many studies^[20-23]. Third, does the gene polymorphism produce a relevant alteration in the level or function of the gene product? *In vitro*, the *TaqI* polymorphism in human IL-1 β gene correlates with IL-1 β secretion^[10]. *In vitro* and *in vivo* studies showed that IL-10-1082 variant significantly influences the secretion of IL-10^[24-27]. With regard to CD14-159 polymorphism, there is mounting evidence that the SNP in CD14 genome significantly influences the production of CD14^[9].

IL-1 and TNF- α are the most prominent inflammatory mediators and regarded as the "first-line" cytokines. Administration of IL-1 β to human beings results in inflammation, tissue injury, and septic shock-like syndrome. Different polymorphisms of the IL-1 β gene have been described^[7,10], and at least two of them could influence the protein production. One is located within the promoter region, and the other is located in exon 5. In our present study, we examined the frequency of IL-1 β A *TaqI* RFLP at the 5th exon and found that it was comparable in patients with mild or severe pancreatitis. Similarly, no significant difference in the allele distribution was noted between patients and controls. In addition, no significant difference in the allele frequency was seen between septic shock patients and nonseptic shock subjects. The results suggest that IL-1 β A may not play a principle role in the onset of SAP or SAP-associated septic shock. Our results are in line with the report by Powell *et al.*^[28].

In the clinical setting, levels of IL-10 showed a steep increase within the first 24 h from disease onset, and the level of IL-10 on the first day was found to be higher in patients with mild AP than in those with severe AP, suggesting that at position-1082 bp from the transcriptional start site, the presence of G is associated with higher and A with lower production of IL-10^[6]. Based on the observation, we postulate that IL-10-1082 polymorphism may have some association with the occurrence or the severity of AP. In our study, no significant difference was found in the frequency of IL-10-1082G between any two groups, but significant difference was found in the distribution of IL-10-1082G between septic shock patients and nonseptic shock patients. The pathophysiology of septic shock is a complex and multifactorial process, involving an imbalance between proinflammatory and anti-inflammatory cytokine release. Our results suggest that in the late stage of SAP, anti-inflammatory cytokine polymorphism likely plays a more important role in the pathogenesis of septic shock than proinflammatory cytokine polymorphism. The ability to identify patients at high risk for developing septic shock may be a critically important factor that will lead to improvements in the management of septic shock.

CD14, a receptor of LPS, plays a vital role in the mechanism of SIRS and sepsis. Because of the important role of CD14 with respect to LPS binding and signaling, we postulate that the polymorphism in the promoter of CD14 gene might be

an important factor in determining the susceptibility to or the severity of AP. In our study, we failed to find an association in CD14-159T frequency between controls and AP or between AP and SAP, indicating that CD14-159T plays no part in disease severity or susceptibility to AP. To the best of our knowledge, there is no report on the association between CD14-159 polymorphism and pancreatitis so far. Our result did not show any difference between patients and controls or between mild pancreatitis and severe pancreatitis. Furthermore, no significant difference was found between CD14-159T frequency and septic shock secondary to severe pancreatitis, indicating that in the late stage of the disease, CD14-159 polymorphism plays little role in the onset of SAP-associated septic shock. This is in line with previous studies^[29,30].

Although SAP has many distinct etiologies, the immune system response appears to be almost identical regardless of the cause^[1]. In our study, we divided SAP patients into three groups: gallstone pancreatitis, alcohol pancreatitis, and idiopathic pancreatitis according to the etiology of the disease. The observed allele frequency of IL-1 β +3594T, IL-10-1082G and CD14-159T was comparable between groups of different etiologies, suggesting that environmental factors may play an important role in the occurrence of SAP.

In conclusion, gene polymorphisms have no association with the occurrence or severity of AP. However, the IL-10-1082G may play an important role in the susceptibility of SAP patients to septic shock.

REFERENCES

- 1 **Frossard JL**, Morel P, Pastor CM. Why clinical trials might succeed in acute pancreatitis when they failed in septic shock. *JOP* 2003; **4**: 11-16
- 2 **Chen CC**, Wang SS, Lu RH, Chang FY, Lee SD. Serum interleukin-10 and interleukin-11 in patients with acute pancreatitis. *Gut* 1999; **45**: 895-899
- 3 **Poli F**, Nocco A, Berra S, Scalamogna M, Taioli E, Longhi E, Sirchia G. Allele frequencies of polymorphisms of TNFA, IL-6, IL-10 and IFNG in an Italian Caucasian population. *Eur J Immunogenet* 2002; **29**: 237-240
- 4 **Zhang D**, Li J, Jiang ZW, Yu B, Tang X. Association of two polymorphisms of tumor necrosis factor gene and with acute severe pancreatitis. *J Surg Res* 2003; **112**: 138-143
- 5 **Dianliang Z**, Jiashou L, Zhiwei J, Baojun Y. Association of plasma levels of tumor necrosis factor (TNF)-alpha and its soluble receptors, two polymorphisms of the TNF gene, with acute severe pancreatitis and early septic shock due to ist. *Pancreas* 2003; **26**: 339-344
- 6 **Schaaf BM**, Boehmke F, Esnaashari H, Seitzer U, Kothe H, Maass M, Zabel P, Dalhoff K. Pneumococcal septic shock is associated with the interleukin-10-1082 gene promoter polymorphism. *Am J Respir Crit Care Med* 2003; **168**: 476-480
- 7 **Pociot F**, Molvig J, Wogensen L, Worsaae H, Nerup J. A *TaqI* polymorphism in the human interleukin-1 beta (IL-1 beta) gene correlates with IL-1 beta secretion *in vitro*. *Enr J Clin Invest* 1992; **22**: 396-402
- 8 **Yamazaki K**, Ueki-Maruyama K, Oda T, Tabeta K, Shimada Y, Tai H, Nakajima T, Yoshie H, Herawati D, Seymour GJ. Single-nucleotide polymorphism in the CD14 promoter and periodontal disease expression in a Japanese population. *J Dent Res* 2003; **82**: 612-616
- 9 **Baldini M**, Lohman IC, Halonen M, Erichson RP, Holt PG, Martinez FD. A polymorphism in the 5' flanking region of the CD14 gene is associated with circulating soluble CD14 levels and with total serum immunoglobulin E. *Am J Respir Cell Mol*

- Biol* 1999; **20**: 976-983
- 10 **Zhang D**, Li J, Jiang Z, Yu B, Tang X, Li W. The relationship between tumor necrosis factor- α gene polymorphism to acute severe pancreatitis. *Chin Med J* 2003; **116**: 1779-1781
 - 11 **Sargen K**, Demaine AG, Kingsnorth AN. Cytokine gene polymorphisms in acute pancreatitis. *JOP* 2000; **1**: 24-35
 - 12 **Dominguez-Munoz JE**, Carballo F, Garcia MJ, de Diego JM, Campos R, Yanguela J, de la Morena J. Evaluation of the clinical usefulness of APACHE[?] and SAPS systems in initial prognostic classification of acute pancreatitis: a multiple study. *Pancreas* 1993; **8**: 682-686
 - 13 **Balthazar EJ**, Robinson DL, Megibow AJ, Ranson JH. Acute pancreatitis: value of CT in establishing prognosis. *Radiology* 1990; **174**: 331-336
 - 14 **Muckart DJ**, Bhagwanjee S. American College of Chest Physicians/Society of Critical Care Medicine Consensus Conference definitions of the systemic inflammatory response syndrome and allied disorders in relation to critically injured patients. *Crit Care Med* 1997; **25**: 1789-1795
 - 15 **Koch W**, Kastrati A, Bottiger C, Mehilli J, von Beckerath N, Schomig A. Interleukin-10 and tumor necrosis factor gene polymorphisms and risk of coronary artery disease and myocardial infarction. *Atherosclerosis* 2001; **159**: 137-144
 - 16 **Huang D**, Pirskanen R, Hjelmstrom P, Lefvert AK. Polymorphisms in IL-1 β and IL-1 receptor antagonist genes are associated with myasthenia gravis. *J Neuroimmunol* 1998; **81**: 76-81
 - 17 **Walley AJ**, Aucan C, Kwiatkowski D, Hill AV. Interleukin-1 gene cluster polymorphisms and susceptibility to clinical malaria in a Gambian case-control study. *Eur J Hum Genet* 2004; **12**: 132-138
 - 18 **Mira JP**, Cariou A, Grall F, Delclaux C, Losser MR, Heshmati F, Cheval C, Monchi M, Teboul JL, Riche F, Leleu G, Arbibe L, Mignon A, Delpech M, Dhainaut JF. Association of TNF2, a TNF- α promoter polymorphism, with septic shock susceptibility and mortality: a multicenter study. *JAMA* 1999; **282**: 561-568
 - 19 **Lander ES**, Schork NJ. Genetic dissection of complex traits. *Science* 1994; **265**: 2037-2048
 - 20 **Norman JG**, Fink G, Franz M, Guffey J, Carter G, Davison B, Sexton C, Glaccum M. Active interleukin-1 receptor required for maximal progression of acute pancreatitis. *Ann Surg* 1996; **223**: 163-169
 - 21 **Rongione AJ**, Kusske AM, Reber HA, Ashley SW, McFadden DW. Interleukin-10 reduces circulating levels of serum cytokines in experimental pancreatitis. *J Gastrointest Surg* 1997; **1**: 159-166
 - 22 **Rongione AJ**, Kusske AM, Kwan K, Ashley SW, Reber HA, McFadden DW. Interleukin 10 reduces the severity of acute pancreatitis in rats. *Gastroenterology* 1997; **112**: 960-967
 - 23 **Landmann R**, Muller B, Zimmerli W. CD14, new aspects of ligand and signal diversity. *Microbes Infect* 2000; **2**: 295-304
 - 24 **Westendorp RG**, Langermans JA, Huizinga TW, Elouali AH, Verweij CL, Boomsma DI, Vandenbroucke JP, Vandenbroucke JP. Genetic influence on cytokine production and fatal meningococcal disease. *Lancet* 1997; **349**: 170-173
 - 25 **van Dissel JT**, van Langevelde P, Westendorp RG, Kwappenberg K, Frolich M. Antiinflammatory cytokine profile and mortality in febrile patients. *Lancet* 1998; **351**: 950-953
 - 26 **Turner DM**, Williams DM, Sankaran D, Lazarus M, Sinnott PJ, Hutchinson IV. An investigation of polymorphism in the interleukin 10 gene promoter. *Eur J Immunogenet* 1997; **24**: 1-8
 - 27 **Eskdale J**, Gallagher G, Verweij CL, Keijsers V, Westendorp RG, Huizinga TW. Interleukin10 secretion in relation to human IL 10 locus haplotypes. *Proc Natl Acad Sci USA* 1998; **95**: 9465-9470
 - 28 **Powell JJ**, Fearon KC, Siriwardena AK, Ross JA. Evidence against a role for polymorphisms at tumor necrosis factor interleukin-1 and interleukin-1 receptor antagonist gene loci in the regulation of disease severity in acute pancreatitis. *Surgery* 2001; **129**: 633-640
 - 29 **Agnese DM**, Calvano JE, Hahm SJ, Coyle SM, Corbett SA, Calvano SE, Lowry SF. Human toll-like receptor 4 mutations but not CD14 polymorphisms are associated with an increased risk of gram-negative infections. *J Infect Dis* 2002; **186**: 1522-1525
 - 30 **Hubacek JA**, Stuber F, Frohlich D, Book M, Wetegrove S, Rothe G, Schmitz G. The common functional C(-159)T polymorphism within the promoter region of the lipopolysaccharide receptor CD14 is not associated with sepsis development or mortality. *Genes Immun* 2000; **1**: 405-407

Effects of magnolol and honokiol derived from traditional Chinese herbal remedies on gastrointestinal movement

Wei-Wei Zhang, Yan Li, Xue-Qing Wang, Feng Tian, Hong Cao, Min-Wei Wang, Qi-Shi Sun

Wei-Wei Zhang, Yan Li, Xue-Qing Wang, Feng Tian, Department of Gastroenterology, the Second Affiliated Hospital of China Medical University, Shenyang 110004, Liaoning Province, China
Hong Cao, Min-Wei Wang, Department of Pharmacology, School of Pharmacy, Shenyang Pharmaceutical University, Shenyang 110016, Liaoning Province, China
Qi-Shi Sun, Department of Chinese Herbs, School of Pharmacy, Shenyang Pharmaceutical University, Shenyang 110016, Liaoning Province, China

Supported by the Natural Science Foundation of Liaoning Province, No. 20032074

Correspondence to: Yan Li, Department of Gastroenterology, the Second Affiliated Clinical Hospital of China Medical University, 36 Sanhao Street, Heping District, Shenyang 110004, Liaoning Province, China. liyan1@medmail.com.cn

Fax: +86-24-83956416

Received: 2004-06-02 Accepted: 2004-06-28

honokiol on contractility of the smooth muscles of isolated gastric fundus strips of rats and isolated ileum of guinea pigs is associated with a calcium-antagonistic effect. Magnolol and honokiol can improve the gastric emptying of a semi-solid meal and intestinal propulsive activity in mice.

© 2005 The WJG Press and Elsevier Inc. All rights reserved.

Key words: Magnolol and honokiol; Gastrointestinal movement

Zhang WW, Li Y, Wang XQ, Tian F, Cao H, Wang MW, Sun QS. Effects of magnolol and honokiol derived from traditional Chinese herbal remedies on gastrointestinal movement. *World J Gastroenterol* 2005; 11(28): 4414-4418

<http://www.wjgnet.com/1007-9327/11/4414.asp>

Abstract

AIM: To study the effects of magnolol and honokiol on isolated smooth muscle of gastrointestinal tract and their relationship with Ca^{2+} , and on the gastric emptying and the intestinal propulsive activity in mice.

METHODS: Routine experimental methods using isolated gastric fundus strips of rats and isolated ileum segments of guinea pigs were adopted to measure the smooth muscle tension. The effects of magnolol 10^{-3} , 10^{-4} , 10^{-5} mol/L, and honokiol 10^{-4} , 10^{-5} , 10^{-6} mol/L on the contractility of gastric fundus strips of rats and ileum of guinea pigs induced by acetylcholine (Ach) and 5-hydroxytryptamine (5-HT) was assessed respectively. The method using nuclein and pigment methylene blue was adopted to measure the gastric retention rate of nuclein and the intestinal propulsive ratio of a nutritional semi-solid meal for assessing the effect of magnolol and honokiol (0.5, 2, 20 mg/kg) on gastric emptying and intestinal propulsion.

RESULTS: Magnolol and honokiol significantly inhibited the contractility of isolated gastric fundus strips of rats treated with Ach or 5-HT and isolated ileum guinea pigs treated with Ach or $CaCl_2$, and both of them behaved as non-competitive muscarinic antagonists. Magnolol and honokiol inhibited the contraction induced by Ach in Ca^{2+} -free medium and extracellular Ca^{2+} -dependent contraction induced by Ach. Each group of magnolol and honokiol experiments significantly decreased the residual rate of nuclein in the stomach and increased the intestinal propulsive ratio in mice.

CONCLUSION: The inhibitory effect of magnolol and

INTRODUCTION

Cortex Magnoliae officinalis is a traditional Chinese herb, belonging to “prokinetic agent” of Chinese herbs. It can improve the symptoms of abdominal distention, dyspepsia, nausea, and vomiting, *etc.*, in gastrointestinal diseases. Magnolol and honokiol are the main components of magnoliae bark. Both can relieve spasm of smooth muscle and stop vomiting, *etc.* Magnolol also has an anti-allergic, anti-asthma and anti-inflammatory effect^[1], and honokiol has an anxiolytic effect^[2-4] and a cardiac muscle protective effect^[5]. We used the isolated gastric fundus strips of rats and isolated ileum segments of guinea pigs to measure the smooth muscle tension for assessing the effects of magnolol and honokiol on the contractility of gastric fundus strips of rats induced by acetylcholine (Ach) and 5-hydroxytryptamine (5-HT), and ileum of guinea pigs induced by Ach and $CaCl_2$. Nuclein and pigment methylene blue were used to measure the gastric retention rate of nuclein and the intestinal propulsive ratio of a nutritional semi-solid meal for assessing the effect of magnolol and honokiol on gastric emptying and intestinal propulsion.

MATERIALS AND METHODS

Preparation of magnolol and honokiol: Magnolia bark (*Magnolia officinalis* Rehd. et Wils.) was purchased from Shenyang Medicinal Material Company. The voucher specimens of *Magnolia officinalis* Rehd. et Wils. was identified by Professor Sun of Shenyang Pharmacy University. Magnolol and honokiol were extracted in Shenyang Pharmacy University.

Magnolol and honokiol were dissolved in a very small amount of ethanol. In isolated and *in vivo* experiments the resultant solution was diluted with a 10% aqueous solution of Tween-80. Subsequently, the solution was diluted with distilled water, so that the final concentration of both ethanol and Tween-80 in the vehicle was 0.5%.

Propulsid (cisapride tablet, 5 mg/tablet) was produced by Xi'an Pharmaceutical Company Ltd (batch number: 030815020). Cisapride was crushed and dissolved in distilled water to make a 0.15 mg/mL cisapride solution.

Methylthioninium chloride injection (20 mg/2 mL) was produced by Beijing Yongkang Pharmaceutical Company Ltd.

Preparation of a semi-solid nutritious meal^[6]: Ten grams of carboxymethylcellulose was added to 250 mL of distilled water. After the mixture was agitated, 16 g of milk powder, 8 g of cane sugar and 8 g of cornstarch were added to the mixture. The resulting mixture was a white semisolid paste.

Animals

Rats (200-300 g) and guinea pigs (200-300 g) of either sex were raised in cages in groups of five male mice (18-22 g) at a constant temperature (22 ± 2 °C) with free access to food and water.

Method

Effects of magnolol and honokiol on contractility of gastric fundus strips of rats induced by Ach and 5-HT

Isolated gastric fundus strips of rats were prepared and mounted on an organ bath (Magnus' bath) containing 30 mL of Krebs' solution bubbled with 95% O₂+50 mL/L CO₂ (pH 7.3-7.4 at 37 °C) under a resting tension of 1 g. The muscular tension, measured with a force transducer, was displayed on a MS-302 biosignal recording and analyzing system. The preparations were allowed to equilibrate for 50 min. After equilibration, 3×10^{-3} mol/L Ach 0.1 mL or 3×10^{-6} mol/L 5-HT 0.2 mL was added in the bath to activate the gastric fundus strips. When it reached its maximum contraction, it was washed with Krebs' solution to regain spontaneous contraction. Then Ach or 5-HT was added to the bath from low to high logarithmic doses to make the final respective concentrations of 10^{-8} , 3×10^{-8} , 10^{-7} , 3×10^{-7} , 10^{-6} , 3×10^{-6} , 10^{-5} , 3×10^{-5} , 10^{-4} , 3×10^{-4} mol/L, or 10^{-10} , 3×10^{-10} , 10^{-9} , 3×10^{-9} , 10^{-8} , 3×10^{-8} , 10^{-7} , 3×10^{-7} , 10^{-6} , 3×10^{-6} mol/L. The accumulated concentration-efficacy curve was made. When the curve reached its peak, the gastric fundus strips were washed thrice at 5-min intervals with Krebs' solution to wash the Ach out. After 15-min equilibration the drugs were added to the organ bath in respective doses (final concentrations of magnolol were 10^{-5} , 10^{-4} or 10^{-3} mol/L, honokiol were 10^{-6} , 10^{-5} or 10^{-4} mol/L). The accumulated concentration-efficacy curve was made after 1 min.

We made the maximum efficacy (E_{max}) of Ach or 5-HT as 100%, and calculated the effect percentage (E/E_{max}) of each concentration of Ach or 5-HT. Then the cumulative concentration-efficacy curves were drawn with E/E_{max} as the ordinates and the negative logarithm of final concentration of Ach or 5-HT ($-\log[A]$) as the abscissae.

Effects of magnolol and honokiol on the contractility of the ileum of guinea pigs induced by Ach Terminal ileum segments from guinea pigs were prepared and

suspended vertically in organ baths containing 30 mL of Tyrode's solution bubbled with 95% O₂+50 mL/L CO₂ (pH 7.3-7.4 at 37 °C) under a resting tension of 1 g. The spontaneous contractions were measured after equilibration for 50 min, 3×10^{-3} mol/L Ach 0.1 mL was added in the bath to activate the ileum. When it reached its maximum contraction, it was washed in Tyrode's solution to regain spontaneous contractions. The cumulative concentration-efficacy curves of Ach were made, then the curve was remade after magnolol and honokiol were added in the organ bath respectively (the final concentrations were the same in method 1).

Effects of magnolol and honokiol on the contractility of the ileum of guinea pigs induced by CaCl₂

After equilibration of guinea pig ileum segments in Ca²⁺-free Tyrode's solution (CaCl₂ was omitted from normal Tyrode's solution) for 40 min they were changed with Ca²⁺-free high K⁺-depolarized Tyrode's solution. Ca²⁺-free Tyrode's solution was (the equal mole NaCl was replaced with 80 mmol/L KCl in the Ca²⁺-free Tyrode's solution) to make the smooth muscle depolarization after 30 min, CaCl₂ was added to the bath from low to high logarithmic doses (final concentrations were 10^{-5} , 3×10^{-5} , 10^{-4} , 3×10^{-4} , 10^{-3} , 3×10^{-3} , 10^{-3} , and 3×10^{-3} mol/L respectively) and the cumulative concentration-efficacy curves were drawn. The ileum segments were washed with the Ca²⁺-free Tyrode's solution till the muscular tension regained the normal contraction. After 30 min, Ca²⁺-free Tyrode's solution was changed with Ca²⁺-free high K⁺ Tyrode's solution and magnolol and honokiol were added respectively. After 30 min, the cumulative concentration-efficacy curves were drawn.

Effects of magnolol and honokiol on the two contractile components of Ach

After equilibration for 1 h in Tyrode's solution, guinea pigs ileum segments were washed with Ca²⁺-free Tyrode's solution thrice and incubated for 30 min, then 3×10^{-3} mol/L Ach 0.2 mL (2×10^{-5} mol/L) was added to the solution and it produced a brief contraction (the first or initial phasic contraction) that was induced by the release of intracellular calcium. When the ileum segments reached maximal contraction, CaCl₂ 0.2 mL (2×10^{-2} mol/L) was added and caused an advanced contraction (the second phasic contraction or sustained tonic component) induced by the extracellular calcium influx evoked by Ach. The ileum segments were washed with Ca²⁺-free Tyrode's solution and incubated in Ca²⁺-free Tyrode's solution for 30 min; meanwhile magnolol (final concentrations were 10^{-5} , 10^{-4} or 10^{-3} mol/L) or honokiol (final concentrations were 10^{-6} , 10^{-5} or 10^{-4} mol/L) was added respectively, then Ach and CaCl₂ were added successively. The guinea pig ileum segments produced the first and second contractions respectively.

Effects of magnolol and honokiol on gastrointestinal movement in mice

Magnolol and honokiol were dispensed as before to the concentrations of 0.5, 2.0, and 20 mg/L. Mice were allocated randomly to a control group (administrated orally with distilled water), a cisapride group, and experimental groups. They were given orally either magnolol 0.5, 2.0, and 20 mg/L, or honokiol 0.5, 2.0, and 20 mg/L, respectively. Nuclide and pigment methylene blue were used to measure the gastric retention rate of nuclide and intestinal propulsive ratio of nutritious semi-solid meal. After having fasted for

12 h, the mice were given orally either 0.2 mL/10 g of each of the above substances or 0.2 mL/10 g of distilled water. After 30 min, each mouse was given orally a semi-solid nutritious meal containing ^{99m}Tc -DTPA 0.05 mCi/10 g and a small quantity of methylthionium chloride. The mice were killed after 20 min, and dissected. Residual nuclide in the gastrointestinal tract was measured by a radioactivity monitor. The gastric residual nuclide rate (%) = (gastric retention nuclide/total nuclide in gastrointestinal tract) $\times 100\%$. Intestinal propulsive ratio (%) = (distance from sphincter of pylorus to the distal pigment methylene/distance from sphincter of pylorus to the ileocecum) $\times 100\%$.

Statistical analysis

Results were expressed as mean \pm SD. Comparisons between groups of data were made by the Student's *t*-test or *t*-test of paired comparison.

RESULTS

Effects of magnolol and honokiol on the contractility of gastric fundus strips of rats induced by Ach and 5-HT (Figure 1)

The data showed that magnolol and honokiol inhibited incompetitively the contraction of gastric fundus strips of rats induced by cumulative concentrations of Ach and 5-HT, and the effect increased with the increase of dosage. The antagonistic parameters ($\text{PD}_{2'}$) of magnolol and honokiol were 3.66 and 4.31 for Ach, and 5.08 and 4.91 for 5-HT respectively.

Effects of magnolol and honokiol on the contractility of guinea pig ileum induced by Ach (Figures 2A and B)

The data showed that magnolol and honokiol antagonized incompetitively the contraction of gastric fundus strips of

rats induced by cumulative concentration of Ach, and the effect increased with the increase of dosage. The $\text{PD}_{2'}$ values of magnolol and honokiol were 5.09 and 4.99 respectively.

Effects of magnolol and honokiol on the contractility of ileum segments of guinea pigs induced by CaCl_2 (Figures 2C and D)

The data showed that magnolol and honokiol antagonized incompetitively the contraction of gastric fundus strips of rats induced by cumulative concentration of CaCl_2 , and the effect increased with the increase of dosage. The $\text{PD}_{2'}$ values of magnolol and honokiol were 4.34 and 4.84 respectively.

Effects of magnolol and honokiol on the two contractile components of Ach (Table 1)

Magnolol and honokiol inhibited the contraction of ileal segments induced by Ach in Ca^{2+} -free medium and the extracellular Ca^{2+} -dependent contraction induced by Ach.

Magnolol 10^{-5} , 10^{-4} or 10^{-3} mol/L and honokiol 10^{-6} , 10^{-5} or 10^{-4} mol/L inhibited significantly the two contractile components induced by Ach.

Table 1 Effects of magnolol and honokiol on the two contractile components of Ach (% , mean \pm SD, *n* = 6)

Group (mol/L)	First phase	Second phase
Magnolol 10^{-3}	89.08 \pm 7.32 ^b	86.89 \pm 8.04 ^b
Magnolol 10^{-4}	83.80 \pm 11.18 ^b	92.97 \pm 4.70 ^b
Magnolol 10^{-5}	66.48 \pm 12.95 ^b	75.39 \pm 10.53 ^b
Honokiol 10^{-4}	74.54 \pm 6.75 ^b	91.11 \pm 3.89 ^b
Honokiol 10^{-5}	68.93 \pm 10.90 ^b	82.11 \pm 5.51 ^b
Honokiol 10^{-6}	45.68 \pm 4.92 ^b	78.95 \pm 5.83 ^b

^b*P* < 0.01 vs others.

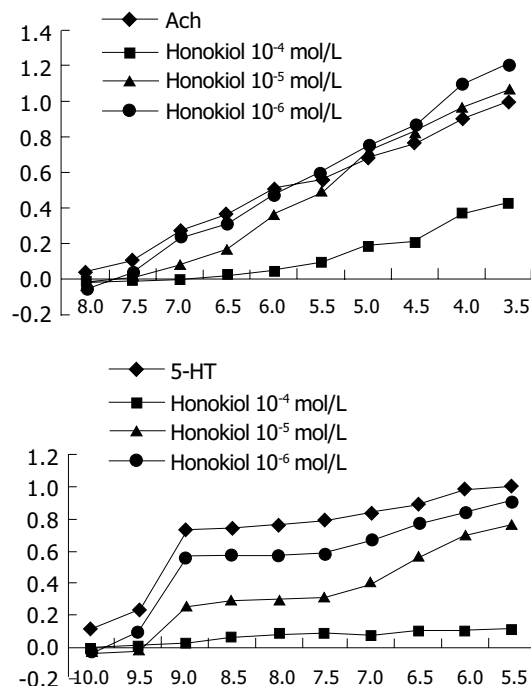
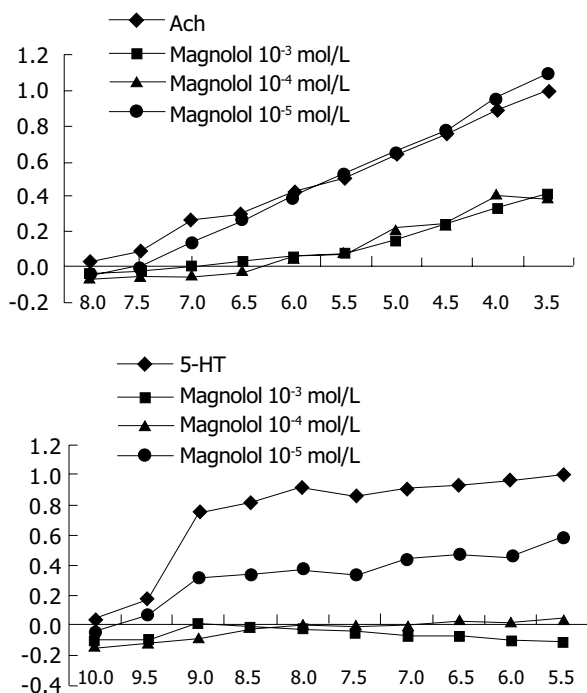


Figure 1 Effect of magnolol and honokiol on the contractility of rat gastric fundus strips induced by Ach and 5-HT. Magnolol effects on contractility of rat

gastric fundus strips induced by Ach (A) and 5-HT (C); Honokiol effects on contractility of rat gastric fundus strips induced by Ach (B) 5-HT (D) (*n* = 6).

Effects of magnolol and honokiol on gastrointestinal movement in mice (Table 2)

In the experimental groups of magnolol 0.5, 2.0, and 20 mg/L, or honokiol 0.5, 2.0, and 20 mg/L, the gastric nuclide retention rate was significantly lower and the intestinal propulsive ratios were significantly higher than those in the control group, indicating that magnolol and honokiol could improve the gastric emptying of a semi-solid meal and intestinal propulsion in mice.

Table 2 Effects of magnolol and honokiol on gastrointestinal movement in mice (mean±SD, *n* = 20)

Group (mg/kg)	Rate of gastric residual nuclide (%)	Intestinal propulsive ratio (%)
Control	50.05±12.74	47.92±8.49
Cisapride	22.26±9.17 ^b	61.92±11.77 ^b
Magnolol 0.5	24.61±10.90 ^b	57.14±13.12 ^b
Magnolol 2	26.40±12.14 ^b	55.46±11.26 ^b
Magnolol 20	25.96±8.44 ^b	60.30±10.52 ^b
Honokiol 0.5	24.91±11.30 ^b	53.57±9.54 ^a
Honokiol 2	34.11±12.25 ^b	54.54±8.29 ^b
Honokiol 20	33.22±13.64 ^b	53.53±9.90 ^a

^a*P*<0.05, ^b*P*<0.01 vs control.

DISCUSSION

Magnolol and honokiol are neolignan-derivatives present in *Magnolia* bark, which is used in the treatment of abdominal distention and vomiting. The experimental results indicated that magnolol and honokiol significantly inhibited the contractility of isolated gastric fundus strips of rats treated with Ach or 5-HT and isolated ileum of guinea pigs treated with Ach or CaCl₂, and both of them behaved as non-

competitive muscarinic antagonists. Magnolol and honokiol inhibited the ileal contraction induced by Ach in Ca²⁺-free medium and extracellular Ca²⁺-dependent contraction induced by Ach.

The contraction of gastrointestinal smooth muscle depends on the mediation of intracellular Ca²⁺, and is accomplished by the process of excitation–contraction coupling (E-C coupling). The free Ca²⁺ originated from the release of intracellular calcium and the restoration of extracellular calcium^[7]. A high-K⁺ medium could depolarize the cellular membrane of ileum longitudinal smooth muscle, activate the potential-dependent calcium channel (PDC), and result in the inflow of calcium and the contraction of smooth muscles. Our experimental results indicated that magnolol and honokiol could block the transmembrane inflow of calcium through PDC, inhibit the contraction of smooth muscle, and relieve the spasm of smooth muscles.

Physical active substances Ach and 5-HT can increase the tension of gastrointestinal smooth muscle, and the agonist Ca²⁺ is derived from various resources. The two components of intracellular and extracellular calcium were involved in the contraction of smooth muscles induced by Ach. The first phasic contraction induced by Ach in Ca²⁺-free medium depended on the release of intracellular calcium. The second phasic contraction based on the first phase after the addition of calcium was caused by Ach facilitating the inflow of extracellular calcium through the receptor-operated calcium channel (ROC). In this study, magnolol and honokiol significantly inhibited the first and the second phasic contractions of smooth muscles induced by Ach, indicating that the two components of magnolia bark not only have an intracellular point of action but also inhibit the contraction of smooth muscles by blocking the inflow of calcium through ROC.

Normal gastric motility involves gastric fundus, corpus,

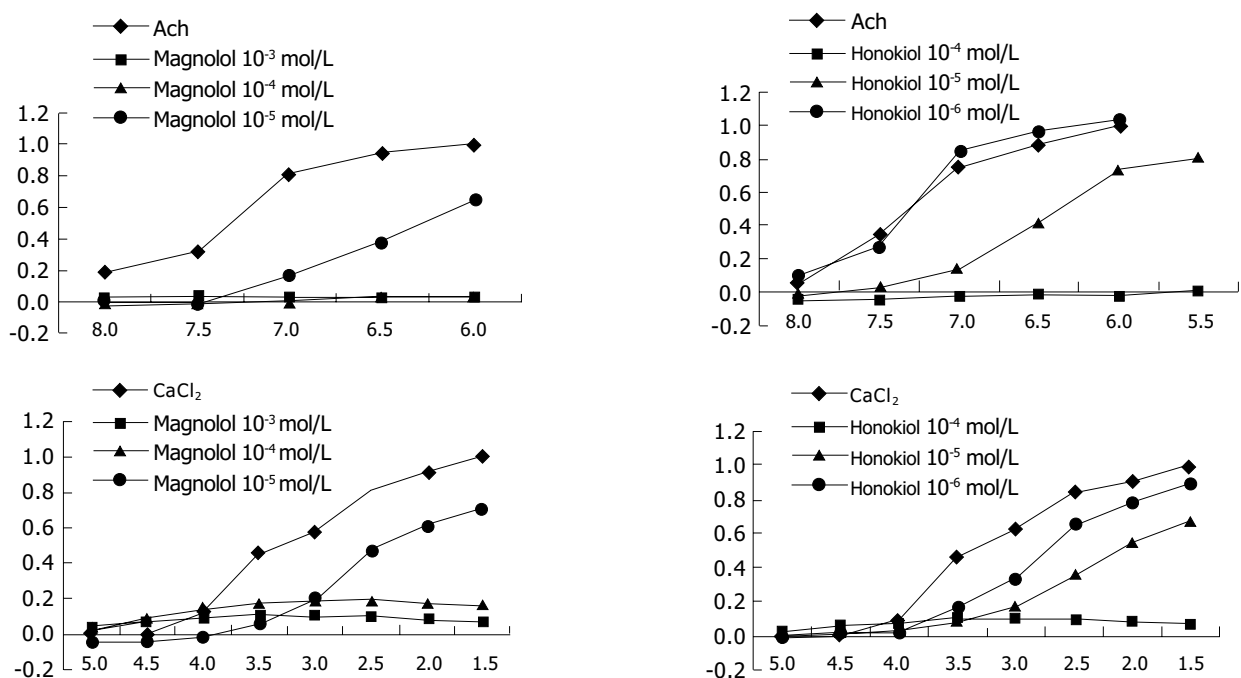


Figure 2 Effect of magnolol and honokiol on the contractility of guinea pig ileum segments induced by Ach and CaCl₂. Magnolol effects on the contractility of

guinea pig ileum induced by Ach (A) and CaCl₂ (C); Honokiol effects on contractility of guinea pig ileum segments induced by Ach (B) and CaCl₂ (D) (*n* = 6).

antrum, pylorus, and antroduodenal coordination. As food is swallowed, the gastric fundus relaxes to accommodate the incoming nutrients. This is termed receptive relaxation, which is coordinated by vagal efferent activity via nonadrenergic, noncholinergic mechanisms. As swallowing during the meal continues, the fundic filling and relaxation continue with little increase in intraluminal pressure. Gastric distention and activation of mechanoreceptor and stretch receptors stimulate vagal afferent nerve activity, which in turn modifies vagal efferent traffic.

The emptying of solid foods is accomplished by complex interplays among intra-gastric pressure, gastric peristalses, pyloroduodenal resistance, and neuroendocrine responses elicited by the specific components of the particular meal. In this study, magnolol and honokiol could significantly decrease the residual rate of nuclein in stomach and increase the intestinal propulsive ratio of semi-solid nutritious meal in mice, and there was no significant difference between them and cisapride. Combined with the study above, the functions in improving the gastric emptying and intestinal propulsive action may relate to their functions of relaxation of gastrointestinal smooth muscles.

Disorders of stomach motility and intestinal propulsion are involved in functional gastroenterological diseases such as gastroesophageal reflux disease, functional dyspepsia, irritable bowel syndrome, chronic constipation, *etc.*^[8], gastroparesis^[9], postoperative gastrointestinal atony^[10], chronic intestinal pseudo-obstruction^[11], and many other diseases. Prokinetic agents such as domperidone and cisapride are important therapeutic drugs^[12,13]. But domperidone and cisapride have some severe side-effects, such as prolongation of the QT interval and cardiac arrhythmias^[14,15]. There are rich resources of natural herbs in China, which may provide a valuable source of effective prokinetic agents.

REFERENCES

- 1 Wang JP, Ho TF, Chang LC, Chen CC. Anti-inflammatory effect of magnolol, isolated from *Magnolia officinalis*, on A23187-induced pleurisy in mice. *J Pharm Pharmacol* 1995; **47**: 857-860
- 2 Kuribara H, Kishi E, Hattori N, Yuzurihara M, Mjaruyama Y. Application of the elevated plus-maze test in mice for evaluation of the content of honokiol in water extracts of magnolia. *Phytother Res* 1999; **13**: 593-596
- 3 Kuribara H, Stavinoha WB, Maruyama Y. Behavioural pharmacological characteristics of honokiol, an anxiolytic agent present in extracts of magnolia bark, evaluated by an elevated plus-maze test in mice. *J Pharm Pharmacol* 1998; **50**: 819-826
- 4 Kuribara H, Kishi E, Hattori N, Okada M, Maruyama Y. The anxiolytic effect of two oriental herbal drugs in Japan attributed to honokiol from magnolia bark. *J Pharm Pharmacol* 2000; **52**: 1425-1429
- 5 Tsai SK, Huang SS, Hong CY. Myocardial protective effect of honokiol: an active component in *Magnolia officinalis*. *Planta Med* 1996; **62**: 503-506
- 6 Francis J, Critchley D, Dourish CT, Cooper SJ. Comparisons between the effects of 5-HT and DL-fenfluramine on food intake and gastric emptying in the rat. *Pharmacol Biochem Behav* 1995; **50**: 581-585
- 7 Bauer V, Holzer P, Ito Y. Role of extra- and intracellular calcium in the contractile action of agonists in the guinea-pig ileum. *Naunyn Schmiedebergs Arch Pharmacol* 1991; **343**: 58-64
- 8 Hunt RH. Evolving concepts in the pathophysiology of functional gastrointestinal disorder. *J Clin Gastroenterol* 2002; **35** (1 Suppl): S2-6
- 9 Tomi S, Plazinska M, Zagorowicz E, Ziolkowski B, Muszynski J. Gastric emptying disorders in diabetes mellitus. *Pol Arch Med Wewn* 2002; **108**: 879-886
- 10 Hep A, Prasek J, Filipinsky J, Navratil P, David L, Dolina J, Dite P. Cisapride (Prepulsid) in the prevention of postoperative gastrointestinal atony. *Rozhl Chir* 1998; **77**: 101-104
- 11 Quigley EM. Chronic Intestinal Pseudo-obstruction. *Curr Treat Options Gastroenterol* 1999; **2**: 239-250
- 12 Veldhuyzen van Zanten SJ, Jones MJ, Verlinden M, Talley NJ. Efficacy of cisapride and domperidone in functional (nonulcer) dyspepsia: a meta-analysis. *Am J Gastroenterol* 2001; **96**: 689-696
- 13 Barone JA. Domperidone: a peripherally acting dopamine2-receptor antagonist. *Ann Pharmacother* 1999; **33**: 429-440
- 14 Drolet B, Rousseau G, Daleau P, Cardinal R, Turgeon J. Domperidone should not be considered a no-risk alternative to cisapride in the treatment of gastrointestinal motility disorders. *Circulation* 2000; **102**: 1883-1885
- 15 Layton D, Key C, Shakir SA. Prolongation of the QT interval and cardiac arrhythmias associated with cisapride: limitations of the pharmacoepidemiological studies conducted and proposals for the future. *Pharmacoepidemiol Drug Saf* 2003; **12**: 31-40

Effect of early nutrition on intestine development of intrauterine growth retardation in rats and its correlation to leptin

Xiao-Shan Qiu, Ting-Ting Huang, Zhen-Yu Shen, Hui-Ying Deng, Zhi-Yong Ke

Xiao-Shan Qiu, Ting-Ting Huang, Zhen-Yu Shen, Zhi-Yong Ke, Pediatric Department, the First Affiliated Hospital of Sun Yat-Sen University, Guangzhou 510080, Guangdong Province, China
Hui-Ying Deng, Guangzhou Children's Hospital, Guangzhou 510120, Guangdong Province, China

Supported by the Science and Technology Bureau Foundation of Guangdong Province, No. 99M04815G

Correspondence to: Dr. Ting-Ting Huang, Department of Pediatrics, the First Affiliated Hospital of Sun Yat-Sen University, Guangzhou 510080, Guangdong Province, China. huangtt.cn@yahoo.com

Telephone: +86-20-88551570

Received: 2004-09-22 Accepted: 2004-11-19

Abstract

AIM: To investigate the intestine and body development of intrauterine growth retardation (IUGR) rats under early different protein diet and to analyze the correlation between leptin and intestine and body development.

METHODS: An IUGR rat model was established by food restriction of pregnant female rats. Fifty-six neonatal IUGR rats and 24 neonatal normal rats were randomly divided into normal control group (C group), IUGR model group (SC group), low protein diet IUGR group (SL group), and high protein diet IUGR group (SH group). Eight rats were killed per group at wk 0, 4, and 12. Serum leptin, body weight (BW), body length (BL), intestinal weight (IW), intestinal length (IL), and intestinal disaccharidase (including lactase, maltase, and saccharase) were detected.

RESULTS: BW (4.50 ± 0.41 g), BL (5.96 ± 0.40 cm), IW (0.05 ± 0.01 g), and IL (15.9 ± 2.8 cm) in neonatal IUGR rats were much lower than those in C group (6.01 ± 0.55 g, 6.26 ± 0.44 cm, 0.10 ± 0.02 g, 21.8 ± 2.7 cm, $P < 0.05$), while intestinal lactase and maltase activities were higher than those in C group. SH group showed the fastest catch up growth and their BW, BL, IW, and IL reached the C group level at wk 4. SC group showed relatively slower catch up growth than SH group, and their BW, BL, IW did not reach the C group level at wk 4. SL group did not show intestine and body catch up growth. Intestinal maltase [344 ± 33 $\mu\text{mol}/(\text{min}\cdot\text{g})$] and saccharase activities [138 ± 32 $\mu\text{mol}/(\text{min}\cdot\text{g})$] in SL group were both markedly lower than those in C group [751 ± 102 , 258 ± 27 $\mu\text{mol}/(\text{min}\cdot\text{g})$, $P < 0.05$]. There were no significant differences in lactase activities at wk 4 and disaccharidase activities at wk 12 among all groups ($P > 0.05$). The leptin level in SL group (0.58 ± 0.12 ng/mL) was the highest in all groups, and much lower in SH group (0.21 ± 0.03 ng/mL) than that in any other IUGR groups at wk 4 ($P < 0.05$). Leptin was negatively related

to BW ($r = -0.556$, $P = 0.001$), IW ($r = -0.692$, $P = 0.001$) and IL ($r = -0.738$, $P = 0.000$) at wk 4, while no correlation was found at wk 12.

CONCLUSION: High protein diet is a reasonable early nutritional mode to IUGR rats in promoting intestine and body catch up growth.

© 2005 The WJG Press and Elsevier Inc. All rights reserved.

Key words: Intrauterine growth retardation; Rat; Intestine development; Disaccharidase; Leptin; Nutritional intervention

Qiu XS, Huang TT, Shen ZY, Deng HY, Ke ZY. Effect of early nutrition on intestine development of intrauterine growth retardation in rats and its correlation to leptin. *World J Gastroenterol* 2005; 11(28): 4419-4422
<http://www.wjgnet.com/1007-9327/11/4419.asp>

INTRODUCTION

The incidence rate of intrauterine growth retardation (IUGR) is about 7.5-8.7% in our country. Development of the stomach and intestine is closely related to the body growth, it affects and is also reversely affected by nutrition. As a protein coded by ob gene (obesity gene), leptin is a neuroendocrine regulatory factor secreted from mature adipocytes into blood. Leptin can pass through blood-brain barrier and has a central effect on feeding behavior. It was reported^[1] that IUGR rats have temporarily high leptin level to regulate growth hormone secretion and growth during catch up growth. Since the infant growth is mainly regulated by nutrition, and nutritional intake is controlled by the development of stomach and intestine and leptin level, our study aimed to investigate the intestine, intestinal disaccharidase and body development and their relation to serum leptin at wk 4 (childhood) and 12 (adulthood) in order to offer some animal research data for early nutritional intervention of IUGR.

MATERIALS AND METHODS

Materials and animals

Leptin kit was purchased from Diagnostic Systems Laboratories (USA). Glucose and disaccharidase enzyme kits were purchased from Great Wall Company (Baoding, Hebei Province, China).

The second class SD female rats were bought from Animal Center of Sun Yat-Sen University and mated with

male rats. IUGR model was established by food restriction of pregnant female rats^[2]. The standard of IUGR was that the birth weight -2SD lower than control normal group (5.1 g). Fifty-six newborn IUGR rats and 24 newborn normal rats were randomly divided into normal control group (C group), IUGR model group (SC group), low protein diet IUGR group (SL group), and high protein diet IUGR group (SH group). The former two groups were fed with 22.5% normal protein diet, while the latter two groups with 11.3% low-protein diet and 28.6% high-protein diet respectively. All the rats were weaned when they were 3 wk old and fed with original diet till the 4th wk and then with normal protein diet till the end of the experiment. Components of the diets are shown in Table 1.

Table 1 Content ratio of different components (g) in 100 g food

Components	Protein	Fat	Carbohydrate	Total energy (kJ/100 g)
Normal diet	22.5	3.9	57.8	1 583.4
High protein diet	28.6	3.9	56.8	1 625.4
Low protein diet	11.3	8.5	58.7	1 558.2
χ^2	10.09	3.04	0.09	-
<i>P</i>	0.006*	0.22	0.96	-

**P*<0.05 vs other.

Methods

Body weight (BW) and body length (BL, from nose to tail) of each rat were measured at wk 0, 4, and 12. Eight newborn female rats of IUGR group and C group were killed right after birth. Another eight female rats were killed per group after being fasted for 10-12 h at wk 4 and 12 respectively. Blood sample was taken from the eyeballs and kept at -30 °C. Serum leptin was monitored by ELISA.

Abdomen was opened right after the rats were killed. Intestinal weight (IW) and intestinal length (IL) were measured from the beginning of jejunum to the end of ileum, and then 10 cm proximal end of the jejunum (about 3 cm from the beginning of jejunum) was cut, weighed, and homogenized. The disaccharidase activities (including lactase, saccharase, and maltase) were measured.

Statistical analysis

Results were expressed as mean±SD. All data were analyzed

by the SPSS 10.0 statistical package. ANOVA test was used to compare these four groups. Least significant difference was used to compare every two groups when variance was regular, while Dunnett T3 test was used when variance was irregular. Pearson's test was used in correlation analysis.

RESULTS

Development of body and intestine and disaccharide activity in newborn IUGR rats and normal rats

The BW, BL, IW, and IL of newborn IUGR rats were significantly lower than those of C group (*P*<0.05), while lactase and maltase activities were higher than those in C group. There was no significant difference in saccharase activity between the two groups (Table 2).

Development of intestine and body of rats

SH group showed the fastest catch up growth, and BW, BL, IW, and IL reached the C group level at wk 4 (*P*>0.05). BW, BL, IW, and IL in SL group at wk 4 and 12 were all markedly lower than those in normal control group (*P*<0.05). BW, BL, and IW in SC group at wk 4 were all significantly lower than those in C group (*P*<0.05). IL in SC group was lower than that in C group at wk 12. There were no significant differences in BW, BL, and IW between the two groups (*P*>0.05).

Intestinal maltase and saccharase activities in SL group were markedly lower than those in C group (*P*<0.05). There was no significant difference in lactase activity between the two groups at wk 4 (*P*>0.05). Maltase activity in SH group was lower than that in C group (*P*<0.05). There were no significant differences in disaccharidase activity between groups at wk 12 (*P*>0.05).

Leptin in SL group was significantly higher than that in SC and C groups, and lower in SH group than that in SC group at wk 4 (*P*<0.05). Leptin in SC group was higher than that in C group and lower in SH and SL group than that in SC group (*P*<0.05). There were no significant differences between these two groups and C group at wk 12 (*P*>0.05). Results are shown in Table 2.

Correlation analysis

The following results were found in correlation analysis of leptin and BW, BL, IW, and IL. Leptin and BW had a negative correlation at wk 4 (*r* = -0.556, *P* = 0.001), while

Table 2 Leptin, BW, BL, IW, IL, and disaccharidase activities in all groups (mean±SD) *n* = 8/group

Age (yr)	Group	Leptin (ng/mL)	BW (g)	BL (cm)	IW (g)	IL (cm)	Lactase	Saccharase	Maltase
0 wk	C	ND	6.01±0.55	6.26±0.44	0.10±0.02	21.8±2.7	315±19	13±6	58±20
	SC	ND	4.50±0.41 ^a	5.96±0.40 ^a	0.05±0.01 ^a	15.9±2.8 ^a	383±39 ^a	15±8	269±17 ^a
4 th wk	C	0.26±0.08	60.8±9.5	23.1±1.4	2.2±0.2	74.8±9.1	54±15	258±27	751±102
	SC	0.36±0.20	52.0±10.9 ^a	21.0±2.5 ^a	1.4±0.3 ^a	70.3±3.4	39±14	254±23	797±95
	SH	0.21±0.03 ^c	70.0±4.5 ^c	23.6±0.5 ^c	1.9±0.2	80.7±9.5	62±8	230±21	368±26 ^{a,c}
	SL	0.58±0.12 ^{a,c}	21.4±3.5 ^{a,c}	16.0±1.3 ^{a,c}	0.8±0.4 ^{a,c}	53.9±3.1 ^{a,c}	66±22	138±32 ^{a,c}	344±33 ^{a,c}
12 th wk	C	0.40±0.23	235.5±43.4	38.5±0.8	4.3±0.7	122.7±12.6	48±3	230±32	713±157
	SC	0.79±0.41 ^a	208.6±21.6	36.9±1.7	3.9±0.9	101.2±5.8 ^a	50±21	262±43	670±157
	SH	0.42±0.15 ^c	254.8±23.5 ^{a,c}	37.1±0.4	4.1±0.4	122.3±13.0	48±12	242±27	682±144
	SL	0.38±0.25 ^c	169.3±6.7 ^{a,c}	33.2±0.8 ^{a,c}	3.3±0.6 ^a	99.6±6.9 ^a	53±12	239±35	568±52

Disaccharidase activity unit: μmol/(min·g) protein. ^a*P*<0.05, IUGR group vs C group; ^c*P*<0.05, SL, and SH groups vs SC group. ND: not determined.

had no correlation at wk 12; leptin and BL had no correlation at wk 4 and 12; leptin and IW had a negative correlation at wk 4 ($r = -0.692$, $P = 0.001$), while had no correlation at wk 12; leptin and IL had a negative correlation at wk 4 ($r = -0.738$, $P = 0.001$), while had no correlation at wk 12.

DISCUSSION

Multiple lines of evidence show that about 20-50% IUGR cannot catch up the growth after birth, and remains small till they become adults. Growth is mainly regulated by heredity, nutrition, and endocrine system. The early postnatal growth (the first year after birth) is mainly regulated by nutrition. Mother malnutrition during pregnancy not only delays the fetal growth, but also impairs many organ and tissue structures and functions of the fetus^[3]. Zhang *et al.*^[2], showed that the weight, length and many morphologic structures of intestine in newborn IUGR rats are significantly lower than those of normal newborn rats. Only few reports about the development of stomach and intestine and disaccharidase activity of IUGR are available at present.

Due to the effect of early nutrition on growth, Lucas^[4] have raised the “nutritional programming” hypothesis: nutritional conditions during the critical or sensitive stage of growth have long-term or life-long effects on organic structure or function. The mechanism is that early nutrition stimulates clone selection and differentiation of blast cells and causes irreversible changes in cell number of organism. Based on the hypothesis, we carried out the early nutritional intervention during the first 4 wk after birth - a sensitive and critical stage of growth. We investigated its effects on the development of intestine and jejunum mucosa disaccharidase activity and their correlations with serum leptin.

Our research showed that the impaired development of intestine recovered quickly in SH group after high protein diet was given after birth. Ziegler *et al.*^[5], found that the development of intestine mainly depends on the proliferation of cells before weaning. Enough nutrition can not only promote intestinal neuron's activity and increase blood supply of viscera but also stimulate the secretion of growth factor. Intestinal epithelium can absorb more nutrition for catch up growth. Although SC group was fed with normal diet after birth, it failed to catch up the normal control group at wk 4. SL group even failed to catch up normal growth at wk 12 and remained small till they became adults, suggesting that early postnatal protein diet has great effects on the development of intestine. Intestine and body catch up growth of IUGR rats depends on sufficient nutrition after birth, especially enough protein.

Intestine is the main organ to absorb sugar and protein. Disaccharidase, gastrin, and intestinal hormones play an important role in this process. Lactase and maltase are often produced at the late stage of gestation, while saccharase activity increases quickly only after intake of solid food. Stomach and intestine develops very fast in neonatal stage. As the stomach and intestine of neonates become mature, their lactase activity decreases, while maltase and saccharase activities increase^[6]. Therefore, it is beneficial to the

understanding of the development of stomach and intestine by detecting disaccharidase activities. Our research suggested that the premature of lactase and maltase activity in newborn IUGR rats was an adaptive compensation to intrauterine malnutrition. Saccharase activity in newborn IUGR rats was not affected, suggesting that saccharase is not regulated by intrauterine nutrition. Our research also demonstrated that maltase and saccharase activities in SL groups were markedly lower than those in C and SC groups at wk 4, which is consistent with the study by Nichol *et al.*^[7]. The relatively higher lactase activity in SL group may be an accommodation response to lack of nutritional supply. The nutrition of neonatal rats is mainly from milk and lactose is the main component of carbohydrate in milk. The high lactase activity is an advantage for neonatal rats to absorb more lactose to compensate for the shortage of protein. But the reason why maltase activity in SH group was markedly lower than that in C and SC groups at wk 4 is still unknown. Gomez *et al.*^[8], gave high protein diet to the rats suffering from abdominal wound and found that its lactase activity is markedly higher than in other rats given normal level protein diet. Further research is needed to test whether the decrease of maltase activity in SH group is related to the increase of lactase activity. There was no significant difference in disaccharidase activity between groups at wk 12, suggesting that disaccharidase activity might change with different kinds of food after birth, such as milk, solid food, and different protein diet.

It was reported that IUGR rats are insensitive to leptin during catch up growth^[9]. Jaquet *et al.*^[10], found that IUGR children are relatively resistant to leptin in order to catch up growth and leptin is closely related to catch up growth and fat tissue development. We know that blood and umbilical leptin level of newborn baby is positively related to birth weight. Leptin reflects not only the body fat level but also nutritional status. Leptin is a medium between neuroendocrine system and fat tissue. It builds a negative loop between fat tissue and neuropeptide Y (NPY). When weight decreases to some extent, the inhibitory effect of leptin on the secretion of NPY from hypothalamus is also weakened^[11]. NPY is a strong stimulator of appetite, high level of NPY is advantageous for IUGR children to take in more nutrition and energy to accumulate body fat.

Correlation analysis showed that leptin was negatively related to BW, IW, and length at wk 4. The BW in SL group was the lowest but leptin level was the highest in all groups at wk 4. We found that IUGR rats were relatively resistant to leptin during catch up growth, but this phenomenon disappeared at wk 12, suggesting that leptin resistance is only related to catch up growth in IUGR children.

In conclusion, high protein diet is a reasonable early nutritional mode for IUGR rats. High leptin level in IUGR rats is related to catch up growth and nutritional status.

REFERENCES

- 1 Hileman SM, Pierroz DD, Flier JS. Leptin, nutrition, and reproduction: timing is everything. *J Clin Endocrinol Metab* 2000; **85**: 804-807
- 2 Zhang Q, Li HS, Zheng HL. The effects of timing and causes

- of IUGR on gastro intestinal tract in newborn rats. *Zhonghua Erke Zazhi* 1997; **35**: 567-570
- 3 **Chui YP**, Wang XL, Ye HM. Low birth weight and insulin resistance. *Guowai Yixue Erkexue Fence* 2003; **30**: 10-13
- 4 **Lucas A**. Programming by early nutrition: an experimental approach. *J Nutr* 1998; **128**(2 Suppl): s401-s406
- 5 **Ziegler TR**, Estivariz CF, Jonas CR, Gu LH, Jones DP, Leader LM. Interactions between nutrients and peptide growth factors in intestinal growth, repair, and function. *J Parenter Enteral Nutr* 1999; **23**(6 Suppl): s174-s183
- 6 **Li ZB**, Wu SW, Qian LH. Regulatory effects of bombesin on the activities of disaccharidase in the intestinal mucosal cells in neonatal rabbits. *Shanghai Yixue Zazhi* 2001; **25**: 656-658
- 7 **Nichols BL**, Nichols VN, Putman M, Avery SE, Fraley JK, Quaroni A, Shiner M, Sterchi EE, Carrazza FR. Contribution of villous atrophy to reduced intestinal maltase in infants with malnutrition. *J Pediatr Gastroenterol Nutr* 2000; **30**: 494-502
- 8 **Gomez de Segura IA**, Vazquez P, Garcia P, Garcia P, Candela CG, Cos A, Gancedo PG, Lopez JM, De Miguel E. Effect of four enteral foods on the small bowel of undernourished rats after midgut resection. *Eur J Surg* 1999; **165**: 491-499
- 9 **Gura T**. Obesity research. Tracing leptin's partners in regulating body weight. *Science* 2000; **287**: 1738-1741
- 10 **Jaquet D**, Leger J, Tabone MD, Czernichow P, Levy-Marchal C. High Serum leptin concentrations during catch-up growth of children born with intrauterine growth retardation. *J Clin Endocri Metab* 1999; **84**: 1949-1952
- 11 **Kalra SP**, Kalra PS. Neuropeptide Y: a physiological orexigen modulated by the feedback action of ghrelin and leptin. *Endocrine* 2003; **22**: 49-56

Science Editor Wang XL and Guo SY Language Editor Elsevier HK

• BRIEF REPORTS •

Protection against hepatic ischemia/reperfusion injury via downregulation of toll-like receptor 2 expression by inhibition of Kupffer cell function

Jin-Xiang Zhang, He-Shui Wu, Hui Wang, Jin-Hui Zhang, Yang Wang, Qi-Chang Zheng

Jin-Xiang Zhang, He-Shui Wu, Yang Wang, Department of Emergency Surgery, Union Hospital, Tongji Medical College, Huazhong University of Science and Technology, Wuhan 430030, Hubei Province, China

Hui Wang, Hereditary Department, Tongji Medical College, Huazhong University of Science and Technology, Wuhan 430030, Hubei Province, China

Jin-Hui Zhang, Qi-Chang Zheng, Department of General Surgery, Union Hospital, Tongji Medical College, Huazhong University of Science and Technology, Wuhan 430030, Hubei Province, China
Supported by the National Natural Science Foundation of China, No. 30200272

Co-first-authors: Jin-Xiang Zhang, He-Shui Wu and Hui Wang

Co-correspondence: He-Shui Wu

Correspondence to: Dr. Jin-Xiang Zhang, Department of Emergency Surgery, Union Hospital, Tongji Medical College, Huazhong University of Science and Technology, Wuhan 430030, Hubei Province, China. camelzjx@yahoo.com.cn
Telephone: +86-27-62707120

Received: 2004-08-18 Accepted: 2004-12-14

Abstract

AIM: To elucidate the mechanism of liver protection by inhibition of Kupffer cells (KCs) function.

METHODS: All the animals were randomly divided into three groups. Blockade group (gadolinium chloride solution (GdCl₃) injection plus ischemia/reperfusion (I/R) injury): GdCl₃ solution was injected once every 24 h for 2 d via the tail vein before I/R injury. Non-blockade group (saline solution injection plus I/R injury): saline instead of GdCl₃ as a control was injected as in the blockade group. Sham group: saline was injected without I/R injury. Liver samples were collected 4 h after blood inflow restoration. The blockade of the function of KCs was verified by immunostaining with an anti-CD68 mAb. Toll-like receptor 2 (TLR2) was immunostained with a goat antimouse polyclonal anti-TLR2 antibody. Membrane proteins were extracted from the liver samples and TLR2 protein was analyzed by Western blot. Portal vein serum and plasma were taken respectively at the same time point for further detection of the levels of tumor necrosis factor- α (TNF- α) and alanine aminotransferase (ALT), an indicator of liver function.

RESULTS: Compared to non-blockade group, CD68⁺ cells significantly reduced in blockade group (OPTDI, optical density integral): 32.97 \pm 10.55 vs 185.65 \pm 21.88, P <0.01) and the liver function impairment was relieved partially (level of ALT: 435.89 \pm 178.37 U/L vs 890.21 \pm 272.91 U/L,

P <0.01). The expression of TLR2 protein in blockade group significantly decreased compared to that in non-blockade group (method of immunohistochemistry, OPDTI: 75.74 \pm 17.44 vs 170.58 \pm 25.14, P <0.01; method of Western blot, A value: 125.89 \pm 15.49 vs 433.91 \pm 35.53, P <0.01). The latter correlated with the variation of CD68 staining ($r = 0.745$, P <0.05). Also the level of portal vein TNF- α decreased in blockade group compared to that in non-blockade group (84.45 \pm 14.73 ng/L vs 112.32 \pm 17.56 ng/L, P <0.05), but was still higher than that in sham group (84.45 \pm 14.73 ng/L vs 6.07 \pm 5.33 ng/L, P <0.01).

CONCLUSION: Inhibition of the function of KCs may protect liver against I/R injury via downregulation of the expression of TLR2.

© 2005 The WJG Press and Elsevier Inc. All rights reserved.

Key words: Toll-like receptor 2; Reperfusion injury; Kupffer cell; Liver

Zhang JX, Wu HS, Wang H, Zhang JH, Wang Y, Zheng QC. Protection against hepatic ischemia/reperfusion injury via downregulation of toll-like receptor 2 expression by inhibition of Kupffer cell function. *World J Gastroenterol* 2005; 11 (28): 4423-4426

<http://www.wjgnet.com/1007-9327/11/4423.asp>

INTRODUCTION

Hepatic ischemia/reperfusion (I/R) injury is one of the major complications of liver resection surgery, transplantation, and hypovolemic shock^[1,2]. Although the detailed biochemical mechanisms are unclear, activation of Kupffer cells (KCs) may play an important role. During the very early phase of I/R injury, the secretion of proinflammatory cytokines by activated KCs, such as TNF- α , interleukin-1, participates in liver I/R injury, which precedes the activation of adhesion factors, chemotactic agents, and the sequestration of neutrophils in liver. Neutrophil accumulation in the liver causes direct hepatocellular damage through exhaustion of hepatic microcirculation by blocking the capillary perfusion and releasing proteases. So that we can see that KCs are among the first and key cells that mediate hepatic I/R injury^[3]. Inhibition of the function of KCs elicits the protection against liver I/R injury. The mechanism of KCs in such an insult remains unclear. Endotoxin or lipopolysaccharide is a strong stimulator inducing KCs to secrete proinflammatory

mediators and ultimately leading to endotoxin-induced liver injury^[4,5]. In order to clarify the mechanism of I/R injury without the effect of endotoxin and the corresponding cytokines evoked by endotoxin^[5,6], we reproduced a lobar rather than total hepatic I/R injury in a mouse model to produce a severe hepatic ischemic insult without mesenteric venous congestion. So that the development of intestinal congestion and leakage of bacteria or bacterial products into the circulation can be avoided^[6,7].

TLR family members, a kind of newly found transmembrane peptides, recognize pathogen-associated molecular patterns derived from both Gram-negative and Gram-positive bacteria such as endotoxin and are capable of sensitizing danger signals in *in vivo* environment^[1,7,8]. TLRs participate in the initiation of the downstream inflammatory cascades^[8,9]. In previous studies, we have proved that TLR2 and TLR4 are involved in the hepatic I/R pathologic process and the activation of them is not related to endotoxin^[10,11]. Whether TLR2 expression is affected by the function of KCs is still unknown. GdCl₃ is a kind of experimental drug, which is capable of blocking KC function specifically, while it has no effect on other macrophages, such as those residing in lung or intestinal canals^[12,13]. CD68 is a pan-macrophage endosomal glycoprotein, which belongs to a family of acidic, highly glycosylated lysosomal glycoproteins and is found in cytoplasmic granules. It is considered as a specific indicator of KC activation^[14]. That is why we used CD68 immunohistological staining to assess the inhibition of KC function.

This experiment aimed to observe the variation of TLR2 expression after the inhibition of the function of KCs and to further clarify the protective mechanism against hepatic I/R injury induced by inhibition of the function of KCs.

MATERIALS AND METHODS

Animal model and grouping

Male BALB/c mice weighing 20-25 g were supplied by Experimental Animal Center in Tongji Medical College. Their age ranged 6-8 wk. The animals were fasted for 12 h with free access to water and randomly divided into GdCl₃ injection plus I/R injury group (blockade group), saline solution injection plus I/R injury group (non-blockade group), and sham operation group (sham group). The animals in blockade group received injections of GdCl₃ solution (0.1 mmol/kg body weight, Sigma, USA) via tail vein once every 24 h for two times. The operation was performed 24 h after the last injection. The animals in non-blockade group were injected saline solution as control. Mice were anesthetized with pentobarbital (60 mg/kg). Laparotomy was performed through a midline incision and an atraumatic clip was placed across the hepatic hilar to interrupt blood supply to the left and median lobes of the liver. After 60 min of partial hepatic ischemia, the clip was removed to initiate hepatic reperfusion. Sham group mice underwent the same protocol as the control group without vascular occlusion. After the tissue was removed, animals were euthanized by injection of an overdose of pentobarbital. All studies were approved by the Institutional Animal Care and Use Committee of Tongji Medical College.

Detection of KC function variation after injection of GdCl₃ by CD68 stain

Liver samples from ischemic lobes were taken after 4 h of blood supply restoration and immediately fixed with 40 g/L formaldehyde, dehydrated, and embedded in paraffin for immuno-histopathologic examination. Four micrometers of thick sections were stained with anti-CD68 Ab (Boster Bio. Co., Wuhan, China). The results were analyzed with a HPIAS pathological image analyzer and expressed as optical density integral (OPTDI).

Detection of TLR2 protein in ischemic hepatic lobes

Membrane proteins of ischemic liver tissues (100 mg) were extracted (1× PBS, 10 mL/L NP40, 5 g/L sodium desoxycholate, 1 g/L sodium dodecyl sulfate, 10 g/L phenylmethylsulfonyl fluoride, 30 mL/L aprotinin, 1 mol/L sodium orthovanadate). After quantification and aliquot, the samples were degenerated by boiling, separated on 85 g/L SDS-PAGE and transferred to nitrocellulose membranes. Filters were blocked 50 g/L nonfat milk in blocking buffer (TBS-T, 50 mmol/L Tris-Cl, pH 7.5, 150 mmol/L NaCl, 0.2 g/L Tween 20), and incubated with anti-TLR2 antibody (Santa Cruz, CA, USA) for 2 h and with peroxidase-conjugated secondary antibody for 1 h at 37 °C. Specific bands were revealed with DAB solution and analyzed by Gel-Pro-Analyzer 4 as the value of *A*.

Other 4- μ m-thick sections were stained with a goat antimouse TLR2 polyclonal antibody (Santa Cruz, CA, USA). The results were expressed as OPTDI and analyzed with a HPIAS pathological image analyzer.

The relationship between the expressions of CD68 and TLR2 was analyzed with Spearman, bivariate assay.

Examination of ALT and TNF- α in portal vein after injection of GdCl₃

Blood samples from portal vein were taken for assay of plasma alanine aminotransferase (ALT) and TNF- α level. The ALT activity was determined by an automatic biochemistry analyzer (HITACHI 2000, Japan) in Laboratory of Union Hospital. TNF- α level was assayed by an ELISA kit (JINGMEI Bio. Co., China).

Statistical analysis

All numeric data were expressed as mean \pm SD. Differences between blockade and non-blockade groups were analyzed by *t*-test with SPSS 10.0 software. The correlation between CD68 staining and TLR2 expression was analyzed with Spearman assay. *P*<0.05 was considered statistically significant.

RESULTS

Variation of KC function after injection of GdCl₃

When KCs were blocked with GdCl₃, the CD68⁺ reaction was weaker in blockade group than in non-blockade group (Figure 1A). CD68 content was shown as absolute value OPTDI (Area \times OPTDM), which was 32.97 \pm 10.55 *vs* 185.65 \pm 21.88. The difference between them was significant (*P*<0.01), suggesting that the function of KCs was inhibited in blockade group.

Detection of TLR2 in ischemic hepatic lobes by immunological stain

The positive immunoreaction of TLR2 in slices was weaker

in blockade group than in non-blockade group (Figure 1B), which was shown as OPDTI (75.74 ± 17.44 vs 170.58 ± 25.14). The difference between them was significant ($P < 0.01$).

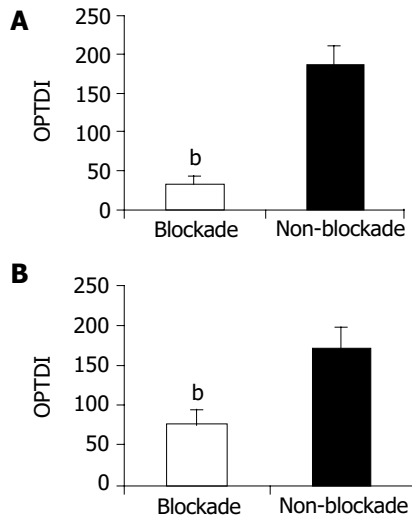


Figure 1 Effect of GdCl₃ injection on CD68 (A) and TLR2 (B) expression in blockade and non-blockade groups. ^b $P < 0.01$ vs non-blockade group.

Variation of TLR2 protein expression in ischemic hepatic lobes

After 4 h restoration of blood supply, the expression of TLR2 protein, which was detected by Western blot increased in the non-blockade group compared to sham group (A : 433.91 ± 35.53 vs 52.86 ± 13.58 , $P < 0.01$). The injection of GdCl₃ significantly down regulated the expression of TLR2 in ischemic lobes compared to the non-blockade group (125.89 ± 15.49 vs 433.91 ± 35.53 , $P < 0.01$, Figure 2). Correlation analysis indicated that the downregulation of TLR2 expression between blockade and non-blockade groups was correlated with that of CD68 ($r = 0.745$, $P < 0.05$).

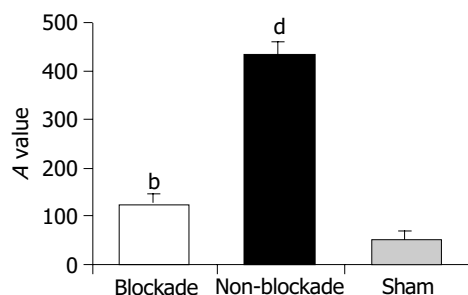


Figure 2 Detection of TLR2 expression by Western blot. ^b $P < 0.01$ vs non-blockade group, ^d $P < 0.01$ vs sham group.

Effect of GdCl₃ injection on portal vein plasma ALT and serum TNF- α

After 4 h restoration of blood supply, the level of ALT in portal vein, an indicator of liver function, was higher in non-blockade group than in sham group (890.21 ± 272.91 U/L vs 40.66 ± 15.42 U/L, $P < 0.01$). The value in blockade

group decreased to 435.89 ± 178.37 U/L. The difference between blockade and non-blockade groups was significant ($P < 0.01$, Figure 3A).

The serum TNF- α level in portal vein was higher in non-blockade group than in sham group (112.32 ± 17.56 ng/L vs 6.07 ± 5.33 ng/L, $P < 0.01$) after 4 h blood supply restoration. When the function of KCs was blocked by injection of GdCl₃, the level of portal vein TNF- α was decreased remarkably (84.45 ± 14.73 ng/L vs 112.32 ± 17.56 ng/L, $P < 0.01$), which might be an indirect indicator of KC inhibition (Figure 3B).

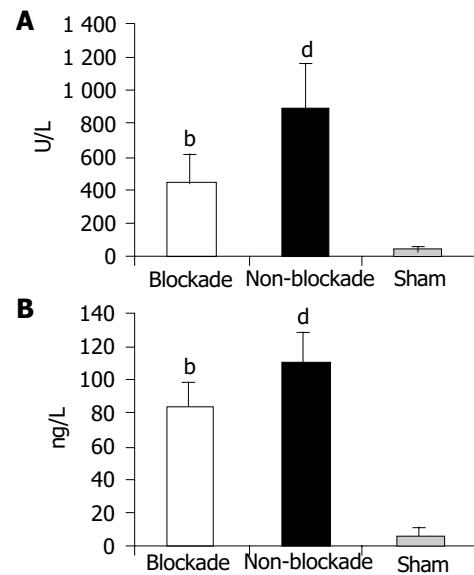


Figure 3 Portal vein ALT (A) and TNF- α (B) levels. ^b $P < 0.01$ vs non-blockade group, ^d $P < 0.01$ vs sham group.

DISCUSSION

KCs play an important part in mediating ischemia and reperfusion injury^[15]. When activated during ischemia and subsequent reperfusion, they generate excessive inflammatory cytokines and oxygen-derived free radicals, which play a particularly important role in the pathogenesis of hepatic ischemia and reperfusion injury with an increased release of TNF- α and histological impairment. GdCl₃, a specific inhibitor of KCs, is often used as a tool for studying the role of KCs^[16]. GdCl₃ is capable of protecting liver from injury mediated by the activation of KCs through depletion of lipid peroxidation. In the present study, injection of GdCl₃ selectively inhibited the activation of KCs, but did not induce hepatotoxicity. On the contrary, the impairment of liver function was relieved.

TLR2 can be activated during the process of hepatic I/R injury^[10]. When TLR2 is activated, its cytoplasmic portion would conduct signals to two distinct signaling pathways, JNK and NF- κ B, resulting in the proinflammatory cascade and excessive production of TNF- α ^[17]. TLRs recognize two kinds of signals. One is related to pathogen-associated molecular pattern molecules, which claims the existence of pathogens^[9]; the other is linked with some danger signals inside or outside the body, which does not need the existence of pathogens^[18]. Hypothesis infers that TLRs may be the

candidate of a key “gate” through which the down stream inflammatory cascade is initiated^[17]. TLR2 and TLR4 are activated in liver I/R injury^[10,11], but the factors regulating the expression of TLRs have not been revealed.

Previous study has proved that NF- κ B activation may be important in “switching off” the cytokine cascade during I/R injury. TNF- α plays a central role in mediating such an insult^[7]. Nevertheless, what happens preceding the NF- κ B activation and TNF- α release? Where is the switch point that starts a crucial inflammatory cascade involving the activation of NF- κ B during the I/R pathological process? Activation of TLR2 results in the activation of NF- κ B^[17], and NF- κ B activation in the liver could be downregulated by KC blockade. In this paper, we confirmed that blocking the function of KCs downregulated the expression of TLR2 in ischemic lobes in mice partial hepatic I/R model, and the levels of TNF- α and ALT in portal vein decreased at the same time, suggesting that inhibition of KC function may protect liver from I/R injury by suppressing the release of TNF- α through downregulation of TLR2 expression. On the other hand, KCs might play an important role in mediating liver injuries and inflammatory disorders in the liver by changing the TLR2 signal transduction pathway. But compared to the sham group, the levels of portal vein TNF- α and ALT were still higher in blockade group, indicating that besides activation of KCs there are other factors regulating the expression of TLR2. Whether KCs themselves or cytokines secreted by KCs regulate the expression of TLR2 in ischemic lobes remains unclear.

KCs are major contributors to cytokine production in hepatic I/R injury^[15]. Although many factors, including reactive oxygen species, Ca⁺⁺ overload, adhesive molecules, nitrogen monoxide, *etc*, contribute to the pathogenesis of hepatic I/R injury, all these factors exert their role after the activation of KCs and the resulting inflammatory cascade^[3]. Further study on inflammatory reaction controlled by TLRs and KCs may resolve the enigma of hepatic I/R injury.

ACKNOWLEDGMENTS

Authors thank Professor Du-Jun Ye, Pathophysiology Department, Tongji Medical College, Huazhong University of Science and Technology, for his helpful discussions. An excellent technical assistance of Dr. Yun Yang is acknowledged.

REFERENCES

- 1 **Fondevila C**, Busuttill RW, Kupiec-Weglinski JW. Hepatic ischemia/reperfusion injury—a fresh look. *Exp Mol Pathol* 2003; **74**: 86
- 2 **Jaeschke H**. Mechanisms of reperfusion injury after warm ischemia of liver. *J Hepatobiliary Pancreat Surg* 1998; **5**: 402
- 3 **Teoh NC**, Farrell GC. Hepatic ischemia reperfusion injury: Pathogenic mechanisms and basis for hepatoprotection. *J Gastroenterol Hepatol* 2003; **18**: 891
- 4 **Enomoto N**, Ikejima K, Yamashina S, Hirose M, Shimizu H, Kitamura T, Takei Y, Sato And N, Thurman RG. Kupffer cell sensitization by alcohol involves increased permeability to gut-derived endotoxin. *Alcohol Clin Exp Res* 2001; **25**: 51S
- 5 **Lukkari TA**, Jarvelainen HA, Oinonen T, Kettunen E, Lindros KO. Short-term ethanol exposure increases the expression of Kupffer cell CD14 receptor and lipopolysaccharide binding protein in rat liver. *Alcohol Alcohol* 1999; **34**: 311
- 6 **Kojima Y**, Suzuki S, Tsuchiya Y, Konno H, Baba S, Nakamura S. Regulation of pro-inflammatory and anti-inflammatory cytokine responses by Kupffer cells in endotoxin-enhanced reperfusion injury after total hepatic ischemia. *Transpl Int* 2003; **16**: 231
- 7 **Colletti LM**, Remick DG, Burtch GD, Kunkel SL, Strieter RM, Campbell DA Jr. Role of tumor necrosis factor- α in the pathophysiologic alterations after hepatic ischemia/reperfusion injury in the rat. *J Clin Invest* 1990; **85**: 1936
- 8 **Frantz S**, Kelly RA, Bourcier T. Role of TLR-2 in the activation of nuclear factor kappaB by oxidative stress in cardiac myocytes. *J Biol Chem* 2001; **276**: 5197
- 9 **Takeuchi O**, Akira S. Toll-like receptors; their physiological role and signal transduction system. *Int Immunopharmacol* 2001; **1**: 625
- 10 **Zhang JX**, Wu HS, Wang L, Zhang JH, Wang H, Zheng QC. TLR2 mRNA upregulation in ischemic lobes in mouse partial hepatic ischemia/reperfusion injury model. *J HUST* 2004; **24**: 144-146
- 11 **Wu HS**, Zhang JX, Wang L, Tian Y, Wang H, Rotstein O. Toll-like receptor 4 involvement in hepatic ischemia/reperfusion injury in mice. *Hepatobiliary Pancreat Dis Int* 2004; **3**: 250
- 12 **Lee CM**, Yeoh GC, Olynyk JK. Differential effects of gadolinium chloride on Kupffer cells *in vivo* and *in vitro*. *Int J Biochem Cell Biol* 2004; **36**: 481
- 13 **Gloor B**, Todd KE, Lane JS, Lewis MP, Reber HA. Hepatic Kupffer cell blockade reduces mortality of acute hemorrhagic pancreatitis in mice. *J Gastrointest Surg* 1998; **2**: 430
- 14 **Ramprasad MP**, Terpstra V, Kondratenko N, Quehenberger O, Steinberg D. Cell surface expression of mouse macrophage and human CD68 and their role as macrophage receptors for oxidized low density lipoprotein. *Proc Natl Acad Sci USA* 1996; **93**: 14833
- 15 **Schumann J**, Wolf D, Pahl A, Brune K, Papadopoulos T, van Rooijen N, Tiegs G. Importance of Kupffer Cells for T-Cell-Dependent Liver Injury in Mice. *Am J Pathol* 2000; **157**: 1671
- 16 **Rivera CA**, Bradford BU, Hunt KJ, Adachi Y, Schrum LW, Koop DR, Burchardt ER, Rippe RA, Thurman RG. Attenuation of CCl4-induced hepatic fibrosis by GdCl3 treatment or dietary glycine. *Am J Physiol Gastrointest Liver Physiol* 2001; **281**: G200
- 17 **Yang RB**, Mark MR, Gray A, Huang A, Xie MH, Zhang M, Goddard A, Wood WI, Gurney AL, Godowski PJ. Toll-like receptor-2 mediates lipopolysaccharide-induced cellular signalling. *Nature* 1998; **395**: 284
- 18 **Matzinger P**. The danger model: a renewed sense of self. *Science* 2002; **296**: 301

• BRIEF REPORTS •

Effect of *c-fos* antisense probe on prostaglandin E₂-induced upregulation of vascular endothelial growth factor mRNA in human liver cancer cells

Yong-Qi Li, Kai-Shan Tao, Ning Ren, Yi-Hu Wang

Yong-Qi Li, Ning Ren, Yi-Hu Wang, Comprehensive Diagnostic and Therapeutic Center, Xijing Hospital, the Fourth Military Medical University, Xi'an 710033, Shaanxi Province, China
Kai-Shan Tao, Department of Hepatobiliary Surgery, Xijing Hospital, the Fourth Military Medical University, Xi'an 710033, Shaanxi Province, China

Correspondence to: Dr. Yong-Qi Li, Comprehensive Diagnostic and Therapeutic Center, Xijing Hospital, the Fourth Military Medical University, Xi'an 710033, Shaanxi Province, China. yongqil33@yahoo.com.cn

Telephone: +86-29-83375151 Fax: +86-29-82516966

Received: 2005-03-01 Accepted: 2005-05-13

Abstract

AIM: To examine the effect of prostaglandin E₂ (PGE₂) on the expression of vascular endothelial growth factor (VEGF) mRNA in the human hepatocellular carcinoma (HCC) HepG2 cells and the possible involvement of *c-fos* protein in this process.

METHODS: Human HCC HepG2 cells were divided into three groups treated respectively with PGE₂, a combination of PGE₂ and *c-fos* antisense oligodeoxynucleotide (ASO), and PGE₂ plus *c-fos* sense oligodeoxynucleotide (SO). The expression of VEGF mRNA in HepG2 cells after different treatments was detected by reverse transcriptase-polymerase chain reaction (RT-PCR). The relative expression level of VEGF mRNA in HepG2 cells in each group was measured.

RESULTS: Administration of PGE₂ resulted in an increased expression of *c-fos* and VEGF mRNA in HepG2 cells. The relative expression level of *c-fos* mRNA reached the peak at 3 h (68.4±4.7%) after PGE₂ treatment, which was significantly higher than that at 0 h (20.6±1.7%, *P*<0.01). Whereas, the highest expression level of VEGF mRNA was observed at 6 h (100.5±6.1%) after PGE₂ treatment, which was significantly higher than that at 0 h (33.2±2.4%, *P*<0.01). *C-fos* ASO significantly reduced PGE₂-induced VEGF mRNA expression in HepG2 cells.

CONCLUSION: PGE₂ increases the expression and secretion of VEGF in HCC cells by activating the transcription factor *c-fos*, promotes the angiogenesis of HCC and plays an important role in the pathogenesis of liver cancer.

© 2005 The WJG Press and Elsevier Inc. All rights reserved.

Key words: Hepatocellular carcinoma; Prostaglandin E₂;

c-fos; Vascular endothelial growth factor; Angiogenesis

Li YQ, Tao KS, Ren N, Wang YH. Effect of *c-fos* antisense probe on prostaglandin E₂-induced upregulation of vascular endothelial growth factor mRNA in human liver cancer cells. *World J Gastroenterol* 2005; 11(28): 4427-4430
<http://www.wjgnet.com/1007-9327/11/4427.asp>

INTRODUCTION

PGE₂ is produced in various kinds of cancer cells and seems to be particularly important for carcinogenesis^[1-3]. PGE₂ activates multiple G-protein-linked receptor subtypes (EP1-EP4) in an autocrine or paracrine fashion, which may lead to tumor growth promotion via growth factors and oncogenes^[4-6]. However, the mechanism of PGE₂ in promoting tumor growth still remains unclear. VEGF is a regulator of pathological angiogenesis and plays an important role in tumor growth. Studies have revealed that VEGF can be produced by liver cancer cells in a paracrine manner, thus promoting the angiogenesis of liver cancer^[7,8]. Studies also indicate that many tumor growth factors stimulate the production of VEGF in tumor cells^[5,9]. This study was undertaken to estimate if PGE₂ could affect the expression of VEGF in HCC HepG2 cells and the possible involvement of the oncogene *c-fos* in this process.

MATERIALS AND METHODS

Cell culture and PGE₂ administration

HepG2 cells were cultured in RPMI-1640 medium (Gibco) containing 10 mL/L fetal bovine serum, 100 kU/L penicillin and 0.1 g/L streptomycin at 37 °C in 50 mL/L CO₂/950 mL/L air for 4-6 d and then put into fresh 35 mm dishes. Twenty-four hours later, PGE₂ (Sigma) was added into each dish in a final concentration of 1 μmol/L. The dose of PGE₂ in the present study was chosen based on the previous reports and our preliminary experiments. The cells were then cultured for 0, 1, 3, 6, 12, and 24 h, respectively (*n* = 4/each time point) and collected for RNA extraction.

C-fos ASO administration

C-fos ASO (5'-GAACATCATCGTGCC-3') was synthesized according to reported human *c-fos* mRNA sequence (GenBank Accession No. M16287). *C-fos* SO (5'-GCCA-CGATGATGTTTC-3') was also synthesized as a control. Both ASO and SO were modified phosphorothioate

oligodeoxynucleotide.

HepG2 cells were cultured as mentioned above and divided into: (1) control group in which 10 μ L physical saline was added, (2) PGE₂-treated groups in which 1 μ mol/L of PGE₂ was added, (3) SO-treated group in which 10 μ L (50 μ g) *c-fos* SO was added followed by addition of 1 μ mol/L of PGE₂ after 30 min, (4) ASO-treated group in which 10 μ L (50 mg) *c-fos* ASO was added followed by addition of 1 μ mol/L of PGE₂ after 30 min. The cells were cultured for 6 h and then collected for RNA extraction.

Primer design and synthesis

Specific primers for human *c-fos* and VEGF were synthesized according to their reported mRNA sequences. The primer pair of *c-fos* were: sense: 5'-TGC TGA AGG AGA AGG AAA AA -3'; antisense: 5'-TGC ATA GAA GGA CCC AGA TA -3' (GenBank Accession No. M16287). The primer pair of VEGF were: sense: 5'-ACC CAT GGC AGA AGG AGG AG -3' antisense 5'-ACG CGA GTC TGT GTT TTT GC-3' (GenBank Accession No. M32977). The primers (sense: 5'-GGC ATC CAC GAA ACT ACC TT-3' antisense 5'-CGT CAT ACT CCT GCT TGC TG -3') for human β -actin (GenBank Accession No. M10277) were also synthesized as internal control in the PCR reaction. The length of PCR product for *c-fos*, VEGF and β -actin was 344 bp, 433 bp and 274 bp, respectively.

RNA extraction

Total cellular RNA was extracted from HepG₂ cells using TRIzol reagent (Invitrogen) according to the manufacturer's instructions. The purity and integrity of the RNA samples were assessed by $A_{260/280}$ spectrophotometric measurement.

RT-PCR

After measurement of the concentration, cDNA was reversely transcribed in a 50 μ L mixture containing 2 μ g total RNA, 10 μ L 5 \times RT buffer, 5 μ L 10 mmol/L dNTPs, 0.5 μ L RNase inhibitor (4 \times 10⁵ U/L, Invitrogen) 0.5 μ L oligo (dT)₁₂₋₁₈ (500 g/L, Invitrogen) 1 μ L SuperScript II reverse transcriptase (2 \times 10⁴ U/L, Invitrogen), 0.5 μ L 0.1 mol/L DTT at 42 $^{\circ}$ C for 60 min followed by enzyme denaturation at 70 $^{\circ}$ C for 10 min. Thirty cycles of PCR were carried out in 25 μ L reaction mixture containing 0.1 μ g synthesized cDNA, 2.5 μ L 10 \times PCR buffer, 2.5 μ L dNTPs (2 mmol/L), 2.5 μ L MgCl₂ (2.5 mmol/L), 1 μ L of each primer (20 μ mol/L), 2.5 u of Taq DNA polymerase (Takara) using a PTC-100 programmed thermal controller (MJ Research), each consisting of denaturation at 94 $^{\circ}$ C for 1 min, annealing at 56 $^{\circ}$ C for 30 s, extension at 72 $^{\circ}$ C for 1 min. Then, 10 μ L of each PCR product was separated by electrophoresis on a 30 g/L agarose gel and visualized by ethidium bromide staining.

Statistical analysis

For each template, PCR amplification was performed 2-3 times. The electrophoresis results were observed through a gel imaging system (UVP) and the density of each positive band was analyzed by Labworks software. The relative expression level of *c-fos* and VEGF mRNA was expressed as a ratio of densitometric measurements (*c-fos*/ β -actin or

VEGF/ β -actin). The data were expressed as mean \pm SE, and analyzed by analysis of variance and Dunnett's test using SPSS10.1 software.

RESULTS

Effect of PGE₂ on expression of *c-fos* and VEGF mRNA in HepG2 cells

Addition of PGE₂ to the HepG2 cells resulted in a time-dependent increase in the expression of *c-fos* and VEGF mRNA (Figure 1A). Compared to the expression level at 0 h (20.6 \pm 1.7%), the expression of *c-fos* mRNA induced by PGE₂ treatment reached the highest level at 1 h (62.3 \pm 4.3%, P <0.01) and 3 h (68.4 \pm 4.7%, P <0.01), and slightly higher level at 6 h (55.3 \pm 3.8%, P <0.05; Figure 1B). The expression level of VEGF mRNA significantly increased at 3 h after PGE₂ administration (87.6 \pm 6.4%, P <0.01) when compared to the expression level at 0 h (33.2 \pm 2.4%). Its expression level reached a maximum at 6 h (100.5 \pm 6.1%, P <0.01). At 24 h, the expression level returned to its level at 0 h (35.2 \pm 2.8%, P >0.05; Figure 1B). The expression level of β -actin mRNA remained unchanged at each time-point, indicating the equal amount of the template used in PCR.

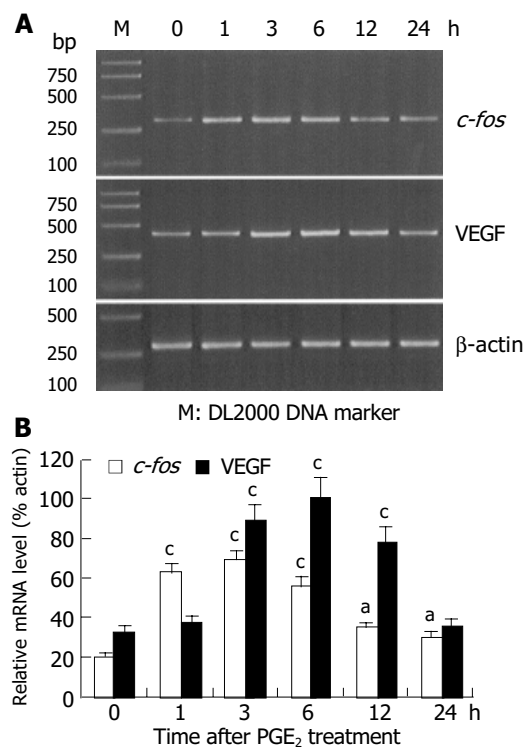


Figure 1 RT-PCR results (A) and histograms (B) showing effect of PGE₂ on expression of *c-fos* and VEGF mRNA in HepG2 cells. ^a P <0.05, ^c P <0.05 vs 0 h.

Effect of *c-fos* ASO on PGE₂-induced upregulation of VEGF mRNA in HepG2 cells

Since the maximal expression level of VEGF mRNA was at 6 h after PGE₂ treatment, this time-point was selected to observe the effect of *c-fos* ASO. The results showed that the expression level of VEGF mRNA significantly decreased in *c-fos* ASO-treated group (39.6 \pm 3.2%) when compared to that in PGE₂-treated group (98.6 \pm 6.4%, P <0.01, Figure 2A

and B). In contrast, no such change in *c-fos* SO-treated group was observed ($95.2 \pm 6.3\%$, $P > 0.05$).

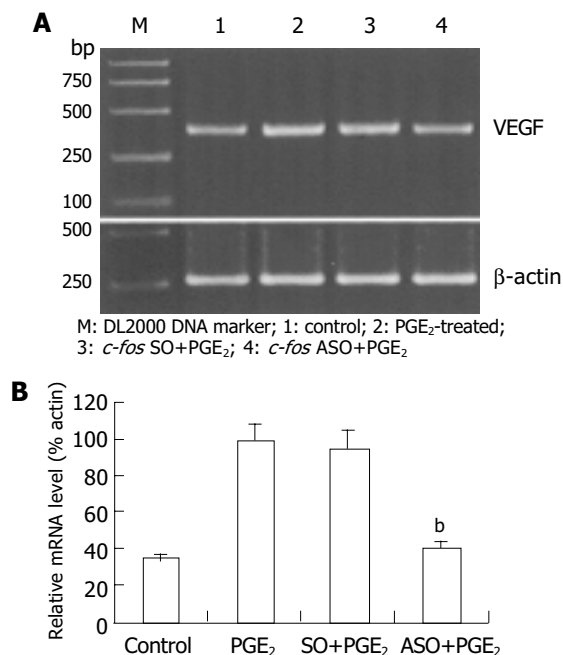


Figure 2 RT-PCR results (A) and histograms (B) showing effect of *c-fos* ASO on PGE₂-induced VEGF mRNA expression in HepG2 cells. ^b $P < 0.01$ vs PGE₂ group.

DISCUSSION

At present, the exact pathological function and mechanism of PGE₂ in tumors are not fully known. Previous studies indicate that PGE₂ can be produced by tumor cells and plays an important role in tumor immune inhibition^[10-12]. Some studies revealed that the PGE₂ level in patients with cancer is higher than that in normal people, and that tumor tissues also contain higher concentration of PGE₂ than normal tissues^[13]. Animal experiments indicate that PGE₂ produced by tumor cells, can promote the growth and development of tumors through its immune inhibitory function^[10]. Further studies have proved that PGE₂ promotes the growth of liver cancer through its receptor EP3^[14]. In the present study, we observed that PGE₂ could stimulate the expression of VEGF mRNA in HepG2 cells in a time-dependent manner, suggesting that PGE₂ may promote the angiogenesis of HCC by increasing the secretion of VEGF from liver cancer cells. This might be one of the mechanisms of PGE₂ in facilitating the growth of liver cancer.

It is well known that the oncogene *c-fos* can function as a third intracellular messenger. Its product Fos protein can form a homo-dimer itself or hetero-dimer with c-Jun protein and then binds to the AP-1 site in the target gene, thus promoting the transcription of target gene. It has been reported that the promoter region for the VEGF gene contains several AP-1 binding motifs^[15] and the expression of VEGF gene is controlled by transcription factors AP-1 and AP-2^[16-18]. In the present study, we observed that PGE₂ increased the expression of *c-fos* mRNA, the maximal level was at 1 and 3 h after PGE₂ administration, earlier than the

PGE₂-induced highest expression of VEGF mRNA. Furthermore, *c-fos* ASO significantly reversed PGE₂-induced VEGF mRNA expression. These results indicate that Fos protein is involved in the PGE₂-induced VEGF expression in HepG2 cells.

The intracellular signaling pathway coupled to PGE₂ is complicated. As a third intracellular messenger, *c-fos* is just located in the downstream of the signaling pathway. Many other molecules should also be involved in the modulation of VEGF expression by PGE₂. In addition, several PGE₂ receptors are present in HCC^[6,19]. Which receptors mediate the role of PGE₂ in tumor growth needs to be investigated.

In conclusion, PGE₂ stimulates VEGF induction in HepG2 cells by activating the transcription factor Fos protein.

ACKNOWLEDGMENT

The authors thank Dr. SX Wu, Department of Anatomy, Faculty of Basic Medicine, Fourth Military Medical University for his technical assistance and help with preparation of the manuscript.

REFERENCES

- 1 **Bishop-Bailey D**, Calatayud S, Warner TD, Hla T, Mitchell JA. Prostaglandins and the regulation of tumor growth. *J Environ Pathol Toxicol Oncol* 2002; **21**: 93-101
- 2 **Ito H**, Duxbury M, Benoit E, Clancy TE, Zinner MJ, Ashley SW, Whang EE. Prostaglandin E2 enhances pancreatic cancer invasiveness through an Ets-1-dependent induction of matrix metalloproteinase-2. *Cancer Res* 2004; **64**: 7439-7446
- 3 **Leung WK**, To KF, Go MY, Chan KK, Chan FK, Ng EK, Chung SC, Sung JJ. Cyclooxygenase-2 upregulates vascular endothelial growth factor expression and angiogenesis in human gastric carcinoma. *Int J Oncol* 2003; **23**: 1317-1322
- 4 **Ushio A**, Takikawa Y, Lin SD, Miyamoto Y, Suzuki K. Induction of Bcl-xL is a possible mechanism of anti-apoptotic effect by prostaglandin E2 EP4-receptor agonist in human hepatocellular carcinoma HepG2 cells. *Hepatol Res* 2004; **29**: 173-179
- 5 **Yamaki T**, Endoh K, Miyahara M, Nagamine I, Thi Thu Huong N, Sakurai H, Pokorny J, Yano T. Prostaglandin E2 activates Src signaling in lung adenocarcinoma cell via EP3. *Cancer Lett* 2004; **214**: 115-120
- 6 **Amano H**, Hayashi I, Endo H, Kitasato H, Yamashina S, Maruyama T, Kobayashi M, Satoh K, Narita M, Sugimoto Y, Murata T, Yoshimura H, Narumiya S, Majima M. Host prostaglandin E(2)-EP3 signaling regulates tumor-associated angiogenesis and tumor growth. *J Exp Med* 2003; **197**: 221-232
- 7 **Imura S**, Miyake H, Izumi K, Tashiro S, Uehara H. Correlation of vascular endothelial cell proliferation with microvessel density and expression of vascular endothelial growth factor and basic fibroblast growth factor in hepatocellular carcinoma. *J Med Invest* 2004; **51**: 202-209
- 8 **Qin LX**, Tang ZY. Recent progress in predictive biomarkers for metastatic recurrence of human hepatocellular carcinoma: a review of the literature. *J Cancer Res Clin Oncol* 2004; **13**: 497-513
- 9 **Casibang M**, Purdom S, Jakowlew S, Neckers L, Zia F, Ben-Av P, Hla T, You L, Jablons DM, Moody TW. Prostaglandin E2 and vasoactive intestinal peptide increase vascular endothelial cell growth factor mRNAs in lung cancer cells. *Lung Cancer* 2001; **31**: 203-212
- 10 **Harris SG**, Padilla J, Koumas L, Ray D, Phipps RP. Prostaglandins as modulators of immunity. *Trends Immunol* 2002; **23**: 144-150
- 11 **Rocca B**, FitzGerald GA. Cyclooxygenases and prostaglandins: shaping up the immune response. *Int Immunopharmacol* 2002;

- 2: 603-630
- 12 **Kaur K**, Harris SG, Padilla J, Graf BA, Phipps RP. Prostaglandin E2 as a modulator of lymphocyte mediated inflammatory and humoral responses. *Adv Exp Med Biol* 1999; **469**: 409-412
- 13 **Majima M**, Amano H, Hayashi I. Prostanoid receptor signaling relevant to tumor growth and angiogenesis. *Trends Pharmacol Sci* 2003; **24**: 524-529
- 14 **Hashimoto N**, Watanabe T, Ikeda Y, Yamada H, Taniguchi S, Mitsui H, Kurokawa K. Prostaglandins induce proliferation of rat hepatocytes through a prostaglandin E2 receptor EP3 subtype. *Am J Physiol* 1997; **272**(3 Pt 1): G597-604
- 15 **Tischer E**, Mitchell R, Hartman T, Silva M, Gospodarowicz D, Fiddes JC, Abraham JA. The human gene for vascular endothelial growth factor. Multiple protein forms are encoded through alternative exon splicing. *J Bio Chem* 1991; **266**: 11947-11954
- 16 **Clifford SC**, Czaplak K, Richards FM, O'Donoghue DJ, Maher ER. Hepatocyte growth factor-stimulated renal tubular mitogenesis: effects on expression of c-myc, c-fos, c-met, VEGF and the VHL tumour-suppressor and related genes. *Br J Cancer* 1998; **77**: 1420-1428
- 17 **Ryuto M**, Ono M, Izumi H, Yoshida S, Weich HA, Kohno K, Kuwano M. Induction of vascular endothelial growth factor by tumor necrosis factor alpha in human glioma cells. Possible roles of SP-1. *J Biol Chem* 1996; **271**: 28220-28228
- 18 **Ben-Av P**, Crofford LJ, Wilder RL, Hla T. Induction of vascular endothelial growth factor expression in synovial fibroblasts by prostaglandin E and interleukin-1: a potential mechanism for inflammatory angiogenesis. *FEBS Lett* 1995; **372**: 83-87
- 19 **Bhattacharya M**, Peri K, Ribeiro-da-Silva A, Almazan G, Shichi H, Hou X, Varma DR, Chemtob S. Location of functional prostaglandin E2 receptors EP3 and EP4 in the nuclear envelope. *J Biol Chem* 1999; **274**: 15719-15724

Science Editor Wang XL and Guo SY Language Editor Elsevier HK

Risk factors for primary liver carcinoma in Chinese population

Rui-Hong Luo, Zhi-Xin Zhao, Xu-Yu Zhou, Zhi-Liang Gao, Ji-Lu Yao

Rui-Hong Luo, Zhi-Xin Zhao, Zhi-Liang Gao, Ji-Lu Yao,
Department of Infectious Diseases, The Third Affiliated Hospital
of Sun Yat-Sen University, Guangzhou 510630, Guangdong Province,
China

Xu-Yu Zhou, Medical Information Institute, Sun Yat-Sen University,
Guangzhou 510089, Guangdong Province, China

Correspondence to: Dr. Rui-Hong Luo, Department of Infectious
Diseases, The Third Affiliated Hospital of Sun Yat-Sen University,
Guangzhou 510630, Guangdong Province,
China. ruihongluo2002@yahoo.com.cn

Telephone: +86-20-85263061

Received: 2004-10-09 Accepted: 2004-11-24

Abstract

AIM: To evaluate the risk factors for primary liver carcinoma (PLC) in Chinese population.

METHODS: Chinese Biomedical Literature Database, China Hospital Knowledge Database and MEDLINE were searched. All the related literatures were screened, and the risk factors for PLC in Chinese population were studied. Heterogeneity was evaluated by odds ratio (OR) q test. Combined OR and its 95% confidence interval (95%CI) were calculated, the association between the investigated risk factors and PLC was determined. Validity and bias of the findings were evaluated by sensitivity analysis and funnel plot analysis respectively.

RESULTS: Fifty-five of one hundred and ninety identified studies were accepted according to the inclusive criteria. Ten factors related to PLC were demonstrated by sensitive analysis and funnel plot analysis. They were cirrhosis (OR = 11.97, P = 0.000), HBV infection (OR = 11.34, P = 0.000), HCV infection (OR = 4.28, P = 0.000), family history of liver cancer (OR = 3.49, P = 0.000), unstable emotion (OR = 2.20, P = 0.000), depressed characters (OR = 3.07, P = 0.000), aflatoxin (OR = 1.80, P = 0.000), alcoholic (OR = 1.88, P = 0.000), intake of musty food (OR = 1.87, P = 0.000) and drinking contaminated water from pond (OR = 1.77, P = 0.003).

CONCLUSION: The main risk factors for PLC in China are liver diseases, family history of liver carcinoma, poor psychic status, aflatoxin, and some unhealthy behaviors.

© 2005 The WJG Press and Elsevier Inc. All rights reserved.

Key words: Primary carcinoma; Liver; Meta-analysis; Risk factor

Luo RH, Zhao ZX, Zhou XY, Gao ZL, Yao JL. Risk factors for primary liver carcinoma in Chinese population. *World J Gastroenterol* 2005; 11(28): 4431-4434
<http://www.wjgnet.com/1007-9327/11/4431.asp>

INTRODUCTION

Primary liver carcinoma (PLC) affects more than 500 000 people globally with 110 000 deaths annually. More than one-half of them were Chinese^[1]. The incidence rate is 14.58-46 per 100 000 people. In Qidong, Jiangsu Province and Fusui, Guangxi Zhuang Autonomous Region, the morbidity is higher than that in any other areas of China.

It is known that persistent hepatitis B virus (HBV) and HCV infection and aflatoxins are the main causes of PLC^[1]. However, most of the investigations were case-control studies. The real risk factors for PLC may be far more than the known causes. The results from different investigated areas are variable. Cohort study on risk factors for PLC in Chinese people is still not available. A meta-analysis confined to case-control studies published from January 1966 to December 2003 was carried out.

MATERIALS AND METHODS

Search strategy

The databases including Chinese Biomedical Literature Database (1979-December 2003), China Hospital Knowledge Database (1994-December 2003) and MEDLINE (1966-December 2003) were searched. The following keywords were used: liver cancer, liver carcinoma, primary liver cancer, primary liver carcinoma, malignant liver tumors, primary liver tumors, hepatocellular carcinoma, hepatocellular cancer, risk factor, cause, etiology, case-control study. In the search of MEDLINE, the keywords of Chinese population, Chinese and China were added. Further studies were identified through scanning reference lists of relevant articles, reviews, and textbooks. Articles published in both English and Chinese were accepted. To eliminate irrelevant studies, the title and abstract of the articles were screened at first, and then the whole texts of selected paper were examined for further screening based the inclusive criteria.

Inclusion and exclusion criteria

Inclusion criteria in the meta-analysis included case-control studies investigating the risk factors for PLC in Chinese population, the data from the articles including the background of population and time investigated, the articles that reported original data or statistical results of odd ratio (OR) and its 95% confidence interval (95%CI), the studies based on similar diagnostic criteria of PLC.

Exclusion criteria in the meta-analysis were poor methodological quality^[2], the republished studies, and no sufficient data and/or results in the article.

Data selection and study appraisal

Data used in this study included year of publication, number of case and control, characteristics of patients and control

(gender, age, native place, and living place), suspected risk factor and its definition of exposure, diagnostic criterion of PLC, and outcomes (OR value and its 95%CI of each factor should be provided, if the article did not report the results in the form of OR, we calculated OR and its 95%CI based on the given data).

Two researchers extracted the data from each study independently and any disagreements were discussed for consensus. Quality of the study was assessed by the guideline of Lichtenstein^[2].

Statistical analysis

OR q test for heterogeneity was used to examine gross statistical heterogeneity among included studies. If K studies were included, $OR_i (i = 1, 2, \dots, K)$ was OR of the investigated factors in each study, OR_{ui} and OR_{li} were the upper and lower limit of its 95%CI respectively. V_i was variance calculated by the formula of $V_i = [\ln(OR_i/OR_{li})/1.96]^2$ or $V_i = [\ln(OR_{ui}/OR_i)/1.96]^2$. Weight (W_i) was calculated by $W_i = 1/V_i$. Supposed $y_i = \ln(OR_i)$ and $y_w = (\sum W_i y_i) / (\sum W_i)$. The heterogeneity among included studies was tested by $q = \sum [W_i (y_i - y_w)^2]$. If the q value was low ($P > 0.05$), the results of the included studies were considered as significant homogeneity, otherwise significant heterogeneity existed among studies^[3,4].

The association between investigated factors and PLC was presented as OR and its 95%CI. If the studies had no significant heterogeneity demonstrated by OR q test, fixed-effect model was used to calculate the combined OR and its 95%CI. Otherwise, random-effect model was used. Combined OR value greater than one indicated a risk factor for PLC. The significance of the combined OR was tested by $\chi^2 = (\sum W_i y_i)^2 / (\sum W_i)$ with $g = 1$ ^[3,4], and the significant level was $P = 0.05$.

Sensitivity analysis was performed through fixed-effect model and random-effect model. Coherence of the results from two models indicated a valid outcome^[4].

Funnel plot analysis was used to assess the potential bias, and its symmetry was tested through linear regression model. Intercept 95%CI of linear regression function spanning 0 and its significant level greater than 0.1 indicated symmetric funnel plot^[4].

RESULTS

Description of studies

Fifty-five of 190 identified studies were included in meta-analysis after the quality assessment of each study. They were published in Chinese in 1984-2002. The investigated people were from 24 cities located in 13 different provinces of China.

The investigated factors included liver diseases, family history, psychic status, past history of exposure to poison and style of living. The factors for liver diseases were from 26 studies of HBV infection, 15 of HCV infection, 9 of liver cirrhosis, and 20 of hepatitis history. There were 25 studies on family history of liver carcinoma. Psychological factors for PLC included 10 for negative living events, 6 for unstable emotions, and 6 for depressed characters. The past history of exposure to poison was from five studies of

pesticide and four of aflatoxin. The living style included nine factors: drinking (22 studies), smoking (15 studies), intake of musty food (3 studies), intake of pickle (5 studies), intake of bean product (4 studies), tea (4 studies), drinking water from pond (8 studies), drinking water from river (2 studies), and drinking water from well (5 studies).

Heterogeneity of studies

OR q test was carried out in included studies (Table 1). No significant heterogeneity existed among the studies on HCV infection, unstable emotion, past history of exposure to aflatoxin, and intake of musty food ($P > 0.05$). The remaining factors in the studies all had significant heterogeneity ($P < 0.05$).

Association of outcomes

Association between the factors and PLC was shown by combined OR and its 95%CI. If heterogeneity was significant, OR was combined with random-effect model, otherwise, fixed-effect model was used (Table 2). The OR and its 95%CI of five factors including past history of exposure to pesticide, intake of bean products, tea, drinking water from river and well had no statistical significance ($P > 0.05$). According to the value of OR, the strength of association in descending turn was liver cirrhosis, HBV infection, history of hepatitis, HCV infection, family history of liver carcinoma, depressed character, negative living events, unstable emotion, alcoholic, intake of musty food, aflatoxin, drinking water from pond, intake of pickle, and smoking, with their OR value greater than one, 95%CI beyond one. There was a statistical significance ($P < 0.05$).

Sensitive analysis

The combined OR and its 95%CI of each factor were calculated by both fixed-effect model and random-effect model, and coherence of the results was assessed. The factors of exposure to pesticide and drinking water from well showed conflicting results from two models (combined OR and its 95%CI of fixed-effect model were 1.69 (1.24 and 2.29) and 0.74 (0.58 and 0.96) respectively). Other factors showed similar results from two models.

Funnel plot

Since only two studies were involved in the factor of drinking water from river, funnel plot analysis was insignificant. According to the linear regression models of funnel plots, four factors including history of hepatitis, negative living events, smoking, and intake of pickle existed as asymmetric funnel plots with their intercept 95%CI beyond 0 and $P < 0.1$. Other factors showed symmetry funnel plots with their intercept 95%CI spanning 0 and $P > 0.1$ in their linear regression models.

DISCUSSION

A considerable number of chemical agents have been proved to be directly carcinogenic for liver malignant tumor in animal experiments, and also most likely in human beings^[5]. But still no evidence is presented as yet. It was reported that the risk factors for PLC include hepatitis viruses, liver

Table 1 Heterogeneity of investigated factors

Factors	Included studies	<i>q</i>	<i>P</i>
Liver diseases			
HBV infection	26	74.72	0.000 ^b
HCV infection	15	10.68	0.711
Liver cirrhosis	9	23.61	0.003 ^b
History of hepatitis	20	104.13	0.000 ^b
Family history			
Family history of PLC	25	96.95	0.000 ^b
Psychological factors			
Negative living events	10	25.54	0.002 ^b
Unstable emotion	6	3.46	0.630
Depressed character	6	12.69	0.027 ^a
Past history of exposure to poison			
Pesticide	5	16.99	0.002 ^b
Aflatoxin	4	3.47	0.325
Living style			
Alcoholic	22	82.13	0.000 ^b
Smoking	15	24.58	0.039 ^a
Intake of musty food	3	3.72	0.156
Intake of pickle	5	23.73	0.000 ^b
Intake of bean products	4	18.56	0.000 ^b
Tea	4	16.03	0.001 ^b
Drinking water from pond	8	649.10	0.000 ^b
Drinking water from river	2	9.05	0.003 ^b
Drinking water from well	5	10.44	0.034 ^a

The values of *q* shown are statistical values of OR *q* test. ^a*P*<0.05 vs significant difference. ^b*P*<0.01 vs very significant difference.

Table 2 Summary of the association between factors and PLC

Factors	Total case/control	Combined OR	95%CI	χ^2 (<i>g</i> = 1)	<i>P</i>
Liver diseases					
HBV infection	3 390/4 604	11.34	8.72-14.75	327.60	0.000 ^b
HCV infection	1 737/2 534	4.28	3.30-5.56	119.93	0.000 ^b
Liver cirrhosis	1 689/2 609	11.97	6.19-23.19	54.46	0.000 ^b
History of hepatitis	3 625/4 903	5.71	4.11-7.92	108.12	0.000 ^b
Family history					
Family history of PLC	3 681/4 932	3.49	2.68-4.53	87.24	0.000 ^b
Psychological factors					
Negative living events	1 688/2 096	2.65	1.69-4.15	17.90	0.000 ^b
Unstable emotion	1 502/2 086	2.20	1.74-2.77	44.48	0.000 ^b
Depressed character	1 355/1 777	3.07	2.10-4.47	33.99	0.000 ^b
Past history of exposure to poison					
Pesticide	755/969	1.55	0.82-2.93	1.84	0.175
Aflatoxin	327/327	1.80	1.44-2.25	26.90	0.000 ^b
Living style					
Alcoholic	3 207/3 983	1.88	1.53-2.32	35.60	0.000 ^b
Smoking	2 408/3 347	1.24	1.09-1.41	10.90	0.001 ^b
Intake of musty food	623/723	1.87	1.42-2.47	19.74	0.000 ^b
Intake of pickle	1 233/1 602	1.69	1.34-2.13	47.56	0.000 ^b
Intake of bean products	814/1 158	0.74	0.29-1.90	0.13	0.718
Tea	656/870	0.69	0.31-1.51	0.88	0.348
Drinking water from pond	1 561/1 614	1.77	1.09-2.87	8.65	0.003 ^b
Drinking water from river	379/437	1.41	0.38-5.19	0.27	0.603
Drinking water from well	636/856	0.79	0.45-1.36	7.99	0.392

The values of χ^2 shown are statistical values of significant test of combined OR. ^b*P*<0.01 vs significant difference.

diseases, mycotoxins or phytotoxins, nutrition, social drugs, metabolic diseases, chemical agents, inorganic substances, medication, and ionizing radiation. However, in 10–15% of patients, there is no risk factor for the development of PLC^[5]. This study investigated the association between possible risk factors and PLC in Chinese population by meta-analysis of case-control studies published in the past 37 years, and demonstrated the risk factors for PLC in Chinese population.

This study analyzed 19 suspected risk factors for PLC.

The combined outcomes showed that liver diseases were the most important factors for PLC with much a greater OR value than any other factor. Both liver cirrhosis and HBV infection were strongly associated with PLC, with their OR being 11.97 and 11.34 respectively (*P*<0.05). The association between HCV infection and PLC was moderate, with its OR being 4.28 (*P*<0.05). Though history of hepatitis was significantly associated with PLC, its funnel plot was asymmetric. Therefore this outcome might have bias, possibly due to the published bias, and heterogeneity from

the different definitions of history of liver diseases in the included studies. Family history of PLC was another risk factor for PLC, with its OR being 3.61 ($P < 0.05$), suggesting that people with family history of PLC have a higher risk. Poor psychological status can strengthen the risk for PLC. In this meta-analysis, the factors for unstable emotion and depressed character were significantly associated with PLC, with their OR being 2.20 and 3.07, respectively ($P < 0.05$). The funnel plot of negative living events was asymmetric though its combined OR was significant. The reason may be the published bias, and the conclusion on negative living events could not be made. In regard to exposure to poison, two factors including exposure to aflatoxin or pesticide were investigated. It was demonstrated that aflatoxin played an important role in PLC^[5]. In this meta-analysis, the outcome showed that aflatoxin was also a risk factor for PLC in Chinese population, with its OR being 1.80 ($P < 0.005$), but it seems to be trivial when compared to the factors for liver diseases, family history of PLC and poor psychological status. The results indicated that there was no significant association between exposure to pesticide and PLC, with its OR being 1.55 ($P > 0.05$). Furthermore, this result was unreliable because it was conflicting in sensitivity analysis. Hence, it is not clear whether exposure to pesticide is a risk factor for PLC. The living habits of drinking, intake of musty food and drinking water from pond were all significantly associated with PLC (OR was 1.88, 1.87, and 1.77 respectively, $P < 0.05$), suggesting that they may enhance the risk for PLC. Though the factors of both smoking and intake of pickle had a significant combined OR (1.24 and 1.69 respectively, $P < 0.05$), it was unable to draw conclusions because of the bias demonstrated by their asymmetric funnel plots ($P < 0.1$). Drinking water from river was not significantly associated with PLC (OR = 1.41, $P > 0.05$) and its bias was difficult to analyze by funnel plot due to its limited number of the included studies. Thus it is unknown whether it is a risk factor. The ORs of intake of bean products, tea and drinking water from well were all less than 1 (OR being 0.74, 0.69, and 0.79 respectively, $P > 0.05$). These results could not demonstrate that they are protective factors for PLC. Furthermore, the result of drinking water from well was unreliable because the results were conflicting in sensitivity analysis.

Meta-analysis is a tool, but bias in meta-analysis can cause invalid results. In this study, case-control studies were included in meta-analysis. Considering the design of the included studies, validity of their results was inferior to that of prospective studies. Thus, the significance of conclusion from this meta-analysis is limited due to the design of the included studies. Since lack of qualified cohort studies on the risk factor for PLC in Chinese population, the result of this meta-analysis is valuable for further research. Test of heterogeneity is a formal statistical analysis for examining if the observed variation in study results is compatible with

the variation expected by chance^[4]. When heterogeneity is statistically significant ($P < 0.05$), the observed different results should be explained individually. Nineteen factors in the included studies were involved in this investigation, fifteen of which had significant heterogeneity. The various risk factors for PLC were possibly interactive. When an investigated factor is involved in the included studies, the difference between other risk factors and their interaction is not easy to control among studies, thus leading to the heterogeneity. Furthermore, different studies are usually undertaken in different ways, but it is hard to attribute heterogeneity to any single factor^[4]. Since the differences in the included studies are of practical significance, random-effect model is used for the factor with significant heterogeneity to make a more conservative estimation of the combined result. In the current study, some original articles were unable to be used because of their deficient data. It is difficult to estimate the effect of these missing data on the combined results. Sensitivity analysis can test the reliability of the outcomes by assessing coherence of the combined results from fixed-effect model and random-effect model. In this study, most factors passed sensitivity analysis successfully (17/19), thus proving the reliability of the results in this meta-analysis. Publication bias is associated with funnel plot asymmetry. However, the reasons for asymmetric funnel plot may include publication bias and others such as selection biases, poor methodology of smaller studies, true heterogeneity and chance^[4]. Since the funnel plots of history of hepatitis, negative living events, smoking, and intake of pickle were found asymmetric, conclusions about these factors should not be drawn due to the bias.

In conclusion, the main risk factors for PLC in Chinese population are related to liver diseases, family history of liver carcinoma, poor psychological status, aflatoxin, and bad living style. Liver diseases are most important in all these factors. Control of HBV infection, HCV infection, and liver cirrhosis is the essential measure for the prevention of PLC. In addition, balanced psychological status, avoidance of musty food or food polluted by aflatoxin-contaminated food, and no alcoholic can reduce the risk for PLC.

REFERENCES

- 1 Hall AJ, Wild CP. Liver cancer in low and middle income countries. *BMJ* 2003; **326**: 994-995
- 2 Lichtenstein MJ, Mulrow CD, Elwood PC. Guidelines for reading case-control studies. *J Chron Dis* 1987; **40**: 893-903
- 3 Me HY, Shi LY. Meta-analysis of the risk factors on lung cancer in Chinese people. *Zhonghua Liuxingbingxue Zazhi* 2003; **24**: 45-48
- 4 Zhou XY, Fang JQ, Yu CH, Xu ZL, Lu Y. Meta analysis In: Lu Y, Fang JQ. Advanced medical statistics. *Singapore World Scientific Publishing Co Pte Ltd* 2003: 233-318
- 5 Erwin Kuntz, Hans-Dieter Kuntz. Malignant liver tumours In: Erwin Kuntz, Hans-Dieter Kuntz, eds. *Hepatology: principles and practice*. New York: Springer-Verlag Berlin Heidelberg 2002: 699-730

• BRIEF REPORTS •

Effects of sulfasalazine on biopsy mucosal pathologies and histological grading of patients with active ulcerative colitis

Ying-Qiang Zhong, Hua-Rong Huang, Zhao-Hua Zhu, Qi-Kui Chen, Jun Zhan, Lian-Chun Xing

Ying-Qiang Zhong, Zhao-Hua Zhu, Qi-Kui Chen, Jun Zhan, Department of Gastroenterology, the Second Affiliated Hospital, Sun Yat-Sen University, Guangzhou 510120, Guangdong Province, China

Hua-Rong Huang, Department of Pediatrics, the Second Affiliated Hospital, Sun Yat-Sen University, Guangzhou 510120, Guangdong Province, China

Lian-Chun Xing, Department of Pathology, the Second Affiliated Hospital, Sun Yat-Sen University, Guangzhou 510120, Guangdong Province, China

Correspondence to: Ying-Qiang Zhong, Department of Gastroenterology, the Second Affiliated Hospital, Sun Yat-Sen University, Guangzhou 510120, Guangdong Province, China. zhongyingqiang@21cn.com

Telephone: +86-20-81332598

Received: 2004-07-19 Accepted: 2004-09-19

Abstract

AIM: To investigate the mechanisms of sulfasalazine (SASP) in the treatment of ulcerative colitis (UC).

METHODS: Changes of pathological signs and histological grading of 106 patients with active UC were observed before and after the treatment with SASP, 1 g, thrice daily for 6 wk.

RESULTS: The effect of SASP on the vasculitis in lamina propria was 48.2% and 17.4% in the mild active UC ($P < 0.001$) and 68% and 26.7% in the moderate active UC ($P < 0.001$) before and after treatment. Fibroid necrosis of vessel wall was found in one case of mild UC and two cases of moderate UC before treatment and was not found after treatment. No thrombosis was found in mild UC before and after treatment, while thrombosis was found in one case of moderate UC before treatment. The effect on mucosal glandular abnormality was 30.4% and 13.0% in mild UC ($P < 0.05$), and 42% and 40% in moderate UC ($P > 0.05$) before and after treatment. The rate of eosinophil infiltration was 98.2% and 80.4% in mild UC ($P < 0.01$), and 100% and 91.1% in moderate UC ($P < 0.05$) before and after treatment. The effect on crypt abscess was 21.4% and 4.4% in mild UC ($P < 0.05$), and 48% and 13.3% in moderate UC ($P < 0.001$) before and after treatment. The effect on mucosal pathohistological grading was 2.00 ± 0.84 and 0.91 ± 0.46 in mild UC ($P < 0.001$), and 2.49 ± 0.84 and 1.31 ± 0.75 in moderate UC ($P < 0.001$) before and after treatment.

CONCLUSION: SASP can improve small vessel lesions and crypt abscesses and reduce neutrophilic and eosinophilic leukocyte infiltration in inflammatory mucosa of UC.

© 2005 The WJG Press and Elsevier Inc. All rights reserved.

Key words: Ulcerative colitis; Biopsy mucosae; Sulfasalazine; Pathology

Zhong YQ, Huang HR, Zhu ZH, Chen QK, Zhan J, Xing LC. Effects of sulfasalazine on biopsy mucosal pathologies and histological grading of patients with active ulcerative colitis. *World J Gastroenterol* 2005; 11(28): 4435-4438
<http://www.wjgnet.com/1007-9327/11/4435.asp>

INTRODUCTION

Ulcerative colitis (UC) is an inflammatory bowel disease mainly characterized by inflammatory changes in mucosa and submucosa of the rectum and colon. The continuous inflammatory lesions commonly involve rectum and extend to the proximal colon and even to pancolitis. The main clinical manifestations are chronic relapsing diarrhea, mucopurulent hematochezia and abdominal pain.

Though sulfasalazine (SASP) has been used to treat active UC for more than 60 years, its mechanisms have not been completely clarified^[1]. The purpose of the present study was to investigate the mechanisms of SASP in treatment of active UC.

MATERIALS AND METHODS

Patients^[2]

Following patients were enrolled in the study: patients aged 14-69 years with chronic or relapsing diarrhea, mucopurulent hematochezia, abdominal pain and systemic symptoms, and extraintestinal presentations of their joints, skin, eyes, mouth, liver, and gall bladder, as well as those with inflammatory lesions of rectum and colon. Patients with bacillary or amoebic dysentery, fungous or tuberculous colitis, ischemic bowel disease, radiation colitis, Crohn's disease and large bowel cancer and those who did not complete the course of treatment due to drug allergy or quitted the study were excluded.

Objects of study

A total of 106 patients (50 males and 56 females) with active UC were enrolled in the study^[2]. The ratio of male to female was 0.98:1. Their age was 20-66 years (41.6 ± 11.4 years). Fifty-six cases (22 males and 34 females) had mild UC, and their age was 22-66 years (41.5 ± 10.6 years). Fifty cases (28 males and 22 females) had moderate UC, and their age was 20-65 years (42.8 ± 12.1 years). There were no significant

differences in their age, ratio of male to female and clinical types between the two groups ($P>0.05$). Forty-six of fifty-six cases of mild UC and 45 of 50 cases of moderate UC were followed up.

Treatment

The patients received 1 g SASP thrice daily for 6 wk. Endoscopy was carried out before and after treatment. Biopsy specimens were taken at the same sites before and after treatment.

Grouping

Patients were divided into two groups according to the criteria of mild and moderate UC^[2].

Endoscopy and mucosal biopsy

The colon and rectum were examined with electronic colonoscope and 3-5 biopsy specimens were taken from the most obvious inflammatory lesions on the left side of colon or rectum. The specimens were fixed in 40 g/L formaldehyde and embedded in paraffin wax, then cut into continuous sections and stained with hematoxylin and eosin. Pathologic morphometry was analyzed by one pathologist with double blind method. The final morphologic results were obtained from the average of three observations under a high power microscope.

Observed pathological items^[3-6]

The following pathological items were observed: small vessel lesions in lamina propria such as vasculitis, fibroid necrosis of vessel wall, thrombosis and focal hemorrhage; mucosal gland lesions including glandular abnormality, epithelial cell regeneration, atypical hyperplasia, goblet cell depletion (GCD) and Paneth cell metaplasia (PCM); inflammatory cell infiltration in mucosal epithelium such as lymphocyte hyperplasia, lymphoid follicular formation, eosinophils (Eos) and plasmacytes; cellular stromal lesions including granulation tissue formation, fiber tissue hyperplasia and pseudo-polyp; crypt abscess.

Pathohistological grading criteria^[7,8]

Grade 0: no neutrophilic leukocyte infiltration in lamina

propria; grade I: a small number of neutrophilic leukocytes (<10 /HPF) in lamina propria with minimal infiltration of crypts; grade II: prominent neutrophilic leukocytes ($10-50$ /HPF) in lamina propria with infiltration of more than 50% of crypts; grade III: a large number of neutrophilic leukocytes (>50 /HPF) in lamina propria with crypt abscesses; grade IV: significant acute inflammation with ulcerations in lamina propria.

Statistical analysis

Results were expressed as mean \pm SD. The data of two groups were analyzed using independent and paired t test. The counted data were expressed as rate or ratio, and analyzed by χ^2 test. All data were analyzed with SPSS10.0 software.

RESULTS

Effects of SASP on small vessel lesions in lamina propria

No significant changes were found in all specimens before and after SASP treatment ($P>0.05$). The effect of SASP on vasculitis in lamina propria was 48.2% and 17.4% in mild active UC ($P<0.001$), and 68% and 26.7% in moderate active UC ($P<0.001$) before and after treatment. Fibroid necrosis of vessel wall was found in one case of mild UC and two cases of moderate UC before treatment but was not found after treatment. Thrombosis was not found in mild UC before and after treatment, but was found in one case of moderate UC before treatment and not found after treatment (Table 1).

Effect of SASP on mucosal gland lesions

The effect of SASP on mucosal glandular abnormality was 30.4% and 13.0% in mild UC ($P<0.05$), and 42% and 40% in moderate UC ($P>0.05$) before and after treatment. No significant effect of SASP on epithelial cell regeneration, atypical hyperplasia, GCD, and PCM was observed before and after treatment ($P>0.05$, Table 2).

Effects of SASP on inflammatory cell infiltration

The rate of Eos infiltration was 98.2% and 80.4% in mild UC ($P<0.01$), and 100% and 91.1% in moderate UC ($P<0.05$)

Table 1 Effect of SASP on small vessel lesions in lamina propria (n%)

	n	Focal hemorrhage	Vessel inflammation	Fibroid necrosis	Thrombosis
Before treatment (mild)	56	41 (73.2)	27 (48.2)	1 (1.8)	0
After treatment (mild)	46	25 (54.3)	8 (17.4)	0	0
Before treatment (moderate)	50	32 (64.0)	34 (68.0)	2 (4.0)	1 (2.0)
After treatment (moderate)	45	22 (48.9)	12 (26.7)	0	0

Table 2 Effect of SASP on mucosal gland lesions (n%)

	n	Glandular abnormality	Epithelial cell regeneration	Atypical hyperplasia	GCD	PCM
Before treatment (mild)	56	17 (30.4)	19 (34.0)	8 (14.3)	3 (5.4)	0 (0)
After treatment (mild)	46	6 (13.0)	13 (28.3)	2 (4.4)	2 (4.4)	1 (2.2)
Before treatment (moderate)	50	21 (42.0)	15 (30.0)	15 (30.0)	12 (24)	2 (4.0)
After treatment (moderate)	45	18 (40.0)	7 (15.6)	8 (17.8)	6 (13.3)	0 (0)

Table 3 Effects of SASP on inflammatory cell infiltration (n%)

	n	Lymphocyte hyperplasia	Lymphoid follicle	Eos infiltration	Plasmacyte infiltration
Before treatment (mild)	56	42 (75.0)	44 (78.6)	55 (98.2)	50 (89.3)
After treatment (mild)	46	30 (65.2)	32 (69.6)	37 (80.4)	37 (80.4)
Before treatment (moderate)	50	37 (74.0)	35 (70.0)	50 (100)	46 (92)
After treatment (moderate)	45	32 (71.1)	26 (57.8)	41 (91.1)	39 (86.7)

before and after treatment. No significant effects of SASP on lymphocyte hyperplasia, lymphoid follicular formation and plasmacyte infiltration were observed before and after treatment ($P>0.05$, Table 3).

Effect of SASP on cellular stromal lesions

No significant effect of SASP on granulation tissue formation, fiber tissue hyperplasia and pseudo-polyp was found before and after treatment ($P>0.05$).

Effect of SASP on crypt abscess

The effect of SASP on crypt abscess was 21.4% and 4.4% in mild UC ($P<0.05$), and 48% and 13.3% in moderate UC ($P<0.001$) before and after treatment.

Effect of SASP on mucosal pathohistological grading

The effect of SASP on mucosal pathohistological grading was 2.00 ± 0.84 and 0.91 ± 0.46 in mild UC ($P<0.001$), and 2.49 ± 0.84 and 1.31 ± 0.75 in moderate UC ($P<0.001$) before and after treatment (Table 4).

Table 4 Effect of SASP on mucosal pathohistological grade (mean \pm SD)

	n	Mild	n	Moderate
Before treatment	46	2.00 ± 0.84	45	2.49 ± 0.84
After treatment	46	0.91 ± 0.46	45	1.31 ± 0.75

DISCUSSION

The common drugs used in treatment of patients with active UC are still SASP and glucocorticoids. Sangfelt *et al.*^[9], used prednisolone enema to treat active UC and showed that the release quantity of neutrophil myeloperoxidase (MPO), eosinophil cationic protein (ECP) and eosinophil peroxidase (EPO) in enema liquid is correlated with their clinical, endoscopic and histological activities before treatment. When the patients respond to the treatment, their MPO markedly decreases, but ECP and EPO do not decrease. The results suggest that glucocorticoids can reduce mucosal neutrophil infiltration, but cannot improve Eos infiltration. The increase of MPO is correlated with neutrophil-activated peptide-interleukin 8 and tumor necrosis factor- α ^[10].

The mechanism of SASP against active UC is that it depresses the production of leukotrienes (LTs), prostaglandin and free radicals^[1,11]. SASP plays a role in the treatment of active UC by interfering with synthesis of inflammatory media^[12]. SASP can depress immune responses of immune cells and prevent relapse of UC. But the mechanisms have not been completely clarified^[1]. Wright *et al.*^[13], used

20 mg/100 mL sucralfate once or twice daily to treat distal active UC for 4 wk and showed that it can improve the clinical, endoscopic and histological scores.

The present study using oral SASP to treat active UC for 6 wk showed that it could improve small vessel inflammation and crypt abscess in lamina propria of inflammatory mucosa, decrease neutrophil and Eos infiltration in mucosal epithelium, and decline the histological grading after treatment. There was no fibroid necrosis of vessel wall and thrombosis in all specimens after treatment. Significant effect of SASP on mucosal glandular abnormality, lymphocyte hyperplasia and lymphoid follicular formation, plasmacytes infiltration and cellular stromal lesions was not observed.

The insufficient mucosal blood supply and submucosal vessel lesions are also the pathogenic factors for active UC. SASP could improve mucosal small vessel lesions, crypt abscess, mucopurulent hematochezia and mucosal inflammation in patients with active UC, thus improving and promoting the healing of inflammatory mucosa.

One cause of inflammatory lesions include all kinds of hydrolase and cationic protein released from neutrophil granules of damaged local tissues, which play an important role in the course of inflammation of type III hypersensitivity^[14]. The activated neutrophils produce active oxygen and several active molecules that promote occurrence and development of inflammation^[15]. SASP could decrease neutrophil infiltration and histological grading, thus decreasing the production of inflammatory factors and improving inflammation.

In this study, SASP obviously decreased mucosal Eos infiltration. Mucosal Eos infiltration is associated with chronic intestine inflammation^[16]. Eos collected from the inflammatory mucosa is attracted by immune complex and Eos chemokine releases from mast cells. Eos could synthesize prostaglandins E and E₂, which restrain the synthesis of histamine, neutralize hypersusceptibility and inflammatory reactants. Eos accompanying degranulation phenomena result from allergic reaction by main degranulation way^[17]. The number of Eos not only reflects the degree of inflammation^[18], but also is an important index of prognosis^[19]. There are more acidophil granules in Eos's cytoplasm, containing four toxic cationic proteins: alkaline protein, ECP, neurotoxin and peroxidase, all of which have toxic effect on normal cells^[14]. Raab *et al.*^[20], also confirmed that there are more Eos infiltrating lamina propria of active UC, and ECP obviously increases. The activation or degranulation of Eos is correlated with mucosal inflammatory responses. The changes in intestinal mucosa resulted from Eos infiltration in the inflammatory mucosa that are activated and cause mucosal lesions during degranulation and release

of ECP^[21].

In conclusion, SASP can effectively treat patients with active UC and improve small vessel lesions, crypt abscesses, and decrease neutrophil and Eos infiltration.

REFERENCES

- 1 **Hu PJ**. Ulcerative colitis. In: Ye RG: Internal medicine, 5nd ed. Beijing: *People Healthy Publishing House* 2000: 428-434
- 2 The digestive academy of Chinese medical academy. Suggestion of diagnosis and treatment regulation of inflammatory bowel disease. *Zhonghua Xiaohua Zazhi* 2001; **21**: 236-239
- 3 **Gong EC**, Liu CL, Shi XY. Pathological diagnosis and the differential diagnosis of inflammatory bowel disease. *Zhonghua Xiaohua Zazhi* 2001; **21**: 233
- 4 **Ou YQ**, Zhang GY, Li SH. Diagnostic study of chronic non-special ulcerative colitis: in 66 cases. *Zhonghua Xiaohua Zazhi* 1987; **7**: 142-144
- 5 **Xia B**, Zhou Y, Luo N, Chen DJ, Zhou ZY. Biopsy and diagnosis of inflammatory bowel disease. *Zhonghua Xiaohua Beijing Zazhi* 1996; **13**: 276-278
- 6 **Qu HS**, Lv YM, Sun YK, Zheng J. Clinical pathological analysis of 35patients with chronic non-special ulcerative colitis. *Beijing Yixueyuan Xuebao* 1981; **13**: 121-124
- 7 **Truelove SC**, Richards WC. Biopsy studies in ulcerative colitis. *Br Med J* 1956; **6**: 1315-1318
- 8 **Pullan RD**, Rhodes J, Ganesh S, Mani V, Morris JS, Willian GT, Newcombe RG, Russell MA, Feyerabend C, Thomos GA. Tansdermal nicotine for active ulcerative colitis. *N Engl J Med* 1994; **330**: 811-815
- 9 **Sangfelt P**, Carlson M, Thorn M, Loof L, Raab Y. Neutrophil and eosinophil granule proteins as markers of response to local prednisolone treatment in distal ulcerative colitis and proctitis. *Am J Gastroenterol* 2001; **96**: 1085-1090
- 10 **Raab Y**, Gerdin B, Ahlstedt S, Hallgren R. Neutrophil mucosal involvement is accompanied by enhanced local production of interleukin-8 in ulcerative colitis. *Gut* 1993; **34**: 1203-1206
- 11 **Li DG**, Liu YL, Liu HB. The abstract of academic conference of chronic non-infective intestinal disease in China. *Zhonghua Xiaohua Zazhi* 1993; **13**: 351-353
- 12 **Zheng JJ**. Ulcerative colitis. In: Zheng JJ, Inflammatory bowel disease, 1nd ed. *Shanghai: Shanghai Publishing House of Literature of Science and Technology* 1998: 24-43
- 13 **Wright JP**, Winter TA, Candy S, Marks IS. Sucralfate and methylprednisolone enemas in active ulcerative colitis: a prospective, single-blind study. *Dig Dig Sci* 1999; **44**: 1899-1901
- 14 **Li BQ**. Immune system, immune organ and immune cell. In: Wu MY, Liu GZ, Medical immunology, 3nd ed. *Hefei: Publishing House of Chinese University of Science and Technology* 1999: 45-46
- 15 **Oshitani N**, SawaY, Hara J, Adachi K, Nakamura S, Matsumoto T, Arakawa T, Kuroki T. Functional and phenotypical activa-tion of leucocytes in inflamed human colonic mucosa. *J Gastroenterol Hepatol* 1997; **12**: 809-814
- 16 **Bischoff SC**, Wedemeyer J, Herrmann A, Meier PN, Trantwein C, Cetin Y, Maschek H, Stolte M, Gebel M, Manns MP. Quantitative assessment of intestinal eosinophils and mast cells in inflammatory bowel disease. *Histopathology* 1996; **28**: 1-13
- 17 **Wang ZM**, Xu YJ, Shi P. Observation on eosinophilic degranulation in chronic ulcerative colitis. *Zhongguo Gangchangbing Zazhi* 1994; **14**: 6-7
- 18 **Zhong YQ**, Huang HR, Zeng ZY, Xing LC. Application of eosinophils grading for the assessment of severity of patients with active ulcerative colitis. *Zhonghua Xiaohua Zazhi* 2004; **24**: 559-560
- 19 **Deng ZH**, Xu DY. Laboratory items of assessment of activity and treatment effect of chronic ulcerative colitis. *Zhonghua Xiaohua Zazhi* 1992; **12**: 292-293
- 20 **Raab Y**, Fredens K, Gerdin B, Hallgren R. Eosinophil activation in ulcerative colitis: studies on mucosal release and localization of eosinophil granule constituents. *Dig Dig Sci* 1998; **43**: 1061-1070
- 21 **Makiyama K**, Kanzaki S, Yamasaki K, Zea-Itiarte W, Tsuji Y. Activation of eosinophils in the pathophysiology of ulcerative colitis. *J Gastroenterol* 1995; **30**(Suppl 8): 64-69

Science Editor Wang XL and Guo SY Language Editor Elsevier HK

Liposome transfected to plasmid-encoding endostatin gene combined with radiotherapy inhibits liver cancer growth in nude mice

Ai-Qing Zheng, Xian-Rang Song, Jin-Ming Yu, Ling Wei, Xing-Wu Wang

Ai-Qing Zheng, Tianjin Medical University, Tianjin 300070, China
Ai-Qing Zheng, Xian-Rang Song, Ling Wei, Xing-Wu Wang, Cancer Research Center, Shandong Cancer Hospital, Jinan 250117, Shandong Province, China

Jin-Ming Yu, Department of Radiation Oncology, Shandong Cancer Hospital, Jinan 250117, Shandong Province, China

Correspondence to: Dr. Ai-Qing Zheng, Cancer Research Center, Shandong Cancer Hospital, Jinan 250117, Shandong Province, China. aiqingzheng@yahoo.com.cn

Telephone: +86-531-7984777-82423

Received: 2004-09-23 Accepted: 2004-10-04

CONCLUSION: Endostatin not only significantly suppresses tumor growth but also enhances the antitumor efficacy of radiation therapy in human carcinoma xenograft.

© 2005 The WJG Press and Elsevier Inc. All rights reserved.

Key words: Endostatin; Human liver carcinoma; Radiotherapy; Gene therapy

Zheng AQ, Song XR, Yu JM, Wei L, Wang XW. Liposome transfected to plasmid-encoding endostatin gene combined with radiotherapy inhibits liver cancer growth in nude mice. *World J Gastroenterol* 2005; 11(28): 4439-4442
<http://www.wjgnet.com/1007-9327/11/4439.asp>

Abstract

AIM: To evaluate whether intratumoral injection of liposome-endostatin complexes could enhance the antitumor efficacy of radiation therapy in human liver carcinoma (BEL7402) model.

METHODS: Recombinant plasmid pcDNA3.End was transfected into human liver carcinoma cell line (BEL7402) with lipofectamine to produce conditioned medium. Then BEL7402 cells and human umbilical vein endothelial cells (HUVECs) were treated with the conditioned medium. Cell cycle and apoptosis were analyzed by flow cytometer and endothelial cell proliferation rates were determined by MTT assay. The antitumor efficacy of endostatin gene combined with ionizing radiation in mouse xenograft liver tumor was observed.

RESULTS: Endostatin significantly suppressed the S phase fraction and increased the apoptotic index in HUVECs. In contrast, endostatin treatment had no effect on BEL7402 cell apoptosis ($2.1 \pm 0.3\%$ vs $8.9 \pm 1.3\%$, $t = 8.83$, $P = 0.009 < 0.01$) or cell cycle distribution ($17.2 \pm 2.3\%$ vs $9.8 \pm 1.2\%$, $t = 4.94$, $P = 0.016 < 0.05$). The MTT assay showed that endostatin significantly inhibited the proliferation of HUVECs by 46.4%. The combination of local endostatin gene therapy with radiation therapy significantly inhibited the growth of human liver carcinoma BEL7402 xenografts, the inhibition rate of tumor size was 69.8% on d 28 compared to the untreated group. The tumor volume in the pcDNA3.End combined with radiation therapy group ($249 \pm 83 \text{ mm}^3$) was significantly different from that in the untreated group ($823 \pm 148 \text{ mm}^3$, $t = 5.86$, $P = 0.009 < 0.01$) or in the pcDNA3 group ($717 \pm 94 \text{ mm}^3$, $t = 6.46$, $P = 0.003 < 0.01$). Endostatin or the radiation alone also inhibited the growth of liver tumor *in vivo*, but their inhibition effects were weaker than those of endostatin combined with radiation, the inhibition rates on d 28 were 44.7% and 40.1%, respectively.

INTRODUCTION

Tumors are dependent on angiogenesis for sustained growth^[1]. Endostatin, an endogenous antiangiogenic agent, is a M_r 20 000 COOH-terminal fragment of collagen XVIII. It is a potent inhibitor of angiogenesis *in vitro*, and has significant antitumor effects in a variety of preclinical tumor models^[2,3]. Endostatin specifically inhibits endothelial cell proliferation without direct effects on tumor cell or non-neoplastic cell growth^[4-7], whose overexpression can lead to primary tumor regression and growth inhibition^[8].

Most therapeutic investigations of endostatin utilized the purified protein, but the protein purification process is difficult and may denature endostatin. For maintaining therapeutically effective serum levels the protein must be repeatedly used because it has a short half-life *in vivo*. One possible approach to overcome this problem may be the utilization of gene therapy strategy. Studies using viral vectors to deliver endostatin gene have demonstrated its efficacy in treatment of mouse tumor models^[9-11].

Although antiangiogenic therapies have shown significant antitumor effects in preclinical investigations, angiogenesis inhibitors cannot achieve tumor cures on their own. Antiangiogenic strategies in combination with conventional anticancer approaches may achieve better results. The involvement of antiangiogenic agents during the course of radiotherapy have been shown to produce significant therapeutic effects^[12-15].

In this study, we investigated whether intratumoral injection of liposome-endostatin complexes could enhance the treatment efficacy of ionizing radiation in a human liver carcinoma (BEL7402) model.

MATERIALS AND METHODS

Plasmid and cell lines

The plasmid pcDNA3.End containing a synthetic rat insulin leader sequence and the full-length mouse endostatin cDNA was kindly provided by Dr. Wang Jianli (Shandong Medical University, Jinan, China). The synthetic rat insulin leader was cloned in front of the endostatin gene. Human liver carcinoma cell line BEL7402 and human umbilical vein endothelial cell line (HUVEC) were kept in our laboratory. HUVECs and BEL7402 cells were maintained in DMEM (Gibco) containing 10% FBS.

In vitro transfection and production of conditioned endostatin medium

BEL7402 cells were grown in 6-well plates at the density of 2×10^5 cells/well to 50-80% confluence, then transfected with 10 μ L of lipofectamine (Invitrogen) mixed with 4 μ g of plasmid (pcDNA3.End or pcDNA3) as described by the Invitrogen protocol. After 24 h transfection, the cells were extensively rinsed with PBS and incubated in serum-free DMEM for another 24 h. The conditioned media were collected, centrifuged and cell debris was cleared off. Endostatin in the culture media was measured with a murine endostatin enzyme immunoassay kit (Chemicon Inc.). The conditioned media were concentrated 20-fold with Amicon membranes (Amicon Inc.), and endostatin protein levels were determined by immunoassay before being stored at -80°C for further use.

Cell cycle assay

BEL7402 cells and HUVECs were plated in 6-well plates at the density of 2×10^5 cells/well and allowed to attach overnight. The cells were treated with conditioned medium containing certain concentration of endostatin and 10% FBS after removal of the medium. Forty-eight hours later, the cells were trypsinized, counted and fixed in 50% ethanol overnight, then treated with PBS (containing 1 g/L RNase) for 30 min. Samples were washed with PBS twice and resuspended in PBS at a concentration of 1×10^6 cells/mL. The cells were stained with PI in darkness for 30 min and cell cycle distribution was analyzed with a flow cytometer (Becton-Dickinson FACS Calibur).

Apoptosis assay

BEL7402 cells and HUVECs were cultured in 6-well plates at the density of 2×10^5 cells/well and incubated for 24 h. The medium was replaced with 2 mL of conditioned medium containing certain concentration of endostatin and 10% FBS. After being incubated for 48 h, the cells were trypsinized, counted, washed twice with cold PBS and then resuspended in $1 \times$ binding buffer at a concentration of 1×10^6 cells/mL. Five microliters of annexin V-FITC and five microliters of PI were added. The cells were gently vortexed and incubated for 15 min at RT in the dark, and then 400 μ L of $1 \times$ binding buffer was added. Apoptosis was analyzed with a flow cytometer.

Endothelial cell proliferation assay

HUVECs were incubated in 96-well dishes at the density of 10^4 cells/well and allowed to attach overnight. The

medium was then replaced with 20 μ L of conditioned medium and incubated for 30 min. Eighty microliters of DMEM containing with 10% FBS and 1 μ g/L bFGF (Sigma) were then added. After the cells were incubated for 48 h, 20 μ L MTT solution (5 g/L) was added. Then, 4 h later, 100 μ L 100 g/L SDS was added. After being vortexed gently for 10 min, the number of cells was quantified by colorimetric MTT assay.

In vivo treatment of tumor cells by liposome-DNA complex injection combined with radiation therapy

Female nude mice aged 4-6 wk were obtained from Animal Center of Shandong Medical University and fed with a standard rodent diet. To establish xenografts, animals were subcutaneously injected into the right flank with 1×10^6 BEL7402 cells suspended in 200 μ L 0.9% saline. Seven days after the injection of tumor cells, the mice were randomly divided into five treatment groups: untreated, empty vector (Lip-pcDNA3), Lip-pcDNA3.End, pcDNA3.End combined with radiation, and radiation. Six mice were enrolled in each group. To deliver the gene therapy, each mouse in groups 2, 3, and 4 received three intratumoral injections of liposome-DNA complex which consisted of 40 μ L lipofectamine and 20 μ g of DNA (1 g/L) and 40 μ L 0.9% saline on d 7, 14, and 21 after the injection of tumor cells. Irradiations were performed using a 6 MV Varian 2100 C linear accelerator, operating a single dose of 10 Gy 7 d after injection of tumor cells. Before irradiation, the mice were confined in plastic containers. The animals' tumor-bearing sites extended through openings in the containers allowing the tumors to be irradiated locally. Tumors were measured every 3-4 d. Tumor response to treatment was determined by growth delay assay. The tumor volume was calculated by the formula: tumor volume = $ab^2 \times 0.52$, where a is the length, and b is the width.

RESULTS

In vitro endostatin quantification

Unconcentrated media (100 μ L) collected from BEL7402 cells transfected with pcDNA3.End and pcDNA3 were measured with a murine endostatin enzyme immunoassay kit. The experiment showed that BEL7402 cells transfected with pcDNA3.End efficiently secreted endostatin protein into the culture media. Endostatin levels were 486.2 ± 56.5 mg/L in conditioned media from BEL7402 cells transfected with pcDNA3.End, and 6.8 ± 2.6 mg/L in conditioned media from BEL7402 cells transfected with pcDNA3. There were significant differences in endostatin levels between the two groups ($t = 14.68$, $P = 0.005 < 0.01$, Figure 1).

Endostatin-affected HUVEC cell cycle and apoptosis

After being treated with conditioned medium, compared to conditioned medium from BEL7402 cells transfected with pcDNA3, conditioned medium from BEL7402 cells transfected with pcDNA3.End significantly suppressed the S phase fraction ($17.2 \pm 2.3\%$ vs $9.8 \pm 1.2\%$, $t = 4.94$, $P = 0.016 < 0.05$) and increased the apoptotic index ($2.1 \pm 0.3\%$ vs $8.9 \pm 1.3\%$, $t = 8.83$, $P = 0.009 < 0.01$) in HUVECs. In contrast, after being treated with the two-conditioned media respectively,

there were no differences in BEL7402 cell apoptosis or cell cycle distribution, suggesting that endostatin treatment had no effect on BEL7402 tumor cell apoptosis or cell cycle distribution.

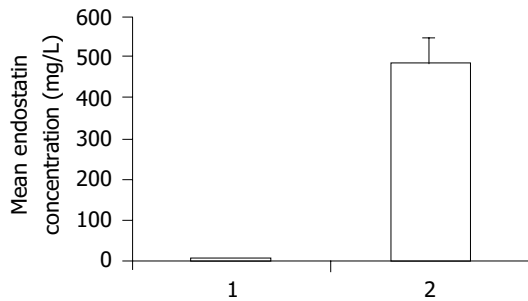


Figure 1 Mean concentration of endostatin protein in supernatant. 1: Secretion of endostatin by BEL-7402 cells transfected with pcDNA3; 2: secretion of endostatin by BEL-7402 cells transfected with pcDNA3.End.

Endostatin-inhibited endothelial cell proliferation

After 24 h incubation with conditioned media, endostatin-inhibited HUVECs proliferation by $46.4 \pm 9.7\%$, while the conditioned media derived from cultures of BEL7402 cells transfected with pcDNA3 control vector did not affect endothelial cell proliferation, the inhibition rate was $8.7 \pm 0.5\%$ ($t = 6.72$, $P = 0.02 < 0.05$, Figure 2).

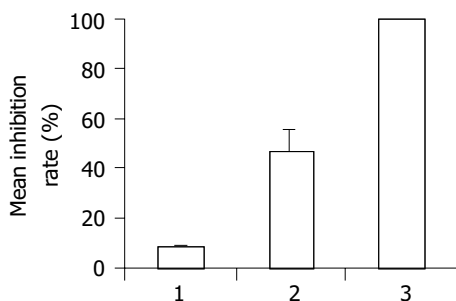


Figure 2 HUVEC proliferation rates inhibited by endostatin. 1: Proliferation rate inhibited by conditioned media derived from cultures of BEL7402 cells transfected with pcDNA3; 2: proliferation rate inhibited by conditioned media derived from cultures of BEL7402 cells transfected with pcDNA3.End; 3: control group.

Endostatin gene therapy combined with radiation-inhibited tumor growth in nude mice

As shown in Figure 3, tumors treated with Lip-pcDNA3. End combined with radiation group grew very slowly in nude mice, the inhibition rate of tumor size was 69.8% on d 28 compared to untreated group. The tumor volume of the pcDNA3.End combined with radiation group ($249 \pm 83 \text{ mm}^3$) was significantly different from that of the untreated group ($823 \pm 148 \text{ mm}^3$, $t = 5.86$, $P = 0.009 < 0.01$) or the pcDNA3 group ($717 \pm 94 \text{ mm}^3$, $t = 6.46$, $P = 0.003 < 0.01$). Tumors of the pcDNA3.End group and radiation group also grew slower than those of the untreated group or the pcDNA3 group, but the inhibitory effects on tumor growth were slightly weaker than those of the pcDNA3.

End combined with radiation group, the inhibitory rates on d 28 were 44.7% and 40.1%, respectively. The tumor volume of the pcDNA3.End group ($492 \pm 97 \text{ mm}^3$) or the radiation group ($455 \pm 124 \text{ mm}^3$) was significantly different from that of the untreated group (the pcDNA3.End group, $t = 3.14$, $P = 0.039 < 0.05$ and the radiation group, $t = 3.30$, $P = 0.03 < 0.05$) or the pcDNA3 group (the pcDNA3.End group, $t = 2.89$, $P = 0.045 < 0.05$ and the radiation group, $t = 2.92$, $P = 0.047 < 0.05$).

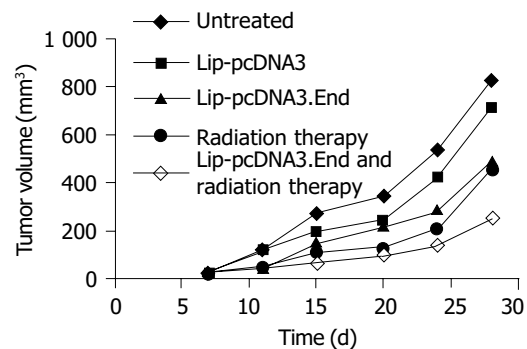


Figure 3 Tumor growth after intratumoral injections of liposome-plasmid complexes or irradiation or both.

DISCUSSION

Radiotherapy is one of the most important treatment modalities for solid tumors. Today, 45-50% of all cancer patients can be cured, and nearly 70% of those who are cured have received radiation either alone or in combination with other modalities, but a large number of patients have no response to radiotherapy treated with curative intent ultimately fail, not only because of metastasis of the disease, but also because of relapse at the local treatment site. One reason responsible for radiotherapy failure may be the tumor vasculature. Numerous studies have shown that tumor cells stop growing when the diameter of tumor exceeds 1-2 mm if new blood vessels supplying the tumor fail to generate^[16]. Hence, the combined radiotherapy with antiangiogenic agents has aroused great concerns^[17,18].

Angiogenesis is a complex process with multiple, sequential, and interdependent steps. Tumor cells promote new vessel formation by releasing endothelial cell growth factors that support endothelial cell proliferation, migration, and survival. Tumor angiogenesis is the consequence of enhanced expression of proangiogenic factors relative to antiangiogenic factors in the tumor microenvironment.

The combination of radiation treatment with endostatin may improve radiotherapy outcome by enhancing antitumor efficacy, reducing the total radiation dose, improving local tumor control rate, alleviating radiation damage. These considerations, along with the extensive clinical use of radiotherapy, make thorough investigation of strategies combining conventional treatment modality with endostatin. It was reported that combined endostatin gene therapy with radiotherapy can improve tumor response^[19-22].

We chose liposome to transfect BEL7402 cells with endostatin gene due to its high transfection efficiency. In

our pre-experiment, we chose lipofectamine to transfect BEL7402 cells with pcDNA3.GFP, the transfection rate was 73.5%. ELISA analysis of conditioned media from BEL7402 cells transfected with pcDNA3.End showed that the level of endostatin protein was 486.2 ± 56.5 mg/L, suggesting that BEL7402 cells transfected with pcDNA3.End plasmids secrete endostatin proteins into the culture media. The conditioned medium significantly suppressed the S phase fraction and increased the apoptotic index in HUVECs. However, it had no effect on BEL7402 cell apoptosis or cell cycle distribution. *In vivo*, endostatin significantly enhanced the treatment efficacy of ionizing radiation. The antitumor inhibition rate of combined endostatin gene therapy with radiation in BEL7402 human liver tumor model was 69.8%, which was significantly different from the untreated group ($t = 5.86, P = 0.009 < 0.01$) or the empty vector group ($t = 6.46, P = 0.003 < 0.01$) on d 28. Tumors of the radiation group and the pcDNA3.End group grew slower than those of the untreated group or the pcDNA3 group. These results indicate that intratumoral injection of liposome-endostatin complex significantly enhances the antitumor efficacy of radiation therapy.

In summary, gene therapy can deliver antiangiogenic polypeptide endostatin. Cationic liposomes transfected to endostatin gene can not only suppress endothelial cell proliferation, but also enhance the treatment efficacy of ionizing radiation.

REFERENCES

- 1 Folkman J. Angiogenesis in cancer, vascular, rheumatoid and other disease. *Nat Med* 1995; **1**: 27-31
- 2 Perletti G, Concaro P, Giardini R, Marras E, Piccinini F, Folkman J, Chen L. Antitumor activity of endostatin against carcinogen-induced rat primary mammary tumors. *Cancer Res* 2000; **60**: 1793-1796
- 3 Chen QR, Kumar D, Stass SA, Mixson AJ. Liposomes complexed to plasmids encoding angiostatin and endostatin inhibit breast cancer in nude mice. *Cancer Res* 1999; **59**: 3308-3312
- 4 Du Z, Hou S. The anti-angiogenic activity of human endostatin inhibits bladder cancer growth and its mechanism. *J Urol* 2003; **170**: 2000-2003
- 5 Wang X, Liu F, Li X, Li JS, Xu GX. Anti-tumor effect of human endostatin mediated by retroviral gene transfer in nude mice. *Chin Med J* 2002; **115**: 1664-1169
- 6 Boehle AS, Kurdow R, Schulze M, Kliche U, Sipos B, Soondrum K, Ebrahimnejad A, Dohrmann P, Kalthoff H, Henne-Bruns D, Neumaier M. Human endostatin inhibits growth of human non-small-cell lung cancer in a murine xenotransplant model. *Int J Cancer* 2001; **94**: 420-428
- 7 Felbor U, Dreier L, Bryant RAR, Ploegh HL, Olsen BR, Mothes W. Secreted cathepsin L generates endostatin from collagen XVIII. *EMBO J* 2000; **19**: 1187-1194
- 8 Herbst RS, Lee AT, Tran HT, Abbruzzese JL. Clinical studies of angiogenesis inhibitors: the University of Texas MD Anderson Center Trial of Human Endostatin. *Curr Oncol Rep* 2001; **3**: 131-140
- 9 Sauter BV, Martinet O, Zhang WJ, Mandeli J, Woo SLC. Adenovirus-mediated gene transfer of endostatin *in vivo* results in high level of transgene expression and inhibition of tumor growth and metastases. *Proc Natl Acad Sci USA* 2000; **97**: 4802-4807
- 10 Ding XQ, Chen Y, Li L, Liu RY, Huang JL, Lai K, Wu XJ, Ke ML, Huang WL. Inhibition of tongue cancer development in nude mice transfected with adenovirus carrying human endostatin gene. *Aizheng* 2003; **22**: 1152-1157
- 11 Chen W, Fu J, Liu Q, Ruan C, Xiao SD. Retroviral endostatin gene transfer inhibits human colon cancer cell growth *in vivo*. *Chin Med J* 2003; **116**: 1582-1584
- 12 Gorski DH, Mauceri HJ, Salloum RM, Gately S, Hellman S, Beckett MA, Sukhatme VP, Soff GA, Kufe DW, Weichselbaum RR. Potentiation of the antitumor effect of ionizing radiation by brief concomitant exposures to angiostatin. *Cancer Res* 1998; **58**: 5686-5689
- 13 Wachsberger P, Burd R, Dicker AP. Tumor response to ionizing radiation combined with antiangiogenesis or vascular targeting agents: exploring mechanisms of interaction. *Clin Cancer Res* 2003; **9**: 1957-1971
- 14 Griscelli F, Li H, Cheong C, Opolon P, Bennaceur-Griscelli A, Vassal G, Soria J, Soria C, Lu H, Perricaudet M, Yeh P. Combined effects of radiotherapy and angiostatin gene therapy in glioma tumor model. *Proc Natl Acad Sci USA* 2000; **97**: 6698-6703
- 15 Harari PM, Huang SM. Head and neck cancer as a clinical model for molecular targeting of therapy: combining EGFR blockade with radiation. *Int J Radiat Oncol Biol Phys* 2001; **49**: 427-433
- 16 Hahnfeldt P, Panigrahy D, Folkman J, Hlatky L. Tumor development under angiogenic signaling: a dynamical theory of tumor growth, treatment response, and postvascular dormancy. *Cancer Res* 1999; **59**: 4770-4775
- 17 Rofstad EK, Henriksen K, Galappathi K, Mathiesen B. Antiangiogenic treatment with thrombospondin-1 enhances primary tumor radiation response and prevents growth of dormant pulmonary micrometastases after curative radiation therapy in human melanoma xenografts. *Cancer Res* 2003; **63**: 4055-4061
- 18 Lund EL, Bastholm L, Kristjansen PEG. Therapeutic synergy of TNP-470 and ionizing radiation: effects on tumor growth, vessel morphology, and angiogenesis in human glioblastoma multiforme xenografts. *Clin Cancer Res* 2000; **6**: 971-978
- 19 Siemann DW, Shi W. Targeting the tumor blood vessel network to enhance the efficacy of radiation therapy. *Semin Radiat Oncol* 2003; **13**: 53-61
- 20 Herbst RS, O'Reilly MS. The rationale and potential of combining novel biologic therapies with radiotherapy: focus on non-small cell lung cancer. *Semin Oncol* 2003; **30** (4 Suppl 9): 113-123
- 21 Shi W, Teschendorf C, Muzyczka N, Siemann DW. Gene therapy delivery of endostatin enhances the treatment efficacy of radiation. *Radiother Oncol* 2003; **66**: 1-9
- 22 Greenberger JS. Antitumor interaction of short course endostatin and ionizing radiation. *Cancer J* 2000; **6**: 279-281

• CASE REPORT •

Small bowel non-Hodgkin's lymphoma remaining in complete remission by surgical resection and adjuvant rituximab therapy

Kenichi Nomura, Koichi Tomikashi, Yosuke Matsumoto, Naohisa Yoshida, Takashi Okuda, Chohei Sakakura, Shoji Mitsufuji, Shigeo Horiike, Hisakazu Yamagishi, Takeshi Okanoue, Masafumi Taniwaki

Kenichi Nomura, Yosuke Matsumoto, Shigeo Horiike, Molecular Hematology and Oncology, Kyoto Prefectural University of Medicine, Graduate School of Medical Science, Kyoto, Japan
Koichi Tomikashi, Naohisa Yoshida, Takashi Okuda, Shoji Mitsufuji, Takeshi Okanoue, Molecular Gastroenterology and Hepatology, Kyoto Prefectural University of Medicine, Graduate School of Medical Science, Kyoto, Japan
Chohei Sakakura, Hisakazu Yamagishi, Department of Surgery, Kyoto Prefectural University of Medicine, Graduate School of Medical Science, Kyoto, Japan
Masafumi Taniwaki, Clinical Molecular Genetics and Laboratory Medicine, Kyoto Prefectural University of Medicine, Graduate School of Medical Science, Kyoto, Japan
Correspondence to: Kenichi Nomura, MD, PhD, Molecular Hematology and Oncology, Kyoto Prefectural University of Medicine, Graduate School of Medical Science, Kawaramachi-Hirokoji, Kamigyoku, Kyoto 602-0841, Japan. nomuken@sun.kpu-m.ac.jp
Telephone: +81-75-251-5521 Fax: +81-75-251-0710
Received: 2004-06-15 Accepted: 2004-07-17

Abstract

A 44-year-old man was referred to our hospital with intermittent abdominal pain. Because distention of fluid- and gas-filled loops of small intestine was proved by X-ray, the patient was diagnosed as having small bowel obstruction. A laparotomy revealed a segmental stenosis in the jejunum, which showed diffuse thickening of the intestinal wall. Some mesenteric lymph nodes were swollen. Pathological examination was defined. We diagnosed diffuse large B-cell lymphoma based on the pathological findings of diffuse transmural infiltration of large lymphoid cells and flow-cytometric analyses. Rituximab was administered as adjuvant therapy at weekly doses of 375 mg/m². Four cycles were performed every 6 mo and he remained CR. Rituximab may be effective as adjuvant therapy.

© 2005 The WJG Press and Elsevier Inc. All rights reserved.

Key words: Intermittent abdominal pain; Rituximab

Nomura K, Tomikashi K, Matsumoto Y, Yoshida N, Okuda T, Sakakura C, Mitsufuji S, Horiike S, Yamagishi H, Okanoue T, Taniwaki M. Small bowel non-Hodgkin's lymphoma remaining in complete remission by surgical resection and adjuvant rituximab therapy. *World J Gastroenterol* 2005; 11(28): 4443-4444
<http://www.wjgnet.com/1007-9327/11/4443.asp>

INTRODUCTION

Primary gastrointestinal lymphoma (PGL) accounts for 4-

20% of all non-Hodgkin's lymphomas (NHL)^[1,2]. The location most frequently involved has been the ileocecal region, followed by small bowel, accounting for 20-40% of PGL^[1]. Small bowel lymphoma tends to be annular in the distal ileum, not proximal^[2]. Jejunal obstruction in a patient with NHL has been exceptionally described.

Regarding treatment, it has been established that the primary surgical treatment had the most favorable influence on failure-free survival in localized diseases and hence the resection may be appropriate as the primary treatment^[3]. On the other hand, the effectiveness of adjuvant therapy for localized NHL remains to be unclear, because some cases could be cured only by surgical resection.

In this study, we have described the primary jejunal NHL with small bowel obstruction, which remained in complete remission by surgical resection followed by rituximab administration.

CASE REPORT

A 44-year-old man was admitted to our hospital in May 2002 because of intermittent abdominal pain. Small bowel series and computed tomography (CT) of the abdomen showed stenosis at jejunum and dilatation of small bowel (Figures 1 and 2), indicating small bowel obstruction. However, the cause of obstruction remained unclear in spite of several workups. Laparotomy disclosed a 3 cm long jejunal segment stenosis at 110 cm from the ligament of Treitz and some mesenteric lymph nodes were swollen.

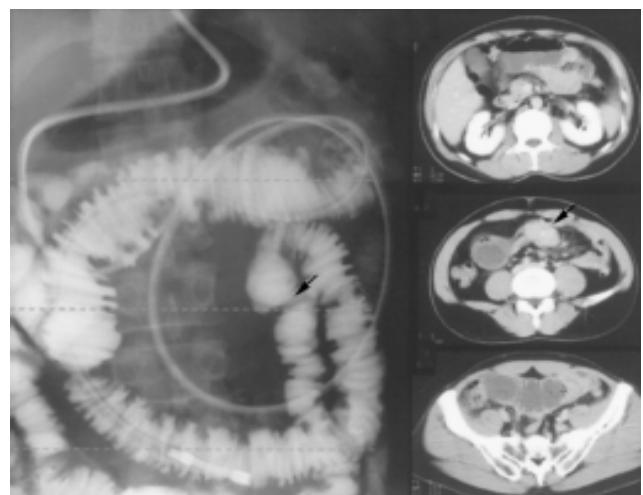


Figure 1 Small bowel series and CT showed both the distention of fluid- and gas-filled loops of small intestine and segmental stenosis indicated by arrow.

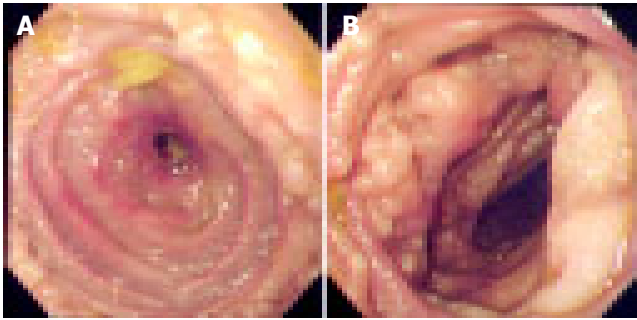


Figure 2 Resected jejunum show. **A:** Resected jejunum showed diffuse thickening of the intestinal wall (oral side); **B:** multiple hyperplastic follicles (anal side).

The resected specimens showed diffuse thickening of the intestinal wall, histopathological analysis of which showed that large lymphoid cells aggregated diffusely. Mesenteric lymph nodes were also involved. Flow-cytometric studies showed that the tumor cells expressed HLA-DR (84.8%), s-IgA (46.6%), γ (69.8%), CD10 (44.7%), CD19 (68.1%), and CD20 (62.4%) with a high-intensity signal. Results for CD5 were negative (26.2%) with a low-intensity signal. Postoperative workup did not demonstrate the evidence of systemic involvement. Thus, the patient was diagnosed having primary jejunal diffuse large B-cell lymphoma at stage II₁. Rituximab was administered as adjuvant therapy at weekly doses of 375 mg/m². Four courses were performed every 6 mo and the patient is in complete remission with a follow-up time of 24 mo with no significant adverse effects.

DISCUSSION

We experienced a rare case of primary jejunal NHL as radiological workup including CT and angiography provided no evidence for final diagnosis, we performed laparotomy and segmental intestinal resection. The recognition of the possibility of jejunal obstruction due to NHL may facilitate

early diagnosis. Yamamoto *et al.*, have recently developed double-balloon endoscopy. This method enables us to survey all intestines with ease^[4]. In future, this method may become the routine mode of study for small bowel obstruction.

Regarding treatment, we performed segmental resection of jejunum and rituximab therapy as adjuvant treatment. The efficacy and toxicity of adjuvant therapy for localized NHL remained unclear because excess chemotherapy may provoke secondary malignancies. On the other hand, a new anti-CD20 mAb, rituximab, is effective in the treatment of B-cell lymphoma with slight adverse effects^[5,6]. Thus we treated the patient under study with rituximab as adjuvant therapy. He tolerated this adjuvant therapy well, with slight nausea. Rituximab may be effective as adjuvant therapy for PGL. The efficacy and toxicity should be examined in large series.

REFERENCES

- 1 **Lee J**, Kim WS, Kim K, Ko YH, Kim JJ, Kim YH, Chun HK, Lee WY, Park JO, Jung CW, Im YH, Lee MH, Kang WK, Park K. Intestinal lymphoma: exploration of the prognostic factors and the optimal treatment. *Leuk Lymphoma* 2004; **45**: 339-344
- 2 **Domizio P**, Owen RA, Shepherd NA, Talbot IC, Norton AJ. Primary lymphoma of the small intestine. A clinicopathological study of 119 cases. *Am J Surg Pathol* 1993; **17**: 429-442
- 3 **Samel S**, Wagner J, Hofheinz R, Sturm J, Post S. Malignant intestinal non-Hodgkin's lymphoma from the surgical point of view. *Onkologie* 2002; **25**: 268-271
- 4 **Yamamoto H**, Sugano K. A new method of enteroscopy--the double-balloon method. *Can J Gastroenterol* 2003; **17**: 273-274
- 5 **Maloney DG**, Grillo-Lopez AJ, Bodkin DJ, White CA, Liles TM, Royston I, Varns C, Rosenberg J, Levy R. IDEC-C2B8: results of a phase I multiple-dose trial in patients with relapsed non-Hodgkin's lymphoma. *J Clin Oncol* 1997; **15**: 3266-3274
- 6 **Maloney DG**, Grillo-Lopez AJ, White CA, Bodkin D, Schilder RJ, Neidhart JA, Janakiraman N, Foon KA, Liles TM, Dallaire BK, Wey K, Royston I, Davis T, Levy R. IDEC-C2B8 (Rituximab) anti-CD20 monoclonal antibody therapy in patients with relapsed low-grade non-Hodgkin's lymphoma. *Blood* 1997; **90**: 2188-2195

Ovarian carcinoma in two patients with chronic liver disease

Mehlika Isildak, Gulay Sain Guven, Murat Kekilli, Yavuz Beyazit, Mustafa Erman

Mehlika Isildak, Murat Kekilli, Yavuz Beyazit, Gülay Sain Guven, Mustafa Erman, Department of Internal Medicine, Faculty of Medicine, Hacettepe University, Sıhhiye, Ankara 06100, Turkey
Gülay Sain Guven, Department of Internal Medicine, Section of General Internal Medicine, Faculty of Medicine, Hacettepe University, Sıhhiye, Ankara 06100, Turkey

Mustafa Erman, Department of Internal Medicine, Section of Medical Oncology, Faculty of Medicine, Hacettepe University, Sıhhiye, Ankara 06100, Turkey

Correspondence to: Dr. Gülay Sain Guven, Department of Internal Medicine, Section of General Internal Medicine, Faculty of Medicine, Hacettepe University, Sıhhiye, Ankara 06100,

Turkey. gsain@tr.net

Telephone: +90-312-305-3029 Fax: +90-312-305-2302

Received: 2004-07-23 Accepted: 2004-12-01

Abstract

Ascites is a common and debilitating complication of cirrhosis. However, patients with chronic liver disease are not spared from other causes of ascites and physicians should be careful not to miss an underlying malignancy. Ovarian cancer is an insidious disease, which is difficult to diagnose and it ranks first in mortality among all gynecological cancers. Here, we present two cases of patients with chronic liver disease that developed ascites not simply because of cirrhosis but as a manifestation of ovarian cancer. We would like to emphasize that the causes of ascites, other than the liver itself, should not be overlooked in patients with chronic liver disease.

© 2005 The WJG Press and Elsevier Inc. All rights reserved.

Key words: Ovarian carcinoma; Ascites; Chronic liver disease

Isildak M, Guven GS, Kekilli M, Beyazit Y, Erman M. Ovarian carcinoma in two patients with chronic liver disease. *World J Gastroenterol* 2005; 11(28): 4445-4446

<http://www.wjgnet.com/1007-9327/11/4445.asp>

INTRODUCTION

Ascites is the most common complication of viral, alcoholic or metabolic liver cirrhosis. Approximately half of the cirrhotic patients are expected to develop ascites within 10 years after the diagnosis^[1]. Development of ascites is an important prognostic sign in the usual course of chronic liver disease since it shortens the 5-year survival rate of a cirrhotic patient^[2-4].

Ascites may develop in 75% of all patients with liver disease. The remaining 25% is due to malignancy (10%), cardiac failure (3%), pancreatitis (1%), tuberculosis (2%) and

other uncommon causes^[5]. However, it is important to comprehend that cirrhotic patients are not spared from these non-cirrhotic causes. Herein we present two patients with chronic liver disease who were diagnosed to have ovarian cancer after a thorough investigation of their ascites.

CASE REPORT

Case 1

A 45-year-old woman with chronic liver disease was seen at the outpatient clinic, because of her recent complaints. She complained of abdominal swelling, in the previous 2 mo. She had abdominal pain radiating to her back, which was aggravated after meals. Famotidine was of no use in relieving the pain. She also complained of weight loss as much as 5 kg in 20 d. The patient had been followed up for chronic hepatitis B infection for 8 years. The diagnosis was confirmed with a liver biopsy, which showed cirrhosis at developmental stage. She underwent esophageal variceal band ligation and transjugular intrahepatic portosystemic shunt (TIPSS) for the management of chronic ascites before 5 years. TIPSS was performed once again before 3 years. She received medical treatment while awaiting liver transplantation. She had no evident family history.

Physical examination revealed that she had massive ascites and was admitted to our hospital for further investigation. Ultrasonographic examination of the abdomen had no remarkable finding except ascites and parenchymal changes in the liver. Hepatic and portal venous systems were normal since the portosystemic shunt functioned well. Diagnostic paracentesis was performed and biochemical analysis was as follows: LDH: 318 U/L (concomitant serum LDH was 337 U/L), albumin: 2.4 g/dL (serum albumin: 2.9 g/dL). Cytological investigation of the ascites showed malignant cells. Abdominal computed tomography (CT) revealed peritoneal carcinomatosis and solid mass lesions of both the ovaries. CT of the thorax showed metastatic nodules on the pleural surface. Serum CA 125 level was 9 853 U/mL.

The patient underwent total abdominal hysterectomy, bilateral salpingo-oophorectomy, omentectomy, and pelvic-paraaortic lymph node dissection. Tumor debulking surgery and histopathological examination of the specimens reported that she had ovarian serous papillary adenocarcinoma (stage III). Paclitaxel-carboplatin therapy was started. Unfortunately, during the first course of chemotherapy she developed acute pneumonia and empyema, which rapidly progressed to septic shock leading to her death.

Case 2

A 40-year-old woman was admitted to hospital because of ascites. She was also suffering from loss of weight and appetite

in the last 10 d. She was known to have had chronic hepatitis B and D. She received interferon treatment for 6 mo, followed by another course of pegylated interferon 2 years later. She had no significant complication of chronic liver disease.

Biochemical analysis of ascites showed an LDH level of 564 U/L and serum-ascites albumin gradient was 0.7. Computed tomography of the abdomen showed massive ascites, omental cake sign and mass lesions of 4-5 cm in both adnexal regions. Serum CA 125 level was 3 028 U/mL. She underwent total abdominal hysterectomy, bilateral oophorectomy, lymph node dissection and tumor debulking surgery. Pathological diagnosis of the tumor was poorly differentiated adenocarcinoma, which was positive for CA 125 and CK7, thus confirming an ovarian origin. Serum CA 125 value of the patient decreased to 25.9 U/mL after the operation.

DISCUSSION

Ovarian carcinoma is difficult to diagnose and it is usually discovered only in its advanced stages. It therefore has the highest mortality among all gynecological malignancies. Cachexia with pelvic mass, ascites and elevated CA125 levels generally lead to its correct diagnosis, but usually there are no pathognomonic radiological or laboratory findings. Therefore, a laparotomy is usually necessary for its final diagnosis.

In the majority of ovarian cancer cases, the etiology is unknown. A small percentage of cases may be attributed to hereditary disorders. Close follow-up with annual transvaginal ultrasound examination and measurement of CA125 levels is advocated for patients with high at genetic risk. Prophylactic oophorectomy after completion of fertility may be a reasonable option for BRCA mutation carriers and might be effective in preventing both ovarian or breast cancers. However, such an approach has not been evaluated^[6]. Multiple pregnancies or the use of oral contraceptives might have a protective effect as they can reduce ovulation and related hormonal effect^[7].

The 5-year survival rate for advanced disease is about 30%. In a study reviewing the general practice records of patients with epithelial ovarian cancer, the most frequent symptoms are abdominal pain, change in bowel habits, abdominal swelling, vaginal bleeding, weight loss, and backache^[8]. The same study revealed that the most significant independent variable for survival is the stage of the disease at surgery^[8].

Ascites is an important clinical finding in ovarian cancer. Any patient who presents with ascites should undergo a thorough investigation of ascites influencing cytological analysis and measurement of amylase level. Though an elevated CA125 level should raise a suspicion of ovarian cancer, its interpretation in patients with any serosal involvement may not be easy, since any type of pleural, peritoneal or pericardial irritation can lead to elevated serum level of this high molecular weight glycoprotein^[9].

CA125 level greater than 35 U/mL has been reported in 35-75% of cirrhotic patients, most commonly in those with ascites. Studies have shown that cirrhotic patients with ascites have different mean serum CA125 levels of 291 and 572 U/mL, respectively^[10-12]. All these data show that CA125 is not a strong diagnostic tool for ovarian cancer in patients with preexisting cirrhotic ascites.

Though it is not possible to define a strict dividing line between "expected" and "alarming" ascites during the course of chronic liver disease, some clues may help physicians to find other underlying causes. We believe that the two cases in our study contribute to this. The first patient had a rapid development of ascites despite a functional TIPSS. The other patient did not have overt signs of cirrhotic changes of the liver, the reason why ascites occurred is not clear. In both cases, the presence of an exudative rather than transudative peritoneal fluid is another underlying cause other than cirrhosis^[13]. As mentioned above, an elevated CA125 level is not a specific diagnostic marker for ovarian cancer as it may be elevated in a cirrhotic patient, due to peritoneal irritation. Thus, extremely high CA125 levels merit further investigation.

We conclude that the development of ascites in patients with chronic liver disease should never be considered as "normal" and a search for other causes should be considered. Prompt diagnosis and surgical intervention may be life-saving in such cases.

REFERENCES

- 1 **Moore KP**, Wong F, Gines P, Bernardi M, Ochs A, Salerno F, Angeli P, Porayko M, Moreau R, Garcia-Tsao G, Jimenez W, Planas R, Arroyo V. The management of ascites in cirrhosis: Report on the consensus conference of the international ascites club. *Hepatology* 2003; **38**: 258-266
- 2 **Saunders JB**, Walters JRF, Davies P, Paton A. A 20-year prospective study of cirrhosis. *Br Med J* 1981; **282**: 263-266
- 3 **Llach J**, Gines P, Arroyo V, Rimola A, Tito L, Badalamenti S, Jimenez W, Gaya J, Rivera F, Rodes J. Prognostic value of arterial pressure, endogenous vasoactive systems and renal function in cirrhotic patients admitted to hospital for the treatment of ascites. *Gastroenterology* 1988; **94**: 482-487
- 4 **Salerno F**, Borroni G, Moser P, Badalamenti S, Cassara L, Maggi A, Fusini M, Cesana B. Survival and prognostic factors of cirrhotic patients with ascites: a study of 134 outpatients. *Am J Gastroenterol* 1993; **88**: 514-519
- 5 **Reynolds TB**. Ascites. *Clin Liver Dis* 2000; **4**: 151-168
- 6 **Anderiesz C**, Quinn MA. Screening for ovarian cancer. *Med J Aust* 2003; **178**: 655-656
- 7 **Molpus KL**, Jones HW 3rd. Gynecological Cancers In: L Goldman, Ausiello D, eds. Cecil Textbook of Medicine. Philadelphia: WB Saunders 2004: 1238-1241
- 8 **Kirwan JM**, Tincello DG, Herod JJ, Frost O, Kingston RE. Effect of delays in primary care referral on survival of women with epithelial ovarian cancer: retrospective audit. *Br Med J* 2002; **324**: 148-151
- 9 **Sevinc A**, Camci C, Turk HM, Buyukberber S. How to interpret serum CA 125 levels in patients with serosal involvement? A clinical dilemma. *Oncology* 2003; **65**: 1-6
- 10 **Bergmann JF**, Bidart JM, George M, Beaugrand M, Levy VG, Bohuon C. Elevation of CA 125 in patients with benign and malignant ascites. *Cancer* 1987; **59**: 213-217
- 11 **Eerdeken MW**, Nouwen EJ, Pollet DE, Briers TW, DeBroe ME. Placental alkaline phosphatase and cancer antigen 125 in sera of patients with benign and malignant diseases. *Clin Chem* 1985; **31**: 687-690
- 12 **Collazos J**, Genolla J, Ruibal A. CA 125 serum levels in patients with nonneoplastic liver diseases. A clinical and laboratory study. *Scand J Clin Lab Invest* 1992; **52**: 201-206
- 13 **Runyon BA**, Montano AA, Akriviadis EA, Antillon MR, Irving MA, McHutchinson JG. The serum-ascites albumin gradient is superior to the exudate-transudate concept in the differential diagnosis of ascites. *Ann Intern Med* 1992; **117**: 215-220

• CASE REPORT •

Acute pancreatitis caused by leptospirosis: Report of two cases

Ekrem Kaya, Adem Dervisoglu, Cafer Eroglu, Cafer Polat, Mustafa Sunbul, Kayhan Ozkan

Ekrem Kaya, Department of Surgery, Uludag University, Bursa, Turkey
Adem Dervisoglu, Cafer Eroglu, Department of Surgery, Ondokuz
Mayis University, Samsun, Turkey
Cafer Polat, Mustafa Sunbul, Department of Infectious Disease,
Ondokuz Mayis University, Samsun, Turkey
Kayhan Ozkan, Department of Surgery, Ondokuz Mayis University,
Samsun, Turkey
Correspondence to: Ekrem Kaya, MD, Department of Surgery,
HPB Unit, Uludag University School of Medicine, Gorukle-Bursa
16059, Turkey. ekremkaya@uludag.edu.tr
Telephone: +90-224-4428598 Fax: +90-224-4428398
Received: 2004-07-31 Accepted: 2004-11-04

Abstract

Two cases of acute pancreatitis with leptospirosis are reported in this article. Case 1: A 68-year-old woman, presented initially with abdominal pain, nausea, vomiting, and jaundice. She was in poor general condition, and had acute abdominal signs and symptoms on physical examination. Emergency laparotomy was performed, acute pancreatitis and leptospirosis were diagnosed on the basis of surgical findings and serological tests. The patient died on postoperative d 6. Case 2: A 62-year-old man, presented with fever, jaundice, nausea, vomiting, and malaise. Acute pancreatitis associated with leptospirosis was diagnosed, according to abdominal CT scanning and serological tests. The patient recovered fully with antibiotic treatment and nutritional support within 19 d.

© 2005 The WJG Press and Elsevier Inc. All rights reserved.

Key words: Acute pancreatitis; Leptospirosis; Infection

Kaya E, Dervisoglu A, Eroglu C, Polat C, Sunbul M, Ozkan K. Acute pancreatitis caused by leptospirosis: Report of two cases. *World J Gastroenterol* 2005; 11(28): 4447-4449
<http://www.wjgnet.com/1007-9327/11/4447.asp>

INTRODUCTION

Leptospirosis is a spirochetal bacterial infection and causes clinical illness in animals and humans. This zoonosis is common in some other parts of the world but rather rare in Turkey^[1,2]. This disease is predominantly seen in farmers, trappers, veterinarians, and rice-field workers. Leptospirosis mainly affects liver and kidney. Rarely, other organs such as lung, heart, gallbladder, brain, and ophthalmic tissues are involved, mainly due to vasculitis^[3,4]. Hyperamylasemia can be present in leptospirosis infection due to renal impairment^[5-7]. Therefore, the diagnosis of acute pancreatitis is controversial in this disease.

Pancreatitis is a rare complication of leptospirosis and only a few cases have been reported in literature^[1,5,8,9]. We report two cases here.

CASE REPORT

Case 1

A 68-year-old woman was referred to Ondokuz Mayis University hospital for abdominal pain, nausea, vomiting, and jaundice with 1-d history. She had no history of contact with jaundiced persons, blood transfusions and drug abuse. She was operated on 3 years ago for hip fracture and occasionally she took some analgesics. On physical examination, she was in poor general condition with dehydration and her scleras were icteric. Her pulse rate was 120/min, blood pressure 14.6/10.6 kPa and she was tachypneic. Urine output was normal. There was a marked tenderness in her whole abdomen with guarding and rebound tenderness. No other abnormalities were noted. Laboratory investigations on admission revealed Hb: 13 g/dL, Htc: 39.7, WBC: 9 000/mm³, platelet count: 120 000/mm³ (*n*: 150×10³-300×10³), BUN: 60 mg/dL (*n*: 5-24), creatinine (Cr): 2.7 mg/dL (*n*: 0.4-1.4), lactate dehydrogenase (LDH): 2 321 U/L (*n*: 95-500), total/direct bilirubin: 6.5/4.7 mg/dL, Ca: 7.8 mg/dL (8-10), amylase: 630 U/L (28-100), lipase: 642 U/L (*n*: 0-190), aspartate transaminase (AST): 2 500 U/L (*n*: 8-46), alanine transaminase (ALT): 1 900 U/L (*n*: 7-46), serum C-reactive protein (CRP): 192 mg/L (*n*: 0-5), PaO₂: 7.71 kPa, base excess (BE): -5 mmol/L, with negative viral hepatitis markers. The Ranson score was 8. Abdominal ultrasonographic examination revealed acute calculus cholecystitis and abdominal fluid collection. Biliary dilatation was not observed in ultrasonographic examination.

The patient was operated on with the diagnosis of surgical acute abdomen. On exploration, 500 mL sero-hemorrhagic fluid was found in the abdominal cavity, and gallbladder and pancreas were found to be markedly edematous. Areas of fatty necrosis were seen on peripancreatic tissues. Cholecystectomy and common bile duct exploration were done. Pre-operative cholangiogram was normal. Histopathologic diagnosis of the gallbladder was acute cholecystitis. Leptospire were seen in blood, intra-abdominal fluid and bile on dark-field microscopy. *Leptospira microagglutination* test was positive (at 1:100 *Leptospira samaranga Patoc* I). Penicillin G, 3 million units four times per day was given to the patient intravenously. Total parenteral nutrition was also started for artificial nutrition. The patient recovered after operation and oral intake was started on postoperative d 5. Although liver function tests and laboratory values returned to normal within 5 d, others included Hb: 11 g/dL, platelet count: 170 000/mm³, BUN: 43 mg/dL, Cr: 0.8 mg/dL, total/direct bilirubin: 1.9/1.56 mg/dL, AST: 47 U/L, ALT:

168 U/L. Six days after the operation the patient died due to a suddenly developed cardiopulmonary arrest.

Case 2

A 62-year-old man was admitted to Ondokuz Mayıs University hospital with fever, marked jaundice, nausea, and vomiting. The patient had also 2 wk' history of malaise, fever, and dizziness before hospital admission. On examination, the patient was icteric and there was conjunctival hyperemia. His temperature was 39 °C and blood pressure was 19.9/11.9 kPa. Urine output was 30 mL/h. The remainder of the physical examination was normal. Laboratory investigations on admission showed Hb: 8.6 g/dL, Htc: 27.8, WBC: 23 000/mm³, platelet count: 53 000/mm³, glucose 140 mg/dL, total/direct bilirubin: 48/44 mg/dL, AST: 70 U/L, ALT: 85 U/L, alkaline phosphatase: 516 U/L (*n*: 95-280), γ -glutamyl transpeptidase: 104 U/L (*n*: 7-49), BUN: 120 mg/dL, Cr: 17 mg/dL, LDH: 1 638 U/L, total protein 4.8 g/dL (*n*: 6-8.5), albumin: 2.2 g/dL (*n*: 3.5-5), amylase 980 U/L, pancreatic amylase: 830 U/L (*n*: 13-53), lipase: 797 U/L, Ca: 7.5 mg/dL, CRP: 68, negative viral hepatitis markers. The Ranson score was 6. Leptospira microagglutination test was positive (at 1/800, *L. icterohemorrhagica*). Leptospire were seen in blood on dark-field microscopy. Abdominal CT examination revealed bilateral pleural effusion, intra-abdominal minimal fluid collection, pancreatic edema and peripancreatic tissues heterogeneity (Figure 1A).

A diagnosis of leptospirosis with acute pancreatitis was made. The patient had renal failure in acute non-oliguric form. Hemodialysis was performed at the beginning of the treatment. Intravenous fluid resuscitation and ampicillin-sulbactam treatment were given. Nasojejunal feeding tube was inserted endoscopically for adequate caloric intake. Four days after the treatment, body temperature decreased to 37.5 °C, amylase levels decreased to normal value 150 U/L and platelet count increased to 150 000/mm³. Bilirubin levels, liver function tests, and creatinine level slowly returned to normal within 2 wk (laboratory tests at the discharge time revealed WBC: 9 000/mm³, Hb: 90 g/L, total/direct bilirubin: 2/1.8 mg/dL, BUN: 30 mg/dL, Cr: 1.2 mg/dL, AST: 24 U/L, ALT: 45 U/L, LDH: 380 U/L). Oral intake was started on d 19 of admission and the patient was discharged. Abdominal CT findings at the discharge time revealed minimal edema in the pancreas (Figure 1B). The patient was examined 2 mo later and he was in a completely healthy condition.

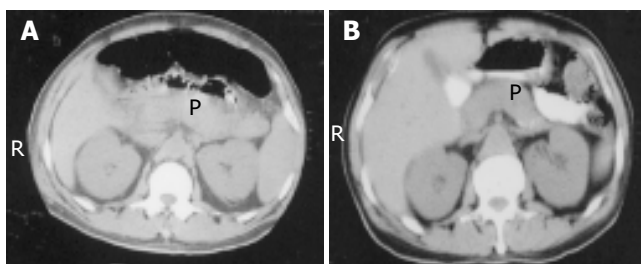


Figure 1 Abdominal CT scan of case 2. **A:** Pancreatic edema, heterogeneity and minimal intra-abdominal fluid collection; **B:** minimal edema in the pancreas after treatment. P: pancreas.

DISCUSSION

Leptospirosis is a spirochetal zoonosis that causes clinical illness in humans as well as in animals. The source of infection in humans is usually either direct or indirect contact with the urine of infected animals. These bacteria infect humans by entering through abraded skin, mucous membrane, conjunctivae. Direct transmission between humans is rare^[3,4]. Leptospirosis is a common disease in rice-field workers due to prevalence of wild rats^[4,8]. Both of our patients were from rural area of the middle Black Sea region of Turkey and have worked in rice fields. Rice field with stagnant water and humid condition is an ideal environment for leptospira.

Leptospirosis is characterized by the development of vasculitis, endothelial damage, and inflammatory infiltration. This disease mostly affects tissues of the liver and kidney. Other tissues such as the pancreas can be affected due to vasculitis^[4].

This disease occurs as two clinically recognizable syndromes: the anicteric leptospirosis (80-90% of all cases) and the remainder icteric leptospirosis^[3,4]. Icteric leptospirosis is known as Weil's disease, which is characterized by hemorrhage, renal failure, and jaundice. Icteric leptospirosis is a much more severe disease than anicteric form. The clinical course is often rapidly progressing. Our cases seemed to be icteric leptospirosis. Serological tests confirmed on blood samples as *L. icterohemorrhagica* and *L. samaranga Patoc*. First of these is responsible for icteric form of the disease. *L. samaranga Patoc* sero-type is not the cause of Weil's disease but cross-reaction is possible between the serotypes of leptospirosis.

Thrombocytopenia is a common finding in leptospirosis, occurring in 40-85% of this disease. But the exact reason for thrombocytopenia is unknown. Vasculitis, increased peripheral destruction and decreased thrombocyte production have been considered as potential causes of thrombocytopenia^[4,10]. Thrombocytopenia was also present in the two cases reported here which were remedied by our treatment.

Oliguric and non-oliguric acute renal failure may be observed in icteric leptospirosis^[7], as also seen in our cases. It was reported that oliguria was a significant predictor of death in leptospirosis^[4]. Urine output was normal in case 1 but case 2 was oliguric. Renal insult was treated with intravenous fluid replacement and other supportive treatment including antibiotic and hemodialysis in case 2.

Jaundice occurring in leptospirosis is not commonly associated with hepatocellular necrosis and impaired liver function. There are moderate rises in transaminase levels, and minor elevation of alkaline phosphatase level usually occurs^[3,4]. Hepatic dysfunction occurs but resolves, and it is rarely the cause of death. The serum bilirubin level is usually <20 mg/dL but can be as high as 60-80 mg/dL. The bilirubin level of case 2 was close to this value (48 mg/dL). In case 1, transaminase levels were very high (more than 2 000 U/dL). The elevation of transaminases that is more than threefold of the normal value is not usual. Some sporadic cases with very high transaminase level were reported in the medical literature^[11]. Furthermore, hepatocyte degeneration and liver cell necrosis have been reported in biliary pancreatitis^[12,13]. So, elevated transaminases levels as high as that in case I may be seen in leptospirotic hepatitis. Pancreatic and bile tree involvement can be additional factors

for liver cell necrosis. Acute cholecystitis was pathologically confirmed and leptospire were seen in bile in case 1. Therefore, we believe that hepatobiliary and pancreatic involvement could be possible in this case.

For the diagnosis of acute pancreatitis, a simultaneous determination of both amylase and lipase is recommended for the evaluation of patient with abdominal pain. The serum amylase test is available in nearly all laboratories and at all hours. Elevation of lipase level with serum amylase is important for the diagnosis of acute pancreatitis. Elevation of pancreatic isoamylase level also supports the diagnosis^[14]. Hyperamylasemia also can be seen in leptospirosis due to renal function alterations or other unknown reasons^[5,6]. The serum amylase and lipase levels were elevated more than threefold of normal level in both cases. Pancreatic isoamylase level was also elevated at diagnostic level in case 2.

CT scan is a gold standard in diagnosis of acute pancreatitis, as shown by many authors who use it. This diagnostic test has 100% specificity and over 90% sensitivity for this disease^[15-17]. We also routinely use CT for both diagnosis and follow-up of the treatment as in case 2. Because abdominal CT scan was not available in the emergency condition in our hospital, we could not use it in case 1. However, the pathologic findings of acute pancreatitis were clearly observed at laparotomy in this case. So, there is no diagnostic dilemma for both of two presented cases.

The treatment of acute pancreatitis in leptospirosis includes antibiotic treatment against leptospira and supportive treatments for acute pancreatitis (including intravenous fluid resuscitation and nutrition). We preferred the nutritional support (parenterally or enterally but mostly enterally) in severe acute pancreatitis. This regime was successful in case 2. Case 1 also completely recovered after d 5 and she could feed orally. We believe that the reason of mortality was pulmonary embolism in case 1.

In conclusion, pancreatitis may be seen in leptospirosis infection. Leptospirosis should also be considered in the differential diagnosis of hyperamylasemia, pancreatitis, and obstructive jaundice in endemic areas. Early diagnosis and appropriate treatment is essential for life saving.

REFERENCES

- 1 **Leblebicioglu H**, Sencan I, Sunbul M, Altintop L, Günaydin M. Weil's disease: Report of 12 cases. *Scand J Infect Dis* 1996; **28**: 637-639
- 2 **Casella G**, Scatena L. Mild pancreatitis in leptospirosis infection (letter to the Ed.). *Am J Gastroenterol* 2000; **95**: 1843-1844
- 3 **Farr RW**. Leptospirosis. State-of-the-art article. *CID* 1995; **21**: 1-6
- 4 **Levett PN**. Leptospirosis. *Clin Microbiol Rev* 2001; **14**: 296-326
- 5 **Edwards CN**, Evarard COR. Hyperamylasemia and pancreatitis in leptospirosis. *Am J Gastroenterol* 1991; **86**: 1665-1668
- 6 **Kameya S**, Hayakawa T, Kemaye A, Wtarabe T. Hyperamylasemia in patients at an intensive care unit. *J Clin Gastroenterol* 1986; **8**: 438-442
- 7 **Cengiz K**, Sahan C, Sunbul M, Leblebicioglu H, Cuner E. Acute renal failure in leptospirosis in the black- sea region in Turkey. *Int Urol Nephrol* 2002; **33**: 133-136
- 8 **Sunbul M**, Esen S, Leblebicioglu H, Hokelek M, Pekbay A, Eroglu C. Rattus acting as reservoir of leptospira interrogans in the middle black sea region of Turkey, as evidenced by PCR and presence of serum antibodies to leptospira strain. *Scand J Infect Dis* 2001; **33**: 896-898
- 9 **O'Brien MM**, Vincent JM, Person DA, Cook A. Leptospirosis and pancreatitis: a report of ten cases. *Pediatr Infect Dis J* 1999; **18**: 399-400
- 10 **Turgut M**, Sunbul M, Bayýrlý D, Bilge A, Leblebicioglu H, Haznedaroglu I. Trombocytopenia complicating the clinical course of leptospiral infection. *J Int Med Res* 2002; **30**: 535-540
- 11 **Kuntz E**, Kuntz HD. Hepatology. 1 st ed. *Hiedelberg: Springer Verlag, Berlin* 2000: 425
- 12 **Tenner S**, Dubner H, Steinberg W. Predicting gallstone pancreatitis with laboratory parameter meta-analysis. *Am J Gastroenterol* 1994; **89**: 1863-1866
- 13 **Isogai M**, Yamagýchi A, Hori A, Nakano S. Hepatic histopathological changes in biliary pancreatitis. *Am J Gastroenterol* 1995; **90**: 449-454
- 14 **Frank B**, Gottlieb K. Amylase normal, lipase elevated : Is it pancreatitis? *Am J Gastroenterol* 1999; **94**: 463-469
- 15 **Clavien PA**, Hauser H, Meyer P, Rohner A. Value of contrast-enhanced computerized tomography in the early diagnosis and prognosis of acute pancreatitis. *Am J Surg* 1988; **155**: 457-463
- 16 **Moossa AR**. Diagnostic tests and procedures in acute pancreatitis. *N Engl J Med* 1984; **311**: 639-643
- 17 **Lott JA**. The value of clinical laboratory studies in acute pancreatitis. *Arch pathol Lab Med* 1991; **115**: 325-326

• ACKNOWLEDGMENTS •

Acknowledgments to Reviewers of *World Journal of Gastroenterology*

Many reviewers have contributed their expertise and time to the peer review, a critical process to ensure the quality of *World Journal of Gastroenterology*. The editors and authors of the articles submitted to the journal are grateful to the following reviewers for evaluating the articles (including those were published and those were rejected in this issue) during the last editing period of time.

Takafumi Ando, M.D.

Nagoya University Graduate School of Medicine, Therapeutic Medicine, 65 Tsurumai-cho, Showa-ku, Nagoya 466-8550, Japan

Zong-Jie Cui, Professor

Institute of Cell Biology, Beijing Normal University, Beijing 100875, China

Er-Dan Dong, Professor

Department of Life Science, Division of Basic Research in Clinic Medicine, National Natural Science Foundation of China, 83 Shuanqing Road, Haidian District, Beijing 100085, China

Sheung-Tat Fan, Professor

Department of Surgery, The University of Hong Kong, Queen Mary Hospital, 102 Pokfulam Road, Hong Kong, China

Xue-Gong Fan, Professor

Xiangya Hospital, Changsha 410008, China

Joachim Labenz, Associate Professor

Jung-Stilling Hospital, Wichernstr. 40, Siegen 57074, Germany

Ansgar W Lohse, Professor

Department of Medicine, Hamburg University, Martinistr. 52, Hamburg 20246, Germany

Giovanni Maconi, M.D.

Department of Gastroenterology, 'L.Sacco' University Hospital, Via G.B.Grassi, 74, Milan 20157, Italy

James Neuberger, Professor

Liver Unit, Queen Elizabeth Hospital, Birmingham B15 2TH, United Kingdom

Bo-Rong Pan, Professor

Department of Oncology, Xijing Hospital, Fourth Military Medical University, No.1, F.8, Bldg 10, 97 Changying East Road, Xi'an 710032, Shaanxi Province, China

Heitor Rosa, Professor

Department of Gastroenterology and Hepatology, Federal University School of Medicine, Rua 126 n.21, Goiania - GO 74093-080, Brazil

Jose Sahel, Professor

Hepato-gastroenterology, Hospital sainti Marevenite, 1270 Boulevard AE Sainti Margrenise, Marseille 13009, France

Tilman Sauerbruch, M.D.

Department of Internal Medicine I, University of Bonn, Sigmund-Freud-Strasse 25, 53105 Bonn, Germany

Rudi Schmid, M.D.

211 Woodland Road, Kentfield, California 94904, United States

Tadashi Shimoyama, M.D.

Hirosaki University, 5 Zaifu-cho, Hirosaki 036-8562, Japan

Yoshio Shirai, Associate Professor

Division of Digestive and General Surgery, Niigata University Graduate School of Medical and Dental Sciences, 1-757 Asahimachidori, Niigata City 951-8510, Japan

Manfred Stolte, Professor

Institute of Pathology, Klinikum Bayreuth, Preuschwitzer Str. 101, Bayreuth 95445, Germany

Simon D Taylor-Robinson, M.D.

Department of Medicine A, Imperial College London, Hammersmith Hospital, Du Cane Road, London W12 0HS, United Kingdom

Frank Ivor Tovey, M.D.

Department of Surgery, University College London, 5 Crossborough Hill, Basingstoke RG21 4AG, United Kingdom

Hong-Yang Wan, M.D.

International Co-operation Laboratory on Signal Transduction Eastern Hepatobiliary Surgery Institute, SMMU, 225 Changhai Road, Shanghai 200438, China

Jia-Yu Xu, Professor

Shanghai Second Medical University, Rui Jin Hospital, 197 Rui Jin Er Road, Shanghai 200025, China

Michael Zenilman, Professor and Chairman

Department of Surgery, SUNY Downstate Medical Center, 450 Clarkson Avenue, Brooklyn NY, United States

Jian-Zhong Zhang, Professor

Department of Pathology and Laboratory Medicine, Beijing 306 Hospital, 9 North Anxiang Road, PO Box 9720, Beijing 100101, China

Zhi-Rong Zhang, Professor

West China School of Pharmacy, Sichuan University, 17 South Renmin Road, Chengdu 610041, Sichuan Pvince, China

Role of stress-activated MAP kinase P38 in cisplatin- and DTT-induced apoptosis of the esophageal carcinoma cell line Eca109

Qian-Xian Zhang, Ruo Feng, Wei Zhang, Yi Ding, Ji-Yao Yang, Guo-Hong Liu

Qian-Xian Zhang, Ruo Feng, Wei Zhang, Yi Ding, Ji-Yao Yang, Guo-Hong Liu, Department of Histology and Embryology, Medical College of Zhengzhou University, Zhengzhou 450052, Henan Province, China

Supported by the Henan Medical Science and Technology Innovation Project, No. 200084

Correspondence to: Professor Qian-Xian Zhang, Department of Histology and Embryology, Medical College of Zhengzhou University, Zhengzhou 450052, Henan Province, China. qxz53@zzu.edu.cn
Telephone: +86-371-6658162 Fax: +86-371-6658162

Received: 2004-11-02 Accepted: 2004-11-19

Abstract

AIM: To study the role of P38 kinase in esophageal cancer cell apoptosis induced by genotoxin, cisplatin and the unfolded protein response (UPR) inducer, dithiothreitol (DTT).

METHODS: Esophageal carcinoma cell line Eca109 was cultured in RPMI 1640 medium to 70% confluency and treated with either cisplatin, DTT, or cisplatin plus DTT in the presence or absence of P38 inhibitor, SB203580. The untreated cells served as the control. The esophageal carcinoma cell apoptosis was detected by agarose gel DNA ladder analysis and quantified by flow cytometry. The P38 phosphorylation was detected by immunohistochemistry using antibodies specific to phosphorylated P38 protein.

RESULTS: (1) Both cisplatin and DTT induced apoptosis in the esophageal cancer cell line Eca109 as shown by DNA ladder formation; (2) As detected by antibodies specific for the phosphorylated P38 protein (p-P38), both cisplatin and DTT treatments activated the stress-activated enzyme, MAP kinase P38. The number of positive cells was about 50% for the treatment groups, comparing to that of 10% for untreated group. DTT treatment, but not cisplatin treatment, induces nuclear localization of p-P38; (3) As measured by flow cytometry, inhibition of P38 activity by SB203580 blocks DTT- and cisplatin-induced apoptosis. The rates for DTT, cisplatin, and DTT plus cisplatin-induced apoptosis were 16.8%, 17.1%, and 21.4%, respectively. Addition of the SB compound during the incubation reduced the apoptotic rate to about 7.6% for all the treatment groups, suggesting that P38 activation is essential for cisplatin- and DTT-induced apoptosis in Eca109 cells.

CONCLUSION: (1) Both DTT and cisplatin were able to induce apoptosis in esophageal cancer cell line Eca109; (2) P38 MAP kinase is essential for DTT- and cisplatin-

induced apoptosis in Eca109 cells; (3) P38 activation may be the common signaling component relaying the multiple upstream signaling events to the downstream cell death program.

© 2005 The WJG Press and Elsevier Inc. All rights reserved.

Key words: P38MAPK; Cisplatin; Dithiothreitol; Apoptosis; Eca109 cell line

Zhang QX, Feng R, Zhang W, Ding Y, Yang JY, Liu GH. Role of stress-activated MAP kinase P38 in cisplatin- and DTT-induced apoptosis of the esophageal carcinoma cell line Eca109. *World J Gastroenterol* 2005; 11(29): 4451-4456
<http://www.wjgnet.com/1007-9327/11/4451.asp>

INTRODUCTION

Apoptosis is a programmed cell death stringently controlled by cell signaling pathways and the expression of pro- and anti-apoptotic genes. Inactivation of pro-apoptotic genes or signaling pathways or activation of anti-apoptotic genes or signaling pathways would compromise the ability of the cell to undergo apoptosis, thus contributing to the genesis and development of cancer. Therefore, a thorough understanding of the signaling events leading to the apoptotic program in tumor cells may assist in the development of novel strategies for cancer therapy.

Mitogen-activated protein kinases (MAPK) are members of a family of serine/threonine protein kinases activated by dual phosphorylation at threonine 188 and tyrosine 190 positions. They mainly consist of ERK, JNK/SAPK, and P38. Despite structural similarities, MAPKs play diverse roles in regulating cell function. The activation of ERK promotes cell proliferation and survival, while activation of the stress-activated protein kinases JNK/P38 can mediate different cell responses ranging from stress-induced cell apoptosis to various inflammatory responses^[1-3]. In different cells, the activation of P38 kinase is reportedly either pro-apoptotic or anti-apoptotic^[6-10], and is likely to be determined by the type of stress stimuli and/or the state of cell proliferation and differentiation. Cisplatin is a genotoxin that causes nuclear damage and nuclear stress. It was found that JNK/P38 MAP kinase is activated during cisplatin-induced apoptosis in human lung and ovarian cancer cells^[11,12], which might play an important role in signaling cancer cell apoptosis during cisplatin therapy. The unfolded protein response (UPR) or ER stress response is an ER-based cell stress response^[13-15], which can be triggered by many agents

such as DTT, tunicamycin, and thapsigargin^[16-20]. These agents induce the UPR by interfering with protein folding in the endoplasmic reticulum (ER), thus resulting in the build up of unfolded proteins in the ER. Activation of the UPR triggers cellular compensatory responses such as slowing down of protein translation and speeding up the production of molecular chaperone and, when the rescue efforts fail, it induces cell apoptosis. Whether the activation of P38 is required for the UPR-mediated cell apoptosis remains to be elucidated.

Esophageal carcinoma is one of the most common and debilitating malignancies in China. It was reported that cisplatin could induce apoptosis in esophageal cancer cells^[21]. However, the role of P38 MAP kinase in cisplatin-induced esophageal cancer cell apoptosis is unclear. In this study, it was tested whether P38 kinase is activated in cisplatin-treated esophageal cancer cells and, if it is, whether the P38 activation is an essential step for cisplatin-induced apoptosis. And it was further investigated whether P38 kinase activation is required for the UPR inducer DTT-induced apoptosis in esophageal cancer cells. This study may provide new insights into the role of P38 kinase in esophageal cancer cell apoptosis triggered by diverse cell stressors.

MATERIALS AND METHODS

Materials

The anti-phosphorylated P38 antibodies were kindly provided by Dr. Tao Zhu, National University of Singapore. SB203580, DTT, RPMI 1640, and FBS were from Sigma. The other reagents were purchased from Beijing Zhongshan Biotechnology Co., Ltd.

Cell culture

Eca109 cells were provided by our department and grown in RPMI 1640 medium supplemented with 10% heat-inactivated fetal calf serum, 100 U/mL penicillin and 100 U/mL streptomycin. All cell cultures were done at 37 °C with 5 mL/L CO₂ in a humidified incubator.

Induction of apoptosis by cisplatin and DTT

Eca109 cells were cultured to 70% confluency in RPMI 1640 medium. The cultures were continued in the RPMI 1640 medium for additional 24 h with or without 10 µg/mL cisplatin, 2 mmol/L DTT, or 10 µg/mL cisplatin plus 2 mmol/L DTT. For testing the effects of P38 inhibitor SB203580 on cell apoptosis, cells were pretreated with 10 µg/mL SB203580 for 2 h before switching to cisplatin, DTT or cisplatin+DTT containing media. Each experimental condition was set up in flask. The untreated cells were the control. At the end of the treatment, the cells were collected from the cell culture flasks and further analyzed either for cell apoptosis by DNA ladder formation, P38 activation by immunostaining or cell apoptosis by flow cytometry.

DNA isolation and gel electrophoresis

DNAs for fragmentation analysis were prepared as previously described^[22]. DNA was analyzed for each condition by 1.5% agarose gel electrophoresis in TBE buffer. The gel was stained with ethidium bromide (0.5% µg/mL) and visualized under UV light.

Immunohistochemistry

Cells were harvested from the flasks, washed with cold PBS and fixed onto glass slides by using 40 g/L paraformaldehyde solution. p-P38 kinase was detected using anti-phosphorylated P38 antibody (1:200 dilution), according to the protocol of Beijing Zhongshan Biotechnology Co., Ltd. Negative control was provided by the untreated Eca109 cells, without the incubation with anti-phosphorylated P38 antibody. DAB staining system was used to demonstrate the amount of p-P38, which is the activated form of P38. The slides were counter-stained by Methyl Green dye to visualize the cell structure. The 100 cells from each condition were scored based on the immunostaining signal intensity as follows: -: 0, -/+ : 0.5, +: 1, ++: 2.

Flow cytometry analysis

The cells were harvested and washed twice with PBS (pH 7.2) and suspended in 80% ethanol at 20 °C for 24 h, then thawed quickly at room temperature and centrifuged to collect the cells. The cells were washed with PBS twice again and resuspended in the extraction buffer (0.2 mol/L Na₂HPO₄ 0.1 mol/L citric acid) for 5 min, and finally resuspended in PBS containing RNase A (100 µg/mL) and 50 µg/mL propidium iodide for 30 min. The cell cycle distribution and quantitation of apoptotic cells were determined by the fluorescence of individual cells measured by flow cytometry (Beckman-Coulter Epics Altra).

Statistical analysis

Biostatistical analyses were done using SPSS10.0 software package. The data from immunohistochemistry and flow cytometry were analyzed by χ^2 and Kruskal-Wallis tests.

RESULTS

Detection of cisplatin- and DTT-induced apoptosis by DNA ladder formation in esophageal cancer cell line Eca109

Cisplatin is known to induce cell death via apoptosis in many cell types, by damaging DNA and disturbing nuclear function. DTT, on the other hand, is a well-known ER stress inducer and induces cell apoptosis via UPR. A biochemical hallmark of apoptosis is the characteristic degradation of the genomic DNA by cleavage at the internucleosomal sites, generating a 'ladder' of DNA fragments, which can be detected by agarose gel electrophoresis^[23-25]. To determine whether cisplatin and DTT induce Eca109 cell apoptosis, Eca109 cells were treated with cisplatin, DTT and cisplatin plus DTT. The total DNA was resolved on agarose gel. DNA ladders were observed for all three treatment groups, while only large molecular weight DNA with no obvious ladder formation was seen for the untreated cells (Figure 1). This result demonstrates that both cisplatin and DTT were able to induce apoptosis in esophageal cancer Eca109 cells. In addition, spontaneous apoptosis of Eca109 cells is minimal under these experimental conditions.

The DNA samples were analyzed by 1.5% agarose gel in TBE buffer and visualized by UV-ethidium bromide method. Lane 1: cisplatin plus DTT; lane 2: DTT; lane 3: cisplatin; lane 4: untreated cells; lane 5: DNA molecular weight marker. The DNA bands of 400, 600, 800, and 1 000 bp were clearly seen on lanes 1-3.

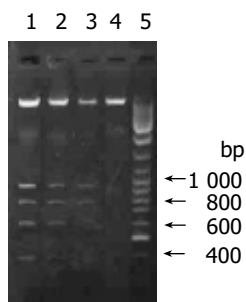


Figure 1 Cisplatin and DTT treatments induce DNA ladder formation in Eca109 cells.

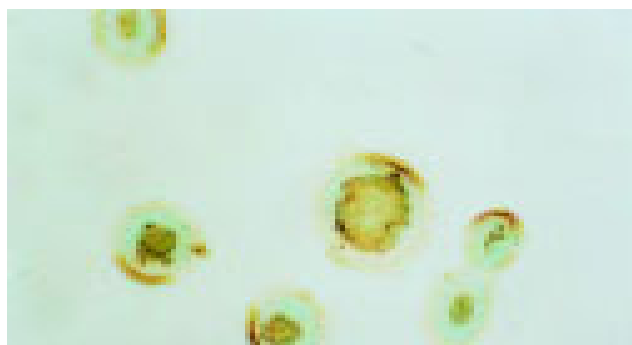


Figure 2 Activation of P38 kinase in DTT-treated Eca109 cells.

Cisplatin and DTT treatments activate P38 kinase in Eca109 cells

Activation of P38 kinase is achieved via the phosphorylation of P38 protein by the upstream kinases, which can be detected by antibodies specifically for the phosphorylated P38 protein (p-P38). To detect the P38 activation upon cell stresses, the Eca109 cells were cultured and treated with cisplatin, DTT, and cisplatin plus DTT for 24 h. The cells were stained with anti-p-P38 antibodies. The untreated Eca109 cells without incubation with anti-p-P38 antibodies were used as negative control. The cells were grouped into four groups, based on their signal intensity for the immunostaining. The percentage of cells positively stained with anti-p-P38 antibodies are summarized in Table 1.

Both cisplatin and DTT treatments markedly increased the number of the cells positive for p-P38 kinase. About 50% of the treated cells were positive for p-P38, when compared to that of 10% for the untreated cells. Few positive cells were observed in negative control (Figure 6). Moreover, comparing with the untreated group, the level of the phosphorylated P38 was dramatically increased upon treatment with cisplatin and DTT ($P < 0.01$). Treatment with DTT in combination with cisplatin showed only a modest increase in the number of the positive cells and the level of p-P38 signal. The difference did not reach statistical significance ($P < 0.05$).

Interestingly, the subcellular localization of p-P38 kinase was markedly different between DTT, and cisplatin-treated cells (Figures 2-5) though both treatments achieved the same level of P38 activation. The p-P38 was largely localized in the nucleus for DTT-treated cells, while the distribution of p-P38 for cisplatin-treated cells was mostly cytoplasmic, accentuated in the peri-plasma membrane region. Addition of DTT to the cisplatin treatment resulted in partial nuclear



Figure 3 Activation of P38 kinase in cisplatin-treated Eca109 cells.

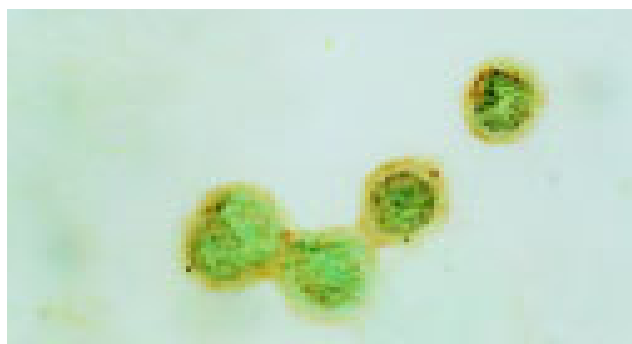


Figure 4 Activation of P38 kinase in DTT- and cisplatin-treated Eca109 cells.

localization of the p-P38 kinase. The significance of the different localization of p-P38 by different death inducers is unclear.

Inhibiting P38 kinase blocks DTT- and cisplatin-induced Eca109 cell apoptosis

To test whether the activation of P38 kinase is required for DTT- and cisplatin-induced Eca109 cell apoptosis, the P38 kinase inhibitor SB203580 was employed to inhibit P38 kinase activity in DTT- and cisplatin-treated cells. The rate of apoptosis was determined by flow cytometry analysis. The data are shown in Figure 6 and summarized in Table 2. The rates of Eca109 cell apoptosis were 16.8%, 17.1%, and 21.4% for DTT, cisplatin, and DTT plus cisplatin, respectively. Consistent with the data of P38 kinase activation, DTT and cisplatin induced apoptosis to a similar

Table 1 Number of cells positive for p-P38 kinase upon cisplatin and DTT treatments

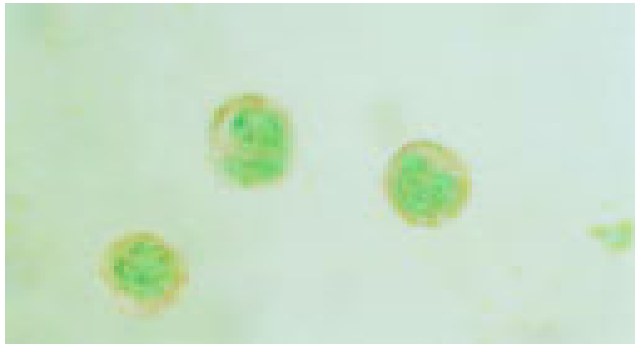
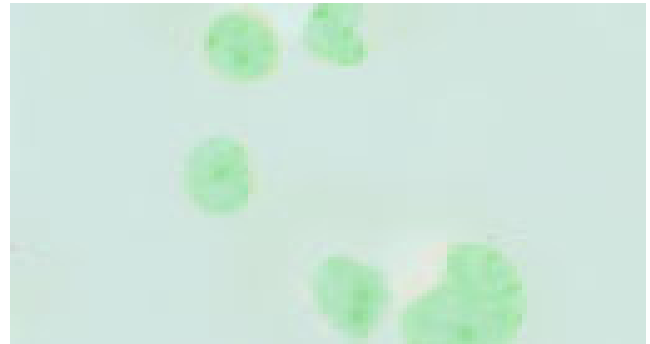
	D	C	D+C	U
-	26	23	15	69
±	29	31	31	21
+	24	25	24	6
++	21	21	30	4
Total scores	80.5 ^b	82.5 ^b	99.5 ^b	24.5

D: DTT, C: cisplatin, D+C: DTT + cisplatin, U: untreated. ^b $P < 0.01$ vs control group.

Table 2 SB203580 blocks DTT- and cisplatin-induced Eca109 cell apoptosis

	D	Di	C	Ci	D+C	D+Ci	U
Number of observed cells	17 925	18 889	18 162	19 220	17 929	18 260	18 430
Number of apoptosis cells	3 026	1 450	3 110	1 504	3 160	1 401	538
Apoptotic rate (%±0.00)	16.8 ^{a,b,d}	7.6 ^b	17.1 ^{b,d}	7.8 ^b	21.4 ^{b,d}	7.6 ^b	2.9

D: DTT, Di: DTT-SB203580, C: cisplatin, Ci: cisplatin-SB203580, D+C: DTT+cisplatin, D+Ci: (DTT+cisplatin)-SB203580, U: untreated. ^a $P < 0.05$ vs group treated with DTT plus cisplatin, ^b $P < 0.01$ vs control group; ^d $P < 0.01$ vs corresponding group in the presence of SB203580.

**Figure 5** Activation of P38 kinase in untreated Eca109 cells.**Figure 6** Negative control.

extent. The rate of apoptosis for DTT plus cisplatin-treated cells was moderately higher. Remarkably, SB203580 compound effectively inhibited Eca109 cell apoptosis in all three treatment groups ($P < 0.01$). These results strongly suggest that P38 activation is essential for both cisplatin- and DTT-induced apoptosis in Eca109 cells. The fact that both DTT- and cisplatin-induced cell apoptosis requires P38 activity implies that P38 kinase might be the common component shared by both stress response pathways (Figure 7).

DISCUSSION

As a commonly used chemotherapeutic agent, cisplatin exerts its cytotoxic effect by intrastrand and interstrand crosslinking of DNA at specific base sequences^[26]. Recent studies have shown that the mechanism of cisplatin-induced cell death is through apoptosis^[21]. It was found that P38 MAP kinase is activated during cisplatin-induced apoptosis in human lung and ovarian cancer cells, which might play an important role in signaling cancer cell apoptosis during cisplatin therapy. However, no reports showed the role of P38 MAP kinase in cisplatin-induced esophageal cancer cell apoptosis. Our studies show that cisplatin treatment strongly activates P38 kinase in esophageal cancer cells. Moreover, inhibition of P38 activity by the specific inhibitor SB203580 almost completely blocked cisplatin-induced apoptosis. Our results and the data reported by others^[11,12] support the notion that P38 activation is a critical step in cisplatin-induced apoptosis.

The exact position of P38 activation in the chain of signaling pathways leading to the execution of cell death program is still undetermined. Previous data suggest that P38 kinase is involved in histone H₃ phosphorylation^[27], nuclear condensation, and cell blebbing^[28] during cisplatin-induced apoptosis. It is conceivable that the activation of

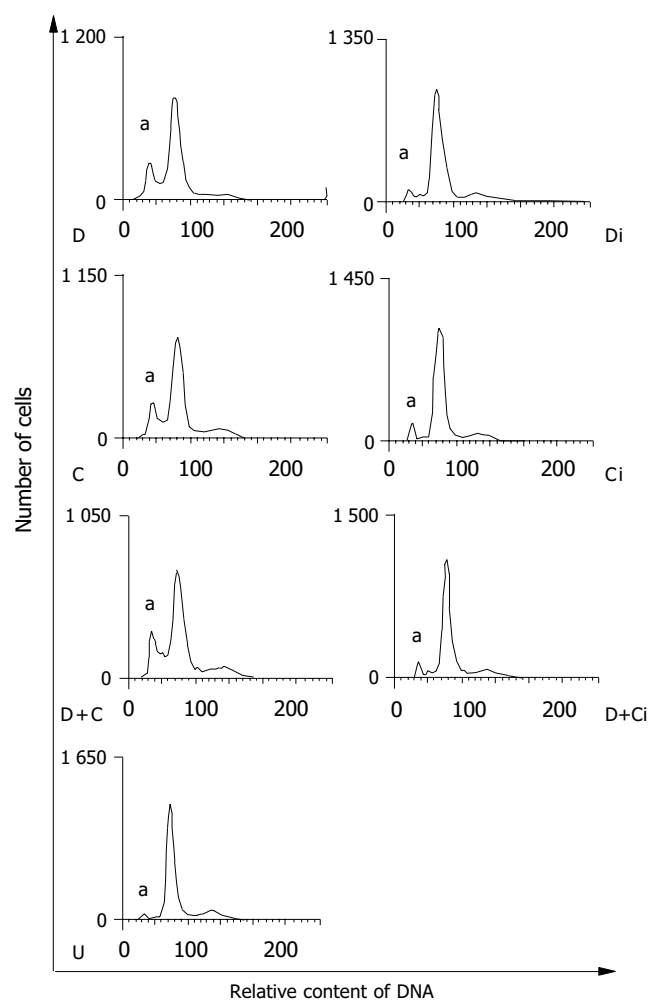


Figure 7 The effects of SB203580 on DTT- and cisplatin-induced Eca109 cell apoptosis – flow cytometry analysis. SB sharply decreased the apoptotic peak of the group treated with DTT or cisplatin or DTT plus cisplatin. D: DTT, Di: DTT-SB203580, C: cisplatin, Ci: cisplatin-SB203580, D+C: DTT+cisplatin, D+Ci: DTT+cisplatin-SB203580, U: untreated, a: apoptotic peak.

P38 kinase is an early intermediate event branching out from the cell stress response pathways but before the execution of cell death program.

DTT is known to induce the unfolded protein response, probably by perturbing the ER oxidoreductive potential, important for disulfide bond formation and protein folding. Several branches of the UPR can lead to cell death program^[29]. Few studies focus on the effects of DTT on apoptosis and none of the reports had showed the relationship between UPR and P38 MAP kinase signaling pathway. Our data indicate that DTT treatment effectively triggered Eca109 cell apoptosis with potency comparable to that of cisplatin. Remarkably, P38 kinase was strongly activated by DTT treatment. This provides the first link between the UPR and P38 kinase activation. Furthermore, inhibition of P38 kinase activity blocks DTT-induced apoptosis, indicating that P38 activation is an indispensable intermediate step for the UPR-mediated cell apoptosis. It was reported previously that Japanese encephalitis virus (JEV) infection triggers the UPR and apoptosis in fibroblast and neuronal cells^[30]. Japanese encephalitis virus-induced apoptosis can be partially blocked by P38 kinase inhibitor SB203580.

An intriguing finding was that the subcellular localization of the activated P38 was markedly different in DTT- and cisplatin-treated cells. In DTT-treated cells, p-P38 was mainly seen in the nucleus, while in cisplatin-treated cells, p-P38 is mostly localized in the cytoplasm. The basis for this observation remains speculative. One possibility is that the nuclear perturbation exerted by cisplatin treatment hinders the p-P38 nuclear entry or retention. Surprisingly, the different localization of p-P38 does not significantly affect the apoptotic rate of the treated cells. This might suggest that p-P38 localization is not essential for p-P38 to relay its signal to the downstream apoptotic pathways. Alternatively, the nuclear fraction and cytoplasmic fraction of the p-P38 might trigger different downstream signaling pathways, which are able to transduce the signal to cell death program with similar efficacies. More studies are needed to address this issue.

The data obtained here raises the possibility that P38 kinase is the common central component relaying multiple cell stress pathways to the cell death program. If this notion proved to be true, then it might be possible to develop anticancer agents, which could specifically activate P38 kinase along with minimal nonspecific toxicities. This might also help to formulate newer drug combinations with synergistic activation of P38 kinase, to achieve better therapeutic efficacy and lesser side effects. Furthermore, DTT might be another apoptosis inducer. More studies should be carried out using different cell lines.

REFERENCES

- 1 **Kim BS**, Yoon KH, Oh HM, Choi EY, Kim SW, Han WC, Kim EA, Choi SC, Kim TH, Yun KJ, Kim EC, Lyou JH, Nah YH, Chung HT, Cha YN, Jun CD. Involvement of P38 MAP kinase during iron chelator-mediated apoptotic cell death. *Cell Immunol* 2002; **220**: 96-106
- 2 **Petrich BG**, Wang Y. Stress-activated map kinases in cardiac remodeling and heart failure; new insights from transgenic studies. *Trends Cardiovasc Med* 2004; **14**: 50-55
- 3 **Hashimoto K**, Farrow BJ, Evers BM. Activation and role of MAP kinases in 15d-PGJ2- induced apoptosis in the human pancreatic cancer cell line MIA PaCa-2. *Pancreas* 2004; **28**: 153-159
- 4 **Scali C**, Giovannini MG, Prosperi C, Bellucci A, Pepeu G, Casamenti F. The selective cyclooxygenase-2 inhibitor rofecoxib suppresses brain inflammation and protects cholinergic neurons from excitotoxic degeneration *in vivo*. *Neuroscience* 2003; **117**: 909-919
- 5 **Choi JA**, Park MT, Kang CM, Um HD, Bae S, Lee KH, Kim TH, Kim JH, Cho CK, Lee YS, Chung HY, Lee SJ. Opposite effects of Ha-Ras and Ki-Ras on radiation-induced apoptosis via differential activation of PI3K/Akt and Rac/p38 mitogen-activated protein kinase signaling pathways. *Oncogene* 2004; **23**: 9-20
- 6 **Schrantz N**, Bourgeade MF, Mouhamad S, Leca G, Sharma S, Vazquez A. P38 mediated regulation of an Fas-associated death domain protein-independent pathway leading to caspase-8 activation during TGF beta- induced apoptosis in human Burkitt lymphoma B cells BL41. *Mol Biol Cell* 2001; **12**: 3139-3151
- 7 **Sanchez-Prieto R**, Rojas JM, Taya Y, Gutkind JS. A role for the P38 mitogen-activated protein kinase pathway in the transcriptional activation of P53 on genotoxic stress by chemotherapeutic agents. *Cancer Res* 2000; **60**: 2464-2472
- 8 **Liu HR**, Tao L, Gao E, Lopez BL, Christopher TA, Willette RN, Ohlstein EH, Yue TL, Ma XL. Anti-apoptotic effects of rosiglitazone in hypercholesterolemic rabbits subjected to myocardial ischemia and reperfusion. *Cardiovasc Res* 2004; **62**: 135-144
- 9 **Lee RJ**, Albanese C, Stenger RJ, Watanabe G, Inghirami G, Haines GK 3rd, Webster M, Muller WJ, Brugge JS, Davis RJ, Pestell RG. ppv-Src induction of cyclinD1 requires collaborative interactions between the extracellular signal-regulated kinase P38 and Jun kinase pathways. A role cAMP response element-binding protein and activating transcription factor-2 in PP60 (V-src) signaling in breast cancer cells. *J Biol Chem* 1999; **274**: 7341-7350
- 10 **Olson JM**, Hallahan AR. p38 MAP kinase: a convergence point in cancer therapy. *Trends Mol Med* 2004; **10**: 125-129
- 11 **Viktorsson K**, Ekedahl J, Lindebro MC, Lewensohn R, Zhivotovsky B, Linder S, Shoshan MC. Defective stress kinase and Bak activation in response to ionizing radiation but not cisplatin in a non-small cell lung carcinoma cell line. *Exp Cell Res* 2003; **289**: 256-264
- 12 **Mansouri A**, Ridgway LD, Korapati AL, Zhang Q, Tian L, Wang Y, Siddik ZH, Mills GB, Claret FX. Sustained activation of JNK/p38 MAPK pathways in response to cisplatin leads to Fas ligand induction and cell death in ovarian carcinoma cells. *J Biol Chem* 2003; **278**: 19245-19256
- 13 **Harding HP**, Calton M, Urano F, Novoa I, Ron D. Transcriptional and translational control in the Mammalian unfolded protein response. *Annu Rev Cell Dev Biol* 2002; **18**: 575-599
- 14 **Rutkowski DT**, Kaufman RJ. A trip to the ER: coping with stress. *Trends Cell Biol* 2004; **14**: 20-28
- 15 **Zhang K**, Kaufman RJ. Signaling the unfolded protein response from the endoplasmic reticulum. *J Biol Chem* 2004; **279**: 25935-25938
- 16 **Gilmore WJ**, Kirby GM. Endoplasmic reticulum stress due to altered cellular redox status positively regulates murine hepatic CYP2A5 expression. *J Pharmacol Exp Ther* 2004; **308**: 600-608
- 17 **Trotter EW**, Grant CM. Thioredoxins are required for protection against a reductive stress in the yeast *Saccharomyces cerevisiae*. *Mol Microbiol* 2002; **46**: 869-878
- 18 **Martinez IM**, Chrispeels MJ. Genomic analysis of the unfolded protein response in Arabidopsis shows its connection to important cellular processes. *Plant Cell* 2003; **15**: 561-576
- 19 **Piccini A**, Fassio A, Pasqualetto E, Vitali A, Borghi R, Palmieri D, Nacmias B, Sorbi S, Sitia R, Tabaton M. Fibroblasts from FAD-linked presenilin 1 mutations display a normal unfolded protein response but overproduce Abeta42 in response to tunicamycin. *Neurobiol Dis* 2004; **15**: 380-386
- 20 **Mulder HJ**, Saloheimo M, Penttila M, Madrid SM. The tran-

- scription factor HACA mediates the unfolded protein response in *Aspergillus niger*, and up-regulates its own transcription. *Mol Genet Genomics* 2004; **271**: 130-140
- 21 **Raouf A**, Evoy D, Carton E, Mulligan E, Griffin M, Sweeney E, Reynolds JV. Spontaneous and inducible apoptosis in oesophageal adenocarcinoma. *Br J Cancer* 2001; **85**: 1781-1786
- 22 **Nasreen N**, Mohammed KA, Dowling PA, Ward MJ, Galffy G, Antony VB. Talc induces apoptosis in human malignant mesothelioma cells *in vitro*. *Am J Respir Crit Care Med* 2000; **161**(2 Pt 1): 595-600
- 23 **Kim JY**, Kim KM, Nan JX, Zhao YZ, Park PH, Lee SJ, Sohn DH. Induction of apoptosis by tanshinone I via cytochrome c release in activated hepatic stellate cells. *Pharmacol Toxicol* 2003; **92**: 195-200
- 24 **Scavo LM**, Newman V, Ertsey R, Chapin CJ, Kitterman JA. Maternally administered dexamethasone transiently increases apoptosis in lungs of fetal rats. *Exp Lung Res* 2003; **29**: 211-226
- 25 **Yeh CH**, Wang YC, Wu YC, Chu JJ, Lin PJ. Continuous tepid blood cardioplegia can preserve coronary endothelium and ameliorate the occurrence of cardiomyocyte apoptosis. *Chest* 2003; **123**: 1647-1654
- 26 **Zamble DB**, Mikata Y, Eng CH, Sandman KE, Lippard SJ. Testis-specific HMG-domain protein alters the responses of cells to cisplatin. *J Inorg Biochem* 2002; **91**: 451-462
- 27 **Wang D**, Lippard SJ. Cisplatin-induced post-translational modification of histones H3 and H4. *J Biol Chem* 2004; **279**: 20622-20625
- 28 **Deschesnes RG**, Huot J, Valerie K, Landry J. Involvement of p38 in apoptosis-associated membrane blebbing and nuclear condensation. *Mol Biol Cell* 2001; **12**: 1569-1582
- 29 **Kudo T**. Involvement of unfolded protein responses in neurodegeneration. *Nihon Shinkei Seishin Yakurigaku Zasshi* 2003; **23**: 105-109
- 30 **Su HL**, Liao CL, Lin YL. Japanese encephalitis virus infection initiates endoplasmic reticulum stress and an unfolded protein response. *J Virol* 2002; **76**: 4162-4171

Science Editor Wang XL and Li WZ Language Editor Elsevier HK

Histological and ultrastructural changes induced by selenium in early experimental gastric carcinogenesis

Yan-Ping Su, Jun-Min Tang, Yan Tang, Hui-Ying Gao

Yan-Ping Su, Hui-Ying Gao, Department of Histology and Embryology, Taishan Medical College, Taian 271000, Shandong Province, China

Jun-Min Tang, Yan Tang, Department of Histology and Embryology, Peking University Health Science Center, Beijing 100083, China
Supported by the Shandong Educational Office, No. J00K67

Correspondence to: Yan-Ping Su, Department of Histology and Embryology, Taishan Medical College, Taian 271000, Shandong Province, China. su-yanping@163.com

Telephone: +86-538-6222080

Received: 2004-10-23 Accepted: 2004-12-26

Abstract

AIM: To investigate the effect and significance of selenium in early experimental gastric carcinogenesis.

METHODS: Weaning male Wistar rats were divided randomly into normal control group, experiment control group, low selenium (2 mg/L) group and high selenium (4 mg/L) group. Wistar rat gastric carcinogenesis was induced by *N*-methyl-*N*-nitro-*N*-nitroso guanidine (MNNG) (20 mg/kg) gavage daily for 10 d. Na₂SeO₃ was given by piped drinking 1 wk prior to MNNG gavage. The rats were killed at the 43rd wk. The surface characteristics of gastric mucosa were observed with naked eyes. Histopathologic changes of rat gastric mucosa were observed by HE staining and AB-PAS methods. The changes of cellular ultrastructure were observed under transmission electron microscope. Statistical analysis was carried out by SPSS.

RESULTS: The incidence rate of gastric mucosa erosion, hemorrhage and intestinal metaplasia was 0, 45.5%, 66.7%, and 92.9%, respectively (92.9% vs 45.5%, $P < 0.05$) in the normal control group, experiment control group, low selenium group, and high selenium group. Leiomyoma formed in the process of inducement of rat gastric carcinoma. Dietary Na₂SeO₃ (2 and 4 mg/L) slightly increased the incidence rate of leiomyoma (0, 23%, 46.6%, and 46.6%). gastric mucosa did not change in the course of rat gastric carcinogenesis. Dietary Na₂SeO₃ by pipe drinking could expand the intracellular secretory canaliculus of parietal cells and increase the number of endocrine cells and lysosomes.

CONCLUSION: Dietary Na₂SeO₃ by pipe drinking aggravates gastric erosion, hemorrhage and promotes intestinal metaplasia of gastric mucosa. The mechanism may be related with the function of parietal cells.

Key words: Selenium; Ultrastructure; Experimental gastric carcinogenesis

Su YP, Tang JM, Tang Y, Gao HY. Histological and ultrastructural changes induced by selenium in early experimental gastric carcinogenesis. *World J Gastroenterol* 2005; 11(29): 4457-4460
<http://www.wjgnet.com/1007-9327/11/4457.asp>

INTRODUCTION

Gastric cancer results from chronic superficial gastritis, atrophic gastritis, intestinal metaplasia, and heterotypic hyperplasia. Previous studies showed that selenium (Se) supplementation or selenium deficiency causes changes in the cellular ultrastructure^[1-4]. Selenium is an essential trace element in mammals. The results of laboratory investigations and cohort studies suggest that selenium exhibits a bivalent effect in cancer, either increasing or decreasing the risk of cancer^[5,6]. We conducted this study to investigate the effect and significance of selenium in experimental gastric carcinogenesis.

MATERIALS AND METHODS

Materials

A total of 62 weaned male Wistar rats, weighing 31-56 g, were purchased from Department of Experimental Animals, Health Science Center of Peking University. The rats were housed in wire-bottomed metal cages at controlled temperature (21-22 °C) with a humidity of 30-50%, and in light-dark cycle. The rats were divided into the normal control group (group 1) which was given dimethyl sulfoxide (DMSO)-0.9% NaCl vehicle gavage with drinking normal tap water, experiment control group (group 2) which was given *N*-methyl-*N*-nitro-*N*-nitroso guanidine (MNNG), 20 mg/kg (presented by Professor Deng-DJ) gavage with drinking normal tap water, low selenium (2 mg/L) group (group 3) which was given MNNG (20 mg/kg) gavage with drinking water containing 2 mg selenium/L as sodium selenite before 1 wk administration of MNNG, or at the beginning of the experiment, and high selenium (4 mg/L) group (group 4) which was given MNNG (20 mg/kg) gavage with drinking water containing 4 mg selenium/L as sodium selenite before 1 wk administration of MNNG (Table 1).

Methods

The rats in groups 2-4 were given MNNG (20 mg/kg) gavage daily for 10 d, 1 wk after the experiment. MNNG was dissolved in DMSO at the concentration of 100 g/L

Table 1 Groups of Wistar rats

Group	Number	Dose of MNNG (mg/kg)	Dose of selenium in water (mg/L)	Time of selenium given
Normal control	10	0	0	/
Experimental control	22	20	0	/
Low selenium	15	20	2	1 wk before MNNG gavage
High selenium	15	20	4	1 wk before MNNG gavage

and kept in a cool, dark place. The stock solution was diluted to 1 g/L with 0.9% physiological saline before use. The rats in normal group were given DMSO-0.9% NaCl vehicle gavage. Selenium containing water was prepared. The low and high selenium groups were given selenium containing water at the beginning of experiment, 1 wk before administration of MNNG. The experiment rats had free access to diet and water. The animals were examined and weighed twice a week.

The animals were killed at the 43rd wk. The rats were starved for 12 h and anesthetized with 2.5% pentobarbitone intraperitoneal injection before they were killed. The stomach and other organs of the rats were carefully examined. Tissues from the stomach were fixed in 10% neutral Phosphate-buffered formalin solution and embedded in paraffin. Serial sections (5-6 μ m thick) were obtained from the stomach and stained with hematoxylin and eosin (HE), or Alcian blue-Periodic acid-Schiff (AB-PAS). Metaplasia of gastric mucosa was found as blue or purple blue granules in gastric mucosa cells after AB-PAS staining. For electron microscopy, the tissues from stomach were fixed for 2 h at 4 $^{\circ}$ C in 2.5 glutaraldehyde solution in 0.1 mol/L phosphate buffer, postfixed in 1.0% osmium tetroxide in the same buffer at 4 $^{\circ}$ C for 1 h, and then embedded in Epoxy resin. Ultrathin sections were stained with uranium acetate and lead acetate according to double stained method. The results were examined under a JEM-JEOL 100 \times electron microscope.

Statistical analysis

The clinicopathological results were statistically analyzed by SPSS software and χ^2 test.

RESULTS

Clinicopathological results

The results are shown in Table 2. The stomachs in the normal control group were smooth on the surface of serosa. Their inner surfaces clearly presented longitudinal branching folds and gastric pits. All the surface cells of rat gastric mucosa in group 1 had violet red granules (Figure 2A). Erosion and hemorrhage of gastric mucosa were found in 10 of 22 rats (45.5%) in the experimental control group (Figure 1A). There were many blue or purple blue granules in the erosive gastric mucosa of group 2 (Figure 2B). Similar erosive, hemorrhagic and intestinal metaplasia of gastric mucosa was found in 10 of 15 rats (66.7%) of low selenium group, 13 of 14 rats (92.9%) of high selenium group. The incidence rate of intestinal metaplasia was significantly higher in low and high selenium groups than in experiment control group ($P < 0.05$). The incidence of intestinal metaplasia was not significantly different between the high and low selenium groups. There were no significant changes by HE staining,

but the glandular cavity of fundic gland was slightly larger in high selenium group than in the other groups. In experimental control group, a single neoplasm was found on the surface of serosa breaching the serosa (Figure 1B). The diameter was about 0.2-1 cm. A similar neoplasm was also found in low and high selenium groups. The incidence of neoplasm was slightly higher in these two groups than in experimental control group. The neoplasm was diagnosed as leiomyoma by HE staining.

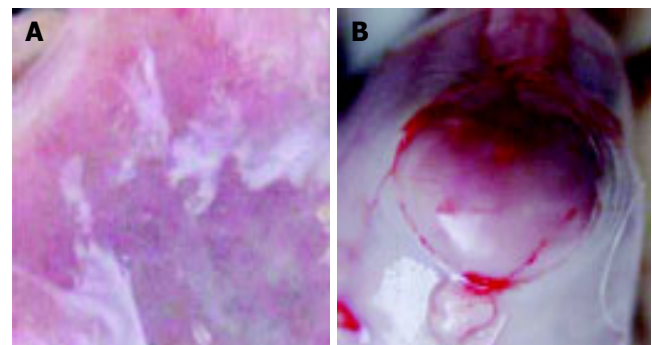


Figure 1 Erosive mucosa of rat stomach (A) and leiomyoma under serosa (B).

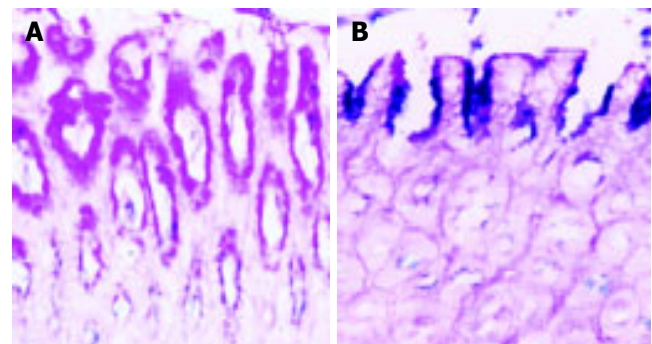


Figure 2 Normal mucosa (A) and erosive mucosa (B) of rat stomach, AB-PAS, $\times 200$.

Table 2 Results of pathologic diagnosis

	Number of rats	Incidence rate of leiomyoma (%)	Incidence rate of intestinal metaplasia (%)
Normal control	10	0	0
Experimental control	22	23	45.5
Low selenium	15	46.6	66.7 ^a
High selenium	14	42.8	92.9 ^a

^a $P < 0.05$ vs experiment control group.

Ultrastructural changes of gastric mucosa

In normal control group, the most distinctive feature in the ultrastructure of gastric mucosa was the presence of a deep invagination of the apical membrane forming a secretory canaliculus. The membrane lining the canaliculus had numerous microvilli projecting into its lumen. About 40% of the cytoplasmic volume was occupied by large mitochondria (Figure 3). Fewer endocrine cells were found in the normal gastric mucosa. Pinosomes distributed in the capillary endothelium of normal control group were large in diameter. Compared to normal control group, the secretory canaliculi in parietal cells were scarce, microvilli projecting into canaliculus lumen were sparse, the pinosomes were more in number and smaller in diameter than in experimental control group. Compared to the normal and experimental control groups, the following characteristics were observed in selenium supplement group: (1) the secretory canaliculus expanded and the microvilli projecting into canaliculus were scarce (Figure 4); (2) endocrine cells scattered in gastric mucosa contained granules with a different diameter and high electron density, there were a few secondary lysosomes in cytoplasm of some endocrine cells (Figure 5); (3) more eosinophils were found in the erosive gastric mucosa (Figure 6); (4) the chief cells had abundant rough endoplasmic reticulum, mitochondria were more in number and larger in volume; (5) the pinosomes in capillary endothelium were slightly less. These characteristics were significant in high selenium group.

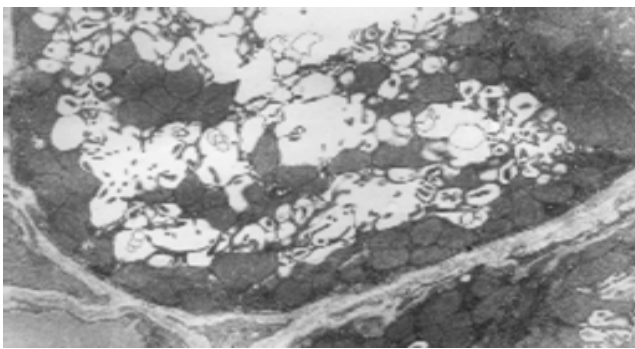


Figure 3 Intracellular secretory canaliculi of parietal cells in normal control group, TEM 5.8×10^3 .

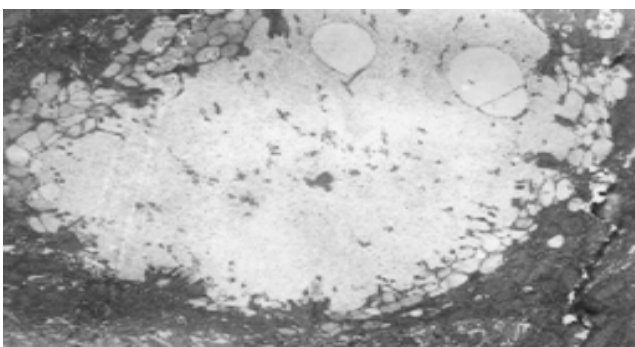


Figure 4 Expansion of intracellular secretory canaliculi of parietal cells in high selenium group, TEM 5.8×10^3 .

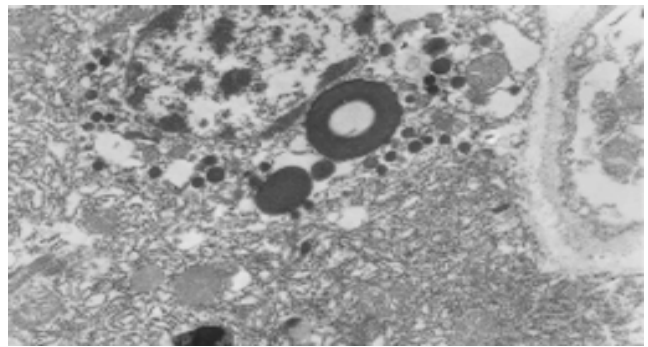


Figure 5 Endocrine cells and secondary lysosomes in high selenium group, TEM 10×10^3 .

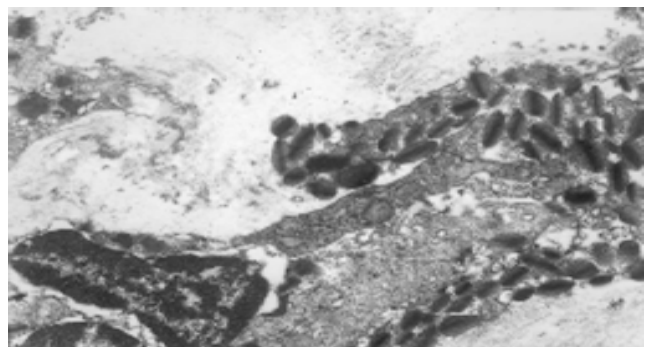


Figure 6 Infiltration of eosinophils in gastric mucosa of high selenium group, TEM 10×10^3 .

DISCUSSION

Selenium, a constituent of antioxidant enzyme, has been proposed as a chemopreventive agent for many kinds of cancer^[7-10]. Selenium supplement to diet or drinking water can prevent tumorigenesis and decrease the incidence rate of cancer^[11-14]. The effect of selenium on carcinoma is still controversial^[5,6]. It was reported that selenium promotes carcinogenesis and tumor development^[15]. Gastric cancer is the second most frequent cause of cancer death in the world and the leading cause of cancer death in China. Studies have been focused on randomized nutritional intervention trial to prevent gastric cancer^[16-20] and epidemiology in serum selenium concentrations and esophageal and gastric cancer^[21]. Wu *et al.*^[22], reported that gastric cancer tissues have significantly higher concentrations of Fe, K, Mg, Na, Rb, Se, and Zn than normal gastric mucosal tissues. At present, the information on the effect of selenium in early experimental gastric carcinogenesis is scarcely available. This experiment was conducted to investigate the effect and significance of selenium on experimental gastric carcinogenesis by morphologic methods. The findings in this study showed that 2.0 and 4.0 g/L selenium in drinking water for 43 wk aggravated gastric mucosa erosion and hemorrhage and promoted intestinal metaplasia of gastric mucosa. Because gastric cancer results from chronic superficial gastritis, atrophic gastritis, intestinal metaplasia, heterotypic hyperplasia, supplement of selenium as sodium selenite does not decrease the risk of gastric cancer induced by MNNG. Furthermore, leiomyoma formed in the process of gastric carcinogenesis

induced by MNNG. Dietary Na₂SeO₃ (2 and 4 mg/L) increased the incidence of leiomyoma. Since the general dose of selenium is 0.5-6 g/mL (or /g)^[23] supplemented to diet and drinking water, the selenium dose in this study did not reach the toxic limits. Consequently the effects of sodium selenite maybe related to the kind of selenium, type of cancer, and different carcinogens.

Selenium induces oxidation and cross-linking of protein thiol groups, mitochondrial permeability transition, decrease in mitochondrial membrane potential, and release of cytochrome C in mitochondria isolated from rat liver, thus possibly inducing tumor cell apoptosis^[1]. Zhong and Oberley^[2] reported that oxidative stress is induced by sodium selenite at high concentrations, but outcomes are different. After acute exposure to selenite, cells display mitochondrial injury and cell death. After chronic exposure to selenite, cells show growth inhibition due to cell cycle arrest, increase the number of mitochondria and the levels of mitochondrial enzymes. Lysosomes in the liver and kidneys of selenium-deficient rats are enlarged and contain electron-dense areas^[3]. Demirel-Yilmaz *et al.*^[4], reported that low or high doses of sodium selenite and vitamin E in diet can alter the microvascular permeability of different organs. Our findings in this study indicate that selenium supplement can lead to the expansion of secretory canalculus, increase in the number of endocrine cells in gastric mucosa, alterations in the mitochondria and changes in the number and shape of pinosomes. Furthermore, our results also indicate that selenium supplement as sodium selenite can alter the ultrastructure of gastric mucosa. Though we did not find gastric cancer and gastric precancerosis, the results indicate that selenium supplement cannot prevent gastric carcinogenesis in early period of MNNG-induced gastric cancer. These mechanisms should be studied by future experiments.

REFERENCES

- 1 **Kim TS**, Jeong DW, Yun BY, Kim IY. Dysfunction of rat liver mitochondria by selenite: induction of mitochondrial permeability transition through thiol-oxidation. *Biochem Biophys Res Commun* 2002; **294**: 1130-1137
- 2 **Zhong W**, Oberley TD. Redox-mediated effects of selenium on apoptosis and cell cycle in the LNCaP human prostate cancer cell line. *Cancer Res* 2001; **61**: 7071-7078
- 3 **Chareonpong-Kawamoto N**, Higasa T, Yasumoto K. Histological study of iron deposits in selenium-deficient rats. *Biosci Biotechnol Biochem* 1995; **59**: 1913-1920
- 4 **Demirel-Yilmaz E**, Dincer D, Yilmaz G, Turan B. The effect of selenium and vitamin E on microvascular permeability of rat organs. *Biol Trace Elem Res* 1998; **64**: 161-168
- 5 **Vinceti M**, Wei ET, Malagoli C, Bergomi M, Vivoli G. Adverse health effects of selenium in humans. *Rev Environ Health* 2001; **16**: 233-251
- 6 **Vinceti M**, Nacci G, Rocchi E, Cassinadri T, Vivoli R, Marchesi C, Bergomi M. Mortality in a population with long-term exposure to inorganic selenium via drinking water. *J Clin Epidemiol* 2000; **53**: 1062-1068
- 7 **Klein EA**. Selenium: epidemiology and basic science. *J Urol* 2004; **171**(2 Pt 2): S50-53
- 8 **Klein EA**, Thompson IM. Update on chemoprevention of prostate cancer. *Curr Opin Urol* 2004; **14**: 143-149
- 9 **Sinha R**, El-Bayoumy K. Apoptosis is a critical cellular event in cancer chemoprevention and chemotherapy by selenium compounds. *Curr Cancer Drug Targets* 2004; **4**: 13-28
- 10 **Prokopczyk B**, Rosa JG, Desai D, Amin S, Sohn OS, Fiala ES, El-Bayoumy K. American Health Foundation, Valhalla, NY 10595, USA. Chemoprevention of lung tumorigenesis induced by a mixture of benzo(a)pyrene and 4-(methylnitrosamino)-1-(3-pyridyl)-1-butanone by the organoselenium compound 1, 4-phenylenebis(methylene)selenocyanate. *Cancer Lett* 2000; **161**: 35-46
- 11 **Nakaji S**, Fukuda S, Sakamoto J, Sugawara K, Shimoyama T, Umeda T, Baxter D. Relationship between mineral and trace element concentrations in drinking water and gastric cancer mortality in Japan. *Nutr Cancer* 2001; **40**: 99-102
- 12 **La Vecchia C**, Franceschi S. Nutrition and gastric cancer. *Can J Gastroenterol* 2000; **14**: 51-54
- 13 **Beno I**, Klvanova J, Magalova T, Brtkova A. Blood levels of natural antioxidants in gastric and colorectal precancerous lesions and cancers in Slovakia. *Neoplasma* 2000; **47**: 37-40
- 14 **Yang CS**. Vitamin nutrition and gastroesophageal cancer. *J Nutr* 2000; **130**(2S Suppl): 338-339
- 15 **Thompson HJ**, Becci PJ. Effect of graded dietary levels of selenium on tracheal carcinomas induced by 1-methyl-1-nitrosourea. *Cancer Lett* 1979; **7**: 215-219
- 16 **Li H**, Li HQ, Wang Y, Xu HX, Fan WT, Wang ML, Sun PH, Xie XY. An intervention study to prevent gastric cancer by micro-selenium and large dose of allitridum. *Chin Med J* 2004; **117**: 1155-1160
- 17 **Taylor PR**, Qiao YL, Abnet CC, Dawsey SM, Yang CS, Gunter EW, Wang W, Blot WJ, Dong ZW, Mark SD. Prospective study of serum vitamin E levels and esophageal and gastric cancers. *J Natl Cancer Inst* 2003; **95**: 1414-1416
- 18 **You WC**, Chang YS, Heinrich J, Ma JL, Liu WD, Zhang L, Brown LM, Yang CS, Gail MH, Fraumeni JF Jr, Xu GW. An intervention trial to inhibit the progression of precancerous gastric lesions: compliance, serum micronutrients and S-allyl cysteine levels, and toxicity. *Eur J Cancer Prev* 2001; **10**: 257-263
- 19 **Mark SD**, Qiao YL, Dawsey SM, Wu YP, Katki H, Gunter EW, Fraumeni JF Jr, Blot WJ, Dong ZW, Taylor PR. Prospective study of serum selenium levels and incident esophageal and gastric cancers. *J Natl Cancer Inst* 2000; **92**: 1753-1763
- 20 **Beno I**, Klvanova J, Magalova T, Brtkova A. Blood levels of natural antioxidants in gastric and colorectal precancerous lesions and cancers in Slovakia. *Neoplasma* 2000; **47**: 37-40
- 21 **Wei WQ**, Abnet CC, Qiao YL, Dawsey SM, Dong ZW, Sun XD, Fan JH, Gunter EW, Taylor PR, Mark SD. Prospective study of serum selenium concentrations and esophageal and gastric cardia cancer, heart disease, stroke, and total death. *Am J Clin Nutr* 2004; **79**: 80-85
- 22 **Wu CW**, Wei YY, Chi CW, Lui WY, P'Eng FK, Chung C. Tissue potassium, selenium, and iron levels associated with gastric cancer progression. *Dig Dis Sci* 1996; **41**: 119-125
- 23 **Jao SW**, Shen KL, Lee W, Ho YS. Effect of selenium on 1, 2-dimethylhydrazine-induced intestinal cancer in rats. *Dis Colon Rectum* 1996; **39**: 628-631

Inhibitory effects of apigenin on the growth of gastric carcinoma SGC-7901 cells

Kun Wu, Lin-Hong Yuan, Wei Xia

Kun Wu, Lin-Hong Yuan, Wei Xia, Department of Nutrition and Food Hygiene, Public Health College, Harbin Medical University, Harbin 150001, Heilongjiang Province, China
Co-first-authors: Kun Wu and Lin-Hong Yuan
Correspondence to: Professor Kun Wu, Department of Nutrition and Food Hygiene, Public Health College, Harbin Medical University, 199 Dongdazhi Street, Nangang District, Harbin 150001, Heilongjiang Province, China. wukun@publichl.hr.cn
Telephone: +86-451-53648665 Fax: +86-451-53648617
Received: 2004-05-27 Accepted: 2004-06-24

Abstract

AIM: To explore the growth inhibition and apoptosis-inducing effect of apigenin on human gastric carcinoma SGC-7901 cells.

METHODS: The effects of apigenin on the growth, clone formation and proliferation of human gastric carcinoma SGC-7901 cells were observed by MTT, clone-forming assay, and morphological observation. Fluorescent staining and flow cytometry analysis were used to detect apoptosis of cells.

RESULTS: Apigenin obviously inhibited the growth, clone formation and proliferation of SGC-7901 cells in a dose-dependent manner. Inhibition of growth was observed on d 1 at the concentration of 80 $\mu\text{mol/L}$, while after 4 d, the inhibition rate (IR) was 90%. The growth IRs at the concentration of 20, 40, and 80 $\mu\text{mol/L}$ were 38%, 71%, and 99% respectively on the 7th d. After the cells were treated with apigenin for 48 h, the number of clone-forming in control, 20, 40, and 80 $\mu\text{mol/L}$ groups was 217 ± 16.9 , 170 ± 11.1 ($P < 0.05$), 98 ± 11.1 ($P < 0.05$), and 25 ± 3.5 ($P < 0.05$) respectively. Typical morphological changes of apoptosis was found by fluorescent staining. The cell nuclei had lost its smooth boundaries, chromatin was condensed, and cell nuclei were broken. Flow cytometry detected typical apoptosis peak. After the cells were treated with apigenin for 48 h, the apoptosis rates were 5.76%, 19.17%, and 29.30% respectively in 20, 40, and 80 $\mu\text{mol/L}$ groups.

CONCLUSION: Apigenin shows obvious inhibition on the growth and clone formation of SGC-7901 cells by inducing apoptosis.

© 2005 The WJG Press and Elsevier Inc. All rights reserved.

Key words: Apigenin; Apoptosis; Anti-cancer effect; Gastric carcinoma

Wu K, Yuan LH, Xia W. Inhibitory effects of apigenin on the

growth of gastric carcinoma SGC-7901 cells. *World J Gastroenterol* 2005; 11(29): 4461-4464
<http://www.wjgnet.com/1007-9327/11/4461.asp>

INTRODUCTION

Apigenin (4', 5, 7-trihydroxyflavone), a phytopolyphenol, is widely distributed in vegetables and fruits such as celery, onion, apple, orange, etc. Recent studies have shown that apigenin exhibits anti-proliferation effects on several forms of cancer cells such as prostate cancer cells^[1], breast cancer cells^[2], leukemia cells^[3], colon cancer cells^[4-6], and enhances gap junctional intracellular communication changes in human liver cells^[7] and induces morphological changes in some cells^[8,9]. In addition, apigenin can suppress tumor-promoting effects of ultraviolet radiation on mouse skin^[10]. Compared with other flavonoid substances, apigenin is characterized by low toxicity and non-mutagenesis^[11]. Besides, it has other bioactivities such as anti-inflammatory^[12] and anti-oxide^[13] effects. Apigenin is a promising cancer inhibitor that may provide a new approach for the treatment of human cancers. In this article, we report the anti-proliferation effect and apoptosis-inducing effect of apigenin on human gastric carcinoma SGC-7901 cells.

MATERIALS AND METHODS

Chemicals

Apigenin (95% purity), 3-[4,5-dimethylthiazol-2-yl]-2,5-diphenyl tetrazolium bromide (MTT) and 4',6-diamidino-2'-phenylindole-dihydrochloride (DAPI) were purchased from Sigma Chemical Co. (St. Louis, MO, USA). RPMI 1640 medium, ethylene diaminetetraacetic acid (EDTA), N²-2-hydroxyethyl piperazine-N²-ethane sulfonic acid were obtained from Gibco Chemical Co. (Rockville, MD, USA).

Cell culture and apigenin treatment

Human gastric cancer SGC-7901 cells, obtained from Cancer Research Institute of Beijing (China), were grown as a monolayer in RPMI 1640 medium containing 1% penicillin/streptomycin, and 0.2% gentamicin sulfate supplemented with 100 mL/L fetal bovine serum (FBS) at 37 °C in a 50 mL/L CO₂ humidified atmosphere. Apigenin was dissolved in dimethyl sulfoxide (DMSO) and mixed with a fresh medium to achieve the desired concentration. The final DMSO concentration in all media was 0.2%. This concentration of DMSO did not alter cell growth and cell cycle measurement when compared with the vehicle-free medium.

Cell growth assay

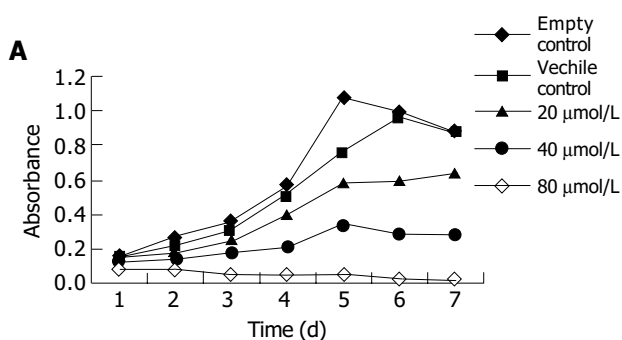
The effect of apigenin on the viability of cells was determined by MTT assay. Near-confluent stock cultures of cells were harvested with 0.2% EDTA and plated at a density of 2.5×10^3 /well in 96-well microtiter plates. After an overnight incubation to allow cell attachment, the medium was replaced by fresh medium containing different concentrations (0, 20, 40, and 80 $\mu\text{mol/L}$) of apigenin. Control wells received DMSO (0.2%). Each concentration of apigenin was repeated in four wells. After incubation for 24 h, one plate was assayed with a microplate reader at the wavelength of 570 nm. Before the assay, MTT (5 mg/mL in PBS) was added to each well and incubated for 4 h, then MTT solution was removed from the wells by aspiration. After careful removal of the medium, 0.1 mL of DMSO was added to each well, and the plate was shaken for 15 min. The data of 7 d were fed into the computer and the growth curve was drawn. The growth inhibition rate (IR) was calculated according to the following formula.

$$\text{Clone efficiency} = \frac{\text{absorbance of vehicle control} - \text{absorbance of apigenin treatment group}}{\text{absorbance of vehicle control group}} \times 100\%$$

Clone formation assay

The cells were plated at a density of 500/well on 24-well microtiter plates. After an overnight incubation to allow cell attachment, the medium was replaced by fresh medium containing DMSO (0.2%) at different concentrations (20, 40, and 80 $\mu\text{mol/L}$) of apigenin, with each concentration repeated in five wells. After being incubated for 24 or 48 h, the medium was replaced by fresh medium containing 10% FBS. The cells were incubated for another 7 d, then washed thrice with PBS and fixed in methanol for 15 min. The cells were stained with Giemsa stain. Then the number of clone-forming cells (>50 cells) was calculated under the microscope. The data were expressed as mean \pm SD. Clone-formation rate was calculated as follows:

$$\text{Clone efficiency} = \frac{\text{average clone number of five wells}}{\text{number of plating cells}} \times 100\%$$



Cell morphological change

The cells were harvested with 0.2% EDTA and plated in 25-mL culture bottles at the density of 1×10^5 . After an overnight incubation to allow cell attachment, the medium was replaced by fresh medium containing DMSO (0.2%) at different concentrations (20, 40, and 80 $\mu\text{mol/L}$) of apigenin. Morphological change of the cells was observed microscopically and photographed at 24 and 48 h after the addition of apigenin.

Besides, the cells were exposed to various concentrations of apigenin (20, 40, and 80 $\mu\text{mol/L}$) for 48 h, then harvested with EDTA and washed twice with PBS. The cells were stained with 2 mg/L DAPI ethanol solution and incubated at 37 °C for 15 min. Morphological changes of the stained cells were observed under fluorescent microscope (300-500 nm) and photographed.

Flow cytometry analysis

The cells (70% confluent) were treated with apigenin (40 and 80 $\mu\text{mol/L}$) for 48 h, then harvested with EDTA, washed twice with PBS, and centrifuged. The pellet was resuspended in 70% cold ethanol for 24 h at 4 °C. The cells were centrifuged at 110 r/min for 5 min, washed twice with PBS, suspended with 200 μL RNase A (20 $\mu\text{g/mL}$ final concentration) and incubated at 37 °C for 30 min. The cells were chilled over ice for 10 min and stained with 800 μL propidium iodide (50 $\mu\text{g/mL}$ final concentration) for 1 h and analyzed by flow cytometry.

Statistical analysis

All data were expressed as mean \pm SD and analyzed with SAS statistic software. $P < 0.05$ was considered statistically significant.

RESULTS

Growth curve and growth inhibition rate of SGC-7901 cells treated with apigenin

Apigenin inhibits the cell proliferation. Previous studies have proved that apigenin can inhibit the growth of several kinds of cancer cells. In our study, we examined whether apigenin exerted a similar anti-proliferative effect on human gastric cancer SGC-7901 cells. As shown in Figure 1, the cells in control group entered the logarithmic growth phase on the 1st d after they were plated and reached their peak on the 6th d. While in the treatment groups, the growth of

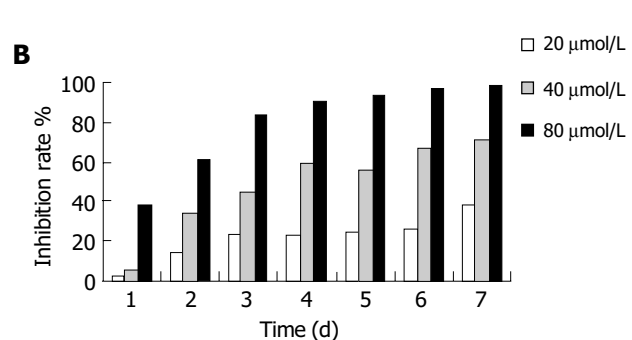


Figure 1 Inhibition effect of apigenin on growth curve (A) and growth IR (B) in

human gastric cancer SGC-7901 cells.

cells was inhibited in a dose- and time-dependent manner. Inhibition of growth was evident on d 1 at the concentration of 80 $\mu\text{mol/L}$, after 4 d the IR was 90%. The growth IR of 20, 40, and 80 $\mu\text{mol/L}$ of apigenin was 38%, 71%, and 99% respectively on the 7th d.

Effect of apigenin on clone formation of SGC-7901 cells

As shown in Figure 2, after exposure to apigenin for 24 or 48 h, the clone formation of SGC-7901 cells was suppressed in a dose- and time-dependent manner. The cloning efficiency in 80 $\mu\text{mol/L}$ was 9.8% and 5% after treatment with apigenin for 24 and 48 h, while in the control group it was 40.4% and 43.4% (Table 1).

Table 1 Effect of apigenin on clone formation in SGC-7901 cells ($n = 5$, mean \pm SD)

Groups ($\mu\text{mol/L}$)	Number of clone-forming cells		Cloning efficiency (%)	
	24 h	48 h	24 h	48 h
Control	202 \pm 12.1	217 \pm 16.9	40.4	43.4
20	192 \pm 10.5	170 \pm 11.1 ^a	38.4	34.0
40	147 \pm 11.3 ^a	98 \pm 11.1 ^a	29.4	19.6
80	49 \pm 6.7 ^a	25 \pm 3.5 ^a	9.8	5.0

^a $P < 0.05$ vs control group.

Morphological changes of SGC-7901 cells

Figure 3 shows the morphological changes of SGC-7901 cells treated for 48 h with 80 $\mu\text{mol/L}$ apigenin or vehicle.

In the vehicle control group, DMSO (0.2%) did not induce any marked morphological change in the cells. In the DMSO group, the cells were transparent and in the great density, the boundaries of the cells were dim, the nucleolus was very clear. While in the treatment group, there was a significant decrease in quantity and transparency of the cells, the cells crumpled and the boundaries became clear, the nucleolus could not be observed clearly.

After being stained with DAPI, the cells were visualized under blue fluorescence. In the control group, the nuclei were almost round in shape with clear and smooth boundaries, the staining was equal. After treatment with apigenin for 48 h, the nuclei of cells were broken and the staining was unequal. The chromatins of cells were condensed, and the nuclei lost their smooth boundaries.

Result of flow cytometry analysis

During apoptosis, the DNA is broken into small fragments and released from cells. In this experiment, apoptosis was induced by apigenin. Flow cytometry analysis results are shown in Figure 4. Apigenin (20, 40, and 80 $\mu\text{mol/L}$) treatment for 48 h induced a significant apoptosis and accumulation of cells in S phase. The apoptosis rates were 5.76%, 19.17%, and 29.30%, respectively.

DISCUSSION

The pathogenesis of cancer is a multi-phase process. Inherited and environmental factors play an important role in the occurrence of cancer. Gastric cancer is one of the most

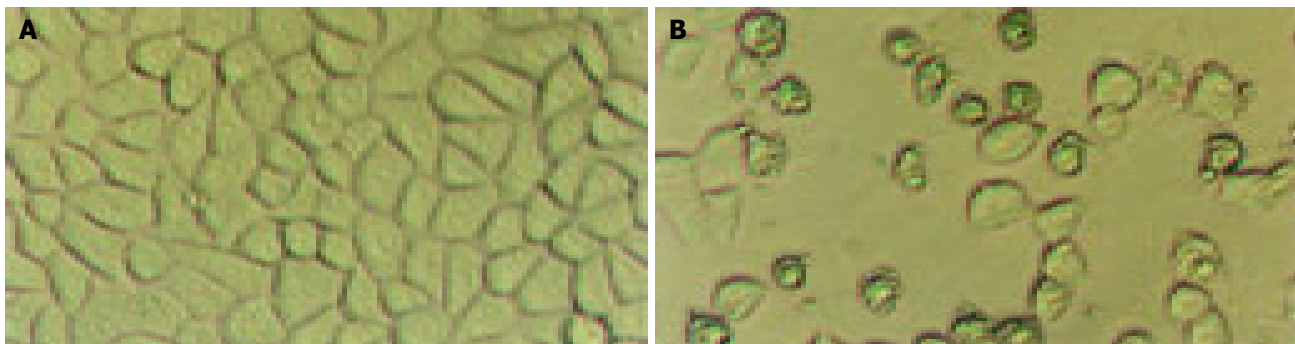


Figure 2 Morphological changes in SGC-7901 cells after treated with vehicle

(A) and apigenin (B) for 48 h ($\times 200$).

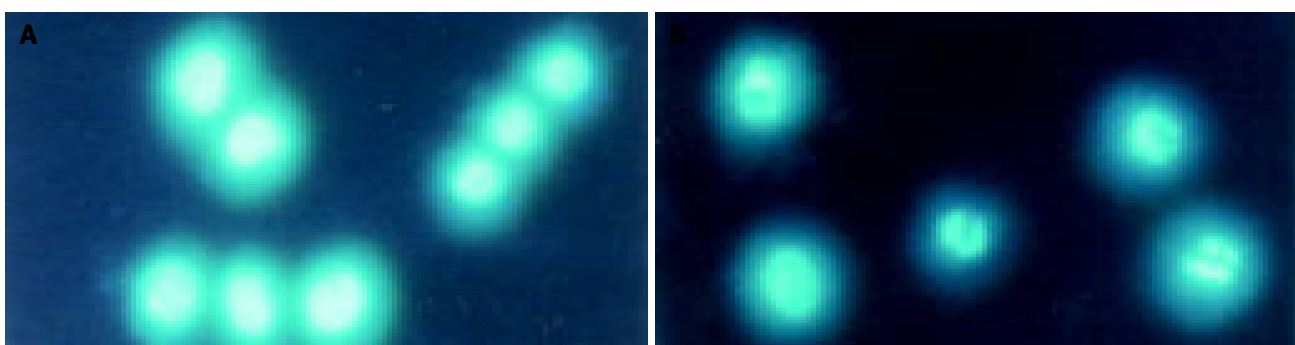


Figure 3 Morphological changes of SGC-7901 cells after being treated with

DMSO (A) and apigenin (B) for 48 h ($\times 400$).

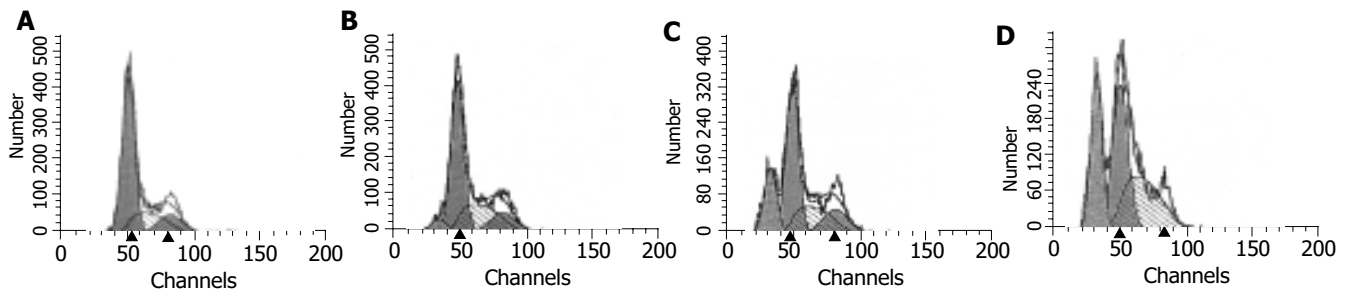


Figure 4 FACS analysis of cells treated with DMSO (A), 20 $\mu\text{mol/L}$ apigenin (B), 40 $\mu\text{mol/L}$ apigenin (C), and 80 $\mu\text{mol/L}$ apigenin (D).

common malignant tumors in China. Some bioactive substances such as polyphenolic and isoflavone exist mainly in plant-based food (fruits and vegetables). Apigenin, one of the most common flavonoids, is widely distributed in many fruits and vegetables. Studies^[14] have proved that apigenin has strong anti-cancer effects.

In our experiment, we used MTT and clone-forming assay to detect the growth inhibition effect of apigenin on human gastric SGC-7901 cells. The results showed that apigenin dramatically suppressed the growth and clone formation of the cells in a dose- and time-dependent manner. After treatment of cells with 80 $\mu\text{mol/L}$ apigenin for 4 d, the growth IR was above 90% and other concentrations of apigenin also suppressed cell growth to different degrees. Clone formation reflects the proliferative ability of tumor stem cells, which is the important target of anticancer treatment. Inhibition of stem cells is more effective than that of common carcinoma cells during the treatment of cancer. With fluorescence microscope, we observed typical morphological changes such as the disintegrity of nuclear membrane, condensation of chromatin and broken nuclei. FACS analysis detected special apoptosis peak, which further supports the results in fluorescence morphological observation.

In conclusion, apigenin can suppress the growth of human gastric cancer SGC-7901 cells, which is associated with its apoptosis-inducing effect.

ACKNOWLEDGMENTS

We thank Yan Zhao, Lan Zhao and Xiao-Hua Zhang for their help and encouragement throughout the whole experiment.

REFERENCES

- Gupta S, Afaq F, Mukhtar H. Selective growth-inhibitory, cell-cycle deregulatory and apoptotic response of apigenin in normal versus human prostate carcinoma cells. *Biochem Biophys Res Commun* 2001; **287**: 914-920
- Yin F, Giuliano AE, Law RE, Van Herle AJ. Apigenin inhibits growth and induces G2/M arrest by modulating cyclin-CDK regulators and ERK MAP kinase activation in breast carcinoma cells. *Anticancer Res* 2001; **21**: 413-420
- Wang IK, Lin-Shiau SY, Lin JK. Induction of apoptosis by apigenin and related flavonoids through cytochrome c release and activation of caspase-9 and caspase-3 in leukaemia HL-60 cells. *Eur J Cancer* 1999; **35**: 1517-1525
- Steinmetz KA, Potter JD. Vegetables, fruits and cancer. *Epidemiology. Cancer Causes Control* 1991; **2**: 325-357
- Block G, Patterson B, Sulbar A. Fruits, vegetables and cancer prevention: A review of the epidemiological evidence. *Nutr Cancer* 1992; **18**: 1-29
- Wang W, Heideman L, Chung CS, Pelling JC, Koehler KJ, Birt DF. Cell-cycle arrest at G2/M and growth inhibition by apigenin in human colon carcinoma cell lines. *Mol Carcinog* 2000; **28**: 102-110
- Chaumontent C, Bex V, Gallard-Sanchez I, Seillan-Heberdeh C, Suschete M, Martel P. Apigenin and tangeretin enhance gap junction intracellular communication in rat liver epithelial cells. *Carcinogenesis* 1994; **15**: 2325-2330
- Kuo ML, Lin JK, Huang TS. Reversion of the transformed phenotypes of v-Ha-ras NIH3T3 cells by flavonoids through attenuating the content of phosphotyrosine. *Biochem Biophys Res Commun* 1995; **212**: 767-775
- Sato F, Matsukawa Y, Matsumoto K, Nishino H, Sakai T. Apigenin induced morphological differentiation and G2-M arrest in rat neuronal cells. *Biochem Biophys Res Commun* 2004; **324**: 578-584
- Lepley DM, Li B, Birt DF, Dellihy JC. The chemopreventive flavonoid apigenin induces G2/M arrest in keratinocytes. *Carcinogenesis* 1996; **17**: 2367-2375
- Nijveldt RJ, van Nood E, van Hoorn DEC. Flavonoids: a review of probable mechanisms of action and potential applications. *Am J Clin Nutr* 2001; **74**: 418-425
- Fuchs J, Milbradt R. Skin anti-inflammatory activity of apigenin-7-glucoside in rats. *Res Commun Chem Pathol Pharmacol* 1989; **64**: 69-78
- Lin CM, Chen CT, Lee HH, Lin JK. Prevention of cellular ROS damage by isovitexin and related flavonoids. *Planta Med* 2002; **68**: 365-367
- Way TD, Kao MC, Lin JK. Apigenin induces apoptosis through proteasomal degradation of HER2/neu in HER2/neu-overexpressing breast cancer cells via the phosphatidylinositol 3-kinase/Akt-dependent pathway. *J Biol Chem* 2004; **279**: 4479-4489

Outcome of transarterial chemoembolization in patients with inoperable hepatocellular carcinoma eligible for radiofrequency ablation

Mike SL Liem, Ronnie TP Poon, Chung Mau Lo, Wai Kuen Tso, Sheung Tat Fan

Mike SL Liem, the Dutch Cancer Society, Queen Wilhelmina Fund, Amsterdam, The Netherlands

Ronnie TP Poon, Chung Mau Lo, Sheung Tat Fan, Centre for the Study of Liver Disease and Departments of Surgery and Radiology, The University of Hong Kong, Pokfulam, Hong Kong, China

Wai Kuen Tso, Department of Radiology, The University of Hong Kong, Pokfulam, Hong Kong, China

Supported by the Sun CY Research Foundation for Hepatobiliary and Pancreatic Surgery of the University of Hong Kong, China

Correspondence to: Dr. Ronnie T Poon, Department of Surgery, The University of Hong Kong, Queen Mary Hospital, 102 Pokfulam Road, Hong Kong, China. poontp@hkucc.hku.hk

Telephone: +852-28553641 Fax: +852-28175475

Received: 2004-09-06 Accepted: 2004-10-06

Abstract

AIM: To evaluate the outcome of transarterial chemoembolization (TACE) in patients with unresectable hepatocellular carcinoma (HCC) <5 cm in diameter eligible for radiofrequency ablation (RFA).

METHODS: The treatment-related mortality, morbidity, long-term survival, and prognostic factors of HCC patients who had TACE and fulfilled the present inclusion criteria for RFA were evaluated.

RESULTS: Of the 748 patients treated with TACE between January 1990 and December 2002, 114 patients were also eligible for RFA. The treatment-related mortality and morbidity were 1% and 19%, respectively. Survival at 1, 3, and 5 years was 80%, 43%, and 23%, respectively. Older age and a high albumin level were associated with a better survival, whereas a high α -fetoprotein level (AFP) and the size of the largest tumor >3 cm in diameter were adverse prognostic factors in multivariate analysis.

CONCLUSION: The morbidity, mortality, and survival data after TACE for small HCCs eligible for RFA are comparable to those reported after RFA in the literature. Our data suggest the need for a randomized comparison of the two treatment modalities for small HCCs.

© 2005 The WJG Press and Elsevier Inc. All rights reserved.

Key words: Hepatocellular carcinoma; Radiofrequency ablation; Transarterial chemoembolization

Liem MSL, Poon RTP, Lo CM, Tso WK, Fan ST. Outcome of transarterial chemoembolization in patients with inoperable hepatocellular carcinoma eligible for radiofrequency ablation. *World J Gastroenterol* 2005; 11(29): 4465-4471
<http://www.wjgnet.com/1007-9327/11/4465.asp>

INTRODUCTION

Hepatocellular carcinoma (HCC) is one of the most common human cancers with poor prognosis if left untreated, and only a small proportion is eligible for intentional curative surgical resection^[1,2]. Transarterial chemoembolization (TACE) has been used as a palliative treatment for patients with inoperable disease and those with recurrence after resection. TACE is also used as a (neo-)adjuvant treatment before or after surgical resection, and before liver transplantation^[3-6]. Hence, TACE is one of the most frequently performed treatment modalities for HCC. However, this treatment is still controversial and unsupported by evidence of early randomized controlled trials^[7-9]. Renewed interest in this form of treatment that has emerged as evidence from recent randomized trials is in favor of this treatment^[10,11]. A systematic review has convincingly shown a significant survival benefit for treatment with chemoembolization compared to no treatment^[12]. Moreover, in some patients, TACE has even shown a similar survival compared to certain patients who underwent hepatic resection^[13].

Local ablative, either open or percutaneous, techniques are considered alternatives for hepatic resection, if HCC is located either bilobar or multifocal rendering the disease unresectable, or if the patient has poor liver function reserve. Radiofrequency ablation (RFA) for HCC is a relatively new and popular local ablative technique. However, the lack of sufficient long-term follow-up data to support the treatment is well recognized. Strict criteria for RFA have not yet been clearly defined, but in general RFA is considered suitable if there are less than four lesions and the largest lesion is 5 cm or less in diameter^[4,14,15]. RFA may not be suitable for tumors with portal vein, hepatic vein or vena cava involvement and in patients with severe cirrhosis^[16,17]. Given these criteria and the reported promising results of RFA, some patients who might have been given TACE treatment prior to the advent of RFA may now be treated with RFA as the preferred alternative. However, TACE is a better documented treatment that is still used in many centers for HCC even if the tumor is eligible for RFA. Currently there are no studies in the literature directly comparing the results of the two treatment modalities. Such comparative studies may not be available in the near future because in most centers, RFA has been employed for a short duration with no long-term follow-up data, and not many centers have abundant experience in both treatment modalities. The results of TACE treatment for unresectable HCCs <5 cm in diameter eligible for RFA are also unknown because previous studies on TACE for

HCC usually included a heterogeneous group of patients, including those with large tumors and vascular invasion.

This study that applied the currently accepted RFA inclusion criteria to our vast experience with TACE in patients with HCC reports the outcome of these patients and the factors associated with poor prognosis of TACE treatment in this particular group.

MATERIALS AND METHODS

A prospective database, which contained the data of all patients with surgical and non-surgical treatments for HCC at the Department of Surgery, Queen Mary Hospital, Hong Kong, was used. All patients with newly diagnosed HCC who had TACE as their initial treatment between January 1990 and December 2002 and had HCC with their largest nodule being <5 cm in diameter were identified and retrospectively analyzed. Other criteria included the number of tumor nodules less than four, absence of severe cirrhosis reflected by a Child's C grading, and absence of portal vein (intrahepatic or main trunk), hepatic vein or inferior vena cava involvement.

Patients who had a diagnosis of HCC, confirmed either by biopsy or needle cytology, by two diagnostic imaging modalities (contrast computed tomography (CT) scan, magnetic resonance imaging or arteriography) showed typical HCC nodules with arterial hypervascularization or one diagnostic a persistently raised serum α -fetoprotein level (AFP) >400 ng/mL according to the Barcelona-2000 EASL conference criteria^[18]. We selected patients for TACE treatment if they had inoperable bilobar disease or unilobar disease in combination with sufficient hepatic function reflected by a bilirubin level <50 μ mol/L and no metastatic disease.

Our technique of TACE has been described elsewhere^[19,20]. Superselective cannulation of the artery supplying the tumor was performed whenever possible. An emulsion of cisplatin (1 mg/mL) and lipiodol (Lipiodol Ultrafluide[®]; Laboratoire Guerbet, Aulnay-Sous-Bois, France) at a volume ratio of 1:1 was injected up to a maximum of 60 mL. Embolization was performed with 1-mm² particles of gelatin-sponge (Spongostan[®], Johnson and Johnson Ltd, Skipton, UK) mixed with 40 mg of gentamycin. Repetition of TACE treatment was tailored to response of tumor and tolerance of liver rather than a fixed regimen. TACE was repeated every 8-12 wk if there was tumor response (\geq 50% decrease in tumor size according to World Health Organization criteria) or if the tumor was static in size (<50% decrease or <25% increase in tumor size). Treatment of TACE was terminated if there was no evidence of tumor on reassessment CT (i.e. complete response), disease progression (\geq 25% increase in tumor size or appearance of new lesions), evidence of liver failure (rise of bilirubin >50 μ mol/L, uncontrollable ascites or hepatic encephalopathy), severe life-threatening complications such as liver abscess, or extrahepatic metastasis.

Patient demographics, laboratory data, and tumor characteristics were used for analysis. The Child-Pugh classification (A or B) was used to categorize the patients according to their status of liver cirrhosis and the new TNM classification according to the American Joint Committee

on Cancer (AJCC)^[21] was used for staging.

Continuous, normally distributed data were expressed as mean \pm SD, and other continuous data were expressed as medians with their interquartile range. Survival was analyzed by Kaplan-Meier survival curves. Prognostic variables for recurrence and survival were studied with univariate and multivariate Cox proportional hazards regression. Variables were categorized according to their quartile distribution wherever possible. This regression yields a hazard ratio, which may be interpreted as a relative risk within the average follow-up period. We used sex, age, laboratory data (bilirubin, albumin, AFP, platelet count) and tumor characteristics (bilobar disease, size of largest tumor, number of tumors, TNM stage) in a univariate Cox proportional hazard analysis. Next, variables for which univariate test had a *P* value less than 0.25 and biologically important variables (sex and age) were included in a multivariate analysis with survival as the outcome^[22]. For model building, we applied backward stepwise elimination of variables. All reported *P* values were two-tailed. *P*<0.05 was considered statistically significant.

RESULTS

In the period between January 1990 and December 2002, a total of 2 850 patients were seen at our outpatient clinic for HCC and included in our database. Of these, 748 patients with newly diagnosed HCC underwent TACE as their initial treatment, and 200 patients had the largest tumor nodule <5 cm in diameter. This group included 15 patients who were considered unresectable during laparotomy and subsequently given TACE as the primary treatment. Patients who had more than three nodules (*n* = 60) subsequently undergoing hepatic resection (*n* = 14), and those who had portal vein (intrahepatic or main portal vein, *n* = 2) were excluded from this study. There were no patients with hepatic vein or inferior vena cava involvement. Of the remaining 124 patients, another 5 patients were excluded because of Child's C cirrhosis and an additional 5 patients did not fulfill the criteria of HCC diagnosis used in this study. Hence, this study involved 114 patients and all analyses were performed in this group of patients.

The diagnosis of 17 patients was confirmed by either histology (*n* = 2) or cytology (*n* = 15). In 93 patients, confirmation of HCC was done by CT and hepatic arteriogram, in 2 patients by magnetic resonance imaging and hepatic arteriogram, and in the remaining 2 patients by an ultrasound of the liver and a consistently increased AFP combined with a hepatic arteriogram.

Patient characteristics are shown in Table 1. One patient died as a direct result of TACE treatment, the treatment-related mortality was 1%. This patient had four previous TACE sessions and developed both a liver abscess and deterioration of liver function after his 5th TACE treatment. He subsequently developed sepsis and pneumonia and died of respiratory failure. The overall treatment morbidity was 18%, the patient who died had two complications. Other complications as a result of TACE were hematoma at the puncture site in the groin (*n* = 1, 1%) and liver failure, defined as elevated bilirubin >50 μ mol/L, development of uncontrolled ascites or hepatic encephalopathy (*n* = 20, 17%).

Table 1 Characteristics of 114 patients eligible for RFA but received TACE treatment

Characteristics	Median	Interquartile range
Age (yr)	63	55-71
Gender: male/female (<i>n</i>)	87/27	76/24
Child's grading (<i>n</i> , %)		
A	90	79
B	24	21
HBsAg status (<i>n</i> , %)		
Positive	82	71
Negative	32	28
TNM stage (<i>n</i> , %)		
Stage I	72	63
Stage II	39	34
Stage IIIA	1	1
Stage IIIC	2	2
Number of tumor nodules (<i>n</i> , %)	1	1-2
1	76	67
2	32	28
3	6	5
Size of largest tumor nodule (cm)	3.0	2.1-4.0
Tumor distribution (<i>n</i> , %)		
Unilobar	88	77
Bilobar	26	23
Platelet count ($\times 10^9/L$)	98	72-128
Albumin (g/L)	37	33-41
Total bilirubin ($\mu\text{mol/L}$)	17	12-24
Prothrombin time (s)	13.2	11.9-14.6
INR	1.1	1.0-1.2
AFP (ng/mL)	80	15-373
Number of TACE procedures	5	3-8

TACE: transarterial chemoembolization; HBsAg: hepatitis B surface antigen; INR: international normalized ratio; values are median with their interquartile range, unless denoted otherwise.

Table 2 Causes of death in 74 patients after TACE treatment

Causes	<i>n</i>	%
Malignant cachexia	45	61
Bleeding	3	4
Hepatic failure	9	12
Respiratory failure	1	1
Multiorgan failure	2	3
Sepsis	4	5
Other	10	14
Total (<i>n</i>)	74	

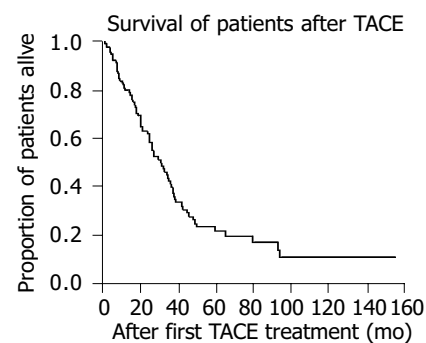
TACE: transarterial chemoembolization.

Seventy-four patients died during our observation period and the reasons for their death are given in Table 2. One patient was lost to follow-up (1%). The 1-, 3-, and 5-year survival rates were 80%, 43%, and 23% respectively (Figure 1). The median survival was 31 months (95%CI: 24-38 mo).

Univariate and multivariate analyses are shown in Tables 3 and 4, respectively. Higher age and a high albumin level (above 41 g/L) were associated with a better survival whereas AFP (above 81.50 ng/mL) and the size of the largest tumor >3 cm in diameter were the risk factors for death in the multivariate analysis.

DISCUSSION

We evaluated the morbidity, mortality and long-term survival, and identified several independent risk factors for

**Figure 1** Kaplan-Meier curve for survival of patients undergoing TACE as treatment.

death in patients who underwent TACE treatment with patient and tumor characteristics that fulfilled all our present criteria for RFA treatment. Although there are numerous reports on the results of TACE for inoperable HCC, many included patients with large or advanced HCC with vascular invasion for which the outcome is expectedly worse^[3,5,6,19]. Such reports may give the impression that results after TACE are worse than those after RFA, because most studies of RFA on HCCs focused on small HCCs and hence reported more favorable results. To our knowledge, the survival and prognostic factors in this specific group of patients with HCC who were eligible for RFA but underwent TACE treatment have not been reported before. As many patients

Table 3 Univariate analysis for prognostic factors of death

Variable	Hazard ratio	95%CI	P
Age (per yr)	1.01	0.99-1.03	0.347
Female sex	0.91	0.51-1.63	0.747
Bilirubin ($\mu\text{mol/L}$) ¹			
5.00-11.75			
11.75-17.00	1.16	0.62-2.17	0.648
17.00-24.00	1.67	0.88-3.18	0.116
24.00-83.00	1.66	0.85-3.25	0.140
Albumin (g/L) ¹			
24-33			
33-37	0.72	0.38-1.37	0.310
37-41	0.92	0.50-1.69	0.786
41-50	0.40	0.20-0.81	0.011
AFP (ng/mL) ¹			
2-14.75			
14.75-81.50	1.42	0.71-2.86	0.320
81.50-366	2.30	1.16-4.57	0.017
366-11 470	1.99	1.03-3.83	0.041
Platelet count ($\times 10^9/\text{L}$) ¹			
36-72			
72-99	1.00	0.54-1.85	0.992
99-128	1.26	0.66-2.39	0.486
128-295	0.81	0.42-1.59	0.539
Bilobar disease	1.06	0.62-1.80	0.841
Largest tumor >3 cm	1.40	0.87-2.24	0.163
Child's B grade ²	1.67	0.97-2.88	0.065
AJCC TNM stage ³			
Stage I			
Stage II	1.08	0.67-1.73	0.763
Stage IIIA	0.00	0.00->100	0.971
Stage IIIC	1.73	0.24-12.65	0.591

CI: confidence interval; AJCC: American Joint Committee on Cancer. ¹Hazard ratio of bilirubin, albumin, AFP, and platelet count is given relative to the lowest quartile. ²Hazard ratio of Child's B grade is given relative to Child's A grade. ³Hazard ratio of AJCC TNM stage is given relative to stage I.

Table 4 Multivariate analysis for prognostic factors of death

Variable	Hazard ratio	95%CI	P
Age (per yr)	0.98	0.95-1.00	0.044
Albumin (g/L) ¹			
24-33			
33-37	0.83	0.42-1.63	0.586
37-41	1.14	0.61-2.13	0.685
41-50	0.21	0.09-0.49	<0.0005
AFP (ng/mL) ¹			
2-14.75			
14.75-81.50	1.57	0.77-3.17	0.209
81.50-366	4.61	2.13-9.98	<0.0005
366-11 470	3.72	1.77-7.85	0.001
Largest tumor >3 cm ²	1.64	1.00-2.69	0.049

CI: confidence interval. ¹Hazard ratio of albumin and AFP is given relative to the lowest quartile. ²Hazard ratio is given relative to the size of the largest tumor smaller than 3 cm in diameter.

who were considered to have unresectable HCC <5 cm in diameter received TACE treatment before the RFA era, this knowledge may be of specific interest to those who are rethinking the concept of TACE and RFA and wish to refine their indications for both TACE and RFA treatments. With the availability of RFA, patients with small HCCs <5 cm in diameter previously treated by TACE are now treated by RFA instead as the preferred treatment in some centers, although there is no direct evidence to show that RFA is superior to TACE in terms of treatment safety and long-

term survival benefit. The exact place of local ablative techniques and TACE in the overall management of HCC still needs to be determined. Offering a strict order of treatment options to the patient, i.e. first hepatic resection, then local ablative techniques and then TACE, may not be fully justified. Indeed, percutaneous ethanol injection appears to acquire similar results as resection for small HCC in terms of treatment efficacy, recurrence, and survival rates^[23]. In addition, Bronowicki *et al.*^[24], found similar survival after surgery and TACE, while the patients who underwent surgery

were younger and had a better staging, and, just recently, TACE has been shown to be as effective as hepatic resection in certain patients^[13]. Moreover, evidence from randomized controlled trials comparing even two local ablative techniques is hardly available, not to mention trials comparing two different treatment modalities such as TACE and RFA. Therefore, one must be careful not to jump to conclusions^[25]. In patients who do not want surgery, which is still necessary in a large proportion of cases for RFA because of tumor location at the superior portion of the liver or close to the adjacent viscera^[26], TACE is still one of the best options. Furthermore, some centers may not have the availability and/or equal expertise of all treatment options and may stick to the use of TACE as the preferred treatment for all unresectable HCC.

Given the potentially curative intent of RFA, many clinicians consider RFA as the treatment of choice for unresectable small HCC, although long-term survival results of RFA are scarce^[27]. In addition, complications and treatment mortality after RFA are generally expected to be fewer than those after TACE, and RFA may result in less deterioration of liver function. The treatment mortality in this study (1%), however, appears comparable to that of RFA^[28]. A recent literature review suggests that the treatment morbidity of RFA in the early reports is probably underestimated^[28]. The treatment morbidity of TACE for small HCC in this study was 18%, which is comparable to the complication rates of 13-20% after RFA for HCC reported in some of the more recent studies^[28,29]. The complication rate is 14% in our preliminary experience with RFA in 86 patients with HCC between May 2001 and December 2002^[30]. The 1-year survival rate of the HCC patients treated by TACE in the current study was 80%, which is comparable to the 1-year survival observed after RFA for HCC in our preliminary experience^[30]. The 3-year survival rate of 43% is also comparable with that of 33-50% in recent reports of more long-term survival results of RFA for HCC^[31,32]. In this study, the 5-year survival after TACE for HCCs <5 cm in diameter that were eligible for RFA was 23%. Data on 5-year survival rate after RFA for HCC are scarce. In a recent study, Buscarini *et al.*^[33], reported a 5-year survival rate of 33% after RFA for HCCs \leq 3.5 cm in diameter, which appears comparable to that after TACE for tumors of a similar size in our study.

In this study, we did not directly compare our TACE results to similar patients who underwent RFA treatment in our institution. We have started RFA only 4 years before, like many others, and long-term follow-up is unavailable yet. Furthermore, most patients in this study were treated with TACE in the era long before the availability of RFA. Naturally, a future comparison between similar patients undergoing TACE and RFA within the same time-frame will be made. Ultimately, however, a randomized controlled trial may be needed. This study may serve as a reference to compare present and future RFA series, as in many centers that perform RFA, TACE is either losing ground or experience with TACE is not so large in the first place. Our results of TACE in patients with HCC <5 cm in diameter suggest that the safety of TACE and survival results may be comparable to those of RFA, which is an important message

for clinicians treating HCCs. This highlights the need for randomized studies to compare the two treatment modalities rather than simply considering RFA as the preferred treatment based on perceived benefits.

RFA is still an evolving technique and it is therefore understandable that there is a large diversity in indications for RFA. Our inclusion criteria for RFA are consistent with the reported criteria^[14-17,27]. A largest tumor size \leq 5 cm in diameter, the number of tumors less than four and tumors not invading or abutting major hepatic veins or portal vein branches have all been reported as the inclusion criteria for RFA. In our database of HCC patients treated with TACE, 114 of 748 patients who underwent TACE treatment (15%) fulfilled the criteria for RFA treatment. We found that a high albumin concentration was associated with better survival. We believe that this reflects the better liver function of these patients compared to those with low albumin concentrations. Indeed, it is reasonable to speculate that patients with poor liver function may do better with local ablative techniques, such as RFA, because these techniques result in less liver damage than TACE. Child's B grade liver function did not appear to be an independent predictor in the multivariate analysis because it possibly interacted with albumin concentration. A higher age results in a risk reduction of 2% per year. Others have found that age is an adverse prognostic factor^[34,35]. We cannot explain this interesting observation but we propose that it might be related to selection or, partially a more malignant behavior of HCC in younger patients. In any case, age may not be a clinically important factor that influences the clinician's decision to treat the patient with RFA or TACE. Both a high AFP, which reflects tumor volume and perhaps also tumor aggressiveness, and tumor size are associated with poorer survival. These risk factors have been identified previously in other prognostic studies of TACE^[35-38]. Patients with tumors measuring between 3 and 5 cm performed worse compared to those with smaller tumors when put on TACE treatment. Perhaps this particular group may do better when treated by local ablative techniques such as RFA. Advances in RFA technology have allowed ablation of larger HCC. RFA may effectively treat tumors up to 5 cm in diameter by using a clustered probe or by inflow occlusion with the Pringle maneuver^[4,30].

This is the first study that investigated the outcomes of TACE for a group of patients with HCC <5 cm in diameter who would now be treated with RFA instead in many centers. TACE for small HCC has been reported before but focused mainly on the technical aspects, and those studies did not specifically look at patients who were also eligible for RFA treatment. Moreover, these are all Japanese studies with mainly hepatitis C patients^[39-41]. Our results compare favorably with the results of Nakao *et al.*^[39], (34% 3-year survival), and are similar to the results of Yamada *et al.*^[40], (47% 3-year survival). Takayasu *et al.*^[41], have reported a 77% 3-year survival in their patients with HCC <5 cm in diameter. However, the mean tumor size was only 1.9 cm in their study.

In conclusion, this study provides the morbidity, mortality and long-term survival results of a group of patients who were otherwise eligible for RFA treatment but received

TACE. Our data, based on a retrospective analysis, suggest that the immediate and at least the short-term and intermediate-term survival results of TACE for small HCC may be comparable to those of RFA reported in the literature. The data may serve as a useful reference for comparison to RFA treatment when long-term survival of the latter treatment becomes available. This study highlights the need for a prospective comparative study of the two treatment modalities rather than simply replacing TACE with RFA for small inoperable HCCs as the treatment of choice, as what many centers are doing with the availability of this new technology. The identification of the prognostic factors may help in better selection of patients for TACE or RFA treatment.

REFERENCES

- 1 Okuda K, Ohtsuki T, Obata H, Tomimatsu M, Okazaki N, Hasegawa H, Nakajima Y, Ohnishi K. Natural history of hepatocellular carcinoma and prognosis in relation to treatment. Study of 850 patients. *Cancer* 1985; **56**: 918-928
- 2 Akriviadis EA, Llovet JM, Efremidis SC, Shouval D, Canelo R, Ringe B, Meyers WC. Hepatocellular carcinoma. *Br J Surg* 1998; **85**: 1319-1331
- 3 Poon RT, Ngan H, Lo CM, Liu CL, Fan ST, Wong J. Transarterial chemoembolization for inoperable hepatocellular carcinoma and postresection intrahepatic recurrence. *J Surg Oncol* 2000; **73**: 109-114
- 4 Poon RT, Fan ST, Tsang FH, Wong J. Locoregional therapies for hepatocellular carcinoma: a critical review from the surgeon's perspective. *Ann Surg* 2002; **235**: 466-486
- 5 Kasugai H, Kojima J, Tatsuta M, Okuda S, Sasaki Y, Imaoka S, Fujita M, Ishiguro S. Treatment of hepatocellular carcinoma by transcatheter arterial embolization combined with intra-arterial infusion of a mixture of cisplatin and ethiodized oil. *Gastroenterology* 1989; **97**: 965-971
- 6 Carr BI. Hepatic artery chemoembolization for advanced stage HCC: experience of 650 patients. *Hepatogastroenterology* 2002; **49**: 79-86
- 7 Miller DL, Lotze MT. A plea for a standard standard. *Radiology* 1993; **188**: 19-20
- 8 Trevisani F, De Notariis S, Rossi C, Bernardi M. Randomized controlled trials on chemoembolization for hepatocellular carcinoma: is there room for new studies? *J Clin Gastroenterol* 2001; **32**: 383-389
- 9 Camma C, Schepis F, Orlando A, Albanese M, Shahied L, Trevisani F, Andreone P, Craxi A, Cottone M. Transarterial chemoembolization for unresectable hepatocellular carcinoma: meta-analysis of randomised controlled trials. *Radiology* 2002; **224**: 47-54
- 10 Llovet JM, Real MI, Montana X, Planas R, Coll S, Aponte J, Ayuso C, Sala M, Muchart J, Sola R, Rodes J, Bruix J. Barcelona Liver Cancer Group. Arterial embolisation or chemoembolisation versus symptomatic treatment in patients with unresectable hepatocellular carcinoma: a randomized controlled trial. *Lancet* 2002; **359**: 1734-1739
- 11 Lo CM, Ngan H, Tso WK, Liu CL, Lam CM, Poon RT, Fan ST, Wong J. Randomized controlled trial of transarterial lipiodol chemoembolization for unresectable hepatocellular carcinoma. *Hepatology* 2002; **35**: 1164-1171
- 12 Llovet JM, Bruix J. Systematic review of randomized trials for unresectable hepatocellular carcinoma: Chemoembolization improves survival. *Hepatology* 2003; **37**: 429-442
- 13 Lee HS, Kim KM, Yoon JH, Lee TR, Suh KS, Lee KU, Chung JW, Park JH, Kim CY. Therapeutic efficacy of transcatheter arterial chemoembolization as compared with hepatic resection in hepatocellular carcinoma patients with compensated liver function in a hepatitis B virus-endemic area: a prospective cohort study. *J Clin Oncol* 2002; **20**: 4459-4465
- 14 Allgaier HP, Deibert P, Zuber I, Olschewski M, Blum HE. Percutaneous radiofrequency interstitial thermal ablation of small hepatocellular carcinoma. *Lancet* 1999; **353**: 1676-1677
- 15 McGhana JP, Dodd GD 3rd. Radiofrequency ablation of the liver: current status. *Am J Roentgenol* 2001; **176**: 3-16
- 16 Curley SA. Radiofrequency ablation of malignant liver tumors. *Ann Surg Oncol* 2003; **10**: 338-347
- 17 Llovet JM, Vilana R, Bru C, Bianchi L, Salmeron JM, Boix L, Ganau S, Sala M, Pages M, Ayuso C, Sole M, Rodes J, Bruix J. Barcelona Clinic Liver Cancer (BCLC) Group. Increased risk of tumor seeding after percutaneous radiofrequency ablation for single hepatocellular carcinoma. *Hepatology* 2001; **33**: 1124-1129
- 18 Bruix J, Sherman M, Llovet JM, Beaugrand M, Lencioni R, Burroughs AK, Christensen E, Pagliaro L, Colombo M, Rodes J. EASL Panel of Experts on HCC. Clinical management of hepatocellular carcinoma. Conclusions of the Barcelona-2000 EASL conference. European Association for the Study of the Liver. *J Hepatol* 2001; **35**: 421-430
- 19 Ngan H, Lai CL, Fan ST, Lai EC, Yuen WK, Tso WK. Treatment of inoperable hepatocellular carcinoma by transcatheter arterial chemoembolization using an emulsion of cisplatin in iodized oil and gelfoam. *Clin Radiol* 1993; **47**: 315-320
- 20 O'Suilleabhain CB, Poon RT, Yong JL, Ooi GC, Tso WK, Fan ST. Factors predictive of 5-year survival after transarterial chemoembolization for inoperable hepatocellular carcinoma. *Br J Surg* 2003; **90**: 325-331
- 21 Greene FL, Page DL, Fleming ID, Fritz AG, Balch CM, Haller DG, Morrow M, eds. AJCC cancer staging manual, 6th ed. Springer-Verlag; 2002
- 22 Hosmer DW, Lemeshow S. Applied logistic regression. New York: John Wiley & Sons, 1989
- 23 Castells A, Bruix J, Bru C, Fuster J, Vilana R, Navasa M, Ayuso C, Boix L, Visa J, Rodes J. Treatment of small hepatocellular carcinoma in cirrhotic patients: a cohort study comparing surgical resection and percutaneous ethanol injection. *Hepatology* 1993; **18**: 1121-1126
- 24 Bronowicki JP, Boudjema K, Chone L, Nisand G, Bazin C, Pflumio F, Uhl G, Wenger JJ, Jaeck D, Boissel P, Bigard MA, Gaucher P, Vetter D, Doffoel M. Comparison of resection, liver transplantation and transcatheter oily chemoembolization in the treatment of hepatocellular carcinoma. *J Hepatol* 1996; **24**: 293-300
- 25 Boyle MJ. Percutaneous ablation of liver tumors. *Arch Surg* 2003; **138**: 809-810
- 26 Curley SA, Izzo F, Delrio P, Ellis LM, Granchi J, Vallone P, Fiore F, Pignata S, Daniele B, Cremona F. Radiofrequency ablation of unresectable primary and metastatic hepatic malignancies. Results in 123 patients. *Ann Surg* 1999; **230**: 1-8
- 27 Ng KK, Lam CM, Poon RT, Ai V, Tso WK, Fan ST. Thermal ablative therapy for malignant liver tumors: a critical appraisal. *J Gastroenterol Hepatol* 2003; **18**: 616-629
- 28 Mulier S, Mulier P, Ni Y, Miao Y, Dupas B, Marchal G, De Wever I, Michel L. Complications of radiofrequency coagulation of liver tumours. *Br J Surg* 2002; **89**: 1206-1222
- 29 Curley SA, Izzo F, Ellis LM, Nicolas Vauthey J, Vallone P. Radiofrequency ablation of hepatocellular cancer in 110 patients with cirrhosis. *Ann Surg* 2000; **232**: 381-391
- 30 Poon RT, Ng KK, Lam CM, Ai V, Yuen J, Fan ST. Effectiveness of radiofrequency ablation for hepatocellular carcinomas greater than 3 cm in diameter. *Arch Surg* 2004; **139**: 281-287
- 31 Vivarelli M, Guglielmi A, Ruzzenente A, Cucchetti A, Bellusci R, Cordiano C, Cavallari A. Surgical resection versus percutaneous radiofrequency ablation in the treatment of hepatocellular carcinoma on cirrhotic liver. *Ann Surg* 2004; **240**: 102-107
- 32 Xu HX, Xie XY, Lu MD, Chen JW, Yin XY, Xu ZF, Liu GJ. Ultrasound-guided percutaneous thermal ablation of hepatocellular carcinoma using microwave and radiofrequency ablation. *Clin Radiol* 2004; **59**: 53-61
- 33 Buscarini L, Buscarini E, Di Stasi M, Vallisa D, Quaretti P, Rocca A. Percutaneous radiofrequency ablation of small hepatocellular carcinoma: long-term results. *Eur Radiol* 2001;

- 11: 914-921
- 34 **Mondazzi L**, Bottelli R, Brambilla G, Rampoldi A, Rezakovic I, Zavaglia C, Alberti A, Ideo G. Transarterial oily chemoembolization for the treatment of hepatocellular carcinoma : a multivariate analysis of prognostic factors. *Hepatology* 1994; **19**: 1115-1123
- 35 **Ikeda M**, Okada S, Yamamoto S, Sato T, Ueno H, Okusaka T, Kuriyama H, Takayasu K, Furukawa H, Iwata R. Prognostic factors in patients with hepatocellular carcinoma treated by transcatheter arterial embolization. *Jpn J Clin Oncol* 2002; **32**: 455-460
- 36 **Llado L**, Virgili J, Figueras J, Valls C, Dominguez J, Rafecas A, Torras J, Fabregat J, Guardiola J, Jaurrieta E. A prognostic index of the survival of patients with unresectable hepatocellular carcinoma after transcatheter arterial chemoembolization. *Cancer* 2000; **88**: 50-57
- 37 **Savastano S**, Miotto D, Casarrubea G, Teso S, Chiesura-Corona M, Feltrin GP. Transcatheter arterial chemoembolization for hepatocellular carcinoma in patients with Child's grade A or B cirrhosis: a multivariate analysis of prognostic factors. *J Clin Gastroenterol* 1999; **28**: 334-340
- 38 **Akashi Y**, Koreeda C, Enomoto S, Uchiyama S, Mizuno T, Shiozaki Y, Sameshima Y, Inoue K. Prognosis of unresectable hepatocellular carcinoma: an evaluation based on multivariate analysis of 90 cases. *Hepatology* 1991; **14**: 262-268
- 39 **Nakao N**, Kamino K, Miura K, Takayasu Y, Ohnishi M, Miura T. Transcatheter arterial embolization in hepatocellular carcinoma: a long-term follow-up. *Radiat Med* 1992; **10**: 13-18
- 40 **Yamada R**, Kishi K, Sonomura T, Tsuda M, Nomura S, Satoh M. Transcatheter arterial embolization in unresectable hepatocellular carcinoma. *Cardiovasc Intervent Radiol* 1990; **13**: 135-139
- 41 **Takayasu K**, Muramatsu Y, Maeda T, Iwata R, Furukawa H, Muramatsu Y, Moriyama N, Okusaka T, Okada S, Ueno H. Targeted transarterial oily chemoembolization for small foci of hepatocellular carcinoma using a unified helical CT and angiography system: analysis of factors affecting local recurrence and survival rates. *Am J Roentgenol* 2001; **176**: 681-688

Science Editor Wang XL and Li WZ Language Editor Elsevier HK

Down-regulation of *PTEN* expression due to loss of promoter activity in human hepatocellular carcinoma cell lines

Dong-Zhu Ma, Zhen Xu, Yu-Long Liang, Jian-Ming Su, Zeng-Xia Li, Wen Zhang, Li-Ying Wang, Xi-Liang Zha

Dong-Zhu Ma, Zhen Xu, Yu-Long Liang, Jian-Ming Su, Zeng-Xia Li, Wen Zhang, Li-Ying Wang, Xi-Liang Zha, Ministry of Health Key Laboratory of Glycocojugate Research, Department of Biochemistry and Molecular Biology, Shanghai Medical College, Fudan University, Shanghai 200032, China

Supported by the National Natural Science Foundation of China, No. 39970338; Shanghai Municipal Government Science and Technology Committee, No. 00JC14042; and Innovation fund of Fudan University, QCF109801

Correspondence to: Professor Xi-Liang Zha, Department of Biochemistry and Molecular Biology, Shanghai Medical College, Fudan University, 138 Yixueyuan Road, Shanghai 200032, China. xlzha@shmu.edu.cn

Telephone: +86-21-54237696 Fax: +86-21-64179832

Received: 2004-03-30 Accepted: 2004-05-13

Abstract

AIM: To investigate the regulation of phosphatase and tensin homolog deleted on chromosome ten (*PTEN*) gene expression in human hepatocellular carcinoma (HCC) cell lines.

METHODS: The mRNA and protein levels of *PTEN* were detected by Northern blot and Western blot in HCC cell lines, respectively. Plasmids containing different fragments of *PTEN* promoter with Luciferase reporter were constructed and transiently transfected into HCC cell lines to study the promoter activity. DNA analysis and RT-PCR were performed to detect the mutation of *PTEN* promoter and *PTEN* cDNA.

RESULTS: Either protein or mRNA levels of *PTEN* in L02 cells (as a control) were significantly higher than that in HCC cell lines. The profile of *PTEN* promoter activity in 8 cell lines was closely correlated with levels of *PTEN* mRNA and *PTEN* protein. Furthermore, the sequence analysis of 8 cell lines showed no mutation in the region of *PTEN* promoter and *PTEN* cDNA.

CONCLUSION: *PTEN* expression is down-regulated in HCC cell lines probably due to loss of activity of *PTEN* promoter.

© 2005 The WJG Press and Elsevier Inc. All rights reserved.

Key words: Phosphatase; Tensin homolog; Hepatocellular carcinoma

Ma DZ, Xu Z, Liang YL, Su JM, Li ZX, Zhang W, Wang LY, Zha XL. Down-regulation of *PTEN* expression due to loss of promoter activity in human hepatocellular carcinoma cell lines. *World J Gastroenterol* 2005; 11(29): 4472-4477
<http://www.wjgnet.com/1007-9327/11/4472.asp>

INTRODUCTION

The tumor suppressor gene phosphatase and tensin homolog deleted on chromosome ten (*PTEN*), mutated in a wide range of human cancers^[1,2], encodes a protein containing 403 amino acids with phospholipid and protein phosphatase activity^[3-6]. Consequently, *PTEN* inhibits the generation of phosphatidylinositol 3,4,5-trisphosphate (PIP3)^[7] and then blocks the activation of proto-oncogene PKB/Akt^[8,9]. The loss of *PTEN* in human tumors leads to an increase in PI(3,4,5)P3 and the uncontrolled stimulation of growth and survival signals^[10]. *PTEN* also dephosphorylated focal adhesion kinase because of its tyrosine phosphatase activity^[11,12], which might lead to the inactivation of Ras/mitogen-activated protein kinase (MAPK) pathway^[12-15]. It is well known that both pathways mentioned above are intimately involved in control of cell growth and survival, so *PTEN* appears to impinge on cell proliferation, adhesion, cell migration, and cell invasion^[14,15]. Moreover, germline mutations in *PTEN* cause Cowden disease, which is characterized by the formation of multiple hamartomas and increased susceptibility to skin, thyroid, and breast tumors^[16]. Together, these findings suggest that loss of *PTEN* activity sensitizes cells to malignant transformation and *PTEN* is an important protein to regulate various physiological pathways. Despite extensive characterization of *PTEN* mutations in human cancers and relatively good understanding of the molecular roles of *PTEN* in the control of cellular processes, little is known about modes of *PTEN* regulation. Recently, scientists have paid more attention to the regulation of *PTEN* expression. It was reported that the transcription of *PTEN* could be regulated by p53 and Sp1^[17,18]. In addition, 5'-untranslated region (5'-UTR) of *PTEN* gene was responsible for constitutive *PTEN* expression in mice^[18]. Salvesen *et al.*^[19], found that *PTEN* promoter methylation was relatively frequent in endometrial carcinoma. Till now, the regulation of *PTEN* expression is still unclear especially in HCC cells. It is well known that the regulation of gene expression is a multi-step process in eukaryotes, and the transcriptional regulation plays a important role in it. So, we attempted to study the transcriptional regulation of *PTEN* expression in HCC cell lines.

MATERIALS AND METHODS

Cell culture

Human hepatocellular carcinoma (HCC) cell lines (SMMC-7721, BEL-7402, BEL-7404, and BEL-7405) and human liver immortal cell line L02, purchased from Institute

of Biochemistry and Cell Biology, Chinese Academy of Sciences (Shanghai, China), were routinely maintained in RPMI 1640 (Gibco BRL, USA) supplemented with 100 mL/L fetal bovine serum (HyClone, USA) at 37 °C in a humidified atmosphere containing 50 mL/L CO₂ in air. HepG2 (human hepatoblastoma) was obtained from American Type Culture Collection (ATCC). HCC cell lines MHCC-97H and MHCC-97L kindly provided by Liver Cancer Institute of Zhongshan Hospital, Fudan University (Shanghai, China), were maintained in Dulbecco's modified Eagle's medium (Gibco BRL, USA) supplemented with 100 mL/L fetal bovine serum (HyClone, USA) at 37 °C in a humidified atmosphere containing 50 mL/L CO₂ in air.

Western blot analysis

After being grown into confluence, cells were washed twice with ice-cold phosphate-buffered saline (PBS) and lysed in cold lysis buffer (50 mmol/L HEPES, pH 7.5, 150 mmol/L NaCl, 1.5 mmol/L MgCl₂, 1 mmol/L EDTA, 0.2 mmol/L EGTA, 10 mL/L NP-40, 100 g/L glycerol, 1 mmol/L dithiothreitol, 1 mmol/L phenylmethylsulfonyl fluoride, 20 mmol/L sodium fluoride, 5 mmol/L sodium orthovanadate, 10 g/L aprotinin, 10 g/L leupeptin, 2 g/L pepstatin, and 1 mmol/L benzamide). Lysates were incubated for 20 min on ice and centrifugated at 12 000 *g* for 20 min. The supernatants were collected and protein concentration was determined by Lowry protein assay. Cell lysates were electrophoresed by SDS-PAGE and then transferred onto polyvinylidene fluoride (PVDF) membrane. The membranes were blocked with 50 g/L nonfat dry milk in PBST (PBS, 0.5 mL/L Tween-20) for 4 h at room temperature and incubated overnight at 4 °C with a mAb against human *PTEN* (Santa Cruz, CA, USA), followed by incubation with HRP-conjugated secondary antibody at room temperature for 3 h. Antibody binding was detected by enhanced chemiluminescence (ECL).

Northern blot analysis

Total RNA was isolated using the TRIzol reagent (Invitrogen, CA, USA) according to the manufacturer's directions. The 20 µg RNA was electrophoresed on a 12 g/L agarose/formaldehyde gel and blotted onto a nylon membrane (Schleicher & Schuell, Germany) by capillary transfer. Hybridization was performed in 0.2 mol/L Na₂HPO₄/NaH₂PO₄ (pH 7.2), 1 mmol/L EDTA, 10 g/L BSA, 70 g/L SDS and 150 mL/L formamide at 50 °C, and the filters were washed extensively with 40 mmol/L Na₂HPO₄/NaH₂PO₄ (pH 7.2), 1 mmol/L EDTA, 10 g/L SDS at 65 °C. A 1.2 kb DNA fragment representing the entire coding region of *PTEN* was used as a probe and was labeled by Prime-a-Gene labeling system (Promega, Madison, WI, USA). Air-dried blots were autoradiographed onto Kodak film (Eastman Kodak, Rochester, NY, USA) and the RNA signal was detected using an ImageMaster VDS system (Pharmacia Biotech, San Francisco, CA, USA) and normalized against the signal for β-actin using ImageMaster TotalLab 1D software.

Isolation of 5'-flanking and promoter region of *PTEN* gene

Based on the published sequence of *PTEN* (accession

number AF067844), a 2.7 kb DNA fragment of *PTEN* containing 5'-flanking region, 5'-untranslated region (5'-UTR) and full-length of *PTEN* promoter region were obtained by PCR using primers 5'-GATAGATCTGGGTG-GGGTGC GGGGTAGGAGTGC-3' and 5'-GAGAAG-CTTGCTGCGGGCGGCTGCTGGATGGTTG-3'. The fragment was subcloned into the luciferase reporter plasmid pGL3-basic (Promega, Madison, WI, USA) which was digested twice with *Bgl*II and *Hind*III restriction enzymes. Positive clones, pGL3-2768, from 8 cell lines were identified by restriction enzymes digest and DNA sequencing, and aligned with the GenBank databases.

Reporter gene plasmids constructions

Several specific primers containing *Bgl*II and *Hind*III restriction enzyme sites (listed below) were designed to amplify serial deletion fragment of *PTEN* using the clone pGL3-2768 (-2 927/-160) as a template.

5'-CGGAGATCTGTGTTTGATGTGGGTGCTTTT-3' (-2 403),
5'-GCTAGATCTTCATTTAGATAGGTGCCCTTTGG-3' (-1 794),
5'-GAGAGATCTGCGTGTCACCTGGTCCCT-3' (-1 389),
5'-CTGAGATCTCTCAGTAGAGCTGCGGCTTGG-3' (-1 118),
5'-GGCAGATCTGCGGTGATGTGGCGGACTCTT-3' (-916),
5'-GCGAGATCTCGCGACTGCGCTCAGTTCTCTCCT-3' (-858),
5'-CCGAAGCTTGGCTCGCCTCACAGCGGCTCAACT-3' (-778),
5'-CAGAGATCTGGTCTGAGTCGCTGTCAACATTT-3' (-458),
5'-GAGAAGCTTGTGCGGCGGCTGCTGGATGGTTG-3' (-160).

Fragments of 2 234 (-2 403/-160), 1 635 (-1 794/-160), 1 230 (-1 389/-160), 1 526 (-2 403/-778), 1 016 (-1 794/-778), 612 (-1 389/-778), 341 (-1 118/-778), 139 (-916/-778), 81 (-858/-778) and 299 (-458/-160) were cloned into the vector pGL3-basic at the *Bgl*II and *Hind*III sites to individually generate pGL3-2234, pGL3-1635, pGL3-1230, pGL3-1526, pGL3-1016, pGL3-612, pGL3-341, pGL3-139, pGL3-81, pGL3-299, respectively. These constructs were sequenced and aligned with the GenBank databases.

Transient transfections and luciferase activity assays

Cells were seeded into 6-well plates at a density of 150 000 cells per well 1 day before transfection. The transfection was performed with the Lipofectamine™ 2000 transfection reagent (Invitrogen, CA, USA) according to the manufacturer's guidelines. Typically, 3 µg of pGL3 vector and 1 µg of pGFP-β-Gal (a gift from Houyan Song, Department of Molecular Genetics, Shanghai Medical College, Fudan University, Shanghai, China) were used per well. After 48 h, cells were lysed with lysis buffer (Promega, Madison, WI, USA). The mixtures were centrifugated at 12 000 *g* for 15 s at 4 °C, and the supernatant was preserved at -70 °C. Activities of firefly luciferases were measured in a luminometer Lumat LB 9507 using the luciferase assay system (Promega, Madison, WI, USA). β-Gal activity was measured by β-galactosidase enzyme assay system (Promega, Madison, WI, USA). Promoter activity was quantified by calculating the ratio of firefly luciferase activity/β-gal activity of the same sample. Transfection efficiency was determined through the positive cells with green fluorescence from the green fluorescence protein (GFP) under fluorescent microscope. All the luciferase assays were carried out at least in triplicate, and the experiments were repeated thrice.

RT-PCR and DNA sequencing of *PTEN* cDNA and *PTEN* promoter

Total RNA was isolated from cell lines using the TRIzol RNA isolation kit (Invitrogen, CA, USA) according to the manufacturer's protocols. After synthesis of first strand cDNA using oligo-d(T)₁₂₋₁₈ primer and moloney murine leukemia virus (M-MuLV) reverse transcriptase (Promega, Madison, WI, USA), *PTEN* cDNA was amplified using PCR with pyrococcus furiosus (Pfu) DNA-polymerase (Promega, Madison, WI, USA). The primer sequences were as follows: upper primer, 5'-ACAGGC-TCCCAGACATGACA-3' and lower primer, 5'-TCAG-ACTTTTGTAATTTGTGTATG-3'. PCR amplification was carried out for 30 cycles under denaturing-annealing-extension conditions of 94 °C for 30 s, 60 °C for 1 min and 72 °C for 1 min, respectively. The PCR product was cloned into the T vector and was identified by DNA sequencing of at least three independent clones and aligned with the GenBank databases.

Statistical analysis

F test was used for statistical analysis.

RESULTS

PTEN protein and mRNA expression in 8 cell lines

Most mammalian cells containing the wild-type *PTEN* gene expressed detectable levels of *PTEN* mRNA and protein under normal growth conditions^[17]. L02, a human liver immortal cell line, was used as a control in the present study. There was one 55 ku *PTEN* protein detected with various levels in 8 cell lines by Western blot analysis (Figure 1). The protein level of *PTEN* in L02 cells was the highest among the 8 cell lines, whereas the *PTEN* protein in HepG2 cells was almost undetectable. Simultaneously, Northern blot analysis showed a major 2.5-kb transcript and a lower abundance 5.0-kb transcript of *PTEN* mRNA in all 8 cell lines, which was consistent with previous reports^[20] (Figure 2). The total mRNA of *PTEN* was calculated in both 5.0-kb and 2.5-kb transcripts. The mRNA level of *PTEN* was much higher in L02 cells than the other 7 HCC

cell lines, especially in HepG2 cells (Figure 2). The mRNA level of *PTEN* in L02 cells was over five-folds than in HepG2 cells. However, the profile of *PTEN* protein level in each of 8 cell lines closely parallelized with its *PTEN* mRNA.

Absence of *PTEN* promoter and *PTEN* cDNA mutation in 8 cell lines

Deletions or mutations of *PTEN* encoding gene are associated with a variety of human cancers^[12]. Furthermore, decreased expression of *PTEN* was associated with advanced glioma, melanoma, and prostate cancer, implicating losses of *PTEN* by mutation involved in tumor progression^[21-23]. To investigate whether the deletion or mutation exists in *PTEN* gene, leading to the lost expression of *PTEN* in HCC cell lines, we analyzed the sequence of *PTEN* cDNA and *PTEN* promoter (-2 927/-160 bp) in 8 cell lines. We found no mutation in *PTEN* cDNA and *PTEN* promoter region of 8 cell lines (data not shown), indicating that the different levels of *PTEN* mRNA and protein in 8 cell lines were not caused by the mutation of *PTEN* cDNA and promoter region. It might be related to *PTEN* transcriptional or post-transcriptional regulation.

Core region of *PTEN* promoter identified in SMMC-7721 and L02 cell lines

It is well known that promoter plays the most important role in gene transcription. In an attempt to analyze the function of *PTEN* promoter, we isolated a DNA fragment containing 5'-flanking region and the 5'-untranslated region (5'-UTR) from *PTEN* gene, and performed a series of promoter deletion. Eleven fragments of *PTEN* gene promoter were constructed into pGL3-basic with luciferase reporter (Figure 3 A) and were transiently transfected into L02 and SMMC-7721 cell lines. It was found that the profiles of luciferase activities of various plasmids were the same in the two cell lines (Figures 3B and C). The 612-bp fragment (-1 389/-778) was sufficient to induce maximum luciferase activity in L02 and SMMC-7721 cell lines. The plasmid pGL3-2768 (-2 927/-160), which

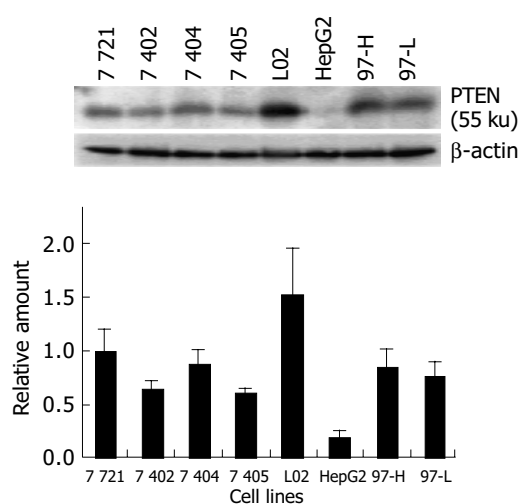


Figure 1 Western blot analysis for *PTEN* protein expression in 8 cell lines under normal growth conditions.

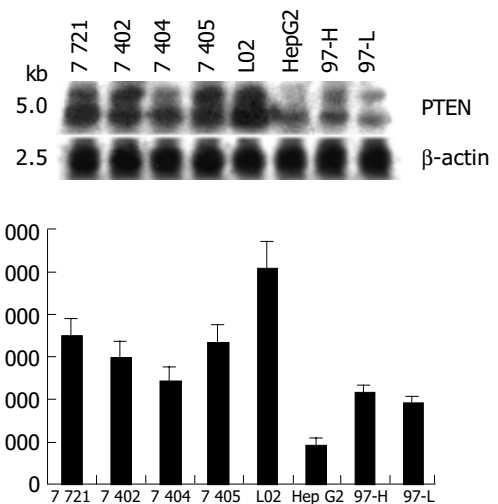


Figure 2 Northern blot analysis of *PTEN* mRNA expression in 8 cell lines under normal growth conditions.

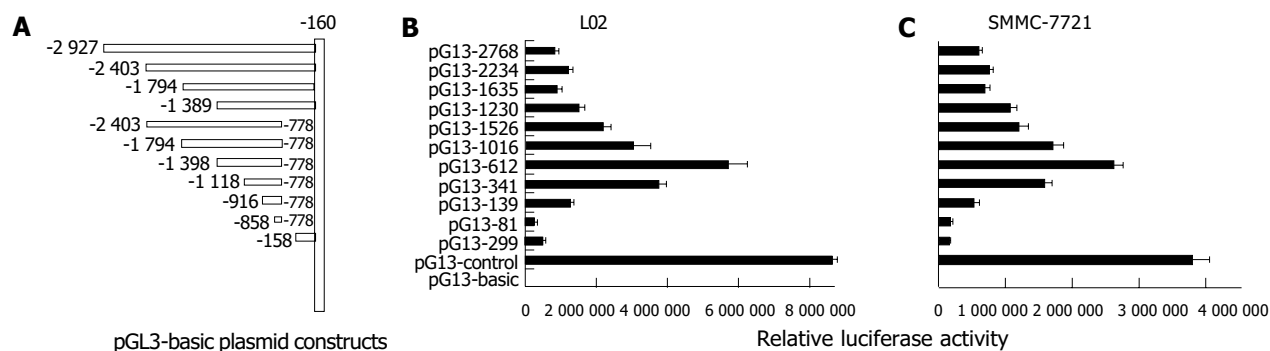


Figure 3 *PTEN* promoter deletion analysis in SMMC-7721 and L02 cell lines. **A:** Schematic representation of serial deletion constructs of human *PTEN* genomic

locus; **B:** promoter activity of serial deletion constructs of *PTEN* in L02 cell lines; **C:** promoter activity of serial deletion constructs of *PTEN* in SMMC-7721 cell lines.

contained full-length promoter, appeared to have lower activity than that of pGL3-612 (-1 389/-778), indicating that the suppressor elements or special DNA structure may exist in double ends, especially in 3' end fragment (-777/-160). The 341 bp fragment (-1 118/-778) possessed over 60% of the promoter activity of the 612 bp fragment. The 81-bp fragment (-858/-778), however, appeared to be insufficient for inducing transcriptional activation of *PTEN*. The 299-bp downstream fragment (-458/-160) possessed no significant promoter activity in L02 and SMMC-7721 cells. No further increase in activity was observed when longer fragments than 612 bp were transfected, which was consistent with previous report^[24]. Taken together, these data showed that the 612-bp fragment (-1 389/-778) had optimal promoter activity and the core region of *PTEN* promoter was located within the -1 118 to -778 region.

Different activities of *PTEN* promoter in 8 cell lines

When transfecting the plasmid pGL3-612 that possessed maximum *PTEN* promoter activity into the 8 cell lines, we found the activity of pGL3-612 in SMMC-7721 and L02 cells were much higher than that in others (Figure 4), while the activity of pGL3-612 in HepG2 cells was the lowest, only 17% of that in L02 cells. The activities of pGL3-612 in BEL-7402, BEL-7404, BEL-7405, MHCC-97H and MHCC-97L were 55%, 65%, 62%, 45%, and 39% of that in L02 cells, respectively. The profile of *PTEN* promoter activity in 8 cell lines was mostly parallelized to

the profiles of *PTEN* protein and *PTEN* mRNA. These results demonstrated that the changes of *PTEN* protein and *PTEN* mRNA in 8 cell lines might result from the function of *PTEN* promoter.

DISCUSSION

Since the isolation of *PTEN/MMAC1/TEP1* (acronyms for phosphatase and tensin homolog^[2], mutated in multiple advanced cancers^[1], and TGF- β (transforming growth factor- β)-regulated and epithelial cell-enriched phosphatase^[25] as a candidate tumor suppressor gene, hundreds of reports have been published focusing on its structure and function, as well as on mutations that cause human diseases^[26]. Mutations of the *PTEN* gene arise during cancer progression in a remarkable variety of cancers, including brain, prostate, breast, endometrial cancers and melanoma^[26]. The frequency of *PTEN* mutations observed in endometrial tumors^[26], malignant glial tumors^[25], malignant melanoma cell lines^[26] and metastatic prostate carcinomas^[27] was about 45%, 24%, 40%, and 10%, respectively. In addition, germline mutations in the *PTEN* gene have been associated with Cowden syndrome and a significantly increased risk of certain tumors, including cancer of the breast and thyroid^[21,28]. These data further support that *PTEN* is a tumor suppressor gene.

The structure of *PTEN* contains a phosphatase domain that has a structure resembling tyrosine phosphatase and a C2 domain appears to bind *PTEN* to the plasma membrane, which might orientate the catalytic domain appropriately for interactions with phosphatidylinositol 3,4,5-trisphosphate (PIP3) and other potential substrates^[29]. A PDZ binding motif in the tail might also play a role in altering the balance of *PTEN* effects on potential downstream signaling targets such as Akt^[16]. *PTEN* is also known to be critically important both during embryonic development and in mature organisms as a tumor suppressor^[30-32]. Studies of *PTEN* functions have provided a novel insight into the regulation of apoptosis, migration and tumor progression. *PTEN* appears to serve as a hub or switchpoint linking complex signaling pathways^[33,34].

HCC presents a major health threat in South-East Asia, especially in China. It ranks the third among all malignancies both in incidence and mortality in China and accounts for approximately 42.5% of the total incidence worldwide^[35].

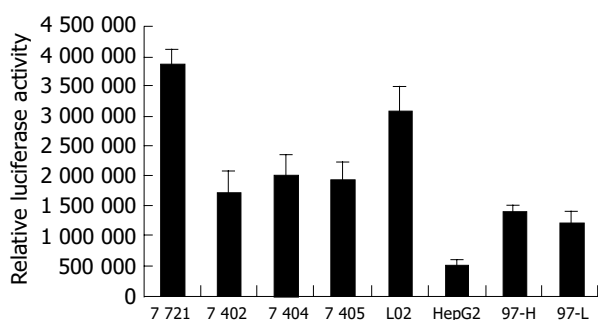


Figure 4 Activity of *PTEN* promoter in 8 cell lines.

As a tumor suppressor gene, *PTEN* expression is downregulated in tumors and tumor cell lines by genetic and epigenetic mechanisms^[26]. Therefore, it is very important to study the regulation of *PTEN* expression in human HCC cell lines. In this study, the results of Western blot analysis demonstrated that the protein level of *PTEN* in L02 cells was the highest among 8 cell lines, whereas there was almost undetectable *PTEN* protein expression in HepG2 cells. Northern blot analysis showed that the profile of *PTEN* mRNA in 8 cell lines almost parallelized to the profile of *PTEN* protein, indicating that the variation of *PTEN* protein was mostly dependent on the change of *PTEN* mRNA. Moreover, deletions or mutations of *PTEN* gene are associated with a variety of human cancers^[12]. Does such deletion or mutation of *PTEN* gene exist in HCC cell lines, causing the cut down of *PTEN* expression in HCC cell lines? The sequence analysis of *PTEN* cDNA and *PTEN* promoter region showed no mutations in these HCC cell lines. Hence the downregulation of *PTEN* expression in HCC cell lines probably existed in transcriptional or post-transcriptional levels.

The deletion analysis of *PTEN* promoter showed that the fragment of 612 bp (-1 389/-778) could produce maximum promoter activity in 8 cell lines and the core region of *PTEN* promoter was within the 341 bp (-1 118/-778) fragment. The full-length fragment possessing low activity indicated that the double ends of the 612 bp fragment contained suppressive elements or special structures. We used the Genomatix Suite/MatInspector software^[36] to analyze the potential binding sites in *PTEN* core promoter region and its downstream DNA sequence (-1 118/-160 bp), and found a variety of binding sites for p53, NF-kappaB, Ap2, MAZ, Sp1, E4F and Egr-1. Particularly, there were five MAZ binding sites in core promoter region (-1 118/-778) area and 11 Egr-1 in its downstream area (-779/-160). Our results suggested that these two transcription factors might play an important role in control of *PTEN* expression. After the transfection of pGL3-612 (-1 389/-778), which could produce maximum promoter activity into 8 cell lines, we found the profile of *PTEN* promoter activity was almost parallelized with the profiles of *PTEN* mRNA and *PTEN* protein in 8 cell lines. Furthermore, a recent study reported that the *PTEN* had no internal ribosome entry site (IRES) that could mediate cap-independent initiation of translation^[18]. Taken together, we conclude that the downregulation of *PTEN* expression in 7 HCC cell lines may not be responsible for the mutation of *PTEN*, but mainly contribute to the loss of *PTEN* promoter activity.

ACKNOWLEDGMENT

We gratefully acknowledge the kind support of Dr. Sui-Quan Wang in our research for the using of luminometer Lumat LB 9507.

REFERENCES

- 1 **Steck PA**, Pershouse MA, Jasser SA, Yung WK, Lin H, Ligon AH, Langford LA, Baumgard ML, Hattier T, Davis T, Frye C, Hu R, Swedlund B, Teng DH, Tavtigian SV. Identification of a candidate tumour suppressor gene, MMAC1, at chromosome 10q23.3 that is mutated in multiple advanced cancers.

- Nat Genet* 1997; **15**: 356-362
- 2 **Li J**, Yen C, Liaw D, Podsypanina K, Bose S, Wang SI, Puc J, Miliareis C, Rodgers L, McCombie R, Bigner SH, Giovannella BC, Ittmann M, Tycko B, Hibshoosh H, Wigler MH, Parsons R. PTEN, a putative protein tyrosine phosphatase gene mutated in human brain, breast, and prostate cancer. *Science* 1997; **275**: 1943-1947
- 3 **Maehama T**, Taylor GS, Dixon JE. PTEN and myotubularin: novel phosphoinositide phosphatases. *Annu Rev Biochem* 2001; **70**: 247-279
- 4 **Simpson L**, Parsons R. PTEN: life as a tumor suppressor. *Exp Cell Res* 2001; **264**: 29-41
- 5 **Waite KA**, Eng C. Protean PTEN: form and function. *Am J Hum Genet* 2002; **70**: 829-844
- 6 **Leslie NR**, Downes CP. PTEN: The down side of PI 3-kinase signalling. *Cell Signal* 2002; **14**: 285-295
- 7 **Myers MP**, Pass I, Batty IH, Van der Kaay J, Stolarov JP, Hemmings BA, Wigler MH, Downes CP, Tonks NK. The lipid phosphatase activity of PTEN is critical for its tumor suppressor function. *Proc Natl Acad Sci USA* 1998; **95**: 13513-13518
- 8 **Maehama T**, Dixon JE. PTEN: a tumour suppressor that functions as a phospholipid phosphatase. *Trends Cell Biol* 1999; **9**: 125-128
- 9 **Stambolic V**, Suzuki A, de la Pompa JL, Brothers GM, Mirtsos C, Sasaki T, Ruland J, Penninger JM, Siderovski DP, Mak TW. Negative regulation of PKB/Akt-dependent cell survival by the tumor suppressor PTEN. *Cell* 1998; **95**: 29-39
- 10 **Furnari FB**, Lin H, Huang HS, Cavenee WK. Growth suppression of glioma cells by PTEN requires a functional phosphatase catalytic domain. *Proc Natl Acad Sci USA* 1997; **94**: 12479-12484
- 11 **Li DM**, Sun H. PTEN/MMAC1/TEP1 suppresses the tumorigenicity and induces G1 cell cycle arrest in human glioblastoma cells. *Proc Natl Acad Sci USA* 1998; **95**: 15406-15411
- 12 **Myers MP**, Stolarov JP, Eng C, Li J, Wang SI, Wigler MH, Parsons R, Tonks NK. P-TEN, the tumor suppressor from human chromosome 10q23, is a dual-specificity phosphatase. *Proc Natl Acad Sci USA* 1997; **94**: 9052-9057
- 13 **Gu J**, Tamura M, Yamada KM. Tumor suppressor PTEN inhibits integrin- and growth factor-mediated mitogen-activated protein (MAP) kinase signaling pathways. *J Cell Biol* 1998; **143**: 1375-1383
- 14 **Tamura M**, Gu J, Matsumoto K, Aota S, Parsons R, Yamada KM. Inhibition of cell migration, spreading, and focal adhesions by tumor suppressor PTEN. *Science* 1998; **280**: 1614-1617
- 15 **Tamura M**, Gu J, Takino T, Yamada KM. Tumor suppressor PTEN inhibition of cell invasion, migration, and growth: differential involvement of focal adhesion kinase and p130Cas. *Cancer Res* 1999; **59**: 442-449
- 16 **Liaw D**, Marsh DJ, Li J, Dahia PL, Wang SI, Zheng Z, Bose S, Call KM, Tsou HC, Peacocke M, Eng C, Parsons R. Germline mutations of the PTEN gene in Cowden disease, an inherited breast and thyroid cancer syndrome. *Nat Genet* 1997; **16**: 64-67
- 17 **Stambolic V**, MacPherson D, Sas D, Lin Y, Snow B, Jang Y, Benchimol S, Mak TW. Regulation of PTEN transcription by p53. *Mol Cell* 2001; **8**: 317-325
- 18 **Han B**, Dong Z, Liu Y, Chen Q, Hashimoto K, Zhang JT. Regulation of constitutive expression of mouse PTEN by the 5'-untranslated region. *Oncogene* 2003; **22**: 5325-5337
- 19 **Salvesen HB**, MacDonald N, Ryan A, Jacobs IJ, Lynch ED, Akslen LA, Das S. PTEN methylation is associated with advanced stage and microsatellite instability in endometrial carcinoma. *Int J Cancer* 2001; **91**: 22-26
- 20 **Wu RC**, Blumenthal M, Li X, Schonthal AH. Loss of cellular adhesion to matrix induces p53-independent expression of PTEN tumor suppressor. *BMC Mol Biol* 2002; **3**: 11
- 21 **Guldborg P**, thor Straten P, Birck A, Ahrenkiel V, Kirkin AF, Zeuthen J. Disruption of the MMAC1/PTEN gene by deletion or mutation is a frequent event in malignant melanoma. *Cancer Res* 1997; **57**: 3660-3663

- 22 **Rasheed BK**, Stenzel TT, McLendon RE, Parsons R, Friedman AH, Friedman HS, Bigner DD, Bigner SH. PTEN gene mutations are seen in high-grade but not in low-grade gliomas. *Cancer Res* 1997; **57**: 4187-4190
- 23 **Suzuki H**, Freije D, Nusskern DR, Okami K, Cairns P, Sidransky D, Isaacs WB, Bova GS. Interfocal heterogeneity of PTEN/MMAC1 gene alterations in multiple metastatic prostate cancer tissues. *Cancer Res* 1998; **58**: 204-209
- 24 **Sheng X**, Koul D, Liu JL, Liu TJ, Yung WK. Promoter analysis of tumor suppressor gene PTEN: identification of minimum promoter region. *Biochem Biophys Res Commun* 2002; **292**: 422-426
- 25 **Li DM**, Sun H. TEP1, encoded by a candidate tumor suppressor locus, is a novel protein tyrosine phosphatase regulated by transforming growth factor beta. *Cancer Res* 1997; **57**: 2124-2129
- 26 **Ali IU**, Schriml LM, Dean M. Mutational spectra of PTEN/MMAC1 gene: a tumor suppressor with lipid phosphatase activity. *J Natl Cancer Inst* 1999; **91**: 1922-1932
- 27 **Liu W**, James CD, Frederick L, Alderete BE, Jenkins RB. PTEN/MMAC1 mutations and EGFR amplification in glioblastomas. *Cancer Res* 1997; **57**: 5254-5257
- 28 **Cairns P**, Okami K, Halachmi S, Halachmi N, Esteller M, Herman JG, Jen J, Isaacs WB, Bova GS, Sidransky D. Frequent inactivation of PTEN/MMAC1 in primary prostate cancer. *Cancer Res* 1997; **57**: 4997-5000
- 29 **Lee JO**, Yang H, Georgescu MM, Di Cristofano A, Maehama T, Shi Y, Dixon JE, Pandolfi P, Pavletich NP. Crystal structure of the PTEN tumor suppressor: implications for its phosphoinositide phosphatase activity and membrane association. *Cell* 1999; **99**: 323-334
- 30 **Nelen MR**, van Staveren WC, Peeters EA, Hassel MB, Gorlin RJ, Hamm H, Lindboe CF, Fryns JP, Sijmons RH, Woods DG, Mariman EC, Padberg GW, Kremer H. Germline mutations in the PTEN/MMAC1 gene in patients with Cowden disease. *Hum Mol Genet* 1997; **6**: 1383-1387
- 31 **Leslie NR**, Gray A, Pass I, Orchiston EA, Downes CP. Analysis of the cellular functions of PTEN using catalytic domain and C-terminal mutations: differential effects of C-terminal deletion on signalling pathways downstream of phosphoinositide 3-kinase. *Biochem J* 2000; **346**(Pt 3): 827-833
- 32 **Di Cristofano A**, Pesce B, Cordon-Cardo C, Pandolfi PP. Pten is essential for embryonic development and tumour suppression. *Nat Genet* 1998; **19**: 348-355
- 33 **Suzuki A**, de la Pompa JL, Stambolic V, Elia AJ, Sasaki T, del Barco Barrantes I, Ho A, Wakeham A, Itie A, Khoo W, Fukumoto M, Mak TW. High cancer susceptibility and embryonic lethality associated with mutation of the PTEN tumor suppressor gene in mice. *Curr Biol* 1998; **8**: 1169-1178
- 34 **Yamada KM**, Araki M. Tumor suppressor PTEN: modulator of cell signaling, growth, migration and apoptosis. *J Cell Sci* 2001; **114**(Pt 13): 2375-2382
- 35 **Yu J**, Ni M, Xu J, Zhang H, Gao B, Gu J, Chen J, Zhang L, Wu M, Zhen S, Zhu J. Methylation profiling of twenty promoter-CpG islands of genes which may contribute to hepatocellular carcinogenesis. *BMC Cancer* 2002; **2**: 29
- 36 **Quandt K**, Frech K, Karas H, Wingender E, Werner T. MatInd and MatInspector: new fast and versatile tools for detection of consensus matches in nucleotide sequence data. *Nucleic Acids Res* 1995; **23**: 4878-4884

Antitumor activity of anti-type IV collagenase monoclonal antibody and its lidamycin conjugate against colon carcinoma

Liang Li, Yun-Hong Huang, Yi Li, Feng-Qiang Wang, Bo-Yang Shang, Yong-Su Zhen

Liang Li, Yun-Hong Huang, Yi Li, Feng-Qiang Wang, Bo-Yang Shang, Yong-Su Zhen, Institute of Medicinal Biotechnology, Chinese Academy of Medical Sciences and Peking Union Medical College, Beijing 100050, China

Supported by the National High Technology Research and Development Program of China, 863 Program, No. 2002AA2Z346D

Correspondence to: Professor Yong-Su Zhen, Institute of Medicinal Biotechnology, Chinese Academy of Medical Sciences and Peking Union Medical College, 1 Tiantan Xili, Beijing 100050, China. zhenys@public.bta.net.cn

Telephone: +86-10-63010985 Fax: +86-10-63017302

Received: 2004-11-01 Accepted: 2004-12-03

CONCLUSION: mAb 3G11 is immunoreactive with human colorectal carcinoma and its conjugate with LDM is highly effective against colon carcinoma in mice.

© 2005 The WJG Press and Elsevier Inc. All rights reserved.

Key words: Type IV collagenase; Monoclonal antibody; Lidamycin; Colon carcinoma

Li L, Huang YH, Li Y, Wang FQ, Shang BY, Zhen YS. Antitumor activity of anti-type IV collagenase monoclonal antibody and its lidamycin conjugate against colon carcinoma. *World J Gastroenterol* 2005; 11(29): 4478-4483
<http://www.wjgnet.com/1007-9327/11/4478.asp>

Abstract

AIM: Type IV collagenase including MMP-2 and -9 plays an important role in cancer cell invasion and metastasis and is an attractive target for mAb-directed therapy. The immunoreactivity of mAb 3G11, a mAb directed against type IV collagenase in human colorectal carcinomas, was studied by immuno-histochemical (IHC) staining. mAb 3G11 was conjugated to an antitumor antibiotic lidamycin (LDM). The antitumor activity of 3G11-LDM conjugate against colon carcinoma was investigated in mice.

METHODS: ELISA, gelatin zymography, and Western blot assay were used for the biological characterization of mAb 3G11. The immunoreactivity of mAb 3G11 with human colorectal carcinomas was detected by IHC staining. The cytotoxicity of LDM and 3G11-LDM conjugate to human colon carcinoma HT-29 cells was examined by clonogenic assay and MTT assay. The therapeutic effect of conjugate 3G11-LDM was evaluated with colon carcinoma 26 in mice.

RESULTS: As shown in ELISA, mAb 3G11 reacted specifically with type IV collagenase, while 3G11-LDM conjugate also recognized specifically its respective antigen. In IHC assay, mAb 3G11 showed positive immunoreactivity in most cases of colorectal carcinoma, and negative immunoreactivity in the adjacent non-malignant tissues. By gelatin zymography, the inhibition effect of mAb 3G11 on the secretion activity of type IV collagenase was proved. In terms of IC_{50} values in MTT assay, the cytotoxicity of LDM to human colon carcinoma HT-29 cells was 10 000-fold more potent than that of mitomycin C (MMC) and adriamycin (ADM). 3G11-LDM conjugate also displayed extremely potent cytotoxicity to human colon carcinoma HT-29 cells with an IC_{50} value of 5.6×10^{-19} mol/L. 3G11-LDM conjugate at the doses of 0.05 and 0.1 mg/kg inhibited the growth of colon carcinoma 26 in mice by 70.3 and 81.2%, respectively.

INTRODUCTION

There were 622 000 deaths of colorectal cancer globally in 2002 according to the World Health Report 2004 of WHO. Colorectal cancer can be considered as a complex disease, with a combination of predisposing genetic variants and environmental factors that contribute to the illness as a whole. Since colorectal carcinoma is a leading cause of cancer death in the world, many therapeutic strategies are being investigated, among which the recent major achievements are Avastin and Erbitux, as antibody therapeutics approved for treatment of refractory and advanced colorectal carcinoma by the FDA of USA in 2004. This indicates that antibody-based drugs are promising for colorectal cancer therapy.

Lidamycin (LDM), also called C-1027, is a member of enediyne antitumor antibiotics family and binds to the minor groove of DNA, causing double-strand breaks and apoptosis. LDM consists of an apoprotein (LDP) of 10.5 ku and an enediyne chromophore (LDC) of 843 Da. These two parts of the molecule, connected each other through non-covalent binding, can be dissociated and reconstituted^[1,2]. Because of its extremely potent cytotoxicity against cancer cells and its remarkable activity of anti-angiogenesis and anti-metastasis, LDM can serve as an "effector" agent or "warhead" molecule to construct immunoconjugates^[3-5]. In addition, as a potential chemotherapeutic agent for cancer treatment, LDM has recently entered phase I clinical trials.

Type IV collagenase (also called gelatinases including MMP-2 and -9), as the main member of MMPs family, is of particular interest in the study of antibody-based drugs because the enzyme plays an important role in cancer invasion and metastasis. Using type IV collagenase as a molecular target, mAb 3G11 directed against MMP-2 and -9 was herein produced, analyzed, and evaluated for targeting

cancer therapy. Previous studies have demonstrated that 3G11-LDM immunoconjugate remarkably suppresses the growth of hepatoma 22 (H22) and increases the survival time of tumor bearing mice. Moreover, the antitumor efficacy of the conjugate was higher than that of free LDM or mAb 3G11 alone⁶. In order to reduce the molecular size of agent, e.g. from the mAb to Fab' and even to the Fv, a series of antibody-based drugs have been studied in our laboratory^{7,8}. Utilizing anti-tumor and anti-metastasis mAb 3G11 as a therapeutic agent or as a carrier in cancer treatment may enhance the selectivity of chemotherapy.

In this study, we observed the immunoreactivity of mAb 3G11 with 32 cases of human colorectal carcinoma specimens by IHC staining. For further characterization of the mAb, Western blot assay, ELISA, and gelatin zymography were performed. mAb 3G11 was used as a targeting carrier for colon cancer as it demonstrated a highly specific immunoreactivity to human colorectal carcinoma. 3G11-LDM immunoconjugate was prepared and its antitumor efficacy against colon carcinoma was examined.

MATERIALS AND METHODS

Materials

Highly purified LDM was prepared in our institute. MTT was obtained from Sigma Chemical Co., (St. Louis, MO, USA). Mitomycin C (MMC) was purchased from Kyowa Hakko Kogyo Co., Ltd.

Preparation of monoclonal antibody and conjugate

mAb 3G11, a murine IgG1-type mAb, was prepared using type IV collagenase (SIGMA Inc.) to immunize BALb/c mice. According to our previous methods, mAb 3G11 was purified by sequential affinity and size-exclusion chromatography on protein G and Superose-12 columns and then used for conjugation with LDM immediately. The 3G11-LDM conjugate was formed by heterobifunctional crosslinking reagent *m*-maleimidobenzoyl-*N*-hydroxy-succinimide ester (MBS) through linkage of the amino group of LDM apoprotein with the 3G11 molecule at molecular ratio of 1:1 in our laboratory.

Cells and cell culture

The following cancer cell lines were used: human colon carcinoma HT-29 cells, human fibrosarcoma HT-1080 cells, human breast carcinoma MCF7 cells, mouse colon carcinoma 26 cells, mouse hepatoma 22 cells. All the cell lines were cultured in RPMI 1640 medium (Gibco BRL Inc.) supplemented with 10% heat-inactivated fetal bovine serum (FBS, Gibco BRL Inc.), 0.03% L-glutamine, 100 µg/mL streptomycin and 100 IU/mL penicillin at 37 °C in a humidified atmosphere containing 50 mL/L CO₂. For use in experiments, cells grown in exponential phase were disaggregated to single cells by treatment with trypsin/EDTA for 2 min.

Specimens of human colorectal carcinomas

Tumor tissue specimens collected by standard surgical oncology procedures were obtained from the Pathology 20% glycerin, 2% SDS, 0.1% bromophenol blue. Samples

Department of Friendship Hospital in Beijing. A total of 32 cases of colorectal carcinoma were examined. The specimens were fixed in 40 mL/L formaldehyde in PBS (pH 7.0) and embedded in paraffin.

Immunohistochemical staining

Paraffin-embedded tissue sections of 4 µm thickness were placed on APES-coated slides. Immunohistochemical (IHC) staining of the sections was performed after dewaxing and rehydrating. Then the sections were incubated in 0.3% H₂O₂ for 15 min, blocked by normal mouse serum for 30 min, and incubated with primary mouse mAb (3G11) overnight at 4 °C. IHC staining was performed by the labeled streptavidin–biotin immunoperoxidase technique with SABC kit (Bostern Inc.). After each step, the sections were washed thrice with PBS. Finally, 3,3'-diaminobenzidine-hydrogen peroxide (DAB, Bostern Inc.) was used as a chromogen for visualized reaction. For negative control, PBS and irrelevant mAb F9 were used instead of the primary antibody.

The IHC intensity of various colorectal carcinoma cases was assessed by image analysis and semiquantitative scoring, respectively. The sections were observed under a microscope. Manual evaluation of staining results was performed according to the general methods by semiquantitative scoring⁹. For quantitative evaluation of mAb 3G11 staining, each tumor section was examined by the image progressing and analysis system (Leica Inc.) in 20 representative high-power fields (×400).

Western blot assay

Total cell extraction from human colon carcinoma HT-29 cells, human fibrosarcoma HT-1080 cells and human breast carcinoma tissue lysate (Prosci Inc.) was performed by Western blot assay. The samples in the cold lysate buffer (50 mmol/L Tris-HCl, 150 mmol/L NaCl, 1% Nonidet P40, 0.5% sodium deoxycholate, 2 mg/L aprotinin, 2 mg/L lupeptin, 2 mmol/L AEBSF, pH 8.0) were electrophoresed on 10% gradient SDS-polyacrylamide gels in the presence of β-mercaptoethanol. The proteins were transblotted onto a PVDF membrane, blocked with 5% BSA/TBS for 2 h and incubated with primary antibody (mAb 3G11) overnight at 4 °C and then with peroxidase-conjugated goat anti-mouse IgG (Zhongsan Inc.) at room temperature for 1 h. The membrane was washed and the antibody reaction was visualized using Western blot luminol reagent: sc-2048. The membrane was scanned and the data were fed into the computer by image analysis system (AIO Inc.).

Gelatin zymography

Gelatinolytic activity of HT-29 cells was analyzed according to the method described previously¹⁰. The cells at the concentration of 1×10⁶/mL were incubated for about 18–24 h with mAb 3G11 in serum-free 1640 medium and PBS. After low-speed centrifugation at 3 000 r/min to remove cellular debris, the condition medium (CM) was collected. All sample volumes were adjusted with PBS to 1 g/L of total protein to obtain a uniform protein content of 20 µg per sample. Then 20 µL of CM was mixed with 10 µL of 3× sample buffer containing 10 mmol/L Tris-HCl (pH 6.8),

(30 μ L) were then separated by electrophoresis on 10% polyacrylamide gel containing 0.1% SDS and 1% gelatin as a substrate. Thereafter, gels were washed in the reaction buffer (50 mmol/L Tris-HCl, pH 7.6, 0.15 mol/L NaCl, 10 mmol/L CaCl₂, 0.02% NaN₃) containing 2.5% Triton-X 100 for 1 h to remove SDS. During this process, progelatinases A and B were autocatalytically activated *in situ*. Gels were then incubated for 24 h at 37 °C in the reaction buffer and stained with 0.1% Coomassie-brilliant blue R-250. The location of gelatinolytic activity was detectable as a clear band in the background of uniform staining. The blank bands were scanned and saved by the image system (AIO Inc.).

Enzyme-linked immunosorbent assay

Above-mentioned single-cell suspension volume was placed into the poly-L-lysine-coated 96-well ELISA plates (Costar Inc.) containing 1×10^5 cells/100 μ L per well at 4 °C overnight. After being blocked with a solution of BSA (1 mg/100 mL in PBS) and washed thrice with 0.05% Tween-20 in PBS (PBST), plates were incubated with primary antibody (mAb 3G11 or 3G11-LDM conjugate) and goat-anti-mouse IgG-conjugated horseradish peroxidase for 1 h at 37 °C, respectively. Following six washes with PBST, *o*-phenylenediamine-hydrogen peroxide (OPD-H₂O₂) substrate was used as a chromogen for visualization. Finally, the reaction was stopped by the addition of 100 μ L of 0.1 mol/L H₂SO₄, and the absorbance readings (490 nm) were taken using a microplate reader (Bio-Rad Inc.).

MTT assay

Cells were detached by trypsinization and seeded at 3 000 cells/well in a 96-well plate (Costar, Cambridge, MA, USA) overnight. Then different concentrations of LDM, adriamycin (ADM), and MMC were added and incubated for an additional 48 h. The effect on cell growth was examined by MTT assay. Briefly, 20 μ L of MTT solution (5 mg/mL) was added to each well and incubated at 37 °C for 4 h. The supernatant was aspirated, and the MTT formazan formed by metabolically viable cells was dissolved in 150 μ L of DMSO, and then monitored by a microplate reader (Bio-Rad) at a wavelength of 560 nm.

Clonogenic assay

Cancer cells at the concentration of 50 cells/well were seeded in 96-well plates and cultured for 24 h, then treated with LDM or 3G1-LDM at 37 °C for 1 h. Subsequently they were incubated for 5-7 d. Colonies formed were scored microscopically and the survival fractions (% control) were calculated using the following formula: survival fraction = (colony number of control well/colony number of treated well)/colony number of control well.

In vivo therapy studies

Female BALB/c mice (20 \pm 2 g, 7 wk of age, obtained from the Institute for Experimental Animals, CAMS) were inoculated subcutaneously with murine colon carcinoma 26 cells (1.5×10^6 cells/mouse). Mice were divided randomly into untreated control group and six treatment groups, and carefully monitored for general well-being, body weight, and

tumor size. Diameter of the tumor was measured twice a week with a caliper. Tumor volume was calculated with the following formula: $v = 1/2ab^2$, where *a* and *b* are the long diameter and its perpendicular short diameter of the tumor, respectively. The data were presented as mean \pm SD. Student's *t*-test was used to determine statistically significant differences.

RESULTS

Immunohistochemical staining of tumors with mAb 3G11

MAb 3G11 showed positive immunoreactivity in 81.3% (26/32) of cases of colorectal carcinoma, 43.8% (7/16) of cases of mammary carcinoma, 63.6% (7/11) of cases of gastric carcinoma, and 66.7% (4/6) of cases of esophageal carcinoma, respectively. Cytoplasmic staining tended to be strongest in the cells at the periphery or invasive margin of the tumors and in the cells at the margin of tumor nests, whereas adjacent non-neoplastic tissues showed negative staining (Figure 1).

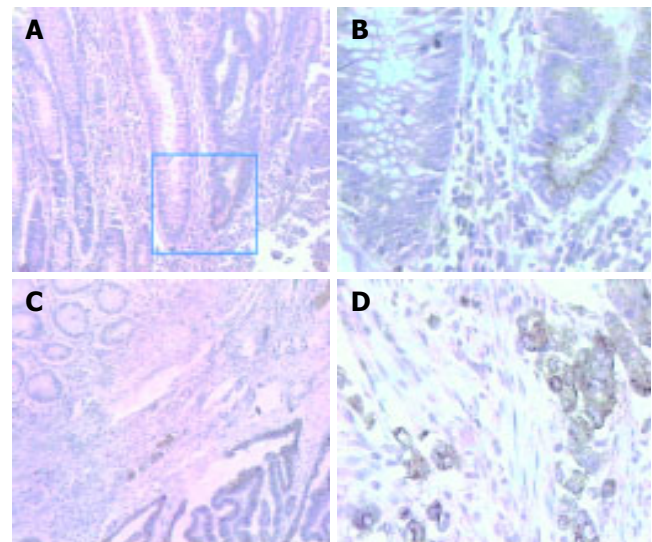


Figure 1 Immunohistochemical staining of mAb 3G11 in human colon carcinoma section. **A:** Colon carcinoma (100 \times , the bar represents 400 μ m in length.); **B:** the same case of A (400 \times , the bar represents 100 μ m in length.); **C:** (100 \times) and **D:** (400 \times): another case of typical colon adenocarcinoma.

Moreover, we found a significant correlation between the evaluation method of 3G11 immunostaining by computer image analysis and by semi-quantitative scoring (Figure 2). The consistent results assessed by both manual methods and quantitative image analysis system proved that 3G11 showed highly specific immunoreactivity with human colon carcinomas and that quantitative estimation might also serve as an useful approach for IHC analysis.

Western blot analysis

MAb 3G11 was characterized by Western blot analysis and two specific electrophoretic bands of 72 and 92 ku in the cell or tissue lysates are shown, supporting the IHC results (Figure 3). The appearance of two bands indicated that other matrix metalloproteinase present in the samples did

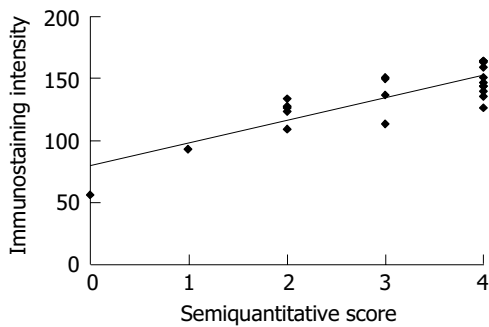


Figure 2 Immunohistochemical intensity of mAb 3G11 in various cases of human colorectal carcinoma assessed by image analysis and semiquantitative scoring.

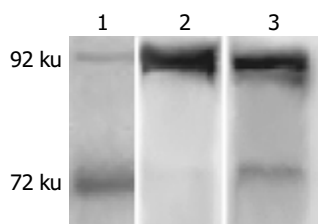


Figure 3 Immunological property of mAb 3G11 by Western blot analysis. Lane 1: human colon cancer HT-29 cell lysate; Lane 2: human fibrosarcoma HT-1080 cell lysate; Lane 3: human breast cancer tissue lysate.

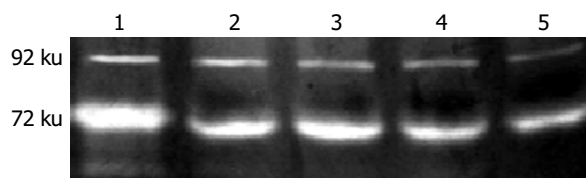


Figure 4 Gelatin-zymography assay of HT-29 cells after treatment with mAb 3G11 at different concentrations.

not cross-react with mAb 3G11. The intensity of two bands of 72 and 92 ku was different in various cell lines and tissue lysates. The results indicated that the expression level of gelatinase was different in various tumors.

Gelatin zymography assay

Both active and latent species could be visualized by using this technique. It showed that the clearance of the gelatin substrate by gelatinases with 72 and 92 ku was detected as a negative staining band, respectively. As shown, both the secreted activity of 72 and 92 ku gelatinases in human colon carcinoma HT-29 cells was inhibited by mAb 3G11 in a dose-dependent manner (Figure 4).

Immunoreactivity of mAb 3G11 and immunoconjugate 3G11-LDM

The binding of mAb 3G11 to antigen-related cancer cells including HT-29, H22, and C26 cells, which expressed type IV collagenases including MMP-2 and -9, is shown in a concentration-dependent manner ranging from 0.01 to 0.3 $\mu\text{mol/L}$ of 3G11 (Figure 5A). The immunoconjugate 3G11-LDM still retained the immunoreactivity at a range

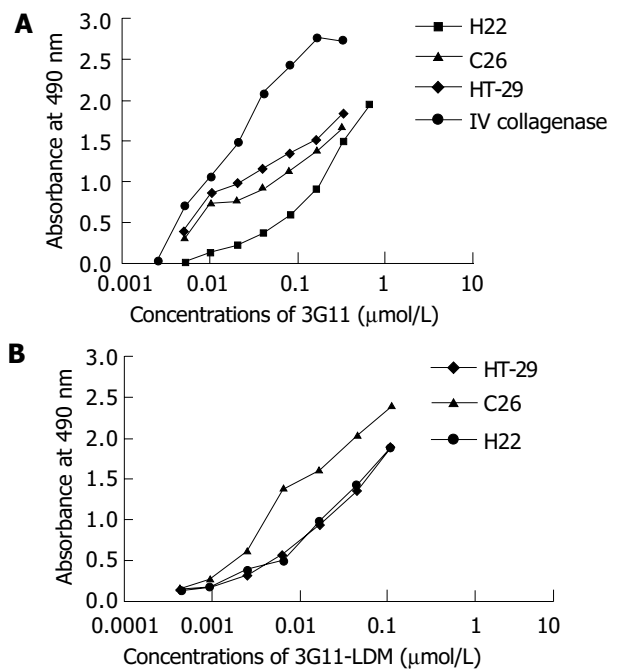


Figure 5 Immunoreactivity of 3G11(A) and 3G11-LDM (B) with type IV collagenase and various cancer cells in ELISA.

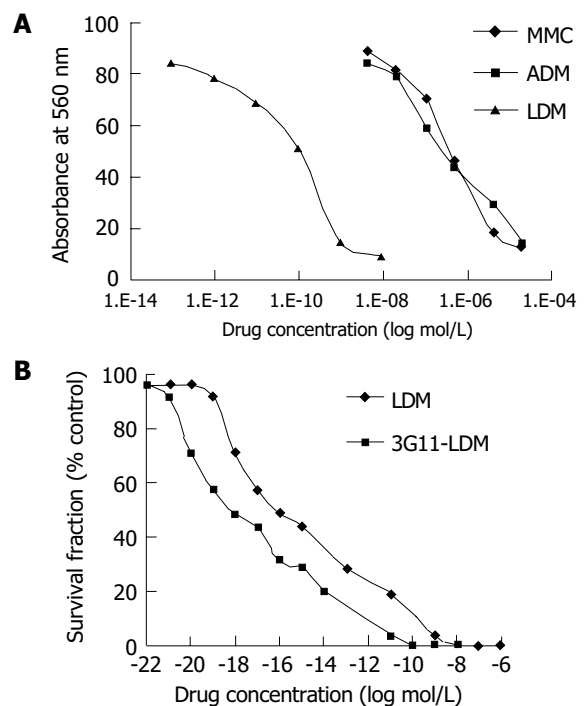


Figure 6 Cytotoxicity of LDM to human colon carcinoma HT-29 cells in comparison to ADM and MMC (A) and 3G11-LDM (B).

of concentrations between 0.01 and 0.1 $\mu\text{mol/L}$ (Figure 5B).

Cytotoxicity of LDM to human colon carcinoma cells

As determined by MMT assay, the IC_{50} values for LDM, ADM, and MMC to human colon carcinoma HT-29 cells were 0.042 ± 0.007 , 528.3 ± 97.7 , and 992.0 ± 93.0 nmol/L, respectively (Figure 6A).

In terms of IC_{50} values, the effect of LDM on HT-29 cells

Table 1 Growth inhibition of colon carcinoma 26 by immunoconjugate 3G11-LDM in mice

Groups	Doses (mg/kg)	Mice number (begin/end)	BWC (g)	Tumor volume (cm ³) mean±SD	Inhibition rate (%)
Control		10/10	+0.5	1.0±0.20	
3G11	0.75	10/10	+0.6	0.8±0.20	25.7 ^b
LDM	0.05	10/10	-0.2	0.4±0.16	56.4 ^b
3G11+	0.75	10/10	-0.3	0.7±0.13	38.6 ^b
LDM	+0.05				
3G11-LDM	0.025	10/10	-0.4	0.5±0.09	54.5 ^{ab}
3G11-LDM	0.05	10/10	-0.3	0.3±0.06	70.3 ^{ab}
3G11-LDM	0.1	10/10	-0.3	0.2±0.06	81.2 ^{ab}

^aP<0.05 vs LDM; ^bP<0.01 vs control; BWC = body weight change.

was 10 000-fold more potent than that of ADM and MMC.

Cytotoxicity of 3G11-LDM to human colon carcinoma cells

By clonogenic assay, the conjugate 3G11-LDM displayed extremely potent cytotoxicity to human colon carcinoma HT-29 cells (Figure 6A). The IC₅₀ value of 3G11-LDM for HT-29 cells was 5.6×10⁻¹⁰ nmol/L and that of the free LDM was 3.48×10⁻⁹ nmol/L.

In vivo therapy with immunoconjugate 3G11-LDM

According to the results on d 10 (Table 1), the tumor growth of colon carcinoma 26 in mice treated with 3G11-LDM was significantly inhibited by 54.5%, 70.3%, and 81.2% at the dose of 0.025, 0.05, and 0.1 mg/kg, respectively. It proved that 3G11-LDM showed higher anti-tumor efficacy against colon carcinoma in mice, as compared to the results of either free LDM or mAb 3G11.

DISCUSSION

Though numerous patients with alimentary tract carcinoma could be successfully induced into first remission by chemotherapy or radiotherapy, most of these patients ultimately have a relapse within 3-5 years. In addition, chemotherapy is accompanied with substantial side effects because of the non-specificity of the cytotoxic drugs. Therefore, it is clear that novel or additional therapy approaches are required. A promising therapy is antibody-targeted chemotherapy, which allows the specific delivery of cytotoxic drugs to the tumor tissues and is likely to have minimal toxic side effects^[11,12]. Owing to its high potency cytotoxicity and molecular constitution, LDM may be successfully applied as a promising "warhead" in the production of antibody-based targeting therapeutics. The FDA-approved Zevalin and Bexxar are radioimmunotherapeutics derived from murine mAb. Their clinical application indicates that murine mAb may be used for cancer therapy under certain circumstances.

MMPs are now known to contribute tumor progression in addition to invasion, including tumor promotion, angiogenesis, and the establishment and growth of metastatic lesions in distant organ sites^[13]. There is evidence that the expression of MMP-2 and -9, two of the most important MMPs, are linked to enhanced tumor angiogenesis, tumor invasion, and metastasis^[14-16]. By IHC staining in our studies, mAb 3G11 showed significant immunoreactivity with gelatinases in various human tumor tissues, especially in human colon carcinoma specimens, and no cross-reaction

with adjacent non-neoplastic tissues was found. The IHC staining of mAb 3G11 was found to localize in most colon carcinoma cells and a few of surrounding fibroblasts. Our IHC results are in accordance with some previous reports^[17]. MMP-2 and MMP-9 expression is more frequently found at the lateral and deep margins of the tumors as observed by immunohistological staining. Among the examined human cancer specimens, mAb 3G11 had the strongest staining intensity and the highest positive rate in colon carcinomas, suggesting that mAb 3G11 has highly specific immunoreactivity with human colon carcinoma and this is the key reason for the use of mAb 3G11 as a carrier for antibody-based therapy.

Inhibitors of MMPs (MMPIs) can be used to halt the spread of cancer. MMPIs do not directly kill cancer cells, but instead targets processes such as cancer cell invasion and metastasis. However, many initial clinical trials using MMPIs proved to be disappointing^[18]. 3G11-LDM is a conjugate composed of a mAb directed against type IV collagenase, including MMP-2 and -9, and LDM displays extremely potent cytotoxicity. This antibody can inhibit the enzyme activity and selectively bind to the target enzyme in tumor tissues. 3G11-LDM conjugate has potent antitumor efficacy both *in vivo* and *in vitro*.

In conclusion, 3G11-LDM is a promising agent for targeted cancer chemotherapy, especially for colorectal carcinoma.

REFERENCES

- Xu YJ, Zhen YS, Goldberg IH. C-1027 chromophore, a potent new enediyne antitumor antibiotic, induces sequence-specific double-strand DNA cleavage. *Biochemistry* 1994; **33**: 5947-5954
- Shao RG, Zhen YS. Relationship between the molecular composition of C-1027, a new macromolecular antibiotic with enediyne chromophore, and its antitumor activity. *Yaoxue Xuebao* 1995; **30**: 336-342
- Wang XH, Wu SY, Zhen YS. Lidamycin inhibits proliferation and induces apoptosis in endothelial cells. *Zhongguo Kangshengsu Zazhi* 2003; **28**: 605-612
- He QY, Liang YY, Wang DS, Li DD. Characteristics of motitic cell death induced by enediyne antibiotic lidamycin in human epithelial tumor cells. *Int J Oncol* 2002; **20**: 261-266
- Liu W, Christenson SD, Standage S, Shen B. Biosynthesis of the enediyne antitumor antibiotic C-1027. *Science* 2002; **297**: 1170-1173
- Wang FQ, Shang BY, Zhen YS. Antitumor effect of the immunoconjugate composed of lidamycin and monoclonal antibody 3G11. *Yaoxue Xuebao* 2003; **38**: 515-519
- Liu XY, Zhen YS. Antitumor effect of lidamycin-containing monoclonal antibody immunoconjugate with downsized molecular.

- Zhongguo Yixue Kexueyuan Xuebao* 2001; **23**: 563-567
- 8 **Li L**, Huang YH, Miao QF, Shang BY, Zhen YS. Fv-LDP-AE, an engineered and enediyne-energized fusion protein, shows highly potent antitumor efficacy and antiangiogenic activity. *Proc Am Assoc Cancer Res* 2004; **45**: 2884
- 9 **Lehr HA**, Jacobs TW, Yaziji H, Schnitt SH, Gown AM. Quantitative evaluation of HER-2/neu status in breast cancer by fluorescence in situ hybridization and by immunohistochemistry with image analysis. *Am J Clin Pathol* 2001; **115**: 814-822
- 10 **Brown PD**, Levy AT, Margulies IM, Liotta LA, Stetler-Stevenson WG. Independent expression and cellular processing of M, 72 000 type IV collagenase and interstitial collagenase in human tumorigenic cell lines. *Cancer Res* 1990; **50**: 6184-6191
- 11 **Zhen YS**. Advances in research of antitumor antibiotics and monoclonal antibody therapeutics. *Zhongguo Kangshengsu Zazhi* 2002; **27**: 1-5
- 12 **Dickman S**. Dickman S. Antibodies stage a comeback in cancer treatment. *Science* 1998; **280**: 1196-1197
- 13 **Stamenkovic I**. Matrix metalloproteinases in tumor invasion and metastasis. *Semin Cancer Biol* 2000; **10**: 415-433
- 14 **Coussens LM**, Fingleton B, Matrisian LM. Matrix metalloproteinase inhibitors and cancer: trials and tribulations. *Science* 2002; **295**: 2387-2392
- 15 **Hoyhtya M**, Fridman R, Komarek D, Porter-Jordan K, Stetler-Stevenson WG, Liotta LA, Liang CM. Immunohistochemical localization of matrix metalloproteinase 2 and its specific inhibitor TIMP-2 in neoplastic tissues with monoclonal antibodies. *Int J Cancer* 1994; **56**: 500-505
- 16 **Jeziorska M**, Haboubi NY, Schofield PF, Ogata Y, Nagase H, Woolley DE. Distribution of gelatinase B (MMP-9) and type IV collagen in colorectal carcinoma. *Int J Colorectal Dis* 1994; **9**: 141-148
- 17 **Bodey B**, Bodey B Jr, Siegel SE, Kaiser HE. Prognostic significance of matrix metalloproteinase expression in colorectal carcinomas. *In Vivo* 2000; **14**: 659-666
- 18 **Rundhaug JE**. Matrix metalloproteinases, angiogenesis, and cancer: commentary re: A. C. Lockhart. Reduction of wound angiogenesis in patients treated with BMS-275291, a broad spectrum matrix metalloproteinase inhibitor. *Clin Cancer Res* 2003; **9**: 551-554

Science Editor Wang XL and Guo SY Language Editor Elsevier HK

• VIRAL HEPATITIS •

Interferon β -1a alone or in combination with ribavirin: A randomized trial to compare efficacy and safety in chronic hepatitis C

Rinaldo Pellicano, Antonio Craxì, Piero Luigi Almasio, Mario Valenza, Giovanna Venezia, Alfredo Alberti, Silvia Boccato, Luigi Demelia, Orazio Sorbello, Antonino Picciotto, Francesco Torre, Gaetano Ideo, Carlo Cattaneo, Mara Berrutti, Mario Rizzetto

Rinaldo Pellicano, Mara Berrutti, Mario Rizzetto, U.O.A.D.U. Gastro-Hepatology, S. Giovanni Battista (Molinette) Hospital, Turin, Italy

Antonio Craxì, Piero Luigi Almasio, Mario Valenza, Giovanna Venezia, Department of Gastroenterology and Hepatology, University of Palermo, Italy

Alfredo Alberti, Silvia Boccato, Department of Internal Medicine, University of Padua, Italy

Luigi Demelia, Orazio Sorbello, Institute of Clinical Medicine, University of Cagliari, Italy

Antonino Picciotto, Francesco Torre, Department of Internal Medicine, University of Genoa, Italy

Gaetano Ideo, Carlo Cattaneo, Department of Hepatology, San Giuseppe Hospital, Milan, Italy

Supported by an Unrestricted Grant From Industria Farmaceutica Sero S.p.A. (Rome, Italy). The Antiviral Drugs Employed in this Study were Also Made Available by Sero

Correspondence to: Professor Mario Rizzetto, U.O.A.D.U. Gastro-Epatologia, Ospedale S. Giovanni Battista (Molinette), Corso Bramante 88-10126 Torino, Italy. mario.rizzetto@unito.it
Telephone: +39-11-6336397 Fax: +39-11-6335927

Received: 2004-05-12 Accepted: 2004-09-20

Key words: Chronic hepatitis C; IFN β -1a; Ribavirin

Pellicano R, Craxì A, Almasio PL, Valenza M, Venezia G, Alberti A, Boccato S, Demelia L, Sorbello O, Picciotto A, Torre F, Ideo G, Cattaneo C, Berrutti M, Rizzetto M. Interferon β -1a alone or in combination with ribavirin: A randomized trial to compare efficacy and safety in chronic hepatitis C. *World J Gastroenterol* 2005; 11(29): 4484-4489

<http://www.wjgnet.com/1007-9327/11/4484.asp>

INTRODUCTION

The safety of current treatments for chronic hepatitis C is still under debate. Studies published to date demonstrate that pegylated interferons (both alpha [α]-2a and α -2b) in combination with ribavirin could eradicate the hepatitis C virus (HCV) in 47-56% of infected subjects^[1,2]. However, a consistent number of patients experience significant adverse events, such as severe gastrointestinal symptoms, psychiatric disorders, dermatological symptoms, autoimmune disorders and significant laboratory abnormalities (neutropenia, anemia, thrombocytopenia)^[3]. The severity of these adverse events has led to treatment discontinuation in both controlled trials and in clinical practice. In the first clinical trial^[1] of pegylated interferon (PEG-IFN) α -2b with ribavirin, side effects prompted withdrawal of therapy in 13-14% of patients. In the first clinical trial of PEG-IFN α -2a with ribavirin^[2], 22% of patients treated with the combination and 32% treated with PEG-IFN α -2a alone, discontinued therapy. The discontinuation rates reported with standard formulations of IFN- α were high. The pivotal IFN- α -2b and ribavirin trial performed by McHutchinson *et al.*^[4], demonstrated a discontinuation rate of 21% in patients treated for 48 wk.

Not surprisingly, the side effects may have pronounced negative impact in the general population than in clinical trial subjects; Gaeta and colleagues found that 24.5% of patients treated with IFN- α plus ribavirin in the regular clinical-practice setting failed to complete treatment due to adverse events^[5]. Therefore, safe and effective alternatives to IFN- α could be of value to patients who cannot tolerate PEG-IFN.

Previous pilot studies have shown that IFN β -1a is effective in HCV eradication^[6] and its use is safe and well tolerated^[7,8]. A trial was performed in patients resistant to a previous treatment with IFN- α treated with recombinant human interferon (IFN) β -1a at different schedules

Abstract

AIM: To compare the efficacy and safety of recombinant human IFN β -1a alone or in combination with ribavirin in treatment-naïve subjects with chronic hepatitis C.

METHODS: Open, randomized trial was performed in 6 Italian tertiary centers: 102 of the 108 patients screened were randomized to receive 6 MIU of recombinant human IFN β -1a subcutaneously daily for 24 wk, alone (Group 1, $n = 51$) or in combination with ribavirin 1 000 to 1 200 mg/d (Group 2, $n = 51$).

RESULTS: The end-of-treatment virologic response rate was 29.4% in Group 1 and 41.2% in Group 2 (non-significant). Twenty-four weeks after stopping therapy, sustained virologic response rate was 21.6% in Group 1 and 27.4% in Group 2 (non-significant). All subjects in Group 1 completed treatment, while two subjects in Group 2 stopped therapy due to treatment-related adverse events.

CONCLUSION: Recombinant human IFN β -1a, alone or in combination with ribavirin, has an excellent safety profile and, may represent an alternative for chronic hepatitis C patients who are unable to tolerate pegylated α -interferon.

(up to 24 MIU every d for 48 wk) but it failed to induce a significant response rate. A post hoc analysis was performed to stratify the patients according to the race and it showed a sustained virological responses of 21.7% in the Chinese subjects enrolled in the trial^[9].

In this open clinical trial, we investigated the safety and efficacy of subcutaneous r-hIFN β -1a alone or in combination with ribavirin in the treatment of chronic hepatitis C patients naïve to therapy.

MATERIALS AND METHODS

Study design

Using a 4-block, centralized randomization list, patients were randomly assigned to receive r-hIFN β -1a 6 MIU/d (22 μ g/d) subcutaneously for 24 wk, either alone (Group 1, $n = 51$) or in combination with ribavirin (Group 2, $n = 51$).

Ribavirin was given at a dose of 1 000 mg/d (five capsules) to patients weighing less than 70 kg and 1 200 mg/d (six capsules) to those weighing 70 kg or over.

Randomized patients who withdrew from the study without taking the first treatment dose were substituted. Patients who withdrew from the study after receiving the first treatment dose were not substituted and were considered as dropouts.

Patient selection

Patients from six tertiary centers in Italy were recruited. Subjects were eligible for inclusion in the trial if they met the following criteria: age between 18 and 70 years; positive serum anti-HCV and HCV-RNA tests; no previous therapy with IFN; alanine-aminotransferase (ALT) level more than 1.5 times the upper normal limit, on two different assessments in the past 12 mo and at the screening visit; and a liver biopsy performed within 36 mo prior to enrollment consistent with a diagnosis of chronic hepatitis C without cirrhosis.

Patients were excluded if they had leukopenia (less than $3.0 \times 10^9/L$), neutropenia (less than $1.5 \times 10^9/L$), anemia (hemoglobin less than 12 g/dL in women and 13 g/dL in men), thrombocytopenia (less than $100 \times 10^9/L$), serum albumin less than 30 g/L, total bilirubin more than three times the upper normal limit, other significant hepatic diseases (including HBV infection), psychiatric disorders requiring treatment, or serious chronic diseases (including tumors and HIV infection). Patients were also excluded if they had received antiviral or immunosuppressive drugs during 6 mo preceding inclusion in the study. Females were included if they were pregnant or breast-feeding, and were not considering childbearing for the entire treatment period.

The therapeutic protocol was approved by the local ethical committee and the study was carried out according to the 1975 Declaration of Helsinki and Good Clinical Practice guidelines. All patients provided written informed consent before treatment was initiated.

Assessment of efficacy

Quantitative viremia was assessed at baseline to allow patient classification on the basis of viral load. A cut-off limit of

800 000 IU/mL (corresponding to 2 million copies/mL) was used to classify patients as having either low or high viral counts. From the fourth week of treatment to the end of follow-up, the virologic assessment was performed using qualitative viremia. Evaluations were performed using a polymerase chain reaction (PCR) assay (Cobas Amplicor HCV test, version 2.0; Roche Diagnostics, Basel, Switzerland; lower limit of detection 100 copies, corresponding to 40 IU/mL).

The trial endpoints were: (1) the rate of sustained virological responses (SVR); (2) the percentage of patients with normal aminotransferase levels at 24 wk of treatment (wk 24) and 24 wk post-treatment (wk 48); and (3) the safety and tolerability of r-hIFN β -1a alone or in combination with ribavirin.

Data were evaluated using an intention-to-treat analysis and included all subjects who received at least one treatment dose. Patients were considered as sustained virologic responders, if the qualitative serum HCV-RNA test performed 24 wk post-treatment (wk 48) was negative. Patients treated with r-hIFN β -1a alone were withdrawn from the trial if HCV viremia persisted after 12 and 18 wk of treatment.

Safety assessment

Patients were examined at baseline, after 4, 8, 12, 18, and 24 wk of treatment and at wk 12 and 24 post treatment. Routine laboratory tests, and autoantibody and IFN- β binding antibody (BAB) assessments were performed at each visit.

The following autoantibody evaluations were conducted at the coordinating center: ANA (anti-nuclear), AMA (anti-mitochondrial), ASMA (anti-smooth muscle), LKM (anti-liver/kidney microsome type 1), APC (anti-parietal cells), ABBA (anti-brush border), MT (anti-thyroid microsomal), TGA (anti-thyroglobulin), MB (anti-basement membrane of tubule/glomerular), R1 (anti-R1 type reticulin) and R2 (anti-R2 type reticulin). Autoantibodies were tested by indirect immunofluorescence on murine liver, kidney and stomach and human thyroid. IgA, IgG, and IgM were detected with fluorescein isothiocyanate^[10]. BABs were determined using a radioimmunobinding assay (RIBA)^[11].

In cases of grade III adverse events (according to the WHO classification), the dose of r-hIFN β -1a was reduced to 3 MIU/d. If anemia occurred, the dose of ribavirin was reduced according to the investigator's judgment.

Statistical analysis

Statistical analyses and data processing were performed using SAS software (version 8 for Windows). Both descriptive analyses and inferential tests were used to analyze the data. The significance level of all tests was set at 5%. The baseline characteristics of the two groups were compared using t -test and χ^2 test. χ^2 test was used to evaluate the significant difference between two treatment groups for end-of-treatment response rate (ETR), SVR rate, and ALT/AST normalization. Logistic regression model was used to evaluate the SVR rate adjusting the ORs for factors predictive of treatment response, like viral levels, genotype, class of age, etc.

The proportion of patients in each treatment group experiencing at least one adverse event that was likely related

to the study drug(s) was compared using the χ^2 test.

RESULTS

Patient characteristics

One-hundred-and-eight patients were enrolled from May 29, 2000 to June 1, 2001. One-hundred-and-two met the inclusion criteria and were randomized to one of the two study groups: 51 patients received r-hIFN β -1a alone and 51 received r-hIFN β -1a in combination with ribavirin. Of the six subjects not admitted into the trial (i.e., not included in the intention-to-treat analysis), two did not meet the inclusion criteria and four refused to sign the informed consent form.

The baseline characteristics were similar in the two groups (Table 1). Twenty-one patients (41.1%) in Group 1 and 24 (47%) in Group 2 had high viral levels. Thirty-one patients (60.8%) treated with r-hIFN β -1a alone and 33 (64.7%) treated with combination therapy were infected with HCV genotype 1.

Table 1 Summary of demographic and clinical characteristics at baseline

	Group 1	Group 2
Patients (n)	51	51
Sex (M/F)	29/22	36/17
Mean age (yr) \pm SD	45 \pm 11.7	43.9 \pm 9.0
Hemoglobin (g/dL)	14.8 \pm 1.3	15 \pm 1.3
Platelets ($\times 10^9$ /L)	195.9 \pm 45	203.9 \pm 54
Leukocytes ($\times 10^9$ /L)	6.7 \pm 1.4	6.8 \pm 1.9
ALT (mean \pm SD)	142.7 \pm 86.2	123.2 \pm 78.7
HCV-RNA quantitation (Meq/mL)		
Low viremia	27	23
High viremia	21	24
Undetermined	3	4
Genotype		
1	31	33
2	6	8
3	12	8
4	2	1
Undetermined	0	1

Virologic response

After 12 wk of treatment, 41.2% (21/51) of patients in Group 1 and 47.1% (24/51) in Group 2 showed clearance of serum HCV-RNA (Table 2). By the end of the treatment period (wk 24), the response rate had diminished to 29.4% (15/51) and 41.2% (21/51) in Groups 1 and 2, respectively. After the 24-wk post-therapy follow-up (wk 48), 11 patients (21.6%) in Group 1 and 14 (27.4%) in Group 2 maintained a SVR. There was no statistically significant difference between the two groups in the percentage of

Table 2 Rate (number responding/total treated) of patients with negative viremia during the course of the trial

	Screening	T4	T8	T12	T18	T24	T48
r-hIFN β -1a (n = 51)	0 (0%)	18 (35.3%)	16 (31.4%)	21 (41.2%)	16 (31.4%)	15 (29.4%)	11 (21.56%)
r-hIFN β -1a + ribavirin (n = 51)	0 (0%)	13 (25.5%)	22 (43.1%)	24 (47.1%)	21 (41.2%)	21 (41.2%)	14 (27.45%)

patients negative for viremia at the end of the treatment period ($P = 0.2138$) or at the completion of follow-up (wk 48) ($P = 0.4898$).

Multivariate analysis showed that genotype (OR = 0.39; 95%CI, 0.21-0.72; $P = 0.0025$) and baseline viremia level (OR = 2.1; 95%CI, 1.17-3.96; $P = 0.0141$) were factors predictive of response. Among patients with genotype 1, the rate of response was 12.9% (4/31) in Group 1 and 12.1% (4/33) in Group 2, respectively *vs* 35% (7/20) in Group 1 and 52.9% (9/17) in Group 2 patients with genotype non-1 (NS, Table 3). The genotype was not determined in one patient in Group 2 who responded to therapy.

Among subjects with high viral loads, the response rate was 4.8% (1/21) and 16.6% (4/24) in Groups 1 and 2, respectively, compared to 33.3% (9/27) and 34.8% (8/23) in patients with low viremia in Groups 1 and 2, ($P = 0.2972$, Table 4). The viral load was not determined in three patients in Group 1 and four patients in Group 2.

Table 3 Rate (number responding/total treated) of patients with negative viremia after the 24-wk post-therapy follow-up according to genotype

	1	Non-1	Not determined
r-hIFN β -1a	12.9% (4/31)	35.0% (7/20)	-
r-hIFN β -1a + ribavirin	12.1% (4/33)	52.9% (9/17)	(1/1)

Between group difference not significant.

Table 4 Rate (number responding/total treated) of patients with negative viremia after the 24-wk post-therapy follow-up according to viral load (cut-off 800 000 IU)

	Low	High	Not determined
r-hIFN β -1a	33.3% (9/27)	4.8% (1/21)	(1/3)
r-hIFN β -1a + ribavirin	34.8% (8/23)	16.6% (4/24)	(2/4)

Between group difference, $P = 0.2972$.

Biochemical response

At the end of the treatment period, 27.5% of patients (14/51) in Group 1 and 39.2% (20/51) in Group 2 exhibited normal aminotransferases associated with a virologic response. At the end of the follow-up period (wk 48), 21.6% (11/51) and 25.5% (13/51) of patients in Groups 1 and 2, respectively, maintained normal aminotransferase levels; the χ^2 test showed no significant difference between

treatment groups ($P = 0.2076$ at wk 24; $P = 0.6406$ at wk 48). Three patients showed abnormal levels of aminotransferase despite the clearance of HCV-RNA in serum, possibly due to concomitant steatohepatitis.

Among the patients who remained viremic, 22.2% (8/36) of those in monotherapy and 36.6% (11/30) of those in combination treatment exhibited normal aminotransferase levels at the end of therapy ($P = 0.1969$); Of these patients, 17.5% (7/40) in Group 1 and 37.8% (14/37) in Group 2 maintained normal levels at wk 48 ($P = 0.0453$).

Safety evaluation

Ninety-nine of the one hundred and two patients enrolled completed treatment according to protocol. Drug discontinuation due to adverse events occurred in three (all in the combination therapy group) of the 102 patients. One patient stopped treatment due to the incidental discovery of ovarian cancer (not related to the study drugs). In the remaining two cases, treatment was discontinued due to depression and acute psychosis; both events were considered to be related to therapy.

At each time-point of the study, between 86.4% and 100% of patients received the expected doses of IFN- β and ribavirin according to protocol. No patient failed to complete the study due to poor compliance.

In patients treated with combination therapy, the mean hemoglobin level dropped from 14.9 to 12.6 g/dL, while in Group 1 from 14.8 to 14.3 g/dL. Treatment interruptions or dose reductions were not required in any subject. In patients treated with monotherapy, there was a mean drop in platelet count from $195.9 \pm 45 \times 10^9/L$ to $175.0 \pm 41.5 \times 10^9/L$; in Group 2, there was a mean increase from $204.1 \pm 54.0 \times 10^9/L$ to $206.1 \pm 66.4 \times 10^9/L$. The leukocyte count dropped from $6.7 \pm 1.4 \times 10^9/L$ to $5.8 \pm 1.3 \times 10^9/L$ and from $6.7 \pm 1.9 \times 10^9/L$ to $5.2 \pm 1.8 \times 10^9/L$ in Groups 1 and 2, respectively.

Thirty-seven percent of subjects (19/51) treated with IFN- β and 49% (25/51) of those in Group 2 reported at least one mild adverse event during the study (Table 5). The difference between the two groups was not significant.

Only mild titer increases of pre-existing autoantibodies were observed. Compared to baseline, ANA increased in two patients and decreased in one; ASMA decreased in two cases and MT as well as MB increased in one patient. None of the patients developed autoimmune disease.

Table 5 Adverse events possibly or probably related to study treatment, occurring with a frequency higher than 5%

	r-hIFN β -1a (n = 24, %)	r-hIFN β -1a + ribavirin (n = 35, %)
Fatigue	4 (16.7)	4 (11.4)
Pyrexia	2 (8.3)	6 (17.1)
Anemia	0 (0.0)	6 (17.1)
Erythema	4 (16.7)	2 (5.7)
Headache	4 (16.7)	0 (0.0)
Thrombocytopenia	3 (12.5)	0 (0.0)
Neutropenia	0 (0.0)	2 (5.7)
Depression	2 (8.3)	0 (0.0)
Insomnia	0 (0.0)	2 (5.7)
Weight loss	0 (0.0)	2 (5.7)

BABs developed in 11 patients (12%) and usually appeared within 8 to 12 wk of treatment; titers ranged between 5.0 and 20 AU in three of these patients and were less than 5.0 AU in eight patients. There was no difference between Group 1 and Group 2 with regards to BAB development and no correlation was found between BABs development and response to treatment.

DISCUSSION

In contrast to the variety of IFN- α , of which there are 25 subtypes with molecular weights ranging from 17.5 to 23 ku^[12], only one type of IFN- β has been identified in human beings. Though its amino-acid sequence differs from IFN- α by as much as 70%, IFN- β shares many antiviral properties of interferon alpha, thereby providing an alternative treatment for chronic hepatitis C.

Three forms of IFN- β are available: (1) the fibroblast-derived natural IFN- β ^[13]; (2) the r-hIFN β -1a produced by mammalian cells (identical to the IFN- β naturally occurring in humans); and (3) r-hIFN β -1b produced by *E. coli*. The r-hIFN β -1a formulation was chosen for this study as it offers several advantages over the other two: it can be produced in unlimited quantities by bioengineering techniques, its batch-to-batch consistency and purity allows for dosage by mass instead of international units, and it is identical to the IFN- β naturally occurring in human beings but more potent and less immunogenic^[14].

Previous experience with IFN- α indicates that the efficacy of these agents is related to the frequency of administration. Therefore, the rationale behind the newest pegylated formulation is that a more steady and sustained release of IFN- α is more effective than the thrice-a-week administration.

The pharmacokinetic data obtained with natural IFN- β have demonstrated the significant bioequivalence of the intramuscular, intravenous, and subcutaneous routes of administration^[15]. Therefore, we have chosen to administer the cytokine via the more convenient subcutaneous route. Since the safety of r-hIFN β -1a in combination with ribavirin has not been previously determined, a 6- rather than 12-mo course of therapy was selected for this initial study.

PEG-IFN with ribavirin is currently the gold standard for the treatment of chronic hepatitis C. Though less efficacious than PEG-IFN, that consents to achieve 47-56% of SVR^[1,2], our findings suggest that r-hIFN β -1a alone or in combination with ribavirin, is as effective as conventional non-PEG-IFN α . The overall 21.6% and 27.5% SVR rates achieved in our patients treated with r-hIFN β -1a alone or in combination with ribavirin, respectively, are comparable to the 6-13% and 31-38% response rates reported with the use of IFN α -2b alone or in combination with ribavirin, respectively, for 24-48 wk^[4].

In both treatment groups, viral response rates were higher at 12 wk of therapy than at the end of the treatment period (wk 24). A possible reason for this decrease, which was more pronounced in Group 1, could be the low dosage of IFN- β used in this trial. Analogous to the results of previous IFN- α studies that assessed the efficacy of IFN monotherapy *vs* the association of the same IFN with ribavirin, combination therapy in this trial yielded better

results for both virologic and biochemical endpoints compared to IFN- β monotherapy.

The major factors influencing the response rate in clinical trials of IFN- α were the genotype of the infecting HCV and the level of baseline viremia: genotype 1 and high viremia were associated with a reduced response, while genotypes 2 or 3 and low viremia had a higher response. This was also the case with r-hIFN β -1a; the end-of-treatment virologic and biochemical response rates were significantly higher in our patients of genotype 2-3 and low viremia, compared to those with genotype 1 and high viremia.

The use of ribavirin, as well as prolongation of IFN treatment up to 48 wk (instead of 24 wk), not only enhances the therapeutic response, but also decreases the relapse rate after the end of treatment. This effect is negligible in patients with easy-to-treat HCV genotype 2 or 3, for whom 24 wk of IFN is sufficient to achieve a maximal SVR. On the other hand, subjects infected with HCV genotype 1 achieve a higher SVR rate after 48 wk of therapy when compared to 24 wk (despite similar end-of-treatment virological response rates after 24 and 48 wk of treatment). Unfortunately, this effect could not be evaluated in the present study, which was designed to provide a 24 wk course of treatment. In fact, several post-therapy relapses occurred in HCV-genotype 1 patients treated with combination therapy for 6 mo, resulting in an off-therapy response rate distinctly lower than that achieved upon completion of treatment.

The overall safety profile of r-hIFN β -1a, both alone and in combination with ribavirin, was remarkably favorable. Compared to previous IFN- α data, the drop-out rate in our study was low (0/51 [0%] in Group 1 and 3/51 [5.9%] in Group 2) and was due primarily to two patients who withdrew from the study as a result of treatment-related psychiatric problems.

In contrast to the 2% of patients treated with IFN- α who had developed autoimmune disorders^[16], none of our patients treated with r-hIFN β -1a developed clinical features of autoimmune diseases. Furthermore, systematic autoantibody monitoring failed to demonstrate the emergence of autoimmune reactivities during therapy or significant titer increases of pre-existing autoantibodies. Likewise, IFN- β BAB titers rose in only 12% of our patients; these increases were in the low titer ranges and were not clinically significant.

Decreases in WBC and platelet counts observed in the present study (two patients on combination therapy and three subjects on IFN monotherapy respectively) were not clinically relevant to induce discontinuation of therapy. On the contrary, IFN- α led to higher reductions in WBC and platelet counts that are often responsible for premature termination of therapy. The fall in hemoglobin level noted in our patients treated with combination therapy was expected as it is a well-recognized, side-effect of ribavirin^[17].

In conclusion, the satisfactory therapeutic effects and excellent tolerability profile of r-hIFN β -1a could represent a treatment option for patients with chronic hepatitis C who cannot tolerate PEG-IFNs. IFN β -1a may also be used as initial therapy in subjects at high risk of significant side effects with IFN- α treatment. Future studies should

evaluate the efficacy and safety of r-hIFN β -1a in subpopulations of patients with chronic hepatitis C and cirrhosis or cryoglobulinemia.

ACKNOWLEDGMENTS

The authors wish to thank Francesca Vannini (Industria Farmaceutica Serono-Rome, Italy) for her assistance in collecting and delivering samples for centralized evaluation and in collecting data for analysis and, Carlo Pellas, Giuliano Ferrucci and Stefania Bellino (Informa Arakne S.r.l. - Rome, Italy) for the statistical analysis. The IBIS Study Group also included: Antonina Smedile and Giovanni Antonio Touscoz (Turin); Antonio Bellobuono and Gianvito Martino (Milan); Gavino Faa and Gabriella Mancosu (Cagliari); Luisa Benvegnù (Padua); Michele Pitaro (Rome).

REFERENCES

- 1 **Manns MP**, McHutchison JG, Gordon SC, Rustgi VK, Shiffman M, Reindollar R, Goodman ZD, Koury K, Ling M, Albrecht JK. Peginterferon alfa-2b plus ribavirin compared with interferon alfa-2b plus ribavirin for initial treatment of chronic hepatitis C: a randomised trial. *Lancet* 2001; **358**: 958-965
- 2 **Fried MW**, Shiffman ML, Reddy KR, Smith C, Marinos G, Goncales FL, Haussinger D, Diago M, Carosi G, Dhumeaux D, Craxi A, Lin A, Hoffman J, Yu J. Peginterferon alfa-2a plus ribavirin for chronic hepatitis C virus infection. *N Engl J Med* 2002; **347**: 975-982
- 3 **Fried MW**. Side effects of therapy of hepatitis C and their management. *Hepatology* 2002; **36**: S237-S244
- 4 **McHutchison JG**, Gordon SC, Schiff ER, Shiffman ML, Lee WM, Rustgi VK, Goodman ZD, Ling MH, Cort S, Albrecht JK. Interferon alfa-2b alone or in combination with ribavirin as initial treatment for chronic hepatitis C. Hepatitis Interventional Therapy Group. *N Engl J Med* 1998; **339**: 1485-1492
- 5 **Gaeta GB**, Precone DF, Felaco FM, Bruno R, Spadaro A, Stornaiuolo G, Stanzione M, Ascione T, De Sena R, Campanone A, Filice G, Piccinino F. Premature discontinuation of interferon plus ribavirin for adverse effects: a multicentre survey in "real world" patients with chronic hepatitis C. *Aliment Pharmacol Ther* 2002; **16**: 1633-1639
- 6 **Habersetzer F**, Boyer N, Marcellin P, Bailly F, Ahmed SN, Alam J, Benhamou JP, Trépo C. A pilot study of recombinant interferon beta-1a for the treatment of chronic hepatitis C. *Liver* 2000; **20**: 437-441
- 7 **Pellicano R**, Palmas F, Cariti G, Tappero G, Boero M, Tabone M, Suriani R, Pontisso P, Pitaro M, Rizzetto M. Retreatment with interferon-beta of patients with chronic hepatitis C virus infection. *Eur J Gastroenterol Hepatol* 2002; **14**: 1377-1382
- 8 **Festi D**, Sandri L, Mazzella G, Roda E, Sacco T, Staniscia T, Capodicasa S, Vestito A, Colecchia A. Safety of interferon beta treatment for chronic HCV hepatitis. *World J Gastroenterol* 2004; **10**: 12-16
- 9 **Cheng PN**, Marcellin P, Bacon B, Farrel G, Parson I, Wee T, Chang TT. Racial differences in response to interferon - β -1a: a better response in Chinese patients. *J Viral Hepat* 2004; **11**: 418-426
- 10 **Strassburg CP**, Obermayer-Straub P, Alex B, Durazzo M, Rizzetto M, Tukey RH, Manns MP. Autoantibodies against glucuronosyltransferases differ between viral hepatitis and autoimmune hepatitis. *Gastroenterology* 1996; **111**: 1576-1586
- 11 **Bonifacio E**, Lampasona V, Bingley PJ. IA-2 is the primary phosphatase-like autoantigen in type 1 diabetes. *J Immunol* 1998; **161**: 2648-2654

- 12 **Blatt LM**, Davis JM, Klein SB, Taylor MW. The biologic activity and molecular characterization of a novel synthetic interferon- α species, consensus interferon. *J Interferon Cytokine Res* 1996; **16**: 489-499
- 13 **Kobayashi Y**, Watanabe S, Konishi M, Yokoi M, Kakehashi R, Kaito M, Kondo M, Hayashi Y, Jomori T, Suzuki S. Quantitation and typing of serum hepatitis C virus RNA in patients with chronic hepatitis C treated with interferon- β . *Hepatology* 1993; **18**: 1319-1325
- 14 **Scagnolari C**, Bellomi F, Turriziani O, Bagnato F, Tomassini V, La Volpe V, Ruggieri M, Bruschi F, Meucci G, Dicuonzo G, Antonelli G. Neutralizing and binding antibodies to IFN-beta: relative frequency in relapsing-remitting multiple sclerosis patients treated with different IFN-beta preparations. *J Interferon Cytokine Res* 2002; **22**: 207-213
- 15 **Salmon P**, Le Cottonnec JY, Galazka A, Abdul-Ahad A, Darragh A. Pharmacokinetics and pharmacodynamics of recombinant human interferon-beta in healthy male volunteers. *J Interferon Cytokine Res* 1996; **16**: 759-764
- 16 **Strader DB**. Understudied population with hepatitis C. *Hepatology* 2002; **36**(Suppl): S226-S236
- 17 **Chang CH**, Chen KY, Lai MY, Chan KA. Meta-analysis: ribavirin-induced haemolytic anaemia in patients with chronic hepatitis C. *Aliment Pharmacol Ther* 2002; **16**: 1623-1632

Science Editor Guo SY Language Editor Elsevier HK

On the origin of cardiac mucosa: A histological and immunohistochemical study of cytokeratin expression patterns in the developing esophagogastric junction region and stomach

Gert De Hertogh, Peter Van Eyken, Nadine Ectors, Karel Geboes

Gert De Hertogh, Peter Van Eyken, Nadine Ectors, Karel Geboes, Department of Morphology and Molecular Pathology, University Hospitals, KU Leuven, Leuven, Belgium
Correspondence to: Dr. Gert De Hertogh, Dienst Pathologische Ontleedkunde, UZ St.-Rafaël, Minderbroedersstraat 12, Leuven 3000, Belgium. gert.dehertogh@uz.kuleuven.ac.be
Telephone: +32-16-336588 Fax: +32-16-336548
Received: 2004-08-27 Accepted: 2004-12-23

Abstract

AIM To examine the fetal and neonatal esophagogastric junction region (EGJ) histologically for the presence of an equivalent to adult cardiac mucosa (CM); to study the expression patterns of all cytokeratins (CK) relevant to the EGJ during gestation; to compare the CK profile of the gestational and the adult EGJ; and to determine the degree of development in the adult EGJ histology and CK profile during gestation.

METHODS: Forty-eight fetal autopsy specimens of the EGJ were step-sectioned and stained with hematoxylin and eosin (H&E) to select sections showing the mucosal lining. Immunohistochemistry for CK5, 7, 8, 13, 18, 19, and 20 was performed. Antibody staining was then graded for location, intensity, and degree.

RESULTS: The distal esophagus was lined by simple columnar epithelium from 12-wk gestational age (GA). The proximal part of this segment consisted of mucus-producing epithelium, devoid of parietal cells. CK5 and 13 were present exclusively in multilayered epithelia and CK8, 18, and 19 predominantly in simple columnar epithelium. There were no differences in the frequencies of the coordinate CK7+/20+ and the CK7-/20- immunophenotypes between different locations. The prevalence of the CK7+/20- immunophenotype decreased, and that of the CK7-/20+ immunophenotype increased significantly from the distal esophagus to the distal stomach.

CONCLUSION: Fetal columnar-lined lower esophagus (fetal CLE) may be the equivalent and precursor of the short segments of columnar epithelium found in the distal esophagus of some normal adult subjects. Esophageal simple columnar epithelium without parietal cells (ESN) may be the precursor of adult CM. The similarities between the fetal and adult EGJ and stomach CK expression patterns support the conclusion that adult CM has an identifiable precursor in the fetus. This would then indicate that at

least a part of the adult CM has a congenital origin.

© 2005 The WJG Press and Elsevier Inc. All rights reserved.

Key words: Cardiac mucosa; Origin; Fetal autopsy; Barrett's CK7/20 pattern

De Hertogh G, Van Eyken P, Ectors N, Geboes K. On the origin of cardiac mucosa: A histological and immunohistochemical study of cytokeratin expression patterns in the developing esophagogastric junction region and stomach. *World J Gastroenterol* 2005; 11(29): 4490-4496

<http://www.wjgnet.com/1007-9327/11/4490.asp>

INTRODUCTION

Since the mid-1970s, there has been a continuing increase in the incidence of gastric cardiac adenocarcinoma in the USA and other Western countries^[1]. This increase is probably genuine, because it cannot be explained by improved diagnostic methods or classification changes^[2]. The pathogenesis of gastric cardiac adenocarcinoma remains unclear. These tumors may arise from foci of intestinal metaplasia, secondary to inflammation of the gastric cardia (carditis)^[3]. It is controversial, however, whether factors like gastroesophageal reflux disease, *Helicobacter pylori* infection or others contribute to the development of inflammation and intestinal metaplasia in the cardia region^[4,5]. Research on this topic is hampered by the limited knowledge of the normal histology of the esophagogastric junction region (EGJ). There is no consensus on the normal histology, location, and length of cardiac mucosa (CM). Histological investigation of hematoxylin and eosin (H&E)-stained sections of the EGJ in adults and children has led some investigators to suggest that CM is actually a metaplasia^[6-9]. Others, however, support the concept that CM is present from birth as a normal structure^[10-14].

Immunohistochemical investigation of the cytokeratin (CK) profile in the EGJ can be used for the study of the origin of adult CM. The keratins are the largest group of intermediate filament proteins expressed by epithelial cells. There are at least 30 different keratins, which are divided into two types. CK filaments are obligate heteropolymers composed of type I and type II proteins. Keratins are typically expressed as pairs in a tissue- and differentiation-specific manner. In 1999, Ormsby *et al.*, described a CK7 and 20 immunoreactivity pattern typical for intestinal metaplasia in long-segment Barrett's esophagus (LSBE)^[15].

This pattern consists of superficial CK20 staining and strong CK7 staining of both superficial and deep glands. It has been claimed by the same group that Barrett's CK7/20 pattern also identifies a subset of patients with suspected short-segment Barrett's esophagus (SSBE) who have a patient profile similar to that seen in LSBE^[16]. Glickman *et al.*, reported that intestinal metaplasia of the EGJ shows a similar pattern of CK7/20 reactivity as LSBE and SSBE. They also found that non-intestinalized CM was diffusely positive for CK7 and showed surface positivity only for CK20, irrespective of its location in LSBE, SSBE or in the most proximal portion of the stomach. This CK7/20 staining pattern was clearly different from that seen in the normal antrum. According to these authors, the results suggest that CM, whether present in the esophagus or at the EGJ, may already represent a form of metaplastic epithelium^[17]. DeMeester *et al.*, found the Barrett's CK7/20 pattern in 85% of CM biopsies^[18]. On the basis of these and other findings, they conclude that there is a strong evidence but no conclusive proof that all CM is acquired.

We have earlier done a histological study on mucosal development in the EGJ of embryos and fetuses^[19]. In this study, CM was defined as a structure composed of columnar foveolar and surface epithelium overlying glandular structures containing no parietal cells. We found that CM develops during pregnancy and we concluded that it is present at birth as a normal structure. The description of the Barrett's CK7/20 pattern in adult CM and the fact that this finding has been used to claim a metaplastic origin for CM have urged us to examine our material for the presence of Barrett's CK7/20 pattern. In addition, we studied the expression patterns of all other CKs relevant to the EGJ during gestation.

MATERIALS AND METHODS

Study group

The study material was derived from 48 embryonic, fetal and neonatal autopsies performed between August 1999 and March 2004 in Leuven University Hospital Gasthuisberg. All autopsies were performed between 6 and 24 h after death. The presence of congenital malformations involving the gastrointestinal tract was considered as an exclusion criterion.

Autopsy protocol

At autopsy, a careful *in situ* examination of the EGJ was carried out. A hiatus hernia was absent in all cases. About 1 cm of the distal esophagus and the whole stomach were excised together as a single piece, with a ring of diaphragmatic muscle. Two specimens were snap-frozen in isopentane, cooled by liquid nitrogen and stored at -80 °C. The other specimens were opened along the greater curvature or transversely and fixed overnight in 10% neutral-buffered formalin. The fixed specimens were routinely processed and embedded in paraffin.

Histology

Five-micrometer-thick step sections of all cases were stained with H&E and evaluated microscopically to select sections

showing the EGJ mucosae. The number of sections selected varied between 10 and 40.

The epithelial lining of the EGJ was classified into five types according to Salenius^[20] and Chandrasoma^[21]. Foregut embryonic epithelium was defined as pseudostratified columnar epithelium consisting of undifferentiated cells; esophageal ciliated epithelium as multilayered epithelium covered by ciliated cells; esophageal squamous epithelium as non-keratinizing multilayered squamous epithelium; esophageal simple columnar epithelium without parietal cells (ESN) as simple columnar epithelium which is either flat or shows crypts, but is devoid of parietal cells; and esophageal simple columnar epithelium with parietal cells (ESP) as simple columnar epithelium with crypts and parietal cells.

The following parameters were measured at four evenly spaced points along the esophageal perimeter: length of abdominal esophagus (defined as the distance between the upper rim of the attachment of the diaphragm to the esophagus and the level of the angle of His); length of esophagus lined by simple columnar epithelium (defined as the distance from the squamocolumnar junction to the level of the angle of His); and length of ESN. These distances were measured along the mucosal surface using a calibrated graticule in the eyepiece of a Leitz DMRB microscope (objectives: Fluotar, eyepieces: L PLAN 10×/25).

Cytokeratin immunohistochemistry

Serial sections were immunostained with mAbs for CK5, 7, 8, 13, 18, 19, and 20. Murine mAbs against human CK7, 18, 19, and 20 were purchased from DakoCytomation (Glostrup, Denmark); mAbs against CK5, 8, and 13 were purchased from Novocastra Laboratories (Newcastle upon Tyne, UK, Table 1). After standard avidin-biotin-peroxidase complex immunostaining, all slides were counterstained with hematoxylin. Positive controls consisted of sections from prostate (CK5, 18, and 19), bile duct (CK7 and 8), tonsil (CK13), and ileum (CK20). Negative controls consisted of slides without application of primary antibody.

Antibody staining was graded for location, intensity (absent, weak, moderate, or strong) and degree (focal = <50% of epithelium, diffuse = ≥50% of epithelium) and compared with controls. The coordinate CK7/CK20 pattern was defined as CK7 positivity at least in surface and pit cells, and CK20 positivity at least in surface cells. The slides were scored independently by two of the authors (GDH and KG), and differences in interpretation were resolved by consensus at a multihead microscope.

Statistical analysis

The Pearson correlation coefficient *r* was calculated to investigate the degree of linear relationship between two continuous variables. A Fisher's *r* to *z* transformation was carried out on the correlation allowing the calculation of a *P*-value for the null hypothesis that the correlation was equal to zero. The ANOVA test was used to study the effect of a nominal independent variable on a continuous dependent variable. To detect relationships between two nominal variables, the χ^2 test or the Fisher's exact test was used, wherever appropriate. *P* values <0.05 were considered significant.

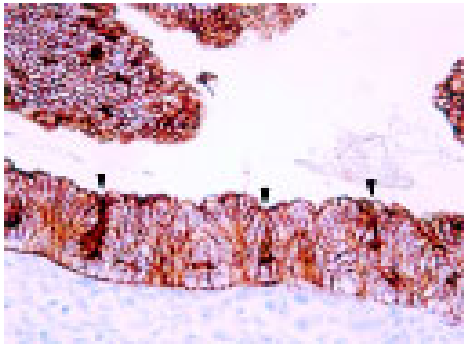


Figure 1 Foregut embryonic epithelium as seen in the esophagus and stomach at 7-wk GA. Note the presence of depressions in the epithelial surface (arrowheads): these may be primitive pits. The immunostaining is for CK19 and shows diffuse moderate to strong positivity (original magnification, OM $\times 400$).

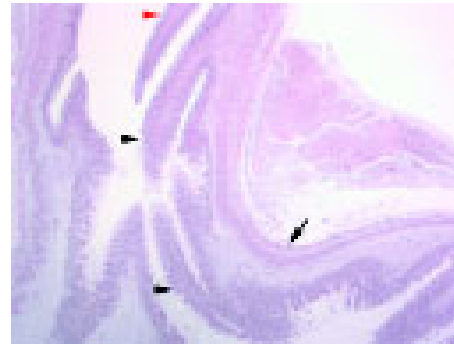


Figure 2 Overview of the fetal EGJ at 20-wk GA. The upper border of the abdominal esophagus is indicated by a red arrowhead. The angle of His (the anatomic boundary between the tubular esophagus and the saccular stomach) is easily recognizable (arrow). The distal end of the esophagus is located at the level of the angle of His. Esophageal simple columnar epithelium is present in the distal esophagus (indicated by black arrowheads at its proximal and distal margins, H&E, OM $\times 125$).

RESULTS

Study group characteristics

Of the 48 autopsy specimens included in this study, 9 were rejected because of epithelial dehiscence, delocalization and fragmentation due to autolysis. The remaining 39 autopsy specimens belonged to 1 embryo of 7 wk gestational age (GA), 35 fetuses (GA: range 12-30 wk, mean \pm SD: 20 \pm 4 wk) and 3 neonates (of 38, 40, and 43 wk GA) (Table 1).

Histology

At 7 wk GA, both esophagus and stomach were lined by foregut embryonic epithelium, which contained depressions surrounded by radially placed cells along the lesser curvature of the stomach (Figure 1).

The distal end of the esophagus was located at the level of the angle of His. This anatomic boundary between the tubular esophagus and the saccular stomach was easily identifiable in the microscopy slides of all cases from 12-wk GA (Figure 2). At this time point, the tubular esophagus was lined by ciliated epithelium (Figure 3A), except in its most distal part. With advancing pregnancy, the ciliated epithelium was progressively replaced by squamous epithelium. Ciliated cells were absent from 40 wk GA (Figure 3B).

The distal esophagus was lined by simple columnar epithelium from 12-wk GA. This segment was between 0.480 and 7.505 mm in length (mean \pm SD: 2.185 \pm 1.619 mm). Its length increased significantly during gestation ($r = 0.344$, $P = 0.0494$), as did the length of the abdominal esophagus ($r = 0.540$, $P = 0.0025$). The length of esophageal simple

columnar epithelium expressed as a percentage of length of the abdominal esophagus ranged between 21.569 and 100.000% (mean \pm SD: 50.884 \pm 18.259%). This percentage remained nearly constant during gestation ($r = -0.140$, $P = 0.4815$).

Throughout gestation, esophageal simple columnar epithelium could be divided into two parts (Figure 3C). The distal part contained parietal cells with roughly triangular shape and highly acidophilic cytoplasm (ESP). This segment was continuous with the stomach fundus. The proximal part of the esophageal simple columnar epithelium, however, was always devoid of parietal cells (ESN). Crypts were present over the entire length of the ESN from 16 wk GA. The length of the ESN ranged between 0.160 and 1.308 mm (mean \pm SD: 0.612 \pm 0.304 mm). There was no significant difference between the lengths of ESN at four evenly spaced points along the esophageal perimeter (ANOVA test, $P = 0.4704$). The length of ESN expressed as a percentage of total length of esophageal simple columnar epithelium ranged between 8.120% and 91.447% (mean \pm SD: 38.499 \pm 24.089%). This percentage decreased significantly during gestation ($r = -0.572$, $P = 0.0004$).

Cytokeratin immunohistochemistry

The CK immunostaining patterns for all locations are summarized in Table 2.

CK5 and CK13 were first detected in a fetus of 14 wk GA. They were seen exclusively in multilayered epithelia.

Table 1 Summary of antibodies used in this study

Antigen	Clone	Antigen retrieval technique ¹	Application of primary Ab ²
CK5	XM26	M	1:50; 1 h; room temperature
CK7	OV-TL 12/30	T	1:50; 1 h; room temperature
CK8	TS1	M	1:50; 1 h; room temperature
CK13	KS-1A3	M	1:50; 1 h; room temperature
CK18	DC 10	M	1:10; 1 h; room temperature
CK19	RCK108	M	1:20; 1 h; room temperature
CK20	Ks20.8	T	1:50; 1 h; room temperature

¹M = heat-induced antigen retrieval by boiling deparaffinized and rehydrated sections in 10 mmol/L citrate buffer (pH 6) in a microwave oven during 20 min; T = antigen retrieval by trypsin digestion. ²Dilution; application time; application temperature.

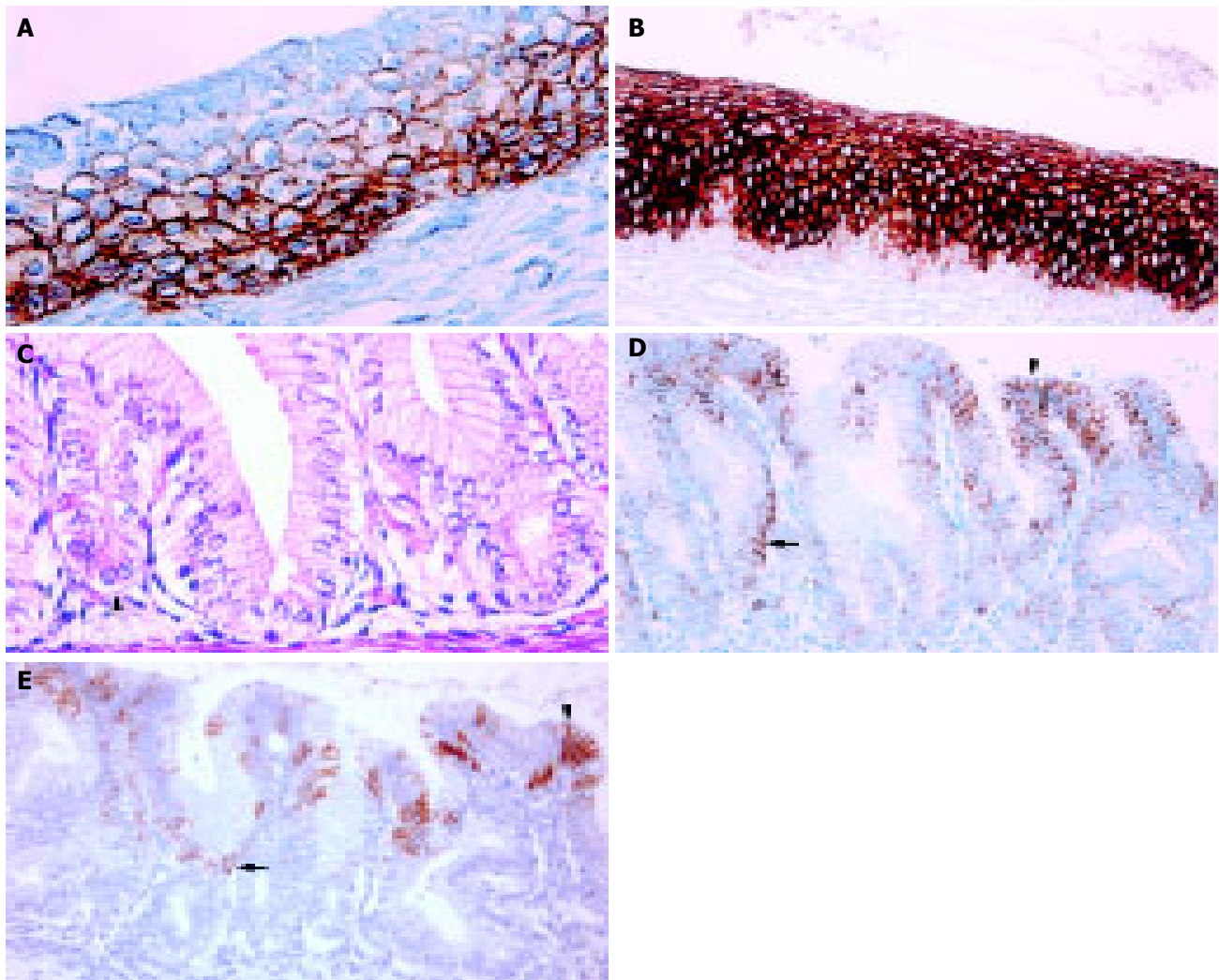


Figure 3 Tubular esophagus. **A:** Esophageal ciliated epithelium at 20-wk GA. The immunostaining is for CK5 and is more intense in the basal and intermediate cell layers than in the superficial cell layer (OM $\times 400$); **B:** Esophageal squamous epithelium in a 3-wk-old neonate. The immunostaining is for CK13 and is absent in the basal cell layer and diffuse moderate to strong in the intermediate and superficial cell layers (OM $\times 200$); **C:** Esophageal simple columnar epithelium at 20-wk GA. To the left: parietal cells with roughly triangular shape and highly acidophilic cytoplasm (ESP, arrowhead). To the right: no discernible parietal

cells are present (ESN, H&E, OM $\times 400$); **D:** Esophageal simple columnar epithelium at 20-wk GA. The immunostaining is for CK7 and shows moderate positivity at the mucosal surface and deep in the glands (arrowhead and arrow, respectively, OM $\times 200$); **E:** Esophageal simple columnar epithelium at 20-wk GA (same case as in Figure 3D). The immunostaining is for CK20 and shows patchy positivity of the superficial part of the mucosa (surface and pit epithelium: arrowhead and arrow, respectively, OM $\times 200$).

CK5 staining was stronger and more diffuse in the basal and intermediate cell layers than in the superficial cell layer (Figure 3A). CK13 staining was diffused in the intermediate and superficial cell layers (Figure 3B). Its staining intensity increased significantly throughout gestation ($r = 0.476$ and 0.523 respectively, $P < 0.0001$).

CK8, CK18, and CK19 were all present in foregut embryonic epithelium (Figure 1). CK8 and CK18 staining were less intense in multilayered epithelia than in simple columnar epithelium. In ciliated epithelium, the basal cell layer was more often negative for these CKs than the other cell layers. In simple columnar epithelium, parietal cells stained weaker for CK8 and CK19 than mucus-secreting cells.

CK7 was first detected at 12-wk GA. Throughout gestation, it was more commonly present in the esophagus than in the stomach (Figure 3D). In multilayered epithelia, basal cells were always negative. Parietal cells contained no

CK7, whereas the deepest crypt cells in the ESN were focally and weakly positive. This was the only statistically significant difference between the CK immunophenotypes of ESN and ESP (χ^2 : $P < 0.0001$).

CK20 was seen in the stomach from 14 wk GA and in the esophagus from 17 wk GA (Figure 3E). It was expressed in the surface or pit cells of simple columnar epithelia. Expression of CK20 was always focal.

Coordinate CK7/20 expression for all locations is summarized in Table 3. We observed no statistically significant differences in the frequencies of the CK7+/20+ and the CK7-/20- immunophenotypes between different locations. The prevalence of the CK7+/20- immunophenotype decreased significantly from proximal to distal (33% in esophageal simple columnar epithelium *vs* 0% in the stomach, Fisher's exact test $P = 0.0039$). The positive predictive value of the CK7+/20- immunophenotype for location in the esophagus (*vs* location in the stomach) was 100%. The usefulness of

Table 2 Summary of intensity and degree of CK immunostaining for all locations¹

Location	CK5	CK7	CK8	CK13	CK18	CK19	CK20
Foregut embryonic epithelium (n = 1)	A	A	M (D)	A	M (D)	M (D)	A
Esophageal ciliated epithelium (n = 36)							
Basal cell layer	S (D)	A	M (F)	A	A	M (D)	A
Columnar cell layer, non-ciliated cells	S (D)	M (D)	M (D)	S (D)	W (F)	M (D)	A
Columnar cell layer, ciliated cells	M (F)	M (D)	M (D)	M (D)	M (F)	M (D)	A
Esophageal squamous epithelium (n = 2)							
Basal cell layer	S (D)	A	A	A	A	M (D)	A
Prickle cell layer	S (D)	W (F)	A	M (D)	A	M (D)	A
Superficial cell layer	M (D)	W (F)	A	S (D)	A	M (D)	A
ESN (n = 38)							
Surface cells	A	M (F)	M (D)	A	M (D)	S (D)	A (1)
Pit cells	A	M (F)	M (D)	A	M (D)	M (D)	A
Deepest crypt cells	A	W (F)	M (D)	A	M (D)	M (D)	A
ESP (n = 38)							
Surface cells	A	M (F)	M (D)	A	M (D)	S (D)	A (2)
Pit cells	A	M (F)	M (D)	A	S (D)	S (D)	A (3)
Parietal cells	A	A	M (D)	A	S (D)	M (D)	A
Stomach body mucosa (n = 38)							
Surface cells	A	M (F)	M (D)	A	M (D)	M (D)	A (4)
Pit cells	A	M (F)	M (D)	A	M (D)	M (D)	A (5)
Glandular cells	A	A	M (D)	A	M (D)	M (D)	A
Stomach antrum mucosa (n = 10)							
Surface cells	A	A	S (D)	A	M (D)	S (D)	S(F)
Pit cells	A	A	S (D)	A	M (D)	S (D)	M(F)
Glandular cells	A	A	M (D)	A	M (D)	M (D)	A

¹Intensity was graded as absent (A), weak (W), moderate (M), or strong (S). Degree was graded as focal (F), or diffuse (D). Degree is indicated in parentheses. (1) 4/20 cases showed focal weak positivity. (2) 10/24 cases showed focal moderate positivity. (3) 9/23 cases showed focal moderate positivity. (4) 8/25 cases showed focal moderate positivity. (5) 7/25 cases showed focal weak positivity.

Table 3 Summary of coordinate CK7 and 20 expression for all locations¹

Location	CK7+/20- (%)	CK7+/20+ (%)	CK7-/20+ (%)	CK7-/20- (%)
Fetal CLE (n = 24)	8 (33)	6 (25)	2 (8)	8 (33)
ESN (n = 22)	8 (36)	4 (18)	0 (0)	10 (45)
ESP (n = 22)	4 (18)	5 (23)	3 (14)	10 (45)
Stomach (n = 23)	0 (0)	4 (17)	4 (17)	15 (65)
Body mucosa (n = 23)	0 (0)	3 (13)	5 (22)	15 (65)
Antrum mucosa (n = 5)	0 (0)	1 (20)	2 (40)	2 (40)

¹CK7+ is positivity at least in surface and pit cells; CK20+ is positivity at least in surface cells.

this feature was limited however, by its low sensitivity (33%). The prevalence of the CK7-/20+ immunophenotype increased significantly from proximal to distal (0% in ESN vs 40% in the stomach antrum, Fisher's exact test $P = 0.0285$).

DISCUSSION

In this study, we examined the histology and CK expression patterns of the esophageal and gastric mucosae in fetuses and neonates, using autopsy material. We believe that the results of such a study may be relevant to the description of the normal adult situation. This is important in view of the current controversy on the origin and significance of CM. Our results can be summarized as follows: (1) the distal esophagus was lined by simple columnar epithelium from 12-wk GA; (2) the proximal part of this segment consisted of mucus-producing epithelium devoid of parietal

cells; and (3) the reported adult CK expression pattern was established during gestation.

We found that the distal esophagus was lined by simple columnar epithelium from 12-wk GA. We propose the term "fetal columnar-lined lower esophagus" (fetal CLE) for this condition. Fetal CLE has been mentioned only infrequently until now. Salenius states that "The gastroesophageal limit is by no means sudden, but the epithelial change occurs quite abruptly. Glands typical of the esophagus are found over a distance of a few millimeters in the cardiac area at the junction of the esophagus and stomach."^[20] Thus, it may be difficult to decide whether simple columnar epithelium is actually located in the distal esophagus or in the proximal stomach of fetuses. Ellison *et al.*, mentioned the presence of "the squamocolumnar junction in the tubular esophagus proximal to the gastric dilatation" in 1 case out of 49 fetal and pediatric autopsies. They considered this

finding suggestive of a hiatus hernia^[22]. We excluded the presence of hiatal hernia by a careful *in situ* examination of the EGJ at autopsy. In our material, fetal CLE had a length ranging between 0.480 and 7.505 mm, with a mean of 2.185 mm. We admit that these segments of simple columnar epithelium are very short. This might influence the decision whether to locate the simple columnar epithelium in the fetal esophagus or stomach. However, we are quite sure that this simple columnar epithelium was in the distal esophagus in our cases. We have two arguments: (1) the angle of His, the level of which marks the distal margin of the tubular esophagus, was always easily identifiable; and (2) the length of esophageal simple columnar epithelium expressed as a percentage of length of the abdominal esophagus ranged between 22% and 100%, with a mean of 51%. The last finding indicates that the fetal squamo-columnar junction was located definitely in the abdominal esophagus, often mid-way between the angle of His and the diaphragm.

The significance of fetal CLE is unclear. It is known since 1953 that the most distal part of the adult tubular esophagus can be lined by columnar epithelium^[23]. Since the 1970 landmark experimental report by Bremner *et al.*, it has been widely accepted that adult columnar-lined esophagus is an acquired condition in which the squamous esophageal epithelium destroyed by gastroesophageal reflux is replaced by columnar cells^[24]. However, even normal subjects may have short segments of columnar epithelium within 2 cm of the proximal margin of the gastric folds^[25,26]. In our material, the length of fetal CLE showed no tendency to decrease during gestation. Moreover, its length expressed as a percentage of abdominal esophagus length remained nearly constant. The fetal squamo-columnar junction thus had an almost constant position. Therefore, the possibility exists that fetal CLE may be the equivalent (and the precursor) of the short segments of columnar epithelium found in the distal esophagus of some normal adult subjects. On the other hand, we cannot formally exclude that fetal CLE may differentiate into squamous epithelium in the esophagus and gastric mucosa in the stomach once the gastroesophageal sphincter is fully developed^[21].

From 12-wk GA, the fetal CLE could be divided into two parts. Parietal cells were present in the distal part, which was continuous with the fundus part of the fetal stomach. We call this part of the fetal CLE as ESP. ESP may be the equivalent of oxyntocardiac mucosa, which was first described by Chandrasoma *et al.*^[7]. Oxyntocardiac mucosa differs from pure oxyntic mucosa by the absence of chief cells in the former.

The proximal part of the fetal CLE was lined circumferentially by a mucus-producing epithelium devoid of parietal cells. We call this part of the fetal CLE as ESN. From 16-wk GA, ESN contained crypts over its entire length at least as deep as those in the ESP. Therefore, we assume that mucus-secreting glandular structures devoid of parietal cells are present proximally in the fetal CLE. This description equates the histological definition of adult CM^[4,7,8]. Consequently, we consider ESN as the equivalent (and forerunner) of adult CM. An alternative name for ESN would thus be "fetal CM". Besides the histologic aspect of the epithelium,

several other arguments are in favor of this conclusion. Like adult CM, ESN is located between multilayered esophageal epithelium and simple columnar epithelium with parietal cells. Also like adult CM, it is very short (range in our material: 0.160–1.308 mm, mean 0.612 mm)^[7,8]. Even its position in the distal esophagus cannot be objected, if one accepts that fetal CLE may be the precursor of the short segments of columnar epithelium found in the distal esophagus in some normal adults. Our view on ESN is shared by other investigators^[14].

Since classical morphological techniques cannot definitely solve the riddle of the origin of adult CM, we also investigated the CK expression patterns of the developing EGJ and stomach. We chose to do this for two reasons: (1) there is a large body of literature on CK expression in the adult EGJ mucosae, particularly on the so-called Barrett's CK7/20 pattern^[15-18]; and (2) Barrett's CK7/20 pattern has also been found in adult CM and this similarity to intestinal metaplastic epithelium in Barrett's esophagus has been used as an argument for its metaplastic origin^[17,18].

CK expression in the adult EGJ mucosae has been investigated by Glickman *et al.*^[27]. CK13 positivity was restricted to esophageal squamous epithelium. The basal layer of this epithelium stained for CK19 in 90% of cases. CK7 and CK8/18 were present focally and weakly in 61% and 18% of cases, respectively. CK7, 8/18, 19, and 20 were present in all biopsies of esophageal columnar and gastric cardiac epithelium. CK20 was only seen in columnar epithelia, where it was present in all cases. The CK expression pattern of adult ciliated respiratory epithelium has been studied by Hicks *et al.*^[28]. Basal cells typically stained for CK5, and columnar cells were positive for CK7, 8, and 18. CK19 was positive in both cell types. CK13 expression was not detected.

We observed similar CK expression patterns in the fetal EGJ mucosae. The only notable difference from the adult situation was the initially weak expression of CK13 in multilayered epithelia. However, CK13 immunostaining increased significantly throughout gestation. This finding may be related to the maturation of ciliated into squamous esophageal epithelium.

The co-ordinated CK7/20 immunophenotypes of the non-intestinalized mucosae of the adult EGJ and stomach have been described and illustrated in several publications^[29-31]. From these data, it seems that in general CK7 positivity is more common and more extensive in CM than in gastric body or antrum mucosa. Conversely, CK20 positivity is more intense and more widespread in the stomach. These observations are concordant with our findings showing that the prevalence of the CK7+/20- immunophenotype decreases significantly from fetal CM to fetal antrum, while the prevalence of the CK7-/20+ immunophenotype increases significantly in the same direction.

The fetal CK7+/20+ immunophenotype in the esophagus is illustrated in Figures 3D and E, showing patchy superficial CK20 positivity and superficial and deep CK7 positivity. This pattern is similar to the expression reported in non-intestinalized CM by DeMeester *et al.*^[18]. The patchy superficial CK20 positivity is slightly different from the adult Barrett's CK7/20 pattern. Ormsby *et al.*, studied CK7/20 expression in LSBE. They described the Barrett's CK7/20

pattern as band-like (i.e., diffuse) CK20 staining of surface epithelium and superficial glands, with moderate to strong CK7 staining of both superficial and deep glands in the specialized mucosa^[15,16].

The fetal equivalent to adult CM thus shows already co-ordinated CK7/20 expression (in our material in 25% of cases). Together with the other similarities between the fetal and adult EGJ and stomach CK expression patterns, this supports the conclusion that a cardia-type mucosa is established during gestation. This would then indicate that at least a part of the adult CM has a congenital origin.

REFERENCES

- 1 **Devesa SS**, Blot WJ, Fraumeni JF Jr. Changing patterns in the incidence of esophageal and gastric carcinoma in the United States. *Cancer* 1998; **83**: 2049-2053
- 2 **Pera M**, Cameron AJ, Trastek VF, Carpenter HA, Zinsmeister AR. Increasing incidence of adenocarcinoma of the esophagus and esophagogastric junction. *Gastroenterology* 1993; **104**: 510-513
- 3 **Spechler SJ**. The role of gastric carditis in metaplasia and neoplasia at the gastroesophageal junction. *Gastroenterology* 1999; **117**: 218-228
- 4 **Oberg S**, Peters JH, DeMeester TR, Chandrasoma P, Hagen JA, Ireland AP, Ritter MP, Mason RJ, Crookes P, Bremner CG. Inflammation and specialized intestinal metaplasia of cardiac mucosa is a manifestation of gastroesophageal reflux disease. *Ann Surg* 1997; **226**: 522-530
- 5 **Goldblum JR**, Vicari JJ, Falk GW, Rice TW, Peek RM, Easley K, Richter JE. Inflammation and intestinal metaplasia of the gastric cardia: the role of gastroesophageal reflux and *H. pylori* infection. *Gastroenterology* 1998; **114**: 633-639
- 6 **Csendes A**, Smok G, Christensen H, Rojas J, Burdiles P, Korn O. Prevalence of cardiac or fundic mucosa and *Helicobacter pylori* in the squamous-columnar mucosa in patients with chronic pathological gastroesophageal reflux without intestinal metaplasia compared with controls. *Rev Med Chil* 1999; **127**: 1439-1446
- 7 **Chandrasoma PT**, Lokuhetty DM, Demeester TR, Bremner CG, Peters JH, Oberg S, Groshen S. Definition of histopathologic changes in gastroesophageal reflux disease. *Am J Surg Pathol* 2000; **24**: 344-351
- 8 **Chandrasoma PT**, Der R, Ma Y, Dalton P, Taira M. Histology of the gastroesophageal junction: an autopsy study. *Am J Surg Pathol* 2000; **24**: 402-409
- 9 **Park YS**, Park HJ, Kang GH, Kim CJ, Chi JG. Histology of gastroesophageal junction in fetal and pediatric autopsy. *Arch Pathol Lab Med* 2003; **127**: 451-455
- 10 **Ormsby AH**, Ksilgore SP, Goldblum JR, Richter JE, Rice TW, Gramlich TL. The location and frequency of intestinal metaplasia at the esophagogastric junction in 223 consecutive autopsies: implications for patient treatment and preventive strategies in Barrett's esophagus. *Mod Pathol* 2000; **13**: 614-620
- 11 **Kilgore SP**, Ormsby AH, Gramlich TL, Rice TW, Richter JE, Falk GW, Goldblum JR. The gastric cardia: fact or fiction? *Am J Gastroenterol* 2000; **95**: 921-924
- 12 **Zhou H**, Greco MA, Daum F, Kahn E. Origin of cardiac mucosa: ontogenic consideration. *Pediatr Dev Pathol* 2001; **4**: 358-363
- 13 **Glickman JN**, Fox V, Antonioli DA, Wang HH, Odze RD. Morphology of the cardia and significance of carditis in pediatric patients. *Am J Surg Pathol* 2002; **26**: 1032-1039
- 14 **Derdoy JJ**, Bergwerk A, Cohen H, Kline M, Monforte HL, Thomas DW. The gastric cardia: to be or not to be? *Am J Surg Pathol* 2003; **27**: 499-504
- 15 **Ormsby AH**, Goldblum JR, Rice TW, Richter JE, Falk GW, Vaezi MF, Gramlich TL. Cytokeratin subsets can reliably distinguish Barrett's esophagus from intestinal metaplasia of the stomach. *Hum Pathol* 1999; **30**: 288-294
- 16 **Ormsby AH**, Vaezi MF, Richter JE, Goldblum JR, Rice TW, Falk GW, Gramlich TL. Cytokeratin immunoreactivity patterns in the diagnosis of short-segment Barrett's esophagus. *Gastroenterology* 2000; **119**: 683-690
- 17 **Glickman JN**, Wang H, Das KM, Goyal RK, Spechler SJ, Antonioli D, Odze RD. Phenotype of Barrett's esophagus and intestinal metaplasia of the distal esophagus and gastroesophageal junction: an immunohistochemical study of cytokeratins 7 and 20, Das-1 and 45 MI. *Am J Surg Pathol* 2001; **25**: 87-94
- 18 **DeMeester SR**, Wickramasinghe KS, Lord RV, Friedman A, Balaji NS, Chandrasoma PT, Hagen JA, Peters JH, DeMeester TR. Cytokeratin and DAS-1 immunostaining reveal similarities among cardiac mucosa, CIM, and Barrett's esophagus. *Am J Gastroenterol* 2002; **97**: 2514-2523
- 19 **De Hertogh G**, Van Eyken P, Ectors N, Tack J, Geboes K. On the existence and location of cardiac mucosa: an autopsy study in embryos, fetuses, and infants. *Gut* 2003; **52**: 791-796
- 20 **Salenius P**. On the ontogenesis of the human gastric epithelial cells. A histologic and histochemical study. *Acta Anat* 1962; **50** (Suppl 46): 1-76
- 21 **Chandrasoma PT**. Fetal "cardiac mucosa" is not adult cardiac mucosa. *Gut* 2003; **52**: 1798
- 22 **Ellison E**, Hassall E, Dimmick JE. Mucin histochemistry of the developing gastroesophageal junction. *Pediatr Pathol Lab Med* 1996; **16**: 195-206
- 23 **Allison PR**, Johnstone AS. The oesophagus lined with gastric mucous membrane. *Thorax* 1953; **8**: 87-101
- 24 **Bremner CG**, Lynch VP, Ellis FH Jr. Barrett's esophagus: congenital or acquired? An experimental study of esophageal mucosal regeneration in the dog. *Surgery* 1970; **68**: 209-216
- 25 **McClave SA**, Boyce HW Jr, Gottfried MR. Early diagnosis of columnar-lined esophagus: a new endoscopic diagnostic criterion. *Gastrointest Endosc* 1987; **33**: 413-416
- 26 **Csendes A**, Maluenda F, Braghetto I, Csendes P, Henriquez A, Quesada MS. Location of the lower esophageal sphincter and the squamous columnar mucosal junction in 109 healthy controls and 778 patients with different degrees of endoscopic oesophagitis. *Gut* 1993; **34**: 21-27
- 27 **Glickman JN**, Chen YY, Wang HH, Antonioli DA, Odze RD. Phenotypic characteristics of a distinctive multilayered epithelium suggests that it is a precursor in the development of Barrett's esophagus. *Am J Surg Pathol* 2001; **25**: 569-578
- 28 **Hicks W Jr**, Ward R, Edelstein D, Hall L 3rd, Albino A, Hard R, Asch B. Cytokeratin expression in human respiratory epithelium of nasal polyps and turbinates. *Cell Biol Int* 1995; **19**: 301-306
- 29 **Jovanovic I**, Tzardi M, Mouzas IA, Micev M, Pesko P, Milosavljevic T, Zois M, Sganzos M, Delides G, Kanavaros P. Changing pattern of cytokeratin 7 and 20 expression from normal epithelium to intestinal metaplasia of the gastric mucosa and gastroesophageal junction. *Histol Histopathol* 2002; **17**: 445-454
- 30 **Mohammed IA**, Streutker CJ, Riddell RH. Utilization of cytokeratins 7 and 20 does not differentiate between Barrett's esophagus and gastric cardiac intestinal metaplasia. *Mod Pathol* 2002; **15**: 611-616
- 31 **Flucke U**, Steinborn E, Dries V, Monig SP, Schneider PM, Thiele J, Holscher AH, Dienes HP, Baldus SE. Immunoreactivity of cytokeratins (CK7, CK20) and mucin peptide core antigens (MUC1, MUC2, MUC5AC) in adenocarcinomas, normal and metaplastic tissues of the distal oesophagus, oesophago-gastric junction and proximal stomach. *Histopathology* 2003; **43**: 127-134

Liver-specific gene expression in mesenchymal stem cells is induced by liver cells

Claudia Lange, Philipp Bassler, Michael V. Lioznov, Helge Bruns, Dietrich Kluth, Axel R. Zander, Henning C. Fiegel

Claudia Lange, Philipp Bassler, Michael V. Lioznov, Axel R. Zander, Center of Bone Marrow Transplantation, University Hospital Hamburg-Eppendorf, Martinistrasse 52, D-20246 Hamburg, Germany
Helge Bruns, Dietrich Kluth, Henning C. Fiegel, Department of Pediatric Surgery, University Hospital Hamburg-Eppendorf, Martinistrasse 52, D-20246 Hamburg, Germany
Supported by the "Rudolf Bartling Foundation" and "Foerdergemeinschaft Kinder-Krebs-Zentrum Hamburg e.V."
Correspondence to: Dr. Claudia Lange, Center of Bone Marrow Transplantation, Universitätsklinikum Hamburg-Eppendorf, Martinistrasse 52, D-20246 Hamburg, Germany. cllange@uke.uni-hamburg.de
Telephone: +49-40-42803-5917 Fax: +49-40-42803-3795
Received: 2004-11-23 Accepted: 2004-12-20

© 2005 The WJG Press and Elsevier Inc. All rights reserved.

Key words: Mesenchymal stem cells; Liver-specific differentiation; Coculture

Lange C, Bassler P, Lioznov MV, Bruns H, Kluth D, Zander AR, Fiegel HC. Liver-specific gene expression in mesenchymal stem cells is induced by liver cells. *World J Gastroenterol* 2005; 11(29): 4497-4504
<http://www.wjgnet.com/1007-9327/11/4497.asp>

Abstract

AIM: The origin of putative liver cells from distinct bone marrow stem cells, e.g. hematopoietic stem cells or multipotent adult progenitor cells was found in recent *in vitro* studies. Cell culture experiments revealed a key role of growth factors for the induction of liver-specific genes in stem cell cultures. We investigated the potential of rat mesenchymal stem cells (MSC) from bone marrow to differentiate into hepatocytic cells *in vitro*. Furthermore, we assessed the influence of cocultured liver cells on induction of liver-specific gene expression.

METHODS: Mesenchymal stem cells were marked with green fluorescent protein (GFP) by retroviral gene transduction. Clonal marked MSC were either cultured under liver stimulating conditions using fibronectin-coated culture dishes and medium supplemented with SCF, HGF, EGF, and FGF-4 alone, or in presence of freshly isolated rat liver cells. Cells in cocultures were harvested and GFP+ or GFP- cells were separated using fluorescence activated cell sorting. RT-PCR analysis for the stem cell marker Thy1 and the hepatocytic markers CK-18, albumin, CK-19, and AFP was performed in the different cell populations.

RESULTS: Under the specified culture conditions, rat MSC cocultured with liver cells expressed albumin-, CK-18, CK-19, and AFP-RNA over 3 weeks, whereas MSC cultured alone did not show liver specific gene expression.

CONCLUSION: The results indicate that (1) rat MSC from bone marrow can differentiate towards hepatocytic lineage *in vitro*, and (2) that the microenvironment plays a decisive role for the induction of hepatic differentiation of rMSC.

INTRODUCTION

The existence of putative liver stem cells in the bone marrow was first demonstrated by Petersen *et al.*, who showed that bone marrow cells transplanted into lethally irradiated mice engrafted in the recipient's liver differentiated into liver stem cells (oval cells) or mature liver cells (hepatocytes)^[1]. These *in vivo* results were confirmed by mouse experiments^[2] and in patients who received a bone marrow transplantation or peripheral blood stem cell transplantation for hematological disorders^[3-5]. Furthermore, Lagasse *et al.*, found liver-specific gene expression and function in FACS-sorted mouse hematopoietic stem cells (HSC, KTLS cells: c-kit^{high}, thy1^{+/-}, lin^{neg}, sca-1⁺) after transplantation into FAH-deficient mice^[6]. Recent studies in the same animal model indicated that cells observed in the recipients' liver after stem cell transplantation bearing donor markers and liver specific markers were rather a product of cell fusion than of a real "transdifferentiation"^[7,8]. However, variable data concerning cellular fusion *vs* transdifferentiation as the mechanism of liver-like differentiated cells derived from bone marrow were found in other animal models: Engraftment of human albumin producing cells in livers of NOD/SCID recipient mice was observed after xenogeneic transplantation of human hematopoietic or umbilical cord blood stem cells. However, fusion events were not ruled out^[9]. In contrast to these results, two studies using similar settings found liver specific differentiation of the transplanted cells occurring without any evidence of cell fusion events after transplantation of human sorted CD34+ or unsorted mononuclear cord blood cells into NOD/SCID mice^[10,11]. These results were supported by a recent report of Jang *et al.*^[12], showing conversion of HSC into viable hepatocytes *in vitro* and *in vivo*, notably without any cell fusion.

Several *in vitro* studies suggested the differentiation potential of various types of bone marrow cells/stem cells towards hepatocytic cells under appropriate culture

conditions. Oh *et al.*, found an expression of the liver specific genes alpha-fetoprotein (AFP) and albumin in cultures of unsorted rat bone marrow cells after 21 d. The liver specific gene expression was induced by hepatocyte growth factor (HGF) and was mediated by the expression of its receptor c-met^[13]. The expression of liver specific genes (albumin, cytokeratins (CK)) in cultured human CD34-positive hematopoietic stem cells or mononuclear cord blood cells was also demonstrated to be induced by HGF in culture^[14,15].

From cultures of mature hepatocytes it is known that important stimuli for an adequate maintenance of cellular function *in vitro* are (1) the addition of growth hormones and cytokines to the culture medium^[16,17], (2) coating culture dishes with extracellular matrix (ECM) molecules^[18,19], and (3) coculturing with other cell types^[20,21]. In stem cell cultures, Miyazaki *et al.*, showed an induction of the liver specific genes, albumin, tryptophan-2, 3-dioxygenase and tyrosine amino-transferase of rat bone marrow cells indicating a maturation towards hepatocytes when cultured in a hepatocyte growth medium supplemented with HGF and epidermal growth factor (EGF)^[22]. Avital *et al.*, demonstrated that β_2 -microglobulin-negative Thy1-positive stem cells residing in rat bone marrow expressed the liver marker albumin. In cocultures of these cells with hepatocytes (separated by a PTFE-membrane), cells were shown to adopt metabolic activity after 7 d in culture^[23]. An important influence of hepatocytes on the differentiation of stem cell enriched bone marrow was also highlighted by Okumoto *et al.*, Here, immuno-selected bone marrow stem cells cultured in the presence of HGF and fetal bovine serum (FBS) expressed the markers, hepatic nuclear factor 1 (HNF1- α) and CK-8 only after 7 d. In cocultures with hepatocytes separated by a semipermeable membrane, the stem cells additionally expressed the liver specific markers-AFP and albumin^[24]. This suggested that cocultured hepatocytes have a stimulatory effect for the differentiation of stem cells toward liver cells, which was mediated by soluble factors. For the culture of adult hepatocytes, it has been shown that cell-to-cell or cell-to-matrix contacts also play an important role for the control of liver specific differentiation^[25]. Thus, an optimal *in vitro* environment for the induction of liver specific differentiation in stem cells should be achieved by cocultures with liver cells.

Besides the HSCs, bone marrow contains nonhematopoietic, i.e. mesenchymal stem cells (MSC) reported to differentiate into cell lineages of all three germ layers^[26-29]. One distinct adherent growing cell population derived from bone marrow was described by Schwartz *et al.*^[30]. The authors isolated CD45- and GlycophorinA-depleted multipotent adult progenitor cells (MAPC) from rat, mouse, or human plastic-adherent bone marrow cells that expressed liver specific markers after 14 d in culture with FGF and HGF, e.g. albumin and CK-18. However, the relation between MSC and MAPC remains unclear. MAPCs were separated differently from bone marrow in comparison to MSCs and appear after long periods of time *in vitro* using low serum concentrations. For cloned MSCs, differentiation in hepatic cells has not been shown yet. Additionally, little evidence for cell fusion in MSC cultures has been published so far. Recently, coculture of MSCs with heatshocked airway

epithelial cells revealed the differentiation into epithelial cells^[31]. Cell fusion in this setting was a rather frequent than a rare event with a frequency of $\approx 10^{-2}$ and has to be expected in other experimental settings as well.

In this study, we investigated the potential of rat mesenchymal stem cells derived from adult bone marrow to differentiate into hepatic lineage cells *in vitro*. Furthermore, we assessed the impact of coculture with adult liver cells permitting cell-cell contacts for the initiation of liver specific gene expression.

MATERIALS AND METHODS

An outline of the experimental design is shown in Figure 1.

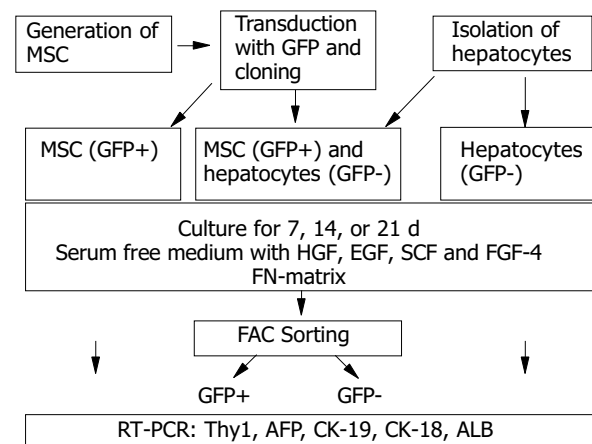


Figure 1 Experimental design. rMSC were harvested from rat bone marrow and were transduced with GFP and cloned. Cloned GFP+ rMSC were expanded and either seeded with hepatocytes in cocultures or alone. Controls included hepatocytes cultured alone. Cells were cultured for 7, 14, or 21 d. Cocultured cells were sorted by FACS into GFP+ (rMSC-derived) or GFP- (hepatocyte-derived) cells. Gene expression analysis for stem cell marker or liver specific genes was performed by RT-PCR.

Isolation, transduction, and cloning of rat mesenchymal stem cells

Bone marrow was harvested from Lewis.1WR2 rats by flushing femurs and tibiae with icecold IMDM (Gibco BRL, Karlsruhe, Germany) and 10% fetal calf serum (FCS, Gibco). Cells were centrifugated at 400 r/min for 10 min at 4 °C. The pellet was suspended in DMEM/Hams-F12 medium (1:1; Biochrom, Berlin, Germany) supplemented with 20% preselected fetal bovine serum (FBS, Biochrom), 2 mol/L L-glutamine (Gibco), 100 U/mL penicillin, and 100 mg/mL streptomycin (both Gibco). Cells of one femur and one tibia were seeded in tissue culture flasks ($A = 75 \text{ cm}^2$, Greiner, Frickenhausen, Germany). Non-adherent cells were removed after 3 d by washing the cultures with PBS (Gibco). Plastic adherent cells were grown to near confluency, and were passaged twice. Retroviral gene transduction with ectropic-packaged GFP was performed as described elsewhere^[32]. In brief, cells were removed from cultures with Trypsin/EDTA (Gibco), and 1×10^5 MSC/well were seeded in six-well culture plates. 2×10^6 virus particles containing the ectropic vector SF α 11-

GFP^[33] and 4 µg/mL protamine sulfate (Gibco) were added, and the culture plates were centrifuged for 1 h with 1 000 r/min at room temperature. Transduction efficiency was 25.5%, as determined by FACS analysis (BD FACScan with CellQuest software, BD Heidelberg, Germany). After transfection, 0.3 cells were seeded per well in 96 well plates for cloning. The clones were checked for GFP expression with a fluorescence microscope. GFP-positive clones were expanded and the clone with the highest proliferation capacity was chosen for further work (IG3 clone). Clonal GFP-marked rMSC were stored frozen at -196 °C until culture for cell differentiation.

Hepatocyte isolation

Hepatocytes were isolated from Sprague-Dawley rats by two step collagenase perfusion described by Seglen^[34] and performed in our laboratory^[35]. Briefly, donor animals received 250 U heparin (Liquemin, Hoffmann La-Roche, Mannheim, Germany) prior to cell isolation. After cannulation of the portal vein, the liver was perfused with a calcium-free buffer solution [1 000 mL distilled water, 8.3 g NaCl, 0.5 g KCl, 2.38 g HEPES (Sigma, Seelzen, Germany); pH 7.4; flow 30 mL/min] at 37.0 °C for 7 min. Then, the liver was perfused with a collagenase solution [1 000 mL distilled water, 8.3 g NaCl, 0.5 g KCl, 2.38 g HEPES, 0.7 g CaCl₂·2H₂O, 7.5 mg trypsin-inhibitor (ICN, Eschwege, Germany) and 500 mg collagenase (Collagenase H, Boehringer Mannheim, Mannheim, Germany); pH 7.35; flow 30 mL/min] at 37 °C for 8-11 min. The perfused liver was resected, and the cells were released by gentle shaking and collected in 20 mL Williams medium E without L-glutamine (Gibco). The cell suspension was filtered using a 200 µm nylon mesh and washed twice with Williams medium E (centrifugation at 50 r/min; 4 °C for 3 min). Cells were purified by Percoll[®] (density 1.13 g/mL; Sigma) gradient centrifugation (400 r/min; 4 °C for 12 min) and washed twice in Williams medium E.

Coculture of rMSC with rat hepatocytes

GFP-transduced and cloned rMSC from passage (*P*) nine or later ($\geq P 9$) were cocultured with freshly isolated rat hepatocytes. As controls, rMSC and rat hepatocytes cultured alone were included. Cultures were analyzed at d 0, 7, 14, and 21. Cells were seeded into culture wells coated with

4 µg/well fibronectin (FN, Sigma) in 24-well plates (Greiner). The culture medium used for the differentiation in cocultures consisted of Stem Span serum-free essential medium (SFEM, Stem Cell Technologies, St. Katherinen, Germany) supplemented with 100 mg/mL penicillin/streptomycin (Gibco), 2.5 nmol/L dexamethasone (Sigma), 100 ng/mL human recombinant stem cell factor (SCF), 20 ng/mL hepatocyte growth factor (HGF, both Immunotools, Friesoythe, Germany), 50 ng/mL epidermal growth factor (EGF), and 10 ng/mL fibroblast growth factor-4 (FGF-4, both R&D, Wiesbaden, Germany).

9×10^4 rMSC were seeded per well for MSC-controls, or 6×10^4 hepatocytes per well for hepatocyte controls. For cocultures of rMSC with rat hepatocytes 9×10^4 rMSC per well were preseeded in 24 well-plates for 2-3 h. Then, 6×10^4 hepatocytes per well were added to the cultures. Medium was changed twice a week.

Separation of GFP-positive and -negative cells in cocultures by fluorescence activated cell sorting (FACS)

After the culture period, cells from cocultures were trypsinized, counted with trypan blue, and resuspended in 3 mL PBS. To get single cell suspension, cells were filtered through a 35 µm filter (BD, Heidelberg, Germany). Cells were sorted using the FACS Aria[™] Cell Sorter (BD) into GFP-positive (GFP+) or GFP-negative (GFP-) cells, focusing on the highest possible purity of GFP+ cells.

RNA extraction from cells, reverse transcription and polymerase chain reaction (RT-PCR)

RNA was extracted using the Invisorb Spin Cell-RNA[™] Mini-kit (Invitek, Berlin, Germany) according to the manufacturer's instructions. RNA was stored at -80 °C. Reverse transcription (RT) of extracted RNA was performed using the bulk first-strand c-DNA synthesis kit (Amersham, Freiburg, Germany). The cDNA was stored at -20 °C. For the semiquantitative PCR reaction, 5 µL cDNA-template was mixed with 2.5 µL 10× PCR-buffer, 0.5 µL 10 mmol/L dNTPs, 0.5 µL of each primer (50 ng/µL), and 0.5 µL polymerase (Ampli-Taq, Gibco) in a total volume of 25 µL for each probe. PCR was carried out in a programmable Biometra Uno-Thermobloc (Biometra, Göttingen, Germany) using the primers and conditions is shown in Table 1. Negative controls were performed for each set of

Table 1 RT-PCR analysis

Primer name	Sequence	PCR conditions	Fragment length	Refer-ence
GAPDH	S: 5'-CCT TCA TTG ACC TCA ACT AC-3' A: 5'-GGA AGG CCA TGC CAG TGA GC-3'	60 °C; 30×	593 bp	14
Thy1	S: 5'-CGC TTT ATC AAG GTC CTT ACT C-3' A: 5'-GCG TTT TGA GAT ATT TGA AGG T-3'	52 °C; 29×	343 bp	39
CK-18	S: 5'-GGA CCT CAG CAA GAT CAT GGC-3' A: 5'-CCA CGA TCT TAC GGG TAG TTG-3'	60 °C; 30×	518 bp	
CK-19	S: 5'-ACC ATG CAG AAC CTG AAC GAT-3' A: 5'-CAC CTC CAG CTC GCC ATT AG-3'	60 °C; 30×	261 bp	30
AFP I.	S I: 5'-AAC AGC AGA GTG CTG CAA AC-3' A I: 5'-AGG TTT CGT CCC TCA GAA AG-3'	55 °C; 35×		13
AFP II. (nested)	S II: 5'-CAC CAT CGA GCT CGC CTA TT-3' A II: 5'-TGA TGC AGA GCC TCC TGT TG-3'	60 °C; 30×	619 bp	13
Albumin	S: 5'-ATA CAC CCA GAA AGC ACC TC-3' A: 5'-CAC GAA TTG TGC GAA TGT CAC-3'	60 °C; 30×	416 bp	13

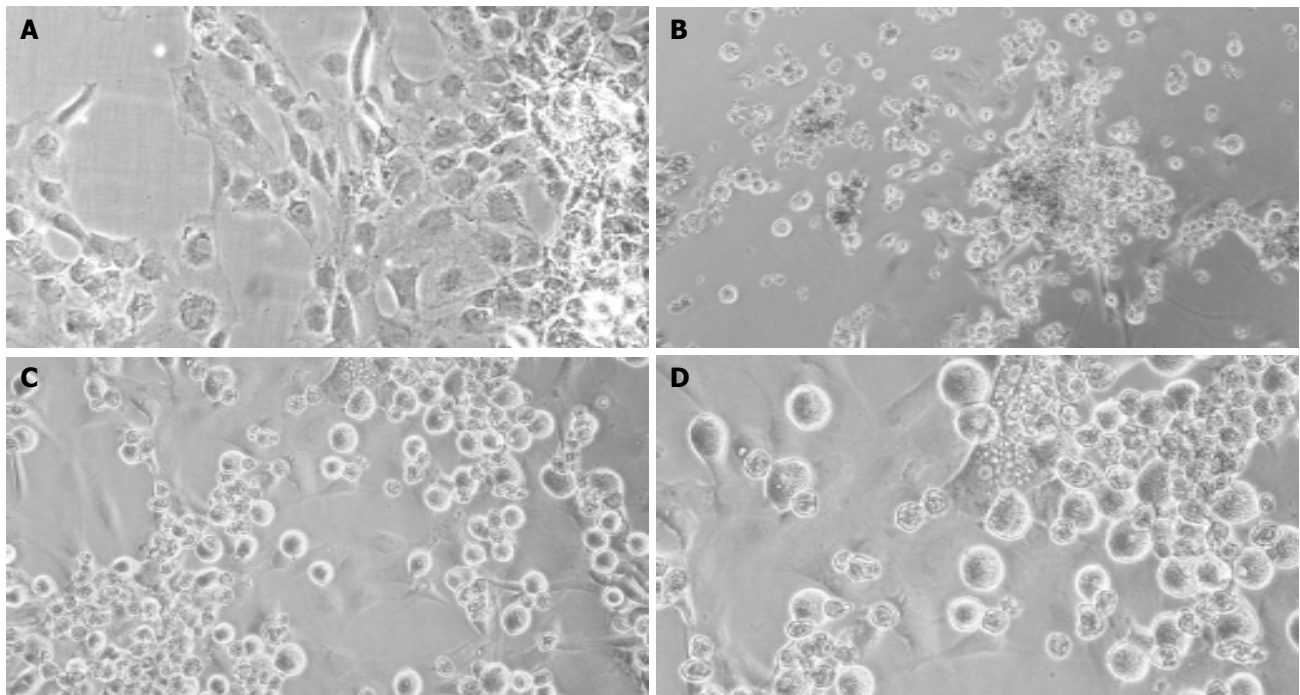


Figure 2 Light-microscopic pictures of cultured cells. Cultured rMSC (A), hepatocyte controls (B), or cocultures of rMSC with hepatocytes (C + enlargement D) after 3 wk. Cultured rMSC grew adherent and adopted a polygonal cell morphology after weeks in culture (A). Hepatocytes formed clumps of rounded cells, and few viable cells were observed after 3 wk in culture (B). In mixed cultures,

mainly MSC attached to the substratum, whereas hepatocytes grew over the MSC-layer forming clusters (C). Binucleated cells were found within the attached layer of the cultured MSC beginning with 1 wk in culture. Shown is one example at wk 2 out of three experiments. Original magnification $\times 200$.

primers. Samples were analyzed on 1% agarose gels. The size of the PCR-fragments was estimated using a 100-base-pair ladder (Gibco BRL).

RESULTS

Culture morphology

rMSC cultured alone attached to the culture substratum within 3 h and grew to confluency within 3 d as long, spindle-shaped cells. Within 3 wk, they adopted a polygonal cell morphology (Figure 2A). Freshly isolated hepatocytes were round in shape and showed a high nuclear to cytoplasm ratio. A minimal proportion of cells attached within the 1st day to the culture substratum. In the first week of culture, the cells tend to form clumps of rounded cells. After 3 wk, only few viable cells were found in the cultures of

hepatocytes alone (Figure 2B). In mixed cultures, mainly mesenchymal cells attached to the culture substratum, whereas hepatocytes attached to the mesenchymal cell layer forming clusters (Figure 2C). Hepatocytes were smaller in size compared to mesenchymal stem cells. From the second week onwards big polygonal shaped diploid (Figure 2D) cells were observed in the attached cell layer. As revealed by morphological studies, attached and adjacent cells were still viable after 21 d in the cocultures.

Gene-expression of GFP+ rMSC

GFP-transduced rat MSC ($\geq P9$) showed no expression of the liver specific genes, CK-18, CK-19, albumin, or AFP, as detected by RT-PCR (Figure 3, lanes M). In contrast, fetal liver cells as positive control cells revealed a constant expression of all markers analyzed (Figure 3, lanes C).

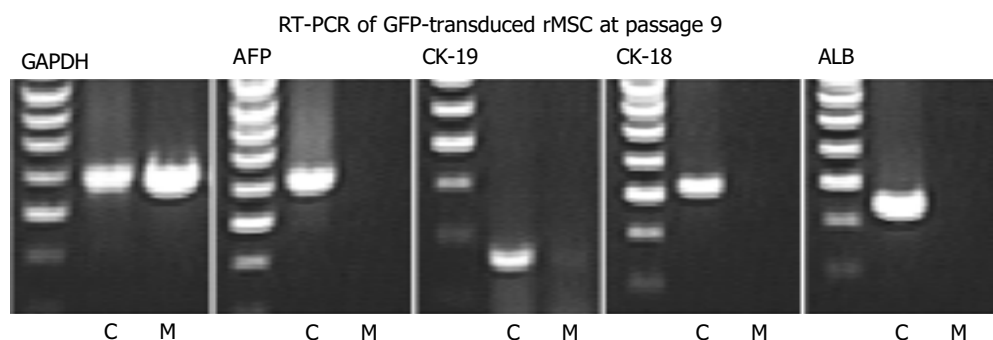


Figure 3 RT-PCR analysis of cloned GFP+ rMSC. rMSC (M) and liver control cells (C) were investigated before differentiation. GAPDH showed a strong signal in both liver controls and rMSC, whereas no liver specific genes (AFP,

CK-19, CK-18, and albumin ALB) were expressed in GFP+rMSC (results from one out of three experiments).

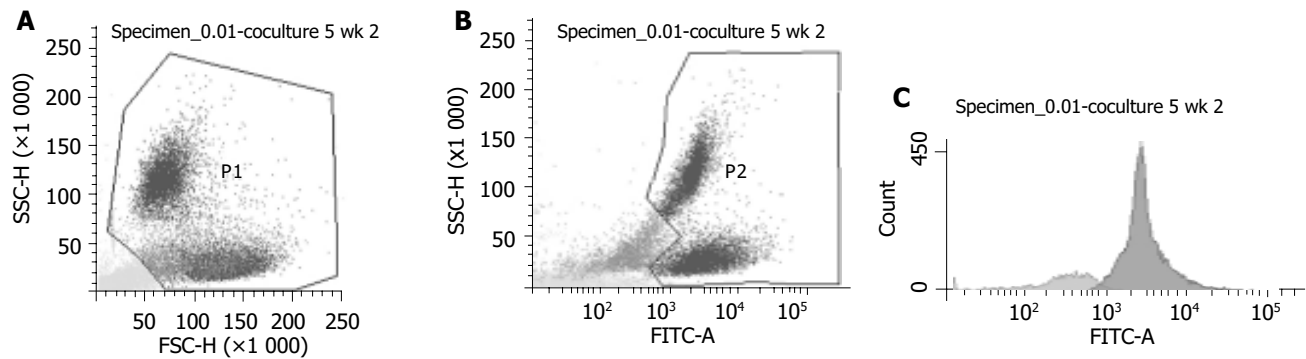


Figure 4 FACS-pictograms. One example out of three experiments from sorting of GFP+ and GFP- cells of cocultures at wk 2 is shown. **A:** Viable cells were gated as P1; **B:** P1 cells were gated in GFP- or GFP+ (P2); **C:** For highest purification of GFP+ cells, P2 was analyzed and only GFP+

cells were sorted in the sample tube for PCR-analysis (dark gray peak). 80.8% of cells from P2 were GFP+(sorted into the GFP+ test tube) and 19.2% were GFP-.

FAC sorting of cocultured cells

The sorting strategy aimed at maximal purity of GFP+ cells to exclude contamination with hepatocyte-derived RNA used in the RT-PCR. A representative example for FACS-sorting 2 wk after coculture from 1 out of 3 experiments is shown in Figure 4. First, the viable cells were gated according to forward and side scatter properties (Figure 4A). Two populations were seen, which varied in size and granulation. GFP-expression of this gated cells were detected in two populations, differing in granulation (Figure 4B) and were gated as P2. From these P2-cells, the contaminating GFP-cells were sorted out (Figure 4C). All non-P1, non-P2 and non-GFP cells were collected as GFP-cells.

Comparing the number of seeded cells set as 100%, recovered cell numbers were decreased at all three time points in two experiments (Figure 5). In one experiment, cocultured cells proliferated between wk 1 and 2 leading to a non-significant increase at d 14 in the mean of all experiments. An identical picture was observed for sorted GFP+ and GFP- cells: in 2 wk a slight increase in the number of GFP-cells and the maintenance of GFP+ counts could be observed. It is important to note that the GFP-cell population contained not only hepatocytes but also all dead/dying cells as well as conflicting events.

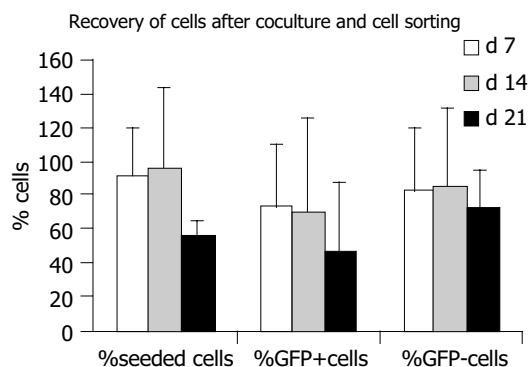


Figure 5 Recovery of cultured cells in cocultures. Recovery of seeded cells decreased from 91.6 ± 28.8 % in the 1st wk towards 56.7 ± 8.6 % in the 3rd wk (data from 3 experiments). Recovery of GFP+ cells decreased from 72.2 ± 38.5 % to 46.3 ± 41.6 %, and recovery of GFP-cells from 81.9 ± 38.2 % to 71.5 ± 24.3 % from the 1st to the 3rd wk in culture, respectively.

Gene-expression of Thy1 in GFP+ rMSC cocultured with hepatocytes

GFP+ and GFP-cells from cocultures showed a stable Thy1 gene-expression (Figure 6A) over the whole observation period (lanes GFP-or GFP+ cocultures). Also, in cultures of rMSC, a stable Thy1 expression was observed (lane rMSC), whereas hepatocytes showed no Thy1 expression (Figure 6A, lane rHep).

Liver specific gene-expression (AFP, CK-19, CK-18, albumin)

GAPDH expression in cultured rMSC, hepatocytes, GFP+ and GFP-FACS-sorted cells was similar at all time points (not shown). Although we used the same amounts of cDNA for all analyses, we found slightly different signals. Therefore, only semiquantitative assessments were possible. Cultures of rMSC alone showed no expression for AFP, CK-19, CK-18, or albumin (Figure 6B-E, lane rMSC). Cultured hepatocytes were found to express AFP and CK-19 weakly, and CK-18 and albumin stable over the whole culture period (Figure 6 B-E, lane rHep). In mixed cultures, the GFP-cells (lane GFP-cocultures) showed a strong expression of AFP (Figure 6B), albumin (Figure 6E) and CK-19 (Figure 6C), and a weak expression of CK-18 (Figure 6D). The GFP+ cells (lane GFP+ cocultures) showed a stable expression of AFP (Figure 6B), CK-18 (Figure 6D), and albumin (Figure 6E), and weak expression of CK-19 (Figure 6C), respectively. Negative controls without template were negative at all times and probes (not shown).

DISCUSSION

In this study, cloned GFP+ rMSC from passage ≥ 9 were used to analyze hepatic differentiation potential of MSC. For liver specific differentiation, cells were cultured on a fibronectin matrix in serum-free medium containing the hepatocytic growth factors- HGF, EGF, FGF-4, and the stem cell growth factor- SCF. The impact of liver cells on hepatic differentiation was assessed in cocultures of GFP+ rMSC with freshly isolated rat hepatocytes (GFP-negative) and was compared to pure cultures of rMSC or hepatocytes, respectively. For gene-expression analysis, cells from cocultures were separated in GFP+ or GFP-cells by FACS-sorting before RT-PCR analysis (Figure 1).

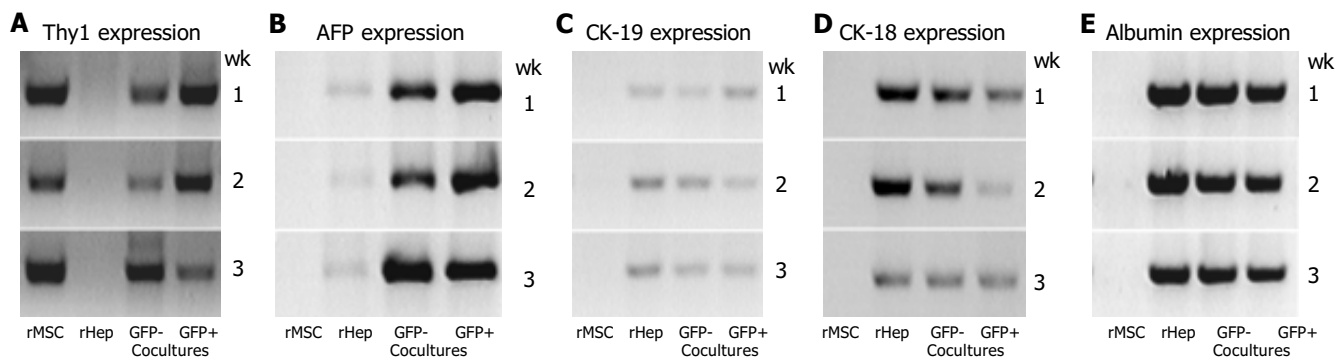


Figure 6 Gene expression profile. Cultured rMSC, hepatocytes (rHep), and GFP+ or GFP- cells of the cocultures after 1-3 wk were investigated for their expression of the stem cell marker Thy1 (A) and of the liver specific markers AFP (B), CK-19 (C), CK-18 (D), or albumin (E). Results from one out of three experiments are shown. rMSC (lane rMSC), GFP- (lane GFP- cocultures) or GFP+ (lane GFP+ cocultures) cells showed a stable Thy1 gene expression over the whole observation period, whereas hepatocytes (lane rHep) showed no signal for Thy1 gene expression in the RT-PCR analysis (A). In cultures of hepatocytes, GFP- or GFP+ cells show, the expression of the studied liver

markers was observed, whereas in cultured rMSC none of the studied liver specific genes was observed at all time points (B-E). Cultured hepatocytes expressed AFP and CK-19 weakly (B and C), and CK-18 (D) and albumin (E) stable. GFP- cells from cocultures showed a stable expression of AFP (B), CK-19 (C) or albumin (E), and a weak signal for CK-18 expression (D). The GFP+ cells showed a stable expression of the liver specific genes AFP (B), CK-18 (D), and albumin (E), and a weak expression of CK-19 (C) over the whole observation period.

AFP in the liver is a marker of immature (e.g. fetal) liver cells or oval cells in adult liver^[36]. CK19 has been shown to be expressed on hepatic oval cells as well as on adult biliary epithelial cells. Albumin is a typical marker of mature hepatocytes, whereas CK18 is expressed by several liver cells types, including biliary epithelial cells and hepatic oval cells^[37]. Our data indicated, that rMSC possess a differentiation potential towards hepatocytic cells *in vitro*; expression of the liver specific genes CK-18, albumin, CK-19, and AFP was demonstrated in GFP+ cells of the cocultures for the observation period of 3 wk. Thy1 is a marker for CD34-positive stem cells, activated endothelial cells and fetal liver cells^[38,39]. In the adult liver, Thy1 is expressed on oval cells but not on mature hepatocytes^[37,40]. It has also been found on mesenchymal stem cells generated from rat bone marrow^[41,42]. Expression of Thy1 in cultured MSC suggests that the rMSC should have the potential to differentiate toward hepatic cells by exhibition of a liver stem cell-like gene expression profile, as it is found in adult liver stem cells (oval cells). Oval cells are tissue residing liver stem cells, which possess a bipotential ability to generate biliary and hepatocytic cells, which can clonally repopulate the regenerating liver under certain conditions (reviewed in Ref.^[37]). Also, for other multipotential stem cell types from bone marrow, a hepatocytic differentiation potential was shown: sorted hematopoietic stem cells^[14,23], side population cells in the liver derived from bone marrow^[43], or multipotential adult progenitor cells^[30] were found to express liver specific genes, when cultured in the presence of certain growth factors. Previous studies in our laboratory have shown the tri-lineage differentiation potential of the cloned rMSC used, e.g. into adipogenic, chondrogenic, or osteogenic cells^[41]. In the present study, an additional differentiation potential towards hepatic progenitor cells was shown for the first time for clonally derived MSC. Thus, MSC seem to possess a multilineage differentiation potential, including a potential to differentiate into hepatocyte-like cells at least *in vitro*.

In our study, we found that hepatocyte-specific gene

expression was induced by the coculture of isolated hepatocytes. Cultured rMSC alone did not express any of the liver specific genes studied in the presence of a FN-coating and hepatic growth factors, suggesting that the added growth factors are not sufficient to induce hepatic differentiation. In contrast, a hepatocyte-like gene expression profile was observed in rMSC-derived cells in cocultures with hepatocytes. Additionally, we found binucleated GFP+ cells beginning with wk 1 (in the adult rat liver $\approx 10\%$ are binucleated cells). Very recently, a first report described the differentiation of rMSC into hepatocytic cells induced by growth factors. However, the authors used non-clonal cells of early passages. According to our experience, MSC isolated from bone marrow of rodents in early passages still contain hematopoietic cells. Thus, in these experiments a differentiation of contaminating cells into hepatic lineages cannot be conclusively excluded. In our experiments, a differentiation of MSC into hepatic cells without coculture was not successful. This could be due to either an impaired differentiation capability of the chosen clonal MSC or the high purity of MSC without contamination of HSC.

It has been shown that MSC express HGF as well as the respective receptor, c-met^[44]. Thus, MSC should be accessible for differentiation induction via this pathway. Furthermore, cocultured liver cells (GFP-) also showed a stable liver specific gene expression and viability over the whole observation period, whereas the hepatocyte controls rapidly lost cell viability and differentiation within the first week of culture. This is consistent with findings of other groups that investigated the differentiation of stem cells into hepatic lineages using coculture models. A positive influence for the induction of hepatocyte-specific genes in stem cells was found to be dependent on the presence of hepatocytes, even in cultures with separation of the cells by a semi-permeable membrane^[23,24]. A coculture of hepatocytes with stromal bone marrow cells allowing cell-cell contacts was first established by Mizuguchi *et al.*^[45]. They found that in cocultures the proliferation of hepatocytes and small hepatocytes was significantly enhanced by marrow stromal

cells compared to controls. Furthermore, a prolonged hepatocyte-specific gene expression was demonstrated by analysis of the markers, albumin^[45] and tryptophan dioxygenase, and activated hepatocyte-specific transcription factors were revealed by Northern blot analysis. By immunolabeling, the presence of Jagged1 protein was found in the cocultured marrow stromal cells^[24] and it was suggested to mediate differentiation events via the Notch signal pathway. However, no analysis of differentiation of the cocultured MSC was performed. Okumoto *et al.*, highlighted the role of the Jagged1 and Notch expression as one pathway of bone marrow cell differentiation towards hepatocytic cells^[24]. Thus, a liver-specific differentiation of stroma cells might be possible but remained unknown from these studies. The cells used in our study were similarly generated from bone marrow, at least they were characterized by plastic adherence and clonal expansion. It is important to note, that the coculture of MSC and hepatocytes seemed also to improve the viability of the cultured hepatocytes.

Our *in vitro* data indicate that mesenchymal stem cells from rat bone marrow possess a differentiation capacity towards hepatocytic cells *in vitro*. Furthermore, we showed a strong influence of cocultures with isolated liver cells permitting cell-to-cell contacts for the induction of liver specific gene expression of cultured stem cells. Bone marrow-derived liver stem cells, and herein the MSC are promising candidates for new cell-based approaches for the treatment of liver diseases^[46]: (1) these cells can easily be harvested from adult bone marrow and expanded tremendously *in vitro*; (2) transduction of MSC may result in the expansion of “cured” daughter cells; (3) the use of adult stem cells is favorable over other stem cells, such as embryonic stem cells or fetal stem cells, regarding ethical issues; (4) MSC have been proven to suppress T-cell activation in unrelated donor-recipient situations and seem to be an alternative in some areas of tissue regeneration^[47]. The differentiation of such cells toward liver cells by cocultures may permit the generation of artificial liver tissue for tissue engineering of the liver or liver cell transplantation^[48]. In our experiments, we have not investigated the influence of fusion on differentiation of MSC into hepatic cells. Still, the debate about fusion or true “transdifferentiation” continues. For liver cells, fusion seems to be a common process. However, for our experimental setting the mechanism remains to be explored in future. But even in the case of fusion, the generated cells would be equipped with two new informations: expansion and hepatic differentiation. Thus, the potential of MSC to differentiate towards potential liver cells should be of high interest for new cell-based therapies. Therefore, coculture of rMSC with hepatocytes is a model worth studying for further characterization of the mechanisms underlying a differentiation of stem cell into the hepatocytic lineage.

ACKNOWLEDGMENTS

We thank Arne Düsedau, Heinrich Pette Institute of the University of Hamburg, for FACS-sorting and Mrs. B. Roth, Department of Pediatric Surgery, for technical assistance.

REFERENCES

- 1 **Petersen BE**, Bowen WC, Patrene KD, Mars WM, Sullivan AK, Murase N, Boggs SS, Greenberger JS, Goff JP. Bone Marrow as a potential Source of Hepatic Oval Cells. *Science* 1999; **284**: 1168-1170
- 2 **Theise ND**, Badve S, Saxena R, Henegariu O, Sell S, Crawford JM, Krause DS. Derivation of hepatocytes from bone marrow cells in mice after radiation induced myeloablation. *Hepatology* 2000; **31**: 2352-2340
- 3 **Alison MR**, Poulosom R, Jeffery R, Dhillon AP, Quaglia A, Jacob J, Novelli M, Prentice G, Williamson J, Wright NA. Hepatocytes from non-hepatic adult stem cells. *Nature* 2000; **406**: 257
- 4 **Theise ND**, Nimmakayalu M, Gardner R, Illei PB, Morgan G, Teperman L, Henegariu O, Krause DS. Liver from bone marrow in humans. *Hepatology* 2000; **32**: 11-16
- 5 **Korbling M**, Katz RL, Khanna A, Ruifrok AC, Rondon G, Albitar M, Champlin RE, Estrov Z. Hepatocytes and epithelial cells of donor origin in the recipients of peripheral blood stem cell transplantation. *N Engl J Med* 2002; **346**: 738-746
- 6 **Lagasse E**, Connors H, Al-Dhalimy M, Reitsma M, Dohse M, Osborne L, Wang X, Finegold M, Weissman IL, Grompe M. Purified hematopoietic stem cells can differentiate into hepatocytes *in vivo*. *Nat Med* 2000; **6**: 1229-1234
- 7 **Wang X**, Willenbring H, Akkari Y, Torimaru Y, Foster M, Al-Dhalimy M, Lagasse E, Finegold M, Olson S, Grompe M. Cell fusion is the principal source of bone marrow derived hepatocytes. *Nature* 2003; **422**: 897-901
- 8 **Vassilopoulos G**, Wang PR, Russell DW. Transplanted bone marrow regenerates liver by cell fusion. *Nature* 2003; **422**: 901-904
- 9 **Wang X**, Ge S, McNamara G, Hao QL, Crooks GM, Nolte JA. Albumin-expressing hepatocyte-like cells develop in the livers of immune-deficient mice that received transplants of highly purified human hematopoietic stem cells. *Blood* 2003; **101**: 4201-4208
- 10 **Ishikawa F**, Drake CJ, Yang S, Fleming P, Minamiguchi H, Visconti RP, Crosby CV, Argraves WS, Harada M, Key LL Jr, Livingston AG, Wingard JR, Ogawa M. Transplanted human cord blood cells give rise to hepatocytes in engrafted mice. *Ann N Y Acad Sci* 2003; **996**: 174-185
- 11 **Newsome PN**, Johannessen I, Boyle S, Dalakas E, McAulay KA, Samuel K, Rae F, Forrester L, Turner ML, Hayes PC, Harrison DJ, Bickmore WA, Plevris JN. Human cord blood-derived cells can differentiate into hepatocytes in the mouse liver with no evidence of cellular fusion. *Gastroenterology* 2003; **124**: 1891-1900
- 12 **Jang YY**, Collector MI, Baylin SB, Diehl AM, Sharkis SJ. Hematopoietic stem cells convert into liver cells within days without fusion. *Nat Cell Biol* 2004; **6**: 532-539
- 13 **Oh SH**, Miyazaki M, Kouchi H, Inoue Y, Sakaguchi M, Tsuji T, Shima N, Higashio K, Namba M. Hepatocyte growth factor induces differentiation of adult rat bone marrow cells into hepatocyte lineage *in vitro*. *Biochem Biophys Res Commun* 2000; **279**: 500-504
- 14 **Fiegel HC**, Lioznov MV, Cortes-Dericks L, Lange C, Kluth D, Fehse B, Zander AR. Liver specific gene expression in cultured human hematopoietic stem cells. *Stem Cells* 2003; **21**: 98-104
- 15 **Kakinuma S**, Tanaka Y, Chinzei R, Watanabe M, Shimizu-Saito K, Hara Y, Teramoto K, Arai S, Sato C, Takase K, Yasumizu T, Teraoka H. Human umbilical cord blood as source of transplantable hepatic progenitor cells. *Stem Cells* 2003; **21**: 217-227
- 16 **Block GD**, Locker J, Bowen WC, Petersen BE, Katyal S, Strom SC, Riley T, Howard TA, Michalopoulos GK. Population expansion, clonal growth, and specific differentiation patterns in primary cultures of hepatocytes induced by HGF/SF, EGF, and TGF alpha in a chemically defined (HGM) medium. *J Cell Biol* 1996; **132**: 1133-1149
- 17 **Reid LM**. Stem cell biology, hormone/matrix synergies and liver differentiation. *Curr Opin Cell Biol* 1990; **2**: 121-130

- 18 **Mooney D**, Hansen L, Vacanti J, Langer R, Farmer S, Ingber D. Switching from differentiation to growth in hepatocytes: Control by extracellular matrix. *J Cell Physiol* 1992; **151**: 497-505
- 19 **Berthiaume F**, Moghe PV, Toner M, Yarmush ML. Effect of extracellular matrix topology on cell structure, function, and physiological responsiveness: hepatocytes cultured in a sandwich configuration. *FASEB J* 1996; **10**: 1471-1484
- 20 **Guguen-Guillouzo C**, Clement B, Baffet G, Beaumont C, Morel-Chany E, Glaize D, Guillouzo A. Maintenance and reversibility of active albumin secretion by adult rat hepatocytes co-cultured with another liver epithelial cell type. *Exp Cell Res* 1983; **143**: 47-54
- 21 **Shimaoka S**, Nakamura T, Ichihara A. Stimulation of growth of primary cultured adult rat hepatocytes without growth factors by coculture with nonparenchymal liver cells. *Exp Cell Res* 1987; **172**: 228-242
- 22 **Miyazaki M**, Akiyama I, Sakaguchi M, Nakashima E, Okada M, Kataoka K, Huh NH. Improved conditions to induce hepatocytes from rat bone marrow cells in culture. *Biochem Biophys Res Commun* 2002; **298**: 24-30
- 23 **Avital I**, Inderbitzin D, Aoki T, Tyan DB, Cohen AH, Ferrareso C, Rozga J, Arnaout WS, Demetriou AA. Isolation, characterization, and transplantation of bone marrow derived hepatocyte stem cells. *Biochem Biophys Res Commun* 2001; **288**: 156-164
- 24 **Okumoto K**, Saito T, Hattori E, Ito JI, Adachi T, Takeda T, Sugahara K, Watanabe H, Saito K, Togashi H, Kawata S. Differentiation of bone marrow cells into cells that express liver-specific genes *in vitro*: implication of the Notch signals in differentiation. *Biochem Biophys Res Commun* 2003; **304**: 691-695
- 25 **Bhatia SN**, Balis UJ, Yarmush ML, Toner M. Effect of cell-cell interactions in preservation of cellular phenotype: cocultivation of hepatocytes and nonparenchymal cells. *FASEB J* 1999; **13**: 1883-1900
- 26 **Friedenstein AJ**, Gorskaja JF, Kulagina NN. Fibroblast precursors in normal and irradiated mouse hematopoietic organs. *Exp Hematol* 1976; **4**: 267-274
- 27 **Caplan AI**. Mesenchymal stem cells. *J Orthop Res* 1991; **9**: 641-650
- 28 **Azizi SA**, Stokes D, Augelli BJ, DiGirolamo C, Prockop DJ. Engraftment and migration of human bone marrow stromal cells implanted in the brains of albino rats-similarities to astrocyte grafts. *Proc Natl Acad Sci USA* 1998; **95**: 3908-3913
- 29 **Pittenger MF**, Mackay AM, Beck SC, Jaiswal RK, Douglas R, Mosca JD, Moorman MA, Simonetti DW, Craig S, Marshak DR. Multilineage potential of adult human mesenchymal stem cells. *Science* 1999; **284**: 143-147
- 30 **Schwartz RE**, Reyes M, Koodie L, Jiang Y, Blackstad M, Lund T, Lenvik T, Johnson S, Hu WS, Verfaillie CM. Multipotent adult progenitor cells from bone marrow differentiate into functional hepatocyte-like cells. *J Clin Invest* 2002; **109**: 1291-1302
- 31 **Spees JL**, Olson SD, Ylostalo J, Lynch PJ, Smith J, Perry A, Peister A, Wang MY, Prockop DJ. Differentiation, cell fusion, and nuclear fusion during *ex vivo* repair of epithelium by human adult stem cells from bone marrow stroma. *Proc Natl Acad Sci USA* 2003; **100**: 2397-2402
- 32 **Li Z**, Schwieger M, Lange C, Kraunus J, Sun H, van den Akker E, Modlich U, Serinsoz E, Will E, von Laer D, Stocking C, Fehse B, Schiedlmeier B, Baum C. Predictable and efficient retroviral gene transfer into murine bone marrow repopulating cells using a defined vector dose. *Exp Hematol* 2003; **31**: 1206-1214
- 33 **Kuhlcke K**, Fehse B, Schilz A, Loges S, Lindemann C, Ayuk F, Lehmann F, Stute N, Fauser AA, Zander AR, Eckert HG. Highly efficient retroviral gene transfer based on centrifugation-mediated vector preloading of tissue culture vessels. *Mol Ther* 2002; **5**: 473-478
- 34 **Seglen PO**. Preparation of rat liver cells. *Methods Cell Biol* 1976; **13**: 29-83
- 35 **Kaufmann PM**, Kneser U, Fiegel HC, Pollok JM, Kluth D, Izbicki JR, Herbst H, Rogiers X. Is there an optimal concentration of cotransplanted islets of Langerhans for stimulation of hepatocytes in three dimensional matrices? *Transplantation* 1999; **68**: 272-279
- 36 **Brill S**, Holst P, Sigal S, Zvibel I, Fiorino A, Ochs A, Somasundaran U, Reid LM. Hepatic progenitor populations in embryonic, neonatal, and adult liver. *Proc Soc Exp Biol Med* 1993; **204**: 261-269
- 37 **Thorgeirsson SS**. Hepatic stem cells in liver regeneration. *FASEB J* 1996; **10**: 1249-1256
- 38 **Fiegel HC**, Park JJ, Lioznov MV, Martin A, Jaeschke-Melli S, Kaufmann PM, Fehse B, Zander AR, Kluth D. Characterization of cell types during rat liver development. *Hepatology* 2003; **37**: 148-154
- 39 **Fiegel HC**, Kluth J, Lioznov MV, Holzhter S, Fehse B, Zander AR, Kluth D. Hepatic lineages isolated from developing rat livers show different ways of maturation. *Biochem Biophys Res Commun* 2003; **305**: 46-53
- 40 **Petersen BE**, Goff JP, Greenberger JS, Michalopoulos GK. Hepatic oval cells express the hematopoietic stem cell marker Thy-1 in the rat. *Hepatology* 1998; **27**: 433-445
- 41 **Lange C**, Jaquet K, Krause K, Kuck KH, Zander AR. Myogenic differentiation of rat mesenchymal stem cells [abstract]. *Exp Hematol* 2003; **31**(Suppl 1): 181
- 42 **Javazon EH**, Colter DC, Schwarz EJ, Prockop DJ. Rat marrow stromal cells are more sensitive to plating density and expand more rapidly from single-cell-derived colonies than human marrow stromal cells. *Stem Cells* 2001; **19**: 219-225
- 43 **Wulf GG**, Luo KL, Jackson KA, Brenner MK, Goodell MA. Cells of the hepatic side population contribute to liver regeneration and can be replenished by bone marrow stem cells. *Haematologica* 2003; **88**: 368-378
- 44 **Neuss S**, Becher E, Woltje M, Tietze L, Jahnen-Dechent W. Functional expression of HGF and HGF receptor/c-met in adult human mesenchymal stem cells suggests a role in cell mobilization, tissue repair, and wound healing. *Stem Cells* 2004; **22**: 405-414
- 45 **Mizuguchi T**, Hui T, Palm K, Sugiyama N, Mitaka T, Demetriou AA, Rozga J. Enhanced proliferation and differentiation of rat hepatocytes cultured with bone marrow stromal cells. *J Cell Physiol* 2001; **189**: 106-119
- 46 **Mitaka T**. Hepatic stem cells: from bone marrow cells to hepatocytes. *Biochem Biophys Res Commun* 2001; **281**: 1-5
- 47 **Maitra B**, Szekely E, Gjini K, Laughlin MJ, Dennis J, Haynesworth SE, Koc ON. Human mesenchymal stem cells support unrelated donor hematopoietic stem cells and suppress T-cell activation. *Bone Marrow Transplant* 2004; **33**: 597-604
- 48 **Mitaka T**. Reconstruction of hepatic organoid by hepatic stem cells. *J Hepatobiliary Pancreat Surg* 2002; **9**: 697-703

Antibody to eosinophil cationic protein suppresses dextran sulfate sodium-induced colitis in rats

Kazuko Shichijo, Kazuya Makiyama, Chun-Yang Wen, Mutsumi Matsuu, Toshiyuki Nakayama, Masahiro Nakashima, Makoto Ihara, Ichiro Sekine

Kazuko Shichijo, Chun-Yang Wen, Mutsumi Matsuu, Toshiyuki Nakayama, Ichiro Sekine, Department of Molecular Pathology, Atomic Bomb Disease Institute, Nagasaki University Graduate School of Biomedical Sciences, 1-12-4 Sakamoto, Nagasaki 852-8523, Japan
Kazuya Makiyama, Department of Endoscopy, Nagasaki University School of Medicine Hospital and Clinics, 1-12-4 Sakamoto, Nagasaki 852-8523, Japan

Chun-Yang Wen, Department of Digestive Disease, the Affiliated Drum Tower Hospital of Nanjing University Medical School, Nanjing 210008, Jiangsu Province, China

Masahiro Nakashima, Tissue and Histopathology Section, Atomic Bomb Disease Institute, Nagasaki University Graduate School of Biomedical Sciences, 1-12-4 Sakamoto, Nagasaki 852-8523, Japan
Makoto Ihara, Radiation Biophysics, Atomic Bomb Disease Institute, Nagasaki University Graduate School of Biomedical Sciences, 1-12-4 Sakamoto, Nagasaki 852-8523, Japan

Supported by a grant-in-aid from the Ministry of Science, Education, Sports and Culture of Japan, No. 14570193

Correspondence to: Kazuko Shichijo, PhD, Department of Molecular Pathology, Atomic Bomb Disease Institute, Nagasaki University Graduate School of Biomedical Sciences, 1-12-4 Sakamoto, Nagasaki 852-8523, Japan. shichijo@net.nagasaki-u.ac.jp

Telephone: +81-95-849-7107 Fax: +81-95-849-7108

Received: 2004-10-25 Accepted: 2004-12-23

Abstract

AIM: To produce an antibody against rat eosinophil cationic protein (ECP) and to examine the effects of the antibody in rats with dextran sulfate sodium (DSS)-induced colitis.

METHODS: An antibody was raised against rat ECP. Rats were treated with 3% DSS in drinking water for 7 d and received the antibody or normal serum. The colons were examined histologically and correlated with clinical symptoms. Immunohistochemistry and Western blot analysis were estimated as a grade of inflammation.

RESULTS: The ECP antibody stained the activated eosinophils around the injured crypts in the colonic mucosa. Antibody treatment reduced the severity of colonic ulceration and acute clinical symptoms (diarrhea and/or blood-stained stool). Body weight gain was significantly greater and the colon length was significantly longer in anti-ECP-treated rats than in normal serum-treated rats. Expression of ECP in activated eosinophils was associated with the presence of erosions and inflammation. The number of Ki-67-positive cells in the regenerated surface epithelium increased in anti-ECP-treated rats compared with normal serum-treated rats. Western blot analysis revealed reduced expression of macrophage migration inhibitory factor (MIF)

in anti-ECP-treated rats.

CONCLUSION: Our results indicate that treatment with ECP antibody, improved DSS-induced colitis in rats, possibly by increasing the regenerative activity of the colonic epithelium and downregulation of the immune response, and suggest that anti-ECP may promote intestinal wound healing in patients with ulcerative colitis (UC).

© 2005 The WJG Press and Elsevier Inc. All rights reserved.

Key words: Ulcerative colitis; Eosinophil cationic protein; Dextran sulfate sodium

Shichijo K, Makiyama K, Wen CY, Matsuu M, Nakayama T, Nakashima M, Ihara M, Sekine I. Antibody to eosinophil cationic protein suppresses dextran sulfate sodium-induced colitis in rats. *World J Gastroenterol* 2005; 11(29): 4505-4510

<http://www.wjgnet.com/1007-9327/11/4505.asp>

INTRODUCTION

Eosinophil accumulation in the gastrointestinal tract is a common feature of numerous gastrointestinal disorders, including classic IgE-mediated food allergy, eosinophilic gastroenteritis, allergic colitis, eosinophilic esophagitis, inflammatory bowel disease (IBD)^[1-3] and gastroesophageal reflux disease. In IBD, eosinophils usually represent only a small percentage of the infiltrating leukocytes^[3,4] but their levels has been proposed as a negative prognostic indicator^[4,5]. Several studies have found an association between allergic colitis and later development of IBD, but this association is controversial^[6].

Eosinophils and one of their granule proteins, eosinophil cationic protein (ECP)^[7] and eosinophil protein X (EPX), are generally recognized as being involved in the host defense against invading parasites. They are markedly cationic proteins with cytotoxic capacities that can potentially cause tissue destruction and could act as modulators of immune response^[8]. The eosinophil may also be involved in the pathogenesis of IBD because we have already reported activation of eosinophils in patients with active ulcerative colitis (UC), using the techniques of indirect immunoenzymatic method and electron microscopic examination of eosinophils, measurement of serum ECP^[9,10], as well as increased percentages of hypodense eosinophils in the peripheral blood. Moreover, bowel biopsies from patients with IBD have demonstrated infiltration of eosinophils in the lamina

propria and marked extracellular deposits of ECP^[11,12]. There is also an excess release of the eosinophil proteins ECP and EPX in the luminal fluid and fecal material of patients with UC or Crohn's disease^[13]. However, the pathophysiological role played by activated eosinophils in the inflammatory process in UC has not yet been elucidated.

The aim of this study was to produce an antibody against rat ECP and to examine the antibody in dextran sulfate sodium (DSS)-induced colitis model. Rats treated with DSS develop severe colorectal damage mimicking IBD in humans^[14,15]. We herein present evidence for the effectiveness of ECP antibody against DSS-induced colitis in rats, possibly by increasing the regenerative activity of the colonic epithelium and downregulation of the immune response.

MATERIALS AND METHODS

Antibody raised against rat ECP

TRAQWFAIQHISLNPPR^[16] was synthesized based on human ECP amino acid sequence^[17], which has homology to rat ECP^[18]. Anti-ECP sera were generated by immunizing New Zealand white rabbits. In brief, rabbits were inoculated intradermally with 100 µg of ECP diluted in complete Freund's adjuvant at weeks 2, 4, 6, 8, 10, 12, and 14. The serum was prepared according to the protocol provided by the manufacturer.

Induction of experimental colitis

Male Wistar rats/IZM (8 wk old) were obtained from Charles River Japan, Inc. Rats were kept in a specific pathogen-free environment at the Animal Center in accordance with the rules and regulations of the Institutional Animal Care and Use Committee of Nagasaki University. Food as well as drinking water with or without DSS (MW 5 000; Wako Pure Chemical Industries, Osaka, Japan) were provided *ad libitum*. The rats were treated with 3% DSS in drinking water for 7 d^[19], and then received either antibodies or normal serum intraperitoneally. The rats were weighed daily and visually inspected for gross rectal bleeding and diarrhea. The colons were examined histologically and correlated with clinical symptoms. Hematoxylin and eosin (HE)-stained sections were prepared from the distal colon. The severity of ulceration was quantified by the Ulcer Index (ulcer length/circumference length, %) in the distal colon. Furthermore, the severity of colitis was evaluated by assessment of colon length and histological examination. Similarly, we evaluated the effect of anti-ECP antibodies with regard to clinical signs and pathologic features.

Administration of antibodies specific for ECP

The polyclonal ECP antibody (0.25 mL/rat at d 0 and 1, 0.5 mL/rat at d 2, 3, 4, 5, 6, and 7 after DSS treatment) or non-immune rabbit serum was injected intraperitoneally.

Immunohistochemical studies

Anti-ECP antibody as eosinophils, anti-ED1 antibody (Serotec, Oxford, UK) as activated macrophages, anti-Ki-67 antibody (MIB-5, Dako Cytomation Denmark A/S, Denmark) as proliferative cells were used. The sections were deparaffinized and rehydrated. Then, they were microwaved

for 10 min in 0.01 mol/L citrate buffer, pH 6.0, to unmask the antigenicity, and trypsin digested for 15 min, for Ki-67 and for ED1 as pre-treatment, respectively. The slides were placed in methanol with 0.3% H₂O₂ for 10 min to block endogenous peroxidase activity. They were then incubated with ECP, Ki-67, and ED1 for 60 min and further processed for immunohistochemistry using the Histofine Simple Stain kit (Nichirei, Tokyo, Japan). Peroxidase activity was developed in diaminobenzidine as a chromogen. In the procedures described above, tissue sections that were not incubated with ECP, ED1, or Ki-67 served as negative controls.

Western blot analysis

Western blots were prepared for expression of ED1 and macrophage migration inhibitory factor (MIF). For this purpose, the colonic tissue was collected from the lesion area, and then suspended in 5 volumes of ice-cold 50 mmol/L Tris-HCl (pH 7.2) containing 150 mmol/L NaCl, 1% NP-40, 1% sodium deoxycholate, and 0.05% SDS, broken into pieces on ice, and subjected to three freeze-thaw cycles. After centrifugation at 15 000 *g* for 10 min at 4 °C, 2-mercaptoethanol and bromophenol blue were added to the supernatant at final concentrations of 2% and 0.001%, respectively. The tissue extracts (30 µg protein) were subjected to 10% sodium dodecyl sulfate-polyacrylamide gel electrophoresis, and the separated proteins transferred onto Hybond ECL nitrocellulose membrane. After blocking nonspecific binding sites with 5% skim milk, the membrane was incubated with 1 000× diluted antibody, against ED1 and MIF (N-20, Santa Cruz Biotechnology, Inc.) at room temperature for 1 h. The bound antibodies were detected using an enhanced chemiluminescence detection kit (ECL Plus, Amersham Life Science, Buckinghamshire, UK) and the amount of each protein was quantified by densitometric analysis^[20].

Statistical analysis

All data were expressed as mean±SE. Differences between groups were examined for statistical significance using the Student's *t*-test or Cochran and Cox test. A *P* value less than 0.05 denoted the presence of a statistically significant difference.

RESULTS

Clinicopathological findings

The body weight gain was significantly greater in anti-ECP-treated rats at d 4 and 7 after DSS treatment compared with normal serum-treated rats (Figure 1). ECP antibody clearly reduced acute clinical symptoms (diarrhea and/or blood-stained stool, Table 1). Moreover, ECP antibody improved various mucosal parameters; it reduced colonic ulceration severity (Ulcer Index) from 61.1±25.5% (DSS) to 43.1±29.4% (DSS+anti-ECP). The colon length was 13.4±0.4 cm in anti-ECP-treated rats and 12.3±0.6 cm in normal serum-treated rats at 7 d after DSS treatment (Table 2). DSS-induced shortening of the colon length was significantly abrogated in anti-ECP-treated rats (*P*<0.05).

ECP expression in normal colonic mucosa and in colitis

HE- and immunohistochemically-stained sections showed

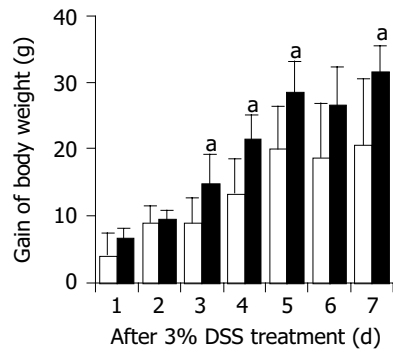


Figure 1 Changes in body weight in normal serum- (open columns), anti-ECP- (closed columns) treated rats during DSS treatment. The body weight gain after DSS treatment was significantly greater in anti-ECP-treated rats compared with normal serum-treated rats. Rats treated with the antibodies or normal serum intraperitoneally were also treated with 3% DSS in drinking water for 7 d ($n = 7$, $^aP < 0.05$ vs DSS+normal serum).

Table 1 Clinical findings

Time (d)	Gross bleeding		Diarrhea	
	NS	Anti-ECP	NS	Anti-ECP
1	0	0	0	0
2	0	14.3	14.3	14.3
3	14.3	0	14.3	14.3
4	0	0	0	0
5	14.3	0	28.6	14.3
6	42.9	14.3	28.6	0
7	42.9	28.6	0	0

Data are percentage of animals ($n = 7$).

Table 2 Effects of anti-ECP antibody on ulcer index and colon length (mean \pm SE, $n = 7$)

Group	Ulcer index (%) ¹	Colon length (cm)
DSS+normal serum	61.1 \pm 25.5	12.3 \pm 0.6
DSS+anti-ECP	43.1 \pm 29.4 ^a	13.4 \pm 0.4 ^b

¹Ulcer length/circumference length \times 100. ^a $P < 0.05$ vs DSS+normal serum. ^b $P < 0.01$ vs DSS+normal serum.

eosinophils and ECP-positive eosinophils in close proximity to damaged crypts in the lamina propria and partially in the extracellular interstitium of the colon of rats with DSS-induced colitis (Figures 2A and B). The ECP antibody stained activated eosinophils. In the normal colon, eosinophil infiltration was hardly observed and ECP-positive activated eosinophils were never seen in the colonic tissue (data not shown).

Histological findings

ECP antibody treatment clearly suppressed DSS-induced colitis as confirmed in HE-stained sections (Figures 2C and D). Moreover, immunohistochemical studies for Ki-67 and ED1 revealed that the ECP antibody treatment increased the regenerative activity of the colonic epithelium and downregulation of immune response (Figure 3). Expression of ECP in activated eosinophils was associated with the presence of erosions and inflammation. The number of Ki-67-positive cells in the regenerative surface epithelium/circumference significantly increased in anti-ECP-treated

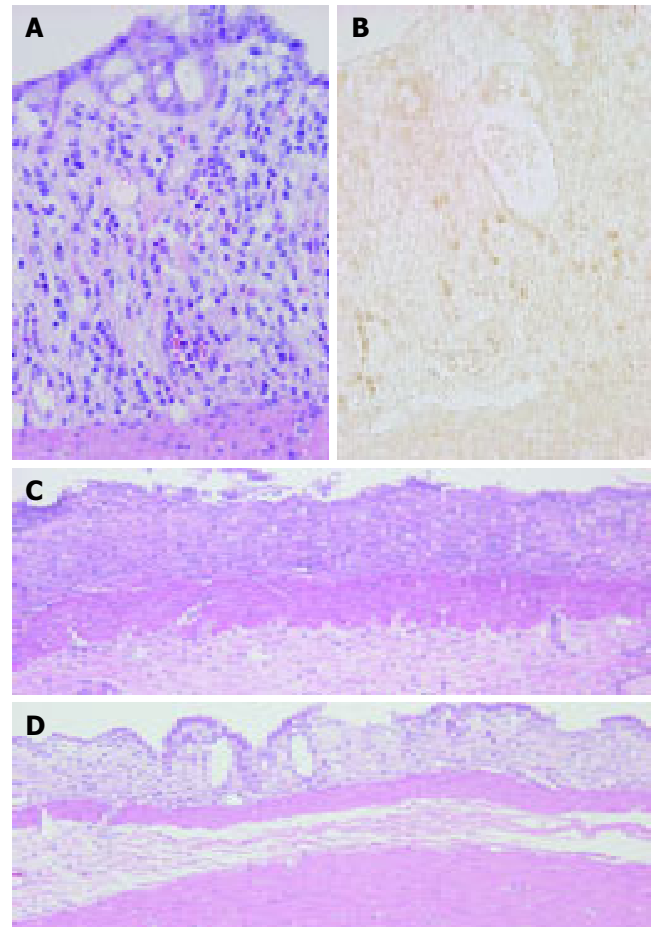


Figure 2 Colonic mucosa at 3 d post-DSS treatment showing eosinophils in the lamina propria. HE staining (A) and immunostaining for ECP (B) as described under Materials and methods. ECP-positive cells (brown) appear in close proximity to damaged crypts in the lamina propria and partially in the extracellular interstitium of DSS-induced colitis. Original magnification, $\times 400$. Colonic mucosa at 7-d treatment of DSS. (C) Colonic ulceration in normal serum-treated rats. (D) Reduced severity of colonic mucosal ulceration in anti-ECP-treated rats. HE stain. Original magnification, $\times 100$.

Table 3 Effects of anti-ECP antibody on the Ki-67-positive cells in the regenerative surface of colonic epithelium at d 7 after DSS treatment (mean \pm SE, $n = 7$)

Group	Ki-67-positive cells ¹
DSS+normal serum	14.0 \pm 6.5
DSS+anti-ECP	21.3 \pm 10.4 ^a

¹Number of Ki-67-positive cells/circumference. ^a $P < 0.05$ vs DSS+normal serum.

rats (21.3 \pm 10.4) compared with normal serum-treated rats (14.0 \pm 6.5) at d 7 after DSS treatment ($P < 0.05$, Table 3 and Figure 3).

The number of ED1-positive macrophages in the lamina propria of anti-ECP-treated rats at d 7 after DSS treatment was less than that in normal serum-treated rats. Moreover, the size of ED1-positive macrophages in the lamina propria of anti-ECP-treated rats at d 7 after DSS treatment was smaller than that of normal serum-treated rats.

Western blot analysis

ECP antibody treatment significantly downregulated

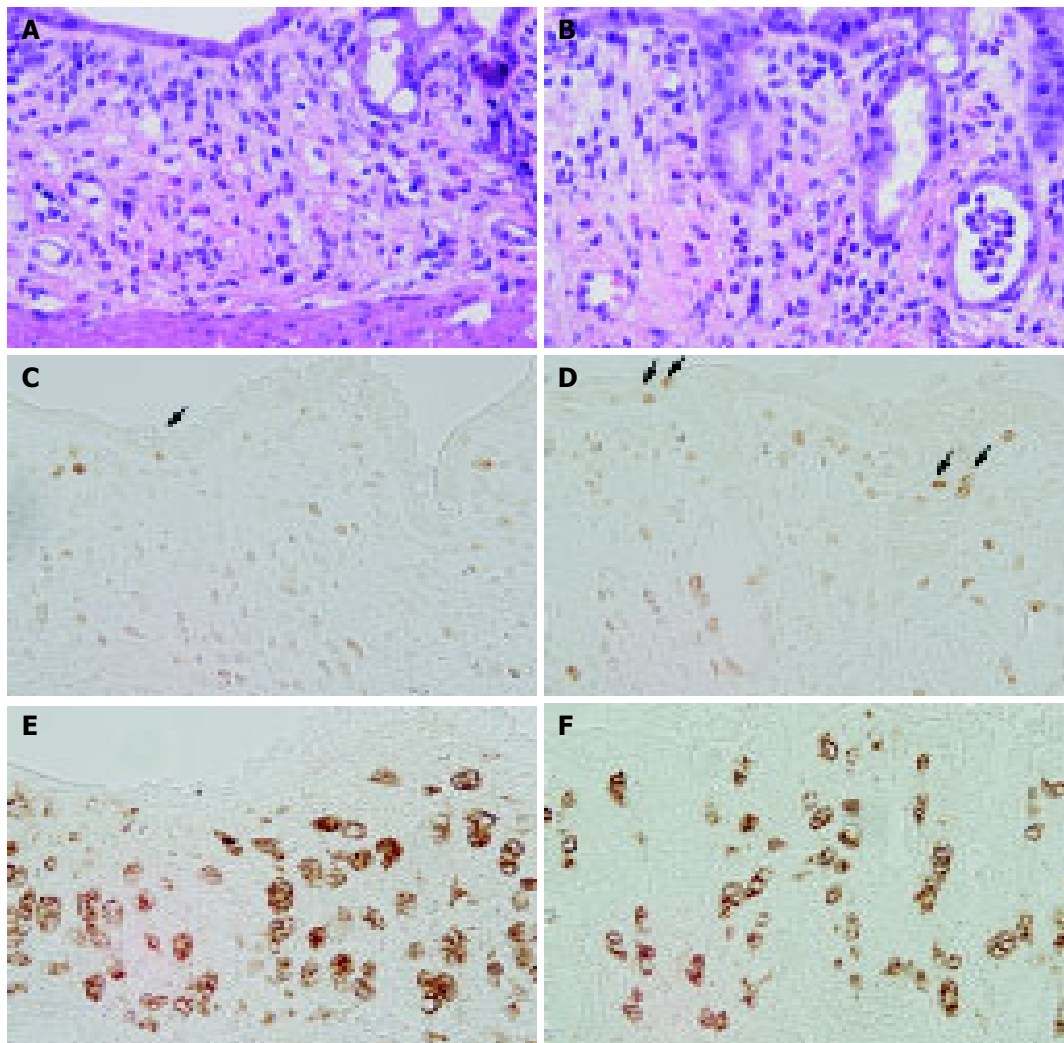


Figure 3 Colonic mucosa in normal serum-treated rats (A, C, and E) and anti-ECP1-treated rats (B, D, and F) at 7-d treatment of DSS. HE staining (A and B), immunostaining for Ki-67 (C and D) and ED1 (E and F) as described under Materials and methods. Treatment with ECP antibody increased the number of

Ki-67-positive cells in the regenerated surface epithelium and reduced the size of activated macrophages present in the lamina propria. Original magnification, $\times 400$.

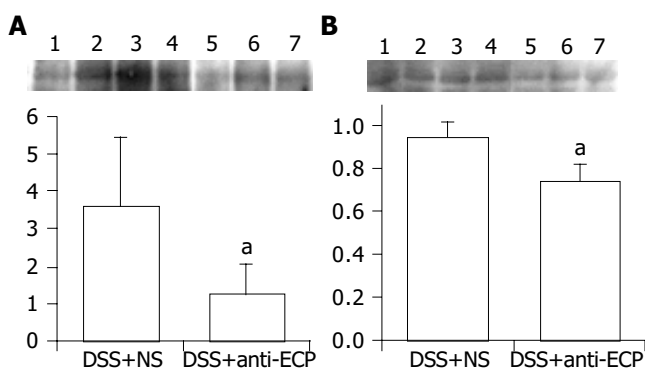


Figure 4 Detection of ED1 (A) and MIF (B) by Western blot analysis in colonic tissues after 7 d of DSS treatment in normal serum-treated rats (lanes 1-4) and anti-ECP-treated rats (lanes 5-7). The colonic tissue was collected from the lesion area and examined by Western blot analysis as described under Materials and methods. The relative expression levels of ED1 and MIF in the damaged colonic tissue were significantly lower in anti-ECP-treated rats than in normal serum-treated rats. The relative protein expression was quantified by densitometric analysis ($n = 7$, $^*P < 0.05$ vs DSS+normal serum).

colonic tissue at d 7 after DSS treatment decreased significantly in anti-ECP-treated rats. The relative ED1 expression was significantly lower in anti-ECP-treated rats (1.25 ± 0.79) than in normal serum-treated rats (3.62 ± 1.83 , $P < 0.05$, $n = 7$). Furthermore, the relative expression of MIF was significantly lower in anti-ECP-treated rats (0.74 ± 0.08) than in normal serum-treated rats (0.94 ± 0.08 , $P < 0.05$, $n = 7$).

DISCUSSION

A variety of clinical and experimental models has revealed that eosinophils promote pro-inflammatory changes mediated by their ability to release various cytotoxic substances and a variety of lipid mediators and cytokines. In type-2 helper T (Th2) cells-associated gastrointestinal inflammatory conditions, increased levels of eosinophils occur in the lamina propria in an eotaxin 1-dependent manner^[21]. After mucosal allergen challenge, eosinophils under the regulation of IL-5 accumulate in the esophagus, an organ normally devoid of eosinophils. However, the main role of IL-5 in DSS-induced colonic inflammation is to attract a population of eosinophils that do not appear to

macrophage activation during 7-d treatment of DSS (Figure 4). The expressions of both ED1 and MIF in the damaged

contribute significantly to the initiation or development of tissue damage in this model of colitis^[22].

In 1974, the existence of an eosinophil-granule protein, ECP, with a highly cytotoxic action, was reported by Olsson and Venge^[7]. ECP is antibacterial^[23], helminthotoxic^[24], elicits the Gordon phenomenon when injected intrathecally into rabbits, and is cytotoxic to tracheal epithelium^[25,26]. Although the mechanism of its cytotoxicity is not completely understood, it is suggested to be due to the pore-forming activity of ECP, which destabilizes lipid membranes^[27], but is unrelated to RNase activity^[28]. We demonstrated here that a polyclonal antibody to eosinophil granule protein ECP exhibits beneficial effects on various mucosal parameters of DSS-induced colitis in rats. ECP expressed in activated eosinophils of the colonic mucosa in DSS-induced colitis were associated with the presence of injured crypts and inflammation. The body weight gain was significantly greater in anti-ECP-treated rats, compared with control rats. The ECP antibody reduced acute clinical symptoms (diarrhea and/or blood-stained stool), severity of colonic ulceration and shortening of the colon length. Immunohistochemical studies for Ki-67 and ED1 revealed that ECP antibody treatment increased the regenerative activity of the colonic epithelium and downregulation of the immune response.

Mucosal repair involves both the rapid migration of cryptal enterocytes into the injured area of the mucosa, and replacement of the mucosa by cell replication^[29]. Various peptide growth factors regulate epithelial cell function within the mucosal epithelium of the gastrointestinal tract. Recently, Sinha *et al.*, reported preliminary data suggesting that epidermal growth factor enemas are effective in the treatment of active left-sided UC^[30]. Furthermore, Dignass *et al.*^[31], demonstrated that hepatocyte growth factor (HGF) modulates intestinal epithelial cell proliferation and migration, thus enhancing epithelial cell restitution, the initial step of gastrointestinal wound healing, in an *in vitro* model. Moreover, it was demonstrated that administration of recombinant human HGF lessened colitis-associated weight loss in rats as well as improved the clinical signs of colitis *in vivo*^[32]. In our rat model, mucosal erosion was observed on d 5 and accelerated on d 7, whereas the colon length was reduced on d 7. Importantly, the ECP antibody enhanced epithelial regeneration, leading to a reduction in size of colonic mucosal erosions, although it was administered concomitantly with DSS. In this regard, enhanced mucosal repair allows for a more rapid recovery of epithelial barrier function leading to reduced exposure to various luminal agents that contribute to persistent colitis. Accordingly, treatment with ECP antibody should reduce the inflammatory response to these luminal stimuli.

MIF was originally identified as a lymphokine derived from activated T cells that inhibits the random migration of macrophages *in vitro* and is involved in delayed-type hypersensitivity^[33]. Moreover, it is postulated that tumor necrosis factor (TNF)- α and interferon (IFN)- γ upregulate MIF production in macrophages and, conversely, MIF induces TNF- α production, forming a proinflammatory loop within the cytokine network^[34]. Gut monocyte macrophages are responsible for production of MIF, which in turn stimulates Th-1-type cytokines and features characteristic

of colitis. Swollen macrophages induced by DSS have been seen in the mucosa with gland dropout and inflammatory cell infiltration even under intact colonic epithelium^[35]. It seems that macrophage dysfunction, alterations of luminal bacteria, and DSS toxic effects on the colonic epithelium acted together to result in inflammatory ulcerative changes of the colonic mucosa. Therefore, in our study, the ECP antibody reduced macrophage activation such as the size of ED1-positive macrophages and the expressions of ED1 and MIF proteins in damaged colonic mucosa induced by DSS, resulting in downregulation of the immune response.

ECP is one of the major components of eosinophilic granules with a molecular mass ranging from 16 to 21.4 ku. It exhibits various biological effects both *in vitro* and *in vivo*^[8,36]. It is classified as a member of the ribonuclease (RNase) A supergene family based on the homology of both nucleotide and amino acid sequences. The homology of amino acid sequence between rat ECP^[18] and human ECP^[37] is 54%. When the amino acid sequence of rat ECP was compared with that of human ECP, eight structural cysteines and three amino acids, H15, K38, and H128, that are required for RNase activity^[37] were found to be highly conserved. The length of the signal peptide of rat ECP is equivalent to that of human ECP. Maeda *et al.*^[38], demonstrated that ECP is growth-inhibitory and this ability of ECP to bind to heparin or other carboxy hydrates on the cell surface is dependent on tryptophan residues, W10 and W35. Interestingly, W10 is located at the P2 subsite of the catalytic domain of RNase and controls the weak RNase activity of the protein^[39]. ECP alters the coagulation cascades^[40], augments fibrinolysis^[41], and regulates the classical pathway of complement^[42]. Our results showed that the ECP antibody clearly reduced acute clinical symptoms of blood-stained stool. Our evaluation of the ECP molecule including W10 and H15 in human ECP enabled us to test the beneficial effects of anti-ECP treatment on inflammatory disease, in which uncontrolled cell growth could contribute to a delay in wound healing. Further studies are needed to investigate this issue.

In summary, we demonstrated that treatment with an antibody to ECP improved DSS-induced colitis in rats possibly by increasing the regenerative activity of the colonic epithelium and downregulation of the immune response. This supports the concept that humanized anti-ECP treatment could also be an effective therapy for IBDs.

REFERENCES

- 1 **Dvorak AM.** Ultrastructural evidence for release of major basic protein-containing crystalline cores of eosinophil granules *in vivo*: cytotoxic potential in Crohn's disease. *J Immunol* 1980; **125**: 460-462
- 2 **Sarin SK, Malhotra V, Sen Gupta S, Karol A, Gaur SK, Anand BS.** Significance of eosinophil and mast cell counts in rectal mucosa in ulcerative colitis. A prospective controlled study. *Dig Dis Sci* 1978; **32**: 363-367
- 3 **Walsh RE, Gaginella TS.** The eosinophil in inflammatory bowel disease. *Scand J Gastroenterol* 1991; **26**: 1217-1224
- 4 **Desreumaux P, Nutten S, Colombel JF.** Activated eosinophils in inflammatory bowel disease: do they matter? *Am J Gastroenterol* 1999; **94**: 3396-3398
- 5 **Nishitani H, Okabayashi M, Satomi M, Shimoyama T, Dohi Y.** Infiltration of peroxidase-producing eosinophils into the lamina propria of patients with ulcerative colitis. *J Gastroenterol*

- 1998; **33**: 189-195
- 6 **Geajardo JR**, Rothenberg ME. Eosinophilic esophagitis, gastroenteritis, gastroenterocolitis, and colitis. In: *Food allergy: adverse reactions to foods and additives. 3rd ed*, edited by Metcalfe DD, Sampson HA, Simon RA, Malden (MA): Blackwell Publishing 2003: 217-226
- 7 **Olsson I**, Venge P. Cationic proteins of human granulocytes. II. Separation of the cationic proteins of the granules of leukemic myeloid cells. *Blood* 1974; **44**: 235-246
- 8 **Giembycz MA**, Lindsay MA. Pharmacology of the eosinophil. *Pharmacol Rev* 1999; **51**: 213-340
- 9 **Yamasaki K**, Makiyama K, Iwanaga S, Mizuta Y, Kubo K. Immunohistochemical study of eosinophil cationic protein on colonic mucosa of patients with ulcerative colitis. *Dig Organ Immunol* 1989; **22**: 74-77
- 10 **Yamasaki K**, Makiyama K. Eosinophil cationic protein (ECP) in ulcerative colitis. *Acta Med Nagasaki* 1994; **39**: 67-71
- 11 **Makiyama K**, Kanzaki S, Yamasaki K, Zea-Iriarte W, Tsuji Y. Activation of eosinophils in pathophysiology of ulcerative colitis. *J Gastroenterol* 1995; **30** (Suppl 8): 64-69
- 12 **Raab Y**, Fredens K, Gerdin B, Hallgren R. Eosinophil activation in ulcerative colitis: Studies on mucosal release and localization of eosinophil granule constituents. *Dig Dis Sci* 1998; **43**: 1061-1070
- 13 **Saitoh O**, Kojima K, Sugi K, Matsuse R, Uchida K, Tabata K, Nakagawa K, Kayazawa M, Hirata I, Katsu K. Fecal eosinophil granule derived proteins reflect disease activity in inflammatory bowel disease. *Am J Gastroenterol* 1999; **94**: 3513-3520
- 14 **Copper HS**, Murthy SN, Shah RS, Sedergran DJ. Clinicopathologic study of dextran sulfate sodium experimental murine colitis. *Lab Invest* 1993; **69**: 238-249
- 15 **Okayasu I**, Hatakeyama S, Yamada M, Ohkusa T, Inagaki Y, Nakaya R. A novel method in the induction of reliable experimental acute and chronic ulcerative colitis in mice. *Gastroenterology* 1990; **98**: 694-702
- 16 **Makiyama K**, Tsuzimura N. Synthesis and evaluation of an ECP polypeptide as a polyclonal antibody for staining of migrating inflammatory cells in the colonic mucosa of patients with ulcerative colitis (in Japanese). *Annual Report of The Research Committee of Inflammatory Bowel Disease The Japan Ministry of Health Labour and Welfare* 2004
- 17 **Barker RL**, Loegering DA, Ten RM, Hamann KJ, Pease LR, Gleich GJ. Eosinophil cationic protein cDNA. Comparison with other toxic cationic proteins and ribonucleases. *J Immunol* 1989; **143**: 952-955
- 18 **Nittoh T**, Hirakata M, Mue S, Ohuchi K. Identification of cDNA encoding rat eosinophil cationic protein/eosinophil-associated ribonuclease. *Biochem Biophys Acta* 1998; **1351**: 42-46
- 19 **Shichijo K**, Gottfried M, Sekine I, Pappas TN. Dextran sulfate sodium-induced colitis in immunodeficient rats. *Dig Dis Sci* 2000; **45**: 2320-2326
- 20 **Shichijo K**, Ihara M, Matsuo M, Ito M, Okumura Y, Sekine I. Overexpression of heat shock protein of stress-induced gastric ulcer-resistant rats. *Dig Dis Sci* 2003; **48**: 340-348
- 21 **Hogan SP**, Mishra A, Brandt EB, Royalty MP, Pope SM, Zimmermann N, Foster PS, Rothenberg ME. A pathological function for eotaxin and eosinophils in eosinophilic gastrointestinal inflammation. *Nat Immunol* 2001; **2**: 353-360
- 22 **Stevceva L**, Pavli P, Husband A, Matthaie KI, Young IG, Doe WF. Eosinophilia is attenuated in experimental colitis induced in IL-5 deficient mice. *Genes Immunity* 2000; **1**: 213-218
- 23 **Lehrer RI**, Szklarek D, Barton A, Ganz T, Hamann KJ, Gleich GJ. Antibacterial properties of eosinophil major basic and eosinophil cationic protein. *J Immunol* 1989; **142**: 4428-4434
- 24 **Ackerman SJ**, Gleich GJ, Loegering DA, Richardson BA, Butterworth AE. Comparative toxicity of purified human eosinophil granule cationic proteins for schistosomula of *Schistosoma mansoni*. *Am J Trop Med Hyg* 1985; **34**: 735-745
- 25 **Fredens K**, Dybdahl H, Dahl R, Baandrup U. Extracellular deposit of the cationic proteins ECP and EPX in Tissue infiltrations of eosinophils related to tissue damage. *APMIS* 1988; **96**: 711-719
- 26 **Motojima S**, Frigas E, Loegering DA, Gleich GJ. Toxicity of eosinophil cationic proteins for guinea pig tracheal epithelium *in vitro*. *Am Rev Respir Dis* 1989; **139**: 801-805
- 27 **Young JD**, Peterson CG, Venge P, Cohn ZA. Mechanism of membrane damage mediated by human eosinophil cationic protein. *Nature* 1986; **321**: 613-616
- 28 **Rosenberg HF**. Recombinant human eosinophil cationic protein. Ribonuclease activity is not essential for cytotoxicity. *J Biol Chem* 1995; **270**: 7876-7881
- 29 **Silen W**, Ito S. Mechanisms for rapid re-epithelialization of the gastric mucosal surface. *Annu Rev Physiol* 1985; **47**: 217-229
- 30 **Sinha A**, Nightingale J, West KP, Berlanga-Acosta J, Playford RJ. Epidermal growth factor enemas with oral mesalazine for mild-to-moderate left sided ulcerative colitis. *N England J Med* 2003; **349**: 350-357
- 31 **Dignass AU**, Lynch-Devaney K, Podolsky DK. Hepatocyte growth factor/scatter factor modulates intestinal epithelial cell proliferation and migration. *Biochem Biophys Res Commun* 1994; **202**: 701-709
- 32 **Tahara Y**, Ido A, Yamamoto S, Miyata Y, Uto H, Hori T, Hayashi K, Tsubouchi H. Hepatocyte growth factor facilitates colonic mucosal repair in experimental ulcerative colitis. *J Pharmacol Exp Ther* 2003; **307**: 146-151
- 33 **Bloom BR**, Bennett B. Mechanism of a reaction *in vitro* associated with delayed-type hypersensitivity. *Science* 1966; **153**: 80-82
- 34 **Calandra T**, Bernhagen J, Mitchell RA, Bucala R. The macrophage is an important and previously unrecognized source of macrophage migration inhibitory factor. *J Exp Med* 1994; **179**: 1895-1902
- 35 **Oshitani N**, Sawa Y, Hara J, Adachi K, Nakamura S, Matsumoto T, Arakawa T, Kuroki T. Functional and phenotypical activation of leucocytes in inflamed human colonic mucosa. *J Gastroenterol Hepatol* 1997; **12**: 809-814
- 36 **Rosenberg HF**. The eosinophil ribonuclease. *Cell Mol Life Sci* 1998; **54**: 795-803
- 37 **Rosenberg HF**, Ackerman SJ, Tenen DG. Human eosinophil cationic protein. Molecular cloning of cytotoxin and helminthotoxin with ribonuclease. *J Exp Med* 1989; **170**: 163-176
- 38 **Maeda T**, Kitazoe M, Tada H, de Llorens R, Salomon DS, Ueda M, Yamada H, Seno M. Growth inhibition of mammalian cells by eosinophil cationic protein. *Eur J Biochem* 2002; **269**: 307-316
- 39 **Boix E**, Leonidas DD, Nikolovski Z, Nogues MV, Cuchillo CM, Achrya KR. Crystal structure of eosinophil cationic protein at 2.4A resolution. *Biochemistry* 1999; **38**: 16794-16801
- 40 **Venge P**, Dahl R, Hallgren R. Enhancement of factor XII dependent reactions by eosinophil cationic protein. *Thromb Res* 1979; **14**: 641-649
- 41 **Dahl R**, Venge P. Enhancement of urokinase-induced plasminogen activation by the cationic protein of human eosinophil granulocytes. *Trom Res* 1979; **14**: 599-608
- 42 **Weiler JM**, Edens RE, Bell CS, Gleich GJ. Eosinophil granule cationic proteins regulate the classical pathway of complement. *Immunology* 1995; **84**: 213-219

• BASIC RESEARCH •

Ephrin-B reverse signaling induces expression of wound healing associated genes in IEC-6 intestinal epithelial cells

Christian Hafner, Stefanie Meyer, Ilja Hagen, Bernd Becker, Alexander Roesch, Michael Landthaler, Thomas Vogt

Christian Hafner, Stefanie Meyer, Ilja Hagen, Bernd Becker, Alexander Roesch, Michael Landthaler, Thomas Vogt, Department of Dermatology, University Hospital of Regensburg, Regensburg D-93042, Germany

Supported by the German Research Society (DFG – SFB 585/A8) and the Dr. Heinz Maurer Grant KFB 1.7

Co-first-authors: Christian Hafner and Stefanie Meyer

Co-correspondent: Christian Hafner

Correspondence to: Professor Dr. Thomas Vogt, Department of Dermatology, University of Regensburg, Regensburg D-93042, Germany. thomas.vogt@klinik.uni-regensburg.de

Telephone: +49-941-944-9606 Fax: +49-941-944-9608

Received: 2004-11-23 Accepted: 2005-01-05

Hafner C, Meyer S, Hagen I, Becker B, Roesch A, Landthaler M, Vogt T. Ephrin-B reverse signaling induces expression of wound healing associated genes in IEC-6 intestinal epithelial cells. *World J Gastroenterol* 2005; 11(29): 4511-4518

<http://www.wjgnet.com/1007-9327/11/4511.asp>

Abstract

AIM: Eph receptors and ephrin ligands play a pivotal role in development and tissue maintenance. Since previous data have indicated an involvement of ephrin-B2 in epithelial healing, we investigated the gene expression and downstream signaling pathways induced by ephrin-B mediated cell-cell signaling in intestinal epithelial cells.

METHODS: Upon stimulation of ephrin-B pathways in IEC-6 cells with recombinant rat EphB1-Fc, gene expression was analyzed by Affymetrix® rat genome 230 high density arrays at different time points. Differentially expressed genes were confirmed by real-time RT-PCR. In addition, MAP kinase pathways and focal adhesion kinase (FAK) activation downstream of ephrin-B were investigated by immunoblotting and fluorescence microscopy.

RESULTS: Stimulation of the ephrin-B reverse signaling pathway in IEC-6 cells induces predominant expression of genes known to be involved into wound healing/cell migration, antiapoptotic pathways, host defense and inflammation. Cox-2, c-Fos, Egr-1, Egr-2, and MCP-1 were found among the most significantly regulated genes. Furthermore, we show that the expression of repair-related genes is also accompanied by activation of the ERK1/2 MAP kinase pathway and FAK, two key regulators of epithelial restitution.

CONCLUSION: Stimulation of the ephrin-B reverse signaling pathway induces a phenotype characterized by upregulation of repair-related genes, which may partially be mediated by ERK1/2 pathways.

© 2005 The WJG Press and Elsevier Inc. All rights reserved.

Key words: Ephrin-B; IEC-6; Wound healing; Gene expression; c-Fos; Egr-1/2; COX-2

INTRODUCTION

Eph receptor tyrosine kinases (RTKs) and their receptor-like ligands, the ephrins, represent the largest family of RTKs and are specialized on directing coordinated cell migration in development and possibly in tissue repair^[1,2]. Based on their sequence homology, structure, and binding affinity, the Eph RTKs and ephrins are divided into two subclasses A and B. Usually, EphA receptors interact with ephrin-A ligands and EphB receptors with ephrin-B ligands. Both the receptors and the ligands are membrane-bound. A-ephrins are tethered to the outer leaflet of the plasma membrane by virtue of a glycosyl-phosphatidylinositol anchor, whereas B-ephrins are transmembrane proteins^[3,4]. As a unique feature, upon receptor-ligand interaction, both receptor mediated “forward” and a “reverse” cellular signaling response are induced. Therefore, Eph/ephrin signaling represents a bidirectional cell-cell signaling system with ephrin ligands taking over receptor-like functions^[5].

The rapid restitution of the intestinal surface after disruption of the epithelial barrier relies on the highly adaptive ability of epithelial wound-edge cells to rapidly form pseudopodial protrusions, reorganize the cytoskeleton, and migrate into a wound defect in a coordinated manner^[6-8]. This fast epithelial healing is particularly important considering the necessity to protect the host against a considerable microbial threat and exposure to a multitude of immunogenic and toxic factors present in the gut^[6].

Recent data suggest a pivotal role of Eph/ephrin signaling in tissue repair and maintenance of the gut. EphA2/ephrinA1 signaling has already been suggested to be involved in the homeostasis of the intestinal barrier in adults^[9]. Moreover, differential expression of ephrin ligands and Eph-RTKs along the crypt-villus axis determines the correct positioning and allocation of the proliferating vs differentiating compartment during development of the intestinal crypts^[10]. Interestingly, knockout of EphB2/B3 in mice leads to intermingling of both compartments and also displacement of Paneth cells to the top of the villi. More recently, the expression of a variety of Eph receptors and ephrin ligands has been demonstrated in the adult human gut by our group, with most prominent expression of EphA2, EphB2, ephrin-A1 and ephrin-B1/2^[11]. Considering the important role of

Eph receptors and ephrins development and their life-long highly organized expression in gut epithelium, a role in epithelial maintenance and repair seems possible. As a further step to understand their role in intestinal physiology, we investigated gene expression profiles in response to the stimulation of the ephrin-B dependent signaling pathways. Since many links between ephrin-B2 and MAP kinase (ERK) as well as focal adhesion kinase (FAK) mediated pathways have already been demonstrated^[12,13], these pathways were also analyzed in more detail.

MATERIALS AND METHODS

Cell culture and total RNA isolation

Non-transformed rat intestinal IEC-6 cells^[14] were cultured in Dulbecco's MEM (Biochrom AG, Berlin, Germany) supplemented with 5% fetal calf serum (FCS PAN Biotech, Aldenbach, Germany). After reaching 80% confluence, cells (passage 6) were starved overnight with 0.1% FCS and stimulated with 0.5 µg/mL (-3.3 nmol/L) rat recombinant EphB1-Fc (R&D Systems, Minneapolis, USA). Doses were determined according to the efficient stimulation of intestinal epithelial wound healing in scratch wound assays. Cells were harvested at 0 (control), 30, and 120 min in RLT buffer (Qiagen, Hilden, Germany). After homogenization, RNA isolation for further array analysis was performed using the RNeasy Mini Kit (Qiagen). RNA quality was assessed with an Agilent 2100 bioanalyzer (Agilent Technologies, Palo Alto, USA) and quantity was measured spectrophotometrically.

High density arrays

For investigation of downstream transcriptional responses of EphB1-Fc stimulated pathways in IEC-6 cells, gene expression was analyzed by the Affymetrix® rat genome expression set 230A (version 2.0). Sample preparation for microarray hybridization was carried out as described in the Affymetrix GeneChip® Expression Analysis Technical Manual. Briefly, 15 µg of total RNA were used to generate double-stranded cDNA (Invitrogen). Synthesis of Biotin-labeled cRNA was performed using the BioArray™ HighYield™ RNA Transcript Labeling Kit (ENZO Diagnostics). The length of the cRNA and fragmentation was confirmed using the Agilent 2100 bioanalyzer (Agilent Technologies, Palo Alto, USA). Affymetrix® Microarray Suite (MAS) 5.1 was used for Single Array and Comparison Analysis. A global scaling strategy was applied, setting the average signal intensity of all arrays to a target value of 100. For RNA quality control and stringent data evaluation, the quality standards were applied as defined at a regional German Affymetrix® Core Facility and Service Provider, the "CFB" (Competence Centre for Fluorescent Bioanalytics, www.kfb-regensburg.de).

Ingenuity® pathway analysis

Analysis of 331 regulated genes with changed *P*-values lower than 0.003 and higher than 0.997 (fold change >1.5) by the Ingenuity® Pathway Analysis Software tool was used to get a better defined concept of the complex downstream events.

Real-time RT-PCR

To confirm the differential expression of a selection of

more than twofold regulated genes, real-time TaqMan® RT-PCR (PE Applied Biosystems, Darmstadt, Germany) was performed on an ABI Prism 7900 HT Sequence Detection System as published elsewhere^[11]. Briefly, cDNA was synthesized using the Reverse Transcription Kit from Promega (Madison, USA) according to the manufacturer's protocol. Rat primers and probes for Cox-2, Egr-1/2, c-Fos, and monocyte chemotactic protein 1 (MCP-1) were obtained as Assays on Demand® (Applied Biosystems). The standard curve method was used for the quantification of the relative amounts of gene expression products. This method provides unit less normalized expression values that can be used for direct comparison of the relative amounts of target mRNA in different samples^[11]. All reactions were performed as triplicates. Probes and primers for TaqMan® analysis for ephrin-B1 and -B2 were designed on the basis of gene-specific non-homologous DNA sequence of the corresponding members^[11]. The sequences were as follows: ephrin-B1 (MGB probe TGTACTGGCTTGGGCC, forward CCTCC CCAGGCTTGTGA, reverse TCCTGGCTGACCACA TCGT), ephrin-B2 (MGB probe TGCTCAGCGCTTAAA, forward GATGTGAAATTCAT-TTGTGGCAAT, reverse CCAGAAGTAGCTGTCA-ATTTGTTT).

Immunocytochemistry

IEC-6 cells were plated on fibronectin coated Lab-Tek chamber glass slides (Nalge Nunc Int., Naperville, USA) (100 000 cells/slide) and grown in Dulbecco's MEM plus 5% FCS overnight. After washing with PBS, cells were fixed with 4% paraformaldehyde and after repeated wash steps with PBS blocked with 3% H₂O₂/CH₃OH. Cells were again washed with PBS and incubated with Super Block (Zytomed, Berlin, Germany). For immunocytochemical staining, the following antibodies were used (30 min, 37 °C): goat EphB2 (1:100), rabbit ephrin-B1 (1:100), and rabbit ephrin-B2 (1:75) (Santa Cruz, CA, USA). Cells were incubated with Anti-Broad Spectrum Biotinylated antibody for 15 min (37 °C), and ZytoChemPlus HRP solution was added for 10 min at room temperature (Zytomed). After washing with PBS, the slides were stained with AEC chromogen for 10 min at room temperature (Dako, Hamburg, Germany). The reaction was stopped with H₂O and counterstained with hemalaun. For negative control, the protocol was performed as mentioned above, but primary antibodies were omitted.

Immunoblotting

IEC-6 cells were grown in Dulbecco's MEM (Biochrom AG, Berlin, Germany) supplemented with 5% FCS to 80% confluence. Cells were starved overnight with 0.1% FCS, then stimulated with 0.25 µg/mL (-1.65 nmol/L) rat recombinant EphB1-Fc (R&D Systems, Minneapolis, USA) and harvested at 0, 5, 10, 20, 30, and 45 min. Protein was isolated from the cells and the protein lysates were analyzed by SDS-PAGE and blotted according to standard protocols.

Activated (phosphorylated) FAK and pan-FAK were detected by the anti-(phosphotyrosine)-pY397 FAK antibody from Sigma (St. Louis, USA) and anti-FAK from Biosource (Camarillo, CA, USA). For detection of MAP-kinase phosphorylation, the following antibodies were used: anti-ERK1/2 (pT185, pY187) 1:1 000, anti-JNK1/2 (pT183,

pY185) 1:2 500, anti-p38 (pT180, pY182) 1:1 000 (Biosource, Camarillo, CA, USA). Rabbit polyclonal anti-protein disulfide isomerase (PDI) antibody (dilution 1:4 000) served as a control for equal protein load (StressGen, Victoria, Canada). As secondary antibody, the anti-Rabbit-HRP (Cell signaling, Beverly, MA, USA) was used.

Immunofluorescence microscopy

IEC-6 cells were plated on fibronectin coated glass cover slips and grown for 16 h in Dulbecco's MEM plus 5% FCS. The monolayer was starved with Dulbecco's MEM plus 0.1% FCS overnight, wounded by a cell scraper and stimulated with 0.5 $\mu\text{g}/\text{mL}$ EphB1-Fc (-3.3 nmol/L). IgG-Fc (R&D Systems, Minneapolis, USA) served as a control. Cells were fixed with 4% paraformaldehyde for 5 min at room temperature and permeabilized with 0.1% Triton-X 100 for 5 min at 37 °C. After washing with PBS, cells were blocked with 1% bovine serum albumin for 15 min at 37 °C. For detection of activated FAK, an anti-(phosphotyrosine)-pY397 antibody (Sigma, St. Louis, USA) was used as primary

and an anti-rabbit FITC-labeled antibody as secondary (Vector, Burlingame, USA). Cell nuclei were stained with DAPI (Chemicon, Temecula, USA). Images from the wound margin were taken on a Leitz microscope equipped with a fluorescence lamp and adequate filters. Cells were photographed at 400 \times magnification.

RESULTS

IEC-6 cells express ephrin-B1/2 ligands

In the human small intestine and colon, coexpression of EphB2 and ephrin-B1/2 ligands has previously been demonstrated by our group^[11]. To evaluate the suitability of IEC-6 cells as a model for investigation of EphB/ephrin-B dependent cell-cell signaling, the expression of both EphB2 receptor and ephrin-B1/2 ligands in IEC-6 cells was investigated. Real-time TaqMan[®] RT-PCR revealed mRNA expression of ephrin-B1 and, more abundantly, ephrin-B2 in IEC-6 cells (Figure 1A). In addition, the expression of the EphB2 receptor and two corresponding high-affinity ligands in IEC-6 cells could be confirmed on the protein

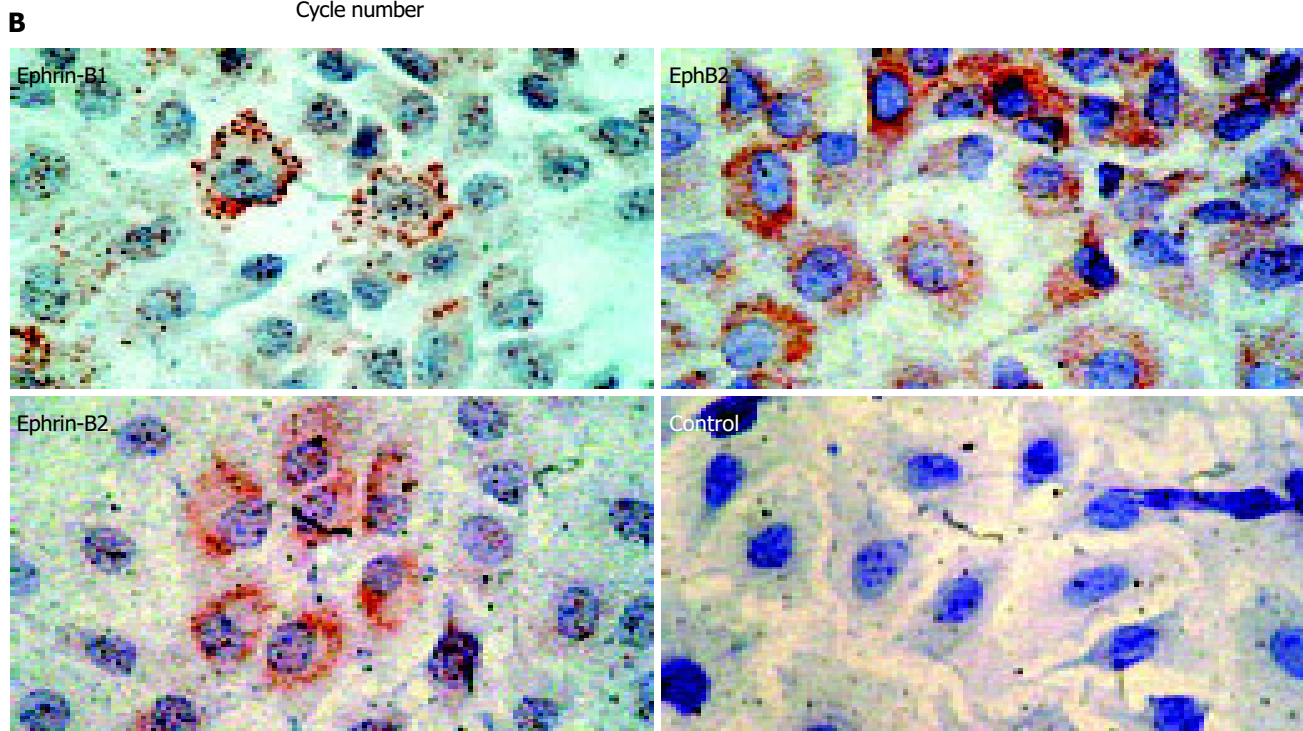
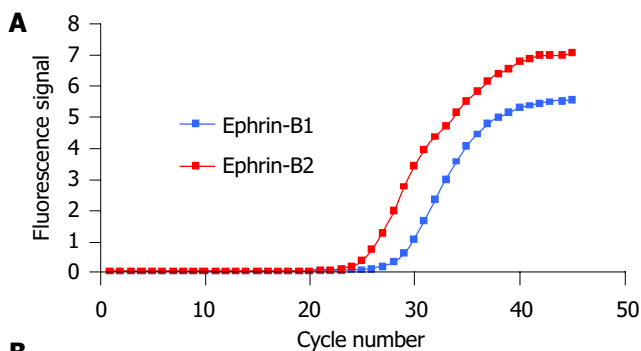


Figure 1 Rat IEC-6 intestinal epithelial cells express ephrin-B ligands on the mRNA and protein level. **A:** Real-time RT-PCR shows expression of ephrin-B1 and -B2 mRNA. As the curve of ephrin-B2 demonstrates lower C_t -values, the amount of ephrin-B2 mRNA starting material was higher than the amount of ephrin-B1 mRNA. The values were normalized by detection of the 18S rRNA

(data not shown); **B:** IEC-6 cells coexpress ephrin-B1/2 and the corresponding EphB2 receptor on the protein level. IEC-6 cells may therefore be able to interchange cell-cell signals via EphB2/ephrin-B1/2 contacts. The coexpression of the EphB2 receptors and ephrin-B1/2 ligands is in accordance with previous data on human adult intestinal tissue in these cells^[11].

level by immunocytochemistry (Figure 1B). Hence, comparable to the human *in vivo* expression^[11], IEC-6 cells coexpress the EphB2 receptor and two ephrin-B ligands *in vitro*. Therefore, cell-cell signaling between these cells seems possible.

High-density cDNA array analysis

Since previous investigations showed that ephrin-B mediated 'reverse' signals generated upon binding of EphB receptors can specifically enhance intestinal wound healing *in vitro*, we were interested in the "downstream" target genes of the corresponding signaling cascades. Therefore, the transcriptional response to ephrin-B reverse signaling induced by recombinant EphB1-Fc was analyzed on the Affymetrix[®] platform. The cells were stimulated with 0.5 $\mu\text{g}/\text{mL}$ (-3.3 nmol/L) rat recombinant EphB1-Fc for 30 and 120 min. To identify the genes with highest possible probability to be truly regulated in these experiments, only genes were collected with significant detection-*P* values (exclusion of any false positives due to mismatch hybridization) and significant change-*P* values according to Affymetrix[®] algorithms. In addition, a minimum twofold change was set as cut-off. Table 1 shows the list of significantly regulated candidate genes after applying these stringent rules. Most of the genes are "early responders", i.e., detectable after 30 min. However, a few of those genes were differentially regulated still after 120 min. Based on the current knowledge on gene function annotated to individual probe sets of the Affymetrix[®] rat chip, the regulated genes fell into seven major categories: Genes with direct links to (I) wound healing, (II) cell migration, (III) wound edge activation, (IV) pleiotrope transcription factors which also can directly participate in cell migration and wound healing, (V) genes that are functionally involved in apoptotic pathways, (VI) genes linked to host defense and inflammation, and (VII) genes that have host defense functions such as osmoregulation and detoxification (Table 1).

Real-time RT-PCR confirms differential regulation of c-Fos, Cox-2, MCP-1, Egr-1 and Egr-2

As real-time TaqMan[®] RT-PCR has been proven to be a sensitive and reliable method for quantitative gene expression analysis^[11], differential mRNA expression of selected candidate genes (c-Fos), cyclooxygenase 2 (Cox-2), early growth response gene 1 and 2 (Egr-1 and -2) and MCP-1 was confirmed using this method. The real-time RT-PCR results confirmed the array data very well (Figure 2). The c-Fos mRNA displayed a 7.1-fold upregulation after 30 min. Likewise, the strong induction of Egr-1, Egr-2, and Cox-2 after 30 min could be confirmed. In addition, RT-PCR revealed a 2.2-fold downregulation of Egr-1 mRNA after 120 min, which was not observed in the array data.

Ingenuity[®] pathway analysis reveals a complex network of interacting genes, which are possibly related to intestinal repair, upon EphB1-Fc stimulation

A total of 331 genes that were more than 1.5-fold regulated after 30 min of EphB1-Fc treatment and with MAS (Affymetrix[®] Microarray Suite) change, *P*-values lower than 0.003 or higher than 0.997 respectively were used for the

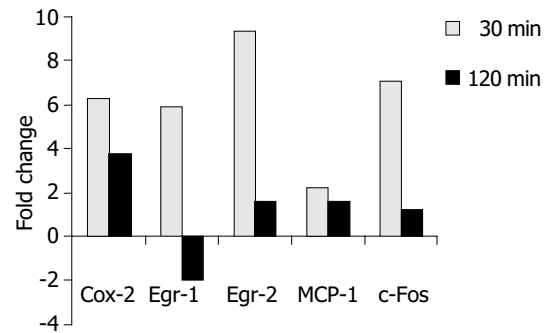


Figure 2 Real-time RT-PCR analysis confirmed the differential expression of COX-2, Egr-1, Egr-2, MCP-1, and c-Fos in accordance to Affymetrix[®] array data. The results are indicated as positive (= upregulation) or negative (= downregulation) fold changes of mRNA amount compared to the control (*t* = 0 min, values normalized to 18S rRNA).

pathway analysis. The Affymetrix[®] ProbeSet IDs were imported together with the fold changes into the Ingenuity[®] Pathway Analysis Software (Ingenuity[®] Systems). One hundred and thirteen genes were eligible for generating networks. All 21 networks found were ranked by score. The score is a numerical value, used to rank networks according to how relevant they are to the genes within the dataset. The network with the highest score contained 28 genes. A functional network of differentially regulated genes could be established including the confirmed candidates c-Fos, Egr-1 and Egr-2 together with further genes related to growth and apoptosis (Figure 3). Interestingly, the pathway tools revealed that the strongly upregulated genes Egr-2 and c-Fos are linked by mutual activation, expression and transcription of each other. Both Egr-1 and c-Fos interact with jun, which obviously has a central position in the demonstrated network. Furthermore, Egr-1 enhances the expression of the growth factor receptor EGFR and is further linked to the cell cycle via CDKN1A. The details of the conceptual ephrin-B dependent network are shown in Figure 3.

Stimulating the ephrin-B reverse signaling pathways in IEC-6 induces temporary activation of ERK 1/2 map kinase stress pathways and FAK

Previous work has shown that signaling responses to changes in the microenvironment regarding the presentation of Eph-RTKs or ephrins on neighboring cells involve major MAP kinase pathways such as JNK and Erk^[13,15,16]. To identify the MAP kinase pathways involved in EphB/ephrin-B signaling in IEC cells, we screened for MAP kinase phosphorylation status in time-course experiments using stimulation with EphB1-Fc (0.25 $\mu\text{g}/\text{mL}$). As shown in Figure 4, there is a temporary induction of ERK1/2 phosphorylation that peaks after 20-30 min before returning to base levels.

Another important biological read-out of ephrin-B activation is the recruitment of FAK^[2]. FAK is a crucial player in integrin-mediated attachment and migration as well as reorganization of focal adhesion complexes, which also protect from anoikis^[17,18]. As shown in Figure 4, blotting with the anti-pY397-FAK indicates a time course of FAK phosphorylation upon EphB1-Fc stimulation in IEC-6 cells, which is almost identical to ERK 1/2 activation.

The latter observations could be further substantiated by immunofluorescence microscopy of wounded IEC-6 cell monolayers. Compared to IgG-Fc controls, EphB1-Fc stimulated IEC-6 cells revealed prominent induction of active pY397-FAK in neighboring cells at the wound margin (Figure 5).

DISCUSSION

Recent data generated by our group had suggested that EphB/ephrin-B cell-cell signaling can enhance epithelial wound closure of IEC-6 intestinal cells. In particular, the ephrin-B reverse signals seem to activate wound closure. *In*

in vivo, such functions could be essential for the protection of the host against microbial antigens and toxic factors abundantly present in the gut. In this context, it is also very interesting that we had observed significant imbalance of the ephrin-B ligand expression in intestinal epithelial cells isolated from patients with Crohn's disease compared to healthy controls. Therefore, to elucidate further details of an assumed protective action of EphB-ephrin-B signal exchange in intestinal cells, we analyzed 'downstream' effects of the ephrin-B pathway. The most important finding of this study is that Affymetrix® gene chip data revealed a significant upregulation of a set of genes known to be fundamentally involved into wound healing, e.g. c-Fos, Egr-1,

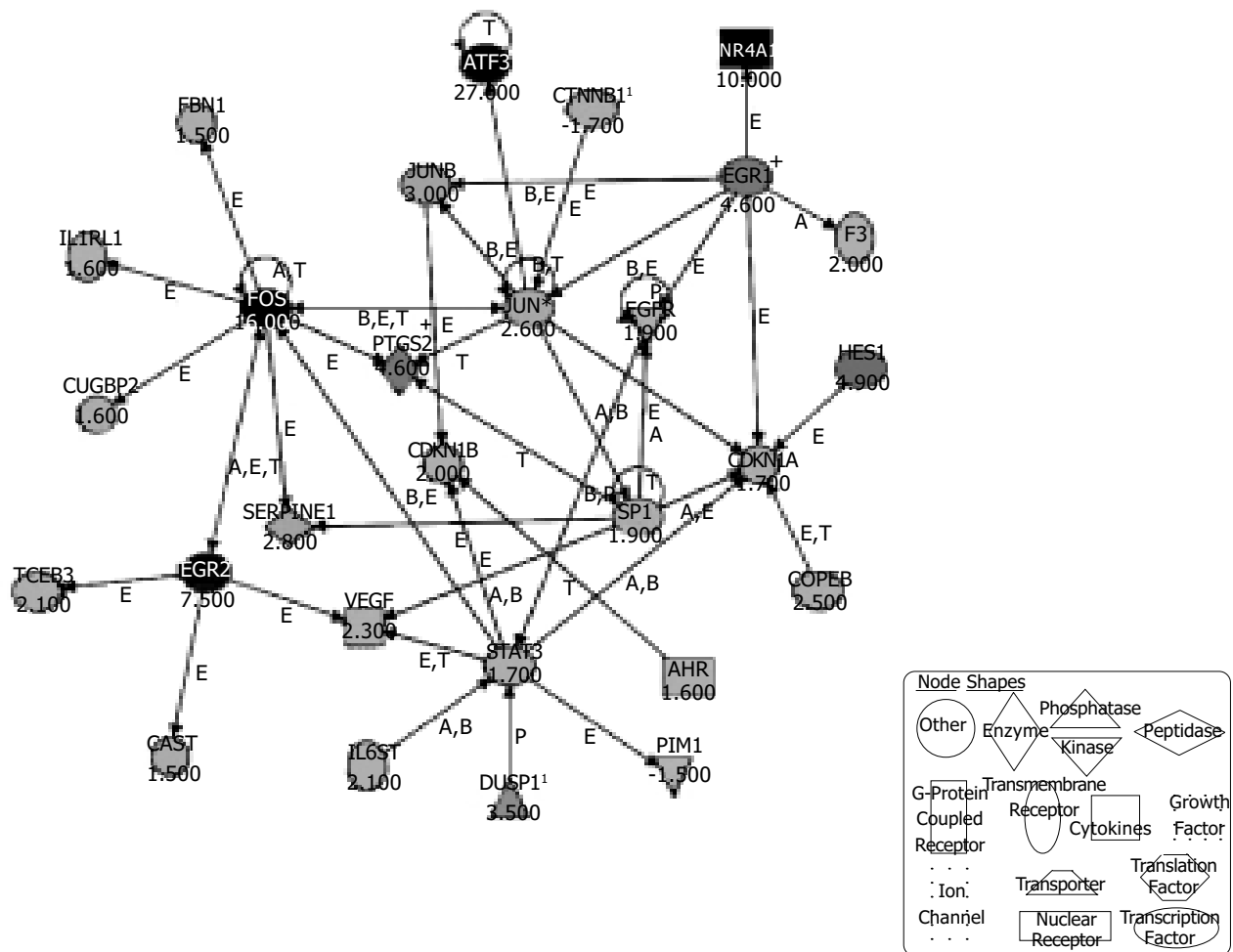


Figure 3 Ingenuity® Pathways Analysis reveals a possible network of genes activated in IEC-6 cells upon induction of the ephrin-B pathway. Three hundred and thirty-one regulated genes with changed *-P* values lower than 0.003 and higher than 0.997 were selected and entered the Ingenuity® pathway analysis. The displayed network features only genes with functional interactions. Many of those genes are associated with cellular growth, proliferation and control of cell death. Arrows pointing from one gene to another indicate that one causes activation of the other one (includes any direct interaction: e.g. binding, phosphorylation, dephosphorylation, etc.). For ligands/receptors arrows pointing from a ligand to a receptor signify that the ligand binds the receptor and subsequently leads to activation of the receptor. The respective fold-changes are given below the gene symbols. Further abbreviations are: A, Activation/deactivation; B, Binding; E, Expression; M, Biochemical Modification; P, Phosphorylation/dephosphorylation; T, Transcription; †Duplicate-user input gene that had duplicate identifiers in the dataset file mapping to a single gene in the Ingenuity® Pathways Knowledge Base. + Indicates there are other networks from the analysis that contain this gene. Gene names are: AHR:

Aryl hydrocarbon receptor; ATF3: Activating transcription factor 3; CAST: Calpastatin; CDKN1A: Cyclin-dependent kinase inhibitor 1A; CDKN1B: Cyclin-dependent kinase inhibitor 1B; COPEB: Core promoter element binding protein; CTNNB1: Catenin (cadherin-associated protein), beta 1; CUGBP2: UG triplet repeat, RNA-binding protein 2; DUSP1: Dual specificity phosphatase 1; EGFR: Epidermal growth factor receptor; EGR1: Early growth response 1; EGR2: Early growth response 2; F3: Coagulation factor 3; FBN1: Fibrillin-1; FOS: v-fos FBJ murine osteosarcoma viral oncogene homolog; HES1: Hairy and enhancer of split 1 (Drosophila); IL1RL1: Interleukin 1 receptor-like 1; IL6ST: Interleukin 6 signal transducer; JUN: v-jun sarcoma virus 17 oncogene homolog (avian); JUNB: Jun-B oncogene; NR4A1: Nuclear receptor subfamily 4, group A, member 1; PIM1: Proviral integration site 1; PTGS2: Prostaglandin-endoperoxide synthase 2; SERPINE1: Serine (or cysteine) proteinase inhibitor, member 1; SP1: Sp1 transcription factor; STAT3: Signal transducer and activator of transcription 3; TCEB3: Transcription elongation factor B (SIII), polypeptide 3; VEGF: Vascular endothelial growth factor.

Table 1 Selection of significantly regulated genes (fold change >2) upon stimulation of ephrin-B pathways in IEC-6 cells

Gene bank accession	Title	Function	FC (30 min ¹)	FC (120 min ¹)
gb:AA944459	Dynein, cytoplasmic, light intermediate chain 1	Migration/polarity/Wound edge	-2.0	NC
gb:AA875047	JQ0866 T-complex protein 1 - rat	Chaperonin/protein folding	-2.0	NC
gb:AI231350	Transcribed sequences	Unknown	-2.0	NC
gb:AI071071	Transcribed sequences	Unknown	-2.0	NC
gb:BE097926	Transcribed sequences	Unknown	-2.1	NC
gb:AA925921	ELV4_RAT ELAV-like protein 4	Binds to the AU-rich element in c-fos and interleukin-3/mRNA degradation	-2.1	NC
gb:AW144020	Transcribed sequences	Unknown	-2.1	NC
gb:U30789.1	Upregulated by 1,25-dihydroxyvitamin D-3	Unknown	-2.3	-2.8
gb:AI230596	Importin alpha S1	Nuclear transport/DNA binding	-2.3	NC
gb:BF389856	Beta-galactosidase, alpha peptide	Metabolism	-2.3	NC
gb:NM_012903.1	Acidic nuc. phosphoprotein 32 family, member A	Apoptosis	-3.2	NC
gb:BF415939	c-fos	Wound healing	16.0	NC
gb:NM_053633.1	Early growth response 2	Apoptosis/EGR2 induces apoptosis	7.5	NC
gb:NM_024360.1	HES-1/hairy and enhancer of split 1 (Drosophila)	Notch pathway target/neurite outgrowth/morphogenesis	4.9	NC
gb:NM_012551.1	Early growth response 1	Apoptosis/EGR2 induces apoptosis	4.6	NC
gb:U03389.1	Cox-2/prostaglandin-endoperoxide synthase 2	Epithelial wound healing	4.6	4.0
gb:BE110108	MAP kinase phosphatase-1/protein tyrosine phosphatase	Signaling/stress	3.5	NC
gb:NM_021836.1	Jun B proto-oncogene	Transcription factor/wound healing cornea	3.0	NC
gb:AI178746	Transcribed sequences	Unknown	3.0	NC
gb:NM_012620.1	PAI-1/serine (or cysteine) proteinase inhibitor, member 1	Affect wound healing by regulating the fibrinolytic environment	2.8	NC
gb:AI710284	Beta-galactosidase, alpha peptide	Unknown	2.8	3.2
gb:BF420059	Immediate-early protein pip92	Unknown	2.6	NC
gb:BI288619	c-jun homolog/v-jun sarcoma virus 17 oncogene homolog (avian)	Transcription factor/wound repair/epithelial migration	2.6	NC
gb:BI298889	RBBP-2	Transcription factor/cell cycle inhibition	2.6	NC
gb:NM_031642.1	Core promoter element binding protein	Unknown	2.5	NC
gb:AB025017	Zinc finger protein 36	Unknown	2.5	NC
gb:AI599423	DNA-damage-inducible protein GADD45 gamma	Cell cycle control	2.5	NC
gb:U02553.1	MAP kinase phosphatase-1/protein tyrosine phosphatase	Signaling/stress	2.3	NC
gb:L81174.1	Ankyrin-like repeat protein	Endothelial activation	2.1	NC
gb:NM_017206.1	Solute carrier family 6, member 6	Protects IECs from osmotic stress	2.1	NC
gb:BM383427	Gp130/Interleukin 6 signal transducer	Host defense/tight junction loosening/proinflammatory lipid production	2.1	2.3
gb:AI179464	Rattus norvegicus RM1 mRNA, partial sequence	Unknown	2.1	3.2
gb:NM_031530.1	MCP-1/small inducible cytokine A2	Monocyte chemotaxis/candidate locus for exp. EM	2.0	NC
gb:NM_022858.1	HNF-3/forkhead homolog-1	Transcription factor/development	2.0	2.6
gb:AA850780	Transcribed sequences	Unknown	2.0	NC
gb:NM_012940.1	Cytochrome P450, subfamily 1B, polypeptide 1	Detoxification	2.0	5.3
gb:NM_013057.1	Coagulation factor 3	Blood coagulation	2.0	NC
gb:BI284349	Myeloid differentiation primary response gene 116	Unknown	2.0	NC
gb:AI176519	DIF-2/lipid responsive gene/Immediate early response 3 protein	Differentiation	2.0	NC
gb:AI169756	G33_rat gene 33 polypeptide	Migration/signaling/adaptor protein binds GTP-Cdc42/activates SAPK/JNK	2.0	NC
gb:BI288619	c-jun homolog/v-jun sarcoma virus 17 oncogene homolog (avian)	Transcription factor/wound repair/epithelial migration	2.0	NC
gb:AA800192	Rattus norvegicus endogenous retrovirus mRNA, partial sequence	Unknown	2.0	NC
gb:AW533292	Similarity to protein ref: NP_073600.1 (<i>H. sapiens</i>)	Unknown	2.0	NC
gb:BF392456	Rattus norvegicus non-erythrocyte beta-spectrin mRNA, partial cds	Unknown	2.0	NC

¹IEC-6 cells were treated with 0.5 mg/mL (- 3.3 nmol/L) rat recombinant EphB1-Fc and RNA was harvested after 30 and 120 min. FC: fold changes; NC: no changes.

Egr-2, and COX-2 (30 min after stimulation with recombinant EphB1-Fc). Egr-1 (4.6-fold) and c-Fos (16-fold) were among the most strongly early-induced genes. Egr-1 is known as a

key activator of injury-induced gene expression^[19]. Egr-1 might also be responsible for the observed induction of NR4A1 (immediate early gene transcription factor NGFI-

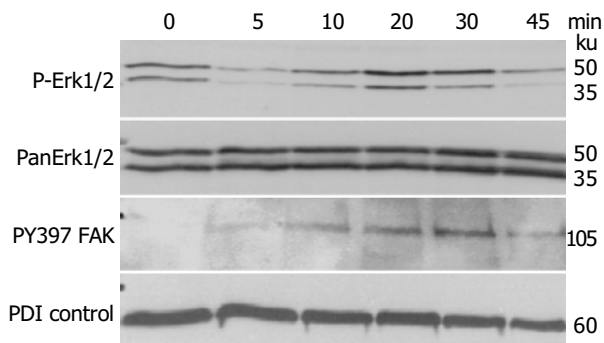


Figure 4 Stimulating the ephrin-B reverse signaling pathway in IEC-6 with recombinant EphB1-Fc induces temporary activation of Erk1/2 map kinase stress pathways and FAK phosphorylation, demonstrated by immunoblotting. PDI served as a loading control.

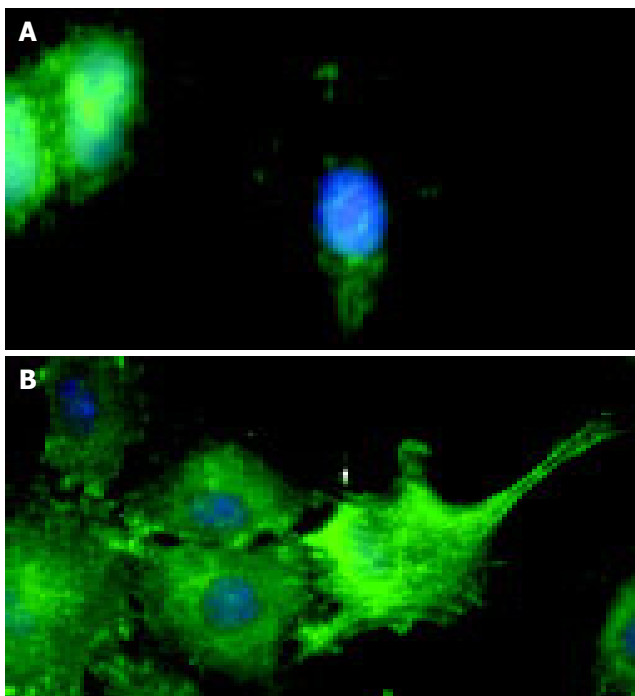


Figure 5 Immunofluorescence microscopy demonstrates that compared to the control (A), stimulation of IEC-6 cells with recombinant EphB1-Fc leads to induction of active pY397-FAK in neighboring cells most prominently at the wound edge (B).

B; 10-fold) and EGFR (epidermal growth factor receptor; 1.9-fold), as well as for the induction of jun B (3.0, fold) and c-jun (2.6, fold) according to the Ingenuity[®] pathway analysis. In turn, the resulting AP-1 activity is known to be responsible for the observed prolonged induction of COX-2 (prostaglandin-endoperoxide synthase 2; 4.6-fold), but also MCP-1 (small inducible cytokine A2, 2.0-fold). COX-2 induction is considered as a further important line of defense for the gastrointestinal mucosa, necessary for maintenance of mucosal integrity and ulcer healing^[20,21]. On the other hand, MCP-1 is a proinflammatory cytokine with a well defined role in inflammatory bowel disease^[22-24]. Taken together, the Ingenuity[®] pathway analysis suggests that stimulation of the ephrin-B signaling can induce a complex network of wound healing associated genes in intestinal

epithelial cells with major interconnections to growth regulation and antiapoptosis, but also inflammation.

The exact anatomy of the signaling pathways activated in order to reseal epithelial defects in the gut remains poorly understood. IEC-6 cells, derived from fetal rat duodenal crypt cells, are one of the best-studied *in vitro* models for epithelial restitution^[19]. Previous work on IEC-6 wounding has implicated the extracellular signal-regulated kinase (ERK), mitogen-activated protein kinase as a central mediator of wound-signal transduction and regulator of epithelial restitution. Monolayer injury results in rapid activation of ERK1/2 (p42 and p44) in IEC-6 cells^[25]. Interestingly, our immunoblotting results are consistent with the view that ephrin-B signaling contributes to this pivotal wound-healing cascade. Moreover, in accordance with our data it has already been shown by another group that wounding of IEC-6 cells leads to ERK-dependent induction of Egr-1 and c-Fos. Both, direct blocking of ERK activation and interference with Egr-1 function resulted in diminished cell migration after injury^[19]. This suggests that stimulation of ephrin-B is a part of the injury response program in intestinal epithelial cells involving ERK1/2, Egr-1, and c-Fos. Interestingly, activation of forward signaling by ligand-mediated stimulation of EphA2 and EphB2 receptors is also linked to the ERK/MAPK signaling cascade^[26,27].

Recently, the receptor-like functions of B-ephrins and their intimate links to cell migration mechanisms could be defined in more detail on the molecular level^[2,13]. Upon binding and dimerization of the cognate receptors of neighboring cells, the cytoplasmic c-terminus of ephrin-B undergoes phosphorylation due to the recruitment of Src-family kinases^[15]. Subsequently, the phosphorylated cytoplasmic domain of ephrin-B provides a binding domain for SH2/SH3-adaptor proteins such as Grb4 (Nck2). In turn, Grb4 has three further SH3-domains that function as a scaffold for binding and activation of a variety of SH3-binding effectors. Some of them directly influence the dynamic control of the cytoskeleton, e.g., FAK, Paxillin, Abi-1, Axin, CAP, dynamin, hnRNPk, and Pak1^[2,28]. Among those effectors, FAK is particularly interesting in this context, because active FAK is essential to control cell spreading, movements and also integrin-dependent survival of IEC^[17,29]. Therefore, we analyzed FAK phosphorylation both by immunoblotting and by fluorescence microscopy. We show that in starved IEC-6 cells ephrin-B activation with nmol/L doses of EphB1-Fc leads to rapid induction of pY397-FAK, which seems to be most prominently detectable in wound-edge cells. The phosphorylation of FAK on Tyr397 is known to correlate with increased catalytic activity and appears to be important for the tyrosine phosphorylation of focal adhesion complex-associated proteins such as paxillin and Cas^[17]. Theoretically, the directed turnover of such complexes finally determines the speed of cell movements and the capacity of an epithelium to reseal defects.

We conclude that ephrin-B signaling induces complex pathways, which are essential for rapid epithelial wound closure in the intestine. Functional links to major determinants of epithelial defense and coordinated cell movement place EphB/ephrin-B into the list of targets for future molecular therapies trying to intervene with such pathways, for instance

in the context of inflammatory bowel disease. However, firstly the specifics of the side-effects such as the production of proinflammatory cytokines like MCP-1 and the complexity of seemingly counteracting downstream targets have to be investigated in more detail.

ACKNOWLEDGMENTS

The skillful technical assistance and support of Mrs. Lydia Künzel and Mrs. Nadine Wandtke is gratefully acknowledged.

REFERENCES

- Drescher U. Eph family functions from an evolutionary perspective. *Curr Opin Genet Dev* 2002; **12**: 397-402
- Cowan CA, Henkemeyer M. Ephrins in reverse, park and drive. *Trends Cell Biol* 2002; **12**: 339-346
- Pasquale EB. The Eph family of receptors. *Curr Opin Cell Biol* 1997; **9**: 608-615
- Murai KK, Pasquale EB. 'Eph'ective signaling: forward, reverse and crosstalk. *J Cell Sci* 2003; **116**: 2823-2832
- Holland SJ, Gale NW, Mbamalu G, Yancopoulos GD, Henkemeyer M, Pawson T. Bidirectional signalling through the EPH-family receptor Nuk and its transmembrane ligands. *Nature* 1996; **383**: 722-725
- Wilson AJ, Gibson PR. Epithelial migration in the colon: filling in the gaps. *Clin Sci* 1997; **93**: 97-108
- Podolsky DK. Healing the epithelium: solving the problem from two sides. *J Gastroenterol* 1997; **32**: 122-126
- Jacinto A, Martinez-Arias A, Martin P. Mechanisms of epithelial fusion and repair. *Nat Cell Biol* 2001; **3**: E117-123
- Rosenberg IM, Goke M, Kanai M, Reinecker HC, Podolsky DK. Epithelial cell kinase-B61: an autocrine loop modulating intestinal epithelial migration and barrier function. *Am J Physiol* 1997; **273**(4 Pt 1): G824-832
- Batlle E, Henderson JT, Beghtel H, van den Born MM, Sancho E, Huls G, Meeldijk J, Robertson J, van de Wetering M, Pawson T, Clevers H. Beta-catenin and TCF mediate cell positioning in the intestinal epithelium by controlling the expression of EphB/ephrinB. *Cell* 2002; **111**: 251-263
- Hafner C, Schmitz G, Meyer S, Bataille F, Hau P, Langmann T, Dietmaier W, Landthaler M, Vogt T. Differential gene expression of Eph receptors and ephrins in benign human tissues and cancers. *Clin Chem* 2004; **50**: 490-499
- Vindis C, Cerretti DP, Daniel TO, Huynh-Do U. EphB1 recruits c-Src and p52Shc to activate MAPK/ERK and promote chemotaxis. *J Cell Biol* 2003; **162**: 661-671
- Huynh-Do U, Vindis C, Liu H, Cerretti DP, McGrew JT, Enriquez M, Chen J, Daniel TO. Ephrin-B1 transduces signals to activate integrin-mediated migration, attachment and angiogenesis. *J Cell Sci* 2002; **115**(Pt 15): 3073-3081
- Quaroni A, Wands J, Trelstad RL, Isselbacher KJ. Epithelioid cell cultures from rat small intestine. Characterization by morphologic and immunologic criteria. *J Cell Biol* 1979; **80**: 248-265
- Palmer A, Zimmer M, Erdmann KS, Eulenburg V, Porthin A, Heumann R, Deutsch U, Klein R. EphrinB phosphorylation and reverse signaling: regulation by Src kinases and PTP-BL phosphatase. *Mol Cell* 2002; **9**: 725-737
- Huynh-Do U, Stein E, Lane AA, Liu H, Cerretti DP, Daniel TO. Surface densities of ephrin-B1 determine EphB1-coupled activation of cell attachment through alphavbeta3 and alpha5beta1 integrins. *Embo J* 1999; **18**: 2165-2173
- Parsons JT, Martin KH, Slack JK, Taylor JM, Weed SA. Focal adhesion kinase: a regulator of focal adhesion dynamics and cell movement. *Oncogene* 2000; **19**: 5606-5613
- Valentinis B, Reiss K, Baserga R. Insulin-like growth factor-I-mediated survival from anoikis: role of cell aggregation and focal adhesion kinase. *J Cell Physiol* 1998; **176**: 648-657
- Dieckgraefe BK, Weems DM. Epithelial injury induces egr-1 and fos expression by a pathway involving protein kinase C and ERK. *Am J Physiol* 1999; **276**(2 Pt 1): G322-330
- Halter F, Tarnawski AS, Schmassmann A, Peskar BM. Cyclooxygenase 2-implications on maintenance of gastric mucosal integrity and ulcer healing: controversial issues and perspectives. *Gut* 2001; **49**: 443-453
- Rodrigues S, Van Aken E, Van Boclaer S, Attouf S, Nguyen QD, Bruyneel E, Westley BR, May FE, Thim L, Mareel M, Gispach C, Emami S. Trefoil peptides as proangiogenic factors *in vivo* and *in vitro*: implication of cyclooxygenase-2 and EGF receptor signaling. *Faseb J* 2003; **17**: 7-16
- Ugucioni M, Gionchetti P, Robbiani DF, Rizzello F, Peruzzo S, Campieri M, Baggiolini M. Increased expression of IP-10, IL-8, MCP-1, and MCP-3 in ulcerative colitis. *Am J Pathol* 1999; **155**: 331-336
- MacDermott RP. Chemokines in the inflammatory bowel diseases. *J Clin Immunol* 1999; **19**: 266-272
- McCormack G, Moriarty D, O'Donoghue DP, McCormick PA, Sheahan K, Baird AW. Tissue cytokine and chemokine expression in inflammatory bowel disease. *Inflamm Res* 2001; **50**: 491-495
- Goke M, Kanai M, Lynch-Devaney K, Podolsky DK. Rapid mitogen-activated protein kinase activation by transforming growth factor alpha in wounded rat intestinal epithelial cells. *Gastroenterology* 1998; **114**: 697-705
- Pratt RL, Kinch MS. Activation of the EphA2 tyrosine kinase stimulates the MAP/ERK kinase signaling cascade. *Oncogene* 2002; **21**: 7690-7699
- Tong J, Elowe S, Nash P, Pawson T. Manipulation of EphB2 regulatory motifs and SH2 binding sites switches MAPK signaling and biological activity. *J Biol Chem* 2003; **278**: 6111-6119
- Cowan CA, Henkemeyer M. The SH2/SH3 adaptor Grb4 transduces B-ephrin reverse signals. *Nature* 2001; **413**: 174-179
- Ray RM, Viar MJ, McCormack SA, Johnson LR. Focal adhesion kinase signaling is decreased in polyamine-depleted IEC-6 cells. *Am J Physiol Cell Physiol* 2001; **281**: C475-485

Science Editor Guo SY Language Editor Elsevier HK

• BASIC RESEARCH •

Apoptosis of pancreatic cancer BXPc-3 cells induced by indole-3-acetic acid in combination with horseradish peroxidase

Chen Huang, Li-Ying Liu, Tu-Sheng Song, Lei Ni, Ling Yang, Xiao-Yan Hu, Jing-Song Hu, Li-Ping Song, Yu Luo, Lu-Sheng Si

Chen Huang, Li-Ying Liu, Tu-Sheng Song, Lei Ni, Ling Yang, Xiao-Yan Hu, Jing-Song Hu, Li-Ping Song, Yu Luo, Department of Cytobiology and Medical Genetics, Xi'an Jiaotong University, Xi'an 710061, Shaanxi Province, China
Lu-Sheng Si, College of Life Science and Technology, Xi'an Jiaotong University, Xi'an 710061, Shaanxi Province, China
Supported by the Natural Science Foundation of Shaanxi Province, No. 2003C215

Correspondence to: Professor Lu-Sheng Si, College of Life Science and Technology, Xi'an Jiaotong University, Xi'an 710061, Shaanxi Province, China. slusheng@yahoo.com

Telephone: +86-29-82655190 Fax: +86-29-82655077

Received: 2004-10-30 Accepted: 2004-12-09

Abstract

AIM: To explore the mechanisms underlying the apoptosis of human pancreatic cancer BXPc-3 cells induced by indole-3-acetic acid (IAA) in combination with horseradish peroxidase (HRP).

METHODS: BXPc-3 cells derived from human pancreatic cancer were exposed to 40 or 80 $\mu\text{mol/L}$ IAA and 1.2 $\mu\text{g/mL}$ HRP at different times. Then, MTT assay was used to detect the cell proliferation. Flow cytometry was performed to analyze cell cycle. Terminal deoxynucleotidyl transferase-mediated dUTP nick end labeling assay was used to detect apoptosis. 2,7-Dichlorofluorescein diacetate uptake was measured by confocal microscopy to determine free radicals. Level of malondialdehyde (MDA) and activity of superoxide dismutase (SOD) were measured by biochemical methods.

RESULTS: IAA/HRP initiated growth inhibition of BXPc-3 cells in a dose- and time-dependent manner. Flow cytometry revealed that the cells treated for 48 h were arrested at G_1/G_0 . After exposure to 80 $\mu\text{mol/L}$ IAA plus 1.2 $\mu\text{g/mL}$ HRP for 72 h, the apoptosis rate increased to 72.5%, which was nine times that of control. Content of MDA and activity of SOD increased respectively after treatment compared to control. Meanwhile, IAA/HRP stimulated the formation of free radicals.

CONCLUSION: The combination of IAA and HRP can inhibit the growth of human pancreatic cancer BXPc-3 cells *in vitro* by inducing apoptosis.

© 2005 The WJG Press and Elsevier Inc. All rights reserved.

Key words: Indole-3-acetic acid; Horseradish peroxidase; BXPc-3 cells; Apoptosis; Free radical

Huang C, Liu LY, Song TS, Ni L, Yang L, Hu XY, Hu JS, Song LP, Luo Y, Si LS. Apoptosis of pancreatic cancer BXPc-3 cells induced by indole-3-acetic acid in combination with horseradish peroxidase. *World J Gastroenterol* 2005; 11 (29): 4519-4523

<http://www.wjgnet.com/1007-9327/11/4519.asp>

INTRODUCTION

Indole-3-acetic acid (IAA) is an important plant growth hormone found in higher plants, and plays a role in the regulation of plant cell division, elongation and differentiation^[1]. It is present in human urine^[2], blood plasma^[3], and central nervous system^[4]. IAA is well tolerated in humans^[5] and not oxidized by mammalian peroxidases. Recent researches suggest that the combination of IAA and horseradish peroxidase (HRP) is cytotoxic to mammalian cells, and can be used as a novel anticancer drug^[6-10], while neither IAA nor HRP alone shows any cytotoxic effect^[6]. HRP is a heme-containing peroxidase and can oxidize a wide variety of substrates including IAA in the presence of hydrogen peroxide. It has been reported that IAA activated by HRP produces free radicals, such as indolyl, skatolyl, and peroxy radicals, which can cause lipid peroxides^[11-13]. There are differences in endurance to the combination of IAA and HRP among the different types of cells^[14]. In the present study, we investigated the effects of IAA/HRP on BXPc-3 cells, a cell line derived from human pancreatic cancer, and found that IAA/HRP treatment could induce an increase of free radicals within the cells and cause apoptosis of BXPc-3 cells.

MATERIALS AND METHODS

Drug and reagents

IAA, HRP, and 3-(4,5-dimethylthiazol)-2,5-diphenyl tetrazolium bromide (MTT) were purchased from Sigma Chemical Co. 2,7-Dichlorofluorescein diacetate (DCFH-DA) was from Molecular Probes Co., and *in situ* cell apoptosis detection kit was from Sino-American Biotechnic Co. Commercial kits used for determining lipid peroxide and superoxide dismutase (SOD) activity were obtained from the Jiancheng Institute of Biotechnology (Nanjing, China).

Cell culture

Cells (1.0×10^5 cells/mL) were cultured in RPMI supplemented with 100 mL/L fetal bovine serum containing 2.0 mmol/L glutamine and 20 μg penicillin-streptomycin/mL in 50 mL/L CO_2 at 37 °C.

Experimental design

The experiments were divided into three groups: control group, 40 $\mu\text{mol/L}$ IAA+1.2 $\mu\text{g/mL}$ HRP (40 $\mu\text{mol/L}$ IAA/HRP) and 80 $\mu\text{mol/L}$ IAA+1.2 $\mu\text{g/mL}$ HRP (80 $\mu\text{mol/L}$ IAA/HRP) treatment groups. All tests were carried out in triplicate.

MTT assay for cell viability

Cells (2×10^4 cells/well) were seeded onto 96-well plates and incubated with test substances for an indicated time at 37 °C in 50 mL/L CO₂. Then, 20 μL /well of MTT solution (5 mg/mL) was added and incubated for another 4 h. Supernatants were removed and formazan crystals were dissolved in 200 μL of dimethylsulfoxide. Finally, optical density was determined at 540 nm by a POLARstar⁺ OPTIMA (BMG Labtechnologies).

Detection of apoptosis

Apoptotic cells were identified using an *in situ* cell apoptosis detection kit. The cells were treated with IAA/HRP for a given time, and processed following the manufacturer's instruction. At least 1 000 cells were counted in each test, and the percentage of terminal deoxynucleotidyl transferase-mediated dUTP nick end labeling (TUNEL)-positive cells was calculated.

Measurement of MDA content and SOD activity in cells

The number of cells was adjusted to 1×10^6 cells/mL, and broken by ultrasonic with PBS. Homogenates were centrifuged (1 000 r/min, 10 min, 4 °C) and the supernatant was used immediately for the assays of malondialdehyde (MDA) and SOD according to the instructions of the kits. MDA content was determined by the thiobarbituric acid method^[15] and expressed in nanomole per milligram protein. The assay for total SOD was based on its ability to inhibit the oxidation of oxyamine by the xanthine-xanthine oxidase system. The red product (nitrite) had an absorbance at 550 nm. One unit of SOD activity was defined as the quantity reducing the absorbance at 550 nm by 50%. The activity of SOD was expressed in nanounit per milligram protein.

Quantitative image analysis of intracellular ROS in live cells by confocal microscopy

Cells (2×10^4 cells/well) were seeded onto 24-well plates with cover slide and incubated with test substances for an indicated time at 37 °C in 50 mL/L CO₂. The cells adhered to the glass flake were incubated with 50 $\mu\text{mol/L}$ of DCFH-DA for 5 min in dark in a CO₂ incubator. DCFH-DA is a nonpolar and nonfluorescent compound, which diffuses into the cells and is hydrolyzed into a polar 2',7'-dichlorofluorescein (DCFH)^[16]. The intracellular DCFH was rapidly oxidized to produce highly fluorescent 2',7'-dichlorofluorescein (DCF) at the presence of ROS or hydrogen peroxide within the cells. After incubation, the remaining dye was removed and the cells were washed twice with RPMI-HEPES before imaging collection. All confocal imaging analyses were performed under a Leica confocal laser scanning microscope using the 488-nm excitation laser line and simultaneous dual display mode (522 nm emission

and phase-contrast) of the BioRad LaserSharp imaging program. Five random images were collected to determine the average fluorescence intensity.

Cell cycle analysis by flow cytometry

DNA content per duplicate was analyzed using a FACStar flow cytometer (Becton Dickinson, Mountainview, CA). The adherent cells were harvested by brief trypsinization, and washed with PBS, fixed in 70% ethanol, stained with 20 $\mu\text{g/mL}$ propidium iodide containing 20 $\mu\text{g/mL}$ RNase (DNase free) for 30 min, and analyzed by flow cytometry. The populations of G₀/G₁, S, and G₂/M cells were quantitated.

Statistical analysis

The data were expressed as mean \pm SD and analyzed by software of SPSS10.0. $P < 0.05$ was considered statistically significant.

RESULTS

Inhibition of cell growth and arrest of cell cycle

The growth of human pancreatic cancer BXPC-3 cells was measured using MTT assay at varying time points after treatment. As shown in Figure 1, the combination of IAA and HRP could inhibit the growth of BXPC-3 cells. The inhibition of cell growth after treatment with 80 $\mu\text{mol/L}$ IAA/HRP was higher than that after treatment with 40 $\mu\text{mol/L}$ IAA/HRP, suggesting that the inhibition was in an IAA dose-dependent manner. Because the inhibition of cell growth was the highest 2 d after the treatment, we checked the cell cycle using a flow cytometer at the time of 2-d treatment. The cell cycle distribution of BXPC-3 cells in control group was 62.28% at G₁/G₀, 0.43% at G₂/M and 37.28% at S. In the IAA/HRP treatment group, the cell cycle distribution of BXPC-3 cells significantly increased at G₁/G₀ phase, and decreased greatly at S phase, implying that IAA/HRP could induce the arrest of cells at G₁/G₀ phase.

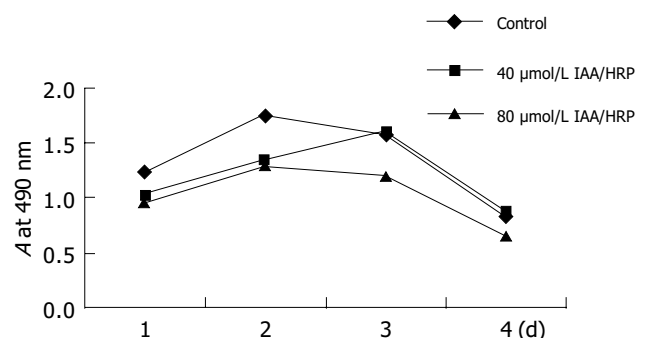


Figure 1 Effect of IAA and HRP treatment on growth of BXPC-3 cells.

Effect of IAA/HRP treatment on apoptosis of BXPC-3 cells

After TUNEL staining, the apoptotic cells markedly increased after IAA/HRP treatment. When the cells were treated with IAA/HRP for 72 h, the apoptosis rate increased to 72.5%, which was nine times that of the control ($P < 0.05$, Figure 2).

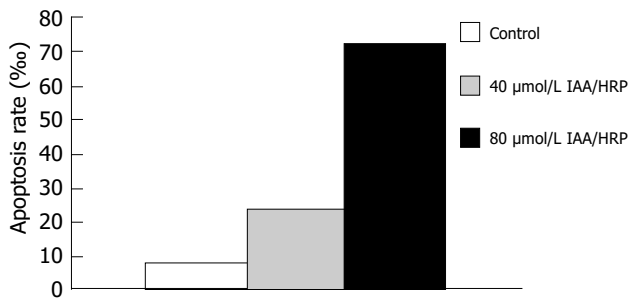


Figure 2 Apoptosis rate of BXPC-3 cells 3 d after IAA and HRP treatment.

Production of free radicals in BXPC-3 cells induced by IAA/HRP

The formation of ROS in BXPC-3 cells treated with IAA/HRP could be detected by confocal microscopy as the product was able to show fluorescence. As shown in Figure 3, DCF fluorescence in cells exposed to IAA/HRP for 3, 6, 24, and 48 h was much brighter compared to that in control group, suggesting that free radicals were formed in a IAA dose- and time-dependent manner (Table 1, Figure 4).

Level of MDA and activity of SOD in BXPC-3 cells treated with IAA/HRP

To investigate the damage of free radicals induced by IAA/HRP in BXPC-3 cells, MDA content and SOD activity were measured. The content of MDA and activity of SOD

Table 1 Cell cycle distribution of BXPC-3 cells 2 d after IAA plus HRP treatment

Treatment	G ₁ /G ₀	G ₂ /M	S
Control	62.28±8.34	0.43±0.57	37.28±8.91
40 μmol/L IAA/HRP	76.68±5.06 ^a	0.85±1.47	22.47±5.83
80 μmol/L IAA/HRP	76.91±5.78 ^a	18.77±1.87 ^a	4.32±6.66 ^a

^aP<0.05 between control vs treated group.

Table 2 SOD activity and MDA content in BXPC-3 cells 3 d after IAA and HRP treatment (mean±SD)

Treatment	Control	40 μmol/L IAA/HRP	80 μmol/L IAA/HRP
SOD (nU/mg protein)	105.60±41.04	135.98±1.46	193.34±37.89 ^b
MDA (μmol/L/mg protein)	20.80±0.33	22.29±1.04	99.53±30.45 ^b

^bP<0.01 control group vs treatment group.

in BXPC-3 cells increased after IAA/HRP treatment (Table 2). There were significant differences between treatment group and control group (P<0.01).

DISCUSSION

Although IAA/HRP-induced cell death and its potential application in cancer therapy has been recognized^[8,17,18], the sensitivity of different cell types to IAA/HRP might not be the same^[14]. We chose human pancreatic cancer BXPC-3 cells to evaluate IAA/HRP, which could be used in treatment of human pancreatic cancer. In this study, the MTT assay showed that the viability of BXPC-3 cells decreased with increase of IAA in the presence of HRP (Figure 1). In addition, TUNEL analysis showed that IAA/HRP induced apoptosis of BXPC-3 cells (Figure 2). In agreement with our results, it was also reported that the photoproducts of IAA induce apoptosis of human HL-60 and murine tumor cells^[19].

There are two important arrest points in cell cycle at G₁/G₀ and G₂/M^[20-23]. Flow cytometric analysis of propidium iodide-stained cells showed that cells accumulated at the G₁/G₀ phase compared to control (Table 1). These cell cycle changes suggest that pancreatic cancer cells have oxidative stress response to IAA/HRP treatment with DNA damage leading to apoptosis.

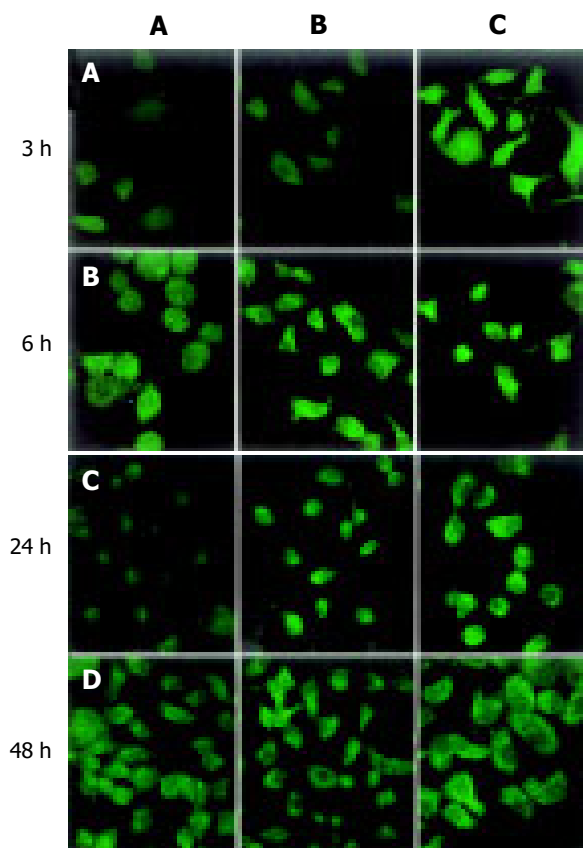


Figure 3 Confocal images of intracellular ROS generation after 3, 6, 24, and 48 h exposure of BXPC-3 cells to IAA/HRP. A: Control; B: 40 μmol/L IAA/HRP; C: 80 μmol/L IAA/HRP.

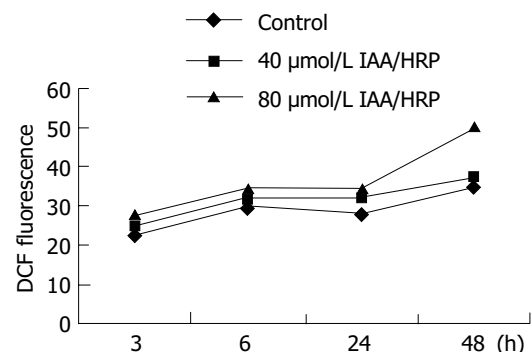


Figure 4 Production of free radicals in BXPC-3 cells exposed to IAA and HRP.

DCFH is widely used to measure the oxidative stress in cells^[24-26]. When the diacetate form of DCFH is added to cells, it diffuses across the cell membrane and is hydrolyzed by intracellular esterases to liberate DCFH, which upon reaction with oxidizing species forms its two-electron oxidation product, the highly fluorescent compound DCF. The fluorescence intensity can be easily measured by confocal microscopy and is the basis of the popular cellular assay for oxidative stress. In this study, DCF was used to investigate the production of free radicals in BXPC-3 cells treated with IAA/HRP. The fluorescence intensity increased in the treatment group in comparison to control group (Figure 3), suggesting that the formation of free radicals increases in an IAA dose- and time-dependent manner (Figure 4).

It is known that tumor cells exhibit metabolic characteristics in terms of oxygen consumption and oxidative metabolism. The fact that tumor tissues are more susceptible to oxidative stress than the surrounding normal cells is supported by the increase of lipid peroxidation and DNA damage^[27] and the decrease of antioxidant enzyme activities^[28]. Folkes *et al.*^[6], found that lipid peroxidation in liposomes is stimulated by the IAA/HRP treatment, but it cannot be measured in mammalian cells. To investigate the damage of free radicals in cells, MDA content, and SOD activity were measured in this study. The results showed that the content of MDA and the activity of SOD in BXPC-3 cells increased when treated with IAA/HRP (Table 2). In agreement with our results, it was also reported that incubation of neutrophils for 24 h in the presence of IAA increases the activities of SOD, catalase (CAT) and glutathione peroxidase^[29]. Recently, it was reported that ROS activates the ERK signaling cascade^[30-32]. Kim *et al.*^[33], proved that IAA/HRP can activate p38 mitogen-activated protein (MAP) kinase and c-Jun N-terminal kinase (JNK) in G361 human melanoma cells, which are almost completely blocked by antioxidants.

In summary, the combination of IAA and HRP can inhibit the growth of human pancreatic cancer BXPC-3 cells *in vitro* by inducing apoptosis, which is associated with the increase of free radicals.

REFERENCES

- Rapparini F, Tam YY, Cohen JD, Slovin JP. Indole-3-acetic acid metabolism in *Lemna gibba* undergoes dynamic changes in response to growth temperature. *Plant Physiol* 2002; **28**: 1410-1416
- Qureshi GA, Baig SM. The role of tryptophan, 5-hydroxy indole-3-acetic acid and their protein binding in uremic patients. *Biochem Mol Biol Int* 1993; **29**: 411-419
- Bertuzzi A, Mingrone G, Gandolfi A, Greco AV, Ringoir S, Vanholder R. Binding of indole-3-acetic acid to human serum albumin and competition with L-tryptophan. *Clin Chim Acta* 1997; **265**: 183-192
- Nilsson GE, Tottmar O. Biogenic aldehydes in brain: characteristics of a reaction between rat brain tissue and indole-3-acetaldehyde. *J Neurochem* 1985; **45**: 744-751
- Diengott D, Mirsky IA. Hypoglycemic action of indole-3-acetic acid by mouth in patients with diabetes mellitus. *Proc Soc Exp Biol Med* 1956; **93**: 109-110
- Folkes LK, Candeias LP, Wardman P. Toward targeted "oxidation therapy" of cancer: peroxidase-catalysed cytotoxicity of indole-3-acetic acids. *Int J Radiat Oncol Biol Phys* 1998; **42**: 917-920
- Greco O, Dachs GU. Gene directed enzyme/prodrug therapy of cancer: historical appraisal and future perspectives. *J Cell Physiol* 2001; **187**: 22-36
- Wardman P. Indole-3-acetic acid and horseradish peroxidase: a new prodrug/enzyme combination for targeted cancer therapy. *Curr Pharm Des* 2002; **8**: 1363-1374
- Greco O, Rossiter S, Kanthou C, Folkes LK, Wardman P, Tozer GM, Dachs GU. Horseradish peroxidase-mediated gene therapy: choice of prodrugs in oxic and anoxic tumor conditions. *Mol Cancer Ther* 2001; **1**: 151-160
- Greco O, Folkes LK, Wardman P, Tozer GM, Dachs GU. Development of a novel enzyme/prodrug combination for gene therapy of cancer: horseradish peroxidase/indole-3-acetic acid. *Cancer Gene Ther* 2000; **7**: 1414-1420
- Folkes LK, Greco O, Dachs GU, Stratford MR, Wardman P. 5-Fluoroindole-3-acetic acid: a prodrug activated by a peroxidase with potential for use in targeted therapy. *Biochem Pharmacol* 2002; **63**: 265-272
- Candeias LP, Folkes LK, Wardman P. Amplification of oxidative stress by decarboxylation: a new strategy in antitumor drug design. *Biochem Soc Trans* 1995; **23**: 262S
- Candeias LP, Folkes LK, Porssa M, Parrick J, Wardman P. Enhancement of lipid peroxidation by indole-3-acetic acid and derivatives: Substituent effects. *Free Radical Res* 1995; **23**: 403-418
- Candeias LP, Folkes LK, Porssa M, Parrick J, Wardman P. Enhancement of peroxidase-induced lipid peroxidation by indole-3-acetic acid: effect of antioxidants. *Free Radic Res* 1996; **2**: 141-147
- Gavino VC, Miller JS, Ikharebha SO, Milo GE, Cornwell DG. Effect of polyunsaturated fatty acids and antioxidants on lipid peroxidation in tissue cultures. *J Lipid Res* 1981; **22**: 763-769
- Chen KC, Zhou Y, Xing K, Krysan K, Lou MF. Platelet derived growth factor (PDGF)-induced reactive oxygen species in the lens epithelial cells: the redox signaling. *Exp Eye Res* 2004; **78**: 1057-1067
- Folkes LK, Wardman P. Oxidative activation of indole-3-acetic acids to cytotoxic species- a potential new role for plant auxins in cancer therapy. *Biochem Pharmacol* 2001; **61**: 129-136
- Greco O, Dachs GU, Tozer GM, Kanthou C. Mechanisms of cytotoxicity induced by horseradish peroxidase/indole-3-acetic acid gene therapy. *J Cell Biochem* 2002; **87**: 221-232
- Edwards AM, Barredo F, Silva E, De Ioannes AE, Becker MI. Apoptosis induction in nonirradiated human HL-60 and murine NSO/2 tumor cells by photoproducts of indole-3-acetic acid and riboflavin. *Photochem Photobiol* 1999; **70**: 645-649
- Chang GC, Hsu SL, Tsai JR, Liang FP, Lin SY, Sheu GT, Chen CY. Molecular mechanisms of ZD1839-induced G1-cell cycle arrest and apoptosis in human lung adenocarcinoma A549 cells. *Biochem Pharmacol* 2004; **68**: 1453-1464
- Abasolo I, Wang Z, Montuenga LM, Calvo A. Adrenomedullin inhibits prostate cancer cell proliferation through a cAMP-independent autocrine mechanism. *Biochem Biophys Res Commun* 2004; **322**: 878-886
- Yang JS, Hour MJ, Kuo SC, Huang LJ, Lee MR. Selective induction of G2/M arrest and apoptosis in HL-60 by a potent anticancer agent, HMJ-38. *Anticancer Res* 2004; **24**: 1769-1778
- Parnaud G, Li P, Cassar G, Rouimi P, Tulliez J, Combaret L, Gamet-Payrastra L. Mechanism of sulforaphane-induced cell cycle arrest and apoptosis in human colon cancer cells. *Nutr Cancer* 2004; **48**: 198-206
- Rota C, Chignell CF, Mason RP. Evidence for free radical formation during the oxidation of evidence for free radical formation during the oxidation of 2'-7'-Dichlorofluorescein to the fluorescent dye 2'-7'-dichlorofluorescein by horseradish peroxidase: possible implications for oxidative stress measurements. *Free Radic Biol Med* 1999; **27**: 873-881

- 25 **Royall JA**, Ischiropoulos H. Evaluation of 2',7'-dichlorofluorescein and dihydrorhodamine 123 as fluorescent probes for intracellular H₂O₂ in cultured endothelial cells. *Arch Biochem Biophys* 1993; **302**: 348–355
- 26 **Huang X**, Frenkel K, Klein CB, Costa M. Nickel induces oxidants in intact cultured mammalian cells as detected by dichlorofluorescein fluorescence. *Toxicol Appl Pharmacol* 1993; **120**: 29–36
- 27 **Jaruga P**, Zastawny TH, Skokowski J, Dizdaroglu M, Olinski R. Oxidative DNA base damage and antioxidant enzyme activities in human lung cancer. *FEBS Lett* 1994; **341**: 59–63
- 28 **Sun Y**. Free radicals, antioxidant enzymes and carcinogenesis. *Free Radic Biol Med* 1990; **8**: 583–599
- 29 **de Melo MP**, de Lima TM, Pithon-Curi TC, Curi R. The mechanism of indole acetic acid cytotoxicity. *Toxicol Lett* 2004; **148**: 103–111
- 30 **Guyton KZ**, Liu Y, Gorospe M, Xu Q, Holbrook NJ. Activation of mitogen-activated protein kinase by H₂O₂. Role in cell survival following oxidant injury. *J Biol Chem* 1996; **271**: 4138–4142
- 31 **Gupta A**, Rosenberger SF, Bowden GT. Increased ROS levels contribute to elevated transcription factor and MAP kinase activities in malignantly progressed mouse keratinocyte cell lines. *Carcinogenesis* 1999; **20**: 2063–2073
- 32 **Tournier C**, Thomas G, Pierre J, Jacquemin C, Pierre M, Saunier B. Mediation by arachidonic acid metabolites of the H₂O₂-induced stimulation of mitogen-activated protein kinases (extracellular-signal-regulated kinase and c-Jun NH₂-terminal kinase). *Eur J Biochem* 1997; **244**: 587–595
- 33 **Kim DS**, Jeon SE, Park KC. Oxidation of indole-3-acetic acid by horseradish peroxidase induces apoptosis in G361 human melanoma cells. *Cell Signal* 2004; **16**: 81–88

Science Editor Wang XL and Li WZ Language Editor Elsevier HK

Role of interleukin 18 in acute lung inflammation induced by gut ischemia reperfusion

Yong-Jie Yang, Yun Shen, Song-Hua Chen, Xi-Rui Ge

Yong-Jie Yang, Institute of Biochemistry and Cell Biology, Shanghai Institutes for Biological Sciences, Chinese Academy of Sciences; Graduate School of the Chinese Academy of Sciences, Shanghai 200031, China

Yun Shen, Department of Traditional Chinese Medicine, Shanghai University of Traditional Chinese Medicine, Shanghai 201023, China
Song-Hua Chen, Xi-Rui Ge, Institute of Biochemistry and Cell Biology, Shanghai Institutes for Biological Sciences, Chinese Academy of Sciences, Shanghai 200031, China

Supported by the CAS Pilot Project of Knowledge Innovation Program, No. KSCX 2-3-04-03

Correspondence to: Professor Xi-Rui Ge, Cell Resources Center, Shanghai Institutes for Biological Sciences, CAS, Shanghai 200031, China. gexirui@sibs.ac.cn

Telephone: +86-21-54920407 Fax: +86-21-54920406

Received: 2004-12-25 Accepted: 2005-01-05

Abstract

AIM: To study the changes of endogenous interleukin 18 (IL-18) levels and evaluate the role of IL-18 on lung injury following gut ischemia/reperfusion.

METHODS: A superior mesenteric artery occlusion model was selected for this research. The mice were randomly divided into four groups: Sham operation (sham), ischemia (0.5 h) followed by different times of reperfusion (I/R), and I/R pretreated with exogenous IL-18 (I/R+IL-18) or IL-18 neutralizing antibody (I/R+IL-18Ab) 15 min before ischemia. Serum IL-18 levels were detected by Western blot and ELISA, and the levels of IL-18 in lung tissue were evaluated by immunohistochemical staining. For the study of pulmonary inflammation, the lung myeloperoxidase (MPO) contents and morphological changes were evaluated.

RESULTS: Gut ischemia/reperfusion induced rapid increase of serum IL-18 levels, peaked at 1 h after reperfusion and then declined. The levels of IL-18 in lung tissue were gradually enhanced as the progress of reperfusion. Compared with I/R group, exogenous administration of IL-18 (I/R+IL-18) further remarkably enhanced the pulmonary MPO activity and inflammatory cell infiltration, and in I/R+IL-18Ab group, the content of MPO were significantly reduced and lung inflammation was also decreased.

CONCLUSION: Gut ischemia/reperfusion induces the increase of IL-18 expression, which may make IL-18 act as an important proinflammatory cytokine and contribute to gut ischemia/reperfusion-induced lung inflammation.

Key words: IL-18; Ischemia; Reperfusion; Inflammation

Yang YJ, Shen Y, Chen SH, Ge XR. Role of interleukin 18 in acute lung inflammation induced by gut ischemia reperfusion. *World J Gastroenterol* 2005; 11(29): 4524-4529
<http://www.wjgnet.com/1007-9327/11/4524.asp>

INTRODUCTION

Multiple organ dysfunction syndrome (MODS) is the leading cause of death in critically ill patients. Although systemic inflammation characteristic of MODS can result in damage to any organ, onset of the syndrome is usually heralded by the development of respiratory insufficiency^[1,2]. Gut ischemia and reperfusion (I/R) is a prime mechanism that results in the pathogenesis of MODS partly dependent on neutrophils^[2]. Neutrophils can be activated in response to reperfusion of ischemia tissue or exposure to endotoxin and pro-inflammatory cytokines^[1]. Activated neutrophils adhere to endothelium through adhesion molecules, resulting in localized release of proteases, reactive oxygen species (ROS) and various cytokines and inflammatory mediators that contribute to tissue injury and failure^[1,2].

Interleukin 18 (IL-18), known initially as an IFN- γ -inducing factor, is a pleiotropic proinflammatory cytokine and it has direct proinflammatory properties. In this respect, IL-18 induces production of proinflammatory cytokines such as TNF- α , IL-1 β and chemokines such as IL-8, MIP-1 α and MCP-1^[3,4], and upregulates expression of adhesion molecules such as ICAM-1, VCAM-1 on endothelial cells^[3,5]. Furthermore, IL-18 is found to activate neutrophils and promote neutrophil migration, adhesion and accumulation *in vivo*^[6]. These data suggest that IL-18 may be involved in the inflammatory injuries associated with I/R^[1,2,7,8]. Therefore, recent evidence showing that some local tissue ischemic injuries are associated with increased IL-18 levels^[9,10], and elevated IL-18 levels have been detected in response to hepatic I/R injury^[11]. A direct correlation has been observed between IL-18 levels and liver neutrophils sequestration and liver injury, which suggests that IL-18 is required for facilitating neutrophil-dependent hepatic I/R injury^[11]. Similarly, increased levels of IL-18 have been detected in isolated atrial trabeculae during I/R injury^[12]. Inhibition of IL-18 or caspase-1 activity attenuated tissue and circulating levels of IL-18 and improved myocardial contractility, suggesting that endogenous IL-18 play a significant role in I/R-induced human myocardial injury^[12]. Furthermore, Melnikov *et al.*, reported that caspase-1 and IL-18 play an important role in the ischemic acute renal failure^[13]; however,

there is also evidence suggesting that activated caspase-1 and its inflammatory products are not crucial to the induction of inflammation after renal I/R^[4]. It is intriguing to consider the role of IL-18 in the I/R-induced local organ injury, and no evidence exists on the role of IL-18 in the MODS following I/R. Therefore, the major aim of present study was to determine the change of expression and role of IL-18 in the acute pulmonary injury after gut ischemia/reperfusion.

MATERIALS AND METHODS

Reagents and mice

C57BL/6J mice (SPF) were obtained from animal center, SIBS, Shanghai. For the experiments, 8-10-wk-old mice weighing 22-26 g were used. rmIL-18 was expressed and purified in our lab (purity >95% by SDS-PAGE) and the activity was confirmed by its ability to induce IFN- γ production by mouse spleen cells. For immunohistochemical analysis, polyclonal rabbit anti-mouse IL-18 antibody was purchased from Boster (Wuhan, China). For immunoprecipitation and Western blot analysis, polyclonal rabbit anti-murine IL-18 antibody was provided by PeproTech (Rocky Hill, NJ, USA).

Ischemia/reperfusion model

Mice were anesthetized by intraperitoneal injection of urethane (250 mg/mL, 1.25 mg/g wt of mouse, Sigma). The abdomen was rinsed with 75% ethanol, a midline laparotomy was performed and the superior mesenteric artery was occluded with an arterial clamp. Intestinal ischemia was confirmed by pulselessness of the mesenteric artery and paleness of the jejunum and ileum. Sham-operated mice underwent the same procedure, but without vascular occlusion. After 30 min, the clamp was removed, sterile saline was injected into the peritoneal cavity for resuscitation, and the mice were sutured.

Experimental protocols

The mice were randomly divided into four groups ($n = 5$ in each): sham, I/R, I/R+IL-18, and I/R+anti-IL-18. For exogenous IL-18 studies, animals were pretreated with either IL-18 (5 μ g/mouse) or sterile saline via the lateral tail vein 15 min before ischemia. For IL-18 neutralization studies, mice received monoclonal anti-IL-18 antibody (25 μ g/mouse, MBL, Nagoya, Japan) or sterile saline 15 min before ischemia. Animals underwent 30 min of superior mesenteric artery occlusion (or sham operation) followed by indicated periods of reperfusion were killed, lung tissues, and blood samples were taken for analysis. Excised lungs were frozen in liquid nitrogen and stored at -70 °C before determination of myeloperoxidase (MPO) activity. For histological or immunohistochemical studies, lungs were immersed in 10% neutral buffered formalin before sectioning. All blood samples were kept at room temperature for 2 h to clot, and serum was removed and stored at -70 °C until the time of assay.

Serum IL-18 measurements

Animals underwent cardiac puncture to obtain blood at the indicated times in the reperfusion period. Systemic levels of IL-18 were evaluated by immunoprecipitation followed by Western blot. Serum was diluted to 1 mL with PBS, and

serum IL-18 was immunoprecipitated with rabbit anti-murine IL-18 antibody. Then, the immunoprecipitates were resolved by SDS-PAGE (12-15% acrylamide) under reducing conditions. Gels were transferred to NC membranes and incubated with primary antibodies (1:1 000) at 4 °C overnight. Then mouse anti-rabbit IgG peroxidase was added and developed by ECL. Serum levels of IL-18 were further measured by ELISA according to the manufacturer's instructions (Boster, Wuhan, China). The detection limit for IL-18 was <5 pg/mL.

MPO assay

MPO activity is an indicator of neutrophil accumulation. The content of MPO in the tissues was measured as previously described with slight modification^[7]. The lungs were homogenized for 30 s in 4 mL 50 mmol/L potassium phosphate buffer (pH 6.0) and then centrifuged for 30 min at 16 000 g at 4 °C. The pellet was resuspended in 1.5 mL 50 mmol/L potassium phosphate buffer (pH 6.0) containing 5 g/L cetrimonium bromide. The samples were sonicated for 90 s and then incubated in a 60 °C water bath for 2 h, and centrifuged for 30 min at 35 000 g at 4 °C. The supernatant 50 μ L was added to 950 μ L of 50 mmol/L potassium phosphate buffer (pH 6.0) containing 0.167 mg/mL *o*-dianisidine (Sigma) and 5 μ L/L hydrogen peroxide. Absorbance of 460 nm was measured at 1 and 3 min. MPO content per gram of wet tissue was calculated as: MPO content (A/g wet tissue) = $(A_{460}(3 \text{ min}) - A_{460}(1 \text{ min})) / \text{tissue weight (g)}$.

Histopathology and immunohistochemistry

Lungs were immersed in 10% neutral buffered formalin before sectioning. Sections (4 μ m) were obtained from paraffin-embedded tissue samples, stained with hematoxylin-eosin (HE), and examined for histological evaluation of tissue damage under a microscope and photographed. For immunohistochemical analyses, paraffin-embedded lung sections of 4 μ m were incubated overnight at 4 °C with polyclonal rabbit anti-mouse IL-18 antibody (dilution 1:100). Biotinylated IgG was added as second antibody. Horseradish peroxidase-labeled streptomycin-avidin complex was used to detect second antibody. Slides were stained with diaminobenzidine, counterstained with hematoxylin, and finally examined under light microscope. The brown or dark brown stain was considered as positive.

Statistical analysis

All data are presented as mean \pm SD. Significant differences between groups were determined using Student's *t*-test. $P < 0.05$ is considered as statistically significant.

RESULTS

Ischemia/reperfusion-induced upregulation of IL-18 levels

IL-18 has been shown to be upregulated after ischemia in the kidney, heart, and liver. Therefore, we investigated whether the levels of IL-18 changed in response to gut ischemia/reperfusion. The serum, obtained from sham and from gut I/R model at different times of reperfusion, was first evaluated by Western blot, and the change of IL-18

levels is shown in Figure 1A. Two bands were detected in all serum samples, which are consistent with the “pro” and “mature” form of IL-18. At time 0, the content of IL-18 from I/R group, for both pro and mature, was elevated as compared with that from sham-operated mice, and the levels of mature IL-18 (mIL-18) was further considerably elevated 1 h after reperfusion, and then decreased at 3 h (Figure 1A).

Mouse serum IL-18 was further detected by ELISA after gut ischemia/reperfusion or sham operation. As shown in Figure 1B, IL-18 levels from normal mouse were <200 pg/mL. Consistent with the previous results, there was a marked increase in serum IL-18 from I/R group, peak at 1 h (at 660 pg/mL), followed by a decline. In the sham group, there was little measurable change in IL-18 levels during all reperfusion time.

Furthermore, lung tissues obtained from normal mouse and I/R mice with 1 or 3 h reperfusion was examined by immunohistochemistry. Besides the constitutive expression of IL-18 in air way epithelium, normal lung tissue lacked immunoreactive IL-18 (Figure 1C, a and b); during 1-3 h of reperfusion, gradually increased levels of IL-18 were observed with prominent IL-18 staining (Figure 1C, c and d). These data indicated that IL-18 is induced at the early phase of ischemia/reperfusion and may participate in the pulmonary inflammation.

Effects of rIL-18 on lung inflammation after gut I/R

Ischemia-induced expression of IL-18 increased remarkably at the early phase of reperfusion, suggesting that IL-18 may be an early inflammatory mediator and involved in the injurious processes in lung after gut I/R, which prompted

us to suppose whether administration of exogenous IL-18 could exert early effects on neutrophil activation and accelerate lung injury. As shown in Figure 2, in the IL-18-nontreated group, gut ischemia/reperfusion induced gradually increased MPO activity in the lungs at 0.5, 1, or 3 h after reperfusion (0.65 ± 0.08 , 0.86 ± 0.19 , or 1.99 ± 0.17 respectively), and IL-18 injection further dramatically enhanced the MPO activity in the lung tissues at each indicated times after reperfusion: the MPO value in IL-18-treated mice was further increased to 1.54 ± 0.38 (a 237% increase), and 2.63 ± 0.20 (a 306% increase) at 0.5 or 1 h after ischemia respectively, as compared with IL-18-nontreated group ($P<0.05$); and IL-18 administration induced much more neutrophils infiltration in lung within 1 h of reperfusion than that of 3 h of reperfusion in IL-18-nontreated group (Figure 2A). Furthermore, after 3 h of reperfusion, the MPO activity was further increased to higher level (3.68 ± 0.45 , a 184% increase) compared with that from IL-18-nontreated mice ($P<0.05$). These data suggested that IL-18 injection enhanced pulmonary MPO activity and augmented the neutrophil accumulation in lung.

Lung inflammation in this model was evident from histological analysis (Figure 2B). As previously reported, massive neutrophil infiltration was observed in the lung tissues from gut I/R model within 3 h of reperfusion (Figure 2B, b). Although the infiltration in IL-18-nontreated mice at 1 h after ischemia was not obvious (Figure 2B, a), IL-18 injection significantly enhanced the pulmonary infiltration after 1 h of reperfusion (Figure 2B, c). Furthermore, treatment of IL-18 induced more serious inflammatory cell infiltration compared with that of IL-18-nontreated mice as the reperfusion

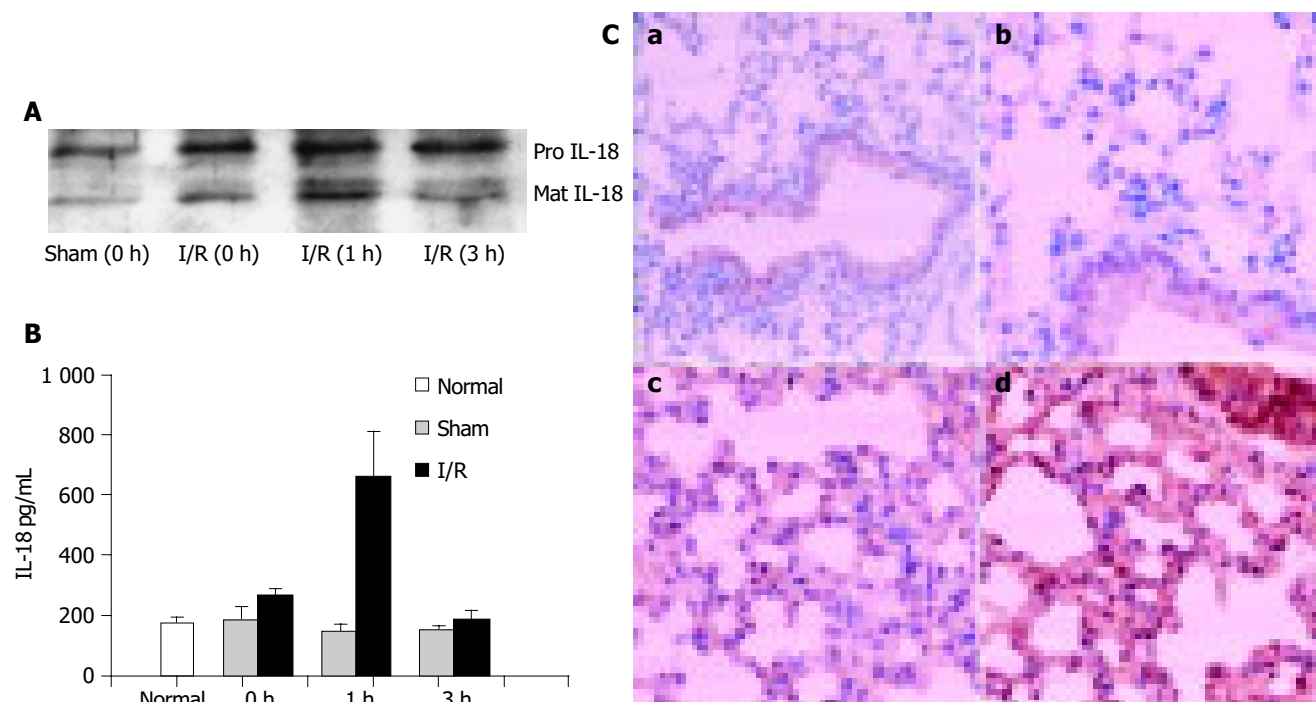


Figure 1 Gut ischemia/reperfusion results in increased levels of IL-18 in serum and lung. (A and B) The circulating levels of IL-18 after gut ischemia/reperfusion. Mice were subjected to gut ischemia/reperfusion or sham. Serum IL-18 at the indicated times after reperfusion was collected, part of which was immunoprecipitated with polyclonal rabbit anti-murine IL-18 antibody and analyzed by immunoblotting

(A), and another part was assayed with ELISA (B) ($n = 5$). (C) Gut ischemia/reperfusion results in elevated levels of IL-18 in lung tissue. Immunohistochemistry of lung sections obtained from normal (a, $\times 100$, and b, $\times 200$), 1 h (c) or 3 h (d) I/R model. The positive staining for IL-18 shows as dark brown. Magnification (c and d) $\times 200$.

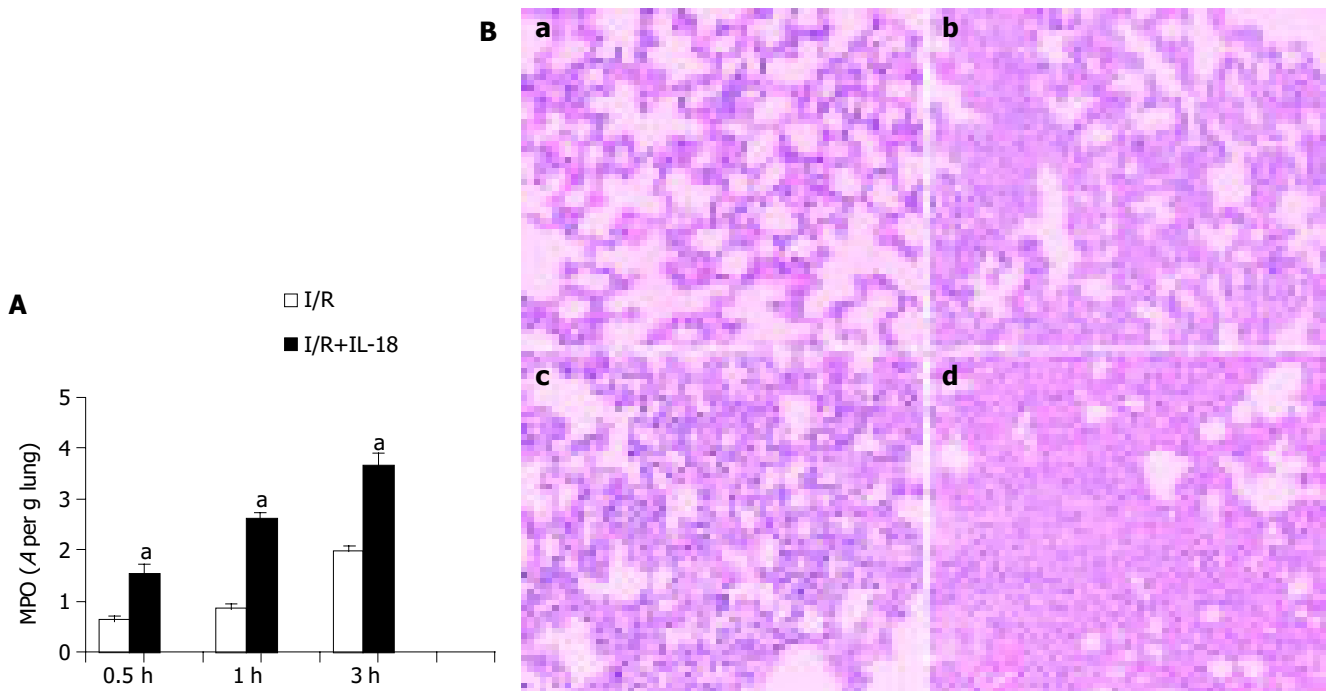


Figure 2 The effect of exogenous IL-18 on the ischemia/reperfusion-induced lung injury. **A:** IL-18 injection further remarkably enhanced the neutrophil sequestration in lung. After indicated times of reperfusion, the MPO activity was determined in lung tissue ($n = 5$), ^a $P < 0.05$ vs I/R. **B:** Comparison of pulmonary

histopathology. Lungs from IL-18-nontreated (a, for 1 h of reperfusion and b, for 3 h) or IL-18-treated (c, for 1 h and d, for 3 h of reperfusion) mice subjected to gut I/R and stained with HE. Magnification $\times 100$.

time extended to 3 h (Figure 2B, b and d), which in accordance with the higher MPO activity in IL-18-treated group. Both indices of lung inflammation, including histological changes and MPO activity, suggest that IL-18 injection may accelerate and augment the lung inflammatory injury in response to gut I/R, and IL-18 may be involved in the lung pathogenesis in this I/R model as an early inflammatory mediator.

Effects of anti-IL-18 on lung inflammatory induced by gut ischemia/reperfusion

To further determine the role of induced IL-18 in the lung pathogenesis, we investigated whether *in vivo* neutralization of IL-18 could modify neutrophil-mediated acute inflammatory response induced by gut I/R. Anti-IL-18Ab (25 μ g/mouse) was administered 15 min before ischemia insult, and after 3 h of reperfusion, the MPO levels were determined and

the lung inflammation was evaluated histopathologically. As shown in Figure 3, anti-IL-18 recipient mice exhibited significantly reduced tissue MPO activity (more than 50% decrease in the lung MPO levels) as compared with the positive control ($P < 0.05$, Figure 3A). Consistent with this, the inflammatory infiltration was significantly reduced in anti-IL-18-treated mice (Figure 3B). These data suggested the IL-18Ab attenuated lung inflammation induced by gut I/R and supported the concept that endogenous IL-18 functioned as an important proinflammatory factor, which may be involved in the neutrophil sequestration and lung injury in this gut I/R model.

DISCUSSION

To date, IL-18 has been known for its role in infectious

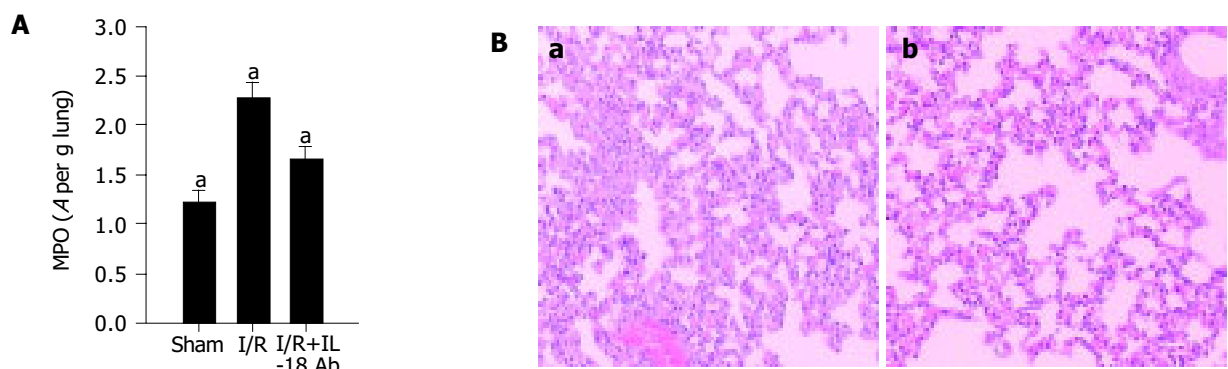


Figure 3 The effect of anti-IL-18 antibody on the ischemia-induced lung injury. **A:** Anti-IL-18 antibody injection remarkably inhibited the lung MPO activity. After 3 h of reperfusion, the MPO activity was determined in lung tissues ($n = 5$),

^a $P < 0.05$ vs others. **B:** Comparison of pulmonary histopathology. Lungs from ischemic mice (a, for 3 h of reperfusion), and ischemic mice treated with IL-18Ab (b, for 3 h of reperfusion) and stained with HE. Magnification $\times 100$.

inflammatory injury. However, few investigations have been accomplished regarding the role of IL-18 during non-infectious acute inflammatory reactions such as those that occur in ischemia/reperfusion. Previous reports have shown that IL-18 have important regulatory role during organ injury induced by local ischemia/reperfusion^[11-13]. In the current study, we used a model of acute lung inflammation induced by gut ischemia/reperfusion, which results in damage of capillary endothelial cells and neutrophil influx, and oxidants, proteases released from inflammatory cells damage lung cells and tissue matrix^[1-3]. The role of IL-18 in this model of lung injury has not been explored. The current study provides evidence that endogenous IL-18 may act as a proinflammatory cytokine and contribute to gut ischemia/reperfusion-induced lung inflammation.

Our results, consistent with the previous reports, have shown that local ischemia may induce the elevation of IL-18 level^[11-13]. It promptly reached peak at 1 h and then declined to baseline. However, the levels of IL-18 in lung tissue were not the same. Constitutively, expression of IL-18 in airway epithelium has been observed by using immunohistochemistry, and as the reperfusion time extended to 3 h, the level of IL-18 in air way epithelium was greatly enhanced and immunoreactive IL-18 dispersed all over the lung tissue, which suggests that pulmonary expression of IL-18 may be enhanced during reperfusion as the inflammatory agents secreted from intestine reached the lung tissue and further, the IL-18 receptor mediated mechanism may also account for the pulmonary accumulation of IL-18, which in accordance with the rapid decline of serum IL-18 level during reperfusion.

IL-18 has been known to be produced as a proform and stored in cytoplasm. After the cleavage of caspase-1, it turns to a functional, mature protein. By Western blot analysis, the IL-18 mature protein was quickly increased after 1 h of reperfusion (Figure 1A), which suggests that gut ischemia may result in the activation of caspase-1 and enhance the maturation and secretion of IL-18. Furthermore, previous reports have shown that ischemia also induces IL-1 β expression. Therefore, it is possible that intestinal caspase-1 may play a key role in expression of both the mature IL-18 and IL-1 β , and ischemic gut may serve as a major source for circulating IL-18 in this model.

Experimental studies have suggested that IL-18 protects against bacterial and viral agents^[3], which is thought to be attributable in part to the infiltration of inflammatory cells after treatment with IL-18. There is also evidence suggesting that IL-18 may activate neutrophils and promote neutrophil migration and accumulation *in vivo*^[6]. In the current studies, we showed that the *in vivo* exogenous administration of IL-18 before gut ischemia greatly enhanced neutrophil recruitment as well as lung inflammation (Figure 2). Conversely, IL-18 blockade reduced the evidence of lung inflammation by neutralizing Ab (Figure 3). These results suggest that IL-18 may, like IL-1 β , be an important early pro-inflammatory cytokine involved in the pathogenesis of acute lung inflammation induced by gut ischemia/reperfusion. Furthermore, these data also suggest that the preoperative levels of serum IL-18 may represent a valuable parameter to aid the postoperative prognostic determinant in clinical

patients with ischemia-induced MODS.

But how IL-18 is activated, and how it enhances the pulmonary inflammation during ischemia/reperfusion is still unknown. There is evidence indicating that NO suppresses IL-18 processing by inhibiting caspase-1 activity^[15,16]. It is likely that ischemia-induced decrease of NO levels may result in the activation of caspase-1 and the further secretion of mature IL-18. Furthermore, it is clear that IL-18, a pleiotropic proinflammatory cytokine, has an endogenous role in enhancing production of several early response cytokines during lung inflammation, such as TNF- α , IFN- γ , and IL-1 β . Previous reports have shown that IL-18 may activate neutrophil and promote neutrophil migration and accumulation *in vivo* via a TNF- α -dependent pathway^[6,17]. However, the mechanism of pulmonary neutrophils sequestration is possibly independent of TNF- α in this lung injury model^[18], which suggests that the function of IL-18 may not be totally dependent on the role of TNF- α . These works are now in progress in our group.

The present data expand our knowledge of the immunoregulatory properties of IL-18. Our findings are clinically applicable to ischemia/reperfusion injury during surgical operation such as small intestinal transplantation, and modulation of IL-18 expression may enhance endogenous protective effects, leading to a reduction in organ injury.

REFERENCES

- 1 Carden DL, Granger DN. Pathophysiology of ischaemia-reperfusion injury. *J Pathol* 2000; **190**: 255-266
- 2 Chen LW, Egan L, Li ZW, Greten FR, Kagnoff MF, Karin M. The two faces of IKK and NF-kappaB inhibition: prevention of systemic inflammation but increased local injury following intestinal ischemia-reperfusion. *Nat Med* 2003; **9**: 575-581
- 3 Nakanishi K, Yoshimoto T, Tsutsui H, Okamura H. Interleukin-18 is a unique cytokine that stimulates both Th1 and Th2 responses depending on its cytokine milieu. *Cytokine Growth Factor Rev* 2001; **12**: 53-72
- 4 Puren AJ, Fantuzzi G, Gu Y, Su MS, Dinarello CA. Interleukin-18 (IFN-gamma-inducing factor) induces IL-8 and IL-1beta via TNFalpha production from non-CD14+ human blood mononuclear cells. *J Clin Invest* 1998; **101**: 711-721
- 5 Gerdes N, Sukhova GK, Libby P, Reynolds RS, Young JL, Schonbeck U. Expression of interleukin (IL)-18 and functional IL-18 receptor on human vascular endothelial cells, smooth muscle cells, and macrophages: implications for atherogenesis. *J Exp Med* 2002; **195**: 245-257
- 6 Leung BP, Culshaw S, Gracie JA, Hunter D, Canetti CA, Campbell C, Cunha F, Liew FY, McInnes IB. A role for IL-18 in neutrophil activation. *J Immunol* 2001; **167**: 2879-2886
- 7 Netea MG, Fantuzzi G, Kullberg BJ, Stuyt RJ, Pulido EJ, McIntyre RC Jr, Joosten LA, Van der Meer JW, Dinarello CA. Neutralization of IL-18 reduces neutrophil tissue accumulation and protects mice against lethal *Escherichia coli* and *Salmonella typhimurium* endotoxemia. *J Immunol* 2000; **164**: 2644-2649
- 8 Jordan JA, Guo RF, Yun EC, Sarma V, Warner RL, Crouch LD, Senaldi G, Ulich TR, Ward PA. Role of IL-18 in acute lung inflammation. *J Immunol* 2001; **167**: 7060-7068
- 9 Zaremba J, Losy J. Interleukin-18 in acute ischaemic stroke patients. *Neurol Sci* 2003; **24**: 117-124
- 10 Hedtjarn M, Leverin AL, Eriksson K, Blomgren K, Mallard C, Hagberg H. Interleukin-18 involvement in hypoxic-ischemic brain injury. *J Neurosci* 2002; **22**: 5910-5919
- 11 Takeuchi D, Yoshidome H, Kato A, Ito H, Kimura F, Shimizu H, Ohtsuka M, Morita Y, Miyazaki M. Interleukin 18 causes hepatic ischemia/reperfusion injury by suppressing anti-in-

- flammatory cytokine expression in mice. *Hepatology* 2004; **39**: 699-710
- 12 **Pomerantz BJ**, Reznikov LL, Harken AH, Dinarello CA. Inhibition of caspase 1 reduces human myocardial ischemic dysfunction via inhibition of IL-18 and IL-1beta. *Proc Natl Acad Sci USA* 2001; **98**: 2871-2876
- 13 **Melnikov VY**, Ecder T, Fantuzzi G, Siegmund B, Lucia MS, Dinarello CA, Schrier RW, Edelstein CL. Impaired IL-18 processing protects caspase-1-deficient mice from ischemic acute renal failure. *J Clin Invest* 2001; **107**: 1145-1152
- 14 **Daemen MA**, Denecker G, van't Veer C, Wolfs TG, Vandenabeele P, Buurman WA. Activated caspase-1 is not a central mediator of inflammation in the course of ischemia-reperfusion. *Transplantation* 2001; **71**: 778-784
- 15 **Kozar RA**, Holcomb JB, Hassoun HT, Macaitis J, DeSoignie R, Moore FA. Superior mesenteric artery occlusion models shock-induced gut ischemia-reperfusion. *J Surg Res* 2004; **116**: 145-150
- 16 **Kim YM**, Talanian RV, Li J, Billiar TR. Nitric oxide prevents IL-1beta and IFN-gamma-inducing factor (IL-18) release from macrophages by inhibiting caspase-1 (IL-1beta-converting enzyme). *J Immunol* 1998; **161**: 4122-4128
- 17 **Canetti CA**, Leung BP, Culshaw S, McInnes IB, Cunha FQ, Liew FY. IL-18 enhances collagen-induced arthritis by recruiting neutrophils via TNF-alpha and leukotriene B4. *J Immunol* 2003; **171**: 1009-1015
- 18 **Caty MG**, Guice KS, Oldham KT, Remick DG, Kunkel SI. Evidence for tumor necrosis factor-induced pulmonary microvascular injury after intestinal ischemia-reperfusion injury. *Ann Surg* 1990; **212**: 694-700

Science Editor Guo SY Language Editor Elsevier HK

CYP2E1-dependent hepatotoxicity and oxidative damage after ethanol administration in human primary hepatocytes

Lie-Gang Liu, Hong Yan, Ping Yao, Wen Zhang, Li-Jun Zou, Fang-Fang Song, Ke Li, Xiu-Fa Sun

Lie-Gang Liu, Hong Yan, Ping Yao, Wen Zhang, Li-Jun Zou, Fang-Fang Song, Ke Li, Xiu-Fa Sun, Department of Nutrition and Food Hygiene, School of Public Health, Tongji Medical College, Huazhong University of Science and Technology, Wuhan 430030, Hubei Province, China

Supported by the National Science Foundation of China, No. 30271130

Correspondence to: Dr. Lie-Gang Liu, Department of Nutrition and Food Hygiene, Tongji Medical College, Huazhong University of Science and Technology, Wuhan 430030, Hubei Province, China. lgliu@mails.tjmu.edu.cn

Telephone: +86-27-83692711 Fax: +86-27-83693307

Received: 2004-05-25 Accepted: 2004-06-17

Abstract

AIM: To observe the relationship between ethanol-induced oxidative damage in human primary cultured hepatocytes and cytochrome P450 2E1 (CYP2E1) activity, in order to address if inhibition of CYP2E1 could attenuate ethanol-induced cellular damage.

METHODS: The dose-dependent (25–100 mmol/L) and time-dependent (0–24 h) exposures of primary human cultured hepatocytes to ethanol were carried out. CYP2E1 activity and protein expression were detected by spectrophotometer and Western blot analysis respectively. Hepatotoxicity was investigated by determination of lactate dehydrogenase (LDH) and aspartate transaminase (AST) level in hepatocyte culture supernatants, as well as the intracellular formation of malondialdehyde (MDA).

RESULTS: A dose- and time-dependent response between ethanol exposure and CYP2E1 activity in human hepatocytes was demonstrated. Moreover, there was a time-dependent increase of CYP2E1 protein after 100 mmol/L ethanol exposure. Meanwhile, ethanol exposure of hepatocytes caused a time-dependent increase of cellular MDA level, LDH, and AST activities in supernatants. Furthermore, the inhibitor of CYP2E1, diallyl sulfide (DAS) could partly attenuate the increases of MDA, LDH, and AST in human hepatocytes.

CONCLUSION: A positive relationship between ethanol-induced oxidative damage in human primary cultured hepatocytes and CYP2E1 activity was exhibited, and the inhibition of CYP2E1 could partly attenuate ethanol-induced oxidative damage.

© 2005 The WJG Press and Elsevier Inc. All rights reserved.

Key words: Ethanol; CYP2E1; Oxidative damage; Human

primary hepatocytes

Liu LG, Yan H, Yao P, Zhang W, Zou LJ, Song FF, Li K, Sun XF. CYP2E1-dependent hepatotoxicity and oxidative damage after ethanol administration in human primary hepatocytes. *World J Gastroenterol* 2005; 11(29): 4530-4535
<http://www.wjgnet.com/1007-9327/11/4530.asp>

INTRODUCTION

The enzymes that are believed to be primarily responsible for the oxidation of ethanol are alcohol dehydrogenase, catalase, and cytochrome P450 2E1 (CYP2E1), all of which appear to be relatively widely distributed in mammalian cell types^[1,2]. Ethanol has long been known to have cytotoxic effects on a wide variety of animal cell types, even at relatively low doses^[3,4]. In several cell types and organs such as liver^[5], it is now believed that the toxicity of ethanol stems principally from free radicals produced during oxidation^[6] that can then damage cellular components such as DNA, proteins, and membrane lipids.

CYP2E1 is of special interest because of its ability to metabolize and activate numerous hepatotoxic substrates in the liver such as ethanol, carbon tetrachloride, acetaminophen, and *N*-nitroso dimethylamine, to more toxic products. CYP2E1 exhibits enhanced reduced form of nicotinamide adenine dinucleotide phosphate oxidase activity and is very reactive in catalysis of lipid peroxidation and production of reactive oxygen intermediates (ROI) such as H₂O₂ in higher amounts relative to other P450 isoforms^[7]. Induction of cytochrome CYP2E1 by ethanol appears to be one of the central pathways by which ethanol generates a state of oxidative stress. In addition, oxidation of ethanol by CYP2E1 produces acetaldehyde, a highly reactive compound that may contribute to the toxic effect of ethanol^[8]. Hence, there is considerable interest in the role of reactive oxygen species (ROS) during ethanol metabolism by which ethanol is hepatotoxic.

CYP2E1 is shown to be more effective in catalyzing lipid peroxidation compared to several other forms of cytochrome P450 enzymes. Increases in formation of ROS by microsomes isolated from ethanol-treated rats were prevented by anti-CYP2E1 IgG, thus linking them to induction of CYP2E1^[9]. In the intragastric ethanol feeding, significant alcoholic injury occurred^[10]. In addition, large increases in lipid peroxidation have been observed, and the ethanol-induced liver pathology has been shown to correlate with CYP2E1 levels and elevated lipid peroxidation, and to be blocked by inhibitors of CYP2E1. Moreover, CYP2E1

inhibitors also reduced ethanol-induced ROS formation, suggesting that CYP2E1 contributes to ROS formation. Inhibitors of CYP2E1 were also shown to prevent ethanol cytotoxicity in transduced HepG2 cells^[11].

However, question arises whether the responses to expression of different forms of cytochromes P450 are similar in rats and humans. The concentrations of ethanol required to increase CYP2E1 in cultured human hepatocytes are dramatically lower than those required to induce these forms of P450 in cultured rat hepatocytes. The activity of alcohol dehydrogenase, a major enzyme involved in ethanol metabolism, is lower in human liver than in rat liver. Thus, in the human hepatocyte cultures, more ethanol may be available intracellularly to induce the P450s due to lower metabolism. Alternatively, the mechanism of induction of these forms of P450s may be different in human than in rat hepatocytes^[12]. In this study, we investigated the effects of ethanol administration on human primary culture hepatocytes in order to determine if there is a correlation between CYP2E1 activity and ethanol-induced oxidative damage in human hepatocytes, and further address if diallyl sulfide (DAS), an inhibitor of CYP2E1^[13], could partly attenuate ethanol-induced oxidative damage.

MATERIALS AND METHODS

Materials

Williams' medium E (with Glutamax-1), HEPES, and penicillin/streptomycin were obtained from Life Technologies (Karlsruhe, Germany), insulin and hydrocortisone were supplied from Sigma (Deisenhofen, Germany), while calf serum was purchased from PAA Ltd (Linz, Austria), anti-mouse CYP2E1 antibody was purchased from Amersham (Germany). Western blot development kits were purchased from Amersham (ECL, Buckinghamshire, UK). All other reagents were obtained from Sigma unless indicated otherwise.

Isolation and culture of human hepatocytes

Human liver tissue weighing 5-10 g was obtained from liver resections of cholecystectomy of patients who had no known liver pathology, nor had they received medication during 4 wk prior to surgery. None of the patients was a habitual consumer of alcohol or other drugs. The collection of tissue was done according to institutional guideline, and the patient's written consent. Immediately after resection, a wedge section of the normal tissue was transferred under sterile conditions to the laboratory in culture media. Human hepatocytes were isolated by a two-step collagenase perfusion technique followed by a Percoll centrifugation step as previously described^[14]. Hepatocyte purity assessed under light microscope was over 95% and viability consistently exceeded 93% by trypan blue exclusion. The freshly harvested human hepatocytes were then seeded onto rat-tail collagen-coated Petri dishes or 12-well culture trays. The medium consisted of Williams' E medium supplemented with 1 μ mol/L insulin, 15 mmol/L HEPES, 1.4 μ mol hydrocortisone, 10% calf serum, penicillin (100 U/mL), and streptomycin (100 μ g/mL). Cells were incubated in a humidified incubator in 950 mL/L air and 50 mL/L CO₂ at 37 °C until cell attachment. On the following day, cells

were exposed to various concentrations of ethanol (25-100 mmol/L) for 9 h. Time-dependent studies were undertaken in human hepatocytes using 100 mmol/L ethanol between 0.5 and 24 h. At the corresponding time intervals, cells and supernatants were collected in agreement with the applied technique.

CYP 2E1 enzyme activity

Human hepatocytes were seeded onto 12-well dishes at a concentration of 0.5×10^6 cells. The cells were cultured overnight, fresh medium alone or medium containing various concentrations of ethanol or DAS (25-100 μ mol/L) was added, and the cells were incubated for various lengths of time. Cells were harvested with a cell scraper and washed with PBS twice. The activity of CYP2E1 was determined by the rate of hydroxylation of *p*-nitrophenol^[15], at 546 nm. Plates were washed with saline to remove traces of phenol red and incubated with 0.5 mmol/L *p*-nitrophenol up to 60 min. The extinction coefficient for *p*-nitrophenol is 10.28 mmol/(L·cm). Results were expressed as formed *p*-nitrophenol pmols/min/mg protein.

Cellular damage

LDH and AST measurement Both enzymes, LDH and AST, were measured using a commercially available test kit. Results were expressed as units per liter.

Lipid peroxidation measurement MDA, formed from the breakdown of polyunsaturated fatty acids, was used as a convenient index for determining the extent of lipid peroxidation reactions. It was assayed in human hepatocytes using the thiobarbituric acid reaction as described by Wrighton *et al.*^[12]. The absorbance of the resulting organic layer was measured spectrophotometrically at 532 nm and calculated in relative to an external standard (1,1,3, 3-tetraethoxypropane) of MDA. Results were expressed as nmol/mg of protein.

Western blot analysis Cells were washed twice with PBS and homogenized in a buffer containing protease inhibitors. Protein concentrations were determined by the method of Lowry, using bovine serum albumin as the standard. Proteins were separated on a 10% SDS polyacrylamide gel, and then transferred onto polyvinylidene difluoride membranes^[16,17]. Nonspecific binding sites were blocked by overnight incubation of membranes in nonfat milk (5/100 g) solution solved in PBS/Tween-20 at 4 °C. After washing with PBS/Tween-20, the membranes were incubated with a CYP2E1 antibody, followed by an incubation with a horseradish-peroxidase-conjugated antibody at room temperature for 1 h. Then, membranes were washed again with PBS/Tween-20 for 1 h, and the immune complexes were developed using a chemiluminescence detection system. Equal loading of total protein was verified using a commercially available antibody against β -actin^[18].

Statistical analysis

Values were expressed as mean \pm SD of three values per experiment and experiments were repeated at least twice. Differences were analyzed by using the ANOVA test. Statistical significance was established at a *P* value <0.05.

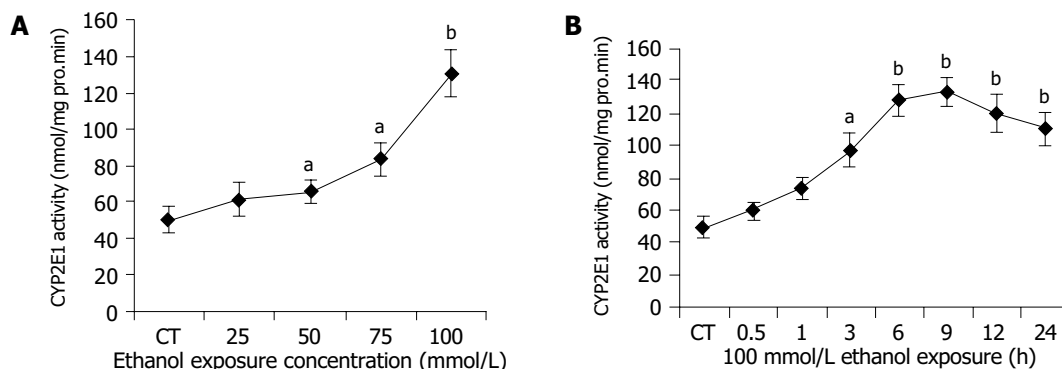


Figure 1 Dose- and time-dependent CYP2E1 activity by ethanol administration. **A:** Ethanol dose-dependent induction of CYP2E1. Hepatocytes were incubated with various concentrations of ethanol (0-100 mmol/L) for 9 h. CYP2E1 enzyme activity was measured as described in Materials and methods. CT: control; ^a $P < 0.05$, ^b $P < 0.01$ vs untreated control cultures. Each point represents the mean \pm SE of triplicates of five independent experiments;

B: Ethanol time-dependent induction of CYP2E1 enzyme activity in human hepatocytes. Hepatocytes were incubated with medium in the presence or absence of 100 mmol/L ethanol for various lengths of time (0-24 h). CYP2E1 enzyme activity was measured. CT: control; ^a $P < 0.05$, ^b $P < 0.01$ vs untreated control cultures. Each point represents the mean \pm SE of triplicates of five independent experiments.

RESULTS

Dose- and time-dependent CYP2E1 activity by ethanol administration

As depicted in Figure 1A, we observed a dose-dependent increase in CYP2E1 activity, which reached its maximum at 100 mmol/L ethanol after 9 h exposure as compared to untreated control cultures (CT: 50.09 ± 6.68 pmol/mg protein per min vs 100 mmol/L ethanol: 130.7 ± 12.61 pmol/mg protein per min; $P < 0.01$). We found that the exposure to 100 mmol/L ethanol led to a continuous increase in CYP2E1 activity in human hepatocytes (Figure 1B). CYP2E1 activity increased rapidly and reached its maximum between 6 and 12 h after ethanol exposure. Then, by 24 h we saw a decline of CYP2E1 activity. CYP2E1 activity between 3 and 24 h was significantly higher compared to untreated control cultures.

Time-dependent CYP2E1 protein expression after ethanol exposure

Figure 2 shows a time-dependent expression of CYP2E1 protein in human hepatocytes. We demonstrated that the exposure to 100 mmol/L ethanol of human hepatocytes induced continuous increase of CYP2E1 protein expression during the investigation period.

Cytotoxicity of ethanol in human hepatocytes

The formation of various radicals was closely linked to

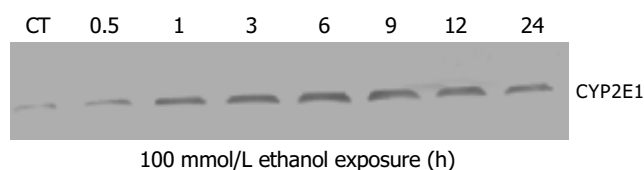


Figure 2 Western blot analysis of time-dependent induction of CYP2E1 protein expression in human hepatocytes. Human hepatocytes were incubated with medium alone or medium containing 100 mmol/L ethanol for 0-24 h. Each was loaded with 100 μ g of the sample. Experiments were carried out as described under Materials and methods (CT: control).

oxidative injury. A typical characteristic of radical formation was lipid peroxidation, where malondialdehyde (MDA) was a by-product that could be easily measured in cells and tissue. Figure 3 shows that MDA levels increased with time, reaching first time significant level already after 3 h ($P < 0.05$ vs controls) of ethanol exposure. The maximum MDA formation in human hepatocytes after ethanol exposure was seen at 9 h and thereafter a slow decline of the lipid peroxidation could be seen. Moreover, there appeared to be a positive relation between CYP2E1 activity and MDA level ($r = 0.9724$, $P < 0.01$).

Further, the degree of cellular injury caused by ethanol can be estimated by the leakage of enzymes from the hepatocytes. In order to evaluate the hepatocellular damage caused by ethanol, supernatants taken from hepatocyte cultures were screened for the presence of LDH and AST. In our experiments, ethanol caused a clear time-dependent release of LDH and AST. (LDH: CT = 15.6 ± 1.66 U/L, 100 mmol/L ethanol (24 h): 84.5 ± 7.86 U/L, $P < 0.01$ vs CT; Figure 4. AST: CT = 94.22 ± 9.52 U/L, 100 mmol/L

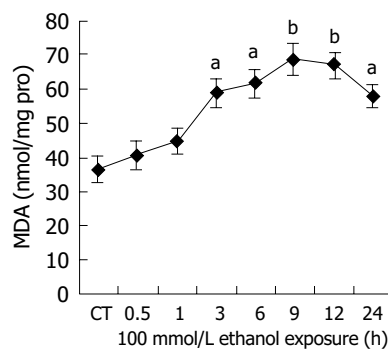


Figure 3 Ethanol-dependent formation of MDA in human hepatocytes. Hepatocytes were incubated with 100 mmol/L ethanol for various lengths of time (0-24 h). MDA formation was measured as described in Materials and methods. CT: control; ^a $P < 0.05$, ^b $P < 0.01$ vs untreated control cultures. Each point represents the mean \pm SE of triplicates of five independent experiments.

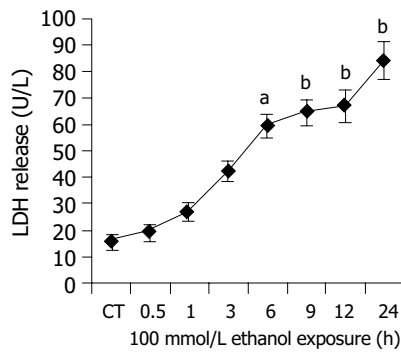


Figure 4 Time course experiments for LDH release after ethanol (100 mmol/L) exposure between 0.5 and 24 h. CT: control; ^a $P < 0.05$, ^b $P < 0.01$ vs untreated control cultures. Each point represents the mean \pm SE of triplicates of five independent experiments.

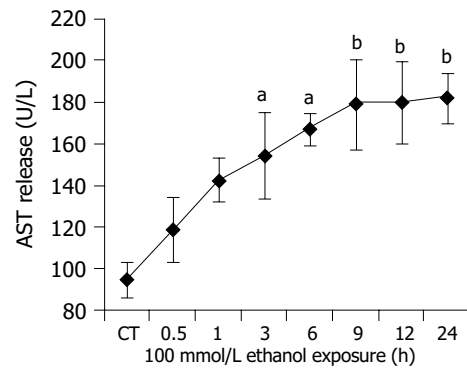


Figure 5 Time course experiments for AST release after ethanol 100 mmol/L exposure between 0.5 and 24 h. CT: control; ^a $P < 0.05$, ^b $P < 0.01$ vs untreated control cultures. Each point represents the mean \pm SD of triplicates of five independent experiments.

ethanol (24 h): 181.91 ± 11.55 U/L, $P < 0.01$ vs CT Figure 5). The above results indicated that ethanol was toxic to human hepatocytes, and there was positive relationship between CYP2E1 activity induced by ethanol and ethanol-induced cellular damage.

Protection from ethanol-induced oxidative damage by CYP2E1 inhibitors

In the following set of experiments we addressed the question whether the inhibition of CYP2E1 could protect human hepatocytes from ethanol-induced cellular damage. First, we found that the co-induction of ethanol with 25 or 50 $\mu\text{mol/L}$ DAS, produced no cellular protection against the ethanol-induced cytotoxicity. In contrast, when cells were co-induced with 100 $\mu\text{mol/L}$ DAS and ethanol for 9 h, we saw a profound reduction of MDA formation caused by ethanol (Table 1). However, MDA formation was still higher than that of untreated control cultures. This reversing effect of DAS was also seen with regard to the release of LDH and AST (Table 1). There was no effect on MDA, LDH, and AST, when 25–100 $\mu\text{mol/L}$ DAS was incubated with ethanol, respectively (Table 1). Thus, the inhibition of CYP2E1 could partly attenuate ethanol-induced cytotoxicity in human primary hepatocytes.

Table 1 Ethanol exposure of hepatocytes causes cellular damage in human hepatocytes

Group	MDA (nmol/mg protein)	LDH (U/L)	AST (U/L)
CT	36.37 \pm 3.64	15.6 \pm 1.66	94.22 \pm 9.52
100 mmol/L ethanol	69.05 \pm 4.41	84.5 \pm 7.86	181.91 \pm 11.55
100 mmol/L ethanol plus 25 $\mu\text{mol/L}$ DAS	65.31 \pm 9.32	80.4 \pm 8.86	174.51 \pm 17.12
100 mmol/L ethanol plus 50 $\mu\text{mol/L}$ DAS	59.54 \pm 7.02	75.5 \pm 7.06	160.42 \pm 17.86
100 mmol/L ethanol plus 100 $\mu\text{mol/L}$ DAS	56.13 \pm 6.32 ^a	70.8 \pm 6.24 ^a	156.42 \pm 15.55 ^a
25 $\mu\text{mol/L}$ DAS	37.43 \pm 3.45	16.7 \pm 1.85	93.056 \pm 9.64
50 $\mu\text{mol/L}$ DAS	36.43 \pm 4.15	15.8 \pm 1.33	92.16 \pm 9.04
100 $\mu\text{mol/L}$ DAS	38.43 \pm 4.05	17.6 \pm 1.95	96.32 \pm 10.08

^a $P < 0.05$ vs 100 mmol/L ethanol ($n = 5$).

DISCUSSION

Ethanol consumption and its effects on CYP2E1 in animals have long been studied in the past. However, reports about the influence of CYP2E1 inhibition on human primary hepatocytes and its possible positive effects on ethanol-induced toxicity are very limited. The concentrations of ethanol required to increase CYP2E1 in cultured human hepatocytes are dramatically lower than those required to induce the same forms of P450 in cultured rat hepatocytes. The activity of alcohol dehydrogenase, a major enzyme involved in ethanol metabolism, is lower in human liver than in rat liver. Thus, in the human hepatocyte cultures, more ethanol may be available intracellularly to induce the P450s due to lower metabolism. Alternatively, the mechanism of induction of these forms of P450s may be different or more sensitive in human than in rat hepatocytes^[12]. It was reported that 25–100 mmol/L ethanol could lead to sustained cellular damage such as teratogenesis in guinea pigs, ethanol-induced unconsciousness or even death in humans^[19]. In the present study, 25–100 mmol/L ethanol was used to investigate the relationship between ethanol exposure and CYP2E1 gene expression. Meanwhile, cellular LDH, AST, and MDA levels were chosen to assess hepatocyte damage caused by ethanol exposure.

CYP2E1 is induced by a broad variety of chemicals, such as ethanol. The production of ROS via CYP2E1 induction may contribute to the development of alcoholic liver disease or at least increase cytotoxic effects of alcohol^[20]. Ethanol is an essential CYP2E1 inducer in human hepatocytes, which was also confirmed in a recent study by Ponsoda *et al.*^[21], showing that human hepatocytes incubated with 100 mmol/L ethanol showed a two- to threefold increase in CYP2E1 enzyme activity compared with untreated control cultures. By use of recombinant retroviral expression, in addition to ethanol (20–100 mmol/L) exposure, the culture medium of the HepG2 cell line exhibited both a large increase of CYP2E1 content and enzyme activity^[22]. Our data confirmed these results, clearly showing a dose-dependent and time-dependent relationship between CYP2E1 enzyme activity in human hepatocytes and ethanol exposure. Western blot analysis further proved ethanol-induced CYP2E1 expression in a time-dependent manner.

Lipid peroxidation (and associated membrane damage) is a key feature in alcoholic liver injury. It resulted in increased excretion of MDA in the urine of rats following short- and long-term administration of relatively low doses of ethanol^[23]. Lipid peroxidation results directly from the increased oxygen radical production induced by CYP2E1. In the present work, we have demonstrated that time-dependent increased MDA levels were directly linked to the presence of ethanol and there was a clear relationship between MDA levels and CYP2E1 changes in hepatocytes after ethanol administration.

The increase in LDH activity is seen in many pathologic conditions. Release of the intracytoplasmic enzyme LDH into cell culture medium is frequently used as a measure of cellular injury. AST is present only in hepatocytes, located in mitochondria and cytoplasm. Like LDH, its increase is an early sign of cellular injury. In the present study, ethanol clearly caused a time-dependent release of LDH and AST, and there was a positive relationship between the induction of CYP2E1 activity and the release of LDH and AST. Ethanol exposure could cause marked cellular damage in human primary cultured hepatocytes.

It was demonstrated that ethanol cytotoxicity was directly related to CYP2E1 enzyme activity. Cytotoxicity of ethanol in rat hepatocytes was prevented either by alcohol/aldehyde dehydrogenase inhibitors or by CYP2E1 inhibitors. Cederbaum observed that ethanol-induced ROI formation was also reduced in the presence of CYP2E1 inhibitors in HepG2 cells, suggesting that CYP2E1 directly contributes to ROI formation^[24]. Leclercq *et al.*^[25], using the knockout mice observed that other CYPs, notably CYP4A10 and CYP4A14, were upregulated in the CYP2E1 knockout but not the wild-type mice; these CYPs were, like CYP2E1, active generators of reactive oxygen and catalysts of lipid peroxidation, and in the absence of CYP2E1 served as alternative initiators of oxidative stress. Furthermore, French and collaborators found that the ethanol-induced oxidative inactivation of the proteasome and increase in oxidized proteins were completely prevented in these CYP2E1 knockout mice^[26]. Our experiments showed that DAS, the inhibitor of CYP2E1, could partly protect human hepatocytes from ethanol-induced cellular injury, or reduce cellular MDA, LDH and AST levels. However, in contrast to these observations, studies by Thurman and colleagues have suggested that CYP2E1 may not play a role in alcoholic liver injury based upon studies in CYP2E1 knockout mice^[1,27,28]. In some cells, ethanol-induced damage may not be the consequence of oxidative reactions, but may result directly from the direct interaction of ethanol with cell membranes or from its non-oxidative incorporation into fatty acid ethyl esters^[29,30]. Clearly, further studies are necessary to resolve the above discrepancies.

In summary, this study revealed that an innocuous concentration of DAS significantly decreased the ethanol-induced oxidative damage in human primary cultured hepatocytes. This protection appeared to be, at least in part, due to the attenuation of oxidative stress. These findings warrant future *in vivo* studies of DAS for the prevention and/or treatment of alcoholic liver disease. The inhibition of CYP2E1 in cells or organs could lead to new strategies

for better prevention and treatment of ethanol-induced oxidative damage in human liver.

ACKNOWLEDGMENT

We thank Professor Andreas K Nussler, Department of General-, Visceral-, and Transplantation Surgery, Humboldt University, Charité, Campus Virchow, Berlin, Germany, for his countless help in the performance of this study.

REFERENCES

- 1 **Oneta CM**, Lieber CS, Li J, Rüttimann S, Schmid B, Lattmann Rosman AS, Seitz HK. Dynamics of cytochrome P4502E1 activity in man: induction by ethanol and disappearance during withdrawal phase. *J Hepatol* 2002; **36**: 47-52
- 2 **Agarwal DP**. Genetic polymorphisms of alcohol metabolizing enzymes. *Pathol Biol* 2001; **49**: 703-709
- 3 **Bailey SM**, Cunningham CC. Contribution of mitochondria to oxidative stress associated with alcoholic liver disease. *Free Radic Biol Med* 2002; **32**: 11-16
- 4 **Person RE**, Chen H, Fantel AG, Juchau MR. Enzymic catalysis of the accumulation of acetaldehyde from ethanol in human prenatal cephalic tissues: evaluation of the relative contributions of CYP2E1, alcohol dehydrogenase, and catalase/peroxidases. *Alcohol Clin Exp Res* 2000; **24**: 1433-1442
- 5 **Diehl AM**. Liver disease in alcohol abusers: clinical perspective. *Alcohol* 2002; **27**: 7-11
- 6 **Albano E**. Free radical mechanisms in immune reactions associated with alcoholic liver disease. *Free Radic Biol Med* 2002; **32**: 110-114
- 7 **Cervino V**, Benaim G, Carafoli E, Guerini D. The effect of ethanol on the plasma membrane calcium pump is isoform-specific. *J Biol Chem* 1998; **273**: 29811-29815
- 8 **Neuman MG**, Shear NH, Jacobson-Brown PM, Katz GG, Neilson HK, Malkiewicz IM, Cameron RG, Abbott F. CYP2E1-mediated modulation of valproic acid-induced hepatocytotoxicity. *Clin Biochem* 2001; **34**: 211-218
- 9 **Kukielka E**, Cederbaum AI. DNA strand cleavage as a sensitive assay for the production of hydroxyl radical by microsomes: roles of CYP2E1 in the increased activity after ethanol treatment. *Biochem J* 1994; **302**: 773-779
- 10 **Nanji AA**, Zhao S, Sadrzadeh SM, Dannenberg AJ, Tahan SR, Waxman DJ. Markedly enhanced cytochrome P4502E1 induction and lipid peroxidation is associated with severe liver injury in fish oil-ethanol-fed rats. *Alcohol Clin Exp Res* 1994; **18**: 1280-1285
- 11 **Cederbaum AI**, Wu D, Mari M, Bai J. CYP2E1-dependent toxicity and oxidative stress in HepG2 cells. *Free Radic Biol Med* 2001; **31**: 1539-1543
- 12 **Kostrubsky VE**, Strom SC, Wood SG, Wrighton SA, Sinclair PR, Sinclair JF. Ethanol and isopentanol increase CYP3A and CYP2E in primary cultures of human hepatocytes. *Arch Biochem Biophys* 1995; **322**: 516-520
- 13 **Wang T**, Shankar K, Bucci TJ, Warbritton A, Mehendale HM. Diallyl sulfide inhibition of CYP2E1 does not rescue diabetic rats from thioacetamide-induced mortality. *Toxicol Appl Pharmacol* 2001; **173**: 27-37
- 14 **Nussler AK**, Liu ZZ, Di Silvio M, Sweetland MA, Geller DA, Lancaster JR Jr, Billiar TR, Freeswick PD, Lowenstein CL, Simmons RL. Hepatocyte inducible nitric oxide synthesis is influenced *in vitro* by cell density. *Am J Physiol* 1994; **267** (2 Pt 1): C394-401
- 15 **Sapone A**, Affatato A, Canistro D, Broccoli M, Trespidi S, Pozzetti L, Biagi GL, Cantelli-Forti G, Paolini M. Induction and suppression of cytochrome P450 isoenzymes and generation of oxygen radicals by procymidone in liver, kidney and lung of CD1 mice. *Mutat Res* 2003; **527**: 67-80
- 16 **Raghavendra V**, Kulkarni SK. Possible antioxidant mechanism in melatonin reversal of aging and chronic ethanol-induced amnesia in plus-maze and passive avoidance memory

- tasks. *Free Radic Biol Med* 2001; **30**: 595-602
- 17 **Hannon-Fletcher MP**, O'Kane MJ, Moles KW, Barnett YA, Barnett CR. Lymphocyte cytochrome P450-CYP2E1 expression in human IDDM subjects. *Food Chem Toxicol* 2001; **39**: 125-132
- 18 **Jung M**, Drapier JC, Weidenbach H, Renia L, Oliveira L, Wang A, Beger HG, Nussler AK. Effects of hepatocellular iron imbalance on nitric oxide and reactive oxygen intermediates production in a model of sepsis. *J Hepatol* 2000; **33**: 387-394
- 19 **Cook MN**, Marks GS, Vreman HJ, Nakatsu K, Stevenson DK, Brien JF. Heme oxygenase activity and acute and chronic ethanol exposure in the hippocampus, frontal cerebral cortex, and cerebellum of the near-term fetal guinea pig. *Alcohol* 1997; **14**: 117-124
- 20 **Cederbaum AI**. Iron and CYP2E1-dependent oxidative stress and toxicity. *Alcohol* 2003; **30**: 115-120
- 21 **Ponsoda X**, Bort R, Jover R, Gomez-Lechon MJ, Castell JV. Increased toxicity of cocaine on human hepatocytes induced by ethanol: role of GSH. *Biochem Pharmacol* 1999; **58**: 1579-1585
- 22 **Carroccio A**, Wu D, Cederbaum AI. Ethanol increases content and activity of human cytochrome P4502E1 in a transduced HepG2 cell line. *Biochem Biophys Res Commun* 1994; **203**: 727-733
- 23 **Goasduff T**, Cederbaum AI. CYP2E1 degradation by *in vitro* reconstituted systems: role of the molecular chaperone hsp90. *Arch Biochem Biophys* 2000; **379**: 321-330
- 24 **Cederbaum AI**. Ethanol-related cytotoxicity catalyzed by CYP2E1-dependent generation of reactive oxygen intermediates in transduced HepG2 cells. *Biofactors* 1998; **8**: 93-96
- 25 **Leclercq IA**, Farrell GC, Field J, Bell DR, Gonzalez FJ, Robertson GR. CYP2E1 and CYP4A as microsomal catalysts of lipid peroxides in murine nonalcoholic steatohepatitis. *J Clin Invest* 2000; **105**: 1067-1075
- 26 **Bardag-Gorce F**, Yuan QX, Li J, French BA, Fang C, Ingelman-Sundberg M, French SW. The effect of ethanol-induced cytochrome P4502E1 on the inhibition of proteasome activity by alcohol. *Biochem Biophys Res Commun* 2000; **279**: 23-29
- 27 **Isayama F**, Froh M, Bradford BU, McKim SE, Kadiiska MB, Connor HD, Mason RP, Koop DR, Wheeler MD, Arteel GE. The CYP inhibitor 1-aminobenzotriazole does not prevent oxidative stress associated with alcohol-induced liver injury in rats and mice. *Free Radic Biol Med* 2003; **35**: 1568-1581
- 28 **Kono H**, Bradford BU, Yin M, Sulik KK, Koop DR, Peters JM, Gonzalez FJ, McDonald T, Dikalova A, Kadiiska MB, Mason RP, Thurman RG. CYP2E1 is not involved in early alcohol-induced liver injury. *Am J Physiol* 1999; **277**(6 Pt 1): G1259-G1267
- 29 **You M**, Crabb DW. Recent advances in alcoholic liver disease II. Minireview: molecular mechanisms of alcoholic fatty liver. *Am J Physiol Gastrointest Liver Physiol* 2004; **287**: G1-6
- 30 **Li J**, Hu W, Baldassare JJ, Bora PS, Chen S, Poulos JE, O'Neill R, Britton RS, Bacon BR. The ethanol metabolite, linolenic acid ethyl ester, stimulates mitogen-activated protein kinase and cyclin signaling in hepatic stellate cells. *Life Sci* 2003; **73**: 1083-1096

Science Editor Zhu LH and Guo SY Language Editor Elsevier HK

Characteristics of benign lymphadenosis of oral mucosa

Shu-Xia Li, Shi-Feng Yu, Kai-Hua Sun

Shu-Xia Li, Shi-Feng Yu, Kai-Hua Sun, Department of Oral Pathology, School of Stomatology, Peking University, Beijing 100081, China

Correspondence to: Shu-Xia Li, Department of Oral Pathology, School of Stomatology, Peking University, Beijing 100081, China. lishuxia@sina.com

Telephone: +86-10-62179977-2201

Received: 2004-06-08 Accepted: 2004-08-05

Abstract

AIM: To investigate the pathological characteristics and carcinogenesis mechanism of benign lymphadenosis of oral mucosa (BLOM).

METHODS: The expressions of Ki-67, CD34 and apoptosis were evaluated by immunohistochemical SP staining in 64 paraffin-embedded tissue samples. Of them, 9 were from BLOM with dysplasia, 15 from BLOM without dysplasia, 15 from oral squamous cell carcinoma (OSCC), 15 from oral precancerosis, and 10 from normal tissues. Cell proliferation, apoptosis and angiogenesis of tissue samples were also analyzed.

RESULTS: The expression of Ki-67 in BLOM with dysplasia, oral precancerosis and OSCC was significantly higher than in BLOM without dysplasia and normal mucosa. The microvascular density (MVD) in BLOM with and without dysplasia, oral precancerosis, and OSCC was significantly higher than in normal mucosa. Apoptosis in BLOM and oral precancerosis was significantly higher than in OSCC and normal mucosa.

CONCLUSION: Benign lymphadenosis of oral mucosa has potentialities of cancerization.

© 2005 The WJG Press and Elsevier Inc. All rights reserved.

Key words: Benign lymphadenosis of oral mucosa; Ki-67; Microvascular density; Apoptosis

Li SX, Yu SF, Sun KH. Characteristics of benign lymphadenosis of oral mucosa. *World J Gastroenterol* 2005; 11(29): 4536-4540

<http://www.wjgnet.com/1007-9327/11/4536.asp>

INTRODUCTION

Benign lymphadenosis of oral mucosa (BLOM), which could be commonly found clinically, usually occurs in the mucosae of lips, cheeks, tongue or gingiva. Sometimes, BLOM may develop in all of the oral mucosa and accompany

other oral diseases. As far as we know, few reports have ever mentioned BLOM, and there has been no international definition about it. Most researchers considered it as a kind of reactive proliferation. Since 1970s, our department have been studying BLOM from the aspects of morphology and immunopathology. Ultrastructural changes of this disease is similar to that of leukoplakia^[1,2]. Clinically, BLOM has a malignant trend^[3,4]. At present, it is regarded as a kind of precancerous lesion^[5]. To investigate the pathological characteristics and carcinogenesis mechanism of BLOM, we studied cell proliferation, cell apoptosis and angiogenesis of different types of oral mucosa diseases, including BLOM with dysplasia and without dysplasia, OSCC, oral precancerosis and normal tissues by immunohistochemistry method.

MATERIALS AND METHODS

Materials

A total of 64 paraffin-embedded tissue samples were from Pathological Research Laboratory, School of Stomatology, Peking University. Of them, 9 were from BLOM with dysplasia, 15 from BLOM without dysplasia, 15 from oral OSCC (8 in stage III, 7 in stage I or II), 15 from oral precancerosis, and 10 from normal tissues around the neoplasms. Streptavidin-biotin-immunoperoxidase system kit was purchased from Fuzhou Maixin Immunotech Corporation, China; mouse monoclonal antihuman Ki-67 antibody was provided by Beijing Immunotech Zhonghshan Corporation, China; and cell death detection kit was from Boehringer Mannheim, Germany.

Immunohistochemistry protocol for Ki-67 and CD34

Five micrometer thick sections were dewaxed with xylene, and rehydrated in graded ethanol. Endogenous peroxidase activity was blocked by immersion of slides in methanol with 0.03% hydrogen peroxide for 10 min. In order to retrieve antigenicity, these sections were then heated in a pressure cooker in 10 mmol/L citrate buffer (pH 6, 90 s after water boiled). After washing in distilled water, these sections were rinsed in phosphate-buffered saline (PBS) and incubated for 60 min at room temperature with CD34 or Ki-67 mAb. Reaction was visualized with a streptavidin-biotin-immunoperoxidase system using diaminobenzidine (DAB) as chromogen. All sections were then counterstained with hematoxylin.

Positive staining for CD34 or Ki-67 was regarded as positive control. For negative control, the primary antibodies were replaced with PBS. Staining was measured as the percentage of positively stained nuclei (Ki-67, labeling index, LI) or cytoplasm (CD34, microvascular density, MVD). Ki-67 reaction was scored at ×400 magnification, a total of 1 000 epithelial cells (normal tissue and BLOM) or tumor cells

(OSCC) were evaluated. Reactive nuclei were considered positive, regardless of staining intensity. The percentage of Ki-67 positive was then calculated and positivity of lymphocytes was not evaluated. Criteria for counting included individual or cluster of cells with or without lumen positivity for CD34 immunoreactivity. Areas of inflammation, necrosis, and fibrosis were excluded. For determination of mean MVD, sections were first observed under low power ($\times 200$) for areas with dense vascularity. These were then counted in three different fields under high power ($\times 400$). The average counts were recorded as MVD for each case.

TUNEL protocol for apoptosis evaluation

Detection of apoptosis in tissue was determined by TUNEL assay, employing in situ. The procedure is based on the detection of chromatin DNA strand breaks, the most characteristic biochemical feature of apoptosis caused by activation of endogenous nuclease activity.

Sections were dewaxed, rehydrated, and washed in distilled water for 10 min. The nuclei in tissue sections were stripped from proteins with 4% pepsin diluted in sterile buffer (10 mm Tris-HCl, pH 7.4) for 60 min at 37 °C, followed by quenching of endogenous peroxidase. The sections were rinsed in 50 μ L of a label mixture containing the labeled nucleotide and enzyme, and incubated in a humidified chamber for 60 min at 37 °C. After washing with PBS, the sections were incubated for 30 min at 37 °C with alkaline phosphatase reagent. The substrate reaction was developed using diethyl chlorophosphite (DECP) and counterstained with nuclei fast red.

Positive staining for CD34 or Ki-67 was regarded as positive control. For negative control, the primary antibodies were replaced with PBS. A cell was considered apoptotic only when unequivocal nuclear labeling was observed in the areas with no inflammation. Cells exhibiting necrotic nuclear karyorrhexis as well as those in necrotic foci were excluded. TUNEL reactivity was always estimated in relation to characteristic histological criteria of apoptosis, including overall shrinkage, homogeneously dark basophilic nuclei, presence of nuclear fragments, sharply delineated cell borders and homogenous eosinophilic cytoplasm. To evaluate the different rates of TUNEL reactivity in each sample, 1 000 cells were counted randomly under high power ($\times 400$) and the percentage of positively stained nuclei (AI) was calculated.

Statistical analysis

The expression of Ki-67, MVD and extent of TUNEL reactive nuclei in different tissue samples was analyzed by *t*-test and χ^2 -test using SPSS10.0 for Windows. $P < 0.05$ was considered significant.

RESULTS

The histological characteristics of BLOM is that lymphoid follicles or dense lymphocytes foci could be seen in the basal cell layer. The expression of Ki-67, which was stained brown in nuclei, could be found in normal tissues, BLOM, BLOM with dysplasia, precancerosis and OSCC. Positive cells distributed dispersedly in epithelium of normal tissues and BLOM without dysplasia (Figure 1A). Meanwhile, many cells appeared positive in lymphoid follicles. The expression of Ki-67 obviously increased in BLOM with dysplasia and in some samples Ki-67 positively stained nuclei were seen in all layers of epithelium (Figure 1B). The expression of Ki-67 also increased in precancerous tissues and OSCC, in the center of which positive cells distributed diffusely (Figure 1C). The positive rates of Ki-67 expression in different groups are shown in Table 1.

Table 1 The positive rates of Ki-67 expression in different groups (mean \pm SD)

Group	Ki-67 positive rate (%)
Normal	14.19 \pm 6.18
BLOM	22.29 \pm 11.39
BLOM with dysplasia	45.42 \pm 9.89 ^a
Precancerosis	47.15 \pm 6.84 ^{a,c}
OSCC	65.89 \pm 9.09 ^{a,c,e}

^a $P < 0.05$ vs normal, ^c $P < 0.05$ vs BLOM, ^e $P < 0.05$ vs BLOM with dysplasia.

The expression of CD34 was positive in all samples, and distributed punctately, located in the cytoplasm of vascular endotheliocytes (Figure 2A). Only a few microvessels in the connective tissues of normal mucosa could be seen. But in BLOM, BLOM with dysplasia and precancerosis, their number increased obviously (Figure 2B). A great amount of microvessels also could be found in OSCC. MVD values in different groups are shown in Table 2.

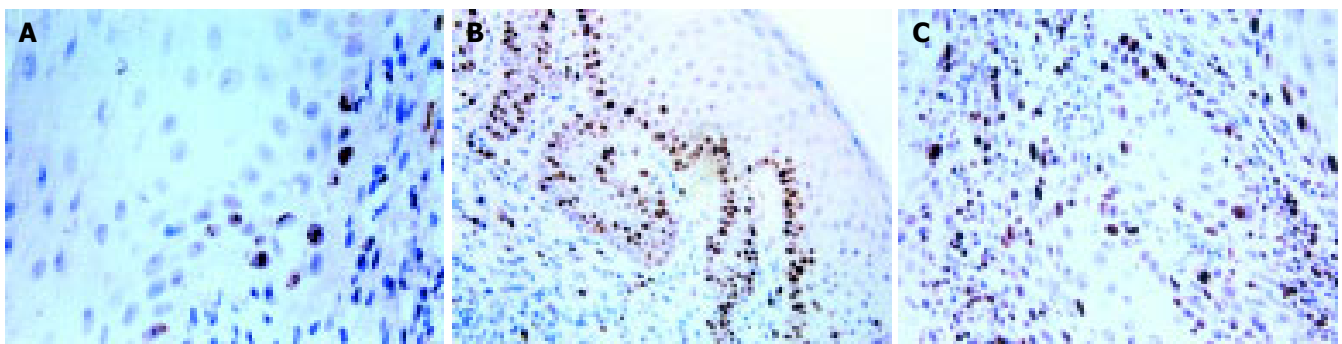


Figure 1 Ki-67 expression in A: BLOM without dysplasia (IHC $\times 400$), B: BLOM with dysplasia (IHC $\times 200$), and C: oral cancer (IHC $\times 200$).

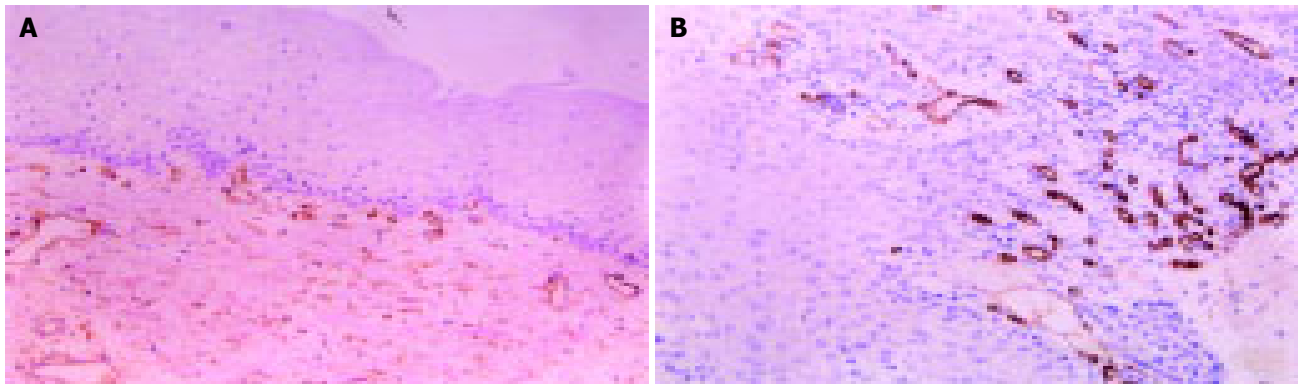


Figure 2 CD34 expression in **A**: BLOM without dysplasia (IHC $\times 100$) and

B: BLOM with dysplasia (IHC $\times 100$).

Table 2 MVD in different groups (mean \pm SD)

Group	MVD value
Normal	14.31 \pm 2.71
BLOM	44.81 \pm 10.20
BLOM with dysplasia	43.89 \pm 8.78 ^a
Precancerosis	45.28 \pm 11.09 ^{a,c}
OSCC	62.73 \pm 8.13 ^{a,c,e}

^aP<0.05 vs normal, ^cP<0.05 vs BLOM, ^eP<0.05 vs BLOM with dysplasia.

Cell apoptosis was found in 2/10 normal tissues, 10/15 BLOM, 8/9 BLOM with dysplasia, 13/15 precancerosis and 8/15 OSCC. Apoptosis was seldom seen in the stromal layer of normal mucosa, but it increased obviously in BLOM, BLOM with dysplasia and precancerosis (Figure 3). At the same time, apoptosis could be found in connective tissues of BLOM, BLOM with dysplasia and precancerosis. The positive rate of apoptosis in OSCC was significantly lower than that in other groups except the normal mucosa.

DISCUSSION

Ki-67 is an acknowledged marker that indicates the proliferation capacity of cells, and many studies demonstrated that it was overexpressed in oral premalignancy and oral cancer^[6-9]. Tabor *et al.*^[10], studied 43 samples from patients who had undergone resection of their squamous cell carcinoma in oral cavity/oropharynx. With the consensus score, 12 samples were classified as normal, and 31 as dysplastic (21 mild, 6 moderate, and 4 severe). They found that there was a high coincidence between loss of heterozygosity (LOH) and the expression of Ki-67. The Ki-67 index in LOH-positive cases was significantly higher than that in LOH-negative cases. It was suggested that the expression of Ki-67 was correlated with other factors (beta-catenin, p53R2, *etc*)^[11-14]. Other scholars found there was a significant correlation between Ki-67 LI, stroma/tumor proportion and the degree of keratinization^[15,16]. In the present study, over-expression was found in the epithelium of BLOM with dysplasia, precancerosis and OSCC. But the expression in epithelium of BLOM without dysplasia was similar to that in the normal mucosa and there was an abundant expression in lymphoid follicles. This suggested that the epithelial cells of BLOM without dysplasia had not undergone genetic

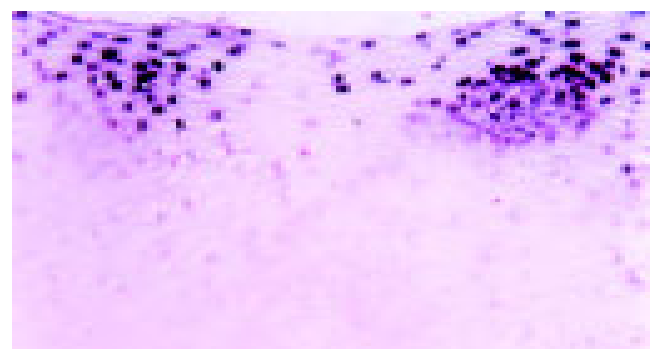


Figure 3 Apoptosis in BLOM with dysplasia (TUNEL $\times 200$).

transformation, and the cells of germinal center had a strong proliferation capacity. In the connective tissues of BLOM and BLOM with dysplasia, a great amount of positive cells could be found in the center of lymphoid follicles. However, no obvious difference was revealed. This indicated that the center had a strong capacity of proliferation, but not a malignant trend, because the proliferation of lymphocytes was a kind of benign and reactive proliferation. Why we considered BLOM benign was also due to this reason. The number of Ki-67 positive cells and the staining in BLOM without dysplasia had no obvious difference from those in normal mucosa, indicating that epithelial cells did not appear abnormal. In the epithelium of BLOM with dysplasia and precancerosis, the number of positive cells obviously increased and the distribution of positive cells extended from the lower basal layer to the upper basal layer and prickle cell layer. In some samples, positive cells were distributed in all the layers of epithelium. This indicated that the proliferation capacity of basal cells was strengthened. Angiogenesis is a process involved in the development of new blood vessels, by the division and migration of existing vasculature^[17-20]. It is an important mechanism to sustain tumorigenic potential in neoplasm and in dysplastic lesions, indicating abundant capillaries leading to intense vascularization in cancer. Therefore, evaluation of angiogenesis may be of prognostic significance in the assessment of tumor progression. Iwasa *et al.*^[21], suggested that negative DNA instability lesions had a higher MVD in proliferating cell nuclear antigen (PCNA)-positive cells than positive DNA instability lesions.

Other scholars proved that in non-small cell lung cancer and oral cancer, the mean AIs of the lower-MVD and the higher-MVD patients were significantly different^[22-24]. Our study has confirmed that insufficient angiogenesis could accelerate apoptotic cell death. The angiogenesis in BLOM with and without dysplasia, and in precancerosis was significantly higher than in normal tissue, and new blood vessels were more abundant. Sauter *et al.*, suggested that the angiogenesis in precancerosis was between oral normal tissue and OSCC^[17].

Apoptosis is a programmed cell death under genetic control. A fine balance between the cell proliferation and cell death is very important to normal development and maintenance of tissue size and shape. In another word, the imbalance between the positive and negative regulation of cell growth could cause a series of diseases including neoplasm. In neoplasm, the disorder of homeostasis may result in the development of tumor^[25-27]. Some studies showed that epidermal growth factor receptor blockade, cyclin dependent kinase inhibitor and 5-FU could induce cell apoptosis^[28-30]. Other scholars also found that the overexpression of p27(Kip1) and retinoic acid receptor could induce growth arrest and apoptosis in an oral cancer cell line^[31,32]. Results of the present study indicated that the apoptosis was significantly higher in BLOM, BLOM without dysplasia, and precancerosis than in normal tissue. However, it was lower in tumor tissue (OSCC). This suggested that the body tried to control the balance of cell number by increasing cell apoptosis with the increase in cell proliferation. However if the body fails, tumor develops. Similar result could be found in the study of Guan *et al.*^[33,34].

Previous studies also showed that BLOM should be regarded as a kind of precancerous lesion. In the present study, the cell proliferation, angiogenesis and apoptosis of BLOM were similar to that of precancerosis, and in BLOM without dysplasia the angiogenesis was significantly higher than that in normal oral tissue. But the expression of Ki-67 was similar to that in normal tissue. Therefore, the changes of cell proliferation, cell apoptosis, and angiogenesis in connective tissue were earlier than in epithelium; BLOM had the potential of carcinogenesis. Many factors may induce the proliferation of cancer cells, enhance their survival by escape of apoptosis, and provide abundant nutrients during early-stage carcinogenesis of oral precancerous lesions. Comparison of gene expression profiles between head and neck squamous cell carcinoma and normal tissues showed that altered expression levels of genes were involved in the control of cell growth and differentiation, angiogenesis, apoptosis, cell cycle, and signaling, most of which had not been previously described in head and neck squamous cell carcinoma^[35]. Which factor contributes to cell proliferation, and inhibits cell apoptosis during the carcinogenesis of BLOM is still a subject to be investigated in future.

REFERENCES

- 1 Sun KH, Wu QG, Zheng LF. Clinicopathological analysis of 70 cases of benign lymphadenosis of oral mucosa. *Zhonghua Kouqiang Yixue Zazhi* 1986; **21**: 137-139
- 2 Sun KH, Yu SF, Wu QG, Zheng LF, Wei MJ. Ultrastructural and immunopathological study of benign lymphadenosis of oral mucosa. *Zhonghua Kouqiang Yixue Zazhi* 1992; **27**: 104-106
- 3 Harsany DL, Ross J, Fee WE Jr. Follicular lymphoid hyperplasia of the hard palate simulating lymphoma. *Otolaryngol Head Neck Surg* 1980; **88**: 349-356
- 4 Wright JM, Dunsworth AR. Follicular lymphoid hyperplasia of the hard palate: A benign lymphoproliferative. *Oral Surg* 1983; **55**: 162-169
- 5 Yu SF. Kouqiang Zuzhi Binglixue(5th edition). Beijing: People's health publishing house 2003: 203-204
- 6 Carlos de Vicente J, Herrero-Zapatero A, Fresno MF, Lopez-Arranz JS. Expression of cyclin D1 and Ki-67 in squamous cell carcinoma of the oral cavity: clinicopathological and prognostic significance. *Oral Oncol* 2002; **38**: 301-308
- 7 Farrar M, Sandison A, Peston D, Gailani M. Immunocytochemical analysis of AE1/AE3, CK 14, Ki-67 and p53 expression in benign, premalignant and malignant oral tissue to establish putative markers for progression of oral carcinoma. *Br J Biomed Sci* 2004; **61**: 117-124
- 8 Alves FA, Pires FR, De Almeida OP, Lopes MA, Kowalski LP. PCNA, Ki-67 and p53 expressions in submandibular salivary gland tumours. *Int J Oral Maxillofac Surg* 2004; **33**: 593-597
- 9 Haffian H, Venteo L, Sukhanova A, Nabiev I, Lefevre B, Pluot M. Immunohistochemical study of DNA topoisomerase I, DNA topoisomerase II alpha, p53, and Ki-67 in oral preneoplastic lesions and oral squamous cell carcinomas. *Hum Pathol* 2004; **35**: 745-751
- 10 Tabor MP, Braakhuis BJ, van der Wal JE, van Diest PJ, Leemans CR, Brakenhoff RH, Kummer JA. Comparative molecular and histological grading of epithelial dysplasia of the oral cavity and the oropharynx. *J Pathol* 2003; **199**: 354-360
- 11 Sato K, Okazaki Y, Tonogi M, Tanaka Y, Yamane GY. Expression of beta-catenin in rat oral epithelial dysplasia induced by 4-nitroquinoline 1-oxide. *Oral Oncol* 2002; **38**: 772-778
- 12 Yanamoto S, Kawasaki G, Yoshitomi I, Mizuno A. Expression of p53R2, newly p53 target in oral normal epithelium, epithelial dysplasia and squamous cell carcinoma. *Cancer Lett* 2003; **190**: 233-243
- 13 Xie X, Clausen OP, Boysen M. Bag-1 expression as a prognostic factor in tongue squamous cell carcinomas. *Laryngoscope* 2004; **114**: 1785-1790
- 14 Bowen SL, Bloor BK, Leigh IM, Waseem A. Adducin expression in cutaneous and oral lesions: alpha- and beta-adducin transcripts down-regulate with keratinocyte differentiation in stratified epithelia. *J Pathol* 2003; **201**: 119-126
- 15 Bettendorf O, Herrmann G. Prognostic relevance of Ki-67 antigen expression in 329 cases of oral squamous cell carcinoma. *ORL J Otorhinolaryngol Relat Spec* 2002; **64**: 200-205
- 16 Kurokawa H, Matsumoto S, Murata T, Yamashita Y, Tomoyose T, Zhang M, Fukuyama H, Takahashi T. Immunohistochemical study of syndecan-1 down-regulation and the expression of p53 protein or Ki-67 antigen in oral leukoplakia with or without epithelial dysplasia. *J Oral Pathol Med* 2003; **32**: 513-521
- 17 Sauter ER, Nesbit M, Watson JC, Klein-Szanto A, Litwin S, Herlyn M. Vascular endothelial growth factor is a marker of tumor invasion and metastasis in squamous cell carcinomas of the head and neck. *Clin Cancer Res* 1999; **5**: 775-782
- 18 Chimenos-Kustner E, Font-Costa I, Lopez-Lopez J. Oral cancer risk and molecular markers. *Med Oral Patol Oral Cir Bucal* 2004; **9**: 377-384
- 19 Shieh YS, Lee HS, Shiah SG, Chu YW, Wu CW, Chang LC. Role of angiogenic and non-angiogenic mechanisms in oral squamous cell carcinoma: correlation with histologic differentiation and tumor progression. *J Oral Pathol Med* 2004; **33**: 601-606
- 20 Sotiriou C, Lothaire P, Dequanter D, Cardoso F, Awada A. Molecular profiling of head and neck tumors. *Curr Opin Oncol* 2004; **16**: 211-214
- 21 Iwasa M, Imamura Y, Noriki S, Nishi Y, Kato H, Fukuda M. Immunohistochemical detection of early-stage carcinogenesis of oral leukoplakia by increased DNA-instability and various malignancy markers. *Eur J Histochem* 2001; **45**: 333-346
- 22 Tanaka F, Otake Y, Yanagihara K, Kawano Y, Miyahara R, Li M, Ishikawa S, Wada H. Correlation between apoptotic index and angiogenesis in non-small cell lung cancer: comparison

- between CD105 and CD34 as a marker of angiogenesis. *Lung Cancer* 2003; **39**: 289-296
- 23 **Hannen EJ**, Riediger D. The quantification of angiogenesis in relation to metastasis in oral cancer: a review. *Int J Oral Maxillofac Surg* 2004; **33**: 2-7
- 24 **Lim JJ**, Kang S, Lee MR, Pai HK, Yoon HJ, Lee JI, Hong SP, Lim CY. Expression of vascular endothelial growth factor in salivary gland carcinomas and its relation to p53, Ki-67 and prognosis. *J Oral Pathol Med* 2003; **32**: 552-561
- 25 **Birchall M**, Winterford C, Tripconi L, Gobe G, Harmon B. Apoptosis and mitosis in oral and oropharyngeal epithelia: evidence for a topographical switch in premalignant lesions. *Cell Prolif* 1996; **29**: 447-456
- 26 **Grabnbauer GG**, Suckorada O, Niedobitek G, Rodel F, Iro H, Sauer R, Rodel C, Schultze-Mosgau S, Distel L. Imbalance between proliferation and apoptosis may be responsible for treatment failure after postoperative radiotherapy in squamous cell carcinoma of the oropharynx. *Oral Oncol* 2003; **39**: 459-469
- 27 **Chrysomali E**, Nikitakis NG, Tosios K, Sauk JJ, Papanicolaou SI. Immunohistochemical evaluation of cell proliferation antigen Ki-67 and apoptosis-related proteins Bcl-2 and caspase-3 in oral granular cell tumor. *Oral Surg Oral Med Oral Pathol Oral Radiol Endod* 2003; **96**: 566-572
- 28 **Holsinger FC**, Doan DD, Jasser SA, Swan EA, Greenberg JS, Schiff BA, Bekele BN, Younes MN, Bucana CD, Fidler IJ, Myers JN. Epidermal growth factor receptor blockade potentiates apoptosis mediated by Paclitaxel and leads to prolonged survival in a murine model of oral cancer. *Clin Cancer Res* 2003; **9**: 3183-3189
- 29 **Mihara M**, Shintani S, Nakashiro K, Hamakawa H. Flavopiridol, a cyclin dependent kinase (CDK) inhibitor, induces apoptosis by regulating Bcl-x in oral cancer cells. *Oral Oncol* 2003; **39**: 49-55
- 30 **Ohtani T**, Hatori M, Ito H, Takizawa K, Kamijo R, Nagumo M. Involvement of caspases in 5-FU induced apoptosis in an oral cancer cell line. *Anticancer Res* 2000; **20**: 3117-3121
- 31 **Supriatno**, Harada K, Hoque MO, Bando T, Yoshida H, Sato M. Overexpression of p27(Kip1) induces growth arrest and apoptosis in an oral cancer cell line. *Oral Oncol* 2002; **38**: 730-736
- 32 **Hayashi K**, Yokozaki H, Naka K, Yasui W, Lotan R, Tahara E. Overexpression of retinoic acid receptor beta induces growth arrest and apoptosis in oral cancer cell lines. *Jpn J Cancer Res* 2001; **92**: 42-50
- 33 **Guan WQ**, Yu SF, Gao Y. Expression of bcl-2, p53 protein in oral leukoplakia and squamous cell carcinoma. *Linchuang Yu Shiyan Binglixue Zazhi* 1999; **4**: 123-125
- 34 **Nikitakis NG**, Sauk JJ, Papanicolaou SI. The role of apoptosis in oral disease: mechanisms; aberrations in neoplastic, autoimmune, infectious, hematologic, and developmental diseases; and therapeutic opportunities. *Oral Surg Oral Med Oral Pathol Oral Radiol Endod* 2004; **97**: 476-490
- 35 **Lin DT**, Subbaramaiah K, Shah JP, Dannenberg AJ, Boyle JO. Cyclooxygenase-2: a novel molecular target for the prevention and treatment of head and neck cancer. *Head Neck* 2002; **24**: 792-799

Science Editor Zhu LH Language Editor Elsevier HK

Visceral response to acute retrograde gastric electrical stimulation in healthy human

Shu-Kun Yao, Mei-Yun Ke, Zhi-Feng Wang, Da-Bo Xu, Yan-Li Zhang

Shu-Kun Yao, Mei-Yun Ke, Zhi-Feng Wang, Da-Bo Xu, Yan-Li Zhang, Department of Gastroenterology, Peking Union Medical College Hospital, Beijing 100730, China
Correspondence to: Mei-Yun Ke, Department of Gastroenterology, Peking Union Medical College Hospital, Beijing 100730, China. mygcn@public3.bta.net.cn
Telephone: +86-10-65295006 Fax: +86-10-65295006
Received: 2004-10-19 Accepted: 2004-12-03

Abstract

AIM: To investigate the visceral response to acute retrograde gastric electrical stimulation (RGES) in healthy humans and to derive optimal parameters for treatment of patients with obesity.

METHODS: RGES with a series of effective parameters were performed via a bipolar mucosal electrode implanted along the great curvature 5 cm above pylorus of stomach in 12 healthy human subjects. Symptoms associated with dyspepsia and other discomfort were observed and graded during RGES at different settings, including long pulse and pulse train. Gastric myoelectrical activity at baseline and during different settings of stimulation was recorded by a multi-channel electrogastrography.

RESULTS: The gastric slow wave was entrained in all the subjects at the pacing parameter of 9 cpm in frequency, 500 ms in pulse width, and 5 mA in amplitude. The frequently appeared symptoms during stimulation were satiety, bloating, discomfort, pain, sting, and nausea. The total symptom score for each subject significantly increased as the amplitude or pulse width was adjusted to a higher scale in both long pulse and pulse train. There was a wide diversity of visceral responses to RGES among individuals.

CONCLUSION: Acute RGES can result in a series of symptoms associated with dyspepsia, which is beneficial to the treatment of obesity. Optimal parameter should be determined according to the individual sensitivity to electrical stimulation.

© 2005 The WJG Press and Elsevier Inc. All rights reserved.

Key words: Visceral response; Retrograde gastric electrical stimulation; Symptom; Obesity

Yao SK, Ke MY, Wang ZF, Xu DB, Zhang YL. Visceral response to acute retrograde gastric electrical stimulation in healthy human. *World J Gastroenterol* 2005; 11(29): 4541-4546
<http://www.wjgnet.com/1007-9327/11/4541.asp>

INTRODUCTION

Motility is one of the most critical physiological functions of the stomach. Coordinated gastric contractions are necessary for the emptying of ingested food, and impairment in gastric motility may result in delayed gastric emptying. Gastric motility (contractile activity) is regulated by the myoelectrical activity of the stomach, called slow waves^[1]. The gastric slow wave originates in the proximal stomach, propagates distally toward the pylorus, and dominates the maximum frequency, propagation velocity and propagation direction of gastric contractions. Abnormalities in gastric slow waves including uncoupling and gastric dysrhythmia lead to gastric motor disorders and are frequently observed in patients with functional disorders of the stomach, such as gastroparesis, functional dyspepsia, anorexia, etc. Gastric myoelectrical abnormalities are believed to be the fundamental factors for gastric hypomotility^[2-5]. Gastric prokinetics are used to treat patients with gastric hypomotility and cisapride has been proved to be effective on both gastric hypomotility and myoelectrical abnormality^[6]. But there are still a lot of patients who are refractory or could not tolerate these drugs.

Gastric electrical stimulation is used to affect gastric motility with the rationale as a forward gastric pacing to trigger the gastric myoelectrical propagation from proximal towards pylorus of stomach. It has been accepted as a therapy for chronic gastroparesis associated with drug refractory nausea and vomiting secondary to diabetic or idiopathic etiology^[7,8]. Researchers adopt its mechanism with converse effects and have developed implantable gastric stimulation (IGS) to treat obesity that is attributed to rapid gastric emptying or hypermotility^[9-11].

IGS for weight loss is an exciting new concept for the treatment of obesity^[12]. It is unique in that it relies on neither gastric restriction nor intestinal malabsorption but instead induces early satiety. IGS is also a relatively invasive procedure that does not alter the gastrointestinal anatomy. The system comprises an electrical pulse generator similar to a cardiac pacemaker and a serosal lead implanted in the muscular layer of the distal gastric wall. Both animal^[13] and human studies^[14-18] revealed that it results in decreased food intake and a substantial weight loss.

Up to now, whether there is responsive diversity among individuals to gastric electrical stimulation is unknown. An optimal parameter, which should be of high efficiency, low energy expenditure and acceptability, has not been determined. This study aimed to investigate the visceral response to RGES with mucosal electrode, and to derive optimal parameter for therapy of obesity.

MATERIALS AND METHODS

Subjects

Twelve healthy volunteers were recruited in this study, including six males and six females, with their age being 29.4 ± 8.6 years, body weight being 62.63 ± 8.29 kg (48-80 kg) and body mass index being 23.18 ± 2.62 kg/m². None of the subjects had gastrointestinal diseases or symptoms or a history of gastrointestinal surgery. All women were studied during their follicular phase of the menses to minimize possible hormonal influences^[19]. No medications were used by any of the participants except for oral contraceptives 2 wk prior to the study. Organic diseases of stomach, such as erosive gastritis, gastric ulcer, esophagitis, etc., were ruled out by endoscopy. Subjects with swallowing disorders such as dysphagia, achalasia, and hypersensitivity to nasal intubation were excluded. Females in pregnancy, or nursing period were also excluded. Written consent form was signed by each subject before the study, and the protocol was approved by the Ethical Committee of the University Hospital.

Implantation of mucosal electrodes

The subjects were fasted for 8 h or more before implantation of the electrodes. A temporary transvenous cardiac pacing lead system (Model 6416, Medtronic, Netherlands) composed of an active fixation, a lead with bipolar electrodes and a soft-tipped, lubricated guide catheter was used (Figure 1). This lead was intubated into the stomach through a nasal cavity before endoscopy. At a good exposure of the antrum under endoscopy, the distal electrode was screwed into the mucosa along the greater curvature 5 cm above the pylorus and fixed with a titanium clamp. The proximal electrode was affixed to the surface of the gastric mucosa with one or two titanium clamps (Figure 2). After the placement, the guide catheter was pulled out of the stomach. An X-ray picture was taken once daily to ensure that the electrodes were located at the original positions in the stomach.

A multi-channel electrogastrograph (POLYGRAM NET™, Medtronic Functional Diagnostics A/S, Denmark) was used to record gastric myoelectrical activity. Two channel gastric myoelectrical recordings were obtained by connecting each of the mucosal electrodes to a common reference electrode placed on the leg of the subject. These myoelectrical recordings were used to further confirm the attachment of electrodes to the gastric mucosa. A recording of rhythmic 3 cpm gastric slow waves would be indicative

of a good attachment of the electrodes. The entrainment of gastric myoelectrical activity by RGEs was also observed to assess its electrophysiological effectiveness.

Experimental protocol

After a baseline recording of gastric slow waves for 30 min, symptomatic responses to gastric electrical stimulation with various parameters were assessed in the fasting state. Visceral sensation (symptomatic response) to gastric electrical stimulation was assessed by three parameters: initial sensation, maximum tolerance, and the symptom score. The initial sensation was defined as the stimulation with which the subject first reported one or more of any symptoms. The maximum tolerance was defined as the stimulation with which the subject reported the maximally tolerable symptoms.

Symptoms, including satiety, bloating, discomfort (the character and location of a symptom could not be described clearly and precisely), upper abdominal pain, sting, belching, nausea, vomiting, were recorded and graded during RGEs at different settings. Each symptom was graded from 0 to 3 (0: no symptom; 1: mild symptoms, requiring intention to feel the symptoms; 2: moderate symptoms, being aware of the symptoms, but not interfering with daily activities; 3: severe symptoms, interfering with daily activities). The total symptom score in each subject was derived and its correlation with the stimulation energy was determined.

Retrograde gastric electrical stimulation

RGEs was performed via the bipolar electrodes attached to the mucosa/submucosa of the distal antrum using a universal pulse generator (Acupulser, model A310, World Precision Instrument, Inc., Sarasota, FL, USA). Two models of electric stimulation, long pulse and pulse train, were applied to the pacing electrodes in the constant current mode. The long pulse was composed of periodic rectangular pulses with a frequency of 9 cpm, pulse width of 500 ms, and adjustable pulse amplitude (current) consisting three settings of 5, 10, and 15 mA. The pulsed train was on for a period of 2 s and off for 3 s. The pulse frequency was 20 Hz, an adjustable pulse width consisting three settings of 5, 10, and 20 ms. The amplitude was adjusted from 10 to 15 mA. If maximal intolerable symptom did not appear, the amplitude was adjusted to 20 mA. Each session of

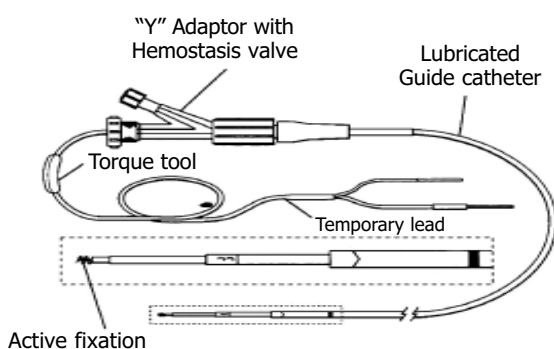


Figure 1 Model 6416 temporary transvenous pacing lead system.



Figure 2 Placement of mucosal electrode. Arrow 1 indicates the distal electrode; arrow 2 indicates the proximal electrode.

Table 1 Symptom scores at different parameters (mean±SE)

	Long pulse 112.5 smA ²	Long pulse 450 smA ²	Long pulse 1 012.5 smA ²	Pulse train 240 smA ²	Pulse train 480 smA ²	Pulse train 960 smA ²	Pulse train 2 160 smA ²
Satiety	0.08±0.08	0	0.08±0.08	0.08±0.08	0.17±0.17	0.25±0.18	0.42±0.23
Bloating	0.08±0.18	0.21±0.17	0.33±0.19	0.25±0.18	0.50±0.19	0.58±0.26	1.00±0.31
Discomfort	0.38±0.18	0.5±0.27	0.67±0.28	0.75±0.12	0.50±0.19	0.50±0.23	0.42±0.26
Pain	0.33±0.18	0.8±0.26	1.54±0.27	0.16±0.21	1.33±0.19	1.92±0.24	2.50±0.27
Sting	0.17±0.17	0.17±0.17	0.25±0.18	0.08±0.17	0.25±0.21	0.25±0.18	0.33±0.22
Nausea	0.17±0.17	0.21±0.21	0.25±0.25	0.08±0.08	0.21±0.17	0.29±0.22	0.75±0.35

stimulation lasted for about 20 min and there was a 10 min or more resting period between consecutive stimulation sessions. For all tests, the subject was blinded about the stimulation and stimulation parameters.

Stimulation energy was calculated for each stimulation session. The stimulation energy was defined as $t \times I^2 R$, where t is stimulation time, I is stimulation current and R is the impedance between two stimulation electrodes. In this study, R was ignored since it was constant for various stimulation sessions, I was the pulse amplitude and t was the total on-time of pulses within a minute. For long pulses, $t = \text{pulse frequency (pulses/min)} \times \text{pulse width}$. For pulse trains, $t = \text{number of trains/min} \times \text{number of pulses/train} \times \text{pulse width}$. The unit of stimulation energy used in this study was s (mA)² or simply smA².

Statistical analysis

Results of specific symptom scores and total symptom score in each subject to different parameters were expressed as mean±SE. Statistical analysis was performed by one-way ANOVA. Pearson's linear correlation and regression method was used to assess the correlation between responsive severity and stimulation energy. $P < 0.05$ was considered statistically significant.

RESULTS

All the 12 subjects completed the study with good compliance. Regular gastric slow waves were recorded from stimulation electrodes attached to the gastric mucosa at baseline. Typical tracings are presented in Figure 3. The dominant frequency of the gastric slow waves was 2.71 ± 0.16 cpm. The gastric slow waves in all the subjects were completely entrained by the signal of RGES at the frequency 9 cpm, pulse width 500 ms and amplitude 5 mA (112.5 smA², Figure 4).

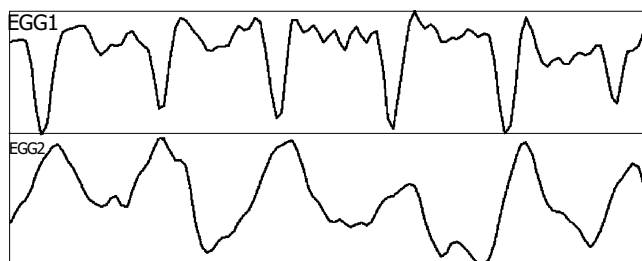


Figure 3 Intrinsic myoelectrical activities from mucosa/submucosa electrodes in stomach.

Frequently appeared symptoms during stimulation were satiety, bloating, discomfort, upper abdominal pain, sting, and nausea. The sum of these six symptoms was used as an overall total symptom score. The severity of specific symptoms to different parameters is shown in Table 1.

The output energy of electrical stimulation for inducing initial sensation showed a wide distribution among individuals. The initial sensation appeared in three subjects at 112.5 smA² (long pulse: 9 cpm, 500 ms, 5 mA), six subjects at 240 smA² (pulse train: 2 s-on, 3 s-off, 20 Hz, 5 ms, 10 mA), one subject at 450 smA² (long pulse: 9 cpm, 500 ms, 10 mA), and two subjects at 480 smA² (pulse train: 2 s-on, 3 s-off, 20 Hz, 10 ms, 10 mA). The maximal energy for inducing initial sensation was more than four times that of the minimum. The initial sensation occurred as different symptoms. Bloating appeared in three subjects, satiety in two, discomfort and pain in five, sting and nausea in one, respectively.

The output energy for inducing maximal tolerable sensation also showed a wide diversity among individuals. The maximal tolerable sensation was recorded at 480 smA² in two subjects, at 2 160 smA² (pulse train: 2 s-on, 3 s-off, 20 Hz, 20 ms, 15 mA) in nine subjects and at 3 840 smA² (pulse train: 2 s-on, 3 s-off, 20 Hz, 20 ms, 20 mA) in one subject. The maximal energy for maximal tolerable sensation was eight times that of the minimum. The major symptoms resulted from the maximally tolerable stimulation included upper abdominal pain in nine subjects, nausea in two subjects, and both pain and nausea in one subject. Some mild to moderate symptoms were simultaneously noted with the maximally tolerable stimulation, including satiety, bloating, discomfort, belching, and nausea.

The most common symptomatic response to stronger RGES was upper abdominal pain. It appeared synchronously with stimulus signals, such as 9 cpm at long pulse, and became

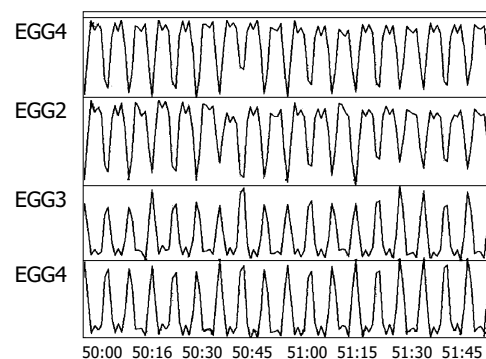


Figure 4 Entrainment of gastric myoelectrical activity by RGES.

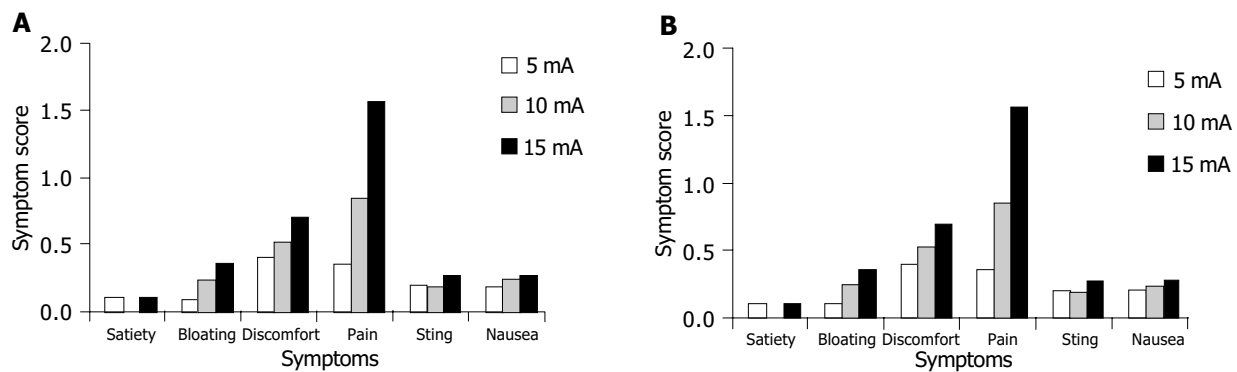


Figure 5 Symptom scores at different parameters of long pulse (A) and pulse

train (B).

persistent in three subjects when the maximal stimulation was applied. It disappeared immediately as the stimulation terminated in seven subjects and gradually ceased within 4 min in five subjects. Other symptoms, such as bloating, discomfort, nausea, etc., also disappeared as soon as the stimulation ended.

During stimulation with long pulse, the severity of the symptoms including bloating, discomfort, and pain significantly increased when the pulse amplitude was adjusted to a higher scale ($P < 0.01$, Figure 5A). The severity of symptoms including satiety, bloating, pain, and nausea also significantly increased when the pulse width or amplitude was set to higher scales during pulse train ($P < 0.05$, Figure 5B). The mean total symptom score for the seven settings of gastric electrical stimulation was linearly correlated with stimulation energy ($r = 0.96$, $P < 0.001$, Figure 6). That is, the total symptom score for each subject significantly increased as the output energy was adjusted to a higher scale in both long pulse and pulse train.

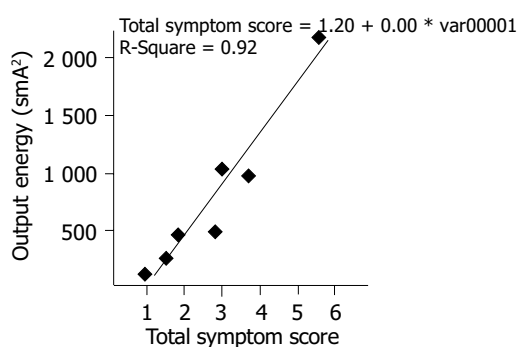


Figure 6 Correlation of total symptom score with output energy of stimulation.

DISCUSSION

Obesity, defined by an excess of body fat, is a highly prevalent disorder in the Western world. In the USA, it has been estimated that one of three adults is obese^[20]. Obesity predisposes to or aggravates many clinical conditions, such as hypertension, hyperlipidemia, diabetes, gout, atherosclerotic heart disease, etc.^[21]. Obesity is of a multifactorial pathogenesis. The basic mechanism is believed that obesity results from food intake greater than energy

needs. The quantity of food intake is directly determined by sensory and motor function of stomach, i.e., gastric accommodation (capacity) and emptying. Previous studies using an intragastric balloon to assess proximal stomach capacity showed that it is larger in both moderate and severe obese individuals^[22,23]. In the studies of gastric capacity in obese people, distal gastric volume is also found larger in obese individuals in the fasting state from imaging with single photon emission computed tomography^[24], suggesting that the increased gastric volume causes changes in the sensation of satiety with a consequent increase of food intake in these subjects.

In addition to stomach capacity, the retaining time of food in stomach also influences mechano- and chemosensitive satiety signals and it is a reasonable hypothesis that an enhanced rate of gastric emptying predisposes to overeating. Although the contribution of changes in gastrointestinal motility to the pathogenesis of obesity is unclear, several noteworthy changes in gastrointestinal motility have been observed in obesity^[25]. For example, some studies suggest more rapid gastric emptying in obesity^[9-11], although normal^[26-29] or even slower^[30-32] emptying has also been reported in other studies. But in a better designed study of 77 subjects including 46 obese and 31 age-, sex-, and racematched nonobese individuals, obese subjects are found to have a more rapid emptying rate than nonobese subjects^[9].

Based on the pathogenesis of obesity, great efforts from different fields have been tried to conquer obesity. Medicines and neuroendocrine agents or analogs are found to be able to inhibit appetite or to delay gastric emptying^[33,34]. Surgical approaches can weaken the gastric capacity, as implantation of balloon in the stomach^[35-37]. By doing this, symptoms associated with dyspepsia, such as satiety, bloating, anorexia, discomfort or pain of upper abdomen, are duplicated in fasting state or postprandial. The occurrence of these symptoms results in reduction of food intake, eventually loss of body weight, which is the goal for the treatment of obesity.

As the stomach contractility is controlled by gastric myoelectrical activity, electrophysiological approaches can alter stomach motility. A recent preliminary study indicates the potential of gastric electrical stimulation for weight loss^[13]. The first human study using a gastric stimulator for the treatment of morbid obesity was performed in 1995, which results in decreased food intake and a substantial

weight loss^[4]. IGS for human obesity has been investigated in different institutes in the world since then^[15-18].

Recently, we have proposed retrograde gastric electrical stimulation (RGES). In this method, electrical stimulation is performed at a tachygastrial frequency and via a pair of mucosal electrodes placed in the distal antrum, mimicking an ectopic pacemaker generating tachygastria. Experiments in dogs have revealed a successful inhibition of antral contractions in the fed state and a delayed gastric emptying of liquid^[38,39]. This study was designed to observe the acute symptomatic responses induced by RGES via bipolar mucosal electrodes. During seven settings of RGES, the frequently appeared symptoms were satiety, bloating, discomfort, pain, sting, and nausea, which are all associated with dyspepsia. These symptoms were typically seen during initial sensation by less energy. Even during maximum stimulation, the frequently appeared symptom was pain of upper abdomen, which is the key symptom of dyspepsia. Furthermore, some mild to moderate symptoms simultaneously occurred such as bloating, discomfort, nausea, satiety, and belching. These symptoms are all associated with dyspepsia. When these symptoms are present with activation of gastric stimulation, the subjects will change their eating behavior and ingest less food, eventually leading to their weight loss. All these are expected for the treatment of obese patients.

In this study, we found that the severity of some symptoms, such as bloating, discomfort and pain, significantly increased when the output energy of stimulation was adjusted to a higher scale. The total symptom score for each subject also simultaneously increased with the increase of energy, suggesting that there is a linear correlation between symptom score and stimulation energy, which is consistent with that of dosage-efficacy seen in pharmacology. In this sense, RGES meets the essential qualification for a potential therapy of obesity.

IGS can induce weight loss in patients with morbid obesity, but its mechanism remains largely unknown. Recent animal studies suggested that this increased satiety is attributed to gastric distention induced by gastric stimulation^[38]. Gastric distention contributes to the feeling of fullness or satiety. The mechanism is unclear, but distending the stomach stimulates gastric stretch receptors, thus triggering vagal discharges that activate hypothalamic neurons^[40] and induce the feeling of satiety^[41]. The stimulation-induced gastric relaxation or distention is mediated by the intrinsic nitrergic pathway, as the inhibitor of nitric oxide synthase blocks the effect whereas vagotomy does not^[42].

Satiety as a signal of reduction of food intake is also regulated by endocrine system especially the peptides in gastrointestinal tract^[43]. Peptides like cholecystokinin (CCK), glucagon-like peptide (GLP)-1, leptin and ghrelin have been shown to evoke satiety, thereby reducing food intake^[43,44]. Cigaina and Hirschberg^[16] have investigated the mechanism behind the changed eating behavior in patients treated with IGS. Gastric electrical stimulation can lead to significant weight loss and decrease in plasma levels of CCK, somatostatin, GLP-1, and leptin. Weight loss correlates significantly with decreased leptin levels. In this study, RGES induced a series of symptoms associated with dyspepsia, suggesting that the stimulation results in gastric distention

via neuroendocrine pathways. As gastric electrical stimulation is a novel and promising therapy for morbid obesity, more studies are necessary to elucidate the correlations between satiety, weight loss, and digestive neuro-hormone changes.

The results of our study reveal a wide diversity of visceral sensitivity to RGES among individuals and we should determine the optimal parameters according to the individual responsive severity. However, we should not select the pulse amplitude that is more than 15 mA, at which it would induce intolerable symptoms to most human subjects. The subjects who get initial sensation with low stimulation energy may be expected to get desirable therapeutic effect from RGES, but those insensitive to RGES may not. As for those insensitive subjects, we should include them in this therapy with deliberation. They may take other effective option such as bariatric surgery.

REFERENCES

- 1 **Chen JD**, McCallum RW. Electrogastrographic parameters and their clinical significance. In: Chen JDZ, McCallum RW, Eds. *The Electrogastrography: principles and clinical applications*. New York: Raven Press 1994: 45-73
- 2 **Chen JD**, McCallum RW. Clinical applications of electrogastrogram. *Am J Gastroenterol* 1993; **88**: 1324-1336
- 3 **Chen JD**, Schirmer BD, McCallum RW. Serosal and cutaneous recordings of gastric myoelectrical activity in patients with gastroparesis. *Am J Physiol* 1994; **266**(1 Pt 1): G90-98
- 4 **You CH**, Lee KY, Chey WY, Menguy R. Electrogastrographic study of patients with unexplained nausea, bloating and vomiting. *Gastroenterology* 1980; **79**: 311-314
- 5 **Chen JD**, Pan J, McCallum RW. Clinical significance of gastric myoelectrical dysrhythmias. *Dig Dis* 1995; **13**: 275-290
- 6 **Chen JD**, Ke MY, Lin XM, Wang Z, Zhang M. Cisapride provides symptomatic relief in functional dyspepsia associated with gastric myoelectrical abnormality. *Aliment Pharmacol Ther* 2000; **14**: 1041-1047
- 7 **Chen JD**, Qian LW, Ouyang H, Yin J. Gastric electrical stimulation with short pulses reduces vomiting but not dysrhythmias in dogs. *Gastroenterology* 2003; **124**: 401-409
- 8 **McCallum RW**, Chen JD, Lin Z, Schirmer BD, Williams RD, Ross RA. Gastric pacing improves emptying and symptoms in patients with gastroparesis. *Gastroenterology* 1998; **114**: 456-461
- 9 **Wright RA**, Krinsky S, Fleeman C, Trujillo J, Teague E. Gastric emptying and obesity. *Gastroenterology* 1983; **84**: 747-751
- 10 **Zahorska-Markiewicz B**, Jonderko K, Lelek A, Skrzypek D. Gastric emptying in obesity. *Hum Nutr Clin Nutr* 1986; **40**: 309-313
- 11 **Sasaki H**, Nagulesparan M, Dubois A, Straus E, Samloff IM, Lawrence WH, Johnson GC, Sievers ML, Unger RH. Hypergastrinemia in obese noninsulin-dependent diabetes: a possible reflection of high prevalence of vagal dysfunction. *J Clin Endocrinol Metab* 1983; **56**: 744-750
- 12 **Shikora SA**. Implantable gastric stimulation for the treatment of severe obesity. *Obes Surg* 2004; **14**: 545-548
- 13 **Xing JH**, Brody F, Brodsky J, Rosen M, Larive B, Ponsky J, Soffer E. Gastric electrical-stimulation effects on canine gastric emptying, food intake, and body weight. *Obes Res* 2003; **11**: 41-47
- 14 **Cigaina V**. Gastric pacing as therapy for morbid obesity: preliminary results. *Obes Surg* 2002; **12**: 421-424
- 15 **D'Argent J**. Gastric electrical stimulation as therapy of morbid obesity: preliminary results from the French study. *Obes Surg* 2002; **12**(Suppl 1): 21S-25S
- 16 **Cigaina V**, Hirschberg AL. Gastric pacing for morbid obesity: plasma levels of gastrointestinal peptides and leptin. *Obes Res* 2003; **11**: 1456-1462
- 17 **Favretti F**, De Luca M, Segato G, Busetto L, Ceoloni A, Magon

- A, Enzi G. Treatment of morbid obesity with the transcend implantable gastric stimulator (IGS): a prospective survey. *Obes Surg* 2004; **14**: 666-670
- 18 **Miller K**, Holler E, Hell E. Intra-gastric stimulation (IGS) for treatment of morbid obesity. *Zentralbl Chir* 2002; **127**: 1049-1054
- 19 **Parkman HP**, Harris AD, Miller MA, Fisher RS. Influence of age, gender, and menstrual cycle on the normal electrogastrogram. *Am J Gastroenterol* 1996; **91**: 127-133
- 20 **Wickelgren I**. Obesity: how big a problem? *Science* 1998; **280**: 1364-1367
- 21 **Seidell JC**. Societal and personal costs of obesity. *Exp Clin Endocrinol Diabetes* 1998; **106**: 7-9
- 22 **Granstrom L**, Backman L. Stomach distension in extremely obese and in normal subjects. *Acta Chir Scand* 1985; **151**: 367-370
- 23 **Geliebter A**. Gastric distension and gastric capacity in relation to food intake in humans. *Physiol Behav* 1988; **44**: 665-668
- 24 **Kim DY**, Camilleri M, Murray JA, Stephens DA, Levine JA, Burton DD. Is there a role for gastric accommodation and satiety in asymptomatic obese people. *Obes Res* 2001; **9**: 655-661
- 25 **Wisén O**, Hellstrom PM. Gastrointestinal motility in obesity. *J Intern Med* 1995; **237**: 411-418
- 26 **Barkin JS**, Reiner DK, Goldberg RI, Phillips RS, Janowitz WR. The effects of morbid obesity and the Garren-Edwards gastric bubble on solid phase gastric emptying. *Am J Gastroenterol* 1988; **83**: 1364-1367
- 27 **French SJ**, Murray B, Rumsey RD, Sepple CP, Read NW. Preliminary studies on the gastrointestinal responses to fatty meals in obese people. *Int J Obes Relat Metab Disord* 1993; **17**: 295-300
- 28 **Verdich C**, Madsen JL, Toubro S, Buemann B, Holst JJ, Astrup A. Effect of obesity and major weight reduction on gastric emptying. *Int J Obes Relat Metab Disord* 2000; **24**: 899-905
- 29 **Horowitz M**, Collins PJ, Harding PE, Shearman DJ. Abnormalities of gastric emptying in obese patients. *Gastroenterology* 1983; **85**: 983-985
- 30 **Horowitz M**, Collins PJ, Shearman DJ. Effect of increasing the caloric/osmotic content of the liquid component of a mixed solid and liquid meal on gastric emptying in obese subjects. *Hum Nutr Clin Nutr* 1986; **40**: 51-56
- 31 **Maddox A**, Horowitz M, Wishart J, Collins P. Gastric and esophageal emptying in obesity. *Scand J Gastroenterol* 1989; **24**: 593-598
- 32 **Geliebter A**, Melton PM, Gage D, McCray RS, Hashim SA. Gastric balloon to treat obesity: a double blind study in non-dieting subjects. *Am J Clin Nutr* 1990; **51**: 584-588
- 33 **Foxx-Orenstein A**, Camilleri M, Stephens D, Burton D. Effect of a somatostatin analogue on gastric motor and sensory functions in healthy humans. *Gut* 2003; **52**: 1555-1561
- 34 **Nozu T**, Martinez V, Rivier J, Taché Y. Peripheral urocortin delays gastric emptying: role of CRF receptor 2. *Am J Physiol* 1999; **276**(4 Pt 1): G867-874
- 35 **Sagar PM**. Surgical treatment of morbid obesity. *Br J Surg* 1995; **82**: 732-739
- 36 NIH conference. Gastrointestinal surgery for severe obesity. Consensus development conference panel. *Ann Intern Med* 1991; **15**: 956-961
- 37 **Geliebter A**, Melton PM, McCray RS, Gage D, Heymsfield SB, Abiri M, Hashim SA. Clinical trial of silicone-rubber gastric balloon to treat obesity. *Int J Obes* 1991; **15**: 259-266
- 38 **Xing JH**, Brody F, Brodsky J, Larive B, Ponsky J, Soffer E. Gastric electrical stimulation at proximal stomach induces gastric relaxation in dogs. *Neurogastroenterol Motil* 2003; **15**: 15-23
- 39 **Ouyang H**, Yin JY, Chen JD. Therapeutic potential of gastric electrical stimulation for obesity and its possible mechanisms: a preliminary canine study. *Dig Dis Sci* 2003; **48**: 698-705
- 40 **Anand BK**, Pillai RV. Activity of single neurons in the hypothalamic feeding centres: effect of gastric distention. *J Physiol* 1967; **192**: 63-67
- 41 **Deutsch JA**, Young WG, Kalogeris TJ. The stomach signals satiety. *Science* 1978; **201**: 165-167
- 42 **McMinn JE**, Baskin DG, Schwartz MW. Neuroendocrine mechanisms regulating food intake and body weight. *Obes rev* 2000; **1**: 37-46
- 43 **Wang L**, Barachina MD, Martinez V, Wei JY, Tache Y. Synergistic interaction between CCK and leptin to regulate food intake. *Regul Pept* 2000; **92**: 79-85
- 44 **Gutzwiller JP**, Goke B, Drewe J, Hildebrand P, Ketterer S, Handschin D, Winterhalder R, Conen D, Beglinger C. Glucagon-like peptide-1: a potent regulator of food intake in humans. *Gut* 1999; **44**: 81-86

Impact of release characteristics of sinomenine hydrochloride dosage forms on its pharmacokinetics in beagle dogs

Jin Sun, Jie-Ming Shi, Tian-Hong Zhang, Kun Gao, Jing-Jing Mao, Bing Li, Ying-Hua Sun, Zhong-Gui He

Jin Sun, Jie-Ming Shi, Tian-Hong Zhang, Kun Gao, Jing-Jing Mao, Bing Li, Ying-Hua Sun, Zhong-Gui He, Department of Biopharmaceutics, School of Pharmacy, Shenyang Pharmaceutical University, Shenyang 110016, Liaoning Province, China
Jie-Ming Shi, Guangzhou Municipal Institute of Drug Control, Guangzhou 510160, Guangdong Province, China
Correspondence to: Professor Zhong-Gui He, Mailbox 59, School of Pharmacy, Shenyang Pharmaceutical University, No. 103 Wenhua Road, Shenyang 110016, Liaoning Province, China. hezhgui@mail.sy.ln.cn
Telephone: +86-24-23986321 Fax: +86-24-23986321
Received: 2004-07-26 Accepted: 2004-12-21

© 2005 The WJG Press and Elsevier Inc. All rights reserved.

Key words: Sinomenine; Release behavior; Pharmacokinetics; Pellets

Sun J, Shi JM, Zhang TH, Gao K, Mao JJ, Li B, Sun YH, He ZG. Impact of release characteristics of sinomenine hydrochloride dosage forms on its pharmacokinetics in beagle dogs. *World J Gastroenterol* 2005; 11(29): 4547-4551
<http://www.wjgnet.com/1007-9327/11/4547.asp>

Abstract

AIM: To investigate the effect of release behavior of sustained-release dosage forms of sinomenine hydrochloride (SM·HCl) on its pharmacokinetics in beagle dogs.

METHODS: The *in vitro* release behavior of two SM·HCl dosage forms, including commercial 12-h sustained-release tablets and 24-h sustained-release pellets prepared in our laboratory, was examined. The two dosage forms were orally administrated to beagle dogs, and then the *in vivo* SM·HCl pharmacokinetics was investigated and compared.

RESULTS: The optimal SM·HCl sustained-release formulation was achieved by mixing slow- and rapid-release pellets (9:1, w/w). The SM·HCl release profiles of the sustained-release pellets were scarcely influenced by the pH of the dissolution medium. Release from the 12-h sustained-release tablets was markedly quicker than that from the 24-h sustained-release pellets, the cumulative release up to 12-h was 99.9% vs 68.7%. From a pharmacokinetic standpoint, the 24-h SM·HCl sustained-release pellets had longer t_{max} and lower C_{max} compared to the 12-h sustained-release tablets, the t_{max} being 2.67 ± 0.52 h vs 9.83 ± 0.98 h and the C_{max} being 1334.45 ± 368.76 ng/mL vs 893.12 ± 292.55 ng/mL, respectively. However, the AUC_{0-t_n} of two SM·HCl dosage forms was comparable and both preparations were statistically bioequivalent. Furthermore, the two preparations had good correlations between SM·HCl percentage absorption *in vivo* and the cumulative percentage release *in vitro*.

CONCLUSION: The *in vitro* release properties of the dosage forms strongly affect their pharmacokinetic behavior *in vivo*. Therefore, managing the *in vitro* release behavior of dosage forms is a promising strategy for obtaining the optimal *in vivo* pharmacokinetic characteristics and safe therapeutic drug concentration-time curves.

INTRODUCTION

Sinomenine [(9 α , 13 α , 14 α)-7,8-didehydro-4-hydroxy-3,7-dimethoxy-17-methyl-morphinan-6-one] is an active alkaloid, which can be extracted from the stems of *Sinomenium acutum* *Rehd. et Wils.* Generally, sinomenine hydrochloride (SM·HCl) is the main chemical form for pharmaceutical purposes. Recent studies have shown that SM·HCl possesses potent anti-inflammatory, analgesic, and immunoinhibitory pharmacological effects, which provide the basis for the treatment of rheumatoid arthritis. Many clinical therapeutical trials have confirmed the effectiveness of SM·HCl in treating rheumatoid arthritis and the efficacy is as high as 90%^[1].

The conventional SM·HCl dosage forms (injection and rapid-release tablets) require frequent administration (3-4 times/d) and even the sustained-release tablets available on the market require administration twice per day, thus leading to poor patient compliance. Additionally, the high fluctuation in the SM·HCl plasma levels during multi-dose therapy with the marketed SM·HCl dosage forms contributes to side effects, such as gastrointestinal tract toxicity and allergic reactions^[2]. Accordingly, it is necessary to develop 24-h SM·HCl sustained-release dosage forms (for once-daily administration) in order to reduce side effects and increase patient compliance.

Currently, many controlled/sustained-release dosage forms are being converted from single unit drug delivery systems (DDS) such as tablets to multiple unit DDS such as pellets for the following reasons. Firstly, pellets seem to be less influenced by physiologic factors such as gastric emptying and intestinal transit than tablets, resulting in less marked inter-individual differences. Secondly, pellets are widely and evenly distributed over the surface of the gastrointestinal tract, increasing drug-gastrointestinal contact, thus improving oral bioavailability. Thirdly, release failures of individual units hardly affect the total release behavior due to the presence of multiple units, unlike the case with

tablets^[3]. Finally, optimal release characteristics can be achieved using a mixing strategy involving pellets with different release properties^[3].

For these reasons, we decided to design SM·HCl sustained-release pellets, and to manage the *in vitro* drug release in a manner that would allow 24-h sustained release. Furthermore, the *in vivo* pharmacokinetic properties of the 24-h sustained-release pellets were compared with those of the marketed 12-h sustained-release tablets in beagle dogs.

MATERIALS AND METHODS

Materials

SM·HCl was obtained from Hunan Zhengqing Pharm. Co. (Changsha, China). Microcrystalline cellulose (MCC, Avicel PH101) was provided by Changshu Pharm. Adjunct Co. (Changshu, China). Eudragit® NE 30D was provided by Röhm Pharma GmbH (Darmstadt, Germany). Reference formulation: SM·HCl sustained-release tablets (Zhengqing Pharm. Co., each tablet containing 60 mg of SM·HCl); Test formulation: SM·HCl 24-h sustained-release pellets in capsules (each containing 120 mg).

Preparation of SM-HCl sustained-release pellets

Preparation of blank core pellets Blank core pellets (0.8-1.1 mm in diameter) were prepared using MCC as a matrix and water as the adhesive by a rotary layering process (BZJ-360IIM rotary processor, 15th Institute of Academy for Chinese Carrier-Rocket Technology, Beijing). Four hundred grams of MCC was placed in the rotary processor chamber. The inlet airflow was 10-20 L/min, the atomizing pressure was 0.1-0.3 MPa and the rotation speed was 200 r/min. Then, the adhesive was sprayed at a flow rate of 15-25 r/min. Finally, the products were dried at 60 °C and then sieved to obtain blank core pellets of the required size.

Preparation of SM·HCl pellets Four hundred grams of blank core pellets were placed in the rotary processor chamber at a rotation speed of 200 r/min. SM·HCl in the drug supply container was added to chamber at 10-20 r/min. One percent of hydroxypropylmethyl cellulose (5 cps) in water was used as an adhesive, and sprayed over the pellets at a rate of 10-15 r/min. Finally, the products were dried at room temperature^[4,5].

Preparation of SM·HCl 24-h sustained-release pellets

The pellets were coated in a fluidized-bed coating apparatus (Shenyang Pharmaceutical University, China). For the coating process, the nozzle port size was 1 mm, the inlet air temperature was 18-23 °C, the atomizing pressure was 1.0 kg/cm², and the coating solution was sprayed onto the pellets at a flow rate of 0.8-1.2 mL/min. The coating solution was an aqueous dispersion of Eudragit® NE 30D. Talc- an antiadherent agent and sodium dodecyl sulfate- an anti-static agent, were added to the coating solution. Finally, the coated pellets were cured by heating at 40 °C for 24 h^[6,7].

Dissolution test Dissolution studies were carried out using the basket method at a rotation speed of 100 r/min at 37 °C in 900 mL dissolution medium according to ChP 2000. The dissolution tests were performed in 0.1 HCl, pH 6.8 or 7.4 PBS and distilled water, respectively. Samples were

collected at predetermined time points, and the SM·HCl content was analyzed using a UV-spectrophotometer (UV-9100, Ruili Co., China) at 365 nm. Then cumulative percentage of SM·HCl release was calculated.

Pharmacokinetic evaluation of SM-HCl sustained-release dosage forms

Experimental protocol All animal studies were performed according to the Guidelines for the Care and Use of Laboratory Animals approved by the Ethics Committee of Animal Experimentation of Shenyang Pharmaceutical University. Six male beagle dogs (weighing 20±2.5 kg) were randomly assigned to one of two crossover experiments with a 7-d washout period. Dogs were fasted for 12 h before administration with free access to water. Each dog was given orally either reference (two sustained-release tablets) or test formulation (one capsule of sustained-release pellets). Blood samples were collected at predetermined times for each protocol: (1) 0, 0.5, 1, 2, 3, 4, 5, 6, 8, 10, 12, 14, and 24 h for the reference; (2) 0, 1, 2, 4, 6, 8, 9, 10, 11, 12, 14, 24, and 36 h for the test. Plasma was immediately obtained by centrifuging blood samples at 3 000 r/min for 10 min. The plasma samples were stored in a freezer at -20 °C until analysis.

Chromatographic conditions Quantitative determination was performed on a high-performance liquid chromatograph (HPLC) equipped with a PU-980 pump (Jasco, Japan) and UV-975 detector (Jasco). An ODS C-18 (4.6 mm×200 mm, 5 μm) was used and the mobile phase consisted of methanol: acetonitrile:0.3% PBS (pH 4.8, 240:80:1 180, v/v)^[7]. The eluates were monitored at 265 nm. The flow rate was 0.9 mL/min and the column temperature was maintained at 30 °C.

Sample preparation Each plasma sample (0.5 mL) was mixed with 100 μL of 1.5 μg/mL caffeine and 200 μL amine-ammonium chloride aqueous solution (pH 11) in a glass centrifuge tube, followed by the addition of 3 mL of a solution of hexane:dichloride methane:isopropyl alcohol (100:50:5, v/v). The mixture was then shaken on a vortex mixer for 3 min and centrifuged at 3 000 r/min for 10 min. The organic layer was transferred to a clean tube and evaporated to dryness under nitrogen at 50 °C. The residue was dissolved in 100 μL of 0.5% phosphoric acid and 20 μL was subjected to HPLC.

Data analysis The term t_{max} denotes the time to reach peak concentration, and C_{max} is the peak concentration, and they were obtained directly from the measured values. The elimination rate constant (K_e) was calculated from the slope of the logarithm of the plasma concentration *vs* time using the final four points. The parameter $t_{0.5}$ was derived from $0.693/K_e$. The area under the plasma concentration-time curve (AUC_{0-t_n}) until the last sampling time (t_n) was calculated by the trapezoidal method. The relative bioavailability ($F^0\%$) was calculated as $AUC_{Test\ formulation}/AUC_{Reference\ formulation}$. The percentage absorption *in vivo* was calculated by Wagner-Nelson method.

RESULTS

Preparation of 24 h SM-HCl sustained-release pellets

The SM·HCl-loaded pellets were coated using the coating

formulation consisting of 117 g/L Eudragit® NE 30D, sodium dodecyl sulfate (1% of Eudragit® NE 30D, w/w) as an antistatic agent and talc (45% of Eudragit® NE 30D, w/w) as an antiadherent agent in aqueous dispersion. The effect of the coating level on the *in vitro* release behavior of SM·HCl sustained-release pellets is shown in Figure 1A. Clearly, higher the coating level, slower the release of SM·HCl from the coated pellets. Judged from the initial release rate and cumulative percentage release up to 20 h, the ideal release behavior was achieved at a coating level of 6.5%. However, drug release was still rather slow in the initial phase, with 2.84% being released up to 2 h. Therefore, SM·HCl rapid-release pellets were prepared with a coating level of 0.1%, and their release profiles are shown in Figure 1B, and almost complete release was obtained within 2 h. When employing a 9:1 (w/w) mixture ratio of slow- and rapid-release pellets, the SM·HCl cumulative release was 10% at 2 h, 48% at 8 h, and more than 85% up to 20 h (Figure 1B). This formulation was regarded as the optimal sustained-release formulation for the following studies.

The effect of the pH of the dissolution medium on the release profiles of SM·HCl sustained-release pellets is shown in Figure 2. The pH had no significant effect on the SM·HCl release properties of the coated pellets. The release profiles of the reference 12-h and test 24-h sustained-release tablets and pellets were compared (Figure 3). The reference formulation released drug completely up to 12 h, while the

test formulation only released 68% up to 12 h with near complete release until 24 h.

In vivo pharmacokinetics of 24 h SM·HCl sustained-release pellets

Either SM·HCl reference formulation (two 60 mg 12-h sustained-release tablets) or SM·HCl test formulation (one capsule containing 120 mg 24-h sustained-release pellets) was orally administered in the two crossover experiments in beagle dogs. The concentration-time curves of SM·HCl in plasma for the two dosage forms are illustrated in Figure 4. The pharmacokinetic parameters were calculated (Table 1). The t_{max} was 2.67 ± 0.21 and 9.83 ± 0.40 h for SM·HCl reference and test formulations, respectively, indicating that the test pellets underwent a slower release and prolonged absorption than the reference tablets. Also, the C_{max} of SM·HCl 24-h sustained-release pellets was 893.1 ± 119.4 ng/mL, which was significantly lower than that of 12-h sustained-release tablets ($1\ 334.5 \pm 150.5$ ng/mL, $P < 0.05$). Furthermore, the AUC_{0-36} of the SM·HCl test formulation (13.50 ± 1.47 mg·h/L) was similar to the AUC_{0-24} of the SM·HCl reference formulation (13.06 ± 9.45 mg·h/L), with the F (%) being 103.4. Hence, the two formulations were statistically bioequivalent ($P < 0.05$).

The percentage absorption *in vivo* of the two formulations was assessed by the Wagner-Nelson method. The percentage absorption ($F(t)$) exhibited a good linear relationship with

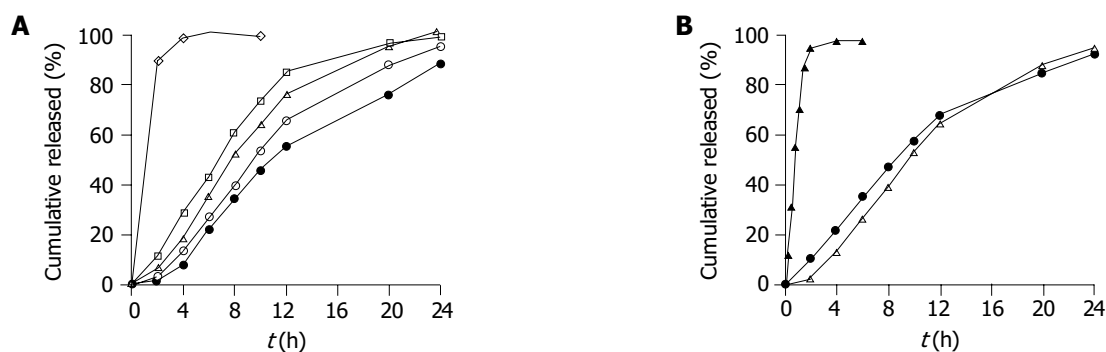


Figure 1 Effect of different coating levels on SM·HCl release behavior from the coated pellets in distilled water ($n = 6$). **A:** Pellets coated at five levels of 0% (\diamond), 3% (\square), 5% (\triangle), 6.5% (\circ), 8% (\bullet , w/w, total solid applied); **B:** rapid-

release pellets (\blacktriangle) and slow-release pellets at a 6.5% coating level (\triangle) and a mixture of slow- and rapid-release pellets (9:1, w/w, \bullet).

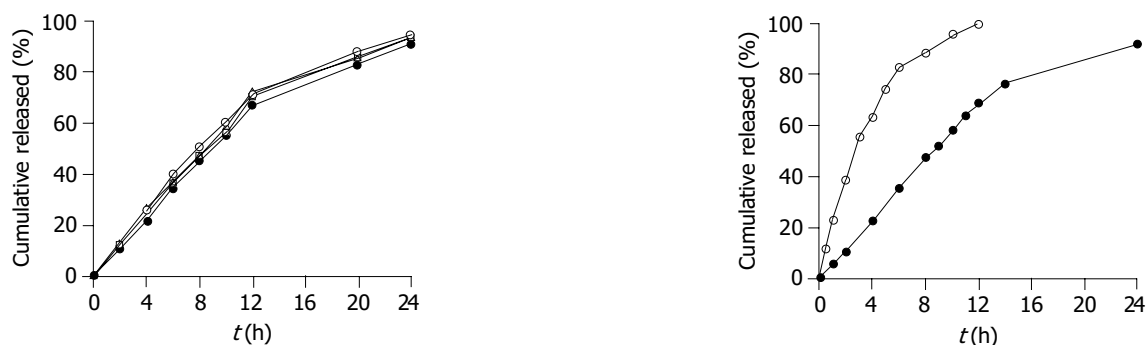


Figure 2 Effect of pH of the dissolution medium on SM·HCl release from coated pellets of the optimal formulation ($n = 6$). Distilled water (\circ), 0.1 mol/L HCl (\bullet), pH 6.8 (\triangle) and pH 7.4 (\square) PBS.

Figure 3 Comparative SM·HCl release profiles of 24-h test sustained-release pellets (\bullet) and 12-h reference sustained-release tablets (\circ , $n = 6$).

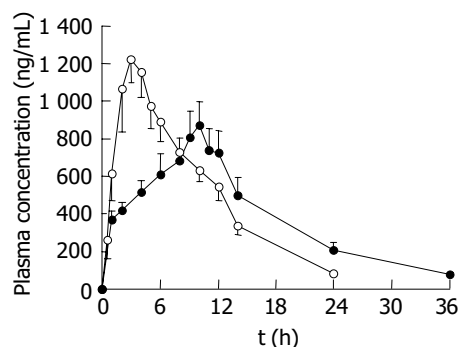


Figure 4 SM-HCl plasma concentration-time profiles after oral administration of 24-h test sustained-release pellets (●) and 12-h reference sustained-release tablets (○) in beagle dogs at a single dose of 120 mg/animal. Each value represents mean±SE ($n = 6$).

Table 1 Pharmacokinetic parameters after oral administration of either SM-HCl 24-h test sustained-release pellets or 12-h reference sustained-release tablets in beagle dogs at a single dose of 120 mg/animal ($n = 6$, mean±SD)

Parameter	Test formulation	Reference formulation
C_{max} (ng/mL)	893.1±119.4	1 334.5±150.5
t_{max} (h)	9.83±0.40	2.67±0.21
K_e (1/h)	0.044±0.01	0.084±0.01
$t_{0.5}$ (h)	20.7±8.7	8.6±1.9
AUC _{0-t_n} (mg·h/L)	13.50±1.47	13.06±9.45
F (%)	103.41	-

the cumulative percentage release ($f(t)$, r being 0.98 and 0.97 for the test and reference formulations, respectively, Figure 5), demonstrating a good correlation between the *in vitro* release and *in vivo* absorption processes.

DISCUSSION

It has been well established that SM-HCl is in an effective treatment for rheumatoid arthritis comparable with another traditional Chinese medicine, total glycosides of *tripterygium Wilfordii* Hook f. However, SM-HCl has markedly reduced side effects and improved safety, compared to the latter in terms of gastrointestinal tract effects and urogenital toxicity^[8]. In spite of this, the conventional SM-HCl dosage forms give rise to higher peak to trough plasma concentration fluctuation, resulting in moderate side effects. For this reason, we attempted to develop a 24-h SM-HCl sustained-release preparation (once daily), and to prolong the absorption phase and reduce the degree of concentration fluctuation *in vivo* by managing the drug release characteristics of dosage forms *in vitro*.

The multiple unit drug DDS and SM-HCl pellets were prepared by a rotary layering process and the sustained-release behavior was obtained by standard industrial coating technology. The coating formulation consisted of an aqueous dispersion of Eudragit® NE 30D^[9], with the addition of talc as the antiadherent agent and sodium dodecyl sulfate as the antistatic agent. The coating layer of Eudragit® NE 30D was moderately permeable to water molecules, which are capable of penetrating into the pellet core. Thus, a

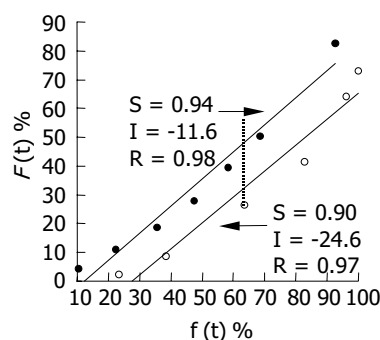


Figure 5 Relationship between cumulative SM-HCl percentage release *in vitro* $f(t)$ and percentage absorption *in vivo* $F(t)$ of the two dosage forms. S , I and R are the abbreviations for the slope, intercept and correlation coefficient for the correlation equation, respectively. Twenty-four-hour test sustained-release pellets (●) and 12-h reference sustained-release tablets (○).

saturable drug solution was formed within the Eudragit® NE 30D coating layer and provided the primary drive for drug release. Two mechanisms were assumed to account for drug release from the coated pellets. Provided the coating layer was a homogenous uninterrupted membrane, the additives were evenly distributed, and there were many interstices of the correct molecular size in the membrane. Drug molecules initially dissolved in the membrane, then diffused down the concentration gradient through these microgaps, and finally released into the outer medium. In addition, if a water-soluble channeling agent was added, a number of aqueous micro-channels formed across the membrane when coming into contact with water, and acted as release paths for soluble drug molecules, such as SM-HCl^[10].

In this study, when a small amount of channeling agent (1% PEG 4000 of Eudragit® NE 30D, w/w) was added to the coating formulation, SM-HCl-coated pellets at the coating level of 6.5% released drug completely up to 12 h (unpublished data). Thus, the channeling agent was absent in the coating formulation, and the former mechanism is responsible for water-soluble SM-HCl release from the coated pellets. Its release behavior corresponds to Fick's diffusion equation: $dC/dt = -DAk\Delta C/b$, where dC/dt is the diffusion rate, D the diffusion coefficient, A the surface area of membrane, k the partition coefficient, ΔC the concentration difference across membrane, and b the thickness of membrane. Since D , k and A were given for SM-HCl and coating membrane, and ΔC was constant in the initial release phase and decreased exponentially in the later phase, dC/dt was inversely related to b , as evidenced in Figure 1A. When the 6.5% coating level was used, ideal release behavior was achieved. Unfortunately, it exhibited a rather slower release in the initial phase up to 2 h. With regard to mixing pellets with different release rates to obtain the desired release behavior, rapid-release pellets with complete release within 2 h were prepared and combined with the above slow-release pellets (1:9, w/w). The final product exhibited optimal release behavior with 10.5% being released up to 2 h (Figure 1B), indicating that mixing pellets with different release rates is a powerful strategy for the management of *in vitro* drug release properties^[11].

The release profile of the final SM-HCl sustained-release

pellets was unaffected by the pH of dissolution medium (Figure 2). This was to be expected because the matrix (Eudragit® NE 30D) of the membrane was insensitive to pH and the drug release was unaffected by the pH. The 24-h SM·HCl sustained-release pellets maintained a zero-rate release up to 14 h, and exhibited prolonged release up to 24 h, in contrast to the 12-h SM·HCl sustained-release tablets (Figure 3). In order to investigate the effect of *in vitro* release behavior on *in vivo* absorption of the coated pellets, an *in vivo* comparative pharmacokinetic evaluation was undertaken using 24-h SM·HCl sustained-release pellets *vs* marketed 12-h sustained-release tablets in beagle dogs.

After oral administration at a single dose of 120 mg to beagle dogs, the t_{max} of the 12-h sustained-release tablets was 2.67 ± 0.52 h, 7 h faster than 9.83 ± 0.98 h for the 24-h sustained-release pellets (Table 1 and Figure 4). In addition, the C_{max} of the 12-h sustained-release tablets (1334.45 ± 368.76 ng/mL) was significantly higher than that of the 24-h sustained-release pellets (893.12 ± 292.55 ng/mL). Combining the C_{max} and t_{max} , the 24-h test pellets exhibited more significant sustained release and prolonged absorption characteristics than the 12-h reference tablets, including a reduced peak concentration and a prolonged time to reach the peak concentration. More importantly, the $t_{0.5}$ of the 24-h test pellets (20.7 ± 8.7 h) was higher than that of the 12-h reference tablets (8.6 ± 1.9 h). This result is obviously inconsistent with the theory that the intrinsic biologic half-time depends on a given drug while being independent of the type of dosage forms. The prolonged $t_{0.5}$ of the 24-h test pellets suggested a reduced apparent K_e compared to the 12-h reference tablets (Table 1), which was accounted for by prolonged absorption to partially counteract the intrinsic elimination capability during the terminal phase. In effect, the absorption of the 24-h test pellets was markedly slower than that of the 12-h reference tablets (Figure 4), due to more prolonged drug release compared to the reference tablets. The aforementioned results clearly indicate that the release characteristics of dosage forms, play a significant role in mediating their pharmacokinetic behavior. As a consequence, an optimal pharmacokinetic performance could be achieved by producing the desired release profiles of dosage forms. The AUC_{0-t_n} of the two SM·HCl dosage forms was comparable and both were statistically bioequivalent preparations ($P < 0.05$). Moreover, the SM·HCl percentage absorption *in vivo* correlated well with the cumulative percentage release *in vitro* as far as two preparations were concerned (Figure 5), validating the *in vitro* dissolution conditions and verifying the utility of the sustained-release dosage forms (Figure 4). In addition, the slopes of two correlation equations for the two dosage forms were similar. In contrast, the intercept of the 24-h test formulation (-11.6%) was greater than that of the 12-h reference tablets (-24.6%), suggesting that the percentage absorption of the 12 h reference tablets is 13% lower than that of the 24-h test formulation when the percentage release

is the same. Ren *et al.*^[12], reported that the permeability of SM·HCl in jejunum and ileum is poorer than that in the colon, which might be responsible for the above relatively reduced absorption of the 12-h reference tablets due to the main site of residence being the jejunum and ileum.

In summary, 24-h SM·HCl sustained-release pellets can be successively prepared by a conventional rotary layering process and standard industrial coating technology. Optimal *in vitro* release properties can be achieved by a mixing strategy involving pellets with different release rates. Moreover, the SM·HCl release characteristics of the dosage forms have a marked effect on their pharmacokinetics *in vivo*. Accordingly, managing the *in vitro* release behavior of dosage forms is a promising strategy for obtaining optimal *in vivo* pharmacokinetic characteristics and safe therapeutic drug concentration–time curves.

REFERENCES

- 1 Wang XH, Qiu SH, Dong SX, Chou P, Wu FC. Studies on the pharmacodynamics of Sinomenine tablets. *Zhongyao Yaoli Yu Linchuang* 1997; **13**: 23-25
- 2 Liu Q, Zhou LL, Li R. Research overview of Sinomenine. *Zhongcaoyao* 1997; **28**: 247-249
- 3 Fan TY, Wei SL, Yan WW, Chen DB, Li J. An investigation of pulsatile release tablets with ethylcellulose and Eudragit L as layer coating materials and cross-linked polyvinylpyrrolidone in the core tablets. *J Control Release* 2001; **77**: 245-251
- 4 Vertommen J, Rombaut P, Michoel A, Kinget R. Estimation of the amount of water removed by gap and atomization air streams during pelletization in a rotary processor. *Pharm Dev Technol* 1998; **3**: 63-72
- 5 Liew CV, Wan LS, Heng PW. Role of base plate rotational speed in controlling spheroid size distribution and minimizing oversize particle formation during spheroid production by rotary processing. *Drug Dev Ind Pharm* 2000; **26**: 953-963
- 6 Lecomte F, Siepmann J, Walther M, MacRae RJ, Bodmeier R. Polymer blends used for the coating of multiparticulates: comparison of aqueous and organic coating techniques. *Pharm Res* 2004; **21**: 882-890
- 7 Bataille B, Rahman L, Jacob M. Parameters for the formulation of physical-technical characteristics of granules of theophylline obtained by extrusion-spheronization. *Pharm Acta Helv* 1991; **66**: 233-236
- 8 Sun X, Zhang SM, Tian CH, Yan L, Wang LM, Li SL. Safety of *tripterygium Wilfordii*. *Zhongguo Xinyao Zazi* 2001; **10**: 539-533
- 9 Vecchio C, Fabiani F, Sangalli ME, Zema L, Gazzaniga A. Rotary tangential spray technique for aqueous film coating of indobufen pellets. *Drug Dev Ind Pharm* 1998; **24**: 269-274
- 10 Radtke G, Knop K, Lippold BC. Manufacture of slow-release matrix granules by wet granulation with an aqueous dispersion of quaternary poly(meth)acrylates in the fluidized bed. *Drug Dev Ind Pharm* 2002; **28**: 1295-1302
- 11 Lippold BC, Monells Pages R. Film formation, reproducibility of production and curing with respect to release stability of functional coatings from aqueous polymer dispersions. *Pharmazie* 2001; **56**: 5-17
- 12 Ren FZ, Sun SY, Jing QF. Study of the absorption character of sinomenine in intestines. *Shenyang Yaoke Daxue Xuebao* 2002; **19**: 165-167

Clinical analysis of surgical treatment of portal hypertension

Xin-Bao Xu, Jing-Xiu Cai, Xi-Sheng Leng, Jia-Hong Dong, Ji-Ye Zhu, Zhen-Ping He, Fu-Shun Wang, Ji-Run Peng, Ben-Li Han, Ru-Yu Du

Xin-Bao Xu, Xi-Sheng Leng, Ji-Ye Zhu, Fu-Shun Wang, Ji-Run Peng, Ru-Yu Du, Department of Hepatobiliary Surgery, People's Hospital, Peking University, Beijing 100044, China
Xin-Bao Xu, Department of Hepatobiliary Surgery, Airforce General Hospital, Beijing 100036, China
Jing-Xiu Cai, Zheng-Ping He, Jia-Hong Dong, Ben-Li Han, Center of Hepatobiliary Surgery, Southwest Hospital, The Third Military Medical University, Chongqing 400038, China
Correspondence to: Xin-Bao Xu, Department of Hepatobiliary Surgery, People's Hospital, Peking University, Beijing 100044, China. x_xb@163.net
Telephone: +86-10-68792703
Received: 2004-06-29 Accepted: 2004-07-11

Abstract

AIM: To review the experience in surgery for 508 patients with portal hypertension and to explore the selection of reasonable operation under different conditions.

METHODS: The data of 508 patients with portal hypertension treated surgically in 1991-2001 in our centers were analyzed. Of the 508 patients, 256 were treated with portaazygous devascularization (PAD), 167 with portasystemic shunt (PSS), 62 with selective shunt (SS), 11 with combined portasystemic shunt and portaazygous devascularization (PSS+PAD), 9 with liver transplantation (LT), 3 with union operation for hepatic carcinoma and portal hypertension (HCC+PH).

RESULTS: In the 167 patients treated with PSS, free portal pressure (FPP) was significantly higher in the patients with a longer diameter of the anastomotic stoma than in those with a shorter diameter before the operation ($P<0.01$). After the operation, FPP in the former patients markedly decreased compared to the latter ones ($P<0.01$). The incidence rate of hemorrhage in patients treated with PAD, PSS, SS, PSS+PAD, and HCC+PH was 21.09% (54/256), 13.77 (23/167), 11.29 (7/62), 36.36% (4/11), and 100% (3/3), respectively. The incidence rate of hepatic encephalopathy was 3.91% (10/256), 9.58% (16/167), 4.84% (3/62), 9.09% (1/11), and 100% (3/3), respectively while the operative mortality was 5.49% (15/256), 4.22% (7/167), 4.84% (3/62), 9.09% (1/11), and 66.67% (2/3) respectively. The operative mortality of liver transplantation was 22.22% (2/9).

CONCLUSION: Five kinds of operation in surgical treatment of portal hypertension have their advantages and disadvantages. Therefore, the selection of operation should be based on the actual needs of the patients.

Key words: Portal hypertension; Surgical operation; Shunt

Xu XB, Cai JX, Leng XS, Dong JH, Zhu JY, He ZP, Wang FS, Peng JR, Han BL, Du RY. Clinical analysis of surgical treatment of portal hypertension. *World J Gastroenterol* 2005; 11 (29): 4552-4559
<http://www.wjgnet.com/1007-9327/11/4552.asp>

INTRODUCTION

In order to discuss operation indications, the data of 508 patients with portal hypertension treated surgically with portaazygous disconnection (PD), portasystemic shunt (PSS), selective shunt (SS), combined portasystemic shunt and portaazygous devascularization (PSS+PAD), liver transplantation (LT), and union operation for hepatic carcinoma and portal hypertension (HCC+PH) in 1991-2002 in our centers were analyzed.

MATERIALS AND METHODS

General data

Of the 508 patients, 425 were males and 83 females, aged 3-71 years (average 40.8 years). Three hundred and fifty-eight patients (70.47%) had a history of bleeding from the upper digestive tract, 150 patients (37.24%) had esophageal varices in different degrees with no history of bleeding from the upper digestive tract. Child-Pugh classification of liver function showed grade I in 260 patients, grade II in 164, grade III in 84. Etiology was posthepatic cirrhosis in 468 patients, biliary cirrhosis with biliary tract stenosis in 22, extrahepatic portal obstruction in 6, alcoholic cirrhosis in 8, schistosomiasis cirrhosis in 3, and idiopathic portal hypertension in 1.

Types of operation

Portaazygous disconnection (PAD) was performed in 256 patients (50.39%); portasystemic shunt (PSS) in 167 patients (32.87%, Table 1); selective shunt (SS) including distal splenorenal shunt (DSRS), distal splenocaval shunt (DSCS), coronary vein-left renal vein shunt and coronary vein-caval shunt in 62 patients (12.20%, Table 2).

Statistical analysis

The data were expressed as mean \pm SD, and analyzed with SPSS 10.0 for Windows. $P<0.05$ was considered statistically significant.

RESULTS

Free portal pressure (FPP)

The changes of free portal pressure (FPP) in 215 cases

Table 1 Patients treated with PSS

Types of operation	Cases
Portacaval shunt (PCS)	14
Portacaval shunt with prosthetic H-graft (PCS-H)	25
Mesocaval shunt (MCS)	66
Inferior mesocaval shunt (IMCS)	26
Splenorenal shunt (SRS)	12
Juxtal splenocaval shunt (SCS)	16
Branch of mesenterico-caval shunt (BMCS)	5
Inferior meso-left renal vein shunt	2
Colonic media vein-caval shunt	1
Total	167

Table 2 Patients treated with selective shunt (SS)

Types of operation	Cases
Distal splenocaval shunt (DSCS)	42
Distal splenorenal shunt (DSRS)	16
Coronary vein-caval shunt	4
Total	62

were observed before and after operation. The results are summarized in Table 3.

The results showed that FPP in the four groups of operation showed a marked post-operative decrease, especially in the PSS group with a diameter of anastomotic stoma in 8-12 mm compared to pre-operation ($P < 0.01$). The pre-operation FPP in the PSS (diameter 8-12 mm) group was notably higher than that in other groups ($P < 0.01$). The decreased absolute value of post-operation FPP in the PSS (diameter 8-12 mm) group (1.23 ± 0.5 kPa) was also much higher than that in the PAD group (0.5 ± 0.47 kPa) and SS group (0.51 ± 0.46 kPa, $P < 0.01$). No significant difference was found in the post-operation FPP of the above-mentioned four groups ($P > 0.05$).

The FPP in 9 of 11 patients who underwent combined PSS+PAD decreased 0.79 kPa (81 cm H₂O) averagely after operation with no change of FPP in the other 2 patients. The degrees of esophageal varices in 7 of the 11 patients were alleviated with no change in the other 4 patients after operation as confirmed by barium meal.

Table 3 Changes of free portal pressure (FPP) in three types of operation (mean±SD)

Types of operation	Cases	Pre-operation (kPa)	Post-operation (kPa)
Portaazygous disconnection (PAD)	81	3.78±0.50	3.26±0.57
PSS (diameter of anastomotic stoma in 8-12 mm)	52	4.29±0.80	3.11±0.63
PSS (diameter of anastomotic stoma in 6-8 mm)	42	3.91±0.48	3.12±0.46
Selective shunt (SS)	62	3.85±0.59	3.26±0.45

Rehemorrhage

Ninety-one of the five hundred and eight cases (16.8%) had rehemorrhage. The incidence rate of hemorrhage in patients treated with PAD, PSS, SS, and PSS+PAD was

21.09% (54/256), 13.77 (23/167), 11.29 (7/62), and 36.36% (4/11), respectively. Twenty-four (44.44%) of the fifty-four rebleeding patients treated with PAD had rebleeding within a year after operation, the incidence rate of rehemorrhage was 9.38% (24/256). Fourteen cases had rebleeding 5 years after PAD. Hepatectomy combined with splenic artery ligation, coronary vein and cardia and fundus varix ligation, or portacaval shunt with H-grafts (8 mm in diameter) was performed in three patients with hepatocellular carcinoma complicated by portal hypertension. The incidence rate of rebleeding was 100% (3/3).

Hepatic encephalopathy

The total incidence rate of hepatic encephalopathy was 6.50% (33/508). The incidence rate of hepatic encephalopathy in patients treated with PAD, PSS, SS, PSS+PAD, and HCC+PH was 3.91% (10/256), 9.58% (16/167), 4.84% (3/62), 9.09% (1/11), and 100% (3/3), respectively.

Operative mortality and its causes

The total operative mortality was 5.91% (30/508).

PAD The operative mortality was 5.86% (15/256). The cause of death was rebleeding. The high mortality was associated with severe disease. After being discharged from hospital, 21 cases died of rebleeding (10 cases), primary hepatocellular carcinoma (5 cases), liver function failure (5 cases) and malignant lymphoma (1 case).

PSS The operative mortality was 4.19% (7/167). Three patients died of severe hepatorenal syndrome, two died of rebleeding after operation, two underwent emergency MCS (12 mm in diameter of the anastomotic stoma), and died of hepatic encephalopathy 5 d after operation due to the improper operation method and large diameter of the anastomotic stoma. After being discharged from hospital, 16 cases died of primary hepatocellular carcinoma (5 cases), liver function failure (7 cases) and of rebleeding (4 cases).

SS The operative mortality was 4.84% (3/62). Three patients died of cerebral hemorrhage 5 d after operation, hepatorenal syndrome, and, rehemorrhage and infection in the subphrenic area and left lung. After discharge, two patients died of primary peritonitis, one of severe hepatitis, one of rebleeding.

PSS+PAD The operative mortality was 9.09% (1/11), this patient died of persistent deterioration of hepatic function and renal failure.

HCC+PH The operative mortality was 66.67% (2/3). One patient died of postoperative hemorrhage, the other died of hepatic failure. The last one succumbed to hepatic function failure 10 mo later after operation.

Liver transplantation We performed liver transplantation in 9 (1.77%) cases. The operative mortality was 2/9 (22.22%). The major reason of death was liver failure and infection after operation.

Portacaval shunt for patients with portal hypertension combining ascites

Nineteen patients with ascites before operation underwent portacaval shunt. They all had hematemesis, dark stools, moderate and severe esophageal varices, ascites, and no hypertension and kidney disease. The liver function of all

the patients was Child's grade B, and their HBsAg was positive. Eleven patients underwent portacaval shunt with H-graft, and eight patients, portacaval side-to-side anastomosis. No ascites were found by B-type ultrasound reexamination in the abdominal cavity before discharge. Hepatic tissue biopsy showed liver cirrhosis. But mild and moderate hepatic coma occurred in three patients with diameter of anastomotic stoma of 8-10 mm after operation.

Emergency operation for massive hemorrhage of gastrointestinal tract due to portal hypertension

Twenty (3.94%) of the above-mentioned patients underwent emergency operation. Ten of the patients (50%) had massive hemorrhage in gastrointestinal tract for the first time, the other 10 patients had a past medical history of massive hemorrhage in the gastrointestinal tract. They received endoscopic sclerotherapy (four cases) and loop ligation of varices (two cases), TIPSS (one case), balloon tamponade compression by a four-lumen tube (three cases). The causes of portal hypertension were cavernous transformation of portal vein, idiopathic portal hypertension, and posthepatic cirrhosis. Liver function was Child's grade A (2 cases), Child's grade B (7 cases), Child's grade C (11 cases). Of the 20 cases, 12 cases received emergency PSS, 8 emergency PAD (gastroesophageal devascularization, 4 cases had ligation of splenic artery without splenectomy). The ratio of preoperative liver function as Child's grade C was 58.33% (7/12) in the PSS group and 50% (4/8) in the PAD group. Postoperative mean loss of FFP was 9.6 cm H₂O in the PSS group and 1.8 cm H₂O in the PAD group. Surgical hemostasis had an effect on all the patients. Of the eight patients who underwent PAD, none had hepatic encephalopathy, five recovered smoothly, three (37.5%) had rehemorrhage within 2 wk after operation. We could not determine whether rupture of varices or hemorrhagic gastritis was the cause of postoperative bleeding. Of 12 patients who received PSS, 3 (25%) had hepatic encephalopathy, 2 (16.67%) rehemorrhage, 4 died of liver failure. The total operative mortality was 25%. The operative mortality was 33.33% in the PSS group and 12.5% in the PAD group.

DISCUSSION

Portal hypertension refers strictly to an increase in the portal venous pressure (>5 mm Hg or 7 cm H₂O). Based on data in China, the normal portal venous pressure ranges from 13 to 24 cm H₂O, its mean value is 18 cm H₂O. Portal hypertension can be diagnosed when free portal venous pressure exceeds 25 cm H₂O, but the term is used to the clinical syndrome associated with an increased portal venous pressure characterized by splenomegaly and the development of abnormal portalsystemic venous anastomosis. Increased resistance to blood flow in the portal venous system is the most important cause, though increased portal blood flow may contribute to it in a few cases. The causes of increased portal venous resistance may lie in the presinusoidal vessels outside the liver or in the intrahepatic vessels at pre-sinusoidal, sinusoidal or post-sinusoidal levels. No consistent therapeutic method has been successful due to its complex etiology, pathophysiology and hemodynamics. Which kind of surgical

treatment should be used depends on portal hemodynamics, etiology, age, liver pathology, liver function, bleeding history of upper digestive tract, size of spleen and hypersplenism.

PAD

PAD has no significant effect on portal perfusion. Nutritional factors such as insulin and glucagons are favorable for maintaining normal liver function^[1,2]. Portal hypertension is important in maintaining hepatopetal blood flow during liver cirrhosis^[3-6]. The present study showed that FPP of the pre-PAD-operation decreased by 0.59 kPa averagely compared to that of post-PAD-operation ($P<0.01$). In a small number of patients treated with PAD, the mean FPP decreased much more than 0.59 kPa, suggesting that PAD is an effective hemostatic method for patients with massive hemorrhage of the upper digestive tract^[7]. A few of the patients with plentiful collateral circulation in gastric fundus and pericardia and recurrent upper gastrointestinal bleeding, had no change of FPP or a slightly elevated FPP after PAD and might have had rehemorrhage shortly after PAD operation.

One typical male patient had a massive hemorrhage of upper digestive tract combined with primary peritonitis, jaundice and ascites, and underwent emergency PAD. His hemorrhage ceased, and liver function and general state improved. Four years later, the patient had a massive rehemorrhage of upper digestive tract without jaundice and ascites, and received emergency MCS with a diameter of the anastomotic stoma in 10 mm. From then on, we followed him up continuously and found no rebleeding and hepatic encephalopathy. Animal experimental study showed that during cirrhotic portal hypertension, the defensive capacity of mucosa is progressively weakened, resulting in pathologic changes of the gastric mucosa^[8]. After disconnection of portaazygous junction, desquamation of the epithelial cells of the gastric mucosa, edema and thickening of the submucosal layer, and narrowing of its capillaries occur^[9]. The epithelium of the gastric mucosa is obviously ischemic and hypoxic, the defensive capability of the gastric mucosa is further deteriorated, indicating that it is one of the causes of high hemorrhage rate after disconnection^[10,11]. A few patients may have rebleeding shortly after PAD^[12,13].

Another typical case, a female, had recurrent bleeding four times (hematemesis and hemafecia) accompanied with hydrothorax and ascites within 3 mo, underwent emergency PAD, then she could take food as her hydrothorax and ascites gradually receded. Seventeen days after operation, hematemesis occurred, she had a massive rehemorrhage of upper digestive tract the next day, balloon tamponade compression had no effect on hemostasis. Two days later, emergency MCS was performed, 1 000 mL ascites was found during operation, then rebleeding ceased. The rebleeding of this case was due to the pathologic changes of the gastric mucosa that resulted from PAD^[14].

Based on the above data about PAD, the operation indications for PAD include: massive bleeding of upper digestive tract which cannot be controlled by non-surgical methods; the FPP<3.92-4.41 kPa (40-45 cm H₂O) after splenectomy; esophageal varicosis, splenomegaly, anteroposterior diameter of the spleen>7 cm and apparent hypersplenism; recurrent

bleeding of the upper digestive tract, debility or poor condition, and poor liver function; rebleeding after DSCS or DSRS, thrombosis of anastomotic stoma of splenic vein; regional portal hypertension.

PSS

PAD combined with small stoma PSS is widely used in the therapy of portal hypertension^[15,16]. The diameter of the anastomosis stoma of PSS mentioned in this paper was from 6 to 8 mm. Small-diameter portacaval shunt for patients is in favor of hepatic reserve^[17,18]. After PSS, the FPP level was (3.15 ± 0.39) kPa and the incidence rate of rehemorrhage of upper digestive tract reduced by alleviating pathological changes of gastric mucosa and prevented the formation of lateral branch circulation. In order to preserve hepatopetal perfusion to support and improve liver function, the FPP should be maintained at the level no more than $(3.92-4.41)$ kPa. The FPP level was as high as 9.58% (16/167) in patients treated with PSS, which might be associated with improper selection of patients and large anastomotic stoma. In recent years, we have performed some kinds of PSS with small caliber and low blood flow discharge such as inferior mesocaval shunt (IMCS)^[19], inferior meso-left renal vein shunt^[20,21] and branch of mesenterico-caval shunt (BMCS), which are technically easy to operate and popularize. Experimental animal study suggested that the portacaval shunt significantly improves the microcirculation of gastric mucosa^[22] and can promote gastric mucosa to synthesize and secrete glycoprotein and prostaglandins, thus increasing the defensive capability of the gastric mucosa^[23,24]. It was reported that the levels of plasma renin activity (PRA), angiotensin converting enzyme (ACE), angiotensin II and portal venous pressure (PVP) decrease significantly in cirrhotic patients with portal hypertension after portacaval shunts, which may be the major causes of ascites disappearance in cirrhotic patients after portacaval shunt^[25]. Surgical PSS might be considered for acute or chronic portal bleeding if medical treatment fails^[26]. Some kinds of diseases must be operated with PSS, such as extrahepatic portal vein obstruction and portal hypertension resulting from biliary cirrhosis of liver due to bile duct stenosis.

The operation indications for PSS include recurrent multiple bleeding of the upper digestive tract and liver function in Child's grades A and B status, no ascites, extrahepatic portal vein obstruction, portal hypertension resulting from biliary cirrhosis of liver due to hepatic duct stenosis, rebleeding after PAD, and rebleeding after PAD combined with PSS.

Selective shunt (SS)

The theoretical bases for designing selective shunt (SS) are as follows^[27,28]. PSS (unselective shunts) is effective in hemostasis of the upper digestive tract, but it decreases portal perfusion leading to deterioration of liver function^[29,30]. PAD aggravates pathologic changes of gastric mucosa and has a high rate of rebleeding. The functional reserve of the liver depends on portal perfusion^[17,31]. These thoughts have led to the development of selective portasystemic shunts. Warren first reported DSRS in 1967^[32], and Inokuchi

designed and reported coronary vein-caval shunt in 1968^[33] and 1969^[34]. Holmin *et al.*^[35], operated DSCS in rats in 1977, Bhalerao *et al.*^[36], firstly reported DSCS in patients in 1978. Since 1984, Cai *et al.*^[37], have begun to operate DSCS in patients in China. Preliminary data indicate that DSRS in a subgroup of patients with good liver function and a correct portaazygous disconnection, more effectively prevents variceal rebleeding than endoscopic sclerotherapy^[38]. It was reported that DSCS selectively improves microcirculation and functions of the gastric mucosa^[39]. DSCS and PAD are better than MCS and PCS (portacaval shunt) in protecting the hepatic reserve function in rats with cirrhotic portal hypertension^[40-44]. Experimental study also revealed that the blood viscosity after DSCS is lower than that after PAD^[45]. DSRS and DSCS have all the advantages of both PAD and PSS, but they are technically difficult. The incidence rates of rebleeding and hepatic encephalopathy in our patients treated with SS were lower compared to the patients treated with other kinds of operation, which might be partly associated with the different conditions of patients. Our results are in accord with other reports^[46-48].

Gradual development of encephalopathy also exists after selective shunts, and is related with loss of hepatic perfusion of portal blood^[49]. Based on other reports, portal blood flows to the liver in the early postoperative period in about 88% of patients but in about 42% after 3 years; no patient with a continuing flow of portal blood to the liver suffers from encephalopathy. Final loss of portal blood flow may be due to continuing superior mesenteric venous hypertension causing the development of collateral vessels which convert the selective shunt to an unselective shunt. The selective shunts have not yet been shown to improve long-term survival, which may in any case be limited by progressive liver disease, but their advantages in the shorter term may allow more patients a better survival.

The role of selective shunts in the treatment of gastrointestinal bleeding due to portal hypertension is still controversial. It has already established that it is not suitable to patients with ascites because it may become uncontrollable after the operation and cannot improve portal flow to the liver. It should never be done when there is centrifugal portal blood flow, as in the Budd-Chiari syndrome.

The operation indications for SS include liver function stabilized in Child's grade A or B, portal blood flow velocity higher than 8-10 cm/s, degree I or II of portal vein displaying during arterial portography^[50], more than 1.96 kPa (20 cm H₂O) of the difference between splanchnic obstructive portal pressure (SOPP) and free portal pressure (FPP), no active hepatitis, esophageal varicosis with history of hemorrhage or severe esophageal varicosis without history of hemorrhage, splenomegaly and anteroposterior diameter of the spleen >7 cm and no apparent hypersplenism, no chronic pancreatitis and splenic phlebitis or periphlebitis, no ascites, no retro-peritoneal edema, no Budd-Chiari syndrome.

Combined PSS+PAD

Compared to PAD, PSS+PAD had a higher operative mortality, but their postoperative hemorrhage incidence rates had no difference. The number of our cases that underwent

PSS+PAD was too small to induce a definite objective evaluation.

PSS+PAD was performed in the early 1980s. Huang Yaoquan^[51] reported the experience of 33 cases operated with PSS+PAD. Then some similar reports showed that this type of operation cannot only decrease free portal pressure to achieve the goal of persistent hemostasis, but also not reduce excessive hepatopetal blood flow^[16,52]. After PAD, spontaneous shunt will be gradually emerged. PSS+PAD, ahead of schedule replaces spontaneous shunt, which slowly occurs after PAD with artificial shunt in operation. Combined devascularization and splenorenal shunt (PAD+PSS) significantly decreases portal venous flow and portal pressure, as well as maintaining hepatopetal flow, thus entailing fewer complications compared to either PAD or PSS, some scholars even advocated that PSS+PAD could be a primary selection in the operations for portal hypertension^[53,54].

Compared to PSS or PAD, PSS+PAD prolongs operation time, aggravates surgical trauma, and damages liver function, which are the reasons why PSS+PAD cannot be generally performed. Based on the incomplete statistics of 24 famous Chinese hospitals in 1998, only 204 (only accounted for 1.7%) cases received PSS+PAD in more than 12 000 cases of operations for portal hypertension^[55].

Prognosis of the patients is mainly dependent on the condition of the whole body and hepatic function. We should select the operations which have minimal adverse effect on the whole condition and liver function in the patients. PSS has few advantages because of a negative effect on hepatic blood perfusion in contrast to PAD. In China, Yang Zhen and Qiu Fazu^[6,56] reported that patients that underwent standard PAD have a postoperative rebleeding incidence rate lower than 10%. Thus, it should be emphasized that surgeons should be careful when choosing PSS+PAD as a treating method for the patients with portal hypertension.

The operation indications for PAD combined with small stoma PSS (usually mesocaval shunt or portacaval shunt) include recurrent or massive bleeding of varices of esophagus and gastric fundus and stable liver function in Child's grades A and B, overt varices of esophagus and gastric fundus and Child's grade A status of hepatic function with FPPs more than 3.92-4.41 kPa (40-45 cm H₂O) after splenectomy in operation and no ascites or small amounts of ascites, and a relatively younger age (generally less than 60 years).

Surgical treatment of primary hepatic carcinoma concurrent with portal hypertension

Surgical treatment of primary hepatic carcinoma complicated by portal hypertension is based on appraisal of hepatosis and prediction of life expectancy of the patients with portal hypertension^[57,58]. The 5-year survival rate of the patients with liver cirrhosis and hemorrhage of upper digestive tract is 25-35%. Pinto *et al.*^[59], reported that 287 patients with hemorrhage of the upper digestive tract have a total 5-year survival rate of 26.2%, and that hepatic function condition of the patients exerts great effects upon their survival. Yang *et al.*^[60], reported that poor liver

function increases postoperative rebleeding and mortality. Zhang *et al.*^[61], showed that onestage hepatocellular carcinoma excision and splenectomy and portal azygous disconnection can be simultaneously performed for patients with good hepatic function. Our datas showed that hepatectomy and portacaval shunt greatly exacerbate the hepatic function, if these two operations are performed simultaneously.

During the treatment of patients with hepatocellular carcinoma and portal hypertension, the following must be considered. Hepatic function of the patients is a fundamental factor in determining the prognosis and long-term survival. In recent years, many domestic hospitals have performed whole liver transplantation in order to treat the liver-function decompensation (Child's grade C or more serious) patients with hepatocellular carcinoma (mainly small HCC) and upper gastrointestinal hemorrhage due to portal hypertension, and have achieved good therapeutic effects. Prophylactic PAD and PSS should not be done for the patients with varices of esophagus and gastric fundus but without upper gastrointestinal hemorrhage. One-stage hepatectomy and PAD (splenectomy and pericardia disconnection) should be a better choice for patients with HCC and portal hypertension^[62]. Interventional therapy (hepatic artery embolism) plus PAD and hepatectomy plus either sclerotherapy or loop ligature can reduce operational risk^[63,64].

Liver transplantation

Liver transplantation can treat portal hypertension, and rehemorrhage, and encephalopathy do not occur in treated patients. Liver transplantation was carried out abroad much earlier. The domestic practice of liver transplantation in recent years indicates that liver transplantation is feasible not only in patients with chronic progressive hepatic failure, refractory ascites and jaundice, but also in patients with recurrent hemorrhage, especially with poor hepatic function, if they are not old and their other vital organs function well. For example, one patient with multiple upper gastrointestinal bleeding received repeated sclerotherapy and TIPS, but no effective results were achieved. He then underwent a whole liver transplantation because of carcinomatous changes in his liver, and his free portal pressure decreased to normal level and conditions were very satisfactory.

In China, most patients who underwent liver transplantation were those with advanced-stage hepatocellular carcinoma and malignant diseases of biliary tract, the few were those with benign irreversible liver diseases including liver failure and recurrent upper gastrointestinal hemorrhage.

The indication for liver transplantation is end-stage liver disease. Not all patients with variceal bleeding have end-stage liver disease, and not every patient with variceal bleeding needs a new liver. Although the availability and increasingly successful outcome of liver transplantation have significantly altered the management of patients with cirrhosis, the question "does this patient really need a transplant now, or is the patient likely to need a transplant in the future?" should always be asked.

We believe that the therapy of hepatic cirrhosis and portal hypertension complicated by upper digestive

hemorrhage will change greatly.

Portacaval shunt for patients with portal hypertension and ascites

Many researches have confirmed that blood renin activity of the patients with liver cirrhosis and portal hypertension, especially those with ascites^[25,65,66], increases obviously. Vice versa, increased renin activity can raise portal vein pressure (PVP) via initiating renin-angiotensin-aldosterone system and plays an important role in ascites due to cirrhosis.

The reasons why their ascites disappear after portacaval shunt are as follows. Portal vein pressure (PVP) decreases significantly. After portacaval shunt, returned blood volume and effective blood volume increase, and then renal blood flow relatively raises, making the juxtaglomerular cells secrete less renin. The blood level of glucagons reduced by portacaval shunt also inhibits the secretion of renin^[30,67], that may weaken the role of renin-angiotensin-aldosterone system and reduce ascites.

It is well known that hepatic coma usually occurs in patients after portacaval shunt operation. We should use a small diameter (6-8 mm) of anastomosis stoma of portacaval shunt as best as we can.

Emergency operation for upper gastroesophageal massive hemorrhage due to portal hypertension

The results in our study demonstrate that emergency operation rank non-negligible position in the treatment of portal hypertension.

Once the varices rupture, the chance of rehemorrhage is very high shortly after the first hemorrhage, and the mortality rate due to rehemorrhage is nearly twice that of the first hemorrhage. Thus, the indications of emergency surgery include massive hemorrhage which cannot be controlled within 12 h, recurrent massive upper gastrointestinal hemorrhage, and no obvious surgical contraindications.

Which surgical procedure should be adopted depends upon the condition of patients, liver function and findings in surgery. Generally, shunt operation can be performed in patients with relatively better condition and liver function, a great quantity of collateral vessels surrounding the spleen and higher portal pressure (>3.43 kPa or 35 cm H₂O). On the contrary, patients with poor body condition and liver function, a few collateral vessels, obvious atrophy of liver volume and portal vein pressure less than 3.43 kPa (35 cm H₂O), are fit for splenectomy and disconnection. Our data showed that only a slight difference in operative mortality between the two groups of patients was found, and that no operative mortality and encephalopathy occurred in the PAD group, suggesting that PAD can be performed when possible.

With regard to emergency operation, we should decide whether the spleen is resected according to the condition of patients. It was reported that splenic artery ligation in these patients achieves the same therapeutic effects as splenectomy^[68]. Therefore, when the patients undergo disconnecting combined with shunting (except for splenorenal shunt), their spleen may not be excised, and splenic artery may be ligated.

It was considered previously that the patients with poor liver function should not be operated because of high operative

mortality. In the shunting group in this article, three of seven patients with Child's grade C died of surgical treatment. In the disconnecting group in this article, none of the three patients with Child's grade C died of PAD operation, suggesting that surgical therapy should be taken and PAD is the proper selection for patients with poor liver function^[69].

In regard to the surgical therapy of patients with portal hypertension, a suitable surgical procedure can achieve satisfactory therapeutic results. Different patients at different stages in their disease may require different therapies. An emphasis of this management is the full evaluation of the underlying liver disease. Our data showed that PAD as a major operation accounted for 50.39% of all the operations in this article. If the diameters of anastomotic stoma of PSS are restricted, favorable therapeutic effects can be achieved. When PSS needs to be conducted, the diameter of the anastomotic stoma should be 6-8 mm and the most usual operative approach is side-to-side meso-caval shunt. Selective shunt is a relatively ideal surgical procedure, but technically it is difficult. Although disconnection plus shunt seems to be a better procedure of choice because it can lower the portal pressure and maintain the portal flow, it will give the patient a big strike and should be carefully selected according to the liver function of patients. Liver transplantation can treat portal hypertension and achieve better long-term results, but it should not be the first choice in treating portal hypertension in China. Doctors should evaluate liver function comprehensively of patients with hepatocellular carcinoma and portal hypertension and carefully select combined operation in order to prolong their survival time. The cirrhotic patients with ascites can be treated with PSS with a small diameter (6-8 mm) of the stoma anastomosis. If acute continuous gastroesophageal variceal bleeding in cirrhotic patients cannot be controlled by medical treatment, and if no operational contraindication exists, emergency surgical treatment should be given immediately.

REFERENCES

- 1 **Isaksson B, Hultberg B, Hansson L, Bengtsson F, Jeppsson B.** Effect of mesocaval interposition shunting and repeated sclerotherapy on blood levels of gastrointestinal regulatory peptides, amino acids, and lysosomal enzymes—a prospective randomised trial. *Liver* 1999; **19**: 3-11
- 2 **Malesci A, Tacconi M, Valentini A, Basilio M, Lorenzano E, Salerno F.** Octreotide long-term treatment in patients with portal hypertension: persistent inhibition of postprandial glucagon response without major changes in renal function. *J Hepatol* 1997; **26**: 816-825
- 3 **Gulberg V, Haag K, Rossle M, Gerbes AL.** Hepatic arterial buffer response in patients with advanced cirrhosis. *Hepatology* 2002; **35**: 630-634
- 4 **Miyamoto Y, Oho K, Kumamoto M, Toyonaga A, Sata M.** Balloon-occluded retrograde transvenous obliteration improves liver function in patients with cirrhosis and portal hypertension. *J Gastroenterol Hepatol* 2003; **18**: 934-942
- 5 **Asakura T, Ohkohchi N, Orii T, Koyamada N, Tsukamoto S, Sato M, Enomoto Y, Usuda M, Satomi S.** Portal vein pressure is the key for successful liver transplantation of an extremely small graft in the pig model. *Transpl Int* 2003; **16**: 376-382
- 6 **Qiu FZ.** Evaluation of the pericardial devascularization in portal hypertension. *Zhonghua Waike Zazhi* 1983; **21**: 275-277
- 7 **Huang YT, Wang WM, Wang JQ, Bai CN.** Surgical treatment

- of portal hypertension:45 year experience. *Zhonghua Waikē Zazhi* 2000; **38**: 85-88
- 8 **Chen FM**, Wang JY, Huang TJ, Hsieh JS. The effect of portal hypertension on the glycoprotein biosynthesis of rat gastric mucosa. *J Invest Surg* 2002; **15**: 311-317
- 9 **Thuluvath PJ**, Yoo HY. Portal Hypertensive gastropathy. *Am J Gastroenterol* 2002; **97**: 2973-2978
- 10 **Ohta M**, Yamaguchi S, Gotoh N, Tomikawa M. Pathogenesis of portal hypertensive gastropathy: a clinical and experimental review. *Surgery* 2002; **131**(1 Suppl): S165-170
- 11 **Liu JK**, Cai JX, Wang AC, Yang HW. Studies of functional and morphological changes of gastric mucosa after portoozygos disconnection in cirrhotic portal hypertension in rats. *Disan Junyi Daxue Xuebao* 1994; **16**: 252-255
- 12 **Chen L**, Yang L, Yang Z, Dai Z. Magnetic resonance angiography in assessing changes of pre-and post-disconnective portal system in patients with portal hypertension. *Zhonghua Waikē Zazhi* 2000; **38**: 92-94
- 13 **Guan H**, Chen Y, Qian H. Expression of endothelin-1 and nitric oxide synthase mRNA in gastric mucosa of rats with cirrhosis and portal hypertensive gastropathy after disconnective operations. *Zhonghua Yixue Zazhi* 1998; **78**: 702-703
- 14 **Kojima K**. Experimental and clinical studies on esophageal hemodynamics in the Sugiura procedure. *Nippon Geka Gakkai Zasshi* 1986; **87**: 488-498
- 15 **Xue H**, Zhang H, Zhang Y, Jiang Q. Portal anticoagulation in preventing thrombosis after portaazygos devascularization for portal hypertension. *Zhonghua Waikē Zazhi* 2000; **38**: 855-857
- 16 **Gao D**, He Z, Wu J, Ma Q, Song H, Mei L, Wu Y. Long-term results of combined splenorenal shunt and portaazygos devascularization in patients with portal hypertension. *Zhonghua Waikē Zazhi* 1998; **36**: 327-329
- 17 **Rosemurgy AS**, Zervos EE, Bloomston M, Durkin AJ, Clark WC, Goff S. Post-shunt resource consumption favors small-diameter prosthetic H-graft portacaval shunt over TIPS for patients with poor hepatic reserve. *Ann Surg* 2003; **237**: 820-827
- 18 **Leng X**, Zhu J, Du R. Portacaval shunt with H-grafts of small diameter in treating cirrhotic patients with portal hypertension. *Zhonghua Waikē Zazhi* 1998; **36**: 330-332
- 19 **Cai J**, Dong J, Gu H. Inferior mesocaval shunt. *Zhonghua Waikē Zazhi* 1996; **34**: 151-153
- 20 **D'Cruz K**, Natarajan A. Emergency inferior mesenteric vein to left renal vein shunt in variceal bleeding: an alternative technique. *Trop Gastroenterol* 2001; **22**: 230-231
- 21 **Rahmani O**, Wolpert LM, Drezner AD. Distal inferior mesenteric veins to renal vein shunt for treatment of bleeding anorectal varices: case report and review of literature. *J Vasc Surg* 2002; **36**: 1264-1266
- 22 **Triger DR**. Portal hypertensive gastropathy. *Baillieres Clin Gastroenterol* 1992; **6**: 481-495
- 23 **Ekelund M**, Hakanson R, Holmin T, Oscarson J, Rehfeld JF, Sundler F, Westrin P. Effects of portacaval shunt on the rat stomach. *Acta Physiol Scand* 1985; **124**: 437-447
- 24 **Liu Jikui**, Cai JX, Duan HC, Yang HW. Effects of portacaval shunt on gastric mucosa in cirrhotic rats with portal hypertension. *Zhonghua Shiyān Waikē Zazhi* 1997; **14**: 18-20
- 25 **Zhang Z**, Feng H, Leng X, Ma F, Wang B, Du R. The levels of renin activity, angiotensin converting enzyme and angiotensin II in cirrhotic patients with ascites undergoing portacaval shunt. *Zhonghua Waikē Zazhi* 1999; **37**: 366-368
- 26 **Primignani M**, Dell'Era A, Fazzini L, Zatelli S, de Franchis R. Portal hypertensive gastropathy in patients with cirrhosis of the liver. *Recenti Prog Med* 2001; **92**: 735-740
- 27 **Gusberg RJ**. Distal splenorenal shunt-premise, perspective, practice. *Dig Dis* 1992; **10**(Suppl 1): 84-93
- 28 **Mercado MA**, Orozco H, Ramirez-Cisneros FJ, Hinojosa CA, Plata JJ, Alvarez-Tostado J. Diminished morbidity and mortality in portal hypertension surgery: relocation in the therapeutic armamentarium. *J Gastrointest Surg* 2001; **5**: 499-502
- 29 **Zhu J**, Liu F, Leng X. Perioperative plasma amino acid spectrum analysis in portal hypertensive cirrhotic patients undergoing portacaval H-graft shunt. *Zhonghua Waikē Zazhi* 1997; **35**: 299-301
- 30 **Feng H**, Zhang Z, Leng X, Li S, Zhu J, Du R. Plasma level of glucagon in cirrhotic patients with portal hypertension during operation of portacaval shunts. *Zhonghua Waikē Zazhi* 1999; **37**: 222-224
- 31 **Weng Y**, Wang Y, Xue J, Zhang Z, Zhou Y, Chen D, Li C. The influence of side-to-side portacaval shunt plus enhancement of perfusion of hepatic artery on cirrhotic liver: an experimental study. *Zhonghua Waikē Zazhi* 1998; **36**: 487-490
- 32 **Warren WD**, Zeppa R, Fomon JJ. Selective trans-splenic decompression of gastroesophageal varices by distal splenorenal shunt. *Ann Surg* 1967; **166**: 437-455
- 33 **Inokuchi K**. A selective portacaval shunt. *Lancet* 1968; **2**: 51-52
- 34 **Inokuchi K**, Kobayashi Y. Selective shunt method for portal hypertension-our method of the left gastric venous-caval shunt. *Shujutsu* 1969; **23**: 138-150
- 35 **Holmin T**, Schroder R, Berchtold R. A technique for distal splenocaval shunt in the rat. *World J Surg* 1977; **1**: 661-665
- 36 **Bhalerao RA**, Pinto AC, Bapat RD, Shetty SV, Bhide PD, Waingankar VS, Kirtane JM, Mehendale VG, Shetty SD. Selective transsplenic decompression of oesophageal varices by distal splenorenal and splenocaval shunt. *Gut* 1978; **19**: 831-837
- 37 **Cai J**, Dong J, Gu H, Bie P, Wang S, Sun W, Liu J, Zhou Y, Peng Z, Wang A. Distal splenocaval shunt in 66 patients with portal hypertension. *Zhonghua Waikē Zazhi* 1998; **36**: 336-338
- 38 **Spina GP**, Santambrogio R, Opocher E, Cosentino F, Zambelli A, Passoni GR, Cucchiario G, Macri M, Morandi E, Bruno S. Distal splenorenal shunt versus endoscopic sclerotherapy in the prevention of variceal rebleeding. First stage of a randomized, controlled trial. *Ann Surg* 1990; **211**: 178-186
- 39 **Liu JK**, Cai JX, Duan HC, Yang HW. Effects of distal splenocaval shunt on gastric mucosa in cirrhotic portal hypertension in rats. *Zhonghua Shiyān Waikē Zazhi* 1997; **14**: 104-105
- 40 **Xu XB**, Cai JX, Dong JH, Han BL. Effects of different operations on mitochondrial respiratory function of cirrhotic liver in rats. *Disan Junyi Daxue Xuebao* 1996; **18**: 48-51
- 41 **Wu G**, Cai JX, Dong JH, Duan HC. Effects of different types of operation on hepatic reserve function in rats with cirrhotic portal hypertension. *Disan Junyi Daxue Xuebao* 1998; **20**: 37-39
- 42 **Xue XB**, Cai JX, Dong JH, Han BL, Lin K, Leng XS. Effects of the different procedures on the Portasystemic shunting and the hepatic function in the rats. *J Dig Surg* 2004; **3**: 46-49
- 43 **Xu XB**, Cai JX, Dong JH, He ZP, Han BL, Leng XS. Effects of different operations on cirrhotic portal hypertensive liver in rats. *Shijie Huaren Xiaohua Zazhi* 2004; **12**: 689-693
- 44 **Xu XB**, Cai JX, Dong JH, He ZP, Han BL, Leng XS. Effects of portaazygos disconnection, portacaval shunt and selective shunts on experimental rat liver cirrhosis. *Zhonghua Ganzangbing Zazhi* 2005; **13**: 113-116
- 45 **Li MX**, Wang AC, Cai JX. Effects of distal splenocaval shunt on hemorheology. *Disan Junyi Daxue Xuebao* 1993; **15**: 532-535
- 46 **Millikan WJ Jr**, Warren WD, Henderson JM, Smith RB 3rd, Salam AA, Galambos JT, Kutner MH, Keen JH. The Emory prospective randomized trial: selective versus nonselective shunt to control variceal bleeding. Ten year follow-up. *Ann Surg* 1985; **201**: 712-722
- 47 **Henderson JM**, Kutner MH, Millikan WJ Jr, Galambos JT, Riepe SP, Brooks WS, Bryan FC, Warren WD. Endoscopic variceal sclerosis compared with distal splenorenal shunt to prevent recurrent variceal bleeding in cirrhosis. A prospective, randomized trial. *Ann Intern Med* 1990; **112**: 262-269
- 48 **Raia S**, da Silva LC, Gayotto LC, Forster SC, Fukushima J, Strauss E. Portal hypertension in schistosomiasis: a long-term follow-up of a randomized trial comparing three types of surgery. *Hepatology* 1994; **20**: 398-403
- 49 **Rikkers LF**, Rudman D, Galambos JT, Fulenwider JT, Millikan

- WJ, Kutner M, Smith RB 3rd, Salam AA, Sones PJ Jr, Warren WD. A randomized, controlled trial of the distal splenorenal shunt. *Ann Surg* 1978; **188**: 271-282
- 50 **Nordlinger BM**, Nordlinger DF, Fulenwider JT, Millikan WJ, Sones PJ, Kutner M, Steele R, Bain R, Warren WD. Angiography in portal hypertension: clinical significance in surgery. *Am J Surg* 1980; **139**: 132-141
- 51 **Huang YQ**, Zhong YF. Evaluation of the remote results of various procedures in the treatment of portal hypertension. *Zhonghua Waike Zazhi* 1986; **24**: 722-724
- 52 **Cao Y**, Cui L, Meng F, Wang M, Wang R, Han W. Treatment of portal hypertension by using pericardial vascular disconnection and mesocaval side-to-side shunting. *Zhonghua Waike Zazhi* 1998; **36**: 339-341
- 53 **Xu CE**, Zhang SG, Yu ZH, Li GX, Cao LL, Ruan CL, Li ZT. Combined devascularization and proximal splenorenal shunt: is this a better option than either procedure alone? *Hepatobiliary Pancreat Surg* 2004; **11**: 129-134
- 54 **Li Z**, Zhao L, Yu Z, Zhong Z. Effect of combined operation including splenorenal shunt as the main technique for portal hypertension in children. *Zhonghua Waike Zazhi* 2000; **38**: 601-603
- 55 **Huang CT**, Wang WM, Dai ZB. Survey of surgical treatment to portal hypertension in China. *Zhonghua Waike Zazhi* 1998; **36**: 324-326
- 56 **Yang Z**, Qiu F. Pericardial devascularization with splenectomy for the treatment of portal hypertension. *Zhonghua Waike Zazhi* 2000; **38**: 645-648
- 57 **Üeo W**, Sung JY, Chung SCS. A prospective study of upper gastrointestinal hemorrhage in patients with hepatocellular carcinoma. *Dig Dis Sci* 1995; **40**: 2516-2521
- 58 **Minagawa N**. Selection criteria for hepatectomy in patients with hepatocellular carcinoma and portal vein tumor thrombus. *Ann Surg* 2001; **233**: 379-384
- 59 **Pinto HC**, Abrantes A, Esteves AV. Long term prognosis of patients with cirrhosis of the liver and upper gastrointestinal bleeding. *Am J Gastroenterol* 1989; **84**: 1239-1243
- 60 **Yang W**, Wang GJ, Ding SQ, Liu QG, Pan CE. Surgical management of liver carcinoma accompanied by portal hypertension. *Zhonghua Putong Waike Zazhi* 2002; **17**: 200-201
- 61 **Zhang ZL**, Hu JK, Jin ZT. Surgical treatment for hepatocellular carcinoma and concomitant portal hypertension. *Zhongguo Shiyong Waike Zazhi* 2002; **22**: 85-87
- 62 **Li H**, Hu YL, Wang Y, Zhang DS, Jiang FX. Simultaneous operative treatment of patients with primary liver cancer associated with portal hypertension. *Hepatobiliary Pancreat Dis Int* 2002; **1**: 92-93
- 63 **Chen WC**, Hou MC, Lin HC. Feasibility and potential benefit of maintenance endoscopic variceal ligation patients with unresectable hepatocellular carcinoma and acute esophageal variceal hemorrhage: a controlled trial. *Gastrointest Endosc* 2001; **54**: 18-23
- 64 **Letier MH**, Krige JE, Lemmer ER, Terblanche J. Injection sclerotherapy for variceal bleeding in patients with irresectable hepatocellular carcinoma. *Hepatogastroenterology* 2000; **47**: 1680-1684
- 65 **Zhang ZM**, Leng XS, Feng HQ, Zhang WF, Pan T, Du RY. The changes of plasma renin activity in cirrhotic patients with ascites undergoing portacavalshunt. *Zhonghua Putong Waike Zazhi* 2001; **16**: 395-396
- 66 **Sola-Vera J**, Minana J, Ricart E, Planella M, Gonzalez B, Torras X, Rodriguez J, Such J, Pascual S, Soriano G, Perez-Mateo M, Guarner C. Randomized trial comparing albumin and saline in the prevention of paracentesis-induced circulatory dysfunction in cirrhotic patients with ascites. *Hepatology* 2003; **37**: 1147-1153
- 67 **Jalan R**, Hayes PC. Sodium handling in patients with well compensated cirrhosis is dependent on the severity of liver disease and portal pressure. *Gut* 2000; **46**: 527-533
- 68 **Orozco H**, Mercado MA, Martinez R, Tielve M, Chan C, Vasquez M, Zenteno-Guichard G, Pantoja JP. Is splenectomy necessary in devascularization procedures for treatment of bleeding portal hypertension? *Arch Surg* 1998; **133**: 36-38
- 69 **Xu R**, Ling Y, Qiu W. The different influences of splenectomy plus ligation of pericardial vein and shunt on portal hypertensive gastropathy. *Zhonghua Waike Zazhi* 1997; **35**: 515-517

Science Editor Wang XL Language Editor Elsevier HK

• CLINICAL RESEARCH •

Hemodynamic analysis of esophageal varices in patients with liver cirrhosis using color Doppler ultrasound

Feng-Hua Li, Jing Hao, Jian-Guo Xia, Hong-Li Li, Hua Fang

Feng-Hua Li, Jian-Guo Xia, Hong-Li Li, Hua Fang, Department of Ultrasound, Renji Hospital, The Second Medical University of Shanghai, Shanghai 200001, China

Jing Hao, Department of Radiology, Ruijin Hospital, The Second Medical University of Shanghai, Shanghai 200001, China

Supported by the Natural Science Foundation of Shanghai, No. 034119921

Co-first-authors: Feng-Hua Li and Jing Hao

Correspondence to: Dr. Feng-Hua Li, Department of Ultrasound, Renji Hospital, The Second Medical University of Shanghai, Shanghai 200001, China. proflihf@sina.com

Telephone: +86-21-63260930 Fax: +86-21-63260930

Received: 2004-07-19 Accepted: 2004-09-04

Abstract

AIM: To study the portal hemodynamics and their relationship with the size of esophageal varices seen at endoscopy and to evaluate whether these Doppler ultrasound parameters might predict variceal bleeding in patients with liver cirrhosis and portal hypertension.

METHODS: One hundred and twenty cirrhotic patients with esophageal varices but without any previous bleeding were enrolled in the prospective study. During a 2-year observation period, 52 patients who had at least one episode of acute esophageal variceal hemorrhage constituted the bleeding group, and the remaining 68 patients without any previous hemorrhage constituted the non-bleeding group. All patients underwent endoscopy before or after color Doppler-ultrasonic examination, and images were interpreted independently by two endoscopists. The control group consisted of 30 healthy subjects, matched to the patient group in age and gender. Measurements of diameter, flow direction and flow velocity in the left gastric vein (LGV) and the portal vein (PV) were done in all patients and controls using color Doppler unit. After baseline measurements, 30 min after oral administration of 75 g glucose in 225 mL, changes of the diameter, flow velocity and direction in the PV and LGV were examined in 60 patients with esophageal varices and 15 healthy controls.

RESULTS: The PV and LGV were detected successfully in 115 (96%) and 105 (88%) of 120 cirrhotic patients, respectively, and in 27 (90%) and 21 (70%) of 30 healthy controls, respectively. Among the 120 cirrhotic patients, 37 had F1, 59 had F2, and 24 had F3 grade varices. Compared with the healthy controls, cirrhotic group had a significantly lower velocity in the PV, a significantly greater diameter of the PV and LGV, and a higher velocity in the LGV. In the cirrhotic group, no difference in portal flow velocity and

diameter were observed between patients with or without esophageal variceal bleeding (EVB). However, the diameter and blood flow velocity of the LGV were significantly higher for EVB (+) group compared with EVB (-) group ($P < 0.01$). Diameter of the LGV increased with enlarged size of varices. There were differences between F1 and F2, F1 and F3 varices, but no differences between F2 and F3 varices ($P = 0.125$). However, variceal bleeding was more frequent in patients with a diameter of LGV > 6 mm. The flow velocity in the LGV of healthy controls was 8.70 ± 1.91 cm/s ($n = 21$). In patients with liver cirrhosis, it was 10.3 ± 2.1 cm/s ($n = 12$) when the flow was hepatopetal and 13.5 ± 2.3 cm/s ($n = 87$) when it was hepatofugal. As the size of varices enlarged, hepatofugal flow velocity increased ($P < 0.01$) and was significantly different between patients with F1 and F2 varices and between patients with F2 and F3 varices. Variceal bleeding was more frequent in patients with a hepatofugal flow velocity > 15 cm/s (32 of 52 patients, 61.5%). Within the bleeding group, the mean LGV blood flow velocity was 16.6 ± 2.62 cm/s. No correlation was observed between the portal blood flow velocity and EVB. In all healthy controls, the flow direction in the LGV was hepatopetal, toward the PV. In patients with F1 varices, flow direction was hepatopetal in 10 patients, to-and-fro state in 3 patients, and hepatofugal in the remaining 18. The flow was hepatofugal in 91% patients with F2 and all F3 varices. Changes in diameter of the PV and LGV were not significant before and after ingestion of glucose (PV: 1.41 ± 1.5 cm before and 1.46 ± 1.6 cm after; LGV: 0.57 ± 1.7 cm before and 0.60 ± 1.5 cm after). Flow direction in the LGV was hepatopetal and to-and-fro in 16 patients and hepatofugal in 44 patients before ingestion of glucose. Flow direction changed to hepatofugal in 9 of 16 patients with hepatopetal and to-and-fro blood flow after ingestion of glucose. In 44 patients with hepatofugal blood flow in the LGV, a significant increase in hepatofugal flow velocity was observed in 38 of 44 patients (86%) with esophageal varices. There was a relationship between the percentage changes in flow velocity and the size of varices. Patients who responded excessively to food ingestion might have a high risk for bleeding. The changes of blood flow velocity in the LGV were greater than those in the PV (LGV: $28.3 \pm 26.1\%$, PV: $7.2 \pm 13.2\%$, $P < 0.01$), whereas no significant changes in the LGV occurred before and after ingestion of glucose in the control subjects.

CONCLUSION: Hemodynamics of the PV is unrelated to the degree of endoscopic abnormalities in patients with liver cirrhosis. The most important combinations are endoscopic findings followed by the LGV hemodynamics. Duplex-Doppler ultrasonography has no value in the identification of patients with cirrhosis at risk of variceal

bleeding. Hemodynamics of the LGV appears to be superior to those of the PV in predicting bleeding.

© 2005 The WJG Press and Elsevier Inc. All rights reserved.

Key words: Hemodynamics; Esophageal varices; Liver cirrhosis; Color Doppler ultrasound

Li FH, Hao J, Xia JG, Li HL, Fang H. Hemodynamic analysis of esophageal varices in patients with liver cirrhosis using color Doppler ultrasound. *World J Gastroenterol* 2005; 11(29): 4560-4565

<http://www.wjgnet.com/1007-9327/11/4560.asp>

INTRODUCTION

Esophageal variceal bleeding (EVB) is a potentially deadly complication in patients with liver cirrhosis and portal hypertension^[1-4]. In patients with cirrhosis, the incidence of esophageal varices ranges from 35% to 80% and approximately a third of patients with esophageal varices experience variceal bleeding, and up to 70% of the survivors have one or more additional episodes of bleeding^[5]. The ultrasonographic examination is a simple, inexpensive, accurate, and noninvasive technique. It has been widely used to investigate the relationship between EVB and hemodynamics associated with portal hypertension and liver cirrhosis^[6-9]. However, no consistent results have been reported yet. In this study, we investigated the hemodynamic features of the portal vein (PV) and left gastric vein (LGV) before and after oral glucose (75 mg), and evaluated whether these Doppler ultrasound parameters might predict variceal bleeding in patients with liver cirrhosis.

MATERIALS AND METHODS

Materials

One hundred and twenty cirrhotic patients with esophageal varices without any previous bleeding (mean age 57.6 ± 6.8 years; 42 females and 78 males) were enrolled in the prospective study. During a 2-year observation period, 52 patients who had at least one episode of acute esophageal variceal hemorrhage constituted the bleeding group, and the remaining 68 patients without any previous hemorrhage constituted the non-bleeding group. The diagnosis of cirrhosis was based on clinical and imaging findings or pathologic findings.

The control group consisted of 30 healthy subjects, matched to the patient group in age (mean age 53.8 ± 6.7 years) and gender (10 females and 20 males). None of the controls had a history or clinical evidence of liver disease. All subjects provided written informed consent prior to participation.

Methods

All patients underwent endoscopy before or after color Doppler-ultrasonic examination, and images were interpreted independently by two endoscopists. Esophageal varices were graded according to the criteria of the Japanese Research Society for Portal Hypertension and endoscopic finding of PV hypertension^[10] in straight and small-calibered varices (F1), moderately enlarged beady varices (F2), or markedly enlarged nodular or tumor-shaped varices (F3).

Ultrasonographic examinations were performed using HDI5000 and HPsono4500 color Doppler units with a 3.75-MHz convex probe. All the patients and controls were kept fasting overnight prior to the procedure. They were examined in the supine position during quiet respiration. Measurements of diameter, flow direction and flow velocity in the LGV and PV were done in all patients and controls. The PV blood flow was measured at the crossing point with the hepatic artery or just distally to it. The LGV usually originates from the portal-splenic vein junction or its vicinity and runs to the esophagogastric junction. It was identified longitudinally by ultrasonography in a left oblique scan in the epigastrium. Blood flow measurement was made in the straight portion of the LGV, usually within 5 cm from its origin^[11,12]. The diameters of the LGV and PV were calculated from the inner surface within the vessel as seen in a longitudinal view. The sample volume was selected from 2 to 5 mm widths to include the width of the vessel. Flow direction was assessed according to the upward or downward position of the Doppler waveform over the baseline. The beam-vessel angle was less than 60° in every patient. Flow velocity was calculated as an average value of three consecutive measurements. The operator was blind to any information on the endoscopic findings of varices and the portal pressure.

After baseline measurements, 30 min after oral administration of 75 g glucose in 225 mL, changes of the diameter, flow velocity and direction in the PV and LGV were examined in 60 patients with esophageal varices and 15 healthy controls.

Statistical analysis

Student's *t*-test was used for single comparison, one-way analysis of variance for multiple comparisons. A *P*-value less than 0.05 was considered statistically significant. Statistical analyses were performed with the SPSS 10.0 software program.

RESULTS

The PV and LGV were detected successfully in 115 (96%) and 105 (88%) of 120 cirrhotic patients, respectively, and in 27 (90%) and 21 (70%) of 30 healthy volunteers, respectively. Among the 120 cirrhotic patients, 37 had F1, 59 had F2, and 24 had F3 grade varices.

Table 1 summarizes the duplex sonography findings. Compared with the healthy controls, cirrhotic group had a significantly lower velocity in the PV, a significantly greater diameter of the PV and LGV, a higher velocity in the LGV. In the cirrhotic group, no difference in portal flow velocity and diameter was observed between patients with or without EVB. However, the diameter and blood flow velocity of the LGV were significantly higher in EVB (+) group compared with EVB (-) group ($P < 0.01$).

Diameter of the LGV increased with enlarged size of varices. In patients with F1, F2, and F3 varices, the diameter was 0.48 ± 0.16 , 0.62 ± 0.23 , and 0.72 ± 0.24 cm, respectively. There were differences between F1 and F2, F1 and F3 varices, but no differences between F2 and F3 varices ($P = 0.125$). However, variceal bleeding was more frequent in patients with a diameter of the LGV > 6 mm, suggesting that the diameter of LGV had a relationship with the size of esophageal varices, but had no value in the identification of patients with cirrhosis at risk for EVB (Table 2).

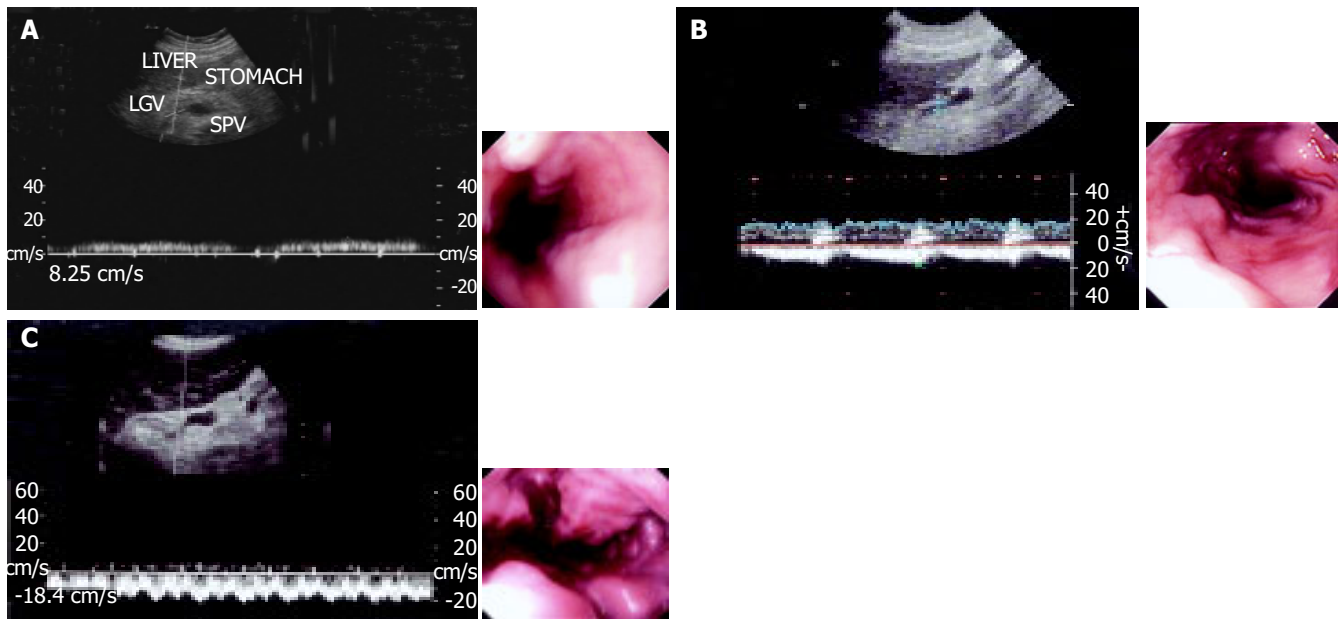


Figure 1 Relationship between hemodynamics of the LGV and the size of esophageal varices. **A:** Hepatopetal blood flow in the LGV; **B:** hepatofugal blood

flow in the LGV; **C:** hepatofugal blood flow in the LGV.

Table 1 Hemodynamics in cirrhotic and healthy groups (mean±SD)

Group	Diameter (cm)		Velocity (cm/s)	
	PV	LGV	PV	LGV
Controls	1.12±0.11	0.40±0.18	15.3±1.41	8.70±1.91
EVB (-)	1.48±0.15 ^b	0.52±0.21 ^{a,b}	13.7±1.54 ^b	14.8±1.11 ^{a,b}
EVB (+)	1.56±0.28 ^b	0.71±0.34 ^b	12.8±1.18 ^b	16.6±2.62 ^b

EVB, esophageal variceal bleeding; PV, portal vein; LGV, left gastric vein. ^a $P<0.05$ compared with EVB (+); ^b $P<0.01$ compared with the healthy controls.

Table 2 Hemodynamics in relation to the development of esophageal varices in cirrhotic group (mean±SD)

Varices	Diameter (cm)		Velocity (cm/s)	
	PV	LGV	PV	LGV
F1	1.47±0.19	0.48±0.16	14.2±2.15	7.80±2.15
F2	1.51±0.18	0.62±0.23	13.1±1.81	11.5±2.03
F3	1.55±0.21	0.72±0.24	12.0±1.72	16.0±3.19

The flow velocity in LGV, in healthy controls, was 8.70 ± 1.91 cm/s ($n = 21$). In patients with liver cirrhosis, it was 10.3 ± 2.1 cm/s ($n = 12$) when the flow was hepatopetal and 13.5 ± 2.3 cm/s ($n = 87$) when the flow was hepatofugal (Figure 1). As the size of varices enlarged, hepatofugal flow velocity increased ($P<0.01$) and was significantly different between patients with F1 and F2 varices, and between patients with F2 and F3 varices. Variceal bleeding was more frequent in patients with a hepatofugal flow velocity >15 cm/s (32 of 52 patients, 61.5%). Within the bleeding group, the mean LGV blood flow velocity was 16.6 ± 2.62 cm/s. No correlation was observed between the portal blood flow velocity and EVB. Hepatofugal flow velocity of the LGV in relation to the development of esophageal varices is shown in Figure 2.

In all healthy controls, the flow direction in the LGV was hepatopetal, toward the PV (Figure 3). In patients with

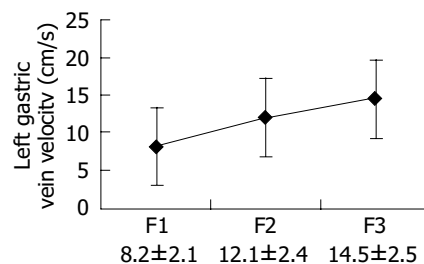


Figure 2 Hepatofugal flow velocity in LGV in relation to the size of esophageal varices.

Table 3 Flow direction in the LGV in relation to the development of esophageal varices in cirrhotic group, n (%)

Varices	n	Flow direction		
		Hepatopetal	Hepatofugal	To-and-fro
F1	31	10 (32)	18 (58)	3 (10)
F2	53	2 (4)	48 (91)	3 (5)
F3	21	0	21 (100)	0
Sum	105	12 (11)	87 (83)	6 (6)

F1 varices, flow direction was hepatopetal in 10 patients, to-and-fro state in 3 patients, and hepatofugal in the remaining 18. The flow direction was hepatofugal in 91% patients with F2 and all F3 varices (Table 3).

Changes in diameter of the PV and LGV were not significant before and after ingestion of glucose (PV: 1.41 ± 1.5 cm before and 1.46 ± 1.6 cm after; LGV: 0.57 ± 1.7 cm before and 0.60 ± 1.5 cm after). Flow direction in the LGV was hepatopetal and to-and-fro in 16 patients and hepatofugal in 44 patients before ingestion of glucose. Flow direction changed to hepatofugal in 9 of 16 patients with hepatopetal and to-and-fro blood flow after ingestion of glucose (Figure 4). In 44 patients with hepatofugal blood flow in the LGV, a

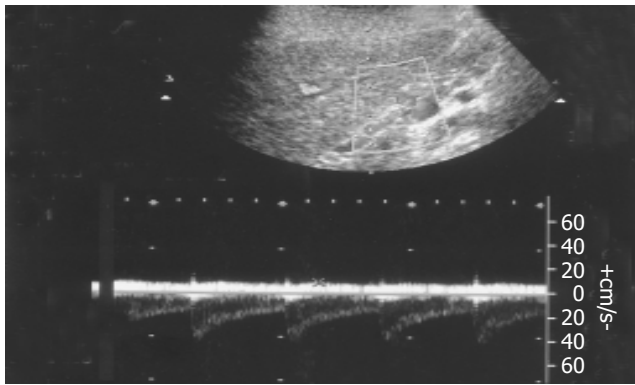


Figure 3 Hepatopetal blood flow in the LGV of normal subjects.

significant increase in hepatofugal flow velocity was observed in 38 of 44 patients (86%) with esophageal varices (Figure 5). The changes of blood flow velocity were greater in the LGV than in the PV (LGV: $28.3 \pm 26.1\%$, PV: $7.2 \pm 13.2\%$, $P < 0.01$). The degree of changes in percentages in the LGV and PV of patients with hepatofugal flow after ingestion of glucose is shown in Figure 6. There was a relationship between the percentage changes in flow velocity and the size of varices. Patients who responded excessively to food ingestion might have a high risk for bleeding, whereas no significant changes occurred in the

LGV before and after ingestion of glucose in the control subjects.

DISCUSSION

EVB is a potentially deadly complication in patients with liver cirrhosis and portal hypertension. Once esophageal varices occur, the risk for EVB ranges from 10% to 60%, and the mortality rate related to EVB ranges from 20% to 60%^[1-4]. Since esophageal varices-induced hemorrhage in patients with cirrhosis can be fatal, these patients must be routinely classified according to their risk status and appropriate prophylactic measures should be taken to prevent hemorrhage. The size of esophageal varices is one of the strongest risk factors for variceal rupture^[1-5]. Differences in connecting venous structures and their underlying hemodynamics may be predisposing factors in the progression of esophageal varices. The ultrasonographic examination is a simple, inexpensive, accurate, and noninvasive technique to evaluate the hemodynamics under physiological conditions and has been widely used experimentally and clinically, but there is a continuing debate concerning the hemodynamics of the PV system in relation to the development of esophageal varices^[6-9].

The notable findings of this study are related to the hemodynamics of the PV. Compared with the healthy controls, cirrhotic group had a significantly lower velocity in the PV and a significantly greater diameter of the PV.

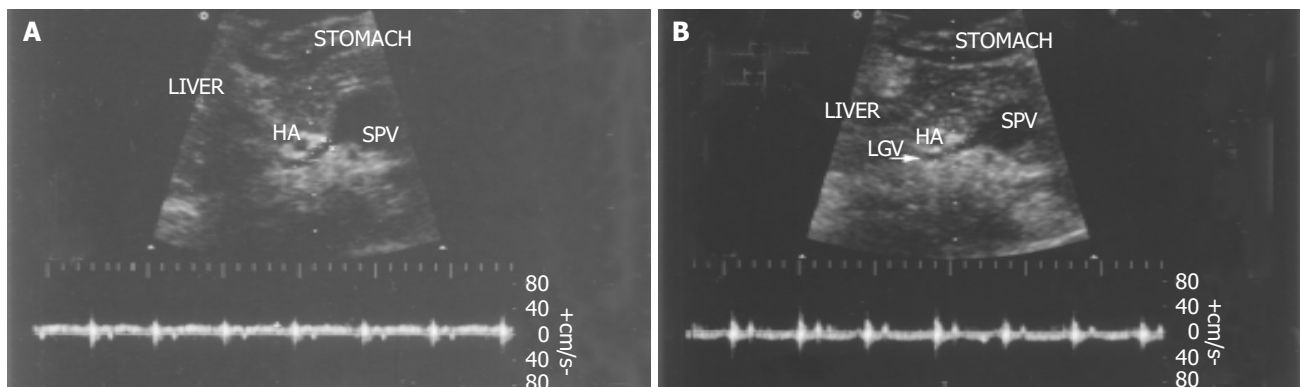


Figure 4 Change in flow direction in the LGV. **A:** Hepatopetal blood flow in the LGV before ingestion of glucose; **B:** changes of flow direction from hepatopetal

to hepatofugal after ingestion of glucose.

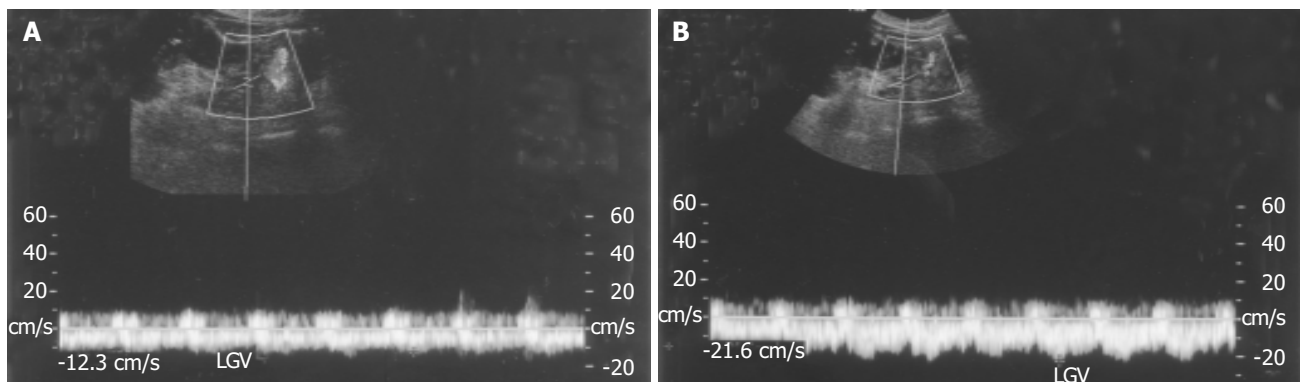


Figure 5 Doppler sonograms in the LGV with hepatofugal blood flow before (A) and

after (B) ingestion of glucose in a patient with a significant response to glucose.

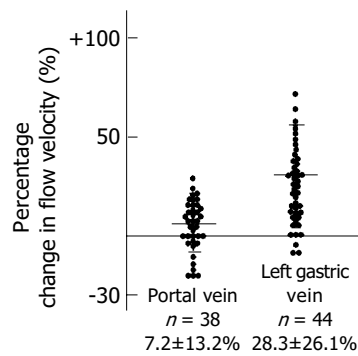


Figure 6 Changes in blood flow in the PV and LGV of patients with hepatofugal blood flow before and after ingestion of glucose.

These findings indicate that the portal venous system in cirrhotic patients with portal hypertension is the site of passive congestion and increased blood flow. During the period of 2 years, 52 (43%) patients had at least one episode of acute esophageal variceal hemorrhage. The portal hemodynamic features had no differences between the EVB (+) and EVB (-) subgroups. It is generally thought that elevated vascular resistance and increased portal blood inflow are the two principal mechanisms involved in the development of portal hypertension secondary to cirrhosis^[13]. The former is an initiating factor, while the latter plays an important role in maintaining a chronic portal hypertensive state. Therefore, portal flow velocity is unrelated to the degree of endoscopic abnormalities in patients with liver cirrhosis and has no value in the identification of patients with cirrhosis at risk for EVB. Therefore, passive congestion of portal blood has no direct relationship with EVB.

In cirrhotic patients, because of portal outflow obstruction (i.e., elevated intrahepatic portal vascular resistance), increased blood flow in the splenic vein cannot enter the liver via the PV, and a considerable percentage of splenic vein flow is forced to bypass the liver. One of the most important shunting routes is the LGV, which may normally arise from the PV and splenic vein. When increased flow in the splenic vein is prominent, the diversion of a large quantity of portal flow via the LGV would result in more severe esophageal varices and might trigger the occurrence of EVB^[14,15].

This study showed a close relationship between the velocity of hepatofugal flow in the LGV and esophageal variceal size. EVB was more frequent in patients with a hepatofugal flow velocity >15 cm/s (32 of 52 patients, 61.5%). Preservation of hepatopetal flow in the LGV in patients with portal hypertension may be associated with a low risk for variceal hemorrhage. Because the LGV is the major source of blood supply to esophageal varices, velocity of hepatofugal flow may be the more important determinant in the development of varices. These results are similar to those of previous studies^[16-18]. Therefore, detection of a high-flow velocity in the LGV may be suggestive of hemodynamically active esophageal varices that carry a high risk for bleeding.

The diameter of the LGV increased as the size of varices enlarged, there were differences between patients with F1 and F2, F1 and F3 varices, but no differences between patients with F2 and F3 varices, suggesting that diameter

of the LGV has a relationship with the size of esophageal varices, but has no value in the identification of patients with cirrhosis at risk for EVB. The diameter of the LGV may measure up to 6 mm on sonograms of normal subjects. However, variceal bleeding is more frequent in patients with a diameter of the LGV >6 mm.

It is generally thought that flow direction in the LGV changes from hepatopetal to hepatofugal during variceal development^[17,18]. However, in our study the flow direction in the LGV was still hepatopetal and LGV did not seem to contribute to the formation of esophageal varices in 32% patients with F1 varices. Blood flow in the stomach wall from the left gastric artery also participates in variceal blood flow^[19-21]. These blood flows in the gastric wall alone possibly contribute to the formation of esophageal varices in its early stage, where LGV flow does not significantly constitute to the variceal flow. In advanced portal hypertension, esophageal varices become large as the LGV flow changes to hepatofugal and drains into the varices. Whereas a to-and-fro flow state is generally considered to be present in the LGV during the period when the flow becomes reversed^[19], which was observed in six patients in the present study. Other studies reported that there is a relationship between esophageal varices and venous collaterals outside the esophageal wall in patients with portal hypertension. Collaterals are divided into periesophageal collateral veins and paraesophageal collateral veins. Periesophageal collateral veins play a more important role in the formation of esophageal varices than paraesophageal collateral veins in the early stage of esophageal varices^[21-24].

Food intake usually increases portal blood flow. In this study, we gave a dose of glucose and an increase of hepatofugal blood flow velocity was observed in the LGV and PV. Also the changes of blood flow velocity were greater in the LGV than in the PV. Out of 44 patients with hepatofugal blood flow in the LGV, a significant increase in hepatofugal flow velocity was observed in 38 patients (86%) with esophageal varices. There was a relationship between the percentage changes in flow velocity and the size of varices. Patients who responded excessively to food ingestion might have a high risk for bleeding. High flow resistance in a portal hypertensive liver may exaggerate the increase in intestinal inflow into the LGV, henceforth into the esophageal varices under such conditions^[17], because blood flow in the LGV tends to increase readily when the portal blood flow increases or portal flow resistance is elevated. In patients with portal hypertension, an increase in variceal blood flow may contribute to bleeding from esophageal varices. The analysis of these factors influencing blood flow in esophageal varices seems to be important to understand the pathophysiology of variceal bleeding and helps us to estimate the risk for variceal hemorrhage^[25-28].

In conclusion, PV is unrelated to the degree of endoscopic abnormalities in patients with liver cirrhosis and its measurement by Duplex-Doppler ultrasonography has no value in the identification of patients with cirrhosis at risk for variceal bleeding. Hemodynamics of the LGV appears to be superior to those of the PV in predicting bleeding, allowing physicians to optimize therapy^[29]. Therefore, the likelihood index, adopted to determine the best parameters related to variceal

bleeding showed that the most important combinations are endoscopic findings followed by the LGV hemodynamics.

REFERENCES

- 1 **Brandenburger LA**, Regenstein FG. Variceal Hemorrhage. *Curr Treat Options Gastroenterol* 2002; **5**: 73-80
- 2 **Seewald S**, Seitz U, Yang AM, Soehendra N. Variceal bleeding and portal hypertension: still a therapeutic challenge? *Endoscopy* 2001; **33**: 126-139
- 3 **Bratovic I**, Lacevic N. Management of esophageal varices. *Med Arh* 2002; **56**(1 Supp1): 11-12
- 4 **Bhasin DK**, Malhi NJ. Variceal bleeding and portal hypertension: much to learn, much to explore. *Endoscopy* 2002; **34**: 119-128
- 5 **Tsokos M**, Turk EE. Esophageal variceal hemorrhage presenting as sudden death in outpatients. *Arch Pathol Lab Med* 2002; **126**: 1197-1200
- 6 **Martins RD**, Szejnfeld J, Lima FG, Ferrari AP. Endoscopic, ultrasonographic, and US-Doppler parameters as indicators of variceal bleeding in patients with schistosomiasis. *Dig Dis Sci* 2000; **45**: 1013-1018
- 7 **Erdozain Sosa JC**, Martin Hervas C, Moreno Blanco MA, Zapata Aparicio I, Herrera Abian A, Conde Gacho P, Madero R, Segura Cabral JM. Color duplex Doppler ultrasonography in the evaluation of the risk of esophageal varices bleeding in cirrhotic patients. *Gastroenterol Hepatol* 2000; **23**: 466-469
- 8 **Piscaglia F**, Donati G, Serra C, Muratori R, Solmi L, Gaiani S, Gramantieri L, Bolondi L. Value of splanchnic Doppler ultrasound in the diagnosis of portal hypertension. *Ultrasound Med Biol* 2001; **27**: 893-899
- 9 **Cioni G**, Tincani E, Cristani A, Ventura P, D'Alimonte P, Sardini C, Turrini F, Abbati GL, Romagnoli R, Ventura E. Does the measurement of portal flow velocity have any value in the identification of patients with cirrhosis at risk of digestive bleeding? *Liver* 1996; **16**: 84-87
- 10 **Liang ZH**, Li shb, portal vein hypertension, publishing company of people's military Dr
- 11 **Roi DJ**. Ultrasound anatomy of the left gastric vein. *Clin Radiol* 1993; **47**: 396-398
- 12 **Xia JG**, Dong SQ, Li FH. Sonography and hemodynamic features of normal left gastric vein. *Shijie Huaren Xiaohua Zazhi* 2003; **11**: 491-493
- 13 **Benoit JN**, Womack WA, Hernandez L, Granger DN. "Forward" and "backward" flow mechanisms of portal hypertension. Relative contributions in the rat model of portal vein stenosis. *Gastroenterology* 1985; **89**: 1092-1096
- 14 **Kotenko OG**. The state of regional hemodynamics after performance of operations of the portogastroesophageal blood flow disconnection in liver cirrhosis. *Klin Khir* 2000; **7**: 19-21
- 15 **Nakano R**, Iwao T, Oho K, Toyonaga A, Tanikawa K. Splanchnic hemodynamic pattern and liver function in patients with cirrhosis and esophageal or gastric varices. *Am J Gastroenterol* 1997; **92**: 2085-2089
- 16 **Wachsberg RH**, Simmons MZ. Coronary vein diameter and flow direction in patients with portal hypertension: evaluation with duplex sonography and correlation with variceal bleeding. *Am J Roentgenol* 1994; **162**: 637-641
- 17 **Hino S**, Kakutani H, Ikeda K, Uchiyama Y, Sumiyama K, Kuramochi A, Kitamura Y, Matsuda K, Arakawa H, Kawamura M, Masuda K, Suzuki H. Hemodynamic assessment of the left gastric vein in patients with esophageal varices with color Doppler EUS: factors affecting development of esophageal varices. *Gastrointest Endosc* 2002; **55**: 512-517
- 18 **Matsutani S**, Furuse J, Ishii H, Mizumoto H, Kimura K, Ohto M. Hemodynamics of the left gastric vein in portal hypertension. *Gastroenterology* 1993; **105**: 513-518
- 19 **Irisawa A**, Shibukawa G, Obara K, Saito A, Takagi T, Shishido H, Odajima H, Abe M, Sugino T, Suzuki T, Kasukawa R, Sato Y. Collateral vessels around the esophageal wall in patients with portal hypertension: comparison of EUS imaging and microscopic findings at autopsy. *Gastrointest Endosc* 2002; **56**: 249-253
- 20 **Widrich WC**, Srinivasan M, Semine MC, Robbins AH. Collateral pathways of the left gastric vein in portal hypertension. *Am J Roentgenol* 1984; **142**: 375-382
- 21 **Irisawa A**, Obara K, Sato Y, Saito A, Takiguchi F, Shishido H, Sakamoto H, Kasukawa R. EUS analysis of collateral veins inside and outside the esophageal wall in portal hypertension. *Gastrointest Endosc* 1999; **50**: 374-380
- 22 **Escorsell A**, Garcia-Pagan JC, Bosch J. Assessment of portal hypertension in humans. *Clin Liver Dis* 2001; **5**: 575-589
- 23 **Bolognesi M**, Sacerdoti D, Merkel C, Bombonato G, Gatta A. Noninvasive grading of the severity of portal hypertension in cirrhotic patients by echo-color-Doppler. *Ultrasound Med Biol* 2001; **27**: 901-907
- 24 **Yin XY**, Lu MD, Huang JF, Xie XY, Liang LJ. Color Doppler velocity profile assessment of portal hemodynamics in cirrhotic patients with portal hypertension: correlation with esophageal variceal bleeding. *J Clin Ultrasound* 2001; **29**: 7-13
- 25 **Matsutani S**, Maruyama H, Sato G, Fukuzawa T, Mizumoto H, Saisho H. Hemodynamic response of the left gastric vein to glucagon in patients with portal hypertension and esophageal varices. *Ultrasound Med Biol* 2003; **29**: 13-17
- 26 **Silva G**, Navasa M, Bosch J, Chesta J, Pilar Pizcueta M, Casamitjana R, Rivera F, Rodes J. Hemodynamic effects of glucagons in portal hypertension. *Hepatology* 1990; **11**: 668-673
- 27 **Okazaki K**, Miyazaki M, Onishi S, Ito K. Effects of food intake and various extrinsic hormones on portal blood flow in patients with liver cirrhosis demonstrated by pulsed Doppler with the Octoson. *Scand J Gastroenterol* 1986; **21**: 1029-1038
- 28 **Lin HC**, Yang MC, Hou MC, Lee FY, Huang YT, Lin LF, Li SM, Hwang SJ, Wang SS, Tsai YT, Lee SD. Hyperglucagonaemia in cirrhotic patients and its relationship to the severity of cirrhosis and haemodynamic values. *J Gastroenterol Hepatol* 1996; **11**: 422-428
- 29 **Schepis F**, Camma C, Niceforo D, Magnano A, Pallio S, Cinquegrani M, D'amico G, Pasta L, Craxi A, Saitta A, Raimondo G. Which patients with cirrhosis should undergo endoscopic screening for esophageal varices detection? *Hepatology* 2001; **33**: 333-338

Circulating adhesion molecules in patients with virus-related chronic diseases of the liver

Cosimo Marcello Bruno, Claudio Sciacca, Danila Cilio, Gaetano Bertino, Anna Elisa Marchese, Gaetana Politi, Lucia Chinnici

Cosimo Marcello Bruno, Claudio Sciacca, Danila Cilio, Gaetano Bertino, Department of Internal Medicine and Systemic Diseases, University of Catania, Italy
Anna Elisa Marchese, Gaetana Politi, Lucia Chinnici, Clinical Laboratory Analysis, S. Bambino Hospital, Catania, Italy
Co-first-author: Cosimo Marcello Bruno
Correspondence to: Professor Cosimo Marcello Bruno, Dip. Medicina Interna e Patologie Sistemiche Osp. S. Marta, via G. Clementi 36, Catania 95124, Italy. cmbruno@unict.it
Telephone: +39-95-7435677
Received: 2004-10-05 Accepted: 2004-12-23

Key words: ICAM-1; VCAM-1; Chronic liver diseases; Hepatocellular necrosis; Liver fibrosis

Bruno CM, Sciacca C, Cilio D, Bertino G, Marchese AE, Politi G, Chinnici L. Circulating adhesion molecules in patients with virus-related chronic diseases of the liver. *World J Gastroenterol* 2005; 11(29): 4566-4569
<http://www.wjgnet.com/1007-9327/11/4566.asp>

Abstract

AIM: In the inflammatory state, intercellular adhesion molecule-1 (ICAM-1) and vascular cellular adhesion molecule-1 (VCAM-1) play a key role in promoting migration of immunological cells from the circulation to target site. Aim of our study was to investigate soluble forms of these molecules in patients with virus-related chronic liver diseases, to assess their behavior in different pathologies and correlation with severity of liver damage.

METHODS: Circulating ICAM-1 and VCAM-1 were assayed by EIA commercial kits (R&D System Co., Abington, UK) in 23 patients with chronic active hepatitis (CH), 50 subjects affected by liver cirrhosis (LC) and 15 healthy controls comparable for sex and age. In patients, serum alanine aminotransferase (ALT) and aspartate aminotransferase (AST) were also detected by autoanalyzer.

RESULTS: LC patients had significantly higher ICAM-1 values than CH patients (38.56 ± 7.4 ng/mL vs 20.89 ± 6.42 ng/mL; $P < 0.001$) and these ones had significantly higher values than controls (12.92 ± 1.08 ng/mL; $P < 0.001$). In CH group, ICAM-1 levels were significantly related to inflammatory activity ($P = 0.041$) and ALT values ($r = 0.77$; $P < 0.05$). VCAM-1 values were significantly increased only in LC patients ($P < 0.001$) and related to severity of liver impairment.

CONCLUSION: These findings suggest that the determination of serum ICAM-1 can be considered as an additional useful marker of hepatocellular necrosis and inflammatory activity in chronic hepatitis, while serum VCAM-1 is an indicator of liver fibrogenesis and severity of disease in cirrhosis.

INTRODUCTION

During inflammation, cytokines enhance the presentation on cell endothelial surface of adhesion molecules, which interact with corresponding leukocyte receptors and promote their adhesion and migration from the circulation to target site^[1].

Intercellular adhesion molecule-1 (ICAM-1) and vascular cellular adhesion molecule-1 (VCAM-1), are single-chain membrane-bound glycoproteins, belonging to the immunoglobulin supergene family. They are expressed on endothelial and other cells and play a crucial role in the trans-migration of inflammatory cells^[2,3].

Cellular expression is associated to the release of soluble forms (sICAM-1 and sVCAM-1) which are detectable in the peripheral blood^[4,5].

Although the biological function of these soluble forms are not clearly established yet, their increased serum concentration reflects cellular overexpression in inflammatory state^[6].

In patients with inflammatory diseases of the liver, increased sICAM-1 and sVCAM-1 values have been reported but their clinical usefulness is still controversial^[7-11].

Aim of the study was to investigate circulating ICAM-1 and VCAM-1 in patients affected by virus-related liver diseases, namely chronic active hepatitis (CH) and liver cirrhosis (LC), compared to healthy control subjects, to verify whether there are differences between these two molecules and to evaluate a possible correlation with severity of liver damage as clinically and histologically assessed.

MATERIALS AND METHODS

We examined three groups of subjects: 23 neodiagnosed and untreated patients with CH, 50 patients with LC and 15 control subjects.

All groups were comparable for sex and age.

Diagnosis, in patients, was based on clinical (medical history, physical examination), instrumental (ultrasonography,

endoscopy) and laboratory (liver function tests) data. In all patients with chronic hepatitis and in 24 cirrhotic subjects, diagnosis was confirmed by liver biopsy (in the remaining cirrhotic subjects the procedure was not necessary, as diagnosis was clinically evident).

Patients with evidence of other chronic or acute infective processes (altered white blood cells count, temperature, urinary tract infection, spontaneous bacterial peritonitis, airway infections) were excluded as well as those with suspected hepatocellular carcinoma (on the basis of ultrasonography, alpha-fetoprotein and carcinoembryonic antigen levels performed during the screening).

In 6 out of 23 CH patients, the etiological agent was HBV while in the remaining 17 hepatitis C virus (HCV). Of the 50 LC subjects, 19 were infected by HBV, and 31 by HCV.

All sections from liver biopsies were examined by a histopathologist who was unaware of the clinical details. With regard to histological findings, all patients with chronic hepatitis had none or mild fibrosis (staging score 0-1); according to grading score, they were classified into two groups: (a) 12 subjects with minimal or mild inflammatory activity (score 1-8); (b) 11 subjects with moderate or severe inflammatory activity (score 9-18).

As liver biopsy was not performed in all cirrhotics, we could not grade severity of histological picture in this group. For this reason we chose the Child-Pugh's classification^[12] to state the seriousness of liver impairment.

Twenty-three cirrhotic patients were in class B and 27 belonged to class C.

Informed consent was obtained for the whole study series and the study confirmed to Helsinki Declaration.

A blood sample was withdrawn, fasting in the morning, from all subjects. Sample was centrifugated and plasma was stored at -20 °C until determination.

Circulating ICAM-1 and VCAM-1 were assayed by EIA commercial kit (R&D System Co., Abington, UK), according to procedures described by the manufacturer and concentrations expressed as nanogram per milliliter. The sensitivity of sVCAM-1 assay was less than 2.0 ng/mL. Intra- and inter-assay variability averaged 4.3% and 8.5%, respectively. For sICAM-1 assay, the sensitivity was <0.35 ng/mL. Intra- and inter-assay variability averaged 4.0% and 7.0%, respectively.

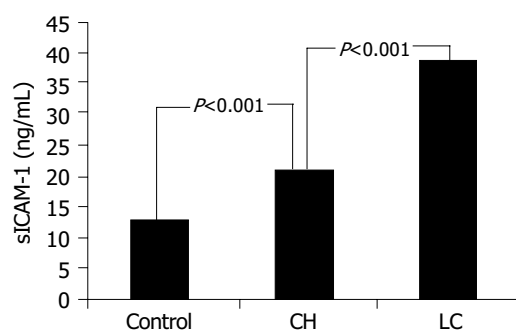


Figure 1 Mean sICAM-1 values in controls, patients affected by chronic hepatitis (CH) and cirrhotic subjects (LC).

In patients, alanine aminotransferase (ALT) and aspartate aminotransferase (AST) were also detected by autoanalyzer.

Analysis of variance and Kruskal-Wallis test were used to compare mean ± SD between various groups. Relationship between continuous variables was investigated by correlation test. Statistical significance was set at $P < 0.05$.

RESULTS

Mean ± SD. ICAM-1 was 12.92 ± 1.08 ng/mL in controls, 20.89 ± 6.42 ng/mL in CH patients and 38.56 ± 7.4 ng/mL in LC patients.

Mean ± SD. VCAM-1 was 15.96 ± 4.02 ng/mL in controls, 17.96 ± 8.43 ng/mL in CH patients and 42.29 ± 5.76 ng/mL in LC patients, respectively.

Mean ± SD. AST was 73.9 ± 9 U/L in CH patients and 62.7 ± 8.5 U/L in LC subjects.

ALT values averaged 84 ± 12 U/L in CH subjects and 58 ± 7.2 U/L in cirrhotic patients.

Statistical analysis showed that LC patients had significantly higher ICAM-1 values than CH patients ($P < 0.001$) and these ones had significantly higher values ($P < 0.001$) than controls (Figure 1). Among CH patients, a significant difference in serum was found between ICAM-1 with score 1-8 and those with score 9-18 (18.1 ± 4.9 ng/mL *vs* 23.5 ± 6.9 ng/mL, respectively; $P = 0.041$).

VCAM-1 values were significantly higher in LC patients than in CH subjects ($P < 0.001$) and controls ($P = 0.000$). There was no significant difference ($P > 0.05$) in VCAM-1 values between controls and CH patients and among these ones with regard to grading score (17.41 ± 8.3 ng/mL *vs* 18.13 ± 8.2 ng/mL; $P > 0.05$).

With regard to Child-Pugh classification, in cirrhotic patients there was no difference in ICAM-1 levels ($P > 0.05$) between class B (37.7 ± 6.1 ng/mL) and class C (40.2 ± 4.3 ng/mL) subjects; circulating VCAM-1 was significantly higher ($P = 0.005$) in class C (43.6 ± 4.1 ng/mL) than in class B (40.5 ± 3.1 ng/mL) patients.

Correlation test showed a significant relationship ($r = 0.77$; $P < 0.001$) between ICAM-1 and ALT values in CH patients (Figure 2). No significant correlation was found between ICAM-1 and AST values in CH patients, as well as between VCAM-1 concentration and ALT and AST values both in CH and in LC patients.

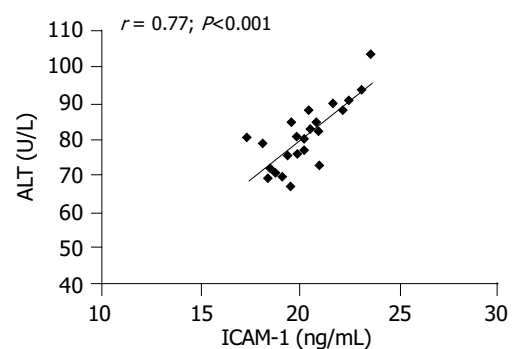


Figure 2 Relationship between ALT and sICAM-1 values in patients with chronic hepatitis.

Main characteristics and findings of our investigated patients are summarized in Table 1.

Table 1 Main characteristics and results of our investigated subjects

	Controls, n = 15	CH patients, n = 23	LC patients, n = 50
Mean age±SD	57.4± 4.1 yr	58.2±5.1 yr	61.1±8.3 yr
Males	8	13	29
Females	7	10	21
ALT (mean±SD)		84±12 U/L	58±7.2 U/L
AST (mean±SD)		73.9±9 U/L	67.2±8.5 U/L
ICAM-1 (mean±SD)	12.92±1.08 ng/mL	20.89±6.42 ng/mL (score 1-8) 18.1±4.9 (score 9-18) 23.5±6.9	38.56±7.4 ng/mL Child B 37.7±6.1 Child C 40.2±4.3
VCAM-1 (mean±SD)	15.96±4.02 ng/mL	17.96±8.43 ng/mL (score 1-8) 17.41±8.3 (score 9-18) 18.13±8.2	42.29±5.76 ng/mL Child B 40.5±3.1 Child C 43.6±4.1

DISCUSSION

Increased serum ICAM-1 and VCAM-1 have been previously described in patients with liver diseases, but such increase does not seem to be able to distinguish among various etiologies and its clinical significance is still controversial.

Some authors reported that circulating levels of these molecules are related to degree of inflammatory activity and to histological score, suggesting a putative role in monitoring the follow-up^[13,14]. Others have declared that their measurement adds little to the information provided by traditional biochemistry^[15].

Recently, it has been reported that treatment with alpha-interferon, in chronic hepatitis, is capable to decrease circulating ICAM-1 in responder but not in non-responder patients, while VCAM-1 does not differentiate between these two groups^[11,16,17].

Our results show that, in patients affected by chronic hepatitis, serum ICAM-1 is increased and mean values in subjects with moderate or severe inflammation (score 9-18) are significantly higher ($P<0.05$) than in those with minimal or mild inflammation (score 1-8).

Conversely, in this group, serum VCAM-1 was similar to controls and no difference was observed with regard to inflammatory activity.

Moreover, we found a significant positive correlation between ICAM-1 and ALT values.

Then, our findings appear in agreement with literature data and suggest that ICAM-1, but not VCAM-1, can be considered, in subjects with chronic hepatitis, a useful marker to assess severity of inflammation and hepatocellular necrosis.

Nevertheless, the relationship between ICAM-1 and ALT values does not implicate a direct involvement of this adhesion molecule in physiopathology of hepatocellular damage but it could only reflect the activation of undergoing immunological mechanisms.

Elevated serum VCAM-1 in chronic hepatitis have been reported by some authors^[16,18], but we found enhanced levels only in cirrhosis, when fibrosis progresses to an irreversible state.

This discordance is likely due to the selection of patients.

Notably, our CH patients had none or mild fibrosis (staging score 0-1). Therefore, we cannot exclude that subjects with chronic hepatitis and more severe fibrosis have increased sVCAM-1.

On the other hand, in cirrhotic patients, both circulating ICAM-1 and VCAM-1 were higher than in CH patients and controls. However, in this group, neither ICAM-1 nor VCAM-1 values correlated to AST and ALT levels.

In advanced phases of evolving liver diseases, the formation of fibrous tissue, stimulated by chronic inflammation, can be predominant on cellular necrosis, leading to structural alterations of hepatic architecture and development of cirrhosis.

In fact, our cirrhotic patients had lower transaminases values than subjects affected by chronic hepatitis.

In these conditions, increased ICAM-1 likely reflects the persistence of inflammation rather than severity of cellular necrosis. This could explain the lack of correlation between serum ICAM-1 and transaminases values in cirrhotic patients.

Interestingly, in our experience, no overlapping resulted in VCAM-1 values between LC and CH patients because the lowest value in LC group was greater than highest value in CH group (Figure 3). Furthermore, mean serum ICAM-1 was similar in classes B and C cirrhotic subjects while in the last ones mean VCAM-1 value was higher than in class B patients ($43.6±4.1$ ng/mL *vs* $40.5±3.1$ ng/mL; $P = 0.005$).

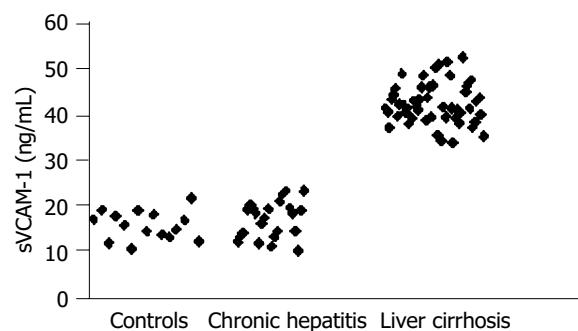


Figure 3 Scatter plot of sVCAM-1 values in controls, chronic hepatitis and liver cirrhosis.

Therefore, cirrhotic subjects with disease in a more advanced phase, belonging to Child-Pugh class C, had a greater VCAM-1 increase.

These findings, altogether considered, suggest the association of VCAM-1 levels to amount of liver fibrosis rather than to severity of inflammation and cellular necrosis.

However, the pathogenic link between VCAM-1 and liver fibrosis remains unclear.

In the liver, the formation of fibrous tissue depends upon the balance between matrix synthesis and its removal. Extra-cellular matrix production and degradation is a complex process involving cells, cytokines and proteinases. The interaction between membrane receptors of stellate cells (also called Ito cells) and proteins, included in the

extra-cellular matrix, is modulated by adhesion molecules. Such interaction determines its effects through cytoplasmic signaling pathways which can influence collagen synthesis and metalloprotease activity, resulting in a raised production and/or a reduced removal of hepatic connective tissue.

Thus, a role in this process can be supposed even though, to date, the expression of VCAM-1 on stellate cell surface has not been demonstrated.

Alternatively, enhanced VCAM-1 values could be the consequence of persistent activation of vascular endothelial cells which are able to produce connective tissue growth factor, a highly profibrogenic molecule involved in several fibrotic disorders, including those of the liver^[9].

Activated endothelial cells may also contribute, by expressing *de novo* integrins in the space of Disse, to the formation of a pathological basement membrane in the capillarized sinusoids of cirrhotic liver^[20].

Even though further investigations are required, from a clinical overview, the serial determination of serum VCAM-1 could be useful to weigh intensity of fibrogenesis and to identify the switch from prevalence of necro-inflammation to prevalence of sclerofibrotic processes, marked by an accentuated increase of values.

In conclusion, our results confirm that, in patients with chronic virus hepatitis, serum ICAM-1 is increased and related to severity of necro-inflammation as assessed by biochemistry and histological score. In cirrhotic patients, ICAM-1 is also augmented but it is not related to transaminase values. Circulating VCAM-1 is increased in cirrhosis and appears related to seriousness of liver impairment.

These findings suggest that serum ICAM-1 is an additional useful marker of cytonecrotic activity in chronic hepatitis. Serum VCAM-1 could be instead considered as a noninvasive indicator of liver fibrosis and severity of disease in cirrhosis.

REFERENCES

- 1 **Springer TA.** Adhesion receptors of the immune system. *Nature* 1990; **346**: 425-434
- 2 **Volpes R, Van den Oord JJ, Desmet VJ.** Immunohistochemical study of adhesion molecules in liver inflammation. *Hepatology* 1990; **12**: 59-65
- 3 **Garcia-Monzon C, Sanchez-Madrid F, Garcia-Buey L, Garcia-Arroyo A, Garcia-Sanchez A, Moreno-Otero R.** Vascular adhesion molecule expression in viral chronic hepatitis: evidence of neoangiogenesis in portal tracts. *Gastroenterology* 1995; **108**: 231-241
- 4 **Rothlein R, Mainolfi E, Czajkowski M, Marlin SD.** A form of circulating ICAM-1 in human serum. *J Immunol* 1991; **1**: 147: 3788-3793
- 5 **Pigott R, Dillon LP, Hemingway IH, Gearing AJH.** Soluble forms of E-selectin, ICAM-1 and VCAM-1 are present in the supernatants of cytokine activated cultured endothelial cells. *Biochem Biophys Res Commun* 1992; **187**: 584-589
- 6 **Gearing AJ, Newman W.** Circulating adhesion molecules in disease. *Immunol Today* 1993; **14**: 506-512
- 7 **Giron-Gonzalez JA, Rodriguez-Ramos C, Elvira J, Galan F, Del Alamo CF, Diaz F, Martin-Herrera L.** Serial analysis of serum and ascitic fluid levels of soluble adhesion molecules and chemokines in patients with spontaneous bacterial peritonitis. *Clin Exp Immunol* 2001; **123**: 56-61
- 8 **Thomson AW, Satoh S, Nussler AK, Tamura K, Woo J, Gavaler J, van Thiel DH.** Circulating intercellular adhesion molecule-1 (ICAM-1) in autoimmune liver disease and evidence for the production of ICAM-1 by cytokine-stimulated human hepatocytes. *Clin Exp Immunol* 1994; **95**: 83-90
- 9 **Tortorella C, Sacco R, Orlando P, Salerno MT, Schiraldi O, Antonaci S.** sICAM-1, sCD95 and sCD95L levels in chronic liver diseases of different etiology. *Immunopharmacol Immunotoxicol* 2000; **22**: 19-33
- 10 **de Caestecker JS.** Bile acid therapy and markers of immune-mediated damage in primary biliary cirrhosis. *Eur J Gastroenterol Hepatol* 1997; **9**: 145-147
- 11 **Granot E, Shouval D, Ashur Y.** Cell adhesion molecules and hyaluronic acid as markers of inflammation, fibrosis and response to antiviral therapy in chronic hepatitis C patients. *Mediators Inflamm* 2001; **10**: 253-258
- 12 **Pugh RNH, Murray-Lyon IM, Dawson JL, Pietrosi MC, Williams R.** Transection of the esophagus for bleeding esophageal varices. *Br J Surg* 1973; **60**: 646
- 13 **Douds AC, Lim AG, Jazrawi RP, Finlayson C, Maxwell DJ.** Serum intercellular adhesion molecule-1 in alcoholic liver disease and its relationship with histological disease severity. *J Hepatol* 1997; **26**: 280-286
- 14 **Lo Iacono O, Garcia-Monzon C, Almasio P, Garcia-Buey L, Craxi A, Moreno-Otero R.** Soluble adhesion molecules correlate with liver inflammation and fibrosis in chronic hepatitis C treated with interferon- α . *Aliment Pharmacol Ther* 1998; **12**: 1091-1099
- 15 **Falletti E, Pirisi M, Fabris C, Bortolotti N, Soardo G, Gonano F, Batoli E.** Circulating standard CD44 isoform in patients with liver disease: relationship with other soluble adhesion molecules and evaluation of diagnostic usefulness. *Clinical Biochemistry* 1997; **30**: 69-73
- 16 **Dejica D, Grigorescu M, Dejica V, Radu C, Neculoiu D.** Serum levels of soluble intercellular-1 and vascular cell-1 adhesion molecules in chronic hepatitis C and the influence of interferon- α + ribavirin therapy. *Rom J Gastroenterol* 2002; **11**: 277-283
- 17 **Radu C, Dejica D, Grigorescu M, Zaharie T, Neculoiu D.** Correlation of sICAM-1 and sVCAM-1 level with biochemical, histological and viral findings in chronic hepatitis C after interferon- α + ribavirin therapy. *Rom J Gastroenterol* 2003; **12**: 91-95
- 18 **Kaplanski G, Farnarier C, Payan MJ, Bongrand P, Durand JM.** Increased levels of soluble adhesion molecules in the serum of patients with hepatitis C. Correlation with cytokine concentrations and liver inflammation and fibrosis. *Dig Dis Sci* 1997; **42**: 2277-2284
- 19 **Rachfal AW, Brigstock DR.** Connective tissue growth factor (CTGF/CCN2) in hepatic fibrosis. *Hepatology* 2003; **26**: 1-9
- 20 **Quondamatteo F, Kempkensteffen C, Miosge N, Sonnenberg A, Herken R.** Ultrastructural localization of integrin subunits α 3 and α 6 in capillarized sinusoids of the human cirrhotic liver. *Histol Histopathol* 2004; **19**: 799-806

Acute upper gastrointestinal bleeding in operated stomach: Outcome of 105 cases

Vassiliki N Nikolopoulou, Konstantinos C Thomopoulos, George I Theocharis, Vassiliki A Arvaniti, Constantine E Vagianos

Vassiliki N Nikolopoulou, Konstantinos C Thomopoulos, George I Theocharis, Vassiliki A Arvaniti, Division of Gastroenterology, Department of Internal Medicine, University Hospital, Patras, Greece

Constantine E Vagianos, Department of Surgery, University Hospital, Patras, Greece

Correspondence to: Vassiliki N Nikolopoulou, Associate Professor of Medicine, University of Patras, Medical School, PO Box 1045, Patras 26110, Greece. bnikolop@med.upatras.gr

Fax: +30-261-0993982

Received: 2004-05-25 Accepted: 2004-07-27

Key words: Operated stomach; Active bleeding; Endoscopic hemostasis

Nikolopoulou VN, Thomopoulos KC, Theocharis GI, Arvaniti VA, Vagianos CE. Acute upper gastrointestinal bleeding in operated stomach: Outcome of 105 cases. *World J Gastroenterol* 2005; 11(29): 4570-4573

<http://www.wjgnet.com/1007-9327/11/4570.asp>

Abstract

AIM: To compare the causes and clinical outcome of patients with acute upper gastrointestinal bleeding (AUGB) and a history of gastric surgery to those with AUGB but without a history of gastric surgery in the past.

METHODS: The causes and clinical outcome were compared between 105 patients with AUGB and a history of gastric surgery, and 608 patients with AUGB but without a history of gastric surgery.

RESULTS: Patients who underwent gastric surgery in the past were older (mean age: 68.1 ± 11.7 years vs 62.8 ± 17.8 years, $P = 0.001$), and the most common cause of bleeding was marginal ulcer in 63 patients (60%). No identifiable source of bleeding could be found in 22 patients (20.9%) compared to 42/608 (6.9%) in patients without a history of gastric surgery ($P = 0.003$). Endoscopic hemostasis was permanently successful in 26 out of 35 patients (74.3%) with peptic ulcers and active bleeding or non-bleeding visible vessel. Nine patients (8.6%) were operated due to continuing or recurrent bleeding, compared to 23/608 (3.8%) in the group of patients without gastric surgery in the past ($P = 0.028$). Especially in peptic ulcer bleeding patients, emergency surgery was more common in the group of patients with gastric surgery in the past [9/73 (12.3%) vs 19/360 (5.3%), $P = 0.025$]. Moreover surgically treated patients in the past required more blood transfusion (3.3 ± 4.0 vs 1.5 ± 1.7 , $P = 0.0001$) and longer hospitalization time (8.6 ± 4.0 vs 6.9 ± 4.9 d, $P = 0.001$) than patients without a history of gastric surgery. Mortality was not different between the two groups [4/105 (3.8%) vs 19/608 (3.1%)].

CONCLUSION: Upper gastrointestinal bleeding seems to be more severe in surgically treated patients than in non-operated patients.

INTRODUCTION

Surgical management of peptic ulcer diseases has steadily decreased over the past 20 years. Several therapeutic improvements, such as the widespread use of acid suppressive drugs and the eradication of *Helicobacter pylori*, are responsible for this decrease^[1-3]. Upper gastrointestinal bleeding, however, remains a common emergency situation presenting a high rate of morbidity and mortality^[4-6]. This, despite the introduction and wide application of endoscopic hemostasis, has significantly reduced the need for emergency surgical hemostasis and improved the mortality and morbidity in these patients^[7-11]. High or subtotal gastrectomy and antrectomy supplemented with vagotomy have been successfully applied in the past to the treatment of bleeding peptic ulcer. Anastomotic ulcer is a post-gastrectomy complication and bleeding of such an ulcer is a particularly frightening complication. Several factors mainly related to surgical inadequacies or uncommonly to the presence of ectopic hormone-producing tumors, are associated with the formation of an anastomotic ulcer after gastric surgery^[12,13]. Few reports are available on the role of endoscopic hemostasis in active ulcer bleeding.

The purpose of this study was to compare the outcome between patients with a history of gastric surgery and active bleeding anastomotic ulcers and those with active upper gastrointestinal bleeding but without gastric surgery in the past.

MATERIALS AND METHODS

During the last 5 years, 105 patients with a history of gastric surgery and active upper gastrointestinal bleeding (AUGB) were admitted to our hospital. The outcome of this group of patients was compared to 608 patients with AUGB but without a history of gastric surgery. No patient was excluded because of age or concurrent diseases. Patients presented with hematemesis and/or melena, as well other clinical or laboratory evidence of acute blood loss, and those with iron deficiency anemia and history of gastric surgery who reported melena and/or hematemesis were included in this

study. All patients underwent emergency endoscopy either during the first 24 h after admission or immediately after resuscitation in case of massive bleeding. Three senior gastroenterologists performed all endoscopic examinations. Pre-medication included local pharyngeal anesthesia with xylocaine spray. Stigmata of active or recent bleeding were classified according to the Forrest classification^[14]: Forrest Ia: active spurting bleeding; Ib: active oozing bleeding; IIa: non-bleeding visible vessel (NBVV); IIb: adherent clot; and IIc: spots. A NBVV was defined as a raised, red spot resistant to washing. Endoscopic injection hemostasis with adrenaline diluted at 1:10 000 in 0.9% saline (A/S) and/or endoclips were performed on all patients with active spurting or oozing bleeding or NBVV.

Endoscopic A/S hemostatic injections were performed via the working channel of an endoscope using a disposable injector. The injections were administered into the ulcer base in a circumferential fashion as close as possible to the visible vessel. As a routine, a total of 15 mL was injected, approaching to 30 mL was injected when control of bleeding was not easily achieved. Marginal ulcer was defined as the recurrent ulceration at or around the gastro-jejunal stoma or within the afferent or efferent loop.

After endoscopic hemostasis, patients were carefully observed and managed by the same medical team of gastroenterologists and surgeons. Blood pressure and pulse rate were checked before endoscopy, during and after injection therapy. After hemostasis, all patients with peptic ulcer bleeding routinely received intravenously the standard doses of proton pump inhibitors (omeprazole 40 mg/d). Blood transfusion was given, if Hb was less than 100 g/L and if there were signs of ongoing bleeding. After early stabilization of the patients, recurrence of bleeding was considered when vomiting of fresh blood and signs of massive melena were found in conjunction with either shock or decrease in hemoglobin concentration by at least 20 g/L over a 24-h period. In case of re-bleeding, endoscopy was repeated and in most cases, a second endoscopic hemostasis either by A/S injection, or by placement of endoclips was carried out. Although the criteria for emergency surgical hemostasis were individualized, in most cases patients received emergency surgery when bleeding was not controlled after endoscopic hemostasis and transfusion of more than 5 U of blood over a 24-h period or 12 U over 48 h, and when intra-hospital re-bleeding occurred while on sufficient medical treatment with hemodynamic evidence of shock (systolic pressure <100 mmHg, pulse rate >100/min).

After discharge, all patients were routinely followed up. A second endoscopy with biopsies was performed after 4-6 wk and if the ulcer was completely healed, a third endoscopy was performed after 1 year.

The patient's age, sex, type of gastric operation, previous consumption of non-steroidal anti-inflammatory drugs (NSAIDs), clinical presentation, initial hemodynamic status, hemoglobin at admission, endoscopic findings, number of blood transfusions, days of hospital stay and clinical outcome were also analyzed.

Differences between groups were tested for significance. Continuous variables were expressed as mean±SD and compared using Student's *t* test. Categorical variables were

expressed as percentages and compared using χ^2 test. A *P* value less than 0.05 was considered statistically significant. Statistical analysis was performed using SPSS version 10.0 for Windows.

RESULTS

A total of 105 patients (96 men and 9 women, mean age 68.1±11.7 years) with a history of gastric surgery were admitted to our hospital due to AUGB. The investigated parameters in this patient group were compared to those in the well-matching group of patients with AUGB but without gastric surgery in the past and the cause of bleeding was due to a benign peptic ulcer. Table 1 provides an overview of the clinical characteristics and emergency endoscopic findings in both patient groups. A marginal ulcer with endoscopic stigmata of hemorrhage was identified in 63 patients (60%) in the first group. Endoscopy failed to show any source of bleeding in 22 patients (21%) and none of these patients received a new surgical intervention for severe bleeding. Spurting bleeding was identified in 10 (13.7%), oozing bleeding in 7 (9.6%) and NBVV in 18 (24.6%) patients (Table 2). Endoscopic hemostasis was permanently successful in 26 out of 35 (74.3%) patients. Twelve patients underwent a second endoscopic hemostasis with injection of A/S and/or endoclips because of re-bleeding while four patients with re-bleeding did not undergo second endoscopic injection therapy or any other hemostatic treatment. Emergency surgical hemostasis for persistent or recurrent bleeding was required in 9 out of 105 patients (8.6%) and in 9 out of 73 patients (12.3%) with peptic ulcer bleeding (Table 3). Four patients died (3.8%), two of them died after surgery with a post-surgical mortality of 22.9%. Causes of death were respiratory failure (*n* = 2, one of them preoperatively), cerebral ischemia (*n* = 1, the patient died post-operatively) and hemorrhagic shock (*n* = 1, the patient died pre-operatively).

Table 1 Characteristics of patients recruited in the study

	Gastric surgery in the past <i>n</i> = 105 group A, <i>n</i> (%)	No surgery in the past <i>n</i> = 608 group B, <i>n</i> (%)	<i>P</i>
Age (yr)	68.1±11.7	62.8±17.8	0.001
Sex: men/women	96/9	470/138	0.0009
NSAIDs	41/105	398/608	<0.0001
Ht at admission (%)	27.9±6.5	26.9±7.8	NS
Gastric ulcers	0	141 (23.1)	
Duodenal ulcers	9 (8.6)	215 (35.3)	0.00019
Marginal ulcers	63 (60)	0	
Dieulafoy's ulcers	1 (1)	4 (0.7)	NS
Varices	1 (1)	83 (13.7)	
Mallory-Weiss	1 (1)	31 (5.1)	
Esophagitis	1 (1)	8 (1.3)	
Gastric cancer	3 (2.9)	18 (2.9)	NS
Erosions	1 (1)	46 (7.5)	
None	22 (20.9)	42 (6.9)	0.0003
Other	1 (2)	5 (0.8)	
Non-cooperative	1 (1)	15 (2.5)	

When the results of patients with a history of gastric surgery were compared with those patients who had no

gastric surgery, there was a statistically significant difference in age, consumption of NSAIDs, number of blood transfusions, length of hospital stay, percentage of patients with spurting bleeding and need for surgical intervention (Tables 1-3). In the control group, endoscopy failed to show any source of bleeding in 42 (6.9%) patients ($P = 0.0003$). Similarly in the control group, the re-bleeding/continued bleeding rate and the mortality rate did not differ statistically from the patients who had gastric surgery in the past. Nineteen patients in the control group (3.1%) died after surgery.

Table 2 Endoscopic stigmata of the patients with bleeding peptic ulcers

	Patients with gastric surgery in the past and benign ulcers <i>n</i> = 73/105, <i>n</i> (%)	Patients without surgery in the past and benign ulcers <i>n</i> = 360/608, <i>n</i> (%)	<i>P</i>
Forrest Ia	10 (13.7)	30 (8.3)	NS
Forrest Ib	7 (9.6)	32 (8.8)	NS
Forrest IIa	18 (24.6)	63 (18.6)	NS
Forrest IIb	8 (11.0)	38 (10.5)	NS
Forrest IIc	3 (4.1)	41 (11.3)	NS
Forrest III	27 (36.9)	152 (42.2)	NS

Table 3 Outcome of patients recruited in the study

	Patients with surgery in the past total <i>n</i> = 105 benign ulcers <i>n</i> = 73	Patients without surgery in the past total <i>n</i> = 608 benign ulcers <i>n</i> = 360	<i>P</i>
Blood transfusions	3.3±4.0	1.5±1.7	0.0001
Hospital d	8.57±4	6.86±4.75	0.001
Re-bleeding	13/105	66/608	NS
Emergency surgery (overall), <i>n</i> (%)	9/105 (8.6)	23/608 (3.8)	0.028
Emergency surgery, <i>n</i> (%) (peptic ulcers)	9/73 (12.3)	19/360 (5.3)	0.025
Duodenal ulcers	1	11	
Gastric ulcers	-	7	
Marginal ulcers	7	-	
Dieulafoy's ulcers	1	1	
Mortality (overall), <i>n</i> (%)	4/105 (3.8)	19/608 (3.1)	NS
Post-surgical mortality, <i>n</i> (%)	2/9 (22.2)	6/23 (26)	NS

DISCUSSION

Gastric surgery has been successfully used in the treatment of peptic ulcer disease; however, the potential complications after gastric surgery are numerous^[15,16]. Ulcer recurrence rate after surgery for peptic ulcer diseases varies according to the nature of the procedure, pathophysiology of the underlying disease, and operator's skill. One of the major complications is bleeding from marginal ulcers^[17,18]. Recurrent ulcers after Billroth II gastrectomy may result in retained antral mucosa in the closed duodenal stump, which can be a source of hypergastrinemia. In patients after vagotomy and pyloroplasty, a recurrent ulcer may be due to an incomplete vagotomy^[19-25].

In this study, recurrent ulcers were found in 70% of patients with AUGB after gastric surgery. Marginal ulcer was detected in 63% of patients, while recurrent duodenal

ulcer was found in 8.6%. All patients with recurrent duodenal ulcers underwent pyloroplasty and elective vagotomy. Two patients in the group had Dieulafoy's ulcer. The majority were male and elderly patients. It is well known that patients after partial gastrectomy are at high risk of developing adenocarcinoma^[26,27]. In our study, three patients (2.9%) after Billroth II gastrectomy were proved to have adenocarcinoma in the anastomotic area. In patients who had gastric surgery in the past, diagnostic failure at emergency endoscopy for AUGB occurred in 22 patients (21%), and 18 of them underwent a new endoscopy check after 24 h, though it failed to detect any lesions. These patients were admitted because of iron deficiency anemia and reported melena and/or hematemesis. None needed emergency surgical intervention. An explanation for this high incidence of missed lesions at the emergency endoscopy stage is that the presumed lesions are superficial and they heal quickly. Anemia is a sequel of gastrectomy. AUGB was not found in 42 (6.9%) of the control group of patients. According to Cheng *et al.*^[27], peptic ulcers including marginal ulcer and Dieulafoy's lesions are the major missed diagnosis during AUGB. Limited endoscopic vision due to excessive blood and clots is a well-known problem which results in inadequate examination during AUGB.

When the two groups of patients were compared, the upper gastrointestinal bleeding seemed to be more severe in patients with a history of gastric surgery. The need for new surgical intervention was greater in this group. This may be due to the differences in blood supply in the anastomotic area. The marginal ulcer receives blood from the jejunal branches of the superior mesenteric artery or gastric branches of the celiac artery^[28]. In this study, the presence of a spurting artery was noted more in patients who had gastric surgery in the past. Similarly, the successful rate of endoscopic intervention was higher in the control group. In a previous study, we also found that an anastomotic ulcer is a factor associated with failure of endoscopic injection hemostasis in bleeding peptic ulcers^[29]. A new surgical intervention was required in 8.6% of patients after gastric surgery, compared to 3.8% of patients in the control group who underwent surgical hemostasis. Seven of the nine operated ulcers in the gastric surgery group were marginal ulcers and located mostly at the saddle area of the jejunal loop. The angulation phenomenon characterizing the saddle area makes it a weak point during food impulsion. Furthermore, it also receives the least supply of blood^[28]. Whether blood supply or other aggressive factors attribute to the development of resistant bleeding marginal ulcers needs to be confirmed. The mortality rate (overall and post-surgery) was the same in the two groups.

In conclusion, upper gastrointestinal bleeding in surgically treated patients seems to be more severe than that in non-operated patients. New surgical intervention is a significant challenge, not only because of the technical difficulties of a further operation, but also because of the requirement of a more radical procedure. More studies are required to confirm our findings.

REFERENCES

- Adkins RB Jr, De Lozier JB 3rd, Scott HW Jr, Sawyers JL. The

- management of gastric ulcers-a current review. *Ann Surg* 1985; **201**: 741-751
- 2 **Feldman M**, Burton M. Histamine 2-receptor antagonists. Standard therapy for acid-peptic diseases (second of two parts). *N Engl J Med* 1990; **323**: 1749-1755
 - 3 **Walan A**, Bader JP, Clasen M, Classen M, Lamers CB, Piper DW, Rutgersson K, Eriksson S. Effect of Omeprazole and ranitidine on ulcer healing and relapse rates in patients with benign gastric ulcer. *N Engl J Med* 1989; **320**: 69-75
 - 4 **Laine L**, Peterson WL. Bleeding peptic ulcer. *N Engl J Med* 1994; **331**: 717-727
 - 5 **Rockall TA**, Logan RF, Devlin HB, Northfield TC. Incidence of and mortality from acute upper gastrointestinal haemorrhage in the United Kingdom. Steering Committee and members of the National Audit of Acute Upper Gastrointestinal Haemorrhage. *Br Med J* 1995; **311**: 222-226
 - 6 **Turner IB**, Jones M, Piper DW. Factors influencing mortality from bleeding peptic ulcers. *Scand J Gastroenterol* 1991; **26**: 661-666
 - 7 **Rajgopal C**, Palmer KR. Endoscopic injection sclerosis: effective treatment for bleeding peptic ulcer. *Gut* 1991; **32**: 727-729
 - 8 **Meier R**, Wettstein A. Treatment of acute nonvariceal upper gastrointestinal hemorrhage. *Digestion* 1999; **60**(Suppl): 47-52
 - 9 **Thomopoulos K**, Nikolopoulou V, Katsakoulis E, Markou S. The effect of endoscopic therapy on the clinical outcome of patients with peptic ulcer bleeding. *Scand J Gastroenterol* 1997; **32**: 212-216
 - 10 **Holman RAE**, Davis M, Gough KR, Smith RB. Value of centralized approach in the management of haematemesis and melaena: experience in a distinct general hospital. *Gut* 1990; **31**: 504-508
 - 11 **Silverstein FE**, Gilbert DA, Tedesco FJ, Buenger NK, Persing J. The national ASGE survey on upper gastrointestinal bleeding. *Gastrointest Endosc* 1981; **27**: 80-93
 - 12 **Shin JS**, Chen KW, Lin XZ, Lin CY, Chang TT, Yang CC. Active, bleeding marginal ulcer of Billroth II gastric resection: A clinical experience of 18 patients. *AJG* 1994; **89**: 1831-1835
 - 13 **Bini E**, Unger J, Weinschel E. Outcomes of endoscopy in patients with iron deficiency anemia after Billroth II partial gastrectomy. *J Clin Gastroenterol* 2002; **34**: 421-426
 - 14 **Feldman M**, Richardson CT, Fordtran JS. Experience with sham feeding as a test for vagotomy. *Gastroenterology* 1980; **79**: 792-795
 - 15 **Forrest JA**, Finlayson NDC, Shearman DJC. Endoscopy in gastrointestinal bleeding. *Lancet* 1974; **2**: 394-397
 - 16 **Holscher AH**, Klingele C, Bollschweiler E, Schroder W, Siewert JR. Postoperative recurrent after gastric resection-results-surgical treatment. *Chirurg* 1996; **67**: 814-820
 - 17 **Printen KJ**, Scott D, Mason EE. Stomal ulcers after gastric bypass. *Arch Surg* 1980; **115**: 525-527
 - 18 **Braley SC**, Nguyen NT, Wolfe BM. Late gastrointestinal hemorrhage after gastric bypass. *Ober Surg* 2002; **12**: 404-407
 - 19 **Erdozain Sosa JC**, Guerrero Vega E, Martin-de-Argila C, Gonzalez Murillo M, Presa Valle M, Munoz Nunez F, Lizasoain Urkola J, Suarez de Parga J, Herrera Abian A, Molina Pere E. Upper digestive hemorrhage in the operated stomach (Billroth I and II): clinical course and prognosis. *Rev Esp Enferm Dig* 1994; **85**: 87-90
 - 20 **Emas S**, Grupcev G, Eriksson B. Ten-year follow-up of a prospective, randomized trial of selective proximal vagotomy with ulcer excision and partial gastrectomy with gastroduodenostomy for treating corpore gastric ulcer. *Am J Surg* 1994; **167**: 596-600
 - 21 **Ogoshi K**, Mitomi T. Recurrent peptic ulcer after surgery in Japan-a nationwide-questionnaire survey of 57 institutions. *Nippon Geka Gakkai Zasshi* 1992; **93**: 393-399
 - 22 **Touchet J**, Orsoni P, Caamano A, Picaud R. Treatment of recurrent ulcers after parietal cell vagotomy. Analysis of 18 cases. *Ann Chir* 1992; **46**: 570-577
 - 23 **Fukushima K**, Sasaki I, Naito H, Matsuno S. Long-term follow-up study after pylorus-preserving gastrectomy for gastric ulcer. *Nippon Geka Gakkai Zasshi* 1991; **92**: 401-410
 - 24 **Bretzke G**, List A. The site of recurrent ulcer following stomach surgery (Billroth I and II). *Z Gesamte Inn Med* 1990; **45**: 78-80
 - 25 **Terismet AC**, Giardiello FM, Tytgat GN, Offerhaus GJ. Carcinogenesis after remote peptic ulcer surgery: the long-term prognosis of partial gastrectomy. *Scand J Gastroenterol* 1995; **212**: 96-99
 - 26 **Greene FL**. Discovery of early gastric remnant carcinoma. Results of a 14-year endoscopic screening program. *Surg Endosc* 1995; **9**: 1199-1203
 - 27 **Cheng CL**, Lee CS, Chen PC, Wu CS. Overlooked lesions at emergency endoscopy for acute nonvariceal upper gastrointestinal bleeding. *Endoscopy* 2002; **34**: 527-530
 - 28 **Oglevie SB**, Smith DC, Mera SS. Bleeding marginal ulcers: angiographic evaluation. *Radiology* 1990; **174**: 943-944
 - 29 **Thomopoulos K**, Mitropoulos I, Katsakoulis E, Vagianos CE, Mimidis KP, Hatzigiriou MN, Nikolopoulou V. Factors associated with failure of endoscopic injection therapy in bleeding peptic ulcers. *Scand J Gastroenterol* 2001; **36**: 664-668

• BRIEF REPORTS •

Kinetics of phytohemagglutinin-induced IFN- γ and TNF- α expression in peripheral blood mononuclear cells from patients with chronic hepatitis B after liver transplantation

Ying-Mei Tang, Min-Hu Chen, Gui-Hua Chen, Chang-Jie Cai, Xiao-Shun He, Min-Giang Lu, Wei-Min Bao

Ying-Mei Tang, Min-Hu Chen, Department of Gastroenterology, the First Affiliated Hospital of Sun-Yat Sen University, Guangzhou 510080, Guangdong Province, China

Gui-Hua Chen, Chang-Jie Cai, Min-Giang Lu, Wei-Min Bao, Department of Liver Transplantation Center, the Third Affiliated Hospital of Sun-Yat Sen University, Guangzhou 510080, Guangdong Province, China

Xiao-Shun He, Department of Organ Transplantation, the First Affiliated Hospital of Sun-Yat Sen University, Guangzhou 510080, Guangdong Province, China

Supported by the Technology Program of Guangdong Province, No. 2004B35001001

Correspondence to: Dr. Min-Hu Chen, Department of Gastroenterology, the First Affiliated Hospital of Sun-Yat Sen University, 58, the Second Road of Zhongshan, Guangzhou 510080, Guangdong Province, China. chenminhu@vip.163.com

Telephone: +86-20-87332200-8172

Received: 2004-08-20 Accepted: 2004-11-24

copies/mL after OLT except for one with 5.72×10^6 copies/mL 4 wk after OLT who was diagnosed as HBV recurrence. The levels of INF- γ and TNF- α were lower in patients with a high HBV load than in those with a low HBV load (HBV DNA detected/undetected in PBMCs: INF- γ 138.08 ± 72.44 ng/L vs 164.24 ± 72.07 ng/L, $t = 1.065$, $P = 0.297 > 0.05$, TNF- α 80.75 ± 47.30 ng/L vs 74.10 ± 49.70 ng/L, $t = 0.407$, $P = 0.686 > 0.05$; HBV DNA positive/negative: INF- γ 136.77 ± 70.04 ng/L vs 175.27 ± 71.50 ng/L, $t = 1.702$, $P = 0.097 > 0.05$; TNF- α 75.37 ± 43.02 ng/L vs 81.53 ± 52.46 ng/L, $t = 0.402$, $P = 0.690 > 0.05$).

CONCLUSION: The yielding of INF- γ and TNF- α from PBMCs is inhibited significantly by immunosuppressive agents following OLT with HBV load increased, indicating that the impaired immunity of host is associated with HBV recurrence after OLT.

© 2005 The WJG Press and Elsevier Inc. All rights reserved.

Key words: Liver transplantation; HBV; Recurrence; PBMC

Tang YM, Chen MH, Chen GH, Cai CJ, He XS, Lu MG, Bao WM. Kinetics of phytohemagglutinin-induced IFN- γ and TNF- α expression in peripheral blood mononuclear cells from patients with chronic hepatitis B after liver transplantation. *World J Gastroenterol* 2005; 11(29): 4574-4578

<http://www.wjgnet.com/1007-9327/11/4574.asp>

Abstract

AIM: To study the association between host immunity and hepatitis B virus (HBV) recurrence after liver transplantation.

METHODS: Peripheral blood mononuclear cells (PBMC) were isolated from 40 patients with hepatitis B and underwent orthotopic liver transplantation (OLT) before and 2, 4, 8 wk after surgery. After being cultured *in vitro* for 72 h, the levels of INF- γ and TNF- α in culture supernatants were detected with ELISA. At the same time, the quantities of HBV DNA in serum and PBMCs were measured by real time PCR.

RESULTS: The levels of INF- γ and TNF- α in PBMC culture supernatants decreased before and 2, 4 wk after surgery in turns (INF- γ 155.52 ± 72.32 ng/L vs 14.76 ± 9.88 ng/L vs 13.22 ± 10.35 ng/L, $F = 6.946$, $P = 0.027 < 0.05$; TNF- α 80.839 ± 46.75 ng/L vs 18.59 ± 17.29 ng/L vs 9.758 ± 7.96 ng/L, $F = 22.61$, $P = 0.0001 < 0.05$). The levels of INF- γ and TNF- α were higher in groups with phytohemagglutinin (PHA) than in those without PHA before surgery. However, the difference disappeared following OLT. Furthermore, INF- γ and TNF- α could not be detected in most patients at wk 4 and none at wk 8 after OLT. The HBV detection rate and virus load in PBMC before and 2, 4 wk after surgery were fluctuated (HBV detected rate: 51.4%, 13.3%, 50% respectively; HBV DNA: 3.55 ± 0.674 log(10) copies/mL vs 3.00 ± 0.329 log(10) copies/mL vs 4.608 ± 1.344 log(10) copies/mL, $F = 7.582$, $P = 0.002 < 0.05$). HBV DNA in serum was 4.48 ± 1.463 log(10) copies/mL before surgery and $< 10^3$

INTRODUCTION

Liver transplantation is the most effective therapy for end-stage liver diseases. The recurrence of primary diseases becomes the main problem, which impedes the long-term survival rate of patients undergoing liver transplantation despite the improvements of surgery and the perioperative management. Chronic hepatitis B virus (HBV) infection is one of the most common diseases leading to a high morbidity and mortality in Asians. In China, there are more than 30 million people suffering from HBV infection. Despite anti-HBs immunoglobulin therapy, HBV infection recurs in a high proportion of patients with HBsAg positive and serum HBV DNA-negative, chronic liver disease after liver transplantation. Therefore, the recurrence of hepatitis B is the critical issue of liver transplantation in China^[1]. It was reported that host immunity is closely related with the prognosis of chronic and acute hepatitis B. Few HBV-specific T cells have been found in peripheral blood mononuclear

cells (PBMCs) of patients with chronic hepatitis B. Lymphocytes are infected with HBV^[2]. However, little is known about the immune condition of HBV-infected patients after orthotopic liver transplantation (OLT). After OLT, the HBV load decreases immediately and dramatically, but HBV hiding in extrahepatic tissues especially in PBMCs can infect the graft again^[3,4]. Since the function of PBMCs is an important indication of the host immunity status^[5], we investigated the function of PBMCs in producing INF- γ and TNF- α , and the association between host immunity and HBV recurrence after liver transplantation.

MATERIALS AND METHODS

Patients

A total of 40 patients with hepatic cirrhosis and hepatocellular carcinoma (HCC) who underwent liver transplantation at Sun-Yat Sen University, Guangzhou, from November 2003 to April 2004 were enrolled. Blood samples were obtained one day before and 2, 4 and 8 wk after surgery.

Immunosuppression consisted of tacrolimus-based/cyclosporin-based dual therapy with prednisolone. The doses were adjusted to maintain desired blood levels (5-15 $\mu\text{g/L}$ tacrolimus, 100-250 $\mu\text{g/L}$ cyclosporin) for the 1st year. Prednisolone was commenced at a daily dose of 60 mg, reduced by 8 mg every 4 d after the 2nd wk, and withdrawn completely at a median of 3 mo. mAbs were used for patients whose ascites >3 000 mL or serum Cr >132.6 $\mu\text{mol/L}$ or were used for those infected with bacteria within 2 wk before surgery. The protocol for prevention of HBV recurrence after liver transplantation was as follows: intra-operative administration of 400 IU hepatitis B immunoglobulin intramuscular injection during the an-hepatic phase, followed by 400 IU intramuscular injection for the first 14 postoperative days, then 400 IU every other day for 2 wk, followed by 400 IU once a week. Immunoprophylaxis was continued indefinitely with monthly administration of 400 IU of HBIg by intramuscular injection. All patients received HBIg and lamivudine (100 mg/d) immuno-noprophylaxis. HBV recurrence following liver transplantation was defined as the reappearance of HBsAg-HBV DNA in serum and/or positive staining for HBsAg on liver biopsy.

Isolation and culture of PBMCs

PBMCs isolated from heparinized venous blood by gradient centrifugation using Ficoll-Hypaque (Shenggong, Ltd, Shanghai, China) were suspended in RPMI-1640 supplemented with 10% heat-inactivated fetal calf serum (RPMI-1640/10% FCS) and penicillin-streptomycin (Sigma). A total of 2×10^6 PBMC were added to each well (48-well plates, Invitrogen, Carlsbad, CA, USA) for stimulation with or without 2 $\mu\text{g/L}$ of phytohemagglutinin (PHA-P, Atlanta, GA, USA) at 37 °C for 72 h. All supernatants were collected and stored at -20 °C until use.

Measurement of cytokine concentration by ELISA

Immunoreactive IFN- γ and TNF- α levels in PBMCs were quantified with human IFN- γ and TNF- α ELISA kits (U-CyTech, Dutch). Optical density was measured at 450 nm with a Bio-Rad 550 microplate reader (Bio-Rad Laboratories

Inc., Hercules, CA, USA). The cytokine concentration was estimated from the standard curve generated by a curve-fitting program. The minimum detectable IFN- γ and TNF- α concentration was 5.0 ng/L.

Quantification of HBV DNA using real-time PCR

HBV DNA was extracted from 200 μL of patient's sera according to the manufacturer's instructions. For total HBV quantification, PCR amplification was performed with a HBV DNA diagnostic kit (DaAn Gene Diagnostic Center, China) using ABI 7000HT sequence detection system. The PCR program consisted of an initial denaturation at 95 °C for 10 min, followed by 40 amplification cycles at 95 °C for 15 s and at 61.5 °C for 1 min.

Statistical analysis

All the data were analyzed with SPSS statistics software version 10.0. Repeated measures analysis of variance was used to measure IFN- γ and TNF- α levels at different time points. Independent sample *t* test was used to assess the differences between groups of various HBV load. $P < 0.05$ was considered statistically significant.

RESULTS

Demographic data of patients before surgery

The mean age of patients was 49.65 ± 9.06 years, the male and female ratio was 36:4, the positive and negative HBeAg ratio was 10:30, HBV DNA >1 000/<1 000 copies/mL was 21/19, Child-Pugh grade of hepatic function (A/B/C) was 12/11/27.

Kinetics of IFN- γ and TNF- α level in culture supernatants of PBMCs

The levels of INF- γ and TNF- α in PBMC culture supernatants decreased before and 2, 4 wk after operation in turn (INF- γ : 155.52 ± 72.32 ng/L *vs* 14.76 ± 9.88 ng/L *vs* 13.22 ± 10.35 ng/L, $P < 0.05$; TNF- α : 80.839 ± 46.75 ng/L *vs* 18.59 ± 17.29 ng/L *vs* 9.758 ± 7.96 ng/L, $P < 0.05$; Tables 1 and 2). The levels of INF- γ and TNF- α were higher in groups with PHA than in those without PHA. However, the difference disappeared following OLT. Furthermore, INF- γ and TNF- α could not be determined in most patients at wk 4 and none at wk 8 after OLT.

HBV DNA in serum before and after surgery

The level of HBV DNA was more than 10^3 copies/mL (2.75×10^3 - 6.95×10^7 copies/mL) in 52.5% (21/40) of patients before surgery. Almost all patients had an undetectable HBV DNA level (< 10^3 copies/mL), except for one patient who had a detectable HBV DNA level at wk 4 after surgery (5.72×10^6 copies/mL). Recurrence of hepatitis B was confirmed by an immunohistochemistry of liver biopsy in this patient.

HBV DNA in PBMCs

The HBV detectable rate and HBV DNA load in PBMCs before and 2, 4 wk after surgery fluctuated (HBV detectable rate: 51.4%, 13.3%, 50% respectively; HBV DNA: 3.55 ± 0.674 *vs* 3.00 ± 0.329 *vs* 4.608 ± 1.344 , $F = 7.582$, $P = 0.002$).

Table 1 IFN- γ levels in PBMC culture supernatants at different time points

Source	DF	SS	MS	F	P
Factor (pre-/2 wk/4 wk)	2	28 770.02	14 385.01	6.946	0.027
Factor treat	2	27 072.82	13 536.409	6.536	0.031
Error	6	12 425.41	2 070.902		
Treat (PHA+/-)	1	26 999.63	26 999.63	10.269	0.049
Partly factor	1	13 665.74	13 665.74	5.169	0.107

Table 2 TNF- α levels in PBMC culture supernatants at different time points

Source	DF	SS	MS	F	P
Factor (pre-/2 wk/4 wk)	1.233	32 186.69	26 113.60	22.612	0.0001
Factor treat	1.233	3 330.98	2 702.48	2.340	0.1350
Error	38	27 045.63	1 154.87		
Treat (PHA+/-)	1	2 363.206	2 363.21	3.192	0.0900
Partly factor	1	62 804.36	62 804.36	84.833	0.0001

Table 3 HBV DNA in serum and PBMCs (mean \pm SD)

		IFN- γ (ng/L)	t	P	TNF- α (ng/L)	t	P
HBV DNA in PBMCs	Detected	138.08 \pm 72.44	1.065	0.297	80.75 \pm 47.30	0.407	0.686
	Undetected	164.24 \pm 72.07			74.10 \pm 49.70		
HBV DNA in serum (copies/mL)	>1 000	136.77 \pm 70.04	1.702	0.097	75.37 \pm 43.02	0.402	0.690
	<1 000	175.27 \pm 71.50			81.53 \pm 52.46		

Effect of HBV DNA on IFN- γ and TNF- α level and PBMC culture supernatants

According to the HBV DNA level in serum and PBMCs before surgery, patients were divided into four groups. HBV DNA was >1 000 and <1 000 copies/mL in two groups respectively. HBV DNA was detected and undetected in the other two groups. Comparing the IFN- γ and TNF- α levels in various groups, we found that the HBV DNA level was higher, the cytokine level was lower (Table 3).

DISCUSSION

Several studies showed that the following factors influence the HBV recurrence after OLT^[6-11]: the HBV infection before surgery, the administration of immunosuppressive agents, the HBV level in extrahepatic tissues and the genotype of HBV. It is generally accepted that patients with active replication of HBV before the surgery and on high dose immunosuppressive agents are easier to be reinfected. In addition, the infection of PBMC might lead to the selection of HBV variants which contribute to immunologic escaping^[4]. Previous studies showed that the pattern of cytokines produced by circulating PBMCs from patients underwent OLT would determine the immunologic state of transplanted allograft^[12]. However, the function of PBMCs of HBV-infected patients who underwent OLT is still unclear.

Cytokines play an important role in antiviral immunity. After infecting the host cells, HBV is eliminated by the host immune system through two pathways^[13,14]. One is the cytolytic pathway characterized by activated HBV-specific T cells, mediating the effect of cellular cytotoxicity and lysis of HBV-infected cells. The other is mediated by

cytokines, especially by IFN- γ and TNF- α , which depress the replication and expression of HBV, degrade HBV^[15-17]. Recently, evidence supports that the non-cytolytic immune-mediated pathway is the principal way to eliminate viruses. Since the function of PBMCs reflects the host immunity to HBV^[18], it is useful to evaluate the graft immunity state and the change of host anti-viral immunity through monitoring the function of PBMCs in producing IFN- γ and TNF- α post OLT.

In our study, the levels of IFN- γ and TNF- α in PBMCs culture supernatants decreased dramatically post operation, consistent with literature reports, 50% cytokine reduction under clinical dose of CsA and FK506^[19]. Other reports showed that the TNF- α plasma level increased in the 1st wk post OLT^[20]. However, we did not detect the cytokine plasma concentrations. Since liver transplantation may lead to changes in the metabolic activity of neutrophils, it is necessary to perform further detailed study about IFN- γ and TNF- α plasma levels.

We also found that there were no differences between the groups with and without PHA, suggesting that PBMCs do not respond to the stimulation of PHA. On the contrary, in Chen's study^[12], the increased IFN- α mRNA expression after stimulated by PHA was reported. TNF- α expression induced by PHA in PBMC was higher in patients with an acute rejection episode. There are several underlined reasons that contributed to the difference between the two studies: first, the patients enrolled in Chen's study had previous rejection episodes, while in our study none had rejection. Second, in China, most patients who underwent OLT had serious complications and the human mAb of Tac was given to inhibit and then impair the function of T cells completely. Third, FK506 is preferred in our immunosuppressive

protocol. Sakuma *et al.*^[21], found that compared with CsA and DEX, FK506 may be most effective in specifically preventing T cell activation mediated inflammatory cytokine production in a clinic setting. We are not clear which immunosuppressive agents were favored in Chen's study.

The present study showed no differences between the groups with and without PHA. It may be because the multi-immunosuppressive agents downregulated the receptors on T cells and fewer signals were transmitted into the cells. However, the function of T cells was partially suppressed in this period and produced cytokines. In clinic, acute rejection occurs within 1 mo and more frequently within 2 wk after surgery^[22], indicating that the cell-mediated immunity is partially depressed during this period. At the same time, HBV DNA in PBMCs decreases, suggesting that it was a relatively safe period to avoid HBV reinfection. Four weeks following surgery, cytokines in culture supernatants cannot be detected in most patients. This may be explained by the following reasons. Firstly, immunosuppressive agents block the activation and proliferation of T cell and the production of cytokines are suppressed. Secondly, these patients are at high risk before surgery and human monoclonal antibody of Tac is given during and 2, 5 d after surgery. Thirdly, lymphocytes die following activation. Therefore, the suppression of T cells is reinforced. In our study, one case of hepatitis B recurrence was found 4 wk after surgery. We suggested that the following reasons contributed. The anti-virus capability was the lowest at this time, the HBV replication was accelerated and the host immunity of anti-virus was impaired. Eight weeks following OLT, no cytokines could be detected in PBMC culture supernatants, indicating that the function of lymphocytes is depressed completely. At the same time, the detectable rate of HBV DNA in PBMCs increased, and the virus load in PBMCs was near to that before surgery.

The HBV DNA level in serum affects the cytokine level in PBMCs. Higher HBV DNA would inhibit the production of IFN- γ induced by IL-12 in chronic hepatitis B patients^[23]. The reduction of virus load and antigen would repair the response function of cytotoxic T lymphocytes^[24,25]. We also found that the IFN- γ and TNF- α level would likely decrease when HBV DNA level increased.

In conclusion, the yielding of IFN- γ and TNF- α from PBMCs is inhibited significantly by immunosuppressive agents following OLT with HBV load increased, indicating that the impaired immunity of host is associated with HBV recurrence after OLT.

ACKNOWLEDGMENTS

The authors thank Chang-You Wu for valuable advice and Nian-Qiang Feng for assistance with the experiment.

REFERENCES

- 1 Wu J, Zheng SS. Liver transplantation in China: problems and their solutions. *Hepatobiliary Pancreat Dis Int* 2004; **3**: 170-174
- 2 Trippler M, Meyer zum Buschenfelde KH, Gerken G. HBV viral load within subpopulations of peripheral blood mononuclear cells in HBV infection using limiting dilution PCR. *J Virol Methods* 1999; **78**: 129-147
- 3 Brind A, Jiang J, Samuel D, Gigou M, Feray C, Brechot C, Kremsdorf D. Evidence for selection of hepatitis B mutants after liver transplantation through peripheral blood mononuclear cell infection. *J Hepatol* 1997; **26**: 228-235
- 4 Trautwein C, Schrem H, Tillmann HL, Kubicka S, Walker D, Boker KH, Maschek HJ, Pichlmayr R, Manns MP. Hepatitis B virus mutations in the pre-S genome before and after liver transplantation. *Hepatology* 1996; **24**: 482-488
- 5 Webster GJ, Reignat S, Maini MK, Whalley SA, Ogg GS, King A, Brown D, Amlot PL, Williams R, Vergani D, Dusheiko GM, Bertolotti A. Incubation phase of acute hepatitis B in man: dynamic of cellular immune mechanisms. *Hepatology* 2000; **32**: 1117-1124
- 6 Samuel D, Muller R, Alexander G, Fassati L, Ducot B, Benhamou JP, Bismuth H. Liver transplantation in European patients with the hepatitis B surface antigen. *N Engl J Med* 1993; **329**: 1842-1847
- 7 Gonzalez RA, de la Mata M, de la Torre J, Mino G, Pera C, Pena J, Munoz E. Levels of HBV-DNA and HBsAg after acute liver allograft rejection treatment by corticoids and OKT3. *Clin Transplant* 2000; **14**: 208-211
- 8 Ho BM, So SK, Esquivel CO, Keeffe EB. Liver transplantation in Asian patients with chronic hepatitis B. *Hepatology* 1997; **25**: 223-225
- 9 Teixeira R, Pastacaldi S, Papatheodoridis GV, Burroughs AK. Recurrent hepatitis C after liver transplantation. *J Med Virol* 2000; **61**: 443-454
- 10 Mazzaferro V, Brunetto MR, Pasquali M, Regalia E, Pulvirenti A, Baratti D, Makoweeka L, Van Thiel D, Bonino F. Preoperative serum levels of wild-type and hepatitis B e antigen-negative hepatitis B virus (HBV) and graft infection after liver transplantation for HBV-related hepatocellular carcinoma. *J Viral Hepat* 1997; **4**: 235-242
- 11 Douglas DD, Rakela J, Wright TL, Krom RA, Wiesner RH. The clinical course of transplantation-associated de novo hepatitis B infection in the liver transplant recipient. *Liver Transpl Surg* 1997; **3**: 105-111
- 12 Chen Y, McKenna GJ, Yoshida EM, Buczkowski AK, Scudamore CH, Erb SR, Steinbrecher UP, Chung SW. Assessment of immunologic status of liver transplant recipients by peripheral blood mononuclear cells in response to stimulation by donor alloantigen. *Ann Surg* 1999; **230**: 242-250
- 13 Guidotti LG, Rochford R, Chung J, Shapiro M, Purcell R, Chisari FV. Viral clearance without destruction of infected cells during acute HBV infection. *Science* 1999; **284**: 825-829
- 14 Suri D, Schilling R, Lopes AR, Mullerova I, Colucci G, Williams R, Naoumov NV. Non-cytolytic inhibition of hepatitis B virus replication in human hepatocytes. *J Hepatol* 2001; **35**: 790-797
- 15 Heise T, Guidotti LG, Chisari FV. La autoantigen specifically recognizes a predicted stem-loop in hepatitis B virus RNA. *J Virol* 1999; **73**: 5767-5776
- 16 Schultz U, Chisari FV. Recombinant duck interferon gamma inhibits duck hepatitis B virus replication in primary hepatocytes. *J Virol* 1999; **73**: 3162-3168
- 17 Guidotti LG, McClary H, Loudis JM, Chisari FV. Nitric oxide inhibits hepatitis B virus replication in the livers of transgenic mice. *J Exp Med* 2000; **191**: 1247-1252
- 18 Webster GJ, Reignat S, Maini MK, Whalley SA, Ogg GS, King A, Brown D, Amlot PL, Williams R, Vergani D, Dusheiko GM, Bertolotti A. Incubation phase of acute hepatitis B in man: dynamic of cellular immune mechanisms. *Hepatology* 2000; **32**: 1117-1124
- 19 Flores MG, Zhang S, Ha A. *In vitro* evaluation of the effects of candidate immunosuppressive drugs: flow cytometry and quantitative real-time PCR as two independent and correlated read-outs. *J Immunol Methods* 2004; **289**: 123-135
- 20 Kubala L, Ciz M, Vondracek J, Cizova H, Cerny J, Nemecek P, Studenik P, Duskova M, Lojek A. Peri- and post-opera-

- tive course of cytokines and the metabolic activity of neutrophils in human liver transplantation. *Cytokine* 2001; **16**: 97-101
- 21 **Sakuma S**, Kato Y, Nishigaki F, Sasakawa T, Magari K, Miyata S, Ohkubo Y, Goto T. FK506 potently inhibits T cell activation induced TNF-alpha and IL-1beta production *in vitro* by human peripheral blood mononuclear cells. *Br J Pharmacol* 2000; **130**: 1655-1663
- 22 **Neuberger J**. Incidence, timing, and risk factors for acute and chronic rejection. *Liver Transpl Surg* 1999; **5** (4 Suppl 1): S30-36
- 23 **Lok AS**, Chung HT, Liu VW, Ma OC. Long-term follow-up of chronic hepatitis B patients treated with interferon alfa. *Gastroenterology* 1993; **105**: 1833-1838
- 24 **Boni C**, Penna A, Ogg GS, Bertolotti A, Pilli M, Cavallo C, Cavalli A, Urbani S, Boehme R, Panebianco R, Fiaccadori F, Ferrari C. Lamivudine treatment can overcome cytotoxic T-cell hyporesponsiveness in chronic hepatitis B: new perspectives for immune therapy. *Hepatology* 2001; **33**: 963-971
- 25 **Kondo Y**, Asabe S, Kobayashi K, Shiina M, Niitsuma H, Ueno Y, Kobayashi T, Shimosegawa T. Recovery of functional cytotoxic T lymphocytes during lamivudine therapy by acquiring multi-specificity. *J Med Virol* 2004; **74**: 425-433

Science Editor Wang XL and Guo SY Language Editor Elsevier HK

Effects of garlicin on apoptosis in rat model of colitis

Xi-Ming Xu, Jie-Ping Yu, Xiao-Fei He, Jun-Hua Li, Liang-Liang Yu, Hong-Gang Yu

Xi-Ming Xu, Jie-Ping Yu, Jun-Hua Li, Liang-Liang Yu, Hong-Gang Yu, Department of Gastroenterology, Renmin Hospital, Wuhan University, Wuhan 430060, Hubei Province, China
Xiao-Fei He, Department of Gastroenterology, the Affiliated Hospital of Xianning Medical College, Xianning 437100, Hubei Province, China

Supported by the Educational Foundation of Hubei Province, No. 2002A04006

Correspondence to: Hong-Gang Yu, Department of Gastroenterology, Renmin Hospital, Wuhan University, Wuhan 430060, Hubei Province, China. doctorxu120@sina.com

Telephone: +86-27-62954290

Received: 2004-10-30 Accepted: 2004-12-26

Abstract

AIM: To investigate the effects of garlicin on apoptosis and expression of bcl-2 and bax in lymphocytes in rat model of ulcerative colitis (UC).

METHODS: Healthy adult Sprague-Dawley rats of both sexes, weighing 180 ± 30 g, were employed in the present study. The rat model of UC was induced by 2,4,6-trinitrobenzene sulfonic acid (TNBS) enema. The experimental animals were randomly divided into garlicin treatment group (including high and low concentration), model control group, and normal control group. Rats in garlicin treatment group and model control group received intracolonic garlicin daily at doses of 10.0 and 30.0 mg/kg and equal amount of saline respectively 24 h after colitis model was induced by alcohol and TNBS co-enema. Rats in normal control group received neither alcohol nor only TNBS but only saline enema in this study. On the 28th d of the experiment, rats were executed, the expression of bcl-2 and bax protein was determined immunohistochemically and the apoptotic cells were detected by the terminal deoxynucleotidyl transferase-mediated deoxyuridine triphosphate fluorescence nick end labeling (TUNEL) method. At the same time, the rat colon mucosal damage index (CMDI) was calculated.

RESULTS: In garlicin treatment group, the positive expression of bcl-2 in lymphocytes decreased and the number of apoptotic cells was more than that in model control group, CMDI was lower than that in model control group. The positive expression of bax in lymphocytes had no significant difference.

CONCLUSION: Garlicin can protect colonic mucosa against damage in rat model of UC induced by TNBS enema.

© 2005 The WJG Press and Elsevier Inc. All rights reserved.

Key words: Garlicin; Ulcerative colitis; Apoptosis; Bcl-2

Xu XM, Yu JP, He XF, Li JH, Yu LL, Yu HG. Effects of garlicin on apoptosis in rat model of colitis. *World J Gastroenterol* 2005; 11(29): 4579-4582

<http://www.wjgnet.com/1007-9327/11/4579.asp>

INTRODUCTION

Ulcerative colitis (UC), one of the chronic nonspecific inflammation diseases of the intestine, is related to infection, heredity, and immunologic inadequacy. In recent years, studies have shown that apoptosis plays an important role in the pathogenesis of UC^[1-3]. Apoptosis of enterocytes and lymphocytes are the main reasons for UC and inflammation^[4,5]. Apoptosis of lymphocytes is closely related with UC^[6-8]. Garlicin is a kind of chemical compound extracted from garlic corn. It has many biological activities against inflammation, fungi, anti-oxidant, and tumor, *etc.*^[9-11]. Therefore, we performed this study to observe the effects of garlicin on expression of bcl-2 and bax protein in rats with UC and its possible mechanism against the damage to colonic mucosa.

MATERIALS AND METHODS

Materials

Healthy adult Sprague-Dawley rats of both sexes, weighing 180 ± 30 g, employed in this study were purchased from the Experimental Animal Center, Hubei Academy of Medical Sciences, housed in a temperature conditioned room ($22-24$ °C) with a 12-h light-dark cycle, allowed free access to standard rat chow and water *ad libitum*, and acclimatized to the surroundings for 1 wk before the experiment. The study protocol was in accordance with the guideline for animal research and approved by the Ethical and Research Committee of the hospital.

Reagents

Garlicin was purchased from Hubei Wusan Drug Manufactory. 2,4,6-Trinitrobenzene sulfonic acid (TNBS) was bought from Sigma Corp. Immunohistochemical assay kits for bcl-2 and bax were provided by Wuhan Boster Reagent Corp. Apoptosis assay kits and S-P assay kits were provided by Roche Reagent Corp.

Experimental protocol

Rat model of UC was induced by TNBS enema as previously described in the literature^[12]. According to different treatment regimens, the experimental animals were randomly divided into garlicin treatment group (including high and low concentration), model control group, and normal control group. Rats in garlicin treatment group and model control group received intracolonic garlicin daily at doses of 10.0 and

30.0 mg/kg and equal amount of saline (8:00 am) 24 h after colitis model was induced by 50% alcohol and TNBS (150 mg/kg) co-enema. Rats in normal control group received neither alcohol nor TNBS but saline enema. On the 28th d of the experiment, rats were executed, the expression of bcl-2 and bax in lymphocytes was determined immunohistochemically and apoptotic cells were detected by the TUNEL method. At the same time, the colon mucosal damage index (CMDI) was evaluated.

Colon mucosal damage index

CMDI was evaluated by the methods as previously reported^[13]. The evaluation standard of CMDI includes adhesion, congestion, ulcer inflammation, and pathological change depth. Adhesion and congestion according to the difference of pathological change degree were scored as 0, 1 and 2 respectively. The inflammation and ulcer of colonic mucosa scored 1; the pathological change of submucous membrane, muscular layer, serous coat layer scored 1, 2, and 3 separately. Each point was added to get the total points.

Immunohistochemistry detection

The expression of bcl-2 and bax protein in colon tissue was determined immunohistochemically as previously described^[14,15], formalin-fixed, paraffin-embedded tissue blocks were cut into 5- μ m-thick sections mounted on glass slides, and then kept in an oven at 4 °C overnight. Immunostaining was performed as previously described with a slight modification^[16]. Sections were deparaffinized in xylene and rehydrated. Endogenous peroxidase activity was blocked with 1% hydrogen peroxide for 20 min. To improve the quality of staining, microwave oven-based antigen retrieval was performed. Slides were probed with either anti-bcl-2 (1:100, mouse mAb) or anti-bax (1:100, mouse mAb). Sections were washed thrice with PBS for 10 min each and incubated with biotin-labeled anti-mouse IgG for 1 h at room temperature. After washing thrice with PBS for 10 min each, sections were stained with a streptavidin-peroxidase detection system. Incubation with PBS instead of the primary antibody served as a negative control. In specimens containing positive cells, the positive cells were counted in 10 randomly selected fields under 200- or 400-fold magnification for each sample, and the average was expressed as the density of positive cells.

Determination of apoptosis

The TUNEL assay, originally described by Gavrieli *et al.*^[17], was used with minor modifications. Briefly, 5- μ m-thick tissue sections were mounted onto glass slides, deparaffinized,

hydrated, and treated with proteinase-K (Roche Corp.; 20 μ g/mL in 10 mmol/L Tris-HCl buffer, pH 7.4) for 15-30 min at 37 °C. Slides were rinsed twice with PBS. Then, 50 μ L of TUNEL reaction mixture (450 μ L nucleotide mixture containing fluoresceinated dUTP in reaction buffer plus 50 μ L enzyme TdT from calf thymus, Roche Corp.) was added to the samples. To ensure homogeneous spread of the TUNEL reaction mixture on tissue sections and to avoid evaporative loss, slides were covered with coverslips during incubation and incubated in a humidified chamber for 60 min at 37 °C. After rinsing, slides were incubated with anti-fluorescein antibody, Fab fragment from sheep, conjugated with horse-radish peroxidase for 30 min at 37 °C. Slides were rinsed twice with PBS. Then, 50-100 μ L of DAB substrate was added and incubated for 10 min at room temperature. Samples were counterstained prior to analysis by light microscopy. Positive signals were defined as presence of a distinct brown nuclear staining of the neoplastic cells or were morphologically defined as apoptotic bodies. The apoptotic index (AI) was determined by counting at least 1 000 neoplastic nuclei in 10 randomly chosen fields at 400-fold magnification. Apoptotic cells were identified by TUNEL assay in conjunction with characteristic morphological changes such as cell shrinkage, membrane blebbing, and chromatin condensation, to distinguish apoptotic cells and bodies from necrotic cells.

Statistical analysis

All statistical analyses were performed with SPSS10.0 statistical package for Microsoft Windows. Measurement data were expressed as mean \pm SD, *t* test and one-way analysis of variance were used to compare continuous variables among groups. *P*<0.05 was considered statistically significant.

RESULTS

Protective effects of garlicin on rat colonic lesion

Pronounced pathological changes of colonic mucosa were similar to those in human IBD which were observed in rats colitis model induced by both alcohol and TNBS co-enema. CMDI significantly increased in experimental animals compared to normal controls (*P*<0.01). Treatment groups with different doses of garlicin could effectively reduce the severity of gut injury and CMDI significantly decreased in a dose-dependent manner in rats treated with garlicin compared to that in model control group (*P*<0.05-0.01, Table 1).

Effects of garlicin on expression of bcl-2 and bax protein

In the present study, the expression of bcl-2 and bax was

Table 1 Effect of garlicin on CMDI in rats with experimental colitis (mean \pm SD, *n* = 10)

Group	CMDI							
	0	1	2	3	4	5	6	7
Normal control	2	5	3					
Model control				1 ^d	2 ^d	3 ^d	3 ^d	1 ^d
Garlicin (10.0 mg/kg)		2 ^a	2 ^a	3 ^a	2 ^a	1 ^a		
Garlicin (30.0 mg/kg)			5 ^b	3 ^b	2 ^b			

^a*P*<0.05, ^b*P*<0.01 vs model control; ^d*P*<0.01 vs normal control.

also investigated by immunohistochemistry. Immunostaining specific for bcl-2 and bax was shown as brown. Positive expression of bcl-2 in lymphocytes significantly increased in rat model of UC induced by alcohol and TNBS enema compared to the normal control group ($P < 0.01$), which were significantly inhibited by different doses of garlicin ($P < 0.01-0.05$ vs model control, Table 2 and Figure 1). Positive expression of bax in lymphocytes was common in normal group, which had no alteration in model control group and garlicin treatment group.

Apoptosis

TUNEL staining was restricted to the nuclei of apoptotic cells. TUNEL-positive staining cells were detected in normal control group, model control group, and garlicin treatment group. The AI significantly decreased ($P < 0.01$) in model control group compared to normal control group, and increased in garlicin treatment group compared to model control group ($P < 0.01-0.05$, Table 2 and Figure 2).

Table 2 Effect of garlicin on expression of bcl-2 and bax and AI in rats with experimental UC (mean±SD, n = 10)

Group	Bcl-2	Bax	AI
Normal control	9.8±1.4	30.1±3.2	20.8±0.7
Model control	41.0±2.5 ^d	9.9±0.8 ^d	2.3±1.6 ^d
Garlicin (10.0 mg/kg)	22.4±0.8 ^a	11.2±4.3	9.8±1.3 ^a
Garlicin (30.0 mg/kg)	10.2±2.5 ^b	13.1±2.5	15.3±0.6 ^b

^a $P < 0.05$, ^b $P < 0.01$ vs model control; ^c $P < 0.01$ vs normal control.

DISCUSSION

The term “apoptosis” describes the change of morphology different from cell necrosis. Hallmarks of apoptosis include chromatin condensation, nuclear segmentation, cytoplasmic shrinkage, blebbing, and formation of apoptotic bodies^[18]. Bcl-2 is a suppressor gene of apoptosis, which was found from follicular B cell lymphoma with t(14,18) chromosome malposition^[19]. Orientating as 18q21, bax, and bcl-2 are homologous proteins, and bax is an induction gene of apoptosis. Bcl-2 and bax can exist in the form of homodimer and form heterodimer too. When the expression of bax increases, the homodimer of bax–bax can induce apoptosis. When the expression of bcl-2 increases, bax can combine with bcl-2 to form more stable heterodimers which can inhibit apoptosis. The ratio of bcl-2/bax can regulate apoptosis^[20].

The important pathological change in UC are inflammatory damage of intestine, during which a large number of inflammatory cells infiltrate the intestinal wall and activate continuously^[21]. Apoptosis of the lymphocytes has a close relation with UC, and apoptosis of lymphocytes in colonic mucosa is the main reason for the development of UC^[6,22-24]. This experiment has proved that apoptosis of lymphocytes is delayed in UC, which is consistent with previous reports^[2,3,20]. The positive expression of Bcl-2 in lymphocytes increased while that of bax was relatively rare, which is in agreement with previous reports^[20]. Garlicin is a kind of chemical compound extracted from garlic corn. It has many biological activities against inflammation, fungi, anti-oxidant, etc.^[9-11].

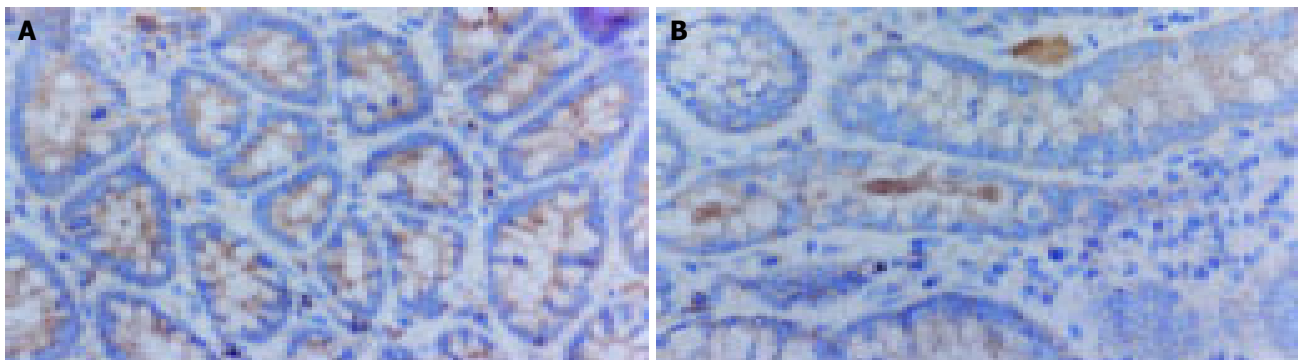


Figure 1 Immunohistochemical staining of bcl-2 in tissue sections of model control group (A) and garlicin treatment group (B).

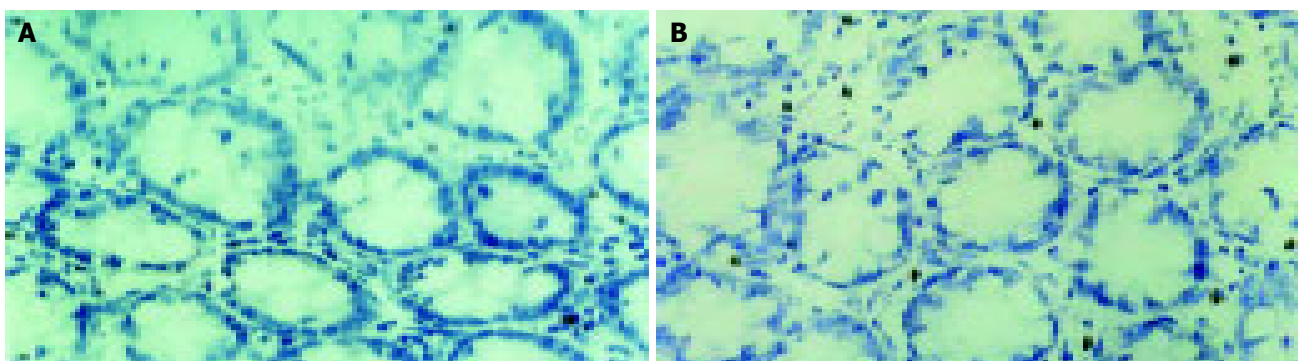


Figure 2 TUNEL staining in tissue sections of model control group (A) and garlicin treatment group (B).

It can protect colonic mucosa against damage. In this study, the apoptosis of lymphocytes increased in garlicin treatment group and the positive expression of bcl-2 in lymphocytes decreased, suggesting that garlicin has protective effects on UC by promoting apoptosis of lymphocytes and reducing expression of bcl-2 protein.

We observed the effects of garlicin on the expression of bcl-2 and bax in lymphocytes in rat model of UC induced by TNBS. The results showed that the CMDI of garlicin treatment group was obviously lower than that of the model control group, indicating that the garlicin can prevent and cure UC. At the same time, the apoptosis of lymphocytes increased in garlicin treatment group, showing that the protective effects of garlicin in rats with UC are related with the induction of apoptosis of lymphocytes. The results of this experiment may open up a new way for the treatment of UC.

REFERENCES

- 1 **Brannigan AE**, O'Connell PR, Hurley H, O'Neill A, Brady HR, Fitzpatrick JM, Watson RW. Neutrophil apoptosis is delayed in patients with inflammatory bowel disease. *Shock* 2000; **13**: 361-366
- 2 **Neurath MF**, Finotto S, Fuss I, Boirivant M, Galle PR, Strober W. Regulation of T-cell apoptosis in inflammatory bowel disease: to die or not to die, that is the mucosal question. *Trends Immunol* 2001; **22**: 21-26
- 3 **Suzuki A**, Sugimura K, Ohtsuka K, Hasegawa K, Suzuki K, Ishizuka K, Mochizuki T, Honma T, Narisawa R, Asakura H. Fas/Fas ligand expression and characteristics of primed CD45RO+ T cells in the inflamed mucosa of ulcerative colitis. *Scand J Gastroenterol* 2000; **35**: 1278-1283
- 4 **Iimura M**, Nakamura T, Shinozaki S, Iizuka B, Inoue Y, Suzuki S, Hayashi N. Bax is downregulated in inflamed colonic mucosa of ulcerative colitis. *Gut* 2000; **47**: 228-235
- 5 **Mallolas J**, Esteve M, Rius E, Cabre E, Gassull MA. Antineutrophil antibodies associated with ulcerative colitis interact with the antigen(s) during the process of apoptosis. *Gut* 2000; **47**: 74-78
- 6 **Yeung MM**, Melgar S, Baranov V, Oberg A, Danielsson A, Hammarstrom S, Hammarstrom ML. Characterisation of mucosal lymphoid aggregates in ulcerative colitis: immunecell phenotype and TcR-gammadelta expression. *Gut* 2000; **47**: 215-227
- 7 **Atreya R**, Mudter J, Finotto S, Mullberg J, Jostock T, Wirtz S, Schutz M, Bartsch B, Holtmann M, Becker C, Strand D, Czaja J, Schlaak JF, Lehr HA, Autschbach F, Schurmann G, Nishimoto N, Yoshizaki K, Ito H, Kishimoto T, Galle PR, Rose-John S, Neurath MF. Blockade of interleukin 6 trans signaling suppresses T-cell resistance against apoptosis in chronic intestinal inflammation: evidence in crohn disease and experimental colitis *in vivo*. *Nat Med* 2000; **6**: 583-588
- 8 **Ueyama H**, Kiyohara T, Sawada N, Isozaki K, Kitamura S, Kondo S, Miyagawa J, Kanayama S, Shinomura Y, Ishikawa H, Ohtani T, Nezu R, Nagata S, Matsuzawa Y. High Fas ligand expression on lymphocytes in lesions of ulcerative colitis. *Gut* 1998; **43**: 48-55
- 9 **Guyonnet D**, Belloir C, Suschetet M, Siess MH, Le Bon AM. Mechanisms of protection against aflatoxin B(1) genotoxicity in rats treated by organosulfur compounds from garlic. *Carcinogenesis* 2002; **23**: 1335-1341
- 10 **Yin MC**, Hwang SW, Chan KC. Nonenzymatic antioxidant activity of four organosulfur compounds derived from garlic. *J Agric Food Chem* 2002; **50**: 6143-6147
- 11 **Munday R**, Munday CM. Relative activities of organosulfur compounds derived from onions and garlic in increasing tissue activities of quinone reductase and glutathione transferase in rat tissues. *Nutr Cancer* 2001; **40**: 205-210
- 12 **Morris GP**, Beck PL, Herridge MS, Depew WT, Szwczuk MR, Wallace JL. Hapten-induced model of chronic inflammation and ulceration in the rat colon. *Gastroenterology* 1989; **96**: 795-803
- 13 **Butzner JD**, Parmar R, Bell CJ, Dalal V. Butyrate enema therapy stimulates mucosal repair in experimental colitis in the rat. *Gut* 1996; **38**: 568-573
- 14 **Bukholm IK**, Nesland JM. Protein expression of p53, p21 (WAF1/CIP1), bcl-2, Bax, cyclin D1 and pRb in human colon carcinomas. *Virchows Arch* 2000; **436**: 224-228
- 15 **Ho YS**, Liu HL, Duh JS, Chen RJ, Ho WL, Jeng JH, Wang YJ, Lin JK. Induction of apoptosis by S-nitrosoglutathione and Cu2+ or Ni2+ ion through modulation of bax, bad, and bcl-2 proteins in human colon adenocarcinoma cells. *Mol Carcinog* 1999; **26**: 201-211
- 16 **Zabel U**, Henkel T, Silva MS, Baeuerle PA. Nuclear uptake control of NF- κ B by MAD-3, an I κ B protein present in the nucleus. *EMBO J* 1993; **12**: 201-211
- 17 **Gavrieli Y**, Sherman Y, Ben-Sasson SA. Identification of programmed cell death in situ via specific labeling of nuclear DNA fragmentation. *J Cell Biol* 1992; **119**: 493-501
- 18 **Sakai T**, Kimura Y, Inagaki-Ohara K, Kasugamu K, Lynch DH, Yoshikai Y. Fas-mediated cytotoxicity by intestinal intraepithelial lymphocytes during acute graft-versus-host disease in mice. *Gastroenterology* 1997; **113**: 168-174
- 19 **Tsujimoto Y**, Gorham J, Cossman J, Jaffe E, Croce CM. The t(14;18) chromosome translocations involved in B-cell neoplasms result from mistakes in VDJ joining. *Science* 1985; **229**: 1390-1393
- 20 **Ina K**, Itoh J, Fukushima K, Kusugami K, Yamoguchi T, Kyokane K, Imada A, Binion DC, Musso A, West GA, Dobrea GM, McCormick TS, Lapetina EG, Levine AD, Ottaway CA, Fiocchi C. Resistance of Crohn's disease T cells to multiple apoptotic signals is associated with a Bcl-2/Bax mucosal imbalance. *J Immunol* 1999; **163**: 1081-1090
- 21 **Sartor RB**. Current concepts of the etiology and pathogenesis of ulcerative colitis and Crohn's disease. *Gastroenterol Clin North Am* 1995; **24**: 475-507
- 22 **Hagiwara C**, Tanaka M, Kudo H. Increase in colorectal epithelial apoptotic cells in patients with ulcerative colitis ultimately requiring surgery. *J Gastroenterol Hepatol* 2002; **17**: 758-764
- 23 **Yukawa M**, Iizuka M, Horie Y, Yoneyama K, Shirasaka T, Itou H, Komatsu M, Fukushima T, Watanabe S. Systemic and local evidence of increased Fas-mediated apoptosis in ulcerative colitis. *Int J Colorectal Dis* 2002; **17**: 70-76
- 24 **Bregenholt S**, Petersen TR, Claesson MH. The majority of lamina propria CD4(+) T-cells from scid mice with colitis undergo Fasmediated apoptosis *in vivo*. *Immunol Lett* 2001; **78**: 7-12

Novel DNA vaccine based on hepatitis B virus core gene induces specific immune responses in Balb/c mice

Yi-Ping Xing, Zu-Hu Huang, Shi-Xia Wang, Jie Cai, Jun Li, Te-Hui W Chou, Shan Lu

Yi-Ping Xing, Zu-Hu Huang, Jie Cai, Jun Li, Department of Infectious Diseases, the First Affiliated Hospital of Nanjing Medical University, 300 Guangzhou Road, Nanjing 210029, Jiangsu Province, China

Shi-Xia Wang, Te-Hui W Chou, Shan Lu, Department of Medicine, University of Massachusetts Medical School, 55 Lake Avenue North, Worcester, MA 01655, United States

Supported by the 135 Project of Jiangsu Province, No. 044

Correspondence to: Associate Professor Yi-Ping Xing, Department of Infectious Diseases, the First Affiliated Hospital of Nanjing Medical University, 300 Guangzhou Road, Nanjing 210029, Jiangsu Province, China. yipingx@public1.ptt.js.cn

Telephone: +86-25-83718836-6394

Received: 2004-11-20 Accepted: 2004-12-03

Abstract

AIM: To investigate the immunogenicity of a novel DNA vaccine, pSW3891/HBc, based on HBV core gene in Balb/c mice.

METHODS: A novel DNA vaccine, pSW3891/HBc, encoding HBV core gene was constructed using a vector plasmid pSW3891. Balb/c mice were immunized with either pSW3891/HBc or empty vector DNA via gene gun. IgG anti-HBc responses in mouse sera were demonstrated by ELISA. Specific cytotoxicity of cytotoxic T lymphocytes (CTLs) of mice was quantitatively measured by lactate dehydrogenase release assay.

RESULTS: HBcAg was expressed effectively in 293T cell line transiently transfected with pSW3891/HBc. Strong IgG anti-HBc responses were elicited in mice immunized with pSW3891/HBc. The end-point titers of anti-HBc reached the highest 1:97 200, 4 wk after the third immunization. The specific CTL killing with the highest specific lysis reached 73.25% at effector:target ratio of 20:1 in mice that received pSW3891/HBc DNA vaccine.

CONCLUSION: pSW3891/HBc vaccination elicits specific anti-HBc response and induces HBc-specific CTL response in immunized Balb/c mice.

© 2005 The WJG Press and Elsevier Inc. All rights reserved.

Key words: DNA vaccine; Hepatitis B virus core antigen; Immunogenicity; Gene gun; CTL; HBV

Xing YP, Huang ZH, Wang SX, Cai J, Li J, Chou THW, Lu S. Novel DNA vaccine based on hepatitis B virus core gene induces specific immune responses in Balb/c mice. *World J Gastroenterol* 2005; 11(29): 4583-4586

<http://www.wjgnet.com/1007-9327/11/4583.asp>

INTRODUCTION

Chronic infection with HBV affects more than 250 million people worldwide, and is considered to be a high risk factor for developing cirrhosis and hepatocellular carcinoma. Although some antiviral drugs for HBV can effectively inhibit viral replication, they rarely eliminate the intra-nuclear viral covalently close circular DNA, which is responsible for the persistence of infection. Recent data indicate that immunotherapeutic strategies stimulating both cellular and humoral immune responses to HBV antigens are essential to cure chronic HBV infection. Since genetic immunization, i.e. *in vivo* transfection of somatic cells with antigen-encoding DNA, effectively induces major histocompatibility complex (MHC) class I-restricted cell-mediated immunity in CD8⁺ cytotoxic T lymphocytes (CTLs) and elicits humoral immune reactions which are dependent on MHC class II-restricted activation of T helper (Th) cells. In this regard, DNA-based vaccination appears to be a particularly pertinent approach for chronic hepatitis B therapy. It has been demonstrated that plasmid DNA encoding HBV surface antigen (HBsAg) and core antigen (HBcAg) elicits vigorous humoral and cellular response in many species^[1-5]. However, the vectors used for animal testing cannot be applied in human studies. On the basis of our previous work, we designed a novel plasmid vector pSW3891. In this study, we investigated the immunogenicity of plasmid pSW3891/HBc encoding HBcAg with this new vector pSW3891 in Balb/c mice.

MATERIALS AND METHODS

Plasmid construction and *in vitro* expression of HBc

To construct plasmid pSW3891/HBc, plasmid pJW4303/HBc^[6] was digested with *Bam*HI and *Pst*I. The HBc gene fragment was isolated by gel electrophoresis and purified with QIAquick gel extraction kit (Qiagen, Valencia, CA, USA). The purified HBc gene was cloned into the *Bam*HI and *Pst*I sites of the pSW3891 vector, resulting in pSW3891/HBc. The pSW3891/HBc DNA vaccine plasmids transformed in *E coli* (HB101 strain) were propagated in LB medium containing kanamycin (0.06 g/L). The pSW3891/HBc plasmid DNA was isolated and verified by restriction enzyme analysis. Large prep of pSW3891/HBc was prepared using the Maxi-plasmid purification kit (Qiagen).

The expression of HBc antigen from DNA vaccine plasmid was confirmed in 293T cells transiently transfected with pSW3891/HBc. The 293T cells were grown in Dulbecco's modified Eagle's medium (Invitrogen, Gaithersburg, MD, USA) supplemented with 10% heat-

inactivated fetal bovine serum, 0.1 g/L of streptomycin, and 100 IU/mL penicillin. Each of the 60-mm tissue culture dishes (2.5×10^6 cells) was transfected with 10 μ g of pSW3891/HBc DNA vaccine plasmid or the empty pSW3891 vector by calcium phosphate precipitation. The levels of HBcAg in the supernatant and the lysate of the 293T cell culture harvested after 48-72 h were detected by Western blot analysis.

Animals and DNA immunization

Seven-week-old female Balb/c mice were purchased from Millbrook Farm (Amherst, MA, USA) and housed in the animal facility at the Department of Animal Medicine of the University of Massachusetts Medical School in accordance with Institutional Animal Care and Use Committee (IACUC) approved protocol. Ten mice were randomly assigned into two groups. Both groups of mice received DNA immunizations by a Bio-Rad Helios gene gun (Bio-Rad, Hercules, CA, USA). The experimental group was vaccinated thrice at 4-wk intervals with pSW3891/HBc, while the control group received only the empty vector pSW3891. The DNA vaccine plasmids were coated onto the 1.0-micron gold beads at a ratio of 2 μ g of DNA per mg of gold. Each gene gun shot delivered 1 μ g of DNA, and a total of six non-overlapping shots were delivered to each mouse on shaved abdominal skin at each immunization. Blood samples before immunization and 4 wk after the last immunization were collected from orbital sinus. The sera were isolated and stored at -70°C until use.

Western blot analysis

The HBc antigens in supernatant from transiently transfected 293T cells were subjected to SDS-PAGE and blotted onto polyvinylidene difluoride membrane (PVDF; Bio-Rad). Blocking was done with 0.1% I-Block (Tropix, Bedford, MA, USA). The membranes were incubated with immunized mouse sera at 1:500 dilution for 45 min and subsequently reacted with AP-conjugated goat anti-rabbit IgG at 1:5 000 dilution for 10 min. Membranes were washed with blocking buffer after each step. Western-light substrate was then applied to the membranes for 5 min. Once the membranes were dried, X-ray films were exposed to the membrane and developed by a Kodak processor.

Measurement of CTL response

HBcAg-specific CTL responses were detected by the CytoTox 96[®] non-radioactive cytotoxicity assay (Promega, Madison, WI, USA) according to the manufacturer's instructions. Briefly, single cell suspensions were prepared from spleens of mice, 4 wk after the last immunization. For specific re-stimulation, 3×10^6 /mL splenocytes were cultured *in vitro* with recombinant human IL-2 (25 U/mL) and 0.01 g/L of the HBc-specific polypeptide SYVNTNMGL (Life Technologies, Gaithersburg, MD, USA). After 7 d of re-stimulation, the splenocytes were used as effector cells in the CTL assays. The effector cells and target cells (P815) at the effector:target ratio of 20:1, 10:1, 5:1, or 2.5:1, respectively were co-cultured with 0.01 g/L specific polypeptide. After 4-h incubation at 37°C with 50 mL/L CO_2 , the absorbance of culture supernatant from each well

was quantitatively measured using a standard 96-well plate reader according to the instructions. The percent cytotoxicity for each effector:target cell ratio was calculated using the following formula: %cytotoxicity = (experimental-effector spontaneous-target spontaneous)/(target maximum-target spontaneous) $\times 100$. The results represented the mean of the triplicate data set.

Enzyme-linked immunosorbent assay

Mouse sera were tested for HBc-specific IgG antibody responses by ELISA. Microtiter plates (Corning, NY, USA) were first coated overnight with 0.005 g/L of purified HBcAg (Aldevron, Fargo, ND, USA) in 0.05 mol/L sodium carbonate buffer at pH 9.2. After coating buffer was removed, 200 μ L/well blocking buffer (5% Marvel skim milk in 0.1% PBS-Triton X100) was added for 1 h at room temperature. Blocking buffer was then removed and primary antibody (100 μ L/well) was added at different dilutions in blocking buffer and plates were incubated at room temperature. Plates were washed thrice in 0.1% PBS-Triton X100 and diluted anti-mouse biotinylated antibodies (Caltag, Burlingame, CA, USA) were added, followed by 1-h incubation. Plates were washed thrice in 0.1% PBS-Triton X100, then streptavidin-horseradish peroxidase (Caltag) was added, and plates were incubated for 1 h. The horseradish peroxidase activity was detected with ortho-phenylenediamine substrate solution. The reaction was stopped by the addition of 50 μ L/well of 3 mol/L H_2SO_4 after 35 min in the dark. The optical density (A) was read at 450 nm in an ELISA reader (BioRad). The end titration titer was determined when the A reading at the last sera dilution was twofold above the A reading of the negative control wells with the normal mouse sera.

RESULTS

Construction of recombinant plasmid pSW3891/HBc

The cloning of the HBc gene into vector pSW3891 was confirmed by restriction enzyme analysis (Figure 1). A small molecular weight band (662 bases) corresponding to the HBc gene insert was observed when the plasmid was restricted with *Bam*HI and *Pst*I. Single band representing the full length plasmid was observed in *Xba*I-digested lane because there was one *Xba*I site in the HBc gene but not in vector pSW3891.

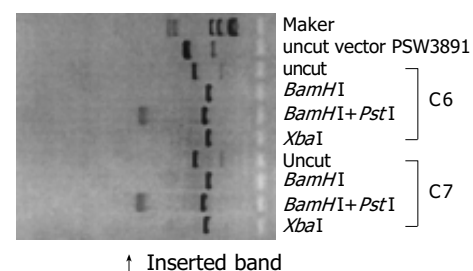


Figure 1 Digestion of pSW3891/HBc. Marker: λ Hind III; C6, C7: clone no.

Expression of pSW3891/HBc in 293T cells

A protein with expected molecular weight of M_r 21 000 was efficiently expressed in the lysate of 293T cells transiently transfected with pSW3891/HBc as shown by Western blotting (Figure 2). No specific bands were detected in the supernatant of 293T cells transfected with pSW3891/HBc, nor in the supernatant and lysate of 293T cells transfected with pSW3891 (Figure 2).

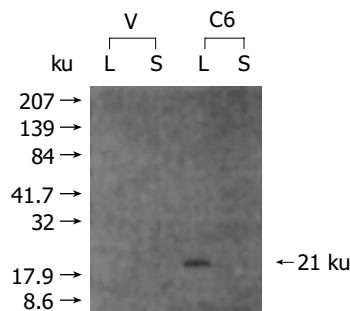


Figure 2 *In vitro* HBc expression in pSW3891/HBc transiently transfected 293T cells. V: pSW3891; L: lysate; C6: pSW3891/HBc/C6; S: supernatant.

Anti-HBc IgG response in Balb/c mice immunized with pSW3891/HBc

Strong anti-HBc IgG responses were elicited in mice immunized with pSW3891/HBc, the end-point titers of anti-HBc reached the highest 1:97 200, 4 wk after the third immunization. The antibody titers were significantly higher in the group immunized with pSW3891/HBc than in the group immunized with empty vector pSW3891 (Figure 3).

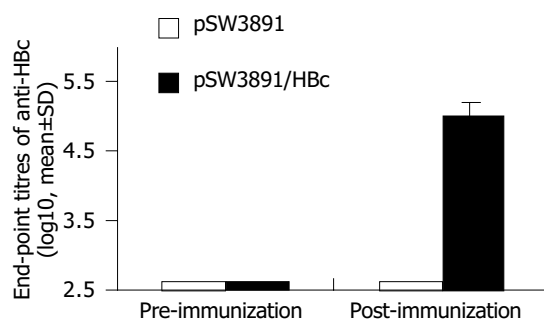


Figure 3 End-point titres of anti-HBc in sera of Balb/c mice immunized with pSW3891/HBc.

HBc-specific CTLs in mice

Four weeks following the last immunization, splenocytes from mice immunized with pSW3891/HBc or vector pSW3891 were isolated and stimulated *in vitro* with the HBc-specific peptide. Specific cell-mediated cytotoxic activities with different effector/target ratios are shown in Figure 4.

Compared to the control group, the specific CTL killing with the highest specific lysis reached 73.25% at effector:target ratio of 20:1 in the experimental group of mice that received pSW3891/HBc DNA vaccine.

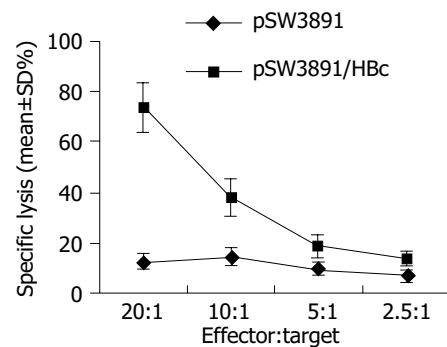


Figure 4 Specific cytotoxicity of splenocytes in Balb/c mice immunized with pSW3891/HBc.

DISCUSSION

It is well known that immune responses play a significant role in both virus clearance and pathogenesis of hepatitis B. The vigorous polyclonal and multi-specific immune responses to HBV have been associated with recovery from acute infection. It has been shown that specific cellular immunity against HBcAg is a key factor for the control of HBV infection^[7]. CTLs and Th cells with specificity for HBcAg are detectable in the circulation during acute infection^[8-10]. In contrast, defective CTL- and Th-cell responses have been observed in chronic HBV carriers^[11].

There is evidence that DNA plasmid encoding HBcAg is a promising vaccine candidate against HBV infection. Our previous data have also shown that plasmid pJW4303/HBc encoding HBc elicits high titer antibodies and CTL responses in mice and monkeys^[6]. However, the plasmids used in these experiments are not suitable for humans because of their vector components. For example, the ampicillin resistant gene for selection may cause antibiotic resistance in clinic, and the sequence derived from SV40 virus promoter region might potentially cause or promote lymphomas and other cancers. We deleted SV40 virus sequence and substituted ampicillin resistant gene in the vector pSW4303 with kanamycin resistant gene to generate a new vector pSW3891. Then the HBc gene was inserted into this new vector to develop a novel DNA vaccine pSW3891/HBc suitable for humans.

Restriction enzyme analysis of pSW3891/HBc confirmed that the HBc gene was inserted correctly into vector pSW3891. The HBc gene could release from pSW3891/HBc with *Bam*HI and *Pst*I, which was not observed in the control vector pSW3891. The expression of pSW3891/HBc *in vitro* was confirmed in transiently transfected 293T cells. Western blotting analysis showed that HBcAg was detectable in the cell lysate but not in supernatant of the transfected 293T cells in accordance with the early reports^[6]. This is consistent with the observation that HBcAg only exists in hepatic cells where capsids of HBV particles have been found in patients with hepatitis B.

To investigate the ability of pSW3891/HBc to elicit humoral responses in vaccinated Balb/c mice, two groups of mice were immunized with different plasmids. The experimental group of mice that received pSW3891/HBc induced a potent anti-HBc response with the titers reaching

1:97-200. In contrast, anti-HBc antibody was undetectable in the control group of mice that received only vector DNA alone. These results suggest that pSW3891/HBc can elicit strong specific anti-HBc humoral responses in Balb/c mice after DNA vaccination.

Lee *et al.*^[12], have shown that specific CTL responses can be induced by a DNA vaccine encoding HBsAg in C57BL/6 mice. Our results are in agreement with this finding. We measured the CTL component of immune response by the specific killing of syngeneic target cells pulsed with a recognized CTL epitope peptide. Our result showed the specific CTL killing with the highest specific lysis reached 73.25% at effector:target ratio of 20:1, suggesting that pSW3891/HBc vaccination induces HBc-specific CTL responses in immunized Balb/c mice.

Clinical studies of DNA vaccine against HBV infection are still in the early stage and focused on investigating the effects of prophylactic immunization in healthy volunteers. Roy *et al.*^[13], demonstrated that all healthy volunteers immunized with 1, 2, or 4 µg of DNA encoding HBsAg using the gene gun deliver system develop protective antibody titers. Volunteers who are positive for HLA-A2 have detectable antigen-specific CD8⁺ T cells identified by flow cytometry analysis following staining with HLA-A2/HBsAg 335-343 tetramers. Tacket *et al.*^[14], conducted the phase I safety and immune response study of an HBV DNA-based vaccine in healthy volunteers who received two immunizations with plasmid DNA encoding HBsAg on d 0 and 56 by gene gun, and found that although volunteers fail to develop protective antibody responses, it is attributed to the extremely low dose of DNA (0.25 µg) used.

In conclusion, pSW3891/HBc vaccination can elicit specific anti-HBc response and induce HBc-specific CTL response in immunized mice.

REFERENCES

- 1 **Rahman F**, Dahmen A, Herzog-Hauff S, Bocher WO, Galle PR, Lohr HF. Cellular and humoral immune responses induced by intradermal or intramuscular vaccination with the major hepatitis B surface antigen. *Hepatology* 2000; **31**: 521-527
- 2 **Davis HL**, McCluskie MJ, Gerin JL, Purcell RH. DNA vaccine for hepatitis B: evidence for immunogenicity in chimpanzees and comparison with other vaccines. *Proc Natl Acad Sci USA* 1996; **93**: 7213-7218
- 3 **Kwissa M**, Unsinger J, Schirmbeck R, Hauser H, Reimann J. Polyvalent DNA vaccines with bidirectional promoters. *J Mol Med* 2000; **78**: 495-506
- 4 **Riedl P**, Stober D, Oehninger C, Melber K, Reimann J, Schirmbeck R. Priming Th₁ immunity to viral core particles is facilitated by trace amounts of RNA bound to its arginine-rich domain. *J Immunol* 2002; **168**: 4951-4959
- 5 **Kwissa M**, Lindblad EB, Schirmbeck R, Reimann J. Codelivery of a DNA vaccine and a protein vaccine with aluminum phosphate stimulates a potent and multivalent immune response. *J Mol Med* 2003; **81**: 502-510
- 6 **Huang ZH**, Lu S, Liu N. Humoral and cellular immunogenicity of genetic vaccine on core gene of hepatitis B virus in mice. *Zhonghua Yixue Zazhi* 1999; **79**: 456-459
- 7 **Ferrari C**, Penna A, Bertoletti A, Valli A, Antoni AD, Giuberti T, Cavalli A, Petit MA, Fiaccadori F. Cellular immune response to hepatitis B virus-encoded antigens in acute and chronic hepatitis B virus infection. *J Immunol* 1990; **145**: 3442-3449
- 8 **Jung MC**, Diepolder HM, Spengler U, Wierenga EA, Zachoval R, Hoffmann RM, Eichenlaub D, Frosner G, Will H, Pape GR. Activation of a heterogeneous hepatitis B (HB) core and e antigen-specific CD4⁺T-cell population during seroconversion to anti-HBe and anti-HBs in hepatitis B virus infection. *J Virol* 1995; **69**: 3358-3368
- 9 **Penna A**, Chisari FV, Bertoletti A, Missale G, Fowler P, Giuberti T, Fiaccadori F, Ferrari C. Cytotoxic T lymphocytes recognize an HLA-A2-restricted epitope within the hepatitis B virus nucleocapsid antigen. *J Exp Med* 1991; **174**: 1565-1570
- 10 **Rehermann B**, Fowler P, Sidney J, Person J, Redeker A, Brown M, Moss B, Sette A, Chisari FV. The cytotoxic T lymphocyte response to multiple hepatitis B virus polymerase epitopes during and after acute viral hepatitis. *J Exp Med* 1995; **181**: 1047-1058
- 11 **Tsai SL**, Chen PJ, Lai MY, Yang PM, Sung JL, Huang JH, Hwang LH, Chang TH, Chen DS. Acute exacerbations of chronic type B hepatitis are accompanied by increased T cell responses to hepatitis B core and E antigens. Implications for hepatitis B e antigen seroconversion. *J Clin Invest* 1992; **89**: 87-96
- 12 **Lee YS**, Yoon SJ, Kwon TK, Kim YH, Woo JH, Suh MH, Suh SI, Baek WK, Kim HJ, Ahn SY, Choe BK, Park JW. *Immunol Lett* 2001; **78**: 13-20
- 13 **Roy MJ**, Wu MS, Barr LJ, Fuller JT, Tussey LG, Speller S, Culp J, Burkholder JK, Swain WF, Dixon RM, Widera G, Vessey R, King A, Ogg G, Gallimore A, Haynes JR, Heydenburg FD. Induction of antigen specific CD8⁺ T cells, T helper cells and protective levels of antibody in humans by particle mediated administration of a hepatitis B virus DNA vaccine. *Vaccine* 2000; **19**: 764-778
- 14 **Tacket CO**, Roy MJ, Widera G, Swain WF, Broome S, Edelman R. Phase I safety and immune response studies of a DNA vaccine encoding hepatitis B surface antigen delivered by a gene gun delivery device. *Vaccine* 1999; **17**: 2826-2829

Expression and hypermethylation of p27^{kip1} in hepatocarcinogenesis

Pu-Ping Lei, Zong-Ji Zhang, Li-Juan Shen, Jin-Yun Li, Qiong Zou, Hua-Xian Zhang

Pu-Ping Lei, Zong-Ji Zhang, Li-Juan Shen, Qiong Zou, Hua-Xian Zhang, Department of Pathology, Kunming Medical College, Kunming 650031, Yunnan Province, China

Jin-Yun Li, Department of Pathology, the Second Affiliated Hospital, Kunming Medical College, Kunming 650032, Yunnan Province, China Supported by the Natural Science Foundation of Yunnan Province, China, No. 2000C0058M, and Scientific Research Foundation of the Education Department of Yunnan Province, No. 0011010

Co-first-authors: Pu-Ping Lei and Zong-Ji Zhang

Correspondence to: Dr. Li-Juan Shen, Department of Pathology, Kunming Medical College, Kunming 650031, Yunnan Province, China. wycslj@public.km.yn.cn

Telephone: +86-871-5338845 Fax: +86-871-5151197

Received: 2004-07-28 Accepted: 2005-01-14

p27mRNA are potentially involved in hepatocarcinogenesis. The hypermethylation of p27 might lead to the loss of p27mRNA transcription.

© 2005 The WJG Press and Elsevier Inc. All rights reserved.

Key words: Hepatocellular carcinoma; p27^{kip1}; Immunohistochemical staining; *In situ* hybridization; Hypermethylation

Lei PP, Zhang ZJ, Shen LJ, Li JY, Zou Q, Zhang HX. Expression and hypermethylation of p27^{kip1} in hepatocarcinogenesis. *World J Gastroenterol* 2005; 11(29): 4587-4591

<http://www.wjgnet.com/1007-9327/11/4587.asp>

Abstract

AIM: To study the expressions of p27^{kip1} protein and p27mRNA, the hypermethylation of p27^{kip1} and the relation between them in various stages of hepatocarcinogenesis.

METHODS: p27 protein and p27mRNA were detected by immunohistochemical staining and *in situ* hybridization respectively in 68 cases of normal liver, liver cirrhosis, pericancerous cirrhosis and hepatocellular carcinoma (HCC). The hypermethylation of p27^{kip1} was detected by methylation-specific PCR (MSP) in 44 cases of normal liver, liver cirrhosis, and HCC.

RESULTS: The positive rate of p27 protein was 66.7% (4/6) in normal liver, 60.0% (6/10) in liver cirrhosis, 50.0% (12/24) in pericancerous cirrhosis and 21.4% (6/28) in HCC. There were no statistical differences in normal liver, liver cirrhosis and pericancerous cirrhosis, but the positive rate of p27 protein significantly decreased in HCC compared to that in the other groups ($P = 0.006$, $\chi^2 = 7.664$). The positive rate of p27^{kip1} mRNA was 83.3% (5/6) in normal liver, 70.0% (7/10) in liver cirrhosis, 75.0% (18/24) in pericancerous cirrhosis and 25.0% (7/28) in HCC. There were no statistical differences in normal liver, liver cirrhosis and pericancerous cirrhosis, but the positive rate of p27^{kip1} mRNA also significantly decreased in HCC compared to that in the other groups ($P = 0.000$, $\chi^2 = 16.600$). In addition, there was a significant correlation between the expression of p27 protein and p27mRNA in the integrated group of normal liver and liver cirrhosis. However, no significant correlation was found between pericancerous cirrhosis and HCC. Using MSP, we found that 1 HCC in 44 cases (including 6 cases of normal liver, 10 cases of liver cirrhosis and 28 cases of HCC) was methylated, whose p27 protein and p27mRNA were negative.

CONCLUSION: The reduction or loss of p27 protein and

INTRODUCTION

Disruption of cell cycle regulation plays a significant role in carcinogenesis. p27^{kip1}, located at chromosome 12p13, is a regulator of the mammalian cell cycle and a tumor suppressor^[1]. It was reported that the expression of p27^{kip1} protein in hepatocellular carcinoma (HCC) is lost or reduced, when compared to that in liver cirrhosis and normal liver^[2,3], as well as the transcription of p27mRNA^[4]. The mechanism of loss and reduction of p27^{kip1} expression during hepatocarcinogenesis still remains unclear. Specific alterations of the p27^{kip1} gene, including mutations and homozygous deletions, are exceedingly rare in HCC, suggesting that p27^{kip1} might be inactivated by transcription rather than genomic aberrations.

In normal tissues, methylation of the promoter region CpG islands is associated with transcriptional silencing of imprinted alleles and genes on the inactive X chromosome^[5,6]. Indeed, aberrant DNA methylation of the promoter region CpG islands can serve as an alternative to mutations in the coding region for the inactivation of tumor suppressor genes, including the APC gene, p16INK4A, and p15INK4B^[7-9]. p27^{kip1} promoter methylation has not been studied in HCC. We focused on analyzing the DNA methylation patterns in CpG islands of the p27^{kip1} gene.

MATERIALS AND METHODS

Specimens

Specimens obtained from surgical resection, autopsy of livers from 1970 to 2003 were fixed in 40 g/L formaldehyde, embedded in paraffin, and stained with routine HE. The specimens were divided into four groups: normal liver tissue specimens used as controls ($n = 6$), liver cirrhosis tissue specimens ($n = 10$), pericancerous tissue specimens ($n = 24$) and HCC tissue specimens ($n = 28$). All specimens were examined by two pathologists.

Immunohistochemical staining

Immunohistochemistry S-P method was used to detect p27^{kip1} protein expression. Mouse monoclonal antibody to human p27^{kip1} was purchased from Fuzhou Maixin Biotechnical Company. The main steps were as follows. The tissues were treated with 3% H₂O₂ to block endogenous peroxidase at room temperature for 10 min, heated to boiling for 5 min in 10 mmol/L sodium citrate (pH 6.0) buffer in a pressure cooker, incubated in endogenous peroxidase blocking solution at room temperature for 10 min, and then incubated in normal nonimmune serum at room temperature for 10 min. The mouse anti p27^{kip1} antibody was added to tissue sections and incubated overnight at 4 °C. Biotin-conjugated secondary antibody was added to the sections and incubated at room temperature for 10 min. S-P complex was added at room temperature for 10 min and then DAB was used for the color reaction. The tissue sections were washed with PBS (0.01 mol/L, pH 7.4) between each step. Positive and negative controls were simultaneously used to ensure specificity and reliability of the staining process. A positive section provided by the company was taken as positive control. In the negative control, PBS was used to replace the primary antibody.

The immunohistochemical staining (IHC) was independently assessed by two experienced pathologists in a double-blind fashion. Positive p27 staining was mainly localized in the cell nuclei and only rarely in the cytoplasm. All fields of each section were observed. If there was no positive cell, the grade was 0; under 30% of positive cells the grade was 1; 31-70% positive cells the grade was 2; >70% positive cells the grade was 3. The criterion of the staining intensity was determined by the staining characteristics of most cells in each section. If there was no staining, the scale was 0; weak yellow staining was grade 1; brown yellow staining was grade 2; brown staining was grade 3. The final staining results were determined by the total of the staining and intensity grade. If the total grade was 0, the result was regarded as negative (-); grades between 1 and 3 as weakly positive (+); grades between 4 and 6 as strongly positive (++)^[10].

In situ hybridization

In situ hybridization (ISH) was used for the detection of p27^{kip1} mRNA. The p27^{kip1} probe with digoxin-labeled and ISH kit was purchased from Wuhan Boster Biological Technology Ltd. The main steps were as follows. All slides were baked overnight at 58-60 °C. The tissues were deparaffinized by xylene and graded alcohols, treated with 3% H₂O₂ at room temperature for 10 min. Proteinase K freshly diluted with 3% citrate acid was added at 37 °C for 10-15 min. The tissues were pre-hybridized for 3 h at 37 °C in pre-hybridization liquid. Digoxin-labeled probe with coverslip was added, the tissues were hybridized at 37 °C for about 16 h. The slides were washed four times with SSC at 37 °C. Block liquid was added for 3 min at 37 °C. Mouse biotin-antidigoxin antibody was applied for 60 min at 37 °C, followed by detection with nitroblue tetrazolium and 5-bromo-4-chloro-3-indolyl phosphate (NBT/BCIP) for 20 min. Positive control provided by the company was used. Hybridization liquid replaced by PBS served as negative control.

ISH staining was evaluated according to the following scales: no positive cell for negative, 1+ for staining in <25% of cells, 2+ for staining in 25-70% of cells, and 3+ for staining in >70% of cells^[11].

Methylation-specific PCR

Tissues were deparaffinized by xylene and graded alcohols. Genomic DNA was then extracted with a standard phenol/chloroform procedure. DNA methylation patterns in the CpG islands of the p27^{kip1} gene were determined by methylation-specific PCR (MSP)^[12]. MSP distinguishes unmethylated from methylated alleles based on sequence changes produced after bisulfite treatment of DNA, which converts unmethylated (but not methylated) cytosine to uracil, and subsequent PCR using primers were designed for either methylated or unmethylated DNA. Sodium bisulfite modification was performed using the CpGenomeTM DNA modification kit (Intergen, Oxford, UK) according to the manufacturer's protocol with minor modifications. Briefly, DNA was denatured by NaOH (final concentration, 0.2 mol/L) for 15 min at 37 °C. Sodium bisulfite solution at pH 5.0, freshly prepared, was added (550 µL), and incubated at 50 °C for 20 h. The modified DNA was treated with NaOH (final concentration, 0.3 mol/L) for 5 min at room temperature. After precipitation by ethanol, the DNA was resuspended in TE buffer (10 mmol/L Tris pH 8.0, 0.1 mmol/L EDTA)^[13]. The primer sequences for the p27^{kip1} methylated reaction were 5'-AAGAGGCGAG-TTAGCGT-3' (sense) and 5'-AAAACGCCGCCGAACGA-3' (antisense); 5'-ATGGAAGAGGTTAGTTAGT-3' (sense) and 5'-AAAACCCCAATTAACA-3' (antisense) for the p27^{kip1} unmethylated reaction^[14]. PCR was carried out in a 10 µL volume containing PCR buffer (10 mmol/L Tris-HCl pH 8.3, 50 mmol/L KCl, 1.5 mmol/L MgCl₂), dNTPs (250 µmol/L each), primers (2.5 pmol each), 0.4 unit of *TaKaRa taq*TM (DR100A, TaKaRa Biotech, Dalian, China) and approximately 10-100 ng bisulfite-modified DNA. Amplification was carried out in a DNA Autorisierter thermocycler (Eppendorf) with initial denaturing at 95 °C for 3 min followed by 34 cycles of denaturing at 94 °C for 1 min, annealing for 1 min at 53 °C (for p27^{kip1} methylated reaction) or at 58 °C (for p27^{kip1} unmethylated reaction), extension for 1 min at 72 °C, and then a final extension for 10 min at 72 °C. DNA extracted from HCC treated with methylase (SssI, New England BioLabs, Beverly, MA, USA) was used as the methylated control and DNA extracted from relatively normal liver was the unmethylated control. Amplified products were electrophoresed on 2% agarose gels and visualized with ethidium bromide staining. In the total, we tested 44 cases including 6 cases of normal liver, 10 cases of liver cirrhosis and 28 cases of HCC.

Statistical analysis

The Fisher's exact test, χ^2 test and Spearman's correlation were used.

RESULTS

p27 protein expression

The positive rate of p27 protein was 66.7% (4/6) in normal

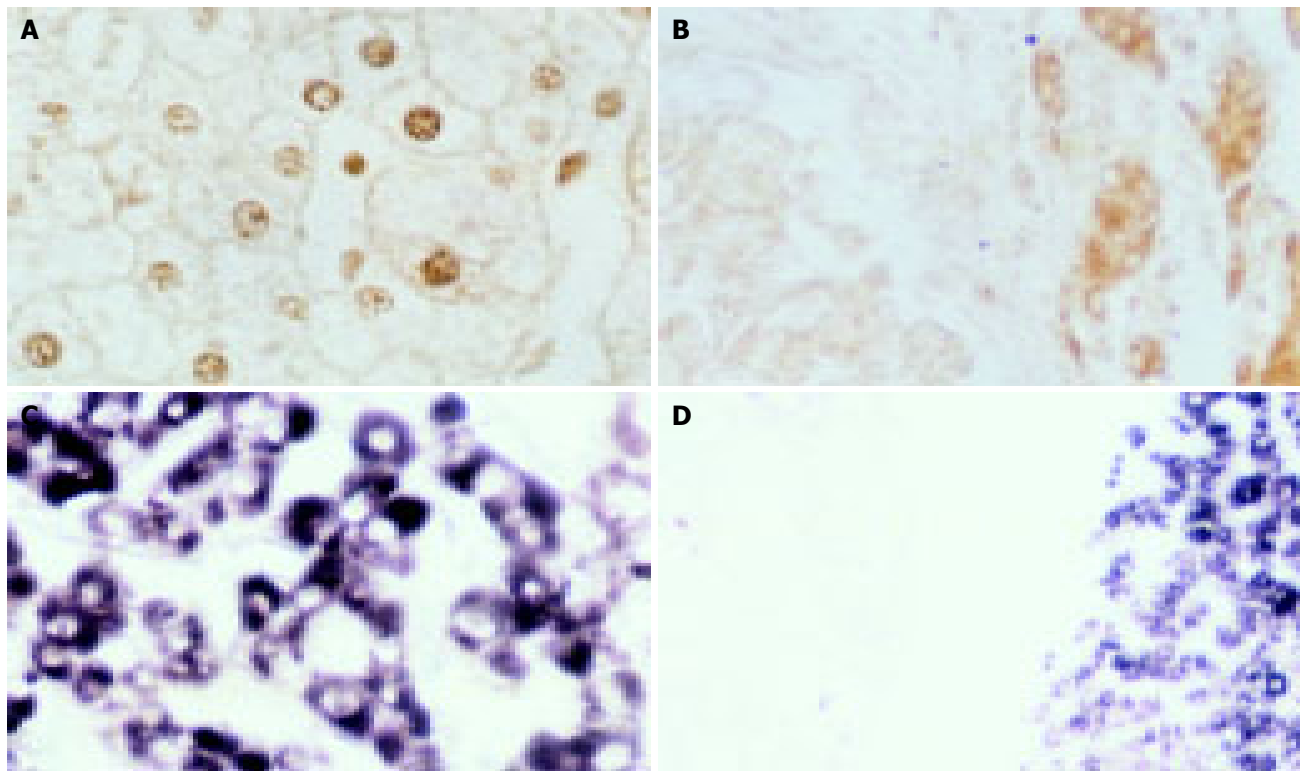


Figure 1 Expressions of p27. **A:** p27 protein was expressed in nuclei of liver cirrhosis (SP $\times 400$); **B:** p27 protein was expressed in pericancerous cirrhosis, but not in HCC (SP $\times 200$); **C:** p27mRNA was positive in liver cirrhosis (ISH $\times 200$);

$\times 200$); **D:** p27mRNA was positive in pericancerous cirrhosis, but negative in HCC (ISH $\times 100$).

liver, 60.0% (6/10) in liver cirrhosis, 50.0% (12/24) in pericancerous cirrhosis and 21.4% (6/28) in HCC. There were no statistical differences in normal liver, liver cirrhosis and pericancerous cirrhosis, but the positive rate of p27 protein significantly decreased in HCC compared to that in the other groups ($P = 0.006$, $\chi^2 = 7.664$). In addition, the positive signals of p27 protein were mainly located in nuclei in normal liver and liver cirrhosis (Figure 1A), while they were located in cytoplasm in pericancerous cirrhosis and HCC (Figure 1B).

Table 1 Correlation between expression of p27mRNA and p27 protein in integrated group of normal liver and liver cirrhosis

p27 protein	p27mRNA		Total
	+	-	
+	9	1	10
-	3	3	6
Total	12	4	16

Table 2 Correlation between expression of p27mRNA and p27 protein in pericancerous cirrhosis group

p27 protein	p27mRNA		Total
	+	-	
+	10	2	12
-	8	4	12
Total	18	6	24

p27^{kip1} mRNA expression

The positive result showed blue coloration in the cytoplasm (Figures 1C and D). The positive rate of p27^{kip1} mRNA was 83.3% (5/6) in normal liver, 70.0% (7/10) in liver cirrhosis, 75.0% (18/24) in pericancerous cirrhosis and 25.0% (7/28) in HCC. There were no statistical differences in normal liver, liver cirrhosis and pericancerous cirrhosis, but the positive rate of p27^{kip1} mRNA also significantly decreased in HCC compared to that in the other groups ($P = 0.000$, $\chi^2 = 16.600$). There was a significant correlation between the expression of p27 protein and p27mRNA in the integrated group of normal liver and liver cirrhosis ($P = 0.082 < 0.1$, $\chi^2 = 0.447$, $r = 0.447$, Table 1). However, no significant correlations were between pericancerous cirrhosis ($P = 0.368$, $\chi^2 = 0.192$, $r = 0.192$) and HCC ($P = 0.611$, $\chi^2 = 0.101$, $r = 0.101$, Tables 2 and 3).

p27^{kip1} hypermethylation

p27^{kip1} promoter hypermethylation was only detected in 1 of 28 HCC cases, which was negative when detected by

Table 3 Correlation between expression of p27mRNA and p27 protein in HCC

p27 protein	p27mRNA		Total
	+	-	
+	2	4	6
-	5	17	22
Total	7	21	28

ISH and IHC. $p27^{kip1}$ methylation was not detected in any of 10 cases of liver cirrhosis and 6 cases of normal livers. Methylated and unmethylated control DNA showed the expected fragment sizes of 195 and 212 bp (Figure 2).

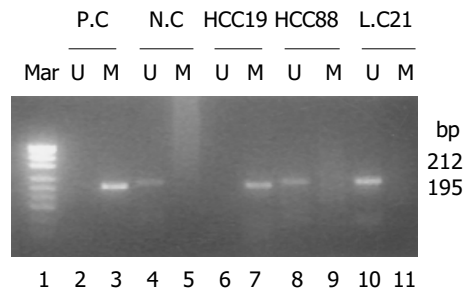


Figure 2 MCP of CpG islands of $p27^{kip1}$ promoter. Lane 1: marker; lanes 2, 4, 6, 8 and 10: PCR products of each case to unmethylated specific primers. Lanes 3, 5, 7, 9 and 11: PCR products of each case to methylated specific primers. In HCC19 case, only methylated DNA (M) was present. HCC88 case and L.C21 case (liver cirrhosis case) showed unmethylated status (U). Positive control (P.C) for methylated DNA was treated with SssI methylase first, normal control (N.C) for unmethylated DNA.

DISCUSSION

$p27$ is involved in cancer because of its essential role in controlling cell cycle progression^[1]. Decreased expression of $p27$ protein is inversely correlated with stage of disease at the time of surgery in HCC, reduced $p27$ is significantly related to advanced locoregional extent of the primary tumor and tumor size^[15]. The expression of $p27$ is a favorable prognostic indicator in patients with HCC^[16] and other tumors^[17,18]. Our results revealed that $p27$ protein was expressed in normal liver, liver cirrhosis, pericancerous cirrhosis and HCC, but the positive expression rate of $p27$ protein significantly decreased in HCC compared to that in the other groups. The loss or decrease of $p27$ protein may lead to reduction or disappearance of its cell cycle negative regulation, thus cells pass the G_1 phase into S phase, resulting in division and autonomous program^[19].

Our results also revealed that the positive rate of $p27$ mRNA was high in the normal liver, liver cirrhosis and pericancerous cirrhosis, and there were no differences in them. But the level of $p27$ mRNA was low in HCC compared to that in the other groups, suggesting that reduced $p27$ expression may be at least partly responsible for human hepatocarcinogenesis^[4]. There was a significant correlation between the expression of $p27$ protein and $p27$ mRNA in the integrated group of normal liver and liver cirrhosis. However, no significant correlations were found between pericancerous cirrhosis and HCC. This phenomenon has not been reported. Whether the expression of $p27$ protein is regulated by $p27$ mRNA before carcinogenesis or by other mechanisms remains to be verified.

After having analyzed 44 cases (including 6 cases of normal liver, 10 cases of liver cirrhosis and 28 cases of HCC) by MSP, we found that one HCC case was hypermethylated, whose $p27$ protein and $p27$ mRNA were negative, suggesting that $p27$ methylation might lead to its

loss of transcription, contributing to cell proliferation. The same result has been reported in a few other tumors^[20-22], but not in HCC^[23]. Because there are few reports on the $p27$ methylation in HCC, only one HCC case was hypermethylated in our study, we could not analyze the relationship between the $p27$ mRNA expression and $p27$ gene methylation.

In conclusion, reduction or loss of $p27$ protein and $p27$ mRNA is potentially involved in hepatocarcinogenesis, and hypermethylation of $p27$ may lead to the loss of $p27$ mRNA transcription^[20-22].

REFERENCES

- 1 Polyak K, Lee MH, Erdjument-Bromage H, Koff A, Roberts JM, Tempst P, Massague J. Cloning of $p27^{kip1}$, a cyclin-dependent kinase inhibitor and a potential mediator of extracellular antimitogenic signals. *Cell* 1994; **78**: 59-66
- 2 Ito Y, Matsuura N, Sakon M, Miyoshi E, Noda K, Takeda T, Umeshita K, Nagano H, Nakamori S, Dono K, Tsujimoto M, Nakahara M, Nakao K, Taniguchi N, Monden M. Expression and prognostic roles of the G1-S modulators in hepatocellular carcinoma: $p27$ independently predicts the recurrence. *Hepatology* 1999; **30**: 90-99
- 3 Chen TC, Ng KF, Lien JM, Jeng LB, Chen MF, Hsieh LL. Mutational analysis of the $p27^{kip1}$ gene in the hepatocellular carcinoma. *Cancer Lett* 2000; **153**: 169-173
- 4 Hui AM, Sun L, Kanai Y, Sakamoto M, Hirohashi S. Reduced $p27^{kip1}$ expression in hepatocellular carcinomas. *Cancer Lett* 1998; **132**: 67-73
- 5 Paulsen M, Ferguson-Smith AC. DNA methylation in genomic imprinting, development and disease. *J Pathol* 2001; **195**: 97-110
- 6 Curradi M, Izzo A, Badaracco G, Landsberger N. Molecular mechanisms of gene silencing mediated by DNA methylation. *Mol Cell Biol* 2002; **22**: 3157-3173
- 7 Tsujie M, Yamamoto H, Tomita N, Sugita Y, Ohue M, Sakita I, Tamaki Y, Sekimoto M, Doki Y, Inoue M, Matsuura N, Monden T, Shiozaki H, Monden M. Expression of tumor suppressor gene p16^{INK4} products in primary gastric cancer. *Oncology* 2000; **58**: 126-136
- 8 Nakamura M, Yonekawa Y, Kleihues P, Ohgaki H. Promoter hyper methylation of the RB1 gene in glioblastomas. *Lab Invest* 2001; **81**: 77-82
- 9 Konishi N, Nakamura M, Kishi M, Nishimine M, Ishida E, Shimada K. DNA hypermethylation status of multiple genes in prostate adenocarcinomas. *Jpn J Cancer Res* 2002; **93**: 767-773
- 10 Zhao JG, Wu AG, Huang ZH, Yang JH. Expression of $p27$ and its clinical significance in colorectal carcinomas. *Chin Ger J Clin Oncol* 2002; **1**: 129-131
- 11 Erickson LA, Jin L, Wollan P, Thompson GB, Heerden JA, Lloyd RV. Parathyroid hyperplasia, adenomas, and carcinomas: differential expression of $p27^{kip1}$ protein. *Am J Surg Pathol* 1999; **23**: 288-295
- 12 Herman JG, Graff JR, Myohanen S, Nelkin BD, Baylin SB. Methylation-specific PCR: a novel PCR assay for methylation status of CpG islands. *Proc Natl Acad Sci USA* 1996; **93**: 9821-9826
- 13 Nakamura M, Watanabe T, Klangby U, Asker C, Wiman K. p14 Deletion and Methylation in genetic Pathways to Glioblastomas. *Brain Pathol* 2001; **11**: 159-168
- 14 Nakamura M, Toshisuke S, Hashimoto H, Nakase H, Ishida E. Frequent alteration of the p14^{ARF} and p16^{INK4a} Genes in primary Central Nervous System Lymphomas. *Cancer Res* 2001; **61**: 6335-6339
- 15 Tannapfel A, Grund D, Katalinic A, Uhlmann D, Kocherling F, Haugwitz U, Wasner M, Hauss J, Engeland K, Wittekind C. Decreased expression of $p27$ protein is associated with advanced tumor stage in hepatocellular carcinoma. *Int J Cancer* 2000; **89**: 350-355

- 16 **Fiorentino M**, Altimari A, D'rrico A, Cukor B, Barozzi C, Loda M, Grifioni WF. Acquired expression of p27 is a favorable prognostic indicator in patients with hepatocellular carcinoma. *Clin Cancer Res* 2000; **6**: 3966-3972
- 17 **Nitti D**, Belluco C, Mammano E, Marchet A, Ambrosi A, Mencarelli R, Segato P, Lise M. Low level of p27(Kip1) protein expression in gastric adenocarcinoma is associated with disease progression and poor outcome. *J Surg Oncol* 2002; **81**: 167-175
- 18 **Anastasiadis AG**, Calvo-Sanchez D, Franke KH, Ebert T, Heydthausen M, Schulz WA, Burchardt M, Gerharz CD. p27KIP1 expression in human renal cell cancers: implications for clinical outcome. *Anticancer Res* 2003; **23**: 217-221
- 19 **Filipits M**, Puhalla H, Wrba F. Low p27Kip1 expression is an independent prognostic factor in gallbladder carcinoma. *Anticancer Res* 2003; **23**: 675-679
- 20 **Qian X**, Jin L, Kulig E, Lloyd RV. DNA methylation regulates p27kip1 expression in rodent pituitary cell lines. *Am J Pathol* 1998; **153**: 1475-1482
- 21 **Worm J**, Bartkova J, Kirkin AF, Straten P, Zeuthen J, Bartek J, Guldberg P. Aberrant p27Kip1 promoter methylation in malignant melanoma. *Oncogene* 2000; **19**: 5111-5115
- 22 **Nakatsuka S**, Liu A, Yao M, Takakuwa T, Tomita Y, Hoshihiko Y, Nishiu M, Aozasa K. Methylation of promoter region in p27 gene plays a role in the development of lymphoid malignancies. *Int J Oncol* 2003; **22**: 561-568
- 23 **Yu J**, Zhang HY, Ma ZZ, Lu W, Wang YF, Zhu JD. Methylation profiling of twenty four genes and the concordant methylation behaviours of nineteen genes that may contribute to hepatocellular carcinogenesis. *Cell Res* 2003; **13**: 319-333

Science Editor Wang XL and Guo SY Language Editor Elsevier HK

• BRIEF REPORTS •

Evaluation of contrast-enhanced helical hydro-CT in staging gastric cancer

Wen-Zhou Wei, Jie-Ping Yu, Jun Li, Chang-Sheng Liu, Xiao-Hua Zheng

Wen-Zhou Wei, Chang-Sheng Liu, Xiao-Hua Zheng, Department of Radiology, Renmin Hospital of Wuhan University, Wuhan 430060, Hubei Province, China

Jie-Ping Yu, Department of Gastroenterology, Renmin Hospital of Wuhan University, Wuhan 430060, Hubei Province, China

Jun Li, Department of Stomatology, Renmin Hospital of Wuhan University, Wuhan 430060, Hubei Province, China

Correspondence to: Assistant Professor Wen-Zhou Wei, Department of Radiology, Renmin Hospital of Wuhan University, Wuhan 430060, Hubei Province, China. weizhou8@msn.com

Telephone: +86-27-88041911-8290

Received: 2004-08-18 Accepted: 2004-12-21

Abstract

AIM: To discuss the helical computed tomography (CT) characteristics of gastric cancer and evaluate the diagnostic value of contrast-enhanced helical hydro-CT (HHCT) in staging gastric cancer.

METHODS: A total of 50 patients with gastric cancer were included in this study. The CT findings in them were retrospectively analyzed and correlated with pathologic findings at surgery. All patients were preoperatively imaged by plain and contrast-enhanced helical CT after orally ingesting 1 000-1 500 mL water. Peristalsis was minimized by intravenous administration of spasmolytics.

RESULTS: The foci of gastric cancer became more prominent in all the 50 patients and showed strong enhancement in contrast-enhanced HHCT. The tumor was located at the gastric cardia in 14 cases, at the gastric fundus in 3 cases, at the gastric body in 8 cases, at the gastric antrum in 4 cases, at the gastric fundus and the body in 8 cases, at the gastric body and antrum in 11 cases, and at three segments of the stomach in 2 cases. The CT features of gastric cancer were focal or diffuse mural thickening, soft tissue mass, cancerous ulcer, stenosis of stomach, infiltration to adjacent tissues, lymph node and distant metastases. Strong contrast enhancement of the gastric wall was closely related to gastric cancer. The accuracy rate of contrast-enhanced HHCT in staging gastric cancer was 86% (43/50). The detection rate of lymph node metastases by CT was 60% (12/20).

CONCLUSION: Contrast-enhanced HHCT is a reliable method to diagnose and stage gastric cancer.

© 2005 The WJG Press and Elsevier Inc. All rights reserved.

Key words: Stomach; Neoplasm; Tomography; X-ray; Staging

Wei WZ, Yu JP, Li J, Liu CS, Zheng XH. Evaluation of contrast-enhanced helical hydro-CT in staging gastric cancer. *World J Gastroenterol* 2005; 11(29): 4592-4595

<http://www.wjgnet.com/1007-9327/11/4592.asp>

INTRODUCTION

Gastric cancer is one of the most common malignancies in China. Its accurate staging contributes to its pre-operative management^[1-4]. In the evaluation of gastric diseases, gastroscopy is used for the detection of gastric abnormality. Computed tomography (CT) is a valuable tool in addition to gastroscopy in the evaluation of gastric diseases^[5-7]. With the clinical application of helical CT and the improvement of CT equipments, helical CT has been used for the detection of gastric abnormality and in staging of gastric cancer^[8-11]. Since January 1999, 50 patients with gastric cancer have been scanned. CT results are correlated with surgical and pathologic findings. This work aimed to analyze the characteristic findings of gastric cancer, stage the tumor and evaluate the clinical value of CT imaging of the stomach.

MATERIALS AND METHODS

Patients

A total of 50 cases of gastric cancer were examined by helical hydro-CT (HHCT) and their clinical data were collected from January 1999 to April 2004. There were 36 male and 14 female patients with an age range of 39-81 years (mean 58.3 years).

CT examination

All patients included in the study were fasting for at least 5 h before CT imaging with a commercially available scanner (Hispeed CT/i unit GE Medical Systems, Milwaukee, WI, USA). Thirty minutes before scanning, the patients ingested 500-1 000 mL of water, and were then examined in the supine position during full inspiration. Immediately before helical scanning, the patients received 20-40 mg of anisodamine (raceanisodamine hydrochloride, Hangzhou, China) intramuscularly to minimize peristalsis. An additional 500 mL of water was then offered to improve distension of the proximal part of the stomach. First, a plain scan of the upper abdomen was obtained using 10-mm sections. If the tumor was located at the antral or pyloric antrum, patients were then examined in the prone position, followed by injection of 80-100 mL of contrast material (Omnipaque, Schering, Germany) at a rate of 2.5-3.0 mL/s (Madrid power injector, SA) into the antecubital vein. Helical scanning of

the stomach was performed at 30, 60-70, 150-180 s after contrast material was injected. It started above the diaphragm to cover the gastric cardia by obtaining contrast images with 5- or 7-mm collimation, a pitch of 1.5:1.0 or 1.1:1.0 (120 kV, 210 mA), and a matrix size of 512×512, then 3-mm axial scans were reconstructed for image evaluation.

Image interpretation

Without prior knowledge of endoscopic, surgical, or histological findings, one reviewer interpreted all CT studies. First, the gastric wall was evaluated for the presence of tumor. Carcinoma of the stomach was suspected if thickening and marked contrast enhancement of the gastric wall were visible on CT. The depth of infiltration and perigastric invasion of gastric tumors were evaluated according to the TNM system^[11].

CT staging of gastric tumor was performed as follows: T1, invasion of the lamina propria or submucosa, when thickening was limited to the inner layer; T2, invasion of the muscularis propria, when all three layers of the gastric wall were grossly thickened and replaced by a homogeneous or inhomogeneous soft tissue mass with no serosal irregularity; T3, tumor invasion of the serosa, when high-density irregularities of the outer layer or micronodularity or strands in the fat planes contiguous to the lesion were evident; T4, invasion of adjacent organs and structures, when cleavage fat planes between neoplastic gastric wall and contiguous organs were replaced by mass or when the invasion was clearly demonstrated.

Soft tissue nodules were classified as lymph nodes, which were divided into loco regional peri-gastric lymph nodes (N1/N2 = 3 cm away from the gastric tumor) and distant nodes which were classified as metastatic disease (M1) according to the TNM system if it has tumor infiltration. All visible lymph nodes were judged to be infiltrated by carcinoma independent of size or contrast enhancement. In abdominal M staging, any hepatic or splenic lesion other than a cyst was regarded as potentially malignant. Nodular thickening of the peritoneum or ascites without signs of liver cirrhosis was assumed to be peritoneal carcinomatosis.

CT-histopathologic correlation

All resected specimens were carefully examined both macroscopically and microscopically. A lesion-by-lesion analysis was performed, and gastric carcinoma was staged according to the American Joint Committee on Cancer (AJCC) classification^[11]. The histological studies were correlated with the CT data, and comparative evaluation of location, size, depth of tumor infiltration, and extent of the primary tumor was performed. The presence of lymph node metastasis was histologically determined, and the histological N stage of the tumor was correlated with CT findings. In all patients who underwent surgery, the abdomen was carefully explored to exclude metastatic disease.

Statistical analysis

According to the AJCC classification, TNM staging criteria were applied to all cases. The accuracy of CT imaging to predict the T, N, and M stage of gastric cancer was determined. The overall detection rate of gastric cancer was determined.

The maximum diameter of each cancer was calculated and compared with the maximum diameter of the tumor determined by pathology. The largest tumor diameter was used for correlation with the pathologic size of the tumor.

RESULTS

All CT studies were successfully completed. A lesion-by-lesion analysis revealed that 43 of 50 (86%) gastric cancer were correctly staged by HHCT. Gastrectomy was performed in 46 patients, 4 patients with T1 tumor underwent partial gastrectomy. In all cases, histology revealed malignant ulcer corresponding to early gastric cancer.

Location and histological classification of the tumor

The maximum diameter of the resected gastric tumors ranged 0.7-15 cm (mean 5.3 cm). Fourteen cancers were located at the gastric cardia, three of them showed infiltration of the distal esophagus, three of them invaded the gastric body, and two of them infiltrated both the distal esophagus and the gastric body. The remaining cancers were located at the gastric fundus ($n = 3$), the gastric body ($n = 8$), the gastric antrum ($n = 4$), the gastric fundus and the body ($n = 8$), and the gastric body and antrum ($n = 11$). In two cases, the gastric cancer involved three segments of the stomach (*limitis plastica*).

The histological classifications were papillary adenocarcinoma (5 cases), mucous carcinoma (2 cases), low-grade adenocarcinoma (35 cases), undifferentiated carcinoma (2 cases), squamous carcinoma (3 cases), and adenosquamous carcinoma (3 cases).

Contrast-enhanced HHCT findings of gastric cancer

In 13 of 50 cases (26%), single layer normal gastric wall was demonstrated. In the remaining 37 cases (74%), two- or three-layer structure was shown at arterial phase of contrast-enhanced HHCT scans. Abnormal local gastric wall thickening and area of strong contrast medium enhancement were found in one of four early gastric cancers confirmed by pathology. Two layers of gastric wall were found in 3 patients with early gastric cancer and in 5 of 46 patients with advanced gastric cancer. In the three advanced gastric cancers, low attenuation was found with no enhancement below the strong enhancement inner layer, their pathological diagnosis was mucous carcinoma. Single or triple layer gastric wall with homogeneous or heterogeneous strong enhancement was shown in the remaining advanced gastric cancer, their mean increase of CT values was 26.47 ± 6.67 HU. Gastric wall thickening was found in 37 cases (Figures 1A and B), intramural soft mass in 23 cases (Figure 1C), lymph node metastasis in 12 cases, tumor spread to perigastric area and infiltration to adjacent organs in 9 cases, and distant metastasis in 7 cases. In our study, the detection rate of lymph node metastasis by CT was 60% (12/20).

Gastric cancer staging by CT and pathology

The TNM staging of gastric cancer by contrast-enhanced HHCT was compared to the pathological results in 50 cases (Table 1). In 43 of 50 cases, HHCT staging of gastric cancer was in accordance with pathological staging. The accurate



Figure 1 Enhancement patterns of gastric cancer on contrast-enhanced HHCT. **A:** Focal wall thickening in gastric antrum with marked enhancement of mucosal layer and narrowing of gastric lumina; **B:** focal wall thickening with marked

enhancement of mucosal layer in greater curvature of the gastric body; **C:** homogeneous enhancement of soft tissue mass in anterior wall of the gastric body.

rate of T staging by HHCT was 86.0% (43/50). Findings at HHCT were concordant with histological findings in 2 of 4 T1 tumors (50%), in 17 of 20 T2 tumors (85%), in 15 of 17 T3 tumors (83.3%), and in 7 of 9 T4 tumors (77.8%). Overstaging occurred in 2 T1 tumors and in 3 T2 tumors on CT images. In addition, 2 T4 tumors were understaged.

Table 1 T staging of gastric carcinoma ($n = 50$)

Staging at CT	Staging at pathology			
	T1	T2	T3	T4
T1	2			
T2	2	17	2	
T3		3	15	2
T4				7

DISCUSSION

Normal architecture of gastric wall and enhancement pattern of gastric cancer on contrast-enhanced HHCT

Normal gastric wall is histologically classified as four slices: mucosa, submucosa, muscular layer, and serosa. The structure of gastric wall is shown as a single slice in conventional CT. The excellent spatial resolution of helical CT makes it possible to identify the triple-layer structure of the gastric wall after contrast material is intravenously injected. The inner layer with high attenuation corresponds to the mucosa and its muscular layer, the middle layer with low attenuation corresponds to the submucosal layer, and the outer layer with slightly high attenuation corresponds to the muscular layer and serosa^[12-15]. The results of our study are concordant with the previous reports^[16,17]. After gastric lumen was sufficiently filled, the mean thickness of normal gastric wall was 2-3 mm on CT image, while it was 4-5 mm at cardia and antrum^[18]. Otherwise it was regarded as abnormal. The thickness of gastric lumen may be equal to 1.0 cm or above, if not being sufficiently filled. Therefore, it is a prerequisite to fill gastric lumen before CT examination.

Significance of contrast-enhanced HHCT in staging gastric cancer

CT is most frequently used in staging gastric cancer. Helical CT in combination with the water-filling method has led to

marked improvements in the detection and characterization of gastric cancer^[19]. The main CT findings of gastric cancer are local or diffuse thickenings of gastric wall with variable enhancement and intraluminal soft tissue mass. In this study, gastric wall thickening was found in 37 cases, intraluminal soft tissue mass in 13 cases, local and distant lymph metastasis in 12 cases. Tumor can also infiltrate into perigastric tissue, encroach on adjacent organs and metastasize to distant places. Contrast-enhanced HHCT can reflect blood supply to gastric cancer.

Reports on staging gastric cancer by conventional CT prior to surgery are available^[20]. Recently more and more studies have been focused on staging gastric cancer by helical CT^[21]. Our study demonstrated that TNM staging by CT was closely related with pathology. The accuracy of HHCT (86.0%) in our study was higher than that of conventional CT (72%)^[13]. TNM staging by HCT depends upon the improvement of CT equipments and stomach filling with water. Contrast-enhanced HHCT can further improve the accuracy of gastric cancer staging before operation.

Our results showed 60.0% of all lymph nodes were detected by HHCT. The sensitivity of detecting lymph node metastasis was not high. The detection of regional lymph nodes can be improved by hypotension of the stomach, because the delineation of regional lymph nodes and gastric wall can be improved^[22]. Enlarged lymph nodes may be missed if they are located close to the gastric cancer. For the assessment of lymph node metastasis, the size of lymph nodes is the most frequently used criterion. But there is no agreement concerning the upper limits of normal lymph node size. The diameter of normal lymph nodes in the upper abdomen may vary from 6 to 11 mm depending on their location^[23-25]. Lymph nodes in the gastro-hepatic ligament region have to be considered as abnormal if they exceed 8 mm in diameter. A diameter of lymph nodes in 8-15 mm is used in studies as the upper limit for normal lymph nodes^[26-28]. However, when these criteria are used, false-negative and false-positive results may occur because micrometastases do not result in enlargement or inflammatory changes in lymph nodes^[4,13,29,30]. Contrast enhancement of lymph nodes can be useful in differentiating lymph nodes with and without metastasis^[11]. Further study is needed to improve methods for the detection of lymph node metastasis such as dynamic CT^[4,31].

In conclusion, the primary pathologic condition of gastric cancer and its metastasis to adjacent or distant structures can be demonstrated by contrast-enhanced HHCT. HHCT can provide more information for surgeons to make an appropriate therapy for gastric cancer patients.

REFERENCES

- 1 **Dehn TC**, Reznek RH, Nockler IB, White FE. The pre-operative assessment of advanced gastric cancer by computed tomography. *Br J Surg* 1984; **71**: 413-417
- 2 **Botet JF**, Lightdale CJ, Zauber AG, Gerdes H, Winawer SJ, Urmacher C, Brennan MF. Preoperative staging of gastric cancer: comparison of endoscopic US and dynamic CT. *Radiology* 1991; **181**: 426-432
- 3 **DElia F**, Zingarelli A, Palli D, Grani M. Hydro-dynamic CT preoperative staging of gastric cancer: correlation with pathological findings. A prospective study of 107 cases. *Eur Radiol* 2000; **10**: 1877-1885
- 4 **Hundt W**, Braunschweig R, Reiser M. Assessment of gastric cancer: value of breathhold technique and two-phase spiral CT. *Eur Radiol* 1999; **9**: 68-72
- 5 **Shirakawa T**, Fukuda K, Tada S. New method for evaluation of perigastric invasion of gastric cancer by right lateral position CT. *Eur Radiol* 1996; **6**: 358-361
- 6 **Lee DH**, Ko YT. Advanced gastric carcinoma: the role of three-dimensional and axial imaging by spiral CT. *Abdom Imaging* 1999; **24**: 111-116
- 7 **Lee DH**. Two-dimensional and three-dimensional imaging of gastric tumors using spiral CT. *Abdom Imaging* 2000; **25**: 1-6
- 8 **Tsuda K**, Hori S, Murakami T, Nakamura H, Tomoda K, Nakanishi K, Shiozaki H. Intramural invasion of gastric cancer: evaluation by CT with water-filling method. *J Comput Assist Tomogr* 1995; **19**: 941-947
- 9 **Dux M**, Richter GM, Hansmann J, Kuntz C, Kauffmann GW. Helical hydro-CT for diagnosis and staging of gastric carcinoma. *J Comput Assist Tomogr* 1999; **23**: 913-922
- 10 **Sohn KM**, Lee JM, Lee SY, Ahn BY, Park SM, Kim KM. Comparing MR imaging and CT in the staging of gastric carcinoma. *Am J Roentgenol* 2000; **174**: 1551-1557
- 11 **Ba-Ssalamah A**, Prokop M, Uffmann M, Pokieser P, Teleky B, Lechner G. Dedicated multidetector CT of the stomach: spectrum of diseases. *Radiographics* 2003; **23**: 625-644
- 12 **Kuntz C**, Herfarth C. Imaging diagnosis for staging of gastric cancer. *Semin Surg Oncol* 1999; **17**: 96-102
- 13 **Rossi M**, Broglio L, Maccioni F, Bezzi M, Laghi A, Graziano P, Mingazzini PL, Rossi P. Hydro-CT in patients with gastric cancer: preoperative radiologic staging. *Eur Radiol* 1997; **7**: 659-664
- 14 **Kadowaki K**, Murakami T, Yoshioka H, Kim T, Takahashi S, Tomoda K, Narumi Y, Nakamura H. Helical CT imaging of gastric cancer: normal wall appearance and the potential for staging. *Radiat Med* 2000; **18**: 47-54
- 15 **Bhandari S**, Shim CS, Kim JH, Jung IS, Cho JY, Lee JS, Lee MS, Kim BS. Usefulness of three-dimensional, multidetector row CT (virtual gastroscopy and multiplanar reconstruction) in the evaluation of gastric cancer: a comparison with conventional endoscopy, EUS, and histopathology. *Gastrointest Endosc* 2004; **59**: 619-626
- 16 **Cho JS**, Kim JK, Rho SM, Lee HY, Jeong HY, Lee CS. Preoperative assessment of gastric carcinoma: value of two-phase dynamic CT with mechanical iv. injection of contrast material. *Am J Roentgenol* 1994; **163**: 69-75
- 17 **Fukuya T**, Honda H, Kaneko K, Kuroiwa T, Yoshimitsu K, Irie H, Maehara Y, Masuda K. Efficacy of helical CT in T-staging of gastric cancer. *J Comput Assist Tomogr* 1997; **21**: 73-81
- 18 **Scatarige JC**, DiSantis DJ. CT of the stomach and duodenum. *Radiol Clin North Am* 1989; **27**: 687-706
- 19 **Takao M**, Fukuda T, Iwanaga S, Hayashi K, Kusano H, Okudaira S. Gastric cancer: evaluation of triphasic spiral CT and radiologic-pathologic correlation. *J Comput Assist Tomogr* 1998; **22**: 288-294
- 20 **Rossi M**, Broglio L, Graziano P, Maccioni F, Bezzi M, Masciangelo R, Rossi P. Local invasion of gastric cancer: CT findings and pathologic correlation using 5-mm incremental scanning, hypotonia, and water filling. *Am J Roentgenol* 1999; **172**: 383-388
- 21 **Lee JH**, Jeong YK, Kim DH, Go BK, Woo YJ, Ham SY, Yang SO. Two-phase helical CT for detection of early gastric carcinoma: importance of the mucosal phase for analysis of the abnormal mucosal layer. *J Comput Assist Tomogr* 2000; **24**: 777-782
- 22 **Davies J**, Chalmers AG, Sue-Ling HM, May J, Miller GV, Martin IG, Johnston D. Spiral computed tomography and operative staging of gastric carcinoma: a comparison with histopathological staging. *Gut* 1997; **41**: 314-319
- 23 **Dorfman RE**, Alpern MB, Gross BH, Sandler MA. Upper abdominal lymph nodes: criteria for normal size determined with CT. *Radiology* 1991; **180**: 319-322
- 24 **De Gaetano AM**, Vecchioli A, Minordi LM, Parrella A, Gaudino S, Masselli G, Savino G. Role of diagnostic imaging in abdominal lymphadenopathy. *Rays* 2000; **25**: 463-484
- 25 **Lee DH**, Ko YT, Park SJ, Lim JW. Comparison of hydro-US and spiral CT in the staging of gastric cancer. *Clin Imaging* 2001; **25**: 181-186
- 26 **Fukuya T**, Honda H, Hayashi T, Kaneko K, Tateshi Y, Ro T, Maehara Y, Tanaka M, Tsuneyoshi M, Masuda K. Lymph-node metastases: efficacy for detection with helical CT in patients with gastric cancer. *Radiology* 1995; **197**: 705-711
- 27 **Tunaci M**. Carcinoma of stomach and duodenum: radiologic diagnosis and Staging. *Eur J Radiol* 2002; **42**: 181- 192
- 28 **Gossios K**, Tsianos E, Prassopoulos P, Papakonstantinou O, Tsimoyiannis E, Gourtsoyiannis N. Usefulness of the non-distension of the stomach in the evaluation of perigastric invasion in advanced gastric cancer by CT. *Eur J Radiol* 1998; **29**: 61-70
- 29 **Balfe DM**, Mauro MA, Koehler RE, Lee JK, Weyman PJ, Picus D, Peterson RR. Gastrohepatic ligament: normal and pathologic CT anatomy. *Radiology* 1984; **150**: 485-490
- 30 **Einstein DM**, Singer AA, Chilcote WA, Desai RK. Abdominal lymphadenopathy: spectrum of CT findings. *Radiographics* 1991; **11**: 457-472
- 31 **Magnusson A**, Andersson T, Larsson B, Hagberg H, Sundstrom CH. Contrast enhancement of pathologic lymph nodes demonstrated by computed tomography. *Acta Radiol* 1989; **30**: 307-310

• BRIEF REPORTS •

Apoptosis induction with polo-like kinase-1 antisense phosphorothioate oligodeoxynucleotide of colon cancer cell line SW480

Yu Fan, Shu Zheng, Ze-Feng Xu, Jia-Yi Ding

Yu Fan, Shu Zheng, Ze-Feng Xu, Jia-Yi Ding, Cancer Institute, 2nd Affiliated Hospital, School of Medicine, Zhejiang University, Hangzhou 310009, Zhejiang Province, China

Correspondence to: Shu Zheng, Cancer Institute, 2nd Affiliated Hospital, School of Medicine, Zhejiang University, Hangzhou 310009, Zhejiang Province, China. zhengshu@zju.edu.cn

Telephone: +86-751-87784527

Received: 2004-09-13 Accepted: 2005-01-14

Abstract

AIM: To investigate the effects of polo-like kinase-1 (PLK1) antisense phosphorothioate oligodeoxynucleotide (ASODN) on apoptosis and cell cycle of human colon cancer cell line SW480.

METHODS: After SW480 colon cancer cells were transfected with PLK1 ASODN, Northern and Western blot analyses were used to examine PLK1 gene expression in cancer cells. We studied apoptosis using terminal uridine deoxynucleotidyl nick end labeling. Apoptosis and cell cycle of SW480 cells were examined by fluorescence-activated cell sorter scan.

RESULTS: The levels of PLK1 mRNA and protein were greatly inhibited by PLK1 ASODN in SW480 cancer cells transfected with PLK1 ASODN. Apoptosis index (AI) induced PLK1 ASODN in a time- and dose-dependent manner. Results from FLM showed that sub-2N DNA content of transfected cancer cells was significantly increased and arrested at G₂/M compared with control groups.

CONCLUSION: PLK1 ASODN can induce apoptosis of human colon cancer cell line SW480.

© 2005 The WJG Press and Elsevier Inc. All rights reserved.

Key words: Polo-like kinase-1; Antisense; Apoptosis; Cell cycle

Fan Y, Zheng S, Xu ZF, Ding JY. Apoptosis induction with polo-like kinase-1 antisense phosphorothioate oligodeoxynucleotide of colon cancer cell line SW480. *World J Gastroenterol* 2005; 11(29): 4596-4599

<http://www.wjgnet.com/1007-9327/11/4596.asp>

INTRODUCTION

The polo kinase family includes mammalian polo-like kinase (PLK) 1, Snk, Fnk, *Xenopus laevis* Plx1, *Drosophila* polo,

fission yeast PLO1, and budding yeast Cdc5^[1]. Genetic and biochemical experiments in various organisms indicate that PLK are important regulators of many cell-cycle-related events, including activation of Cdc2, chromosome segregation, centrosome maturation, bipolar spindle formation, regulation of anaphase-promoting complex, and execution of cytokinesis^[1,2]. The importance of PLK1 as a measure for the aggressiveness of a tumor seems to result from its different functions during mitotic progression in particular, its role in the G₂/M transition (phosphorylation of cyclin B1, a component of the mitosis-promoting factor)^[3-5]. PLK1 also phosphorylates substrates that are involved in several additional steps of mitotic progression, including components of the anaphase-promoting complex and the cytokinesis machinery^[6,7]. The activity of PLK1 is elevated in tissues and cells with a high mitotic index, including cancer cells^[8,9]. An increasing body of evidence suggests that the level of PLK1 expression has prognostic value for predicting outcomes in patients with different cancers, including non-small cell lung cancer, squamous cell carcinoma of the head and neck, esophageal carcinoma, oropharyngeal carcinoma, ovarian cancer, breast cancer, endometrial carcinoma, colorectal cancer, and glioma^[10-18]. Takahashi *et al.*^[18], found that some crypt cells in normal colon mucosa show weakly positive staining for PLK1, and PLK1 overexpresses in most of colorectal cancers. Moreover, PLK1 expression is associated with pT (primary tumor invasion) ($P < 0.0006$), pN (regional lymph nodes, $P < 0.008$) and the Dukes' classification ($P < 0.0005$). The results suggest that overexpression of PLK1 might be of pathogenic, prognostic and proliferative importance, so that this kinase might have potential as an invasion and metastasis marker for colorectal cancer. But whether PLK1 plays a role in colon cancer cell is not clear.

In this article, we used ASODN to inhibit the expression of PLK1 in human cancer cell lines SW480 and determined the role of PLK1 in tumorigenesis.

MATERIALS AND METHODS

Cell culture

New fetal calf serum, RPMI-1640, phosphate-buffered saline (PBS), oligofectamine, penicillin and streptomycin, and trypsin were obtained from Invitrogen (Karlsruhe, Germany). Colon cancer line SW480 was obtained from the Institute of Cell Biology, Shanghai, China. Cells were maintained in RPMI 1640 supplemented with 10% newborn bovine serum at 37 °C in 50 mL/L CO₂ atmosphere. The sequence of antisense phosphorothioate oligodeoxynucleotide (ASODN) target PLK1 was 5'-GCAGACCTCGATCC-GAGCAG-3', 20-mer^[20].

***In vitro* transfection with ASODN**

Cancer cells were transfected with ASODN using the oligofectamine protocol (Invitrogen). In brief, 1 d prior to transfection, cancer cells were seeded without antibiotics onto 24-well plates, 1×10^5 cells/well, corresponding to a density of 40–50% at the time of transfection. Cancer cells were transfected with ASODN at different doses (25, 50, 100 nmol/L). There were two control groups: control cells were incubated with RPMI 1640 alone without ASODN or oligofectamine. Cells were harvested 12, 24, 48, and 72 h after the transfection. All transfections were performed in triplicate at each time point.

Northern blot

At 12, 24, 26, 48, 72 h after transfection, total RNAs was isolated using TRIzol according to the manufacturer's protocol (Invitrogen). 18 and 28 S were used as an inner standard. Probes for Northern blots were generated by radiolabeling using 250 μ Ci of [α - 32 P] dCTP (6 000 Ci/mmol) according to the Prime-a-gene labeling System's protocol for each reaction. Northern blotting and hybridizations were carried out routinely.

Western blot

Protein level was determined with Western blot. At 12, 24, 26, 48, and 72 h after transfection, total protein of cancer cells of controls and each transfected group was extracted and protein concentration was determined. Western blot assay was performed with routine methods.

Terminal deoxynucleotidyltransferase-mediated dUTP nick-end labeling (TUNEL) assay

Terminal uridine deoxynucleotidyl nick end labeling (TUNEL) assay was performed by using the *in situ* cell detection kit (FITC) following the manufacturer's instructions (Roche Molecular Biochemicals). In brief, cells grown on glass coverslips were fixed by a freshly prepared paraformaldehyde solution (4% in PBS, pH 7.4) for 1 h at room temperature. Coverslips were then washed with PBS and incubated in permeabilization solution (0.1% Triton X-100, 0.1% sodium citrate) for 2 min in ice. Then, 50 μ L of TUNEL reaction mixture was added on coverslips and incubated in a humidified chamber for 1 h at 37 °C in the dark. Finally, cells were mounted and examined by microscopy as described above. TUNEL-positive (apoptotic) cells were stained bright green. Apoptosis index (AI) was calculated by apoptosis cells/total cell \times 100%.

FACScan analysis

Cell cycle distribution and apoptosis were analyzed using a fluorescence-activated cell sorter (FACS) scan apparatus (BD Biosciences, Heidelberg, Germany). For the determination of cell cycle distribution, cells were harvested, washed with PBS and probed with CycleTEST™ PLUS DNA reagent kit (BD Biosciences) according to the manufacturer's protocol. For each transfection (control and different doses of ASODN), 30 000 cells were analyzed in triplicate. The percentage of cells in different cell cycle phases was calculated using ModFit LT for Mac (BD Biosciences). For the detection of apoptotic phenotypes, harvested cells were fixed

with ice-cold 70% ethanol and treated for 20 min at 37 °C with RNase A at 5 μ g/mL and propidium iodide (PI) at 50 μ g/mL. Subsequent analyses of cell cycle distribution and apoptosis were performed using CELLQuest software (BD Biosciences).

Statistical analysis

SPSS 10.0 was performed to assay the data. Data were analyzed using SPSS. $P < 0.05$ was considered statistically significant.

RESULTS

Inhibition of PLK1 mRNA and protein expression by ASODN

We first tested the ability of ASODN to reduce the endogenous level of PLK1 mRNA and protein in the SW480 cancer cell line. PLK1 mRNA and protein levels in untransfected control cells were not significantly influenced. Transfection with PLK1 ASODN at a concentration of 50 nmol/L led to a statistically significant loss of PLK1 mRNA at 12 h after the beginning of transfection (Figure 1). We found that SW480 cancer cells transfected with ASODN showed a statistically significant reduction in PLK1 protein levels 24 h after ASODN transfection as compared with untransfected control cells. The results showed that ASODN could exert inhibitory effects on mRNA and protein expression of PLK1 gene in SW480 cancer cells at 50 nmol/L.

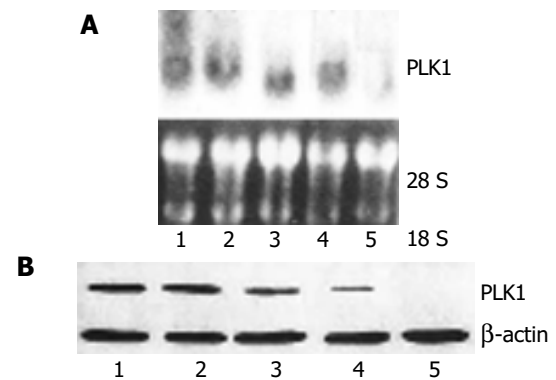


Figure 1 Inhibition of PLK1 mRNA and protein expression by ASODN demonstrated in Northern blot (A) and Western blot (B) analyses. Lane 1: control group; lane 2–5: groups treated by ASODN (50 nmol/L) after 12, 24, 48 and 72 h.

AI induced by ASODN

As shown in Figure 2, apoptosis was observed in cancer cells transfected with PLK1 ASODN. AI increased in a time- and dose-dependent manner. These data suggested that ASODN could induce apoptosis of colon cancer cell line SW480.

FACScan results

To study the apoptosis induced by ASODN, we investigated whether PLK1 levels were associated with apoptosis in all cancer cell lines by determining the sub-2N DNA content with FACScan analysis. Untransfected cells contained 1.9% cells with sub-2N DNA, transfection with ASODN was associated with 16.5% sub-2N DNA content in SW-480

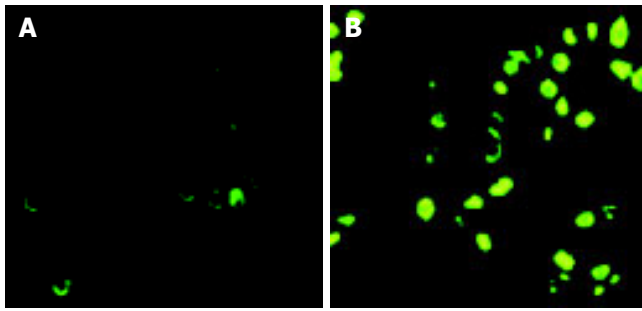


Figure 2 AI induced by ASODN in control group (A) and PLK1 group (B).

cells. Next, we analyzed the effect of PLK1 depletion on cell-cycle progression using FACSscan. As shown in Figure 3, no substantial change in cell cycle distribution was detected in control (untransfected or oligofectamine-treated alone) cells. Transfection of PLK1 ASODN induced significant G₂/M arrest 48 h after transfection with 50 nmol/L ASODN: SW-480 cells showed a fivefold increase in the percentage of cells in G₂/M compared to untransfected cancer cells. These data suggested that ASODN could induce apoptosis and G₂/M arrest in human colon cancer cell line SW480.

DISCUSSION

The polo family of protein kinases is an important group of cell cycle regulators^[1]. PLK1 is one of mammalian members of this gene family. In lower organisms, members of the polo family have been shown to control centrosomal function, chromosomal segregation, and cytokinesis^[8]. A close correlation between mammalian PLK1 expression and carcinogenesis was recently documented. Mammalian PLK1 was found to be overexpressed in various human tumors^[10-17]. It has been proposed that PLK1 could be used as a novel diagnostic marker for several types of cancers^[9,19]. Furthermore, constitutive expression of PLK1 in NIH 3T3 cells causes oncogenic focus formation and induces tumor growth in nude mice^[20]. Therefore, inhibition of PLK1 function is important for cancer therapy.

Immunohistochemical analyses showed that PLK1 is expressed in 78 primary colorectal cancers as well as 15 normal colorectal specimens^[18]. In normal colon mucosa, some crypt cells showed weakly positive staining for PLK1 in 13 out of 15 cases, the remaining cases being negative. Elevated expression of PLK1 was observed in 57 (73.1%)

of colorectal cancers, which was significantly associated with pT ($P < 0.0006$), pN ($P < 0.008$) and the Dukes' classification ($P < 0.0005$). The results suggest overexpression of PLK1 might be of pathogenic, prognostic and proliferative importance, and might have potential as a marker for colorectal cancer. In this study, PLK1 is upregulated in colon cancer cell line SW480, suggesting that PLK1 was overexpressed in colon cancer and may play an important role in colon cancer development and progression.

Antisense oligonucleotides can downregulate some oncogenes associated with malignant tumor, and synthetic oligonucleotides have been currently evaluated in clinical trials for the treatment of cancer, inflammation, and viral diseases^[21]. Li *et al.*^[19], tested some ASODN, ASODN 9 that is most effective in blocking PLK1 expression in liver carcinoma cell line HepG2. But no studies of PLK1 ASODN are available on colon cancer. In the present study, SW480 cancer cells were transfected with ASODN 9. mRNA and protein expression of PLK1 gene could be induced significantly by Western and Northern blot. Our results suggest that transfection of ASODN is efficient in suppressing PLK1 expression in SW480 colon cancer cells.

After PLK1 expression was downregulated, we detected apoptosis of cancer cells by TUNEL assay. We observed that transfection with PLK1 ASODN significantly induced AI in a time- and dose-dependent manner. To further confirm the induction of apoptosis in SW480 cells was through the activation of an apoptotic program, we detected apoptosis program by sub-2N DNA content by flow cytometry. It was found that sub-2N DNA content of cancer cells transfected with ASODN increased significantly compared with untransfected cells. Results from flow cytometry analysis further confirmed that ASODN could induce significant apoptosis in SW480 cells. All these data indicate that downregulation of PLK1 expression with ASODN may induce apoptosis in colon cancer cell line SW480.

Meanwhile, cell viability was significantly decreased in cells after ASODN treatment as compared with untreated controls, suggesting that apoptosis may be related to inhibition of SW480 colon cancer cell line.

In addition, we examined the cell cycle distribution changes in ASODN-transfected SW480 cells by flow cytometry. Forty-eight hours after transfection with ASODN, SW480 cancer cells showed a stronger G₂/M arrest compared with control cells.

In conclusion, targeting PLK1 expression using ASODN

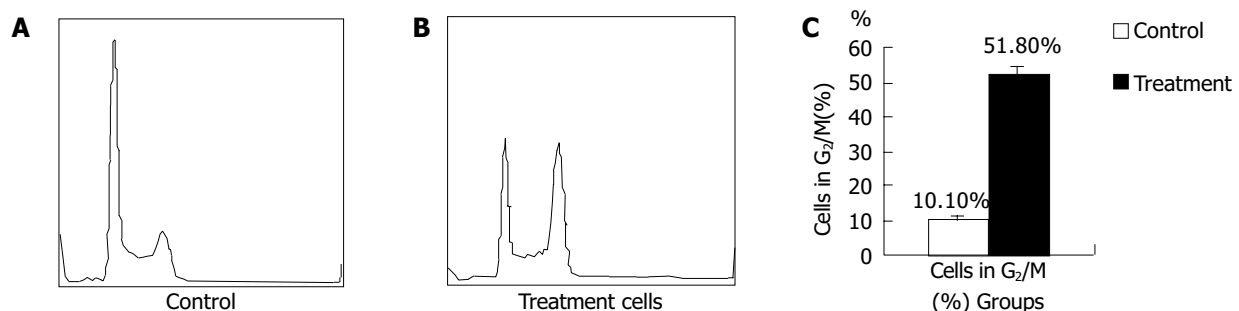


Figure 3 Effect of ASODN on cell cycle distribution of cancer cells. A: Control; B: Treatment cells; C: Cells in G₂/M.

may hold promise as one of the effective therapies for colon cancer. It is hoped that application of this strategy in clinic may improve the efficacy of treatment of patients with colon cancer.

REFERENCES

- 1 **Glover DM**, Hagan IM, Tavares AA. Polo-like kinases: a team that plays throughout mitosis. *Genes Dev* 1998; **2**: 3777-3787
- 2 **Nigg EA**. Polo-like kinases: positive regulators of cell division from start to finish. *Curr Opin Cell Biol* 1998; **10**: 776-783
- 3 **Toyoshima-Morimoto F**, Taniguchi E, Shinya N, Iwamatsu A, Nishida E. Polo-like kinase 1 phosphorylates cyclin B1 and targets it to the nucleus during prophase. *Nature* 2001; **410**: 215-220
- 4 **Yuan J**, Eckerdt F, Bereiter-Hahn J, Kurunci-Csacsco E, Kaufmann M, Strebhardt K. Cooperative phosphorylation including the activity of polo-like kinase 1 regulates the subcellular localization of cyclin B1. *Oncogene* 2002; **21**: 8282-8292
- 5 **Qian YW**, Erikson E, Taieb FE, Maller JL. The polo-like kinase Plx1 is required for activation of the phosphatase Cdc25C and cyclin B-Cdc2 in *Xenopus* oocytes. *Mol Biol Cell* 2001; **12**: 1791-1799
- 6 **Shirayama M**, Zachariae W, Ciosk R, Nasmyth K. The Polo-like kinase Cdc5p and the WD-repeat protein Cdc20p/fizzy are regulators and substrates of the anaphase promoting complex in *Saccharomyces cerevisiae*. *EMBO J* 1998; **17**: 1336-1349
- 7 **Ohkura H**, Hagan IM, Glover DM. The conserved Schizosaccharomyces pombe kinase plo1, required to form a bipolar spindle, the actin ring, and septum, can drive septum formation in G1 and G2 cells. *Genes Dev* 1995; **9**: 1059-1073
- 8 **Golsteyn RM**, Schultz SJ, Bartek J, Ziemiecki A, Ried T, Nigg EA. Cell cycle analysis and chromosomal localization of human Plk1, a putative homologue of the mitotic kinases *Drosophila* polo and *Saccharomyces cerevisiae* Cdc5. *J Cell Sci* 1994; **107**: 1509-1517
- 9 **Holtrich U**, Wolf G, Brauninger A, Karn T, Bohme B, Rubsamen-Waigmann H. Induction and down-regulation of PLK, a human serine/threonine kinase expressed in proliferating cells and tumors. *Proc Natl Acad Sci USA* 1994; **91**: 1736-1740
- 10 **Wolf G**, Elez R, Doermer A, Holtrich U, Ackermann H, Stutte HJ, Altmannberger HM, Rubsamen-Waigmann H, Strebhardt K. Prognostic significance of polo-like kinase (PLK) expression in non-small cell lung cancer. *Oncogene* 1997; **14**: 543-549
- 11 **Knecht R**, Elez R, Oechler M, Solbach C, von Ilberg C, Strebhardt K. Prognostic significance of polo-like kinase (PLK) expression in squamous cell carcinomas of the head and neck. *Cancer Res* 1999; **59**: 2794-2797
- 12 **Tokumitsu Y**, Mori M, Tanaka S, Akazawa K, Nakano S, Niho Y. Prognostic significance of polo-like kinase expression in esophageal carcinoma. *Int J Oncol* 1999; **15**: 687-692
- 13 **Knecht R**, Oberhauser C, Strebhardt K. PLK (polo-like kinase), a new prognostic marker for oropharyngeal carcinomas. *Int J Cancer* 2000; **89**: 535-536
- 14 **Takai N**, Miyazaki T, Fujisawa K, Nasu K, Hamanaka R, Miyakawa I. Expression of polo-like kinase in ovarian cancer is associated with histological grade and clinical stage. *Cancer Lett* 2001; **164**: 41-49
- 15 **Wolf G**, Hildenbrand R, Schwar C, Grobholz R, Kaufmann M, Stutte HJ, Strebhardt K, Bleyl U. Polo-like kinase: a novel marker of proliferation: correlation with estrogen-receptor expression in human breast cancer. *Pathol Res Pract* 2000; **196**: 753-759
- 16 **Macmillan JC**, Hudson JW, Bull S, Dennis JW, Swallow CJ. Comparative expression of the mitotic regulators SAK and PLK in colorectal cancer. *Ann Surg Oncol* 2001; **8**: 729-740
- 17 **Dietzmann K**, Kirches E, von Bossanyi, Jachau K, Mawrin C. Increased human polo-like kinase-1 expression in gliomas. *J Neurooncol* 2001; **53**: 1-11
- 18 **Takahashi T**, Sano B, Nagata T, Kato H, Sugiyama Y, Kunieda K, Kimura M, Okano Y, Saji S. Polo-like kinase 1 (PLK1) is overexpressed in primary colorectal cancers. *Cancer Sci* 2003; **94**: 148-152
- 19 **Li L**, Sheng QW, Wei G, Bing HY, Xiao DH. Antitumor activity of antisense oligonucleotides targeted at Plk1 in HepG2 cell *in vivo* and *in vitro*. *Aizheng* 2001; **20**: 1233-1236
- 20 **Smith MR**, Wilson ML, Hamanaka R, Chase D, Kung H, Longo DL, Ferris DK. Malignant transformation of mammalian cells initiated by constitutive expression of the polo-like kinase. *Biochem Biophys Res Commun* 1997; **234**: 397-405
- 21 **Monteith DK**, Levin AA. Synthetic oligonucleotides: the development of antisense therapeutics. *Toxicol Pathol* 1999; **27**: 8-13

Clinical characteristics of fulminant hepatitis in pregnancy

Xiao-Mao Li, Lin Ma, Yue-Bo Yang, Zhong-Jie Shi, Shui-Sheng Zhou

Xiao-Mao Li, Lin Ma, Yue-Bo Yang, Zhong-Jie Shi, Shui-Sheng Zhou, Department of Obstetrics and Gynecology, Third Affiliated Hospital, Sun Yat-Sen University, Guangzhou 510630, Guangdong Province, China

Correspondence to: Professor Xiao-Mao Li, Department of Obstetrics and Gynecology, Third Affiliated Hospital, Sun Yat-Sen University, Guangzhou 510630, Guangdong Province, China. tigerlee777@163.net

Telephone: +86-20-85515609 Fax: +86-20-87565575

Received: 2004-10-19 Accepted: 2004-12-26

Abstract

AIM: To investigate the clinical characteristics of fulminant hepatitis in pregnancy.

METHODS: We compared and analyzed the etiology, clinical characteristics, and laboratory examinations of 25 cases of fulminant hepatitis in pregnancy and 30 cases of fulminant hepatitis not in pregnancy.

RESULTS: HBV infection and chronic fulminant hepatitis were most common both in the pregnant and in the non-pregnant groups. Jaundice, digestive tract symptoms, increase of bilirubin and thrombinogen activity were the main manifestations. The incidence of hepatic encephalopathy (HE) and hepato-renal syndrome (HRS) was significantly different between the two groups. The incidence of preterm labor, dead fetus and neonatal asphyxia was high.

CONCLUSION: Fulminant hepatitis is likely to occur in late pregnancy with more severe complications, which significantly influences maternity, perinatal fetus, and newborn.

© 2005 The WJG Press and Elsevier Inc. All rights reserved.

Key words: Pregnancy; Fulminant hepatitis; Clinical characteristics

Li XM, Ma L, Yang YB, Shi ZJ, Zhou SS. Clinical characteristics of fulminant hepatitis in pregnancy. *World J Gastroenterol* 2005; 11(29): 4600-4603

<http://www.wjgnet.com/1007-9327/11/4600.asp>

INTRODUCTION

Fulminant hepatitis (FH) refers to a kind of severe clinical type of hepatitis characterized by acute onset, fast progression, complicated manifestations and poor prognoses. The average mortality rate of FH in our country is over

60%. Hepatitis A virus (HAV), hepatitis B virus (HBV), hepatitis C virus (HCV), hepatitis D virus (HDV), hepatitis E virus (HEV), transfusion transmitted virus (TTV), herpes simplex virus (HSV) and cytomegalo virus (CMV) can all lead to FH, with HBV being the commonest cause (accounting for about 85%). The basic pathologic changes are massive necrosis and degeneration of hepatocytes. The main clinical manifestations are icteric sclera and xanthochromia, hypodynamia and loss of appetite, nausea and vomiting. Bilirubin increases to more than 171 mmol/L, prothrombin time (PT) decreases to less than 40%, progressive shrinkage of liver, significant deterioration of liver function, deviation of enzyme and bilirubin, and inversion of albumin/globulin ratio. The severe complications include hepatic encephalopathy (HE) and hepato-renal syndrome (HRS). The incidence of FH in pregnancy (FHP) is 66 times that of patients not in pregnancy^[1]. The former is more dangerous with a significantly higher incidence of dead fetus, preterm labor and neonatal asphyxia because of interactions of pregnancy and liver disease. It is also among the major causes of maternal and perinatal death and is still left to be solved in the field of liver disease.

We compared 25 cases of FHP and 30 cases of FH not in pregnancy (FHNP) retrospectively to enhance our knowledge about FHP.

MATERIALS AND METHODS

A total of 55 female reproductive-age patients who met the clinical diagnostic criteria approved by Chinese Medical Association (2000, Xi' an)^[2] were admitted in our hospital from January 1993 to February 2004. In the FHP group, there were 25 cases aged from 23 to 37 years, with an average age of 26.7 ± 3.8 years. There were 30 cases in the FHNP group, aged from 18 to 39 years, with an average age of 28.1 ± 5.6 years. There were no significant differences in age distribution ($t = 1.053, P > 0.05$), etiology and clinical classification ($P > 0.05$) between the two groups.

In the improved FHP group, there were eight cases of primipara and three cases of multipara with an average gestational period of 29.8 ± 6.3 wk. Four cases were simple virus infection, four cases had co-infection and three cases had infection of unknown causes. In the death group, there were 10 primipara and 4 cases of multipara with an average gestational period of 30.6 ± 7.0 wk. Nine cases were simple virus infection, one case had co-infection and four cases had infection with unknown causes. There was no significant difference between the two groups in general conditions.

We compared the etiological markers, clinical groups, symptoms and signs, complications, biochemical indices, B-ultrasonography and pregnancy outcomes. The results were analyzed by “*t* test”, “ χ^2 test”, “fidelity rate test” and

Table 1 Laboratory findings of FHP group and FHNP group (mean±SD)

Items	FHP group	FHNP group	<i>t</i>	<i>P</i>
Glutamate-pyruvate transaminase (ALT, U/L)	424.05±285.12	747.04±621.23	1.996	>0.05
Glutamic-oxalacetic transaminase (AST, U/L)	436.92±304.52	534.93±525.73	1.657	>0.05
ALT/AST	0.89±0.96	1.32±1.56	1.201	>0.05
Alkaline phosphatase (ALP, U/L)	199.42±101.02	142.23±50.03	-2.716	<0.05
Total bilirubin (Tbil, μmol/L)	403.11±162.32	460.54±246.45	0.998	>0.05
Direct bilirubin (Dbil, μmol/L)	240.05±111.69	230.44±112.85	-0.316	>0.05
Bile acid (TBA, μmol/L)	105.92±72.17	205.96±37.20	3.053	<0.05
Serum albumin (ALB, g/L)	28.00±4.45	33.49±5.92	3.818	<0.05
Cholesterol (CHOL, mmol/L)	1.70±0.75	1.91±1.00	0.838	>0.05
Cholinephospholipid (CHE, U/L)	3 132.55±983.57	3 885.81±1 510.60	1.490	>0.05
Blood glucose (GLU, mmol/L)	3.03±1.50	5.25±3.82	2.728	<0.05
Blood urea nitrogen (BUN, mmol/L)	9.66±9.07	4.34±4.02	-2.888	<0.05
Creatinine (Cr, mmol/L)	230.99±205.46	60.55±37.47	-4.459	<0.05
Serum calcium (Ca, mmol/L)	2.00±0.24	2.14±0.21	2.100	<0.05
Alpha-fetoprotein (AFP, ng/mL)	186.11±135.74	456.47±1 374.12	0.805	>0.05
Blood ammonia (NH ₃ , μmol/L)	92.05±55.39	127.71±83.30	1.263	>0.05
PT (s)	43.93±43.66	44.10±26.32	0.018	>0.05
PTA (%)	25.33±12.30	20.81±9.44	-1.513	>0.05

“sum of ranks test” through SPSS software. $P < 0.05$ was considered statistically significant.

RESULTS

Etiological markers

The infection rate of HBV was 68% (17/25), HDV 4% (1/25), HEV 24% (6/25) and unidentified type 28% (7/25) in the FHP group. The infection rate of HAV was 3.3% (1/30), HBV 63.3% (19/30), HEV 20% (6/30) and unidentified type 20% (6/30) in the FHNP group. There was no significant difference in etiology between the two groups ($\chi^2 = 3.249$, $P > 0.05$).

Clinical groups

In the FHP group, there were 7 cases of acute FH, 3 cases of sub-acute FH, and 15 cases of chronic FH. In the FHNP group, there were 4 cases of acute FH, 5 cases of sub-acute FH, and 21 cases of chronic FH. There was no significant difference between the two groups ($\chi^2 = 1.879$, $P > 0.05$).

Hepatitis history

Seven cases had hepatitis history in the FHP group and four died. While 17 cases had hepatitis history in the FHNP group and 8 died. There was a significant difference in hepatitis history between the two groups ($\chi^2 = 4.556$, $P < 0.05$).

Clinical manifestations

The main clinical manifestations of FHP were icteric sclera and xanthochromia (100%), yellow urine (100%), hypodynamia and loss of appetite (96%), nausea and vomiting (64%), abnormal behavior (44%), edema of lower limbs (40%), fever, abdominal pain, oliguria (24%), abdominal distention (16%), tarry stools (12%), skin pruritus, gingival bleeding, and loss of weight.

We compared the clinical symptoms of the two groups and found no significant differences except for abdominal distention ($P > 0.05$).

Laboratory findings

Between the two groups, there were significant differences in such indices as alkaline phosphatase (ALP), bile acid (TBA), serum albumin (ALB), blood urea nitrogen (BUN), creatinine (Cr), blood glucose (GLU) and serum calcium (Ca, $P < 0.05$). In the FHP group, ALP, BUN, Cr were higher while TBA, ALB, GLU, and Ca were lower (Table 1).

B-ultrasonography

In the FHP group, 1 case had liver enlargement, 9 cases liver shrinkage, 15 cases spleen enlargement, 15 cases ascites, and 3 cases had no B-ultrasonography results. In the FHNP group, 2 cases had liver enlargement, 6 cases liver shrinkage, 18 cases spleen enlargement, 16 cases ascites, and 2 cases had no B-ultrasonography results. There were no significant differences in B-ultrasonography results between the two groups (χ^2 liver = 1.190, χ^2 spleen = 0.000, χ^2 ascites = 0.246, $P > 0.05$).

Complications

The most common complication was HE (76%). Others were HRS (64%), peritonitis (56%), hemorrhage (56%), and pulmonary infection (16%). Compared to the FHNP group, there were significant differences in the incidence rates of HE, HRS and hemorrhage ($P < 0.05$). Complications were more likely to develop in the FHP group (Table 2).

Table 2 Comparison of complications between FHP group and FHNP group

Complications	FHP (n = 25, %)	FHNP (n = 30, %)	χ^2	<i>P</i>
Peritonitis	14 (56)	13 (43.3)	0.875	>0.05
HE	19 (76)	15 (50.0)	3.905	<0.05
HRS	16 (64)	4 (13.3)	15.128	<0.01
Hemorrhage	14 (56)	1 (3.3)	13.221	<0.01
Pulmonary infection	4 (16)	4 (13.3)	0.000	>0.05
DIC	6 (24)	0 (0)	5.801	<0.05

Gestational period of FHP onset and pregnancy outcome

Onset of FHP in 25 cases was all in middle (28%, 7/25) or late pregnancy (72%, 18/25).

Two cases had spontaneous abortion, five cases dead fetus, six cases preterm labor, seven cases term labor, and four cases had no labor in our hospital. One patient died before labor. The incidence rate of preterm labor and neonatal asphyxia was 33.3% (6/18) and 27.7% (5/18), respectively.

DISCUSSION

HBV infection is the most common cause of both FHP and FHNP, because China is an area with a high incidence of HBV infection^[4,5]. It was reported in national epidemiologic survey from 1992 to 1995 that 9.57% of Chinese are hepatitis B surface antigen positive^[4]. While the carrier state of HBV infection may be the underlying cause of chronic liver diseases^[6-8]. Once triggered, massive liver necrosis or FH will occur. In our study, chronic FH was most common both in FHP group (60%, 15/25) and in FHNP (70%, 21/30). During pregnancy, the vigorous metabolism puts heavy burden on liver and makes it hard to recover^[9,10]. Infection with HBV during pregnancy is more likely to lead to FH with a fast progression.

The onset of FHP is more rapid, which can develop during the whole pregnancy, and most common during late pregnancy^[11] due to heavy burden in late pregnancy^[12]. Because of the interaction between pregnancy and hepatitis, severe immune response and damage caused by multi-factors, a large number of liver cells will undergo necrosis in a short period. Therefore, the conditions of FHP can aggravate very quickly and complications are more likely to develop^[13]. In our study, the main clinical manifestations were as follows: extreme hypodynamia, digestive tract symptoms such as loss of appetite and frequent vomiting, yellow urine, icteric sclera and xanthochromia, liver shrinkage, hepatic odour and early stage of ascites. Whereas abdominal distention was rare, which may be due to the insensitiveness caused by enlarged uterus, HE was most common. The incidence of other complications, such as hemorrhage^[14,15] and HRS^[16] was significantly higher in the FHP group^[17-20], and influenced the prognoses of FHP^[21,22], especially postpartum hemorrhage and disseminated intravascular coagulation (DIC)^[21,23-25], suggesting that postpartum hemorrhage and DIC are common death causes of FHP.

Bilirubin rose, PT prolonged, prothrombin activity (PTA) decreased, hypoproteinemia occurred, albumin/globulin reversed and cholesterol-enzyme separated. Between FHP and FHNP, there were significant differences in ALP, TBA, ALB, BUN, Cr, GLU, and Ca ($P < 0.05$). Since ALP can be produced not only by liver, but also by placebo, ALP is higher in FHP than in FHNP and returns to normal after labor. During pregnancy, progesterone can suppress smooth muscle to weaken gallbladder contractions and relax bile tract smooth muscle. Evacuation of gall bladder is longer, thus leading to cholestasis. Less TBA is discharged, causing decrease of TBA in blood. During pregnancy, the metabolism is high, serum protein and storage of glucogen reduced, while the blood volume increased. Therefore

hypoproteinemia and hypoglycemia are more notable than in FHNP. The fetus in pregnancy needs calcium for development of bones, causing increase of Ca in maternity, meanwhile, ALB and protein-bound Ca decrease. The incidence of higher BUN and Cr is caused by the development of HRS in FHP.

The main dangers of FHP are fetal malformation, preterm labor, abortion, dead fetus in uterus and stillbirth. The incidence of fetal distress and perinatal death is higher^[26]. In our study, such labor outcomes as dead fetus in uterus (20%, 5/25), preterm labor (33.3%, 6/18) and fetal distress (27.7%, 5/13) were significantly higher in FHP group. In normal pregnancy, the incidence of preterm labor is 5-15% and asphyxia is 3-10%^[11]. In FH, there are metabolic disorders all over the body and insufficient energy generation, blood and oxygen supply through placenta. Accordingly, fetal distress, fetus death in uterus and preterm labor are likely to develop, increasing the rate of perinatal distress and mortality.

In order to decrease maternal and perinatal death rate and increase obstetrical quality, we should recognize FHP comprehensively to the make right diagnosis and treat FHP in its early stage.

REFERENCES

- 1 **Cao ZY.** Chinese Obstetrics and Gynecology. Beijing: *People's Medical Publishing House* 1999: 486
- 2 Infectious diseases branch, parasitic diseases branch and liver disease branch of Chinese Medical Association. Prevention and cure program for viral hepatitis. *Zhonghua Ganzangbing Zazhi* 2000; **8**: 324-329
- 3 **Li XM, Liu SL, Li X, Huang HJ, Lu JX, Gao ZL.** The relative study of hepatitis B virus DNA in maternal blood umbilical blood and breast milk. *Zhongshan Yike Daxue Xuebao* 2000; **21**: 233-235
- 4 **Merle P, Trepo C, Zoulim F.** Current management strategies for hepatitis B in the elderly. *Drugs Aging* 2001; **18**: 725-735
- 5 **Hamdani-Belghiti S, Bouazzaou NL.** Mother-child transmission of hepatitis B virus. State of the problem and prevention. *Arch Pediatr* 2000; **7**: 879-882
- 6 **Ogasawara J, Watanabe-Fukunaga R, Adachi M, Matsuzawa A, Kasugai T, Kitamura Y, Itoh N, Suda T, Nagata S.** Lethal effect of the anti-fas antibody in mice. *Nature* 1993; **364**: 806-809
- 7 **Leist M, Gantner F, Bohlinger I, Tiegs G, Germann PG, Wendel A.** Tumor necrosis factor-induced hepatocyte apoptosis precedes liver failure in experimentae marine shock models. *Am J Pathol* 1995; **146**: 1220-1234
- 8 **Zang GQ, Zhou QX, Yu H, Xie Q, Wang B, Zhao GM, Guo Q, Xiang YQ, Liao D.** The role of TNF- α induced hepatic apoptosis in fulminant hepatic failure. *Zhonghua Xiaohua Zazhi* 2000; **20**: 163-166
- 9 **Wang DZ.** Diagnosis and treatment of fulminant hepatitis. *Zhongguo Shiyong Fuke Yu Chanke Zazhi* 2001; **17**: 325-327
- 10 **Jaiswal SP, Jain AK, Naik G, Soni N, Chitnis DS.** Viral hepatitis in pregnancy. *Int J Gynaecol Obstet* 2001; **72**: 103-108
- 11 **Zhuang YL.** Obstetrical diagnoses and treatments of fulminant hepatic failure. *Zhongguo Shiyong Fuke Yu Chanke Zazhi* 1996; **12**: 79-80
- 12 **Riely CA.** Hepatic disease in pregnancy. *Am J Med* 1994; **96** (1A): 18s-22s
- 13 **Zhang DF.** Etiopathogenesis of hepatitis B virus and clinic. Chongqing: *Chongqing Publishing House* 1998: 264
- 14 **Qiu DK.** Complications of chronic liver disease-Current conception of diagnosis and treatment. Shanghai: *Shanghai Science and Technology Publishing House* 2001: 76

- 15 **Xu JZ**, Liu GZ. Preventive and treatment measures of digestive tract hemorrhage in fulminant hepatitis. *Zhongguo Shiyong Neike Zazhi* 1995; **15**: 131-132
- 16 **Luo CY**, Zhang XY. Preventive and treatment measures of hepatorenal symptom in fulminant hepatitis. *Zhongguo Shiyong Neike Zazhi* 1995; **15**: 137-139
- 17 **Khuroo MS**, Kamili S. Aetiology, clinical course and outcome of sporadic acute viral hepatitis in pregnancy. *J Viral Hepat* 2003; **10**: 61-69
- 18 **Duff P**. Hepatitis in pregnancy. *Semin Perinatol* 1998; **22**: 277-283
- 19 **Fink CG**, Read SJ, Hopkin J, Peto T, Gould S, Kurtz JB. Acute herpes hepatitis in pregnancy. *J Clin Pathol* 1993; **46**: 968-971
- 20 **Coursaget P**, Buisson Y, N'Gawara MN, Van Cuyck-Gandre H, Roue R. Role of hepatitis E virus in sporadic cases of acute and fulminant hepatitis in an endemic area (Chad). *Am J Trop Med Hyg* 1998; **58**: 330-334
- 21 **Hussaini SH**, Skidmore SJ, Richardson P, Sherratt LM, Cooper BT, O'Grady JG. Severe hepatitis E infection during pregnancy. *J Viral Hepat* 1997; **4**: 51-54
- 22 **Hamid SS**, Jafri SM, Khan H, Shah H, Abbas Z, Fields H. Fulminant hepatic failure in pregnant women: acute fatty liver or acute viral hepatitis? *J Hepatol* 1996; **25**: 20-27
- 23 **Xu H**. Analysis of 18 cases of postpartum haemorrhagic shock in pregnancy with virus hepatitis. *Zhonghua Fuchanke Zazhi* 1992; **27**: 150-152
- 24 **Yang YB**, Li XM, Zhou SS, Shi ZJ, Shen HM. The relation between hepatitis B virus infection complicated with pregnancy and prognoses of maternity and newborns. *Zhongguo Shiyong Fuke Yu Chanke Zazhi* 2004; **20**: 371-372
- 25 **Yang YB**, Li XM, Zhou SS, Shi ZJ, Teng BQ. The relation between indices of liver function and the prognoses of fulminant hepatitis in pregnancy. *Zhongshan Daxue Xuebao* 2004; **25**: 133-134
- 26 **Yao ZW**, Wu WX. Pregnancy complicated with hepatitis. *Shiyong Fuchanke Zazhi* 1999; **15**: 185

Science Editor Wang XL and Guo SY Language Editor Elsevier HK

Alterations of serum cholinesterase in patients with gastric cancer

Shan-Zhi Gu, Xin-Han Zhao, Ping Quan, Sheng-Bin Li, Bo-Rong Pan

Shan-Zhi Gu, Xin-Han Zhao, Ping Quan, Sheng-Bin Li, Key Laboratory of Environment and Genes Related to Diseases of Ministry of Education, Medical College of Xi'an Jiaotong University, Xi'an 710061, Shaanxi Province, China

Bo-Rong Pan, Department of Oncology, Xijing Hospital, Fourth Military Medical University, Xi'an 710032, Shaanxi Province, China

Co-first-authors: Shan-Zhi Gu and Xin-Han Zhao

Correspondence to: Xin-Han Zhao, Key Laboratory of Environment and Genes Related to Diseases of Ministry of Education, Department of Medical Oncology, First Hospital of Xi'an Jiaotong University, Xi'an 710061, Shaanxi Province, China. zhxinhan@pub.xaonline.com

Telephone: +86-29-85324136 Fax: +86-29-82655472

Received: 2004-10-09 Accepted: 2004-11-26

Abstract

AIM: To understand the correlation of serum cholinesterase (CHE) activity with gastric cancer and to assess their clinical significance.

METHODS: The velocity method was adopted to detect the activity of serum CHE in patients with gastric cancer and in patients with non-malignant tumor as controls.

RESULTS: The serum CHE activity in the treatment group was significantly lower than that in the control group with a very significant difference between the two groups (83.3 ± 113.1 , $P = 0.0003$). Age was significantly associated with the incidence of gastric cancer.

CONCLUSION: Serum CHE activity has a close relation with the incidence of gastric cancer.

© 2005 The WJG Press and Elsevier Inc. All rights reserved.

Key words: Cholinesterase activity; Gastric cancer

Gu SZ, Zhao XH, Quan P, Li SB, Pan BR. Alterations of serum cholinesterase in patients with gastric cancer. *World J Gastroenterol* 2005; 11(29): 4604-4606

<http://www.wjgnet.com/1007-9327/11/4604.asp>

INTRODUCTION

CHE is a type of glycoprotein^[1-4], existing *in vivo* in multiple forms of isozyme^[5-7]. The decrease of serum CHE activity is often observed in patients with organic phosphorus poisoning^[8] and damage of parenchymal cells^[9-12]. In clinical practice, we have discovered that there is a decrease of serum CHE activity in patients with gastric cancer. This study aimed to detect the serum CHE activity in patients with gastric cancer, and to observe the correlation of serum CHE activity with the incidence of gastric cancer.

MATERIALS AND METHODS

Subjects

The treatment group included 81 patients (61 males and 20 females aged 30-80 years with an average age of 58.8 ± 12.0 years) with gastric cancer hospitalized from January 1998 to June 2002. The disease was confirmed by gastroscopic examination and/or pathological examination. Clinical and pathologic classifications followed the General Rules for Gastric Cancer Study in Surgery and Pathology in Japan. The control group included 80 patients (44 males and 36 females) with non-malignant tumor hospitalized during the same period. Their age ranged 26-86 years with an average age of 57.7 ± 15.3 years. Patients with organic phosphorus poisoning or damage of parenchymal cells were excluded.

Methods

All the patients were fasted for more than 12 h, then venous blood was taken. After centrifugation, serum was subjected to detection on the same day. Serum CHE activity was measured by the velocity method with Hitachi 7170 full automatic biochemical instrument and Hitachi 7170 special reagent. The normal reference value was 75-217 $\mu\text{kat/L}$.

Statistical analysis

All the data were fed into a computer. The SPSS10.0 software package was employed for analysis and processing. The chi-square test was conducted. With the CHE difference between the gastric cancer group and the control group, *F* test was adopted. For the purpose of reviewing the relation between sex, age and CHE, the multi-factor regression analysis was conducted with respect to the above three factors. The statistical significance level was defined as <0.05 with two-sided detection.

RESULTS

Serum CHE activity in gastric cancer

The age of the gastric cancer group and control group both expressed abnormal distribution with the mid-value being 60.5 and 61.5 years respectively. The χ^2 was performed ($\chi^2 = 22.265$, $P = 0.0002$), suggesting that the age distribution in the two groups was overbalanced. The result from the χ^2 detection for the sex distribution was $\chi^2 = 25.138$ and $P = 0.0003$, showing that the sex distribution in the two groups was out of balance as well. Tables 1 and 2 respectively show the co-variance analysis results.

The age and nature of gastric cancer patients had a linear correlation with the CHE level ($r = 0.8$, $P = 0.031$), suggesting that the difference in CHE level between gastric cancer patients and controls was significant ($F = 79.069$,

$P = 0.0004$). The serum CHE level of gastric cancer patients ($81.6 \pm 31.5 \mu\text{kat/L}$) was significantly lower than that in the control group ($114.8 \pm 30.8 \mu\text{kat/L}$), indicating that age was also an important factor affecting the incidence of gastric cancer ($F = 18.481, P = 0.0003$).

With the age distribution, χ^2 was performed ($\chi^2 = 5.281, P = 0.383$), showing that the age was evenly distributed. In gastric cancer patients and controls, CHE had a normal distribution and the variance was in order. Therefore, single-factor variance analysis could be made. The average value, standard deviation and single-factor variance are listed in Tables 1 and 2.

The difference in CHE levels of the two groups was significant ($F = 29.884, P = 0.0006$). The serum CHE level in gastric cancer patients ($85.0 \pm 34.5 \mu\text{kat/L}$) was significantly lower than that in the control group ($111.4 \pm 25.8 \mu\text{kat/L}$, Figure 1).

Table 1 Serum CHE distribution in gastric cancer patients ($\mu\text{kat/L}$)

Sex	Group	n	Average	Standard error	95%CI	
					Lower limit	Upper limit
Male	Gastric cancer	61	81.6	31.5	77.2	86.1
	Control	44	114.8	30.8	108.9	120.6
Female	Gastric cancer	20	85.0	34.5	76.2	93.9
	Control	36	111.4	25.8	106.2	116.7

Table 2 Covariance analysis results of CHE in gastric cancer patients and controls

Sex	Variation source	Df	Mean square	F	P
Male	Within group	1	849 712 857.157	256.718	0.000
	Age (yr)	4	6 116 906.471	18.481	0.000
	Between groups	1	261 709 135.862	79.069	0.000
	Error	79	3 309 902.711		
	Total	85			
Female	Within group	1	93 519 230.733	29.884	0.000
	Age (yr)	3	732 546.506	16.372	0.000
	Between groups	1	3 129 425.453	54.081	0.000
	Error	61	430 763.233		
	Total	66			

Multi-factor logistic regressive analysis

The three variables (sex, age, and CHE) were put into the Logistic model. After being fitted with the backward method, the final model was expressed (Table 3). The factors put into the model were only sex and CHE. The adaptive regressive equation was $P(1) = 1/[1 + e^{-(0.129) + 2.542X_1 + 1.006X_3}]$ or $\text{CHE} = 12.701$. Therefore, after removing the influence of other factors, the reduction of the CHE activity was a dangerous factor for gastric cancer.

Table 3 The Logistic analysis of sex and CHE

Variable	B	SE	Wald	df	Sig.	Exp (B)	95.0 (%) CI for exp (B)	
							Lower	Upper
Sex	1.066	0.234	20.825	1	0.000	2.905	1.837	4.592
CHE	2.542	0.313	66.131	1	0.000	12.701	6.883	24.435
Constant	16.129	0.697	77.303	1	0.000	0.002		

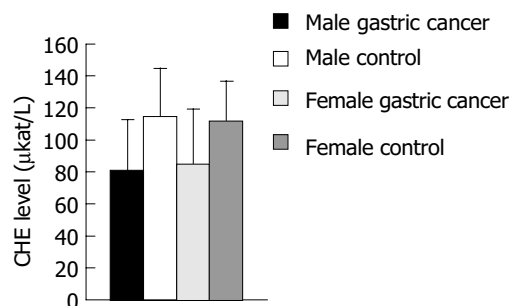


Figure 1 Different CHE levels in gastric cancer patients.

DISCUSSION

Cholinesterase can be divided into true cholinesterase (acetylcholinesterase, AChE) and pseudocholinesterase (PChE). AChE exists mainly in the vesicles of cholinergic nerve peripheral synapse where there is a comparatively large amount of AChE in the folding of the terminal synapse back membranes. It also exists in the cholinergic neurons^[13,14], red cells^[15], sera^[16], livers^[17], kidneys^[18], intestines, white mass of brain^[19], *etc.* In the activity center on the surface of the molecules of CHE protein, there are two places to be combined with acetylcholine, namely the anion place with negative charges and the place with ester decomposition. The place with ester decomposition has an acidic action point formed by serine hydroxide and an alkaline action point formed by histidine imidazole ring. They are combined by means of hydrogen bonds. PChE reduces when the parenchymal cells are damaged, as the liver synthesizes PChE^[20-22]. Organophosphorus toxicant is a powerful inhibitor of AChE and PChE^[23-26]. Measuring serum CHE activity can help diagnose organophosphorus poisoning and evaluate the condition after recovery. The results of this experiment indicate that human serum CHE activity has a significant correlation with gastric cancer.

Anic *et al.*^[27], discovered that the serum CHE activity in hepatitis B patients is relatively low. Khan *et al.*^[28], detected serum CHE and lactic dehydrogenase (LDH) activity in 40 cases of mammary cancer patients, 25 cases of benign tumor patients and 30 cases of healthy persons, and found that there is a significant difference in serum CHE activity between malignant and benign tumor patients.

If the ratio between CHE activity and serum CHE activity is less than 0.42, the malignant source should be considered^[29]. A number of studies have been conducted on the relation between serum CHE activity and acute leukemia and cervical cancer^[30,31].

Among the 81 cases of gastric cancer in the present study, there were 39 cases (48.2%) whose serum CHE activity was less than $75.0 \mu\text{kat/L}$. Among the 80 cases of

controls, there were only five cases (6.3%) whose serum CHE activity was less than 50.0 $\mu\text{kat/L}$. In the gastric cancer group, there were 14 cases whose serum CHE activity was less than 75.0 $\mu\text{kat/L}$. However, in the control group, there were no such cases. The results suggest that if a patient with gastric pathological changes whose serum CHE activity is less than 50.0 $\mu\text{kat/L}$, sharp vigilance on the existence of gastric cancer should be maintained after organophosphorous poisoning and damages of parenchymal cells, etc., are excluded.

In conclusion, the determination of serum CHE activity is a rapid, simple, convenient, inexpensive and reliable method to diagnose gastric cancer. Its exact mechanism remains to be further explored.

REFERENCES

- 1 **Fukumoto H**, Tennis M, Locascio JJ, Hyman BT, Growdon JH, Irizarry MC. Age but not diagnosis is the main predictor of plasma amyloid beta-protein levels. *Arch Neurol* 2003; **60**: 958-964
- 2 **Luo ZB**, Xu CP, Wang D, Wang G, Xiao SQ, Zhu GY, Fang DC. Immunotherapy of dendritic cells and its exosomes transfected with mRNA of gastric cancer cells in tumor-carried mice. *World Chin J Digestol* 2004; **12**: 9-12
- 3 **Valbonesi P**, Sartor G, Fabbri E. Characterization of cholinesterase activity in three bivalves inhabiting the North Adriatic sea and their possible use as sentinel organisms for biosurveillance programmes. *Sci Total Environ* 2003; **312**: 79-88
- 4 **Pelizzi N**, Puccini P, Riccardi B, Acerbi D, Catinella S. Characterization of Ganstigmine metabolites in hepatocytes by low- and high-resolution mass spectrometry coupled with liquid chromatography. *Rapid Commun Mass Spectrom* 2003; **17**: 1691-1698
- 5 **Sagi Y**, Weinstock M, Youdim MB. Attenuation of MPTP-induced dopaminergic neurotoxicity by TV3326, a cholinesterase-monoamine oxidase inhibitor. *J Neurochem* 2003; **86**: 290-297
- 6 **Luo ZB**, Xu CP, Zhu GY, Zhang PB, Guo CH, Luo YH, Fang DC, Luo CJ. Immunotherapy of dendritic cells transfected with mRNA of gastric cancer cells in carried-tumor mice. *World Chin J Digestol* 2004; **12**: 13-15
- 7 **Marco JL**, Carreiras MC. Recent developments in the synthesis of acetylcholinesterase inhibitors. *Mini Rev Med Chem* 2003; **3**: 518-524
- 8 **Pascuzzi RM**. The edrophonium test. *Semin Neurol* 2003; **23**: 83-88
- 9 **Xin SJ**, Zhang LX, Zhu CL, Hu JH, Duan XZ, You SL, Hu LP, Zou ZS, Mao YL, Huangpu YS. Correlation of clinical features with pathology in chronic viral hepatitis. *Zhonghua Shiyan He Linchuang Bingduxue Zazhi* 2003; **17**: 88-90
- 10 **Pepin JL**, Myressiotis S, Ceulemans S. Prevention of dementia: is it possible? *Rev Med Liege* 2003; **58**: 220-224
- 11 **Androne AS**, Hryniewicz K, Goldsmith R, Arwady A, Katz SD. Acetylcholinesterase inhibition with pyridostigmine improves heart rate recovery after maximal exercise in patients with chronic heart failure. *Heart* 2003; **89**: 854-858
- 12 **Migliaccio-Walle K**, Getsios D, Caro JJ, Ishak KJ, O'Brien JA, Papadopoulos G. AHEAD Study Group. Economic evaluation of galantamine in the treatment of mild to moderate Alzheimer's disease in the United States. *Clin Ther* 2003; **25**: 1806-1825
- 13 **Grossberg G**, Irwin P, Satlin A, Mesenbrink P, Spiegel R. Rivastigmine in Alzheimer disease: efficacy over two years. *Am J Geriatr Psychiatry* 2004; **12**: 420-431
- 14 **Loewenstein DA**, Acevedo A, Czaja SJ, Duara R. Cognitive rehabilitation of mildly impaired Alzheimer disease patients on cholinesterase inhibitors. *Am J Geriatr Psychiatry* 2004; **12**: 395-402
- 15 **Darvesh S**, Arora RC, Martin E, Magee D, Hopkins DA, Armour JA. Cholinesterase inhibitors modify the activity of intrinsic cardiac neurons. *Exp Neurol* 2004; **188**: 461-470
- 16 **Zdrzilova P**, Stepankova S, Komers K, Ventura K, Cegan A. Half-inhibition concentrations of new cholinesterase inhibitors. *Z Naturforsch* 2004; **59**: 293-296
- 17 **Van Dyck CH**. Understanding the latest advances in pharmacologic interventions for Alzheimer's disease. *CNS Spectr* 2004; **9**(7 Supp 5): 24-28
- 18 **Eskenazi B**, Harley K, Bradman A, Weltzien E, Jewell NP, Barr DB, Furlong CE, Holland NT. Association of in utero organophosphate pesticide exposure and fetal growth and length of gestation in an agricultural population. *Environ Health Perspect* 2004; **112**: 1116-1124
- 19 **Arai H**. Current therapies in dementia. *Nippon Ronen Igakkai Zasshi* 2004; **41**: 310-313
- 20 **Kurz A**, Van Baelen B. Ginkgo biloba Compared with Cholinesterase Inhibitors in the Treatment of Dementia: A Review Based on Meta-Analyses by the Cochrane Collaboration. *Dement Geriatr Cogn Disord* 2004; **18**: 217-226
- 21 **Fu G**, Wang GB, Lu XM, Huang QX, Zheng H. MAPK signal transduction and apoptosis of human gastric carcinoma cells induced by liposomes of survivin antisense oligonucleotide. *World Chin J Digestol* 2004; **12**: 1034-1039
- 22 **Khang P**, Weintraub N, Espinoza RT. The Use, Benefits, and Costs of Cholinesterase Inhibitors for Alzheimer's Dementia in Long-Term Care. Are the Data Relevant and Available? *J Am Med Dir Assoc* 2004; **5**: 249-255
- 23 **Sormani MP**, Oneto R, Bruno B, Fiorone M, Lamparelli T, Gualandi F, Raiola AM, Dominiotto A, Van Lint MT, Frassoni F, Bruzzi P, Bacigalupo A. A revised day +7 predictive score for transplant-related mortality: serum cholinesterase, total protein, blood urea nitrogen, gamma glutamyl transferase, donor type and cell dose. *Bone Marrow Transplant* 2003; **32**: 205-211
- 24 **Lu CJ**, Tune LE. Chronic exposure to anticholinergic medications adversely affects the course of Alzheimer disease. *Am J Geriatr Psychiatry* 2003; **11**: 458-461
- 25 **Pang YP**, Kollmeyer TM, Hong F, Lee JC, Hammond PI, Haugabouk SP, Brimijoin S. Rational design of alkylene-linked bis-pyridiniumaldoximes as improved acetylcholinesterase reactivators. *Chem Biol* 2003; **10**: 491-502
- 26 **Tariot PN**, Jakimovich L. Donepezil use for advanced Alzheimer's disease—a case study from a long-term care facility. *Am Med Dir Assoc* 2003; **4**: 216-219
- 27 **Anic K**, Ivandic A, Volaric M, Peric L, Getto L, Bacun T. Cholinesterase in the differential diagnosis of parenchymal and obstructive icterus and in the differentiation between malignant and benign obstruction. *Wien Med Wochenschr* 1999; **149**: 355-358
- 28 **Khan SA**, Stewart AK, Morrow M. Does aggressive local therapy improve survival in metastatic breast cancer? *Surgery* 2002; **132**: 620-626
- 29 **Cabello G**, Juarranz A, Botella LM, Calaf GM. Organophosphorous pesticides in breast cancer progression. *J Submicrosc Cytol Pathol* 2003; **35**: 1-9
- 30 **Yi Z**, Wang Z, Li H, Liu M. Inhibitory effect of tellimagrandin I on chemically induced differentiation of human leukemia K562 cells. *Toxicol Lett* 2004; **147**: 109-119
- 31 **Bradamante V**, Smigovec E, Bukovic D, Geber J, Matanic D. Plasma cholinesterase activity in patients with uterine cervical cancer during radiotherapy. *Coll Antropol* 2000; **24**: 373-380

Heart-touching Chilaiditi's syndrome

Dario Sorrentino, Massimo Bazzocchi, Luigi Badano, Francesco Toso, Pietro Giagu

Dario Sorrentino, Massimo Bazzocchi, Luigi Badano, Pietro Giagu, Francesco Toso, Ester Zearo, GI Unit-Internal Medicine of the Department of Clinical and Experimental Pathology and Department of Radiology, University of Udine School of Medicine and Division of Cardiology, Udine General Hospital, Udine, Italy
Correspondence to: Professor Dario Sorrentino, Medicina Interna, Policlinico Universitario, P.zza SMM 1, Udine 33100, Italy. sorrentino@uniud.it
Telephone: +39-0432559803
Received: 2004-09-20 Accepted: 2004-12-01

Abstract

Symptomatic hepato-diaphragmatic interposition of a bowel loop or Chilaiditi's syndrome is a peculiar anatomical condition most often found by chance. Its described symptoms range from intermittent, mild abdominal pain and dyspepsia to acute intestinal obstruction. We report a case of hepato-diaphragmatic migration of the hepatic flexure of the colon associated to an unusual, heretofore unreported, angina-like pain exclusively evoked by the left lateral decubitus. To maximize the chance of observing anatomical changes in different postures, computed tomography of the chest and abdomen was performed after air insufflation into the colon. While frank herniation into the chest was excluded, the scan showed that the hepatic flexure-with the interposition of the diaphragm-came in contact with the right side of the heart in the left lateral, but not in the supine, decubitus. This finding was reproduced by echocardiography which also showed virtually unaltered hemodynamics after the change of posture. ECG, left and right ventricular global and regional function as well as cardiac injury markers also remained unchanged during the maneuver, indicating that the pain evoked by the latter was unlikely due to myocardial ischemia. This case suggests that Chilaiditi's syndrome should be included among the possible, although rare, causes of unexplained angina-like symptoms.

© 2005 The WJG Press and Elsevier Inc. All rights reserved.

Key words: Chilaiditi's syndrome; Hepatodiaphragmatic interposition; Precordial pain

Sorrentino D, Bazzocchi M, Badano L, Toso F, Giagu P. Heart-touching Chilaiditi's syndrome. *World J Gastroenterol* 2005; 11(29): 4607-4609
<http://www.wjgnet.com/1007-9327/11/4607.asp>

INTRODUCTION

The radiological finding of hepato-diaphragmatic

interposition of a bowel segment, also known as Chilaiditi's sign, defines an uncommon and typically asymptomatic anatomical abnormality. When associated with symptoms, it is termed as Chilaiditi's syndrome^[1]. Although a number of different symptoms have been attributed to this condition they are almost always related to the digestive tract itself such as, most commonly, abdominal pain, dyspepsia and intestinal obstruction due to volvulus.

In the case described in this paper, the hepato-diaphragmatic migration of the hepatic flexure of the colon was associated with an angina-like pain, exclusively evoked by the left lateral decubitus. The investigations conducted in our patient clearly showed that the symptom was associated to the contact between the heart and the intestine. Although the precise mechanism at the basis of this phenomenon remains unknown it is, to our knowledge, the first time that precordial pain has been attributed to such a peculiar anatomical condition.

CASE REPORT

A 69-year-old white male was admitted to the hospital with a history of retrosternal oppressive pain radiating to the left arm, mild dyspnea, and a state of prostration for the past 2 years.

These symptoms were present with the patient lying on his left side, and subsided in the supine position and in orthostatism.

For this reason, he had been previously referred to a cardiologist. However, an ECG failed to show overt signs of ischemia; a stress test and a Holter monitoring were within limits and a trial with calcium antagonists proved ineffective. At this point, a diagnosis of anxiety/depression syndrome was considered likely but a therapeutic trial with benzodiazepines was without effect.

The only relevant episodes in his past medical history were an apparent pleural effusion at the age of 18 which spontaneously resolved; and an NSAID-related gastric ulcer at the age of 46 which was treated with H₂-antagonists with complete healing.

On admittance, the patient was in good general condition. He was overweight (BMI 27.5 kg/m²) but physical examination was otherwise unremarkable. The pulse rate was 72, and the blood pressure was 130/70 mmHg. Laboratory tests showed increased values of ferritin (635 ng/dL), γ -GT (75 U/L) and total cholesterol (295 mg/dL). The ECG tracing at rest was normal. During the hospital stay, the symptoms mentioned above took place on two separate episodes: in each occasion they immediately subsided by changing decubitus. The physical examination during the crisis was unremarkable; the ECG and cardiac injury markers remained unchanged. Cardiac involvement at this point seemed unlikely. Since he reported, during his symptoms, the subjective feeling of a mass moving from the abdomen

toward the chest, subsequent studies focused on the gastrointestinal tract.

An abdominal ultrasound showed a severe hypotrophism of the liver with marked stretching of the intrahepatic vessels, while the portal hilum and the gallbladder were not identifiable at all. The general picture was not incompatible with chronic liver disease, even in the absence of parenchymal and focal lesions. However, liver disease became unlikely once the diagnosis of Chilaiditi's sign was established by a double contrast barium enema (not shown) and a CT scan of the abdomen which showed the interposition of the hepatic flexure of the colon between the right liver lobe and the homolateral rib cage (Figure 1) while excluding frank herniation into the chest.

Subsequently, we sought a correlation between this anatomic finding and the patient's symptoms. To maximize the chances of observing anatomical changes in different postures, a CT scan of the abdomen and chest was performed with a Toshiba Aquilion 16 Multi-Slice CT (Toshiba AMS, Tustin, CA, USA) after air insufflation into the colon. The latter involved an amount of air (approximately 800 cm³) that caused mild discomfort to the patient, roughly equivalent to the sensation provoked by naturally occurring meteorism. The scan demonstrated

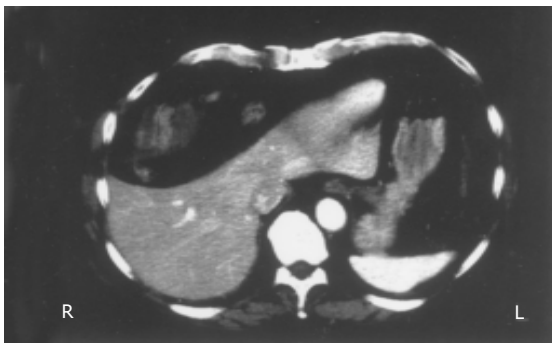


Figure 1 Axial CT scan of the abdomen. The image shows interposition of the colon (with fecal content) between the rib cage and the liver (Chilaiditi's sign). The latter appears compressed and dislocated in the absence of parenchymal and focal lesions.

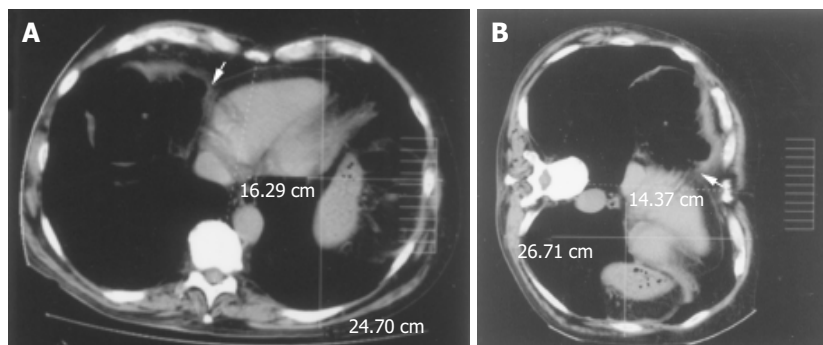


Figure 2 CT scan of the chest after air insufflation into the colon. **A:** Supine position: the arrow shows the close vicinity of the hepatic flexure (asterisk) to the right side of the heart with the interposition of the diaphragm. However, the pericardium and the intestinal wall are clearly demarcated. The left hemithorax appears symmetrical compared to the right one; **B:** Left lateral decubitus: upon changing position the colon moves forward and medially, coming into contact with the vena cava and the right side of the heart (arrow). Compared to the

the close vicinity of the colon to the right side of the heart in the supine position (Figure 2A, arrow). When the same scan was taken with the patient lying on his left side (Figure 2B) it showed that the colon had moved forward and medially, coming into contact with the vena cava and the right side of the heart. In this position, the patient complained of his typical precordial pain. The change of posture also caused migration of the diaphragm and its attached organs (i.e., the heart) toward the left side of the chest (Figures 2A and B). At the same time, the left hemithorax anteroposterior diameter increased, while the transverse diameter decreased (Figures 2A and B).

Finally, the patient was subjected to multiplane transesophageal echocardiography (SONOS 5500, Philips, Best, Holland) before and after air insufflation into the colon as above. The latter did not produce echos different from the exam conducted under basic conditions. However, the change of posture from the supine (Figure 3A) to the left lateral decubitus (Figure 3B) resulted again in frank contact between the heart and the colon with blurring of each other's contours. Blood pressure, heart rate, right and left ventricular global and regional function and oxygen saturation remained unchanged indicating no alteration in cardiac hemodynamics.

Thus, the mechanism provoking pain, as well as being reversible, did not appear to involve true ischemia. In addition, the patient refused to take surgery into consideration. Therefore, we opted for careful observation recommending the patient to lose weight. After 8 mo he did lose 8 kg of body weight and his symptoms have now become much less frequent and intense.

DISCUSSION

Hepato-diaphragmatic interposition of a bowel loop, usually the hepatic flexure of the colon, described by Chilaiditi^[2] in 1910, is a peculiar anatomical condition most often found by chance. When associated with symptoms-usually from mild abdominal pain and dyspepsia to acute intestinal obstruction-it is termed Chilaiditi's syndrome^[1].

Congenital anatomical abnormalities such as colonic

supine position, the left hemithorax anteroposterior diameter is increased while the transverse diameter is decreased. This phenomenon may, at least in part, be associated to partial migration of the diaphragm and its attached organs and vessels toward the left side of the chest. This is also underlined by the change in the position of the heart in this radiogram in relation to the broken line (drawn from the sternum to the vertebra) compared to the radiogram in Figure 1. In this posture the patient complained of his typical precordial pain.

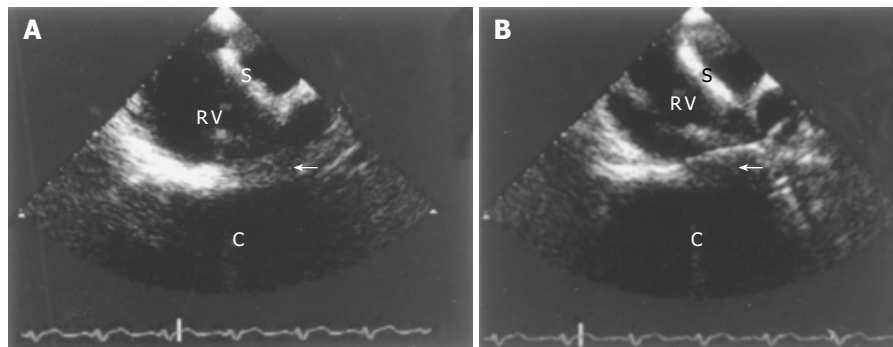


Figure 3 Multiplane trans-esophageal echocardiography after air insufflation into the colon. **A:** supine position; **B:** left lateral decubitus. Confirming the CT scan findings, the change of posture resulted in frank contact (arrow) between the heart and the colon with blurring of each other's contours. However, blood

pressure, heart rate and oxygen saturation remained unchanged during the maneuver, indicating no alteration in cardiac hemodynamics. (RV: right ventricle; S: interventricular septum; C: air space corresponding to the colon).

elongation and laxity of colonic and hepatic suspensory ligaments have been postulated as the principal predisposing factors^[3]. Other predisposing situations can be acquired such as an enlarged lower thoracic outlet (e.g., in pregnancy, emphysema, and cirrhosis with ascites), or organ shrinkage (e.g., atrophic cirrhosis of the liver)^[4]. Fat deposition between the liver and the colon, in obese individuals, widens the space between the two organs and can also favor the migration of the colon^[5].

The case of Chilaiditi's syndrome reported in this paper is peculiar with regard to its symptoms angina of like pain with left arm irradiation and their likely origin, i.e., the motion of the colon into the chest. Although a case of *right* rib cage pain has been attributed to Chilaiditi's syndrome^[6] the latter has never been causally associated to precordial pain.

Our patient had a few known predisposing factors for the migration of the hepatic flexure, i.e., he was overweight and, likely, had an abnormally thin and lax diaphragm. In addition, he had a hypotrophic liver even though the latter could have been a consequence rather than the cause of his bowel displacement.

Guided by the absence of cardiologic abnormalities and by the patient's subjective feeling of a moving abdominal mass, we made an initial diagnosis of Chilaiditi's sign by barium enema and CT scan. We then elected to perform both CT scan and cardiac ultrasound after air insufflation into the colon to study in detail the expected anatomical changes associated with the patient's symptom. It should be emphasized that the amount of insufflated air was small and only produced a typical subjective feeling of meteorism. Although the colon (with the interposition of the diaphragm) was very close to the heart in the supine position (Figures 2A and 3A) it was in the left lateral decubitus, that the two organs clearly touched each other and the heart moved to the left of the chest (Figures 2B and 3B). Since the ECG, the cardiac function and the cardiac enzymes remained within limits during the maneuver, it is unlikely that the pain originated from true cardiac ischemia. Blood pressure, heart rate, and oxygen saturation also did not change. Indeed, cardiac hemodynamics were not expected to be affected since the pressure inside the heart chambers far exceeds

that inside the colon. Thus, it is possible that the pain felt by the patient, concomitant to the migration of the hepatic flexure, was simply due to the transient stimulation of cardiac nervous fibers or to the internal compression of the chest or to overstretching of the major vessels-including the aorta and vena cava, or to a combination of these last two factors^[7]. Indeed, the CT scan showed a movement of the heart with the diaphragm toward the left side of the chest upon changing position (Figures 2A and B). This partial migration might have caused the hypothetical stretching of the vessels as well as (at least in part) the change in the anteroposterior and transverse diameters of the left hemithorax.

Based on patient's choices and given the apparent absence of a life threatening situation, we did not recommend surgery but only careful observation and weight loss. Indeed, losing weight has gradually decreased the frequency and intensity of the patient's symptoms.

In conclusion, we have shown a case of Chilaiditi's syndrome presenting with an unusual symptom-precordial pain-associated to the unusual contact between the colon and the heart and the movement of the heart to the left of the chest. Hence, Chilaiditi's syndrome should be included among the possible, although rare, causes of unexplained angina-like symptoms.

REFERENCES

- 1 **Lekkas CN, Lentino W.** Symptom-producing interposition of the colon. *JAMA* 1978; **240**: 747-750
- 2 **Chilaiditi D.** Zur frage der hepatoptose und ptose im allgemeinen im Anschluss an drei Falle von temporarer, partieller Leberverlagerung. *Fortchr Geb Rontgenstr Nuklearmed Ergänzungsband* 1910; **16**: 173-208
- 3 **Walsh SD, Cruikshank JG.** Chilaiditi's syndrome. *Age Ageing* 1976; **6**: 51-57
- 4 **Pritchard GA, Price-Thomas JM.** Internal hernia of the transverse colon. A new syndrome. *Dis Colon Rectum* 1986; **29**: 657-658
- 5 **Murphy JM, Maibaum A, Alexander G, Dixon AK.** Chilaiditi's syndrome and obesity. *Clin Anat* 2000; **13**: 181-184
- 6 **Schubert SR.** Chilaiditi's syndrome: an unusual cause of chest or abdominal pain. *Geriatrics* 1998; **53**: 85-88
- 7 **Braunwald E.** The History. In: Braunwald E. ed: Heart Disease, Philadelphia, PA WB Saunders 2000: 1-13

• ACKNOWLEDGMENTS •

Acknowledgments to Reviewers of *World Journal of Gastroenterology*

Many reviewers have contributed their expertise and time to the peer review, a critical process to ensure the quality of *World Journal of Gastroenterology*. The editors and authors of the articles submitted to the journal are grateful to the following reviewers for evaluating the articles (including those were published and those were rejected in this issue) during the last editing period of time.

Andrew Seng Boon Chua, M.D.

Department Of Gastroenterology, Gastro Centre Ipoh, 31, Lebuhraya Taman Ipoh, Ipoh Garden South, 32400, Ipoh, Perak, Malaysia

Curt Einarsson, Professor

Department of Medicine, Karolinska institute, Karolinska University Hospital Huddinge, Dept of Gastroenterology and Hepatology, K 63, Huddinge SE-141 86, Sweden

Xue-Gong Fan, Professor

Xiangya Hospital, Changsha 410008, Hunan Province, China

Jin Gu, Professor

Peking University School of Oncology, Beijing Cancer Hospital, Beijing 100036, China

Ichiro Hirata, Professor

Internal Medicine II, Osaka Medical College, Takatsuki, Osaka 569-8686, Japan

Keiji Hirata, M.D.

Surgery 1, University of Occupational and Environmental Health, 1-1 Iseigaoka, Yahatanishi-ku, Kitakyushu 807-8555, Japan

Zhi-Qiang Huang, Professor

Abdominal Surgery Institute of General Hospital of PLA, Fuxing Road, Beijing 100853, China

Shunji Ishihara, M.D.

Department of Gastroenterology and Hepatology, Shimane University, School of Medicine, 89-1, Enya-cho, Izumo 693-8501, Japan

Hong-Xiang Liu, PhD

Department of Pathology, Division of Molecular Histopathology, University of Cambridge, Box 231, Level 3, Lab Block, Addenbrooke's Hospital, Hills Road, Cambridge CB2 2QQ, United Kingdom

Ai-Ping Lu, Professor

China Academy of Traditional Chinese Medicine, Dongzhimen Nei, 18 Beixincang, Beijing 100700, China

You-Yong Lu, Professor

Beijing Molecular Oncology Laboratory, Peking University School

of Oncology and Beijing Institute for Cancer Research, #1, Da-Hong-Luo-Chang Street, Western District, Beijing 100034, China

Reza Malekzadeh, Professor

Director, Digestive Disease Research Center, Tehran University of Medical Sciences, Shariati Hospital, Kargar Shomali Avenue, 19119 Tehran, Iran

Jing-Yun Ma, M.D.

Managing Director, *World Journal of Gastroenterology*, PO Box 2345, Beijing 100023, China

Yuji Naito, Professor

Kyoto Prefectural University of Medicine, Kamigyo-ku, Kyoto 602-8566, Japan

Julian Panes, Professor

Department of Gastroenterology, Hospital Clinic of Barcelona, Villarroel 170, Barcelona 08036, Spain

Qin Su, Professor

Department of Pathology, Cancer Hospital and Cancer Institute, Chinese Academy of Medical Sciences and Peking Medical College, PO Box 2258, Beijing 100021, China

Eddie Wisse, Professor

Irisweg 16, Keerbergen 3140, Belgium

Jian Wu, Assistant Professor of Medicine

Internal Medicine/Transplant Research Program, University of California, Davis Medical Center, 4635 2nd Ave. Suite 1001, Sacramento CA 95817, United States

Harry H-X Xia, M.D.

Department of Medicine, The University of Hong Kong, Pokfulam Road, Hong Kong, China

Jia-Yu Xu, Professor

Shanghai Second Medical University, Rui Jin Hospital, 197 Rui Jin Er Road, Shanghai 200025, China

Yuan Yuan, Professor

Cancer Institute of China Medical University, 155 North Nanjing Street, Heping District, Shenyang 110001, Liaoning Province, China

Jian-Zhong Zhang, Professor

Department of Pathology and Laboratory Medicine, Beijing 306 Hospital, 9 North Anxiang Road, PO Box 9720, Beijing 100101, China

Xiao-Hang Zhao, Professor

State Key Laboratory of Molecular Oncology, Cancer Institute of Chinese Academy of Medical Sciences, 17 Panjiayuan, Chaoyangqu, Beijing 100021, China

Liver alveolar echinococcosis in China: Clinical aspect with relative basic research

Ci-Peng Jiang, McManus Don, Malcolm Jones

Ci-Peng Jiang, Hydatidosis Research Laboratory of Basic Medical School, Lanzhou University, Lanzhou 730000, Gansu Province, China
McManus Don, Malcolm Jones, Post Office Royal Brisbane Hospital, Q 4029 Australia

Supported by England Wellcome Trust, 2002

Correspondence to: Ci-Peng Jiang, MD, Professor of Parasitology, Hydatidosis Research Laboratory of Basic Medical School, Lanzhou University, Western Dong Gang Road, Lanzhou 730000, Gansu Province, China

Telephone: +86-931-8616759 Fax: +86-931-8611355

Received: 2004-09-23 Accepted: 2004-11-12

Abstract

This paper deals with all aspects of liver alveolar echinococcosis (AE) including epidemiology, pathology, clinical manifestations, imaging examinations, diagnosis and differential diagnosis, surgical treatment and chemotherapy. The review is not only based on personal clinical experiences but also in combination with relative basic research such as proliferation and growth of alveococcus, preclinical studies of a novel compound extracted from TCM for treatment of liver AE, and molecular immunology used for specific AE diagnosis, etc.

© 2005 The WJG Press and Elsevier Inc. All rights reserved.

Key words: Echinococcosis; Alveolar echinococcosis; Liver; Clinical aspect; Basic research; China

Jiang CP, Don M, Jones M. Liver alveolar echinococcosis in China: Clinical aspect with relative basic research. *World J Gastroenterol* 2005; 11(30): 4611-4617

<http://www.wjgnet.com/1007-9327/11/4611.asp>

INTRODUCTION

Echinococcosis is a parasitic zoonosis, consisting of cystic echinococcosis (CE) and alveolar echinococcosis (AE). These two types differ in parasitology, epidemiology, pathology, clinical aspects, treatment and prognosis. They are respectively caused by the larval stage of *Echinococcus granulosus* (Eg) and *E. multilocularis* (Em) (Figure 1). Over one hundred years, the disease had been misdiagnosed as liver colloid cancer. The cause of AE was not confirmed until 1856. In China, liver AE was reported respectively in Ningxia, Xinjiang autonomous regions and Gansu Province during 1950s to 1970s^[1-3]. Up to now, at least one thousand cases of AE have been reported throughout China, but most of them

were mistaken as liver cancer. In order to improve the diagnostic level of AE, a review is comprehensively introduced as follows.

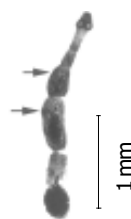


Figure 1 Adult of *E. multilocularis*.

EPIDEMIOLOGY

Em needs two mammalian hosts for completion of its life cycle. They are respectively called the definite host, arnivore and the intermediate host, mainly rodents. Proglottid containing eggs or free eggs are excreted in the feces of the definite hosts, e.g. dog or fox. Once eggs are ingested by the intermediate hosts including rodents and human beings, AE may occur in liver or other organs. In China, fox, dog and wolf have been found to be as definite hosts and a few species of the rodent such as *Citellus dauricus*, *Myospalax fontanieri*, *Microtus brandti*, were confirmed to be as intermediate hosts. Human body affected by AE is chiefly due to contacting the animals: fox, dog, or occasionally cat. Especially, ladies, herdsmen and hunters are higher risk populations. AE has been found mainly in the west of China including eight provinces or autonomous regions (Figure 2)^[4].

Gansu province

During a period from 1985 to 2000, of 89 AE cases originating from Gansu Province, 63 came from Zhang County, which may be considered as a hyper-endemic area^[5]. In the three neighbouring counties of central eastern Gansu (Figure 3), human AE epidemiological surveys were conducted four times respectively in three counties^[6-9] (Table 1). The results of comparative analysis showed that the prevalent rate was higher in Zhang County and Ming County than in Lintao County. Factors were also investigated regarding natural geographical condition, local climate, parasitic life cycle, and our experimental study^[10].

Xinjiang uygur autonomous region

AE was more common in northern Xinjiang with a total of 100 cases.



Figure 2 Distribution of AE in eight provinces in west China.

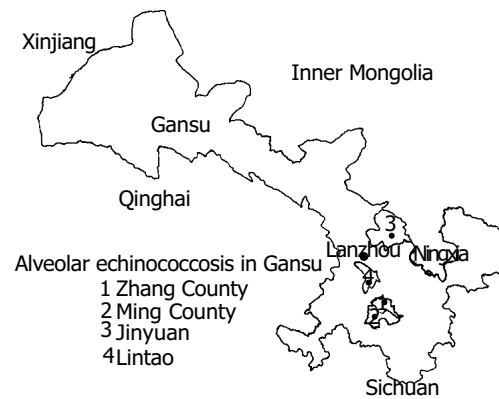


Figure 3 AE endemic counties in central eastern Gansu. (1) Zhang County, (2) Ming County, (3) Lintao, (4) Jinyuan.

Table 1 Human AE epidemiological survey in three counties of central eastern Gansu

Yr	County	Persons investigated	Positive rate of immuno-test(%)		Ultrasonic morbidity(%)
			Intradermal test	ELISA	
1986 ^[6]	Zhang County	380	19.2		2.4
1992 ^[7]	Zhang County	1 312		2.8	5.0
1998 ^[8]	Ming County	1 200		2.2	5.6
2003 ^[9]	Lintao	1 071	1.8		0.7

Ningxia Hui autonomous region

Distribution of AE was limited to a specific endemic area, and chiefly found in Xi Hai Gu's three Counties which were situated bilaterally along branches of Liupan Mountain. In 1989 during human ultrasonic investigation in Xiji County, AE morbidity was 5.9%(141/2 389). The positive rate by ELISA was 5.8%(138/2 389). In 2003, 263 cases of AE in the past 17 years were followed up in Xiji, of whom the positive rate of intradermal test was 90.2%(174/193) and ELISA in 137 patients were all positive^[11].

Qinghai province

Until 2000, 1 748 cases with echinococcosis were reviewed and 143 of them belonged to AE (8.3%). Another survey was made in 3 702 individuals, of whom 23 (0.62%) were ultrasonically diagnosed as liver AE. The distribution of AE appeared with a scattered tendency. During an investigation of human AE in three counties under the jurisdiction of Qingnan plateau, the average morbidity was 0.35%. From 1959 to 1998, 111 cases of AE were surgically treated^[12].

West Sichuan province

AE severely affected three counties of Ganzi, Shiqu, and Seda. According to investigations of 3 998 individuals in Ganzi and Shiqu from 1997 to 1998, AE morbidity was 7.78% and 2.33% respectively.

Tibet autonomous region

In 1993, 12 cases of AE originating from Larsa and three prefectural hospitals of Naqu, Shannan, and Changdu were discovered surgically and pathologically.

Inner Mongolia autonomous region

Although animals of definite host and intermediate host

were found in Hulunbeier grassland in 1988, the patient of AE was not clinically reported until 1998^[13].

Heilongjiang province

Two scattered patients of liver AE were identified surgically and pathologically. One of them was a native of Nahe County^[14] and another case was from Jiamusi city^[15].

PROLIFERATION AND GROWTH OF ALVEOCOCCUS AND HISTOGENESIS OF PROTOSCOLEX

Proliferation and growth of alveococcus is very significant as it bears practical relation with clinical aspects especially chemotherapy. As early as in 1950s to 1980s, a few Euro-american authors^[16-21] observed the proliferation and growth phenomenon of experimental alveococcus respectively in white mice, cotton mice, and jirds (*Meriones unguiculatus*). Our study was partially carried out microscopically on the pathological sections of human AE^[22]. Two modes of proliferation were found, i.e. endogenous budding and exogenous budding (Figure 4). The former (Figure 4A) was characterized by internally protrusive hyperplasia from the mother alveolar wall into the alveolar cavity and then proliferation extending continuously to reach the opposite wall of the cavity. So, septum-like budding was named. Sometimes two or more proliferative sites on the alveolar wall propagated simultaneously into the cavity in opposite directions, and mingled with each other to form a septum dividing the mother to form two or more small alveoli (Figure 4B). Externally protrusive proliferation occurred at one or several sites of the mother alveolar wall, producing single or multiple daughter and granddaughter alveoli under the name of exogenous budding (Figure 4C). These two buddings may coexist not only in one

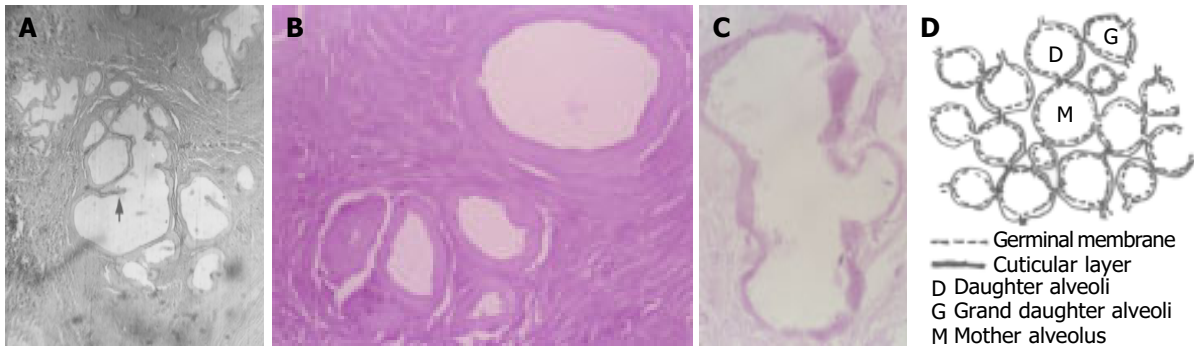


Figure 4 Modes of proliferation. **A:** Endogenous budding of alveococcus (HE stain $\times 200$). Arrow: Septum; **B:** One mother alveolus (left lower side)

dividing into four daughter alveoli (HE stain $\times 400$); **C:** Exogenous budding of alveococcus (HE stain $\times 400$); **D:** Model of alveococcus exogenous budding.

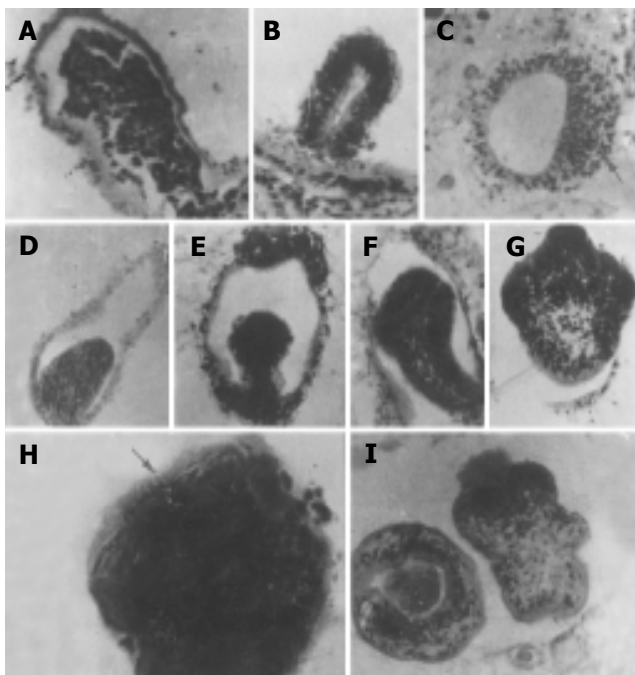


Figure 5 The entire process of mouse AE protoscolex histogenesis (HE stain $\times 200-800$). **A:** local cellular hyperplasia of germinal membrane of alveococcus wall; **B:** re-arrangement of hyperplastic cells and formation of brood capsule; **C:** local cellular hyperplasia of brood capsule wall; **D:** elliptical protrusion into cavity; **E:** mushroom protrusion; **F:** lingual protrusion; **G:** showing rostellum and suckers of protoscolex; **H:** Hooklets on rostellum; **I:** mature protoscolex (right: evaginated type. Left: invaginated type).

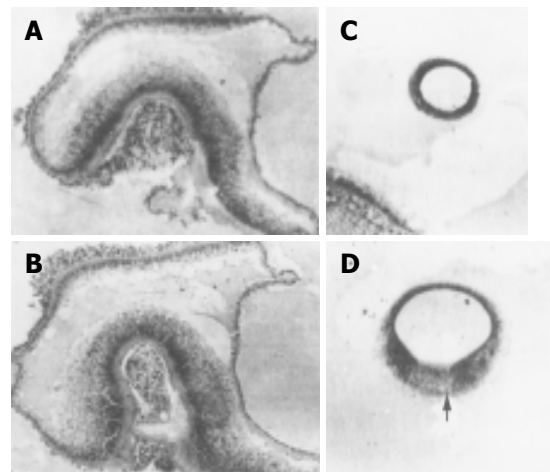


Figure 6 Histogenesis process of brood capsule of liver AE protoscolex in *Mus musculus* (HE stain $\times 200$). **A:** local hyperplasia of alveococcus wall into the cavity, looking like a reversed pocket; **B:** gradually approximating and finally closing of two pocket edges; **C:** formation of brood capsule; **D:** local cellular hyperplasia of brood capsule wall.

section of liver AE but also in that of metastatic lung or brain AE and metastatic lymph node AE. To date, the mechanism of AE proliferation and growth is not understood completely although it has been studied for decades. In the exogenous proliferative course of liver AE, the daughter alveoli of 1st grade budding and the grand-daughter alveoli of 2nd grade budding were respectively named. Proliferating grade by grade, a mother alveolus may propagate into numerous new alveoli of multi-grades just like infiltrative dissemination of carcinoma, or it further affects neighbouring organs such as porta hepatis, inferior vena cava or pancreas, rendering radical surgical operation impossible. Euzeby^[21] explained that exogenous budding was due to discontinuity of the alveolar cuticular layer, allowing the germinal membrane to escape from the mother alveolus (Figure 4D). As concerns the entire

process of protoscolex histogenesis, a stage of the formation of brood capsule must be passed through. Local cellular hyperplasia began in the wall of brood capsule, and elliptical, mushroom-shaped or lingual protrusion protruded into the cavity of brood capsule. After that, the protrusion gradually developed into rostellum and suckers, finally changing from embryonic protoscolex to mature protoscolex of evaginated or invaginated type (Figure 5). The formation of brood capsule expressed two modes. The first was local hyperplasia of germinal membrane of alveococcus wall, forming cellular group. By means of cellular rearrangement, the cells accumulated towards the periphery and a cell-free space appeared in the center, developing further into brood capsule^[23] (Figure 5). This is basically similar to other reports at home and abroad^[19,25]. The second mode of brood capsule formation was found by us from liver AE of *Mus musculus* in Zhang County, Gansu Province^[24] (Figure 6). Similar report has not been seen yet.

PATHOLOGY (Figure 7)

Macroscopical appearance

The lesion was yellowish or gray and felt as firm as cartilage. Superficially, it showed numerous noduli or minute cysts

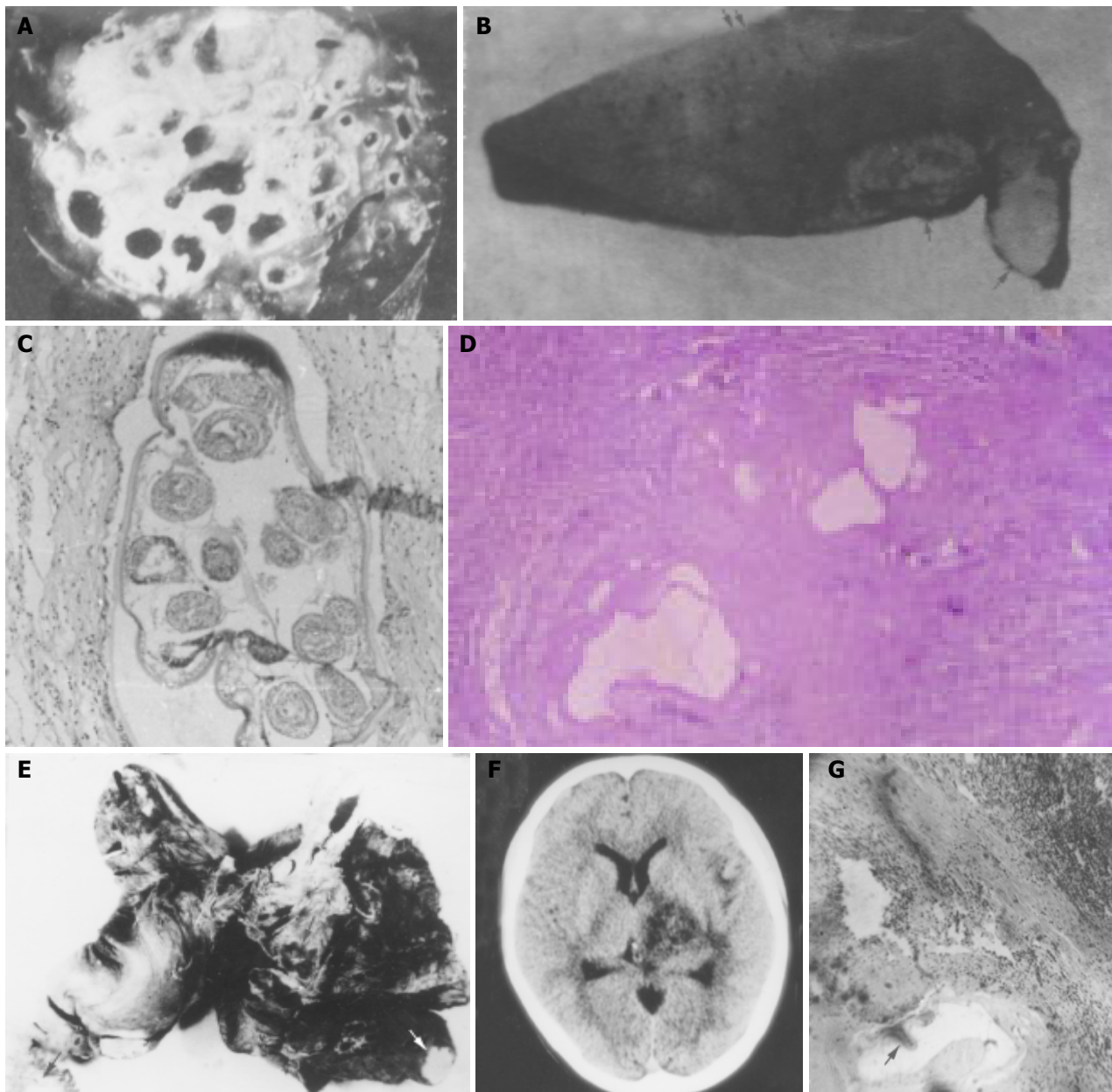


Figure 7 Pathology. **A:** A cross section of human liver AE showed alveolate appearance; **B:** Types of liver AE. ↑: Nodular type, ↑↑: Mixed type; **C:** Protoscolices inside brood capsule (HE stain×100); **D:** Alveococcus nodule

(HE stain×200); **E:** Three arrows indicating metastatic bilateral lung AE; **F:** ↑: metastatic right brain AE; **G:** lymph node metastasis near porta hepatis (HE stain×200). ↑: AE. The left upper side: Metastatic lymph nodes.

without definite encapsulation, but with alveolate structure on cross section (Figure 7A). It was usually classified into three types, of which large circumscribed mass type was more common (67.8%) and the other two were nodular type (16.7%) and mixed type (15.5%) (Figure 7B)^[26]. The central area of alveococcus may be complicated by coagulated necrosis due to poor blood supply.

Microscopic finding The lesion was characterized by many alveoli with different sizes and shapes. Observation of alveolus wall showed that the thick, acellular, laminated outer layer looked bank-like, sometimes folding within the alveolar cavity. The thin, germinal inner membrane lined by a single-layer cell was usually deficient due to detachment. Brood capsule or protoscolices were occasionally seen (Figure 7C). The lesion may be complicated by central necrosis, producing a cavity or pseudocyst after liquidization. In the

periphery of alveoli group it showed hyperplasia of fibro-connective tissue and cellular infiltration of eosinocytes, lymphocytes, plasma cells and giant cells, forming a typical alveococcus nodule (Figure 7D).

Metastasis According to a collective analysis of 270 cases with liver AE from five provinces of China (Table 2)^[27], general metastatic rate was 3.7%(10/270). The commonest metastatic organ was lung (4.7%)(Figure 7E) and the next one was brain (3.3%) (Figure 7F).

Three modes of metastasis were found. The first was direct infiltrative dissemination. The alveococcus lesion infiltrated gradually into the liver parenchyma and formed a large mass. The neighbouring organs outside the liver such as the porta hepatis, diaphragm, pancreas or inferior vena cava were further involved. The second was blood metastasis. A small portion of detached proliferating bud, if involving

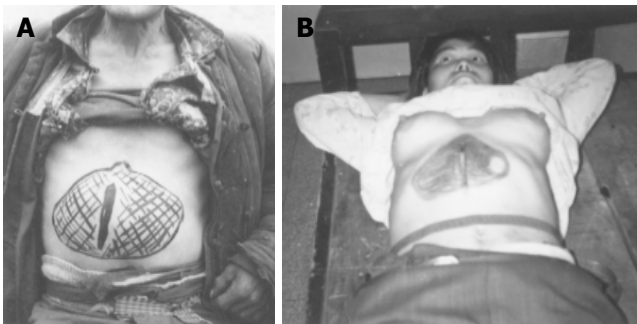


Figure 8 The size of upper abdominal mass with the largest reaching the umbilicus level. **A:** After external drainage of pseudocyst, the patient survived for 23 years. **B:** The patient survived only for 3 years.

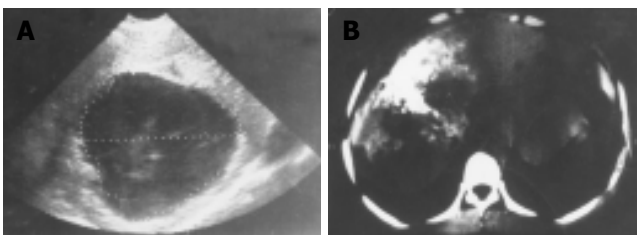


Figure 9 Imaging examinations. **A:** Ultrasonic scanning of liver AE showed a central necrotic pseudocystic cavity, but the cystic wall was irregular; **B:** Liver CT showed partial AE calcification (left) and pseudocyst (right) on the left upper side. The patient was confirmed surgically and pathologically.

the branches of portal vein, extensively disseminated within the liver parenchyma resulted in multiple noduli. Involving the branches of hepatic vein, the alveococcus spread along systemic circulation to distal organs such as lung or/and brain. The third was lymphatic metastasis. The liver alveococcus may spread to lymph nodes of the porta hepatis (Figure 7G), peritoneal cavity and colonic mesentery. According to the results of animal experiment in Japan^[28], the mechanism of metastasis was due to the detached proliferated bud, even very small or only a few nuclei entering the blood vessels. Nevertheless, it was incapable of causing metastasis if protoscolices were injected into the vessels.

CLINICAL MANIFESTATIONS

Generally speaking, sex difference is not obvious, sometimes males slightly outnumbered females. Most patients were young and in robust years of their life. According to clinical features^[29], four types, i.e. simple hepatic enlargement, obstructive jaundice, liver giant node (cancer-like) and remote metastasis were classified. According to clinical course, we divided AE into the early stage with only mild hepatic enlargement, middle stage with progressive hepatomegaly and the advanced stage associated with impaired liver function, portal hypertension, or metastasis^[30]. The main symptom was upper abdominal mass or liver mass with stiff and nodular feeling on palpation. The size of the mass varied, with the smallest being not felt or only palpated below right sub-costal margin and the largest reaching the umbilicus level (Figures 8A and B). Another symptom was abdominal pain, but usually not severe. Jaundice was found

in some cases, usually due to the impairment of liver function or the invasion and compression of bile duct by liver mass at the advanced stage. Extensive infiltration of the alveococcus lesion or fibrosis caused liver cirrhosis with subsequent portal hypertension such as the superficial varicosity of the thoracic or abdominal wall, ascites and splenomegaly. In case of liver AE associated with lung or brain metastasis, the patient manifested corresponding respiratory or neuropathic symptoms and signs.

IMAGING EXAMINATIONS (Figure 9)

X-ray films

Enlargement of liver and elevation of right diaphragm were shown on abdominal plain film. The shadows of spotted or clustered calcification were visible in the hepatic region. But they must be carefully observed as their appearances were usually not distinct. If multiple shadows of bilateral lung showed on chest film, the possibility of liver AE associated with lung metastasis ought to be considered.

Ultrasonic scanning

In a series of 141 cases with liver AE^[31], the ultrasonic features revealed solid mass in 96 and solid-cystic degeneration in 45. The former comprised 23 cases with local type, 21 with diffuse nodular type and 52 with large circumscribed mass type. If the liver alveococcus was complicated by central necrotic pseudocyst, the ultrasonic scanning showed echo-free area with irregular cystic wall (Figure 9A).

Computerized tomography (CT)

Liver CT showed single or multiple, intrahepatic, hypodense areas with irregular margin, or occasionally partial calcification of alveococcus (Figure 9B).

IMMUNOLOGICAL EXAMINATIONS

As hydatid intradermal test was simple and cheap, it was commonly used, especially in our country. Although the sensitivity was high, false positive reaction may occur. Therefore indirect hemagglutination test and ELISA were reliable methods for immunological diagnosis due to their higher specificity. Along with current advancement of molecular immunology, purification of a specific antigen from *Echinococcus multilocularis* (Em) has been successful. As early as in 1983, Gottstein *et al.*^[32,33], prepared an antigen fraction (Em2) from alveococcus tissue using affinity chromatography. Owing to a high specificity of Em2 for *E. multilocularis*, a correct serological differential diagnosis was achieved in 95% of 57 confirmed cases of human CE or AE. However, Em2 was isolated from laminated layer of alveococcus, a higher or lower level of antibody titer did not reflect whether the focus was active or not. Em2-ELISA test still showed positive result with a high titer even though the focus became stable or calcified after chemotherapy. As the protoscolex is the most active component of the alveococcus tissues, it was used to isolate protoscolex antigens designated as Em16 and Em18 using Western blotting in a cooperative study between China and Japan^[34]. Em18 and Em16, especially the former showed not only a higher sensitivity but also stronger specificity for immunodiagnosis

Table 2 Remote metastases of 270 cases with liver AE in China

Province or autonomous region (yr)	n	Number of cases of blood-stream metastasis (%)				Number of cases of lymphatic metastasis (%)		
		Lung	Brain	Lung+brain	Spleen	Lymph node of porta hepatis	Lymph node of peritoneal cavity	Lymph node of colonic mesentery
Xinjiang (1985)	43	3	2					
Ningxia (1991)	22						1	
Sichuan (1994)	24	2		1				
Gansu (1995)	70	3	2	1		1		1
Qinghai (2000)	111	2	7		2		1	
Total	270	10 (3.7)	11 (4.1)	2 (0.7)	2 (0.7)	1 (0.4)	2 (0.7)	1 (0.4)

of human AE. We also used the alveococcus protoscolices for isolating Em16 and Em18 by isoelectric focusing analysis^[35]. These protein antigens could not show the best diagnostic value and cross reaction which possibly occurred between AE and CE or between AE and cysticercosis^[36]. In short, molecular immunological diagnosis for human AE needs further studies.

DIAGNOSIS

Until now, liver AE is always mis-diagnosed. To make a correct diagnosis of liver AE, we should not ignore the past histories of the patients. First, where did the patient come from, AE endemic area? Next, did the patient contact dog, cat, or fox-fur? Thirdly, what is the occupation of the patient, fox-hunter or dog-raiser? These data would be helpful for the diagnosis of liver AE.

DIFFERENTIAL DIAGNOSIS

Liver cancer

In our collective review of 274 cases with liver AE, the determination of serum AFP was negative in all the patients^[27]. So it is significant for differential diagnosis of AE. As a rule, liver AE pursues a slow, but progressive course. It obviously differs from liver carcinoma which develops faster or very rapidly, leading to patient death in a short time. AFP test is a reliable differential diagnostic method. Sometimes, gross findings of liver AE may be confused with carcinoma on the operation table and frozen section is necessary. When the diagnosis of liver AE is still difficult before operation, liver needle biopsy may be considered (Figure 10). Occasionally liver AE also needs to be differentiated from cystic echinococcosis (CE) or some nonparasitic diseases such as tuberculosis. If chest X-ray film showed multiple shadows of bilateral lung or brain CT showed cerebral lesion, it might be possible that liver AE was associated with lung or/and brain metastasis^[37]. Clinically unknown nature of malignant tumor was always determined.

TREATMENT

Surgical operation

The rational treatment for liver AE is radical hepatectomy and the prognosis of the patient may be good. An individual case had been postoperatively followed up for 21 years without recurrence^[2]. However, the rate of hepatectomy is very low due to the difficulty of early diagnosis. According

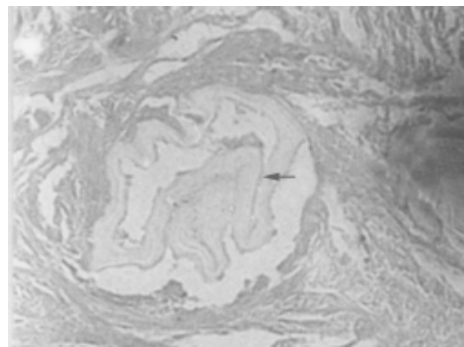


Figure 10 Liver needle biopsy. Arrow: alveococcus (HE stain×200).

to our collective analysis of 258 cases of liver AE in China^[27], only 27(10.5%) and 16 (6.2%) had performed radical liver lobectomy and partial hepatectomy respectively. In order to increase the percentage of hepatectomy, an epidemiological survey in AE endemic area is very significant to screen out early cases. For liver unresectable case, a palliative operation may be indicated such as surgical drainage for a large pseudocyst in order to decompress pericystic liver tissues. As in Figure 8A, the patient was alive for 23 years after external drainage of liver pseudocyst.

Chemotherapy

Albendazole (ABZ) is considered by WHO as the best anti-AE drug. Experimental studies showed that ABZ was able to inhibit alveococcus proliferation and growth. Considering the clinical effects, it was shown to alleviate the symptoms, to prolong the survival, and diminish lung or/and brain metastasis after therapy. In our 23 cases of liver AE treated with ABZ, symptoms were improved, appetite increased, jaundice relieved, and liver enlargement decreased in 15 (65.2%)^[38] cases. Liu *et al.*^[39], reported that in 11 cases of liver AE followed-up for 2-7 years after long-term continuous ABZ therapy, 7 showed calcification on liver CT film. Thus ABZ may be lethal to the parasite. In addition, we found a novel compound extracted from traditional Chinese medicine, Xiao-Bao capsule for treatment of AE. Experimental results showed that the inhibitory rate of mouse AE was 65.7% and 80.6% respectively in two groups of mice, i.e., 1-week and 10-weeks after inoculative infection^[40]. In our 21 cases of liver AE, symptoms improved in 16 (76.1%)^[27] cases. Both acute toxicity test in mice and chronic toxicity test in rats showed no toxic reactions^[41]. We

postulate that combination of Xiao-Bao capsule and ABZ would be more effective than single medication.

REFERENCES

- 1 **Qi ZY**, Zhang ZZ, Wei XY, Han F, Lin XL. A clinical analysis of 15 cases with alveolar echinococcosis. *Zhonghua Yixue Zazhi* 1965; **15**: 28-29
- 2 **Yao BL**, Huang IC, Fu LM, Fang SH. Liver alveolar echinococcosis. *Zhonghua Waike Zazhi* 1965; **13**: 460-461
- 3 **Jiang CP**. Report of 3 cases with alveolar echinococcosis. *Zhonghua Neike Zazhi* 1997; **16**: 374
- 4 **Jiang CP**. Today's regional distribution of echinococcosis in China. *Chin Med J* 2002; **115**: 1244-1247
- 5 **Jiang CP**. Present epidemic situation of liver alveolar echinococcosis in Gansu Province, China. *Chin Med J* 2005; **118**: 327-328
- 6 **Jiang CP**, Wang HX, Wang ZR, Ma YC, Shi HY. Epidemiological survey of alveolar echinococcosis in Zhang County, Gansu Province. *Difangbing Tongbao* 1991; **6**: 83-85
- 7 **Craig PS**, Liu DS, Mepheron CNL. A large focus of alveolar echinococcosis in central China. *Lancet* 1992; **340**: 826-830
- 8 **Shin DZ**, Wang NQ, Bao GS, Li WK. Epidemiological survey of alveolar echinococcosis in Ming County. Gansu Province. *Difangbing Tongbao* 1998; **13**: 61-63
- 9 **Jiang CP**. Report of seven cases with liver alveolar echinococcosis and infective rate of human population in Lintao County, Gansu Province. *Difangbing Tongbao* 2003; **18**: 33-34
- 10 **Jiang CP**. Preliminary observation on infectivity of isolated alveolar hydatid after cryopreservation. *Zhongguo Jishengchongxue Yu Jishengchongbing Zazhi* 1992; **10**: 307-310
- 11 **Li M**, Li JL, Liu XZ, Yang YR, Wang H, Chen G. A retrospect on the diagnosis and treatment of 263 cases of hepatic alveolar echinococcosis in 17 years. *Zhongguo Jishengchongxue Yu Jishengchongbing Zazhi* 2003; **21**: 192
- 12 **Wang H**, Schantz PM, Liu FJ, Ito A, Chai JJ. Infections of larval and adult *Echinococcus multilocularis* in human and animals in Qinghai Province. *Zhongguo Jishengchongbing Fangzhi Zazhi* 2000; **13**: 120-122
- 13 **Bai G**, Ma YG. One case of liver alveolar echinococcosis. *Zhongguo Jishengchongxue Yu Jishengchongbing Zazhi* 1998; **16**: 20
- 14 **Li G**, Shi XQ. One case of liver alveolar echinococcosis. *Zhongguo Jishengchongxue Yu Jishengchongbing Zazhi* 1985; **3**: 8
- 15 **Wen GZ**, Wang GZ, Zhang YF. A case report of liver alveolar echinococcosis. *Zhongguo Renshou Gonghuanbing Zazhi* 1990; **6**: 62
- 16 **Mankau SK**. Studies on *Echinococcus sibiricensis* in laboratory mice. *J Parasitol* 1995; **41**: 29
- 17 **Mankau SK**. Studies in *Echinococcus alveolaris* from ST. Lawrence Island, Alaska. Histogenesis of the alveolar cyst in white mice. *J Parasitol* 1957; **43**: 453
- 18 **Likashenko HI**. Studies on histogenesis of protoscolices from *Alveococcus multilocularis* (Ieuckart,1983). *Rus J Med Parasitol Parasit Dis* 1964; **33**: 584-587
- 19 **Eckert J**. Proliferation and metastases formation of larval *Echinococcus multilocularis*. I. Animal model, macroscopical and histological findings. *Z Parasitenkd* 1983; **69**: 37
- 20 **Mehlhorn H**, Eckert J, Thompson RC. Proliferation and metastases formation of larval *Echinococcus multilocularis*. II. Ultrastructural investigations. *Z Parasitenkd* 1983; **69**: 749-763
- 21 **Euzeby JA**. Zoonotic cestodes. In: Soubry EJL, ed. Parasitic zoonoses: clinical and experimental studies. New York: Academic Press 1974; **160**: 163
- 22 **Jiang CP**. Studies on echinococcosis in China. In: Xu KD. Science and technology at the frontier in China, 2004. Beijing: Higher Education Press 2004: 374-378
- 23 **Jiang CP**. Light microscopic observations in the proliferation and growth of human echinococcus. *Chin Med J* 1987; **100**: 17-21
- 24 **Jiang CP**, Liu YH. Histogenesis of protoscolices from alveococcus cyst wall in mice. *Zhongguo Jishengchongxue Yu Jishengchongbing Zazhi* 1995; **13**: 229
- 25 **Qiu JM**, Chen HC. Histologic observation on developmental process of alveococcus in mice. *Sichuan Dongwuxue* 1985; **4**: 17-20
- 26 **Jiang CP**. Liver alveolar echinococcosis in the northwest: Report of 15 patients and collective analysis of 90 cases. *Chin Med J* 1981; **94**: 771-778
- 27 **Jiang CP**. Progress of alveolar echinococcosis in China. *Chin Med J* 1998; **111**: 470-475
- 28 **Matsuhisa T**, Uchino J, Sato N, Furuya K, Fujioka Y. Which component makes distant metastasis of alveolar echinococcosis, germinal cells or protoscolices? In: Uchino J, Sato N. eds. Strategy for Eradication of Alveolar Echinococcosis of the Liver, 1996. Sapporo Fuji Shoin Publishers 1996: 233-237
- 29 **Yao YQ**, Liu YH, Wang XG. Clinical analysis of 24 cases of liver alveolar hydatidosis. *Shiyong Jishengchongbing Zazhi* 1994; **2**: 13-15
- 30 **Jiang CP**. Clinical nomenclature of echinococcosis based on 20 selected cases. *Chin M J* 1986; **99**: 597-598
- 31 **Wang HL**, Yin YC, Ma C, Zhang CY, Zhang XP, Cheng RP, Jing RF, Li M. Preliminary investigation of liver alveolar echinococcosis and cystic echinococcosis in Xiji, Ningxia. *Zhongguo Jishengchongxue Yu Jishengchongbing Zazhi* 1991; **9**: 143-145
- 32 **Gottstein B**, Eckert J, Fey H. Serological differentiation between *Echinococcus granulosus* and *E. multilocularis* infection in man. *Z Parasitenkd* 1983; **69**: 347-356
- 33 **Gottstein B**. Purification and Characterization of a specific antigen from *Echinococcus multilocularis*. *Parasitol Immunol* 1985; **7**: 201-202
- 34 **Ma L**, Ito A, Liu YH, Wang XG, Yao YQ, Yu DG. Evaluation of the diagnostic value of Em 18 KDa and Em 16 KDa antigens in *Echinococcus multilocularis* by Western blotting. *Zhongguo Jishengchongxue Yu Jishengchongbing Zazhi* 1997; **15**: 65-68
- 35 **Li SP**, Chen YT, Jiang CP, Qiu JM, Yu DG. Isoelectric focusing analysis of *Echinococcus multilocularis* protoscolelex antigens. *Zhongguo Jishengchongxue Yu Jishengchongbing Zazhi* 2000; **18**: 107-108
- 36 **Li SP**, Chen YT, Jiang CP, Qiu JM, Yu DG. Immuno-diagnostic value of protein antigens from *Echinococcus multilocularis* protoscolelex. *Zhongguo Jishengchongxue Yu Jishengchongbing Zazhi* 2001; **19**: 56-57
- 37 **Jiang CP**. Two cases of liver alveolar echinococcosis associated with simultaneous lung and brain metastases. *Chin Med J* 2002; **115**: 1898-1901
- 38 **Jiang CP**, Liu YH. A further study on liver alveolar echinococcosis, report of 70 cases. *Chin Med J* 1995; **108**: 551-554
- 39 **Liu YH**, Wang XG, Chen YT, Yao YQ. Computerized tomography of liver alveolar echinococcosis treated with albendazole. *Zhonghua Neike Zazhi* 1993; **32**: 733-735
- 40 **Jiang CP**. Experimental study on a novel compound extracted from Traditional Chinese Medicine for treatment of alveolar echinococcosis. *Chin Med J* 2002; **115**: 1576-1578
- 41 **Li SP**, Jiang CP. Acute toxicity test of Xiao-Bao decoction extracted from Traditional Chinese Medicine. *Zhongyiyao Keji* 1996; **3**: 13-14

Mutation of DNA polymerase β in esophageal carcinoma of different regions

Guo-Qiang Zhao, Tao Wang, Qin Zhao, Hong-Yan Yang, Xiao-Hui Tan, Zi-Ming Dong

Guo-Qiang Zhao, Tao Wang, Qin Zhao, Hong-Yan Yang, Xiao-Hui Tan, Zi-Ming Dong, Basic Medical College, Zhengzhou University, Zhengzhou 450052, Henan Province, China
Supported by the National Natural Science Foundation of China, No. 39870287

Correspondence to: Dr. Guo-Qiang Zhao, Basic Medical College, Zhengzhou University, Zhengzhou 450052, Henan Province, China. zhaogq@zzu.edu.cn

Telephone: +86-371-66912523

Received: 2004-11-02 Accepted: 2004-12-26

Abstract

AIM: To observe the variation of DNA polymerase β (pol β) in esophageal carcinoma.

METHODS: Thirty specimens containing adjacent normal epithelial tissues were collected from patients in Linzhou region (a high risk area for esophageal squamous carcinoma) and 25 specimens were from a non-high risk area. Total RNA was extracted from the samples and reverse transcription polymerase chain reaction (RT-PCR) was performed. PCR products were cloned and sequenced to investigate the pol β gene with DNASIS and OMIGA. Statistical significance was evaluated using the χ^2 test.

RESULTS: High-incidence area group: pol β gene variation was detected in 13 of 30 esophageal carcinoma tissue specimens, and only one variation was found in 30 corresponding adjacent normal tissue specimens. Non high-incidence area group: pol β gene variation was detected in 5 of 25 esophageal carcinoma tissue specimens, and no variation was found in 25 corresponding adjacent normal tissue specimens. The incidence of pol β gene variation observed in the high-incidence area group was significantly higher than in the non-high incidence area group. Two mutation hot spots (454-466 and 648-670 nt) and a 58 bp deletion (177-234 nt) were found.

CONCLUSION: Variations of pol β perform different functions between the high-incidence areas and the other areas, and may play a more important role in the high-incidence areas.

© 2005 The WJG Press and Elsevier Inc. All rights reserved.

Key words: DNA polymerase β ; Esophageal carcinoma; Gene mutation

Zhao GQ, Wang T, Zhao Q, Yang HY, Tan XH, Dong ZM. Mutation

of DNA polymerase β in esophageal carcinoma of different regions. *World J Gastroenterol* 2005; 11(30): 4618-4622
<http://www.wjgnet.com/1007-9327/11/4618.asp>

INTRODUCTION

Esophageal carcinoma occurs frequently in China, especially in the mountainous Taihang area. Epidemiology and laboratory studies suggest that the carcinogenesis and progression of esophageal carcinoma are probably associated with some gene mutations^[1,2]. Some researches indicate that the ability of pol β to repair DNA damage reduces in peripheral blood of esophageal carcinoma patients and that obvious chromosome changes occur in tumor cells^[3-5]. Therefore, there must be DNA damage repair in the development of esophageal carcinoma. However, variations of DNA replication and repair enzymes in esophageal carcinoma, especially the mutation of pol β is rare. Thus, we made a preliminary analysis on the mutation of pol β in esophageal carcinoma.

MATERIALS AND METHODS

Specimens

High-incidence area group: Specimens of 30 esophageal squamous carcinomas (serial numbers H1-H30) and matched adjacent normal tissues were obtained from patients in Linzhou region of northern China, a well-recognized high-risk area for esophageal carcinoma.

Non-high incidence area group: Specimens of 25 esophageal squamous carcinomas (serial numbers N1-N25) and corresponding adjacent normal tissues were obtained from patients who underwent surgery at Cancer Hospital of Henan Province and the First Affiliated Hospital of Zhengzhou University.

All patients were histopathologically diagnosed to be infiltrative squamous carcinoma cases. The tissues were frozen in liquid nitrogen immediately after surgery.

RT-PCR

A pair of primers for PCR was designed to amplify the total pol β gene according to the sequence of M13140 in GenBank. Primer P1 (sense): 5' ATGAGCAAACG GAG-GGCGCCG 3'; Primer P2 (antisense): 5' TCATTCGCT-CCGTCCTTGG 3'. The primer was synthesized by Shanghai Sangon Co., Ltd.

Total RNA was extracted with the QIAGEN RNA extraction kit. Five microliters of total RNA was transcribed into cDNA using 0.2 μ mol/L primer P2, 0.2 μ mol/L dNTP,

RNasin 40 U, 1 \times buffer (Promega), and 2 U AMV in a final volume of 30 μ L. In PCR assay, the PCR reaction mixture consisted of 1 \times PCR buffer (PE), 200 μ mol/L dNTP, 20 pmol of each primer, 2 U of Golden Taq DNA polymerase (PE). The mixture was pre-incubated for 5 min at 94 $^{\circ}$ C, followed by amplification at 94 $^{\circ}$ C for 50 s, 56 $^{\circ}$ C for 50 s, and at 72 $^{\circ}$ C for 60 s, for 30 cycles. A final extension was performed at 72 $^{\circ}$ C for 7 min.

DNA cloning and sequencing

The PCR products from all specimens were excised from 0.8% agarose gels, and the desired fragments were purified using a DNA gel extraction kit (Promega). The purified fragments were cloned into a pGEM-T plasmid vector, and then transformed into *E. coli* JM109 competent cells. Plasmid DNA was extracted from the positive clones and sequenced using a PE 377 sequencer. The sequences were analyzed by DNASIS and OMEGA.

Statistical analysis

Statistical significance was evaluated using the χ^2 test. $P < 0.05$ was considered statistically significant. Statistical analysis was performed with SPSS 11.0.

RESULTS

PT-PCR analysis of whole pol β gene

In the high-incidence group, PCR products were obviously smaller than 1 008 bp in six carcinoma specimens. The correct length of pol β gene was obtained by amplifying the other specimens (Figure 1).

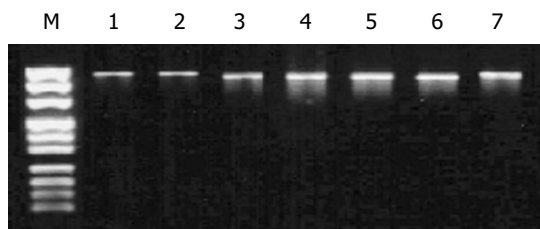


Figure 1 RT-PCR amplification of pol β gene. Lanes 1, 2 and 7: Normal size of PCR products of H1, H2 and H3; lanes 3-6: shorter size of PCR product of H5, H8, H10, and H16; M: DNA marker (from top to bottom: 1 000, 900, 800, 700, 600, 500, 400, 300, 200, 100 bp).

Result of sequencing

Point mutations and deletion of pol β gene were detected in the high-incidence area group (Table 1 and Figure 2). Overall, pol β gene variations were found in 13 of 30 esophageal carcinoma tissue specimens. A 58 bp(177-234 nt) deletion was detected in six tumor tissue specimens (Figure 3). Only one variation was found in the corresponding adjacent normal tissue (Table 1).

Pol β gene point mutations were detected in 5 of 25 esophageal carcinoma tissue specimens, and no variation was found in corresponding adjacent normal tissues in the non-high incidence area group (Table 2).

The incidence of pol β gene variation observed in the high-incidence area group was significantly higher than that

in the non-high incidence area group ($P = 0.007$, χ^2 test).

Table 1 Mutation analysis of pol β in high-incidence areas

Specimen	Gene mutation	
	Carcinoma	Corresponding adjacent normal tissue
H1	-	-
H2	-	-
H3	-	-
H4	660 nt A→G	-
H5	462 nt G→T, 177-234 nt deletion	-
H6	-	-
H7	64 nt G→C, 665 nt T→C	-
H8	462 nt G→T, 660 nt A→G, 177-234 nt deletion	660 nt A→G
H9	-	-
H10	177-234 nt deletion, 454 nt T→C 466 nt G→A	-
H11	-	-
H12	375 nt A→G 177-234 nt deletion	-
H13	-	-
H14	-	-
H15	454 nt T→C, 466 nt G→A	-
H16	177-234 nt deletion	-
H17	737 nt A→T, 740 nt A→G	-
H18	-	-
H19	-	-
H20	-	-
H21	462 nt G→T	-
H22	-	-
H23	-	-
H24	-	-
H25	177-234 nt deletion, 660 nt A→G	-
H26	177-234 nt deletion	-
H27	-	-
H28	613 nt A→T	-
H29	-	-
H30	-	-

Table 2 Mutation analysis of pol β in low-incidence areas

Specimen	Gene mutation	
	Carcinoma	Corresponding adjacent normal tissue
N1	670 nt A→G	-
N2	660 nt A→G	-
N8	660 nt A→G	-
N16	613 nt A→T	-
N22	670 nt A→G	-

Variation of amino acid caused by gene mutations

Twelve kinds of variation in the pol β gene were found in the present study, including 11 point mutations and a 58 bp deletion (Table 3). The translation of pol β was interrupted due to the emergence of a termination codon at 117 nt caused by 462 nt G→T mutation. Mutations at 665, 737, and 740 nt were synonymous mutations, which would not change the amino acids. The other seven point mutations caused replacement of amino acids.

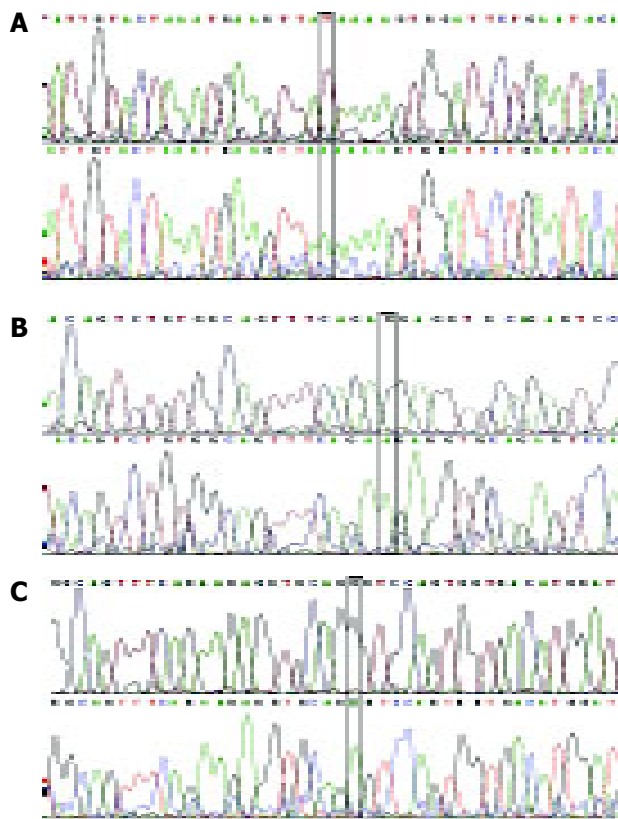


Figure 2 Mutations in the polβ gene. **A:** 660 nt A→G mutation in H4 carcinoma; **B:** 670 nt A→G mutation in N1 carcinoma; **C:** 613 nt A→T mutation in H28 carcinoma.

Table 3 Gene and amino acid variations in polβ

Mutation code	Gene variation	Amino acid variation	Mutation
1	375 nt A→G	88 nt Ile→Val	
2	454 nt T→C	114 nt Phe→Ser	
3	462 nt G→T	117 nt Glu→termination codon	Termination mutation
4	466 nt G→A	118 nt Gly→Glu	
5	613 nt A→T	167 nt Lys→Ile	
6	648 nt G→C	179 nt Gly→Arg	
7	660 nt A→G	183 nt Arg→Gly	
8	665 nt T→C	184 nt Gly→Gly	Synonymous mutation
9	670 nt A→G	186 nt Glu→Gly	
10	737 nt A→T	208 nt Pro→Pro	Synonymous mutation
11	740 nt A→G	209 nt Lys→Lys	Synonymous mutation
12	177-234 nt deletion		Frameshift mutation Termination mutation

		110	120	130	140	150	
BATE. SEQ	101	GGTGCAGGCC	GCCATGAGCA	AACGGAAGGC	GCCGCAGGAG	ACTCTCAACG	150
H10. SEQ	101	GGTGCAGGCC	GCCATGAGCA	AACGGAAGGC	GCCGCAGGAG	ACTCTCAACG	150
H16. SEQ	101	GGTGCAGGCC	GCCATGAGCA	AACGGAAGGC	GCCGCAGGAG	ACTCTCAACG	150
H25. SEQ	101	GGTGCAGGCC	GCCATGAGCA	AACGGAAGGC	GCCGCAGGAG	ACTCTCAACG	150
H26. SEQ	101	GGTGCAGGCC	GCCATGAGCA	AACGGAAGGC	GCCGCAGGAG	ACTCTCAACG	150
H5. SEQ	101	GGTGCAGGCC	GCCATGAGCA	AACGGAAGGC	GCCGCAGGAG	ACTCTCAACG	150
H8. SEQ	101	GGTGCAGGCC	GCCATGAGCA	AACGGAAGGC	GCCGCAGGAG	ACTCTCAACG	150
		160	170	180	190	200	
BATE. SEQ	151	GGGGAATCAC	CGACATGCTC	ACAGAACTCG	CAAACITTTGA	GAAGAACGTG	200
H10. SEQ	151	GGGGAATCAC	CGACATGCTC	ACAGAA	_____	_____	200
H16. SEQ	151	GGGGAATCAC	CGACATGCTC	ACAGAA	_____	_____	200
H25. SEQ	151	GGGGAATCAC	CGACATGCTC	ACAGAA	_____	_____	200
H26. SEQ	151	GGGGAATCAC	CGACATGCTC	ACAGAA	_____	_____	200
H5. SEQ	151	GGGGAATCAC	CGACATGCTC	ACAGAA	_____	_____	200
H8. SEQ	151	GGGGAATCAC	CGACATGCTC	ACAGAA	_____	_____	200
		210	220	230	240	250	
BATE. SEQ	201	AGCCAAGCTA	TCCACAAGTA	CAATGCTTAC	AGAAAAGCAG	CATCTGTTAT	250
H10. SEQ	201	_____	_____	_____	AAGCAG	CATCTGTTAT	250
H16. SEQ	201	_____	_____	_____	AAGCAG	CATCTGTTAT	250
H25. SEQ	201	_____	_____	_____	AAGCAG	CATCTGTTAT	250
H26. SEQ	201	_____	_____	_____	AAGCAG	CATCTGTTAT	250
H5. SEQ	201	_____	_____	_____	AAGCAG	CATCTGTTAT	250
H8. SEQ	201	_____	_____	_____	AAGCAG	CATCTGTTAT	250
		260	270	280	290	300	
BATE. SEQ	251	AGCAAAATAC	CCACACAAAA	TAAAGAGTGG	AGCTGAAGCT	AAGAAATTGC	300
H10. SEQ	251	AGCAAAATAC	CCACACAAAA	TAAAGAGTGG	AGCTGAAGCT	AAGAAATTGC	300
H16. SEQ	251	AGCAAAATAC	CCACACAAAA	TAAAGAGTGG	AGCTGAAGCT	AAGAAATTGC	300
H25. SEQ	251	AGCAAAATAC	CCACACAAAA	TAAAGAGTGG	AGCTGAAGCT	AAGAAATTGC	300
H26. SEQ	251	AGCAAAATAC	CCACACAAAA	TAAAGAGTGG	AGCTGAAGCT	AAGAAATTGC	300
H5. SEQ	251	AGCAAAATAC	CCACACAAAA	TAAAGAGTGG	AGCTGAAGCT	AAGAAATTGC	300
H8. SEQ	251	AGCAAAATAC	CCACACAAAA	TAAAGAGTGG	AGCTGAAGCT	AAGAAATTGC	300

Figure 3 Comparison between wild type polβ gene fragment and six gene fragments with deletion (177→234 nt).

DISCUSSION

DNA pol β is one of the four recognized, vertebrate, cellular, DNA polymerizing enzymes. Two features of pol β from various species may play a key role. First, the structure of pol β is highly conserved from the standpoint of both polypeptide size and amino acid sequence. Second, in cultured mammalian cells, the level of pol β enzymatic activity is low and independent of cell-cycle stage^[6,7]. Hence, pol β is considered as a constitutively expressed “housekeeping” enzyme required for DNA metabolic events other than replicative synthesis of genomic DNA. DNA synthesis during DNA repair and recombination are examples of such events, and the idea that pol β is involved in some types of DNA repair is supported by various studies with DNA polymerase inhibitors^[8-11]. Recent observations have shown that the variation of pol β occurs in some tumors such as colorectal carcinoma, bladder carcinoma, breast carcinoma, prostate carcinoma and non-small cell lung cancer. The variation rate is particularly high in colon carcinoma, being more than 80% (5/6)^[12-17,20]. Some studies indicate that the accumulation of proto-oncogene and tumor suppressor gene variations perhaps leads to tumor. However, the initial molecular defects causing accumulated mutations and inducing cancer are not well understood. Interestingly, there is a higher mutation rate of pol β , p53 and ras in colorectal carcinoma. A genetic disease, xeroderma pigmentosum, is associated with ERCC, a kind of DNA repair gene^[18-21], and these patients are more susceptible to skin carcinoma^[22,23]. The above findings suggest that there is a correlation between human tumors and the damage, maladjustment and defects in the DNA repair system.

The present results showed that some mutations, such as 462 nt G \rightarrow T and deleting 177-234 nt, could lead to the abnormal amino acid of pol β followed by abnormal protein structure and lack of DNA repair activity. From the histopathological diagnosis, we found that cancer cells involving the two mutations were more malignant. In addition, there were three synonymous mutations at 665 nt (T \rightarrow G), 737 nt (A \rightarrow T) and 740 nt (A \rightarrow G), which may be the single nucleotide polymorphism (SNP)^[24-29].

Pol β gene variation in the high-incidence area group was detected in 13 of 30 esophageal carcinoma tissue specimens. The mutation rate of this group was 43.3%. Pol β gene variation in the non-high incidence area group was found in 5 of 25 esophageal carcinoma tissue specimens, and the mutation rate was 20%. Thus, there was a significant difference in mutation rates between these two groups ($P < 0.05$). Twelve types of pol β gene variation were found in high-incidence area, but only three types were found in the non-high incidence area, suggesting that damage of the DNA repair system via alteration of this gene may contribute to the development of esophageal carcinoma, and that pol β may play a more important role in the high-incidence area.

By analyzing the variation site of pol β , we found that three point mutations were located in one region (454-466 nt), and four point mutations were located in another region (648-670 nt). The two regions are probably the mutation hot spots of the pol β gene of esophageal carcinoma. Moreover, the deletion of 58 bp was found in 6 of 20 specimens

from the high-incidence area (31.6% frequency), but was not found in the non-high incidence area. Hence, this deletion may be one of the main variations of pol β gene in esophageal carcinoma. Our results prove that pol β mutations do exist in esophageal carcinoma, and are probably correlated to the development of esophageal carcinoma.

It is suggested that during such genetic evolution, the DNA repair system plays an important role in cancer development^[30-32]. Although the relationship between mutations of pol β and alterations in proto-oncogenes or tumor suppressor genes is currently not clear, pol β gene mutation is involved in a subset of human esophageal carcinoma, especially in the high-incidence area.

REFERENCES

- 1 **Okuda E**, Osugi H, Morimura K, Takada N, Takemura M, Fukushima S, Higashino M, Kinoshita H. Detection of p53 gene mutations in human esophageal squamous cell carcinomas using a p53 yeast functional assay: possible difference in esophageal carcinogenesis between the young and the elderly group. *Clin Cancer Res* 2001; **7**: 600-606
- 2 **Nie Y**, Yang G, Song Y, Zhao X, So C, Liao J, Wang LD, Yang CS. DNA hypermethylation is a mechanism for loss of expression of the HLA class I genes in human esophageal squamous cell carcinomas. *Carcinogenesis* 2001; **22**: 1615-1623
- 3 **Kokoska RJ**, Bebenek K, Boudsocq F, Woodgate R, Kunkel TA. Low fidelity DNA synthesis by a γ family DNA polymerase due to misalignment in the active site. *J Biol Chem* 2002; **277**: 19633-19638
- 4 **Ito T**, Shimada Y, Hashimoto Y, Kaganoi J, Kan T, Watanabe G, Murakami Y, Imamura M. Involvement of TSLC1 in progression of esophageal squamous cell carcinoma. *Cancer Res* 2003; **63**: 6320-6326
- 5 **Kuroki T**, Trapasso F, Yendamuri S, Matsuyama A, Alder H, Mori M, Croce CM. Allele loss and promoter hypermethylation of VHL, RAR-beta, RASSF1A, and FHIT tumor suppressor genes on chromosome 3p in esophageal squamous cell carcinoma. *Cancer Res* 2003; **63**: 3724-3728
- 6 **Kim SJ**, Beard WA, Harvey J, Shock DD, Knutson JR, Wilson SH. Rapid segmental and subdomain motions of DNA polymerase beta. *J Biol Chem* 2003; **278**: 5072-5081
- 7 **Widen SG**, Kedar P, Wilson SH. Human beta-polymerase gene. Structure of the 5'-flanking region and active promoter. *J Biol Chem* 1988; **263**: 16992-16998
- 8 **Cabelof DC**, Raffoul JJ, Yanamadala S, Guo Z, Heydari AR. Induction of DNA polymerase beta-dependent base excision repair in response to oxidative stress *in vivo*. *Carcinogenesis* 2002; **23**: 1419-1425
- 9 **Lavrik OI**, Kolpashchikov DM, Prasad R, Sobol RW, Wilson SH. Binary system for selective photoaffinity labeling of base excision repair DNA polymerases. *Nucleic Acids Res* 2002; **30**: e73
- 10 **Servant L**, Cazaux C, Bieth A, Iwai S, Hanaoka F, Hoffmann JS. A role for DNA polymerase beta in mutagenic UV lesion bypass. *J Biol Chem* 2002; **277**: 50046-50053
- 11 **Idriss HT**, Al-Assar O, Wilson SH. DNA polymerase beta. *Int J Biochem Cell Biol* 2002; **34**: 321-324
- 12 **SenGupta DN**, Zmudzka BZ, Kumar P, Cobianchi F, Skowronski J, Wilson SH. Sequence of human DNA polymerase beta mRNA obtained through cDNA cloning. *Biochem Biophys Res Commun* 1986; **136**: 341-347
- 13 **Bergoglio V**, Pillaire MJ, Lacroix-Triki M, Raynaud-Messina B, Canitrot Y, Bieth A, Gares M, Wright M, Delsol G, Loeb LA, Cazaux C, Hoffmann JS. Deregulated DNA polymerase beta induces chromosome instability and tumorigenesis. *Cancer Res* 2002; **62**: 3511-3514
- 14 **Muniappan BP**, Thilly WG. The DNA polymerase beta replication error spectrum in the adenomatous polyposis coli

- gene contains human colon tumor mutational hotspots. *Cancer Res* 2002; **62**: 3271-3275
- 15 **Thompson TE**, Rogan PK, Risinger JI, Taylor JA. Splice variants but not mutations of DNA polymerase beta are common in bladder cancer. *Cancer Res* 2002; **62**: 3251-3256
- 16 **Tompkins JD**, Nelson JL, Hazel JC, Leugers SL, Stumpf JD, Foster PL. Error-prone polymerase, DNA polymerase IV, is responsible for transient hypermutation during adaptive mutation in *Escherichia coli*. *J Bacteriol* 2003; **185**: 3469-3472
- 17 **Miyamoto H**, Miyagi Y, Ishikawa T, Ichikawa Y, Hosaka M, Kubota Y. DNA polymerase beta gene mutation in human breast cancer. *Int J Cancer* 1999; **83**: 708-709
- 18 **Selfridge J**, Hsia KT, Redhead NJ, Melton DW. Correction of liver dysfunction in DNA repair-deficient mice with an ERCC1 transgene. *Nucleic Acids Res* 2001; **29**: 4541-4550
- 19 **Lehmann AR**. The xeroderma pigmentosum group D (XPD) gene: one gene, two functions, three diseases. *Genes Dev* 2001; **15**: 15-23
- 20 **Dobashi Y**, Shuin T, Tsuruga H, Uemura H, Torigoe S, Kubota Y. DNA polymerase beta gene mutation in human prostate cancer. *Cancer Res* 1994; **54**: 2827-2829
- 21 **Lindstrom UM**, Chandrasekaran RA, Orbai L, Helquist SA, Miller GP, Oroudjev E, Hansma HG, Kool ET. Artificial human telomeres from DNA nanocircle templates. *Proc Natl Acad Sci USA* 2002; **99**: 15953-15958
- 22 **Yamada NA**, Farber RA. Induction of a low level of microsatellite instability by overexpression of DNA polymerase. *Beta Cancer Res* 2002; **62**: 6061-6064
- 23 **Saxowsky TT**, Matsumoto Y, Englund PT. The mitochondrial DNA polymerase beta from *Crithidia fasciculata* has 5'-deoxyribose phosphate (dRP) lyase activity but is deficient in the release of dRP. *J Biol Chem* 2002; **277**: 37201-37206
- 24 **Hartenstine MJ**, Goodman MF, Petruska J. Weak strand displacement activity enables human DNA polymerase beta to expand CAG/CTG triplet repeats at strand breaks. *J Biol Chem* 2002; **277**: 41379-41389
- 25 **Kedar PS**, Kim SJ, Robertson A, Hou E, Prasad R, Horton JK, Wilson SH. Direct interaction between mammalian DNA polymerase beta and proliferating cell nuclear antigen. *J Biol Chem* 2002; **277**: 31115-31123
- 26 **Jezewska MJ**, Galletto R, Bujalowski W. Dynamics of gapped DNA recognition by human polymerase beta. *J Biol Chem* 2002; **277**: 20316-20327
- 27 **Prasad R**, Bebenek K, Hou E, Shock DD, Beard WA, Woodgate R, Kunkel TA, Wilson SH. Localization of the deoxyribose phosphate lyase active site in human DNA polymerase iota by controlled proteolysis. *J Biol Chem* 2003; **278**: 29649-29654
- 28 **Matsuda T**, Vande Berg BJ, Bebenek K, Osheroff WP, Wilson SH, Kunkel TA. The base substitution fidelity of DNA polymerase beta-dependent single nucleotide base excision repair. *J Biol Chem* 2003; **278**: 25947-25951
- 29 **Le Page F**, Schreiber V, Dherin C, De Murcia G, Boiteux S. Poly(ADP-ribose) polymerase-1 (PARP-1) is required in murine cell lines for base excision repair of oxidative DNA damage in the absence of DNA polymerase beta. *J Biol Chem* 2003; **278**: 18471-18477
- 30 **Harrigan JA**, Opresko PL, von Kobbe C, Kedar PS, Prasad R, Wilson SH, Bohr VA. The Werner syndrome protein stimulates DNA polymerase beta strand displacement synthesis via its helicase activity. *J Biol Chem* 2003; **278**: 22686-22695
- 31 **Heidenfelder BL**, Topal MD. Effects of sequence on repeat expansion during DNA replication. *Nucleic Acids Res* 2003; **31**: 7159-7164
- 32 **Sobol RW**, Kartalou M, Almeida KH, Joyce DF, Engelward BP, Horton JK, Prasad R, Samson LD, Wilson SH. Base excision repair intermediates induce p53-independent cytotoxic and genotoxic responses. *J Biol Chem* 2003; **278**: 39951-39959

Gastric cancer surgery in cirrhotic patients: Result of gastrectomy with D2 lymph node dissection

Jun Ho Lee, Junuk Kim, Jae Ho Cheong, Woo Jin Hyung, Seung Ho Choi, Sung Hoon Noh

Jun Ho Lee, Research Institute and Hospital, National Cancer Center, Goyang, South Korea
Junuk Kim, Jae Ho Cheong, Woo Jin Hyung, Seung Ho Choi, Sung Hoon Noh, Department of Surgery, Yonsei University College of Medicine, Seoul, South Korea
Jae Ho Cheong, Woo Jin Hyung, Sung Hoon Noh, Cancer Metastasis Research Center, Yonsei University College of Medicine, Seoul, South Korea
Woo Jin Hyung, Sung Hoon Noh, Brain Korea 21 Project for the Medical Sciences, Yonsei University College of Medicine, Seoul, South Korea
Correspondence to: Dr. Sung Hoon Noh, Department of Surgery, College of Medicine, Yonsei University, C.P.O. Box 8044, Seoul, South Korea. sunghoonn@yumc.yonsei.ac.kr
Telephone: +82-2-361-5540 Fax: +82-2-313-8289
Received: 2004-11-23 Accepted: 2004-12-08

Abstract

AIM: To explore the feasibility of performing gastrectomy with D2 lymphadenectomy in gastric cancer patients with liver cirrhosis.

METHODS: A total of 7 178 patients were admitted with a diagnosis of liver cirrhosis from January 1993 to December 2003. We reviewed the records of 142 patients who were diagnosed with liver cirrhosis and gastric adenocarcinoma during the same period. Gastrectomy with D2 lymph node dissection for carcinoma of the stomach was performed in 94 patients with histologically proven hepatic cirrhosis.

RESULTS: All but 12 patients were classified as Child's class A. Only 35 patients (37.2%) were diagnosed with cirrhosis before operation. Seventy-three patients underwent a subtotal gastrectomy (77.7%) and 21 patients (22.3%) underwent a total gastrectomy, each with D2 or more lymph node dissection. Two patients (3.8%) who had prophylactic intra-operative drain placement, died of postoperative complications from hepatorenal failure with intractable ascites. Thirty-seven patients (39.4%) experienced postoperative complications. The extent of gastric resection did not influence the morbidity whereas serum aspartate aminotransferase level ($P = 0.011$) and transfusion did ($P = 0.008$). The most common postoperative complication was ascites (13.9%) followed by wound infection (10.6%).

CONCLUSION: We concluded that the presence of compensated cirrhosis, i.e. Child class A, is not a contraindication against gastrectomy with D2 or more lymph node dissection, when curative resection for gastric cancer is possible. Hepatic reserve and meticulous hemostasis

are the likely determinants of operative prognosis.

© 2005 The WJG Press and Elsevier Inc. All rights reserved.

Key words: Gastric cancer; Liver cirrhosis; D2 lymph node dissection; Morbidity; Mortality

Lee JH, Kim J, Cheong JH, Hyung WJ, Choi SH, Noh SH. Gastric cancer surgery in cirrhotic patients: Result of gastrectomy with D2 lymph node dissection. *World J Gastroenterol* 2005; 11(30): 4623-4627

<http://www.wjgnet.com/1007-9327/11/4623.asp>

INTRODUCTION

Although the prognosis of gastric cancer has improved significantly as a result of early diagnosis, radical operation, and advances in adjuvant therapy, gastric cancer remains the most common cause of cancer-related death in Korea^[1]. Extended lymph node dissection is regarded as an essential criterion for the treatment of gastric cancer^[2-4]. It not only makes the surgical therapy more radical but also provides adequate lymph node staging.

Liver cirrhosis is another major health problem in Korea, where it is the fourth most common cause of death, and is probably linked to the high prevalence of HBV infection and a culture that encourages high alcohol consumption^[5]. Because of the high prevalence, cirrhosis of the liver is not infrequently encountered among candidates for gastric cancer surgery in Korea. Most surgeons are reluctant to perform a D2 lymph node dissection in patients with liver cirrhosis due to the risk of liver dysfunction^[6].

Recent advances in peri-operative patient care and surgical techniques, however, have reduced the morbidity and mortality rates associated with gastric cancer surgery even after a D2 lymph node dissection. This study was conducted to explore the feasibility of performing gastrectomy with D2 lymphadenectomy in gastric cancer patients with liver cirrhosis, in terms of the morbidities and mortalities.

MATERIALS AND METHODS

Patients

A total of 7 178 patients were admitted with a diagnosis of liver cirrhosis to Yonsei University Medical Center from January 1993 to December 2003. We reviewed the records of 142 patients who were diagnosed with liver cirrhosis and gastric adenocarcinoma at the Department of Surgery, Yonsei University College of Medicine during the same

period. All patients had no previous history of abdominal surgery or other malignancies. Thirty-four patients who had palliative surgery and 14 patients who did not have surgery due to impaired liver function were excluded from the study. The remaining 94 gastric cancer patients with liver cirrhosis who underwent curative gastric resection for gastric cancer were included in this study.

Cirrhosis was diagnosed primarily by liver biopsy. In patients in whom liver biopsy was not performed, the diagnosis was made by gross findings during the operation, a history of liver disease, with impaired liver function tests and CT scan or ultrasonography imaging.

Characteristics of the patients including age, sex, Child-Pugh classification, extent of gastric resection, stage of the tumor, and postoperative outcomes including operation time, the number of retrieved lymph nodes, complications, hospital stay, survival rates were analyzed. The χ^2 test was used for discrete variables and Student's *t* test for continuous variables. Survival rates were estimated using the Kaplan-Meier method and the difference between the curves was assessed using the log-rank test. *P* values less than 0.05 indicated statistical significance.

Operative technique

Gastric cancer surgery in our institution is done according to the following standardized operative protocol: (1) A total or distal subtotal gastrectomy is performed depending on the location and the macroscopic type of gastric cancer. (2) A D2 or more lymph node dissection is preferred regardless of the clinical stage^[7]. Lymph nodes along the hepato-duodenal ligament and common hepatic artery were retrieved and tied with #3 silk. After gastric resection, the gastrointestinal continuity is restored by either a gastro-duodenostomy or a gastro-jejunostomy, depending on the location of the tumor after a distal subtotal gastrectomy. A Roux-en-Y esophago-jejunostomy is done after a total gastrectomy. Gastro-duodenostomy is done using interrupted 3-0 silk Lembert

sutures for the outer layer and interrupted 3-0 polyglycolic sutures for the transmural inner layer. The gastro-jejunostomy is performed using interrupted 3-0 silk Lembert sutures for the outer layer and a running 3-0 polyglycolic suture for the transmural inner layer. Esophago-jejunostomy is done using an EEA stapler (Ethicon, Somerville, NJ, USA). Before the abdominal wall is closed, a two-armed suction drain (Hemovac, Sewoon Medical Co., Seoul, South Korea) is inserted through a new stab wound on the right flank toward the subhepatic area after a subtotal gastrectomy. An additional suction drain is inserted through the left flank toward the left sub-diaphragmatic space after a total gastrectomy. The abdominal fascia is closed with continuous polydioxanone sutures reinforced by interrupted 1-0 silk sutures. The subcutis and cutis are restored with interrupted 3-0 silk sutures and skin staplers.

RESULTS

Characteristics of the patients, tumors, and surgeries

There were 73 (77.7%) males and 21 (22.3%) females. The median age was 59 years (range, 36-76 years). All but 12 patients were classified as Child's class A. Thirty-five patients (37.2%) were diagnosed with cirrhosis before the operation and the other 59 (62.8%) patients were diagnosed with liver cirrhosis during the operation. Cirrhosis was related to HBV in 52 (55.3%) patients, HCV in 8 (8.5%) patients, and alcohol abuse in 30 (31.9%) patients. Cirrhosis was cryptogenic in 4 (4.3%) patients.

Seventy-three (77.7%) patients had a subtotal gastrectomy and 21 (22.3%) patients underwent a total gastrectomy. All patients underwent D2 or more lymph dissection. The mean number of the retrieved lymph nodes was 35 (range, 15-71). The mean operation time was 195 min (range, 110-345 min). Prophylactic drainage was done in 51 (73.9%) patients. The median hospital stays in this cohort of 94 patients was 13.5 d (range, 7-90 d). The characteristics of patients, tumors, and surgeries are summarized in Table 1.

Table 1 Characteristics of patients, tumors, and surgeries

Variables	Patients		Variables	
	Number	%		
Sex			Age (yr)	
Male	73	77.7	Median	59
Female	21	22.3	Range	36-76
Diagnosis of cirrhosis			Retrieved nodes	
Preoperative	35	37.2	Median	35
Intraoperative	59	62.8	Range	15-71
Cause of cirrhosis			Positive nodes	
HBV-related	52	55.3	Mean	3.5
Alcohol	30	31.9	Range	0-27
HCV-related	8	8.5	Operation time (min)	
Cryptogenic	4	4.3	Mean	194.6
Extent of gastric resection			Range	110-345
Subtotal	73	77.7	Hospital stay (d)	
Total	21	22.3	Median	13.5
TNM stage			Range	7-90
I	51	54.3		
II	25	26.6		
III	10	10.6		
IV	8	8.5		

Mortality and morbidity

Two patients who had prophylactic intra-operative drains died after the operation (2.1%) as a result of hepato-renal failure related with intractable ascites. One patient was classified as Child's class B and the other patient as Child's class C. The most common post-operative complication was ascites (13 patients, 13.9%) followed by wound infection (10 patients, 10.6%). Ascites was well controlled with medications in nine patients (six patients had prophylactic intra-operative drain placement and three patients had not) and with paracentesis in four patients who had prophylactic intra-operative drain placement. All the patients who experienced post-operative bleeding (four patients) and anastomotic leakage (two patients) were managed conservatively (Table 2).

Table 2 Morbidities and mortalities

	Patients		Total (%)
	No drainage (n = 37, %)	Drainage (n = 57, %)	
Morbidities			
Absent	27 (73.0)	30 (52.6)	57 (60.6)
Present	10 (27.0)	27 (47.4)	37 (39.4)
Wound infection	2 (5.4)	8 (14.0)	10 (10.6)
Ascending infection	0 (0.0)	3 (5.3)	3 (3.2)
Pneumonia	2 (5.4)	3 (5.3)	5 (5.3)
Bleeding	1 (2.7)	3 (5.3)	4 (4.3)
Anastomosis leakage	1 (2.7)	1 (1.8)	2 (2.1)
Ascites	3 (8.1)	10 (17.5)	13 (13.9)
Mortalities	0 (0.0)	2 (3.8) ¹	2 (2.1)

¹Mortalities were caused by hepatorenal syndrome.

The association between clinico-pathological parameters and the risk of post-operative complications are summarized in Table 3. Transfusion and serum aspartate aminotransferase levels were the independent predictive factors of morbidity ($P < 0.05$) (Table 4). The extent of gastric resection or tumor stage did not influence the morbidity, while intra-operative drain placement showed marginal significance ($P = 0.055$). Ten out of the thirty-seven patients, who had no prophylactic drains (27.0%) experienced postoperative complications, whereas 27 out of the 57 patients who had prophylactic drains (47.4%) experienced complications.

Survival of the patients

The overall 5-year survival rate of the patients was 65.9%. The overall 5-year survival rate of the Child's class A patients was 69.1% and 44.4% for the Child's class B and C patients. There was a significant difference between the survival rates at Child's class ($P = 0.0195$).

DISCUSSION

Postoperative complications in cirrhotic patients after gastrectomy with D2 lymph node dissection were associated with serum aspartate aminotransferase levels and transfusion. We observed that the post-operative morbidity was more common among patients with prophylactic drains after gastrectomy with D2 lymph node dissection, than among patients without prophylactic drains. Two patients who had

prophylactic intra-operative drain placement died of postoperative complications from hepato-renal failure with intractable ascites.

The prevalence of gastric cancer among cirrhotic patients in this study was higher than other reports (2.0%, 142 patients out of 7 178 cirrhotic patients). Gastric cancer among cirrhotic patients have been rarely reported in the literature^[8]. A recent nationwide cohort study from Denmark revealed that the risk of gastric carcinoma in cirrhotic patients is not low compared to other cancers, except for hepatocellular carcinoma^[9]. The study identified 40 gastric carcinoma patients (0.34%) among 11 605 cirrhotic patients during a 12-year follow-up. A group of Italian endoscopists has made similar observations^[10]. Zullo *et al.*, reported that the prevalence of latent gastric cancer in liver cirrhosis patients could be significantly higher than that expected in the general population (a 2.6-fold increase). The reasons for the high prevalence of gastric cancer in our study remain unclear but probably are associated with the generally high prevalence of gastric cancer and a culture that encourages high alcohol consumption in Korea^[5,11].

The data presented here demonstrates that gastrectomy with D2 lymph node dissection in cirrhotic patients is feasible. Abdominal operations in cirrhotic patients have been a technical challenge with mortality rates around 30%^[12-14]. Therefore, gastric cancer surgery for cirrhotic patients remains controversial. Our peri-operative morbidity and mortality rates compared favorably with most series on abdominal procedures in the literature. The Child-Pugh classification has proven to be a reliable tool in identifying patients at risk of post-operative complications. In our series, the morbidity rate was related to serum aspartate aminotransferase levels and peri-operative transfusion status. Peri-operative transfusion has been reported to be associated with morbidities in gastric cancer patients due to immunosuppressive effects^[15]. Lowering the serum aspartate aminotransferase levels and meticulous hemostasis during operation are probably the best way to decrease post-operative complication rate in patients with liver cirrhosis.

Our data showed that D2 lymph node dissection in cirrhotic patients is feasible without drains, if the hepatic reserve is not severely compromised and no usage of prophylactic drain. All the patients underwent D2 lymph node dissection and the mean number of retrieved lymph nodes was 35 in this study. This result is comparable to the results of other studies concerning D2 lymph node dissection^[3,6]. Prophylactic drain placement showed no beneficial effect in terms of post-operative morbidity in this study. Although three patients, who did not have intraoperative drain placement, developed ascites after surgery, they were easily controlled with medications. Three out of ten patients who needed paracentesis were all patients who had intra-operative drain placement. Similar results were reported by Urbach *et al.*, who performed a metaanalysis on colorectal cancer patients and concluded that they could not find any benefit of routine intra-operative drain placement after colon and rectal anastomoses in reducing the rate of anastomotic leakage or other complications^[16].

Lymph node dissection around the hepato-duodenal ligament (station number 12 according to the classification

Table 3 Factors associated with complications

Variables	Complication		P
	Absent (n, %)	Present (n, %)	
Sex			0.351
Male	42 (57.5)	31 (42.5)	
Female	15 (71.4)	6 (28.6)	
Age (yr)			0.138
<55	34 (66.7)	17 (33.3)	
≥55	23 (53.4)	20 (46.6)	
Causes of cirrhosis			0.188
HBV-related	36 (69.2)	16 (30.8)	
Alcohol	14 (46.7)	16 (53.3)	
HCV-related	4 (50.0)	4 (50.0)	
Cryptogenic	3 (75.0)	1 (25.0)	
Anemia (<100 g/L)			0.370
Absent	46 (62.2)	28 (37.8)	
Present	11 (55.0)	9 (45.0)	
Thrombocytopenia (<10 ⁵ /U)			0.619
Absent	45 (62.5)	27 (37.5)	
Present	12 (54.5)	10 (45.5)	
Albumin (g/L)			0.386
≥36	38 (64.4)	21 (35.6)	
<36	19 (54.3)	16 (45.7)	
Aspartate aminotransferase (IU/L)			0.030
≤40	40 (70.2)	17 (29.8)	
>40	17 (63.0)	20 (37.0)	
Bilirubin (mg/dL)			0.819
≤1.4	40 (59.7)	27 (40.3)	
>1.4	17 (63.0)	10 (37.0)	
Prothrombin (%)			0.656
≥80	39 (62.9)	23 (37.1)	
<80	18 (56.3)	14 (43.7)	
Child-Pugh class			0.207
A	52 (63.4)	30 (36.6)	
B or C	5 (41.7)	7 (58.3)	
Transfusion			<0.001
No	46 (75.4)	15 (24.6)	
Yes	11 (33.3)	22 (66.7)	
Extent of gastric resection			0.450
Subtotal	46 (63.0)	27 (37.0)	
Total	11 (52.4)	10 (47.6)	
Stage			0.835
EGC	26 (61.9)	16 (38.1)	
AGC	31 (59.6)	21 (40.4)	
Prophylactic drainage			0.055
No	27 (73.0)	10 (27.0)	
Yes	30 (52.6)	27 (47.4)	

Table 4 Logistic regression analysis of risk factors for postoperative complication

Covariate (observed value)	Coefficient	SE	RR (95%CI)	P
Causes of cirrhosis (Postnecrotic vs others)	0.9744	0.5543	2.6496 (0.8941-7.8517)	0.079
GPT (IU/L) (≤40 vs >40)	1.3899	0.5446	4.0143 (1.3807-11.672)	0.011
Transfusion (no vs yes)	1.6837	0.5000	5.3856 (2.0214-14.3485)	0.008

SE: standard deviation; RR: relative risk; CI: confidence interval.

by the Japanese Research Society on Gastric Cancer) and common hepatic artery (station number 8) in cirrhotic gastric cancer patients has been reported to be limited^[6,17]. The lymphatic systems in these two lymph node stations are

extensive and well developed, making these two lymph node stations as the frequent sites of lymphorrhea especially after lymph node dissection that is not easy to control^[6]. Cirrhotic patients often suffer from ascites after gastric cancer surgery,

which can be aggravated by insertion of a drainage catheter [12,18]. Two patients who had prophylactic intra-operative drain placement died of post-operative complications from hepato-renal failure with intractable ascites. Downstaging Child's class B and C patients to Child's class A patients and meticulous tying of the lymphatic systems should be attempted first, instead of limiting the extent of lymph node dissection.

Since more than half of the patients in our study were diagnosed with liver cirrhosis during the operation and this study was a retrospective study with inherent sampling bias, the association of Child's class with morbidities and mortalities was not always clear. Therefore, it is difficult to compare our results against other reports in the literature. The reason why more than half of the patients in this study had been diagnosed as liver cirrhosis during the operations is unclear.

In conclusion, patients with compensated cirrhosis, i.e., Child's class A, may safely undergo gastrectomy with D2 lymph node dissection. Downstaging the Child's class and performing a D2 lymph node dissection with meticulous hemostasis and without a prophylactic drain placement appear to be the most reasonable treatment plan for gastric cancer patients with liver cirrhosis.

REFERENCES

- 1 **Shin HR**, Ahn YO, Bae JM, Shin MH, Lee DH, Lee CW, Ohrr HC, Ahn DH, Ferlay J, Parkin DM, Oh DK, Park JG. Cancer incidence in Korea. *Cancer Res Treatment* 2002; **34**: 405-408
- 2 **Sano T**, Sasako M, Yamamoto S, Nashimoto A, Kurita A, Hiratsuka M, Tsujinaka T, Kinoshita T, Arai K, Yamamura Y, Okajima K. Gastric cancer surgery: morbidity and mortality results from a prospective randomized controlled trial comparing D2 and extended para-aortic lymphadenectomy—Japan Clinical Oncology Group study 9501. *J Clin Onco* 2004; **22**: 2767-2773
- 3 **Siewert JR**, Bottcher K, Stein HJ, Roder JD. German Gastric Carcinoma Study Group. Relevant prognostic factors in gastric cancer: ten-year results of the German Gastric Cancer Study. *Ann Surg* 1998; **228**: 449-461
- 4 **Yoo CH**, Noh SH, Shin DW, Choi SH, Min JS. Recurrence following curative resection for gastric carcinoma. *Br J Surg* 2000; **87**: 236-242
- 5 **Kim YS**, Um SH, Ryu HS, Lee JB, Lee JW, Park DK, Kim YS, Jin YT, Chun HJ, Lee HS, Lee SW, Choi JH, Kim CD, Hyun JH. The prognosis of liver cirrhosis in recent years in Korea. *J Korean Med Sci* 2003; **18**: 833-841
- 6 **Isozaki H**, Okajima K, Ichinona T, Fujii K, Nomura E, Izumi N. Surgery for gastric cancer in patients with liver cirrhosis. *Surg Today* 1997; **27**: 17-21
- 7 **Nishi M**, Omori Y, Miwa K, eds. Japanese classification of gastric carcinoma (1st English ed.). Japanese research society for gastric cancer (JRSJC). Tokyo Kanehara 1995: 6-15
- 8 **Takeda J**, Hashimoto K, Tanaka T, Koufujii K, Kakegawa T. Review of operative indication and prognosis in gastric cancer with hepatic cirrhosis. *Hepatogastroenterology* 1992; **39**: 433-436
- 9 **Sorensen HT**, Friis S, Olsen JH, Thulstrup AM, Møller M, Linet M, Trichopoulos D, Vilstrup H, Olsen J. Risk of liver and other types of cancer in patients with cirrhosis: a nationwide cohort study in Denmark. *Hepatology* 1998; **28**: 921-925
- 10 **Zullo A**, Romiti A, Tomao S, Hassan C, Rinaldi V, Giustini M, Morini S, Taggi F. Gastric cancer prevalence in patients with liver cirrhosis. *Eur J Cancer Prev* 2003; **12**: 179-182
- 11 **Vigneri S**, Termini R, Piraino A, Scialabba A, Pisciotto G, Fontana N. The stomach in liver cirrhosis. Endoscopic, morphological, and clinical correlations. *Gastroenterology* 1991; **101**: 472-478
- 12 **Liu CL**, Fan ST, Lo CM, Wong Y, Ng IO, Lam CM, Poon RT, Wong J. Abdominal drainage after hepatic resection is contraindicated in patients with chronic liver diseases. *Ann Surg* 2004; **239**: 194-201
- 13 **Gervaz P**, Pak-art R, Nivatvongs S, Wolff BG, Larson D, Ringel S. Colorectal adenocarcinoma in cirrhotic patients. *J Am Coll Surg* 2003; **196**: 874-879
- 14 **Mansour A**, Watson W, Shayani V, Pickleman J. Abdominal operations in patients with cirrhosis: still a major surgical challenge. *Surgery* 1997; **122**: 730-735
- 15 **Karl RC**, Schreiber R, Boulware D, Baker S, Coppola D. Factors affecting morbidity, mortality, and survival in patients undergoing Ivor Lewis esophagogastrectomy. *Ann Surg* 2000; **231**: 635-643
- 16 **Urbach DR**, Kennedy ED, Cohen MM. Colon and rectal anastomoses do not require routine drainage. *Ann Surg* 1999; **229**: 174-180
- 17 **Takeda J**, Toyonaga A, Koufujii K, Kodama I, Tsuji Y, Aoyagi K, Kakegawa T. Surgical management of gastric cancer patients with liver cirrhosis. *Kurume Med J* 1994; **41**: 205-213
- 18 **Kumagai K**. Intractable ascites following surgery for gastric carcinoma. *Dig Surg* 1998; **15**: 236-240

Altered profiles of nuclear matrix proteins during the differentiation of human gastric mucous adenocarcinoma MGc80-3 cells

Chun-Hong Zhao, Qi-Fu Li

Chun-Hong Zhao, Qi-Fu Li, Laboratory of Cell Biology, the Key Laboratory of Ministry of Education for Cell Biology and Tumor Cell Engineering, School of Life Sciences, Xiamen University, Xiamen 361005, Fujian Province, China

Supported by the National Natural Science Foundation of China, No. 30470877, and the Natural Science Foundation of Fujian Province, No. C0310003

Correspondence to: Professor Qi-Fu Li, Laboratory of Cell Biology, School of Life Sciences, Xiamen University, Xiamen 361005, Fujian Province, China. chifulee@xmu.edu.cn

Telephone: +86-592-2185363 Fax: +86-592-2181015

Received: 2004-11-08 Accepted: 2005-01-05

Abstract

AIM: To find and identify specific nuclear matrix proteins associated with proliferation and differentiation of carcinoma cells, which will be potential markers for cancer diagnosis and targets in cancer therapy.

METHODS: Nuclear matrix proteins were selectively extracted from MGc80-3 cells treated with or without hexamethylamine bisacetamide (HMBA), and subjected to 2-D gel electrophoresis. The resulted protein patterns were analyzed by Melanie software. Spots of nuclear matrix proteins differentially expressed were excised and subjected to *in situ* digestion with trypsin. Peptide masses were obtained by matrix-assisted laser-desorption/ionization time of flight mass spectrometry (MALDI-TOF-MS) analysis and submitted for database searching using Mascot tool.

RESULTS: The MGc80-3 cells were induced into differentiation by HMBA. There were 22 protein spots which changed remarkably in the nuclear matrix, from differentiation of MGc80-3 cells compared to control. Eleven of which were identified. Seven proteins - actin, prohibitin, porin 31HL, heterogeneous nuclear ribonucleoprotein A2/B1, vimentin, ATP synthase, and heat shock protein 60 were downregulated, whereas three proteins - heat shock protein gp96, heat shock protein 90-beta, and valosin-containing protein were upregulated, and the oxygen-regulated protein was only found in the differentiated MGc80-3 cells.

CONCLUSION: The induced differentiation of carcinoma cells is accompanied by the changes of nuclear matrix proteins. Further characterization of those proteins will show the mechanism of cellular proliferation and differentiation, as well as cancer differentiation.

Key words: Nuclear matrix proteins; Cell differentiation; Human gastric mucous adenocarcinoma MGc80-3; Hexamethylamine bisacetamide

Zhao CH, Li QF. Altered profiles of nuclear matrix proteins during the differentiation of human gastric mucous adenocarcinoma MGc80-3 cells. *World J Gastroenterol* 2005; 11(30): 4628-4633

<http://www.wjgnet.com/1007-9327/11/4628.asp>

INTRODUCTION

Nuclear matrix (nuclear skeleton) is the filamentous protein framework in eukaryotic cell nucleus. Nuclear matrix plays an important role in life activities such as maintaining the cell morphology, dimensional localization, DNA replication and transcription. Thereby, it is intensely associated with cell proliferation and differentiation, as well as carcinogenesis^[1,2].

The role of nuclear matrix in cell activities has drawn increasing attention recently. Most of its components, besides the fibrins, are proteins and/or enzyme in DNA replication, transcription and gene expression^[3,4]. The nuclear matrix in cancer cells is not only abnormal in morphology, but also apparently different in its composition. Tumor-associated nuclear matrix proteins have been identified in cancers of the breast, colon, bone, bladder, and larynx using 2-D gel electrophoresis^[5-9]. But nuclear matrix proteins associated with the differentiation of carcinoma cells were unexplored.

Previously, we found that the morphology of nuclear matrix in differentiated human gastric cancer cells, induced by hexamethylamine bisacetamide (HMBA) and retinoic acid^[10], showed similar characteristics with that in normal cells. It is implied that further study on the differential expressed nuclear matrix proteins in response to differentiation reagent will be able to reveal the mechanism of carcinogenesis and phenotypic reversion, as well as cell growth and differentiation.

This study was designed to find and identify specific nuclear matrix proteins, associated with the proliferation and differentiation of carcinoma cells. The human gastric mucous adenocarcinoma MGc80-3 cell was selected as a subject to undergo differentiation induced by HMBA. The nuclear matrix proteins from MGc80-3 cells were selectively extracted, and subjected to 2-D gel electrophoresis. The changed nuclear matrix proteins during the differentiation process were identified by matrix-assisted laser-desorption/ionization time of flight mass spectrometry (MALDI-TOF-MS) combined with database searching.

MATERIALS AND METHODS

Materials

HMBA (Sigma Chemical Company) were used to induce the differentiation of MGc80-3 cells. Sequence grade, modified trypsin (Promega) and iodoacetamide (Sigma) were used in the in-gel digestion. ReadyStrip IPG strips (pH 3-10, 11 cm) and IPG buffer pH 3-10 were from Amersham Biosciences. Other reagents used in 2-D gel electrophoresis and Coomassie blue R250 were from Shanghai Sangon Biological Engineering Technology and Service Co., Ltd.

Cell culture

MGc80-3 cells were cultured in the RPMI-1640 supplemented with 15% new born bovine serum at 37 °C. The cells were seeded in a constant density overnight, and treated with 5 mmol/L HMBA for 7 d. Fresh culture media were added to the cells every 48 h, and cells were harvested at subconfluency. The obtained cells were then stored at -80 °C.

Purification of nuclear matrix proteins

The nuclear matrix proteins were extracted by a method of Fey *et al.*^[11]. The MGc80-3 cells were washed with PBS and extracted with cytoskeleton buffer (CSK100) (10 mmol/L PIPES pH 6.8, 300 mmol/L sucrose, 100 mmol/L NaCl, 4 mmol/L CaCl₂, 1.0 mmol/L PMSF, 0.5% Triton X-100) at 0 °C for 10 min. The nuclei were sheared through a 16-gauge needle, and subjected to centrifugation for 5 min at 400 r/min. The deposition was washed twice with CSK50 (10 mmol/L PIPES pH 6.8, 300 mmol/L sucrose, 50 mmol/L NaCl, 4 mmol/L CaCl₂, 1.0 mmol/L PMSF, 0.5% Triton X-100) and digested for 30 min at 25 °C in the same buffer containing 500 U/mL DNase I. One mole per liter ammonium sulfate was added dropwise to a final concentration of 0.25 mmol/L. After incubation for 15 min, the nuclear matrix proteins were pelleted by centrifugation at 1 000 r/min for 5 min, and washed once with the CSK50 buffer, then stored at -80 °C. Protein concentrations were determined by Bradford's method.

Two-dimensional gel electrophoresis

To solubilize nuclear matrix proteins, the pellet of purified nuclei was resuspended in 2-D buffer containing 7 mol/L urea, 2 mol/L thiourea, 4% CHAPS, 50 mmol/L DTT and ultrasonicated for 2 min. The supernatant was centrifuged for 30 min at 16 000 *g* at 4 °C. IEF was performed in ReadyStrip IPG strips. ReadyStrip IPG strips were rehydrated overnight in a reswelling tray with 2-D buffer containing 0.5% IPG buffer pH 3-10 and nuclear matrix proteins in a final volume of 250 μ L (200 μ g). IEF was carried out on a Protean IEF Cell (Investigator) at 19 °C with a maximum current setting of 80 mA/strip. Focusing was performed for a total of 70 000 V·h.

Before carrying out second dimensional SDS-PAGE, the strips were equilibrated in an equilibration buffer consisting of 20% glycerol, 2% SDS, 65 mmol/L Tris-HCl, pH 6.8 and 20 mmol/L DTT for 10 min at room temperature, then transferred into the second equilibration buffer consisting of 20% glycerol, 2% SDS, 65 mmol/L Tris-HCl, pH 6.8 and 2.5% iodoacetamide. The strips were transferred onto 1-mm thick SDS-PAGE gels and sealed in place with

1% agarose. SDS-PAGE was performed on a 12.5% acrylamide/bisacrylamide gel at 50 V for 30 min followed by 170 V for 8 h. The gels were run in the following electrode buffer: 25 mmol/L Tris, 192 mmol/L glycine, 0.1% SDS. SDS-PAGE standards were used for gel calibration. The gels were stained with Coomassie blue R250 and destained with 5% methanol, 7.5% acetic acid. 2-DE maps of nuclear matrix proteins were subjected to analysis with Melanie software. Protein spots were manually excised for mass spectrometry.

Protein identification by matrix-assisted laser-desorption/ionization time of flight mass spectrometry (MALDI-TOF-MS) analysis

In-gel digestion Spots were cut into about 1 cm \times 1 cm \times 1 cm pieces, and washed twice with 80 μ L of 25 mmol/L NH₄HCO₃, 50% acetonitrile for 5 min, then dehydrated with 80 μ L of acetonitrile. Gel pieces were completely dried. Reduction was achieved by 1 h treatment with 10 mmol/L DTT/100 mmol/L NH₄HCO₃ at 57 °C. Alkylation was performed with 25 mmol/L iodoacetamide/100 mmol/L NH₄HCO₃ for 45 min in the dark at 25 °C. Finally, gel pieces were washed thrice for 5 min alternatively with 100 mmol/L ammonium carbonate and acetonitrile, and then completely dried with a Speed Vac before trypsin digestion. Appropriate volumes of trypsin (12.5 ng/ μ L, freshly diluted in 50 mmol/L NH₄HCO₃) were added to the dried gel pieces. The digestion was performed at 37 °C overnight. After being centrifuged for 5 min in a Speed Vac, the gel pieces were incubated in 10 μ L 20 mmol/L NH₄HCO₃ for 20 min at room temperature, and then incubated in 10 μ L 5% TFA/50% acetonitrile for 5 min at room temperature. The supernatant was mixed, and completely dried with a Speed Vac.

MALDI-TOF-MS analysis For MALDI-TOF-MS analysis, samples were dissolved in 2 μ L 0.1% TFA. Mass measurements were carried out on a Bruker ULTRAFLEX™ TOF/TOF mass spectrometer. This instrument was used at a maximum accelerating potential of 20 kV (in positive mode) and was operated in reflector mode. 0.5 μ L of saturated solution of α -cyano-4-hydroxy cinnamic acid in 0.1% TFA/30% acetonitrile was mixed with 0.5 μ L sample solution, and added to the target. Internal calibration was performed with tryptic peptides coming from autodigestion of trypsin (monoisotopic masses at m/z 842.51, and m/z 2 211.10). Monoisotopic peptide masses were assigned and used for database search.

Database search

The MALDI-TOF-MS data were searched against a NCBI nonredundant protein sequence database using Mascot tool from Matrix Science. All proteins present in the NCBI database were taken into account without any *pI* or *M_r* restrictions. Search parameters included a maximum allowed peptide mass error of 100 ppm with a consideration of one incomplete cleavage per peptide. Accepted modifications included carbamidomethylation of cysteine residues (from iodoacetamide exposure) and methionine oxidation, a common modification occurring during SDS-PAGE. Protein identifications were assigned when three criteria were met:

(1) Statistical significance ($P < 0.05$) of the match when tested by Mascot (matrixscience.com); (2) $>20\%$ sequence coverage by the tryptic peptides; (3) Concordance ($\pm 15\%$) with the molecular weight and pI of the parent 2-D PAGE protein spot; and (4) Protein identifications not fulfilling criterion 2 were still assigned, if criteria 1 and 3 were fulfilled and no other *Homo sapiens* proteins with peptide mass-matched P values < 0.05 were identified by Mascot; identified protein was inferred.

RESULTS

Changes in nuclear matrix proteins upon addition of 5 mmol/L HMBA

Samples of nuclear matrix proteins extracted from MGc80-3 cells treated with or without 5 mmol/L HMBA were subjected to 2-D gel electrophoresis for at least three repeats per experimental condition. Analysis of proteins was based on evaluation of at least two gels. Typical 2-DE map of nuclear matrix proteins from MGc80-3 cells in the presence or absence of HMBA is shown in Figure 1. There were 22 protein spots that were changed remarkably, whereas most of the spots were similar in the expression patterns of nuclear matrix proteins from differentiated MGc80-3 cells compared to that from control. Among the changed spots,

12 spots were downregulated, one spot disappeared in the differentiated MGc80-3 cells, whereas 8 spots were upregulated, and 1 spot emerged as a new protein spot that appeared in the differentiated cells (Figures 1 and 2). Relative expression levels of the changed proteins were shown using Melanie software (Figure 3), relative volume (%vol) of spot was employed to make the data independent of uninteresting variation between gels, such as differences in protein loading or staining (Table 1).

Identification of the altered proteins

In the 22 differentially expressed protein spots, 15 were identified as 11 proteins by peptide mass fingerprinting according to the criteria, while 8 spots failed to be identified by peptide mass fingerprinting. The Spot C33 that disappeared in the HMBA-treated MGc80-3 cells was identified as hnRNP A2/B1. Nine of the twelve spots downregulated in the HMBA-treated cells were actin, vimentin, prohibitin, porin 31HL, hnRNP A2/B1, ATP synthase and heat shock protein 60. The new spot present after HMBA treatment was oxygen-regulated protein. In the eight upregulated spots, four spots were matched with heat shock protein gp96, heat shock protein 90-beta, ubiquitin thiolesterase (EC 3.1.2.15) and valosin-containing protein individually.

Table 1 Nuclear matrix proteins from the 2-DE map of MGc80-3 cells identified by peptide mass fingerprinting

Number Accession Protein name	Sequence coverage (%)	Theoretical values		Experimental values		Number of matched peptides
		M_r (Da)	pI	M_r (Da)	pI	
Disappeared proteins:						
C33 gi 4504447 Heterogeneous nuclear ribonucleo-protein A2/B1	26	36 041	8.67	37 100	8.47	7
Downregulated proteins:						
C19 gi 15277503 ACTB protein	37	40 536	5.55	29 000	5.51	10
C20 gi 4505773 Prohibitin	40	29 843	5.57	31 500	5.58	8
C29 gi 238427 Porin 31HL	34	30 737	8.63	34 500	8.78	7
C30 gi 4504447 Heterogeneous nuclear ribonucleo-protein A2/B1	43	37 429	8.97	36 600	8.85	11
C38 gi 15277503 ACTB protein	35	40 536	5.55	48 400	5.13	10
C39 gi 5030431 Vimentin	34	41 651	4.82	46 800	4.82	11
C40 gi 2119204 Vimentin	20	53 676	5.06	52 800	4.98	9
C41 gi 32189394 ATP synthase	29	56 525	5.26	55 200	5.05	15
C70 P10809 Heat shock protein 60	17	61 187	5.70	59 400	5.51	6
Newly emerged proteins:						
S78 gi 5453832 oxygen regulated protein	14	111 494	5.16	92 300	5.50	12
Upregulated proteins:						
S72 gi 15010550 heat shock protein gp96 precursor	14	90 309	4.73	98 000	4.62	12
S74 gi 72222 heat shock protein 90-beta	27	83 584	4.97	79 700	5.16	19
S73 gi 2134982 ubiquitin thiolesterase (EC 3.1.2.15)	12	96 596	4.90	82 000	5.14	9
S75 gi 6005942 valosin-containing protein	34	89 950	5.14	82 000	5.50	20
Unidentified proteins						

Downregulated: C23, C27, C28; Upregulated: S41, S44, S53, S66, S54.

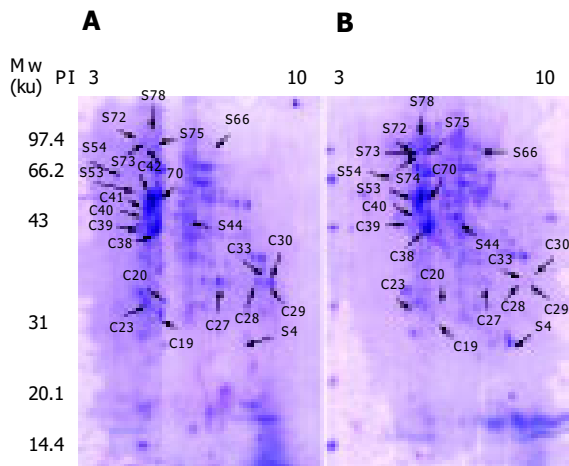


Figure 1 2-D PAGE gels of nuclear matrix proteins from MGc80-3 cells, Coomassie blue-stained **A:** MGc80-3 cells; **B:** MGc80-3 cells exposed to 5 mmol/L HMBA for 7 d. Arrows pointed to changed proteins. Disappeared protein: C33; downregulated proteins: C19, C20, C23, C27, C28, C29, C30, C38, C39, C40, C41, C70; new protein: S78; upregulated proteins: S4, S44, S53, S54, S72, S74, S75.

DISCUSSION

In the present study, nuclear matrix proteins extracted from differentiated MGc80-3 cells induced by HMBA were compared with those from MGc80-3 cells using 2-D gel electrophoresis. 2-D gel image analysis software was used to confirm the identification of specific nuclear matrix proteins associated with the differentiation of carcinoma cells combined with the visual observation. The protein patterns were highly reproducible. There were 22 spots that were changed remarkably during the differentiation process. Most of interested proteins differed qualitatively between control and differentiated MGc80-3 cells, except for two proteins, in which one was absent, while the other was only present in the HMBA-treated cells. The differentially expressed proteins confirm that specific nuclear matrix proteins are accompanied with the differentiation of MGc80-3 cells.

Fifteen of the twenty-two changed proteins were identified. The identified proteins that associated with proliferation and/or differentiation of MGc80-3 cells were grouped into six classes: (1) common nuclear matrix proteins:

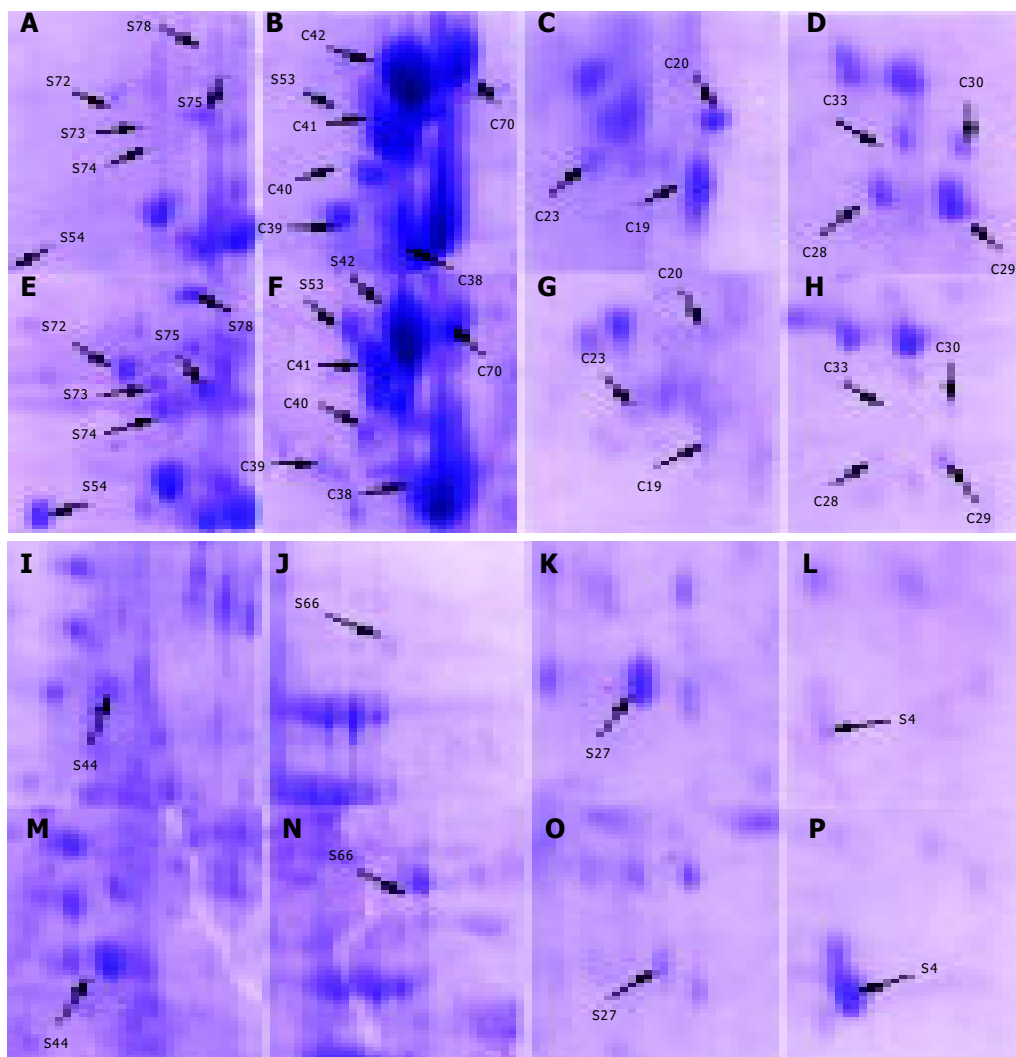


Figure 2 Enlarged maps of changed nuclear matrix proteins from MGc80-3 cells, Coomassie blue-stained **A-H:** nuclear matrix from control cells; **I-P:** nuclear matrix from HMBA-treated cells. Arrows pointed to changed proteins. C33 disappeared, while C19, C20, C23, C27, C28, C29, C30, C38, C39, C40,

C41, C70 were downregulated in the HMBA-treated cells; S78 was a new protein, whereas S4, S44, S53, S54, S72, S74, S75 were upregulated after HMBA treatment.

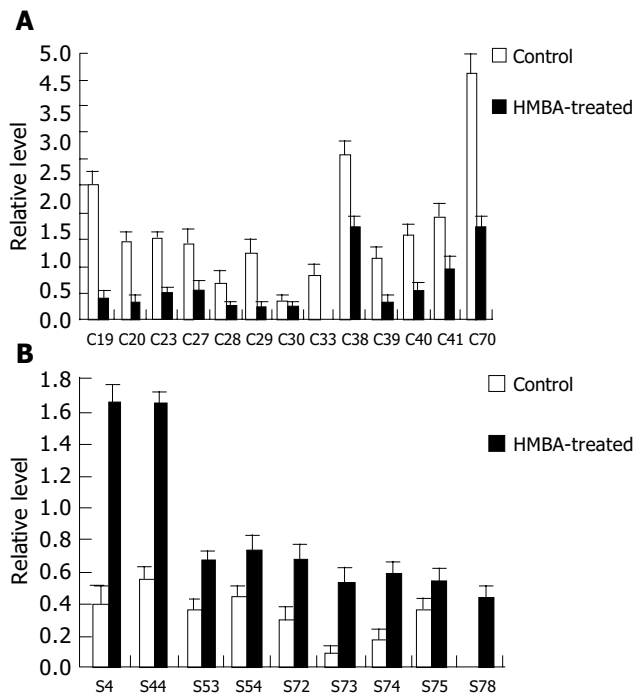


Figure 3 Relative expression level of changed nuclear matrix proteins. **A:** Relative expression level of disappeared or downregulated proteins in the nuclear matrix fractions of MGc80-3 cells treated with HMBA; **B:** Relative expression level of new or upregulated proteins in the nuclear matrix fractions of MGc80-3 cells treated with HMBA. C33 was disappeared, while C19, C20, C23, C27, C28, C29, C30, C38, C39, C40, C41, C70 were downregulated in the HMBA-treated cells; S78 was a new protein, whereas S4, S44, S53, S54, S72, S74, S75 were upregulated after HMBA treatment. Relative expression levels were shown using Melanie software. Values are mean \pm SE for two experiments.

vimentin and actin; (2) heterogenous nuclear ribonucleoprotein family: hnRNP A2/B1; (3) heat shock proteins; heat shock protein 60, heat shock protein gp 96, heat shock protein 90-beta, oxygen-regulated protein; (4) enzymes: ATP synthase, ubiquitin thiolesterase, and valosin-containing protein; (5) tumor suppressor protein: prohibitin; and (6) chloride channel protein: porin 31HL^[12].

Previously, several nuclear matrix proteins identified in this study, such as hnRNP A2/B1^[13], vimentin, actin^[14], prohibitin^[15], heat shock protein 60^[16], heat shock protein gp96^[17], and heat shock protein 90-beta^[18], were reported previously to be associated with cell growth and/or differentiation, although the roles they played in cell differentiation remain unclear.

In the downregulated proteins, vimentin and hnRNP A2/B1 have drawn intense attention to their relationship with cellular differentiation^[12,13]. In accordance to the result in this study, vimentin and hnRNP A2/B1 were highly expressed in cancer cell lines, but not detected or expressed in a lower level in well differentiated cells. Low expression of vimentin was reported to be correlated with the decreased mobility of cell, while the expression level of hnRNP A2/B1 was associated with cell proliferation ability. Inhibition on mobility and proliferation ability are the characteristics of differentiated cells, it is sure that vimentin and hnRNP A2/B1 are involved in the differentiation process, but the roles they play in cell growth and differentiation remain unknown.

In the upregulated or newly-emerged five proteins, there were three belonging to the heat shock protein family, while another member of the family, HSP60, was downregulated in the differentiated MGc80-3 cells. All the involved HSP proteins were reported to be associated with cell growth and differentiation^[16-19]. The deep involvement of heat shock protein family in the differentiation of MGc80-3 was consistent with the reports that heat shock proteins played an important role in the gastric tumors.

The proteins found in this study may be directly or indirectly involved in altered gene expression associated with the differentiation of carcinoma cells.

The findings described here will facilitate the understanding of the signal pathways and the mechanism of HMBA-induced differentiation. Further characterization of these proteins is now underway. These specific proteins are potential markers for tumor development or therapeutic target.

In this study, proteomic methods were used to systematically analyze the altered protein profiles in differentiated cancer cells. Specific nuclear matrix proteins associated with the differentiation of carcinoma cells were found and identified. It is of significance for revealing the signal pathway and mechanism of cell growth and differentiation, as well as carcinogenesis. Further characterization of those proteins will show the mechanism of cellular proliferation and differentiation, as well as cancer differentiation.

REFERENCES

- 1 Pederson T. Half a century of "the nuclear matrix". *Mol Biol Cell* 2000; **11**: 799-805
- 2 Berezney R, Mortillaro MJ, Ma H, Wei X, Samarabandu J. The nuclear matrix: a structural milieu for nuclear genomic function. *Int Rev Cytol* 1995; **162**: 1-65
- 3 S'iakste NI, S'iakste TG. Transcription factors and the nuclear matrix. *Mol Biol* 2001; **35**: 739-749
- 4 Gooden MD, Vernon RB, Bassuk JA, Sage EH. Cell cycle-dependent nuclear location of the matricellular protein SPARC: association with the nuclear matrix. *J Cell Biochem* 1999; **74**: 152-167
- 5 Khanuja PS, Lehr JE, Soule HD, Gehani SK, Noto AC, Choudhury S, Chen R, Pienta KJ. Nuclear matrix proteins in normal and breast cancer cells. *Cancer Res* 1993; **53**: 3394-3398
- 6 Keese SK, Meneghini MD, Szaro RP, Wu YJ. Nuclear matrix proteins in human colon cancer. *Proc Natl Acad Sci USA* 1994; **91**: 1913-1916
- 7 Bidwell JP, Fey EG, van Wijnen AJ, Penman S, Stein JL, Lian JB, Stein GS. Nuclear matrix proteins distinguish normal diploid osteoblasts from osteosarcoma cells. *Cancer Res* 1994; **54**: 28-32
- 8 Getzenberg RH, Konety BR, Oeler TA, Quigley MM, Hakam A, Becich MJ, Bahnson RR. Bladder cancer-associated nuclear matrix proteins. *Cancer Res* 1996; **56**: 1690-1694
- 9 Donat TL, Sakr W, Lehr JE, Pienta KJ. Unique nuclear matrix protein alterations in head and neck squamous cell carcinomas: Intermediate biomarker candidates. *Otolaryngol Head Neck Surg* 1996; **114**: 387-393
- 10 Huang ZP, Li QF, Wang L. Differentiation in human gastric adenocarcinoma cells induced by combination of HMBA and sodium selenite. *Xiamen Daxue Xuebao* 1996; **15**: 20-24
- 11 Fey EG, Capco DG, Krochmalnic G, Penman S. Epithelial structure revealed by chemical dissection and unembedded electron microscopy. *J Cell Biol* 1984; **99**(1 Pt 2): 203S-208

- 12 **Jentsch TJ**, Stein V, Weinreich F, Zdebik AA. Molecular structure and physiological function of chloride channels. *Physiol Rev* 2002; **82**: 503-568
- 13 **Zhou J**, Allred DC, Avis I, Martinez A, Vos MD, Smith L, Treston AM, Mulshine JL. Differential expression of the early lung cancer detection marker, heterogeneous nuclear ribonucleoprotein-A2/B1 (hnRNP-A2/B1) in normal breast and neoplastic breast cancer. *Breast Cancer Res Treat* 2001; **66**: 217-224
- 14 **Yoon WH**, Song IS, Lee BH, Jung YJ, Kim TD, Li G, Lee TG, Park HD, Lim K, Hwang BD. Differential regulation of vimentin mRNA by 12-O-tetradecanoylphorbol 13-acetate and all-trans-retinoic acid correlates with motility of Hep 3B human hepatocellular carcinoma cells. *Cancer Lett* 2004; **203**: 99-105
- 15 **Fusaro G**, Dasgupta P, Rastogi S, Joshi B, Chellappan S. Prohibitin induces the transcriptional activity of p53 and is exported from the nucleus upon apoptotic signaling. *J Biol Chem* 2003; **278**: 47853-47861
- 16 **Cappello F**, Bellafiore M, Palma A, David S, Marciano V, Bartolotta T, Sciume C, Modica G, Farina F, Zummo G, Bucchieri F. 60KDa chaperonin (HSP60) is over-expressed during colorectal carcinogenesis. *Eur J Histochem* 2003; **47**: 105-110
- 17 **Peibin Y**, Shude Y, Changzhi H. Heat shock protein gp96 and cancer immunotherapy. *Chin Med Sci J* 2002; **17**: 251-256
- 18 **Liu X**, Ye L, Wang J, Fan D. Expression of heat shock protein 90 beta in human gastric cancer tissue and SGC7901/VCR of MDR-type gastric cancer cell line. *Chin Med J* 1999; **112**: 1133-1137
- 19 **Miyagi T**, Hori O, Koshida K, Egawa M, Kato H, Kitagawa Y, Ozawa K, Ogawa S, Namiki M. Antitumor effect of reduction of 150-kDa oxygen-regulated protein expression on human prostate cancer cells. *Int J Urol* 2002; **9**: 577-585

Science Editor Guo SY Language Editor Elsevier HK

• GASTRIC CANCER •

Histochemical studies on intestinal metaplasia adjacent to gastric cardia adenocarcinoma in subjects at high-incidence area in Henan, north China

She-Gan Gao, Li-Dong Wang, Zong-Min Fan, Ji-Lin Li, Xin He, Rui-Feng Guo, Dong-Ling Xie, Xin-Wei He, Shan-Shan Gao, Hua-Qin Guo, Jun-Kuan Wang, Xiao-Shan Feng, Bao-Gen Ma

She-Gan Gao, Li-Dong Wang, Zong-Min Fan, Xin He, Rui-Feng Guo, Dong-Ling Xie, Xin-Wei He, Shan-Shan Gao, Hua-Qin Guo, Jun-Kuan Wang, Laboratory for Cancer Research, College of Medicine, Zhengzhou University, Zhengzhou 450052, Henan Province, China

Ji-Lin Li, Department of Pathology, Linzhou Esophageal Cancer Hospital, Linzhou, Henan Province, China

She-Gan Gao, Xiao-Shan Feng, Department of Clinical Oncology, The First Affiliated Hospital of Henan Science and Technology University, Luoyang 471001, Henan Province, China

Bao-Gen Ma, Department of Oncology, Henan Tumor Hospital, Zhengzhou 450003, Henan Province, China

Supported by the National Outstanding Young Scientist Award of China, No. 30025016, State Key Project for Basic Research, No. G1998051206, Foundation of Henan Education Committee 1999125 and the US NIH Grant, No. CA65871

Correspondence to: Li-Dong Wang, MD, Laboratory for Cancer Research, College of Medicine, Zhengzhou University, Zhengzhou 450052, Henan Province, China. lidong0823@sina.com

Telephone: +86-371-6658335 Fax: +86-371-6658335

Received: 2004-09-09 Accepted: 2004-12-21

Abstract

AIM: To characterize the histochemical type and pattern of intestinal metaplasia (IM) adjacent to gastric cardia adenocarcinoma (GCA) and distal gastric cancer (GC) in Linzhou, Henan Province, China.

METHODS: Alcian-blue-periodic acid Schiff and high iron diamine-Alcian blue histochemical methods were performed on 142 cases of IM, including 49 cases of GCA and 93 cases of GC. All the patients were from Linzhou, Henan Province, China, the highest incidence area for both GCA and squamous cell carcinoma. Radio- or chemotherapy was not applied to these patients before surgery.

RESULTS: The detection rate of IM in tissues adjacent to GCA tissues was 44.9%, which was significantly lower than that in GC tissues (80.64%, $P < 0.01$). The rates of both incomplete small intestinal and colonic IM types identified by histochemistry in GCA tissues (31.82% and 63.64%, respectively) were significantly higher than those in GC (5.33% and 21.33%, respectively, $P < 0.01$).

CONCLUSION: IM in GCA and GC should be considered as a separate entity. Further research is needed to evaluate whether neoplastic progression of IM is related to its mucin profile in GCA.

© 2005 The WJG Press and Elsevier Inc. All rights reserved.

Key words: Gastric cardia; Intestinal metaplasia; Histochemistry

Gao SG, Wang LD, Fan ZM, Li JL, He X, Guo RF, Xie DL, He XW, Gao SS, Guo HQ, Wang JK, Feng XS, Ma BG. Histochemical studies on intestinal metaplasia adjacent to gastric cardia adenocarcinoma in subjects at high-incidence area in Henan, north China. *World J Gastroenterol* 2005; 11(30): 4634-4637

<http://www.wjgnet.com/1007-9327/11/4634.asp>

INTRODUCTION

In China, epidemiologically, gastric cardia adenocarcinoma (GCA) shares a very similar geographic distribution with esophageal squamous cell carcinoma (SCC), especially in Linzhou (formerly Linxian County), Henan Province, north China, the highest incidence area of SCC in the world^[1,2]. However, the incidence of adenocarcinoma arising from the distal stomach is very low in this area^[3,4]. In the last two decades, the incidence of primary adenocarcinoma of the lower esophagus, esophagogastric junction and GCA has increased dramatically in North America and Western European countries^[5-6]. In contrast, the incidence of gastric cancer (GC) has decreased steadily in recent years.

In Linzhou, China, GCA has been classified as esophageal cancer by the local registry for the past several decades, because of their similar clinical symptoms, such as dysphagia^[7]. Approximately 60% of patients with dysphagia are found to have a diagnosis of SCC, the remaining 40% are found to have adenocarcinomas of the lower esophagus or gastric cardia^[8]. A case-control study performed on patients with presumed distal esophageal or gastric cardia cancer in Linzhou found that one-third of all these tumors are adenocarcinomas of the gastric cardia^[9].

The histogenesis and carcinogenesis for malignant transformation of GCA, however, are still not clear. Intestinal metaplasia (IM) is documented in the gastro-esophageal junction and cardia, but the etiology remains unclear^[10,11]. It has been believed that IM is closely related with the distal stomach cancer^[12]. However, whether IM is a premalignant lesion for GCA is still not clear. Studies on the histochemical features of IM arising from gastric cardia

Table 1 Criteria for IM classification based on histology and histochemistry

Types of IM	Histology			Histochemical staining		
	Structure of glands	Columnar cell	Paneth cell	AB	PAS	HID
Complete	Regular	-	+	+	-	-
Incomplete	Irregular	+	-	+	+	-
Complete colonic	Regular	-	-	+	-	+
Incomplete colonic	Irregular	+	-	+	+	+
Incomplete gastric	Irregular	+	-	-	+	-

Revised from Ref. [11].

and distal stomach and their relationship are very limited. Thus, the present study was undertaken to characterize the histological and histochemical types of IM in tissues adjacent to GCA and GC from patients in Linzhou, a high-incidence area of SCC and GCA in north China with Alcian-blue-periodic acid Schiff (AB-PAS) and High Iron Diamine-Alcian blue (HID-AB) staining methods.

MATERIALS AND METHODS

Collection and processing of surgically resected GCA and GC specimens

One hundred and forty-two surgically resected GCA and AC specimens were collected from Linzhou People's Hospital, Linzhou Center Hospital and Yaocun Esophageal Cancer Hospital in Henan Province from 2000 to 2001. All the patients were from Linzhou, Henan Province, the highest incidence area of both GCA and SCC. There were 49 patients with GCA, including 26 males and 23 females with an average age of 59.96 ± 10.29 years (range 36-80 years) and 93 patients with GC, including 49 males and 44 females with an average age of 58.96 ± 9.38 years (range 33-82 years). None of the cases received chemotherapy or radiotherapy before surgery. The surgically resected specimens were immediately fixed in 85% ethanol, and embedded with paraffin. Ten to fifteen pieces of tissue adjacent to cancer foci were obtained from each sample, dehydrated routinely with graded ethanol, embedded with paraffin, and cut into 5- μ m-thick sections. For each block, three slides were prepared, one slide was stained with hematoxylin and eosin (HE) for pathological diagnosis and another two slides were histochemically stained for histochemical analysis.

AB-PAS and HID-AB staining

The protocols for AB-PAS and HID-AB staining established previously in our laboratory were used [11]. Briefly, for AB-PAS staining, the paraffin slides were deparaffinized with xylene. One hundred microliters of AB staining solution (Fluka Company) was added to the slides for staining in wet boxes for 20-30 min, washed with distilled water for 3-5 min; 100 mL 0.5% periodic acid solution was applied for oxidation for 10 min, washed with distilled water for 3-5 min; Schiff solution staining for 10 min, washed with distilled water for 5-10 min. Finally, the slides were sealed with neutral gum. For HID-AB staining (Sigma Company, USA), the paraffin slides were deparaffinized with xylene. The slides reacted with high iron diamine solution at room temperature for 24 h and then were washed with distilled water. One hundred

microliters of AB solution was applied for staining in wet boxes for 20-30 min and washed with distilled water, 0.5% neutral red solution (No. 3 Reagent Factory, Shanghai) was stained for 1-2 min and then washed with distilled water for 3-5 min. Finally, the slides were sealed with neutral gum.

Criteria for diagnosis and classification of IM

Based on the morphology and histochemistry findings, IM was classified as five types: complete intestinal IM, incomplete intestinal IM, complete colonic IM, incomplete colonic IM, and incomplete gastric IM (Table 1). In complete IM, the epithelial cells were composed of goblet cells, Paneth cells, mucous columnar cells, and absorptive cells; in incomplete IM, the epithelial cells were composed of goblet and mucous columnar cells.

Statistical analysis

The data were processed with SPSS 8.0 and χ^2 test was used for the difference among different IM types. $P < 0.05$ was considered statistically significant.

RESULTS

Histological findings

The histological analysis showed that the detection rate in both complete and incomplete IM adjacent to GCA (44.9%) was lower than that in both complete and incomplete IM adjacent to GC (80.64%, $P < 0.01$, Table 2). IM could be identified in a single acinus, or in several acini (Figure 1A).

Table 2 Prevalence and distribution of different types of IM in tissues adjacent to GCA and GC in Linzhou, Henan Province, China

Type	Incomplete IM		
	Complete IM n (%)	Small intestinal n (%)	Colonic n (%)
GCA (44.90%, 22/49)	1/22 (4.55)	7/22 (31.82)	14/22 (63.64)
GC (80.64%, 75/93)	55/75 (73.33)	4/75 (5.33)	16/75 (21.33)

Histochemical findings

By AB-PAS staining, complete type of IM was stained blue (Figure 1B), the incomplete type of IM was stained blue and red (Figure 1C), the gastric type of IM was stained red, the intestinal type of IM was stained blue. But, by HID-AB staining, the intestinal type of IM was stained blue (Figure 1D), the colonic type of IM was stained brown or black (Figure 1E).

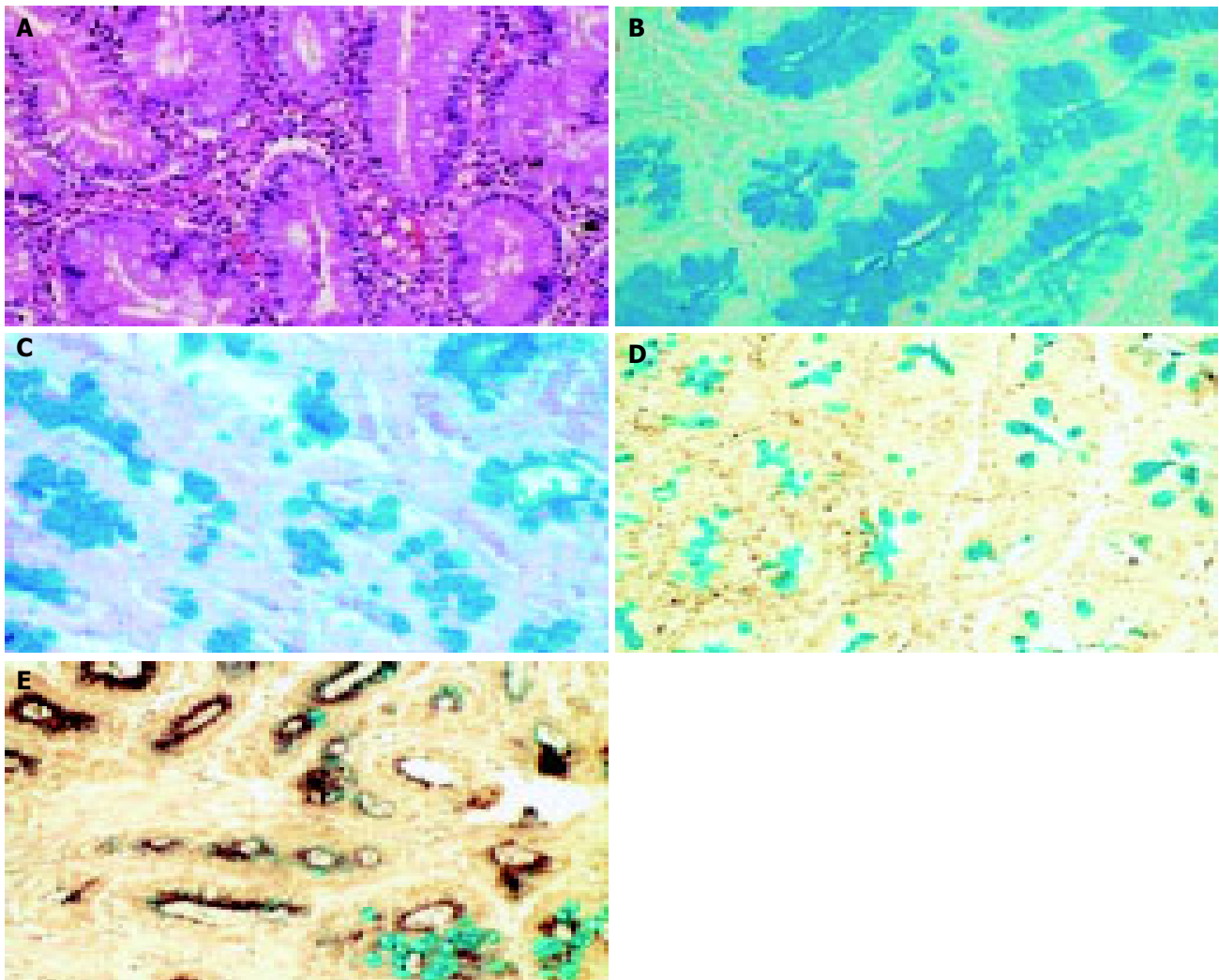


Figure 1 Histological and histochemical findings in different types of IM. **A:** Microphotograph of chronic carditis with IM; **B:** Microphotograph of histochemical stain on complete IM at gastric cardia; **C:** Microphotograph of histochemical

stain on incomplete IM at gastric cardia; **D:** Microphotograph of histochemical stain on intestinal type of IM at gastric cardia; **E:** Microphotograph of histochemical stain on colonic type of IM at gastric cardia.

The histochemical pattern and type of IM were different between GCA and GC and most types of IM in GCA were incomplete type (95.45%), especially in the incomplete colonic type (63.64%); In contrast, complete IM occurred more frequently in GC (73.33%, $P < 0.01$, Table 2). Incomplete colonic and small intestinal IM could be observed in the same microscopic field or different fields on the same sample. In other words, blue acid mucous and brown-black sulfuric acid mucous co-existed in one acinus in some cases. The detection rate of co-existence for both colonic and small intestinal types on the same slide was 22.73% ($n = 5$). IM mostly occurred in the deep glands of gastric cardia.

DISCUSSION

The present study showed that IM was a frequent event in gastric cardia non-cancerous tissue adjacent to GCA (44.9%) in Linzhou, Henan Province, the highest incidence area of SCC and GCA. Goblet cells were invariably identified on HE-stained specimens. Only 0.7% symptom-free subjects in Linzhou are identified with IM in gastric cardia biopsies^[4]. These results suggest that IM may be a precancerous lesion

of GCA in this area.

Another interesting observation in the present study is that incomplete type of IM, especially the colonic type, is the predominant form of IM found in the gastric cardia. In contrast, the complete type of IM is the major form of IM found in GC. These results suggest that IM in GCA and GC should be considered as a separate entity. In stomach, IM frequently forms at the antrum (22.9%) but rarely at the fundus (2.8%)^[13]. Likewise, most GCs arise from the distal part of the stomach and infrequently from the near part. It is believed that GC correlates with IM closely, particularly with the intestinal type of GC based on the fact that the risk for GC and IM shares the same epidemiological characteristics^[14]. It was reported that the incomplete IM in which columnar cells secrete sulfuric acid mucous relates with GC^[12,15,16]. The present study indicated that the detection rate of IM adjacent to GCA was lower than that adjacent to GC. But the IM adjacent to GCA belonged to the incomplete IM, and the percentage of incomplete IM is much higher, suggesting that GCA correlates with incomplete IM closely and incomplete IM may be precancerous lesions of GCA. Reports with respect to the relationship between

IM and GCA are inconsistent^[17]. Further characterization of molecular changes of IM in nearby cancer foci and cancer tissue will shed light on the relationship of IM and GCA.

The prevalence of IM in gastric cardia is an understudied subject, especially in symptom-free subjects at the high-risk area of GCA. Only 0.7% symptom-free subjects in Linzhou, Henan Province, the high incidence area for GCA are identified with IM in gastric cardia biopsy, which is much lower than that in gastric cardia tissue adjacent to GCA (64-folds lower, 44.9% *vs* 0.7%)^[4]. The possibility for this difference may be that the prevalence of IM in symptom-free subjects is lower than that in GCA patients. Recent studies in Western countries indicate that IM in Barrett's esophagus and at the gastroesophageal junction seems to occur more apparently in old subjects. GCA patients are usually 5-10 years older at the time of diagnosis than symptom-free subjects in the same area. Another reason may be due to the sampling procedure. IM occurs with a patchy, irregular distribution in flat mucosa that is usually invisible at endoscopy. Presently, we lack methods to target biopsy for IM lesions, the chance to identify IM lesions in small biopsy is much less than that in surgically resected GCA specimen. Methylene blue selectively stains specialized columnar epithelia in Barrett's esophagus with a high accuracy. Chromoendoscopy with methylene blue stain may help to direct biopsies in subjects with IM in gastric cardia^[17-19].

IM has been recognized as a key point in Barrett's esophagus. Goblet cells are invariably identified on HE-stained Barrett's esophagus. It has been hypothesized that Barrett's adenocarcinoma follows the metaplasia-dysplasia-adenocarcinoma sequence^[10]. At present, however, the importance of IM at gastric cardia remains unclear. Apparently, reflux esophagitis is not correlated with IM at gastric cardia in Chinese population. Chronic carditis may contribute to the development of IM at gastric cardia. Further research in large scale and long-term follow-up are needed to evaluate whether neoplastic progression of GCA is related to IM and its mucin profile.

The present study showed that incomplete IM and colonic IM coexisted in the same area or different areas of one sample. Some stomach glands presented blue acid mucous of intestinal IM and brown-black sulfuric acid mucous of colonic IM. The possible explanation is the multipotent stem cells in the neck of gastric glands are to differentiate different types of epithelium due to the irritation of various initial agents, leading to different mucous reaction.

ACKNOWLEDGMENTS

We would like to thank Dr. Zhe Sun and Dr. Xiao-Dong Lv for helpful discussions and preparation of this manuscript.

REFERENCES

- 1 Wang LD, Zhou Q, Yang CS. Esophageal and gastric cardia epithelial cell proliferation in northern Chinese subjects living in a high-incidence area. *J Cell Biochem Suppl* 1997; **28-29**:

- 159-165
- 2 Wang LD, Shi ST, Zhou Q, Goldstein S, Hong JY, Shao P, Qiu SL, Yang CS. Changes in p53 and cyclin D1 protein levels and cell proliferation in different stages of human esophageal and gastric-cardia carcinogenesis. *Int J Cancer* 1994; **59**: 514-519
- 3 Wang LD, Zheng S. Mechanisms of human esophageal and gastric cardia cancer on the subjects in Henan, the high incidence area for esophageal cancer. *Zhengzhou Daxue Xuebao* 2002; **37**: 717-729
- 4 Wang LD, Feng CW, Zhou Q, Chen YL, Li YX, Zhuang Y, Xie BH, Qiu SL, Liu BC, Zhao YZ, Wu JP, Yang WC, Zou JX, Li XF, Li J, Wang DC, Guao SS, Pai YM, Yang GY. Analysis of the screening result of esophageal disease in high risk urban and rural areas of esophageal carcinoma. *Henan Yike Daxue Xuebao* 1997; **32**: 6-8
- 5 Powell J, McConkey CC. Increasing incidence of adenocarcinoma of the gastric cardia and adjacent sites. *Br J Cancer* 1990; **62**: 440-443
- 6 Blot WJ, Devesa SS, Kneller RW, Fraumeni JF. Rising incidence of adenocarcinoma of the esophagus and gastric cardia. *JAMA* 1991; **265**: 1287-1289
- 7 Blot WJ, Devesa SS, Fraumeni JF. Continuing climb in rates of esophageal adenocarcinoma: An update. *JAMA* 1993; **270**: 1320-1322
- 8 Wang LD, Gao WJ, Yang WC, Li XF, Li J, Zou JX, Wang DC, Guo RX. Preliminary analysis of the statistics on 3,933 cases with esophageal cancer and gastric cardia cancer from the subjects in people's Hospital of Linzhou in 9 years. *Henan Yike Daxue Xuebao* 1997; **32**: 9-11
- 9 Li JY, Ershaw AG, Chen ZJ, Wacholder S, Li GY, Guo W, Li B, Blot WJ. A case-control study of cancer of the esophagus and gastric cardia in Linzhou. *Int J Cancer* 1989; **43**: 755-761
- 10 Clouston AD. Timely topic: premalignant lesions associated with adenocarcinoma of the upper gastrointestinal tract. *Pathology* 2001; **33**: 271-277
- 11 Chen H, Wang LD, Fan ZM, Gao SG, Guo HQ, Guo M. The comparison study of the three histochemical staining methods in gastric cardia intestinal metaplasia staining. *Henan Yixue Yanjiu* 2003; **12**: 10-13
- 12 Conio M, Lapertosa G, Bianchi S, Filiberti R. Barrett's esophagus: an update. *Critical Rev Oncol Hematol* 2003; **46**: 187-206
- 13 Eidt S, Stolte M. Prevalence of intestinal metaplasia in *Helicobacter pylori* gastritis. *Scand J Gastroenterol* 1994; **29**: 607-610
- 14 Ruol A, Parenti A, Zaninotto G, Merigliano S, Costantini M, Cagol M, Alfieri R, Bonavina L, Peracchia A, Ancona E. Intestinal metaplasia is the probable common precursor of adenocarcinoma in Barrett esophagus and adenocarcinoma of the gastric cardia. *Cancer* 2000; **88**: 2520-2528
- 15 El-Serag HB, Sonnenberg A, Jamal MM, Kunkel D, Crooks L, Feclerseh RM. Characteristics of intestinal metaplasia in the gastric cardia. *Am J Gastroenterol* 1999; **94**: 622-627
- 16 Morales CP, Spechler SJ. Intestinal metaplasia at the gastroesophageal junction: Barrett's, bacteria, and biomarkers. *Am J Gastroenterol* 2003; **98**: 759-762
- 17 Sharma P, Weston AP, Morales T, Topalovski M, Mayo MS, Sampliner RE. Relative risk of dysplasia for patients with intestinal metaplasia in the distal oesophagus and in the gastric cardia. *Gut* 2000; **46**: 9-13
- 18 Canto MIF, Setrakian S, Willis JE, Chak A, Petras RE, Sivak MV. Methylene blue staining of dysplastic and nondysplastic Barrett's esophagus: an *in vivo* and *ex vivo* study. *Endoscopy* 2001; **33**: 391-400
- 19 Olliver JR, Wild CP, Sahay P, Dexter S, Hardie LJ. Chromoendoscopy with methylene blue and associated DNA damage in Barrett's oesophagus. *Lancet* 2003; **362**: 373-374

Correlation between expression of cyclooxygenase-2 and the presence of inflammatory cells in human primary hepatocellular carcinoma: Possible role in tumor promotion and angiogenesis

Melchiorre Cervello, Daniela Foderà, Ada Maria Florena, Maurizio Soresi, Claudio Tripodo, Natale D'Alessandro, Giuseppe Montalto

Melchiorre Cervello, Daniela Foderà, Institute of Biomedicine and Molecular Immunology "Alberto Monroy", National Research Council, Palermo, Italy

Ada Maria Florena, Claudio Tripodo, Institute of Pathologic Anatomy, University of Palermo, Palermo, Italy

Maurizio Soresi, Giuseppe Montalto, Department of Clinical Medicine, University of Palermo, Palermo, Italy

Natale D'Alessandro, Department of Pharmacological Science, University of Palermo, Palermo, Italy

Supported by the MIUR and Progetto Strategico Oncologia "Terapia Preclinica Molecolare Oncologia" MIUR-CNR

Correspondence to: Melchiorre Cervello, Istituto di Biomedicina e Immunologia Molecolare "Alberto Monroy", C.N.R., Via Ugo La Malfa 153, Palermo 90146, Italy. cervello@ibim.cnr.it
Telephone: +39-91-6809534 Fax: +39-91-6809548

Received: 2004-07-26 Accepted: 2004-11-04

cells. Moreover, there was a positive correlation between CD34 and COX-2 expression in tumor tissues. Comparison between well- and poorly-differentiated HCC showed that the number of CD34-positive cells decreased with dedifferentiation. However, COX-2 was the only independent variable showing a positive correlation with CD34 in a multivariate analysis.

CONCLUSION: The presence of inflammatory cells and COX-2 expression in liver tumor suggests a possible relationship with tumor angiogenesis. COX-2 expressing cells and the number of macrophages/Kupffer cells and mast cells decrease with progression of the disease.

© 2005 The WJG Press and Elsevier Inc. All rights reserved.

Key words: COX-2; HCC; Angiogenesis; Mast cells; Macrophages

Cervello M, Foderà D, Florena AM, Soresi M, Tripodo C, D'Alessandro N, Montalto G. Correlation between expression of cyclooxygenase-2 and the presence of inflammatory cells in human primary hepatocellular carcinoma: Possible role in tumor promotion and angiogenesis. *World J Gastroenterol* 2005; 11(30): 4638-4643

<http://www.wjgnet.com/1007-9327/11/4638.asp>

Abstract

AIM: To investigate the association of cyclooxygenase-2 (COX-2) expression with angiogenesis and the number and type of inflammatory cells (macrophages/Kupffer cells; mast cells) within primary hepatocellular carcinoma (HCC) tissues and adjacent non-tumorous (NT) tissues.

METHODS: Immunohistochemistry for COX-2, CD34, CD68 and mast cell tryptase (MC_T) was performed on 14 well-characterized series of liver-cirrhosis-associated HCC patients. COX-2 expression and the number of inflammatory cells in tumor lesions and surrounding liver tissues of each specimen were compared. Moreover, COX-2, CD34 staining and the number of inflammatory cells in areas with different histological degrees within each tumor sample were comparatively analyzed.

RESULTS: The percentage of COX-2 positive cells was significantly higher in NT tissues than in tumors. COX-2 expression was higher in well-differentiated HCC than in poorly-differentiated tissues. Few mast cells were observed within the tumor mass, whereas a higher number was observed in the surrounding tissue, especially in peri-portal spaces of NT tissues. Abundant macrophages/Kupffer cells were observed in NT tissues, whereas the number of cells was significantly lower in the tumor mass. However, a higher cell number was observed in the well-differentiated tumor and progressively decreased in relation to the differentiation grade. Within the tumor, a positive correlation was found between COX-2 expression and the number of macrophages/Kupffer cells and mast

INTRODUCTION

Cyclooxygenase-2 (COX-2) is an inducible immediate early gene associated with inflammation, cell growth and differentiation, prevention of apoptosis and tumorigenesis^[1]. A substantial body of evidence supports the role of COX-2 in the angiogenesis of a variety of human malignancies^[2-5]. Recent studies have already shown an increased expression of COX-2 in patients with liver disease, suggesting the role of COX-2 in chronic liver disease and during the progression of HCC^[6-8]. In addition, COX-2 expression is reported to correlate with tumor angiogenesis in patients with hepatitis C or B virus-associated HCC^[9,10].

Macrophages are an important source of angiogenic activity in wound healing, cancer, and chronic inflammation. They can produce various growth factors and cytokines that promote angiogenesis. The presence of infiltrating macrophages is closely associated with angiogenesis in several types of malignancies, including melanoma^[11], breast^[12], prostate^[13] and lung^[14] cancer, glioma^[15], cervical^[16] and esophageal carcinoma^[17]. In the liver, infiltrating macrophages

and Kupffer cells which are considered as resident macrophages, play an essential role not only in host defense but also in homeostatic responses of tissue^[18-20]. However, their role in the process of tumor progression and angiogenesis is not well understood.

Mast cells (MCs) circulate in blood as progenitors and undergo terminal differentiation into mature cells only when they enter the tissues. Mast cells release a variety of factors known to enhance angiogenesis, namely heparin, histamine and tryptase, as well as cytokines, such as transforming growth factor- β (TGF- β), tumor necrosis factor- α (TNF- α), interleukin-8 (IL-8), fibroblast growth factor-2 (FGF-2) and vascular endothelial growth factor (VEGF). MC density is highly correlated with the extent of both normal and pathological angiogenesis in chronic inflammatory diseases and tumors^[21,22]. MCs are present in both normal and pathological livers^[23,24]. Their role in tumor angiogenesis is not entirely clear, although MCs are of primary importance in the transition from sinusoidal to capillary-type endothelial cells during HCC growth.

Although, as quoted above, some studies on the liver have evaluated the relationship between COX-2 and angiogenesis, or the relationship between the presence of macrophages and mast cells and the different liver pathologies, no studies are available to date on the possible relationship between the various parameters. Therefore, we investigated the association of COX-2 expression with the number of microvessels, the number and type of inflammatory cells in primary hepatocellular carcinoma and adjacent non-tumorous tissues; compared within the same tumor specimen of the two areas with the greatest difference in differentiation grade, and evaluated which of the parameters analyzed could play a prominent role in the neoangiogenesis of HCC.

MATERIALS AND METHODS

Patients and tissue samples

The study included 14 primary HCC patients whose main clinical characteristics are shown in Table 1. Diagnosis was made according to the pathological findings in all cases. All the patients with known cirrhosis were enrolled in a prospective study for HCC screening. The disease was associated with the presence of serum HCV antibodies in all cases. None of the patients was positive for HBsAg. HCC was histologically

graded by two pathologists (AMF and CT) and divided into well-differentiated (WD), moderately-differentiated (MD) or poorly-differentiated (PD) types. Nine of the fourteen patients showed different histological grades (WD+MD+PD) in a single nodule (Table 1). However, a total of 23 tumor sites (11 well-differentiated and 12 poorly-differentiated) were analyzed (Table 1). In order to analyze the different parameters during tumor progression and to avoid variability between the different patients, we compared the two areas with the greatest difference in differentiation grade (i.e. well-differentiated *vs* poorly-differentiated, $n = 9$) within the same tumor specimen.

Histochemical staining

Specimens were fixed in formalin and embedded in paraffin. Four micrometer-thick sections were cut, dewaxed and hydrated. In the case of COX-2 and mast cell tryptase (MC_T) staining, the sections were first heated in a microwave oven (3-4 cycles of 5 min each) in 10 mmol/L citrate buffer (pH 6.0) and then washed twice with PBS for 5 min. All sections were incubated with 30 mL/L hydrogen peroxide in methanol for 5 min to inhibit endogenous peroxidase. Immunohistochemistry was performed by the streptavidin-biotin complex (StreptABC) using the following antibodies: rabbit polyclonal antibody against COX-2 (Cayman, Chemical, MI, USA) at a dilution of 1:100 for 2 h at 37 °C, and mouse mAb against CD68 (clone PG-M1, Dako, Copenhagen, Denmark) at a dilution of 1:50 and CD34 (Clone Qbend/10, Menarini, Florence, Italy) at a dilution of 1:30, or anti-human mast cell tryptase (clone AA1, Dako, Copenhagen, Denmark) at a dilution of 1:150 for 30 min at room temperature. Sections were then incubated for 30 min at room temperature with biotinylated anti-rabbit or anti-mouse immunoglobulin diluted in PBS and streptavidin-biotin complex for 30 min at room temperature. The color was developed with 3-amino-9-ethyl-carbazole (AEC) (Dako, Copenhagen, Denmark) for 5-10 min at room temperature and counterstained with Mayer hematoxylin for 3 min.

Evaluation of COX-2 expression, determination of the number of macrophages/Kupffer cells, mast cells and microvessels

Immunohistochemical staining for COX-2 was semi-quantitative

Table 1 Patient characteristics and histological features of HCC

n	Age (yr)	Sex	Child	ALT	AST	Tumor size (cm)	Histology pattern	Histology grading
1	65	F	A5	26	55	2.8	PS	WD
2	64	M	A6	21	17	3	TR+PS+COM	WD+MD+PD
3	62	M	A5	53	44	7	TR	WD+MD+PD
4	63	M	B7	91	334	3	TR	PD
5	66	M	B7	145	302	1	TR+PS	WD
6	77	M	A5	32	24	3	TR+PS	WD+MD+PD
7	53	F	A6	161	186	2	TR+PS+COM	WD+MD+PD
8	70	F	A6	25	38	3	TR+PS+COM	WD+MD+PD
9	75	F	B7	42	55	2	TR	PD
10	65	M	A5	41	37	2.5	TR+COM	WD+MD+PD
11	56	F	A5	28	57	3.5	TR+PS+COM	WD+MD+PD
12	77	M	A6	44	47	2.7-2.2	TR+PS+COM	PD
13	61	M	A6	21	17	2.5-4.5	TR+PS+COM	WD+MD+PD
14	78	M	A5	210	388	6	TR+PS	WD+MD+PD

TR: trabecular; PS: pseudoglandular; COM: compact. WD: well-differentiated; MD: moderately-differentiated; PD: poorly-differentiated.

tatively evaluated by two independent observers (AMF, CT) using a scale of 0-5, according to both degree and intensity of staining, in which 0: negative, 1: positive staining in 1-20% of cells, 2: in 21-40%, 3: in 41-60%, 4: in 61-80% and 5 \geq 81%.

When the number of macrophages and mast cells was determined, the CD68-positive and MC_T-positive cells were counted respectively. Intra-tumoral microvessels were assessed by immunostaining with anti-CD34. All stained endothelial cells or cell clusters were counted as one microvessel. Branching structures were counted as a single vessel. The same two evaluators (AMF and CT) performed the counts. Briefly, stained sections were observed at 100 \times magnification to identify the areas with the highest number of positive cells. Counts were performed in five regions at 200 \times magnification. A scale of 0-5 was used for CD68, in which 0: negative, 1: 1-15 positive cells, 2: 16-30, 3: 31-45, 4: 45-60 and 5 \geq 61. In the case of CD34, a scale of 0-4 was used, in which 0: negative, 1: 1-20 microvessels, 2: 21-40, 3: 41-60, 4: \geq 61. For MC_T, the mean of the five counts was used directly because a small number of cells were observed.

Statistical analysis

Data were expressed as median and range (min-max). The Mann-Whitney *U* test and Spearman's rank correlation test were used when appropriate. Multiple linear regression analysis was used to study the association between increased values of CD34 and values of COX-2, CD68, and MC_T. The linear regression equation was used to describe a linear

relationship between the dependent variable (CD34) and one or more explanatory variables. $P < 0.05$ was considered statistically significant.

RESULTS

Expression of COX-2

COX-2 expression was detected in all the HCCs studied by immunohistochemical analysis. The percentage of COX-2 positive cells was significantly higher in non-tumor (NT) tissues than in tumors ($P < 0.0001$) (Figure 1 and Table 2). COX-2 showed a diffuse cytoplasmic localization in NT hepatocytes, whereas it showed a cytoplasmic dot-like pattern in tumor cells. COX-2 expression tended to be higher in well-differentiated than in poorly-differentiated HCC tissues ($z = 4.2, P < 0.0001$). As shown in Figures 1B and C, a clear difference in COX-2 staining was observed at the boundary of HCC tissues with different histological grades.

Immunostaining of macrophages

In this study, anti-CD68, an anti-human macrophage antibody, was used to identify the macrophages. However, in the CD68-positive (CD68+) cells, short spindle cells were considered to be Kupffer cells, whereas migrating macrophages were those with oval shape and abundant cytoplasm. The total number of CD68+ cells was calculated in all cases. The expression of CD68+ cells was significantly higher in non-tumor tissue than in tumor itself ($P < 0.0001$, Figure 2 and Table 2). In addition, the number of CD68+ cells reduced as the histological grade decreased

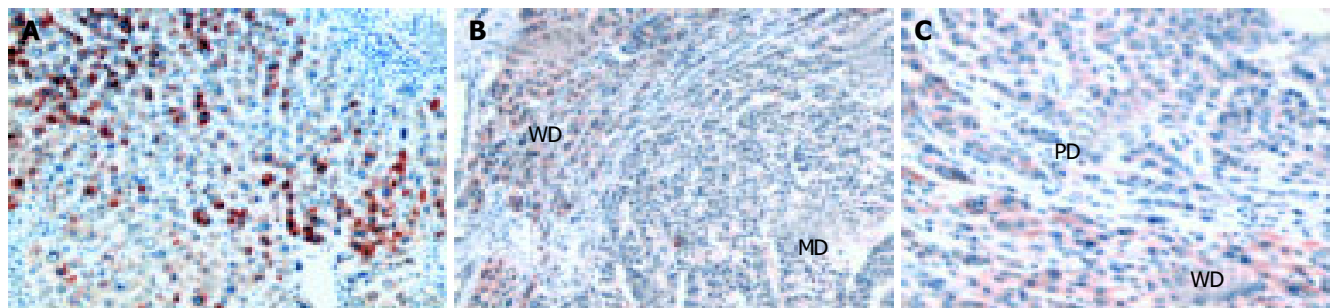


Figure 1 Immunohistochemical expression of COX-2 in cirrhotic liver area (A), well- and moderately-differentiated HCC areas (B), well-differentiated

HCC with trabecular arrangement and poorly-differentiated HCC with loose cohesive pattern (C) ($\times 250$).

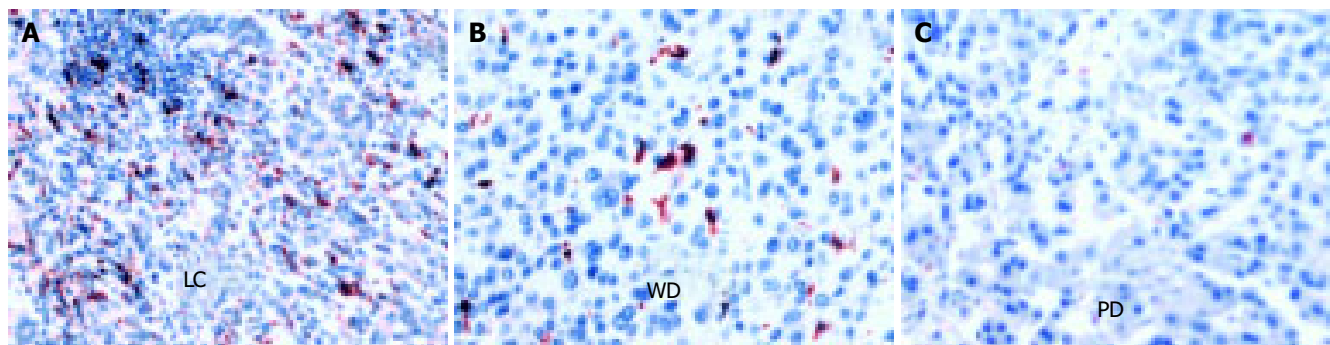


Figure 2 Immunohistochemical staining with anti-CD68 highlights the number of histiocytes in cirrhotic liver cells (A), well-differentiated HCC (B) and poorly-

differentiated HCC (C). (A, C $\times 250$; B $\times 400$).

Table 2 Mann-Whitney analysis of score representing immunostaining for COX-2, CD68 and number of MCs in liver cirrhosis and HCC tissues

	LC	HCC	z	P
COX-2	5 (3-5)	1 (0-5)	3.7	<0.0001
CD68	5 (3-5)	3 (0-4)	4.2	<0.0001
MC _T	4 (2-18)	1 (0-10)	4	<0.0001

LC: liver cirrhosis; HCC: hepatocellular carcinoma.

(Figures 2B and C) and was completely absent in some cases of poorly-differentiated HCC.

Immunostaining of mast cells

Mast cells were recognized by using anti-human tryptase mAb. Tryptase is a neutral protease contained in the secretory granules of MCs. Tryptase-positive mast cells (MC_T) were abundant and mainly localized in the portal tracts of non-tumorous liver tissues (Figure 3A). The number of MCs was significantly lower in HCC tissue than in surrounding cirrhotic liver tissue ($P < 0.0001$, Figure 3A and Table 2). However, different histological grades of HCC showed different number of MCs (Figure 3B), well-differentiated HCC showed the highest number of MCs which tended to decrease in less-differentiated HCC ($z = 4.1$, $P < 0.0001$).

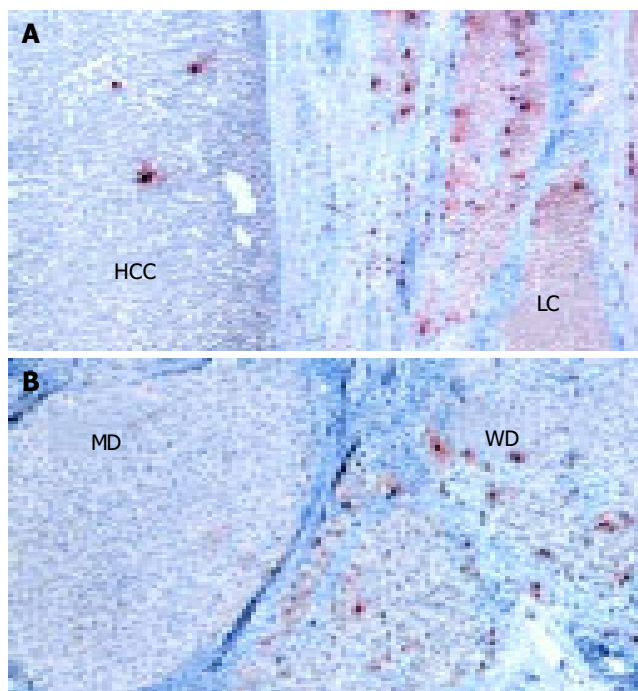


Figure 3 Immunohistochemical staining with anti-human mast cell tryptase in cirrhotic and HCC tissues (A) and in well-differentiated HCC and moderately-differentiated HCC (B). (x 250).

Immunostaining of endothelial cells

The presence of microvessels inside the tumor mass was evaluated by staining endothelial cells with anti-CD34 antibody. In the surrounding cirrhotic tissue CD34-positive

cells were found only in the portal tracts and septa. As shown in Figure 4, CD34+ cells were clearly found in well-differentiated HCC, whereas poorly-differentiated HCC showed few or no vessels (Figure 4B). The mean score was 2 (0-14) in well- and 0 (0-2) in poorly-differentiated HCC ($z = 3.3$, $P < 0.001$).

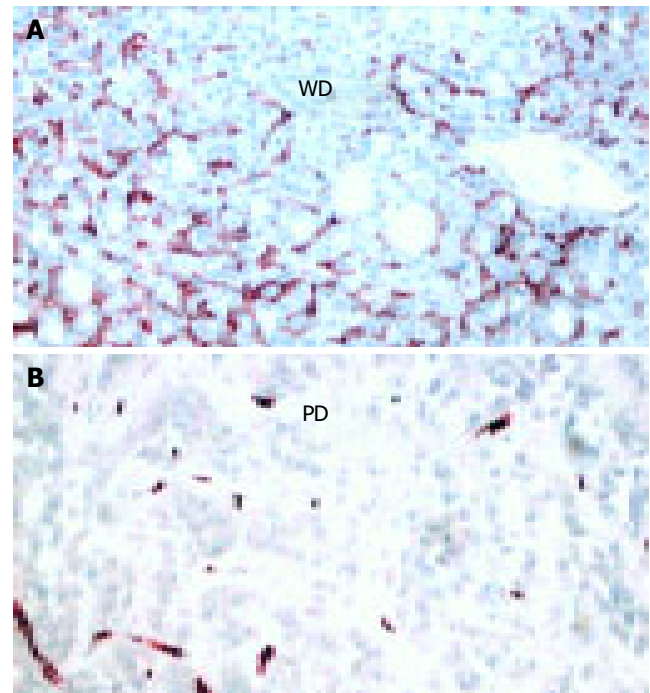


Figure 4 Immunohistochemical expression of CD34 underlining striking differences between well-differentiated HCC (A) and poorly-differentiated HCC (B). (x250).

COX-2 expression as evaluated in all HCC sites (WD-HCC+PD-HCC, $n = 23$) significantly correlated with the presence of macrophages ($P < 0.001$), mast cells ($P < 0.0001$) and CD34 expression ($P < 0.0001$). The presence of CD68+ cells significantly correlated with the number of MC_T ($P < 0.0001$) and CD34 expression ($P < 0.001$). The number of MC_T in HCC significantly correlated with CD34 expression ($P < 0.001$).

To confirm the relationship between angiogenesis expressed as CD34 (dependent variable) and other parameters (independent variables), multiple linear regression analysis was performed. A close association was found between CD34 and COX-2 ($\beta = 0.69$, $P < 0.002$, $R^2 = 0.65$), while no association was found between CD68 ($P < 0.07$) and MC_T ($P =$ not significant).

DISCUSSION

Tumor angiogenesis is essential for tumor growth, and depends on angiogenic factors produced by tumor cells and/or infiltrating cells in tumor tissue. The tumor microenvironment largely orchestrated by inflammatory cells is an indispensable participant factor in the neoplastic process. The inflammatory component of a developing neoplasm includes a varied leukocyte population, e.g., macrophages, neutrophils, eosinophils, and mast cells, all of which are variably loaded

with an assorted array of cytokines, cytotoxic mediators including reactive oxygen species, serine-, cysteine-, and metalloproteases, membrane-perforating agents, and soluble cell killing mediators, such as TNF- α , interleukines, and interferons^[24,25].

In recent years, a number of studies have correlated COX-2 expression with tumor angiogenesis^[2-5]. In addition, accumulation of inflammatory cells, macrophage and mast cells coupled with angiogenesis can be found in the literature^[11-17,20,21].

In this study, we evaluated the association of COX-2 expression with angiogenesis and the number and type of inflammatory cells in primary HCC and surrounding NT tissues, as well as their association with differentiation grades in HCC tissues. A previous study demonstrated that dedifferentiation occurs with time and tumor growth^[26]. In our study, a single tumor node showing areas with different histological grades was found in most HCC tissues. This allowed us to compare well-differentiated tumors with poorly-differentiated tumors in the same subject, and therefore to determine the role of molecules and cells analyzed during HCC progression.

We found that COX-2 expression and the number of macrophages/Kupffer cells and MCs were higher in adjacent NT tissues than in tumors. However, due to our limited patient population ($n = 14$) no correlation was observed by comparing each parameter in NT and tumor tissues in the same patient (data not shown). In addition, no correlation was found between the presence of inflammatory cells and COX-2 expression in peri-tumorous cirrhotic liver (data not shown).

We found that COX-2 was expressed in all HCC cases, which is in agreement with the results reported by Koga^[6] and Bae^[8]. COX-2 expression was higher in well-differentiated HCC than in poorly-differentiated HCC, suggesting that COX-2 may be involved in the early stages of hepatocarcinogenesis. The reduction of COX-2 expression during tumor progression is not common in all types of cancer. A possible explanation of this different behavior is that, in some cell types COX-2 over-expression may cause a growth disadvantage during tumor progression. This is in agreement with the results of Trifan *et al.*^[27], who reported that COX-2 overexpression is able to induce cell cycle arrest in a variety of cell types.

Although the functions of intra-tumor macrophages/Kupffer cells and MCs are still unclear, two hypotheses have been advanced about their possible role in tumor lesions. One hypothesis suggests that both cell types are important in the host defense mechanism and anti-tumor effects, the other postulates that they may directly promote tumor growth, invasion and neovascularity. Our results, in agreement with previous observations, show that there is a significant difference in the number of CD68+ cells between well- and poorly-differentiated HCC, and that the latter contains few of these cells. Similarly, the number of MC_T decreases significantly with tumor dedifferentiation. These results suggest that the decrease in inflammatory cells is closely related to the differentiation grade and tumor progression. In view of these results, it is reasonable to hypothesize that both cell types may have an inhibitory effect on HCC cell proliferation.

Moreover, the data of this study seem to suggest a correlation between both cell types and COX-2 expression and tumor angiogenesis, although COX-2 expression is the only independent variable that shows a significant positive correlation with CD34.

In conclusion, there is a relationship between COX-2 expression and the neovasculature of human HCC. Therefore, it is likely that COX-2 inhibition may block HCC-associated angiogenesis, thus providing a rationale for the use of selective COX-inhibitors in the treatment of this malignancy.

ACKNOWLEDGMENTS

We thank Dr. Lydia Giannitrapani, Nadia Lampiasi and Professor Vito Franco for their valuable discussion.

REFERENCES

- 1 **Cao Y**, Prescott SM. Many actions of cyclooxygenase-2 in cellular dynamics and in cancer. *J Cell Physiol* 2002; **190**: 279-286
- 2 **Joo YE**, Rew JS, Seo YH, Choi SK, Kim YJ, Park CS, Kim SJ. Cyclooxygenase-2 overexpression correlates with vascular endothelial growth factor expression and tumor angiogenesis in gastric cancer. *J Clin Gastroenterol* 2003; **37**: 28-33
- 3 **Chapple KS**, Scott N, Guillou PJ, Coletta PL, Hull MA. Interstitial cell cyclooxygenase-2 expression is associated with increased angiogenesis in human sporadic colorectal adenomas. *J Pathol* 2002; **198**: 435-441
- 4 **Davies G**, Salter J, Hills M, Martin LA, Sacks N, Dowsett M. Correlation between cyclooxygenase-2 expression and angiogenesis in human breast cancer. *Clin Cancer Res* 2003; **9**: 2651-2656
- 5 **Chu J**, Lloyd FL, Trifan OC, Knapp B, Rizzo MT. Potential involvement of the cyclooxygenase-2 pathway in the regulation of tumor-associated angiogenesis and growth in pancreatic cancer. *Mol Cancer Ther* 2003; **2**: 1-7
- 6 **Koga H**, Sakisaka S, Ohishi M, Kawaguchi T, Taniguchi E, Sasatomi K, Harada M, Kusaba T, Tanaka M, Kimura R, Nakashima Y, Nakashima O, Kojiro M, Kurohiji T, Sata M. Expression of cyclooxygenase-2 in human hepatocellular carcinoma: relevance to tumor dedifferentiation. *Hepatology* 1999; **29**: 688-689
- 7 **Kondo M**, Yamamoto H, Nagano H, Okami J, Ito Y, Shimizu J, Eguchi H, Miyamoto A, Dono K, Umeshita K, Matsuura N, Wakasa K, Nakamori S, Sakon M, Monden M. Increased expression of COX-2 in nontumor liver tissue is associated with shorter disease-free survival in patients with hepatocellular carcinoma. *Clin Cancer Res* 1999; **5**: 4005-4012
- 8 **Bae SH**, Jung ES, Park YM, Kim BS, Kim BK, Kim DG, Ryu WS. Expression of cyclooxygenase-2 (COX-2) in hepatocellular carcinoma and growth inhibition of hepatoma cell lines by a COX-2 inhibitor, NS-398. *Clin Cancer Res* 2001; **7**: 1410-1418
- 9 **Rahman MA**, Dhar DK, Yamaguchi E, Maruyama S, Sato T, Hayashi H, Ono T, Yamanoi A, Kohno H, Nagasue N. Coexpression of inducible nitric oxide synthase and COX-2 in hepatocellular carcinoma and surrounding liver: possible involvement of COX-2 in the angiogenesis of hepatitis C virus-positive cases. *Clin Cancer Res* 2001; **7**: 1325-1332
- 10 **Cheng AS**, Chan HL, To KF, Leung WK, Chan KK, Liew CT, Sung JJ. Cyclooxygenase-2 pathway correlates with vascular endothelial growth factor expression and tumor angiogenesis in hepatitis B virus-associated hepatocellular carcinoma. *Int J Oncol* 2004; **24**: 853-860
- 11 **Shimizu T**, Abe R, Nakamura H, Ohkawara A, Suzuki M, Nishihira J. High expression of macrophage migration inhibitory factor in human melanoma cells and its role in tumor cell growth and angiogenesis. *Biochem Biophys Res Commun* 1999; **264**: 751-758

- 12 **Leek RD**, Lewis CE, Whitehouse R, Greenall M, Clarke J, Harris AL. Association of macrophage infiltration with angiogenesis and prognosis in invasive breast carcinoma. *Cancer Res* 1996; **56**: 4625-4629
- 13 **Lissbrant IF**, Stattin P, Wikstrom P, Damber JE, Egevad L, Bergh A. Tumor associated macrophages in human prostate cancer: relation to clinicopathological variables and survival. *Int J Oncol* 2000; **17**: 445-451
- 14 **Takanami I**, Takeuchi K, Kodaira S. Tumor-associated macrophage infiltration in pulmonary adenocarcinoma: association with angiogenesis and poor prognosis. *Oncology* 1999; **57**: 138-142
- 15 **Nishie A**, Ono M, Shono T, Fukushi J, Otsubo M, Onoue H, Ito Y, Inamura T, Ikezaki K, Fukui M, Iwaki T, Kuwano M. Macrophage infiltration and heme oxygenase-1 expression correlate with angiogenesis in human gliomas. *Clin Cancer Res* 1999; **5**: 1107-1113
- 16 **Davidson B**, Goldberg I, Gotlieb WH, Lerner-Geva L, Ben-Baruch G, Agulansky L, Novikov I, Kopolovic J. Macrophage infiltration and angiogenesis in cervical squamous cell carcinoma - clinicopathologic correlation. *Acta Obstet Gynecol Scand* 1999; **78**: 240-244
- 17 **Ohta M**, Kitadai Y, Tanaka S, Yoshihara M, Yasui W, Mukaida N, Haruma K, Chayama K. Monocyte chemoattractant protein-1 expression correlates with macrophage infiltration and tumor vascularity in human esophageal squamous cell carcinomas. *Int J Cancer* 2002; **102**: 220-224
- 18 **Tanaka M**, Nakashima O, Wada Y, Kage M, Kojiro M. Pathomorphological study of Kupffer cells in hepatocellular carcinoma and hyperplastic nodular lesions in the liver. *Hepatology* 1996; **24**: 807-812
- 19 **Bortolami M**, Venturi C, Giacomelli L, Scalerta R, Bacchetti S, Marino F, Floreani A, Lise M, Naccarato R, Farinati F. Cytokine, infiltrating macrophage and T cell-mediated response to development of primary and secondary human liver cancer. *Dig Liver Dis* 2002; **34**: 794-801
- 20 **Ribatti D**, Vacca A, Nico B, Crivellato E, Roncali L, Dammacco F. The role of mast cells in tumour angiogenesis. *Br J Haematol* 2001; **115**: 514-521
- 21 **Norrby K**. Mast cells and angiogenesis. *APMIS* 2002; **110**: 355-371
- 22 **Hagmann W**, Hacker HJ, Buchholz U. Resident mast cells are the main initiators of anaphylactic leukotriene production in the liver. *Hepatology* 1992; **16**: 1477-1484
- 23 **Terada T**, Matsunaga Y. Increased mast cells in hepatocellular carcinoma and intrahepatic cholangiocarcinoma. *J Hepatol* 2000; **33**: 961-966
- 24 **Kuper H**, Adami HO, Trichopoulos D. Infections as a major preventable cause of human cancer. *J Int Med* 2000; **248**: 171-183
- 25 **Wahl LM**, Kleinman HK. Tumor-associated macrophages as targets for cancer therapy. *J Natl Cancer Inst* 1998; **90**: 1583-1584
- 26 **Sugihara S**, Nakashima O, Kojiro M, Majima Y, Tanaka M, Tanikawa K. The morphologic transition in hepatocellular carcinoma. A comparison of the individual histologic features disclosed by ultrasound-guided fine-needle biopsy with those of autopsy. *Cancer* 1992; **70**: 1488-1492
- 27 **Trifan OC**, Smith RM, Thompson BD, Hla T. Overexpression of cyclooxygenase-2 induces cell cycle arrest. Evidence for a prostaglandin-independent mechanism. *J Biol Chem* 1999; **274**: 34141-34147

Nitrative and oxidative DNA damage in intrahepatic cholangiocarcinoma patients in relation to tumor invasion

Somchai Pinlaor, Banchob Sripa, Ning Ma, Yusuke Hiraku, Puangrat Yongvanit, Sopit Wongkham, Chawalit Pairojkul, Vajarabhongsa Bhudhisawasdi, Shinji Oikawa, Mariko Murata, Reiji Semba, Shosuke Kawanishi

Somchai Pinlaor, Department of Parasitology, Faculty of Medicine, Khon Kaen University, Khon Kaen 40002, Thailand
Banchob Sripa, Chawalit Pairojkul, Department of Pathology, Faculty of Medicine, Khon Kaen University, Khon Kaen 40002, Thailand
Puangrat Yongvanit, Sopit Wongkham, Department of Biochemistry, Faculty of Medicine, Khon Kaen University, Khon Kaen 40002, Thailand

Vajarabhongsa Bhudhisawasdi, Department of Surgery, Faculty of Medicine, Khon Kaen University, Khon Kaen 40002, Thailand
Somchai Pinlaor, Banchob Sripa, Puangrat Yongvanit, Sopit Wongkham, Chawalit Pairojkul, Vajarabhongsa Bhudhisawasdi, Liver Fluke and Cholangiocarcinoma Research Center, Faculty of Medicine, Khon Kaen University, Khon Kaen 40002, Thailand
Ning Ma, Reiji Semba, Department of Anatomy, Mie University School of Medicine, Tsu, Mie 514-8507, Japan
Somchai Pinlaor, Yusuke Hiraku, Shinji Oikawa, Mariko Murata, Shosuke Kawanishi, Department of Environmental and Molecular Medicine, Mie University School of Medicine, Tsu, Mie 514-8507, Japan
Supported by the Khon Kaen University Research Fund in Thailand and Grants-in-Aid for Scientific Research from the Ministry of Education, Science, Sports and Culture of Japan

Correspondence to: Professor Shosuke Kawanishi, Department of Environmental and Molecular Medicine, Mie University School of Medicine, 2-174, Edobashi, Tsu, Mie 514-8507, Japan. kawanishi@doc.medic.mie-u.ac.jp
Telephone: +81-59-231-5011 Fax: +81-59-231-5011
Received: 2004-10-09 Accepted: 2004-12-01

HIF-1 α co-localized in cancerous tissues. Notably, the formation of 8-oxodG was correlated significantly with lymphatic invasion ($r = 0.386$ and $P = 0.018$). Moreover, 8-nitroguanine and 8-oxodG in non-cancerous tissues were associated significantly with neural invasion ($P = 0.042$ and $P = 0.026$, respectively). These results suggest that reciprocal activation between HIF-1 α and iNOS mediates persistent DNA damage, which induces tumor invasiveness via mutations, resulting in poor prognosis.

CONCLUSION: The formation of 8-nitroguanine and 8-oxodG plays an important role in multiple steps of genetic changes leading to tumor progression, including invasiveness.

© 2005 The WJG Press and Elsevier Inc. All rights reserved.

Key words: 8-Nitroguanine; 8-Oxo-7,8-dihydro-2'-deoxyguanosine; Hypoxia-inducible factor-1 α ; Cholangiocarcinoma; Tumor invasion

Pinlaor S, Sripa B, Ma N, Hiraku Y, Yongvanit P, Wongkham S, Pairojkul C, Bhudhisawasdi V, Oikawa S, Murata M, Semba R, Kawanishi S. Nitrative and oxidative DNA damage in intrahepatic cholangiocarcinoma patients in relation to tumor invasion. *World J Gastroenterol* 2005; 11(30): 4644-4649
<http://www.wjgnet.com/1007-9327/11/4644.asp>

Abstract

AIM: Nitrative and oxidative DNA damage such as 8-nitroguanine and 8-oxo-7,8-dihydro-2'-deoxyguanosine (8-oxodG) formation has been implicated in initiation and/or promotion of inflammation-mediated carcinogenesis. The aim of this study is to clarify whether these DNA lesions participate in the progression of intrahepatic cholangiocarcinoma.

METHODS: We investigated the relation of the formation of 8-nitroguanine and 8-oxodG and the expression of hypoxia-inducible factor-1 α (HIF-1 α) with tumor invasion in 37 patients with intra-hepatic cholangiocarcinoma.

RESULTS: Immunohistochemical analyses revealed that 8-nitroguanine and 8-oxodG formation occurred to a much greater extent in cancerous tissues than in non-cancerous tissues. HIF-1 α could be detected in cancerous tissues in all patients, suggesting low oxygen tension in the tumors. HIF-1 α expression was correlated with inducible nitric oxide synthase (iNOS) expression ($r = 0.369$ and $P = 0.025$) and 8-oxodG formation ($r = 0.398$ and $P = 0.015$). Double immunofluorescence study revealed that iNOS and

INTRODUCTION

Intra-hepatic cholangiocarcinoma (ICC), an adenocarcinoma originating from intra-hepatic bile duct epithelium, presents in most cases with an extremely poor prognosis^[1]. The highest proportional incidence of ICC is observed in the north-east region of Thailand, in which *Opisthorchis viverrini* (OV) infection is endemic^[2,3]. Thus, molecular markers serving as predictive factors are needed to provide effective therapy as well as to understand the underlying mechanisms of ICC carcinogenesis.

Infections are well accounted for association with several types of cancer including ICC through chronic inflammation^[4,5]. Production of a large amount of reactive oxygen species (ROS) and reactive nitrogen species (RNS), such as nitric oxide (NO), is associated with an increased risk of human cancer^[6-8]. 8-Oxo-7,8-dihydro-2'-deoxyguanosine (8-oxodG), a marker of DNA damage by ROS^[9], is a mutagenic lesion leading to G \rightarrow T transversions^[10,11], which are frequently found in tumor relevant genes in a variety of cancers. NO generation by inducible nitric oxide synthase (iNOS) is triggered

during infection and inflammation^[12]. Overproduction of NO leads to the generation of various RNS, causing nitrate DNA damage such as 8-nitroguanosine formation^[13]. 8-nitroguanine undergoes spontaneous depurination, which leads to apurinic sites in DNA^[13]. The resulting apurinic sites in DNA can also lead to G→T transversions^[14]. Recently, we have reported 8-nitroguanine formation in the liver of hamsters re-infected with OV^[15-17]. We have also demonstrated the accumulation of 8-nitroguanine in human gastric epithelium induced by *Helicobacter pylori* infection, which is associated with gastric cancer^[18]. Thus, we have proposed that 8-nitroguanine and 8-oxodG can be biomarkers of initiation and/or promotion in cases of carcinogenesis mediated by inflammation. However, the role of 8-nitroguanine and 8-oxodG in tumor progression in ICC has not been elucidated.

Tumor growth induces hypoxia, which is associated with poor prognosis^[19]. Tumor cells adapt to hypoxia by increasing the synthesis of hypoxia-inducible factor-1 α (HIF-1 α), which mediates transcription of various genes, including vascular endothelial growth factor, glucose transporter 1, lactate dehydrogenase and iNOS^[19], in solid tumors. It remains to be clarified whether HIF-1 α is associated with DNA base lesions and tumor invasion, resulting in poor prognosis with ICC patients.

To evaluate prognostic factors in ICC carcinogenesis, we investigated the formation of 8-nitroguanine and 8-oxodG, and the expression of iNOS and HIF-1 α in the liver of ICC patients by immunohistochemistry. We raised a highly specific antibody against 8-nitroguanine without cross reaction by immunizing with an 8-nitroguanine-aldehyde-rabbit serum albumin conjugate. We investigated the association of DNA damage in the liver tissue with neural and lymphatic invasion in ICC patients.

MATERIALS AND METHODS

Subjects

This study was approved by the Ethics Group of the Human Research Committee, Khon Kaen University, Thailand. Patients undergoing surgical resection of hepatogastrointestinal cancer in 1998 and 1999 at the Department of Surgery, Faculty of Medicine, Khon Kaen University, Thailand, were asked to volunteer for this study. Informed consent was obtained from each subject. Gross appearance of 37 surgical specimens was classified as periductal-infiltrating (11 patients) or mass-forming (26 patients) types. In addition, nine healthy individuals of accidental cause of death were used as controls.

Specimen collection and storage

ICC cases were clarified by physicians using clinical finding and laboratory investigation such as tumor markers, including α -fetoprotein, carcinoembryonic antigen and carbohydrate antigen 19-9, X-ray and histological examination. Liver tissues in both cancerous and adjacent non-cancerous region were obtained from the same patients in all cases. Sections were immediately frozen in liquid nitrogen and stored at -80 °C until analysis. The International Union against Cancer TNM classification and staging system were used for tumor assessment. Liver function test and complete blood count were performed

by the hospital laboratory using standard protocols.

Reagents

Highly sensitive and specific anti-8-nitroguanine rabbit polyclonal antibody was raised as described previously^[17]. Mouse monoclonal anti-8-oxodG antibody was purchased from Japan Institute for the Control of Aging (Fukuroi, Japan). Rabbit polyclonal anti-iNOS antibody and mouse monoclonal anti-HIF-1 α antibody were purchased from Calbiochem-Novabiochem Corporation (Darmstadt, Germany). Alexa 594-labeled antibody against rabbit IgG and Alexa 488-labeled antibody against mouse IgG were obtained from Molecular Probes Inc. (Eugene, OR, USA).

Immunohistological staining

Immunohistochemical staining was performed by using immunoperoxidase methods. Sections (thickness, 6 μ m) were deparaffinized in xylene and rehydrated in descending gradations of ethanol. To enhance the immunostaining, sections were placed in citrate buffer (pH 6) and microwaved intermittently for up to 10 min for antigen unmasking. Endogenous peroxidase was quenched by immersion in 30 mL/L hydrogen peroxide (H₂O₂) for 30 min, and then blocked with 10 mg/L skimmed milk for 30 min. These sections were treated with the primary antibodies (2 μ g/mL for 8-nitroguanine and 5 μ g/mL for 8-oxodG) overnight at room temperature. The slides were then washed, and incubated for 3 h with goat anti-rabbit IgG antibody, followed by the treatment with peroxidase-anti-peroxidase complex (1:200) for 1 h for detection of 8-nitroguanine. To detect 8-oxodG, the slides were treated with HRP-conjugated goat anti-mouse IgG antibody (1:200). The immunostaining were developed by using 3,3-diaminobenzidine tetrahydrochloride as a chromogen for 15 min.

The expression of iNOS and HIF-1 α was assessed by using double immunofluorescence technique as described previously^[18]. Briefly, the sections were treated with anti-iNOS antibody (1:300) and anti-HIF-1 α antibody (1:500) and then treated with Alexa 594-labeled antibody against rabbit IgG and Alexa 488-labeled antibody against mouse IgG (1:400 each). The results were analyzed by using a laser scanning microscope.

The following scores were assigned to each specimen according to the degree of staining: 0, negative; +, less than 25% (minimal); ++, 25-50% (moderate); and +++, more than 50% (strong) in the cells of tissue sections.

Histopathological study

Histopathological study was performed by hematoxylin and eosin staining in paraffin sections as described previously^[20]. Neural invasion and lymphatic invasion were assessed by standard method^[21].

Examination of specific IgG antibody against OV antigen and OV eggs

OV-specific IgG antibody was determined by ELISA technique^[22]. Crude somatic antigen of OV was prepared from hamsters infected with 100 metacercariae after 4 mo as described previously^[20]. The OV egg count was determined from 1 g of feces using the formalin-ethyl acetate concentration technique^[22].

Statistical analysis

Significant differences were analyzed by the χ^2 -test. Spearman's rank correlation coefficient served to analyze correlations for qualitative data, while Pearson's correlation coefficient was used for quantitative data. *P* values less than 0.05 were considered to be statistically significant.

RESULTS

Clinical data of ICC patients

ICC samples, comprising 37 matched cancerous and adjacent noncancerous tissues and 9 healthy subjects who died from accidental cases, were collected at the time of surgery. ICC patients included 26 men and 11 women with the mean age 53 ± 11 years. These subjects were verified by histopathological study and comprised of well (15 patients, including 2 patients of papillary), moderately (11 patients) and poorly (11 patients) differentiated adenocarcinoma. The gross appearance was periductal infiltrating (11 patients) and mass forming (26 patients). Tumor size was 3-6 cm (22 patients), 7-10 cm (4 patients) and >10 cm (4 patients). The average of hemoglobin and hematocrit of all patients was $11.7 \pm 2.3\%$ and $34.7 \pm 6.5\%$, respectively. Most of the patients (22 out of 37, 59.5%) had total bilirubin less than 1 mg% without jaundice, and other patients had total bilirubin of 1-10 mg% (5 patients) and >14 mg% (10 patients). Sixty percent was positive for OV antibody and 30% was positive for OV egg, without adult worm in the liver. All patients had no history of infection with hepatitis virus and exposure to aflatoxin.

Formation of 8-oxodG and 8-nitroguanine

Immunohistochemical staining demonstrated that 8-oxodG and 8-nitroguanine formation was observed in inflammatory cells within the liver to a greater extent in cancer patients than in healthy subjects. 8-oxodG and 8-nitroguanine were formed to a much greater extent in cancerous tissues than that in non-cancerous tissues. 8-oxodG formation was observed in tumor cells and inflammatory cells, whereas 8-nitroguanine was formed mainly in inflammatory cells and weakly in tumor cells in cancerous tissues (Figure 1). We have confirmed that the anti-8-nitroguanine antibody is highly sensitive and specific by a dot immunobinding assay and absorption test^[17].

Expression of HIF-1 α and iNOS

Double immunofluorescence staining revealed that HIF-1 α and iNOS expression could be detected in all cancerous tissues and was found to a greater extent than in non-cancerous tissues. Expression of HIF-1 α and iNOS was found in the tumor tissues especially bile duct epithelial cells (Figure 2). Slight immunoreactivity of iNOS was observed in inflammatory cells, especially Kupffer cells, in healthy subjects.

The correlation of 8-oxodG and 8-nitroguanine formation and iNOS expression with tumor invasion

Table 1 exhibits the relationship of DNA damage with lymphatic and neural invasion in ICC patients. Immunoreactivity for 8-oxodG and 8-nitroguanine was stronger in

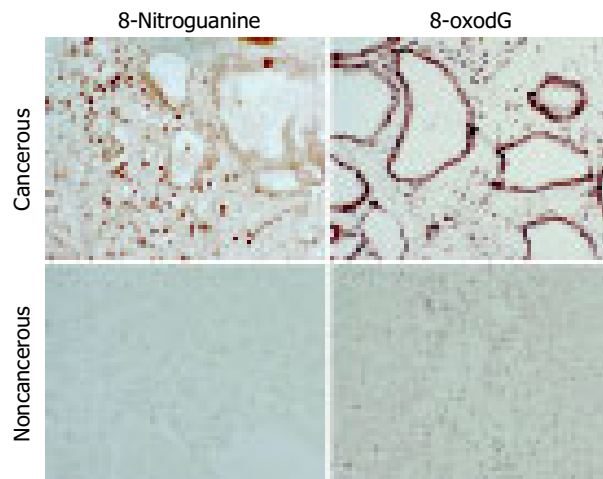


Figure 1 Localization of 8-oxodG and 8-nitroguanine in cancerous and noncancerous liver tissues in an ICC patient with a well-differentiated adenocarcinoma. Formation of 8-oxodG and 8-nitroguanine was assessed by immunohistochemistry using an immunoperoxidase method. Paraffin sections (6 μ m thickness) were incubated with a rabbit polyclonal anti-8-nitroguanine antibody and a mouse monoclonal anti-8-oxodG antibody. The original magnification is 200 \times .

cancerous tissues than in the adjacent non-cancerous tissues ($P < 0.05$). HIF-1 α could be detected in all cancerous tissues. HIF-1 α expression was correlated with iNOS expression ($r = 0.369$ and $P = 0.025$) and 8-oxodG formation ($r = 0.398$ and $P = 0.015$) in cancerous tissues. Furthermore, iNOS expression was significantly correlated with the formation of 8-oxodG ($r = 0.584$ and $P = 0.00015$) and 8-nitroguanine ($r = 0.328$ and $P = 0.047$). 8-oxodG formation in cancerous tissues was also significantly correlated with increased lymphatic invasion ($r = 0.386$, $P = 0.018$). The formation of 8-nitroguanine and 8-oxodG in non-cancerous tissues was significantly associated with neural invasion ($P = 0.042$ and $P = 0.026$, respectively). Neural invasion was associated with poor survival by generalized Wilcoxon test ($P = 0.021$) using the Kaplan-Meier method (Figure 3). In addition, in cancerous tissues, formation of 8-oxodG and 8-nitroguanine was positively correlated with serum ALT, AST and alkaline phosphatase (ALP) ($r = 0.76$, 0.58 , and 0.96 for 8-oxodG and $r = 0.63$, 0.58 , and 0.86 for 8-nitroguanine, respectively). Moreover, iNOS expression was also associated with ALT, AST, ALP ($r = 0.71$, 0.97 and 0.82 , respectively).

DISCUSSION

Our results showed that both 8-nitroguanine and 8-oxodG were formed in cancerous tissues to a much greater extent than the adjacent non-cancerous tissues. Moreover, the formation of these DNA lesions was correlated with neural and lymphatic invasion. 8-oxodG was formed in tumor cells and inflammatory cells, whereas 8-nitroguanine was observed mainly in inflammatory cells and weakly in tumor cells. These results are consistent with a model in which tumor cells encourage inflammatory cell infiltration in cancerous areas; inflammatory cells then induce 8-nitroguanine and 8-oxodG formation via NO and superoxide anion radical production^[23].

The present study revealed that 8-nitroguanine and 8-oxodG formation was related with serum ALT, AST, and

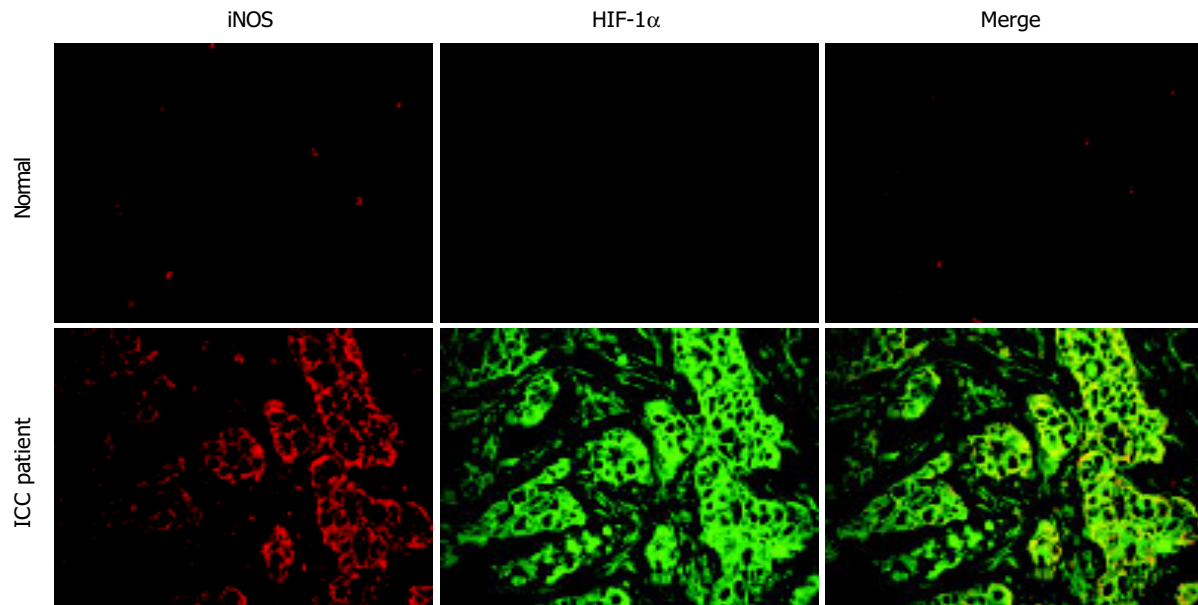


Figure 2 Localization of iNOS and HIF-1 α in cancerous liver tissues in an ICC patient with poorly-differentiated adenocarcinoma. The expression of iNOS and HIF-1 α was assessed by using double immunofluorescence technique. Paraffin

sections were treated with anti-iNOS and anti-HIF-1 α antibodies. The original magnification is 400 \times .

ALP activity. This result is supported by the report showing that the number of 8-oxodG-positive hepatocytes was correlated with ALT and AST in liver diseases^[24]. These findings can be explained by assuming that increase in NO and ROS not only causes DNA damage, but also induces epithelial bile duct and hepatocyte injury, resulting in an increase in hepatobiliary enzyme activities.

Our results showed that HIF-1 α was associated with iNOS expression and 8-oxodG formation in cancerous tissues. This result is confirmed by immunohistochemistry showing that iNOS and HIF-1 α co-localized in cancerous tissues. HIF-1 α could be detected in all cancerous tissues, suggesting low oxygen consumption in tumor tissues. Tumor cells adapt to hypoxia by increasing the synthesis of HIF-1 α ,

which mediates transcription of various genes, including iNOS^[19]. iNOS expression was correlated with both 8-nitroguanine and 8-oxodG formation. Therefore, we hypothesize that tumor hypoxia induces HIF-1 α expression, and then HIF-1 α mediates iNOS expression, resulting in nitrative and oxidative DNA damage. On the other hand, an increase in NO production through iNOS expression not only causes DNA damage^[25] but also induces the accumulation and activation of HIF-1 α ^[26,27]. Therefore, these findings lead to an idea that reciprocal activation between HIF-1 α and iNOS mediates persistent DNA damage. Hypoxia in tumor cells increases the generation of mitochondrial H₂O₂ at complex III^[28], which may lead to 8-oxodG formation. Interestingly, we found that 8-oxodG formation in cancerous

Table I Relationship of DNA damage with lymphatic and neural invasion in ICC patients

Immuno-histological grading	8-oxodG Number of patients (%)		8-Nitroguanine Number of patients (%)		HIF-1 α Number of patients (%)	Number (%) of patients with lymphatic invasion (8-oxodG)	Number (%) of patients with lymphatic invasion (8-nitroguanine)	Number (%) of patients with neural invasion (8-oxodG)	Number (%) of patients with neural invasion (8-nitroguanine)
	Cancerous	Non-cancer	Cancerous	Non-cancer					
ICC (37)									
0	-	5 (13.51)	11 (29.73)	17 (45.95)	-	-	9/11 (81.82)	1/5 (20)	8/17 (47.1)
+	11 (29.73)	17 (45.94)	13 (35.14)	19 (51.35)	10 (27.03)	6/11 (54.55)	10/13 (76.92)	14/17 (82.4)	16/19 (84.2)
++	11 (29.73)	10 (27.03)	8 (21.62)	1 (2.70)	18 (48.65)	10/11 (90.91)	6/8 (75)	5/10 (50)	0/1 (0)
+++	15 (40.54)	5 (13.51)	5 (13.51)	-	9 (24.32)	14/15 (93.33)	5/5 (100)	4/5 (80)	
P-value	P = 0.004		P = 0.007			P = 0.018	P = 0.679	P = 0.042	P = 0.026
Healthy (9)									
0		2 (22.22)		7 (77.77)					
+		7 (77.77)		2 (22.22)					

Non-cancer = noncancerous tissues. 0 = no positive cell, + = positive in few areas or cells, ++ = moderately positive and +++ = predominately positive. ICC samples, comprising 37 matched cancerous and adjacent noncancerous tissues and 9 healthy subjects who died from accidental cases were collected at the time of surgery. ICC patients included 26 men and 11 women with the mean age 53 \pm 11 years. These subjects were verified by histopathological study and comprised well- (15 patients, including 2 patients of papillary), moderately- (11 patients) and poorly (11 patients) differentiated adenocarcinoma. The International Union Against Cancer TNM classification and staging system were used for tumor assessment.

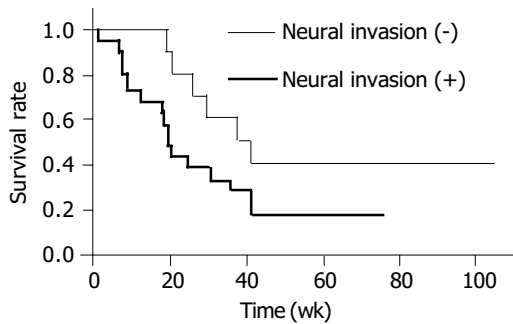


Figure 3 Overall survival curve of ICC patients. *Thin line*, neural invasion evaluated as -; *thick line*, neural invasion evaluated as + (Kaplan-Meier method).

tissues was significantly correlated with lymphatic invasion. In addition, the formation of 8-nitroguanine and 8-oxodG in non-cancerous tissues was significantly associated with neural invasion. These results suggest that DNA damage participates in tumor invasion and/or poor survival. The accumulation of DNA base lesions may contribute to genetic instability and mutations, leading to tumor progression^[14,29]. Recent data have expanded the concept that inflammation is a critical component of tumor progression^[4]. It has been reported that iNOS expression is associated with poor survival in cancer patients^[30,31]. Tumor-derived NO promoted tumor growth and metastasis by enhancing invasive, angiogenic and migratory capacities of tumor cells^[32-34]. Our findings raise the idea that NO-mediated DNA damage plays the key role in tumor progression and poor survival. Together, HIF-1 α may contribute to tumor progression^[35] and subsequent poor prognosis^[36] via a nitrative and oxidative DNA damage-dependent mechanism. Therefore, our results and these reports lead to an idea that tumor hypoxia mediates HIF-1 α expression, followed by iNOS expression, and nitrative and oxidative DNA damage, which induces tumor invasiveness via mutations. Tumor growth facilitates tumor hypoxia and subsequent expression of HIF-1 α and iNOS to cause DNA damage in addition to DNA damage mediated by inflammatory cells, resulting in tumor development. Tumor tissues may undergo development through repetition of this process, resulting in invasion and metastasis, leading to poor prognosis.

The combination of previous data with the results of this study, proposes a model in which 8-nitroguanine and 8-oxodG induced by inflammation and hypoxia may participate in tumor invasion, functioning in combination with DNA damage-independent mechanisms, including NO-mediated promotion of migratory, invasive and angiogenic properties^[37]. We previously reported that OV infection induced the formation of 8-oxodG and 8-nitroguanine through chronic inflammation at the initiation and/or promotion step of carcinogenesis^[16]. In addition, we hypothesize that 8-nitroguanine and 8-oxodG may also contribute to progression of carcinogenesis mediated by chronic OV infection. In this study, we demonstrated earlier that 8-nitroguanine was formed by cancerous tissues in humans, and this observation strongly supports our hypothesis. In conclusion, the formation of 8-nitroguanine and 8-oxodG is mediated by reactive

species generated endogenously in the process of tumor hypoxia. These DNA lesions could contribute to multiple steps of carcinogenesis, leading to tumor progression, including invasiveness.

ACKNOWLEDGMENTS

The author also thanks all members of the Liver Fluke and Cholangiocarcinoma Research Centers' staff at the Faculty of Medicine, Khon Kaen University, Khon Kaen, Thailand, for their kind help in the collection of samples.

REFERENCES

- Gores GJ. Cholangiocarcinoma: current concepts and insights. *Hepatology* 2003; **37**: 961-969
- IARC Working Group. Infection with liver flukes (*Opisthorchis viverrini*, *Opisthorchis felineus* and *Clonorchis sinensis*) In: IARC Monographs on the Evaluation of Carcinogenic Risks to Humans vol. 61. Lyon IARC Press 1994: 121-175
- Sripa B. Pathobiology of opisthorchiasis: an update. *Acta Trop* 2003; **88**: 209-220
- Coussens LM, Werb Z. Inflammation and cancer. *Nature* 2002; **420**: 860-867
- Hussain SP, Hofseth LJ, Harris CC. Radical causes of cancer. *Nat Rev Cancer* 2003; **3**: 276-285
- Wiseman H, Halliwell B. Damage to DNA by reactive oxygen and nitrogen species: role in inflammatory disease and progression to cancer. *Biochem J* 1996; **313**(Pt 1): 17-29
- Hofseth LJ, Hussain SP, Wogan GN, Harris CC. Nitric oxide in cancer and chemoprevention. *Free Radic Biol Med* 2003; **34**: 955-968
- Dedon PC, Tannenbaum SR. Reactive nitrogen species in the chemical biology of inflammation. *Arch Biochem Biophys* 2004; **423**: 12-22
- Kasai H, Crain PF, Kuchino Y, Nishimura S, Ootsuyama A, Tanooka H. Formation of 8-hydroxyguanine moiety in cellular DNA by agents producing oxygen radicals and evidence for its repair. *Carcinogenesis* 1986; **7**: 1849-1851
- Shibutani S, Takeshita M, Grollman AP. Insertion of specific bases during DNA synthesis past the oxidation-damaged base 8-oxodG. *Nature* 1991; **349**: 431-434
- Bruner SD, Norman DP, Verdine GL. Structural basis for recognition and repair of the endogenous mutagen 8-oxoguanine in DNA. *Nature* 2000; **403**: 859-866
- Ohshima H, Tatemichi M, Sawa T. Chemical basis of inflammation-induced carcinogenesis. *Arch Biochem Biophys* 2003; **417**: 3-11
- Yermilov V, Rubio J, Ohshima H. Formation of 8-nitroguanine in DNA treated with peroxyntirite *in vitro* and its rapid removal from DNA by depurination. *FEBS Lett* 1995; **376**: 207-210
- Loeb LA, Loeb KR, Anderson JP. Multiple mutations and cancer. *Proc Natl Acad Sci USA* 2003; **100**: 776-781
- Pinlaor S, Yongvanit P, Hiraku Y, Ma N, Semba R, Oikawa S, Murata M, Sripa B, Sithithaworn P, Kawanishi S. 8-Nitroguanine formation in the liver of hamsters infected with *Opisthorchis viverrini*. *Biochem Biophys Res Commun* 2003; **309**: 567-571
- Pinlaor S, Ma N, Hiraku Y, Yongvanit P, Semba R, Oikawa S, Murata M, Sripa B, Sithithaworn P, Kawanishi S. Repeated infection with *Opisthorchis viverrini* induces accumulation of 8-nitroguanine and 8-oxo-7, 8-dihydro-2'-deoxyguanine in the bile duct of hamsters via inducible nitric oxide synthase. *Carcinogenesis* 2004; **25**: 1535-1542
- Pinlaor S, Hiraku Y, Ma N, Yongvanit P, Semba R, Oikawa S, Murata M, Sripa B, Sithithaworn P, Kawanishi S. Mechanism of NO-mediated oxidative and nitrative DNA damage in hamsters infected with *Opisthorchis viverrini*: A model of inflammation-mediated carcinogenesis. *Nitric Oxide* 2004; **11**: 175-183
- Ma N, Adachi Y, Hiraku Y, Horiki N, Horiike S, Imoto I, Pinlaor S, Murata M, Semba R, Kawanishi S. Accumulation

- of 8-nitroguanine in human gastric epithelium induced by *Helicobacter pylori* infection. *Biochem Biophys Res Commun* 2004; **319**: 506-510
- 19 **Harris AL**. Hypoxia-a key regulatory factor in tumour growth. *Nat Rev Cancer* 2002; **2**: 38-47
 - 20 **Sripa B**, Kaewkes S. Localisation of parasite antigens and inflammatory responses in experimental opisthorchiasis. *Int J Parasitol* 2000; **30**: 735-740
 - 21 **Nakanuma Y**, Harada K, Ishikawa A, Zen Y, Sasaki M. Anatomic and molecular pathology of intrahepatic cholangiocarcinoma. *J Hepatobiliary Pancreat Surg* 2003; **10**: 265-281
 - 22 **Elkins DB**, Sithithaworn P, Haswell-Elkins M, Kaewkes S, Awacharagan P, Wongratanacheewin S. *Opisthorchis viverrini*: relationships between egg counts, worms recovered and antibody levels within an endemic community in northeast Thailand. *Parasitology* 1991; **102**(Pt 2): 283-288
 - 23 **Chazotte-Aubert L**, Oikawa S, Gilibert I, Bianchini F, Kawanishi S, Ohshima H. Cytotoxicity and site-specific DNA damage induced by nitroxyl anion (NO⁻) in the presence of hydrogen peroxide. Implications for various pathophysiological conditions. *J Biol Chem* 1999; **274**: 20909-20915
 - 24 **Ichiba M**, Maeta Y, Mukoyama T, Saeki T, Yasui S, Kanbe T, Okano J, Tanabe Y, Hirooka Y, Yamada S, Kurimasa A, Murawaki Y, Shiota G. Expression of 8-hydroxy-2'-deoxyguanosine in chronic liver disease and hepatocellular carcinoma. *Liver Int* 2003; **23**: 338-345
 - 25 **Jadeski LC**, Chakraborty C, Lala PK. Role of nitric oxide in tumour progression with special reference to a murine breast cancer model. *Can J Physiol Pharmacol* 2002; **80**: 125-135
 - 26 **Mateo J**, Garcia-Lecea M, Cadenas S, Hernandez C, Moncada S. Regulation of hypoxia-inducible factor-1 α by nitric oxide through mitochondria-dependent and -independent pathways. *Biochem J* 2003; **376**: 537-544
 - 27 **Thomas DD**, Espey MG, Ridnour LA, Hofseth LJ, Mancardi D, Harris CC, Wink DA. Hypoxic inducible factor 1 α , extracellular signal-regulated kinase, and p53 are regulated by distinct threshold concentrations of nitric oxide. *Proc Natl Acad Sci USA* 2004; **101**: 8894-8899
 - 28 **Chandel NS**, McClintock DS, Feliciano CE, Wood TM, Melendez JA, Rodriguez AM, Schumacker PT. Reactive oxygen species generated at mitochondrial complex III stabilize hypoxia-inducible factor-1 α during hypoxia: a mechanism of O₂ sensing. *J Biol Chem* 2000; **275**: 25130-25138
 - 29 **Olinski R**, Gackowski D, Rozalski R, Foksinski M, Bialkowski K. Oxidative DNA damage in cancer patients: a cause or a consequence of the disease development? *Mutat Res* 2003; **531**: 177-190
 - 30 **Ekmekcioglu S**, Ellerhorst J, Smid CM, Prieto VG, Munsell M, Buzaid AC, Grimm EA. Inducible nitric oxide synthase and nitrotyrosine in human metastatic melanoma tumors correlate with poor survival. *Clin Cancer Res* 2000; **6**: 4768-4775
 - 31 **Aaltoma SH**, Lipponen PK, Kosma VM. Inducible nitric oxide synthase (iNOS) expression and its prognostic value in prostate cancer. *Anticancer Res* 2001; **21**: 3101-3106
 - 32 **Jadeski LC**, Chakraborty C, Lala PK. Nitric oxide-mediated promotion of mammary tumour cell migration requires sequential activation of nitric oxide synthase, guanylate cyclase and mitogen-activated protein kinase. *Int J Cancer* 2003; **106**: 496-504
 - 33 **Lala PK**, Orucevic A. Role of nitric oxide in tumor progression: lessons from experimental tumors. *Cancer Metastasis Rev* 1998; **17**: 91-106
 - 34 **Siegert A**, Rosenberg C, Schmitt WD, Denkert C, Hauptmann S. Nitric oxide of human colorectal adenocarcinoma cell lines promotes tumour cell invasion. *Br J Cancer* 2002; **86**: 1310-1315
 - 35 **Semenza GL**. Hypoxia, clonal selection, and the role of HIF-1 in tumor progression. *Crit Rev Biochem Mol Biol* 2000; **35**: 71-103
 - 36 **Koukourakis MI**, Giatromanolaki A, Brekken RA, Sivridis E, Gatter KC, Harris AL, Sage EH. Enhanced expression of SPARC/osteonectin in the tumor-associated stroma of non-small cell lung cancer is correlated with markers of hypoxia/acidity and with poor prognosis of patients. *Cancer Res* 2003; **63**: 5376-5380
 - 37 **Lala PK**, Chakraborty C. Role of nitric oxide in carcinogenesis and tumour progression. *Lancet Oncol* 2001; **2**: 149-156

Functional expression of a proliferation-related ligand in hepatocellular carcinoma and its implications for neovascularization

Hiroshi Okano, Katsuya Shiraki, Yutaka Yamanaka, Hidekazu Inoue, Tomoyuki Kawakita, Yukiko Saitou, Yumi Yamaguchi, Naoyuki Enokimura, Keiichi Ito, Norihiko Yamamoto, Kazushi Sugimoto, Kazumoto Murata, Takeshi Nakano

Hiroshi Okano, Katsuya Shiraki, Yutaka Yamanaka, Hidekazu Inoue, Tomoyuki Kawakita, Yukiko Saitou, Yumi Yamaguchi, Naoyuki Enokimura, Keiichi Ito, Norihiko Yamamoto, Kazushi Sugimoto, Kazumoto Murata, Takeshi Nakano, First Department of Internal Medicine, Mie University School of Medicine, Tsu 514-8507, Japan

Correspondence to: Katsuya Shiraki, MD, PhD, First Department of Internal Medicine, Mie University School of Medicine, 2-174 Edobashi, Tsu, Mie 514-8507, Japan. katsuyas@clin.medic.mie-u.ac.jp
Telephone: +81-592-31-5015 Fax: +81-592-31-5201
Received: 2004-08-30 Accepted: 2004-10-07

Abstract

AIM: To detect the expression of a proliferation-related ligand on human hepatocellular carcinoma (HCC) cell lines (SK-Hep1, HLE and HepG2) and in culture medium.

METHODS: APRIL expression was analyzed by Western blotting in HCC cell lines. Effects of APRIL to cell count and angiogenesis were analyzed, too.

RESULTS: Recombinant human APRIL (rhAPRIL) increased cell viability of HepG2 cells and, in HUVEC, rhAPRIL provided slight tolerance to cell death from serum starvation. Soluble APRIL (sAPRIL) from HLE cells increased after serum starvation, but did not change in SK-Hep1 or HepG2 cells. These cells showed down-regulation of VEGF after incubation with anti-APRIL antibody. Furthermore, culture medium from the HCC cells treated with anti-APRIL antibody treatment inhibited tube formation of HUVECs.

CONCLUSION: Functional expression of APRIL might contribute to neovascularization via an upregulation of VEGF in HCC.

© 2005 The WJG Press and Elsevier Inc. All rights reserved.

Key words: A proliferation-inducing ligand; HCC; VEGF; Cell proliferation; Neovascularization

Okano H, Shiraki K, Yamanaka Y, Inoue H, Kawakita T, Saitou Y, Yamaguchi Y, Enokimura N, Ito K, Yamamoto N, Sugimoto K, Murata K, Nakano T. Functional expression of a proliferation-related ligand in hepatocellular carcinoma and its implications for neovascularization. *World J Gastroenterol* 2005; 11(30): 4650-4654

<http://www.wjgnet.com/1007-9327/11/4650.asp>

INTRODUCTION

Cytokines regulate cellular proliferation and differentiation by binding to their specific receptors on target cells^[1]. Tumor necrosis factor (TNF) is the prototypic member of a family of cytokines playing an important role in immune regulation and cancer^[2,3].

A proliferation-inducing ligand (APRIL), a new member of the TNF family, is reported to stimulate tumor cell growth^[4-6], modulate tumor cell apoptosis^[7-9], or activate nuclear factor-kappa B (NF- κ B)^[10,11]. APRIL also is associated with regulation of humoral immunity^[6,12]. APRIL is a type II membrane protein, which is typical of the TNF ligand family member^[4]. The sequence of the extracellular domain of APRIL shows homology with FasL, TNF α , LT β , TRAIL, TWEAK, and TRANCE^[4]. In particular, APRIL shares significant homology with B-lymphocyte stimulator (BLys)^[13]. Though the TNF ligand family is synthesized into membrane-bound proteins, of which several are cleaved into a soluble form, APRIL is processed intracellularly and secreted from the cell surface^[14].

The expression of APRIL mRNA or protein has been detected in many tumor cells and tissues^[4,5,7], but is almost undetectable in normal tissues^[5]. Hence, APRIL may provide a significant growth advantage to malignant cells. Because soluble APRIL can stimulate tumor cell growth^[1], APRIL may provide its signal in an autocrine and/or paracrine mode^[5].

APRIL binds to two TNF receptor families, transmembrane activator and CAML interactor (TACI) and B cell maturation antigen (BCMA) with relatively high affinity^[6,10,15]. It is clear that TACI and BCMA intracellular signaling is similar to that of other TNF receptor homologs without a death domain^[16,17]. However, the signaling transduction pathway triggered by APRIL that prolongs lymphocyte survival is still not characterized^[18]. A soluble form of BCMA inhibits APRIL activity and decreases tumor cell proliferation^[19]. NZB/WF1 mice, which develop chronic autoimmune disease, can inhibit development of proteinuria and prolongation of survival after being treated with soluble TACI-Ig fusion protein treatment^[20]. These observations imply the importance of APRIL via these receptors with tumor cell or lymphocyte survival. However, in Jurkat cells, APRIL induces cell death and binds to other TNF family receptors^[7]. An additional APRIL-specific receptor expressed on cell surfaces other than TACI or BCMA, is implied adenocarcinoma or fibroblast tumor cells lacking any detectable BCMA or TACI expression even though

these cells respond to growth stimulatory effects of APRIL^[5,19]. However, the function of APRIL in tumor cells is not well elucidated.

Therefore, we investigated the function of APRIL in HCC cell lines and human umbilical vein endothelial cells (HUVEC). We further investigated the expression of APRIL in HCC cells and evaluated the effects of APRIL on neovascularization.

MATERIALS AND METHODS

Cell lines and reagents

Human umbilical vein endothelial cells (HUVECs), and human HCC cell lines, HepG2 and SK-Hep1 cells were purchased from American Type Culture Collection (Rockville, MD, USA). Human HCC cell line, HLE was purchased from the Health Science Research Resource Bank (Osaka, Japan). HCC cell lines were cultured in Dulbecco's modified Eagle's medium (Dainippon Pharmaceutical Co., Ltd., Osaka, Japan) at 37 °C. All media were supplemented with 1% penicillin/streptomycin (GIBCO BRL, Grand Island, NY, USA) and 10% heat-inactivated fetal calf serum (GIBCO BRL). HUVECs were cultured in HuMedia-EG2 (KURABO, Osaka, Japan). Recombinant human APRIL (rhAPRIL) was purchased from ALEXIS Biochemicals (Switzerland). Anti-APRIL polyclonal antibody was purchased from Ψ ProSci Incorporated (Poway, CA, USA). Anti-vascular endothelial growth factor (VEGF) mAb and anti- α -tubulin mAb were purchased from Oncogene Research Products (Boston, MA, USA). Normal rabbit IgG was purchased from Santa Cruz Biotechnology, Inc. (Santa Cruz, CA, USA). Recombinant human VEGF (rhVEGF) was purchased from Peprotech EC Ltd. (London, UK).

Assessment of count of HCC cells and HUVECs

To assess the viability of HCC cells and HUVECs, the 3-(4,5-dimethylthiazol-2-yl)-2,5-diphenyl tetrazolium bromide (MTT) assay was performed. The cells were plated at a density of 5×10^3 cells/well in 96-well microtiter plates (Corning Glass Works, Corning, NY, USA) and each plate was incubated for 24 h at 37 °C in 50 mL/L CO₂. Reagents were added and the plates were incubated for the indicated time. The live-cell count was determined using a Cell Titer 96 assay kit (Promega, Madison, WI, USA) according to the manufacturer's instructions. The absorbance of each well was measured at 570 nm with a microtiter plate reader (Bio-Rad Laboratories, Hercules, CA, USA).

Western blotting

Expression of APRIL was analyzed by Western blotting. HCC cells were harvested and lysed in lysis buffer (50 mmol/L Tris-HCl, pH 8, 150 mmol/L NaCl, 5 mmol/L EDTA, 1% NP-40, 1 mmol/L phenylmethyl-sulfonyl fluoride) on ice. Protein content was measured using a Bio-Rad protein assay kit (Bio-Rad Laboratories). Equal amounts of protein from each extract were separated by 14% sodium dodecyl sulfate-polyacrylamide gel electrophoresis (SDS-PAGE) and transferred onto nitrocellulose membranes (Toyo Roshi, Tokyo, Japan). Blots were blocked by incubation in 5% non-fat dried milk in Tris buffered saline (TBS)

overnight at 4 °C and probed for 2 h at room temperature with primary antibody. The immunoblots were then probed with horseradish peroxidase-conjugated immunoglobulin (Ig) G (1:2 000 diluted with 5% non-fat dried milk in Tris-HCl; pH 7.5 and 0.05% Tween 20). Signal was detected with an ECL kit (Amersham Pharmacia Biotech, Buckinghamshire, UK).

Angiogenesis assay

Matrigel (BD Biosciences, MA) was placed in an 8-well Lab-tek II chamber slide (NUNC™ Brand Products, Denmark) (100 μ L/well) and allowed to set at 37 °C for 30 min. HUVECs were added to each well (4×10^4) and incubated in the culture medium of HCC cells with rabbit IgG or anti-APRIL polyclonal antibody at 37 \times for 6 h in a 50 mL/L CO₂ atmosphere. Tube formation was observed by microscopy (OLYMPUS, Tokyo, Japan).

RESULTS

APRIL expressions in human HCC cell lines

APRIL expression in 3 human HCC cell lines (SK-Hep1, HLE, HepG2) was investigated. Bands corresponding to the expression in 42 ku unprocessed form of APRIL were observed in all human HCC cell lines (Figure 1). SK-Hep1 or HepG2 cells, were similar, but weaker in HLE cells. In addition to the unprocessed form, a lower molecular weight form (17 ku) was observed in HCC cell lysates and supernatants (Figure 1). This was thought to be a soluble form of APRIL. The soluble form of APRIL was observed in the three HCC cell lysates and supernatants. The soluble form of APRIL was most strongly expressed in supernatant from SK-Hep1 cells.

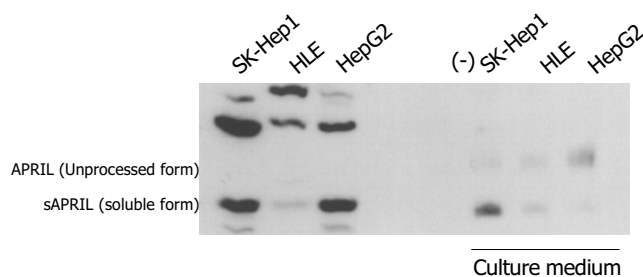


Figure 1 APRIL expression in human HCC cell lines and their supernatants by Western blotting. Closed arrowhead indicates the expression of unprocessed form of APRIL (42 ku) and open arrowhead indicates the soluble form of APRIL (17 ku).

Effect of recombinant human APRIL (rhAPRIL) in human HCC cell lines and HUVECs

We analyzed the effect of rhAPRIL on proliferation of human HCC cells. After 72-h incubation, the HCC cell counts slightly increased at the concentrations of 1, 10, or 100 ng/mL (Figure 2A), the greatest effects were observed at concentration of 1 ng/mL in HepG2 cells.

Since HCC is generally a hypervascular tumor^[21] and gains its hypervascularity during dedifferentiation and progression^[22], we investigated the effect of rhAPRIL stimulation on the proliferation of HUVECs.

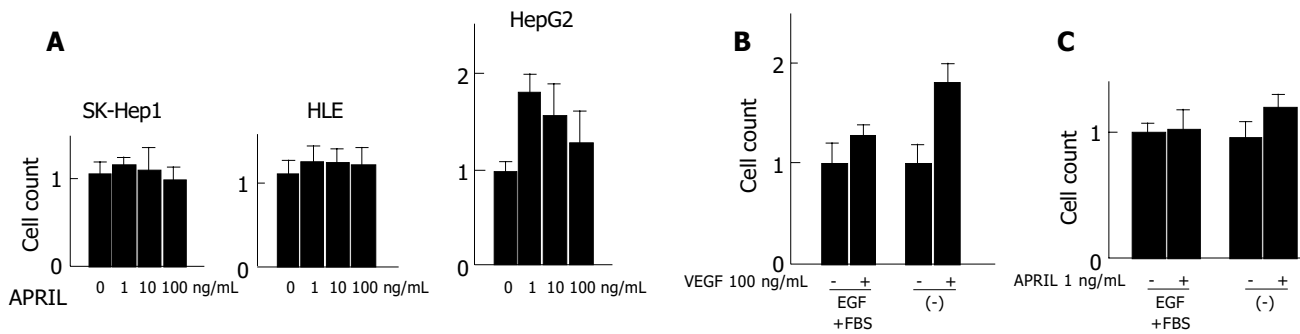


Figure 2 Effects of rhAPRIL stimulation on viability of human HCC cells (A) and

HUVECs (B and C) incubated at different time periods.

An increase in proliferation at the concentration of 100 ng/mL rhVEGF was observed in the presence or absence of FBS and EGF (Figure 2B). In particular, rhVEGF effectively inhibited cell death induced by cell starvation. The cell viability of HUVECs slightly increased with the stimulation of 1 ng/mL rhAPRIL and the same concentration of rhAPRIL inhibited cell death with starvation (Figure 2C). From these results, we confirmed that APRIL could induce cell proliferation and cell death inhibition in HCC cells and HUVECs, but we also observed that the effect of APRIL on HCC cell lines was not so potent.

APRIL could mediate regulation of cell growth, induce XIAP expression and decrease caspase activity^[23]. We examined the expression of apoptosis-related proteins, including FLICE/caspase-8 inhibitory protein (FLIP), X-chromosome-linked inhibitor of apoptosis (XIAP), BclL, Apaf-1, and smac in HCC cell lines and HUVECs after APRIL stimulation. However, these apoptosis-related proteins did not show changes in expression levels after APRIL stimulation (data not shown).

Regulation of APRIL in human HCC cell lines

We examined the expression of APRIL after serum starvation in HCC cells and HUVECs (Figure 3). Serum starvation increased the expression of both the unprocessed and soluble forms of APRIL in HLE. In SK-Hep1 and HepG2 cells, serum starvation did not induce upregulation of APRIL, however its expression was maintained. sAPRIL eventually disappeared after 24 h of serum starvation in SK-Hep1 cells, whereas HepG2 cells maintained sAPRIL expression.

APRIL was associated with VEGF expression in HCC cell lines

We observed APRIL expression and regulation by serum starvation in human HCC cell lines. In particular, the serum starvation induced APRIL expression in HLE cells. VEGF might be associated with angiogenesis or tumor progression^[24-31] and VEGF expression could be induced by stress, for example hypoxia or ischemia, in HCC cells^[24,25,28,29]. All HCC cell lines showed expression of VEGF with serum starvation, although the modulation of VEGF expression differed among three cell lines (Figure 4A). In SK-Hep1 and HepG2 cells, VEGF expression was stable for 12 h. In contrast, VEGF expression in HLE cells was not observed until 48 h and was less than that in SK-Hep1 or HepG2 cells.

Because APRIL was expressed constitutively in SK-Hep1 and HepG2 and upregulated in HLE cells after starvation,

we considered that APRIL might be associated with VEGF expression in HCC cells. So, we used anti-APRIL antibody to bind to sAPRIL in culture medium and to inhibit APRIL effects mediated by an autocrine or paracrine system. As shown in Figure 4B, blockade of APRIL by anti-APRIL antibody induced downregulation of VEGF expression in SK-Hep1 and HepG2 cells, compared to controls with normal IgG.

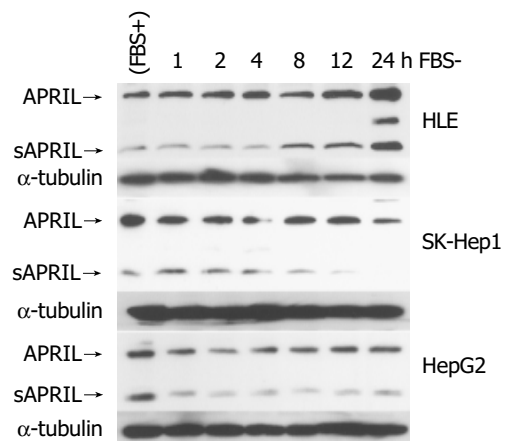


Figure 3 Regulation of APRIL expression in HCC cells. Closed arrowhead indicates the expression of unprocessed form of APRIL. Open arrowhead indicates soluble form of APRIL.

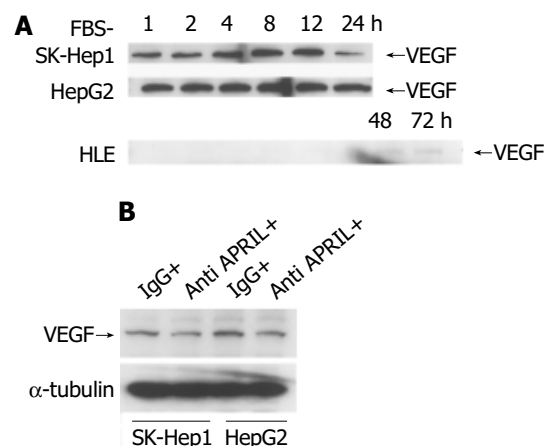


Figure 4 Regulation of VEGF expression with starvation in HCC cells incubated with FBS-negative culture (A) and 10 μg/mL anti-APRIL polyclonal antibody or normal rabbit IgG (B).

Finally, we observed that culture medium from the HCC cells incubated with anti-APRIL polyclonal antibody inhibited endothelial cell tube formation in matrigel (Figure 5).

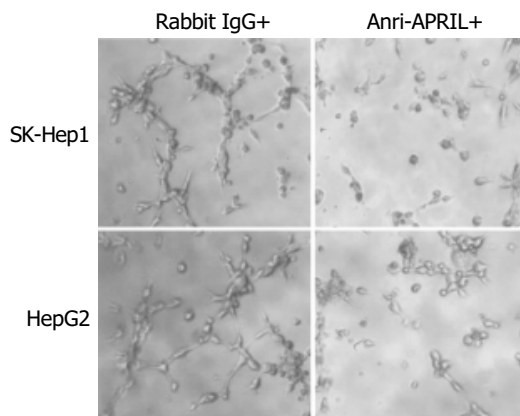


Figure 5 Effect of APRIL on *in vitro* endothelial cell tube formation.

DISCUSSION

Though HCC is the most common primary cancer of the liver and preceded by chronic hepatitis and cirrhosis, the mechanism of hepatocarcinogenesis or tumor progression is complex and not well understood. Cell killing and stimulation of mitosis leading to cell transformation or chromosomal instability induced by recombinogenic proteins during chronic hepatitis may cause carcinogenesis of HCC^[32].

HCC is resistant to conservative chemotherapy and difficult to induce apoptosis with TNF family members^[33]. On the other hand, TNF families, including TNF, TRAIL or Fas, can induce activation of NF- κ B^[33-41] and the tumor itself expresses these ligands^[42,43]. These phenomena suggest that TNF families contribute to tumor progression by autocrine or paracrine systems. In this study, we demonstrated that APRIL, a TNF family member, expressed in HCC cell lines, including SK-Hep1, HLE and HepG2, and sAPRIL was detected in culture medium of these HCC cell lines. However, addition of rhAPRIL did not induce any significant effect on viability of HCC cell lines, except for HepG2 cells stimulated with 1 ng/mL rhAPRIL. Because APRIL can induce both cell proliferation^[4,5,19] and death^[7] of malignant tumors, the result of present study may reflect that APRIL does not induce cell death so much as proliferation in HCC cells. In contrast to other TNF members, which are processed from the cell surface, APRIL is processed intracellularly and sAPRIL is purified^[14]. sAPRIL is used to stimulate tumor cells and induce cell proliferation in previous studies^[4,14]. The unprocessed form of APRIL may have less ability to induce tumor cell proliferation than sAPRIL.

APRIL enhances the growth of several tumor lines, however, the effect is more prominent at the point of tumor implantation than established tumor^[23]. Because expanding solid tumors, including HCC, are advanced with insufficient nutrition or oxygen, they have to get new vascular support to grow. In this study, HUVECs did not show significant cell proliferation or apoptosis inhibition after APRIL

stimulation. But HLE cells showed upregulation of APRIL after 24 h starvation, and further prolonged starvation induced upregulation of VEGF. In SK-Hep1 and HepG2 cells, starvation did not significantly induce the expression of APRIL, however, starvation promptly induced upregulation of VEGF. These results suggest that APRIL may be associated with expression of VEGF and induction of neovascularization in HCC. Further more, blockade of APRIL activity by anti-APRIL antibody induced downregulation of VEGF and inhibited tube formation of HUVECs. These results support the notion that neovascularization and progression of HCC may be induced by APRIL via VEGF expression.

Until now, some factors including VEGF have been identified as mediators of angiogenesis associated with tumors. With regard to HCC, recent studies indicate that angiopoietin^[44,45] is a target of angiogenesis. APRIL may not be critical for HCC progression as a direct effector, but plays an important role in neovascularization of HCC.

REFERENCES

- 1 Nagata S. Apoptosis by death factor. *Cell* 1997; **88**: 355-365
- 2 Beutler B. TNF, immunity, and inflammatory disease: lessons of the past decade. *J Investig Med* 1995; **43**: 227-235
- 3 Bazzoni F, Beutler B. The tumor necrosis factor ligand and receptor families. *N Engl J Med* 1996; **334**: 1717-1725
- 4 Hahne M, Kataoka T, Schröter M, Hofmann K, Irmeler M, Bodmer JL, Schneider P, Bornand T, Holler N, French LE, Sordat B, Rimoldi D, Tschopp J. APRIL, a new ligand of the tumor necrosis factor family, stimulate tumor cell growth. *J Exp Med* 1998; **188**: 1185-1190
- 5 Ware CF. APRIL and BAFF connect autoimmunity and cancer. *J Exp Med* 2000; **192**: F35-37
- 6 Yu G, Boone T, Delaney J, Hawkins N, Kelley M, Ramakrishnan M, McCabe S, Qiu WR, Kornuc M, Xia XZ, Guo J, Stolina M, Boyle WJ, Sarosi I, Hsu H, Senaldi G, Theill LE. APRIL and TALL-1 and receptors BCMA and TACI: system for regulating humoral immunity. *Nature Immunol* 2000; **1**: 253-256
- 7 Kelly K, Manos E, Jensen G, Nadauld L, Jones DA. APRIL/TRDL-1, a tumor necrosis factor-like ligand, stimulate cell death. *Cancer Res* 2000; **60**: 1021-1027
- 8 Roth W, Wagenknecht B, Klumpp A, Naumann U, Hahne M, Tschopp J, Weller M. APRIL, a new member of the tumor necrosis factor family, modulates death ligand-induced apoptosis. *Cell Death Differ* 2001; **8**: 403-410
- 9 Novak AJ, Bram RJ, Kay NE, Jelinek DF. Aberrant expression of B-lymphocyte stumulator by B chronic lymphocytic leukemia cells: a mechanism for survival. *Blood* 2002; **100**: 2973-2979
- 10 Marster SA, Yan M, Pitti RM, Haas PE, Dixit VM, Ashkenazi A. Interaction of the TNF homologues BLys and APRIL with the TNF receptor homologues BCMA and TACI. *Curr Biol* 2000; **10**: 785-788
- 11 Litinskiy MB, Nardelli B, Hilbert DM, He B, Schaffer A, Casali P, Cerutti A. DCS induce CD40-independent immunoglobulin class smitchiny through BLyS and APRIL. *Nat Immunol* 2002; **3**: 822-829
- 12 Stein JV, López-Fraga M, Elustondo FA, Carvalho-Pinto CE, Rodríguez D, Gómez-Care R, Jong JD, Martínez AC, Medema JP, Hahne M. APRIL modulates B and T cell immunity. *J Clin Invest* 2002; **109**: 1587-1598
- 13 Moore PA, Belvedere O, Orr A, Pieri K, LaFleur DW, Feng P, Soppet D, Charters M, Gentz R, Parmelee D, Li Y, Galperina O, Giri J, Roschke V, Nardelli B, Carrell J, Sosnovtseva S, Greenfield W, Ruben SM, Olsen HS, Fikes J, Hilbert DM. BLys: member of the tumor necrosis factor family and B lymphocyte stimulator. *Science* 1999; **285**: 260-263
- 14 López-Fraga M, Fernández R, Albar JP, Hahne M. Biologically active APRIL is secreted following intracellular process-

- ing in the Golgi apparatus by furin convertase. *EMBO Reports* 2001; **2**: 945-951
- 15 **Wu Y**, Bressette D, Carrell JA, Kaufman T, Feng P, Taylor K, Gan Y, Cho YH, Garcia AD, Gollatz E, Dimke D, LaFleur D, Migone TS, Nardelli B, Wei P, Ruben SM, Ullrich SJ, Olsen HS, Kanakaraj P, Moore PA, Baker KP. Tumor necrosis factor (TNF) receptor superfamily member TACI is a high affinity receptor for TNF family member APRIL and Blys. *J Biol Chem* 2000; **275**: 35478-35485
 - 16 **Xia XZ**, Treanor J, Senaldi G, Khare SD, Boone T, Kelley M, Theill LE, Colombero A, Solovyev I, Lee F, McCabe S, Elliott R, Miner K, Hawkins N, Guo J, Stolina M, Yu G, Wang J, Delaney J, Meng SY, Boyle WJ, Hsu H. TACI is a TRAF-interacting receptor for TALL-1, a tumor necrosis factor family member involved in B cell regulation. *J Exp Med* 2000; **192**: 137-143
 - 17 **Hatzoglou A**, Rousset J, Bourgeade MF, Rogier E, Madry C, Inoue J, Devergne O, Tsapis A. TNF receptor family member BCMA (B cell maturation) associates with TNF receptor-associated factor (TRAF) 1, TRAF2, and TRAF3 and activates NF- κ B, Elk-1, c-jun N-terminal kinase, and p38 mitogen-activated protein kinase. *J Immunol* 2000; **165**: 1322-1330
 - 18 **MacLennan ICM**, Vinuesa CG. Dendritic cells, BAFF, and APRIL: innate players in adaptive antibody responses. *Immunity* 2002; **17**: 235-238
 - 19 **Rennert P**, Schneider P, Cachero TG, Thompson J, Trabach L, Hertig S, Holler N, Qian F, Mullen C, Strauch K, Browning JL, Ambrose C, Tschopp J. A soluble form of B cell maturation antigen, a receptor for tumor necrosis factor family member APRIL, inhibits tumor cell growth. *J Exp Med* 2000; **192**: 1677-1683
 - 20 **Gross JA**, Johnston J, Mudri S, Enselman R, Dillon SR, Madden K, Xu W, Parrish-Novak J, Foster D, Loffton-Day C, Moore M, Littau A, Geossmann A, Haugen H, Foley K, Blumberg H, Harrison K, Kindsvogel W, Clegg CH. TACI and BCMA are receptors for a TNF homologue implicated in B-cell autoimmune disease. *Nature* 2000; **404**: 995-999
 - 21 **Francis IR**, Agha FP, Thompson NW, Keren DF. Fibrolamellar hepatocarcinoma: clinical, radiologic, and pathologic features. *Gastrointest Radiol* 1986; **11**: 67-72
 - 22 **Sugimachi K**, Tanaka S, Terashi T, Taguchi K, Rikimaru T, Sugimachi K. The mechanisms of angiogenesis in hepatocellular carcinoma: angiogenic switch during tumor progression. *Surgery* 2002; **131**: S135-141
 - 23 **Mackay F**, Schneider P, Rennert P, Browning J. BAFF and APRIL: A tutinal on B cell survival. *Annu Rev Immunol* 2003; **21**: 231-264
 - 24 **Mise M**, Arii S, Higashitani H, Furutani M, Niwano M, Harada T, Ishigami S, Toda Y, Nakayama H, Fukumoto M, Fujita J, Imamura M. Clinical significance of vascular endothelial growth factor and basic fibroblast growth factor gene expression in liver tumor. *Hepatology* 1996; **23**: 455-464
 - 25 **Suzuki H**, Seto K, Shinoda Y, Mori M, Ishimura Y, Suematsu M, Ishii H. Paracrine upregulation of VEGF receptor mRNA in endothelial cells by hypoxia-exposed HepG2 cells. *Am J Physiol* 1999; **276**: G92-97
 - 26 **Yoshiji H**, Kuriyama S, Hicklin DJ, Huber J, Yoshii J, Miyamoto Y, Kawata M, Ikenaga Y, Nakatani T, Tsujinoue H, Fukui H. KDR/Flk-1 is a major regulator of vascular endothelial growth factor-induced tumor development and angiogenesis in murine hepatocellular carcinoma cells. *Hepatology* 1999; **30**: 1179-1186
 - 27 **Kang MA**, Kim KY, Seol JY, Kim KC, Nam MJ. The growth inhibition of hepatoma by gene transfer of antisense vascular endothelial growth factor. *J Gene Med* 2000; **2**: 289-296
 - 28 **Baek JH**, Jang JE, Kang CM, Chung HY, Kim ND, Kim KW. Hypoxia-induced VEGF enhances tumor survivability via suppression of serum deprivation -induced apoptosis. *Oncogene* 2000; **19**: 4621-4631
 - 29 **von Marschall Z**, Cramer T, Hocker M, Finkenzeller G, Wiedenmann B, Rosewicz S. Dual mechanism of vascular endothelial growth factor upregulation by hypoxia in human hepatocellular carcinoma. *Gut* 2001; **48**: 87-96
 - 30 **Ng IO**, Poon RT, Lee JM, Fan ST, Ng M, Tso WK. Microvessel density, vascular endothelial growth factor and its receptors Flt-1 and Flk-1/KDR in hepatocellular carcinoma. *Am J Clin Pathol* 2001; **116**: 838-845
 - 31 **Shimamura T**, Saito S, Morita K, Kitamura T, Morimoto M, Kiba T, Numata K, Tanaka K, Sekihara H. Hepatocellular carcinoma and vascular endothelial growth factor receptors. Detection of vascular endothelial growth factor and its receptor expression in human hepatocellular carcinoma biopsy specimens. *J Gastroenterol Hepatol* 2000; **15**: 640-646
 - 32 **Hino O**, Kajino K, Umeda T, Arakawa Y. Understanding the hypercarcinogenic state in chronic hepatitis: a clue to the prevention of human hepatocellular carcinoma. *J Gastroenterol* 2002; **37**: 883-887
 - 33 **Yamanaka T**, Shiraki K, Sugimoto K, Ito T, Fujikawa K, Ito M, Takase K, Moriyama M, Nakano T, Suzuki A. Chemotherapeutic agents augment TRAIL-induced apoptosis in human hepatocellular carcinoma cell lines. *Hepatology* 2000; **32**: 482-490
 - 34 **Hsu H**, Xiong J, Goeddel DV. The TNF receptor 1-associated protein TRADD signals cell death and NF-kappa B activation. *Cell* 1995; **81**: 495-504
 - 35 **Hsu H**, Shu HB, Pan MG, Goeddel DV. TRADD-TRAF2 and TRADD-FADD interactions define two distinct TNF receptor 1 signal transduction pathways. *Cell* 1996; **299**: 299-308
 - 36 **Wajant H**, Haas E, Schwenzer R, Mühlenbeck F, Kreuz S, Schubert G, Grell M, Smith C, Scheurich P. Inhibition of Death Receptor-mediated Gene Induction by a Cycloheximide-sensitive Factor Occurs at the Level of or Upstream of Fas-associated Death Domain Protein (FADD). *J Biol Chem* 2000; **275**: 24357-24366
 - 37 **Bodmer JL**, Burns K, Schneider P, Hofmann K, Steiner V, Thome M, Bornand T, Hahne M, Schroter K, Wilson A, French LE, Browning JL, MacDonald HR, Tschopp J. TRAMP, a novel apoptosis-mediating receptor with sequence homology to tumor necrosis factor receptor 1 and Fas (APO-1/CD95). *Immunity* 1997; **6**: 79-88
 - 38 **Chinnaiyan AM**, O'Rourke K, Yu GL, Lyons RH, Garg M, Duan DR, Xing L, Gentz R, Ni J, Dixit VM. Signal transduction by DR3, a death domain-containing receptor related to TNF-R1 and CD95. *Science* 1996; **274**: 990-992
 - 39 **Ponton A**, Clement MV, Stamenkovic I. The CD95 (APO-1/Fas) receptor activates NF- κ B independently of its cytotoxic function. *J Biol Chem* 1996; **271**: 8991-8995
 - 40 **Okano H**, Shiraki K, Inoue H, Kawakita T, Saitou Y, Enokimura N, Yamamoto N, Sugimoto K, Murata K, Nakano T. Fas stimulation activates NF- κ B in SK-Hep1 hepatocellular carcinoma (HCC) cells. *Oncol Report* 2003; **10**: 1145-1148
 - 41 **Shiraki K**, Takase K, Nakano T. The emerging role of caspase inhibitors in gastrointestinal cancers. *J Gastroenterol* 2002; **37**: 323-331
 - 42 **Shiraki K**, Tsuji N, Shioda T, Isselbacher KJ, Takahashi H. Expression of Fas ligand in liver metastasis of human colonic adenocarcinomas. *Proc Natl Acad Sci USA* 1997; **94**: 6420-6425
 - 43 **Inoue H**, Shiraki K, Yamanaka T, Ohmori S, Sakai T, Deguchi M, Okano H, Murata K, Sugimoto K, Nakano T. Functional expression of tumor necrosis factor-related apoptosis-inducing ligand in human colonic adenocarcinoma cells. *Lab Invest* 2002; **82**: 1111-1119
 - 44 **Mitsunashi N**, Shimizu H, Ohtsuka M, Wakabayashi Y, Ito H, Kimura F, Yoshidome H, Kato A, Nukui Y, Miyazaki M. Angiopoietins and Tie-2 expression in angiogenesis and proliferation of human hepatocellular carcinoma. *Hepatology* 2003; **37**: 1105-1113
 - 45 **Tanaka S**, Sugimachi K, Yamashita Y, Shirabe K, Shimada M, Wands JR, Sugimachi K. Angiogenic switch as a molecular target of malignant tumors. *J Gastroenterol* 2003; **38** (Suppl 15): 93-97

Expression and alteration of insulin-like growth factor II-messenger RNA in hepatoma tissues and peripheral blood of patients with hepatocellular carcinoma

Zhi-Zhen Dong, Deng-Fu Yao, Deng-Bing Yao, Xin-Hua Wu, Wei Wu, Li-Wei Qiu, Dao-Rong Jiang, Jian-Hua Zhu, Xian-Yong Meng

Zhi-Zhen Dong, Department of Internal Medicine, Affiliated Hospital of Nantong University, Nantong 226001, Jiangsu Province, China

Deng-Fu Yao, Xin-Hua Wu, Wei Wu, Li-Wei Qiu, Research Center of Clinical Molecular Biology, Affiliated Hospital of Nantong University, Nantong 226001, Jiangsu Province, China

Deng-Bing Yao, Institute of Neurosciences, Nantong University, Nantong 226001, Jiangsu Province, China

Dao-Rong Jiang, Jian-Hua Zhu, Xian-Yong Meng, Department of Internal Medicine, Affiliated Hospital of Nantong University, Nantong 226001, Jiangsu Province, China

Supported by a grants-in-aid from the Key Project of Medical Science from Jiangsu Province, China, No. RC2003100

Correspondence to: Professor Deng-Fu Yao, Research Center of Clinical Molecular Biology, Affiliated Hospital of Nantong University, 20 Xisi Road, Nantong 226001, Jiangsu Province, China. dfyrcmb@yahoo.com

Telephone: +86-513-5861539 Fax: +86-513-5052523

Received: 2004-05-27 Accepted: 2004-06-17

Abstract

AIM: To investigate the clinical values of serum free insulin-like growth factor II (IGF-II) levels and IGF-II mRNA in hepatocellular carcinoma (HCC) tissues and peripheral blood for diagnosis of HCC and monitoring of extrahepatic metastasis.

METHODS: Total RNAs were extracted from HCC tissues or peripheral blood mononuclear cells from patients with HCC, liver diseases devoid of cancer, non-hepatic tumors, and healthy controls, respectively. IGF-II cDNAs were synthesized through random primers and reverse-transcriptase, amplified by polymerase chain reaction (PCR), and confirmed by DNA sequencing analysis. Serum free IGF-II levels in patients with different liver diseases were analyzed by an enzyme-linked immunosorbent assay.

RESULTS: The amplified fragments of IGF-II mRNA by RT-PCR were identical to originally designed ones with a size of 170 bp and confirmed by sequencing analysis. The dilution experiments revealed that the lowest sensitivity of our system was 2 ng/L of total RNA. The positive frequencies of IGF-II mRNA were 100% in HCC tissues, 53.3% in para-cancerous tissues, and 0% in non-cancerous tissues, respectively. The serum free IGF-II levels were significantly higher in HCC than those in chronic hepatitis or liver cirrhosis. The positive frequency of circulating IGF-II mRNA was 34.2% in HCC, no amplified fragment

was found in other liver diseases, extrahepatic tumors, and normal controls, respectively. The circulating IGF-II mRNA correlated with the stage of HCC, and its positive rate was 100% in HCC with extrahepatic metastasis and 35.5% in HCC with AFP-negative. No significant correlation was found between tumor sizes and circulating IGF-II mRNA fragment.

CONCLUSION: The abnormal expressions of free IGF-II and IGF-II mRNA are useful tumor markers for HCC diagnosis, differentiation of extrahepatic metastasis and monitoring postoperative recurrence.

© 2005 The WJG Press and Elsevier Inc. All rights reserved.

Key words: IGF-II; Hepatocellular carcinoma

Dong ZZ, Yao DF, Yao DB, Wu XH, Wu W, Qiu LW, Jiang DR, Zhu JH, Meng XY. Expression and alteration of insulin-like growth factor II-messenger RNA in hepatoma tissues and peripheral blood of patients with hepatocellular carcinoma. *World J Gastroenterol* 2005; 11(30): 4655-4660

<http://www.wjgnet.com/1007-9327/11/4655.asp>

INTRODUCTION

Hepatocellular carcinoma (HCC) is one of the most common and rapidly fatal malignancies worldwide, and has been ranked as the second cancer killer in China since the 1990s, particularly in the eastern and southern areas, including the inshore area of the Yangtze River^[1,2]. Major risk factors for HCC in these areas are exposure to aflatoxin B1 (AFB1) and infection by hepatitis viruses^[3]. HCC prognosis is poor and early detection is of utmost importance^[4]. Treatment options are severely limited by the frequent presence of metastases^[2]. Although serum α -fetoprotein (AFP) is a useful tumor marker for the detection and monitoring of HCC development, the false-negative rate with AFP level alone may be as high as 40% for patients with small size HCC^[5]. However, if hepatocyte-specific mRNAs are detected in the circulation, it is possible to infer the presence of circulating, presumably malignant liver cells and to predict the likelihood of hematogenous metastasis^[6,7].

Insulin-like growth factor II (IGF-II) is a mitogenic polypeptide closely related to insulin. Its gene has complex regulation of transcription, resulting in multiple mRNAs initiated by different promoters^[8,9]. IGF-II is speculated to

serve as an autocrine growth factor in various cancers, because they often coexpress IGF-II and IGF-I receptors. IGF-II is a kind of fetal growth factor and highly expressed during hepatocarcinogenesis^[10,11] and reexpression of IGF-II gene has recently been described in HCC^[12,13]. HCC is generally considered to be a hypervascular tumor. Although hepatic arterial embolization is widely used as an effective treatment of HCC on the basis of hypervascularization of HCC, IGF-II may play an important role in the development of neovascularization of HCC, because IGF-II substantially increases vascular endothelial growth factor (VEGF) mRNA and protein levels in a time-dependent manner in human hepatoma cells^[14]. The induction of VEGF by IGF-II was further increased by hypoxia, and IGF-II may be a hypoxia-inducible angiogenic factor in HCC and stimulates the growth of HCC cells *in vitro*^[15,16]. Park *et al.*, reported that most of the cirrhotic and HCC tissues express IGF-II^[17]. However, little is known of the circulating IGF-II in HCC.

In order to investigate the expression of IGF-II-mRNA in patients with liver diseases, we analyzed IGF-II-mRNA in tissues and peripheral blood of patients with HCC by reverse-transcriptase polymerase chain reaction (RT-PCR), and estimated the clinical values of circulating IGF-II mRNA as a peripheral blood tumor marker in diagnosis, differential diagnosis, and hematogenous metastasis of HCC.

MATERIALS AND METHODS

Patients

We studied 111 patients (100 males and 11 females) with HCC treated at Affiliated Hospital of Nantong University, China. The patients' ages ranged from 25 to 80 years (median, 48.3 years). Ninety patients (81%) had a history of cirrhosis, and 32 (29%) had a history of chronic hepatitis. Moreover, 85.6% (95/111) had hepatitis B surface antigen (HBsAg) carriers, 10.8% (12/111) had antibody to hepatitis C virus (anti-HCV, second generation antibody, Shanghai, China) and 14.4% (16/111) antibody to hepatitis G virus by enzyme-linked immunosorbent assay (ELISA, Beijing, China), respectively. Other cases studied included 30 patients with chronic viral hepatitis (23 males and 7 females), 30 patients with acute hepatitis (18 males and 12 females), 25 patients with cirrhosis (16 males and 9 females), 25 patients with non-liver tumors (6 with lung cancer, 6 with gastric cancer, 3 with esophageal cancer, 3 with breast cancer, 3 with colon cancer, 2 with cervical cancer, 2 with pancreatic cancer), and 25 healthy individuals with hepatitis B markers (HBsAg, HBcAb, HBV-DNA, and anti-HCV)-negative and normal serum alanine aminotransferase (ALT) levels from the Nantong Central Blood Bank as a control group.

All patients were diagnosed by blood biochemical tests, viral histology and B-ultrasonic examination. All peripheral blood samples were collected in the morning, with anti-clot heparin, and peripheral blood mononuclear cells were separated immediately, according to the method as described previously^[18]. Serum AFP concentrations ranged from 30 to 2 600 µg/L (median, 418 µg/L) and exceeding 50 µg/L was taken as a positive result. AFP-mRNA in peripheral blood

was also detected in this study as described elsewhere^[7]. The diagnosis of HCC and viral hepatitis was based on the criteria proposed by Chinese National Collaborative Cancer Research Group^[19] and the 2000 Prevention and Cure Scheme of Viral Hepatitis^[20], respectively.

Tissue specimens

Fresh tissue specimens including cancerous, paracancerous, and non-cancerous tissues were collected from 30 patients who underwent operations for liver cancers at the Affiliated Hospital of Nantong University, China. The tissue specimens were immediately frozen in liquid nitrogen and kept at -85 °C until used. The patients included 25 men and 5 women, ranging from 22 to 70 years.

Isolation of total RNA and synthesis of cDNA

Total RNAs were isolated from peripheral blood mononuclear cells and from liver tissues by the guanidine thiocyanate method with RNazole reagent (Promega) and purified as described elsewhere^[21]. RNAs were dissolved in tromethamine-HCl buffer (10 mmol/L, pH 8.0) containing EDTA 10 mmol/L. The concentration of total RNAs was measured by optical density at 260 nm in an ultraviolet spectrophotometer (Shimadzu UV-2201 type, Kyoto, Japan), and calculated µg/mg wet tissue, and it was stored at -85 °C. For synthesis of cDNA, 2 µg of total RNAs was denatured in the presence of random hexamers (200 pmol/L, Promega, Madison, WI, USA) at 95 °C for 5 min and incubated with moloney murine leukemia virus reverse-transcriptase (GIBCO, BRL) at 23 °C for 10 min, 42 °C for 60 min and 95 °C for 10 min, then on ice for 5 min, and stored at -20 °C for PCR analysis.

Amplification of nested polymerase chain reaction

The resulting cDNA was amplified by a nested PCR with two pairs of primers. The oligonucleotides were designed according to IGF-II sequence^[22] and synthesized with synthesizer (Model 381 A, Applied Biosystems, Foster City, CA, USA). The sequences of the 2 external primer pairs used for the initial PCR amplification were IGF-II-1(sense), 5'-ATGGGAATGCCAATGGGGAAG-3' (nt 251-271) and IGF-II-2(antisense), 5'-CTTGCCACGGGGTATC-TGGG-3' (nt 566-586), the size of amplified gene fragment was 336 bp. The sequences of the two internal primer pairs used for the second PCR amplification were IGF-II-3 (sense), 5'-TGCTGCATTGCTGCTTACCG-3' (nt 311-330) and IGF-II-4 (anti-sense), 5'-AGGTCACAGCTGCGG AAACA-3' (nt 461-480). PCR amplification consisted of initial denaturation at 94 °C for 5 min, followed by 94 °C for 25 s, 55 °C for 30 s, and 72 °C for 90 s for 30 cycles. The final product of nested PCR was 170 bp. Human glyceraldehyde-3-phosphate dehydrogenase (GAPDH) genome^[23] was used as a control. Primer sequence for GAPDH was GAPDH-1 (sense), 5'-ACCACAGT-CCATGCCATCAC-3' (nt 601-620) and GAPDH-2 (antisense), 5'-TCCACCACCCTGTTGCTGT A-3' (nt 1 033-1 052), the product of PCR was 452 bp (GAPDH gene transcript, 40 pmol/L). The PCR products were electrophoresed on 2% agarose gels with ethidium bromide staining. The fragment sizes were evaluated using PCR markers (Promega) as molecular weight standards.

Sequencing of PCR products

The 170 bp amplified product of human IGF-II genome was purified with the Montage PCR centrifugal filter devices (Millipore, MA, USA) according to the instruction of protocol. One microgram DNA was used for preparation of sequencing reaction and directly sequenced using the MegaBACE DNA analysis system in MegaBACE DNA sequencer with the DYEnamic ET Dye Terminator Cycle Sequencing Kit (Amersham Biosciences, NJ, USA), following their protocol. The sequences were edited using the MegaBACE Sequence Analyzer Version 3.0 program (Amersham Biosciences) and aligned with the amplified sequences of IGF-II genome, HCC tissue and circulating IGF-II.

Detection of serum free IGF-II protein level

The levels of serum free IGF-II protein in patients with chronic diseases were detected by an enzymatically amplified two-step sandwich-type immunoassay (ACTIVE™ Free IGF-II ELISA, TX). In this assay, standards, controls and serum samples were incubated in microtitration wells, which had been coated with anti-IGF-II antibody. After incubation and washing, the wells were treated with another anti-free IGF-II detection antibody labeled with the enzyme horseradish peroxidase (HRP). After a second incubation and washing step, the wells were incubated with the substrate tetramethylbenzidine (TMB). An acidic stopping solution was then added and the degree of enzymatic turnover of the substrate was determined by dual wavelength absorbance measurement at 450 nm and 620 nm. The absorbance measured was directly proportional to the concentration of free IGF-II present. A set of free IGF-II standards was used to draw a standard curve of absorbance *vs* free IGF-II concentration from which the free IGF-II concentrations in the serum samples can be calculated according to the ELISA routine method.

Statistical analysis

All patients were divided into six groups: HCC, acute hepatitis, chronic hepatitis, cirrhosis, extrahepatic tumor, and normal subjects. Hepatoma tissues were divided into three groups: cancerous, para-cancerous and non-cancerous tissues. Results are expressed as mean±SD. Differences between different groups were assessed by the Student's *t* test or the χ^2 test. *P*<0.05 was considered to be significant.

RESULTS

Amplification of IGF-II mRNA and sensitivity of detection

The fragments of IGF-II genome were amplified by a nested PCR assay from human hepatoma tissues and circulating blood of patients with HCC (Figure 1). The sizes of amplified fragments were identical to the original designed ones, which were 336 bp in single-step PCR, and 170 bp in nested-PCR. Differences between single-step PCR and nested PCR for amplified IGF-II mRNA were compared in 111 peripheral blood samples. The detecting frequency of IGF-II-mRNA was 6.3% (7/111) by single-step PCR and 34.2% (38/111) by nested-PCR. The incidence of nested PCR for IGF-II mRNA amplification was significantly higher than that in single-step PCR (*P*<0.05). Total RNAs (2 mg/L) extracted from hepatoma tissues were

diluted 10⁻²-10⁻⁸ times and amplified by nested-PCR, and the lowest sensitivity of the assay was 2 ng/L of total RNA (Figure 1A). The positive fragments of IGF-II genome were found distinctly from HCC tissues or peripheral blood of patients with HCC (Figure 1C) and could not be detected from non-cancerous tissues of HCC patients or from peripheral blood of patients with acute hepatitis, chronic hepatitis, liver cirrhosis, and extrahepatic tumors. By sequence analysis, the nucleotide homologies of amplified IGF-II gene fragments from HCC tissue and peripheral blood were identical to the cited sequence of human IGF-II genome (Figure 2)^[22].

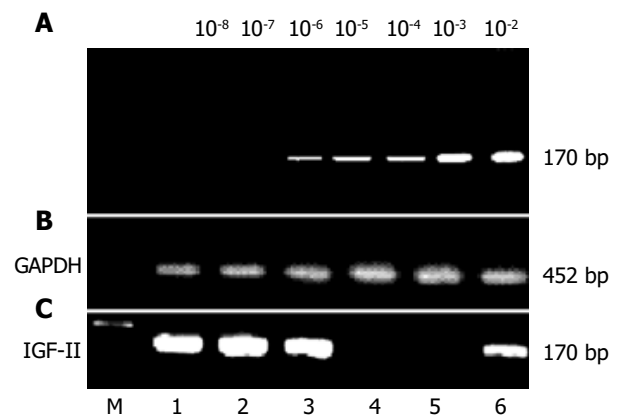


Figure 1 Amplification of IGF-II genomes from human hepatoma tissues or circulating blood samples of patients with hepatocellular carcinoma. IGF-II mRNAs were synthesized according to IGF-II cDNA with random hexamers and moloney murine leukemia virus reverse-transcriptase, and detected with different primer pairs by nested PCR (170 bp). The positive fragments of IGF-II genome were found distinctly in hepatoma tissues or in peripheral blood of patients with hepatocellular carcinoma. **A:** the sensitive limitation of our detection system (2 ng/L), using total RNA with 10⁻²-10⁻⁸ fold dilution and then amplified by nested PCR; **B:** the amplified fragments (452 bp) of glyceraldehyde-3-phosphate dehydrogenase genome from liver tissues or peripheral blood as controls; **C:** the amplification of IGF-II genomes in liver tissues (No. 1-4) or circulating blood (No. 5-6). No. 1-2, the positively amplified fragments of IGF-II mRNA from cancerous tissues of patients with hepatocellular carcinoma; No. 3, the positively amplified fragments of IGF-II mRNA from para-cancerous tissue of patients with hepatocellular carcinoma; No. 4, no positively amplified fragment from non-cancerous tissue of patients with hepatocellular carcinoma; No. 5, no positively amplified fragment from circulating blood of patients with liver cirrhosis, and No. 6, the positively amplified fragment from peripheral blood of patients with hepatocellular carcinoma. GAPDH: glyceraldehyde-3-phosphate dehydrogenase. M: DNA molecular weight marker.

	311				360
Origin	tgctgcattg	ctgcttaccg	ccccagttag	accctgtgcg	gcggggagct
Hepatoma	-----	-----	-----	-----	-----
PB	-----	-----	-----	-----	-----
	361				410
Origin	ggtggacacc	ctccagttcg	tctgtgggga	ccgcggcttc	tacttcagca
Hepatoma	-----	-----	-----	-----	-----
PB	-----	-----	-----	-----	-----
	411				460
Origin	ggcccgcaag	ccgtgtgagc	cgctgcagcc	gtggcatcgt	tgaggagtgc
Hepatoma	-----	-----	-----	-----	-----
PB	-----	-----	-----	-----	-----
	461		480		
Origin	tgtttccgca		gctgtgacct		
Hepatoma	-----	-----	-----	-----	-----
PB	-----	-----	-----	-----	-----

Figure 2 Alignment of nucleotide sequences of the amplified fragments of IGF-II genome from cancerous tissue or circulating blood in patients with HCC by sequence analysis. Origin: the cited sequence (170 bp, nt 311-480) of human IGF-II genome²²; Hepatoma: the amplification fragment of IGF-II genome from human hepatoma tissue; PB: the amplified fragment of peripheral blood IGF-II genome from patients with hepatocellular carcinoma.

Expression of total RNA and IGF-II mRNA in HCC

Different expression of total RNA was found in different parts of HCC tissues. The total RNA concentrations were significantly lower in HCC tissues than in self-control surrounding tissues ($P<0.05$) or non-cancerous tissues ($P<0.01$), respectively (Table 1). However, the expression of IGF-II mRNA amplified by nested-PCR was 100% in cancerous tissues, 53.3% in its surrounding tissues, and 0% in its non-cancerous tissues, respectively. The positive frequencies of IGF-II mRNA in HCC tissues or its para-cancerous tissues were significantly higher than those in its non-cancerous tissues ($P<0.01$), respectively.

Table 1 Alterations of total RNA (mean±SD) and amplification of IGF-II mRNA in cancerous, para-cancerous, and non-cancerous liver tissues

Groups	n	Total RNA level (µg/mg wet tissue)	IGF-II mRNA	
			Positive	%
Cancerous tissues	30	13.4±8.4	30	100
Para-cancerous tissues	30	20.7±14.6 ^a	16	53.3 ^b
Non-cancerous tissues	30	25.0±20.2 ^b	0	0 ^b

^a $P<0.05$, ^b $P<0.01$ vs the cancerous tissue group.

Circulating free IGF-II level in patients with chronic liver diseases

The levels of serum free IGF-II protein in patients with chronic liver diseases were investigated in this study, and the results are shown in Table 2. Of the 166 cases with chronic liver disease, the level of circulating free IGF-II protein was significantly higher ($P<0.01$) in HCC patients (75.7%, 84/111) than in patients with liver cirrhosis (28%, 7/25) or with chronic hepatitis (26.7%, 8/30). Also, the levels of serum AFP in patients with HCC (64.9%, 72/111) were significantly higher ($P<0.01$) than in patients with liver cirrhosis (36%, 9/25) or with chronic hepatitis (23.3%, 7/30).

Table 2 Levels of serum free IGF-II and AFP in patients with chronic liver diseases

Groups	n	Free IGF-II (µg/L)		AFP (µg/L)	
		mean±SD	>6.0 (%)	mean±SD	>50 (%)
CH	30	4.1±2.4	8 (26.7)	32.0±23.7	7 (23.3)
LC	25	5.5±1.7	7 (28.0)	34.7±39.8	9 (36.0)
HCC	111	6.7±1.8	84 (75.7) ^b	417.5±274.1	72 (64.9) ^b

^b $P<0.01$ vs the chronic hepatitis group or the liver cirrhosis group. HCC: hepatocellular carcinoma; LC: liver cirrhosis; CH: chronic hepatitis.

Detection of circulating IGF-II mRNA in HCC

Amplification of IGF-II mRNA in peripheral blood of patients with liver diseases or with extrahepatic tumors in comparison with AFP mRNA is shown in Table 3. Although the serum free IGF-II level increased in patients with chronic hepatitis or with liver cirrhosis, the circulating IGF-II mRNAs only were detected in HCC patients. The frequency of peripheral blood IGF-II mRNA was 34.2% in patients with HCC, no amplified fragments of circulating IGF-II

mRNA could be detected in patients with benign liver diseases, extrahepatic tumors, and normal controls, respectively. The incidence of circulating IGF-II mRNA was lower than that of AFP mRNA in patients with HCC, but it was a more specific circulating marker for HCC diagnosis. Of the 111 cases with HCC, both of AFP mRNA and IGF-II mRNA were detected in 28 patients (25.2%, 28/111), and only 27.0% of HCC cases were positive for AFP mRNA (30/111) or only IGF-II mRNA was detected in 10 patients (9%, 10/111). The combined analysis of circulating AFP mRNA and IGF-II mRNA was useful for diagnosis and differential diagnosis of HCC.

Table 3 Analysis of IGF-II-mRNA and AFP-mRNA in peripheral blood of patients with different liver diseases or non-liver tumors

Groups	n	IGF-II mRNA		AFP mRNA		Both	
		Positive	%	Positive	%	Positive	%
HCC	111	38	34.2	58	52.3	68	61.3
LC	25	0	0 ^b	5	20.0 ^b	5	20.0 ^b
CH	30	0	0 ^b	2	6.7 ^b	2	6.7 ^b
AH	30	0	0 ^b	0	0 ^b	0	0 ^b
ET	25	0	0 ^b	0	0 ^b	0	0 ^b
NC	25	0	0 ^b	0	0 ^b	0	0 ^b

^b $P<0.01$ vs the hepatocellular carcinoma group. HCC: hepatocellular carcinoma; LC: liver cirrhosis; CH: chronic hepatitis; AH: acute hepatitis; ET: extrahepatic tumor; NC: normal control.

Circulating IGF-II mRNA in HCC metastasis

Of the 111 patients with HCC, the relationship between circulating IGF-II mRNA and HCC stages and metastasis is analyzed in Table 4. The fragments of circulating IGF-II mRNA could be detected in any stage of HCC development. No significant differences of IGF-II mRNA were found between HCC stage I and II. The incidence of IGF-II mRNA in HCC stage III was 45.5% (30/66), significantly higher than that in early-stage (stage I or II) HCC. The fragments of IGF-II mRNA could be detected in all HCC patients with extrahepatic metastasis (100%). However, no significant difference of peripheral blood IGF-II mRNA was found between HCC with intra-hepatic metastasis and without intra-hepatic metastasis ($P>0.05$).

Table 4 Relationship between peripheral blood IGF-II mRNA or AFP mRNA and HCC stage or metastasis

Groups	n	IGF-II mRNA		AFP mRNA	
		Positive	%	Positive	%
HCC Stage I	14	2	14.3 ^a	5	35.7 ^a
Stage II	31	6	19.4 ^a	8	25.8 ^a
Stage III	66	30	45.5	47	71.2
Intra-hepatic metastasis					
With	67	27	40.3	44	65.7 ^c
Without	44	11	25.0	18	40.9
Extrahepatic metastasis					
With	13	13	100 ^b	13	100 ^b
Without	98	25	25.5	53	54.1

^a $P<0.05$ vs the HCC stage III group. ^b $P<0.01$, ^c $P<0.05$ vs the non-metastasis group. HCC: hepatocellular carcinoma.

Circulating IGF-II mRNA with AFP level and tumor size

We divided the 111 HCC patients into two groups according to serum AFP level: the positive frequency of circulating IGF-II mRNA fragment was 35.3% (6/17) in cases with AFP less than 50 µg/L, and 34.0% (32/94) in cases with AFP more than or equal to 50 µg/L, without significant differences between the two groups ($P>0.05$). In addition, we found that the incidence of peripheral blood IGF-II mRNA was 31.8% (7/22) in cases with diameters of tumor less than 5 cm, and 34.8% (31/89) in cases with diameters of tumor more than or equal to 5 cm, respectively.

DISCUSSION

Hepatocellular carcinoma is one of the most common forms of malignant cancer with the 4th highest mortality rate worldwide^[24]. Major risk factors for the development of HCC include chronic infections with hepatitis B or C virus, alcohol consumption, exposure to dietary aflatoxin B1, hereditary liver disease or liver cirrhosis of any etiology^[25]. Recent studies have discovered changes in the IGF axis that affect the molecular pathogenesis of HCC, including the autocrine production of IGFs, IGF binding proteins (IGFBPs), IGFBP proteases, and IGF receptor expression. Characteristic alterations detected in HCC and hepatoma cell lines comprise the overexpression of IGF-II and IGF-I receptor emerging as critical events in malignant transformation and growth of tumors^[26,17]. IGF-II is a polypeptide hormone secreted by many organs of the fetus. Very little information is available on the expression of IGF-II mRNA in HCC. In the present study, the total RNA levels and IGF-II mRNA in different parts of HCC tissues, the expression of peripheral blood IGF-II mRNA, and the level of serum free IGF-II protein were investigated in patients with various liver diseases.

The sinusoidal cells in para-cancerous cirrhotic nodule tissues and the malignant hepatocytes in HCC tissues expressed IGF-II. As we know, liver cirrhotic nodules are the precancerous lesion of HCC, so it is suggested that, in the precancerous condition, IGF-II mediated hepatocyte proliferation mainly via IGF1R by a paracrine mechanism. IGF-II mRNA was distributed in the cytoplasm of hepatocytes and overexpressed in HCC tissues^[27,28]. IGF-II could be secreted by hepatoma cells themselves and stimulate their proliferation via an autocrine mechanism^[29,30]. In order to analyze IGF-II expression, the fragments of IGF-II genome in HCC tissues were amplified by the sensitive nested PCR and confirmed by analysis of IGF-II sequences. Although different expression levels of total RNA were found in different parts of HCC tissues, the expression of IGF-II mRNA was detected in all of HCC tissues, half in its para-cancerous cirrhotic tissues, and none in its non-cancerous tissues (Table 1), respectively. Some differences in RNA level between tumor and cirrhotic tissues were quite informative.

The observations that HCC cells expressed less IGF-I than control liver cells, whereas IGF-II expression was higher in a high proportion of HCC cells^[31,32], are consistent with previous reports^[33,34] which showed that IGF-I mRNA levels were lower in HCC as compared with adjacent non-tumorous hepatic tissue, whereas IGF-II mRNA was higher in tumor tissues compared with normal liver tissues. The molecular

mechanisms responsible for reduction in IGF-I and reactivation of IGF-II in HCC remain to be determined. These results support growth factor-dependent HCC development and provide novel prognosis markers after HCC surgery.

IGFs are potent autocrine and paracrine mitogens for liver cancer cell proliferation, and their bioactivity is reduced by IGFBP-3. Human embryonic liver cell lines expressed IGF-II also, suggesting that hepatoma cells may regain some embryonic development characteristics like AFP secretion^[35,36]. A smaller proportion of IGF-II is associated with other IGFBPs, while less than 5% of IGF-II exists as unbound or free IGF-II that is believed to be the biologically active fraction of IGF-II^[37], capable of binding the type 2 IGF receptor^[38]. IGF-II present in the ternary complex is not easily dissociated, however IGF-II contained in low molecular weight binding complexes has a rapid turnover and may be the source of much of the detected free IGF-II. The levels of serum free IGF-II protein were significantly higher in HCC group than those in liver cirrhosis or in chronic hepatitis group (Table 2). The data indicated that serum free IGF-II secreted from HCC cells may act as an angiogenic factor for the hypervascularization of HCC.

Serum AFP is a diagnostic marker of HCC, but its significance in the early diagnosis of HCC is unclear and the positive rate is not high^[5,7,39]. The fragments of peripheral blood IGF-II mRNA were amplified by PCR and its clinical significances in patients with liver diseases were analyzed in the present study (Table 3). Although the serum free IGF-II level increased in patients with chronic hepatitis or liver cirrhosis, the circulating IGF-II mRNA only was detected in HCC patients. The frequency of IGF-II mRNA was not so high in patients with HCC, yet it was more specific (100%) for HCC diagnosis than that of peripheral blood AFP mRNA. No amplified fragments of circulating IGF-II mRNA could be detected in patients with benign liver diseases, extrahepatic tumors, and normal controls. The fragments of circulating IGF-II mRNA could be detected in all HCC patients with extrahepatic metastasis (100%), and like circulating AFP mRNA, could provide markers of severity and prognosis after HCC resection. The analyses of peripheral blood AFP-mRNA and IGF-II mRNA were more specific and more sensitive tumor markers for detecting and monitoring a few of circulating HCC hepatocytes.

In conclusion, the present data indicate that the expression levels of IGF-II mRNA were different in different parts of HCC liver tissues, and IGF-II mRNA could only be detected in peripheral blood of HCC patients. The frequency of circulating IGF-II mRNA and its diagnostic value increased with clinical stage of HCC and with distant metastases of HCC. The circulating IGF-II mRNA could be a useful molecular marker for HCC diagnosis, especially in monitoring extrahepatic metastases of tumor cells. Further studies will allow us to quantitate IGF-II mRNA in liver tissues and peripheral blood, and to explore the molecular mechanisms responsible for reactivation of IGF-II in development of HCC.

REFERENCES

- 1 Peto J. Cancer epidemiology in the last century and the next decade. *Nature* 2001; **411**: 390-395

- 2 **Qin LX**, Tang ZY. The prognostic molecular markers in hepatocellular carcinoma. *World J Gastroenterol* 2002; **8**: 385-392
- 3 **Yao DF**, Horie C, Horie T, Shimizu I, Meng XY, Ito S. Virological features of hepatitis C virus infection in patients with liver diseases in the inshore area of the Yangtze river. *Tokushima J Exp Med* 1994; **41**: 49-56
- 4 **Shimizu I**, Yao DF, Horie C, Yasuda M, Shiba M, Horie T, Nishikado T, Meng XY, Ito S. Mutations in a hydrophilic part of the core gene of hepatitis C virus from patients with hepatocellular carcinoma in China. *J Gastroenterol* 1997; **32**: 47-55
- 5 **Yao DF**, Jiang DR, Huang ZW, Lu JX, Tao QY, Yu ZJ, Meng XY. Abnormal expression of hepatoma specific γ -glutamyl transferase and alteration of γ -glutamyl transferase gene methylation status in patients with hepato-cellular carcinoma. *Cancer* 2000; **88**: 761-769
- 6 **Kar S**, Carr BI. Detection of liver cells in peripheral blood of patients with advanced-stage hepatocellular carcinoma. *Hepatology* 1995; **21**: 403-407
- 7 **Yao DF**, Dong ZZ, Yang DM, Zhu YS, Jiang DR, Lu JX. Peripheral blood AFP mRNA amplification in the diagnosis and differential diagnosis of hepatocellular carcinoma. *Zhonghua Putong Waike Zazhi* 2000; **15**: 474-477
- 8 **Kim KW**, Bae SK, Lee OH, Bae MH, Lee MJ, Park BC. Insulin-like growth factor II induced by hypoxia may contribute to angiogenesis of human hepatocellular carcinoma. *Cancer Res* 1998; **58**: 348-351
- 9 **Lee YI**, Lee S, Das GC, Park US, Park SM, Lee YI. Activation of the insulin-like growth factor II transcription by aflatoxin B1 induced p53 mutant 249 is caused by activation of transcription complexes; implications for a gain-of-function during the formation of hepatocellular carcinoma. *Oncogene* 2000; **19**: 3717-3726
- 10 **Thorgeirsson SS**, Grisham JW. Molecular pathogenesis of human hepatocellular carcinoma. *Nat Genet* 2002; **31**: 339-346
- 11 **Aihara T**, Noguchi S, Miyoshi Y, Nakano H, Sasaki Y, Nakamura Y, Monden M, Imaoka S. Allelic imbalance of insulin-like growth factor II gene expression in cancerous and precancerous lesions of the liver. *Hepatology* 1998; **28**: 86-89
- 12 **Fiorentino M**, Grigioni WF, Baccarini P, D'Errico A, De Mitri MS, Pisi E, Mancini AM. Different in situ expression of insulin-like growth factor type II in hepatocellular carcinoma. An in situ hybridization and immuno-histochemical study. *Diagn Mol Pathol* 1994; **3**: 59-65
- 13 **Scharf JG**, Dombrowski F, Ramadori G. The IGF axis and hepato-carcinogenesis. *Mol Pathol* 2001; **54**: 138-144
- 14 **Bae MH**, Lee MJ, Bae SK, Lee OH, Lee YM, Park BC, Kim KW. Insulin-like growth factor II (IGF-II) secreted from HepG2 human hepatocellular carcinoma cells shows angiogenic activity. *Cancer Lett* 1998; **128**: 41-46
- 15 **Kang-Park S**, Lee YI, Lee YI. PTEN modulates insulin-like growth factor II (IGF-II)-mediated signaling; the protein phosphatase activity of PTEN downregulates IGF-II expression in hepatoma cells. *FEBS Lett* 2003; **545**: 203-208
- 16 **Carmeliet P**. Angiogenesis in health and disease. *Nature Med* 2003; **9**: 653-660
- 17 **Park BC**, Huh MH, Seo JH. Differential expression of transforming growth factor alpha and insulin-like growth factor II in chronic active hepatitis B, cirrhosis and hepatocellular carcinoma. *J Hepatol* 1995; **22**: 286-294
- 18 **Ijichi M**, Takayama T, Matsumura M, Shiratori Y, Omata M, Makuuchi M. alpha-Fetoprotein mRNA in the circulation as a predictor of postsurgical recurrence of hepatocellular carcinoma: a prospective study. *Hepatology* 2002; **35**: 853-860
- 19 The Liver Cancer Committee of Chinese Anticancer Association. Diagnostic criteria of primary hepatocellular carcinoma. *Zhonghua Ganzangbing Zazhi* 2000; **8**: 135
- 20 The Group of Viral Hepatitis Research (2000, Xian). The Prevention and Cure Scheme of Viral Hepatitis. *Zhonghua Ganzangbing Zazhi* 2000; **8**: 324-329
- 21 **Kanashiro CA**, Schally AV, Groot K, Armatas P, Bernardino AL, Varga JL. Inhibition of mutant p53 expression and growth of DMS-153 small cell lung carcinoma by antagonists of growth hormone-releasing hormone and bombesin. *Proc Natl Acad Sci USA* 2003; **100**: 15836-15841
- 22 **Rall LB**, Scott J, Bell GI. Human insulin-like growth factor I and II messenger RNA: isolation of complementary DNA and analysis of expression. *Meth Enzymol* 1987; **146**: 239-248
- 23 **Benham FJ**, Povey S. Members of the human glyceraldehyde-3-phosphate dehydrogenase-related gene family map to dispersed chromosomal locations. *Genomics* 1989; **5**: 209-214
- 24 **Ito S**, Yao DF, Nii C, Horie T, Kamamura M, Nishikada T, Honda H, Shibata H, Shimizu I, Meng XY. Incidence of hepatitis C virus (HCV) antibodies and HCV-RNA in blood donors and patients with liver diseases in the inshore area of the Yangtze River. *J Gastroenterol Hepatol* 1994; **9**: 245-249
- 25 **Orito E**, Mizokami M. Hepatitis B virus genotypes and hepatocellular carcinoma in Japan. *Intervirology* 2003; **46**: 408-412
- 26 **Scharf JG**, Bralulke T. The role of the IGF axis in hepatocarcinogenesis. *Horm Metab Res* 2003; **35**: 685-693
- 27 **Zhang J**, Chan EK. Autoantibodies to IGF-II mRNA binding protein p62 and overexpression of p62 in human hepatocellular carcinoma. *Autoimmun Rev* 2002; **1**: 146-153
- 28 **Huynh H**, Chow PK, Ooi LL, Soo KC. A possible role for insulin-like growth factor-binding protein-3 autocrine/paracrine loops in controlling hepatocellular carcinoma cell proliferation. *Cell Growth Differ* 2002; **13**: 115-122
- 29 **Lee S**, Park U, Lee YI. Hepatitis C virus core protein transactivates insulin-like growth factor II gene transcription through acting concurrently on Egr1 and Sp1 sites. *Virology* 2001; **283**: 167-177
- 30 **Ng IO**, Lee JM, Srivastava G, Ng M. Expression of insulin-like growth factor II mRNA in hepatocellular carcinoma. *J Gastroenterol Hepatol* 1998; **13**: 152-157
- 31 **Zhang N**, Siegel K, Odenthal M, Becker R, Oesch F, Dienes HP, Schirmacher P, Steinberg P. The role of insulin-like growth factor II in the malignant transformation of rat liver oval cells. *Hepatology* 1997; **25**: 900-905
- 32 **Su Q**, Liu YF, Zhang JF, Zhang SX, Li DF, Yang JJ. Expression of insulin-like growth factor II in hepatitis B, Cirrhosis and hepatocellular Carcinoma: its relationship with hepatitis B virus antigen expression. *Hepatology* 1994; **19**: 788-799
- 33 **Scharf JG**, Ramadori G, Dombrowski F. Analysis of the IGF axis in preneoplastic hepatic foci and hepatocellular neoplasms developing after low-number pancreatic islet transplantation into the livers of streptozotocin diabetic rats. *Lab Invest* 2000; **80**: 1399-1411
- 34 **Su JJ**, Qin GZ, Yan RQ, Huang DR, Yang C, Lotlikar PD. The expression of insulin-like growth factor II, hepatitis B virus X antigen and p21 in experimental hepatocarcinogenesis in tree shrews. *Ann Acad Med Singapore* 1999; **28**: 62-66
- 35 **Sohda T**, Iwata K, Soejima H, Kamimura S, Shijo H, Yun K. In situ detection of insulin-like growth factor II (IGF2) and H19 gene expression in hepatocellular carcinoma. *J Hum Genet* 1998; **43**: 49-53
- 36 **Uchida K**, Kondo M, Takeda S, Osada H, Takahashi T, Nakao A, Takahashi T. Altered transcriptional regulation of the insulin-like growth factor 2 gene in human hepatocellular carcinoma. *Mol Carcinog* 1997; **18**: 193-198
- 37 **Ooasa T**, Karasaki H, Kanda H, Nomura K, Kitagawa T, Ogawa K. Loss of imprinting of the insulin-like growth factor II gene in mouse hepatocellular carcinoma cell lines. *Mol Carcinog* 1998; **23**: 248-253
- 38 **Seo JH**, Kim KW, Murakami S, Park BC. Lack of colocalization of HBxAg and insulin like growth factor II in the livers of patients with chronic hepatitis B, cirrhosis and hepatocellular carcinoma. *J Korean Med Sci* 1997; **12**: 523-531
- 39 **Funaki NO**, Tanaka J, Seto SI, Kasamatsu T, Kaido T, Imamura M. Hematogenous spreading of hepatocellular carcinoma cells: possible participation in recurrence in the liver. *Hepatology* 1997; **25**: 564-568

Expression of MUC1 and its significance in hepatocellular and cholangiocarcinoma tissue

Shi-Fang Yuan, Kai-Zong Li, Ling Wang, Ke-Feng Dou, Zhen Yan, Wei Han, Ying-Qi Zhang

Shi-Fang Yuan, Ling Wang, Department of Vascular and Endocrine Surgery, Xijing Hospital, The Fourth Military Medical University, Xi'an 710033, Shaanxi Province, China

Kai-Zong Li, Ke-Feng Dou, Department of Hepatobiliary Surgery, Xijing Hospital, The Fourth Military Medical University, Xi'an 710033, Shaanxi Province, China

Zhen Yan, Wei Han, Ying-Qi Zhang, Biotechnology Center, The Fourth Military Medical University, Xi'an 710033, Shaanxi Province, China

Supported by the National Natural Science Foundation of China, No. 39470683

Correspondence to: Professor Shi-Fang Yuan, Department of Vascular and Endocrine Surgery, Xijing Hospital, The Fourth Military Medical University, Xi'an 710033, Shaanxi Province, China. shifangy@fmmu.edu.cn

Telephone: +86-29-83375271 Fax: +86-29-83375267

Received: 2004-09-03 Accepted: 2004-12-09

Abstract

AIM: To investigate the relation between MUC1 expression, distribution, and prognosis in hepatocellular and cholangiocarcinoma (HCC and CC) and cirrhotic liver tissues, and their significance in HCC and CC diagnosis.

METHODS: Expression and distribution of MUC1 were examined by immunohistochemical assay with anti-MUC1 mAb in 59 samples of HCC and 37 samples of CC, 20 samples of cirrhotic liver tissues, and 10 samples of normal liver tissues, seeking possible associations between MUC1 positive expression, distribution in HCC and CC (primary liver cancer, PLC) cases and the studied clinical data.

RESULTS: Immunohistochemical analysis of MUC1 expression showed that in the 96 PLC samples, 68 (70.8%) were strong positive, and 6 (6.2%) were weak positive. Only 4 in the 20 cirrhotic liver tissues were found to be weak positive, while no expression of MUC1 was detected in normal liver tissues. Apparently, the high expression rate of MUC1 in PLC tissues was statistically significant in comparison to that in cirrhotic and normal liver tissues. The expressed MUC1 protein, stained in dark brownish or brownish-yellow particles, chiefly localized on the cancer cell membranes or in cytoplasm. In the 68 strong positive samples, 40 were detected on cell membrane and the other 28 were in cytoplasm. In addition, follow-up studies of those PLC cases demonstrated that MUC1 expression on cell membrane or in cytoplasm was closely associated with PLC prognosis. The expression of MUC1 in PLC had little statistical significance in respect of the pathological types and sizes of the tumors, but a strong

relationship regarding histological differentiation, metastasis of lymph nodes, portal canal emboli, and post-operational recurrence of the carcinomas. After 3 years of tumor excision, the metastasis rate in MUC1 positive expression group (67.6%) was much higher than that in MUC1 weak expression group (33.3%) and negative expression group (31.8%), and thus the survival rate in MUC1-positive expression group was significantly different from that in weak and negative expression groups.

CONCLUSION: Expression and localization of MUC1 proteins in primary liver carcinomas (PLCs) may act as prognostic markers, and MUC1 molecules might be helpful in differential diagnosis.

© 2005 The WJG Press and Elsevier Inc. All rights reserved.

Key words: MUC1; Primary liver carcinoma; Prognosis; Immunohistochemistry

Yuan SF, Li KZ, Wang L, Dou KF, Yan Z, Han W, Zhang YQ. Expression of MUC1 and its significance in hepatocellular and cholangiocarcinoma tissue. *World J Gastroenterol* 2005; 11(30): 4661-4666

<http://www.wjgnet.com/1007-9327/11/4661.asp>

INTRODUCTION

Primary liver carcinoma (PLC) is one of the most frequent malignant tumors in clinics, and its tendency to invade and metastasize is the paramount reason for high recurrence after excision, greatly affecting the survival rate of PLC suffers. Even with the developments in PLC therapies, the overall effect is far from radical cure on demand^[1]. Thus, it is quite necessary and important to explore new approaches for early diagnosis and immunological treatment of PLC.

MUC1, also known as polymorphic epithelial mucin, is a group of glycoproteins with high molecular mass. One important characteristic of MUC1 gene is the polymorphism. The second expressed exon within the MUC1 coding genes contains a variable number of tandem repeats (VNTRs), and every VNTR is composed of a 20-amino acid peptide motif as VTSAPDTRPAPGSTAPPAHG, constituting main antigenic determinants in this region. Usually MUC1 is expressed at a very low level on normal adenocytes, chiefly localized on gland cell surfaces or in gland cavities by excretion, and thus not recognized by the host immune system^[2-4]. It has been found that MUC1 is aberrantly expressed in the forms of misglycolization or incomplete

glycolization, in many tumor tissues like breast, stomach, and colon cancers. These abnormal MUC1 molecules reveal new protein epitopes or carbohydrate antigens, distributed all around the cancer cell surface, and may be recognized by the immune system as notable tumor-associated antigens^[5-9]. As a tumor marker, MUC1 has been applied in breast cancer and other tumors for their diagnosis and biological treatment^[10-13].

During the process of malignant transformation and invasion of tumor cells, the changes of MUC1 glycolization influence the biological behavior of tumor cells^[14]. It was also reported that MUC1 positive expression is an important prognostic indicator in breast cancer and other tumor patients^[15-17]. However, the expression levels of MUC1 in PLC and cirrhotic liver tissues and their correlation with carcinogenesis still remain to be elucidated. In this study, we used immunohistochemical assay to detect MUC1 expression in PLC and cirrhotic liver tissues, and further investigated the potential significance of MUC1 in PLC diagnosis and immunological treatment.

MATERIALS AND METHODS

Clinical data

Ninety-six paraffin-embedded PLC samples were collected from patients undergoing surgery in our hospital from 1990 to 2001. Hepatocellular carcinoma (HCC) was found in 59 patients, and cholangiocarcinoma (CC) in 37 patients. Sixty-six samples were from male patients and 30 from female patients, aged 35-68 years (averaged 41.5 years). Lymph node metastasis was confirmed by pathological examination. No chemotherapy or radiotherapy was given before tumor excision. In the 20 samples of cirrhotic tissues, 12 were from male patients and 8 female patients, aged 19-70 years (averaged 40.7 years). Ten samples of normal liver tissues from 10 cases of hepatic angiomas served as normal controls. All tissue sections were stained with hematoxylin and eosin (H&E).

The diagnosis of HCC was primarily based on history of chronic hepatitis, results of AFP detection, and space occupying lesions in the liver on ultrasonography and CT. The pathological diagnosis of HCC and CC was confirmed by H&E staining of the tissue sections. Patients were regularly examined by ultrasonography and CT after PLC surgery. Tumor recurrence was defined as new focus was detected, and metastasis was defined when lymph nodes of hepatic portal vein became swollen or new foci were found in distal organs.

Preparation of tissue samples

For routine sections, tissue samples were immersion-fixed in 40 g/L buffered formaldehyde for hours, and dehydrated through graded alcohols. After paraffin wax embedding, sections of 5 μ m thickness were cut and mounted on coated glass slides. Then H&E as well as immunohistochemical staining were performed.

Immunohistochemical assay

Endogenous peroxidase blocker and normal house serum were added to all sections for 30-min incubation at room

temperature to minimize non-specific staining, and antigen restoration was performed by microwave method. Mouse anti-human MUC1 mAb working at 1:100 dilution was purchased from Antibody Diagnostica Inc., USA, and ABC diagnostic kit was purchased from Santa Cruz, USA. Detection procedures were performed according to the kit instructions. The cover slide was treated with goat anti-mouse bridging antibody (1:200) for 30 min at 37 °C. Finally, diaminobenzidine tetrachloride was used for color development and the slides were counterstained with hematoxylin. Dehydration, clearing, covering, and light microscopy were performed routinely. Blank test and replacement test were set for negative controls.

Result determination

Brownish-yellow particles under light microscope were considered positive. Three positive levels according to positive cell percentage in five high power, randomized, observation fields were classified: Level 0: cells without stained particles (negative MUC1 expression, -), Level 1: positive cell percentage less than 25% (weak MUC1 expression, +), and Level 2: positive cell percentage more than 25% (strong MUC1 expression, ++).

Statistical analysis

All data were analyzed by SPSS 11.0 (SPSS Inc., USA). Statistical methods included χ^2 -test, Fisher's exact test, and the Kruskal-Wallis test. $P < 0.05$ was considered statistically significant.

RESULTS

MUC1 expression in primary liver carcinoma, cirrhotic liver, and normal liver tissues

In the 96 tested PLC samples, 68 were strong positive (Figures 1A and B) and 6 were weak positive. Only 4 in the 20 cirrhotic liver tissues were found to be weak positive (Figure 1C), while no expression of MUC1 was detected in normal liver tissues (Figure 1D). Apparently, the high expression rate of MUC1 in PLC tissues was statistically significant in comparison to that in cirrhotic and normal liver tissues ($P < 0.05$, Table 1).

Table 1 Expression of MUC1 in PLC, cirrhotic, and normal liver tissues

Group	n	Expression of MUC1		
		-	+	++
Normal liver	10	10	0	0
Cirrhotic liver	20	16	4	0
PLC	96	22	6	68 ^a

^a $P < 0.05$ vs cirrhotic and normal liver tissues.

MUC1 expression was associated with PLC pathology

MUC1 was both expressed in HCC (Figure 2) and CC tissues with no statistical difference between them ($P > 0.05$), demonstrating that MUC1 gene expression was not associated with histological classification of the hepatic tumors. The

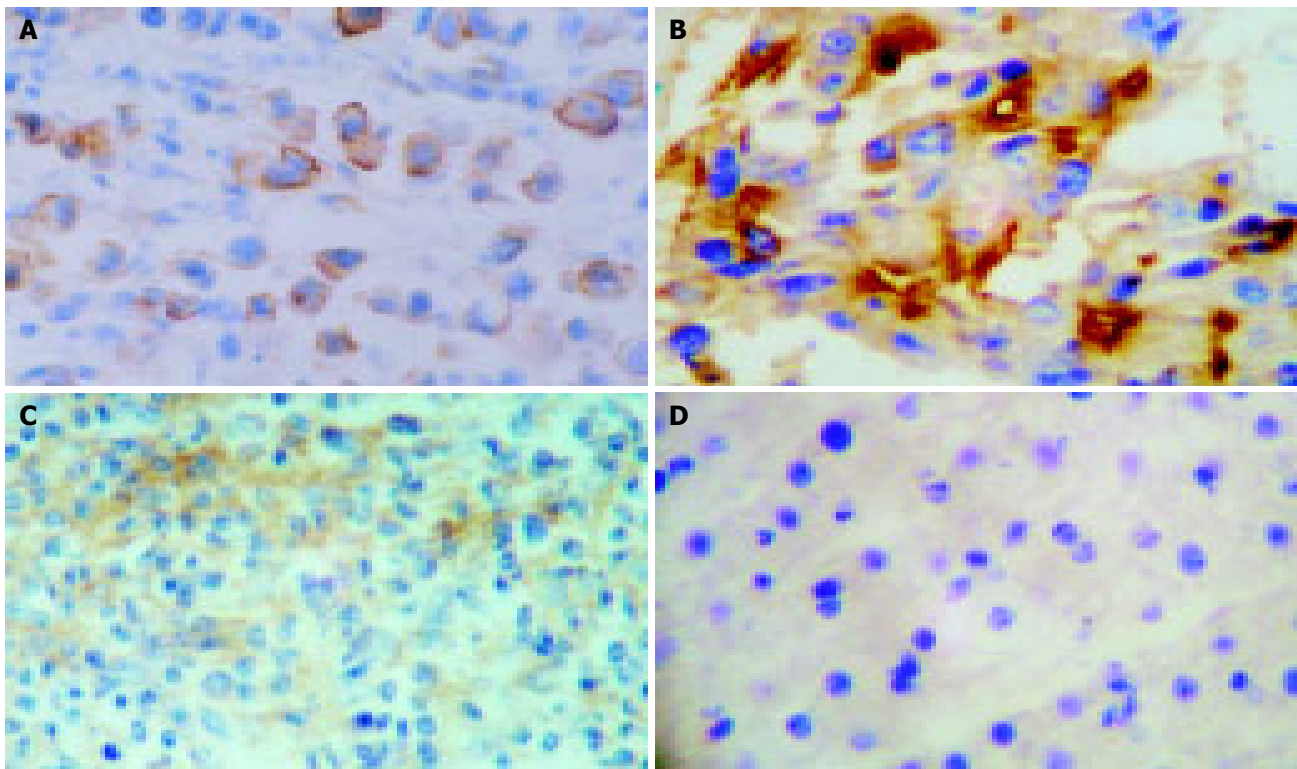


Figure 1 Characterization of MUC1 expression in PLC and cirrhotic liver tissues as well as normal liver tissues by immunohistochemical staining. **A:** Overexpression of MUC1 on cell membranes ($\times 400$); **B:** positive staining of

MUC1 in cytoplasm ($\times 400$); **C:** MUC1 weak expression in cirrhotic liver tissues ($\times 400$); **D:** MUC1 negative expression in normal liver tissues ($\times 400$).

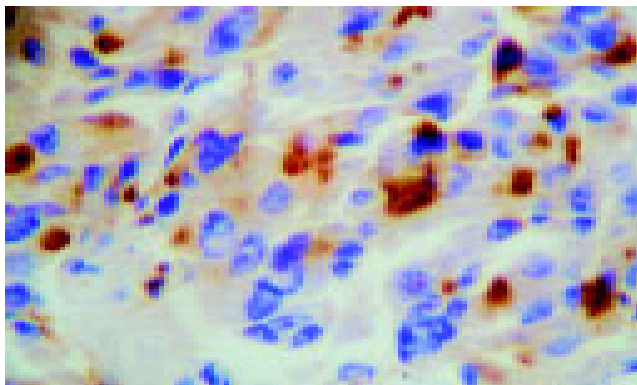


Figure 2 Positive expression of MUC1 protein in HCC samples ($\times 400$).

sizes of solid tumors were not different in the MUC1 expression either ($P > 0.05$). However, MUC1 expression in well differentiated tumor tissues were significantly different from that in moderately and poorly differentiated tissues ($P < 0.05$), and so did in lymph node metastases, portal vein embolis, and 3-year post-operation recurrence ($P < 0.05$). The association of MUC1 expression and PLC clinical pathology behavior is illustrated in Table 2.

Localization of MUC1 in PLC tissues and prognosis

By immunohistochemical assay, the expressed MUC1 proteins in liver carcinoma tissues were stained as dark brownish or brownish-yellow particles, and mainly localized on the cancer cell membranes (Figure 1A) or in cytoplasm (Figure 1B). Table 3 shows the association of strong MUC1

expression and the prognosis of 68 cases of hepatic tumor.

MUC1 expression and PLC metastasis

Three years after surgery, metastasis occurred in 55 out of

Table 2 MUC1 expression and PLC clinical pathology behavior

Clinical pathology	n	MUC1 expression			P
		-	+	++	
Histological classification					
HCC	59	17	4	38	>0.05
CC	37	5	2	30	
Histological differentiation					
Well ^{a,c}	30	14	2	14	<0.01
Moderate	40	6	2	32	
Poor	26	2	2	22	
Lymph node metastasis					
Yes	52	5	2	45	<0.01
No	44	17	4	23	
Portal vein embolism					
Yes	32	1	2	29	<0.01
No	64	21	4	39	
Size of solid tumor (cm)					
<5	49	15	2	32	>0.05
≥ 5	47	7	4	36	
Recurrence (3 yr)					
Yes	65	9	4	52	<0.01
No	31	13	2	16	

^a $P < 0.05$ vs moderately differentiated HCC. ^c $P < 0.05$ vs poorly differentiated HCC.

the 96 PLC patients: intra-hepatic metastasis in 30 cases, pulmonary metastasis in 12 cases, osseous metastasis in 4 cases, and lymph node metastasis in 9 cases. The metastasis rate in MUC1 strong positive expression group (67.6%) was much higher than that in MUC1 negative expression group (31.8%, $P < 0.01$, Table 4).

Table 3 MUC1 localization in PLC tissues and prognosis of PLC

Clinical pathology	n	MUC1 expression		P
		Membrane	Cytoplasm	
Lymph node metastasis				
Yes	45	23	22	<0.05
No	23	17	6	
Portal vein embolism				
Yes	29	11	18	<0.01
No	39	29	10	
Survival rate (yr)				
<3	50	17	33	<0.01
≥3	18	13	5	

Table 4 MUC1 expression and post-operation metastasis

MUC1 expression	n	Rate of metastasis (%)
Negative	22	31.8
Weak positive	6	33.3
Strong positive ^b	68	67.6

^b $P < 0.01$ vs negative.

Positive MUC1 expression in PLC tissues and survival rate

Follow-up data were collected from 86 of the 96 PLC patients (89.6%). The survival rate in MUC1 strong positive expression group was significantly different from that in MUC1 weak positive or negative expression group ($P < 0.05$, Table 5).

Table 5 Positive MUC1 expression in PLC tissues and survival of PLC patients

MUC1 expression	n	Survival rate (%)			
		6 mo	12 mo	24 mo	36 mo
Negative	22	86.4	72.7	59.1	50.0
Weak positive ^a	6	50.0	33.3	33.3	33.3
Strong positive ^a	68	51.5	44.1	29.4	26.4

^a $P < 0.05$ vs negative.

DISCUSSION

To investigate the possible correlation among MUC1 expression and localization and prognosis in PLC and cirrhotic liver tissues, we carried out immunohistochemical assay to detect the MUC1 expression in 96 samples of PLC hepatic tissues. The results showed that MUC1 was strongly expressed on PLC cell membrane or in cytoplasm, while weak and negative expressions were found in human

cirrhotic liver tissues, and no expression was found in normal liver tissues. The difference was of statistical significance. In addition, MUC1 expression increased during the process of transformation from benign cells to malignant cells, which is in accordance with the common understanding of hepatic carcinoma resulting from liver cirrhosis.

There are discrepant results in reports on MUC1 expression and PLC histological differentiation types. Sasaki and Nakanuma^[18] reported that MUC1 core protein is expressed in intrahepatic bile duct carcinoma, but not in HCC. Cao *et al.*^[19] demonstrated that MUC1 is remarkably expressed in HCC cells and can be considered as an indicator of HCC prognosis. In our test, MUC1 expression was not associated with either histological classification or size of the tumors. Based on our testing data, we take it that MUC1 can be used as one of the helping indicators early diagnosis of PLC, by hepatic puncture biopsy before PLC surgery.

In previous studies, it was suggested that high-level MUC1 expression is reversely correlated with prognosis of tumor patients. For example, MUC1 expression is closely related with prognosis of breast cancer sufferers^[3,20]. However, possible association(s) of MUC1 expression levels in PLC liver tissues with the prognosis still remains uncertain. From our test results, it is clear that MUC1 expression levels are quite different in well-differentiated tumor tissues and moderately- or poorly-differentiated tumor tissues, and so are the differences among MUC1 expression and lymph node metastasis, portal vein embolism, and post-operation recurrence. Expression and localization of MUC1 proteins in PLC may act as different prognostic markers of PLC. We also found that the prognosis was worse in cytoplasm expression group than in cell surface expression group. It is reasonable to deduce that MUC1 molecule on cell surface may stimulate protective immunities (for instance, specific cytotoxic T lymphocytes) from the body to fight against the tumor cells.

Intra-hepatic tumor invasion in portal vein system with subsequent metastasis is the major cause of morbidity and mortality in patients with PLC. In our work, it was apparent that MUC1 expression was associated with PLC cell infiltration and metastasis as well. The possible mechanisms might be as follows. (1) E-cadherin is a transmembrane glycoprotein that mediates calcium-dependent, inter-cellular adhesion and is specifically involved in epithelial cell-to-cell adhesion. In cancers, decreased E-cadherin expression is one of the alterations that characterize the invasive phenotype, and the data support its role as a tumor suppressor. Studies have shown that aberrant E-cadherin expression is associated with the acquisition of invasiveness and more advanced tumor stage for many cancers including lung cancer, prostate cancer, gastric cancer, and breast cancer, indicating that MUC1 promotes tumor metastasis by downregulating E-cadherin expression and its binding to beta-catenin^[21-23]. (2) MUC1 acts as anti-cell adhesion molecules. High density of filamentous MUC1 molecules expressed on tumor cell surface might prevent binding between membrane-anchored ligands and corresponding receptors, minimize intercellular interactions induced by integrin in extracellular matrix, thus facilitating cancer cell invasion^[24,25]. (3) Sialyl Lewis epitopes on MUC1 molecules function as

ligands to E-selectin in injured or inflammatory vascular endothelial cells, and facilitate tumor cell adhesion, infiltration, and metastasis^[26].

Currently, carcinectomy is still one of the major treatments for PLC, but has limitations for PLC patients of life expansion and quality promotion. MUC1 molecules play a double role in tumor genesis and development^[4]. On one hand, aberrant MUC1 expression influences inter-cellular adhesions via surface molecule interactions, and makes easier for tumor cell growth and metastasis. On the other hand, as a hapten with newly formed glycan or peptide epitopes because of incomplete glycolization, MUC1 induces anti-tumor immune responses, and may be a target for tumor immunotherapy. It was reported that clinical MUC1 vaccination trials for breast cancer are in progress^[27]. We also discovered that MUC1 gene vaccination induces specific cytotoxic T lymphocyte responses in mice^[28]. MUC1-targeted tumor therapeutical vaccination may be effective for PLC treatment.

To conclude, we used immunohistochemical assay to detect MUC1 expression in PLC, cirrhotic and normal liver tissues, and the results show that MUC1 may be an indicator for PLC diagnosis and prognosis. As HCC is common in China^[29-31] and most Asian countries^[32-35], further investigations on MUC1 roles in PLC genesis and development are of particular significance in providing new ways of PLC treatment.

REFERENCES

- 1 **Aoki T**, Imamura H, Hasegawa K, Matsukura A, Sano K, Sugawara Y, Kokudo N, Makuuchi M. Sequential preoperative arterial and portal venous embolizations in patients with hepatocellular carcinoma. *Arch Surg* 2004; **139**: 766-774
- 2 **Croce MV**, Isla-Larrain MT, Demichelis SO, Gori JR, Price MR, Segal-Eiras A. Tissue and serum MUC1 mucin detection in breast cancer patients. *Breast Cancer Res Treat* 2003; **81**: 195-207
- 3 **Rahn JJ**, Dabbagh L, Pasdar M, Hugh JC. The importance of MUC1 cellular localization in patients with breast carcinoma: an immunohistologic study of 71 patients and review of the literature. *Cancer* 2001; **91**: 1973-1982
- 4 **von Mensdorff-Pouilly S**, Snijdwint FG, Verstraeten AA, Verheijen RH, Kenemans P. Human MUC1 mucin: a multifaceted glycoprotein. *Int J Biol Markers* 2000; **15**: 343-356
- 5 **Chu PG**, Weiss LM. Immunohistochemical characterization of signet-ring cell carcinomas of the stomach, breast, and colon. *Am J Clin Pathol* 2004; **121**: 884-892
- 6 **Baldus SE**, Monig SP, Huxel S, Landsberg S, Hanisch FG, Engelmann K, Schneider PM, Thiele J, Holscher AH, Dienes HP. MUC1 and nuclear beta-catenin are coexpressed at the invasion front of colorectal carcinomas and are both correlated with tumor prognosis. *Clin Cancer Res* 2004; **10**: 2790-2796
- 7 **Levi E**, Klimstra DS, Adsay NV, Andea A, Basturk O. MUC1 and MUC2 in pancreatic neoplasia. *J Clin Pathol* 2004; **57**: 456-462
- 8 **Sakamoto H**, Yonezawa S, Utsunomiya T, Tanaka S, Kim YS, Sato E. Mucin antigens expression in gastric carcinomas of young and old adult. *Hum Pathol* 1997; **28**: 1056-1065
- 9 **Utsunomiya T**, Yonezawa S, Sakamoto H, Kitamura H, Hokita S, Aiko T, Tanaka S, Irimura T, Kim YS, Sato E. Expression of MUC1 and MUC2 mucins in gastric carcinomas: its relationship with the prognosis of the patients. *Clin Cancer Res* 1998; **4**: 2605-2614
- 10 **Mukherjee P**, Madsen CS, Ginardi AR, Tinder TL, Jacobs F, Parker J, Agrawal B, Longenecker BM, Gendler SJ. Mucin 1-specific immunotherapy in a mouse model of spontaneous breast cancer. *J Immunother* 2003; **26**: 47-62
- 11 **Chen D**, Xia J, Tanaka Y, Chen H, Koido S, Wernet O, Mukherjee P, Gendler SJ, Kufe D, Gong J. Immunotherapy of spontaneous mammary carcinoma with fusions of dendritic cells and mucin 1-positive carcinoma cells. *Immunology* 2003; **109**: 300-307
- 12 **Johnen H**, Kulbe H, Pecher G. Long-term tumor growth suppression in mice immunized with naked DNA of the human tumor antigen mucin (MUC1). *Cancer Immunol Immunother* 2001; **50**: 356-360
- 13 **Snijdwint FG**, von Mensdorff-Pouilly S, Karuntu-Wanamarta AH, Verstraeten AA, Livingston PO, Hilgers J, Kenemans P. Antibody-dependent cell-mediated cytotoxicity can be induced by MUC1 peptide vaccination of breast cancer patients. *Int J Cancer* 2001; **93**: 97-106
- 14 **Byrd JC**, Bresalier RS. Mucins and mucin binding proteins in colorectal cancer. *Cancer Metastasis Rev* 2004; **23**: 77-99
- 15 **Hiraga Y**, Tanaka S, Haruma K, Yoshihara M, Sumii K, Kajiyama G, Shimamoto F, Kohno N. Immunoreactive MUC1 expression at the deepest invasive portion correlates with prognosis of colorectal cancer. *Oncology* 1998; **55**: 307-319
- 16 **Kocer B**, Soran A, Kiyak G, Erdogan S, Eroglu A, Bozkurt B, Solak C, Cengiz O. Prognostic significance of mucin expression in gastric carcinoma. *Dig Dis Sci* 2004; **49**: 954-964
- 17 **Yonezawa S**, Sato E. Expression of mucin antigens in human cancers and its relationship with malignancy potential. *Pathol Int* 1997; **47**: 813-830
- 18 **Sasaki M**, Nakanuma Y. Expression of mucin core protein of mammary type in primary liver cancer. *Hepatology* 1994; **20**: 1192-1197
- 19 **Cao Y**, Karsten U, Otto G, Bannasch P. Expression of MUC1, Thomsen-Friedenreich antigen, Tn, sialosyl-Tn, and alpha2, 6-linked sialic acid in hepatocellular carcinomas and preneoplastic hepatocellular lesions. *Virchows Arch* 1999; **434**: 503-509
- 20 **Vgenopoulou S**, Lazaris AC, Markopoulos C, Boltetsou E, Kyriakou V, Kavantzias N, Patsouris E, Davaris PS. Immunohistochemical evaluation of immune response in invasive ductal breast cancer of not-otherwise-specified type. *Breast* 2003; **12**: 172-178
- 21 **Fujita K**, Denda K, Yamamoto M, Matsumoto T, Fujime M, Irimura T. Expression of MUC1 mucins inversely correlated with post-surgical survival of renal cell carcinoma patients. *Br J Cancer* 1999; **80**: 301-308
- 22 **Wesseling J**, Van der Valk SW, Vos HL, Sonnenberg A, Hilkens J. Episialin (MUC1) overexpression inhibits integrin-mediated cell adhesion to extracellular matrix components. *J Cell Biol* 1995; **129**: 255-265
- 23 **Kondo K**, Kohno N, Yokoyama A, Hiwada K. Decreased MUC1 expression induces E-cadherin-mediated cell adhesion of breast cancer cell lines. *Cancer Res* 1998; **58**: 2014-2019
- 24 **Steelant WF**, Goeman JL, Philippe J, Oomen LC, Hilkens J, Krzewinski-Recchi MA, Huet G, Van der Eycken J, Delannoy P, Bruyneel EA, Mareel MM. Alkyl-lysophospholipid 1-O-octadecyl-2-O-methyl-glycerophosphocholine induces invasion through episialin-mediated neutralization of E-cadherin in human mammary MCF-7 cells *in vitro*. *Int J Cancer* 2001; **92**: 527-536
- 25 **Satoh S**, Hinoda Y, Hayashi T, Burdick MD, Imai K, Hollingsworth MA. Enhancement of metastatic properties of pancreatic cancer cells by MUC1 gene encoding an anti-adhesion molecule. *Int J Cancer* 2000; **88**: 507-518
- 26 **Takao S**, Uchikura K, Yonezawa S, Shinchi H, Aikou T. Mucin core protein expression in extrahepatic bile duct carcinoma is associated with metastases to the liver and poor prognosis. *Cancer* 1999; **86**: 1966-1975
- 27 **Musselli C**, Ragupathi G, Gilewski T, Panageas KS, Spinat Y, Livingston PO. Reevaluation of the cellular immune response in breast cancer patients vaccinated with MUC1. *Int J Cancer* 2002; **97**: 660-667

- 28 **Yuan SF**, Li KZ, Wang L, Yan Z, Han W, Zhang YQ. Induction of specific cytotoxic T lymphocytes and humoral immune response by MUC1 DNA vaccine in mice. *Xibao Yu Fenzi Mianyixue Zazhi* 2003; **19**: 343-345
- 29 **Yuen MF**, Cheng CC, Lauder IJ, Lam SK, Ooi CG, Lai CL. Early detection of hepatocellular carcinoma increases the chance of treatment: Hong Kong experience. *Hepatology* 2000; **31**: 330-335
- 30 **Chen TH**, Chen CJ, Yen MF, Lu SN, Sun CA, Huang GT, Yang PM, Lee HS, Duffy SW. Ultrasound screening and risk factors for death from hepatocellular carcinoma in a high risk group in Taiwan. *Int J Cancer* 2002; **98**: 257-261
- 31 **Yuan SF**, Wang L, Li KZ, Yan Z, Han W, Zhang YQ. Inhibitory effect of MUC1 gene immunization on H22 hepatocellular carcinoma growth. *Shijie Huaren Xiaohua Zazhi* 2003; **11**: 1322-1325
- 32 **Zhou J**, Tang ZY, Fan J, Wu ZQ, Li XM, Liu YK, Liu F, Sun HC, Ye SL. Expression of platelet-derived endothelial cell growth factor and vascular endothelial growth factor in hepatocellular carcinoma and portal vein tumor thrombus. *J Cancer Res Clin Oncol* 2000; **126**: 57-61
- 33 **Sun HC**, Tang ZY, Li XM, Zhou YN, Sun BR, Ma ZC. Microvessel density of hepatocellular carcinoma: its relationship with prognosis. *J Cancer Res Clin Oncol* 1999; **125**: 419-426
- 34 **Shuto T**, Hirohashi K, Kubo S, Tanaka H, Yamamoto T, Higaki I, Takemura S, Kinoshita H. Treatment of adrenal metastases after hepatic resection of a hepatocellular carcinoma. *Dig Surg* 2001; **18**: 294-297
- 35 **Huang YH**, Wu JC, Lui WY, Chan GY, Tsay SH, Chiang JH, King KL, Huo TI, Chang FY, Lee SD. Prospective case-controlled trial of adjuvant chemotherapy after resection of hepatocellular carcinoma. *World J Surg* 2000; **24**: 551-555

Science Editor Wang XL and Li WZ Language Editor Elsevier HK

Role of cell adhesion signal molecules in hepatocellular carcinoma cell apoptosis

Jian-Min Su, Li-Ying Wang, Yu-Long Liang, Xi-Liang Zha

Li-Ying Wang, Yu-Long Liang, Xi-Liang Zha, Department of Biochemistry and Molecular Biology, Shanghai Medical College of Fudan University, Shanghai 200032, China

Jian-Min Su, Department of Chemistry, Fudan University, Shanghai 200032, China

Supported by the National Natural Science Foundation of China, No. 30400224 and 30370342, the Major State Basic Research Development Program of China, 973 Program, No. 2004CB520802

Correspondence to: Professor Xi-Liang Zha, Department of Biochemistry and Molecular Biology, Shanghai Medical College of Fudan University, Yixueyuan Road 138, Shanghai 200032, China. xlzha@shmu.edu.cn

Telephone: +86-21-54237696 Fax: +86-21-64179832

Received: 2004-10-28 Accepted: 2004-12-26

Su JM, Wang LY, Liang YL, Zha XL. Role of cell adhesion signal molecules in hepatocellular carcinoma cell apoptosis. *World J Gastroenterol* 2005; 11(30): 4667-4673

<http://www.wjgnet.com/1007-9327/11/4667.asp>

INTRODUCTION

Apoptosis or programmed cell death is critical for normal development and tissue homeostasis^[1]. However uncontrolled apoptosis may occur after treatment with cytostatic chemicals. It is a pathophysiological process and is associated with the occurrence of various human diseases^[2]. Maintenance of cell-matrix or cell-cell contact is an important cell survival factor^[3-6] and loss of these contacts, or rounding up, is a hallmark of apoptosis. Cell-matrix interactions occur at the closest contact between the cell and the substratum. It was called as focal adhesion. Integrins are mainly engaged in cell-matrix adhesion. Integrin ligated with the extracellular matrix results in activation of focal adhesion kinase (FAK) and integrin linked kinase (ILK). FAK is a 125-ku protein tyrosine kinase, that is critical in transmission of signals from the focal adhesion to the cytoplasm after cell attachment^[7,8]. ILK is another integrin cytoplasmic-binding protein that has been implicated in the regulation of cell adhesion and extracellular matrix deposition as well as the activation of cell survival and proliferative pathways, including those involving MAP kinase, PKB/Akt and GSK-3 β ^[9,10]. Similarly, E-cadherin is a calcium-dependent transmembrane cell-cell adhesion protein, mainly involved in cell-cell adhesion^[11]. When the homophilic interaction in their specific extra-cellular regions occurred, their intra-cellular linked protein, β -catenin, was activated and mediated signal transduction^[12,13]. It seems clear that FAK, ILK, and β -catenin are important for signaling, cell attachment and cell survival. Despite the importance of these proteins in signal transduction and cell survival, there is little evidence about the role of FAK, ILK, and β -catenin in chemically induced models of apoptotic cell death. Therefore, we have investigated the role of FAK, ILK, β -catenin and other related signal molecule such as PKB in SMMC-7721 hepatocellular carcinoma cell using the characterized nephrotoxicant, *S*-(1,2-dichlorovinyl)-L-cysteine (DCVC)^[14,15]. DCVC is metabolized by a β -lyase to a reactive acylating metabolite that covalently modifies cellular macromolecules^[16-18]. The apoptosis of renal proximal tubule epithelial cell (RPTE) induced by DCVC had been reported. Cell death of primary cultured RPTE caused by DCVC treatment is preceded by disorganization of the cytoskeletal network and dissolution of focal adhesion^[14,15]. Thus, this compound is a useful agent to study the role of

Abstract

AIM: Cell adhesion molecules and their signal molecules play a very important role in carcinogenesis. The aim of this study is to elucidate the role of these molecules and the signal molecules of integrins and E-cadherins, such as (focal adhesion kinase) FAK, (integrin linked kinase) ILK, and β -catenin in hepatocellular carcinoma cell apoptosis.

METHODS: We first synthesized the small molecular compound, *S*-(1,2-dichlorovinyl)-L-cysteine (DCVC), and identified it, by element analysis and ¹H NMR. To establish the apoptosis model of the SMMC-7721 hepatocellular carcinoma cell, we treated cells with DCVC in EBSS for different concentrations or for various length times in the presence of 20 μ mol/L *N,N*-diphenyl-*p*-phenylenediamine, which blocks necrotic cell death and identified this model by flow cytometry and DNA ladder. Then we studied the changes of FAK, ILK, β -catenin, and PKB in this apoptotic model by Western blot.

RESULTS: We found that the loss or decrease of cell adhesion signal molecules is an important reason in apoptosis of SMMC-7721 hepatocellular carcinoma cell and the apoptosis of SMMC-7721 cell was preceded by the loss or decrease of FAK, ILK, PKB, and β -catenin or the damage of cell-matrix and cell-cell adhesion.

CONCLUSION: Our results suggested that the decrease of adhesion signal molecules, FAK, ILK, PKB, and β -catenin, could induce hepatocellular carcinoma cell apoptosis.

© 2005 The WJG Press and Elsevier Inc. All rights reserved.

Key words: Cell adhesion signal molecule; Hepatocellular carcinoma; Cell apoptosis

cell-cell or cell-matrix adhesion in apoptosis of epithelial cells.

To study the relationship between the cell adhesion signal molecules and cell apoptosis, we found the apoptosis model of the SMMC-7721 hepatocellular carcinoma cell using DCVC and examined the role of FAK, ILK, β -catenin and other related signal molecules in this model.

MATERIALS AND METHODS

Chemicals and antibodies

SMMC-7721 cells were obtained from the Department of Pathology, Shanghai No. 2, Military Medical University (Shanghai, China)^[19]. Anti-FAK and anti-ILK polyclonal antibodies were purchased from Santa Cruz. Anti- β -catenin and anti-PKB mAb were purchased from Sigma. Secondary antibodies conjugated with HRP were purchased from Watson Biotech. (Shanghai). *N,N'*-Diphenyl-*p*-phenylenediamine (DPPD) was from Sigma-Aldrich (St. Louis, MO, USA). DCVC was synthesized by us.

Cell culture and DCVC treatment

SMMC-7721 cells were grown in RPMI medium 1640 supplemented with penicillin and 10% heat inactivated fetal bovine serum in 37 °C and 50 mL/L CO₂. Confluent monolayers of SMMC-7721 in 10-cm dishes were washed with Earle's balanced salt solution (EBSS) twice. Thereafter, cells were treated with DCVC in EBSS for different concentrations or for various lengths of time. To find the apoptosis model, cells were treated with DCVC in the presence of 20 μ mol/L DPPD (stocked in dimethyl sulfoxide), which blocks necrotic cell death but allows the onset of apoptosis^[15,20]. Following treatment with DCVC, cells were allowed to recover in a complete medium containing 20 μ mol/L DPPD.

Western blot analysis

After treatment of DCVC and recovery in complete medium, confluent cells were washed twice with ice-cold PBS and lysed in modified loading buffer containing 50 mmol/L Tris-HCl, pH 6.8, 2% SDS, 10% glycerol and protease inhibitors (1 mmol/L PMSF). The samples were boiled for 10 min and centrifuged at 12 000 *g* for 10 min, and insoluble material was removed. Equal amount of protein were separated on a SDS-PAGE and transferred to PVDF membrane. After being blocked with 3% BSA in PBS (containing 0.05% Tween 20), the membrane was incubated with the appropriate primary antibodies, followed by HRP-conjugated secondary antibodies. Proteins were visualized by fluorography using an enhanced chemiluminescence system (Perfect Biotech, Shanghai).

Synthesis and identification of *S*-(1,2-dichlorovinyl)-*L*-cysteine (DCVC)

Dry *L*-cysteine (0.1 mol) and sodium were added in portions to 300 mL of dry ammonia contained in a flask equipped with a magnetic stirrer and a drying tube. The reaction flask was set in a dish, so that alcohol could be applied to prevent frosting. Sodium was added first to give the characteristic blue color, which disappeared when cysteine was added to form the disodium salt. Trichloroethylene (8.96 mL, 0.1 mole) was dissolved slowly in liquid ammonia (25 mL). After 30 min, a stream of air was directed on the reaction flask to

speed up evaporation of ammonia, which required about 2 h. The slightly colored residue was dissolved in 300 mL of water, free from traces of ammonia *in vacuo* and, by the addition of glacial acetic acid, adjusted to pH 5.0 from an initial pH 11.9. The resulting copious precipitate was diluted with one volume of ethanol, cooled overnight in a refrigerator and isolated by filtration. The crude precipitate was dissolved in 600 mL of water at 70 °C, 1 g of activated carbon was added, and the mixture was filtered while it was still hot. An equal volume of ethanol was added to the clear filtrate and, after overnight at 4 °C, 9.1 g of needle-like crystals were obtained. MP 158-159 °C.

DCVC analysis, calculated for C₅H₇NO₂SCl₂: C, 27.79; H, 3.27; N, 6.48; S, 14.84; Cl, 32.82. Found: C, 27.82; H, 3.28; N, 6.47; S, 14.94; Cl, 32.80. ¹H NMR (deuterium replaced DMSO as solvent 300 mol/L) δ : 3.35 (*t*, *J* = 15.50 Hz, *J* = 7.42 Hz, 1 H), 3.53 (*t*, *J* = 15.50 Hz, *J* = 4.05 Hz, 1 H), 3.91 (*t*, *J* = 4.05 Hz, *J* = 7.42 Hz, 1 H), 6.71 (*s*, 1 H). FAB MS: 217 ([MH⁺]).

Detection of cell apoptosis

DNA laddering was determined by agarose gel electrophoresis. Cells were harvested by scraping the adherent cells which were then combined with floating cells present in the culture medium. After centrifugation, the cell pellet was washed once with ice-cold PBS by centrifugation, lysed with lysis buffer (10 mmol/L Tris, 1 mmol/L EDTA, and 2 g/L Triton X-100, pH 7.4), and incubated on ice for 20 min. Cell debris was removed by centrifugation; the supernatant was treated with RNase (60 μ g/mL) for 1 h at 50 °C. The DNA was precipitated with 0.5 mol/L NaCl and equal volume of isopropyl alcohol and separated by electrophoresis on 1% agarose gels.

SMMC-7721 hepatocellular carcinoma cell nuclear fragmentation treated with DCVC was stained with 1 μ g/mL Hoechst 33258 in PBS. After washing with PBS, coverslips were mounted and viewed using a Nikon epifluorescence microscope.

Apoptosis was also determined by cell cycle analysis. Both floating and adherent cells that were trypsinized were pooled and fixed in 100% ethanol (-20 °C). After washing the cells twice with PBS, cells were resuspended in PBS containing 10 μ g/mL RNase A and 7.5 μ mol/L propidium iodide. After 30 min incubation at room temperature, the cell cycle was analyzed by flow cytometry (FAC Scan, Becton Dickinson) and the percentage of cells present in sub-G₀/G₁ was calculated using the LYSIS software (Becton Dickinson).

RESULTS

DCVC induces apoptosis of SMMC-7721 hepatocellular carcinoma cell

SMMC-7721 hepatocellular carcinoma cells were induced into apoptosis in the presence of DCVC (Figure 1). When SMMC-7721 hepatocellular carcinoma cells were treated with 0.02 mmol/L DPPD and various DCVC concentrations for 6 h and then harvested for flow cytometry assay, it was found that the cell apoptosis was induced by DCVC in a dose-dependent manner in the presence of DPPD and when the concentration of DCVC is larger than 0.05 mmol/L, the percentage of cell apoptosis increased rapidly (Figure 2).

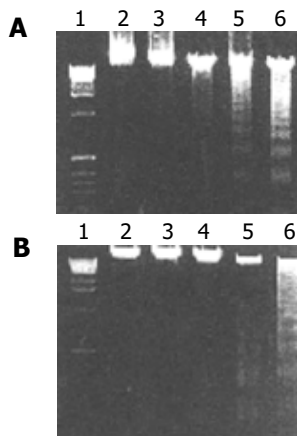


Figure 1 Measurement of apoptosis by DNA fragmentation upon treatment with DCVC/DPPD. **A:** SMMC-7721 Hepatocellular carcinoma cells were treated with 0.1 mmol/L DCVC and 0.02 mmol/L DPPD for various time duration, then harvested for DNA fragmentation assay to estimate apoptosis. Lane 1, DNA marker; lane 2, absent DCVC; lanes 3–6 represent tumor cells treated for 1, 2, 4, 6, and 8 h, respectively; **B:** SMMC-7721 hepatocellular carcinoma cells were treated with 0.02 mmol/L DPPD and various DCVC concentrations for 6 h, then harvested for DNA fragmentation assay to estimate apoptosis. Lane 1, DNA marker; lane 2, absent DCVC; lanes 3–6 represent tumor cells treated for 0.02, 0.05, 0.1, and 0.2 mmol/L, respectively.

Similarly, the effect of DCVC on apoptosis was also time-dependent. At the first 4 h, the percentage of cell apoptosis was very low and after that it increased rapidly (Figure 3).

These data demonstrate that the effective apoptosis had not happened until the DCVC concentration and treatment time was high and long enough. We also demonstrate that DPPD alone could not cause cell apoptosis (Figure 4).

DCVC-induced loss of FAK expression in SMMC-7721 hepatocellular carcinoma cell

FAK, as an important cell survival factor, has been implicated in apoptosis induced by various stimuli^[21–23]. Until now, no reports have described the role of FAK in DCVC/DPPD-induced malignant cell apoptosis. We investigated the FAK expression in DCVC-induced SMMC-7721 hepatocellular carcinoma cell by Western blot analysis and found that the level of FAK protein was almost lost (Figure 5).

Interestingly, we found that the FAK expression decreased in a dose-dependent and time-dependent manner. When the cells were treated for 1 h, the protein level of FAK began to decrease, but at that time the percentage of cell apoptosis had no significant decrease. After the treatment time gets

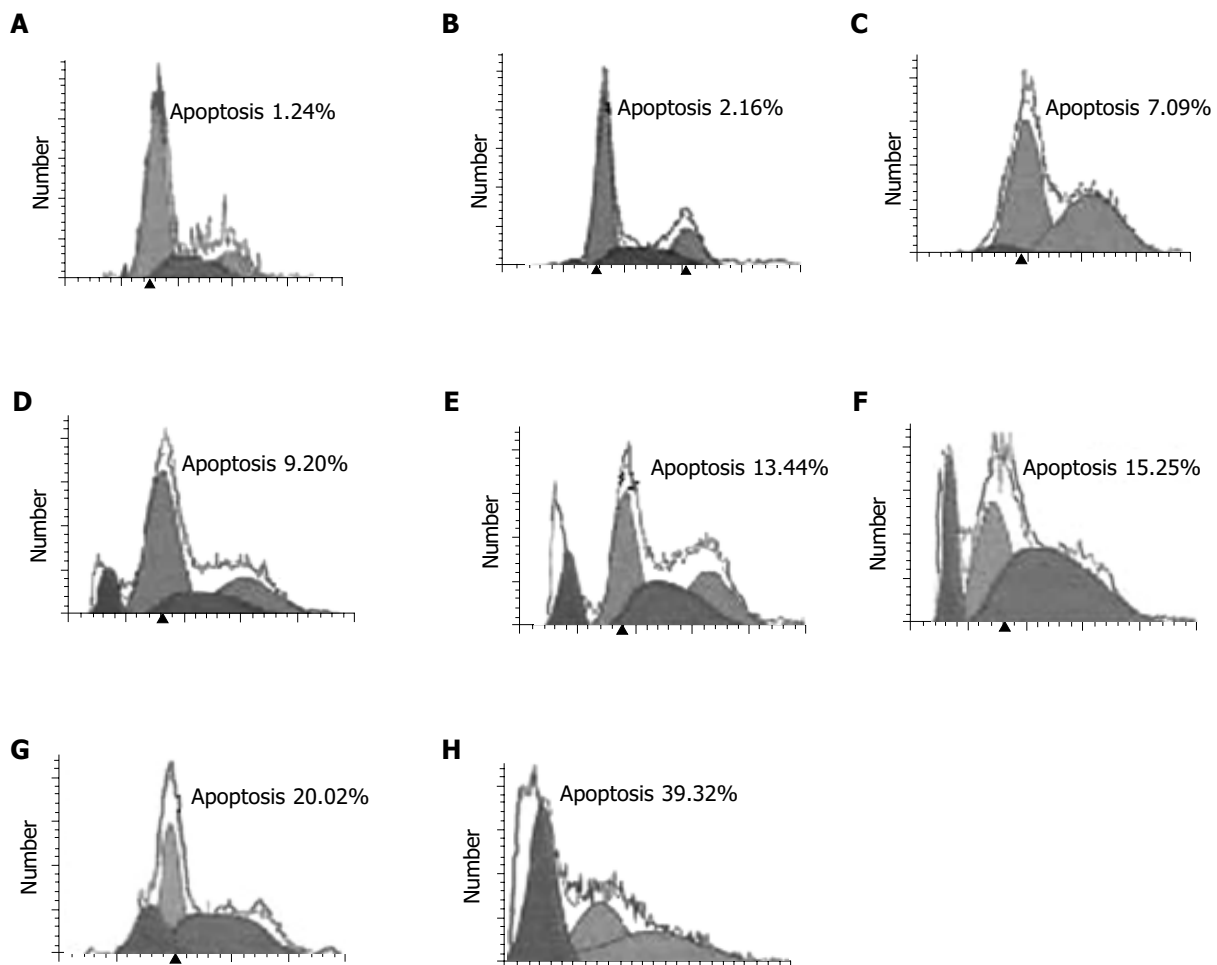


Figure 2 Dose effect on cell apoptosis induced by DCVC co-treated with DPPD. SMMC-7721 hepatocellular carcinoma cells were treated with 0.02 mmol/L DPPD and various DCVC concentration for 6 h, then harvested for flow cytometry

assay to estimate apoptosis. **A:** Absent both DCVC and DPPD; **B:** absent DCVC; **C:** DCVC (0.005 mmol/L); **D:** DCVC (0.01 mmol/L); **E:** DCVC (0.02 mmol/L); **F:** DCVC (0.05 mmol/L); **G:** DCVC (0.1 mmol/L); **H:** DCVC (0.2 mmol/L).

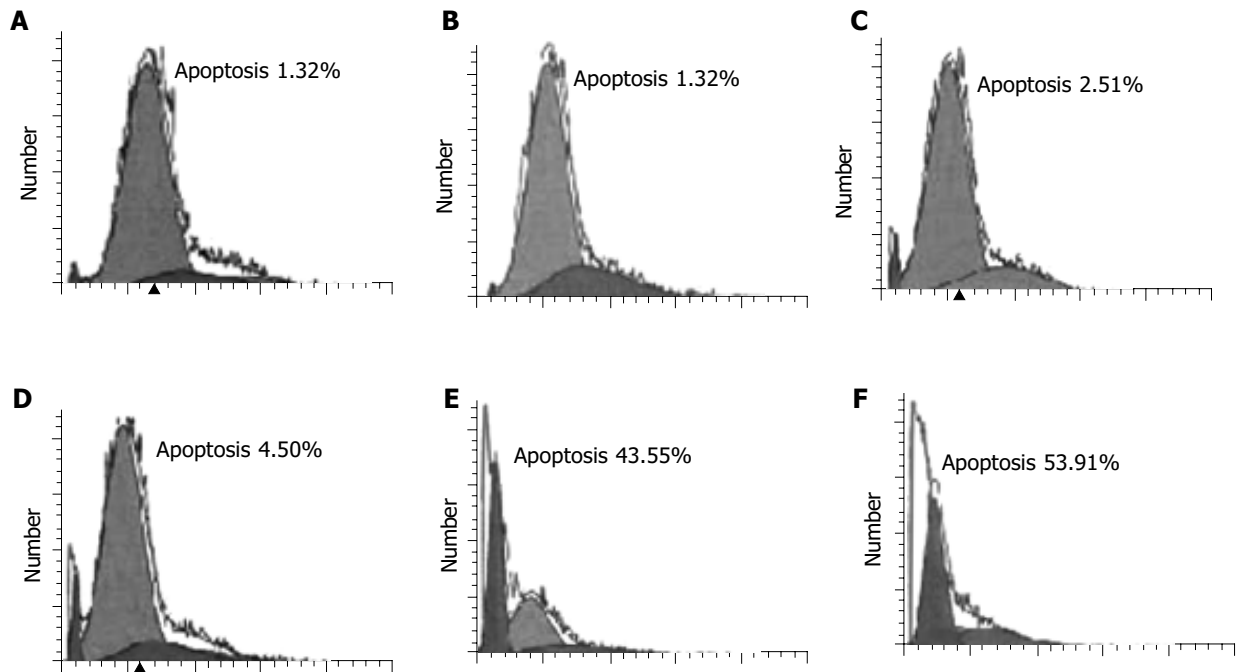


Figure 3 Time effect on cell apoptosis induced by DCVC co-treated with DPPD. SMMC-7721 hepatocellular carcinoma cells were treated with 0.1 mmol/L DCVC and 0.02 mmol/L DPPD for various time, then harvested for flow cytometry

assay to estimate apoptosis. A: absent DCVC, for 8 h; B: for 1 h; C: 2 h; D: 4 h; E: 6 h; F: 8 h.

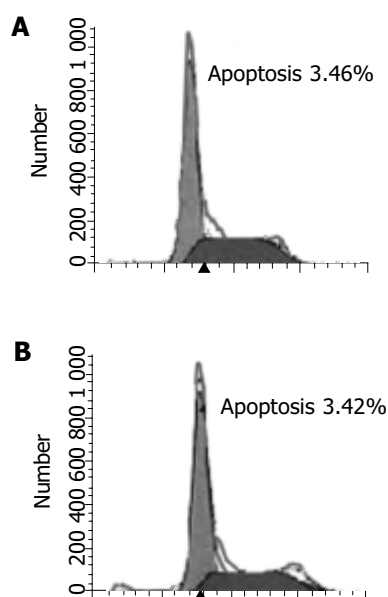


Figure 4 Role of DPPD in apoptosis of SMMC-7721 hepatocellular carcinoma cell. Cells were cultured in completed medium for 12 h. A: In the absence of DPPD; B: in the presence of 0.02 mmol/L DPPD, then cells were carried out in FCM to estimate apoptosis.

longer than 4 h, the FAK protein was almost lost (Figure 5A) and the percentage of cell apoptosis began to increase rapidly. When the concentration of DCVC was larger than 0.05 mmol/L, the FAK expression almost was not observed (Figure 5B). These results were consistent with the process of cell apoptosis and suggested that cell apoptosis occurred after the cleavage of FAK and the damage of cell-matrix interaction or the focal adhesion.

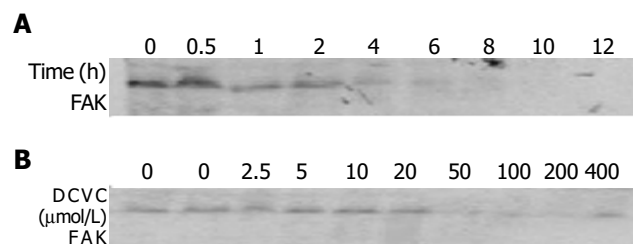


Figure 5 DCVC effects on FAK protein expression. A: SMMC-7721 hepatocellular carcinoma cells were treated with 0.1 mmol/L DCVC and 0.02 mmol/L DPPD for various time duration; B: SMMC-7721 hepatocellular carcinoma cells were treated with 0.02 mmol/L DPPD and various DCVC concentrations for 6 h, from right the first lane both DCVC and DPPD were absent, the second lane had DPPD but no DCVC. Cells were harvested with 1× SDS loading buffer, followed by Western blot analysis. Equal amounts of cell protein (60 μg) were added to each lane, these studies were repeated thrice with similar results.

ILK level was decreased after the DCVC treatment

ILK is another newly identified, integrin cytoplasmic-binding protein. Overexpression of ILK in cultured intestinal and mammary epithelial cells has been previously shown to induce changes characteristic of oncogenic transformation, including anchorage-independent growth, invasiveness, suppression of anoikis and tumorigenicity in nude mice^[9]. For this reason, we measured the expression of ILK in DCVC-induced SMMC-7721 hepatocellular carcinoma cell by Western blot analysis and found that the level of ILK was also decreased (Figure 6). These findings further demonstrated that the disruption of focal adhesion was taking place in this apoptosis model.

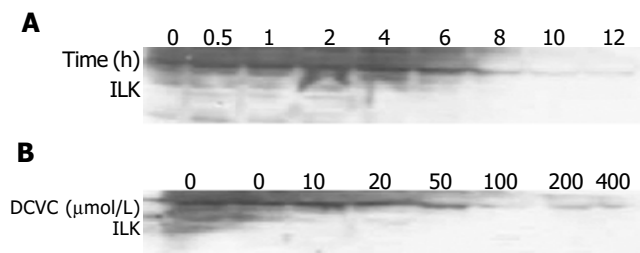


Figure 6 DCVC effects on ILK protein expression. **A:** SMMC-7721 hepatocellular carcinoma cells were treated with 0.1 mmol/L DCVC and 0.02 mmol/L DPPD for various time duration; **B:** SMMC-7721 hepatocellular carcinoma cells were treated with 0.02 mmol/L DPPD and various DCVC concentrations for 6 h, from left the both DCVC and DPPD were absent, the second lane had DPPD but no DCVC. Cells were harvested with 1× SDS loading buffer, followed by Western blot analysis. Equal amounts of cell protein (60 μg) were added to each lane, these studies were repeated thrice with similar results.

β-catenin level was down-regulated in the apoptosis induced by DCVC

E-cadherin-mediated cell-cell adhesion plays a crucial role in intercellular communication, which is related to the regulation of cell proliferation, differentiation, and apoptosis^[24]. β -Catenin regulates cadherin-mediated cell-cell adhesion and also functions as a signaling molecule^[25]. For this reason, we measured the expression of β -catenin in DCVC-induced SMMC-7721 hepatocellular carcinoma cell by Western blot analysis and interestingly found that the level of β -catenin began to decrease for an hour of DCVC treatment and after that, the level of β -catenin decreased further (Figure 7A). Similarly when the dose of DCVC was larger than 0.05 mmol/L, β -catenin also decreased (Figure 7B). These findings suggest that, the cell apoptosis occurred after the decrease of β -catenin and the damage of intercellular adhesion.

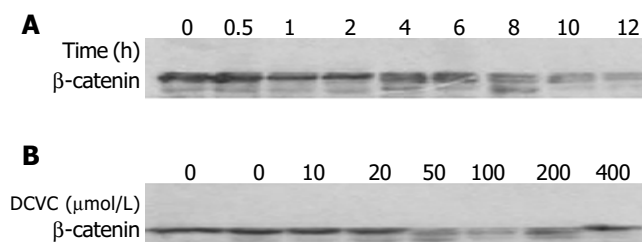


Figure 7 DCVC effects on β -catenin protein expression. **A:** SMMC-7721 hepatocellular carcinoma cells were treated with 0.1 mmol/L DCVC and 0.02 mmol/L DPPD for various time duration; **B:** SMMC-7721 hepatocellular carcinoma cells were treated with 0.02 mmol/L DPPD and various DCVC concentrations for 6 h, from left the first lane both DCVC and DPPD were absent, the second lane had DPPD but no DCVC. Cells were harvested with 1× SDS loading buffer, followed by Western blot analysis. Equal amounts of cell protein (60 μg) were added to each lane, these studies were repeated thrice with similar results.

PKB level was downregulated in the apoptosis induced by DCVC

PKB has been demonstrated to play a suppressive role in cell apoptosis^[26]. We therefore investigated the PKB level in

response to DCVC in the presence of DPPD. We found when the time of DCVC treatment was longer or the dose of DCVC was increased, the level of PKB decreased. Particularly, after 4 h of DCVC treatment, PKB obviously decreased and after 8 h, PKB protein almost disappeared (Figure 8).

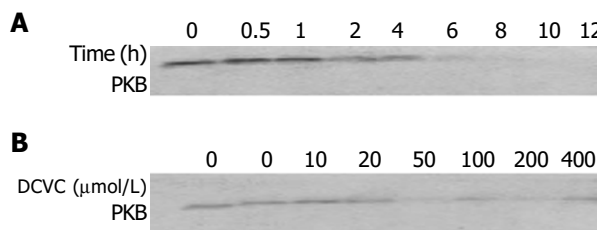


Figure 8 DCVC effects on PKB protein expression. **A:** SMMC-7721 hepatocellular carcinoma cells were treated with 0.1 mmol/L DCVC and 0.02 mmol/L DPPD for various time duration; **B:** SMMC-7721 hepatocellular carcinoma cells were treated with 0.02 mmol/L DPPD and various DCVC concentration for 6 h, from left both DCVC and DPPD were absent in the first lane, the second lane had DPPD but without DCVC. Cells were harvested with 1× SDS loading buffer, followed by Western blot analysis. Equal amounts of cell protein (60 μg) were added to each lane, these studies were repeated thrice with similar results.

DISCUSSION

In this study, we investigated the level of FAK, ILK, PKB, and β -catenin during apoptosis of SMMC-7721 hepatocellular carcinoma cell induced by DCVC in the presence of DPPD. It was found that the level of each protein mentioned above dramatically decreased. These results suggest that the loss or decrease of cell adhesion signal molecules is an important reason in apoptosis of SMMC-7721 hepatocellular carcinoma cell. The apoptosis of SMMC-7721 was preceded by the loss or decrease of FAK, ILK, PKB, and β -catenin or the damage of cell-matrix and cell-cell adhesion.

FAK has been shown to play a suppressive role in apoptosis induced by various stimuli including H_2O_2 and c-myc, and apoptosis induced by keeping cell in suspension, termed anoikis, which disrupts the interactions between normal epithelial cells and the extracellular matrix^[21,27,28]. Our findings strongly support the view that FAK play a suppressive role in apoptosis. Furthermore, decrease of FAK seems to precede cell apoptosis.

ILK is another integrin cytoplasmic-binding protein that has been identified as a potential PDK-2. ILK is capable of phosphorylating PKB/Akt on Ser-473 and stimulating its activity. Attwell found that overexpression of ILK in SCP2 mouse mammary epithelial cells results in a profound inhibition of anoikis^[29]. Until the present day, no reports have described the role of ILK in the apoptosis of human hepatocellular carcinoma cell. We found that the level of ILK was decreased in DCVC/DPPD-induced apoptosis. This finding is in accordance with that of Attwell's reports^[29].

β -catenin has emerged as an important oncogene in the transformation of a number of epithelial cancers^[30]. It acts as a downstream transcriptional activator of the Wnt signaling pathway. The β -catenin-Tcf complex transactivates the downstream genes that regulate cell proliferation or inhibit

apoptosis^[31]. But Kim *et al.*, reported that overexpressed β -catenin induces apoptosis in NIH 3T3 fibroblasts, corneal fibroblasts, corneal epithelia, uveal melanoma cells, and several carcinoma cell lines^[32]. In this study, we found that the level of β -catenin was dramatically decreased in DCVC-induced SMMC-7721 cell apoptosis and the reason needs to be elucidated by further research.

PKB acted as a common downstream signal protein of FAK, and ILK has been demonstrated to play a suppressive role in cell apoptosis^[21,26,29]. Our results showed that the PKB level was decreased with increased DCVC concentration or treatment time, as well as the percentage of apoptotic cells during the apoptosis induced by DCVC in the presence of DPPD.

Our findings indicate that DCVC cause the cleavage of FAK, ILK, β -catenin, and PKB. Cleavage of these proteins may actually ensure that the cell does not attach to matrix or other cells. It blocks the cell-matrix and cell-cell adhesion-mediated signal transduction and gives rise to cell apoptosis. It demonstrates the importance of cell adhesion signal molecules in cell survival. However, the exact way of cleavage of these proteins is still unclear. FAK and β -catenin may be cleaved by caspases, as both have been identified as substrates for caspases^[33,34]. Whether ILK and PKB are also cleaved by caspases or other enzymes, remains to be determined.

In conclusion, the present findings demonstrate that the cell apoptosis occurred after the damage of cell-matrix interaction and cell-cell contact. Cell-matrix and cell-cell adhesion-mediated signal transduction is fundamental for cell survival and many cell adhesion signal molecules such as FAK, ILK, and β -catenin have oncogenic potential and have anti-apoptotic function.

ACKNOWLEDGMENTS

We gratefully appreciate Dr. Hong-Xing Zhang for the assistance of DCVC synthesis. We thank all people in the Flow Cytometry Core Facility of Tumor Hospital at Fudan University for processing the cell apoptosis analysis.

REFERENCES

- Sanders EJ, Wride MA. Programmed cell death in development. *Int Rev Cytol* 1995; **163**: 105-173
- Osborne BA. Induction of genes during apoptosis: examples from the immune system. *Semin Cancer Biol* 1995; **6**: 27-33
- Zachary I, Rozengurt E. Focal adhesion kinase (p125FAK): a point of convergence in the action of neuropeptides, integrins, and oncogenes. *Cell* 1992; **71**: 891-894
- Schwartz MA. Integrins, oncogenes, and anchorage independence. *J Cell Biol* 1992; **139**: 575-578
- Re F, Zanetti A, Sironi M, Polentarutti N, Lanfrancone L, Dejana E, Colotta F. Inhibition of anchorage-dependent cell spreading triggers apoptosis in cultured human endothelial cells. *J Cell Biol* 1994; **127**: 537-546
- Zhang Z, Vuori K, Reed JC, Ruoslahti E. The alpha 5 beta 1 integrin supports survival of cells on fibronectin and up-regulates Bcl-2 expression. *Proc Natl Acad Sci USA* 1995; **92**: 6161-6165
- Kornberg L, Earp HS, Parsons JT, Schaller M, Juliano RL. Cell adhesion or integrin clustering increases phosphorylation of a focal adhesion-associated tyrosine kinase. *J Biol Chem* 1992; **267**: 23439-23442
- Schaller MD, Borgman CA, Cobb BS, Vines RR, Reynolds AB, Parsons JT. pp125FAK a structurally distinctive protein-tyrosine kinase associated with focal adhesions. *Proc Natl Acad Sci USA* 1992; **89**: 5192-5196
- White DE, Cardiff RD, Dedhar S, Muller WJ. Mammary epithelial-specific expression of the integrin linked kinase (ILK) results in the induction of mammary gland hyperplasias and tumors in transgenic mice. *Oncogene* 2001; **20**: 7064-7072
- Guo L, Sanders PW, Woods A, Wu C. The distribution and regulation of integrin-linked kinase in normal and diabetic kidneys. *Am J Pathol* 2001; **159**: 1735-1742
- Nose A, Nagafuchi A, Takeichi M. Isolation of placental cadherin cDNA: Identification of a novel gene family of cell-cell adhesion molecules. *EMBO J* 1987; **6**: 3655-3661
- Yap AS, Brieher WM, Gumbiner BM. Molecular and functional analysis of cadherin-based adherens junctions. *Annu Rev Cell Dev Biol* 1997; **13**: 119-146
- Yap AS, Brieher WM, Pruschy M, Gumbiner BM. Lateral clustering of the adhesive ectodomain: a fundamental determinant of cadherin function. *Curr Biol* 1997; **7**: 308-315
- Van de Water B, Jaspers JJ, Maasdam DH, Mulder GJ, Nagelkerke JF. *In vivo* and *in vitro* detachment of proximal tubular cells and F-actin damage: consequences for renal function. *Am J Physiol* 1994; **267** (5 Pt 2): F888-899
- Van de Water B, Kruidering M, Nagelkerke JF. F-actin disorganization in apoptotic cell death of cultured rat renal proximal tubular cells. *Am J Physiol* 1996; **270** (4 Pt 2): F593-F603
- Stevens JL, Robbins JD, Byrd RA. A purified cysteine conjugate beta-lyase from rat kidney cytosol. Requirement for an alpha-keto acid or an amino acid oxidase for activity and identity with soluble glutamine transaminase K. *J Biol Chem* 1986; **261**: 15529-15537
- Hayden PJ, Stevens JL. Cysteine conjugate toxicity, metabolism, and binding to macromolecules in isolated rat kidney mitochondria. *Mol Pharmacol* 1990; **37**: 468-476
- Chen Q, Jones TW, Brown PC, Stevens JL. The mechanism of cysteine conjugate cytotoxicity in renal epithelial cells. Covalent binding leads to thiol depletion and lipid peroxidation. *J Biol Chem* 1990; **265**: 21603-21611
- Cai T, Lei QY, Wang LY, Zha XL. TGF-beta 1 modulated the expression of alpha 5 beta 1 integrin and integrin-mediated signaling in human hepatocarcinoma cells. *Biochem Biophys Res Commun* 2000; **274**: 519-525
- Zhan Y, Cleveland JL, Stevens JL. A role for c-myc in chemically induced renal-cell death. *Mol Cell Biol* 1997; **17**: 6755-6764
- Sonoda Y, Watanabe S, Matsumoto Y, Aizu-Yokota E, Kasahara T. FAK is the upstream signal protein of the phosphatidylinositol 3-kinase-Akt survival pathway in hydrogen peroxide-induced apoptosis of a human glioblastoma cell line. *J Biol Chem* 1999; **274**: 10566-10570
- Xu LH, Owens LV, Sturge GC, Yang X, Liu ET, Craven RJ, Cance WG. Attenuation of the expression of the focal adhesion kinase induces apoptosis in tumor cells. *Cell Growth Differ* 1996; **7**: 413-418
- Crouch DH, Fincham VI, Frame MC. Targeted proteolysis of the focal adhesion kinase pp125FAK during c-MYC-induced apoptosis is suppressed by integrin signaling. *Oncogene* 1996; **12**: 2689-2696
- Yang SZ, Kohno N, Kondo K, Yokoyama A, Hamada H, Hiwada K, Miyake M. Adriamycin activates E-cadherin-mediated cell-cell adhesion in human breast cancer cells. *Int J Oncol* 1999; **15**: 1109-1115
- Ninomiya I, Endo Y, Fushida S, Sasagawa T, Miyashita T, Fujimura T, Nishimura G, Tani T, Hashimoto T, Yagi M, Shimizu K, Ohta T, Yonemura Y, Inoue M, Sasaki T, Miwa K. Alteration of beta-catenin expression in esophageal squamous-cell carcinoma. *Int J Cancer* 2000; **85**: 757-761
- Ozes ON, Mayo LD, Gustin JA, Pfeffer SR, Pfeffer LM, Donner DB. NF- κ B activation by tumor necrosis factor requires the PKB serine-threonine kinase. *Nature* 1999; **401**: 82-85
- Frisch SM, Vuori K, Ruoslahti E, Chan-Hui PY. Control of adhesion-dependent cell survival by focal adhesion. *J Cell Biol*

- 1996; **134**: 793-799
- 28 **Ilic D**, Almeida EA, Schlaepfer DD, Dazin P, Aizawa S, Damsky CH. Extracellular matrix survival signals transduced by focal adhesion kinase suppress p53-regulated apoptosis. *J Cell Biol* 1998; **143**: 547-560
- 29 **Attwell S**, Roskelley C, Dedhar S. The integrin-linked kinase (ILK) suppresses anoikis. *Oncogene* 2000; **19**: 3811-3815
- 30 **Wright K**, Wilson P, Morland S, Campbell I, Walsh M, Hurst T, Ward B, Cummings M, Chenevix-Trench G. beta-catenin mutation and expression analysis in ovarian cancer: exon 3 mutations and nuclear translocation in 16% of endometrioid tumours. *Int J Cancer* 1999; **82**: 625-629
- 31 **Kim YS**, Kang YK, Kim JB, Han SA, Kim KI, Paik SR. beta-catenin expression and mutational analysis in renal cell carcinomas. *Patho Int* 2000; **50**: 725-730
- 32 **Kim K**, Pang KM, Evans M, Hay ED. Overexpression of beta-catenin induces apoptosis independent of its transactivation function with LEF-1 or the involvement of major G1 cell cycle regulators. *Mol Biol Cell* 2000; **11**: 3509-3523
- 33 **Wen LP**, Fahrni JA, Troie S, Guan JL, Orth K, Rosen GD. Cleavage of focal adhesion kinase by caspases during apoptosis. *J Biol Chem* 1997; **272**: 26056-26061
- 34 **Brancolini C**, Lazarevic D, Rodriguez J, Schneider C. Dismantling cell-cell contacts during apoptosis is coupled to a caspase-dependent proteolytic cleavage of beta-catenin. *J Cell Biol* 1997; **139**: 759-771

Science Editor Guo SY Language Editor Elsevier HK

• COLORECTAL CANCER •

Anticancer effects of oligomeric proanthocyanidins on human colorectal cancer cell line, SNU-C4

Youn-Jung Kim, Hae-Jeong Park, Seo-Hyun Yoon, Mi-Ja Kim, Kang-Hyun Leem, Joo-Ho Chung, Hye-Kyung Kim

Youn-Jung Kim, Department of Dental Hygiene, Hanseo University, Seosan, South Korea

Hae-Jeong Park, Seo-Hyun Yoon, Joo-Ho Chung, Department of Pharmacology, Kohwang Medical Research Institute, College of Medicine, Kyung Hee University, Seoul, South Korea

Mi-Ja Kim, Department of Obesity Management, Graduate School of Obesity Science, Dongduk Women's University, Seoul, South Korea
Kang-Hyun Leem, College of Oriental Medicine, Semyung University, Jecheon, South Korea

Hye-Kyung Kim, Department of Food and Biotechnology, Hanseo University, Seosan, South Korea

Co-first-authors: Hae-Jeong Park

Correspondence to: Hye-Kyung Kim, Department of Food and Biotechnology, Hanseo University, Seosan 356-705, South Korea. hkkim111@hanseo.ac.kr

Telephone: +82-41-660-1454 Fax: +82-41-660-1119

Received: 2004-09-18 Accepted: 2004-10-08

Key words: Oligomeric pranthocyanidins; Apoptosis; Anticancer effects; Colorectal cancer

Kim YJ, Park HJ, Yoon SH, Kim MJ, Leem KH, Chung JH, Kim HK. Anticancer effects of oligomeric proanthocyanidins on human colorectal cancer cell line, SNU-C4. *World J Gastroenterol* 2005; 11(30): 4674-4678

<http://www.wjgnet.com/1007-9327/11/4674.asp>

INTRODUCTION

Oligomeric proanthocyanidins are some of the most abundant polyphenolic substances in the plant kingdom. Proanthocyanidins are an integral part of the human diet, found in high concentration in fruits, vegetables and seeds as well as in most types of tea and red wine^[1]. Numerous studies have reported that flavonoids have potent antioxidant effects through scavenging of superoxide and hydroxyl radicals^[2] and anti-proliferative actions via inhibition of metabolic pathways and inhibition of intra-cellular signal transduction^[3]. In addition, a variety of proanthocyanidins have been shown to be anti-bacterial, anti-viral^[4], anti-carcinogenic^[3-6], anti-inflammatory^[7,8], anti-allergic^[9-11] and consequently reduce the concentration of reactive oxygen species^[12] and low density lipoprotein oxidation^[13], and cardioprotective effects in human beings^[14].

Despite their beneficial effects, the great extent of polyphenolics are not absorbed and metabolized easily due to their chemical structures and the glycosylation, acylation, conjugation, polymerization and the solubility of the compound. Monomeric flavonoids are absorbed in the small intestine. However, polymeric polyphenolics may be degraded by intestinal and colonic microflora, and then excreted in the feces, and the monomers appear to be absorbed in a dose-dependent manner^[15].

Apoptosis, a programmed cell death, also plays an essential role as a protective mechanism against cancer cells^[16]. Induction of apoptosis is a highly desirable mode as a therapeutic strategy for cancer control. In fact, many chemopreventive agents act through the induction of apoptosis as a mechanism to suppress carcinogenesis^[17]. Recently, cancer chemotherapy has gradually improved with the development and discovery of novel anti-tumor drugs, but sometimes these drugs have been limited in clinical application by drug resistance of tumor and by serious damage to the normal tissues and cells.

Oligomeric proanthocyanidins incubated with several human cancer cell lines (breast, lung, gastric, and skin) revealed a selective cytotoxicity for the cancerous cells.

Abstract

AIM: Oligomeric proanthocyanidins (OPC), natural polyphenolic compounds found in plants, are known to have antioxidant and anti-cancer effects. We investigated whether the anti-cancer effects of the OPC are induced by apoptosis on human colorectal cancer cell line, SNU-C4.

METHODS: Colorectal cancer cell line, SNU-C4 was cultured in RPMI 1640 medium supplemented with 10% fetal bovine serum. The cytotoxic effect of OPC was assessed by 3-(4, 5-dimethylthiazol-2-yl)-2, 5-diphenyltetrazolium bromide (MTT) assay. To find out the apoptotic cell death, 4, 6-diamidino-2-phenylindole (DAPI) staining, terminal deoxynucleotidyl transferase (TdT)-mediated dUTP nick end labeling (TUNEL) assay, reverse transcription-polymerase chain reaction (RT-PCR), and caspase-3 enzyme assay were performed.

RESULTS: In this study, cytotoxic effect of OPC on SNU-C4 cells appeared in a dose-dependent manner. OPC treatment (100 µg/mL) revealed typical morphological apoptotic features. Additionally OPC treatment (100 µg/mL) increased level of *BAX* and *CASPASE-3*, and decreased level of *BCL-2* mRNA expression. Caspase-3 enzyme activity was also significantly increased by treatment of OPC (100 µg/mL) compared with control.

CONCLUSION: These data indicate that OPC caused cell death by apoptosis through caspase pathways on human colorectal cancer cell line, SNU-C4.

However OPC has not been tested for colorectal cancer which is one of the major cause of cancer-related mortality in the West.

In this study, we examined the inhibitory effects of OPC on cancer cell proliferation, and pharmacological mechanism for anti-tumor effects on human colorectal cancer cell line SNU-C4.

MATERIALS AND METHODS

Materials

Grape seed OPC was donated by Doosan Biotech (Yongin, Korea). According to the manufacturer, this OPC extract contained essentially, dimeric (17.4%), trimeric (16.3%), tetrameric (13.3%) and oligomeric (5-13 Units) (53.0%) proanthocyanidins. DAPI and caspase-3 assay kit were obtained from Sigma (St. Louis, MO, USA). MTT and TUNEL assay kits were purchased from Roche (Roche, Basal, Switzerland).

Cell culture

The SNU-C4 cell line was obtained from Korean Cell Line Bank (KCLB, Seoul, Korea). Cells were cultured in RPMI 1640 medium (Gibco, Grand Island, NY, USA) supplemented with 10% heat-inactivated fetal bovine serum (Gibco). Cultures were maintained in a humidified incubator with 5% CO₂-95% O₂ air at 37 °C, and the medium was changed every 2 d.

MTT assay

Cell viability was determined using the MTT assay kit according to a previously described protocol^[18]. In order to detect the cytotoxicity of OPC, SNU-C4 cells were treated with OPC at the concentrations of 10, 50, 100, and 500 µg/mL for 24 h. The control group was treated with the same amount of vehicle. After the MTT, labeling reagent (5 mg/mL) was added to each group and incubated for 4 h at 37 °C, they were incubated for 12 h with the solubilization solution in which the formazan crystals formed by MTT will be dissolved. The absorbance was measured with a microtiter plate reader (Bio-Tek, Winooski, VT, USA) at a test wavelength of 595 nm with a reference wavelength of 690 nm. The optical density (*A*) was calculated as the difference between the reference wavelength and the test wavelength. Percent viability was calculated as (*A* of drug-treated sample/*A* of none-treated control) ×100.

DAPI staining

The nucleic condensation of apoptosis was determined by DAPI staining. SNU-C4 cells treated with OPC (100 µg/mL) for 24 h were cultured on four-chamber slides (Nalge Nunc International, Rochester, NY, USA). The cells were fixed in 40 g/L paraformaldehyde for 30 min, and were incubated for 30 min in the dark, including 1 µg/mL DAPI solution. They were observed through a fluorescence microscope (Zeiss, Oberkochen, Germany).

TUNEL assay

For detection of apoptotic cells, TUNEL assay was performed by ApoTag[®] peroxidase *in situ* cell death

detection kit (Roche, Basal, Switzerland). After 24 h exposure to OPC (100 µg/mL), cultured SNU-C4 cells were fixed in acetic acid at -20 °C for 5 min. Incubated with digoxigenin-conjugated dUTP in a terminal deoxynucleotidyl transferase-catalyzed reaction for 1 h at 37 °C in a humidified atmosphere. The fixed cells were immersed in stop/wash buffer for 10 min at room temperature, and the cells were again incubated with an anti-digoxigenin antibody conjugating peroxidase for 30 min. The nuclei fragments were stained using 3,3'-diaminobenzidine (DAB) as a substrate for the peroxidase.

RT-PCR analysis

Total RNA was isolated from SNU-C4 cells with RNazol[™] (TEL-TEST, Friendswood, TX, USA) according to the manufacturer's instruction. cDNA was produced using random hexamer primers and reverse transcriptase (Promega, Madison, WI, USA). The corresponding cDNA was amplified in PCR reactions with following primers for *BCL-2* (5'-TCC GTG CCT GAC TTT AGC AAG CTG-3'; 5'-GGA ATC CCA ACC AGA GAT CTC AA-3'), *BAX* (5'-AGA TGA ACT GGA TAG CAA TAT GGA-3', 5'-CCA CCC TGG TCT TGG ATC CAG ACA-3'), and for *CASPASE-3* (5'-CTT GGT AGA TCG GCC ATC TGA AAC-3'; 5'-GGT CCC GTA CAG GTG TGC TTC GAC-3'). *CYCLOPHILIN* (5'-ACC CCA CCG TGT TCT TCG AC-3', 5'-CAT TTG CCA TGG ACA AGA TG-3') was used as an internal standard. The annealing temperature was 50 °C for *BCL-2* and *BAX*, 57 °C for *CASPASE-3*, and 56 °C for *CYCLOPHILIN*. The amplified fragment sizes were respectively 333 bp (for *BCL-2*), 260 bp (for *BAX*), 405 bp (for *CASPASE-3*), and 300 bp (for *CYCLOPHILIN*). The PCR products were electrophoresed on a 1.2% agarose gel, and stained with ethidium bromide. The PCR amplification was performed in 30 cycles for *BCL-2*, *BAX*, *CASPASE-3*, and 24 cycles for *CYCLOPHILIN*.

Caspase-3 enzyme activity

Because caspase-3 is a key step in the regulation of apoptosis, caspase-3 activity was measured using a commercially available kit. Cells were incubated with OPC (100 µg/mL) for 24 h, and were washed with phosphate-buffered saline (PBS) and lysed. Then the lysates were incubated overnight with caspase-3 substrate (Ac-DVED-pNA) at 37 °C, and absorbance at 405 nm was measured using a 96-well microtiter plate reader. As a positive control, recombinant caspase-3 protein was incubated with a substrate. As an inhibitor of caspase-3, Ac-DVED-CHO was used.

Statistical analysis

Results were expressed as mean±SE. All experiments were done in triplicate. The data were analyzed by one-way ANOVA followed by Dunnett's post-hoc analysis using SPSS. Differences were considered significant at *P*<0.05.

RESULTS

Cytotoxic effects of OPC on colorectal cancer cell line, SNU-C4

The MTT assay was used to measure the viability of SNU-

C4 cells exposed to OPC. As shown in Figure 1, the viabilities of cells exposed to OPC at concentrations of 10, 50, 100, and 500 $\mu\text{g}/\text{mL}$ for 24 h, were $94.03\pm 0.21\%$, $81.17\pm 0.35\%$, $35.61\pm 5.53\%$, and $21.24\pm 1.31\%$ of control value, respectively. The cytotoxic effect of OPC on SNU-C4 cells appeared in a dose-dependent manner (Figure 1).

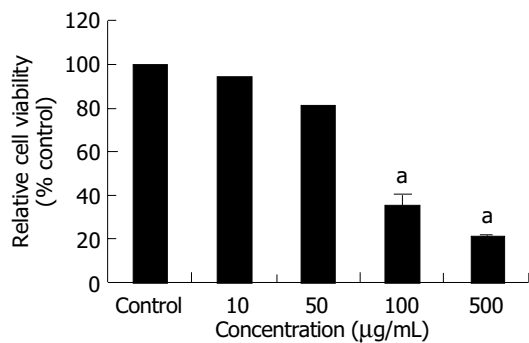


Figure 1 Cytotoxic effects of OPC. SNU-C4 cells were treated with various concentrations of OPC for 24 h prior to the determination of cellular viability. Results are presented as mean \pm SE. ^a $P<0.05$ vs control group.

Morphological changes in OPC-induced cytotoxicity

The morphological changes, DAPI staining, and TUNEL reaction were studied to investigate whether cell death was a result of apoptosis in SNU-C4 cells. Cells treated with OPC (100 $\mu\text{g}/\text{mL}$) for 24 h revealed shrinkage of cells through phase-contrast microscope (Figure 2B). To

characterize the cell death induced by OPC, nuclear morphology of dying cells were examined with a fluorescent DNA-binding agent, DAPI. Cells treated with OPC displayed typical morphological features of apoptotic cells, with condensed and fragmented nuclei (Figure 2D). The induction of apoptosis by OPC was examined by *in situ* apoptosis detection. TUNEL assay, based on labeling of DNA strand breaks generated during apoptosis, confirmed that OPC induces apoptosis in SNU-C4 cells (Figure 2F).

Involvement of BCL-2 and BAX genes in OPC-induced cytotoxicity

To examine the role of these *BCL-2* family genes in OPC-induced apoptosis, the expression of *BCL-2* and *BAX* genes were evaluated in SNU-C4 cells using RT-PCR. As shown in Figure 3, *BCL-2* gene expression was markedly decreased and *BAX* gene expression was highly increased with OPC treatment.

Involvement of caspase-3 in OPC-induced cytotoxicity

Since caspase-3 plays the critical role in apoptosis, the *CASPASE-3* gene expression and caspase-3 enzyme activity were determined through RT-PCR and caspase-3 activity assay. The expression of *CASPASE-3* was markedly increased after OPC treatment (Figure 3). The caspase-3 activity was measured using specific substrate (Ac-DEVD- ρ NA). Caspase-3 protein was used as the positive control, and a caspase inhibitor, Ac-DEVD-CHO was the negative control. As illustrated in Figure 4, caspase-3 specific activity was increased by OPC treatment.

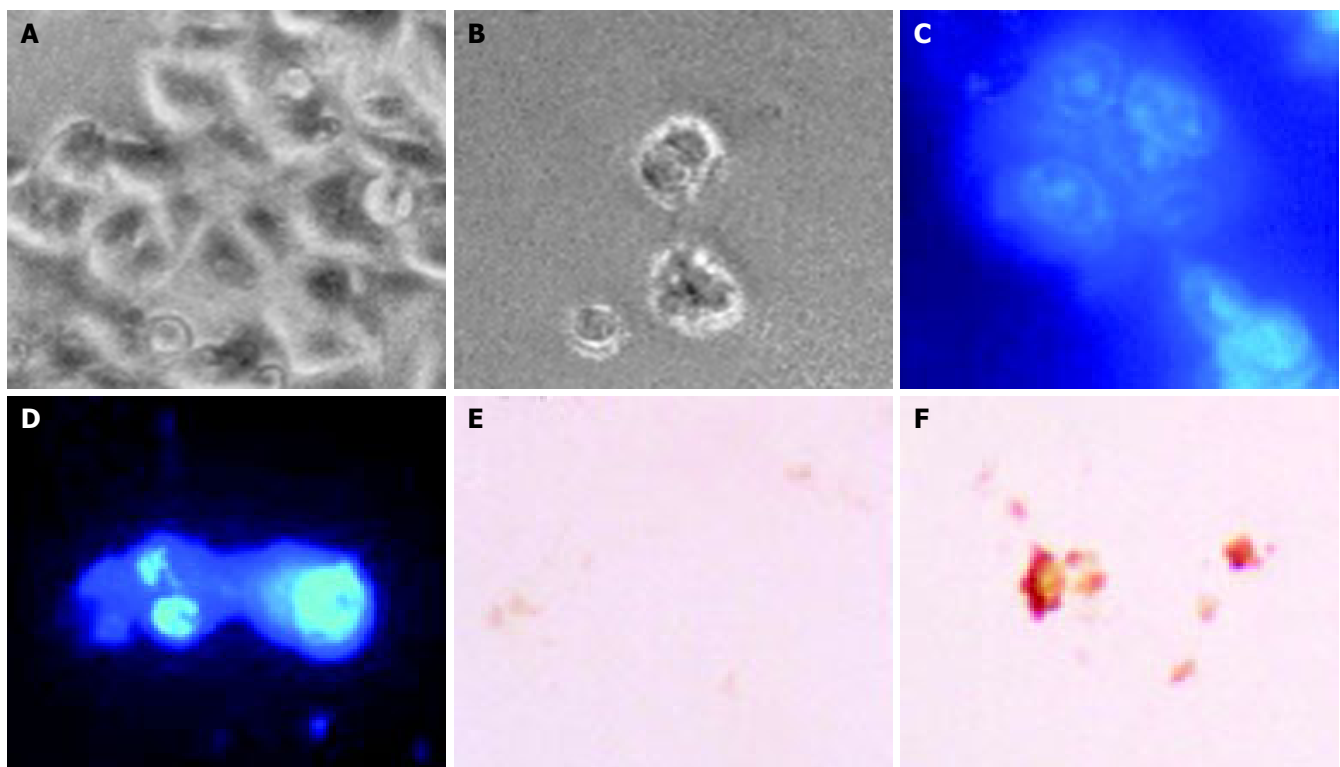


Figure 2 Characterization of OPC-induced cell death in SNU-C4 cells. Cells were cultured without OPC (A, C and E) or with 100 $\mu\text{g}/\text{mL}$ OPC (B, D and F). Morphology (top): phase-contrast microscopy shows cell shrinkage, bubble

like bleb in cell membrane and cellular detachment in OPC-treated cultures (B). SNU-C4 cells stained with DAPI staining (D). SNU-C4 cells stained with TUNEL staining (F): Scale bar, 10 μm .

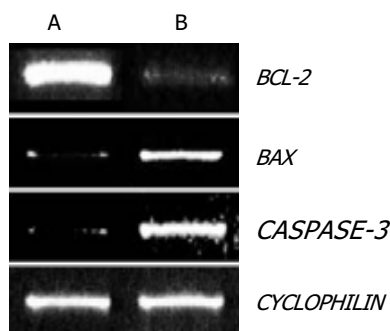


Figure 3 Results of RT-PCR analysis of *BCL-2*, *BAX*, and *CASPASE-3*. As internal control, *CYCLOPHILIN* mRNA was also reverse-transcribed and amplified. (A) Control, (B) 100 µg/mL OPC treated group.

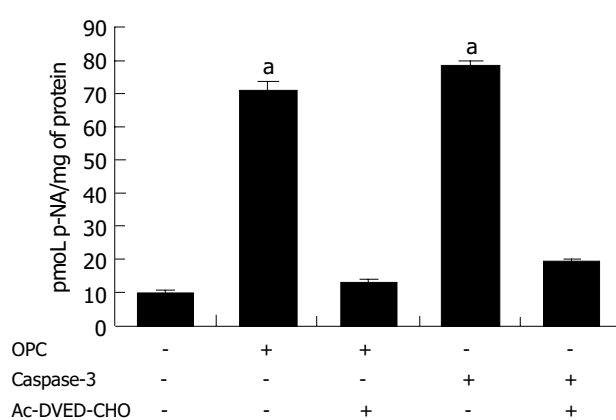


Figure 4 Result of caspase-3 enzyme activity assay. The rate of Ac-DEVD-pNA cleavage was measured at 405 nm. OPC was used as concentration of 100 µg/mL. Caspase-3 was a positive control and Ac-DEVD-CHO was a caspase inhibitor. ^a $P < 0.05$ vs control group.

DISCUSSION

Colorectal cancer is the most common of visceral malignancies with the third most common cause of cancer-related mortality in the West^[19]. Despite improvements in the management of the colon cancer patient, there is little change in survival rates over the past 50 years^[20]. Tumor cells differ from normal cells in their non-responsiveness to normal growth-controlling mechanisms. Current chemotherapeutic drugs try to change the biological properties of cancer cells that continuously divide and grow^[21].

In the present study, we investigated the effect of OPC-induced apoptosis on human colorectal cancer cell line SNU-C4 to define the pharmacological basis for anticancer effects and its mechanism of OPC. OPC, extracted from grape seed showed potent anti-oxidant effects in numerous studies^[22-25]. Additionally, proanthocyanidins exhibit anti-carcinogenic^[3-6], anti-inflammatory^[7,8], anti-allergic^[9,10], cardioprotective activities^[14], as well as being inhibitors of the phospholipase A2, cyclooxygenase and lipoxygenase^[26].

Recently, Carnéscechi *et al.*^[6], reported anti-proliferative effects of procyanidins from cocoa extracts on the growth inhibition of human colonic cancer cell with a blockade of the cell cycle at the G2/M phase. OPC have demonstrated the anti-proliferative effect in murine Hepa-1c1c7^[26],

cytotoxic effects on selected human cancer cells, including cultured MCF-7 breast cancer, CRL 1739 gastric adenocarcinoma and A-427 lung cancer cells^[5]. These reports demonstrated that OPC influences cancer cell proliferation and growth.

The results of present study demonstrated that OPC induce cytotoxic effect measured by the cell viability on SNU-C4 cells in a dose-dependent manner (Figure 1). SNU-C4 cells also showed apoptotic morphological change of nuclear shrinkage, chromatin condensation, irregularity in shape and retraction by the OPC treatment (Figure 2). In this study, we observed the apoptotic morphology of cellular bodies and the chromatin condensation by DAPI staining (Figure 2). It is known that DNA strand breaks occur during the process of apoptosis, and the nicks in DNA molecules can be detected by the apoptotic status of cells through TUNEL assay^[27]. In the present study, typical TUNEL distinction of apoptosis was observed in OPC-treated cells (Figure 2).

In a number of studies, it has been documented that the progress of apoptosis is regulated by the expression of several genes, one of these genes is a member of the *BCL-2* family^[28]. The *BCL-2* family can be classified into two functionally different groups: anti-apoptotic genes and pro-apoptotic genes. *BCL-2*, an anti-apoptotic gene, is known for regulating the apoptotic pathways and protecting cell death, while *BAX*, a pro-apoptotic gene of the family, is expressed abundantly and selectively during apoptosis, promoting cell death^[29]. Our data showed that OPC altered the expression of apoptosis-regulating genes. *BCL-2* gene expression decreased and *BAX* gene expression increased after OPC-treatment (Figure 3).

At the execution phase of apoptosis, a series of morphological and biochemical changes appear to have resulted from the action of caspases^[30]. Caspase-3, in particular, is believed to be most commonly involved in the execution of apoptosis in various cell types^[31], because it cleaves most of caspase-related substrates, including key proteins such as the nuclear enzyme PARP^[32]. In our data, it is shown that the *CASPASE-3* gene expression was increased (Figure 3) and the activity of caspase-3 was increased after OPC treatment (Figure 4). Based on the results, OPC appears to activate intracellular death-related pathways, leading to caspase-3 activation in SNU-C4 cells. Ye *et al.*^[5], revealed cytotoxicity of proanthocyanidins from grape seed compared between the human cancer cells with two normal cells, proanthocyanidins demonstrated selective cytotoxicity toward several cancer cells at the concentration of 25, 50 mg/L, while it enhances the growth and viability of the normal cells at the same concentration. Moreover, Joshi *et al.*^[33], demonstrated that grape seed proanthocyanidin, ameliorates the toxic effects associated with chemotherapeutic agents such as, 30 nmol/L idarubicin and 1 µg/mL 4-hydroxyperoxycyclophosphamide (4-HC) on normal human hepatocyte, Chang liver cells. These findings suggest that the treatment with OPC show low toxicity on normal cells, and it might have a novel anti-tumor effect on human colorectal cancer cells.

In conclusion, inhibitory effect of OPC on the proliferation of human colorectal cancer cells, SNU-C4 is mainly through apoptosis induced by *CASPASE-3* related to *BCL-2* families.

ACKNOWLEDGMENT

The authors are grateful to Doosan Biotech Institute (Yong-in, Korea).

REFERENCES

- Middleton E, Kandaswami C, Theoharides TC. The effects of plant flavonoids on mammalian cells: Implications for inflammation, heart disease, and cancer. *Pharmacol Rev* 2000; **52**: 673-751
- Jorge M, Silva RC, Darmon N, Fernandez Y, Mitjavila S. Oxygen free radical scavenger capacity in aqueous models of different procyanidins from grape seeds. *J Agric Food Chem* 1991; **39**: 1549-1552
- Jang M, Cai L, Udeani GO, Slowing KV, Thomas CF, Beecher CW, Fong HH, Farnsworth NR, Hinghorn AD, Mehta RG, Moon RC, Pezzuto JM. Cancer chemopreventive activity of resveratrol, a natural product derived from grapes. *Science* 1997; **275**: 218-220
- De Bruyne T, Pieters L, Witvrouw M, De Clercq E, Vanden Berghe D, Vlietinck AJ. Biological evaluation of proanthocyanidin dimers and related polyphenols. *J Nat Prod* 1999; **62**: 954-958
- Ye X, Krohn RL, Liu W, Joshi SS, Kuszynski CA, McGinn TR, Bagchi M, Preuss HG, Stohs SJ, Bagchi D. The cytotoxic effects of a novel IH636 grape seed proanthocyanidin extract on cultured human cancer cells. *Mol Cell Biochem* 1999; **196**: 99-108
- Carnecchi S, Schneider Y, Lazarus AS, Coehlo D, Gossé F, Raul F. Flavanols and procyanidins of cocoa and chocolate inhibit growth and polyamine biosynthesis of human colonic cancer cells. *Cancer Lett* 2002; **175**: 147-155
- Subarnas A, Wagner H. Analgesic and anti-inflammatory activity of the proanthocyanidin shelleagueain A from *Polypodium feei* METT. *Phytomedicine* 2000; **7**: 401-405
- Li WG, Zhang XY, Wu YJ, Tian X. Anti-inflammatory effect and mechanism of proanthocyanidins from grape seeds. *Acta Pharmacol Sin* 2000; **22**: 1117-1120
- Middleton E, Drzewiecki G. Flavonoid inhibition of human basophil histamine release stimulated by various agents. *Biochem Pharmacol* 1984; **33**: 3333-3338
- Pearce F, Befus AD, Bienenstock J. Mucosal mast cells, effects of quercetin and other flavonoids on antigen-induced histamine secretion from rat intestinal mast cells. *J Allergy Clin Immunol* 1984; **73**: 819-823
- Mao TK, Powell JJ, Van De Water, Keenz CL, Schmitz HH, Hammerstone JF, Gershwin ME. The effect of cocoa procyanidins on the transcription and secretion of interleukin 1 beta in peripheral blood mononuclear cell. *Life Sci* 2000; **66**: 1377-1386
- Bagchi D, Garg A, Krohn RL, Bagchi M, Tran MX, Stohs SJ. Oxygen free radical scavenging abilities of vitamins C and E, and a grape seed proanthocyanidin extract *in vitro*. *Res Commun Mol Pathol Pharmacol* 1997; **95**: 179-189
- Fremont L, Belguendouz L, Delpal S. Antioxidant activity of resveratrol and alcohol-free wine polyphenols related to LDL oxidation and polyunsaturated fatty acids. *Life Sci* 1999; **64**: 2511-2521
- Rein D, Paglieroni TG, Wun T, Pearson DA, Schmitz HH, Gosselin R, Keen CL. Cocoa inhibits platelet activation and function. *Am J Clin Nutr* 2000; **72**: 30-35
- Depeint F, Gee JM, Williamson G, Johnson IT. Evidence for consistent patterns between flavonoid structures and cellular activities. *Proc Nutr Soc* 2002; **61**: 97-103
- Schmitt E, Sane AT, Steyaert A, Cimoli G, Bertrand R. The Bcl-xL and Bax-alpha control points: modulation of apoptosis induced by cancer chemotherapy and relation to TPCK-sensitive protease and caspase activation. *Biochem Cell Biol* 1997; **75**: 301-314
- Galati G, Teng S, Moridani MY, Chan TS, O'Brien PJ. Cancer chemoprevention and apoptosis mechanisms induced by dietary polyphenolics. *Drug Metabol Drug Interact* 2000; **17**: 311-349
- Je JJ, Shin HT, Chung SH, Lee JS, Kim SS, Shin HD, Jang MH, Kim YJ, Chung JH, Kim EH, Kim CJ. Protective effects of *Wuyao* against H₂O₂-induced apoptosis on hippocampal cell line HiB5. *American J Chin Med* 2002; **30**: 561-570
- Landis SH, Murray T, Bolden S, Wingo PA. Cancer statistics, 1999. *CA Cancer J Clin* 1999; **49**: 8-31
- Yeatman TJ, Chambers AF. Osteopontin and colon cancer progression. *Clin Exp Metastasis* 2003; **20**: 85-90
- Kelloff GJ, Boone CW, Steele VC, Crowell JA, Lubet RA, Greenwald P, Hawk ET, Fay JR, Sigman CC. Mechanistic considerations in the evaluation of chemopreventive data. *IARC Sci Pub* 1996; **139**: 203-219
- Shi J, Yu J, Pohorly JE, Kakuda Y. Polyphenolics in grape seeds-Biochemistry and functionality. *J Med Food* 2003; **6**: 291-299
- Scalbert A, Williamson G. Dietary intake and bioavailability of polyphenols. *J Nutr* 2000; **130**: 2073S-2085S
- Cos P, De Bruyne T, Hermans N, Apers S, Berghe DV, Vlietinck AJ. Proanthocyanidins in health care: current and new trends. *Curr Med Chem* 2004; **11**: 1345-1359
- Fine AM. Oligomeric proanthocyanidin complexes: history, structure, and phytopharmaceutical applications. *Altern Med Rev* 2000; **5**: 144-151
- Matito C, Mastorakou F, Centelles JJ, Torres JL, Cascante M. Antiproliferative effect of antioxidant polyphenols from grape in murine Hepa-1c1c7. *Eur J Nutr* 2003; **42**: 43-49
- Qiao L, Hanif R, Sphicas E, Shiff SJ, Rigas B. Effect of aspirin on induction of apoptosis in HT-29 human colon adenocarcinoma cells. *Biochem Pharmacol* 1998; **55**: 53-64
- Korsmeyer SJ. Bcl-2 gene family and the regulation of programmed cell death. *Cancer Res Suppl* 1999; **59**: 1693-1700
- Oltvai ZN, Milliman CL, Korsmeyer SJ. Bcl-2 heterodimerizes *in vivo* with a conserved homolog, bax, that accelerates programmed cell death. *Cell* 1993; **74**: 609-619
- Thornberry NA, Lazebnik Y. Caspases: enemies within. *Science* 1998; **281**: 1312-1316
- Izban KF, Wrone-Smith T, His ED, Schnitzer B, Quevedo ME, Alkan S. Characterization of the interleukin-1 beta-converting enzyme/ced-3-family protease, caspase-3/ CPP32, in Hodgkin's disease: lack of caspase-3 expression in nodular lymphocyte predominance Hodgkin's disease. *Am J Pathol* 1999; **154**: 1439-1447
- Nicholson DW, Ali A, Thornberry NA, Vaillancourt JP, Ding CK, Gallant M, Gareau Y, Griffin PR, Labelle M, Lazebnik YA. Identification and inhibition of the ICE/CED-3 protease necessary for mammalian apoptosis. *Nature* 1995; **376**: 37-43
- Joshi SS, Kuszynski CA, Bagchi M, Bagchi D. Chemopreventive effects of grape seed proanthocyanidin extract on Chang liver cells. *Toxicology* 2000; **155**: 83-90

• COLORECTAL CANCER •

Identification of proteins of human colorectal carcinoma cell line SW480 by two-dimensional electrophoresis and MALDI-TOF mass spectrometry

Ying-Tao Zhang, Yi-Ping Geng, Le Zhou, Bao-Chang Lai, Lv-Sheng Si, Yi-Li Wang

Ying-Tao Zhang, Yi-Ping Geng, Le Zhou, Bao-Chang Lai, Lv-Sheng Si, Yi-Li Wang, The Key Laboratory of Biomedical Information Engineering of Education Ministry, Institute of Cancer Research, School of Life Science and Technology, Xi'an Jiaotong University, Xi'an 710061, Shaanxi Province, China

Ying-Tao Zhang, Department of Gastroenterology, First Hospital, Xi'an Jiaotong University, Xi'an 710061, Shaanxi Province, China

Supported by the Natural Science Foundation, Y100-573006 and Doctoral Foundation of Xi'an Jiaotong University, DFXJTU2002-11

Correspondence to: Yi-Li Wang, The Key Laboratory of Biomedical Information Engineering of Education Ministry, Institute of Cancer Research, School of Life Science and Technology, Xi'an Jiaotong University, Xi'an 710061, Shaanxi Province, China. wangyili@mail.xjtu.edu.cn

Telephone: +86-29-82655499 Fax: +86-29-82655499

Received: 2004-07-05 Accepted: 2004-09-04

Abstract

AIM: To conduct the proteomic analysis of human colorectal carcinoma cell line, SW480 by using two-dimensional electrophoresis (2-DE) and matrix-assisted laser desorption/ionization-time of flight mass spectrometry (MALDI-TOFMS).

METHODS: The total proteins of human colorectal carcinoma cell line, SW480 were separated with 2-DE by using immobilized pH gradient strips and visualized by staining with silver nitrate. The gel images were acquired by scanner and 2-DE analysis software, Image Master 2D Elite. Nineteen distinct protein spots were excised from gel randomly and digested in gel by TPCK-trypsin. Mass analysis of the tryptic digest peptides mixture was performed by using MALDI-TOF MS. Peptide mass fingerprints (PMFs) obtained by the MALDI-TOF analysis were used to search NCBI, SWISS-PROT and MSDB databases by using Mascot software.

RESULTS: PMF maps of all spots were obtained by MALDI-TOF MS and thirteen proteins were preliminarily identified.

CONCLUSION: The methods of analysis and identification of protein spots of tumor cells in 2-DE gel with silver staining by MALDI-TOF MS derived PMF have been established. Protein expression profile of SW480 has been obtained. It is demonstrated that a combination of proteomics and cell culture is a useful approach to comprehend the process of colon carcinogenesis.

Key words: Colorectal carcinoma; SW480 cell line; Two-dimensional electrophoresis; MALDI-TOF MS; Peptide mass fingerprinting

Zhang YT, Geng YP, Zhou L, Lai BC, Si LS, Wang YL. Identification of proteins of human colorectal carcinoma cell line SW480 by two-dimensional electrophoresis and MALDI-TOF mass spectrometry. *World J Gastroenterol* 2005; 11(30): 4679-4684

<http://www.wjgnet.com/1007-9327/11/4679.asp>

INTRODUCTION

Colorectal cancer (CRC) is one of the three leading causes of morbidity and mortality worldwide^[1]. It is believed that CRC develops through a multistep process involving the accumulation of genetic alterations. The genetic changes involved in colon carcinogenesis, including changes in proto-oncogenes, tumor suppressor genes, and DNA repair genes were well studied. But the exact mechanisms involved in this process are not well understood. Recently, changes in the transcriptome of colon tissues were studied by using DNA microarray analysis^[2]. However, the value of mRNA changes may be limited in terms of understanding changes in cellular physiology. Instead, genetic alterations lead to altered expression patterns, modifications in protein structures and functions. Alterations in the proteome may reflect cellular changes more accurately since proteins are the actual mediators of intracellular processes as opposed to mRNAs. Proteomics is the study and analysis of the proteins of living organisms. In recent years, the development of research entailing the protein complement of the genome, the proteome, has evolved significantly as a result of improved technology for two-dimensional gel electrophoresis (2-DE) and mass spectrometry (MS) for protein identification. With these technologies, it is now possible to obtain a more holistic view of protein changes associated with colon carcinogenesis. Here, for the first time, a proteomic approach is used to display the protein profile of human colorectal carcinoma cell line, SW480 to understand the basis of colon carcinogenesis.

MATERIALS AND METHODS

Chemicals and materials

Immobilized pH gradient (IPG) strips (pH3-10, linear, 13 cm), IPG buffer (pH3-10, linear) were purchased from Amersham Biosciences (Uppsala, Sweden). Dithiothreitol (DTT),

iodoacetamide (IAA), TPCK-trypsin, Trifluoroacetic acid (TFA), CHAPS, α -cyano-4-hydroxycinnamic acid (CHCA) were purchased from Sigma company (St. Louis, MO, USA). All the buffers were made by using high purity MilliQ water. IPGphor electrophoresis unit, Hoefer SE 600 vertical chambers, electrophoresis apparatus, Image Master 2D Elite 4.01 software and image scanner were purchased from Amersham Biosciences. Voyager-DE MALDI-TOF MS was product of Applied Biosystems (USA).

Cell line culture and sample preparation

The cell line, SW480 was purchased from Institute of Biochemistry and Cell Biology, Chinese Academy of Sciences (Shanghai, China). The cells were cultured in RPMI 1640 medium supplemented with 10 mL/L fetal bovine serum (FBS) and antibiotics. The cells were maintained in an incubator at 37 °C in 50 mL/L CO₂ humidified atmosphere. The cells grown at the exponential growth phase were harvested with trypsinization. After washing in Hanks' solution and ice-cold PBS, the cells were counted, lysated in a cocktail of 9 mol/L urea, 40 g/L CHAPS, 40 mmol/L Tris and 40 mmol/L DTT and centrifuged at 12 000 *g* for 1 h at 4 °C. Protein concentrations were determined by the method of Bradford.

2-DElectrophoresis

2-DE was performed by using IPG strips. Briefly, first-dimensional isoelectric focusing (IEF) was performed on 13 cm strips (pH 3-10, linear) by using an Amersham IPGphor unit. IEF was carried out by using an IPGphor electrophoresis unit (Amersham Biosciences). Separation in the second dimension (SDS-PAGE) was carried out on a 1.0 mm-thick 125 g/L polyacrylamide gels at a constant current (20 mA/gel) and temperature (15 °C) by using the Hoefer SE 600 vertical chambers. After 2-D separation, the gels were stained with silver nitrate. Image analysis was performed by using the Image Master 2D Elite software 4.01.

In-gel trypsin digestion of proteins

Proteins were in-gel digested as previously described by Wilm *et al.*, (Nature 1996; 379: 466-469) with some modification. Silver-stained spots were excised and washed with a 50 μ L fresh bleaching liquid (100 mmol/L Na₂S₂O₃; 30 mmol/L K₃Fe (CN)₆ = 1:1). Gel spots were dried in a vacuum centrifuge and reswelled in 50 μ L of solution containing 10 mol/L DTT/100 mol/L NH₄HCO₃ and incubated at 57 °C for 1 h. This solution was subsequently replaced with 50 μ L of solution containing 55 mol/L IAA/100 mol/L NH₄HCO₃ and incubated at room temperature for 30 min. The gel spots were dried again and digested with TPCK-trypsin at 37 °C overnight. After the incubation, the liquid was removed from the gel piece and the liquid was transferred to a new-labeled tube. This solution contains the extracted tryptic peptides.

MALDI-TOF -MS analysis of tryptic peptide

Mass analysis was performed by using a Voyager-DE MALDI-TOF MS (Framingham, MA, USA), operated in the delayed extraction and linear mode. The tryptic digest mixture was mixed with CHCA matrix. The MALDI spectra

averaged over 50 laser shots. All mass spectra were calibrated externally by using a standard peptide mixture (angiotensin II and ACTH 18-39). Internal calibration was performed by using auto digestion peaks of trypsin.

Database searching and identification of proteins

Peptide mass fingerprints obtained by the MALDI-TOF MS were used to search NCBIInr, SWISS-PROT and MSDB databases by using Mascot software (<http://www.matrixscience.com>). The parameters used for the search were as follows: peptide mass ranged from 1 000 to 3 000 U; modifications were allowed for carboxy-amidomethylation of cysteine and oxidation of methionine; one missed cleavage site was allowed; mass accuracy was ± 1 U; restriction was placed on the species of *Homo sapiens*. The criteria for positive identification of proteins were set as follows: (1) the MS match consisted of a minimum of four peptides; (2) the matched peptides covered at least 20% of the whole protein sequence; (3) 50 ppm or better mass accuracy.

RESULTS

Proteomic pattern of SW480 by 2-DE

Proteins of human colorectal cancer cell line SW480 were separated by 2-DE. Spots were visualized with silver staining. Three pairs of gels from SW480 were analyzed by using the Image Master 2D Elite software 4.01. Figure 1 shows a representative example of cell proteins separated on a 2-DE gel, where 100 μ g of total protein was applied. Nearly 1 000 proteins spots were obtained in the range of *M_r* 14 400-9 4000 u, *PI* 3-10.

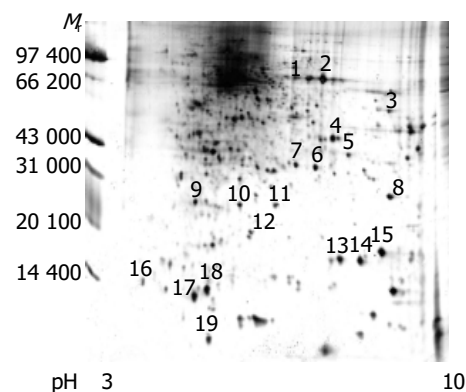


Figure 1 2-DE map of human colorectal cancer cell line SW480 proteome (silver staining).

MALDI-TOF MS analysis of proteins

Nineteen distinct protein spots were excised from gels randomly and marked with Arabic numbers at the corresponding sites in Figure 1. All spots obtained the PMF maps by MALDI-TOF MS following in-gel digestion with TPCK-trypsin. Figure 2 shows the spectrum of trypsin digestion of protein spot 2.

Database searching and identification of proteins

PMFs obtained by the MALDI-TOF MS were used to search NCBIInr, SWISS-PROT and MSDB databases by using

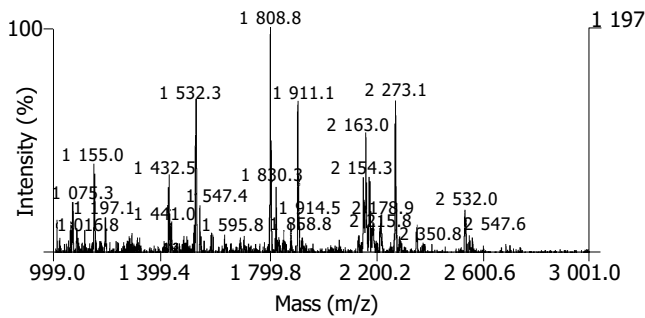


Figure 2 PMF of protein spot 2 in SW480 2-DE map.

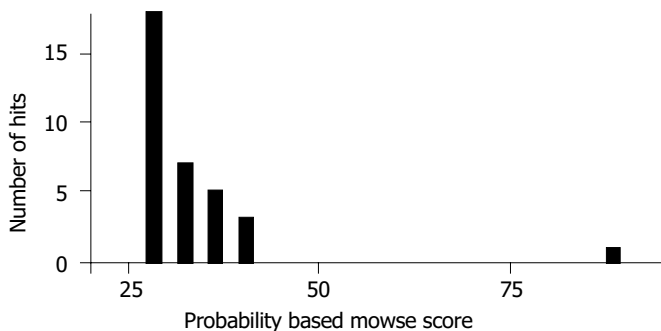
Mascot software (<http://www.matrixscience.com>). Figure 3 shows the searching result of spot 2.

Thirteen proteins were preliminarily identified on the basis of peptide mass matching by database searching. Some PMFs such as 1, 8, 9, 10, 11, 16 were not searched by the satisfactory proteins. Table 1 lists the identified proteins. Among these proteins, some were correlated with signal transduction (e.g. zinc finger protein 79 and PR-domain zinc finger protein 7

isoform B), some with cell metabolism (e.g. enolase 1, phosphopyruvate hydratase, carboxypeptidase A5 precursor and peptidylprolyl isomerase), some with cell growth and adhesion (e.g. paired box transcription factor and intermediate filament-binding fragments of Desmoplakin), and some with the immunological function of tumor cells (e.g. MHC class I promoter binding protein, immunoglobulin heavy chain VHDJ region and human B7-1 CTLA-4 co-stimulatory complex).

DISCUSSION

To further understand cellular functioning, the next logical level of analysis is proteomics. Proteomics is the study of global protein expression patterns in a cell, tissue, or organism. In general, it deals with the large-scale determination of gene and cellular function directly at the protein level^[3]. The most commonly used method is a combination of two-dimensional electrophoresis (2-DE) and mass spectrometry (MS)^[4]. Protein mixtures from cells are separated by 2-DE, stained, and each observed protein spot is quantified by its staining intensity. Selected spots are excised, digested and



Probability Based Mowse Score: Score is $-10 \log(P)$, where P is the probability that the observed match is a random event. Protein scores greater than 63 are significant ($P < 0.05$).

Concise protein summary report:

Accession	Mass (U)	Score	Peptides matched	Protein description
1. gi 4503571	47 511	88	14	Enolase 1; Phosphopyruvate hydratase; MYC promoter-binding protein 1; Non-neural enolase; 2-phospho-D-glycerate hydro-lyase; Tau-crystallin [<i>Homo sapiens</i>]
2. gi 31873302	47 435	88	14	Hypothetical protein [<i>Homo sapiens</i>]
3. gi 2661039	36 651	75	12	Alpha enolase [<i>Homo sapiens</i>]
4. gi 13279239	30 168	74	11	ENO1 protein [<i>Homo sapiens</i>]
5. gi 693933	47 451	68	12	2-phosphopyruvate-hydratase alpha-enolase; Carbonate dehydratase [<i>Homo sapiens</i>]
6. gi 3282243	29 853	62	10	Alpha enolase like 1 [<i>Homo sapiens</i>]
7. gi 39644728	29 204	61	10	ENO1 protein [<i>Homo sapiens</i>]
8. gi 39644850	20 700	44	7	ENO1 protein [<i>Homo sapiens</i>]
9. gi 1022782	25 872	42	7	Ca ²⁺ -dependent activator protein for secretion
10. gi 37540705	16 508	40	6	Hypothetical protein XP_353015 [<i>Homo sapiens</i>]

Matched peptides shown in bold red:

1	MSILKIHARE	IFDSRGNPTV	EVDLFTSKGL	FRAAVPSGAS	TGIYEALRLR	
51	DNDKTRYMGK	GVSKAVEHIN	KTIAPALVSK	KLNVTEQEKI	DKLMIEMDGT	
101	ENKSKFGANA	ILGVSLAVCK	AGAVEKGVPL	YRHIADLAGN	SEVILPVPAF	
151	NVINGGSHAG	NKLAMQEFMI	LPVGAANFRE	AMRIGAEVYH	NLKNVIKEY	
201	GKDATNVGDE	GGFAPNILEN	KEGLELLKTA	IGKAGYTDKV	VIGMDVAASE	
251	FFRSGKYDLD	FKSPDDPSRY	ISPDQLADLY	KSFIDYPVW	SIEDPFQDD	
301	WGAWQKFTAS	AGIQVGDLL	TVTNPKRIAK	AVNEKSCNCL	LLKVNQIGSV	
351	TESLQACKLA	QANGWVMVS	HRSGETEDTF	IADLWGLCT	GQIKTGAPCR	
401	SERLAKYNQL	LRIEELGSK	AKFAGRNFNRN	PLAK		
Start-End	Observed	Mr (expt)	Mr (calc)	Delta	Miss	Sequence
10-28	2 154.79	2 153.78	2 154.36	-0.58	1	EIFDSRGNPTVEVDLFTSK
33-50	1 805.65	1 804.64	1 805.02	-0.38	0	AAVPSGASTGIYEALRLR
106-120	1 520.21	1 519.20	1 519.83	-0.63	0	FGANAILGVSLAVCK
163-179	1 908.54	1 907.53	1 908.31	-0.77	0	LAMQEFMILPVGAANFR
203-221	1 962.05	1 961.05	1 961.07	-0.03	0	DATNVGDEGGFAPNILENK
234-253	2 176.80	2 175.79	2 176.47	-0.68	1	AGYTDKVVIGMDVAASEFFR
240-253	1 541.52	1 540.51	1 540.80	-0.29	0	VVIGMDVAASEFFR
254-262	1 073.12	1 072.11	1 072.18	-0.07	1	SGKYDLDFK
270-281	1 426.28	1 425.27	1 425.60	-0.33	0	YISPDQLADLYK
270-285	1 901.22	1 900.21	1 901.19	-0.98	1	YISPDQLADLYKSFID
336-343	1 008.03	1 007.03	1 007.24	-0.21	0	SCNCLLLK
344-358	1 634.29	1 633.28	1 633.84	-0.56	0	VNQIGSVTESLQACK
359-372	1 527.20	1 526.19	1 525.75	0.44	0	LAQANGWGMVSHR
373-394	2 353.91	2 352.90	2 353.63	-0.73	0	SGETEDTFIADLWGLCTGQIK

Figure 3 Searching results of spot 2.

analyzed by MS^[5]. 2-DE was the first technique capable of supporting the concurrent quantitative analysis of large numbers of gene products. Proteins are separated by charge in the first dimension and then by size in the second dimension, yielding spots on a polyacrylamide gel. Then, each protein spot was individually recovered and cleaved into short peptide fragments. 2-DE has been a mature technique for more than 25 years. Compared to classical 2-DE with carrier ampholytes (O' Farrell 1975), the employment of immobilized pH gradient (IPG) gel strips as the first dimension, isoelectric focusing (IEF), has produced significant improvements in 2-D electrophoretic separation, permitting higher resolution and greater reproducibility. It become an effective method for separation of complex proteomes such as human cancer cells and tissues, facilitating spot identification by peptide mass fingerprinting (PMF), MALDI or tandem mass spectrometry, amino acid composition analysis, N-terminal and/or internal peptide microsequencing. We have developed a comprehensive strategy for reproducible, robust, gel-based separation of >1 000 protein components for quantitative protein profile. This strategy uses improved sample preparation methods and an optimized in-gel proteolysis protocol.

Protein identification is the most important step in expression proteomics. MS has increasingly become the method of choice for analysis of complex protein samples. MS-based proteomics is a discipline made possible by the availability of gene and genome sequence databases and technical and conceptual advances in many areas, most notably the discovery and development of protein ionization methods, as recognized by the 2002 Nobel prize in chemistry.

The two most widely used ion-producing methods are called Electro Spray Ionization (ESI) and Matrix-Assisted Laser Desorption Ionization (MALDI)^[6]. The method of choice for rapid, high-volume sequence analysis is MALDI, developed in 1987 by Hillenkamp and Karas^[7]. In this process, peptides are first made soluble in a solvent containing an organic acid, such as nicotinic acid, and are then deposited onto a metal stage, as the solvent is evaporated. The organic acid plays a dual role - it is capable of absorbing light energy and it serves as a matrix that holds the protein molecules in place. Energy from a short laser pulse is absorbed by the matrix, which vaporizes, releasing stable precharged peptide ions into the ion chamber. Ionized molecules released in this manner may remain intact or break down into smaller pieces en route to the detector. MALDI's tendency to deliver intact protein masses to the detector is very useful for determining the full molecular weight of a protein, but provides little information about the amino acid sequence that composes it. This limitation can be overcome by enzymatically or chemically cleaving the protein to obtain a mixture of peptides that is then analyzed by mass spectrometry. The peptide mass pattern obtained in this manner is characteristic of the original protein and constitutes a sort of "fingerprint" that can aid in its identification. Each peptide in the fingerprint can be further analyzed by fragmentation to yield complex patterns of ion mass that may be used to identify the molecule. Once a suitable mass spectrum is obtained, it is compared against a protein mass spectral database to see if the sample pattern matches the fingerprint of any known peptides. Commonly used protein sequence

databases include the SWISSPROT, OWL and NCBItr databases, which are publicly available. Several software programs for protein identification are available online such as Mascot (<http://www.matrixscience.com>), MOWSE (<http://srs.hgmp.mrc.ac.uk/cgi-bin/mowse>), PeptIdent2, and ProFound (<http://prowl.rockefeller.edu/cgi-bin/ProFound> or <http://www.proteometrics.com/prowl-cgi/ProFound.exe>), Prowl (<http://prowl.rockefeller.edu/contents/resource.htm>), and Protein Prospector (<http://prospector.ucsf.edu/>). PMF by MALDI-TOF has become highly efficient in the identification of gel-separated proteins^[8].

The identified proteins were abundantly expressed in SW480 cells including enzymes (enolase), cytoskeletal components (intermediate filaments, IF), transcription factors (PR-domain family), and immunological molecules (MHC class and human B7-1 CTLA-4 co-stimulatory complex). These proteins maybe involved in colorectal carcinogenesis. Enolase is a key enzyme of glycolysis related with the energy metabolism^[9]. This gene encodes one of three enolase isoenzymes found in mammals. It encodes alpha-enolase, a homodimeric soluble enzyme, and also encodes a shorter monomeric structural lens protein, tau-crystallin. The two proteins are made from the same message. The full-length protein, the isoenzyme, is found in the cytoplasm. The shorter protein is produced from an alternative translation start, is localized to the nucleus, and has been found to bind to an element in the c-myc promoter. A pseudogene has been identified, that is located on the other arm of the same chromosome. Intermediate filaments are the most abundant cytoskeletal proteins in cells and regulate the migration of normal and transformed epithelial cells and can be used to define a specific cancer tissue^[10]. The PR domain (PRDI-BF1-RIZ homology region), a distant relative of the SET

domain functioning in chromatin-mediated gene expression, defines a small family of zinc-finger type DNA-binding transcription factors. Three human members are presently known, and they are RIZ, MDS1-EVI1, and PRDI-BF1 or BLIMP1. A characteristic feature of these genes is the unusual yin-yang involvement in human cancers. Two products are normally produced from PR-domain family members who differ by the presence or absence of the PR domain; the PR-plus product is disrupted or under expressed whereas the PR-minus product is present or over expressed in cancer cells. This imbalance in the amount of the two products, a result of either genetic or epigenetic events, appears to be an important cause of malignancy^[11].

Cancer cells can be detected and destroyed by cytotoxic T lymphocytes in many tumors. In humans however, most diagnosed tumors are not eliminated by T cells but grow steadily, invading and metastasizing until the host is destroyed. Evidence is accumulating that progressive tumor growth occurs not because the immune system is defective or deteriorated, but because the cancer cell is capable of developing a variety of strategies to escape immune recognition. Major histocompatibility complex (MHC) molecules are of central importance in regulating the immune response against tumors. Proper HLA class I antigen processing and presentation is a prerequisite for the recognition of tumor cells by cytotoxic T lymphocytes^[12]. MHC II molecules are designated DP, DQ or DR and consist of two transmembrane polypeptides: an alpha (α) chain and a beta (β) chain. HLA-DPB1 is located on chromosome 6p12.3 and codes for Human Leukocyte Antigen, a Major Histocompatibility Class II (MHC II) molecule. MHC II molecules are heterodimeric, having α and β chains, DPB1 codes for the β chain. These molecules are responsible for initiation of the immune

Table 1 Database searching results of proteins of SW480 cell line

Spot ID	NCBI ID	Peptides matched	Sequence covered (%)	Theoretic M_r /pI	Protein name
1	Unidentified				
2	gi 4503571	14/40	44	47 511/7.01	Enolase 1; Phosphopyruvate hydratase; MYC promoter-binding protein 1; Non-neural enolase; 2-phospho-D-glyceratehydro-lyase; Tau-crystallin
3	gi 24307937	19/35	26	56 918/8.48	Zinc finger protein 79 (pT7)
4	gi 37723146	4/11	24	33 130/7.04	Paired box transcription factor
5	SwissProt ID:	3/12	15	394 787.81	Carboxypeptidase A5 precursor (EC 3.4.17.1) Q8WXQ8-01-00-00
6	gi 22219251	4/13	21	23 385/6.23	Chain A, structures of two intermediate filament-binding fragments of Desmoplakin
7	gi 2135648	6/38	31	25 794/6.42	MHC class I promoter binding protein (fragment)
8	Unidentified				
9	Unidentified				
10	Unidentified				
11	Unidentified				
12	gi 13786754	4/24	34	24 093/5.38	Chain A, human B7-1 CTLA-4 co-stimulatory complex
13	MSDB ID: 1AK4B	6/36	33	18 010/7.85	Peptidylprolyl isomerase (EC 5.2.1.8) A, chain B
14	gi 21670535	3/19	50	13 285/8.64	Immunoglobulin heavy chain VH DJ region [Homo sapiens]
15	gi 8575802	5/26	35	18 715/8.29	PR-domain zinc finger protein 7 isoform B; PR-domain family protein 4 isoform B; PRDM7B; PFM4B
16	Unidentified				
17	gi 2222804	4/31	55	10 467/4.85	HLA-DPB1
18	gi 24475861	4/25	42	14 004/5.65	Phosphohistidine phosphatase; Sex-regulated protein janus-a
19	gi 2134526	3/43	52	9 785/5.02	Gene MHC DQ-beta 1 protein (fragment)

response through antigen presentation to T cells^[13,14]. B7 family members play a central co-stimulatory role in T cell activation^[15]. These two signals are necessary for T cell activation. It is generally accepted that human and experimental tumor cells can lose Major Histocompatibility Complex (MHC) class I molecules and this represents the major mechanism of tumor escape from T-cell immune responses. This is now mandatory, considering the high frequency of total or partial MHC class I losses observed in different tumor types as a result of escape mechanism from infiltrating-infiltrating lymphocytes: 90% in cervical carcinomas^[16], 73% in colorectal carcinomas^[17], 88% in breast carcinomas^[18,19], 51% in melanomas^[20,21], and 66% in laryngeal carcinomas^[22] and renal cell carcinoma^[23]. The expression of MHC I, MHC II and B7-1 molecules by SW480 cells might imply that such a kind of tumor cells had all the components necessary for evoking T lymphocyte activation and generating a positive anti-tumor immune response. Why the hosts cannot eliminate the malignancies? Recent findings discovered that the lymphocyte population of a patient with CRC contained at least two types of lymphocytes with tumor specificity, i.e., CTLs and regulatory T cells. They might be induced by a tumor-associated self antigen(s)^[24,25]. However, the exact immunological pathomechanism(s) of these immunological molecules remains to be established. The regulatory T cells may suppress autologous CTL functions, resulting in escape of the tumor from immune surveillance by CTLs. This may explain why tumors often grow despite the presence of CTLs in the same individual.

Peptide mass fingerprinting (PMF) is a powerful tool for identification of proteins separated by 2-DE. However, there are several limitations to peptide mass fingerprinting, including a lack of complete and accurately annotated genome- and protein-sequence databases for a great number of highly homologous human proteins. Beyond identification, confirmation and validation of the protein of interest are also important steps in proteomic approaches.

REFERENCES

- 1 Crawford NP, Colliver DW, Galandiuk S. Tumor markers and colorectal cancer: utility in management. *J Surg Oncol* 2003; **84**: 239-248
- 2 Bertucci F, Salas S, Eysteris S, Nasser V, Finetti P, Ginestier C, Charafe-Jauffret E, Loriod B, Bachelart L, Montfort J, Victorero G, Viret F, Ollendorff V, Fert V, Giovaninni M, Delpero JR, Nguyen C, Viens P, Monges G, Birnbaum D, Houlgatte R. Gene expression profiling of colon cancer by DNA microarrays and correlation with histoclinical parameters. *Oncogene* 2004; **23**: 1377-1391
- 3 Mann M, Hendrickson RC, Pandey A. Analysis of proteins and proteomes by mass spectrometry. *Annu Rev Biochem* 2001; **70**: 437-473
- 4 Long YZ, Fan XG, Li N. Progress in tumor proteomics. *Shijie Huaren Xiaohua Zazhi* 2002; **10**: 1436-1440
- 5 Katayama H, Nagasu T, Oda Y. Improvement of in-gel digestion protocol for peptide mass fingerprinting by matrix-assisted laser desorption/ionization time-of-flight mass spectrometry. *Rapid Commun Mass Spectrom* 2001; **15**: 1416-1421
- 6 Aebersold R, Mann M. Mass spectrometry-based proteomics. *Nature* 2003; **422**: 198-207
- 7 Karas M, Hillenkamp F. Laser desorption ionization of proteins with molecular masses exceeding 10 000 daltons. *Anal Chem* 1988; **60**: 2299-2301
- 8 Berndt P, Hobohm U, Langen H. Reliable automatic protein identification from matrix-assisted laser desorption/ionization mass spectrometric peptide fingerprints. *Electrophoresis* 1999; **20**: 3521-3526
- 9 Thoden JB, Taylor Ringia EA, Garrett JB, Gerlt JA, Holden HM, Rayment I. Evolution of enzymatic activity in the enolase superfamily: structural studies of the promiscuous o-succinylbenzoate synthase from amycolatopsis. *Biochemistry* 2004; **43**: 5716-5727
- 10 Herzig KH, Altmannsberger M, Folsch UR. Intermediate filaments in rat pancreatic acinar tumors, human ductal carcinomas, and other gastrointestinal malignancies. *Gastroenterology* 1994; **106**: 1326-1332
- 11 Jiang GL, Huang S. The yin-yang of PR-domain family genes in tumorigenesis. *Histol Histopathol* 2000; **15**: 109-117
- 12 Cabrera T, Lopez-Nevot MA, Gaforio JJ, Ruiz-Cabello F, Garrido F. Analysis of HLA expression in human tumor tissues. *Cancer Immunol Immunother* 2003; **52**: 1-9
- 13 Edelshtein D, Sidebottom D, Chen DF, Baxter-Lowe LA. A novel HLA-DPB1 allele identified by sequence-based typing and confirmed by SSP. *Hum Immunol* 2003; **64**(10 Suppl): S162
- 14 Zino E, Frumento G, Markt S, Sormani MP, Ficara F, Di Terlizzi S, Parodi AM, Sergeant R, Martinetti M, Bontadini A, Bonifazi F, Lisini D, Mazzi B, Rossini S, Servida P, Ciceri F, Bonini C, Lanino E, Bandini G, Locatelli F, Apperley J, Bacigalupo A, Ferrara GB, Bordignon C, Fleischhauer K. A T-cell epitope encoded by a subset of HLA-DPB1 alleles determines nonpermissive mismatches for hematologic stem cell transplantation. *Blood* 2004; **103**: 1417-1424
- 15 Chen L. Co-inhibitory molecules of the B7-CD28 family in the control of T-cell immunity. *Nat Rev Immunol* 2004; **4**: 336-347
- 16 Ryu KS, Lee YS, Kim BK, Park YG, Kim YW, Hur SY, Kim TE, Kim IK, Kim JW. Alterations of HLA class I and II antigen expression in preinvasive, invasive and metastatic cervical cancers. *Exp Mol Med* 2001; **33**: 136-144
- 17 Cabrera T, Collado A, Fernandez MA, Ferron A, Sancho J, Ruiz-Cabello F, Garrido F. High frequency of altered HLA class I phenotypes in invasive colorectal carcinomas. *Tissue Antigens* 1998; **52**: 114-123
- 18 Palmisano GL, Pistillo MP, Capanni P, Pera C, Nicolo G, Salvi S, Perdelli L, Pasciucco G, Ferrara GB. Investigation of HLA class I downregulation in breast cancer by RT-PCR. *Hum Immunol* 2001; **62**: 133-139
- 19 Redondo M, Garcia J, Villar E, Rodrigo I, Perea-Milla E, Serrano A, Morell M. Major histocompatibility complex status in breast carcinogenesis and relationship to apoptosis. *Hum Pathol* 2003; **34**: 1283-1289
- 20 Ferrone S, Marincola FM. Loss of HLA class I antigens by melanoma cells: molecular mechanisms, functional significance and clinical relevance. *Immunol Today* 1995; **16**: 487-494
- 21 Marincola FM, Ferrone S. Immunotherapy of melanoma: the good news, the bad ones and what to do next. *Semin Cancer Biol* 2003; **13**: 387-389
- 22 Cabrera T, Salinero J, Fernandez MA, Garrido A, Esquivias J, Garrido F. High frequency of altered HLA class I phenotypes in laryngeal carcinomas. *Hum Immunol* 2000; **61**: 499-506
- 23 Atkins D, Ferrone S, Schmahl GE, Storkel S, Seliger B. Downregulation of HLA class I antigen processing molecules: an immune escape mechanism of renal cell carcinoma? *J Urol* 2004; **171**: 885-859
- 24 Jordan MS, Boesteanu A, Reed AJ, Petrone AL, Holenbeck AE, Lerman MA, Naji A, Caton AJ. Thymic selection of CD4⁺CD25⁺ regulatory T cells induced by an agonist self-peptide. *Nat Immunol* 2001; **2**: 301-306
- 25 Sakaguchi S. Regulatory T cells: key controllers of immunologic self-tolerance. *Cell* 2000; **101**: 455-458

• COLORECTAL CANCER •

Changing patterns of colorectal cancer in China over a period of 20 years

Ming Li, Jin Gu

Ming Li, Jin Gu, Department of Surgery, Beijing Cancer Hospital, Peking University School of Oncology, Beijing Institute for Cancer Research, Beijing 100036, China

Correspondence to: Dr. Jin Gu, Department of Surgery, No. 52 Fucheng Road, Beijing Cancer Hospital, Beijing 100036, China. zlguj@bjmu.edu.cn

Telephone: +86-10-88141032 Fax: +86-10-88122437

Received: 2004-07-09 Accepted: 2004-11-17

Abstract

AIM: To determine whether any changes have occurred on the patterns of colorectal cancer in China.

METHODS: Data from 21 Chinese articles published from 1980 to 1999, were used to analyze the time trend of colorectal cancer according to the patients' age at diagnosis, sex, the site of the tumor, stage, and the pathology.

RESULTS: From 1980s to 1990s, the mean age of the colorectal cancer patients has increased. The percentage of the female patients rose. The distribution of colorectal carcinoma shows a predominance of rectal cancer. However, the proportion of proximal colon cancer (including transverse and ascending colon) increased significantly accompanied by a decline in the percentage of rectal cancer. Similarity in the percentage of distal colon cancer between two decades was revealed. In the 1990s, statistically more Stage B patients were found than those in 1980s. In addition, databases show a significant decrease in the Stage D cases. The proportion of adenocarcinoma increased, but the mucinous adenocarcinoma decreased during two decades.

CONCLUSION: These findings indicate that the pattern of colorectal cancer in China has been changing. Especially, a proximal shift due to the increasing proportion of ascending and transverse colon cancer has occurred in China.

© 2005 The WJG Press and Elsevier Inc. All rights reserved.

Key words: Colorectal carcinoma; Time trends; Age; Sex; Subsite; Pathology

Li M, Gu J. Changing patterns of colorectal cancer in China over a period of 20 years. *World J Gastroenterol* 2005; 11(30): 4685-4688

<http://www.wjgnet.com/1007-9327/11/4685.asp>

INTRODUCTION

Colorectal carcinoma (CRC) is one of the most common

tumor types in the world, with approximately 400 000 deaths annually^[1]. It is a frequent cause of cancer death in the developed world^[2]. For example, in the USA, despite a slight decrease in its incidence and mortality during the past two decades, CRC has remained the third most common cancer, affecting approximately 140 000 people and causing approximately 50 000 cancer-related deaths per year^[3]. In China, the incidence rate was initially low, but in recent years, due to the changes of life style and nutritional habits, the rate is increasing. The most impressive increase in the incidence rates of CRC was observed from 1972-1974 to 1987-1989, being 85% in males and 79% in females. The average rate of increase in incidence is 4.2% per year^[4]. According to the report of the Ministry of Health PR China in 2002, the incidence rate of CRC has ranked third in 1990s, from the sixth most common cancer in 1970s, and the death rate of CRC has increased to 10.25/10⁵ annually, which is the fifth leading cause of cancer mortality^[5].

Recent epidemiologic studies have suggested that the anatomic distribution of colorectal cancer may have undergone a distal to proximal shift over several decades. Lev^[6] has reported that during 1986 to 1992, cecal and ascending colon tumors increased in incidence from 33.9% to 36%, tumors of the transverse colon increased from 15.8% to 17.2%, and tumors of the sigmoid colon decreased from 36.0% to 33.4%.

So besides the increasing incidence rate and mortality rate, we still want to know whether there are some changes on patterns of CRC in China. But because a National Colorectal Cancer Registry system has not been established yet in China, so we compiled all the Chinese articles on CRC in order to compare the changing patterns between 1980s and 1990s. These articles were published on the journals included by the Chinese S&T Journal Citation Reports (CJCR). It is difficult to collect only articles in SCI, because in 1980s, few Chinese journals were included by SCI.

MATERIALS AND METHODS

Data were obtained from 21 Chinese articles published from 1980 to 1999 in CJCR. The articles involved 25 hospitals and 11 geographic areas of China. The study was based on the records of 10 201 patients reported during 20 years. According to the time of falling ill, they were divided into two groups, 1980s and 1990s. The former included 3 420 patients, and the latter had 6 781. These cases were recorded under sex, age, the subsites distribution of the CRC, Dukes' classification and the pathologic data. The distribution of the CRC was categorized into five segments: rectum (excluding

anal canal cancer), sigmoid, descending colon, transverse colon, and ascending colon (including cecum cancer but excluding appendicular neoplasm). On the other hand, we classified as proximal colon (ascending and transverse colon), distal colon (descending and sigmoid colon) and rectum. The patients without these detailed data were excluded.

Statistical analysis

Statistical analysis was performed using the SPSS 10.0 program. Independent samples' *t* test was used to compare the difference of age between two groups. Other data was examined by χ^2 test and statistical significance was accepted at $P < 0.05$.

RESULTS

Incidence and patient characteristics

In the 1980s group, 3 420 patients were reported, including 2 053 men and 1 367 women. The ratio was 1.50:1. But in the 1990s group, 6 781 patients were registered, among them there were 3 780 men and 3 001 women, and the ratio was 1.26:1. There is a significant difference between the two groups on the gender constituent ratio ($P < 0.05$). The mean age of 1980s group was 56.83, which was lower than 59.66 in 1990s (Table 1).

Table 1 Epidemiologic results

	1980s (%)	1990s (%)	<i>P</i>
Total number of CRCs	3 420	6 781	
Male	2 053 (60.03)	3 780 (55.74)	
Female	1 367 (39.97)	3 001 (44.26)	
Male/female ratio	1.50:1	1.26:1	0.02
Mean age (yr)	56.83	59.66	

Distribution of CRC

The CRC localization changed in the two decades. The distribution of CRC shows a predominance of rectal cancer. However, the proportion of rectal cancer in CRC has decreased significantly from 71.2% in 1980s to 66.7% in 1990s ($P < 0.001$). The proportion of transverse colon and ascending colon individually increased significantly ($P < 0.001$). Meanwhile, the percentage of patients with proximal colon cancer among those with colorectal cancer certainly increased significantly (10.9% *vs* 15.2% $P < 0.001$). But the data revealed similarity in the percentage of distal colon cancer between two groups ($P > 0.05$, Table 2).

Table 2 Distribution of CRC

Localization	1980s (%)	1990s (%)	<i>P</i>
Rectum	2 484 (72.6)	4 539 (66.9)	<0.001
Colon	936 (27.4)	2 242 (33.1)	<0.001
Distal			
Sigmoid	337 (9.9)	844 (12.4)	<0.001
Descending colon	226 (6.6)	366 (5.4)	0.02
Total distal CRCs	563 (16.5)	1 210 (17.85)	
Proximal			
Transverse colon	87 (2.5)	275 (4.1)	<0.001
Ascending colon	286 (8.4)	757 (11.2)	<0.001
Total proximal CRCs	373 (10.9)	1 032 (15.2)	<0.001
Others			
Total number of CRCs	3 420	6 781	

Dukes' classification

Of all CRCs, complete tumor staging is available in 2 300 and 3 772 patients in 1980s and 1990s respectively. Distributions among different categories of the Dukes' classification are shown in Table 3. In 1990s statistically more Stage B CRCs were found than in 1980s ($P < 0.001$) and databases show a statistically significant decrease in the Stage D cases.

Table 3 Dukes' staging

Stage	1980s (%)	1990s (%)	<i>P</i>
A	306 (13.3)	416 (11.0)	0.01
B	679 (29.5)	1 399 (37.1)	<0.001
C	823 (35.8)	1 379 (36.6)	
D	492 (21.4)	578 (15.3)	<0.001
Total	2 300	3 772	

Pathologic classification

The pathologic data of the CRCs were classified into adenocarcinoma, mucinous adenocarcinoma and others which mean carcinoid, adenosquamous carcinoma, and so on. We can see in Table 4, that recent pathologic classification in CRC in China has significantly changed. The proportion of adenocarcinoma increased but the mucinous adenocarcinoma decreased ($P < 0.001$).

Table 4 Pathologic classification

Pathologic classification	1980s (%)	1990s (%)	<i>P</i>
Adenocarcinoma	1 251 (82.1)	3 838 (85.6)	<0.001
Mucinous adenocarcinoma	231 (15.2)	465 (10.4)	<0.001
Others	42 (2.8)	180 (4.0)	
Total	1 524	4 483	

DISCUSSION

Rates of CRC vary considerably with geography. The disease is common in USA, Australia, Western Europe, and Scandinavia and is relatively uncommon in Asia, Africa, and South America^[7,8]. In recent years, there were some changes on the pattern of CRC, such as increasing incidence rate in Japan and Eastern Europe^[9-11], continued rightward shift of CRC^[11-13] and so on. Compared with Western countries, the incidence of CRC in China is low, but the dietary habits and lifestyle of Chinese have changed greatly, and the incidence is increasing rapidly. Thus, it is worthwhile to study the time trends for the changing patterns on CRC in China. This study collected 10 201 cases to investigate the age, male/female ratio, subsite distribution and pathologic changes on CRC in China over a period of 20 years.

CRC is primarily a cancer of the older population and risk for it increases with age^[7,8]. The increase of mean age may contribute to the population aging during 20 years in China. But we failed to show that there is a significance between the two decades.

It is clearly shown that the proportion of the female patients on CRC in China increased significantly from 1.50:1 in 1980s to 1.26:1 in 1990s. One possible explanation for the role of

gender may be the effect of female hormones^[14]. Some suggested that hormonal replacement therapy may decrease the incidence of CRC in females^[15,16]. Female sex hormones are known to affect cholesterol metabolism, which in turn affects bile acid production, a pathway linked to the development of colorectal cancer^[17].

In low-risk countries, rectal cancer accounts for the largest proportion of all colorectal cancers^[18]. The proportion of rectal cancer among all colorectal cancers is generally less than 40% in Europe and North America, in contrast to the 50% or more in Asia^[19]. In our study, rectal cancer is the main part of the colorectal cancer in China, no matter what was in 1980s or 1990s. However, the ratio of patients with colon cancer to all CRC cases has increased greatly in both sexes. In 1980s, the proportion of the colon cancer is 27.4%, but 33.1% in 1990s. Correspondingly, the percentage of rectal cancer decreased obviously. Likewise, several recent studies reported consistent results^[19-24]. The reason for this is not clear. It may be continued anatomic rightward shift of CRC, which were mentioned as follows, improved diagnostic accuracy for lesions in colon^[19], and varying etiologic factors^[21,23,24].

In the past 40 years, since the first description on CRC shift toward the proximal colon by Axtell and Chiazze^[25], many investigators confirmed it from various countries^[14,24,26-34]. The present study indicates the distribution of colon cancer in China changed greatly in 20 years, a significant increase in proximal colon cancer including transverse and ascending colon. The ratio of proximal colon cancer to all CRCs increased about 4.3%. Nevertheless the proportion of total distal colon cancer (sigmoid and descending) remains static. To exclude the possible question that the rightward shift may be due to the decreasing proportion of rectal cancer among all CRC, we limited our further analysis to data for the colon alone. It also concluded that there was an actual increase in right-sided cancer. So the proximal shift may be a reason for the increased ratio of colon cancer to rectal cancer as mentioned before.

There may be several potential causes for the rightward shift in CRC. The proximal and distal colon has different embryologic origins, morphology, physiology, and function^[35]. Cecum, ascending colon, and proximal two-thirds of the transverse colon derives from the midgut, whereas the segment comprising the splenic flexure to the upper anal canal derives from the hindgut. The distinct embryologic origins of each segment are reflected in the dual blood supply of the normal colon. The proximal colon is primarily involved with water absorption and solidification of fecal contents, but the distal colon functions primarily for storage^[19]. The metabolic pathways such as that of glucose, butyrate, and polyamines are also different. It has therefore been hypothesized that proximal and distal colons are two different organs^[36]. It may mean differences in differential sensitivities and exposures to carcinogens for the proximal and distal sections of colon and rectum.

The colon cancer is associated with genetic factors. Some studies reported that high-frequency microsatellite instability was significantly associated with tumors occurring in the proximal colon^[37,38]. Also Gervaz showed that distal colon cancer were more likely to express a nonfunctional p53

protein and a p53 gene mutation than proximal tumors^[31]. In the future, such genetic variations by cancer site may provide more clues to understanding the reasons of rightward shift of CRC.

The fecal occult blood test, digital examination of rectum, rigid and flexible sigmoidoscopy, barium enema X-ray as well as colonoscopy are particularly geared toward the diagnosis and screening of colorectal cancer. In 1980s, the colonoscopy was not popular in China especially in the suburban. So the rectal and sigmoid cancers are inclined to be found and diagnosed. Following the increased use of colonoscopy, more and more was the detection of proximal lesions with the observed time trends in 1990s. Although sigmoidoscope has been proven as an effective tool for screening against colorectal cancer^[39,40] and detects almost 80% CRC in China, it has the limitation that it would miss the proximal cancer for 20%. Accompanying the continuing rightward shift, the miss rate (meaning the ratio of miss out diagnosis cases to all CRC patients) may rise, especially on symptomatic patients. The miss rate may even be higher when one takes into account that approximately 25% of all patients who underwent sigmoidoscopy, the entire sigmoid is not adequately visualized^[41]. So the use of barium enema X-rays and total colonoscopy appears more appropriate for symptomatic patients, especially elderly people and women.

There are some other theories to explain the rightward shift of CRC. Gonzalez^[14] considered that five co-morbid conditions were associated with a greater likelihood of proximal lesions: congestive heart failure, cerebrovascular disease, chronic pulmonary disease, ulcer disease, and diabetes mellitus. West *et al.*^[42] demonstrated that a high-fat diet increased the risk for proximal colon cancer, whereas a high-protein diet increases the risk for distal neoplasm.

Screening seems attractive because of the difference in prognosis between early and late stage of CRC. During 20 years, China has developed the screening system. So the Dukes' D stage CRC has shrunk significantly and Dukes' B has been the main part of all cases.

Finally, our data indicated that the proportion of adenocarcinoma increased, correspondingly, mucinous adenocarcinoma decreased. The reasons for it needs further study.

Future studies should examine the subsites of CRC to clarify further analytical epidemiological findings, carcinogenic mechanisms, various risk factors, and prognosis to reduce the mortality.

REFERENCES

- 1 **Pisani P**, Parkin DM, Bray F, Ferlay J. Erratum: Estimates of the worldwide mortality from 25 cancers in 1990. *Int J Cancer* 1999; **83**: 18-29
- 2 **Bourt RW**, DiSario JA, Cannon-Albright L. Genetics of colon cancer: impact of inheritance on colon cancer risk. *Annu Rev Med* 1995; **46**: 371-379
- 3 **Greenlee RT**, Hill-Harmon MB, Murray T, Thun M. Cancer statistics 2001. *CA Cancer J Clin* 2001; **51**: 15-36
- 4 **Zheng S**. Recent study on colorectal cancer in China: early detection and novel related gene. *Chin Med J* 1997; **110**: 309-310
- 5 **Statistic bulletin on the development of Chinese health service 2001**. The information center on health statistics of Ministry of Health P.R China. 2002, 4 Beijing

- 6 **Lev R.** The National Cancer Data Base report on colorectal cancer. *Cancer* 1995; **76**: 538-539
- 7 **Coleman MP,** Esteve J, Damiecki P, Arslan A, Renard H. Trends in cancer incidence and mortality. *IARC Sci Publ* 1993; **121**: 1-806
- 8 **Parkin DM,** Muir CS. Cancer incidence in the Five Continents. Comparability and quality of data. *IARC Sci Publ* 1992; **120**: 45-173
- 9 **Lands WE,** Hamazaki T, Yamazaki K, Okuyama H, Sakai K, Goto Y, Hubbard VS. Changing dietary patterns. *Am J Clin Nutr* 1990; **51**: 991-993
- 10 **Kotake K,** Koyama Y, Nasu J, Fukutomi T, Yamaguchi N. Relation of family history of cancer and environmental factors to the risk of colorectal cancer: a case-control study. *Jpn J Clin Oncol* 1995; **25**: 195-202
- 11 **Levin KE,** Dozois RR. Epidemiology of large bowel cancer. *World J Surg* 1991; **15**: 562-567
- 12 **Wilmink AB.** Overview of the epidemiology of colorectal cancer. *Dis Colon Rectum* 1997; **40**: 483-493
- 13 Trends in colorectal cancer incidence-United States, 1973-1986. *MMWR* 1989; **38**: 728
- 14 **Gonzalez EC,** Roetzheim RG, Ferrante JM, Campbell R. Predictors of proximal vs. distal colorectal cancers. *Dis Colon Rectum* 2001; **44**: 251-258
- 15 **Hebert-Croteau N.** A meta-analysis of hormone replacement therapy and colon cancer in women. *Cancer Epidemiol Biomarkers Prev* 1998; **7**: 653-659
- 16 **Paganini-Hill A.** Estrogen replacement therapy and colorectal cancer risk in elderly women. *Dis Colon Rectum* 1999; **42**: 1300-1305
- 17 **Fleshner P,** Slater G, Aufses AH Jr. Age and sex distribution of patients with colorectal cancer. *Dis Colon Rectum* 1989; **32**: 107-111
- 18 **Waterhouse JA,** Muir CS, Shanmugaratnam K, Powell J. IARC Scientific Publication No42. International Agency for Research on Cancer: Lyon, 1982
- 19 **Devesa SS,** Chow WH. Variation in colorectal cancer incidence in the United States by subsite of origin. *Cancer* 1993; **71**: 3819-3826
- 20 **Koyama Y,** Kotake K. Overview of colorectal cancer in Japan: report from the Registry of the Japanese Society for Cancer of the Colon and Rectum. *Dis Colon Rectum* 1997; **40** (10 Suppl): S2-9
- 21 **Levi F,** Randimbison L, La Vecchia C. Trends in subsite distribution of colorectal cancers and polyps from the Vaud Cancer Registry. *Cancer* 1993; **72**: 46-50
- 22 **Dubrow R,** Bernstein J, Holford TR. Age-period-cohort modeling of large-bowel-cancer incidence by anatomic subsite and sex in Connecticut. *Int J Cancer* 1993; **53**: 907-913
- 23 **Kee F,** Wilson RH, Gilliland R, Sloan JM, Rowlands BJ, Moorehead RJ. Changing site distribution of colorectal cancer. *BMJ* 1992; **305**: 158
- 24 **Jass JR.** Subsite distribution and incidence of colorectal cancer in New Zealand, 1974-1983. *Dis Colon Rectum* 1991; **34**: 56-59
- 25 **Axtell LM,** Chiazzie L Jr. Changing relative frequency of cancers of the colon and rectum in the United States. *Cancer* 1966; **19**: 750-754
- 26 **Rhodes JB,** Holmes FF, Clark GM. Changing distribution of primary cancers in the large bowel. *JAMA* 1977; **238**: 1641-1643
- 27 **Mamazza J,** Gordon PH. The changing distribution of large intestinal cancer. *Dis Colon Rectum* 1982; **25**: 558-562
- 28 **Beart RW,** Melton LJ 3rd, Maruta M, Dockerty MB, Frydenberg HB, O'Fallon WM. Trends in right and left sided colon cancer. *Dis Colon Rectum* 1983; **26**: 393-398
- 29 **Schub R,** Steinheber FU. Rightward shift of colon cancer. A feature of the aging gut. *J Clin Gastroenterol* 1986; **8**: 630-634
- 30 **Demers RY,** Severson RK, Schottenfeld D, Lazar I. Incidence of colorectal adenocarcinoma by anatomic subsite. An epidemiologic study of time trends and racial differences in the Detroit, Michigan area. *Cancer* 1997; **79**: 441-447
- 31 **Gervaz P,** Bouzourene H, Cerottini JP, Chaubert P, Benhattar J, Secic M, Wexner S, Givel JC, Belin B. Dukes B colorectal cancer: distinct genetic categories and clinical outcome based on proximal or distal tumor location. *Dis Colon Rectum* 2001; **44**: 364-372
- 32 **Cucino C,** Buchner AM, Sonnenberg A. Continued rightward shift of colorectal cancer. *Dis Colon Rectum* 2002; **45**: 1035-1040
- 33 **Mensink PB,** Kolkman JJ, Van Baarlen JV, Kleibeuker JH. Change in anatomic distribution and incidence of colorectal carcinoma over a period of 15 years. *Dis Colon Rectum* 2002; **45**: 1393-1396
- 34 **Takada H,** Ohsawa T, Iwamoto S, Yoshida R, Nakano M, Imada S, Yoshioka K, Okuno M, Masuya Y, Hasegawa K, Kamano N, Hioki K, Muto T, Koyama Y. Changing site distribution of colorectal cancer in Japan. *Dis Colon Rectum* 2002; **45**: 1249-1254
- 35 **Bufill JA.** Colorectal cancer: evidence for distinct genetic categories based on proximal or distal tumor location. *Ann Intern Med* 1990; **113**: 779-788
- 36 **Distler P,** Holt PR. Are right- and left- sided neoplasms distinct tumors? *Dig Dis* 1997; **15**: 302-311
- 37 **Kim H,** Jen J, Vogelstein B, Hamilton SR. Clinical and pathological characteristics of sporadic colorectal carcinomas with DNA replication errors in microsatellite sequences. *Am J Pathol* 1994; **145**: 148-156
- 38 **Thibodeau SN,** French AJ, Cunningham JM, Tester D, Burgart LJ, Roche PC, McDonnell SK, Schaid DJ, Vockley CW, Michels VV, Farr GH Jr, O'Connell MJ. Microsatellite instability in colorectal cancer: different mutator phenotypes and the principal involvement of hMLH1. *Cancer Res* 1998; **58**: 1713-1718
- 39 **Newcomb PA,** Norfleet RG, Storer BE, Surawicz TS, Marcus PM. Screening sigmoidoscopy and colorectal cancer mortality. *J Natl Cancer Inst* 1992; **84**: 1572-1575
- 40 **Selby JV,** Friedman GD, Quesenberry CP Jr, Weiss NS. A case-control study of screening sigmoidoscopy and mortality from colorectal cancer. *N Engl J Med* 1992; **326**: 653-657
- 41 **Painter J,** Saunders DB, Bell GD, Williams CB, Pitt R, Bladen J. Depth of insertion at flexible sigmoidoscopy: implications for colorectal cancer screening and instrument design. *Endoscopy* 1999; **31**: 227-231
- 42 **West DW,** Slattery ML, Robison LM, Schuman KL, Ford MH, Mahoney AW, Lyon JL, Sorensen AW. Dietary intake and colon cancer: sex- and anatomic site-specific associations. *Am J Epidemiol* 1989; **130**: 883-894

• COLORECTAL CANCER •

Expression of a novel apoptosis inhibitor-survivin in colorectal carcinoma

Hai-Yan Tan, Jun Liu, Shan-Min Wu, He-Sheng Luo

Hai-Yan Tan, Shan-Min Wu, Department of General surgery, Renmin Hospital of Wuhan University, Wuhan 430060, Hubei Province, China

Jun Liu, He-Sheng Luo, Department of Gastroenterology, Renmin Hospital of Wuhan University, Wuhan 430060, Hubei Province, China

Correspondence to: Dr. Hai-Yan Tan, Department of General Surgery, Renmin Hospital of Wuhan University, Jiefang Road No. 238, Wuhan 4300 60, Hubei Province, China. liu9861jun@yahoo.com.cn

Telephone: +86-27-88054316

Received: 2004-08-30 Accepted: 2004-11-04

Abstract

AIM: To investigate the role of survivin expression in the pathogenesis of colorectal carcinoma.

METHODS: Immunohistochemistry S-P method and terminal deoxynucleotidyl transferase-mediated dUTP nick end labeling (TUNEL) were used to detect the expression of survivin and apoptotic cell *in situ* in colorectal cancerous tissues, para-cancerous tissues and normal tissues of 48 cases of colorectal carcinoma.

RESULTS: The survivin positive unit (PU) was higher in cancerous tissues (38.76 ± 5.14) than in para-cancerous (25.17 ± 7.26) or normal tissues (0.57 ± 0.03) ($P < 0.05$). The apoptosis index (AI) of para-cancerous tissues was ($7.51 \pm 2.63\%$) higher than cancerous tissues ($4.65 \pm 1.76\%$). The expression of survivin was associated with pathological grade, lymph node metastasis and Dukes stage of colorectal carcinoma.

CONCLUSION: Survivin expression may play an important role in carcinogenesis of colorectal carcinoma and may be associated with malignant biological behaviors of colorectal carcinoma.

© 2005 The WJG Press and Elsevier Inc. All rights reserved.

Key words: Survivin; Colorectal carcinoma; Cell apoptosis

Tan HY, Liu J, Wu SM, Luo HS. Expression of a novel apoptosis inhibitor-survivin in colorectal carcinoma. *World J Gastroenterol* 2005; 11(30): 4689-4692

<http://www.wjgnet.com/1007-9327/11/4689.asp>

INTRODUCTION

Survivin is a new member of inhibitors of apoptosis proteins (IAP) gene family that has been found recently. The survivin

gene lies in the 17q25 of human chromosome with unique structure and characteristics, coding a 16.5 KD protein^[1]. Survivin protein contains only one BIR (baculovirus IAP repeat) domain and does not have the zinc-binding fold terminated with carboxyl. Furthermore, under normal circumstances survivin is expressed in embryonic and fetal tissues, but completely downregulated in normal adult tissues. Interestingly, this protein is found to be prominently reexpressed in a variety of human malignant transformation cell lines and tumorous tissues^[2,3]. And its unique structure and biological function have interested so many scholars during their researches on the molecular biology of tumors.

Colorectal carcinoma has a high incidence in China. The deficiency of cell apoptosis plays an important role in the pathogenesis of this carcinoma. It is still uncertain about the role of survivin expression in colorectal carcinoma. In the present study, the expression of survivin and cell apoptosis were detected. The correlation between survivin expression and cell apoptosis and the role of survivin in the pathogenesis of colorectal carcinoma were also investigated.

MATERIALS AND METHODS

Study materials

Forty-eight cases of colorectal carcinoma who received rectectomy were obtained from the Department of General Surgery, Renmin Hospital of Wuhan University. Twenty-six of them were male and 22 female. The mean age was 55.8 years ranged from 37 to 75 years. All the cases did not receive radiation treatment or chemotherapy before surgery and had been diagnosed by two doctors at the department of pathology. Three pieces of tissues were taken respectively from cancerous tissues, para-cancerous tissues (5 cm away from cancerous tissues) and normal tissues (10 cm away from cancerous tissues). All the specimens were fixed in 10% neutral-buffered formalin, dehydrated in ascending series of ethanol and routinely embedded in paraplast. Sections were cut at 4 μ m, stained with hematoxylin and eosin for histopathological and immunohistochemical evaluation as well as TUNEL. The clinicopathological parameters are summarized in Table 1.

Immunohistochemical analysis

All the specimens were incubated in 3% hydrogen peroxide for 15 min to inactivate the endogenous peroxidase and then heated in 0.01 mol/L citrate buffer for antigen retrieval through 12 min microwave pre-treatment. Incubated with 10% goat serum, all the specimens were subsequently reacted with rabbit-anti-human survivin polyclonal antibody (Neomarkers, USA, 1:1 000 dilution) at 4 °C overnight.

Table 1 Relationship between survivin PU and pathological parameter in 48 cases with colorectal carcinoma (mean±SD)

Subjects	Clinical pathological index	n	Survivin PU	P
Gender	Male	26	42.95±16.87	P>0.05
	Female	22	30.96±16.06	
Age (yr)	<55	14	36.95±19.86	P>0.05
	≥55	34	38.96±15.37	
Tumor Diameter	<3 cm	14	36.15±16.29	P>0.05
	≥3 cm	34	38.28±18.16	
Pathological Grade	High and intermedium differentiated	24	33.16±14.28	P<0.05
	Cannular adenocarcinoma	10	51.93±20.89	
	Low differentiated tubular adenocarcinoma			
	Other types	14	35.61±17.22	
Lymph node	Negative	26	30.12±13.33	P<0.05
	Positive	22	56.21±11.95	
Dukes stage	A	16	20.16±5.16	P<0.05
	B	4	24.85±3.12	
	C	10	45.13±10.21	
	D	14	59.66±10.21	

Immunohistological staining was performed according to SP detection kit.

TUNEL staining

Apoptotic cells were detected, according to the procedure recommended by *in situ* cell apoptosis detection kit (Boehringer Mannheim Company, Germany).

Evaluation criteria

Immunohistochemical quantitative evaluation All the analyses were performed using the HIPAS-2000 computer image analysis system (produced by Tongji Qianping Image Engineering Company) Images were captured at ×400 magnification by micrographic system. Image analysis system separated staining positive area from background. Then the gray level units as well as areas of positive staining and background could be measured. According to Shen's method, positive unit represents the relative concentration of positive staining^[4]. Each section was observed randomly at five areas and the mean PU was calculated.

Evaluation criteria for cell apoptosis

The apoptotic cells were located sporadically with nuclei stained yellow or brownish yellow. A mean percentage of positive cells among 500 cells was determined in five areas at ×400 magnification. The results could be recorded as apoptosis index (AI).

Statistical analysis

All analyses were performed with *t* test and ANOVA using SPSS 9.0 software (Statistical Package for Social Science). *P* values<0.05 were considered to indicate statistical significance.

RESULTS

Survivin PU and apoptosis index of cancerous, paracancerous and normal tissues

Survivin PU were mainly in the cytoplasm of para-cancerous or cancer cells. The nuclei could be stained equally light yellow or brownish yellow, located sporadically or in the

form of sheets (Figure 1A). Survivin PU was rarely expressed in normal large intestinal mucosa (Figure 1B). Quantitative analysis of immunohistochemistry is summarized in Table 2. The apoptotic cells were distributed sporadically or in clusters with brownish yellow nuclei. apoptotic cells were found to be rare and weak stained in normal large intestinal mucosa, most of which were located in epithelium (Figure 2A), but scattered sporadically in cancerous (Figure 2B) and para-cancerous tissues. Survivin PU in cancerous tissues 38.76±5.14 was significantly higher than in para-cancerous 25.17±7.26 and normal tissues 0.57±0.03 (*P*<0.05). And the AI in para-cancerous tissues, (7.51±2.63)% was significantly higher than in cancerous tissues, (4.65±1.76)%(*P* = 0.0075).

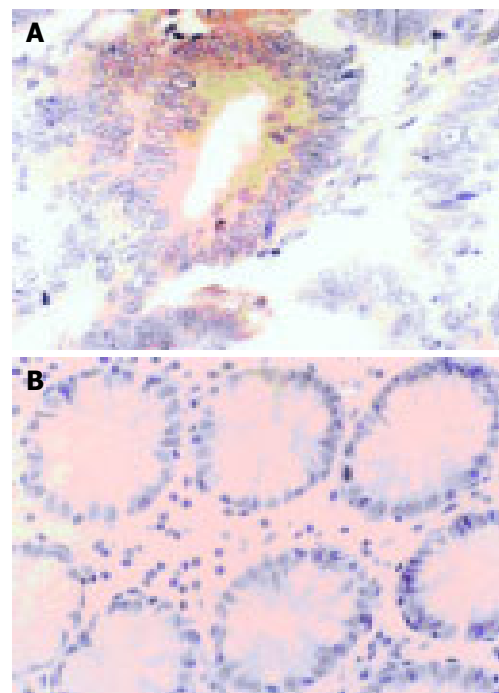


Figure 1 Expression of survivin in colorectal cancerous and normal tissues by S-P method. (x400). **A:** colorectal cancerous tissues; **B:** normal colorectal tissues.

Table 2 The comparison of survivin PU and AI in cancerous, paracancerous and normal tissues (mean±SD)

Subjects	Cancerous tissues	Paracancerous tissues	Normal tissues	P
Survivin PU	38.76±5.14	25.17±7.26 ^a	0.57±0.03 ^a	<i>P</i>
AI (%)	4.65±1.76	7.51±2.63	1.75±0.49	<i>P</i>

^a*P*<0.05, Survivin PU of cancerous tissue vs paracancerous or normal tissue; *P* = 0.0075, AI of paracancerous tissue vs cancerous tissue.

Relationship between survivin PU and clinicopathological parameters

Survivin PU was not correlated with sex, age and tumor diameter of patients, but correlated with pathological grade, lymph node and Dukes stage. Survivin PU in cancerous tissues with low differentiation, lymph node positive and Dukes C/D stage was higher than in cancerous tissues with high differentiation, lymph node negative, and Dukes A/B stage.

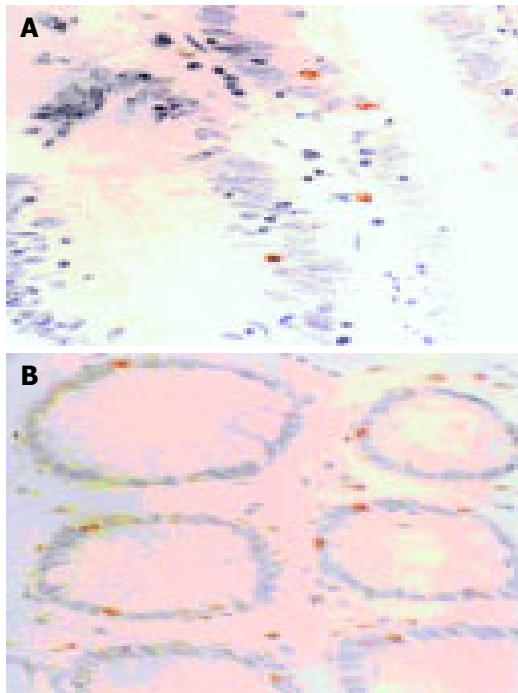


Figure 2 Apoptotic cells in normal colorectal epithelial and cancerous tissues by TUNEL method. (x400). **A:** normal colorectal epithelial tissues; **B:** colorectal epithelial tissues.

DISCUSSION

According to recent clinical and statistical data, there was a gradually increasing incidence in colorectal carcinoma. carcinogenesis can be regarded as a complex process with multi-gene participation and multi-steps. As we all know, most colorectal carcinomas originate from adenoma. Abnormalities in the control of programmed cell death (apoptosis) play an important role in the pathogenesis of colorectal carcinoma during the process from adenoma to cancer. It has been proved that the genes closely related with the control of colorectal cell apoptosis include bcl-2, c-myc, p53 and IAP gene family. So the research and application of those apoptosis-related genes is of great importance in the diagnosis, treatment and prognosis judgement of colorectal carcinoma.

Survivin is a new member of IAP gene family, which was obtained by Altieri in Yale University through hybridization and filtration of human genome^[5]. It can combine with microtubules of mitotic spindle, and through interaction with caspases it can inhibit cell apoptosis^[6]. Survivin affects various terminal effect factors and might be one of the strongest apoptosis inhibitory factors till now. This research using immunohistochemical staining showed that survivin was very weak in normal epithelial cells and partially expressed in para-cancerous tissues. But positive cells in para-cancerous tissues were less than in cancerous tissues with a weaker staining, suggesting that survivin expression could be an early event during the pathogenesis of colorectal carcinoma. This is in accordance with the researches on pancreatic and hepatocellular cancers. Evidence showed that survivin could be expressed in early stage of pancreatic cancer or precancerous lesions^[6,7]. Sarela found survivin mRNA mainly existed in survivin positive cancerous tissues,

but hardly in survivin negative cancerous tissues^[8]. Thus, it is proposed that, survivin is an oncogene, and also a marker with great potential for tumor diagnosis. Survivin antibody could also be taken as a common marker for early diagnosis of colorectal carcinoma^[9,10].

This research proved that survivin PU had no significant correlation with sex, age, and tumor diameter, but correlated with differentiation stage, lymph node and Dukes stage of colorectal carcinoma. Survivin PU in cancerous tissues with low differentiation, lymph node positive and Dukes C/D stage was higher than in cancerous tissues with high differentiation, lymph node negative and Dukes A/B stage. It indicated that survivin PU was related with malignant biological behaviors. Its continuous expression might be associated with the development of malignant tumor. Researches on gastric carcinoma, lung cancer, breast cancer revealed that survivin PU was not only correlated with malignant biological behaviors such as invasion, metastasis, etc, but also correlated with recurrence, reduced survival time after surgery. It might be taken as an independent index for judging the prognosis^[11-13]. Therefore, survivin is of great value for diagnosis and prognosis judgement of malignant tumors.

Survivin has the feature of selective expression in various malignant tumors, which might be essential for carcinogenesis of those tumors. But the mechanism for survivin to contribute to carcinogenesis of tumors is not clear yet. It is probably involved in cell apoptosis, proliferation, etc.^[14]. Our research showed that the apoptotic cells mainly located in epithelium of normal large intestinal mucosa, but distributed sporadically in cancerous and para-cancerous tissues. AI of paracancerous tissues was higher than cancerous tissues, indicating that survivin could inhibit apoptosis of colorectal carcinoma cells. This might be regarded as part of mechanisms for its participation in carcinogenesis of colorectal carcinoma. But the precise pathway for survivin to inhibit apoptosis still needs further investigation. According to the present study, survivin had various pathways to inhibit apoptosis, which could also be found in other malignant tumors^[15]. It might play an important role in the carcinogenesis of various tumors.

REFERENCES

- 1 **Reed JC.** The survivin saga goes *in vivo*. *J Clin Invest* 2001; **108**: 965-969
- 2 **Adida C, Crotty PL, McGrath J, Berrebi D, Diebold J, Altieri DC.** Developmentally regulated expression of the novel cancer anti-apoptosis gene survivin in human and mouse differentiation. *Am J Pathol* 1998; **152**: 43-49
- 3 **Xu Y, Fang F, Ludewig G, Jones G, Jones D.** A mutation found in the promoter region of the human survivin gene is correlated to overexpression of survivin in cancer cells. *DNA Cell Biol* 2004; **23**: 527-537
- 4 **Hong S.** Research on quantitative methods of immunohistochemical staining. *Zhongguo Zuzhi Huaxue Yu Xibaohuaxue Zazhi* 1995; **4**: 89-91
- 5 **Altieri DC.** Molecular cloning of effector cell protease receptor-1, a novel cell surface receptor for the protease factor Xa. *J Biol Chem* 1994; **269**: 3139-3142
- 6 **Satoh K, Kaneko K, Hirota M, Masamune A, Satoh A, Shimosegawa T.** Expression of survivin is correlated with cancer cell apoptosis and is involved in the development of human pancreatic duct cell tumors. *Cancer* 2001; **92**:

271-278

- 7 **Sarela AI**, Verbeke CS, Ramsdale J, Davies CL, Markham AF, Guillou PJ. Expression of survivin, a novel inhibitor of apoptosis and cell cycle regulatory protein, in pancreatic adenocarcinoma. *Br J Cancer* 2002; **86**: 886-892
- 8 **Sarela AI**, Macadam RC, Farmery SM, Markham AF, Guillou PJ. Expression of the antiapoptosis gene, survivin, predicts death from recurrent colorectal carcinoma. *Gut* 2000; **46**: 645-650
- 9 **Zhang JY**, Casiano CA, Peng XX, Koziol JA, Chan EK, Tan EM. Enhancement of antibody detection in cancer using panel of recombinant tumor-associated antigens. *Cancer Epidemiol Biomarkers Prev* 2003; **12**: 136-143
- 10 **Yagihashi A**, Asanuma K, Nakamura M, Araya J, Mano Y, Torigoe T, Kobayashi D, Watanabe N. Detection of anti-survivin antibody in gastrointestinal cancer patients. *Clin Chem* 2001; **47**: 1729-1731
- 11 **Tamm I**, Wang Y, Sausville E, Scudiero DA, Vigna N, Oltersdorf T, Reed JC. IAP-family protein survivin inhibits caspase activity and apoptosis induced by Fas (CD95), Bax, caspases, and anticancer drugs. *Cancer Res* 1998; **58**: 5315-5320
- 12 **Span PN**, Sweep FC, Wiegerinck ET, Tjan-Heijnen VC, Manders P, Beex LV, de Kok JB. Survivin is an independent prognostic marker for risk stratification of breast cancer patients. *Clin Chem* 2004; **50**: 1986-1993
- 13 **Johnson ME**, Howerth EW. Survivin: a bifunctional inhibitor of apoptosis protein. *Vet Pathol* 2004; **41**: 599-607

Science Editor Zhu LH and Guo SY Language Editor Elsevier HK

• VIRAL HEPATITIS •

Mutations in hepatitis B virus core regions correlate with hepatocellular injury in Chinese patients with chronic hepatitis B

Hiroto Tanaka, Hiroki Ueda, Hiroko Hamagami, Susumu Yukawa, Masakazu Ichinose, Motoshige Miyano, Keiji Mimura, Iwao Nishide, Bo-Xin Zhang, Su-Wen Wang, Shi-Oing Zhou, Bei-Hai Li

Hiroto Tanaka, Hiroki Ueda, Hiroko Hamagami, Susumu Yukawa, Masakazu Ichinose, The Third Department of Internal Medicine, Wakayama Medical University, 811-1 Kimiidera Wakayama City, Wakayama 641-0012, Japan
Motoshige Miyano, Keiji Mimura, Iwao Nishide, Nishide Hospital, 236 Umizuka, Kaizuka City, Osaka 597-0083, Japan
Bo-Xin Zhang, Su-Wen Wang, Shi-Oing Zhou, Bei-Hai Li, Jinan Central Hospital, 105 Jiefang Road, Jinan 250013, Shandong Province, China
Correspondence to: Hiroto Tanaka, MD, PhD, Horidomenishi 1-4-28, Wakayama city, Japan. h-tana@yf6.so-net.ne.jp
Telephone: +81-73-426-4467 Fax: +81-73-426-4467
Received: 2004-10-29 Accepted: 2004-12-20

Abstract

AIM: To elucidate the relationship between the frequency of core mutations and the clinical activity of hepatitis B virus (HBV)-related liver disease and to characterize the amino acid changes in the core region of HBV.

METHODS: We studied 17 Chinese patients with chronic hepatitis B according to their clinical courses and patterns of the entire core region of HBV.

RESULTS: Amino acid changes often appeared in the HBV core region of the HBV gene in patients with high values of alanine aminotransferase (ALT) or with the seroconversion from HBeAg to anti-HBe. The HBV core region with amino acid changes had high frequency sites that corresponded to HLA I/II restricted recognition epitopes reported by some investigators.

CONCLUSION: The core amino acid changes of this study occur due to influence of host immune system. The presence of mutations in the HBV core region seems to be important for predicting the clinical activity of hepatitis B in Chinese patients.

© 2005 The WJG Press and Elsevier Inc. All rights reserved.

Key words: Hepatitis B virus; Core region; Mutation; Serum ALT; DNA sequences; HBe antigen; Chronic hepatitis B; Activity

Tanaka H, Ueda H, Hamagami H, Yukawa S, Ichinose M, Miyano M, Mimura K, Nishide I, Zhang BX, Wang SW, Zhou SO, Li BH. Mutations in hepatitis B virus core regions correlate with hepatocellular injury in Chinese patients with chronic hepatitis B. *World J Gastroenterol* 2005; 11(30): 4693-4696
<http://www.wjgnet.com/1007-9327/11/4693.asp>

INTRODUCTION

Individuals infected with hepatitis B virus (HBV) may display asymptomatic, acute, fulminant, or chronic hepatitis. Previous studies have suggested that liver disorders due to HBV are immune-mediated and that hepatitis B envelope antigen (HBeAg) and hepatitis B core antigen (HBcAg) could be immunological targets^[1-3]. Furthermore, several antigenic regions have been identified in the HBV core region using recombinant antigens or synthetic peptides. Some reports have revealed that amino acids (aa) 78-83 and aa 127-133 are exposed on the surface of HBcAg^[4,5]. Others have also reported that aa 120-140 are related to the recognition of helper T-cells, and forms of the HBV core and e antigens influence cytokine release in mouse models^[6-8]. Thus, liver disorder in hepatitis B is influenced by the host immune system, which attacks core peptides as the main target. Given this, the pattern of amino acid changes in the HBV core region might predict the clinical course according to the level of serum ALT (sALT) values and the presence of HBeAg. In other words, mutations in the HBV core region may help to predict the outcome of liver disorders. To identify one cause of hepatitis B activity, we analyzed the HBV core sequence and the frequency of core mutations.

MATERIALS AND METHODS

Patients

Serum samples were taken from 17 Chinese patients, who were consistently positive for hepatitis B surface antigen (HBsAg). HBsAg and anti-hepatitis B surface antibody (HBsAb) were determined by immunoassay, while HBeAg, anti-hepatitis B envelope antibody (HBeAb), and HBcAb were determined by passive hemagglutination (PHA) assay. Patients were first divided according to the presence of HBeAg into positive (eAg-Po) and negative (eAg-Ne) groups, and then divided, according to the sALT values measured twice or thrice a year into high activity (HA) and low activity (LA) groups. The HA group had sALT over 100 IU/L at least once a year and the LA group had sALT consistently below 100 IU/L. This study was approved by the ethics committee and informed consent was obtained from all patients.

Extraction and amplification of HBV DNA by polymerase chain reaction (PCR)

HBV DNA was extracted from 100 µL of serum. In brief, after the serum samples were diluted to 400 µL with distilled water, the DNA was extracted with 1 mL of phenol/

chloroform (1/1:v/v) and precipitated with 1/10 volume of 3 mol/L sodium acetate and 2 volumes of 100% ethanol. The precipitates were dried under vacuum and dissolved with 20 μ L of Tris-HCL and EDTA buffer (pH 7.4). PCR was performed to amplify a 609-bp DNA fragment using specific primers (the 1st PCR primers: sense primer H: 5'-GGGAGGAGATTAGGTTA-3', anti-sense primer I: 5'-GTACAGTAGAAGAATAAAG C-3'; /the 2nd PCR primers: sense primer D: 5'-CAAGCCTCCAAGCTGTG-CCT-3', anti-sense primer F: 5'-ACCTTATG AGTCCA-AGGGAT-3') corresponding to the outside of the core region in the HBV genome. A reaction mixture containing 50 mmol/L KCl, 10 mmol/L Tris-HCl (pH 8.0), 2.5 mmol/L MgCl₂, 1 μ mol/L each of the two primers, 200 μ mol/L dNTP, 200 μ g/mL gelatin, and 5 U of *Taq* DNA polymerase (Amersham Life Science, Cleveland, OH, USA) was added into a 200- μ L tube containing 10 μ L DNA solution. Amplification was performed for 35 cycles as follows: denaturation at 94 °C for 1 min, annealing at 58 °C for 1 min, extension at 72 °C for 2 min. In the last cycle, incubation at 72 °C was continued for 10 min to complete the extension. Electrophoresis of 10- μ L aliquots of PCR products was performed on a 3.5 % agarose gel subsequently stained with ethidium bromide. To avoid contamination, we performed amplification under the stringent conditions recommended by Kwok and Higuchi, with one positive and one negative control for each sample^[9].

Cloning and DNA sequencing

After the primers were removed from the amplification products by the commercial product SUPREC-02TM (TAKARA, Otsu, Japan), the products were ligated to pT7BlueT vectors (Novagen Inc., WI, USA). The ligated phagemid vector was transfected into competent JM109 cells (Toyobo, Osaka, Japan). Several independent colonies were examined to find appropriate clones from PCR using D and F primers. At least three clones for each case were subjected to 2 mL of liquid culture and small-scale preparation of phagemid DNA. Each clone was reacted with the DyeDeoxyTM terminator cycle sequencing kit and sequenced with a DNA sequencing system (Model 373A, Perkin Elmer, Urayasu, Japan), and the consensus sequences were adopted. The amino acid (aa) sequences deduced from the DNA consensus sequences in the HBV core region were compared to the wild type, subtype adr^[10] for all subjects.

Statistical analysis

Data values were presented as mean \pm SD. Statistical studies were achieved by Fisher's exact probability test and unpaired Student's *t*-test or Welch's *t*-test. *P*<0.05 was considered statistically significant.

RESULTS

Clinical and laboratory data on 17 patients with chronic hepatitis B

Of the 17 patients in the study, 7 were in the eAg-Po group and 10 were in the eAg-Ne group. Similarly, 10 were in the HA group and 7 were in the LA group. The percentage of HBeAg/anti-HBe seroconversion was 80% in the HA group and 28.6% in the LA group. The percentage of females in

HA group (50%) was greater than that in LA group (28.6%). More eAg-Po members were found in the HA group than in the LA group.

Mutation at HBV core region

The DNA sequences in the HBV core region samples from 17 patients were analyzed and compared to the adr subtype (Figures 1A and B). Figure 1A shows the HBV core regions in the eAg-Po and eAg-Ne groups, whereas Figure 1B shows those in the HA and LA groups. As shown in Figures 1A and B, many amino acid changes were detected in the HBV core regions of the eAg-Ne group and the HA group. The frequency of DNA mutations and the amino acid changes in the HBV core region are summarized in Table 1. No significant difference was found in the number of DNA mutations between the LA and HA groups, whereas the number of DNA mutations in the eAg-Ne group tended to be higher than that in the eAg-Po group (*P* = 0.06). The number of amino acid changes in the HA group was significantly greater than that in the LA group (*P*<0.05). The number of amino acid changes in the eAg-Ne group was also significantly greater than that in the eAg-Po group (*P*<0.05).

Table 1 Comparison of DNA mutation number and amino acid changes (mean \pm SD)

Group	DNA mutations	Amino acid changes
eAg-Po (<i>n</i> = 7)	8.9 \pm 3.7	0.9 \pm 0.9
eAg-Ne (<i>n</i> = 10)	13.7 \pm 5.4	5.0 \pm 2.4 ^b
HA (<i>n</i> = 10)	12.8 \pm 5.8	4.3 \pm 2.6 ^a
LA (<i>n</i> = 7)	10.1 \pm 4.1	1.7 \pm 2.1

^a*P*<0.05 eAg-Po group, ^b*P*<0.001 vs LA group.

Hot mutation spots of amino acid changes in HBV core region

As shown in Figures 1A and B, unique amino acid changes were detected in 30 of the 183 residues of the HBV core region. Of these 30 residues, six had an especially high mutation rate (more than 30%). The amino acid changes included replacements. Proline (Pro)-5 was replaced by threonine (Thr)-5, valine (Val)-5, and histidine (His)-5. Serine (Ser)-87 was replaced by glycine (Gly)-87 and asparagine (Asn)-87. Isoleucine (Ile)-97 was replaced by leucine (Leu)-97. Pro-130 was replaced by glutamine (Gln)-130 and Thr-130. Pro-135 was replaced by Gln-135 and Gly-153 was replaced by cysteine (Cys)-153.

DISCUSSION

Several virus factors and host factors have been reported to affect the activity of chronic hepatitis B^[11-14]. In this study, we analyzed Chinese patients with chronic hepatitis B according to the level of sALT values and the presence of HBeAg, and then investigated the entire core region of HBV to characterize the amino acid changes in this region and to elucidate the relationship between the frequency of core mutations and the clinical activity of HBV-related liver diseases. We found that many amino acid changes in the HBV core region occurred in the HBV DNA of patients with high sALT values and with the seroconversion from

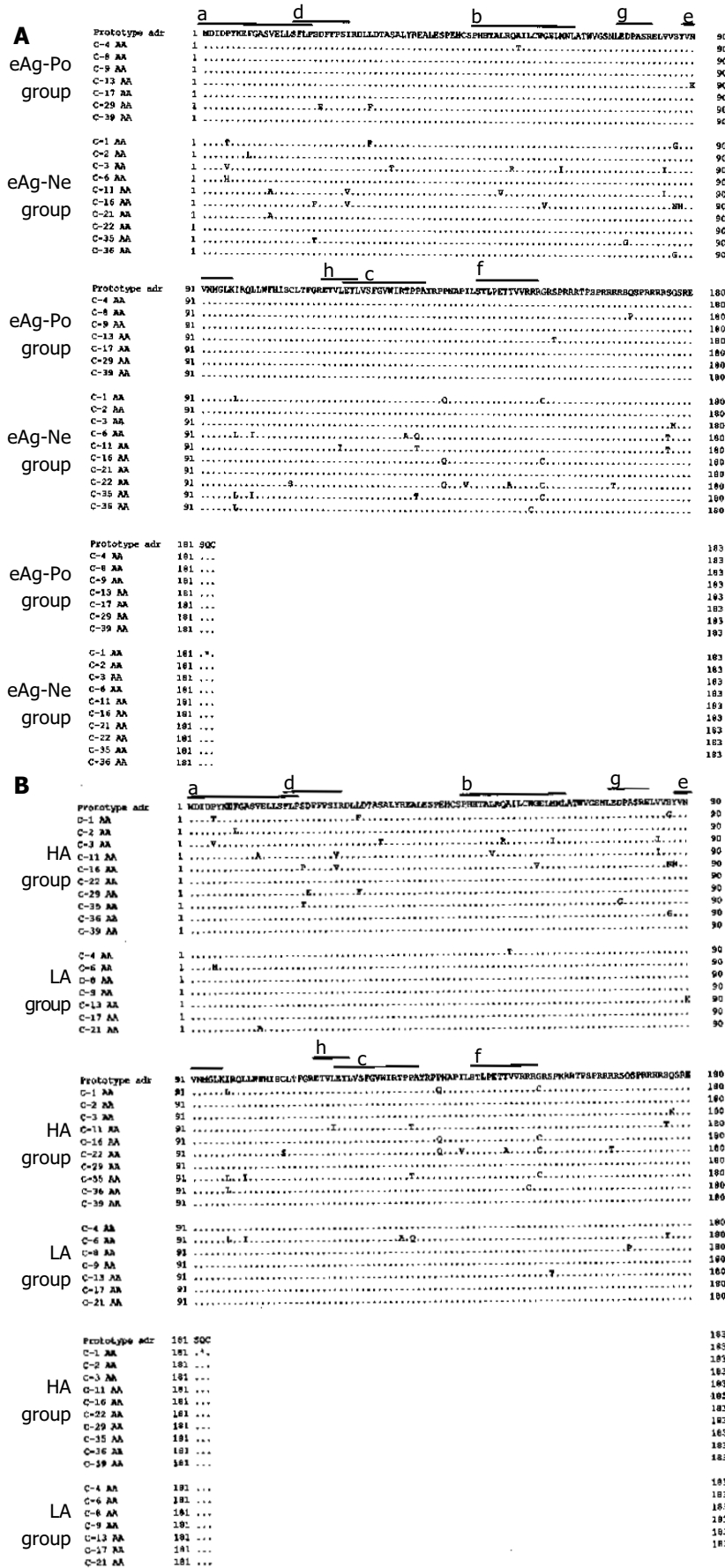


Figure 1 Comparison of core amino acid sequences between eAg-Po and eAg-Ne groups. (A) and between HA and LA groups (B). The top line is the core amino acid sequence of the HBV adr subtype. Core amino acid sequences of the HA group are C-1, C-2, C-3, C-11, C-16, C-22, C-29, C-35, C-36, and C-39, and those of the LA group are C-4, C-6, C-8, C-9, C-13, C-17, and C-21,

Each dot denotes an identical match to the top sequence. An asterisk denotes that this codon is a stop codon. a,b,c are HLA class II-restricted T cell recognition sites. d, e, f are HLA class I-restricted CTL epitopes. g, h are the lesion exposed at the surface of HBcAg.

HBeAg to anti-HBe. Increased activity of hepatitis and decreased time of seroconversion from HBeAg to anti-HBe may be attributed to increased immunological attacks against the HBV core region. Indeed, it has been reported that both B and T lymphocytes [helper T lymphocytes and cytotoxic T lymphocytes (CTL)] recognize core peptides. Some studies have reported that aa 78-83 and aa 127-133 are exposed on the surface of HBcAg^[4,5]. Penna *et al.*^[15], and Ferrari *et al.*^[16], have identified three major HLA class II-restricted T cell recognition sites within HBcAg: aa 1-20, aa 50-69, and aa 117-131. Furthermore, it has been reported that the HLA-A2.1-restricted CTL epitope is mapped to aa 18-27, HLA-A31- and HLA-AW68-restricted-CTLs recognize aa 141-151^[17], and HLA-A11-restricted-CTLs including HLA-A11 binding motifs recognize aa 88-96^[18]. To our surprise, these recognition epitopes correspond to the HBV core region involving the most sites of amino acid changes, suggesting that the amino acid changes are not randomly distributed, but selectively generated. From these data, we can also suggest that core amino changes are influenced by the host immune system. Regarding the mechanism of the relationship between virus mutations and host immunity, it has been recently reported that amino acid changes in epitopes of T and B lymphocytes in the HBV core region may markedly influence T lymphocyte function or subsequent cytokine release. Therefore, we speculate that such amino acid changes affect the viral antigenicity against the host immunity and may be associated with the clinical severity of hepatitis. This study suggests that the frequency of core mutations may be associated with the severity of hepatitis and the HBV seroconversion from HBeAg to anti-HBe. On the other hand, we could not find any difference in the HBV core protein among several HBV viruses. To differentiate HBV among groups, it may be necessary to examine not only various HBV proteins including surface protein and polymerase protein, but also the type of HLA in the host. Further investigation is needed regarding other causes of activity in chronic hepatitis B.

We conclude that identifying mutations in the HBV core region is important for predicting the clinical course of hepatitis B.

REFERENCES

- 1 **Carman WF**, Jacyna MR, Hadziyannis S, Karayiannis P, McGarvey MJ, Makris A, Thomas HC. Mutation-preventing formation of hepatitis B e antigen in patients with chronic hepatitis B infection. *Lancet* 1989; **2**: 588-591
- 2 **Omata M**, Ehata T, Yokosuka O, Hosoda K, Ohto M. Mutations in the precore region of hepatitis B virus DNA in patients with fulminant and severe hepatitis. *N Engl J Med* 1991; **324**: 1699-1704
- 3 **Ehata T**, Omata M, Chuang WL, Yokosuka O, Ito Y, Hosoda K, Ohto M. Mutations in the core nucleotide sequence of hepatitis B virus correlate with fulminant and severe hepatitis. *J Clin Invest* 1993; **91**: 1206-1213
- 4 **Pushko P**, Sallenberg M, Borisova G, Ruden U, Bichko V, Wahren B, Pumpens P, Magnus L. Identification of hepatitis B virus core protein regions exposed or internalized at the surface of HBcAg particles by scanning with monoclonal antibodies. *Virology* 1994; **202**: 912-920
- 5 **Sallberg M**, Pushko P, Berzinshi I, Bichko V, Sillekens P, Noah M, Pumpens P, Grens E, Wahren B. Immunochemical structure of the carboxy-terminal part of hepatitis B e antigen: identification of internal and surface-exposed sequences. *J Gen Virol* 1993; **74**: 1335-1340
- 6 **Milich DR**, Peterson DL, Schodel F, Jones JE, Hughes JL. Preferential recognition of hepatitis B nucleocapsid antigens by Th1 or Th2 cells is epitope and major histocompatibility complex dependent. *J Virol* 1995; **69**: 2776-2785
- 7 **Milich DR**, Schodel F, Hughes JL, Jones JE, Peterson DL. The hepatitis B virus core and e antigens elicit different Th cell subsets: antigen structure can affect Th cell phenotype. *J Virol* 1997; **71**: 2192-2201
- 8 **Sallberg M**, Ruden U, Wahren B, Noah M, Magnus LO. Human and murine B-cells recognize the HBeAg/beta (or HBe2) epitopes as a linear determinant. *Mol Immunol* 1991; **28**: 719-726
- 9 **Kwok S**, Higuchi R. Avoiding false positives with PCR. *Nature* 1989; **339**: 237-238
- 10 **Okamoto H**, Tsuda F, Sakugawa H, Sastrosoewignjo RI, Imai M, Miyakawa Y, Mayumi M. Typing hepatitis B virus by homology in nucleotide sequence: Comparison of surface antigen subtypes. *J Gen Virol* 1988; **69**: 2575-2583
- 11 **Okamoto H**, Tsuda F, Akahane Y, Sugai Y, Yoshida M, Moriyama K, Tanaka T, Miyakawa Y, Mayumi M. Hepatitis B virus with mutations in the core promoter for an e antigen-negative phenotype in carriers with antibody to e antigen. *J Virol* 1994; **68**: 8102-8110
- 12 **Sato S**, Suzuki K, Akamatsu K, Akiyama K, Yunomura K, Tsuda F, Tanaka T, Okamoto H, Miyakawa Y, Mayumi M. Hepatitis B virus strains with mutations in the core promoter in patients with fulminant hepatitis. *Ann Intern Med* 1995; **122**: 241-248
- 13 **Inoue K**, Yoshida M, Sekiyama K, Okamoto H, Mayumi M. Clinical and molecular virological differences between fulminant hepatic failures following acute and chronic infection with hepatitis B virus. *J Med Virol* 1998; **55**: 35-41
- 14 **Peters M**, Vierling J, Gershwin ME, Milich D, Chisari FV, Hoofnagle JH. Immunology and the liver. *Hepatology* 1991; **13**: 977-994
- 15 **Penna A**, Bertolotti A, Cavalli A, Valli A, Missale G, Pilli M, Marchelli S, Giuberti T, Fowler P, Chisari FV, Fieccadori F, Ferrari C. Fine specificity of the human T cell response to hepatitis B virus core antigen. *Arch Virol* 1992; **4**: 23-28
- 16 **Ferrari C**, Bertolotti T, Pena A, Cavalli A, Valli A, Missale G, Pilli M, Fowler P, Giuberti T, Chisari F, Fieccadori F. Identification of immunodominant T cell epitopes of the hepatitis B virus nucleocapsid antigen. *J Clin Invest* 1991; **88**: 214-222
- 17 **Missale G**, Redeker A, Person J, Fowler P, Guilhot S, Schlicht HJ, Ferrari C, Chisari FV. HLA-A31- and HLA-AW68-restricted cytotoxic T cell responses to a single hepatitis B virus nucleocapsid epitope during acute viral hepatitis. *J Exp Med* 1993; **177**: 751-762
- 18 **Tsai SL**, Chen MH, Yeh CT, Chu CM, Lin AN, Chiou FH, Chang TH, Liaw YF. Purification and characterization of a naturally processed hepatitis B virus peptide recognized by CD8+cytotoxic T lymphocytes. *J Clin Invest* 1996; **97**: 577-584

• VIRAL HEPATITIS •

Blood micronutrient, oxidative stress, and viral load in patients with chronic hepatitis C

Wang-Sheng Ko, Chih-Hung Guo, Maw-Sheng Yeh, Li-Yun Lin, Guoo-Shyng W. Hsu, Pei-Chung Chen, Mei-Ching Luo, Chia-Yeh Lin

Wang-Sheng Ko, Department of Food and Nutrition, Hung Kuang University; Department of Internal Medicine, Kuang-Tien General Hospital, Taichung 433, Taiwan, China
Chih-Hung Guo, Maw-Sheng Yeh, Li-Yun Lin, Mei-Ching Luo, Chia-Yeh Lin, Department of Food and Nutrition, Hung Kuang University, Taichung 433, Taiwan, China
Guoo-Shyng W. Hsu, Department of Nutrition and Food Sciences, Fu Jen University, Taipei 242, Taiwan, China
Pei-Chung Chen, Department of Biotechnology, Hung Kuang University, Taichung 433, Taiwan, China
Supported by the Kuang-Tien General Hospital, Taichung, Taiwan, China

Co-first-authors: Wang-Sheng Ko and Chih-Hung Guo

Co-correspondents: Wang-Sheng Ko

Correspondence to: Chih-Hung Guo, Department of Food and Nutrition, Hung Kuang University, Taichung 433, Taiwan, China. eillyguo@sunrise.hk.edu.tw

Telephone: +886-42631-8652-5037 Fax: +886-42631-9176

Received: 2004-10-10 Accepted: 2004-12-23

CONCLUSION: The levels of Zn, Se, Cu, and oxidative stress (MDA), as well as related anti-oxidative enzymes (GR and GPX) in blood have important impact on the viral factors in chronic hepatitis C. The distribution of these parameters might be significant biomarkers for HCV.

© 2005 The WJG Press and Elsevier Inc. All rights reserved.

Key words: Micronutrient; Oxidative stress; Viral load; Plasma and erythrocytes; Hepatitis C

Ko WS, Guo CH, Yeh MS, Lin LY, Hsu GSW, Chen PC, Luo MC, Lin CY. Blood micronutrient, oxidative stress, and viral load in patients with chronic hepatitis C. *World J Gastroenterol* 2005; 11(30): 4697-4702

<http://www.wjgnet.com/1007-9327/11/4697.asp>

Abstract

AIM: To assess the extent of micronutrient and oxidative stress in blood and to examine their linkages with viral loads in chronic hepatitis C patients.

METHODS: Hepatitis C virus (HCV)-RNA levels were quantified in the serum from 37 previously untreated patients with chronic hepatitis C. The plasma and erythrocyte micronutrients (zinc, selenium, copper, and iron) were estimated, and malondialdehyde (MDA) contents were determined as a marker to detect oxidative stress. Antioxidant enzymes, superoxide dismutase (SOD), glutathione peroxidase (GPX) and glutathione reductase (GR) activities in blood were also measured. The control group contained 31 healthy volunteers.

RESULTS: The contents of zinc (Zn), and selenium (Se) in plasma and erythrocytes were significantly lower in hepatitis C patients than in the controls. On the contrary, copper (Cu) levels were significantly higher. Furthermore, plasma and erythrocyte MDA levels, and the SOD and GR activities in erythrocytes significantly increased in hepatitis C patients compared to the controls. However, the plasma GPX activity in patients was markedly lower. Plasma Se ($r = -0.730$, $P < 0.05$), Cu ($r = 0.635$), and GPX ($r = -0.675$) demonstrated correlations with HCV-RNA loads. Significant correlation coefficients were also observed between HCV-RNA levels and erythrocyte Zn ($r = -0.403$), Se ($r = -0.544$), Cu ($r = 0.701$) and MDA ($r = 0.629$) and GR ($r = 0.441$).

INTRODUCTION

Essential micronutrients are involved in many metabolic pathways in the liver, such as enzymatic functions and protein synthesis, oxidative damage and anti-oxidant defense, immunological competence, interferon therapy response regulations, and alterations of the virus genomes^[1-5]. Reactive oxygen species (ROS) have also been implicated in a number of hepatic pathologies in exacerbating liver diseases^[6-10]. The oxidant production associated with immune reactions against viral hepatitis leads to the formation of hepatocellular carcinoma (HCC)^[8]. Therefore, the changes in micronutrients and their demolishing effects against oxidative stress are factors for viral hepatitis pathogenesis.

HCV is a major cause of chronic liver disease. HCV infection frequently leads to chronic hepatitis with increasing risk of developing liver cirrhosis and HCC. Interferon with or without ribavirin is the only drug with proven efficacy in treating chronic HCV infections^[11-13]. Unfortunately, these therapeutic models maintain the rate of sustained virologic response (SVR) to approximately 10-40%^[14-16]. The effective advancement in the antiviral treatments against chronic hepatitis C is necessary.

There are several factors that attribute to the failure in achieving a SVR for the majority of patients^[17-19]. Hepatic iron deposit has been identified as one of these factors^[20-23]. Iron depletion and zinc supplementation^[24,25] may improve the response of chronic hepatitis C patients to interferon treatment. Moreover, viral factors may affect the outcome of the therapy. Zhang *et al.*^[26], indicated that selenium-dependent glutathione peroxidase (GPX) modules are

encoded in the RNA viruses. The presence of zinc ion also decreases the HIV-1 reverse transcriptase activity^[27]. It is conceivable that the micronutrient status may affect the HCV load and viral replication, leading to significant changes in reported SVR rates. However, there is limited information about the distribution of micronutrients and their effects on viral production.

Our present study aimed to examine the levels of micronutrients (zinc, copper, iron, selenium), and malondialdehyde (MDA) which is an indirect marker for oxidative stress in blood. Moreover, superoxide dismutase (SOD), glutathione reductase (GR) and GPX activities were assessed. In addition, the relationships among these parameters and HCV-RNA levels in patients with chronic hepatitis C were investigated.

MATERIALS AND METHODS

Subjects

This study contained 33 patients with chronic hepatitis C including 20 men and 13 women (from 2002 to 2003). The mean age of the patients was 49.5 ± 2.4 years. All patients underwent serological and biochemical analyses. Diagnosis of chronic hepatitis C was based on elevated serum alanine aminotransferase levels for at least 6 mo, and consistent detection of serum HCV-RNA. All patients were negative for hepatitis B surface antigen and HIV, and none had liver cirrhosis or renal disease.

A control group of 31 healthy volunteers (17 men and 14 women) was recruited from blood donors aged 43.2 ± 1.7 years. They underwent a routine medical examination prior to the blood collection.

Biochemical determinations and HCV-RNA analysis

Venous blood samples were collected from patients prior to treatment. Erythrocytes were pelleted by centrifugation and washed thrice with cold isotonic saline. The plasma and erythrocyte zinc (Zn), copper (Cu), and iron (Fe) levels were determined by flame atomic absorption spectrophotometry (932 plus, GBC, Australia) as previously described^[28]. The accessory hydride formation system (HG3000), also from GBC, was used for determining selenium (Se) concentrations. All samples were analyzed in triplicate. Serum "second-generation" reference materials (Seronorm™ Trace Elements Serum) were purchased from Nycomed, Oslo, Norway.

Thiobarbituric acid substances reacted with products of lipid peroxidation, mainly MDA, producing a pink color compound that could be measured at 535 nm. Following the protocol in Richard *et al.*^[29], thiobarbituric acid levels were determined in plasma and erythrocytes of patients and controls. Results were expressed as nanomoles of MDA per milliliter in plasma and as nanomoles of MDA per gram protein in erythrocytes. Protein concentration was determined using the Coomassie protein assay (Pierce, Rockford, IL, USA) with bovine serum albumin as the standard.

Erythrocyte SOD and GPX activities in plasma were determined with RANSOD kits (Randox, San Diego) and Cayman GPx assay kits (Cayman Chemical, USA) respectively. All values were expressed as units per gram hemoglobin or

units per milliliter. One unit of SOD was defined as the amount of enzyme necessary to produce 50% inhibition in the *p*-iodonitrotetrazolium reduction rate. The activity of GR in erythrocytes was also measured at 340 nm using the commercial kits (GR340, OxisResearch). One GR activity unit was defined as the amount of enzyme catalyzing the reduction of 1 mmol of GSSG.

Additionally, viral RNA was detected and quantitative HCV-RNA was determined by Amplicor (Roche Molecular Diagnostics) and expressed as the log of copies of RNA per milliliter. RNA was extracted from serum samples following the manufacturer's instructions (QIAamp viral RNA kit from Qiagen Inc.). This assay had a lower limit of 100 copies/mL.

Statistical analysis

Data were expressed as mean \pm SE. Significant differences in variables between two groups were tested by Student's *t*-test. $P < 0.05$ was considered statistically significant. Linear regressions were used to analyze the correlation among variables.

RESULTS

Blood micronutrient levels

Table 1 shows the values of specific micronutrients in plasma of chronic hepatitis C patients and healthy subjects. There was a significant decrease in Zn and Se and a statistical increase in Cu concentrations of the patients ($P < 0.05$). However, plasma Fe levels revealed no significant difference ($P > 0.05$).

The erythrocyte concentration of Cu in the patients was significantly higher than that in the healthy controls, and the Fe concentrations were not significantly different between two groups. Furthermore, Se and Zn levels were significantly lower in erythrocytes of the patients (Table 2).

Table 1 Plasma concentrations of Zn, Cu, Fe, and Se in patients with chronic hepatitis C and healthy controls (mean \pm SE)

Groups	Plasma			
	Zn (mg/L)	Cu (mg/L)	Fe (mg/L)	Se (μ g/L)
Patients	0.13 \pm 0.01 ^a	1.68 \pm 0.08 ^a	0.56 \pm 0.04	159.12 \pm 5.30 ^a
Healthy controls	0.55 \pm 0.06	0.53 \pm 0.03	0.57 \pm 0.03	216.69 \pm 7.44

^a $P < 0.05$ vs healthy controls.

Table 2 Erythrocyte levels of Zn, Cu, Fe, and Se in patients with chronic hepatitis C and healthy controls (mean \pm SE)

Groups	Erythrocytes			
	Zn (mg/L)	Cu (mg/L)	Fe (mg/L)	Se (μ g/L)
Patients	0.79 \pm 0.05 ^a	0.52 \pm 0.05 ^a	1 369.8 \pm 88.6	55.09 \pm 3.79 ^a
Healthy controls	1.40 \pm 0.10	0.09 \pm 0.01	1 075.9 \pm 96.7	139.08 \pm 5.76

^a $P < 0.05$ vs healthy controls.

Evidence of oxidative stress

Table 3 summarizes the values of parameters related to oxidative stress. Erythrocyte and plasma MDA increased

Table 3 MDA levels, SOD, GR, and GPX activities in patients with chronic hepatitis C and healthy controls (mean±SE)

Group	Parameters ¹				
	MDA		SOD (U/g Hb)	GR (mU/g Hb)	GPX [nmol/(min·mL)]
	Plasma (nmol/mL)	RBC (nmol/g protein)			
Patients	0.41±0.02 ^a	0.33±0.02 ^a	17.95±0.51 ^a	40.10±2.48 ^a	38.95±1.99 ^a
Healthy controls	0.15±0.01	0.19±0.02	15.24±0.45	30.15±2.69	51.26±2.66

^a $P < 0.05$ vs healthy controls. ¹MDA: malondialdehyde; SOD: superoxide dismutase; GR: glutathione reductase; GPX: glutathione peroxidase.

significantly in patients. Also, the erythrocyte Cu, Zn-SOD, and GR activities increased significantly in the patients compared to the controls. In contrast, the plasma Se-dependent GPX activity in hepatitis C patients was markedly lower.

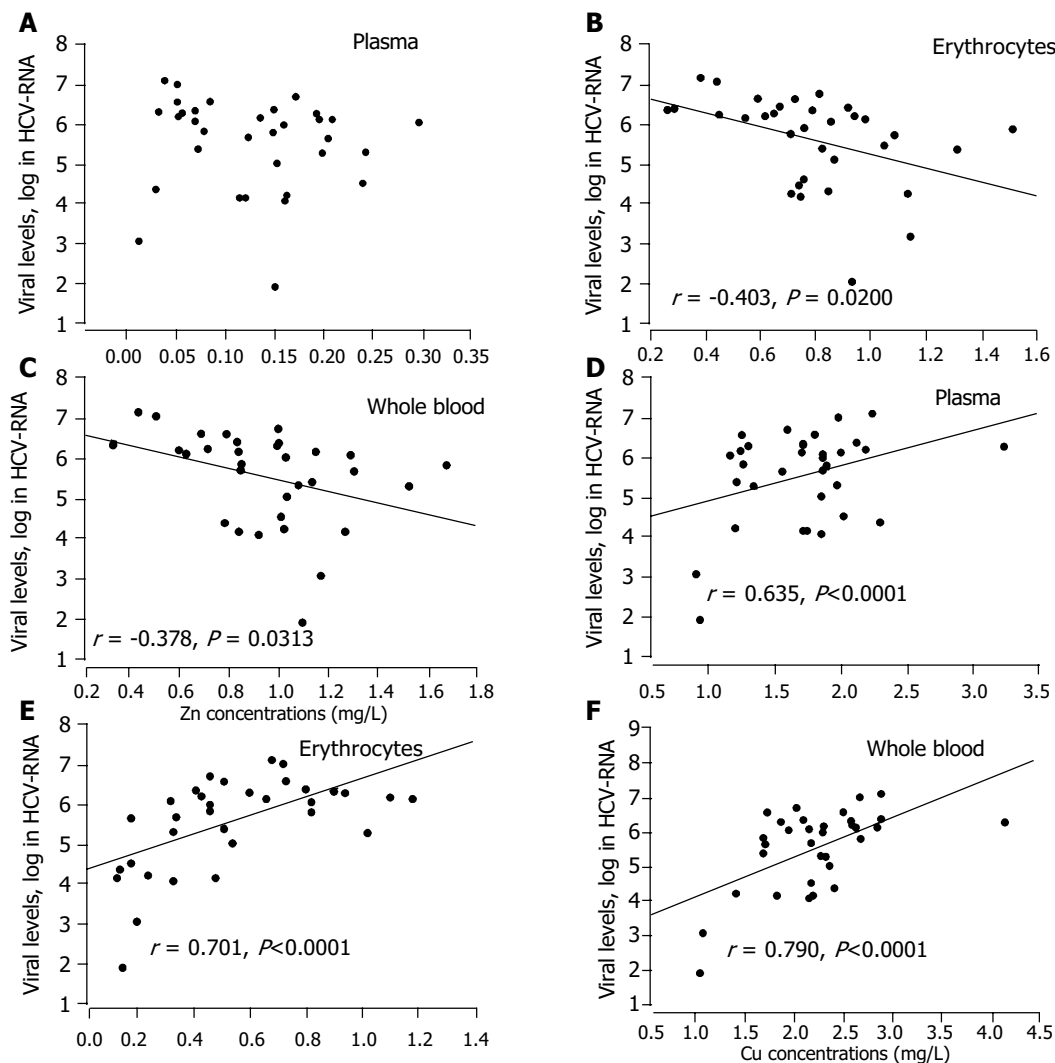
Correlation of micronutrient concentrations with HCV-RNA levels

Figures 1A-C shows that there was a significant negative relationship between Zn contents in erythrocytes/whole blood and HCV-RNA levels (by log) in patients. In plasma, however, no significant correlation was observed. A positive correlation was noted between plasma Cu and HCV-RNA levels in patients, and an even stronger correlation between the Cu in erythrocytes/whole blood and HCV-RNA levels (Figures 1D-F).

The Se levels in plasma/erythrocytes/whole blood had a statistically significant negative correlation with HCV-RNA levels, whereas a better correlation was found in plasma or whole blood (Figures 1G-I, $r = -0.730, -0.742, P < 0.0001$).

Relationship between oxidative stress and HCV-RNA levels

No significant correlation was found between MDA in plasma and HCV-RNA levels ($P > 0.05$, data not presented). However, erythrocyte MDA production was positively correlated with HCV-RNA concentration (Figure 1J, $r = 0.629, P < 0.0001$). Additionally, HCV-RNA levels correlated with both erythrocyte GR (Figure 1K, $r = 0.441, P = 0.01$) and plasma GPX (Figure 1L, $r = -0.675, P < 0.0001$) activities. The activities of SOD did not correlate with the HCV-RNA levels ($P > 0.05$, data not shown).



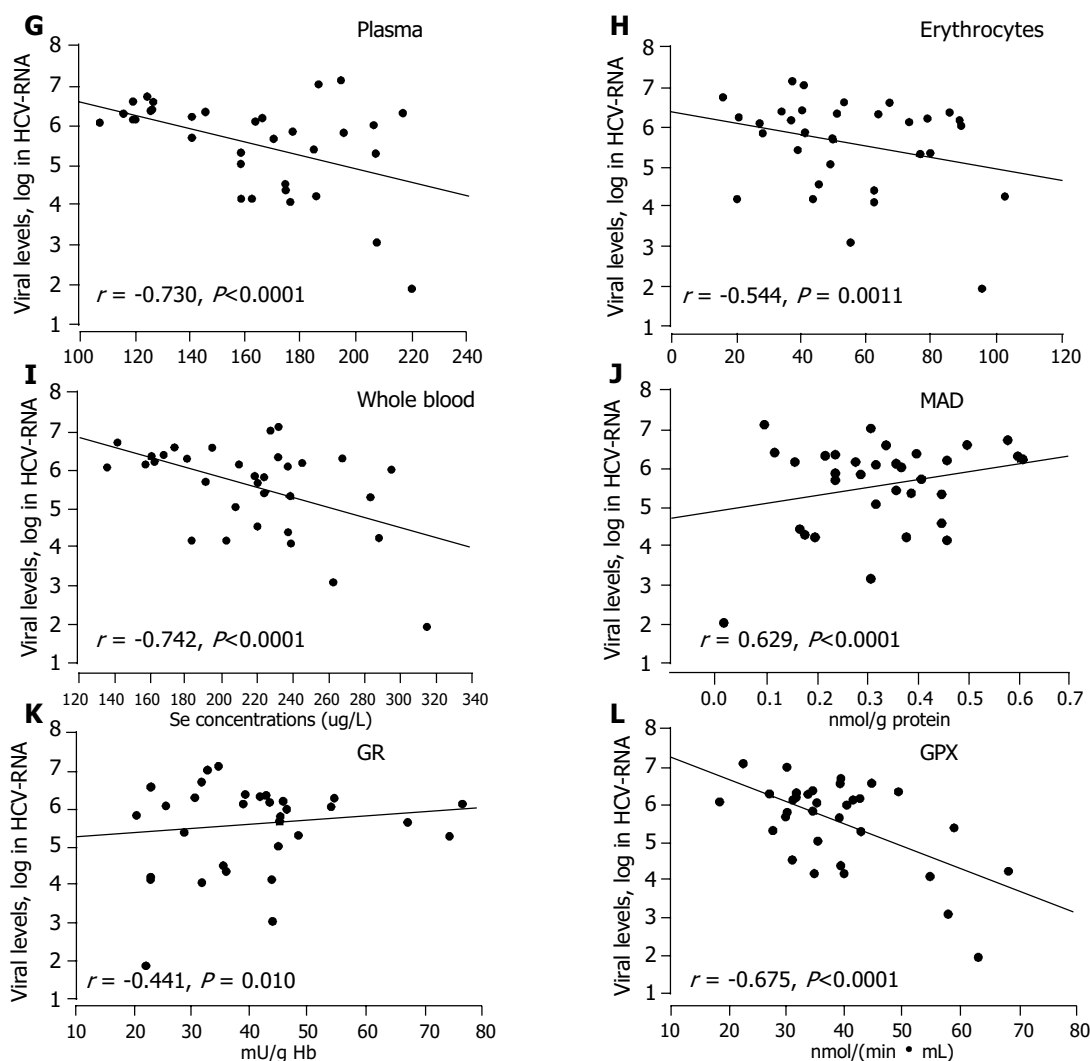


Figure 1 Correlations between viral levels and plasma zinc (A), erythrocytes zinc (B), or whole blood zinc (C), plasma copper (D), erythrocyte copper (E), whole blood copper (F), plasma selenium (G), erythrocyte selenium (H), whole

blood selenium (I), erythrocyte MDA (J), GR (K), and plasma GPX activities (L) in chronic hepatitis C patients.

DISCUSSION

The purpose of our study was to find the levels of blood micronutrient and oxidative stress in patients with chronic hepatitis C, and to search for linkages between the HCV-RNA levels and micronutrient status, as well as between oxidative stress and the presence of antioxidant enzymes.

The essential micronutrients (Zn, Cu, Fe, and Se) might exacerbate liver disease in case of deficiency, imbalance, or toxicity^[5,30]. They are also linked to the process of oxidation during chronic liver damage^[6,7,31]. In the present investigation, the levels of Zn and Se in plasma and erythrocytes of HCV-infected patients decreased significantly compared to healthy subjects. On the contrary, the Cu levels in patients were significantly higher than those in the control group. Nevertheless, alterations of these micronutrients in plasma and erythrocytes varied in different magnitudes.

Decreasing levels of Zn, Se, or increasing Cu levels were also noted in sera of hepatitis cases^[31-33]. HCV- and HIV-co-infected patients showed markedly lower blood Se levels compared to HIV-infected patients without concomitant HCV infection^[34]. However, no significant difference in blood Zn and Se concentrations was observed between chronic

hepatitis C patients and controls^[35,36]. One possible explanation for this discrepancy is that, the subjects in the above two studies could not be distinguished by the type of hepatitis, and patients with hepatitis A-D may have different blood concentrations of Zn and Se. The present study did not find significantly higher values of erythrocyte Fe in the patients to coincide with the results in Loguercio *et al.*^[36], whereas some data in the literature show an obvious increase of Fe contents both in the liver and in the serum of these patients^[37,38]. Thus, the pretreatment levels of blood Fe might not be a proper marker for the iron status in patients with chronic hepatitis C infection.

Although the precise causes remain to be elucidated, there is evidence that cytokines might alter the levels of serum trace elements in viral hepatitis^[32]. It was reported that inflammatory cytokines are higher in HCV-infected individuals than in normal individuals^[39,40]. Increased Cu levels might result from inflammatory responses^[32]. Therefore, the present results suggest that changes of Zn, Cu, and Se levels in plasma and erythrocytes of patients with chronic hepatitis C are directly related to the pathology developed in the liver.

ROS plays a crucial role in the induction and progression of liver disease, and are involved in the transcription and activation of a large series of cytokines that could induce production of ROS. Some studies indicate that treatment of high serum Se and Zn levels leads to reduction of inflammatory reaction in hepatitis patients^[41,42]. In addition to the anti-inflammatory reaction, Se or Zn has antioxidant and immuno-modulatory effects^[43-45]. Copper is also associated with the inflammatory response and oxidative stress^[46,47]. In the present study, decreased activity of Se-dependent GPX and increased Cu, Zn-SOD, and GR activities either in plasma or in erythrocytes suggest that anti-oxidative capability is limited during circulation. The presence of significant increase in MDA levels also indicates a possible oxidative insult in these patients. Liver cirrhosis induces a significant decrease in Se and Zn levels, another indication of presence of oxidative stress^[36]. The levels of MDA have been correlated with the severity of chronic hepatitis^[45]. There is evidence that the production of free radicals increases while anti-oxidant defense decreases significantly in all types of liver damage^[6-9]. Therefore, supportive nutrients, Zn, Cu, and Se, and oxidative stress might be sensitive indicators for the degree of liver injuries and the sustained response to therapy in chronic hepatitis C patients.

The outcome of HCV infection is also thought to depend on the balance between the rate of viral replication, rapidity, and specificity and the effectiveness of the host immune response. Few studies have focused on the relationship between circulating pool of these immune-regulated micronutrients and HCV-RNA contents. Our present results suggest that there is a markedly negative relationship between HCV-RNA titer (in log) and either erythrocyte or whole blood Zn concentrations. Similarly, the inverse correlations between HCV-RNA and blood Se levels observed in this study suggest that significant higher viral loads are correlated with lower blood Zn and Se levels in HCV-infected patients.

In addition, higher levels of blood Cu are markedly correlated with higher HCV-RNA concentrations. Little is known about the possible regulatory mechanism of micronutrients in the pathogenesis of HCV infection. However, these nutrients are known to assist in immune-mediated response and involve in the alteration of virus genomes^[5,27,45,48]. It is suggested that the distribution of Zn, Se, and Cu might affect sustained response to therapy in patients with chronic hepatitis C. Therefore, these micronutrients may be involved in multiple points in the immune pathogenesis of HCV infection that is essential for viral clearance.

The oxidative stress is high in hepatitis patients, and there are significant correlations among HCV-RNA and erythrocyte MDA, erythrocyte GR and plasma GPX activities. Zhang *et al.*^[26], reported that Se-dependent GPX modules are encoded in a number of RNA viruses, including HIV-1, HCV, Coxsackie's virus B3, and HIV-2 virus. A HCV-encoded GPX gene might demonstrate that oxidant stress is associated with HCV disease progression. In HIV-infected patients, the decline in Se levels is greater than that in those with HCV co-infection^[34]. Se deficiency increases the virulence of CVB3 infection, which is encoded

by the GPX gene within Keshan disease's cofactor^[26,49]. It has been proposed that Se-dependent GPX participates directly in immune cytotoxicity, enabling neutrophils and macrophages to complete intracellular lysis of phagocytosed cells. In previous investigations, an inverse relationship between Se level and HBV infection incidence was found^[50]. Zn has also been studied for its antiviral effect against HIV, rhinovirus, and herpes virus^[24]. Moreover, Zn supplementation enhances the response to interferon therapy in chronic hepatitis C patients^[25]. Zn is necessary for the dimerization of interferon, which activates the interferon receptor^[51]. It is apparent that erythrocyte and plasma Zn, Se, and Cu levels and oxidative stress are associated with HCV-RNA levels.

In conclusion, the distribution of Zn, Cu, Se levels and MDA product, GPX and GR activities in blood may be an additional host-specific parameter (outside of predictive viral factors) with a predictive value for the responsiveness of patients to interferon/ribavirin therapy. Furthermore, these results may be affected by immunocytokines as a host-defense system during HCV infection.

ACKNOWLEDGMENT

Great appreciation is extended to Miss Anna Hsu of Oregon State University for the English editing of the manuscript.

REFERENCES

- 1 **Beisel WR.** Single nutrients and immunity. *Am J Clin Nutr* 1982; **35**(2 Suppl): 417-468
- 2 **Evans GW.** Zinc and its deficiency diseases. *Clin Physiol Biochem* 1986; **4**: 94-98
- 3 **Bray TM, Bettger WJ.** The physiological role of zinc as an antioxidant. *Free Rad Biol Med* 1990; **8**: 281-291
- 4 **Bhaskaram P.** Micronutrient malnutrition, infection, and immunity: an overview. *Nutr Rev* 2002; **60**: S40-S45
- 5 **Ozcelik D, Ozaras R, Gurel Z, Uzun H, Aydin S.** Copper-mediated oxidative stress in rat liver. *Biol Trace Elem Res* 2003; **96**: 209-215
- 6 **Halliwell B, Gutteridge JMC.** Role of free radicals and catalytic metal ions in human disease: an overview. *Methods Enzymol* 1990; **186**: 1-85
- 7 **Peterhans E.** Reactive oxygen species and nitric oxide in viral diseases. *Biol Trace Elem Res* 1997; **56**: 107-116
- 8 **Jain SK, Pemberton PW, Smith A, McMahon RF, Burrows PC, Aboutwerat A, Warnes TW.** Oxidative stress in chronic hepatitis C: not just a feature of late stage disease. *J Hepatol* 2002; **36**: 805-811
- 9 **Loguercio C, Federico A.** Oxidative stress in viral and alcoholic hepatitis. *Free Radic Biol Med* 2003; **34**: 1-10
- 10 **Toubi E, Kessel A, Goldstein L, Slobodin G, Sabo E, Shmuel Z, Zuckerman E.** Enhanced peripheral T-cell apoptosis in chronic hepatitis C virus infection: association with liver disease severity. *J Hepatol* 2001; **35**: 774-780
- 11 National institutes of health consensus development conference panel statement: management of hepatitis C. *Hepatology* 1997; **15**: 1-41
- 12 **McHutchison JG, Gordon SC, Schiff ER, Shiffman ML, Lee WM, Rustgi VK, Goodman ZD, Ling MH, Cort S, Albrecht JK.** Interferon alfa-2b alone or in combination with ribavirin as initial treatment for chronic hepatitis C. *N Engl J Med* 1998; **339**: 1485-1492
- 13 **Poynard T, Leroy V, Cohard M, Thevenot T, Mathurin P, Opolon P, Zarski JP.** Meta-analysis of interferon randomized trials in the treatment of viral hepatitis: effects of dose and duration. *Hepatology* 1996; **24**: 778-789

- 14 **Poynard T**, Marcellin P, Lee SS, Niederau C, Minuk GS, Ideo G, Bain V, Heathcote J, Zeuzem S, Trepo C, Albrecht J. Randomised trial of interferon alpha 2b plus ribavirin for 48 wk or for 24 wk virus interferon with hepatitis C virus. *Lancet* 1998; **352**: 1426-1432
- 15 **Thevenot T**, Regimbeau C, Ratzu V, Leroy V, Opolon P, Poynard T. Meta-analysis of interferon randomized trials in the treatment of viral hepatitis C in naïve patients. *J Viral Hepat* 1999; **8**: 48-62
- 16 **Hoofnagle JH**. Management of hepatitis C: current and future perspectives. *J Hepatol* 1999; **31**(Suppl 1): 264-268
- 17 **Neuman MG**, Benhamou JP, Malkiewicz IM, Akremi R, Shear NH, Asselah T, Ibrahim A, Boyer N, Martinot-Peignour M, Jacobson-Brown P, Katz GG, Le Breton V, Le Guludee G, Suneja A, Marcellin P. Cytokines as predictors for sustained response and as markers for immunomodulation in patients with chronic hepatitis C. *Clin Biochem* 2001; **34**: 173-182
- 18 **Ho SB**, Nguyen H, Tetrick LL, Opitz GA, Basara ML, Dieperink E. Influence of psychiatric diagnoses on interferon- α treatment for chronic hepatitis C in a veteran population. *Am J Gastroenterol* 2001; **96**: 157-164
- 19 **Kumar D**, Wallington-Beddoe C, George J, Lin R, Samarasinghe D, Liddle C, Farrell GC. Effectiveness of interferon alfa-2b/ribavirin combination therapy for chronic hepatitis C in a clinic setting. *Med J Aust* 2003; **178**: 267-271
- 20 **Van Thiel DH**, Friedlander L, Fagioli S, Wright HI, Irish W, Gavaler JS. Response to interferon therapy is influenced by the iron content of the liver. *J Hepatol* 1994; **20**: 410-415
- 21 **Olynyk JK**, Reddy KR, Di Bisceglie AM, Jeffers LJ, Parker TI, Radick JL, Schiff ER, Bacon BR. Hepatic iron concentration as a predictor of response to interferon α therapy in chronic hepatitis C. *Gastroenterology* 1995; **108**: 1104-1109
- 22 **Kageyama F**, Kobayashi Y, Murohisa G, Shimizu E, Suzuki F, Kikuyama M, Souda K, Kawasaki T, Nakamura H. Failure to respond to interferon- α 2a therapy is associated with increased hepatic iron levels in patients with chronic hepatitis C. *Biol Trace Elem Res* 1998; **64**: 185-196
- 23 **Carlo C**, Daniela P, Giancarlo C. Iron depletion and response to interferon in chronic hepatitis C. *Hepatogastroenterology* 2003; **50**: 1467-1471
- 24 **Nagamine T**, Takagi H, Takayama H, Kojima A, Kakizaki S, Mori M, Nakajima K. Preliminary study of combination therapy with interferon- α and zinc in chronic hepatitis C patients with genotype 1b. *Biol Trace Elem Res* 2000; **75**: 53-63
- 25 **Takagi H**, Nagamine T, Abe T, Takayama H, Sato K, Otsuka T, Kakizaki S, Hashimoto Y, Matsumoto T, Kojima A, Takezawa J, Suzuki K, Sato S, Mori M. Zinc supplementation enhances the response to interferon therapy in patients with chronic hepatitis C. *J Viral Hepatol* 2001; **8**: 367-371
- 26 **Zhang W**, Ramanathan CS, Nadimpalli RG, Bhat AA, Cox AG, Taylor EW. Selenium-dependent glutathione peroxidase modules encoded by RNA viruses. *Biol Trace Elem Res* 1999; **70**: 97-116
- 27 **Sabbioni E**, Blanch N, Baricevic K, Serra MA. Effects of trace metal compounds on HIV-1 reverse transcriptase. An *in vitro* study. *Biol Trace Elem Res* 1999; **68**: 107-119
- 28 **Guo CH**, Huang CJ, Chiou YL, Hsu GSW. Alteration of trace element distribution and testis ACE activity in mice with high peritoneal aluminum. *Biol Trace Elem Res* 2002; **86**: 145-158
- 29 **Richard MJ**, Portal B, Meo J, Coudray C, Hadjian A, Favier A. Malondialdehyde kit evaluated for determining plasma and lipoprotein fractions that react with thiobarbituric acid. *Clin Chem* 1992; **38**: 704-709
- 30 **Buck WB**, Ewan RC. Toxicology and adverse effects of mineral imbalance. *Clin Toxicol* 1973; **6**: 459-485
- 31 **Pramoolsinsap C**, Promvanit N, Komindr S, Lerdverasirikul P, Sriyanujata S. Serum trace metals in chronic viral hepatitis and hepatocellular carcinoma in Thailand. *J Gastroenterol* 1994; **29**: 610-615
- 32 **Kalkan A**, Bulut V, Avci S, Celik I, Bingol NK. Trace elements in viral hepatitis. *J Trace Elem Med Biol* 2002; **16**: 227-230
- 33 **Czuczejko J**, Zachara BA, Staubach-Topczewska E, Halota W, Kedziora J. Selenium, glutathione and glutathione peroxidase in blood of patients with chronic liver diseases. *Acta Biochim Polon* 2003; **50**: 1147-1154
- 34 **Look MP**, Rockstroh JK, Rao GS, Kreuzer KA, Barton S, Lemoch H, Sudhop T, Hoch J, Stockinger K, Spengler U, Sauerbruch T. Serum selenium, plasma glutathione (GSH) and erythrocyte glutathione peroxidase (GSH-Px)-levels in asymptomatic versus symptomatic human immunodeficiency virus-1 (HIV-1)-infection. *Eur J Clin Nutr* 1997; **51**: 266-272
- 35 **Loguercio C**, de Girolamo V, Federico A, Feng SL, Cataldi V, Del Vecchio Blanco C, Gialanella G. Trace elements and chronic liver diseases. *J Trace Elem Med Biol* 1997; **11**: 158-161
- 36 **Loguercio C**, de Girolamo V, Federico A, Feng SL, Crafa E, Cataldi V, Gialanella G, Moro R, del Vecchio BC. Relationship of blood trace elements to liver damage, nutritional status, and oxidative stress in chronic nonalcoholic liver disease. *Biol Trace Elem Res* 2001; **81**: 245-254
- 37 **Sikorska K**, Stalke P, Lakomy EA, Michalska Z, Witczak-Malinowska K, Stolarczyk J. Disturbances of iron metabolism in chronic liver diseases. *Med Sci Monit* 2003; **9**(Suppl 3): 64-67
- 38 **Metwally MA**, Zein CO, Zein NN. Clinical significance of hepatic iron deposition and serum iron values in patients with chronic hepatitis C infection. *Am J Gastroenterol* 2004; **99**: 286-291
- 39 **Malaguarnera M**, Di Fazio I, Romeo MA, Restuccia S, Laurino A, Trovato BA. Elevation of IL6 levels in patients with chronic hepatitis due to hepatitis C virus. *J Gastroenterol* 1997; **32**: 211-215
- 40 **Neuman MG**, Benhamou JP, Martinot M, Boyer N, Shear NH, Malkiewicz I, Katz GG, Suneja A, Singh S, Marcellin P. Predictors of sustained response to alpha interferon therapy in chronic hepatitis C. *Clin Biochem* 1999; **32**: 537-545
- 41 **Sartori M**, Andorno S, Rigamonti C, Boldorini R. Chronic hepatitis C treated with phlebotomy alone: biochemical and histological outcome. *Dig Liver Dis* 2001; **33**: 157-162
- 42 **Selimoglu MA**, Aydogdu S, Unal F, Yuce G, Yagci RV. Serum zinc status in chronic hepatitis B and its relationship to liver histology and treatment results. *Pediat Intern* 2001; **43**: 396-399
- 43 **Tanasescu C**, Baldescu R, Chirulescu Z. Interdependence between Zn and Cu serum concentrations and serum immunoglobulins (IgA, IgM, IgG) in liver diseases. *Rom J Intern Med* 1996; **34**: 217-224
- 44 **Takagi H**, Nagamine T, Abe T, Takayama H, Sato K, Otsuka T, Kakizaki S, Hashimoto Y, Matsumoto T, Kojima A, Takezawa J, Suzuki K, Sato S, Mori M. Zinc supplementation enhances the response to interferon therapy in patients with chronic hepatitis C. *J Viral Hepatol* 2001; **8**: 367-371
- 45 **Cunningham-Rundles S**, Ahrn S, Abuav-Nussbaum R, Dnistrian A. Development of immunocompetence: Role of micronutrients and microorganisms. *Nutr Rev* 2002; **60**: S68-S72
- 46 **Fisher AE**, Naughton DP. Vitamin C contributes to inflammation via radical generating mechanisms: a cautionary note. *Med Hypotheses* 2003; **61**: 657-660
- 47 **Klein D**, Lichtmannegger J, Finckh M, Summer KH. Gene expression in the liver of Long-Evans cinnamon rats during the development of hepatitis. *Arch Toxicol* 2003; **77**: 568-575
- 48 **Taylor EW**, Nadimpalli RG, Ramanathan CS. Genomic structures of viral agents in relation to the biosynthesis of selenoproteins. *Biol Trace Elem Res* 1997; **56**: 63-91
- 49 **Beck MA**, Shi Q, Morris VC, Levander OA. Rapid genomic evolution of a non-virulent Coxsackievirus B3 in selenium-deficient mice results in selection of identical virulent isolates. *Nature Med* 1995; **1**: 433-436
- 50 **Yu SY**, Zhu YJ, Li WG. Protective role of selenium against hepatitis B virus and primary liver cancer in Qidong. *Biol Trace Elem Res* 1997; **56**: 117-124
- 51 **Radhakrishnan R**, Walter LJ, Hruza A, Reichert P, Trotta PP, Nagabhushan TL, Walter MR. Zinc mediated dimmer of human interferon-alpha 2b revealed by X-ray crystallography. *Structure* 1996; **4**: 1453-1463

• VIRAL HEPATITIS •

Biological impacts of "hot-spot" mutations of hepatitis B virus X proteins are genotype B and C differentiated

Xu Lin, Xiao Xu, Qing-Ling Huang, Yu-Qing Liu, Da-Li Zheng, Wan-Nan Chen, Jian-Yin Lin

Xu Lin, Xiao Xu, Qing-Ling Huang, Da-Li Zheng, Wan-Nan Chen, Jian-Yin Lin, Research Center of Molecular Medicine, Fujian Medical University, Fuzhou 350004, Fujian Province, China
Yu-Qing Liu, Centre for the Study of Liver Disease and Department of Surgery, The University of Hong Kong, Pokfulam, Hong Kong, China

Supported by the Foundation for the Author of National Excellent Doctoral Dissertation of PR China, No. 200359, Fujian Natural Science Key Foundation, No. 2002F005, and Fujian Science and Technology Innovation Foundation for Young Scientists, No. 2001J058

Correspondence to: Xu Lin, Research Center of Molecular Medicine, Fujian Medical University, Fuzhou 350004, Fujian Province, China. linxu70@hotmail.com

Telephone: +86-591-83569300 Fax: +86-591-83574535

Received: 2004-07-23 Accepted: 2004-12-29

Abstract

AIM: To investigate the biological impacts of "hot-spot" mutations on genotype B and C HBV X proteins (HBx).

METHODS: Five types of "hot-spot" mutations of genotype B or C HBV X genes, which sequentially lead to the amino acid substitutions of HBx as I127T, F132Y, K130M+V131I, I127T+K130M+V131I, or K130M+V131I+F132Y, respectively, were generated by means of site-directed mutagenesis. To evaluate the anti-proliferative effects, HBx or related mutants' expression vectors were transfected separately to the Chang cells by lipofectamine, and the cells were cultured in hygromycin selective medium for 14 d, drug-resistant colonies were fixed with cold methanol, stained with Giemsa dyes and scored (increase of the colonies indicated the reduction of the anti-proliferation activity, and vice versa). Different types of HBx expression vectors were co-transfected separately with the reporter plasmid pCMV β to Chang cells, which were lysed 48 h post-transfection and the intra-cellular β -galactosidase activities were monitored (increase of the β -galactosidase activities indicated the reduction of the transactivation activity, and vice versa). All data obtained were calculated by paired-samples *t*-test.

RESULTS: As compared to standard genotype B HBx, mutants of I127T and I127T+K130M+V131I showed higher transactivation and anti-proliferative activities, while the mutants of F132Y, K130M+V131I, and K130M+V131I+F132Y showed lower activities. As compared to standard genotype C HBx, I127T mutant showed higher transactivation activity, while the other four types of mutants showed no differences. With regard to anti-proliferative activity, compared to standard genotype C HBx, F132Y and K130M+

V131I mutants showed lower activities, and K130M+V131I+F132Y mutant, on the other hand, showed higher activity, while the mutants of I127T and I127T+K130M+V131I showed no differences.

CONCLUSION: "Hot-spot" mutations affect the anti-proliferation and transactivation activities of genotype B and/or C HBx, and the biological impacts of most "hot-spot" mutations on HBx are genotype B and C differentiated.

© 2005 The WJG Press and Elsevier Inc. All rights reserved.

Key words: Hepatitis B virus; Genotype; X gene; Mutation

Lin X, Xu X, Huang QL, Liu YQ, Zheng DL, Chen WN, Lin JY. Biological impacts of "hot-spot" mutations of hepatitis B virus X proteins are genotype B and C differentiated. *World J Gastroenterol* 2005; 11(30): 4703-4708

<http://www.wjgnet.com/1007-9327/11/4703.asp>

INTRODUCTION

HBV belongs to the hepadnaviridae family, which has a double-stranded DNA genome with a single-stranded gap. The genome of HBV encodes four kinds of proteins including the envelope protein (S/Pre-S), the core protein (C/pre-C), the polymerase (P), and the X protein (HBx). HBx is a multi-functional transcriptional transactivator^[1] and has been shown to be crucial in the pathogenesis of HBV-related diseases^[2].

Based on an intergroup divergence of 8% or more in the complete or partial nucleotide sequences, HBV can be classified presently into eight genotypes^[3,4], termed A-H, in which B and C genotypes are prevalent in East Asia including China^[5]. Recent studies^[6,7] revealed that the infection of genotype B or C HBV brought about quite different clinical manifestations and liver histological changes, yet the exact mechanisms involved remain largely obscure. Considering the important role HBx plays in the pathogenesis of HBV, it is reasonable to speculate that the clinical and histological differences of the infection of genotype B and C HBV may be partially related with the functional differentiations between these two genotypes of HBx due to the genetic variability.

Genetic variability^[8] of HBx includes both of the genotype-specific variations and the mutations emerged during chronic infection. We had shown in our previous study^[9] that there were 16 amino acid genotype-specific

variations between genotype B and C HBx, and the biological functions including transactivation activities and anti-proliferation capacities were different between these two HBx genotypes. It was also demonstrated that during chronic infection, genotype B and C HBx shared the same “hot-spot” mutations in the amino acid positions of 127, 130, 131, and 132^[10], we wondered whether these “hot-spot” mutations effected HBx, and more importantly, whether the influences of the same type of mutation on HBx showed genotype B or C specificity. To address these issues, we constructed HBx mutants of each genotype (B or C) with the same “hot-spot” mutations, and comparatively analyzed their differences in biological functions.

MATERIALS AND METHODS

Plasmids

pcDNA3.1-XB and pcDNA3.1-XC were recombinant pcDNA3.1/Hygro(-) (Invitrogen, USA) vectors harboring either genotype B or genotype C HBV X gene with conserved sequences (the amino acid alignment of these two genotypes of HBx is shown in Figure 1) and could express HBx in transfected Chang cells, as detected by immunohistochemistry.

Generation of genotype B or C HBV X mutants with “hot-spot” mutations

pcDNA3.1-XB or pcDNA3.1-XC was used as the template and the mutagenesis was carried out using GeneTailor site-directed mutagenesis system (Invitrogen, USA) following the manufacturer’s instructions. In brief, 200 ng of pcDNA3.1-XB or pcDNA3.1-XC DNA was methylated by 8 U methylase in a total volume of 32 μ L, and 2 μ L of methylated DNA was used as the template for PCR using paired primers (reverse primer R was used together with one of the forward primers F1-F5 to generate nucleotide mutation, sequentially resulting in amino acid substitution) (Table 1). After amplification, 5 μ L of PCR product was used to transform *E. coli* DH5 α -T1, and transformants were screened by growth on bacterial culture plates with ampicillin for selection. All mutants were sequenced to confirm the correctness of the induced mutations.

Cell culture and transfection

The human liver cell line, CCL13 (Chang cells) was cultured in Dulbecco’s modified Eagle minimal essential medium with penicillin (100 U/mL) and streptomycin (100 μ g/mL), supplemented with 10% fetal calf serum. Recombinant plasmid DNA was extracted and purified with Qiagen maxiprep kits, and used to transfect Chang cells in 60-mm plates or six-well plates by lipofectamine 2000. Duplicate plates/wells were used for all samples. Empty vector pcDNA3.1/Hygro(-) was used as a mock transfection control.

Colony formation assay

Chang cells (3×10^5) in six-well plates were transfected with 2.5 μ g of HBx constructs or empty vector. Forty-eight hours after transfection, the cells were subcultured at a ratio of 1:3, and cultured in 200 μ g/mL hygromycin (Roche, Germany) selective medium for 14 d. Drug-resistant colonies were fixed with cold methanol, stained with Giemsa, and then scored.

β -galactosidase test

Two micrograms of HBx constructs and 2.0 μ g reporter pCMV β plasmids (Promega, USA) were co-transfected into Chang cells in 60-mm plates (5×10^5 cells per plate). Cells were harvested and lysed at 48 h post-transfection. After protein normalization by the Bradford assay (Bio-Rad Laboratories, Hercules, CA, USA), equal amounts of protein (30 ng) were used for β -galactosidase assay following the manufacturer’s instructions.

Statistical analysis was performed using a paired *t*-test. $P < 0.05$ was taken as significant.

RESULTS

Generation of genotype B or C HBx mutants

Mutations at HBV nucleotides 1 753, 1 762, 1 764, and 1 768 resulted in amino acid substitution of HBx at positions 127, 130, 131, and 132, respectively. In this study, nucleotide mutations were generated in each genotype of HBx with five types of combinations as 1 753^{T→C}, 1 762^{A→T}+1 764^{G→A}, 1 753^{T→C}+1 762^{A→T}+1 764^{G→A}, 1 762^{A→T}+1 764^{G→A}

Table 1 Sequences and related applications of the primers used for site-directed mutagenesis and nomenclature of HBx mutants

Primers	Sequences (5'→3')	Applications		Nomenclature of the HBx mutants
		Nucleotide mutation ²	Amino acid substitution ³	
R	CTCCTCCCCAACTCTTCCCACTCAGTAAAC			
F1	GAAGAGTTGGGGGAGGAGAC ¹ TAGGTTAAAGGTC	1 753 ^{T→C}	I127T	XB/XC-127
F2	GAAGAGTTGGGGGAGGAGACTAGGTTA ATGATCTTTGACTAGG	1 753 ^{T→C} +1 762 ^{A→T} +1 764 ^{G→A}	I127T+K130M+V131I	XB/XC-127-130-131
F3	GAAGAGTTGGGGGAGGAGATTAGGTTA ATGATCTTTGACTAGG	1 762 ^{A→T} +1 764 ^{G→A}	K130M+V131I	XB/XC-130-131
F4	GAAGAGTTGGGGGAGGAGATTAGGTTA ATGATCTATGACTAGGAGGC	1 762 ^{A→T} +1 764 ^{G→A} +1 768 ^{T→A}	K130M+V131I+F132Y	XB/XC-130-131-132
F5	GAAGAGTTGGGGGAGGAGATTAGGTTA AAGTCTATGACTAGGAGGC	1 768 ^{T→A}	F132Y	XB/XC-132

¹Mutated nucleotides are shown as underlined; ²1 753, 1 762, 1 764, 1 768 indicate the positions of mutated nucleotides in HBV genome; ³127, 130, 131, 132 are positions of substituted amino acids in HBx.

+1 768^{T→A} and 1 768^{T→A}, which sequentially resulted in amino acid substitutions as I127T, K130M+V131I, I127T+K130M+V131I, K130M+V131I+F132Y, and F132Y, respectively (Table 1 and Figure 1). The X mutants were named according to their genotype belongings (B or C) and the position of the substituted amino acids, for example, XB-127 for I127T mutant of genotype B HBx, while XC-127 for I127T mutant of genotype C HBx.

	5	15	25	35	45	55
XB	MAARLCCQLD	PARDVLCRLP	VGAESRGRPL	PGPLGALPPA	SPPVVPTDHG	AHLSLRGLPV
XCV.....V	S..F.P..SP	.SSA..A...
	65	75	85	95	105	115
XB	CAFSSAGPCA	LRFTSARRME	TTVNAHRNLP	KVLHKRTLGL	SAMSTTDLEA	YFKDCVFTWE
XCQV..L.KD.
	125	135	145			
XB	EELGEE	RKIV	VLGGCRHK	LVCSPAPCNF	FTSA	
XC

Figure 1 There were 16 amino acid variations between genotype B and C HBx, which were located at amino acid positions 5, 30, 31, 34, 36, 39, 40, 42, 43, 44, 47, 87, 88, 116, 118, and 119, respectively. Four boxed amino acids, located at the positions of 127, 130, 131, 132, respectively, were to be substituted by site-directed mutagenesis.

Anti-proliferation activities of genotype B or C HBx mutants

To study the anti-proliferation activities of HBx mutants, we performed colony formation assay^[11], in which the increasing anti-proliferation activities should be paralleled with the reduction of cell colonies, and vice versa. Chang cells were transfected separately with parental vector pcDNA3.1/Hygro(-) or recombinant vectors harboring different types of HBx; cells were subcultured in hygromycin selective medium 48 h post-transfection, and the drug-resistant colonies formed 14 d later were stained with Giemsa and scored. The results showed that, as compared with XB (standard genotype B HBx), expression of mutants XB-127 and XB-127-130-131 caused the reduction in the number of colonies, and expression of mutants XB-132, XB-130-131, or XB-130-131-132 caused the elevation (Figure 2). As for genotype C HBx, expression of mutant XC-130-131-132 caused the sharp reduction of colonies to zero, and mutants of XC-132 and XC-130-131, on the other hand, caused the elevation in the number of colonies as compared with XC (standard genotype C HBx), while XC-127 and XC-127-130-131 showed no differences from XC (Figure 3). It indicated that effects of three types of “hot spot” mutations, i.e., I127T, I127T+K130M+V131I, and K130M+V131I+F132Y, on anti-proliferation of HBx were

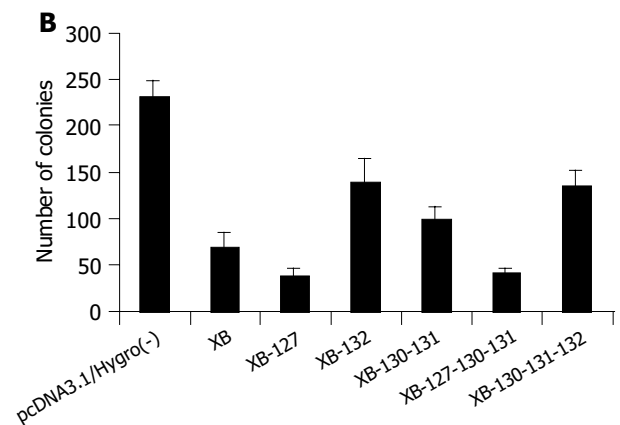
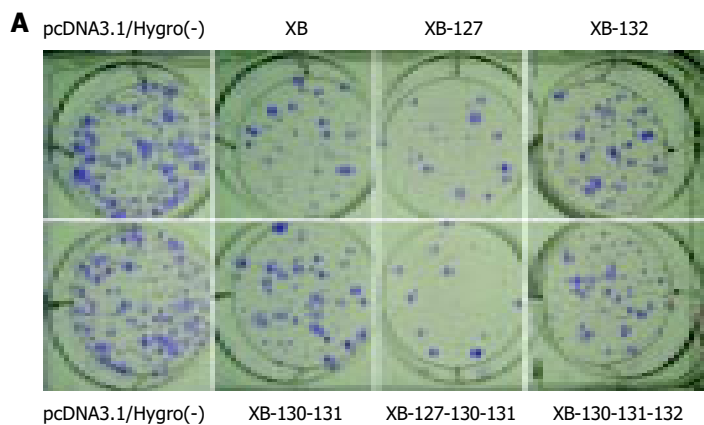


Figure 2 Chang cells were transfected by genotype B X gene expression vectors and screened by hygromycin, the drug-resistant colonies formed 14 d

post-transfection were fixed by cold methanol, stained with Giemsa (A) and counted (B). The results are shown as mean±SD of six separate experiments.

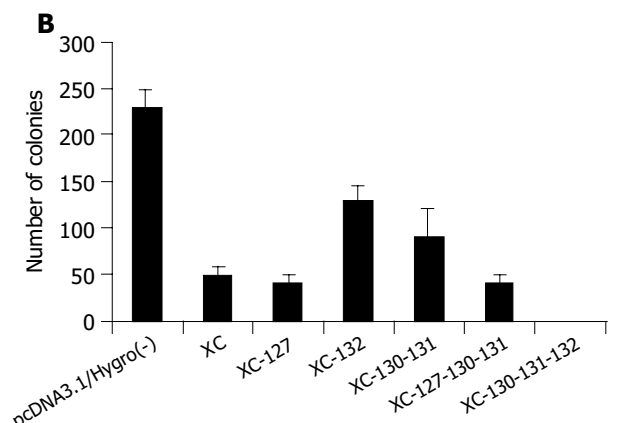
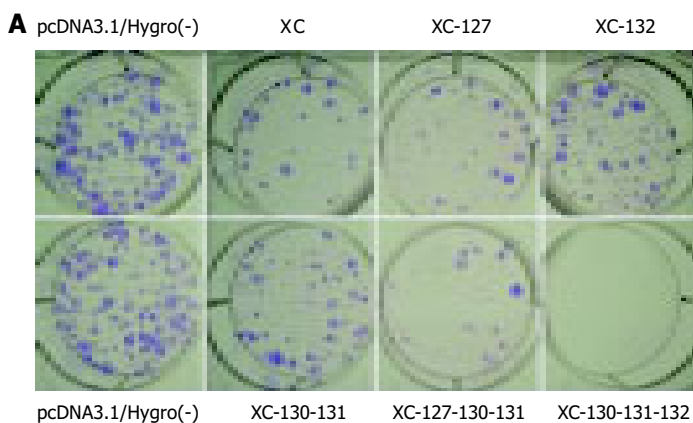


Figure 3 Chang cells were transfected by genotype C X gene expression vectors and screened by hygromycin, the drug-resistant colonies formed 14 d

post-transfection were fixed by cold methanol, stained with Giemsa (A) and scored (B). The results are shown as mean±SD of six separate experiments.

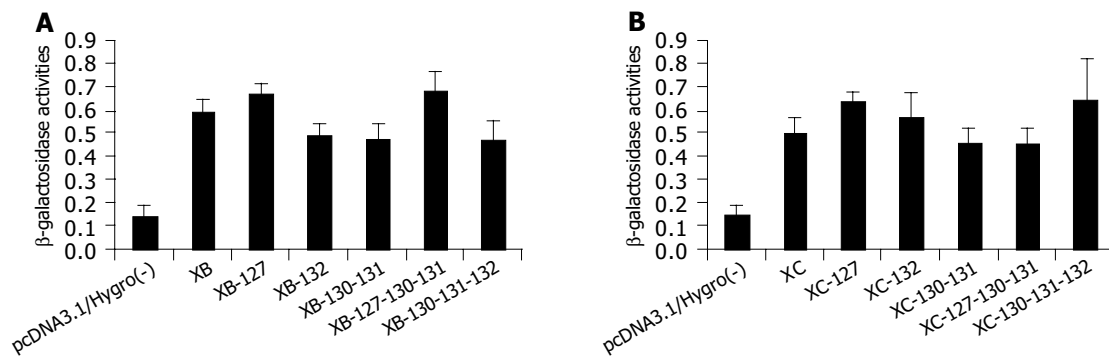


Figure 4 Chang cells were co-transfected by pCMVβ together with the X gene or related mutants with genotype B (A) or genotype C (B). Forty-eight hours post-transfection, the cells were lysed and the intracellular β-galactosidase

activities were monitored after protein normalization. The results are shown as mean ± SD of six separate experiments.

genotype B and C differentiated. In addition, it was also demonstrated that all HBx caused dramatic reduction of colonies as compared with the empty vector pcDNA3.1/Hygro(-), irrespective of genotypes (B or C) or the types (the standard or the mutants), indicating the retaining of anti-proliferation activities of all HBx.

Transactivation activities of genotype B or C HBx mutants

It was reported previously that HBx could transactivate the CMV immediate early promoter^[12], so plasmid pCMVβ containing the CMV immediate early promoter and expressing β-galactosidase was used as the indicator to evaluate the transactivation activities of HBx mutants. In our study, pCMVβ was co-transfected with an HBx construct to Chang cells, which were lysed 48 h post transfection, and intra-cellular β-galactosidase activities were monitored. The results showed that, as for genotype B HBx, expression of mutants XB-127 and XB-127-130-131 induced increase in β-galactosidase activities as compared with XB, and three other mutants, i.e., XB-132, XB-130-131, and XB-130-131-132 induced decreased activities (Figure 4A and Table 2), as for genotype C HBx, XC-127 induced the increase in β-galactosidase activities as compared with XC, while the other four types of mutants showed no differences (Figure 4B and Table 2). The results revealed that effects

of four types of “hot spot” mutations, i.e., I127T+K130M+V131I, K130M+V131I, K130M+V131I+F132Y, and F132Y, on transactivation of HBx were genotype B and C differentiated. In addition, the results also showed that expression of HBx, irrespective of genotypes (B or C) or the mutant types, induced the increase in intra-cellular β-galactosidase activities as compared with the empty vector pcDNA3.1/Hygro(-), indicating the retaining of transactivation activities of all HBx.

DISCUSSION

There are increasing evidences that the clinical manifestations, the long-term prognosis, the liver histological changes, and the response to treatment of interferon and nucleosidic inhibitors may differ depending on which genotype of HBV the patient has been infected with^[13]. In Taiwan, where the genotypes of HBV were predominantly B and C, genotype C is associated with more severe liver disease and genotype B is associated with the development of hepatocellular carcinoma (HCC) in young non-cirrhotic patients^[6]. In contrast, genotype B has a relatively good prognosis in Japan and China and is rarely associated with the development of HCC^[7]. However, the impact of genotypes on HBV pathogenesis remains largely obscure.

HBx is a promiscuous activator^[1] and considered to be of importance in the pathogenesis of HBV, it can indirectly activate miscellaneous viral and cellular genes^[14], induce or block apoptosis of the infected cells^[15,16], and induce HCC in certain lines of transgenic mice^[17,18]. We demonstrated previously that there were 16 amino acid differences between standard genotype B and C HBx, and the activities including transactivation and anti-proliferation were different between these two genotypes of HBx. These results indicated that the B, C genotype-specific structural and functional differentiations of HBx may partially contribute to the different clinical outcomes and histological changes of the infection with genotype B or C HBV.

In addition to the genotype-specific variations, both of B and C genotypes of HBx also showed the same gene mutations within their coding regions (nt1 376-1 840), i.e., nt1 753^{T→C}, nt1 762^{A→T}, nt1 764^{G→A}, and nt1 768^{T→A}, which accordingly led to the amino acid variations as I127T, K130M, V131I, and F132Y. These “hot-spot” mutations

Table 2 Intracellular β-galactosidase activities of transfected Chang cells by pCMVβ and X gene expression vectors

DNA transfected	β-galactosidase activities ¹	P ²	P ³
pcDNA3.1/Hygro(-)	0.147±0.039	-	-
XB	0.593±0.051	<0.01	-
XB-127	0.666±0.054	<0.01	<0.05
XB-132	0.492±0.052	<0.01	<0.01
XB-130-131	0.477±0.065	<0.01	<0.01
XB-127-130-131	0.680±0.090	<0.01	<0.05
XB-130-131-132	0.472±0.081	<0.01	<0.05
XC	0.505±0.064	<0.01	-
XC-127	0.641±0.044	<0.01	<0.01
XC-132	0.571±0.104	<0.01	>0.05
XC-130-131	0.459±0.065	<0.01	>0.05
XB-127-130-131	0.457±0.067	<0.01	>0.05
XB-130-131-132	0.646±0.177	<0.01	>0.05

¹All data are expressed as mean ± SD of six separate experiments; ²Paired-samples *t*-test between pcDNA3.1/Hygro(-) and all HBx; ³Paired-samples *t*-test between genotype B(XB)/genotype C(XC) and the relative mutants.

Table 3 Summary of the biological impact of “hot-spot” mutations on genotype B and C HBx

HBx mutants	Genotype B ¹		Genotype C ²	
	Transactivation	Antiproliferation	Transactivation	Antiproliferation
I127T	↑ ³	↑	↑	- ⁵
I127T+K130M+V131I	↑	↑	-	-
K130M+V131I	↓ ⁴	↓	-	↓
K130M+V131I+F132Y	↓	↓	-	↑
F132Y	↓	↓	-	↓

¹Changes of biological functions were compared with XB; ²Changes of biological functions were compared with XC. ³, ⁴, and ⁵ accordingly indicate increased, decreased and equal activities of HBx mutants as compared with XB/XC.

emerged due to the error-prone reverse transcriptase activity of HBV polymerase^[19] and the long-term virus-host interaction, and occurred mainly during chronic infection including different clinical stages of chronic hepatitis^[20] and HBV-associated HCC as well^[21]. In fact, these “hot-spot” mutations appeared predominantly in five types: I127T, F132Y, K130M+V131I, I127T+K130M+V131I, or K130M+V131I+F132Y. Our results demonstrated that these mutations affected the anti-proliferation and transactivation activities of genotype B and/or C HBx, and more importantly, the impacts of most types of the “hot-spot” mutations on HBx were genotype B and C differentiated, i.e., as concerning the anti-proliferation activities, impacts of HBx mutants of I127T, I127T+K130M+V131I, and K130M+V131I+F132Y showed genotype B and C differentiated, and regarding the transactivation activities, impacts of mutants of I127T+K130M+V131I, K130M+V131I, K130M+V131I+F132Y, and F132Y showed genotype B and C differentiated (Table 3).

It was also revealed that all HBx mutants, irrespective of genotypes or mutant types, retained their biological functions. It may be therefore concluded that the effects of the mutations on HBx was relatively mild and was in strong contrast to the distal COOH-terminal deletion mutants isolated from the integrated chromosomes of HCC tissues, which completely abrogated the transactivation or anti-proliferation activities^[22,23]. In addition, it was previously reported that the transactivation activities of HBx are often linked to anti-proliferation function^[24]. Our results strikingly showed that the linkage of these two activities only occurred in genotype B HBx, in which the increasing activation activities of HBx mutants were coupled with the enhanced anti-proliferation activities, and vice versa, while it seemed that the activities of anti-proliferation and transactivation were completely separated in genotype C HBx (Table 3). Therefore, it was concluded that association of transactivation with anti-proliferation activities was a common feature of HBx with genotype B rather than genotype C.

There is no indisputable evidence showing that the transactivation activity of HBx contributes to liver disease. However, reduction of the anti-proliferation effect may endow a growth advantage on cells containing these particular HBx mutants, while increase of anti-proliferation effects will lead to cell disruption and hence accelerate intracellular spread of HBV^[25]. So in this point, any functional changes of anti-proliferation are pathogenic.

In summary, “hot-spot” mutations affect the anti-proliferation and transactivation activities of genotype B

and/or C HBx, and the biological impacts of most “hot-spot” mutations on HBx are genotype B and C differentiated. Together with our previous findings demonstrating the different biological functions between genotype B and C HBx^[9,26], we conclude that genetic variability results in functional differentiations between genotype B and C HBx. Nevertheless, considering the sophisticated mechanism of HBV pathogenesis^[27], whether these genotype B and C specific functional differentiations of HBx are responsible for the different clinical outcomes and liver histological changes between two genotypes of HBV, and more importantly, the exact mechanisms involved await further studies.

REFERENCES

- 1 **Rossner MT.** Review: hepatitis B virus X-gene product: a promiscuous transcriptional activator. *J Med Virol* 1992; **36**: 101-117
- 2 **Feitelson MA.** Hepatitis B virus in hepatocarcinogenesis. *J Cell Physiol* 1999; **181**: 188-202
- 3 **Vieth S, Manegold C, Drosten C, Nippraschk T, Gunther S.** Sequence and phylogenetic analysis of hepatitis B virus genotype G isolated in Germany. *Virus Gene* 2002; **24**: 153-156
- 4 **Arauz-Ruiz P, Norder H, Robertson BH, Magnus LO.** Genotype H: a new Amerindian genotype of hepatitis B virus revealed in Central America. *J Gen Virol* 2002; **83**(Pt 8): 2059-2073
- 5 **Ding X, Mizokami M, Yao G, Xu B, Orito E, Ueda R, Nakanishi M.** Hepatitis B virus genotype distribution among chronic hepatitis B virus carriers in Shanghai, China. *Intervirology* 2001; **44**: 43-47
- 6 **Kao JH, Chen PJ, Lai MY, Chen DS.** Basal core promoter mutations of hepatitis B virus increase the risk of hepatocellular carcinoma in hepatitis B carriers. *Gastroenterology* 2003; **124**: 327-334
- 7 **Orito E, Mizokami M, Sakugawa H, Michitaka K, Ishikawa K, Ichida T, Okanoue T, Yotsuyanagi H, Iino S.** A case control study for clinical and molecular biological differences between hepatitis B viruses of genotypes B and C. Japan HBV Genotype Research Group. *Hepatology* 2001; **33**: 218-223
- 8 **Gunther S.** Naturally occurring mutations of hepatitis B virus and outcome of chronic infection: is there an association? *Eur J Clin Invest* 2000; **30**: 751-753
- 9 **Lin X, Xu X, Huang QL, Zheng DL, Lin JY.** Difference in structural and transactivating capacity between X proteins of genotype B and C hepatitis B virus. *Zhonghua Weishengwuxue He Miyanixue Zazhi* 2004; **24**: 559-563
- 10 **Gunther S, Fischer L, Pult I, Sterneck M, Will H.** Naturally occurring variants of hepatitis B virus. *Adv Virus Res* 1999; **52**: 25-137
- 11 **Sirma H, Giannini C, Poussin K, Paterlini P, Kremsdorf D, Brechot C.** Hepatitis B virus X mutants, present in hepatocellular carcinoma tissue abrogate both the antiproliferative and transactivation effects of HBx. *Oncogene* 1999; **18**: 4848-4859

- 12 **Assogba BD**, Choi BH, Rho HM. Transcriptional activation of the promoter of human cytomegalovirus immediate early gene (CMV-IE) by the hepatitis B viral X protein (HBx) through the NF-kappaB site. *Virus Res* 2002; **84**: 171-179
- 13 **Sumi H**, Yokosuka O, Seki N, Arai M, Imazeki F, Kurihara T, Kanda T, Fukai K, Kato M, Saisho H. Influence of hepatitis B virus genotypes on the progression of chronic type B liver disease. *Hepatology* 2003; **37**: 19-26
- 14 **Caselmann WH**, Koshy R. Transactivators of HBV, signal transduction and tumorigenesis In: Caselmann WH and Koshy R eds. *Hepatitis B Virus: Molecular Mechanisms in Disease and Novel Strategies for Therapy*, London: Imperial College Press 1998: 161-181
- 15 **Elmore LW**, Hancock AR, Chang SF, Wang XW, Chang S, Callahan CP, Geller DA, Will H, Harris CC. Hepatitis B virus, X protein and p53 tumor suppressor interactions in the modulation of apoptosis. *Proc Natl Acad Sci USA* 1997; **94**: 14707-14712
- 16 **Gottlob K**, Fulco M, Levrero M, Graessmann A. The hepatitis B virus HBx protein inhibits caspase 3 activity. *J Biol Chem* 1998; **273**: 33347-33353
- 17 **Kim CM**, Koike K, Saito I, Miyamura T, Jay G. HBx gene of hepatitis B virus induces liver cancer in transgenic mice. *Nature* 1991; **351**: 317-320
- 18 **Yu DY**, Moon HB, Son JK, Jeong S, Yu SL, Yoon H, Han YM, Lee CS, Park JS, Lee CH, Hyun BH, Murakami S, Lee KK. Incidence of hepatocellular carcinoma in transgenic mice expressing the hepatitis B virus X-protein. *J Hepatol* 1999; **31**: 123-132
- 19 **Kao JH**. Hepatitis B viral genotypes: clinical relevance and molecular characteristics. *J Gastro Hepatol* 2002; **17**: 643-650
- 20 **Hunt CM**, McGill JM, Allen MI, Condreay LD. Clinical relevance of hepatitis B viral mutations. *Hepatology* 2000; **31**: 1037-1044
- 21 **Takahashi K**, Akahane Y, Hino K, Ohta Y, Mishiro S. Hepatitis B virus genomic sequence in the circulation of hepatocellular carcinoma patients: comparative analysis of 40 full-length isolates. *Arch Virol* 1998; **143**: 2313-2326
- 22 **Sirma H**, Giannini C, Poussin K, Paterlini P, Kremsdorf D, Brechot C. Hepatitis B virus, X mutants, present in hepatocellular carcinoma tissue abrogate both the antiproliferative and transactivation effects of HBx. *Oncogene* 1999; **18**: 4848-4859
- 23 **Tu H**, Bonura C, Giannini C, Mouly H, Soussan P, Kew M, Paterlini-Brechot P, Brechot C, Kremsdorf D. Biological impact of natural COOH-terminal deletions of hepatitis B virus X protein in hepatocellular carcinoma tissues. *Cancer Res* 2001; **61**: 7803-7810
- 24 **Bergametti F**, Prigent S, Luber B, Benoit A, Tiollais P, Sarasin A, Transy C. The proapoptotic effect of hepatitis B virus HBx protein correlates with its transactivation activity in stably transfected cell lines. *Oncogene* 1999; **18**: 2860-2871
- 25 **Soussan P**, Garreau F, Zylberberg H, Ferray C, Brechot C, Kremsdorf D. *In vivo* expression of a new hepatitis B virus protein encoded by a spliced RNA. *J Clin Invest* 2000; **105**: 55-60
- 26 **Xu X**, Chen WN, Zheng DL, Huang QL, Lin X. X protein variations of genotype B and C hepatitis B virus isolated from the patients with hepatocellular carcinoma. *Aizheng* 2004; **23**: 756-761
- 27 **Rapicetta M**, Ferrari C, Levrero M. Viral determinants and host immune responses in the pathogenesis of HBV infection. *J Med Virol* 2002; **67**: 454-457

Science Editor Zhu LH and Guo SY Language Editor Elsevier HK

• VIRAL HEPATITIS •

Screening of genes of proteins interacting with p7 protein of hepatitis C virus from human liver cDNA library by yeast two-hybrid system

Yan-Ping Huang, Shu-Lin Zhang, Jun Cheng, Lin Wang, Jiang Guo, Yan Liu, Yuan Yang, Li-Ying Zhang, Gui-Qin Bai, Xue-Song Gao, Dong Ji, Shu-Mei Lin, Yan-Wei Zhong, Qing Shao

Yan-Ping Huang, Shu-Lin Zhang, Yuan Yang, Gui-Qin Bai, Shu-Mei Lin, The First Hospital of Xi'an Jiaotong University, Xi'an 710061, Shaanxi Province, China

Jun Cheng, Lin Wang, Jiang Guo, Yan Liu, Li-Ying Zhang, Xue-Song Gao, Dong Ji, Yan-Wei Zhong, Qing Shao, Institute of Infectious Diseases, Ditan Hospital, Anwai Street, Beijing 100011, China
Supported by the National Natural Scientific Foundation, No. C03011402, No. C30070690; the Research and Technique Foundation of PLA during the 9th-five year plan period, No. 98D063; the Launching Foundation for Student Studying Abroad of PLA, No. 98H038; and the Youth Research and Technique Foundation of PLA during the 10th-five year plan period, No. 01Q138; and the Research and Technique Foundation of PLA during the 10th-five year plan period, No. 01MB135

Correspondence to: Yan-Ping Huang, Department of Pediatrics, the First Hospital of Xi'an Jiaotong University, Xi'an 710061, Shaanxi Province, China. huangyp423@126.com
Telephone: +86-29-85324065

Received: 2004-10-19 Accepted: 2004-12-26

Abstract

AIM: To investigate the biological function of p7 protein and to look for proteins interacting with p7 protein in hepatocytes.

METHODS: We constructed p7 protein bait plasmid by cloning the gene of p7 protein into pGBKT7, then transformed it into yeast AH109 (a type). The transformed yeast was mated with yeast Y187 (α type) containing liver cDNA library plasmid, pACT2 in 2 \times YPDA medium. Diploid yeast was plated on synthetic dropout nutrient medium (SD/-Trp-Leu-His-Ade) containing α -gal for selection and screening. After extracting and sequencing of plasmids from blue colonies, we performed sequence analysis by bioinformatics.

RESULTS: Fifty colonies were selected and sequenced. Among them, one colony was *Homo sapiens* signal sequence receptor, seven colonies were *Homo sapiens* H19, seven colonies were immunoglobulin superfamily containing leucine-rich repeat, three colonies were spermatid peri-nuclear RNA binding proteins, two colonies were membrane-spanning 4-domains, 24 colonies were cancer-associated antigens, four colonies were nucleoporin 214 ku and two colonies were CLL-associated antigens.

CONCLUSION: The successful cloning of gene of protein interacting with p7 protein paves a way for the study of the

physiological function of p7 protein and its associated protein.

© 2005 The WJG Press and Elsevier Inc. All rights reserved.

Key words: Hepatitis C virus; p7 protein; Interacting proteins; Yeast two-hybrid system

Huang YP, Zhang SL, Cheng J, Wang L, Guo J, Liu Y, Yang Y, Zhang LY, Bai GQ, Gao XS, Ji D, Lin SM, Zhong YW, Shao Q. Screening of genes of proteins interacting with p7 protein of hepatitis C virus from human liver cDNA library by yeast two-hybrid system. *World J Gastroenterol* 2005; 11(30): 4709-4714

<http://www.wjgnet.com/1007-9327/11/4709.asp>

INTRODUCTION

Hepatitis C virus (HCV) is a major cause of chronic hepatitis, liver cirrhosis, and hepatocellular carcinoma throughout the world. Although HCV cannot be incubated efficiently *in vitro*, several of its key features have been elucidated in the past few years. HCV, cloned successfully via molecule biological technology^[1,2], is an enveloped, positive single-stranded RNA (9.6-kb) virus belonging to the Flaviviridae. The HCV genome has only one ORF which is flanked by a 5' and 3' noncoding region. The ORF encodes for a large polyprotein precursor of about 3 000 amino acid residues, and this precursor protein is cleaved by the host and viral proteinases to generate at least 10 proteins in the following order: NH2-C-E1-E2-p7-NS2-NS3-NS4A-NS4B-NS5A-NS5B-COOH. HCV proteins not only function in viral replication but also affect a variety of cellular functions^[3-6]. HCV p7, which is located between the E2 and NS2 proteins, is a 63 residue peptide encoded by HCV genome between 2 580-2 768 nt^[7]. Although there are studies on the genomic structure, synthesis and function of p7 protein, the role of the HCV p7 protein in the virus life cycle is not known. To gain more information on the HCV p7 protein, and provide some new clues for elucidating the potential biological function of p7, we looked for proteins interacting with p7 protein by screening human liver cDNA library with yeast two-hybrid system.

MATERIALS AND METHODS

Bacteria, yeast strains and plasmids

All yeast strains and plasmids for yeast two-hybrid experiments

were obtained from Clontech (Palo Alto, CA, USA) as components of the MATCHMAKER two hybrid system 3. Yeast strain AH109 (MATa, *trp1-901*, *leu2-3,112*, *ura3-52*, *bis3-200*, *gal4Δ*, *gal80Δ*, *LYS2:GAL1_{UAS}-GAL1_{TATA}-HIS3*, *GAL2_{UAS}-GAL2_{TATA}-ADE2*, *URA3: MEL1_{UAS}-MEL1_{TATA}-LacZ*) containing pGBKT7-53, coding for DNA-BD/mouse p53 fusing protein and AH109 was used for cloning of bait plasmids, yeast strain Y187 (MATa, *ura3-52*, *bis3-200*, *Ade2-101*, *trp1-901*, *leu2-3, 112*, *gal4Δ*, *gal80Δ*, *met-*, *URA3: GAL1_{UAS}-GAL1_{TATA}-lacZ MEL1*) containing pTD1-1, in which pACT2 codes for AD/SV40 large T antigen fusing protein and Y187 was used for cloning of library plasmids. Bacterial strain DH5a was used for cloning of every shuttle plasmid. pGBKT7 DNA-BD cloning plasmid, pGADT7 AD cloning plasmid, pGBKT7-53 control plasmid, pGADT7, pGBKT7-Lam control plasmid, pCL1 plasmid were from Clontech Ltd Company (K1612-1). pGEM T vector was from Promega Company, USA.

Chemical agents and culture media

Taq DNA polymerase was purchased from MBI Company. T4 DNA ligase, *EcoRI* and *BamHI* restriction endonuclease were from Takara. c-Myc mAb secreted by 1-9E10.2 hybridoma (ATCC), and goat anti-mouse IgG conjugated with horseradish peroxidase were from Zhongshan Company, China. Lithium acetate, semi-sulfate adenine, acrylamide, and *N,N*-bis-acrylamide were from Sigma. TEMED was from Boehringer Mannheim. Tryptone and yeast extracts were from Oxoid. X- α -gal and culture media: YPDA, SD/-Trp, SD/-Leu, SD/-Trp/-Leu, SD/-Trp/-Leu/-His, SD/-Trp/-Leu/-His/-Ade were from Clontech Ltd Company. Protein-G agarose were from Roche. pEGM-T vector was from Promega. RT-PCR kit was from Isotope Company of China. Others were from Sigma Company.

Construction of "bait" plasmid and expression of HCV p7 protein

To make the bait plasmid, HCV-p7 sequences were generated by PCR amplification of HCV plasmid (HCV strain 1b). The plasmid containing coding sequences of all the structural and non-structural proteins was used as the template. The sequence of the primers containing the *EcoRI* and *BamHI* restriction enzyme sites are sense primer: 5'-GAA TTC ATG GCT TTG GAG AAC CTC G-3' and anti-sense primer: 5'-GGA TCC TTA CGC GTA CGC CCG CTG G-3'. The PCR conditions were as follows: at 94 °C for 30 s, at 60 °C for 30 s, at 72 °C for 30 s. Ten nanograms of the 189-bp PCR product were cloned with pGEM-T vector. The primary structure of insert was confirmed by direct sequencing. The fragment of encoding p7 was released from the pEGM-T-p7 by digestion with *EcoRI* and *BamHI*, and ligated to pGBKT7. Vector pGBKT7-expressing proteins were fused with amino acids 1-147 of the GAL4 DNA binding domain (DNA-BD), pGADT7-expressing proteins were fused with amino acids 768-881 of the GAL4 activation domain (AD). Plasmid pGBKT7-p7 (Figure 1) containing full-length HCV p7 gene could directly express DNA binding domain, c-Myc and p7 fusion protein. The plasmid was transformed into yeast strain AH109 by using lithium acetate method^[8]. Transformed AH109 (bait) was cultured on quadruple dropout media to exclude the auto-activity.

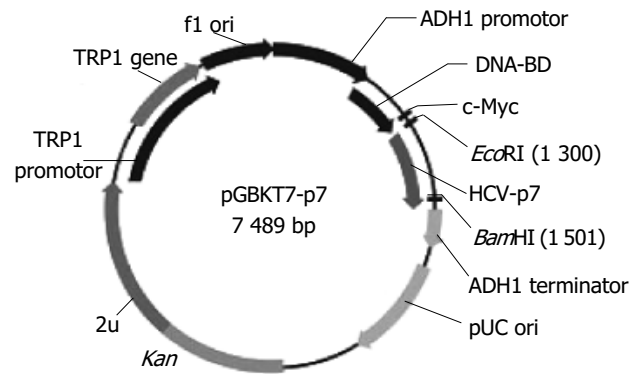


Figure 1 Map of "bait" plasmid pGBKT7-p7.

Western blot analysis

A single isolated colony (1-2 mm in diameter, not older than 5 d) of yeast AH109 transformed with pGBKT7-p7 selected by lithium acetate method was inoculated into 5 mL of SD/-Trp and incubated at 30 °C overnight with shaking at 220-250 r/min. The entire overnight culture was inoculated into 50 mL YPDA medium and incubated at 30 °C with shaking at 220-250 r/min until the A_{600} reached 0.4-0.6. The culture was chilled and centrifuged for cell pellets. The yeast protein extracts of p7 were prepared according to urea/SDS method. A part of protein extract was resolved on SDS-polyacrylamide gel and transferred onto nitrocellulose membrane. After being blocked with nonfat dried milk, the membrane was treated with c-Myc mAb for 90 min, then with HRP-goat anti-mouse IgG at the dilution of 1:500 for 60 min. Subsequently the blot was developed by 4-chloro-1-naphthol and H₂O₂. The yeast AH109 cells with transformed pGBKT7 were used for positive control and the untransformed yeast, AH109 cells were used for negative control.

Screening of liver cell cDNA library by yeast two-hybrid system

One large (2-3 mm), fresh (<2 mo old) colony of AH109 (bait) was inoculated into 50 mL of SD/-Trp and incubated at 30 °C overnight (16-24 h) with shaking at 250-270 r/min. Then the cells were spun by centrifuging the entire 50 mL culture at 1 000 r/min for 5 min. After supernatant was decanted, the cell pellet was resuspended in the residual liquid by vortexing. A human liver cDNA library was cloned into pACT2 and yeast reporter strain Y187 (Clontech Co.). The entire AH109 (bait) culture and 1 mL human liver cDNA library (1×10⁶ CFU/mL) were combined and cultured in a 2-L sterile flask and 45 mL of 2 YPDA/Kan was added and swirled gently. After 20 h mating, the cells were spun re-suspended and spread on 50 large (150 mm) plates containing 100 mL of SD/-Ade/-His/-Leu/-Trp (QDO). After growth for 6-15 d, the yeast colonies were transferred onto the plates containing X- α -gal to check for expression of the MEL1 reporter gene (blue colonies).

Plasmid isolation from yeast and transformation of E. coli with yeast plasmid

Approximately 1×10⁶ colonies were screened and 50 positive clones were identified. Yeast plasmid was isolated from

positive yeast colonies with lyticase method (Clontech Co.), and transformed into super-competence *E. coli* DH5 α by a chemical method. Transformants were plated on ampicillin SOB selection media and grown under selection. Subsequently, pACT2-cDNA constructs were re-isolated following the standard protocol, analyzed by restriction digestion and sequencing in.

Bioinformatic analysis

After the positive colonies were sequenced, the sequences were blasted with GenBank to analyze the function of the genes (<http://www.ncbi.nlm.gov/blast>).

Confirmation of the true interaction in yeast

To confirm the true protein–protein interaction and exclude false positives, the plasmids of positive colonies were transformed into yeast strain Y187, and then mating experiments were carried out by mating with yeast strain AH109 containing pGBKT7-p7 or pGBKT7-Lam. After mating, the diploids of yeast were plated on SD/-Ade-His-Leu-Trp (QDO) covered with X- α -gal to test the specificity of interactions.

RESULTS

Identification of recombinant plasmid

The full length sequences of HCV p7 were generated by PCR amplification of HCV plasmid (HCV strain 1b), sequenced and analyzed by comparing to vector NT1 6 and BLAST database homology search (<http://www.ncbi.nlm.nih.gov/blast>). After being cut by *EcoRI*/*Bam*HI, the fragment was in-frame ligated into pGBKT7 *EcoRI*/*Bam*HI site. Restriction enzyme analysis of pGBKT7-p7 plasmid with *EcoRI*/*Bam*HI yielded two bands: 7 300 bp empty pGBKT7 and 189 bp HCV p7. The product of plasmid was amplified by PCR. Analysis of the PCR reaction products by agarose gel electrophoresis showed the clear bands with the expected size (189 bp of p7). Sequences of the PCR products were correct (Figures 2A and B).

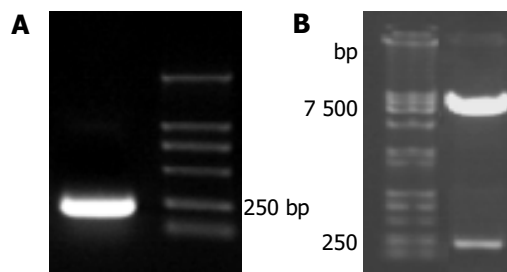


Figure 2 Fragment-p7 amplified by PCR (A) and pGBKT7-p7 cut by *EcoRI*/*Bam*HI (B).

Expression of “bait” fusion protein

Yeast strain AH109 transformed with pGBKT7-p7 could stably express the fusion protein at high level (Figure 3) and could only grow on SD/-Trp medium but not on QDO medium. Thus, the transformed yeast could be used for yeast hybrid analysis.

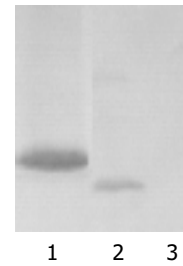


Figure 3 Expression of HCV p7 in yeast shown by Western blotting. Lane 1: HCV p7 protein; lane 2: positive control; lane 3: negative control.

Screening of liver cell cDNA library

We isolated the plasmids from the blue colonies containing only pGBKT7-p7 and one library plasmid other than other plasmids. Because plasmid pACT2-cDNA contains two restriction endonuclease sites of *Bgl*II on both sides of multiple cloning sites, the gene fragments of the liver cell cDNA library (pACT2-cDNA) screened were released by *Bgl*II digestion (Figure 4). The gene fragments of different lengths in Figure 4 proved, that these screened clones were positive colonies growing on SD/-Trp/-Leu/-His/-Ade culture medium after mating.

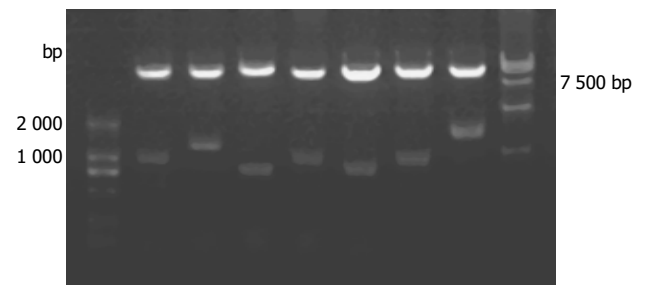


Figure 4 Identification of different colonies with *Bgl*II digestion.

Analysis of cDNA sequence and homology

We obtained a total of 50 positive colonies growing on the selective SD/-trp-leu-his-ade/X- α -gal medium. These colonies were prescreened by *Bgl*II digestion to make sure that only colonies with different inserts were subjected to sequencing. Fifty colonies from cDNA library were sequenced. Using the BLAST program at the National Center for Biotechnology Information, the 50 sequences had a high similarity to known genes. The data are presented in Table 1.

DISCUSSION

The precise mechanism of early HCV infection remains largely unknown. We tried to obtain a sufficient amount of free virions from the plasma of infected individuals and to establish a robust *in vitro* system for virus propagation. In HCV polyprotein, HCV p7 is located downstream of the envelope glycoprotein, E2 and upstream of the NS2 protein and begins at the position 747 of HCV H strain polyprotein. The generation of HCV p7 is supposed to be catalyzed by

Table 1 Comparison between positive clones and similar sequences in GenBank

High similarity to known genes	Number of similar	Homolog (%)
<i>Homo sapiens</i> signal sequence receptor, delta	1	100
<i>Homo sapiens</i> H19, imprinted maternally expressed untranslated mRNA	7	96-99
<i>Homo sapiens</i> immunoglobulin superfamily containing leucine-rich repeat	7	98
<i>Homo sapiens</i> spermatid perinuclear RNA binding protein	3	100
<i>Homo sapiens</i> membrane-spanning 4-domains, subfamily A, member 6A (MS4A6A)	2	97-98
<i>Homo sapiens</i> colon cancer-associated antigen	24	94-100
<i>Homo sapiens</i> nucleoporin 214 ku	4	86
<i>Homo sapiens</i> CLL-associated antigen KW-13	2	99

a host signal peptidase localized in the endoplasmic reticulum^[9]. The p7 polypeptide of HCV is a small hydrophobic polyprotein of unknown function and contains 63 amino acids. Its encoding gene is present between structural and non-structural proteins, but it is still not clear whether p7 is a structural protein or a non-structural protein. Studies on the subcellular localization of HCV proteins indicate that most of them associate with ER membranes^[10-12]. HCV p7 comprising two transmembrane alpha helices linked by a small charged cytoplasmic loop, is indeed membrane-associated and mostly located in the endoplasmic reticulum^[7]. HCV p7 is an integral membrane polypeptide. Pulse-chase analysis showed that a large proportion of p7 stays in an early compartment of the secretory pathway. Carrere-Kremer *et al.*'s studies^[7] showed that p7 has a double membrane-spanning topology, the amino- and carboxyl-terminal tails are oriented toward the ER and should therefore also be accessible from the extracellular environment. The C-terminal transmembrane domain of p7 is a signal sequence and the amino- and/or carboxyl-terminal intraluminal tails of p7 contain sequences with genotype-specific function^[13]. The data indicate that p7 is a polytopic membrane protein that could play a functional role in several compartments of the secretory pathway.

At present, studies are carried on the biological functions of HCV p7 protein in the virus life cycle. HCV p7 protein forms hexamer cation ion channels in black lipid membranes. The function of p7 is supposed to be similar to viroporin, which mediates cation permeability across membranes and are important for virion release or maturation^[14,15]. Mutants with deletions of all or part of p7 and a mutant with substitutions of two conserved residues in the cytoplasmic loop are not viable. Thus, p7 is essential for infectivity of HCV^[13]. HCV p7 regulates the internalization properties of HCV structural proteins^[16]. It has been hypothesized that lack of p7 may lead to conformational changes of envelope proteins, as reported for closely related virus, that are perhaps important for cell binding and entry of the HCV virion. Studies of HCV subgenomic replicons showed that p7 is not critical for RNA replication^[17,18].

Transfection with RNA transcripts from an infectious BVDV cDNA clone with in-frame deletions or point mutations of p7 could not produce infectious virus, but the infectivity could be restored by providing p7 in transmembrane. HCV p7 has characteristics similar to those of a group of proteins called viroporins^[13,15]. These proteins form ion channels that might be of importance for virus assembly and/or release or maturation. Mutation of a conserved basic loop located between the two predicted

transmembrane alpha helices rendered HCV p7 non-functional as an ion channel. The intra-cellular localization of p7 was unaffected by this mutation^[19,20]. The HCV-like particles (HCV-LPs) without p7 (p7-HCV-LP) have been shown to be more potent in inducing cellular immune responses with a Th1 bias than HCV-LP with p7^[21]. The study showed that p7-HCV-LP can also induce both humoral and cellular immunities in AAD mice^[22].

Protein-protein interactions occur in a wide variety of biological processes and essentially control the cell fate from division to death. Yeast two-hybrid assays represent a versatile tool to study protein interactions *in vivo*. Yeast two-hybrid system 3 based on the system originally designed by Fields and Song, takes advantage of the properties of the GAL4 protein of the yeast *Saccharomyces cerevisiae*. GAL4-based assay uses yeast transcription factor, GAL4 for detection of protein interactions by transcriptional activation. GAL4 possesses a characteristic phenomenon that the transactivation function can be restored when the factor's DNA-binding domain (DBD) and its transcription-AD are brought together by two interacting heterologous proteins. GAL4-yeast two-hybrid assay uses two expression vectors, one uses DBD and the other uses AD. The GAL4-DBD fuses to a protein 'X' and a GAL4-AD fuses to a protein 'Y' to form the bait and the target of the interaction trap, respectively. A selection of host cells with different reporter genes and different growth selection markers provides a means to detect and confirm protein-protein interactions and has significantly fewer false positives^[23-26].

To investigate the role of HCV p7 in pathogenesis of HCV and physiologic function in hepatocytes, yeast two hybrid system 3 is used to screen the proteins interacting with p7 protein. In this study, the "bait" plasmid pGBKT7-p7 was transformed into yeast strain AH109. In order to further confirm the expression of HCV p7 protein in AH109 yeast strain, we performed the experiment of Western blot and a strong expression of the HCV p7 protein was observed. After the "bait" plasmid pGBKT7-p7 yeast strain AH109 was mated with liver cDNA library yeast strain Y187, the diploid yeast cells were plated on QDO media containing X- α -gal, 50 true positives were obtained. By sequencing analysis of isolated library plasmids, we got the sequences of 50 genes with known functions. Eight of them were respectively associated with genesis of tumor and immunity, regulation of cell life cycle, and the way of signal transmission.

We screened *Homo sapiens* membrane-spanning 4-domains, subfamily A (MS4A6A). Tetraspanins are a large superfamily of cell surface membrane proteins characterized by their

four transmembrane domains, and expressed in a wide variety of cell types and formed two different circularity structures outside cellular membrane. Tetraspanins interact with diverse important proteins, such as integrins, immunoreceptors, and signaling molecules and have functional roles in processes. They promote cellular growth and signal transduction and are possibly related to viral adhesion and entry, cellular cancerization, tumor cell invasion, and metastasis^[27,28]. The tetraspanin web refers to a network of molecular interactions involving tetraspanins and other molecules. The functions of net are complex and multiple. The CD81 is one of the tetraspanins and widely expressed in a variety of cell types. Todres *et al.*^[29], and Bartosch *et al.*^[30], showed that CD81 is likely to be the receptor protein of HCV infecting target cells, and the structures of CD81 and other subfamilies of tetraspanins are partly homologous. Because CD37 can regulate directly B cell function and interact between T and B cells, and regulate humoral immunity^[31,32]. CD53 relates to apoptosis and tumor formation. CD63 relates to maturation of human dendritic cells and modulates differential distribution of associated MHC class II molecules during maturation of dendritic cells^[33]. Migration of activated hepatic stellate cells (HSC) is a key event in the progression of liver fibrosis. The tetraspanin CD151 molecule plays a key role as a regulator of $\alpha6\beta1$ integrin adhesion strengthening and involves in HSC migration, adhesion, and proliferation^[34,35]. Human CD81 directly enhances Th1 and Th2 cell activation, but preferentially induces proliferation of Th2 cells upon long-term stimulation. CD81 cross-linking can also induce adhesion in B and T cells and decrease the threshold for B cell activation via the immunoglobulin (Ig) receptor, which produces autoantibodies and form corresponding immunopathologic damage^[36]. In this study, it was shown that HCV p7 could bind to tetraspanins and the functions of p7 are complex.

Another important protein interacting with p7 protein from liver cDNA library is *Homo sapiens* nucleoporin 214 ku (NUP214). Nuclear pore complexes (NPCs) are large protein structures spanning the double membrane of the eukaryotic nucleus that serves as a site for translocation of macromolecules between the nucleus and the cytoplasm. NPCs include a family of 50-100 proteins termed as nucleoporins (Nups). Studies in the past several years have demonstrated that individual Nups play a unique role in regulating NPC function and nucleocytoplasmic transport of proteins and RNAs. The functions of individual Nups are associated with specific human diseases. NUP214, also named as CAN protein, is an oncogene and one of the components of NPCs in eukaryotic cells. It contains FG repeat sequences of special proteins of NPCs, which bind directly to receptors that transport substrates through the NPC. NUP214 is located at cytoplasmic side of the NPC and plays a role in numerous pathways, including cell cycle progression, control of gene expression, oncogenesis, and transport of nucleoplasmic. 3' extremity of the gene forms an integral gene with DEK gene on chromosome 6, which is correlative to acute myelocytic leukemia and myelodysplastic syndrome^[37-39].

We also screened *Homo sapiens* Ig superfamily (IgSF) containing leucine-rich repeat. The IgSF is one of the largest families of protein domains in this genome and one of the

major families in other multicellular eukaryotes. The members of the superfamily are involved in a variety of functions including cell-cell recognition, cell-surface receptors, muscle structure and the immune system^[40]. The IgSF containing a leucine-rich repeat (LRR) is named as ISLR. The ISLR gene is mapped on human chromosome 15q23-q24 by fluorescence *in situ* hybridization. It is a protein with a molecular mass of 46 ku and contains a LRR, with conserved flanking sequences and a C2-type Ig-like domain. These domains are important for protein-protein interaction or cell adhesion, therefore it is possible that the ISLR may also interact with other proteins or cells^[41].

HCV p7 protein also interacts with *Homo sapiens* signal sequence receptor δ , *Homo sapiens* H19, imprinted maternally-expressed untranslated mRNA, *Homo sapiens* spermatid perinuclear RNA binding protein, *Homo sapiens* colon cancer-associated antigen and *Homo sapiens* CLL-associated antigen KW-13. The significance of interactions of the proteins with HCV p7 should be further studied *in vivo* and *in vitro*.

REFERENCES

- 1 **Choo QL**, Kuo G, Weiner AJ, Overby LR, Bradley DW, Houghton M. Isolation of a cDNA clone derived from a blood-borne non-A, non-B viral hepatitis genome. *Science* 1989; **244**: 359-362
- 2 **Kato N**. Molecular virology of hepatitis C virus. *Acta Med Okayama* 2001; **55**: 133-159
- 3 **De Francesco R**, Neddermann P, Tomei L, Steinkuhler C, Gallinari P, Folgori A. Biochemical and immunologic properties of the nonstructural proteins of the hepatitis C virus: implications for development of antiviral agents and vaccines. *Semin Liver Dis* 2000; **20**: 69-83
- 4 **Taniguchi H**, Kato N, Otsuka M, Goto T, Yoshida H, Shiratori Y, Omata M. Hepatitis C virus core protein upregulates transforming growth factor-beta 1 transcription. *J Med Virol* 2004; **72**: 52-59
- 5 **Hofmann H**. Virology of hepatitis C virus. *Wien Med Wochenschr* 2000; **150**: 463-466
- 6 **Kato N**. Genome of human hepatitis C virus (HCV): gene organization, sequence diversity, and variation. *Microb Comp Genomics* 2000; **5**: 129-151
- 7 **Carrere-Kremer S**, Montpellier-Pala C, Cocquerel L, Wychowski C, Penin F, Dubuisson J. Subcellular localization and topology of the p7 polypeptide of hepatitis C virus. *J Virol* 2002; **76**: 3720-3730
- 8 **Gietz RD**, Triggs-Raine B, Robbins A, Graham KC, Woods RA. Identification of proteins that interact with a protein of interest: applications of the yeast two-hybrid system. *Mol Cell Biochem* 1997; **172**: 67-69
- 9 **Reed KE**, Rice CM. Overview of hepatitis C virus genome structure, polyprotein processing, and protein properties. *Curr Top Microbiol Immunol* 2000; **242**: 55-84
- 10 **Hugle T**, Fehrmann F, Bieck E, Kohara M, Krausslich HG, Rice CM, Blum HE, Moradpour D. The hepatitis C virus nonstructural protein 4B is an integral endoplasmic reticulum membrane protein. *Virology* 2001; **284**: 70-81
- 11 **Itakura J**, Sakamoto N, Enomoto N. Structure and functions of HCV non-structural proteins. *Nippon Rinsho* 2004; **62**(Suppl 7 Pt 1): 64-68
- 12 **Op De Beeck A**, Voisset C, Bartosch B, Ciczora Y, Cocquerel L, Keck Z, Foug S, Cosset FL, Dubuisson J. Characterization of functional hepatitis C virus envelope glycoproteins. *J Virol* 2004; **78**: 2994-3002
- 13 **Sakai A**, Claire MS, Faulk K, Govindarajan S, Emerson SU, Purcell RH, Bukh J. The p7 polypeptide of hepatitis C virus is critical for infectivity and contains functionally important genotype-specific sequences. *Proc Natl Acad Sci USA* 2003;

- 100:** 11646-11651
- 14 **Pavlovic D**, Neville DC, Argaud O, Blumberg B, Dwek RA, Fischer WB, Zitzmann N. The hepatitis C virus p7 protein forms an ion channel that is inhibited by long-alkyl-chain minosugar derivatives. *Proc Natl Acad Sci USA* 2003; **100**: 6104-6108
- 15 **Griffin SD**, Beales LP, Clarke DS, Worsfold O, Evans SD, Taeger J, Harris MP, Rowlands DJ. The p7 protein of hepatitis C virus forms an ion channel that is blocked by the antiviral drug, Amantadine. *FEBS Lett* 2003; **535**: 34-38
- 16 **Saunier B**, Triyatni M, Ulianich L, Maruvada P, Yen P, Kohn LD. Role of the asialoglycoprotein receptor in binding and entry of hepatitis C virus structural proteins in cultured human hepatocytes. *J Virol* 2003; **77**: 546-559
- 17 **Harada T**, Tautz N, Thiel HJ. E2-p7 region of the bovine viral diarrhea virus polyprotein: processing and functional studies. *J Virol* 2000; **74**: 9498-9506
- 18 **Pietschmann T**, Lohmann V, Kaul A, Krieger N, Rinck G, Rutter G, Strand D, Bartenschlager R. Persistent and transient replication of full-length hepatitis C virus genomes in cell culture. *J Virol* 2002; **76**: 4008-4021
- 19 **Griffin SD**, Harvey R, Clarke DS, Barclay WS, Harris M, Rowlands DJ. A conserved basic loop in hepatitis C virus p7 protein is required for amantadine-sensitive ion channel activity in mammalian cells but is dispensable for localization to mitochondria. *J Gen Virol* 2004; **85**: 451-461
- 20 **Fischer WB**, Sansom MS. Viral ion channels: structure and function. *Biochim Biophys Acta* 2002; **1561**: 27-45
- 21 **Lechmann M**, Murata K, Sato J, Vergalla J, Baumert TF, Liang TJ. Hepatitis C virus-like particles induce virus-specific humoral and cellular immune responses in mice. *Hepatology* 2001; **34**: 417-423
- 22 **Murata K**, Lechmann M, Qiao M, Gunji T, Alter HJ, Liang TJ. Immunization with hepatitis C virus-like particles protects mice from recombinant hepatitis C virus-vaccinia infection. *Proc Natl Acad Sci USA* 2003; **100**: 6753-6758
- 23 **Meng JJ**, Rojas M, Bacon W, Stickney JT, Ip W. Methods to study protein-protein interactions. *Methods Mol Biol* 2005; **289**: 341-358
- 24 **Osman A**. Yeast two-hybrid assay for studying protein-protein interactions. *Methods Mol Biol* 2004; **270**: 403-422
- 25 **Gietz RD**, Woods RA. Screening for protein-protein interactions in the yeast two-hybrid system. *Methods Mol Biol* 2002; **185**: 471-486
- 26 **Zhen Z**. Progress in proteomics. *Shengwu Gongcheng Xuebao* 2001; **17**: 491-493
- 27 **Tarrant JM**, Robb L, van Spriel AB, Wright MD. Tetraspanins: molecular organisers of the leukocyte surface. *Trends Immunol* 2003; **24**: 610-617
- 28 **Carlioni V**, Mazzocca A, Ravichandran KS. Tetraspanin CD81 is linked to ERK/MAPKinase signaling by Shc in liver tumor cells. *Oncogene* 2004; **23**: 1566-1574
- 29 **Todres E**, Nardi JB, Robertson HM. The tetraspanin superfamily in insects. *Insect Mol Biol* 2000; **9**: 581-590
- 30 **Bartosch B**, Vitelli A, Granier C, Gouion C, Dubuisson J, Pascale S, Scarselli E, Cortese R, Nicosia A, Cosset FL. Cell entry of hepatitis C virus requires a set of co-receptors that include the CD81 tetraspanin and the SR-B1 scavenger receptor. *J Biol Chem* 2003; **278**: 41624-41630
- 31 **van Spriel AB**, Puls KL, Sofi M, Pouniotis D, Hochrein H, Orinska Z, Knobloch KP, Plebanski M, Wright MD. A regulatory role for CD37 in T cell proliferation. *J Immunol* 2004; **172**: 2953-2961
- 32 **Knobloch KP**, Wright MD, Ochsenbein AF, Liesenfeld O, Lohler J, Zinkernagel RM, Horak I, Orinska Z. Targeted inactivation of the tetraspanin CD37 impairs T-cell-dependent B-cell response under suboptimal costimulatory conditions. *Mol Cell Biol* 2000; **20**: 5363-5369
- 33 **Engering A**, Kuhn L, Fluitsma D, Hoefsmit E, Pieters J. Differential post-translational modification of CD63 molecules during maturation of human dendritic cells. *Eur J Biochem* 2003; **270**: 2412-2420
- 34 **Lammerding J**, Kazarov AR, Huang H, Lee RT, Hemler ME. Tetraspanin CD151 regulates alpha6beta1 integrin adhesion strengthening. *Proc Natl Acad Sci USA* 2003; **100**: 7616-7621
- 35 **Mazzocca A**, Carlioni V, Sciammetta S, Cordella C, Pantaleo P, Caldini A, Gentilini P, Pinzani M. Expression of transmembrane 4 superfamily (TM4SF) proteins and their role in hepatic stellate cell motility and wound healing migration. *J Hepatol* 2002; **37**: 322-330
- 36 **Maecker HT**. Human CD81 directly enhances Th1 and Th2 cell activation, but preferentially induces proliferation of Th2 cells upon long-term stimulation. *BMC Immunol* 2003; **4**: 1
- 37 **Cronshaw JM**, Matunis MJ. The nuclear pore complex: disease associations and functional correlations. *Trends Endocrinol Metab* 2004; **15**: 34-39
- 38 **Marg A**, Shan Y, Meyer T, Meissner T, Brandenburg M, Vinkemeier U. Nucleocytoplasmic shuttling by nucleoporins Nup153 and Nup214 and CRM1-dependent nuclear export control the subcellular distribution of latent Stat1. *J Cell Biol* 2004; **165**: 823-833
- 39 **Cronshaw JM**, Krutchinsky AN, Zhang W, Chait BT, Matunis MJ. Proteomic analysis of the mammalian nuclear pore complex. *J Cell Biol* 2002; **158**: 915-927
- 40 **Teichmann SA**, Chothia C. Immunoglobulin superfamily proteins in *Caenorhabditis elegans*. *J Mol Biol* 2000; **296**: 1367-1383
- 41 **Yoon IK**, Kim HK, Kim YK, Song IH, Kim W, Kim S, Baek SH, Kim JH, Kim JR. Exploration of replicative senescence-associated genes in human dermal fibroblasts by cDNA microarray technology. *Exp Gerontol* 2004; **39**: 1369-1378

• *Helicobacter pylori* •

Implications of anti-parietal cell antibodies and anti-*Helicobacter pylori* antibodies in histological gastritis and patient outcome

Ching-Chu Lo, Ping-I Hsu, Gin-Ho Lo, Kwok-Hung Lai, Hui-Hwa Tseng, Chiun-Ku Lin, Hoi-Hung Chan, Wei-Lun Tsai, Wen-Chi Chen, Nan-Jing Peng

Ching-Chu Lo, Ping-I Hsu, Gin-Ho Lo, Kwok-Hung Lai, Chiun-Ku Lin, Hoi-Hung Chan, Wei-Lun Tsai, Wen-Chi Chen, Division of Gastroenterology, Department of Internal Medicine, Kaohsiung Veterans General Hospital and St. Martin De Porres Hospital, National Yang-Ming University, Kaohsiung, Taiwan, China
Hui-Hwa Tseng, Department of Pathology, Kaohsiung Veterans General Hospital and National Yang-Ming University, Kaohsiung, Taiwan, China

Nan-Jing Peng, Department of Nuclear Medicine, Kaohsiung Veterans General Hospital and National Yang-Ming University, Kaohsiung, Taiwan, China

Supported by Research Grant VGHKS-92-20 and VGHKS-93-28 from Kaohsiung Veterans General Hospital, Kaohsiung, Taiwan, China

Correspondence to: Ping-I Hsu, MD, Division of Gastroenterology, Department of Internal Medicine, Kaohsiung Veterans General Hospital, 386, Ta-Chung 1st Road, Kaohsiung 813, Taiwan, China. williamhsup@yahoo.com.tw

Telephone: +886-7-3422121-2075 Fax: +886-7-3468237
Received: 2004-12-22 Accepted: 2005-01-05

with glandular atrophy in corpus and the presence of positive AHPA correlates with glandular atrophy in antrum. The existence of serum APCA and AHPA betokens glandular atrophy and requires further examination for gastric cancer.

© 2005 The WJG Press and Elsevier Inc. All rights reserved.

Key words: Glandular atrophy; Intestinal metaplasia; Gastric cancer; Anti-parietal cell antibody; Anti-*Helicobacter pylori* antibodies

Lo CC, Hsu PI, Lo GH, Lai KH, Tseng HH, Lin CK, Chan HH, Tsai WL, Chen WC, Peng NJ. Implications of anti-parietal cell antibodies and anti-*Helicobacter pylori* antibodies in histological gastritis and patient outcome. *World J Gastroenterol* 2005; 11(30): 4715-4720

<http://www.wjgnet.com/1007-9327/11/4715.asp>

Abstract

AIM: To develop a serum or histological marker for early discovery of gastric atrophy or intestinal metaplasia.

METHODS: This study enrolled 44 patients with gastric adenocarcinoma, 52 patients with duodenal ulcer, 14 patients with gastric ulcer and 42 consecutive healthy adults as controls. Each patient received an endoscopy and five biopsy samples were obtained. The degrees of histological parameters of gastritis were categorized following the Updated Sydney System. Anti-parietal cell antibodies (APCA) and anti-*Helicobacter pylori* (*H pylori*) antibodies (AHPA) were analyzed by immunoassays. *H pylori* infection was diagnosed by rapid urease test and histological examination.

RESULTS: Patients with gastric cancer and gastric ulcer are significantly older than healthy subjects, while also displaying higher frequency of APCA than healthy controls. Patients with positive APCA showed higher scores in gastric atrophy and intestinal metaplasia of corpus than patients with negative APCA. Patients with positive AHPA had higher scores in gastric atrophy, intestinal metaplasia, and gastric inflammation of antrum than those patients with negative AHPA. Elderly patients had greater prevalence rates of APCA. Following multivariate logistic regression analysis, the only significant risk factor for antral atrophy is positive AHPA, while that for corpus atrophy is positive APCA.

CONCLUSION: The existence of positive APCA correlates

INTRODUCTION

Statistics from the American Cancer Society indicated around 22 000 new cases of gastric carcinoma in the USA for 2001^[1]. Gastric cancer, a disease with high mortality, is the second leading cause of cancer death worldwide^[2]. An important factor concerning the high mortality rate is the high frequency of advanced gastric cancer at diagnosis. Early diagnosis is difficult because gastric cancer tends to manifest initially with non-specific symptoms and signs.

Helicobacter pylori (*H pylori*) was categorized as class I carcinogen of gastric cancer by the International Agency for Research on Cancer in 1994^[3]. However, most patients with *H pylori* gastritis are clinically silent and only a fraction of them will develop gastric cancer^[4]. Which histological elements would raise the risk of gastric cancer is disputable. Chronic atrophic gastritis was reported in 80-90% and intestinal metaplasia appeared in 70% of patients with gastric carcinoma^[5]. Glandular atrophy and intestinal metaplasia are now considered as risk factors for gastric cancer. The identification of both conditions, however, demands invasive procedures and biopsy. To develop a non-invasive, diagnostic tool is an important challenge to all gastroenterologists.

There are no sufficiently sensitive serum markers to enable an early diagnosis of gastric cancer^[6]. A low serum pepsinogen I and raised serum gastrin levels were found in patients with gastric cancer^[7,8]. However, they lack adequate sensitivity and specificity. The levels of anti-parietal cell antibody (APCA) expression were associated with the

histological degree of atrophy^[9]. The presence of APCA may represent an early marker of gastric atrophy.

This study attempted to assess differences in histological parameters of gastritis among patients with gastric cancer and other controls. The effectiveness of serum APCA and anti-*H pylori* antibodies (AHPA) in predicting glandular atrophy and even gastric cancer was also assessed.

MATERIALS AND METHODS

Patients

This study enrolled 152 consecutive subjects with epigastric discomfort between July 2002 and June 2003. The subjects comprised 44 patients with histologically documented gastric adenocarcinoma, 52 patients with duodenal ulcer, 14 patients with gastric ulcer, and 42 consecutive healthy adults as controls. Those subjects with history of major systemic diseases including diabetes mellitus, adrenal insufficiency, iron deficiency anemia, thyrotoxicosis, myxedema, and Hashimoto's thyroiditis were excluded.

All subjects were recruited at our hospital and gave informed consent for endoscopic biopsies. Biopsies were executed with jumbo forceps from cancer and non-cancer sites. At least six specimens were obtained from the neoplastic lesions for histological verification. Only those who were histologically documented as gastric adenocarcinoma were included in this study.

In addition, five specimens were collected from antrum and corpus following the standard protocol. These five specimens were classified with a visual analog scale proposed by the Updated Sydney System^[10]. This study was approved by the Human Medical Research Committee of the Kaohsiung Veterans General Hospital, Kaohsiung, Taiwan.

Biopsy protocol

A standardized biopsy protocol was done in all subjects. All subjects underwent endoscopic biopsies and five specimens were extracted from A3 (lesser curvature site of angularis), A1 (lesser curvature site of antrum), A4 (greater curvature site of antrum), B5 (lesser curvature site of mid-body), and B6 (greater curvature site of mid-body). Only cases from whom all five specimens were available were included in this study.

Histology

The specimens for histological examinations were fixed in 10% buffered formalin, embedded in paraffin, and sectioned. The sections were stained with a hematoxylin and eosin stain and a modified Giemsa stain^[11,12]. The biopsied specimens were assessed by a histopathologist who was unaware of the endoscopic features and clinical data. The morphological variables, including *H pylori* density, neutrophils (AIS: acute inflammatory score), monocytes (CIS: chronic inflammatory score), lymphoid follicles, glandular atrophy and intestinal metaplasia, were graded with a visual analog scale according to the Updated Sydney System. The scores of all histological parameters in antrum were calculated from means of A1 and A4 and those in corpus from B5 and B6.

Rapid urease test

The rapid urease test was performed according to our

previous studies^[13]. Each biopsied specimen was placed immediately in 1 mL of a 10% solution of urea in deionized water (pH 6.8) to which two drops of 1% phenol red solution had been added and incubated at 37 °C for up to 24 h. If the yellowish color around the area of inserted specimen changed to bright pink within the 24-h limit, the urease test was considered positive. In our laboratory, the sensitivity and specificity of the rapid urease test were 96% and 91%, respectively^[14].

Questionnaire

Complete medical history and demographic data was gathered from each patient, comprising age, sex, blood type, residence area, marital status, cigarette and alcohol consumption, beverage of tea or coffee, and drug history.

Helicobacter pylori infection

The presence of *H pylori* infection was defined as both positivity of rapid urease test and histology.

Anti-parietal cell antibodies (APCA)

Serum APCA was determined with indirect fluorescent antibody tests employing the commercial kit FLUORO-KIT™ (DiaSorin Inc. Stillwater, USA) test systems utilizing rat stomach for detection and differentiation of circulating autoantibodies in human serum. Patient's serum samples were diluted in phosphate buffered saline and overlaid onto tissue cryostat sections fixed on a microscope slide. If APCA appeared in patients' serum, stable antigen-antibody complexes would be formed. The complexes bound fluorescein labeled anti-human immunoglobulin. The consequent positive reaction, observed with a properly equipped fluorescence microscope, appeared as apple green fluorescence.

Anti-*Helicobacter pylori* antibodies (AHPA)

Immunoglobulin G (IgG) antibodies to *H pylori* were measured with an inhouse enzyme immunoassay (EIA). The antigen employed was an acid glycine extract from *H pylori* strain NCTC 11637. Absorbance readings were converted to reciprocals of the end point titers.

Statistical analysis

Statistical tests were performed with SPSS system. The χ^2 test or the Fisher exact test was used for nominal scale and between groups. Two independent samples were compared by the Student test or the Mann-Whitney/Wilcoxon rank sum test. The stepwise logistic regression analysis was performed with various items and a *P* value < 0.05 was considered to be significant.

RESULTS

Demographic data

The demographic data for all groups of patients are shown in Table 1. The mean age of patients with gastric cancer (68.8±13.7) and gastric ulcer (71.6±10.7) was significantly higher than that in healthy controls (48.2±13.3). Males had distinctively higher rates of gastric cancers than females. (84% vs 45%, *P* < 0.05) Patients with gastric ulcer had greater

rates of smoking than controls. (71% vs 29%, $P<0.05$) No significant differences emerged in other demographic variables between patients with gastric cancer and controls.

***Helicobacter pylori* infection**

H pylori infection was defined as, both positivity of rapid urease test and histology. The positive rates of *H pylori* infection of patients with gastric cancer (53%), gastric ulcer (57%), and duodenal ulcer (75%) were notably higher than in controls (24%, Table 2).

Anti-parietal cell antibodies (APCA)

The prevalence rates of APCA in patients with gastric cancer (70%) and gastric ulcer (79%) were much higher than those of controls (36%, $P<0.05$, Table 2). Host and bacterial factors related to the presence of APCA in serum were also evaluated. (Table 3) Old age (≥ 60 years) was the only significant factor correlated with the presence of APCA.

Anti-Helicobacter pylori antibodies (AHPA)

The presence of AHPA was detected by serum IgG. The investigation assessed host and bacterial factors associated with the presence of AHPA in serum. (Table 4) No significant difference was found between patients with and without AHPA.

APCA and scores of histological gastritis (Figure 1)

All degrees of histological parameters of gastritis were graded with a visual analog scale according to the Updated Sydney System. The correlation between APCA and histological

gastritis is shown in Figure 1. For the histological parameters in antrum, the scores of CIS and atrophy were significantly higher in patients with positive APCA than in those with negative APCA. For the parameters in corpus, the scores of CIS, glandular atrophy, and intestinal metaplasia were significantly higher in patients with positive APCA than in those without. There were no significant differences in scores of other parameters.

AHPA and scores of histological gastritis (Figure 2)

The correlation between AHPA and histological gastritis is shown in Figure 2. For the histological parameters in antrum, the scores for AIS, CIS, glandular atrophy, intestinal metaplasia, and *H pylori* density were significantly higher in patients with positive AHPA than in those without. ($P<0.05$) For parameters in corpus, the scores of CIS and *H pylori* density were significantly higher in patients with positive AHPA than in those without. There were no significant differences in other parameters.

Table 3 Host and bacterial factors related to the presence of anti-parietal cell antibodies (APCA) in serum

	Anti-parietal cell antibodies			P
	Positive (n = 80, %)	Negative (n = 72, %)	Absolute difference (95%CI)	
Age ≥ 60 (yr)	48 (60) ^a	17 (24)	0.36 (0.22–0.51)	0.000
Sex (male)	58 (73)	42 (58)	0.14 (–0.01–0.29)	0.07
Blood type				
A	23 (29)	23 (32)	–0.03 (–0.18–0.12)	0.67
B	21 (26)	19 (26)	–0.00 (–0.14–0.14)	0.99
O	32 (40)	26 (36)	0.04 (–0.12–0.20)	0.63
AB	4 (5)	4 (6)	–0.01 (–0.08–0.07)	0.88
Smoking	34 (43)	22 (31)	0.12 (–0.03–0.27)	0.13
Daily alcohol use	13 (16)	6 (8)	0.08 (–0.03–0.19)	0.14
Daily coffee use	3 (4)	9 (13)	–0.09 (–0.17–0.00)	0.05
Daily tea use	24 (30)	17 (24)	0.06 (–0.08–0.21)	0.38

^a $P<0.05$ vs APCA (–) group.

Table 4 Host and bacterial factors related to the presence of anti-*H pylori* antibodies (AHPA) in serum

	Anti- <i>H pylori</i> antibodies			P
	Positive (n = 82, %)	Negative (n = 70, %)	Absolute difference (95%CI)	
Age ≥ 60 (yr)	30 (37)	35 (50)	–0.13 (–0.29–0.02)	0.10
Sex (male)	59 (72)	41 (58)	0.13 (–0.02–0.29)	0.08
Blood type				
A	25 (30)	21 (30)	0.00 (–0.14–0.15)	0.95
B	22 (27)	18 (26)	0.01 (–0.13–0.15)	0.88
O	31 (38)	27 (39)	–0.01 (–0.16–0.15)	0.92
AB	4 (5)	4 (6)	–0.01 (–0.08–0.06)	0.82
Smoking	31 (38)	25 (36)	0.02 (–0.14–0.18)	0.79
Daily alcohol use	13 (16)	6 (9)	0.07 (–0.03–0.18)	0.18
Daily coffee use	9 (11)	3 (4)	0.07 (–0.02–0.15)	0.13
Daily tea use	24 (29)	17 (24)	0.05 (–0.09–0.19)	0.49

Table 1 Baseline characteristics of all patients

	¹ HC (n = 42, %)	² DU (n = 52, %)	³ GU (n = 14, %)	⁴ GC (n = 44, %)
Age (mean \pm SD) (yr)	48.2 \pm 13.3	51.2 \pm 14.3	71.6 \pm 10.7 ^a	68.8 \pm 13.7 ^a
Sex: male	19 (45)	34 (65)	10 (71)	37 (84) ^a
Blood type				
A	15 (36)	13 (25)	6 (42)	12 (27)
B	11 (26)	16 (31)	2 (14)	11 (25)
O	13 (31)	21 (40)	5 (36)	17 (39)
AB	3 (7)	2 (4)	1 (7)	4 (9)
Smoking	12 (29)	19 (37)	10 (71) ^a	15 (34)
Daily alcohol use	4 (10)	5 (10)	4 (29)	6 (14)
Daily coffee use	6 (14)	3 (6)	1 (7)	2 (5)
Daily tea use	11 (26)	17 (33)	5 (36)	8 (18)

¹HC: healthy control; ²DU: duodenal ulcer; ³GU: gastric ulcer; ⁴GC: gastric cancer.

^a $P<0.05$ vs healthy control group.

Table 2 Prevalence rate of *H pylori* infection and anti-parietal cell antibodies among various groups of patients

	¹ HC (n = 42, %)	² DU (n = 52, %)	³ GU (n = 14, %)	⁴ GC (n = 44, %)
<i>H pylori</i> infection	10 (24)	39 (75) ^a	8 (57) ^a	23 (53) ^a
⁵ APCA	15 (36)	23 (44)	11 (79) ^a	31 (70) ^a

¹HC: healthy control; ²DU: duodenal ulcer; ³GU: gastric ulcer; ⁴GC: gastric cancer;

⁵APCA: anti-parietal cell antibodies. ^a $P<0.05$ vs healthy control group.

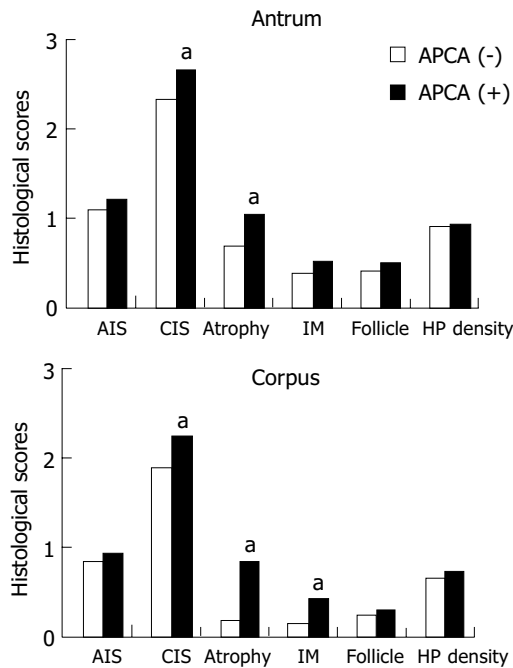


Figure 1 Correlation between anti-parietal cell antibodies (APCA) and histological parameters of gastritis. (AIS: acute inflammatory score; CIS: chronic inflammatory score; IM: intestinal metaplasia, HP: *H pylori*). ^a $P < 0.05$ vs APCA(-).

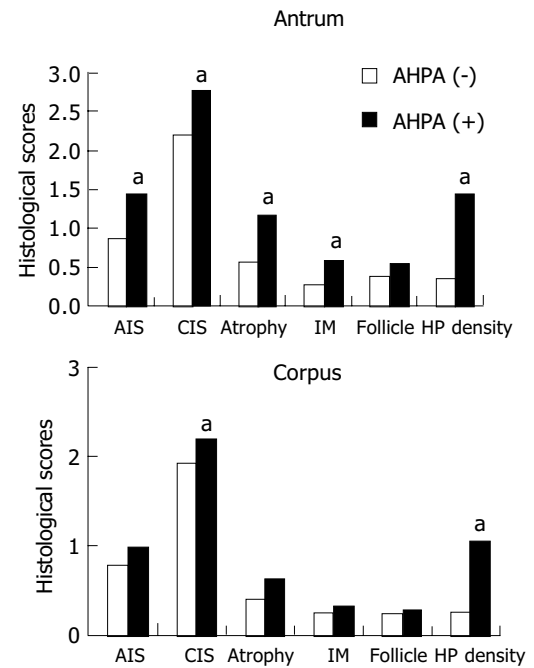


Figure 2 Correlation between anti-*H pylori* antibodies (AHPA) and histological parameters of gastritis. (AIS: acute inflammatory score; CIS: chronic inflammatory score; IM: intestinal metaplasia, HP: *H pylori*). ^a $P < 0.05$ vs AHPA(-).

Multivariate logistic regression analysis (Tables 5 and 6)

Multivariate logistic regression analysis of factors affecting severe atrophy (score of glandular atrophy > 2) was also executed. The only factor affecting severe atrophy in antrum was positive AHPA and that in corpus was positive APCA.

DISCUSSION

Discovery of *H pylori* led to a widely accepted hypothesis of a multi-step sequence that begins with gastritis and, through atrophy, metaplasia, dysplasia, finally leads to gastric cancer^[15]. An odds ratio of 3.6 was reported for gastric cancer among patients infected with *H pylori* vs those non-

infected^[16]. The seropositive rate of *H pylori* infection ranged from 65% to 84% in patients with gastric cancer^[17]. In the present study, the infection rate with *H pylori* was significantly higher in the gastric cancer group (53%) than in controls (24%). ($P < 0.05$) The positive rate was lower than that reported previously. The reason may relate to the strict policy that presence of *H pylori* infection was defined as both positivity of rapid urease test and histology.

Glandular atrophy and intestinal metaplasia have been demonstrated to be linked with gastric cancer^[5]. An earlier study claimed that in patients with intestinal-type early gastric cancer, more severe glandular atrophy and intestinal metaplasia was noted in all biopsy sites of the stomach^[18].

Table 5 Multivariate logistic regression analysis of factors influencing severe atrophy in antrum

Variables	Exp(B)	SE	Wald	Sig
Age (yr)	1.0003	0.0165	0.0004	0.98
Sex	0.8724	0.5639	0.0586	0.81
Blood_A	0.6916	0.5468	0.4547	0.50
Blood_B	0.5688	0.5129	1.2106	0.27
Blood_O	0.6418	0.5042	0.7736	0.38
Blood_AB	1.1187	0.3705	0.0917	0.76
Smoking	1.0790	0.5127	0.0220	0.88
Alcohol	2.0850	0.6279	1.3694	0.24
Coffee	1.352	0.8278	0.1328	0.72
Tea	0.9952	0.4880	0.0001	0.99
¹ AHPA	2.8104	0.4768	4.6965	0.03
² APCA	1.5004	0.4863	0.6961	0.40

¹AHPA: anti-*H pylori* antibodies; ²APCA: anti-parietal cell antibodies.

Table 6 Multivariate logistic regression analysis of factors influencing severe atrophy in corpus

Variables	Exp(B)	SE	Wald	Sig
Age (yr)	1.0272	0.0301	0.7907	0.37
Sex	3.1120	1.2611	0.8104	0.37
Blood_A	0.5556	0.8903	0.4358	0.51
Blood_B	0.5490	0.7726	0.6023	0.44
Blood_O	0.3659	0.8854	1.2890	0.26
Blood_AB	0.6659	0.3478	1.3675	0.24
Smoking	1.0528	0.8430	0.0037	0.95
Alcohol	3.3423	0.8884	1.8446	0.17
Coffee	0.0003	1.4524	2.3234	0.13
Tea	3.8250	0.8091	2.7494	0.10
¹ AHPA	1.8250	0.8418	0.5106	0.47
² APCA	25.1000	1.3096	6.0565	0.01

¹AHPA: anti-*H pylori* antibodies; ²APCA: anti-parietal cell antibodies.

However, another study revealed that both glandular atrophy and intestinal metaplasia were more severe in distal stomach^[19,20]. The present study disclosed that scores for glandular atrophy were statistically higher in antrum and corpus of patients with gastric cancer. These results imply that if glandular atrophy occurs, either in antrum or corpus, the risk of developing gastric cancer is greater. The investigation also discovered that scores of intestinal metaplasia and CIS in antrum were significantly higher in patients with gastric cancer. Scores of AIS, CIS, glandular atrophy, intestinal metaplasia, and lymphoid follicles were also higher in corpus. All these results imply that severe degrees of CIS, glandular atrophy and intestinal metaplasia may herald the development of gastric cancer.

Strickland and Mackay even reported in 1973 that APCA was associated with chronic atrophic gastritis of corpus^[21]. The levels of APCA expression are connected with the histological degree of atrophy^[9], whose presence closely paralleled gastric atrophic status. In the present study, the presence of APCA was significantly higher in patients with gastric cancer than among controls. Evaluation of the histological parameters revealed that the scores of CIS, intestinal metaplasia and glandular atrophy were markedly higher in patients with positive APCA, particularly in corpus. Following multivariate logistic regression analysis, positive APCA was the only significant factor affecting severe atrophy in corpus. These results suggest that the presence of APCA represents an early marker for glandular atrophy in corpus and even for the development of gastric cancer.

When assessing host factors related to the presence of APCA, this study identified old age (>60 years) as the only factor for developing APCA. Although host factors have been thought important for the promotion of atrophic gastritis, the factor that actually triggers these changes remains unknown^[22]. Results of this study suggest that age may be the factor promoting atrophic changes. However, the small sample size precludes a definite conclusion at this stage.

The correlations between AHPA and histological gastritis indicated that AHPA correlated well with AIS, CIS, glandular atrophy, intestinal metaplasia, and *H. pylori* density in the antrum. ($P < 0.05$) These correlation results conform to many previous studies^[23]. Following multivariate logistic regression analysis, AHPA emerged as the only significant factor affecting severe atrophy in the antrum. The occurrence of AHPA may act as a predictive marker for glandular atrophy in antrum.

Chronic atrophic gastritis is an independent risk factor for gastric cancer. Timely recognition of these patients was difficult without endoscopic biopsy. If any factor predicting gastric atrophy can be found, these high-risk patients may be diagnosed earlier. Patients with gastric cancer were found to have higher prevalence of APCA and AHPA. (Table 2) The existence of positive APCA correlates well with glandular atrophy in corpus, whereas the presence of positive AHPA correlates with atrophy in antrum. The results of the present work imply that both APCA and AHPA can predict glandular atrophy in corpus and antrum. However, this sample size is small and large-scale age-matched prospective studies are

awaited to determine the definite correlation between APCA, AHPA and glandular atrophy.

ACKNOWLEDGMENTS

The authors would like to express their deep appreciation to Dr. Chang-Bih Shie, Yuh-Chyi Chou, Chia-Lin Yeh, Chao-Ming Wu, Lung-Chih Cheng, Miss Yu-San Chen for their invaluable support in this study.

REFERENCES

- 1 American Cancer Society. Statistics for 2001. Available at: http://www.cancer.org/eprise/main/docroot/STT/stt_02001. Accessed March 21, 2002
- 2 Pisani P, Parkin DM, Muñoz N, Ferlay J. Cancer and infection: estimates of the attributable fraction in 1990. *Cancer Epidemiol Biomarkers Prev* 1997; **6**: 387-400
- 3 International Agency for Research on Cancer. Monographs on the evaluation of carcinogenic risks to humans. Schistosomes, Liver flukes and *Helicobacter pylori*. Lyon: International Agency for Research on Cancer 1994: 177-240
- 4 Dooley CP, Fitzgibbons PL, Cohen H, Fitzgibbons PL, Bauer M, Appleman MD, Perez-Perez GI, Blaser MJ. Prevalence of *Helicobacter pylori* infection and histological gastritis in asymptomatic persons. *N Engl J Med* 1989; **321**: 1562-1566
- 5 Kuipers EJ, Klinkenberg-Knol EC, Vandenbroucke-Grauls CM, Applemelk BJ, Scheuk BE, Meuwissen SG. Role of *Helicobacter pylori* in the pathogenesis of atrophic gastritis. *Scand J Gastroenterol* 1997; **223**: 28-34
- 6 Ellis DJ, Speirs C, Kingston RD, Brookes VS, Leonard J, Dykes PW. Carcinoembryonic antigen levels in advanced gastric carcinoma. *Cancer* 1978; **42**: 623-625
- 7 Nomura AHY, Stemmermann GN, Samloff IM. Serum pepsinogen I as a predictor of stomach cancer. *Ann Intern Med* 1980; **93**: 537-540
- 8 McGuigan JE, Trudeau WKL. Serum and tissue gastrin concentration in patients with carcinoma of stomach. *Gastroenterology* 1973; **64**: 22-25
- 9 Ito M, Haruma K, Kaya S, Kamada T, Kim S, Sasaki A, Sumii M, Tanaka S, Yoshihara M, Chayama K. Role of anti-parietal cell antibody in *Helicobacter pylori*-associated atrophic gastritis: evaluation in a country of high prevalence of atrophic gastritis. *Scand J Gastroenterol* 2002; **37**: 287-293
- 10 Dixon MF, Genta RM, Yardley JH, Correa P. Classification and grading of gastritis. The updated Sydney System. International workshop on the histopathology of gastritis. *Am J Surg Pathol* 1996; **20**: 1161-1181
- 11 Hsu PI, Lai KH, Tseng HH, Lo GH, Lo CC, Lin CK, Cheng JS, Chan HH, Ku MK, Peng NJ, Chien EJ, Chen W, Hsu PN. Eradication of *Helicobacter pylori* prevents ulcer development in patients with ulcer-like functional dyspepsia. *Aliment Pharmacol Ther* 2001; **15**: 195-201
- 12 Hsu PI, Lai KH, Tseng HH, Lin CK, Lo GH, Cheng JS, Chan HH, Chen GC, Jou HS, Peng NJ, Ger LP, Chen W, Hsu PJ. Risk factors for presentation with bleeding in patients with *Helicobacter pylori*-related peptic ulcer diseases. *J Clin Gastroenterol* 2000; **30**: 386-391
- 13 Peng NJ, Lai KH, Liu RS, Lee SC, Tsay DG, Lo CC, Tseng HH, Huang WK, Lo GH, Hsu PI. Endoscopic 13C-urea breath test for the diagnosis of *Helicobacter pylori* infection. *Dig Liver Dis* 2003; **35**: 73-77
- 14 Hsu PI, Lai KH, Tseng HH, Lin YC, Yen MY, Lin CK, Lo GH, Huang RL, Cheng JS, Huang WK, Ger LP, Chen W, Hsu PN. Correlation of serum immunoglobulin G *Helicobacter pylori* antibody titers with histologic and endoscopic findings in patients with dyspepsia. *J Clin Gastroenterol* 1997; **25**: 587-591

- 15 **Kuipers EJ**, Uytterlinde AM, Pena AS, Poosendaal R, Nelis GF, Festen HP, Meuwissen SG. Long-term sequelae of *Helicobacter pylori* gastritis. *Lancet* 1995; **345**: 1525-1528
- 16 **Parsonnet J**, Friedman GD, Vandersteen DP, Chang Y, Vogelman JH, Orentreich N, Sibley RK. *Helicobacter pylori* infection and the risk of gastric carcinoma. *N Engl J Med* 1991; **325**: 1127-1131
- 17 **Talley NJ**, Zinsmeister AR, Weaver A, DiMagno EP, Carpenter HA, Perez-perez GI, Blaser MJ. Gastric adenocarcinoma and *Helicobacter pylori* infection. *J Natl Cancer Inst* 1991; **83**: 1734-1739
- 18 **Craanen ME**, Dekker W, Blok P, Ferwerda J, Tytgat GN. Intestinal metaplasia and *Helicobacter pylori*: An endoscopic bioptic study of the gastric antrum. *Gut* 1992; **33**: 16-20
- 19 **Yoshimura T**, Shimoyama T, Fukuda S, Tanaka M, Axon ATR, Munakata A. Most gastric cancer occurs on the distal side of the endoscopic atrophic border. *Scand J Gastroenterol* 1999; **34**: 1077-1081
- 20 **Stolte M**, Meining A. *Helicobacter pylori* gastritis of the gastric carcinoma phenotype: Is histology capable of identifying high-risk gastritis? *J Gastroenterol* 2000; **35**(Suppl 12): 98-101
- 21 **Strickland RG**, Machay A. A reappraisal of the nature and significance of chronic atrophic gastritis. *Am J Dig Dis* 1973; **18**: 426-440
- 22 **Azuma T**, Konishi J, Tanaka Y, Hirai M, Ito S, Kato T, Kohli Y. Contribution of HLA-DQA gene to host's response against *Helicobacter pylori*. *Lancet* 1994; **343**: 542-543
- 23 **Kukao A**, Komatsu S, Tsubono Y, Hisamichi S, Ohori H, Ohsato N, Fujino N, Endo N, Iha M. *Helicobacter pylori* infection and chronic atrophic gastritis among Japanese blood donors-a cross-sectional study. *Cancer Causes Control* 1993; **4**: 307-312

Science Editor Guo SY Language Editor Elsevier HK

• BRIEF REPORTS •

Long-term omeprazole and esomeprazole treatment does not significantly increase gastric epithelial cell proliferation and epithelial growth factor receptor expression and has no effect on apoptosis and p53 expression

Istvan Hritz, Laszlo Herszenyi, Bela Molnar, Zsolt Tulassay, Laszlo Pronai

Istvan Hritz, Laszlo Herszenyi, Bela Molnar, Zsolt Tulassay, Laszlo Pronai, 2nd Department of Medicine, Semmelweis University, Hungarian Academy of Sciences, Clinical Gastroenterology Research Unit, Budapest, Hungary

Supported by the National Science Foundation (OTKA Grant No: T 034345)

Correspondence to: Dr. Istvan Hritz, 2nd Dept Medicine, Semmelweis University, 1088 Budapest, Szentkirályi u. 46, Hungary. hritz.istvan@freemail.hu

Telephone: +36-1-266-0901 Fax: +36-1-266-0816

Received: 2004-05-25 Accepted: 2004-07-15

growth factor receptor

Hritz I, Herszenyi L, Molnar B, Tulassay Z, Pronai L. Long-term omeprazole and esomeprazole treatment does not significantly increase gastric epithelial cell proliferation and epithelial growth factor receptor expression and has no effect on apoptosis and p53 expression. *World J Gastroenterol* 2005; 11(30): 4721-4726

<http://www.wjgnet.com/1007-9327/11/4721.asp>

Abstract

AIM: To study the effect of proton pump inhibitor (PPI) treatment on patients with reflux esophagitis and its *in vivo* effect on apoptosis, p53- and epidermal growth factor receptor (EGFR) expression.

METHODS: After informed consent was obtained, gastric biopsies of the antrum were taken from patients with reflux oesophagitis prior to and after 6 mo of 20 mg omeprazole ($n = 14$) or 40 mg esomeprazole ($n = 12$) therapy. Patients did not take any other medications known to affect the gastric mucosa. All patients were *Helicobacter pylori* negative as confirmed by rapid urease test and histology, respectively. Cell proliferation, apoptosis, EGFR, and p53 expression were measured by immunohistochemical techniques. At least 600 glandular epithelial cells were encountered and results were expressed as percentage of total cells counted. Was considered statistically significant.

RESULTS: Although there was a trend towards increase of cell proliferation and EGFR expression both in omeprazole and esomeprazole treated group, the difference was not statistically significant. Neither apoptosis nor p53 expression was affected.

CONCLUSION: Long-term PPI treatment does not significantly increase gastric epithelial cell proliferation and EGFR expression and has no effect on apoptosis and p53 expression.

© 2005 The WJG Press and Elsevier Inc. All rights reserved.

Key words: Proton pump inhibitor; Omeprazole; Esomeprazole; Cell proliferation; Apoptosis; p53 expression; Epidermal

INTRODUCTION

Long-term PPI therapy is suggested to be the best treatment for gastro-esophageal reflux disease. Administration of PPI causes profound and continuous hypochlorhydria by selective inhibition of the proton pump (H^+/K^+ -ATPase) in gastric parietal cells^[1]. It has been shown in animal studies that long-term omeprazole treatment reversibly increases epidermal cell proliferation and suppresses its differentiation in rats^[2,3].

Apoptosis normally plays a role complementing proliferation and is also considered to be essential for the maintenance of gastro-intestinal homeostasis and health^[4]. Disturbance in the balance between these two processes may predispose to either cell loss with mucosal damage or cell accumulation and cancer development^[5].

However, several studies have investigated the effects of omeprazole on gastric mucosa, but there is no information available about the effect of the first single-isomer, esomeprazole, on gastric epithelial cell proliferation, apoptosis, p53- and EGFR expression.

The proliferating cell nuclear antigen (PCNA) technique is an accepted method for measurement of cell proliferation. PCNA is the co-factor of DNA-polymerase and can be detected mostly in the late G₁ and S phases, but it is also present in every phase of the cell cycle.

The terminal deoxynucleotidyl (TdT)-mediated deoxyuridine triphosphate (dUTP) nick end labelling (TUNEL) method has been accepted for the detection of apoptotic cells^[6].

Abnormalities in p53 expression represent the most common molecular change not only in cancer, but also in precancerous gastric lesions, including gastric dysplasia^[7,8]. An increased wild-type p53 expression may also represent a cellular response to DNA damage.

Epithelial growth factor (EGF) is a potent mitogenic peptide, which plays a crucial role in promoting gastric epithelial cell migration, proliferation and differentiation. The increased local production of EGF leads to over expression of EGFR^[9-11].

The aim of the present study was to measure the cell turnover (cell proliferation and apoptosis), p53- and EGFR expression by immunohistochemistry in gastric biopsy samples during long-term omeprazole and esomeprazole treatment.

MATERIALS AND METHODS

Patients

To analyze the effect of PPI therapy on cell kinetics pattern of the gastric mucosa, we studied patients with gastroesophageal reflux disease. A total of 26 patients (14 males and 12 females, mean age 46.2 ± 16.5 years) took part in the study. All patients gave written informed consent.

Biopsies were taken in each subject during upper endoscopy from the antrum (lesser curvature, 3 cm from the pylorus). Additional biopsies were taken during endoscopy for the histological evaluation of their *Helicobacter pylori* (*H pylori*) status^[12].

Patients were treated in an open label study continuously with omeprazole (20 mg/d) or esomeprazole (40 mg/d) for 6 mo. Fourteen patients were on omeprazole and 12 patients on esomeprazole therapy.

Patients did not receive any other medication known to affect the gastric mucosa, but stable medication for hypertension or other diseases such as hypercholesterinemia, non-insulin dependent diabetes mellitus, *etc.* was allowed.

Patients were classified by the Los Angeles classification (15 patients had grade A, and 11 had grade B). None of the patients had Los Angeles grades C, D, or Barrett esophagus. Exclusion criteria were active *H pylori* infection and presence of intestinal metaplasia, since it has been established in previous studies that gastric epithelial cell proliferation is enhanced, if intestinal metaplasia or *H pylori* infection is present^[13-15]. Since histology may miss initial focal microscopical lesions of intestinal metaplasia, small intestine mucus antigen (SIMA) and large intestine mucus antigen (LIMA), each indicates intestinal metaplasia in the gastric biopsy samples, were measured by immunohistochemical technique in all samples. To exclude *H pylori* infection, in addition to histology, both rapid urease test during endoscopy and urease breath test were performed.

Biopsies taken at 0 and 6 mo in both the omeprazole- and esomeprazole-treated groups were assessed.

Neither patients treated with omeprazole nor patients on esomeprazole therapy had endoscopic changes in the stomach or duodenum or *H pylori* infection when biopsy was taken. No intestinal metaplasia was found in the samples.

For immunohistochemistry, all biopsy specimens were fixed in buffered formalin and embedded in paraffin. Four micron thick sections were cut and mounted on glass slides.

Proliferation-PCNA immunohistochemistry

The four micron thick tissue sections were dewaxed and rehydrated. Antigen unmasking was carried out in citrate buffer pH 6.0 by microwave heat treatment (3 min 750 W

and 3 min 370 W), and samples were cooled down in PBS for 20 min. Endogenous peroxidase activity was blocked by incubation for 30 min at room temperature in 3% hydrogen peroxide. After being washed thrice in PBS for 3 min, the slides were incubated with optimally diluted PCNA antibody (Clone: PC10, DAKO) for 15 min at room temperature in a humidified chamber. After being washed thrice in PBS, signal conversion was carried out with the LSAB2 system (DAKO: K0672) as described in the manual. Hematoxylin co-staining was done.

Apoptosis-TUNEL immunohistochemistry

After deparaffinization in xylene and rehydration through graded ethanol, antigen unmasking was carried out in citrate buffer pH 6.0 by microwave heat treatment (5 min 750 W), and samples were cooled down in PBS for 20 min. Samples were digested with nuclease free proteinase K for 20 min at room temperature. After being washed twice in PBS, samples were covered with 30 μ L TUNEL dilution label and 50 μ L TUNEL reaction mixture (5 μ L Tdt enzyme solution and 45 μ L dUTP label solution). Samples were incubated for 120 min at 37 °C in a dark humidified chamber. After being washed thrice in PBS, endogenous peroxidase activity was blocked by incubation for 30 min in 3% hydrogen peroxide at room temperature in a dark humidified chamber. After being washed twice in PBS, non-specific blocking was carried out with 1% BSA-PBS solution for 10 min at room temperature in a dark humidified chamber. After redundant BSA was removed with pipette, samples were covered with 50 μ L converter-POD antibody and incubated for 60 min at 37 °C in a dark humidified chamber. After being washed thrice with PBS, 50 μ L DAB solution (5 μ L DAB substrate and 45 μ L peroxide buffer) was added to each sample and signal conversion was checked by light microscopy. Finally, haematoxylin co-staining was done.

P53 immunohistochemistry

The four micron thick tissue sections were deparaffinized in xylene, rehydrated through graded ethanol. Antigen unmasking was carried out by microwave heat treatment (samples in plastic jars containing citrate buffer pH 6.0 were put into a preheated (95-99 °C) plastic water bath and heated with 500 W for 15 min), and samples were cooled down in PBS for 20 min. Endogenous peroxidase activity was blocked by incubation for 30 min at room temperature in 3% hydrogen peroxide. After being washed thrice in PBS for 3 min, the slides were incubated with optimally diluted p53 antibody (Clone: DO-7, DAKO) at 37 °C for 30 min in a humidified chamber. After being washed thrice in PBS, signal conversion was carried out with the LSAB2 system (DAKO) as described in the manual. Hematoxylin co-staining was done.

EGFR immunohistochemistry

After deparaffinization, antigen unmasking was carried out by nuclease free proteinase K digestion for 20 min at room temperature. After being washed twice in PBS, endogenous peroxidase activity was blocked by incubation for 30 min at room temperature in 3% hydrogen peroxide. After being washed thrice in PBS for 3 min, non-specific blocking was

done with 1% BSA-PBS solution for 10 min at room temperature. Then, the slides were incubated with diluted EGFR antibody (1 μ L EGFR antibody and 40 μ L PBS) (Clone: H-11, DAKO) at 37 °C for 60 min in a humidified chamber. After being washed thrice in PBS, signal conversion was carried out with the LSAB2 system (DAKO) as described in the manual. Hematoxylin co-staining was done.

Counting

Known immunohistochemically-positive tissue sections were used as positive controls, and negative control sections were processed immunohistochemically after the primary antibody was replaced by PBS. None of these control sections exhibited immunoreactivity.

Axially, at least 800 (mainly 1 000) crypt epithelial cells within well-oriented crypts were counted in each sample under light microscope (40X objective). The labelling index (LI) was defined as a percentage of the positive nuclei over the total nuclei counted. The evaluation of staining intensity (i.e. number of positive cells) for PCNA, TUNEL, p53 and EGFR was performed by two investigators independently, without knowledge of the histology and the results of the other investigator. There was less than 5 % variance between the results of two counts.

SIMA, LIMA immunohistochemistry

The four micron thick tissue sections were dewaxed and rehydrated, reacted with anti-SIMA and -LIMA mAbs, stained by indirect immunoperoxidase methods, and counterstained with hematoxylin, including appropriate controls. The deparaffinized sections were blocked with 5% BSA (diluted in PBS) for 5 min, drained and incubated with the diluted mouse antibodies for 20 min. After two 5-min washings with PBS, the sections were covered with horseradish-peroxidase-labelled rabbit anti-mouse immunoglobulin (Serotec, UK), then washed twice for 5 min with PBS. Sections from all blocks were also stained with hematoxylin-eosin (H&E) for 2-10 min.

The immunoperoxidase-stained slides were then viewed under a light microscope, and assessed under code, by two observers. Scores of 0-3 were assigned to intensity of reactivity (weak, 1; moderate, 2; strong, 3) and distribution (restricted, <25% positive, 1; patchy, 25-75%, 2; and diffuse, >75%, 3) for each of the antibodies, in serial sections of specimens.

Statistical analysis

Statistical analysis with one-way ANOVA, LSD test and

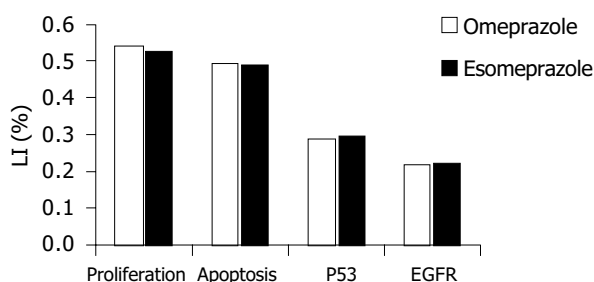


Figure 1 No difference between the effects of omeprazole and esomeprazole on cell turnover of gastric mucosa.

correlation analysis were performed by the Statistica for Windows 4.3 program package. $P < 0.05$ was considered statistically significant.

RESULTS

Proliferation index, apoptosis, p53- and EGFR expression prior to and after 6 mo of omeprazole or esomeprazole therapy are shown in Tables 1 and 2, respectively.

Table 1 Effect of long-term omeprazole therapy on gastric epithelial cell kinetics (mean \pm SD)

Endoscopy (mo)	Omeprazole (n = 14)	
	0	6
Proliferation index (%)	40.9 \pm 13.8	54.1 \pm 16.6
Apoptosis (%)	45.3 \pm 8.7	49.5 \pm 10.3
P53 (%)	28.7 \pm 4.3	28.9 \pm 12.7
EGFR (%)	17.6 \pm 11.9	21.9 \pm 7.9

Table 2 Effect of long-term esomeprazole therapy on gastric epithelial cell kinetics (mean \pm SD)

Endoscopy (mo)	Esomeprazole (n = 12)	
	0	6
Proliferation index (%)	39.6 \pm 8.7	52.8 \pm 10.4
Apoptosis (%)	43.5 \pm 9.8	48.9 \pm 9.8
P53 (%)	29.2 \pm 10.7	29.6 \pm 11.5
EGFR (%)	16.8 \pm 8.1	22.3 \pm 8.1

There was no difference between the effects of omeprazole and esomeprazole therapy on gastric epithelial cell kinetics (Figure 1). There was no statistically significant difference in any of the investigated parameters between the samples taken at the beginning and those taken after 6 mo of PPI treatment. Cell parameters were not significantly affected by age and sex (data not shown).

Although there was a trend towards increase of cell proliferation and EGFR expression in both omeprazole- and esomeprazole-treated groups, the difference was not statistically significant.

We found alterations only in the localization of immunohistochemical staining density prior to and after PPI therapy.

In a non-affected normal gastric mucosa, the greatest density of PCNA positive cells was found in the neck cell compartment (Figure 2). The greatest increment in cell

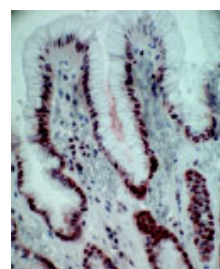


Figure 2 Greatest density of PCNA positive cells (brown colored cells) found in neck cell compartment of non-affected gastric mucosa (400x magnification).

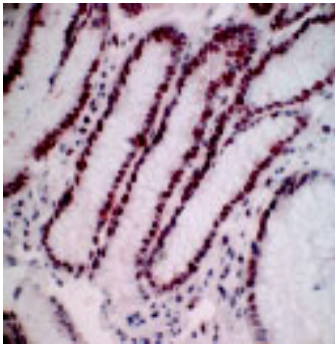


Figure 3 Greatest increase in PCNA positive cells (brown colored cells) observed in gland compartment of gastric mucosa after PPI therapy (400x magnification).

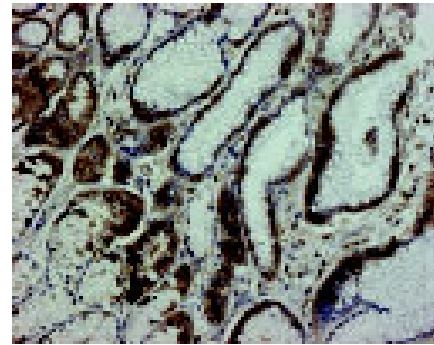


Figure 4 Positive EGFR immunoreactivity (brown color) in parietal cells and mucous neck cells of fundic glands (200x magnification).

proliferation in response to PPI therapy, occurred in the gland compartment of the gastric mucosa. The increase was limited to the deepest portions of the crypts (Figure 3). In both, prior to and after PPI administration, parietal cells did not express PCNA.

In a non-affected normal gastric mucosa, positive EGFR immunoreactivity was observed in parietal cells and mucous neck cells of the gastric fundic glands. EGFR was localized to the basolateral cell membrane, but not to the apical luminal membrane (Figure 4). After PPI administration, a strong positive EGFR immunoreactivity was observed at the basolateral membrane, in cytoplasm and supranuclear area of mucosal cells (Figure 5A). Positive EGFR expression was also found in some parietal cells (in cytoplasm and plasma membrane), but it was generally weaker compared to the neck cells (Figure 5B).

No dysplasia was observed after 6 mo of follow-up in any of the patients receiving either omeprazole or esomeprazole therapy.

DISCUSSION

Maintaining cell turnover is a key feature in organs with high metabolism such as the gastric mucosa. Higher cell turnover may lead to tumor formation while the suppressed state results in ulcer development^[4].

Omeprazole-induced potent acid suppression may lead to sustained and profound hypochlorhydria, which is often associated with hypergastrinemia^[16]. In majority of animal studies, it has been shown that long-term omeprazole

treatment reversibly increases epithelial cell proliferation and suppresses its differentiation^[2,3]. In other studies, however, neither cell proliferation is higher^[17,18], nor increased gastrinoma or other tumor formation is observed during long-term PPI treatment^[19]. Additional data suggest that gastrin enhances growth of normal and malignant colonic cells *in vitro* and may be linked to the development of colorectal cancer^[20-24]. On the other hand, animal and clinical studies do not support the role of omeprazole-induced hypergastrinemia in gastro-intestinal neoplasia development^[25,26] and no increased incidence of colon cancer has been found in patients with either pernicious anemia or gastrinomas^[27-29].

The risk of hypergastrinemia induced by long-term PPI therapy is still ambiguous and of concern to many clinicians.

This study analyzed the gastric epithelial cell kinetics in patients with gastro-esophageal reflux disease during long-term PPI treatment using immunohistochemical techniques. We investigated the effect of two different proton pump inhibitors: omeprazole and esomeprazole.

Although esomeprazole has a higher bio-availability than omeprazole and provides more pronounced inhibition of acid secretion compared to all other clinically available proton pump inhibitors, we found no difference between these drugs in terms of their effects on the gastric epithelium.

Our results confirmed the previous observations^[17,18] that cell proliferation is not significantly altered during long-term PPI therapy. Although there was a trend towards increase of both cell proliferation and EGFR expression, the difference was not statistically significant. Previous studies

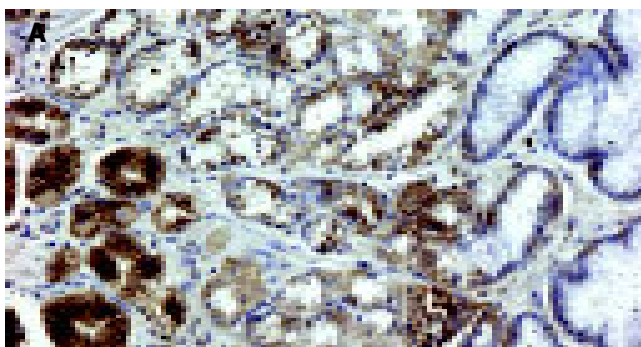


Figure 5 EGFR immunostaining (A) and immunoreactivity (B) after PPI therapy

(200x magnification).

have indicated that PCNA positive cells are nearly always positive for EGFR^[10]. The accompanied increase of EGFR expression to a higher PCNA activity in this study has therefore been expected.

The fact that the trend towards increase in gastric cell proliferation and EGFR expression is not accompanied with a parallel increase in apoptosis and p53 expression also supports the conclusion that there is no significant change in cell turnover during chronic administration of any PPI. No dysplasia or neoplasia was observed in any of the samples obtained during this study.

In the present study, in a non-affected normal gastric mucosa, positive EGFR immunoreactivity was identified in the mucous neck cells and parietal cells of the fundic glands, and the staining was localized only on the basolateral cell membrane, which is in agreement with previous studies^[3,11].

Gray *et al.*^[3], suggested that the greatest increment in cell proliferation in response to the increased gastrin drive occurs in the gland compartment of gastric mucosa. Our findings have confirmed their observations. After long-term PPI administration, we observed the greatest increase in PCNA positive cells mainly in the gland compartment. Although there is a proportionally greater increase in proliferation in the gland compartment compared to that in the mucous neck cell compartment, the neck cell compartment remains the main source of new cell formation.

Several studies have shown an intense EGFR expression during ulcer healing^[10,11]. In our study, after administration of PPI a strong positive EGFR immunoreactivity was observed predominantly in some mucous neck cells of the proliferative zone compared to the weaker staining density in parietal cells. The EGFR immunoreactivity was localized not only on the basolateral membrane of these cells, but also appeared in cytoplasm and supranuclear area.

EGFR is a good immunohistochemical marker for the detection of altered gastric epithelial cell function. The presence of EGFR on cells of the proliferative zone clearly indicates that they are the targets for the proliferation-stimulating action of EGF.

Parietal cells express EGFR but not PCNA. Presence of EGFR in the parietal cells is not associated with cell proliferation, but is consistent with a potent inhibitory action of EGF on gastric acid secretion.

We demonstrated that long-term PPI treatment did not significantly increase gastric epithelial cell proliferation and EGFR expression and had no effect on apoptosis and p53 expression. We found alterations only in the localization of immunohistochemical staining density during chronic PPI administration.

Our results have confirmed the previous observations that cell proliferation is not significantly altered during long-term PPI therapy. In addition no alterations in cellular response and no disturbance in the balance between cell proliferation and apoptosis are found, the maintenance of gastro-intestinal hemostasis is ensured and there is no risk for progression of hyperplasia to dysplasia in patients during chronic PPI administration.

These data suggest that 6-mo treatment with proton pump inhibitors is not associated with cell proliferation abnormalities of the gastric antral mucosa, which is a further

argument for the safety of PPIs.

REFERENCES

- 1 **Iijima K**, Sekine H, Koike T, Imatani A, Ohara S, Shimosegawa T. Long-term effect of *Helicobacter pylori* eradication on the reversibility of acid secretion in profound hypochlorhydria. *Aliment Pharmacol Ther* 2004; **19**: 1181-1188
- 2 **Takei N**, Ichinose M, Tatematsu M, Shimizu M, Oka M, Yahagi N, Matsushima M, Kurokawa K, Yonezawa S, Furihata C. Effects of long-term omeprazole treatment on adult rat gastric mucosa-enhancement of the epithelial cell proliferation and suppression of its differentiation. *Biochem Biophys Res Commun* 1995; **214**: 861-868
- 3 **Gray MR**, Darnton SJ, Hunt JA, Irlam RW, Nemeth J, Wallace HM. Accelerated gastric epithelial proliferation. *Gut* 1995; **36**: 522-527
- 4 **Que FG**, Gores GJ. Cell death by apoptosis: basic concepts and disease relevance for the gastroenterologist. *Gastroenterology* 1996; **110**: 1238-1243
- 5 **Yoshimura T**, Shimoyama T, Tanaka M, Sasaki Y, Fukuda S, Munakata A. Gastric mucosal inflammation and epithelial cell turnover are associated with gastric cancer in patients with *Helicobacter pylori* infection. *J Clin Pathol* 2000; **53**: 532-536
- 6 **Labat-Moleur F**, Guillermet C, Lorimier P, Robert C, Lantuejoul S, Brambilla E, Negoescu A. TUNEL apoptotic cell detection in tissue sections: critical evaluation and improvement critical evaluation and improvement. *J Histochem Cytochem* 1998; **46**: 327-334
- 7 **Sasano H**, Date F, Imatani A, Asaki S, Nagura H. Double immunostaining for c-erb-B2 and p53 in human stomach cancer cells. *Hum Pathol* 1993; **24**: 584-589
- 8 **Shiao YH**, Rugge M, Correa P, Lehmann HP, Scheer WD. p53 alterations in gastric precancerous lesions. *Am J Pathol* 1994; **144**: 511-517
- 9 **Playford RJ**, Boulton R, Ghatei MA, Bloom SR, Wright NA, Goodlad RA. Comparison of the effects of transforming growth factor-alpha and epidermal growth factor on gastrointestinal proliferation and hormone release. *Digestion* 1996; **57**: 362-367
- 10 **Abe S**, Sasano H, Katoh K, Ohara S, Arikawa T, Noguchi T, Asaki S, Yasui W, Tahara E, Nagura H, Toyota T. Immunohistochemical studies on EGF family growth factors in normal and ulcerated human gastric mucosa. *Dig Dis Sci* 1997; **42**: 1199-1209
- 11 **Tarnawski A**, Stachura J, Durbin T, Sarfeh IJ, Gergely H. Increased expression of epidermal growth factor receptor during gastric ulcer healing in rats. *Gastroenterology* 1992; **102**: 695-698
- 12 **Dixon MF**, Genta RM, Yardley JH, Correa P. Classification and grading of gastritis. The updated Sydney System. International Workshop on the Histopathology of Gastritis, Houston 1994. *Am J Surg Pathol* 1996; **20**: 1161-1181
- 13 **Unger Z**, Molnar B, Szaleczky E, Torgykes E, Muller F, Zagoni T, Tulassay Z, Pronai L. Effect of *Helicobacter pylori* infection and eradication on gastric epithelial cell proliferation and apoptosis. *J Physiol Paris* 2001; **95**: 355-360
- 14 **Ruzovics A**, Unger Z, Molnar B, Pronai L, Tulassay Z. Effect of *Helicobacter pylori* infection on epidermal growth factor receptor (EGFR) expression and cell proliferation of gastric epithelial mucosa: correlation to macroscopic and microscopic diagnosis. *Int J Exp Pathol* 2002; **83**: 257-263
- 15 **Fan XG**, Kelleher D, Fan XJ, Xia HX, Keeling PW. *Helicobacter pylori* increases proliferation of gastric epithelial cells. *Gut* 1996; **38**: 19-22
- 16 **Ligumsky M**, Lysy J, Siguencia G, Friedlander Y. Effect of long-term, continuous versus alternate-day omeprazole therapy on serum gastrin in patients treated for reflux esophagitis. *J Clin Gastroenterol* 2001; **33**: 32-35
- 17 **Biasco G**, Mordenti P, Brandi G, Paganelli GM, Santuci R, Miglioli M. Cell kinetics of the gastric mucosa of patients treated with omeprazole. *Am J Gastroenterol* 1996; **91**: 621-622
- 18 **Li H**, Helander HF. Parietal cell kinetics after administration

- of omeprazole and ranitidine in the rat. *Scand J Gastroenterol* 1995; **30**: 205-209
- 19 **Klinkenberg-Knol EC**, Nelis F, Dent J, Snel P, Mitchell B, Prichard P, Lloyd D, Havu N, Frame MH, Roman J, Walan A, Group LT. Long-term omeprazole treatment in resistant gastroesophageal reflux disease: efficacy, safety, and influence on gastric mucosa. *Gastroenterology* 2000; **118**: 661-669
- 20 **Sirinek KR**, Levine BA, Moyer MP. Pentagastrin stimulates *in vitro* growth of normal and malignant human colon epithelial cells. *Am J Surg* 1985; **149**: 35-39
- 21 **Smith JP**, Wood JG, Solomon TE. Elevated serum gastrin levels in patients with colon cancer or adenomatous polyps. *Dig Dis Sci* 1989; **34**: 171-174
- 22 **Seitz JF**, Giovannini M, Gouvernet J, Gauthier AP. Elevated serum gastrin levels in patients with colorectal neoplasia. *J Clin Gastroenterol* 1991; **13**: 541-545
- 23 **Chu M**, Nielsen FC, Franzen L, Rehfeld JF, Holst JJ, Borch K. Effect of endogenous hypergastrinemia on gastrin receptor expressing human colon carcinoma transplanted to athymic rats. *Gastroenterology* 1995; **109**: 1415-1420
- 24 **Renga M**, Brandi G, Paganelli GM, Calabrese C, Papa S, Tosti A, Tomassetti P, Miglioli M, Biasco G. Rectal cell proliferation and colon cancer risk in patients with hypergastrinemia. *Gut* 1997; **41**: 330-332
- 25 **Graffner H**, Singh G, Chaudry I, Milsom JW. Omeprazole-induced hypergastrinemia does not influence growth of colon carcinoma. *Dig Dis Sci* 1992; **37**: 485-489
- 26 **Pinson DM**, Havu N, Sztern MI, Mattsson H, Looney GA, Kimler BF, Hurwitz A. Drug-induced hypergastrinemia: absence of trophic effects on colonic carcinoma in rat. *Gastroenterology* 1995; **108**: 1068-1074
- 27 **Brinton LA**, Gridley G, Hrubec Z, Hoover R, Fraumeni JF Jr. Cancer risk following pernicious anemia. *Br J Can* 1989; **59**: 810-813
- 28 **Talley NJ**, Chute CG, Larson DE, Epstein R, Lydick EG, Melton LJ 3rd. Risk for colorectal adenocarcinoma in pernicious anemia. A population-based cohort study. *Ann Intern Med* 1989; **111**: 738-742
- 29 **Orbuch M**, Venzon DJ, Lubensky IA, Weber HC, Gibril F, Jensen RT. Prolonged hypergastrinemia does not increase the frequency of colonic neoplasia in patients with Zollinger-Ellison syndrome. *Dig Dis Sci* 1996; **41**: 604-613

Science Editor Wang XL Language Editor Elsevier HK

• BRIEF REPORTS •

Prevalence of porcine endogenous retrovirus in Chinese pig breeds and in patients treated with a porcine liver cell-based bioreactor

Qing Liu, Zheng Liu, Evangelos Dalakas

Qing Liu, Artificial Liver Treatment and Training Center, Beijing Youan Hospital, Capital University of Medical Sciences, Beijing 100054, China
Zheng Liu, Department of General Surgery, Shen Zheng Hospital, Peking University, Shenzheng 518036, Guangdong Province, China
Evangelos Dalakas, Department of Hepatology, Chancellor's Building, University of Edinburgh, Edinburgh EH16 4SB, Scotland, UK
Correspondence to: Dr. Qing Liu, Artificial Liver Treatment and Training Center, Beijing Youan Hospital, Beijing 100054, China. liuqing7@yahoo.com
Telephone: +86-10-63295285 Fax: +86-10-63295285
Received: 2004-06-28 Accepted: 2004-07-22

Abstract

AIM: To determine the prevalence of porcine endogenous retrovirus (PERV) in various pig breeds raised in China including Chinese experimental mini-pigs by PERV-reverse transcriptase (PERV-RT enzyme). Moreover, the potential for infection of PERV was investigated in patients treated with a bioreactor based on porcine liver cells ($n = 3$).

METHODS: Pig serum, liver and muscle cell-free supernatants were collected from various Chinese pig breeds. Porcine hepatocytes were isolated with a two-step perfusion method. Three patients with acute or chronic liver failure were treated with a bioartificial liver support system (BALSS) for 8-12 h and serum samples were collected from the patients before, immediately after and 30 d after treatment.

RESULTS: The activities of PERV-RT enzyme in pig liver and muscle cell-free supernatants were higher than in normal human controls. PERV-TR enzyme activity did not increase in patients before and after 1 mo of treatment. PERV-RT activities were not significantly different when compared with pre-treatment group (1.544 ± 0.155576), the post-treatment groups (1.501 ± 0.053507 , 1.461 ± 0.033808 and 1.6006667 ± 0.01963 for 0, 14 and 30 d post-treatment, respectively, $P > 0.05$), and normal control group (1.440 ± 1.0641 , $P > 0.05$). RT enzyme activity in Chinese experimental mini-pigs was higher than in normal human control group (1.440 ± 1.0641 U/mL, $P < 0.05$), and not significantly different ($P > 0.05$) when compared with the pig breeds except in the muscle supernatants. All the samples including muscle and liver cell supernatants from the Chinese mini-experimental pigs and the four domestic Chinese pig breeds contained PERVs.

CONCLUSION: These results suggest that the risk of PERV infection through BALSS containing porcine liver cells without immunosuppressants may be quite low. Although

there were PERVs in Chinese experimental mini-pigs and porcine liver cell culture suspensions, we did not find any evidence of persistent PERV infection in patients treated with this porcine hepatocyte-based bioartificial liver.

© 2005 The WJG Press and Elsevier Inc. All rights reserved.

Key words: Porcine endogenous retrovirus; Bioartificial liver support system; Porcine endogenous retrovirus-reverse transcriptase

Liu Q, Liu Z, Dalakas E. Prevalence of porcine endogenous retrovirus in Chinese pig breeds and in patients treated with a porcine liver cell-based bioreactor. *World J Gastroenterol* 2005; 11(30): 4727-4730
<http://www.wjgnet.com/1007-9327/11/4727.asp>

INTRODUCTION

Acute or chronic liver failure is still one of the most challenging clinical syndromes in modern medicine. Survival rate in patients with acute or chronic liver failure caused by hepatitis B virus (HBV) is less than 20%^[1]. Various non-biological approaches including plasma exchange, hemodialysis and hemofiltration have had limited success, presumably because of the role of the synthetic and metabolic functions of the liver that are inadequately replaced in these systems. The liver is an organ with an extensive regenerative potential and has a remarkable capacity to meet replacement demands of cellular loss^[2] If a system is designed to maintain normal liver functions for a bridging period until liver transplantation or liver recovery, then the survival rate of patients with acute liver failure (ALF) could be dramatically improved. Bioartificial liver support systems, which combine living cells of the liver in an extracorporeal circuit, have been successfully used in primary clinical trials and serve as a potent therapy and bridge to liver transplantation^[3]. The shortage of human organs to be used for bioreactors and the lack of safe and effective human liver cell lines have resulted in pigs becoming an important hepatic cell source. Primary porcine hepatocytes are most commonly used in devices undergoing pre-clinical and clinical evaluation. However, using these cells may be associated with the risk of transmission of PERVs^[4]. PERVs are present in the genome of all pigs and are able to infect human cells *in vitro*^[5]. However, the prevalence of PERV in Chinese pig breeds and whether PERVs infect patients who undergo bioartificial liver treatments based on Chinese experimental mini-pig liver

cells remains unclear. The objective of the study was to detect the prevalence of PERVs in the serum, liver and muscle cell-free supernatants of different pig breeds and in the serum of patients with acute or chronic liver failure, treated with a bioreactor based on porcine liver cells

MATERIALS AND METHODS

Samples collection and treatment

Pig liver and muscle cell-free supernatant collection

Muscle and liver samples (20 g) were collected from three Chinese experimental mini-pigs (the Institute of Experimental Animals, Beijing Agriculture University, China), weighing 10-15 kg each and from four domestic Chinese pigs of different breeds (Taihu pig, Wuzhishan pig, Dabai pig and Dahei pig-Beijing pig market), weighing approximately 60 kg each. The samples were taken and ground, pulverized with an SPS-3 Ultrasonic Pulverizer (working frequency 23 kHz; pulse 50% for 5 min). The pulverized samples were collected and centrifuged for 3 min at 80 r/min at room temperature. The cell-free supernatant was collected and resuspended in a solution provided by the C-type RT activity kit (Cavidi Tech AB, Uppsala, Sweden). The solution was then incubated for 30 min at room temperature and stored at -70 °C until used.

Serum samples collection Serum samples (1.5 mL) were collected from domestic Chinese pigs ($n = 4$) and Chinese experimental mini-pigs ($n = 3$). Human serum samples (1.5 mL) were collected from normal adult controls ($n = 4$) and from patients ($n = 3$) undergoing bioartificial liver treatments with samples taken at pre-treatment, d 0, 14 and 30 post-treatment. All serum samples were stored at -70 °C until used.

Liver cell isolation

Pig hepatocytes were harvested from three Chinese experimental mini-pigs using a two-step *in situ* collagenase perfusion technique that was modified from the original method developed by Aiken^[6]. The pig was initially anesthetized with ketamine (40 mg/kg). The liver was first perfused *in vivo* with oxygenated perfusion solution I (143 mmol/L sodium chloride, 6.7 mmol/L potassium chloride, 10 mmol/L Hepes, and 1 g/L EDTA, pH 7.4) at 300 mL/min for 20-40 min. The liver was then perfused *ex vivo* at 300 mL/min with oxygenated perfusion solution II (100 mmol/L Hepes, 67 mmol/L sodium chloride, 6.7 mmol/L potassium chloride, 4.8 mmol/L calcium chloride, 10 mL/L bovine albumin, and 1 g/L collagenase-D (Sigma), pH 7.6). Once the liver was visually dissolved (after 20-30 min), it was broken and irrigated with cold William's E medium (Gibco) supplemented with 15 mmol/L Hepes, 0.2 U/mL insulin, 2 mmol/L L-glutamine (Gibco), 100 U/mL penicillin, and 100 mg/mL streptomycin. The released cells were filtered through nylon mesh with 100- μ m openings and washed via three centrifugations (50 r/min) and resuspended in William's E medium. Viability for the harvests as determined using trypan blue exclusion ranged from 90% to 95%.

Patients

Three patients (2 males, 1 female, age 32-54) suffering from

acute on chronic liver failure were recruited into the study. Informed consent was obtained from all the patients or their relatives and approved by the Beijing Youan Hospital Ethics Committee. All the patients involved in the study were treated with HBL (*Cell Biotech Bioartificial Liver BIOLIV A3 device*) in our center from March 2000 to June 2001. The criteria^[7] for acute or chronic liver failure are as follows: (1) Evidence of chronic liver disease (chronic hepatitis and cirrhosis; cutaneous features of chronic liver disease; investigations demonstrating splenomegaly and hypoalbuminemia; evidence of chronic hepatitis/cirrhosis; chronic HBV carrier status by liver biopsy; chronic HBV/HCV overlapping with HAV, HDV, HEV or other viral infection). (2) All of the following: Prolonged prothrombin time and PTA < 40%, bilirubin rise > 17.1 μ mol/L per day or total bilirubin > 171 μ mol/L, Grade III/IV hepatic encephalopathy and ascites alone, or both simultaneously.

PERV-RT activity

Liver and muscle cell-free supernatants and serum samples filtered through membranes (0.45- μ m pore size) were analyzed for RT activity using the C-type RT activity assay (Cavidi Tech AB, Uppsala, Sweden) according to the instructions of the manufacturer (protocol B). One hundred and sixty microliters of sample dilution buffer was added to all wells of 96-well microtiter plate. Then 40 μ L of various samples was added to wells. A series of MuLV RT standard dilutions served as the positive controls, with normal human serum and sample dilutions as the negative controls. The PolyA Plate was sealed with adhesive tape. The plate was incubated at 33 °C for 3 h for the first plate and overnight for the second plate on an orbital shaker set at gentle agitation. The PolyA Plate was washed according to the protocol. Residual fluid in the wells was removed by tapping the plate upside down on absorbing cloth or paper. Two hundred microliters of AP substrate solution was added to each well of the PolyA plate and incubated at room temperature under dark cover on an orbital shaker set at gentle agitation. The filter of the plate reader was set at 405 nm. The absorbance of every well in the plate was read.

Statistical analysis

Data were expressed as the mean \pm SD. An unpaired Student's *t* test was used to compare mean between two groups and ANOVA was used for multiple comparisons. $P < 0.05$ was considered significant.

RESULTS

Yield and survival rate of porcine hepatocytes

Freshly isolated porcine hepatocytes were assessed for viability and function by trypan blue dye exclusion. The yield of cells was 5×10^9 cells/liver and cell viability was (95 \pm 5)%. During HBL treatment, porcine hepatocyte viability was monitored every 30 min and viability was maintained at 80%.

Enzymatic activity of PERV-RT

Standard curve and regression analysis The regression line was calculated with the use of SPSS10.0 software. A

Table 1 PERV-RT activities of patient's sera and Chinese experimental mini-pig tissues (U/mL)

	Pre-treatment	0 d after treatment	14 d after treatment	30 d after treatment
Patient 1	1.366	1.540	1.500	1.612
Patient 2	1.612	1.440	1.440	1.612
Patient 3	1.654	1.523	1.443	1.578
Mean±SD	1.544±0.155576 ¹	1.501±0.053507 ¹	1.461±0.033808 ¹	1.6006667±0.01963 ¹
Normal control (Mean±SD)	1.441±0.10 ²	1.451667±0.119801 ²	1.525667±0.085031 ²	1.468333±0.085031 ²

¹PERVs-RT activities before treatment were not significantly different when compared with post-treatment; ²normal control groups ($P>0.05$).

strong correlation was found between absorbance (A_{405}) and the various concentrations of MuLV RT standard dilution (Figure 1). The regression equation was obtained as follows: $Y = 0.098617 - 0.131297X$, the relative coefficient (r) was 0.95491, the regression coefficient comparison was done by an unpaired Student's t test ($t = 3.795$, $P < 0.0035$) and both the absorbance and concentrations of MuLV RT were linear. RT activity for wells giving an A_{405} within the linear measuring range of the reader was determined by taking the A values of the samples into the regression equation. The results of each sample's RT activity are shown in Tables 1 and 2.

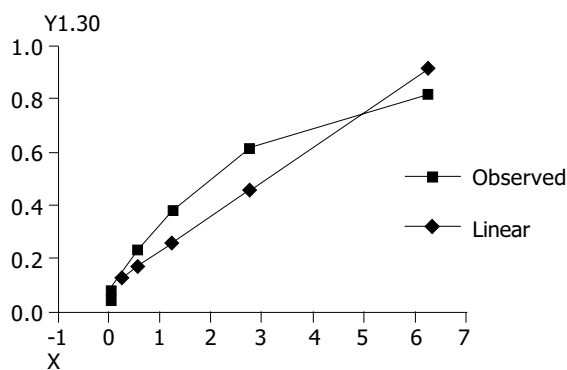


Figure 1 Correlation between absorbance of A_{405} (Y) and the various concentrations of MuLV RT standard dilution (X).

PERV-RT activities in patients' serum and Chinese experimental mini-pig tissues

Serum RT activities result from the three patients were: 1.544 ± 0.155576 pre-treatment, 1.501 ± 0.053507 at 0 d post-treatment, 1.461 ± 0.033808 at 14 d post-treatment and 1.6006667 ± 0.01963 at 30 d post-treatment. The difference of PERV-RT activities was not significant between the pre-treatment, post-treatment and normal control groups (Table 1). The patients treated for acute hepatic failure with a bioreactor based on porcine cells were shown to be free of PERV infections, with a follow-up period of 1 mo.

PERV-RT activities of pig tissues from Chinese experimental mini-pigs and domestic pig breeds

RT activities results from the Chinese experimental mini-pigs were 2.443333 ± 0.09609 U/mL in muscle cell-free supernatants, 2.256667 ± 0.188237 U/mL in liver cell-free supernatants and 2.503333 ± 0.032146 U/mL in serum, respectively. RT activities in the four domestic pig breeds were 3.645 ± 0.205 U/mL in muscle cell-free supernatants,

3.6375 ± 0.523983 U/mL in liver cell-free supernatants and 3.0425 ± 0.378979 U/mL in serum, respectively. Serum RT activity in the Chinese experimental mini-pigs was higher than in normal human control group 1.440 ± 1.0641 U/mL ($P < 0.05$), but not significantly different from the domestic pig breeds ($P > 0.05$). RT activity in the muscle cell-free supernatant in the Chinese experimental mini-pigs was higher than that of the domestic pig breeds ($P < 0.05$) (Table 2). All of the samples including muscle and liver cell-free supernatants from either the Chinese mini-experimental pigs or the four domestic Chinese pigs demonstrated high PERV-RT activity, implicating that PERVs not only existed in these tissues but was also actively replicating.

Table 2 PERV-RT activities of pig tissues of Chinese experimental mini-pig and domestic pig breeds (U/mL)

	Muscle supernatants	Liver supernatants	Serum
Chinese experimental mini-pig 1	2.34	2.04	2.49
Chinese experimental mini-pig 2	2.53	2.35	2.48
Chinese experimental mini-pig 3	2.46	2.38	2.54
mean±SD	2.443333±0.09609 ^a	2.256667±0.188237 ^a	2.503333±0.032146 ^a
Taihu pig	4.0	3.4	3.44
Wuzhishan pig	3.7	4.3	2.56
Dabai pig	3.49	3.08	2.95
Dahei pig	3.39	3.77	3.22
mean±SD	3.4950±1.43875	3.6375±0.523983	3.0425±0.378979
Human normal control	-	-	1.440±1.0641

^a $P < 0.05$ vs normal human control group.

DISCUSSION

According to the literature published from 1964 to 2000, a total of 270 patients worldwide with acute, sub-acute or chronic liver failure have been treated by 527 extracorporeal liver perfusions in 49 medical centers with livers from six different animal species, the pig being the most frequently used source^[8]. In addition, swine organs are amongst the most likely source species of xenografts for clinical use to date^[9-12]. The extracorporeal pig liver perfusion might provide the opportunity for a virus to evolve into a pathogen that can be transmitted from one individual to another efficiently enough to create a new epidemic disease. PERVs are a special risk, because they are part of the normal genetic material of mammalian cells except humans. Laboratory assays have been developed which target many aspects of the PERV replication/transmission cycle: PERV pro-viral DNA sequences, mRNA expression, RT activity, and the presence

of proteins, as well as the detection of anti-PERV immune responses^[13-15]. Among various assays, only enzymatic RT-activity is highly sensitive and specific for all PERV-A, PERV-B and PERV-C types, since RT is a generic marker of retroviruses. The presence of RT activity can be used to identify the presence of virus particles and, failure to detect it in these patient's sera points to the absence of any other, unrecognized retrovirus of porcine origin^[16].

This study showed that the RT activities from four domestic pig breeds were 2.445 U/mL in muscle cell-free supernatants, 2.508 U/mL in liver cell-free supernatants and 2.264 U/mL (range 2.048-2.387 U/mL) in serum respectively. All samples from the Chinese experimental mini-pigs and four domestic pig breeds contained PERVs that actively replicated in the tissues.

Breeding and keeping pigs under specific-pathogen-free or qualified-pathogen-free conditions is generally assumed to reduce the potential risk of transmitting exogenous viral, bacterial, fungal, and parasitic agents by xenotransplantation. Viral transmission, in a particular PERV is still a major obstacle, since PERVs are capable of infecting human cells *in vitro*. In a worse scenario, it is feared that PERV transmission to humans might be the starting point of a man-made pandemic threatening the health not only of BLASS patients, but also of the general public. A recent example of a rapid worldwide spread of an animal-borne disease was highlighted with the outbreak of severe acute respiratory syndrome (SARS), which spread in a matter of weeks from mainland China and Hong Kong to Vietnam, Singapore, Australia, Europe, and North America. This virus was the "common cold" virus of the Himalayan masked palm civet, an exotic species sold at live-animal markets in southern China where their meat is considered as a traditional delicacy. The transmission of SARS from animal to humans was traced back to civet chefs from Guangdong Province who contracted the disease, while handling infected meat.

The diameter of the 3A bioreactor membrane pore is about 200 nm and the diameter of PERV RNA is about 100 nm. Thus, it is quite possible for the PERV to pass through the bioreactor membrane. However, we did not find any evidence of infection with PERV in the patient's serum soon after treatment or within 1 mo of follow-up. Like all investigations published to date, in patients who have been treated with porcine cells, tissues and organs, there has been no evidence for PERV infection. Although the results are encouraging, it has to be stated that the human immune system through a variety of specific and non-specific mechanisms can clear PERV particles effectively. As humans do not express functional α 1, 3-galactosyl transferase, high titers of natural anti-gal-antibodies develop in their circulation because of continuous contact with gal- α 1, 3-gal bearing microorganisms. These pre-formed or natural antibodies also effectively neutralize the α -gal-bearing γ -retroviruses including PERV. Since PERVs are produced by pig cells that have gal- α 1, 3-gal-epitopes, they are sensitive to serum-mediated virolysis via the classical complement pathway *in vivo*. Thus, if immunosuppressed patients are treated with porcine liver cell bioreactor therapy then the potential risk of PERV infection will enhance. In this study the patient's sera were not in direct contact with the pig cells and the time of treatment was limited to only 8-10 h. Clearly, with an increase in the duration of

treatment by BLASS, the potential for PERV transmission will also increase. Therefore, it remains to be determined whether PERV transmission might occur in future trials and necessitates the continuation of strict monitoring regimens. The ability to monitor clinical trials closely using these assays will be of great benefit to the microbiological safety of clinical BLASS and xenotransplantation. This study sets one possible standard for laboratory surveillance of PERV infection after exposure to cellular xenografts from pigs.

REFERENCES

- 1 **Schioldt FV**, Davern TJ, Shakil AO, McGuire B, Samuel G, Lee WM. Viral hepatitis-related acute liver failure. *Am J Gastroenterol* 2003; **98**: 448-453
- 2 **Thorgeirsson SS**. Hepatic stem cells in liver regeneration. *FASEB J* 1996; **10**: 1249-1256
- 3 **Demetriou AA**, Brown RS Jr, Busuttill RW, Fair J, McGuire BM, Rosenthal P, Am Esch JS 2nd, Lerut J, Nyberg SL, Salizzoni M, Fagan EA, de Hemptinne B, Broelsch CE, Muraca M, Salmer JM, Metselaar HJ, Pratt D, De La Mata M, Mcchesney LP, Everson GT, Lavin PT, Stevens AC, Pitkin Z, Solomon BA. Prospective, randomized, multicenter, controlled trial of a bioartificial liver in treating acute liver failure. *Ann Surg* 2004; **239**: 660-670
- 4 **Irgang M**, Sauer IM, Karlas A, Zeilinger K, Gerlach JC, Kurth R, Neuhaus P, Denner J. Porcine endogenous retroviruses: no infection in patients treated with a bioreactor based on porcine liver cells. *J Clin Virol* 2003; **28**: 141-154
- 5 **Martin U**, Kiessig V, Blusch JH, Haverich A, von der Helm K, Herden T, Steinhoff G. Expression of pig endogenous retrovirus by primary porcine endothelial cells and infection of human cells. *Lancet* 1998; **352**: 692-694
- 6 **Aiken J**, Cima L, Schloo B, Mooney D, Johnson L, Langer R, Vacanti JP. Studies in rat liver perfusion for optimal harvest of hepatocytes. *J Pediatric Surg* 1990; **25**: 140-144
- 7 Chinese Association for liver diseases and for contagious and parasitic disease. Guideline of prevention and treatment of virus hepatitis. *Zhonghua Ganzangbing Zazhi* 2000; **6**: 324
- 8 **Pascher A**, Sauer IM, Hammer C, Gerlach JC, Neuhaus P. Extracorporeal liver perfusion as hepatic assist in acute liver failure: a review of world experience. *Xenotransplantation* 2002; **9**: 309-324
- 9 **MacKenzie DA**, Hullett DA, Sollinger HW. Xenogeneic transplantation of porcine islets: an overview. *Transplantation* 2003; **76**: 887-891
- 10 **Denner J**. Porcine endogenous retroviruses (PERVs) and xenotransplantation: screening for transmission in several clinical trials and in experimental models using non-human primates. *Ann Transplant* 2003; **8**: 39-48
- 11 **Magre S**, Takeuchi Y, Bartosch B. Xenotransplantation and pig endogenous retroviruses. *Rev Med Virol* 2003; **13**: 311-329
- 12 **Mollnes TE**, Fiane AE. Role of complement in xenotransplantation. *Allergy* 2002; **57**(Suppl 72): 75-78
- 13 **Kuddus R**, Patzer JF 2nd, Lopez R, Mazariegos GV, Meighen B, Kramer DJ, Rao AS. Clinical and laboratory evaluation of the safety of a bioartificial liver assist device for potential transmission of porcine endogenous retrovirus. *Transplantation* 2002; **73**: 420-429
- 14 **Switzer WM**, Shanmugam V, Chapman L, Heneine W. Polymerase chain reaction assays for the diagnosis of infection with the porcine endogenous retrovirus and the detection of pig cells in human and nonhuman recipients of pig xenografts. *Transplantation* 1999; **68**: 183-188
- 15 **Clemenceau B**, Jegou D, Martignat L, Sai P. Long-term follow-up failed to detect *in vitro* transmission of full-length porcine endogenous retroviruses from specific pathogen-free pig islets to human cells. *Diabetologia* 2001; **44**: 2044-2055
- 16 **Blusch JH**, Patience C, Martin U. Pig endogenous retroviruses and xenotransplantation. *Xenotransplantation* 2002; **9**: 242-251

Prevalence of advanced colonic polyps in asymptomatic Chinese

Hui-Hsiung Liu, Meng-Chen Wu, Yeh Peng, Ming-Shiang Wu

Hui-Hsiung Liu, Graduate Institute of Public Health, Taipei Medical University, Taipei, Taiwan, China

Meng-Chen Wu, Yeh Peng, Taipei Institute of Pathology, Taipei, Taiwan, China

Ming-Shiang Wu, Division of Gastroenterology, Department of Internal Medicine, National Taiwan University Hospital; Department of Primary Care medicine, School of Medicine, National Taiwan University, Taipei, Taiwan, China

Correspondence to: Dr. Ming-Shiang Wu, Department of Internal Medicine, National Taiwan University Hospital, No. 7, Chung San S. Road, Taipei, Taiwan, China. stanley@ha.mc.ntu.edu.tw

Telephone: +886-2-23123456-5410 Fax: +886-2-23947899

Received: 2004-03-09 Accepted: 2005-02-15

Chinese with advanced proximal polyps is not associated with any distal sentinel lesions. These data have implications for screening policy of colon cancers in Taiwanese Chinese.

© 2005 The WJG Press and Elsevier Inc. All rights reserved.

Key words: Colon polyp; Colonoscopy; Screening; Epidemiology

Liu HH, Wu MC, Peng Y, Wu MS. Prevalence of advanced colonic polyps in asymptomatic Chinese. *World J Gastroenterol* 2005; 11(30): 4731-4734

<http://www.wjgnet.com/1007-9327/11/4731.asp>

Abstract

AIM: To investigate the prevalence of advanced polyps in asymptomatic Chinese and to determine the risk of proximal advanced colonic polyps in subjects with and without polyps in the distal colon.

METHODS: Data were collected prospectively during colonoscopic examinations performed in 5 973 subjects as part of health evaluation at our unit from December 1997 to December 2003. Polyps were considered advanced, if they were larger than 10 mm or were tubovillous, villous or malignant. Proximal colon was defined as the splenic flexure and more proximal portions of the colon.

RESULTS: Colon polyps were detected in 971 (16.3%) subjects (613 males and 358 females) with their mean age being 56.6±10.7 years. Advanced polyps were noted in 199 (3.3%) individuals. Subjects were sub-classified according to the location of polyps into three groups: distal (569, 58.6%), proximal (284, 29.2%), and combined proximal and distal (118, 12.2%) groups. Subjects with advanced polyps in these three groups were 95 (9.8%), 56 (5.8%), and 48 (4.9%) respectively. In the 48 subjects with advanced combined polyps, 13 advanced polyps were distributed at the distal colon, 17 at the proximal colon, and 18 at both. Eighteen colon cancers including 12 at sigmoid and 6 at ascending colon were confirmed by final pathology. The relative risk for advanced proximal polyp according to distal findings was 3.1 (95%CI: 1.3-7.4) for hyperplastic polyp, 2.7 (95%CI: 1.4-5.3) for tubular polyp and 13.5 (95%CI: 5.1-35.4) for advanced polyp as compared to that for no polyp. However, 56 (28.2%) of 199 subjects with advanced polyps had no index polyps at the distal colon and might go undetected under sigmoidoscopic screening.

CONCLUSION: Although distal lesions can predict the risk of advanced proximal polyps, a substantial portion of

INTRODUCTION

Colorectal cancer (CRC) is an important health problem that carries high morbidity and mortality in the developed and Western countries^[1]. The majority of CRCs arise from pre-existing adenomas^[2]. This adenoma-adenocarcinoma sequence in colorectal carcinogenesis has provided an opportunity for screening asymptomatic individuals to prevent CRC. Indeed, accumulating evidence has indicated that the screening policy may greatly reduce the mortality and incidence of CRC^[3]. Currently, CRC screening is suggested for those with 50 years of age and above. Standard recommendations include annual testing for fecal occult blood and periodic sigmoidoscopy. Colonoscopy is generally reserved for patients with positive screening tests or those with a high average risk^[4].

Early detection and removal of potentially malignant polyps is the central element of CRC screening^[3]. In this respect, efforts to control and prevent CRC lie in the reliable detection and resection of advanced adenomas before they become malignant. Atkin *et al.*^[5], investigated the long-term risk of CRC after excision of recto-sigmoid adenomas and found that 88% of cancers develop in patients with high risk (namely villous, tubovillous histology, or >10 mm in diameter) recto-sigmoid adenomas. This study has led them to propose that a single examination with a sigmoidoscopy leading to full colonoscopy in patients with high risk recto-sigmoid adenomas is a cost effective and safe screening protocol^[6]. The UK flexible sigmoidoscopy screening trial further supports that population screening by sigmoidoscopy is a worthwhile screening tool^[7]. However, sigmoidoscopy is a sub-optimal approach for colon screening, and proximal adenomas without associated distal polyps may not benefit from early detection. The intrinsic risk of underdiagnosis by sigmoidoscopy has been illustrated by evidence of an increasing rightward trend of colon polyps and CRC^[8]. It was also reported that 46-52% of proximal advanced adenomas are not accompanied with distal polyps^[9,10]. Even

addition of fecal occult blood testing to sigmoidoscopy cannot significantly increase the detection of advanced neoplasia^[11]. Similar observations have also been reported from other countries^[12-15]. Therefore, another school of thought has advocated use of an ordinary colonoscope instead of a sigmoidoscope for screening^[16].

Racial differences in the anatomical distribution of colorectal neoplasia exist between Western and Oriental countries. Variations in prevalence of proximal adenomas could influence the choice of colonoscopy *vs* sigmoidoscopy for screening in different populations. It remains uncertain whether clinical findings from Western countries are applicable to Chinese. In Taiwan, CRC ranks the third leading cancer death and its incidence has increased rapidly due to westernization of lifestyle^[17]. The information regarding the prevalence of colorectal polyps in asymptomatic Chinese remains limited^[14,15]. Our unit has provided self-paid screening for CRC since December 1997^[18]. Taking this advantage, we performed a prospective study to investigate the prevalence of advanced polyps in asymptomatic subjects and to determine the risk of proximal advanced polyps in subjects with and without distal polyps.

MATERIALS AND METHODS

Since December 1997, our center has started to provide full colonoscopic service for all subjects who attended health checkup with a request for a colonoscopy. All colonoscopies were performed with Olympus Model CF200 or CF240 colonoscopes by experienced colonoscopists^[18]. Patients were prepared by oral administration of balanced electrolyte solution with polyethylene glycol on the day before the examination. All lesions identified were removed for histologic examination by either biopsy, polypectomy, or conventional surgery. The exact size of the polyp was determined immediately after polyp removal or by comparing the known width of opened biopsy forceps. The location and size of all polypoid lesions were recorded. The distal colon was defined as the rectum, sigmoid, and descending colon, whereas proximal colon was splenic flexure and more proximal portions of the colon. Polyps were considered advanced, if they were larger than 10 mm or were tubovillous, villous, or malignant.

The exclusion criteria included presence of colorectal symptoms, previous history of colorectal neoplasia, colonic surgery, inflammatory bowel disease, family history of colon cancer or first-degree relatives with related neoplasms of the breast, ovary or uterus, inability to give informed consent, and incomplete colonoscopic examinations. From December 1997 to December 2003, a total of 5 973 subjects who fulfilled the above criteria were enrolled for further analysis. Categorical data were analyzed by χ^2 test and relative risk of advanced proximal polyps was evaluated by logistic regression analysis.

RESULTS

Colonoscopy was successfully performed in the cecum in 5 973 subjects. The baseline characteristics of patients and colonoscopic findings are described in Table 1. Colon polyps were detected in 971 (16.3%) subjects (613 males and 358

females) with a mean age of 56.6 ± 10.7 years. Among them, 199 (3.3%) subjects had advanced polyps. The prevalence of colorectal polyps in relation to demographic parameters is listed in Table 2. The prevalence of polyps (682/3 317, 20.6% *vs* 289/2 656, 10.9%, $P < 0.01$) and advanced polyps (165/3 317, 3.0% *vs* 34/2 656, 1.3%, $P < 0.01$) was significantly higher in subjects older than 50 years as compared to those younger than 50 years. Overall, male subjects had a significantly higher prevalence of polyps (613/3 125, 19.6% *vs* 358/2 848, 12.6%, $P < 0.01$) and advanced polyps (124/3 125, 3.9% *vs* 75/2 848, 2.6%, $P < 0.01$) than female subjects. The 971 subjects with polyps were subclassified according to the location of polyps into distal (567, 58.6%), proximal (284, 29.2%) and combined proximal and distal (118, 12.2%) groups. Advanced polyps in these three groups were 95 (9.8%), 56 (5.8%), and 48 (4.9%), respectively. In the 48 subjects with advanced combined groups, 13 advanced polyps were distributed at the distal colon, 17 at the proximal colon, and 18 at both. Eighteen colon cancers including 12 at sigmoid and 6 at ascending colon were confirmed by final pathology. The relative risk for advanced proximal polyp according to distal findings was 3.1 (95%CI: 1.3-7.4) for hyperplastic polyp, 2.7 (95%CI: 1.4-5.3) for tubular polyp and 13.5 (95%CI: 5.1-35.4) for advanced polyps as compared to that for no polyp (Table 3).

Table 1 Baseline characteristics of patients and colonoscopic findings

Characteristics	Patients, n (%)
Gender	
Female	2 848 (47.7)
Male	3 125 (52.3)
Age (yr)	
40-49	2 656 (44.4)
50-59	1 903 (31.9)
60-69	942 (15.8)
≥ 70	472 (7.9)
Colonoscopic findings	
No polyp	5 002 (83.7)
Proximal polyp	284 (4.8)
Distal polyp	569 (9.5)
Combined	118 (2.0)

DISCUSSION

The reported prevalence of colonic polyps varies widely due to differences in structure of the studies and sensitivities of the test used to define prevalence^[19]. Referred and symptomatic patients cannot represent screening setting, but true incidence is difficult to calculate in symptom-free and unselected populations. It was estimated that 30% of the Western population have colonic polyps while a lower rate (10-15%) is noted in Asia and Africa^[16]. Cross-sectional studies indicate that 5-10% of asymptomatic subjects (50-75 years old) have advanced colonic neoplasia^[9,10]. Colonoscopy is the most sensitive imaging study for assessment of colonic polyps. Prior to our study, there were two studies dealing with the prevalence of colonic polyps in asymptomatic Chinese. Sung *et al.*^[14], enrolled 505 subjects older than 50 years through health exhibitions and documented

Table 2 Prevalence of colorectal polyps in relation to demographic parameters, *n* (%)

Age group (yr)	Male			Female		
	Total no. of cases	Polyps	Advanced polyps	Total no. of cases	Polyps	Advanced polyps
40-49	1 348	186 (13.8)	18 (1.3)	1 308	103 (7.9)	16 (1.2)
50-59	1 067	217 (20.3)	38 (3.6)	836	104 (12.4)	23 (2.8)
60-69	480	140 (29.2)	40 (8.3)	462	84 (18.2)	19 (4.1)
≥70	230	70 (30.4)	28 (12.2)	242	67 (27.7)	17 (7.0)
Total	3 125	613 (19.6)	124 (4.0)	2 848	358 (12.6)	75 (2.6)

Table 3 Prevalence of advanced proximal polyps according to distal findings

Distal finding	Total	Advanced proximal polyp	Relative risk
No polyp	5 286	56	1.0
Hyperplastic polyp	181	6	3.1 (1.3-7.4)
Tubular adenoma	380	11	2.7 (1.4-5.3)
Advanced adenoma	126	18	13.5 (5.1-35.4)

12.5% of advanced polyps in Hong Kong Chinese. In contrast, Cheng *et al.*^[15], detected only 1.3% of advanced polyps in Taiwanese Chinese. We found 16.3% of colonic polyps and 3.3% of advanced polyps respectively in 5 973 asymptomatic subjects older than 40 years. All these three studies were performed by colonoscopy, indicating that factors other than screening methods are responsible for the difference. The low prevalence in the later two studies may in part reflect the relatively large number of individuals younger than 50 years. In addition, inherent selection bias of enrolled subjects, geographic or dietary factors, and different incidence rates are among the plausible explanations but remain to be investigated by future studies.

Results from previous studies have shown that colonic polyps are more common in men than in women and increase in frequency with increasing age^[13,19]. In agreement with these observations, subjects ≥50 years old and males tend to have a higher prevalence of both colonic polyps and advanced adenoma. To our knowledge, none of the studies have addressed the prevalence of colonic polyps in asymptomatic Chinese younger than 50 years. Overall, in subjects aged ≥50 years, colonic polyps and advanced adenomas are present in 20.6% and 3.0%, respectively, whereas 10.9% and 1.3% are found in patients aged <50 years. Taken together, these studies support the notion that age and gender may also influence the prevalence of colonic polyps^[13,19]. Furthermore, our data suggest that in Chinese the optimal cut-off point of age for screening of average risk is similar to Western guideline because the incidence of colorectal polyps begins to rise above the age of 50 years^[4].

From the standpoint of screening accuracy, colonoscopy is the only reliable way for detection of all colorectal polyps. However, current guidelines recommend sigmoidoscopy as the first-line CRC screening in view of expense, complication and patient's acceptability^[4]. A crucial assumption underlying the practice of sigmoidoscopy is that, there exists an association between distal and proximal colonic neoplasia. Therefore, sigmoidoscopy may function as a gatekeeper and colonoscopy could be reserved for individuals with index polyps at the distal colon. Two recent systematic reviews

support this notion and point out that distal polyps, irrespective of size or histology, are associated with an increased prevalence of synchronous proximal neoplasia^[20,21]. In keeping with these observations, our results have demonstrated that distal hyperplastic, tubular, and advanced polyps are associated with 3- to 13-fold risk of synchronous, proximal advanced polyp.

Although distal colonic polyps can predict the risk of advanced proximal lesion, a clean rectum and sigmoid colon cannot guarantee any significant adenomas in the proximal colon. The proximal colon is not routinely examined when an index lesion is not detected in sigmoidoscopy. Consequently, the proportion of patients with adenoma in the proximal colon but without distal colonic neoplasia may influence the effectiveness of screening sigmoidoscopy^[20,21]. The issue is becoming increasingly important, since several reports have revealed a rightward shift of CRC^[8]. Moreover, available data from recent colonoscopic screening indicate that 46-52% of proximal advanced adenomas are not accompanied with distal polyps^[9,10]. In the present study, we found 199 subjects had advanced polyps and 56 (28.1%) were isolated proximal lesions. Taken together, these findings implicate that a substantial portion of individuals with proximal neoplasia will go undetected by screening sigmoidoscopy and are at increased risk of cancer.

In summary, this study provides data on the background prevalence of colonic polyps in asymptomatic Chinese aged ≥40 years. The varied prevalence as compared to previous studies may be explained by variation of screening methods, selection criteria of enrolled subjects and different etiologic factors. About 30% of advanced proximal polyps are not associated with sentinel lesions, and might be missed by screening sigmoidoscopy. For the motivated individuals older than 50 years, whole colon screening by colonoscopy will detect more proximal lesions and give the greatest reassurance. The cost-effectiveness of colonoscopy needs to be evaluated further in future studies.

REFERENCES

- 1 Landis SH, Murray T, Bolden S, Wingo PA. Cancer statistics 1998. *CA Cancer J Clin* 1998; **48**: 6-30
- 2 Bond JH. Clinical evidence for the adenoma-carcinoma sequence, and the management of patients with colorectal adenomas. *Semin Gastrointest Dis* 2000; **11**: 176-184
- 3 Winawer S, Zauber A, O'Brien M, Ho M, Gottlieb L, Sternberg S. Prevention of colorectal cancer by colonoscopic polypectomy. *N Engl J Med* 1993; **329**: 1977-1981
- 4 Smith RA, Cokkinides V, Eyre HJ. American cancer society guidelines for the early detection of cancer, 2003. *CA Cancer J Clin* 2003; **53**: 27-43
- 5 Atkin WS, Morson BC, Cuzick J. Long-term risk of colorectal

- cancer after excision of rectosigmoid adenomas. *N Engl J Med* 1992; **326**: 658-662
- 6 **Atkin WS**, Cuzick J, Northover JM, Whynes DK. Prevention of colorectal cancer by once-only sigmoidoscopy. *Lancet* 1993; **341**: 736-740
- 7 Single flexible sigmoidoscopy screening to prevent colorectal cancer: baseline findings of a UK multicenter randomized trial. *Lancet* 2002; **359**: 1291-1300
- 8 **Cucino C**, Buchner AM, Sonnenberg A. Continued rightward shift of colorectal cancer. *Dis Colon Rectum* 2002; **45**: 1035-1040
- 9 **Lieberman DA**, Weiss DG, Bond JH, Ahren DJ, Garewal H, Chejfec G. Use of colonoscopy to screen asymptomatic adults for colorectal cancer. *N Engl J Med* 2000; **343**: 162-168
- 10 **Imperiale TF**, Wagner DR, Lin CY, Larkin G, Rogge JD, Ransohoff DF. Risk of advanced proximal neoplasms in asymptomatic adults according to the distal colorectal findings. *N Engl J Med* 2000; **343**: 169-174
- 11 **Lieberman DA**, Weiss DG. One-time screening for colorectal cancer with combined fecal occult-blood testing and examination of the distal colon. *N Engl J Med* 2001; **345**: 555-560
- 12 **Gondal G**, Grotmol T, Hofstad B, Bretthauer M, Eide TJ, Hoff G. Grading of distal colorectal adenomas as predictors for proximal colonic neoplasia and choice of endoscopy in population screening: experience from the Norwegian Colorectal Cancer Prevention Study. *Gut* 2003; **52**: 398-403
- 13 **Betes M**, Munoz-Navas MA, Duque JM, Angos R, Macias E, Subtil JC, Herraiz M, De La Riva S, Delgado-Rodriguez M, Martinez-Gonzalez MA. Use of colonoscopy as a primary screening test for colorectal cancer in average risk people. *Am J Gastroenterol* 2003; **98**: 2648-2654
- 14 **Sung JJ**, Chan FK, Leung WK, Wu JC, Lau JY, Ching J, To KF, Lee YT, Luk YW, Kung NN, Kwok SP, Li MK, Chung SC. Screening for colorectal cancer in Chinese: comparison of fecal occult blood test, flexible sigmoidoscopy, and colonoscopy. *Gastroenterology* 2003; **124**: 608-614
- 15 **Cheng TI**, Wong JM, Hong CF, Cheng SH, Cheng JT, Shieh MJ, Lin YM, Tso CY, Huang AT. Colorectal cancer screening in asymptomatic adults: comparison of colonoscopy, sigmoidoscopy and fecal occult blood test. *J Formos Med Assoc* 2002; **101**: 685-690
- 16 **Rex DK**, Lieberman DA. Feasibility of colonoscopy screening: discussion of issues and recommendations regarding implementation. *Gastrointest Endosc* 2001; **54**: 662-667
- 17 **Chen CJ**, You SL, Lin LH, Hsu WL, Yang YW. Cancer epidemiology and control in Taiwan: a brief review. *Jpn J Clin Oncol* 2002; **32**(Suppl 1): 66-81
- 18 **Liu HH**, Kudo SE, Juch JP. Pit pattern analysis by magnifying chromoendoscopy for the diagnosis of colorectal polyps. *J Formos Med Assoc* 2003; **102**: 178-182
- 19 **Johnson DA**, Gurney MS, Volpe RJ, Jones DM, VanNess MM, Chobanian SJ, Avalos JC, Buck JL, Kooyman G, Cattau EL Jr. A prospective study of the prevalence of colonic neoplasms in asymptomatic patients with an age-related risk. *Am J Gastroenterol* 1990; **85**: 969-974
- 20 **Dave S**, Hui S, Kroenke K, Imperiale TF. Is the distal hyperplastic polyps a marker for proximal neoplasia? A systematic review. *J Gen Intern Med* 2003; **18**: 128-137
- 21 **Lewis JD**, Ng K, Hung KE, Bilker WB, Berlin JA, Brensinger C, Rustgi AK. Detection of proximal adenomatous polyps with screening sigmoidoscopy: a systemic review and meta-analysis of screening colonoscopy. *Arch Intern Med* 2003; **163**: 413-420

Science Editor Wang XL Language Editor Elsevier HK

Effect of ligand of peroxisome proliferator-activated receptor γ on the biological characters of hepatic stellate cells

Yan-Tong Guo, Xi-Sheng Leng, Tao Li, Ji-Run Peng, Sheng-Han Song, Liang-Fa Xiong, Zhi-Zhong Qin

Yan-Tong Guo, Xi-Sheng Leng, Tao Li, Ji-Run Peng, Sheng-Han Song, Liang-Fa Xiong, Zhi-Zhong Qin, Department of General Surgery, Peking University People's Hospital, Beijing 100044, China
Supported by the National Natural Science Foundation of China, No. 30371387

Correspondence to: Professor Xi-Sheng Leng, Department of General Surgery, Peking University People's Hospital, Beijing 100044, China. lengxs2003@yahoo.com.cn

Telephone: +86-10-68792703

Received: 2004-05-29 Accepted: 2004-06-24

Abstract

AIM: To study the effect of rosiglitazone, which is a ligand of peroxisome proliferator-activated receptor gamma (PPAR γ), on the expression of PPAR γ in hepatic stellate cells (HSCs) and on the biological characteristics of HSCs.

METHODS: The activated HSCs were divided into three groups: control group, 3 μ mol/L rosiglitazone group, and 10 μ mol/L rosiglitazone group. The expression of PPAR γ , α -smooth muscle actin (α -SMA), and type I and III collagen was detected by RT-PCR, Western blot and immunocytochemical staining, respectively. Cell proliferation was determined with methylthiazolyltetrazolium (MTT) colorimetric assay. Cell apoptosis was demonstrated with flow cytometry.

RESULTS: The expression of PPAR γ at mRNA and protein level markedly increased in HSCs of 10 μ mol/L rosiglitazone group (t value was 10.870 and 4.627 respectively, $P < 0.01$ in both). The proliferation of HSCs in 10 μ mol/L rosiglitazone group decreased significantly ($t = 5.542$, $P < 0.01$), α -SMA expression level and type I collagen synthesis ability were also reduced vs controls (t value = 10.256 and 14.627 respectively, $P < 0.01$ in both). The apoptotic rate of HSCs significantly increased in 10 μ mol/L rosiglitazone group vs control ($\chi^2 = 16.682$, $P < 0.01$).

CONCLUSION: By increasing expression of PPAR γ in activated HSCs, rosiglitazone, an agonist of PPAR γ , decreases α -SMA expression and type I collagen synthesis, inhibits cell proliferation, and induces cell apoptosis.

© 2005 The WJG Press and Elsevier Inc. All rights reserved.

Key words: Peroxisome proliferator-activated receptor gamma; Hepatic stellate cell; Rosiglitazone

Guo YT, Leng XS, LI T, Peng JR, Song SH, Xiong LF, Qin

ZZ. Effect of ligand of peroxisome proliferator-activated receptor γ on the biological characters of hepatic stellate cells. *World J Gastroenterol* 2005; 11(30): 4735-4739
<http://www.wjgnet.com/1007-9327/11/4735.asp>

INTRODUCTION

It is well established that hepatic fibrosis is the pathological basis on which chronic liver diseases further progress to hepatic cirrhosis^[1]. Multiple factors produce hepatic lesions, contributing to hepatic fibrosis^[2]. Studies show that reversing hepatic fibrosis may block the progression of hepatic cirrhosis^[3]. Hepatic stellate cell (HSC) is now well established as the key cellular element involved in the development of hepatic fibrosis^[4]. When the liver is attacked by pathogenic factors, HSCs, a pericyte-like mesenchymal liver cell population, transform from a "quiescent" status ("resting" HSC) into myofibroblast-like cells ("activated" HSC) with the latter synthesizing and secreting extracellular matrix (ECM), tissue inhibitor of matrix metalloproteinases and multiple cytokines, which contribute to collagen deposition, leading to fibrosis^[5-7]. Recently, it has been reported that resting HSC expresses peroxisome proliferator-activated receptor gamma (PPAR γ); the expression of PPAR γ gradually decreases during the course of activation of HSC cultured *in vitro*, indicating that certain expression level of PPAR γ may be a crucial element that inhibits the natural activation of HSC^[8-14]. The present study was designed to investigate whether activated HSCs (myofibroblast-like cells) treated by PPAR γ -specific ligands were able to enhance the expression of PPAR γ and its effect on HSC proliferation, collagen secretion, and cell apoptosis.

MATERIALS AND METHODS

HSCs of rats

HSCs of rats were obtained from HSC strain rHSC-99 produced by the Department of Hepatobiliary Surgery, Peking University People's Hospital and this strain had the characteristics of activated HSCs^[15].

Rosiglitazone

A high-affinity specific ligand of PPAR γ , was purchased from GlaxoSmithKline Investment Co., Ltd.

Experimental groups

Three groups were set up in the study, blank control group, 3 μ mol/L rosiglitazone, and 10 μ mol/L rosiglitazone groups, respectively.

Semi-quantitative RT-PCR detection of PPAR γ

The extraction and reverse transcription of RNA were performed according to the directions of the kits (Taq PCR MasterMix, TW-Biotech Co.); PPAR γ primer was synthesized by Shanghai Bioengineering Co., Ltd, with an upstream fragment of CCCTGGCAAAGCATTGTAT, a downstream fragment of ACTGGCACCCCTTGAAAAATG and an extension fragment of 222 bp. The internal reference β -actin was designed with an upstream fragment of TGGGACG-ATATGGAGAAGAT, a downstream fragment of ATTG-CCGATAGTGATGACCT and an extension fragment of 522 bp. PCR reaction is as follows. PPAR γ primers were added to reaction systems, which conditions were set at 95 °C for 5 min; 94 °C for 20 s, 55 °C for 30 s, 72 °C for 40 s, totally 29 cycles; finally at 72 °C for 5 min. The products of PCR were photographed after electrophoresis on 2% agarose gel and the gray scale values determined through image analysis. The sample quantities were adjusted to make the gray scale value in each β -actin group stay at a relatively identical level and then the gray scale values of PPAR γ between groups were compared.

Detection of PPAR β protein by western blot

In each electrophoresis lane, a sample of 30 μ g protein was added and after polyacrylamide gel electrophoresis at a volume fraction of 30%, the electrophoretic proteins were transferred onto nitrocellulose membranes, blocked with 5% fat-free milk in TBST buffer (20 mmol/L Tris-HCl, 137 mmol/L NaCl, and 0.05% Tween 20). The membranes were incubated with the first and second antibody, respectively. Antigen-antibody complexes were visualized using the enhanced chemiluminescence detection system according to the manufacturer's instructions (Santa Cruz Biotechnology, Inc.). Membranes were exposed to autoradiography, and signals were scanned for quantitation. Image analysis was done on the straps to determine the gray scale value. The expression quantity of PPAR γ by HSC in each group was expressed relative to that of the control group.

Detection of PPAR γ protein by immunocytochemistry method

After HSCs were cultured on the slides, they were fixed in neutralized 40 g/L formaldehyde, then detected with SP method (Santa Cruz Biotechnology, Inc.) and examined under a microscope. Those cells whose nuclei were brown were defined as positive.

Effect of rosiglitazone on HSC proliferation

Cells were incubated in a 96-well plate. The cells grew in DMEM culture medium containing a volume fraction of 16% calf serum until the logarithmic growth phase, and were then incubated for 24 h in DMEM culture medium that contained a volume fraction of 1% calf serum, which could stop the growth of cells. After that, cells were incubated in culture media respectively containing a volume fraction of 16% calf serum, as blank control group, and rosiglitazone groups of a final concentration of 3 and 10 μ mol/L. And the absorbance value of A570 was read on the microplate reader for each well using MTT colorimetric assay at 0, 24, and 48 h.

Effect of rosiglitazone on the synthesis of α -SMA of HSC, and collagen I and III

HSCs from control group, 3 μ mol/L rosiglitazone group and 10 μ mol/L rosiglitazone group were detected by Western blot and immunocytochemistry respectively.

Effect of rosiglitazone on HSCs apoptosis

The apoptotic index was determined by flow cytometry (Applied Biosystems). A total of 1×10^6 /mL cells in a suspension were fixed with precooled 70% ethanol solution and stained, and analyzed by a flow cytometer and the apoptotic index was determined by Multicycles software.

Statistical analysis

t-Test and χ^2 test were employed to analyze all the data concerned. $P < 0.05$ was taken as significant.

RESULTS

10 μ mol/L rosiglitazone enhanced the expression of HSC PPAR γ mRNA

At 3 μ mol/L of rosiglitazone, no significant difference was seen in the expression of PPAR γ mRNA in HSCs compared with the control group. There was a significant increase in the expression of PPAR γ mRNA in HSCs by 10 μ mol/L rosiglitazone compared with the control group ($t = 10.87$, $P < 0.01$, Figure 1). Meanwhile obvious expression of all β -actin was observed.

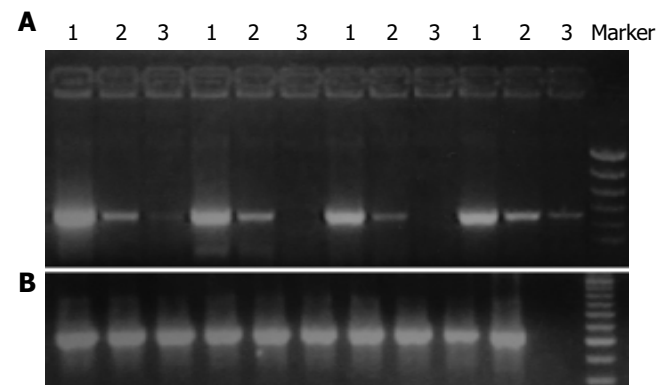


Figure 1 PPAR γ mRNA level. **A:** Expression of PPAR γ mRNA. Lane 1, 10 μ mol/L rosiglitazone group; lane 2, 3 μ mol/L rosiglitazone group; lane 3, control group; **B:** Expression of β -actin.

Western blot demonstrated that the expression of PPAR γ protein increased by 10 μ mol/L rosiglitazone

At 3 μ mol/L rosiglitazone, no significant difference was seen in the expression of PPAR γ protein in HSCs compared with control group. The expression of PPAR γ protein in HSCs by 10 μ mol/L rosiglitazone was significantly increased compared with that of the control group ($t = 4.627$, $P < 0.01$, Figure 2).

Immunocytochemistry demonstrated enhanced expression of PPAR γ protein in HSCs in 10 μ mol/L rosiglitazone group

In the blank control group and 3 μ mol/L rosiglitazone

group, no evident expression of PPAR γ protein was found by immunocytochemistry. In the 10 $\mu\text{mol/L}$ rosiglitazone group, there was a relatively increased expression of PPAR γ protein in the nucleus of most HSCs and in the cytoplasm of some HSCs (Figure 3A). The expression of PPAR γ protein seen in the cytoplasm in some of the HSCs might be proteins not entering into the cell nucleus, and the precursor of PPAR γ proteins in cytoplasm.

10 $\mu\text{mol/L}$ rosiglitazone markedly inhibited HSCs proliferation

There was no significant difference in the proliferation activity of HSCs between 3 $\mu\text{mol/L}$ rosiglitazone group and the control group. After a 24 and 48 h culture period, the proliferation activity of 10 $\mu\text{mol/L}$ rosiglitazone group was lower than that in both the control group (t value = 5.542 and 19.293, respectively, $P < 0.01$ in both) and the 3 $\mu\text{mol/L}$ rosiglitazone group (t value = 6.880 and 10.502 respectively, $P < 0.01$ in both, Table 1).

Table 1 Effect of rosiglitazone on proliferation of rHSC-99

Groups	0 h	24 h	48 h
Controls	0.21 \pm 0.041	0.62 \pm 0.088	1.00 \pm 0.045
3 $\mu\text{mol/L}$	0.22 \pm 0.038	0.63 \pm 0.060	0.93 \pm 0.049
10 $\mu\text{mol/L}$	0.22 \pm 0.064	0.33 \pm 0.085 ^b	0.49 \pm 0.060 ^b

^b $P < 0.01$ vs controls or 3 $\mu\text{mol/L}$ treatment group.

10 $\mu\text{mol/L}$ rosiglitazone decreased synthesis of α -SMA, collagen I in HSCs

Detection of synthesis of α -SMA, collagen I and III in HSCs by immunocytochemistry indicated that cytoplasmic

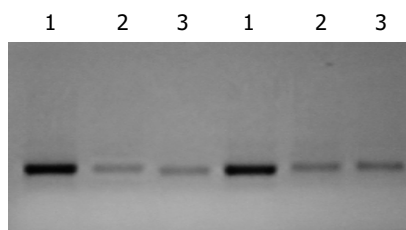


Figure 2 PPAR γ protein was assessed with Western blotting. Lane 1, 10 $\mu\text{mol/L}$ rosiglitazone group; lane 2, 3 $\mu\text{mol/L}$ rosiglitazone group; lane 3, control group.

staining of α -SMA and collagen I and III in both the blank control group and 3 $\mu\text{mol/L}$ rosiglitazone group was strongly positive. In 10 $\mu\text{mol/L}$ rosiglitazone group, the expression of α -SMA and collagen I decreased significantly while there was no distinct change in the expression of collagen III. Through gray-scale scanning analysis, the quantity of α -SMA and collagen I decreased 48% and 42%, respectively compared with the blank control group (t value = 10.256 and 14.627, respectively, $P < 0.01$ in both). Western blot detection of α -SMA showed that there was no significant difference between 3 $\mu\text{mol/L}$ rosiglitazone group and blank control group. The gray-scale value of α -SMA strap of 10 $\mu\text{mol/L}$ rosiglitazone group significantly decreased compared with the blank control group ($t = 4.627$, $P < 0.01$).

10 $\mu\text{mol/L}$ rosiglitazone accelerated HSC apoptosis

Flow cytometry analysis revealed that HSC apoptosis index in 10 $\mu\text{mol/L}$ rosiglitazone group was 23.8%, significantly higher than that in the control group (3.6%, $\chi^2 = 16.682$, $P < 0.01$).

DISCUSSION

Excessive production and deposition of extracellular matrix is one of the main characteristics of hepatic fibrosis, in which type I collagen is an essential component^[16]. Type I collagen mainly comes from activated myofibroblast HSC^[17]. At present, studies on hepatic fibrosis are increasingly concentrating on HSC, in order to find specific and efficient approaches to inhibit and reverse hepatic fibrosis^[1,2,18,19].

Several studies demonstrated that resting HSCs express PPAR γ and when resting HSCs are activated to become myofibroblast HSCs, they lose the ability to transcribe and express PPAR γ ^[8,9,12,20,21]. PPAR γ is a member of nuclear receptor superfamily^[22]. When combined with its ligand, PPAR γ forms heterodimer with retinoid X receptor, which is then combined with peroxisome proliferator response element (PPRE) at the upstream of regulated gene promoter to play a role in transcription and regulation^[23]. Rosiglitazone is widely used in clinical practice as an insulin sensitizer, and at present, it is identified as a high-affinity specific ligand of PPAR γ , which can promote the expression of PPAR γ in cells and enhance the transcription activity of PPAR γ ^[24-28]. According to the change of blood drug level after rosiglitazone is taken, 2-3 $\mu\text{mol/L}$ rosiglitazone is believed



Figure 3 Immunocytochemistry of rHSC-99 $\times 100$. A: Positive of PPAR γ in 10 $\mu\text{mol/L}$ rosiglitazone group; B: positive of α -SMA in control group; C: weak

positive of α -SMA in 10 $\mu\text{mol/L}$ rosiglitazone group.

to be at a relatively high level, but in a preliminary experiment, only 10 $\mu\text{mol/L}$ rosiglitazone displayed a notable effect. Therefore, we set up a blank control group, 3 $\mu\text{mol/L}$ rosiglitazone group, and 10 $\mu\text{mol/L}$ rosiglitazone group. It was shown that 10 $\mu\text{mol/L}$ rosiglitazone markedly increased the transcription activity and expression level of PPAR γ in HSC, indicating that using PPAR γ -specific ligand was able to recover the expression and transcription activity of PPAR γ to a certain extent.

HSC strain rHSC-99 has been established by serial passage of rat HSC. This strain has the characteristics of activated myofibroblast HSC and highly expresses α -SMA and collagen I and III^[15]. The results of our experiment demonstrate that while 10 $\mu\text{mol/L}$ rosiglitazone remarkably enhances the transcription activity and expression level of PPAR γ in HSCs, the PPAR γ inhibits the expression of α -SMA and collagen I and the proliferation of HSCs.

At present, the mechanism that enhances the transcription activity and expression level of PPAR γ in HSC can inhibit the expression of α -SMA and collagen I and HSC proliferation has not been well elucidated^[30]. PPAR γ has a regulatory effect on multiple genes, but little research has been done regarding the effect of changes in PPAR γ expression and transcription activity on related genes of HSCs^[9,12,13,21,29]. Researches have shown that the enhancement of PPAR γ transcription activity can inhibit the expression of TGF- β 1 mRNA induced by TGF- β 1, suggesting that the activation of PPAR γ might block the autocrine loop of TGF- β 1 and further reduce TGF- β 1 induced secretion of collagen and HSCs proliferation^[30-32]. In researches on human and mouse macrophages^[33-36], it was found that there existed an interaction between PPAR γ and AP-1 signal pathway and the activation of PPAR γ could inhibit the activity of transcription factor AP-1, STAT, and NF- κ B. It is assumed that, there may be similar mechanism in HSC that PPAR γ , through inhibiting the activity of transcription factor AP-1, STAT, and NF- κ B, further plays an inhibitory role in HSC proliferation and expression of collagen.

HSC apoptosis can reduce the absolute quantity of activated HSC, thus not only reducing the synthesis of collagen, but also weakening the inhibitory effect on collagen degradation through decreasing activated HSCs to reduce the expression of matrix tissue inhibitor of metalloproteinases^[5]. Therefore, induction of HSC apoptosis has been considered as an efficient countermeasure to postpone or reverse hepatic fibrosis^[19]. Rosiglitazone, as a specific ligand of PPAR γ , can significantly increase HSC apoptosis rate.

The results of our experiment indicate that PPAR γ -specific ligand rosiglitazone, through activating the expression of PPAR γ , can inhibit the expression of α -SMA and collagen I in activated HSCs, the proliferation of activated HSCs and induce apoptosis of activated HSCs.

REFERENCES

- 1 **Friedman SL.** Seminars in medicine of the Beth Israel Hospital, Boston. The cellular basis of hepatic fibrosis. Mechanisms and treatment strategies. *N Engl J Med* 1993; **328**: 1828-1835
- 2 **Olaso E, Friedman SL.** Molecular regulation of hepatic

- fibrogenesis. *J Hepatol* 1998; **29**: 836-847
- 3 **Brenner DA.** Signal transduction during liver regeneration. *J Gastroenterol Hepatol* 1998; **13**(Suppl): S93-95
- 4 **Friedman SL.** Molecular regulation of hepatic fibrosis, an integrated cellular response to tissue injury. *J Biol Chem* 2000; **275**: 2247-2250
- 5 **Han YP, Zhou L, Wang J, Xiong S, Garner WL, French SW, Tsukamoto H.** Essential role of matrix metalloproteinases in interleukin-1-induced myofibroblastic activation of hepatic stellate cell in collagen. *J Biol Chem* 2004; **279**: 4820-4828
- 6 **Eng FJ, Friedman SL.** Fibrogenesis I. New insights into hepatic stellate cell activation: the simple becomes complex. *Am J Physiol Gastrointest Liver Physiol* 2000; **279**: G7-G11
- 7 **Casini A, Pinzani M, Milani S, Grappone C, Galli G, Jezequel AM, Schuppan D, Rotella CM, Surrenti C.** Regulation of extracellular matrix synthesis by transforming growth factor beta 1 in human fat-storing cells. *Gastroenterology* 1993; **105**: 245-253
- 8 **Kersten S, Desvergne B, Wahli W.** Roles of PPARs in health and disease. *Nature* 2000; **405**: 421-424
- 9 **Pinzani M, Marra F, Carloni V.** Signal transduction in hepatic stellate cells. *Liver* 1998; **18**: 2-13
- 10 **Xu J, Fu Y, Chen A.** Activation of peroxisome proliferator-activated receptor-gamma contributes to the inhibitory effects of curcumin on rat hepatic stellate cell growth. *Am J Physiol Gastrointest Liver Physiol* 2003; **285**: G20-30
- 11 **Miyahara T, Schrum L, Rippe R, Xiong S, Yee HF Jr, Motomura K, Anania FA, Willson TM, Tsukamoto H.** Peroxisome proliferator-activated receptors and hepatic stellate cell activation. *J Biol Chem* 2000; **275**: 35715-35722
- 12 **Hazra S, Xiong S, Wang J, Rippe RA, Krishna V, Chatterjee K, Tsukamoto H.** Peroxisome proliferator-activated receptor gamma induces a phenotypic switch from activated to quiescent hepatic stellate cells. *J Biol Chem* 2004; **279**: 11392-11401
- 13 **Mann DA, Smart DE.** Transcriptional regulation of hepatic stellate cell activation. *Gut* 2002; **50**: 891-896
- 14 **Marra F, Efsen E, Romanelli RG, Caligiuri A, Pastacaldi S, Batignani G, Bonacchi A, Caporale R, Laffi G, Pinzani M, Gentilini P.** Ligands of peroxisome proliferator-activated receptor gamma modulate profibrogenic and proinflammatory actions in hepatic stellate cells. *Gastroenterology* 2000; **119**: 466-478
- 15 **Leng XS, Weng SG, Li T, Wei YH, Peng JR, Du RY.** Establishment of a new rat hepatic stellate cell line rHSC-99 with characteristics of myofibroblast cell. *ACTA ANATOMICA SINICA* 2003; **34**: 269-274
- 16 **Rojkind M, Giambrone MA, Biempica L.** Collagen types in normal and cirrhotic liver. *Gastroenterology* 1979; **76**: 710-719
- 17 **Milani S, Herbst H, Schuppan D, Hahn EG, Stein H.** *In situ* hybridization for procollagen types I, III and IV mRNA in normal and fibrotic rat liver: evidence for predominant expression in nonparenchymal liver cells. *Hepatology* 1989; **10**: 84-92
- 18 **Galli A, Crabb DW, Ceni E, Salzano R, Mello T, Svegliati-Baroni G, Ridolfi F, Trozzi L, Surrenti C, Casini A.** Antidiabetic thiazolidinediones inhibit collagen synthesis and hepatic stellate cell activation *in vivo* and *in vitro*. *Gastroenterology* 2002; **122**: 1924-1940
- 19 **Solis-Herruzo JA, de la Torre P, Munoz-Yague MT.** Hepatic stellate cells (HSC): architects of hepatic fibrosis. *Rev Esp Enferm Dig* 2003; **95**: 436-439
- 20 **Everett L, Galli A, Crabb D.** The role of hepatic peroxisome proliferator-activated receptors (PPARs) in health and disease. *Liver* 2000; **20**: 191-199
- 21 **Galli A, Crabb D, Price D, Ceni E, Salzano R, Surrenti C, Casini A.** Peroxisome proliferator-activated receptor gamma transcriptional regulation is involved in platelet-derived growth factor-induced proliferation of human hepatic stellate cells. *Hepatology* 2000; **31**: 101-108
- 22 **Ferre P.** The biology of peroxisome proliferator-activated receptors: relationship with lipid metabolism and insulin sensitivity. *Diabetes* 2004; **53**(Suppl 1): S43-50

- 23 **Tontonoz P**, Hu E, Spiegelman BM. Regulation of adipocyte gene expression and differentiation by peroxisome proliferator activated receptor gamma. *Curr Opin Genet Dev* 1995; **5**: 571-576
- 24 **Saltiel AR**, Olefsky JM. Thiazolidinediones in the treatment of insulin resistance and type II diabetes. *Diabetes* 1996; **45**: 1661-1669
- 25 **Greene DA**. Rosiglitazone: a new therapy for Type 2 diabetes. *Expert Opin Investig Drugs* 1999; **8**: 1709-1719
- 26 **Miller JL**. Rosiglitazone approved for treatment of type 2 diabetes. *Am J Health Syst Pharm* 1999; **56**: 1292-1294
- 27 **Balfour JA**, Plosker GL. Rosiglitazone. *Drugs* 1999; **57**: 921-932
- 28 **Lehmann JM**, Moore LB, Smith-Oliver TA, Wilkison WO, Willson TM, Kliewer SA. An antidiabetic thiazolidinedione is a high affinity ligand for peroxisome proliferator-activated receptor gamma (PPAR gamma). *J Biol Chem* 1995; **270**: 12953-12956
- 29 **Kawaguchi K**, Sakaida I, Tsuchiya M, Omori K, Takami T, Okita K. Pioglitazone prevents hepatic steatosis, fibrosis, and enzyme-altered lesions in rat liver cirrhosis induced by a choline-deficient L-amino acid-defined diet. *Biochem Biophys Res Commun* 2004; **315**: 187-195
- 30 **Sung CK**, She H, Xiong S, Tsukamoto H. Tumor necrosis factor-alpha inhibits peroxisome proliferator-activated receptor gamma activity at a posttranslational level in hepatic stellate cells. *Am J Physiol Gastrointest Liver Physiol* 2004; **286**: G722-729
- 31 **Kon K**, Ikejima K, Hirose M, Yoshikawa M, Enomoto N, Kitamura T, Takei Y, Sato N. Pioglitazone prevents early-phase hepatic fibrogenesis caused by carbon tetrachloride. *Biochem Biophys Res Commun* 2002; **291**: 55-61
- 32 **Parkes JG**, Templeton DM. Effects of retinol and hepatocyte-conditioned medium on cultured rat hepatic stellate cells. *Ann Clin Lab Sci* 2003; **33**: 295-305
- 33 **Jiang C**, Ting AT, Seed B. PPAR-gamma agonists inhibit production of monocyte inflammatory cytokines. *Nature* 1998; **391**: 82-86
- 34 **Ricote M**, Li AC, Willson TM, Kelly CJ, Glass CK. The peroxisome proliferator-activated receptor-gamma is a negative regulator of macrophage activation. *Nature* 1998; **391**: 79-82
- 35 **Frungieri MB**, Weidinger S, Meineke V, Kohn FM, Mayerhofer A. Proliferative action of mast-cell tryptase is mediated by PAR2, COX2, prostaglandins, and PPARgamma: Possible relevance to human fibrotic disorders. *Proc Natl Acad Sci USA* 2002; **99**: 15072-15077
- 36 **Marra F**. Hepatic stellate cells and the regulation of liver inflammation. *J Hepatol* 1999; **31**: 1120-1130

Science Editor Zhu LH Language Editor Elsevier HK

Dynamic expression of apoptosis-related genes during development of laboratory hepatocellular carcinoma and its relation to apoptosis

Xiao-Xian Duan, Jing-Sheng Ou, Yuan Li, Jian-Jia Su, Chao Ou, Chun Yang, Hui-Fen Yue, Ke-Chen Ban

Xiao-Xian Duan, Jing-Sheng Ou, Yuan Li, Jian-Jia Su, Chao Ou, Chun Yang, Hui-Fen Yue, Ke-Chen Ban, Department of Pathology, Affiliated Tumor Hospital of Guangxi Medical University, Laboratory Center of Medical Sciences of Guangxi Medical University, Guangxi Zhuang Autonomous Region, China
Supported by the Science and Technology Department of Guangxi, No. 0143058, No. 0144002; and the National Natural Science Foundation of China, No. 39860072

Correspondence to: Xiao-Xian Duan, Department of Pathology, Affiliated Tumor Hospital of Guangxi Medical University, 71 Hedi Lu, Nanning 530021, Guangxi Zhuang Autonomous Region, China. casyduan@yahoo.com.cn

Telephone: +86-771-5331100 Fax: +86-771-5312000

Received: 2004-07-19 Accepted: 2004-12-18

anti-apoptosis effect of bcl-2 is influenced by bax, and ratio bcl/bax reflects more correctly the extent of cell apoptosis.

© 2005 The WJG Press and Elsevier Inc. All rights reserved.

Key words: Hepatocellular carcinoma; Apoptosis; Gene

Duan XX, Ou JS, Li Y, Su JJ, Ou C, Yang C, Yue HF, Ban KC. Dynamic expression of apoptosis-related genes during development of laboratory hepatocellular carcinoma and its relation to apoptosis. *World J Gastroenterol* 2005; 11 (30): 4740-4744

<http://www.wjgnet.com/1007-9327/11/4740.asp>

Abstract

AIM: To explore the expression of p53, bcl-2, bax, survivin and the cell apoptosis during the development of tree shrew hepatocellular carcinoma (HCC), the relationship between expression of these genes, its impact on HCC development, and its relation to cell apoptosis.

METHODS: Tree shrew HCC was induced with aflatoxin B1 (AFB1), and regular biopsy of liver tissues was carried out and the biopsy tissues were collected during cancer inducement. Liver biopsy tissue and HCC tissue were collected from 35 pre-cancerous experimental animals at wk 30 and 60 and at the 30th-, 60th-, and 90th-wk. Liver biopsy tissues were collected from 13 blank control animals at wk 30, 60, and 90. Expression of p53, bcl-2, bax, and survivin at each stage was examined by immunohistochemistry method. Apoptotic cells were detected *in situ* by the terminal deoxynucleotidyl transferase-mediated nick end labeling (TUNEL) technique.

RESULTS: The apoptosis rate of normal hepatic cells was extremely low, whereas it increased during the formation of HCC. Expression of the apoptosis-related genes p53, bcl-2, bax, and survivin during the formation of HCC presented an increasing tendency. Expression of p53 did not noticeably relate to that of bcl-2, bax, and survivin, whereas expression of bcl-2 and bax was closely related. In HCC, p53 did not present a distinct relation to cell apoptosis, whereas its high level expression was probably related to liver cell proliferation. Survivin negatively correlated apoptosis index, and its overexpression could inhibit cell apoptosis.

CONCLUSION: Apoptosis-related genes p53, bcl-2, bax, and survivin are all related to the occurrence of HCC. The

INTRODUCTION

Occurrence and biological characteristics of tumors are related not only to over-proliferation of carcinoma cells but also to decrease of apoptosis. Investigation of apoptosis helps to disclose the biological characteristics of tumors, and seeks new methods of diagnosis and treatment for tumors. Product of gene bax (bcl-2 associated X gene) expression is a 21-ku protein, which is able to combine bcl-2 protein to form a heterogeneous dimer, thus inhibiting the function of bcl-2 and promoting the occurrence of apoptosis. p53 is universally accepted as a tumor suppressor, whose mutation and deficiency accelerate cancer growth. Survivin is a new member of the inhibitor of apoptosis inhibiting protein family. It is believed that cell apoptosis induced by most of apoptosis signals is realized through the effect of a cascade proteinase, namely caspase. Survivin can act directly on caspase, thus inhibiting the activity of caspase-3 and caspase-7^[1] and eventually blocking the terminal pathway of apoptosis. In this research, expression of p53, bcl-2, bax, survivin, and cell apoptosis in different stage liver tissues during the development of laboratory tree shrew HCC were explored by the immunohistochemistry method and the terminal deoxyn-ucleotidyl transferase-mediated nick end labeling (TUNEL) technique. The relationship between expression of these genes, its impact on HCC formation, and its relation to cell apoptosis were discussed.

MATERIALS AND METHODS

Animal experiment

Adult laboratory tree shrews, weighing 100-160 g, were raised in separate stainless cages under a laboratory temperature of 25±2 °C. After 2-4 wk of feeding, all animals were examined for serum ALT and HBsAg. Thus, 61 healthy animals were

selected and divided into experimental group and control group.

Forty-eight tree shrews in the experimental group received aflatoxin B1 (AFB1) at the beginning of the experiment, 150 µg/(kg·d), five times/wk. AFB1 was solved into dimethyl sulfoxide, then added into milk for lapping by the animals. The animals received AFB1 for 105 wk then common animal food for 45 wk when the experiment was completed.

Thirteen tree shrews in the control group did not receive AFB1 but common animal food, milk and fruits.

Liver tissue biopsy

During the whole experiment, liver tissue biopsy was carried out in both groups of tree shrews once in every 15 wk. Biopsy tissues were fixed in 10% formaldehyde solution.

Tissue specimens

Specimens of liver biopsy tissues taken at wk 30 and 60 and HCC tissues from the experimental animals and those of the liver biopsy tissues taken at wk 30, 60, and 90 were embedded with paraffin wax and cut into 5-µm consecutive sections, then subjected to the routine HE staining. Expression of p53, bcl-2, bax, and survivin was detected by immunohistochemistry method. Apoptotic cells were subjected to *in situ* detection by the TUNEL technique.

Reagents

Mouse anti-human p53, bcl-2, bax, and survivin mAbs were from Beijing Zhongshan Company. Streptavidin-peroxidase (S-P) kits and DAB developers were from Fuzhou Maixin Company; TUNEL staining kits (Cat. No. 1684809) were from Boehringer Mannheim GmbH, Deutschland. DNAase I, proteinase K, and 3% bovine serum albumin were from Dalian Baosheng Company.

Immunohistochemistry staining and in situ detection of apoptosis

S-P method was applied. Sections before addition of mAb were subjected to microwave antigen repairing, all other procedures were according to the kit manual. PBS was substituted for the first antibody to act as the negative contrast, and the positive contrast sections from Fuzhou Maixin Company were used as the positive contrast. *In situ* detection of apoptosis was carried out as previously described^[2]. Positive contrast sections were subjected to a 30-min digestion with DNAase I before TUNEL reacting solution was added, whereas negative contrast sections were subjected to TDT-free TUNEL reacting solution.

Result assessment and statistical analysis

p53 and survivin protein positive reactions were located in nuclei, presenting light or dark brown. Bcl-2 and bax protein positive reactions were located in cytoplasm, appearing as dark brown.

Immunohistochemical staining was divided into five grades: grade 0: <5%; grade I: 5-25%; grade II: 25-50%; grade III: 50-75%; and grade IV: >75%. Five percent was taken as the criterion for the judgment of positive cells.

Staining intensity of positive cells was divided into three grades: grade I: low; grade II: medium; grade III: strong. The staining intensity of all the positive contrast sections was

determined as grade III for reference. Immunohistochemical staining score = grading for percentage of positive cells × staining intensity^[3].

Apoptotic cells were calculated under five high power fields randomly selected, at least than 1 000 cells per field. Percentage of positive cells to total cells was taken as apoptosis index.

Statistical analysis was carried out by variance analysis, χ^2 test, etc., with the statistical software package PEMS.

RESULTS

Occurrence of HCC

At the 150th wk of the experiment, all dead animals were subjected to etiological diagnosis of HCC. The result showed that occurrence of HCC was seen in 35 of 48 experimental tree shrews, with an incidence rate of 72.9%, and in none of 13 control tree shrews. The earliest time of carcinoma occurrence was 88 wk, and the latest time was 150 wk. The average time was 117 wk.

Pathological tissues' change at each stage

In the liver biopsy tissues from the control animals at each stage, liver cells were arrayed in good order, lobular structure was clear and complete, and no inflammation and hepatocyte hyperplasia appeared. In the experimental animals, the liver biopsy tissues taken at wk 30 and 60 appeared with hepatocellular degeneration and hyperplasia change. The former was primarily vacuole degenerative, the latter presented hepatocyte array in two lines, multi-lines, even pieces, with clear lobular structure. In HCC animals, liver cells were poorly and moderately differentiated presenting diffusive, nodular, or girder-like types.

Expression of apoptosis-related genes and cell apoptosis

The expression of p53, bcl-2, bax, and survivin in HCC and other liver tissues is listed in Table 1; the apoptosis indices in HCC and other liver tissues are shown in Table 2; the relationship between expression of p53, bcl-2, bax, survivin, and cell apoptosis in HCC tissues is summarized in Table 3.

DISCUSSION

Studies^[3,15,18,20] have shown that genes p53, bcl-2, bax, and survivin play an important role in HCC formation, but these studies are confined to the resected HCC, employing carcinoma-adjacent tissues as control liver tissues. This study was carried out in the tree shrew HCC model established at the Department of Pathology of the Affiliated Tumor Hospital of Guangxi Medical University. The HCC model allows repeated biopsy with no animals being killed during the induction of HCC, so that liver tissues at different stages of carcinogenesis are available. These tissues were utilized for the investigation on the dynamic expression of p53, bcl-2, bax, and survivin during the development of HCC, and for the exploration of its impact on HCC development.

Relationship between cell apoptosis and HCC

Apoptosis is a process of programmed cell death under certain physiological or pathological conditions. This process is active, highly ordered, multi-gene controlled, and serial-

Table 1 Expression of p53, bcl-2, bax, and survivin in HCC and other liver tissues

Groups	Biopsy at	Cases	p53	Bcl-2	Bax	Survivin
			Positive (%)	Positive (%)	Positive (%)	Positive (%)
Control	30 th wk	13	0 (0)	0 (0)	0 (0)	4 (30.8)
	60 th wk	13	0 (0)	0 (0)	0 (0)	5 (38.4)
	90 th wk	13	0 (0)	0 (0)	0 (0)	5 (38.4)
Trial	30 th wk	35	0 (0)	3 (8.6)	2 (5.7)	14 (40)
	60 th wk	35	21 (60) ^{b,d}	7 (20)	10 (28.6) ^{a,c}	13 (37.1)
	HCC	35	25 (71.4) ^{b,d}	14 (40)	25 (71.4) ^{b,d,e}	19 (57.1)

^a*P*<0.05, ^b*P*<0.01 vs each stage control; ^c*P*<0.05, ^d*P*<0.01 vs experiment for 30 wk; ^e*P*<0.05 vs experiment for 30 wk.

Table 2 Apoptosis indices in HCC and other liver tissues

Groups	Biopsy at	cases	Apoptosis indices		
			Maximum	Minimum	Average
Control	30 th wk	13	0.25	0	0.01±0.02
	60 th wk	13	0.25	0	0.01±0.02
	90 th wk	13	0.3	0	0.02±0.04
Trial	30 th wk	35	1.5	0	0.57±0.47 ^b
	60 th wk	35	2.1	0	0.70±0.60 ^b
	HCC	35	2.5	0.1	0.71±0.51 ^b

^b*P*<0.01 vs same stage control.

Table 3 Relationship between expression of p53, bcl-2, bax, survivin, and cell apoptosis in HCC tissues

Observation indications	Cases	Apoptosis indices (%)			<i>P</i>	
		Maximum	Minimum	Average		
p53	+	25	2.5	0.1	0.70±0.57	>0.05
	-	10	1.0	0.2	0.72±0.31	
Bcl-2	+	14	2.5	0.4	1.02±0.45	<0.05
	-	21	1.5	0.1	0.50±0.40	
Bax	+	25	2.5	0.2	0.74±0.25	<0.01
	-	10	0.5	0.1	0.24±0.16	
Survivin	+	19	1.5	0.1	0.51±0.40	<0.05
	-	16	2.5	0.2	0.86±0.54	
Bcl-2 Bax	+	14	2.5	0.5	1.02±0.45	<0.01
Bcl-2 Bax	-	10	0.5	0.1	0.25±0.15	

enzyme catalyzed^[4]. As an important modulating mechanism maintaining the stability of organ itself, apoptosis not only plays a role in physiological courses such as embryo developing, tissue shaping, hematopoiesis modulating, growing and ageing, but also has a close relation to cancer occurrence and development^[5]. The occurrence of cancer is related to the over-proliferation of carcinoma cells and the relative destitution of apoptosis.

It was reported that the apoptosis index in HCC is apparently lower than that in tissues of normal liver, chronic hepatitis, hepato-cirrhosis, and adjacent cancer tissues^[6-9]. It has also been found that the cell proliferation augment usually accompanies increased apoptosis during HCC development^[10]. The result of this study is consistent with the latter case with a result indicating that the natural incidence rate of apoptosis in normal hepatic cells is low (1-0.3%). The averaged apoptosis indices of pre-HCC tissues and carcinoma-adjacent tissues taken at wk 30 and 60 were 0.57, 0.70%, and 0.71% respectively. Though no significant

difference was found when intra-group comparison was made, these indications were higher than those at the same stage of the control group suggesting that cell apoptosis during the development of HCC increases. The possible reason for the different reports mentioned above is that invariableness of cell number of multi-cell organisms depends upon the dynamic equilibrium between cell proliferation and apoptosis. Cancer occurrence and development are the results of destruction of the equilibrium. Therefore, besides the blockade of cell proliferation and apoptosis, cell apoptosis may increase. In the latter case, the speed of apoptosis is lower than that of malignant cell proliferation, thus resulting in a net augment of cell number. It is believed that this is related to blood supply deficiency that results in anoxemia of tumor cells and induces apoptosis increment.

Relationship between p53, bcl-2, bax, and survivin expression, HCC, and apoptosis

Fifty percent of human tumors are related to p53 mutation.

The wild-type p53 has a very short half life, and cannot be detected by immunohistochemistry method. The half life of mutant p53 is long enough to allow detection by the same method^[11]. The possible reason is that the control animals are free from cancer-inducible factors so that the liver tissues do not present any substantial change. At the late stage of our experiment, p53 was significantly expressed (0.60% and 71.4%), showing that the mutant p53 participate in occurrence of liver cancer. It is also found that p53 protein expression does not relate to apoptosis index level. The reason may be that during the development of idiopathic HCC, liver cell apoptosis increases with the augment of liver cell proliferation. In addition, in this experiment p53-positive tissues accompanied the expression of the apoptosis-promoting gene bax, which may counteract the influence of p53 on apoptosis. Therefore, in AFB1-induced HCC p53 expression does not inhibit cell apoptosis but stimulates cell proliferation, thus promoting the malignant conversion of cells.

It was reported that bax can significantly promote cell apoptosis^[12], yet bcl-2 has anti-apoptosis effects. Bax distributes in tissues and cells in human body, and its expression is high in liver and kidney tissues, but low in most carcinoma tissues. This study found that bax did not express in tissues of the control animals, but expressed apparently with an increasing tendency in tissues of the HCC-infected animals. Presently, there are still some controversies over the relationship between bcl-2 and HCC. Results from this study indicate that bcl-2 is significantly expressed in HCC tissues but not in tissues of control animals. The scores of bcl-2 expression present an increasing trend, suggesting that both bax and bcl-2 proteins take part in the formation of HCC.

The anti-apoptosis effect of bcl-2 is affected by bax. The bcl-2/bax ratio is a key factor for determining apoptosis. When bcl-2 expresses excessively, bcl-2-bax heterogeneous dimer predominates, thus inhibiting apoptosis^[13]. When bax expresses excessively, bax-bax homogeneous dimer or monomer predominates, thus promoting apoptosis. This study found that apoptosis index for bcl-2-positive HCC tissues was higher than that for bcl-2-negative tissues. In bcl-2-positive tissues, bax appeared positive. Because of the overexpression of bax, bax-bax homogeneous dimer predominates, thus speeding up apoptosis.

Survivin, a recently discovered anti-apoptosis gene, bears the following anti-apoptosis mechanisms: (1) directly inhibiting the activity of the terminal-responsive enzymes caspase-3 and caspase-7, which act during the apoptosis process, thus blocking up apoptosis^[14]; (2) combining the cell cycle modulator CDK4 to form survivin-CDK4 complex, thus causing CDK4 complex releasing p21 that further combines with caspase-3 within mitochondrion, so as to inhibit the activity of caspase-3, eventually blocking apoptosis^[15].

Although survivin inhibits various kinds of stimulant-induced apoptosis through a direct action on caspase, survivin does not significantly present any anti-apoptosis effect in HCC. This study found that survivin rendered high expression in normal liver tissues, experimental animal liver tissues, and HCC tissues, showing no significant difference between these three tissues. This is in accordance

with the previous report^[16]. In HCC, apoptosis index for survivin-positive tissues is higher than that for survivin-negative tissues, suggesting that during the formation of HCC, enhancement of survivin expression is a late incident. The possible reason is that tumor formation activates through a certain mechanism, then holds down apoptosis of carcinoma cells, and at last results in consecutive proliferation and differentiation of carcinoma cells. Therefore, the primary effect of survivin in HCC is to inhibit cell apoptosis and promote cell proliferation and malignant conversion.

Interrelationship between p53, bcl-2, bax, and survivin in HCC

Carcinoma occurrence is an extremely complicated course. Though it is known that genes have a close relation to carcinoma occurrence, but whether they relate to each other is still unknown. p53 is an important apoptosis-regulating gene and modulates apoptosis through many pathways. It was reported that p53 serves as a very important regulator bax, that promotes apoptosis through the bax pathway^[17,18]. p53 also causes downregulation of bcl-2^[19,20] and survivin^[21] at protein and mRNA level. This study showed that there was no significant interrelation between p53, bcl-2, bax, and survivin in HCC. This may result from the fact that the mutation of p53 has lost effect on expression of bax, bcl-2, and survivin. In HCC tissues of 14 bcl-2-positive cases, bax was positive for all cases; in HCC tissues of 21 bcl-2-negative cases, bax was positive for 10 cases; in HCC tissues of 25 bax-positive cases, bcl-2 was positive for 14 cases; in HCC tissues of 11 bax-negative cases, bcl-2 negative for all cases. Inter-group comparison showed that the difference was rather significant, suggesting that there is a mechanism of co-transcript or mutual activation between bcl-2 and bax.

In conclusion, apoptosis rate in normal liver cells is extremely low and increases during the development of HCC. Apoptosis-related genes p53, bcl-2, bax, and survivin are all related to HCC occurrence, and their expression renders an increasing tendency during the formation of HCC. There is no distinct relationship between bcl-2, bax, and survivin, but there is a close relationship between bcl-2 and bax. Bax can facilitate apoptosis, and the anti-apoptosis effect of bcl-2 is affected by bax. Therefore, the bax/bcl-2 ratio reflects more accurately the extent of cell apoptosis. Survivin relates negatively to the apoptosis index, and its expression inhibits apoptosis. In HCC, p53 is not noticeably related to cell apoptosis, and its high expression may relate to the proliferation of liver cells.

REFERENCES

- 1 **Shin S, Sung BJ, Cho YS, Kim HJ, Ha NC, Hwang JI, Chung CW, YK, Oh BH.** An anti-apoptotic protein human survivin is a direct inhibitor of caspase-3 and -7. *Biochemistry* 2001; **40**: 1117-1123
- 2 **Cuello-Carrion FD, Ciocca DR.** Improved detection of apoptotic cells using a modified *in situ* TUNEL technique. *J Histochem Cytochem* 1999; **47**: 837-839
- 3 **Sinicropo FA, Ruan SB, Cleary KR, Stephens LG, Lee JJ, Levin B.** Bcl-2 and p53 oncoproteins expression during colorectal tumorigenesis. *Cancer Res* 1995; **55**: 237-241
- 4 **Stewart BW.** Mechanisms of apoptosis: integration of genetic, biochemical, and cellular indicators. *J Natl Cancer Inst* 1994; **86**: 1286-1296

- 5 **Carson DA**, Ribeiro JM. Apoptosis and disease. *Lancet* 1993; **341**: 1251-1254
- 6 **Feng DY**, Zheng H, Shen M, Cheng RX, Yan YH. Regulation of p53 and bcl-2 proteins to apoptosis and cell proliferation in liver cirrhosis and hepatocellular carcinoma. *Hunan Yike Daxue Xuebao* 1999; **24**: 325-328
- 7 **Xu HY**, Han JW, Song G, Guan XL, Mei HL. Relationship between regulating apoptosis gene and apoptosis index in human hepatocellular carcinoma. *Harbin Yike Daxue Xuebao* 1999; **33**: 436-438
- 8 **Lü YY**, Yuan MB. Expression of bax and bcl-2 and their relationship with cell apoptosis index in human hepatocellular carcinoma. *Shandong Daxue Xuebao* 2002; **40**: 310-311
- 9 **Gras1-Kraupp B**, Ruttkay-Nedecky B, Mullauer L, Taper H, Hut-Bursch W, Schulte-Hermann R. Inherent increase of apoptosis in liver tumors: implications for carcinogenesis and tumor regression. *Hepatology* 1997; **25**: 906-912
- 10 **Meki AR**, Abdel-Ghaffar SK, El-Gibaly I. Aflatoxin B1 induces apoptosis in rat liver: protective effect of melatonin. *Neuroendocrinol Lett* 2001; **22**: 417-426
- 11 **Sturm I**, Papadopoulos S, Hillebrand T, Benter T, Luck T, Luck HJ, Wolff G, Dorken B, Daniel PT. Impaired BAX proteins expression in breast cancer; mutational analysis of the BAX and the p53 gene. *Int J Cancer* 2000; **87**: 517-521
- 12 **Chong MJ**, Murray MR, Gosink EC, Russell HR, Srinivasan A, Kapasetaki M, Korsmeyer SJ, Mckinnon PJ. Atm and Bax cooperate in ionizing radiation-induced apoptosis in the central nervous system. *Proc Natl Acad Sci USA* 2000; **97**: 889-894
- 13 **Oltvai ZN**, Milliman CL, Korsmeyer SJ. Bcl-2 heterodimerizes *in vivo* with a conserved homolog, Bax, that accelerates programmed cell death. *Cell* 1993; **74**: 609-619
- 14 **Sela B**. Survivin: anti-apoptosis proteins and a prognostic marker for tumor progression and recurrence. *Harefuah* 2002; **141**: 103-107
- 15 **Ito T**, Shiraki K, Sugimoto K, Yamanaka T, Fujikawa K, Ito M, Takase K, Moriyama M, Kawana H, Hayashida M, Nakano T, Suzuki A. Survivin promotes cell proliferation in human hepatocellular carcinoma. *Hepatology* 2000; **31**: 1080-1085
- 16 **Gianani R**, Jarboe E, Orlicky D, Frost M, Bobak J, Lehner R, Shroyer KR. Expression of surviving in normal, hyperplastic, and neoplastic colonic mucosa. *Hum Pathol* 2001; **32**: 119-125
- 17 **Miyashita T**, Krajewski S, Krajewska M, Wang HG, Lin HK, Liebermann DA, Hoffman B, Reed JC. Tumor suppressor p53 is a regulator of bcl-2 and bax gene expression *in vitro* and *in vivo*. *Oncogene* 1994; **9**: 1799-1805
- 18 **Miyashita T**, Reed JC. Tumor suppressor p53 is a direct transcriptional activator of the human bax gene. *Cell* 1995; **80**: 293-299
- 19 **Haldar S**, Negrini M, Monne M, Sabbioni S, Croce CM. Down-regulation of bcl-2 by p53 in breast cancer cells. *Cancer Res* 1994; **54**: 2095-2097
- 20 **Nakamura S**, Akazawa K, Kinukawa N, Yao T, Tsuneyoshi M. Inverse correlation between the expression of bcl-2 and p53 proteins in primary gastric lymphoma. *Hum Pathol* 1996; **27**: 225-233
- 21 **Mirza A**, McGuirk M, Hockenberry TN, Wu Q, Ashar H, Black S, Wen SF, Wang L, Kirschmeier P, Bishop WR, Nielsen LL, Pickett CB, Liu S. Human survivin is negatively regulated by wild-type p53 and participates in p53-dependent apoptotic pathway. *Oncogene* 2002; **21**: 2613-2622

Science Editor Wang XL and Guo SY Language Editor Elsevier HK

Resveratrol prolongs allograft survival after liver transplantation in rats

Sheng-Li Wu, Liang Yu, Ke-Wei Meng, Zhen-Hua Ma, Cheng-En Pan

Sheng-Li Wu, Liang Yu, Ke-Wei Meng, Zhen-Hua Ma, Cheng-En Pan, Department of Hepatobiliary Surgery, First Hospital of Xi'an Jiaotong University, Xi'an 710061, Shaanxi Province, China
Correspondence to: Dr. Sheng-Li Wu, Department of Hepatobiliary Surgery, First Hospital of Xi'an Jiaotong University, Xi'an 710061, Shaanxi Province, China. victorywu2000@163.com
Telephone: +86-29-5324009 Fax: +86-29-5323536
Received: 2004-10-04 Accepted: 2004-12-03

Wu SL, Yu L, Meng KW, Ma ZH, Pan CE. Resveratrol prolongs allograft survival after liver transplantation in rats. *World J Gastroenterol* 2005; 11(30): 4745-4749
<http://www.wjgnet.com/1007-9327/11/4745.asp>

Abstract

AIM: To study the immuno-modulatory effect of resveratrol (RES) on allograft rejection after liver transplantation in rats.

METHODS: Male Sprague-Dawley (SD) rats were selected as donors and male Wistar rats as recipients for a rejection model. The recipients were divided into four groups after orthotopic liver transplantation (OLTx). In the RES A, B, and C groups, RES was given intra-peritoneally once a day (25, 50, and 100 mg/kg, respectively) after OLTx, whereas in the control group, vehicle buffer was given intra-peritoneally once a day. The survival time, serum chemistry, production of cytokines, activation of transcription factor NF- κ B, and histopathologic findings were then compared among these groups.

RESULTS: The mean survival time after OLTx in the RES C group was significantly longer than that in the control group (16.7 \pm 1.2 d vs 9.3 \pm 0.6 d, P <0.01). On the 7th post-transplant day the serum albumin level significantly improved in the RES C group, the serum total bile acid and alanine aminotransferase (ALT) levels were significantly lower in the RES C group, the serum IL-2 and INF- γ levels were significantly lower in the RES C group, and the activation of transcription factor NF- κ B in peripheral blood T lymphocytes was significantly suppressed in the RES A, B, and C groups in comparison to those in the control group. On the 7th post-transplant day, a histological examination revealed apparent difference in the severity of rejection between the RES C group and control group.

CONCLUSION: RES has an immuno-suppressive property as well as protective effect on hepatocytes under allograft rejection. It might serve as a novel agent for reducing the severity of hepatic allograft rejection in rats.

© 2005 The WJG Press and Elsevier Inc. All rights reserved.

Key words: Resveratrol; Liver; Transplantation; Rat

INTRODUCTION

Since the introduction of cyclosporine and tacrolimus for the control of post-operative rejection, liver transplantation has become an established surgical technique and is now performed on patients with various terminal liver diseases. Most instances of mortality after liver transplantation are still attributed to infection, and such infection is apt to occur as a result of over-immunosuppression to severe rejection^[1-3]. Rejection is still a leading cause of morbidity and mortality after liver transplantation. To improve the survival after liver transplantation, novel strategies are still needed for the treatment of the rejection.

Resveratrol (3,5,4'-trihydroxystilbene, RES) is a polyphenol present in a limited number of plants^[4], mainly in grapes with levels up to tens of grams per kg^[5], where it is synthesized in response to stress conditions such as fungal infections and trauma^[4]. Many studies have demonstrated that this molecule exhibits a wide range of biological and pharmacological activities both *in vitro* and *in vivo*^[6]. A series of studies showed that resveratrol has anti-oxidant properties^[7], anti-inflammatory properties^[8,9], and cancer-chemopreventive activity^[10,11]. Many of the biological activities of resveratrol, like the inhibition of cyclooxygenase^[8], induction of CD95 signaling-dependent apoptosis^[12], effects on the cell division cycle^[13] and modulation of NF- κ B activation^[14], indicate a possible effect on immune response and many *in vitro* experiments have proven that resveratrol has immuno-modulatory activity^[15-17].

To our knowledge, there has not been a report on the *in vivo* immuno-modulatory effect of RES on hepatic allograft after transplantation. We therefore investigated whether RES might have any beneficial effect on hepatic allograft after transplantation.

MATERIALS AND METHODS

Materials

Male Sprague-Dawley (SD) rats 9-10 wk old weighing 190-210 g as donors and male Wistar rats 7-8 wk old weighing 190-210 g as recipients were purchased from the Animal Center of Xi'an Jiaotong University (Xi'an, China) and Animal Center of Shanxi Medical College (Shanxi, China), respectively. All rats were allowed free access

to water and standard laboratory chow. Before operation the rats were fasted for 12 h and only allowed free access to water. All animal protocols were approved by the Xi'an Jiaotong University Institutional Animal Care and Use Committee.

Resveratrol, dimethyl sulfoxide (DMSO), and IL-2 and INF- γ ELISA kits were purchased from Sigma Chemical Co. RPMI-1640, HEPES, EDTA, EGTA, DTT, PMSF, and NP-40 were from Gibco BRL. NF- κ B consensus oligonucleotide and single base pair mutant were from Promega. Fetal bovine serum was from SiJiQing Co., Hangzhou, China. 32 P-ATP was from Beijing Isotope Co., China.

Orthotopic liver transplantation

Orthotopic rat liver transplantation (OLTx) was performed by the cuff technique as described by Kamada and Calne^[18], with some slight modifications. With the rat under ketamine anesthesia (75 mg/kg), the liver was gently skeletonized and flushed with chilled lactated Ringer's solution through the abdominal aorta. Special care was taken for minimal manipulation of the graft and portal vein and bile duct for reconstruction. The liver was harvested and stored at 4 °C in lactated Ringer's solution until transplantation. OLTx was performed without hepatic artery reconstruction. The suprahepatic vena cava was anastomosed with 7-0 Prolene continuous suture (Ethicon, Somerville, NJ) and portal vein and inferior vena cava reconstruction was performed by the cuff technique. The bile duct connection was made with an intra-luminal epidural catheter stent. In rat liver transplantation, the cold ischemic time and anhepatic phase were 40-50 min and 14-16 min, respectively, and no significant difference was recognized among these groups.

RES administration and graft survival

The RES was dissolved and sterilized in DMSO and then diluted in RPMI-1640 to 5, 10, and 20 mg/mL. The recipients were randomly divided into four groups after OLTx. In the RES A, B, and C groups, 1 mL of these preparations was administered by intra-peritoneal route once a day after OLTx (25, 50, and 100 mg/kg, respectively) and in the control group, vehicle buffer was given by intraperitoneal route once a day after OLTx.

Six rats were left in each group until they died. The rats used to evaluate graft survival were given RES or vehicle buffer until they died.

Liver function test and ELISA

Six animals in each group were killed on the 7th posttransplant day for blood collection. A 6-mL blood sample was obtained from the vena cava. Two milliliters blood was centrifuged immediately at 3 000 r/min at 4 °C for 10 min and stored at -80 °C until analysis. Albumin, total bile acid, and alanine aminotransferase (ALT) were assayed by standard enzymatic methods, while serum IL-2 and INF- γ levels were assayed by ELISA.

EMSA

The remaining 4 mL of blood was used for the detection of NF- κ B activation in peripheral blood T lymphocytes. First, the peripheral blood mononuclear cells were separated

by standard Ficoll-Hypaque gradient centrifugation, and then incubated in RPMI-1640 culture medium containing 10% calf serum. The cell suspension was separated from the adherent cells the next day and T-lymphocyte subpopulation was obtained by magnetic separation column according to the instructions of the manufacturer (Miltenyi Biotec, Germany). The purity of the cell population was confirmed by FACScan analysis and cell viability was determined by trypan blue dye exclusion.

Then T-lymphocyte nuclear extracts were prepared by the modified procedure of Dignam *et al.*^[19]. Following treatment, cells were washed thrice with PBS, resuspended, and incubated on ice for 15 min in hypotonic buffer A (10 mmol/L HEPES, pH 7.9, 10 mmol/L KCl, 0.1 mmol/L EDTA, 0.1 mmol/L EGTA, 1 mmol/L DTT, 0.5 mmol/L PMSF, and 0.6% NP-40). Cells were vortexed gently for lysis, and nuclei were separated from cytosolic components by centrifugation at 12 000 *g* for 1 min at 25 °C. Nuclei were resuspended in buffer C (20 mmol/L HEPES, pH 7.9, 25% glycerol, 0.4 mol/L NaCl, 1 mmol/L EDTA, 1 mmol/L EGTA, 1 mmol/L DTT, 0.5 mmol/L PMSF) and shaken for 30 min at 4 °C. Nuclear extracts were obtained by centrifugation at 12 000 *g* for 10 min at 25 °C. Protein concentration was measured by the Bradford assay (Bio-Rad).

For binding reactions, nuclear extracts (10 μ g of protein) were incubated in a 25- μ L total reaction volume containing 20 μ mol/L HEPES, pH 7.9, 60 mmol/L NaCl, 0.1 mmol/L EDTA, 1 mmol/L DDT, 8% glycerol, and 2.55 μ g/mL of poly (dl-dC, Pharmacia). Double-stranded radiolabeled NF- κ B oligonucleotide probe (5'-CGCTT-GATGAGTCAGC-CGGAA-3') was added to the mixture after pre-incubation for 15 min at 4 °C, and the reaction mixture was then incubated for 20 min at room temperature. Samples were loaded on 6% polyacrylamide gels in low-ionic-strength 0.25 \times TBE buffer (22.3 mmol/L Tris, 22.2 mmol/L borate, 0.5 mmol/L EDTA) and run at 150 V/cm with cooling. The gels were dried and analyzed by autoradiography.

Histopathologic examination

Liver specimens were collected from five animals in each group on the 7th post-transplant day and fixed in 10% neutral buffered formalin. Then, the specimens were embedded in paraffin and 3 μ m thick sections were cut and stained with hematoxylin and eosin (H&E). A single blinded pathologist examined the liver graft specimens.

Statistical analysis

All data were expressed as mean \pm SD, and Student's *t*-test was used to evaluate the significance of the difference between experimental groups and control group. The survival time were compared according to the Kaplan-Meier and log rank analysis. *P*<0.05 was considered statistically significant.

RESULTS

Graft survival

The mean survival time was 8.3 \pm 0.6, 11.7 \pm 1.5, and 16.7 \pm 1.2 d in the RES A, B, and C groups, respectively,

and 9.3 ± 0.6 d in the control group. The difference between the RES C group and control group was statistically significant ($P < 0.01$). The survival rates in the four groups are shown in Figure 1.

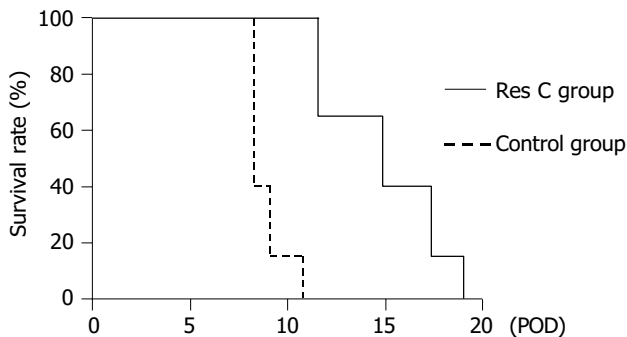


Figure 1 Survival rate of rats after liver transplantation.

Liver function tests

Table 1 shows the serum chemistry data that reflected the liver functions after OLTx. On the 7th posttransplant day the albumin level was 2.0 ± 0.1 , 2.2 ± 0.1 , and 2.7 ± 0.2 g/dL in the RES A, B, and C groups, respectively, whereas it was 2.1 ± 0.3 g/dL in the control group. The difference between the RES C group and control group was statistically significant ($P < 0.05$). The total bile acid was 314.7 ± 97.5 , 270.4 ± 93.7 , and 155.4 ± 34.2 μ mol/L in the RES A, B, and C groups respectively, whereas it was 353.9 ± 84.4 μ mol/L in the control group. The difference between the RES C group and the control group was significant ($P < 0.05$). ALT was 1112.1 ± 159.4 , 806.5 ± 135.2 , and 482.7 ± 101.2 U/L in the RES A, B, and C groups respectively, whereas it was 1137.5 ± 235.4 U/L in the control group. The difference between the RES C group and the control group was significant ($P < 0.05$).

Table 1 Effect of RES on liver function in rats after OLTx (mean \pm SD)

Group	Dose (mg/kg)	n	Albumin level (g/dL)	Total bile acid (μ mol/L)	ALT (U/L)
Control	0.0	6	2.1 ± 0.3	353.9 ± 84.41	1137.5 ± 235.4
RES A	25.0	6	2.0 ± 0.1	314.7 ± 97.5	1112.1 ± 159.4
RES B	50.0	6	2.2 ± 0.1	270.4 ± 93.7	806.5 ± 135.2
RES C	100.0	6	2.7 ± 0.2^a	155.4 ± 34.2^a	482.7 ± 101.2^a

^a $P < 0.05$ vs control.

ELISA

The IL-2 level was 305.1 ± 82.8 , 241.7 ± 38.1 , and 195.7 ± 42.4 ng/L in the RES A, B, and C groups respectively, whereas it was 294.4 ± 38.0 ng/L in the control group. The difference between the RES C group and the control group was significant ($P < 0.05$). The INF- γ level was 96.5 ± 6.5 , 82.8 ± 14.9 , and 66.6 ± 15.7 ng/L in the RES A, B, and C groups respectively, whereas it was 101.3 ± 14.1 ng/L in the control group. The difference between the RES C group and the control group was

significant ($P < 0.05$). The serum cytokine levels on the 7th post-transplant day in the four groups are shown in Table 2.

Table 2 Effect of RES on IL-2 and INF- γ production in rats after OLTx (mean \pm SD)

Group	Dose (mg/kg)	n	IL-2 (ng/L)	INF- γ (ng/L)
Control	0.0	6	294.4 ± 38.0	101.3 ± 14.1
RES A	25.0	6	305.1 ± 82.8	96.5 ± 6.5
RES B	50.0	6	241.7 ± 38.1	82.8 ± 14.9
RES C	100.0	6	195.7 ± 42.4^a	66.6 ± 15.7^a

^a $P < 0.05$ vs control.

Activation of NF- κ B

The activation of NF- κ B DNA binding activity in peripheral blood T lymphocytes was 57.00 ± 3.00 , 52.33 ± 2.08 , and 41.67 ± 1.53 U in the RES A, B, and C groups respectively, whereas it was 100.33 ± 7.57 U in the control group, being significantly lower in the RES A, B, and C groups than in the control group ($P < 0.05$). Figure 2 demonstrates the measurable NF- κ B DNA binding activity in the four groups on the 7th post-transplant day.

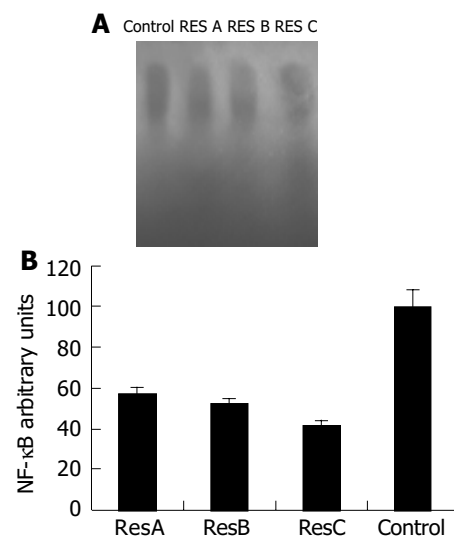


Figure 2 Levels of NF- κ B in peripheral T lymphocytes analyzed by EMSA (A) AND quantitation of NF- κ B activity by PhosphorImager (B).

Histopathologic examination

All the four groups showed the typical signs of severe graft rejection with intense portal infiltrate. There was an apparent difference in the severity of rejection between the RES C group (Banff score 4.3 ± 1.5) and control group (Banff score 7.3 ± 0.6) on the basis of Banff schema by a blinded pathologist ($P < 0.05$). Figure 3 shows the H&E staining of histologic sections in the RES C group and control group on the 7th posttransplant day.

DISCUSSION

The immuno-modulatory effect of resveratrol has been reported

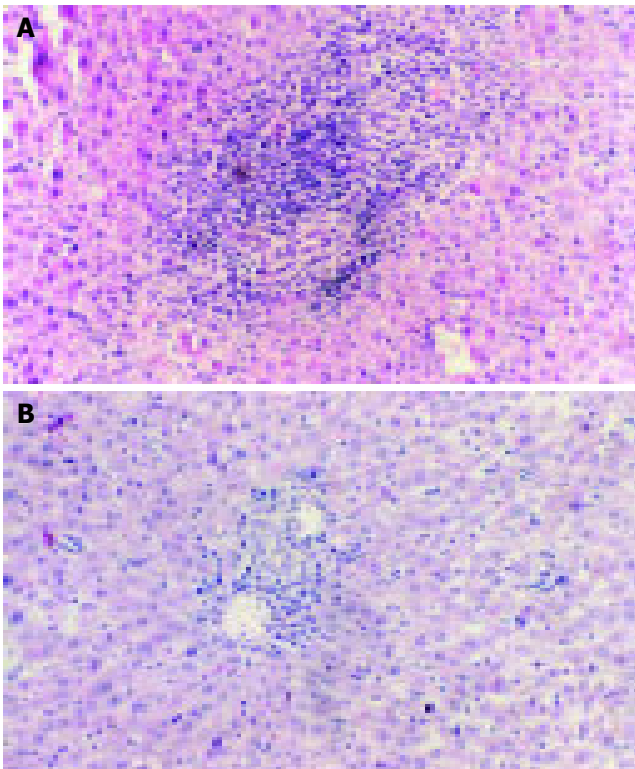


Figure 3 Typical signs of severe graft rejection in control group (A) and RES C group (B).

with use of mouse splenic lymphocytes, lymphokine activated killer (LAK) cells, mouse macrophage-like cell line RAW 264.7, and human peripheral blood T lymphocytes^[15,20-23]. Gao *et al.*^[15], reported that RES inhibits splenic lymphocyte proliferation, induction of cytotoxic T lymphocytes, and cytokine production, at least in part through the inhibition of NF- κ B activation. Yu *et al.*^[20], reported that RES can suppress notably the proliferation and transformation of human lymphocytes and the combination of resveratrol at a given concentration with cyclosporine-A can enhance immune suppression. Although most of these studies focused on the immunosuppressive effects of RES, a few experiments showed that low dose RES could enhance cell-mediated immune response. Feng *et al.*^[23], reported that RES (4 mg/kg, ig) promotes DTH response of mouse. However, the detailed mechanisms of the bi-phasic modulatory effects of RES remain to be studied. Our study revealed that RES could downregulate NF- κ B activation of peripheral T lymphocytes and IL-2 and INF- γ serum levels and decrease portal infiltrate of T lymphocytes in rats with severe rejection. RES has also been shown to promote albumin synthesis and prevent elevation of total bile acid and ALT and prolong the survival time of rats after liver transplantation.

As rejection occurs in the graft, hepatocytes are destroyed by infiltrating T lymphocytes. Hepatic function deteriorates as the number of hepatocytes decreases, and rejection eventually kills the recipient unless immuno-suppressants are given. In this hepatic allograft rejection model, RES decreased the number of accumulated mononuclear cells around the Glissonian triad in the H&E stained section on the 7th posttransplant day. RES may influence lymphocytes in the

hepatic allograft because of its influence on NF- κ B of T lymphocytes^[24].

Transcription factor NF- κ B, and other members of the Rel homology family of transcription factors play a pivotal role in the transcription of genes involved in immune and inflammatory responses^[25], and in cell proliferation and transformation^[26,27]. It is possible that suppression of lymphocyte infiltration and cytokine production by resveratrol may result from suppression of NF- κ B activation. In resting cells, NF- κ B remains sequestered in the cytoplasm in a functionally inactive form, non-covalently bound to an inhibitory protein, I κ B. Upon stimulation of cells with mitogens, antigens, or cytokines, I κ B dissociates from the NF- κ B complex, allowing NF- κ B to translocate to the nucleus where it binds to κ B motifs in the promoter region of the response genes. In our study, peripheral T lymphocytes expressed high levels of activated NF- κ B. However, after administration of RES, the NF- κ B activation due to the stimulation of heterogeneous antigens was blocked partly. These results are consistent with those of other investigators^[14,28].

It has been generally accepted that the immune response leading to graft rejection is accompanied with an increase of cytokine production by the primed T cells. Cytokines are essential for the differentiation, proliferation and amplification of the T cells^[29]. The most important cytokine is IL-2, which is essential for activated T cell proliferation^[30,31], and INF- γ is mainly secreted by activated T cells^[32] and induces MHC class I antigen expression in several kinds of cells such as lymphocytes^[33], myocytes^[34], endothelial cells^[35] and fibroblasts^[36]. Some studies have shown that the gene expression of IL-2 and INF- γ by intragraft is specific to acute rejection, which precedes histopathologic manifestations in liver transplantation^[37,38]. We also investigated the effect of resveratrol on the production of INF- γ and IL-2, and found that RES could suppress the serum IL-2 and INF- γ levels in rats after liver transplantation when it was administered at a dosage of 100 mg/kg body weight. The results are consistent with other reports^[15,22].

In conclusion, resveratrol downregulates the serum IL-2 and INF- γ levels, decreases the lymphocyte infiltration in allograft liver, prolongs the mean survival time after OLTx. Suppression of the activation of transcription factor NF- κ B in peripheral T lymphocytes appears to be a part of the mechanism by which resveratrol inhibits the *in vivo* development of immunological responses.

ACKNOWLEDGMENTS

The authors thank Tzakis AG, Division of Transplantation, Department of Surgery, University of Miami School of Medicine, and Phillip Ruiz, Department of Immunopathology, School of Medicine, University of Miami, for their invaluable assistance in critical reading and expert comments.

REFERENCES

- 1 Klintmalm GB. Rejection therapies. *Dig Dis Sci* 1991; **36**: 1431-1433
- 2 Kusne S, Dummer JS, Singh N, Iwatsuki S, Makowka L, Esquivel C, Tzakis AG, Starzl TE, Ho M. Infections after liver transplantation. An analysis of 101 consecutive cases.

- Medicine* 1988; **67**: 132-143
- 3 **Berlakovich GA**, Rockenschaub S, Taucher S, Kaserer K, Muhlbacher F, Steiniger R. Underlying disease as a predictor for rejection after liver transplantation. *Arch Surg* 1998; **133**: 167-172
 - 4 **Krasnow MN**, Murphy TM. Polyphenol glucosylating activity in cell suspension of grapes (*Vitis vinifera*). *J Agric Food Chem* 2004; **52**: 3467-3472
 - 5 **Soleas GJ**, Diamandis EP, Goldberg DM. Resveratrol: a molecule whose time has come? And gone? *Clin Biochem* 1997; **30**: 91-113
 - 6 **Frémont L**. Biological effects of resveratrol. *Life Sci* 2000; **66**: 663-673
 - 7 **Fauconneau B**, Waffo-Teguo P, Huguet F, Barrier L, Decendit A, Merillon JM. Comparative study of radical scavenger and antioxidant properties of phenolic compounds from *Vitis vinifera* cell cultures using *in vitro* tests. *Life Sci* 1997; **61**: 2103-2110
 - 8 **Jang M**, Cai L, Udeani GO, Slowing KV, Thomas CF, Beecher CW, Fong HH, Farnsworth NR, Kinghorn AD, Mehta RG, Moon RC, Pezzuto JM. Cancer chemopreventive activity of resveratrol, a natural product derived from grapes. *Science* 1997; **275**: 218-220
 - 9 **Subbaramaiah K**, Chung WJ, Michaluart P, Telang N, Tanabe T, Inoue H, Jang M, Pezzuto JM, Dannenberg AJ. Resveratrol inhibits Cyclo-oxygenase-2 transcription and activity in phorbol ester-treated human mammary epithelial cells. *J Biol Chem* 1998; **273**: 21875-21882
 - 10 **Hsieh TC**, Burfeind P, Laud K, Backer JM, Traganos F, Darzynkiewicz Z, Wu JM. Cell cycle effects and control of gene expression by resveratrol in human breast carcinoma cells lines with different metastatic potential. *Int J Oncol* 1999; **15**: 245-252
 - 11 **Hsieh TC**, Wu JM. Differential effects on growth, cell cycle arrest, and induction of apoptosis by resveratrol in human prostate cancer cell lines. *Exp Cell Res* 1999; **249**: 109-115
 - 12 **Clément MV**, Hirpara JL, Chawdhury SH, Pervaiz S. Chemopreventive agent resveratrol, a natural product derived from grapes, triggers CD95 signaling-dependent apoptosis in human tumor cells. *Blood* 1998; **92**: 996-1002
 - 13 **Ragione FD**, Cucciolla V, Borriello A, Pietra VD, Racioppi L, Soldati G, Manna C, Galletti P, Zappia V. Resveratrol arrests the cell division cycle at S/G2 phase transition. *Biochem Biophys Res Commun* 1998; **250**: 53-58
 - 14 **Holmes-McNary M**, Baldwin AS Jr. Chemopreventive properties of trans-resveratrol are associated with inhibition of activation of the I κ B kinase. *Cancer Research* 2000; **60**: 3477-3483
 - 15 **Gao X**, Xu YX, Janakiraman N, Chapman RA, Gautam SC. Immunomodulatory activity of resveratrol: suppression of lymphocyte proliferation, development of cell-mediated cytotoxicity, and cytokine production. *Biochem Pharmacol* 2001; **62**: 1299-1308
 - 16 **Wadsworth TL**, Koop DR. Effects of the wine polyphenolics quercetin and resveratrol on pro-inflammatory cytokine expression in RAW 264.7 macrophages. *Biochem Pharmacol* 1999; **57**: 941-949
 - 17 **Gao X**, Deeb D, Media J, Divine G, Jiang H, Chapman RA, Gautam SC. Immunomodulatory activity of resveratrol: discrepant *in vitro* and *in vivo* immunological effects. *Biochem Pharmacol* 2003; **66**: 2427-2435
 - 18 **Kamada N**, Calne RY. Orthotopic liver transplantation in the rat. Technique using cuff for portal vein anastomosis and biliary drainage. *Transplantation* 1979; **28**: 47-50
 - 19 **Dignam JD**, Lebovitz RM, Roeder RG. Accurate transcription initiation by RNA polymerase II in a soluble extract from isolated mammalian nuclei. *Nucleic Acids Res* 1983; **11**: 1475-1489
 - 20 **Yu L**, Wu SL, Zhang M, Pan CE. Effect of resveratrol alone and its combination with cyclosporin A on the immune function of human peripheral blood T lymphocytes. *Xibao Yu Fenzi Mianyixue Zazhi* 2003; **19**: 549-551
 - 21 **Boscolo P**, del Signore A, Sabbioni E, Di Gioacchino M, Di Giampaolo L, Reale M, Conti P, Paganelli R, Giaccio M. Effects of resveratrol on lymphocyte proliferation and cytokine release. *Ann Clin Lab Sci* 2003; **33**: 226-231
 - 22 **Falchetti R**, Fuggetta MP, Lanzilli G, Tricarico M, Ravagnan G. Effects of resveratrol on human immune cell function. *Life Sci* 2001; **70**: 81-96
 - 23 **Feng YH**, Zhou WL, Wu QL, Li XY, Zhao WM, Zou JP. Low dose of resveratrol enhanced immune response of mice. *Acta Pharmacol Sin* 2002; **23**: 893-897
 - 24 **Kochel I**, Strzadala L. FK506-binding proteins in the regulation of transcription factors activity in T cells. *Postepy Hig Med Dosw* 2004; **58**: 118-127
 - 25 **Lenardo MJ**, Baltimore D. NF- κ B: a pleiotrophic mediator of inducible, and tissue-specific gene control. *Cell* 1989; **58**: 227-229
 - 26 **Bargou RC**, Emmerich F, Krappmann D, Bommert K, Mapara MY, Arnold W, Royer HD, Grinstein E, Greiner A, Scheidereit C, Dorken B. Constitutive nuclear factor- κ B-RelA activation is required for proliferation and survival of Hodgkin's disease tumor cells. *J Clin Invest* 1997; **100**: 2961-2969
 - 27 **Reuther JY**, Reuther GW, Cortez D, Pendergast AM, Baldwin AS Jr. A requirement for NF- κ B activation in Bcr-Abl-mediated transformation. *Genes Dev* 1998; **12**: 968-981
 - 28 **Manna SK**, Mukhopadhyay A, Aggarwal BB. Resveratrol suppresses TNF-induced activation of nuclear transcription factors NK-KappaB, activator protein-1, and apoptosis: potential role of reactive oxygen intermediates and lipid peroxidation. *J Immunol* 2000; **164**: 6509-6519
 - 29 **Schwartz RH**. Costimulation of T lymphocytes: the role of CD28, CTLA-4, and B7/BB1 in interleukin-2 production and immunotherapy. *Cell* 1992; **71**: 1065-1068
 - 30 **Fitch FW**, McKisic MD, Lancki DW, Gajewski TF. Differential regulation of murine T lymphocyte subsets. *Annu Rev Immunol* 1993; **11**: 29-48
 - 31 **Seder RA**, Paul WE. Acquisition of lymphokine-producing phenotype by CD4⁺ T cells. *Annu Rev Immunol* 1994; **12**: 635-673
 - 32 **Halloran PF**, Wadgymar A, Autenried P. The regulation of expression of major histocompatibility complex products. *Transplantation* 1986; **41**: 413-420
 - 33 **Walrand F**, Picard F, McCullough K, Martinod S, Levy D. Recombinant bovine interferon-gamma enhances expression of class I and class II bovine lymphocyte antigens. *Vet Immunol Immunopathol* 1989; **22**: 379-383
 - 34 **Kalovidouris AE**. The role of cytokines in polymyositis: interferon-gamma induces class II and enhances class I major histocompatibility complex antigen expression on cultured human muscle cells. *J Lab Clin Med* 1992; **120**: 244-251
 - 35 **Doukas J**, Pober JS. IFN-gamma enhances endothelial activation induced by tumor necrosis factor but not IL-1. *J Immunol* 1990; **145**: 1727-1733
 - 36 **Morris AG**, Ward GA, Bateman WJ. Instability of expression of major histocompatibility antigens in fibroblasts expressing activated ras oncogene: constitutive and interferon-gamma induced class I and class II antigens in a series of clonal isolates of murine fibroblasts transformed by v-Ki-ras. *Br J Cancer* 1989; **60**: 211-215
 - 37 **Martinez OM**, Villanueva JC, Lake J, Roberts JP, Ascher NL, Krams SM. IL-2 and IL-5 gene expression in response to alloantigen in liver allograft recipients and *in vitro*. *Transplantation* 1993; **55**: 1159-1166
 - 38 **Gaweco AS**, Otto G, Otto HF, Meuer S, Geisse T, Hofmann WJ. Common and sequential overexpression patterns of T-helper cytokines during acute (cellular) rejection and correlation of proinflammatory cytokine expression with chronic (dactypenic) rejection of human liver allografts: a study under cyclosporine, FK506, and quadruplet BT563 immunosuppression. *Transplant proc* 1995; **27**: 1152-1154

Expression of interferon inducible protein-10 in pancreas of mice

Dong Li, Su-Wen Zhu, Dong-Juan Liu, Guo-Liang Liu

Dong Li, Department of Infectious Disease, the First Affiliated Hospital of China Medical University, Shenyang 110001, Liaoning Province, China

Su-Wen Zhu, Dong-Juan Liu, Department of Histology and Embryology, the College of Basic Science, China Medical University, Shenyang 110001, Liaoning Province, China

Guo-Liang Liu, Department of Endocrinology, the First Affiliated Hospital of China Medical University, Shenyang 110001, Liaoning Province, China

Correspondence to: Dr. Dong Li, Department of Infectious Disease, the First Affiliated Hospital of China Medical University, 155 Nanjing Beijie, Shenyang 110001, Liaoning Province, China. ldcmu@yahoo.com.cn

Telephone: +86-24-23256666-6213

Received: 2005-03-28 Accepted: 2005-04-11

Abstract

AIM: To investigate the expression of interferon inducible protein-10 (IP-10) in pancreas of mice and to discuss its possible role in the pathogenesis of type 1 diabetes.

METHODS: Non-obese diabetic (NOD) mice were used as experiment group and BALB/c mice as non-diabetic prone model. Immunohistochemistry method was used to evaluate the expression of IP-10 in the pancreas of NOD mice and BALB/c mice. Immunoelectron microscope was used to show the location of IP-10 in pancreatic islet β cells.

RESULTS: Pancreatic islets were positively stained in all the NOD mice. Insulinitis could be found in mice at the age of 4 wk. The weakly positive results were found in control group with no insulinitis. Immunoelectron microscopy further demonstrated that IP-10 was produced by pancreatic β cells and stored in cytoplasm of the cells.

CONCLUSION: IP-10 can be largely produced in pancreatic islets of NOD mice at the age of 2 wk when there is no significant insulinitis, and may play an important part in the pathogenesis of type 1 diabetes by attracting immune cells to infiltrate the pancreatic islets.

© 2005 The WJG Press and Elsevier Inc. All rights reserved.

Key words: Interferon inducible Protein-10; Type 1 diabetes; Insulinitis

Li D, Zhu SW, Liu DJ, Liu GL. Expression of interferon inducible protein-10 in pancreas of mice. *World J Gastroenterol* 2005; 11(30): 4750-4752

<http://www.wjgnet.com/1007-9327/11/4750.asp>

INTRODUCTION

Type 1 diabetes has been recognized as an organ specific autoimmune disease due to the immune destruction of pancreatic islet β cells in genetically susceptible individuals^[1]. In both human and rodent models of Type 1 diabetes, the disease has a distinct stage characterized by infiltration of immune cells in the pancreas (insulinitis). The major populations of infiltrating cells are macrophages and lymphocytes. Therefore, immune cell infiltration in pancreatic islets may be a crucial step in the pathogenesis of type 1 diabetes^[2]. Experiments have shown that interferon induced protein-10 (IP-10), an important member of CXC chemokine subfamily, has chemoattractant effects on monocytes and activated lymphocytes^[3]. Thus, we hypothesize that IP-10 may recruit immune cells into the pancreas by binding to the chemokine receptor, CXCR4 expressed on the target cells, thus leading to type 1 diabetes. In this study, we evaluated the expression of IP-10 in the pancreas of animal model of type 1 diabetes and discussed its possible role in the pathogenesis of type 1 diabetes.

MATERIALS AND METHODS

Experimental animals and samples

Experimental NOD mice were obtained from Shanghai Laboratory Animal Center, Chinese Academy of Sciences. Pancreatic islet infiltration of immune cells appeared and insulinitis developed in the mice at the age of 4 wk. Insulinitis became most serious at the age of 9-10 wk. The remaining pancreatic β cells decreased to 10% of normal levels and diabetes developed. The incidence of diabetes in female NOD mice was higher than that in males. BALB/c mice were used as non-diabetes and non-autoimmune-prone control. Blood glucose in all the mice was measured before death. If the blood glucose concentrations exceeded 300 mg/L, diabetes could be considered.

The mice were killed by decollation. Pancreases were fixed in 40 g/L formaldehyde and embedded in paraffin. Paraffin-embedded tissues were sectioned and stained with hematoxylin-eosin and analyzed by light microscopy.

Expression of IP-10

Dewaxed sections were stained using streptavidin-biotin-peroxidase complex (SABC) method (Wuhan Boster Biological Technology Co., Ltd). Primary antibody was goat anti-mouse polyclonal antibody (Santa Cruz Biotechnology, Inc.). The color of the complex was developed using 3,3'-diaminobenzidine tetrahydrochloride (DAB) kit (AR1022). The sections were counterstained with hematoxylin, dehydrated and mounted, examined microscopically.

Immunoelectron microscopy

The samples were fixed with 1% osmic acid, after the color reaction using DAB. Sections were dehydrated in graded ethanol solutions and embedded in Epon 872. Ultra-thin (70 nm) sections were made and stained with uranyl acetate, and then examined under JEM-1200EX (JEOL) electron microscope.

RESULTS

Expression of IP-10 in NOD mice

Pancreatic islets were positively stained in all NOD mice. Insulinitis could be found at the age of 4 wk (Figures 1A-D)

Expression of IP-10 in BALB/C mice

Weakly positive results were found in the pancreatic islets of BALB/c mice, which were stained light brown (Figure 2). No insulinitis could be found.

Immunoelectron microscopy in NOD mice

Immunoelectron microscopy demonstrated that IP-10 was

produced by pancreatic β cells and stored in cytoplasm of the cells (Figure 3).

DISCUSSION

Type 1 diabetes is a chronic disease, severely affecting the health of children. Its incidence has been increasing continuously from 1980s. In both human and rodent models of Type 1 diabetes, the disease has a distinct stage characterized by immune cell infiltration in pancreas (insulinitis). The major populations of infiltrating cells are macrophages and lymphocytes. Therefore, the infiltration of macrophages and lymphocytes may be a crucial step in the auto-immune response of type 1 diabetes. IP-10 is a member of CXC chemokine subfamily and has chemoattractant effects on monocytes and activated lymphocytes. Thus, we suppose that it may play an important part in the immune cell infiltration of pancreatic islets.

We demonstrated in this study that the expression of IP-10 was positive in the pancreas of both NOD mice and

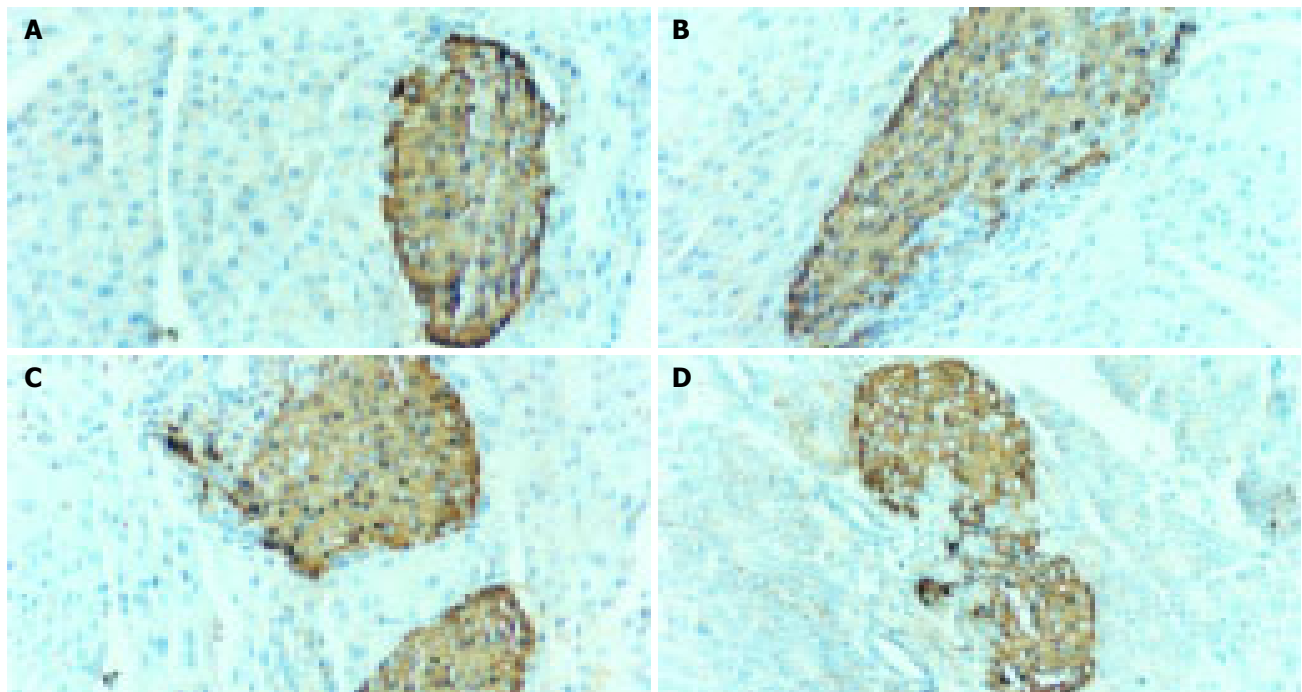


Figure 1 Expression of IP-10 in pancreatic islets of NOD mice at the age of 2

wk (A), 4 wk (B), 8 wk (C), and 14 wk (D).

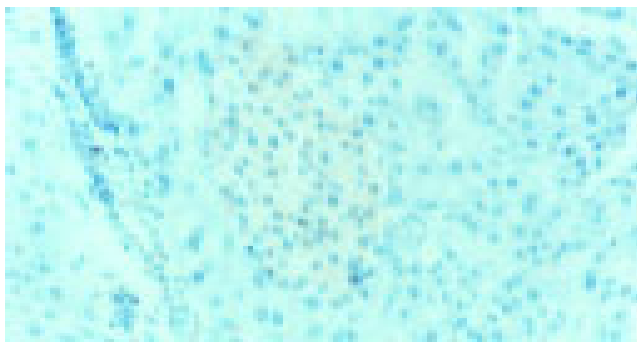


Figure 2 Expression of IP-10 in pancreatic islets of BALB/C mice at the age of 4 wk.

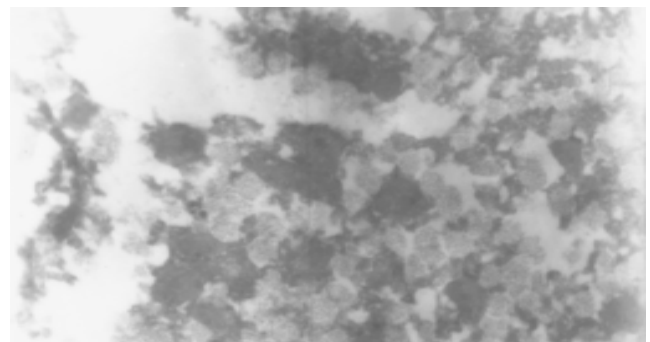


Figure 3 Various shapes of IP-10 crystal in pancreatic islet β cells.

BALB/c mice, which agrees well with the findings of Arimilli *et al.*^[4], suggesting that IP-10 is constitutively produced by the pancreatic islets in mice. But the production of IP-10 is small because weak expression of IP-10 has been shown in BALB/c mice, and IP-10 produced has no chemoattractant effect as no infiltration of immune cells could be found in the control group. It has long been known that chemokines have many functions in addition to chemo-attractant effect. IP-10 is involved in delayed-type allergy and the suppression of angiogenesis. Therefore, IP-10 has other biological functions in normal pancreatic tissues other than chemoattractant effect. Few studies on expressions of IP-10 in pancreas are available. The acute functions of the constitutive expressions of IP-10 in pancreatic tissues need further study. But, the pancreatic islets of diabetic mice produce high level of IP-10 and accompanied insulinitis, which supports our hypothesis that abundant IP-10 can be produced in a pathological environment and attract immune cells into pancreatic tissues. Our study also proved that IP-10 could be found in the pancreatic islets of NOD mice at the age of 2 wk when there was no significant insulinitis, suggesting that IP-10 is produced at the onset of diabetes. Its concentration may not be high enough to cause insulinitis at first. As IP-10 accumulates, more immune cells can be recruited into the pancreatic islets and finally result in insulinitis.

Viral infections and inflammatory cytokines including IL-1 β and interferon- γ are important factors triggering type 1 diabetes. Double stranded RNA (dsRNA) produced by virus cooperated with IL-1 β and Interferon- γ or IL-1 β could induce high levels of IP-10 in human and NOD mice pancreatic β cells *in vitro*^[5,6]. Our study also showed that IP-10 existed in the pancreatic β cells. These results indicate that pancreatic β cells can produce IP-10, and that virus and inflammatory cytokines can initiate expression of IP-10 *in vivo*. Pancreatic β cells are possibly one of the main sources of IP-10. It has been reported that pancreatic islet specific Th1 cells can produce IP-10 and may be another source^[7].

We can speculate about the possible mechanism of viral infections causing diabetes based on the present studies. Viruses induce the expression of IP-10 in pancreatic β cells, and IP-10 is secreted into the pancreatic islets. Then, peripheral

immune cells migrate into the pancreatic islets along with the IP-10 concentration gradient and result in insulinitis.

Since few studies on the role of IP-10 in type 1 diabetes are available, our data are necessary to be confirmed by more studies. There is no study on the expression of IP-10 in the pancreas of patients with type 1 diabetes. Although the serum IP-10 levels in newly diagnosed patients with type 1 diabetes are much higher than those in healthy subjects^[8], chemokines tend to form high concentration grade in local secretion point that attract target cells. The serum chemokine level cannot reflect the true conditions of expressions of chemokine in human pancreas.

In conclusion, IP-10 may play an important part in the pathogenesis of type 1 diabetes by attracting immune cells to infiltrate the pancreatic islets.

REFERENCES

- 1 **Devendra D**, Liu E, Eisenbarth GS. Type 1 diabetes: recent developments. *BMJ* 2004; **328**: 750-754
- 2 **Atkinson MA**, Eisenbarth GS. Type 1 diabetes: new perspectives on disease pathogenesis and treatment. *LANCET* 2001; **358**: 221-229
- 3 **Atkinson MA**, Wilson SB. Fatal attraction: chemokines and type 1 diabetes. *J Clin Invest* 2002; **110**: 1611-1613
- 4 **Arimilli S**, Ferlin W, Solvason N, Deshpande S, Howard M, Mocchi S. Chemokines in autoimmune diseases. *Immunol Rev* 2000; **177**: 43-51
- 5 **Liu D**, Cardozo AK, Darville MI, Eizirik DL. Double-stranded RNA cooperates with interferon- γ and IL-1 β to induce both chemokine expression and nuclear factor- κ B-dependent apoptosis in pancreatic β -cells: potential mechanisms for viral-induced insulinitis and β -cell death in type 1 diabetes mellitus. *Endocrinology* 2002; **143**: 1225-1234
- 6 **Cardozo AK**, Proost P, Gysemans C, Chen MC, Mathieu C, Eizirik DL. IL-1 β and IFN- γ induce the expression of diverse chemokines and IL-15 in human and rat pancreatic islet cells, and in islets from pre-diabetic NOD mice. *Diabetologia* 2003; **46**: 255-266
- 7 **Bradley LM**, Asensio VC, Schioetz LK, Harbertson J, Krahl T, Patstone G, Woolf N, Campbell IL, Sarvetnick N. Islet-specific Th1, But Not Th2, cells secrete multiple chemokines and promote rapid induction of autoimmune diabetes. *J Immunol* 1999; **162**: 2511-2520
- 8 **Shimada A**, Morimoto J, Kodama K, Suzuki R, Oikawa Y, Funae O, Kasuga A, Saruta T, Narumi S. Elevated serum IP-10 levels observed in type 1 diabetes. *Diabetes Care* 2001; **24**: 510-515

Influence of HLA-DRB1 alleles and HBV genotypes on interferon- α therapy for chronic hepatitis B

Rui-Hai Chu, Li-Xian Ma, Gang Wang, Li-Hua Shao

Rui-Hai Chu, Li-Xian Ma, Gang Wang, Li-Hua Shao, Department of Infectious Diseases, Qilu Hospital of Shandong University, Jinan 250012, Shandong Province, China

Correspondence to: Dr. Rui-Hai Chu, Department of Infectious Diseases, Qilu Hospital of Shandong University, Jinan 250012, Shandong Province, China. rhchu@163.com

Telephone: +86-531-8380313

Received: 2004-07-12 Accepted: 2004-08-25

Abstract

AIM: To investigate the influence of HLA-DRB₁ alleles and HBV genotypes on interferon- α therapy for chronic hepatitis B.

METHODS: HLA-DRB₁*03, *07, *09, *12, *15 alleles were determined using polymerase chain reaction/sequence specific primer (PCR/SSP) technique in 126 patients with chronic hepatitis B and 76 normal control subjects in Shandong Province, and HBV genotypes were determined by nested-PCR analysis using type-specific primers in 126 patients.

RESULTS: The positivity of HLA-DRB₁*07 allele in chronic hepatitis B group was significantly higher than that in normal control group ($\chi^2 = 6.33$, $P < 0.025$, $RR = 2.37$). Among the 126 patients, genotype B was found in 38 (30.2%), genotype C in 69 (54.8%), and mixed genotype (B+C) in 19 (15.0%), genotypes D-F were not found. Among the 46 DRB₁*07(+) patients, 7 were responders and 39 were non-responders among them ($\chi^2 = 6.71$, $P < 0.05$). The positivity of HLA-DRB₁*07 and prevalence of HBV genotype C were significantly higher in non-responders than in responders.

CONCLUSION: High positivities of HLA-DRB₁*07 allele and HBV genotype C are closely associated with the lower response to interferon- α therapy for chronic hepatitis B.

© 2005 The WJG Press and Elsevier Inc. All rights reserved.

Key words: HLA-DRB₁ alleles; HBV genotypes; Interferon- α therapy; Chronic hepatitis B

Chu RH, Ma LX, Wang G, Shao LH. Influence of HLA-DRB₁ alleles and HBV genotypes on interferon- α therapy for chronic hepatitis B. *World J Gastroenterol* 2005; 11(30): 4753-4757
<http://www.wjgnet.com/1007-9327/11/4753.asp>

INTRODUCTION

Hepatitis B virus (HBV) is a well-known agent of acute and

chronic hepatitis. Seventy-five percent of the estimated 400 million patients with chronic HBV infection in the world are Asians^[1]. Transient infections may cause fatal, fulminant hepatitis and chronic infections may lead to liver cirrhosis and even hepatocellular carcinoma.

Interferon- α (IFN- α) has anti-viral, immuno-modulatory, anti-proliferative, and gene induction properties. Treatment with interferon- α results in the clearance of HBeAg, and is associated with improved clinical outcomes^[2]. It is well-known that several factors influence the response, including viral factors (particularly serum HBV-DNA loads), host factors, which may be genetic (sex, cytokine polymorphism), other factors such as age, serum aminotransferase activities, grade of inflammatory activity in liver, presence of cirrhosis, and race. The aim of this study was to identify the influence of HLA-DRB₁ alleles and HBV genotypes on the response to interferon- α therapy.

MATERIALS AND METHODS

Subjects

A total of 126 patients (94 males, 32 females, mean age: 33.2±10.6 years) with chronic hepatitis B and 76 healthy controls (54 males, 22 females, mean age: 33.8±9.8 years) were enrolled in this study. These patients received treatment in the Department of Infectious Diseases, Qilu Hospital of Shandong University, China. The diagnoses of these patients were made according to the criteria established in the National Viral Hepatitis Conference of China (2000). All the patients and controls were Chinese Han people from Shandong Province. HCV infection, auto-immune hepatitis and metabolic disorders were excluded by appropriate clinical and laboratory evaluations. They had no histories of malignancy or depression, immunodeficiency virus infection, liver cirrhosis, decompensated liver diseases, use of IFN and thyroid abnormality, chemotherapy, or other agents that could influence treatment outcomes. HLA-DRB₁*03, *07, *09, *12, *15 alleles were determined in all patients and healthy controls. HBV genotypes were detected only in patients.

The 126 patients received IFN- α treatment subcutaneously at a dose of 3 MU thrice weekly for 24 wk. The response to IFN- α therapy was defined as loss of HBeAg, sero-conversion to anti-HBe, normalization of serum ALT levels and HBV-DNA (-). The patients with a response were described as 'responders' and those without response as 'non-responders' in this report.

Serological tests

Sera were tested for ALT, HBeAg, anti-HBeAg, and HBV-

DNA. The remaining sera were stored at $-70\text{ }^{\circ}\text{C}$.

Genotyping of HLA alleles

Genomic DNA was extracted from frozen blood clots by proteinase K digestion followed by phenol/chloroform extraction and ethanol precipitation. DNA was typed for HLA class II alleles DRB1*03, *07, *09, *12, *15 by polymerase chain reaction (PCR), using published sequence-specific primers^[2]. A total amount of 50 μL PCR reaction solution contained 1 μL of each sequence specific primer (10 $\mu\text{mol/L}$), 2 μL of genomic DNA (60-80 ng/ μL), 5 μL of 10 \times buffer, 5 μL of MgCl_2 (15 mmol/L), 5 μL of dNTP (2 mmol/L), 0.4 μL of Taq polymerase (5 U/ μL) and 30.6 μL of deionized H_2O . The PCR cycling parameters of HLA-DRB1 alleles were as follows: pre-denaturation at $94\text{ }^{\circ}\text{C}$ for 5 min, denaturation at $94\text{ }^{\circ}\text{C}$ for 30 s, annealing at $55\text{ }^{\circ}\text{C}$ for 1 min, extension at $72\text{ }^{\circ}\text{C}$ for 50 s, repetition for 30 cycles and final extension at $72\text{ }^{\circ}\text{C}$ for 5 min.

Genotyping of HBV

Nucleic acid of HBV was extracted from 200 μL serum samples by heating at $100\text{ }^{\circ}\text{C}$ for 10 min and the HBV genome was amplified by nested PCR using universal primers for the outer primers, followed by two different mixtures containing type-specific inner primers^[3]. The first round of PCR was carried out in a tube containing 40 μL of a reaction buffer containing 4 μL of HBV-DNA, 4 μL of 10 \times buffer, 4 μL of MgCl_2 (15 mmol/L), 4 μL of dNTPs (10 mmol/L), 0.2 μL of Taq polymerase (5 U/ μL), 4 μL of each outer primer (12.5 $\mu\text{g/mL}$), and 15.8 μL of deionized H_2O . The thermocycler was programmed to incubate the samples for 2 min at $94\text{ }^{\circ}\text{C}$, followed by 35 cycles, each at $94\text{ }^{\circ}\text{C}$ for 15 s, at $58\text{ }^{\circ}\text{C}$ for 30 s, at $72\text{ }^{\circ}\text{C}$ for 30 s, and final extension at $72\text{ }^{\circ}\text{C}$ for 7 min. Two second rounds of PCR were performed for each sample, with the common universal anti-sense primers for mixA and mixB. Two microliters of the first PCR product was added to two tubes containing the second sets of each of the inner primer pairs, each of the deoxynucleotides, Taq polymerase and PCR buffer, as in the first reaction, then amplified with the following parameters: preheating at $94\text{ }^{\circ}\text{C}$ for 2 min, then followed by 35 cycles, each at $94\text{ }^{\circ}\text{C}$ for 15 s, at $60\text{ }^{\circ}\text{C}$ for 30 s, at $72\text{ }^{\circ}\text{C}$ for 30 s, and final extension at $72\text{ }^{\circ}\text{C}$ for 7 min.

HLA-DRB1*03, *07, *09, *12, *15 alleles and genotypes of HBV for each sample were determined by identifying the genotype-specific DNA bands. All the primers were synthesized by Shanghai Branch, Canadian Sangon Company.

Taq DNA polyenzyme and dNTPs were also purchased from Shanghai Branch, Canadian Sangon Company. pUC19 DNA/*MspI* (*HpaII*) marker 23 was purchased from MBI Fermentas. Amplifications of all samples were performed in a GeneAmp PCR system (GeneAmp PCR system 9600; Perkin Elmer).

Detection of PCR products

PCR products were electrophoresed on 2% agarose gel, stained with ethidium bromide, and evaluated under ultraviolet light. The sizes of PCR products were estimated according to the pUC19 DNA/*MspI* (*HpaII*) marker 23.

Statistical analysis

The positivity of HLA-DRB1 alleles was calculated by direct count. The positive number (PN) of the study group was compared with that of the control group using χ^2 -test. Relative risk frequencies (RR) were calculated according to Wolf formula. $P < 0.05$ was considered statistically significant.

RESULTS

HLA-DRB1 alleles in patients with chronic hepatitis B and healthy controls

The distribution of HLA-DRB1*03, *07, *09, *12, *15 alleles in patients with chronic hepatitis B and healthy controls is shown in Table 1. The positivity of HLA-DRB1*07 allele in patients with chronic hepatitis B group was markedly higher than that in normal controls, there was a significant difference between them. The positivity of HLA-DRB1*03, *09, *12, *15 alleles in patients with chronic hepatitis B was not different from that in normal controls. The electrophoresis of HLA-DRB1*03, *07, *09, *12, *15 alleles is shown in Figure 1.

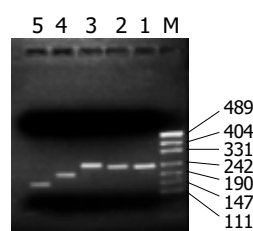


Figure 1 Electrophoresis of HLA-DRB1*03, *07, *09, *12, *15 alleles. M: pUC19 DNA/*MspI* (*HpaII*) marker 23; 1: DRB1*0701/0702, 232 bp; 2: DRB1*0901, 236 bp; 3: DRB1*1201/1202, 248 bp; 4: DRB1*1501/1502, 197 bp; 5: DRB1*0301/0302, 151 bp.

Table 1 Distribution of HLA-DRB1*03, *07, *09, *12, *15 alleles in patients with chronic hepatitis B and healthy controls

DRB1 Allele	Chronic hepatitis (n = 126)		Normal control (n = 76)		RR	χ^2	P
	PN	PR (%)	PN	PR (%)			
0301/0302	10	7.9	5	6.6	1.24	0.13	>0.75
0701/0702	46	36.5	15	19.7	2.37	6.33	<0.025
0901	31	24.6	22	28.9	0.80	0.46	>0.50
1201/1202	17	13.5	12	15.8	0.85	0.20	>0.75
1501/1502	16	12.7	9	11.8	1.08	0.03	>0.90
Blank	19	15.0	8	10.5	1.51	0.85	>0.50

PN: positive number, PR: positive rate, RR: relative risk.

Prevalence of HBV genotypes in patients with chronic hepatitis B

The prevalence of different HBV genotypes in patients with chronic hepatitis B is shown in Table 2. Genotype B was found in 38 patients (30.2%), genotype C in 69 (54.8%), mixed genotype (B+C) in 19 (15.0%), genotypes D- F were not found. Genotypes C and B were the major genotypes in this area. The electrophoresis of HBV genotypes is shown in Figure 2.

Table 2 Prevalence of different HBV genotypes in patients with chronic hepatitis B

Genotype	Number	%
B	38	30.2
C	69	54.8
B+C	19	15.0
D	0	0
E	0	0
F	0	0

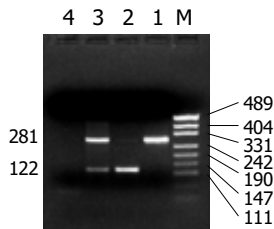


Figure 2 Electrophoresis of HBV genotypes. M: pUC19 DNA/*MspI* (*HpaII*) marker 23; lane 1: genotype B (281 bp); lane 2: genotype C (122 bp); lane 3: genotype B+C; lane 4: negative control.

No response of HLA-DRB1*07 to IFN- α therapy

Among the 46 DRB1*07(+) patients, 7 were responders and 39 were non-responders. Compared with the DRB1*07 (-) patients, the positivity of DRB1*07 in responder group was significantly lower than that in non-responder group ($\chi^2 = 4.51, P < 0.05$), indicating that DRB1*07 had no response to IFN- α therapy (Table 3).

Table 3 Correlation between DRB1*07 and IFN- α therapy, n (%)

	Responder (n=33)	Non-responder (n=93)	Total (126)	χ^2	P
HLA-DRB1*07(+)	7 (15.2)	39 (84.8)	46	4.51	<0.05
HLA-DRB1*07(-)	26 (32.5)	54 (67.5)	80		

Response of HBV genotypes C and B to interferon- α therapy

Patients with HBV genotype C had a significantly lower response to IFN- α , only 13% *vs* 50% among patients with genotype B and 26.3% with genotype B+C ($\chi^2 = 17.3, P < 0.005$, Table 4).

Response to interferon- α therapy in patients with HLA-DRB1*07 (+) and genotype C (+)

The patients with both HLA-DRB1*07(+) and genotype C (+) were compared with those with HLA-DRB1*07(+) or

genotype C(+), significant difference was found among them ($\chi^2 = 6.71, P < 0.05$, Table 5).

Table 4 Response to interferon- α therapy in patients with different genotypes, n (%)

	Responder	Non-responder	Total	χ^2	P
Genotype				17.3	<0.005
B	19 (50)	19 (50)	38		
C	9 (13)	60 (87)	69		
B+C	5 (26.3)	14 (73.7)	19		

Table 5 Response to interferon- α therapy in patients with HLA-DRB1*07 and genotype C, n (%)

	Responder	Non-responder	Total	χ^2	P
HLA-DRB1*07+				6.36	<0.05
genotype C					
+ +	2 (7.7)	24 (92.3)	26		
+ -	7 (35)	13 (65)	20		
- +	14 (32.6)	29 (67.4)	43		

DISCUSSION

Currently, two therapeutic agents, interferon and lamivudine, are used in treatment of chronic hepatitis B in most countries, and the only agent known to have a lasting beneficial effect on chronic hepatitis B is interferon- α . It was reported that IFN treatment can result in sustained clearance of HBeAg in approximately 25-40% of patients, and a loss of HBsAg in 10% of Western patients^[4]. The response of chronic hepatitis B to IFN- α is generally determined by a combination of virological factors, host immunological factors and genetic factors^[5-10].

The present study aimed to investigate the role of HBV genotypes and HLA-DRB1 alleles in response to IFN- α in Chinese Han hepatitis B patients. Until now, HBV can be classified into eight genotypes (A-H)^[11-14]. HBV genotypes have a characteristic geographic distribution^[13-18]. Genotype A is more common in North America and northwestern Europe, genotypes B and C are the two most common genotypes prevailing in Asia. Genotype D is predominant in the Mediterranean area, the Middle East, and in India. The distribution of genotype H is less studied. Studies suggested that genotype A is associated with a higher rate of IFN- α -induced HBeAg sero-conversion than genotype D^[19], and genotype B is associated with a higher rate of IFN- α -induced HBeAg clearance than genotype C^[20,21]. Our study showed that HBV genotype C was associated with a lower rate of anti-viral response to IFN- α treatment in Chinese Han patients with HBeAg-positive chronic hepatitis B than genotype B and genotype B+C (50% *vs* 13% *vs* 26.3%, $P < 0.005$). Further studies are needed to determine if HBV genotypes also play a role in response to IFN- α treatment of chronic hepatitis B patients from other geographic regions where other HBV genotypes prevail.

Great inconsistencies exist in studies about the association between HLA-DRB1 alleles and chronic hepatitis B. Jiang *et al.*, suggested that the allele frequencies of HLA-DRB1*0301

in chronic hepatitis B group (17.31%) are markedly higher than those in normal control group (5.67%), and that HLA-DRB1*0301 is closely associated with susceptibility to chronic hepatitis B. They also found that the allele frequencies of HLA-DRB1*1101/1104 in chronic hepatitis B group were markedly lower than those in acute hepatitis B group, and that HLA-DRB1*1101/1104 is closely associated with resistance to chronic hepatitis B. Shen *et al.*^[9] suggested that susceptibility to chronic hepatitis B is strongly associated with HLA-DRB1*10 allele in northern Chinese patients. Cotrina *et al.*^[22], reported that HLA-DRB1*1301 and -DRB1*1302 alleles are associated with the clearance of HBV infection and protect people against chronic hepatitis B. Diepolder *et al.*^[10], found that a strong virus-specific CD4⁺ and CD8⁺ T lymphocyte response to HBV is associated with viral clearance, patients with acute hepatitis B carrying HLA-DR13 have a more vigorous CD4⁺ T cell response to HBV core than patients not carrying HLA-DR13, suggesting that HLA-DR13 is associated with a self-limited course of HBV infection. In the present study, we did not examine HLA-DRB1*11 and HLA-DRB1*13, but there was no significant difference in HLA-DRB1*03 between the control group and the chronic hepatitis B group, which is inconsistent with Jiang's report. On the contrary, we found that HLA-DRB1*07 was significantly higher in chronic hepatitis B group than in control group, the response to IFN- α therapy was significantly lower in HLA-DRB1*07(+) group than in HLA-DRB1*07(-) group ($P < 0.05$), suggesting that susceptibility to persistent infection and lower response to interferon- α are significantly associated with the presence of HLA-DRB1*07^[23-25].

It is more important that the response to IFN- α therapy in patients with both HLA-DRB1*07(+) and genotype C (+) was even lower than that in patients with HLA-DRB1*07 (+) or genotype C (+, $P < 0.05$), suggesting that HBV genotype C and HLA-DRB1*07 are closely associated with lower response of chronic hepatitis B to IFN- α therapy. Therefore, early exclusion of their existence before anti-viral therapy is very important for selection of patients and judgment of their prognosis.

ACKNOWLEDGMENTS

The authors thank XR Song and AQ Zheng (Tumor Research Center, Shandong Tumor Hospital) for their assistance with the PCR and serologic assays, and all patients for participating in this research.

REFERENCES

- 1 Merican I, Guan R, Amarapukaa D, Alexander MJ, Chutaputti A, Chien RN, Hasnain SS, Leung N, Lesmana L, Phiet PH, Sjalfoellah Noer HM, Sollano J, Sun HS, Xu DZ. Chronic hepatitis B virus infection in Asian countries. *J Gastroenterol Hepatol* 2000; **15**: 1356-1361
- 2 Olerup O, Zetterquist H. HLA-DR typing by PCR amplification with sequence-specific primers (PCR-SSP) in 2 h: an alternative to serological DR typing in clinical practice including donor-recipient matching in cadaveric transplantation. *Tissue Antigen* 1992; **39**: 225-235
- 3 Naito H, Hayashi S, Abe K. Rapid and specific genotyping system for hepatitis B virus corresponding to six major genotypes by PCR using type-specific primers. *J Clin Microbiol* 2001; **39**: 362-364
- 4 Wong DK, Cheung AM, O'Rourke K, Naylor CD, Detsky AS, Heathcote J. Effect of alpha-interferon treatment in patients with hepatitis B e antigen-positive chronic hepatitis B. A metaanalysis. *Ann Intern Med* 1993; **119**: 312-323
- 5 Lindh M, Hannoun C, Horal P, Krogsgaard K. Interpret Study Group. Virological response to interferon therapy of chronic hepatitis B as measured by a highly sensitive assay. *J Viral Hepat* 2001; **8**: 349-357
- 6 Brunetto MR, Oliveri F, Coco B, Leandro G, Colombatto P, Gorin JM, Bonino F. Outcome of anti-HBe positive chronic hepatitis B in alpha-interferon treated and untreated patients: a long term cohort study. *J Hepatol* 2002; **36**: 263-270
- 7 Carreno V, Marchllin P, Hadziyannis S, Salmeron J, Diago M, Kitis GE, Vafiadis I, Schalm SW, Zahm F, Manzarbeitia F, Jimenez FJ, Quiroga JA. Retreatment of chronic hepatitis B e antigen-positive patients with recombinant interferon alpha-2a. The european concerted action on viral hepatitis (EUROHEP). *Hepatology* 1999; **30**: 277-282
- 8 Tatulli I, Francavilla R, Rizzo GL, Vinciguerra V, Ierardi E, Amoroso A, Panella C, Francavilla A. Lamivudine and alpha-interferon in combination long term for precore mutant chronic hepatitis B. *J Hepatol* 2001; **35**: 805-810
- 9 Shen JJ, Ji Y, Gu XL, Huang RJ, Sun YP. The association of HLA-DRB1*10 with chronic hepatitis B in Chinese patients. *Zhonghua Weishengwuxue He Mianyixue Zazhi* 1999; **19**: 58-59
- 10 Diepolder HM, Jung MC, Keller E, Schraut W, Gerlach JT, Gruner N, Zachoval R, Hoffmann RM, Schirren CA, Scholz S, Pape GR. A vigorous virus-specific CD4⁺ T cell response may contribute to the association of HLA-DR13 with viral clearance in hepatitis B. *Clin Exp Immunol* 1998; **113**: 244-251
- 11 Okamoto H, Tsuda F, Sakugawa H, Sastrosowignjo RI, Imai M, Miyakawa Y, Mayumi M. Typing hepatitis B virus by homology in nucleotide sequence: comparison of surface antigen subtypes. *J Gen Virol* 1988; **69**(Pt 10): 2575-2583
- 12 Norder H, Courouce AM, Magnus LO. Complete genomes, phylogenetic relatedness, and structural proteins of six strains of the hepatitis B virus, four of which represent two new genotypes. *Virology* 1994; **198**: 489-503
- 13 Stuyver L, De Gendt S, Van Geyt C, Zoulim F, Fried M, Schinazi RF, Rossau R. A new genotype of hepatitis B virus: complete genome and phylogenetic relatedness. *J Gen Virol* 2000; **81**(Pt 1): 67-74
- 14 Arauz-Ruiz P, Norder H, Robertson BH, Magnus LO. Genotype H: a new Amerindian genotype of hepatitis B virus revealed in Central America. *J Gen Virol* 2002; **83**(Pt 8): 2059-2073
- 15 Lindh M, Gonzalez JE, Norkrans G, Horal P. Genotyping of hepatitis B virus by restriction pattern analysis of a pre-S amplicon. *J Virol Methods* 1998; **72**: 163-174
- 16 Swenson PD, Van Geyt C, Alexander WR, Hagan H, Freitag-Koomtz JM, Wilson S, Norder H, Magnus LO, Stuyver L. Hepatitis B virus genotypes and HbsAg subtypes in refugees and injection drug users in the United States determined by LiPA and monoclonal EIA. *J Med Virol* 2001; **64**: 305-311
- 17 Blitz L, Pujol FH, Swenson PD, Porto L, Atercio R, Araujo M, Costa L, Monsalve DC, Torres JR, Fields HA, Lambert S, Van Geyt C, Norder H, Magnus LO, Echevarria JM, Stuyver L. Antigenic diversity of hepatitis B virus strains of genotype F in Amerindians and other population groups from Venezuela. *J Clin Microbiol* 1998; **36**: 648-651
- 18 Kao JH, Chen PJ, Lai MY, Chen DS. Hepatitis B genotypes correlate with clinical outcomes in patients with chronic hepatitis B. *Gastroenterology* 2000; **118**: 554-559
- 19 Erhardt A, Reineke U, Blondin D, Gerlich WH, Adams O, Heintges T, Niederau C, Haussinger D. Mutations of the

- core promoter and response to interferon treatment in chronic replicative hepatitis B. *Hepatology* 2000; **31**: 716-725
- 20 **Wai CT**, Chu CJ, Hussain M, Lok AS. HBV genotype B is associated with better response to interferon therapy in HBeAg (+) chronic hepatitis than genotype C. *Hepatology* 2002; **36**: 1425-1430
- 21 **Kao JH**, Wu NH, Chen PJ, Lai MY, Chen DS. Hepatitis B genotypes and the response to interferon therapy. *J Hepatol* 2000; **33**: 998-1002
- 22 **Cotrina M**, Buti M, Jardi R, Rodriguez-Frias F, Campins M, Esteban R, Guardia J. Study of HLA-II antigens in chronic hepatitis C and B and in acute hepatitis B. *Gastroenterol Hepatol* 1997; **20**: 115-118
- 23 **Liu PB**, Xu HW, Wang XL, Li H, Zhuang GH, Wu ZL, Zhang KL. Field epidemiological and experimental study on relationship between genetic factor and non-response or hyporesponse to hepatitis B vaccine. *Zhonghua Yixue Zazhi* 2000; **113**: 547-550
- 24 **Wang C**, Tang J, Song W, Lobashevsky E, Wilson CM, Kaslow RA. HLA and cytokine gene polymorphisms are independently associated with responses to hepatitis B vaccination. *Hepatology* 2004; **39**: 978-988
- 25 **Qian Y**, Zhang L, Liang XM, Hou JL, Lou KX. Association of immune response to hepatitis B vaccine with HLA-DRB1*02, 07, 09 genes in the population of Han nationality in Guangdong Province. *Diyi Junyi Daxue Xuebao* 2002; **22**: 67-69

Science Editor Wang XL and Guo SY Language Editor Elsevier HK

Hepatotoxicity of NONI juice: Report of two cases

Vanessa Stadlbauer, Peter Fickert, Carolin Lackner, Jutta Schmerlaib, Peter Krisper, Michael Trauner, Rudolf E Stauber

Vanessa Stadlbauer, Peter Fickert, Peter Krisper, Michael Trauner, Rudolf E Stauber, Department of Internal Medicine, Medical University Graz, Graz, Austria
Carolin Lackner, Institute of Pathology, Medical University Graz, Graz, Austria

Jutta Schmerlaib, Department of Internal Medicine, Landeskrankenhaus, Wolfsberg, Austria

Correspondence to: Rudolf E Stauber, MD, Department of Internal Medicine, Division of Gastroenterology and Hepatology, Medical University Graz, Auenbruggerplatz 15, Graz A-8036, Austria. rudolf.stauber@meduni-graz.at

Telephone: +43-316-385-2863 Fax: +43-316-385-3062

Received: 2004-12-21 Accepted: 2005-01-26

Abstract

AIM: NONI juice (*Morinda citrifolia*) is an increasingly popular wellness drink claimed to be beneficial for many illnesses. No overt toxicity has been reported to date. We present two cases of novel hepatotoxicity of NONI juice. Causality of liver injury by NONI juice was assessed. Routine laboratory tests and transjugular or percutaneous liver biopsy were performed. The first patient underwent successful liver transplantation while the second patient recovered spontaneously after cessation of NONI juice. A 29-year-old man with previous toxic hepatitis associated with small doses of paracetamol developed sub-acute hepatic failure following consumption of 1.5 L NONI juice over 3 wk necessitating urgent liver transplantation. A 62-year-old woman without evidence of previous liver disease developed an episode of self-limited acute hepatitis following consumption of 2 L NONI juice for over 3 mo. The most likely hepatotoxic components of *Morinda citrifolia* were anthraquinones. Physicians should be aware of potential hepatotoxicity of NONI juice.

© 2005 The WJG Press and Elsevier Inc. All rights reserved.

Key words: Herbal hepatotoxicity; Drug-induced hepatitis; NONI juice; Acute liver failure

Stadlbauer V, Fickert P, Lackner C, Schmerlaib J, Krisper P, Trauner M, Stauber RE. Hepatotoxicity of NONI juice: Report of two cases. *World J Gastroenterol* 2005; 11 (30): 4758-4760

<http://www.wjgnet.com/1007-9327/11/4758.asp>

INTRODUCTION

Due to the known side effects of approved pharmaceuticals, patients often turn to alternative medicine which is considered "natural" and "healthy". Herbal medicine is thus gaining popularity, but lack of knowledge of the mechanisms and

side effects of these preparations as well of safety regulations for their preparation may have serious consequences^[1]. Reports of hepatotoxicity associated with the use of herbal medicines are accumulating, ranging from mild elevations of liver enzymes to fulminant liver failure requiring liver transplantation^[2]. Healthcare professionals should be made aware of the potential dangers of herbal preparations. We present two cases of acute drug-induced hepatitis associated with the consumption of NONI juice.

CASE REPORT

Case 1

A 29-year-old male patient presented in March 2003 with acute hepatitis following treatment of an upper respiratory tract infection with paracetamol (4 g daily for 5 d followed by lower doses over 4 wk, cumulative dose of 40 g) associated with reduced food intake. Laboratory abnormalities included a bilirubin concentration of 26.3 mg/dL (normal: 0.1-1.2 mg/dL), ASAT 2 926 U/L (normal: <35 U/L), ALAT 2 665 U/L (normal: <45 U/L), γ -glutamyl transpeptidase 75 U/L (normal: <55 U/L), and alkaline phosphatase 209 U/L (normal: 40-130 U/L). Besides, the patient had allergic asthma treated with inhalative β_2 -agonists and glucocorticoids and eosinophilia of up to 12% in his peripheral blood smear. During military service at the age of 18, liver function tests were normal except for bilirubin (1.8 mg/dL) attributed to Gilbert's syndrome. Viral hepatitis, autoimmune hepatitis, hemochromatosis, α_1 -antitrypsin deficiency, Wilson's disease as well as other infections (leptospirosis, toxoplasmosis, coxsackie, and brucellosis) were ruled out and his abnormal liver tests were interpreted as low-dose paracetamol toxicity facilitated by fasting. Three months later, aminotransferase and bilirubin levels improved (ASAT 222, ALAT 300 U/L, bilirubin 4.8 mg/dL) and the patient was lost to follow-up. From April 2003 until June 2004, he treated himself with various homeopathic preparations containing small amounts of ethanol (<1 g/d). In June 2004 he was readmitted with acute liver failure. During the 3 wk prior to readmission, he ingested 1.5 L Tahitian NONI[®] juice and for 9 d prior to admission, approximately 7 g/d of a Chinese herbal mix containing bupleuri, pinellia, scutellaria, codonopsis, glycyrrhizae, schizonepeta, and paeonia. He denied any other medication over the past year. Other etiologies for acute liver failure such as fulminant hepatitis A or B, acute Wilson's disease, mushroom poisoning, and Budd-Chiari syndrome were ruled out. On re-admission, he showed grade 1 hepatic encephalopathy, ASAT 1 557, ALAT 1 626 U/L, bilirubin 45.3 mg/dL, INR 1.4 (normal: 0.85-1.15), albumin 3.3 g/dL (normal: 3.5-5.3 g/dL), and ammonia 90 μ mol/L (normal: 15-55 μ mol/L). A transjugular liver biopsy was performed and revealed acute hepatitis consistent with an

idiosyncratic drug reaction (Figure 1A). Over the next 3 d, liver failure progressed rapidly. On d 4, the patient fulfilled King's College criteria for emergency liver transplantation and was listed for urgent liver transplantation. During the waiting time, he underwent two consecutive sessions of extra-corporeal liver support using fractionated plasma separation, adsorption and dialysis (FPAD, Prometheus™, Fresenius Medical Care, Bad Homburg, Germany) which resulted in temporary improvement of hepatic encephalopathy from grade 3 to grade 2 and a decrease of arterial ammonia levels from 144 to 97 μmol/L. On d 6, liver transplantation was performed. On d 11, hepatic artery thrombosis necessitated re-transplantation. Thereafter, the patient recovered completely and was discharged on d 30.

Case 2

A 62-year-old woman was admitted in September 2003 with vomiting and diarrhea. On admission, routine laboratory tests revealed acute hepatitis (ASAT 1 415, ALAT 2 381 U/L, γ-glutamyl transpeptidase 241, alkaline phosphatase 292 U/L, bilirubin 2.9 mg/dL). In 1999, she was diagnosed with chronic B-cell leukemia which was treated with fludarabine in 2002 resulting in remission. Throughout that time, liver function tests were normal and the patient did not take any other regular medication. From April to July 2003, she ingested 2 L of Tahitian NONI® juice. Viral hepatitis, auto-immune hepatitis, hemochromatosis, α₁-antitrypsin deficiency, and Wilson's disease were

ruled out. There was no evidence of biliary obstruction or Budd-Chiari syndrome on ultrasound. The patient did not take any other potentially hepatotoxic drugs during that period. A percutaneous liver biopsy revealed acute hepatitis consistent with an idiosyncratic drug reaction (Figure 1B). Laboratory values peaked at ASAT 2 022, ALAT 3 570 U/L, and bilirubin 4.9 mg/dL and gradually improved over the next 30 d (ASAT 194, ALAT 645 U/L, and bilirubin 3.9 mg/dL). Nine months later, aminotransferases and bilirubin normalized and the patient remained asymptomatic.

DISCUSSION

We present two cases of toxic hepatitis associated with NONI juice (*Morinda citrifolia*) which represent the first reports of hepatotoxicity of this herbal preparation. To our knowledge, only one further case of NONI hepatotoxicity observed at the Medical University Innsbruck, Austria, has been published to date^[3]. Case 1 developed fulminant liver failure requiring emergency liver transplantation while liver function was preserved in case 2 and the patient recovered spontaneously after cessation of NONI juice. The temporal relationship between NONI intake and liver dysfunction (Figures 2A and B) and extensive exclusion of alternative causes of acute hepatitis confirmed herbal hepatotoxicity in both cases. Causality of liver injury by NONI juice was assessed using the Council for International Organizations of Medical Sciences scale^[4]

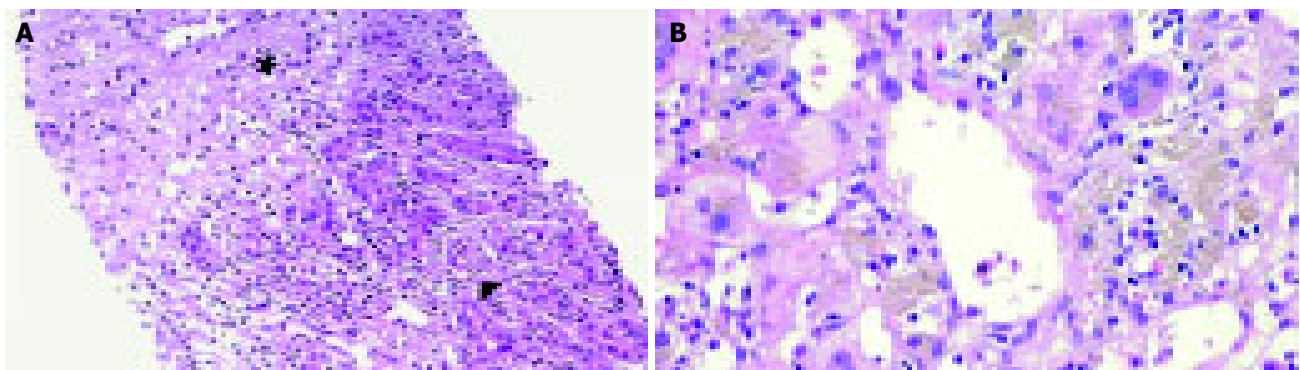


Figure 1 Confluent liver cell necrosis (asterisk), ductular reaction and metaplasia as well as mild inflammatory infiltrate (arrow head) in case 1 (A) and centrolobular

area with liver cell necrosis, ballooned hepatocytes and mild inflammatory infiltrate in case 2 (B).

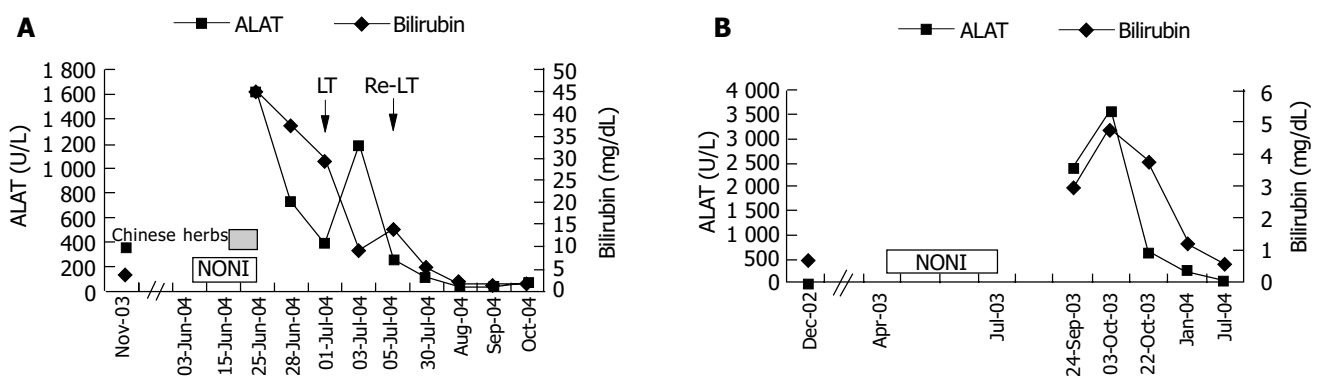


Figure 2 Time course of NONI intake and elevation of ALAT and bilirubin in

case 1 (A) and case 2 (B). LT: Liver transplantation.

and yielded a score of +5 (“possible”) in case 1 and a score of +7 (“probable”) in case 2. Histology revealed acute hepatitis with centrilobular necrosis consistent with acute drug-induced hepatotoxicity of idiosyncratic type in both cases (Figures 1A and B). However, we could not exclude concomitant pre-existing liver damage by paracetamol and/or an additional hepatotoxic effect of components of the Chinese herbal mix in case 1.

NONI juice is prepared from the fruit of *Morinda citrifolia*, a Polynesian plant with a long history of medicinal applications^[5]. Since 1996, various preparations of NONI juice have been sold as wellness drinks. Short-term safety studies in rats have not yielded overt toxicity^[5]. One case of hyperkalemia due to self medication with NONI juice is reported in a patient with renal failure^[6]. So far, no detailed pharmacological studies were reported on the putative active ingredients of the NONI plant, which include scopoletin, including scopoletin, potassium, ascorbic acid, terpenoids, alkaloids, anthraquinones, β -sitosterol, carotene, vitamin A, flavone glycosides, linoleic acid, alizarin, amino acids, acubin, L-asperuloside, caproic acid, caprylic acid, ursolic acid, rutin, and several volatile components such as acids (mainly octanoic acid and hexanoic acid), alcohols, esters, ketones, and lactones^[5,7]. The most likely hepatotoxic components are anthraquinones such as nordamnacanthal, moridone, and rubiadin. Anthraquinones in other herbal remedies have been reported to cause hepatotoxicity^[8-12]. A possible mechanism of hepatotoxicity of anthraquinones has been described for rhein (4,5-dihydroxyanthraquinone-2-carboxylic acid) which produces oxygen-derived free radicals by redox cycling resulting in depletion of intracellular reduced glutathione, decreased mitochondrial membrane potential, initiation of lipid peroxidation, and cell death^[13]. Further studies are required to evaluate the exact mechanism of toxicity. Physicians should be aware of potentially serious hepatotoxicity of NONI juice.

REFERENCES

- 1 **Boullata JI**, Nace AM. Safety issues with herbal medicine. *Pharmacotherapy* 2000; **20**: 257-269
- 2 **Stedman C**. Herbal hepatotoxicity. *Semin Liver Dis* 2002; **22**: 195-206
- 3 **Millonig G**, Stadlmann S, Vogel W. Herbal hepatotoxicity: acute hepatitis caused by a Noni preparation (*Morinda citrifolia*). *Eur J Gastroenterol Hepatol* 2005; **17**: 445-447
- 4 **Danan G**, Benichou C. Causality assessment of adverse reactions to drugs. I. A novel method based on the conclusions of international consensus meetings: application to drug-induced liver injuries. *J Clin Epidemiol* 1993; **46**: 1323-1330
- 5 **Wang MY**, West BJ, Jensen CJ, Nowicki D, Su C, Palu AK, Anderson G. *Morinda citrifolia* (Noni): a literature review and recent advances in Noni research. *Acta Pharmacol Sin* 2002; **23**: 1127-1141
- 6 **Mueller BA**, Scott MK, Sowinski KM, Prag KA. Noni juice (*Morinda citrifolia*): hidden potential for hyperkalemia? *Am J Kidney Dis* 2000; **35**: 310-312
- 7 **Farine JP**, Legal L, Moreteau B, Le Quere JL. Volatile components of ripe fruits of *Morinda citrifolia* and their effects on *Drosophila*. *Phytochemistry* 1996; **41**: 433-438
- 8 **Li FK**, Lai CK, Poon WT, Chan AY, Chan KW, Tse KC, Chan TM, Lai KN. Aggravation of non-steroidal anti-inflammatory drug-induced hepatitis and acute renal failure by slimming drug containing anthraquinones. *Nephrol Dial Transplant* 2004; **19**: 1916-1917
- 9 **Park GJ**, Mann SP, Ngu MC. Acute hepatitis induced by Shou-Wu-Pian, a herbal product derived from *Polygonum multiflorum*. *J Gastroenterol Hepatol* 2001; **16**: 115-117
- 10 **Nadir A**, Reddy D, Van Thiel DH. Cascara sagrada-induced intrahepatic cholestasis causing portal hypertension: case report and review of herbal hepatotoxicity. *Am J Gastroenterol* 2000; **95**: 3634-3637
- 11 **Beuers U**, Spengler U, Pape GR. Hepatitis after chronic abuse of senna. *Lancet* 1991; **337**: 372-373
- 12 **Itoh S**, Marutani K, Nishijima T, Matsuo S, Itabashi M. Liver injuries induced by herbal medicine, syo-saiko-to (xiao-chai-hu-tang). *Dig Dis Sci* 1995; **40**: 1845-1848
- 13 **Bironaite D**, Ollinger K. The hepatotoxicity of rhein involves impairment of mitochondrial functions. *Chem Biol Interact* 1997; **103**: 35-50

• CASE REPORT •

Giant appendiceal mucocele: Report of a case and brief review

Bernardino Rampone, Franco Roviello, Daniele Marrelli, Enrico Pinto

Bernardino Rampone, Franco Roviello, Daniele Marrelli, Enrico Pinto, Department of General Surgery and Surgical Oncology, University of Siena, Italy

Correspondence to: Dr. Franco Roviello, Via De Gasperi, 5, Siena 53100, Italy. roviello@unisi.it

Telephone: +39-577585157 Fax: +39-577585157

Received: 2004-10-19 Accepted: 2005-01-05

Abstract

Mucocele of the appendix is a rare lesion, characterized by distension of the lumen due to accumulation of mucoid substance. This disease is often asymptomatic and pre-operative diagnosis is rare. If untreated, one type of mucocele may rupture producing a potentially fatal entity known as pseudomyxoma peritonei. The type of surgical treatment is related to the dimensions and to histology of the mucocele. Appendectomy is used for simple mucocele or for cystadenoma. Right hemi-colectomy is recommended for cystadenocarcinoma. In this paper, we report a case of a 51-year-old woman with a mobile, painless mass in the right lower quadrant of abdomen caused by a giant appendiceal mucocele. Imaging showed a large, tubular, cystic structure extending below from the inferior wall of the cecum. Surgery revealed a giant retro-cecal appendix measuring 17 cm in length and 4 cm in diameter. The final pathologic diagnosis was mucocele caused by mucinous cystadenoma.

© 2005 The WJG Press and Elsevier Inc. All rights reserved.

Key words: Appendix; Mucocele; Pseudomyxoma peritonei; Surgical treatment

Rampone B, Roviello F, Marrelli D, Pinto E. Giant appendiceal mucocele: Report of a case and brief review. *World J Gastroenterol* 2005; 11(30): 4761-4763

<http://www.wjgnet.com/1007-9327/11/4761.asp>

INTRODUCTION

Mucocele is a rare pathology of the appendix, characterized by a cystic dilation of the lumen with stasis of mucus. The incidence ranges between 0.2% and 0.3% of all appendectomies, with a higher frequency in females (4/1) and in people more than 50 years^[1]. It demonstrates an inflammatory or a tumoral cause; most important for the surgeon, however, the mucoceles are caused by mucinous cystadenomas and cystadenocarcinomas. In the latter case, a possible rupture of the mucocele, either spontaneous or accidental, may result in the clinical condition of pseudomyxoma peritonei, a spread of malignant

cells throughout the peritoneal cavity in the form of multiple mucinous deposits^[2,3]. A correct diagnosis may help to avoid iatrogenic rupture during surgery. We describe a case of a giant appendiceal mucocele and present the diagnostic aspects, surgical options and prognosis of this disease.

CASE REPORT

A 51-year-old woman was admitted to our department on April 21, 2004 due to the appearance of a mass in the right lower quadrant of abdomen, with nausea and decreased appetite. No urinary dysfunction or changes in her intestinal transit was reported. Her blood pressure was 130/80 mmHg with regular pulse of 80/min. She had a body temperature of 36.8 °C. On admission, physical examination of chest revealed no abnormalities and superficial lymph nodes were not palpable. A mobile, painless mass was palpated at the right lower abdomen. No liver or spleen enlargements were noted.

Laboratory tests, including CEA, CA 19-9, CA 125, CA 15-3 and CA 72-4, were unremarkable.

Abdominal ultrasonography revealed the presence of a non-homogeneous oval mass. Computed tomography scan of the abdomen showed a large, hypodense, tubular, cystic structure extending below the inferior wall of the cecum (Figure 1). Coronal view of computed tomography disclosed a mass, which measured about 13 cm in length (Figure 2).

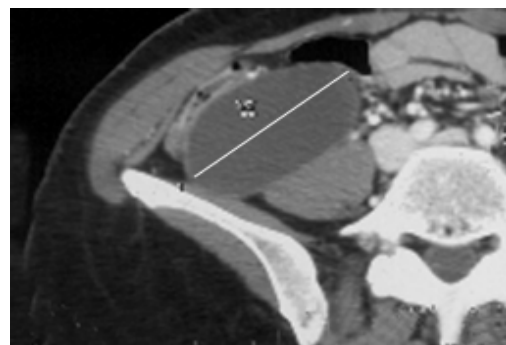


Figure 1 Large, hypodense, tubular, cystic structure extending below the inferior wall of the cecum revealed in a computed tomography scan of the abdomen.

On April 24 the patient had a laparotomy. At surgery, a giant retro-cecal appendix was found (Figure 3). There was no lymphadenopathy or hepatic metastases. No other tumors were noted in the abdominal or pelvic cavities. The appendix was bent behind the ascending colon. After adhesiotomy, a standard appendectomy was performed.

The mass, which measured 17 cm in length and 4 cm in diameter, showed a thin fibrous wall and viscous hemorrhagic mucoid content without any mucosal lesion. The final pathologic diagnosis was mucocele caused by mucinous cystadenoma. There was no evidence of malignancy. The patient's post-operative course was unremarkable and she was discharged 5 d post-operatively.

At present, about 7 mo post-operatively, the patient is asymptomatic, and abdominal ultrasonography did not reveal any abdominal lesion.

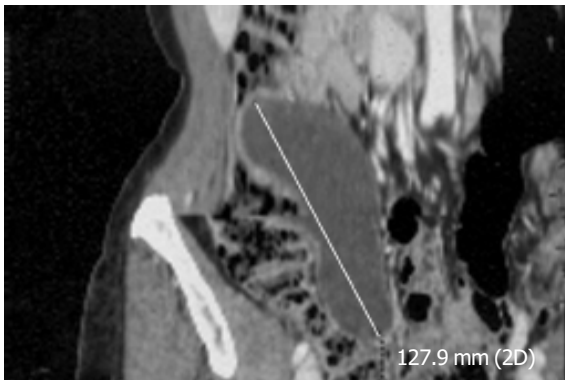


Figure 2 Mass of about 13 cm in length disclosed in a coronal view of computed tomography scan.



Figure 3 Intraoperative finding of a giant appendix, which measured 17 cm in length and 4 cm in diameter.

DISCUSSION

The term mucocele is often used as a general descriptive term for dilatation of the appendiceal lumen by mucinous secretions. Four subgroups of the disease can be identified, according to the characteristics of the epithelium: (1) simple or retention mucoceles resulting from obstruction of the appendiceal outflow, usually by a fecalith, and characterized by normal epithelium and mild luminal dilatation up to 1 cm. (2) Mucoceles with hyperplastic epithelium where luminal dilatation is also mild; these constitute 5-25% of mucoceles. (3) Benign mucoceles, the most common form, accounting for 63-84% of cases. These exhibit mostly epithelial villous adenomatous changes with some degree of epithelial atypia, and are characterized by marked distention of the lumen

up to 6 cm. Our patient belongs to this group. (4) Malignant mucinous cystadenocarcinomas, representing 11-20% of cases. They are distinguished from the previous group by their glandular stromal invasion and/or presence of epithelial cells in the peritoneal implants. The luminal distention is usually severe^[1-4].

Mucinous cystadenomas and cystadenocarcinomas are often referred to as neoplastic mucoceles. In cystadenomas, which are the most common form, the luminal dilatation reaches up to 6 cm and is associated with appendiceal perforation in 20% of instances. This results in mucinous spillage into the peri-appendicular area and peritoneal cavity. Histological examination of the mucus does not reveal any neoplastic cells and appendectomy is usually curative^[5]. Mucinous cystadenocarcinomas, on the other hand, are less common than mucinous cystadenomas and may present with spontaneous rupture in 6% of cases. Macroscopically, they produce mucin-filled cystic dilatation of the appendix indistinguishable from cystadenomas. However, neoplastic cells may penetrate the appendiceal wall and spread beyond the appendix in the form of peritoneal implants. In its fully developed state, the peritoneal cavity becomes distended with adhesive, semi-solid mucin in which neoplastic adenocarcinomatous cells can be found; this condition is termed as pseudomyxoma peritonei. The intraperitoneal spread of this mucin-secreting cancer is identical to that of intra-peritoneal ovarian mucinous cystadenocarcinomas^[2-5].

Symptomatology of appendiceal mucoceles is not specific: very large lesions are asymptomatic in 25% of patients. The most common presentation is right lower quadrant pain, similar to an acute appendicitis; a palpable mass can be found in 50% of cases, whereas urinary dysfunction or hematuria is rarely related^[6]. Increase of tumor markers indicate a probable neoplastic origin^[7,8]. The rare complications include intestinal obstruction, frequently caused by intussusception, or intestinal bleeding. Pseudomyxoma is the worst complication, characterized by peritoneal dissemination caused by spontaneous or iatrogenic perforation of the appendix. In benign mucocele, the pseudomyxoma is confined to the peri-appendicular area. In malignant cases, this dissemination is considered a real metastatic entity; retro-peritoneal or pleural implants are occasionally reported^[7-9].

Preoperative diagnosis is difficult, due to the nonspecific nature of the disease. The lesion may be identified by radiologic, sonographic, or endoscopic means. Elevated carcino-embryonic antigen levels have been described in neoplastic mucoceles^[10,11].

Computed tomography scan of the abdomen is important in the diagnosis and evaluation of the extent of the disease. A typical computed tomography scan finding of an appendiceal mucocele is a round, low-density, thin-walled, encapsulated mass, communicating with the cecum. Ultrasonography shows a cystic, encapsulated lesion, firmly attached to the cecum, with liquid content and an internal variable echogenicity related to mucus density. Colonoscopy may show a pathognomonic image, the 'sign of the volcano', i.e., an erythematous, soft mass with a central crater, from which mucus is discharged^[12-15].

Therapy is surgical, but laparoscopic approach is not advised because of the risk of rupture^[16].

The type of surgical treatment is related to the dimensions and to histology of the mucocele. Appendectomy is used for simple mucocele or for cystoadenoma, when the appendiceal base is intact. Cecal resection is indicated for cystoadenoma with a large base, and a right hemi-colectomy is recommended for cystadenocarcinoma. Intra-operative histologic examination is not always definitive. An accurate exploration of the abdomen during laparotomy is advised, because of the association between the appendiceal mucocele and other tumors, particularly carcinoma of the colon (11-20 %) and tumors of the ovary^[17].

If exploration reveals a ruptured appendiceal mucocele, the primary resection should be accompanied by removal of all gross implants^[16,17].

Postoperatively, patients with simple or benign neoplastic mucoceles have shown an excellent prognosis with 5-year survival rates of 91-100%, even in cases with extension of mucus into the extra-appendiceal spaces. In malignant mucoceles, however, the 5-year survival rate is markedly diminished (25%) due to complications of pseudomyxoma peritonei^[18].

In conclusion, patients with mucoceles can present with various symptoms, but may also be asymptomatic. Preoperative diagnosis is rare, but it is possible using appropriate tests. These uncommon and potentially lethal entities are usually surgically curable, if diagnosed in an early phase. Therefore, pre-operative recognition with a carefully planned resection to remove the mass is required.

REFERENCES

- 1 **Aho AJ**, Heinonen R, Lauren P. Benign and malignant mucocele of the appendix. *Acta Chir Scand* 1973; **139**: 392-400
- 2 **Crawford J**. Tumors of the appendix. In: Cotran R, Kumar V, Robbins S, eds. *Pathologic basis of disease*. Philadelphia Saunders 1994; 824-825
- 3 **Landen S**, Bertrand C, Maddern GJ, Herman D, Pourbaix A, de Neve A, Schmitz A. Appendiceal mucoceles and pseudomyxoma peritonei. *Sur Gynecol Obstet* 1992; **175**: 401-404
- 4 **Higa E**, Rosai J, Pizzimbono CA, Wise L. Mucosal hyperplasia, mucinous cystadenoma, and mucinous cystadenocarcinoma of the appendix: A re-evaluation of appendiceal mucocele. *Cancer* 1973; **32**: 1525-1541
- 5 **Gibbs NM**. Mucinous cystadenoma and cystadenocarcinoma of the vermiform appendix with particular reference to mucocele and pseudomyxoma peritonei. *J Clin Pathol* 1973; **26**: 413-421
- 6 **Merran S**. Tumeur muco-secretante de l'appendice (mucocele appendiculaire). *Presse Med* 1997; **26**: 933
- 7 **Peek DF**, Beets GL. Pseudomyxoma peritonei in the pleural cavity: report of a case. *Dis Colon Rectum* 1999; **42**: 113-116
- 8 **Takahashi S**, Furukawa T, Ueda J. Case report: mucocele of the tip of the appendix. *Clin Radiol* 1998; **53**: 149-150
- 9 **Stevens KJ**, Dunn K, Balfour T. Pseudomyxoma extra-peritonei: a lethal complication of mucinous adenocarcinoma of the appendix. *Am J Gastroenterol* 1997; **92**: 1920-1922
- 10 **Dachman AH**, Linchtenstein JE, Friedman AC. Mucocele of the appendix and pseudomyxoma peritonei. *Am J Roentgenol* 1985; **144**: 923-929
- 11 **Soweid AM**, Clarkston WK, Andrus CH, Janney CG. Diagnosis and management of appendiceal mucoceles. *Dig Dis* 1998; **16**: 183-186
- 12 **Kim SH**, Lim HK, Lee WJ, Lim JH, Byun JY. Mucocele of the appendix: ultrasonographic and CT findings. *Abdom Imaging* 1998; **23**: 292-296
- 13 **Zissin R**, Gayer G, Kotos E, Apter S, Peri M, Sharipo-Feinberg M. Imaging of mucocele of the appendix with emphasis on the CT findings: a report of 10 cases. *Clin Radiol* 1999; **54**: 826-832
- 14 **Isaacs KL**, Warshauer DM. Mucocele of the appendix: computer tomographic, endoscopic, and pathologic correlation. *Am J Gastroenterol* 1992; **87**: 787-789
- 15 **Hamilton DL**, Stormont JM. The volcano sign of appendiceal mucocele. *Gastrointest Endosc* 1989; **35**: 453-456
- 16 **Gonzales Moreno S**, Shmookler BM, Sugarbaker PH. Appendiceal mucocele. Contraindication to laparoscopic appendectomy. *Surg Endosc* 1998; **12**: 1177-1179
- 17 **Kahn M**, Friedman IH. Mucocele of the appendix: Diagnosis and surgical management. *Dis Colon Rectum* 1979; **22**: 267-269
- 18 **Aho AJ**, Heinonen R, Lauren P. Benign and malignant mucocele of the appendix: Histological types and prognosis. *Acta Chir Scand* 1973; **139**: 392-400

• CASE REPORT •

Biloma following repeated transcatheter arterial embolization and complicated by intrahepatic duct stones: A case report

Ming-Jen Chen, Ching-Chung Lin, Wen-Hsiung Chang, Fei-Shih Yang

Ming-Jen Chen, Ching-Chung Lin, Wen-Hsiung Chang, Division of Gastroenterology, Department of Internal medicine, Mackay Memorial Hospital, Mackay Medicine, Nursing and Management College, Taipei, Taiwan, China

Fei-Shih Yang, Department of Radiation, Mackay Memorial Hospital, Mackay Medicine, Nursing and Management College, Taipei, Taiwan, China

Correspondence to: Dr. Ming-Jen Chen, Division of Gastroenterology, Department of Internal Medicine, Mackay Memorial Hospital, No. 92, Sec. 2, Chungshan North Road, Taipei, Taiwan, China. mingjen.ch@msa.hinet.net

Telephone: +886-2-25433535-2260 Fax: +886-2-25433642

Received: 2004-05-25 Accepted: 2004-06-18

Abstract

Biloma is an encapsulated bile collection outside the biliary tree due to a bile leak. It is occasionally found following traumatic liver injury or iatrogenic injury to the biliary tract, induced either during an endoscopic or surgical procedure. It is a rare complication of transcatheter arterial embolization (TAE). Although biloma can be shrunk by appropriate aspiration or drainage in majority of cases, we report a case of intrahepatic biloma following repeated TAE for hepatocellular carcinoma (HCC) and complicated by infection and intrahepatic stones. This particular constellation of problems has not been reported before and the intrahepatic stones need to be removed by percutaneous procedure.

© 2005 The WJG Press and Elsevier Inc. All rights reserved.

Key words: Biloma; Biliary tract; Transcatheter; Arterial embolization

Chen MJ, Lin CC, Chang WH, Yang FS. Biloma following repeated transcatheter arterial embolization and complicated by intrahepatic duct stones: A case report. *World J Gastroenterol* 2005; 11(30): 4764-4765

<http://www.wjgnet.com/1007-9327/11/4764.asp>

CASE REPORT

A 69-year-old woman was diagnosed with cryptogenic liver cirrhosis 15 years ago, but had well-compensated liver function. In October 2000, she was found to have a 8-cm tumor in the left lobe of the liver. HCC was diagnosed on pathological examination. Surgical resection was not attempted because of the large size of the tumor and atrophy of the right lobe. Therefore, she was treated with transcatheter arterial

embolization (TAE) and percutaneous ethanol injection (PEI). TAE was performed with 6 cm³ of iodized oil (lipiodol) injected through the catheter and embolization with gelfoam sponge. Four weeks after TAE, enhanced CT was used to access the effects. If the response was not satisfactory, pure ethanol was injected under ultrasound guidance. By May 2003, the patient received five courses of combined TAE and PEI. Her cirrhosis was assessed as Child-Pugh class A, and HCC was maintained at 7 cm in diameter. No major complications were noted till that point.

Three weeks after the sixth TAE procedure, the patient complained of nausea, epigastric pain, and poor appetite. She denied fever or chills. A tender mass was palpable in the epigastric area. Her bilirubin was elevated at 2.8 mg/dL. An abdominal CT disclosed an encapsulated fluid collection in the left lobe of the liver. Echo-guided aspiration of bile from the lesion confirmed the diagnosis of biloma. Several days later, the culture of the aspirated bile culture was reported as growing *K. pneumoniae*. On the same day, the patient developed fever and leukocytosis. She was treated with intravenous antibiotics, and a 10 F pig-tail catheter was placed percutaneously to drain the biloma. Two days later, contrast media was injected through the catheter for a fluoroscopic evaluation. A communication was found between the biloma and the left biliary tree (Figure 1). Small filling defects were seen in one dilated branch of the IHD, consistent with stones. Some of these fell into the biloma. The biloma drain continued to put out a large volume of bile along with sandy stones for 5 d, without any shrinkage the size of the cavity. However, the fever did subside. Concerned that the stones were preventing collapse of the biloma, we decided to remove the stones percutaneously. The fistula track was gradually dilated to 16 F by changing the drainage

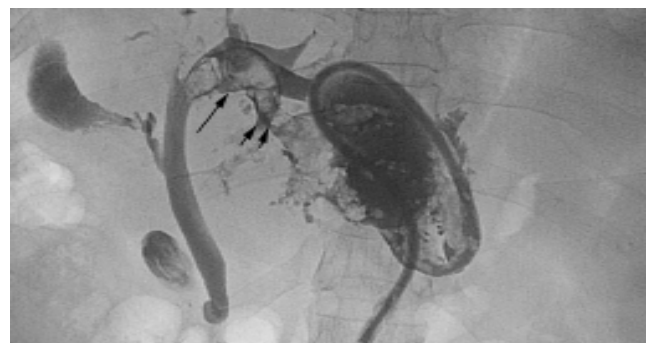


Figure 1 Communication between the biloma and the left biliary tree (short arrows) on injection contrast via the percutaneous pig-tail catheter and small filling defects (long arrow) seen in one dilated branch of the IHD, consistent with stones.

catheter. The IHD stones were removed with a basket over several sessions. Two months later, the biloma shrunk.

DISCUSSION

Biloma is occasionally found following traumatic liver injury or iatrogenic injury to the biliary tract, induced either during an endoscopic^[1] or surgical procedure. Peripheral bile duct necrosis caused by microvascular damage and ductal stenosis after TAE might lead to a bile leak^[2,3]. Our patient has already undergone five courses of TAE and PEI before, and the biloma developed 3 wk after the sixth TAE. We do not think that the PEI could directly influence this biloma, although there is one case report in the literature of a biloma after PEI^[4]. The incidence of biloma after TAE in several series has been reported to be around 0.8-1.1%^[5-7]. These often occurred only after more than five courses of TAE^[5,6]. Recent reports indicate the advantage of the usage of embolization materials which have a suitable size only for the feeding artery, but largely for occlusion of bile duct microplexus. It is in terms of effective tumor embolization as well as prevention of possible complications.

Biloma is usually a simple cyst without septum. Percutaneous needle aspiration with chemical analysis could confirm the diagnosis. It may be asymptomatic or present with a variety of manifestations, such as gastric outlet obstruction, jaundice, or fever. The presentation depends on the size and location of the lesion and the presence or absence of infection. Asymptomatic patients may be treated conservatively. In a series reported by Kohno *et al.*^[4], in 15 of 20 patients, the biloma shrank spontaneously during a 6-mo follow-up period. A biloma that fails to decrease in size should be drained, as infection is a common complication if the condition persists. If there is no communication with the biliary tree, and the proximal biliary tree has neither stricture nor stones, percutaneous drainage and intravenous antibiotics may achieve resolution. Intra-hepatic duct strictures may require insertion of a stent in order to relieve pressure that might reopen a tract to the biloma. However, IHD stones are often difficult to be removed. A biloma connected to a biliary tree containing stones has not been previously reported. It appeared in our patient that peripheral bile outflow was blocked by the IHD stones, causing a high pressure in biliary system and thus, led to a persistent bile leak. Given the difficulty of reaching IHD stones endoscopically, percutaneous removal of the stones seemed advisable, and ultimately, the biloma did shrink.

The proposed therapies for HCC, beyond TAE and PEI are increasing and include hepatic artery infusion of chemotherapy agents^[8], microwave coagulation^[9], and high frequency radioablation. Any of these may cause peripheral bile duct damage, so that it is conceivable that the incidence of biloma will increase. Clinicians must be aware of this possible complication. The prophylactic administration of antibiotics may be employed in these procedures, since biloma can be a result of focal infection. But the real necessity of prophylactic antibiotics remains to be identified.

REFERENCES

- 1 **Ranjeev P**, Goh KL, Rosmawati M, Tan YM. Intrahepatic biloma: an unusual complication of cholangiocarcinoma treated endoscopically. *Gastrointest Endosc* 1999; **50**: 711-713
- 2 **Kobayashi S**, Nakanuma Y, Terada T, Matsui O. Postmortem survey of bile duct necrosis and biloma in hepatocellular carcinoma after transcatheter arterial chemoembolization therapy: relevance to microvascular damage of peribiliary capillary plexus. *Am J Gastroenterol* 1993; **88**: 1410-1415
- 3 **Koda M**, Murawaki Y, Mitsuda A, Oyama K, Okamoto K, Idobe Y, Suou T, Kawasaki H. Combination therapy with transcatheter arterial chemoembolization and percutaneous ethanol injection compared with percutaneous ethanol injection alone for patients with small hepatocellular carcinoma: a randomized control study. *Cancer* 2001; **92**: 1516-1524
- 4 **Kohno E**, Chen S, Numata K, Nakamura S, Tanaka K, Endo O, Inoue S, Takamura Y. A case of biloma: complication of percutaneous ethanol injection therapy for hepatocellular carcinoma (in Japanese with English abstract). *Nippon Shokakibyo Gakkai Zasshi* 1992; **89**: 2719-2724
- 5 **Chen C**, Tsang YM, Hsueh PR, Huang GT, Yang PM, Sheu JC, Lai MY, Chen PJ, Chen DS. Bacterial infections associated with hepatic arteriography and transarterial embolization for hepatocellular carcinoma: a prospective study. *Clin Infect Dis* 1999; **29**: 161-166
- 6 **Chung JW**, Park JH, Han JK, Choi BI, Han MC, Lee HS, Kim CY. Hepatic tumors: predisposing factors for complications of transcatheter oily chemoembolization. *Radiology* 1996; **198**: 33-40
- 7 **Sakamoto I**, Aso N, Nagaoki K, Matsuoka Y, Uetani M, Ashizawa K, Iwanaga S, Mori M, Morikawa M, Fukuda T, Hayashi K, Matsunaga N. Complications associated with transcatheter arterial embolization for hepatic tumors. *Radiographics* 1998; **18**: 605-619
- 8 **Seno H**, Ito K, Kojima K, Nakajima N, Chiba T. Efficacy of an implanted drug delivery system for advanced hepatocellular carcinoma using 5-fluorouracil, epirubicin and mitomycin C. *J Gastroenterol Hepatol* 1999; **14**: 811-816
- 9 **Shimada S**, Hirota M, Beppu T, Matsuda T, Hayashi N, Tashima S, Takai E, Yamaguchi K, Inoue K, Ogawa M. Complications and management of microwave coagulation therapy for primary and metastatic liver tumors. *Surg Today* 1998; **28**: 1130-1137

Science Editor Wang XL Language Editor Elsevier HK

• CASE REPORT •

Acute pancreatitis as an initial symptom of systemic lupus erythematosus: A case report and review of the literature

Feng Wang, Nian-Song Wang, Bing-Hui Zhao, Ling-Quan Tang

Feng Wang, Nian-Song Wang, Ling-Quan Tang, Department of Nephrology, the Sixth Hospital attached to Shanghai Jiaotong University, 600 Yishan Road, Shanghai 200233, China
Bing-Hui Zhao, Department of Radiology, the Sixth Hospital attached to Shanghai Jiaotong University, 600 Yishan Road, Shanghai 200233, China

Correspondence to: Feng Wang, Department of Nephrology, the Sixth Hospital attached to Shanghai Jiaotong University, 600 Yishan Road, Shanghai 200233, China. zyzwq1030@sohu.com

Telephone: +86-21-64369181-8379

Received: 2004-05-25 Accepted: 2004-07-22

Abstract

Acute pancreatitis as an initial symptom of systemic lupus erythematosus (SLE) is rare. We present a report of a 46-year-old female patient who had fever, abdominal pain and vomiting, elevated pancreatic enzyme levels, hypocalcemia, hypoxemia, and various other laboratory abnormalities. She was first diagnosed with acute severe pancreatitis and then with SLE after further investigations. After a 2-mo treatment with somatostatin, the patient recovered.

© 2005 The WJG Press and Elsevier Inc. All rights reserved.

Key words: Systemic lupus erythematosus; Pancreatitis

Wang F, Wang NS, Zhao BH, Tang LQ. Acute pancreatitis as an initial symptom of systemic lupus erythematosus: A case report and review of the literature. *World J Gastroenterol* 2005; 11(30): 4766-4768

<http://www.wjgnet.com/1007-9327/11/4766.asp>

INTRODUCTION

Systemic lupus erythematosus (SLE) is a multi-system, autoimmune disorder characterized by a broad range of manifestations, including presence of antibodies against cell nuclei. The initial manifestations of SLE, however, can involve many organ systems either singly or in combination, which frequently makes diagnosis difficult. The American Rheumatism Association recommends that the diagnosis of SLE can be confirmed if it meets 4 of the following 11 revised criteria: malar rash, discoid rash, photo-sensitivity, oral ulcers, arthritis, serositis, renal disorder, neurologic disorder, hematologic disorder, immunologic disorder, and antinuclear antibodies.

We report a 46-year-old female patient with fever, abdominal pain and vomiting, elevated levels of pancreatic enzyme, hypocalcemia, hypoxemia, and other laboratory

abnormalities. She was first diagnosed with acute severe pancreatitis and then with SLE, after further investigations.

CASE REPORT

A 46-year-old woman came to the Sixth Hospital attached to Shanghai Jiaotong University, complaining of a 6-d history of persistent abdominal pain, loss of appetite, occasional nausea and vomiting without obvious reasons. She also had a 3-d history of fever and generalized weakness.

She reported bilateral thigh pain, finger pain and swelling 5 mo ago, which were abated after 7-d treatment with hydroxy-chloroquine. Four months ago, she had elevated alanine aminotransferase, and received no treatment. She also reported some thinning of her hair and a weight loss of 5 kg in the past 2 mo. Her family history was unremarkable for auto-immune disorders.

Her body temperature was 38 °C, pulse rate 100 beats per minute, blood pressure 120/80 mmHg. She had no skin lesions, but had swollen and painless lymph nodes. She had fine rales on bilateral lungs, and 3-degree systolic murmur in the mitral valve area and a pericardial friction sound. Her abdomen was soft with mild epigastric tenderness, minimal guarding, and no rebound tenderness.

Her blood chemistry was as follows: 126 mmol/L sodium, 4.4 mmol/L potassium, 97 mmol/L chloride, 22.5 mmol/L bicarbonate, 1.6 mmol/L blood urea nitrogen, 31 µmol/L creatinine, 5.1 mmol/L glucose, 83 U/L aspartate aminotransferase, 16 U/L alanine aminotransferase, 66 g/L protein, 37 g/L albumin, 1.70 mmol/L calcium, and 18 µmol/L total bilirubin. A complete blood count showed a white cell count of $3.0 \times 10^9/L$ with 78.9% neutrophils, 19.8% lymphocytes, 2.3% monocytes. Hemoglobin was 89 g/L, hematocrit 33.8%, and platelets $112 \times 10^9/L$. Pancreatic enzyme determinations disclosed a blood amylase level of 1 000 U/L (normal 20-115 U/L) and urine amylase level of 830 U/L, and a lipase level of 690 U/L. Urinalysis showed cloudy urine with a protein level of 260 mg/dL, a white cell count of 3-4/µL, granular casts 0. Nitrite and leukocyte esterase were negative. Blood culture was negative.

Computed tomographic (CT) scan and ultrasonic scan of the abdomen with contrast, showed swollen pancreas but no gallbladder stones (Figure 1A). Another CT scan of the bosom showed effusion both in right and in left pleurae (Figure 1B).

Connective tissue showed an antinuclear antibody (ANA) titer of 1:640, positive anti-double-stranded DNA (dsDNA) antibody, negative anti-Smith antibody, anti-ribonucleoprotein, anti-SSA, and anti-SSB. The erythrocyte sedimentation rate was 92, complement 3 (C₃) was 0.75 g/L (normal 1.0-1.8 g/L),

anti-cardiolipin antibodies and lupus anti-coagulant were negative.

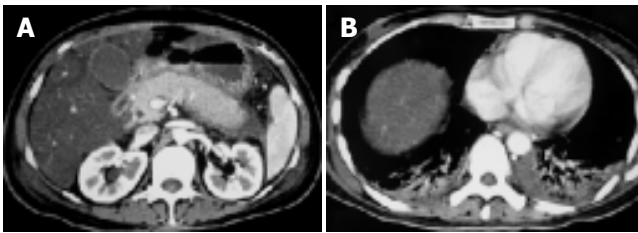


Figure 1 Swollen pancreas (A) and pleural effusion (B) before treatment with somatostatin.

After a 2-mo treatment with somatostatin, the pancreatic enzyme was 29 U/L. Repeated CT scan revealed a less swollen pancreas (Figure 2A) and still bilateral pleural effusion (Figure 2B). But the patient still had fever and palpitation. A diagnosis of SLE pancreatitis was made on the 66th d of admission, and 40 mg methylprednisolone intravenous injection qd was started. Once steroid therapy began, the heart rate declined to 90 beats per minute. Two weeks after continuous steroid therapy, the heart rate was 78 beats per minute and the temperature was 36.6 °C. Pleural effusion disappeared.

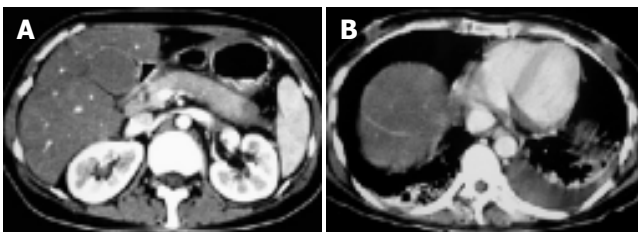


Figure 2 Less swollen pancreas (A) and pleural effusion (B) after treatment with somatostatin.

DISCUSSION

Although the patient on admission was positive for ANA and anti-dsDNA, arthritic, serositic and blood cells reduced, which fulfills the American Rheumatism Association criteria for the diagnosis of SLE. Our case illustrates the protean manifestations of SLE and a rare initial manifestation as acute pancreatitis. Over 50% SLE patients have manifestations of digestive system, but pancreatitis is few, and such acute pancreatitis as an initial manifestation is even rare. The association between SLE and pancreatitis was first documented in 1939^[1]. Since then, only 70 cases of SLE pancreatitis have been documented in the literature, and only 10 of these cases, including this one, have pancreatitis as their initial manifestation^[2-5].

The mechanisms involved in the origin of SLE pancreatitis are not clear. SLE pancreatitis might result from vasculitis, microthrombi, anti-pancreas autoantibody, side-effects of medicine, intimal thickening and virus infection. Most lupus

pancreatitis is found in patients with long-standing SLE who have multi-organ involvement and are already on steroid, diuretic, or immunosuppressive therapy, all of which have been implicated in the etiology of pancreatitis. Since the initial description of SLE pancreatitis, whether steroid or SLE is the primary cause has been controversial. Recent studies support that SLE is the primary etiologic factor of SLE pancreatitis, and drug toxicity may also play a role^[5-9].

Pathological changes of SLE pancreatitis bear similarities to those of pancreatitis due to other causes. SLE pancreatitis can occur during a generalized flare-ups and disease quiescence, though the latter seems more likely^[3]. Its manifestation can be acute, severe, or chronic, self-limiting or fulminant. It is believed that subclinical pancreatitis which has an elevation of pancreatic enzymes without clinical symptoms is much more frequent than symptomatic pancreatitis^[10-14]. About 30.5% of asymptomatic SLE patients have hyperamylasemia; therefore subclinical pancreatic damage might occur very frequently in SLE^[15].

Within the context of SLE, the diagnosis of SLE pancreatitis is usually based on clinical findings as abdominal pain, nausea, and vomiting as well as laboratory findings like abnormal pancreatic enzymes and suggestive tomographic findings. Etiology diagnosis is fairly important, which decides whether steroid can be used. If drug toxicity is not considered as the origin, SLE pancreatitis is treated with steroid. Of course, steroid or other drugs should be stopped once they are regarded as the cause^[16,17].

In conclusions, it is important to determine whether drug toxicity is the cause of SLE pancreatitis. If the condition of patients with SLE pancreatitis can be improved with somatostatin, steroid might not be necessary during the acute episode.

REFERENCES

- 1 **Jaspersen D.** Gastrointestinal manifestations of systemic lupus erythematosus: symptoms, diagnosis and differential diagnosis. *Fortschr Med* 1992; **110**: 167-169
- 2 **Penalva JC, Martinez J, Pascual E, Palanca VM, Lluís F, Peiro F, Perez H, Perez-Mateo M.** Chronic pancreatitis associated with systemic lupus erythematosus in a young girl. *Pancreas* 2003; **7**: 275-277
- 3 **Duncan HV, Achara G.** A rare initial manifestation of systemic lupus erythematosus-acute pancreatitis: case report and review of the literature. *J Am Board Fam Prac* 2003; **16**: 334-338
- 4 **Swol-Ben J, Bruns CJ, Muller-Ladner U, Hofstadter F, Link J, Hechenrieder C, Jauch KW.** Leukoencephalopathy and chronic pancreatitis as concomitant manifestations of systemic lupus erythematosus related to anticardiolipin antibodies. *Rheumatol Int* 2004; **24**: 177-181
- 5 **Le Thi Huong D, Papo T, Laraki R, Wechsler B, Bletry O, Chapelon C, Cabane J, Godeau P.** Pancreatitis in systemic lupus erythematosus. Review of the literature apropos of 5 cases. *Rev Med Interne* 1994; **15**: 89-94
- 6 **Yeh TS, Wang CR, Lee YT, Chuang CY, Chen CY.** Acute pancreatitis related to anticardiolipin antibodies in lupus patients visiting an emergency department. *Am J Emerg Med* 1993; **11**: 230-232
- 7 **Kolk A, Horneff G, Wilgenbus KK, Wahn V, Gerharz CD.** Acute lethal necrotising pancreatitis in childhood systemic lupus erythematosus-possible toxicity of immunosuppressive therapy. *Clin Exp Rheumatol* 1995; **13**: 399-403
- 8 **Saab S, Corr MP, Weisman MH.** Corticosteroids and systemic lupus erythematosus pancreatitis: a case series. *J*

- Rheumatol* 1998; **25**: 801-806
- 9 **Ikura Y**, Matsuo T, Ogami M, Yamazaki S, Okamura M, Yoshikawa J, Ueda M. Cytomegalovirus associated pancreatitis in a patient with systemic lupus erythematosus. *J Rheumatol* 2000; **27**: 2715-2717
- 10 **Al-Mayouf SM**, Majeed M, Al-Mehaidib A, Alsuhaibani H. Pancreatic pseudocyst in paediatric systemic lupus erythematosus. *Clin Rheumatol* 2002; **21**: 264-266
- 11 **Singh R**, Saunders B, Scopelitis E. Pancreatitis leading to thrombotic thrombocytopenic purpura in systemic lupus erythematosus: a case report and review of literature. *Lupus* 2003; **12**: 136-139
- 12 **Langlet P**, Karmali R, Deprez C, Brandelet B, Kleynen P, Dratwa M, de Koster E, Denis P, Deltenre M. Severe acute pancreatitis associated with peliosis hepatis in a patient with systemic lupus erythematosus. *Acta Gastroenterol Belg* 2001; **64**: 298-300
- 13 **Singh M**, Wani S, Murtaza M, Joglekar S, Kasubhai M. Systemic lupus erythematosus presenting with acute fatal pancreatitis as an initial manifestation. *Am J Gastroenterol* 2001; **96**: 2280- 2281
- 14 **Marum S**, Veiga MZ, Silva F, Vasconcelos T, Ferreira A, Viegas J. Lupus pancreatitis. *Acta Med Port* 1998; **11**: 779-782
- 15 **Ranson JH**. Diagnostic standards for acute pancreatitis. *World J Surg* 1997; **21**: 136-142
- 16 **Frank B**, Gottlieb K. Amylase normal, lipase elevated: is it pancreatitis? A case series and review of the literature. *Am J Gastroenterol* 1999; **94**: 463-469
- 17 **Eaker EY**, Toskes PP. Systemic lupus erythematosus presenting initially with acute pancreatitis and a review of the literature. *Am J Med Sci* 1989; **297**: 38-41

Science Editor Wang XL Language Editor Elsevier HK

• LETTERS TO THE EDITOR •

Is the severity of obstructive sleep apnea or the magnitude of respiratory effort associated with gastroesophageal reflux?

Levent Ozturk, Zerrin Pelin

Levent Ozturk, Department of Physiology, Faculty of Medicine, Trakya University Edirne, Turkey
Zerrin Pelin, Electroencephalography and Sleep Laboratory, Neurology Department, Pendik State Hospital, Istanbul, Turkey
Correspondence to: Levent Ozturk, MD, Associate Professor, Trakya Universitesi Tip Fakültesi, Fizyoloji Anabilim Dalı, Edirne 22030, Turkey. leventozturk@trakya.edu.tr
Telephone: +90-284-2357641-1304 Fax: +90-284-2357652
Received: 2005-03-07 Accepted: 2005-03-31

© 2005 The WJG Press and Elsevier Inc. All rights reserved.

Key words: Sleep apnea; Respiratory effort; Gastroesophageal reflux

Ozturk L, Pelin Z. Is the severity of obstructive sleep apnea or the magnitude of respiratory effort associated with gastroesophageal reflux?. *World J Gastroenterol* 2005; 11(30): 4769

<http://www.wjgnet.com/1007-9327/11/4769.asp>

TO THE EDITOR

In a recent issue of *World Journal of Gastroenterology*, Demeter *et al.*^[1], reported that in patients having both gastro-esophageal reflux disease (GERD) and obstructive sleep apnea (OSA), there was a positive correlation between endoscopic findings of GERD and the number of apneas and hypopneas per hour, namely apnea hypopnea index. They proposed that the severity of OSA and GERD are parallel to each other. The study of Demeter and colleagues is very important, not only for assessing reflux-induced esophageal damage in OSA, but also for determining therapeutic approaches for patients with OSA and GERD. Because both conditions are very common in general population and are associated with morbidity and deterioration of quality of life^[2,3].

However, causative relationship underlying the association may be complicated. One proposed mechanism is that greater respiratory effort increases the pressure gradient across the lower esophageal sphincter and eventually facilitates the retrograde movement of gastric content^[4]. The point is that classification of OSA is traditionally based on the apnea-hypopnea index (AHI) and, severity of OSA, which is defined by higher score of AHI, does not necessarily reflect the magnitude of respiratory effort during obstruction. Therefore, it is not easy to conclude that the occurrence of gastro-esophageal reflux is related to the number of apneas

and hypopneas rather than respiratory effort during each breathing cessation period. Besides the magnitude of respiratory effort, repetitive stimulation of lower esophageal sphincter via phreno-esophageal ligament may also be linked with a threshold value of respiratory effort. Interestingly, there is another sleep-disordered breathing called "Upper Airway Resistance Syndrome", which is described by excessive daytime sleepiness, increased respiratory effort without oxyhemoglobin desaturation during sleep and absence of apneas or hypopneas. Inspiratory effort is an important characteristic and determinant of sleepiness and other symptomatology in UARS patients^[5]. Considering the same mechanism, patients with UARS should also complain from reflux-related symptoms. We are not aware of any study reporting GERD in UARS. Another mechanism involves increased arousals in patients with OSA, together with reduced sleep efficiency, which may trigger transient lower esophageal sphincter relaxation and thus, promote acid reflux^[6]. We have recently reported that there is no sufficient evidence to accept arousals and obstructive respiratory events during sleep as primary causes of gastroesophageal reflux and vice versa^[7]. Indeed, we failed to find any timely relation between reflux episodes and respiratory events on the simultaneous recordings of dual probe esophageal pH monitoring and polysomnography. We think that controversy will remain until placebo-controlled studies focusing on the timely relation between respiratory effort and reflux episodes will be performed.

REFERENCES

- 1 Demeter P, Visy KV, Magyar P. Correlation between severity of endoscopic findings and apnea-hypopnea index in patients with gastroesophageal reflux disease and obstructive sleep apnea. *World J Gastroenterol* 2005; **11**: 839-841
- 2 Reimer MA, Flemons WW. Quality of life in sleep disorders. *Sleep Med Rev* 2003; **7**: 335-349
- 3 Kulig M, Leodolter A, Vieth M, Schulte E, Jaspersen D, Labenz J, Lind T, Meyer-Sabellek W, Malfertheiner P, Stolte M, Willich SN. Quality of life in relation to symptoms in patients with gastro-oesophageal reflux disease- an analysis based on the ProGERD initiative. *Aliment Pharmacol Ther* 2003;**18**: 767-776
- 4 Fields SK, Flemons WW. Is the relationship between obstructive sleep apnea and gastroesophageal reflux clinically important? *Chest* 2002; **121**: 1730-1733
- 5 Pelin Z, Karadeniz D, Ozturk L, Gozukirmizi E, Kaynak H. The role of mean inspiratory effort on daytime sleepiness. *Eur Respir J* 2003; **21**: 688-694
- 6 Ing AJ, Ngu MC, Breslin AB. Obstructive sleep apnea and gastroesophageal reflux. *Am J Med* 2000; **108**: 120S-125
- 7 Ozturk O, Ozturk L, Ozdogan A, Oktem F, Pelin Z. Variables affecting the occurrence of gastroesophageal reflux in obstructive sleep apnea patients. *Eur Arch Otorhinolaryngol* 2004; **261**: 229-232

• ACKNOWLEDGMENTS •

Acknowledgments to Reviewers of *World Journal of Gastroenterology*

Many reviewers have contributed their expertise and time to the peer review, a critical process to ensure the quality of *World Journal of Gastroenterology*. The editors and authors of the articles submitted to the journal are grateful to the following reviewers for evaluating the articles (including those were published and those were rejected in this issue) during the last editing period of time.

Takafumi Ando, M.D.

Nagoya University Graduate School of Medicine, Therapeutic Medicine, 65 Tsurumai-cho, Showa-ku, Nagoya 466-8550, Japan

Zong-Jie Cui, Professor

Institute of Cell Biology, Beijing Normal University, Beijing 100875, China

Er-Dan Dong, Professor

Department of Life Science, Division of Basic Research in Clinic Medicine, National Natural Science Foundation of China, 83 Shuanqing Road, Haidian District, Beijing 100085, China

Sheung-Tat Fan, Professor

Department of Surgery, The University of Hong Kong, Queen Mary Hospital, 102 Pokfulam Road, Hong Kong, China

Xue-Gong Fan, Professor

Xiangya Hospital, Changsha 410008, Hunan Province, China

Joachim Labenz, Associate Professor

Jung-Stilling Hospital, Wichernstr. 40, Siegen 57074, Germany

Ansgar W Lohse, Professor

Department of Medicine, Hamburg University, Martinistr. 52, Hamburg 20246, Germany

Giovanni Maconi, M.D.

Department of Gastroenterology, 'L.Sacco' University Hospital, Via G.B.Grassi, 74, Milan 20157, Italy

James Neuberger, Professor

Liver Unit, Queen Elizabeth Hospital, Birmingham B15 2TH, United Kingdom

Bo-Rong Pan, Professor

Department of Oncology, Xijing Hospital, Fourth Military Medical University, No.1, F.8, Bldg 10, 97 Changying East Road, Xi'an 710032, Shaanxi Province, China

Heitor Rosa, Professor

Department of Gastroenterology and Hepatology, Federal University School of Medicine, Rua 126 n.21, Goiania - GO 74093-080, Brazil

Jose Sahel, Professor

Hepato-gastroenterology, Hospital sainti Marevenite, 1270 Boulevard AE Sainti Margrenise, Marseille 13009, France

Tilman Sauerbruch, M.D.

Department of Internal Medicine I, University of Bonn, Sigmund-Freud-Strasse 25, 53105 Bonn, Germany

Rudi Schmid, M.D.

211 Woodland Road, Kentfield, California 94904, United States

Tadashi Shimoyama, M.D.

Hirosaki University, 5 Zaifu-cho, Hirosaki 036-8562, Japan

Yoshio Shirai, Associate Professor

Division of Digestive and General Surgery, Niigata University Graduate School of Medical and Dental Sciences, 1-757 Asahimachidori, Niigata City 951-8510, Japan

Manfred Stolte, Professor

Institute of Pathology, Klinikum Bayreuth, Preuschwitzer Str. 101, Bayreuth 95445, Germany

Simon D Taylor-Robinson, M.D.

Department of Medicine A, Imperial College London, Hammersmith Hospital, Du Cane Road, London W12 0HS, United Kingdom

Frank Ivor Tovey, M.D.

Department of Surgery, University College London, 5 Crossborough Hill, Basingstoke RG21 4AG, United Kingdom

Hong-Yang Wan, M.D.

International Co-operation Laboratory on Signal Transduction Eastern Hepatobiliary Surgery Institute, SMMU, 225 Changhai Road, Shanghai 200438, China

Jia-Yu Xu, Professor

Shanghai Second Medical University, Rui Jin Hospital, 197 Rui Jin Er Road, Shanghai 200025, China

Michael Zenilman, Professor and Chairman

Department of Surgery, SUNY Downstate Medical Center, 450 Clarkson Avenue, Brooklyn NY, United States

Jian-Zhong Zhang, Professor

Department of Pathology and Laboratory Medicine, Beijing 306 Hospital, 9 North Anxiang Road, PO Box 9720, Beijing 100101, China

Zhi-Rong Zhang, Professor

West China School of Pharmacy, Sichuan University, 17 South Renmin Road, Chengdu 610041, Sichuan Pvince, China

• REVIEW •

Bio-feedback treatment of fecal incontinence: Where are we, and where are we going?

Giuseppe Chiarioni, Barbara Ferri, Antonio Morelli, Guido Iantorno, Gabrio Bassotti

Giuseppe Chiarioni, Gastroenterological Rehabilitation Division of the University of Verona, Valeggio sul Mincio Hospital, Azienda Ospedaliera of Verona, Italy

Barbara Ferri, Gastroenterology and Digestive Endoscopy Institute, Policlinico "GB Rossi", University of Verona Medical School, Italy
Antonio Morelli, Gabrio Bassotti, Gastroenterology and Hepatology Section, Department of Clinical and Experimental Medicine, University of Perugia Medical School, Italy

Guido Iantorno, Digestive Motility Unit, Gastroenterology Municipal Hospital "Dr. C. Bonorino Udaondo", Buenos Aires, Argentina

Correspondence to: Dr. Gabrio Bassotti, Strada del Cimitero, 2/a 06131 San Marco (Perugia), Italy. gabassot@tin.it

Fax: +39-75-584-7570

Received: 2004-12-03 Accepted: 2005-02-18

Abstract

Fecal incontinence is a disabling disease, often observed in young subjects, that may have devastating psycho-social consequences. In the last years, numerous evidences have been reported on the efficacy of bio-feedback techniques for the treatment of this disorder. Overall, the literature data claim a success rate in more than 70% of cases in the short term. However, recent controlled trials have not confirmed this optimistic view, thus emphasizing the role of standard care. Nonetheless, many authors believe that this should be the first therapeutic approach for fecal incontinence due to the efficacy, lack of side-effects, and scarce invasiveness. Well-designed randomized, controlled trial are eagerly awaited to solve this therapeutic dilemma.

© 2005 The WJG Press and Elsevier Inc. All rights reserved.

Key words: Biofeedback; Fecal incontinence

Chiarioni G, Ferri B, Morelli A, Iantorno G, Bassotti G. Bio-feedback treatment of fecal incontinence: Where are we, and where are we going? *World J Gastroenterol* 2005; 11 (31): 4771-4775

<http://www.wjgnet.com/1007-9327/11/4771.asp>

INTRODUCTION

Fecal incontinence is a common health care problem, with modest physical but important psychosocial consequences that can be distressful and incapacitating, up to complete social isolation^[1]. Fecal incontinence is one of the fields in which bio-feedback techniques are thought to be most

successful, and owing to the fact that bio-feedback procedures have had a strong impact in gastro-enterology, behavioral research in this area has greatly increased in recent years^[2,3]. The term bio-feedback training refers to the use of various devices (mechanical, electrical) that are supposedly able to increase the awareness of a biological response, so that patients can learn, through a process of "trial and error", to improve their voluntary control of this response^[4]. Bio-feedback training sessions are usually supplemented by home practice training (Kegel exercises), with the purpose of enforcing muscle strength through an increase of the number of muscle fibers innervated by existing nerves. It is commonly thought that bio-feedback is not able to repair or generate new neural pathways.

The increase of patient's awareness of somatic sensations, and the improvement of motor skills, which represent the basis of biologic self-regulation, are critical points for bio-feedback training. For instance, a cause of fecal incontinence is the loss of the ability to feel rectal fullness, a major point for contracting the pelvic floor muscles to avoid incontinence^[5]. In these patients, the goal of bio-feedback training is to improve the ability to detect rectal filling through sensory re-training^[6,7].

Types of bio-feedback training for fecal incontinence

Bio-feedback treatment of fecal incontinence was proposed by Engel and coworkers, 30 years ago^[8]. Patients were taught to improve their ability to voluntarily contract the external anal sphincter during rectal filling, either by improving the strength of the sphincter (motor skills training) or by increasing the ability to perceive weak rectal distention (discrimination training) or by combining the previous two mechanisms (training in the coordination of sphincter contractions with rectal sensation). No side effects were reported and the treatment was generally well accepted. Further trials had shown that therapeutic goals can be achieved through training, that employs measurements of pressures (manometry) or electrical activity (electromyography, EMG) in the anal canal^[2,3].

Manometric bio-feedback

Bio-feedback training aimed at increasing the strength of the external anal sphincter has usually been carried out by recording anal canal pressures, coupled to visual/auditory signals proportional to the pressures themselves. Anal pressure may be recorded by balloon probes or by perfused catheters^[4]. During manometric recording, the patient is required to squeeze as to prevent defecation while being given visual feedback and verbal guidance on how to reach

this goal. The patients may also be taught to inhibit wrong responses such as contraction of the abdominal muscles. Asking the patient to squeeze may be obtained in response to balloon distention of the rectum^[9] or without rectal distention^[10]. Some authors have suggested that improving squeeze duration is more important than maximizing anal strength. Therefore, patients are taught to pursue this therapeutic goal as a part of the bio-feedback protocol^[10,11].

EMG bio-feedback

Strengthening the pelvic floor muscle may also be achieved by showing the patient, a recording of the integrated (average) EMG activity from the striated muscles which surround the anal canal^[12]. In EMG training, the patient is asked to squeeze and relax without rectal distention, and home exercises in which the patient is required to repeatedly squeeze the pelvic floor muscles (Kegel exercises) are usually added to the training to further strengthen these muscles. Other methods of EMG recording of the pelvic floor employ an anal plug with surface electrodes^[13], very easy to use and requiring no preparation.

Sensory discrimination training

This is aimed at increasing the patient's ability to perceive and respond to rectal distention^[14]. After inserting within the rectum a catheter-mounted balloon, the latter is inflated with different air volumes; the patient is then asked to signal when the feeling of distention is perceived, or to contract the pelvic floor muscles in response to the distention. For these purposes, easily perceived distention with large volumes of air is firstly given, the volumes of distention are gradually decreased until the patient is able to perceive them with difficulty. Repeated distention slightly above and below the sensory threshold of the patient, coupled to the investigator's feedback on the accuracy of detection, teach the patient to recognize distention of even weaker intensity^[3,4]. This type of sensory training is often coupled to sphincter strength training, asking the patient always to contract (as strongly as possible) in response to rectal distention and providing feedback on the strength of contraction and accuracy of detection^[3,4]. Several evidences suggest that sensory discrimination training (aimed at reducing the threshold for perception of rectal distention) is very important for an effective bio-feedback procedure^[6-8,15]. We have recently evaluated 24 patients with severe, solid-stool fecal incontinence^[16] by teaching them to squeeze in response to rectal distention; the patients were evaluated 3 mo after bio-feedback training, and were classified as responders (>75% decrease of incontinence episodes) or non-responders. Comparison of the two groups showed that responders displayed significantly lower sensory thresholds after training with respect to non-responders, but squeeze pressures were not significantly different between groups. Sensory thresholds measured before bio-feedback training were good predictors of which patients would respond to it; in fact, patients with more severe sensory impairment had poor response to bio-feedback training^[16]. Sphincter strength and severity of fecal incontinence before bio-feedback training were not useful as predictors of outcome.

METHODS

An internet-based comprehensive search strategy of the Medline and Science Citation Index was performed using the keywords bio-feedback and fecal incontinence, in various combinations with the Boolean operators AND, OR, and NOT. Only articles related to human studies were used, and manual cross-referencing was also performed. Articles published in English between January 1965 and September 2004 were selected; however, a search in non-English languages and in journals was also older than 1965 performed in our library. Letters were excluded, and abstracts were quoted only when the full papers were unavailable.

Usefulness of bio-feedback in fecal incontinence

Most of the available studies concerning the use of bio-feedback to treat fecal incontinence have been carried out by manometric means; however, a clear superiority of pressure *vs* EMG feedback has not surfaced^[17], and only one study aimed at comparing pressure *vs* EMG feedback training showed no significant differences between the two techniques^[18].

Looking at all the studies available in literature regardless of etiology, it is found that about 2/3 of patients display at least a 75% decrease of their episodes of fecal incontinence^[19,20], although only about 50% of them developed complete continence. However, it must be stressed that (1) no uniform criteria for defining improvement or assessing outcome have been adopted; (2) inclusion criteria differed; (3) treatment protocols varied and (4) only few prospective, randomized, parallel-group studies have been published, not enough to draw conclusions on the overall efficacy of bio-feedback training. In addition, recent randomized studies have not confirmed the optimistic outcome of previous open studies. These trials will be examined in detail in the following paragraph.

In a first randomized controlled study, bio-feedback plus behavioral management was compared to behavioral management alone in children with fecal incontinence due to myelomeningocele^[21]; both groups displayed significant improvement, suggesting that bio-feedback has the same effects as behavioral management for most children with myelomeningocele. However, it must be stressed that patients with spinal cord defects show commonly worst responses to bio-feedback than patients with incontinence due to other causes^[22]. In a second controlled study, van der Plas and coworkers studied 71 children with fecal incontinence without constipation and randomized them to standard care and laxatives or standard care and laxatives plus bio-feedback. At 12-18 mo follow-up, approximately 50% of children in both groups showed significant symptoms improvement. A trend toward better outcome was shown in the bio-feedback group, but statistical significance was not reached^[23]. In the first randomized study of bio-feedback in adults with fecal incontinence, a complex cross-over design was employed making interpretation of results quite difficult^[24]. Twenty-five patients were initially randomized to either three sessions, sensory discrimination training without bio-feedback on sphincter strength or equivalent distention without feedback on the accuracy of their

detection of the strength of contractions. Patients in the sensory training group had significant decrease of frequency of episodes of incontinence with respect to controls, but between-group differences did not reach statistical significance (probably due to small sample size). Control patients were then given sensory training, and displayed improvement in continence. Thereafter, all patients were randomized again to sphincter-strengthening exercises without bio-feedback or to squeeze in response to rectal distention with feedback. Overall, the patients had further improvement of continence in this second step of the study, but no significant differences were observed between groups, suggesting that sensory training is important for the treatment of incontinence, although the results are not definitive due to the small size samples. Recently, the St. Mark group reported a large, randomized, controlled study on 171 adults with fecal incontinence^[25]. Patients were randomized into four groups: (1) standard care with advice; (2) standard care with advice plus anal sphincter exercises taught verbally and via digital examinations; (3) same as group 2 plus bio-feedback therapy run at the clinic; (4) same as group 3 plus sphincter exercises guided by a home bio-feedback device. Approximately half of patients in all groups reported improvement of symptoms at one year follow-up. Interestingly, quality of life measurements, bowel symptoms and anal sphincter pressures were improved in similar percentage in all groups. Bio-feedback therapy yielded no greater benefit than did standard care with advice on an intention-to-treat analysis.

This trial appears methodologically sound in most instances with few, relevant limitations mostly related to the lack of details of the bio-feedback protocol used. Type and dosage of anti-diarrheal medications used in all the groups were also not provided. The results of this trial are at variance with a previous open study coming from the same Center, where bio-feedback therapy was reported to improve symptoms in the majority of patients with fecal incontinence^[26]. Moreover, another prospective, randomized, controlled study comparing pelvic floor exercises plus anal exercises taught via digital examination with either manometry or anal ultrasound-guided bio-feedback in 120 adults with fecal incontinence had failed to show any additional benefit of behavior therapy over Kegel exercises in terms of clinical outcome, quality of life measurements, and anal pressures^[27]. In this trial, a clinical benefit was evident in the short term in approximately 70% of all patients. The same group then reported this clinical benefit as substantially preserved in the long term follow-up^[28]. Interestingly, quality of life measurements and subjective perception of "catching up" with incontinence improved even in patients whose incontinence scores worsened. Therefore, intervention "*per se*" seems to improve subjective symptoms perception in fecal incontinence.

Do predictors of outcome exist

Although it is traditionally thought that subgroups of patients (demented, mentally retarded, young children, severely depressed, mobility impaired) are less prone to respond to bio-feedback training, there are few data to support these concepts as guidelines^[29]. The available data may be

summarized as follows: (1) severe mechanical damage of the anal sphincters is generally associated with poor bio-feedback responses^[30,31]; (2) major sensory impairment determines a poor response to bio-feedback training^[16,26,32]; (3) although many studies have not found the response to bio-feedback predictable on the basis of pretreatment findings^[33-35], there are reports showing that a low basal pressure of the internal anal sphincter is associated with poor outcomes^[36]; (4) abnormally prolonged pudendal nerve conduction times are employed to identify subjects with pudendal nerve injuries as a cause of incontinence; these measurements correlate poorly with the response to bio-feedback^[37]; (5) there is no significant association between fecal incontinence and anxiety or depression^[38,39], the latter, however, may decrease the patient's ability to learn and to comply with home practice^[40]; (6) the association of constipation by outlet dysfunction may affect outcome unfavorably^[41].

Associate treatments

There are several reports of miscellaneous combinations of bio-feedback with surgical procedures to treat fecal incontinence. Results described as positive have been reported for high imperforate anus repair^[42], gracilis muscle transposition^[43], and anterior resection of the rectum and total colectomy with ileo-anal anastomosis^[44]; however, all these were uncontrolled studies, and the patient sample's were small. Other studies associated electrical stimulation with pelvic floor bio-feedback in a miscellaneous group of patients (including subjects with fecal incontinence and subjects with constipation due to pelvic floor dysfunction), and claimed that this association was more effective than a single approach^[45]. Real-time ultrasonographic imaging of the pelvic floor muscles has also been employed to teach patients with fecal incontinence to squeeze the external anal sphincter^[46], but the trials with this technique are still ongoing. Loening-Baucke implemented standard medical care with a pressure bio-feedback protocol in a small group of adults with fecal incontinence. No additional benefit could be evidenced compared to standard medical care alone^[47].

Conclusions

Although fecal incontinence is a socially devastating disorder, many physicians are still unaware that it is often amenable to treatment^[48]. Recently, well-designed, randomized trials have shown that standard medical care implemented with simple pelvic floor exercises is effective in a large percentage of patients with fecal incontinence. Attention to diet, scheduled defecations and judicious use of anti-diarrheal medications seem to preserve a relevant role in this "untreatable" disease. Traditionally, bio-feedback techniques have been rated to offer a suitable non-invasive method of approaching the problem superior to conservative simpler therapeutic measurements. This has not been confirmed by randomized, controlled trials. Notwithstanding the reported symptoms improvement in over 2/3 of fecally incontinent patients shown in open trials, and the common belief that behavior therapy is a safe and effective therapeutic option for many patients with fecal incontinence, experimental evidence is giving conflicting results. Properly

designed and carefully analyzed bio-feedback trials are actually needed to prove the effectiveness of this treatment in fecal incontinence. Meanwhile, it is reassuring to know that simple therapeutic measurements may effectively help these individuals affected by such a disabling disorder.

REFERENCES

- Bharucha AE.** Fecal incontinence. *Gastroenterology* 2003; **124**: 1672-1685
- Bassotti G, Whitehead WE.** Biofeedback as a treatment approach to gastrointestinal tract disorders. *Am J Gastroenterol* 1994; **89**: 158-164
- Bassotti G, Chiarioni G.** Terapia conductual, relajación, y biorretroalimentación en los trastornos funcionales del tracto digestivo inferior. In Montoro Hugueta MA, ed. Principios básicos de Gastroenterología para médicos de familia. Madrid: Jarpay Editores 2002: 377-390
- Whitehead WE, Heymen S, Schuster MM.** Motility as a therapeutic modality: bio-feedback treatment of gastrointestinal disorders. In Schuster MM, Crowell MD, Koch KL, eds. Schuster Atlas of Gastrointestinal Motility, Second edition. Hamilton: BC Decker Inc 2002: 381-397
- Sun WM, Read NW, Miner PB.** Relation between sensation and anal function in normal subjects and patients with faecal incontinence. *Gut* 1990; **31**: 1056-1061
- Wald A, Tunuguntla AK.** Anorectal sensorimotor dysfunction in fecal incontinence and diabetes mellitus. Modification with bio-feedback therapy. *N Engl J Med* 1984; **310**: 1282-1287
- Buser WD, Miner PB.** Delayed rectal sensation with fecal incontinence. Successful treatment using anorectal manometry. *Gastroenterology* 1986; **91**: 1186-1191
- Engel BT, Nikoomeanesh P, Schuster MM.** Operant conditioning of rectosphincteric responses in the treatment of fecal incontinence. *N Engl J Med* 1974; **290**: 646-649
- Glia A, Gyllin M, Akerlund JE, Lindfors U, Lindberg G.** Bio-feedback training in patients with fecal incontinence. *Dis Colon Rectum* 1998; **41**: 359-364
- Patankar SK, Ferrara A, Larach SW, Williamson PR, Perozo SE, Levy JR, Mills J.** Electromyographic assessment of bio-feedback training for fecal incontinence and chronic constipation. *Dis Colon Rectum* 1997; **40**: 907-911
- Chiarioni G, Scattolini C, Bonfante F, Vantini I.** Liquid stool incontinence with severe urgency: anorectal function and effective bio-feedback therapy. *Gut* 1993; **34**: 1576-1580
- Cox DJ, Sutphen J, Borowitz S, Dickens MN, Singles J, Whitehead WE.** Simple electromyographic bio-feedback treatment for chronic pediatric constipation/encopresis: preliminary report. *Biofeedback Self Regul* 1994; **19**: 41-50
- Eisman E, Tries J.** A new probe for measuring electromyographic activity from multiple sites in the anal canal. *Dis Colon Rectum* 1993; **36**: 946-952
- Whitehead WE, Wald A, Diamant NE, Enck P, Pemberton JH, Rao SSC.** Functional disorders of the anus and rectum. In Drossman DA, Corazziari E, Talley NJ, Thompson WG, Whitehead WE, eds. Rome II. The functional gastrointestinal disorders, second edition. Mc Lean, VA: Degnon Associates 2000: 483-532
- Latimer PR, Campbell D, Kasperski J.** A component analysis of bio-feedback in the treatment of fecal incontinence. *Biofeedback Self Regul* 1984; **9**: 311-324
- Chiarioni G, Bassotti G, Stanganini S, Vantini I, Whitehead WE.** Sensory retraining is key to bio-feedback therapy for formed stool fecal incontinence. *Am J Gastroenterol* 2002; **97**: 109-117
- Heymen S, Jones KR, Ringel Y, Scarlett Y, Whitehead WE.** Biofeedback treatment of fecal incontinence: a critical review. *Dis Colon Rectum* 2001; **44**: 728-736
- Heymen S, Wexner SD, Vickers D, Noguera JJ, Weiss EG, Pikarsky AJ.** Prospective, randomized trial comparing four bio-feedback techniques for patients with constipation. *Dis Colon Rectum* 1999; **42**: 1388-1393
- Enck P.** Biofeedback training in disordered defecation: a critical review. *Dig Dis Sci* 1993; **38**: 1953-1960
- Rao SS, Enck P, Loenig-Baucke V.** Biofeedback therapy for defecation disorders. *Dig Dis* 1997; **15**(Suppl 1): 78-92
- Whitehead WE, Parker L, Bosmajian L, Morrill-Corbin ED, Middaugh S, Garwood M, Cataldo MF, Freeman J.** Treatment of fecal incontinence in children with spina bifida: comparison of bio-feedback and behavioral modification. *Arch Phys Med Rehabil* 1986; **67**: 218-224
- Cerulli MA, Nikoomeanesh P, Schuster MM.** Progress in bio-feedback conditioning for fecal incontinence. *Gastroenterology* 1979; **76**: 742-746
- van der Plas RN, Benninga MA, Redekop WK, Taminiou JA, Buller HA.** Randomised trial of bio-feedback training for encopresis. *Arch Dis Childh* 1996; **75**: 367-374
- Miner PB, Donnelly TC, Read NW.** Investigation of mode of action of bio-feedback in treatment of fecal incontinence. *Dig Dis Sci* 1990; **35**: 1291-1298
- Norton C, Chelvanayagam S, Wilson-Barnett J, Redfern S, Kamm MA.** Randomized controlled trial of bio-feedback for fecal incontinence. *Gastroenterology* 2003; **125**: 1320-1329
- Norton C, Kamm MA.** Outcome of bio-feedback for faecal incontinence. *Br J Surg* 1999; **86**: 1159-1163
- Solomon MJ, Pager CK, Rex J, Roberts RA, Manning J.** Randomized, controlled trial of bio-feedback with anal manometry, transanal ultrasound, or pelvic floor retraining with digital guidance alone in the treatment of mild to moderate fecal incontinence. *Dis Colon Rectum* 2003; **46**: 703-710
- Pager CK, Solomon MJ, Rex J, Roberts RA.** Long-term outcomes of pelvic floor exercises and bio-feedback treatment for patients with fecal incontinence. *Dis Colon Rectum* 2002; **45**: 997-1003
- Whitehead WE, Wald A, Norton NJ.** Treatment options for fecal incontinence. *Dis Colon Rectum* 2001; **44**: 131-144
- Iwai N, Nagashima S, Shimotake T, Iwata G.** Biofeedback therapy for fecal incontinence after surgery for anorectal malformations: preliminary results. *J Pediatr Surg* 1993; **28**: 863-866
- Leroi AM, Dorival MP, Lecoturier MF, Saiter C, Welter ML, Touchais JY, Denis P.** Pudendal neuropathy and severity of incontinence but not presence of an anal sphincter defect may determine the response to bio-feedback therapy in fecal incontinence. *Dis Colon Rectum* 1999; **42**: 762-769
- Kraemer M, Ho YH, Tan W.** Effectiveness of anorectal bio-feedback therapy for faecal incontinence: medium-term results. *Tech Coloproctol* 2001; **5**: 125-129
- Sangwan YP, Collier JA, Barrett RC, Roberts PL, Murray JJ, Schoetz DJ.** Can manometric parameters predict response to bio-feedback therapy in fecal incontinence? *Dis Colon Rectum* 1995; **38**: 1021-1025
- Keck JO, Staniunas RJ, Collier JA, Barrett RC, Oster ME, Schoetz DJ, Roberts PL, Murray JJ, Veidenheimer MC.** Biofeedback training is useful in fecal incontinence but disappointing in constipation. *Dis Colon Rectum* 1994; **37**: 1271-1276
- Ferrara A, De Jesus S, Gallagher JT, Williamson PR, Larach SW, Pappas D, Mills J, Sepulveda JA.** Time-related decay of the benefits of bio-feedback therapy. *Tech Coloproctol* 2001; **5**: 131-135
- Hamalainen KJ, Raivio P, Antila S, Palmu A, Mecklin JP.** Biofeedback therapy in rectal prolapse patients. *Dis Colon Rectum* 1996; **39**: 262-265
- Diamant NE, Kamm MA, Wald A, Whitehead WE.** AGA technical review on anorectal testing technique. *Gastroenterology* 1999; **116**: 735-760
- Nelson R, Furner S, Jesudason V.** Fecal incontinence in Wisconsin nursing homes: prevalence and association. *Dis Colon Rectum* 1998; **41**: 1226-1229
- Heymen S, Wexner SD, Gullledge AD.** MMPI assessment of patients with functional bowel disorders. *Dis Colon Rectum*

- 1993; **36**: 593-596
- 40 American Psychiatric Association. Diagnostic and statistical manual of mental disorders, 4th ed rev. American Psychiatric Association, Washington (DC), 1999
- 41 **Fernandez-Fraga X**, Azpiroz F, Aparici A, Casaus M, Malagelada JR. Predictors of response to bio-feedback treatment in anal incontinence. *Dis Colon Rectum* 2003; **46**: 1218-1225
- 42 **Arnbjorsson E**, Breland U, Kullendorff CM, Michaelsson C, Okmian L. Physiotherapy to improve faecal control after Stephen's rectoplasty in high imperforate anus. *Z Kinderchirurgie* 1986; **41**: 101-103
- 43 **Sielezneck I**, Bauer S, Bulgare JC, Sarles JC. Gracilis muscle transposition in the treatment of faecal incontinence. *Int J Colorect Dis* 1996; **11**: 15-18
- 44 **Ho YH**, Chiang JM, Tan M, Low JY. Biofeedback therapy for excessive stool frequency and incontinence following anterior resection or total colectomy. *Dis Colon Rectum* 1996; **39**: 1289-1292
- 45 **Menard C**, Trudel C, Cloutier R. Anal reeducation for post-operative fecal incontinence in congenital diseases of the rectum and anus. *J Pediatr Surg* 1997; **32**: 867-869
- 46 **Solomon MJ**, Rex J, Eysers AA, Stewart P, Roberts R. Biofeedback for fecal incontinence using transanal ultrasonography. *Dis Colon Rectum* 2000; **43**: 788-792
- 47 **Loening-Baucke V**. Efficacy of bio-feedback training in improving faecal incontinence and anorectal physiologic function. *Gut* 1990; **31**: 1395-1402
- 48 **Rudolph W**, Galandiuk S. A practical guide to the diagnosis and management of fecal incontinence. *Mayo Clin Proc* 2002; **77**: 271-275

Science Editor Guo SY Language Editor Elsevier HK

Preventing prolonged post-operative ileus in gastric cancer patients undergoing gastrectomy and intra-peritoneal chemotherapy

De-Chuan Chan, Yao-Chi Liu, Cheng-Jueng Chen, Jyh-Cherng Yu, Heng-Cheng Chu, Fa-Chang Chen, Teng-Wei Chen, Huan-Fa Hsieh, Tzu-Ming Chang, Kuo-Liang Shen

De-Chuan Chan, Yao-Chi Liu, Cheng-Jueng Chen, Jyh-Cherng Yu, Teng-Wei Chen, Kuo-Liang Shen, Division of General Surgery, Tri-Service General Hospital, National Defense Medical Center, National Defense University, Taipei, Taiwan, China
Heng-Cheng Chu, Division of Gastroenterology and Hepatology, Department of Internal Medicine, Tri-Service General Hospital, National Defense Medical Center, National Defense University, Taipei, Taiwan, China
Fa-Chang Chen, Department of Anesthesiology, Tri-Service General Hospital, National Defense Medical Center, National Defense University, Taipei, Taiwan, China
Huan-Fa Hsieh, Yee-Zen General Hospital, Taoyuan, Taiwan, China
Tzu-Ming Chang, Department of Surgery, Shalu Tungs' Memorial Hospital, Tai-Chung, Taiwan, China
Correspondence to: Dr. De-Chuan Chan, Division of General Surgery, National Defense Medical Center, National Defense University, Taipei 114, Taiwan, China. chrischan1168@yahoo.com.tw
Telephone: +886-2-87927191 Fax: +886-2-87927372
Received: 2005-01-11 Accepted: 2005-01-26

Abstract

AIM: To assess the efficacy of metoclopramide (Met) for prevention of prolonged post-operative ileus in advanced gastric cancer patients undergoing D2 gastrectomy and intra-peritoneal chemotherapy (IPC).

METHODS: Thirty-two advanced gastric cancer patients undergoing D2 gastrectomy and IPC were allocated to two groups. Sixteen patients received Met immediately after operation (group A), and 16 did not (group B). Another 16 patients who underwent D2 gastrectomy without IPC were enrolled as the control group (group C). All patients had received epidural pain control. The primary endpoints were time to first post-operative flatus and time until oral feeding with a soft diet without discomfort. Secondary endpoints were early complications during hospitalization.

RESULTS: Gender, the type of resection, operating time, blood loss, tumor status and amount of narcotics were comparable in the three groups. However, the group C patients were older than those in groups A and B (67.5 ± 17.7 vs 56.8 ± 13.2 , 57.5 ± 11.7 years, $P = 0.048$). First bowel flatus occurred after 4.35 ± 0.93 d in group A, 4.94 ± 1.37 d in group B, and 4.71 ± 1.22 d in group C ($P > 0.05$). Oral feeding of a soft diet was tolerated 7.21 ± 1.92 d after operation in group A, 10.15 ± 2.17 d in group B, and 7.53 ± 1.35 d in group C (groups A and C vs group B, $P < 0.05$). There was no significant difference in respect to the first flatus among the three groups. However, the time of tolerating oral intake with soft food in groups A and C patients was significantly

shorter than that in group B patients. Levels of C-reactive protein (CRP) were significantly lower in group C and there was a more prominent and prolonged response in CRP level in patients undergoing IPC. The incidence of post-operative complications was similar in the three groups except for prolonged post-operative ileus. There was no increased risk of anastomotic leakage in patients receiving Met.

CONCLUSION: The results suggest that a combination of intravenous Met and epidural pain control may be required to achieve a considerable decrease in time to resumption of oral soft diet in advanced gastric cancer patients who underwent gastrectomy and IPC. Furthermore, the administration of Met did not increase anastomotic leakage. Met has a role in the prevention of prolonged post-operative ileus.

© 2005 The WJG Press and Elsevier Inc. All rights reserved.

Key words: Metoclopramide; C-reactive protein; Gastric cancer; Intraperitoneal chemotherapy

Chan DC, Liu YC, Chen CJ, Yu JC, Chu HC, Chen FC, Chen TW, Hsieh HF, Chang TM, Shen KL. Preventing prolonged post-operative ileus in gastric cancer patients undergoing gastrectomy and intra-peritoneal chemotherapy. *World J Gastroenterol* 2005; 11(31): 4776-4781
<http://www.wjgnet.com/1007-9327/11/4776.asp>

INTRODUCTION

The long-term results of treatment for resectable gastric cancer have not shown any significant improvement in recent decades^[1]. Analyses of surgical treatment failure after curative resection have indicated intra-peritoneal recurrence is the major pattern of tumor recurrence^[2]. Large randomized trials of intravenous or radiotherapy have failed to demonstrate any benefit for lowering intra-peritoneal recurrence^[3,4].

Therefore, intra-peritoneal chemotherapy (IPC) as an adjuvant to surgery, may be considered as a rational therapeutic modality.

Although the role of IPC in treating peritoneal seeding or preventing peritoneal recurrence for advanced gastric cancer is still controversial, its use in prophylactic treatment in potentially curative gastric cancer resection has shown improved survival and lower peritoneal recurrence rates in Japan and Korea^[5,6]. There are some prospective randomized trials that have shown a patient with surgery plus IPC was

1.3 more times more likely to survive 5 years than a patient with surgery alone^[6]. However, prolonged post-operative ileus (POI) is one of the most commonly reported complications of IPC^[7-9]. In the situation of an immunocompromised condition induced by surgical trauma, cancer, and chemotherapy, prolonged gastro-intestinal (GI) tract stasis can increase the potential for bacterial overgrowth and translocation, potentially leading to systemic sepsis and multiple organ failure, both of which are the most prevalent post-operative complications causing death^[10,11].

To our knowledge, there are few reports concerning aggressive treatment or prevention of POI in patients undergoing IPC. Most treatments for this problem are largely supportive, including naso-gastric (NG) decompression, intravenous hydration and parenteral nutrition.

Metoclopramide (Met) antagonizes central and peripheral dopamine receptors and sensitizes GI tract receptors to acetylcholine^[12-14]. These actions increase peristalsis in the antrum, duodenum, and jejunum and increase the lower esophageal pressure. In previous studies about the effect of Met on intestinal motility, major surgical procedures have not been combined with intensive regional chemotherapy. The incidence of prolonged POI was reported as relatively low and the prophylactic use of Met as seemingly unnecessary or ineffective^[15-19].

The present study was a prospective, controlled trial in which only gastric cancer patients who underwent sub-total or total gastrectomy were enrolled. The aim of the study was to assess the effects of Met on the IPC-induced ileus.

MATERIALS AND METHODS

This study was approved by the institutional review board of Tri-Service General Hospital and informed consent was obtained from patients and family members. It was a prospective, controlled study conducted in the above hospital from March 2001 to October 2004, involving patients lesser than 70 years who had undergone R0 curative gastrectomy with D2 lymph node, i.e., N1 and N2, dissection^[20] followed by IPC for advanced gastric cancer, including T3 (serosal penetration) or T4 (invasion of adjacent organs), according to the Japanese Classification of Gastric Carcinoma^[21]. The type of resection, total or sub-total gastrectomy, depended on the location and Bormann type of primary tumor. After the potentially curative operation was performed, the peritoneal cavity was extensively washed, using seven liters of physiologic saline (1 L, seven times), followed by IPC with mitomycin-C (MMC) 10 mg in 1 L normal saline, for 60 min for all patients. The patients were allocated into two groups of 16 patients each. Patients in group A received intravenous Met 10 mg, every 8 h, commencing immediately after completion of the operation and continued until oral feeding with soft diet was resumed or abdominal cramping pain developed. Patients in group B received an equivalent volume of 5% dextrose in water, and did not receive Met. A control group (group C) of further 16 patients did not receive IPC and Met. All patients had received epidural pain control for the first three post-operative days, and then pain control was changed to intramuscular meperidine

on post-operative day (POD) four in three groups.

Epidural pain control

Before surgery, a thoracic epidural catheter was inserted at T₈-T₁₀ and advanced 5 cm into the epidural space. A test dose of 3 mL of 2% lidocaine containing epinephrine (5 µg/mL) was administered to rule out intra-thecal or intravascular misplacement. After pre-operative assessment of the epidural block, general anesthesia was induced with fentanyl (2 µg/kg), cisatracurium (2 mg), thiamylal (3-5 mg/kg), and lidocaine (1.5 mg/mg) by intravenous (IV) administration, and tracheal intubation was facilitated with succinylcholine (1.5 mg/mg). General anesthesia was maintained with desflurane in oxygen (300 mL/min) in a totally closed circuit system where the end-tidal desflurane concentration was maintained at 7.5±0.5%. Cisatracurium was used for muscle relaxation. No additional intravenous opioid was given during operation. Standard monitors included pulse oximetry, electrocardiography, central venous pressure measurement, and intra-arterial pressure measurement via a radial artery catheter. At the end of surgery, the residual neuromuscular block was antagonized with edrophonium (4 mg) and atropine (0.6 mg); the endotracheal tube was removed when the patient breathed spontaneously. After surgery, all patients received a uniform epidural pain control regimen consisting of morphine (1 mg) in 10 mL of 0.095% bupivacaine every 8 h until 72 h. If pain relief was insufficient, meperidine (50 mg every 6 h) was given. Acetaminophen tablets or meperidine were administered after termination of epidural pain control.

Postoperative care

Serum electrolytes were monitored and corrected in the first seven post-operative days for all patients. Serum C-reactive protein (CRP) levels and abdominal drainage fluid amylase levels were determined post-operatively in all patients. Pancreatic leakage was suspected if the amylase levels of abdominal drainage fluid rose to more than 4 000 U/L^[22]. NG tubes were removed immediately after operation in patients receiving a total gastrectomy and maintained for one day in patients receiving a sub-total gastrectomy. Indication of NG tube reinsertion was biliary vomiting or abdominal distension. Oral intake with 5% glucose solution resumed immediately after the first bowel flatus, and then progressed to a soft diet two days later, if no abdominal discomfort developed. Patients who could not resume oral intake of a soft diet beyond the seventh POD and have generalized ileus shown in plain abdominal x-ray film (KUB) (Figure 1), were defined as having prolonged POI. The epidural catheter was removed routinely on the third POD (approximately 72 h after surgery). The main aim of the study was to compare the length of time of IPC-induced ileus. Therefore, data collected included time to the first post-operative bowel flatus, and number of days required for patients to tolerate a soft oral diet. Narcotic use was recorded for comparison among the three groups. Other information analyzed included operation time, type of resection, blood loss, and complications.

Student's *t*-test, Fisher exact test or the Mann-Whitney *U*-test were used in the statistical analysis. Probabilities of less than 0.05 were accepted as significant.

RESULTS

There were no major differences among the three groups with regard to clinico-pathological characteristics (Table 1). However, patients receiving IPC were younger than those not receiving IPC (56.8 ± 13.2 , 57.5 ± 11.7 years *vs* 67.5 ± 17.7 years, $P = 0.048$). All three groups had an increase of serum CRP post-operatively (Figure 2). Group A and B patients, however, had much higher levels of CRP, which were significantly raised at the first day post IPC, compared with the group C patients ($P < 0.05$). There was a more prominent and prolonged response in patients undergoing IPC.

The mean time of first flatus and resumption of glucose solution was not different among the three groups (Table 2). Regarding a soft oral diet, however, there was a significantly shorter mean time in group A patients compared with group

B patients (7.21 ± 1.92 d *vs* 10.15 ± 2.17 d, $P < 0.05$) and no difference between group A and group C (7.21 ± 1.92 d *vs* 7.53 ± 1.35 d, $P > 0.05$). There was one death (6.25%) secondary to aspiration pneumonia and sepsis in group B. Several complications (prolonged POI, wound infection, pneumonia, anastomotic leakage, pancreatic leakage) are shown in Table 3. The patients in group B have a higher incidence of prolonged POI. All complications were successfully treated with medical therapy, except for one case of aspiration pneumonia leading to the only death.

DISCUSSION

Prolonged POI is a significant problem after abdominal surgery, especially when accompanied by IPC. This study indicates that intravenous Met, combined with thoracic epidural pain

Table 1 Clinicopathological characteristics of patients in three groups

	Group A (n = 16)	Group B (n = 16)	Group C (n = 16)	P
Sex (M/F)	11/5	12/4	10/6	NS
Age (yr)	56.8 ± 13.2	57.5 ± 11.7	67.5 ± 17.7	0.048
Sub-total/total gastrectomy	11/5	10/6	10/6	NS
Operation time (min)	272 ± 60	312 ± 69	259 ± 43	NS
Blood loss (mL)	216 ± 106	235 ± 92	196 ± 137	NS
Meperidine use (mg/d)	83.3 ± 21.6	91.4 ± 31.2	79.3 ± 15.9	NS
Primary tumor ¹				NS
pT3	14	13	14	
pT4	2	3	2	
Stage ²				NS
II	4	4	3	
IIIa	4	3	4	
IIIb	5	6	6	
IV	3	3	3	

Gender was assessed by χ^2 test, others were assessed by *t*-test. Significant difference in age ($P = 0.048$) between group C and groups A and B. ¹T classification according to the Japanese Classification of Gastric Carcinoma (22). ²Staging classification according to the 1997 TNM staging system. NS: not significant. All patients had received R0 gastrectomy with D2 lymph node dissection.

Table 2 Bowel motility recovery (mean days and standard deviation)

	Group A ^a (n = 16)	Group B ^a (n = 16)	Group C ^a (n = 16)	P
First bowel flatus	4.35 ± 0.93	4.94 ± 1.37	4.71 ± 1.22	NS
Time elapsed to glucose solution	5.43 ± 1.15	6.67 ± 2.71	5.81 ± 1.35	NS
Time elapsed to soft diet	7.21 ± 1.92	10.15 ± 2.17	7.53 ± 1.35	<0.05
NG tube reinsertion (%)	1 (6.25)	9 (56.25)	1 (6.25)	<0.01

Significant difference in days to soft diet (^a $P < 0.05$) between group B and groups A and C. NG tube: nasogastric tube. NS: not significant.

Table 3 Postoperative complications and mortality

	Group A ^b (n = 16)	Group B ^b (n = 16)	Group C ^b (n = 16)	P
Death	0	1 ¹	0	NS
Prolonged POI	1 (6.25)	9 (56.26)	1 (6.25)	<0.01
Wound infection	2	1	2	NS
Pneumonia	2	3	2	NS
Anastomotic leak	0	0	1	NS
Pancreatic leak	3	3	2	NS

¹The patient died of aspiration pneumonia and sepsis. Significant difference in prolonged POI (^b $P < 0.01$) between group B and groups A and C. Prolonged POI was defined as intolerance to oral soft diet more than 7 d and generalized ileus shown in KUB. Pancreatic leakage was defined as amylase level of abdominal fluid more than 4 000 U/L. POI: post-operative ileus. NS: not significant.



Figure 1 One patient in group B developed biliary vomiting on the 7th post-operative d. The supine abdominal plain x-ray film showed generalized ileus. (Arrow: dilated colonic air; arrow head: water-soluble contrast media retention in proximal jejunum).

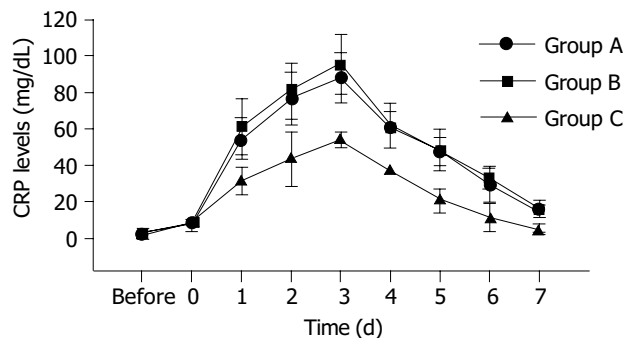


Figure 2 Serial measurement of CRP levels in three groups of patients (group A, with IPC and Met treatment; group B, with IPC but without Met treatment; group C, without IPC and Met) at eight different time points. The change of serum CRP were found to be prominent and prolonged in groups A and B. The data are expressed as mean \pm SD.

control, could effectively prevent prolonged IPC-induced ileus in gastric cancer patients. Further it is indicated that the administration of intravenous Met in patients receiving GI resection does not increase the risk of leakage of the newly constructed GI anastomosis.

IPC, with or without hyperthermia, has been used successfully for a variety of intra-abdominal malignancies, especially ovarian and GI tract cancer^[23,24]. Although it has many advantages, such as a high cytotoxic level of intra-peritoneal drug and less systemic toxicity, it is associated with morbidity. Prolonged POI is one of the most consistent and common side effect^[7,8,25,26]. Prolonged POI was also observed in our study in which intra-peritoneal infusion of MMC was performed in 32 patients. Of these patients, 10 (31.2%) developed prolonged POI, especially in group B (56.25%). This is a higher incidence compared with a previous report that indicated an incidence of 42%. The reason of the higher incidence might partly be due to us giving a more clear definition of prolonged POI in our study.

POI is a poorly understood complication in post-surgical patients. The autonomic nervous system, inflammatory mediators, neurotransmitters, and opioid receptors have all been implicated in the pathophysiology of POI^[27-32]. With

respect to the inflammatory response to surgery, Cannon and Murphy demonstrated in 1906 that opening the peritoneum in dogs and surgical manipulation of the bowel resulted in decreased peristalsis^[33]. More recently Kalfff *et al.*^[31], showed an association between bowel manipulation and impaired contractile activity, noting increased neutrophil infiltration of the muscularis. Surgical manipulation of the bowel and subsequent ileus has been linked to the release of inflammatory mediators from WBC. The inflammatory mediators released as part of a stress response contributes to the development of POI. In general, it is characterized as a temporary impairment of intestinal motility after surgery. Usually different areas of the GI tract resume function at different times. The stomach can take 24-48 h to recover, whereas the colon requires 72-120 h to resume normal motility patterns. Thus, uncomplicated POI resolves spontaneously after approximately 3-5 d^[34,35]. Moreover, some studies indicated that after 7 d of fasting, the intestinal mass decreased by nearly 50%, which might increase the risk of bacterial translocation and septic complications^[36-38]. Therefore, we made a definition of prolonged POI as intolerance of soft diet exceeding 7 d after operation and generalized ileus in KUB. Abdominal surgical procedures may be responsible for the uncomplicated POI. However, extensive surgical procedures, IPC, or a combination of both, may be responsible for prolonged ileus. Stimulation in the small intestine, such as mechanical inflammation after surgical manipulation, may be enhanced by chemical inflammation after IPC, and thus prolong reasonably predictable uncomplicated POI. This was clearly observed in our study which indicated that more patients receiving IPC developed prolonged POI than patients not receiving IPC. Indeed, the concentration of acute phase protein (CRP) in the blood samples of the patients receiving IPC exceeded the level in patients not receiving IPC, suggesting IPC may worsen POI by increasing an inflammatory response.

Prolonged POI and GI tract stasis, in the situation of an immuno-compromised condition induced by cancer, surgical trauma and chemotherapy, will increase the potential for bacterial overgrowth and translocation, which could lead to systemic sepsis and multiple organ failure. Both these post-operative complications are the most prevalent causes of death^[9,10]. Clearly, it is important to find a strategy for preventing or treating these problems.

Met has been used as a prokinetic agent for many years and may potentially influence motility throughout the GI tract^[11-13]. It has both a central and peripheral anti-dopamine effect as well as a direct and indirect stimulatory effect on cholinergic receptors. Dopaminergic receptors have been identified throughout the GI tract. It has also been suggested that the prokinetic effect of Met may be due to the stimulatory effect on cholinergic receptors and the blockade of dopamine receptors that inhibit the release of acetylcholine. This inhibition of dopamine and augmentation of acetylcholine release are thought to sensitize the muscarinic receptors of the GI smooth muscle, allowing for coordinated intestinal motor function. However, results of several studies on the effect of Met on POI have been varied. Some studies have supported the hypothesis that Met reduces the length of POI^[39,40], whereas others refute it^[14-19]. In this study, the effect of Met on preventing prolonged POI was obvious. There

were some differences in our study compared to previous studies about the effect of Met on POI. Firstly, our study focused on prolonged POI, not uncomplicated POI. Moreover, we have a more clear definition of prolonged POI. Met may not change the course of uncomplicated POI, however, it could prevent IPC-induced prolonged POI. Theoretically, prolonged POI has more important and deleterious effect on clinical outcome than uncomplicated POI. However, there was no obvious effect of Met on clinical outcome. Small sample of this study might be the reason. Secondly, all our patients received thoracic epidural pain control. Thoracic epidural analgesia shortens POI via this mechanism by not only blocking pain and lessening stress, but also by inhibiting sympathetic efferent nerve transmission to the gut while preserving motility-promoting parasympathetic stimulation in the sacral region. Parasympathetic innervation via both the vagus nerve and sacral nerve roots can be spared, while sympathetic innervations to the gut (T5-L2) can be selectively blocked when local anesthetics are delivered through a mid-thoracic epidural catheter^[41-43]. In our study, however, most of the patients in group B who received IPC without Met administration developed prolonged ileus, even though they all had epidural pain control. This might be due to epidural anesthesia could not completely abolish IPC-induced inflammatory inhibition of intestinal motility. In contrast, additional administration of Met in group A patients can sensitize the muscarinic receptors of the GI smooth muscle, allowing for coordinated intestinal motor function even though these patients had undergone IPC and vagotomy. Therefore, the time to resumption of soft diet was significantly reduced by Met when compared without Met (Table 3). It is believed that the combination of Met and epidural pain control has a synergic effect on the motility of the GI tract.

An important consideration is whether it is safe to promote intestinal motility by epidural anesthesia or intravenous Met immediately after operation. Some authors have questioned whether Met or epidural anesthesia might be harmful to healing of GI anastomoses because of the increased bowel motility^[44,45]. In the present study, however, no patient developed anastomotic leakages after administration of Met and epidural anesthesia. Our findings do not support the common fear that disturbance to healing of GI anastomoses and an increased risk of anastomotic leakages are linked with early increase of GI motility. Similar results to ours have been reported by some authors^[46,47]. Moreover, early removal or no use of an NG tube after operation is safe in patients receiving Met, only one patient needed reinsertion of the tube in our patients. The concept has been speculated by some investigators^[48,49].

Prolonged POI occurs frequently in patients undergoing extended gastrectomy and IPC, increasing the time needed to achieve nutritional goals, and limiting the benefit of early enteral feedings. This study was the first to examine the role of Met in a group of advanced gastric cancer patients undergoing extended gastrectomy and IPC. Our results demonstrated a clear improvement in the resumption of oral soft diet in the Met-treatment group during the 1st wk post-operatively compared with the no-treatment group (7.21 ± 1.92 d *vs* 10.15 ± 2.17 d, $P < 0.05$). There is a theoretical

possibility that improvement in nutritional intake might improve outcome. We found no significant differences among three groups in infectious risk, or mortality. This study, however, was not powered to detect small differences in outcome. Further studies with more patients are needed to determine whether patient outcomes can be improved by the administration of Met in clinical outcome.

In conclusion, Met with epidural pain control prevents prolonged POI at an early post-operative stage in advanced gastric cancer patients undergoing gastrectomy and IPC. We conclude that Met can be used as a safe prokinetic drug for post-operative intestinal dysmotility worsened by IPC.

REFERENCES

- 1 Akoh JA, Macintyre IM. Improving survival in gastric cancer: review of 5-year survival rates in English language publications from 1970. *Br J Surg* 1992; **79**: 293-299
- 2 Landry J, Tepper JE, Wood WC, Moulton EO, Koerner F, Sullinger J. Patterns of failure following curative resection of gastric carcinoma. *Int J Radiat Oncol Biol Phys* 1990; **19**: 1357-1362
- 3 Hermans J, Bonenkamp JJ, Boon MC, Bunt AM, Ohyama S, Sasako M, Van de Velde CJ. Adjuvant therapy after curative resection for gastric cancer: meta-analysis of randomized trials. *J Clin Oncol* 1993; **11**: 1441-1447
- 4 Hallisay MT, Dunn JA, Ward LC, Allum WH. The second British stomach cancer group trial of adjuvant radiotherapy or chemotherapy in resectable gastric cancer: five-year follow-up. *Lancet* 1994; **343**: 1309-1312
- 5 Hall JJ, Loggie BW, Shen P, Beamer S, Douglas Case L, McQuellon R, Geisinger KR, Levine EA. Cytoreductive surgery with intra-peritoneal hyperthermic chemotherapy for advanced gastric cancer. *J Gastrointest Surg* 2004; **8**: 454-463
- 6 Sugarbaker PH, Yu W, Yonemura Y. Gastrectomy, peritonectomy, and perioperative intra-peritoneal chemotherapy: the evolution of treatment strategies for advanced gastric cancer. *Semin Surg Oncol* 2003; **21**: 233-248
- 7 Sarnaik AA, Sussman JJ, Ahmad SA, Lowy AM. Technology of intra-peritoneal chemotherapy administration: a survey of techniques with a review of morbidity and mortality. *Surg Oncol Clin N Am* 2003; **12**: 849-863
- 8 Rossi CR, Pilati P, Mocellin S, Foletto M, Ori C, Innocente F, Nitti D, Lise M. Hyperthermic intra-peritoneal intraoperative chemotherapy for peritoneal carcinomatosis arising from gastric adenocarcinoma. *Suppl Tumori* 2003; **2**: S54-57
- 9 Fujiwara Y, Taniguchi H, Kimura Y, Takiguchi S, Yasuda T, Yano M, Monden M. Two advanced gastric cancer patients who showed malignant ileus soon after administration of combination therapy of preoperative intra-peritoneal chemotherapy and gastrectomy. *Gan To Kagaku Ryoho* 2003; **30**: 1614-1617
- 10 Livingston EH, Passaro EP Jr. Postoperative ileus. *Dig Dis Sci* 1990; **35**: 121-132
- 11 Holte K, Kehlet H. Postoperative ileus: a preventable event. *Br J Surg* 2000; **87**: 1480-1493
- 12 Jenner P, Marsden CD. The substituted benzamides—a novel class of dopamine antagonists. *Life Sci* 1979; **25**: 479-485
- 13 Albibi R, McCallum RW. Metoclopramide: pharmacology and clinical application. *Ann Intern Med* 1983; **98**: 86-95
- 14 Beani L, Bianchi C, Cremer C. Effects of metoclopramide on isolated guinea pig colon. 1. Peripheral sensitization to acetylcholine. *Eur J Pharmacol* 1970; **12**: 220-231
- 15 Bonacini M, Quiason S, Reynolds M, Gaddis M, Pemberton B, Smith O. Effect of intravenous erythromycin on post-operative ileus. *Am J Gastroenterol* 1993; **88**: 208-211
- 16 Heimbach DM, Crout JR. Treatment of paralytic ileus with adrenergic neuronal blocking drugs. *Surgery* 1971; **69**: 582-587
- 17 Furness JB, Costa M. Adynamic ileus, its pathogenesis and treatment. *Med Biol* 1974; **52**: 82-89
- 18 Kreis ME, Kasperek M, Zittel TT, Becker HD, Jehle EC.

- Neostigmine increases post-operative colonic motility in patients undergoing colorectal surgery. *Surgery* 2001; **130**: 449-456
- 19 **Jepsen S**, Klaerke A, Nielsen PH, Simonsen O. Negative effect of Metoclopramide in post-operative adynamic ileus. A prospective, randomized, double blind study. *Br J Surg* 1986; **73**: 290-291
- 20 **Maruyama K**, Okabayashi K, Kinoshita T. Progress in gastric cancer surgery in Japan and its limits of radicality. *World J Surg* 1987; **11**: 418-425
- 21 Japanese Gastric Cancer Association. Gastric cancer. In: *Japanese Classification of Gastric Carcinoma*. 2nd English ed. 1998: 10-24
- 22 **Sano T**, Sasako M, Katai H, Maruyama K. Amylase concentration of drainage fluid after total gastrectomy. *Br J Surg* 1997; **84**: 1310-1312
- 23 **Zanon C**, Clara R, Chiappino I, Bortolini M, Cornaglia S, Simone P, Bruno F, De Riu L, Airolidi M, Pedani F. Cytoreductive surgery and intra-peritoneal chemohyperthermia for recurrent peritoneal carcinomatosis from ovarian cancer. *World J Surg* 2004; **28**: 1040-1045
- 24 **Yano M**, Yasuda T, Fujiwara Y, Takiguchi S, Miyata H, Monden M. Preoperative intra-peritoneal chemotherapy for patients with serosa-infiltrating gastric cancer. *Surg Oncol* 2004; **88**: 39-43
- 25 **van der Vange N**, van Goethem AR, Zoetmulder FA, Kaag MM, van de Vaart PJ, ten Bokkel Huinink WW, Beijnen JH. Extensive cytoreductive surgery combined with intra-operative intra-peritoneal perfusion with cisplatin under hyperthermic conditions (OVHIPEC) in patients with recurrent ovarian cancer: a feasibility pilot. *Eur J Surg Onco* 2000; **26**: 663-668
- 26 **Gilly FN**, Beaujard A, Glehen O, Grandclement E, Caillet JL, Francois Y, Sadeghi-Looyeh B, Gueugniaud PY, Garbit F, Benoit M, Bienvu J, Vignal J. Peritonectomy combined with intra-peritoneal chemohyperthermia in abdominal cancer with peritoneal carcinomatosis: phase I-II study. *Anticancer Res* 1999; **19**: 2317-2321
- 27 **Bauer AJ**, Boeckxstaens GE. Mechanisms of post-operative ileus. *Neurogastroenterol Motil* 2004; **16** (Suppl 2): 54-60
- 28 **Luckey A**, Livingston E, Tache Y. Mechanisms and treatment of post-operative ileus. *Arch Surg* 2003; **138**: 206-214
- 29 **Barquist E**, Bonaz B, Martinez V, Rivier J, Zinner MJ, Tache Y. Neuronal pathways involved in abdominal surgery-induced gastric ileus in rats. *Am J Physiol* 1996; **270**: R888-R894
- 30 **Tache Y**, Monnikes H, Bonaz B, Rivier J. Role of CRF in stress-related alterations of gastric and colonic motor function. *Ann N Y Acad Sci* 1993; **697**: 233-243
- 31 **Kalff JC**, Schraut WH, Simmons RL, Bauer AJ. Surgical manipulation of the gut elicits an intestinal muscularis inflammatory response resulting in postsurgical ileus. *Ann Surg* 1998; **228**: 652-663
- 32 **Kalff JC**, Buchholz BM, Eskandari MK, Hierholzer C, Schraut WH, Simmons RL, Bauer AJ. Biphasic response to gut manipulation and temporal correlation of cellular infiltrates and muscle dysfunction in rat. *Surgery* 1999; **126**: 498-509
- 33 **Kalff JC**, Carlos TM, Schraut WH, Billiar TR, Simmons RL, Bauer AJ. Surgically induced leukocytic infiltrates within the rat intestinal muscularis mediate post-operative ileus. *Gastroenterology* 1999; **117**: 378-387
- 34 **Cannon W**, Murphy F. The movements of the stomach and intestines in some surgical conditions. *Ann Surg* 1906; **43**: 512-536
- 35 **Prasad M**, Matthews J. Deflating post-operative ileus. *Gastroenterology* 1999; **117**: 489-492
- 36 **Dou Y**, Gregersen S, Zhao J, Zhuang F, Gregersen H. Morphometric and biomechanical intestinal remodeling induced by fasting in rats. *Dig Dis Sci* 2002; **47**: 1158-1168
- 37 **Baue AE**. The role of the gut in the development of multiple organ dysfunction in cardiothoracic patients. *Ann Thorac Surg* 1993; **55**: 822-829
- 38 **Deitch EA**, Berg R. Bacterial translocation from the gut: a mechanism of infection. *J Burn Care Rehabil* 1987; **8**: 475-482
- 39 **Jooste CA**, Mustoe J, Collee G. Metoclopramide improves gastric motility in critically ill patients. *Intensive Care Med* 1999; **25**: 464-468
- 40 **MacLaren R**. Intolerance to intragastric enteral nutrition in critically ill patients: complications and management. *Pharmacotherapy* 2000; **20**: 1486-1498
- 41 **Liu S**, Carpenter RL, Neal JM. Epidural anesthesia and analgesia. *Anesthesiology* 1995; **82**: 1474-1506
- 42 **Carpenter RL**. Gastrointestinal benefits of regional anesthesia/analgesia. *Reg Anesth* 1996; **21**: 13-17
- 43 **Steinbrook RA**. Epidural anesthesia and gastrointestinal motility. *Anesth Analg* 1998; **86**: 837-844
- 44 **Garcia-Olmo D**, Paya J, Lucas FJ, Garcia-Olmo DC. The effects of the pharmacological manipulation of post-operative intestinal motility on colonic anastomoses. An experimental study in a rat model. *Int J Colorectal Dis* 1997; **12**: 73-77
- 45 **Jansen M**, Fass J, Tittel A, Mumme T, Anurov M, Titkova S, Polivoda M, Ottinger A, Schumpelick V. Influence of post-operative epidural analgesia with bupivacaine on intestinal motility, transit time, and anastomotic healing. *World J Surg* 2002; **26**: 303-306
- 46 **Holte K**, Kehlet H. Epidural analgesia and risk of anastomotic leakage. *Reg Anesth Pain Med* 2001; **26**: 111-117
- 47 **Fotiadis RJ**, Badvie S, Weston MD, Allen-Mersh TG. Epidural analgesia in gastrointestinal surgery. *Br J Surg* 2004; **91**: 828-841
- 48 **Chung HY**, Yu W. Reevaluation of routine gastrointestinal decompression after gastrectomy for gastric cancer. *Hepatogastroenterology* 2003; **50**: 1190-1192
- 49 **Yoo CH**, Son BH, Han WK, Pae WK. Nasogastric decompression is not necessary in operations for gastric cancer: prospective randomised trial. *Eur J Surg* 2002; **168**: 379-383

• *Helicobacter pylori* •

High concentrations of human β -defensin 2 in gastric juice of patients with *Helicobacter pylori* infection

Hajime Isomoto, Hiroshi Mukae, Hiroshi Ishimoto, Yoshito Nishi, Chun-Yang Wen, Akihiro Wada, Ken Ohnita, Toshiya Hirayama, Masamitsu Nakazato, Shigeru Kohno

Hajime Isomoto, Hiroshi Mukae, Hiroshi Ishimoto, Yoshito Nishi, Ken Ohnita, Shigeru Kohno, Second Department of Internal Medicine, Nagasaki University School of Medicine, Sakamoto 1-7-1, Nagasaki, Japan

Chun-Yang Wen, Department of Molecular Pathology, Atomic Bomb Disease Institute, Nagasaki University School of Medicine, Sakamoto 12-4, Nagasaki, Japan

Akihiro Wada, Toshiya Hirayama, Department of Bacteriology, Institute of Tropical Medicine, Nagasaki University School of Medicine, Sakamoto 12-4, Nagasaki, Japan

Masamitsu Nakazato, Third Department of Internal Medicine, Miyazaki Medical College, Kiyotake, Miyazaki, Japan

Correspondence to: Dr. Hajime Isomoto, Second Department of Internal Medicine, Nagasaki University School of Medicine, 1-7-1 Sakamoto, Nagasaki 852-8501, Japan. hajime2002@yahoo.co.jp
Telephone: +81-95-849-7567 Fax: +81-95-849-7568

Received: 2004-09-19 Accepted: 2005-01-05

HBD-2, in the front line of innate immune defence. Moreover, HBD-2 may be involved in the pathogenesis of *H. pylori*-associated gastritis, possibly through its function as immune and inflammatory mediator.

© 2005 The WJG Press and Elsevier Inc. All rights reserved.

Key words: β -Defensin 1; β -Defensin 2; *Helicobacter pylori*

Isomoto H, Mukae H, Ishimoto H, Nishi Y, Wen CY, Wada A, Ohnita K, Hirayama T, Nakazato M, Kohno S. High concentrations of human β -defensin 2 in gastric juice of patients with *Helicobacter pylori* infection. *World J Gastroenterol* 2005; 11(31): 4782-4787

<http://www.wjgnet.com/1007-9327/11/4782.asp>

Abstract

AIM: Human β -defensin (HBD)-1 and HBD-2 are endogenous antimicrobial peptides. Unlike HBD-1, the HBD-2 expression is augmented by *Helicobacter pylori* (*H. pylori*). We sought to determine HBD-1 and HBD-2 concentrations in gastric juice during *H. pylori* infection.

METHODS: HBD-1 and HBD-2 concentrations were measured by radioimmunoassay in plasma and gastric juice of 49 *H. pylori*-infected and 33 uninfected subjects and before and after anti-*H. pylori* treatment in 13 patients with *H. pylori*-associated gastritis. Interleukin (IL)-1 β and IL-8 concentrations in gastric juice were measured by enzyme-linked immunosorbent assay (ELISA). Histological grades of gastritis were determined using two biopsy specimens taken from the antrum and corpus. Reverse phase high performance liquid chromatography (RP-HPLC) was used to identify HBD-2.

RESULTS: HBD-2 concentrations in gastric juice, but not in plasma, were significantly higher in *H. pylori*-positive than -negative subjects, albeit the post-treatment levels were unchanged. Immunoreactivity for HBD-2 was exclusively identified in *H. pylori*-infected mucosa by RP-HPLC. HBD-2 concentrations in gastric juice correlated with histological degree of neutrophil and mononuclear cell infiltration in the corpus. IL-1 β levels correlated with those of IL-8, but not HBD-2. Plasma and gastric juice HBD-1 concentrations were similar in *H. pylori*-infected and uninfected subjects.

CONCLUSION: Our results place the β -defensins, especially

INTRODUCTION

Helicobacter pylori (*H. pylori*) infection is the major cause of chronic gastritis and peptic ulcer disease and is a risk factor for gastric cancer^[1,2]. The non-invasive organism colonizes the gastric epithelium and elicits specific antibodies against various immunogenic proteins derived from the bacteria^[3]. *H. pylori*-associated gastritis is characterized by intense infiltration of neutrophils and mononuclear cells into the lamina propria^[4,5]. However, despite these humoral and cellular immune responses, the infection usually lasts a lifetime in the absence of antibiotic treatment^[5]. Moreover, current anti-*H. pylori* combination regimens are rather complicated and do not always result in cure of the infection because *H. pylori* strains often develop resistance to antibiotic drugs^[3,6].

Recently, various endogenous anti-microbial peptides have been identified as key elements of innate host defence against infection^[7,9]. Defensins, single chain cationic peptides of molecular weight ranging from 3 000 to 4 500 Da, are one of the most extensively studied classes of such naturally occurring antibiotics^[7,9]. They exhibit a wide variety of microbicidal activities against Gram-positive and -negative bacteria, mycobacteria, fungi and certain enveloped viruses^[7,9]. Human defensins are divided into α - and β -defensins, based on the arrangements of three intra-molecular disulfide bridges^[7,9]. At present, four members of β -defensins have been isolated in humans^[7-11]. They are essentially synthesized in the epithelial compartment at various mucosal sites^[7-11].

Recent *in vitro* studies showed the constitutive expression of human β -defensin (HBD)-1 and induced expression of HBD-2 in several gastric cancer cell lines in response to

H pylori infection^[12-14]. Exclusive enhancement of HBD-2 expression upon *H pylori* infection was also noted in patients with chronic gastritis^[15,16]. However, there is no information on the secretion of HBD-2 into the gastric lumen *in vivo* or its concentrations in gastric juice during *H pylori* infection.

We have developed a sensitive, specific radioimmunoassay (RIA) for HBD^[17]. Employing this assay system, we measured HBD-2 concentrations in gastric juice of *H pylori*-infected and uninfected individuals. This study paves the way for further understanding of the mechanisms involved in host immune response to this pathogen.

MATERIALS AND METHODS

Patients and sampling

A total of 82 patients referred for diagnostic upper gastro-intestinal endoscopy between September 2002 and August 2003 were enrolled in the present study. The following exclusion criteria were applied for enrollment in the study. (1) The use of non-steroidal anti-inflammatory drugs, proton pump inhibitors, histamine H₂-receptor antagonists or antibiotics within 4 wk prior to the present study; (2) History of severe concomitant diseases, upper gastro-intestinal surgery, peptic ulcer diseases and gastric cancer. On the day of endoscopy, blood samples were taken, transferred into tubes containing EDTA-2Na and aprotinin, centrifuged, plasma separated, and stored at -80 °C until assay.

At the beginning of endoscopy (XQ 200; Olympus Optical Co., Tokyo, Japan), a sample of the gastric juice was aspirated into collection tube containing EDTA-2Na and aprotinin using an aspiration instrument (PW-6P-1, Olympus) under endoscopic guidance. Gastric juice samples were immediately neutralized to pH 7.0 with 1 N NaOH and frozen at -80 °C until measurement. Two biopsy specimens were endoscopically obtained from both the antrum within 2 cm of the pyloric ring and the middle portion of the corpus along the greater curvature, fixed in 10% buffered formalin and embedded in paraffin. One was used for rapid urease test (Helicocheck, Otsuka Pharmaceutical Co., Tokushima, Japan) and another for histopathological and immunohistochemical assessments.

Fourteen patients with *H pylori*-associated gastritis were treated with eradication therapy consisting of lansoprazole (30 mg twice daily), amoxicillin (750 mg twice daily) and clarithromycin (400 mg twice daily) for 7 d^[18]. Four weeks after cessation of the treatment, patients were examined by endoscopy again, and gastric juice and biopsy specimens were taken in a similar fashion to that performed before treatment.

Eradication of *H pylori* was considered successful when ¹³C-urea breath test was negative^[18].

Histopathological examination

Paraffin-embedded biopsy specimens were cut into 4- μ m thick sections and stained with hematoxylin and eosin. Each histological parameter of activity (neutrophils), chronic inflammation (mononuclear cells), glandular atrophy and intestinal metaplasia in the antrum and corpus of patients with *H pylori* infection was scored as 0, 1, 2 or 3 corresponding to none, mild, moderate or severe, respectively, based on

the Sydney system^[19,20]. Intestinal metaplasia was defined by the presence of goblet cells in glandular mucosa with Alcian blue (pH 2.50)/periodic acid-Schiff staining^[21].

Furthermore, the density of *H pylori* colonization assessed with Giemsa staining was also scored from 0 to 3, based on the above classification system^[19,20]. The biopsy specimens were examined blindly without knowledge of the results of β -defensins measurement.

Diagnosis of *H pylori* infection

H pylori status was assessed by serology (anti-*H pylori* immunoglobulin G antibody, HEL-p TEST, AMRAD Co., Melbourne, Australia), rapid urease test and histology with Giemsa staining. Patients were considered positive for *H pylori* infection when at least two of these examinations yielded positive results^[20,22]. On the other hand, patients were defined as *H pylori*-negative, if all test results were negative^[23].

Measurement of interleukin (IL)-1 β and -8 levels in gastric juice

The concentrations of interleukin (IL)-1 β and -8 in gastric juice were measured as described previously^[20,22,24]. The samples were assayed for total protein by a modified Lowry method, diluted to 0.5 mg/mL total protein concentration, and frozen at -80 °C until assay. Measurement of the two cytokines in the aliquots was performed using commercially available assay kits (Research and Diagnostics, Minneapolis, MN, USA), which employ the quantitative immunometric sandwich enzyme immunoassay technique. These assays were performed in duplicate according to the instructions provided by the manufacturer. In our study, inter- and intra-assay variabilities were <10%, respectively^[20,22].

Measurement of HBD-1 and -2 levels in plasma and gastric juice

The concentrations of HBD-2 in plasma and gastric juice samples were measured by RIA established in our laboratory^[17]. Briefly, full-length HBD-2 was synthesized using a peptide synthesizer (model 430, Applied Biosystems, Foster City, CA, USA) and purified by reverse phase high performance liquid chromatography (RP-HPLC). Synthetic HBD-2 was used for immunizing New Zealand white rabbits by multiple intracutaneous and subcutaneous injections. It was radio-iodinated and the ¹²⁵I-labelled peptide was purified by RP-HPLC on a TSK ODS 120A column (Tosoh Co., Tokyo). The diluted sample or a standard peptide solution (100 μ L) was incubated for 24 h with 100 μ L antiserum diluent (final dilution 1:4 200 000). The ¹²⁵I-labelled solution (16 000 cpm in 100 μ L) was added and the mixture was incubated again for another 24 h. Normal rabbit serum and anti-rabbit IgG goat serum were then added and stored for 16 h. Bound and free ligands were separated by centrifugation. All procedures were performed at 4 °C and duplicate assays were carried out. Volumes of 0.5 mL plasma and 1-2 mL gastric juice were used to determine the levels of HBD-2. The concentrations of HBD-1 were also measured in similar fashions. The intra-assay and inter-assay coefficients of variation were <10%, respectively, in both the RIA analyses^[15,23].

Chromatographic characterization of HBD-2

Chromatographic characterization of HBD-2 was performed as described previously^[26,27]. Each 10 mg wet weight of non-cancerous mucosal tissue was sampled from surgically resected stomach of three patients with gastric cancer and *H pylori* infection. The samples were immediately homogenized and aliquots of homogenate supernatants, obtained by centrifugation (10 000 g for 10 min), were used for RP-HPLC on a TSK ODS SIL 120A column (Tosoh Co.). A linear gradient of acetonitrile (CH₃CN) from 10% to 60% in 0.1% trifluoroacetic acid (pH 2.0) was used at a flow rate of 1.0 mL/min for 50 min. All fractions were analyzed for HBD-2 employing RIA.

Statistical analysis and ethical considerations

Statistical analyses were performed using Fisher's exact, χ^2 , Student's *t*, Mann-Whitney *U*, Kruskal-Wallis, Spearman rank and Wilcoxon signed ranks tests, as appropriate. A *P* value of less than 0.05 was accepted as statistically significant. Data were expressed as mean \pm SD.

All examinations were conducted according to Good Clinical Practice and the Declaration of Helsinki, and were approved by the university ethics committees. All samples were obtained with written informed consent of the patients prior to their inclusion in the study. All experiments involving animals were approved by the ethics review committees for animal experimentation of participating universities.

RESULTS

Patient demographics

The study population consisted of 49 *H pylori*-positive and 33 *H pylori*-negative subjects. They included 38 men and 44 women, with mean age of 50 years (range, 25-78 years). There were no significant differences between the *H pylori*-positive and -negative groups in background data on age, sex, body mass index, current tobacco use and alcohol intake (Table 1).

Table 1 Baseline characteristics

	<i>H pylori</i> -positive (n = 49)	<i>H pylori</i> -negative (n = 33)
Mean age, ys (range)	49.9 (25-72)	49.6 (28-78)
Male/female	24/25	14/19
Smoker	17 (34.7%)	12 (36.4%)
Alcohol drinker	16 (32.7%)	10 (30.3%)
Body mass index (range)	24.4 (17.1-29.0)	23.7 (16.4-28.8)

Plasma and gastric juice β -defensins concentrations according to *H pylori* status

HBD-2 levels in gastric juice of patients with *H pylori* infection were significantly higher than those of *H pylori*-negative subjects ($P < 0.0005$, Table 2), whereas infection had no significant impact on plasma concentrations of HBD-2 (Table 2). There were no significant differences in HBD-1 concentrations both in plasma and gastric juice with respect to *H pylori* status (Table 2). The levels of β -defensins in gastric juice did not correlate with those in plasma

(correlation coefficient, $r = 0.036$ and -0.005 for each HBD-1 and HBD-2). In addition, there were no significant correlations between HBD-1 and HBD-2 levels in plasma ($r = -0.077$) and gastric juice ($r = -0.092$).

Correlation between HBD-2 and cytokine levels in gastric juice

There were significant differences in IL-1 β and IL-8 concentrations in gastric juice between *H pylori*-positive and -negative subjects ($P < 0.05$ and $P < 0.005$, respectively, Table 2). HBD-2 concentrations in gastric juice did not correlate with IL-1 β and IL-8 levels ($r = -0.055$ and $r = 0.121$, respectively). There was a positive correlation between IL-1 β and IL-8 concentrations ($r = 0.575$, $P < 0.0001$).

Table 2 Plasma and gastric juice HBD-1 and HBD-2 levels and gastric juice IL-1 β and -8 concentrations

	<i>H pylori</i> -positive (n = 49)	<i>H pylori</i> -negative (n = 33)	<i>P</i>
Plasma			
HBD-1 levels (ng/mL)	10.1 \pm 0.9	9.6 \pm 1.8	NS
HBD-2 levels (pg/mL)	276.2 \pm 61.0	257.2 \pm 56.0	NS
Gastric juice			
HBD-1 levels (pg/mL)	384.2 \pm 101.5	357.9 \pm 79.6	NS
HBD-2 levels (pg/mL)	230.3 \pm 77.4	118.1 \pm 87.7	<0.0005
Interleukin 1 β levels (mg/mL)	53.6 \pm 16.9	5.3 \pm 4.4	<0.05
Interleukin 8 levels (pg/mL)	17.9 \pm 3.1	8.6 \pm 1.7	<0.005

¹Human β -defensin, NS: not significant.

Correlation between gastric juice HBD-2 concentrations and histopathological parameters

As shown in Table 3, HBD-2 concentrations in gastric juice correlated positively with the scores of activity and chronic inflammation in the corpus ($P < 0.005$ and $P < 0.05$, respectively), but not with glandular atrophy and intestinal metaplasia scores in the corpus. On the other hand, there were no significant correlations between HBD-2 concentrations and each score of gastritis in the antrum. In addition, *H pylori* density in the antrum and corpus did not correlate with HBD-2 concentrations in gastric juice.

Table 3 Correlation coefficients between gastric human- β -defensin 2 levels and each histological parameter

	Correlation coefficient	<i>P</i>
Antrum		
Activity	0.048	NS
Chronic inflammation	0.258	NS
Glandular Atrophy	0.148	NS
Intestinal Metaplasia	-0.063	NS
<i>H pylori</i> density	0.011	NS
Corpus		
Activity	0.499	<0.005
Chronic inflammation	0.341	<0.05
Glandular Atrophy	0.294	NS
Intestinal Metaplasia	0.081	NS
<i>H pylori</i> density	0.237	NS

NS: not significant.

Table 4 Gastric juice HBD-2 and IL-1 β and -8 levels before and after anti-*H pylori* therapy

	Successful eradication of <i>H pylori</i> (n = 10)		P	Failed eradication (n = 4)		P
	Before therapy	After therapy		Before therapy	After therapy	
Gastric juice						
HBD ¹ -2 levels (pg/mL)	182.2 \pm 57.6	210.1 \pm 66.4	NS	137.4 \pm 65.2	112.9 \pm 79.3	NS
Interleukin 1 β levels (pg/mL)	17.7 \pm 10.2	0.5 \pm 0.3	<0.05	88.5 \pm 80.9	64.7 \pm 64.1	NS
Interleukin 8 levels (pg/mL)	22.3 \pm 2.1	12.8 \pm 1.8	<0.005	18.1 \pm 6.1	18.6 \pm 4.5	NS

¹Human β -defensin, NS: not significant.

Effects of eradication treatment on gastric juice concentrations of HBD-2, IL-1 β and IL-8

Successful eradication of *H pylori* was achieved in 10 of 14 (71%) with the triple therapy. At 4 wk after completion of the 7-d treatment, HBD-2 concentrations in gastric juice of these patients were not significantly different from those measured before eradication therapy (Table 4). However, *H pylori* eradication was associated with a significant fall in IL-1 β , and IL-8 levels of gastric juice compared with pre-treatment levels ($P < 0.05$ and $P < 0.005$, respectively, Table 4).

In patients who were still infected with *H pylori* after antibiotic treatment, HBD-2, IL-1 β and IL-8 levels in gastric juice remain unchanged compared to the pre-treatment concentrations (Table 4).

Chromatographic characterization of HBD-2

Immunoreactive HBD-2 was identified in the gastric mucosa infected with *H pylori* on RP-HPLC coupled with RIA (Figure 1). The peak was situated at a position identical to that of synthetic HBD-2 peptide. Each sample prepared yielded the same chromatographic pattern.

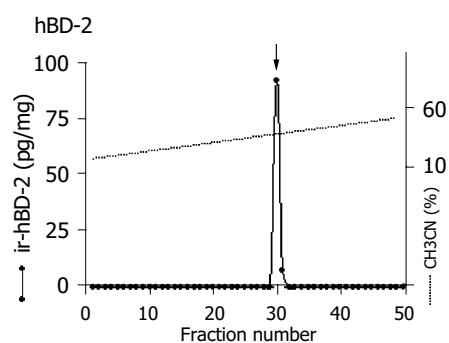


Figure 1 Representative RP-HPLC profiles of the HBD-2 molecules in *H pylori*-infected gastric mucosa.

DISCUSSION

Recent studies have shown the inducible expression of HBD-2 messenger ribonucleic acid (mRNA) in response to *H pylori* infection in cultured gastric epithelial cells^[12-14]. In clinical setting of gastritis, the HBD-2 mRNA and peptide expression is evidently increased in gastric mucosa infected with the organism^[15,16]. There are a few *in vitro* observations of the secretion of HBD-2 peptide upon *H pylori* infection. George *et al.*^[26], showed its enhanced release in supernatants from

infected gastric cancer cell lines by Western blotting. However, the actual concentrations of such antimicrobial peptides at the local site of human stomach during *H pylori* infection remain unknown. Our sensitive RIA system allowed us to determine the HBD-2 concentrations in gastric juice, as well as in other body fluids and blood^[17,25]. Thus, we demonstrated, for the first time, that the HBD-2 levels in gastric juice of *H pylori*-infected patients were significantly higher than those of uninfected ones, suggesting its physio-pathological significance in the bacterial infection. In contrast, *H pylori* status did not have a significant impact on plasma HBD-2 levels. Immunoreactivity for HBD-2 was identified in *H pylori*-infected gastric mucosa by RT-HPLC combined with RIA. In agreement with the results of previous studies^[15,16], immunohistochemical staining against anti-HBD-2 antibody within the infected mucosa was confined to the superficial epithelial cells. Taken together, we believe that *H pylori* infection stimulates the biosynthesis of HBD-2 in gastric mucosa, primarily in epithelia confronting this organism^[15], and the product is mainly released into the gastric lumen.

In the present study, however, there was no significant difference in gastric juice, HBD-2 levels before and 4 wk after cure of the infection, and in certain cases, post-treatment HBD-2 levels were rather increased compared to the pre-treatment ones. In contrast, Hamanaka *et al.*^[15], reported that epithelial HBD-2 expression assessed by immunohistochemistry was markedly decreased in gastric specimens obtained 4 wk after eradication of *H pylori*, concomitant with the pronounced reduction of its transcripts to undetectable levels by reverse transcription-polymerase chain reaction (RT-PCR). These results must be interpreted within the context of studies' limitations including their small sample sizes, differences in samples assessed-gastric biopsy tissues *vs* gastric juice- and diverse methodological approaches to HBD-2. Nevertheless, one might postulate the mingling of HBD-2 secreted by the other cells than gastric epithelial cells, such as esophageal squamous cells, in the gastric juice. In fact, more than 95% of biopsy specimens from the esophagus were positive for the β -defensin mRNA on RT-PCR analysis^[16]. Several recent studies have shown that elimination of *H pylori* infection would lead to the development of gastro-esophageal reflux disease, probably in some cases, in association with post-treatment increase in acid secretion^[27-29]. At present, however, there is no information available as to whether the esophageal HBD-2 expression is altered during this condition or upon such stimuli as refluxates with increased acidity.

We found the association of HBD-2 concentrations in gastric juice with histological degree of mucosal infiltration of neutrophils and mononuclear cells in the corpus, but not in the antrum. In line with this, Wehkamp *et al.*^[16], reported that *H pylori* colonization was significantly related to higher percentage of positive biopsies taken from the corpus with respect to HBD-2 transcripts. The sparse distribution and confined localization to cells of the apical foveolae of this peptide^[15,16] may be attributable to the topographical differences in HBD-2 expression. In addition to the direct anti-microbial activity, evidence is accumulating for the role of defensins as immune and inflammatory mediators^[7-9,30]. In fact, β -defensins display chemotactic activities for dendritic cells and T lymphocytes through the chemokine receptor CCR6^[30]. It is possible that β -defensins, especially HBD-2, may be involved in the pathogenesis of *H pylori*-associated gastritis, in part, via their action as chemoattractant. Again, the HBD-2 levels in gastric juice can provide useful information on histological severity of corporal mucosal inflammation.

Recent *in vitro* studies have demonstrated that HBD-2 mRNA expression is stimulated by pro-inflammatory cytokines such as IL-1 β and tumor necrosis factor α in various cell lines including gastric epithelial cells^[9,12,13]. We have also reported a positive correlation between IL-1 β and HBD-2 concentrations in broncho-alveolar lavage fluid of patients with pneumonia and diffuse panbronchiolitis^[17,23]. In the present study, however, there was no significant correlation between gastric juice HBD-2 and IL-1 β concentrations, whereas the IL-1 β levels strongly correlated with those of IL-8. IL-1 β is known to activate nuclear factor kappa B (NF- κ B)^[31], an important transcription factor regulating a plethora of genes including those of IL-8 and HBD-2^[9,31,32]. In this regard, we demonstrated that mucosal IL-8 levels of patients with *H pylori*-associated gastritis correlated strongly with the grades of activated NF- κ B expression in gastric epithelial cells^[20,22]. Considered together, these data suggest that IL-8 expression is probably enhanced by IL-1 β -induced NF- κ B activation within the *H pylori*-infected mucosa. On the other hand, we suggest that the increased expression of HBD-2 in the gastric epithelium may result from the direct contact between this pathogen and epithelial cells *in vivo*.

H pylori status had no impact on HBD-1 concentrations in gastric juice, providing further evidence for its constitutive nature^[12-14,16]. Since ingestion of contaminated food or water exposes the gastric mucosa to a wide variety of microbial pathogens, the constitutive expression of HBD-1 could play a 'surveillance-like' role during normal homeostasis of human stomach^[33].

The *in vitro* minimal inhibitory concentrations against a panel of micro-organisms range from 0.1 to 100 μ g/mL for defensin peptides^[9]. Hamanaka *et al.*^[15], reported that the growth rate of cultured *H pylori* was suppressed by 50% on incubation with 0.3 μ g/mL of HBD-2 and was completely inhibited at 30 μ g/mL of this peptide. It remains to be determined whether β -defensins are microbicidal for the organism in gastric milieu *in vivo*. However, it is tempting to speculate that the *H pylori* strains that are able to establish persistent infection may be rather insensitive to such innate

mucosal defense machinery.

In conclusion, we demonstrated the presence of significantly high levels of HBD-2 in gastric juice in patients with *H pylori* infection. The enhanced production/release of HBD-2 may contribute to the perpetuation of mucosal inflammation of the corpus. Our results highlight the importance of β -defensins, especially HBD-2, not only in innate defense but also in adaptive immune response to the organism.

REFERENCES

- 1 **Blaser MJ.** *Helicobacter pylori* and the pathogenesis of gastroduodenal inflammation. *J Infect Dis* 1990; **161**: 626-633
- 2 **Ernst PB, Gold BD.** The disease spectrum of *Helicobacter pylori*: the immunopathogenesis of gastroduodenal ulcer and gastric cancer. *Ann Rev Microbiol* 2000; **54**: 615-640
- 3 **Zevering Y, Jacob L, Meyer TF.** Naturally acquired human immune responses against *Helicobacter pylori* and implications for vaccine development. *Gut* 1999; **45**: 465-474
- 4 **Shimoyama T, Crabtree JE.** Bacterial factors and immune pathogenesis in *Helicobacter pylori* infection. *Gut* 1998; **43** (Suppl 1): S2-S5
- 5 **Allen LA.** The role of the neutrophils and phagocytosis in infection caused by *Helicobacter pylori*. *Curr Opin Infect Dis* 2001; **14**: 273-277
- 6 **Isomoto H, Inoue K, Furusu H, Enjoji A, Fujimoto C, Yamakawa M, Hirakata Y, Omagari K, Mizuta Y, Murase K, Shimada S, Murata I, Kohno S.** High-dose rabeprazole/amoxicillin vs rabeprazole/amoxicillin/metronidazole as second-line treatment after failure of the Japanese standard regimen for *Helicobacter pylori* infection. *Aliment Pharmacol Ther* 2003; **18**: 101-107
- 7 **van Wetering S, Sterk PJ, Rabe KF, Hiemstra PS.** Defensins: Key players or bystanders in infection, injury, and repair in the lung. *J Allergy Clin Immunol* 1999; **104**: 1131-1138
- 8 **Chertov O, Yang D, Howard OMZ, Oppenheim JJ.** Leukocyte granule proteins mobilize innate host defenses and adaptive immune responses. *Immunol Rev* 2000; **177**: 68-78
- 9 **Bals R.** Epithelial antimicrobial peptides in host defense against infection. *Respir Res* 2000; **1**: 141-150
- 10 **Harder J, Bartels J, Christophers E, Schroder JM.** Isolation and characterization of human beta -defensin-3, a novel human inducible peptide antibiotic. *J Biol Chem* 2001; **276**: 5707-5713
- 11 **Garcia JR, Krause A, Schulz S, Rodriguez-Jimenez FJ, Kluver E, Adermann K, Forssmann U, Frimpong-Boateng A, Bals R, Forssmann WG.** Human β -defensin 4: a novel inducible peptide with a specific salt-sensitive spectrum of antimicrobial activity. *FASEB J* 2001; **15**: 1819-1821
- 12 **O'Neil DA, Cole SP, Martin-Porter E, Housley MP, Liu L, Ganz T, Kagnoff MF.** Regulation of human β -defensins by gastric epithelial cells in response to infection with *Helicobacter pylori* or stimulation with interleukin-1. *Infect Immun* 2000; **68**: 5412-5415
- 13 **Bajaj-Elliott M, Smith GV, Domizio P, Maher L, Ali RS, Quinn AG, Farthing MJG.** Modulation of host antimicrobial peptide (β -defensins 1 and 2) expression during gastritis. *Gut* 2002; **51**: 356-361
- 14 **Uehara N, Yagihashi A, Kondoh K, Tsuji N, Fujita T, Hamada H, Watanabe N.** Human β -defensin-2 induction in *Helicobacter pylori*-infected gastric mucosal tissues: antimicrobial effect of overexpression. *J Med Microbiol* 2003; **52**: 41-45
- 15 **Hamanaka Y, Nakashima M, Wada A, Ito M, Kurazono H, Hoji H, Nakahara Y, Kohno S, Hirayama T, Sekine I.** Expression of human β -defensin 2 (hBD-2) in *Helicobacter pylori* induced gastritis: antibacterial effect of hBD-2 against *Helicobacter pylori*. *Gut* 2001; **49**: 481-487
- 16 **Wehkamp J, Schmidt K, Herrlinger KR, Baxmann S, Behling S, Wohlschlagel C, Feller AC, Stange EF, Fellermann K.**

- Defensin pattern in chronic gastritis: HBD-2 is differentially expressed with respect to *Helicobacter pylori* status. *J Clin Pathol* 2003; **56**: 352-357
- 17 **Hiratsuka T**, Nakazato M, Date Y, Ashitani JI, Minematsu T, Chino N, Matsukura S. Identification of human beta-defensin-2 in respiratory tract and plasma and its increase in bacterial pneumonia. *Biochem Biophys Res Commun* 1998; **249**: 943-947
- 18 **Isomoto H**, Inoue K, Furusu H, Nishiyama H, Shikuwa S, Omagari K, Mizuta Y, Murase K, Murata I, Kohno S. Lafutidine, a novel histamine H₂-receptor antagonist, versus lansoprazole in combination with amoxicillin and clarithromycin for eradication of *Helicobacter pylori*. *Helicobacter* 2003; **8**: 111-119
- 19 **Price AB**. The Sydney system; histological division. *J Gastroenterol Hepatol* 1991; **6**: 209-222
- 20 **Isomoto H**, Miyazaki M, Mizuta Y, Takeshima F, Murase K, Inoue K, Yamasaki K, Murata I, Koji T, Kohno S. Expression of nuclear factor κ B in *Helicobacter pylori*-infected gastric mucosa detected with Southwestern histochemistry. *Scand J Gastroenterol* 2000; **35**: 247-254
- 21 **Morini S**, Zullo A, Hassan C, Lorenzetti R, Stella F, Martini MT. Gastric cardiac inflammation: Role of *Helicobacter pylori* infection and symptoms of gastroesophageal reflux disease. *Am J Gastroenterol* 2001; **96**: 2337-2340
- 22 **Isomoto H**, Mizuta Y, Miyazaki M, Takeshima F, Omagari K, Murase K, Nishiyama T, Inoue K, Murata I, Kohno S. Implication of NF- κ B in *Helicobacter pylori*-associated gastritis. *Am J Gastroenterol* 2000; **95**: 2768-2776
- 23 **Isomoto H**, Furusu H, Morikawa T, Mizuta Y, Nishiyama T, Omagari K, Murase K, Inoue K, Murata I, Kohno S. 5-d vs 7-day triple therapy with rabeprazole, clarithromycin and amoxicillin for *Helicobacter pylori* eradication. *Aliment Pharmacol Ther* 2000; **14**: 1619-1623
- 24 **Isomoto H**, Wang A, Mizuta Y, Akazawa Y, Ohba K, Omagari K, Miyazaki M, Murase K, Hayashi T, Inoue K, Murata I, Kohno S. Elevated levels of chemokines in esophageal mucosa of patients with reflux esophagitis. *Am J Gastroenterol* 2003; **98**: 551-556
- 25 **Hiratsuka T**, Mukae H, Iiboshi H, Ashitani J, Nabeshima K, Minematsu T, Chino N, Ihi T, Kohno S, Nakazato M. Increased concentrations of human β -defensins in plasma and bronchoalveolar lavage fluid of patients with diffuse panbronchiolitis. *Thorax* 2003; **58**: 425-430
- 26 **George JT**, Boughan PK, Karageorgiou H, Bajaj-Elliott M. Host anti-microbial response to *Helicobacter pylori* infection. *Mol Immunol* 2003; **40**: 451-456
- 27 **Labenz J**, Blum AL, Bayerdorffer E, Meining A, Stolte M, Borsch G. Curing *Helicobacter pylori* infection in patients with duodenal ulcer may provoke reflux esophagitis. *Gastroenterology* 1997; **112**: 1442-1447
- 28 **Fallone CA**, Barkun AN, Friedman G, Mayrand S, Loo V, Beech R, Best L, Joseph L. Is *Helicobacter pylori* eradication associated with gastroesophageal reflux disease? *Am J Gastroenterol* 2000; **95**: 914-920
- 29 **Iijima K**, Ohara S, Sekine H, Koike T, Kato K, Asaki S, Shimosegawa T, Toyota T. Changes in gastric acid secretion assayed by endoscopic gastrin test before and after *Helicobacter pylori* eradication. *Gut* 2000; **46**: 20-26
- 30 **Raj PA**, Dentino AR. Current status of defensins and their role in innate and adaptive immunity. *FEMS Microbiol Lett* 2002; **206**: 9-18
- 31 **Barnes PJ**, Karin M. Nuclear factor- κ B-a pivotal transcription factor in chronic inflammatory diseases. *N Engl J Med* 1997; **336**: 1066-1071
- 32 **Wada A**, Ogushi K, Kimura T, Hojo H, Mori N, Suzuki S, Kumatori A, Se M, Nakahara Y, Nakamura M, Moss J, Hirayama T. *Helicobacter pylori*-mediated transcriptional regulation of the human β -defensin 2 gene requires NF κ B. *Cell Microbiol* 2001; **3**: 114-123
- 33 **Zhao C**, Wang I, Lehrer RI. Widespread expression of β -defensin hBD-1 in human secretory glands and epithelial cells. *FEBS Lett* 1996; **396**: 319-322

Effect of IL-10 on the expression of HSC growth factors in hepatic fibrosis rat

Mei-Na Shi, Wei-Da Zheng, Li-Juan Zhang, Zhi-Xin Chen, Xiao-Zhong Wang

Mei-Na Shi, Wei-Da Zheng, Li-Juan Zhang, Zhi-Xin Chen, Xiao-Zhong Wang, Department of Gastroenterology, Union Hospital of Fujian Medical University, Fuzhou 350001, Fujian Province, China

Supported by Technology and Science Foundation of Fujian Province, No. 2003 D05

Correspondence to: Xiao-Zhong Wang, Department of Gastroenterology, Union Hospital of Fujian Medical University, Fuzhou 350001, Fujian Province, China. drwangxz@pub6.fz.fj.cn
Telephone: +86-591-83357896-8482

Received: 2004-08-30 Accepted: 2004-12-08

Abstract

AIM: To study the effect of IL-10 on the expression of growth factors - transforming growth factor- β 1 (TGF- β 1), epidermal growth factor (EGF), hepatocyte growth factor (HGF) and platelet-derived growth factor (PDGF) of hepatic stellate cells (HSCs) of hepatic fibrosis rat and the anti-fibrogenic role of exogenous IL-10.

METHODS: Hepatic fibrosis was induced by CCl₄ administration intra-peritoneally. Sixty clean male Sprague-Dawley (SD) rats were randomly divided into three groups: normal control group (GN, 8 rats), hepatic fibrosis model group (GC, 28 rats) and IL-10 treated group (GI, 24 rats). At the beginning of the 7th and 11th wk, rats in each group were routinely perfused with pronase E and type IV collagenase through a portal vein catheter and the suspension obtained from the liver was spun by centrifugation with 11% Nycodenz density gradient to isolate HSCs. Histological examination was used to determine the degree of hepatic fibrosis. RT-PCR was employed to analyze mRNA expression from freshly isolated cells. Immunocytochemistry was performed to detect protein expression in primary cultured HSCs.

RESULTS: Rat hepatic fibrosis was developed with the increase of injection frequency of CCl₄, and HSCs were successfully isolated. At the 7th and 11th wk, TGF- β 1, EGF, and HGF mRNA in GC increased obviously compared with GN ($P = 0.001/0.042$, $0.001/0.001$, $0.001/0.001$) and GI ($P = 0.001/0.007$, $0.002/0.001$, $0.001/0.001$). For TGF- β 1, no difference was observed between GI and GN. For EGF, mRNA level in GI increased compared with GN during the 7th wk ($P = 0.005$) and 11th wk ($P = 0.049$). For HGF, mRNA level in GI decreased compared with GN at the 7th wk ($P = 0.001$) and 11th wk ($P = 0.021$). Between these two time points, TGF- β 1 expression at the 7th wk was higher than that of the 11th wk ($P = 0.049$), but for EGF, the former was lower than the latter ($P = 0.022$). As for PDGF mRNA, there was no significant difference between these

groups, but difference seemed to exist in protein levels. Results by immunocytochemistry of TGF- β 1 and EGF were paralleled with the above findings.

CONCLUSION: The expression of TGF- β 1, EGF and HGF increased in HSC of hepatic fibrosis rat and decreased after treatment with IL-10. IL-10 plays an anti-fibrogenic role by suppressing growth factors expression.

© 2005 The WJG Press and Elsevier Inc. All rights reserved.

Key words: Hepatic fibrosis; Hepatic stellate cells; Interleukin-10; Transforming growth factor- β 1; Epidermal growth factor; Hepatocyte growth factor; Platelet-derived growth factor

Shi MN, Zheng WD, Zhang LJ, Chen ZX, Wang XZ. Effect of IL-10 on the expression of HSC growth factors in hepatic fibrosis rat. *World J Gastroenterol* 2005; 11(31): 4788-4793
<http://www.wjgnet.com/1007-9327/11/4788.asp>

INTRODUCTION

Hepatic fibrosis, which represents the wound healing response of the liver is a common sequel to diverse liver injuries, characterized by increased deposition and altered composition of extracellular matrix (ECM). Hepatic stellate cells (HSCs) are the major source of ECM, and believed to be the crucial cell type in the development of hepatic fibrosis^[1,2] and growth factors were considered to exert their effects through autocrine or paracrine on HSCs during the process^[3]. It has been reported that interleukin-10 (IL-10) could relieve the degree of rat hepatic fibrosis induced by carbon tetrachloride (CCl₄). In the present study, based on the established hepatic fibrosis rat model and IL-10 treated model, we isolated HSCs, detected the expression of TGF β 1, EGF, HGF and PDGF of HSC, and tried to explore the relationship between growth factors and hepatic fibrosis and the possible mechanisms of the anti-fibrogenic activities of exogenous IL-10 *in vivo*.

MATERIALS AND METHODS

Establishment of animal models

Sixty clean male SD rats, weighing 200-300 g, were divided randomly into three groups: normal control group (GN, 8 rats), hepatic fibrosis model group (GC, 28 rats) and IL-10 treated group (GI, 24 rats). All rats were bred under routine conditions (room temperature, 22±2 °C; humidity, 55±5%; light, 12 h per day; drinking tap water and food

ad libitum. Animal food was provided by BK Company in Shanghai, China. Rats in GN were injected intra-peritoneally with saline at a dose of 2 mL/kg twice a wk; rats in the other two groups received intra-peritoneal injection of 500 ml/L CCl₄ dissolved in castor oil 2 mL/kg twice a week as described previously^[4]. From the 3rd wk, rats in the treated group were given intra-peritoneally IL-10 dissolved in saline 4 ug/kg, 20 min before CCl₄ administration, as proposed by Nelson *et al.*^[5]. The intervention stated above lasted to the end of the experiment.

Histological examination

At the beginning of the 7th and 11th wk, two rats of each group were selected randomly for histological examination. The liver tissues were fixed in 40 g/L formaldehyde and embedded with paraffin. Sections were stained with hematoxylin and eosin (HE) and examined under a light microscope.

Isolation, culture and identification of HSCs

Isolation, culture and identification of HSCs have been described thoroughly in our previous experiments^[6]. Briefly, at the beginning of the 7th and 11th wk, five rats of each group were selected randomly to perfuse successively with 0.13% pronase E and 0.025% type-IV collagenase through a portal vein catheter. The liver tissue suspension was incubated with 0.02% pronase E and 0.025% type-IV collagenase with agitation. Then the suspension obtained from the digested liver was spun by centrifugation with 11% Nycodenz density gradient to purify HSCs. Thereafter, HSCs were seeded at approximately 1×10⁶ cells/mL of Dulbecco's modified eagle medium (DMEM) with 20% fetal calf serum in 96-well plates. Then HSCs were kept in culture at 37 °C in a 50 mL/L CO₂ atmosphere for 72 h. They were identified by their typical phase-contrast microscopic appearance and by immunocytochemistry using antibody directed against desmin. Cell vitality was checked by trypan blue exclusion.

RNA extraction and RT-PCR

Total RNA was extracted from freshly isolated HSCs, according to the RNA isolation kit instructions (Jingmei Biotechnology Company of Shenzhen). Its quantity and purity were assessed by measuring the optical density at 260 and 280 nm. After measurement of RNA amount, samples were either used immediately for reverse transcription (RT) or stored at -70 °C.

For RT, 1 µg total RNA was reversely transcribed following the instructions of first strand cDNA synthesis kit (Jingmei Biotechnology Company of Shenzhen). Reaction mixtures of 20 µL were transcribed using the following program: at 42 °C for 60 min, 99 °C for 5 min, and stored at -20 °C.

For PCR, primers coding for the house-keeping gene β-actin was added to the reaction mixture spontaneously to standardize the results. Reactive systems contained cDNA 2 µL, 10×buffer 5 µL, 25 mmol/L MgCl₂ 5 µL, 10 mmol/L d NTP 1 µL, 20 mmol/L target gene sense and anti-sense primers 1 µL, 20 mmol/L β-actin primer pairs 1 µL, Taq DNA polymerase 3 U, with a total volume of 50 µL by adding aqua. Then PCR was performed with cycle parameters of 45 s at 94 °C, 30 s at 55 °C (TGF-β1) or 58 °C (EGF) or 66 °C (HGF) or 62 °C (PDGF) and 60 s at 72 °C after pre-denaturation for 5 min at 94 °C; final elongation time was 7 min at 72 °C. The number of corresponding cycles for TGF-β1, EGF, HGF and PDGF were 30, 32, 34 and 34, respectively. Primers were designed with reference to GenBank (Table 1). PCR products were immediately analyzed by 2% agarose gel electrophoresis and the density of resultant bands was semi-quantified by scanning densitometry with the ratio of TGF-β1/β-actin2, EGF/β-actin1, HGF/β-actin1 and PDGF/β-actin2.

Immunocytochemistry

Most of HSCs were attached to the dishes after 72 h of primary culture. Then the 96-well plates were washed twice with 0.1 mol/L PBS and fixed with poly-formaldehyde at 4 °C overnight. The following procedures were performed according to the instructions of streptavidin-peroxidase (S-P) kit (Beijing Zhongshan Company). Briefly, cells were washed with PBS, incubated with bovine serum albumin in PBS, reacted with primary antibody dissolved in PBS, washed, incubated with peroxidase-conjugated second antibody, washed, and reacted for 20 min with S-P. Color reaction was developed by incubation with DAB. For negative controls, the primary antibody was replaced by PBS. Table 2 summarizes the characteristics of the antibodies used in this study.

Statistical analysis

All data were expressed as mean±SE. The significance for the difference between the groups was analyzed with SPSS10.0 by one-way ANOVA.

RESULTS

Histological examination

Hepatic fibrosis, as shown histologically, became remarkable with the treatment of CCl₄. During the 7th wk, specimens from GC showed steatosis and ballooning degeneration, the collagen fibers increased and began to extend to the parenchyma, a great number of mononuclear cells and unusual neutrophils surrounded the centrilobular veins and fibrotic septa (Figure 1A), while only a few inflammatory

Table 1 Primer sequences used in this study

mRNA	Sense primers	Antisense primers	Product length (bp)
TGF-β1	CTC TGC AGG CGC AGC TCT G	GGA CTC TCC ACC TGC AAG AC	392
EGF	GAC AAC TCC CCT AAG GCT TA	CATGCA CAC GCC ACC ATT	567
GAG		GCA GTA CCC ATC GTA CGA	
HGF	TCTTGA CCC TGA CAC CCC	GTG ATT CAG CCC CAT CCG G	269
PDGF	GAT CCG CTC CTT TGA TGA TC	GTC TCA CAC TTG CAT GCC AG	435
β-actin1	AGC ACT TGC GGT CCA CGA	GAG CTA TGA GCT GCC TGA	410
β-actin2	CCA ACC GTG AAA AGA TGA CC	CAG GAG GAG CAA TGA TCT TG	660

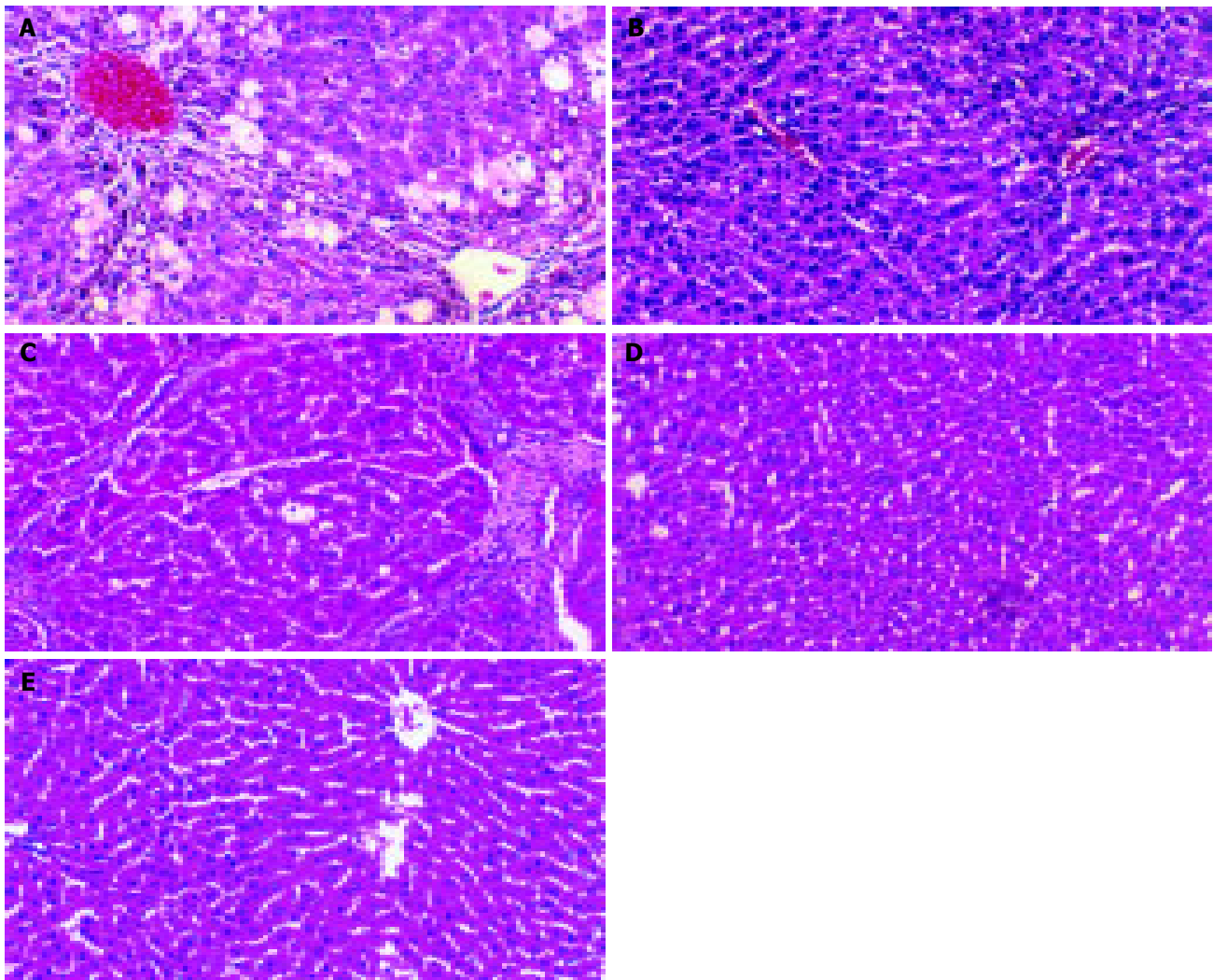


Figure 1 Effect of IL-10 on liver histology of hepatic fibrosis rats. **A:** Rat liver in group C at the 7th wk (HE×100); **B:** Rat liver in group I at the 7th wk (HE×100); **C:**

Rat liver in group C at the 11th wk (HE×100); **D:** Rat liver in group I at the 11th wk (HE×100); **E:** Rat liver in group N (HE×100).

Table 2 Antibodies used for immunocytochemistry

Antibody	Type	Source	Working solution
Desmin	Polyclonal, mouse	Beijing Zhongshan Co.	1:100
TGF-β1	Polyclonal, rabbit	BOSTER Co.	1:20
EGF	Polyclonal, rabbit	BOSTER Co.	1:50
PDGF	Polyclonal, rabbit	Beijing Zhongshan Co.	1:20
Antibody to rabbit IgG	Goat	Beijing Zhongshan Co.	Ready to use
Antibody to mouse IgG	Goat	Beijing Zhongshan Co.	Ready to use

cells infiltrated around centrilobular veins without evident changes of lobular structure in GI (Figure 1B). At the 11th wk, the reticular fibers extended into hepatic plate and full delimitation was developed in GC (Figure 1C), while less fibrous and inflammatory infiltrates were seen in GI (Figure 1D). Specimens from GN showed normal lobular structure (Figure 1E). Due to the limit of samples, no statistical data could be obtained to present disparity between the two groups, but it still illustrated the trend that fibrogenesis of GI was much less severe than that of GC.

Isolation and identification of HSCs

Totally 2-4.5×10⁷ cells per rat were harvested by the present

method. HSCs were identified by immunoreaction for desmin (Figure 2), the mean purity of freshly isolated HSCs was (95±5)%. Cell vitality checked by trypan blue exclusion was higher than 95%.

Expression of mRNA

RNA purity was determined by the ratio of A_{260}/A_{280} , which ranged from 1.8 to 2.0. At the 7th and 11th wk, TGF-β1, EGF, and HGF mRNA in GC increased obviously compared with GN and GI ($P<0.01$). For TGF-β1, no difference was seen between GI and GN. For EGF, mRNA level in GI increased compared with GN at the 7th wk ($P<0.01$) and 11th wk ($P<0.05$). For HGF, mRNA level in GI



Figure 2 Desmin expression of HSCs from primary culture for 5 d by immunochemistry (SP \times 100).

decreased compared with GN at the 7th wk ($P<0.01$) and 11th wk ($P<0.05$). Between these two time points, TGF- β 1 expression at the 7th wk was higher than that of the 11th wk; but for EGF, the former was lower than the latter. As for PDGF mRNA, there was no significant difference between these groups (Tables 3-5, Figure 3 A-C).

Table 3 Expression of TGF- β 1 mRNA in HSCs (mean \pm SE)

Wk	n	Group N	Group C	Group I
7 th wk	5	0.143 \pm 0.009	0.267 \pm 0.025 ^b	0.140 \pm 0.008 ^d
11 th wk	5	0.141 \pm 0.004	0.207 \pm 0.029 ^{a,b}	0.123 \pm 0.009 ^d

^a $P<0.05$ vs 7th wk; ^b $P<0.01$ vs group N; ^d $P<0.01$ vs group C.

Table 4 Expression of EGF mRNA in HSCs (mean \pm SE)

Wk	n	Group N	Group C	Group I
7 th wk	5	0.181 \pm 0.012	0.425 \pm 0.013 ^b	0.293 \pm 0.024 ^{b,d}
11 th wk	5	0.179 \pm 0.004	0.514 \pm 0.008 ^{a,b}	0.258 \pm 0.021 ^{c,d}

^a $P<0.05$ vs 7th wk; ^b $P<0.01$ vs group N; ^c $P<0.05$ vs group N; ^d $P<0.01$ vs group C.

Table 5 Expression of HGF mRNA in HSCs (mean \pm SE)

Wk	n	Group N	Group C	Group I
7 th	5	0.364 \pm 0.015	0.636 \pm 0.009 ^b	0.210 \pm 0.010 ^{b,d}
11 th	5	0.383 \pm 0.004	0.622 \pm 0.022 ^b	0.265 \pm 0.028 ^{a,d}

^a $P<0.05$ vs group N; ^b $P<0.01$ vs group N; ^d $P<0.01$ vs group C.

Protein expression and immunophenotyping of cells

TGF- β 1, EGF and PDGF positive expressions were localized in cytoplasm and nuclei of HSCs in all groups by immunocytochemistry after primary culture for 72 h. By then, most of the cells were attached and spread over the plastic sub-stratum. At the 7th wk, the size of HSCs in GC and GI was slightly larger than GN, as well as the number and length of pseudopodium. At the 11th wk, cell phenotype in GI was in the form of a circle or an ellipse and slightly smaller than the 7th wk, no obvious change of phenotype was seen in GC compared to the 7th wk. Despite the small number of samples and lack of statistical data, we could still find the tendency that the expression of TGF- β 1, EGF and PDGF in GC was higher than that of GN and decreased after treatment with IL-10 (Figure 4A-F).

DISCUSSION

Although significant progress has been made in understanding the pathogenesis of hepatic fibrosis, a rational therapy that prevents the progression or even reverses established fibrosis remains elusive^[7-9]. IL-10 is produced mainly by TH₂ cells and inhibits functions of TH₁ cells. It downregulates pro-cytokine synthesis and is associated with amelioration of the inflammatory response^[10-12] and fibrosis. The present study also found the trend of IL-10 relieving the degree of inflammation. Then, except for anti-inflammation, is there any other mechanism to fulfill its anti-fibrotic role? In this experiment, we detected the mRNA level of TGF- β 1, EGF, HGF and PDGF of HSCs of rat in hepatic fibrosis group and IL-10 treated group at the 7th and 11th wk.

TGF- β 1 is the most important growth factor involved in the fibrotic and cirrhotic liver. It is known to promote the development of liver fibrosis by inducing synthesis of ECM proteins and downregulating the expression of matrix degrading enzymes and stimulating the synthesis of their respective inhibitors^[13-16]. The present study showed that with the development of hepatic fibrosis, TGF- β 1 mRNA increased in GC compared to GN, and decreased after treatment with IL-10. Specifically, TGF- β 1 mRNA level did not parallel with the progression of hepatic fibrosis. These illustrated further that TGF- β 1 correlated closely with hepatic fibrosis, and it could not be regarded as a predictable factor of the degree of hepatic fibrosis and HSCs' capacity of producing TGF- β 1 declined when fibrosis developed to

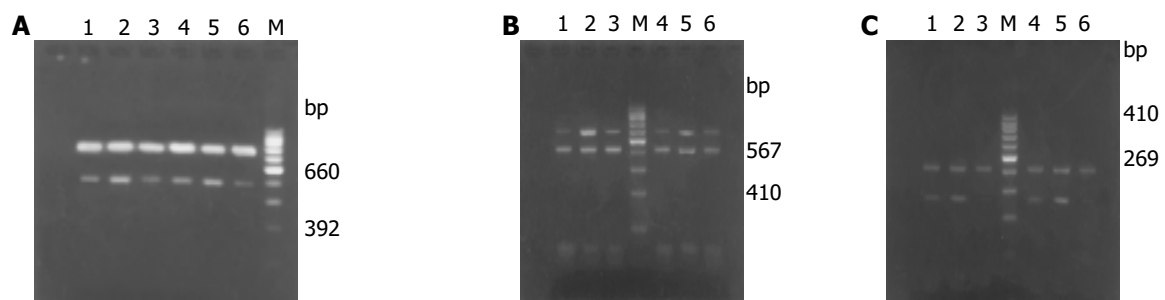


Figure 3 RT-PCR analysis of growth factor gene expression of HSC before and after intervention. **A:** Electrophoretogram of PCR for TGF- β 1 gene of HSCs. 1-3: groups N, C, I of 11th wk; 4-6: groups N, C, I of 7th wk; M: DNA ladder of 100 bp; **B:** Electrophoretogram of PCR for EGF gene of HSCs. 1-3:

groups N, C, I of 11th wk; 4-6: groups N, C, I of 7th wk; M: DNA ladder of 100 bp; **C:** Electrophoretogram of PCR for HGF gene of HSCs. 1-3 groups N, C, I of 11th wk; 4-6: groups N, C, I of 7th wk; M: DNA ladder of 100 bp.

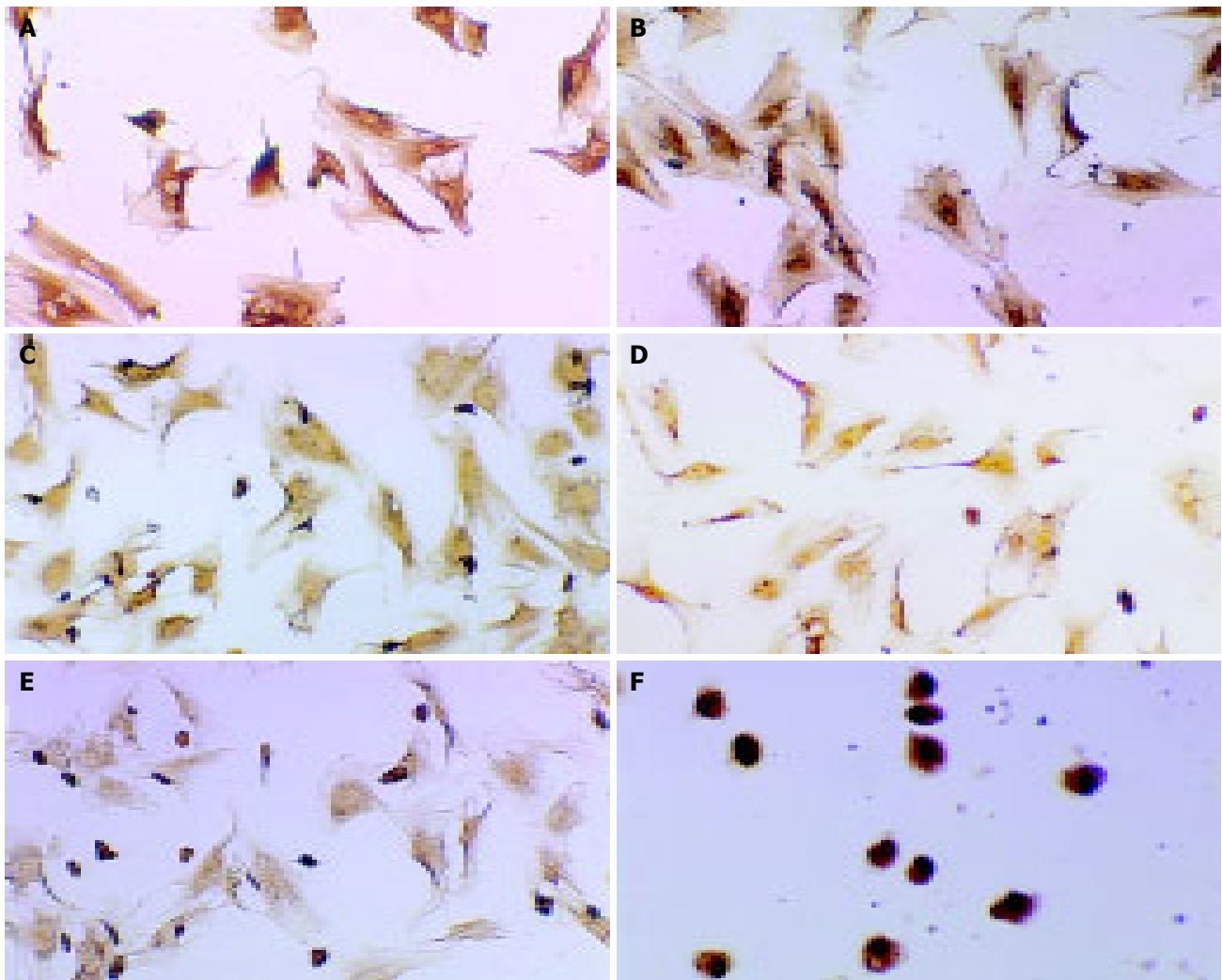


Figure 4 Expression of growth factor protein of HSCs in different groups. **A:** Expression of PDGF protein of HSCs in group C at the 7th wk (SP×100); **B:** Expression of PDGF protein of HSCs in group I at the 7th wk (SP×100); **C:** Expression of TGF-β1 protein of HSCs in group C at the 7th wk (SP×100);

D: Expression of TGF-β1 protein of HSCs in group I at the 7th wk (SP×100); **E:** Expression of EGF protein of HSCs in group C at the 11th wk (SP×100); **F:** Expression of EGF protein of HSCs in group I at the 11th wk (SP×100).

a certain extent and that IL-10 exerted its anti-fibrotic activities by attenuating the expression of TGF-β1 of HSCs.

EGF is a potent mitogen for many cells. EGF up-regulation is a characteristic feature of fibrotic liver disease^[17]. Apart from stimulating hepatocyte and bile duct epithelial proliferation, EGF also has a chemotactic mitogen effect on HSCs^[18]. A recent study demonstrated that direct stimulation with TGF-β1 and EGF results in an increased migratory response of activated HSCs^[19]. In the present study, EGF level increased with the presence of hepatic fibrosis or cirrhosis and dropped after intervention with IL-10. It showed that IL-10 inhibited HSCs from proliferating and migrating by reducing autocrine secretion of EGF, thus it limited the spread of disease, and retarded the progression of hepatic fibrosis.

HGF is secreted as a precursor polypeptide that requires proteolytic cleavage to a disulfide-linked heterodimer and binds to a specific receptor known as c-Met^[20] for biological activity. Physiologically, HGF has potent hepatotrophic and cytoprotective functions^[21]. Reports have shown treatment with HGF suppressed the increase of TGF-beta1, reduced

mRNA levels of procollagen, inhibited fibrogenesis and cell apoptosis, and produced complete resolution of fibrosis in the cirrhotic liver, thereby improving the survival rate of rats with this severe illness^[22-26]. In the present experiment, HGF mRNA level of HSCs increased in hepatic fibrosis rats which might reflect intra-hepatic inflammation or the compensation of steatosis of hepatocytes. After intervention with IL-10, HGF mRNA level dropped. So we postulated that IL-10 probably suppressed some cytokines that positively regulated HGF expression by anti-inflammation or immunoreaction or that it indicated normal liver function, or a manifestation of decreased degree of steatosis and degeneration.

PDGF has been identified as the most potent-polypeptide growth factor able to stimulate the proliferation of HSCs^[27-29], which play a critical role in the development of hepatic fibrosis. Although no statistical data were obtained to prove any difference of PDGF mRNA in these groups, which probably resulted from the difference in experimental animals, drugs, reagents and methods, PDGF protein level seemed to show the disparity that it increased in GC and

decreased in GI compared to GN.

Our experiment showed IL-10 exerted anti-fibrotic effect not only by anti-inflammatory reaction but by suppressing the expression of growth factors. Whether IL-10 plays an adverse role in liver regeneration by downregulating the expression of HGFmRNA awaits further studies. Based on the biological effect model of HGF, it is necessary to elucidate its activities at protein and receptor levels, which should provide a promising prospect for the therapy of hepatic fibrosis.

REFERENCES

- 1 **Bataller R**, Bremmer DA. Hepatic stellate cells as a target for the treatment of liver fibrosis. *Semin Liver Dis* 2001; **21**: 437-451
- 2 **Wang FS**, Wu ZZ. Current situation in studies of gene therapy of liver cirrhosis and liver fibrosis. *Shijie Huaren Xiaohua Zazhi* 2000; **8**: 371-373
- 3 **Xiang DD**, Wei YL, Li QF. Molecular mechanism of transforming growth factor b1 on Ito cell. *Shijie Huanren Xiaohua Zazhi* 1999; **7**: 980-981
- 4 **Morrow JD**, Awad JA, Kato T, Takahashi K, Badr KF, Robert LJ 2nd, Burk KF. Formation of novel non-cyclooxygenase-derived prostanoids (F2-isoprostanes) in carbon tetrachloride hepatotoxicity. An animal model of lipid peroxidation. *J Clin Invest* 1992; **90**: 2502-2507
- 5 **Nelson DR**, Lauwers GY, Lau JY, Davis GL. Interleukin 10 treatment reduces fibrosis in patients with chronic hepatitis C: a pilot trial of interferon nonresponders. *Gastroenterology* 2000; **118**: 655-660
- 6 **Zheng WD**, Wang XZ, Zhang LJ, Shi MN. A simple and reliable method of isolating rat hepatic stellate cells. *Fujian Yikedaxue Xuebao* 2002; **38**: 71-73
- 7 **Schuppan D**, Strobel D, Hahn EG. Hepatic fibrosis therapeutic strategies. *Digestion* 1998; **59**: 385-390
- 8 **Pinzane M**, Marra F, Carloni V. Signal transduction in hepatic stellate cells. *Liver* 1998; **18**: 2-13
- 9 **Gressner AM**. The cell biology of liver fibrogenesis: an imbalance of proliferation, growth arrest and apoptosis of myofibroblasts. *Cell Tissue Res* 1998; **292**: 447-452
- 10 **Ledeboer A**, Breve JJ, Poole S, Tilders FJ, Van Dam AM. Interleukin-10, interleukin-4, and transforming growth factor-beta differentially regulate lipopolysaccharide-induced production of pro-inflammatory cytokines and nitric oxide in co-cultures of rat astroglial and microglial cells. *Glia* 2000; **30**: 134-142
- 11 **Marques CP**, Hu S, Sheng W, Cheeran MC, Cox D, Lokensgard JR. Interleukin-10 attenuates production of HSV-induced inflammatory mediators by human microglia. *Glia* 2004; **47**: 358-366
- 12 **Mitchell MD**, Simpson KL, Keelan JA. Paradoxical proinflammatory actions of interleukin-10 in human amnion: potential roles in term and preterm labour. *J Clin Endocrinol Metab* 2004; **89**: 4149-4152
- 13 **Xu XB**, He ZP, Liang ZQ, Leng XS. Obstruction of TGF- β 1 signal transduction by anti-Smad4 gene can therapy experimental liver fibrosis in the rat [Article in Chinese. *Zhonghua Ganzangbing Zazhi* 2004; **12**: 263-266
- 14 **Wu XR**, Lv MH, Wang Q, Shi SS, Guo WD. The plasma levels of transforming growth factor beta1 and the protein expressions of alpha-SMA, urokinase plasminogen activator and plasminogen activator inhibitor-1 in liver of patients with different grades of hepatic fibrosis. *Zhonghua Ganzangbing Zazhi* 2004; **12**: 400-402
- 15 **Ma C**, Chegini N. Regulation of matrix metalloproteinases (MMPs) and their tissue inhibitors in human myometrial smooth muscle cells by TGF- β 1. *Mol Hum Reprod* 1999; **5**: 950-954
- 16 **Knittel T**, Mehde M, Kobold D, Saile B, Dinter C, Ramadori G. Expression patterns of matrix metalloproteinases and their inhibitors in parenchymal and non-parenchymal cells of rat liver: regulation by TNF- α and TGF- β 1. *J Hepatol* 1999; **30**: 48-60
- 17 **Komuves LG**, Feren A, Jones AL, Fodor E. Expression of epidermal growth factor and its receptor in cirrhotic liver disease. *J Histochem Cytochem* 2000; **48**: 821-830
- 18 **Liu X**, Zhang J, Zhang Y. Effects of platelet-derived growth factor on the proliferation of hepatic stellate cells and their expression of genes of collagens and platelet-derived growth factor. *Zhonghua Binglixue Zazhi* 2000; **29**: 27-29
- 19 **Yang C**, Zeisberg M, Mosterman B, Sudhakar A, Yerramalla U, Holthaus K, Xu L, Eng F, Afdhal N, Kalluri R. Liver fibrosis: insights into migration of hepatic stellate cells in response to extracellular matrix and growth factors. *Gastroenterology* 2003; **124**: 147-159
- 20 **Mars WM**, Zarnegar R, Michalopoulos GK. Activation of hepatocyte growth factor by the plasminogen activators uPA and tPA. *Am J Pathol* 1993; **143**: 949-958
- 21 **Kosai K**, Matsumoto K, Nagata S, Tsujimoto Y, Nakamura T. Abrogation of Fas-induced fulminant hepatic failure in mice by hepatocyte growth factor. *Biochem Biophys Res Commun* 1998; **244**: 683-690
- 22 **Sato M**, Kakubari M, Kawamura M, Sugimoto J, Matsumoto K, Ishii T. The decrease in total collagen fibers in the liver by hepatocyte growth factor after formation of cirrhosis induced by thioacetamide. *Biochem Pharmacol* 2000; **59**: 681-690
- 23 **Ueki T**, Kaneda Y, Tsutsui H, Nakanishi K, Sawa Y, Morishita R, Matsumoto K, Nakamura T, Takahashi H, Okamoto E, Fujimoto J. Hepatocyte growth factor gene therapy of liver cirrhosis in rats. *Nat Med* 1999; **5**: 226-230
- 24 **Goda K**, Fujisawa M, Shirakawa T, Dobashi M, Shiota G, Zhang ZJ, Gotoh A, Kamidono S. Adenoviral-mediated HGF expression inhibits germ cell apoptosis in rats with cryptorchidism. *J Gene Med* 2004; **6**: 869-876
- 25 **Okada M**, Sugita K, Inukai T, Goi K, Kagami K, Kawasaki K, Nakazawa S. Hepatocyte growth factor protects small airway epithelial cells from apoptosis induced by tumor necrosis factor- α or oxidative stress. *Pediatr Res* 2004; **56**: 336-344
- 26 **Liu Y**. Hepatocyte growth factor in kidney fibrosis: therapeutic potential and mechanisms of action. *Am J Physiol Renal Physiol* 2004; **287**: F7-16
- 27 **Kuter DJ**. Future directions with platelet growth factors. *Semin Hematol* 2000; **37**(2 Suppl 4): 41-49
- 28 **Pinzani M**. Pdgf and signal transduction in hepatic stellate cells. *Front Biosci* 2002; **7**: D1720-1726
- 29 **Yuan N**, Wang P, Wang Z. Expression and significance of platelet derived growth factor and its receptor in liver tissues of patients with liver fibrosis. *Zhonghua Ganzangbing Zazhi* 2002; **10**: 58-60

Vitamin D receptor gene *Tru9I* polymorphism and risk for incidental sporadic colorectal adenomas

You-Ling Gong, Da-Wen Xie, Zong-Lin Deng, Roberd M Bostick, Xi-Jiang Miao, Jin-Hui Zhang, Zhi-Hong Gong

You-Ling Gong, Tumor Center, West China Hospital, Sichuan University, Chengdu 610041, Sichuan Province, China
You-Ling Gong, Da-Wen Xie, Zong-Lin Deng, Jin-Hui Zhang, Zhi-Hong Gong, Department of Epidemiology and Biostatistics, School of Public Health and South Carolina Cancer Center, University of South Carolina, Columbia, SC 29203, USA
Roberd M Bostick, Department of Epidemiology, Rollins School of Public Health, Emory University, Atlanta, GA 30322, USA
Xi-Jiang Miao, Department of Computer Science and Engineering, University of South Carolina, Columbia, SC 29203, USA
Supported by the Public Health Service grants, No. R01CA-51932 to RMB (National Cancer Institute), and Center for Colon Cancer Research grant, No. RR017698 to FGB from National Institutes of Health, Department of Health and Human Services
Co-first-authors: You-Ling Gong and Da-Wen Xie
Correspondence to: Dr. Da-Wen Xie, University of South Carolina, 14 Richland Medical Park, Suite 500, Columbia, SC 29203, USA. dawen.xie@palmettohealth.org
Telephone: +01-803-434-3707 Fax: +01-803-434-3795
Received: 2005-12-03 Accepted: 2005-01-05

CONCLUSION: Our findings suggest that the VDR *Tru9I* polymorphism may be associated with lower risk for colorectal adenoma, particularly in interaction with various risk factors, but not with calcium or vitamin D.

© 2005 The WJG Press and Elsevier Inc. All rights reserved.

Key words: Case-control study; Colorectal adenoma; Colorectal neoplasia; Vitamin D receptor; Genetic polymorphism

Gong YL, Xie DW, Deng ZL, Bostick RM, Miao XJ, Zhang JH, Gong ZH. Vitamin D receptor gene *Tru9I* polymorphism and risk for incidental sporadic colorectal adenomas. *World J Gastroenterol* 2005; 11(31): 4794-4799
<http://www.wjgnet.com/1007-9327/11/4794.asp>

Abstract

AIM: Recent laboratory and epidemiological studies suggest that vitamin D is a potential agent for colorectal cancer prevention. Its function is partially mediated by the vitamin D receptor (VDR). The aim of this study was to investigate whether a novel G (allele 'U')>A (allele 'u') polymorphism (*Tru9I*) in the VDR intron 8 region is associated with risk for colorectal adenoma in a colonoscopy-based case-control study.

METHODS: Genotyping for a total of 391 subjects was carried out through PCR and restriction fragment length polymorphism.

RESULTS: The frequencies of 'U' and 'u' alleles were 89.3% and 10.7%, respectively. The 'Uu' and 'uu' genotypes were associated with decreased risk for adenoma (OR, 0.71; 95%CI, 0.40-1.25). The inverse association was more pronounced for multiple adenomas and adenomas that were larger had moderate or greater dysplasia, or were sessile: the odds ratios (ORs) were, 0.51 (95%CI, 0.21-1.24), 0.37 (95%CI, 0.11-1.28), 0.68 (95%CI, 0.33-1.41), and 0.36 (95%CI, 0.13-0.97) respectively. In joint/combined analyses, inverse associations were more obvious among those who had at least one 'u' allele and also were younger (OR, 0.60; 95%CI, 0.26-1.37), women (OR, 0.38; 95%CI, 0.17-0.88), did not smoke (OR, 0.39; 95%CI, 0.13-1.23), or took NSAID (OR, 0.38; 95%CI, 0.12-1.25), but no evidence existed for interactions with calcium or vitamin D intake.

INTRODUCTION

Colorectal cancer (CRC) is one of the most common cancers in the USA, with an annual incidence of 146 940 cases and 56 730 deaths^[1]. It has been reported that in USA, CRC morbidity is greater in northern latitudes, which may in part be due to lower sun exposure^[2]. Several epidemiological studies support the hypothesis that dermal vitamin D synthesis mediated by sunlight may protect against colorectal cancer; several found decreased risk for this disease with higher serum levels of vitamin D or with increasing dietary vitamin D intake^[3-5]. The vitamin D receptor (VDR), a member of the steroid/thyroid receptor family, mediates genomic actions of the active metabolite of vitamin D [1, 25(OH)₂D₃], and thus regulates cellular proliferation and differentiation^[6-8] and induces apoptosis^[9]. Recent studies show that VDR functions as a sensor of the colorectal carcinogen, lithocholic acid (LCA), inducing *in vivo* expression of the CYP3A family that detoxifies LCA in the liver and intestine^[10]. Based on such findings, there has been increased interest in an interaction between vitamin D and the VDR gene and risk for colorectal cancer. Although contradictory results have been reported^[11-13], evidence suggests that at least some VDR gene polymorphisms are related to the risk of CRC or adenoma^[14-17].

Recently, a novel G>A polymorphism in the 3'-UTR region of the VDR gene was identified and designated as VDR *Tru9I*^[18]. It is thought that the polymorphisms in this region of the VDR gene may affect its mRNA stability, possibly through linkage to other variants^[19]. So far, no previous study has been reported on investigating the function of this polymorphism. In a epidemiological

study, Gyorffy *et al.*^[20], found that the presence of the variant 'u' allele, combined with VDR *ApaI* 'a' and *BsmI* 'b' alleles, is associated with increased risk for type I diabetes mellitus in girls. To our knowledge, there has been no previously published study on a potential association between the VDR *Tru9I* polymorphism and colorectal adenoma risk. Previously, we found that different genetic polymorphisms might affect risk for colorectal adenoma: the *cyclinD1 A/G* polymorphism was associated with increased risk^[21], and the p53-inducible ribonucleotide reductase small subunit 2 (p53R2) 'AA' genotype was strongly associated with increased risk in those with lower dietary nutrients including vitamins and calcium intakes (paper submitted). Herein, we report data from this same North Carolina case-control study on the association of the VDR *Tru9I* polymorphism and colorectal adenoma risk, alone and in interaction with various environmental risk factors for colorectal neoplasms.

MATERIALS AND METHODS

Study design

From 1994 to 1997, the markers of adenomatous polyps (MAP) case-control study were conducted to assess the validity of colonic epithelial cell proliferation as a biomarker of risk for incident sporadic colorectal adenomatous polyps. Prior to beginning the study, MAP was approved by the Institutional Review Board of Wake Forest University, Bowman Gray School of Medicine in accordance with an assurance filed with and approved by the Department of Health and Human Services. Informed consent was obtained from each participant. Eligibility criteria for study subjects consisted of English speaking adults from 30 to 74 years of age, either sex or any race who were scheduled for elective outpatient colonoscopy by four large gastro-enterology practices in Winston-Salem and Charlotte, North Carolina. Patients were recruited for over 24 mo. Cases were identified as eligible colonoscopy patients who were determined to have study index pathologist-confirmed incident adenomatous polyps according to criteria adapted from the National Polyp Study^[22]. Controls consisted of all eligible colonoscopy patients with no previous history of adenomatous polyps and who were found to be free of adenomatous polyps. Persons with familial polyposis, Gardner's syndrome, ulcerative colitis, Crohn's Disease, bowel resection, newly diagnosed recurrent adenomatous polyps, and incident colon cancer were excluded, as they were patients with past or prevalent cancer other than non-melanoma skin cancer.

Patients completed mailed questionnaires prior to their colonoscopies (to avoid bias) regarding family history of polyps or colon cancer, medical history, dietary information (via a semi-quantitative Willett 153-item Food Frequency Questionnaire), physical activity (via a modified Paffenbarger questionnaire), reproductive variables, body fat distribution, and their reasons for and the sequence of events leading to colonoscopy. Blood was drawn and stored at -70 °C for possible later measurement of various genotypes.

Preparation for colonoscopy included a 12 h fast and bowel cleansing with polyethylene glycol (GoLYTELY). Subjects willing to undergo biopsies had four quadrant

biopsies taken from normal appearing mucosa in the rectum (10 cm above the anus), sigmoid colon, and cecum for a total of 16 biopsies. Information recorded included number of polyps, polyp size, polyp type (adenoma, hyperplastic, or mixed), adenoma subtype (tubular, villous, tubulo-villous), and the degree of dysplasia.

Subjects

Among all four clinical sites, 2 246 colonoscopy patients were identified. Of these, 669 were eligible on initial screening (eligibility rate 29.8%), and of these 633 were willing to discuss the study, 617 of these were contacted, and 417 of these signed consent and had study colonoscopies (consent rate 63.1%). Of the 417 participants, 259 had some type of polyp, and of these 179 had adenomatous polyps. Nine of the 417 patients were subsequently determined ineligible for the study, and an additional eight patients had incident colon cancer and were not eligible for the primary case-control analyses; thus, 400 possible patients were available for genotypic analysis. Of these 400 patients, viable DNA was isolated from 391 (171 cases and 220 controls) for genotyping.

Genotyping

Genomic DNA was obtained from stored WBCs digested in 500 µL of lysis buffer (50 mmol/L Tris-HCl, pH 8.5, 1 mmol/L EDTA, 0.2% SDS, 200 g/mL proteinase K) over night at 55 °C with shaking. The digestion was precipitated directly with isopropanol and the pellets were washed with 70% ethanol. The genomic DNA pellets (50-100 µg) were dissolved in 300-800 µL of TE buffer, of which about 1 µL was used for each PCR reaction. DNA was amplified following the primers designed for the exon 8 region of the VDR gene following the published DNA sequence (GenBank number: AY342401). An isoschizomer of *Tru9I*, *MseI*, was used in this study. The PCR (50 µL volume) was carried out in 20 mmol/L Tris-HCl, pH 8.4, 50 mmol/L KCl, 1.5 mmol/L MgCl₂, 0.2 mmol/L dNTP, 0.5 mmol/L of each primer (5'-GCA GGG TAC AAA ACT TTG GAG -3' as forward and a 5'-CCT CAT CAC CGA CAT CAT GTC -3' as reverse), 80-120 ng of DNA template, and 2.5 units Taq polymerase (Gibco-Invitrogen). The solution was heated to 94 °C for 2 min, followed by 35 cycles of 30 s at 94 °C, 30 s at 69 °C, and 30 s at 72 °C. The final reaction was extended 7 min at 72 °C. The PCR products (5 µL) were loaded onto a 3% 2:1 NuSieve-SeaKem gel for confirmation. The PCR products (10 µL) were then subjected to *MseI* restriction enzyme at 37 °C overnight. Bands for the wild-type ('UU') allele were not cut (177 bp); the 'uu' genotype was showed at 91 and 86 bp; and the heterozygote ('Uu') allele was cut into 177-, 91-, and 86-bp fragments.

Statistical analysis

Allelic frequencies for polymorphic VDR *Tru9I* G>A alleles were compared to those in previous study populations. VDR *Tru9I* G>A genotype (UU, Uu, uu) distributions for cases and controls were tested for adherence to the Hardy-Weinberg equilibrium.

All statistical inquiries were conducted using R language

version 1.9.0 from <http://www.R-project.org>. Descriptive comparisons (i.e., mean \pm SD, frequencies as percents) of cases and controls were conducted utilizing χ^2 tests for categorical variables, and *t* test for continuous variables.

Multiple logistic regressions were utilized to calculate odds ratios (ORs) and corresponding 95%CI, adjusted for potential confounding factors, to estimate the strength of an association between VDR *Tru9I* genotype and risk for incident sporadic colorectal adenomas. The effect of VDR *Tru9I* genotype was analyzed utilizing a priori hypothesized low risk, common 'UU' genotype as the referent group. A 'P' test for trend was calculated across genotypes to detect a pattern of association.

Several risk factors were scrutinized as possible confounders or effect modifiers of the VDR *Tru9I* genotype-colorectal adenoma association. Among these were age, sex, race, body mass index, family history of colon cancer (FHCC), smoking, alcohol consumption, non-steroidal anti-inflammatory drug (NSAID) use, and total dietary intake of calcium and vitamin D. Criteria for inclusion of any covariate in the final model included: (1) biological plausibility; (2) whether it fits the model at $P \leq 0.1$; and (3) whether it altered the OR for the primary exposure variable by 10% or more. Final models for genotype main effects included age, sex, smoking status, drinking status, and FHCC.

Models involving in the assessment of possible interactions between genotypes and various anti- and pro-proliferative and other key risk factors included age, sex, FHCC, NSAIDs, smoking status, and total intake of calcium and alcohol.

To examine potential gene-environment interactions of VDR *Tru9I* genotype and certain risk factors, stratified analyses were conducted. Continuous variables were dichotomized on median values for controls; furthermore, continuous dietary variables were categorized as sex-specific. Criteria for assessing effect modifiers were based on previous literature, biological plausibility, and whether or not risk estimates differed substantially across strata.

RESULTS

Adenoma cases were similar to the controls in respect to race, education status, and most dietary intakes (Table 1). However, cases were more likely to be a little older, male, and current drinkers or smokers. Controls were more likely to have histories of colon cancer in first-degree relatives.

There were significant differences in NSAID use and dietary calcium intake between cases and controls. The polymorphism distribution in present population was in Hardy-Weinberg equilibrium ($\chi^2 = 3.41$, $P = 0.07$).

Table 2 presents the associations between VDR *Tru9I*

Table 1 Selected characteristics of cases and controls, MAP study, 1994-1997¹

	Cases (n = 171)	Controls (n = 220)	P ^a
Demographic factors			
Age (yr) ²	58.4 (8.4)	55.8 (10.2)	0.006
Male (%)	60	36	<0.001
White (%)	89	89	0.98
College education (%)	19	23	0.38
Major risk factors			
Family history of colon cancer (%)	14	31	<0.001
Currently smoke cigarettes (%)	30	20	0.02
Currently drink alcohol (%)	75	55	<0.001
NSAID ³ use (%)	19	30	0.007
Dietary intakes			
Total energy (kcal/d)	2 010 (30)	2 169 (1 999)	0.27
Total fat (g/d)	71.3 (39.9)	72.6 (65.9)	0.80
Total meat (serve/wk)	4.4 (1.4)	4.5 (1.4)	0.57
Total fruits and vegetables (serve/wk)	6.1 (3.6)	7.4 (10.2)	0.09
Total calcium (mg/d)	736 (406.6)	871 (757)	0.02
Total vitamin D (IU/d)	315 (258.2)	359 (374)	0.16
Total folate (mg/d)	416.7 (241.6)	467 (402)	0.12
Total alcohol (g/d)	7.4 (15.1)	4.8 (20.8)	0.14

¹Adjusted for age, sex, total energy intake, history of colon cancer in a first degree relative, nonsteroidal anti-inflammatory drug use, current smoking status, and total calcium and alcohol intakes; ²mean \pm SD presented unless otherwise indicated, except for age, all other means are age adjusted; ³non-steroidal anti-inflammatory drug.

Table 2 Frequencies of VDR *Tru9I* genotypes and associations with incident sporadic colorectal adenomas (MAP study), 1994-1997

VDR <i>Tru9I</i> genotype	Cases (n = 171)		Controls (n = 220)		Adjusted OR ¹	95%CI ²
	n	%	n	%		
UU	144	84.2	171	77.8	1.00	
Uu	23	13.5	45	20.4	0.88	(0.17-4.55) ³
uu	4	2.3	4	1.8	0.69	(0.38-1.25)
Uu+uu	27	15.8	49	22.2	0.71	(0.40-1.25)
P-trend					0.24	

¹Odds ratio; ²95% confidence interval; ³adjusted for age, sex, total energy intake, history of colon cancer in a first degree relative, nonsteroidal anti-inflammatory drug use, current smoking status, and total calcium and alcohol intake.

genotypes and colorectal adenoma risk. The frequencies of VDR *Tru9I* 'UU', 'Uu', and 'uu' genotypes were 84.2%, 13.5%, and 2.3% in cases, and 77.8%, 20.3%, and 1.9% in controls, respectively. There were equivalent allele distributions for cases ('U' = 90.9%, 'u' = 9.1%) and controls ('U' = 88%, 'u' = 12%). A 29% decreased multivariable-adjusted OR (0.71; 95%CI, 0.40-1.25) was observed in 'Uu' and 'uu' carriers, compared to 'UU' carriers.

We investigated the association of the polymorphism with colorectal adenoma risk according to characteristics

of adenomatous polyps (Table 3). The inverse association of having at least one 'u' allele with risk for colorectal adenoma was more pronounced for adenoma that were multiple (OR, 0.51; 95%CI, 0.21-1.24), larger (OR, 0.37; 95%CI, 0.11-1.28), sessile (OR, 0.36; 95%CI, 0.13-0.97), and perhaps for adenomas with higher levels of dysplasia (OR, 0.68; 95%CI, 0.33-1.41).

Potential interactions of VDR *Tru9I* polymorphism and other risk factors for colorectal neoplasms and risk for adenomas are shown in Table 4. Compared to the 'UU'

Table 3 Age-, sex-adjusted associations of VDR *Tru9I* genotypes and risk for incident sporadic colorectal adenomas according to adenoma characteristics, MAP Study, 1994-1997

Adenoma characteristics	<i>Tru9I</i> genotypes			
	UU		Uu+uu	
	Cases/controls (n)	OR ¹ /95%CI ²	Cases/controls (n)	OR/95%CI
Multiplicity				
1	85/171	1.00	20/49	0.88 (0.48-1.60)
>1	59/171	1.00	7/49	0.51 (0.21-1.24)
Shape				
Sessile	51/171	1.00	5/49	0.36 (0.13-0.97)
Pedunculated	97/171	1.00	22/49	0.93 (0.51-1.68)
Size (cm) ³				
<1.0	111/171	1.00	24/49	0.84 (0.47-1.49)
≥1.0	33/171	1.00	3/49	0.37 (0.11-1.28)
Dysplasia ⁴				
Mild	73/171	1.00	15/49	0.79 (0.41-1.53)
≥Moderate	71/171	1.00	12/49	0.68 (0.33-1.41)
Morphology ⁵				
Tubular	131/171	1.00	27/49	0.80 (0.46-1.38)
Any villous	13/171	1.00	0/49	NA ⁶

¹Odds ratio; ²95% confidence interval; ³greatest diameter of largest adenoma; ⁴dysplasia in adenoma with greatest degree of dysplasia; ⁵if multiple adenomas, classified as "Any villous" if any adenoma villous or tubulovillous; ⁶not available.

Table 4 Multivariate-adjusted¹ joint and combined associations of VDR *Tru9I* genotypes and various risk factors for colorectal neoplasms and risk for incident sporadic colorectal adenomas, MAP study, 1994-1997

	UU			Uu+uu		
	Cases (n)	Controls (n)	OR ² /95%CI ³	Cases (n)	Controls (n)	OR/95%CI
Age (yr)						
≤57	58	83	1.00	12	31	0.60 (0.26-1.37)
>57	86	89	1.41 (0.86-2.31)	15	18	1.09 (0.46-2.56)
Sex						
Male	85	60	1.00	15	16	0.65 (0.28-1.53)
Female	59	112	0.51 (0.30-0.85)	12	33	0.38 (0.17-0.88)
Current smoker						
No	35	77	1.00	6	25	0.39 (0.13-1.23)
Yes	105	94	1.84 (1.07-3.17)	20	24	1.56 (0.69-3.53)
Current drinker						
No	63	99	1.00	13	26	0.96 (0.44-2.08)
Yes	77	71	1.65 (1.01-2.69)	12	22	0.90 (0.39-2.06)
NSAID ⁴ use						
No	118	117	1.00	21	38	0.64 (0.34-1.23)
Yes	23	54	0.48 (0.26-0.86)	5	11	0.38 (0.12-1.25)
Total calcium intake ⁵						
Lower	92	84	1.00	13	23	0.53 (0.23-1.20)
Higher	49	86	0.53 (0.32-0.87)	14	26	0.52 (0.23-1.14)
Total vitamin D intake ⁶						
Lower	76	83	1.00	14	25	0.59 (0.26-1.33)
Higher	65	87	0.78 (0.48-1.27)	13	24	0.60 (0.27-1.38)

¹Adjusted for age, sex, total energy intake, history of colon cancer in a first degree relative, nonsteroidal anti-inflammatory drug use, current smoking status, and total calcium and alcohol intakes; ²odds ratio; ³95% confidence interval; ⁴nonsteroidal anti-inflammatory drug; ⁵sex-specific median calcium intakes for males 701.3 mg/d, for females 754.1 mg/d; ⁶sex-specific median vitamin D intakes for males 257.2 IU/d, for females 229.7 IU/d.

genotype carriers, having a 'u' allele was inversely associated with risk for colorectal adenoma among those who were younger (OR, 0.60; 95%CI, 0.26-1.37), women (OR, 0.38; 95%CI, 0.17-0.88), did not smoke (OR, 0.39; 95%CI, 0.13-1.23), or took NSAID (OR, 0.38; 95%CI, 0.12-1.25). Dietary calcium and vitamin D intake were observed to be related to decreased risk for adenoma; however, there was no evidence suggesting an interaction with the VDR *Tru9I* polymorphism.

DISCUSSION

VDR polymorphisms have been evaluated as risk factors for CRC or adenoma; however, their impact remains unclear. In the present study, we assessed, for the first time, VDR *Tru9I* variants as risk factor for colorectal adenoma. Our data suggest that the *Tru9I* mutant 'u' allele was associated with decreased risk for colorectal adenoma, particularly for adenomas that were larger, multiple, had moderate or greater dysplasia, or were sessile. Also, the 'u' allele was related to decreased risk for adenoma, particularly among persons who were younger, female, NSAID users or did not smoke.

Vitamin D is obtained from the diet or sunlight-induced synthesis, and hydroxylated first in the liver [forming 25-(OH)D], then subsequently in the kidney [forming 1,25-(OH)₂D]. The hypothesis that vitamin D may provide reduced colorectal adenoma risk was first proposed in the early 1980s in light of an inverse ecologic association between CRC morbidity and solar exposure^[23]. *In vivo* and *in vitro* studies found that vitamin D₃ promotes differentiation of colon carcinoma cells by inducing E-cadherin and inhibiting β-catenin signaling^[7]. Experimental data also suggest that the active metabolite of vitamin D and its analogs can induce apoptosis in a colorectal adenoma cell line^[9]. Vitamin D interacts with the VDR, which upregulates CYP3A expression, which in turn increases detoxification of secondary bile acids, including LCA^[10]. Recent epidemiological studies have suggested inverse associations among calcium, vitamin D and CRC or adenoma risk; but results are mixed. In the present study, higher calcium and vitamin D intake were associated with lower risk for colorectal adenomas; however, there was no support for the hypothesis that the VDR *Tru9I* polymorphism may interact with these dietary micronutrients.

VDR is thought to mediate most vitamin D effects, and six common polymorphisms of the VDR gene have been identified. It has been reported that the polymorphisms in the 3'UTR-region (*BsmI*, *TaqI*, *ApaI*, *Tru9I* and *Poly-A*) might alter transcriptional activity and mRNA degradation^[19]; and *FokI*, located at the VDR start codon, affects the length of the N-terminal VDR transactivation domain, resulting in a three-amino acid longer protein^[24]. Several epidemiological studies have addressed associations between VDR polymorphisms and different cancer types including colorectal cancers^[11-15,25-31]. The *FokI* polymorphism, which is a potential functional variant, has been extensively studied. Under various exposures, inconsistent results were obtained from different investigators: Wong *et al.*^[14], reported, that the mutant 'f' allele was associated with increased risk of colorectal cancer; while another study by Ingles *et al.*, found that the 'f' allele was related to decreased risk^[13]; but null associations

also have been observed^[12,17]. The association of VDR *BsmI* polymorphism with cancer risk has also been investigated. Two previous studies found that the VDR *BsmI* 'BB' genotype may reduce risk for colorectal adenoma; in one, the association was modified by NSAID use, and in the other, the association was associated with reduced risk among those who had lower calcium intake and used NSAIDs^[11,16]. Also, we previously reported that the VDR *BsmI* variant 'b' allele was associated with colorectal adenoma risk in the same study population as the current study^[32]. The VDR *Poly-A* polymorphism has been associated with decreased risk for colorectal adenoma, modified by NSAID use^[11]. So far, there have been no previous reports of investigations of an association of the *Tru9I* polymorphism with any cancer.

Many studies have reported that the VDR polymorphisms are associated with susceptibility for and prognosis of different cancers^[13,33,34]. Hutchinson *et al.*^[33], found that the VDR 'ttff' genotype (according to *TaqI* and *FokI* polymorphisms) was significantly associated with thicker malignant melanoma tumors. It has also been reported that the *FokI* polymorphism was more strongly related to large adenoma risk among subjects with lower dietary calcium intake^[13].

Some limitations in this study should be considered in interpreting our results. First, the small sample size and consequent low power preclude drawing strong conclusions. Second, this study is colonoscopy-based, and the population may not be representative of the general population. People who worried about their positive family history were more likely to seek colonoscopy examination, leading to a family history bias that may have attenuated associations. Another potential limitation is that ultraviolet radiation exposure was not assessed in the present study; therefore, the dietary vitamin D intake may not reflect the true exposure to vitamin D. In light of the relationship between vitamin D and calcium, this may also impact the estimated calcium-adenoma association.

In conclusion, this is the first study to investigate an association between the VDR *Tru9I* polymorphism and risk for incident sporadic colorectal adenoma. Our data suggest that the VDR *Tru9I* polymorphism may be more related to progression than initiation of colorectal adenoma. Our study also focused on the interaction between the VDR gene polymorphism, *Tru9I*, and dietary calcium and vitamin D intakes; however, no such interaction was found. On the other hand, our data suggest possible interactions of VDR *Tru9I* genotypes with age, sex, smoking, drinking, and NSAID use. Further, larger studies are needed to verify the present data, to understand the biological mechanisms of VDR gene/calcium/vitamin D interactions.

REFERENCES

- 1 Jemal A, Tiwari RC, Murray T, Ghafoor A, Samuels A, Ward E, Feuer EJ, Thun MJ. American Cancer Society. Cancer statistics, 2004. *CA Cancer J Clin* 2004; **54**: 8-29
- 2 Garland CF, Garland FC, Gorham ED. Can colon cancer incidence and death rates be reduced with calcium and vitamin D? *Am J Clin Nutr* 1991; **54**(1 Suppl): 193S-201S
- 3 Platz EA, Hankinson SE, Hollis BW, Colditz GA, Hunter DJ, Speizer FE, Giovannucci E. Plasma 1,25-dihydroxy- and 25-hydroxyvitamin D and adenomatous polyps of the dis-

- tal colorectum. *Cancer Epidemiol Biomarkers Prev* 2000; **9**: 1059-1065
- 4 **Garland CF**, Comstock GW, Garland FC, Helsing KJ, Shaw EK, Gorham ED. Serum 25-hydroxyvitamin D and colon cancer: eight-year prospective study. *Lancet* 1989; **2**: 1176-1178
 - 5 **Braun MM**, Helzlsouer KJ, Hollis BW, Comstock GW. Colon cancer and serum vitamin D metabolite levels 10-17 years prior to diagnosis. *Am J Epidemiol* 1995; **142**: 608-611
 - 6 **Pence BC**, Buddingh F. Inhibition of dietary fat-promoted colon carcinogenesis in rats by supplemental calcium or vitamin D3. *Carcinogenesis* 1988; **9**: 187-190
 - 7 **Palmer HG**, Gonzalez-Sancho JM, Espada J, Berciano MT, Puig I, Baulida J, Quintanilla M, Cano A, de Herreros AG, Lafarga M, Munoz A. Vitamin D(3) promotes the differentiation of colon carcinoma cells by the induction of E-cadherin and the inhibition of beta-catenin signaling. *J Cell Biol* 2001; **154**: 369-387
 - 8 **Sadava D**, Remer T, Petersen K. Hyperplasia, hyperproliferation and decreased migration rate of colonic epithelial cells in mice fed a diet deficient in vitamin D. *Biol Cell* 1996; **15**: 113-115
 - 9 **Diaz GD**, Paraskeva C, Thomas MG, Binderup L, Hague A. Apoptosis is induced by the active metabolite of vitamin D3 and its analogue EB1089 in colorectal adenoma and carcinoma cells: possible implications for prevention and therapy. *Cancer Res* 2000; **60**: 2304-2312
 - 10 **Makishima M**, Lu TT, Xie W, Whitfield GK, Domoto H, Evans RM, Haussler MR, Mangelsdorf DJ. Vitamin D receptor as an intestinal bile acid sensor. *Science* 2002; **296**: 1313-1316
 - 11 **Peters U**, Hayes RB, Chatterjee N, Shao W, Schoen RE, Pinsky P, Hollis BW, McGlynn KA. Prostate, lung, colorectal and ovarian cancer screening project team. Circulating vitamin D metabolites, polymorphism in vitamin D receptor, and colorectal adenoma risk. *Cancer Epidemiol Biomarkers Prev* 2004; **13**: 546-552
 - 12 **Grau MV**, Baron JA, Sandler RS, Haile RW, Beach ML, Church TR, Heber D. Vitamin D, calcium supplementation, and colorectal adenomas: results of a randomized trial. *J Natl Cancer Inst* 2003; **95**: 1765-1771
 - 13 **Ingles SA**, Wang J, Coetzee GA, Lee ER, Frankl HD, Haile RW. Vitamin D receptor polymorphisms and risk of colorectal adenomas (United States). *Cancer Causes Control* 2001; **12**: 607-614
 - 14 **Wong HL**, Seow A, Arakawa K, Lee HP, Yu MC, Ingles SA. Vitamin D receptor start codon polymorphism and colorectal cancer risk: effect modification by dietary calcium and fat in Singapore Chinese. *Carcinogenesis* 2003; **24**: 1091-1095
 - 15 **Speer G**, Cseh K, Fuszek P, Dworak O, Vargha P, Takacs I, Nagy Z, Lakatos P. The role of estrogen receptor, vitamin D receptor and calcium receptor genotypes in the pathogenesis of colorectal cancer. *Orv Hetil* 2001; **142**: 947-951
 - 16 **Kim HS**, Newcomb PA, Ulrich CM, Keener CL, Bigler J, Farin FM, Bostick RM, Potter JD. Vitamin D receptor polymorphism and the risk of colorectal adenomas: evidence of interaction with dietary vitamin D and calcium. *Cancer Epidemiol Biomarkers Prev* 2001; **10**: 869-874
 - 17 **Peters U**, McGlynn KA, Chatterjee N, Gunter E, Garcia-Closas M, Rothman N, Sinha R. Vitamin D, calcium, and vitamin D receptor polymorphism in colorectal adenomas. *Cancer Epidemiol Biomarkers Prev* 2001; **10**: 1267-1274
 - 18 **Ye WZ**, Reis AF, Velho G. Identification of a novel Tru9 I polymorphism in the human vitamin D receptor gene. *J Hum Genet* 2000; **45**: 56-57
 - 19 **Beelman CA**, Parker R. Degradation of mRNA in eukaryotes. *Cell* 1995; **81**: 179-183
 - 20 **Gyorffy B**, Vasarhelyi B, Krikovszky D, Madacsy L, Tordai A, Tulassay T, Szabo A. Gender-specific association of vitamin D receptor polymorphism combinations with type 1 diabetes mellitus. *Eur J Endocrinol* 2002; **147**: 803-808
 - 21 **Lewis RC**, Bostick RM, Xie D, Deng Z, Wargovich MJ, Fina MF, Roufail WM, Geisinger KR. Polymorphism of the cyclin D1 gene, CCND1, and risk for incident sporadic colorectal adenomas. *Cancer Res* 2003; **63**: 8549-8553
 - 22 **O'Brien MJ**, Winawer SJ, Zauber AG, Gottlieb LS, Sternberg SS, Diaz B, Dickersin GR, Ewing S, Geller S, Kasimian D. The National Polyp Study. Patient and polyp characteristics associated with high-grade dysplasia in colorectal adenomas. *Gastroenterology* 1990; **98**: 371-379
 - 23 **Garland C**, Shekelle RB, Barrett-Connor E, Criqui MH, Ross AH, Paul O. Dietary vitamin D and calcium and risk of colorectal cancer: a 19-year prospective study in men. *Lancet* 1985; **1**: 307-309
 - 24 **Gross C**, Eccleshall TR, Malloy PJ, Villa ML, Marcus R, Feldman D. The presence of a polymorphism at the translation initiation site of the vitamin D receptor gene is associated with low bone mineral density in postmenopausal Mexican-American women. *J Bone Miner Res* 1996; **11**: 1850-1855
 - 25 **Tayeb MT**, Clark C, Haites NE, Sharp L, Murray GI, McLeod HL. Vitamin D receptor, HER-2 polymorphisms and risk of prostate cancer in men with benign prostate hyperplasia. *Saudi Med J* 2004; **25**: 447-451
 - 26 **Cheteri MB**, Stanford JL, Friedrichsen DM, Peters MA, Iwasaki L, Langlois MC, Feng Z, Ostrander EA. Vitamin D receptor gene polymorphisms and prostate cancer risk. *Prostate* 2004; **59**: 409-418
 - 27 **Huang SP**, Chou YH, Wayne Chang WS, Wu MT, Chen YY, Yu CC, Wu TT, Lee YH, Huang JK, Wu WJ, Huang CH. Association between vitamin D receptor polymorphisms and prostate cancer risk in a Taiwanese population. *Cancer Lett* 2004; **207**: 69-77
 - 28 **Ruza E**, Sotillo E, Sierrasesumaga L, Azcona C, Patino-Garcia A. Analysis of polymorphisms of the vitamin D receptor, estrogen receptor, and collagen Ialpha1 genes and their relationship with height in children with bone cancer. *J Pediatr Hematol Oncol* 2003; **25**: 780-786
 - 29 **Guy M**, Lowe LC, Bretherton-Watt D, Mansi JL, Colston KW. Approaches to evaluating the association of vitamin D receptor gene polymorphisms with breast cancer risk. *Recent Results Cancer Res* 2003; **164**: 43-54
 - 30 **Schondorf T**, Eisberg C, Wassmer G, Warm M, Becker M, Rein DT, Gohring UJ. Association of the vitamin D receptor genotype with bone metastases in breast cancer patients. *Oncology* 2003; **64**: 154-159
 - 31 **Ikuyama T**, Hamasaki T, Inatomi H, Katoh T, Muratani T, Matsumoto T. Association of vitamin D receptor gene polymorphism with renal cell carcinoma in Japanese. *Endocr J* 2002; **49**: 433-438
 - 32 **Boyapati SM**, Bostick RM, McGlynn KA, Fina MF, Roufail WM, Geisinger KR, Wargovich M, Coker A, Hebert JR. Calcium, vitamin D, and risk for colorectal adenoma: dependency on vitamin D receptor BsmI polymorphism and nonsteroidal anti-inflammatory drug use? *Cancer Epidemiol Biomarkers Prev* 2003; **12**: 631-637
 - 33 **Hutchinson PE**, Osborne JE, Lear JT, Smith AG, Bowers PW, Morris PN, Jones PW, York C, Strange RC, Fryer AA. Vitamin D receptor polymorphisms are associated with altered prognosis in patients with malignant melanoma. *Clin Cancer Res* 2000; **6**: 498-504
 - 34 **Xu Y**, Shibata A, McNeal JE, Stamey TA, Feldman D, Peehl DM. Vitamin D receptor start codon polymorphism (FokI) and prostate cancer progression. *Cancer Epidemiol Biomarkers Prev* 2003; **12**: 23-27

Effects of four regulating-intestine prescriptions on pathology and ultrastructure of colon tissue in rats with ulcerative colitis

Heng Fan, Ming-Yi Qiu, Jia-Jun Mei, Guan-Xin Shen, Song-Lin Liu, Rui Chen

Heng Fan, Rui Chen, Department of Integrated Traditional Chinese and Western Medicine, Union Hospital, Tongji Medical College, Huazhong University of Science and Technology, Wuhan 430022, Hubei Province, China

Ming-Yi Qiu, Jia-Jun Mei, Song-Lin Liu, Hubei College of Traditional Chinese Medicine, Wuhan 430061, Hubei Province, China

Guan-Xin Shen, Tongji Medical College, Huazhong University of Science and Technology, Wuhan 430022, Hubei Province, China

Supported by the Hubei Provincial Department of Education, No. 99Z014

Correspondence to: Professor Heng Fan, Department of Integrated Traditional Chinese and Western Medicine, Union Hospital, Tongji Medical College, Huazhong University of Science and Technology, Wuhan 430022, Hubei Province, China. fanheng001@hotmail.com
Telephone: +86-27-85726395

Received: 2004-07-23 Accepted: 2004-10-11

CONCLUSION: The model made with DNCB and acetic acid was successful, and FRIP had better curative effect and WMW was the best curative effect, BTW, SLBSS and TXYF were similar to SASP, and we discovered that apoptosis was possibly related to UC.

© 2005 The WJG Press and Elsevier Inc. All rights reserved.

Key words: Ulcerative colitis; TCM therapy; Experimental research; Pathology; Ultrastructure; Apoptosis

Fan H, Qiu MY, Mei JJ, Shen GX, Liu SL, Chen R. Effects of four regulating-intestine prescriptions on pathology and ultrastructure of colon tissue in rats with ulcerative colitis. *World J Gastroenterol* 2005; 11(31): 4800-4806
<http://www.wjgnet.com/1007-9327/11/4800.asp>

Abstract

AIM: To observe different histomorphologic changes of ulcerative colitis (UC) rats that were treated with four regulating-intestine prescriptions (FRIP), to investigate the curative effects of FRIP and to analyze their treatment mechanism.

METHODS: The UC rat model was made by the method of 2,4-dinitro chloro benzene (DNCB) immunity and acetic acid local enema. Ninety-eight SD rats were randomly divided into seven groups, namely, the normal control group, model group, salicylazosulfapyridine (SASP) group, Wumeiwan (WMW) group, Baitouwengtang (BTWT) group, Senglingbaishusan (SLBSS) group, and Tongxieyaofang (TXYF) group. Each group had 14 rats (with equal ratio of male and female). The six animal model groups of UC -SASP, TXYF, WMW, BTWT, SLBSS, TXYF-were treated by distilled water except the normal control group. Changes of the rat's general conditions after treatment were respectively observed, the colon tissue damage scores were given out, the pathology of colonic mucosa and changes of ultrastructure were analyzed.

RESULTS: Different pathological changes on histology were shown after treatment by FRIP. The colon tissue damage score in model group was higher than that of FRIP groups and SASP group ($q = 4.59, 4.77, P < 0.05$ or $q = 5.48, 6.25, 5.97, P < 0.01$). The scores of WMW group, BTWT group and SLBSS group were lower than that of SASP ($q = 4.13, P < 0.05$ or $q = 5.31, 5.12, P < 0.01$). There was no remarkable difference between the damage score of TXYF group and SASP group ($q = 3.75, P > 0.05$). In addition, some apoptosis cells were found in the pathologic control group.

INTRODUCTION

Ulcerative colitis (UC) is a non-specific inflammatory intestinal disease. The pathogenesis of UC is affected by a variety of factors, but its pathogenesis is still unknown at present^[1]. A rat model of UC was established by the methods of DNCB immunity and acetic acid local enema. This subject is about the treatment effect of four regulating-intestine prescriptions (FRIP) by making rat model of UC, especially they were observed by scoring the gross morphologic damage and the change on the pathological section of colon tissue under light and electron microscope by treating with traditional Chinese medicine (TCM), and compared the different curative effect of Wumeiwan (WMW) group, Baitouwengtang (BTWT) group, Senglingbaishusan (SLBSS) group and Tongxieyaofang (TXYF) group.

MATERIALS AND METHODS

Materials

Herbs in FRIP (WMW, BTWT, SLBSS, TXYF) and their quantity are as follows: WMW: 16 g dark plum, 6 g asarum herb, 10 g dried ginger, 16 g Chinese goldthread, 4 g Chinese angelica root, 6 g aconite root, 4 g pricklyash peel, 6 g cassia twig, 6 g sun-dried ginseng, 6 g bark of cork tree; BTWT: 30 g Chinese pulsatilla root, 24 g bark of amur corktree, 10 g Chinese goldthread, 24 g ash bark; SLBSS: 10 g pulp of lotus seed, 10 g coix seed, 10 g dried amomum fruit, 10 g balloon flower root, 15 g bean of white hyacinth, 20 g white Tuckahoe, 20 g sun-dried ginseng, 20 g licorice root, 20 g big head atractylodes rhizome, 20 g Chinese yam; TXYF:

30 g parched white atractylodes rhizome, 20 g white peony root, 15 g dried old orange peel, 20 g ledebouriella root.

Salicylazosulfapyridine (SASP) with batch no. 200111002 is produced by Shanghai Sanwei Pharmaceutical Company (250 mg/tablet).

TNF- α ISH detection kit, ISH special cover glass, DBA chromogenic kit, poly-L-lysine, DEPC and 20% glycerin were supplied by Wuhan Boster Biological Technology Co., Ltd.

Transmission electron microscope (Hitachi H-600), photomicroscope (Japan), ultramicrotome (LKB-V), magnifier and microscope, *etc.*, were used.

Ninety-eight SD rats (male rats and female rats separately account for 50% and a rat weighed 300 ± 50 g) were supplied by Test Animal Center of Tongji Medical School, Huazhong University of Science and Technology. They were raised in the SPF environment (constant temperature, humidity and sterilized water, food and padding) and acclimatized to the surrounding for 7 d before the experiments.

Methods

Animal groups Ninety-eight SD rats (male rats and female rats separately account for 50%) were randomly divided into seven groups as males and females, and each group contained 14 rats (male rats and female rats separately account for 50%), of which group 7 was normal group. Groups 1-6 were modeled, which were respectively WMW group, BTWT group, SLBSS group, TXYF group, SASP group, and model group. Body weight of rats in each group showed no significant difference on statistics ($P > 0.05$).

Preparation of the animal model Model of UC rat was established with 2,4-dinitro chloro benzene (DNCB) immunity and acetic acid local enema^[1-5]. After hair on the rats' nape was removed with Na₂S of 100 g/L, 0.25 mL acetone solution with DNCB content of 20 g/L (five drops) was dripped on the rats' back once a day and continuously dripped for 14 d. On the 15th d, a ϕ 3-mm urinary catheter was put into at 8 mm of a rat's colon via its anus to fill 0.25 mL ethanol containing 0.1% DNCB. On the 16th d, 2 mL 8% acetate solution was filled in the same position. After accurately timing for 10 s, this position was flushed with 5 mL physiological saline. After that, they were fed for 2 wk, to continue observing the rats' stool characters, dietetics, hair and activity conditions, *etc.*, every day. It could be seen from observation that the rats gradually produced typical symptom of UC active period. After 30 d, the modeling was finished. After modeling was finished (after the 30th d), two rats were randomly taken in each group and their colons were examined after they were killed to pathologically confirm a series of changes occurring in their colons such as hyperemia, hydrops, inflamed cellular infiltration, crypt abscess, fewer goblet cells, body of gland destroyed and apthous formed.

Means for drugs For each rat in WMW group, BTWT group, SLBSS group, TXYF group, gastric lavage was conducted respectively with 3 mL prepared WMW liquid (0.515 g/mL), BTWT liquid (0.562 g/mL), SLBSS liquid (0.987 g/mL) and TXYF liquid (0.216 g/mL) once a day. For each rat in SASP group, gastric lavage was conducted with 3 mL SASP suspension (0.026 g/mL) liquid once a

week. For each rat in model control group and normal group, gastric lavage was conducted with 3 mL distilled water. The drug feeding period was 15 d.

Collection and treatment of specimens After the feeding of drugs in all groups of rats ended, they were weighed and killed by the mode of cutting off their heads. After that, they were immediately dissected to take 6-8 mm colons upward at 2 mm of the anus. The intestine cavities were opened along the longitudinal axis of the intestinal mucosa and cleaned thoroughly with 0.9% saline and pure water, and assigned a code number. Then they were spread on the wax plate with the intestinal mucosa pointing upward. After they were fastened with the pins, occurring conditions of inflammation and ulcer were observed with a dissecting microscope. The colon was immediately examined under a stereomicroscope and any visible damage was scored on a 0-5 scale (Table 1).

Table 1 Criteria for scoring the gross morphologic damage of colon tissue^[6-9]

Score	Gross morphology
0	No damage
1	Localized hyperemia with no ulcers
2	Linear ulcers with no significant inflammation
3	Linear ulcers with inflammation at one site
4	More site of ulcers and inflammation, the size of ulcers <1 cm
5	Multiple inflammation and ulcers, the size of ulcers ≥ 1 cm

After modeling was finished (30 d), two rats were randomly selected from each group and killed by the mode of cutting off their heads to take part of the intestine tissues, which were immobilized with 40 g/L formaldehyde, embedded with paraffin, pathological section was taken and HE staining was performed. And then, colon conditions after modeling were observed and investigated.

After ending of the above tests (45 d), a small piece of colon tissue (3 mm) was taken from the colon of each rat. They were immobilized with 40 g/L formaldehyde (grouped and numbered with the penicillin bottles), embedded with paraffin, pathological section was taken and HE staining was performed. And then, pathological changes in each group of colons were observed (the above work was finished with the help of Pathology Department of Hubei Hospital of Traditional Chinese Medicine).

A rat was randomly selected in each group and the above procedures were executed until cleaning procedure. The colonic mucosa with ulcer was taken immediately and cut into 1-mm bits, which was immobilized with 2.5% glutaraldehyde, washed with 1% paraformaldehyde and immobilized after it was put in 1% osmic acid. Then, they were dehydrated in steps with ethanol and acetone, embedded with vegetable wax, cut into super-thin sections and doubly stained with uranium acetate and lead nitrate. After that, they were observed with a transmission electron microscope (finished with the help of Electron Microscope Department of Medical School of Wuhan University).

Statistical analysis

The weights of rats and tissue damage scores were expressed

as mean±SD, and analyzed with the Student's *t*-test or *F* test (*q* test).

RESULTS

Changes of symptoms and signs

The study of the rats in the model had symptoms of mucous thin stool after about 2 wk and worsened gradually. After about 4 wk, the symptoms were more serious and some symptoms such as pus and blood stool, thinner, less weight, hair having no gloss, significantly less appetite, intolerance of cold and action and less movement occurred. After gastric lavage was conducted with FRIP and SASP, their symptoms were improved differently (no statistical analysis except for weights). Weight changes are shown in Table 2.

Table 2 Effect on weights in rats of FRIP (mean±SD)

Group	Case (n)	Weights (g)
Normal control group	12	352.5±20.7 ^b
Model group	10	307.8±15.3 ^d
SASP group	9	321.5±18.7 ^{a,d}
WMW group	11	340.3±16.8 ^{b,c}
BTWT group	10	331.4±13.8 ^{b,d}
SLBSS group	9	325.6±18.4 ^{a,d}
TXYF group	10	328.7±10.5 ^{a,d}

^a*P*<0.05, ^b*P*<0.01 vs model group; ^c*P*<0.05, ^d*P*<0.01 vs normal control group.

Visual observing results of colonic mucosal damage

The degree of colonic mucosal damage in rats of FRIP was scored according to the criteria in Table 1. The colon tissue damage score in model group was higher than that of FRIP groups and SASP group (*P*<0.05 or *P*<0.01). The scores of WMW group, BTWT group, and SLBSS group was lower than that of SASP (*P*<0.05 or *P*<0.01). There was no remarkable difference between the damage score of TXYF group and SASP group (*P*>0.05). The scores were roughly given out according to the inflammation and injury level, observation results of which are shown in Table 3.

Table 3 Scoring the gross morphologic damage of colon tissue in rats of FRIP (mean±SD)

Group	Case (n)	Scoring the gross morphologic damage
Normal control group	12	0 ^b
Model group	10	5.5±0.45
SASP group	9	3.8±0.39 ^a
WMW group	11	1.8±0.34 ^{b,d}
BTWT group	10	2.5±0.38 ^{b,d}
SLBSS group	9	1.9±0.35 ^{b,c}
TXYF group	10	3.7±0.47 ^a

^a*P*<0.05, ^b*P*<0.01 vs model group; ^c*P*<0.05, ^d*P*<0.01 vs SASP group.

Observation results of pathological sections (HE dye)

Normal control group: The colonic mucosa of rats was in good condition without inflammatory cell infiltration or ulceration of mucosa; the epithelial mucosae was intact and continuous; the bodies of gland arranged regularly with clear

structure and active secreting function; the epithelial mucosae, the blood vessel in the membrana propria and fibers were normal; muscularis had no abnormal conditions. Model group: The colonic mucosa of the rats showed erosion and ulcers; the most of mucosa produced coloboma and some produced deep and large erosions, mucous gland bodies were destroyed; remaining mucosa was hyperemic and dropsical and formed polyp-like appearance (false polyp) due to hyperplasia; a lot of inflammatory cells (lymphocytes, plasma cells, and macrophages) infiltrated; some cells were scattered and were in multiplication conditions (more plasma, large nucleus, and sparse chromatin); mucous layer became thinner and the lamina propria beneath the mucosa showed local hyperemia, dropsy, and fiber hyperplasia. SASP group: The epithelial mucosae of the rat colon produced the local defects; the bodies of gland arranged less regularly with slight hyperemia beneath the mucosa and more inflammatory cells infiltrated. WMW group: The epithelial mucosae of the rat was basically sound; the bodies of gland arranged more regularly without significant hyperemia beneath the mucosa; a few inflammatory cells infiltrated. BTWT group: The epithelial mucosae of the rat was basically sound; the bodies of gland arranged more regularly without significant hyperemia beneath the mucosa; and inflammatory cell infiltration could be seen. SLBSS group: The epithelial mucosae of the rat was basically sound; the bodies of gland arranged more regularly without significant hyperemia beneath the mucosa; and a few inflammatory cell infiltration could be seen. TXYF group: The epithelial mucosae of the rat was less sound; the bodies of gland arranged less regularly with significant hyperemia beneath the mucosa; and inflammatory cell infiltration could be seen (Figures 1A-H).

Observation results of ultrastructure

Normal control group: The microvilli on the surface of the mucosal epithelium of the rat colon was integral with neat arrangement, identical sizes, and regular mitochondrion shape and showed approximate roundness and ellipse, inner matrixes of which were of medium density; endoplasmic reticulum and nucleus were all up to snuff; epithelia linked tightly; space between cells was found to be wider (normal linking); the intestine gland was composed of the goblet cells. Model group: The microvilli on the surface of the mucosal epithelium of the rat colon were sparse, became shorter and irregularly curled with visible vacuoles, even epithelium cell membrane produced defects; organelles became fewer; cytoplasm liquefied and dissolved; inner matrixes in the mitochondria were clear with fewer inner cristae and significant swelling; endoplasmic reticulum expanded; chromatic agglutination and pyknosis could be seen; nucleoplasm proportion became less, some congregated beneath karyolemma and showed goblet with clear boundaries, even apoptosis corpusculum, karyo-pyknosis, and lymphocyte infiltration could be seen. SASP group: The microvilli on the surface of the mucosal epithelium of the rat colon partly dropped off and became less regular; mitochondria shape became less regular and some were with slight swelling with destroyed cytoarchitecture; fat particles and endoplasmic reticulum expanding could be seen. WMW group: The microvilli on the surface of the mucosal

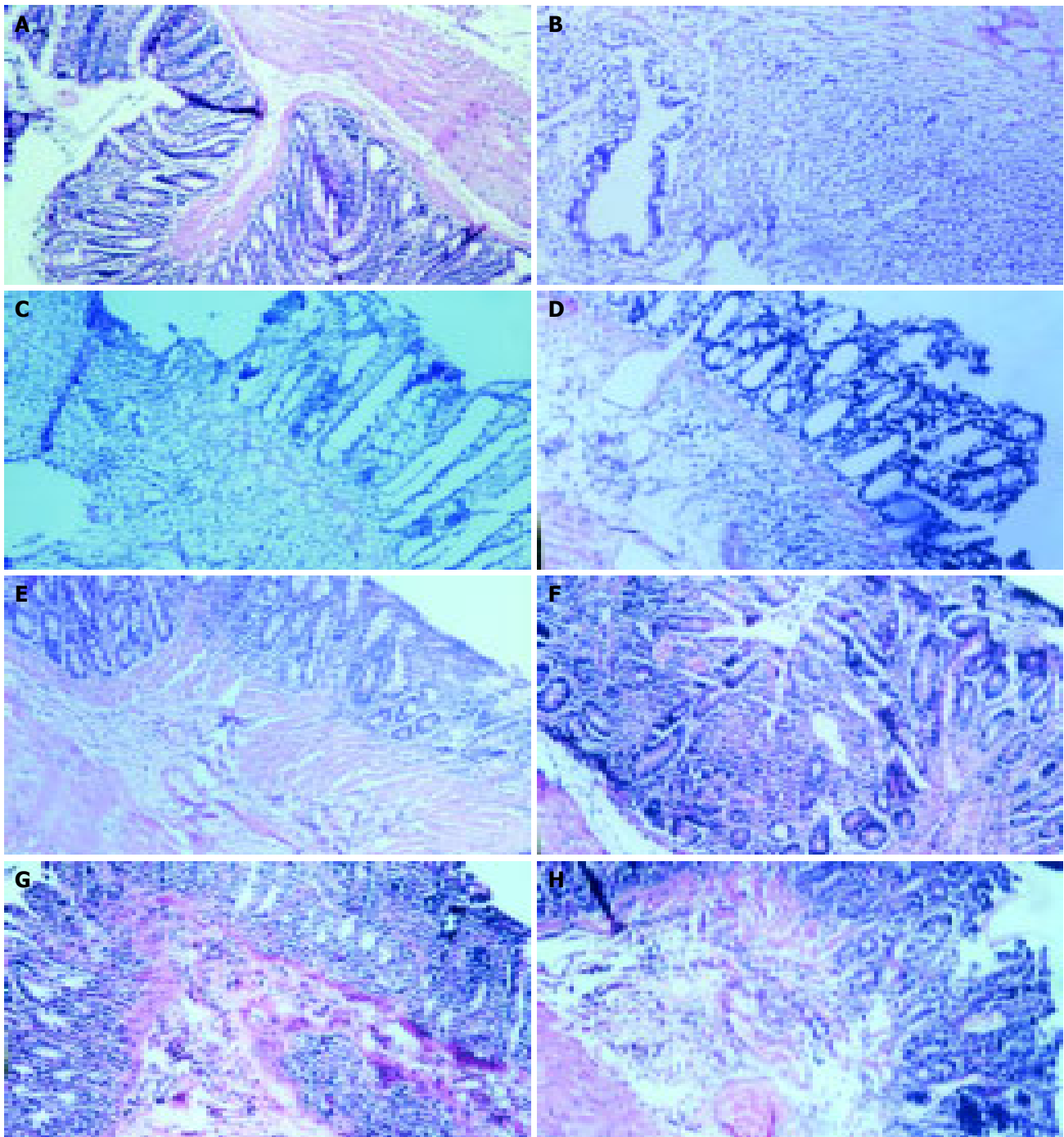


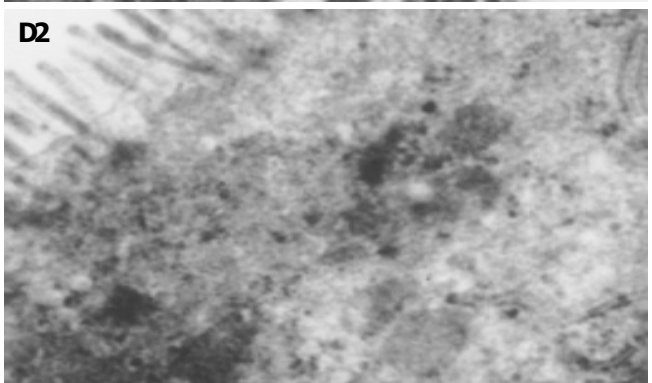
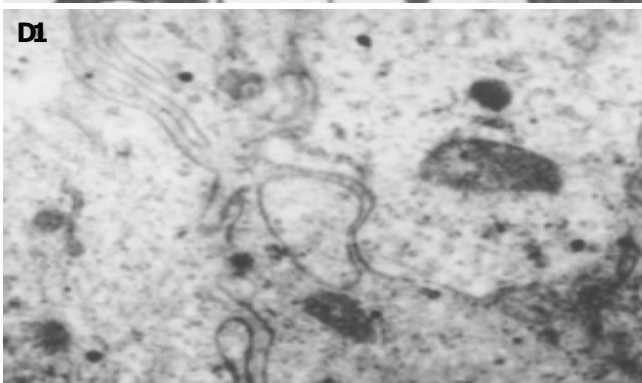
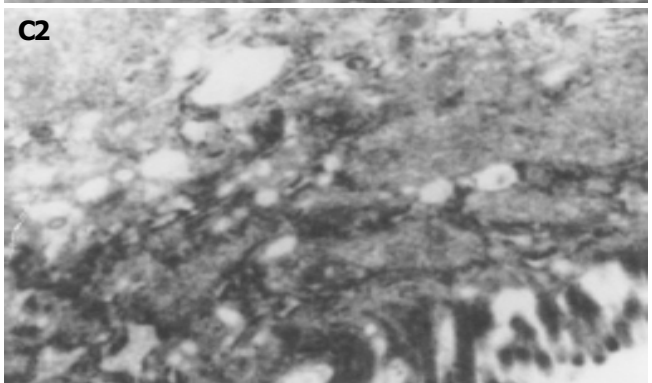
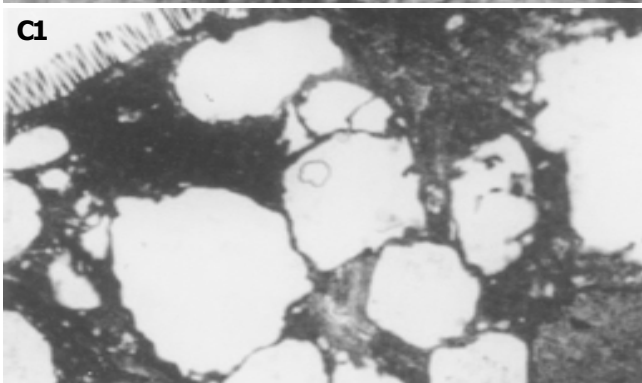
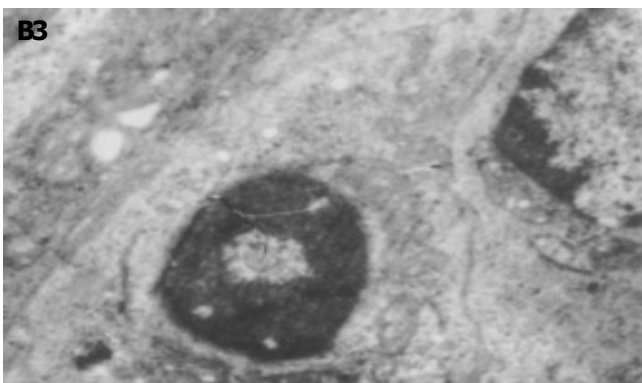
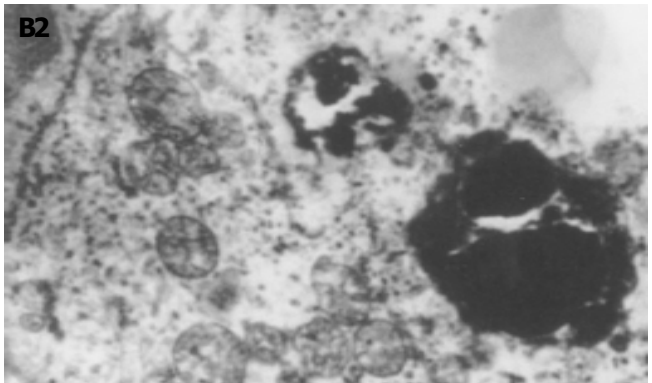
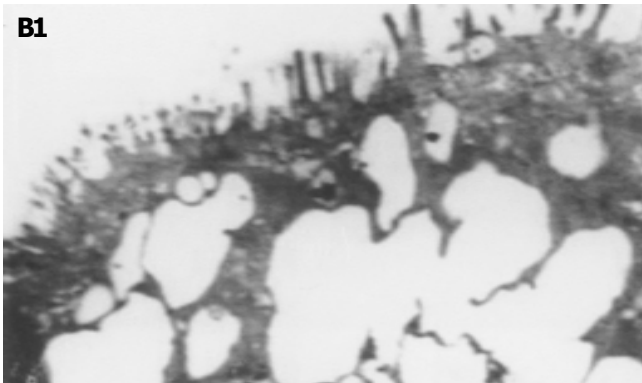
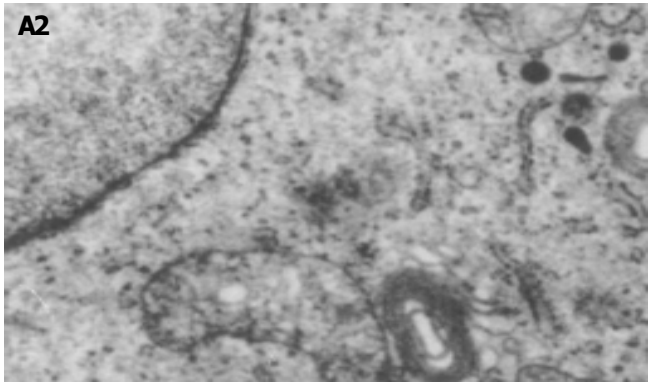
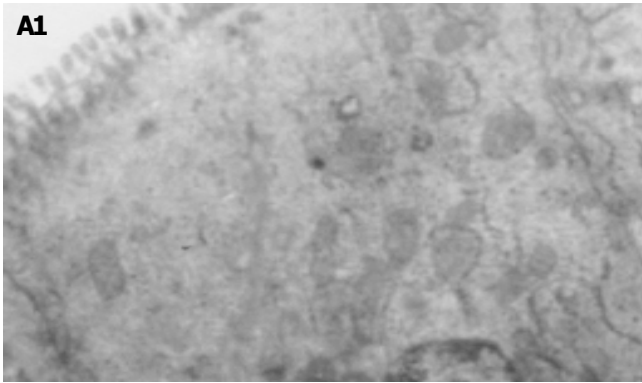
Figure 1 Pathology of colon tissue in rats. **A:** normal control group; **B** and **C:** model group; **D:** SASP group; **E:** WMW group; **F:** BTWT group; **G:** SLBSS

group; **H:** TXYF group (HE $\times 200$).

epithelium of the rat colon were basically intact with normal cytoarchitecture; after observing under the electron microscope ($\times 12\,000$), it could be found that their endoplasmic reticulum and mitochondria were clearer, and the organelles such as mitochondria and elder with cytorcytes could be seen with clear cytoarchitecture as well as dropping-off of the microvilli could be seen. BTWT group: The microvilli on the surface of the mucosal epithelium of the rat colon was basically regular and intact; mitochondria in the cytoplasm was abundant with regular mitochondria and showed approximate roundness or ellipse; the matrixes were basically even. SLBSS group: The microvilli on the surface of the mucosal epithelium

of the rat colon were less irregular and a few microvilli dropped off; mitochondria were swelling with normal cytoarchitecture. TXYF group: More microvilli on the surface of the mucosal epithelium of the rat colon dropped off or they were sparse and expanding; staining of nucleus was a little dark; destroyed cytoarchitecture and wider chromatin margin could be seen; cellular nucleus became smaller (Figures 2A-G).

The results of pathological sections under electron microscope showed that UC was related to apoptosis and the curative effect of WMW was better than that of the other groups and SASP groups.



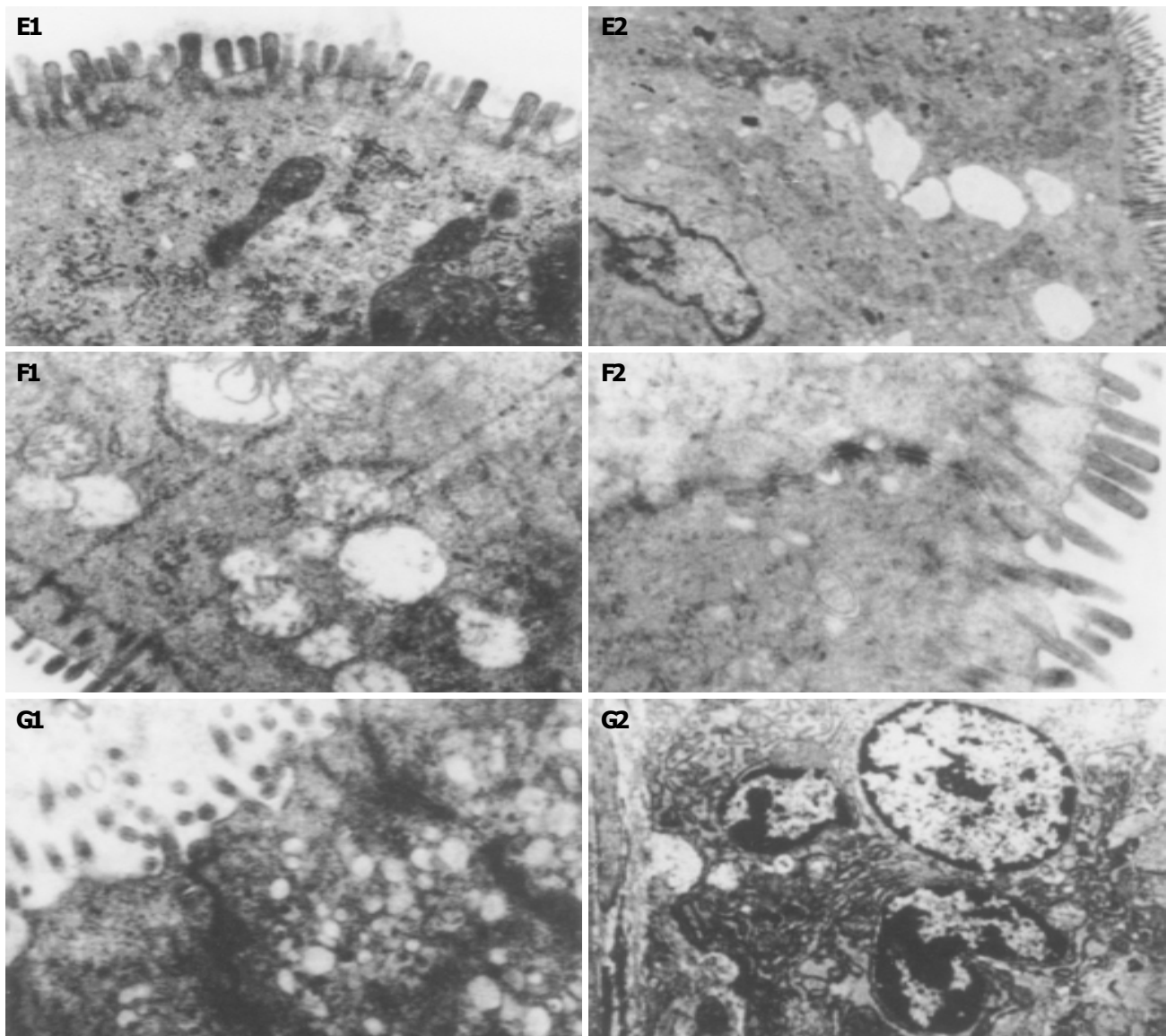


Figure 2 Ultrastructure of colon tissue in rats. **A:** Normal control group, A1 ($\times 10\,000$), A2 ($\times 17\,000$); **B:** model group, B1 ($\times 8\,000$), B2 ($\times 12\,000$), B3 ($\times 10\,000$), B4 ($\times 10\,000$); **C:** SASP group, C1 ($\times 5\,000$), C2 ($\times 17\,000$); **D:**

WMW group, D1 ($\times 12\,000$), D2 ($\times 17\,000$); **E:** BTWT group, E1 ($\times 17\,000$), E2 ($\times 5\,000$); **F:** SLBSS group, F1 ($\times 10\,000$), F2 ($\times 200\,000$); **G:** TXFY group, G1 ($\times 17\,000$), G2 ($\times 17\,000$).

DISCUSSION

Normal colonic tissue consists of mucous membrane layer (including epidermis layer, lamina propria, muscular layer of mucous membrane), mucous membrane substrate layer, muscular layer (inner ring and outer race), chorion layer and so on. Pathological changes of UC affects mucous membrane and substrate layer. The best characteristic changes of histology included diffuse and severe inflammatory cell infiltration in all layers of inhesion membrane, serious and comprehensive mucous configuration abnormality, crypt lymph in recess (namely crypt abscess), inhesion membrane with a great number of plasma cells, lymphocyte, mononuclear cells, neutrophils and eosinophils infiltration. Because of inflammatory irritation, there were epithelial hyperplasia of gland, which were shown as goblet cells and mucilage in the body of the gland reduced but nucleus expanded and nuclear fusion increased in various extents. Cytoplasm had a liking for alkalinescence; epithelial hyperplasia of gland sometime

became false compound. Further observation showed that the capillary vessel dilatation caused congestion and blood vessel swelling further. In a serious case, the inflammation could develop into the mucous membrane substrate layer, even perforation, which broke to form the pilosity granular light ulcer or merged into various sizes and shapes to become irregular ulcer. Serious cases had large range of mucous membrane peeling. More normal mucous membrane between the ulcer turn into prowling form (there are boundary between sick mucous membrane and normal mucous membrane), taking on hydronics and polyp (false polyp), so the mucous membrane took the form of particle coarsely, the blood vessels were so fuzzy and fragile that they were apt to bleed with purulence secretion when touched. But there was seldom involvement of the deep layer of intestine wall, so the incrassation and fibrosis intestine wall were not remarkable, but few breaking out types and poisoning type colon cases come out of a hole because of

piercing through intestine wall.

In recent years, many studies to the change of colonic mucus were carried out. It was suggested that it might be the prodromal change of carcinoma of large intestine. As we all know, UC is a pre-cancerous lesion of colon carcinoma. The mucosa in this region also showed certain histologic characteristics: the goblet cells in the glandular body decreased remarkably or disappeared with appearance of simple columnar cells, which lack mucin secretion. The lumen of some mucosal glands became dilated, branched or irregularly arranged. We found that the important characteristic of UC was inflammation in this experiment and cell apoptosis under electron microscope. We also found that the presentation was hyperemia and edema with a great number of plasma cells, lymphocytes, mononuclear cells, neutrophils, and eosinophils infiltration^[10-12], the characteristic that pathology changes and ultrastructure was different in all groups was associated with the treatment.

This model made with DNCB and acetic acid was successful by the changes of symptoms and signs, damage scores of the colonic mucosa and the pathology sections and ultrastructure of colon tissue. At the same time, their symptoms and signs and pathology differently improved after treatment (not statistically significant, $P > 0.05$). In this study, we discovered that FRIP had better curative effect on UC and WMWs was the best, BTWs and SLBSSs were the second of best. TXYFs were worst (they were as same as SASPs). At the same time, this implies, that we must have BianzhengLunzhi in the treatment of UC^[13]. According to TCM, UC belongs to the category of "Xiouxili" (diarrhea), the mucosal inflammatory lesions result from not only deficiency and hypofunction of spleen and stomach, but also accumulation of damp heat, the pathogenesis of UC is similar with the prescription characteristic of WMW. Therefore, in this study, the best curative effect was achieved by the treatment of the WMW. The results showed that this WMW had the function of strengthening the spleen and reinforcing Qi and eliminating damp-heat pathogen, promoting flow of Qi and blood, improving luminal blood circulation, and was helpful for hemostasis and the absorption of inflammatory products, eventually attained the goal of the neogenesis of granulated tissue in the region of ulceration, and the repair of mucosal epithelium. But BTW concentrated on eliminating damp-heat pathogen, SLBSS was good at strengthening the spleen and reinforcing Qi, the former had the function of reducing the excess, the latter had the function of reinforcing the deficiency, so two

formulae of BTW and SLBSS had some therapeutic effects, and they were the second curative effect; the prescription characteristic of TXYF, which had the function of smoothing the liver-Qi to normalize the stomach, was different with the pathogenesis of UC and it had the worst curative effect.

In addition, we discovered that apoptosis was possibly related to UC^[13] and FRIP could decrease apoptosis, block inflammation and induce remission.

REFERENCES

- 1 **Bicks RO**, Rosenberg EW. A chronic delayed hypersensitivity reaction in the guinea pig colon. *Gastroenterology* 1964; **46**: 543-549
- 2 **Li Y**. Methods on making rat experiment model of ulcerative colitis. *New Drugs TCM Clinical Pharmacol* 1999; **10**: 120-122
- 3 **Jiang XL**, Quan QZ, Wang D, Sun ZQ, Wang YJ. A new ulcerative colitis model induced by compound method and the change of immunity and ultrastructures. *Shijie Huaren Xiaohua Zazhi* 1999; **7**: 381
- 4 **Jiang XL**, Quan QZ, Wang D, Sun ZQ, Wang YJ, Qi F. Effect of heartleaf houttuynia herb on colonic pressure in rats with ulcerative colitis. *Shijie Huaren Xiaohua Zazhi* 1999; **7**: 786
- 5 **Fan H**, Qiu MY. Evaluating on making rat experiment model of ulcerative colitis. *Chinese Archives Traditional Chinese Med* 2004; **22**: 865-866
- 6 **Wallace JL**, Keenan CM. An orally active inhibitor of Leukotriene synthesis accelerates healing in a rat model of colitis. *Am J Physiol* 1990; **258**(4 Pt 1): G527-534
- 7 **Zheng HB**, Hu HY, Lu X, Ma GT. Morphological observation of intestine-clearing suppository in preventing and treating rats, ulcerative colitis. *J Zhejiang College TCM* 2001; **25**: 47-51
- 8 **Morris GP**, Beck PL, Herridge MS, Depew WT, Szewczuk MR, Wallace JL. Hapten-induced model of chronic inflammation and ulceration in the rat colon. *Gastroenterology* 1989; **96**: 795-803
- 9 **Padol I**, Huang JQ, Hogaboam CM, Hunt RH. Therapeutic effects of the endothelin receptor antagonist Ro 48-5695 in the TNBS/DNBS rat model of colitis. *Eur J Gastroenterol Hepatol* 2001; **12**: 257-265
- 10 **Tjandra K**, Le T, Swain MG. Experimental colitis attenuates development of toxin-induced cholangitis in rats. *Dig Dis Sci* 2002; **47**: 1216-1223
- 11 **Ji XL**, Shen MS, Yin W. Key of Pathological Diagnosis on ulcerative colitis and colon disease. *J Diag Pathol* 2002; **9**: 245-247
- 12 **Nosalova V**, Cerna S, Schunack W, Grandi D, Coruzzi G. Effects of (R) alpha-methylhistamine on experimental colitis. *Inflamm Res* 2001; **50**(Suppl 2): S108-109
- 13 **Fan H**, Qiu MY, Mei JJ, Shen GX, Liu SL. Effect of Lichangshifang on cellular apoptosis and expression of the related regulatory genes in rats with ulcerative colitis. *Shijie Huaren Xiaohua Zazhi* 2004; **12**: 1119-1124

Screening and identification of proteins interacting with nucleostemin

Hai-Xia Yang, Geng-Lin Jin, Ling Meng, Jian-Zhi Zhang, Wen-Bin Liu, Cheng-Chao Shou

Hai-Xia Yang, Geng-Lin Jin, Ling Meng, Jian-Zhi Zhang, Wen-Bin Liu, Cheng-Chao Shou, Department of Biochemistry and Molecular Biology, Peking University School of Oncology and Beijing Institute for Cancer Research, Beijing 100034, China
Supported by the National High Technology Research and Development Program of China, No. 200BA711A11A06 and Beijing Science and Technology Project, No. H020220020310
Correspondence to: Dr. Cheng-Chao Shou, Department of Biochemistry and Molecular Biology, Peking University School of Oncology and Beijing Institute for Cancer Research, Beijing 100034, China. cshou@vip.sina.com
Telephone: +86-10-66160960 Fax: +86-10-66175832
Received: 2004-12-25 Accepted: 2005-01-26

Abstract

AIM: To identify the proteins interacting with nucleostemin (NS), thereby gaining an insight into the function of NS.

METHODS: Yeast two-hybrid assay was performed to screen a human placenta cDNA library with the full length of NS as a bait. X-Gal assay and β -galactosidase filter assay were subsequently conducted to check the positive clones and the gene was identified by DNA sequencing. To further confirm the interaction of two proteins, the DNA fragment coding NS and the DNA fragment isolated from the positive clone were inserted into the mammalian expression vector pcDNA3 and pcDNA3-myc, respectively. Then, two plasmids were cotransfected into the COS-7 cells by DEAE-dextran. The total protein from the cotransfected cells was extracted and coimmunoprecipitation and Western blot were performed with suitable antibodies sequentially.

RESULTS: Two positive clones that interacted with NS were obtained from human placenta cDNA library. One was an alpha isoform of human protein phosphatase 2 regulatory subunit B (B56) (PPP2R5A) and the other was a novel gene being highly homologous to the gene associated with spondylo paralysis. The co-immunoprecipitation also showed that NS specifically interacted with PPP2R5A.

CONCLUSION: NS and PPP2R5A interact in yeast and mammalian cells, respectively, which is helpful for addressing the function of NS in cancer development and progression.

© 2005 The WJG Press and Elsevier Inc. All rights reserved.

Key words: Nucleostemin; Yeast two-hybrid; Co-IP

Yang HX, Jin GL, Meng L, Zhang JZ, Liu WB, Shou CC. Screening and identification of proteins interacting with nucleostemin. *World J Gastroenterol* 2005; 11(31): 4812-4814
<http://www.wjgnet.com/1007-9327/11/4812.asp>

INTRODUCTION

There is evidence that cancer originates from cancerous stem cells^[1-7]. Nucleostemin (NS) is a novel protein found in the nucleoli of CNS stem cells, embryonic stem cells, and several cancer cell lines, and plays a critical role in controlling the proliferation of stem cells and some cancer cells^[7]. NS contains a N-terminal basic domain and two GTP-binding motifs. Mutation analysis indicates that excessive NS, particularly mutant NS that lacks the GTP-regulatory domain, prevents cells from mitosis and causes apoptosis in a p53-dependent manner. The N-terminal basic domain specifies nucleolus localization, p53 interaction, and is required for cell death caused by NS overexpression. To investigate the function of NS in cancer development and progression, yeast two-hybrid assay was used to screen the proteins associated with NS from a human placenta cDNA library, and the interaction between the alpha isoform of human protein phosphatase 2 regulatory subunit B (B56) known as PPP2R5A and NS was identified in yeast and COS-7 cells, thus providing new clues to the functional study of NS as well as related proteins.

MATERIALS AND METHODS

Cell culture and reagents

Monkey *Cercopithecus Aethiops* COS-7 cells provided by American Type Culture Collection (Manassas, VA, USA) were cultured in Dulbecco's modified Eagle's medium (Invitrogen Corporation, Carlsbad, CA, USA) supplemented with 10% fetal bovine serum (Sigma Chemical Co., St. Louis, MO, USA), and maintained in a humidified chamber with 50 mL/L CO₂ at 37 °C.

Plasmid pGBKT7, matchmaker 3 pretransformed human placenta cDNA library, X-Gal and all other yeast two-hybrid components were purchased from Clontech. Various restriction endonucleases were products of New England Biolabs. T4 DNA ligase was purchased from Promega. The kits for PCR and purification reagents of PCR products were obtained from Qiagen. Antibody against NS or c-myc tag and other reagents were all kept in our laboratory.

Plasmid construction

The full length of NS cDNA was cut by *Bam*HI and *Xba*I restriction endonucleases from pcDNA3-NS, then inserted into the downstream of the Gal4 DNA-binding domain of the bait vector pGBKT7 (Clontech Laboratories) with T4 DNA ligase. The recombinant vector pGBKT7-NS was sequenced and NS protein was in the reading frame. The expression of NS fusion protein with yeast Gal4 DNA-binding domain was checked by Western blot with antibody against NS.

To construct the eukaryotic vector expressing the protein

of the positive clone, DNA of the positive clone was digested by restriction endonucleases *Bam*HI and *Xho*I, and the DNA fragment was inserted into the pCDNA-myc vector.

Screening of clones interacted with NS

The experiments were carried out according to the protocols described in the MATCHMAKER Libraries User Manual (PT3042-1)^[8-11]. Briefly, the pGBKT7-NS plasmid was initially introduced into the AH109 yeast strains using a modified lithium acetate protocol and the transformed clones were selected on SD/-Trp plates. The mating between the selected AH109 and human placenta cDNA library was performed and co-transformed clones were selected on SD/-Leu-Trp-His plates and SD/-Leu-Trp-His-Ade pulsing 3AT (DO) plates with X-Gal to detect the transcription of reporter genes (HIS, LEU, TRP, and ADE). Colonies growing at 30 °C and having turned into blue in 8 h were selected as positive clones. Plasmid DNA from the single positive clones was extracted and sequenced with the primer provided with the kit. The clone was identified by DNA sequence and compared with GenBank. To further exclude the false positives, plasmid was transformed into yeast strain AH109 to rule out its self-activation.

In order to further confirm the positive clones in yeast system, experiments were performed in AH109 yeast strain to detect the transcription of LacZ reporter gene according to the protocols. Colony-lift filter assay was used to check the activity of β-galactosidase. Briefly, fresh colonies growing to about 1-3 mm in diameter were transferred completely to a sterile filter and submerged in liquid nitrogen for 10 s and thawed at room temperature, then put on a pre-soaked filter with Z buffer (Na₂HPO₄·7H₂O 16.1 g/L, NaH₂PO₄·H₂O 5.50 g/L, KCl 0.75 g/L, and MgSO₄·H₂O 0.246 g/L, pH 7.0) containing 0.27 mL β-mercaptoethanol and 1.67 mL X-Gal stock solution (20 mg/mL) in 100 mL volume. The filters were incubated at 30 °C and the colors of colonies were checked periodically.

Co-immunoprecipitation

When COS-7 cells reached 50-70% confluence on the dish, the plasmids expressing NS and interacted protein of NS were cotransfected into COS-7 cells with DEAE-dextran as described^[12], and total plasmid DNA was 8 μg/100 mm/dish. After 48 h, the cells were washed with PBS, then scraped and collected by spinning down. The cell pellet was lysed in 0.5 mL HEDL buffer (50 mmol/L HEPES pH 8.0, 150 mmol/L NaCl, 2 mmol/L EDTA, 1% Triton X-100, 10 mmol/L MgCl₂, 1 mmol/L Na₃VO₄, 25 mmol/L NaF, 1 mmol/L PMSF) and shaken for 2 h at 4 °C, centrifuged at 12 000 *g* for 15 min at 4 °C. The resulting supernatants were immunoprecipitated with various antibodies (mouse anti-c-myc, mouse anti-nucleostemin and mouse non-specific antibodies) respectively as described^[12]. SDS-PAGE and Western blot were performed with suitable antibodies and the signal was detected with ECL (Pulilai Co.).

RESULTS

Plasmids construction

The constructed plasmid pGBKT7-NS was identified by

restriction endonucleases *Bam*HI/*Xho*I and DNA sequence analysis. As shown in Figure 1A, there was an expected DNA band about 1.7 kb released from the digested plasmid pGBKT7-NS and the DNA sequence was completely identical with NS in GenBank. Western blot showed that the NS protein fused with yeast Gal4 DNA-binding domain was expressed in yeast (Figure 1B). The recombinant plasmids PPP2R5A/pCDNA3-myc and pCDNA3-NS were identified by restriction endonucleases *Bam*HI/*Xho*I and DNA sequencing, respectively (Figure 2). As shown in Figure 3, there was an expected band about 2.3 or 1.7 kb released from the digested plasmid and the DNA sequence was completely identical with PPP2R5A or NS in GenBank.

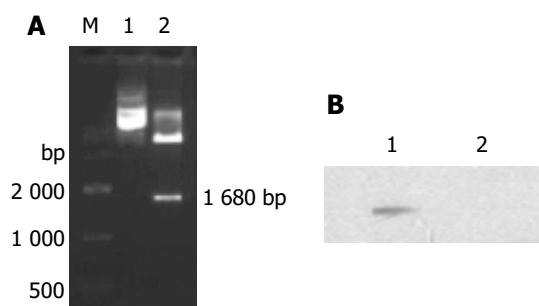


Figure 1 Identification of the recombinant clone of NS and its expression in yeast cell. **A:** Analysis of pGBKT7-NS with restriction enzyme digestion. M: DNA markers; lane 1: undigested pGBKT7-NS; lane 2: digestion of pGBKT7-NS with *Bam*HI/*Xho*I and 1 680-bp fragment was released; **B:** Western blotting analysis of NS expression by pGBKT7-NS in yeast. Total protein from yeast AH109 transferred with pGBKT7-NS was subjected to Western blot and the NS mAb was used to detect the NS protein. Lane 1: total proteins from pGBKT7-NS transferred AH109; lane 2: total proteins from pGBKT7 transferred AH109.

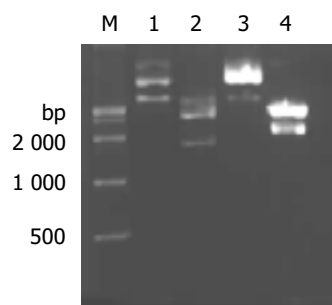


Figure 2 Restriction enzyme analysis of recombinant pcDNA₃-NS and pcDNA₃-myc-PPP2R5A. M: DNA markers; lane 1: undigested pcDNA₃-NS; lane 2: digestion of pcDNA₃-NS by *Bam*HI/*Xho*I and 1 680-bp fragment was released; lane 3: undigested pcDNA₃-myc-PPP2R5A; lane 4: digestion of pcDNA₃-myc-PPP2R5A with *Bam*HI/*Xho*I and 2 300 bp fragment was released.

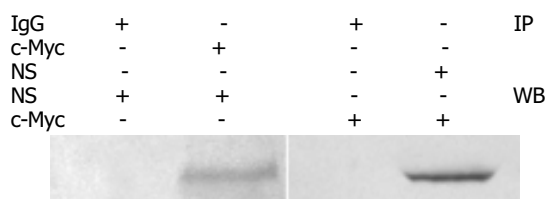


Figure 3 Co-immunoprecipitation of protein NS and PPP2R5A. Total proteins from cells co-transferred with plasmids pcDNA₃-NS and pcDNA₃-myc-PPP2R5A were used for immunoprecipitation with antibody against NS or c-myc and antibody against c-myc or NS was used in Western blot. Mouse IgG was used in immunoprecipitation as negative control.

Screening of clones interacted with NS

To rule out the transcription activity of NS, the bait plasmid pGBKT7-NS was transformed into yeast AH109 and the transcription initiation of HIS and MEL1 reporter genes was tested. The results showed that the self-activation of NS was negative.

Amplification of human placenta cDNA library was pre-performed and transformed into the AH109 yeast strain containing pGBKT7-NS plasmids using modified lithium acetate. The transformants of pGBKT7 and pCL1 were used as negative and positive control respectively in the experiment. There were two positive clones, which were subjected to DNA sequence analysis. The results showed that one clone was identical to gene PPP2R5A (GenBank, GI: 30795205), the other was a novel gene being highly homologous to the gene associated with spondylo paralysis. To identify the specificity of the protein interaction, PPP2R5A/pACT2 was co-transformed into yeast cells with plasmids pGBKT7-NS or pGBKT7. The results showed that PPP2R5A/pACT2 interacted with pGBKT7-NS, but not with pGBKT7.

Co-immunoprecipitation

To further testify the two protein interaction in mammalian cells, eukaryotic plasmids expressing NS or PPP2R5A were cotransfected into COS-7 cells and the total protein was extracted and used for immunoprecipitation and Western blot sequentially. The proteins precipitated with NS antibody could be recognized by c-myc tag antibody, and vice versa, indicating the interaction between NS and PPP2R5A in mammalian cell.

DISCUSSION

Yeast two-hybrid assay is an effective method to isolate interacted proteins^[8], and can screen all protein-protein interactions *in vivo*. The proteins obtained by yeast two-hybrid assay are more likely in their native conformations^[12]. However, the yeast two-hybrid assay also has its limitations, and false positive clones may occur. In this study, more sensitive and credible yeast strain AH109 was used, which has three reporter genes regulated by different promoters, such as GAL1-HIS3, GAL2-ADE2, and MEL1-LacZ. By using this system, a novel binding protein PPP2R5A of NS was obtained from human placenta cDNA library and its interaction with NS and PPP2R5A was further characterized in mammalian cells using co-immunoprecipitation.

P53 plays an important role in the physiological or pathological processes, including cell growth regulation and cell cycle progress. It was reported that the p53 protein can bind to NS protein by GST pull-down and co-immunoprecipitation, respectively^[7]. In our study, a novel NS binding protein was identified as an alpha isoform of human protein phosphatase 2 regulatory subunit B (B56) (PPP2R5A). PPP2R5A belongs to the phosphatase 2A regulatory subunit B family. Phosphatase 2A is one of the four major Ser/Thr phosphatases, and plays an important role in negative control of cell growth and division as well as cell cycle progress^[13]. According to Gene Database,

PPP2R5A is located in cytoplasm^[14-18]. It was found in our study that NS was expressed in cytoplasm and nucleoli (data not shown). NS expression in gastric cancer tissue is higher than that in other gastric tissues (data not shown), suggesting that NS may play a role in the carcinogenesis of gastric cancer. In conclusion, the results of our study help to investigate the functions of NS.

REFERENCES

- 1 **Lessard J, Sauvageau G.** *Bmi-1* determines the proliferative capacity of normal and leukaemic stem cells. *Nature* 2003; **423**: 255-260
- 2 **Marx J.** Mutant stem cells may seed cancer. *Science* 2003 **301**: 1308-1310
- 3 **Jamieson CHM, Ailles LE, Dylla SJ, Muijtjens M, Jones C, Zehnder JL, Gotlib J, Li K, Manz MG, Keating A, Sawyers CL, Weissman IL.** Granulocyte-macrophage progenitors as candidate leukemic stem cells in blast-crisis CML. *N Engl J Med* 2004; **351**: 657-667
- 4 **Reya T, Morrison SJ, Clarke MF, Weissman IL.** Stem cell, cancer and cancer stem cell. *Nature* 2001; **414**: 105-111
- 5 **Normile D.** Cell proliferation: common control for cancer, stem cells. *Science* 2002; **298**: 1869
- 6 **Bernardi R, Pandolfi PP.** The nucleolus: at the stem of immortality. *Nat Med* 2003; **9**: 24-25
- 7 **Tsai RY, McKay RD.** A nuclear mechanism controlling cells proliferation in stem cells and cancer cells. *Genes Dev* 2002; **16**: 2991-3003
- 8 **Fields S, Song O.** A novel genetic system to detect protein-protein interactions. *Nature* 1989; **340**: 245-246
- 9 **Bartel P, Chien CT, Sternglanz R, Fields S.** Elimination of false positives that arise in using the two-hybrid system. *Biotechniques* 1993; **14**: 920-924
- 10 **Ye Q, Worman HJ.** Protein-protein interactions between human nuclear lamins expressed in yeast. *Exp Cell Res* 1995; **219**: 292-298
- 11 **Shou CC, Wurmser A, Ling K, Barbacid M, Feig LF.** Differential response of the Ras exchange factor, Ras-GRF to tyrosine kinase and G protein mediated signals. *Oncogene* 1995; **10**: 1887-1893
- 12 **Phizicky EM, Fields S.** Protein-protein interactions: methods for detection and analysis. *Microbiol Rev* 1995; **59**: 94-123
- 13 **Kuner R.** Identifizierung differenziell exprimierter Gene bei Brust- und Ovarialkarzinomen in den chromosomalen Regionen 1q32-q41 und 11q12-q23. *MetaGen Pharmaceuticals GmbH* 2002; **23**: 1
- 14 **Sijin L, Ziwei C, Yajun L, Meiyu D, Hongwei Z, Guofa H, Siguo L, Hong G, Zhihong Z, Xiaolei L, Yingyun W, Yan X, Weide L.** The effect of knocking-down nucleostemin gene expression on the *in vitro* proliferation and *in vivo* tumorigenesis of HeLa cells. *J Exp Clin Cancer Res* 2004; **23**: 529-538
- 15 **Tsai RY, McKay RD.** A multistep, GTP-driven mechanism controlling the dynamic cycling of nucleostemin. *J Cell Biol* 2005; **168**: 179-184
- 16 **Martens E, Stevens I, Janssens V, Vermeesch J, Gotz J, Goris J, Van Hoof C.** Genomic organisation, chromosomal localisation tissue distribution and developmental regulation of the PR61/B' regulatory subunits of protein phosphatase 2A in mice. *J Mol Biol* 2004; **336**: 971-986
- 17 **McCright B, Brothman AR, Virshup DM.** Assignment of human protein phosphatase 2A regulatory subunit genes b56alpha, b56beta, b56gamma, b56delta, and b56epsilon (PPP2R5A-PPP2R5E), highly expressed in muscle and brain, to chromosome regions 1q41, 11q12, 3p21, 6p21.1, and 7p11.2-> p12. *Genomics* 1996; **36**: 168-170
- 18 **McCright B, Virshup DM.** Identification of a new family of protein phosphatase 2A regulatory subunits. *J Biol Chem* 1995; **270**: 26123-26128

Influence of continuous veno-venous hemofiltration on the course of acute pancreatitis

Hong-Li Jiang, Wu-Jun Xue, Da-Qing Li, Ai-Ping Yin, Xia Xin, Chun-Mei Li, Ju-Lin Gao

Hong-Li Jiang, Wu-Jun Xue, Da-Qing Li, Ai-Ping Yin, Xia Xin, Chun-Mei Li, Ju-Lin Gao, Department of Hemodialysis Center, The First Hospital of Xi'an Jiaotong University, Xi'an 710061, Shaanxi Province, China

Supported by the Natural Science Foundation of Shaanxi Province, No. 2002C257

Correspondence to: Dr. Hong-Li Jiang, Department of Hemodialysis Center, The First Hospital of Xi'an Jiaotong University, No.1 Jankang Lu, Xi'an 710061, Shaanxi Province, China. j92106@sina.com

Telephone: +86-29-85323255

Received: 2005-04-14 Accepted: 2005-06-06

Abstract

AIM: To investigate whether continuous veno-venous hemofiltration (CVVH) in different filtration rate to eliminate cytokines would result in different efficiency in acute pancreatitis, whether the saturation time of filter membrane was related to different filtration rate, and whether the onset time of CVVH could influence the survival of acute pancreatitis.

METHODS: Thirty-seven patients were classified into four groups randomly. Group 1 underwent low-volume CVVH within 48 h of the onset of abdominal pain (early CVVH, $n = 9$). Group 2 received low-volume CVVH after 96 h of the onset of abdominal pain (late CVVH, $n = 10$). Group 3 underwent high-volume CVVH within 48 h of the onset of abdominal pain (early CVVH, $n = 9$). Group 4 received high-volume CVVH after 96 h of the onset of abdominal pain (late CVVH, $n = 9$). CVVH was sustained for at least 72 h. Blood was taken before hemofiltration, and ultrafiltrate was collected at the start of CVVH and every 12 h during CVVH period for the purpose of measuring the concentrations of TNF- α , IL-1 β and IL-6. The concentrations of TNF- α , IL-1 β and IL-6 were measured by swine-specific ELISA. The Solartron 1 255 B frequency response analyzer (British) was used to observe the resistance of filter membrane.

RESULTS: The survival rate had a significant difference (94.44% vs 68.42%, $P < 0.01$) high-volume and low-volume CVVH patients. The survival rate had also a significant difference (88.89% vs 73.68%, $P < 0.05$) between early and late CVVH patients. The hemodynamic deterioration (MAP, HR, CVP) was less severe in groups 4 and 1 than that in group 2, and in group 3 than in group 4. The adsorptive saturation time of filters membranes was 120-180 min if the filtration rate was 1 000-4 000 mL/h. After the first, second and third new hemofilters were changed, serum TNF- α concentrations had a negative correlation

with resistance (r : -0.91, -0.89, and -0.86, respectively in group 1; -0.89, -0.85, and -0.76, respectively in group 2; -0.88, -0.92, and -0.82, respectively in group 3; -0.84, -0.87, and -0.79, respectively in group 4). The decreasing extent of TNF- α , IL-1 β and IL-6 was significantly different between group 3 and group 1 (TNF- α $P < 0.05$, IL-1 β $P < 0.05$, IL-6 $P < 0.01$), between group 4 and group 2 (TNF- α $P < 0.05$, IL-1 β $P < 0.05$, IL-6 $P < 0.01$), between group 1 and group 2 (TNF- α $P < 0.05$, IL-1 β $P < 0.05$, IL-6 $P < 0.05$), and between group 3 and group 4 (TNF- α $P < 0.01$, IL-1 β $P < 0.01$, IL-6 $P < 0.05$), respectively during CVVH period. The decreasing extent of TNF- α and IL-1 β was also significantly different between survival patients and dead patients (TNF- α $P < 0.05$, IL-1 β $P < 0.05$). In survival patients, serum concentration of TNF- α and IL-1 β decreased more significantly than that in dead patients.

CONCLUSION: High-volume and early CVVH improve hemodynamic deterioration and survival in acute pancreatitis patients. High-volume CVVH can eliminate cytokines more efficiently than low-volume CVVH. The survival rate is related to the decrease extent of TNF- α and IL-1 β . The adsorptive saturation time of filter membranes are different under different filtration rate condition. The filter should be changed timely once filter membrane adsorption is saturated.

© 2005 The WJG Press and Elsevier Inc. All rights reserved.

Key words: Venovenous hemofiltration; Acute pancreatitis; TNF- α ; IL-1 β ; IL-6

Jiang HL, Xue WJ, Li DQ, Yin AP, Xin X, Li CM, Gao JL. Influence of continuous veno-venous hemofiltration on the course of acute pancreatitis. *World J Gastroenterol* 2005; 11(31): 4815-4821

<http://www.wjgnet.com/1007-9327/11/4815.asp>

INTRODUCTION

Excessive activation of inflammatory mediator cascade during severe acute pancreatitis is a major cause of multiple organ dysfunction associated with a high mortality^[1]. Non-selective elimination of pancreatitis-related mediators is a preventive measure against the systemic complications of the disease. Continuous veno-venous hemofiltration (CVVH) has been shown to have considerable benefit for the treatment of multiple organ dysfunction secondary to sepsis^[2,3]. Clinical and experimental studies indicate that CVVH is able to eliminate small and medium-sized inflammatory mediators such as cytokines^[4-6]. These data suggest that the mechanisms of

mediator elimination are convective filtration through the filters and adsorption of mediators to the filter membrane. Whether different filtration rate can induce different efficiency in removing inflammatory mediators is controversial^[7,8]. If filter membrane adsorption reaches saturation, the filter should be changed timely. However, little is known about the saturation time of filter membrane. Whether the filtrate rate can change membrane saturation time is unclear. The present study therefore investigated whether low-volume and high-volume CVVH could eliminate cytokines in acute pancreatitis, and whether the onset time of CVVH could affect the survival of acute pancreatitis patients. By measuring electrical resistance of filter membranes with the impedance method, we studied the adsorptive saturation time of filter membranes. Furthermore, we investigated whether the saturation time of filter membrane was related to different filtration rates.

MATERIALS AND METHODS

Patients

Thirty-seven patients (21 males, 16 females, averaging 51.4±11.6 years in age with a range of 36-70 years) with acute pancreatitis were studied. Prior to the study, all patients or their relatives were informed in detail, and consent was obtained. The diagnosis was based on typical abdominal pain associated with an increase in serum amylase and lipase concentration. All the patients studied also had morphologic abnormalities compatible with acute pancreatitis demonstrated by contrast-enhanced computed tomography and/or ultrasonography. Pancreatitis was biliary origin in 31 patients, alcoholic origin in 4 patients, and unknown origin in 2 patients.

Diagnostic criteria for severe acute pancreatitis (SAP) standardized by the British Society of Gastroenterology Working Party on the management of acute pancreatitis in 1995^[9] and diagnostic criteria for multiple organ dysfunction syndrome (MODS) standardized by American College of Chest Physicians (ACCP) and Society of Critical Care Medicine (SCCM) were applied^[10]. The frequencies of various complications observed in patients with severe pancreatitis are reported in Table 1. All patients initially received standard conservative treatment. Two patients with severe pancreatitis underwent surgery for infection of pancreatic necrosis. Mean arterial blood pressure (MAP), central venous pressure (CVP), and heart rate (HR) were monitored continuously. The primary end point was mortality on d 14.

Table 1 Complications in 37 patients with acute pancreatitis

Complication	Patients (n)
Pancreatic necrosis	20
Pulmonary involvement (pleural effusion, atelectasis)	16
Pancreatic fluid collection	12
Renal failure	6
Pseudocyst	5
Infection	4
Multi-organ failure	4

Patients were classified into four groups randomly by the onset of acute pancreatitis and the intensity of CVVH.

Group 1: Nine cases underwent low-volume CVVH within 48 h of the onset of abdominal pain (early CVVH);

Group 2: Ten cases underwent low-volume CVVH after 96 h of the onset of abdominal pain (late CVVH);

Group 3: Nine cases received high-volume CVVH within 48 h of the onset of abdominal pain (early CVVH);

Group 4: Nine cases received high-volume CVVH after 96 h of the onset of abdominal pain (late CVVH).

Procedures of CVVH

A double lumen catheter was inserted into the internal jugular vein of 23 patients and into the femoral vein of 14 patients to establish vascular access. The blood flow rate ranged 250-300 mL/min. CVVH was sustained for at least 72 h. The substitution fluid was infused at a rate of 1 000 mL/h in low-CVVH group and at a rate of 4 000 mL/h in high-CVVH group^[11] in a pre-diluted manner (before hemofiltration). The substitution fluid rate was equal to the ultrafiltrate rate. An AN69 hemofilter (HOSPAL, Industrie-69 330 Meyzieu, France, 1.2 m²) was used and changed every 24 h. To prevent clotting, low molecular weight heparin (Fraxi, 0.4 mL) was given at the start of CVVH. Then Fraxi was infused into the blood circuit before filtration every four hours, and ceased when the patient displayed hemorrhagic tendencies, such as hematemesis, hemafecia and emorrhagia nasalis.

Application of frequency response analyzer

The Solartron 1 255 B frequency response analyzer (UK) was used to observe the resistance of filter membrane. Filters were holed near the inlet and outlet of dialysate. Two ends of pyrogen-free electrode (alloy of nickel chromium thread coated with pvc. diameter: 0.5 mm) of the Solartron 1 255 B frequency response analyzer were fixed to the periphery of filter membranes through the holes. Then the holes were sealed up by pyrogen-free gel bar gun. The resistance of filter membrane was constantly observed and recorded every 10 min.

Cytokine measurement

Blood was taken before hemofiltration, the ultrafiltrate was collected at the start of CVVH and every 12 h during CVVH for the purpose of measuring the concentration of TNF- α , IL-1 β , and IL-6. To analyze the correlation of serum inflammatory mediators with resistance of filter membrane, blood samples for measuring TNF- α were collected every 10-min when a new filter was used until the resistance of filter membrane reached the plateau. The concentrations of TNF- α , IL-1 β , and IL-6 were measured by swine-specific ELISA (Sigma, USA).

Statistical analysis

Student's *t*-test was used to compare the data between groups. The data were expressed as mean±SD. The survival time was calculated by the Kaplan-Meier analysis and compared by the log-rank test. Hemodynamic parameters were evaluated by one-way analysis of variance (ANOVA). The change of hemodynamic parameters, cytokines, and electrical resistance of filter membrane was evaluated and by ANOVA. The correlation between serum TNF- α and the resistance of filter membrane was determined by Pearson correlation analysis. *P*<0.05 was considered statistically significant.

RESULTS

Survival

Among the 19 patients in groups 1 and 2 who underwent low-volume CVVH, 13 patients were still alive at the end of the observation period. In groups 3 and 4, among the 18 patients who underwent high-volume CVVH, 17 patients were still alive at the end of the observation period (Figure 1A). The survival rate was significantly different between the patients undergone high-volume and low-volume CVVH (94.44% *vs* 68.42%, $P<0.01$). The data showed that the survival could be improved significantly by high-volume CVVH.

In groups 1 and 3, among the 18 patients who underwent early CVVH, 16 patients were still alive at the end of the observation period. In groups 2 and 4, among the 19 patients who received late CVVH, 14 patients were still alive at the end of the observation period (Figure 1B). The survival rate was significantly different between the patients who had undergone early and late CVVH (88.89% *vs* 73.68%, $P<0.05$). The results suggested that early CVVH could improve survival of acute pancreatitis patients.

Hemodynamic parameters

Seventy-two hours after CVVH, MAP and CVP had no significant difference between group 1 and group 3 ($P>0.05$). MAP and CVP significantly decreased in group 2 compared to group 4 ($P<0.05$, Table 2). The hemodynamic diversity (MAP, HR, CVP) was different between group 2 and group 4 ($P<0.05$). The hemodynamic deterioration (MAP, HR, CVP) was less severe in group 4 than in group 2 ($P<0.05$). The data demonstrated that high-volume CVVH significantly improved hemodynamic deterioration compared to low-volume CVVH.

MAP and CVP had a significant difference in groups 2 and 4 compared to groups 1 and 3 ($P<0.01$), 72 h after

CVVH (Table 2). The hemodynamic diversity (MAP, HR, CVP) was different between groups 1 and 2 ($P<0.05$) and between groups 3 and 4 ($P<0.01$). The hemodynamic deterioration (MAP, HR, CVP) was less severe in groups 1 and 3 than in groups 2 and 4 ($P<0.05$). These data showed that CVVH could improve hemodynamic parameters in pancreatitis, and that early CVVH significantly improved hemodynamic deterioration than compared to late CVVH.

Resistance of filter membrane in different filtration flow rate

The filter membrane is an insulator before it contacts with blood or substitution fluid. In our study, when pyrogen-free saline passed through the blood compartment of filter, the resistance of filter membranes did not change at different time points. Electrical resistance tended to change in all treatment groups ($P<0.05$, Table 3). The highest resistance of filter membrane demonstrated at 120 min in groups 1 and 2, and at 180 min in groups 3 and 4. It also showed that the adsorptive saturation time of filter membranes was at 120 and 180 min in 1 000 mL/h filtration rate and in 4 000 mL/h filtration rate, respectively. The resistance at the same time point was significantly different ($P<0.01$) between groups 4 and 2, and groups 3 and 1. The data demonstrated that the adsorptive saturation time of filter membranes was different under different filtration rate conditions. The adsorptive saturation time of filter membranes was 120-180 min if the filtration rate was 1 000-4 000 mL/h.

Serum TNF- α levels and relationship between TNF- α and resistance

Serum TNF- α levels decreased significantly ($P<0.01$) until the resistance reached the plateau (120 min in group 2 and 180 min in group 4) after a new filter was exchanged (Table 4). Then, TNF- α concentrations decreased slowly in groups 1

Table 2 Clinical outcome parameters of acute pancreatitis (mean \pm SD)

Parameter	Group	Pre-CVVH	12 h	24 h	36 h	48 h	60 h	72 h
MAP (kPa)	1	14.00 \pm 1.60	14.13 \pm 1.87	14.13 \pm 2.00	13.33 \pm 1.87	13.07 \pm 2.00	13.07 \pm 1.60	13.20 \pm 2.13
	2	12.13 \pm 1.87	12.10 \pm 1.65	12.10 \pm 1.87	11.20 \pm 2.13	11.14 \pm 1.60	10.27 \pm 1.58	9.33 \pm 2.13 ^{ab}
	3	14.13 \pm 2.00	14.17 \pm 1.60	13.87 \pm 1.87	13.85 \pm 1.85	13.87 \pm 2.13	13.60 \pm 1.62	13.87 \pm 2.00
	4	12.13 \pm 1.60	12.15 \pm 1.86	12.00 \pm 1.88	12.13 \pm 1.47	11.73 \pm 2.00	11.47 \pm 1.87	10.80 \pm 1.89 ^{ac}
HR (beats/min)	1	105 \pm 20	106 \pm 18	102 \pm 24	93 \pm 21	90 \pm 22	91 \pm 25	88 \pm 19
	2	120 \pm 24	116 \pm 20	110 \pm 22	112 \pm 18	114 \pm 19	120 \pm 20	118 \pm 25
	3	106 \pm 22	104 \pm 21	96 \pm 24	88 \pm 19	84 \pm 21	84 \pm 18	86 \pm 20
	4	119 \pm 18	110 \pm 24	102 \pm 22	104 \pm 25	101 \pm 20	96 \pm 20	90 \pm 18
CVP (kPa)	1	0.77 \pm 0.15	0.77 \pm 0.14	0.79 \pm 0.13	0.81 \pm 0.11	0.84 \pm 0.16	0.80 \pm 0.17	0.81 \pm 0.15
	2	0.67 \pm 0.17	0.68 \pm 0.13	0.71 \pm 0.12	0.73 \pm 0.14	0.69 \pm 0.13	0.64 \pm 0.14	0.55 \pm 0.14 ^{ab}
	3	0.77 \pm 0.14	0.80 \pm 0.14	0.81 \pm 0.13	0.81 \pm 0.14	0.80 \pm 0.12	0.83 \pm 0.13	0.81 \pm 0.14
	4	0.69 \pm 0.12	0.64 \pm 0.11	0.67 \pm 0.14	0.67 \pm 0.14	0.69 \pm 0.13	0.64 \pm 0.10	0.60 \pm 0.14 ^{ac}

^a $P<0.05$ vs Pre-CVVH; ^b $P<0.01$ vs group 1; ^c $P<0.05$ vs group 2.

Table 3 Resistance level of different groups of acute pancreatitis patients (mean \pm SD)

Group	0 min	30 min	60 min	90 min	120 min	150 min	180 min	210 min
1	0.37 \pm 0.07	0.93 \pm 0.08	1.32 \pm 0.15	1.59 \pm 0.10	1.72 \pm 0.11	1.72 \pm 0.10	1.70 \pm 0.09	1.72 \pm 0.13
2	0.37 \pm 0.09	0.94 \pm 0.07	1.35 \pm 0.08	1.60 \pm 0.07	1.72 \pm 0.10	1.72 \pm 0.13	1.71 \pm 0.14	1.72 \pm 0.10
3	0.37 \pm 0.05	1.67 \pm 0.11	2.68 \pm 0.14	3.58 \pm 0.15	4.11 \pm 0.12	4.27 \pm 0.11	4.29 \pm 0.15	4.27 \pm 0.11
4	0.37 \pm 0.07	1.66 \pm 0.09	2.70 \pm 0.11	3.57 \pm 0.15	4.09 \pm 0.14	4.28 \pm 0.15	4.29 \pm 0.16	4.28 \pm 0.15
Saline	0.37 \pm 0.05	0.38 \pm 0.09	0.35 \pm 0.08	0.36 \pm 0.12	0.37 \pm 0.11	0.36 \pm 0.13	0.36 \pm 0.15	0.36 \pm 0.13

Table 4 TNF α concentration after changing filter of acute pancreatitis (mean \pm SD, ng/L)

Group	Filter	0 min	30 min	60 min	90 min	120 min	150 min	180 min	210 min
2	1 st	1 932 \pm 248	1 825 \pm 292	1 711 \pm 254	1 603 \pm 268	1 562 \pm 247	1 543 \pm 224	1 532 \pm 248	1 520 \pm 228
	2 nd	1 449 \pm 237	1 362 \pm 215	1 295 \pm 239	1 221 \pm 281	1 208 \pm 272	1 201 \pm 268	1 197 \pm 274	1 191 \pm 272
	3 rd	1 173 \pm 253	1 107 \pm 213	1 035 \pm 246	1 018 \pm 274	982 \pm 237	978 \pm 226	962 \pm 225	954 \pm 225
4	1 st	1 893 \pm 248	1 786 \pm 292	1 676 \pm 254	1 592 \pm 268	1 501 \pm 247 ^b	1 468 \pm 224	1 440 \pm 248	1 431 \pm 247
	2 nd	1 365 \pm 237	1 280 \pm 215	1 205 \pm 239	1 136 \pm 281	1 093 \pm 272	1 082 \pm 268	1 067 \pm 274	1 060 \pm 238
	3 rd	985 \pm 253	903 \pm 213	846 \pm 346	784 \pm 274	751 \pm 237	730 \pm 226	718 \pm 345	711 \pm 235

^bP<0.01 vs group 2 1st.

and 3 compared to groups 2 and 4 ($P < 0.05$). When the first filter was used, TNF- α concentration decreased significantly in groups 4 and 3 compared to groups 2 and 1 ($P < 0.05$). The data suggested that there was a correlation between resistance and serum TNF- α concentration. When the resistance increased, serum TNF- α concentration decreased significantly in the same group after a new filter was installed. After the first, second, and third new hemofilters were exchanged, serum TNF- α concentration was negatively correlated with the resistance (r : -0.91, -0.89, and -0.86 in group 1; -0.89, -0.85, and -0.76 in group 2; -0.88, -0.92, and -0.82 in group 3; -0.84, -0.87, and -0.79 in group 4). The data showed that the time point at which the resistance reached plateau was the membrane adsorptive saturation time, and the resistance could reflect the mass of inflammatory mediators for membrane adsorption.

Cytokine levels in different groups

Before CVVH, serum concentrations of TNF- α , IL-1 β ,

and IL-6 had no significant difference between groups 3 and 1, and between groups 4 and 2 ($P > 0.05$). Serum concentrations of TNF- α , IL-1 β and IL-6 tended to decrease in all treatment groups during CVVH. The decreasing extent of TNF- α , IL-1 β and IL-6 was different between groups 3 and 1 (TNF- α $P < 0.05$, IL-1 β $P < 0.05$, IL-6 $P < 0.01$), between groups 4 and 2 (TNF- α $P < 0.05$, IL-1 β $P < 0.05$, IL-6 $P < 0.01$), (Figure 2A-C). The data demonstrated that the diversity of TNF- α , IL-1 β and IL-6 levels increased 72 h after CVVH. The results showed that high-volume CVVH could eliminate cytokines more effectively than low-volume CVVH.

The decreasing extent of TNF- α , IL-1 β and IL-6 was different between groups 1 and 2 (TNF- α $P < 0.05$, IL-1 β $P < 0.05$, IL-6 $P < 0.05$), between groups 3 and 4 (TNF- α $P < 0.01$, IL-1 β $P < 0.01$, IL-6 $P < 0.05$) during CVVH (Figure 2A-C). Serum concentrations of TNF- α , IL-1 β , and IL-6 decreased more significantly in groups 1 and 3

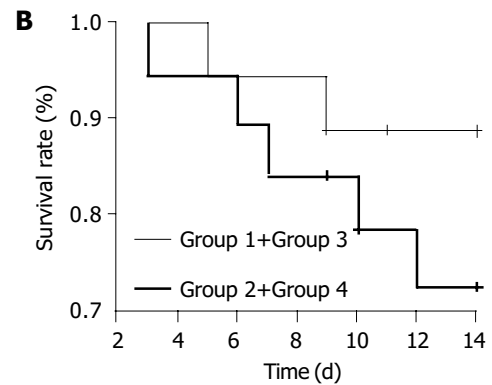
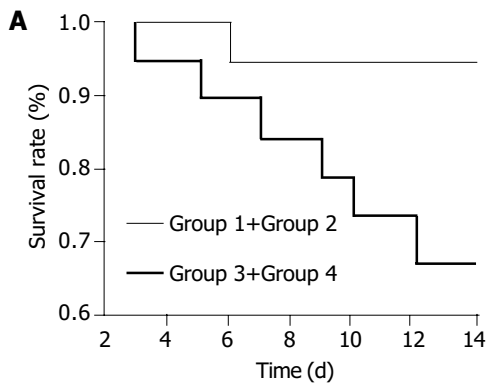


Figure 1 Survival rate of different intensifying CVVH (A) and different start time of CVVH (B).

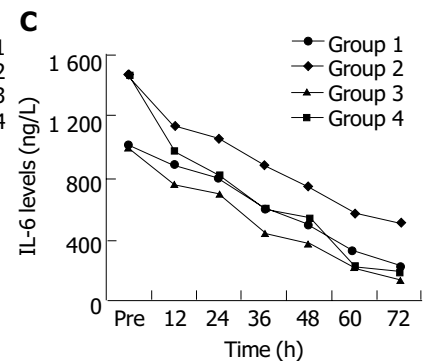
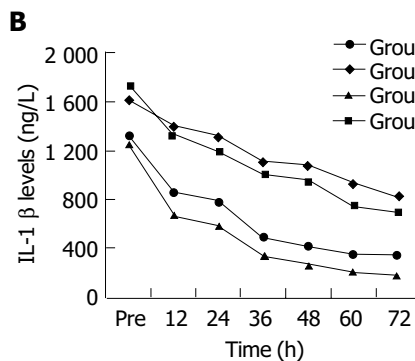
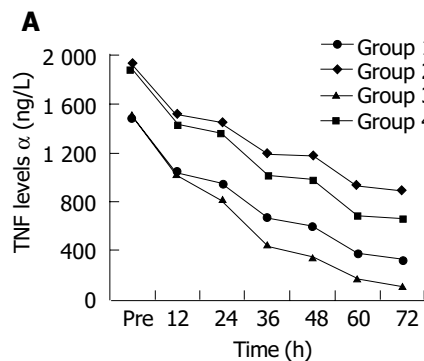


Figure 2 Serum level of TNF α (A), IL-1 β (B), and IL-6 (C) in different groups of acute pancreatitis patients.

than in groups 2 and 4 (TNF- α $P < 0.05$, IL-1 β $P < 0.05$, IL-6 $P < 0.01$). Early CVVH decreased serum concentrations of TNF- α , IL-1 β and IL-6 more efficiently than late CVVH. The data showed that early CVVH could decrease the excessive activation of inflammatory mediator cascade by reducing TNF- α , IL-1 β and IL-6.

The decreased extent of TNF- α and IL-1 β had no significant difference ($P > 0.05$), but was significantly different between IL-6 and TNF- α , and between IL-6 and IL-1 β ($P < 0.01$, Figure 3) in group 4. The data showed that IL-6 decreased more significantly during high-volume CVVH. TNF- α , IL-1 β and IL-6 were detectable in the ultrafiltrate.

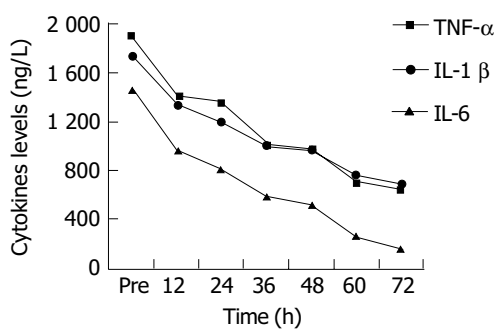


Figure 3 Different cytokine levels in group 4 of acute pancreatitis patients.

Relationship between survival rate and cytokine levels

Before CVVH, serum concentrations of TNF- α and IL-1 β had a difference between survival and dead patients (TNF- α $P < 0.05$, IL-1 β $P < 0.05$, Figure 4). TNF- α and IL-1 β levels were higher in dead patients. Serum concentrations of TNF- α and IL-1 β decreased in both survival and dead patients during CVVH. The decreasing extent of TNF- α and IL-1 β was different between survival and dead patients (TNF- α $P < 0.05$, IL-1 β $P < 0.05$). In survival patients, serum concentrations of TNF- α and IL-1 β decreased more significantly than that in dead patients (Figure 4). The data demonstrated that survival patients had lower serum levels of TNF- α and IL-1 β . Survival rate might be related to the decreasing extent of TNF- α and IL-1 β .

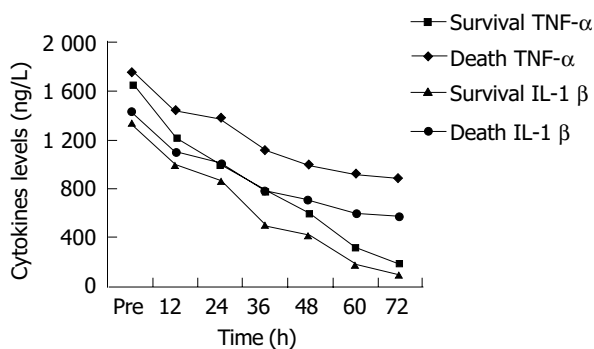


Figure 4 Cytokine levels in survival and dead patients of acute pancreatitis.

DISCUSSION

There is evidence that secondary multiple organ failure resulting from septic complications, is the main cause of mortality in severe pancreatitis. The final pathway of pancreatitis-induced sepsis shares many characteristics with other septic diseases, including systemic histopathological abnormalities, excessive release of pro-and anti-inflammatory cytokines. It has been suggested that patients with severe pancreatitis at the risk to develop septic complications might benefit from early application of CVVH irrespective of the presence of acute renal failure (ARF)^[12,13].

Clinical studies have shown that cumulative ultrafiltrate volume is directly correlated with survival rate in patients with sepsis-associated acute renal failure and acute pancreatitis^[13,14]. In our study, high-volume CVVH could significantly improve the survival compared to low-volume CVVH. Joannes-Boyau *et al.*^[15], evaluated the effect of high volume CVVH on hemodynamic and outcome in patients with septic shock, and found that the mortality in the hemofiltration group decreases significantly. Yekebas *et al.*^[16], examined the impact of CVVH on the course of experimental pancreatitis in pigs, and found that the survival time is significantly prolonged by high-volume CVVH. Most likely, this is due to a more effective removal of sepsis mediators. Furthermore, our data show that early CVVH improves survival significantly compared to late CVVH. In a non-randomized trial, it has been hypothesized that early CVVH prior to overt ARF might result in considerable reduction of morbidity in patients with necrotizing pancreatitis^[12]. Xie *et al.*^[17], studied whether initial time of CVVH could influence survival in acute pancreatitis, and found that the average interval is significantly longer in the mortality group than in the survival group from the onset of acute pancreatitis to CVVH. Yekebas *et al.*^[18], reported that animals receiving prophylactic CVVH have a longer survival period, than those receiving CVVH after clinical impairment, suggesting that the improved survival is also due to the fact that early CVVH improves hemodynamic deterioration better than late CVVH. Improved hemodynamic parameters may be due to the application of high-volume CVVH as it was shown in our study. The results are similar to those reported by other studies^[15,19]. As Ronco *et al.*^[20], argued that it is the time to move from the simple goal of achieving adequate renal support, the proper goal of CVVH in ICU should be multi-organ support therapy.

The resistance of filter membrane was constantly measured by means of the electrical impedance technique during CVVH in the present study. The resistance level reached the plateau at 120 min in 1 000 mL/h filtration rate and at 180 min in 4 000 mL/h filtration rate, respectively. The results demonstrate that the adsorptive saturation time of filter membranes is different in different filtration rate. The adsorptive saturation time of filter membranes is 120 -180 min, if the filtration rate is 1 000-4 000 mL/h. De Vriese *et al.*^[21], calculated the cytokine mass balance during hemofiltration in septic patients with acute renal failure, and demonstrated that the adsorption is most prominent immediately after the installation of a new hemofilter (at $t = 1$ and $t = 13$) with a steady decrease thereafter. The

adsorption and the convective elimination increased in a higher blood flow rate and filtration rate. Kellum *et al.*^[22], performed CVVH in patients with severe systemic inflammatory response syndrome, and deduced that the adsorptive saturation time of filter membranes is at 6 h after exchanging a new hemofilter by measuring the decreasing extent of serum cytokines. By delivering a large amount of blood per a unit of time or higher transmembrane pressure to push the molecules deeper into the membrane, the adsorptive surface area increases. The higher convection driving force may increase the surface area accessible to adsorption, by pushing the molecules deeper into the hydrogel. In this respect, only minimal adsorption occurs when the ultrafiltrate line is clamped^[23]. Therefore, increasing filtration rate can increase the adsorption mass and prolong adsorptive saturation time of filter membranes. Our results showed that serum TNF α concentration decreased significantly in the same group after new filters were installed. After the first, second and third new hemofilters were exchanged, serum TNF- α concentration was negatively correlated with the resistance, demonstrating that the time point at which the resistance reached plateau was the membrane adsorptive saturation time. The resistance could reflect the mass of membrane adsorption of inflammatory mediators. To eliminate more inflammatory mediators, the filter should be changed timely when the filter membrane adsorption is saturated. Compared to that reported by De Vriese *et al.*^[21], the method we used to measure the adsorptive saturation time of filter membranes by electrical impedance technique is convenient. The impedance technique has also been used by Rapoza *et al.*^[25], to evaluate the permeability of dentin. Several studies have shown that proteins are denatured and desorbed with increasing treatment time^[21,24]. Clark *et al.*^[26], demonstrated that the desorption of denatured proteins into the blood may be deleterious, indicating that it is very important to change filter timely once filter membrane adsorption is saturated.

In our study, we particularly focused on whether the removal of cytokines, such as TNF- α , IL-1 β and, IL-6 was related to different filtration rate and the onset of CVVH. The impact of CVVH on serum cytokine levels is controversial^[18,19]. Some investigators have not detected significant decreases of inflammatory mediators in the bloodstream, although relevant concentrations are measured in ultrafiltrate^[27,28]. This may be due to the fact that CVVH was performed with low filtration rates. In contrast, De Vriese *et al.*^[21], reported that in septic patients with ARF, plasma cytokine levels decrease significantly after hemofiltration and found that there is a close relationship between the filtration rate and the efficiency of CVVH in removing cytokines. Other studies have confirmed the benefits of increasing the filtration rate in terms of improved survival or accelerated recovery from ARF^[14,29]. In our study, the filtration rate was 4 000 mL/h which is recommended by Uchino *et al.*^[11], as high-volume CVVH. Our data show that high-volume CVVH could eliminate more cytokines than low-volume CVVH. The results are similar to those of some previous clinical studies^[17,30]. Watanabe *et al.*^[31], found that extremely high interleukin-6 blood levels and bad outcome in critically ill patients are associated with tumor necrosis factor- α and interleukin-1, suggesting that activation of

inflammatory mediator is a kind of excessive cascade effect during acute pancreatitis. In the present study, early CVVH decreased serum concentrations of TNF- α , IL-1 β , and IL-6 more efficiently than late CVVH, demonstrating that early CVVH can decrease the excessive activation of inflammatory mediator cascade through reduced TNF- α , IL-1 β , and IL-6, especially in high CVVH patients. We found that IL-6 decreased more significantly than TNF- α and IL-1 β during high-volume CVVH. This may be due to the fact that pro-inflammatory cytokines, such as TNF- α and IL-1 β , are removed efficiently by high-volume CVVH and the causative factors increasing the serum IL-6 level are reduced. Gomez-Cambronero *et al.*^[1], reported that serum levels of pro-inflammatory cytokines, such as TNF-alpha and IL-1beta, increase during acute pancreatitis and appear to be the driving force for the initiation and propagation of the systemic response. The excessive inflammatory response could be down regulated by removing cytokines and other mediators as Lonneman *et al.*^[32], reported. Early CVVH could prevent inflammatory mediators from increasing.

SAP mortality is associated with organ failure. In the early course, organ failure results from inflammatory mediators released by systemic inflammatory response syndrome even in the absence of infection. In the septic phase, since organ failure occurs because of sepsis, it is common in SAP. Inflammatory cytokines play an important role in the progress of acute pancreatitis. In our study, serum concentration of TNF- α and IL-1 β decreased more significantly in survival patients than in dead patients 72 h after CVVH, and similar studies in MODS field are available^[2,3,5], suggesting that the survival rate is related to the decreasing extent of TNF- α and IL-1 β in acute pancreatitis. IL-1 β and its mRNA do not exist in the normal pancreas, but are released immediately after pancreatitis is induced. Blockage of the IL-1 receptor significantly decreases intrinsic pancreatic damage and mortality^[1,33]. Elevated levels of TNF α may contribute to the pathophysiological sequelae of the disease, and pretreatment with anti-TNF α antibody before induction of the disease can prevent release of TNF α ^[34], lessen disease severity and increase survival time^[35]. Blocking the network of cytokines and eliminating cytokines can improve the prognosis and survival rate of pancreatitis.

In summary, CVVH, especially high-volume CVVH, offers several therapeutic options for patients with acute pancreatitis experiencing multiple organ dysfunction. It can improve the hemodynamic parameters and survival rate of pancreatitis patients by removing inflammatory mediators. CVVH can be performed at the early stage of acute pancreatitis. The adsorptive saturation time of filter membranes is different in different filtration rate. The filter should be changed timely once filter membrane adsorption is saturated.

REFERENCES

- 1 Gomez-Cambronero LG, Sabater L, Pereda J, Cassinello N, Camps B, Vina J, Sastre J. Role of cytokines and oxidative stress in the pathophysiology of acute pancreatitis: therapeutic implications. *Curr Drug Targets Inflamm Allergy* 2002; 1: 393-403
- 2 Tetta C, Bellomo R, Ronco C. Artificial organ treatment for multiple organ failure, acute renal failure, and sepsis: recent new trends. *Artif Organs* 2003; 27: 202-213

- 3 **Schetz M.** Non-renal indications for continuous renal replacement therapy. *Kidney Int Suppl* 1999; S88-94
- 4 **Oda S,** Hirasawa H, Shiga H, Nakanishi K, Matsuda K, Nakamura M. Continuous hemofiltration/hemodiafiltration in critical care. *Ther Apher* 2002; **6**: 193-198
- 5 **Ronco C,** Ricci Z, Bellomo R. Importance of increased ultrafiltration volume and impact on mortality: sepsis and cytokine story and the role for CVVH. *Edtna Erca J* 2002; (Suppl 2): 13-18
- 6 **Pupelis G,** Austrums E, Snippe K. Blood purification methods for treatment of organ failure in patients with severe pancreatitis. *Zentralbl Chir* 2001; **126**: 780-784
- 7 **Rogiers P.** Hemofiltration treatment for sepsis: is it time for controlled trials? *Kidney Int Suppl* 1999; **56**: S99-103
- 8 **Ronco C,** Bellomo R, Kellum JA. Continuous renal replacement therapy: opinions and evidence. *Adv Ren Replace Ther* 2002; **9**: 229-244
- 9 **Norton SA,** Cheruvu CV, Collins J, Dix FP, Eyre-Brook IA. An assessment of clinical guidelines for the management of acute pancreatitis. *Ann R Coll Surg Engl* 2001; **83**: 399-405
- 10 **Bone RC,** Balk RA, Cerra FB, Dellinger RP, Fein AM, Knaus WA, Schein RM, Sibbald WJ. Definitions for sepsis and organ failure and guidelines for the use of innovative therapies in sepsis. The ACCP/SCCM consensus conference committee. American college of chest physicians/society of critical care medicine. *Chest* 1992; **101**: 1644-1655
- 11 **Uchino S,** Bellomo R, Goldsmith D, Davenport P, Cole L, Baldwin I, Panagiotopoulos S, Tipping P. Super high flux hemofiltration: a new technique for cytokine removal. *Intensive Care Med* 2002; **28**: 651-655
- 12 **Gebhardt C,** Bödeker H, Blinzler L, Kraus D, Hergdt G. Wandel in der Therapie der schweren akuten Pankreatitis. *Chirurg* 1994; **65**: 33-40
- 13 **Pupelis G.** Renal failure in acute pancreatitis. Timing of dialysis and surgery. *Przegl Lek* 2000; **57** (Suppl 5): 29-31
- 14 **Kellum JA,** Bellomo R, Mehta R, Ronco C. Blood purification in non-renal critical illness. *Blood Purif* 2003; **21**: 6-13
- 15 **Joannes-Boyau O,** Rapaport S, Bazin R, Fleureau C, Janvier G. Impact of high volume hemofiltration on hemodynamic disturbance and outcome during septic shock. *ASAIO J* 2004; **50**: 102-109
- 16 **Yekebas EF,** Eisenberger CF, Ohnesorge H, Saalmüller A, Elsner HA, Engelhardt M, Gillesen A, Meins J, The M, Strate T, Busch C, Knoefel WT, Bloechle C, Izbicki JR. Attenuation of sepsis-related immunoparalysis by continuous veno-venous hemofiltration in experimental porcine pancreatitis. *Crit Care Med* 2001; **29**: 1423-1430
- 17 **Xie H,** Ji D, Gong D, Liu Y, Xu B, Zhou H, Liu Z, Li L, Li W, Quan Z, Li J. Continuous veno venous hemofiltration in treatment of acute necrotizing pancreatitis. *Chin J Med* 2003; **116**: 549-553
- 18 **Yekebas EF,** Strate T, Zolmajd S, Eisenberger CF, Erbersdobler A, Saalmuller A, Steffani K, Busch C, Elsner HA, Engelhardt M, Gillesen A, Meins J, The M, Knoefel WT, Izbicki JR. Impact of different modalities of continuous veno-venous hemofiltration on sepsis-induced alterations in experimental pancreatitis. *Kidney Int* 2002; **62**: 1806-1818
- 19 **Ullrich R,** Roeder G, Lorber C, Quezado ZM, Kneifel W, Gasser H, Schlag G, Redl H, Germann P. Continuous veno-venous hemofiltration improves arterial oxygenation in endotoxin-induced lung injury in pigs. *Anesthesiology* 2001; **95**: 428-436
- 20 **Ronco C,** Bellomo R. Acute renal failure and multiple organ dysfunction in the ICU: from renal replacement therapy (RRT) to multiple organ support therapy (MOST). *Int J Artif Organs* 2002; **25**: 733-747
- 21 **De Vriese AS,** Colardyn FA, Philippe JJ, Vanholder RC, De Sutter JH, Lameire NH. Cytokine removal during continuous hemofiltration in septic patients. *J Am Soc Nephrol* 1999; **10**: 846-853
- 22 **Kellum JA,** Johnson JP, Kramer D, Palevsky P, Brady JJ, Pinsky MR. Diffusive vs convective therapy: effects on mediators of inflammation in patient with severe systemic inflammatory response syndrome. *Crit Care Med* 1998; **26**: 1995-2000
- 23 **Tetta C,** Mariano F, Buades J, Ronco C, Wratten ML, Camussi G. Relevance of platelet-activating factor in inflammation and sepsis: mechanisms and kinetics of removal in extracorporeal treatments. *Am J Kidney Dis* 1997; **30** (5 Suppl 4): S57-65
- 24 **Pradelle-Plasse N,** Wenger F, Colon P. Effect of conditioners on dentin permeability using an impedance method. *J Dent* 2002; **30**: 251-257
- 25 **Rapoza RJ,** Horbett TA. Changes in the SDS elutability of fibrinogen adsorbed from plasma to polymers. *J Biomater Sci Polym Ed* 1989; **1**: 99-110
- 26 **Clark WR,** Macias WL, Molitoris BA, Wang NH. Membrane adsorption of beta 2-microglobulin: equilibrium and kinetic characterization. *Kidney Int* 1994; **46**: 1140-1146
- 27 **Rogiers P,** Zhang H, Smail N, Pauwels D, Vincent JL. Continuous veno-venous hemofiltration improves cardiac performance by mechanisms other than tumor necrosis factor alpha attenuation during endotoxic shock. *Crit Care Med* 1999; **27**: 1848-1855
- 28 **van Bommel EF,** Hesse CJ, Jutte NH, Zietse R, Bruining HA, Weimar W. Impact of continuous hemofiltration on cytokines and cytokine inhibitors in oliguric patients suffering from systemic inflammatory response syndrome. *Ren Fail* 1997; **19**: 443-454
- 29 **Ronco C,** Bellomo R, Homel P, Brendolan A, Dan M, Piccinni P, La Greca G. Effects of different doses in continuous veno-venous hemofiltration on outcomes of acute renal failure: a prospective randomised trial. *Lancet* 2000; **356**: 26-30
- 30 **Ronco C,** Tetta C, Lupi A, Galloni E, Bettini MC, Sereni L, Mariano F, DeMartino A, Montrucchio G, Camussi G. Removal of platelet-activating factor in experimental continuous arteriovenous hemofiltration. *Crit Care Med* 1995; **23**: 99-107
- 31 **Watanabe E,** Hirasawa H, Oda S, Matsuda K, Hatano M, Tokuhisa T. Extremely high interleukin-6 blood levels and outcome in the critically ill are associated with tumor necrosis factor- and interleukin-1-related gene polymorphisms. *Crit Care Med* 2005 **33**: 89-97
- 32 **Lonnemann G,** Koch KM, Shaldon S, Dinarello CA. Studies on the ability of hemodialysis membranes to induce, bind, and clear human interleukin-1. *J Lab Clin Med* 1988; **112**: 76-86
- 33 **Norman JG,** Franz MG, Fink GS, Messina J, Fabri PJ, Gower WR, Carey LC. Decreased mortality of severe acute pancreatitis after proximal cytokine blockade. *Ann Surg* 1995; **221**: 625-631
- 34 **Hughes CB,** Gaber LW, Mohey el-Din AB, Grewal HP, Kotb M, Mann L, Gaber AO. Inhibition of TNF alpha improves survival in an experimental model of acute pancreatitis. *Am Surg* 1996; **62**: 8-13
- 35 **Eubanks JW 3rd,** Sabek O, Kotb M, Gaber LW, Henry J, Hijjiya N, Britt LG, Gaber AO, Goyert SM. Acute pancreatitis induces cytokine production in endotoxin-resistant mice. *Ann Surg* 1998; **227**: 904-911

Leptin administration exacerbates thioacetamide-induced liver fibrosis in mice

Kai Dai, Jun-Ying Qi, De-Ying Tian

Kai Dai, Jun-Ying Qi, De-Ying Tian, Department of Infectious Diseases, Tongji Hospital, Tongji Medical College, Huazhong University of Science and Technology, Wuhan 430030, Hubei Province, China

Correspondence to: Dr. Jun-Ying Qi, Department of Infectious Diseases, Tongji Hospital, Tongji Medical College, Huazhong University of Science and Technology, Jiefang Street 1 095, Wuhan 430030, Hubei Province, China. daikai@126.com
Telephone: +86-27-83662815

Received: 2004-12-17 Accepted: 2005-02-14

Abstract

AIM: To investigate the effects of leptin administration on liver fibrosis induced by thioacetamide (TAA).

METHODS: Twenty-four male C57Bl/6 mice were randomly allocated into four groups, which were intra-peritoneally given saline (2 mL/kg), leptin (1 mg/kg), TAA (200 mg/kg), TAA (200 mg/kg) plus leptin (1 mg/kg) respectively, thrice a week. All mice were killed after 4 wk. The changes in biochemical markers, such as the levels of alanine aminotransferase (ALT) and aspartate aminotransferase (AST) in serum and superoxide dismutase (SOD), malondialdehyde (MDA) in liver were determined. For histological analysis, liver tissues were fixed with 10% buffered formalin, embedded with paraffin. Hematoxylin-eosin (HE) staining and picric acid-Sirius red dyeing were performed. The level of $\alpha 1(I)$ procollagen mRNA in liver tissues was analyzed by RT-PCR.

RESULTS: Apparent liver fibrosis was found in TAA group and TAA plus leptin group. Compared to saline group, the levels of ALT and AST in serum and MDA in liver increased in TAA group (205.67±27.69 U/L vs 50.67±10.46 U/L, 177.50±23.65 U/L vs 76.33±12.27 U/L, 2.60±0.18 nmol/mg pro vs 1.91±0.14 nmol/mg pro, $P<0.01$) and in TAA plus leptin group (256.17±22.50 U/L vs 50.67±10.46 U/L, 234.17±27.37 U/L vs 76.33±12.27 U/L, 2.97±0.19 nmol/mg pro vs 1.91±0.14 nmol/mg pro, $P<0.01$). The level of SOD in livers decreased (51.80±8.36 U/mg pro vs 81.52±11.40 U/mg pro, 35.78±6.11 U/mg pro vs 81.52±11.40 U/mg pro, $P<0.01$) and the level of $\alpha 1(I)$ procollagen mRNA in liver tissues also increased (0.28±0.04 vs 0.11±0.02, 0.54±0.07 vs 0.11±0.02, $P<0.01$). But no significant changes were found in leptin group and saline group. Compared to TAA group, ALT, AST, MDA, and $\alpha 1(I)$ procollagen mRNA and grade of liver fibrosis in TAA plus leptin group increased (256.17±22.50 U/L vs 205.67±27.69 U/L, $P<0.05$; 234.17±27.37 U/L vs 177.50±23.65 U/L, $P<0.05$; 2.97±0.19 nmol/mg pro vs 2.60±0.18 nmol/mg

pro, $P<0.05$; 0.54±0.07 vs 0.28±0.04, $P<0.01$; 3.17 vs 2.00, $P<0.05$), and the level of SOD in liver decreased (35.78±6.11 U/mg pro vs 51.80±8.36 U/mg pro, $P<0.05$). There were similar changes in the degree of type I collagen deposition confirmed by picric acid-Sirius red dyeing.

CONCLUSION: Leptin can exacerbate the degree of TAA-induced liver fibrosis in mice. Leptin may be an important factor in the development of liver fibrosis.

© 2005 The WJG Press and Elsevier Inc. All rights reserved.

Key words: Liver fibrosis; Leptin; $\alpha 1(I)$ procollagen

Dai K, Qi JY, Tian DY. Leptin administration exacerbates thioacetamide-induced liver fibrosis in mice. *World J Gastroenterol* 2005; 11(31): 4822-4826
<http://www.wjgnet.com/1007-9327/11/4822.asp>

INTRODUCTION

Leptin, an obese gene product, is a 16-ku peptide hormone expressed and secreted predominantly by adipose tissue^[1], and plays an essential role in the regulation of body weight mainly by reducing food intake and increasing energy expenditure^[2]. In addition to the effect of controlling body fat mass, leptin has a variety of other biological functions, such as wound healing, angiogenesis, immune response, etc.^[3-6], thus exerting its effects on many tissues or organs, including the liver. Potter *et al.*^[7], found that isolated hepatic stellate cells (HSCs) also produce leptin during the *in vitro* transactivation process in 1998. Since then researchers have paid more attention to the correlation between leptin and liver diseases. Recently, it was reported that the serum leptin levels are elevated in patients with chronic viral hepatitis, alcohol-induced cirrhosis, or non-alcoholic steatohepatitis (NASH)^[8-11]. These observations suggest that leptin may be involved in the progression of liver fibrosis. Accordingly, in the present study we investigated the effect of leptin administration on liver fibrosis caused by thioacetamide (TAA).

MATERIALS AND METHODS

Animals and treatment

Twenty-four, 6-wk-old male C57Bl/6 mice, weighing 18.4-24.2 g, were obtained from Institute of Transplantation, Tongji Medical College, Huazhong University of Science and Technology. All mice were housed in a temperature-humidity-controlled environment in a 12 h light-dark cycle

with free access to food and water. The mice were randomly divided into four groups with six mice in each, which were given an intra-peritoneal injection of saline (2 mL/kg), recombinant murine leptin (1 mg/kg, R&D Systems Inc., USA), TAA (200 mg/kg), TAA (200 mg/kg) plus leptin (1 mg/kg) thrice a week. All mice were killed after 4 wk. Blood and livers were collected for further examination.

Histological examination

Liver tissues were fixed with 10% buffered formalin, embedded with paraffin, and then hematoxylin-eosin (HE) staining and picric acid-Sirius red dyeing were performed. Liver fibrosis was evaluated by a semi-quantitative method to assess the degree of histological injury using the following criteria: grade 0: normal liver; grade 1: few collagen fibrils extended from the central vein to the portal tract; grade 2: apparent collagen fibril extension without encompassing the whole lobule; grade 3: collagen fibrils extended into and encompassed the whole lobule; grade 4: diffuse extension of collagen fibrils and formation of pseudo-lobule.

Estimation of liver function

Blood was obtained at the time of killing. The serum aspartate aminotransferase (AST) and alanine aminotransferase (ALT) levels were measured by the Olympus AU-1000 biochemical autoanalyzer, as markers of hepatic damage.

Level of malondialdehyde and superoxide dismutase

Malondialdehyde (MDA) and superoxide dismutase (SOD) contents in liver tissue were assayed by assay kits (Jiancheng Biotech Ltd, Nanjing, China).

RNA extraction and RT-PCR assay

Expression of $\alpha 1$ (I) procollagen mRNA was evaluated with RT-PCR. Total RNA was isolated from liver specimens with RNAex reagent (Watson Biotechnologies, Inc., Shanghai, China) according to the manufacturer's descriptions. Total RNA was quantified spectrometrically at 260 nm, and the quality of isolated RNA was analyzed on agarose gels under standard conditions. Two-step RT-PCR was performed as recommended by the suppliers. Primer sequences were $\alpha 1$ (I) procollagen: forward 5'-CCT GGA CGC CAT CAA GGT CTA C-3' and reverse 5'-CCA AGT TCC GGT GTG ACT CG-3', fragment length 419 bp; β -actin: forward 5'-ACC ACA GCT GAG AGG GAA ATC G-3' and reverse 5'-AGA GGT CTT TAC GGA TGT CAA CG-3', fragment length 277 bp. Amplification conditions were as follows: pre-denaturation at 95 °C for 2 min, then in a thermal controller for 35 cycles (denaturation at 95 °C for 45 s,

annealing at 56 °C for 45 s and extension at 72 °C for 1 min), and a final extension at 72 °C for 7 min after the last cycle. Ten milliliters of the PCR products was analyzed on 2% agarose gel containing ethidium bromide with TAE buffer at 80 V for 30 min and photographed under UV illumination. The band intensities were quantified by densitometry. $\alpha 1$ (I) procollagen/ β -actin quotient indicated the relative expression of $\alpha 1$ (I) procollagen.

Statistical analysis

The results were expressed as mean \pm SD. One-way analysis of variance (ANOVA) with LSD post hoc comparison was used to test for differences in means of variables between groups. $P < 0.05$ was considered statistically significant. All data were analyzed by SPSS 11.0 software.

RESULTS

Animal model and liver histology

Compared to saline group and leptin group, the mice in TAA group and TAA plus leptin group were thin and less haired. The surface of liver was rough and formation of small nodules was observed, indicating that liver fibrosis developed as expected. The degree of type I collagen deposition was confirmed by liver histology stained with picric acid-Sirius red. As anticipated, liver tissue specimens from both the saline group and leptin group showed no significant picric acid-Sirius red staining, indicating a lack of type I collagen deposition outside of central and portal blood vessels. Apparent hepatocyte degeneration, necrosis, infiltration of inflammatory cells, expanded portal tracts and collagen deposition were found in TAA group and TAA plus leptin group. The degree of liver fibrosis in these two groups significantly increased compared to that in saline group or leptin group ($P < 0.01$). But compared to TAA group, the deposition of type I collagen in TAA plus leptin group was more apparent and the degree of liver fibrosis also increased ($P < 0.05$). The details about the degree of liver fibrosis in each group are shown in Table 1. Type I collagen deposition in each group is shown in Figure 1.

Serum ALT and AST level

At the end of the study, there was no difference in serum ALT and AST levels between saline group and leptin group. But serum ALT and AST levels in TAA group and TAA plus leptin group significantly increased compared to those in saline group and leptin group ($P < 0.01$). Furthermore, treatment with TAA plus leptin increased the ALT and AST levels compared to treatment with TAA ($P < 0.05$, Table 2).

Table 1 Degree of liver fibrosis in each group of mice

Group	n	Grade of liver fibrosis					Average
		0	I	II	III	IV	
Saline	6	6	0	0	0	0	0
Leptin	6	6	0	0	0	0	0
TAA	6	0	1	4	1	0	2.00 ^{b,d}
TAA+leptin	6	0	0	0	5	1	3.17 ^{a,b,d}

^a $P < 0.05$ vs TAA group; ^b $P < 0.01$ vs saline group; ^d $P < 0.01$ vs leptin group.

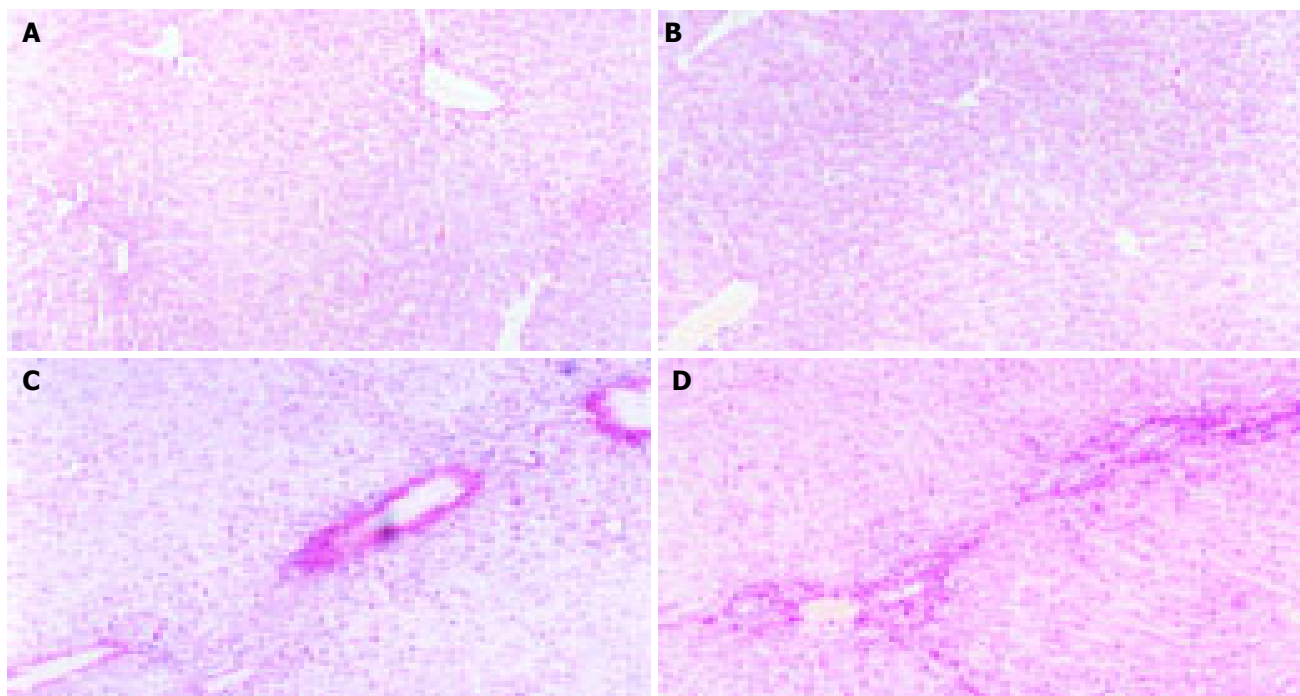


Figure 1 Type I collagen deposition in saline group (A), leptin group (B), TAA (C), and TAA plus leptin group (D). 200 \times (red color indicates picric acid-Sirius

red staining for collagen).

Table 2 Serum ALT and AST level (mean \pm SD)

Group	<i>n</i>	ALT (U/L)	AST (U/L)
Saline	6	50.67 \pm 10.46	76.33 \pm 12.27
Leptin	6	47.50 \pm 11.78	71.67 \pm 14.39
TAA	6	205.67 \pm 27.69 ^{b,d}	177.50 \pm 23.65 ^{b,d}
TAA+leptin	6	256.17 \pm 22.50 ^{a,b,d}	234.17 \pm 27.37 ^{a,b,d}

^a*P*<0.05 vs TAA group; ^b*P*<0.01 vs saline group; ^d*P*<0.01 vs leptin group.

Changes of MDA and SOD in liver tissue

The amount of MDA and SOD did not obviously change in leptin group, compared to that in the saline group. The amount of MDA in TAA group and TAA plus leptin group was significantly higher than that in saline group (*P*<0.01), while SOD in the two groups was significantly lower than that in saline group (*P*<0.01). But MDA was higher in TAA plus leptin group than in TAA group (*P*<0.05), while SOD was lower in TAA plus leptin group than in TAA group (*P*<0.05, Table 3).

Table 3 Changes of MDA and SOD in liver tissue (mean \pm SD)

Group	<i>n</i>	SOD (U/mg pro)	MDA (nmol/mg pro)
Saline	6	81.52 \pm 11.40	1.91 \pm 0.14
Leptin	6	83.63 \pm 10.68	1.93 \pm 0.13
TAA	6	51.80 \pm 8.36 ^{b,d}	2.60 \pm 0.18 ^{b,d}
TAA+leptin	6	35.78 \pm 6.11 ^{a,b,d}	2.97 \pm 0.19 ^{a,b,d}

^a*P*<0.05 vs TAA group; ^b*P*<0.01 vs saline group; ^d*P*<0.01 vs leptin group.

α 1(I) procollagen mRNA expression

To determine the expressions of collagen, mRNA transcripts

Table 4 Level of α 1(I) procollagen mRNA in relation to β -actin (mean \pm SD)

Group	<i>n</i>	Ratio
Saline	6	0.11 \pm 0.02
Leptin	6	0.13 \pm 0.02
TAA	6	0.28 \pm 0.04 ^{b,d}
TAA+leptin	6	0.54 \pm 0.07 ^{b,d,f}

^b*P*<0.01 vs saline group; ^d*P*<0.01 vs leptin group; ^f*P*<0.01 vs TAA group.

for α 1(I) procollagen were assessed. RNA extracts from livers were analyzed by reverse transcription PCR. Furthermore, the band intensity ratio of α 1(I) procollagen to β -actin was evaluated and presented as percentage of β -actin. As shown in Table 4 and Figure 2, the expression of α 1(I) procollagen in leptin group did not obviously change, compared to that in the saline group, but significantly increased in TAA group and TAA plus leptin group (*P*<0.01). The expression of α 1(I) procollagen in TAA plus leptin group was much higher than that in TAA group (*P*<0.01, Table 4 and Figure 2).

DISCUSSION

In the present study, chronic administration of TAA or TAA plus leptin caused liver fibrosis as indicated by the changes of serum markers, histopathological changes, and molecular biological changes. But more overt liver fibrosis was observed, when leptin was used in combination with TAA. Our results are in line with other findings that leptin-deficient *ob/ob* mice do not develop fibrosis during steatohepatitis or in response to chronic toxic liver injury^[12,13], indicating that leptin can exacerbate the degree of fibrosis in mouse liver induced by TAA, and may be an important

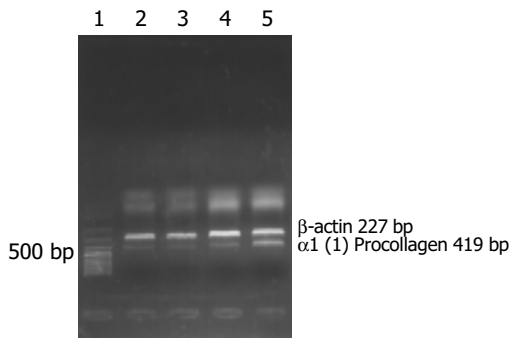


Figure 2 Expression of $\alpha 1(I)$ procollagen mRNA. M: 100-bp DNA marker; lane 1: saline group; lane 2: leptin group; lane 3: TAA group; and lane 4: TAA plus leptin group.

factor in the development of liver fibrosis.

The activities of serum fibrosis-associated enzymes, namely ALT and AST, significantly increased along with the increased expression of $\alpha 1(I)$ procollagen mRNA in TAA group and TAA plus leptin group. But leptin could augment TAA-induced inflammatory response and increase the expression of $\alpha 1(I)$ procollagen mRNA. The histological examination also found that leptin increased the TAA-induced deposition of type I collagen. Specific increase in procollagen mRNAs in liver fibrosis parallels increase in tissue collagen content. Since increased synthesis of procollagen contributes to the increase of collagen content in fibrotic liver, the expression of $\alpha 1(I)$ procollagen mRNA can reflect the degree of hepatic fibrosis^[14,15]. Activation of HSCs is the essential event in hepatic fibrogenesis, because HSCs transactivate to myofibroblast-like cells that produce a large, excess amount of matrix proteins (e.g., fibrillar collagen, fibronectin, laminin, and proteoglycans) in injured liver^[16]. It was reported that HSCs express short forms of the leptin receptor (Ob-Ra), but not the functional long form of the leptin receptor Ob-Rb. Since the sinusoidal endothelial cells and Kupffer cells in the liver express the long form of the leptin receptor Ob-Rb^[17,18], leptin may exert an indirect effect on the activation of HSCs mediated by TGF- β_1 . As Ob-Rb leptin can increase TGF- β_1 expression in the sinusoidal endothelial cells and Kupffer cells, TGF- β_1 activates type I collagen promoters, and upregulates the extracellular matrix such as collagen and fibronectin from HSCs^[19]. Recently, it was reported that leptin also can activate HSCs directly^[20]. However, the role of leptin in the activation of HSCs needs to be further analyzed.

TAA is a typical hepatotoxin and causes centrilobular necrosis by generation of ROS. ROS triggers lipid peroxidation chain reaction. MDA is the production of lipid peroxidation, the amount of MDA can express the degree of lipid peroxidation. SOD is a ubiquitous chain breaking anti-oxidant found in all aerobic organisms. It is a metalloprotein widely distributed in all cells and protects cells against ROS-induced oxidative damage. Oxidative stress contributes to the pathogenesis of hepatic fibrosis induced by alcohol and virus infection^[21,22]. Furthermore, oxidative stress is involved in activation of HSCs and promotion of their proliferation, collagen synthesis, and migration^[23]. The activation of

quiescent HSCs plays an important role in the process of liver fibrosis^[16,24]. In our experiment, MDA was higher in TAA plus leptin group than in TAA group ($P < 0.05$), while SOD was lower in TAA plus leptin group than in TAA group. The results suggest leptin can augment TAA-induced lipid peroxidation by lowering the level of enzymic antioxidant. But leptin administration alone has no apparent effect on lipid peroxidation. Whether leptin is just a co-factor needs to be further studied. On the other hand, leptin can regulate macrophage function^[25] and augment endotoxin-stimulated TNF production by macrophages^[3]. Hematopoietic cells including macrophages and lymphocytes contain a functional leptin receptor^[26], through which leptin regulates proliferation and maturation of immune cells^[27,28] and elicits release of pro-inflammatory cytokines from macrophages^[3]. These pro-inflammatory cytokines and immune responses play a critical role in the development of liver fibrosis. The above findings may explain, at least in part, why leptin increases the degree of liver fibrosis in mice induced by TAA.

It has been reported that hepatic cirrhosis is six fold more prevalent in obese individuals than in the general population^[29,30], and obesity is an independent risk factor for the development of chronic liver diseases caused by alcohol, chronic hepatitis C, and NASH^[31-34]. These observations indicate that there could be a pathogenic link between obesity and liver fibrosis. But the reason why obesity accelerates the development of hepatic fibrosis has not been elucidated. Circulating levels of leptin correlate well with body fat mass^[35]. Obese people have remarkably high serum leptin levels. Increased serum leptin presumably enhances pro-inflammatory and pro-fibrogenic responses in the liver, and generate oxidative stress. Leptin may be a determinant of hepatic inflammation and fibrosis in obese individuals, especially in those with NASH. Our findings support the hypothesis that leptin is involved in the progression of liver fibrosis. However, additional studies are needed to elucidate the role of leptin in the progression of chronic liver fibrosis in obese patients.

REFERENCES

- Zhang Y**, Proenca R, Maffei M, Barone M, Leopold L, Friedman JM. Positional cloning of the mouse obese gene and its human homologue. *Nature* 1994; **372**: 425-432
- Halaas JL**, Gajiwala KS, Maffei M, Cohen SL, Chait BT, Rabinowitz D, Lallone RL, Burley SK, Friedman JM. Weight-reducing effects of the plasma protein encoded by the obese gene. *Science* 1995; **269**: 543-546
- Loffreda S**, Yang SQ, Lin HZ, Karp CL, Brengman ML, Wang DJ, Klein AS, Bulkley GB, Bao C, Noble PW, Lane MD, Diehl AM. Leptin regulates proinflammatory immune responses. *FASEB J* 1998; **12**: 57-65
- Goren I**, Kampfer H, Podda M, Pfeilschifter J, Frank S. Leptin and wound inflammation in diabetic ob/ob mice: differential regulation of neutrophil and macrophage influx and a potential role for the scab as a sink for inflammatory cells and mediators. *Diabetes* 2003; **52**: 2821-2832
- Murad A**, Nath AK, Cha ST, Demir E, Flores-Riveros J, Sierra-Honigsmann MR. Leptin is an autocrine/paracrine regulator of wound healing. *FASEB J* 2003; **17**: 1895-1897
- Frankenberry KA**, Somasundar P, McFadden DW, Vona-Davis LC. Leptin induces cell migration and the expression of growth factors in human prostate cancer cells. *Am J Surg*

- 2004; **188**: 560-565
- 7 **Potter JJ**, Womack L, Mezey E, Anania FA. Transdifferentiation of rat hepatic stellate cells results in leptin expression. *Biochem Biophys Res Commun* 1998; **244**: 178-182
- 8 **Henriksen JH**, Holst JJ, Moller S, Brinch K, Bendtsen F. Increased circulating leptin in alcoholic cirrhosis: relation to release and disposal. *Hepatology* 1999; **29**: 1818-1824
- 9 **Testa R**, Franceschini R, Giannini E, Cataldi A, Botta F, Fasoli A, Tenerelli P, Rolandi E, Barreca T. Serum leptin levels in patients with viral chronic hepatitis or liver cirrhosis. *J Hepatol* 2000; **33**: 33-37
- 10 **Wang XQ**, Zhang WW, Li Y. Serum leptin levels in patients with liver cirrhosis. *Shijie Huaren Xiaohua Zazhi* 2002; **10**: 1177-1179
- 11 **Chalasanani N**, Crabb DW, Cummings OW, Kwo PY, Asghar A, Pandya PK, Considine RV. Does leptin play a role in the pathogenesis of human nonalcoholic steatohepatitis? *Am J Gastroenterol* 2003; **98**: 2771-2776
- 12 **Leclercq IA**, Farrell GC, Schriemer R, Robertson GR. Leptin is essential for the hepatic fibrogenic response to chronic liver injury. *J Hepatol* 2002; **37**: 206-213
- 13 **Honda H**, Ikejima K, Hirose M, Yoshikawa M, Lang T, Enomoto N, Kitamura T, Takei Y, Sato N. Leptin is required for fibrogenic responses induced by thioacetamide in the murine liver. *Hepatology* 2002; **36**: 12-21
- 14 **Goddard CJ**, Smith A, Hoyland JA, Baird P, McMahon RF, Freemont AJ, Shomaf M, Haboubi NY, Warnes TW. Localisation and semiquantitative assessment of hepatic procollagen mRNA in primary biliary cirrhosis. *Gut* 1998; **43**: 433-440
- 15 **Pierce RA**, Glaug MR, Greco RS, Mackenzie JW, Boyd CD, Deak SB. Increased procollagen mRNA levels in carbon tetrachloride-induced liver fibrosis in rats. *J Biol Chem* 1987; **262**: 1652-1658
- 16 **Friedman SL**. Seminars in medicine of the Beth Israel Hospital, Boston. The cellular basis of hepatic fibrosis. Mechanisms and treatment strategies. *N Engl J Med* 1993; **328**: 1828-1835
- 17 **Ikejima K**, Takei Y, Honda H, Hirose M, Yoshikawa M, Zhang YJ, Lang T, Fukuda T, Yamashina S, Kitamura T, Sato N. Leptin receptor-mediated signaling regulates hepatic fibrogenesis and remodeling of extracellular matrix in the rat. *Gastroenterology* 2002; **122**: 1399-1410
- 18 **Tang M**, Potter JJ, Mezey E. Leptin enhances the effect of transforming growth factor beta in increasing type I collagen formation. *Biochem Biophys Res Commun* 2002; **297**: 906-911
- 19 **Penttinen RP**, Kobayashi S, Bornstein P. Transforming growth factor β increases mRNA for matrix proteins both in the presence and in the absence of changes in mRNA stability. *Proc Natl Acad Sci USA* 1988; **85**: 1105-1108
- 20 **Saxena NK**, Saliba G, Floyd JJ, Anania FA. Leptin induces increased $\alpha 2(I)$ collagen gene expression in cultured rat hepatic stellate cells. *J Cell Biochem* 2003; **89**: 311-320
- 21 **Kurose I**, Higuchi H, Miura S, Saito H, Watanabe N, Hokari R, Hirokawa M, Takaishi M, Zeki S, Nakamura T, Ebinuma H, Kato S, Ishii H. Oxidative stress-mediated apoptosis of hepatocytes exposed to acute ethanol intoxication. *Hepatology* 1997; **25**: 368-378
- 22 **Lieber CS**. Alcohol and hepatitis C. *Alcohol Res Health* 2001; **25**: 245-254
- 23 **Lee KS**, Lee SJ, Park HJ, Chung JP, Han KH, Chon CY, Lee SI, Moon YM. Oxidative stress effect on the activation of hepatic stellate cells. *Yonsei Med J* 2001; **42**: 1-8
- 24 **Okuyama H**, Shimahara Y, Kawada N. The hepatic stellate cell in the post-genomic era. *Histol Histopathol* 2002; **17**: 487-495
- 25 **Lee FY**, Li Y, Yang EK, Yang SQ, Lin HZ, Trush MA, Dannenberg AJ, Diehl AM. Phenotypic abnormalities in macrophages from leptin-deficient, obese mice. *Am J Physiol* 1999; **276**: C386-394
- 26 **Bennett BD**, Solar GP, Yuan JQ, Mathias J, Thomas GR, Matthews W. A role for leptin and its cognate receptor in hematopoiesis. *Curr Biol* 1996; **6**: 1170-1180
- 27 **Gainsford T**, Willson TA, Metcalf D, Handman E, McFarlane C, Ng A, Nicola NA, Alexander WS, Hilton DJ. Leptin can induce proliferation, differentiation, and functional activation of hemopoietic cells. *Proc Natl Acad Sci USA* 1996; **93**: 14564-14568
- 28 **Santos-Alvarez J**, Goberna R, Sanchez-Margalet V. Human leptin stimulates proliferation and activation of human circulating monocytes. *Cell Immunol* 1999; **194**: 6-11
- 29 **Ratziu V**, Giral P, Charlotte F, Bruckert E, Thibault V, Theodorou I, Khalil L, Turpin G, Opolon P, Poynard T. Liver fibrosis in overweight patients. *Gastroenterology* 2000; **118**: 1117-1123
- 30 **McCullough AJ**, Falck-Ytter Y. Body composition and hepatic steatosis as precursors for fibrotic liver disease. *Hepatology* 1999; **29**: 1328-1330
- 31 **Chitturi S**, Farrell GC. Etiopathogenesis of nonalcoholic steatohepatitis. *Semin Liver Dis* 2001; **21**: 27-41
- 32 **Naveau S**, Giraud V, Borotto E, Aubert A, Capron F, Chaput JC. Excess weight risk factor for alcoholic liver disease. *Hepatology* 1997; **25**: 108-111
- 33 **Hourigan LF**, Macdonald GA, Purdie D, Whitehall VH, Shorthouse C, Clouston A, Powell EE. Fibrosis in chronic hepatitis C correlates significantly with body mass index and steatosis. *Hepatology* 1999; **29**: 1215-1219
- 34 **Adinolfi LE**, Gambardella M, Andreana A, Tripodi MF, Utili R, Ruggiero G. Steatosis accelerates the progression of liver damage of chronic hepatitis C patients and correlates with specific HCV genotype and visceral obesity. *Hepatology* 2001; **33**: 1358-1364
- 35 **Frederich RC**, Hamann A, Anderson S, Lollmann B, Lowell BB, Flier JS. Leptin levels reflect body lipid content in mice: evidence for diet-induced resistance to leptin action. *Nat Med* 1995; **1**: 1311-1314

GFAP and Fos immunoreactivity in lumbo-sacral spinal cord and medulla oblongata after chronic colonic inflammation in rats

Yi-Ning Sun, Jin-Yan Luo, Zhi-Ren Rao, Li Lan, Li Duan

Yi-Ning Sun, Jin-Yan Luo, Department of Gastroenterology, The Second Hospital of Xi'an Jiaotong University, Xi'an 710004, Shaanxi Province, China

Zhi-Ren Rao, Li Lan, Li Duan, Department of Neurosciences, the Fourth Military Medical University, Xi'an 710032, Shaanxi Province, China

Correspondence to: Professor Jin-Yan Luo, Department of Gastroenterology, The Second Hospital of Xi'an Jiaotong University, Xi'an 710004, Shaanxi Province, China. lly18272@163.com

Telephone: +86-29-87678758

Received: 2004-08-26 Accepted: 2004-12-08

Abstract

AIM: To investigate the response of astrocytes and neurons in rat lumbo-sacral spinal cord and medulla oblongata induced by chronic colonic inflammation, and the relationship between them.

METHODS: Thirty-three male Sprague-Dawley rats were randomly divided into two groups: experimental group ($n = 17$), colonic inflammation was induced by intra-luminal administration of trinitrobenzenesulfonic acid (TNBS); control group ($n = 16$), saline was administered intra-luminally. After 3, 7, 14, and 28 d of administration, the lumbo-sacral spinal cord and medulla oblongata were removed and processed for anti-glial fibrillary acidic protein (GFAP), Fos and GFAP/Fos immunohistochemistry.

RESULTS: Activated astrocytes positive for GFAP were mainly distributed in the superficial laminae (laminae I-II) of dorsal horn, intermediolateral nucleus (laminae V), posterior commissural nucleus (laminae X) and anterolateral nucleus (laminae IX). Fos-IR (Fos-immunoreactive) neurons were mainly distributed in the deeper laminae of the spinal cord (laminae III-IV, V-VI). In the medulla oblongata, both GFAP-IR astrocytes and Fos-IR neurons were mainly distributed in the medullary visceral zone (MVZ). The density of GFAP in the spinal cord of experimental rats was significantly higher after 3, 7, and 14 d of TNBS administration compared with the controls (50.4 ± 16.8 , 29.2 ± 6.5 , 24.1 ± 5.6 , $P < 0.05$). The density of GFAP in MVZ was significantly higher after 3 d of TNBS administration (34.3 ± 2.5 , $P < 0.05$). After 28 d of TNBS administration, the density of GFAP in the spinal cord and MVZ decreased and became comparable to that of the controls (18.0 ± 4.9 , 14.6 ± 6.4 , $P > 0.05$).

CONCLUSION: Astrocytes in spinal cord and medulla oblongata can be activated by colonic inflammation. The activated astrocytes are closely related to Fos-IR neurons. With the recovery of colonic inflammation, the activity of

astrocytes in the spinal cord and medulla oblongata is reduced.

© 2005 The WJG Press and Elsevier Inc. All rights reserved.

Key words: Astrocytes; Neurons; Glial fibrillary acidic protein; Fos; Spinal cord; Medulla oblongata; Colonic inflammation

Sun YN, Luo JY, Rao ZR, Lan L, Duan L. GFAP and Fos immunoreactivity in lumbo-sacral spinal cord and medulla oblongata after chronic colonic inflammation in rats. *World J Gastroenterol* 2005; 11(31): 4827-4832

<http://www.wjgnet.com/1007-9327/11/4827.asp>

INTRODUCTION

Recent studies have shown that astrocytes, being in intimate contact with neurons, may respond to various kinds of stimulation. Both peripheral inflammation and nerve injuries are able to induce astrocytic activation in the spinal cord and brain stem. Moreover, astrocytic activation was shown to be involved in central nervous system (CNS) responses leading to hypersensitivity and persistent pain states^[1-3]. Glial fibrillary acidic protein (GFAP) is an intermediate filament component in astrocytes of nervous tissue. The expression of GFAP may increase with astrocytic activation^[4]. By using GFAP and Fos immunoreactivity (IR) as markers, we aimed to determine the response of astrocytes and neurons in rat lumbo-sacral spinal cord and medulla oblongata induced by chronic colonic inflammation, and the relationship between them.

MATERIALS AND METHODS

Animals

Thirty-three adult male Sprague-Dawley rats (The Fourth Military Medical University) weighing 220-250 g were used in this study. The animals were housed in a quiet room with a constant ambient temperature of 20 °C, and free access to rat chow and water. They were divided randomly into experimental group ($n = 17$) and control group ($n = 16$).

Experimental protocol

After 24 h fast, trinitrobenzenesulfonic acid (TNBS, 100 mg/kg in 300 mL/L ethanol) was administered intra-luminally through a silicone rubber catheter introduced 7 cm into the anus with light diethyl-ether anesthesia, as previously described^[5]. To keep TNBS in the colon for a longer time and to avoid leakage, the tubing was slowly

withdrawn and the tail of the rat was kept elevated for 8-10 min. After intra-luminal administration of TNBS, rats in the experimental group were allowed to live 3 ($n = 4$), 7 ($n = 4$), 14 ($n = 4$) and 28 ($n = 5$) d, respectively.

After intra-luminal administration of 0.5 mL saline, rats in the control group were allowed to live 3 ($n = 4$), 7 ($n = 4$), 14 ($n = 4$) and 28 ($n = 4$) d, respectively.

Immunohistochemistry

The animals were deeply anesthetized with pentobarbital Na (80 mg/kg, intraperitoneal) and perfused intracardially with 100 mL saline followed by 500 mL fixative of 4% paraformaldehyde in 0.1 mol/L phosphate buffer (pH 7.4). L₃-S₂ segments of the spinal cord and medulla oblongata were removed post-fixed in the same fixative at 4 °C for 2-4 h and then cryoprotected in 20% sucrose overnight. Serial frozen sections of 40 μm thick were cut on a Leitz cryocut. Sections were collected in 0.01 mol/L PBS for immunohistochemistry.

The spinal cord and medulla oblongata sections from each rat were randomly divided into three sets. Two sets were processed for anti-GFAP and anti-Fos immunohistochemical staining by using avidin-biotin-peroxidase complex (ABC) method. Briefly, free-floating tissue sections were treated in 800 mL/L methanol containing 0.3% H₂O₂ to block endogenous peroxidase activity for 30 min at room temperature. They were treated with 0.01 mol/L PBS containing 0.1% Triton X100 for 20 min at room temperature. The sections were then incubated with a polyclonal rabbit anti-Fos antibody (1:3 000, Santa Cruz) or rabbit anti-GFAP antibody (1:3 000 Dako) for 48 h at 4 °C. After that, the sections were incubated with biotinylated goat anti-rabbit IgG (1:500, Sigma), and subsequently with the ABC complex (1:500, Sigma) at room temperature for 2 h each. The antigen-antibody reaction sites were visualized by incubation with glucose oxidase-DAB-nickel method for 15-30 min at room temperature. The sections were rinsed in 0.01 mol/L PBS for 3 min×10 min during the transition of these steps. The other set group of sections was stained for GFAP and Fos by using double immunohistochemical labeled method. Finally, the sections were mounted onto gelatin-coated slides, dried, dehydrated, cleared and coverslipped.

Histopathological analysis

Colon specimens that were 1 cm long and 7 cm proximal to the anus were taken for histological assessment. They were rapidly immersed in cold 100 mL/L neutral buffered formalin, fixed overnight. Then they were processed routinely and embedded in paraffin blocks, and 3-5 μm-thick cross sections were stained with H&E and examined by light microscope.

Measurement of the density of GFAP staining and Fos immunoreactive neuronal counts

The density of GFAP staining and the numbers of neuronal nuclear profiles expressing Fos were analyzed with computer assisted QUIC Menu System. The ratio of the area of stained GFAP to the area of outlined regions was presented as the density of GFAP. Fos counting was done by outlining specific regions and then, particles (stained nuclei) were counted in

the outlined regions.

For each animal, the average for density measurements and number counts in the spinal cord was obtained unilaterally from five randomly selected sections. In the medulla oblongata, four sections were selected from above the obex, obex, the area postrema, and pyramidal decussation levels respectively. The average for density measurements and number counts was obtained unilaterally in the nucleus of the solitary tract (NTS), ventrolateral medulla (VLM) and intermediate reticular zone (IRt) from those four section levels.

Statistical analysis

Pictures were taken under BX-60 microscope with the support of IM50 software. All results are expressed as mean±SD. An unpaired *t*-test was used to compare GFAP density and Fos-IR cell count data between the groups. A difference was accepted as significant, if the probability was less than 5% ($P < 0.05$).

RESULTS

Histopathological changes in the inflamed colon

After 3, 7, and 14 d of TNBS administration, macroscopic and histological examination of the rat colon showed that TNBS-induced colitis was uniform, with submucosal and mucosal infiltration with numerous inflammatory cells, signs of extensive ulceration, and dilated blood vessels (Figures 1A and 1B). The colon appeared macroscopically normal in rats that received TNBS for 28 d (Figure 1C). The presence of inflammatory cells was minimal in the colon of the control rats treated with saline (Figure 1D).

GFAP and Fos protein expression in the spinal cord

In the experimental animals, colonic inflammation induced robust astrocytic activation responses after 3, 7, and 14 d of TNBS administration. The activated glial cells were characterized by decreased ramification, hypertrophy and proliferation. Most activated astrocytes positive for GFAP were distributed bilaterally in the superficial laminae (laminae I-II) of dorsal horn, intermediolateral nucleus (laminae V), posterior commissural nucleus (laminae X) and anterolateral nucleus (laminae IX, Figure 2A). Mild GFAP-IR astrocytes exhibited in the spinal cord of the rats treated with saline (Figure 2B). The density of GFAP in the spinal cord of experimental rats was significantly higher after 3, 7, and 14 d of TNBS administration compared with that of the controls ($P < 0.05$). After 28 d of TNBS administration, the density of GFAP in the spinal cord decreased and was comparable to that of the control group ($P > 0.05$, Table 1).

The majority of Fos-IR neurons were distributed bilaterally in L₅, L₆, and S₁ segments of lumbo-sacral spinal cord after TNBS administration. At various post-inflammatory days, Fos-IR cells were mainly localized in deeper laminae III-IV and laminae V-VI in the spinal dorsal horn (Figure 2C). Only a few Fos-IR neurons were sparsely distributed in the dorsal horn of the rats treated with saline (Figure 2D). After 3 d following TNBS administration, the number of Fos-IR neurons in the dorsal horn did not increase significantly

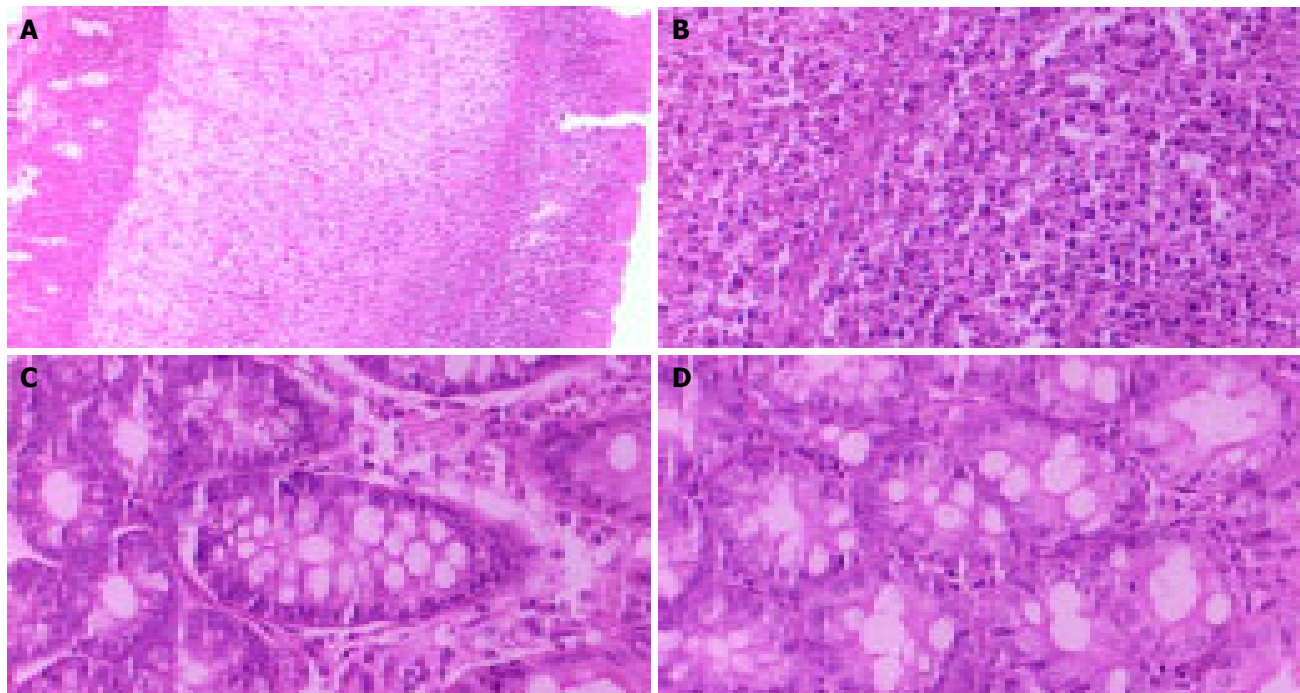


Figure 1 Histopathological changes of the colon. **A:** After 3 d of TNBS administration, the structure of the colon was destroyed ($\times 10$); **B:** Numerous inflammatory cells were infiltrated in the submucosa and mucosa of the colon

($\times 40$); **C:** After 28 d of TNBS administration, only a few inflammatory cells were infiltrated in submucosa and mucosa of the colon ($\times 40$); **D:** The inflammatory cells were minimal in the colon of the rats after 3 d of saline administration ($\times 40$).

($P > 0.05$). With the aggravation of colonic inflammation, the number of Fos-IR cells in the dorsal horn increased after 7 and 14 d following TNBS injection, a significant difference compared with that of the control group ($P < 0.05$). It was noted that Fos expression in the spinal cord displayed two patterns after 28 d of TNBS administration. Few Fos-IR neurons exhibited in the spinal dorsal horn in two rats (12.0 and 13.3, 12.7 ± 0.9), without significant difference from the control ($P > 0.05$). However, many Fos-IR neurons presented in the spinal dorsal horn in three rats (56.7, 69.0 and 36.7 , 54.1 ± 16.3), with a significant difference compared with that in control rats ($P < 0.05$, Table 2).

Table 1 Density of GFAP in the spinal cord and MVZ at various post-inflammatory days (%)

	Spinal cord		MVZ	
	Experimental	Control	Experimental	Control
3 d	50.4 ± 16.8^a	17.7 ± 0.4	34.3 ± 2.5^a	15.9 ± 3.9
7 d	29.2 ± 6.5^a	15.5 ± 0.6	15.6 ± 1.8	13.0 ± 1.6
14 d	24.1 ± 5.6^a	14.9 ± 1.1	16.3 ± 1.6	13.5 ± 2.9
28 d	18.0 ± 4.9	15.9 ± 1.3	14.6 ± 6.4	12.8 ± 1.8

^a $P < 0.05$ vs the control.

GFAP and Fos protein expression in the medulla oblongata

In the control animals, only few GFAP-IR astrocytes exhibited in the medulla oblongata. After TNBS administration, GFAP-IR astrocytes increased and were primarily localized in MVZ, which was composed of NTS, VLM, and IRt, from the level of pyramidal decussation to the level rostral to the obex (Figure 2E). The density of GFAP in MVZ was

significantly increased after 3 d of TNBS administration compared with that of the control group ($P < 0.05$). After 7, 14, and 28 d of TNBS administration, the density of GFAP in MVZ decreased gradually and became comparable to the control group ($P > 0.05$, Table 1).

Similarly, Fos-IR neurons were primarily localized in MVZ in the experimental animals. Fos-IR neurons in MVZ did not increase significantly after 3 d of TNBS administration ($P > 0.05$). After 7 and 14 d of TNBS administration, Fos-IR neurons in MVZ increased significantly compared with those in control animals ($P < 0.05$). Fos-IR cells in MVZ decreased significantly and were comparable to those in the control group after 28 days of TNBS administration (41.2 ± 31.4 , $P > 0.05$, Table 2).

In the medulla oblongata, activated astrocytes positive for GFAP enveloped activated neurons stained for Fos (Figure 2F).

Table 2 Number of Fos-IR neurons in the spinal cord and MVZ at various post-inflammatory days

	Spinal cord		MVZ	
	Experimental	Control	Experimental	Control
3 d	31.8 ± 7.1	23.7 ± 4.9	47.8 ± 17.1	40.5 ± 15.6
7 d	56.7 ± 12.3^a	13.5 ± 2.6	78.5 ± 13.8^a	52.1 ± 17.6
14 d	57.9 ± 14.6^a	13.3 ± 2.4	81.9 ± 27.0^a	48.8 ± 2.2
28 d	37.5 ± 25.5	12.2 ± 2.6	41.2 ± 31.4	47.9 ± 11.9

^a $P < 0.05$ vs the control.

DISCUSSION

It is well known that gut afferent signals reach conscious

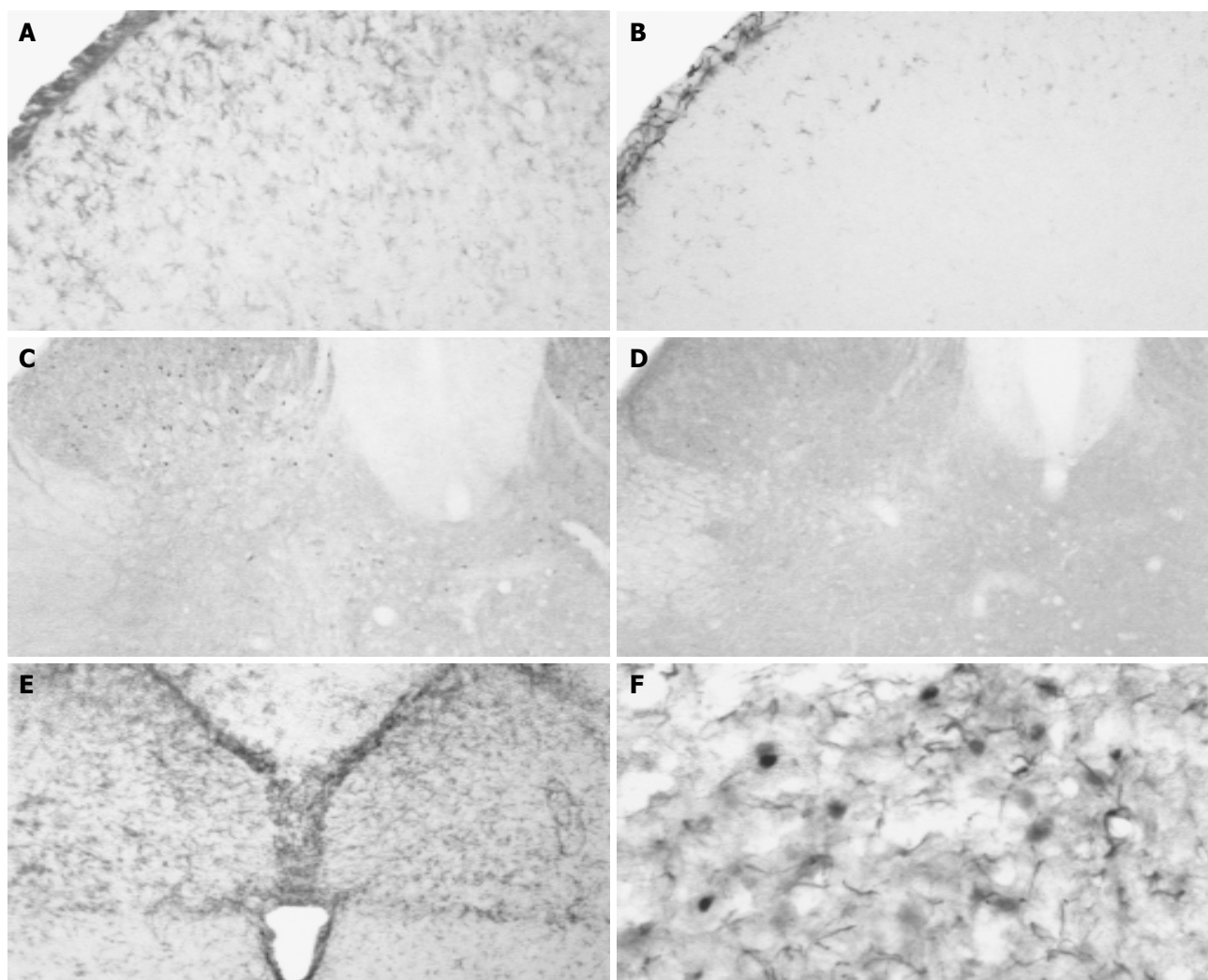


Figure 2 GFAP and Fos expression in the spinal cord and NTS. **A:** After 3 d of TNBS administration, most activated astrocytes positive for GFAP were distributed in the superficial laminae (laminae I-II) of dorsal horn ($\times 20$); **B:** Mild GFAP-IR astrocytes exhibited in the spinal cord of rats after 3 d of saline administration ($\times 20$); **C:** After 14 d of TNBS administration, Fos-IR cells were mainly localized in deeper laminae III-IV and laminae V-VI in the spinal dorsal

horn ($\times 10$); **D:** Only a few Fos-IR neurons were sparsely distributed in the dorsal horn after 7 d of saline administration ($\times 10$); **E:** After 3 d of TNBS administration, GFAP-IR glial cells increased and were primarily localized in NTS ($\times 10$); **F:** After 3 d of TNBS administration, activated astrocytes positive for GFAP enveloped activated neurons stained for Fos in the medulla oblongata ($\times 40$).

perception through a three-neuron chain. The second-order neuron, whose cell body is in the dorsal horn of the spinal cord, converge visceral and somatic afferents^[6]. In the rat, the descending colon is innervated by sensory afferent fibers in the pelvic nerve projecting to the lumbar-sacral (L₆-S₂) spinal cord^[7]. MVZ is an arch zone extending from the dorsomedial area across reticular formation to VLM. It is situated in the middle-caudal segment of the medulla oblongata, from the level of the pyramidal decussation to the level, rostral to the obex. MVZ is a relay station predominantly transmitting visceral sensory information, and takes part in perception of noxious stimulation^[8]. Because of the importance of the lumbo-sacral spinal cord segments and MVZ in transmitting visceral signals, we studied the responses of astrocytes and neurons induced by colonic inflammation in these tissues.

Studies have shown that astrocytes may respond to a number of stimulations, such as somatic and visceral inflammation^[3,9], nerve injuries^[10] and bone cancer^[11]. Activated astrocytes may involve in mediating hyperalgesia

and chronic pain. The activated astrocytes are characterized by decreased ramification, hypertrophy, proliferation, and the up-regulation of immunoregulatory molecules^[12]. GFAP are distributed in the cytoplasm of many types of glial cells. GFAP expression is low in the intact adult CNS, but increases after astrocytic activation^[13]. Sweitzer *et al.*, reported that acute peripheral inflammation induced by subcutaneous injection of formalin and zymosan resulted in increased expression of GFAP in astrocytes. Astrocytic activation has been implicated in regenerative processes and synaptic remodeling that may be detrimental when aberrant processing ensues, leading to chronic pain states^[1].

In our experiment, colonic inflammation induced robust astrocytic activation responses after 3, 7, and 14 d of TNBS administration. Most activated astrocytes positive for GFAP were distributed bilaterally in the superficial laminae (laminae I-II) of dorsal horn. These results are consistent with other studies. In a rat model of bone cancer, significant enhancement of GFAP staining was described in the superficial laminae of the ipsilateral spinal cord^[11]. Watkins

et al., have shown that astrocytes were able to release nerve growth factor (NGF), which exerts its pain modulatory actions on primary afferents. Furthermore, primary afferents expressing high affinity NGF receptors terminate exclusively in laminae I and the outer region of laminae II. Astrocytes in the intermediolateral nucleus (laminae V), posterior commissural nucleus (laminae X) and anterolateral nucleus (laminae IX) were also activated after 3, 7, and 14 d of TNBS administration. In the lumbo-sacral spinal cord, cell bodies of parasympathetic nerve are located in intermediolateral nucleus i.e., is parasympathetic sacral nucleus. Somatic and visceral afferents converge at posterior commissural nucleus. Therefore, astrocytic responses in these nuclei were directly activated by colonic inflammation. Astrocytic activation in anterolateral nucleus might be related to diarrhea induced by TNBS administration.

The timing of the changes of GFAP is relevant to the mode by which astrocytes are activated. A rapid increase in GFAP-IR has been reported to occur between 30 min and 3 h and then a secondary increase which follows approximately 3 d later. GFAP-IR in the trigeminal ganglion in response to dental injury reported by Stephenson *et al.*, appeared by 3 d and was most intense by 7 d^[4]. Astrocytic activation in the spinal cord segments increased 42 d after lumbar root injury^[4]. Chudler *et al.*, proposed that the persistence of GFAP-IR 59 d after nerve injury suggested GFAP was involved in the long-term recovery of injured neurons^[5]. In the experimental rats, the density of GFAP in lumbo-sacral spinal cord and MVZ was most intense by 3 d and decreased gradually after TNBS administration. After 7 and 14 d of TNBS administration, the density of GFAP in the spinal cord was still significantly higher compared with that of the controls ($P < 0.05$). However, the density of GFAP in MVZ became comparable to that of the control group ($P > 0.05$). This result suggested that astrocytic activation in the spinal cord lasted much longer than that in MVZ. The response of astrocytes in both the spinal cord and MVZ decreased significantly with the recovery of colonic inflammation.

The evoked expression of the immediate-early-gene-encoded protein, Fos, serves as a quantifiable marker to identify neuronal populations activated by noxious somatic and visceral stimulation^[6]. Fos protein is thought to be a nuclear third messenger coupling short-term extracellular signals with long-term alterations in cell function^[7]. Thus, Fos protein expression can be used to study long-term changes in stimulus-induced neuronal activity^[8]. We found that Fos-IR cells were mainly localized in deeper laminae III-IV and laminae V-VI in the spinal dorsal horn over time in experimental groups. Only a few Fos-IR neurons were sparsely distributed in the superficial laminae I-II in the dorsal horn. This suggested that persistent noxious visceral stimulation induced Fos expression to a greater extent in deeper laminae than in the superficial ones in the spinal dorsal horn. These results are in line with the spatial distribution of Fos protein in the lumbar spinal dorsal horn in rats following chronic adjuvant-induced arthritis^[9] and chronic constriction injury to the sciatic nerve^[20]. The study of Imbe *et al.*, showed that Fos-IR cells might spread from the superficial laminae to deeper ones in the dorsal horn

when deep tissue inflammation persisted^[8].

The timing changes of Fos expression differed from that of GFAP. After 3 d following TNBS administration, the number of Fos-IR neurons in the spinal dorsal horn and MVZ did not increase significantly. With intensification of colonic inflammation, the number of Fos-IR cells both in the dorsal horn and in MVZ increased significantly after 7 and 14 d following TNBS administration. After 28 d of TNBS administration when colonic inflammation recovered, Fos-IR cells in MVZ decreased significantly and were comparable to those in the control group. However, a lot of Fos-IR neurons still presented in the spinal dorsal horn in three experimental rats. Although it is not known exactly whether increased central hyperexcitability contributes to greater Fos protein expression following inflammation. The study of Zimmerman and Herdegen suggested that the increase in Fos may be a necessary pre-requisite for the development of chronic pain and allodynia, because increased expression of the gene product renders the neurons susceptible to subsequent stimuli^[21]. The development of neuronal activation in the lumbo-sacral dorsal horn may play a role in visceral hypersensitivity.

Astrocytes display an intimate structural relationship with the neurons that they envelope in the CNS. Gap junctions between astrocytes have been demonstrated using the freeze-fracture technique and adherents junctions between neurons and astrocytes have been observed in many species^[4]. In addition to the morphological associations between neurons and astrocytes, there appears to be a wide range of functional interactions between these cells. Duan *et al.*, reported that the number of connexin32/connexin43 gap junction (HGJ) between neurons and astrocytes in rat supraoptic nuclei was significantly increased following hyperosmotic stimuli. They proposed HGJ may be a rapid adaptive signal structure between neurons and astrocytes in response to stimulation. Apart from playing roles in synaptic remodeling and providing neurotrophic support for regenerating neurons, astrocytes which are known to express both voltage gated sodium channels and glutamate receptors could serve as sensors for neuronal activity or injury^[22]. The present study has shown that GFAP-IR astrocytes and Fos-IR neurons distributed similarly in deeper laminae of the spinal dorsal horn and MVZ, especially in the commissural subnucleus inside NTS. This suggested that colonic inflammation could not only induce neuronal activation in visceral transmitting chain, but also induce astrocytic responses via signal interactions between neurons and astrocytes.

REFERENCES

- 1 **Sweitzer SM, Colburn RW, Rutkowski M, Deleo JA.** Acute peripheral inflammation induces moderate glial activation and spinal IL-1 β expression that correlates with pain behavior in the rat. *Brain Res* 1999; **829**: 209-221
- 2 **Winkelstein BA, Deleo JA.** Nerve root injury severity differentially modulates spinal glial activation in a rat lumbar radiculopathy model: considerations for persistent pain. *Brain Res* 2002; **956**: 294-301
- 3 **Wang Y, Qiu JY, Duan L, Chen LW, Rao ZR.** Expression of GFAP in rat brain stem astrocytes induced by stomachic nociception and relationship to neurons. *Zhongguo Zuzhi*

- Huaxue He Xibao Huaxue Zazhi* 2001; **10**: 219-223
- 4 **Stephenson JL**, Byers MR. GFAP immunoreactivity in trigeminal ganglion satellite cells after tooth injury in rats. *Exp Neurol* 1995; **131**: 11-22
 - 5 **Zhou SY**, Mei QB, Liu L, Guo X, Qiu BS, Zhao DH, Cho CH. Delivery of glucocorticoid conjugate in rat gastrointestinal tract and its treatment for ulcerative colitis. *Acta Pharmacol Sin* 2001; **22**: 761-764
 - 6 **Camilleri M**, Coulie B, Tack JF. Visceral hypersensitivity: facts, speculations, and challenges. *Gut* 2001; **48**: 125-131
 - 7 **Traub RJ**, Murphy A. Colonic inflammation induces fos expression in the thoracolumbar spinal cord increasing activity in the spinoparabrachial pathway. *Pain* 2002; **95**: 93-102
 - 8 **Rao ZR**, Ju G. Morphology of the medullary visceral zone. *Chinese Science Bulletin* 1999; **44**: 1-10
 - 9 **Watkins LR**, Martin D, Ulrich P, Tracey KJ, Maier SF. Evidence for the involvement of spinal cord glia in subcutaneous formalin induced hyperalgesia in the rat. *Pain* 1997; **71**: 225-235
 - 10 **Colburn RW**, Rickman AJ, Deleo JA. The effect of site and type of nerve injury on spinal glial activation and neuropathic pain behavior. *Exp Neurol* 1999; **157**: 289-304
 - 11 **Medhurst SJ**, Walker K, Bowes M, Kidd BL, Glatt M, Muller M, Hattenberger M, Vaxelaire J, O'Reilly T, Wotherspoon G, Winter J, Green J, Urban L. A rat model of bone cancer pain. *Pain* 2002; **96**: 129-140
 - 12 **Ma W**, Quirion R. Partial sciatic nerve ligation induces increase in the phosphorylation of extracellular signal-regulated kinase (ERK) and c-Jun N-terminal kinase (JNK) in astrocytes in the lumbar spinal dorsal horn and the gracile nucleus. *Pain* 2002; **99**: 175-184
 - 13 **Ramer MS**, Kawaja MD, Henderson JT, Roder JC, Bisby MA. Glial overexpression of NGF enhances neuropathic pain and adrenergic sprouting into DRG following chronic sciatic constriction in mice. *Neurosci Lett* 1998; **251**: 53-56
 - 14 **Hashizume H**, Deleo JA, Colburn RW, Weinstein JN. Spinal glial activation and cytokine expression after lumbar root injury in the rat. *Spine* 2000; **25**: 1206-1217
 - 15 **Chudler EH**, Anderson LC, Byers MR. Trigeminal ganglion neuronal activity and glial fibrillary acidic protein immunoreactivity after inferior alveolar nerve crush in the adult rat. *Pain* 1997; **73**: 141-149
 - 16 **Lu Y**, Westlund KN. Effects of baclofen on colon inflammation-induced Fos, CGRP and SP expression in spinal cord and brainstem. *Brain Res* 2001; **889**: 118-130
 - 17 **Dai Y**, Iwata K, Kondo E, Morimoto T, Noguchi K. A selective increase in Fos expression in spinal dorsal horn neurons following graded thermal stimulation in rats with experimental mononeuropathy. *Pain* 2001; **90**: 287-296
 - 18 **Imbe H**, Iwata K, Zhou QQ, Zou S, Dubner R, Ren K. Orofacial deep and cutaneous tissue inflammation and trigeminal neuronal activation. Implications for persistent temporomandibular pain. *Cell Tis Org* 2001; **169**: 238-247
 - 19 **Abbadie C**, Besson JM. C-fos expression in rat lumbar spinal cord following peripheral stimulation in adjuvant-induced arthritic and normal rats. *Brain Res* 1993; **607**: 195-204
 - 20 **Yamazaki Y**, Maeda T, Someya G, Wakisaka S. Temporal and spatial distribution of Fos protein in the lumbar spinal dorsal horn neurons in the rat with chronic constriction injury to the sciatic nerve. *Brain Res* 2001; **914**: 106-114
 - 21 **Zimmerman M**, Herdegen T. Plasticity of the nervous system at the systemic, cellular and molecular levels: a mechanism of chronic pain and hyperalgesia. *Prog Brain Res* 1996; **110**: 233-259
 - 22 **Colburn RW**, Deleo JA, Rickman AJ, Yeager MP, Kwon P, Hickey WF. Dissociation of microglial activation and neuropathic pain behaviors following peripheral nerve injury in the rat. *J Neuroimmunol* 1997; **79**: 163-175

• CLINICAL RESEARCH •

Crohn's disease in Japanese is associated with a SNP-haplotype of *N*-acetyltransferase 2 gene

Haruhisa Machida, Kazuhiro Tsukamoto, Chun-Yang Wen, Saburo Shikuwa, Hajime Isomoto, Yohei Mizuta, Fuminao Takeshima, Kunihiko Murase, Naomichi Matsumoto, Ikuo Murata, Shigeru Kohno, Chen-Yang Wen

Haruhisa Machida, Hajime Isomoto, Yohei Mizuta, Fuminao Takeshima, Kunihiko Murase, Shigeru Kohno, Second Department of Internal Medicine, Nagasaki University School of Medicine, 1-7-1 Sakamoto, Nagasaki 852-8501, Japan

Kazuhiro Tsukamoto, Ikuo Murata, Department of Pharmacotherapeutics, Nagasaki University Graduate School of Biomedical Sciences, 1-14 Bunkyo-machi, Nagasaki 852-8521, Japan

Chun-Yang Wen, Department of Molecular Pathology, Atomic Bomb Disease Institute, Nagasaki University Graduate School of Biomedical Sciences, 1-12-4 Sakamoto, Nagasaki 852-8523, Japan

Chen-Yang Wen, Department of Digestive Disease, The Affiliated Drum Tower Hospital of Nanjing University Medical School, Nanjing 210008, Jiangsu Province, China

Saburo Shikuwa, Department of Gastroenterology, National Hospital Organization Nagasaki Medical Center, 2-1001-1 Kubara, Omura 856-8562, Japan

Naomichi Matsumoto, Department of Human Genetics, Nagasaki University Graduate School of Biomedical Sciences, 1-12-4 Sakamoto, Nagasaki 852-8523, Japan

Kazuhiro Tsukamoto, Naomichi Matsumoto, CREST, JST, Kawaguchi, Japan

Correspondence to: Kazuhiro Tsukamoto, MD, PhD, Department of Pharmacotherapeutics, Nagasaki University Graduate School of Biomedical Sciences, 1-14 Bunkyo-machi, Nagasaki 852-8521, Japan. ktsuka@net.nagasaki-u.ac.jp

Telephone: +81-95-819-2448 Fax: +81-95-819-2895

Received: 2004-12-20 Accepted: 2004-12-30

Abstract

AIM: To investigate the frequency and distribution of *N*-acetyltransferase 2 (*NAT2*) and uridine 5'-diphosphate (UDP)-glucuronosyltransferase 1A7 (*UGT1A7*) genes in patients with ulcerative colitis (UC) and Crohn's disease (CD).

METHODS: Frequencies and distributions of *NAT2* and *UGT1A7* SNPs as well as their haplotypes were investigated in 95 patients with UC, 60 patients with CD, and 200 gender-matched, unrelated, healthy, control volunteers by PCR-restriction fragment length polymorphism (RFLP), PCR-denaturing high-performance liquid chromatography (DHPLC), and direct DNA sequencing.

RESULTS: Multiple logistic regression analysis revealed that the frequency of haplotype, *NAT2**7*B*, significantly increased in CD patients, compared to that in controls ($P = 0.0130$, OR = 2.802, 95%CI = 1.243-6.316). However, there was no association between *NAT2* haplotypes and UC, or between any *UGT1A7* haplotypes and inflammatory bowel disease (IBD).

CONCLUSION: It is likely that the *NAT2* gene is one of

the determinants for CD in Japanese. Alternatively, a new CD determinant may exist in the 8p22 region, where *NAT2* is located.

© 2005 The WJG Press and Elsevier Inc. All rights reserved.

Key words: Crohn's disease; *N*-acetyltransferase 2 gene; Polymorphism; Disease-susceptible gene; Association study; Japanese population

Machida H, Tsukamoto K, Wen CY, Shikuwa S, Isomoto H, Mizuta Y, Takeshima F, Murase K, Matsumoto N, Murata I, Kohno S, Wen CY. Crohn's disease in Japanese is associated with a SNP-haplotype of *N*-acetyltransferase 2 gene. *World J Gastroenterol* 2005; 11(31): 4833-4837

<http://www.wjgnet.com/1007-9327/11/4833.asp>

INTRODUCTION

Chronic inflammatory bowel disease (IBD) is a multi-factorial disorder characterized by non-specific inflammation of the gastrointestinal tract with an increase in the permeability to xenobiotics in the intestinal mucosa, finally resulting in intestinal malabsorption and immune defense abnormalities^[1,2]. Ulcerative colitis (UC) and Crohn's disease (CD) are the major forms of IBD. Although the precise etiology of IBD remains unknown, not only several environmental factors, such as dietary components and microorganisms, but also genetic factors may contribute to the occurrence of this disorder^[3,4]. Recently, extensive molecular genetic studies have been launched to identify genes underlying the etiology^[5]. One of them is the caspase activating recruitment domain 15/nucleotide oligomerization domain 2 gene (*CARD15/NOD2*) located at 16q12. Although mutations in *NOD2* are observed frequently in Caucasian patients with CD, but not with UC^[6,7], they have rarely been found in Japanese CD patients^[8,9], suggesting that *NOD2* is not a major determinant for CD in Japanese.

We have particularly focused on genes for *N*-acetyltransferase 2 (*NAT2*) and uridine 5'-diphosphate (UDP)-glucuronosyltransferase 1A7 (*UGT1A7*) as candidates susceptible to IBD, because they are expressed in the gastrointestinal tract and play a role in biochemical barriers against internal and external xenobiotics^[10-12]. Diminution or disturbance of these barriers might result in increased permeability to xenobiotics in the gastrointestinal tract, and subsequently their accumulation in the body, probably leading to the development of IBD. *N*-acetyltransferases (NATs)

are the enzymes catalyzing *N*-acetylation (deactivation) of a variety of carbocyclic and heterocyclic arylamines by means of transferring acetyl-CoA to the amino or hydroxyl side chain of arylamines in metabolism of the phase II reaction^[10]. NATs are encoded by two genes, *NAT1* and *NAT2*, both are located at 8p22. *NAT1* is ubiquitously expressed, while the expression of *NAT2* is confined to the gastrointestinal tract and liver^[10]. The UDP-glucuronosyltransferase 1 family genes located at 2q37 consist of nine functional genes, *UGT1A1*, *UGT1A3-10*, which catalyze the glucuronidation of small lipophilic agents by means of conversion of hydrophobic substrates to inactive hydrophilic UDP-glucuronides, and are expressed in a tissue-specific fashion in the gastrointestinal tract and liver. In particular, *UGT1A7* is expressed exclusively in the gastrointestinal tract and lung, but not in the liver^[13-15]. The degree of metabolism with regard to both *NAT2* and *UGT1A7* varies among individuals, suggesting the presence of genetic variations contributing to the metabolic activation capacity. Current studies have shown an association between *NAT2* or *UGT1A7* polymorphisms and various diseases, i.e., systemic sclerosis and systemic lupus erythematosus^[16], drug toxicity^[17,18], orolaryngeal cancer^[19], esophageal cancer^[20], colorectal cancer^[21,22], pancreas cancer^[23], hepatocellular carcinoma^[15,24], or bladder cancer^[25].

Here we report the results of studies on association between *NAT2* or *UGT1A7* and IBD in Japanese using six and three polymorphic haplotypes in the two genes, respectively.

MATERIALS AND METHODS

Subjects

The subjects studied comprised 95 patients with UC, 60 patients with CD, and 200 gender-matched, unrelated, healthy volunteers, and were further characterized as listed in Table 1. All participants were Japanese, who were randomly recruited from eight general health clinics in the Nagasaki area in Japan. The study protocol was approved by the Committee for the Ethical Issue on Human Genome and Gene Analysis in Nagasaki University, and written informed consent was obtained from each participant. Diagnosis of IBD was made according to endoscopic, radiological, histological, and clinical criteria provided by both the Council for International Organizations of Medical Sciences in WHO and the International Organization for the Study of Inflammatory Bowel Disease^[26-28]. Patients with indeterminate colitis, multiple sclerosis, systemic lupus erythematosus, or other recognized autoimmune diseases were excluded from the subjects studied.

Table 1 Clinical characteristics of study subjects

Characteristic	Disease		Control
	UC	CD	
Number of subjects	95	60	200
Age range (yr)	14-83	17-75	20-60
Age (mean±SD)	44.4±16.4 ^b	35.0±12.6	32.5±11.1
Male/female (%)	53 (55.8)/42 (44.2)	35 (58.3)/25 (41.7)	125 (62.5)/75 (37.5)

^bP<0.01 vs control.

Determination of *NAT2* polymorphisms

Genomic DNA was extracted from peripheral whole blood of each individual using the DNA Extractor WB-rapid Kit (Wako, Osaka, Japan) according to the manufacturer's protocol. Single nucleotide polymorphisms (SNPs) of *NAT2* deposited in SNP-database^[29] were determined with the PCR-restriction fragment length polymorphism (RFLP) method using primer pairs and protocol described by Leff *et al.*^[30]. The PCR-RFLP method was modified in order to distinguish among all known *NAT2* SNPs^[29]. In brief, polymorphic region in *NAT2* was amplified by PCR with a GeneAmp PCR system 9700 thermal cycler (Applied Biosystems, Foster City, CA, USA) using 250 ng of genomic DNA in a 50- μ L reaction containing 10 mmol/L Tris-HCl, pH 8.3, 50 mmol/L KCl, 1.5 mmol/L MgCl₂, 0.2 mmol/L each dNTP, 500 ng of forward primer: 5'-GGCTATAA-GAACTCTAGGAAC-3', 500 ng of reverse primer: 5'-AAGGGTTTATTTTGTTTCCTTATTCTAAAT-3', and 2.0 U *Taq* DNA polymerase. The amplification protocol comprised initial denaturation at 94 °C for 5 min; 35 cycles of denaturation at 94 °C for 30 s, annealing at 55 °C for 30 s, and extension at 72 °C for 30 s; and a final extension at 72 °C for 5 min. PCR product of 896 bp was digested by restriction enzymes (TaKaRa Biomedical, Shiga, Japan). Three SNPs, C190T, G191A, and A434C, were detected by digestion with *MspI*. Likewise, C282T, C481T, or G857A was detected by digestion with *FokI*, *KpnI*, or *BamHI*, respectively. T111C, G590A, and C759T were detected by digestion with *TaqI*. These fragments were subjected to electrophoresis on 2% agarose or 5% polyacrylamide gel, and visualized with UV transilluminator (Alpha Innotech, CA, USA) after ethidium bromide staining. Moreover, T341C, A803G, and A845C were detected by further nested PCR. Amplified *NAT2* product (1 μ L) was used as a template in a 25- μ L reaction containing 10 mmol/L Tris-HCl, pH 8.3, 50 mmol/L KCl, 1.5 mmol/L MgCl₂, 0.2 mmol/L each dNTP, 250 ng of forward primer: 5'-CACCTTCT-CCTGCAGGTGACCG-3' and reverse primer: 5'-TGTC AAGCAGAAAATGCAAGGC-3' for T341C and A803G, or 250 ng of forward primer: 5'-TGAGGAA-GAGGTTGAAGAAGTGCT-3' and reverse primer: 5'-AAGGGTTTATTTTGTTTCCTTATTCTAAAT-3' for A845C, and 0.5 U *Taq* DNA polymerase. The amplification protocol comprised initial denaturation at 94 °C for 5 min; 35 cycles of denaturation at 94 °C for 30 s, annealing at 62 °C for 30 s, and extension at 72 °C for 30 s; and a final extension at 72 °C for 5 min. The former nested PCR products were digested with *AclI* and *DdeI* (New England BioLabs Inc., MA, USA) to detect T341C and A803G, respectively. The latter products were digested with *DraIII* (New England BioLabs Inc.) to detect A845C. All these products were subjected to electrophoresis on 6% polyacrylamide gel, and visualized as described above.

Determination of *UGT1A7* polymorphisms

Four SNPs have been known within *UGT1A7*-exon 1^[15]. A SNP at codon 11 is a silent mutation. SNPs at codons 129 and 131 lying in a linkage disequilibrium (LD) block were detected by PCR-denaturing high-performance liquid chromatography (DHPLC) with an automated HPLC

instrument (WAVE™, Transgenomic, CA, USA), and by direct DNA sequencing with ABI 310 (Applied Biosystems, Foster City, USA). A DNA fragment containing codons 129 and 131 was amplified by PCR using 125 ng of genomic DNA in a 25- μ L reaction containing 10 mmol/L Tris-HCl, pH 8.3, 50 mmol/L KCl, 1.5 mmol/L MgCl₂, 0.2 mmol/L each dNTP, 500 ng of forward primer: 5'-CCGGGAGTTCATGGTTTTT-3', 250 ng of reverse primer: 5'-CACAGAGGGGAGGGAGAAAT-3', and 1.0 U *Taq* DNA polymerase, generating a 260-bp fragment. Amplification protocol comprised initial denaturation at 94 °C for 5 min; 35 cycles of denaturation at 94 °C for 30 s, annealing at 55 °C for 30 s, and extension at 72 °C for 30 s; and a final extension at 72 °C for 5 min. PCR products were used for DHPLC analysis. The temperature required for successful resolution of heteroduplex molecules was determined to be 56.8 °C according to the manufacturer's protocol. Another SNP at codon 208 was detected by PCR-RFLP using primer pair of 5'-GCATGAGGTGGTTCGTCGTC-3'/5'-CATCACGGGTTTGGGATACT-3', as in the *NAT2* SNP-detection. After digestion of PCR products by *RsaI* (Promega, WI, USA), the fragments were subjected to electrophoresis on 2% agarose gel, and visualized as described above.

Statistical analysis

Gender and age value among the subjects were evaluated by χ^2 test and unpaired Student's *t* test, respectively. Allele frequencies were estimated by the gene-counting method, and χ^2 test was used to identify significant departures from the Hardy-Weinberg equilibrium. Subsequently, the odds ratio (OR) with 95% confidence interval (95%CI) was calculated by multiple logistic regression analysis using the JMP program package (version 5, SAS Institute, Cary, NC, USA) and the StatView program package (version 5, SAS Institute). Haplotype and genotype frequencies were compared between individuals with and without haplotype or genotype, using χ^2 test. A *P* value of 0.05 or less was considered statistically significant.

RESULTS

Haplotype frequencies of *NAT2*

We identified six haplotypes composed of six SNPs among the subjects examined (Table 2). The haplotype "*NAT2*4*" comprising 69.5% of controls was wild-type, while five other haplotypes were variants. Distributions of the haplotypes in our study population were well corresponded to the Hardy-Weinberg equilibrium (Table 2). The results implied that the population we studied had a homogeneous genetic background, being consistent with the previous observations^[31-33]. However, since the frequencies of three haplotypes, *NAT2*5B*, *NAT2*11*, and *NAT2*13*, were very low, they were not considered for subsequent multiple logistic regression analysis.

The frequency of haplotype "*NAT2*7B*" composed of two SNPs (C282T and G857A) significantly increased in patients with CD, compared to that in controls (*P* = 0.0130, OR = 2.802, 95%CI: 1.243-6.316, Table 3). In contrast, there was no difference in frequency of *NAT2*7B* between

patients with UC and controls (*P* = 0.3338, OR = 1.436, 95%CI: 0.689-2.992). Of the 60 CD patients, 17 (28.3%) had *NAT2*7B*, the incidence being significantly higher than that (32/200, 16.0%) in controls (*P* = 0.032, OR = 2.076, Table 4). These results indicated that the haplotype *NAT2*7B* was associated with the susceptibility to CD, but not to UC.

Cascorbi *et al.*^[34], and Gross *et al.*^[35], have shown a relationship between genotypes of *NAT2* polymorphism and phenotypes. The haplotypes *NAT2*4*, *NAT2*11*, and *NAT2*13*, code for the rapid acetylator phenotype, while *NAT2*5B*, *NAT2*6A*, and *NAT2*7B*, code for the slow acetylators. According to their reports, we divided the subjects in to two groups: the rapid acetylators comprised homozygous and heterozygous carriers of the haplotypes *NAT2*4*, *NAT2*11*, or *NAT2*13* and the slow acetylators comprised all homozygous carriers of the other haplotypes. The frequency and distribution were compared between these groups, but there were no significant differences in frequencies of these estimated phenotypes among patients with UC, CD, and controls (data not shown).

Table 2 Distributions of six *NAT2*-haplotypes in patients with UC/CD and controls

Haplotype	SNP	Number (%) of subjects with haplotype		
		UC (allele = 190)	CD (allele = 120)	Control (allele = 400)
<i>NAT2*4</i>	None	122 (64.2)	77 (64.2)	278 (69.5)
<i>NAT2*5B</i>	T341C, C481T, A803G	3 (1.6)	1 (0.8)	2 (0.5)
<i>NAT2*6A</i>	C282T, G590A	43 (22.6)	21 (17.5)	79 (19.75)
<i>NAT2*7B</i>	C282T, G857A	20 (10.5)	18 (15.0)	35 (8.75)
<i>NAT2*11</i>	C481T	0 (0)	1 (0.8)	1 (0.25)
<i>NAT2*13</i>	C282T	2 (1.1)	2 (1.7)	5 (1.25)

Table 3 Comparisons of frequencies of *NAT2*-haplotypes among study subjects by multiple logistic regression analysis

Haplotype	<i>P</i>	Odds ratio	95% confidence interval
UC patients vs controls			
<i>NAT2*4</i>	0.6823	0.809	0.293-2.232
<i>NAT2*6A</i>	0.5621	1.183	0.671-2.084
<i>NAT2*7B</i>	0.3338	1.436	0.689-2.992
CD patients vs controls			
<i>NAT2*4</i>	0.2616	2.162	0.563-8.304
<i>NAT2*6A</i>	0.3898	1.349	0.682-2.670
<i>NAT2*7B</i>	0.0130	2.802	1.243-6.316

Table 4 Number of subjects with or without haplotype *NAT2*7B*

<i>NAT2*7B</i>	UC (n = 95, %)	CD (n = 60, %)	Control (n = 200, %)
Presence	19 (20.0)	17 (28.3)	32 (16.0)
Absence	76 (80.0)	43 (71.7)	168 (84.0)

CD patients vs controls: *P* = 0.032, OR = 2.076.

Haplotype frequencies of *UGT1A7*

We detected two SNPs at codons 129 and 131 of *UGT1A7* by DHPLC with 100% accuracy, as confirmed by direct

DNA sequencing. Subsequently, on the basis of the results by PCR-DHPLC and PCR-RFLP, three haplotypes, *UGT1A7*1*, *UGT1A7*2*, and *UGT1A7*3*, were determined in the Japanese population studied (Table 5). The *UGT1A7*1* haplotype was wild-type, *UGT1A7*2* and *UGT1A7*3* were identified as variants, while another haplotype, *UGT1A*4*, was not observed, indicating that it was very rare in Japanese. There were no significant differences in frequencies of haplotypes and genotypes among patients UC, CD, and controls (data not shown).

Table 5 Distributions of three *UGT1A7* haplotypes among study subjects

Haplotype	SNP	Number (%) of subjects with haplotype		
		UC (allele = 190)	CD (allele = 120)	Control (allele = 400)
<i>UGT1A7*1</i>	None	120 (63.2)	69 (57.5)	242 (60.5)
<i>UGT1A7*2</i>	T387G, C391A, G392A	29 (15.3)	24 (20.0)	55 (13.8)
<i>UGT1A7*3</i>	T387G, C391A, G392A, T622C	41 (21.6)	27 (22.5)	103 (25.7)
<i>UGT1A7*4</i>	T622C	0 (0)	0 (0)	0 (0)

DISCUSSION

We have shown that a *NAT2* haplotype, *NAT2*7B*, is associated with CD, and thus, *NAT2* could be one of the genetic factors for the predisposition to the onset and/or development of CD, although its contribution to this disease appears relatively small. In contrast, we could not find any association between *UGT1A7* polymorphism and IBD, suggesting that *UGT1A7* never confers to these diseases. Although there are previous reports demonstrating an association between certain *NAT2* variants and diseases, they deal with phenotypical variations, such as rapid, intermediate, and slow acetylators in different conditions such as systemic sclerosis, systemic lupus erythematosus, and drug-induced agranulocytosis^[16,17]. Therefore, the present study is the first report documenting an association between *NAT2* genetic variation and CD.

Three *NAT2* haplotypes, *NAT2*5B*, *NAT2*6A*, and *NAT2*7B*, are estimated to show slow acetylator phenotypes^[34,35]. The present study showed that slow acetylator carrying these haplotypes was not associated, with CD (data not shown). Although a role of the *NAT2*7B* haplotype in the susceptibility to CD is unknown, Fretland *et al.*, demonstrated, that this haplotype is functionally related to low activity of *N*-acetylation^[36]. It is likely, that low activity of *N*-acetylation due to *NAT2*7B* might fail to metabolite xenobiotics in the state of increased permeability in the gastrointestinal tract and subsequently accumulates them in the body since *NAT2* functions as a biochemical barrier against xenobiotics including dietary intake, intestinal bacteria, and toxins^[10-12,15]. Our hypothesis may be partly supported by clinical evidence that total parenteral nutrition and elemental diet placing the gastrointestinal tract "at rest" can successfully improve CD, and refeeding by oral conventional diet aggravates the activity of CD^[37].

Recent genome-wide linkage analyses and candidate gene-based association studies have shown possible IBD

susceptibility regions at 16q12 (IBD1), 12p13 (IBD2), 6p21 (IBD3), 14q11 (IBD4), 19p13 (IBD5), 5q31-q33 (IBD6), 1p36 (IBD7), and at 16p (IBD8)^[5,38,39]. Our results indicate the existence of a new CD determinant at an LD region of 8p22, even if it is not *NAT2* it-self. It remains to be confirmed whether the association is reproducible in larger Japanese samples as well as in other populations.

ACKNOWLEDGMENTS

We are grateful to physicians, patients, and volunteers for participating in this study. We thank Miss Naoko Sakemi, Dr. Hiroshi Soda, and Professor Norio Niikawa for their support.

REFERENCES

- 1 **Fiocchi C**. Inflammatory bowel disease: etiology and pathogenesis. *Gastroenterology* 1998; **115**: 182-205
- 2 **Farrell RJ**, Peppercorn MA. Ulcerative colitis. *Lancet* 2002; **359**: 331-340
- 3 **Yang H**, Taylor KD, Rotter JJ. Inflammatory bowel disease. I. Genetic epidemiology. *Mol Genet Metab* 2001; **74**: 1-21
- 4 **Watts DA**, Satsangi J. The genetic jigsaw of inflammatory bowel disease. *Gut* 2002; **50**(Suppl 3): s31-36
- 5 **Taylor KD**, Yang H, Rotter JJ. Inflammatory bowel disease. II. Gene mapping. *Mol Genet Metab* 2001; **74**: 22-44
- 6 **Hugot JP**, Chamaillard M, Zouali H, Lesage S, Cezard JP, Belaiche J, Almer S, Tysk C, O'Morain CA, Gassull M, Binder V, Finkel Y, Cortot A, Modigliani R, Laurent-Puig P, Gower-Rousseau C, Macry J, Colombel JF, Sahbatou M, Thomas G. Association of NOD2 leucine-rich repeat variants with susceptibility to Crohn's disease. *Nature* 2001; **411**: 599-603
- 7 **Ogura Y**, Bonen DK, Inohara M, Nicolae DL, Chen FF, Ramos R, Britton H, Moran T, Karaliuskas R, Duerr RH, Achkar JP, Brant SR, Bayless TM, Kirschner BS, Hanauer SB, Nunez G, Cho JH. A frameshift mutation in NOD2 associated with susceptibility to Crohn's disease. *Nature* 2001; **411**: 603-606
- 8 **Inoue N**, Tamura K, Kinouchi Y, Fukuda Y, Takahashi S, Ogura Y, Inohara N, Nunez G, Kishi Y, Koike Y, Shimosegawa T, Shimoyama T, Hibi T. Lack of common NOD2 variants in Japanese patients with Crohn's disease. *Gastroenterology* 2002; **123**: 86-91
- 9 **Yamazaki K**, Takazoe M, Tanaka T, Kazumori T, Nakamura U. Absence of mutation in the NOD2/CARD15 gene among 483 Japanese patients with Crohn's disease. *J Hum Genet* 2002; **47**: 469-472
- 10 **Hein DW**, Doll MA, Rustan TD, Gray K, Feng Y, Ferguson RJ, Grant DM. Metabolic activation and deactivation of arylamine carcinogens by recombinant human NAT1 and polymorphic NAT2 acetyltransferases. *Carcinogenesis* 1993; **14**: 1633-1638
- 11 **Turesky RJ**, Land NP, Butler MA, Teitel CH, Kadlubar FF. Metabolic activation of carcinogenic heterocyclic aromatic amines by human liver and colon. *Carcinogenesis* 1991; **12**: 1839-1845
- 12 **Tukey RH**, Strassburg CP. Human UDP-glucuronosyltransferases: metabolism, expression, and disease. *Annu Rev Pharmacol Toxicol* 2000; **40**: 581-616
- 13 **Strassburg CP**, Kneip S, Topp J, Obermayer-Straub P, Barut A, Tukey RH, Manns MP. Polymorphic gene regulation and interindividual variation of UDP-glucuronosyltransferase activity in human small intestine. *J Biol Chem* 2000; **275**: 36164-36171
- 14 **Tukey RH**, Strassburg CP. Genetic multiplicity of the human UDP-glucuronosyltransferases and regulation in the gastrointestinal tract. *Mol Pharmacol* 2001; **59**: 405-414
- 15 **Vogel A**, Kneip S, Barut A, Ehmer U, Tukey RH, Manns MP, Strassburg CP. Genetic link of hepatocellular carcinoma with polymorphisms of the UDP-glucuronosyltransferase

- UGT1A7 gene. *Gastroenterology* 2001; **121**: 1136-1144
- 16 **von Schmiedeberg S**, Fritsche E, Rönnau AC, Specker C, Golka K, Richter-Hintz D, Schuppe HC, Lehmann P, Ruzicka T, Esser C, Abel J, Gleichmann E. Polymorphisms of the xenobiotic-metabolizing enzymes CYP1A1 and NAT-2 in systemic sclerosis and lupus erythematosus. *Adv Exp Med Biol* 1999; **455**: 147-152
 - 17 **Wadelius M**, Stjernberg E, Wiholm BE, Rane A. Polymorphisms of NAT2 in relation to sulphasalazine-induced agranulocytosis. *Pharmacogenetics* 2000; **10**: 35-41
 - 18 **Huang YS**, Chern HD, Su WJ, Wu JC, Lai SL, Yang SY, Chang FY, Lee SD. Polymorphism of the *N*-acetyltransferase 2 gene as a susceptibility risk factor for antituberculosis drug-induced hepatitis. *Hepatology* 2002; **35**: 883-889
 - 19 **Zheng Z**, Park JY, Guillemette C, Schantz SP, Lazarus P. Tobacco carcinogen-detoxifying enzyme UGT1A7 and its association with orolaryngeal cancer risk. *J Natl Cancer Inst* 2001; **93**: 1411-1418
 - 20 **Strassburg CP**, Strassburg A, Nguyen N, Li Q, Manns MP, Tukey RH. Regulation and function of family 1 and family 2 UDP-glucuronosyltransferase genes (UGT1A, UGT2B) in human oesophagus. *Biochim J* 1999; **338**: 489-498
 - 21 **Brockton N**, Little J, Sharp L, Cotton SC. *N*-acetyltransferase polymorphisms and colorectal cancer: a HuGE review. *Am J Epidemiol* 2000; **151**: 846-861
 - 22 **Strassburg CP**, Vogel A, Kneip S, Tukey RH, Manns MP. Polymorphisms of the human UDP-glucuronosyltransferase (UGT) 1A7 gene in colorectal cancer. *Gut* 2002; **50**: 851-856
 - 23 **Ockenga J**, Vogel A, Teich N, Keim V, Manns MP, Strassburg CP. UDP glucuronosyltransferase (UGT1A7) gene polymorphisms increase the risk of chronic pancreatitis and pancreatic cancer. *Gastroenterology* 2003; **124**: 1802-1808
 - 24 **Huang YS**, Chern HD, Wu JC, Chao Y, Huang YH, Chang FY, Lee SD. Polymorphism of the *N*-acetyltransferase 2 gene, red meat intake, and the susceptibility of hepatocellular carcinoma. *Am J Gastroenterol* 2003; **98**: 1417-1422
 - 25 **Risch A**, Wallace DM, Bathers S, Sim E. Slow *N*-acetylation genotype is a susceptibility factor in occupational and smoking related bladder cancer. *Hum Mol Genet* 1995; **4**: 231-236
 - 26 **Podolsky DK**. Inflammatory bowel disease (1). *N Eng J Med* 1991; **325**: 928-937
 - 27 **Podolsky DK**. Inflammatory bowel disease (2). *N Eng J Med* 1991; **325**: 1008-1016
 - 28 **Lennard-Jones JE**. Classification of inflammatory bowel disease. *Scand J Gastroenterol* 1989; **170**: 2-6
 - 29 <http://www.louisville.edu/medschool/pharmacology/NAT2.html/>
 - 30 **Leff MA**, Fretland AJ, Doll MA, Hein DW. Novel human *N*-acetyltransferase 2 alleles that differ in mechanism for slow acetylator phenotype. *J Biol Chem* 1999; **274**: 34519-34522
 - 31 **Sekine A**, Saito S, Iida A, Mitsunobu Y, Higuchi S, Harigae S, Nakamura Y. Identification of single-nucleotide polymorphisms (SNPs) of human *N*-acetyltransferase genes NAT1, NAT2, AANAT, ARD1 and L1CAM in the Japanese population. *J Hum Genet* 2001; **46**: 314-319
 - 32 **Yokogawa K**, Nakaharu T, Ishizaki J, Ozaki E, Takeda Y, Mabuchi H, Matsushita R, Kimura K, Nakashima E, Ichimura F, Miyamoto K. Kinetic phenotypic diagnosis of *N*-acetylation polymorphism in patients based on ratio of urinary metabolites of salicylazosulfapyridine. *Int J Pharm* 2001; **229**: 183-191
 - 33 **Ando M**, Ando Y, Sekido Y, Ando M, Shimokata K, Hasegawa Y. Genetic polymorphisms of the UDP-glucuronosyltransferase 1A7 gene and irinotecan toxicity in Japanese cancer patients. *Jpn J Cancer Res* 2002; **93**: 591-597
 - 34 **Cascorbi I**, Drakoulis N, Bröckmoller J, Maurer A, Sperling K, Roots I. Arylamine *N*-acetyltransferase (*NAT2*) mutations and their allelic linkage in unrelated Caucasian individuals: correlation with phenotypic activity. *Am J Hum Genet* 1995; **57**: 581-592
 - 35 **Gross M**, Kruißelbrink T, Anderson K, Lang N, McGovern P, Delongchamp R, Kadlubar F. Distribution and concordance of *N*-acetyltransferase genotype and phenotype in an American population. *Cancer Epidemiol Biomarkers Prev* 1999; **8**: 683-692
 - 36 **Fretland AJ**, Leff MA, Doll MA, Hein DW. Functional characterization of human *N*-acetyltransferase 2 (*NAT2*) single nucleotide polymorphisms. *Pharmacogenetics* 2001; **11**: 207-215
 - 37 **Glickman RM**. Inflammatory bowel diseases: ulcerative colitis and Crohn's disease. In: Isselbacher KJ, Braunwald E, Wilson JD, eds. *Harrison's principles of internal medicine*, 13th ed. New York: McGraw-Hill, Inc 1994: 1403-1417
 - 38 **Cho JH**, Nicolae DL, Ramos R, Fields CT, Rabenau K, Corradino S, Brant SR, Espinosa R, LeBeau M, Hanauer SB, Bodzin J, Bonen DK. Linkage and linkage disequilibrium in chromosome band 1p36 in American Chaldeans with inflammatory bowel disease. *Hum Mol Genet* 2000; **9**: 1425-1432
 - 39 **Hampe J**, Frenzel H, Mirza MM, Croucher PJ, Cuthbert A, Mascheretti S, Huse K, Platzer M, Bridger S, Meyer B, Nurnberg P, Stokkers P, Krawczak M, Mathew CG, Curran M, Schreiber S. Evidence for a NOD2-independent susceptibility locus for inflammatory bowel disease on chromosome 16p. *Proc Natl Acad Sci USA* 2002; **99**: 321-326

• CLINICAL RESEARCH •

Sonographic fatty liver, overweight and ischemic heart disease

Yu-Cheng Lin, Huey-Ming Lo, Jong-Dar Chen

Yu-Cheng Lin, Jong-Dar Chen, Department of Family Medicine and Center for Environmental and Occupational Medicine, Shin Kong Wu Ho-Su Memorial Hospital, Taipei 111, Taiwan, China

Huey-Ming Lo, Department of Internal Medicine, Shin Kong Wu Ho-Su Memorial Hospital; School of Medicine, Fu Jen Catholic University, Taipei 111, Taiwan, China

Correspondence to: Dr. Jong-Dar Chen, Department of Family Medicine and Center for Environmental and Occupational Medicine, Shin Kong Wu Ho-Su Memorial Hospital, 95, Wen Chang Road, Shih Lin, Taipei 111, Taiwan, China. jdarchen@ms28.hinet.net

Telephone: +886-2-2833-2211-2626 Fax: +886-2-2838-9420

Received: 2004-12-01 Accepted: 2004-12-20

Abstract

AIM: To demonstrate the prevalence of sonographic fatty liver, overweight and ischemic heart disease (IHD) among the male workers in Taiwan, and to investigate the possible association of these three factors.

METHODS: From July to September 2003, a total of 2 088 male aircraft-maintenance workers aged from 22 to 65 years (mean 40.5) underwent an annual health examination, including anthropometrical evaluation, blood pressure measurement, personal medical history assessment, biochemical blood analysis, abdominal ultrasonographic examination and digital electrocardiography (ECG). The Student's *t*-test, χ^2 test and multivariate logistic regression analysis were utilized to evaluate the relationship between IHD and salient risk factors.

RESULTS: The all-over prevalence of overweight was 41.4%, and that of fatty liver was 29.5% (mild, moderate and severe fatty liver being 14.5%, 11.3%, and 3.7%, respectively); while the prevalence of ischemic changes on ECG was 17.1% in this study. The abnormal rates for conventional IHD risk factors including hypertension, dyslipidemia, hyperglycemia and overweight increased in accordance with the severity of fatty liver. Overweight and severity of fatty liver were independently associated with increased risks for developing IHD. Overweight subjects had a 1.32-fold (95%CI: 1.01-1.73) increased IHD risk. Participants with mild, moderate, and severe fatty liver had a 1.88-fold (95%CI: 1.37-2.6), 2.37-fold (95%CI: 1.66-3.37) and 2.76-fold (95%CI: 1.62-4.72) increased risk for developing IHD. The prevalence of ischemic ECG for the fatty liver-affected subjects with or without overweight was 30.1% and 19.1%, while that of overweight subjects free from fatty liver was 14.4%. Compared to the subjects without fatty liver nor overweight, IHD risk for the three subgroups above was as follows: OR: 2.95 (95%CI: 2.31-4.09), OR: 1.60 (95%CI: 1.07-2.39) and OR: 1.11 (95%CI: 0.78-1.56), respectively.

CONCLUSION: The presence of fatty liver and its severity should be carefully considered as independent risk factors for IHD. Results of the study suggest the synergistic effect between fatty liver and overweight for developing IHD. Abdominal sonographic examination may provide valuable information for IHD risk assessment in addition to limited report about liver status, especially for overweight males.

© 2005 The WJG Press and Elsevier Inc. All rights reserved.

Key words: Fatty liver; Ischemic heart disease; Overweight; Male; Middle-aged

Lin YC, Lo HM, Chen JD. Sonographic fatty liver, overweight and ischemic heart disease. *World J Gastroenterol* 2005; 11(31): 4838-4842

<http://www.wjgnet.com/1007-9327/11/4838.asp>

INTRODUCTION

Fatty change in the liver is closely associated with overweight status and metabolic impairments such as hyperglycemia, and dyslipidemia^[1-3] which are also regarded as factors for atherosclerosis^[1,4,5] and ischemic heart disease (IHD)^[6-9]. However, the association between fatty liver and IHD is waiting for epidemiological investigation.

Since resting electrocardiogram (ECG) and abdominal sonographic examination are two routine, non-invasive health examinations used in medical check-ups in Taiwan^[10-15], we had the opportunity to examine the association between fatty liver and ischemic ECG changes, the hallmark of IHD and strong predictor for cardiac events^[16-18].

The purpose of this study was to evaluate the relationships between fatty liver and IHD utilizing epidemic data. Data analyses were controlled for conventional risk factors, especially overweight.

MATERIALS AND METHODS

Subjects

Records from a total of 2 088 male aircraft maintenance workers who underwent a periodic health examination from July to September 2003.

Methods

The health examinations included anthropometrical evaluation, measurement of weight and height, systolic and diastolic blood pressure. Definition of overweight was BMI ≥ 25 kg/m², based on WHO criteria^[19]. A questionnaire about personal medical history, including alcohol (usage more than once a week: yes *vs* no) and tobacco (current usage: yes *vs* no) consumption was filled by the examinees.

Biochemical blood tests were conducted by Hitachi autoanalyzer model 7150 (Hitachi Corp, Tokyo, Japan), including fasting plasma glucose, levels of triglyceride, and total, low, and high-density lipoprotein (LDL, HDL) cholesterol. The definition of hypertension was systolic blood pressure ≥ 18.7 kPa or diastolic blood pressure ≥ 12 kPa. The cut points of hyperglycemia, hypocholesterolemia, hypercholesterolemia, and hypertriglyceridemia were fasting sugar ≥ 6.1 mmol/L, HDL < 1.0 mmol/L, total cholesterol ≥ 5.2 mmol/L and triglyceride ≥ 17.0 mmol/L.

Abdominal ultrasonographic examinations were performed using convex-type real-time electronic scanners (Toshiba SSA-340 with 3.75 MHz convex-type transducer) by three gastrointestinal specialists who were blind to the medical history and blood test results of the examinees. The definition of ultrasonic fatty liver was based on a comparative assessment of image brightness relative to the kidneys, in line with previously reported diagnostic criteria^[10,20-23]. Severity of fatty liver was classified according to the following modified scoring system^[10,13,15,22,23]: brightness compared to kidneys (0-3), blurring of gall bladder wall (0-3), blurring of hepatic veins (0-3), blurring of portal vein (0-3), far gain attenuation (0-3). Severity was defined as mild (total scores of 2-6), moderate (7-10), and severe (11-15) fatty liver.

A digital electrocardiograph recorder (Kenz Cardico 1207; Suzuken Co., Ltd 8, Higashi Kataha-machi, Higashi-ku Nagoya 461-8701, Japan.) was used for IHD assessment. IHD was defined based on evidence of resting ECG ischemic abnormalities, as expressed in computerized Minnesota code (1.1. \times -1.3. \times , 4.1. \times -4.4. \times , 5.1. \times -5.3. \times)^[12,16-18].

The Student's *t* and χ^2 tests were used for analyzing continuous variables and categorical variables, respectively. Multivariate logistic regression was utilized to evaluate the relationship between IHD and salient risk factors. SAS software was used for statistical analysis (Version 8.0; SAS Institute, Cary, NC, USA).

RESULTS

After 63 cases whose data were incomplete (e.g., biochemical blood test, questionnaire) were excluded, a total of 2 025

subjects were enrolled in the final analysis. The excluded subjects had a similar distribution of anthropometric measurement and biochemical data as subjects in final analysis.

As shown in Table 1, the age for this sample population ranged from 22 to 63 years (mean, 40.5), the mean value of BMI was 24.6 kg/m². The over-all prevalence of overweight was 41.4%, while that of fatty liver was 29.5%. The prevalence of ischemic changes in the resting ECG was 17.1%. The means and standard deviations for serum blood sugar and atherogenic lipid profile were 5.7 \pm 1.1 mmol/L of fasting sugar, 5.1 \pm 0.9 mmol/L of total cholesterol, 1.3 \pm 0.3 mmol/L of HDL cholesterol, 3.3 \pm 0.8 mmol/L of LDL cholesterol, and 17.1 \pm 13.9 mmol/L of triglyceride.

Table 1 Baseline characteristics of middle-aged male workers in Taiwan from a periodic health examination (mean \pm SD, *n* = 2 025)

Risk factor	Value	Range
Age (yr)	40.5 \pm 9.9	22.0-63.0
Height (cm)	169.6 \pm 6.3	150.1-191.1
Body weight (kg)	70.9 \pm 10.6	42.8-121.9
BMI (body mass index) (kg/m ²)	24.6 \pm 3.3	15.6-40.6
Systolic blood pressure (kPa)	17.1 \pm 2.2	11.7-27.5
Diastolic blood pressure (kPa)	10.6 \pm 1.6	6.7-17.3
Fasting sugar (mmol/L)	5.7 \pm 1.1	3.0-24.5
Cholesterol total (mmol/L)	5.1 \pm 0.9	2.6-9.3
Cholesterol HDL (mmol/L)	1.3 \pm 0.3	0.2-4.0
Cholesterol LDL (mmol/L)	3.3 \pm 0.8	1.2-7.1
Triglyceride (mmol/L)	17.1 \pm 13.9	3.1-171.1
ECG with ischemic changes (<i>n</i> , %)	347	(17.1)
Fatty liver (<i>n</i> , %)	597	(29.5)
Overweight (<i>n</i> , %)	839	(41.4)
Smoking (<i>n</i> , %)	702	(34.7)
Alcohol use (<i>n</i> , %)	444	(21.9)

Risk-factor distribution among subgroups stratified according to the severity of fatty liver, is presented in Table 2. The prevalence of mild, moderate and severe fatty liver was 14.5%, 11.3%, and 3.7%, respectively. The abnormal rates for conventional IHD risk factor including hypertension, dyslipidemia, hyperglycemia and overweight increased in accordance with the severity of fatty liver (Figure 1).

Table 2 Assessment of risk factors stratified according to severity of fatty liver (FL)

Risk factors	<i>n</i> = 2 025			
	Non FL 1 428 (70.5%)	Mild FL 294 (14.5%)	Moderate FL 228 (11.3%)	Severe FL 75 (3.7%)
Age (yr)	39.8 \pm 9.9	41.8 \pm 9.9 ^a	42.7 \pm 9.4 ^c	42.6 \pm 9.5 ^e
BMI (body mass index) (kg/m ²)	23.9 \pm 3.1	25.0 \pm 2.6 ^a	26.9 \pm 2.7 ^c	29.0 \pm 3.1 ^e
Systolic blood pressure (kPa)	16.9 \pm 2.2	17.2 \pm 2.1 ^a	17.5 \pm 2.2 ^c	18.3 \pm 2.6 ^e
Diastolic blood pressure (kPa)	10.5 \pm 1.6	10.6 \pm 1.4 ^a	10.9 \pm 1.5 ^c	11.4 \pm 1.7 ^e
Fasting sugar (mmol/L)	5.6 \pm 1.0	5.8 \pm 1.2 ^a	6.0 \pm 1.5 ^c	6.1 \pm 1.6 ^e
Cholesterol total (mmol/L)	5.0 \pm 0.9	5.2 \pm 0.9 ^a	5.3 \pm 0.9 ^c	5.3 \pm 0.9 ^e
Cholesterol HDL (mmol/L)	1.3 \pm 0.3	1.2 \pm 0.2 ^a	1.1 \pm 0.2 ^c	1.1 \pm 0.2 ^e
Cholesterol LDL (mmol/L)	3.3 \pm 0.8	3.5 \pm 0.8 ^a	3.4 \pm 0.8 ^c	3.4 \pm 0.9 ^e
Triglyceride (mmol/L)	15.0 \pm 11.1	18.2 \pm 13.1 ^a	26.3 \pm 20.9 ^c	27.3 \pm 22.3 ^e
ECG with ischemic changes (<i>n</i> , %)	191 (13.4)	67 (22.8) ^a	64 (28.1) ^c	25 (33.3) ^e
Overweight (<i>n</i> , %)	457 (32.0)	143 (48.6) ^a	170 (74.6) ^c	69 (92.0) ^e
Smoking (<i>n</i> , %)	491 (34.4)	106 (36.1)	84 (36.8)	21 (28.0)
Alcohol use ^a (<i>n</i> , %)	304 (21.3)	73 (24.8)	54 (23.7)	13 (17.3)

^a*P*<0.05 vs non FL group; ^c*P*<0.05 vs non FL group; ^e*P*<0.05 vs non FL group.

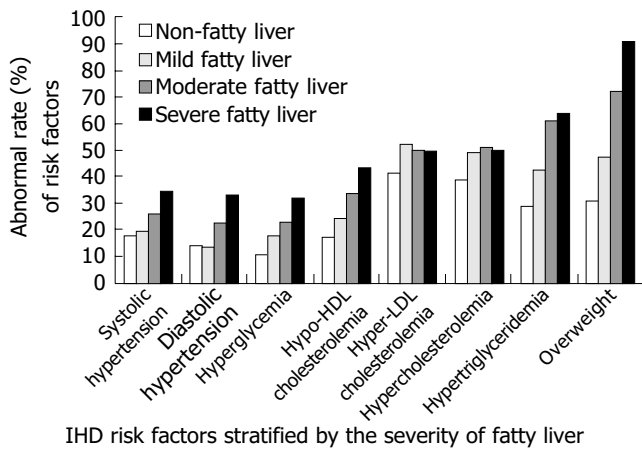


Figure 1 Abnormal rates of IHD risk factors for middle-aged male workers in Taiwan.

Multivariable analysis and odds ratios for IHD are summarized in Table 3. Results showed that overweight, increased systolic blood pressure and fatty liver severity were independently associated with IHD risk. Overweight subjects had a 1.32-fold (95%CI: 1.01-1.73) increased IHD risk. Participants with mild, moderate, and severe fatty liver experienced a 1.88-fold (95%CI: 1.37-2.60), 2.37-fold (95%CI: 1.66-3.37), and 2.76-fold (95%CI: 1.62-4.72) increased risk for developing IHD.

The prevalence of ischemic ECG and odds ratios (OR) for IHD of the middle-aged male workers in Taiwan, stratified according to overweight and fatty liver status, are presented in Table 4. The prevalence of ischemic ECG and the risk for IHD of the fatty liver-affected subjects with or without overweight and the overweight subjects free from fatty liver was 30.1%, OR: 2.95 (95% CI: 2.31-4.09), 19.1%, OR:1.60 (95% CI: 1.07-2.39) and 14.4%, OR: 1.11 (95% CI: 0.78-1.56), respectively, compared to the subjects without fatty liver nor overweight. Result of test for interaction between fatty liver and overweight was significant ($P < 0.05$).

DISCUSSION

Stress test or even coronary catheterization examination naturally has better specificity in IHD diagnosis, and biopsy of liver is the gold standard for hepatosteatosis. However, in the viewpoints of safety, ethic and screening purpose, resting ECG and abdominal sonographic examination have acceptable reliability and are practical tools of epidemiological survey^[10,16-18,21].

Our study indicates that adult male workers with fatty liver are more likely to develop IHD compared to subjects

Table 3 Multivariate logistic regression analysis for the risk factors for IHD

Risk factors	Odds ratio	95% CI
Age (yr)	0.99	0.97-1.00
Systolic blood pressure	1.01 ^a	1.003-1.03
Diastolic blood pressure	0.99	0.97-1.01
Fasting sugar	1.00	1.00-1.006
Cholesterol total	0.99	0.98-1.007
Cholesterol HDL	1.01	1.00-1.03
Cholesterol LDL	1.01	0.99-1.02
Triglyceride	1.00	1.00-1.003
Overweight	1.32 ^a	1.01-1.73
Fatty liver ^b		
Mild fatty liver	1.88 ^a	1.37-2.60
Moderate fatty liver	2.37 ^a	1.66-3.37
Severe fatty liver	2.76 ^d	1.62-4.72
Smoking	0.85	0.65-1.10
Alcohol consumption	1.054	0.79-1.41

^a $P < 0.05$ vs Non FL group; ^b $P < 0.001$ vs Non FL group; ^d $P < 0.0001$ vs Non FL group.

without fatty liver. This finding is compatible to previous studies demonstrating that fatty liver, as a developer of oxidative stress plays a cardinal role in cardiac dysfunction^[24,25]. Of particular significance is the fact that non-overweight subjects with fatty liver experience a significantly increased IHD risk (OR: 1.6). As Park *et al.*^[26], concluded, for non-obese men with fatty liver, systemic inflammatory response increases, and systemic inflammatory response is the integral part of the atherosclerotic process^[27,28]. IHD prevention for non-overweight subjects having fatty liver should be emphasized in clinical practice.

Findings of this study show a synergistic interaction between fatty liver and overweight, this combination makes middle-aged males have significantly highest IHD risk (OR: 2.95) in the four entities (Table 4). Similar findings have been shown in studies about insulin resistance^[7,10,26,29-31], these studies manifested that both overweight and fatty liver are closely correlated with insulin resistance, which aggravates the atherogenic metabolic process^[32,33], accelerating the development of atherosclerosis^[34] and IHD^[35]. For overweight middle-aged male workers with fatty liver, a comprehensive management for IHD risk reduction is needed.

Serum sugar and lipids had insignificant effects on developing IHD in this study, these findings are similar to our previous study based on Eastern population^[36]. Genetic differences^[37] and differences in diet components^[38] may have affected these findings.

Smoking and drinking did not show significant effects on developing IHD in this study, the partial explanation

Table 4 Odds ratio for IHD stratified according to fatty liver (FL) and overweight status

	Non-overweight (n = 1 186)		Overweight (n = 839)	
	Non-FL (n = 970)	FL (n = 216)	Non-FL (n = 458)	FL (n = 381)
Ischemic ECG (%)	125 (12.9)	41 (19.1)	66 (14.4)	115 (30.1)
¹ OR (95%CI)	1.0 ^a (-)	1.60 ^a (1.07-2.39)	1.11 (0.78-1.56)	2.95 ^b (2.31-4.09)

^a $P < 0.05$ vs overweight and fatty, adjusted for age, blood pressure, blood sugar and lipid profile; ^b $P < 0.001$ vs non-overweight and non-FL group; ^c $P < 0.05$ vs non-overweight and non-FL group; ¹OR: adjusted odds ratio; CI: confidence interval.

might be that binary questionnaire could provide only limited information about the dose-effect, which is important in the development of IHD, and then leads to the unsteady results^[36,39].

The findings of this study demonstrate that fatty liver is an independent risk factor for IHD. Abdominal sonographic examination may not only provide limited report about the liver status, but also can provide valuable information for IHD risk assessment, especially for those who are overweight.

ACKNOWLEDGMENTS

The authors would like to acknowledge the personnel of the Department of Family Medicine and Internal Medicine, Shin Kong Wu Ho-Su Memorial Hospital for their full support and generous assistance.

REFERENCES

- 1 Akahoshi M, Amasaki Y, Soda M, Tominaga T, Ichimaru S, Nakashima E, Seto S, Yano K. Correlation between fatty liver and coronary risk factors: a population study of elderly men and women in Nagasaki, Japan. *Hypertens Res* 2001; **24**: 337-343
- 2 Angelico F, Del Ben M, Conti R, Francioso S, Feole K, Maccioni D, Antonini TM, Alessandri C. Non-alcoholic fatty liver syndrome: a hepatic consequence of common metabolic diseases. *J Gastroenterol Hepatol* 2003; **18**: 588-594
- 3 Knobler H, Schattner A, Zhornicki T, Malnick SD, Keter D, Sokolovskaya N, Lurie Y, Bass DD. Fatty liver-an additional and treatable feature of the insulin resistance syndrome. *QJM* 1999; **92**: 73-79
- 4 Chilton RJ. Recent discoveries in assessment of coronary heart disease: impact of vascular mechanisms on development of atherosclerosis. *J Am Osteopath Assoc* 2001; **101**: S1-5
- 5 Ganz P, Creager MA, Fang JC, McConnell MV, Lee RT, Libby P, Selwyn AP. Pathogenic mechanisms of atherosclerosis: effect of lipid lowering on the biology of atherosclerosis. *Am J Med* 1996; **101**(4A): 10S-16S
- 6 Bonora E, Kiechl S, Willeit J, Oberhollenzer F, Egger G, Bonadonna RC, Muggeo M. Bruneck study. Carotid atherosclerosis and coronary heart disease in the metabolic syndrome: prospective data from the Bruneck study. *Diabetes Care* 2003; **26**: 1251-1257
- 7 Indulski JA, Lutz W. Ischaemic heart disease as an effect of obesity-related metabolic disturbances. *Cent Eur J Public Health* 1999; **7**: 122-129
- 8 Jeppesen J, Hein HO, Suadicani P, Gyntelberg F. High triglycerides/low high-density lipoprotein cholesterol, ischemic electrocardiogram changes, and risk of ischemic heart disease. *Am Heart J* 2003; **145**: 103-108
- 9 Lamarche B, Despres JP, Moorjani S, Cantin B, Dagenais GR, Lupien PJ. Triglycerides and HDL-cholesterol as risk factors for ischemic heart disease. Results from the Quebec cardiovascular study. *Atherosclerosis* 1996; **119**: 235-245
- 10 Hsiao TJ, Chen JC, Wang JD. Insulin resistance and ferritin as major determinants of nonalcoholic fatty liver disease in apparently healthy obese patients. *Int J Obesity* 2004; **28**: 167-172
- 11 Lai SW, Tan CK, Ng KC. Epidemiology of fatty liver in a hospital-based study in Taiwan. *Southern Med J* 2002; **95**: 1288-1292
- 12 Chen CH, Chuang JH, Kuo HS, Chang MS, Wang SP, Chou P. Prevalence of coronary heart disease in Kin-Chen, Kinmen. *Int J Cardiol* 1996; **55**: 87-95
- 13 Leung KW, Liu JD, Chen PH, Wang CS, Wang CK, Huang MJ, Siauw CP, Yuan CY, Chen TY. Clinical significance and diagnosis of fatty liver in Taiwan. Taiwan i Hsueh Hui Tsa Chih. *J Formos Med Assoc* 1986; **85**: 149-160
- 14 Lu SN, Wang LY, Chang WY, Chen CJ, Su WP, Chen SC, Chuang WL, Hsieh MY. Abdominal sonographic screening in a single community. *Kaohsiung J Med Sci* 1990; **6**: 643-646
- 15 Yang PM, Huang GT, Lin JT, Sheu JC, Lai MY, Su JJ, Hsu HC, Chen DS, Wang TH, Sung JL. Ultrasonography in the diagnosis of benign diffuse parenchymal liver diseases: a prospective study. *J Formos Med Assoc* 1988; **87**: 966-977
- 16 Hampton JR. The importance of minor abnormalities in the resting electrocardiogram. *Eur Heart J* 1984; **5** (Suppl A): 61-63
- 17 Okin PM, Devereux RB, Kors JA, van Herpen G, Crow RS, Fabsitz RR, Howard BV. Computerized ST depression analysis improves prediction of all-cause and cardiovascular mortality: the strong heart study. *Annals Noninvasive Electrocardiol* 2001; **6**: 107-116
- 18 Kannel WB, Anderson K, McGee DL, Degatano LS, Stampfer MJ. Nonspecific electrocardiographic abnormality as a predictor of coronary heart disease: the Framingham Study. *Am Heart J* 1987; **113**: 370-376
- 19 Anonymous. Obesity: preventing and managing the global epidemic. Report of a WHO consultation. *WHO Technical Report Series* 2000; **894**: 1-253
- 20 Saadeh S, Younossi ZM, Remer EM, Gramlich T, Ong JP, Hurley M, Mullen KD, Cooper JN, Sheridan MJ. The utility of radiological imaging in nonalcoholic fatty liver disease. *Gastroenterology* 2002; **123**: 745-750
- 21 Steinmaurer HJ, Jirak P, Walchshofer J, Clodi PH. Accuracy of sonography in the diagnosis of diffuse liver parenchymal diseases-comparison of sonography and liver histology. *Ultraschall Der Medizin* 1984; **5**: 98-103
- 22 Tam KM, Wu JS. Ultrasonographic diagnosis of fatty liver. *J Formos Med Assoc* 1986; **85**: 45-53
- 23 Yajima Y, Ohta K, Narui T, Abe R, Suzuki H, Ohtsuki M. Ultrasonographical diagnosis of fatty liver: significance of the liver-kidney contrast. *Tohoku J Exp Med* 1983; **139**: 43-50
- 24 Videla LA, Rodrigo R, Orellana M, Fernandez V, Tapia G, Quinones L, Varela N, Contreras J, Lazarte R, Csendes A, Rojas J, Maluenda F, Burdiles P, Diaz JC, Smok G, Thielemann L, Poniachik J. Oxidative stress-related parameters in the liver of non-alcoholic fatty liver disease patients. *Clin Sci* 2004; **106**: 261-268
- 25 Koenig W. Heart disease and the inflammatory response. *BMJ* 2000; **321**: 187-188
- 26 Park SH, Kim BI, Yun JW, Park DI, Cho YK, Sung IK, Park CY, Sohn CI, Jeon WK, Kim H, Rhee EJ, Lee WY, Kim SW. Insulin resistance and C-reactive protein as independent risk factors for non-alcoholic fatty liver disease in non-obese Asian men. *J Gastroenterol Hepatol* 2004; **19**: 694-698
- 27 Bandyopadhyay D, Chattopadhyay A, Ghosh G, Datta AG. Oxidative stress-induced ischemic heart disease: protection by antioxidants. *Curr Med Chem* 2004; **11**: 369-387
- 28 Rothenbacher D, Hoffmeister A, Brenner H, Koenig W. Physical activity, coronary heart disease, and inflammatory response. *Arch Intern Med* 2003; **163**: 1200-1205
- 29 Goto T, Onuma T, Takebe K, Kral JG. The influence of fatty liver on insulin clearance and insulin resistance in non-diabetic Japanese subjects. *Int J Obesity* 1995; **19**: 841-845
- 30 Strang BD, Bertics SJ, Grummer RR, Armentano LE. Relationship of triglyceride accumulation to insulin clearance and hormonal responsiveness in bovine hepatocytes. *J Dairy Sci* 1998; **81**: 740-747
- 31 Grundy SM. Metabolic complications of obesity. *Endocrine* 2000; **13**: 155-165
- 32 Cohn G, Valdes G, Capuzzi DM. Pathophysiology and treatment of the dyslipidemia of insulin resistance. *Current Cardiol Rep* 2001; **3**: 416-423
- 33 Garg A. Insulin resistance in the pathogenesis of dyslipidemia. *Diabetes Care* 1996; **19**: 387-389
- 34 Dandona P. Insulin resistance and endothelial dysfunction in

- atherosclerosis: implications and interventions. *Diabetes Technol Ther* 2002; **4**: 809-815
- 35 **Lamarque B**, Tcherno A, Mauriege P, Cantin B, Dagenais GR, Lupien PJ, Despres JP. Fasting insulin and apolipoprotein B levels and low-density lipoprotein particle size as risk factors for ischemic heart disease. *JAMA* 1998; **279**: 1955-1961
- 36 **Lin YC**, Chu FY, Fu CC, Chen JD. Prevalence and risk factors for angina in elderly Taiwanese. *J Gerontol A Biol* 2004; **59**: 161-165
- 37 **Mitchell BD**, Hazuda HP, Haffner SM, Patterson JK, Stern MP. High prevalence of angina pectoris in Mexican-American men. A population with reduced risk of myocardial infarction. *Ann Epidemiol* 1991; **1**: 415-426
- 38 **Burchfiel CM**, Abbott RD, Sharp DS, Curb JD, Rodriguez BL, Yano K. Distribution and correlates of lipids and lipoproteins in elderly Japanese-American men. The Honolulu Heart Program. *Arterioscler Thromb Vasc Biol* 1996; **16**: 1356-1364
- 39 **Gaziano JM**, Buring JE, Breslow JL, Goldhaber SZ, Rosner B, Van Denburgh M, Willett W, Hennekens CH. Moderate alcohol intake, increased levels of high-density lipoprotein and its subfractions, and decreased risk of myocardial infarction. *New Eng J Med* 1993; **329**: 1829-1834

Science Editor Wang XL and Guo SY Language Editor Elsevier HK

• CLINICAL RESEARCH •

Value of CT-guided core-needle biopsy in diagnosis and classification of malignant lymphomas using automated biopsy gun

Li Li, Qiu-Liang Wu, Li-Zhi Liu, Yun-Xian Mo, Chuan-Miao Xie, Lie Zheng, Lin Chen, Pei-Hong Wu

Li Li, Li-Zhi Liu, Yun-Xian Mo, Chuan-Miao Xie, Lie Zheng, Lin Chen, Pei-Hong Wu, State Key Laboratory of Oncology in Southern China, Imaging Diagnosis and Interventional Center, Cancer Center, Sun Yat-Sen University, Guangzhou 510060, Guangdong Province, China
Qiu-Liang Wu, State Key Laboratory of Oncology in Southern China, Department of Pathology, Cancer Center, Sun Yat-Sen University, Guangzhou 510060, Guangdong Province, China

Co-first-authors: Qiu-Liang Wu

Correspondence to: Dr. Pei-Hong Wu, Imaging Diagnosis and Interventional Center, Cancer Center, Sun Yat-Sen University, 651 Dongfeng Road East, Guangzhou 510060, Guangdong Province, China. jrkzl@gzsums.edu.cn

Telephone: +86-20-87343270 Fax: +86-20-87343392

Received: 2004-12-02 Accepted: 2005-02-18

classification of malignant lymphomas using automated biopsy gun. *World J Gastroenterol* 2005; 11(31): 4843-4847
<http://www.wjgnet.com/1007-9327/11/4843.asp>

INTRODUCTION

CT-guided percutaneous needle biopsy has become an important diagnostic tool and can minimize the need for open biopsy^[1,2]. However, satisfactory sampling is essential for the diagnosis and classification of malignant lymphoma^[3-5]. Percutaneous core-needle biopsy under the guidance of CT or ultrasound in evaluation of malignant lymphomas has a limited value^[6-8]. The advantage of CT guidance is that the whole mediastinum or abdomen is visualized, allowing accurate planning of biopsy for deep and small lesions and avoiding damage to important organs and greater vessels^[9,10]. In recent years, with the advance in new needle biopsy systems and technology of needle biopsy^[11,12], CT-guided core-needle biopsy is widely used in the diagnosis and classification of malignant lymphoma^[13,14]. Since 1999, CT-guided core-needle biopsy has been used as one of the routine sampling techniques for malignant lymphomas in our hospital. This study aimed to retrospectively evaluate the reliability of CT-guided core-needle biopsy for the diagnosis and classification of malignant lymphoma using an automated biopsy gun.

MATERIALS AND METHODS

Patients

From January 1999 to October 2004, 80 patients (51 men, 29 women) with suspected malignant lymphomas underwent CT-guided core-needle biopsy. They aged from 2.8 to 72 years (mean age, 48.5 years). In our series, six patients (7.5%) had a history of malignant lymphoma including two diffuse large B-cell non-Hodgkin's lymphoma (NHLs), one peripheral T-cell NHL, one anaplastic large cell (T/null cell) NHL, one follicular B-cell NHL and one nodular sclerosis Hodgkin's disease (HD). The sites of core-needle biopsy are shown in Table 1. Repeated core-needle biopsies were performed in five patients (6.25%). Nineteen patients (23.75%) with non-diagnostic core-needle biopsy underwent surgery depending on the sites, dimensions, and clinical diagnosis (Table 2). The histological classification in our group was according to 2001 World Health Organization classification of malignant lymphoma^[15].

CT scanning

CT scanning was performed for all patients with incremental

Abstract

AIM: To evaluate the value of CT-guided core-needle biopsy in diagnosis and classification of malignant lymphomas.

METHODS: From January 1999 to October 2004, CT-guided core-needle biopsies were performed in 80 patients with suspected malignant lymphoma. Biopsies were performed with an 18-20 G biopsy-cut (CR Bard, Inc., Covington, GA, USA) needle driven by a spring-loaded Bard biopsy gun.

RESULTS: A definite diagnosis and accurate histological subtype were obtained in 61 patients with a success rate of 76.25% (61/80). Surgical sampling was performed in 19 patients (23.75%) with non-diagnostic core-needle biopsies. The success rate of CT-guided core-needle biopsy varied with the histopathologic subtypes in our group. The relatively high success rates of core-needle biopsy were noted in diffuse large B-cell non-Hodgkin's lymphoma (NHL, 88.89%) and peripheral T-cell NHL (90%). However, the success rates were relatively low in anaplastic large cell (T/null cell) lymphoma (ALCL, 44.44%) and Hodgkin's disease (HD, 28.57%) in our group.

CONCLUSION: CT-guided core-needle biopsy is a reliable means of diagnosing and classifying malignant lymphomas, and can be widely applied in the management of patients with suspected malignant lymphoma.

© 2005 The WJG Press and Elsevier Inc. All rights reserved.

Key words: Malignant lymphoma; Biopsy; Computed tomography

Li L, Wu QL, Liu LZ, Mo YX, Xie CM, Zheng L, Chen L, Wu PH. Value of CT-guided core-needle biopsy in diagnosis and

Table 1 Sites of CT-guided core-needle biopsy in patients with lymphoma

	Number of patients	%
Mediastinum	42	52.5
Retroperitoneum	14	17.5
Abdominal mass	9	11.25
Spleen	2	2.5
Liver	2	2.5
Lung	1	1.25
Kidney	1	1.25
Chest wall	4	5
Pelvic wall	4	5
Extremity	1	1.25
Total	80	100.0

#: percentage of total biopsies.

scanning in cranial-to-caudal direction with 2.7-5 mm collimation on a CT twin flash scanner (Philips Co.). Before biopsies, all patients were subjected to enhanced CT to determine the exact tumor location, its degree of vascularity and the presence of necrosis. The optimal approach of needle was decided for deep or small lesions and lesions with extensive necrotic areas, avoiding damage to the important organs and relatively large vessels near the tumor (Figures 1A-C).

Biopsies

Biopsies were performed during the scanning with an 18-20 G biopsy-cut (CR Bard, Inc., Covington, GA, USA) needle driven by the spring-loaded Bard biopsy gun. The Bard biopsy gun consists of a hand-held device that triggers rapid firing of an 18 (20)-G cutting needle. When the gun is fired, an inner trocar with its 1.7 cm sample notch thrusts forward, followed by its outer cannula which shears a core of tissue with minimum crushing of the specimen^[11,16]. For a satisfactory sampling, an average of three specimens was obtained during each CT-guided core-needle biopsy.

CT scanning was performed immediately after the biopsies to evaluate the possible complications such as bleeding or pneumothorax. Patients were kept under observation for 2 h and discharged, if there were no significant complications, and encouraged to contact their

Table 2 Management of non-diagnostic CT-guided core-needle biopsy

	Number of patients	%
Mediastinoscopy	3	15.79
Mediastinotomy	4	21.05
Lymphadenectomy	6	31.58
Exploratory laparotomy	6	31.58
Total	19	100.00

#: percentage of total biopsies.

physicians if any evidence of complications developed subsequently.

Histologic analysis

All the samples were fixed in 40 g/L formaldehyde and embedded in paraffin and stained with hematoxylin and eosin. Routine immunohistochemical studies were performed using antibodies to leukocyte common antigen, cytokeratin, and vimentin. Histological subtyping of NHL was made using antibodies (CD3, CD8, CD15, CD30, CD43, CD79a, L26, UCHL-1, ALK, EMA).

A biopsy was considered successful, if the definite diagnosis and accurate classification of malignant lymphoma could be established and sufficient information was provided for a therapeutic decision.

RESULTS

No serious complications were noted in all the 80 patients who underwent CT-guided core-needle biopsy. A definite diagnosis and an accurate histological subtype were made in 61 patients with a success rate of 76.25%, including 80.82% (59/73) in NHL and 28.57% (2/7) in HD (Table 3). Nineteen patients (23.75%) with non-diagnostic core-needle biopsies were subjected to surgical interventions including mediastinoscopy, mediastinotomy, lymphadenectomy, and exploratory laparotomy. The main reasons for unsuccessful biopsy were extensive necrosis and unsatisfactory sampling.

The final histopathologic subtypes in 80 patients are listed in Table 4, including 63 NHLs and 7 HDs. In the diagnostic patient group, the majority of NHL subtypes were diffuse large B-cell NHL ($n = 32$) and peripheral T-cell NHL ($n = 9$). The remaining subtypes included one

**Figure 1** CT-guided core-needle biopsy for paratracheal mass (A), large anterior

mediastinal mass (B), and retroperitoneal mass (C).

lymphocyte-predominant HD, one lymphocytic depletion HD, six marginal zone B-cell NHLs, two diffuse small lymphocytic NHLs, three mantle B-cell NHLs, one follicular B-cell NHL, two angioimmunoblastic T-cell NHLs, and four anaplastic large cell (T/null cell) NHLs (ALCL).

The non-diagnostic patient group included two lymphocyte-predominant HDs, three nodular sclerosis HDs, four diffuse large B-cell NHLs, one mantle B-cell NHL, one follicular B-cell NHL, one Burkitt's NHL, one peripheral T-cell NHL, one angioimmunoblastic T-cell NHL, and five anaplastic large cell NHLs (ALCL, Table 4).

In our group, the success rates varied with the histopathologic subtypes. A relatively high success rate was obtained in diffuse large B-cell NHL (88.89%) and peripheral T-cell NHL (90%). However, the success rate was relatively low in anaplastic large cell lymphoma (ALCL, 44.44%) and HD (28.57%) in our group.

Table 3 Success rate of CT-guided core-needle biopsy

	Number of patients	%
HD	2/7	28.57
NHL	59/73	80.82
Total	61/80	76.25

HD: Hodgkin's disease; NHL: non-Hodgkin's lymphoma.

Table 4 Histologic classification in CT-guided core-needle biopsies

	Number of diagnoses	Number of non-diagnoses
HD	2	5
Lymphocyte-predominant	1	2
Lymphocytic depletion	1	–
Nodular sclerosis	–	3
B-cell NHL	44	7
Diffuse large B-cell	32	4
Marginal zone B-cell	6	1
Small lymphocytic	2	–
Mantle B-cell	3	–
Burkitt's	–	1
Follicular NHL	1	1
T-cell NHL	15	7
Peripheral T-cell	9	1
Anaplastic large cell (T/null cell)	4	5
Angioimmunoblastic	2	1
Total	61	19

HD: Hodgkin's disease; NHL: non-Hodgkin's lymphoma.

DISCUSSION

A satisfactory sampling for histological examination is fundamental to the diagnosis and management of malignant lymphomas^[5,17]. Fine-needle aspiration (FNA) biopsies in the diagnosis of malignant lymphomas have been reported^[18–20]. Core-needle biopsies were superior to FNA since histology is more reliable than cytology^[21–23]. The use of CT guidance and improved histological diagnostic techniques have promoted the development of non-surgical sampling of tumor masses in almost any location^[4,9]. Silverman *et al.*^[24],

reported that image-guided biopsy of abdominal lymphoma provided an adequate tissue sample that enables treatment in 72% of patients. Pappa *et al.*^[14], have achieved a diagnostic rate of 83% lymphomas, and suggested that image-guided core-needle biopsy should become the procedure of choice for histological sampling in the absence of peripheral lymphadenopathy. de Kerviler *et al.*^[25], have reported, a relatively high success rate of 88%. Recently, Agid *et al.*^[4], reported, that CT-guided core-needle biopsies are sufficient to establish a diagnosis of 82.5% patients with lympho-proliferative disorders and suggested that it should be used as the first step in diagnosis of lymphomas. In our group, 61 of 80 (76.25%) patients had a definite diagnosis and histological classification, and subsequent treatment was performed on the basis of the results of core-needle biopsy. CT-guided core-needle biopsy is therefore widely regarded as a quick, safe, and efficient alternative to excisional biopsy in patients without enlarged superficial lymph nodes^[10,14].

The core-needle can acquire a relatively large specimen, which allows a better immunohistochemical staining^[26,27]. CT-guided core-needle biopsy obviates the need for surgical biopsy in the majority of cases^[4,9,25]. Automated biopsy systems such as Bard biopsy gun (CR, Inc., Covington, GA, USA) are rapid, simple, and highly efficient in sampling^[11] and have been used as the commonest tool for percutaneous CT-guided biopsy in our hospital. Guided by CT, an 18–20 G needle is driven forward by the spring-loaded gun, and a biopsy specimen with a size of about 1.5-cm in length is rapidly cut, which is sufficient for imm-ohistochemistry staining for complete subtyping^[14,16]. The reliability of CT-guided core-needle biopsy in diagnosis and classification of malignant lymphomas has largely been confirmed, and the opportunity of open biopsy or exploratory operation is greatly reduced^[9,26].

In our study, 76.25% (61/80) of patients with malignant lymphoma underwent CT-guided core-needle biopsies and treated on the basis of biopsy results alone. However, the definite diagnosis and explicit histological classifications were not obtained by core-needle biopsy alone in 19 patients with malignant lymphomas. The most common reason for the failure of core-needle biopsy diagnosis is that satisfactory sampling is not obtained due to the extensive necrosis of the lesions^[1,10]. In diagnosis of follicular lymphoma, very large follicular structures might potentially be missed by core-needle biopsy. However, this theoretical drawback is rarely encountered^[16,28]. Also, primary diagnosis of uncommon lymphomas may be compromised by small samples obtained by needle biopsy, and as with biopsies negative for lymphoma, surgical intervention may be required^[16,29]. Indeed, some subtypes of malignant lymphoma might not be definitely diagnosed and categorized by CT-guided core-needle biopsy alone^[29,30]. Ben-Yehuda *et al.*^[31], suggested that the most problematic category is mixed small- and large-cell NHL, because of the difficulty in making a reliable assessment of the relative number of large cells present and distinguishing diffuse from nodular patterns in these cases.

Due to its morphologic variations, anaplastic large cell (T/null cell) lymphoma (ALCL) might be mistaken for

other lymphoid or non-lymphoid malignancies^[32]. In general, ALCL is of T-cell phenotype and characterized by the classic "anaplastic" morphology and a peculiar CD30 expression. Its diagnosis relies on recognition of distinctive morphologic clues, such as the presence of occasional "hallmark" cells, especially around small vessels, as well as immunopositivity for CD30 and occasionally ALK protein. Therefore, a definitive diagnosis of ALCL is possibly based on careful interpretation of immunohistochemical features^[32,33]. If the explicit diagnosis of ALCL cannot be made on the basis of a small size of samples obtained by core-needle biopsy, the relatively larger specimen obtained by open biopsy may be needed for definite diagnosis.

A common subtype of lymphomas such as diffuse large B cell lymphoma often yields a predominant population of large lymphoid cells with a high mitotic activity and a relatively high rate of diagnosis^[13,32]. The success rate was as high as 88.89% (32/36) in our group. However, there were nine patients (11.25%) with ALCL in our group, and a definite diagnosis by core-needle biopsy alone was made in only four (44.44%). The main reason for this failure is due to the small size of samples obtained by core-needle biopsy.

Zinzani *et al.*^[13], and Pappa *et al.*^[14], have reported, relatively high success rates in diagnosis of HD using core-needle biopsy. However, there were a relatively small number of patients with HD in our group (8.75%), and only 28.57% (2/7) of patients with HD were definitely diagnosed by core-needle biopsy. Except for unsatisfactory sampling^[25], our low success rate may largely be due to lack of experience of pathological diagnosis of HD on the basis of core-needle biopsy in our hospital.

In conclusion, CT-guided core-needle biopsy is a reliable diagnostic procedure for malignant lymphoma, and can be widely used in patients with suspected malignant lymphoma in absence of palpable, enlarged superficial lymph nodes.

REFERENCES

- 1 Sklair-Levy M, Polliack A, Shaham D, Applbaum YH, Gillis S, Ben-Yehuda D, Sherman Y, Libson E. CT-guided core-needle biopsy in the diagnosis of mediastinal lymphoma. *Eur Radiol* 2000; **10**: 714-718
- 2 Mintzer DM, Mason BA. On the need for biopsy confirmation at suspected first recurrence of cancer. *Am J Clin Oncol* 2003; **26**: 192-196
- 3 Demharter J, Muller P, Wagner T, Schlimok G, Haude K, Bohndorf K. Percutaneous core-needle biopsy of enlarged lymph nodes in the diagnosis and subclassification of malignant lymphomas. *Eur Radiol* 2001; **11**: 276-283
- 4 Agid R, Sklair-Levy M, Bloom AI, Lieberman S, Polliack A, Ben-Yehuda D, Sherman Y, Libson E. CT-guided biopsy with cutting-edge needle for the diagnosis of malignant lymphoma: experience of 267 biopsies. *Clin Radiol* 2003; **58**: 143-147
- 5 Gupta RK, Naran S, Lallu S, Fauck R. The diagnostic value of fine needle aspiration cytology (FNAC) in the assessment of palpable supraclavicular lymph nodes: a study of 218 cases. *Cytopathology* 2003; **14**: 201-207
- 6 Zeppa P, Marino G, Troncone G, Fulciniti F, De Renzo A, Picardi M, Benincasa G, Rotoli B, Vetrani A, Palombini L. Fine-needle cytology and flow cytometry immunophenotyping and subclassification of non-Hodgkin lymphoma: a critical review of 307 cases with technical suggestions. *Cancer* 2004; **102**: 55-65
- 7 Jimenez-Heffernan JA, Vicandi B, Lopez-Ferrer P, Hardisson D, Viguer JM. Value of fine needle aspiration cytology in the initial diagnosis of Hodgkin's disease. Analysis of 188 cases with an emphasis on diagnostic pitfalls. *Acta Cytol* 2001; **45**: 300-306
- 8 Gong JZ, Williams DC Jr, Liu K, Jones C. Fine-needle aspiration in non-Hodgkin lymphoma: evaluation of cell size by cytomorphology and flow cytometry. *Am J Clin Pathol* 2002; **117**: 880-888
- 9 Libicher M, Noldge G, Radeleff B, Gholipur F, Richter GM. Value of CT-guided biopsy in malignant lymphoma. *Radiologe* 2002; **42**: 1009-1012
- 10 Goldschmidt N, Libson E, Bloom A, Amir G, Paltiel O. Clinical utility of computed tomography-guided core needle biopsy in the diagnostic re-evaluation of patients with lymphoproliferative disorders and suspected disease progression. *Ann Oncol* 2003; **14**: 1438-1441
- 11 Haramati LB. CT-guided automated needle biopsy of the chest. *Am J Roentgenol* 1995; **165**: 53-55
- 12 Hopper KD, Abendroth CS, Sturtz KW, Matthews YL, Hartzel JS, Potok PS. CT percutaneous biopsy guns: comparison of end-cut and side-notch devices in cadaveric specimens. *Am J Roentgenol* 1995; **164**: 195-199
- 13 Zinzani PL, Corneli G, Cancellieri A, Magagnoli M, Lacava N, Gherlinzoni F, Bendandi M, Albertini P, Baruzzi G, Tura S, Boaron M. Core needle biopsy is effective in the initial diagnosis of mediastinal lymphoma. *Haematologica* 1999; **84**: 600-603
- 14 Pappa VI, Hussain HK, Reznik RH, Whelan J, Norton AJ, Wilson AM, Love S, Lister TA, Rohatiner AZ. Role of image-guided core-needle biopsy in the management of patients with lymphoma. *J Clin Oncol* 1996; **14**: 2427-2430
- 15 Jaffe ES, Harris NL, Stein H, Vardiman JW. World health organization classification of tumours. Pathology and genetics of tumours of haemopoietic and lymphoid tissues. *Lyon: IARC Press* 2001: 111-235
- 16 Whelan JS, Reznik RH, Daniell SJ, Norton AJ, Lister TA, Rohatiner AZ. Computed tomography (CT) and ultrasound (US) guided core biopsy in the management of non-Hodgkin's lymphoma. *Br J Cancer* 1991; **63**: 460-462
- 17 Wakely P Jr, Frable WJ, Kneisl JS. Soft tissue aspiration cytopathology of malignant lymphoma and leukemia. *Cancer* 2001; **93**: 35-39
- 18 Landgren O, Porwit MacDonald A, Tani E, Czader M, Grimfors G, Skoog L, Ost A, Wedelin C, Axedorph U, Svedmyr E, Bjorkholm M. A prospective comparison of fine-needle aspiration cytology and histopathology in the diagnosis and classification of lymphomas. *Hematol J* 2004; **5**: 69-76
- 19 Civardi G, Vallisa D, Berte R, Giorgio A, Filice C, Caremani M, Caturelli E, Pompili M, De Sio I, Buscarini E, Cavanna L. Ultrasound-guided fine needle biopsy of the spleen: high clinical efficacy and low risk in a multicenter Italian study. *Am J Hematol* 2001; **67**: 93-99
- 20 Singh NG, Kapila K, Dawar R, Verma K. Fine needle aspiration cytology diagnosis of lymphoproliferative disease of the breast. *Acta Cytol* 2003; **47**: 739-743
- 21 Varadarajulu S, Fraig M, Schmulewitz N, Roberts S, Wildi S, Hawes RH, Hoffman BJ, Wallace MB. Comparison of EUS-guided 19-gauge Trucut needle biopsy with EUS-guided fine-needle aspiration. *Endoscopy* 2004; **36**: 397-401
- 22 Wotherspoon AC, Norton AJ, Lees WR, Shaw P, Isaacson PG. Diagnostic fine needle core biopsy of deep lymph nodes for the diagnosis of lymphoma in patients unfit for surgery. *J Pathol* 1989; **158**: 115-121
- 23 Lieberman S, Libson E, Maly B, Lebensart P, Ben-Yehuda D, Bloom AI. Imaging-guided percutaneous splenic biopsy using a 20- or 22-gauge cutting-edge core biopsy needle for the diagnosis of malignant lymphoma. *Am J Roentgenol* 2003; **181**: 1025-1027
- 24 Silverman SG, Lee BY, Mueller PR, Cibas ES, Seltzer SE. Impact of positive findings at image-guided biopsy of lymphoma on patient care: evaluation of clinical history, needle size, and pathologic findings on biopsy performance. *Radiology* 1994; **190**: 759-764

- 25 **de Kerviler E**, Guermazi A, Zagdanski AM, Meignin V, Gossot D, Oksenhendler E, Mariette X, Brice P, Fria J. Image-guided core-needle biopsy in patients with suspected or recurrent lymphomas. *Cancer* 2000; **89**: 647-652
- 26 **Gong JZ**, Snyder MJ, Lagoo AS, Vollmer RT, Dash RR, Madden JF, Buckley PJ, Jones CK. Diagnostic impact of core-needle biopsy on fine-needle aspiration of non-Hodgkin lymphoma. *Diagn Cytopathol* 2004; **31**: 23-30
- 27 **Quinn SF**, Sheley RC, Nelson HA, Demlow TA, Wienstein RE, Dunkley BL. The role of percutaneous needle biopsies in the original diagnosis of lymphoma: a prospective evaluation. *J Vasc Interv Radiol* 1995; **6**: 947-952
- 28 **West RB**, Warnke RA, Natkunam Y. The usefulness of immunohistochemistry in the diagnosis of follicular lymphoma in bone marrow biopsy specimens. *Am J Clin Pathol* 2002; **117**: 636-643
- 29 **Mayall F**, Darlington A, Harrison B. Fine needle aspiration cytology in the diagnosis of uncommon types of lymphoma. *J Clin Pathol* 2003; **56**: 821-825
- 30 **Jimenez-Heffernan JA**, Gonzalez-Peramato P, Perna C, Alvarez-Ferreira J, Lopez-Ferrer P, Viguer JM. Fine-needle aspiration cytology of extranodal natural killer/T-cell lymphoma. *Diagn Cytopathol* 2002; **27**: 371-374
- 31 **Ben-Yehuda D**, Polliack A, Okon E, Sherman Y, Fields S, Lebenshart P, Lotan H, Libson E. Image-guided core-needle biopsy in malignant lymphoma: experience with 100 patients that suggests the technique is reliable. *J Clin Oncol* 1996; **14**: 2431-2434
- 32 **Ng WK**, Ip P, Choy C, Collins RJ. Cytologic and immunocytochemical findings of anaplastic large cell lymphoma: analysis of ten fine-needle aspiration specimens over a 9-year period. *Cancer* 2003; **99**: 33-43
- 33 **Creager AJ**, Geisinger KR, Bergman S. Neutrophil-rich Ki-1-positive anaplastic large cell lymphoma: a study by fine-needle aspiration biopsy. *Am J Clin Pathol* 2002; **117**: 709-715

Science Editor Wang XL and Guo SY Language Editor Elsevier HK

Modulation of gastric accommodation by duodenal nutrients

Mauricio Carrasco, Fernando Azpiroz, Juan-R. Malagelada

Mauricio Carrasco, Fernando Azpiroz, Juan-R. Malagelada, Digestive System Research Unit, Hospital General Vall d'Hebron, Autonomous University of Barcelona, Barcelona 08035, Spain
Supported by the Spanish Ministry of Education (Dirección General de Enseñanza Superior del Ministerio de Educación y Cultura, BFI 2002-03413), the Instituto de Salud Carlos III, No. C03/02, and the National Institutes of Health, USA, No. DK 57064
Correspondence to: Fernando Azpiroz, MD, Digestive System Research Unit, Hospital General Vall d'Hebron, Barcelona 08035, Spain. fernando.azpiroz@wol.es
Telephone: +34-93-274-62-59 Fax: +34-93-489-44-56
Received: 2004-12-15 Accepted: 2005-01-05

Carrasco M, Azpiroz F, Malagelada JR. Modulation of gastric accommodation by duodenal nutrients. *World J Gastroenterol* 2005; 11(31): 4848-4851

<http://www.wjgnet.com/1007-9327/11/4848.asp>

Abstract

AIM: To determine the relative potency and contribution of intestinal nutrients to net gastric accommodative relaxation and conscious perception.

METHODS: In 12 healthy subjects, we randomly tested duodenal loads of lipids and carbohydrates (12 mL administered in 4 min) at various caloric concentrations (0.0125-0.8 kcal/mL) separated by 12-24 min wash-out periods of saline infusion. Maximal gastric relaxation was induced at the end of each experiment by i.v glucagon (5 µg/kg), as reference. The reflex gastric response was measured by a barostat, and symptom perception by a 0-6 score questionnaire.

RESULTS: Lipids induced a dose-response gastric relaxation with a steep and early rise. Maximal effect (179±42 mL relaxation) reached at a relatively low concentration (0.2 kcal/mL), maximal lipid-induced relaxation was 61±6% of the glucagon effect. By contrast, duodenal infusion of carbohydrates induced weaker relaxation that became significant only at the high end of the physiological concentration range (65±14 mL with 0.8 kcal/mL). Intestinal nutrient loads, either of lipid or carbohydrates, did not induce significant changes in perception (0.6±0.4 and 0.1±0.4 score increase for the highest concentrations, respectively).

CONCLUSION: Chyme entering the small bowel induces nutrient-specific gastric relaxatory reflexes by a physiologically saturable mechanism. Normally, neither the intestinal nutrient load nor the gastric accommodative response is perceived.

© 2005 The WJG Press and Elsevier Inc. All rights reserved.

Key words: Gastric accommodation; Enterogastric reflex; Postprandial symptoms; Intestinal nutrients; Gastric relaxation; Gastric barostat; Gut perception

INTRODUCTION

The intestine exerts a feedback control on gastric emptying, and thereby regulates the rate of nutrient delivery into the intestine. The duodenum, in particular, plays a key role in this process, by modulating the level of gastric tone via entero-gastric reflexes. The mechanisms that control the gastric relaxatory response to intestinal nutrients have been extensively studied in experimental animal models^[1]. Human data are relatively scarce. Although it has been shown that duodenal nutrients induce a gastric relaxation, and that this effect depends on the type of nutrient^[2-4], comparative dose-related responses to various nutrients are not available. Our aim was to compare the relative potency of duodeno-gastric relaxatory reflexes induced physiologically by different types of nutrients, namely, lipids *vs* carbohydrates in healthy humans employing a combination of enteric nutrient infusion and measurement of gastric tone responses by the barostat.

MATERIALS AND METHODS

Participants

Twelve healthy subjects without gastrointestinal symptoms (seven women, five men; 20-26 years of age) participated in the study after giving written informed consent. The protocol for the study was previously approved by the Institutional Review Board of the University Hospital Vall d'Hebron.

Duodenal nutrient infusion

Using an intra-luminal polyvinyl tube (2 mm outer diameter) located into the duodenum, either saline solution, carbohydrates (Maxijul[®]; Scientific Hospital Supplies, Barcelona, Spain) or lipids (Intralipid[®], Pharmacia and Upjohn, St Cugat del Valles, Spain) were continuously infused at 2 mL/min rate using a perfusion pump (Asid Bonz PP50-300; Lubratronics, Unterschleissheim, Germany). Nutrients were diluted in saline to various caloric concentrations. All perfusates were adjusted to 300 mOsm/L and pH 7.

Gastric tone measurement

Gastric tone was continuously measured using a barostat connected by a double lumen tube (127 Argyle; Sherwood Medical, St. Louis, MO, USA) to an intra-gastric bag (1 L capacity, 36 cm maximal diameter, made of ultrathin

polyethylene). Tone was measured as changes in intra-gastric volume at a constant pressure level, 2 mmHg above the intra-abdominal pressure. The intra-abdominal pressure was determined at the beginning of each study as the minimal distending pressure that detected respiratory variations, by increasing intrabag pressure in 1 mmHg steps every minute^[5]. Detailed description of the barostat has been previously published^[5,6].

Perception measurements

Subjective perception was measured using a graded questionnaire to measure the intensity and the type of sensations perceived^[7]. The graded questionnaire included four graphic rating scales graded from 0 (no perception) to 6 (pain), specifically for scoring the following abdominal sensations: (1) pressure; (2) fullness; (3) nausea; and (4) other type of sensation (to be specified), respectively.

Procedure and experimental design

Participants were orally intubated after 6 h fast. The intestinal infusion tube was positioned under fluoroscopic control in the duodenum, 10 cm distal to the pylorus, and the bag of the barostat was introduced into the stomach. The studies were conducted in a quiet, isolated room with participants sitting on an ergonomic chair with the trunk erect.

The barostat was connected to the intra-gastric bag, and gastric tone was continuously recorded on a paper polygraph (model 6006; Letica, Barcelona, Spain). The duodenal tube was connected to the perfusion pump, and saline solution was infused. Nutrient tests were started after 10 min basal recording. In each subject the following nutrient solutions (12 mL administered as 4 mL bolus plus 4 min infusion at 2 mL/min) were tested in random order: (1) lipids at 0.0125, 0.05, 0.2, and 0.8 kcal/mL; and (2) carbohydrates at 0.2 and 0.8 kcal/mL. After each nutrient perfusion, the saline perfusion was restored. In preliminary studies, the duration of the effects of duodenal nutrients on gastric tone depended on the type of nutrient and the caloric load. Hence, to assure the lack of carry-over effects, we adjusted the duration of the saline wash-out periods between nutrients tests, allowing 24 min after the 0.8 kcal/mL lipid dose, 16 min after the 0.2 kcal lipid dose, and 12 min after the rest. At the end of each nutrient perfusion, subjects were asked to fill in the perception questionnaire. After the nutrient tests were completed, glucagon (Glucagon Novo, Laboratorios Novo, Madrid, Spain) was administered as a 5 µg/kg iv bolus, and gastric tone was recorded for another 20 min.

Data analysis

The response of gastric tone to duodenal nutrients was measured as the difference of mean intra-gastric volume recorded by the barostat during the 2 min before and during the last 2 min of each nutrient perfusion. Perception was measured by the highest score (rather than by the mean or cumulative scores) marked on the scales.

Statistical analysis

Mean±SE of the parameters measured for each nutrient concentration tested was calculated. Comparison of normally

distributed data was performed by the paired Student's *t* test.

RESULTS

Lipids induced a dose-related gastric relaxation with a steep and early rise (Figure 1). The lowest lipid load (0.0125 kcal/mL) did not modify gastric tone. However, the 0.05 kcal/mL load produced a significant relaxation ($P<0.05$ vs 0.0125 kcal/mL), exceeding half of the relaxation induced by the maximal lipid concentration (0.8 kcal/mL). A full effect was achieved with a relatively low concentration (0.2 kcal/mL), and no further gastric relaxation was produced by the highest load (0.8 kcal/mL). The maximal effect achieved by lipids was $61\pm6\%$ of the pharmacological effect of glucagon. The gastric relaxatory response developed rapidly after the lipid administration was started, so that a plateau effect was reached 2 min later (Figure 2). Conversely, during the washout period after the lipid infusion, the relaxation faded and gastric tone reverted to the previous baseline.

Duodenal carbohydrate infusion produced a significantly weaker relaxation than lipids (Figure 1). The 0.2 kcal/mL carbohydrate concentration did not modify gastric tone, though the equicaloric lipid load produced a maximal effect ($P<0.05$ vs lipids). The highest carbohydrate concentration (0.8 kcal/mL) produced a significant ($P<0.05$ kcal/mL vs 0.2 kcal/mL) but modest gastric relaxation of only about one-third than that induced by the equicaloric lipid load ($P<0.05$ vs lipids). The maximal effect achieved by carbohydrates reached only 19% of the glucagon effect.

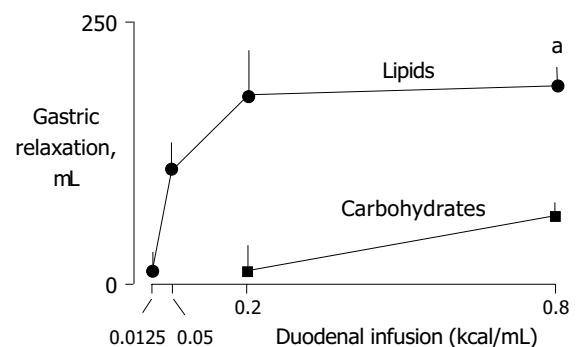


Figure 1 Gastric relaxatory response to duodenal nutrients. Values are mean±SE. Note the saturable dose-related gastric relaxation with lipids, and a significantly weaker response with carbohydrates. ^a $P<0.05$ vs carbohydrates.

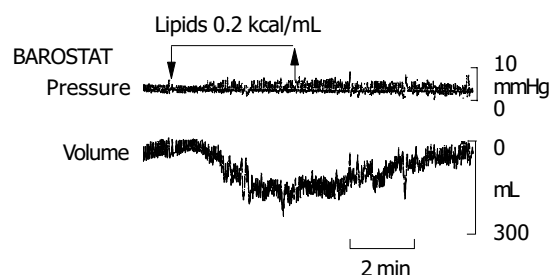


Figure 2 Example of gastric relaxation induced by duodenal lipid infusion (0.2 kcal/mL). Gastric relaxation was measured as intra-gastric volume increment at constant pressure by a barostat. Note rapid relaxation and complete recovery after the infusion.

None of the nutrient loads tested or their reflex effects on gastric tone induced significant conscious perception (Figure 3).

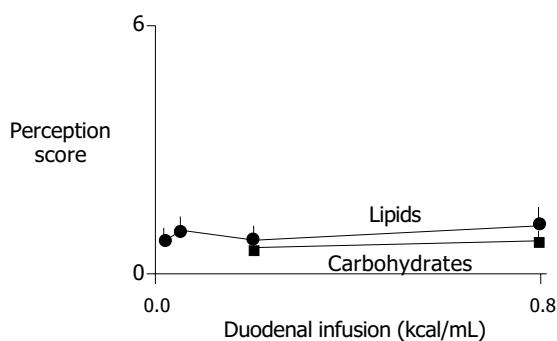


Figure 3 Perception of duodenal nutrient loads. All nutrient loads were unperceived, despite the prominent gastric accommodative response associate to some of them.

DISCUSSION

In our study, chyme entering the small bowel induced nutrient-specific gastric relaxatory reflexes by a physiologically saturable mechanism. In healthy subjects, neither the intestinal nutrient load nor the gastric accommodative response was perceived.

As previously shown, lipids in the duodenum induce a gastric relaxatory reflex^[2-4]. We have further shown that this effect is concentration-related. Indeed low lipid concentration induced marked effects. Full effect was achieved with a very low concentration, and one fourth of this concentration induced a gastric relaxation which was half of the full effect. This mechanism seems saturable, because a four-fold increase of the full-effect concentration did not increase the magnitude of gastric relaxation. Furthermore, we administered at the end of the study, a pharmacological dose of glucagon to produce a maximal gastric relaxation^[8,9], evidenced that the full effect produced by even a very small lipid concentration was about two thirds of the glucagon effect.

By contrast to lipids, intra-duodenal carbohydrates had minor gastric relaxatory effects. Equicaloric amounts of carbohydrates induced significantly smaller gastric relaxation. The same concentration of carbohydrates as that of lipids producing full effect was ineffective, and the maximal concentration tested, achieved only one fifth of the glucagon effect.

The effect of nutrients on gastric tone has been studied on an experimental dog model with isolated intestinal loops^[10]. These studies indicate that nutrient specificity depends on the region of intestine stimulated. When infused into the proximal small bowel, lipids are significantly more potent than carbohydrates, which is consistent with that observed in the present study, but in the distal small bowel, carbohydrates elicit a much stronger response. At variance with humans, in this canine model, carbohydrates into the proximal intestine failed to induce a gastric relaxation, but this could be related to the different regions that were exposed. However, in the present study, nutrients were infused directly into the duodenum and a more distal loop was

isolated in dogs.

Additional experimental studies in animals have further characterized this nutrient-dependent entero-gastric reflex. In a model of isolated vagus, it was that reflex gastric relaxation is mediated by non-adrenergic, non-cholinergic, vagal fibers^[11]. It has also been shown that CCK may be involved in lipid-induced reflexes^[12]. However, CCK is only released by long chain fatty acids, but not by the short-medium length acids^[13,14]. Furthermore, the rapid onset and reversible response, without appreciable carry-over effects, all point toward a neural rather than a humoral type of response. Hence, the different effects of lipids and carbohydrates seem related to the specific reflex pathways activated.

Detection of the reflex relaxation in the present experiments was possible by an artificial manipulation of intra-gastric conditions. During basal conditions, the stomach is empty and contracted. The barostat applies a small, constant intra-gastric pressure insufficient to expand the gastric walls. However, when the stomach relaxes in response to experimental administration of nutrients directly into the intestine, the intra-gastric volume expands and the barostat makes this relaxation visible by the intra-gastric volume increment. Interestingly, this isobaric expansion does not induce conscious sensations.

It has been shown that intra-gastric volumes are perceived via activation of tension receptors^[9], and the present data confirm that expansion and wall elongation do not elicit perception. Nutrients, particularly lipids, have been shown to sensitize mechanoreceptors and heighten perception of gastric distension^[2-4], but in the present experimental conditions, nutrients did not modify perception, conceivably because tension receptors were not activated. The gastric expansion measured by the barostat mimics the normal accommodation process, during which gastric filling by food is associated to an accommodative relaxation^[1,15]. Indeed, this type of nutrient-mediated reflexes, by modulating the level of contraction/relaxation of the gastric wall, plays a dual role, contributing, both, to the unperceived accommodation of the stomach to the meal, and to the control of the gastric emptying rate. In the present study, even high lipid concentration produced only a partial relaxation, as evidenced by the comparison to the effect of glucagon, suggesting that the stomach still exerts some degree of contraction. This residual contraction, similar to that produced during meal accommodation, is enough to gently force intra-gastric content distally and initiate gastric emptying. Subsequently, the emptying profile is controlled by a net of reflexes depending on the nutrient composition of chyme along the small intestine, to adapt the gastric delivery of nutrients to the intestinal processing capability^[1].

The characterization of the nutrient-induced reflexes described in this paper may contribute to a better understanding of the pathophysiology of accommodation-related symptomatic disorders, such as functional dyspepsia. Indeed, it has been shown that dyspeptic patients have impaired entero-gastric reflexes^[16,17] that result in impaired gastric accommodation and post-prandial symptoms^[18,19], but the specific effects of individual nutrients have not been characterized. Hence, evaluation of the full dose-response to different nutrient elements may help to clarify the reflex

dysfunction in functional dyspepsia.

ACKNOWLEDGMENT

The authors thank Gloria Santalieu for secretarial assistance.

REFERENCES

- 1 **Mayer EA**, Gebhart GF. Basic and clinical aspects of visceral hyperalgesia. *Gastroenterology* 1994; **107**: 271-293
- 2 **Barbera R**, Feinle C, Read NW. Nutrient-specific modulation of gastric mechanosensitivity in patients with functional dyspepsia. *Dig Dis Sci* 1995; **40**: 1636-1641
- 3 **Feinle C**, Grundy D, Read NW. Effects of duodenal nutrients on sensory and motor responses of the human stomach to distension. *Am J Physiol* 1997; **273**: G721-G726
- 4 **Feinle C**, Grundy D, Fried M. Modulation of gastric distension-induced sensations by small intestinal receptors. *Am J Physiol Gastrointest Liver Physiol* 2001; **280**: G51-G57
- 5 **Azpiroz F**, Malagelada JR. Gastric tone measured by an electronic barostat in health and postsurgical gastroparesis. *Gastroenterology* 1987; **92**: 934-943
- 6 **Azpiroz F**, Salvioli B. Barostat measurements. In: Schuster MM, Crowl MD, and Koch KL, eds. *Schuster Atlas of Gastrointestinal Motility in Health and Disease*. 2nd Edition ed. Hamilton, Ontario: BC Decker 2002: 151-170
- 7 **Azpiroz F**. Gastrointestinal perception: pathophysiological implications. *Neurogastroenterol Mot* 2002; **14**: 229-239
- 8 **Notivol R**, Coffin B, Azpiroz F, Mearin F, Serra J, Malagelada JR. Gastric tone determines the sensitivity of the stomach to distension. *Gastroenterology* 1995; **108**: 330-336
- 9 **Distritti E**, Azpiroz F, Soldevilla A, Malagelada JR. Gastric wall tension determines perception of gastric distention. *Gastroenterology* 1999; **116**: 1035-1042
- 10 **Azpiroz F**, Malagelada JR. Intestinal control of gastric tone. *Am J Physiol* 1985; **249**: G501-G509
- 11 **Azpiroz F**, Malagelada JR. Vagally mediated gastric relaxation induced by intestinal nutrients in the dog. *Am J Physiol* 1986; **251**: G727-G735
- 12 **Feinle C**, D'Amato M, Read NW. Cholecystokinin-A receptors modulate gastric sensory and motor responses to gastric distension and duodenal lipid. *Gastroenterology* 1996; **110**: 1379-1385
- 13 **Feinle C**, Rades T, Otto B, Fried M. Fat digestion modulates gastrointestinal sensations induced by gastric distention and duodenal lipid in humans. *Gastroenterology* 2001; **120**: 1100-1107
- 14 **Lal S**, McLaughlin J, Barlow J, D'Amato M, Giacobelli G, Varro A, Dockray GJ, Thompson DG. Cholecystokinin pathways modulate sensations induced by gastric distension in humans. *Am J Physiol Gastrointest Liver Physiol* 2004; **287**: G72-G79
- 15 **Moragas G**, Azpiroz F, Pavia J, Malagelada JR. Relations among intragastric pressure; postcibal perception and gastric emptying. *Am J Physiol* 1993; **264**: G1112-G1117
- 16 **Coffin B**, Azpiroz F, Guarner F, Malagelada JR. Selective gastric hypersensitivity and reflex hyporeactivity in functional dyspepsia. *Gastroenterology* 1994; **107**: 1345-1351
- 17 **Caldarella MP**, Azpiroz F, Malagelada JR. Antro-fundic dysfunctions in functional dyspepsia. *Gastroenterology* 2003; **124**: 1220-1229
- 18 **Tack J**, Caenepeel P, Fischler B, Piessevaux H, Janssens J. Symptoms associated with hypersensitivity to gastric distention in functional dyspepsia. *Gastroenterology* 2001; **121**: 526-535
- 19 **Tack J**, Bisschops R, Sarnelli G. Pathophysiology and treatment of functional dyspepsia. *Gastroenterology* 2004; **127**: 1239-1255

Science Editor Wang XL and Guo SY Language Editor Elsevier HK

Overexpression of S100A4 is closely associated with progression of colorectal cancer

Yong-Gu Cho, Chang-Jae Kim, Suk-Woo Nam, Shin-Hee Yoon, Sug-Hyung Lee, Nam-Jin Yoo, Jung-Young Lee, Won-Sang Park

Yong-Gu Cho, Chang-Jae Kim, Suk-Woo Nam, Sug-Hyung Lee, Nam-Jin Yoo, Jung-Young Lee, Won-Sang Park, Department of Pathology, College of Medicine, The Catholic University of Korea, 505 Banpo-dong, Seocho-gu, Seoul 137-701, South Korea

Shin-Hee Yoon, Department of Physiology, College of Medicine, The Catholic University of Korea, 505 Banpo-dong, Seocho-gu, Seoul 137-701, South Korea

Supported by the Korea Science and Engineering Foundation, No. R13-2002-005-01004-0

Correspondence to: Dr. Won-Sang Park, Department of Pathology, College of Medicine, The Catholic University of Korea, 505 Banpo-dong, Seocho-gu, Seoul 137-701, South Korea. wonsang@catholic.ac.kr
Telephone: +82-2-590-1192 Fax: +82-2-537-6586

Received: 2005-01-11 Accepted: 2005-01-26

Abstract

AIM: To investigate whether S100A4 played an important role in the development or progression of colorectal cancer.

METHODS: A total of 124 colorectal adenocarcinoma tissue specimens were analyzed by immunohistochemistry for the expression of S100A4 protein and subsequently investigated for the gene mutations in the coding region of *S100A4* gene. The specimens were collected over a 3-year period in the laboratories at our large teaching hospital in Seoul, Republic of Korea.

RESULTS: Normal colonic epithelium either failed to express or showed focal weak expression of S100A4. Moderate to strong cytoplasmic expression of S100A4 was seen in 69 (55.6%) of the 124 colorectal carcinoma tissue specimens. S100A4 expression was detected in 43 (69.4%) of 62 specimens with lymph node metastasis. Statistically, overexpression of S100A4 was significantly associated with Dukes' stage and lymph node metastasis. Nuclear staining was also observed in 24 (19.4%) of 124 samples and closely associated with Dukes' stage. However, there was no significant correlation between overexpression of S100A4 and other investigated clinico-pathologic parameters, including tumor localization, tumor size, and survival period. In mutational analysis, no gene mutation was found in the analyzed genomic area of colorectal cancer.

CONCLUSION: Overexpression of S100A4 may be closely related with the aggressiveness of colorectal carcinoma.

Key words: S100A4; Mutation; Immunohistochemistry; Colorectal cancer; Tumor stage

Cho YG, Kim CJ, Nam SW, Yoon SH, Lee SH, Yoo NJ, Lee JY, Park WS. Overexpression of S100A4 is closely associated with progression of colorectal cancer. *World J Gastroenterol* 2005; 11(31): 4852-4856

<http://www.wjgnet.com/1007-9327/11/4852.asp>

INTRODUCTION

Colorectal cancer remains one of the most frequent malignant neoplasms worldwide. In Korea, it accounts for an estimated 9.9% of all malignancies, with 9.7% in the male population and 10.2% in the female population^[1]. The major cause of death is the metastatic spread of the disease from the primary tumor to distant sites, especially to the liver^[2]. Research into colorectal cancer has highlighted the prognostic significance of TNM tumor staging including depth of tumor invasion, involvement of regional lymph nodes, and infiltration to distant organs. Although there are a lot of reports showing the significance of many other prognostic parameters such as histological grade, serum carcino-embryonic antigen levels and flow cytometric DNA analysis, none of them has been widely used in the clinic^[3-5].

The concept of multi-stage carcinogenesis has been widely accepted as a consequence of multiple genetic alterations accumulated in cancer cells^[6]. Interestingly, stepwise accumulation of genetic alterations during progression has been observed in several tumor types, particularly in tumors of epithelial origin like colorectal cancer. It is also well known that highly metastatic cells often acquire more genetic alterations than non-metastatic cells. Therefore, it is indispensable to identify the genes, whose alterations accumulate during cancer progression as well as the genes, whose expression is responsible for the acquisition of invasive and/or metastatic potential in cancer cells.

The S100 family of calcium binding proteins has been shown to be involved in a variety of physiological functions, such as cell proliferation, extracellular signal transduction, intercellular adhesion, and motility as well as cancer metastasis^[7-9]. Of these, S100A4 (mts1, p9Ka, calvasculin) has been identified as a cytoplasmic protein in normal cells, which is associated with the actin/myosin cytoskeleton in fixed cells^[10]. Interestingly, elevated levels of S100A4 are closely associated with the process of metastasis in several human solid cancers including gastric cancer^[11,12], colorectal adenocarcinoma^[13-15], and breast cancer^[16]. Recently,

Flatmark *et al.*^[15], reported, that nuclear localization of S100A4 is correlated with tumor stage in colorectal cancer. Furthermore, S100A4 secreted from tumor cells can increase endothelial cell motility and hence induce angiogenesis^[17]. All these findings suggest that S100A4 may exert its effect on metastasis formation not only by stimulating the motility of tumor cells but also by affecting their invasive properties through deregulation of the extracellular matrix^[18]. In the present study, to investigate whether S100A4 played an important role in the development and/or progression of Korean colorectal cancers, the expression patterns of S100A4 in 124 colorectal adenocarcinoma tissues were examined. We also performed mutational analysis of the *S100A4* gene, one of the possible overexpression mechanisms of oncogenic proteins.

MATERIALS AND METHODS

Tissue samples

One hundred and twenty-four colorectal cancer patients between 2001 and 2002 were enrolled in this study and their tissue samples were formalin-fixed and paraffin-embedded. No patient had a family history of colorectal cancer. Tumor stage was classified according to Dukes' criteria. Thirteen patients were classified as Dukes' A, 47 as Dukes' B, 56 as Dukes' C and 8 as Dukes' D. The observation time was 14-38 mo for the survivors. Among the 113 patients who were followed up, 15 patients showed relapse of cancer and 11 patients died of cancer during this time. Two pathologists screened histological sections and selected areas of the representative tumor cells. Three tissue cores (0.6 mm in diameter) were taken from each tumor sample and placed in a new recipient paraffin block using a commercially available microarray instrument (Beecher Instruments, Micro-Array Technologies, Silver Spring, MD, USA), according to the established methods^[19]. One cylinder of normal colonic mucosa adjacent to each tumor was also transferred to the recipient block.

Microdissection

The histological section were stained with hematoxylin and eosin (H and E) and reviewed. Malignant cells were selectively procured from H and E stained slides without normal cell contamination using a laser micro-dissection device (ION LMD, Jungwoo International Co, Seoul, South Korea). Corresponding normal cells were obtained from non-metastatic lymph nodes. DNA was extracted by a modified single-step DNA extraction method, as described previously^[20].

Single strand conformation polymorphism (SSCP) analysis

Genomic DNAs from tumor cells and corresponding normal cells were amplified with 2 primer pairs covering exons 2 and 3, the coding region of *S100A4*. The primer sequences were as follows: 5'-CCAGATCCTGACTGCTGTC-3' and 5'-GACTCACTCAGGCACTACCC-3' for exon 2, and 5'-GGGCTTCTGTTTTCTATC TGT-3' and 5'-CCAACCACA TCAGAG GAG-3' for exon 3. Each PCR was performed under standard conditions in a 10 μ L reaction mixture containing 1 μ L of template DNA, 0.5 μ mol/L

of each primer, 0.2 μ mol/L of each deoxynucleotide triphosphate, 1.5 mmol/L MgCl₂, 0.4 unit of Ampli Taq gold polymerase (Perkin-Elmer, Foster City, CA, USA), 0.5 μ Ci of [³²P]dCTP (Amersham, Buckinghamshire, UK), and 1 μ L of 10X buffer. The reaction mixture was denatured for 1 min at 94 °C and amplified for 35 cycles (denaturing for 40 s at 94 °C, annealing for 40 s at 56 °C, and extending for 40 s at 72 °C). Final extension was continued for 5 min at 72 °C. After amplification, PCR products were denatured for 5 min at 95 °C at a 1:1 dilution of sample buffer containing 98% formamide/5 mmol/L NaOH and loaded onto a SSCP gel (FMC mutation detection enhancement system; Intermountain Scientific, Kaysville, UT, USA) with 10% glycerol. After electrophoresis, the gels were transferred to 3-mm Whatman paper and dried, and autoradiography was performed with Kodak X-OMAT film (Eastman Kodak, Rochester, NY, USA). We repeated the experiment three times, including tissue micro-dissection, PCR, SSCP, and sequencing, and found that the data were consistent.

Immunohistochemistry for S100A4

The primary polyclonal rabbit anti-S100A4 antibody (DAKO, Carpinteria, CA, USA, dilution 1/200) was used. Immunostaining was performed on microarray tissue sections with a tyramide signal amplification kit (NEN Life Science, Boston, MA, USA) for signal intensification. Antigen retrieval was performed by microwave heating in a citrate buffer (pH 6.0). Other procedures were performed as previously described^[21]. The reaction products were developed with diaminobenzidine (Sigma, St Louis, MO, USA) and counterstained with hematoxylin. As a negative control, we used non-immune rabbit serum instead of the S100A4 antibody. Three pathologists independently reviewed the results. For statistical analysis, the stained sections were scored microscopically. The number of tumor cells stained in the cytoplasm was semi-quantitatively estimated and classified into negative and positive: negative $0 \leq 30\%$ and positive $\geq 30\%$ labeling in tumor cells.

RESULTS

Mutational analysis

We analyzed mutations of the *S100A4* gene in 124 colorectal carcinoma tissue specimens. There was no aberrant SSCP pattern in DNAs extracted from cancer cells, suggesting that there were no somatic mutations in the coding regions of the *S100A4* gene in colorectal carcinoma. We found a single nucleotide polymorphism, which was an A to G transition at nucleotide number 99 in both corresponding normal and tumor DNAs of cases No. 10 and No. 67 (data not shown). The variation was an identical single nucleotide polymorphism found in our previous report^[11] and showed no amino acid change at codon 33 (Glu→Glu, GAA→GAG). The data were consistent with triplicate experiments.

Expression of S100A4

One hundred and twenty-four colorectal carcinoma tissue specimens were screened for S100A4 protein expression. The expression was mainly faint or negative in normal colonic

Table 1 Relationship between expression of S100A4 and tumor stage of colorectal carcinoma

	Cytoplasm		Positive (%)	<i>P</i>	Nuclear		Positive (%)	<i>P</i>
	+	-			+	-		
Stage				0.0001 ¹				<0.05 ²
A	4	9	30.8		1	12	7.7	
B	21	26	44.6		7	40	14.9	
C	37	19	66.1		12	44	21.4	
D	7	1	87.5		4	4	50.0	
L/N metastasis				0.0255 ³				0.5184 ³
+	39	20	66.1		10	49	16.9	
-	30	35	46.1		14	51	21.5	
Site				0.5154 ³				0.2719 ³
Right	12	14	46.2		7	19	26.9	
Left	57	41	53.4		17	81	17.3	
Tumor size				0.6421 ³				1.0000 ³
<5 cm	33	24	57.9		11	46	19.2	
≥5 cm	36	31	53.7		13	54	19.4	
Survival period				0.7719 ³				0.9563 ³
<24 mo	6	4	60.0		2	8	20.0	
≥24 mo	63	51	55.3		22	92	19.3	
Total	69	55			24	100		

¹Cochran's linear trend test; ²Bartholomew test; ³ χ^2 test.

mucosa, but moderate to strong in lymphocytes and smooth muscle cells, concordant with previous report^[14]. In the present study, overexpression of S100A4 was found in 69 (55.6%) of the 124 colorectal carcinoma tissue specimens, in which immunostaining was predominantly marked on the cytoplasm of tumor cells (Figure 1). Cytoplasmic staining was seen in 30.8% (4 of 13) stage A cases, 44.6% (21 of 47) stage B cases, 66.1% (37 of 56) stage C cases, and 87.5% (7 of 8) stage D cases, respectively (Table 1).

Statistically, overexpression of S100A4 was closely associated with Dukes' stage ($P<0.01$) and lymph node metastasis ($P<0.01$). However, there was no significant correlation between over-expression of S100A4 and other investigated clinico-pathologic parameters, including tumor localization, tumor size, and survival period (Table 1). Interestingly, 12 of 15 patients with recurrence of cancer demonstrated cytoplasmic staining at diagnosis. Nine of them died of cancer and 2 died of cardio-vascular disease.

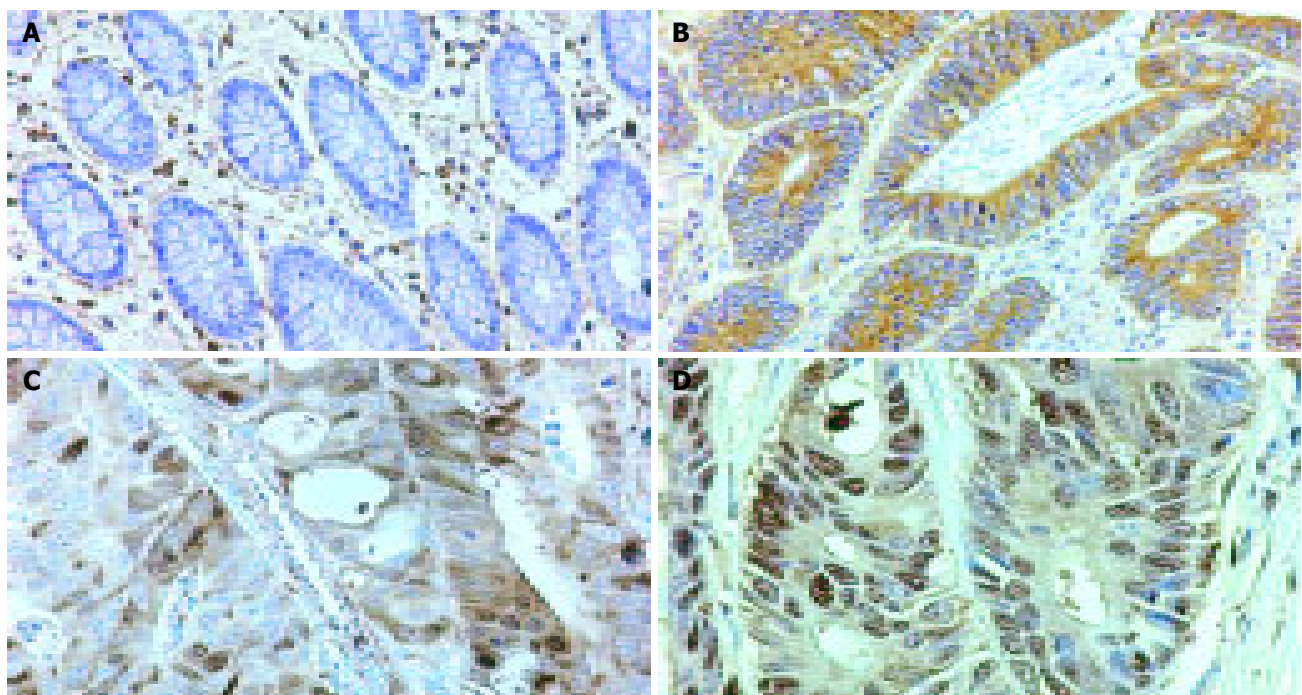


Figure 1 Expression of S100A4 in colonic mucosa (A), tubular adenocarcinoma (B, C), and nuclear staining of S100A4 (D). (Original magnifications: A-C, $\times 200$; D, $\times 400$).

Nuclear staining was also observed in 24 (19.4%) of 124 samples and the percentage of S100A4 positive cases was closely associated with Dukes' stage ($P < 0.05$, Table 1). However, there was no correlation between nuclear staining of S100A4 and pathologic parameters, including lymph node metastasis, tumor localization, tumor size, and survival period (Table 1). Additionally, nuclear staining was found in 4 of 15 patients with relapse and 3 of them died of cancer.

DISCUSSION

Oncogene amplification usually occurs late in tumor progression and correlates well with clinical aggressiveness of tumors^[21]. Over-expression of S100A4 has been reported in several human cancers, including gastric^[11,12], colorectal^[13-15], and breast cancers^[16]. Recently, it has been suggested that nuclear localization of S100A4 is related to tumor stage of colorectal cancer, and S100A4 may be involved in gene regulatory pathways related to the metastatic phenotype of cancer cells^[15].

In the present study, cytoplasmic over-expression of S100A4 was found in 69 (55.6%) of the 124 colorectal adenocarcinoma tissue specimens. Interestingly, the cytoplasmic expression of S100A4 was statistically associated with Dukes' stage and lymph node metastasis (Table 1). Additionally, 12 of 15 patients with recurrence of cancer demonstrated cytoplasmic staining and 9 of them died of cancer. It was reported that over-expression of S100A4 is closely correlated with a number of factors for tumor aggressiveness, such as lymph node metastasis, depth of invasion, and peritoneal dissemination^[11]. Overexpression of S100A4 is more frequently found in cancer cells than in normal colonic mucosa, as well as more in liver metastasis than in primary tumors^[14,15]. Furthermore, S100A4 expression has been proved to be a highly significant and independent prognostic marker in colorectal cancer^[22]. These data further support the significant correlation between over-expression of S100A4 and progression of colorectal cancer, and the putative role of S100A4 in tumor cell aggressiveness^[3,6,15].

In this study, nuclear staining of S100A4 was seen in 24 (19.4%) of 124 samples (Figure 1) and showed a significant association with higher Dukes' stage (Table 1). Previously, Flatmark *et al.*^[15], examined the nuclear expression of S100A4 in colorectal cancer and reported that nuclear location of S100A4 is associated with tumor stage. Our results also suggest that nuclear translocation of S100A4 protein might be involved in the process of invasion and metastasis of colorectal cancer. It is possible that S100A4 regulates transcription of other genes either through direct DNA binding to or through interaction with other DNA-binding proteins. Further large-scale and functional studies are necessary to elucidate the effect of nuclear translocation of S100A4 on the progression of human cancers, including colorectal cancer.

Generally, activation of a proto-oncogene results from mutation, rearrangement or manifold amplification of the DNA sequences, like *N-myc* in neuroblastoma and *c-erb B2* in breast cancer^[23-25]. Since there was no detectable somatic mutation of *S100A4* gene in the primary tumors in this

study, we considered that the S100A4 over-expression might not result from genetic mutation in colorectal carcinogenesis. However, we cannot completely rule out the possibility of a genetic alteration in other regions, such as the promoter, non-coding exon, and splice sites. Another possibility is the amplification or hypo-methylation of the *S100A4* gene in colorectal cancer, as in pancreatic ductal adenocarcinoma^[26]. In addition, our results may underestimate the prevalence of *S100A4* somatic mutations in colorectal cancer, as the sensitivity rate of SSCP analysis for the detection of single base substitutions is about 80%^[27].

In conclusion, S100A4 is overexpressed in colorectal cancer, cytoplasmic and nuclear expression is closely associated with a number of factors for tumor aggressiveness, such as tumor stage and lymph node metastasis.

REFERENCES

- 1 **Suh CI**, Suh KA, Park SH, Chang HJ, Ko JW, Ahn DH. Annual report of the central cancer registry in Korea-1998. *J Korean Cancer Assoc* 2002; **32**: 827-834
- 2 **Soong R**, Grieu F, Robbins P, Dix B, Chen D, Parsons R, House A, Lacopetta B. p53 alterations are associated with improved prognosis in distal colonic carcinomas. *Clin Cancer Res* 1997; **3**: 1405-1411
- 3 **Hutter RV**, Sobin LH. A universal staging system for cancer of the colon and rectum. Let there be light. *Arch Pathol Lab Med* 1986; **110**: 367-378
- 4 **McLeod HL**, Hurray GI. Tumor markers of prognosis in colorectal cancer. *Br J Cancer* 1999; **79**: 191-203
- 5 **Akbulut H**, Dincol D, Aydintug O, Icli F, Karaoguz H, Demirkazik A. The prognostic significance of flow cytometric DNA content determination in patients with colorectal carcinoma. *Turk J Cancer* 1998; **28**: 51-58
- 6 **Fearon ER**, Vogelstein B. A genetic model for colorectal tumorigenesis. *Cell* 1990; **61**: 759-767
- 7 **Schafer BW**, Heizmann CW. The S100 family of EF-hand calcium-binding proteins: functions and pathology. *Trends Biochem Sci* 1996; **21**: 134-140
- 8 **Sherbet GV**, Lakshmi MS. S100A4 (MTS1) calcium binding protein in cancer growth, invasion and metastasis. *Anticancer Res* 1998; **18**: 2415-2422
- 9 **Davies BR**, Davies MP, Gibbs FEM, Barraclough R, Rudland PS. Induction of the metastatic phenotype by transfection of a benign rat mammary epithelial cell line with the gene for p9Ka, a rat calcium-binding protein, but not with the oncogene EJ-ras-1. *Oncogene* 1993; **8**: 999-1008
- 10 **Gibbs FEM**, Barraclough R, Platt-Higgins A, Rudland P, Wilkinson MC, Parry EW. Immunohistochemical distribution of the calcium-binding protein p9Ka in normal rat tissue: variation in the cellular location in different tissues. *J Histochem Cytochem* 1995; **43**: 169-180
- 11 **Cho YG**, Nam SW, Kim TY, Kim YS, Kim CJ, Park JY, Lee JH, Kim HS, Lee JW, Park CH, Song YH, Lee SH, Yoo NJ, Lee JY, Park WS. Overexpression of S100A4 is closely related to the aggressiveness of gastric cancer. *APMIS* 2003; **111**: 539-545
- 12 **Yonemura Y**, Endou Y, Kimura K, Fushida S, Bandou E, Taniguchi K, Kinoshita K, Ninomiya I, Sugiyama K, Heizmann CW, Schafer BW, Sasaki T. Inverse expression of S100A4 and E-cadherin is associated with metastatic potential in gastric cancer. *Clin Cancer Res* 2000; **6**: 4234-4242
- 13 **Taylor S**, Herrington S, Prime W, Rudland PS, Barraclough R. S100A4 (p9Ka) protein in colon carcinoma and liver metastases: association with carcinoma cells and T-lymphocytes. *Br J Cancer* 2002; **86**: 409-416
- 14 **Takenaga K**, Nakanishi H, Wada K, Suzuki M, Matsuzaki O, Matsuura A, Endo H. Increased expression of S100A4, a metastasis-associated gene, in human colorectal adenocarcinomas. *Clin Cancer Res* 1997; **3**: 2309-2316

- 15 **Flatmark K**, Pedersen KB, Nesland JM, Rasmussen H, Aamodt G, Mikalsen SO, Bjørnland K, Fodstad O, Mælandsmo GM. Nuclear localization of the metastasis-related protein S100A4 correlates with tumour stage in colorectal cancer. *J Pathol* 2003; **200**: 589-595
- 16 **Rudland PS**, Platt-Higgins A, Renshaw C, West CR, Winstanley JH, Robertson L, Barraclough R. Prognostic significance of the metastasis-inducing protein S100A4 (p9Ka) in human breast cancer. *Cancer Res* 2000; **60**: 1595-1603
- 17 **Ambartsumian N**, Klingelhofer J, Grigorian M, Christensen C, Kriajevska M, Tulchinsky E, Georgiev G, Berezin V, Bock E, Rygaard J, Cao R, Cao Y, Lukanidin E. The metastasis-associated Mts1 (S100A4) protein could act as an angiogenic factor. *Oncogene* 2001; **20**: 4685-4695
- 18 **Bjørnland K**, Winberg JO, Odegaard OT, Hovig E, Loennechen T, Aasen AO, Fodstad O, Mælandsmo GM. S100A4 involvement in metastasis: deregulation of matrix metalloproteinases and tissue inhibitors of matrix metalloproteinases in osteosarcoma cells transfected with an anti-S100A4 ribozyme. *Cancer Res* 1999; **59**: 4702-4708
- 19 **Kononen J**, Bubendorf L, Kallioniemi A, Barlund M, Schraml P, Leighton S, Torhorst J, Mihatsch MJ, Sauter G, Kallioniemi OP. Tissue microarrays for high-throughput molecular profiling of tumor specimens. *Nat Med* 1998; **4**: 844-847
- 20 **Lee JY**, Dong SM, Kim SY, Yoo NJ, Lee SH, Park WS. A simple, precise and economical microdissection technique for analysis of genomic DNA from archival tissue sections. *Virchows Arch* 1998; **433**: 305-309
- 21 **Park WS**, Oh RR, Kim YS, Park JY, Shin MS, Lee HK, Lee SH, Yoo NJ, Lee JY. Absence of mutations in the kinase domain of the Met gene and frequent expression of Met and HGF/SF protein in primary gastric carcinomas. *APMIS* 2000; **108**: 195-200
- 22 **Gongoll S**, Peters G, Mengel M, Piso P, Klempnauer J, Kreipe H, von Wasielewski RV. Prognostic significance of calcium-binding protein S100A4 in colorectal cancer. *Gastroenterology* 2002; **123**: 1478-1484
- 23 **Yokota J**, Tsunetsugu-Yokota Y, Battifora H, Le Fevre C, Cline MJ. Alterations of myc, myb and ras^{Ha} proto-oncogenes in cancers are frequent and show clinical correlation. *Science* 1986; **231**: 261-265
- 24 **Brodeur GM**, Seeger RC, Schwab M, Varmus HE, Bishop JM. Amplification of N-myc in untreated human neuroblastomas correlates with advanced disease stage. *Science* 1984; **224**: 1121-1124
- 25 **Slamon DJ**, Godolphin W, Jones LA, Holt JA, Wong SG, Keith DE, Levin WJ, Stuart SG, Udove J, Ullrich A, Press MF. Studies of the HER2/neu proto-oncogene in human breast and ovarian cancer. *Science* 1989; **244**: 707-712
- 26 **Rosty C**, Ueki T, Argani P, Jansen M, Yeo CJ, Cameron JL, Hruban RH, Goggins M. Overexpression of S100A4 in pancreatic ductal adenocarcinomas is associated with poor differentiation and DNA hypomethylation. *Am J Pathol* 2002; **160**: 45-50
- 27 **Sheffield VC**, Beck JS, Kwitek AE, Sandstrom DW, Stone EM. The sensitivity of single-strand conformation polymorphism analysis for the detection of single base substitutions. *Genomics* 1993; **16**: 325-332

Science Editor Wang XL and Guo SY Language Editor Elsevier HK

Intra-familial prevalence of hepatitis B virologic markers in HBsAg positive family members in Nahavand, Iran

Amir Houshang Mohammad Alizadeh, Mitra Ranjbar, Shahin Ansari, Seyed Moayed Alavian, Hamid Mohaghegh Shalmani, Leila Hekmat, Mohammad Reza Zali

Amir Houshang Mohammad Alizadeh, Shahin Ansari, Hamid Mohaghegh Shalmani, Mohammad Reza Zali, Research Center for Gastroenterology and Liver Disease, Shaheed Beheshti University of Medical Sciences, Tehran, Iran
Mitra Ranjbar, Leila Hekmat, Hamedan University of Medical Sciences, Iran
Seyed Moayed Alavian, Baghiatallah University of Medical Sciences, Tehran, Iran
Correspondence to: Amir Houshang, Mohammad Alizadeh, Research Center for Gastroenterology and Liver Disease, Shaheed Beheshti University of Medical Sciences, 7th Floor, Taleghani Hospital, Yaman Street, Evin, Tehran 19857, Iran. article@rcgld.org
Telephone: +98-21-2418871 Fax: +98-21-2402639
Received: 2004-12-20 Accepted: 2005-01-05

Key words: Intra-familial prevalence; Hepatitis B; Nahavand; Iran

Alizadeh AHM, Ranjbar M, Ansari S, Alavian SM, Shalmani HM, Hekmat L, Zali MR. Intrafamilial prevalence of hepatitis B virologic markers in HBsAg positive family members in Nahavand, Iran. *World J Gastroenterol* 2005; 11(31): 4857-4860
<http://www.wjgnet.com/1007-9327/11/4857.asp>

Abstract

AIM: To determine the prevalence of hepatitis B in Nahavand and evaluate the HBsAg positive prevalence in families with a member who was confirmed to have HBV infection.

METHODS: This study was performed in two phases. In the first phase, 1 824 subjects in Nahavand city were selected. The interviewers visited the houses of chosen families to fill the questionnaire and take the blood samples. All subjects signed an informed consent before interviews and blood sampling. The samples were evaluated for HBV virologic markers. In the second phase, 115 HBsAg-positive cases were enrolled and evaluated for HBV virologic markers.

RESULTS: The prevalence of positive HBsAg in Nahavand was 2.3%. The most frequent relatives of index cases were sons and daughters (32.2% and 23.5% respectively). Twelve (11%) of all family members were HBsAg positive. Fifty (56.2%) were isolated HBsAb positive and only one person (2.5%) was isolated HBcAb positive. The higher rates of HBsAg marker were detected in the brothers (1-25%) and fathers (1-12.5%). The infection rate in husbands and wives of index cases was 10%. Only two (16.7%) of all HBsAg-positive participants reported previous HBV vaccination.

CONCLUSION: The prevalence of intra-familial HBV infection is lower in Nahavand of Iran compared to other studies. More attention should be paid to HBV vaccination and risk-lowering activities.

INTRODUCTION

Middle East countries including Iran have an intermediate prevalence of hepatitis B. In Iran, hepatitis B prevalence is low as 1.07% in Shiraz and as high as 8.96% in Toiserkan^[1]. There are three main routes of HBV transmission including blood, sexual contacts, and horizontal. In endemic regions of the world such as Africa, Greece, and Hong Kong, vertical transmission from mother to newborn infant and horizontal transmission among children play an important role in intra-familial transmission of HBV. In North America and Western Europe, however, the main route of transmission is intimate sexual contacts^[2-4].

A study of general population in Hamadan of Iran^[5] reported that HBV infection is low in unmarried men and women (18.26%) and high in widows and divorcees (51.59%), suggesting that horizontal transmission is likely to be the primary mode of acquisition of HBV infection in children and young adults. Also, infection is partly transmitted before or soon after birth to babies of HBsAg-carrier mothers. Socio-economic and demographic variables have a greater impact on the prevalence of HBV infection than blood or medical care variables in this population.

In a study in Spain, 848 of family members of 285 HBsAg-positive patients were evaluated and reported that 33.5% of them were positive for at least one HBV virologic marker^[6]. In the other study in Australia, family members of 145 HBV patients were studied and the results showed that 16% of them were HBsAg positive, and that HBV transmission within families is greater, if the index case has a HBsAg and HBeAg-positive mother rather than a HBeAg-negative one^[7].

The city of Nahavand in Hamedan Province (in west of Iran) has always been considered to have high prevalence of hepatitis B without any definitive study. This study aimed to determine the prevalence of hepatitis B in Nahavand and evaluate the HBsAg positive prevalence in families with a member who was confirmed to have HBV infection.

MATERIALS AND METHODS

This cross-sectional study was conducted during a 2-mo period (February-March 2003) in people aged 6 years and over in the city of Nahavand, located in the western part of Iran with a population of 72 000. In Nahavand there are 5 health care centers and 1 health site, and 304 participations were randomly selected from each of them.

This research was carried out in two phases. First, we studied the prevalence of hepatitis B in population of Nahavand (2002) and after identifying the HBsAg-positive cases, all of their families were enrolled into the second phase. The population less than 5 years old was not included in our study because blood sampling was difficult.

A questionnaire including demographic data, marital status and history of vaccination was developed. After taking the approval of health authorities of the city and city council, the educational sessions for data collection teams and directors of health care centers were held to train them on the details of interviewing, questionnaire filling, and blood sampling. Demographic data on eligible families were obtained from 1999 health registry.

The selected families were contacted at their residence. The family members older than 5 years were interviewed and informed consent was obtained. For those under 15 the parents also signed the consent forms. The questionnaires were filled by interviewers, who also took blood samples. The blood samples were sent to the laboratory of research center for gastro-enterology and liver disease, Shaheed Beheshti University of Medical Sciences at the end of each day. The virologic markers of hepatitis B were assessed.

After revealing HBsAg-positive cases, we collected demographic data of their families. The selected families were contacted at their residence and given description of the second phase by the interviewers. After signing the consent forms by the family members, the interviewers took blood samples and sent them to the laboratory (as above mentioned). All the virologic markers of hepatitis B were assessed.

It should be explained that HBsAg detection was carried out by Diasorin kit with lot no. 0370790/1A through sandwiched

ELISA. HBsAb and HBcAb levels were measured by Diasorin kit with lot no. 9230320/A through sandwiched non-competitive ELISA and Diasorin kit with lot no. 8540480/1B through competitive ELISA, respectively. All data were fed into an access data bank. SPSS version 11 was used for the analysis of data.

RESULTS

Of all subjects, 85 (4.6%) did not participate in study, 1 005 (55.1%) were married. The mean family population was 4.8 ± 1.9 , the smallest family had 1 member while biggest family had 13 members. The prevalence of HBsAg-positive cases in Nahavand was 2.3%. The hepatitis B serologic markers in the study subjects are shown in Table 1.

One hundred and fifteen family members including 8 (7%) mothers, 8 (7%) fathers, 11 (9.6%) sisters, 4 (3.5%) brothers, 27 (23.5%) daughters, and 37 (32.2%) sons, 10 (8.7%) husbands, and 10 (8.7%) wives were enrolled. Seventy-one (61.7%) of them were married.

In the participants, 23 (20.2%) had the education of literacy, 19 (16.7%) diploma and 15 (13.2%) higher than diploma, 33 (28.9%) were students and 26 (22.8%) were housekeepers. Twelve (11%) of all family members were HBsAg positive. Fifty (56.2%) were isolated HBsAb positive and only one person (2.5%) was isolated HBcAb positive.

Table 2 shows the relevance of HBV virologic markers to the index case. Higher rates of HBsAg marker were detected in the brothers (1-25%) and fathers (1-12.5%). The prevalence of HBsAg-positive cases in sons and daughters was identical (1.1%). The infection rate in husbands and wives was 10%.

The most frequent relatives with HBsAb positive were husbands and wives (5-71.4%) and then daughters (17-70.8%). There was no positive HBsAb in fathers. Only one person (son) was HBcAb positive.

It should be mentioned that the HBsAg-positive family members were evaluated for HBeAg and HBeAb and all of them were HBeAg negative and HBeAb positive. Also

Table 1 Frequency distribution of hepatitis B serologic markers in participants

	HBsAg positive	Isolated HBcAb positive	Isolated HBsAb positive	HBcAb and HBsAb positive
Number (%)	42 (2.3)	143 (7.84)	212 (11.62)	217 (11.9)
Sex (male%)	54.8	44.1	41.5	53.9
Age (mean \pm SD)	40.2 \pm 18	55.2 \pm 16	37.3 \pm 22	52.8 \pm 17
Marriage (%)	66.7	71.3	51.4	80.2

Table 2 Frequency distribution of hepatitis B virologic markers in family members of index cases, *n* (%)

	HBsAg positive	Isolated HBsAb positive	Isolated HBcAb positive
Mother	0 (0)	2/8 (25)	0 (0)
Father	1/8 (12.5)	0 (0)	0 (0)
Sister	1/8 (10)	5/8 (62.5)	0 (0)
Brother	1/4 (25)	1/4 (25)	0 (0)
Daughter	3/27 (1.1)	17/27 (63)	0 (0)
Son	4/37 (1.1)	15/37 (40.5)	1/37 (2.7)
Husband	1/10 (10)	5/10 (50)	0 (0)
Wife	1/10 (10)	5/10 (50)	0 (0)

they had normal liver function test.

Only 2 (16.7%) of the HBsAg-positive participants reported previous HBV vaccination, while 23 (46.9%) of the subjects with isolated HBsAb had previous HBV vaccination.

DISCUSSION

Among the 115 family members studied, sons and daughters were the most frequent relatives. We had some limitations in categorizing the data for discussion, because the number of positive HBsAg cases in children was low (three daughters and four sons). Sex proportion was identical in HBsAg-positive cases and others. Single participants were about twice of married ones. The most frequent level of education of family members was illiteracy and the most frequent occupations were students and housekeepers. The population less than 5 years old was not included in our study because blood sampling was difficult. This can underestimate the true frequency of hepatitis B in our population.

The mean age of HBsAg-positive cases was 40.2 ± 18 years. The phenomenon of e-seroconversion in this age group may be responsible for the low transmission rate of HBV in our study in comparison to some other regions because marriage age during recent years has increased in Iran. There is no population-based study about genotypes of HBV in Iran. In a limited study, genotype D is found to be the most common genotype in patients with chronic hepatitis B^[8].

In overall, 11% of family members were HBsAg positive. There are different studies about HBV intra-familial transmission in the world that in the strongest ones, phylogenetic sequence analysis and amino-acid variation of the HBV core gene were performed. It is obvious that this way is the only way to confirm HBV intra-familial transmission, but due to lack of sufficient resources in present study, this procedure was not possible^[8-10].

In a study in 2002 in Italy^[9], 49 individuals from 13 families with sibling clusters of positive HBsAg carriers are investigated, HBV isolates are genotyped following amplification of the surface gene region of the viral genome, thus providing convincing evidence that viral isolates within a family originate from the same source. It was reported that the prevalence of HBsAg is significantly higher in family members than in the control group ($P < 0.001$)^[10]. A study in South Korea also reported that among 71 non-vaccinated HBsAg carriers, 10 are positive for HBsAg (14.1%), but none of the controls is positive for HBsAg^[11]. In a study in Spain, among 330 relatives of 145 HBsAg carriers observed over a mean period of 20.1 mo, 284 were positive for at least one HBV marker^[6]. It was reported that relatives of 26 positive HBsAg cases present an intra-familial prevalence of HBV infection of 28.8%^[12]. In other countries, variable results have been reported^[13-18].

In this study, the highest prevalence of HBsAg was in the fathers and sons, and infection rate in the husbands and wives was identical. A Turkey study showed that the husbands had a higher rate of HBsAg than wives (70.0% *vs* 21.9%, $P < 0.01$)^[10]. The high prevalence of HBsAg infection among spouses may be due to sexual transmission in menstrual period in other countries. In Iran, because of cultural and

religious aspects, this way of intra-familial transmission has a low prevalence. HBV transmission within families is greater, if they have a HBsAg positive mother rather than a HBsAg positive father^[6]. The current results show that most of the family members are not vaccinated for HBV infection, so the necessity of HBV vaccination in HBsAg-positive family members must be considered. It has been shown that only half of the isolated HBsAb-positive persons have a history of HBV vaccination. Some people might have insufficient information about vaccines. Coexistence of HBsAg and hepatitis B surface antibody (anti-HBs) has been reported in approximately 24% of HBsAg-positive individuals^[19] and low level of HBsAg in some of our people with isolated positive HBsAb may describe the above finding. We think that repeat testing for HBeAb in people with isolated positive HBsAb during a long time of follow-up may be helpful.

In conclusion, the prevalence of intra-familial HBV infection is low in Nahavand of Iran. More attention should be paid to HBV vaccination and risk-lowering activities.

REFERENCES

- 1 **Zali MR**, Mohammad K, Farhadi A, Masjedi MR, Zargar A, Nowroozi A. Epidemiology of hepatitis B in the Islamic Republic of Iran. *East Mediterr Health J* 1996; **2**: 290-298
- 2 **Yeoh EK**. Hepatitis B virus infection in children. *Vaccine* 1990; **8** (Suppl): S29-30
- 3 **Werner GT**, Frosner GG, Fresenius K. Prevalence of serological hepatitis A and B markers in a rural area of northern Zaire. *Am J Trop Med Hyg* 1985; **34**: 620-624
- 4 **Lionis C**, Frangoulis E, Koulentakis M, Biziagos E, Kouroumalis E. Prevalence of hepatitis A, B, and C markers in school children of a rural area of Crete, Greece. *Eur J Epidemiol* 1997; **13**: 417-420
- 5 **Amini S**, Mahmoodi MF, Andalibi S, Solati AA. Seroepidemiology of hepatitis B, delta and human immunodeficiency virus infections in Hamadan province, Iran: a population based study. *J Trop Med Hyg* 1993; **96**: 277-287
- 6 **Porres JC**, Carreno V, Bartolome J, Gutierrez J, Castillo I. A dynamic study of the intra-familial spread of hepatitis B virus infection: relation with the viral replication. *J Med Virol* 1989; **28**: 237-242
- 7 **Williams SJ**, Craig PI, Liddle C, Batey RG, Farrell GC. Hepatitis B in Australia: determinants of intrafamily spread. *Aust N Z J Med* 1987; **17**: 220-227
- 8 **Amini-Bavil-Olyae S**, Sarrami-Forooshani R, Mahboudi F, Sabahi F, Adeli A, Noorinayer B, Azizi M, Reza Zali M. Genotype characterization and phylogenetic analysis of hepatitis B virus isolates from Iranian patients. *J Med Virol* 2005; **75**: 227-234
- 9 **Zampino R**, Lobello S, Chiamonte M, Venturi-Pasini C, Dumpis U, Thursz M, Karayiannis P. Intra-familial transmission of hepatitis B virus in Italy: phylogenetic sequence analysis and amino-acid variation of the core gene. *J Hepatol* 2002; **36**: 248-253
- 10 **Erol S**, Ozkurt Z, Ertek M, Tasyaran MA. Intrafamilial transmission of hepatitis B virus in the eastern Anatolian region of Turkey. *Eur J Gastroenterol Hepatol* 2003; **15**: 345-349
- 11 **Kim YS**, Ahn YO, Kim DW. Familial clustering of hepatitis B and C viruses in Korea. *J Korean Med Sci* 1994; **9**: 444-449
- 12 **Aristegui J**, Perez A, Cisterna R, Suarez D, Delgado A. Characteristics of intra-familial transmission of the hepatitis B virus: a case load contribution and review of the literature [in Spanish]. *Enferm Infecc Microbiol Clin* 1989; **7**: 18-22
- 13 **Ordog K**, Szendroi A, Szarka K, Kugler Z, Csire M, Kapusinszky B, Xie J, Cszizmadia K, Brojnas J, Rusvai E, Tempfli A, Berencsi G. Perinatal and intrafamily transmis-

- sion of hepatitis B virus in three generations of a low-prevalence population. *J Med Virol* 2003; **70**: 194-204
- 14 **Pastore G**, Dentico P, Angarano G, Lapedota E, Schiraldi O. Infectivity markers in HBsAg chronic carriers and intra-familial spread of hepatitis B virus infection. *Hepatogastroenterology* 1981; **28**: 20-22
- 15 **Thakur V**, Guptan RC, Malhotra V, Basir SF, Sarin SK. Prevalence of hepatitis B infection within family contacts of chronic liver disease patients-does HBeAg positivity really matter? *J Assoc Physicians India* 2002; **50**: 1386-1394
- 16 **Craxi A**, Tine F, Vinci M, Almasio P, Camma C, Garofalo G, Pagliaro L. Transmission of hepatitis B and hepatitis delta viruses in the households of chronic hepatitis B surface antigen carriers: a regression analysis of indicators of risk. *Am J Epidemiol* 1991; **134**: 641-650
- 17 **Dhorje SP**, Pavri KM, Prasad SR, Sehgal A, Phule DM. Horizontal transmission of hepatitis B virus infection in household contacts, Pune, India. *J Med Virol* 1985; **16**: 183-189
- 18 **Abdool Karim SS**, Thejpal R, Coovadia HM. Household clustering and intra-household transmission patterns of hepatitis B virus infection in South Africa. *Int J Epidemiol* 1991; **20**: 495-503
- 19 **Tsang TK**, Blei AT, O'Reilly DJ, Decker R. Clinical significance of concurrent hepatitis B surface antigen and antibody positivity. *Dig Dis Sci* 1986; **31**: 620-624

Science Editor Wang XL and Guo SY Language Editor Elsevier HK

Non-steroidal anti-inflammatory drug-induced small bowel injuries identified by double-balloon endoscopy

Yoshikazu Hayashi, Hironori Yamamoto, Hiroto Kita, Keiji Sunada, Hiroyuki Sato, Tomonori Yano, Michiko Iwamoto, Yutaka Sekine, Tomohiko Miyata, Akiko Kuno, Takaaki Iwaki, Yoshiyuki Kawamura, Hironari Ajibe, Kenichi Ido, Kentaro Sugano

Yoshikazu Hayashi, Hironori Yamamoto, Hiroto Kita, Keiji Sunada, Hiroyuki Sato, Tomonori Yano, Michiko Iwamoto, Yutaka Sekine, Tomohiko Miyata, Akiko Kuno, Takaaki Iwaki, Yoshiyuki Kawamura, Hironari Ajibe, Kenichi Ido, Kentaro Sugano, Department of Internal Medicine, Division of Gastroenterology, Jichi Medical School, 3311-1 Yakushiji, Minamikawachi, Tochigi 329-0498, Japan

Correspondence to: Hironori Yamamoto, MD, Department of Internal Medicine, Division of Gastroenterology, Jichi Medical School, Yakushiji, Minamikawachi, Tochigi 329-0498, Japan. yamamoto@jichi.ac.jp
Telephone: +81-285-58-7348 Fax: +81-285-44-8297
Received: 2004-12-14 Accepted: 2005-01-05

Abstract

AIM: To clarify clinical features of the NSAID-induced small bowel lesions using a new method of endoscopy.

METHODS: This is a retrospective study and we analyzed seven patients with small bowel lesions while taking NSAIDs among 61 patients who had undergone double-balloon endoscopy because of gastro-intestinal bleeding or anemia between September 2000 and March 2004, at Jichi Medical School Hospital in Japan. Neither conventional EGD nor colonoscopy revealed any lesions of potential bleeding sources including ulcerations. Double-balloon endoscopy was carried out from oral approach in three patients, from anal approach in three patients, and from both approaches in one patient.

RESULTS: Ulcers or erosions were observed in the ileum in six patients and in the jejunum in one patient, respectively. The ulcers were multiple in all the patients with different features from tiny punched out ulcers to deep ulcerations with oozing hemorrhage or scar. All the patients recovered uneventfully and had full resolution of symptoms after suspension of the drug.

CONCLUSION: NSAIDs can induce injuries in the small bowel even in patients without any lesions in both the stomach and colon.

© 2005 The WJG Press and Elsevier Inc. All rights reserved.

Key words: Double-balloon endoscopy; NSAIDs-induced small bowel injuries

Hayashi Y, Yamamoto H, Kita H, Sunada K, Sato H, Yano T,

Iwamoto M, Sekine Y, Miyata T, Kuno A, Iwaki T, Kawamura Y, Ajibe H, Ido K, Sugano K. Nonsteroidal anti-inflammatory drug-induced small bowel injuries identified by double-balloon endoscopy. *World J Gastroenterol* 2005; 11(31): 4861-4864
<http://www.wjgnet.com/1007-9327/11/4861.asp>

INTRODUCTION

Adverse effects of non-steroidal anti-inflammatory drugs (NSAIDs) in the upper and lower gastro-intestinal tract are well known^[1]. In addition, NSAIDs can induce and exacerbate damage in the small bowel^[2,3]. There is a study showing that 8.4% of patients taking NSAIDs developed small bowel ulcerations^[4]. Evidence that those lesions may also cause perforation, strictures or hemorrhage stems from a case-control study and several case reports^[5-14]. Despite the necessity, endoscopic observation of the small intestine was technically difficult because of its long length and multiple complex looped configurations. Recently, a video capsule endoscopy, which enables observation of the entire small bowel, was developed and this novel technology provided an outstanding progress for the diagnosis of small bowel diseases^[15-19]. In addition, we have developed a new method of endoscopy using a double-balloon technique (Fujinon EN-450P5/20, Fujinon Corp., Saitama, Japan), which also allows observations of small bowel under controlled movement even from a retrograde approach^[20-23]. The aim of this study was to delineate clinical features of the NSAID-induced small bowel mucosal injuries using the double-balloon endoscopy.

MATERIALS AND METHODS

The records of all the patients who underwent double-balloon endoscopy at Jichi Medical School Hospital, Japan between September 2000 and March 2004 were reviewed. Patients were identified from endoscopy case logs and cross-referenced with pathology database. Charts were also reviewed for NSAID prescription in those patients. Necessary telephone interview was also carried out. Patients with pre-existing or concomitant risk factors for possible small bowel complications, including Crohn's disease and mesenteric vascular disease, were excluded and all the patients with evidence of other small bowel pathology were also excluded. Reasons for exclusion on review of pathology included inflammatory bowel disease, small bowel lymphoma, primary or metastatic carcinoma, small bowel gastro-intestinal stromal

tumor, small bowel granuloma, small bowel diverticulum, angiodysplasia, and post-operative lesions. Two patients who have been on NSAIDs, were excluded and seven patients, in whom small bowel injuries were found while still on NSAIDs, were selected among 61 patients with obscure gastro-intestinal bleeding. These seven patients, two men and five women, with ages ranging 65-89 years (73.7 years on an average), were enrolled and subjected to the analysis.

RESULTS

Of these seven patients, six had melena and one had undetermined anemia with positive fecal occult blood tests during NSAID medications. Underlying disease of these patients included knee joint pain, back pain, headache, and rheumatoid arthritis. Neither conventional EGD nor colonoscopy revealed any lesions of possible cause of bleeding including ulcerations except for one patient (patient 1) in whom gastric ulcer scar was observed. Drug usage by these patients consisted of diclofenac in four patients (57%), and either ampiroxicam, aspirin, or loxoprofen in each of the remaining three patients, respectively (Table 1). Duration of the medication was different for patients, ranging from 7 d to 10 years. More than five units of packed red blood cell was required on an average for blood transfusion before diagnosis.

Double-balloon endoscopy was carried out from oral approach alone in three patients and from anal approach alone in three patients. The approach route was chosen, based on the clinical information including color of the stool. The depth of insertion estimated from the number of pleating procedures and the fluoroscopic images of the small intestine and endoscope in these patients was difficult but approximately 1/2-2/3 of the entire length of the small intestine with rough estimation, although we have succeeded in examining the entire small intestine from oral approach alone in one patient. In addition, another patient underwent total enteroscopy by both approaches. Patient's demographics are delineated in Table 1. Whether the lesions were located in the jejunum or ileum was determined radiographically based on a distance from either pylorus ring or ileocecal valve in each case. Ulcers or erosions were observed in the ileum in six patients (86%) and in the jejunum in one patient (14%). The ulcers were multiple in all the patients with different features from tiny punched out ulcers (Figure 1) to deep ulcerations with oozing hemorrhage (Figure 2A) or scar. Edematous villi around the ulcers were prominent features

by the endoscopic observation. Oozing hemorrhage from the ulcer, observed in one patient, was treated endoscopically using coagulator (ERBE, German, Figure 2B). Of interest, both circular ulcers (Figure 3A) and circular scars (Figure 3B) were observed in a different part of the small bowel in the same patient. Biopsies, taken from the edge of the ulcer in two patients, revealed non-specific inflammation. All the patients recovered uneventfully and had full resolution of the symptoms in accordance with their hemoglobin levels after suspension of the drug.

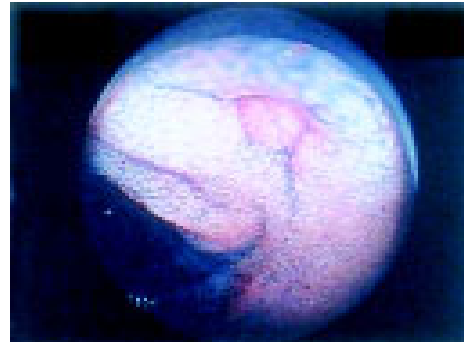


Figure 1 Endoscopic view of the punched-out ulcer in the ileum in a 65-year-old woman (patient 3). Edematous villi were observed around the ulcer.

DISCUSSION

This is a report to delineate NSAID-induced small bowel injuries using double-balloon endoscopy. NSAID-induced injuries were identified in seven out of 61 patients with obscure gastro-intestinal bleeding (11.5%). Despite limitation of this study due to the lack of observation of the entire small bowel in most patients, NSAID-induced ulcers were observed more frequently in the ileum than in the jejunum in consistent with a previous report by Kessler *et al.*^[13]. Further prospective study intended for evaluation of the entire small bowel, if substantiated, will clarify the exact distribution of NSAIDs-induced lesions. NSAIDs-induced lesions, identified by endoscopy, were multiple with different features from tiny ulcers to hemorrhagic ulcers or circular ulcers. These different features of ulcers, even observed in different parts of the small intestine in the same patient, may represent different stages of ulcers. The ulcers may be healing, because NSAIDs were suspended on the day of

Table 1 Clinical Features of the patients with nonsteroidal anti-inflammatory drug-induced small bowel lesions

Patient	Age/sex	Approach	Partial/total	Findings	Location	Dose (mg/d)	NSAIDs	Duration	Serum albumin (g/dL)	Blood transfusion (unit ¹)
1 ²	89/M	Oral	Partial, -middle ileum	Ulcers and erosions	Ileum	27	Ampiroxicam	10 yr	2.1	10
2	69/F	Oral	Total	Ulcers	Ileum	25	Diclofenac	7 yr	3.1	12
3	65/M	Anal	Partial, -upper jejunum	Ulcers and erosions	Ileum	75	Diclofenac	1 wk	3.9	0
4	76/F	Anal	Partial, -middle ileum	Ulcers	Ileum	25	Diclofenac	8 yr	2.7	7
5	74/F	Anal	Partial, -upper ileum	Erosions	Ileum	100	Aspirin	4 yr	3.5	0
6	76/F	Oral	Partial, -upper ileum	Ulcers	Jejunum	120	Loxoprofen	4 yr	1.9	8
7	67/F	Oral+anal	Total	Ulcers	Ileum	75	Diclofenac	1 yr	3.0	0

¹1 unit = Packed blood cells separated from 450 mL of whole blood. ²Gastric ulcer scar was observed in this patient.

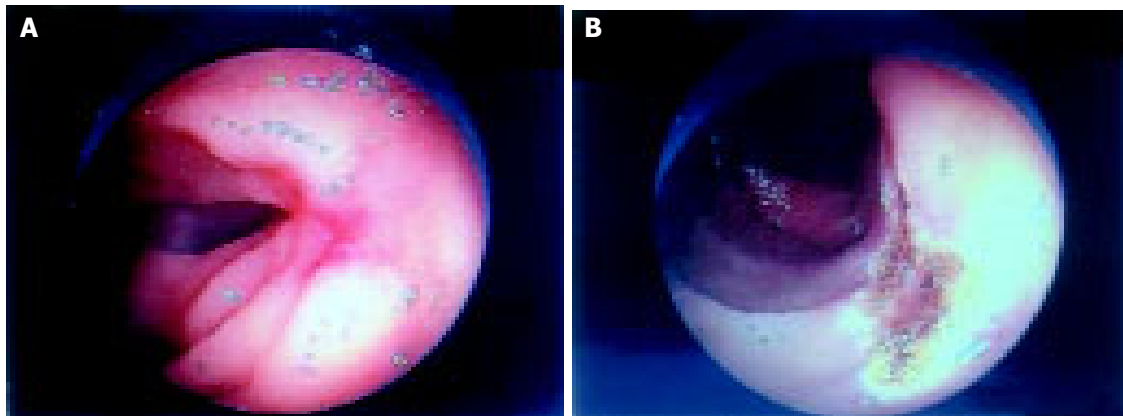


Figure 2 Endoscopic view of the ulcer with oozing hemorrhage in the ileum in a 74-year-old woman (patient 4). **A:** Before coagulation therapy; **B:** After

coagulation therapy.

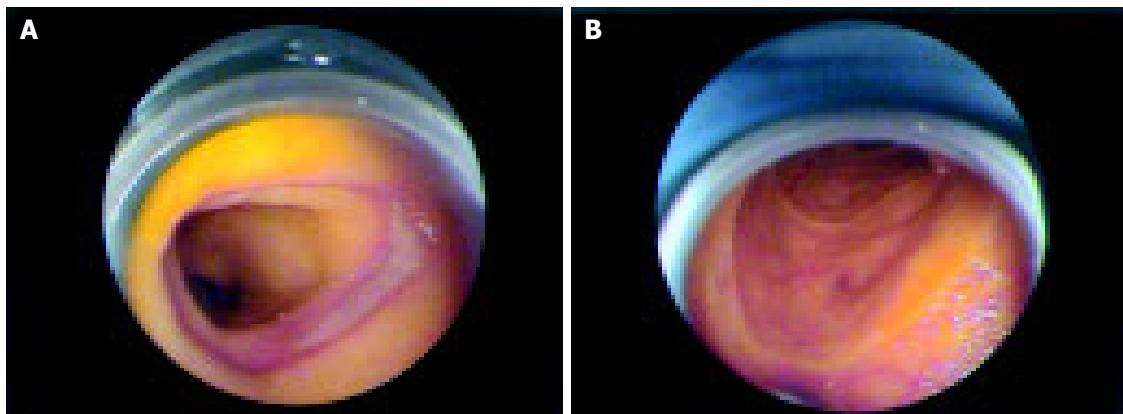


Figure 3 Endoscopic view of the (A) circular ulcer and (B) circular ulcer scar

in the ileum in a 67-year-old woman (patient 7).

admission in all patients. Alternatively, either the dose of NSAIDs or the length that NSAIDs that was given, could attribute to the difference in size and shape of the ulcers, although such tendency was not observed in our study. Of interest, we could observe circular ulcers and even circular scars in the same patients. This observation may reinforce the association between ulcers and severe strictures in the small bowel after NSAID therapy. Further study describing the feature of circular ulcers is warranted for better understanding of these relationships.

In conclusion, NSAID-induced injuries in the small bowel were endoscopically observed and described using double-balloon endoscopy. NSAIDs-induced ulcers were found in the small bowel even in patients without any ulcers and erosions in the stomach as well as colon. Although this was a preliminary study, double-balloon endoscopy was useful for the direct observation and description of each lesion in detail by antegrade as well as retrograde approach.

REFERENCES

- 1 **Bjarnason I**, Hayllar J, MacPherson AJ, Russell AS. Side effects of nonsteroidal anti-inflammatory drugs on the small and large intestine in humans. *Gastroenterology* 1993; **104**: 1832-1847
- 2 **Davies NM**, Saleh JY, Skjodt NM. Detection and prevention of NSAID-induced enteropathy. *J Pharm Sci* 2000; **3**: 137-155
- 3 **de Sanctis S**, Qureshi T, Stebbing JF. Clinical and pathological overlap in nonsteroidal anti-inflammatory drug-related small bowel diaphragm disease and the neuromuscular and vascular hamartoma of the small bowel. *Am J Surg Pathol* 2001; **25**: 539-541
- 4 **Allison MC**, Howatson AG, Torrance CJ, Lee FD, Russell RI. Gastrointestinal damage associated with the use of nonsteroidal anti-inflammatory drugs. *N Engl J Med* 1992; **327**: 749-754
- 5 **Madhok R**, MacKenzie JA, Lee FD, Bruckner FE, Terry TR, Sturrock RD. Small bowel ulceration in patients receiving non-steroidal anti-inflammatory drugs for rheumatoid arthritis. *Q J Med* 1986; **58**: 53-58
- 6 **Langman MJ**, Morgan L, Worrall A. Use of anti-inflammatory drugs by patients admitted with small or large bowel perforations and haemorrhage. *Br Med J* 1985; **290**: 347-349
- 7 **Bjarnason I**, Zanelli G, Prouse P, Smethurst P, Smith T, Levi S, Gumpel MJ, Levi AJ. Blood and protein loss via small-intestinal inflammation induced by non-steroidal anti-inflammatory drugs. *Lancet* 1987; **2**: 711-714
- 8 **Bjarnason I**, Price AB, Zanelli G, Smethurst P, Burke M, Gumpel JM, Levi AJ. Clinicopathological features of nonsteroidal anti-inflammatory drug-induced small intestinal strictures. *Gastroenterology* 1988; **94**: 1070-1074
- 9 **Lang J**, Price AB, Levi AJ, Burke M, Gumpel JM, Bjarnason I. Diaphragm disease: pathology of disease of the small intestine induced by non-steroidal anti-inflammatory drugs. *J Clin Pathol* 1988; **41**: 516-526
- 10 **Matsushashi N**, Yamada A, Hiraishi M, Konishi T, Minota

- S, Saito T, Sugano K, Yazaki Y, Mori M, Shiga J. Multiple strictures of the small intestine after long-term nonsteroidal anti-inflammatory drug therapy. *Am J Gastroenterol* 1992; **87**: 1183-1186
- 11 **Speed CA**, Bramble MG, Corbett WA, Haslock I. Non-steroidal anti-inflammatory induced diaphragm disease of the small intestine: complexities of diagnosis and management. *Br J Rheumatol* 1994; **33**: 778-780
- 12 **Davies NM**, Jamali F, Skeith KJ. Nonsteroidal antiinflammatory drug-induced enteropathy and severe chronic anemia in a patient with rheumatoid arthritis. *Arthritis Rheum* 1996; **39**: 321-324
- 13 **Kessler WF**, Shires GT 3rd, Fahey TJ 3rd. Surgical complications of nonsteroidal antiinflammatory drug-induced small bowel ulceration. *J Am Coll Surg* 1997; **185**: 250-254
- 14 **Zalev AH**, Gardiner GW, Warren RE. NSAID injury to the small intestine. *Abdom Imaging* 1998; **23**: 40-44
- 15 **Iddan G**, Meron G, Glukhovsky A, Swain P. Wireless capsule endoscopy. *Nature* 2000; **405**: 417
- 16 **Appleyard M**, Fireman Z, Glukhovsky A, Jacob H, Shreiver R, Kadirkamanathan S, Lavy A, Lewkowicz S, Scapa E, Shofti R, Swain P, Zaretsky A. A randomized trial comparing wireless capsule endoscopy with push enteroscopy for the detection of small-bowel lesions. *Gastroenterology* 2000; **119**: 1431-1438
- 17 **Costamagna G**, Shah SK, Riccioni ME, Foschia F, Mutignani M, Perri V, Vecchioli A, Brizi MG, Piccicocchi A, Marano P. A prospective trial comparing small bowel radiographs and video capsule endoscopy for suspected small bowel disease. *Gastroenterology* 2002; **123**: 999-1005
- 18 **Lewis BS**, Swain P. Capsule endoscopy in the evaluation of patients with suspected small intestinal bleeding: Results of a pilot study. *Gastrointest Endosc* 2002; **56**: 349-353
- 19 **Van Gossom A**. Capsule endoscopy in patients with obscure GI bleeding. *Gastrointest Endosc* 2003; **57**: 629-630
- 20 **Yamamoto H**, Sekine Y, Sato Y, Higashizawa T, Miyata T, Iino S, Ido K, Sugano K. Total enteroscopy with a nonsurgical steerable double-balloon method. *Gastrointest Endosc* 2001; **53**: 216-220
- 21 **Yamamoto H**, Sugano K. A new method of enteroscopy-the double-balloon method. *Can J Gastroenterol* 2003; **17**: 273-274
- 22 **Hashimoto A**, Yamamoto H, Yano T, Hashimoto N, Kita H, Kawakami S, Miyata T, Sunada K, Ohnishi N, Iwamoto M, Kuno A, Sugano K. A case of malignant lymphoma of the small intestine with successful endoscopic hemostasis using double-balloon enteroscopy. *Progress Dig Endoscopy* 2003; **62**: 104-105
- 23 **Yamamoto H**, Kita H, Sunada K, Hayashi Y, Sato H, Yano T, Iwamoto M, Sekine Y, Miyata T, Kuno A, Ajibe H, Ido K, Sugano K. Clinical outcomes of double-balloon endoscopy for the diagnosis and treatment of small-intestinal diseases. *Clin Gastroenterol Hepatol* 2004; **2**: 1010-1016

Science Editor Guo SY Language Editor Elsevier HK

Effect of oral erythromycin on gastric and small bowel transit time of capsule endoscopy

Wai K Leung, Francis KL Chan, Sara SL Fung, Mei-Yin Wong, Joseph JY Sung

Wai K Leung, Francis KL Chan, Sara SL Fung, Mei-Yin Wong, Joseph JY Sung, Digestive Diseases Center, The Chinese University of Hong Kong, Prince of Wales Hospital, Shatin, Hong Kong, China
Correspondence to: Dr. Wai K Leung, Department of Medicine and Therapeutics, Prince of Wales Hospital, 30-32 Ngan Shing Street, Shatin, Hong Kong, China. wkleung@cuhk.edu.hk
Telephone: +852-2632-3140 Fax: +852-2637-3852
Received: 2004-12-10 Accepted: 2005-01-05

Abstract

AIM: To determine the effect of oral erythromycin on gastric and small bowel transit time of capsule endoscopy.

METHODS: Consecutive patients who underwent capsule endoscopy during the 16-mo study period were either given 250 mg oral erythromycin, 1 h prior to swallowing the capsule endoscope or nothing. The gastric and small bowel transit time, and the small bowel image quality were compared.

RESULTS: Twenty-four patients received oral erythromycin whereas 14 patients were not given any prokinetic agent. Patients who received erythromycin had a significantly lower gastric transit time than control (16 min vs 70 min, $P = 0.005$), whereas the small bowel transit time was comparable between the two groups (227 min vs 183 min, $P = 0.18$). Incomplete small bowel examination was found in three patients of the control group and in one patient of the erythromycin group. There was no significant difference in the overall quality of small bowel images between the two groups. A marked reduction in gastric transit time was noted in two patients who had repeat capsule endoscopy after oral erythromycin.

CONCLUSION: Use of oral erythromycin significantly reduces the gastric transit time of capsule endoscopy.

© 2005 The WJG Press and Elsevier Inc. All rights reserved.

Key words: Capsule endoscopy; Erythromycin; Prokinetic

Leung WK, Chan FKL, Fung SSL, Wong MY, Sung JY. Effect of oral erythromycin on gastric and small bowel transit time of capsule endoscopy. *World J Gastroenterol* 2005; 11(31): 4865-4868

<http://www.wjgnet.com/1007-9327/11/4865.asp>

INTRODUCTION

The introduction of wireless capsule endoscopy, which

has made direct visualization of the small bowel possible, has opened up a new chapter on small bowel imaging. Initial comparative studies showed that wireless capsule endoscopy is superior to push enteroscopy^[1-4] or conventional radiological imaging^[5]. The wireless capsule endoscopy is approved by the Food and Drug Administration of USA and is particularly useful for the diagnosis of obscure gastrointestinal bleeding.

With the limited battery life, the current capsule endoscope could take images for up to 8 h. Any delay in gastric transit may inadvertently result in incomplete small bowel examination. Whilst the capsule endoscope is passively propelled by peristalsis down the intestinal lumen, it is impossible to predict the time required for the capsule endoscope to navigate through the stomach. Although the use of prokinetic agents may potentially speed up the gastric emptying time, the effect of prokinetic agents on the outcome of wireless capsule endoscopy remains undetermined. Among various prokinetic agents, erythromycin, a motilin agonist, has been used to speed up gastric emptying in patients with gastroparesis^[6-8]. Moreover, the use of intravenous erythromycin has been shown to improve the quality of upper gastro-intestinal endoscopy in patients with upper gastro-intestinal bleeding, possibly via emptying of the blood contents within the stomach^[9]. Here, we determined the effects of oral erythromycin on the gastric and small bowel transit time of the capsule endoscope as well as the quality of small bowel images in patients undergoing capsule endoscopy.

MATERIALS AND METHODS

Patients

Consecutive patients who underwent capsule endoscopy in the Prince of Wales Hospital of Hong Kong between December 2002 and March 2004 were included. The use of prokinetic agents in these patients was based on the date of the procedure. All patients who had this examination after October 2003 received oral erythromycin (250 mg) 1 h prior to swallowing the capsule endoscope. In contrast, patients who had capsule endoscopy before October 2003 did not receive any prokinetic agent and were used as controls. Exclusion criteria included patients with swallowing difficulties, previous gastric or small bowel surgery, allergic to erythromycin, use of other prokinetic agents, and known or suspected bowel obstruction. All patients gave informed consent for undergoing the procedure.

A total of 38 patients had capsule endoscopy during the 16-mo study period. There were 17 males and 21 females with a mean age of 60.3 (SD 18.1) years. Twenty-four

(63%) patients were given oral erythromycin (250 mg) prior to swallowing the capsule endoscope (erythromycin group) whereas 14 (37%) patients did not receive any prokinetic agent (control group). None of the patients in the erythromycin group experienced any abdominal discomfort or gastrointestinal upset.

The indications of capsule endoscopy were as follows: unexplained iron deficiency anemia in 11, obscure gastro-intestinal bleeding in 20, recurrent abdominal pain in 6, and Crohn's disease in 1. Ten patients had diabetes mellitus and none of them was taking medications that would alter the gastric or intestinal motility. There was no significant difference in the demographic data, body build, history of diabetes or thyroid disease, and indications of capsule endoscopy between the two groups of patients (Table 1).

Table 1 Baseline characteristics of patients

	Erythromycin (n = 24)	Control (n = 14)
Mean age±SD (yr)	62.7±17.8	56.3±18.6
Male (%)	9 (37.5)	8 (57.1)
Mean body mass index (±SD)	22.9±3.8	22.3±3.2
Diabetes mellitus (%)	7 (29.2)	3 (21.4)
Indication		
Iron deficiency anemia (%)	6 (25)	5 (36)
Obscure gastro-intestinal bleeding (%)	12 (50)	8 (57)
Recurrent abdominal pain (%)	5 (21)	1 (7)
Crohn's disease (%)	1 (4)	0 (0)

Capsule endoscopy

Capsule endoscopy was performed after 12 h of fasting. Eight aeriels, which were connected to a battery-powered portable data recorder, were attached to the chest and abdominal wall of the patients prior to the procedure. Patients were asked to swallow the M2A[®] capsule endoscope (Given Imaging, Yoqneam, Israel) with plenty of water mixed with simethicone to eliminate small bubbles in the gastrointestinal tract. No bowel cleansing agent was used. Patients were allowed to resume clear fluid diet, 4 h after swallowing the capsule endoscope. The sensor array and recorder were removed from the patients after 8 h of recording. The recorded images were then downloaded to the workstation and viewed by the RAPID software (Given Imaging). Patients were monitored for any abdominal discomfort and pain during and after the examination. The time of spontaneous passage of the capsule endoscope was recorded. Patients who were uncertain of the natural passage of the capsule endoscope were called back for abdominal x-ray to check for possible retention of the capsule endoscope.

Gastric and small bowel transit time

All capsule images were independently viewed by two endoscopists who were unaware of the use of prokinetic agents. Gastric transit time was defined as the time taken from the first gastric image to the first duodenal image. Due to the potential difficulty in accurately identifying the

ileo-cecal valve, small bowel transit time was defined as the time taken between the first duodenal image and the first cecal image. Cases having capsules passed to the cecum were considered to be complete small bowel examination. The overall quality of small bowel images was graded as satisfactory or unsatisfactory by the viewers according to the percentage of good and clear images that were not obscured by food particles or bile. Satisfactory image was defined when more than 90% of the images were optimal and clear. All discrepant findings between the two viewers were resolved on discussion.

Statistical analysis

Categorical data were analyzed by Pearson χ^2 test whereas numerical data were analyzed by Student's *t*-test. All statistical analyses were made by the statistical software SPSS version 11.5 (SPSS Inc., Chicago, IL, USA). A two-sided *P* value of less than 0.05 was considered statistically significant.

RESULTS

Effects of erythromycin on gastric transit time

There was no retention of the capsule endoscope in these 38 examinations. The mean gastric and small intestinal transit time in all patients was 35.9 and 218 min respectively. Notably, the gastric transit time was significantly lower in the erythromycin group. The mean gastric transit was 15.8 min (range <1-60 min) in the erythromycin group and 70.2 min (range 1-298 min) in the control group (*P* = 0.005). While the longest gastric transit time in the erythromycin group was 60 min, five (36%) patients in the control group had gastric transit time of more than 1 h. On the other hand, there was no significant difference in the gastric transit time between diabetic and non-diabetic patients (mean 34.2 *vs* 36.4 min, *P* = 0.92). There was also no significant association between gastric transit time and age (*P* = 0.88), gender (*P* = 0.73), or body mass index (*P* = 0.22) of the patients.

Effects of erythromycin on small bowel examination

One (4%) patient in the erythromycin group had incomplete small bowel examination due to the prolonged small bowel transit time of more than 7 h. In contrast, 3 (21%) patients in the control group had incomplete small bowel examination (*P* = 0.13 *vs* erythromycin group). The reasons were the prolonged gastric and small bowel transit time in two and technical failure in one. For those who had complete small bowel examination, the small bowel transit time was comparable in the erythromycin (mean 227 min, range 85-446 min) and control groups (183 min, range 117-401 min; *P* = 0.18, Table 2). Unsatisfactory images were obtained in 46% patients of the erythromycin group and in 36% of patients of the control group (*P* = 0.74).

Effects of erythromycin on repeat capsule endoscopy

Four patients had repeat capsule endoscopy due to incomplete or sub-optimal examination. The minimal interval between the two examinations was 4 d. Two patients received erythromycin only on the second examination while the other two patients received erythromycin in both

examinations. As shown in Figure 1, there was a marked reduction in gastric transit time of the two patients who were given erythromycin in the second examination. In contrast, there was no apparent change in gastric transit time of the two patients who were given erythromycin in both examinations. The gastric transit time was less than 50 min in all examinations pre-treated with oral erythromycin.

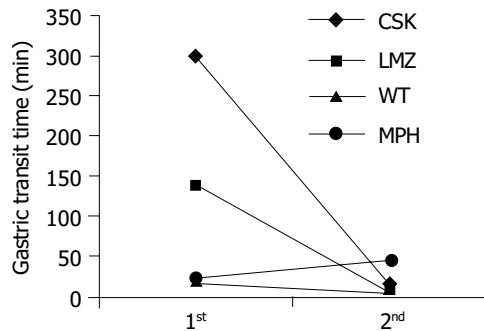


Figure 1 Changes in gastric transit time in patients undergoing repeated capsule endoscopy. Four patients had repeat capsule endoscopy examinations. Two patients (CSK and LMZ), as shown by the black lines, received only erythromycin on the second examination and there was a marked reduction in gastric transit time in the second examination after the use of oral erythromycin. The other patients (WT and MPH), as illustrated by the dotted lines, received erythromycin in both examinations and the gastric emptying time was less than 50 min in both examinations.

Table 2 Gastric and small bowel transit of capsule endoscopy in two groups of patients (mean±SD)

	Erythromycin (n = 24)	Control (n = 14)	P
Gastric transit time (min)	15.8±16.8	70.3±88.1	0.005
Small bowel transit time (min)	226.5±84.0	183.0±91.2	0.18
Incomplete small bowel examination (%)	1 (4)	3 (21)	0.13
Image quality (%)			
Satisfactory	13 (54)	9 (64)	0.74
Unsatisfactory	11 (46)	5 (36)	

DISCUSSION

As gastric and small bowel transit time shows considerable inter-individual variations and the prime interest of the capsule endoscopy is to examine the small bowel only, ways to enhance gastric transit time without compromising small bowel examination would potentially improve the outcome of this investigation. However, the effect of prokinetic agent on this relatively new examination remains elusive. In this study, we specifically addressed the effect of oral erythromycin on gastric and small bowel transit time in patients undergoing capsule endoscopy.

Erythromycin promotes gastric emptying by binding to motilin receptors and acts as a motilin agonist. The use of low dose intravenous erythromycin has been shown to improve gastric emptying in patients with diabetic gastroparesis^[7]. Moreover, erythromycin infusion prior to endoscopy in patients with recent hematemesis has been shown to make endoscopy easier, and reduces the need for a repeat procedure by enhancing the emptying of blood

within the stomach^[9]. Results from this study showed that the use of low dose oral erythromycin could enhance gastric transit time of the wireless capsule endoscopy. The gastric transit time in the 24 patients who received erythromycin was all within 60 min. In contrast, 5 (36%) patients in the control group had gastric transit time of more than 1 h. In a previous volunteer study, it was noted that the mean gastric transit time of capsule endoscopy is 63 min (range 10-319 min)^[10]. This result is comparable to the findings in our control group. To further support our findings, there was a marked reduction in gastric transit time in the two patients who used oral erythromycin on the second examination only.

Other than speeding up the gastric transit time, the use of erythromycin was not associated with any significant changes in small bowel transit time. On the other hand, patients receiving erythromycin tended to have a higher rate of complete small bowel examination. This is probably due to the shortened gastric transit time instead of alterations in small bowel passage by the use of erythromycin. More importantly, the use of erythromycin did not appear to alter the overall quality of small bowel images. The percentage of “unsatisfactory” small bowel images reported in this study was relatively high, which may be related to the use of very stringent criteria for satisfactory images, i.e., >90% clear and optimal images. Moreover, we did not use any bowel cleansing agent in this study, which may further improve the quality of small bowel images^[11]. It was shown in a small uncontrolled study that the use of polyethylene glycol may also shorten the transit time of the capsule endoscopy through the stomach and small bowel^[12]. It remains to be determined whether the combined use of prokinetic agents and bowel cleansing agent has synergistic effect on small bowel transit time.

Erythromycin is a safe and cheap antibiotic, which can be conveniently given via oral route. It is also relatively free of adverse reactions including drug sensitivity. Although most published data used an intravenous preparation of erythromycin, we found that the use of oral dosage was also effective for this purpose. Apart from erythromycin, there are several other prokinetic agents that may be used in reducing gastric transit time during capsule endoscopy. Cisapride, which was previously used as a gastric prokinetic agent, is associated with fatal arrhythmia in susceptible individuals^[13,14] and has been withdrawn by the Food and Drug Administration in 1999^[15]. Domperidone and metoclopramide are also used in treating symptomatic patients with gastroparesis. However, the latter is not infrequently associated with extra-pyramidal side effects. Recently, the 5-HT₄ receptor partial agonist, tegaserod, is found to accelerate gastric emptying and gastro-intestinal transit time in healthy male subjects^[16]. Whether these drugs can also be used as prokinetic agents for capsule endoscopy remains to be determined and it is interesting to compare the effects of different prokinetic agents in future studies.

Although this was a non-randomized study, most of the potential confounding factors were comparable in the two groups. All demographic and clinical details of the two groups were matched. Moreover, all viewers were blinded to the clinical information of the patients. With the shortened

gastric transit time, it is not difficult to anticipate that the time spent by the examiners on reviewing the images would be reduced accordingly. This may be another advantage of using prokinetic agents in this rather time-consuming examination.

In summary, erythromycin given orally prior to swallowing capsule endoscope significantly reduces the gastric emptying time without compromising small bowel transit time and image quality. Further randomized study is necessary to evaluate the role of various prokinetic agents in the performance of capsule endoscopy.

REFERENCES

- 1 **Ell C**, Remke S, May A, Helou L, Henrich R, Mayer G. The first prospective controlled trial comparing wireless capsule endoscopy with push enteroscopy in chronic gastrointestinal bleeding. *Endoscopy* 2002; **34**: 685-689
- 2 **Costamagna G**, Shah SK, Riccioni ME, Foschia F, Mutignani M, Perri V, Vecchioli A, Brizi MG, Piccicocchi A, Marano P. A prospective trial comparing small bowel radiographs and video capsule endoscopy for suspected small bowel disease. *Gastroenterology* 2002; **123**: 999-1005
- 3 **Mylonaki M**, Fritscher-Ravens A, Swain P. Wireless capsule endoscopy: a comparison with push enteroscopy in patients with gastroscopy and colonoscopy negative gastrointestinal bleeding. *Gut* 2003; **52**: 1122-1126
- 4 **Pennazio M**, Santucci R, Rondonotti E, Abbiati C, Beccari G, Rossini FP, De Franchis R. Outcome of patients with obscure gastrointestinal bleeding after capsule endoscopy: Report of 100 consecutive cases. *Gastroenterology* 2004; **126**: 643-653
- 5 **Hara AK**, Leighton JA, Sharma VK, Fleischer DE. Small Bowel: Preliminary Comparison of Capsule Endoscopy with Barium Study and CT. *Radiology* 2004; **230**: 260-265
- 6 **Minocha A**, Katragadda R, Rahal PS, Ries A. Erythromycin shortens oro-caecal transit time in diabetic male subjects: a double-blind placebo-controlled study. *Aliment Pharmacol Ther* 1995; **9**: 529-533
- 7 **Janssens J**, Peeters TL, Vantrappen G, Tack J, Urbain JL, De Roo M, Muls E, Bouillon R. Improvement of gastric emptying in diabetic gastroparesis by erythromycin. Preliminary studies. *N Engl J Med* 1990; **322**: 1028-1031
- 8 **Maganti K**, Onyemere K, Jones MP. Oral erythromycin and symptomatic relief of gastroparesis: a systematic review. *Am J Gastroenterol* 2003; **98**: 259-263
- 9 **Frossard JL**, Spahr L, Queneau PE, Giostra E, Burckhardt B, Ory G, De Saussure P, Armenian B, De Peyer R, Hadengue A. Erythromycin intravenous bolus infusion in acute upper gastrointestinal bleeding: a randomized, controlled, double-blind trial. *Gastroenterology* 2002; **123**: 17-23
- 10 **Appleyard MN**, Glukhovskiy A, Jacob J, Gat D, Lewkowicz S, Swain P. Transit times of the wireless capsule endoscope. *Gastrointest Endosc* 2001; **53**: AB122
- 11 **Viazis N**, Sgouros S, Papaxoinis K, Vlachogiannakos J, Bergele C, Sklavos P, Panani A, Avgerinos A. Bowel preparation increases the diagnostic yield of capsule endoscopy: A prospective, randomized, controlled study. *Gastrointest Endosc* 2004; **60**: 534-538
- 12 **Fireman Z**, Kopelman Y, Fish L, Sternberg A, Scapa E, Mahaina E. Effect of oral purgatives on gastric and small bowel transit time in capsule endoscopy. *Isr Med Assoc J* 2004; **6**: 521-523
- 13 **Bran S**, Murray WA, Hirsch IB, Palmer JP. Long QT syndrome during high-dose cisapride. *Arch Intern Med* 1995; **155**: 765-768
- 14 **Wysowski DK**, Bacsanyi J. Cisapride and fatal arrhythmia. *N Engl J Med* 1996; **335**: 290-291
- 15 **Wysowski DK**, Corken A, Gallo-Torres H, Talarico L, Rodriguez EM. Postmarketing reports of QT prolongation and ventricular arrhythmia in association with cisapride and Food and Drug Administration regulatory actions. *Am J Gastroenterol* 2001; **96**: 1698-1703
- 16 **Degen L**, Matzinger D, Merz M, Appel-Dingemanse S, Osborne S, Luchinger S, Bertold R, Maecke H, Beglinger C. Tegaserod, a 5-HT₄ receptor partial agonist, accelerates gastric emptying and gastrointestinal transit in healthy male subjects. *Aliment Pharmacol Ther* 2001; **15**: 1745-1751

Science Editor Wang XL and Guo SY Language Editor Elsevier HK

Appendix is a priming site in the development of ulcerative colitis

Mitsunobu Matsushita, Hiroshi Takakuwa, Yuji Matsubayashi, Akiyoshi Nishio, Susumu Ikehara, Kazuichi Okazaki

Mitsunobu Matsushita, Kazuichi Okazaki, Third Department of Internal Medicine, Kansai Medical University, Osaka, Japan
Susumu Ikehara, First Department of Pathology, Kansai Medical University, Osaka, Japan
Hiroshi Takakuwa, Yuji Matsubayashi, Department of Gastroenterology, Tenri Hospital, Nara, Japan
Akiyoshi Nishio, Department of Gastroenterology and Endoscopic Medicine, Faculty of Medicine, Kyoto University, Kyoto, Japan
Supported by the Grant-in-Aid for Scientific Research (C) from the Ministry of Culture and Science of Japan No. 16560645; Grant-in-Aid for "Research for the Future" Program from The Japan Society for the Promotion of Science, No. JSPS-RFTF97I00201; Supporting in Research Funds from The Japanese Foundation for Research and Promotion of Endoscopy, No. JFE-1997; Shimidzu Immunology Foundation, 2000; Tenri Foundation for Medical Research, 1997-2000; Health and Labour Science Research Grants from the Japanese Ministry of Health, Labour and Welfare, and Research on Measures for Intractable Disease (Inflammatory Bowel Disease); a Grant from the "The 21st Century Center of Excellence (COE)" Program of the Ministry of Education, Culture, Sports, Science and Technology
Correspondence to: Dr. Mitsunobu Matsushita, Third Department of Internal Medicine, Kansai Medical University, 10-15 Fumizono-cho, Moriguchi, Osaka 570-8506, Japan. matsumit@takii.kmu.ac.jp
Telephone: +81-6-6992-1001 Fax: +81-6-6996-4874
Received: 2004-12-13 Accepted: 2005-01-05

Abstract

AIM: The role of the appendix has been highlighted in the pathogenesis of ulcerative colitis (UC). The aims of this study were to elucidate the immuno-imbalance in the appendix of UC patients, and to clarify the role of the appendix in the development of UC.

METHODS: Colonoscopic biopsy specimens of the appendix, transverse colon, and rectum were obtained from 86 patients with UC: active pancolitis (A-Pan; $n = 15$), active left-sided colitis (A-Lt; $n = 25$), A-Lt with appendiceal involvement (A-Lt/Ap; $n = 10$), inactive pancolitis (I-Pan; $n = 14$), and inactive left-sided colitis (I-Lt; $n = 22$), and from controls. In the isolated mucosal T cells, the CD4/CD8 ratio and proportion of activated CD4+ T cells were investigated, and compared with controls.

RESULTS: In the appendix, the CD4/CD8 ratio significantly increased in A-Lt and A-Lt/Ap. The ratio in the appendix also tended to increase in A-Pan. In the rectum, the ratio significantly increased in all UC groups. In the appendix, the proportion of CD4+CD69+ (early activation antigen) T cells significantly increased in all UC groups. In the rectum, the proportion of CD4+CD69+ T cells significantly increased only in A-Pan. The proportion of CD4+HLA-DR+ (mature activation antigen) T cells significantly increased only in the rectum of A-Pan, but not in the other

areas of any groups.

CONCLUSION: The increased CD4/CD8 ratio and predominant infiltration of CD4+CD69+ T cells in the appendix suggest that the appendix is a priming site in the development of UC.

© 2005 The WJG Press and Elsevier Inc. All rights reserved.

Key words: Appendix; Appendectomy; Ulcerative colitis; Activated T cell; CD4+ T cell

Matsushita M, Takakuwa H, Matsubayashi Y, Nishio A, Ikehara S, Okazaki K. Appendix is a priming site in the development of ulcerative colitis. *World J Gastroenterol* 2005; 11(31): 4869-4874

<http://www.wjgnet.com/1007-9327/11/4869.asp>

INTRODUCTION

Although the triggering factor for ulcerative colitis (UC) is still unknown, cytokine imbalance and the production of inflammatory mediators by activated CD4+ T cells play an important role in the pathogenesis of UC. T helper type 2 cells and their cytokines, particularly interleukin (IL)-4, have been suggested to enhance the development of UC^[1]. Recently, regulatory T cells, characterized by the expression of cell surface markers CD4 and CD25, have been shown to actively suppress immune responses, and lack of regulatory T cells leads to organ-specific autoimmunity^[2]. On the other hand, a sub-population of CD8+ T cells also suppresses the response of activated CD4+ T cells and B cells through an interaction that depends on expression of the major histocompatibility complex class Ib molecule Qa-1, the mouse homolog of human leukocyte antigen (HLA)-E^[3]. However, the precise role of these regulatory T cells in UC remains unclear.

Although human appendix is considered as a vestigial remnant^[4], recent observations have focused attention on the role of the appendix in the pathogenesis of UC. Many case-control studies suggest that previous appendectomy is rare in UC patients^[5-7], raising the possibility that appendectomy protects against the subsequent development of UC^[8-11]. Patients with previous appendectomy also have a delayed onset of UC^[8,9], a reduced need for immunosuppression therapy and proctocolectomy^[8,10], and a reduced relapse rate and extent of UC^[11]. Appendectomy in T-cell receptor (TCR)- α deficient mice suppresses the development of experimental colitis^[12]. Moreover, we first reported a patient with improvement of left-sided UC after appendectomy^[13]. Although these findings support that the appendix may be

related to the pathogenesis of UC, the immunological role of human appendix is unknown.

Extensive infiltration of lymphocytes, especially CD4+ T cells^[14], has been observed in the inflamed mucosa of UC patients^[15]. Activated CD4+ T cells exhibit increased cytotoxic activity^[16] and secrete cytokines that enhance the inflammatory state resulting in tissue injury^[17,18]. Several studies concerning T-cell subsets in the resected appendix have been performed previously^[19], but very few have focused on the activation status of the immune cells in the appendix as well as in the uninflamed mucosa. In this study, we investigated the CD4/CD8 ratio and proportion of activated CD4+ T cells in the inflamed and uninflamed colonic mucosa, especially in the appendiceal mucosa, of UC patients in order to clarify the role of the appendix in the development of UC.

MATERIALS AND METHODS

Subjects

UC patients with toxic megacolon, coexistence of known cancer, complication of extra-intestinal disease, past colectomy, poor general condition, and no consent to participate in the study were excluded. A total of 86 patients with UC and 27 control subjects were subsequently enrolled in the study. Informed consent to participate in this study was obtained from each patient. The diagnosis of UC was based on the established clinical, endoscopic, histological, and/or radiological criteria^[20]. Patients with no malignant or inflammatory colonic disorders, including adenomatous polyps ($n = 8$), diverticular disease ($n = 6$), non-specific abdominal pain ($n = 5$), family history of colorectal cancer ($n = 4$), and chronic constipation ($n = 4$) served as the control subjects. Patients receiving non-steroidal anti-inflammatory drugs or immuno-regulatory drugs, such as corticosteroids and azathioprine were excluded from controls. There was no history of appendectomy both in the patients and controls.

Scoring system of disease activity

The disease activity was evaluated based on the endoscopic findings according to the scoring system as reported previously^[21]: grade 0, normal vascular pattern; grade 1, erythema with loss of vascular pattern; grade 2, grade 1 plus contact bleeding; grade 3, grade 1 plus spontaneous bleeding; and grade 4, grade 1 plus obvious ulceration. We defined the grades 0 and 1 as inactive disease, and the other grades as active disease. The disease extent was also classified endoscopically into three subgroups: pancolitis and left-sided colitis (involvement up to the splenic flexure) with and without appendiceal involvement (skipped erosions in the appendiceal orifice).

Disease activity and patients

A total of 86 patients with UC were divided into six groups according to the activity and extent of the disease: active pancolitis (A-Pan; $n = 15$), active left-sided colitis without appendiceal involvement (A-Lt; $n = 25$), active left-sided colitis with appendiceal involvement (A-Lt/Ap; $n = 10$), inactive pancolitis (I-Pan; $n = 14$), inactive left-sided colitis

without appendiceal involvement (I-Lt; $n = 22$), and inactive left-sided colitis with appendiceal involvement (I-Lt/Ap; $n = 0$). Because the inflamed mucosa in the appendiceal orifice may be restructured by the normal mucosa after treatment, there were no patients with I-Lt/Ap. The characteristics of each group are summarized in Table 1. There was no significant difference in sex (the χ^2 test or Fisher's exact test) and age (Student's *t*-test) among groups.

At the time of the study, 27 patients with active UC and 3 patients with inactive UC had received no medications. Twenty-five patients were treated with salazosulfapyridine (SASP) (1 000-6 000 mg/d) only, 12 were treated with mesalazine (5-ASA) (1 000-2 250 mg/d) only, 2 were treated with prednisolone (PDN) (10 mg/d) only, 12 were treated with PDN (5-20 mg/d) plus SASP (1 500-4 500 mg/d), and 5 were treated with PDN (5-20 mg/d) plus 5-ASA (1 000-2 250 mg/d).

Cell isolation

We obtained colonic mucosal samples from UC patients and control subjects. At diagnostic or follow-up total colonoscopy when the activity and extent of the disease were evaluated, biopsy specimens from the appendix near the appendiceal orifice, transverse colon, and rectum (four specimens in each area) were obtained. We isolated mucosal mononuclear cells from biopsy specimens, as previously described^[22]. The initial viability of the cellular suspensions exceeded 95% in all instances when estimated by the trypan blue dye exclusion test. The viability was maintained at >80% during the entire assay period.

Flow cytometric analysis

Mucosal mononuclear cells were analyzed by two-color or three-color flow cytometry with the following mAbs: anti-CD4-PE/anti-CD8-FITC (Coulter Immunology, Tokyo, Japan), anti-CD45 (leukocyte common antigen)-PE-Cy5 (Immunotech, Cedex, France), anti-CD4-PE (Nichirei, Tokyo, Japan), anti-CD69 (early activation antigen)-FITC (Becton-Dickinson, Tokyo, Japan), and anti-HLA-DR (mature activation antigen)-FITC (Immunotech). The isolated cells were incubated with antibodies at 4 °C for 30 min, and washed thrice in FACS buffer (PBS, sodium azide 0.01%, and bovine serum albumin 0.1%, Sigma, St. Louis, USA), and applied for flow cytometry (EPICS XL system II, Coulter Company).

We first analyzed the phenotyped cells by two-color flow cytometry. After the cell suspensions were initially visualized in the forward scatter/side scatter profile, lymphocyte populations were gated to exclude monocytes. The proportion of CD4+ and CD8+ T cells in the total lymphocyte populations was expressed as CD4/CD8 ratio.

By three-color flow cytometry, we also analyzed the activated CD4+ T cells. In the process of T cell activation, CD69, CD25, CD71, and HLA-DR antigens are serially expressed on the surface of T cells. To identify this process, we investigated the expressions of CD69 (early activation antigen) and HLA-DR (mature activation antigen). After the cell suspensions were visualized, lymphocyte populations were gated as defined by CD45 (leukocyte common antigen) expression. The proportion of CD4+CD69+ and CD4+HLA-

Table 1 Characteristics of patients with ulcerative colitis and normal subjects

	A-Pan	A-Lt	A-Lt/Ap	I-Pan	I-Lt	Normal subjects
Number of patients	15	25	10	14	22	27
Sex (M/F)	7/8	13/12	6/4	9/5	11/11	15/12
Age (yr)						
Mean	36.4	40.3	35.5	41.4	50.7	43.6
Range	11-69	22-76	18-64	17-78	23-73	16-65
Medications						
None	7	11	9	1	2	27
SASP	2	7	0	5	11	0
5-ASA	2	5	1	1	3	0
PDN	1	0	0	0	1	0
SASP+PDN	3	2	0	3	4	0
5-ASA+PDN	0	0	0	4	1	0

A-Pan, active pancolitis; A-Lt, active left-sided colitis; A-Lt/Ap, active left-sided colitis with appendiceal involvement; I-Pan, inactive pancolitis; I-Lt, inactive left-sided colitis; PDN, prednisolone; SASP, salazosulfapyridine; 5-ASA, mesalazine.

Table 2 CD4/CD8 ratio in the colon (mean±SD)

	A-Pan	A-Lt	A-Lt/Ap	I-Pan	I-Lt	Controls
Rectum	2.3±2.0 ^a	3.6±1.6 ^b	4.9±2.2 ^b	1.8±1.0 ^a	2.4±2.0 ^b	1.0±0.6
Transverse	1.5±0.7	1.1±0.4	1.8±0.4 ^a	0.9±0.5	1.3±0.9	1.2±0.8
Appendix	3.2±1.3	3.5±1.3 ^a	3.9±0.9 ^a	2.9±1.9	2.6±1.4	2.6±1.1

^a*P*<0.05, ^b*P*<0.01 vs controls. A-Pan, active pancolitis; A-Lt, active left-sided colitis; A-Lt/Ap, active left-sided colitis with appendiceal involvement; I-Pan, inactive pancolitis; I-Lt, inactive left-sided colitis.

DR+ T cells in the total lymphocyte populations was calculated.

Prior to the present study, we performed a pilot study with immuno-flow cytometric analysis in UC patients (A-Pan: *n* = 7 and A-Lt/Ap: *n* = 3), ascending colon cancer patients (*n* = 5), and ascending colon diverticulitis patients (*n* = 5). The population of T cells, expressing CD4, CD8, CD69, and HLA-DR antigens, in pre-operative biopsy samples of the appendix near the appendiceal orifice and in mucosal samples of resected appendix, was similar in each patient. The results of the pilot study suggested that the analysis of biopsy samples of the appendix near the appendiceal orifice represented those of the appendix.

Statistical analysis

All values were expressed as mean±SD. The Student's *t*-test for comparisons among groups was used for statistical analysis. *P*<0.05 (two-tailed) was considered statistically significant.

RESULTS

CD4/CD8 ratio in appendix

In the appendix, the CD4/CD8 ratio both in A-Lt (*P* = 0.0166) and A-Lt/Ap (*P* = 0.0445) significantly increased compared with that in controls (Table 2). Moreover, the CD4/CD8 ratio significantly increased both in A-Lt (*P* = 0.0452) and A-Lt/Ap (*P* = 0.0445) compared with that in I-Lt. The ratio in A-Pan tended to increase compared with that in controls (*P* = 0.1654) and in I-Pan (*P* = 0.6890). The ratio tended to increase in A-Lt/Ap compared with that in A-Lt (*P* = 0.7370). Interestingly, as the CD4/CD8 ratio in the appendix increased, the ratio in the rectum tended to increase, suggesting that some relations might be present in the immune responses between the appendix and the rectum.

CD4/CD8 ratio in transverse colon

In the normal appearance transverse colon of A-Lt/Ap, the CD4/CD8 ratio significantly increased compared with that in controls (*P* = 0.0374, Table 2). The ratio tended to increase in A-Lt/Ap compared with that in I-Lt (*P* = 0.3051). The ratio significantly increased in A-Lt/Ap compared with that in A-Lt (*P* = 0.0064), and in A-Pan compared with that in I-Pan (*P* = 0.0442).

CD4/CD8 ratio in rectum

In the rectum, the CD4/CD8 ratio significantly increased in all UC groups (A-Pan; *P* = 0.0102, A-Lt; *P*<0.0001, and A-Lt/Ap; *P*<0.0001), even in I-Pan (*P* = 0.0109) and I-Lt (*P* = 0.0046), compared with that in controls (Table 2). The ratio also significantly increased both in A-Lt (*P* = 0.0343) and A-Lt/Ap (*P* = 0.0236) compared with that in I-Lt. The ratio tended to increase in A-Lt/Ap compared with that in A-Lt (*P* = 0.1436), and in A-Pan compared with that in I-Pan (*P* = 0.4682). These findings suggested that the CD4/CD8 ratio might represent the inflammation degree in the mucosa.

Early activated T cells

In the appendix, the proportion of CD4+CD69+ (early activation antigen) T cells significantly increased in all UC groups (A-Pan; *P* = 0.0013, A-Lt; *P* = 0.0042, and A-Lt/Ap; *P* = 0.0245), even in I-Pan (*P*<0.0001) and I-Lt (*P* = 0.0357), compared with that in controls (Table 3), but there were no significant differences among UC groups. In the transverse colon, the proportion did not significantly increase in any UC groups compared with that in controls. In the rectum, the proportion significantly increased only in A-Pan (*P* = 0.0497), but not in the other groups, compared with that in controls.

Table 3 Activated T cells in the colon (mean±SD, %)

	A-Pan	A-Lt	A-Lt/Ap	I-Pan	I-Lt	Controls
CD4+CD69+ T cells						
Rectum	27.8±4.6 ^a	23.2±5.0	24.0±7.6	24.5±6.2	28.2±8.6	23.1±4.1
Transverse	25.0±5.7	20.4±7.8	23.4±4.3	21.5±7.3	22.1±6.2	21.0±9.1
Appendix	26.6±3.0 ^b	28.0±7.0 ^b	26.0±4.0 ^a	28.9±3.9 ^b	25.4±7.3 ^a	19.6±4.1
CD4+HLA-DR+ T cells						
Rectum	15.2±6.2 ^a	10.1±3.8	7.3±2.4	11.6±4.1	11.1±6.0	8.6±4.7
Transverse	13.2±5.0	7.9±4.0	9.1±4.9	14.9±6.7	9.5±3.7	9.5±5.3
Appendix	8.9±2.4	9.9±4.1	9.9±2.4	12.6±2.8	10.9±4.3	8.8±3.6

^a $P < 0.05$, ^b $P < 0.01$ vs controls. A-Pan, active pancolitis; A-Lt, active left-sided colitis; A-Lt/Ap, active left-sided colitis with appendiceal involvement; I-Pan, inactive pancolitis; I-Lt, inactive left-sided colitis.

Late activated T cells

The proportion of CD4+HLA-DR+ (mature activation antigen) T cells in the rectum significantly increased only in A-Pan compared with that in controls ($P = 0.0299$), while the proportion of CD4+HLA-DR+ T cells in the appendix did not significantly increase in any UC groups, compared with that in controls (Table 3). The proportion in the transverse colon also did not significantly increase in any UC groups compared with that in controls.

Effects of drugs on CD4/CD8 ratio and activated T cells

To identify the effects of drug treatment on the profiles of T cells, we analyzed the CD4/CD8 ratio and proportions of CD4+CD69+ and CD4+HLA-DR+ T cells in active UC patients with medication (A-Pan; $n = 8$, and A-Lt; $n = 14$) and those without medication (A-Pan; $n = 7$, and A-Lt; $n = 11$). Although the CD4/CD8 ratio in the transverse colon of A-Pan significantly increased in the patients without medication compared with those with medication ($P = 0.0306$), the other ratios and proportions were not significant between the patients with medication and those without medication. Our results were therefore not so influenced with medical therapy.

DISCUSSION

Although the pathogenesis of UC has not been determined, an abnormal mucosal immune response plays a major role in the development and pathophysiology of UC^[23,24]. There are few studies investigating the immune-regulatory cells in the appendix of patients with UC, especially with left-sided UC. Most studies have used cells isolated from colectomy specimens involving the disease to detect local immune abnormality^[23,24]. Because colectomy is usually performed in severe and refractory cases, mostly in pancolitis cases, but not in other active or inactive cases after a period of medical therapy, these studies may not cover the whole spectrum of disease activity^[25]. We therefore used cells isolated from colonoscopic biopsy specimens of UC patients with a wide range of disease activity, but the appendiceal mucosa is usually hard to obtain by biopsy. In this study, biopsy specimens of the appendix near the appendiceal orifice were used, instead of specimens of the appendix itself, because our prior pilot study showed that the analysis of biopsy samples of the appendix near the appendiceal orifice represented those of the appendix.

Although CD4+ and CD8+ T cells contain counterpart functions, such immuno-activation as helper/inducer T cells and immuno-suppression as regulatory T cells, the CD4/CD8 ratio is one of the most reflective markers for immune activation^[14,26]. In the present study, the CD4/CD8 ratio in the appendix significantly increased both in A-Lt and A-Lt/Ap compared with that in controls (Table 2). The ratio in the appendix also tended to increase in A-Pan compared with that in controls. Interestingly, as the CD4/CD8 ratio in the appendix increased, the ratio in the rectum tended to increase, suggesting that some relationships might be present in the immune responses between the appendix and the rectum.

In the normal appearance transverse colon of A-Lt/Ap, the CD4/CD8 ratio significantly increased compared with that in controls (Table 2). In the entire colon, the CD4/CD8 ratio tended to increase in A-Lt/Ap compared with that in A-Lt, but it was significant only in the transverse colon. Matsumoto *et al.*^[27], also reported that the histological inflammation grade in the entire colon was higher in A-Lt/Ap than that in A-Lt. The grade was significant both in the inflamed appendiceal orifice ($P < 0.001$) and in the uninflamed ascending colon ($P < 0.05$). The CD4/CD8 ratio therefore may represent the inflammation degree in the mucosa.

Even in the inactive UC groups, the CD4/CD8 ratio significantly increased in the rectum compared with that in controls. Most patients with inactive UC have low-grade inflammation, and it is possible that symptomatic relapse occurs only when the inflammatory process reaches a critical intensity^[28]. Also, because inflammation is a continuous process, direct assessment of the level of inflammatory activity may provide a quantitative pre-symptomatic measure of imminent clinical relapse of the disease^[28]. In our study, the increased CD4/CD8 ratio suggested that the significant immuno-imbalance was persistent in the inactive rectum. Because patients with inactive UC even receiving maintenance therapy are easy to relapse^[29], we suspect that the disease can relapse when the immuno-imbalance is persistent in the rectum.

Recent investigations including TCR- α deficient mice colitis models suggest that non-pathogenic enteric bacterial flora may be involved in the induction of colitis^[12,30]. However, it is unclear which part of the colon is involved in priming luminal antigens as the inductive site. To identify the priming site, we compared early- and late-activated CD4+ T cells with CD69 as an early activation antigen and HLA-DR as a late activation antigen, respectively. In the

appendix, the proportion of CD4+CD69+ T cells significantly increased in all UC groups, even in the inactive UC groups, compared with that in controls (Table 3). In the transverse colon, the proportion did not significantly increase in any UC groups compared with that in controls. In the rectum, the proportion significantly increased only in A-Pan, but not in the other groups, compared with that in controls. The proportion of CD4+HLA-DR+ T cells significantly increased only in the rectum of A-Pan, but not in the other areas of any groups compared with that in controls (Table 3). These findings suggest that the appendix may be a priming site in the development of UC. In A-Pan, the CD4/CD8 ratio tended to increase in all areas compared with that in controls, but it was significant only in the rectum (Table 2), where the proportions of CD4+CD69+ and CD4+HLA-DR+ T cells significantly increased compared with those in controls (Table 3). The findings suggest that the appendix may not play a major role in extended colitis.

In TCR- α -deficient mice, the pathological T cells are initially concentrated in the appendix^[31]. Mucosal TCR- $\alpha\beta$ + T cells, including CD4+ T cells, in IL-2-deficient mice appear in the colon prior to the manifestation of colitis^[16]. An increase of identical T cell clones involved in the development of inflammation is detectable in the uninfamed appendix and the inflamed colon of UC patients as well as in TCR- α -deficient mice^[32,33]. Therefore, the increased CD4+CD69+ T cells indicate that CD4+ T cells may be initially activated in the appendix, and may re-circulate to the entire colon and rectum (increased CD4/CD8) prior to the manifestation of UC, and inflammation originating from the rectum extends to the entire colon. The reason why the inflammation begins in the rectum is unknown.

We first reported the improvement of UC (A-Lt/Ap) without medication during the 3 years after appendectomy in a young patient (21-year-old), and proposed that appendectomy may have a place as a therapeutic strategy in UC patients^[13]. Ja³rnerot *et al.*^[34], also performed laparoscopic appendectomy in six patients with refractory UC (two A-Pan and four A-Lt), and found that one young patient (26-years old) was in remission with continued maintenance treatment, but five patients (mean age: 50.8 years, range: 44-56 years) had relapse of the disease. Histological analysis of the resected appendix showed mucosal erosions and moderate infiltrations of CD4+ T cells in our patient^[13], but did not show any inflammation in all patients as reported by Ja³rnerot *et al.*^[34]. They concluded that appendectomy does not influence the course of established UC in a consistent way, which supports our results in this study. Eri *et al.*^[35], also reported the clinical course of six patients (mean age: 30.5 years) with refractory UC (five A-Lt and one A-Lt/Ap) after laparoscopic appendectomy, and found that five patients were in complete clinical remission, and one patient had improved. Histological analysis of the resected appendix showed colitis-type inflammation (ulcerative appendicitis), containing a highly activated lymphocyte population, in the five patients. Recently, Jo *et al.*^[19], reported the clinical course of nine patients (mean age; 32.5 years, range; 13-48 years) with mildly activated UC (four A-Pan and five A-Lt) after appendectomy, and found that two A-Lt patients with ulcerative appendicitis had improved, but

the disease remained active in the other patients (three A-Lt without ulcerative appendicitis and four A-Pan). Hallas *et al.*^[36], reported the nationwide study with complete follow-up of 202 patients (mean age; 43.3 years) with UC who underwent appendectomy after their onset of UC, and concluded that appendectomy has no beneficial effect on admission rates in UC patients. Although appendectomy is associated with a low risk for subsequent UC only in young patients^[13,19,34,35], especially before the age of 20 years^[7], no stratification of data for any age had been performed^[36]. Later, Hallas *et al.*^[37], supported that appendectomy would be useful against UC in young subjects by analyzing those who underwent appendectomy before the age of 30 years. These findings and our results indicate that appendectomy may be performed in young UC patients with ulcerative appendicitis.

In conclusion, our study suggests that the CD4/CD8 ratio represents the inflammation degree in the mucosa. Appendectomy may be a benefit therapy in young UC patients with ulcerative appendicitis. Apart from the rectum, the appendix is a priming site in the development of UC, and should no longer be considered as an evolutionary redundancy. Further studies including analysis of CD4+ and CD8+ T cells are necessary to clarify the role of the appendix in the pathogenesis of UC.

ACKNOWLEDGMENT

The authors thank Dr. Tsutomu Chiba (Department of Gastroenterology and Endoscopic Medicine, Kyoto University, Kyoto, Japan) for critically reading the manuscript and his helpful advices.

REFERENCES

- 1 **Rachmilewitz D**, Karmeli F, Takabayashi K, Hayashi T, Leider-Trejo L, Lee J, Leoni LM, Raz E. Immunostimulatory DNA ameliorates experimental and spontaneous murine colitis. *Gastroenterology* 2002; **122**: 1428-1441
- 2 **Walker MR**, Kasprovicz DJ, Gersuk VH, Be'nard A, Van Landeghen M, Buckner JH, Ziegler SF. Induction of FoxP3 and acquisition of T regulatory activity by stimulated human CD4+CD25- T cells. *J Clin Invest* 2003; **112**: 1437-1443
- 3 **Hu D**, Ikizawa K, Lu L, Sanchirico ME, Shinohara ML, Cantor H. Analysis of regulatory CD8 T cells in Qa-1-deficient mice. *Nat Med* 2004; **5**: 516-523
- 4 **Panaccione R**, Sandborn WJ. The appendix in ulcerative colitis: a not so innocent bystander. *Gastroenterology* 1999; **117**: 272-273
- 5 **Rutgeerts P**, D'haens G, Hiele M, Geboes K, Vantrappen G. Appendectomy protects against ulcerative colitis. *Gastroenterology* 1994; **106**: 1251-1253
- 6 **Russel MG**, Dorant E, Brummer RJM, Van De Kruus MA, Muris JW, Bergers JM, Goedhard J, Stockbrugger RW. Appendectomy and the risk of developing ulcerative colitis or Crohn's disease: results of a large case-control study. *Gastroenterology* 1997; **113**: 377-382
- 7 **Andersson RE**, Olaison G, Tysk C, Ekblom A. Appendectomy and protection against ulcerative colitis. *N Engl J Med* 2001; **344**: 808-814
- 8 **Radford-Smith GL**, Edwards JE, Purdie DM, Pandeya N, Watson M, Martin NG, Green A, Newman B, Florin THJ. Protective role of appendectomy on onset and severity of ulcerative colitis and Crohn's disease. *Gut* 2002; **51**: 808-813
- 9 **Selby WS**, Griffin S, Abraham N, Solomon MJ. Appendectomy protects against the development of ulcerative colitis but

- not affect its course. *Am J Gastroenterol* 2002; **97**: 2834-2838
- 10 **Cosnes J**, Carbonnel F, Beaugerie L, Blain A, Reijasse D, Gendre JP. Effects of appendectomy on the course of ulcerative colitis. *Gut* 2002; **51**: 803-807
 - 11 **Naganuma M**, Iizuka B, Torii A, Ogihara T, Kawamura Y, Ichinose M, Kojima Y, Hibi T. Appendectomy protects against the development of ulcerative colitis and reduces its recurrence: results of a multicenter case-controlled study in Japan. *Am J Gastroenterol* 2001; **96**: 1123-1126
 - 12 **Mizoguchi A**, Mizoguchi E, Chiba C, Bhan AK. Role of appendix in the development of inflammatory bowel disease in TCR- α mutant mice. *J Exp Med* 1996; **184**: 707-715
 - 13 **Okazaki K**, Onodera H, Watanabe N, Nakase H, Uose S, Matsushita M, Kawanami C, Imamura M, Chiba T. A patient with improvement of ulcerative colitis after appendectomy. *Gastroenterology* 2000; **119**: 502-506
 - 14 **Mu"ller S**, Lory J, Corazza N, Griffiths GM, Z'graggen K, Mazzucchelli L, Kappeler A, Mueller C. Activated CD4+ and CD8+ cytotoxic cells are present in increased numbers in the intestinal mucosa from patients with active inflammatory bowel disease. *Am J Pathol* 1998; **152**: 261-268
 - 15 **Ueyama H**, Kiyohara T, Sawada N, Isozaki K, Kitamura S, Kondo S, Miyagawa J, Kanayama S, Shinomura Y, Ishikawa H, Ohtani T, Nezu R, Nagata S, Matsuzawa Y. High Fas ligand expression on lymphocytes in lesions of ulcerative colitis. *Gut* 1998; **43**: 48-55
 - 16 **Simpson SJ**, Mizoguchi E, Allen D, Bhan AK, Terhorst C. Evidence that CD4+, but not CD8+ T cells are responsible for murine interleukin-2-deficient colitis. *Eur J Immunol* 1995; **25**: 2618-2625
 - 17 **Fiocchi C**. Inflammatory bowel disease: etiology and pathogenesis. *Gastroenterology* 1998; **115**: 182-205
 - 18 **Bhan AK**, Mizoguchi E, Smith RN, Mizoguchi A. Colitis in transgenic and knockout animals as models of human inflammatory bowel disease. *Immunol Rev* 1999; **169**: 195-207
 - 19 **Jo Y**, Matsumoto T, Yada S, Nakamura S, Yao T, Hotokezaka M, Mibu R, Iida M. Histological and immunological features of appendix in patients with ulcerative colitis. *Dig Dis Sci* 2003; **48**: 99-108
 - 20 **Schachter H**, Kirsner JB. Definitions of inflammatory bowel disease of unknown etiology. *Gastroenterology* 1975; **68**: 591-600
 - 21 **Riley SA**, Mani V, Goodman MJ, Herd ME, Dutt S, Turnberg LA. Comparison of delayed-release 5-aminosalicylic acid (mesalazine) and sulfasalazine as maintenance treatment for patients with ulcerative colitis. *Gastroenterology* 1988; **94**: 1383-1389
 - 22 **Meenan J**, Spaans J, Grool TA, Pals ST, Tytgat GNJ, van Deventer SJH. Altered expression of $\alpha 4\beta 7$, a gut homing integrin, by circulating and mucosal T cells in colonic mucosal inflammation. *Gut* 1997; **40**: 241-246
 - 23 **Scott IS**, Sheaff M, Coumbe A, Feakins RM, Rampton DS. Appendiceal inflammation in ulcerative colitis. *Histopathology* 1998; **33**: 168-173
 - 24 **Kroft SH**, Stryker SJ, Rao MS. Appendiceal involvement as a skip lesion in ulcerative colitis. *Mod Pathol* 1994; **7**: 912-914
 - 25 **Haruta J**, Kusugami K, Kuroiwa A, Ina K, Shinoda M, Morise K, Iokawa H, Morita M, Ishihara A, Sarai S. Phenotypic and functional analysis of lamina propria mononuclear cells from colonoscopic biopsy specimens in patients with ulcerative colitis. *Am J Gastroenterol* 1992; **87**: 448-454
 - 26 **Sasakawa T**, Takizawa H, Bannai H, Narisawa R, Asakura H. Activated CD4+ and CD8+ cells in the colonic mucosa of ulcerative colitis patients: their relationship to HLA-DR antigen expression on the colonic epithelium and serum soluble CD25 levels. *Digestion* 1995; **56**: 516-522
 - 27 **Matsumoto T**, Nakamura S, Shimizu M, Iida M. Significance of appendiceal involvement in patients with ulcerative colitis. *Gastrointest Endosc* 2002; **55**: 180-185
 - 28 **Tibble JA**, Sigthorsson G, Bridger S, Fagerhol MK, Bjarnason I. Surrogate marker of intestinal inflammation are predictive of relapse in patients with inflammatory bowel disease. *Gastroenterology* 2000; **119**: 15-22
 - 29 **Bitton A**, Peppercorn MA, Antonioli DA, Niles JL, Shah S, Bousvaros A, Ransil B, Wild G, Cohen A, Edwardes MD, Stevens AC. Clinical, biological, and histologic parameters as predictors of relapse in ulcerative colitis. *Gastroenterology* 2001; **120**: 13-20
 - 30 **Taurog JD**, Richardson JA, Croft JT, Simmons WA, Zhou M, Fernandez-Sueiro JL, Balish E, Hammer RE. The germfree state prevents development of gut and joint inflammatory disease in *HLA-B27* transgenic rats. *J Exp Med* 1994; **180**: 2359-2364
 - 31 **Takahashi I**, Kiyono H, Hamada S. CD4+ T-cell population mediates development of inflammatory bowel disease in T-cell receptor α chain-deficient mice. *Gastroenterology* 1997; **112**: 1876-1886
 - 32 **Mizoguchi A**, Mizoguchi E, Saubermann LJ, Higaki K, Blumberg RS, Bhan AK. Limited CD4 T-cell diversity associated with colitis in T-cell receptor α mutant mice requires a T helper 2 environment. *Gastroenterology* 2000; **119**: 983-995
 - 33 **Probert CS**, Chott A, Turner JR, Saubermann LJ, Stevens AC, Bodinaku K, Elson CO, Balk SP, Blumberg RS. Persistent clonal expansions of peripheral blood CD4+ lymphocytes in chronic inflammatory bowel disease. *J Immunol* 1996; **157**: 3183-3191
 - 34 **Ja"rnerot G**, Andersson M, Franzen L. Laparoscopic appendectomy in patients with refractory ulcerative colitis. *Gastroenterology* 2001; **120**: 1562-1563
 - 35 **Eri RD**, Cross S, Misko I, Rickard M, Lumley J, Stitz R, Stevenson A, Lewindon P, Radford-Smith GL. Appendectomy for refractory ulcerative colitis: targeting the right patient. *Gastroenterology* 2002; **122**: A61
 - 36 **Hallas J**, Gaist D, Vach W, Sorensen HT. Appendectomy has no beneficial effect on admission rates in patients with ulcerative colitis. *Gut* 2004; **53**: 351-354
 - 37 **Hallas J**, Gaist D, Vach W, Sorensen HT. The role of age in the protection of appendectomy against ulcerative colitis: author's reply. *Gut* 2004; **53**: 1719-1720

Ursodeoxycholic acid and superoxide anion

Predrag Ljubuncic, Omar Abu-Salach, Arieh Bomzon

Predrag Ljubuncic, Omar Abu-Salach, Arieh Bomzon, Department of Pharmacology, Ruth and Bruce Rappaport Faculty of Medicine, Technion-Israel Institute of Technology, Haifa, Israel
Correspondence to: Arieh Bomzon, Department of Pharmacology, Ruth and Bruce Rappaport Faculty of Medicine, Technion-Israel Institute of Technology, Efron Street, Po Box 9649, Haifa 31096, Israel. bomzon@tx.technion.ac.il
Telephone: +972-4-8295259 Fax: +972-4-8524978
Received: 2004-12-24 Accepted: 2005-01-13

Abstract

AIM: To investigate the ability of ursodeoxycholic acid (UDCA) to scavenge superoxide anion (O_2^-).

METHODS: We assessed the ability of UDCA to scavenge (O_2^-) generated by xanthine-xanthine oxidase (X-XO) in a cell-free system and its effect on the rate of O_2^- -induced ascorbic acid (AA) oxidation in hepatic post-mitochondrial supernatants.

RESULTS: UDCA at a concentration as high as 1 mmol/L did not impair the ability of the X-XO system to generate O_2^- , but could scavenge O_2^- at concentrations of 0.5 and 1 mmol/L, and decrease the rate of AA oxidation at a concentration of 100 μ mol/L.

CONCLUSION: UDCA can scavenge O_2^- , an action that may be beneficial to patients with primary biliary cirrhosis.

© 2005 The WJG Press and Elsevier Inc. All rights reserved.

Key words: Ursodeoxycholic acid; Superoxide anion; Antioxidant

Ljubuncic P, Abu-Salach O, Bomzon A. Ursodeoxycholic acid and superoxide anion. *World J Gastroenterol* 2005; 11(31): 4875-4878

<http://www.wjgnet.com/1007-9327/11/4875.asp>

INTRODUCTION

Ursodeoxycholic acid (UDCA) is a naturally occurring tertiary dihydroxy hydrophilic bile acid used with considerable success in the treatment of primary biliary cirrhosis (PBC)^[1-5]. Traditional mechanisms whereby UDCA is beneficial to the diseased liver center on its ability to block the deleterious actions and encourage the choleresis of toxic bile acids^[6]. We have reported that UDCA has antioxidant properties. This finding is based on our observation that 100 μ mol/L

UDCA could prevent oxidative activation of cultured macrophages by the pro-oxidant hydrophobic bile acid, deoxycholic acid^[7]. In a follow-up *in vivo* study, we demonstrated that the therapeutic dose of 15 mg/kg UDCA administered for 24 d, suppresses the augmented extent of lipid peroxidation in the diseased liver of bile duct-ligated (BDL) rats, a widely used animal model of cholestatic liver disease^[8]. Accordingly, we proposed the antioxidant action of UDCA could contribute to its beneficial effect in patients with PBC^[7,8]. This proposal was recently confirmed by Serviddio and his colleagues who reported UDCA administered for 28 d minimized oxidative damage in the diseased liver of BDL rats^[9]. Other studies have established that UDCA can augment the biosynthesis of glutathione (GSH) and thiol-containing proteins in hepatocytes^[10,11] and could scavenge the hydroxyl radical (OH) in a cell-free system^[12]. Collectively, these findings have contributed to our current awareness that UDCA is a binary antioxidant possessing direct and indirect antioxidant properties.

Superoxide anion (O_2^-) is a reactive oxygen species (ROS) generated in microsomal and mitochondrial electron transport systems when oxygen is reduced by a single electron. It can also be generated by numerous oxidative enzymes including cytosolic xanthine oxidase (XO) during oxidation of xanthine (X) to uric acid. The generation of O_2^- is important, because its biotransformation can lead to formation of hydrogen peroxide through the activity of superoxide dismutase, generation of OH radical in the presence of transition metals such as Fe^{2+} or formation of the reactive peroxynitrite radical by interacting with nitric oxide. Any intervention reducing or preventing excessive generation of O_2^- would result in decreased production of reactive oxygen and nitroxy species thereby lowering the extent of oxidative stress.

Mitsuyoshi *et al.*^[10], reported that UDCA increases hepatocyte levels of GSH and thiol-containing proteins. In this experiment, they spectrophotometrically measured the rate of oxidation of ascorbic acid (AA) by O_2^- and reported that the difference of absorbance before and after the addition of XO was lower in UDCA-treated hepatocytes than in controls. Since bile acids are enzyme inhibitors^[13,14], the difference in absorbance may be due to UDCA inhibiting the ability of the X-XO system to generate O_2^- . Because Mitsuyoshi *et al.*, did not assess the effect of UDCA on the generation of O_2^- by X-XO system in their investigation, we evaluated the ability of UDCA to scavenge O_2^- generated in the X-XO system and its effect on the activity of XO.

MATERIALS AND METHODS

Chemicals and reagents

All chemicals and reagents of the highest purity were

purchased from the Sigma Chemical Co. (St. Louis, MO, USA), except for UDCA that was purchased as its sodium salt from Megapharm Ltd, the Israeli agent of Calbiochem-Novabiochem Corporation.

Preparation of hepatic post-mitochondrial supernatants

The livers were harvested from healthy rats used as "healthy untreated controls" in institute-approved animal-based investigations. The harvested livers were washed in normal ice-cold saline, weighed and then cut into small pieces using scissors before their homogenization in 100 mmol/L ice-cold phosphate buffer, pH 7.4 at 4 °C with a Potter-Elvehjem glass homogenizer. The crude liver homogenates were centrifuged (1 000 r/min×10 min) at 4 °C. The resultant supernatants were then centrifuged at 10 000 g×10 min at 4 °C to pellet mitochondria and the supernatant was collected. The protein content in the supernatants was determined by the method of Lowry *et al.*^[15].

Analytical procedures

Ability of UDCA to scavenge superoxide anion Using the xanthine-xanthine oxidase (X-XO) reaction to generate $O_2^{\cdot-}$ ^[16], we evaluated the ability of 0.01-1 mmol/L UDCA to scavenge $O_2^{\cdot-}$ by the nitroblue tetrazolium (NBT) reduction assay^[17]. The reaction mixture contained 100 μmol/L Na_2EDTA , 40 μmol/L X, and 40 μmol/L NBT in 10 mmol/L phosphate buffer pH 7.4. The reaction was started by adding 10 mU/mL XO and its rate was continuously monitored spectrophotometrically at A_{560} nm for 15 min at 25 °C in the absence and presence of different concentrations of UDCA. The specificity of the reaction was confirmed by 300 mU/mL superoxide dismutase. The ability of UDCA to scavenge $O_2^{\cdot-}$, as expressed as percentage of inhibition of NBT reduction in UDCA-present samples compared to NBT reduction in UDCA-absent samples. The experiment was repeated between 9 and 11 times at each UDCA concentration.

Effect of UDCA on activity of xanthine oxidase

Compounds interacting with XO could affect the kinetics of reaction of oxidation of xanthine to uric acid^[18]. Accordingly, we assessed the effect of 0.01-1 mmol/L UDCA on XO activity by spectrophotometrically monitoring the rate of uric acid formation at A_{295} nm for 3 min at 25 °C in the absence and presence of UDCA^[19]. The rate of uric acid formation was compared in the absence and presence of UDCA. The specificity of the reaction was confirmed by 100 μg/mL allopurinol. The experiment was repeated nine times at each UDCA concentration.

Effect of UDCA on hepatic antioxidant capacity

The effect of 100 μmol/L UDCA on hepatic antioxidant capacity was determined by monitoring the rate of oxidation of AA by the $O_2^{\cdot-}$ generated by the X-XO according to the original method of Nishikimi^[20] with modifications described by Mitsuyoshi *et al.*^[10]. Liver supernatants were incubated for 120 min at 37 °C in shaking water bath in the absence and presence of 100 μmol/L UDCA. Upon completion of the incubation, the change in the rate of oxidation of AA was monitored in a quartz cuvette containing 1 mL reaction

mixture. The post-mitochondrial liver supernatant contained 100 μmol/L X, 100 μmol/L EDTA, 22 μg/mL catalase, 100 μmol/L AA and 0.1 mol/L phosphate buffer pH 7.4. The assay reaction was commenced by adding 10 mU/mL XO. The reaction was monitored spectrophotometrically at A_{250} nm for 10 min at 25 °C. The differences in absorbance between UDCA-absent and UDCA-added samples were compared. The results were expressed as the reaction rate of AA oxidation (Δ absorbance/mg protein). The experiment was repeated thrice.

Experimental design and statistical analysis

The data were analyzed using a two-tailed *t*-test. The sample size for each experiment was determined by power analysis arbitrarily set between 80-90% in order to detect the effect at the 5% significance level using Statmate™ version 1 (GraphPad Software Inc., San Diego, CA, USA). All figures were prepared using Prism™ version 3.02 (GraphPad Software Inc., San Diego, CA, USA). All data were expressed as mean±SD.

RESULTS

Ability of UDCA to scavenge $O_2^{\cdot-}$ and effect of UDCA on activity of xanthine oxidase

Figure 1A summarizes the experiments to establish whether UDCA could scavenge $O_2^{\cdot-}$ using the NBT reduction assay. UDCA (10 μmol/L and 100 μmol/L) had no effect on NBT reduction (Figures 1 A1 and A2). Higher concentrations of UDCA (500 μmol/L and 1 mmol/L) slowed the rate of NBT reduction by 11% and 16% respectively (Figure 1A3 and A4). In order to eliminate the possibility that UDCA suppressed the rate of conversion of X to uric acid to account for this $O_2^{\cdot-}$ scavenging ability, we also measured the effects of the identical concentrations of UDCA on XO activity. None of the UDCA concentrations affected the rate of formation of uric acid (Figure 1B). Overall, these experiments demonstrated UDCA could scavenge $O_2^{\cdot-}$ without affecting the activity of XO.

Effect of UDCA on rate of oxidation of ascorbic acid

UDCA (100 μmol/L) significantly ($P<0.002$) decreased the rate of AA oxidation (Figure 2).

DISCUSSION

The aim of the present study was to assess the ability of UDCA to scavenge $O_2^{\cdot-}$ and its effects on the activity of XO in a cell-free system and post-mitochondrial supernatants prepared from rat livers. In the cell-free experiments, we used UDCA concentrations not greater than 1 mmol/L in order to avoid the problems when extrapolating data to cell-containing systems in which millimolar concentrations of bile acids solubilize membranes to form micellar poly-aggregates (critical micellar concentration)^[21-23]. On the other hand, we used 100 μmol/L UDCA in the experiments conducted in post-mitochondrial supernatants because this is the concentration used by Mitsuyoshi *et al.*^[10], and that found in the plasma of patients treated with UDCA^[24]. Using NBT reduction in the cell-free X-XO system to evaluate the ability of UDCA to scavenge $O_2^{\cdot-}$, we found UDCA

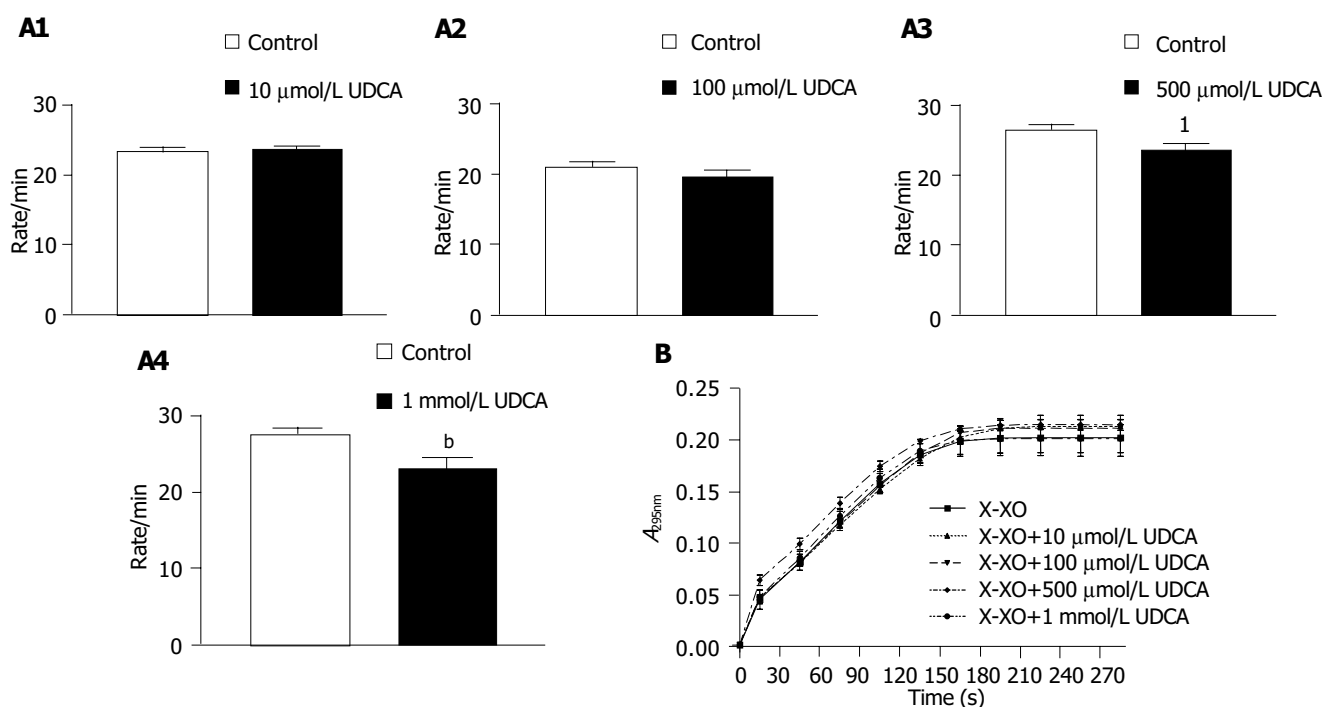


Figure 1 Ability of UDCA to scavenge O_2^- (A) and effect of UDCA on activity

of xanthine oxidase (B) in a cell-free system. ¹ $P < 0.02$, ^b $P < 0.01$ vs control.

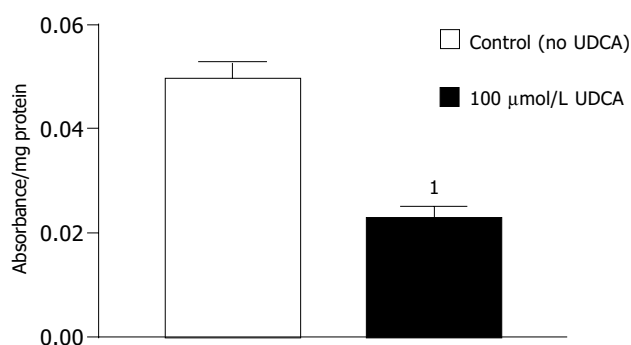


Figure 2 Effect of 100 $\mu\text{mol/L}$ UDCA on rate of oxidation of AA by O_2^- generated by X-XO in post-mitochondrial hepatic supernatants. ¹ $P < 0.002$ vs control.

could scavenge O_2^- at concentrations of 0.5 and 1 mmol/L, respectively. Given the knowledge that bile acids can inhibit enzyme activity^[13,14], we checked the possibility that suppression of the activity of XO accounted for ability of UDCA to scavenge O_2^- . We found that UDCA at concentrations as high as 1 mmol/L did not inhibit the rate of conversion of X to uric acid. After establishing that UDCA could not impair the ability of the X-XO system to generate O_2^- , we then evaluated the effect of 100 $\mu\text{mol/L}$ UDCA on the rate of O_2^- -induced AA oxidation in hepatic post-mitochondrial supernatants. We found that UDCA decreased the rate of AA oxidation. This result agrees with that of Mitsuyoshi *et al.*^[10].

Is the scavenging of O_2^- by UDCA therapeutically relevant? Free-radical-induced peroxidation of phospholipids has been implicated in the pathogenesis of the formation of cholesterol gallstones^[25-27]. In addition, Liu and Hu demonstrated that O_2^- can attack the bilirubin molecule to

generate cytotoxic bilirubin radicals. ROS can also be generated in bile because hydrophobic bile acids are pro-oxidants^[28,29]. It was reported that the concentration of UDCA in bile may reach as high as 29 mmol/L in individuals given 750 mg UDCA daily for 2-3 wk^[30]. In our experiments, UDCA scavenged O_2^- at the concentrations of 0.5 and 1 mmol/L suggesting that the ability of UDCA to scavenge O_2^- may be beneficial in bile.

Lapenna *et al.*^[12], reported that UDCA is an efficient OH^\cdot scavenger. We have confirmed their finding and established the second order rate constant (k_2) for the reaction of UDCA with OH^\cdot in the D-ribose oxidation assay exceeded the rate constants of other OH^\cdot radical scavengers, such as mannitol or dimethylsulfoxide (Ljubuncic, Abu-Salach and Bomzon, *unpublished results*). In conclusion, UDCA is a direct scavenger of superoxide anion and hydroxyl radicals.

REFERENCES

- 1 **Poupon R**, Chretien Y, Poupon RE, Ballet F, Calmus Y, Darnus F. Is ursodeoxycholic acid an effective treatment for primary biliary cirrhosis. *Lancet* 1987; **1**: 834-836
- 2 **Oka H**, Toda G, Ikeda Y. A multi-center double-blind controlled trial of ursodeoxycholic acid for primary biliary cirrhosis. *Gastroenterol Jpn* 1990; **25**: 774-780
- 3 **Heathcote EJ**, Cauch-Dudek K, Walker V, Bailey RJ, Blendis LM, Ghent CN, Michieletti P, Minuk GY, Pappas SC, Scully LJ, Steinbrecher UP, Sutherland LR, Williams CN, Witt-Sullivan H, Worobetz LJ, Milner RA, Wanless IR. The Canadian multicenter double-blind randomized controlled trial of ursodeoxycholic acid in primary biliary cirrhosis. *Hepatology* 1994; **19**: 1149-1156
- 4 **Lindor KD**, Dickson ER, Baldus WP, Jorgensen RA, Ludwig J, Murtaugh PA, Harrison JM, Wiesner RH, Anderson ML, Lange SM, LeSage G, Rossi SS, Hofmann AF. Ursodeoxycholic acid in the treatment of primary biliary cirrhosis. *Gastroenterology* 1994; **106**: 1284-1290
- 5 **Leuschner U**, Güldütüna S, Imhof M, Hubner K, Benjaminov

- A, Leuschner M. Effects of ursodeoxycholic acid after 4 to 12 years of therapy in early and late stages of primary biliary cirrhosis. *J Hepatol* 1994; **21**: 624-633
- 6 **Paumgartner G**, Beuers U. Ursodeoxycholic acid in cholestatic liver disease. mechanisms of action and therapeutic use revisited. *Hepatology* 2002; **36**: 525-531
- 7 **Ljubuncic P**, Fuhrman B, Oiknine J, Aviram M, Bomzon A. Effect of deoxycholic acid and ursodeoxycholic acid on lipid peroxidation in cultured macrophages. *Gut* 1996; **39**: 475-478
- 8 **Ljubuncic P**, Tanne Z, Bomzon A. Ursodeoxycholic acid suppresses extent of lipid peroxidation in diseased liver in experimental cholestatic liver disease. *Dig Dis Sci* 2000; **45**: 1921-1928
- 9 **Serviddio G**, Pereda J, Pallardo FV, Carretero J, Borrás C, Cutrin J, Vendemiale G, Poli G, Vina J, Sastre J. Ursodeoxycholic acid protects against secondary biliary cirrhosis in rats by preventing mitochondrial oxidative stress. *Hepatology* 2004; **39**: 711-720
- 10 **Mitsuyoshi H**, Nakashima T, Sumida Y, Yoh T, Nakajima Y, Ishikawa H, Inaba K, Sakamoto Y, Okanoue T, Kashima K. Ursodeoxycholic acid protects hepatocytes against oxidative injury via induction of antioxidants. *Biochem Biophys Res Comm* 1999; **263**: 537-542
- 11 **Rodriguez-Ortigosa CM**, Cincu RN, Sanz S, Ruiz F, Quiroga J, Prieto J. Effect of ursodeoxycholic acid on methionine adenosyltransferase activity and hepatic glutathione metabolism in rats. *Gut* 2002; **50**: 701-706
- 12 **Lapenna D**, Ciofani G, Festi D, Neri M, Pierdomenico SD, Giamberardino MA, Cucurullo F. Antioxidant properties of ursodeoxycholic acid. *Biochem Pharmacol* 2002; **64**: 1661-1667
- 13 **Parkinson TM**, Olson JA. Inhibitory effects of bile acids on adenosine triphosphatase, oxygen consumption, and the transport and diffusion of water soluble substances in the small intestine of the rat. *Life Sci* 1964; **3**: 107-112
- 14 **Krahenbuhl S**, Stucki J, Reichen J. Reduced activity of the electron transport chain in liver mitochondria isolated from rats with secondary biliary cirrhosis. *Hepatology* 1992; **15**: 1160-1166
- 15 **Lowry OH**, Rosebrough NJ, Farr AL, Randall RJ. Protein measurement with the Folin phenol reagent. *J Biol Chem* 1951; **193**: 265-275
- 16 **McCord JM**, Fridovich I. The reduction of cytochrome c by milk xanthine oxidase. *J Biol Chem* 1968; **243**: 5753-5760
- 17 **Aruoma OI**, Halliwell B, Hoey BM, Butler J. The antioxidant action of N-acetylcysteine: its reaction with hydrogen peroxide, hydroxyl radical, superoxide, and hypochlorous acid. *Free Radic Biol Med* 1989; **6**: 593-597
- 18 **Fridovich I**. Quantitative aspects of the production of superoxide anion radical by milk xanthine oxidase. *J Biol Chem* 1970; **245**: 4053-4057
- 19 **Marcocci L**, Suzuki YJ, Tsuchiya M, Packer L. Antioxidant activity of nitecapone and its analog OR-1246: effect of structural modification on antioxidant action. *Methods Enzymol* 1994; **234**: 525-541
- 20 **Nishikimi M**. Oxidation of ascorbic acid with superoxide anion generated by the xanthine-xanthine oxidase system. *Biochem Biophys Res Comm* 1975; **63**: 463-468
- 21 **Heaton KW**. The importance of keeping bile salts in their place. *Gut* 1969; **10**: 857-863
- 22 **Heuman DM**. Quantitative estimation of the hydrophilic-hydrophobic balance of mixed bile salt solutions. *J Lipid Res* 1989; **30**: 719-730
- 23 **Roda A**, Minutello A, Angellotti MA, Fini A. Bile acid structure-activity relationship: evaluation of bile acid lipophilicity using 1-octanol/water partition coefficient and reverse phase HPLC. *J Lipid Res* 1990; **31**: 1433-1444
- 24 **Stiehl A**, Rudolph G, Raedsch R, Moller B, Hopf U, Lotterer E, Bircher J, Folsch U, Klaus J, Endeke R, Senn M. Ursodeoxycholic acid-induced changes of plasma and urinary bile acids in patients with primary biliary cirrhosis. *Hepatology* 1990; **12**: 492-497
- 25 **Lichtenberg D**, Ragimova S, Peled Y, Halpern Z. Phospholipid peroxidation as a factor in gallstone pathogenesis. *FEBS Lett* 1988; **228**: 179-181
- 26 **Eder MI**, Miquel JF, Jungst D, Paumgartner G, Von Ritter C. Reactive oxygen metabolites promote cholesterol crystal formation in model bile: Role of lipid peroxidation. *Free Radic Biol Med* 1996; **20**: 743-749
- 27 **Leo MA**, Aleynik SI, Siegel JH, Kasmin FE, Aleynik MK, Lieber CS. F₂-isoprostane and 4-hydroxynonenal excretion in human bile of patients with biliary tract and pancreatic disorders. *Am J Gastroenterol* 1997; **92**: 2069-2072
- 28 **Sokol RJ**, Devereaux M, Khandwala R, O'Brien K. Evidence for involvement of oxygen free radicals in bile acid toxicity to isolated rat hepatocytes. *Hepatology* 1993; **17**: 869-881
- 29 **Sokol RJ**, Winkhofer-Roob BM, Devereaux MW, McKim JM. Generation of hydroperoxides in isolated rat hepatocytes and hepatic mitochondria exposed to hydrophobic bile acids. *Gastroenterology* 1995; **109**: 1249-1256
- 30 **Fischer S**, Neubrand M, Paumgartner G. Biotransformation of orally administered ursodeoxycholic acid in man as observed in gallbladder bile, serum and urine. *Eur J Clin Invest* 1993; **23**: 28-36

• BRIEF REPORTS •

HBeAg negative serological status and low viral replication levels characterize chronic hepatitis B virus-infected women at reproductive age in Greece: A one-year prospective single center study

Ioannis S. Elefsiniotis, Irene Glynou, Ioanna Magaziotou, Konstantinos D. Pantazis, Nikolaos V. Fotos, Hero Brokalaki, Helen Kada, George Saroglou

Ioannis S. Elefsiniotis, Konstantinos D. Pantazis, Nikolaos V. Fotos, Hero Brokalaki, George Saroglou, Department of Internal Medicine, Faculty of Nursing, University of Athens, Maternal Hospital 'Helena Venizelou', Athens, Greece
Irene Glynou, Helen Kada, Department of Microbiology, Maternal Hospital 'Helena Venizelou', Athens, Greece
Ioanna Magaziotou, Department of Neonatology, Maternal Hospital 'Helena Venizelou', Athens, Greece
Correspondence to: Ioannis S. Elefsiniotis, MD, Carchidonos 9, A. Glyfada GR-16562, Greece. ielefs@acn.gr
Telephone: +30-210-9630312 Fax: +30-210-7787807
Received: 2005-01-15 Accepted: 2005-01-26

that only a small proportion of HBsAg(+) women in Greece exhibit a high risk for vertical transmission of the infection.

© 2005 The WJG Press and Elsevier Inc. All rights reserved.

Key words: Hepatitis B; Reproductive age; Vertical transmission; HBeAg; HBV-DNA

Elefsiniotis IS, Glynou I, Magaziotou I, Pantazis KD, Fotos NV, Brokalaki H, Kada H, Saroglou G. HBeAg negative serological status and low viral replication levels characterize chronic hepatitis B virus-infected women at reproductive age in Greece: A one-year prospective single center study. *World J Gastroenterol* 2005; 11(31): 4879-4882
<http://www.wjgnet.com/1007-9327/11/4879.asp>

Abstract

AIM: To evaluate the seroprevalence of hepatitis B surface antigen (HBsAg) in 13 581 women at reproductive age and the hepatitis B e antigen (HBeAg)/anti-HBe status as well as serum hepatitis B virus (HBV)-DNA levels in a subgroup of HBsAg(+) pregnant women at labor in Greece.

METHODS: Serological markers were detected using enzyme immunoassays. Serum HBV-DNA was determined by a sensitive quantitative PCR assay. Statistical analysis of data was based on parametric methodology.

RESULTS: Overall, 1.156% of women were HBsAg(+) and the majority of them (71.3%) were Albanian. The prevalence of HBsAg was 5.1% in Albanian women, 4.2% in Asian women and 1.14% in women from Eastern European countries. The prevalence of HBsAg in African (0.36%) and Greek women (0.29%) was very low. Only 4.45% of HBsAg(+) women were also HBeAg(+) whereas the vast majority of them were HBeAg(-)/anti-HBe(+). Undetectable levels of viremia (<200 copies/mL) were observed in 32.26% of pregnant women at labor and 29.03% exhibited extremely low levels of viral replication (<400 copies/mL). Only two pregnant women exhibited extremely high serum HBV-DNA levels (>10 000 000 copies/mL), whereas 32.26% exhibited HBV-DNA levels between 1 500 and 40 000 copies/mL.

CONCLUSION: The overall prevalence of HBsAg is relatively low among women at reproductive age in Greece but is higher enough among specific populations. The HBeAg(-)/anti-HBe(+) serological status and the extremely low or even undetectable viral replicative status in the majority of HBsAg(+) women of our study population, suggest

INTRODUCTION

Worldwide, about 350 million people are chronically infected with hepatitis B virus (HBV)^[1]. Vertical transmission of the infection occurs usually in peri-natal period and is the major cause of HBV transmission in endemic countries of the world. Mother to infant transmission represents a basic factor in maintaining chronic HBV infection and usually depends on the degree of maternal infectivity, especially in peri-natal period^[2]. Vertical transmission of the infection is mainly seen in infants born from hepatitis B e antigen (HBeAg)(+) mothers with very high levels of viremia and maternal serum HBV-DNA levels are positively associated with immunoprophylaxis failure^[2,3].

Hepatitis B has long been a serious public health problem in Greece. Historically, Greece has had the highest burden of HBV infection in the European Union and unfortunately a hepatitis B prevention program aimed at high-risk groups in 1982, had little impact on disease incidence or prevalence^[4]. In recent years, HBV vaccination programs, demographic and socio-economic changes, medical precautions and screening of blood donors have resulted in a significant decline in chronic HBV infection in our country^[4,5]. However, the entrance of a great number of refugees, especially from endemic countries of HBV infection in the last decade, has possibly led to alteration of the epidemiological data, so these data have to be re-evaluated.

In our study we examined the seroprevalence of hepatitis B surface antigen (HBsAg) in a large multinational group of women at reproductive age and evaluated the presence

of HBeAg, antibody to HBeAg (anti-HBeAg) as well as antibody to hepatitis C virus (anti-HCV) in HBsAg(+) individuals. Moreover we measured the serum HBV-DNA levels in a subgroup of HBsAg(+)/anti-HCV(-) pregnant women at labor, in order to gain information about maternal viral load at this important period, a factor positively correlated with vertical transmission of the infection.

MATERIALS AND METHODS

Between August 2003 and August 2004, a total of 13 581 women at reproductive age (range 16-45 years) were prospectively evaluated at the Department of Obstetrics and Gynecology of the Maternal Hospital 'Helena Venizelou' of Athens, Greece. HBsAg, HBeAg, anti-HBeAg, and antibody to hepatitis B core antigen (anti-HBcAg) as well as anti-HCV were detected by routine commercially available enzyme immunoassays (Abbott Laboratories, Abbott Park, IL, USA). All women of the study were screened for HBsAg whereas the rest of the serological markers were evaluated only in HBsAg(+) ones. Antibody to hepatitis D virus (anti-HDV) and antibody to HIV (anti-HIV) were not detected. Serum HBV-DNA was determined by a sensitive, commercially available quantitative PCR assay (COBAS-Amplificor HBV Monitor, Version 2, Roche, Basel, Switzerland), with a lower limit of quantification of 200 copies/mL in a subgroup of HBsAg(+)/anti-HCV(-) pregnant women of the study population, with available serum samples, at labor.

Statistical analysis of data was based on parametric methodology. Student's *t*-test and χ^2 test were used. $P < 0.05$ was statistically significant. The study was reviewed and approved by the local ethics committee. The study protocol conforms to the ethical guidelines of the Declaration of Helsinki.

RESULTS

The majority of the study population came from Greece (70.31%) whereas 15.96% came from Albania, 7.06% from Eastern European countries (Russia, Romania, and Bulgaria), 4.09% from African countries, 0.69% from Asian countries, 0.99% from countries of Northwestern Europe, 0.46% from Australia and 0.43% from North American countries. Overall, 157 of 13 581 females (1.156%) were HBsAg(+) and the vast majority of them (112/157, 71.3%) were Albanian. The participation of each national group in HBsAg(+) cases of the study population is presented in Figure 1. None of the females from countries of North America, Northwestern Europe, and Australia (countries of low prevalence of HBV infection) was HBsAg(+).

The seroprevalence of HBsAg was 5.1% in women from Albania, representing the higher seroprevalence rate among the national groups of the study population, followed by 4.2% in Asian women and 1.14% in women from Eastern European countries. The seroprevalence of HBsAg in African (0.36%) and Greek women (0.29%) was very low, compared to the mean seroprevalence rate of the study population ($P < 0.05$). Overall, only 4.45% of HBsAg(+) women were also HBeAg(+) whereas the vast majority of them were HBeAg(-)/anti-HBeAg(+). HBeAg(+) cases represented 10.7% and 3.6% of Greek and Albanian HBsAg

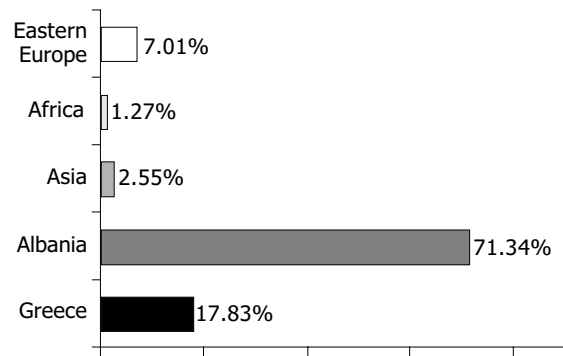


Figure 1 Participation of each national group in HBsAg(+) cases of the study population.

(+) women respectively, whereas 92.9% of Greek and Albanian HBsAg(+) women, 90.9% of Eastern European countries HBsAg(+) women and all Asian/African HBsAg(+) women were HBeAg(-)/anti-HBeAg(+). Only 3 of 157 women (1.91%) with chronic HBV infection were HBV/HCV coinfecting.

Serum HBV-DNA was quantified in 31 HBsAg(+)/anti-HCV(-) pregnant women of our study population with available serum samples at labor. Only one of them was HBeAg(+) whereas the vast majority of them were HBeAg(-)/anti-HBeAg(+), as it was the majority of HBsAg(+) cases of the study population. Twenty-two of them were Albanian (22/31, 70.96%), six of them (6/31, 19.35%) were Greek and the rest three were from an Eastern European, an Asian and an African country, respectively. Undetectable levels of serum HBV-DNA (<200 copies/mL) were observed in 10 of 31 (32.26%) pregnant women at labor and 9 of 31 (29.03%) pregnant women exhibited extremely low levels of viral replication (lower than 400 copies/mL) during this important period. Only two, one HBeAg(-) and one HBeAg(+), of 31 pregnant women (6.45%) evaluated for HBV viral load, exhibited extremely high serum HBV-DNA levels (19 800 000 and 85 500 000 copies/mL, respectively) whereas the rest of the 10 women evaluated (32.26%) exhibited HBV-DNA levels between 1 500 and 40 000 copies/mL. Serum HBV-DNA levels in this subgroup of our study population are presented in Figure 2. As we can see from this figure, the majority (61.29%) of chronic HBV-infected pregnant women evaluated for serum HBV-DNA levels at labor by a very sensitive PCR assay, exhibited undetectable (<200 copies/mL) or extremely low (<400 copies/mL) levels.

DISCUSSION

Epidemiological data on the prevalence of serological markers of HBV infection in women at reproductive age in Greece are limited. It is estimated from previous studies that in Greece, the HBsAg carrier rate in pregnant women is 2.8-3.0%^[6]. In our study we found that the mean prevalence of HBsAg in 13 581 women at reproductive age from multinational origin, was relatively low (1.156%) and the vast majority of HBsAg-positive women (71.3%) came from Albania, representing the 5.1% of the Albanian women of the study population.

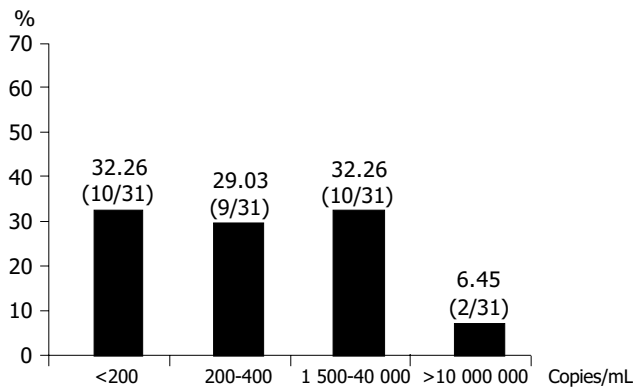


Figure 2 Serum HBV-DNA levels in 31 HBsAg(+)/anti-HCV(-) pregnant women at labor.

Although the seroprevalence rate of HBsAg in Albanian (5.1%) and Asian (4.2%) women was significantly higher than in Greek women (0.29%, $P < 0.001$), which was significantly lower than the mean rate of the study population (1.156%, $P < 0.05$), suggesting that there is a significant decline in seroprevalence of HBsAg in the refugees living in Greece in the last decade. In 1995 Malamitsi-Puchner *et al.*^[7], reported that 13.4% of 500 Albanian pregnant women evaluated in a Greek Maternal Hospital are HBsAg(+) and 7.5% of them are also HBeAg(+), representing an endemic and highly infective group of HBV infection. Significant socio-economic changes, specific precautions due to the knowledge of the modes of transmission of the infection and HBV vaccination programs may have possibly led to this decline observed nowadays in these specific populations.

Maternal HBeAg-positivity in peri-natal period is of great importance for the vertical transmission of HBV infection resulting in extremely higher rates of mother to infant transmission compared to infant born from HBeAg(-) mothers^[2,3,8]. In our study, the vast majority (>90%) of HBsAg(+) women were HBeAg(-)/anti-HBeAg(+), resulting possibly in the low rates of peri-natal transmission of HBV infection and passive/active immunoprophylaxis failure observed in our country, a finding that needs further investigation. Moreover, maternal serum HBV-DNA at labor was undetectable or extremely low in the majority of pregnant women of the study population evaluated, by a sensitive PCR assay. The predominance of HBeAg(-)/anti-HBeAg(+) serological status in combination with the low levels of viremia observed in the majority of chronic HBV-infected women of our study population, suggests that chronic HBV-infected women at reproductive age in Greece represent a group of low infectivity, resulting possibly in low vertical transmission and passive/active immunoprophylaxis failure rates.

Intra-uterine/transplacental transmission of HBV infection in infants born from HBsAg(+) mothers observed in endemic countries is positively correlated to HBeAg(+) maternal serological status and high levels of maternal serum HBV-DNA. It is believed that transplacental transmission of HBV infection is a major cause of immunoprophylaxis failure and this mode of transmission can be effectively

reduced by administration of hepatitis B immune globulin (HBIG) or lamivudine in the third trimester of HBsAg(+) pregnant women^[9]. It seems that this problem is not of clinical significance in our country, because of the relatively low seroprevalence rates of HBsAg observed in our study population, and the serological and virological data of chronic HBV-infected women at reproductive age in Greece, as previously noted.

In Greece, both active (HBV vaccine) and passive (HBIG) immunoprophylaxis are the current clinical practice in newborns from HBsAg(+) mothers, irrespective of maternal serological (HBeAg(+) or HBeAg(-)) and/or virological status. Studies from hyper-endemic countries of HBV infection suggest that there is no clear benefit of passive-active *vs* active immunization alone for chronic HBV infection in infants born from HBsAg(+)/HBeAg(-) mothers^[10]. The estimated efficacy of HBV vaccination alone without HBIG is 84% in infants born from HBeAg(+) mothers and 100% in those born from HBeAg(-) ones, according to a study from endemic Vietnam^[11]. The high cost of HBIG and the serological and virological data of women at reproductive age in our study, may suggest that passive-active immunoprophylaxis of infants born from chronic HBV-infected mothers in our country, possibly represents an over-protection strategy, at least in a significant proportion of them, especially from HBeAg(-)/anti-HBeAg(+) mothers with HBV-DNA <400 copies/mL at labor. This possibility needs further investigation in large-scale clinical trials. Moreover, more than one third (38.7%) of HBsAg(+)/anti-HBeAg(+) women of our study population exhibited active viral replication at labor and some of them exhibited extremely high viral load levels, representing possibly an infection with a mutant HBV variant (precore mutant), a finding that needs further investigation.

In conclusion, the overall seroprevalence rate of HBsAg is relatively low in women at reproductive age in Greece but is rather higher in specific populations (Albanian, Asian) who need screening, vaccination, and immunoprophylaxis programs in order to decline further the rates of peri-natally acquired HBV infection. The HBeAg(-)/anti-HBeAg(+) serological status and the extremely low or even undetectable viral replicative status in the majority of HBsAg(+) women suggest that only a small proportion of HBsAg(+) women in Greece exhibit an extremely high risk for vertical transmission of the infection.

REFERENCES

- 1 The World Health Report. WHO 1998
- 2 Soderstrom A, Norkrans G, Lindh M. Hepatitis B virus DNA during pregnancy and post partum: aspects on vertical transmission. *Scand J Infect Dis* 2003; **35**: 814-819
- 3 Wang Z, Zhang J, Yang H, Li X, Wen S, Guo Y, Sun J, Hou J. Quantitative analysis of HBV DNA level and HBeAg titer in hepatitis B surface antigen positive mothers and their babies: HBeAg passage through the placenta and the rate of decay in babies. *J Med Virol* 2003; **71**: 360-366
- 4 Papaevangelou G. Hepatitis B immunization programme: lessons learnt in Greece. *Vaccine* 1998; **16** (Suppl): S45-S47
- 5 Stamouli M, Gizaris V, Totos G, Papaevangelou G. Decline of hepatitis B infection in Greece. *European J Epidemiol* 1999; **15**: 447-449

- 6 **Papaevangelou G**, Farmaki G, Kada H. Hepatitis B maternal-fetal transmission in Southern Europe. *Intervirology* 1998; **41**: 197-200
- 7 **Malamitsi-Puchner A**, Papacharitonos S, Sotos D, Tzala L, Psychogiou M, Hatzakis A, Evangelopoulou A, Michalas S. Prevalence study of different hepatitis markers among pregnant Albanian refugees in Greece. *Eur J Epidemiol* 1996; **12**: 297-301
- 8 **Stevens CE**, Neurath RA, Beasley RP, Szmuness W. HBeAg and anti-HBs detection by radioimmunoassay: correlation with vertical transmission of hepatitis B virus in Taiwan. *J Med Virol* 1979; **3**: 237-241
- 9 **van Zonneveld M**, van Nunen AB, Niesters HG, de Man RA, Schalm SW, Janssen HL. Lamivudine treatment during pregnancy to prevent perinatal transmission of hepatitis B virus infection. *J Viral Hepat* 2003; **10**: 294-297
- 10 **Yang YJ**, Liu CC, Chen TJ, Lee MF, Chen SH, Shih HH, Chang MH. Role of hepatitis B immunoglobulin in infants born to hepatitis B e antigen-negative carrier mothers in Taiwan. *Pediatr Infect Dis J* 2003; **22**: 584-588
- 11 **Milne A**, West DJ, Chinh DV, Moyes CD, Poerschke G. Field evaluation of the efficacy and immunogenicity of recombinant hepatitis B vaccine without HBIG in newborn Vietnamese infants. *J Med Virol* 2002; **67**: 327-333

Science Editor Wang XL and Guo SY **Language Editor** Elsevier HK

α -Lipoic acid protects against cholecystokinin-induced acute pancreatitis in rats

Sung-Joo Park, Sang-Wan Seo, Ok-Sun Choi, Cheung-Seog Park

Sung-Joo Park, Sang-Wan Seo, Department of Pharmacology, College of Oriental Medicine, Kyung Hee University #1 Hoegi-dong, Dongdaemun-gu, Seoul 130-701, South Korea

Ok-Sun Choi, Cheung-Seog Park, Department of Microbiology, College of Medicine, Kyung Hee University #1 Hoegi-dong, Dongdaemun-gu, Seoul 130-701, South Korea

Supported by the Next Generation Growth Engine Program grant from the Ministry of Science and Technology (2004-00075), South Korea

Correspondence to: Dr. Cheung-Seog Park, Department of Microbiology, College of Medicine, Kyung Hee University #1 Hoegi-dong, Dongdaemun-gu, Seoul 130-701, South Korea

Telephone: +82-2-961-0294 Fax: +82-2-962-6189

Received: 2005-01-11 Accepted: 2005-01-26

Abstract

AIM: α -Lipoic acid (ALA) has been used as an antioxidant. The aim of this study was to investigate the effect of α -lipoic acid on cholecystokinin (CCK)-octapeptide induced acute pancreatitis in rats.

METHODS: ALA at 1 mg/kg was intra-peritoneally injected, followed by 75 μ g/kg CCK-octapeptide injected thrice subcutaneously after 1, 3, and 5 h. This whole procedure was repeated for 5 d. We checked the pancreatic weight/body weight ratio, the secretion of pro-inflammatory cytokines and the levels of lipase, amylase of serum. Repeated CCK octapeptide treatment resulted in typical laboratory and morphological changes of experimentally induced pancreatitis.

RESULTS: ALA significantly decreased the pancreatic weight/body weight ratio and serum amylase and lipase in CCK octapeptide-induced acute pancreatitis. However, the secretion of IL-1 β , IL-6, and TNF- α were comparable in CCK octapeptide-induced acute pancreatitis.

CONCLUSION: ALA may have a protective effect against CCK octapeptide-induced acute pancreatitis.

© 2005 The WJG Press and Elsevier Inc. All rights reserved.

Key words: α -Lipoic acid; Acute pancreatitis; Proinflammatory cytokines; Cholecystokinin

Park SJ, Seo SW, Choi OS, Park CS. α -Lipoic acid protects against cholecystokinin-induced acute pancreatitis in rats. *World J Gastroenterol* 2005; 11(31): 4883-4885
<http://www.wjgnet.com/1007-9327/11/4883.asp>

INTRODUCTION

Acute pancreatitis (AP) is a clinical entity that is believed to have intracellular activation of digestive enzymes and autodigestion of the pancreas as its central patho-physiologic cause. This non-infectious destruction of pancreatic parenchyma quickly induces an inflammatory reaction at the site of injury. AP usually occurs as a result of alcohol abuse. Histologically, acute pancreatitis is characterized by interstitial edema, vacuolization, inflammation and acinar cell necrosis^[1,2]. The diagnosis of acute pancreatitis is usually based on pancreatic edema index (pancreatic weight/ body weight), pancreatic serum enzymes (e.g. pancreatic amylase, lipase, immunoreactive trypsin or elastase) at animal models^[3,4].

Cytokines are important immunoregulatory mediators. Their contribution to the pathogenesis of acute and chronic gastroenterological disorders is obvious. Increased expression of interleukin-1 (IL-1), interleukin-6 (IL-6), tumor necrosis factor (TNF)- α can be detected in AP. These cytokines are involved in the pathogenesis of pancreatitis-associated multiple organ dysfunction.

Among the neurohormonal regulators, Cholecystokinin (CCK) is well known gastrointestinal hormone and neural agonist for inducing the release of pancreatic digestive enzymes. At supra-maximal doses (dose greater than those that cause maximal secretion of digestion enzyme by the pancreatic acinar cell) CCK are able to cause the pancreatic responses^[5,6].

Oxidative stress has been shown to be involved in the pathophysiology of AP^[7,8]. α -Lipoic acid (ALA) is a thiol antioxidant compound with demonstrated direct free-radical scavenging properties^[9,10]. However, the effects of ALA on AP have not yet been investigated. Therefore, in this study, we investigated whether ALA can ameliorate the severity of AP using CCK-octapeptide induced AP system.

MATERIALS AND METHODS

Animals

Male Wistar rats weighing 240-260 g were used. The animals were kept at a constant room temperature of 25 °C with a 12 h light-dark cycle, and allowed free access to water and standard laboratory chow. The rats were fasted for 16 h before the induction of AP. In each experimental group five rats were used.

Reagents

Avidin-peroxidase and 2'-AZINO-bis (3-ethylbenzothiazoline 6-sulfonic acid) tablet substrate were purchased from Sigma (St. Louis, MO, USA). Anti-rat TNF- α , IL-1 β and IL-6 antibodies

was purchased from R&D Systems (Minneapolis, MN, USA).

CCK-induced acute pancreatitis

ALA at 1 mg/kg was intraperitoneally injected, followed by CCK injected subcutaneously at 75 μ g/kg thrice after 1, 3, and 5 h. This whole procedure was repeated for 5 d ($n = 5$). Other rodents ($n = 5$) received saline as control. The animals were killed by exanginations through the abdominal aorta 12 h, after the last CCK injection. The pancreas was quickly removed, cleaned from fat and lymph nodes, weighed, and frozen at -70°C until use. Rats were treated in accordance with the current law and NIH Guide for Care and Use of Laboratory Animals.

Pancreatic weight/body weight ratio

This ratio (pancreatic weight g/body weight g $\times 1000$) was utilized to evaluate the degree of pancreatic edema.

Enzyme-linked immunosorbent assay (ELISA)

ELISA for IL-6 and TNF- α was carried out in duplicate in 96-well plates (Nunc, Denmark) coated with each of 100 μ L aliquots of anti-rat IL-6, IL-1 β and TNF- α mAb at 1.0 μ g/mL in PBS at pH 7.4 and was incubated overnight at 4°C . The plates were washed in PBS containing 0.05% Tween-20 (Sigma, St. Louis, MO, USA) and blocked with PBS containing 1% BSA, 5% sucrose and 0.05% NaN₃ for 1 h. After additional washes, standards were added and incubated at 37°C for 2 h. After 2 h incubation at 37°C , the wells were washed and then each of 0.2 μ g/mL of biotinylated anti-rat IL-6, IL-1 β , and TNF- α were added and again incubated at 37°C for 2 h. After the wells were washed, avidin-peroxidase was added and plates were incubated for 20 min at 37°C . Wells were again washed and ABTS substrate was added. Color development was measured at 405 nm using an automated microplate ELISA reader. A standard curve was run on each assay plate using recombinant IL-6, IL-1 β and TNF- α in serial dilutions.

Measures of serum amylase and lipase

Serum amylase was measured by using an ADIVA 1650 (BAYER, USA). Serum lipase was measured by using a Cobas-mira (Roche, USA).

Statistical analysis

Results are expressed as mean \pm SE. The significance of changes was evaluated using Student's t -test. Differences between the experimental groups were evaluated by using analysis of variance. Values of $P < 0.05$ were accepted as significant.

RESULTS

Effect of ALA on pancreatic weight/body weight ratio

To assess the effect of ALA on the pancreatic weight/body weight ratio, pancreatic weight was divided by the body weight of the rats. As shown in Figure 1, in ALA treated group, pancreatic weight/body weight ratio (3.676 ± 0.63) was significantly decreased compared to the DMSO treated group (6.46 ± 0.66 , $P < 0.05$, Figure 1).

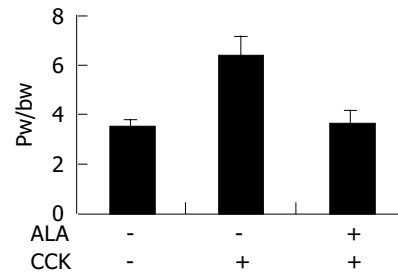


Figure 1 Effect of ALA on the pancreatic weight/body weight ratio (pw/bw) in CCK-induced AP. Groups were treated as indicated in the Materials and method. mean \pm SE for 5 animals are shown. Significant difference ($P < 0.05$) vs the saline treated group.

Effect of ALA on IL-6, IL-1 β , and TNF- α secretion in CCK-induced AP

Secretion of pro-inflammatory cytokines to serum were increased during CCK-induced AP. Then, we investigated whether ALA reduces the serum levels of pro-inflammatory cytokines such as TNF- α , IL-1 β , and IL-6. ALA pre-treatment did not change the level of IL-1 β , IL-6 and TNF- α production during CCK-induced AP (Table 1).

Table 1 Effects of ALA on IL-1 β , IL-6, and TNF- α secretion in CCK-induced AP (mean \pm SE)

Treatment		IL-1 β	IL-6	TNF- α
CCK	ALA		(pg/mL)	
-	-	165.0 ± 26	61 ± 3	140 ± 51
+	-	334.7 ± 15	85 ± 4	289 ± 9
+	+	334.7 ± 14	83 ± 5	238 ± 25

Effect of ALA on serum amylase and lipase activity in CCK-induced AP

The levels of serum amylase and lipase are commonly used as a marker of AP. Pre-treatment of ALA significantly decreased the serum amylase and lipase activity CCK-induced AP (Figure 2).

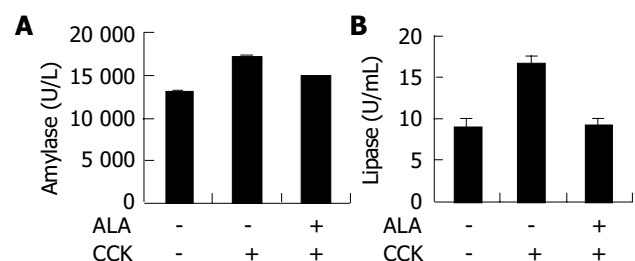


Figure 2 ALA inhibits hyperlipasemia on CCK-induced pancreatitis in rats. **A** and **B**: serum amylase and lipase levels in control rats and with pancreatitis induced by CCK. CCK was applied as described in the Materials and method. Values are mean \pm SE from at least five animals for each group. In lipase measurement, values for animals with AP receiving ALA were significantly lower than for those without ALA $P < 0.05$.

DISCUSSION

Our findings showed that ALA reduced CCK-induced AP. Furthermore, we showed that pancreatic weight/body

weight ratio and serum amylase and lipase were not correlated with the level of cytokines in the rat model. Many previous reports have suggested that ROS may play an important role in the initiation and development of pancreatitis^[11,12]. Anti-oxidant, N-acetyl cysteine (NAC) reduced the severity of AP^[13,14]. ALA is also a potent anti-oxidant and has anti-inflammatory effect^[9,10]. Therefore, in this study, we investigated the effects of ALA on CCK-induced AP. ALA decreased pancreatic weight/body weight ratio in CCK-induced AP. The levels of amylase and lipase usually rise after the onset of symptoms of acute pancreatitis. Compared with serum amylase, serum lipase rises slightly later and remains elevated longer^[15]. We found ALA decreased serum level of amylase, lipase in CCK-induced AP (Figure 2). Furthermore, we also examined several kinds of cytokines. IL-1 β , IL-6, and TNF- α levels are not attenuated by ALA after CCK treatment (Table 1). Recent study suggest that COX (Cyclooxygenase)-2 inhibition by selective inhibitor (SC-58125), induced alteration of serum amylase and lipase level but not IL-6 and IL-1 production on Caerulein (CAE) induced AP^[16]. In the previous report, ALA markedly inhibited radiation or H₂O₂-induced COX-2 upregulation^[17]. On the basis of this report, ALA maybe ameliorates AP via COX-2 inhibition. However, it is needed to investigate its mechanism whether inhibition of COX-2 is involve in the ALA-mediated decrease of AP. Despite of previous studies which link between IL-6 levels and increased severity of AP, recent studies suggest that IL-6 may have an anti-inflammatory role during pancreatitis^[18]. IL-6 KO mice exhibited a more severe pancreatitis after CAE injections than wild type mice^[18]. Our results indicate that pro-inflammatory cytokine levels are elevated in mice treated with or without ALA despite attenuated pancreatitis. This finding suggests that the stimulus for pro-inflammatory cytokines secretion remains intact; however, it is still unclear whether pro-inflammatory cytokines are mechanistically linked to the amelioration of pancreatitis.

In conclusion, this study showed that ALA pr-treatment ameliorated the severity of CCK induced pancreatitis in rats.

REFERENCES

- 1 **Baron TH**, Morgan DE. Acute necrotizing pancreatitis. *N Engl J Med* 1999; **340**: 1412-1417
- 2 **Berger HG**, Rau B, Mayer J, Pralle U. Natural course of acute pancreatitis. *World J surg* 1997; **21**: 130-135
- 3 **Koehler DF**, Eckfeldt JH, Levitt MD. Diagnostic value of routine isoamylase assay of hyperamylasemic serum. *Gastroenterology* 1982; **82**(5 Pt 1): 887-890
- 4 **Smotkin J**, Tenner S. Laboratory diagnostic tests in acute pancreatitis. *J Clin Gastroenterol* 2002; **34**: 459-462
- 5 **Beglinger C**. Potential role of cholecystokinin in the development of acute pancreatitis. *Digestion* 1999; **60**(Suppl 1): 61-63
- 6 **Tachibana I**, Shirohara H, Czako L, Akiyama T, Nakano S, Watanabe N, Hirohata Y, Otsuki M. Role of endogenous cholecystokinin and cholecystokinin-A receptors in the development of acute pancreatitis in rats. *Pancreas* 1997; **14**: 113-121
- 7 **Rau B**, Poch B, Gansauge F, Bauer A, Nussler AK, Nevalainen T, Schoenberg MH, Beger HG. Pathophysiologic role of oxygen free radicals in acute pancreatitis: initiating event or mediator of tissue damage? *Ann Surg* 2000; **231**: 352-360
- 8 **Weber CK**, Adler G. From acinar cell damage to systemic inflammatory response: current concepts in pancreatitis. *Pancreatology* 2001; **1**: 356-362
- 9 **Park KG**, Kim MJ, Kim HS, Lee SJ, Song DK, Lee IK. Prevention and treatment of macroangiopathy: focusing on oxidative stress. *Diabetes Res Clin Pract* 2004; **66**(Suppl 1): S57-62
- 10 **Atmaca G**. Antioxidant effects of sulfur-containing amino acids. *Yonsei Med J* 2004; **45**: 776-788
- 11 **Sanfey H**, Bulkley GB, Cameron JL. The role of oxygen-derived free radicals in the pathogenesis of acute pancreatitis. *Ann Surg* 1984; **200**: 405-413
- 12 **Fu K**, Sarras MP Jr, De Lisle RC, Andrews GK. Expression of oxidative stress-responsive genes and cytokine genes during caerulein-induced acute pancreatitis. *Am J Physiol* 1997; **273** (3 Pt 1): G696-705
- 13 **Kim H**, Seo JY, Roh KH, Lim JW, Kim KH. Suppression of NF-kappaB activation and cytokine production by N-acetylcysteine in pancreatic acinar cells. *Free Radic Biol Med* 2000; **29**: 674-683
- 14 **Sevillano S**, de Dios I, de la Mano AM, Manso MA. N-acetylcysteine induces beneficial changes in the acinar cell cycle progression in the course of acute pancreatitis. *Cell Prolif* 2003; **36**: 279-289
- 15 **Smotkin J**, Tenner S. Laboratory diagnostic tests in acute pancreatitis. *J Clin Gastroenterol* 2002; **34**: 459-462
- 16 **Slogoff MI**, Ethridge RT, Rajaraman S, Evers BM. COX-2 inhibition results in alterations in nuclear factor (NF)-kappaB activation but not cytokine production in acute pancreatitis. *J Gastrointest Surg* 2004; **8**: 511-519
- 17 **Li L**, Steinauer KK, Dirks AJ, Husbeck B, Gibbs I, Knox SJ. Radiation-induced cyclooxygenase 2 up-regulation is dependent on redox status in prostate cancer cells. *Radiat Res* 2003; **160**: 617-621
- 18 **Cuzzocrea S**, Mazzon E, Dugo L, Centorrino T, Ciccolo A, McDonald MC, de Sarro A, Caputi AP, Thiemermann C. Absence of endogenous interleukin-6 enhances the inflammatory response during acute pancreatitis induced by cerulein in mice. *Cytokine* 2002; **18**: 274-285

There is no association between K469E ICAM-1 gene polymorphism and biliary atresia

Paisarn Vejchapipat, Naruemol Jirapanakorn, Nutchanart Thawornsuk, Apiradee Theamboonlers, Voranush Chongsrisawat, Soottiporn Chittmittrapap, Yong Poovorawan

Paisarn Vejchapipat, Soottiporn Chittmittrapap, Pediatric Surgery Unit, Department of Surgery, Faculty of Medicine, Chulalongkorn University, Bangkok 10330, Thailand
Naruemol Jirapanakorn, Nutchanart Thawornsuk, Apiradee Theamboonlers, Voranush Chongsrisawat, Yong Poovorawan, Center of Excellence in Viral Hepatitis Research, Department of Pediatrics, Faculty of Medicine, Chulalongkorn University, Bangkok 10330, Thailand

Supported by the Thailand Research Fund

Correspondence to: Professor Yong Poovorawan, MD, Center of Excellence in Viral Hepatitis Research, Department of Pediatrics, Chulalongkorn Hospital, Rama IV Road, Patumwan, Bangkok 10330 Thailand. yong.p@chula.ac.th

Telephone: +66-2-256-4909 Fax: +66-2-256-4929

Received: 2005-01-11 Accepted: 2005-01-26

Abstract

AIM: To determine whether there was an association between inter-cellular adhesion molecule-1 (ICAM-1) gene polymorphism and biliary atresia (BA), and to investigate the relationship between serum soluble ICAM-1 (sICAM-1) and clinical outcome in BA patients after surgical treatment.

METHODS: Eighty-three BA patients and 115 normal controls were genotyped. *K469E ICAM-1* polymorphism was analyzed using PCR assay. Serum sICAM-1 was determined using ELISA method from 72 BA patients. In order to evaluate the association between these variables and their clinical outcome, the patients were categorized into two groups: patients without jaundice and those with persistent jaundice.

RESULTS: There were no significant differences between BA patients and controls in terms of gender, *K469E ICAM-1* genotypes, and alleles. The proportion of patients having serum sICAM-1 ≥ 3 500 ng/mL in persistent jaundice group was significantly higher than that in the other group. In addition, there was no association between *K469E ICAM-1* polymorphism and the status of jaundice in BA patients after Kasai operation.

CONCLUSION: ICAM-1 possibly plays an important and active role in the disease progression. However, the process is not associated with genetic variation of *K469E ICAM-1* polymorphism.

© 2005 The WJG Press and Elsevier Inc. All rights reserved.

Key words: Biliary atresia; Adhesion molecule; ICAM-1

Vejchapipat P, Jirapanakorn N, Thawornsuk N, Theamboonlers A, Chongsrisawat V, Chittmittrapap S, Poovorawan Y. There is no association between *K469E ICAM-1* gene polymorphism and biliary atresia. *World J Gastroenterol* 2005; 11(31): 4886-4890

<http://www.wjgnet.com/1007-9327/11/4886.asp>

INTRODUCTION

Biliary atresia (BA), the obliteration of extra- and intra-hepatic biliary system, remains one of the most intractable liver diseases in children. When patients with BA are left untreated, the majority of them will die of complications of biliary cirrhosis^[1,2]. At present, it is accepted that hepatic porto-enterostomy or Kasai operation is the first choice of treatment. Surgical correction at an early age is therefore the key to a successful management of infants with BA^[3], especially in countries where liver transplantation program is not widely available. So far, liver transplantation is preserved for BA patients who have gross cirrhosis at diagnosis or who failed Kasai operation^[1]. Since BA is a serious liver disease with poor long-term outcome, extensive research for its exact cause in order to understand the disease has been carried out^[4]. Nevertheless, its etiology is still unclear. A number of hypotheses have been proposed to explain the origin of the disease including peri-natal infection^[5], immune-mediated disorders^[2], and defect of morphogenesis^[6]. It has also been suggested by some research groups that susceptibility to BA is influenced by genetic factors via pro-inflammatory cytokines^[7-9].

Inter-cellular adhesion molecule-1 (ICAM-1) is a transmembrane glycoprotein involved in cell adhesion and acts as a cell surface ligand for members of the leukocyte integrin family. The interaction of leukocyte integrins with endothelial ICAM-1 leads to leukocyte adherence, transendothelial migration and cell activation, which are fundamental to the recruitment of leukocytes to the tissue leading to inflammatory process^[10]. A soluble form of ICAM-1 (sICAM-1) can release into the circulation during the course of an inflammatory reaction^[11,12]. Recently, it has been shown that the elevated serum sICAM-1 is associated with primary biliary cirrhosis. The levels correlate with the disease activity and the degree of cholestasis^[13].

ICAM-1 gene is located on chromosome 19p13. The gene encoding ICAM-1 is affected by a common, functionally important, genetic polymorphism^[14]. The *K469E* polymorphism of the ICAM-1 gene has already been described^[15,16]. This polymorphism occurs in exon 6 of the ICAM-1 gene and results in a change from lysine to glutamic acid in Ig-like

domain 5. The ICAM-1 gene polymorphism can affect the interaction between ICAM-1 and its receptor, namely leukocyte function-associated antigen-1, and influence B-cell activation^[17]. ICAM-1 plays a pivotal role in the migration of leukocytes to inflammatory sites. Therefore, it may be involved in various inflammatory diseases.

As far as we are concerned, there is no investigation regarding ICAM-1 gene polymorphism in BA. Since progressive inflammatory process within the liver is an important feature of BA^[18,19], there may be some links between the pathophysiology of BA and ICAM-1 gene polymorphism. Therefore, the study aimed to evaluate the ICAM-1 gene polymorphism in BA patients and to investigate whether there was an association between serum sICAM-1 and clinical outcome in BA patients after surgical treatment.

MATERIALS AND METHODS

This study was approved by the Ethical Committee of the Faculty of Medicine, Chulalongkorn University, Thailand. All parents of the children with BA and healthy controls had been informed of the purpose of the study. The written informed consents were obtained.

Study of ICAM-1 gene polymorphism in biliary atresia

BA patients were recruited into the study during annual follow-ups between January 2002 and July 2003. All patients were diagnosed as BA by exploratory laparotomy with intra-operative cholangiography during early infancy period. The control group, whose ethnicity is similar to the BA patients (Thai), comprised healthy teenagers among, those who participated in an evaluation of hepatitis B vaccination during the same period. Eighty-three BA patients participated in the study. Six out of eighty-three patients received liver transplantation. The healthy control group comprised 115 teenagers.

ICAM-1 DNA detection

Peripheral whole blood from BA patients and controls was collected in tubes containing EDTA. Genomic DNA was extracted from samples according to the manufacturer's protocol. Single base polymorphism at codon 469 (K469E) in exon 6 of ICAM-1 was determined using a method based on polymerase chain reaction-restriction fragment length polymorphism for the detection of K469E ICAM-1 gene, as previously described^[14,17]. The ICAM-1 F 5'CCCCGAC-TGGACGAGAGG3' is a sense primer and ICAM-1 R 5'GGGGCTGTGGGAGGATA3' is an anti-sense primer. We combined 2 mL of DNA sample with a reaction mixture containing 20 mL of 2.5X Eppendorf MasterMix (Hamburg, Germany), 1 mmol/L P1, 1 mmol/L P2, and sterile water, in a final volume of 25 mL. PCR was performed under the following conditions: after an initial 4 min denaturation step at 95 °C, 37 cycles of amplification were performed, each including 30 s denaturation at 95 °C, 30 s annealing at 60 °C and 30 s extension at 72 °C, followed by a final 4 min extension at 72 °C. Each amplified DNA sample (10 mL) was added to loading buffer and run on a 2% agarose gel (FMC Bioproducts, Rockland, ME, USA) at 100 V for 60 min. The 331-bp product stained with ethidium bromide on preparation was visualized on a UV transilluminator.

PCR-RFLP analysis

PCR products were subjected to RFLP analysis, using restriction endonuclease *Bst*UI (New England Biolabs, Beverly, MA, USA) to determine the ICAM-1 polymorphism. Briefly, 10 mL of PCR product was mixed with 1.5 mL of 10× buffer, 3 mL of sterile water and 0.5 mL (5 U) of *Bst*UI incubated at 60 °C for 4 h. After incubation, the samples were run on a composite gel containing 2% NuSieve agarose (FMC BioProducts, Rockland, ME, USA) and 1% standard agarose. The clusters of PCR products were visible under UV light, as a result of prior ethidium bromide staining.

Study of serum sICAM-1 in biliary atresia

Seventy-two serum samples of BA patients were available for the study of sICAM-1. All patients underwent hepatic porto-jejunostomy with Roux-en-Y (original Kasai operation) during infancy period. Patients who received liver transplantation were excluded from the study to avoid confounding effects of different therapeutic modalities. Briefly, peripheral venous whole blood was drawn with a sterile syringe, transferred to a centrifuge tube, allowed to clot and then centrifuged at 4 °C. The sera were stored at -70 °C until they could be assayed. Serum sICAM-1 levels were determined by a commercially available ELISA kit (Quantikine, R&D Systems, USA). This assay employs the quantitative sandwich enzyme immunoassay technique. The serum sICAM-1 levels were expressed as nanogram per milliliter. In addition, liver function tests including serum albumin, total bilirubin (TB), direct bilirubin (DB), alkaline phosphatase (AP), aspartate aminotransferase (AST), alanine aminotransferase (ALT), and γ -glutamyl transpeptidase (GGT) were performed using an automated chemical analyzer (Hitachi 911) at the central laboratory of the hospital.

Out of 72 BA patients, none in this study exhibited symptoms and signs of fever or ascending cholangitis at the time of blood sampling. None received liver transplantation. In order to compare the outcome among the BA patients, they were subsequently divided into two groups according to the status of jaundice and levels of TB: patients with no jaundice (TB < 2.0 mg%) and patients with persistent jaundice (TB \geq 2.0 mg%). In addition, subgroup analysis between BA patients as per the presence of jaundice and ICAM-1 gene polymorphism was carried out.

Statistical analyses

Demographic data between groups were compared by Fisher's exact and unpaired *t*-tests. Genotype and allele frequencies were compared by χ^2 test. Significant differences were established at $P < 0.05$. Odds ratios were also calculated. For all statistical analyses, either GraphPad Prism version 3.02 (GraphPad Software Inc., CA, USA) or SPSS software version 10.0 (SPSS Inc., Chicago, IL, USA) was used. Data were expressed as mean \pm SD.

RESULTS

Study of ICAM-1 gene polymorphism in biliary atresia

The distribution of ICAM-1 genotypes and alleles in 83 BA patients and 115 controls is shown in Table 1. There

Table 1 ICAM-1 genotypic and allele distribution in BA patients and controls

	BA patients, n (%) n = 83	Controls, n (%) n = 115	Odds ratio (95% CI)	P
Age (yr)	6.09±4.67	13.07±2.13		<0.0005
Male	37:46	57:58		0.49
Genotype				
E/E	28 (33.74)	41 (35.65)	0.92 (0.51-1.66)	0.78
E/K	7 (8.43)	11 (9.57)	0.87 (0.32-2.35)	0.78
K/K	48 (57.83)	63 (54.78)	1.13 (0.64-2.00)	0.67
Alleles				
E	63 (37.95)	93 (40.43)	0.90 (0.60-1.36)	0.62
K	103 (62.05)	137 (59.57)	1.11 (0.74-1.67)	
E/K ratio	0.61	0.68		

were no significant differences between two groups in terms of gender, K469E ICAM-1 genotypes, and K469E ICAM-1 alleles.

Study of serum sICAM-1 in biliary atresia

Serum sICAM-1 levels in 72 BA patients were determined. The demographic data between patients with no jaundice and patients with persistent jaundice are shown in Table 2. There was no difference in age and gender between the two groups. Patients with persistent jaundice had lower levels of albumin and higher levels of AST, ALT, AP, and GGT compared to patients without jaundice.

We also found that 24 out of 72 patients had sICAM-1 levels above the upper limit detected by the ELISA kit (3 500 ng/mL), therefore, the cut point of 3 500 ng/mL was selected to subdivide the patients. By using χ^2 test, the proportion of patients having serum sICAM-1 levels $\geq 3 500$ ng/mL in persistent jaundice group was significantly higher than that of patients having serum sICAM-1 levels

$\geq 3 500$ ng/mL in the other group ($P < 0.0005$), as shown in Table 2.

Association between K469E ICAM-1 gene polymorphism and status of jaundice

After excluding the BA patients who had undergone liver transplantation, 63 out of 83 BA patients had both data of genotype and total bilirubin levels. Therefore, an analysis of the association between ICAM-1 gene polymorphism and the status of jaundice after Kasai operation was conducted in 63 patients. The analysis showed that there was no difference in terms of age, gender, K469E ICAM-1 genotypes, and alleles between patients with no jaundice and with persistent jaundice (Table 3).

DISCUSSION

BA remains one of the major hepatic causes of death in early childhood. Although a number of hypotheses have

Table 2 Demographic data, liver function test, and serum sICAM-1 levels between BA patients without jaundice and with persistent jaundice (mean±SD)

BA patients	No jaundice (n = 41)	Persistent jaundice (n = 31)	P
Age (yr)	6.41±4.05	6.00±5.91	0.73
Male:female	22:19	11:20	0.12
Albumin (g/dL)	4.41±0.56	3.71±0.83	<0.0005
Total bilirubin (mg%)	0.79±0.44	12.04±10.53	<0.0005
DB (mg%)	0.24±0.26	9.36±7.85	<0.0005
AST (IU/L)	84.12±67.28	228.26±130.45	<0.0005
ALT (IU/L)	96.93±93.83	161.84±97.93	0.006
AP (IU/L)	380.90±249.80	593.20±293.49	0.002
GGT (IU/L)	163.16±175.49	384.65±404.72	0.004
sICAM-1 (<3 500: $\geq 3 500$ ng/mL)	37:4	11:20	<0.0005

Table 3 ICAM-1 genotypic and allele distribution in BA patients without jaundice and with persistent jaundice

	No jaundice, n (%) n = 34	Jaundice, n (%) n = 29	Odds ratio (95%CI)	P
Age (yr)	5.91±3.92	5.66±5.17		0.84
Male	18:16	11:18		0.23
Genotype				
E/E	9 (26.47)	10 (34.48)	0.68 (0.23-2.01)	0.49
E/K	3 (8.82)	3 (10.34)	0.83 (0.15-4.52)	0.84
K/K	22 (64.71)	16 (55.18)	1.49 (0.52-4.11)	0.44
Alleles				
E	21 (30.88)	23 (39.66)	0.68 (0.32-1.42)	0.30
K	47 (69.12)	35 (60.34)	1.47 (0.70-3.07)	
E/K ratio	0.45	0.66		

been proposed to account for the disease, its etio-pathogenesis is poorly understood. One possibility is that BA is an immune-mediated disease, which occurs following either a toxic or an infectious insult on a genetically susceptible host^[20]. Therefore, a number of studies have investigated whether bile duct epithelial cells are susceptible to immune or inflammatory attack because of abnormal expression of human leukocyte antigens (HLA) or ICAM-1 on their cell surface^[18]. It has been demonstrated that the expression of ICAM-1 and HLA-DR antigen in BA patients increases compared to that in controls^[21]. In addition to immune-mediated theory, a role of inflammation in the pathophysiology of BA has long been proposed. Histopathologic studies of the hepatic bile duct demonstrate various stages of inflammation causing progressive destruction of biliary system^[3]. This process might be caused by an overexpression of ICAM-1^[22]. The ICAM-1 gene is located on chromosome 19p13 and two non-synonymous single nucleotide polymorphisms are known as 12959G>A (G241R) and 13848A>G (K469E)^[23].

Several investigators have demonstrated the genetic association between ICAM-1 gene polymorphism and chronic inflammation diseases including inflammatory bowel disease^[14], multiple sclerosis^[16], Behcet's disease^[24], and endometriosis^[25]. Although there is a lot of information supporting the role of ICAM-1 gene polymorphism as a risk factor for diseases characterized by inflammatory process, the study of genetic susceptibility to BA, however, receives little attention. Donaldson *et al.*^[8], suggested that BA is not a HLA-associated disease, and that IL-1 and IL-10 gene polymorphisms are not risk factors for BA. Since inflammatory process and obliterative cholangiopathy within the liver are important features of BA, together with the fact that ICAM-1 molecule plays a major role in initiating inflammation, it is of our interest to evaluate whether ICAM-1 gene polymorphism is associated with BA. According to our knowledge, such a study has not been carried out.

The present study revealed that there was no association between K469E ICAM-1 gene polymorphism and BA in Thai population. Our results suggest that K469E ICAM-1 gene polymorphism is not a risk factor for both the etiopathogenesis and the prediction of success after Kasai operation. However, another study of serum sICAM-1 in BA patients showed that high levels of serum sICAM-1 are associated with the presence of jaundice and poor liver function, as illustrated by lower levels of serum albumin as well as higher levels of serum ALT, AST, and GGT^[26]. Our findings support the results from other research groups. Kobayashi *et al.*^[27], demonstrated that serum sICAM-1 levels can be used as a marker of end-stage liver disease in BA. Serum sICAM-1 also increases in BA patients but does not correlate with liver function^[28]. Davenport *et al.*^[2], reported, that a reduction in ICAM-1 expression on infiltrating cells in the biliary remnants is associated with a better post-operative prognosis. It might be possible that elevated sICAM-1 levels in BA patients with persistent jaundice found in this study reflect the impaired clearance of ICAM-1 from significant liver damage or, alternatively that the elevated sICAM-1 levels are caused by the increased ICAM-1 expression or by either mechanisms. Thus, the regulatory mechanisms of serum sICAM-1 seem to be complex. It is not easy to explain

the mechanisms of our observation from the study of serum sICAM-1 levels alone. At least, however, our findings show that the association between serum sICAM-1 and liver function in BA patients is significant enough to bring about a serious consideration.

According to our findings that high serum sICAM-1 levels are associated with poor outcome in BA patients following Kasai operation and the fact that ICAM-1 signaling is responsible for the initiation of inflammation, sICAM-1 levels in BA patients might have a prognostic role. In the study of serum sICAM-1, we recruited only patients who did not receive liver transplantation, in order to avoid the confounding effects from different therapeutic modalities.

It has been demonstrated that serum sICAM-1 levels in normal controls are low (less than 500 ng/mL)^[27,28]. Although there was no normal control group in our study, at least we found that the proportion of BA patients having serum sICAM-1 ≥ 3 500 ng/mL was significantly higher than that of patients without jaundice. Together with evidence supporting the role of ICAM-1 signaling pathway in inflammation, the manipulation of ICAM-1 expression might benefit BA patients. Therefore, apart from the prognostic role of serum sICAM-1 levels in BA, the therapeutic potential for BA using the immunomodulation of BA deserves attention. However, the specific mechanism requires further investigation.

In conclusion, the absence of association between K469E polymorphism of ICAM-1 and BA in Thai population has been demonstrated. BA patients with persistent jaundice following Kasai operation have higher serum sICAM-1 levels than those without jaundice. These findings suggest that ICAM-1 signaling is involved in the immunopathology of BA. Although ICAM-1 plays an important and active role in the disease progression, the process is not influenced by genetic susceptibility of K469E ICAM-1 gene polymorphism.

ACKNOWLEDGMENTS

We are grateful to the Thailand Research Fund and Center of Excellence of Thailand for generous support. Also we would like to express our gratitude to the entire staff of the Viral Hepatitis Research Unit, Chulalongkorn University and Hospital for their efforts in the present study. We would like to thank Rachadaphisek Somphot Endowment, Chulalongkorn University for supporting the research work. Lastly, we thank Venerable Dr. Mettanando Bhikkhu for reviewing the manuscript.

REFERENCES

- 1 **Ohi R.** Surgical treatment of biliary atresia in the liver transplantation era. *Surg Today* 1998; **28**: 1229-1232
- 2 **Davenport M, Gonde C, Redkar R, Koukoulis G, Tredger M, Mieli-Vergani G, Portmann B, Howard ER.** Immunohistochemistry of the liver and biliary tree in extrahepatic biliary atresia. *J Pediatr Surg* 2001; **36**: 1017-1025
- 3 **Nio M, Ohi R.** Biliary atresia. *Semin Pediatr Surg* 2000; **9**: 177-186
- 4 **Narkewicz MR.** Biliary atresia: an update on our understanding of the disorder. *Curr Opin Pediatr* 2001; **13**: 435-440
- 5 **Riepenhoff-Talty M, Gouvea V, Evans MJ, Svensson L, Hoffenberg E, Sokol RJ, Uhnoo I, Greenberg SJ, Schakel K, Zhaori G, Fitzgerald J, Chong S, el-Yousef M, Nemeth A,**

- Brown M, Piccoli D, Hyams J, Ruffin D, Rossi T. Detection of group C rotavirus in infants with extrahepatic biliary atresia. *J Infect Dis* 1996; **174**: 8-15
- 6 **Miyano T**, Fujimoto T, Ohya T, Shimomura H. Current concept of the treatment of biliary atresia. *World J Surg* 1993; **17**: 332-336
- 7 **Bezerra JA**, Tiao G, Ryckman FC, Alonso M, Sabla GE, Shneider B, Sokol RJ, Aronow BJ. Genetic induction of proinflammatory immunity in children with biliary atresia. *Lancet* 2002; **360**: 1653-1659
- 8 **Donaldson PT**, Clare M, Constantini PK, Hadzic N, Mieli-Vergani G, Howard ER, Kelley D. HLA and cytokine gene polymorphisms in biliary atresia. *Liver* 2002; **22**: 213-219
- 9 **A-Kader HH**, El-Ayyouti M, Hawas S, Abdalla A, Al-Tonbary Y, Bassiouny M, Boneberg A, El-Sallab S. HLA in Egyptian children with biliary atresia. *J Pediatr* 2002; **141**: 432-434
- 10 **Springer TA**. Traffic signals on endothelium for lymphocyte recirculation and leukocyte emigration. *Annu Rev Physiol* 1995; **57**: 827-872
- 11 **Gearing AJH**, Newmann W. Circulating adhesion molecules in disease. *Immunol Today* 1993; **14**: 506-524
- 12 **Etzioni A**. Adhesion molecules-their role in health and disease. *Pediatr Res* 1996; **39**: 191-198
- 13 **Bloom S**, Fleming K, Chapman RW. Adhesion molecule expression in primary sclerosing cholangitis and primary biliary cirrhosis. *Gut* 1995; **36**: 604-608
- 14 **Matsuzawa J**, Sugimura K, Matsuda Y, Takazoe M, Ishizuka K, Mochizuki T, Seki SS, Yoneyama O, Bannai H, Suzuki K, Honma T, Asakura H. Association between K469E allele of intercellular adhesion molecule 1 gene and inflammatory bowel disease in a Japanese population. *Gut* 2003; **52**: 75-78
- 15 **Braun C**, Zahn R, Martin K, Albert E, Folwaczny C. Polymorphisms of the ICAM-1 gene are associated with inflammatory bowel disease, regardless of the p-ANCA status. *Clin Immunol* 2001; **101**: 357-360
- 16 **Nejentsev S**, Laaksonen M, Tienari PJ, Fernandez O, Cordell H, Ruutinen J, Wikstrom J, Pastinen T, Kuokkanen S, Hillert J, Ilonen J. Intercellular adhesion molecule-1 K469E polymorphism: study of association with multiple sclerosis. *Human Immunol* 2003; **64**: 345-349
- 17 **Borozdenkova S**, Smith J, Marshall S, Yacoub M, Rose M. Identification of ICAM-1 polymorphism that is associated with protection from transplant associated vasculopathy after cardiac transplantation. *Human Immunol* 2001; **62**: 247-255
- 18 **Kobayashi H**, Stringer MD. Biliary atresia. *Semin Neonatol* 2003; **8**: 383-391
- 19 **Balistreri WF**, Grand R, Hoofnagle JH, Suchy FJ, Ryckman FC, Perlmutter DH, Sokol RJ. Biliary atresia: current concepts and research directions. *Hepatology* 1996; **23**: 1682-1692
- 20 **Sokol RJ**, Mack C. Etiopathogenesis of biliary atresia. *Semin Liver Dis* 2001; **21**: 517-524
- 21 **Broome U**, Nemeth A, Hultcrantz E, Scheynius A. Different expression of HLA-DR and ICAM-1 in livers from patients with biliary atresia and Byler's disease. *J Hepatol* 1997; **26**: 857-862
- 22 **Dillon PW**, Belchis D, Minnick K, Tracy T. Differential expression of the major histocompatibility antigens and ICAM-1 on bile duct epithelial cells in biliary atresia. *Tohoku J Exp Med* 1997; **181**: 33-40
- 23 **Vora DK**, Rosenbloom CL, Beaudet AL, Cottingham RW. Polymorphism and linkage analysis for ICAM-1 and the selectin gene cluster. *Genomics* 1994; **21**: 473-477
- 24 **Boiardi L**, Salvarani C, Casali B, Olivieri I, Ciancio G, Cantini F, Salvi F, Malatesta R, Govoni M, Trotta F, Filippini D, Paolazzi G, Nicoli D, Farnetti E, Macchioni L. Intercellular adhesion molecule-1 gene polymorphisms in Behcet's disease. *J Rheumatol* 2001; **28**: 1283-1287
- 25 **Vigano P**, Infantino M, Lattuada D, Lauletta R, Ponti E, Somigliana E, Vignali M, DiBlasio AM. Intercellular adhesion molecule-1 (ICAM-1) gene polymorphisms in endometriosis. *Mol Hum Reprod* 2003; **9**: 47-52
- 26 **Adams DH**, Mainolfi E, Burra P, Neuberger JM, Ayres R, Elias E, Rothlein R. Detection of circulating intercellular adhesion molecule-1 in chronic liver disease. *Hepatology* 1992; **16**: 810-814
- 27 **Kobayashi H**, Horikoshi K, Long L, Yamataka A, Lane GJ, Miyano T. Serum concentration of adhesion molecules in post-operative biliary atresia patients: relationship to disease activity and cirrhosis. *J Pediatr Surg* 2001; **36**: 1297-1301
- 28 **Minnick KE**, Kreisberg R, Dillon PW. Soluble ICAM-1 (sICAM-1) in biliary atresia and its relationship to disease activity. *J Surg Res* 1998; **76**: 53-56

Lewis blood genotypes of peptic ulcer and gastric cancer patients in Taiwan

Chi-Jung Yei, Jan-Gowth Chang, Mu-Chin Shih, Sheng-Fung Lin, Chao-Sung Chang, Fu-Tsong Ko, Kuang-Yang Lin, Ta-Chih Liu

Chi-Jung Yei, Blood Bank, Kaohsiung Medical University Hospital, Kaohsiung, Taiwan, China
Jan-Gowth Chang, Mu-Chin Shih, Department of Laboratory Medicine, China Medical University and Hospital, Taichung, Taiwan, China
Sheng-Fung Lin, Chao-Sung Chang, Ta-Chih Liu, Division of Hematology/Oncology, Department of Internal Medicine, Kaohsiung Medical University Hospital, Kaohsiung, Taiwan, China
Fu-Tsong Ko, Kuang-Yang Lin, Department of Internal Medicine, Taipei Municipal Jen-Ai Hospital, Taipei, Taiwan, China
Correspondence to: Ta-Chih Liu, MD, Division of Hematology/Oncology, Department of Internal Medicine, Kaohsiung Medical University Hospital, 100 Shih-Chuan 1st Road, Kaohsiung, Taiwan, China. d730093@cc.kmu.edu.tw
Telephone: +886-7-3121101-6113 Fax: +886-7-3162429
Received: 2005-01-04 Accepted: 2005-01-26

CONCLUSION: Lewis blood genotype or phenotype may not play a role in the pathogenesis of *H pylori* infection. However, bacterial strain differences and the presence of more than one attachment mechanism may limit the value of epidemiological studies in elucidating this matter.

© 2005 The WJG Press and Elsevier Inc. All rights reserved.

Key words: Lewis histoblood group; *Helicobacter pylori*; Peptic ulcer; Gastric cancer

Yei CJ, Chang JG, Shih MC, Lin SF, Chang CS, Ko FT, Lin KY, Liu TC. Lewis blood genotypes of peptic ulcer and gastric cancer patients in Taiwan. *World J Gastroenterol* 2005; 11(31): 4891-4894

<http://www.wjgnet.com/1007-9327/11/4891.asp>

Abstract

AIM: The Lewis b (Le^b) antigen has been implicated as a possible binding site for attachment of *Helicobacter pylori* (*H pylori*) to gastric mucosa. However, studies both supporting and denying this association have been reported in the literature. Differences in secretor (Se) genotype have been suggested as a possible reason for previous discrepancies. Therefore, we investigated the relationship between Le and Se genotypes and *H pylori* infection rates in people with peptic ulcer or gastric cancer.

METHODS: Peripheral blood samples were obtained from 347 patients with endoscopic evidence of peptic ulcer disease (235 cases of duodenal ulcer, 62 of gastric ulcer, and 50 of combined duodenal ulcer/ gastric ulcer) and 51 patients with gastric cancer on endoscopy. Peripheral blood specimens from 101 unrelated normal volunteers were used as controls. Lewis phenotype was determined using an antibody method, whereas Le and Se genotypes were determined by DNA amplification and restriction enzyme analysis. Gastric or duodenal biopsies taken from patients with endoscopic evidence of peptic ulcer or gastric cancer were cultured for *H pylori*. Isolates were identified as *H pylori* by morphology and production of urease and catalase. The *H pylori* infection status was also evaluated by rapid urease test (CLO test), and urea breath test (¹³C-UBT). Results of studies were analyzed by chi-square test (taken as significant).

RESULTS: *H pylori* was isolated from 83.7% (303/347) of patients with peptic ulcer disease. Statistical analysis did not show any significant difference in Lewis phenotype or genotype between patients with and without *H pylori* infection. No significant association was found between Lewis genotype and peptic ulcer or gastric cancer.

INTRODUCTION

The Lewis blood group determinants are structurally related to the antigens of the ABO and H/h blood group systems. They are made by sequential addition of specific monosaccharides onto terminal saccharide precursor chains on glycolipids or glycoproteins. The glycolipids on which they reside on the erythrocyte surface are not synthesized in erythroid tissues, but are acquired by erythrocyte membranes from other tissues through circulating soluble forms that are bound to lipoproteins^[1].

The synthesis of the epitopes is dependent on the interaction of two different fucosyltransferases: alpha(1,2) fucosyltransferase encoded by the *FUT2* or secretor (Se) locus of the H/h blood group system, and alpha(1,3,1,4) fucosyltransferase (*FUT3*) encoded by the *FUT3* locus. Fucosylation by *FUT3* gives rise to the Le^a epitope, whereas the action of both enzymes results in Le^b.

If *FUT3* is not expressed, the phenotype is Le^{a-b-} regardless of whether *FUT2* (Se) is expressed or not. If *FUT3* and *FUT2* are both expressed, the phenotype is Le^{a-b+}. If *FUT3*, but not *FUT2* is expressed, the phenotype is Le^{a+b-}. A Le^{a+b+} phenotype may occur, if there is reduced expression of *FUT2*.

The Le^b glycan has been reported to mediate the attachment of *Helicobacter pylori* (*H pylori*) to human gastric mucosa^[2,3]. However, the clinical significance of this reported association remains a topic of debate. It has also been reported that people who do not secrete soluble Lewis b antigen are more susceptible to *H pylori* infection than people with secretor phenotypes^[4].

This study aimed to explore the association among Lewis antigen phenotypes and genotypes, infection with *H pylori*,

and consequent development of peptic ulcer or gastric cancer.

MATERIALS AND METHODS

Peripheral blood samples were collected as previously described^[4] from 347 patients with endoscopic evidence of peptic ulcer disease (235 cases of duodenal ulcer, 62 cases of gastric ulcer, 50 cases of duodenal ulcer and gastric ulcer) and 51 patients diagnosed with gastric cancer on endoscopy. Peripheral blood specimens from 101 unrelated healthy volunteers were used as normal controls. Subjects were enrolled from the Division of Gastroenterology, Department of Internal Medicine, Taipei Municipal Jen-Ai Hospital from August 1998 to December 2002.

The erythrocyte Lewis phenotype was determined by a tube method using monoclonal antibody (Gamma-CloneR, anti-Le^a, anti-Le^b Gamma Biologicals, Inc. Houston, TX, USA) at Taipei Municipal Jen-Ai Hospital.

Total genomic DNA was isolated from peripheral blood leukocytes as described previously^[5], and Le and Se genotypes were determined by DNA amplification (polymerase chain reaction, PCR) and restriction enzyme analysis^[6,7]. Oligonucleotide primer design and restriction enzyme analysis were carried out as previously described^[5]. The primer sequences and restriction enzymes used in this study are shown in Table 1. The amplified products were digested with appropriate restriction enzymes, followed by electrophoresis on 1.5-4% agarose gels. Direct sequencing of the PCR products in selected cases provided a check on the validity of the procedure.

Gastric or duodenal biopsies were taken from all patients with endoscopic evidence of peptic ulcer or gastric cancer and cultured for *H pylori*. Bacterial isolates were identified as *H pylori* by morphology and production of urease and

catalase^[8]. The *H pylori* infection status was also evaluated by rapid urease test (CLO test), and urea breath test (¹³C-UBT). *H pylori* infection was defined as positive results by culture or two positive test results on histology, rapid urease test, and ¹³C-urea breath test^[9].

Results were analyzed by the chi-square test, $P < 0.05$ was considered statistically significant.

RESULTS

H pylori was isolated from 83.7% (303/347) of patients with peptic ulcer disease. Statistical analysis did not show a significant difference in Lewis phenotype (Table 2) or Lewis genotype (Table 3) between peptic ulcer patients with *H pylori* infection and those without infection. Among the 51 gastric cancer patients, *H pylori* infection prevalence in the different Lewis phenotypes was Le^{a+b}, 30/33 (90.9%); Le^{a-b}, 7/8 (87.5%); Le^{a+b}, 3/3 (100%); and Le^{a+b+}, 6/7 (85.7%).

H pylori was detected in 109/124 (87.9%) of peptic ulcer patients with Se/Se genotype, 148/174 (85%) of those with Se/se genotype, and 53/58 (91.3%) of those with se/se genotype. The difference in proportion of infected patients was not significant ($P = 0.436$).

Similarly, no significant difference ($P = 0.440$) was found for presence of *H pylori* infection in peptic ulcer patients with Le/Le (86/97, 88.6%), Le/le (182/215, 84.6%) or le/le (31/34, 91.3%) genotypes.

No significant association was found between Lewis genotype and presence of peptic ulcer disease or gastric cancer (Table 4). Again, an analysis by Se genotype showed no significant difference between patients with peptic ulcer disease and normal controls ($P = 0.915$) or between patients with gastric cancer and normal controls ($P = 0.741$), whereas analysis by Le genotype gave similar, non-significant results

Table 1 Primer sequences and restriction enzymes of mutation in Se and Le genes

Mutation	Primer sequence	Enzyme
Se gene		
A385T	UP ¹ : GATGGAGGAGGAATACCGCTC DP ² : GATCTCTGGCGGAGGTGGTGTAGAAGATC	Ear I
G428A	Identical to A385T primer pairs	Bgl II
C571T	UP: AGGAGATCCTCCAGGAGTTCA DP: AGAAGGAGAAAAGGTCTCAAAGG	Dde I
G849A	Identical to C571T primer pairs	Dde I
C628T	UP: AGTGTGGAAGGGGTGGTGCC DP: CCACTCTGGCAGGAAGGC	Bgl I
Fusion gene	UP: CTGCCCTCTGACCATGTCC DP: identical to reverse primer of C628T	Pst I
Le genes		
T202C and C314T	UP: CCACCCTCTGATCTGCTC DP: GATATCCCAGTGGTGCACGATGATGATC	Msp I (T202C) Bcl I (C314T)
C445A	UP: identical to UP of T202 C and C314 T DP: GAGATTGAAGTATCTGTCCAAGGC	BstNI
G508A	UP: TCAACTTGGAGCCACACCCT DP: AGTTGGACACCGCCAGGCCACCAG	Alu I
A1007C	UP: GCTCCTCCGCTGGGCACTAG DP: TGGCCACAAAGGACTCCAGC	Alu I
T1067A	UP: GTACCAGACGGTGCATGCA DP: identical to DP of A1007 C	Nsi I

¹UP: upstream primer; ²DP: downstream primer; The mutated base is underlined.

Table 2 Correlation between Lewis phenotype and *H pylori* infection in peptic ulcer disease

Phenotypes	Le ^{a+b+} (n = 230)	Le ^{a+b-} (n = 59)	Le ^{a-b+} (n = 14)	Le ^{a+b+} (n = 44)	P
<i>H pylori</i> status					0.5662
Positive	195	54	12	39	
Negative	35	5	2	5	
Prevalence %	84.7	91.5	85.7	88.5	

Table 3 Correlation between Lewis genotype and *H pylori* infection in peptic ulcer disease

Genotypes	SeLe/SeLe (n = 33)	SeLe/seLe (n = 65)	SeLe/Sele (n = 42)	SeLe/Sele (n = 90)	SeLe/Sele (n = 3)	SeLe/Sele (n = 19)	SeLe/Sele (n = 37)	SeLe/Sele (n = 46)	SeLe/Sele (n = 12)	P
<i>H pylori</i> status										0.446
Positive	28	59	36	72	2	17	33	41	12	
Negative	5	6	6	18	1	2	4	5	0	
Prevalence %	84.8	90.7	85.7	80	66.6	89.4	89.1	89.1	100	

Table 4 Lewis genotypes in peptic ulcer and gastric cancer

Genotypes	Peptic ulcer n = 347	Gastric cancer n = 51	Normal n = 101
SeLe/SeLe	33	2	7
SeLe/seLe	65	11	25
SeLe/Sele	42	4	10
SeLe/sele	90	15	21
Sele/Sele	3	3	5
Sele/sele	19	4	7
seLe/seLe	37	3	12
seLe/sele	46	5	9
sele/sele	12	4	5
P	0.129 ¹	0.881 ²	

¹P = 0.129 peptic ulcer vs normal controls; ²P = 0.881 gastric cancer vs normal controls.

(P = 0.067 and P = 0.344 respectively).

Finally, no significant correlation was obtained between ABO blood group type and *H pylori* infection (Table 5).

DISCUSSION

H pylori is the main causative agent of gastric and duodenal ulcers^[10] and gastric adenocarcinoma^[11]. Attachment is a pre-requisite for microbial colonization of epithelial surfaces and is mediated through interaction of adhesins on the bacterial surface and proteins or glycoconjugates on the surface of the epithelial cells^[12,13]. Borén *et al.*^[2], reported that the attachment of *H pylori* to gastric mucosa is mediated by the Lewis^b (Le^b) antigen and that the availability of receptors might therefore be reduced in individuals of blood groups A and B compared to people with blood group O.

Carneiro *et al.*^[14], found that there is a significant relationship between ABO blood group in combination with Lewis phenotype on the one hand and *H pylori* infection on the other. *H pylori* is present in 100% of those with Le^{b+}/O phenotype but in only 57% of Le^{b-}/A or B phenotype. However, infection is also present in 92% of Le^{b-}/O individuals and 86% of Le^{b+}/A or B individuals. Nonetheless, the Carneiro

group challenged the finding of Niv *et al.*^[15], that positivity for *H pylori* is not associated with blood group O and their conclusion that their observations do not support the contention that the receptor for *H pylori* in the gastric mucosa is the Le^b antigen.

However, Clyne and Drumm^[16] found that adherence of *H pylori* to isolated human gastric cells is not dependent on Lewis antigen expression on the cells, and Umlauf *et al.*^[17], could not demonstrate any *in vivo* correlation between *H pylori* infection or disease and Le^b antigen. Taylor *et al.*^[18], also found that there is no correlation between Lewis antigen expression by *H pylori* and gastric epithelial cells in infected patients.

More recently, Keller *et al.*^[19], found that there is no significant association between secretor status or specific ABO blood group and *H pylori* infection or occurrence of gastro-duodenal ulcer. Aguiar^[20] also found that there is no significant association between the presence of *H pylori* and ABO, Lewis or secretor phenotype, while Nogueira *et al.*^[21], actually found that Le^b expression is nearly twice as common among children without *H pylori* (15/23, 65%) as in those with *H pylori* (16/47, 34%).

However, Yang *et al.*^[22], found that there are significant

Table 5 ABO blood types and susceptibility to *H pylori* infection (n = 230)

Blood types	A (n = 44)	B (n = 54)	O (n = 122)	AB (n = 10)	P
<i>H pylori</i> status					0.255
Positive	34	49	106	8	
Negative	10	5	16	2	
Prevalence %	77.2	90.7	86.8	80	

relationships between Lewis phenotype and *H pylori* infection. Expression of Le^a antigen (whether Le^{a+b}- or Le^{a+b+}) is associated with a higher infection rate but a lower bacterial density, a lower severity of chronic inflammation, and a lower frequency of lymphoid follicles in the gastric cardia. To complicate things even further, *H pylori*-infected patients expressing the Le^b antigen have a lower rate of gastro-duodenal ulcers but a higher bacterial density and inflammation severity in the gastric cardia. It is difficult to know how to interpret these results.

In vitro studies by Lindén *et al.*^[23], and Van de Bovenkamp *et al.*^[24], showed that binding of *H pylori* to human gastric MUC5AC mucin is blood group antigen-binding adhesin dependent and mediated by the Le^b structure in the mucin. However, it has also been shown that *H pylori* bacteria that do not express Lewis antigens but do express other complex carbohydrates that may still have the ability to form long-term colonies in the stomach^[25,26].

It may be that differences in reported results are due to strain differences in *H pylori*. Hennig *et al.*^[27], found that there is considerable heterogeneity among *H pylori* isolates in expression of the BabA adhesion, which is thought to bind to Le^b antigen present on the surface of gastric epithelial cells. Sheu *et al.*^[28], in a study of 188 dyspeptic patients with *H pylori* infection in Taiwan, found that all isolates have a positive babA2 genotype and that, among 139 patients with Le^b expression, *H pylori* density increases with Le^b intensity. In the 49 patients without gastric Le^b expression, *H pylori* density is positively correlated with Le^x and Le^a expression.

In conclusion, Lewis blood genotype or phenotype may not play a role in the pathogenesis of *H pylori* infection. However, bacterial strain differences and the presence of more than one attachment mechanism may limit the contribution of epidemiological studies toward elucidating this matter.

REFERENCES

- Marcus DM, Cass L. Glycosphingolipids with Lewis blood group activity: uptake by human erythrocytes. *Science* 1969; **164**: 553-555
- Borén T, Falk P, Roth KA, Larson G, Normark S. Attachment of *Helicobacter pylori* to human gastric epithelium mediated by blood group antigens. *Science* 1993; **262**: 1892-1895
- Ilver D, Arnqvist A, Ogren J, Frick IM, Kersulyte D, Incecik ET, Berg DE, Covacci A, Engstrand L, Borén T. *Helicobacter pylori* adhesion binding fucosylated histo-blood group antigens revealed by retagging. *Science* 1998; **279**: 373-377
- Borén T, Normark S, Falk P. *Helicobacter pylori*: molecular basis for host recognition and bacterial adherence. *Trends Microbiol* 1994; **2**: 221-228
- Chang JG, Chiou SS, Perng LI, Chen TC, Liu TC, Lee LS, Chen PH, Tang TK. Molecular characterization of glucose-6-phosphate dehydrogenase (G6PD) deficiency by naturally and amplification created restriction sites: five mutations account for most G6PD deficiency cases in Taiwan. *Blood* 1992; **80**: 1079-1082
- Chang JG, Yang TY, Liu TC, Lin TP, Hu CJ, Kao MC, Wang NM, Tsai FJ, Peng CT, Tsai CH. Molecular analysis of secretor type a (1,2)-fucosyltransferase gene mutations in the Chinese and Thai populations. *Transfusion* 1999; **39**: 1013-1017
- Liu TC, Chang JG, Lin SF, Chang WC, Yang TY, Lin CL, Wang NM. Lewis (FUT3) genotypes in Taiwanese, Thai, and Filipino populations. *Ann Hematol* 2000; **79**: 599-603
- Hazell SL, Evans DJ, Graham DY. *Helicobacter pylori* catalase. *J Gen Microbiol* 1991; **137**: 57-61
- Wang WM, Lee SC, Wu DC, Chen LT, Liu CS, Peng CF, Ding HJ, Chen CY, Jan CM. Simplified ¹³C-urea breath test for the diagnosis of *Helicobacter pylori* infection-the availability of without fasting and without test meal. *Kaohsiung J Med Sci* 2000; **16**: 607-613
- Graham DY. *Helicobacter pylori*: its epidemiology and its role in gastroduodenal ulcer disease. *J Gastroenterol Hepatol* 1991; **6**: 105-113
- Eurogast Study Group. An international association between *Helicobacter pylori* infection and gastric cancer. *Lancet* 1993; **341**: 1359-1362
- Ofek I, Sharon N. Adhesins as lectins: specificity and role in infection. *Curr Top Microbiol Immunol* 1990; **151**: 91-113
- Karlsson KA. Animal glycosphingolipids as membrane attachment sites for bacteria. *Annu Rev Biochem* 1989; **58**: 309-350
- Carneiro F, Amado M, Lago P, Taveira-Gomes A, Amil M, Barreira R, Soares J, Pinho C. *Helicobacter pylori* infection and blood groups. *Am J Gastroenterol* 1996; **91**: 2646-2647
- Niv Y, Fraser G, Delpre G, Neeman A, Leiser A, Samra Z, Scapa E, Gilon E, Bar-Shany S. *Helicobacter pylori* infection and blood groups. *Am J Gastroenterol* 1996; **91**: 101-104
- Clyne M, Drumm B. Absence of effect of Lewis A and Lewis B expression on adherence of *Helicobacter pylori* to human gastric cells. *Gastroenterology* 1997; **113**: 72-80
- Umlauf F, Keeffe EB, Offner F, Weiss G, Feichtinger H, Lehmann E, Kilga-Nogler S, Schwab G, Propst A, Grünwald K, Judmaier G. *Helicobacter pylori* infection and blood group antigens: lack of clinical association. *Am J Gastroenterol* 1996; **91**: 2135-2138
- Taylor DE, Rasko DA, Sherburne R, Ho C, Jewell LD. Lack of correlation between Lewis antigen expression by *Helicobacter pylori* and gastric epithelial cells in infected patients. *Gastroenterology* 1998; **115**: 1113-1122
- Keller R, Dinkel KC, Christl SU, Fischbach W. Interrelation between ABH blood group O, Lewis (B) blood group antigen, *Helicobacter pylori* infection, and occurrence of peptic ulcer. *Z Gastroenterol* 2002; **40**: 273-276
- Aguiar DC, Corvelo TC, Arajo M, Cruz EM, Daibes S, Assumpcao MB. Expression of ABH and Lewis antigens in chronic gastritis and pre-neoplastic alterations in gastric mucosa. *Arq Gastroenterol* 2002; **39**: 222-232
- Nogueira AM, Marques T, Soares PC, David L, Reis CA, Serpa J, Queiroz DM, Rocha GA, Rocha AC. Lewis antigen expression in gastric mucosa in children: relationship with *Helicobacter pylori* infection. *J Pediatr Gastroenterol Nutr* 2004; **38**: 85-91
- Yang HB, Sheu BS, Chen RC, Wu JJ, Lin XZ. Erythrocyte Lewis antigen phenotypes of dyspeptic patients in Taiwan-correlation of host factor with *Helicobacter pylori* infection. *J Formos Med Assoc* 2001; **100**: 227-232
- Lindén S, Nordman H, Hedenbro J, Hurtig M, Borén T, Carlstedt I. Strain- and blood group-dependent binding of *Helicobacter pylori* to human gastric MUC5AC glycoforms. *Gastroenterology* 2002; **123**: 1923-1930
- Van de Bovenkamp JH, Mahdavi J, Korteland-Van Male AM, Buller HA, Einerhand AW, Boren T, Dekker J. The MUC5AC glycoprotein is the primary receptor for *Helicobacter pylori* in the human stomach. *Helicobacter* 2003; **8**: 521-532
- Rasko DA, Wilson TJ, Zopf D, Taylor DE. Lewis antigen expression and stability in *Helicobacter pylori* isolated from serial gastric biopsies. *J Infect Dis* 2000; **181**: 1089-1095
- Altman E, Smironova N, Li H, Aubry A, Logan SM. Occurrence of a nontypable *Helicobacter pylori* strain lacking Lewis blood group O antigens and DD-heptoglycan: evidence for the role of the core alpha-1,6-glucan chain in colonization. *Glycobiology* 2003; **13**: 777-783
- Hennig EE, Mernaugh R, Edl J, Cao P, Cover TL. Heterogeneity among *Helicobacter pylori* strains in expression of the outer membrane protein BabA. *Infect Immun* 2004; **72**: 3429-3435
- Sheu BS, Sheu SM, Yang HB, Huang AH, Wu JJ. Host gastric Lewis expression determines the bacterial density of *Helicobacter pylori* in babA2 genopositive infection. *Gut* 2003; **52**: 927-932

• BRIEF REPORTS •

Etoposide sensitizes CT26 colorectal adenocarcinoma to radiation therapy in BALB/c mice

Chia-Yuan Liu, Hui-Fen Liao, Tsang-En Wang, Shee-Chan Lin, Shou-Chuan Shih, Wen-Hsuing Chang, Yuh-Cheng Yang, Ching-Chung Lin, Yu-Jen Chen

Chia-Yuan Liu, Tsang-En Wang, Shee-Chan Lin, Shou-Chuan Shih, Wen-Hsuing Chang, Ching-Chung Lin, Division of Gastroenterology, Department of Internal Medicine, Mackay Memorial Hospital, Taipei, Taiwan, China

Chia-Yuan Liu, Hui-Fen Liao, Yuh-Cheng Yang, Yu-Jen Chen, Department of Medical Research, Mackay Memorial Hospital, Taipei, Taiwan, China

Hui-Fen Liao, Department of Molecular Biology and Biochemistry, National Chiayi University, Chiayi, 300 Taiwan, China

Shou-Chuan Shih, Yuh-Cheng Yang, Mackay Medicine, Nursing and Management College, Taipei, Taiwan, China

Yu-Jen Chen, Department of Radiation Oncology, Mackay Memorial Hospital, Taipei, Taiwan, China

Supported by the Grant, No. MMH 9352 from Mackay Memorial Hospital, Taipei, Taiwan, China

Correspondence to: Yu-Jen Chen, Department of Radiation Oncology, Mackay Memorial Hospital, No. 92, Section 2, Chung San North Road, Taipei 104, Taiwan, China. chenmdphd@yahoo.com

Telephone: +886-2-28094661 Fax: +886-2-28096180

Received: 2004-12-13 Accepted: 2005-01-26

Key words: Etoposide (VP-16); Colorectal adenocarcinoma; CT26; BALB/c mice; Radiosensitization

Liu CY, Liao HF, Wang TE, Lin SC, Shih SC, Chang WH, Yang YC, Lin CC, Chen YJ. Etoposide sensitizes CT26 colorectal adenocarcinoma to radiation therapy in BALB/c mice. *World J Gastroenterol* 2005; 11(31): 4895-4898

<http://www.wjgnet.com/1007-9327/11/4895.asp>

INTRODUCTION

Colorectal cancer (CRC) is one of the most common malignancies worldwide, accounting for a significant percentage of cancer mortality. The incidence in both developing and developed countries has been increasing over the past few decades. Concurrent chemo-radiation therapy (CCRT) plays an important role in controlling CRC and palliating symptoms. This is particularly true when aiming for anal preservation in locally advanced disease, and it therefore offers an attractive alternative to surgery, the current mainstay of treatment^[1].

Radiation therapy (RT), either as a definitive treatment along with chemotherapy for unresectable disease or as a post-operative adjuvant for resectable disease, plays an important role in the management of CRC^[2,3]. However, large portions of the colorectum, small intestine, and urinary bladder are inevitably included within the radiation field in order to treat the areas of pelvic lymphatic drainage. Therefore, radiation-induced toxicity limits the use of RT in treating this malignancy, either alone or as part of a CCRT protocol. Moreover, some tumor clones are resistant to RT or chemotherapy. Currently, CCRT using a 5-fluorouracil (5-FU)-based regimen is the mainstay of CRC therapy. 5-FU is known to be a radiosensitizer, but some cancer cell clones are resistant to it^[4,5]. Given these limitations, it is desirable to look for radiosensitizers that augment the efficacy of RT, thus allowing a lower RT dose, and have acceptably low toxicity.

Etoposide (VP-16) is a semi-synthetic derivative of the naturally occurring antibiotic podophyllotoxin, which poisons type II topoisomerase without binding to DNA^[6]. Etoposide has been widely used in the treatment of lung and ovarian cancer, given either intravenously or orally^[7-9]. The combination of etoposide and cisplatin given concurrently with RT for lung cancer has yielded promising results^[10]. Etoposide-based CCRT also appears to be effective in newly diagnosed malignant glioma^[11]. Chemotherapy with etoposide as a single agent, however, is not very successful in a phase II trial for colorectal cancer^[12], which may explain why there

Abstract

AIM: To investigate the combined effect of etoposide and radiation on CT26 colorectal adenocarcinoma implanted into BALB/c mice.

METHODS: We evaluated the radiosensitizing effect of etoposide on CT26 colorectal adenocarcinoma in a syngeneic animal model. BALB/c mice were subcutaneously implanted with CT26 cells and divided into four groups: control (intra-peritoneal saline×2) group, etoposide (5 mg/kg intra-peritoneally×2) group, radiation therapy (RT 5 Gy×2 fractions) group, and combination therapy with etoposide (5 mg/kg intra-peritoneally 1 h before radiation) group.

RESULTS: Tumor growth was significantly inhibited by RT and combination therapy. The effect of combination therapy was better than that of RT. No significant changes were noted in body weight, plasma alanine aminotransferase, or creatinine in any group. The leukocyte count significantly but transiently decreased in the RT and combination therapy groups, but not in the etoposide and control groups. There was no skin change or hair loss in the RT and combination therapy groups.

CONCLUSION: Etoposide can sensitize CT26 colorectal adenocarcinoma in BALB/c mice to RT without significant toxicity.

is little interest in this drug for this disease. However, Shigematsu *et al.*^[13], reported, that a combination of low dose etoposide and radiation, arrests V79 (Chinese hamster fibroblasts) and T24 (human bladder cancer) cells in the G₂/M phase of the cell cycle, decreasing their survival. Since G₂/M is a radiosensitive phase of cell cycle, it is possible that etoposide functions as a radiosensitizer rather than a cytotoxic agent.

In this study, we investigated the combined effect of etoposide and radiation on CT26 colorectal adenocarcinoma implanted into BALB/c mice. Both the therapeutic effect and safety profile were evaluated.

MATERIALS AND METHODS

Cell culture and mice

CT26 cells, *N*-nitroso-*N*-methyl urethane-induced mouse colon carcinoma cells of BALB/c origin^[14], were purchased from the American Type Culture Collection (ATCC, Manassas, VA, USA). Cells were cultured in RPMI1640 medium (GIBCO, Grand Island, NY, USA) supplemented with 10% heat-inactivated fetal calf serum (Hyclone, Logan, UT, USA) at 37 °C in a humidified 50 mL/L CO₂ incubator. The cell cultures were passaged every 2-3 d with TEG solution (0.25% trypsin, 0.1% EDTA and 0.05% glucose in Hanks' balanced salt solution) and maintained in exponential growth. Male BALB/c mice, aged from 6 to 8 wk, were obtained from the National Laboratory Animal Center (Taipei, Taiwan) and housed in a rodent facility at 22±1 °C in a 12-h light-dark cycle. Four groups of animals of 9-11 mice each were implanted with CT26 cells (2×10⁵ cells) by subcutaneous injection into the right gluteal region. Treatment was started when the tumors grew to 0.5 cm in diameter. All experiments were performed in accordance with the regulations of the NIH *Guide for the Care and Use of Laboratory Animals* (DHHS publication no. NIH 85-23, revised 1996).

Drug preparation

Etoposide was purchased from Sigma-Aldrich Co. (St. Louis, MO, USA). It was dissolved in dimethyl sulfoxide (DMSO) at 10 mmol/L as a stock solution and stored at -20 °C. For experimental use, the stock solution was diluted to the appropriate concentration with growth medium, with a final DMSO concentration of less than 0.1%. This concentration of DMSO has been previously proven to be nontoxic to cells.

Drug administration and radiation delivery

There were four groups of mice in our study. The first group received intra-peritoneal (i.p.) saline for 2 consecutive days, and served as controls. The second group received daily i.p. injections of etoposide, 5 mg/kg for 2 consecutive days. The third group received RT, 5 Gy daily for 2 consecutive days. The fourth group received a combination of etoposide, followed by RT 1 h later. The doses of etoposide and RT were the same as used in the previous two groups. The mice were anesthetized with pentobarbital (50 mg/kg i.p.) before RT. The gluteal region, including both femurs and tumor, was irradiated with a total of 10 Gy in two daily fractions (6 MV photon beam at source-to-axis

distance of 100 cm, dose rate 2.4 Gy/min) by an accelerator (Clinac[®] 1800, Varian Associates Inc., CA, USA, dose rate 2.4 Gy/min). Two tissue-equivalent polystyrene plates (1.3 cm thick upward and 5.0 cm thick downward) were used to provide adequate build-up. Dosimetry was measured using a N30001 ionization chamber (PTW-FREIBURG, Germany) prior to radiation.

Evaluation of tumor volume, liver and renal function, leukocyte count, and skin changes

The total body weight of each mouse and size of implanted tumors were determined every other day by a single observer. Calipers were used to measure the largest (*a*) and smallest (*b*) diameter, and the tumor volume was estimated according to the formula $0.5ab^{2[19]}$. The leukocyte count was estimated by retro-orbital blood sampling every other day after treatment. Animals were killed when the first mouse expired after treatment. The plasma levels of alanine aminotransferase (ALT) and creatinine were measured with a SYNCHRON LX20 spectrophotometer (Beckman Coulter, San Diego, CA, USA) by heart blood sampling after being killed. Skin changes and hair loss in the mice were evaluated by a single observer after RT every other day.

Statistical analysis

Data were expressed as mean±SE or percentage. Analysis of variance was used to compare tumor size, body weight, ALT, and creatinine, and leukocyte count among the groups and controls. We used Sigma Stat software (version 2.03, SPSS Inc., Chicago, IL, USA) to perform the statistical analysis. $P<0.05$ was considered statistically significant.

RESULTS

Tumor growth

As shown in Figure 1, low-dose etoposide alone had no significant effect on tumor growth compared to the control group. However, RT alone and the combination therapy resulted in significant decrease in tumor size compared to controls ($P<0.05$). Combination therapy yielded the best results among the four groups. The tumor size at the end of the study in the combination therapy group was only 54% that of the RT group (1.27 cm³ vs 2.35 cm³).

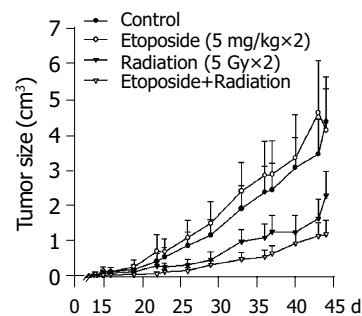


Figure 1 Tumor size in BALB/c mice implanted with CT26 colorectal adenocarcinoma cells. (●) control group, saline only; (○) etoposide group, 5 mg/kg×2; (▼) RT group, 5 Gy×2; (▽) combination therapy group (etoposide plus RT).

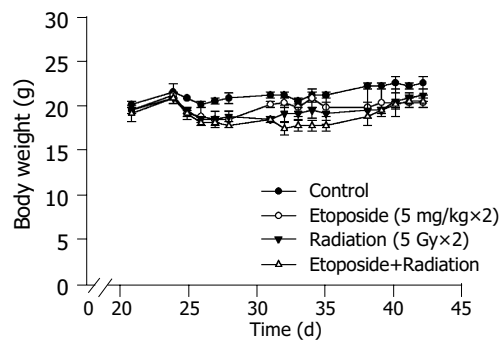


Figure 2 Changes in body weight of BALB/c mice implanted with CT26 colorectal adenocarcinoma cells. (●) control group, saline only; (○) etoposide group, 5 mg/kg \times 2; (▼) RT group, 5 Gy \times 2; (△) combination therapy group (etoposide plus RT).

Changes in body weight, liver, renal function, and skin

There were no significant changes in body weight in any of the four groups (Figure 2). Similarly, there were no significant differences in the plasma ALT and creatinine levels among the four groups (Figure 3). There was no obvious skin change or hair loss in any of the mice after RT or combination therapy except for tumor-related destruction.

Changes in leukocyte count

The leukocyte count decreased significantly but transiently after treatment with RT or combination therapy ($P < 0.05$). As shown in Figure 4, the nadir of the leukocyte count occurred 8 d after treatment. In contrast, the leukocyte counts in the control and etoposide groups had no evident change.

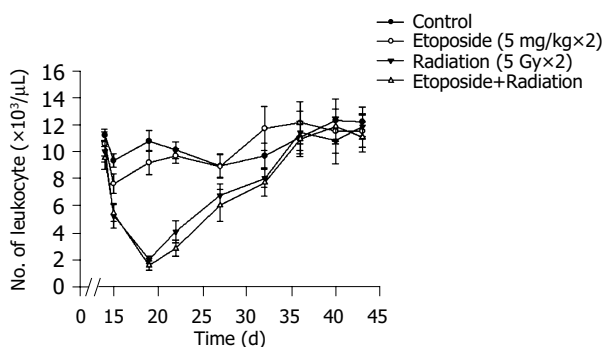


Figure 4 Serial changes in leukocyte counts of BALB/c mice implanted with CT26 colorectal adenocarcinoma cells. (●) control group, saline only; (○) etoposide group, 5 mg/kg \times 2; (▼) RT group, 5 Gy \times 2; (△) combination therapy group (etoposide plus RT).

DISCUSSION

Our findings indicate that etoposide is a potent radiosensitizer in murine CT-26 colorectal adenocarcinoma cells without evident toxicity *in vivo*. This supports the contention that the role of etoposide in CRC treatment is as a radiosensitizer rather than as a cytotoxic agent.

Body weight and plasma ALT and creatinine were unaffected by any of the treatment modalities. The fact that transient leukopenia was found in both the RT and combination therapy groups but not in the etoposide group

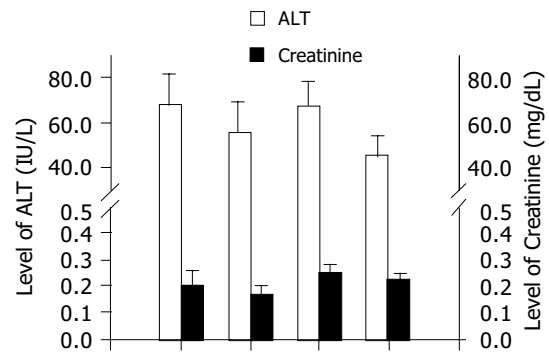


Figure 3 Plasma ALT and creatinine levels after killing of BALB/c mice implanted with CT26 colorectal adenocarcinoma cells. From left to right are: control group, etoposide group, RT group, and combination therapy group.

suggests that the bone marrow suppression may be caused by the radiation alone. The RT regimen used in this study may therefore needs to be adjusted to avoid myelosuppression. O'Dwyer *et al.*^[16], reported, that etoposide-related leukopenia is dose-dependent. The low dose we used was apparently successful in avoiding bone marrow suppression. Low-dose etoposide therefore may have little toxicity *per se*, but in our study, even this low dose appeared to have significant radiosensitizing activity.

One advantage of etoposide is that it comes in an oral form. Long term oral administration of etoposide improves the prognosis of ovarian cancer in patients who tolerate it well^[8,17]. This suggests that oral etoposide might be a good candidate for a daily radiosensitizer. One study has shown that there is no significant difference between intravenous and oral administration of etoposide in terms of median response duration, time to progression, and survival when used to treat small cell lung cancer^[18]. Shigematsu *et al.*^[13], also reported that the killing effect of low dose etoposide *in vitro*, seems to depend on the duration of exposure rather than the concentration. This duration-dependent rather than concentration-dependent also supports the use of lower dose etoposide as a radiosensitizer, as we found in our study.

Newer chemotherapeutic and biological agents, such as irinotecan (CPT-11)^[19], oxaliplatin^[20], and cyclooxygenase-2 inhibitors (e.g. celecoxib)^[21] have been studied for their radiosensitizing potential in rectal cancer. These agents are particularly attractive because they have a favorable safety profile^[22]. According to our results, low dose etoposide also appears to be safe and effective in the mouse model. It would therefore be worth conducting a clinical trial of etoposide-based CCRT for 5-FU resistant rectal cancer.

Although CCRT for CRC has promising clinical results, the mechanism of conventional radiosensitizers such as 5-FU remains unclear^[23]. This is true for etoposide as well. Shigematsu *et al.*^[13], have reported a significant increase in cells in the G₂/M phase after exposure to low-dose etoposide *in vitro*. This phenomenon is similar to our preliminary results (data not shown). Since cells in the G₂/M phase are radiosensitive, etoposide may act to arrest CT26 cells in that phase, thus sensitizing them to RT. Another possibility is that the drug upregulates p53 and Bcl-2 expression, as has been reported in CT26 cells *in vivo*^[24], an effect that

may induce apoptosis. Apoptosis may play an important role in the mechanism of radiosensitization. In the future, we are planning to assess apoptosis in tumors by annexin V/propidium iodide or the TUNEL test.

In conclusion, the results of this study indicate that low-dose etoposide can sensitize CT26 cells to RT *in vivo* without evident toxicity. Further studies to identify the mechanism of etoposide-related radiosensitization are needed.

ACKNOWLEDGMENT

The authors wish to thank Dr. Mary Jeanne Buttrey for critical reading and correction of the manuscript.

REFERENCES

- 1 **Midgley R**, Kerr D. Colorectal cancer. *Lancet* 1999; **353**: 391-399
- 2 **Fisher B**, Wolmark N, Rockette H, Redmond C, Deutsch M, Wickerham DL, Fisher ER, Caplan R, Jones J, Lerner H. Post-operative adjuvant chemotherapy or radiation therapy for rectal cancer: results from NSABP protocol R-01. *J Nat Cancer Inst* 1988; **80**: 21-29
- 3 **O'Connell MJ**, Martenson JA, Wieand HS, Krook JE, Macdonald JS, Haller DG, Mayer RJ, Gunderson LL, Rich TA. Improving adjuvant therapy for rectal cancer by combining protracted-infusion fluorouracil with radiation therapy after curative surgery. *N Engl J Med* 1994; **331**: 502-507
- 4 **Garufi C**, Brienza S, Pugliese P, Aschelter AM, Bensmaine, Bertheault-Cvitkovic F, Nistico C, Giunta S, Caterino M, Giannarelli D, Cosimelli M, Levi F, Terzoli E. Overcoming resistance to chronomodulated 5-fluorouracil and folinic acid by the addition of chronomodulated oxaliplatin in advanced colorectal cancer patients. *Anticancer Drugs* 2000; **11**: 495-501
- 5 **Hughes LL**, Luengas J, Rich TA, Murray D. Radiosensitization of cultured human colon adenocarcinoma cells by 5-fluorouracil: effects on cell survival, DNA repair, and cell recovery. *Int J Radiat Oncol Biol Phys* 1992; **23**: 983-991
- 6 **Ross W**, Rowe T, Glisson B, Yalowich J, Liu L. Role of topoisomerase II in mediating epipodophyllotoxin-induced DNA cleavage. *Cancer Res* 1984; **44**(12 Pt 1): 5857-5860
- 7 **Johnson DH**, Greco FA, Strupp J, Hande KR, Hainsworth JD. Prolonged administration of oral etoposide in patients with relapsed or refractory small-cell lung cancer: a phase II trial. *J Clin Oncol* 1990; **8**: 1613-1617
- 8 **Takeda S**, Takada S, Kojima T, Kinoshita K, Sakamoto S. Oral etoposide therapy in stage III-IV ovarian carcinoma. *Nippon Gan Chiryō Gakkai Shi* 1990; **25**: 2562-2566
- 9 **Tucker RD**, Ferguson A, Van WC, Sealy R, Hewitson R, Levin W. Chemotherapy of small cell carcinoma of the lung with V. P. 16-213. *Cancer* 1978; **41**: 1710-1714
- 10 **Lee JS**, Komaki R, Fossella FV, Glisson BS, Hong WK, Cox JD. A pilot trial of hyperfractionated thoracic radiation therapy with concurrent cisplatin and oral etoposide for locally advanced inoperable non-small-cell lung cancer: a 5-year follow-up report. *Int J Radiat Oncol Biol Phys* 1998; **42**: 479-486
- 11 **Beauchesne P**, Soler C, Boniol M, Schmitt T. Response to a phase II study of concomitant-to-sequential use of etoposide and radiation therapy in newly diagnosed malignant gliomas. *Am J Clin Oncol* 2003; **26**: e22-27
- 12 **Perry MC**, Moertel CG, Schutt AJ, Reitemeier RJ, Hahn RG. Phase II studies of dianhydrogalactitol and VP-16-213 in colorectal cancer. *Cancer Treat Rep* 1976; **60**: 1247-1250
- 13 **Shigematsu N**, Kawata T, Ihara N, Kawaguchi O, Kutsuki S, Ishibashi R, Kubo A, Ito H. Effect of combined treatment with radiation and low dose etoposide on cell survival. *Anti-cancer Res* 2001; **21**: 325-328
- 14 **Brattain MG**, Strobel-Stevens J, Fine D, Webb M, Sarrif AM. Establishment of mouse colonic carcinoma cell lines with different metastatic properties. *Cancer Res* 1980; **40**: 2142-2146
- 15 **Yang EB**, Tang WY, Zhang K, Cheng LY, Mack PO. Norcantharidin inhibits growth of human HepG2 cell-transplanted tumor in nude mice and prolongs host survival. *Cancer Lett* 1997; **117**: 93-98
- 16 **O'Dwyer PJ**, LaCreta FP, Daugherty JP, Hogan M, Rosenblum NG, O'Dwyer JL, Comis RL. Phase I pharmacokinetic study of intraperitoneal etoposide. *Cancer Res* 1991; **51**: 2041-2046
- 17 **Yasumizu T**, Kato J. Clinical trial of daily low-dose oral etoposide for patients with residual or recurrent cancer of the ovary or uterus. *J Obstet Gynaecol* 1995; **21**: 569-576
- 18 **Johnson DH**, Ruckdeschel JC, Keller JH, Lyman GH, Kallas GJ, Macdonald J, DeConti RC, Lee J, Ringenberg QS, Patterson WP. A randomized trial to compare intravenous and oral etoposide in combination with cisplatin for the treatment of small cell lung cancer. *Cancer* 1991; **67**(1 Suppl): 245-249
- 19 **Wang DS**, Ueno Y, Oyamada H, Kojima S. Enhancement of the antitumor effect of gamma-ray irradiation in combination with camptothecin against human colorectal adenocarcinoma. *Biol Pharm Bull* 1996; **19**: 354-359
- 20 **Gerard JP**, Chapet O, Nemoz C, Romestaing P, Mornex F, Coquard R, Barbet N, Atlan D, Adeleine P, Freyer G. Preoperative concurrent chemoradiotherapy in locally advanced rectal cancer with high-dose radiation and oxaliplatin-containing regimen: the Lyon R0-04 phase II trial. *J Clin Oncol* 2003; **21**: 1119-1124.
- 21 **Kishi K**, Petersen S, Petersen C, Hunter N, Mason K, Masferrer JL, Tofilon PJ, Milas L. Preferential enhancement of tumor radioresponse by a cyclooxygenase-2 inhibitor. *Cancer Res* 2000; **60**: 1326-1331
- 22 **Zhu AX**, Willett CG. Chemotherapeutic and biologic agents as radiosensitizers in rectal cancer. *Semin Radiat Oncol* 2003; **13**: 454-468
- 23 **Lawrence TS**, Blackstock AW, McGinn C. The mechanism of action of radiosensitization of conventional chemotherapeutic agents. *Semin Radiat Oncol* 2003; **13**: 13-21
- 24 **Wang C**, Yang YG, Wang XL. Expressions of HTERT, P53, C-ErbB-2 and Bcl-2 in colonic adenocarcinoma mouse models with liver metastases: effects of classical traditional chinese medicine prescriptions for promoting circulation and removing blood stasis. *Diyi Junyi Daxue Xuebao* 2004; **24**: 758-760

Disulfide-stabilized single-chain antibody-targeted superantigen: Construction of a prokaryotic expression system and its functional analysis

Jian-Li Wang, Yu-Ling Zheng, Ru Ma, Bao-Li Wang, Ai-Guang Guo, Yong-Qiang Jiang

Jian-Li Wang, Bao-Li Wang, Ai-Guang Guo, Department of Life Science, Northwest Sci-Tech University of Agriculture and Forestry, No. 22 Xinong Road, Yangling 712100, Shaanxi Province, China
Yong-Qiang Jiang, Yu-Ling Zheng, Ru Ma, Institute of Microbiology and Epidemiology, Academy of Military Medical Sciences, No. 20 Dongda Street, Fengtai District, Beijing 100071, China

Supported by the National Natural Science Foundation of China, No. 30271478

Correspondence to: Yong-Qiang Jiang, Institute of Microbiology and Epidemiology, Academy of Military Medical Sciences, No. 20 Dongda Street, Fengtai District, Beijing 100071, China. jiangyq@nic.bmi.ac.cn

Telephone: +86-10-6694-8487

Received: 2004-12-22 Accepted: 2005-02-18

system and its functional analysis. *World J Gastroenterol* 2005; 11(31): 4899-4903

<http://www.wjgnet.com/1007-9327/11/4899.asp>

INTRODUCTION

Bacterial superantigen *Staphylococcal enterotoxin A* (SEA) is an efficient activator of cytotoxic T cells when presented on MHCII antigens and shows a potential ability in cancer immunotherapy^[1-3]. But SEA also has cytotoxicity against the normal cells when used to kill carcinoma cells and has no effect on MHCII⁻ carcinoma cells. The monoclonal antibody (mAb) preparation technique has brought about a new method for cancer therapy known as tumor-targeting therapy. Which therapy can solve the two problems mentioned above? The mAb B3 is a murine antibody directed against a carbohydrate antigen in the Le^Y family, that is found on the surface of many mucinous carcinomas of the colon, stomach, ovaries, breast, and lung as well as some epidermal carcinomas. Because mAbB3 reacts with a limited number of normal tissues, it is an ideal candidate for the treatment and diagnosis of cancer^[4]. Immunotoxins made from mAb B3 are cytotoxic to various human cancer cell lines that express B3 antigen on their surface, and some of them have been evaluated in clinical or preclinical trials^[5].

Antibodies penetrate tumors slowly and take several days to mix completely within a tumor because of their large size^[6]. Fv fragments of antibodies are heterodimers of the heavy chain variable domain (VH) and the light chain variable domain (VL), and the smallest functional modules of antibodies required for high affinity antigen binding. The polypeptide chains of whole IgG or Fab fragments are joined by a disulfide bond, but Fv fragments have no such inter-chain disulfide bridge and are therefore unstable^[7]. Stable Fv fragments can be produced by making recombinant molecules in which the VH and VL domains are connected by a peptide linker (ScFv) or a disulfide bond (DsFv), so that the antigen binding site is regenerated in a single protein. However, many single-chain Fvs are unstable. When they are fused to toxins, the resulting recombinant immunotoxins are also unstable, presumably owing to aggregation during the transient separation of VH from VL by the peptide linker. DsFv is more stable than ScFv, but the low yield after renaturation limits its application^[8]. A new type of engineered antibody, known as scdsFv has a linker and a disulfide bond between VH and VL, and is more stable than dsFv^[8].

Abstract

AIM: To construct the expression vector of B3 (scdsFv)-SEA (D227A) and to identify its binding and cytotoxic ability to B3 antigen positive carcinoma cell lines.

METHODS: This fusion protein was produced by a bacterial expression system in this study. It was expressed mainly in the inclusion body. The gene product was solubilized by guanidine hydrochloride, refolded by conventional dilution method, and purified using SP-sepharose cation chromatography.

RESULTS: The expression vector B3 (scdsFv)-SEA-PET was constructed, the expression product existed mainly in the inclusion body, the refolding product retained the binding ability of the single-chain antibody and had cytotoxic effect on HT-29 colon carcinoma cells. The stability assay showed that the resulting protein was stable at 37 °C.

CONCLUSION: This genetically engineered B3 (scdsFv)-SEA fusion protein has bifunction of tumor targeting and tumor cell killing and shows its promises as an effective reagent for tumor-targeted immunotherapy.

© 2005 The WJG Press and Elsevier Inc. All rights reserved.

Key words: B3 monoclonal antibody; Single-chain disulfide-stabilized Fv; Superantigen

Wang JL, Zheng YL, Ma R, Wang BL, Guo AG, Jiang YQ. Disulfide-stabilized single-chain antibody-targeted superantigen: Construction of a prokaryotic expression

In this study, scdsFv of B3mAb (B3scdsFv) was fused to the SEA (D227A) by genetic engineering method and expressed in *E. coli*. The refolding protein has been proved to be stable at 37 °C. It can bind to tumor surface antigen and is cytotoxic to HT-29 colon cells, thus SEA can be used in tumor targeting therapy.

MATERIALS AND METHODS

Plasmids and cell lines

Template plasmids B3scFv-pET32a and SEA (D227A)-pET32a were constructed by our laboratory. Expression plasmid pET22b, *E. coli* TOP10, human colon carcinoma cell line HT-29, human hepatoma cell line SMMC-7721, human breast carcinoma cell line MCF-7 were all kept in our laboratory.

Reagents

LATaqDNA polymerase and restricted enzymes were purchased from Takara Biotechnology Co., Ltd (Dalian, China). T4 DNA ligase and non-radioactive cell proliferation assay kit were obtained from Promega (USA). AKTA FPLC and Hitrap-SP sepharose column were products of Amersham Biosciences (Switzerland). Primer synthesizing and DNA sequencing were completed by Bioasia Co., Ltd (Shanghai, China).

Construction of plasmid B3scdsFv-pET22b

Mutated disulfide bond sites in B3VH (Cys⁴⁴) and B3VL (Cys¹⁰⁵) were designed as previously described^[9,10]. A mutation in the linker between VH and VL was found in the template plasmid B3scdsFv-pET32a after DNA sequencing. Since the 6th base in GGGGSGGGGSGGGGS (linker) was mutated from G to S, we corrected the mutation by overlap PCR and ligated B3VH and B3VL at the same time. Four primers were designed according to the gene sequence in GenBank and the linker sequence (Table 1). Part of the linker sequence was involved in P₂ and P₃. Primers 1 and 2 were used for amplification of B3VH and primers 3 and 4 for B3VL. The purified B3VH and B3VL products were mixed at the ratio of 1:1 and then applied as the template for the amplification of B3scdsFv with primers 1 and 4. Then the purified B3scdsFv fragment was cloned into the DNA sequencing vector pMD-18T. The full length B3scdsFv was excised from pMD-18T-vector containing correct insert with *Nde*I and *Bam*HI and subcloned into a similarly digested pET22b vector to produce the recombinant plasmid B3scdsFv-pET22b.

Table 1 Oligonucleotide primers for construction of B3scdsFv-pET22b

Number	Long oligonucleotide sequences
1	5'-ggc cat atg gat gtg aag ctg gtg-3'
2	5'-acc tcc acc tga acc gcc tcc acc gga gac agt gac cag-3'
3	5'-ctg gtc act gtc tcc ggt gga ggc ggt tca ggt gga-3'
4	5'-ccg gga tcc gcc ccc ttt aat ttc cag ctt tgt-3'
5	5'-attggatcggagggttaacgagcgaagcgaagaata-3'
6	5'-cacgtgacttaactgtatataaatatagcaaatatgcatg-3'

Restriction enzyme is underlined.

Construction of expression plasmid B3scdsFv-SEA-pET22b

The SEA gene was amplified by PCR using primer pair P₅ and P₆ and template SEA (D227A)-pET32a. The PCR products were purified and directly cloned into pMD-18T-vector and further cloned into pET22b (Figure 1).

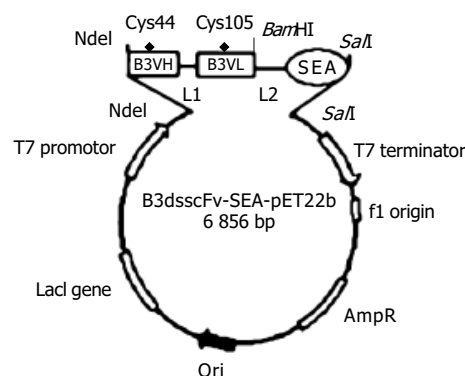


Figure 1 Schematic representation of B3scdsFv-SEA-pET22b expression plasmid. L: polypeptide linker; L1: (GlyGlyGlyGlySer)₃; L2: (GlyGlyGlySer-GlyGlySer).

Expression of B3scdsFv-SEA

The bacterial strain BL21 (DE₃) pLysS was used to express the fusion protein. Briefly, one positive clone was grown in LB medium containing 100 µg/mL ampicillin and induction was started by addition of IPTG (final concentration, 1 mmol/L) when the culture reached A₆₀₀ = 0.5. After the culture was induced for 3 h at 37 °C, the cells were harvested. The bacterial pellet was resuspended in 50 mmol/L Tris-HCl, 5 mmol/L EDTA, pH 8.5, 0.8% NaCl, and sonicated, then centrifuged at 12 000 g for 15 min at 4 °C to separate the supernatant and the inclusion body, and analyzed on 15% SDS-PAGE.

Western blotting analysis

Western blotting was performed to confirm B3scdsFv-SEA identity. Protein samples were dissolved by 15% SDS-PAGE under reducing conditions and using duplicate gels. One gel was Coomassie stained while the other was used for semi-dry electrophoretic transfer (Jim-X Biotechnology Co., Ltd, Dalian, China) of the proteins onto nitrocellulose membrane. The membrane was then blocked with 0.05 mol/L Tris-HCl, pH 7.4, 0.5 mol/L NaCl, 3% BSA and incubated with the rabbit polyclonal antibody against SEA for 1 h and followed by the incubation of HRP-coupled goat anti-rabbit IgG as secondary antibody. Finally, the recombinant B3scdsFv-SEA was visualized with Fast DAB peroxidase substrate. In this part, the B3scdsFv-SEA-pET22b before induction (total protein) was used as a negative control.

Refolding and purification of B3scdsFv-SEA

The inclusion body was washed twice in 0.05 mol/L Tris-HCl, pH 8.0, 20 mmol/L EDTA, 2% Triton X-100, 0.5 mol/L NaCl, then dissolved in 6 mol/L guanidine hydrochloride, 2 mmol/L EDTA, 0.05 mol/L Tris-HCl, pH 8.5, 10 mmol/L DTT and incubated for 3 h at room temperature. The denatured products were centrifuged for 10 min at 12 000 g at 4 °C. The supernatant was slowly

diluted into the refolding solution containing 0.1 mol/L Tris-HCl, pH 8.0, 0.5 mol/L L-Arg, 2 mmol/L EDTA, 0.9 mmol/L oxidized glutathione at the ratio 1:30, refolded for 48 h at 10 °C.

The refolding solution was concentrated by hollow fiber cartridges, and buffer exchange was carried out at the same time. The denatured protein in 5 mmol/L phosphate buffer, pH 5.8 (buffer A) was loaded into a 5 mL sp-sepharose column pre-equilibrated by buffer A. The protein was eluted with a linear gradient from 0 to 0.5 mol/L NaCl in 0.04 mol/L phosphate buffer, pH 7.4 (buffer B). The eluted protein was analyzed on 15% SDS-PAGE.

Binding assay

Analysis for the binding of B3scdsFv-SEA to B3 positive tumor cells (including human colon carcinoma cell line HT-29, human hepatoma cell line SMMC-7721, human breast carcinoma cell line MCF-7) was performed as described previously^[11]. Briefly, the prepared tumor cells were seeded in a 96-well plate containing 5×10^3 cells per well. Cells were cultured for 48 h at 37 °C and the plate was washed thrice with PBS. After fixation with pre-cooled fixing solution (methanol/acetone solution, v/v = 1:1) for 30 min, the reaction was ended by addition of PBS containing 1% H₂O₂. Blocking was performed with 1% bovine serum albumin in PBS with 0.05% Tween-20. After blocking, the purified B3scdsFv-SEA was added to each well. PBS served as the negative control. The plate was incubated at 37 °C for 1 h. After being washed with PBST, the rabbit polyclonal antibody against SEA (1:1 000 diluted by PBST) was added and incubated at 37 °C for 1 h followed by incubation with HRP-coupled goat anti-rabbit IgG for 30 min. At last, the substrate TMB was applied for 3 min and the absorbance at 450 nm was measured when the reaction was stopped by the addition of 2 mol/L H₂SO₄.

Tumor cell growth inhibition assay

Growth inhibition assay was performed in 96-well plates as described previously^[11]. Briefly, 5×10^3 HT-29 cells were added to each well, followed by B3scdsFv-SEA dilutions and 4×10^4 effector cells (human peripheral blood T lymphocytes) in a total volume of 200 μ L. Cells were cultured for 5 d at 37 °C in a humidified atmosphere containing 50 mL/L CO₂. After the culture, the number of remaining tumor cells was determined using a non-radioactive cell proliferation assay kit (Promega, USA) and the A_{490} was measured using a SPECTRA max Plus spectrophotometer (Molecular Device Corp., USA). Data were expressed as percentage of tumor growth inhibition, which was calculated as $(1 - A_{\text{test}}/A_{\text{C}}) \times 100\%$, where A_{test} indicates the absorbance of tumor cells grown in the presence of effector cells and B3scdsFv-SEA dilutions, A_{C} indicates the absorbance of tumor cells grown in medium with the effector cells.

Stability assay

The stability of recombinant toxin was determined by incubating for different periods at 37 °C in PBS, and the remaining activity was determined by testing the binding to the HT-29 cell line.

RESULTS

Expression of B3scdsFv-SEA in *E. coli*

The expression products in bacterial strain BL21 (DE3) pLysS was mainly found in the inclusion body as shown in Figure 2A. The relative mass of targeted protein was approximately 50 ku, and its expression level was approximately 30% of the total cellular protein as determined by TotalLab 2.01 software analysis. Western blotting was performed to test the identity of B3scdsFv-SEA. The rabbit polyclonal antibody could recognize the B3scdsFv-SEA protein at around 50 ku, but the same reaction was not observed at lane 2 (the negative control) (Figure 2B).

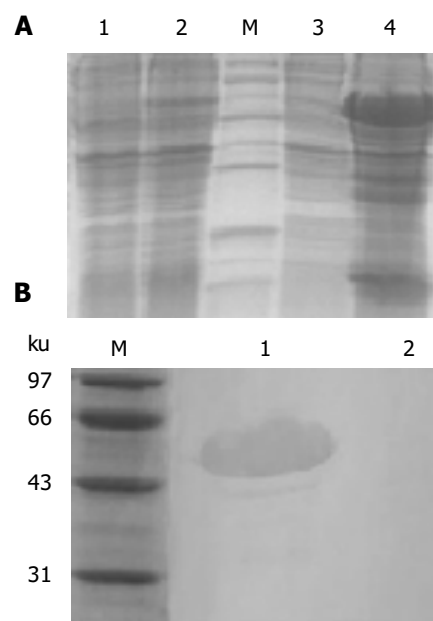


Figure 2 The SDS-PAGE analysis of expression products (A) and Western blot of inclusion body (B). A: Lane 1: B3scdsFv-SEA- pET22b before induction; lane 2: total protein after induction; lane 3: ultrasonic supernatant of B3scdsFv-SEA-pET22b induced by 1 mmol/L IPTG; lane 4: ultrasonic deposit after induction; lane M: low molecular weight protein marker; B: Lane 1: Western blot of B3scdsFv-SEA; lane 2: negative control (total protein before induction); lane M: low molecular weight protein marker.

Refolding and purification of B3scdsFv-SEA

In order to generate protein with a native conformation, we solubilized and reduced the inclusion body in guanidine hydrochloride and DTT, and refolded the protein by dilution in a buffer containing arginine at 10 °C. The refolded product was purified through SP-sepharose column after concentration and buffer exchange.

The fraction of B3scdsFv-SEA molecules could be determined by SDS-PAGE. Figure 3 shows, that the gel mobility of B3scdsFv-SEA was more rapid under non-reducing condition than under reducing condition, indicating that the disulfide bond might be formed during the refolding process.

Binding assay

The binding affinity of B3scdsFv-SEA was measured on B3 antigen expressing cell lines HT-29, MCF-7, and SMMC-

7721. Figure 4 shows, that the binding affinity increased with the protein concentration, and had a better binding ability on MCF-7 cells because the expression level of B3 antigen on MCF-7 was higher than that of the other two cell lines^[12].



Figure 3 Gel mobility of B3scdsFv-SEA under reducing (lane 1) and non-reducing condition (lane 2).

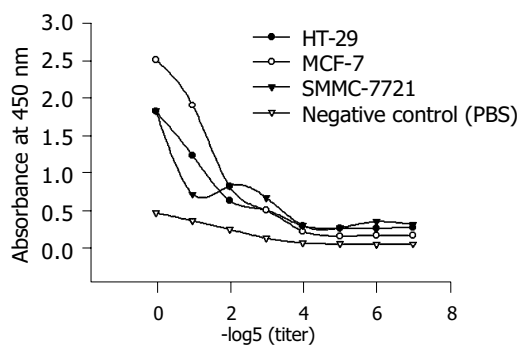


Figure 4 Binding assay of B3scdsFv-SEA to B3 antigen positive carcinoma cell lines.

Stability assay

B3scdsFv-SEA was very stable at 37 °C in PBS. The binding activity of B3scdsFv-SEA at different time points was determined by ELISA. The recombinant toxin retained 85% of its activity after 16 h incubation at 37 °C (Figure 5).

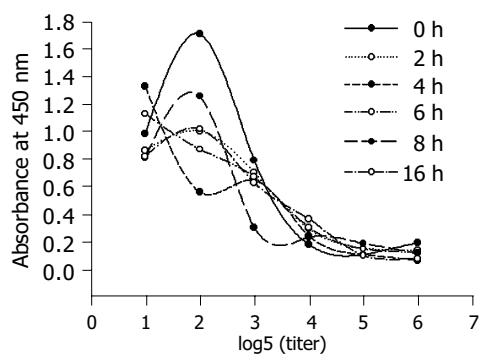


Figure 5 Stability of B3scdsFv-SEA.

Cytotoxic effect on tumor cells of B3scdsFv-SEA

The toxicity of B3scdsFv-SEA to human colon carcinoma

cell line HT-29 was determined by the MTT assay. The results of a representative experiment are shown in Figure 6. The maximum killing effect could achieve 95% when the protein concentration was 1 μg/mL. But the cytotoxic potency was a bit lower than native SEA. No killing effect on tumor cells was observed when the effector cells were added alone (data not shown).

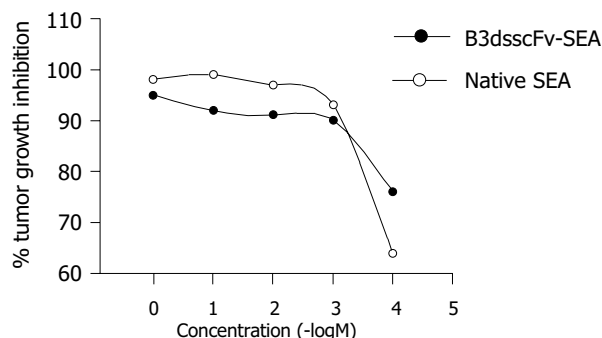


Figure 6 Cytotoxic effects of B3scdsFv-SEA on HT-29 cell line.

DISCUSSION

The Fv fragment of an antibody can penetrate tumors more quickly than the intact antibody because of its small size^[13]. Because of this advantage, different types of Fv fragments such as ScFv and dsFv have been extensively applied in tumor targeting therapy. But the instability of the ScFv and the low yield of dsFv become the obstacles in their clinical application. It was reported that the ScdsFv which has a peptide linker and a disulfide bond between VH and VL is stable at least after 1 wk exposure to human plasma at 37 °C, even under denaturing urea (6 mol/L) conditions, and it has a higher yield after renaturation than dsFv^[8].

In this study, the ScdsFv of B3 mAb was fused to SEA (D227A). The fusion protein was expressed as inclusion body in *E. coli*. Small-scale preparations were performed in order to determine the optimal denaturing conditions, and we found that the maximum protein activity could be achieved in the presence of 0.5 mol/L L-Arg and 0.9 mmol/L GSSG in the refolding solution and the optimal denaturing temperature was 10 °C. The refolded products were purified to get rid of the renaturation agents, the purified B3scdsFv-SEA (D227A) had excellent binding affinity when incubated with B3 antigen positive tumor cell lines. The cytotoxic results indicate that the B3scdsFv-targeted superantigen suppresses the tumor cell growth successfully by activating the T lymphocytes. Moreover, the resulting protein is stable when incubated at 37 °C. All the SEA show that the binding and cytotoxic ability is not affected by the presence of both a linker and a disulfide bond between B3VH and B3VL.

In conclusion, B3scdsFv-targeted superantigen can be constructed in a bacterial system and this fusion protein shows its promise as a good reagent for cancer immunotherapy.

REFERENCES

- 1 Kalland T, Dohlsten M, Abrahmsen L, Hedlund G, Bjork P, Lando PA, Sundstedt A, Akerblom E, Lind P. Targeting of

- superantigens. *Cell Biophys* 1993; **22**: 147-164
- 2 **Hansson J**, Ohlsson L, Persson R, Andersson G, Ilback NG, Litton MJ, Kalland T, Dohlsten M. Genetically engineered superantigens as tolerable antitumor agents. *Proc Natl Acad Sci USA* 1997; **94**: 2489-2494
- 3 **Dohlsten M**, Hedlund G, Akerblom E, Lando PA, Kalland T. Monoclonal antibody-targeted superantigens: a different class of anti-tumor agents. *Proc Natl Acad Sci USA* 1991; **88**: 9287-9291
- 4 **Brinkmann U**, Pai LH, FitzGerald DJ, Willingham M, Pastan I. B3(Fv)-PE38KDEL, a single-chain immunotoxin that causes complete regression of a human carcinoma in mice. *Proc Natl Acad Sci USA* 1991; **88**: 8616-8620
- 5 **Pai LH**, Batra JK, FitzGerald DJ, Willingham MC, Pastan I. Antitumor effects of B3-PE and B3-LysPE40 in a nude mouse model of human breast cancer and the evaluation of B3-PE toxicity in monkeys. *Cancer Res* 1992; **52**: 3189-3193
- 6 **Rajagopal V**, Pastan I, Kreitman RJ. A form of anti-Tac(Fv) which is both single-chain and disulfide stabilized: comparison with its single-chain and disulfide-stabilized homologs. *Protein Eng* 1997; **10**: 1453-1459
- 7 **Reiter Y**, Brinkmann U, Jung SH, Lee B, Kasprzyk PG, King CR, Pastan I. Improved binding and antitumor activity of a recombinant anti-erbB2 immunotoxin by disulfide stabilization of the Fv fragment. *J Biol Chem* 1994; **269**: 18327-18331
- 8 **Bera TK**, Onda M, Brinkmann U, Pastan I. A bivalent disulfide-stabilized Fv with improved antigen binding to erbB2. *J Mol Biol* 1998; **281**: 475-483
- 9 **Jung SH**, Pastan I, Lee B. Design of interchain disulfide bonds in the framework region of the Fv fragment of the monoclonal antibody B3. *Proteins* 1994; **19**: 35-47
- 10 **Brinkmann U**, Reiter Y, Jung SH, Lee B, Pastan I. A recombinant immunotoxin containing a disulfide-stabilized Fv fragment. *Proc Natl Acad Sci USA* 1993; **90**: 7538-7542
- 11 **Dohlsten M**, Lando PA, Bjork P, Abrahmsen L, Ohlsson L, Lind P, Kalland T. Immunotherapy of human colon cancer by antibody-targeted superantigens. *Cancer Immunol Immunother* 1995; **41**: 162-168
- 12 **Pastan I**, Lovelace ET, Gallo MG, Rutherford AV, Magnani JL, Willingham MC. Characterization of monoclonal antibodies B1 and B3 that react with mucinous adenocarcinomas. *Cancer Res* 1991; **51**: 3781-3787
- 13 **Kuan CT**, Pastan I. Improved antitumor activity of a recombinant anti-Lewis(y) immunotoxin not requiring proteolytic activation. *Proc Natl Acad Sci USA* 1996; **93**: 974-978

Science Editor Wang XL and Guo SY Language Editor Elsevier HK

Microsatellite instability in gastric cancer and pre-cancerous lesions

Ping Liu, Xiao-Yong Zhang, Yun Shao, Dao-Fu Zhang

Ping Liu, Department of Oncology, the First Affiliated Hospital of Nanjing Medical University, Nanjing 210029, Jiangsu Province, China

Xiao-Yong Zhang, Yun Shao, Dao-Fu Zhang, Department of Gastroenterology, the First Affiliated Hospital of Nanjing Medical University, Nanjing 210029, Jiangsu Province, China

Supported by the Science and Technology Committee Foundation of Jiangsu Province, No. BS98028

Correspondence to: Dr. Ping Liu, Department of Oncology, the First Affiliated Hospital of Nanjing Medical University, 300 Guangshou Road, Nanjing 210029, Jiangsu Province, China. liupinga@yahoo.com

Telephone: +86-25-83718836-6415 Fax: +86-25-83724440

Received: 2004-12-24 Accepted: 2005-01-12

© 2005 The WJG Press and Elsevier Inc. All rights reserved.

Key words: Stomach neoplasms; Gastric dysplasia; Intestinal metaplasia; Microsatellite instability; PCR-SSCP

Liu P, Zhang XY, Shao Y, Zhang DF. Microsatellite instability in gastric cancer and pre-cancerous lesions. *World J Gastroenterol* 2005; 11(31): 4904-4907

<http://www.wjgnet.com/1007-9327/11/4904.asp>

Abstract

AIM: To investigate the microsatellite instability (MSI) in cancer and pre-cancerous lesions of the stomach and its mechanisms underlying the development of gastric cancer.

METHODS: Thirty-six gastric cancer samples were obtained from patients undergoing surgery. Forty-one gastric mucosa samples with dysplasia and 51 with intestinal metaplasia (IM) were obtained from patients with chronic gastritis undergoing gastro-endoscopy. Genomic DNA was extracted from the samples. Silver staining single strand conformation polymorphis-polymerize chain reaction (SSCP-PCR) was used to screen MSI markers at 5 loci (Bat-25, Bat-26, D5S346, D17S250, and D2S123) in fresh tissues and formalin-fixed, paraffin-embedded samples and their corresponding normal gastric mucosa.

RESULTS: The abnormal shifting of the single-strand DNA (MSI) was identified in 21 out of 36 (58.3%) gastric cancers. Seven cases showed high-level MSI (two or more loci altered) and 14 showed low-level MSI (one locus altered). Gastric cancer with MSI had a tendency to be located in the distal stomach. MSI was also detected in 11 out of 41 (26.8%) dysplasia samples and in 9 of 51 (17.6%) IM samples respectively. Three cases of dysplasia and one case of IM showed high-level MSI. Eight cases of dysplasia and 8 cases of IM displayed low-level MSI. MIS in IM was found only in moderate or severe-grade IM. No association was detected between MSI and dysplasia grade.

CONCLUSION: Accumulation of MSI in dysplasia and intestinal metaplasia of gastric mucosa may be an early molecular event during gastric carcinogenesis and may contribute to the acquisition of transformed cell phenotype and the development of gastric cancer.

INTRODUCTION

There is evidence that gastric carcinogenesis is a long-term, multistep process associated with abnormal alterations in cellular oncogenes, tumor suppressor genes and other genes or factors necessary for cell malignant transformation^[1-4]. Genetic instability is strongly involved in neoplastic transformation and progression^[5-9]. Microsatellite instability (MSI), an important form of genetic instability associated with defective DNA mismatch repair in tumors, was first described in hereditary non-polyposis colorectal cancer (HNPCC) in 1993^[6]. Since then, the presence of MSI has been reported in a variety of sporadic cancers including gastric cancer^[5,10-14], suggesting that MSI may play an important role in the development of gastric cancer^[15]. Intestinal metaplasia and dysplasia predisposed in gastric mucosa have been regarded as pre-cancerous lesions of the stomach and are closely related to the gastric carcinogenesis^[16-19]. However, there are few reports concerning the changeable patterns of MSI in the two pre-cancerous lesions. In this study, we investigated MSI alterations by use of SSCP-PCR technique in gastric mucosa with intestinal metaplasia and dysplasia, and gastric cancer samples to explore the potential role of MSI in gastric carcinogenesis.

MATERIALS AND METHODS

Stomach specimens

Thirty-six gastric cancer samples were obtained from patients undergoing surgery. Forty-one gastric mucosa samples with dysplasia and 51 with intestinal metaplasia were obtained from patients with chronic gastritis undergoing gastro-endoscopy in Jiangsu Provincial Hospital, Nanjing, China. The tumors were graded as well, moderately and poorly differentiated. Lesions of intestinal metaplasia and dysplasia were graded as mild, moderate and severe according to the WHO criteria. Tissues from non-tumor or non-inflammatory gastric mucosa were used as a control in analysis of MSI.

Tissue DNA extraction

Serial 5- μm -thick sections were obtained from formalin-fixed and paraffin-embedded tissue blocks. After tissue deparaffinization, genomic DNA was isolated by standard proteinase-K digestion and phenol-chloroform extraction protocol as previously described^[20].

PCR-SSCP analysis

All samples were analyzed using five markers (Bat-25, Bat-26, D5S346, D17S250, and D2S123) recommended by America National Cancer Institute (NCI) workshop on MSI^[21]. Oligonucleotides of five pair primers were synthesized by Sangon Technologies, Shanghai, China. The primer sequences are listed in Table 1.

Polymerase chain reaction (PCR) was performed as described by Fleisher *et al.*^[11] with some modifications. In brief, 25 μL reaction mixture containing 200 ng of DNA, 2.5 μL 10 \times PCR buffer, 1 $\mu\text{mol/L}$ primer, 1.5-2.0 mmol/L MgCl_2 , 200 $\mu\text{mol/L}$ dNTPs, and 0.5 U Taq DNA polymerase (Takara, Japan), was amplified for one cycle at 95 $^\circ\text{C}$ for 5 min followed by 35 cycles at 94 $^\circ\text{C}$ for 30 s, at

55-58 $^\circ\text{C}$ for 30 s, at 72 $^\circ\text{C}$ for 15 s, and 72 $^\circ\text{C}$ for 1 min.

Single strand conformation polymorphism (SSCP) was carried out. In brief, 12 μL of each PCR product was mixed with 12 μL denaturing buffer, denatured at 97 $^\circ\text{C}$ for 7 min, loaded onto a non-denaturing 7% polyacrylamide gel and electrophoresed for 3 h at 20 $^\circ\text{C}$. The bands were visualized by silver staining.

Existence of MSI was defined as an band mobility shift from either alleles or as appearance of a new band with a different size in the testing sample compared to the control one. The analysis was performed once more in samples displaying MSI for confirmation of the results. High-level MSI (MSI-H) was recognized, when more than 30% of the markers showed instability and low-level MSI (MSI-L) was recognized, if less than 30% of the markers displayed instability. None of the markers showing MSI indicated microsatellite stability (MSS)^[21].

Statistical analysis

Statistical analysis was performed using the *t* test or Fisher's exact test. $P < 0.05$ was considered statistically significant.

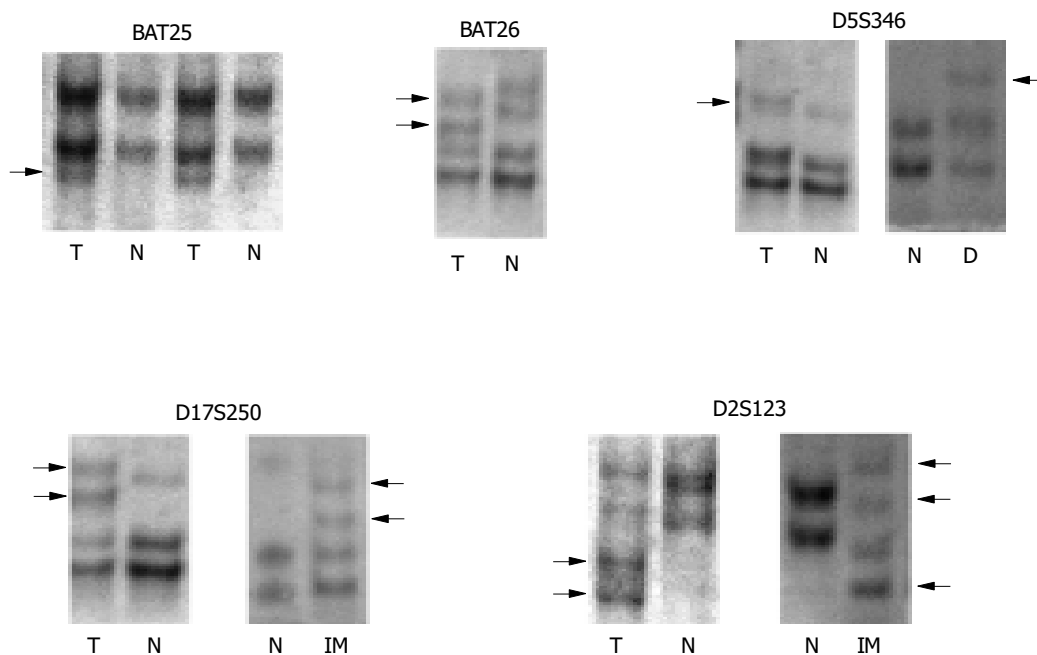


Figure 1 Detection of microsatellite instability (MSI) with five markers in tissues of gastric cancer, dysplasia and intestinal metaplasia by PCR-SSCP.

Arrows show abnormal bond of MSI. T: tumor; IM: intestinal metaplasia; D: dysplasia; N: normal mucosa.

Table 1 Sequences of primers for PCR analysis

Repeat sequence	Primers	Amplicated fragment (bp)
BAT-25	5'-TCGCCTCCAAGAATGTAAGT-3' 5'-TCTGCATTTTAACTATGGCTC-3'	-90
BAT-26	5'-TGACTACTTTTGACTTCAGCC-3' 5'-AACCATTC AACATTTTAAACCC-3'	80-100
D5S346	5'-ACTCACTCTAGTGATAAATCG-3' 5'-AGCAGATAAGACAGTATTACTAGTT-3'	96-122
D17S250	5'-GGAAGAATCAAATAGACAA-3' 5'-GCTGGCCATATATATATTTAAACC-3'	-150
D2S123	5'-AAACAGGATGCCTGCCTTTA-3' 5'-GGACTTTCACCTATGGGAC-3'	197-227

RESULTS

MSI in gastric cancer

None of the 36 gastric cancer patients had a family history of gastric cancer. MSI was observed in 21 out of 36 (58.3%) gastric cancers. Among the 21 MSI⁺ cases, 7 showed MSI-H and 14 showed MSI-L. Figure 1 displays a representative MSI band compared to control counterpart. No association was observed between MSI status and age, gender, tumor grade, tumor location or lymph node spread. Gastric cancer with MSI had a tendency to be located in the distal stomach compared to gastric cancer with MSS (Table 2).

Table 2 Characteristics of 36 gastric cancer patients

Characteristic	MSS (n = 15)	MSI-L (n = 14)	MSI-H (n = 7)
Average age	58	62	58
Sex			
Male	10	11	4
Female	5	3	3
Differentiation grade			
well-moderate	7	9	6
poor	8	5	1
Tumor location			
Distal	8	8	5
Proximal	7	6	2
Lymph node spread			
Absent	9	7	4
Present	6	8	3

MSI in dysplasia

MSI was detected in 11 out of 41 (26.8%) dysplasia samples. Among the 11 MSI⁺ samples, three showed MSI-H and 8 displayed MSI-L. The frequency of MSI in moderate to severe dysplasia was higher (33.3%) than that in mild dysplasia (20%), but the difference was not significant. Notably, four out of five severe dysplasia samples presented MSI, suggesting MSI tended to develop frequently in mucosa with severe dysplasia (Table 3).

Table 3 Characteristics of 41 patients with dysplasia

Characteristic	MSS (n = 30)	MSI-L (n = 8)	MSI-H (n = 3)
Histological grade			
Mild	16	3	1
Moderate	13	2	1
Poor	1	3	1

MSI in intestinal metaplasia

MSI was detected in 9 of 51 (17.6%) intestinal metaplasia samples. Among the nine samples, one showed MSI-H and the other eight showed MSI-L. Notably, MSI was found only in moderate or severe-grade IM (9/14) other than in mild-grade IM (0/28, $Z = 3.630$, $P = 0.001$). Moreover, IM samples from female patients had a higher frequency of MSI compared to IM tissues from males (29.2% vs 7.4%), but the P value was more than 0.05 (Table 4).

DISCUSSION

The mechanisms of carcinogenesis in gastric mucosa remain

Table 4 Characteristics of 51 patients with intestinal metaplasia

Characteristic	MSS (n = 42)	MSI-L (n = 8)	MSI-H (n = 1)
Sex			
Male	25	2	0
Female	17	6	1
Histological grade			
Mild	28	0	0
Moderate	13	7	0
Poor	1	0	1

unclear, and may involve multiple genetic and epigenetic changes in susceptible cells of the stomach. Genetic instability including chromosomal instability and microsatellite instability is an important factor for the accumulation of these genetic changes.

Microsatellites are ubiquitous, short, repetitive DNA sequences widely and randomly distributed throughout the human genome, with unknown function. MSI is a form of genetic instability characterized by expansions and contractions of simple sequence repeats in DNA. It represents an important form of genomic instability associated with defective DNA mismatch repair in tumors. MSI can be identified in tumors when alleles of novel sizes are detected in microsatellite sequences derived from cancer DNA that are not present in normal tissues of the same individual. MSI has been observed in a subset of gastric carcinoma ranging from 13% to 44%, even more than 70% in some individual reports^[10-14]. The discrepancy in different researches is probably due to different types and numbers of microsatellite markers used in different studies.

In the present study, we have screened three groups of patients with the reference set of five markers (two mono- and three di-nucleotide repeats) recommended by American National Cancer Institute (NCI) and the criteria for identification of MSI. In our study, the incidence of MSI in gastric cancer was 58.3%. Leung *et al.*^[12], reported, that MSI in gastric cancer is 76.7%, while Halling *et al.*^[14], reported, that MSI in gastric cancer is 19% with 32 markers, and Wang *et al.*^[13], reported, that MSI is 33.9% with 42 markers in Chinese. We therefore postulate that different MSI rates in gastric cancer may be associated with the markers used in study, the criteria chosen for definition of MSI, the number of samples, race and different geographic regions.

The association between MSI and clinicopathologic characteristics of gastric cancer remains unknown. Wu *et al.*^[22], reported, that MSI-H gastric tumors are statistically associated with location of the tumor (distal area of the stomach), fewer lymph node metastases and better prognosis. Wirtz *et al.*^[23], reported, that no association is observed between MSI and gender, tumor invasion, pathological grade, lymph node metastases, Lauren's classification and prognosis, which is similar to our results.

IM and dysplasia are considered as early phenotypic changes in cascade of events leading to gastric cancer. Development of some gastric cancer may be the result of an accumulation of abnormal gene change in these precancerous lesions^[12, 16-19]. In our study, the MSI incidence of IM was 17.6%, lower than that previously reported (30-44.5%)^[15,19]. The discrepancy might be due to the IM samples

collected from the patients with chronic gastritis, other than gastric cancer and the histological grade of IM. Different markers used in different studies may be another explanation for the discrepancy. MSI is connected with moderate-grade, which is of importance in grading of IM. We detected MSI in 26.8% samples with dysplasia in the present study. Lee *et al.*^[24], reported, that there is no significant association between MSI and histological grade of dysplasia.

Investigating the occurrence of MSI in gastric cancer and pre-cancerous lesions may help us to explore the mechanisms of gastric carcinogenesis. Being detected in gastric cancer, IM and dysplastic mucosa, MSI might play a role in the multistep process of carcinogenesis of the stomach. It was reported that a well-differentiated adenocarcinoma develops 3 years later at the IM mucosa displaying MSI^[25]. In conclusion, early involvement and continuous accumulation of MSI in susceptible cells of the stomach may trigger the multi-step carcinogenesis pathway. Detection of MSI in pre-cancerous lesions may help us to investigate the stomach carcinogenesis and to identify patients at risk of developing gastric malignancies.

REFERENCES

- 1 **Fang DC.** Role of genetic instability in development of gastric cancer. *Shijie Huaren Xiaohua Zazhi* 2003; **11**: 1-5
- 2 **Yasui W,** Yokozaki H, Fujimoto J, Naka K, Kuniyasu H, Tahara E. Genetic and epigenetic alterations in multistep carcinogenesis of the stomach. *J Gastroenterol* 2000; **35** (Suppl 12): 111-115
- 3 **Tamura G.** Genetic and epigenetic alterations of tumor suppressor and tumor-related genes in gastric cancer. *Histol Histopathol* 2002; **17**: 323-329
- 4 **Wang RQ,** Fang DC, Liu WW. MUC2 gene expression in gastric cancer and preneoplastic lesion tissues. *Shijie Huaren Xiaohua Zazhi* 2000; **8**: 285-288
- 5 **Fearon ER,** Vogelstein B. A genetic model for colorectal tumorigenesis. *Cell* 1990; **61**: 759-767
- 6 **Aaltonen LA,** Peltomaki P, Leach PS, Sistonen P, Pylkkanen L, Mecklin JP, Jarvinen H, Powell SM, Jen J, Hamilton SR. Clues to the pathogenesis of familial colorectal cancer. *Science* 1993; **260**: 812-816
- 7 **Thibodeau SN,** Bren G, Schaid D. Microsatellite instability in cancer of the proximal colon. *Science* 1993; **260**: 816-819
- 8 **Ionov Y,** Peinado MA, Malkhosyan S, Shibata D, Perucho M. Ubiquitous somatic mutations in simple repeated sequences reveal a new mechanism for colonic carcinogenesis. *Nature* 1993; **363**: 558-561
- 9 **Lengauer C,** Kinzler KW, Vogelstein B. Genetic instability in colorectal cancers. *Nature* 1997; **368**: 623-627
- 10 **Fang DC,** Jass JR, Wang DX, Zhou XD, Luo TH, Young J. Infrequent loss of heterozygosity of APC/MCC and DCC genes in gastric cancer showing DNA microsatellite instability. *J Clin Pathol* 1999; **52**: 504-508
- 11 **Fleisher AS,** Esteller M, Tamura G, Rashid A, Stine OC, Yin J, Zou TT, Abraham JM, Kong D, Nishizuka S, James SP, Wilson KT, Herman JG, Meltzer SJ. Hypermethylation of the hMLH1 gene promoter is associated with microsatellite instability in early human gastric neoplasia. *Oncogene* 2001; **20**: 329-335
- 12 **Leung WK,** Kim JJ, Kim JG, Graham DY, Sepulveda AR. Microsatellite instability in gastric intestinal metaplasia in patients with and without gastric cancer. *Am J Pathol* 2000; **56**: 537-543
- 13 **Wang YX,** Ke Y, Ning T, Feng LY, Lu GR, Liu WL. Studies of microsatellite instability in Chinese gastric cancer tissues. *Chinese J Med Genetics* 1998; **15**: 155-157
- 14 **Halling KC,** Harper H, Moskaluk CA, Thibodeau SN, Petroni GR, Yustein AS, Tosi P, Minacci C, Roviello F, Piva P, Hamilton SR, Jackson CE, Powell SM. Origin of microsatellite instability in gastric cancer. *Am J Pathol* 1999; **155**: 205-211
- 15 **Semba S,** Yokozaki H, Yamamoto S, Yasui W, Tahara E. Microsatellite instability in pre-cancerous lesions and adenocarcinomas of the stomach. *Cancer* 1996; **77**(Suppl 8): 1620-1627
- 16 **Hao DM,** Sun XJ, Zheng ZH, He G, Ma MC, Xu HM, Wang MX, Sun KL. Screening and expression of associated genes in gastric dysplasia. *Shijie Huaren Xiaohua Zazhi* 2003; **11**: 6-9
- 17 **Chen SY,** Wang JY, Ji Y, Zhang XD, Zhu CW. Effects of *Helicobacter pylori* and protein kinase C on gene mutation in gastric cancer and pre-cancerous lesions. *Shijie Huaren Xiaohua Zazhi* 2001; **9**: 302-307
- 18 **Ruol A,** Parenti A, Zaninotto G, Merigliano S, Costantini M, Cagol M, Alfieri R, Bonavina L, Peracchia A, Ancona E. Intestinal metaplasia is the probable common precursor of adenocarcinoma in Barrett esophagus and adenocarcinoma of the gastric cardia. *Cancer* 2000; **88**: 2520-2528
- 19 **Kobayashi K,** Okamoto T, Takayama S, Akiyama M, Ohno T, Yamada H. Genetic instability in intestinal metaplasia is a frequent event leading to well-differentiated early adenocarcinoma of the stomach. *Er J Cancer* 2000; **36**: 1113-1119
- 20 **Burton MP,** Schneider BG, Brown R, Escamilla-Ponce N, Gully ML. Comparison of histologic stains of use in PCR analysis of microdissected paraffin-embedded tissues. *Biotechniques* 1998; **24**: 86-92
- 21 **Boland CR,** Thibodeau SN, Hamilton SR, Sidransky D, Eshleman JR, Burt RW, Meltzer SJ, Rodriguez-Bigas MA, Fodde R, Ranzani GN, Srivastava S. A national cancer institute workshop on microsatellite instability for cancer detection and familial predisposition: development of international criteria for the determination of microsatellite instability in colorectal cancer. *Cancer Res* 1998; **58**: 5248-5257
- 22 **Wu MS,** Lee CW, Chun CT, Wang HP, Lee WJ, Chang MC, Shen JC, Lin JT. Distinct clinicopathologic and genetic profiles in sporadic gastric cancer with different mutator phenotypes. *Genes Chromosomes Cancer* 2000; **27**: 403-411
- 23 **Wirtz HC,** Muller W, Noguchi T, Scheven M, Ruschoff J, Hommel G, Gabbert HE. Prognostic value and clinicopathological profile of microsatellite instability in gastric cancer. *Clin Cancer Res* 1998; **4**: 1749-1754
- 24 **Lee JH,** Abraham SC, Kim HS, Nam JH, Choi C, Lee MC, Park CS, Juhng SW, Rachid A, Hamilton SR, WU TT. Inverse relationship between APC gene mutation in gastric adenomas and development of adenocarcinoma. *Am J Pathol* 2002; **161**: 611-618
- 25 **Kashiwagi K,** Watanabe M, Ezaki T, Kanai T, Ishii H, Mukai M, Hibi T. Clinical usefulness of microsatellite instability for the prediction of gastric adenoma or adenocarcinoma in patients with chronic gastritis. *Br J Cancer* 2000; **82**: 1814-1818

Expression of cyclooxygenase-2 in gastric cancer and its relation to liver metastasis and long-term prognosis

Ji-Ren Yu, Yi-Jun Wu, Qi Qin, Ke-Zheng Lu, Sheng Yan, Xiao-Sun Liu, Shu-Sen Zheng

Ji-Ren Yu, Yi-Jun Wu, Ke-Zheng Lu, Sheng Yan, Xiao-Sun Liu, Shu-Sen Zheng, Department of Gastrointestinal Surgery, First Affiliated Hospital, Medical School, Zhejiang University, Hangzhou 310003, Zhejiang Province, China

Qi Qin, Department of General Surgery, Children Hospital, Medical School, Zhejiang University, Hangzhou 310003, Zhejiang Province, China

Supported by the Natural Science Foundation of Zhejiang Province, No. 302048

Correspondence to: Dr. Ji-Ren Yu, Department of Gastrointestinal Surgery, First Affiliated Hospital, Medical School, Zhejiang University, Hangzhou 310003, Zhejiang Province, China. wu1jun@sina.com.cn
Telephone: +86-571-87236852

Received: 2004-10-09 Accepted: 2004-11-24

Abstract

AIM: To investigate the expression of cyclooxygenase-2 (COX-2) in gastric cancer and its relation with the liver metastasis and prognosis.

METHODS: Expression of COX-2 mRNA and protein was examined in gastric cancer and its paired substantial normal tissue by semi-quantitative reverse transcription-polymerase chain reaction and immunohistochemistry. The relation between COX-2 expression and prognosis was investigated in 195 cases.

RESULTS: The expression of COX-2 mRNA in gastric cancer tissue was significantly higher than that in normal tissue in 47 cases ($w = 792, P < 0.01$). The COX-2 mRNA in pT3-4 tissue expressed higher than that in pT1-2 tissue ($w = 204, P < 0.05$). The positive expression rate of COX-2 protein was 57.9% (113/195). The COX-2 expression was significantly related to histological type, lymphnode metastasis, venous invasion and liver metastasis ($P < 0.05$). No relation was found between COX-2 expression and invasion depth, peritoneal metastasis and International Union against Cancer TNM stage. The multiple regression analysis showed that the COX-2 expression and venous invasion were obviously associated with liver metastasis ($P < 0.05$). However, there was no significant correlation between COX-2 immunoreactivity and prognosis.

CONCLUSION: COX-2 may play an important role in the development of gastric cancer, and the over-expression of COX-2 protein may be a high risk factor for liver metastasis.

Key words: Gastric cancer; Cyclooxygenase-2; Neoplasm metastasis; Long-term prognosis

Yu JR, Wu YJ, Qin Q, Lu KZ, Yan S, Liu XS, Zheng SS. Expression of cyclooxygenase-2 in gastric cancer and its relation to liver metastasis and long-term prognosis. *World J Gastroenterol* 2005; 11(31): 4908-4911

<http://www.wjgnet.com/1007-9327/11/4908.asp>

INTRODUCTION

Gastric cancer is one of the most common malignancies worldwide, and yet little is known about its molecular process of development and progression. Epidemiological studies showed that non-steroidal anti-inflammatory drugs (NSAID) can reduce the incidence of cancer of digestive tract^[1-4]. Although the mechanism of NSAID remains unclear, it may inhibit COX^[5]. COX, a key enzyme in conversion of arachidonic acid to prostaglandin, has two isoforms, namely COX-1 and cyclooxygenase-2 (COX-2). COX-1 is constitutively expressed in various tissues and involved in various physiological processes, whereas COX-2 is induced by pathological stimuli, such as inflammation, growth factors and cytokines produced by tumor cells^[6,7]. Abnormal expression of COX-2 has been supposed to be related to the pathogenesis of human cancers^[6,8,9].

We attempted to determine the expression of COX-2 in gastric cancer, and the relation between COX-2 and the pathological features of gastric cancer. In addition, the role of COX-2 in liver metastasis of gastric cancer and its prognostic value were explored.

MATERIALS AND METHODS

Patients and tissue samples for RT-PCR

Tissue specimens were taken from 47 gastric cancer patients who underwent resection (15 women and 32 men, aged 29-82 years). Paired samples of cancer tissue and normal gastric mucosa were obtained from each patient during surgery. Resected specimens were snap frozen in liquid nitrogen and stored at -80 °C. All patients were treated at Department of General Surgery, First Affiliated Hospital, Medical College of Zhejiang University, in 2001-2002. According to the criteria of International Union against Cancer (UICC), the depth of invasion was divided into pT1, pT2, pT3, and pT4.

Patients and tissue samples for immunohistochemistry

One hundred and ninety-five patients undergoing resection

for primary gastric cancer were examined at Department of Gastrointestinal Surgery, First Affiliated Hospital, Medical School, Zhejiang University in 1993-1997 (57 women and 138 men, aged 27-85 years). Resected specimens were fixed in 40 g/L formaldehyde and embedded in paraffin. The cancers were reviewed according to the rules of clinical and pathological studies on gastric cancer for histological type, depth of invasion, lymphatic invasion, and venous invasion. Liver metastasis was found in 25 cases (12.8%). Peritoneal metastasis was found in 35 cases (17.9%).

Reverse transcription-PCR analysis for COX-2

Total RNA was isolated using TRIzol reagent (Life Technologies, Inc., Gaithersburg, MD, USA) according to standard acid-guanidium-phenol-chloroform method. About 2 µg of RNA from each sample was reverse transcribed at 42 °C for 60 min in a 20 µL reaction volume using RevertAid™ M-MuLV reverse transcriptase (MBI Fermentas). cDNA was incubated at 95 °C for 5 min to inactivate the reverse transcriptase, and served as template DNA for 32 cycles of amplification using the GeneAmp PCR System 2400 (Perkin-Elmer Applied Biosystems, CA, USA). PCR was performed in a standard 25 µL reaction mixture containing 1.5 µL of 25 mmol/L magnesium chloride, 1 µL 10 mmol/L dNTP, 25 µmol/L of each sense and antisense primer and 1.5 U of Taq DNA polymerase (Promega). Amplification was performed (at 94 °C for 1 min, at 57 °C for 1 min and at 72 °C for 1.5 min) after heat-start for 5 min. Finally, an additional extension step was carried out for 10 min. As a negative control, the DNA template was omitted in the reaction. The primer sequences and PCR product sizes were as follows. COX-2: forward primer, 5'-TGA AAC CCA CTC CAA ACA CAG-3'; reverse primer, 5'-TCA TCA GGC ACA GGG AGG AAG-3', 232 bp; β-actin: forward primer, 5'-TCG TGA TGG ACT CCG GTG AC-3'; reverse primer, 5'-TCG TGG ATG CCA CAG GAC TC-3', 370 bp. The amplified products were evaluated in 2% agarose gel and visualized by ethidium bromide staining under UV light. The stained bands were analyzed with a digital gel documentation system and associated densitometry software (EDAS 290 and 1D software; Kodak Digital Science, Rochester, NY, USA). To estimate COX-2 expression levels, the expression ratio was designated as a band density ratio of COX-2 to β-actin.

Immunohistochemistry

The EnVision™ method was used for immunohistochemical staining. Five micrometer-thick sections were deparaffinized with xylene and progressively dehydrated in decreasing concentrations of alcohol. Endogenous peroxidase activity was blocked by hydrogen peroxidase (3%) in Tris-buffered saline (TBS) for 30 min. Sections were boiled (pressure-cooking) in citrate buffer, pH 6.0, for 3 min for antigen retrieval. Non-specific binding was blocked with 5% goat serum in TBS for 15 min, and the tissues were incubated with monoclonal antibody to COX-2 (1:200; Cayman Chemical, Ann Arbor, MI, USA; catalog no. 160112) in TBS containing 2% rabbit serum and 1% bovine serum albumin for 1 h. The sections were washed with TBS, and incubated with EnVision (goat anti-mouse/HRP) for 60 min.

The color was developed in diaminobenzidine solution (Sigma Chemical Co., St. Louis, MO, USA) and counterstained with Mayer's hematoxylin. Tissues were incubated with TBS containing 2% rabbit serum and 1% bovine serum albumin without the primary antibody as control. Furthermore, each run included a positive control side, which was shown previously to be strongly positive for COX-2. The scientists who performed the immunohistochemical analysis were blinded to pathological features. Tissues stained more than 10% were classified as COX-2 protein-positive^[11].

Statistical analysis

Statistical analysis was performed by use of Wilcoxon signed-ranks, χ^2 test and Kaplan-Meier test. The risk factors for liver metastasis were evaluated by a multivariate logistic regression analysis, variables with a *P*-value less than 0.1 in univariate analysis were included. *P*<0.05 was considered statistically significant.

RESULTS

RT-PCR analysis

The expression of COX-2 mRNA in gastric cancer was apparently elevated in comparison to the normal gastric mucosa (1.08 ± 0.65 vs 0.33 ± 0.21 , *P*<0.01). In addition, the COX-2 mRNA in pT3, pT4 tissues was significantly higher than that in pT1, pT2 (0.75 ± 0.43 vs 1.14 ± 0.67 , *P*<0.05) (Figure 1).

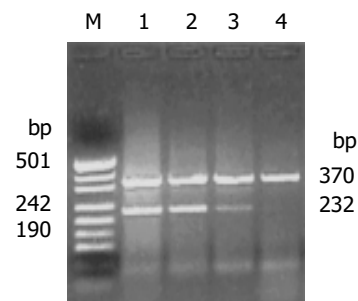


Figure 1 Expression of COX-2 mRNA in gastric cancer. M: pUC19 DNA/*Msp*I marker; lanes 1 and 2: gastric cancer tissues; lanes 3 and 4: matched normal gastric mucosal tissue.

Relation between COX-2 expression and clinicopathological features

As shown in Figure 2, the COX-2 protein was expressed intensely, mainly in cytoplasm and nuclear membrane of cancer cells. In the 195 specimens, 113 (58%) tumor tissue specimens showed positive immunoreactivity for the mAb COX-2. The COX-2 protein was expressed more frequently and intensely in differentiated adenocarcinoma than in diffuse-type carcinoma. The samples with lymph node metastasis, venous invasion and liver metastasis were significantly stained by COX-2, compared to those without lymph node metastasis. No statistical correlation was revealed between COX-2 immunoreactivity and depth of invasion, peritoneal metastasis and UICC TNM stage (Table 1).

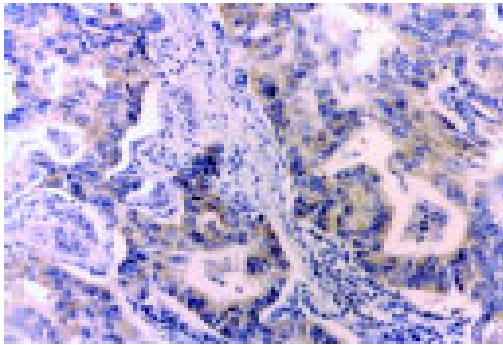


Figure 2 Immunostaining of COX-2 in gastric cancer.

Table 1 Correlation between clinicopathologic features of gastric cancer and COX-2 expression

Variable	n	COX-2 positive cases (%)	P (χ^2)
Histologic type			
Differentiated	84	59 (70.2)	0.002 (9.15)
Diffuse	111	54 (48.6)	
Depth of invasion			
T2	84	47 (60.0)	0.483 (1.46)
T3	88	50 (56.8)	
T4	23	16 (69.6)	
UICC stage			
I	14	6 (42.8)	0.410 (2.88)
II	23	11 (47.8)	
III	61	38 (62.3)	
IV	97	58 (59.8)	
Venous invasion			
Negative	80	39 (48.8)	0.030 (4.71)
Positive	115	74 (64.3)	
Lymph node metastasis			
Negative	20	7 (35.0)	0.028 (4.82)
Positive	175	106 (60.6)	
Liver metastasis			
Negative	170	93 (54.7)	0.017 (5.72)
Positive	25	20 (80.0)	
Peritoneal metastasis			
Negative	160	95 (59.4)	0.388 (0.74)
Positive	35	18 (51.4)	

Risk factors for liver metastasis of gastric cancer

Based on the results of the univariate analysis, histological type ($P = 0.066$), depth of invasion ($P = 0.601$), venous invasion ($P = 0.011$), lymph node metastasis ($P = 0.810$), COX-2 immunoreactivity ($P = 0.008$), and venous invasion were included as covariables in the multivariate regression analysis. The result revealed that COX-2 immunoreactivity and venous invasion were the significant risk factors for liver metastasis (Table 2).

Table 2 Multivariate logistic regression analysis of independent risk factors for liver metastasis in 195 gastric cancer patients

Independent risk factor	Relative risk	95%CI	P
Venous invasion			
Negative	1		0.031
Positive	2.698	1.093-6.660	
COX-2 immunoreactivity			
Negative	1		0.023
Positive	2.857	1.159-7.041	

Expression of COX-2 and prognosis

According to the expression of COX-2, the Kaplan-Meier survival curves showed no significant correlation between COX-2 immunoreactivity and prognosis of gastric cancer (Figure 3).

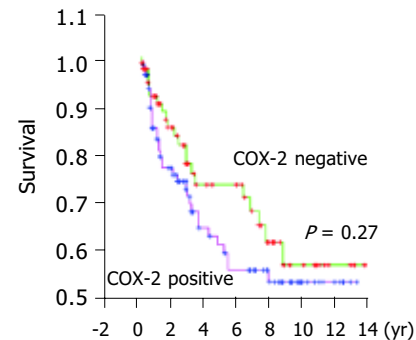


Figure 3 Overall survival curves of patients with gastric cancer.

DISCUSSION

In the current study, we demonstrated that both COX-2 mRNA and protein were expressed in gastric cancer tissue. The COX-2 mRNA level was associated with the depth of tumor invasion. Ristimaki *et al.*^[8], initially reported, that COX-2 mRNA level is elevated in gastric cancer. Uefuji *et al.*^[11], found that the level of COX-2 protein is higher in gastric cancer than in paired normal gastric mucosa by Western blot analysis. Furthermore, Ohno *et al.*^[12], revealed, that COX-2 mRNA level increases gradually with the depth of gastric cancer invasion. But the exact mechanism is still unknown. The COX-2 specific antibody identified that COX-2 protein is located in cytoplasm and nuclear membrane of gastric cancer cells, but not in stroma surrounding cancerous tissues, the COX-2 protein is also observed in smooth muscle cells, fibroblasts, and inflammatory mononuclear cells^[12-14]. Additionally, epithelial cells showing intestinal metaplasia and adenoma are also strongly immunoreactive to anti-COX-2 Ab. The above data demonstrate that COX-2 is upregulated in gastric cancer, and high COX-2 expression may be an early event in the carcinogenesis of stomach.

In our study, the COX-2 protein was expressed higher in differentiated adenocarcinoma than in diffuse-type carcinoma. Yamagata *et al.*^[15], reported, that COX-2 expression increases in early intestinal-type gastric cancer, and is significantly higher than that in diffuse-type carcinoma. However, no correlation is found between the histologic type of gastric cancer and COX-2 protein in other reports^[12].

Recent studies have shown that COX-2 expression is correlated with lymph node metastasis and lymphatic invasion in gastric carcinoma. Murata *et al.*^[17], showed that COX-2 overexpression is associated significantly with tumor invasion of gastric wall lymphatic vessels and lymph node metastasis. The same results are also disclosed in other reports^[13,17]. Taken together, these results suggest that COX-2 may influence lymphatic involvement and promote tumor invasion.

Our study showed that COX-2 expression was associated with venous invasion and liver metastasis of gastric cancer. The multivariate analysis revealed that the COX-2 immunoreactivity was an independent risk factor for liver metastasis of gastric carcinoma. COX-2 can enhance the adhesive ability of endothelial cells in colonic carcinoma cells, and fortify liver metastatic potential via secretion of sialyl Lewis antigens^[18,19]. Nagatsuka *et al.*^[16], also discovered that the selective COX-2 inhibitor (JTE 522) has inhibitory effects on liver metastasis of colon cancer. On the contrary, some reports showed that COX-2 does not play a major role in the process of distant metastasis of gastric cancer^[11,12,17]. The reason why there is such a discrepancy is not clear, but the differences in methods (antibody, results evaluation) might be an important reason.

It was reported that COX-2 protein overexpression is significantly associated with the UICC TNM stage and the prognosis of gastric cancer patients^[16,17]. Ristimaki *et al.*^[20], have connected COX-2 overexpression to an unfavorable distant disease-free survival in breast cancer patients ($n = 1\ 576$). However, no significant correlation was found between COX-2 immunoreactivity and peritoneal metastasis, UICC TNM stage and prognosis in our study. Joo *et al.*^[21], also have not found any significant correlation between them. A large group and long term follow-up are necessary to assess the prognostic value of COX-2 in gastric cancer.

Our results suggest that COX-2 is overexpressed in gastric cancer, and COX-2 may play an important role in liver and lymphatic metastasis of gastric cancer. Inhibiting the activity of COX-2 may provide therapeutic benefit to gastric cancer.

REFERENCES

- 1 **Farrow DC**, Vaughan TL, Hansten PD, Stanford JL, Risch HA, Gammon MD, Chow WH, Dubrow R, Ahsan H, Mayne ST, Schoenberg JB, West AB, Rotterdam H, Fraumeni JF Jr, Blot WJ. Use of aspirin and other nonsteroidal anti-inflammatory drugs and risk of esophageal and gastric cancer. *Cancer Epidemiol Biomarkers Prev* 1998; **7**: 97-102
- 2 **Garcia-Rodriguez LA**, Huerta-Alvarez C. Reduced risk of colorectal cancer among long-term users of aspirin and nonsteroidal antiinflammatory drugs. *Epidemiology* 2001; **12**: 88-93
- 3 **Morgan G**. Beneficial effects of NSAIDs in the gastrointestinal tract. *Eur J Gastroenterol Hepatol* 1999; **11**: 393-400
- 4 **Funkhouser EM**, Sharp GB. Aspirin and reduced risk of esophageal carcinoma. *Cancer* 1995; **76**: 1116-1119
- 5 **Taketo MM**. Cyclooxygenase-2 inhibitors in tumorigenesis (Part II). *J Natl Cancer Inst* 1998; **90**: 1609-1620
- 6 **Sano H**, Kawahito Y, Wilder RL, Hashiramoto A, Mukai S, Asai K, Kimura S, Kato H, Kondo M, Hla T. Expression of cyclooxygenase-1 and -2 in human colorectal cancer. *Cancer Res* 1995; **55**: 3785-3789
- 7 **Williams CS**, DuBois RN. Prostaglandin endoperoxide synthase: why two isoforms? *Am J Physiol* 1996; **270**(3 Pt 1): G393-G400
- 8 **Ristimaki A**, Honkanen N, Jankala H, Sipponen P, Harkonen M. Expression of cyclooxygenase-2 in human gastric carcinoma. *Cancer Res* 1997; **57**: 1276-1280
- 9 **Tucker ON**, Dannenberg AJ, Yang EK, Zhang F, Teng L, Daly JM, Soslow RA, Masferrer JL, Woerner BM, Koki AT, Fahey TJ 3rd. Cyclooxygenase-2 expression is up-regulated in human pancreatic cancer. *Cancer Res* 1999; **59**: 987-990
- 10 **Saukkonen K**, Nieminen O, van Rees B, Vilkki S, Harkonen M, Juhola M, Mecklin JP, Sipponen P, Ristimaki A. Expression of cyclooxygenase-2 in dysplasia of the stomach and in intestinal-type gastric adenocarcinoma. *Clin Cancer Res* 2001; **7**: 1923-1931
- 11 **Uefuji K**, Ichikura T, Mochizuki H, Shinomiya N. Expression of cyclooxygenase-2 protein in gastric adenocarcinoma. *J Surg Oncol* 1998; **69**: 168-172
- 12 **Ohno R**, Yoshinaga K, Fujita T, Hasegawa K, Iseki H, Tsunozaki H, Ichikawa W, Nihei Z, Sugihara K. Depth of invasion parallels increased cyclooxygenase-2 levels in patients with gastric carcinoma. *Cancer* 2001; **91**: 1876-1881
- 13 **Lim HY**, Joo HJ, Choi JH, Yi JW, Yang MS, Cho DY, Kim H, Nam DK, Lee KB, Kim HC. Increased expression of cyclooxygenase-2 protein human gastric carcinoma. *Clin Cancer Res* 2000; **6**: 519-525
- 14 **van Rees BP**, Saukkonen K, Ristimaki A, Polkowski W, Tytgat GN, Drillenburger P, Offerhaus GJ. Cyclooxygenase-2 expression during carcinogenesis in the human stomach. *J Pathol* 2002; **196**: 171-179
- 15 **Yamagata R**, Shimoyama T, Fukuda S, Yoshimura T, Tanaka M, Munakata A. Cyclooxygenase-2 expression is increased in early intestinal-type gastric cancer and gastric mucosa with intestinal metaplasia. *Eur J Gastroenterol Hepatol* 2002; **14**: 359-363
- 16 **Nagatsuka I**, Yamada N, Shimizu S, Ohira M, Nishino H, Seki S, Hirakawa K. Inhibitory effect of a selective cyclooxygenase-2 inhibitor on liver metastasis of colon cancer. *Int J Cancer* 2002; **100**: 515-519
- 17 **Murata H**, Kawano S, Tsuji S, Tsuji M, Sawaoka H, Kimura Y, Shiozaki H, Hori M. Cyclooxygenase-2 overexpression enhances lymphatic invasion and metastasis in human gastric carcinoma. *Am J Gastroenterol* 1999; **94**: 451-455
- 18 **Yamamoto H**, Itoh F, Fukushima H, Hinoda Y, Imai K. Overexpression of cyclooxygenase-2 protein is less frequent in gastric cancers with microsatellite instability. *Int J Cancer* 1999; **84**: 400-403
- 19 **Kakiuchi Y**, Tsuji S, Tsujii M, Murata H, Kawai N, Yasumaru M, Kimura A, Komori M, Irie T, Miyoshi E, Sasaki Y, Hayashi N, Kawano S, Hori M. Cyclooxygenase-2 activity altered the cell-surface carbohydrate antigens on colon cancer cells and enhanced liver metastasis. *Cancer Res* 2002; **62**: 1567-1572
- 20 **Ristimaki A**, Sivula A, Lundin J, Lundin M, Salminen T, Haglund C, Joensuu H, Isola J. Prognostic significance of elevated cyclooxygenase-2 expression in breast cancer. *Cancer Res* 2002; **62**: 632-635
- 21 **Joo YE**, Oh WT, Rew JS, Park CS, Choi SK, Kim SJ. Cyclooxygenase-2 expression is associated with well-differentiated and intestinal-type pathways in gastric carcinogenesis. *Digestion* 2002; **66**: 222-229

Anti-inflammatory mechanism of oxymatrine in dextran sulfate sodium-induced colitis of rats

Ping Zheng, Feng-Li Niu, Wen-Zhong Liu, Yao Shi, Lun-Gen Lu

Ping Zheng, Feng-Li Niu, Wen-Zhong Liu, Yao Shi, Lun-Gen Lu, Shanghai Institute of Digestive Disease, Renji Hospital, Shanghai Second Medical University, Shanghai 200127, China
Supported by the University Science and Technology Development Foundation of Shanghai, No. 00B07

Correspondence to: Professor Ping Zheng, Shanghai Institute of Digestive Disease, Renji Hospital, Shanghai Second Medical University, Shanghai 200127, China. yxfan@danfoss.com.cn
Telephone: +86-21-63364118 Fax: +86-21-63364118
Received: 2004-03-06 Accepted: 2004-07-15

Abstract

AIM: To investigate the anti-inflammatory mechanism of oxymatrine in dextran sulfate sodium (DSS)-induced colitis of rats.

METHODS: Acute colitis was induced by giving 2% DSS orally in drinking water for 8 d. Twenty-six male rats were randomized into oxymatrine-treated group (group A, 10 rats), DSS control (group B, 10 rats) and normal control (group C, 6 rats). The rats in group A were injected muscularly with oxymatrine at the dosage of 63 mg/(kg·d) from d 1 to 11 and drank 2% DSS solution from d 4 to 11. The rats in group B were treated with 0.9% saline in an equal volume as group A and drank 2% DSS solution from d 4 to 11. The rats in group C were treated with 0.9% saline as group B from d 1 to 11 and drank water normally. Diarrhea and bloody stool as well as colonic histology were observed. The levels of serum tumor necrosis factor- α (TNF- α) and interleukin-6 (IL-6) were determined by ELISA, and nuclear factor- κ B (NF- κ B) activity and the expression of inter-cellular adhesion molecule-1 (ICAM-1) in colonic mucosa were detected by immunohistochemistry method.

RESULTS: Compared with DSS control group, the inflammatory symptoms and histological damages of colonic mucosa in oxymatrine-treated group were significantly improved, the serum levels of TNF- α , IL-6, and the expression of NF- κ B, ICAM-1 in colonic mucosa were significantly reduced.

CONCLUSION: The fact that oxymatrine can reduce the serum levels of TNF- α , IL-6, and the expression of NF- κ B and ICAM-1 in colonic mucosa in DSS-induced colitis of rats indicates that oxymatrine may ameliorate the colonic inflammation and thus alleviate diarrhea and bloody stool.

Key words: Oxymatrine; Colitis; Colonic mucosa

Zheng P, Niu FL, Liu WZ, Shi Y, Lu LG. Anti-inflammatory mechanism of oxymatrine in dextran sulfate sodium-induced colitis of rats. *World J Gastroenterol* 2005; 11(31): 4912-4915
<http://www.wjgnet.com/1007-9327/11/4912.asp>

INTRODUCTION

The symptoms and colonic histopathology of rodent colitis model induced by dextran sulfate sodium salt (DSS) resemble more the human ulcerative colitis (UC) than other chemically induced colitis, which has become a research tool for the pathogenesis of UC and the development of new drugs in our country and abroad. *Sophora flavescens* Ait has distinct anti-inflammatory effect and, several mixture formulas with *Sophora flavescens* Ait are effectively used to treat UC in the clinic^[1]. Oxymatrine, as the main efficacy component of light yellow sophora root, has been reported to be effective in the treatment of viral hepatitis and bronchial asthma. Our previous experiments suggested that oxymatrine might significantly improve the colonic inflamed damage in rat colitis induced by DSS, but its exact mechanism is unclear^[2]. The present experiment aimed to elicit the anti-inflammatory mechanism of oxymatrine in terms of the regulation of nuclear factor- κ B (NF- κ B) to tumor necrosis factor- α (TNF- α), interleukin-6 (IL-6), and inter-cellular adhesion molecule-1 (ICAM-1)^[3-5]. The inflamed damage of DSS colitis in rats appears early, so many researches reported to administer studied drugs along with or ahead of DSS administration to obtain predicated efficacy^[6-10]. As diarrhea and bloody stool alleviate rapidly after the withdrawal of DSS, which may affect the observation of drug effect, the present study administered oxymatrine 3 d earlier than DSS and terminated oxymatrine and DSS at the same time according to the literature mentioned above and preliminary experiments.

MATERIALS AND METHODS

Materials

Healthy male SD rats ($n = 26$, 4-5 wk) were obtained from Shanghai Experiment Center of Chinese Academy of Science, Shanghai, China. DSS (Sigma) was prepared as 2% solution with distilled water. Injection oxymatrine (kurorinone) was obtained from Ningxia Pharmaceutical Factory, Ningxia, China, with purity of more than 98%. TNF- α and IL-6 ELISA kits were purchased from R&D Corporation (Cat. R6000 and RTA00). NF- κ Bp65 (F-6) monoclonal antibody

was from Santa Cruz Co., Ltd (Cat. Sc-8008). Mouse CD54 monoclonal antibody was from Cedarlane Laboratory Co., Ltd (Cat. 01010603). Pepsin (Cat. DIG3009) and SP immunohistological staining hypersensitive kit (Cat. 9702) were obtained from Fuzhou Maixin Biotechnological Co., Ltd, Fujian, China.

Methods

Experimental design Rats ($n = 26$) were randomized into three groups: oxymatrine treatment group (group A, $n = 10$), DSS control (group B, $n = 10$) and normal control (group C, $n = 6$). In group A, oxymatrine was injected intramuscularly at the dose of 63 mg/(kg·d) on d 1-11 and 2% DSS solution was given from d 4-11; in group B, equal volume of 0.9% saline was used to take oxymatrine and other procedures referred to group A; in group C, only an equal volume of 0.9% saline was given intramuscularly on d 1-11 and drinking water was obtainable freely. Drinking volume of DSS in group A was controlled to near group B. The symptoms of rats were assessed by disease activity index (DAI) based on stool consistency and incidence of stool hemorrhage^[11]. After blood sampling from inferior vena cava to obtain serum stored in -20°C for detection on d 12, all rats were killed and the intact colons were taken and excised longitudinally to be fixed in 40 g/L formaldehyde. On d 13, colonic segments (8 cm) up from the anus were removed, embedded in paraffin and placed on lysine slices^[2]. Sections were stained with hematoxylin and eosin for assessment of histological changes and scoring^[6].

Detection of serum TNF- α and IL-6 ABC-ELISA assay of double antibodies sandwich were adopted.

Immunohistochemical detection of ICAM-1 SP immunohistological staining hypersensitive kit was used. The sections were deparaffinized and hydrated as routine and digested with pepsin for 15 min at 37°C . A solution (50 μL) was added and kept for 15 min at room temperature followed by a B solution (50 μL) for 30 min at room temperature; 50 μL of the primary antibody (diluted in 1:75) was added and kept at 37°C for 1 h, then placed at room temperature for 15 min and kept at 4°C overnight (no primary antibody added samples were used for negative control); C solution (50 μL) was added, and kept for 1.5 h at room temperature followed by a D solution (50 μL) for another 1 h. Finally, the sections were processed with DAB, stained with hematoxylin followed by routine dehydration and slice-sealing.

Assessment criteria of the results: positive cells presented as buffy, located on cell membrane. Positive vessel was defined as one more positive vascular endothelial cells that were observed in the vessels of mucosa and submucosa. Then the positive vessels of distal colon (about 4 cm up from the anus) and the number of positive vessels of single colonic segment were counted (positive vessels/cm).

Immunohistochemical detection of NF- κB activity After digestion with pepsin, the sections were rinsed thrice with 0.1% PBS Triton X-100 for 5 min respectively, primary antibody diluted in 1:100.

Assessment criteria of the results: positive cells presented as buffy, located on nuclei and cytoplasm. The counting method of positive endothelial cells refers to procedures

above. The counting criteria of positive epithelia cells are as follows: 50 crypts were randomly observed in the distal colon (about 4 cm up from anus) and the percent of positive cells per crypt was counted, then the scores were counted according to the standards: 0 score for $\leq 5\%$; 1 score for 6-25%, presented as +; 2 scores for 26-50%, presented as ++; 3 scores for 51-75%, presented as +++; 4 scores for 76-100%, presented as ++++. Finally, the mean score of each rat was obtained.

Statistical analysis

Statistical analysis was performed according to one factor analysis of variance and Wilcoxon rank sum test. $P < 0.05$ was considered to be statistically significant.

RESULTS

Comparison of DAI and histological scores

Eight days after drinking 2% DSS, SD rats appeared to have diarrhea, bloody stool; erosion and superficial ulcer of colonic mucosa; epithelial damage; inflammatory cell infiltration and proliferation of lymph follicles in mucosa and submucosa; dilatation and proliferation of capillaries and small vessels, which resembled human UC^[11]. Each colon existed with mucosal damage that was located in distal colon. Compared with B group, both DAI and histological scores in group A decreased significantly ($P < 0.05$, Table 1).

Table 1 Scores of DAI and mucosal damage in group A and B ($n = 10$) (mean \pm SD)

Group	DAI	Scores of mucosal damage
A	6.0 \pm 1.2 ^a	5.9 \pm 1.1 ^a
B	7.3 \pm 1.1	7.1 \pm 0.7

^a $P < 0.05$ vs group B.

Comparison of serum levels of TNF- α and IL-6

The serum levels of TNF- α and IL-6 in rat DSS-colitis increased distinctly than normal rats and declined obviously after treatment with oxymatrine. The serum levels of TNF- α and IL-6 in groups A-C were as follows: (9.49 \pm 1.01) and (55.50 \pm 12.13) ng/L, (13.70 \pm 1.33) and (77.80 \pm 14.03) ng/L, (8.32 \pm 1.15) and (40.57 \pm 4.79) ng/L. Compared with B group, the levels of serum TNF- α and IL-6 in group A were significantly reduced ($P < 0.01$, $P < 0.05$, Table 2).

Table 2 Serum levels of TNF- α and IL-6 in three groups (ng/L) (mean \pm SD)

Group	TNF- α	IL-6
A ($n = 10$)	9.49 \pm 1.01 ^b	55.50 \pm 12.13 ^a
B ($n = 10$)	13.70 \pm 1.33 ^d	77.80 \pm 14.03 ^f
C ($n = 6$)	8.32 \pm 1.15	40.57 \pm 4.79

^a $P < 0.05$ vs group C; ^b $P < 0.01$ vs group B; ^c $P < 0.01$, ^f $P < 0.01$ vs group C.

Expression of colonic ICAM-1

In rat DSS-colitis, ICAM-1 expressed on vascular endothelial

cells and macrophages and its expressions in capillaries and venules were higher than arterioles and most frequently appeared in mucosa and submucosa. The positive rates were high in sites and nearby of colonic erosion and superficial ulcer, and became more and more low following the alleviation of inflammatory damage up from 3 cm distance to the anus. Both the stainings of crypt epithelia in mucosa and lymphocytes were negative.

After administration of oxymatrine, the amount of positive vessels in rat DSS-colitis reduced obviously; only small amount of positive vessels were observed in colons of group C. The mean amount of positive cells in groups A-C were as follows: (82.75 ± 19.46) , (137.27 ± 23.31) , (12.97 ± 1.53) /cm with significant differences by comparison between any two groups ($P < 0.01$). The amount in group A decreased obviously compared to group B.

Expression or activation of NF- κ B

In rat DSS-colitis, NF- κ B expressed on vascular endothelial cells and mucosal epithelial cells located in nuclei and/or cytoplasm. Its expressions in capillaries and venules were higher than arterioles, and most frequently appeared in mucosa and submucosa. The positive rates were high in sites and nearby of colonic erosion and superficial ulcer, and became more and more low following the alleviation of inflammatory damage from 3 cm distance to the anus.

After administration of oxymatrine, the amount of positive vessels and positive rates of epithelial cells in rat DSS-colitis reduced obviously; the mean amount of positive cells of endothelial and epithelial cells in distal distant colon were (24.09 ± 4.39) and (0.86 ± 0.17) /cm in group A, (30.49 ± 6.07) and (1.19 ± 0.36) /cm in group B. The amount in group A decreased obviously compared to group B. None or only little amount of positive cells were observed in colons of group C with amount of (3.83 ± 1.00) /cm of positive endothelial cells. The amount of positive cells of vessels in distal colon in group A decreased obviously compared to group B ($P < 0.05$).

DISCUSSION

The present experiment indicates that the serum levels of TNF- α and IL-6 in rat DSS colitis increased distinctly than normal rats and declined obviously after treatment with oxymatrine, which suggests that oxymatrine may inhibit the expression of the above pro-inflammatory cytokines and therefore ameliorate the colonic damage related to them. TNF- α can recruit leukocytes in the inflammatory sites, stimulate monocytes, and vascular endothelial cells to express cytokines, induce the cascade effects for other cytokines and finally result in inflamed lesion of tissues. So it is necessary to inhibit the expression of TNF- α in the early stage of DSS colitis, prevent and alleviate the development of colitis^[12,13]. IL-6 is capable of promoting lymphocyte proliferation and leading to the production of acute phase proteins in liver^[9], also plays an important role in the development of colonic inflammation. The anti-inflammatory effect of oxymatrine may be associated with its inhibitory role to the expression of TNF- α and IL-6^[14,15].

The experiment also demonstrated that expression of

ICAM-1 by vascular endothelial cells and macrophages were enhanced greatly than normal in DSS-induced colonic sites; prophylactic treatment with oxymatrine reduced the inflamed, infiltration and ICAM-1 expression in rat colons, which indicates that oxymatrine may ameliorate DSS colitis by inhibiting ICAM-1 production. Bendjelloul *et al.*^[16], reported that expression of ICAM-1 in ICAM-1 defected mice appears as negative or mild positive, its interaction with leukocytes and inflammatory activity were alleviated. ICAM-1 plays a key role in the trans-endothelial migration and immunological cell activation of leukocytes and prophylactic administration of ICAM-1 mAb could lighten the inflamed damage^[7,17].

The present study also showed that no expression of NF- κ B was observed in non-inflammatory colonic epithelial cells in rat and only mild positive was observed among vascular endothelial cells. However, NF- κ B activation presented in both colonic epithelial cells and vascular endothelial cells; prophylactic treatment with oxymatrine reduced the colonic inflammation and NF- κ B activation, which indicates that oxymatrine may ameliorate DSS colitis by downregulating NF- κ B activation. Marrero *et al.*^[18], also reported, that DSS colitis was related to the high activation of NF- κ B. Inducers of NF- κ B include TNF- α , oxidative stress and so on; NF- κ B is capable of activating many genes such as adhesion molecule ICAM-1 and cytokine TNF- α , IL-1, IL-6, etc.^[3-5,19,20] and therefore it is possible to block the key initial step of inflammation and its secondary effect by inhibiting NF- κ B activity^[21].

REFERENCES

- Zheng P, Wang WW. 28 cases of ulcerative colitis treated with matrine mixture rectum enema. *Weichang Bingxue* 2001; **6**: 54-55
- Zheng P, Niu FL, Peng YS, Zeng MD. Effect of oxymatrine on dextran sulfate sodium induced colitis: A preliminary study. *Weichang Bingxue* 2001; **6**: 209-210
- Baldwin AS. The transcription factor NF- κ B and human disease. *J Clin Invest* 2001; **107**: 3-6
- Wahl C, Liptay S, Adler G, Schmid RM. Sulfasalazine: a potent and specific inhibitor of nuclear factor κ B. *J Clin Invest* 1998; **101**: 1163-1174
- Yamamoto Y, Gaynor RB. Therapeutic potential of inhibition of the NF- κ B pathway in the treatment of inflammation and cancer. *J Clin Invest* 2001; **107**: 135-142
- Kanauchi O, Nakamura T, Agata S, Mitsuyama K, Iwanaga T. Effects of germinated barley foodstuff on dextran sulfate sodium-induced colitis in rats. *J Gastroenterol* 1998; **33**: 179-188
- Taniguchi T, Tsukada H, Nakamura H, Kodama M, Fukuda K, Saito T, Miyasaka M, Seino Y. Effects of the anti-ICAM-1 monoclonal antibody on dextran sodium sulphate-induced colitis in rats. *J Gastroenterol Hepatol* 1998; **13**: 945-949
- Murano M, Maemura K, Hirata I, Toshina K, Nishikawa T, Hamamoto N, Sasaki S, Saitoh O, Katsu K. Therapeutic effect of intracolonicly administered nuclear factor κ B (p65) antisense oligonucleotide on mouse dextran sulphate sodium (DSS)-induced colitis. *Clin Exp Immunol* 2000; **120**: 51-58
- Moriguchi M, Urabe K, Norisada N, Ochi C, Stalc A, Urleb U, Muraoka S. Therapeutic effects of LK 423, a phthalimido-desmursamyl-dipeptide compound, on dextran sulfate sodium-induced colitis in rodents through restoring their interleukin-10 producing capacity. *Arzneimittelforschung* 1999; **49**: 184-192
- Yoshida Y, Iwai A, Itoh K, Tanaka M, Kato S, Hokari R, Miyahara T, Koyama H, Miura S, Kobayashi M. Role of induc-

- ible nitric oxide synthase in dextran sulphate sodium-induced colitis. *Aliment Pharmacol Ther* 2000; **14** (Suppl): 126-132
- 11 **Porter SN**, Howarth GS, Butler RN. An orally administered growth factor extract derived from bovine when suppresses breath ethane in colitic rats. *Scand J Gastroenterol* 1998; **33**: 967-974
- 12 **Myers KJ**, Murthy S, Flanigan A, Witchell DR, Butler M, Murray S, Siwkowski A, Goodfellow D, Madsen K, Baker B. Antisense oligonucleotide blockade of tumor necrosis factor- α in two murine models of colitis. *J Pharmacol Exp Ther* 2003; **304**: 411-424
- 13 **Murthy S**, Flanigan A, Coppola D, Buelow R. RDP58, a locally active TNF inhibitor, is effective in the dextran sulphate mouse model of chronic colitis. *Inflamm Res* 2002; **51**: 522-531
- 14 **Lin W**, Zhang JP, Hu ZL, Qian DH. Inhibitory effect of matrine on lipopolysaccharide-induced tumor necrosis factor and interleukin-6 production from rat Kupffer cells. *Yaoxue Xuebao* 1997; **32**: 93-96
- 15 **Hu ZL**, Zhang JP, Qian DH, Lin W, Xie WF, Zhang XR, Chen WZ. Effects of matrine on mouse splenocyte proliferation and release of interleukin-1 and -6 from peritoneal macrophages *in vitro*. *Zhongguo Yaoli Xuebao* 1996; **17**: 259-261
- 16 **Bendjelloul F**, Rossmann P, Maly P, Mandys V, Jirkovska M, Prokesova L, Tuckova L, Tlaskalova-Hogenova H. Detection of ICAM-1 in experimentally induced colitis of ICAM-1-deficient and wild-type mice: an immunohistochemical study. *Histochem J* 2000; **32**: 703-709
- 17 **Farkas S**, Herfarth H, Rossle M, Schroeder J, Steinbauer M, Guba M, Beham A, Scholmerich J, Jauch KW, Anthuber M. Quantification of mucosal leucocyte endothelial cell interaction by *in vivo* fluorescence microscopy in experimental colitis in mice. *Clin Exp Immunol* 2001; **126**: 250-258
- 18 **Marrero JA**, Matkowskyj KA, Yung K, Hecht G, Benya RV. Dextran sulfate sodium-induced murine colitis activates NF- κ B and increases galanin-1 receptor expression. *Am J Physiol Gastrointest Liver Physiol* 2000; **278**: G797-804
- 19 **Herfarth H**, Brand K, Rath HC, Rogler G, Scholmerich J, Falk W. Nuclear factor- κ B activity and intestinal inflammation in dextran sulphate sodium (DSS)-induced colitis in mice is suppressed by gliotoxin. *Clin Exp Immunol* 2000; **120**: 59-65
- 20 **Jobin C**, Hellerbrand C, Licato LL, Brenner DA, Sartor RB. Mediation by NF- κ B of cytokine induced expression of intercellular adhesion molecule 1 (ICAM-1) in an intestinal epithelial cell line, a process blocked by proteasome inhibitors. *Gut* 1998; **42**: 779-787
- 21 **Spiik AK**, Ridderstad A, Axelsson LG, Midtvedt T, Bjork L, Pettersson S. Abrogated lymphocyte infiltration and lowered CD14 in dextran sulfate induced colitis in mice treated with p65 antisense oligonucleotides. *Int J Colorectal Dis* 2002; **17**: 223-232

• BRIEF REPORTS •

Expression of heparanase mRNA in anti-sense oligonucleotide-transfected human esophageal cancer EC9706 cells

Kui-Sheng Chen, Lan Zhang, Lin Tang, Yun-Han Zhang, Dong-Ling Gao, Liang Yan, Lei Zhang

Kui-Sheng Chen, Lan Zhang, Lin Tang, Yun-Han Zhang, Dong-Ling Gao, Liang Yan, Lei Zhang, Department of Pathology, the First Affiliated Hospital, Zhengzhou University, Key Laboratory of Henan Tumor Pathology, Zhengzhou 450052, Henan Province, China Supported by the Natural Science Foundation of Henan Province, No. 0311043700 and the Foundation for Young Mainstay Teachers in Colleges and universities of Henan Province, No.100(2003) and the Building Foundation for 211 Key Fields during the 15th Five-year Plan Period of Ministry of Education, No. 2(2002)

Correspondence to: Kui-Sheng Chen, Department of Pathology, the First Affiliated Hospital, Zhengzhou University, Key Laboratory of Henan Tumor Pathology, Zhengzhou 450052, Henan Province, China. chenks2002@yahoo.com.cn

Telephone: +86-371-6912412 Fax: +86-371-6658175

Received: 2005-02-17 Accepted: 2005-04-02

Abstract

AIM: To investigate the effects of anti-sense oligonucleotides (ASODNs) on mRNA expression of heparanase in human esophageal cancer EC9706 cells.

METHODS: One non-sense oligonucleotide (N-ODN) and five ASODNs against different heparanase mRNA sites were transfected into EC9706 cells, then the expression of heparanase mRNA in EC9706 cells was studied by *in situ* hybridization.

RESULTS: The expression of heparanase mRNA could be inhibited by ASODNs. There was no significant difference among five ASODNs ($P > 0.05$), but there was a significant difference between ASODNs and N-ODN or non-transfected group (ASODN1: 2.25 ± 0.25 , ASODN2: 2.21 ± 0.23 , ASODN3: 2.23 ± 0.23 , ASODN4: 2.25 ± 0.24 vs N-ODN: 3.47 ± 2.80 or non-transfected group: 3.51 ± 2.93 respectively, $P < 0.05$).

CONCLUSION: The expression of heparanase mRNA in EC9706 cells can be inhibited by ASODNs *in vivo*, and heparanase ASODNs can inhibit metastasis of esophageal squamous cell carcinoma or other tumors by inhibiting the expression of heparanase.

© 2005 The WJG Press and Elsevier Inc All rights reserved.

Key words: Esophageal cancer EC9706 cells; Heparanase; Anti-sense oligonucleotides; *In situ* hybridization

Chen KS, Zhang L, Tang L, Zhang YH, Gao DL, Yan L, Zhang L. Expression of heparanase mRNA in anti-sense oligonucleotide-transfected human esophageal cancer EC9706 cells. *World J Gastroenterol* 2005; 11(31): 4916-4917
<http://www.wjgnet.com/1007-9327/11/4916.asp>

INTRODUCTION

Heparanase (HPA) is closely associated with cell proliferation, differentiation, adhesion and exudation, and may play a crucial role not only in tumor development and progression but also in tumor invasion and metastasis^[1]. Studies indicate that HPA is expressed in tumor tissues, such as liver carcinoma, ovarian adenocarcinoma, cervical squamous carcinoma, colonic adenocarcinoma, lymphoma, fibrosarcoma and melanoma^[1,2]. We detected the expression of HPA mRNA in anti-sense oligonucleotide (ASODN) transfected by *in situ* hybridization, so as to provide the basic theory for esophageal carcinoma target therapy by heparanase ASODN technique.

MATERIALS AND METHODS

Materials

Human esophageal carcinoma EC9706 cell line was provided by Chinese Academy of Medical Sciences Heparanase ASODNs1-4, N-ODN and biotin-labeled HPA cDNA probe were synthesized by DaLian Bao Bio Co., Ltd. SA-Bio-AP and BCIP/NBT were purchased from Promega Company, USA RPMI-1640 was obtained from Gibco Company, USA.

Cell culture

Human esophageal carcinoma EC9706 cells (a adherent cell line) were cultured in RPMI-1640 and divided into six groups until formation of monolayer on the bottle wall. Groups 1 to 4 were treated with 20 $\mu\text{mol/L}$ ASDON1, ASDON2, ASDON3, ASDON4, respectively. Control group 1 was treated with N-ODN at the same concentration. Neither ASDON nor N-ODN was added to control group 2. All groups were cultured for another 48 h, and then the cells were harvested after trypsinization. The cells were adjusted to a concentration of $10^6/\text{mL}$ and added to the prepared slides for hybridization.

In situ hybridization

The samples were fixed in 40 g/L paraformaldehyde for 30 min. After being washed in distilled water, samples were pre-treated with fresh 0.5% H_2O_2 /formaldehyde to block endogenous peroxidases for 30 min at room temperature. The samples were treated with 30 g/L proteinase k diluted freshly by citric acid for 10 min at 37 °C, pre-hybridized in pre-hybridized solution without probe for 4 h, and then for an additional 12 h at 42 °C. The final concentration of the labeled heparanase probe was 1 $\mu\text{g/L}$. After hybridization, excess probes were removed through rinsing in $0.1 \times \text{SSC}$ at 42 °C, and samples were treated with SA-Bio-AP for 10 min

at 37 °C, and rinsed again. Color reaction was performed with new BCIP/NBT in dark for 2-4 h. The samples without probe were used as negative control.

Result assessment

Ten fields of each section were observed under oil microscope and 100 cells of each field were counted. Scores were obtained according to the staining intensity and count degree of *in situ* hybridization [3].

Statistical analysis

The SPSS 10.0 statistical package was used for all analyses. Data were expressed as mean±SD, and analyzed by ANOVA $P<0.05$ was considered statistically significant.

RESULTS

Expression of heparanase mRNA in EC9706 cells

Heparanase mRNA (blue-purple granule) was located in cytoplasm. There was no positive signal in the cell sample without probe (Figure 1).

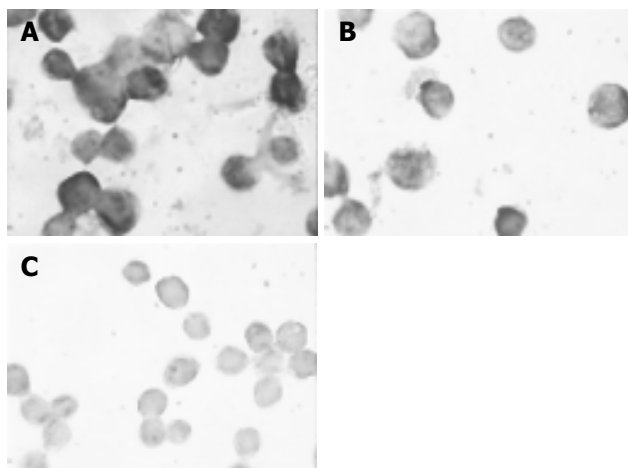


Figure 1 Expression of heparanase mRNA in human esophageal cancer EC9706 cells. **A:** non- transfected group; **B:** ASODNs-transfected group; **C:** control group without probe.

Influence of ASODN on expression of heparanase mRNA in EC9706 cells

The level of heparanase mRNA expression in ASODNs1-4-transfected EC9706 cells was 2.25 ± 0.25 , 2.21 ± 0.23 , 2.23 ± 0.23 , 2.25 ± 0.24 , respectively. There was a significant difference between experimental group and control group 1 (3.47 ± 2.80 , $P<0.05$). But there was no significant difference between control groups 1 and 2 (3.51 ± 2.93). There was no significant difference in different ASODNs.

DISCUSSION

Heparanase is a kind of endoglycosidase. It can degrade heparan sulfate glycoprotein, damage the basement membrane and

promote invasion and metastasis of tumors. It expresses in tissues of spleen, lymph nodes, peripheral blood, bone marrow and infant liver, but not in tissues of heart, encephalon, lung, liver, kidney and pancreas of normal adults^[1,4]. Studies indicate that the level of heparanase expression in liver carcinoma, ovarian adenocarcinoma, colonic adenocarcinoma and melanoma is high^[4,5]. Its activity correlates with the metastatic potential of mouse lymphoma, fibrosarcoma and melanoma cells. The level of heparanase expression in tumor cells with high metastatic potential is higher than that in tumor cells with little or no metastatic potential^[6-9], suggesting that heparanase gene expression is closely associated with metastasis of tumors.

To explore new methods of inhibiting the metastasis of tumor we transfected human esophageal carcinoma EC9706 cells with four heparanase anti-sense oligodeoxynucleotides (ASODNs1-4) and observed the effect of ASODN on the expression of HPA gene in EC9706 cells. The results indicate that heparanase can express in human esophageal carcinoma EC9706 cell line and the expression of heparanase mRNA in EC9706 cells were effectively depressed by transfected ASODNs1-4 suggesting that ASODNs may inhibit the invasion and expression of heparanase gene. These results may provide the basic theory for preventing the invasion and metastasis of esophageal carcinoma.

REFERENCES

- 1 **Vlodavsky I**, Friemann Y, Elkin M, Aingorn H, Atzmon R, Ishai-Michaeli R, Bitan M, Pappo O, Peretz T, Michal I, Spector L, Pecker I. Mammalian heparanase: gene cloning, expression and function in tumor progression and metastasis. *Nat Med* 1999; **5**: 793-802
- 2 **Nakajima M**, Irimura T, Di Ferrante D, Di Ferrante N, Nicolson GL. Heparan sulfate degradation: relation to tumor invasion and metastatic properties of mouse B16 melanoma sublines. *Science* 1983; **220**: 611-613
- 3 **Chen KS**, Zheng NG, Wu JL, Ding Y, Wang YL. Effects of 8-Br-cAMP on growth related gene expression of human esophageal cancer cell line Eca-109. *Jieyou Xuebao* 1999; **30**: 227-229
- 4 **Vaday GG**, Lider O. Extracellular matrix moieties, cytokines, and enzymes: dynamic effects on immune cell behavior and inflammation. *J Leukoc Biol* 2000; **67**: 149-159
- 5 **Graham LD**, Underwood PA. Comparison of the heparanase enzymes from mouse melanoma cells, mouse macrophages and human platelets. *Biochem Mol Biol* 1996; **39**: 563-571
- 6 **Miao HQ**, Ornitz DM, Aingorn E, Ben-Sasson SA, Vlodavsky I. Modulation of fibroblast growth factor-2 receptor binding, dimerization, signaling, and angiogenic activity by synthetic heparinmimicking polyanionic compound. *J Clin Invest* 1997; **99**: 1565-1575
- 7 **Vlodavsky I**, fuks Z, Bar-Ner M, Ariav Y, Schirrmacher V. Lymphoma cell mediated degradation of sulfated proteoglycans in the subendothelial extracellular matrix: relationship to tumor cell metastasis. *Cancer Res* 1983; **43**: 2704-2711
- 8 **Vlodavsky I**, Elkin M, Pappo O, Aingorn H, Atzmon R, Ishai-Michaeli R, Aviv A, Pecker I, Friedmann Y. Mammalian heparanase as mediator of tumor metastasis and angiogenesis. *Isr Med Assoc J* 2000; **2**(Suppl): 37-45
- 9 **Walch ET**, Marchetti D. Role of neurotrophins and neurotrophins receptors in the *in vitro* invasion and heparanase production of human prostate cancer cells. *Clin Exp Metastasis* 1999; **17**: 307-314

Increased expression of cyclooxygenase-2 in first-degree relatives of gastric cancer patients

Jin-Ting Zhang, Ming-Wei Wang, Zhen-Long Zhu, Xiao-Hui Huo, Jian-Kun Chu, Dong-Sheng Cui, Liang Qiao, Jun Yu

Jin-Ting Zhang, Ming-Wei Wang, Zhen-Long Zhu, Xiao-Hui Huo, Jian-Kun Chu, Dong-Sheng Cui, Jun Yu, Department of Medicine, the First Affiliated Hospital of Hebei Medical University, Shijiazhuang 050017, Hebei Province, China
Liang Qiao, Jun Yu, Storr Liver Unit, Westmead Millennium Institute, University of Sydney at Westmead Hospital, NSW 2145, Sydney, Australia

Supported by the National Natural Science Foundation of China, No. 30370637

Co-first-authors: Jin-Ting Zhang and Ming-Wei Wang
Correspondence to: Dr. Jun Yu, Storr Liver Unit, Westmead Millennium Institute, University of Sydney at Westmead Hospital, NSW 2145, Sydney, Australia. jun_yu@wmi.usyd.edu.au
Telephone: +61-2-98459142 Fax: +61-2-98459103
Received: 2005-01-04 Accepted: 2005-01-26

Abstract

AIM: To study the expression of cyclooxygenase-2 (COX-2) in human gastric cancer tissues and their paired adjacent mucosa, as well as mucosa from gastric antrum and corpus of the first-degree relatives of the recruited cancer patients.

METHODS: The expression of COX-2 mRNA in 38 patients with gastric cancer and their 29 first-degree relatives and 18 healthy controls was assessed by the real time RT-PCR. The expression of COX-2 protein was determined by Western blot.

RESULTS: A marked increase in COX-2 mRNA expression was found in 20 of 37 (54%) cancerous tissues compared to their respective paired normal mucosa ($P < 0.001$). Interestingly, increased COX-2 mRNA expression was also found in mucosa of the corpus (6/29) and antrum (13/29) of their first-degree relatives. Increased COX-2 mRNA expression was more frequently observed in the antrum biopsies from cancer patients than in the antrum biopsies from healthy controls ($P < 0.05$). In addition, 3 of 23 (13%) patients with atrophic mucosa and 6 of 35 (17%) patients with intestinal metaplasia showed increased COX-2 mRNA expression. Furthermore, COX-2 expression increased in *H pylori*-positive tissues, especially in antrum mucosa.

CONCLUSION: Increased COX-2 expression is involved in gastric carcinogenesis, and may be necessary for maintenance of the malignant phenotype and contribute to *Helicobacter pylori*-associated malignant transformation.

© 2005 The WJG Press and Elsevier Inc. All rights reserved.

Key words: Gastric cancer; First-degree relatives; COX-2; *H pylori*

Zhang JT, Wang MW, Zhu ZL, Huo XH, Chu JK, Cui DS, Qiao L, Yu J. Increased expression of cyclooxygenase-2 in first-degree relatives of gastric cancer patients. *World J Gastroenterol* 2005; 11(31): 4918-4922

<http://www.wjgnet.com/1007-9327/11/4918.asp>

INTRODUCTION

Gastric cancer is one of the most common malignancies in China and the most frequent cause of cancer-related death^[1]. Although its incidence is increasing, it is still the second most commonly diagnosed fatal cancer worldwide^[2]. Unfortunately, gastric tumors are usually diagnosed at their advanced stage and the current 5-year survival rate is only 17%. Development of gastric cancer, like many other malignancies, is a multi-step process involving the accumulation of genetic alterations. However, much remains to be learned about the molecular pathogenesis of gastric cancer progression and new molecular targets are needed for the prevention and treatment of gastric cancer, especially in its early stage.

Previous studies showed that about 10% of gastric cancer patients exhibit familial clustering^[3,4], and a high prevalence of intestinal metaplasia has been found to be in the first-degree relatives of patients with gastric cancer in contrast to age-matched controls. Thus, the first-degree relatives are considered to be in pre-malignant state^[5]. Therefore, identification of genes predisposing to familial cancer is an essential step towards understanding the molecular events underlying tumorigenesis and is critical for the clinical management of affected families.

Prostaglandins play an important role in the protection of the upper gastrointestinal tract mucosa against injurious agents. Prostaglandin production in the gastro-duodenal mucosa is due to a single isoform of cyclooxygenase (COX)^[6]. Two COX isoforms, COX-1 and -2, have been identified^[7]. COX-1 is a housekeeping gene that is constantly expressed in a number of cell types, whereas COX-2 is an early responsive gene that is rapidly induced by growth factors, tumor promoters, oncogenes, and carcinogens^[8]. COX-2 products have also been shown to be mutagenic^[9] and tumorigenic^[10]. Multiple lines of evidence suggest that COX-2 plays an important role in the malignant transformation of cells^[11] including various cancer cells^[12]. In contrast, levels of COX-1 are relatively constant. Recently, the importance of COX-2 in gastro-intestinal carcinogenesis has been recognized. In humans, COX-2 is frequently detected in the majority of colon tumor samples and is involved in early events of colon carcinogenesis^[13,14]. Indeed, increased COX-2 expression has been observed in gastric carcinoma

with no alteration in the levels of COX-1^[5]. Whether COX-2 is associated with early gastric carcinogenesis in humans, especially in gastric mucosa of the first-degree relatives of gastric cancer patients, remains unclear. In this study, we aimed to detect the expression level of COX-2 in gastric cancer and non-cancerous tissues to look for a possible relationship between the development of gastric cancer and COX-2 expression.

MATERIALS AND METHODS

Subjects

Fifty patients with gastric cancer (mean age 66 years, range 50-87 years), 29 of their first-degree relatives (mean age 50 years, range 27-74 years) and 18 healthy subjects without gastric cancer family history (mean age 58 years, range 24-86 years) were recruited in this study. Tissues were collected from tumor area and their adjacent non-tumor corpus and antrum of cancer patients, their first-degree relatives and healthy subjects. Two or three biopsies were snap-frozen in liquid nitrogen for mRNA and protein analysis, and two additional specimens were fixed in 10% buffered formalin for routine histology. Written informed consent was obtained from all participants before commencement of the study.

Histology

Formalin fixed tissues were processed and stained with hematoxylin and eosin, for routine histological evaluation. *Helicobacter pylori* (*H. pylori*) was detected by Warthin-Starry staining^[6]. Histological classification of gastric cancer type was based upon Lauren system which divides gastric cancer into intestinal or diffuse type. The severity of gastritis and *H. pylori* colonization status of the non-tumorous gastric mucosa were determined by updated Sydney System^[7]. All histological sections were reviewed by an experienced gastrointestinal pathologist.

RNA and protein isolation

Gastric tissue specimens were homogenized with an ultrasonographic homogenizer. Total RNA and proteins were sequentially extracted using TRIzol reagents (CINNA/MRC, Cincinnati, OH, USA), according to the manufacturer's instructions.

RT-PCR

One microgram of total RNA was reverse transcribed using dNTPs (1 mol/L), 5× reverse transcription (RT) buffer (500 mol/L Tris-HCl, pH 8.3, 250 mol/L KCl, 50 mol/L MgCl₂ and 50 mol/L DTT), 16 units RNasin, and 2.5 units of AMV reverse transcriptase (Gibco-BRL, Life Technologies). mRNA expression of COX-2 was first determined by conventional RT-PCR. One microliter of reverse-transcription product (cDNA) was amplified by PCR using 1 U of Ampli-Taq DNA polymerase (Gibco-BRL), and 6 pmol each of COX-2 forward and reverse primers, with 6 pmol each of forward and reverse β-actin primers included in the same multiplex PCR reaction, as an internal control for efficiency of RT and amount of RNA. Each PCR cycle consisted of a denaturation at 94 °C for 28 s, an annealing at 60 °C for 48 s and an elongation at 72 °C for 1 min. A

total of 30 cycles were performed with an additional extension at 72 °C for 5 min. The primer sequences and PCR product sizes were as follows: *cox-2*, sense 5'-AGATCATCTCTGCCTGAGTATCTT-3', anti-sense 5'-TTCAAATGAGATTGTGGGAAAAT-3', with a 305-bp amplification; β-actin, sense, 5'-TGACGGGGTCACCC-ACACTGTGCCCATCTA-3', anti-sense, 5'-CTAGAAGC-ATTTGCGGTGGACGATGGAGGG-3' with a 654-bp amplification. PCR products were separated on 1.5% agarose gels with 0.5 μg/mL of ethidium bromide, and stained bands were visualized under UV light, photographed, and digitized with a scanner.

Real-time quantitative PCR was then performed on ABI PRISM 7000 sequence detection system using Sybrgreen, PCR mastermix (Perkin Elmer, Branchburgh, NJ, USA) and primers. Primer sequences were designed from the GenBank as follows: COX-2, (forward) 5'-GCCCTTCC-TCCCTGTGCC-3', (reverse) 5'-AATCAGGAAGCTGC-TTTTAC-3'; and β-actin, (forward), 5'-CTAATGGGCA-CCCAGCACAATG-3', (reverse) 5'-GCCGATCCACA-CGGAGTACT-3'. A 24-μL reaction mix was aliquot with 1 μL/replicate of cDNA. A DNA-free template control (containing water) was included and each sample was added in duplicate. Reaction tubes were sealed with optical caps, and the PCR reaction was run at 50 °C for 2 min, at 95 °C for 10 min, followed by 40 cycles at 96 °C for 45 s, at 60 °C for 45 s and at 72 °C for 1 min. Specificity of PCR products was characterized by melting curve analysis and followed by gel electrophoresis. Quantification was determined by the threshold cycle. Actin was used as a housekeeping gene to normalize mRNA levels and compared to mRNA expression levels in normal control stomach.

Western blotting

Total protein concentration was determined by the method of Bradford (DC protein assay, Bio-Rad, Hercules, CA, USA). Fifteen micrograms of protein was separated by 12% sodium dodecyl sulfate-polyacrylamide gel electrophoresis and then transferred onto equilibrated polyvinylidene difluoride membrane (Amersham Biosciences, Buckinghamshire, UK) by electroblotting. Membranes were blocked using 5% skim milk, and then incubated with primary antibodies (Santa Cruz Biotechnology, Santa Cruz, CA, USA) against COX-2 (1:1 000) or β-actin (1:1 000) overnight at 4 °C. After incubation with secondary antibody, proteins were detected by enhanced chemiluminescence (ECL, Amersham Corporation), and bands were quantified by scanning densitometry using the SCAN Control (Scanco~1.lnk) imaging system.

Statistical analysis

Statistical association between COX-2 expression and various clinicopathological factors was determined using the χ^2 test. An exact comparison densitometric analysis of COX-2 PCR products was performed by Student's *t*-test. *P*<0.05 was considered statistically significant.

RESULTS

COX-2 expression in gastric cancer

Increased COX-2 mRNA expression was detected in 37 of

50 (74%) gastric cancer tissues, COX-2 mRNA expression was found to be at very low levels in adjacent gastric mucosa, with 6 of 34 (18%) corpus tissues and 2 of 35 (6%) antrum tissues showing positive COX-2 expression (Table 1 and Figure 1). Quantitative analysis showed that tumor tissues expressed significantly higher levels of COX-2 mRNA compared to the adjacent antrum or corpus samples (Figure 2). COX-2 mRNA was expressed in both intestinal and diffuse types of gastric cancer and did not show any significant difference. By Western blot, COX-2 protein expression was found in 15 of 24 (62.5%) cancers and 4 of 24 (16.7%) adjacent non-tumor specimens (Figure 3). There was a significant correlation between COX-2 mRNA and COX-2 protein expression in gastric tumor samples ($r = 0.522$; $P = 0.001$).



Figure 1 RT-PCR analysis of COX-2 mRNA in gastric tissues. Lanes 1-4: gastric cancer; lanes 5 and 6: first-degree relatives; lanes 7 and 8: healthy control; lane 9: negative control; lane 10: 100-bp DNA ladder. T: Tumor; NT: adjacent non-tumor; C: corpus, and A: antrum.

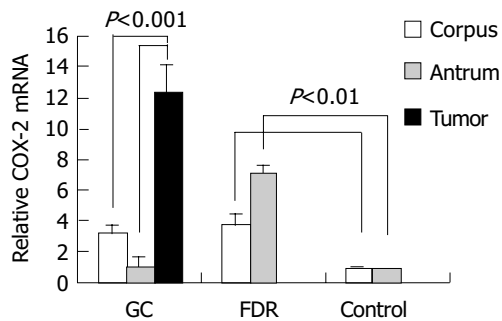


Figure 2 Quantitative RT-PCR analysis of COX-2 mRNA in gastric tissues. GC: gastric cancer; FDR: first degree relatives.

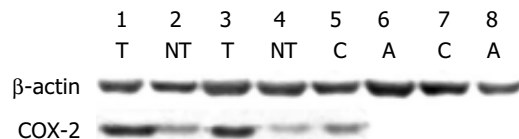


Figure 3 COX-2 protein expression in gastric tissues. T: Tumor; NT: adjacent non-tumor; C: corpus, and A: antrum.

Expression of COX-2 in gastric mucosa of first degree relatives

We also studied the COX-2 expression in 29 first-degree relatives of gastric cancer patients, and in 18 normal subjects without family history of gastric cancer. Increased COX-2 mRNA expression was observed in 6 of 29 (20.1%) corpus tissues and in 13 of 29 (44.8%) antrum tissues of

first-degree relatives (Figure 1). In contrast, only 1 of 18 normal controls exhibited very low COX-2 mRNA expression in both corpus and antrum tissues. Quantitative analysis showed that expression of COX-2 mRNA increased in corpus and antrum tissues of first-degree relatives compared to healthy controls ($P < 0.01$, Figure 2). Weakly positive COX-2 protein was detected in the mucosa of first degree relatives (Figure 3), whereas it was undetectable in normal controls.

We then proceeded to investigate the COX-2 expression in two pre-cancerous conditions: atrophic mucosa and mucosa with intestinal metaplasia, to determine whether upregulation of this gene occurred at an earlier stage in malignant transformation. COX-2 mRNA was upregulated in 3 of 23 (13%) cases of mucosal atrophy and 6 of 35 (17%) cases of intestinal metaplasia.

Table 1 COX-2 mRNA expression in gastric tissues

Tissues	COX-2 mRNA expression		%
	+	-	
Gastric cancer	20	17	54
Paired adjacent corpus	6	28	18
Paired adjacent antrum	2	33	6
Corpus of first-degree relatives	6	23	21
Antrum of first-degree relatives	13	16	45
Corpus of healthy control	1	17	6
Antrum of healthy control	1	17	6

Correlation of COX-2 expression with H pylori infection

We compared the COX-2 mRNA expression in *H pylori* infected and *H pylori*-negative tissues (Table 2). RT-PCR analysis of the gastric tissues showed that the expression of COX-2 was significantly upregulated in *H pylori* infected tissues compared to *H pylori*-negative tissues ($P < 0.05$). Because *H pylori* is most commonly colonized in gastric antrum^[18], we also compared the levels of COX-2 expression in *H pylori* infected antrum and corpus tissues, and found that the expression of COX-2 mRNA was significantly higher in the antrum ($P < 0.05$).

Table 2 Correlation between COX-2 mRNA expression and *H pylori* infection

<i>H pylori</i>	COX-2 mRNA expression					
	Antrum	%	Corpus	%	Total	%
Positive	12/34	35	8/36	22	20/70	29
Negative	4/44	9	4/39	10	8/83	10
<i>P</i>		<0.005		>0.05		<0.005

DISCUSSION

Gastric cancer is one of the most commonly encountered malignancies worldwide. Several of its pre-cancerous conditions, such as atrophic gastritis and intestinal metaplasia, have been well recognized. The concern with these gastric cancer precursor conditions or lesions is related to the attempt to prevent carcinoma or to detect it at an early

stage. Atrophic gastritis is defined as the loss of gastric glands, which can occur either in antrum or in corpus. Increased prevalence of this type of gastritis has been found in subjects who are at high risk for gastric cancer^[19]. Intestinal metaplasia is defined as the replacement of gastric mucosa by glands that have the characteristics of the small intestine^[20], and this condition has been strongly associated with development of gastric cancer. Atrophic gastritis and intestinal metaplasia have been accepted as pre-cancerous conditions for some years. Generalized genetic instability has been shown to occur early in this process^[21,22]. In contrast, the relative contributions of inherited susceptibility and environmental effects to familial gastric cancer are poorly understood, because little is known about the genetic events that predispose to gastric cancer. The first-degree relatives of gastric cancer patients have a three-fold risk for developing gastric carcinoma^[3,9]. Therefore, the identification of genes predisposing to familial cancer is an essential step towards understanding the molecular events underlying tumorigenesis and critical for the clinical management of affected families.

In our study, COX-2 gene expression was undetectable in normal control gastric mucosa. In the majority of gastric carcinomas studied, COX-2 expression was clearly upregulated compared to the levels of expression in accompanying antrum and corpus mucosa devoid of cancer cells. A similar pattern of COX-2 mRNA expression has previously been found in human gastric carcinoma^[23]. More importantly in this study, upregulation of COX-2 mRNA and protein was found in first-degree relatives. Furthermore, we detected COX-2 expression in atrophic mucosa and in intestinal metaplasia. These results suggest that COX-2 overexpression constitutes an early event in the gastric neoplastic transformation process which occurs at the pre-cancerous stage. Similarly, expression of COX-2 is found in some non-malignant hyperplastic gastric glands that may represent pre-malignant lesions stained for the COX-2 protein^[23]. Expression of COX-2 is also found in rat epidermis during hyperplastic transformation^[24]. In addition, colonic epithelium expresses only low levels of COX-2 mRNA and elevated levels are found in more than 40% of pre-malignant colonic adenomas. COX-2 expression is detected in hyperplastic bronchial epithelium and atypical alveolar epithelium in lung specimens^[25]. COX-2 is involved in Barrett's-associated metaplastic and dysplastic specimens^[17]. All these findings strongly suggest that COX-2 may play a role in early carcinogenesis.

H. pylori has been epidemiologically linked to gastric cancer and classified as a class I carcinogen by the World Health Organization^[26]. In the present study, expression of COX-2 mRNA was upregulated in gastric mucosa from *H. pylori*-positive tissues compared to *H. pylori*-negative tissues, suggesting that induction of COX-2 may be a specific response to *H. pylori* infection. COX-2 mRNA expression was significantly correlated with *H. pylori* infected antrum tissues, but not with *H. pylori* infected corpus tissues. A more important factor may be the consistent finding that *H. pylori* infection density is greater in gastric antrum than in corpus^[27,28]. Therefore, the overexpression of COX-2 may be a direct effect of *H. pylori*.

In conclusion, gastric cancer and pre-cancerous lesions

express COX-2. COX-2 mRNA is detectable in gastric mucosa of first-degree relatives of cancer patients. COX-2 may contribute to *H. pylori* associated neoplastic transformation. Further investigation is necessary to determine the putative role of this gene in gastric carcinogenesis.

REFERENCES

- 1 **Parkin DM**, Laara E, Muir CS. Estimates of the worldwide frequency of sixteen major cancers in 1980. *Int J Cancer* 1988; **41**: 184-197
- 2 **Dixon MF**. Histological responses to *Helicobacter pylori* infection: gastritis, atrophy and preneoplasia. *Baillieres Clin Gastroenterol* 1995; **9**: 467-486
- 3 **Zanghieri G**, Di Gregorio C, Sacchetti C, Fante R, Sassatelli R, Cannizzo G, Carriero A, Ponz de Leon M. Familial occurrence of gastric cancer in the 2-year experience of a population-based registry. *Cancer* 1990; **66**: 2047-2051
- 4 **La Vecchia C**, Negri E, Franceschi S, Gentile A. Family history and the risk of stomach and colorectal cancer. *Cancer* 1992; **70**: 50-55
- 5 **Sipponen P**, Seppala K, Varis K, Hjelt L, Ihamaki T, Kekki M, Siurala M. Intestinal metaplasia with colonic-type sulphomucins in the gastric mucosa; its association with gastric carcinoma. *Acta Pathol Microbiol Scand* 1980; **88**: 217-224
- 6 **Scheiman JM**. NSAIDs, gastrointestinal injury, and cytoprotection. *Gastroenterol Clin North Am* 1996; **25**: 279-298
- 7 **Hla T**, Neilson K. Human cyclooxygenase-2 cDNA. *Proc Natl Acad Sci USA* 1992; **89**: 7384-7388
- 8 **Herschman HR**. Prostaglandin synthase 2. *Biochim Biophys Acta* 1996; **1299**: 125-140
- 9 **Plummer SM**, Hall M, Faux SP. Oxidation and genotoxicity of fecapentaene-12 are potentiated by prostaglandin H synthase. *Carcinogenesis* 1995; **16**: 1023-1028
- 10 **Boolbol SK**, Dannenberg AJ, Chadburn A, Martucci C, Guo XJ, Ramonetti JT, Abreu-Goris M, Newmark HL, Lipkin ML, De Cosse JJ, Bertagnolli MM. Cyclooxygenase-2 overexpression and tumor formation are blocked by sulindac in a murine model of familial adenomatous polyposis. *Cancer Res* 1996; **56**: 2556-2560
- 11 **Subbaramaiah K**, Telang N, Ramonetti JT, Araki R, De Vito B, Weksler BB, Dannenberg AJ. Transcription of cyclooxygenase-2 is enhanced in transformed mammary epithelial cells. *Cancer Res* 1996; **56**: 4424-4429
- 12 **Tucker ON**, Dannenberg AJ, Yang EK, Zhang F, Teng L, Daly JM, Soslow RA, Masferrer JL, Woerner BM, Koki AT, Fahey TJ 3rd. Cyclooxygenase-2 expression is up-regulated in human pancreatic cancer. *Cancer Res* 1999; **59**: 987-990
- 13 **Eberhart CE**, Coffey RJ, Radhika A, Giardiello FM, Ferrenbach S, DuBois RN. Up-regulation of cyclooxygenase 2 gene expression in human colorectal adenomas and adenocarcinomas. *Gastroenterology* 1994; **107**: 1183-1188
- 14 **Oshima M**, Dinchuk JE, Kargman SL, Oshima H, Hancock B, Kwong E, Trzaskos JM, Evans JF, Taketo MM. Suppression of intestinal polyposis in Apc delta716 knockout mice by inhibition of cyclooxygenase 2 (COX-2). *Cell* 1996; **87**: 803-809
- 15 **Soydan AS**, Gaffen JD, Weech PK, Tremblay NM, Kargman S, O'Neill G, Bennett A, Tavares IA. Cytosolic phospholipase A2, cyclo-oxygenases and arachidonate in human stomach tumours. *Eur J Cancer* 1997; **33**: 1508-1512
- 16 **Brown KE**, Peura DA. Diagnosis of *Helicobacter pylori* infection. *Gastroenterol Clin North Am* 1993; **22**: 105-115
- 17 **Dixon MF**, Genta RM, Yardley JH, Correa P. Classification and grading of gastritis: the updated Sydney System. *Am J Surg Pathol* 1996; **20**: 1161-1181
- 18 **Peng HB**, Rajavashisth TB, Libby P, Liao JK. Nitric oxide inhibits macrophage-colony stimulating factor gene transcription in vascular endothelial cells. *J Biol Chem* 1995; **270**: 17050-17055
- 19 **Nomura A**, Stemmermann GN. *Helicobacter pylori* and gastric cancer. *J Gastroenterol Hepatol* 1993; **8**: 294-303

- 20 **Stemmermann GN**, Ishidate T, Samloff IM, Masuda H, Walsh JH, Nomura A, Yamakawa H, Guber G. Intestinal metaplasia of the stomach in Hawaii and Japan. A study of its relation to serum pepsinogen I, gastrin, and parietal cell antibodies. *Am J Dig Dis* 1978; **23**: 815-820
- 21 **Yu J**, Miehke S, Ebert MP, Hoffmann J, Breidert M, Alpen B, Starzynska T, Stolte Prof M, Malfertheiner P, Bayerdorffer E. Frequency of TPR-MET rearrangement in patients with gastric carcinoma and in first-degree relatives. *Cancer* 2000; **88**: 1801-1806
- 22 **Yu J**, Ebert MP, Miehke S, Rost H, Lendeckel U, Leodolter A, Stolte M, Bayerdorffer E, Malfertheiner P. alpha-catenin expression is decreased in human gastric cancers and in the gastric mucosa of first degree relatives. *Gut* 2000; **46**: 639-644
- 23 **Murata H**, Kawano S, Tsuji S, Tsuji M, Sawaoka H, Kimura Y, Shiozaki H, Hori M. Cyclooxygenase-2 overexpression enhances lymphatic invasion and metastasis in human gastric carcinoma. *Am J Gastroenterol* 1999; **94**: 451-455
- 24 **Wolff H**, Saukkonen K, Anttila S, Karjalainen A, Vainio H, Ristimaki A. Expression of cyclooxygenase-2 in human lung carcinoma. *Cancer Res* 1998; **58**: 4997-5001
- 25 **Wilson KT**, Fu S, Ramanujam KS, Meltzer SJ. Increased expression of inducible nitric oxide synthase and cyclooxygenase-2 in Barrett's esophagus and associated adenocarcinomas. *Cancer Res* 1998; **58**: 2929-2934
- 26 **Parsonnet J**, Friedman GD, Vandersteen DP, Chang Y, Vogelman JH, Orentreich N, Sibley RK. *Helicobacter pylori* infection and the risk of gastric carcinoma. *N Engl J Med* 1991; **325**: 1127-1131
- 27 **Khulusi S**, Mendall MA, Patel P, Levy J, Badve S, Northfield TC. *Helicobacter pylori* infection density and gastric inflammation in duodenal ulcer and non-ulcer subjects. *Gut* 1995; **37**: 319-324
- 28 **Genta RM**, Graham DY. Comparison of biopsy sites for the histopathologic diagnosis of *Helicobacter pylori*: a topographic study of *H pylori* density and distribution. *Gastrointest Endosc* 1994; **40**: 342-345

Science Editor Wang XL and Guo SY Language Editor Elsevier HK

• CASE REPORT •

Klatskin tumor treated by inter-disciplinary therapies including stereotactic radiotherapy: A case report

Gerhild Becker, Felix Momm, Henning Schwacha, Norbert Hodapp, Henning Usadel, Michael Geißler, Annette Barke, Annette Schmitt-Gräff, Karl Henne, Hubert E. Blum

Gerhild Becker, Henning Schwacha, Henning Usadel, Michael Geißler, Hubert E. Blum, Department of Medicine II, Freiburg University Hospital, Hugstetter Str. 55, Freiburg D-79106, Germany

Felix Momm, Norbert Hodapp, Annette Barke, Karl Henne, Department of Radiotherapy, Freiburg University Hospital, Robert-Koch-Str. 3, Freiburg D-79106, Germany

Annette Schmitt-Gräff, Institute of Pathology, Freiburg University Hospital, Albertstr. 19, Freiburg D-79106, Germany

Co-first-authors: Gerhild Becker and Felix Momm

Correspondence to: Gerhild Becker, MD, Department of Medicine II, Freiburg University Hospital, Hugstetter Str. 55, Freiburg D-79106, Germany. becker@medizin.ukl.uni-freiburg.de

Telephone: +49-761-270-3213 Fax: +49-761-270-3213

Received: 2004-12-10 Accepted: 2005-01-05

Gastroenterol 2005; 11(31): 4923-4926

<http://www.wjgnet.com/1007-9327/11/4923.asp>

INTRODUCTION

Cholangiocarcinoma (CCC) is the second most common primary liver cancer after hepatocellular carcinoma^[1]. Its prognosis is poor. The 5-year survival after surgical treatment with curative intention is 10-30%^[2], but at the time of diagnosis less than one-third of tumors are resectable^[3,4]. Single agent or combination chemotherapy and conventional radiation therapy are so far not effective, neither as primary treatment nor as adjuvant treatment after resection^[1,5]. The majority of patients survive less than 12 mo after diagnosis^[5,6]. Thus, there is a strong need for new therapeutic strategies. Here we report a 45-year-old patient with inoperable hilar CCC, who was treated using an inter-disciplinary concept including stereotactic radiotherapy. This highly precise technique also known as *extracranial stereotactic radiotherapy*^[7], was first developed for the treatment of brain tumors. Using a body frame, it is applicable to the whole body. By this technique, an adequate radiation dose can be delivered to the tumor, while sparing normal structures in the liver hilus and the upper abdomen that are highly radiosensitive. A total dose of 48 Gy (3×4 Gy/wk) could be given and therapy is well tolerated. Although the tumor is locally advanced at the time of diagnosis and prognosis was extremely poor, an unusual long survival of more than 4 years with a good quality of life could be achieved. Stereotactic radiotherapy seems to be a promising choice of treatment for hilar CCC.

Abstract

In view of the poor prognosis of patients with cholangiocarcinoma (CCC), there is a need for new therapeutic strategies. Inter-disciplinary therapy seems to be most promising. Radiotherapy is an effective alternative to surgery for hilar CCC (Klatskin tumors) if an adequate radiation dose can be delivered to the liver hilus. Here, we describe a patient for whom we used a stereotactic radiotherapy technique in the context of an inter-disciplinary treatment concept. We report a 45-year-old patient with a locally advanced Klatskin tumor. Explorative laparotomy showed that the tumor was not resectable. A metallic stent was implanted and the patient was treated by stereotactic radiotherapy using a body frame. A total dose of 48 Gy (3×4 Gy/wk) was administered. Therapy was well tolerated. After 32 mo, local tumor recurrence and a chest wall metastasis developed and were controlled by radio-chemotherapy. After more than 56 mo with a good quality of life, the patient died of advanced neoplastic disease. Stereotactic radiotherapy led to a long-term survival of this patient with a locally advanced Klatskin tumor. In the context of inter-disciplinary treatment concepts, this radiotherapy technique is a promising choice of treatment for patients with hilar CCC.

© 2005 The WJG Press and Elsevier Inc. All rights reserved.

Key words: Klatskin tumor; Stereotactic radiotherapy; Inter-disciplinary treatment

Becker G, Momm F, Schwacha H, Hodapp N, Usadel H, Geißler M, Barke A, Schmitt-Gräff A, Henne K, Blum HE. Klatskin tumor treated by inter-disciplinary therapies including stereotactic radiotherapy: A case report. *World J*

CASE REPORT

In December 1998, a 45-year-old male patient was admitted to our hospital. The only pathologic finding at clinical examination was a generalized, painless jaundice. The patient reported itching, but no abdominal pain, no fever, and no weight loss. Laboratory tests showed elevated levels of alkaline phosphatase (591 U/L; normal 35-104 U/L), γ -glutamyltransferase (75 U/L; normal <39 U/L) and bilirubin (22.8 mg/dL; normal <1.2 mg/dL). C-reactive protein increased slightly (15 mg/L; normal <5 mg/L). The tumor antigen CA 19-9 was elevated (405 U/L; normal <37 U/L). All other routine biochemical tests were normal. Abdominal ultrasound examination showed dilation of intra-hepatic and extra-hepatic bile ducts. Computer

tomography (CT) and magnetic resonance imaging (MRI) revealed a 6 cm×7 cm tumor in hepatic duct bifurcation and cholestasis predominantly in the atrophic left lobe of the liver. Several enlarged lymph nodes were detected in the hepato-duodenal ligament and one retro-pancreatic lymph node in contact to the inferior vena cava. Endoscopic retrograde cholangiopancreatography (ERCP) showed a stenosis of the hepatic duct bifurcation. A biopsy was taken and using percutaneous transhepatic cholangial drainage (PTCD), an external-internal Yamakawa drainage was placed. Histological examination revealed a highly differentiated CCC. Chest X-ray showed no evidence for metastases. Explorative laparotomy showed a non-resectable tumor. The tumor was classified as American Joint Committee on Cancer stage III according to the staging system for CCC^[8] and as type IV according to modified Bismuth-Corlette classification for hilar CCC^[9,10]. The biliary drain was internalized post-operatively by implanting a metallic Memotherm stent (60 mm/10 mm, Fa. Bard-Angiomed, Karlsruhe, Germany). Subsequently a stereotactic radiotherapy with 48 Gy was performed for over 4 wk (3×4 Gy/wk) using the technique of Lax *et al.*^[7,11], with slight modifications. After careful fixation of the patient in a body frame, treatment planning was performed in series of 45 axial CT slices with a distance and thickness of 5 mm. The planning target volume^[12,13], including the clinical target volume (tumor and involved structures/lymphatic nodes) at a distance between 3 and 5 mm to compensate for organ motion and repositioning errors, was 370 cm³. To check the repositioning accuracy in the body frame, a second CT series was performed few days after the first. The maximum positioning deviation in the region of the target volume was less than 3 mm. An optimal dose distribution could be achieved with seven coplanar conformal photon beams from a 6 MV linear accelerator (Figure 1). Using this technique, the mean dose values to liver, right kidney, spleen, and duodenum could be kept at 20.2, 3.2, 8.7, and 22.2 Gy, respectively. The patient developed cholangitis 2 mo after radiotherapy. An ERCP showed a stenosis close to the papilla Vateri. A biopsy was not conclusive and could not determine whether the stenosis was caused by tumor or radiation. The patient was treated with antibiotics. An internal plastic stent (10F/7 cm, Endo-Flex GmbH, Voerde, Germany) was placed to relieve the distal biliary obstruction. Jaundice and associated symptoms resolved. The patient was followed up at 3-mo intervals. Because transhepatic biliary stents have a 1-year patency rate of only 50%^[14,15], the stent was replaced endoscopically every 3 mo between May 1999 and July 2003. MRI, in November 1999, showed no contrast medium enhancement in the tumor region and stable size of the lymph nodes. MRI, one year later (October 2000), showed constant size of the tumor, but a slightly contrast medium enhancement and enlargement of one retro-pancreatic lymph node consistent with a slowly growing residual tumor. In addition, a metastasis was detected in the right lobe of the liver. The patient refused chemotherapy. MRI, in April 2001, showed stable disease. In July 2001, the patient reported a weight loss of 18 kg in 2 mo and pain in the right chest. MRI revealed tumor progression and a metastasis in the right chest wall. Therefore, a combined palliative

radiochemotherapy was initiated in September 2001. The chest wall metastasis was irradiated with a photon beam of a 6 MV linear accelerator with a total dose of 24 Gy (3×4 Gy/wk). Chemotherapy with gemcitabine 1 000 mg/m² was initiated. MRI, after three cycles of chemotherapy in December 2001, showed partial remission with regression of all lesions. Therefore, chemotherapy was continued. Because of thrombocytopenia and anemia, only two additional cycles of gemcitabine at a reduced dose could be given and chemotherapy had to be stopped in March 2002. After tumor progression, the patient received four cycles of 5-fluorouracil/leucovorin/oxaliplatin FOLFOX^[7] and two cycles of 5-fluorouracil/leucovorin/irinotecan FOLFIRI. In July 2003, MRI showed significant progression of the tumor. Though the tumor had such a final progression, the patient had a good quality of life for more than 4 years. Four years and six months after diagnosis he died of liver failure. The treatment course of the patient is shown in Figure 2.



Figure 1 CT slice of radiotherapy treatment plan in the drainage area (planning system: TMS Helax). 1-7: Coplanar beams. Isodoses: green: 100% = 48.0 Gy; light blue 1: 90% = 43.2 Gy; light blue 2: 80% = 38.4 Gy; light blue 3: 70% = 33.6 Gy; dark blue: 50% = 24.0 Gy. A: PTV (planning target volume): outer red line includes a safety rim. B: Body frame (low density materials to avoid shielding) with positioning marks. C: Vacuum cushion for reproducible fixation of the patient (low density materials to avoid shielding: not visible in CT scan). D: Drainage. E: Radio-opaque fiducials for the coordinate read out in longitudinal direction.

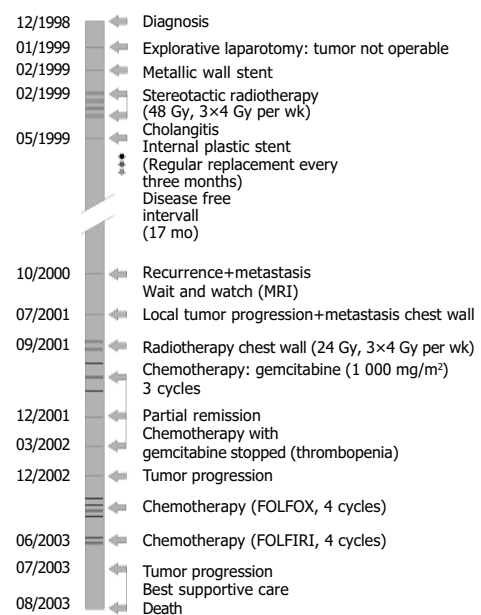


Figure 2 Patient's treatment course from 12/1998 to 08/2003.

DISCUSSION

Patients with CCC have an extremely poor prognosis. Because of the high recurrence rate of CCC, there is no indication for liver transplantation^[14,16,17]. Thus, surgical resection remains the only potentially curative treatment with a 5-year survival rate of 0-22% (mean 14%) for hilar CCC and 0-39% (mean 25%) for distal CCC^[18]. At the time of diagnosis, however, resection is possible in less than a third of the patients^[3]. If the tumor is unresectable, therapeutic interventions are directed toward the relief of biliary obstruction and its associated symptoms. Palliative options include ERC, PTCD, or a bilio-digestive anastomosis. Endoscopic biliary drainage with self-expandable metal stents has become the favored palliative drainage procedure and can be successfully performed on most patients with hilar CCC^[5]. Metallic wall stents are preferred over plastic stents because of their longer patency^[19-21]. In a small number of patients with unresectable CCC and failed endoscopic stents, photodynamic therapy (PDT) has been used. This technique involves the intravenous application of a photosensitizer followed by intra-luminal cholangioscopic photoactivation and generation of oxygen free radicals that harm cancer cells preferentially. Therapy decreases bilirubin levels and leads to a slightly better survival rate^[22,23]. It was reported that biliary stenting with and without PDT shows a survival benefit for patients receiving PDT^[24]. However, a puzzling aspect of the study is the failure to relieve bile duct obstruction with stenting alone. Therefore the observed survival benefit is probably caused by relief of cholestasis rather than by a reduction of tumor and it remains unclear, if PDT prolongs survival in patients responding to conventional biliary stenting procedures. Although this new technique appears promising, further studies are needed. Chemotherapy has not been shown to have a significant impact on survival^[25]. The majority of reports use 5-FU alone or in combination with leucovorin, methotrexate, cisplatin, mitomycin C, or interferon alpha^[5]. In some phase II studies, a response rate of about 20% is reported for gemcitabine^[26,27]. The majority of reports concerning chemotherapy in patients with CCC are retrospective and include only few patients. In intra-hepatic CCC, transarterial chemoperfusion in combination with temporary embolization of the feeding artery can be performed. But randomized controlled trials demonstrating an impact on survival are lacking. Few studies have reported benefits of primary or adjuvant standard radiation therapy^[28,29]. There are no randomized controlled trials demonstrating a therapeutic effect of brachytherapy or external beam radiotherapy^[5]. The main problem of radiation therapy of the upper abdomen is to deliver an adequate dose to the tumor without serious side effects. Using a conforming, stereotactic radiation technique, a steep dose gradient can be obtained^[30]. This means that a high radiation dose reaches the tumor while the normal tissue around the target volume is irradiated with comparatively low doses. Such a highly precise dose distribution is a need in radiotherapy of the liver hilus. Apart from the dose distribution the repositioning accuracy of the target volume is central to a successful radiation therapy. The high repositioning accuracy by a body frame^[7,11] can explain the differences between our patient and published

series with respect to side effects and tumor regression. Thus, stereotactic radiotherapy using a body frame is a valuable option for non-invasive treatment of inoperable tumors in critical regions as the liver hilus. Further technical developments as image guided radiotherapy or breath-triggered radiotherapy should further increase the repositioning accuracy and may make this technique available for routine use.

In conclusion, considering the generally poor prognosis of patients with Klatskin tumor, the long-term survival of our patient treated by stereotactic radiotherapy should encourage a systematic evaluation of this therapeutic strategy by prospective and randomized protocols.

REFERENCES

- 1 **Martin R**, Jarnagin W. Intrahepatic cholangiocarcinoma. Current management. *Minerva Chir* 2003; **58**: 469-478
- 2 **Klempnauer J**, Ridder GJ, Werner M, Weimann A, Pichlmayr R. What constitutes long-term survival after surgery for hilar cholangiocarcinoma? *Cancer* 1997; **79**: 26-34
- 3 **Burke E**, Jarnigan WR, Hochwald SN, Pisters PW, Fong Y, Blumgart LH. Hilar cholangiocarcinoma: patterns of spread, the importance of hepatic resection for curative operation, and a presurgical clinical staging system. *Ann Surg* 1998; **228**: 385-394
- 4 **Reding R**, Buard JL, Lebeau G, Launois B. Surgical management of 552 carcinomas of the bile duct (gall bladder and periampullary excluded). *Ann Surg* 1991; **213**: 236-241
- 5 **Anderson CD**, Pinson CW, Berlin J, Chari RS. Diagnosis and treatment of cholangiocarcinoma. *Oncologist* 2004; **9**: 43-57
- 6 **Chamberlain RS**, Blumgart LH. Hilar cholangiocarcinoma: a review and commentary. *Ann Surg Oncol* 2000; **7**: 55-66
- 7 **Lax I**, Blomgren H, Naslund I, Svanstrom R. Stereotactic radiotherapy of malignancies in the abdomen. Methodological aspects. *Acta Oncol* 1994; **33**: 677-683
- 8 American Joint Committee on Cancer, eds. *AJCC Cancer Staging Manual*. 5th ed. Philadelphia: Lippincott-Raven 1997
- 9 **Bismuth H**, Corlette MB. Intrahepatic cholangioenteric anastomosis in carcinoma of the hilus of the liver. *Surg Gynecol Obstet* 1975; **140**: 170-178
- 10 **Bismuth H**, Nakache R, Diamond T. Management strategies in resection for hilar cholangiocarcinoma. *Ann Surg* 1992; **215**: 31-38
- 11 **Blomgren H**, Lax I, Naslund I, Svanstrom R. Stereotactic high dose fraction radiation therapy of extracranial tumors using an accelerator. Clinical experience of the first thirty-one patients. *Acta Oncol* 1995; **34**: 861-870
- 12 ICRU Report No. 50: Prescribing, Recording and Reporting Photon Beam Therapy, 1993
- 13 ICRU Report No. 62: Prescribing, Recording and Reporting Photon Beam Therapy (Supplement to ICRU Report 50), 1999
- 14 **Jeyarajah DH**, Klintmalm GB. Is liver transplantation indicated for cholangiocarcinoma? *J Hepatobil Pancreat Surg* 1998; **5**: 48-51
- 15 **Shapiro MJ**. Management of malignant biliary obstruction: nonoperative and palliative techniques. *Oncology* 1995; **9**: 493-496
- 16 **Goldstein RM**, Stone M, Tillery GW, Senzer N, Levy M, Husberg BS, Gonwa T, Klintmalm G. Is liver transplantation indicated for cholangiocarcinoma? *Am J Surg* 1993; **166**: 768-771
- 17 **Meyer CG**, Penn I, James L. Liver transplantation for cholangiocarcinoma: results in 207 patients. *Transplantation* 2000; **69**: 1633-1637
- 18 **Thuluvath PJ**, Rai R, Venbrux AC, Yeo CJ. Cholangiocarcinoma: a review. *Gastroenterologist* 1997; **5**: 306-315
- 19 **Daivids PH**, Groen AK, Rauws EA, Tytgat GN, Huibregtse K. Randomised trial of self-expanding metal stents versus

- polyethylene stents for distal malignant biliary obstruction. *Lancet* 1992; **340**: 1488-1492
- 20 **Kaassis M**, Boyer J, Dumas R, Ponchon T, Coumaros D, Delcenserie R, Canard JM, Fritsch J, Rey JF, Burtin P. Plastic or metal stents for malignant stricture of the common bile duct? Results of a randomized prospective study. *Gastrointest Endosc* 2003; **57**: 178-182
- 21 **Prat F**, Chapat O, Ducot B, Ponchon T, Pelletier G, Fritsch J, Choury AD, Buffet C. A randomized trial of endoscopic drainage methods for inoperable malignant strictures of the common bile duct. *Gastrointest Endosc* 1998; **47**: 1-7
- 22 **Ortner MA**, Liebetrueth J, Schreiber S, Hanft M, Wruck U, Fusco V, Muller JM, Hortnagl H, Lochs H. Photodynamic therapy of non resectable cholangiocarcinoma. *Gastroenterology* 1998; **114**: 536-542
- 23 **Dumoulin FL**, Gerhardt T, Furchs S, Scheurlen C, Neubrand M, Layer G, Sauerbruch T. Phase II study of photodynamic therapy and metal stent as palliative treatment for nonresectable hilar cholangiocarcinoma. *Gastrointest Endosc* 2003; **57**: 860-867
- 24 **Ortner ME**, Caca K, Berr F, Liebetrueth J, Mansmann U, Huster D, Voderholzer W, Schachschal G, Mössner J, Lochs H. Successful Photodynamic Therapy for Nonresectable Cholangiocarcinoma: A Randomized Prospective Study. *Gastroenterology* 2003; **125**: 1355-1363
- 25 **Gores GJ**. A spotlight on cholangiocarcinoma. *Gastroenterology* 2003; **125**: 1536-1538
- 26 **Penz M**, Kornek GV, Raderer M, Ulrich-Pur H, Fiebiger W, Lenauer A, Depisch D, Krauss G, Schneeweiss B, Scheithauer W. Phase II trial of two-weekly gemcitabine in patients with advanced biliary tract cancer. *Ann Oncol* 2001; **12**: 183-186
- 27 **Raderer M**, Hejna MH, Valencak JB, Kornek GV, Weinlander GS, Bareck E, Lenauer J, Brodowicz T, Lang F, Scheithauer W. Two consecutive phase II studies of 5-fluorouracil/leucovorin/mitomycin C and of gemcitabine in patients with advanced biliary cancer. *Oncology* 1999; **56**: 177-180
- 28 **Schleicher UM**, Staatz G, Alzen G, Andreopoulos D. Combined external beam and intraluminal radiotherapy for irresectable Klatskin tumors. *Strahlenther Onkol* 2002; **178**: 682-687
- 29 **Todoroki T**, Ohara K, Kawamoto T, Koike N, Yoshida S, Kashiwagi H, Otsuka M, Fukao K. Benefits of adjuvant radiotherapy after radical resection of locally advanced main hepatic duct carcinoma. *Int J Radiat Oncol Biol Phys* 2000; **46**: 581-587
- 30 **Haedinger U**, Thiele W, Wulf J. Extracranial stereotactic radiotherapy: Evaluation of PTV coverage and dose conformity. *Z Med Phys* 2002; **12**: 221-229

Science Editor Wang XL and Guo SY Language Editor Elsevier HK

Calcified reticulate rind sign: A characteristic feature of gossypiboma on computed tomography

Yi-Ying Lu, Yun-Chung Cheung, Sheung-Fat Ko, Shu-Hang Ng

Yi-Ying Lu, Yun-Chung Cheung, Sheung-Fat Ko, Shu-Hang Ng, Department of Diagnostic Radiology, Chang Gung Memorial Hospital, Taiwan, China

Yun-Chung Cheung, Sheung-Fat Ko, Shu-Hang Ng, College of Medicine and School of Medical Technology, Chang Gung University, Taiwan, China

Correspondence to: Shu-Hang Ng, MD, Department of Diagnostic Radiology, Chang Gung Memorial Hospital at Linkou, 5-Fu-Shing Street, Kwei Shan, TaoYuan, Taiwan, China. shng@adm.cgmh.org.tw

Telephone: +886-3-3281200-2574 Fax: +886-2-25469220

Received: 2004-12-17 Accepted: 2005-01-13

Abstract

We herein report a gossypiboma resulting from a retained surgical swab, which had been left in peritoneum for 20 years after appendectomy. CT revealed a cystic mass with a calcified reticulate rind. Subsequent surgery and pathological examination showed a gossypiboma. A simple experiment, using a barium-soaked surgical swab demonstrating similar CT appearance, supported our postulation that calcium deposition on the reticulated fibers of a surgical swab could generate such a characteristic "calcified reticulate rind" sign. We believe that identification of this CT sign facilitates the diagnosis of gossypibomas.

© 2005 The WJG Press and Elsevier Inc. All rights reserved.

Key words: Gossypiboma; Textiloma; Retained surgical swab; CT

Lu YY, Cheung YC, Ko SF, Ng SH. Calcified reticulate rind sign: A characteristic feature of gossypiboma on computed tomography. *World J Gastroenterol* 2005; 11(31): 4927-4929 <http://www.wjgnet.com/1007-9327/11/4927.asp>

INTRODUCTIONS

Gossypiboma (also called textiloma), an infrequent complication of surgery, is a mass lesion owing to a retained surgical swab surrounded by foreign-body reaction. Because the symptoms of gossypiboma usually are non-specific and may appear years after surgery, awareness of a gossypiboma usually comes from imaging studies^[1,2]. The most specific imaging finding of a gossypiboma is a radiopaque marker on plain radiography, followed by entrapment of air bubbles in a spongiform pattern on CT^[1,2]. However, it is difficult to diagnose some long-lasting gossypibomas with these two

imaging findings because the surgical swabs used long time ago may not contain radiopaque markers, surrounding calcifications increased with time may mask radiopaque markers, and gas bubbles within a gossypiboma do not last for years. Herein, we describe a long-lasting gossypiboma with the "calcified reticulate rind" on CT which may ascribe to long-standing deposition of calcifications along the network architecture of a surgical swab. Identification of this novel CT feature may help doctors to diagnose some long-lasting gossypibomas.

CASE REPORT

A 43-year-old man sought medical attention due to progressive abdominal fullness and right flank pain for 2 mo. He denied fever, chill, nausea, vomiting, constipation, dysuria, gross hematuria, or body weight loss. Physical examination revealed a soft mass at the right lower quadrante of his abdomen. The blood cell count, blood chemistries, and urinalysis were all within the normal range. He received appendectomy at another hospital 20 years ago and also underwent bilateral vasectomy for contraception at our hospital 4 mo prior to this admission.

Abdominal radiograph revealed a round pelvic mass with a calcified rim (Figure 1). Intravenous urogram revealed right moderate hydronephrosis due to distal ureteral compression by the pelvic mass. Pre-enhanced CT scan demonstrated a 10-cm cystic lesion, with a thick calcified rind, which exhibited a reticulate pattern (Figures 2 and 3). Enhanced CT showed no abnormal contrast enhancement. During laparotomy, a 10 cm×10 cm cystic lesion with a well-defined fibrotic wall was disclosed in the pelvic cavity. Adhesion of the lesion to the right lower ureter was also noted. On gross examination, a piece of gauze of about 10 cm×4 cm×0.2 cm containing necrotic debris was removed from the thick-wall cystic lesion. Microscopic examination revealed suture granuloma, cholesterol clefts, fibrinoid necrosis, fibrosis, and calcification on the capsule. The final diagnosis was gossypiboma, plausibly resulted from the retained gauze during the appendectomy performed 20 years ago.

We postulated that the "calcified reticulate rind" in this gossypiboma might result from a gradual calcium deposition along the fiber network of the surgical swab. A simple experiment was performed for correlation. We soaked a piece of surgical swab with radiopaque marker in diluted barium. After drying the swab and wrapping it into a mass, we scanned it with CT. CT revealed a reticulate rind pattern (Figures 2 and 3), similar to that of the "calcified reticulate rind" of the gossypiboma noted in our case.



Figure 1 A round mass in pelvis with rim calcification on the abdominal plain radiograph.

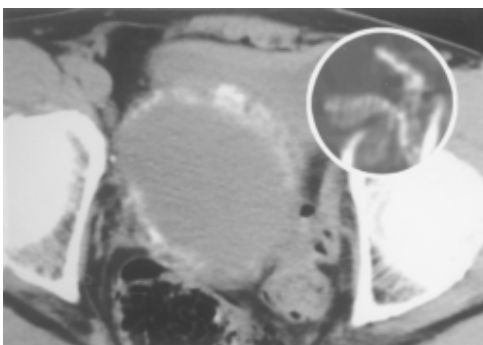


Figure 2 A cystic lesion in pelvic cavity with a thick "calcified reticulate rind" demonstrated by pre-enhanced CT scan.

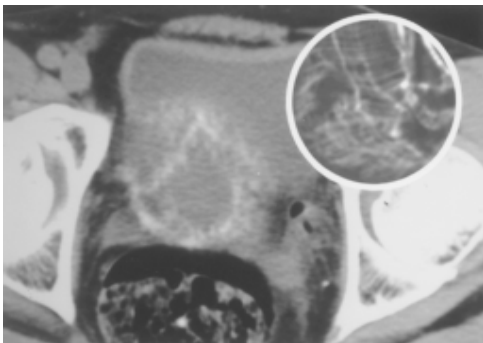


Figure 3 "Calcified reticulate rind" on another level (2 cm below Figure 2) demonstrated by pre-enhanced CT scan.

DISCUSSION

The term gossypiboma is derived from the Latin word gossypium, meaning cotton, and Kiswahili word boma, meaning place of concealment. This is an uncommon surgical complication with an estimated incidence of 1/1 500^[3]. Gossypibomas are most frequently discovered in the abdomen. However, their occurrences in the thorax^[4], extremity^[5], central nervous system^[6], and breast^[7] have also been reported. Pathologically, there are two types of foreign body reactions in gossypibomas. One is an aseptic fibrous response resulting in adhesion, encapsulation, and

granuloma, and the other is an exudative reaction leading to cyst or abscess formation^[8].

The most impressive imaging finding of gossypibomas is the curved or banded radiopaque lines on plain radiograph or CT, which represent the radiopaque markers of the surgical swabs. However, calcification depositions over the surgical gauze may mask the characteristic radiopaque markers, and some surgical swabs used long time ago may not have radiopaque markers. Hence, such radiographic finding may not be seen in every gossypiboma. On CT, a gossypiboma may manifest as a cystic lesion with internal spongiform appearance with mottled gas bubbles, hyperdense capsule, concentric layering, or mottled mural calcifications^[4,9-12]. In a series of 13 cases of gossypiboma found 3 mo to 8 years after surgery, Lars Kopka *et al.*^[2] suggested that the spongiform pattern with entrapped gas bubbles is the most specific CT finding for gossypibomas with an incidence of 54%. They also found that gas bubbles within a gossypiboma decrease slowly with time in an experiment. On MRI, gossypibomas may appear as a low-signal-intensity lesion on T2-weighted images with wavy, striped or spotted appearances^[13-15].

In our case, the gossypiboma might be due to the retention of the gauze during appendectomy 20 years ago. We could not find the conventional characteristic imaging findings of gossypibomas, such as the radiopaque markers and the spongiform pattern with entrapped air bubbles. The plausible explanations are that most surgical swabs at that moment usually contain no radiopaque markers while the air bubbles are completely absorbed after such a long duration of 20 years. Instead, this unique case demonstrated a novel imaging feature of gossypiboma, so-called the "calcified reticulate rind" sign which is probably formed by gradual deposition of calcifications along the fiber network of the surgical gauze. To our knowledge, this CT feature of gossypiboma has not been previously reported.

In summary, this report documents a unique case of gossypiboma that exhibits a "calcified reticulate rind", a characteristic feature of gossypiboma.

REFERENCES

- 1 Willian RG, Bragg DG, Nelson JA. Gossypiboma-the problem of the retained surgical sponge. *Radiology* 1978; **129**: 323-326
- 2 Kopka L, Fischer U, Gross AJ, Funke M, Oestmann JW, Grabbe E. CT of retained surgical sponges (textilomas): pitfalls in detection and evaluation. *J Comput Assist Tomogr* 1996; **20**: 919-923
- 3 Rappaport W, Haynes K. The retained surgical sponge following intra-abdominal surgery: a continuing problem. *Arch Surg* 1990; **125**: 405
- 4 Sheehan RE, Sheppard MN, Hansell DM. Retained intrathoracic surgical swab: CT appearances. *J Thorac Imaging* 2000; **15**: 61-64
- 5 Abdul-Karim FW, Benevenia J, Pathria MN, Makley JT. Case report 736: Retained surgical sponge (gossypiboma) with a foreign body reaction and remote and organizing hematoma. *Skeletal Radiol* 1992; **21**: 466-469
- 6 Mathew JM, Rajshekhar V, Chandy MJ. MRI features of neurosurgical gossypiboma: report of two cases. *Neuroradiology* 1996; **38**: 468-469
- 7 El Khoury M, Mignon F, Tardivon A, Mesurolle B, Rochard F, Mathieu MC. Retained surgical sponge or gossypiboma of

- the breast. *Eur J Radiol* 2002; **42**: 58-61
- 8 **Olnick HM**, Weens HS, Robers JV Jr. Radiological diagnosis of retained surgical sponges. *JAMA* 1955; **159**: 1525-1527
- 9 **Buy JN**, Hubert C, Ghossain MA, Malbec L, Bethoux JP, Ecoiffier J. Computed tomography of retained abdominal sponges and towels. *Gastrointest Radiol* 1989; **14**: 41-45
- 10 **Kokubo T**, Itai Y, Ohtomo K, Yoshikawa K, Ilio M, Atomi Y. Retained surgical sponges: CT and US appearance. *Radiology* 1987; **165**: 415-418
- 11 **Choi BI**, Kim SH, Yu ES, Chung HS, Han MC, Kim CW. Retained surgical sponge: diagnosis with CT and sonography. *Am J Roentgenol* 1988; **150**: 1047-1050
- 12 **Parienty RA**, Pradel J, Lepreux JF, Nicodeme CH, Dologa M. Computed tomography of sponges retained after laparotomy. *J Comput Assist Tomogr* 1981; **5**: 187-189
- 13 **Kuwashima S**, Yamato M, Fujioka M, Ishibashi M, Kogure H, Tajima Y. MR findings of surgically retained sponges and towels: report of two cases. *Radiat Med* 1993; **11**: 98-101
- 14 **Sugimura H**, Tamura S, Kakitsubata Y, Kakitsubata S, Uwada O, Kihara Y, Nagatomo M, Watanabe K. Magnetic resonance imaging of retained surgical sponges. Case report. *Clin Imaging* 1992; **16**: 259-262
- 15 **Roumen RM**, Weerdenburg HP. MR features of a 24-year-old gossypiboma, a case report. *Acta Radiol* 1998; **39**: 176-178

Science Editor Wang XL and Guo SY Language Editor Elsevier HK

• ACKNOWLEDGMENTS •

Acknowledgments to Reviewers of *World Journal of Gastroenterology*

Many reviewers have contributed their expertise and time to the peer review, a critical process to ensure the quality of *World Journal of Gastroenterology*. The editors and authors of the articles submitted to the journal are grateful to the following reviewers for evaluating the articles (including those were published and those were rejected in this issue) during the last editing period of time.

Takafumi Ando, M.D.

Nagoya University Graduate School of Medicine, Therapeutic Medicine, 65 Tsurumai-cho, Showa-ku, Nagoya 466-8550, Japan

Gabrio Bassotti, M.D.

Department of Clinical and Experimental Medicine, University of Perugia, Via Enrico dal Pozzo, Padiglione W, Perugia 06100, Italy

Ramon Bataller, M.D.

Liver Unit, Hospital Clinic, Villarroel 170, Barcelona 08036, Spain

Josep M Bordas, M.D.

Department of Gastroenterology IMD, Hospital Clinic, Llusanes 11-13 at, Barcelona 08022, Spain

Pierre Brissot, Professor

Liver Disease Unit And Inserm U-522, University Hospital Pontchaillou, 2, Rue Henri Le Guilloux, Rennes 35033, France

Vincent Coghlan, Professor

Neurological Sciences Institute, 505 NW 185th Avenue, Beaverton, Oregon 97006, United States

Jacques Cosnes, Professor

Department of Gastroenterology, Hospital St. Antoine, Hospital St. Antoine, 184 rue du Faubourg St-Antoine, PARIS 75012, France

Radha K Dhiman, Associate Professor

Department of Hepatology, Postgraduate Institute of Medical Education and Research, Chandigarh 160012, India

Alfred Gangl, Professor

Department of Medicine 4, Medical University of Vienna, Allgemeines Krankenhaus, Währinger Gürtel 18-20, Vienna A-1090, Austria

Toru Ishikawa, M.D.

Department of Gastroenterology, Saiseikai Niigata Second Hospital, Teraji 280-7, Niigata, Niigata 950-1104, Japan

Michael A Kamm, Professor

Department of Gastroenterology, St Mark's Hospital, St Mark's

Hospital, Watford Road, Harrow HA1 3UJ, United Kingdom

Seigo Kitano, Professor

Department of Surgery I, Oita University Faculty of Medicine, 1-1 Idaigaoka Hasama-machi, Oita 879-5593, Japan

Chris Jacob Johan Mulder, Professor

VUMC, PO Box 7057, Amsterdam 1007, Netherlands

Hiroki Nakamura, M.D.

Department of Gastroenterology and Hepatology, 1-1-1, Minami Kogushi, Ube, Yamaguchi 755-8505, Japan

Curtis T Okamoto, Associate Professor

Department of Pharmaceutical Sciences, University of Southern California, 1985 Zonal Ave. PSC 404A, Los Angeles CA 90089-9121, United States

Piero Portincasa, Professor

Internal Medicine - DIMIMP, University of Bari Medical School, Hospital Policlinico Piazza G. Cesare 11, Bari 70124, Italy

Bruno Stieger, Professor

Department of Medicine, Division of Clinical Pharmacology and Toxicology, University Hospital, Zurich 8091, Switzerland

Qin Su, Professor

Department of Pathology, Cancer Hospital and Cancer Institute, Chinese Academy of Medical Sciences and Peking Medical College, PO Box 2258, Beijing 100021, China

Koji Takeuchi, Professor

Department of Pharmacology and Experimental Therapeutics, Kyoto Pharmaceutical University, Misasagi, Yamashina, Kyoto 607-8414, Japan

Kam-Meng Tchou-Wong, Assistant Professor

Departments of Environmental Medicine and Medicine, NYU School of Medicine, 57 Old Forge Road, Tuxedo, New York 10987, United States

Anton Vavrecka, M.D.

Clinic Of Gastroenterology, SZU, NSP SV.CAM, Antolska 11, Bratislava 85107, Slovakia

Shinichi Wada, M.D.

Department of Gastroenterology, Jichi Medical School, Minamikawachi-machi, Kwachi-gun, Tochigi-ken, Tochigi 329-0498, Japan

Jia-Yu Xu, Professor

Shanghai Second Medical University, Rui Jin Hospital, 197 Rui Jin Er Road, Shanghai 200025, China



World Journal of Gastroenterology®



Volume 11 Number 32
August 28, 2005



National Journal Award
2005

Contents

BASIC RESEARCH

- 4931** Thiazolidinedione treatment inhibits bile duct proliferation and fibrosis in a rat model of chronic cholestasis
Marra F, DeFranco R, Robino G, Novo E, Efsen E, Pastacaldi S, Zamara E, Vercelli A, Lottini B, Spirli C, Strazzabosco M, Pinzani M, Parola M
- 4939** MUC1 and MUC5AC mucin expression in liver fluke-associated intrahepatic cholangiocarcinoma
Boonla C, Sripa B, Thuwajit P, Cha-On U, Puapairoj A, Miwa M, Wongkham S
- 4947** Hepatocytes targeting of cationic liposomes modified with soybean sterylglucoside and polyethylene glycol
Qi XR, Yan WW, Shi J
- 4953** Effect of Danshao Huaxian capsule on expression of matrix metalloproteinase-1 and tissue inhibitor of metalloproteinase-1 in fibrotic liver of rats
Yang Q, Xie RJ, Geng XX, Luo XH, Han B, Cheng ML
- 4957** Effects of dietary supplementation with vitamin E and selenium on rat hepatic stellate cell apoptosis
Shen XH, Cheng WF, Li XH, Sun JQ, Li F, Ma L, Xie LM
- 4962** Effects of acupuncture Tsusanli (S₇36) on expression of nitric oxide synthase in hypothalamus and adrenal gland in rats with cold stress ulcer
Sun JP, Pei HT, Jin XL, Yin L, Tian QH, Tian SJ
- 4967** IFN- γ increases efficiency of DNA vaccine in protecting ducks against infection
Long JE, Huang LN, Qin ZQ, Wang WY, Qu D
- 4974** Time-dependent viscoelastic properties along rat small intestine
Smith JB, Zhao JB, Dou YL, Gregersen H
- 4979** CXCL16 participates in pathogenesis of immunological liver injury by regulating T lymphocyte infiltration in liver tissue
Xu HB, Gong YP, Cheng J, Chu YW, Xiong SD
- 4986** Protective effect of *Astragalus membranaceus* on intestinal mucosa reperfusion injury after hemorrhagic shock in rats
Hei ZQ, Huang HQ, Zhang JJ, Chen BX, Li XY
- 4992** Angiostatin inhibits pancreatic cancer cell proliferation and growth in nude mice
Yang DZ, He J, Zhang JC, Wang ZR

BRIEF REPORTS

- 4997** Impact of antithrombin III on hepatic and intestinal microcirculation in experimental liver cirrhosis and bowel inflammation: An *in vivo* analysis
Maksan SM, Ülger Z, Gebhard MM, Schmidt J
- 5002** Misperceptions among patients with chronic hepatitis B in Singapore
Wai CT, Mak B, Chua W, Tan MH, Ng S, Cheok A, Wong ML, Lim SG
- 5006** Pin1 overexpression in colorectal cancer and its correlation with aberrant β -catenin expression
Kim CJ, Cho YG, Park YG, Nam SW, Kim SY, Lee SH, Yoo NJ, Lee JY, Park WS
- 5010** Effect of NCPB and VSPL on pain and quality of life in chronic pancreatitis patients
Basinski A, Stefaniak T, Vingerhoets A, Makarewicz W, Kaska L, Stanek A, Lachinski AJ, Sledzinski Z

Contents

BRIEF REPORTS

- 5015** Alpha-fetoprotein expression is a potential prognostic marker in hepatocellular carcinoma
Görög D, Regöly-Mérei J, Paku S, Kopper L, Nagy P
- 5019** Replication of hepatitis B virus in primary duck hepatocytes transfected with linear viral DNA
Yao YQ, Zhang DF, Tang N, Huang AL, Zou XY, Xiao JF, Luo Y, Zhang DZ, Wang B, Zhou WP, Ren H, Liu Q, Guo SH
- 5022** Expression of early growth response factor-1 in rats with cerulein-induced acute pancreatitis and its significance
Gong LB, He L, Liu Y, Chen XQ, Jiang B
- 5025** Ca²⁺ cytochemical changes of hepatotoxicity caused by halothane and sevoflurane in enzyme-induced hypoxic rats
Yu WF, Yang LQ, Zhou MT, Liu ZQ, Li Q
- 5029** Effect of *Helicobacter pylori* infection on gastric mucosal pathologic change and level of nitric oxide and nitric oxide synthase
Wang YF, Guo CL, Zhao LZ, Yang GA, Chen P, Wang HK
- 5032** Expression and correlation of CD44v6, vascular endothelial growth factor, matrix metalloproteinase-2, and matrix metalloproteinase-9 in Krukenberg tumor
Lou G, Gao Y, Ning XM, Zhang QF
- 5037** Gene expression profiles in peripheral blood mononuclear cells of SARS patients
Yu SY, Hu YW, Liu XY, Xiong W, Zhou ZT, Yuan ZH
- 5044** Inositol hexaphosphate-induced enhancement of natural killer cell activity correlates with suppression of colon carcinogenesis in rats
Zhang Z, Song Y, Wang XL
- 5047** Level of proinsulin in association with cardiovascular risk factors and sleep snoring
Jia EZ, Yang ZJ, Chen SW, Qi GY, You CF, Ma JF, Zhang JX, Wang ZZ, Qian WC, Wang HY, Ma WZ
- 5053** Effect of lactulose on establishment of a rat non-alcoholic steatohepatitis model
Fan JG, Xu ZJ, Wang GL
- 5057** Expression of cell cycle regulator p57^{kip2}, cyclinE protein and proliferating cell nuclear antigen in human pancreatic cancer: An immunohistochemical study
Yue H, Jiang HY

CASE REPORTS

- 5061** Pneumoscotum: A rare manifestation of perforation associated with therapeutic colonoscopy
Fu KI, Sano Y, Kato S, Fujii T, Sugito M, Ono M, Saito N, Kawashima K, Yoshida S, Fujimori T
- 5064** Recurrent thrombotic occlusion of a transjugular intrahepatic portosystemic stent-shunt due to activated protein C resistance
Siewert E, Salzmann J, Purucker E, Schürmann K, Matern S
- 5068** EUS diagnosis of ectopic opening of the common bile duct in the duodenal bulb: A case report
Krstic M, Stimec B, Krstic R, Ugljesic M, Knezevic S, Jovanovic I
- 5072** Colonic duplication in adults: Report of two cases presenting with rectal bleeding
Fotiadis C, Genetzakis M, Papandreou I, Misiakos EP, Agapitos E, Zografos GC
- 5075** Difficulty with diagnosis of malignant pancreatic neoplasms coexisting with chronic pancreatitis
Leung TK, Lee CM, Wang FC, Chen HC, Wang HJ
- 5079** Sigmoid schwannoma: A rare case
Fotiadis CI, Kouerinis IA, Papandreou I, Zografos GC, Agapitos G
- 5082** Prenatal diagnosis of choledochal cyst using magnetic resonance imaging: A case report
Wong AMC, Cheung YC, Liu YH, Ng KK, Chan SC, Ng SH

Contents

CASE REPORTS	5084 Cystic lymphangioma of the jejunal mesentery in an adult: A case report <i>Chen CW, Hsu SD, Lin CH, Cheng MF, Yu JC</i>
	5087 Preoperative diagnosis of colonic angiolipoma: A case report <i>Chen YY, Soon MS</i>

ACKNOWLEDGMENTS	5090 Acknowledgments to reviewers for this issue
------------------------	---

APPENDIX	5091 Meetings
	5092 Instructions to authors
	5094 <i>World Journal of Gastroenterology</i> standard of quantities and units

FLYLEAF	I-V Editorial Board
----------------	---------------------

INSIDE FRONT COVER	Online Submissions
---------------------------	--------------------

INSIDE BACK COVER	International Subscription
--------------------------	----------------------------

Editorial Coordinator for this issue: Anitha Kumaran

World Journal of Gastroenterology (*World J Gastroenterol*, *WJG*), a leading international journal in gastroenterology and hepatology, has an established reputation for publishing first class research on esophageal cancer, gastric cancer, liver cancer, viral hepatitis, colorectal cancer, and *Helicobacter pylori* infection, providing a forum for both clinicians and scientists, and has been indexed and abstracted in Index Medicus, MEDLINE, PubMed, Chemical Abstracts, EMBASE, Abstracts Journals, Nature Clinical Practice Gastroenterology and Hepatology, CAB Abstracts and Global Health. *WJG* is a weekly journal published jointly by The *WJG* Press and Elsevier Inc. The publication date is on 7th, 14th, 21st, and 28th every month. The *WJG* is supported by The National Natural Science Foundation of China, No. 30224801 and No.30424812, which was founded with a name of *China National Journal of New Gastroenterology* on October 1,1995, and renamed as *WJG* on January 25, 1998.

HONORARY EDITORS-IN-CHIEF

Ke-Ji Chen, *Beijing*
 Dai -Ming Fan, *Xi'an*
 Zhi-Qiang Huang, *Beijing*
 Nicholas F LaRusso, *Rochester*
 Jie-Shou Li, *Nanjing*
 Geng-Tao Liu, *Beijing*
 Fa-Zu Qiu, *Wuhan*
 Eamonn M Quigley, *Cork*
 David S Rampton, *London*
 Rudi Schmid, *California*
 Nicholas Joseph Talley, *Rochester*
 Zhao-You Tang, *Shanghai*
 Guido NJ Tytgat, *Amsterdam*
 Meng-Chao Wu, *Shanghai*
 Xian-Zhong Wu, *Tianjin*
 Hui Zhuang, *Beijing*
 Jia-Yu Xu, *Shanghai*

PRESIDENT AND EDITOR-IN-CHIEF

Lian-Sheng Ma, *Beijing*

EDITOR-IN-CHIEF
 Bo- Rong Pan, *Xi'an*

ASSOCIATE EDITORS-IN-CHIEF

Bruno Annibale, *Roma*
 Henri Bismuth, *Villeshuif*
 Jordi Bruix, *Barcelona*
 Roger William Chapman, *Oxford*
 Alexander L Gerbes, *Munich*
 Shou-Dong Lee, *Taipei*
 Walter Edwin Longo, *New Haven*
 You-Yong Lu, *Beijing*
 Masao Omata, *Tokyo*
 Harry H-X Xia, *Hong Kong*

EDITORIAL BOARD

See full details flyleaf I-V

DEPUTY EDITOR

Michelle Gabbe, Xian-Lin Wang

ASSOCIATE MANAGING EDITORS

Jian-Zhong Zhang, Shi-Yu Guo

EDITORIAL OFFICE MANAGER

Jing-Yun Ma

EDITORIAL ASSISTANT

Juan Li

TECHNICAL EDITORS

Meng Li, Shao-Hua Li, Xi Li, Hu Wang

PROOFREADERS

Hong Li, Wen-Jian Mei, Shi-Yu Guo

PUBLISHED JOINTLY BY

The *WJG* Press and Elsevier Inc

PRINTING GROUP

Printed in Beijing on acid-free paper by Beijing Kexin Printing House

COPYRIGHT

© 2005 Published jointly by The *WJG* Press and Elsevier Inc. All rights reserved; no part of this publication may be reproduced, stored in a retrieval system, or transmitted in any form or by any means, electronic, mechanical, photocopying, recording, or otherwise without the prior permission of

The *WJG* Press and Elsevier Inc. Author are required to grant *WJG* an exclusive licence to publish. Print ISSN 1007-9327 CN 14-1219/R.

SPECIAL STATEMENT

All articles published in this journal represent the viewpoints of the authors except where indicated otherwise.

EDITORIAL OFFICE

Editor: *World Journal of Gastroenterology*, The *WJG* Press, Apartment 1066 Yishou Garden, 58 North Langxinzhuang Road, PO Box 2345, Beijing 100023, China
 Telephone: +86-(0)10-85381901-1023
 Fax: +86-10-85381893
 E-mail: wjg@wjgnet.com
<http://www.wjgnet.com>

Public Relationship Manager

Shi-Yu Guo
 The *WJG* Press, Apartment 1066 Yishou Garden, 58 North Langxinzhuang Road, PO Box 2345, Beijing 100023, China
 Telephone: +86-(0)10-85381901-1023
 Fax: +86-10-85381893
 E-mail: s.y.guo@wjgnet.com
<http://www.wjgnet.com>

SUBSCRIPTION INFORMATION

Foreign
 Elsevier (Singapore) Pte Ltd, 3 Killiney Road #08-01, Winsland House I, Singapore 239519
 Telephone: +65-6349 0200
 Fax: +65-6733 1817

E-mail: r.garcia@elsevier.com
<http://asia.elsevierhealth.com>
 Institutional Rates Print-2005 rates: USD1 500.00
 Personal Rates Print-2005 rates: USD700.00

Domestic

Local Post Offices Code No. BM 82-261

Author Reprints

The *WJG* Press, Apartment 1066 Yishou Garden, 58 North Langxinzhuang Road, PO Box 2345, Beijing 100023, China
 Telephone: +86-(0)10-85381901-1023
 Fax: +86-10-85381893
 E-mail: wjg@wjgnet.com
<http://www.wjgnet.com>

ADVERTISING

Rosalia Da Garcia
 Elsevier Science
 Journals Marketing & Society Relations
 Health Science Asia
 3 Killiney Road #08-01, Winsland House 1
 Singapore 239519
 Telephone: +65-6349 0200
 Fax +65- 6733 1817
 E-mail: r.garcia@elsevier.com
<http://asia.elsevierhealth.com>

INSTRUCTIONS TO AUTHORS

Full instructions are available online at <http://www.wjgnet.com/wjg/help/instructions.jsp> If you do not have web access please contact the editorial office.

Thiazolidinedione treatment inhibits bile duct proliferation and fibrosis in a rat model of chronic cholestasis

Fabio Marra, Raffaella DeFranco, Gaia Robino, Erica Novo, Eva Efsen, Sabrina Pastacaldi, Elena Zamara, Alessandro Vercelli, Benedetta Lottini, Carlo Spirli, Mario Strazzabosco, Massimo Pinzani, Maurizio Parola

Fabio Marra, Raffaella DeFranco, Eva Efsen, Sabrina Pastacaldi, Benedetta Lottini, Massimo Pinzani, Dipartimento di Medicina Interna and Center for Research, Transfer, and High Education 'DENOTHE', University of Florence, Italy

Gaia Robino, Erica Novo, Elena Zamara, Maurizio Parola, Dipartimento di Medicina e Oncologia Sperimentale, University of Turin, Italy

Alessandro Vercelli, Dipartimento di Anatomia, Farmacologia e Medicina Legale, University of Turin, Italy

Carlo Spirli, Mario Strazzabosco, Istituto Veneto di Medicina Molecolare, Padua, Italy

Supported by the Italian MIUR Grant, No. MM_06315722, by the University of Florence and by the Italian Liver Foundation. Eva Efsen was Supported in Part by the Tode Travel Grant, the Direktør Madsen's Grant and Fhv. Direktør Nielsen's Grant (Denmark)

Correspondence to: Professor Fabio Marra, Dipartimento di Medicina Interna, University of Florence, Viale Morgagni 85, Florence I-50134, Italy. f.marra@dmi.unifi.it

Telephone: +39-55-4296475 Fax: +39-55-417123

Received: 2004-10-16 Accepted: 2004-12-23

© 2005 The WJG Press and Elsevier Inc. All rights reserved.

Key words: Cholangiocytes; Ductular reaction; PPAR- γ ; Hepatic stellate cells; Myofibroblasts; Troglitazone

Marra F, DeFranco R, Robino G, Novo E, Efsen E, Pastacaldi S, Zamara E, Vercelli A, Lottini B, Spirli C, Strazzabosco M, Pinzani M, Parola M. Thiazolidinedione treatment inhibits bile duct proliferation and fibrosis in a rat model of chronic cholestasis. *World J Gastroenterol* 2005; 11(32): 4931-4938
<http://www.wjgnet.com/1007-9327/11/4931.asp>

INTRODUCTION

A number of conditions characterized by chronic liver damage are associated with the development of liver fibrosis, ultimately leading to cirrhosis and functional alterations^[1]. Although fibrotic progression represents the final outcome of the liver 'wound healing' response in several conditions of chronic injury, different types of fibrosis show relatively unique features. Biliary fibroses, such as the one observed in conditions of chronic obstruction of the biliary tree, are characterized by the accumulation of extracellular matrix at portal tracts, surrounding newly formed bile ducts emerging during the course of the so-called 'typical' ductular reaction and originated from proliferation of pre-existing bile duct epithelial cells^[2,3]. If the obstruction persists, fibrosis bridging different portal tracts develops, ultimately leading to biliary cirrhosis. Common bile duct ligation (BDL) and scission in rats represents a classical experimental model for the analysis of the events leading the initial injury of the bile ducts to the organization of a fibrotic reaction, which involves different matrix-producing cells of mesenchymal origin, including α -smooth muscle actin (SMA)-positive portal myofibroblasts and activated hepatic stellate cells (HSC)^[2,4-6]. This model has been widely used to investigate the molecular and cellular mechanisms of liver fibrosis and to assess potential treatments for this disorder. In addition, due to the close anatomical and functional contacts between cholangiocytes and matrix-producing cells, the BDL model represents an optimal tool for the study of epithelial-mesenchymal interactions.

Peroxisome proliferator-activated receptors (PPARs) belong to the nuclear hormone receptor superfamily^[7]. All these molecules share the ability to function as transcription factors by binding to target DNA elements, and change their transcriptional activity after binding to specific ligands. Three different PPAR isoforms have been cloned and

Abstract

AIM: To investigate the effects of troglitazone (TGZ), an anti-diabetic drug which activates peroxisome proliferator-activated receptor- γ (PPAR- γ), for liver tissue repair, and the development of ductular reaction, following common bile duct ligation (BDL) in rats.

METHODS: Rats were supplemented with TGZ (0.2% w/w in the pelleted food) for 1 wk before BDL or sham operation. Animals were killed at 1, 2, or 4 wk after surgery.

RESULTS: The development of liver fibrosis was reduced in rats receiving TGZ, as indicated by significant decreases of procollagen type I gene expression and liver hydroxyproline levels. Accumulation of α -smooth-muscle actin (SMA)-expressing cells surrounding newly formed bile ducts following BDL, as well as total hepatic levels of SMA were partially inhibited by TGZ treatment, indicating the presence of a reduced number and/or activation of hepatic stellate cells (HSC) and myofibroblasts. Development of the ductular reaction was inhibited by TGZ, as indicated by histochemical evaluation and hepatic activity of γ -glutamyl-transferase (GGT).

CONCLUSION: Treatment with thiazolidinedione reduces ductular proliferation and fibrosis in a model of chronic cholestasis, and suggests that limiting cholangiocyte proliferation may contribute to the lower development of scarring in this system.

characterized. PPAR- α binds to fatty acids and fibrates and is known to induce transcription of genes involved in ω - and β -oxidation of fatty acids^[7]. PPAR- β (or - δ) is expressed ubiquitously, and could be involved in fatty acid and lipid metabolism^[8]. Finally, the ligands for PPAR- γ include anti-diabetic drugs of the thiazolidinedione group and arachidonic acid metabolites, such as prostaglandins of the D series and its derivatives such as 15deoxy- $\Delta^{12,14}$ PGJ₂. PPAR- γ is expressed at high levels in the adipose tissue, where it regulates lipid storage and modulates the action of insulin^[9-11].

Agonists of PPAR- γ have been shown to regulate multiple and critical functions in diverse pathophysiologic conditions, including type 2 diabetes and the metabolic syndrome, cancer, and inflammation^[12]. In the liver, considerable attention has been directed to the modulation of the development of fibrosis through actions on HSC and liver myofibroblasts^[13-15]. In this study, we investigated the effects of treatment with troglitazone (TGZ), the first thiazolidinedione introduced in clinical practice, on the development of ductular reaction and fibrosis in the BDL model. The results indicate that TGZ not only limits extracellular matrix deposition and HSC activation, but also inhibits the formation of newly formed bile ducts, thus acting on both epithelial and mesenchymal cells involved in the response to this type of chronic liver injury.

MATERIALS AND METHODS

In vivo model

Male Wistar rats (Harlan-Nossan, Correnzana, Italy), weighing 180-200 g, were used according to the national and local ethical guidelines. For experimental purposes, animals were divided into two experimental groups and fed for 2 wk either with a standard pelleted diet (rat diet No. 48, Piccioni, Gessate Milanese, Italy) and water *ad libitum* (control diet) or with the same pelleted diet containing 0.2% (w/w) troglitazone (TGZ diet), according to previously described procedures^[16,17]. In the animals from both experimental groups, permanent extrahepatic cholestasis was induced by common BDL and scission under light ether anesthesia as previously described^[18,19]. Animals receiving sham operation were subjected only to the manipulation of the common bile duct, and served as controls. After BDL or sham operation, the animals continued to receive the same diet according to the following experimental groups: (1) Sham (control, receiving normal diet), (2) TGZ (sham, receiving TGZ-supplemented diet), (3) BDL (operated, receiving normal diet), and (4) BDL/TGZ (operated, receiving TGZ-supplemented diet). The amount of consumed food in each experimental group was recorded throughout the study. The animals were then killed after 1, 2, and 4 wk of surgery ($n = 6-8$ animals for each experimental group at any time point). The liver was promptly removed, and portions of the organ were either immediately used or frozen in liquid nitrogen and stored at -80°C for further determinations or processed for histological and histochemical examination. Blood samples were also collected from individual animals before they were killed.

Serum and liver biochemistry

Serum activities of glutamic oxalacetic transaminase (GOT) and alkaline phosphatase (AP) were determined using a commercial kit (Sigma Diagnostics, Sigma, Milan, Italy). L-Hydroxyproline concentration in liver samples was determined according to standard procedures^[20]. γ -Glutamyltransferase (GGT) activity was evaluated on diluted liver homogenate samples using a modified standard procedure^[21] as previously described^[22].

RNase protection assay

Total RNA was isolated from frozen liver tissues using Nucleospin columns (Mackerey-Nagel, Dürer, Germany). Integrity of RNA was checked by agarose electrophoresis. ³²P-labeled cRNA probes were transcribed from templates encoding for rat α_1 (I) procollagen (kindly provided by Dr. Jackie J. Maher, University of California at San Francisco) and housekeeping gene 36B4. After hybridization, protected fragments were separated on a sequencing gel and autoradiographed. All procedures for probe labeling, hybridization, and digestion have been described in detail elsewhere^[23].

Western blotting

Liver tissue was homogenized in an Ultra-Turrax homogenizer in RIPA buffer containing 1% Nonidet P40 and protease inhibitors. Insoluble proteins were discarded by high-speed centrifugation at 4°C . The protein concentration in the supernatant was measured using a commercially available kit (Pierce, Rockford, IL, USA). Fifty micrograms of protein was separated by 10% SDS-PAGE, and electroblotted on a PVDF membrane. After transfer, the membrane was stained with a Ponceau red solution (Sigma) to ensure an equal protein loading. The staining was then removed by washing in PBS-Tween and the membrane was blocked with 3% BSA in PBS-Tween overnight. After an additional washing, the blots were sequentially incubated with monoclonal anti- α -SMA antibodies and anti-mouse horseradish peroxidase-conjugated antibodies. Detection was performed by chemiluminescence, according to the manufacturer's protocol (Amersham, Arlington Heights, IL, USA).

Immunohistochemistry

Experiments were conducted on frozen sections as described in detail elsewhere^[24]. Dried sections were sequentially incubated with the primary antibody followed by affinity-purified rabbit anti-mouse antibodies after washing. At the end of incubation, sections were washed twice in TBS, incubated with APAAP and developed. Negative controls were treated with omission of the primary antibody or its substitution with non-immune rabbit immunoglobulins.

Histology and histochemistry

Frozen liver specimens or specimens fixed in 4% formaldehyde in phosphate buffer (pH 7.2) and embedded in paraffin were used for morphological analysis. Standard liver sections (4-6- μm thick) embedded in paraffin were stained with hematoxylin and eosin. Biliary epithelial cells of the newly formed ductular structures were identified by histochemical staining for GGT activity as previously described^[18].

RESULTS

In vivo administration of TGZ-supplemented diet to control animals (TGZ group) did not significantly affect either the liver morphology or the serum chemistry (Table 1 and

Figures 1A and B). Following BDL, an increase in serum transaminase and AP was observed in all animals (BDL group, Table 1).

Comparison of the BDL and BDL/TG groups showed

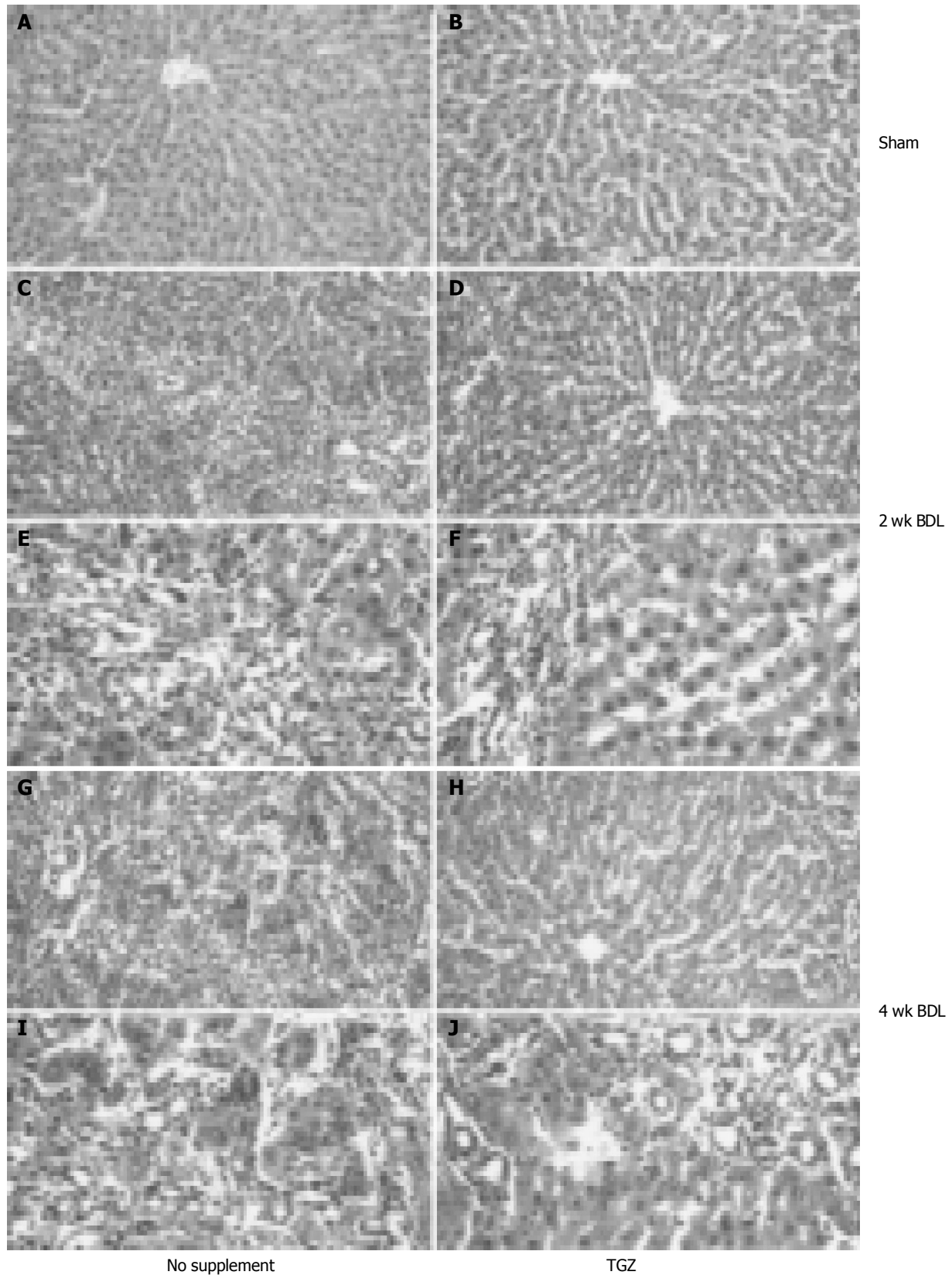


Figure 1 Effects of oral supplementation with TGZ on liver pathology in control rats (A and B) and bile duct-ligated rats (C-J). Animals received sham operation

(A and B) or were subjected to BDL for 2 wk (C-F) or for 4 wk (G-J).

no significant differences in serum enzyme levels or in liver weight, while body weight was significantly lower in BDL animals (Table 1). No difference in food consumption was found between the two groups undergoing BDL. Histological examination of rats undergoing BDL revealed bile duct proliferation in the portal tract (Figure 1), already evident after 1 wk and progressively worsening thereafter. This 'typical' ductular reaction was associated with progressive deposition of extracellular matrix surrounding the newly formed bile ducts. After 4 wk, alteration of liver structure was evident, with bridging fibrosis encircling most of the newly formed bile ducts. These histological alterations were considerably less evident in the group of BDL/TGZ rats (Figure 1). Thus, at 2 wk, only moderate fibrosis was present, and the area occupied by proliferating bile ducts was more limited than in rats not undergoing TGZ supplementation (Figures 1C-F). Similarly, after 4 wk, less fibrosis and a more limited disarray of liver structure were observed in BDL/TGZ animals (Figures 1G-J).

Table 1 Serum biochemical parameters, body, and liver weight in the different experimental groups (mean±SD)

	Sham	TGZ	BDL	BDL/TGZ
ALT (U/L)				
1 wk	35±5	22±2	90±19 ^b	81±7 ^b
4 wk	23±7	21±5	102±34 ^b	75±12 ^b
ALP (U/L)				
1 wk	83±5	76±12	176±19 ^b	168±22 ^b
4 wk	88±7	82±9	137±14 ^b	142±27 ^b
Body weight (g)	332±7	319±9	293±5 ^b	337±12 ^a
Liver weight (g)	9.7±0.6	9.9±0.7	24.4±2.2 ^b	20.2±1.9 ^b

^a*P*<0.05 vs BDL, ^b*P*<0.01 vs Sham.

To establish whether these morphologic changes were associated with reduced fibrogenesis, gene expression levels of procollagen I were measured at different time points. In all animals undergoing BDL, a marked increase in procollagen I gene expression was observed, as indicated by RNase protection assay (Figure 2). In BDL/TGZ rats, the increase in procollagen expression was less marked at 1st and 2nd wk after surgery (Figure 2). Interestingly, the inhibitory effects on procollagen type I expression were no longer evident 4 wk after BDL. We next evaluated whether reduced fibrosis and procollagen expression were associated with modified collagen levels, by measuring hepatic hydroxyproline levels. As expected, a progressive increase in hepatic hydroxyproline was evident in animals undergoing BDL, with a peak at 4 wk, when mean values were approximately five times higher than in controls (Figure 3). Administration of TGZ resulted in a marked inhibition of hydroxyproline accumulation after BDL. At 4 wk, hepatic hydroxyproline levels were inhibited more than 50% in BDL/TGZ rats, being comparable to those measured after 2 wk in BDL animals not receiving the drug. These data indicate that TGZ could effectively reduce hepatic fibrosis caused by BDL.

In vitro studies indicated that thiazolidinediones could inhibit HSC activation and related phenotypic responses,

including proliferation and migration. We analyzed the expression of SMA as an index of the number and activation state of HSC and other fibrogenic mesenchymal cells in the different groups of animals.

Immunohistochemical analysis showed that there was a progressive accumulation of SMA-expressing cells around the expanded portal tracts, in close proximity to bile duct epithelial cells of the ductular reaction. At 4 wk after BDL, SMA-positive cells occupied a significant portion of the hepatic lobule, being a part of the porto-portal septae (Figure 4). This picture was clearly modified in BDL/TGZ rats, where a less marked abundance of cells expressing SMA was present. To substantiate and quantify the inhibitory effect of TGZ on activated matrix-producing cells, SMA expression in the whole liver was analyzed by Western blotting. The progressive increase in SMA expression observed in the BDL group (up to fivefold at 4 wk) was markedly reduced by TGZ treatment (Figure 5). Taken together, these data indicate that TGZ treatment was associated with a reduction in the number of matrix-producing cells accumulated in close contact with cells of the ductular reaction.

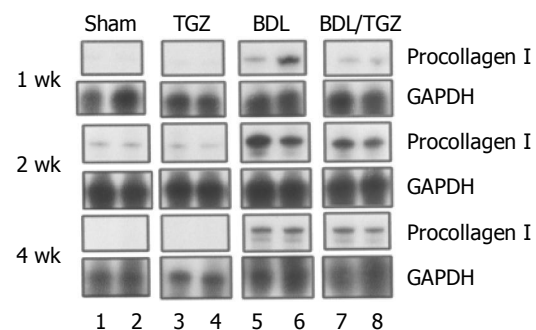


Figure 2 Effects of TGZ on type I procollagen expression in bile duct-ligated rats.

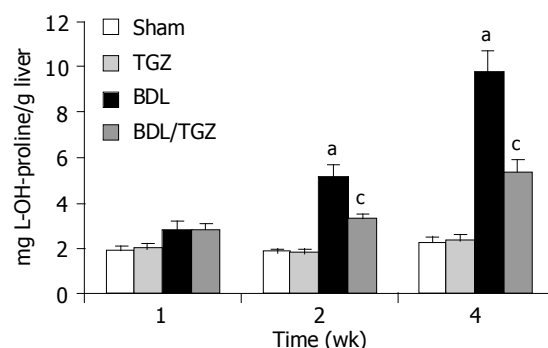


Figure 3 TGZ inhibits collagen accumulation in bile duct-ligated rats in different experimental groups. ^a*P*<0.05 vs Sham, ^b*P*<0.05 vs BDL.

Morphological analysis of tissue samples from BDL/TGZ animals suggested a reduction of the extent of the ductular reaction in this group. We estimated the number of bile duct epithelial cells in the different groups of animals by performing a histochemical staining for GGT, which allowed to identify this cell type (Figure 6). In BDL rats, a progressive accumulation of newly formed bile ducts was

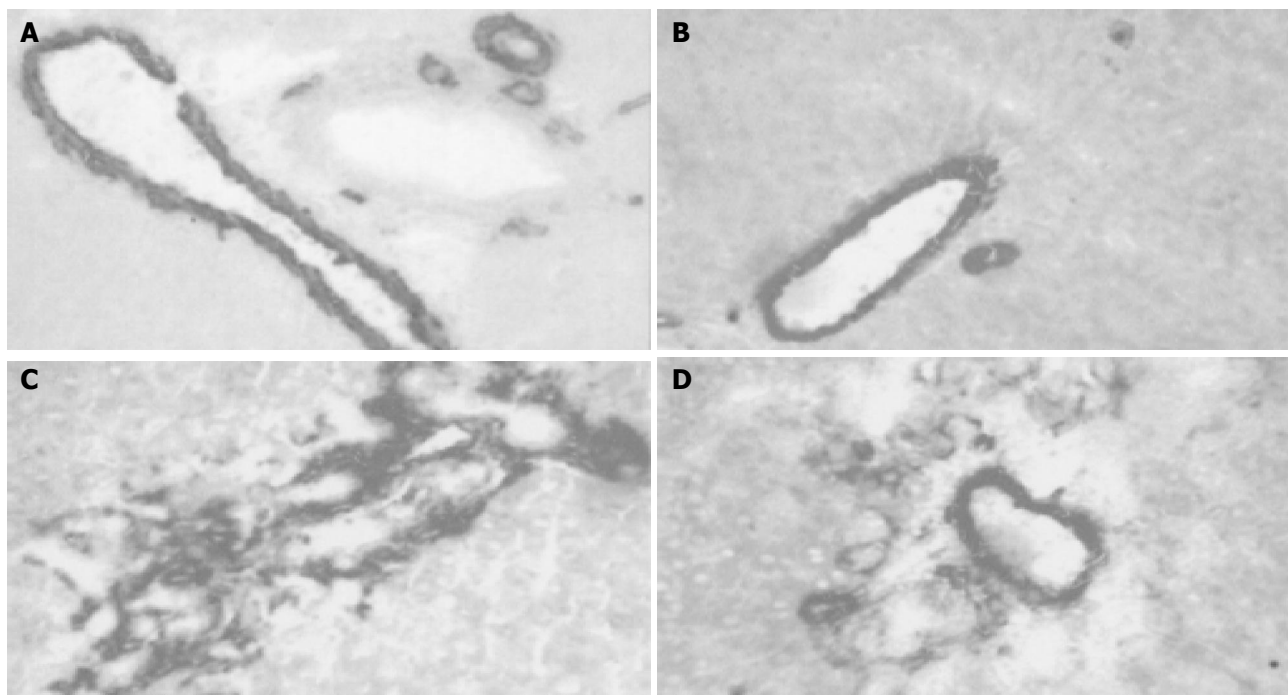


Figure 4 TGZ reduces accumulation of SMA-positive cells after BDL in different experimental groups. **A:** Sham; **B:** TGZ; **C:** BDL; **D:** BDL/TGZ.

evident, reaching a maximum after 4 wk. At all time points after BDL, TGZ treatment reduced the number of GGT-expressing cells, indicating a marked inhibition on the development of the ductular reaction (Figure 6). To quantify this effect, the enzymatic GGT activity was measured in total liver tissue lysates obtained from control and BDL rats (Figure 7). We observed a progressive increase in GGT activity in the BDL group, which was in parallel to the accumulation of newly formed bile ducts. A significant reduction of GGT activity was present in rats treated with TGZ at 2nd and 4th wk after BDL, confirming the inhibitory action shown by histochemical analysis. Thus, treatment with TGZ was also associated with a reduction in the severity of the ductular reaction caused by BDL.

DISCUSSION

Biliary fibrosis is a reproducible and reliable model for the study of experimental liver fibrogenesis^[25]. Long-standing cholestasis leads to an ordered bile duct proliferation, or

typical ductular reaction^[3], associated with progressive accumulation of extracellular matrix, starting from the portal tracts and extending to the other areas of the lobule. This model is characterized by low-grade inflammation, activation of HSC and other mesenchymal cells, including portal myofibroblasts participating in the deposition of extracellular matrix components and contributing to the development of fibrosis^[5,6,26]. In this study, we have provided evidence that TGZ, which activates the nuclear hormone receptor PPAR- γ , reduces the development of fibrosis and the extent of bile duct proliferation following BDL in rats. In the past 3 years, the potential role of PPAR- γ agonists as negative modulators of liver fibrosis has received considerable attention. We and others have shown that thiazolidinediones and 15deoxy- $\Delta^{12,14}$ PGJ₂ inhibit HSC activation and downregulate several biologic actions of activated HSC, which are important for liver wound healing and fibrogenesis, including cell proliferation, migration, extracellular matrix synthesis, and expression of chemokines^[13-15]. 15deoxy- $\Delta^{12,14}$ PGJ₂ also induces apoptosis and reduces matrix

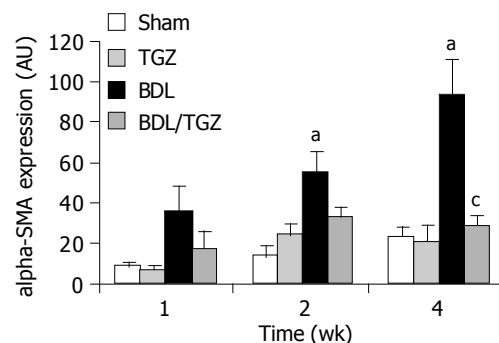
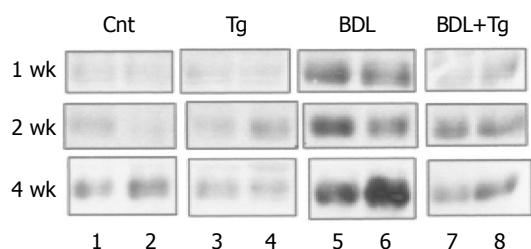


Figure 5 Effects of TGZ on SMA expression in rats undergoing BDL. **P*<0.05

vs Sham, ^a*P*<0.05 vs BDL.

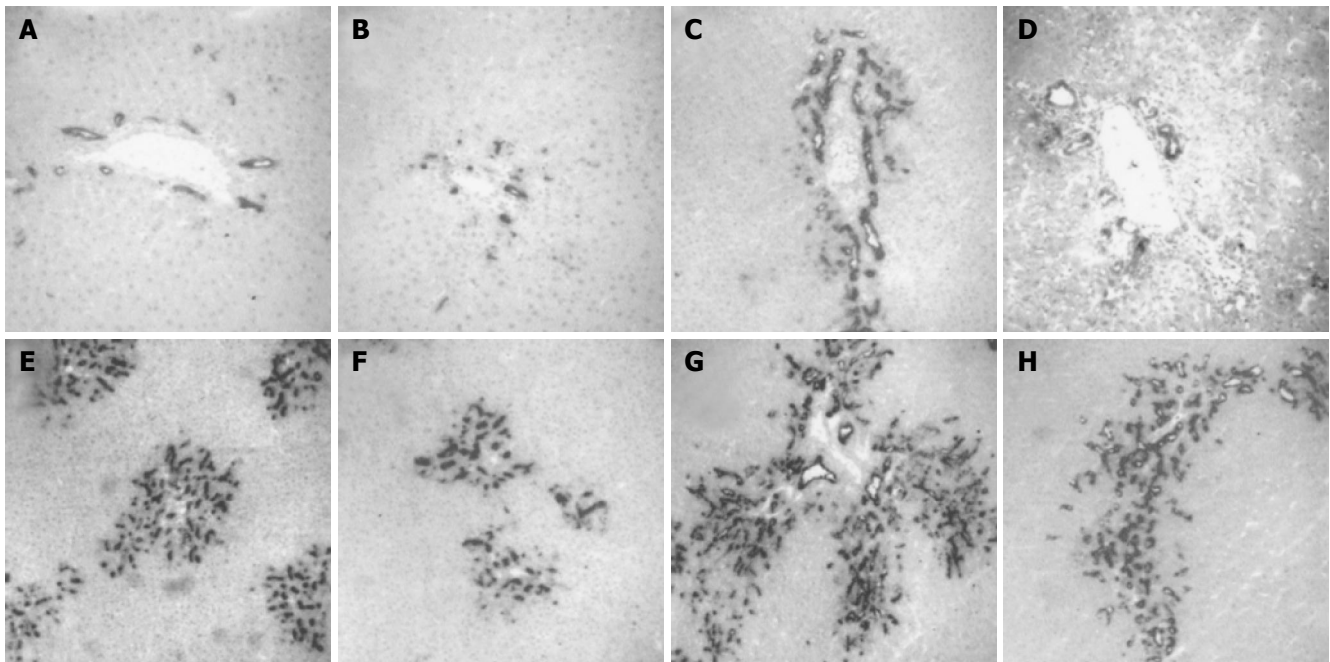


Figure 6 Development of ductular reaction is inhibited in bile duct ligated and TGZ-treated rats in different experimental groups. (A: Sham; B: TGZ; C, E and

G: BDL; D, F, and H: BDL/TGZ) for different periods of time (C and D: 1 wk; E and F: 2 wk; A, B, G, and H: 4 wk).

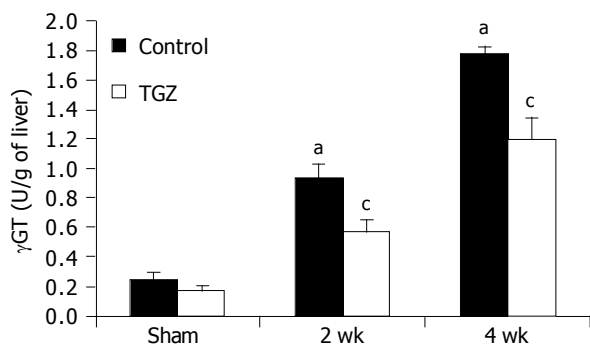


Figure 7 Effects of TGZ on liver GGT activity in bile duct-ligated rats. ^a $P < 0.05$ vs Sham, ^c $P < 0.05$ vs BDL.

expression in cultured liver myofibroblasts, which contribute to extracellular matrix production during injury, although this effect seems to be mediated by PPAR- γ -independent mechanisms^[27]. These mechanisms highlighted in *in vitro* studies are likely to contribute to the observed inhibition of the development of liver fibrosis in this *in vivo* model. Moreover, data from the present study are in agreement with recently reported findings, demonstrating that other thiazolidinediones inhibit collagen deposition in several models of chronic liver damage, including chronic intoxication with carbon tetrachloride or dimethylnitrosamine, or BDL^[28,29]. In our study, collagen accumulation was evaluated using liver hydroxyproline content, which is considered as the 'gold standard' for measuring matrix deposition. We used TGZ, the prototype of thiazolidinediones, as a PPAR- γ agonist. Although TGZ has been withdrawn from the market because of its severe hepatotoxicity^[30], it is still currently used in animal models or in cell culture systems, to establish a 'proof of concept' that may be expanded to other drugs

of the same class, such as rosiglitazone or pioglitazone^[31,32]. Thiazolidinediones also exert a protective role in other conditions of liver injury, as indicated by the recent findings, showing amelioration of ethanol- or diet-induced liver injury by pioglitazone^[33-35].

The most novel and relevant finding of the present work is the observation that treatment with TGZ inhibits bile duct proliferation or typical ductular reaction in this model and in some cases of chronic cholestasis in humans. At the level of portal tract, newly formed bile ducts progressively invade the other parts of the lobule and are surrounded by fibrous tissue. TGZ reduces formation of bile ducts as indicated by histochemical analysis of GGT that is known to be selectively expressed by bile duct cells^[36]. In addition, analysis of the enzymatic activity of GGT in total tissue homogenates has confirmed that this observation is not due to focal changes, but is the result of a general inhibitory action exerted by thiazolidinedione. The reported inhibitory effect on bile duct proliferation is indirectly in agreement with the report of Han *et al.*^[37]. Although these data may not be directly extrapolated to normal cells, they are consistent with the involvement of the PPAR- γ system in growth control of cholangiocytes. Further studies are needed to establish if the molecular mechanisms mediating the effects of TGZ on cholangiocarcinoma cells, such as elevated expression of p53, also operate in non-transformed cholangiocytes.

The intriguing findings on bile duct proliferation provide further insight on the mechanisms of reduced fibrogenesis and epithelial-mesenchymal interactions in this model. Bile duct epithelial cells express soluble mediators affecting the biology of matrix-producing cells. We have previously reported that in the BDL model, cholangiocytes express platelet-derived growth factor (PDGF)^[19], which may contribute to local accumulation of matrix-producing cells

in proximity to newly formed bile ducts, as the result of chemotaxis and proliferation^[26,38-40]. There is evidence that PDGF stimulates the conversion of peri-biliary cells to matrix-producing myofibroblasts, and that an inhibitor of PDGF receptor's tyrosine kinase activity reduces fibrosis in BDL rats^[6]. In addition, bile duct segments isolated from cholestatic rats exert a potent chemotactic action on HSC^[38]. Along these lines, secretion of endothelin-1 by cholangiocytes may induce proliferation and contraction of HSC, and inhibition of endothelin's activity is associated with reversal of fibrosis following BDL^[41-43]. Chemokines produced by cholangiocytes, such as monocyte chemoattractant protein-1 and interleukin-8^[44] are responsible for the recruitment of inflammatory cells that may amplify the fibrogenic stimulus through secretion of additional mediators. Moreover, monocyte chemoattractant protein-1 is chemotactic for activated HSC, providing an additional mechanism leading to local accumulation of fibrogenic cells^[45]. On the other hand, it is also possible that the inhibitory effects of TGZ on HSC and myofibroblasts lead to reduced secretion of mitogenic factors for cholangiocytes. Indeed, liver pro-fibrogenic cells have been shown to secrete cytokines such as interleukin-6 and hepatocyte growth factor modulating cholangiocyte survival and growth^[46,47]. Thus, a bi-directional modulation of the biology of epithelial and mesenchymal cells by soluble factors is likely to occur in this model system.

In conclusion, TGZ can affect not only the development of fibrosis through direct action on matrix-producing cells, but also may modulate the epithelial-mesenchymal interactions characterizing chronic obstructive cholestasis.

ACKNOWLEDGMENTS

The authors thank Wanda Delogu and Nadia Navari for excellent technical assistance, Dr. Jackie J. Maher for kindly providing the plasmid for RNase protection assay of rat procollagen, Dr. Hidekuni Takahagi (Sankyo Co., Tokyo, Japan) for the kind gift of TGZ, and Dr. Stefano Milani for his help with immunohistology.

REFERENCES

- Friedman SL.** Liver fibrosis-from bench to bedside. *J Hepatol* 2003; **38**: S38-S53
- Cassiman D, Roskams T.** Beauty is in the eye of the beholder: emerging concepts and pitfalls in hepatic stellate cell research. *J Hepatol* 2002; **37**: 527-535
- Desmet V, Roskams T, Van Eyken P.** Ductular reaction in the liver. *Pathol Res Pract* 1995; **191**: 513-524
- Knittel T, Kobold D, Piscaglia F, Saile B, Neubauer K, Mehde M, Timpl R, Ramadori G.** Localization of liver myofibroblasts and hepatic stellate cells in normal and diseased rat livers: distinct roles of (myo-)fibroblast subpopulations in hepatic tissue repair. *Histochem Cell Biol* 1999; **112**: 387-401
- Cassiman D, Libbrecht L, Desmet V, Denef C, Roskams T.** Hepatic stellate cell/ myofibroblast subpopulations in fibrotic human and rat livers. *J Hepatol* 2002; **36**: 200-209
- Kinnman N, Francoz C, Barbu V, Wendum D, Rey C, Hultcrantz R, Poupon R, Housset C.** The myofibroblastic conversion of peribiliary fibrogenic cells distinct from hepatic stellate cells is stimulated by platelet-derived growth factor during liver fibrogenesis. *Lab Invest* 2003; **83**: 163-173
- Shearer BG, Hoekstra WJ.** Recent advances in peroxisome proliferator-activated receptor science. *Curr Med Chem* 2003; **10**: 267-280
- Gilde AJ, Van Bilsen M.** Peroxisome proliferator-activated receptors (PPARs): regulators of gene expression in heart and skeletal muscle. *Acta Physiol Scand* 2003; **178**: 425-434
- Kliwer SA, Lenhard JM, Willson TM, Patel I, Morris DC, Lehmann JM.** A prostaglandin J2 metabolite binds peroxisome proliferator-activated receptor gamma and promotes adipocyte differentiation. *Cell* 1995; **83**: 813-819
- Forman BM, Tontonoz P, Chen J, Brun RP, Spiegelman BM, Evans RM.** 15-Deoxy-delta 12, 14-prostaglandin J2 is a ligand for the adipocyte determination factor PPAR gamma. *Cell* 1995; **83**: 803-812
- Nagy L, Tontonoz P, Alvarez JG, Chen H, Evans RM.** Oxidized LDL regulates macrophage gene expression through ligand activation of PPARgamma. *Cell* 1998; **93**: 229-240
- Murphy GJ, Holder JC.** PPAR-gamma agonists: therapeutic role in diabetes, inflammation and cancer. *Trends Pharmacol Sci* 2000; **21**: 469-474
- Galli A, Crabb D, Price D, Ceni E, Salzano R, Surrenti C, Casini A.** Peroxisome proliferator-activated receptor gamma transcriptional regulation is involved in platelet-derived growth factor-induced proliferation of human hepatic stellate cells. *Hepatology* 2000; **31**: 101-108
- Marra F, Efsen E, Romanelli RG, Caligiuri A, Pastacaldi S, Batignani G, Bonacchi A, Caporale R, Laffi G, Pinzani M, Gentilini P.** Ligands of peroxisome proliferator-activated receptor gamma modulate profibrogenic and proinflammatory actions in hepatic stellate cells. *Gastroenterology* 2000; **119**: 466-478
- Miyahara T, Schrum L, Rippe R, Xiong S, Yee HF, Motomura K, Anania FA, Willson TM, Tsukamoto H.** Peroxisome proliferator-activated receptors and hepatic stellate cell activation. *J Biol Chem* 2000; **275**: 35715-35722
- Miles PD, Higo K, Romeo OM, Lee MK, Razaat K, Olefsky JM.** Troglitazone prevents hyperglycemia-induced but not glucosamine-induced insulin resistance. *Diabetes* 1998; **47**: 395-400
- Mizushige K, Noma T, Yao L, Yu Y, Kiyomoto H, Hosomi N, Fukui T, Kimura S, Abe Y, Matsuo H.** Effects of troglitazone on collagen accumulation and distensibility of aortic wall in prestage of non-insulin-dependent diabetes mellitus of Otsuka Long-Evans Tokushima Fatty rats. *J Cardiovasc Pharmacol* 2000; **35**: 150-155
- Parola M, Leonarduzzi G, Robino G, Albano E, Poli G, Dianzani MU.** On the role of lipid peroxidation in the pathogenesis of liver damage induced by long-standing cholestasis. *Free Radic Biol Med* 1996; **20**: 351-359
- Grappone C, Pinzani M, Parola M, Pellegrini G, Caligiuri A, DeFranco R, Marra F, Herbst H, Alpini G, Milani S.** Expression of platelet-derived growth factor in newly formed cholangiocytes during experimental biliary fibrosis in rats. *J Hepatol* 1999; **31**: 100-109
- Boigk G, Stroedter L, Herbst H, Waldschmidt J, Riecken EO, Schuppan D.** Silymarin retards collagen accumulation in early and advanced biliary fibrosis secondary to complete bile duct obliteration in rats. *Hepatology* 1997; **26**: 643-649
- Persijn JP, van der Slik W.** A new method for the determination of gamma-glutamyltransferase in serum. *J Clin Chem Clin Biochem* 1976; **14**: 421-427
- Parola M, Cheeseman KH, Biocca ME, Dianzani MU, Slater TF.** Biochemical studies on bile duct epithelial cells isolated from rat liver. *J Hepatol* 1990; **10**: 341-345
- Marra F, Choudhury GG, Pinzani M, Abboud HE.** Regulation of platelet-derived growth factor secretion and gene expression in human liver fat-storing cells. *Gastroenterology* 1994; **107**: 1110-1117
- Marra F, DeFranco R, Grappone C, Milani S, Pastacaldi S, Pinzani M, Romanelli RG, Laffi G, Gentilini P.** Increased expression of Monocyte Chemoattractant Protein-1 during active hepatic fibrogenesis: correlation with monocyte infiltration. *Am J Pathol* 1998; **152**: 423-430
- Kountouras J, Billing BH, Scheuer PJ.** Prolonged bile duct

- obstruction: a new experimental model for cirrhosis in the rat. *Br J Exp Pathol* 1984; **65**: 305-311
- 26 **Kinnman N**, Gorla O, Wendum D, Gendron MC, Rey C, Poupon R, Housset C. Hepatic stellate cell proliferation is an early platelet-derived growth factor-mediated cellular event in rat cholestatic liver injury. *Lab Invest* 2001; **81**: 1709-1716
- 27 **Li L**, Tao J, Davaille J, Feral C, Mallat A, Rieusset J, Vidal H, Lotersztajn S. 15-deoxy-Delta 12,14-prostaglandin J2 induces apoptosis of human hepatic myofibroblasts. A pathway involving oxidative stress independently of peroxisome-proliferator-activated receptors. *J Biol Chem* 2001; **276**: 38152-38158
- 28 **Kon K**, Ikejima K, Hirose M, Yoshikawa M, Enomoto N, Kitamura T, Takei Y, Sato N. Pioglitazone prevents early-phase hepatic fibrogenesis caused by carbon tetrachloride. *Biochem Biophys Res Commun* 2002; **291**: 55-61
- 29 **Galli A**, Crabb DW, Ceni E, Salzano R, Mello T, Svegliati-Baroni G, Ridolfi F, Trozzi L, Surrenti C, Casini A. Antidiabetic thiazolidinediones inhibit collagen synthesis and hepatic stellate cell activation *in vivo* and *in vitro*. *Gastroenterology* 2002; **122**: 1924-1940
- 30 **Chitturi S**, George J. Hepatotoxicity of commonly used drugs: nonsteroidal anti-inflammatory drugs, antihypertensives, antidiabetic agents, anticonvulsants, lipid-lowering agents, psychotropic drugs. *Semin Liver Dis* 2002; **22**: 169-183
- 31 **Wang MY**, Unger RH. Role of PP2C in cardiac lipid accumulation in obese rodents and its prevention by troglitazone. *Am J Physiol Endocrinol Metab* 2005; **288**: E216-221
- 32 **Wakino S**, Hayashi K, Kanda T, Tatematsu S, Homma K, Yoshioka K, Takamatsu I, Saruta T. Peroxisome proliferator-activated receptor gamma ligands inhibit Rho/Rho kinase pathway by inducing protein tyrosine phosphatase SHP-2. *Circ Res* 2004; **95**: e45-55
- 33 **Enomoto N**, Takei Y, Hirose M, Konno A, Shibuya T, Matsuyama S, Suzuki S, Kitamura KI, Sato N. Prevention of ethanol-induced liver injury in rats by an agonist of peroxisome proliferator-activated receptor-gamma, pioglitazone. *J Pharmacol Exp Ther* 2003; **306**: 846-854
- 34 **Kawaguchi K**, Sakaida I, Tsuchiya M, Omori K, Takami T, Okita K. Pioglitazone prevents hepatic steatosis, fibrosis, and enzyme-altered lesions in rat liver cirrhosis induced by a choline-deficient L-amino acid-defined diet. *Biochem Biophys Res Commun* 2004; **315**: 187-195
- 35 **Tomita K**, Azuma T, Kitamura N, Nishida J, Tamiya G, Oka A, Inokuchi S, Nishimura T, Suematsu M, Ishii H. Pioglitazone prevents alcohol-induced fatty liver in rats through up-regulation of c-Met. *Gastroenterology* 2004; **126**: 873-885
- 36 **Rutenburg AM**, Kim H, Fischbein JW, Hanker JS, Wasserkrug HL, Seligman AM. Histochemical and ultrastructural demonstration of gamma-glutamyl transferase activity. *J Histochem Cytochem* 1969; **17**: 517-526
- 37 **Han C**, Demetris AJ, Michalopoulos GK, Zhan Q, Shelhamer JH, Wu T. PPARgamma ligands inhibit cholangiocarcinoma cell growth through p53-dependent GADD45 and p21 pathway. *Hepatology* 2003; **38**: 167-177
- 38 **Pinzani M**, Gesualdo L, Sabbah GM, Abboud HE. Effects of platelet-derived growth factor and other polypeptide mitogens on DNA synthesis and growth of cultured rat liver fat-storing cells. *J Clin Invest* 1989; **84**: 1786-1793
- 39 **Marra F**, Gentilini A, Pinzani M, Choudhury GG, Parola M, Herbst H, Dianzani MU, Laffi G, Abboud HE, Gentilini P. Phosphatidylinositol 3-kinase is required for platelet-derived growth factor's actions on hepatic stellate cells. *Gastroenterology* 1997; **112**: 1297-1306
- 40 **Kinnman N**, Hultcrantz R, Barbu V, Rey C, Wendum D, Poupon R, Housset C. PDGF-mediated chemoattraction of hepatic stellate cells by bile duct segments in cholestatic liver injury. *Lab Invest* 2000; **80**: 697-707
- 41 **Pinzani M**, Milani S, De Franco R, Grappone C, Caligiuri A, Gentilini A, Tosti-Guerra C, Maggi M, Failli P, Ruocco C, Gentilini P. Endothelin 1 is overexpressed in human cirrhotic liver and exerts multiple effects on activated hepatic stellate cells. *Gastroenterology* 1996; **110**: 534-548
- 42 **Pinzani M**, Failli P, Ruocco C, Casini A, Milani S, Baldi E, Giotti A, Gentilini P. Fat-storing cells as liver-specific pericytes. Spatial dynamics of agonist-stimulated intracellular calcium transients. *J Clin Invest* 1992; **90**: 642-646
- 43 **Cho JJ**, Hoher B, Herbst H, Jia JD, Ruehl M, Hahn EG, Riecken EO, Schuppan D. An oral endothelin-A receptor antagonist blocks collagen synthesis and deposition in advanced rat liver fibrosis. *Gastroenterology* 2000; **118**: 1169-1178
- 44 **Morland CM**, Fear J, McNab G, Joplin R, Adams DH. Promotion of leukocyte transendothelial cell migration by chemokines derived from human biliary epithelial cells *in vitro*. *Proc Assoc Am Physicians* 1997; **109**: 372-382
- 45 **Marra F**, Romanelli RG, Giannini C, Failli P, Pastacaldi S, Arrighi MC, Pinzani M, Laffi G, Montalto P, Gentilini P. Monocyte chemoattractant protein-1 as a chemoattractant for human hepatic stellate cells. *Hepatology* 1999; **29**: 140-148
- 46 **Park J**, Gores GJ, Patel T. Lipopolysaccharide induces cholangiocyte proliferation via an interleukin-6-mediated activation of p44/p42 mitogen-activated protein kinase. *Hepatology* 1999; **29**: 1037-1043
- 47 **Ishida Y**, Smith S, Wallace L, Sadamoto T, Okamoto M, Auth M, Strazzabosco M, Fabris L, Medina J, Prieto J, Strain A, Neuberger J, Joplin R. Ductular morphogenesis and functional polarization of normal human biliary epithelial cells in three-dimensional culture. *J Hepatol* 2001; **35**: 2-9

MUC1 and MUC5AC mucin expression in liver fluke-associated intrahepatic cholangiocarcinoma

Chanchai Boonla, Banchob Sripa, Peti Thuwajit, Ubon Cha-On, Anucha Puapairoj, Masanao Miwa, Sopit Wongkham

Chanchai Boonla, Peti Thuwajit, Ubon Cha-On, Sopit Wongkham, Department of Biochemistry, Liver Fluke and Cholangiocarcinoma Research Center, Faculty of Medicine, Khon Kaen University, Khon Kaen 40002, Thailand

Banchob Sripa, Anucha Puapairoj, Department of Pathology, Liver Fluke and Cholangiocarcinoma Research Center, Faculty of Medicine, Khon Kaen University, Khon Kaen 40002, Thailand
Masanao Miwa, Institute of Basic Medical Sciences, University of Tsukuba, Tsukuba, Ibaraki 305-8575, Japan

Supported by the Thailand Research Fund, No. BRG/06/2544 and Royal Golden Jubilee PhD Program Grant, No. PHD/0045/2542 to Boonla C and Wongkham S

Co-first-authors: Chanchai Boonla and Sopit Wongkham

Correspondence to: Dr. Sopit Wongkham, Department of Biochemistry, Faculty of Medicine, Khon Kaen University, Khon Kaen 40002, Thailand. sopit@kku.ac.th

Telephone: +66-43-348-386 Fax: +66-43-348-375

Received: 2004-11-23 Accepted: 2005-01-26

© 2005 The WJG Press and Elsevier Inc. All rights reserved.

Key words: Cholangiocarcinoma; Mucin; MUC1; MUC5AC; Invasion; Survival; Immunohistochemistry

Boonla C, Sripa B, Thuwajit P, Cha-On U, Puapairoj A, Miwa M, Wongkham S. MUC1 and MUC5AC mucin expression in liver fluke-associated intrahepatic cholangiocarcinoma. *World J Gastroenterol* 2005; 11(32): 4939-4946
<http://www.wjgnet.com/1007-9327/11/4939.asp>

Abstract

AIM: To investigate the expressions of MUC1 and MUC5AC in intrahepatic cholangiocarcinoma (ICC). Association of expressions of mucins MUC1 and MUC5AC with clinical findings, metastasis, and survival of the liver fluke-associated ICC patients was determined.

METHODS: The expressions of MUC1 and MUC5AC mucins were examined by immunohistochemical staining in 87 cases of histologically-proven ICC. The expressions of mucins in relationship between clinicopathological significance and prognosis of the patients were evaluated.

RESULTS: Fifty-two patients (60%) exhibited both MUC1 and MUC5AC expressions, whereas 31% expressed either MUC1 or MUC5AC, and 9% expressed neither. High MUC1 immunoreactivity displayed a significant correlation with tumor progression as reflected by vascular invasion ($P < 0.001$), whereas high expression of MUC5AC significantly correlated with neural invasion ($P = 0.022$) and advanced ICC stage ($P = 0.008$). Patients with high expression of MUC1 had a significantly shorter survival ($P = 0.0002$). According to multivariate analyses, MUC1 reactivity ($P = 0.026$), histological grading and stage of tumor represented the least probability of survival.

CONCLUSION: MUC1 is overexpressed in liver fluke-associated cholangiocarcinoma and relates to vascular invasion and poor prognosis, whereas MUC5AC mucin is neoexpressed and relates to neural invasion and advanced ICC stage. High MUC1 expression in tumor may be useful for predicting the poor outcome of ICC patients.

INTRODUCTION

Cholangiocarcinoma (CC), malignancy of bile duct epithelia, is a relatively rare cancer in Western countries, but it is found frequently in Southeast Asia, especially in Northeast Thailand. The cancer is still a challenging public health problem in the region.

Risk factors for CC in Asia are obviously different from those in the Western countries, according to epidemiological and experimental studies. In Western countries, primary sclerosing cholangitis is the most strong predisposing factor, with a relative risk of 10-30% to develop CC as compared to the general population^[1,2]. In Asia, the animal studies^[3-5] and epidemiological evidence^[6] support the association of liver fluke infection with the development of cancer in this region. The different risk factors and etiology of CC among different geographic regions may lead to different carcinogenesis and pathogenesis of CC in these regions.

Liver fluke (*Opisthorchis viverrini*) infection is a major risk in Thai, Laos, and Malaysia, while *Clonorchis sinensis* infection is prominent in Japanese, Korean and Vietnamese^[7-9]. Liver flukes chronically inhabit in the biliary tree, leading to chronic inflammation, bile duct proliferation, dysplasia, and eventually, development of CC. Liver fluke *per se*, however, is not a sufficient cause to develop cancer^[3]. Potent carcinogens such as nitrosamine compounds enhance the carcinogenic effect of flukes^[10]. These compounds can be obtained from both exogenous and endogenous sources^[11,12]. The former is mostly from diet, while the latter is the byproduct of endogenous nitrosation of nitrogenous compounds, such as nitric oxides and derivatives.

CC is a slowly-growing tumor and frequently diagnosed, when the tumor is big enough to obstruct the biliary tract and produce signs and symptoms. Most of the patients are thus diagnosed at the late stage of tumor and their survival is poor, due to the original as well as disseminated tumors. At present, there is no effective tool or specific biomarkers that can indicate the early stage and status of

CC. A specific marker for either early detection or monitoring of the tumor may significantly improve the prognosis and therapeutic management of such patients.

Mucins are heavily O-glycosylated proteins, mainly expressed by ductal and glandular epithelial tissues. To date, 19 human mucin genes have been identified and designated, according to their distinct structures and functions as transmembrane mucins or secreted gel-forming mucins. Mucin genes are expressed in a cell- and tissue-specific manner, for instances, MUC2 and MUC3 in bowel^[13], MUC5AC and MUC6 in gastric tissue^[14].

Vast production of mucus is frequently found in various carcinomas. The alterations in quantity and quality of mucins have been demonstrated in cancer tissues, including CC^[15-18]. Neoexpressed and overexpressed mucins are of clinical values as a maker for supportive diagnosis, prognosis or monitoring therapy^[19-21]. In this study, we investigated the expressions of two aberrant apomucins, namely MUC1 and MUC5AC in CC tissues obtained from 87 intrahepatic cholangiocarcinoma (ICC) patients who had an active or past history of *O. viverrini* infection. The correlation between mucin expressions and their malignant potential, clinicopathological findings, and patient survival was analyzed.

MATERIALS AND METHODS

Tissue samples

Between January 1998 and December 2000, 87 surgically resected specimens of ICC were selected from the files of the Liver Fluke and Cholangiocarcinoma Research Center, Khon Kaen University, Thailand. Informed consent was obtained from each subject before surgery and the Human Research Ethics Committee, Khon Kaen University approved the research protocol (#HE43210).

Of the 87 ICC patients, 67% had a high titer of antibody against *O. viverrini*, of which 30% had active infection of *O. viverrini* as determined by the presence of parasite eggs in the bile, the others had a past history of liver fluke infection. The age, gender, tumor location, histological grading, and pTNM stage^[22] were evaluated by reviewing the medical charts and pathologic records. Tumor size was evaluated using the greatest perpendicular diameter of each liver lesion. Survival of each CC patient was recorded from the date of surgery to the date of death or to December 31, 2000. Twenty-three patients were (26.4%) lost to follow-up.

Immunohistochemistry

All specimens were fixed in 10% neutral formalin buffer, embedded in paraffin, and cut into 4- μ m-thick sections. Immunohistochemical staining was performed by an immunoperoxidase method using a mAb MUC-1-Core (Clone Ma695, Novocastra Laboratories, Newcastle-Upon-Tyne, UK) or a polyclonal anti-serum MAN-5ACI^[23].

Each section was deparaffinized and the endogenous peroxidase was blocked with 0.3% hydrogen peroxide. The sections were incubated with 1:100 MUC-1-core protein antibody, followed by 1:300 biotin-conjugated goat anti-mouse immunoglobulin (Zymed, San Francisco, CA, USA), or with 1:1 000 MUC-5ACI antisera followed by 1:300 biotin-conjugated goat anti-rabbit immunoglobulin (Zymed, San Francisco, CA, USA). The sections were then incubated

with 1:300 peroxidase-conjugated streptavidin. After being washed, the sections were reacted with 0.05% 3,3'-diaminobenzidine tetrahydrochloride (DAB, Sigma Chemical Co., St. Louis, MO, USA) and 0.1% H₂O₂ in 50 mol/L Tris-HCl pH 7.8. The positive staining was counteracted, when PBS was applied instead of the primary antibody.

The intensity of mucin expression was semi-quantitatively classified into four groups, on the basis of the percentage of positive tumor cells: 0, negative; +1, 1–25%; +2, 26–50%; and +3 >50%. For statistical analysis, the 0 and +1 were categorized as low expression, +2 and +3 as high expression.

Tumor invasion of lymphatic, vascular, or nerve tissues was identified in both tumorous and non-tumorous liver tissues. Lymphatic and vascular invasion was so accounted by the presence of infiltrating cancer cells within the lymphatic or blood vessels, respectively. Neural invasion was presented as positive cancer cells in the perineurium and/or neural fascicle.

Real-time PCR

ICC tissues with either none, low or high expressions of MUC1 or MUC5AC mucin were analyzed by real-time PCR. Total RNA was extracted from the CC tissues, using the standard acid guanidinium thiocyanate-phenol-chloroform protocol. RT-PCR was done using TaqMan[®] Gold RT-PCR Kit in a two-step reaction. The reverse transcription step was performed in 50 μ L reaction for 1 μ g total RNA. The reaction mixture was composed of 5.5 mmol/L MgCl₂, 500 μ mol/L of each dNTP, 2.5 μ mol/L random hexamers, 20 U RNase inhibitor and 62.5 U of MultiScribe[®] reverse transcriptase in regular strength TaqMan RT Buffer[®]. Incubation was at 25 °C for 10 min, at 48 °C for 30 min and at 95 °C for 5 min. The cDNA was stored in solution at -20 °C until use.

Primers and probes were originally designed by Primer Express[®] software. The DNA and cDNA sequences were obtained from the GenBank database. The sequence of the primers and TaqMan[®] probes for MUC1 and MUC5AC are presented in Table 1. The real-time PCR step was done using an ABI7700 machine (Applied Biosystems) in a 25 μ L reaction using the TaqMan[®] Gold RT-PCR Kit (GAPDH was used as the internal control). Each reaction mixture was composed of 25 ng cDNA, 5.5 mmol/L MgCl₂, 200 μ mol/L of dGTP, dATP, dCTP, and 400 μ mol/L dUTP, 100 nmol/L of the TaqMan[®] probe, 200 nmol/L of each primer, 0.25 U of AmpErase[®] enzyme and 0.625 U of AmpliTaq Gold DNA polymerase[®] enzyme in regular strength TaqMan Buffer A[®]. The reaction mixture was incubated at 50 °C for 2 min and at 95 °C for 10 min before the PCR step. The PCR cycle was performed at 95 °C for 15 s at 60 °C for 15 s and at 72 °C for 30 s. The total number of cycles for GAPDH and MUC1 mucin was 40 and 50 for MUC5AC. The comparative temperature was determined by the PCR machine and Sequence Detector 1.7[®] program.

Statistical analysis

Statistical analyses for comparisons between clinicopathologic findings, survival and MUC1 or MUC5AC expression were performed using SPSS software (Chicago, IL, USA). Association among a variety of variables, including age,

Table 1 Sequences of primers and TaqMan® probe for MUC1 and MUC5AC apomucins

Mucin	Primer or probe	Sequence	Product size
MUC1	Forward	GCTATGTGCCCCCTAGCAGTAC	73
	Reverse	AGGCTGTGCCACCGTTA	
	Probe	TCGTAGCCCCTATGAGAAGGTTTCTGCAG	
MUC5AC	Forward	CCCCAACATCAGGAACAGCTT	147
	Reverse	GAGTAGTAGGTTCCCGGCTTCA	
	Probe	AGCGTGGAGAATGAGAAGTATGCTCAGCAC	

Table 2 Expression of MUC1 and MUC5AC apomucins, demographic data, cancer histopathology, and clinical staging of ICC patients

	Variables	n (87)	%
Age (yr)	≤56	42	48.3
	>56	45	51.7
Sex	Male	59	67.8
	Female	28	32.2
Tumor staging	I-III	14	16.1
	IVA	16	18.4
	IVB	57	65.5
Histological grading	Papillary	20	22.9
	Well-differentiated	26	29.8
	Moderately differentiated	11	12.6
	Poorly differentiated	20	22.9
Tumor size	Unclassified	10	11.5
	≤5 cm	24	27.6
Vascular invasion	>5 cm	63	72.4
	No	30	34.5
Neural invasion	Yes	57	65.5
	No	46	52.9
Lymphatic invasion	Yes	41	47.1
	No	23	26.4
Mucin expression	Yes	64	73.6
	MUC1 and MUC5AC	52	59.7
	MUC1 only	15	17.3
	MUC5AC only	12	13.8
MUC1 expression	None	8	9.2
	Low (0, 1+)	53	60.9
MUC5AC expression	High (2+, 3+)	34	39.1
	Low (0, 1+)	41	47.1
	High (2+, 3+)	46	52.8

gender, tumor histology, tumor stage, tumor size, and invasion, was evaluated using the χ^2 test for heterogeneity or the Fisher's exact test. Multivariate analyses for variables influenced by the presence of MUC1 and MUC5AC mucins in the bile duct epithelium were carried out using a logistic regression model.

Patient survival was calculated from the time of resection to either death or the last follow-up. The Kaplan-Meier analysis was used to assess the relation of disease-free survival to the expression of mucins using the log-rank test. Several prognostic factors were evaluated for their association with the overall and disease-free survival in a multivariate analysis using Cox's regression model. $P < 0.05$ was considered statistically significant.

RESULTS

Patient characteristics

Of the 87 ICC patients explored, 59 were male and 28 were female with male to female ratio = 2:1. The mean age was 56.7 ± 8.6 years (range, 36-73 years). Most of the patients

were at advance ICC stage, with 73% lymphatic, 65% vascular, and 47% neural invasion. Thirty percent of the tumors had well-differentiated histopathological grading and 10 specimens (11%) could not be classified. The majority of patients (70%) possessed a tumor size >5 cm (Table 2).

Real-time PCR and immunohistochemistry of MUC1 and MUC5AC expressions

Alteration in glycosylation of mucin epitopes is frequent in carcinomas and this alters the assessment of mucins by a particular antibody^[24,25]. Therefore, immunohistochemical studies using different antibodies against a particular mucin have produced conflicting and inconclusive results^[26,27]. To exclude ambiguity, a semi-quantitative analysis of MUC1 and MUC5AC mucins using antibodies in the immunohistochemical staining study was checked first for their reliabilities with the mRNA transcripts obtained by real-time PCR.

The semi-quantitative immunohistochemistry of ICC tissues with none, low or high expressions of MUC1 or MUC5AC mucin using the antibodies selected in this study corresponded to the quantitative analyses of MUC1 and

MUC5AC mucin transcripts by real-time PCR. MUC1 and MUC5AC transcripts were not detectable in the tumor tissues with negative immunohistochemistry for either MUC1 or MUC5AC mucin. The levels of MUC1 and MUC5AC transcripts matched well with those of immunohistochemistry.

The immunohistochemistry demonstrated that MUC1 and MUC5AC mucins were frequently expressed in ICC (Table 2). Fifty-two patients (60%) exhibited both MUC1 and MUC5AC expressions, whereas 31% expressed either MUC1 or MUC5AC, and only 9% expressed neither. The frequency of MUC1 and MUC5AC expressions in ICC was not significantly different.

Expression of MUC1 and clinicopathological findings

MUC1 was expressed on the luminal surface, cell membrane and cytoplasm of cholangiocarcinoma cells (Figure 1A). Expression of MUC1 was observed in 77% (67/87) of ICC patients, 39.1% (34/87) of the patients had high expression. Increased expression of MUC1 did not show a preference to any histological subtypes of tumor, tumor size, or tumor stage (Table 3). However, statistical analysis showed that high expression of MUC1 significantly correlated with poor prognosis. There was a positive correlation between MUC1 expression and vascular invasion ($P < 0.001$, Figure 1B).

Expression of MUC5AC and clinicopathological findings

The site of MUC5AC expression was mainly in the cytoplasm and luminal mucin (Figure 1C). MUC5AC mucin was frequently detected in 73% (64/87) ICC tissues, 52.8% (46/87) of which were highly expressed.

Increased expression of MUC5AC showed a preference to advanced stage of the tumor ($P = 0.008$) but not to histological grading, tumor size, or tumor stage (Table 3). Tumor invasion of neighboring vascular, lymphatic and

neural tissues was common in ICC patients with MUC5AC expression. However, only neural invasion significantly correlated with high MUC5AC expression ($P = 0.022$, Figure 1D).

Expressions of MUC1 and MUC5AC mucins and cumulative survival

The median length of survival for patients with low MUC1 expression was 294 d (95%CI, 214-507 d) whereas it was 151 d (95%CI, 90-202 d) for patients with high MUC1 expression. The survival rate of patients with high MUC1 expression was significantly lower than that of patients with low MUC1 expression ($P = 0.0002$, log-rank test, Figure 2A).

The median length of survival for patients with low MUC5AC expression was 256 d (95%CI, 169-430 d) whereas it was 195 d (95%CI, 138-285 d) for patients with high MUC5AC expression. The ICC patients with high MUC5AC expression had a shorter survival than those with low MUC5AC expression, but without statistical significance (Figure 2B). There was no significant difference in survival between ICC patients with either MUC1 expression or MUC5AC expression and those with expressions of both MUC1 and MUC5AC.

The multivariate Cox's regression model showed that MUC1 (but not MUC5AC) expression ($P = 0.026$), histological grading ($P < 0.05$), and tumor stage ($P < 0.05$) statistically correlated with patient survival independent of age and gender (Table 4).

DISCUSSION

Alterations of epithelial mucin expression have been described in different malignant localizations. Varying degrees of glycosylation of MUC1 mucin between normal

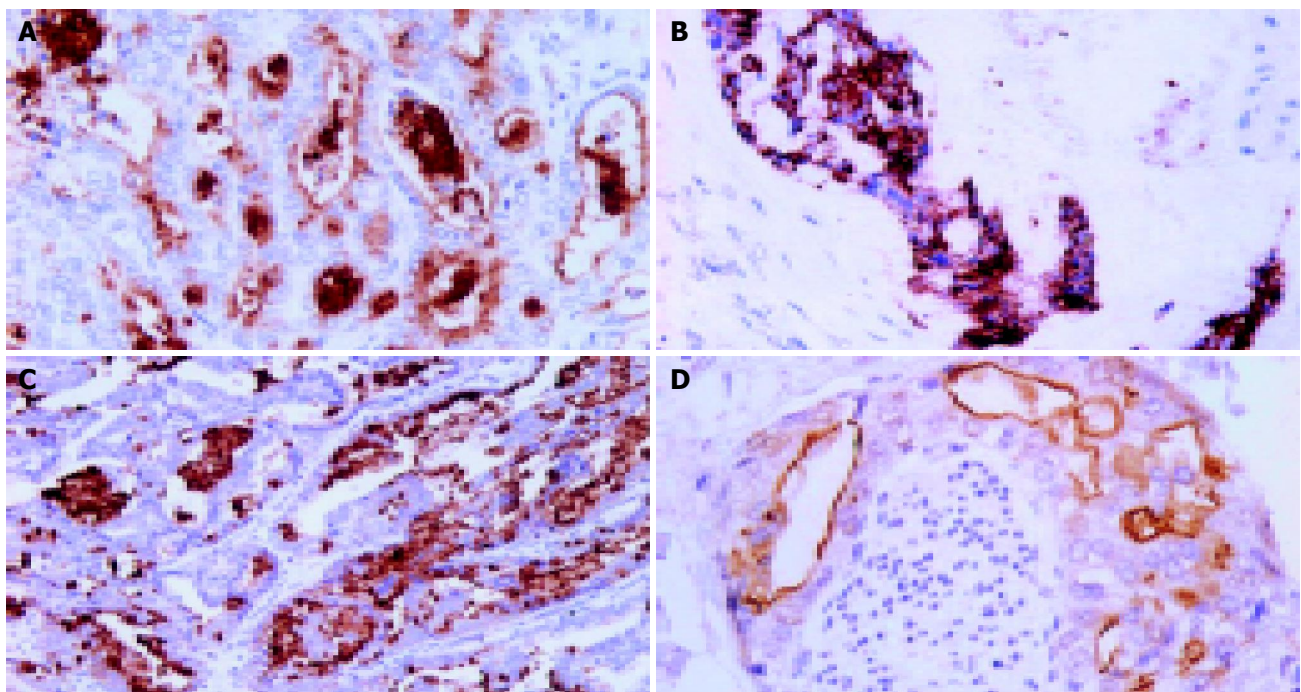


Figure 1 Staining patterns of MUC1 and MUC5AC core proteins. **A** and **C**: Immunohistochemical staining of MUC1 and MUC5AC apomucins expressed

in tumor tissues, respectively. **B** and **D**: MUC1 and MUC5AC staining of vascular and neural-invaded tumor cells.

Table 3 Expressions of MUC1 and MUC5AC apomucins in ICC in relation to patients' cancer histopathology and clinical staging

Variables	MUC1		P	MUC5AC		P
	Low	High		Low	High	
Age (yr)	53	34	0.894	41	46	0.065
≤56	26	17		15	27	
>56	27	17		26	19	
Gender	53	34	0.698	41	46	0.058
Male	34	24		32	26	
Female	19	10		9	20	
Histological grading	43	24	0.575	34	33	0.095
Papillary	13	7		11	9	
Well-diff.	18	8		9	17	
Moderately diff.	5	6		6	5	
Poorly diff.	7	3		8	2	
Tumor size	51	31	0.964	38	44	0.502
≤5 cm	15	9		13	11	
>5 cm	36	22		25	33	
Staging	50	32	0.940	39	43	0.008
I-III	8	5		6	7	
IVA	6	5		10	1	
IVB	36	22		23	35	
Vascular invasion	53	34	<0.001	41	46	0.284
No	27	2		17	14	
Yes	26	30		24	32	
Lymphatic invasion	53	34	0.995	41	46	0.124
No	14	9		14	9	
Yes	39	25		27	37	
Neural invasion	53	34	0.384	41	46	0.022
No	30	16		27	19	
Yes	23	18		14	24	

diff. = differentiation.

Table 4 Significant prognostic factors for disease-free survival by multivariate analysis

Variables	Crude HR (95%CI)	Adjusted HR (95%CI)	P
MUC1 expression			0.026
Low	1	1	
High	2.59 (1.54-4.35)	2.19 (1.11-4.32)	
MUC5AC expression			0.059
Low	1	1	
High	1.36 (0.83-2.24)	2.06 (0.96-4.41)	
Age (yr)			0.571
≤56	1	1	
>56	0.86 (0.53-1.42)	1.19 (0.65-2.17)	
Gender			0.128
Male	1	1	
Female	0.63 (0.37-1.09)	0.60 (0.31-1.18)	
Histological grading			<0.050
Papillary	1	1	
Well-differentiated	1.86 (0.91-3.83)	1.92 (0.82-4.49)	
Moderately differentiated	3.65 (1.59-8.41)	3.00 (1.10-8.20)	
Poorly differentiated	1.78 (0.70-4.53)	3.02 (0.97-9.41)	
Staging			<0.050
I-III	1	1	
IVA	2.49 (0.81-7.62)	5.10 (1.27-20.43)	
IVB	3.57 (1.41-9.00)	3.93 (1.47-10.51)	

and tumor cells are documented in various cancers. The carbohydrate side chains of MUC1 from breast adenocarcinomas are shorter and less densely distributed than those produced by normal breast cells^[28-30], whereas those of advanced stage or metastatic colorectal carcinomas had a high level of fully glycosylated mucin^[31]. Since different

antibodies may require different carbohydrates for their actions, the discrepancies in the immunoreactivity may be obtained, when different mucin antibodies are used^[28,29]. In our study, we have shown that the immunoreactivity obtained using MUC1 (Ma695) and MUC5AC (MAN-5AC1) antibodies corresponds to the levels of the mucin transcripts obtained

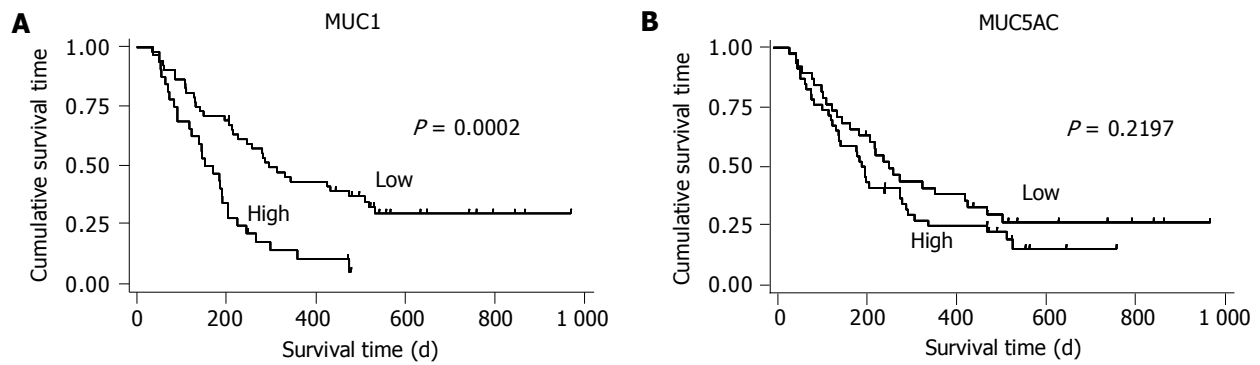


Figure 2 Survival curves using Kaplan-Meier method. **A:** Significant unfavorable prognosis of tumors with high expression of MUC1 compared to low-expression carcinoma ($P = 0.0002$); **B:** Poor survival of patients with tumors having a high

expression of MUC5AC as opposed to patients having a low-expression carcinoma.

by real-time PCR, suggesting that these antibodies are appropriate for semi-quantitative analysis of MUC1 and MUC5AC expressions in the study of immunohistochemistry.

MUC1 is a transmembrane glycoprotein found frequently in the developing intrahepatic bile ducts in fetal liver^[32] but not in the normal adult intrahepatic biliary tree^[33,34]. Overexpression of MUC1 has been reported continuously in various cancers including CC^[35,36]. Therefore, MUC1 apomucin is proposed as an oncofetal antigen in the intrahepatic biliary tree^[32]. In contrast, MUC5AC, a gel-forming phenotype of secretory mucin, is rarely expressed in the intrahepatic biliary tree^[32,35,37], and only aberrantly in CC tissues^[38,39].

In the current study, MUC1 and MUC5AC were significantly expressed in ICC patients. These ectopically expressing mucins showed a significant correlation with poor prognosis. High MUC1 immunoreactivity was associated with vascular invasion, whereas high MUC5AC expression was related to neural invasion. The results suggest that the expression of these two mucins may be influenced by different modulators and may acquire different biological pathways and different clinical courses of ICC.

Association between mucin expression and prognosis of patient outcome has been repeatedly reported in several cancers^[17,40,41] including CC. Expressions of mucin MUC4 is a statistically significant risk factor, affecting the survival of patients with ICC^[42]. Extensive expression of MUC1 apomucin is an independent risk factor for poor outcome of patients with ICC^[35,36,42] and extrahepatic CC^[43]. Our study on MUC1 expression in ICC agrees well with the previous reports. However, the association between high expression of MUC5AC mucin in tumor tissue and unfavorable survival observed here is not statistically significant. The result disagrees with our previous finding that the detection of MUC5AC mucin in the serum of CC patients^[44] correlates with shorter survival outcomes^[39]. This discrepancy may be due to the small number of samples used in the present study.

The link between MUC1 expression and malignant progression is significant in three ways. First, MUC1 is negatively charged and cells expressing high levels may repel each other^[45,46]. Cell repulsion is a pivotal event in metastasis. Decreased carbohydrate epitope on MUC1 mucin and other surface molecules markedly increases tumor cells to tumor cell adhesion and hence reduces the ability of these tumor

cells to adhere to the surrounding endothelium.

Vascular invasion involves the binding to a ligand (E-selectin) of endothelial cells and epitopes (sialyl Lewis^{x/a}) on tumor cells^[47,48]. The association between high MUC1 expression and vascular invasion found in our study may indicate the role of MUC1 in tumor adhesion to endothelial cells. This suggestion is supported by the fact that sialyl Lewis^a, a carbohydrate epitope which is present at high level in tumor and serum of CC patients, has been identified as an epitope on MUC1^[49]. In addition, our previous study indicates that CC patients with positive sialyl Lewis^a expression in tumor tissue have a significantly poorer prognosis and the expression of sialyl Lewis^a is associated with vascular invasion^[50].

Overexpression of MUC1 on the membrane of tumor cells can suppress the immunity of patients. Tumor cells with high expression of MUC1 could inhibit the interaction between cytotoxic lymphocytes and tumor cells^[51], and high levels of MUC1 correlate with immunosuppression in adenocarcinoma patients^[52]. At present, MUC1 mucin is known to serve as a target molecule for killing particular cancer cells by cytotoxic T-lymphocytes and as an antigen for cancer vaccine^[53,54]. Attempts to eliminate or control metastasis of tumor cells via anti-MUC1 and phase I/II trials of cancer vaccines using antigen MUC1 are now underway^[53].

Perineural invasion is one of the most crucial factors, which tend to yield the poor outcome after resection for biliary tract cancer, because cancer cells in the perineural space often remain on the surgical margin of the tumor after an assumed curative resection^[55,56]. In our study, MUC5AC was aberrantly expressed in ICC patients, correlated with neural invasion and advanced stage of tumor, suggesting that MUC5AC mucin plays a role in the late stage carcinogenesis and the poor prognosis of ICC patients is due to neural metastasis.

Even the presently available evidence for the association between MUC5AC mucin expression and neural invasion is limited; however, we can postulate the possible role of MUC5AC mucous layer surrounding the cancer cells in the invasion of cancer cells in several ways. First, the MUC5AC mucin layer may shield the tumor cells from immune recognition by the cellular arm of the immune system, thus favoring metastasis. Second, a number of tumor cells may

cluster as tumor emboli within the mucin layer, which may result in tumor dissemination to distant organ sites. Finally, specific epitopes of carbohydrate ligand on MUC5AC may manipulate specific adherence of tumor cells via some adhesion molecules, e.g., NCAM^[57]. Further investigation, including expression of NCAM in ICC patients with positive MUC5AC mucin expression and neural invasion is needed.

In summary, high expressions of MUC1 mucin significantly correlate with poor survival of ICC patients according to the Kaplan-Meier method. Expression of MUC1 and MUC5AC mucins is associated with metastasis, and is thus considered to be a useful prognostic marker for a poor outcome in ICC patients. We suggest that MUC1 and MUC5AC mucin immunohistochemistry may augment the classic histochemistry for diagnosis and prognosis of ICC as well as prediction of the patient outcome.

ACKNOWLEDGMENT

The authors thank Mr. Bryan Roderick Hamman for his assistance with the English-language presentation of the manuscript.

REFERENCES

- 1 **de Groen PC.** Cholangiocarcinoma in primary sclerosing cholangitis: who is at risk and how do we screen? *Hepatology* 2000; **31**: 247-248
- 2 **Rosen CB,** Nagorney DM, Wiesner RH, Coffey RJ, LaRusso NF. Cholangiocarcinoma complicating primary sclerosing cholangitis. *Ann Surg* 1991; **213**: 21-25
- 3 **Thamavit W,** Bhamarapavati N, Sahaphong S, Vajrasthira S, Angsubhakorn S. Effects of dimethylnitrosamine on induction of cholangiocarcinoma in *Opisthorchis viverrini*-infected Syrian golden hamsters. *Cancer Res* 1978; **38**: 4634-4639
- 4 **Ohshima H,** Bandaletova TY, Brouet I, Bartsch H, Kirby G, Ogunbiyi F, Vatanasapt V, Pipitgool V. Increased nitrosamine and nitrate biosynthesis mediated by nitric oxide synthase induced in hamsters infected with liver fluke (*Opisthorchis viverrini*). *Carcinogenesis* 1994; **15**: 271-275
- 5 **Pinlaor S,** Ma N, Hiraku Y, Yongvanit P, Semba R, Oikawa S, Murata M, Sripa B, Sithithaworn P, Kawanishi S. Repeated infection with *Opisthorchis viverrini* induces accumulation of 8-nitroguanine and 8-oxo-7, 8-dihydro-2'-deoxyguanine in the bile duct of hamsters via inducible nitric oxide synthase. *Carcinogenesis* 2004; **25**: 1535-1542
- 6 **Haswell-Elkins MR,** Mairiang E, Mairiang P, Chaiyakum J, Chamadol N, Loapaiboon V, Sithithaworn P, Elkins DB. Cross-sectional study of *Opisthorchis viverrini* infection and cholangiocarcinoma in communities within a high-risk area in north-east Thailand. *Int J Cancer* 1994; **59**: 505-509
- 7 **de Groen PC,** Gores GJ, LaRusso NF, Gunderson LL, Nagorney DM. Biliary tract cancers. *N Engl J Med* 1999; **341**: 1368-1378
- 8 **Kullavanijaya P,** Tangkijvanich P, Poovorawan Y. Current status of infection-related gastrointestinal and hepatobiliary diseases in Thailand. *Southeast Asian J Trop Med Public Health* 1999; **30**: 96-105
- 9 **Sithithaworn P,** Haswell-Elkins MR, Mairiang P, Satarug S, Mairiang E, Vatanasapt V, Elkins DB. Parasite-associated morbidity: liver fluke infection and bile duct cancer in north-east Thailand. *Int J Parasitol* 1994; **24**: 833-843
- 10 **Thamavit W,** Pairojkul C, Tiwawech D, Itoh M, Shirai T, Ito N. Promotion of cholangiocarcinogenesis in the hamster liver by bile duct ligation after dimethylnitrosamine initiation. *Carcinogenesis* 1993; **14**: 2415-2417
- 11 **Satarug S,** Haswell-Elkins MR, Sithithaworn P, Bartsch H, Ohshima H, Tsuda M, Mairiang P, Mairiang E, Yongvanit P, Esumi H, Elkins DB. Relationships between the synthesis of N-nitrosodimethylamine and immune responses to chronic infection with the carcinogenic parasite, *Opisthorchis viverrini*, in men. *Carcinogenesis* 1998; **19**: 485-491
- 12 **Satarug S,** Haswell-Elkins MR, Tsuda M, Mairiang P, Sithithaworn P, Mairiang E, Esumi H, Sukprasert S, Yongvanit P, Elkins DB. Thiocyanate-independent nitrosation in humans with carcinogenic parasite infection. *Carcinogenesis* 1996; **17**: 1075-1081
- 13 **Chang SK,** Dohrman AF, Basbaum CB, Ho SB, Tsuda T, Toribara NW, Gum JR, Kim YS. Localization of mucin (MUC2 and MUC3) messenger RNA and peptide expression in human normal intestine and colon cancer. *Gastroenterology* 1994; **107**: 28-36
- 14 **Buisine MP,** Devisme L, Degand P, Dieu MC, Gosselin B, Copin MC, Aubert JP, Porchet N. Developmental mucin gene expression in the gastroduodenal tract and accessory digestive glands. II. Duodenum and liver, gallbladder, and pancreas. *J Histochem Cytochem* 2000; **48**: 1667-1676
- 15 **Jass JR,** Walsh MD. Altered mucin expression in the gastrointestinal tract: a review. *J Cell Mol Med* 2001; **5**: 327-351
- 16 **Kim GE,** Bae HI, Park HU, Kuan SF, Crawley SC, Ho JJ, Kim YS. Aberrant expression of MUC5AC and MUC6 gastric mucins and sialyl Tn antigen in intraepithelial neoplasms of the pancreas. *Gastroenterology* 2002; **123**: 1052-1060
- 17 **Lee HS,** Lee HK, Kim HS, Yang HK, Kim YI, Kim WH. MUC1, MUC2, MUC5AC, and MUC6 expressions in gastric carcinomas: their roles as prognostic indicators. *Cancer* 2001; **92**: 1427-1434
- 18 **Pereira MB,** Dias AJ, Reis CA, Schmitt FC. Immunohistochemical study of the expression of MUC5AC and MUC6 in breast carcinomas and adjacent breast tissues. *J Clin Pathol* 2001; **54**: 210-213
- 19 **Higashi M,** Yonezawa S, Ho JJ, Tanaka S, Irimura T, Kim YS, Sato E. Expression of MUC1 and MUC2 mucin antigens in intrahepatic bile duct tumors: its relationship with a new morphological classification of cholangiocarcinoma. *Hepatology* 1999; **30**: 1347-1355
- 20 **Kawamoto T,** Shoda J, Irimura T, Miyahara N, Furukawa M, Ueda T, Asano T, Kano M, Koike N, Fukao K, Tanaka N, Todoroki T. Expression of MUC1 mucins in the subserosal layer correlates with postsurgical prognosis of pathological tumor stage 2 carcinoma of the gallbladder. *Clin Cancer Res* 2001; **7**: 1333-1342
- 21 **Lee KT,** Liu TS. Altered mucin gene expression in stone-containing intrahepatic bile ducts and cholangiocarcinomas. *Dig Dis Sci* 2001; **46**: 2166-2172
- 22 **Sobin LH,** Wittekind CH. *TNM classification of malignant tumours*. 5th ed. New York: John Wiley Sons 1997: 136-143
- 23 **Thornton DJ,** Carlstedt I, Howard M, Devine PL, Price MR, Sheehan JK. Respiratory mucins: identification of core proteins and glycoforms. *Biochem J* 1996; **316** (Pt 3): 967-975
- 24 **Reis CA,** David L, Seixas M, Burchell J, Sobrinho-Simoes M. Expression of fully and under-glycosylated forms of MUC1 mucin in gastric carcinoma. *Int J Cancer* 1998; **79**: 402-410
- 25 **Baldus SE,** Zirbes TK, Engel S, Hanisch FG, Monig SP, Lorenzen J, Glossmann J, Fromm S, Thiele J, Pichlmaier H, Dienes HP. Correlation of the immunohistochemical reactivity of mucin peptide cores MUC1 and MUC2 with the histopathological subtype and prognosis of gastric carcinomas. *Int J Cancer* 1998; **79**: 133-138
- 26 **Sakamoto H,** Yonezawa S, Utsunomiya T, Tanaka S, Kim YS, Sato E. Mucin antigen expression in gastric carcinomas of young and old adults. *Hum Pathol* 1997; **28**: 1056-1065
- 27 **Utsunomiya T,** Yonezawa S, Sakamoto H, Kitamura H, Hokita S, Aiko T, Tanaka S, Irimura T, Kim YS, Sato E. Expression of MUC1 and MUC2 mucins in gastric carcinomas: its relationship with the prognosis of the patients. *Clin Cancer Res* 1998; **4**: 2605-2614
- 28 **Burchell J,** Taylor-Papadimitriou J. Effect of modification of carbohydrate side chains on the reactivity of antibodies with core-protein epitopes of the MUC1 gene product. *Epithelial Cell Biol* 1993; **2**: 155-162

- 29 **Girling A**, Bartkova J, Burchell J, Gendler S, Gillett C, Taylor-Papadimitriou J. A core protein epitope of the polymorphic epithelial mucin detected by the monoclonal antibody SM-3 is selectively exposed in a range of primary carcinomas. *Int J Cancer* 1989; **43**: 1072-1076
- 30 **Hull SR**, Bright A, Carraway KL, Abe M, Hayes DF, Kufe DW. Oligosaccharide differences in the DF3 sialomucin antigen from normal human milk and the BT-20 human breast carcinoma cell line. *Cancer Commun* 1989; **1**: 261-267
- 31 **Nakamori S**, Ota DM, Cleary KR, Shirotani K, Irimura T. MUC1 mucin expression as a marker of progression and metastasis of human colorectal carcinoma. *Gastroenterology* 1994; **106**: 353-361
- 32 **Sasaki M**, Nakanuma Y, Terada T, Kim YS. Biliary epithelial expression of MUC1, MUC2, MUC3 and MUC5/6 apomucins during intrahepatic bile duct development and maturation. An immunohistochemical study. *Am J Pathol* 1995; **147**: 574-579
- 33 **Sasaki M**, Nakanuma Y. Expression of mucin core protein of mammary type in primary liver cancer. *Hepatology* 1994; **20**: 1192-1197
- 34 **Yamashita K**, Yonezawa S, Tanaka S, Shirahama H, Sakoda K, Imai K, Xing PX, McKenzie IF, Hilken J, Kim YS. Immunohistochemical study of mucin carbohydrates and core proteins in hepatolithiasis and cholangiocarcinoma. *Int J Cancer* 1993; **55**: 82-91
- 35 **Sasaki M**, Nakanuma Y, Kim YS. Characterization of apomucin expression in intrahepatic cholangiocarcinomas and their precursor lesions: an immunohistochemical study. *Hepatology* 1996; **24**: 1074-1078
- 36 **Matsumura N**, Yamamoto M, Aruga A, Takasaki K, Nakano M. Correlation between expression of MUC1 core protein and outcome after surgery in mass-forming intrahepatic cholangiocarcinoma. *Cancer* 2002; **94**: 1770-1776
- 37 **Vandenhoute B**, Buisine MP, Debailleul V, Clement B, Moniaux N, Dieu MC, Degand P, Porchet N, Aubert JP. Mucin gene expression in biliary epithelial cells. *J Hepatol* 1997; **27**: 1057-1066
- 38 **Sasaki M**, Nakanuma Y, Kim YS. Expression of apomucins in the intrahepatic biliary tree in hepatolithiasis differs from that in normal liver and extrahepatic biliary obstruction. *Hepatology* 1998; **27**: 54-61
- 39 **Boonla C**, Wongkham S, Sheehan JK, Wongkham C, Bhudhisawasdi V, Tepsiri N, Pairojkul C. Prognostic value of serum MUC5AC mucin in patients with cholangiocarcinoma. *Cancer* 2003; **98**: 1438-1443
- 40 **Kashiwagi H**, Kijima H, Dowaki S, Ohtani Y, Tobita K, Yamazaki H, Nakamura M, Ueyama Y, Tanaka M, Inokuchi S, Makuuchi H. MUC1 and MUC2 expression in human gallbladder carcinoma: a clinicopathological study and relationship with prognosis. *Oncol Rep* 2001; **8**: 485-489
- 41 **Akyurek N**, Akyol G, Dursun A, Yamac D, Gunel N. Expression of MUC1 and MUC2 mucins in gastric carcinomas: their relationship with clinicopathologic parameters and prognosis. *Pathol Res Pract* 2002; **198**: 665-674
- 42 **Shibahara H**, Tamada S, Higashi M, Goto M, Batra SK, Hollingsworth MA, Imai K, Yonezawa S. MUC4 is a novel prognostic factor of intrahepatic cholangiocarcinoma-mass forming type. *Hepatology* 2004; **39**: 220-229
- 43 **Takao S**, Uchikura K, Yonezawa S, Shinchi H, Aikou T. Mucin core protein expression in extrahepatic bile duct carcinoma is associated with metastases to the liver and poor prognosis. *Cancer* 1999; **86**: 1966-1975
- 44 **Wongkham S**, Sheehan JK, Boonla C, Patrakitkomjorn S, Howard M, Kirkham S, Sripa B, Wongkham C, Bhudhisawasdi V. Serum MUC5AC mucin as a potential marker for cholangiocarcinoma. *Cancer Lett* 2003; **195**: 93-99
- 45 **Wesseling J**, van der Valk SW, Vos HL, Sonnenberg A, Hilken J. Episialin (MUC1) overexpression inhibits integrin-mediated cell adhesion to extracellular matrix components. *J Cell Biol* 1995; **129**: 255-265
- 46 **Wesseling J**, van der Valk SW, Hilken J. A mechanism for inhibition of E-cadherin-mediated cell-cell adhesion by the membrane-associated mucin episialin/MUC1. *Mol Biol Cell* 1996; **7**: 565-577
- 47 **Regimbald LH**, Pilarski LM, Longenecker BM, Reddish MA, Zimmermann G, Hugh JC. The breast mucin MUC1 as a novel adhesion ligand for endothelial intercellular adhesion molecule 1 in breast cancer. *Cancer Res* 1996; **56**: 4244-4249
- 48 **Nath D**, Hartnell A, Happerfield L, Miles DW, Burchell J, Taylor-Papadimitriou J, Crocker PR. Macrophage-tumour cell interactions: identification of MUC1 on breast cancer cells as a potential counter-receptor for the macrophage-restricted receptor, sialoadhesin. *Immunology* 1999; **98**: 213-219
- 49 **Yamashita Y**, Ho JJ, Farrelly ER, Hirakawa K, Sowa M, Kim YS. Forskolin and phorbol ester have opposite effects on the expression of mucin-associated sialyl-Lewis(a) in pancreatic cancer cells. *Eur J Cancer* 2000; **36**: 113-120
- 50 **Juntavee A**, Sripa B, Pugkhem A, Khuntikeo N, Wongkham S. Expression of sialyl Lewis^x relates to poor prognosis in cholangiocarcinoma. *World J Gastroenterol* 2005; **11**: 249-254
- 51 **van de Wiel-van Kemenade E**, Ligtenberg MJ, de Boer AJ, Buijs F, Vos HL, Melief CJ, Hilken J, Figdor CG. Episialin (MUC1) inhibits cytotoxic lymphocyte-target cell interaction. *J Immunol* 1993; **151**: 767-776
- 52 **Hamanaka Y**, Suehiro Y, Fukui M, Shikichi K, Imai K, Hinoda Y. Circulating anti-MUC1 IgG antibodies as a favorable prognostic factor for pancreatic cancer. *Int J Cancer* 2003; **103**: 97-100
- 53 **Musselli C**, Livingston PO, Ragupathi G. Keyhole limpet hemocyanin conjugate vaccines against cancer: the Memorial Sloan Kettering experience. *J Cancer Res Clin Oncol* 2001; **127** (Suppl 2): R20-26
- 54 **Kontani K**, Taguchi O, Ozaki Y, Hanaoka J, Tezuka N, Sawai S, Inoue S, Fujino S, Maeda T, Itoh Y, Ogasawara K, Sato H, Ohkubo I, Kudo T. Novel vaccination protocol consisting of injecting MUC1 DNA and nonprimed dendritic cells at the same region greatly enhanced MUC1-specific antitumor immunity in a murine model. *Cancer Gene Ther* 2002; **9**: 330-337
- 55 **Koyama K**, Tanaka J, Kato S, Asanuma Y. New strategy for treatment of carcinoma of the hilar bile duct. *Surg Gynecol Obstet* 1989; **168**: 523-530
- 56 **Koyama K**, Tanaka J, Sato Y, Seki H, Kato Y, Umezawa A. Experience in twenty patients with carcinoma of hilar bile duct treated by resection, targeting chemotherapy and intracavitary irradiation. *Surg Gynecol Obstet* 1993; **176**: 239-245
- 57 **De Bolos C**, Garrido M, Real FX. MUC6 apomucin shows a distinct normal tissue distribution that correlates with Lewis antigen expression in the human stomach. *Gastroenterology* 1995; **109**: 723-734

Hepatocytes targeting of cationic liposomes modified with soybean sterylglucoside and polyethylene glycol

Xian-Rong Qi, Wen-Wei Yan, Jing Shi

Xian-Rong Qi, Wen-Wei Yan, Jing Shi, Department of Pharmaceutics, School of Pharmaceutical Sciences, Peking University, Beijing 100083, China
Supported by the National Natural Science Foundation of China, No. 30371265

Correspondence to: Professor Xian-Rong Qi, Department of Pharmaceutics, School of Pharmaceutical Sciences, Peking University, Beijing 100083, China. qixr2001@yahoo.com.cn
Telephone: +86-10-82801584 Fax: +86-10-62015584
Received: 2004-11-15 Accepted: 2005-02-18

Abstract

AIM: In this study, a hepatocyte-specific targeting technology was developed by modifying cationic liposomes with soybean sterylglucoside (SG) and polyethylene glycol (PEG) (C/SG/PEG-liposomes).

METHODS: The liposomal transfection efficiencies in HepG₂ 2.2.15 cells were estimated with the use of fluorescein sodium (FS) as a model drug, by flow cytometry. The antisense activity of C/SG/PEG-liposomes entrapped antisense oligonucleotides (ODN) was determined as HBsAg and HBeAg in HepG₂ 2.2.15 cells by ELISA. The liposome uptake by liver and liver cells in mice was carried out after intravenous injection of ³H-labeled liposomes.

RESULTS: C/SG-liposomes entrapped FS were effectively transfected into HepG₂ 2.2.15 cells *in vitro*. C/SG/PEG-liposomes entrapped ODN, reduced the secretion of both HBsAg and HBeAg in HepG₂ 2.2.15 cells when compared to free ODN. After *in vivo* injection of ³H-labeled C/SG/PEG-liposomes, higher radiation accumulation was observed in the hepatocytes than non-parenchymal cells of the liver.

CONCLUSION: C/SG/PEG-liposomes mediated gene transfer to the liver is an effective gene-delivery method for hepatocytes-specific targeting, which appears to have a potential for gene therapy of HBV infections.

© 2005 The WJG Press and Elsevier Inc. All rights reserved.

Key words: Hepatocytes targeting; Cationic liposomes; Soybean sterylglucoside

Qi XR, Yan WW, Shi J. Hepatocytes targeting of cationic liposomes modified with soybean sterylglucoside and polyethylene glycol. *World J Gastroenterol* 2005; 11 (32): 4947-4952
<http://www.wjgnet.com/1007-9327/11/4947.asp>

INTRODUCTION

Cationic liposomes have been accepted as effective non-viral vectors for gene delivery with a lower immunogenicity than the viral ones. However, the lack of organ or cell specificity sometimes hampers their applications. In the case of cationic liposomes, the highest gene expression is observed in the lung after intravenous injection of their plasmid DNA complexes in most cases, because the lung capillaries are the first traps to be encountered^[1,2]. Development of cell-specific targeting technology for cationic liposomes attracts great interest in gene therapy.

Since the liver is one of most important target organs in the body, and Kupffer cells in the liver are a part of the reticular endothelial system (RES), relatively high accumulation of administered liposomes is observed in the liver, mostly in non-parenchymal cells^[3]. However, preferential incorporation of liposomes into liver hepatocytes is required for therapeutic situations. Thus, reducing the Kupffer cell uptake and enhancing hepatocyte uptake, are challenges of research in liposome-targeting.

For cell specific delivery, the receptor-mediated endocytosis systems endowed to various cell types would be useful and a number of gene delivery systems have been developed to introduce gene into specific cells with receptor-mediated endocytosis. Ligands currently being investigated include galactose^[4,5], lactose^[6], transferrin^[7], etc. Among these receptors, asialoglycoprotein receptor (ASGP-R) is the most promising for gene targeting, since it exhibits high affinity and a rapid internalization rate^[8].

It was reported that liposomes with soybean sterylglucoside (SG) gets accumulated in the liver, especially in hepatocytes^[9,10]. Doxorubicin (DXR) entrapped in liposomes contained SG (SG-liposomes) showed a high therapeutic effect for its selective delivery of drugs to hepatocytes in animals with liver cancer^[11]. SG-liposomes have glucose residue on the surface of liposomes^[12], which is essential for selective accumulation in liver cells.

Hepatitis B is a disease of global importance with more than 300 million carriers of the hepatitis B virus (HBV) worldwide^[13]. Unfortunately, treatment of chronic HBV infection is far from satisfactory. The most successful therapeutic agent so far available is interferon-alpha, which shows a 40% response rate for patients after completion of the therapy^[14,15]. Since several viruses have become successful targets of the ODN approach, this strategy may be promising in targeting chronic HBV infection, and several studies have now shown that ODN are capable of suppressing HBV *in vitro*^[16,17] and *in vivo*^[18,19]. ODN are synthetic single chain DNA molecules that can inhibit gene expression within cells

by their capability to bind a complementary mRNA sequence, and prevent translation of mRNA, thus providing potentially powerful therapeutic tools against viral diseases and cancer^[20]. For an ODN delivery system towards HBV infection, the SG may be useful for targeting hepatocytes of the liver.

This study describes a specific targeting approach which results in increased hepatocytes uptake. A cationic liposome carrier modified with SG and encapsulated 15-mer ODN for the HBV therapy *in vitro* was constructed. The influence of SG on facilitating the uptake of liposomes by hepatocytes was investigated *in vivo*. The value of the surface modified cationic liposomes as a delivery vehicle, mainly for hepatocytes targeting antisense agent *in vitro* and *in vivo* was assessed.

MATERIALS AND METHODS

Synthesis of ODN

ODN with phosphorothioate backbone encoding the cap site of SP II promoter transcribed mRNA (cap site/SP II) sequences were synthesized using standard phosphoramidite chemistry by Aoke (Beijing, China) and purified by SDS-PAGE. The complementary ODN sequences were: 5' GAT GAC TGT CTC TTA 3'.

Animals and cell line

Male KM mice (18-23 g) were obtained from the Institute of Zoology, Chinese Academy of Sciences (Beijing, China). All animals received good care. A human hepatoblastoma cell line, HepG₂ 2.2.15 was provided by the Institute of Hepatology of the People's Hospital, Peking University (Beijing, China).

Materials

N, N-dimethylethylenediamine (99%) and cholesteryl chloroformate (97%) were obtained from ACROS (USA); dipalmitoylphosphatidylcholine (DPPC) and polyethylene glycol-distearoylphosphatidylethanolamine (PEG-DSPE) were purchased from NOF (Tokyo, Japan); SG was generously supplied by Ryukakusan Co. Ltd. (Tokyo, Japan); cholesterol (Ch) was purchased from Wako Pure Chemical Industries (Tokyo, Japan); ³H-Ch and ¹²⁵I-ODN was provided by China Institute of Atomic Energy (Beijing, China). FS was obtained from the Third Chemical Reagent Factory of Shanghai (Shanghai, China); DMEM medium and fetal bovine serum (FBS) was purchased from Life Technologies (NY, USA). 2, 5-Diphenyloxazole (PPO) and 1, 4-bis (5-phenyl-2-oxazolyl)-benzene (POPOP) were provided by Fluka (Buchs, Switzerland). Collagenase (II) was purchased from Sigma (St. Louis, MO, USA). All other chemicals were of reagent grade.

Synthesis of DC-cholesterol

DC-cholesterol was synthesized according to the method described by Gao^[21]. The production was confirmed by thin-layer chromatogram (TLC), melting point, ¹H nuclear magnetic resonance (NMR) (500 MHz, CDCl₃), mass spectrum (MS), etc.

Preparation of liposomes

The FS or ODN encapsulated liposomes used in the present

study were prepared according to the compositions in Table 1, respectively. A mixture of lipids in chloroform was dried under a stream of nitrogen and additionally dried under vacuum for 3 h to remove all chloroform. The dry lipid film was resuspended with FS or ODN solution (solution in 50 g/L glucose) by vortexing and sonicating, and then **extruded through 0.2 μm pore size polycarbonate filters** to generate the FS and ODN encapsulated liposomes, respectively. The concentration of lipids was 20 μmol/L. To prepare lipid-radioactive labeled liposomes, ³H-Ch was added to the lipid mixture at the beginning of the liposomes preparation and the dry lipid film was resuspended with 5% glucose. The ³H-labeled C-liposomes and C/SG/PEG-liposomes were prepared. The radioactivity of liposomes was 4 μCi/200 μL.

Determination of encapsulation efficacy of liposomes

Free ODN was separated from ODN encapsulated liposomes by equilibrium dialysis, in a dialysis tubing (SpectraPor 12 000 to 14 000 MWCO) at 4 °C for 12 h in 10 mL of 5% glucose solution. The incubation liquid was taken and the concentration of ODN was detected by UV spectro-photometer at 260 nm. Free FS was separated from encapsulated FS by passing through a Sephadex G-50 column (1 cm×20 cm). The concentration of FS was determined by measuring the fluorescence intensity of FS with excitation and emission wavelengths at 490 and 512 nm, respectively. According to the amount of ODN or FS entrapped in the liposomes, the encapsulation efficiency was calculated.

Morphology and size analysis

The size of liposomes was determined by dynamic light scattering using a Zetasizer 3 000HS (Malvern Instruments, Ltd., UK). The morphologies of these liposomes were also observed by the transmission electron microscope.

Cell culture and transfection efficiency measurement

HepG₂ 2.2.15 was maintained in DMEM medium supplemented with 100 mL/L FBS at 37 °C with 50 mL/L CO₂. The cells were scraped by 0.25% trypsin and planted in 96-well tissue culture plates (5×10³/well) for 2 d before the experiment, until the percentage of adherent cells reached approximately 70% confluence. The upper medium was removed and fresh DMEM medium was added with 100 mL/L FS encapsulated liposome. When the liposomes were incubated with cells for 3, 6, and 24 h, respectively, the cells were detached with 0.25% trypsin and washed thrice with 10 mmol/L PBS. The transfection efficiency was determined by counting the amount of cells transferred by FS with flow cytometry (BD, USA). The transfection efficiency was calculated according to the following equation: amount of FS transferred cells/amount of total cells×100%. The means of transfection efficiency were calculated from two independent experiments.

Antisense activity of ODN encapsulated in liposomes

For lipofection, HepG₂ 2.2.15 cells were seeded at an initial concentration of 1×10⁴ per well for 96-well plates. The cells were allowed to grow for about 24 h, until the percentage

of adherent cells reached approximately 80% confluence. Then the cells were washed extensively to remove the previously secreted HBsAg and HBeAg in the medium. After washing, 100 μ L free ODN or C/SG/PEG-liposomes entrapped ODN with an ODN concentration at 1.25, 2.5 or 5.0 μ mol/L, together with 100 μ L DMEM containing 10% serum, were added. The secretion of HBsAg and HBeAg into the culture supernatants was measured daily for 3 d, using ELISA immunoassay kits. The means of HBsAg and HBeAg immunoassay measurements were calculated from two independent experiments.

Liver uptake in vivo and scintillation counting

Liposomes labeled with ^3H -Ch (C-liposomes and C/SG/PEG-liposomes) were injected into the tail vein of three male mice with a dose of 200 μ L/20 g. At 0.5 and 4 h after injection, the mice were killed. The liver tissue was collected and washed with saline. About 100 mg of liver samples were decolorized in a solution, containing 200 μ L HClO_4 and 300 μ L 60% H_2O_2 . Radiation scintillation fluid was added and mixed thoroughly. The radioactivity (dpm) of samples was counted on a scintillation counter (Pharmacia WALAC 1410, Turku, Finland).

Isolation of liver cells

Mice were injected intravenously by tail vein with ^3H -labeled C-liposomes and C/SG/PEG-liposomes, respectively. At 0.5 and 4 h after administration, the mice were anesthetized, and the liver was perfused via the portal vein with isotonic saline to remove the blood. Then the liver was excised, minced and digested in 0.5 g/L collagenase for 30 min at 37 $^\circ\text{C}$. The suspended cells were filtered through cotton mesh sieves, followed by centrifugation at 500 r/min for 3 min. The pellets containing hepatocytes were washed thrice with saline solution by centrifugation at 500 r/min for 3 min. The supernatant containing non-parenchymal cells were similarly centrifuged and washed thrice at 1 500 r/min for 15 min. The radioactivity (dpm) of hepatocytes and non-parenchymal samples was counted on a scintillation counter, as described previously.

RESULTS

Characteristics of liposomes

The entrapment efficiencies, size, polydispersity index of all kinds of FS or ODN encapsulated liposomes are shown in Table 1. The results indicated that FS could hardly be

entrapped in the N-liposomes, with an entrapment efficiency only at 0.64%. By adding DC-chol to the N-liposomes, the entrapment efficiencies of FS and ODN were increased to more than 83%, when the charge ratio of anionic FS or ODN/cationic lipid was 1:1. The C-liposomes, C/SG-liposomes and C/SG/PEG-liposomes had small size (155.0, 117.8, and 96.2 nm for FS entrapped in liposomes, 71.0, 75.4, and 183.0 nm for ODN entrapped in liposomes, respectively). The polydispersity index indicated the uniformity in size distribution. Transmission electron micrographs of these liposomes showed spherical vesicles (data not shown).

Transfection efficiency of liposome in HepG₂ 2.2.15 cells

Figure 1 showed the transfection of FS entrapped in N-liposomes, C-liposomes and C/SG-liposomes when they were incubated for 3, 6, and 24 h with HepG₂ 2.2.15 cells at 37 $^\circ\text{C}$, respectively. FS served as a fluorescent marker because the cell uptake of free FS was almost negligible. As shown in Figure 1A, the transfection of C-liposomes entrapped FS was significantly higher than that of N-liposomes, and the transfection of C/SG-liposomes entrapped FS was the highest. The enhancement of transfection efficiency was about 7.7-fold for the C/SG-liposomes than that of C-liposomes when incubated with cells for 6 h. When different types of liposomes were incubated with HepG₂ 2.2.15 cells at 37 $^\circ\text{C}$ for 24 h, the C/SG-liposomes showed the highest transfection efficiencies, while the C-liposomes and C/PEG-liposomes did not show significant differences (Figure 1B).

Effect of cationic liposomes entrapped ODN on HepG₂ 2.2.15 expression

Figure 2 showed the effect of cellular treatment with free ODN and C/SG/PEG-liposomes entrapped ODN on the expression level of HBsAg and HBeAg protein in HepG₂ 2.2.15 cells. The antisense effect (percent of inhibition on HBsAg and HBeAg secretion) of free ODN and C/SG/PEG-liposomes entrapped ODN was affected by the concentration of ODN and the cultured times. When the concentration of ODN that was added increased from 1.25 to 5.0 μ mol/L, the inhibition percentage of HBsAg by C/SG/PEG-liposomes entrapped ODN increased from 59.15% to 90.37% at 72 h, meanwhile, the inhibition of HBeAg increased from 42.9% to 73.43%. The inhibition effects of free ODN on HBsAg and HBeAg were decreased

Table 1 Entrapment efficiencies (EE), mean intensity diameter (D) of vesicle and polydispersity index (PI) of FS entrapped in liposomes and ODN entrapped in liposomes

Sample	Liposome compositions (molar ratio)	Entrapment of FS			Entrapment of ODN		
		EE (%)	D (nm)	PI	E (%)	D (nm)	PI
N-liposomes	DPPC/Ch(10:10)	0.64	-	-	-	-	-
C-liposomes	DPPC/Ch/DC-chol(10:1:10)	88.58 \pm 4.48 ¹	155.0	0.44	91.11 \pm 5.11 ²	71.0	1.00
C/SG-liposomes	DPPC/Ch/DC-chol/SG (10:1:10:1.34)	88.46 \pm 2.29 ¹	117.8	0.31	-	75.4	0.44
C/SG/PEG-liposomes	DPPC/Ch/DC-chol/SG/PEG- DSPE (10:1:10:1.34:1.34)	83.12 \pm 3.63 ¹	96.2	0.22	89.54 \pm 1.24 ²	183.0	0.35

¹Values represent as mean \pm SD, $n = 4$. ²Values represent as mean \pm SD, $n = 3$.

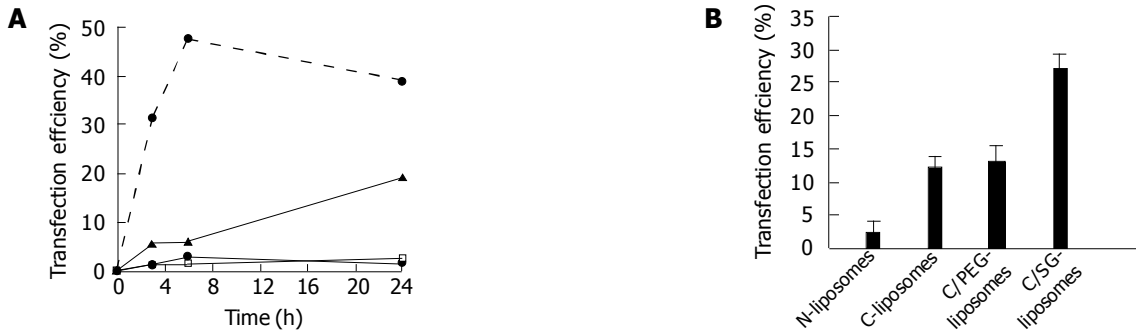


Figure 1 Transfection efficiencies. **A:** Transfection efficiencies of FS entrapped in different types of liposomes incubated with HepG2 2.2.15 cells at 37 °C. --□--: free FS solution as control; -○-: N-liposomes; -▲-: C-liposomes;

---●---: C/SG-liposomes. Data represents the average of two wells; **B:** Transfection efficiencies of FS entrapped in different types of liposomes incubated with HepG2 2.2.15 cells at 37 °C for 24 h. Data represents mean±SD, n = 3.

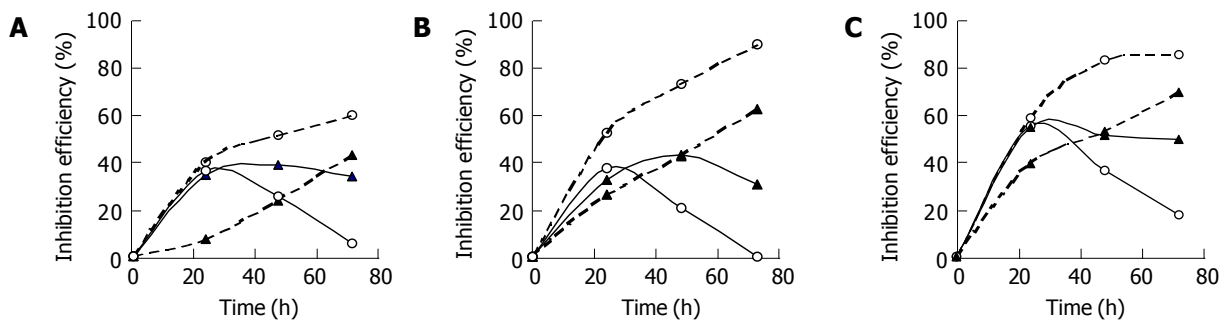


Figure 2 Percent of inhibition on HBsAg and HBeAg secretion of free ODN and C/SG/PEG-liposomes entrapped ODN in HepG2 2.2.15 cells culture medium incubated at 37 °C. The ODN concentration was 1.25 (A), 2.5 (B) and 5.0 μmol/L(C).

___: free ODN; ---: C/SG/PEG-liposomes encapsulated ODN; ○: HBsAg; ▲: HBeAg. Experimental values are given as the mean of two independent experiments.

and the inhibition effects of C/SG/PEG-liposomes entrapped ODN were increased when incubation time was increased from 24 to 72 h. The inhibition on HBeAg secretion brought by free ODN and C/SG/PEG-liposomes entrapped ODN showed lower tendency compared to the HBsAg. The cells remained viable throughout the experiments and no morphological abnormalities were observed.

Distribution in liver and intrahepatic cells in vivo

³H-Ch labeled C-liposomes and C/SG/PEG-liposomes were injected in mice at a dose of 4 μCi/20 g. At 0.5 and 4 h after injection, the radioactivity in 100 mg of liver tissue is shown in Figure 3. The distribution amount in liver tissue

(total hepatocyte and non-parenchymal cells) was not significantly different for C-liposomes and C/PEG/SG-liposomes. The uptake amounts of liposomes at 0.5 and 4 h in hepatocytes and non-parenchymal cells are also shown in Figure 3. After separating liver cells into hepatocytes and non-parenchymal cells, it was found that the uptake of C/SG/PEG-liposomes was higher than that of C-liposomes by hepatocytes at 0.5 h (P<0.01) and the uptake of C/SG/PEG-liposomes was lower than that of C-liposomes by non-parenchymal cells at 0.5 and 4 h (P<0.01). These results indicated that the C/SG/PEG-liposomes have more appety to hepatocytes than non-parenchymal cells in the liver.

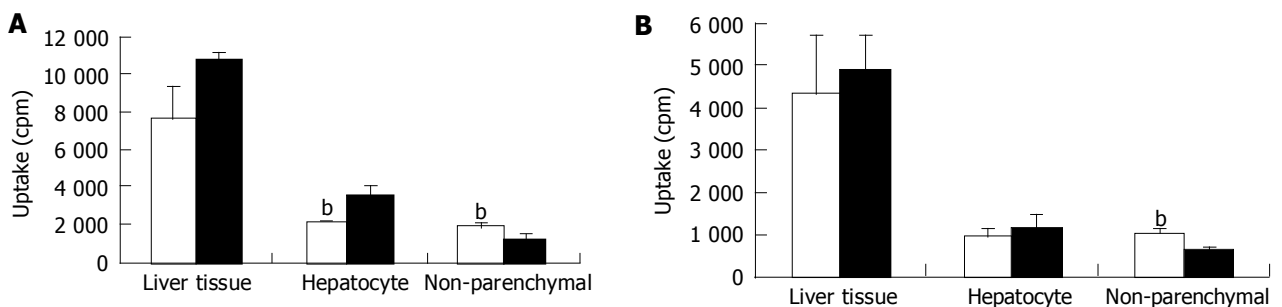


Figure 3 Distribution in liver tissue and uptake amounts in hepatocytes and non-parenchymal cells of liver of ³H-labeled liposomes, after intravenous administration by tail vein in mice, at different time periods. **A:** 0.5; **B:** 4.0 h. The open bar

represents C-liposomes and the filled bar represents C/PEG/SG-liposomes. Data represent mean±SD, n = 3. The statistical significance of differences was analyzed by Student's t-test. ^bP<0.01 vs C/PEG/SG-liposomes.

DISCUSSION

Among various types of non-viral vector systems, cationic liposomes seem to be promising, because of their high gene expression efficiency. When using simple cationic liposomes by both intravenous and intraportal administration^[19,22], it is difficult to transfect into hepatocytes because liposomes prefer targeting the lung and RES. A great challenge faces the investigator who wishes to target liposomes to hepatocytes, for some disorders such as hepatitis B or metabolic diseases which require that the liposomes be steered away from their natural targets. In this study, the characteristics of SG modified liposomes and its inhibition on HBsAg and HBeAg secretion was investigated. In addition, the liver uptake and intrahepatic distribution of a labeled cationic liposome and SG modified cationic liposome were also evaluated.

To investigate the effect of DC-chol, SG and PEG-DSPE on the entrapment and transfection efficiency, FS was used as a marker. DC-chol (positively charged) can bind with FS or ODN (both negatively charged) by electrostatic interaction. Typical cationic liposomes that carry excess positive charge will interact with plasma proteins, and would be rapidly taken up into the mononuclear phagocytic system. In order to decrease the adsorption of plasma proteins and interaction with non-target cells, 6% PEG-DSPE was added into the cationic liposomes.

Entrapment of FS and ODN to cationic liposomes was very efficient, even when containing a relatively high amount of SG and PEG-DSPE (6%, Table 1). Evidently, SG and PEG coating seldom shields the positively charged liposome surface from interaction with FS and ODN.

Receptors for carbohydrates such as the ASGP-R on hepatocytes and the mannose receptor on macrophages and liver endothelial cells produce opportunities for cell-specific gene delivery with liposomal carriers. The presence of a glucoside on the surface of electrically neutral FS entrapped in C/SG-liposomes, resulted in more than a 2-fold increased transfection efficiency of HepG₂ cells, which is a human hepatoblastoma cell line that is known to express ASGP-R, when compared to C-liposomes encapsulated FS (Figure 1). It was surmised that such glucoside in SG could be identified by ASGP-R present on the surface of the HepG₂ cells, leading to liposome entry into cells through endocytosis.

The major HBsAg, and in some cases, the HBeAg, is detectable in the serum of individuals with chronically infected HBV. Serological detection of HBeAg usually correlates well with the presence of circulating virions and is commonly used clinically as an indicator of active HBV replication. Elimination of HBsAg and HBeAg from the supernatant is associated with resolution of infection with a wild-type strain of HBV. Synthetic ODN (15-mers), complementary to the cap site of SP II promoter transcribed mRNA, showed a sequence-specific, dose-dependent inhibitory effect on HBV gene expression from a concentration of 1.25-5.0 $\mu\text{mol/L}$. A previous study showed that, such ODN could inhibit the expression of HBsAg without a significant effect on total synthesized protein in the cells^[23]. According to the results of this study, it is found that the initial concentration of ODN and incubation time appeared to be important factors in obtaining a desired inhibition effect. As the ODN concentration and incubation time increased, the inhibition

efficiency of C/SG/PEG-liposomes entrapped ODN also increased (Figure 2). However, it is demonstrated that larger amounts of ODN and cationic lipid would lead to a higher toxicity to the cells; therefore, concentration of liposome-ODN complexes should be restricted at a certain level^[24]. As for the present ODN encapsulated C/SG/PEG-liposomes, a concentration of DC-chol lower than 10 $\mu\text{g/mL}$ with a cationic lipid/ODN at 1:1 of charge ratio was regarded suitable.

In the study of liver uptake of ³H labeled cationic liposomes, no significant difference was found between C-liposomes and C/SG/PEG-liposomes. These results indicated that the PEG chain and glucose residue in SG did not necessarily improve the *in vivo* behavior of cationic liposomes. Kirby *et al.*, showed that when the cationic liposomes contain only 5% of charged lipid with small zeta potential, the behavior of the cationic liposomes are not different from that of neutral liposomes^[22,25]. Our results agree with these findings. These results could be attributed to the special hepatocytes targeting behavior of SG. A previous study showed that the glucose residue on the surface of liposomes could selectively recognize the ASGP-R of hepatocytes cells^[9]. The result also demonstrated that the liver targeting effect of SG is not diminished by the PEG chain on the surface of liposomes.

In conclusion, this study established a highly efficient receptor-mediated delivery system for ODN to hepatocytes by using SG and PEG modified cationic liposomes. By utilizing this delivery system, an ODN targeting the encapsidation site of the HBV pregenome causes a strong inhibition of HBV replication *in vitro*. Therefore, SG modified liposomes may be effective vehicles to improve the delivery of ODN to the liver for the therapy of hepatotropic viruses.

ACKNOWLEDGMENTS

We would like to thank Professor Lai Wei and his research group at the Institute of Hepatology, Peking University for assistance in cell culture and transfection efficiency measurement.

REFERENCES

- 1 **Zhu N**, Liggitt D, Liu Y, Debs R. Systemic gene expression after intravenous DNA delivery into adult mice. *Science* 1993; **261**: 209-211
- 2 **Huang L**, Li S. Liposomal gene delivery: a complex package. *Nat Biotechnol* 1997; **15**: 620-621
- 3 **Dasgupta P**, Bachhawat BK. Receptor-mediated uptake of asialoganglioside liposomes: sub-cellular distribution of the liposomal marker in isolated liver cell types. *Biochem Int* 1985; **10**: 327-336
- 4 **Hara T**, Aramaki Y, Takada S, Koike K, Tsuchiya S. Receptor-mediated transfer of pSV2CAT DNA to a human hepatoblastoma cell line HepG2 using asialofetuin-labeled cationic liposomes. *Gene* 1995; **159**: 167-174
- 5 **Remy JS**, Kichler A, Mordvinov V, Schuber F, Behr JP. Targeted gene transfer into hepatoma cells with lipopolyamine-condensed DNA particles presenting galactose ligands: a stage toward artificial viruses. *Proc Natl Acad Sci USA* 1995; **92**: 1744-1748
- 6 **Choi YH**, Liu F, Park JS, Kim SW. Lactose-poly-(ethylene glycol)-grafted poly-L-lysine as hepatoma cell-targeted gene carrier. *Bioconjug Chem* 1998; **9**: 708-718

- 7 **Kirchheis R**, Kichler A, Wallner G, Kursa M, Ogris M, Felzmann T, Buchberger M, Wagner E. Coupling of cell-binding ligands to polyethylenimine for targeted gene delivery. *Gene Ther* 1997; **4**: 409-418
- 8 **Wagner E**. Application of membrane-active peptides for nonviral gene delivery. *Adv Drug Deliv Rev* 1999; **38**: 279-289
- 9 **Shimizu K**, Maitani Y, Takayama K, Nagai T. Evaluation of dipalmitoylphosphatidylcholine liposomes containing a soybean-derived sterylglucoside mixture for liver targeting. *J Drug Target* 1996; **4**: 245-253
- 10 **Shimizu K**, Maitani Y, Takayama K, Nagai T. Formulation of liposomes with a soybean-derived sterylglucoside mixture and cholesterol for liver targeting. *Biol Pharm Bull* 1997; **20**: 881-886
- 11 **Shimizu K**, Qi XR, Maitani Y, Yoshii M, Kawano K, Takayama K, Nagai T. Targeting of soybean-derived sterylglucoside liposomes to liver tumors in rat and mouse models. *Biol Pharm Bull* 1998; **21**: 741-746
- 12 **Shimizu K**, Maitani Y, Takayama K, Nagai T. Characterization of dipalmitoylphosphatidylcholine liposomes containing a soybean-derived sterylglucoside mixture by differential scanning calorimetry, Fourier transform infrared spectroscopy, and enzymatic assay. *J Pharm Sci* 1996; **85**: 741-744
- 13 **Maynard JE**. Hepatitis B: global importance and need for control. *Vaccine* 1990; **8**(Supp1): S18-20
- 14 **Hoofnagle JH**. Chronic hepatitis B. *New Engl J Med* 1990; **323**: 337-339
- 15 **Dusheiko GM**. Treatment and prevention of chronic viral hepatitis. *Pharmacol Ther* 1995; **65**: 47-73
- 16 **Goodarzi G**, Gross SC, Tewari A, Watabe K. Antisense oligodeoxyribonucleotides inhibit the expression of the gene for hepatitis B virus surface antigen. *J Gen Virol* 1990; **71**(Pt 12): 3021-3025
- 17 **Wu GY**, Wu CH. Specific inhibition of hepatitis B viral gene expression *in vitro* by targeted antisense oligonucleotides. *J Biol Chem* 1992; **267**: 12436-12439
- 18 **Offensperger WB**, Offensperger S, Walter E, Teubner K, Igloi G, Blum HE, Gerok W. *In vivo* inhibition of duck hepatitis B virus replication and gene expression by phosphorothioate modified antisense oligodeoxynucleotides. *EMBO J* 1993; **12**: 1257-1262
- 19 **Soni PN**, Brown D, Saffie R, Savage K, Moore D, Gregoriadis G, Dusheiko GM. Biodistribution, stability, and antiviral efficacy of liposome-entrapped phosphorothioate antisense oligodeoxynucleotides in ducks for the treatment of chronic duck hepatitis B virus infection. *Hepatology* 1998; **28**: 1402-1410
- 20 **Wagner RW**. Gene inhibition using antisense oligodeoxynucleotides. *Nature* 1994; **372**: 333-335
- 21 **Gao X**, Huang L. A novel cationic liposome reagent for efficient transfection of mammalian cells. *Biochem Biophys Res Commun* 1991; **179**: 280-285
- 22 **Ross PC**, Hui SW. Lipoplex size is a major determinant of *in vitro* lipofection efficiency. *Gene Ther* 1999; **6**: 651-659
- 23 **Li S**, Huang L. *In vivo* gene transfer via intravenous administration of cationic lipid-protamine-DNA (LPD) complexes. *Gene Ther* 1997; **4**: 891-900
- 24 **Allen TM**, Austin GA, Chonn A, Lin L, Lee KC. Uptake of liposomes by cultured mouse bone marrow macrophages: influence of liposome composition and size. *Biochim Biophys Acta* 1991; **1061**: 56-64
- 25 **Huang SK**, Martin FJ, Friend DS, Papahadjopoulos D. Mechanism of stealth liposome accumulation in some pathological tissues, In: D. Lasic, F. Martin (Eds.), *Stealth Liposomes*, Boca Raton CRC Press FL 1995: 119-125

Science Editor Wang XL and Guo SY Language Editor Elsevier HK

Effect of Danshao Huaxian capsule on expression of matrix metalloproteinase-1 and tissue inhibitor of metalloproteinase-1 in fibrotic liver of rats

Qin Yang, Ru-Jia Xie, Xiao-Xia Geng, Xin-Hua Luo, Bing Han, Ming-Liang Cheng

Qin Yang, Ru-Jia Xie, Bing Han, Department of Pathophysiology, Guiyang Medical College, Guiyang 550004, Guizhou Province, China

Xiao-Xia Geng, Ming-Liang Cheng, Department of Infectious Diseases, Affiliated Hospital of Guiyang Medical College, Guiyang 550004, Guizhou Province, China

Xin-Hua Luo, Department of Infectious Diseases, People's Hospital of Guizhou Province, Guiyang 550004, Guizhou Province, China
Supported by the Foundation of Traditional Chinese Medicine Modernization Project of Guizhou Province, No. 200409

Co-first-authors: Qin Yang and Ming-Liang Cheng

Co-correspondents: Qin Yang

Correspondence to: Dr. Ming-Liang Cheng, Department of Infectious Diseases, Affiliated Hospital of Guiyang Medical College, 4 Beijing road, Guiyang 550004, Guizhou Province, China. chengml@21.cn.com

Telephone: +86-851-6855119-3193

Received: 2004-10-30 Accepted: 2004-11-19

CONCLUSION: DSHX enhances the expression of MMP-1 but decreases that of TIMP-1 in liver tissues of CCl₄-induced hepatic fibrotic rats, which may result in its elevated activity that contributes to fighting against hepatic fibrosis.

© 2005 The WJG Press and Elsevier Inc. All rights reserved.

Key words: Danshao Huaxian capsule; Hepatic fibrosis; MMP-1; TIMP-1; Collagen

Yang Q, Xie RJ, Geng XX, Luo XH, Han B, Cheng ML. Effect of Danshao Huaxian capsule on expression of matrix metalloproteinase-1 and tissue inhibitor of metalloproteinase-1 in fibrotic liver of rats. *World J Gastroenterol* 2005; 11 (32): 4953-4956

<http://www.wjgnet.com/1007-9327/11/4953.asp>

Abstract

AIM: To investigate the effects of Danshao Huaxian (DSHX) capsules, a preparation of traditional Chinese medicine, on the expression of matrix metalloproteinase-1 (MMP-1), and tissue inhibitor of metalloproteinase-1 (TIMP-1) in the fibrous livers of rats.

METHODS: Eighty male Wistar rats were randomly divided into normal control group (group A), CCl₄-induced hepatic fibrosis group (group B), non-DSHX-treated group (group C), low dose-treated group (group D), and high dose-treated group (group E). Fibrous liver models in rats were induced by subcutaneous injection of CCl₄, oral administration of alcohol and high-lipid/low-protein diet for 8 wk. After the models were established, the rats in groups D and E were orally given a low dose (0.5 g/kg) and a high dose (1.0 g/kg) of DSHX daily for 8 wk, respectively. Then, the liver indexes, serum hyaluronic acid (HA) and alanine aminotransferase (ALT) were examined. The degree of hepatic fibrosis was evaluated by optical microscopy. Hydroxyproline (Hyp) in the urine was determined, and the expression of MMP-1 and TIMP-1 was detected by immunohistochemical techniques.

RESULTS: In groups D and E, the liver indexes, levels of serum HA and ALT reduced and development of hepatic fibrosis weakened significantly. The urinary Hyp and expression of MMP-1 in the liver tissues elevated, but the expression of TIMP-1 decreased obviously, as compared to groups B and C.

INTRODUCTION

Hepatic fibrosis is a common result of any chronic injury to the liver. It is characterized by excessive deposition of extracellular matrix (ECM), especially collagens I and III^[1-4]. Matrix metalloproteinase (MMP), is a member of zinc-dependent endopeptidase family, that degrades various components of ECM. In liver tissues, 8 members of MMP have been discovered^[5]. One of them is matrix metalloproteinase-1 (MMP-1) with its specific inhibitor, tissue inhibitor of metalloproteinase-1 (TIMP-1) closely correlated with liver fibrosis due to the accumulation and degradation balance of collagens I and III^[6-8]. In this study, we examined the therapeutic effect of Danshao Huaxian (DSHX) capsule on CCl₄-induced hepatic fibrosis in rats and explored its mechanism.

MATERIALS AND METHODS

Experimental animals

Eighty male Wistar rats weighing 180-220 g were provided by the Experimental Animal Center of Guiyang Medical College. The rats were randomly divided into five groups: normal control group (group A), CCl₄-induced hepatic fibrosis group (group B), non-DSHX-treated group (group C), low dose DSHX-treated group (group D), and high dose DSHX-treated group (group E). Each group consisted of 16 rats.

Chemicals and reagents

DSHX capsule containing five Chinese herbal medicines (Tetrandrine, *Radix Salviae Miltiorrhizae*, *Radix Paeoniae Rubra*,

Astragalus Membranaceus and Ginkgo leaf) was supplied by Guiyang Pharmaceutical Company. Carbon tetrachloride (CCl₄) was obtained from Chongqing Inorganic Chemistry Factory and cholesterol was from Beijing Chemical Reagent Company. Immunohistochemical kits for MMP-1 and TIMP-1, hyaluronic acid (HA) and hydroxyproline (Hyp) kits were purchased from Wuhan Boster Biological Engineering Ltd Co., Beijing Northern Biological Technical Research Institute and Nanjing Jiancheng Biological Engineering Research Institute, respectively.

Instruments

Automatic biochemical analytic instrument (Hitachi 7170A) and Olympus BX41 Microimage Collecting System were employed in the study.

CCl₄-induced liver fibrosis and sample collection

Liver fibrosis was induced in four groups by a complex method^[9]. The rats in groups B, C, D, and E received subcutaneous injections of 40% CCl₄ solution (a mixture of pure CCl₄ and peanut oil) and 0.3 mL/100 g, twice a week for 8 wk (the first dose was pure CCl₄ 0.5 mL/100 g). Meanwhile, they were fed with high-lipid/low-protein diet (79.5% corn farina, 20% fat, and 0.5% cholesterol) daily, and orally supplemented with 30% alcohol every other day. Rats in group A were fed only with normal diet. After liver fibrosis was produced, the rats in group B (by this time, only 12 rats survived) were killed and their blood and livers were collected. The wet livers were weighed and liver samples were fixed in 40 g/L formaldehyde. The serum was centrifuged at 1 500 r/min for 5 min and stored at -80 °C. DSHX capsules were then given to the rats in group D (0.5 g/kg, p.o., daily) and group E (1.0 g/kg, p.o., daily) for 8 wk. The rats in group C were given normal saline instead of DSHX. At the end of the experiment (by this time, the rat survivors in group A and groups C-E were 16, 10, 10, and 10, respectively), all the rats were killed, the liver and serum samples were handled in the same way as mentioned above.

Liver index calculation

Liver index was calculated according to the formula (liver weight/body weight)×100%.

Measurements of serum HA and ALT

Concentrations of serum HA and alanine aminotransferase (ALT) were measured by radioimmunoassay or automatic biochemical analytic instrument (Hitachi 7170A).

Histopathological examination

An equal portion of liver from each rat (1 cm×1 cm×0.5 cm) was fixed in 40 g/L formaldehyde for 48 h, embedded in paraffin, and sectioned with a microtome. The 5-μm-thick sections were stained with hematoxylin and eosin for general histopathology examination. Van-Gieson staining was performed for evaluating the severity of liver fibrosis. Liver fibrosis was classified as previously described^[10].

Urinary Hyp determination

The 24 h urine of the rats in each experimental group was collected for determination of urinary Hyp in the 8th wk

and at the end of the experiment, respectively.

Expression of MMP-1 and TIMP-1

The expressions of MMP-1 and TIMP-1 were detected by the streptavidin-biotin complex (SABC) immunohistochemical technique strictly following the directions offered. PBS was used as the negative control to produce MMP-1 and TIMP-1 polyclonal rabbit IgG. Finally, the number of positive cells per field of vision at 400× magnification was counted.

Statistical analysis

Quantitative data were expressed as mean±SD and subjected to one-way analysis of variance, followed by *t* test for multiple comparisons. Ordinal data were analyzed by Radit analysis. *P*<0.05 was considered statistically significant.

RESULTS

Effect of DSHX on liver index, concentration of serum HA and ALT in rats

As shown in Table 1, compared to group A, the liver index and concentrations of serum HA and ALT of rats in group B and group C increased greatly (*P*<0.05). After 8 wk of treatment with DSHX, the liver index and concentration of serum HA and ALT in groups D and E, reduced obviously compared to those in groups B and C (*P*<0.05).

Table 1 Liver index, serum HA, and ALT in rats of each group (mean±SD)

Group	<i>n</i>	Liver index (relative liver weight)	HA (ng/mL)	ALT (U/L)
A	16	0.0249±0.0027	192.52±41.97	32.40±2.30
B	12	0.0423±0.0044 ^b	316.17±78.48 ^a	174.50±6.02 ^b
C	10	0.0295±0.0019 ^{b,d}	300.86±72.73 ^a	104.75±6.54 ^{b,d}
D	10	0.0268±0.0028 ^{d,e}	224.92±36.62 ^{c,e}	96.13±4.94 ^{d,e}
E	10	0.0267±0.0017 ^{d,f}	200.78±31.71 ^{c,e}	93.13±5.79 ^{d,f}

^a*P*<0.05, ^b*P*<0.01 vs normal control group; ^c*P*<0.05, ^d*P*<0.01 vs hepatic fibrosis group; ^e*P*<0.05, ^f*P*<0.01 vs non-DSHX-treated group.

Effect of DSHX on degree of hepatic fibrosis

After HE and V-G staining, hepatocytes of the normal control rats were arrayed radially along the central vein and there were no collagen fibers. The lobular structure of the liver was destroyed and the hepatic cords were disordered in the rats of group B. Also, the fibrous connective tissues containing numerous inflammatory cells regenerated in the portal area. Meanwhile, collagen fibers expanded into the hepatic parenchyma and there appeared fibrous septa surrounding and separating the normal lobules. The degree of hepatic fibrosis in this group was significantly serious compared to that in group A (*P*<0.01). The hepatic fibrosis in group C was alleviated and the fibrous septa were thinner than those in group B. Except for the obvious expansion of collagen fibers, pseudo lobules were also found in some severe samples from group C. The lobular structure in groups D and E was ameliorated significantly, and regeneration of fibrous connective tissues and septa reduced as compared to that in groups B and C. The degree of the hepatic fibrosis in each group is shown in Table 2.

Table 2 Degree of hepatic fibrosis in rats of each group

Group	n	Degree of hepatic fibrosis					Average
		0	I	II	III	IV	
A	16	16	0	0	0	0	0
B	12	0	0	0	1	7	4
C	10	0	1	4	3	2	0
D	10	1	3	5	1	0	0
E	10	1	6	2	1	0	0

^a*P*<0.05 and ^b*P*<0.01 vs non-DSHX-treated group; ^d*P*<0.01 vs normal control group; ^f*P*<0.01 vs hepatic fibrosis group.

Effect of DSHX on urinary excretion of Hyp

Urinary Hyp is an useful index to evaluate the degradation of hepatic collagen. Compared to group A, the Hyp excretion increased in groups B and C. After being treated with DSHX, Hyp in the urine of groups D and E was more than that in groups B and C, suggesting that DSHX capsule could facilitate degradation of collagen (Table 3).

Table 3 Urinary excretion of Hyp (µg/24 h) in rats of each group (mean±SD)

Group	n	Urinary excretion of Hyp
A	16	47.80±5.76
B	12	62.00±6.40 ^b
C	10	182.44±30.83 ^b
D	10	242.76±49.76 ^d
E	10	541.09±73.39 ^{d,f}

^b*P*<0.01 vs normal control group; ^d*P*<0.01 vs hepatic fibrosis group; ^f*P*<0.01 vs non-DSHX-treated group.

Effect of DSHX on expression of MMP-1 and TIMP-1

Immunohistochemical (SABC) study showed that there were only a small number of cells with positive light yellow staining of MMP-1 and TIMP-1 in the normal livers. MMP-1 was observed only in some hepatocytes and stromal cells, whereas TIMP-1 was mainly distributed in vascular endothelial cells and some fibroblasts in the portal area. In the livers of groups B, C, D, and E, the cells with MMP-1 and TIMP-1 positive staining were detected in the fibrous septa and stained dark yellow. The expression of MMP-1 and TIMP-1 in group B was higher than that in group A (*P*<0.01). Compared to groups B and C, the expression of MMP-1 in groups D and E increased significantly, whereas that of TIMP-1 decreased sharply. The results are shown in Table 4.

Table 4 Percentage of expression of MMP-1 and TIMP-1 in each group (mean±SD)

Group	n	MMP-1 (%)	TIMP-1 (%)
A	16	0.595±0.87	1.08±0.68
B	12	5.956±1.85 ^f	9.04±1.60 ^f
C	10	5.104±2.20 ^f	6.46±1.77 ^{b,f}
D	10	8.271±3.29 ^{a,d}	5.07±0.69 ^{b,c}
E	10	8.518±1.88 ^{a,d}	4.32±0.63 ^{b,d}

^a*P*<0.05 and ^b*P*<0.01 vs the hepatic fibrosis group; ^c*P*<0.05 and ^d*P*<0.01 vs non-DSHX-treated group; ^f*P*<0.01 vs normal control group.

DISCUSSION

DSHX capsule is a mixed preparation, composed of five traditional Chinese herbal medicines. We previously reported that DSHX is effective in prevention of hepatic fibrosis^[11]. In this study, we found that after DSHX treatment of rats with liver fibrosis for 8 wk, the relative liver weight and concentration of serum HA and ALT significantly reduced and liver fibrosis was alleviated, suggesting that DSHX possesses a therapeutic effect on CCl₄-induced hepatic fibrosis in rats by attenuating liver inflammation, preventing necrosis of hepatocytes and promoting their generation.

Hepatic fibrosis is a common consequence of enhanced ECM synthesis and weakened breakdown of proteins in the connective tissue, which lead to increased deposition of ECM in the extracellular matrix. The main component of ECM in normal liver is collagen, which is divided into types I, III-VI. Except for these collagen fibers, there are many other non-collagen components, including fibronectin, laminin, tenascin, and entactin^[12]. In fibrous liver, overaccumulated ECM is mainly interstitial collagens (types I and III). Activated hepatic stellate cells (HSCs) are the main source of ECM^[13-17] during liver fibrosis. HSCs in the space of Disse are in a quiescent form without fibrogenic activity, in part because they are in contact with a complex ECM composed of collagen type IV, laminin, and proteoglycans^[18]. When separated from these factors, they are activated into a pro-fibrogenic myofibroblastic phenotype. The expression of MMP-2 increases obviously after liver injury, which may result in excess degradation of type IV collagen and disorder of the microenvironment of the space of Disse, and then HSCs become activated. Meanwhile, Kupffer cells generate cytokines in response to liver injury, in which HSCs are activated and ECM is overexpressed. Normally, deposition of matrix components in liver is well controlled through constant remodeling by matrix-degrading enzymes. MMP is the most important among ECM-degrading enzymes. MMP, a zinc-dependent endopeptidase, can degrade specific components of ECM and its biological activity can be suppressed by TIMPs^[19]. MMPs are released by a variety of cells (macrophages, neutrophils, endothelial cells, etc.) and participate in such physiological and pathological processes as ECM degradation, tissue remodeling, angiogenesis, and tumor invasion^[20-22].

Till now, 26 members of the family of MMPs have been identified^[22] and with the following characteristics^[23-25]. (1) Structurally, there is a zinc atom at the active site; (2) they are often in an inactivated form, when produced; (3) their primary structures contain two highly conserved sequences, a N-terminal peptide domain and a catalytic domain; and (4) they can be inhibited by specific inhibitors known as TIMPs. The activities of MMPs are regulated at the transcriptional level, through zymogen activation and suppression by a family of inhibitory proteins, TIMPs. Four members of the TIMP family have been identified so far, including TIMPs 1-4, which are named in the order of their discovery. Their sequences possess a highly conserved secondary structure interacting with proteins via six conserved disulfide bonds. It seems that there are two domains in the TIMP molecule, a N-terminal domain that is endowed with inhibition of metalloproteinase and a C-terminal domain

that may be important in protein location or combination with progelatinases^[26]. TIMPs act widely and their most important action is to inhibit the activity of MMPs. TIMPs can interact with MMPs to inhibit their activities at 1:1 stoichiometry^[27-29]. MMP-1, a member of the MMP family that specifically degrades native collagen types III and I, plays an important role in the accumulation and degradation balance of ECM. The level of MMP-1 increases transiently in the early stage of liver fibrosis, but becomes undetectable in the stage of cirrhosis^[30]. In contrast, the level of TIMP-1, a specific tissue inhibitor of MMP-1, elevates consistently in the fibrosis process and reaches its peak in the stage of cirrhosis. Upregulation of TIMP-1 and downregulation of MMP-1 result in the inhibition of degradation of collagen types I and III, which leads to overexpression and deposition of ECM in the extracellular matrix.

In addition to inhibiting the degradation of matrix, TIMP-1 plays a significant role in regulation of the apoptosis of such cells such as B lymphocytes, breast epithelial cells and HSCs. TIMP-1 inhibits the apoptosis of HSCs, indicating another possible mechanism whereby it is implicated in the pathogenesis of liver fibrosis. In this study, we found that MMP-1 in the two groups treated with DSHX was overexpressed, whereas the expression of TIMP-1 reduced significantly. We conclude that DSHX can reverse the process of liver fibrosis by upregulating the gene expression and generation of MMP-1 and downregulating the TIMP-1 expression. These results may provide a therapeutic strategy to combat hepatic fibrosis by targeting MMP-1 and TIMP-1.

REFERENCES

- Iredale JP, Benyon RC, Pickering J, McCullen M, Northrop M, Pawley S, Hovell C, Arthur MJ. Mechanisms of spontaneous resolution of rat liver fibrosis. Hepatic stellate cell apoptosis and reduced hepatic expression of metalloproteinase inhibitors. *J Clin Invest* 1998; **102**: 538-549
- Yang CQ, Wang JY, Guo JS, Liu JJ, Zhang C. Effects of the recombinant plasmid of rat interstitial collagenase on experimental liver fibrosis. *Zhonghua Xiaohua Zazhi* 2000; **20**: 297-300
- Yang CQ, Hu GL, Tan DM, Zhang Z. Effects of matrix metalloproteinase-1 and antisense tissue inhibitor of metalloproteinase-1 recombinant plasmid on rat liver fibrosis. *Zhonghua Chuanranbing Zazhi* 2000; **18**: 29-32
- Yang CQ, Hu GL, Tan DM, Zhang Z. Relativity of expression of MMP-1, TIMP-1 and variability of type I, III collagen during experimental liver fibrosis. *Linchuang Gandanbing Zazhi* 2000; **16**: 222-224
- Huang YQ, Gao Y, Chen ZH, Wang Y, Fang SG, Yang JZ, Li CL. Relationship of imbalanced expression of interstitial collagenase and its inhibitors, metalloproteinase-1 gene, to liver fibrosis. *Diyi Junyi Daxue Xuebao* 1999; **19**: 208-210
- Zhang ZA, Shi SX, Lin JG, Huang YC. The expression of MMP-1 and TIMP-1 mRNA in patients with viral hepatitis gravis. *Linchuang Neike Zazhi* 2002; **19**: 258-260
- Gomez DE, De Lorenzo MS, Alonso DF, Andrade ZA. Expression of metalloproteinases (MMP-1, MMP-2, and MMP-9) and their inhibitors (TIMP-1 and TIMP-2) in schistosomal portal fibrosis. *Am J Trop Med Hyg* 1999; **61**: 9-13
- Meng EH, Zhao JM, Wang SS, Liu WX, Liu P, Zhou GD, Zhang TH. Expression of matrix metalloproteinases in liver tissues with nonalcoholic steatohepatitis. *Shijie Huaren Xiaohua Zazhi* 2002; **10**: 1257-1260
- Li CX, Li L, Lou J, Yang WX, Lei TW, Li YH, Liu J, Cheng ML, Huang LH. The protective effects of traditional Chinese medicine prescription, han-dan-gan-le, on CCl4-induced liver fibrosis in rats. *Am J Chin Med* 1998; **26**: 325-332
- Cheng ML, Yang CQ. The basic study and clinical research on hepatic fibrosis. *Beijing Renmin Weisheng Chubanshe* 2002: 269-270
- Cheng ML, Lu YY, Wu J, Luo TY, Ding YS. Clinical Study on Reversing Hepatic Fibrosis with Handan Ganle Capsule. *Chinese J Integrated Traditional Western Med* 2001; **7**: 16-18
- Kossakowska AE, Edwards DR, Lee SS, Urbanski LS, Stabber AL, Zhang CL, Phillips BW, Zhang Y, Urbanski SJ. Altered balance between matrix metalloproteinases and their inhibitors in experimental biliary fibrosis. *Am J Pathol* 1998; **153**: 1895-1902
- Bennett RG, Kharbada KK, Tuma DJ. Inhibition of markers of hepatic stellate cell activation by the hormone relaxin. *Biochem Pharmacol* 2003; **66**: 867-874
- Lemos QT, Magalhaes-Santos IF, Andrade ZA. Immunological basis of septal fibrosis of the liver in Capillaria hepatica-infected rats. *Braz J Med Biol Res* 2003; **36**: 1201-1207
- Benyon RC, Arthur MJ. Extracellular matrix degradation and the role of hepatic stellate cells. *Semin Liver Dis* 2001; **21**: 373-384
- Song LL, Luo HS, Yu BP. Effects of hepatocyte growth factor on fibrosis and hepatic expression of MMP-1 and TIMP-1. *Shijie Huaren Xiaohua Zazhi* 2003; **11**: 209-213
- Xu JW, Gong J, Feng XL, Chang XM, Luo JY, Dong L, Jia K, Xu GP. Effects of estradiol on type I, III collagens and TGF β 1 in hepatic fibrosis in rats. *Shijie Huaren Xiaohua Zazhi* 2003; **11**: 1185-1188
- Wu YJ, Zhai WR, Zhuang L, Zhang YE, Zhu HG. Expression of matrix metalloproteinase-2 and its tissue inhibitor in rat liver fibrosis model. *Shanghai Yike Daxue Xuebao* 1999; **26**: 261-264
- Li W, Cao L, Chen Z, Li W, Du Q, Chen G. Study on the effects of FCu-IUD and FICu-IUD on matrix metalloproteinases in human uterine flushing and endometrium. *J Huazhong Univ Sci Technolog Med Sci* 2002; **22**: 9-11
- Zhang J, Cao YJ, Liu WM, Zhao BS, Zeng GQ, Duan EK. Expression of matrix metalloproteinase-28 in human normal cytotrophoblast cells and a choriocarcinoma cell line, JEG-3. *Chinese Sci Bulletin* 2002; **47**: 732-736
- Lichtinghagen R, Bahr MJ, Wehmeier M, Michels D, Haberkorn CL, Arndt B, Flemming P, Manns MP, Boeker KH. Expression and coordinated regulation of matrix metalloproteinases in chronic hepatitis C and hepatitis C virus-induced liver cirrhosis. *Clin Sci* 2003; **105**: 373-382
- Zhao H, Cai G, Du J, Xia Z, Wang L, Zhu T. Expression of Matrix Metalloproteinase-9 mRNA in osteoporotic bone tissue. *J Tongji Med Univ* 1997; **17**: 28-31
- Li KQ, Li CH. Matrix metalloproteinase and their inhibitors: molecular aspects of their roles in the tumor metastasis. *Chinese J Cancer Res* 2000; **12**: 239-243
- Bai JT, Lu FX. Matrix metalloproteinases in relation to cardiovascular diseases. *Xinxueguanbingxue Jinzhan* 2003; **24**: 43-47
- Yao GY, Yang MT. Matrix metalloproteinases and breast cancer. *Ai zheng* 2002; **21**: 1029-1034
- Zhu F, Liu XG, Liang NC. The relationship of matrix metalloproteinases and its tissue inhibitors to tumor invasion and metastasis. *Guowai Yixue Linchuang Shengwu Huaxue Yu Jianyanxue Fence* 2001; **22**: 229-231
- Zhao YD, Liu NF, He QL, Xu GM. Expression of MMP-3 mRNA in hypertrophic scar fibroblasts and MMP-3 gene transfection. *J Med Coll PLA* 1998; **13**: 244-248
- Li L, Zhang S, Lin H, Lin JY. Relationship of expression unbalance of matrix metalloproteinase and tissue inhibitor of metalloproteinase to invasiveness and metastasis in gastric carcinomas. *Aizheng* 2002; **21**: 305-310
- Lv J, Hu MJ, Cai WM. The expression of MMP-1 and TIMP-1 in peripheral mononucleocytes of patients with chronic hepatitis. *Linchuang Gandanbing Zazhi* 2002; **18**: 31-32
- Arthur MJ. Fibrogenesis II. Metalloproteinases and their inhibitors in liver fibrosis. *Am J Physiol Gastrointest Liver Physiol* 2000; **279**: G245-G249

Effects of dietary supplementation with vitamin E and selenium on rat hepatic stellate cell apoptosis

Xiu-Hua Shen, Wu-Feng Cheng, Xuan-Hai Li, Jian-Qin Sun, Feng Li, Ling Ma, Liang-Min Xie

Xiu-Hua Shen, Wu-Feng Cheng, Xuan-Hai Li, Feng Li, Ling Ma, Department of Nutrition, Shanghai Second Medical University, Shanghai 200025, China

Liang-Min Xie, Department of Nutrition, Shanghai East Hospital, Shanghai 200120, China

Jian-Qin Sun, Department of Nutrition, Huadong Hospital, Shanghai 200040, China

Supported by the Science Research Foundation of Ministry of Public Health of China, No. 98-2-280

Co-correspondent: Liang-Min Xie

Correspondence to: Dr. Xiu-Hua Shen, Department of Nutrition, Shanghai Second Medical University, 280 South Chongqin Road, Shanghai 200025, China. srachel@sina.com

Telephone: +86-210-63846590-776507

Received: 2004-08-18 Accepted: 2004-12-03

Abstract

AIM: To evaluate the effects of dietary supplementation with vitamin E and selenium on proliferation and apoptosis of hepatic stellate cells (HSCs), in acute liver injury induced by CCl₄, and to explore their role in the recovery from hepatic fibrosis phase.

METHODS: An acute liver damage model of rats was established by intraperitoneal injection of carbon tetrachloride (0.3 mL/100 g body weight) twice a week, then the rats were killed at 6, 24, 48, and 72 h after the first and third injection, respectively. A liver fibrosis model was established by the same injection for 8 wk. Then three rats were killed at 3, 7, 14, and 28 d after the last injection, respectively. The rats from the intervention group were fed with chow supplemented with vitamin E (250 mg/kg) and selenium (0.2 mg/kg), and the rats in the normal control group and pathological group were given standard chow. Livers were harvested and stained with hematoxylin and eosin, Sirius red. Activated HSCs were determined by α -smooth muscle actin immunohistochemistry staining. Apoptotic HSCs were determined by dual staining with the terminal deoxynucleotidyl transferase UTP nick end labeling (TUNEL) and α -smooth muscle actin immunohistochemistry. Serum alanine aminotransferase and aspartate aminotransferase were also analyzed.

RESULTS: In the acute liver damage model, the degree of liver injury was more serious in the pathological group than in the intervention group. At each time point, the number of activated HSCs was less in the intervention group than in the pathological group, while the number of apoptotic HSCs was more in the intervention group than in the pathological group. In the liver fibrosis model, the degree of liver fibrosis was more serious in the

pathological group than in the intervention group. At each time point, the number of activated HSCs was less in the intervention group than in the pathological group, and the number of apoptotic HSCs was more in the intervention group than in the pathological group.

CONCLUSION: Vitamin E and selenium supplementation at the given level can inhibit CCl₄-induced activation and proliferation of HSCs and promote the apoptosis of activated HSCs in acute damage phase. Vitamin E and selenium can also effectively decrease the degree of hepatic fibrosis and promote the recovery process.

© 2005 The WJG Press and Elsevier Inc. All rights reserved.

Key words: Vitamin E; Selenium; Hepatic stellate cell; Apoptosis

Shen XH, Cheng WF, Li XH, Sun JQ, Li F, Ma L, Xie LM. Effects of dietary supplementation with vitamin E and selenium on rat hepatic stellate cell apoptosis. *World J Gastroenterol* 2005; 11(32): 4957-4961

<http://www.wjgnet.com/1007-9327/11/4957.asp>

INTRODUCTION

Liver fibrosis is characterized by increased deposition of extracellular matrix, and its mechanism is extremely complex. The common understanding about liver fibrosis is that the activation and proliferation of HSCs, a major source of extracellular matrix, play a key role in liver fibrogenesis^[1,2]. Activated HSCs express α -SMA and are the major source of collagens and other matrix proteins which result in fibrosis. Resolution of liver fibrosis is associated with a net loss of activated HSCs mediated by apoptosis. Therefore, promoting HSC apoptosis may be a viable method to facilitate matrix degradation in fibrotic liver^[3,4].

Studies have shown that oxidative stress is one of the mechanisms in the development of liver fibrosis^[5-8], it is worth investigating the therapeutic role of antioxidative nutrients in hepatic fibrosis. A wealth of evidence indicates that antioxidative nutrients such as vitamin E and selenium can prevent liver fibrosis induced by carbon tetrachloride (CCl₄)^[9,10]. The major mechanism by which CCl₄ induces rat liver fibrosis is that CCl₃• results in a series of lipid peroxidation reactions. The activation of HSCs is enhanced with the increasing CCl₄ concentration^[11]. The results from our previous study confirmed, that dietary supplementation with vitamin E and selenium can protect hepatocytes and prevent liver fibrosis induced by CCl₄ in rat model^[12]. However, the mechanism of the effects is still not clear.

Therefore, rat acute liver injury and hepatic fibrosis models were established by intraperitoneal injection of CCl₄. Dietary supplementation with proper doses of vitamin E and selenium was given to rats in order to determine whether the antioxidative nutrients had an effect on the proliferation and apoptosis of activated HSCs during liver injury or recovery from liver fibrosis *in vivo*.

MATERIALS AND METHODS

Animal model of acute liver damage and liver fibrosis

One hundred and fifty-six male Sprague Dawley rats (Shanghai Xipuer-bikai Company) weighing 250-300 g were randomly divided into normal control group, pathological group, and intervention group, 52 rats each group. The rats were fed with chow supplemented with vitamin E (250 mg/kg) and selenium (0.2 mg/kg diet) in the intervention group, and the rats in the other two groups were given standard chow. After 2 wk, the rats were injected with saline in the normal control group, and those in the other two groups were intraperitoneally injected with 0.3 mL/100 g body weight sterile CCl₄ at 1:1 with olive oil twice a week. In the acute liver damage model, five rats were killed at 6, 24, 48, and 72 h after the first and third injection. In the liver fibrosis model, the same dose of CCl₄ was given to rats for 6 wk, then the dose of CCl₄ was reduced to 0.15 mL/100 g body weight for another 2 wk. Starting from the 8th wk, three rats were killed at 3, 7, 14, and 28 d after the last injection. Livers and serum were collected, one lobe from each liver was fixed in buffered formalin for histological observation. Serum alanine aminotransferase and aspartate aminotransferase were analyzed.

Pathological observation of liver

Liver sections were stained with hematoxylin and eosin, Sirius red. Pathological changes of the liver were observed. Five low power fields (×4) of each slide were randomly selected. The IMS color image integrate system was used to get the total area with Sirius red positive changes of these 5 views. The mean of area was calculated at each time point.

Measurement of serum alanine aminotransferase and aspartate aminotransferase during acute liver damage phase

Serum was collected at each time point in the model of acute liver damage. Alanine aminotransferase and aspartate aminotransferase were tested by Beckman automatic clinic biochemistry system.

Quantification of activated HSCs during acute liver damage and recovery from fibrosis

Activation of HSCs was associated with expression of

α-smooth muscle actin (α-SMA). Immunostaining for α-SMA was used to detect and quantify activated HSCs in each specimen of the liver. The liver section of each rat at each time point was immunostained with horseradish peroxidase-conjugated secondary antibody (monoclonal anti α-SMA, Envision™, DAKO Company) for its expression of α-SMA, and identified by DAB(brown). The number of α-SMA positive cells of each liver slide was counted in 30 randomly selected high power fields (×40) by two observers, one of whom was blinded. If the difference in results between the two observers was higher than 10%, the slides were recounted.

Determination of activated HSCs undergoing apoptosis by double stain with TUNEL and α-SMA

The liver section of each rat was treated with 0.3% H₂O₂, 180 μg/mL proteinase K, then fragmented DNA in apoptotic cells was detected by TUNEL technique. The Boehringer TUNEL staining kit(German) was used following the manufacturer's instructions. TUNEL positive nuclei were identified by NBT/BCIP (violet) and immunostaining for α-SMA with horseradish peroxidase-conjugated secondary antibody (brown). Cells expressed both in TUNEL (with violet nuclei) and in immunostaining for α-SMA (with brown cell plasma) were considered as apoptotic HSCs. Each slide was then analyzed by two researchers as described above.

Statistical analysis

The data were expressed as mean±SD and analyzed by ANOVA. *P*<0.05 was considered statistically significant. All analyses were conducted by SPSS 10.0 statistical package. All the charts were drawn by excel 2000.

RESULTS

Histology of acute liver damage

After injection of CCl₄, livers of the rats were damaged and swollen and became yellow, perivenular ballooning degeneration was present, the pathological changes increased with the increase of time. At each time point, the lesion was more serious in the pathological group than in the intervention group.

Serum alanine aminotransferase and aspartate aminotransferase levels during acute liver damage

Because there was no significant difference at different time points after the first or third injection of CCl₄, the data were regrouped into one group for statistical analysis. The lesion in the pathological group was more serious than that in the intervention group, and became worse with the increase of time (Table 1).

Table 1 Comparison between ALT and AST (mean±SD)

	ALT (IU/L)		AST (IU/L)	
	After the first injection	After the third injection	After the first injection	After the third injection
Intervention group (n = 20)	289.6±80.7 ^{a,b}	446.4±136.5 ^b	63±16.9 ^{a,b}	219.9±98.2 ^a
Pathological group (n = 20)	396.5±134.4 ^b	781.6±295.7	85.3±57.9 ^b	362.5±129.6
Normal control group (n = 20)	256.4±71.6	194.1±69.7	53.9±20.1	58.5±25.0

^a*P*<0.05 vs pathological group; ^b*P*<0.01 vs third injection.

Histology of liver fibrosis recovery

Three days after the last injection of CCl₄, the livers of rats were swollen, yellow, hard and had hepatocyte fatty degeneration with many fibrotic septae. The changes were more serious in the pathological group than in the intervention group. After 28 d of the last injection, the degree and areas of hepatocyte fatty degeneration decreased, compared to those in the normal control group.

Quantification of collagen fiber during acute liver damage (Sirius red staining)

Also, because there was no significant difference at different time points after the first or third injection of CCl₄, the data were regrouped into one group for statistical analysis. Collagen fibers in the intervention group were significantly more than those in the pathological group after the first and third injection of CCl₄, but no significant difference was observed between the first and the third injection (Table 2).

Table 2 Quantitative analysis of collagen fibers during acute liver damage (Sirius red staining, mean±SD)

	After the first injection (pixel)	After the third injection (pixel)
Pathological group (n = 20)	2 686.3±1 109.4 ^b	1 843.5±706.7 ^a
Intervention group (n = 20)	6 351.3±524.2	5 992.0±2 637.2
Normal control group (n = 20)	2 785.5±294.1	2 978.5±214.8

^aP<0.05 vs intervention group; ^bP<0.01 vs intervention group.

Quantification analysis of collagen fibers during liver fibrosis recovery (Sirius red staining)

In the liver fibrosis recovery model, the amount of collagen

fibers 3, and 7 d after the last injection of CCl₄ was much more than that in the model of acute liver injury. The amount of collagen fibers decreased with the changes of time, but was still more than that in the normal control group on d 28. At each time point, the amount of collagen fibers in the pathological group was more than that in the intervention group (Table 2, Figure 1).

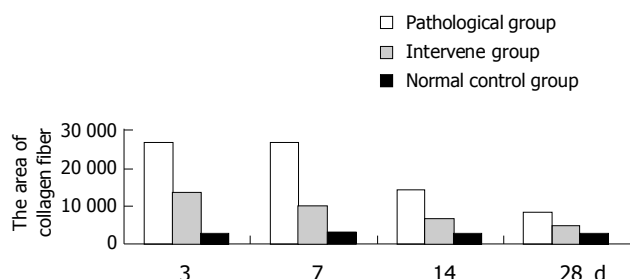


Figure 1 Area of collagen fiber at each time point during recovery of liver fibrosis.

Change of activated HSCs during acute liver damage

Twenty-four hours after the first injection of CCl₄, the number of activated HSCs in the pathological and intervention groups began to increase, and reached the peak after 72 h. The number of activated HSCs began to decrease, 6 h after the third injection. The number of activated HSCs in the intervention group was less than that in the pathological group and more than that in the normal control group (Figures 2A, B).

Change of activated HSCs during liver fibrosis recovery

In the pathological and intervention groups, the activated

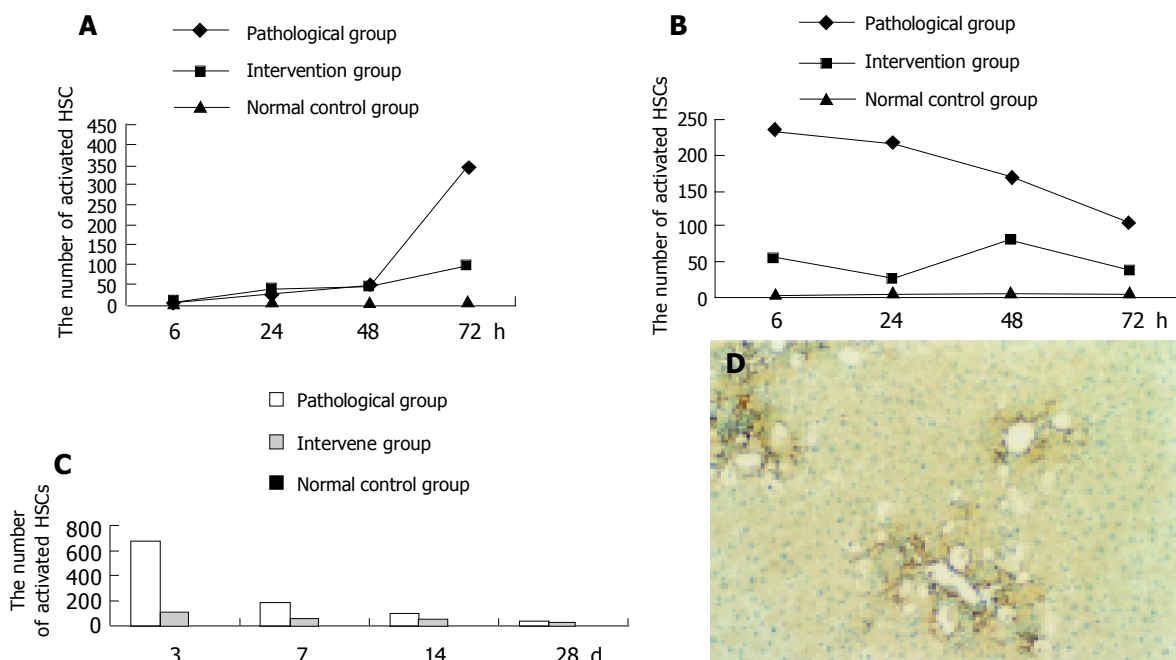


Figure 2 Change of activated HSCs after the first (A) and third (B) injection, during liver fibrosis recovery (C) and positive for α -SMA Immunohistochemistry

staining (D).

HSCs were clustered around the fibrotic septae. The number of activated HSCs decreased gradually 7 d after injection of CCl₄, and was still more than that in the normal control group 28 d after injection of CCl₄. At each time point, the number of activated HSCs in the intervention group was less than that in the pathological group (Figures 2C and D).

Apoptosis of activated HSCs during acute liver damage

Twenty-four hours after the first injection of CCl₄, the apoptotic HSCs began to increase gradually, and the number of apoptotic HSCs in the intervention group was more than that in the pathological group. As expected, 6, 24, 48 h after the first injection, the number of apoptotic HSCs in the intervention and pathological groups was less than that in the normal control group (Figure 3).

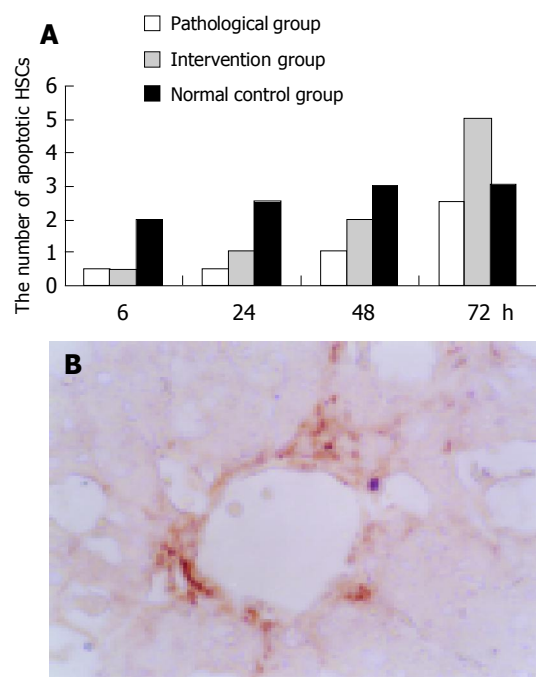


Figure 3 Apoptosis of activated HSCs after the first injection (A) and apoptotic HSCs positive for both TUNEL staining (violet) and α -SMA immunohistochemistry staining (brown) (B).

Apoptosis of activated HSCs during liver fibrosis recovery

The apoptotic HSCs decreased gradually in the pathological and intervention groups after injection of CCl₄, but was still more than that in the normal control group, 28 d after injection of CCl₄. The number of apoptotic HSCs in the intervention group was more than that in the pathological group at each time point during liver fibrosis recovery, and was much more in the intervention and pathological groups than in the normal control group (Figure 4).

DISCUSSION

Experiment design

The dosage of CCl₄, vitamin E, and selenium used in the study was selected as previously described^[12-14]. Tests were carried out at different time points during acute damage

and recovery, because it was reported that this is the best way to observe the continual changes of HSCs *in vivo*^[15].

Vitamin E and selenium protect hepatocytes and promote recovery from liver fibrosis

The results from histology and serum ALT and AST showed that vitamin E and selenium reduced liver damage during acute liver injury and had the effect of decreasing collagen fibers, thus preventing liver fibrosis. Hepatocyte damage or liver fibrosis as shown by many variables at each time point was different.

In the model of acute liver injury, although α -SMA immunostaining showed that the number of HSCs in the intervention group was less than that in the pathological group at each time point, Sirius red staining showed that the number of collagen fibers in the intervention group was more than that in the pathological and normal control groups, suggesting that vitamin E and selenium may promote the synthesis of collagen fibers. Since the synthesis of collagen also is a positive repairing response to hepatocyte injury, vitamin E and selenium can prevent liver damage during acute liver injury, not only by affecting HSCs but also by other ways. This needs to be confirmed by further studies.

Effect of vitamin E and selenium on proliferation and apoptosis of HSCs during acute liver damage

The number of activated HSCs in the intervention group was less than that in the pathological group and more than that in the normal control group during acute damage phase. Meanwhile, the number of apoptotic activated HSCs in the intervention group was more than that in the pathological group and less than that in the normal control group, suggesting that CCl₄ breaks the normal balance between activation and apoptosis of HSCs, resulting in more activation and lesser apoptosis. When the injury continues, more and more activated HSCs are generated thus producing more and more collagen fibers and leads to fibrosis. Vitamin E and selenium can inhibit the activation of HSCs and promote their apoptosis during acute damage phase, which helps to rebuild the balance between activation and apoptosis of HSCs, thus preventing liver fibrosis.

Effect of vitamin E and selenium on proliferation and apoptosis of HSCs during recovery from liver fibrosis

As expected, the number of apoptotic HSCs was more and that of activated HSCs was less than in the pathological

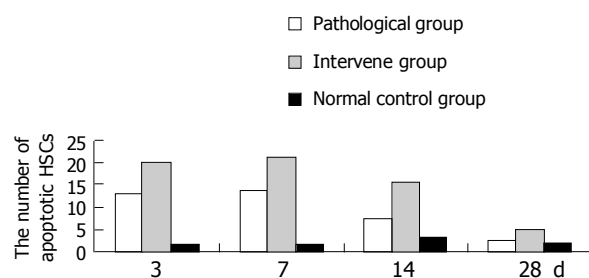


Figure 4 Number of apoptotic HSCs during recovery from liver fibrosis.

group, suggesting that vitamin E and selenium can promote apoptosis of HSCs during recovery from liver fibrosis. During this stage, both activated and apoptotic HSCs in the pathological and intervention groups were more than those in the normal control group.

Iredale *et al.*^[15], have examined an experimental model of fibrosis during progressive and recovery phase to determine whether activated HSCs underwent apoptosis during spontaneous resolution of fibrosis *in vivo*, which is consistent with our results in the pathological group, suggesting that HSCs play a central role in the development and resolution of liver fibrosis.

Furthermore, the data in our study demonstrate that it needs more than 28 d for the rats to recover from hepatic fibrosis.

Activation and proliferation of HSC are the key to the formation of hepatic fibrosis, and apoptosis of HSCs is the crux of the recovery of fibrosis. Therefore, the disease can be intervened by inhibiting the activation of HSCs and inducing apoptosis. Our data show that vitamin E and selenium supplementation may be one of the mechanisms underlying the recovery of fibrosis^[12]. Meanwhile, vitamin E and selenium may be an effective anti-fibrotic approach.

REFERENCES

- 1 **Friedman SL.** Seminars in medicine of the Beth Israel Hospital, Boston. The cellular basis of hepatic fibrosis. Mechanisms and treatment strategies. *N Engl J Med* 1993; **328**: 1828-1835
- 2 **Friedman SL.** Molecular regulation of hepatic fibrosis, an integrated cellular response to tissue injury. *J Biol Chem* 2000; **275**: 2247-2250
- 3 **Lee JI, Lee KS, Paik YH, Nyun Park Y, Han KH, Chon CY, Moon YM.** Apoptosis of hepatic stellate cells in carbon tetrachloride induced acute liver injury of the rat: analysis of isolated hepatic stellate cells. *J Hepatol* 2003; **39**: 960-966
- 4 **Wright MC, Issa R, Smart DE, Trim N, Murray GI, Primrose JN, Arthur MJ, Iredale JP, Mann DA.** Gliotoxin stimulates the apoptosis of human and rat hepatic stellate cells and enhances the resolution of liver fibrosis in rats. *Gastroenterology* 2001; **121**: 685-698
- 5 **Svegliati-Baroni G, Saccomanno S, Van Goor H, Jansen P, Benedetti A, Moshage H.** Involvement of reactive oxygen species and nitric oxide radicals in activation and proliferation of rat hepatic stellate cells. *Liver* 2001; **21**: 1-12
- 6 **Zhan Y, Wang Y, Wei L, Chen H.** Effects of vitamin E on the proliferation and collagen synthesis of rat hepatic stellate cells treated with IL-2 or TNF-alpha. *Chin Med J* 2003; **116**: 472-474
- 7 **Nieto N, Friedman SL, Cederbaum AI.** Stimulation and proliferation of primary rat hepatic stellate cells by cytochrome P450 2E1-derived reactive oxygen species. *Hepatology* 2002; **35**: 62-73
- 8 **Lee KS, Lee SJ, Park HJ, Chung JP, Han KH, Chon CY, Lee SI, Moon YM.** Oxidative stress effect on the activation of hepatic stellate cells. *Yonsei Med J* 2001; **42**: 1-8
- 9 **Parola M, Leonarduzzi G, Biasi F, Albano E, Biocca ME, Poli G, Dianzani MU.** Vitamin E dietary supplementation protects against carbon tetrachloride-induced chronic liver damage and cirrhosis. *Hepatology* 1992; **16**: 1014-1021
- 10 **Bjorneboe A, Nenseter MS, Hagen BF, Bjorneboe GE, Prydz K, Dreven CA.** Effect of dietary deficiency and supplementation with all-rac- α -tocopherol on hepatic content in rats. *J Nutr* 1991; **121**: 1208-1213
- 11 **Kim KY, Choi I, Kim SS.** Progression of hepatic stellate cell activation is associated with the level of oxidative stress rather than cytokines during CCl₄-induced fibrogenesis. *Mol Cells* 2000; **10**: 289-300
- 12 **Li F, Li XH, Cheng WF, Xie LM.** Effects of antifibrosis and antioxidation of dietary supplement vitamin E and selenium on experimental model of rats. *Yingyang Xuebao* 2003; **25**: 60-65
- 13 **Tsukamoto H, Matsuoka M, French SW.** Experimental models of hepatic fibrosis: a review. *Semin Liver Dis* 1990; **10**: 56-65
- 14 **Zhang M, Song G, Minuk GY.** Effects of hepatic stimulator substance, herbal medicine, selenium/vitamin E, and ciprofloxacin on cirrhosis in the rat. *Gastroenterology* 1996; **110**: 1150-1155
- 15 **Iredale JP, Benyon RC, Pickering J, McCullen M, Northrop M, Pawley S, Hovell C, Arthur MJ.** Mechanisms of spontaneous resolution of rat liver fibrosis Hepatic stellate cell apoptosis and reduced hepatic expression of metalloproteinase inhibitors. *J Clin Invest* 1998; **102**: 538-549

Effects of acupuncturing Tsusanli (S_T36) on expression of nitric oxide synthase in hypothalamus and adrenal gland in rats with cold stress ulcer

Jin-Ping Sun, Hai-Tao Pei, Xiang-Lan Jin, Ling Yin, Qing-Hua Tian, Shu-Jun Tian

Jin-Ping Sun, Hai-Tao Pei, Emergency Neurology Department, Affiliated Hospital of Qingdao University Medical College, Qingdao 266003, Shandong Province, China

Xiang-Lan Jin, Ling Yin, Qing-Hua Tian, Shu-Jun Tian, Center of Neuroinformatics, General Hospital of PLA, Beijing 100853, China

Supported by the National Natural Science Foundation of China, No. 30171135

Correspondence to: Dr. Ling Yin, No.28 Fuxing Road, Center of Neuroinformatics, General Hospital of PLA, Beijing 100853, China. sunjinping@sina.com

Telephone: +86-10-66937546

Received: 2004-11-20 Accepted: 2005-01-26

Abstract

AIM: To study the protective effect of acupuncturing Tsusanli (S_T36) on cold stress ulcer, and the expression of nitric oxide synthase (NOS) in hypothalamus and adrenal gland.

METHODS: Ulcer index in rats and RT-PCR were used to study the protective effect of acupuncture on cold stress ulcer, and the expression of NOS in hypothalamus and adrenal gland. Images were analyzed with semi-quantitative method.

RESULTS: The ulcer index significantly decreased in rats with stress ulcer. Plasma cortisol concentration was up regulated during cold stress, which could be depressed by pre-acupuncture. The expression of NOS1 in hypothalamus increased after acupuncture. The increased expression of NOS2 was related with stress ulcer, which could be decreased by acupuncture. The expression of NOS3 in hypothalamus was similar to NOS2, but the effect of acupuncture was limited. The expression of NOS2 and NOS3 in adrenal gland increased after cold stress, only the expression of NOS1 could be repressed with acupuncture. There was no NOS2 expression in adrenal gland in rats with stress ulcer.

CONCLUSION: The protective effect of acupuncturing Tsusanli (S_T36) on the expression of NOS in hypothalamus and adrenal gland can be achieved.

© 2005 The WJG Press and Elsevier Inc. All rights reserved.

Key words: Acupuncture; Cold stress; Ulcer; Rats; NOS

Sun JP, Pei HT, Jin XL, Yin L, Tian QH, Tian SJ. Effects of

acupuncturing Tsusanli (S_T36) on expression of nitric oxide synthase in hypothalamus and adrenal gland in rats with cold stress ulcer. *World J Gastroenterol* 2005; 11(32): 4962-4966
<http://www.wjgnet.com/1007-9327/11/4962.asp>

INTRODUCTION

Hypothalamus is a higher vegetative nerve center, which can accommodate not only the viscera activation, but also some important physiological functions, such as body temperature regulation, endocrine regulation and emotional response. Damage to this region would lead to acute gastric mucosal lesion.

Glands play an important role in the processes of stress. Psychological and physical stress may result in acute gastric mucosal lesions. It was reported that stress relates to nitric oxide (NO) catalyzed by nitric oxide synthase (NOS)^[1,2]. Studies have demonstrated that NO also plays an important role in the healing process of both gastric and duodenal ulcers^[3].

In this study, we focused on the protective effect of acupuncturing Tsusanli (S_T36) on cold stress ulcer and the expression of NOS in hypothalamus and adrenal gland.

MATERIALS AND METHODS

Animals

Twenty-two adult male Sprague-Dawley (SD) rats weighting 250±25 g were provided by Experimental Animal Center of PLA General Hospital.

The rats were divided into three groups randomly, 6 in control group, 8 in cold stress group (stress group), and 8 in pre-acupuncture group (pre-acupuncture group). Cold stress was induced in rats of stress group, pre-acupuncture group received pre-acupuncture treatment for 1 wk, before cold stress was induced. Control group received no treatment. Rats were housed at controlled temperature and humidity in 12 h light/dark cycle. The animals had free access to food and water.

Cold stress ulcer rat model

SD rats were fasted for 24 h and water was deprived for 1 h before the experiments. The rats were fixed on board after being anesthetized with ether and then they were put into the cold room for 3 h.

The cold stress ulcer rat model was success fully established. There were point and line hemorrhage or superficial ulcer (1-2 mm in diameter).

Electro-acupuncture treatment

The rats were placed into tailor-made mouse cages, and their bilateral legs were sufficiently exposed. Acupuncture at Tsusanli (S₇₃₆) was performed.

The rats were acupunctured with electrical needles (WQ1002K, electro-acupuncture equipment company, China) at 9-10 am, 30 min each time for 7 d. The frequency was 2-20 Hz. The original intensity was 2 V, and increased by 1 V every 10 min. No stimulation was given to the control group.

Rats were killed, hypothalamus and adrenal gland were preserved in liquid nitrogen for expression of NOS by reverse transcriptase-polymerase chain reaction (RT-PCR). Plasma cortisol levels were measured by specific radioimmunoassay (RIA). Biopsy mucosal samples were taken for the measurement of ulcer size, preserved and fixed in 40 mg/L formaldehyde solution for HE staining and then photographed under microscope.

Ulcer index (UI)

The ulcer index calculation was expressed as^[4] 1 score, if there was blotch erosion, 2 scores, when the erosion length was less than 1 mm, 3 scores, when the erosion length was 1-2 mm, 4 scores, when the erosion length was 2-3 mm, and 5 scores, when the erosion length was greater than 4 mm.

Total RNA extraction from hypothalamus and adrenal gland

Total RNA was extracted using TRIzol one-step extraction method. Ultraviolet spectrophotometer was used to determine its concentration and purity.

RT-PCR protocol

All laboratory chemicals were obtained from Sigma Chemical Company.

cDNA was reverse transcribed using 20 µg total RNA, including Oligo dT (1.5 µL), dNTPs [25 mmol/(L µL), 2 µL] and DEPC water (26 µL). In PCR procedure, 30 µL of the reaction system was used including 10× buffer (3 µL), dNTPs [2.5 mmol/(L µL), 1.8 µL], sense primer [10 pmol/(L µL), 1.2 µL], anti-sense primer [10 pmol/(L µL), 1.2 µL], cDNA (1.2 µL/per tube) and MilliQ H₂O (20.3 µL). Thirty-two cycles of RT-PCR were amplified at 94 °C for 30 s, at 58 °C for 30 s, and at 72 °C for 1 min.

The following primer sequences were used (Beijing SBS Company, China): rNOS1-sense: 5' > CGC AGA ACA CAT CAC AGG < 3'; rNOS1-antisense: 5' > AGA ACG GGG AGA AAT TCG < 3' (450-bp product);

rNOS2-sense: 5' > TGT TCC ATG CAG ACA ACC < 3'; rNOS2-antisense: 5' > TTC AGA AGC AGA ATG TGA CC < 3' (407-bp product);

rNOS3-sense: 5' > CCT TTG ATC TCA ATG TCG < 3'; rNOS3-antisense: 5' > TAC GAA GAA TGG AAG TGG < 3' (374-bp product);

β-actin was used as control, its primer sequences: 5' > AAC CCT AAG GCC AAC CTG GAA AAG < 3', and 5' > TCG TGA GGT AGT CTG TCA GGT < 3' (241-bp product).

After completion of the PCR amplifications, 10 µL of each PCR reaction was added to each lane of 2% agarose gel. The gel was then stained with 1 µg/mL ethidium

bromide, viewed with a transilluminator, and photographed using UVP-GDS7600 gel image system to perform semi-quantitative analysis.

Statistical analysis

SPSS was used to perform statistical analysis and mapping. The data in experiments for ulcer index and plasma cortisol were presented as mean ± SE, and analyzed by Student's *t*-test for unpaired samples. Data for RT-PCR were analyzed by one-way analysis of variance (ANOVA) followed by a post hoc Duncan's test. *P* < 0.05 was considered statistically significant.

RESULTS

Plasma cortisol concentration (nmol/L)

Plasma cortisol concentration was 104.38 ± 8.31 in stress group, 66.83 ± 12.25 in pre-acupuncture group, and 79.1 ± 11.07 in control group. Difference was statistically significant in three groups (*P* < 0.01 or *P* < 0.05, Figure 1).

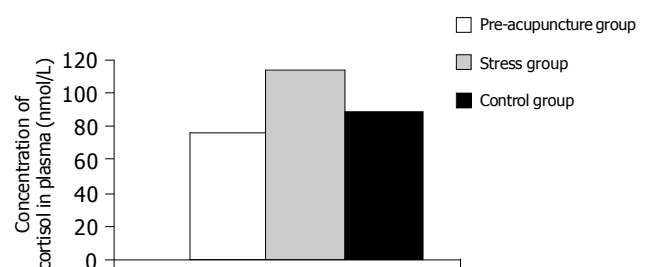


Figure 1 Effects of acupuncture at Tsusanli (S₇₃₆) on plasma cortisol concentration in rats with stress ulcer.

Result of UI

UI was 26.25 ± 4.40 in stress group, 9.75 ± 1.91 in pre-acupuncture group and 0 in control group (*P* < 0.01).

Data for NOS mRNA expression in hypothalamus (Figure 2)

Expression of NOS1 mRNA The ratio of NOS1 mRNA to β-actin mRNA was 0.69 ± 0.05 in control group, 0.77 ± 0.09 in stress group, and 1.87 ± 0.15 in pre-acupuncture group. There was a significant difference compared between acupuncture group and control group (*P* < 0.01), but no significant difference was found between stress group and control group.

Expression of NOS2 mRNA The ratio of NOS2 mRNA to β-actin mRNA was 0.06 ± 0.02 in control group, 0.24 ± 0.05 in stress group, and 0.12 ± 0.06 in pre-acupuncture group. There was a significant difference between pre-acupuncture group and stress group (*P* < 0.01), as well as between stress group and control group (*P* < 0.01).

Expression of NOS3 mRNA The ratio of NOS3 mRNA to β-actin mRNA was 0.30 ± 0.08 in control group, 0.63 ± 0.14 in stress group, and 0.45 ± 0.14 in pre-acupuncture group. There was a significant difference between pre-acupuncture group and stress group (*P* < 0.05), as well as between pre-acupuncture group and control group, stress group, and control group (*P* < 0.05).

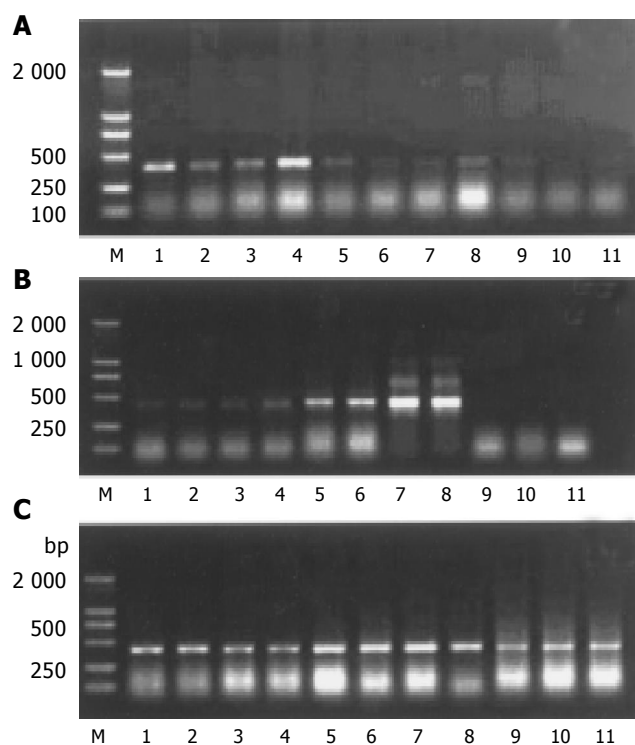


Figure 2 Effects of acupuncture at Tsusanli (S₇36) on expression of NOS1 (A), NOS2 (B), and NOS3 (C) in rats with stress ulcer. M: marker; lanes 1-4: pre-acupuncture group; lanes 5-8: stress group; lanes 9-11: control group.

Data for NOS mRNA expression in adrenal gland (Figure 3)

Expression of NOS1 mRNA The ratio of NOS1 mRNA to β -actin mRNA was 0.43 ± 0.09 in control group, 0.98 ± 0.23 in stress group, and 0.77 ± 0.22 in pre-acupuncture group. There was a significant difference between pre-acupuncture group and stress group ($P < 0.05$), as well as between stress group and control group ($P < 0.01$), pre-acupuncture group and control group ($P < 0.01$).

Expression of NOS2 mRNA There was no expression of NOS2 mRNA.

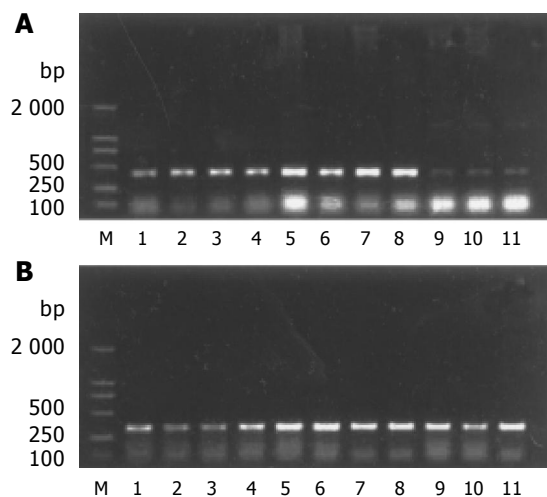


Figure 3 Effects of acupuncture at Tsusanli (S₇36) on expression of NOS1 (A) and NOS3 (B) in rats with stress ulcer. M: marker; lanes 1-4: pre-acupuncture group; lanes 5-8: stress group; lanes 9-11: control group.

Expression of NOS3 mRNA The ratio of NOS3 mRNA to β -actin mRNA was 0.71 ± 0.25 in control group, 2.54 ± 1.15 in stress group, and 1.70 ± 0.86 in pre-acupuncture group. There was a significant difference between stress group and control group ($P < 0.01$), but no significance difference was found between pre-acupuncture group and stress group and between pre-acupuncture group and control group ($P < 0.05$).

Demonstration of gastric mucosa with HE Staining (Figure 4)

Interruption of continuity in gastric mucosa and submucosa, as well as damage in muscular layer were found in stress group. The continuity in gastric mucosa was slightly damaged, and its tissue morphology was relatively normal in pre-acupuncture group.

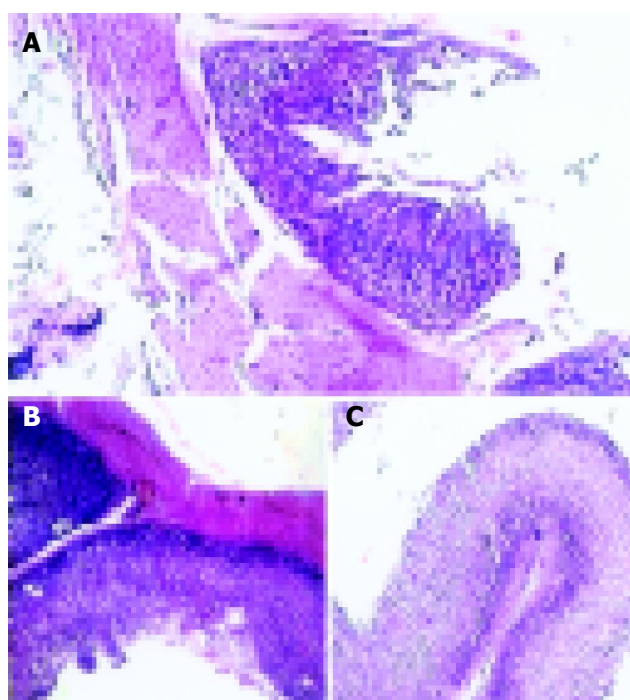


Figure 4 Effects of acupuncture at Tsusanli (S₇36) on gastric mucosa of stress group (A), pre-acupuncture group (B) and control group (C).

DISCUSSION

Studies have shown that the imbalance between NO and ET, decreases the gastric mucosal blood flow (GBF) and accelerates the gastric lesions^[5,6]. NO has both protective and deleterious effects on gastric mucosa by different physiological and pathological mechanisms in various diseases. This double effect depends on the type of NOS involved in these pathological conditions^[7].

It was reported that NO, as a neurotransmitter and a sensory neuropeptide, takes part in the physiological and pathological hyperemia reaction in gastric mucosa, increases gastric mucosal blood flow, thus protecting gastric mucosa^[8,9]. Endogenous NO plays an important role in maintaining vascular integrity and promoting the ulcer healing^[10]. NO catalyzed by NOS, can function both as a second messenger and as a neurotransmitter, and also performs numerous physiological functions as an effective

molecule. In pathological status, superfluous NO can increase vascular permeability, neuron decrease, neurotransmitter release and transitive obstacle, thus affecting organic physiological functions^[11,12]. The damage of NO to gastric mucosa indicates, that higher concentrations of NO exhibit toxic effects through nitrosative and oxidative stress. The mechanism responsible for water immersion stress-induced gastric lesions in aged is related with the activity decrease of NOS in gastric mucosa^[13].

Three types of NOS including neuronal NOS (NOS1), inducible NOS (NOS2) and endothelial NOS (NOS3) have been identified^[14,15].

NOS1 is primarily expressed in neural cells and relates to many physiological functions of the central nervous system, such as synapse plasticity, neural regeneration, nerve conduction, neural development, and neuroendocrine regulation^[16,17]. NOS2, also known as inducible NOS is typically expressed only after induction by pro-inflammatory cytokines and /or lipopolysaccharide (LPS). In a wide variety of pathological conditions, there is a notable biosynthesis of large quantities of NO, due to the increased expression of NOS2^[18-20]. Both NOS2 and COX2 result in stress of rats^[21]. NOS3 is primarily expressed in endothelial cells.

Both NOS1 and NOS3, also named as constitutive NOS (eNOS), are expressed in physiological status. NO catalyzed by NOS, mainly functions as a second messenger and a neurotransmitter. eNOS are related with gastric mucosa protection and the process of ulcer healing. In contrast, NOS2 affects the ulceration^[22-24].

Stress could cause mucosal damage and increase vascular permeability. NOS inhibitor can aggravate these kinds of changes. L-arginine or endotoxin lipopolysaccharide can restrain the increase of vascular permeability^[25,26]. In contrast, some studies reported that L-NAME (a nonspecific inhibitor of NOS) can delay mucosal lesions^[27] by depressing bile acid secretion and ulcer index in stomach^[28].

Results from the present studies, show that cold stress can differently affect NOS in hypothalamus. Acupuncture regulation for NOS is also different.

There was no significant difference in NOS1 in hypothalamus between stress group and control group, suggesting that NOS1 does not take part in stress reaction.

NOS1 expression in pre-acupuncture group was higher than that in control and stress groups, suggesting that puncturing Tsusanli (S₇36) can upregulate the expression of NOS1, leading to synthesizing more NO, and protecting gastric mucosa against the damage induced by cold stress.

Different from NOS1, cold stress caused high expression of NOS3 compared to control group. Moreover, acupuncture Tsusanli (S₇36) could inhibit high expression of NOS3, suggesting that the mechanism of acupuncture in inhibiting NOS3 is different from NOS1. Acupuncture Tsusanli (S₇36) can, in part, downregulate the expression of NOS3, instead of those previously completely inhibiting its injurious expression. The above results are different from reported. Whether the peripheral reaction of NOS3 is different from that in central reaction needs to be confirmed.

The results of this study also showed that NOS in adrenal gland did not play a role as in hypothalamus. NOS3 takes part in the pathological process of cold stress ulcer,

both in adrenal gland and in hypothalamus. Acupuncture can decrease the expression of NOS3. Although it can only be decreased in part, there is no statistical difference. The difference is that NOS1 takes part in the pathological stress process in adrenal gland. Acupuncture can down-regulate the pathological reaction.

The present experimental results display that NOS2 is highly expressed in hypothalamus, which is induced by cold stress. High expression of NOS2 leads to pathological changes in gastric mucosa^[29,30]. Acupuncture Tsusanli (S₇36) can depress the overexpression of NOS2, thus leading to the protection of the body against injury. Studies have demonstrated that the expression of NOS2 is markedly upregulated after ulceration.

In the present study, we have confirmed that NOS2 participates in the pathological stress reaction, whereas NOS1 does not. NOS3 also participates in the pathological stress reaction, which is different from the previous reports^[31,32]. It was reported that NOS1, NOS2, and NOS3 affect the healing of gastric ulcer^[3].

In conclusion, NOS2 and NOS3 in hypothalamus participate in the pathological process of cold stress ulcer. Acupuncture Tsusanli (S₇36) can modulate the expression of NOS1 upward and depress the expression of NOS2 and NOS3, thus playing a role in protecting gastric mucous.

ACKNOWLEDGMENTS

The authors thank Drs. Yi-Ming Mu and Ming Li for their help and advice.

REFERENCES

- 1 Masood A, Banerji B, Vijayan VK, Ray A. Pharmacological and biochemical studies on the possible role of nitric oxide in stress adaptation in rats. *Eur J Pharmacol* 2004; **493**: 111-115
- 2 McLeod TM, Lopez-Figueroa AL, Lopez-Figueroa MO. Nitric oxide, stress, and depression. *Psychopharmacol Bull* 2001; **35**: 24-41
- 3 Dixit C, Rastogi L, Dikshit M. Effect of nitric oxide modulators on pylorus-ligation-induced ulcers in the rat. *Pharmacol Res* 1999; **39**: 33-39
- 4 Guth PH, Aures D, Paulsen G. Topical aspirin plus HCl gastric lesions in the rat. Cytoprotective effect of prostaglandin, cimetidine, and probanthine. *Gastroenterology* 1979; **76**: 88-93
- 5 Zhang GF, Chen YR, Zhang MA. Nitrogen monoxide, endothelins and injury in gastric mucous membrane. *Weichang Bingxue He Ganbingxue Zazhi* 1999; **8**: 293-296
- 6 Brzozowski T, Konturek PC, Konturek SJ, Sliwowski Z, Drozdowicz D, Stachura J, Pajdo R, Hahn EG. Role of prostaglandins generated by cyclooxygenase-1 and cyclooxygenase-2 in healing of ischemia-reperfusion-induced gastric lesions. *Eur J Pharmacol* 1999; **385**: 47-61
- 7 Cho CH. Current roles of nitric oxide in gastrointestinal disorders. *J Physiol Paris* 2001; **95**: 253-256
- 8 Salomone S, Caruso A, Cutuli VM, Mangano NG, Prato A, Amico-Roxas M, Bianchi A, Clementi G. Effects of adrenomedullin on the contraction of gastric arteries during reserpine-induced gastric ulcer. *Peptides* 2003; **24**: 117-122
- 9 Mohanakumar KP, Thomas B, Sharma SM, Muralikrishnan D, Chowdhury R, Chiueh CC. Nitric oxide: an antioxidant and neuroprotector. *Ann N Y Acad Sci* 2002; **962**: 389-401
- 10 Ma L, Chow JY, Liu ES, Cho CH. Cigarette smoke and its extract delays ulcer healing and reduces nitric oxide synthase activity and angiogenesis in rat stomach. *Clin Exp Pharmacol*

- Physiol* 1999; **26**: 828-829
- 11 **Mishra OP**, Delivoria-Papadopoulos M. Nitric oxide-mediated Ca⁺⁺-influx in neuronal nuclei and cortical synaptosomes of normoxic and hypoxic newborn piglets. *Neurosci Lett* 2002; **318**: 93-97
 - 12 **Xie Z**, Wei M, Morgan TE, Fabrizio P, Han D, Finch CE, Longo VD. Peroxynitrite mediates neurotoxicity of amyloid beta-peptide1-42- and lipopolysaccharide-activated microglia. *J Neurosci* 2002; **22**: 3484-3492
 - 13 **Goto H**, Tachi K, Hisanaga Y, Kamiya K, Ohmiya N, Niwa Y, Hayakawa T. Exacerbatory mechanism responsible for water immersion stress-induced gastric lesions in aged rats compared with young rats. *Clin Exp Pharmacol Physiol* 2001; **28**: 659-662
 - 14 **Bolanao JP**, Almeida A. Roles of nitric oxide in brain hypoxia-ischemia. *Biochim Biophys Acta* 1999; **1411**: 415-436
 - 15 **Barrachina MD**, Panes J, Esplugues JV. Role of nitric oxide in gastrointestinal inflammatory and ulcerative diseases: perspective for drugs development. *Curr Pharm Des* 2001; **7**: 31-48
 - 16 **Drew B**, Leeuwenburgh C. Aging and the role of reactive nitrogen species. *Ann N Y Acad Sci* 2002; **959**: 66-81
 - 17 **Sanchez S**, Martin MJ, Ortiz P, Motilva V, Herreras JM, Alarcon de la Lastra C. Role of prostaglandins and nitric oxide in gastric damage induced by metamizol in rats. *Inflamm Res* 2002; **51**: 385-392
 - 18 **Higuchi Y**, Hattori H, Hattori R, Furusho K. Increased neurons containing neuronal nitric oxide synthase in the brain of a hypoxia-ischemic neonatal rat model. *Brain Dev* 1996; **18**: 369-375
 - 19 **Wada K**, Chatzipanteli K, Busto R, Dietrich WD. Role of nitric oxide in traumatic brain injury in the rat. *J Neurosurg* 1998; **89**: 807-818
 - 20 **Chavez AM**, Morin MJ, Unno N, Fink MP, Hodin RA. Acquired interferon gamma responsiveness during Caco-2 cell differentiation: effects on iNOS gene expression. *Gut* 1999; **44**: 659-665
 - 21 **Madrigal JL**, Garcia-Bueno B, Moro MA, Lizasoain I, Lorenzo P, Leza JC. Relationship between cyclooxygenase-2 and nitric oxide synthase-2 in rat cortex after stress. *Eur J Neurosci* 2003; **18**: 1701-1705
 - 22 **West SD**, Helmer KS, Chang LK, Cui Y, Greeley GH, Mercer DW. Cholecystokinin secretagogue-induced gastroprotection: role of nitric oxide and blood flow. *Am J Physiol Gastrointest Liver Physiol* 2003; **284**: G399-410
 - 23 **Brzozowska I**, Konturek PC, Brzozowski T, Konturek SJ, Kwiecien S, Pajdo R, Drozdowicz D, Pawlik M, Ptak A, Hahn EG. Role of prostaglandins, nitric oxide, sensory nerves and gastrin in acceleration of ulcer healing by melatonin and its precursor, L-tryptophan. *J Pineal Res* 2002; **32**: 149-162
 - 24 **Ohta Y**, Nishida K. L-arginine protects against stress-induced gastric mucosal lesions by preserving gastric mucus. *Clin Exp Pharmacol Physiol* 2002; **29**: 32-38
 - 25 **Hsieh JS**, Wang JY, Lin SR, Lian ST, Chen FM, Hsieh MC, Huang TJ. Overexpression of inducible nitric oxide synthase in gastric mucosa of rats with portal hypertension: correlation with gastric mucosal damage. *J Surg Res* 2003; **115**: 24-32
 - 26 **Araki H**, Komoike Y, Matsumoto M, Tanaka A, Takeuchi K. Healing of duodenal ulcers is not impaired by indomethacin or rofecoxib, the selective COX-2 inhibitor, in rats. *Digestion* 2002; **66**: 145-153
 - 27 **Fan YP**, Chakder S, Gao F, Rattan S. Inducible and neuronal nitric oxide synthase involvement in lipopolysaccharide-induced sphincter dysfunction. *Am J Physiol* 2001; **280**: G32-42
 - 28 **Chen M**, Luo HS, Tong QY, Chen JH, Li XZ. Effects of pyloric local CGRP and NO on bile reflux in rat stomach with stress ulcer. *Shijie Huaren Xiaohua Zazhi* 2004; **12**: 2131-2134
 - 29 **Chen K**, Hirota S, Wasa M, Okada A. Expression of NOS II and its role in experimental small bowel ulceration in rats. *Surgery* 1999; **126**: 553-561
 - 30 **Calatayud S**, Ramirez MC, Sanz MJ, Moreno L, Hernandez C, Bosch J, Pique JM, Esplugues JV. Gastric mucosal resistance to acute injury in experimental portal hypertension. *Br J Pharmacol* 2001; **132**: 309-317
 - 31 **Nishida K**, Ohta Y, Ishiguro I. Preventive effect of teprenone on stress-induced gastric mucosal lesions and its relation to gastric mucosal constitutive nitric oxide synthase activity. *Pharmacol Res* 1999; **39**: 325-332
 - 32 **Li Y**, Wang WP, Wang HY, Cho CH. Intra-gastric administration of heparin enhances gastric ulcer healing through a nitric oxide-dependent mechanism in rats. *Eur J Pharmacol* 2000; **399**: 205-214

IFN- γ increases efficiency of DNA vaccine in protecting ducks against infection

Jian-Er Long, Li-Na Huang, Zhi-Qiang Qin, Wen-Yi Wang, Di Qu

Jian-Er Long, Li-Na Huang, Zhi-Qiang Qin, Wen-Yi Wang, Di Qu, Department of Molecular Virology, Shanghai Medical College, Fudan University, Shanghai 200032, China
Jian-Er Long, Shanghai Institute of Medical Genetics, Shanghai Children's Hospital, Shanghai Jiaotong University, Shanghai 200040, China

Supported by the Major State Basic Research Development Program of China, 973 Program, No. G2002CB512803; the National Natural Science Foundation of China, No. 30070693; the Science and Technology Foundation of Shanghai, No. 02DJ14002
Correspondence to: Dr. Di Qu, Department of Molecular Virology, Shanghai Medical College, Fudan University, 138 Fenglin R. Shanghai 200032, China. dqu@shmu.edu.cn
Telephone: +86-21-54237524
Received: 2004-11-15 Accepted: 2005-01-26

DHBpreS/S DNA than in other groups.

CONCLUSION: DHBV preS/S DNA vaccine can protect ducks against DHBV infection, DuIFN- γ gene as an immune adjuvant enhances its efficacy.

© 2005 The WJG Press and Elsevier Inc. All rights reserved.

Key words: Duck IFN- γ ; DHBV; DNA vaccine; Immune adjuvant

Long JE, Huang LN, Qin ZQ, Wang WY, Qu D. IFN- γ increases efficiency of DNA vaccine in protecting ducks against infection. *World J Gastroenterol* 2005; 11(32): 4967-4973
<http://www.wjgnet.com/1007-9327/11/4967.asp>

Abstract

AIM: To detect the effects of DNA vaccines in combination with duck IFN- γ gene on the protection of ducks against duck hepatitis B virus (DHBV) infection.

METHODS: DuIFN- γ cDNA was cloned and expressed in COS-7 cells, and the antiviral activity of DuIFN- γ was detected and neutralized by specific antibodies. Ducks were vaccinated with DHBpreS/S DNA alone or co-immunized with plasmid expressing DuIFN- γ . DuIFN- γ mRNA in peripheral blood mononuclear cells (PBMCs) from immunized ducks was detected by semi-quantitative competitive RT-PCR. Anti-DHBpreS was titrated by enzyme-linked immunosorbent assay (ELISA). DHBV DNA in sera and liver was detected by Southern blot hybridization, after ducks were challenged with high doses of DHBV.

RESULTS: DuIFN- γ expressed by COS-7 was able to protect duck fibroblasts against vesicular stomatitis virus (VSV) infection in a dose-dependent fashion, and anti-DuIFN- γ antibodies neutralized the antiviral effects. DuIFN- γ in the supernatant also inhibited the release of DHBV DNA from LMH-D2 cells. When ducks were co-immunized with DNA vaccine expressing DHBpreS/S and DuIFN- γ gene as an adjuvant, the level of DuIFN- γ mRNA in PBMCs was higher than that in ducks vaccinated with DHBpreS/S DNA alone. However, the titer of anti-DHBpreS elicited by DHBpreS/S DNA alone was higher than that co-immunized with DuIFN- γ gene and DHBpreS/S DNA. After being challenged with DHBV at high doses, the load of DHBV in sera dropped faster, and the amount of total DNA and cccDNA in the liver decreased more significantly in the group of ducks co-immunized with DuIFN- γ gene and

INTRODUCTION

An estimated 350 million people are chronically infected with hepatitis B virus (HBV). Cytotoxic T lymphocytes (CTLs) play a critical role in the clearance of HBV from patients by lysis of virus-infected hepatocytes^[1]. However, IFN- γ and TNF- α have been shown to inhibit HBV replication in HBV transgenic mice, without lysing infected hepatocytes^[2,3]. An *in vitro* model in which lymphocytes from HBsAg positive patients are co-cultured with HBV replicating hepatocytes, shows that the secretion of IFN- γ from lymphocytes inhibits HBV replication^[4]. Consequently, in addition to enhancing the cytotoxicity of CTLs, IFN- γ also mediates the non-cytolytic inhibition of HBV replication, and shows its significance in the host defense against HBV infection and recovery from virus infection.

Recombinant woodchuck IFN- γ up-regulates MHC class I molecule transcription, but hardly inhibits or clears woodchuck hepatitis virus replicating intermediates and RNAs in persistently infected woodchuck primary hepatocytes^[5]. However, treatment of primary duck hepatocytes with recombinant duck IFN- γ can inhibit DHBV replication in a dose-dependent manner^[6]. The role of IFN- γ in hepadnavirus infection is still controversial.

DHBV and HBV share common genomic and structural features, with an envelope surrounding a spherical nucleocapsid that contains a similar viral DNA genome in terms of size, structure, and organization. This is why DHBV-infected ducks have become a useful animal model to explore the molecular mechanism of host defense against HBV infection^[7-9]. Animals immunized with antigen and IFN- γ gene develop Th1-biased immune responses, and it has been reported that IFN- γ , as a genetic adjuvant has

stronger effects on the nature of immune response in neonates than in adults^[10]. To date, whether IFN- γ inhibits DHBV replication *in vivo* has not been reported. Whether DNA vaccine protects ducks against DHBV infection is still controversial^[11-14]. To test the function of IFN- γ as an immune adjuvant and to validate the efficacy of DHBV vaccines, ducks were immunized with the mixture of plasmid expressing DHBV preS/S protein and IFN- γ . The results support the view that DuIFN- γ inhibits DHBV replication and increases the protective efficacy of DNA vaccines expressing DHBV preS/S protein.

MATERIALS AND METHODS

Animals and cells

Cherry valley ducks (*Anas platyrhynchos*) were supplied by Breeding Center of Shanghai Institute of Veterinary Medical Sciences, China. Duck embryo fibroblasts were prepared as previously described^[15], and maintained in Dulbecco's Modified Eagle's Medium (DMEM) containing 2 mmol/L glutamine, 100 U/mL penicillin and streptomycin, supplemented with 2% duck sera (prepared from DHBV-free ducks and filtered through a 0.22 μ m membrane) and 8% fetal calf sera (FCS). COS-7 cells were cultured in DMEM containing 10% FCS. LMH-D2, a chicken hepatoma cell line and a gift from Dr. William S. Mason (Fox Chase Cancer Center), was incubated in DMEM/F12 medium supplemented with 2% chicken sera and 8% FCS.

Separation of duck PBMCs and amplification of DuIFN- γ mRNA by RT-PCR

Blood was taken from adult ducks and diluted by an equal volume of heparinized PBS. PBMCs were separated with Ficoll as described previously^[16], 5×10^6 PBMCs in 1 mL of RPMI 1 640 supplemented with 10% FCS were transferred into 24-well plates and stimulated with PHA at 10 mg/mL for 24 h. Total RNA was extracted from PBMCs with TRIzol reagent (Gibco BRL, USA) and 4 μ g of total RNA was reverse transcribed into cDNA by Superscript IITM and hexamer random primer (Gibco BRL). The sequences of sense and anti-sense primers are 5-CGCCGATCCAT-GACTTGCCAGACCTACTGCTT-3 and 5-CGCCG-ATATCTCATTAACATCTGCATCTCTTTGG-3. cDNA of DuIFN- γ was amplified for 30 cycles at 94 $^{\circ}$ C for 5 min, 94 $^{\circ}$ C for 1 min, 54 $^{\circ}$ C for 1 min, and at 72 $^{\circ}$ C for 2 min.

Expression of recombinant DuIFN- γ in COS-7 cells

For expression of recombinant DuIFN- γ , the amplified DuIFN- γ DNA fragment was cloned into eukaryotic expression vector pcDNA3.1 (Invitrogen) at the *EcoRV*/*Bam*HI sites. Transfection was performed by the method of calcium phosphate precipitation. At 72 h post-transfection, the culture supernatant were harvested and centrifuged to remove the cell debris.

Titration of recombinant DuIFN- γ

Duck embryo fibroblasts were seeded into 96-well plates and incubated in the presence of serial four-fold dilution of DuIFN- γ in the supernatant. After 12 h incubation, the cells were challenged with VSV at 100 TCID₅₀ for 36 h.

Under microscope, the cytopathic effects (CPE) were observed and MTT was added for another 8 h. MTT could be degraded by mitochondrial enzymes and developed blue color. Consequently, the optical density could indicate the course of virus infection and cellular pathogenesis^[17]. DuIFN- γ titers were expressed as reciprocals of the dilutions that resulted in 50% protection against virus-induced cell CPE. The role of DuIFN- γ in protecting cells against virus infection also was confirmed by specific IgG of anti-DuIFN- γ provided by Dr. C.J. Burrell (University of Adelaide, Australia).

Treatment of LMH-D2 cells with DuIFN- γ

LMH-D2 cells were seeded at 1×10^6 cells/flask at 37 $^{\circ}$ C in 50 mL/L CO₂, and incubated with 10% of recombinant DuIFN- γ supernatant (titrated as 4⁷-4⁸) or the same volume of supernatant derived from transfected pcDNA3.1 vector. After the culture supernatant was collected, fresh DMEM/F12 was refilled everyday or every other day, the collected culture supernatant was centrifuged at 5 000 r/min \times 10 min, and 5 μ L of the supernatant was spotted onto positively charged nylon membranes and the DHBV DNA was detected by dot hybridization.

Subcloning of DHBV-preS/S gene into eukaryotic expression vector and detection of gene expression in COS-7 cells

The full length of DHBV genome clone (pCMV-DHBV9) was also a gift from Dr. William S. Mason. DHBV preS/S gene was subcloned into pcDNA3.1 with *A*fII/*E*coRI restriction sites introduced by PCR primers. The sequences of sense and antisense primers are 5-CGCCCTAAGA-TGGGGCAACATCCAGCAAATC-3 and 5-CGCG-AATTCAGTTTATTCCTTATTCCTAACTCTT-3, respectively. The subcloned DHBV preS/S gene was transfected into COS-7 cells by calcium phosphate precipitation. The expressed protein was detected by indirect immunofluorescence (IMF) staining with mAb against DHBV-preS/S protein as previously described^[11]. A reporter gene secreting alkaline phosphatase (SEAP)^[18] was transfected into COS-7 cells simultaneously for detection of the efficacy.

Vaccination protocol

Three-day-old ducks were vaccinated intramuscularly in the quadriceps anterior muscle. DHBpreS/S DNA and DuIFN- γ DNA were extracted with a kit (QIAGEN Mega DNA extracted kit) following the manufacturer's instructions. All ducks were grouped. Group 1 was vaccinated with plasmid pcDNA3.1-DHBpreS/S at 200 μ g/duck, group 2 with DHBpreS/S DNA at 200 μ g and plasmid pcDNA3.1-DuIFN- γ at 200 μ g/duck, group 3 was injected with an equal volume of PBS. The same procedure for DNA vaccination was repeated after 4 wk.

Detection of mRNA of DuIFN- γ in PBMCs after being stimulated with DHBsAg by competitive RT-PCR

Competitive RT-PCR method has been described^[19]. Briefly, β -actin gene functioned as a housekeeping gene. Competitive internal control (IC) was constructed by deleting the partial segment of DuIFN- γ cDNA using a pair of specific PCR

primers. The sequences of sense and anti-sense primers are 5-GGATGTAGCTGATGGCAATCC-3 and 5-TCATTAACATCTGCATCTCTTTGGGACAGTTCC-ACGAGGTC-3, respectively. The sequence of anti-sense primer for amplification of the target segment of DuIFN- γ cDNA is 5-TCATTAACATCTGCATCTCTTTGG-3 (partial sequences of anti-sense primer for IC), and the sequence of sense primer is the same as the one used for constructing IC. After peripheral blood was separated using Ficoll, PBMCs were transferred into 24-well plates at 5×10^6 cells/well, and then stimulated with purified DHBsAg at 1 $\mu\text{g}/\text{mL}$ for 24 h. IC (1.25×10^{-5} $\mu\text{g}/\text{mL}$) was used to quantify the samples. The conditions of amplification were at 94 $^{\circ}\text{C}$ for 4 min, 94 $^{\circ}\text{C}$ for 1 min, 60 $^{\circ}\text{C}$ for 45 s, at 72 $^{\circ}\text{C}$ for 1 min. In the next five cycles, the temperature for annealing was decreased at 1 $^{\circ}\text{C}$ per cycles and another 25 cycles were performed at 94 $^{\circ}\text{C}$ for 1 min, 55 $^{\circ}\text{C}$ for 45 s, 72 $^{\circ}\text{C}$ for 1 min, at 72 $^{\circ}\text{C}$ for 10 min.

Serological assay

DHBV preS protein was expressed in *E. coli* and 100 μL of purified protein (1 $\mu\text{g}/\text{mL}$) was coated on 96-well microdilution plates at 4 $^{\circ}\text{C}$ overnight. Non-specific sites were blocked with 200 μL skim milk (Shanghai Guangming Milk Co., Ltd) in PBS-0.05% Tween 20. The plates were incubated with 2-fold serially diluted serum sample and then with 100 μL of HRP-goat anti-duck immunoglobulin Y at 1/1 000 dilution (KPL). The color was developed by substrate of TMB system in darkness for 15 min and terminated by 50 μL 2 N H_2SO_4 . The optical density at 450 nm (A_{450}) was read on an automatic ELISA reader. The antibody titer in each serum sample was defined as the highest serum dilution that resulted in $S/N > 3$ (S for A_{450} of serum sample, N for A_{450} of control normal duck serum sample at the same dilution).

Viral challenge and DHBV DNA assay

All vaccinated ducks were boosted again at wk 7, vaccinated ducks were challenged with DHBV at a high-titer dosage (1.0×10^{10} DHBV DNA genomes/mL) at wk 13. The volume for injection was adjusted according to the body weight of ducks: volume (mL) = weight (g) $\times 7\% \times 10\%$. The ducks were cannulated via the jugular vein. Blood samples were collected before virus challenge and at 1, 5, 15, 30, 45, 60, 90, 120 min post-challenge. After being challenged

with virus for 5 d, the ducks were killed and livers were taken out for extraction of DHBV DNA. DHBV DNA in sera and liver was detected by Southern blot as previously described^[20]. The whole DHBV genome from pCMV-DHBV9 was used as DNA template for producing specific probes labeled by [α - ^{32}P] dCTP with a random primer.

RESULTS

Expression of recombinant DuIFN- γ in vitro and biological assay

Monolayer of duck embryo skin fibroblast cells was incubated with the supernatant from recombinant plasmid pcDNA3.1-DuIFN- γ transfected COS-7 cells, and then infected with VSV at 100 TCID₅₀. The results indicated that the supernatant from pcDNA3.1-DuIFN- γ transfected cell culture could protect the duck embryo fibroblast cells against VSV infection, while the supernatant from pcDNA3.1 transfected cells showed no antiviral effect (Figure 1A). The protective effect was dose-dependent. The antiviral effect of DuIFN- γ in the supernatant was titrated in a series of four-fold dilution, and titer was expressed as 4^7 - 4^8 (Figure 2 and Table 1). The antiviral activity of the supernatant from pcDNA3.1-DuIFN- γ transfected cells could be neutralized by anti-DuIFN- γ (Figure 1B), indicating that recombinant DuIFN- γ played a role in the control of viral infection.

Inhibition of the DHBV replication by DuIFN- γ

For investigation of anti-DHBV effect of recombinant DuIFN- γ , LMH-D2 cells continuously producing DHBV, were incubated with the supernatant from pcDNA3.1-DuIFN- γ transfected cells, culture fluid was collected everyday or every other day. DHBV in the supernatant was spotted on the nylon membrane and detected by hybridization with a DHBV DNA probe. The results showed that the amount of DHBV DNA decreased dramatically 1 d after treatment with DuIFN- γ and the anti-DHBV effect lasted for 4 d, while no anti-DHBV effect of recombinant DuIFN- γ on the supernatant from pcDNA3.1 transfected cell culture was observed. After treatment for 4 d, no apparent difference was observed between cells treated with the recombinant DuIFN- γ and the control supernatant (Figure 3). The results demonstrated that the recombinant DuIFN- γ temporally inhibited the DHBV replication in LMH-D2 cells.

Table 1 CPE inhibition assay to quantify recombinant DuIFN- γ

IFN- γ (Diluted by log4)	CPE (Four wells)	Average of CPE	Inhibition of CPE	Accumulation of inhibitory CPE	Accumulation of CPE	Inhibition of CPE	Inhibition of CPE (%)
1	0, 0, 0, 0	0	4.00	27.25	0	27.25/27.25	100
2	0, 0, 0, 0	0	4.00	23.25	0	23.25/23.25	100
3	1, 0, 0, 0	0.25	3.75	19.25	0.25	19.25/19.50	98.70
4	0, 1, 0, 0	0.25	3.75	15.50	0.50	15.50/16.00	96.90
5	1, 0, 1, 0	0.50	3.50	11.75	1.00	11.75/12.75	92.20
6	1, 1, 2, 3	1.75	2.25	8.25	2.75	8.25/11.00	75
7	1, 2, 2, 1	1.50	2.50	6.00	4.25	6.00/10.25	58.50
8	2, 1, 2, 3	2.00	2.00	3.50	6.25	3.50/9.75	35.90
9	3, 3, 3, 2	2.75	1.25	1.50	9.00	1.50/10.50	14.30
10	3, 4, 4, 4	3.75	0.25	0.25	12.75	0.25/13.00	1.90

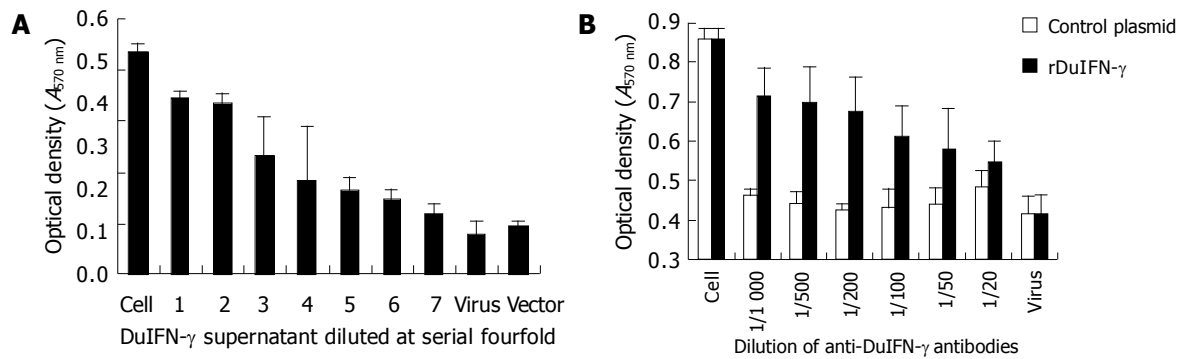


Figure 1 Titration of recombinant DuIFN- γ by MTT (A) and neutralization of

antiviral activity by anti-DuIFN- γ (B).

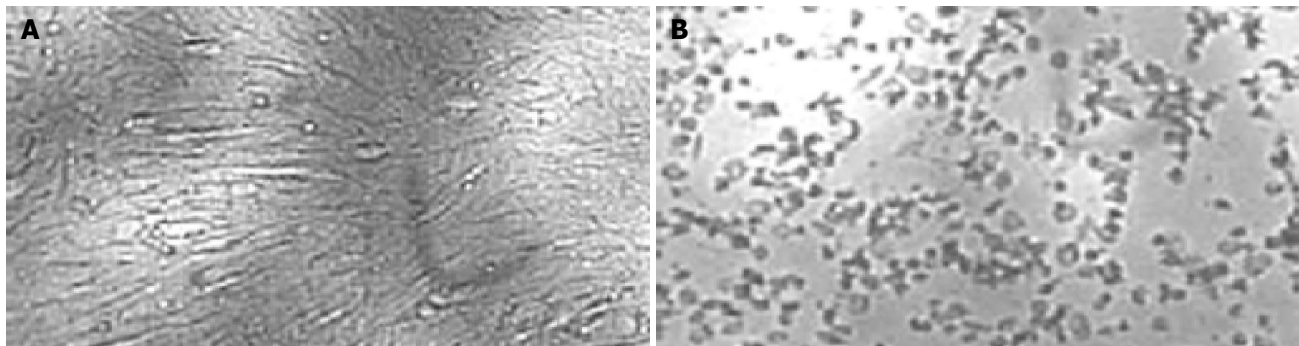


Figure 2 Morphology of normal duck fibroblasts (A) and cytopathic effect

(CPE) of duck fibroblasts when infected with VSV (B).

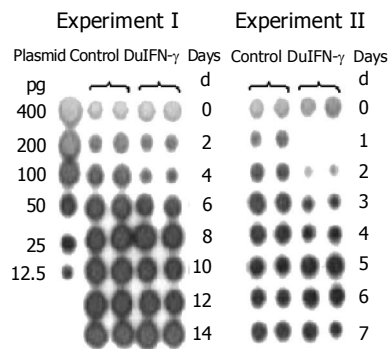


Figure 3 Effects of recombinant DuIFN- γ on release of DHBV DNA from LMH-D2 cells.

Effects of DuIFN- γ as adjuvant of DNA vaccine on DuIFN- γ mRNA transcription in duck PBMCs

Three-day-old ducks were immunized with plasmids expressing DHBV-preS/S gene alone (group 1) or expressing DHBV-preS/S gene and DuIFN- γ DNA (group 2), or PBS alone (group 3), and boosted at wk 4 and 7 after the first immunization. The blood was taken and separated PBMCs were incubated with purified DHBsAg at 1 $\mu\text{g}/\text{mL}$ for 24 h. The cellular total RNA was extracted and DuIFN- γ mRNA was quantified by competitive RT-PCR. The ducks co-vaccinated with plasmids expressing DHBV-preS/S and DuIFN- γ showed a higher ratio of DuIFN- γ T/IC (1.56 \pm 0.08) than those immunized with plasmid expressing DHBV-preS/S alone (the ratio is 1.29 \pm 0.09), or normal ducks (0.92 \pm 0.06) 3 wk after immunization ($P<0.05$)

(Table 2 and Figure 4). The effects were more significant at wk 5 and 7 post-immunization ($P<0.01$), the ratios of DuIFN- γ T/IC were 2.51 \pm 0.11 and 1.81 \pm 0.10 in group 2, 1.96 \pm 0.17 and 1.26 \pm 0.11 in group 1, 1.33 \pm 0.11 and 0.94 \pm 0.04 in group 3 at wk 5 and 7, respectively. These results suggested that DuIFN- γ mRNA transcription of duck PBMCs was enhanced by DuIFN- γ as an immuno-adjuvant co-immunized with DNA vaccines.

Table 2 Detection of DuIFN- γ mRNA of PBMCs from ducks after immunization (mean \pm SD)

Immunized groups	Ratio of DuIFN- γ /IC (weeks after first vaccination)			
	1 wk	3 wk	5 wk	7 wk
Group 1 (DHBpreS/S DNA)	1.10 \pm 0.06	1.29 \pm 0.09 ^{a,b}	1.96 \pm 0.17 ^{a,b}	1.26 \pm 0.11 ^{a,b}
Group 2 (DHBpreS/S DNA+DuIFN- γ)	1.15 \pm 0.08	1.56 \pm 0.08 ^b	2.51 \pm 0.11 ^b	1.81 \pm 0.10 ^b
Group 3 (PBS)	1.04 \pm 0.03	0.92 \pm 0.06	1.33 \pm 0.11	0.94 \pm 0.04

^a $P<0.05$ vs group 2; ^b $P<0.01$ vs group 3.

Effects of DuIFN- γ as an adjuvant of DNA vaccine on anti-DHBpreS antibody responses in ducks

Anti-DHBpreS antibody responses in immunized ducks were detected by ELISA after the first vaccination (Figure 5), the titers of anti-DHBpreS antibody increased gradually after boost at wk 4 and 7. The titer of anti-DHBpreS in ducks vaccinated with DHBV preS/S DNA alone, gradually increased to 2^{7.4}-2^{10.6} from wk 4 to wk 13, and was higher than that in ducks co-immunized with plasmid expressing

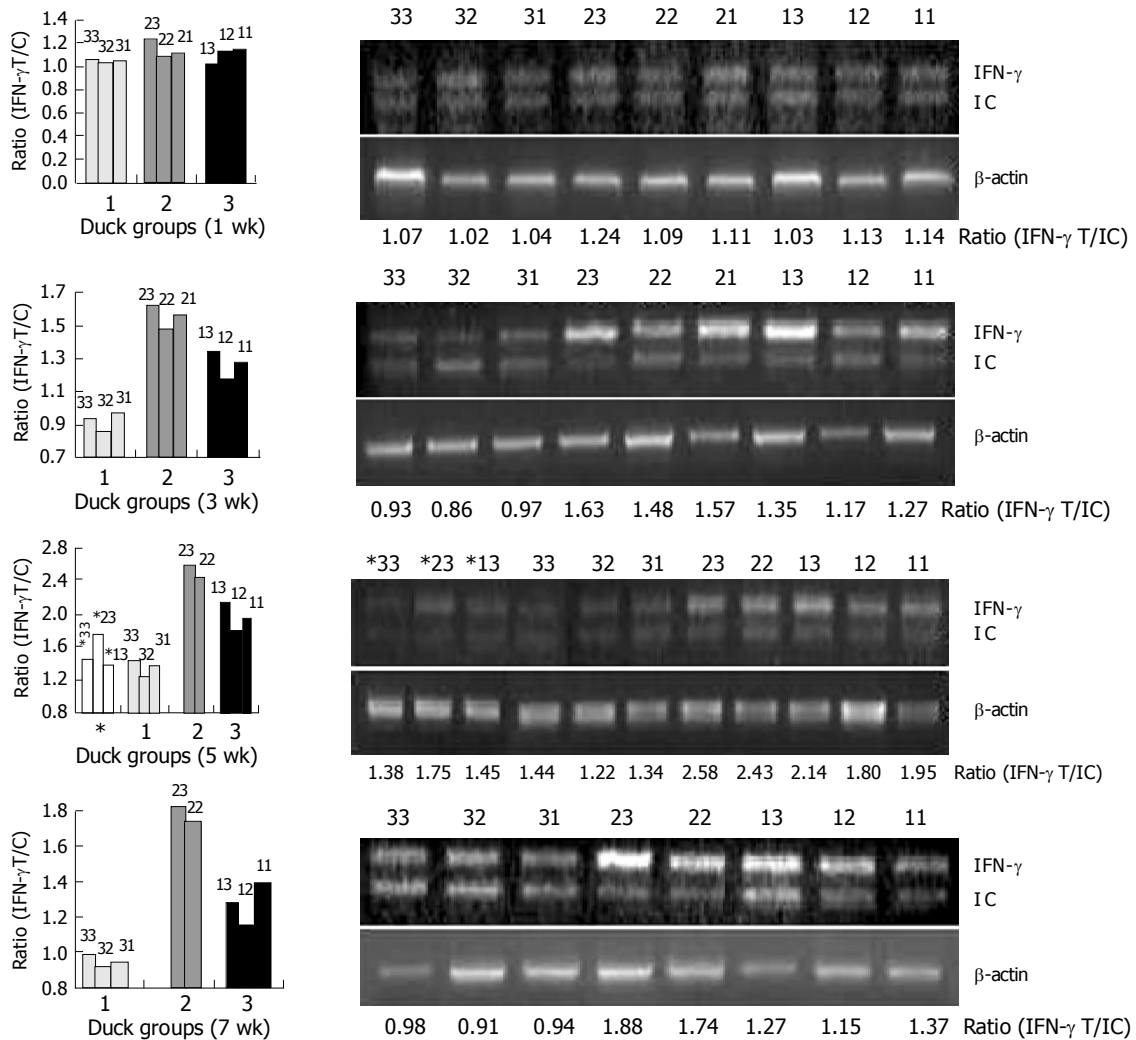


Figure 4 Detection of DuIFN- γ mRNA of PBMCs from ducks after immunization.

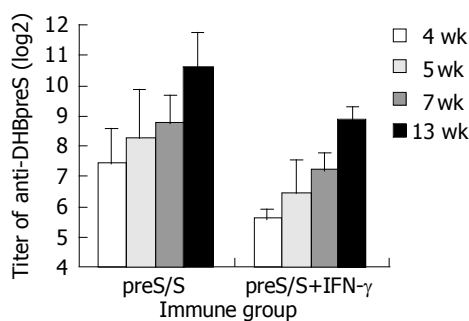


Figure 5 Anti-DHBpreS antibody responses following DNA immunization of DHBV-free ducks.

DuIFN- γ and DHBV preS/S DNA, whose titer of anti-DHBpreS was $2^{5.6}$ - $2^{8.8}$ from wk 4 to wk 13. The results showed that DHBV vaccine expressing DHBV preS/S induced antibody responses, but DuIFN- γ DNA down-regulated the elicitation of IgY against DHBV preS.

Clearance of viremia in vaccinated-ducks after being challenged with DHBV

To investigate the role of DuIFN- γ as an adjuvant of DNA

vaccines in protecting ducks against DHBV infection, 6 wk after the second boost, the vaccinated ducks were challenged with a high dose of DHBV according to their body weight (7.0×10^{10} /kg). The peripheral blood was collected from ducks at different time points after being challenged to detect DHBV DNA. The results showed that ducks co-vaccinated with plasmids expressing DuIFN- γ and DHBV preS/S had a stronger competence to remove DHBV from bloodstream than ducks immunized with DHBV preS/S DNA alone (Figure 6). After DHBV challenge, more than 50% of DHBV DNA in the blood of co-vaccinated ducks was removed in 5 min, whereas DHBV DNA in the ducks immunized with DHBV preS/S DNA alone decreased only a little in 45 min, and DHBV in both groups was undetectable at the last observation time point (120 min after virus challenge). As a viral infection control, the ducks immunized with PBS did not show significant viremia clearance in 120 min. We further detected the DHBV in liver 5 d after the challenge. Although total and ccc DHBV DNA could be detected in the liver, DHBV DNA was much lower in the ducks co-immunized with DuIFN- γ DNA than that in ducks injected only with DHBV preS/S DNA or PBS. The results indicated that DNA vaccine expressing DHBV preS/S protein enhanced the ability of ducks to exclude the DHBV

from bloodstream and remove the DHBV from liver. The capability of ducks was much more significantly upregulated by co-immunization with DuIFN- γ DNA than simple immunization with DHBV preS/S DNA (Figure 7).

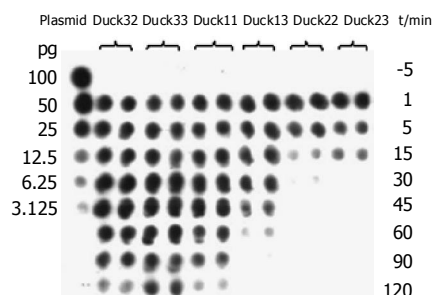


Figure 6 Exclusion of DHBV from bloodstream in DNA-vaccinated ducks following challenge with viruses.

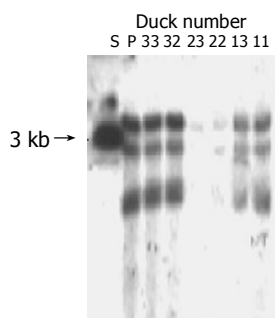


Figure 7 Detection of DHBV cccDNA in ducks' liver tissues after being challenged with high dose of DHBV. S: Full length fragment of DHBV genome, 3.0 kb. P: Positive control ducks infected DHBV.

DISCUSSION

IFN- γ plays a critical role in the host defense against virus infection. It was reported that IFN- γ regulates immune responses and induces strong Th1 biased responses, which are weak in persistent infection and immune tolerance^[21-23]. Transfer of specific CTLs to HBV transgenic mice could inhibit HBV replication in a non-cytolytic way and the CTL capacity of inhibiting HBV infection contributes to IFN- γ and TNF- α ^[2,3]. The efficacy of IFN- γ in inhibiting HBV replication is also observed by Suri *et al.*^[4]. Lu *et al.*^[5] showed that woodchuck IFN- γ *in vitro* upregulates the expression of MHC class I molecules, but does not inhibit the formation of WHV intermediates. Schultz and Chisari^[6], reported that duck IFN- γ inhibits DHBV replication in a dose-dependent fashion. In the present study, we found that recombinant duck IFN- γ could inhibit the release of DHBV from LMH-D2 cells, suggesting that duck IFN- γ can inhibit DHBV replication.

It has been reported that cytokines function as an efficient immuno-adjuvant, when animals are immunized with DNA vaccines^[24-26], but it is unknown whether DuIFN- γ gene also enhances the activity of DNA vaccine in protecting ducks against DHBV infection. Whether DNA vaccine expressing DHBV preS/S protein elicits neutralizing antibodies is still

controversial. Triyatni *et al.*^[11], reported that, DNA vaccine expressing DHBV preS/S induces high titer anti-DHBV preS/S, but shows less protection against virus infection than plasmid pCI/Amp expressing DHBV S protein. Plasmids expressing DHBV preS/S elicits high neutralizing antibodies and the protection could be transferred to offsprings through specific IgY^[12-14]. We have also proved the protective efficacy of DNA vaccine expressing DHBV preS/S, and showed that it could promote DuIFN- γ mRNA transcription of duck PBMCs and quicken the removal of virus from bloodstream and inhibit virus replication in liver, after being challenged with high titer viruses, when the plasmid expressing DuIFN- γ functioned as an immuno-adjuvant.

Little is known about the specific mechanism of DuIFN- γ enhancing the protective capacity of DNA vaccine. Since the titer of anti-DHBpreS elicited by DHBV preS/S DNA vaccine was down-regulated by DuIFN- γ in the present study, the affinity of antibody against antigen may be enhanced and more Th1 cytokines are induced to take effects synergistically. Furthermore, the number and killing capacity of specific cytotoxic lymphocytes could also increase. Further studies are necessary to clarify these important issues.

Thermet *et al.*^[27], have shown that DHBV preS/S DNA vaccine has some protective activity and early administration of anti-DHBV drugs such as lamivudine, significantly increases the protection and clears virus from chronic infection patient. However, it was not the case in our experiments and no significant differences were observed in virus-carriers between non-vaccinated and vaccinated ducks, including the ducks co-administered with plasmid expressing DuIFN- γ (data not shown). Many factors may affect the efficacy of vaccines, such as pathway of vaccination, DNA dosage and protocol. It is possible that the antigens in different pathways of vaccination recruit different antigen presenting cells. If the co-stimulatory signals are lost, immune tolerance but not viral clearance occurs^[28-30]. When animals are vaccinated at different growth phases, their ability to respond to antigens is significantly different. Also the distribution of the same antigen may affect the pathway of antigen presentation, which might be the reason, why viral antigen in circulating bloodstream cannot be cleared by host itself but DNA vaccines expressing antigen induces the efficacy of immune protection and exclude the viruses, when host is re-infected. Consequently, there is a long way to go for defining the molecular mechanism of DNA immunization and developing efficient vaccines.

REFERENCES

- 1 Bertoletti A, Maini M, Williams R. Role of hepatitis B virus specific cytotoxic T cells in liver damage and viral control. *Antiviral Res* 2003; **60**: 61-66
- 2 Guidotti LG, Ishikawa T, Hobbs MV, Matzke B, Schreiber R, Chisari FV. Intracellular inactivation of the hepatitis B virus by cytotoxic T lymphocytes. *Immunity* 1996; **4**: 25-36
- 3 Guidotti LG, Rochford R, Chung J, Shapiro M, Purcell R, Chisari FV. Viral clearance without destruction of infected cells during acute HBV infection. *Science* 1999; **284**: 825-829
- 4 Suri D, Schilling R, Lopes AR, Mullerova I, Colucci G, Williams R, Naoumov NV. Non-cytolytic inhibition of hepatitis B

- virus replication in human hepatocytes. *J Hepatol* 2001; **35**: 790-797
- 5 **Lu M**, Lohregel B, Hilken G, Kemper T, Roggendorf M. Woodchuck gamma interferon upregulates major histocompatibility complex class I transcription but is unable to deplete woodchuck hepatitis virus replication intermediates and RNAs in persistently infected woodchuck primary hepatocytes. *J Virol* 2002; **76**: 58-67
 - 6 **Schultz U**, Chisari FV. Recombinant duck interferon-gamma inhibits duck hepatitis B virus replication in primary hepatocytes. *J Virol* 1999; **73**: 3162-3168
 - 7 **Cova L**, Zoulim F. Duck hepatitis B virus model in the study of hepatitis B virus. *Methods Mol Med* 2004; **96**: 261-268
 - 8 **Jilbert AR**, Botten JA, Miller DS, Bertram EM, Hall PM, Kotlarski J, Burrell CJ. Characterization of age- and dose-related outcomes of duck hepatitis B virus infection. *Virology* 1998; **244**: 273-282
 - 9 **Jilbert AR**, Kotlarski I. Immune responses to duck hepatitis B virus infection. *Dev Comp Immunol* 2000; **24**: 285-302
 - 10 **Pertmer TM**, Oran AE, Madorin CA, Robinson HL. Th1 genetic adjuvants modulate immune responses in neonates. *Vaccine* 2001; **19**: 1764-1771
 - 11 **Triyatni M**, Jilbert AR, Qiao M, Miller DS, Burrell CJ. Protective efficacy of DNA vaccines against duck hepatitis B virus infection. *J Virol* 1998; **72**: 84-94
 - 12 **Rollier C**, Sunyach C, Barraud L, Madani N, Jamard C, Trepo C, Cova L. Protective and therapeutic effect of DNA-based immunization against hepadnavirus large envelope protein. *Gastroenterology* 1999; **116**: 658-665
 - 13 **Rollier C**, Charollos C, Jamard C, Trepo C, Cova L. Maternally transferred antibodies from DNA-immunized avians protect offspring against hepadnavirus infection. *J Virol* 2000; **74**: 4908-4911
 - 14 **Rollier C**, Charollos C, Jamard C, Trepo C, Cova L. Early life humoral response of ducks to DNA immunization against hepadnavirus large envelope protein. *Vaccine* 2000; **18**: 3091-3096
 - 15 **Schultz U**, Kock J, Schlicht HJ, Staeheli P. Recombinant duck interferon: a new reagent for studying the mode of interferon action against hepatitis B virus. *Virology* 1995; **212**: 641-649
 - 16 **Long JE**, Huang LN, Wang WY, Cheng MJ, Wen YM, Yuan ZH, Qu D. Cloning and Expression of Chinese Duck Interferon-gamma Gene. *Shengwuhuaxue Yu Shengwuwuli Xuebao* 2001; **33**: 707-712
 - 17 **Berg K**, Hansen MB, Nielsen SE. A new sensitive bioassay for precise quantification of interferon activity as measured via the mitochondrial dehydrogenase function in cells (MTT-method). *APMIS* 1990; **98**: 156-162
 - 18 **Berger J**, Hauber J, Hauber R, Geiger R, Cullen BR. Secreted placental alkaline phosphatase: a powerful new quantitative indicator of gene expression in eukaryotic cells. *Gene* 1988; **66**: 1-10
 - 19 **Long JE**, Huang LN, Qin ZJ, Wang WY, Cheng MJ, Qu D. Quantitation of IFN- γ mRNA in duck PBMC and Its Application. *Zhonghua Chuanranbing Zazhi* 2003; **23**: 529-533
 - 20 **Moraleda G**, Wu TT, Jilbert AR, Aldrich CE, Condreay LD, Larsen SH, Tang JC, Colacino JM, Mason WS. Inhibition of duck hepatitis B virus replication by hypericin. *Antiviral Res* 1993; **20**: 235-247
 - 21 **Tsai SL**, Sheen IS, Chien RN, Chu CM, Huang HC, Chuang YL, Lee TH, Liao SK, Lin CL, Kuo GC, Liaw YF. Activation of Th1 immunity is a common immune mechanism for the successful treatment of hepatitis B and C: tetramer assay and therapeutic implications. *J Biomed Sci* 2003; **10**: 120-135
 - 22 **Infante-Duarte C**, Kamradt T. Th1/Th2 balance in infection. *Springer Semin Immunopathol* 1999; **21**: 317-338
 - 23 **Jacobson Brown PM**, Neuman MG. Immunopathogenesis of hepatitis C viral infection: Th1/Th2 responses and the role of cytokines. *Clin Biochem* 2001; **34**: 167-171
 - 24 **Sasaki S**, Takeshita F, Xin KQ, Ishii N, Okuda K. Adjuvant formulations and delivery systems for DNA vaccines. *Methods* 2003; **31**: 243-254
 - 25 **Leclercq S**, Harms JS, Oliveira SC. Enhanced efficacy of DNA vaccines against an intracellular bacterial pathogen by genetic adjuvants. *Curr Pharm Biotechnol* 2003; **4**: 99-107
 - 26 **Chow YH**, Chiang BL, Lee YL, Chi WK, Lin WC, Chen YT, Tao MH. Development of Th1 and Th2 populations and the nature of immune responses to hepatitis B virus DNA vaccines can be modulated by codelivery of various cytokine genes. *J Immunol* 1998; **160**: 1320-1329
 - 27 **Thermet A**, Rollier C, Zoulim F, Trepo C, Cova L. Progress in DNA vaccine for prophylaxis and therapy of hepatitis B. *Vaccine* 2003; **21**: 659-662
 - 28 **Kiefer F**, Vogel WF, Arnold R. Signal transduction and costimulatory pathways. *Transpl Immunol* 2002; **9**: 69-82
 - 29 **Dennert G**. Elimination of virus-specific cytotoxic T cells in the liver. *Crit Rev Immunol* 2002; **22**: 1-11
 - 30 **Sebille F**, Vanhove B, Soullillou JP. Mechanisms of tolerance induction: blockade of co-stimulation. *Philos Trans R Soc Lond B Biol Sci* 2001; **356**: 649-657

Time-dependent viscoelastic properties along rat small intestine

James B Smith, Jing-Bo Zhao, Yan-Ling Dou, Hans Gregersen

James B Smith, Yan-Ling Dou, Hans Gregersen, Institute of Experimental Clinical Research, Aarhus University, Denmark
Jing-Bo Zhao, Hans Gregersen, Center of Excellence in Visceral Biomechanics and Pain, Aalborg Hospital and Center of SMI, Aalborg University, Aalborg, Denmark

Yan-Ling Dou, Department of Gastroenterology, China-Japan Friendship Hospital, Beijing 100029, China

Supported by the Karen Elise Jensens Foundation and the Danish Technical Research Council

Correspondence to: Dr. Hans Gregersen, MD, MSc, Director and Professor, Center of Excellence in Visceral Biomechanics and Pain, Aalborg Hospital, Hobrovej 42 A, Aalborg DK-9100, Denmark. hag@smi.auc.dk

Telephone: +45-99322064 Fax: +45-98133060

Received: 2004-12-01 Accepted: 2005-01-26

diseased intestinal tissue or intestinal tissue exposed to drugs or chemicals.

© 2005 The WJG Press and Elsevier Inc. All rights reserved.

Key words: Biomechanics; Standard linear solid; Creep; Opening angle

Smith JB, Zhao JB, Dou YL, Gregersen H. Time-dependent viscoelastic properties along rat small intestine. *World J Gastroenterol* 2005; 11(32): 4974-4978

<http://www.wjgnet.com/1007-9327/11/4974.asp>

Abstract

AIM: To measure the time-dependent (viscoelastic) behavior in the change of the small intestinal opening angle and to test how well the behavior could be described by the Kelvin model for a standard linear solid.

METHODS: Segments from the duodenum, jejunum, and ileum were harvested from 10 female Wistar rats and the luminal diameter, wall thickness, and opening angle over time ($\theta(t)$) were measured from rings cut from these segments.

RESULTS: Morphometric variations were found along the small intestine with an increase in luminal area and a decrease in wall thickness from the duodenum to the ileum. The opening angle obtained after 60 min was highest in the duodenum ($220.8 \pm 12.9^\circ$) and decreased along the length of the intestine to $143.9 \pm 8.9^\circ$ in the jejunum and $151.4 \pm 9.4^\circ$ in the ileum. The change of opening angle as a function of time, fitted well to the Kelvin model using the equation $\theta(t)/\theta_0 = [1 - \eta \exp(-\lambda t)]$ after the ring was cut. The computed creep rate λ did not differ between the segments. Compared to constant calculated from pig aorta and coronary artery, it showed that α agreed well (within 5%), η was three times larger than that for vascular tissue, and λ ranged $\pm 40\%$ from the value of the pig coronary artery and was a third of the value of pig aorta.

CONCLUSION: The change of opening angle over time for all the small intestine segments fits well to the standard linear spring-dashpot model. This viscoelastic constant of the rat small intestine is fairly homogenous along its length. The data obtained from this study add to a base set of biomechanical data on the small intestine and provide a reference state for comparison to other tissues,

INTRODUCTION

The small intestine, like other hollow organs such as heart, blood vessels, bladder and urethra, is functionally subjected to dimensional changes depending on active and passive biomechanical properties. Hence, the biomechanical properties of the small intestine are of particular functional importance.

Most of the data relating to the mechanical aspects of the gastrointestinal (GI) tract deal with motility patterns, flow rates, peristaltic reflexes, and tone in sphincter regions^[1-7]. Data in the literature pertaining to the passive mechanical properties of small intestine are concerned with the length-tension relationship in circular and longitudinal tissue strips *in vitro*^[8-11], the compliance^[12], and the stress-strain relationship of the intact wall^[13,14]. These studies have provided valuable information on some mechanical properties of small intestinal tissue and the distensibility of the intact intestinal wall. However, we still lack a complete database of mechanical parameters to fulfill detailed biomechanical analysis of small intestinal physiology.

In biomechanical analysis, it is important to determine the stress-free state as the reference for the strain analysis. Residual stress and strain are the internal stress and strain that reside in the organ when external forces are removed (the no-load state). Residual strain has been demonstrated in the small intestine^[15-18]. Residual stress reduces transmural stress and strain variations at physiological loads in biological tissues and hence may optimize the mechanical function. The opening angle is commonly used to characterize residual stresses in hollow organs, such as the cardiovascular system and the GI tract. When a hollow organ is cut into rings perpendicular to the central axis, and the rings are then cut radially, the rings will open over a period of time into sectors. When the opening angle has reached a final, static angle, the tissue is considered to have attained a "zero-stress state". Since zero-stress configuration serves as the reference state for computing stress and strain under physiological or

pathophysiological conditions, knowing it is essential in any mechanical analysis. It was reported that the opening angle of rat small intestine reached steady state opening angles after 30-60 min^[15-18].

Viscoelastic properties have been described for the normal and diseased human rectum using pressure data^[19,20]. The viscoelastic behavior of the intestinal wall during diabetes has been investigated by Zhao *et al.*^[21]. However, information is lacking in the time-dependent course of the opening angle. The gradual increase of opening angle over time, until reaching steady state is defined as creep and reflects the viscoelastic properties of the organ wall. The aims of the current study were: (1) to provide the data on the morphometry of the small intestine in rats, (2) to study the time-dependent changes of the opening angle (creep) along the length of the intestine and (3) to model this relationship based on the assumption that the small intestine behaves like a standard linear solid and derives viscoelastic constants to allow for comparison with other tissue types in the literature.

MATERIALS AND METHODS

Sample preparation

Ten female Wistar rats weighing 220-240 g were included in this study. The rats were anesthetized with pentobarbital sodium (50 mg/kg ip). Following laparotomy, the calcium antagonist, papaverine (60 mg/kg) was injected into the lower thoracic aorta through an iv cannula (22 G/25 mm), in order to abolish contractile activity in the GI tract. Once muscular relaxation was achieved, three 6 cm long segments were harvested from the duodenum, jejunum and ileum. The duodenum was taken from the descending part starting 1 cm from the pylorus, the jejunum from 5 cm distal to the ligament of Treitz, and the ileum from 5 cm proximal to the ileo-cecal valve. The residual contents in the lumens were gently cleared using saline and the segments were then placed immediately into cold Krebs solution containing 6% dextran and 10⁻² mol/L MgCl and aerated with a gas mixture (95% O₂ and 50 mL/L CO₂, pH 7.4) for 30 min.

From the proximal end of each segment, rings of 1-2 mm in length were cut for the morphometric measurement and zero-stress state experiment. Each ring was placed into a separate Petri dish filled with cold Krebs solution as mentioned above. The rings were placed into the dishes with a portion of the ring running between two metal pins planted into the surface of the dish in order to assist in keeping the rings upright after opening. Three successive rings from each of the three intestinal segments were arranged in series and the rings were cut radially opposite to the mesentery (at 90° relative to the horizontal plane) with a pair of microsurgery scissors, while in the solution. Successive rings were cut open, each after 5 min. Each series of rings was filmed using a video camera (SONY CCD Camera, Japan) and a videocassette recorder for later analysis.

Data analysis

The morphometric data were obtained from digitized images captured from videocassette at 10, 20, 30, 40, 50 s, 1, 2, 3, 4, 10 min, and every 5 min afterwards until 60 min after

the initial cut (Optimas 5.2 image capture software, Optimas Corp., USA). Measurements of inner diameter (d), wall thickness (w), and opening angle (θ) were made using dedicated software (Sigmascan 4.1, Jandel Scientific). The opening angle θ was defined as the angle subtended by two radii drawn from the midpoint of the inner wall to the inner tips of two ends of the specimen (Figure 1). The measured data were used to model the change of opening angle as a function of time, primarily by fitting the observed data to the Kelvin model for a standard linear solid (Figure 2). Thus, the data were fitted to the exponential function^[22]

$$\theta(t) = \theta_0 [1 - \eta e^{-\lambda t}] \quad (1)$$

where θ_0 = asymptotic steady state value of the opening angle, λ = the creep rate (s⁻¹), t = time after the initial cut (s), η = the creep fraction (nondimensional).

This equation relates to the Kelvin body as follows. In the model, μ_1 and μ_2 are spring constants and η_1 is a coefficient of viscosity. By letting

$$\tau_\epsilon = \frac{\eta_1}{\mu_1}, \tau_\sigma = \frac{\eta_1}{\mu_0} \left(1 + \frac{\mu_0}{\mu_1}\right), E_R = \mu_0, \quad (2)$$

where τ_ϵ = relaxation time for constant strain, τ_σ = relaxation time for constant stress, E_R = relaxed elastic modulus.

We obtained the equation describing this model:

$$c(t) = \frac{1}{E_R} \left[1 - \left(1 - \frac{\tau_\epsilon}{\tau_\sigma}\right) e^{-\frac{t}{\tau_\sigma}} \right]. \quad (3)$$

We defined

$$\alpha = \frac{1}{E_R}; \eta = 1 - \frac{\tau_\epsilon}{\tau_\sigma}; \lambda = \frac{1}{\tau_\sigma}. \quad (4)$$

The empirical constants η and λ could then be used to plot predicted creep curves and for comparison with other tissues.

For most rings, the opening angle reached 90% of its maximum value in 45 min. Subsequently, the opening angle data were normalized by the angle at 45 min before fitting the data to the exponential function. In order to take this normalization into account, the equation modeling a standard linear solid was modified as follows. Taking Equation (1) and letting $\theta(45 \text{ min}) = \alpha\theta_0$, we have

$$\frac{\theta(t)}{\theta(45 \text{ min})} = \frac{1}{\alpha} [1 - \eta e^{-\lambda t}]. \quad (5)$$

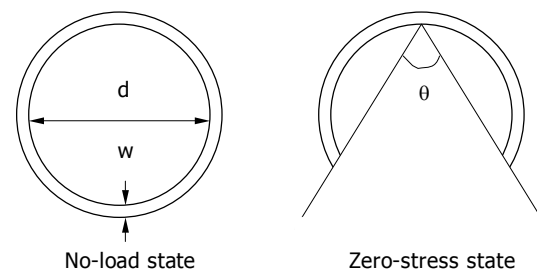


Figure 1 Schematic diagram of wall thickness (w), inner diameter (d), and opening angle (θ) for a ring radially cut into a sector.

The empirical constants α , η , and λ were calculated for the data obtained in this study and are presented in Table 2.

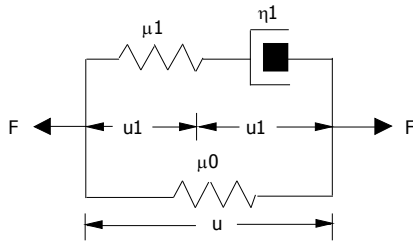


Figure 2 Kelvin body, a mechanical model for a standard linear solid viscoelastic material. μ_1 and μ_0 are spring constants; η_1 is a coefficient of viscosity; u is the displacement including u_1 for dashpot and u_1' for spring; F is the sum of the force.

Statistical analysis

The data were representative of a normal distribution and results were subsequently expressed as mean±SE. Analysis of variance (ANOVA) was used to test for the differences in the viscoelastic constants (α , η , and λ) for the various intestinal segments (Sigmastat 2.0™). In case of significance, data were evaluated in pairs by a multiple comparison procedure (Student-Newman-Keuls method). If the normality test or the equal variance test failed, Kruskal-Wallis one-way analysis of variance on ranks was used. $P < 0.05$ was considered statistically significant.

RESULTS

Morphometry data

Seventy-eight intestinal rings, and 30 duodenal, 18 jejunal, and 30 ileal rings were obtained from 10 rats. There were fewer jejunal rings because the jejunum was implemented in the study after the fourth rat was completed. This was done in order to obtain a more complete dataset. The highest wall thickness of 0.88 ± 0.03 mm was found in the duodenum. The wall thickness decreased to 0.72 ± 0.06 mm in jejunum and 0.66 ± 0.02 mm in ileum ($P < 0.05$). The biggest inner diameter was in the ileal rings and the smallest in the jejunal rings ($P < 0.05$). The maximum opening angle was achieved within 60 min, and it was highest in the duodenum ($220.8 \pm 12.9^\circ$) and decreased along the length of small intestine ($P < 0.01$).

Table 1 Average opening angle at 45 and 60 min and maximal luminal area and wall thickness for rings cut from rat duodenum, jejunum, and ileum from rat intestine (mean±SE)

	Duodenum	Jejunum	Ileum
Angle (45 min)	211.1±17.2	128.5±10.1 ^b	145.9±9.2 ^b
Angle (60 min)	220.8±12.9	143.9±8.9 ^b	151.4±9.3 ^b
Lumen diameter (mm)	0.86±0.03	0.73±0.04 ^a	0.89±0.03
Wall thickness (mm)	0.88±0.03	0.72±0.06 ^a	0.66±0.02 ^b

^a $P < 0.05$, ^b $P < 0.01$ vs duodenum.

Creep of opening angle

The changes of opening angle and normalized opening

angle as function of time (creep) are shown in Figure 3. The opening angles became bigger as function of time. The opening angle was significantly bigger in the duodenal rings than in the other two segmental rings at all time points (Figure 3 top, $P < 0.01$). However, the opening angles did not differ between the jejunal and ileal rings (Figure 3 top, $P > 0.05$). After the opening angle data were normalized by the angle at 45 min, the normalized opening angles as function of time did not differ between the duodenal, jejunal and ileal rings (Figure 3 bottom, $P > 0.05$).

The empirical constants α , η , and λ from a standard linear model analysis did not differ between the different segments (Table 2, $P > 0.05$). Experimental data and predicted data are shown in Figure 4. The solid points represent experimental data of $\theta(t)/\theta(45 \text{ min})$, and the hollow points represent calculated values of $\theta(t)/\theta_0$ using the empirical constants α , η , and λ . It showed that the predicted creep curves agreed well with data obtained from this study.

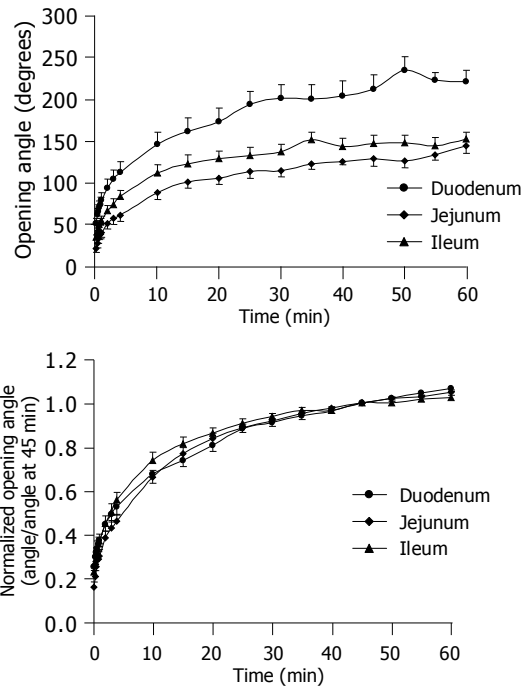


Figure 3 Changes of opening angle and normalized opening angle as function of time.

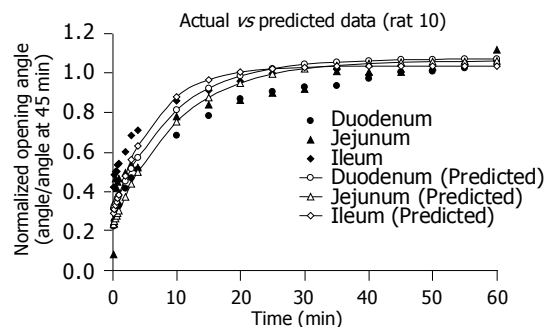


Figure 4 Experimental data and predicted data in rat 10.

Table 2 Standard linear solid coefficients determined for duodenum, jejunum, and ileum of rat small intestine (mean±SE)

	α	η	λ (s ⁻¹)	R ²
Duodenum	0.954±0.023	0.710±0.013	1.04×10 ⁻³ ±1.09 ⁻⁰⁴	0.989
Jejunum	0.978±0.017	0.779±0.012	1.29×10 ⁻³ ±1.05 ⁻⁰⁴	0.992
Ileum	1.005±0.013	0.720±0.012	1.63×10 ⁻³ ±1.33 ⁻⁰⁴	0.992

DISCUSSION

The time-dependent change of the intestinal opening angle reflects viscoelastic properties (creep). The major finding in this study is that the opening angles at all time points are bigger in the duodenum than in the jejunum and ileum in the normal rats. The change of opening angle for all the small intestine segments showed a slow creep phase and the behavior fitted well to the standard linear spring-dashpot model. The empirical constants α , η , and λ calculated from the standard linear solid model did not differ among the three intestinal segments. Furthermore, we have confirmed previous data that both opening angle and the wall thickness decrease from the duodenum to the ileum, whereas the lumen area increases.

Axial variations of morphometric parameters of small intestine

Our results and previous study^[15] has demonstrated substantial axial variations of the morphometric parameters. A decrease in wall thickness is in line with findings in prior studies^[24]. Several zero-stress state studies have been done in the GI tract^[15-18]. All GI studies done so far showed that the rings open into sectors when cut radially. When radial cuts are made, the duodenal rings are more likely to turn inside out producing large opening angles and therefore indicate a larger residual strain than the jejunal and ileal rings^[15]. From a mechanical point of view, a large residual strain may be a natural way of efficiently resisting luminal pressures. Thus, it is likely that the compressed duodenal mucosa may be better protected against injury from pressure changes produced by frequent contractions and the luminal contents ejected at intervals from stomach. In contrast, the less compressed ileal mucosa represents a region under a relatively lower and stable pressure.

Creep of opening angle of intestinal segments

Creep occurs when the material is suddenly stressed and the stress is maintained constant. Hence, the material continues to deform^[25]. Creep is a feature of viscoelasticity that is found in most materials including those in the GI tract. Mechanical models, such as the Maxwell model, the Voigt model, and the Kelvin model (also called the standard linear solid)^[25,26] are often used to describe the visco-elastic behavior of materials. We assumed that the intestine was a standard linear solid and described the change of opening angles of intestine as function of time using this model. A slow creep phase was found and the behavior fitted well to the standard linear spring-dashpot model. Bharucha *et al.*^[27], developed a technique to assess quasi-static colonic P-V curves in the human descending colon and demonstrated that colonic P-V curves approximate to a power exponential function and are reproducible within subjects. In the present

study, the experimental data also fit to the exponential function^[22]. The predicted creep curves were plotted using the empirical constants α , η , and λ calculated for standard linear solid model. The constants were relatively similar for all three intestinal segments, indicating that the viscoelastic properties of the rat small intestine are fairly homogenous. This is consistent with the relaxation data of normal small intestine reported by Zhao *et al.*^[21], (unpublished data). Using these constants, it was also found that $\theta(t)/\theta_0$ reached 95% of the full amplitude after 35 min for the duodenum and jejunum and after 30 min for the ileum. The data obtained from this study add to a base set of morphometric and biomechanical data on the small intestine. These data also provide a reference state for comparison to other tissues, diseased intestine or intestine exposed to drugs or chemicals.

Comparison to other studies

The research by Han and Fung^[22] on the pig aorta showed that the opening angle reaches 95-98% of the steady-state value after 10-15 min. The constants α , η , and λ obtained in the present study were compared to those calculated from work done by Han and Fung^[22] and Frobert *et al.*^[23], for pig aorta and coronary artery (Table 3). The results for α agreed very well, η was three times larger than that for vascular tissue and λ ranged $\pm 40\%$ of the value found by Frobert *et al.*^[23], for the pig coronary artery and was a third of the value that was found by Han and Fung^[22] for the pig aorta. It is likely that the differences are caused by structural differences between tissues^[25]. Studies using enzymatic digestion of structural components have been carried out on the zero-stress state analysis of the cardiovascular system^[28]. Similar studies may shed more light on the viscoelastic properties of different tissue components in the intestine.

In conclusion, the geometric parameters and biomechanical properties of the different segments of small intestine are different. The results obtained from this study add to a base set of morphometric and biomechanical data on the small intestine. The data obtained in this study provide a reference state for future comparison to other tissues, diseased intestinal tissue or intestinal tissue exposed to drugs or chemicals.

Table 3 Comparison of standard linear solid coefficients obtained in this study and from the literature

	Rat duodenum	Rat jejunum	Rat ileum	Pig aorta ^[22]	Pig coronary artery ^[23]
α	0.954	0.978	1.005	0.981	0.971
η	0.710	0.779	0.720	0.263 ^b	0.274 ^b
λ (s ⁻¹)	1.04×10 ⁻³	1.29×10 ⁻³	1.63×10 ⁻³	3.31×10 ^{-3b}	1.17×10 ⁻³

^b $P < 0.01$ vs rat intestine.

REFERENCES

- 1 **Bueno L**, Fioramonti J, Ruckebusch Y. Rate of flow of digesta and electrical activity of the small intestine in dogs and sheep. *J Physiol* 1975; **249**: 69-85
- 2 **Ehrlein HJ**, Schemann M, Siegle ML. Motor patterns of small intestine determined by closely spaced extraluminal transducers and videofluoroscopy. *Am J Physiol* 1987; **253**: G259-G267

- 3 **Kellow JE**, Borody TJ, Phillips SF, Tucker RL, Haddad AC. Human interdigestive motility: variations in patterns from esophagus to colon. *Gastroenterology* 1986; **91**: 386-395
- 4 **Quigley EM**, Borody TJ, Phillips SF, Wienbeck M, Tucker RL, Haddad A. Motility of the terminal ileum and ileocecal sphincter in healthy humans. *Gastroenterology* 1984; **87**: 857-866
- 5 **Quigley EM**, Phillips SF, Dent J. Distinctive patterns of interdigestive motility at the canine ileocolonic junction. *Gastroenterology* 1984; **87**: 836-844
- 6 **Schulze-Delrieu K**. Intrinsic differences in the filling response of the guinea pig duodenum and ileum. *J Lab Clin Med* 1991; **117**: 44-50
- 7 **Weems WA**, Seygal GE. Fluid propulsion by cat intestinal segments under conditions requiring hydrostatic work. *Am J Physiol* 1981; **240**: G147-G156
- 8 **Meiss RA**. Some mechanical properties of cat intestinal muscle. *Am J Physiol* 1971; **220**: 2000-2007
- 9 **Price JM**, Patitucci PJ, Fung YC. Mechanical properties of resting taenia coli smooth muscle. *Am J Physiol* 1979; **236**: C211-C220
- 10 **Yamada H**. Strength of biological materials. *Gaynor Evans, Williams & Wilkins Company, Baltimore* 1970
- 11 **Elbrond H**, Tottrup A, Forman A. Mechanical properties of isolated smooth muscle from rabbit sphincter of Oddi and duodenum. *Scand J Gastroenterol* 1991; **26**: 289-294
- 12 **Storkholm JH**, Villadsen GE, Jensen SL, Gregersen H. Mechanical properties and collagen content differ between isolated guinea pig duodenum, jejunum, and distal ileum. *Dig Dis Sci* 1998; **43**: 2034-2041
- 13 **Duch BU**, Petersen JA, Vinter-Jensen L, Gregersen H. Elastic properties in the circumferential direction in isolated rat small intestine. *Acta Physiol Scand* 1996; **157**: 157-163
- 14 **Storkholm JH**, Villadsen GE, Jensen SL, Gregersen H. Passive elastic wall properties in isolated guinea pig small intestine. *Dig Dis Sci* 1995; **40**: 976-982
- 15 **Dou Y**, Zhao J, Gregersen H. Morphology and stress-strain properties along the small intestine in the rat. *J Biomech Eng* 2003; **125**: 266-273
- 16 **Gao C**, Zhao J, Gregersen H. Histomorphometry and strain distribution in pig duodenum with reference to zero-stress state. *Dig Dis Sci* 2000; **45**: 1500-1508
- 17 **Gregersen H**, Kassab G. Biomechanics of the gastrointestinal tract. *Neurogastroenterol Motil* 1996; **8**: 277-297
- 18 **Gregersen H**, Kassab G, Pallencaoe E, Lee C, Chien S, Skalak R, Fung YC. Morphometry and strain distribution in guinea pig duodenum with reference to the zero-stress state. *Am J Physiol* 1997; **273**: G865-G874
- 19 **Arhan P**, Faverdin C, Persoz B, Devroede G, Dubois F, Dornic C, Pellerin D. Relationship between viscoelastic properties of the rectum and anal pressure in man. *J Appl Physiol* 1976; **41**: 677-682
- 20 **Arhan P**, Devroede G, Danis K, Dornic C, Faverdin C, Persoz B, Pellerin D. Viscoelastic properties of the rectal wall in Hirschsprung's disease. *J Clin Invest* 1978; **62**: 82-87
- 21 **Zhao J**, Liao D, Yang J, Gregersen H. Viscoelastic behavior of small intestine in streptozotocin-induced diabetic rats. *Dig Dis Sci* 2003; **48**: 2271-2277
- 22 **Han HC**, Fung YC. Species dependence of the zero-stress state of aorta: pig versus rat. *J Biomech Eng* 1991; **113**: 446-451
- 23 **Frobert O**, Gregersen H, Bjerre J, Bagger JP, Kassab GS. Relation between zero-stress state and branching order of porcine left coronary arterial tree. *Am J Physiol* 1998; **275**: H2283-2290
- 24 **Gabella G**. Hypertrophy of visceral smooth muscle. *Anat Embryol* 1990; **182**: 409-424
- 25 **Fung YC**. Biomechanics: Mechanical properties of living tissues. 2nd ed. *New York, Springer Verlag* 1993: 41-52
- 26 **Gregersen H**. Biomechanics of the Gastrointestinal Tract. First ed. *London, Springer Verlag* 2002: 66-67
- 27 **Bharucha AE**, Hubmayr RD, Ferber IJ, Zinsmeister AR. Viscoelastic properties of the human colon. *Am J Physiol Gastrointest Liver Physiol* 2001; **281**: G459-G466
- 28 **Zeller PJ**, Skalak TC. Contribution of individual structural components in determining the zero-stress state in small arteries. *J Vasc Res* 1998; **35**: 8-17

CXCL16 participates in pathogenesis of immunological liver injury by regulating T lymphocyte infiltration in liver tissue

Huan-Bin Xu, Yan-Ping Gong, Jin Cheng, Yi-Wei Chu, Si-Dong Xiong

Huan-Bin Xu, Yan-Ping Gong, Jin Cheng, Yi-Wei Chu, Si-Dong Xiong, Department of Immunology and Key Laboratory of Molecular Medicine of Ministry of Education, Shanghai Medical College of Fudan University; Immunology Division, E-Institute of Shanghai Universities, Shanghai 200032, China

Supported by the National Natural Science Foundation of China, No. 30230320, National Science Fund for Distinguished Young Scholars from NSFC, No. 39925031, National High Technology Research and Development Program of China, 863 grant 2004 AA215242, Major State Basic Research Development Program of China, No. 2001CB510005 and partially by E-Institute of Shanghai Universities

Correspondence to: Dr. Si-Dong Xiong, Department of Immunology, Shanghai Medical College of Fudan University, 138 Yixueyuan Road, Shanghai 200032, China. sdxiong@shmu.edu.cn

Telephone: +86-21-54237749 Fax: +86-21-54237749

Received: 2004-10-21 Accepted: 2004-12-26

Abstract

AIM: To investigate the role of CXCL16 in the pathogenesis of immunological liver injury and to explore the possible mechanism of T lymphocyte infiltration regulated by CXCL16.

METHODS: Immunological liver injury in murine model was induced by Bacille Calmette-Guerin and lipopolysaccharide. Expression pattern and distribution of CXCL16 were examined by real-time quantitative RT-PCR and immunohistochemical analysis. Anti-CXCL16 antibody was administered *in vivo* to investigate its effect on T-cell recruitment and acute hepatic necrosis. The survival of murine model was also evaluated.

RESULTS: The murine immunological liver injury model was successfully established. CXCL16 expression increased and predominantly distributed in periportal areas and vascular endothelia in injured liver tissues. Administration of anti-CXCL16 Ab protected the mice from death and acute liver damage. Approximately 70% of the mice survived for 72 h in the anti-CXCL16 Ab treatment group, whereas 80% died within 72 h in control Ab group. The number of liver-infiltrating T lymphocytes was significantly reduced from 1.01×10^7 to 3.52×10^6 /liver, compared with control Ab treatment.

CONCLUSION: CXCL16 is involved in immunological liver injury by regulating T lymphocyte infiltration in liver tissue.

© 2005 The WJG Press and Elsevier Inc. All rights reserved.

Key words: Chemokines; CXCL16; T lymphocytes; Infiltration; Immunological liver injury

Xu HB, Gong YP, Cheng J, Chu YW, Xiong SD. CXCL16 participates in pathogenesis of immunological liver injury by regulating T lymphocyte infiltration in liver tissue. *World J Gastroenterol* 2005; 11(32): 4979-4985

<http://www.wjgnet.com/1007-9327/11/4979.asp>

INTRODUCTION

Immunological liver injury is a key pathological change in liver disease, with a high mortality rate and histopathologically characterized by diffuse intrahepatic infiltration of inflammatory cells with massive multilobular necrosis. The details of the mechanisms involved in immunological liver injury remain to be elucidated. It was reported that injection of a small dose of lipopolysaccharide (LPS) into mice primed with Bacille Calmette-Guerin (BCG) causes lethal acute hepatic necrosis^[1], mimicking fulminant hepatic failure. There is evidence that activated macrophages and T lymphocytes are essential for the induction of liver damage^[2-5].

The current paradigm of T lymphocytes recruited to the inflamed liver is a multiple-step model, which describes the sequence of tethering/rolling, firm adhesion, and diapedesis/extravasation^[6,7]. The chemokine family is a small secreted protein, that directs migration of various types of leukocytes and is involved in inflammatory and immunological processes including lymphocyte homing, angiogenesis and enhancement of cytotoxic T lymphocyte (CTL) responses^[8,9]. Chemokines have been classified into four subfamilies, C, CC, CXC and CX₃C, based on the motif formed by the conserved cysteine residues in the N-terminal region. The selective interaction of chemokines and their receptors in part contributes to the specificity by which leukocyte subsets might be preferentially determined^[10,11].

CXCL16, with its structure similar to that of FKN^[12], containing both membrane-anchored and soluble forms, is a ligand for CXC chemokine receptor 6 (CXCR6), which is expressed on natural killer T (NKT) cells, and type 1-polarized, activated CD4+ and CD8+ T cells. CXCL16 is markedly expressed in lung, small intestine and kidney, and weakly expressed in liver^[13-18]. Because the pathological characteristics of immunological liver injury are associated with T-lymphocyte infiltration, and CXCL16 is chemotactic for T-lymphocyte migration to the liver tissue damage^[4,5,19-21], we could reason that CXCL16 might play a crucial role in the pathogenesis of immunological liver injury. In the present study, we investigated the expression pattern and distribution of CXCL16, and studied the role of CXCL16 in liver T-cell infiltration, and the effect of anti-CXCL16 antibody on the pathogenesis of immunological liver injury.

MATERIALS AND METHODS

Mice

Specific pathogen-free BALB/c mice (6-7 wk old) obtained from Shanghai Animal Center of Chinese Academy of Sciences (Shanghai, China) were bred in pathogen-free conditions and allowed free access to food and water.

Reagents

LPS (*Escherichia coli* 055:B5) was purchased from Sigma (St. Louis, MO). BCG was from Institute of Biological Product (Shanghai, China). Rat immunoglobulin (goat IgG) was gifted by Dr. XL Wang. Rat anti-mouse CXCL16 mAb (clone 142417, rat IgG2a) was obtained from R&D systems. PE-labeled anti-CD4 mAb and FITC-conjugated anti-CD8 mAb were obtained from PharMingen (San Diego, CA, USA). TRIzol RNA extraction kit was purchased from Gibco. All other chemicals used were of analytical grade.

Induction of liver injury by BCG and LPS

BCG was suspended in pyrogen-free physiological saline. To induce liver injury, mice were primed with intravenous injection of BCG (5×10^7 viable bacilli) via tail veins. After 12 d, they were given an intravenous injection of LPS (7.5 $\mu\text{g}/\text{mouse}$) suspended in pyrogen-free phosphate-buffered saline (PBS). To examine the effect of anti-CXCL16 antibodies on BCG-LPS-induced liver injury, monoclonal anti-CXCL16 antibody (0.2 mg/mouse) or nonimmune rat isotype IgG (0.2 mg/mouse) was administered intravenously 1-2 h before LPS challenge. Mice were killed to collect sera and liver specimens, and stored at -70°C until use. Survival rate was determined 72 h after the LPS challenge.

Determination of serum alanine transferase (ALT)

Serum was collected for the measurement of ALT levels at various time points after LPS challenge.

Histology

Liver specimens were fixed in 10% neutrally buffered formalin and embedded in paraffin. Deparaffinized thin sections from each paraffin block were stained with hematoxylin and eosin for histologic examination and analyzed by light microscopy.

Analysis of specific gene expression in liver tissue by real-time quantitative RT-PCR

Total RNA was isolated from liver specimens using TRIzol, according to the manufacturer's instructions. The specific mRNA level was quantified by real-time quantitative PCR using a LightCycler instrument (Roche Molecular Biochemicals, Germany) with the DNA binding dye SYBR Green I as described with minor modifications^[22]. The sense primer for CXCL16 was 5'-AAC CAG GGC AGT GTC GC-3', and the antisense primer was 5'-AGG CAA ATG TTT TTG GTG G-3' (position: 79-342). The sense primer for β -actin was 5'-GCT ACA GCT TCA CCA CCA CAG-3', and the antisense primer was 5'-GGT CTT TAC GGA TGT CAA CGT C-3' (position: 590-877). Expression of mRNA was normalized by β -actin. In brief, external standards were

plasmids containing CXCL16 gene fragment (and β -actin). Plasmid DNA was purified and quantified photometrically and serially diluted. One microgram total RNA was reverse transcribed to cDNA. One microliter cDNA or external standard was added to capillary to a final reaction volume of 20 μL . The primer final concentration was adjusted to 0.5 $\mu\text{mol}/\text{L}$. The amplification conditions were initial denaturation at 95°C for 30 s, 45 cycles at 95°C for 0 s, at 60°C for 3 s, at 72°C for 12 s. Melting curve analysis was performed at the end of amplification. The acquisition temperature for the fluorescence signal was adjusted to 84°C . PCR products were electrophoresed on 2% agarose gels and photos were taken under ultraviolet light to identify their specificity and sensitivity.

Immunohistochemistry

Experiments were conducted on frozen sections as described in detail elsewhere^[23]. Sections were incubated with primary antibody, and then with HRP-conjugated anti-rat IgG antibodies. After being visualized using DAB containing 0.01% hydrogen peroxide and counterstained with hematoxylin, sections were microscopically examined. Control sections were treated with omission of the primary antibody.

Preparation of intrahepatic infiltrating leukocytes and FACS analysis

Liver-infiltrating leukocytes were prepared as previously described^[24]. In brief, livers were taken from mice, pressed through the nylon mesh, and suspended in 2% fetal calf serum (FCS). The cell suspension was treated with Percoll density (1.09) gradient centrifugation. Mononuclear cells (MNCs) were isolated from parenchymal hepatocytes by centrifugation at 2 500 r/min for 30 min. The pellet was washed thrice in DMEM and resuspended in 10% FCS-DMEM. Flow cytometric immunofluorescence analysis of liver-infiltrating cells was performed with FACS caliber (BD Corp.). In brief, 4×10^5 cells were incubated with a PE-labeled anti-CD4 Ab and FITC-conjugated anti-CD8 Ab or FITC-conjugated anti-CD3 Ab at 4°C for 30 min after washing twice with PBS solution.

Statistical analysis

All statistical calculations were performed using GraphPad PRISMTM (Graphpad Software Inc.). The survival rates were analyzed using the log-rank test. Student's *t* test was used to test for significance. $P < 0.05$ was considered statistically significant.

RESULTS

Establishment of immunological liver injury model in mice

BCG treatment alone induced MNC infiltration into hepatic lobes and formed granuloma (Figure 1B). Subsequent LPS challenge in BCG-primed mice induced diffuse infiltration of MNCs and multilobular hepatocellular necrosis in liver tissue (Figure 1C). The ALT level dramatically increased in BCG-primed mice after LPS challenge (Figure 2) compared to BCG treatment alone ($P < 0.05$). All these data confirmed that the murine immunological liver injury model was successfully conducted.

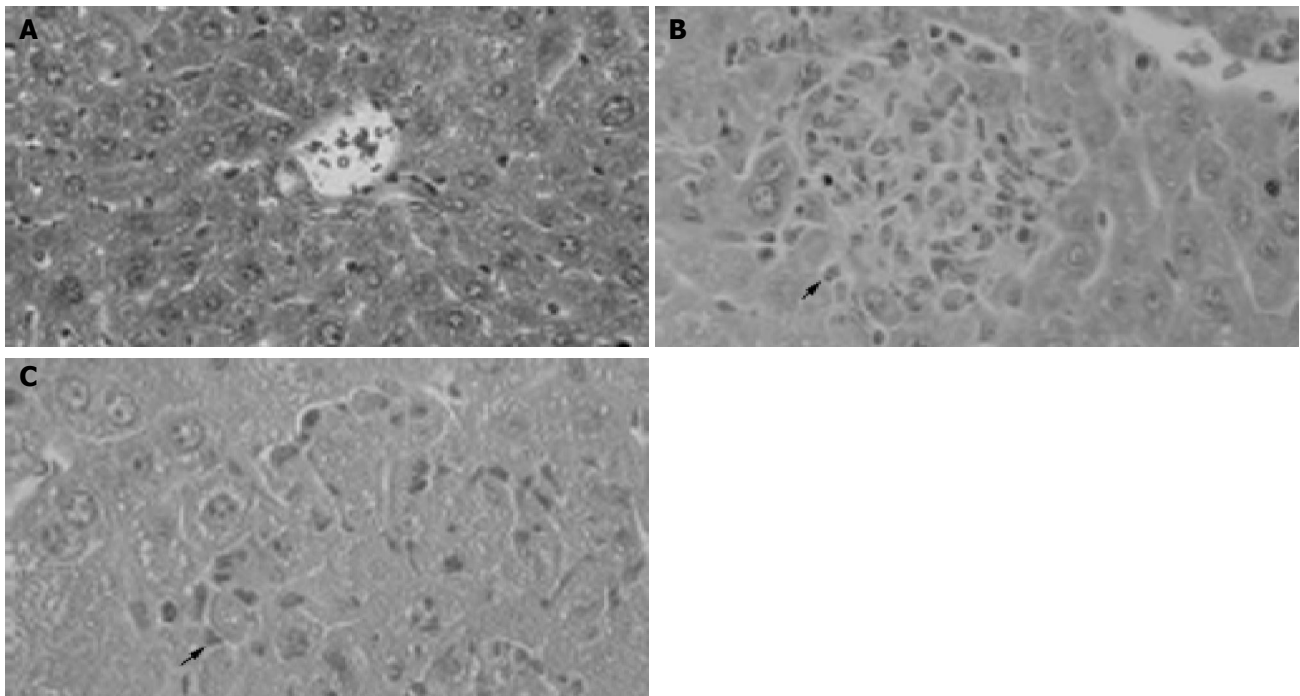


Figure 1 Pathological examination showing granuloma formation with BCG administration and hepatocellular necrosis followed by LPS injection. H&E staining

of cross-sections of normal liver (A), 12 d after BCG injection (B) and BCG-primed mice sequentially challenged with LPS (C). Bars = 20 μ m.

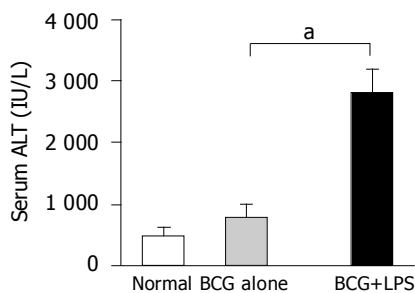


Figure 2 Levels of serum ALT in mice. The serum ALT levels of mice ($n = 5$ at each group) were measured as described in Materials and methods. Data represent mean \pm SD. ^a $P < 0.05$ vs BCG-primed mice.

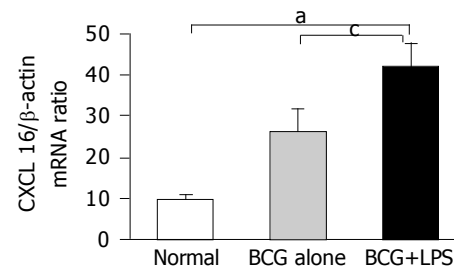


Figure 3 Detection of CXCL16 mRNA in the injured liver by real-time quantitative RT-PCR analysis. Total RNA was isolated from the liver tissues at the different group as indicated and then reverse transcribed with reverse transcriptase and amplified by real-time quantitative PCR specific for CXCL16. Amplification of β -actin by same approach was used as control. The results represent three independent experiments. ^a $P < 0.05$ vs normal mice, ^c $P < 0.05$ vs BCG-primed mice.

Expression pattern and distribution of CXCL16 in murine injured liver model

Total RNA were isolated from liver tissue of normal, BCG-treated and BCG-primed mice after LPS challenge. CXCL16 mRNA was quantified by real-time quantitative PCR. CXCL16 was expressed in BCG-primed mice and strongly upregulated after LPS challenge, compared to that in normal liver tissue (Figure 3). These results suggested that upregulation of CXCL16 expression might be associated with liver injury.

Immunohistochemical analysis further showed that expression of CXCL16 in the liver significantly increased after LPS challenge in BCG-primed mice, compared to that in normal mice (Figure 4). CXCL16 was predominantly distributed in periportal area, hepatic sinusoids and vascular endothelia (Figure 4).

Infiltration of T lymphocytes in injured liver tissue

To investigate the characteristics of circulating T lymphocyte recruitment and infiltration in immunological liver injury,

cell surface expressions of CD3, CD4 and CD8 in the infiltrated MNCs were analyzed using a flow cytometer. The results revealed that the CD4⁺ T lymphocyte population increased from 0.92% to 2.93%, and further increased to 11.2% in BCG-primed mice after LPS challenge. CD8⁺ T lymphocyte population also increased from 0.16% to 1.56%, and reached 2.35% after LPS challenge (Figure 5A). The total absolute number of T lymphocytes increased from 0.399×10^6 to 3.179×10^6 /liver and reached 1.01×10^7 /liver in BCG-primed mice injected with LPS (Figure 5B). These findings demonstrated that T lymphocytes might be involved in the pathogenesis of immunological liver injury.

Anti-CXCL16 antibody increased survival of mice with immunological liver injury

Neutralizing anti-CXCL16 antibody could protect mice

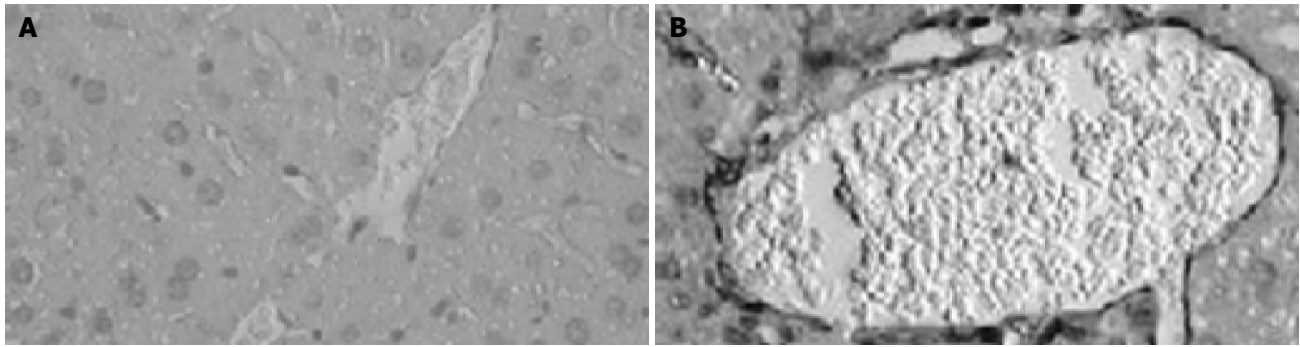


Figure 4 Immunohistochemical examination of CXCL16 expression in liver tissue. Sections of livers were obtained from normal mice without any treatment (A) and BCG-primed mice sequentially injected with LPS (B). CXCL16-positive

(brown) cells are shown in the liver tissue with hematoxylin counterstaining. Bars = 20 μm.

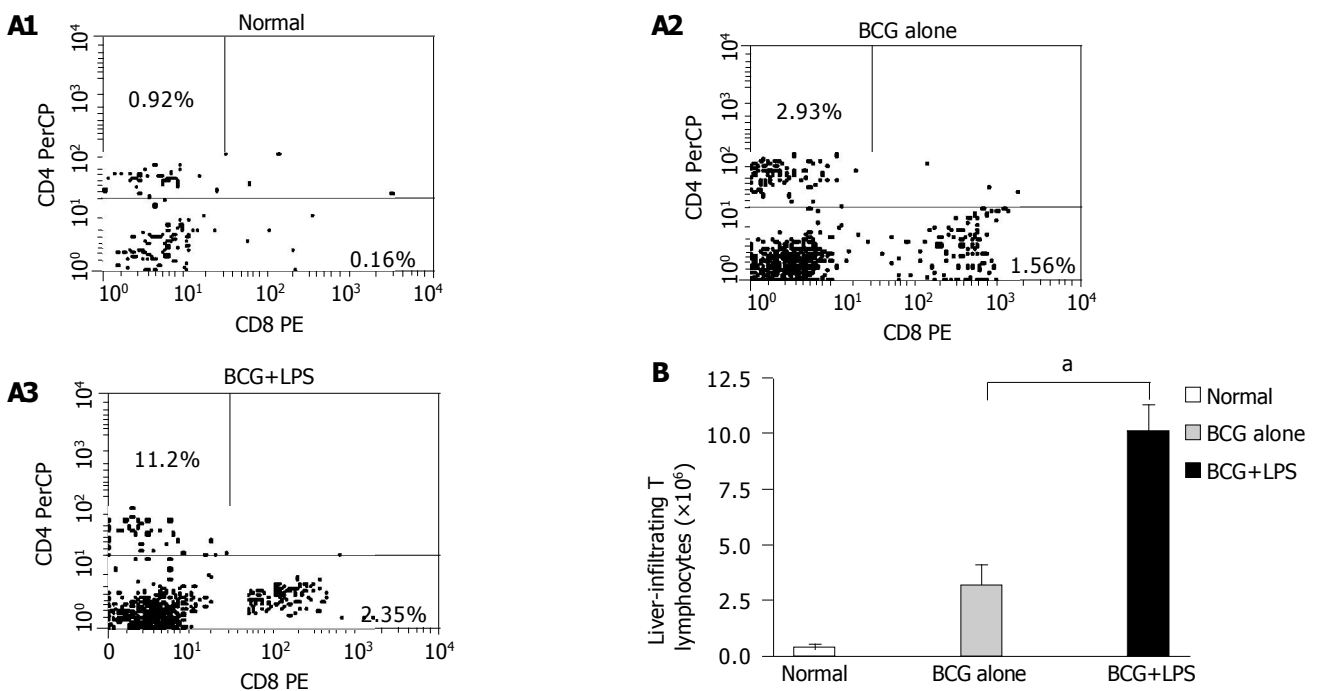


Figure 5 Analysis of liver-infiltrating CD4⁺ and CD8⁺T lymphocytes population in liver injury induced by BCG and LPS. Mice were primed with BCG and sequentially challenged by LPS, 12 d after priming. MNCs derived from normal (without any treatment, open bars); BCG-primed (horizontal bars) and BCG-primed plus LPS challenged mice (hatched bars) were harvested for FACS

analysis. **A₁-A₃**: The CD4⁺ and CD8⁺T lymphocytes population were analyzed with FACS; **B**: the absolute number of T lymphocytes was determined by multiplying the total MNC number by the fraction of CD4⁺, CD8⁺T-lymphocytes population. ^aP<0.05 vs BCG-primed mice.

against lethal liver failure induced by BCG and LPS. Approximately 70% of the mice (n = 10) survived for 72 h, whereas most (80%) of the mice treated with control Ab died within 72 h (Figure 6).

Anti-CXCL16 antibody reduced infiltration of T lymphocytes in liver injury

Infiltrated MNCs in the liver were observed and granuloma formed after BCG treatment. The diffuse infiltration of MNCs resulted in multilobular necrosis after LPS challenge. To investigate the effects of anti-CXCL16 antibody on intrahepatic infiltrating T lymphocytes, liver MNCs were isolated and T lymphocytes were analyzed. The results revealed that anti-CXCL16 antibody *in vivo* significantly decreased the number of T-infiltrating lymphocytes from

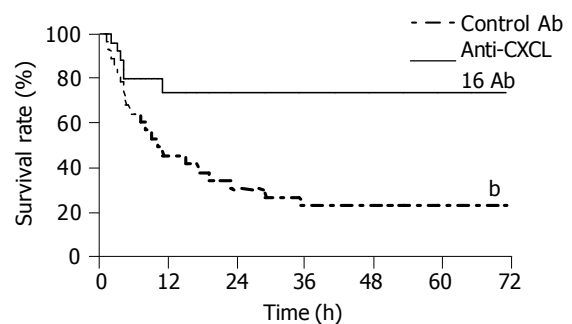


Figure 6 Protective effect of anti-CXCL16 antibody on survival rate for murine lethal hepatic failure. Immunological liver injury was induced by BCG and LPS treatment and anti-CXCL16 Ab (solid line, n = 10) or control Ab (dashed line, n = 10) was injected as indicated in Materials and methods. The anti-CXCL16 antibody significantly protected the mice from lethality (^bP<0.01 vs control Ab).

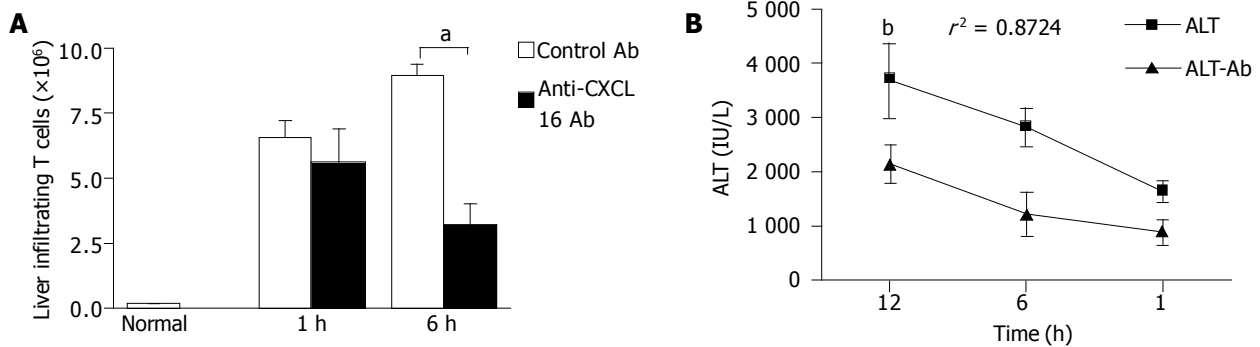


Figure 7 Effects of anti-CXCL16 antibody on intrahepatic infiltration of T lymphocytes and serum ALT level in the mice. Mice were primed with BCG and sequentially challenged by LPS 12 d after priming. Anti-CXCL16 antibody and isotype antibody were administrated into the mice, respectively. **A:** T lymphocytes derived from the mice treated with either anti-CXCL16 antibody (closed bars) or isotype antibody (hatched bars) was harvested for FACS

analysis. The absolute number of T lymphocytes was determined by multiplying the total MNC number by the fraction of CD3⁺T lymphocytes population. ^a $P < 0.05$ vs control Ab treatment. **B:** Anti-CXCL16 antibody significantly suppressed the elevation of serum ALT. ^b $P < 0.01$ vs control Ab group. Results were obtained from three independent experiments.

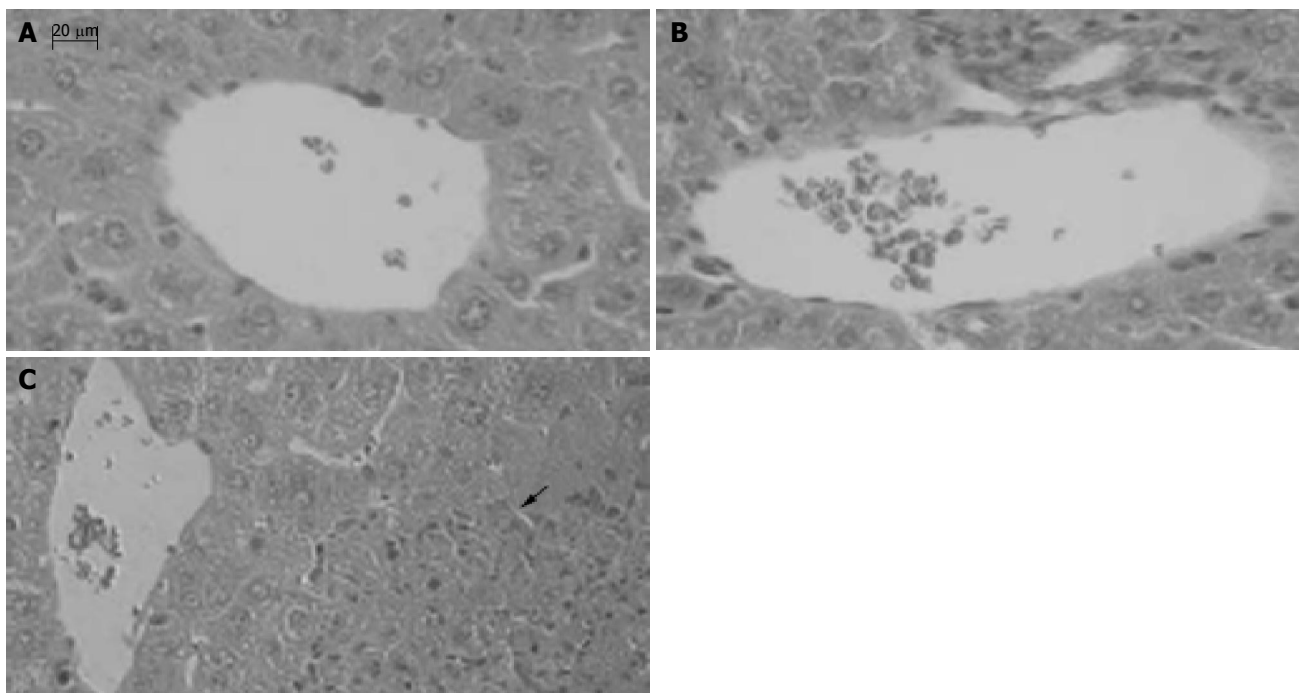


Figure 8 Effect of anti-CXCL16 antibody on the formation of hepatic lesion in liver injury induced by BCG and LPS. Sections of livers were obtained as follows: **A:** The liver tissue without any treatment; **B:** The liver tissue of mice primed with BCG was treated with the anti-CXCL16 Ab followed by LPS

challenge; **C:** The liver tissue of mice primed with BCG was treated with nonimmune rat IgG followed by LPS challenge. An arrow shows a necrotic lesion. Tissues were stained with H&E and examined histologically. Bars = 20 μ m.

1.01×10^7 to 3.52×10^6 /liver in BCG-primed mice after LPS challenge (Figure 7A, $P < 0.05$).

Change in serum ALT levels was characteristic of the immunological liver injury model in mice. The serum ALT level significantly decreased, when anti-CXCL16 antibody was applied *in vivo* compared to that after treatment with control Ab. The correlation coefficient of specific Ab and control Ab was 0.8724 ($P < 0.01$, Figure 7B). These data indicated that T cells might play a key role in the BCG and LPS-induced immunological liver injury.

Anti-CXCL16 antibody protected mice against multilobular necrosis in liver injury

MNCs infiltrated into liver lobes and formed granuloma in

liver 12 d after BCG treatment, compared to the normal mice (Figure 8A). Massive necrosis with diffuse infiltration of MNCs was observed in the livers of BCG-primed mice after LPS challenge (Figure 8C). In contrast, liver necrosis was significantly reduced by anti-CXCL16 Ab administration, and the specific Ab blocked the infiltration of MNCs infiltration in liver lobes and portal areas (Figure 8B).

DISCUSSION

In the present study, accumulation of T lymphocytes and massive hepatic necrosis were found and CXCL16 was strongly upregulated in the injured liver tissue in murine model. Upregulation of CXCL16 might be associated with

necrosis and liver injury. Administration of anti-CXCL16 antibody markedly inhibited the intrahepatic infiltration of T lymphocytes, and prevented lethal hepatic failure. These findings demonstrate that CXCL16 may play an important role in T lymphocyte infiltration and hepatic necrosis in immunological liver injury.

Serum ALT level is an important characteristic of hepatitis accompanied with pathologic changes of liver. Our results demonstrate that intravenous administration of anti-CXCL16 Ab can significantly decrease serum ALT level and hepatic necrosis, suggesting that CXCL16 plays a role in liver injury through some mechanisms. CXCL16 is predominantly expressed on APCs, existing in both secretory and transmembrane forms, and selectively chemoattracts CXCR6+T lymphocytes, which are potential cytotoxic effector cells, such as CD4+Th1, activated CD8+T cells and NKT cells^[13,14]. It was reported that these effector cells are closely associated with massive liver injury^[25-28]. These effector T lymphocytes, perhaps accompanying other leukocytes, might be recruited and involved in the pathogenesis of acute liver injury.

Activated CD4+T, CD8+T and NKT cells express TNF- α and FasL molecules associated with liver injury^[3,15,21,29-31]. Therefore, infiltrated T lymphocytes may mediate cytotoxicity to Fas-expressing hepatocytes and cause liver damage. Injection of LPS activates lymphocytes and triggers the release various soluble factors such as TNF- α , IFN- γ and IL-1, resulting in hepatocyte apoptosis and severe liver injury^[2,31,32]. All these and sequential cytokine production are the key factors in the pathogenesis of acute hepatic failure. Anti-CXCL16 antibody can decrease the number of intrahepatic infiltrating T lymphocytes, especially CD4+ and CD8+T-lymphocyte population. These might explain in part the reason, why specific antibody can rescue mice from death. Some leukocytes, such as neutrophils, are involved in liver injury. However, available evidence suggests that a small dose of LPS, that does not cause overt organ injury, can effectively inhibit extravascular recruitment of neutrophils^[33,34].

It is well known that many chemokines contribute to chemoattraction to trafficking leukocytes during liver inflammation^[8,35,36]. However, anti-CXCL16 antibody could significantly reduce the number of intrahepatic T lymphocytes and liver necrosis, indicating that CXCL16 might play other roles besides chemotactic function. There is evidence that supports these functions^[17,37]. Our experiments have confirmed that macrophages infected with *Mycobacterium tuberculosis* significantly increase the expression of CXCL16 and release chemokines and cytokines (data not shown). CXCL16 function in macrophages needs to be further studied.

Anti-CXCL16 Ab could not completely protect mice against death, suggesting that other chemokines or cytokines can also induce liver injury. Recently, it was reported that chemokines such as migration inhibitory factor, macrophage inflammatory protein-2 and thymus and activation-regulated chemokine are involved in the pathogenesis of liver injury^[1,38,39]. Although these facts can explain in part the possible reason why anti-CXCL16 Ab can protect mice from death, the precise mechanism needs to be elucidated further.

REFERENCES

- 1 Kobayashi S, Nishihira J, Watanabe S, Todo S. Prevention of lethal acute hepatic failure by antimacrophage migration inhibitory factor antibody in mice treated with bacille Calmette-Guerin and lipopolysaccharide. *Hepatology* 1999; **29**: 1752-1759
- 2 Nagakawa J, Hishinuma I, Hirota K, Miyamoto K, Yamanaka T, Tsukidate K, Katayama K, Yamatsu I. Involvement of tumor necrosis factor-alpha in the pathogenesis of activated macrophage-mediated hepatitis in mice. *Gastroenterology* 1990; **99**: 758-765
- 3 Tsutsui H, Matsui K, Kawada N, Hyodo Y, Hayashi N, Okamura H, Higashino K, Nakanishi K. IL-18 accounts for both TNF-alpha and Fas ligand-mediated hepatotoxic pathways in endotoxin-induced liver injury in mice. *J Immunol* 1997; **159**: 3961-3967
- 4 Matsui K, Yoshimoto T, Tsutsui H, Hyodo Y, Hayashi N, Hiroishi K, Kawada N, Okamura H, Nakanishi K, Higashino K. *Propionibacterium acnes* treatment diminishes CD4+NK1.1+T cells but induces type I T cells in the liver by induction of IL-12 and IL-18 production from Kupffer cells. *J Immunol* 1997; **159**: 97-106
- 5 Yajima T, Nishimura H, Saito K, Kuwano H, Yoshikai Y. Overexpression of interleukin-15 increases susceptibility to lipopolysaccharide-induced liver injury in mice primed with *Mycobacterium bovis* bacillus calmette-guerin. *Infect Immun* 2004; **72**: 3855-3862
- 6 Rossi D, Zlotnik A. The biology of chemokines and their receptors. *Annu Rev Immunol* 2000; **18**: 217-242
- 7 Luster AD. Chemokines-chemotactic cytokines that mediate inflammation. *N Engl J Med* 1998; **338**: 436-445
- 8 Baggiolini M. Chemokines and leukocyte traffic. *Nature* 1998; **392**: 565-568
- 9 Ward SG, Bacon K, Westwick J. Chemokines and T lymphocytes: more than an attraction. *Immunity* 1998; **9**: 1-11
- 10 Campbell JJ, Butcher EC. Chemokines in tissue-specific and microenvironment-specific lymphocyte homing. *Curr Opin Immunol* 2000; **12**: 336-341
- 11 Gunn MD, Ngo VN, Ansel KM, Eklund EH, Cyster JG, Williams LT. A B-cell-homing chemokine made in lymphoid follicles activates Burkitt's lymphoma receptor-1. *Nature* 1998; **391**: 799-803
- 12 Bazan JF, Bacon KB, Hardiman G, Wang W, Soo K, Rossi D, Greaves DR, Zlotnik A, Schall TJ. A new class of membrane-bound chemokine with a CX3C motif. *Nature* 1997; **385**: 640-644
- 13 Matloubian M, David A, Engel S, Ryan JE, Cyster JG. A transmembrane CXC chemokine is a ligand for HIV-coreceptor Bonzo. *Nat Immunol* 2000; **1**: 298-304
- 14 Wilbanks A, Zondlo SC, Murphy K, Mak S, Soler D, Langdon P, Andrew DP, Wu L, Briskin M. Expression cloning of the STRL33/BONZO/TYMSTRligand reveals elements of CC, CXC, and CX3C chemokines. *J Immunol* 2001; **166**: 5145-5154
- 15 Johnston B, Kim CH, Soler D, Emoto M, Butcher EC. Differential chemokine responses and homing patterns of murine TCR alpha beta NKT cell subsets. *J Immunol* 2003; **171**: 2960-2969
- 16 Nakayama T, Hieshima K, Izawa D, Tatsumi Y, Kanamaru A, Yoshie O. Cutting edge: profile of chemokine receptor expression on human plasma cells accounts for their efficient recruitment to target tissues. *J Immunol* 2003; **170**: 1136-1140
- 17 Shimaoka T, Nakayama T, Fukumoto N, Kume N, Takahashi S, Yamaguchi J, Minami M, Hayashida K, Kita T, Ohsumi J, Yoshie O, Yonehara S. Cell surface-anchored SR-PSOX/CXC chemokine ligand 16 mediates firm adhesion of CXC chemokine receptor 6-expressing cells. *J Leukoc Biol* 2004; **75**: 267-274
- 18 Yamauchi R, Tanaka M, Kume N, Minami M, Kawamoto T, Togi K, Shimaoka T, Takahashi S, Yamaguchi J, Nishina T, Kitaichi M, Komeda M, Manabe T, Yonehara S, Kita T. Upregulation of SR-PSOX/CXCL16 and recruitment of CD8+ T cells in cardiac valves during inflammatory valvular heart disease. *Arterioscler Thromb Vasc Biol* 2004; **24**: 282-287
- 19 Tsuji H, Harada A, Mukaida N, Nakanuma Y, Bluethmann H, Kaneko S, Yamakawa K, Nakamura SI, Kobayashi KI, Matsushima K. Tumor necrosis factor receptor p55 is essential for intrahepatic granuloma formation and hepatocellular

- apoptosis in a murine model of bacterium-induced fulminant hepatitis. *Infection Immun* 1997; **65**: 1892-1898
- 20 **Heydtmann M**, Adams DH. Understanding selective trafficking of lymphocyte subsets. *Gut* 2002; **50**: 150-152
- 21 **Kim CH**, Kunkel EJ, Boisvert J, Johnston B, Campbell JJ, Genovese MC, Greenberg HB, Butcher EC. Bonzo/CXCR6 expression defines type 1-polarized T-cell subsets with extralymphoid tissue homing potential. *J Clin Invest* 2001; **107**: 595-601
- 22 **Dumoulin FL**, Nischalke HD, Leifeld L, von dem Bussche A, Rockstroh JK, Sauerbruch T, Spengler U. Semi-quantification of human C-C chemokine mRNAs with reverse transcription/real-time PCR using multi-specific standards. *J Immunol Methods* 2000; **241**: 109-119
- 23 **De Clerck LS**, Bridts CH, Mertens AM, Moens MM, Stevens WJ. Use of fluorescent dyes in the determination of adherence of human leucocytes to endothelial cells and the effect of fluorochromes on cellular function. *J Immunol Methods* 1994; **172**: 115-124
- 24 **Watanabe H**, Ohtsuka K, Kimura M, Ikarashi Y, Ohmori K, Kusumi A, Ohteki T, Seki S, Abo T. Details of an isolation method for hepatic lymphocytes in mice. *J Immunol Methods* 1992; **146**: 145-154
- 25 **Tanaka Y**, Takahashi A, Watanabe K, Takayama K, Yahata T, Habu S, Nishimura T. A pivotal role of IL-12 in Th1-dependent mouse liver injury. *Int Immunol* 1996; **8**: 569-576
- 26 **Takahashi M**, Ogasawara K, Takeda K, Hashimoto W, Sakihara H, Kumagai K, Anzai R, Satoh M, Seki S. LPS induces NK1.1+ alpha beta T cells with potent cytotoxicity in the liver of mice via production of IL-12 from Kupffer cells. *J Immunol* 1996; **156**: 2436-2442
- 27 **Ando K**, Moriyama T, Guidotti LG, Wirth S, Schreiber RD, Schlicht HJ, Huang SN, Chisari FV. Mechanisms of class I restricted immunopathology. A transgenic mouse model of fulminant hepatitis. *J Exp Med* 1993; **178**: 1541-1554
- 28 **Nakagawa R**, Nagafune I, Tazunoki Y, Ehara H, Tomura H, Iijima R, Motoki K, Kamishohara M, Seki S. Mechanisms of the antimetastatic effect in the liver and of the hepatocyte injury induced by α -galactosylceramide in mice. *J Immunol* 2001; **166**: 6578-6584
- 29 **Lowin B**, Hahne M, Mattmann C, Tschopp J. Cytolytic T-cell cytotoxicity is mediated through perforin and Fas lytic pathways. *Nature* 1994; **370**: 650-652
- 30 **Ogasawara J**, Watanabe-Fukunaga R, Adachi M, Matsuzawa A, Kasugai T, Kitamura Y, Itoh N, Suda T, Nagata S. Lethal effect of the anti-Fas antibody in mice. *Nature* 1993; **364**: 806-809
- 31 **Fujioka N**, Mukaida N, Harada A, Akiyama M, Kasahara T, Kuno K, Ooi A, Mai M, Matsushima K. Preparation of specific antibodies against murine IL-1ra and the establishment of IL-1ra as an endogenous regulator of bacteria-induced fulminant hepatitis in mice. *J Leukoc Biol* 1995; **58**: 90-98
- 32 **Okamura H**, Tsutsi H, Komatsu T, Yutsudo M, Hakura A, Tanimoto T, Torigoe K, Okura T, Nukada Y, Hattori K. Cloning of a new cytokine that induces IFN-gamma production by T cells. *Nature* 1995; **378**: 88-91
- 33 **Kajdacsy-Balla A**, Doi EM, Lerner MR, Bales WD, Archer LT, Wunder PR, Wilson MF, Brackett DJ. Dose-response effect of *in vivo* administration of endotoxin on polymorphonuclear leukocytes oxidative burst. *Shock* 1996; **5**: 357-361
- 34 **Wagner JG**, Roth RA. Neutrophil migration during endotoxemia. *J Leukoc Biol* 1999; **66**: 10-24
- 35 **Springer TA**. Traffic signals for lymphocyte recirculation and leukocyte emigration, the multistep paradigm. *Cell* 1994; **76**: 301-314
- 36 **Butcher EC**, Picker LJ. Lymphocyte homing and homeostasis. *Science* 1996; **272**: 60-66
- 37 **Shimaoka T**, Nakayama T, Kume N, Takahashi S, Yamaguchi J, Minami M, Hayashida K, Kita T, Ohsumi J, Yoshie O, Yonehara S. Cutting edge: SR-PSOX/CXC chemokine ligand 16 mediates bacterial phagocytosis by APCs through its chemokine domain. *J Immunol* 2003; **171**: 1647-1651
- 38 **Lentsch AB**, Yoshidome H, Cheadle WG, Miller FN, Edwards MJ. Chemokine involvement in hepatic ischemia/reperfusion injury in mice: roles for macrophage inflammatory protein-2 and KC. *Hepatology* 1998; **27**: 1172-1177
- 39 **Yoneyama H**, Harada A, Imai T, Baba M, Yoshie O, Zhang Y, Higashi H, Murai M, Asakura H, Matsushima K. Pivotal role of TARC, a CC chemokine, in bacteria-induced fulminant hepatic failure in mice. *J Clin Invest* 1998; **102**: 1933-1941

Science Editor Wang XL and Guo SY Language Editor Elsevier HK

Protective effect of *Astragalus membranaceus* on intestinal mucosa reperfusion injury after hemorrhagic shock in rats

Zi-Qing Hei, He-Qing Huang, Jing-Jun Zhang, Bing-Xue Chen, Xiao-Yun Li

Zi-Qing Hei, Jing-Jun Zhang, Bing-Xue Chen, Xiao-Yun Li, Department of Anesthesiology, Third Affiliated Hospital, Sun Yat-Sen University, Guangzhou 510080, Guangdong Province, China
He-Qing Huang, School of Pharmaceutical Sciences of Sun Yat-Sen University, Guangzhou 510080, Guangdong Province, China
Supported by the Chinese Traditional Medicine Foundation of Guangdong Province, China, No. 102061

Correspondence to: Dr. Zi-Qing Hei, Department of Anesthesiology, Third Affiliated Hospital, Sun Yat-Sen University, Guangzhou 510630, Guangdong Province, China. heiziqing@sina.com
Telephone: +86-20-85516867-3132

Received: 2004-10-29 Accepted: 2005-01-12

Abstract

AIM: To study the protective effect of *Astragalus membranaceus* on intestinal mucosa reperfusion injury and its mechanism after hemorrhagic shock in rats.

METHODS: A total of 32 SD rats were randomly divided into four groups ($n = 8$, each group): normal group, model group, low dosage group (treated with 10 g/kg *Astragalus membranaceus*) and high dosage group (treated with 20 g/kg *Astragalus membranaceus*). The model of hemorrhagic shock for 60 min and reperfusion for 90 min was established. Therapeutic solution (3 mL) was administered before reperfusion. At the end of the study, the observed intestinal pathology was analyzed. The blood concentrations of lactic acid (LD), nitric oxide (NO), endothelin-1 (ET-1), malondialdehyde (MDA) and the activity of superoxide dismutase (SOD), glutathione peroxidase (GSH-PX) in intestinal mucosa were determined.

RESULTS: The intestinal mucosa pathology showed severe damage in model group and low dosage group, slight damage in high dosage group and no obvious damage in normal group. The Chiu's score in low dose group and high dose group was significantly lower than that in model group. The content of MDA in model group was higher than that in low and high dose groups, while that in high dose group was almost the same as in normal group. The activity of SOD and GSH-PX was the lowest in model group and significantly higher in high dose group than in normal and low dose groups. The concentrations of LD and ET-1 in model group were the highest. The concentrations of NO in model group and low dose group were significantly lower than those in high dose group and normal group.

CONCLUSION: High dose *Astragalus membranaceus* has

much better protective effect on hemorrhagic shock-reperfusion injury of intestinal mucosa than low dose *Astragalus membranaceus*. The mechanism may be that *Astragalus membranaceus* can improve antioxidative effect and regulate NO/ET level during hemorrhagic reperfusion.

© 2005 The WJG Press and Elsevier Inc. All rights reserved.

Key words: Hemorrhage shock; Intestinal reperfusion injury; *Astragalus membranaceus*

Hei ZQ, Huang HQ, Zhang JJ, Chen BX, Li XY. Protective effect of *Astragalus membranaceus* on intestinal mucosa reperfusion injury after hemorrhagic shock in rats. *World J Gastroenterol* 2005; 11(32): 4986-4991

<http://www.wjgnet.com/1007-9327/11/4986.asp>

INTRODUCTION

Under normal conditions, the integrity of intestinal mucosa as a barrier, can prevent bacterial translocation^[1,2]. Bacterial and endotoxin can enter into blood across the barrier when the intestinal mucosal barrier is demolished due to anoxia, ischemic and reperfusion injury. It is possible to induce systemic inflammatory response syndrome (SIRS) or multiple organ dysfunction syndrome (MODS), leading to the hemorrhagic shock^[3-6].

Free oxygen radical is one of the major activating factors in ischemia/reperfusion injury of intestinal mucosa^[7]. The maladjustment of NO/ET can not only aggravate oxidative damage, but also lead to dysfunction of the microcirculation of intestinal mucosa^[8-11]. Many drugs have been tried to palliate the ischemia-reperfusion injury of intestinal mucosa after hemorrhagic shock^[8,12,13]. However the results are still controversial and unsatisfactory.

Astragalus membranaceus is a traditional Chinese medicine which can improve microcirculation and has good curative effect. The main purpose of our study was to investigate whether *Astragalus membranaceus* could protect intestinal mucosa against ischemia-reperfusion injury after hemorrhagic shock, and to observe the effect of *Astragalus membranaceus* on intestinal oxidative damage, NO and ET levels.

MATERIALS AND METHODS

Animal experimental protocol

Approved by the University Animal Study Committee, 32 healthy male Sprague-Dawley rats (200-300 g, provided by

Animal Center of Sun Yat-Sen University) were randomly divided into four groups: normal group ($n = 8$, sham-operation, no shock and reperfusion), model group ($n = 8$, with hemorrhagic shock and treated only with 3 mL normal saline intravenously prior to reperfusion), low dose group ($n = 8$, with hemorrhagic shock and treated with 10 mg/kg *Astragalus membranaceus* which was five times of the human clinical dose) and high dose group ($n = 8$, with hemorrhagic shock and treated with 20 mg/kg of *Astragalus membranaceus* which was 10 times of the human clinical dose). The latter three groups were experimental groups.

Astragalus membranaceus (provided by Dioujiuhong Pharmaceutical Co., Ltd, Chengdu, China) was diluted in 3 mL normal saline and infused intravenously for 3 min prior to reperfusion.

Experimental model of hemorrhagic shock and resuscitation

Laboratory temperature was kept at 25-27 °C. The rats were anesthetized by intraperitoneal injection of urethane (5.0 mL, 20%) after they were fasted for 24 h. Tracheotomy was performed for ventilation. The right cervical vein was cannulated for monitoring central venous pressure and fluid infusion and drugs. The left carotid artery and femoral artery were catheterized for monitoring arterial pressure. The femoral artery was used to withdraw blood samples and to create hemorrhagic shock model.

Preparation of hemorrhagic shock model

Hemorrhagic shock model was established by withdrawing blood by femoral artery until mean arterial blood pressure (MABP) reached about 5.3 kPa (40 mmHg) and maintained for 60 min.

Rat resuscitation

Rats were administrated with 3 mL solution/drugs. Then their blood was reinfused for approximately 5 min and observed for 90 min. The segment samples of small intestinal mucosa were taken. The rats were killed at the end of the experiment.

The parameters included room temperature, rat weight and blood loss.

Mean arterial pressure and pulse rate were recorded every 10 min during the hemorrhagic shock and resuscitation period.

Preparation of specimens and measurements

After successful establishment of experimental model, the rats were killed and paunched rapidly. A segment of 0.5-1.0 cm intestine was cut from 5 cm to terminal ileum, fixed in 4% formaldehyde polymerisatum and embedded in paraffin for section. Another segment of small intestine was washed with frozen saline. The intestinal mucosa was scraped off, dried with suction paper and preserved at -70 °C.

The segment of small intestine was stained with hematoxylin-eosin. The damages of intestinal mucosa were evaluated by criteria of modified Chius method. Criteria of modified Chiu grading system were divided into 10 subdivisions according to the changes of villus and gland of intestinal mucosa: 0, normal villus and gland; 1, changes

in top of villus and initial formation of subepidermal Gruenhagen's antrum; 2, formation of subepidermal Gruenhagen's antrum and slightly injured gland; 3, enlargement of subepidermal gap and engorgement of capillary vessel; 4, epidermis moderately isolated with lamina propria and injured gland; 5, top villus shedding; 6, obvious villus shedding and capillary vessel dilating; 7, lamina propria villus shedding, and distinct injured gland; 8, initially decomposed lamina propria; 9, hemorrhage and ulcer.

Detection of lactic acid content in intestinal mucosa

Intestinal mucosal tissues were weighed and made into 10% homogenate. The lactic acid content in tissues was determined by the method of minim quick measurement (Jiancheng Bioengineering Ltd, Nanjing, China) and the concentration of protein was determined by Coomassie brilliant blue. The results were expressed as mmol/gpro.

Detection of content of MDA (malondialdehyde) in intestinal mucosa

Intestinal mucosal tissues (100 mg) were homogenized with normal saline. MDA content was determined by TBA method (Jiancheng Bioengineering Ltd, Nanjing, China). Homogenate (0.1 mL) was taken to detect MDA content. Briefly, 0.1 mL 8.1% SDS, 0.8 mL acetic acid buffer, 0.8 mL 0.8% TBA and 0.2 mL distilled water were added into the sample tubes and one standard tube (containing 0.1 mL tetraethoxypropane). Then all the tubes were incubated at 100 °C for 1 h. After cooled at -20 °C for 5 min, 2 mL n-butyl alcohol was added into the sample, which was then vibrated for 1 min and centrifuged for 10 min at 3 000 r/min. The supernatant of the samples was taken to detect absorbance at 533 nm with spectrophotometer (content of MDA (nmol/100 mg) = absorbance of each sample/absorbance of standard×dilution times).

Detection of activity of superoxide dismutase (SOD) in intestinal mucosa

Intestinal mucosal tissues (100 mg) were weighed and made into 10% homogenate with 0.9 mL normal saline, frozen in refrigerator at -20 °C for 5 min and centrifuged for 15 min at 4 000 r/min. Supernatants were transferred into fresh tubes for the evaluation of SOD activity. SOD activity was evaluated with SOD detection kit according to the manufacturer's instructions (Kits were provided by Jiancheng Bioengineering Ltd, Nanjing, China). SOD activity (μmL) = $(A_0 - A_1) / A_0 \times 360 \times V$ (A_0 : absorbance of self-oxidation rate per minute; A_1 : absorbance of each sample per minute; V : volume of extracted tissues).

Detection of activity of glutathione peroxidase (GSH-PX) in intestinal mucoa

Intestinal mucosal tissues (100 mg) were weighed and made into 10% homogenate with 0.9 mL normal saline. The activity of GSH-PX was detected according to the manufacturer's instructions (reagents were purchased from Jiancheng Bioengineering Ltd, Nanjing, China). Protein of homogenates was detected with Coomassie brilliant blue. The calculated results were expressed by U/100 mg protein.

Detection of content of NO in intestinal mucosa

Intestinal mucosal tissues (100 mg) were weighed and made into 10% homogenate with 0.9 mL normal saline. After being centrifuged for 10 min at 10 000 *g*, the supernatants were placed in boiling water for 3 min and then centrifuged for 5 min at 10 000 *g*. Supernatant (0.1 mL) was taken for detection, 0.2 mL 35% sulfosalicylic acid was added into the sample to make protein deposits. The sample was homogenized and centrifuged at 10 000 *g* for 10 min. The supernatants were taken again and preserved at -20 °C in refrigerator. One hundred μ L supernatant was detected by indirect nitric acid deoxidized enzyme method (Kits were provided by Jingmei Bioengineering Ltd). After 100 μ L nitrate reductase was homogenized gently, the sample was placed in water at 37 °C for 1 h with KNO₂ standard succi homogenized. After being placed in ambient temperature for 10 min and with zero setting with blank tube at 530 nm wavelength and 0.5 cm colorimetric cylinder, *A* value of detection tube and standard tube was read respectively.

Detection of ET-1 concentration in intestinal mucosa

Intestinal mucosal tissues (100 mg) were weighed and made into 10% homogenate with 0.9 mL normal saline. Homogenate ET-1 levels were measured by radioimmunoassay (Kits were obtained from Beijing East Asian Radioimmunoassay Technology Institute, Beijing, China).

Statistical analysis

Data were expressed as mean \pm SD and analysis of variance was performed using SPSS10.0 software. One-way analysis of variance was used for multiple comparisons and least significant difference test (LSD-t) was used for intra-group comparison. *P*<0.05 was considered statistically significant.

RESULTS

Basic status of each group

There was no difference in the four groups (*P*>0.05). The amount of withdrawn blood in three groups was similar, except in normal group (Table 1).

Table 1 Status of animals in each group (mean \pm SD)

Group	<i>n</i>	Weight (g)	Ambient temperature (°C)	Bloodletting volume (mL)
Normal	8	265 \pm 18	26.38 \pm 1.06	-----
Model	8	281 \pm 20	26.67 \pm 0.52	5.10 \pm 1.80
Low dose	8	269 \pm 14	25.88 \pm 1.13	5.20 \pm 1.60
High dose	8	272 \pm 16	26.20 \pm 1.10	4.80 \pm 1.50

Table 2 Changes of MBP (kPa) and HR (bpm) during shock and reperfusion period (mean \pm SD)

Groups/ <i>n</i>		Pre-shock	30 min of shock	10 min after reperfusion	30 min after reperfusion	60 min after reperfusion	90 min after reperfusion
Normal (<i>n</i> = 8)	MABP	12.66 \pm 1.28	-----	-----			
	HR	316.50 \pm 22.12	-----	-----			
Model (<i>n</i> = 8)	MABP	12.68 \pm 0.82	5.33 \pm 0.25 ^d	12.66 \pm 1.35	12.83 \pm 1.60	11.65 \pm 0.68	11.60 \pm 1.82
	HR	322.50 \pm 28.12	239.75 \pm 35.50 ^d	256.40 \pm 35.63 ^b	292.55 \pm 41.96	325.36 \pm 36.81	309.25 \pm 38.68
Low dose (<i>n</i> = 8)	MABP	13.07 \pm 1.27	5.32 \pm 0.20 ^d	13.21 \pm 1.17	12.46 \pm 1.46	12.21 \pm 0.82	12.05 \pm 1.58
	HR	320.87 \pm 38.83	221.75 \pm 49.89 ^d	250.00 \pm 45.63 ^b	282.76 \pm 45.63	319.50 \pm 42.28	300.62 \pm 32.28
High dose (<i>n</i> = 8)	MABP	13.00 \pm 1.36	5.30 \pm 0.20 ^d	12.16 \pm 1.35	12.90 \pm 1.60	12.05 \pm 0.82	11.82 \pm 1.42
	HR	310.83 \pm 25.63	236.16 \pm 51.67 ^b	266.00 \pm 38.10 ^b	316.83 \pm 30.91	306.66 \pm 22.11	298.50 \pm 22.11

^b*P*<0.01 vs pre-shock, ^d*P*<0.01 vs pre-shock.

Changes of animals' vital signs

There was no difference in MAP and HR in four groups before the experiment (*P*>0.05). The MAP in experimental groups was maintained at 5.33 kPa (40 mmHg), but the HR decreased during hemorrhage shock period. There was no significant difference after resuscitation in experimental group (*P*>0.05, Table 2).

Changes of intestinal mucosa under light microscope

The villus and glands were normal and no inflammatory cell infiltration was observed in mucosal epithelial layer in normal group. Severe edema of mucosa villus and infiltration of necrotic epithelial and inflammatory cells were found, indicating that damage was severe in model group. Light edema of mucosa villus and infiltration of few necrotic epithelial inflammatory cells were found in mucosa epithelial layer in low dosage group. No significant edema and necrotic mucosa villus were observed, but infiltration of a few inflammatory cells in mucosal epithelial layer was found in high dosage group, which was also the same as those in normal intestinal mucosa (Figures 1-4).

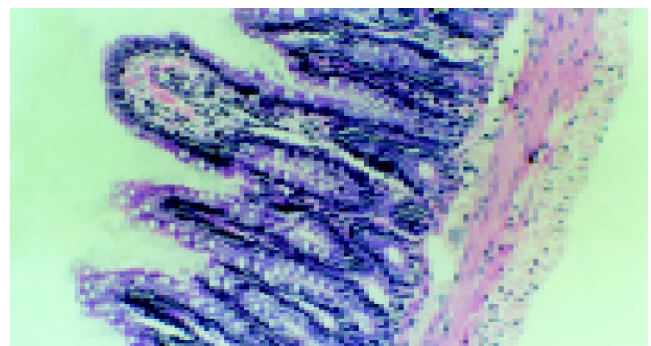


Figure 1 Normal villus and glands in normal group.

Chiu's score of small intestinal structure

The Chiu's score was the lowest in normal group and the highest in model group. Compared to model group, the Chiu's score was significantly lower in high dose group (*P*<0.05, Table 3).

Changes of MDA in small intestinal mucosa

The content of MDA in intestinal mucosa was the highest in model group, compared to that in normal, high and low dose groups. However there was no difference in Chiu's

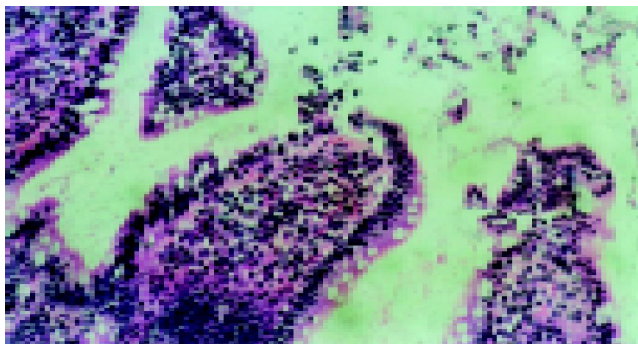


Figure 2 Severe edema of mucosa villus and infiltration of necrotic epithelial cells and inflammatory cells in model group.



Figure 4 No significant edema and necrotic mucosa villus and infiltration of a few inflammatory cells in high dose group.

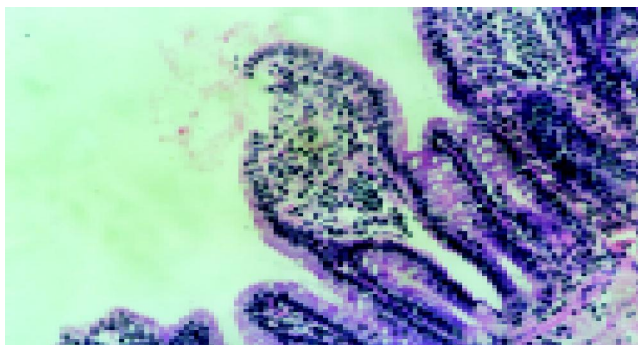


Figure 3 Light edema of mucosa villus and few necrotic epithelial cells and infiltration of few inflammatory cells in low dose group.

score among normal, low and high dose groups ($P>0.05$, Table 3).

Changes of activity of SOD

The activity of SOD in intestinal mucosa was the highest in high dose group ($P<0.05$ or 0.01), and the lowest in model group ($P<0.05$, Table 3).

Change of activity of GSH-PX in intestinal mucosa

The activity of GSH-PX was the lowest in model group ($P<0.05$) compared to that in the other three groups. There was no difference between normal group and low dose group ($P>0.05$, Table 3).

Lactic acid content in intestinal mucosa

The content of lactic acid in model group and low dose group was significantly higher than that in normal and high dose groups ($P<0.05$), There was no significant difference

among model group, low and high dose groups ($P>0.05$, Table 3).

Change of NO content in small intestinal mucosa

The content of NO in small intestinal mucosa in model group and low dosage group was significantly lower than that in normal group and high dosage group ($P<0.05$ or 0.01). There was no significant difference between model group and low dosage group ($P>0.05$) and between normal group and high dosage group ($P>0.05$, Table 3).

Changes of ET-1 content in intestinal mucosa

The content of ET-1 in intestinal mucosa was significantly higher in three experimental groups ($P<0.01$). The content of ET-1 in model group was higher than that in low and high dose groups ($P<0.05$ or 0.01 , Table 3).

DISCUSSION

Blood supply of small intestine from celiac branch of superior mesenteric artery accounts for 20% of total body blood volume. The blood flow in mucous layer is about 70-80% of total intestine blood flow, while the blood flow in muscular layer and serosa is about 15-25% of intestine blood flow. The blood flow in submucous layer is less than 5% of intestine blood flow. But 60% of blood flow in mucous layer is concentrated on the top of mucosa which provides enough hemoperfusion of endotheliocytes and villus^[14]. When shock occurs, the blood flow in intestinal mucosa decreases sharply. That is why the small intestinal mucosa is most easily subjected to ischemia and reperfusion injury^[15,16].

Studies have proved that ischemia reperfusion injury of intestinal mucosa plays an important role in inducing

Table 3 Effects of *Astragalus membranaceus* on LD, NO, MDA and SOD GSH-PX during hemorrhagic shock-resuscitation (mean±SD)

Group	n	Chiu's score	Lactic acid nmol/gpro	NO nmol/100 mg	ET Pg/100 mg	MDA content nmol/100 mg	SOD activity (U/100 mg)	GSH-PX activity (U/100 mg)
Normal	8	0.90±0.86	2.62±0.45	41.27±8.60	274.62±44.2	28.89±4.90	42.42±4.37	58.04±7.18
Model	8	6.25±2.75 ^b	3.11±0.53 ^a	20.21±4.14 ^b	481.50±109.98 ^b	62.70±15.37 ^b	27.85±10.75 ^b	42.92±10.62 ^a
Low dosage	8	4.05±1.96 ^{b,c}	3.00±0.36 ^a	26.86±5.33 ^{a,c}	414.53±26.15 ^{b,c,e}	36.80±9.35 ^{b,d}	39.13±7.62 ^{a,c,e}	55.91±11.27 ^{a,e}
High dosage	8	3.27±1.82 ^{a,c}	2.69±0.19 ^a	42.41±9.89 ^d	353.51±31.90 ^{a,d}	31.31±11.45 ^d	54.38±6.84 ^{a,d}	77.78±13.56 ^{b,d}

^a $P<0.05$, ^b $P<0.01$ vs normal group, ^c $P<0.05$, ^d $P<0.01$ vs low dose group and high dose group, ^e $P<0.05$ vs low dose group.

multiple organ dysfunction syndrome (MODS)^[3-6]. Therefore prevention of intestinal mucosal barrier from hemorrhagic shock is very important. The results of our study showed that small intestinal mucosa was severely injured after simple hemorrhagic shock. However, the injury of small intestinal villus was alleviated after *Astragalus membranaceus* was administered. The best result was obtained with high dose *Astragalus membranaceus* treatment, indicating that *Astragalus membranaceus* can protect intestinal mucosa against reperfusion injury, after hemorrhagic shock in a dose-dependant manner.

NO and ET-1 are active substances released by vascular endothelial cells (especially in lung) and the most important endogenous regulatory factors. It is most important to keep the dynamic balance between NO and ET in order to maintain tissue and organ hemoperfusion. Some studies^[9,17,18] reported that NO and ET-1 increase in plasma sharply during hemorrhagic shock and after resuscitation. At the same time, the intestinal barrier is also damaged.

NO/ET imbalance and endothelial disorder can induce intestinal mucosal hypoperfusion or ischemic injury, when hemorrhagic shock occurs.

Our study showed lactic acid content in intestinal mucosa in model group increased markedly, suggesting that anaerobic metabolism of intestinal mucosa occurs. NO level decreased and ET level increased sharply, suggesting that microcirculation of the intestinal mucosa is destroyed during and after hemorrhagic shock / reperfusion injury.

Bauer *et al.*^[19,20], found that intestinal damage can be relieved by drugs, when endogenous NO release is evoked. Oktar *et al.*^[21], and Anadol *et al.*^[22], used ET receptor antagonists to suppress endogenous ET activity, and found that they can relieve the damage due to intestine ischemic reperfusion, demonstrating that ET receptor antagonists can relieve ischemia reperfusion injury of intestine by modulating NO/ET level.

We found that *Astragalus membranaceus* could increase endogenous NO level and decrease endogenous ET level in intestinal mucosa, suggesting that *Astragalus membranaceus* can relieve endothelial dysfunction and ameliorate microcirculation via regulating NO/ET level during hemorrhagic-reperfusion.

Oxygen free radical is another major factor in inducing ischemia reperfusion injury. It could damage the structure of cell membrane and mitochondrial membrane through lipid peroxidation and result in cellular structure destroy and cell dysfunction^[7,8]. MDA is the direct products of lipid peroxidation^[7,8]. The extent of lipid peroxidation could be accessed by measuring MDA level in tissues. Our study also showed that the content of MDA in intestinal mucosa in model group was significantly higher than that in other groups, suggesting that significant lipid peroxidation occurs in small intestinal mucosa during hemorrhagic shock and reperfusion period. Some previous studies found^[23,24] that peroxide dismutase significantly relieves small intestine mucosal injury after 3 h ischemia, demonstrating that oxygen free radical plays an important role in ischemic injury of small intestinal mucosa.

SOD and GSH-PX are the major enzymes for scavenging oxygen free radical, whose activity could reflect its functional

status^[25-27]. The activity of SOD and GSH-PX in *Astragalus membranaceus*-treated groups was markedly higher than that in normal group and model group, which would be beneficial to scavenging oxygen free radical.

The content of MDA in intestinal mucosa in *Astragalus membranaceus*-treated groups was obviously lower than that in model group, demonstrating that *Astragalus membranaceus* has powerful antioxidative effects and protects small intestinal mucosa against hemorrhagic- reperfusion injury.

In conclusion, *Astragalus membranaceus* protects intestinal mucosa against hemorrhagic-reperfusion injury in a dose-dependant manner by regulating NO/ET level of intestinal mucosa after ischemia-reperfusion.

ACKNOWLEDGMENTS

The authors thank Professor Wei-Kan Wu for his good advice and Hui-Lan Sun for assistance to the experiments.

REFERENCES

- 1 Guarnier F, Malagelada JR, Girling KJ. Gut flora in health and disease. *Lancet* 2003; **361**: 512-519
- 2 Farhadi A, Banan A, Fields J, Keshavarzian A. Intestinal barrier: an interface between health and disease. *J Gastroenterol Hepatol* 2003; **18**: 479-497
- 3 Meng ZH, Dyer K, Billiar TR, Tweardy DJ. Essential role for IL-6 in postresuscitation inflammation in hemorrhagic shock. *Am J Physiol Cell Physiol* 2001; **280**: C343-C351
- 4 Guo W, Magnotti LJ, Ding J, Huang Q, Xu D, Deitch EA. Influence of gut microflora on mesenteric lymph cytokine production in rats with hemorrhagic shock. *J Trauma* 2002; **52**: 1178-1185
- 5 Pape HC, Grotz M, Remmers D, Dwenger A, Vaske R, Wisner D, Tscherne H. Multiple organ failure (MOF) after severe trauma-a sheep model. *Intensive Care Med* 1998; **24**: 590-598
- 6 Mitsuoka H, Kistler EB, Schmid-Schonbein GW. Protease inhibition in the intestinal lumen: attenuation of systemic inflammation and early indicators of multiple organ failure in shock. *Shock* 2002; **17**: 205-209
- 7 Bedirli A, Sozuer EM, Muhtaroglu S, Alper M. The role of oxygen free radicals and nitric oxide in organ injury following hemorrhagic shock and reinfusion. *Int J Surg Investig* 2000; **2**: 275-284
- 8 Mota-Filipe H, McDonald MC, Cuzzocrea S, Thiemermann C. A membrane-permeable radical scavenger reduces the organ injury in hemorrhagic shock. *Shock* 1999; **12**: 255-261
- 9 Hierholzer C, Kalff JC, Billiar TR, Bauer AJ, Tweardy DJ, Harbrecht BG. Induced nitric oxide promotes intestinal inflammation following hemorrhagic shock. *Am J Physiol Gastrointest Liver Physiol* 2004; **286**: G225-233
- 10 Massberg S, Boros M, Leiderer R, Baranyi L, Okada H, Messmer K. Endothelin (ET)-1 induced mucosal damage in the rat small intestine: role of ET(A) receptors. *Shock* 1998; **9**: 177-183
- 11 Denizbasi A, Yegen C, Ozturk M, Yegen B. Role of nitric oxide in gastric injury induced by hemorrhagic shock in rats. *Pharmacology* 2000; **61**: 106-112
- 12 Izumi M, McDonald MC, Sharpe MA, Chatterjee PK, Thiemermann C. Superoxide dismutase mimetics with catalase activity reduce the organ injury in hemorrhagic shock. *Shock* 2002; **18**: 230-235
- 13 Wattanasirichaigoon S, Menconi MJ, Fink MP. Lisofylline ameliorates intestinal and hepatic injury induced by hemorrhage and resuscitation in rats. *Crit Care Med* 2000; **28**: 1540-1549
- 14 Matheson PJ, Wilson MA, Garrison RN. Regulation of intestinal blood flow. *J Surg Res* 2000; **93**: 182-196
- 15 Morrini S, Yacoub W, Rastellini C, Gaudio E, Watkins SC, Cicalese L. Intestinal microvascular patterns during hemor-

- rhagic shock. *Dig Dis Sci* 2000; **45**: 710-722
- 16 **Nakijma Y**, Baudry N, Duranteau J, Vicaut E. Microcirculation in intestinal villi: a comparison between hemorrhagic and endotoxin shock. *Am J Respir Crit Care Med* 2001; **164**(8 Pt 1): 1526-1530
- 17 **Fruchterman TN**, Spain DA, Wilson MA, Harris PD, Garrison RN. Selective microvascular endothelial cell dysfunction in the small intestine following resuscitated hemorrhagic shock. *Shock* 1998; **10**: 417-422
- 18 **Mailman D**. Modulation of hemorrhagic shock by intestinal mucosal NG-nitro-L-arginine and L-arginine in the anesthetized rat. *Shock* 1999; **12**: 155-160
- 19 **Bauer C**, Kuntz W, Ohnsmann F, Gasser H, Weber C, Redl H, Marzi I. The attenuation of hepatic microcirculatory alterations by exogenous substitution of nitric oxide by s-nitroso-human albumin after hemorrhagic shock in the rat. *Shock* 2004; **21**: 165-169
- 20 **Kawata K**, Takeyoshi I, Iwanam K, Sunose Y, Aiba M, Ohwada S, Matsumoto K, Morishita Y. A spontaneous nitric oxide donor ameliorate small bowel ischemia-reperfusion injury in dogs. *Dig Dis Sci* 2001; **46**: 1748-1756
- 21 **Oktar BK**, Gulpinar MA, Bozkurt A, Ghandour S, Cetinel S, Moini H, Yegen BC, Bilsel S, Granger DN, Kurtel H. Endothelin receptor blockers reduce I/R-induced intestinal mucosal injury: role of blood flow. *Am J Physiol Gastrointest Liver Physiol* 2002; **282**: G647-G655
- 22 **Anadol AZ**, Bayram O, Dursun A, Ercan S. Role of endogenous endothelin peptides in intestinal ischemia-reperfusion injury in rats. *Prostaglandins Leukot Essent Fatty Acids* 1998; **59**: 279-283
- 23 **Akcakaya A**, Alimoglu O, Sahin M, Abbasoglu SD. Ischemia-reperfusion injury following superior mesenteric artery occlusion and strangulation obstruction. *J Surg Res* 2002; **108**: 39-43
- 24 **Riaz AA**, Wan MX, Schafer T, Dawson P, Menger MD, Jeppsson B, Thorlacius H. Allopurinol and superoxide dismutase protect against leucocyte-endothelium interactions in a novel model of colonic ischaemia-reperfusion. *Br J Surg* 2002; **89**: 1572-1580
- 25 **Cuzzocrea S**, Mazzon E, Dugo L, Caputi AP, Aston K, Riley DP, Salvemini D. Protective effects of a new stable, highly active SOD mimetic, M40401 in splanchnic artery occlusion and reperfusion. *Br J Pharmacol* 2001; **132**: 19-29
- 26 **Muzakova V**, Kandar R, Vojtisek P, Skalicky J, Cervinkova Z. Selective antioxidant enzymes during ischemia/reperfusion in myocardial infarction. *Physiol Res* 2000; **49**: 315-322
- 27 **Akcil E**, Tug T, Doseyen Z. Antioxidant enzyme activities and trace element concentrations in ischemia-reperfusion. *Biol Trace Elem Res* 2000; **76**: 13-17

Science Editor Wang XL and Guo SY Language Editor Elsevier HK

Angiostatin inhibits pancreatic cancer cell proliferation and growth in nude mice

Ding-Zhong Yang, Jing He, Ji-Cheng Zhang, Zhuo-Ren Wang

Ding-Zhong Yang, Department of Surgery, The First Hospital, Xi'an Jiaotong University, Xi'an 710065, Shaanxi Province, China
Jing He, Department of Pharmacology, University of Texas Medical Branch, Galveston 77555, Texas State, USA
Ji-Cheng Zhang, Department of Surgery, Union Hospital, Fujian Medical University, Fuzhou 350001, Fujian Province, China
Zhuo-Ren Wang, Department of Surgery, The First Hospital, Xi'an Jiaotong University, Xi'an 710065, Shaanxi Province, China
Correspondence to: Ding-Zhong Yang, Zhuque Garden of Shaanxi Province Hospital, Qinsong Road, Xi'an 710065, Shaanxi Province, China. doctoryang8@126.com
Telephone: +86-29-85272432
Received: 2005-05-30 Accepted: 2005-06-11

Abstract

AIM: To observe the biologic behavior of pancreatic cancer cells *in vitro* and *in vivo*, and to explore the potential value of angiostatin gene therapy for pancreatic cancer.

METHODS: The recombinant vector pcDNA3.1(+)-angiostatin was transfected into human pancreatic cancer cells PC-3 with Lipofectamine 2000, and paralleled with the vector and mock control. Angiostatin transcription and protein expression were determined by immunofluorescence and Western blot. The stable cell line was selected by G418. The supernatant was collected to treat endothelial cells. Cell proliferation and growth *in vitro* were observed under microscope. Cell growth curves were plotted. The transfected or untransfected cells overexpressing angiostatin vector were implanted subcutaneously into nude mice. The size of tumors was measured, and microvessel density count (MVD) in tumor tissues was assessed by immunohistochemistry with primary anti-CD34 antibody.

RESULTS: After transfected into PC-3 with Lipofectamine 2000 and selected by G418, macroscopic resistant cell clones were formed in the experimental group transfected with pcDNA 3.1(+)-angiostatin and vector control. But untreated cells died in the mock control. Angiostatin protein expression was detected in the experimental group by immunofluorescence and Western-blot. Cell proliferation and growth *in vitro* in the three groups were observed respectively under microscope. After treatment with supernatant, significant differences were observed in endothelial cell (ECV-304) growth *in vitro*. The cell proliferation and growth were inhibited. In nude mice model, markedly inhibited tumorigenesis and slowed tumor expansion were observed in the experimental group as compared to controls, which was parallel to the decreased

microvessel density in and around tumor tissue.

CONCLUSION: Angiostatin does not directly inhibit human pancreatic cancer cell proliferation and growth *in vitro*, but it inhibits endothelial cell growth *in vitro*. It exerts the anti-tumor functions through antiangiogenesis in a paracrine way *in vivo*.

© 2005 The WJG Press and Elsevier Inc. All rights reserved.

Key words: Angiostatin; Pancreatic cancer; Endothelial cell; Nude mice

Yang DZ, He J, Zhang JC, Wang ZR. Angiostatin inhibits pancreatic cancer cell proliferation and growth in nude mice. *World J Gastroenterol* 2005; 11(32): 4992-4996
<http://www.wjgnet.com/1007-9327/11/4992.asp>

INTRODUCTION

Angiogenesis means the formation of new blood vessels and is indispensable to various physiological processes including reproduction, development, wound repair, and tissue regeneration. There is evidence that tumor growth and metastasis are accompanied with the growth of new blood vessels, which proves the rationality and feasibility of anti-angiogenic therapy for tumor^[1,2].

Pancreatic cancer is the second most common cause of death from any type of gastrointestinal diseases in the United States^[3]. The common treatment of pancreatic cancer is suboptimal and the prognosis of patients is poor^[4].

Although pancreatic cancer is not a grossly vascular tumor, this malignancy often exhibits enhanced foci of endothelial cell proliferation. But several^[5-7] studies have reported a positive correlation between blood vessel density. Angiogenesis may play an important role in this disease. Angiostatin plays a key role in regulating endothelial cell proliferation and migration during the process of angiogenesis^[8,9] and inhibits the growth of a variety of murine and human tumors^[10].

We transfected eukaryotic vector encoding mouse angiostatin into human pancreatic cancer cells to observe the anti-tumor function of angiostatin and to explore the potential activity in gene therapy for pancreatic cancer.

MATERIALS AND METHODS

Cell lines and reagents

Recombinant vector pcDNA3.1(+)-angiostatin was

identified by restriction endonuclease digestion and sequencing. The human pancreatic cancer cell line PC-3 and endothelial cell line ECV-304 were purchased from China Center for Type Culture Collection. *Pvu*I was purchased from Bioson Corporation. Lipofectamine™ 2000 and G418 were purchased from Gibco Company; Rabbit anti-HA tag multiclonal antibody was presented by Jicheng Zhang doctor; FITC was purchased from Boster Biological Technology Co. CD-34 was purchased from Beijing Zhongshan Golden Bridge Biotechnology Co.

Cell culture

Pancreatic cancer cells and endothelial cells were cultured in RPMI1640 (Gibco) supplemented with 10% fetal bovine serum (FBS) (Sijiqing, Hangzhou, China), penicillin (100 U/mL) and streptomycin (100 mg/mL) in a humidified atmosphere of 50 mL/L CO₂ at 37 °C.

Transfection

Pancreatic cancer cells (PC-3) in logarithmic growth phase were implanted in 24-well plates at 2×10^5 cells/well, and approximately 80% confluence was obtained, after overnight incubation. pcDNA3.1(+)-angiostatin was digested by *Pvu*I according to the protocol of the manufacturer, and the recombinant was linearized. DNA/Lipofectamine 2000 complexes were prepared and transfected according to the protocol of the manufacturer. The experimental group and the vector control was designed with pcDNA3.1(+) and the mock control with Lipofectamine 2000. After 12 h of transfection, the selective medium containing G418 (50 mg/L) was used to culture cells for 14 d. Then the isolated resistant cell clones were selected and amplified.

Analysis of angiostatin by immunofluorescence cytochemistry and Western blot

PC-3 with pcDNA3.1(+) angiostatin in logarithmic growth phase was implanted in 6-well plates. After 24 h, the glass flake was taken out and immunofluorescence cytochemistry was carried out according to manufacturer's instructions, and the expression was detected under fluorescent microscope.

The cells were cultured in a conditioned media for 5 d. Cell supernatant was mixed with lysine-sepharose and incubated at 4 °C overnight. Detection was performed by the enhanced chemiluminescence (ECL) Western blotting analysis system according to the manufacturer's instructions.

Inhibitory on vascular endothelial cells

In logarithmic growth phase, the supernatant was collected. Endothelial cells ECV-304 were treated with supernatant separately for 7 d (supernatant/medium = 1/9), and counted under microscope.

Viable cell number counting and growth curve

Pancreatic cancer cells (PC-3) and endothelial cells (ECV-304) were plated on 24-well plates at 1×10^4 cells/well and cultured for 7 d. Viable cells was counted under microscope and growth curves were plotted.

Tumor models

Balb/c nude mice were randomly divided into three groups,

5 in each group. The experimental group with pcDNA3.1(+)-*angio*/PC-3, the vector control with pcDNA3.1(+)/PC-3 and the mock control with untransfected PC-3 were separately injected subcutaneously with pancreatic cancer cells PC-3 at 1.0×10^6 cells each mouse. After 56 d, the mice were killed to measure the size of tumor formed and to calculate the percentage of inhibition on tumorigenesis *in vivo*.

Quantitative analysis for microvessel densities (MVD)

Tumor tissues were fixed and embedded in paraffin. MVD was detected by immunohistochemistry SP method, and counted in four fields under light microscope (200× selected randomly).

Statistical analysis

To determine statistical significance, data were analyzed by statistical software of SPSS 10.0, Student's *t* test and χ^2 test.

RESULTS

Vector-mediated expression and secretion of angiostatin *in vitro*

Pancreatic cancer cells (PC-3) transfected with the corresponding vectors were selected by G418 for 14 d. The experimental and vector control groups formed macroscopic cell clones, but the mock group of cells was dead completely after 8 d of selection. Immunofluorescence showed signals of angiostatin in the experimental group of cell clones genetically engineered, but not in the controls (Figure 1A). Western blot analysis of cell supernatants (Figure 1B) revealed the detected protein with the size (5 800 kb) being consistent with angiostatin in the experimental group, whereas no specific band was observed in the controls.

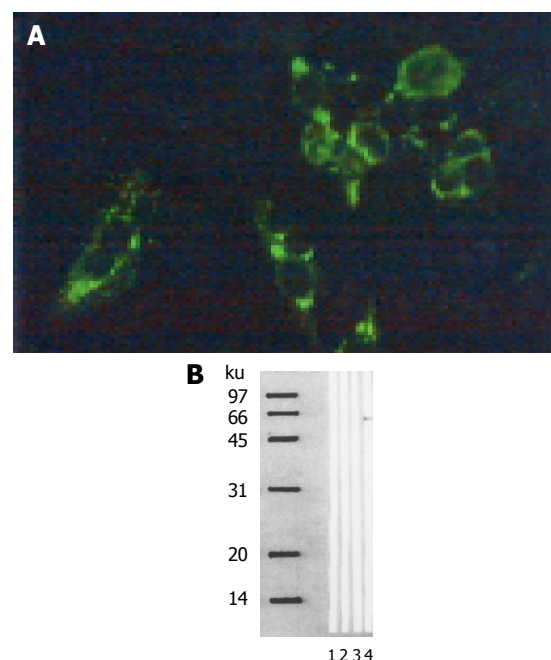


Figure 1 Angiostatin protein expression by immunofluorescence (A) Western blot analysis (B). M: Marker; lane 1: PBS control; lane 2: PC-3; lane 3: PC-3/pcDNA3.1(+); lane 4: PC-3/pcDNA3.1(+).

Biological activity of angiostatin protein expression in vitro

To detect biological activity of the encoded angiostatin *in vitro*, tumor cells transduced with and without the corresponding vectors were cultured for 7 d to make cell growth curve (Figure 2A). Under microscope, no obvious difference was observed in the cell morphology among the three groups of cells. Cell growth curves indicated no change in cell growth speed and doubling time among the three groups. These results indicated that upregulated angiostatin expression could neither directly inhibit cell growth and proliferation, nor affect cell cycle *in vitro*. But biological activity of the cell treated with supernatant of PC-3/pcDNA3.1(+)-angiostatin, the growth was obviously inhibited. The growth of the vector and mock control groups was similar to that of normal (Figure 2B). These results indicated that angiostatin expression could directly inhibit endothelial cell growth and proliferation *in vitro*.

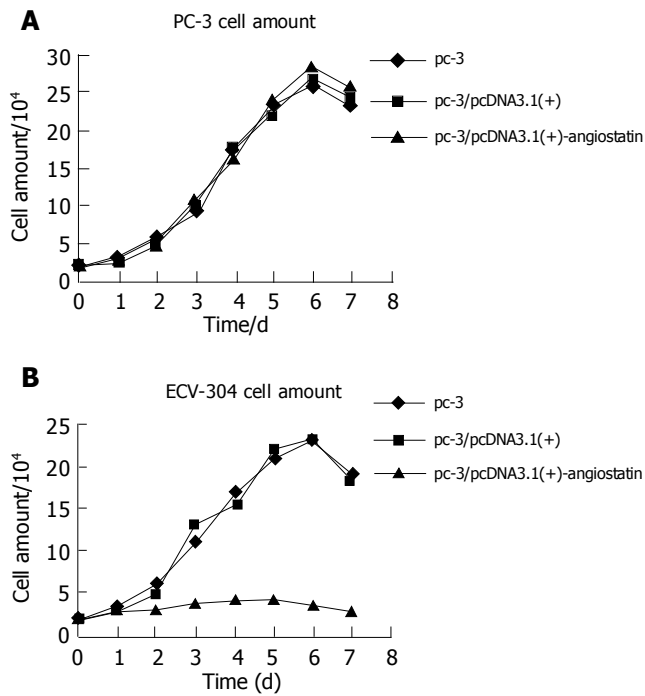


Figure 2 Cell growth curves of PC-3 (A) and ECV-304 (B).

Biological activity of angiostatin protein expression in vivo

Macroscopic tumors were observed on d 10, after injection

of angiostatin developed fast in the vector and mock control groups of nude mice. However, no macroscopic tumors were observed until 14 d, after injection of angiostatin in the experimental group and tumors developed slowly. After 56 d of injection of angiostatin, no mice died in the three groups and the tumors were resected and measured. Small pale tumor nodules were observed in the angiostatin-transfected tumors, whereas red and hypervascularized large tumors were present in the vector-transfected control and mock control tumor cells. The average size of tumors in the experimental group was $6.2 \times 10^{-2} \text{ cm}^3$, much less than the average size of the vector control $1.4 \times 10^{-2} \text{ cm}^3$ and the mock control (Figure 3). The inhibition of angiostatin overexpression reached 77%.

Tumor tissue in the experimental group was more vascularized than in the control groups. Greater microvascular density were found by immunohistochemical staining in tumors in the experimental group than in the vector or mock control groups respectively ($P < 0.01$, Figure 4). The results indicated that overexpression of angiostatin could decrease tumorigenesis by inhibiting neovascularization in tumors *in vivo*. Angiostatin might have inhibitory actions on surrounding tumor tissues and indirectly inhibit tumorigenesis.

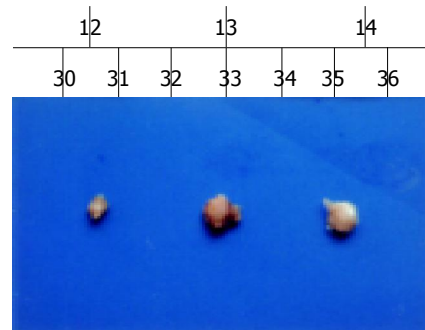


Figure 3 Tumors formed in nude mice by PC-3/pcDNA-angio, PC-3/pcDNA, and PC-3 cells (n = 5). A: PC-3/pcDNA3.1(+)-angio; B: PC-3/pcDNA3.1(+); C: PC-3.

DISCUSSION

Angiogenesis is critical for normal and pathologic processes in new blood vessel formation and plays an important role in the growth and spread of cancer. New blood vessels “feed” cancer cells with oxygen and nutrients, allow these

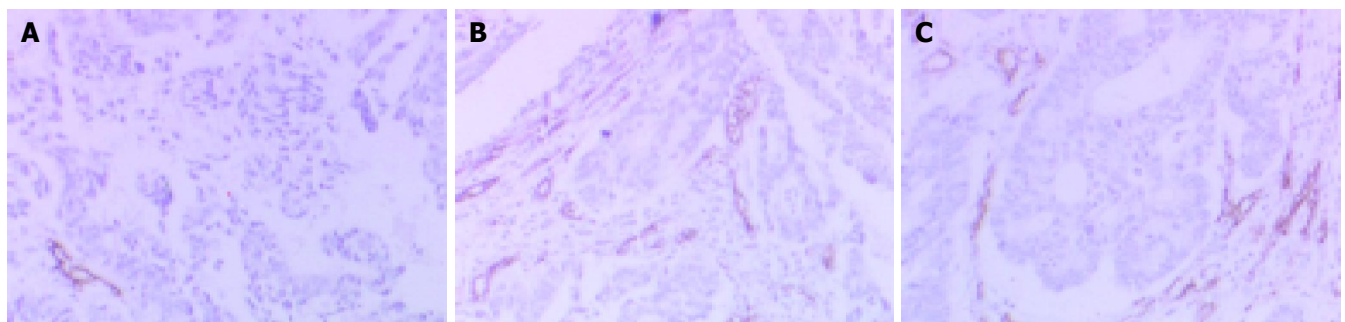


Figure 4 MVD in immunochemistry staining. A: PC-3/pcDNA-angiostatin; B: PC-3/pcDNA3.1; C: PC-3. SP×200.

cells to grow, invade nearby tissue, spread to other parts of the body, and form new colonies of cancer cells. At the prevascular stage, tumor is unable to grow to a size beyond 2-3 mm³ and remains in its dormant state. However, once the angiogenic phenotype of the tumor is switched on, tumor growth rate changes from linear to exponential^[11-14].

Angiogenesis begins, when a fibrin clot forms on the adventitial surface of an existing blood vessel^[15], followed by sprouting of new capillaries. The initial phase begins with increased vascular permeability and local degradation of the vessel wall. Endothelial cells enter the tumor stroma and proliferate. At this time, the cells may be most vulnerable to agents that interfere with their proliferation, since they lack protection from other cell types^[16]. The next step in vessel formation is recruitment of pericytes, followed by smooth muscle cells.

Angiogenesis is a process controlled by certain chemicals produced in the body. These chemicals stimulate cells to repair damaged blood vessels or form new ones such as vascular endothelial growth factor (VEGF)^[17], basic fibroblast growth factor (bFGF)^[18], acidic fibroblast growth factor (aFGF), Interleukin-8, angiogenin, placental growth factor (PGF)^[19], transforming growth factor- α , β ^[20], other chemicals are inhibitors such as angiostatin^[21], thrombospondin-1^[22], 16-kd prolactin fragment^[23], Interferon- α , β ^[24], Endostatin^[25]. Because cancer cannot grow or spread without the formation of new blood vessels^[26], scientists are trying to find ways to stop angiogenesis.

Tumor angiogenesis is often the consequence of an angiogenic imbalance in which pro-angiogenic factors predominate over anti-angiogenic factors^[27]. Furthermore, angiogenesis is essential for growth and metastasis of most solid cancers. Pancreatic cancer is not a grossly vascular tumor, but is related to angiogenesis^[28]. Anti-angiogenic treatment may be necessary and has potential for treatment of pancreatic cancer.

Angiostatin was first isolated as a circulating angiogenesis inhibitor. The structure of angiostatin includes the first four-kringle domains of plasminogen. Amino acid sequence analysis of kringle domains of human angiostatin has shown that K1, K2, K3, and K4 display considerable similarity (about 50% identity). Among these individual kringles, K1 has been identified as the most potent inhibitor of endothelial cell growth. K3 has higher inhibitory potency than K2. Surprisingly, K4 is virtually inactive in suppression of endothelial cell growth. Indeed, a short version of angiostatin only containing the first three kringle domains without K4 (K1-3) seems to be more active than K1-4 in inhibition of endothelial cell growth^[29]. Angiostatin inhibits proliferation of endothelial lineages in a dose-dependent manner, but not in the proliferation of normal and neoplastic nonendothelial cell lines^[30]. Human angiostatin inhibits the growth of transplanted human breast carcinoma, colon carcinoma and prostate carcinoma in mice, without obvious weight loss or other toxicity observed. It causes human primary carcinomas to regress to a dormant state by a net balance of tumor cell proliferation and apoptosis^[31]. Although angiostatin is a potent inhibitor of angiogenesis and tumor growth, the need of high dosages, repeated injections and long-term administration of this protein has made it less attractive for clinical trials.

In our study, mouse angiostatin cDNA was transfected into human pancreatic cancer cells PC-3, and stable cell lines expressing the secreted angiostatin were proved by immunofluorescence and Western-blot. Although angiostatin has no direct effect on pancreatic cancer cell PC-3 growth *in vitro*, the supernatant of stable cells inhibited the growth of endothelial cells ECV-304. The stable cell clones were implanted in the back of nude mice and the tumor growth inhibition rate of primary tumor growth was 77%, tumor growth inhibition is related to vascularization. According to the observation, angiostatin exerted its anti-tumor effect through anti-angiogenesis. These results are consistent with previous reports^[31]. By transfecting angiostatin into pancreatic cancer cells PC-3, we have gotten the protein. Thus angiostatin gene therapy is for pancreatic cancer. However, long-term, high-level, and sustained expression of angiostatin, are necessary to prevent dormant tumors from becoming active again. To achieve this objective, Xu *et al.*^[32], engineered a recombinant adeno-associated virus (AAV) vector encoding mouse angiostatin, and found that it suppresses metastatic liver cancer in mice. In our study, we used Lipofectamine-2000 for transfection and got the similar result. These results support that angiostatin-gene therapy is a potential strategy in the treatment of pancreatic cancer.

In conclusion, angiostatin inhibits pancreatic cancer cell proliferation and growth, and may provide a new way for its treatment.

REFERENCES

- 1 **Rosen LS.** Angiogenesis inhibition in solid tumors. *Cancer J* 2001; 7(Suppl 3): S120-128
- 2 **Gasparini G, Longo R, Fanelli M, Teicher BA.** Combination of antiangiogenic therapy with other anticancer therapies: results, challenges, and open questions. *J Clin Oncol* 2005; 23: 1295-1311
- 3 **Lowenfels AB, Sullivan T, Fiorianti J, Maisonneuve P.** The epidemiology and impact of pancreatic diseases in the United States. *Curr Gastroenterol Rep* 2005; 7: 90-95
- 4 **Horvat-Karajz K.** Modern diagnosis and treatment of pancreatic cancer-from the viewpoint of the internist. *Orv Hetil* 2005; 146: 305-308
- 5 **Ohshima T, Yamaguchi T, Ishihara T, Yoshikawa M, Kobayashi A, Sakaue N, Baba T, Yamada S, Saisho H.** Evaluation of blood flow in pancreatic ductal carcinoma using contrast-enhanced, wide-band Doppler ultrasonography: correlation with tumor characteristics and vascular endothelial growth factor. *Pancreas* 2004; 28: 335-343
- 6 **Seo Y, Baba H, Fukuda T, Takashima M, Sugimachi K.** High expression of vascular endothelial growth factor is associated with liver metastasis and a poor prognosis for patients with ductal pancreatic adenocarcinoma. *Cancer* 2000; 88: 2239-2245
- 7 **Ikeda N, Adachi M, Taki T, Huang C, Hashida H, Takabayashi A, Sho M, Nakajima Y, Kanehiro H, Hisanaga M, Nakano H, Miyake M.** Prognostic significance of angiogenesis in human pancreatic cancer. *Br J Cancer* 1999; 79: 1553-1563
- 8 **Peeters CF, de Geus LF, Westphal JR, de Waal RM, Ruiter DJ, Wobbes T, Oyen WJ, Ruers TJ.** Decrease in circulating anti-angiogenic factors (angiostatin and endostatin) after surgical removal of primary colorectal carcinoma coincides with increased metabolic activity of liver metastases. *Surgery* 2005; 137: 246-249
- 9 **Cao Y.** Antiangiogenic cancer therapy. *Semin Cancer Biol* 2004; 14: 139-145
- 10 **Papetti M, Herman IM.** Mechanisms of normal and tumor-derived angiogenesis. *Am J Physiol Cell Physiol* 2002; 282:

C947-C970

- 11 **Ellis LM**, Liu W, Ahmad SA, Fan F, Jung YD, Shaheen RM, Reinmuth N. Overview of angiogenesis: Biologic implications for antiangiogenic therapy. *Semin Oncol* 2001; **28**(5 Suppl 16): 94-104
- 12 **Cavallaro U**, Christofori G. Molecular mechanisms of tumor angiogenesis and tumor progression. *J Neurooncol* 2000; **50**: 63-70
- 13 **Giuliani N**, Colla S, Rizzoli V. Angiogenic switch in multiple myeloma. *Hematology* 2004; **9**: 377-381
- 14 **van Hinsbergh VW**, Collen A, Koolwijk P. Role of fibrin matrix in angiogenesis. *Ann N Y Acad Sci* 2001; **936**: 426-437
- 15 **Egginton S**, Zhou AL, Brown MD, Hudlicka O. The role of pericytes in controlling angiogenesis *in vivo*. *Adv Exp Med Biol* 2000; **476**: 81-99
- 16 **Sun FY**, Guo X. Molecular and cellular mechanisms of neuroprotection by vascular endothelial growth factor. *J Neurosci Res* 2005; **79**: 180-184
- 17 **Sauer G**, Deissler H. Angiogenesis: prognostic and therapeutic implications in gynecologic and breast malignancies. *Curr Opin Obstet Gynecol* 2003; **15**: 45-49
- 18 **Dalal S**, Berry AM, Cullinane CJ, Mangham DC, Grimer R, Lewis IJ, Johnston C, Laurence V, Burchill SA. Vascular endothelial growth factor: a therapeutic target for tumors of the Ewing's sarcoma family. *Clin Cancer Res* 2005; **11**: 2364-2378
- 19 **Folkman J**. Looking for a good endothelial address. *Cancer Cell* 2002; **1**: 113-115
- 20 **Canfield AE**, Schor AM, Schor SL, Grant ME. The biosynthesis of extracellular -matrix components by bovine retinal endothelial cells displaying distinctive morphological phenotypes. *Biochem J* 1986; **235**: 375-383
- 21 **Narizhneva NV**, Razorenova OV, Podrez EA, Chen J, Chandrasekharan UM, Dicorleto PE, Plow EF, Topol EJ, Byzova TV. Thrombospondin-1 up-regulates expression of cell adhesion molecules and promotes monocyte binding to endothelium. *FASEB J* 2005; **19**: 1158-1160
- 22 **Okamoto R**, Ueno M, Yamada Y, Takahashi N, Sano H, Suda T, Takakura N. Hematopoietic cells regulate the angiogenic switch during tumorigenesis. *Blood* 2005; **105**: 2757-2763
- 23 **Izawa JI**, Sweeney P, Perrotte P, Kedar D, Dong Z, Slaton JW, Karashima T, Inoue K, Benedict WF, Dinney CP. Inhibition of tumorigenicity and metastasis of human bladder cancer growing in athymic mice by interferon-beta gene therapy results partially from various antiangiogenic effects including endothelial cell apoptosis. *Clin Cancer Res* 2002; **8**: 1258-1270
- 24 **Folkman J**. Endogenous angiogenesis inhibitors. *APMIS* 2004; **112**: 496-507
- 25 **Carmeliet P**, Jain RK. Angiogenesis in cancer and other diseases. *Nature* 2000; **407**: 249-257
- 26 **Castellino FJ**, Ploplis VA. Structure and function of the plasminogen/plasmin system. *Thromb Haemost* 2005; **93**: 647-654
- 27 **Onizuka S**, Kawakami S, Taniguchi K, Fujioka H, Miyashita K. Pancreatic carcinogenesis: apoptosis and angiogenesis. *Pancreas* 2004; **28**: 317-319
- 28 **Geiger JH**, Cnudde SE. What the structure of angiostatin may tell us about its mechanism of action. *J Thromb Haemost* 2004; **2**: 23-34
- 29 **van Moorselaar RJ**, Voest EE. Angiogenesis in prostate cancer: its role in disease progression and possible therapeutic approaches. *Mol Cell Endocrinol* 2002; **197**: 239-250
- 30 **Fukumori T**, Nishitani Ma, Naroda T, Onishi T, Oka N, Kanayama Ho, Kagawa S. Expression of angiostatin cDNA in a murine renal cell carcinoma suppresses tumor growth *in vivo*. *Urology* 2002; **59**: 973-977
- 31 **Jung SP**, Siegrist B, Wang YZ, Wade MR, Anthony CT, Hornick C, Woltering EA. Effect of human Angiostatin protein on human angiogenesis *in vitro*. *Angiogenesis* 2003; **6**: 233-240
- 32 **Xu R**, Sun X, Tse LY, Li H, Chan PC, Xu S, Xiao W, Kung HF, Krissansen GW, Fan ST. Long-term expression of angiostatin suppresses metastatic liver cancer in mice. *Hepatology* 2003; **37**: 1451-1460

Science Editor Wang XL and Guo SY Language Editor Elsevier HK

Impact of antithrombin III on hepatic and intestinal microcirculation in experimental liver cirrhosis and bowel inflammation: An *in vivo* analysis

Sasa-Marcel Maksan, Zilfi Ülger, Martha Maria Gebhard, Jan Schmidt

Sasa-Marcel Maksan, Department of Surgery, University of Mainz, Germany
Zilfi Ülger, Martha Maria Gebhard, Jan Schmidt, Department of Surgery, University of Heidelberg, Germany
Correspondence to: Sasa-Marcel Maksan, MD, Department of Surgery, University of Mainz, Langenbeckstrasse 1, Mainz D-55131, Germany. maksan@ach.klinik.uni-mainz.de
Telephone: +49-6131-171
Received: 2004-10-29 Accepted: 2004-11-23

inflammation; Liver; Antithrombin III

Maksan SM, Ülger Z, Gebhard MM, Schmidt J. Impact of antithrombin III on hepatic and intestinal microcirculation in experimental liver cirrhosis and bowel inflammation: An *in vivo* analysis. *World J Gastroenterol* 2005; 11(32): 4997-5001
<http://www.wjgnet.com/1007-9327/11/4997.asp>

Abstract

AIM: To analyze the hepatic and intestinal microcirculation in an animal model of liver cirrhosis and inflammatory bowel disease (IBD) and to characterize the anti-inflammatory action of antithrombin III (ATIII) on leukocyte kinetics and liver damage.

METHODS: Hepatic and intestinal microcirculation was investigated by intravital videomicroscopy. Standardized models of experimental chronic liver cirrhosis and bowel inflammation were employed. Animals were divided into four groups ($n = 6/\text{group}$): controls, animals with cirrhosis, animals with cirrhosis and IBD, animals with cirrhosis and IBD treated with ATIII.

RESULTS: Cirrhosis facilitated leukocyte rolling and sticking in hepatic sinusoids (1.91 ± 0.28 sticker/ μm vs 0.5 ± 0.5 sticker/ μm in controls, $P < 0.05$). The effect enhanced in animals with cirrhosis and IBD (5.4 ± 1.65 sticker/ μm), but reversed after ATIII application (3.97 ± 1.04 sticker/ μm , $P < 0.05$). Mucosal blood flow showed no differences in cirrhotic animals and controls (5.3 ± 0.31 nL/min vs 5.4 ± 0.25 nL/min) and was attenuated in animals with cirrhosis and IBD significantly (3.49 ± 0.6 nL/min). This effect was normalized in the treatment group (5.13 ± 0.4 nL/min, $P < 0.05$). Enzyme values rose during development of cirrhosis and bowel inflammation, and reduced after ATIII application ($P < 0.05$).

CONCLUSION: Liver cirrhosis in the presence of IBD leads to a significant reduction in mucosal blood flow and an increase in hepatic leukocyte adherence with consecutive liver injury, which can be prevented by administration of ATIII.

© 2005 The WJG Press and Elsevier Inc. All rights reserved.

Key words: Liver cirrhosis; Microcirculation; Bowel

INTRODUCTION

Liver cirrhosis is a well-known immunocompromised state, with a high susceptibility to infection and organ dysfunction^[1]. Cirrhotic patients are prone to develop a progressive impairment in local and systemic hemodynamics, leading to renal and hepatic failure. The gut mucosa plays an important role in the pathogenesis of complications of cirrhosis. However, little is known about the exact mechanisms promoting severe septic complications and liver failure in cirrhotic patients. Among other pathophysiological mechanisms, hypoperfusion of the gut mucosa has been implicated as an important mechanism contributing to mucosal injury^[2]. Likewise changes in the intestinal flora and in the intestinal barrier as well as leukocyte dysfunction are presumed to be responsible for infective complications of cirrhosis^[3].

Any inflammatory process is characterized by tissue infiltration of leukocytes mediated by cytokines and cell adhesion molecules expressed on the endothelial surface^[4]. By intravital videomicroscopy, leukocyte-endothelial interaction can be visualized and quantitated. Furthermore, the effects of therapeutic agents can be investigated in the same setting.

Patients with progressive liver disease are known to have low plasma concentrations of antithrombin III (ATIII)^[5,6]. ATIII is synthesized in liver parenchymal cells and plays a central role in regulating hemostasis^[7]. In addition, ATIII has been reported to have some influence on the inflammatory process, which is independent of its effects on coagulation. This effect is thought to be indirect via enhanced prostacyclin release from endothelial cells^[8]. We have previously shown that hepatic reperfusion injury could be attenuated by administration of ATIII in an animal model of warm hepatic ischemia and reperfusion^[9].

The aim of this study was to analyze the intestinal and hepatic microcirculation in cirrhotic animals with inflammatory bowel disease (IBD) and to evaluate the effects of ATIII application during the onset of bowel

inflammation on microcirculation, leukocyte-endothelium interaction and liver function.

Data of control and cirrhotic animals without bowel inflammation published recently by our group were considered for statistical comparison in the present study.

MATERIALS AND METHODS

All experiments were performed in accordance with the Governmental Animal Protection Committee.

Experimental protocol

Twenty-four male Wistar rats weighing 200-220 g were eligible for analysis in this study. Two rats died during induction of liver cirrhosis. Animals were divided into four groups, six animals each: controls, animals with cirrhosis, animals with cirrhosis and IBD, and animals with cirrhosis and IBD treated with ATIII.

Induction of liver cirrhosis

Chronic progressive liver cirrhosis was induced by gavage with carbon tetrachloride (CCl₄) as previously described^[10]. In brief, animals had free access to tap water containing barbitural sodium (100 mg/dL) 2 wk before the first CCl₄ dose. The CCl₄ doses were calibrated weekly from an initial dose of 0.04 mL, to a maximum dose of 0.4 mL after 10 wk.

Induction of bowel inflammation

Bowel inflammation was induced by the protocol of Yamada, described in detail elsewhere^[11]. Indomethacin at a dose of 7.5 mg/kg body weight (Sigma, Germany) was injected subcutaneously in the lower abdomen. Drug application was repeated after 24 h, and intravital videomicroscopy was performed 7 d, after induction of bowel inflammation.

Antithrombin III application

A group of six animals received intravenously 250 IU/kg body weight ATIII (Kybernin HS 1000, Centeon Pharma, Germany) 24 h, after the last indomethacin application.

Monitoring

Mean arterial blood pressure and heart rate were recorded continuously via an arterial catheter placed in the left carotid artery. In addition, arterial blood samples were obtained to perform blood-gas analysis (ABL 5, Radiometer GmbH, Willich, Germany) and venous samples to measure liver enzymes (AST, ALT, GGT, and alkaline phosphatase) and clotting (ATIII levels and prothrombin time) using commercial assays.

Intravital videomicroscopy

Animals were fasted overnight, but received water *ad libitum*. Experiments were performed under general anesthesia with ketamine/pentobarbital (Ketanest, Park-Davis, Germany and Narcoren, Merial, Germany), administered via a catheter (B. Braun, Melsungen, Germany) placed in the left jugular vein. A midline incision was made and intravital fluorescence microscopy was performed using a Leitz orthoplan microscope (Leitz, Wetzlar, Germany). With different excitation filters

(wavelengths 450-490 and 530-560 nm), selective visualization of FITC-labeled erythrocytes and rhodamine 6G stained leukocytes was possible. For contrast enhancement, FITC-labeled albumin was administered intravenously.

Liver microcirculation

The left liver lobe was exteriorized onto a specially designed stage and videomicroscopy was performed according to the technique described by Menger *et al.*^[12]. Ten liver lobules were observed for 30-60 s. Vessels with a diameter between 20 and 40 μ m were eligible for analysis.

Small intestine microcirculation

In the same animal, the terminal ileum was exteriorized and placed on a glass slide. Videomicroscopy of mean mesenteric vessels was performed. Then the bowel was opened along the anti-mesenteric border and fixed at the incision margins. Continuous superfusion with buffered Ringer's solution was provided. Mesenteric microcirculation was investigated in 10 fields of ileal arteries and corresponding veins following the technique described in detail elsewhere^[13]. Mucosal microcirculation was measured in the main arteriole of five single villi. Each vessel was observed for 30 s.

Data analysis

Microcirculatory parameters were quantified by off-line analysis of video-recorded microscopic images using the computer-assisted image analysis system Capimage (Capimage, Zeintl, Heidelberg, Germany)^[14]. Vessel diameter and erythrocyte velocity were evaluated. Leukocyte-endothelium interaction (LEI) was characterized by leukocyte adherence measurements as the number of leukocytes that remained stationary or temporary on the vessel wall. Leukocytes that adhered for at least 30 s were considered as stickers, whereas leukocyte rolling was based on endothelial lining that was less than 66% of the erythrocyte velocity. Microvascular blood flow was derived from erythrocyte velocity (V_c) and vessel diameter (D) using the following equation^[15]: $V_b = V_c \times \pi \times (D/2)^2$.

Histology

After microscopy, animals were killed. One part of the liver and one part of the small intestine were obtained for histopathological investigations. Specimens were fixed in buffered formalin (4%), embedded in paraffin and stained with hematoxylin and eosin.

Statistical analysis

All data were expressed as mean \pm SD. Inter-group comparisons were made using the Mann-Whitney U test. $P < 0.05$ was considered statistically significant.

RESULTS

Hemodynamics and laboratory data

There were no significant differences in hemodynamic variables between the groups. Signs of sepsis were not observed in any of the animals (Table 1). Analysis of laboratory data demonstrated significant differences in all groups (Table 4). In summary, transaminase values rose

during development of cirrhosis and bowel inflammation. This effect was withdrawn after ATIII treatment. Prothrombin time showed comparable characteristics.

Table 1 Cardiorespiratory parameters at the beginning of intravital videomicroscopy (mean±SD)

	Cirrhosis	Cirrhosis and IBD	ATIII treatment group (cirrhosis and IBD)	Controls
Mean arterial blood pressure (mmHg)	107±8.4	102±8.7	106±7.8	112±7.3
Heart rate (bpm)	310±9.2	318±7.4	312±8.2	304±8.4
paO ₂ (mmHg)	89.1±5.3	86.4±4.3	88.6±5.4	92.3±4.8

Microcirculation

Table 2 compares the vessel diameter, RBC velocity and blood flow of the liver, mesentery, and ileal mucosa. Blood flow analysis showed significant differences between the groups. Liver cirrhosis was associated with a reduction of volumetric blood flow in mesenteric vessels, compared to control animals (135.1±3.56 nL/min *vs* 156.5±4.3 nL/min). However, an inverse effect was observed in the presence of bowel inflammation: mesentery blood flow increased significantly (149.8±2.41 nL/min) and rose further in the ATIII treatment group (243.1±3.71 nL/min). Mucosal blood flow in central arterioles showed no differences in cirrhotic animals and controls (5.3±0.31 nL/min *vs* 5.4±0.25 nL/min), but was significantly attenuated in the inflammation group (3.49±0.6 nL/min). This effect was normalized in the treatment group (5.13±0.4 nL/min). Hepatic blood flow increased in the IBD group and remained stable under ATIII substitution.

Table 2 Microcirculatory parameters of the liver, mesentery and ileal mucosa (mean±SD)

	Cirrhosis	Cirrhosis and IBD	ATIII treatment group (cirrhosis and IBD)	Controls
Vessel diameter (μm)				
Liver	27.86±2.03 ^a	28.15±1.72	28.08±1.27	23.03±0.62
Mesentery	32.06±8.91	33.51±5.16	42.51±7.04 ^c	33.46±11.66
Mucosa	7.51±0.30	6.32±0.41	7.21±0.52	7.20±0.23
RBC velocity (mm/s)				
Liver	0.93±0.09 ^a	1.08±0.13 ^c	1.16±0.11	1.22±0.18
Mesentery	2.81±0.49	3.28±0.42	2.93±0.41	3.11±0.35
Mucosa	2.03±0.15	1.81±0.13 ^c	2.11±0.12	2.18±0.16
Volumetric blood flow (nL/min)				
Liver	32.1±0.43	39.5±0.43 ^c	40.9±0.62	31.2±0.6
Mesentery	135.1±3.56 ^a	149.8±2.41 ^c	243.1±3.71 ^e	156.5±4.3
Mucosa	5.3±0.31	3.49±0.6 ^c	5.13±0.4 ^e	5.4±0.25

^a*P*<0.05 cirrhosis *vs* controls; ^c*P*<0.05 cirrhosis+IBD *vs* cirrhosis; ^e*P*<0.05 ATIII *vs* cirrhosis+IBD.

Leukocyte-endothelium interaction

Analysis of leukocyte kinetics showed marked differences

in hepatic leukocyte adherence. Cirrhosis facilitated leukocyte rolling and sticking in hepatic sinusoids (1.91±0.28 sticker/100 μm *vs* 0.5±0.5 sticker/100 μm in control, *P*<0.05). The effect was enhanced in bowel inflammation (5.4±1.65 sticker/100 μm), but reversed in the ATIII group (3.97±1.04 sticker/100 μm, *P*<0.05). LEI in mesenteric vessels was characterized by a significant increase of adherent leukocytes during bowel inflammation (5.24±1.23 sticker/100 μm *vs* 2.54±1.19 sticker/100 μm, *P*<0.05) with no substantial difference in the ATIII treatment group (Table 3).

Table 3 Results of intravital videomicroscopy: LEI in the liver and mesentery (mean±SD)

	Cirrhosis	Cirrhosis and IBD	ATIII treatment group (cirrhosis and IBD)	Controls
Adherent leukocytes (n/100 μm)				
Liver	1.91±0.28 ^a	5.40±1.65 ^c	3.97±1.04 ^e	0.5±0.5
Mesentery	2.54±1.19	5.24±1.23 ^c	4.36±1.19	1.62±0.85
Rolling leukocytes (n/100 μm)				
Liver	4.80±0.90 ^a	5.32±1.29	3.40±0.54 ^e	2.33±0.75
Mesentery	7.68±3.18	10.34±8.94	10.82±7.29	6.88±1.94

^a*P*<0.05 cirrhosis *vs* controls; ^c*P*<0.05 cirrhosis+IBD *vs* cirrhosis; ^e*P*<0.05 ATIII *vs* cirrhosis+IBD.

Table 4 Data of blood samples taken at the end of experiments (mean±SD)

	Cirrhosis	Cirrhosis and IBD	ATIII treatment group (cirrhosis and IBD)	Controls
ASOT (U/L)	63.67±10.42 ^a	109.5±39.18 ^c	29.17±7.62 ^e	28.67±4.85
ALT (U/L)	31.83±4.84 ^a	84.67±32.95 ^c	21.17±13.61 ^e	16.67±1.11
GGT (U/L)	5.33±1.49	14.83±3.48 ^c	7.67±1.25 ^e	3.17±0.69
AP (U/L)	130.5±35.75 ^a	268.83±53.25 ^c	69.83±12.21 ^e	56.83±2.67
Prothrombin	75.3±5.4 ^a	58.7±4.3 ^c	74.6±4.9 ^e	102.4±2.7
Time (%)				
ATIII (IU)	108.5±14.59	71.67±8.94 ^c	138.50±2.29 ^e	125.0±8.96

^a*P*<0.05 cirrhosis *vs* controls; ^c*P*<0.05 cirrhosis+IBD *vs* cirrhosis; ^e*P*<0.05 ATIII *vs* cirrhosis+IBD.

Histology

At the time of videomicroscopy, all animals had evidence of ascites. Light microscopy examination showed that features of cirrhosis were evident in the liver of all rats. The overall impression of the liver was nodular with extensive deposits of fibrous tissue. Sections of ileum revealed macroscopic inflammation. Necrotic areas were not assessed in any group and network of lymphatic vessels was extended in cirrhotic animals and influenced markedly by ATIII treatment.

DISCUSSION

Portal hypertension caused by cirrhosis is characterized by multiple complications, including development of ascites, disturbance of the mucosal barrier, thrombotic, and intestinal derangements^[16,17]. Microcirculation is of

heterogeneous nature in cirrhosis^[18,19]. As portal hypertension develops, local production of vasodilators, mainly nitric oxide, increases, leading to splanchnic arterial vasodilatation^[20]. Clinical observations revealed that there was a close relationship between circulatory dysfunction in portal hemodynamic and the impairment in hepatic function. The results of our study indicate that liver cirrhosis is associated with a significant increase of liver enzymes and hepatic vessel diameter, but has no influence on hepatic blood flow. There was a marked decrease in mesenteric blood flow and this effect was significantly reversed by bowel inflammation. This observation has led to the hypothesis that increased portal pressure may in part depend upon an increased splanchnic inflow and may be related to the overactivity of the endogenous vasoconstrictor systems^[21]. Mucosal blood flow on the other hand, showed a significant decrease in animals with cirrhosis and bowel inflammation. Our data are consistent with the hypothesis that mucosal inflammation may induce shunting in the villus microcirculation, with a depression in capillary perfusion, though the levels of central arteriolar blood flow are normal^[22]. However, the magnitude of mucosal hemodynamic alterations in rats treated with ATIII was not as pronounced as in cirrhotic rats with IBD without this treatment.

LEI and microvascular perfusion changes are known to play a crucial role in the development of organ dysfunction and failure. Leukocyte-endothelial cell adhesion is modulated by a variety of adhesion glycoproteins expressed on the surface of leukocytes and endothelial cells^[23,24]. It has been shown that both leukocyte and endothelial cell adhesion molecules contribute to the granulocyte accumulation in a chronic model of intestinal inflammation^[25]. As venous drainage of the intestine occurs via the portal vein in the liver, intestinal inflammation may lead to an upregulation of the liver LEI and contribute to liver injury. This phenomenon is also described for gut ischemia and reperfusion^[26].

In addition, endothelium plays a key role in the pathogenesis of inflammation and coagulation disorders in infectious diseases^[27]. Though the exact mechanism is not known, there is evidence that intervention in the coagulation pathway may have some beneficial influence on the course of infections^[28]. It has been shown that small intestine injury and LEI are significantly reduced in endotoxemic rats after application of ATIII^[29]. Our group has previously described the same effect in an animal model of hepatic ischemia-reperfusion injury^[9], which is in agreement with the observation of the present study, indicating that application of ATIII reduces both intestinal and hepatic microcirculation failure in bowel inflammation with coexisting liver cirrhosis. The extent of leukocyte adherence to the endothelium and the course of liver enzymes can significantly improve.

In conclusion, though vessel morphology is changed during liver cirrhosis, systemic effects of bowel inflammation in cirrhosis can be attenuated by substitution of dropped ATIII levels subsequently to the onset of inflammation. Maintenance of gut perfusion seems to prevent enhancement of LEI and hepatic damage.

REFERENCES

- 1 **Cirera I**, Bauer TM, Navasa M, Vila J, Grande L, Taura P, Fuster J, Garcia-Valdecasas JC, Lacy A, Suarez MJ, Rimola A, Rodes J. Bacterial translocation of enteric organism in patients with cirrhosis. *J Hepatol* 2001; **34**: 32-37
- 2 **Fink MP**, Antonsson JB, Wang HL, Rothschild HR. Increased intestinal permeability in endotoxic pigs. Mesenteric hypoperfusion as an etiologic factor. *Arch Surg* 1991; **126**: 211-218
- 3 **Navasa M**, Rodes J. Bacterial infections in cirrhosis. *Liver Int* 2004; **24**: 277-280
- 4 **Granger DN**, Kubes P. The microcirculation and inflammation: modulation of leukocyte-endothelial cell adhesion. *J Leukoc Biol* 1994; **55**: 662-675
- 5 **Ben-Ari Z**, Osman E, Hutton RA, Burroughs AK. Disseminated intravascular coagulation in liver cirrhosis: fact or fiction? *Am J Gastroenterol* 1999; **94**: 2977-2982
- 6 **Papathodoridis GV**, Papakonstantinou E, Andrioti E, Cholongitas E, Petraki K, Kontopoulou I, Hadziyannis SJ. Thrombotic risk factors and extent of liver fibrosis in chronic viral hepatitis. *Gut* 2003; **52**: 404-409
- 7 **Bauer KA**, Rosenberg RD. Role of antithrombin III as a regulator of *in vivo* coagulation. *Semin Hematol* 1991; **28**: 10-18
- 8 **Hoffmann JN**, Vollmar B, Inthorn D, Schildberg FW, Menger MD. Antithrombin reduces leukocyte adhesion during chronic endotoxemia by modulation of the cyclooxygenase pathway. *Am J Physiol Cell Physiol* 2000; **279**: C98-C107
- 9 **Maksan SM**, Maksan MO, Gebhard MM, Herfarth C, Klar E. Reduction of hepatic reperfusion injury by antithrombin III and aprotinin. *Transpl Int* 2000; **13**: S562-S564
- 10 **Proctor E**, Chatamra K. High yield micronodular cirrhosis in the rat. *Gastroenterology* 1982; **83**: 1183-1190
- 11 **Yamada T**, Deitch E, Specian RD, Perry MA, Sartor RB, Grisham MB. Mechanisms of acute and chronic intestinal inflammation induced by indomethacin. *Inflammation* 1993; **17**: 641-662
- 12 **Menger MD**, Marzi I, Messmer K. *In vivo* fluorescence microscopy for quantitative analysis of the hepatic microcirculation in hamsters and rats. *Eur Surg Res* 1991; **23**: 158-169
- 13 **Ruh J**, Ryschich E, Secchi A, Gebhard MM, Glaser F, Klar E, Herfarth C. Measurement of blood flow in the main arteriole of the villi in rat small intestine with FITC labeled erythrocytes. *Microvasc Res* 1998; **56**: 62-69
- 14 **Zeintl H**, Sack FU, Intaglietta M, Messmer K. Computer assisted leukocyte adhesion measurement in intravital microscopy. *Int J Microcirc Clin Exp* 1989; **8**: 293-302
- 15 **Gross JF**, Aroesty J. Mathematical models of capillary flow: a critical review. *Biorheology* 1972; **9**: 225-264
- 16 **Foreman MG**, Mannino DM, Moss M. Cirrhosis as a risk factor for sepsis and death: analysis of the National Hospital Discharge Survey. *Chest* 2003; **124**: 1016-1020
- 17 **Misra V**, Misra SP, Dwivedi M, Singh PA, Kumar V. Colonic mucosa in patients with portal hypertension. *J Gastroenterol Hepatol* 2003; **18**: 302-308
- 18 **Vollmar B**, Siegmund S, Menger MD. An intravital fluorescence microscopic study of hepatic microvascular and cellular derangements in developing cirrhosis in rats. *Hepatology* 1998; **27**: 1544-1553
- 19 **Sherman IA**, Pappas SC, Fisher MM. Hepatic microvascular changes associated with development of liver fibrosis and cirrhosis. *Am J Physiol* 1990; **258**: H460-H465
- 20 **Martin PY**, Gines P, Schrier RW. Nitric oxide as a mediator of hemodynamic abnormalities and sodium and water retention in cirrhosis. *N Engl J Med* 1998; **339**: 533-541
- 21 **Ruiz-del-Arbol L**, Urman J, Fernandez J, Gonzales M, Navasa M, Monescillo A, Albillos A, Jimenez W, Arroyo V. Systemic, renal, and hepatic hemodynamic derangement in cirrhotic patients with spontaneous bacterial peritonitis. *Hepatology* 2003; **38**: 1210-1218

- 22 **Sielenkamper AW**, Meyer J, Kloppenburg H, Eicker K, van Aken H. The effects of sepsis on gut mucosal blood flow in rats. *Eur J Anaesthesiol* 2001; **18**: 673-678
- 23 **Elangbam CS**, Qualls CW, Dahlgren RR. Cell adhesion molecules-update. *Vet Pathol* 1997; **34**: 61-73
- 24 **Smith CW**. Leukocyte-endothelial cell interactions. *Semin Hematol* 1993; **30**: 45-53
- 25 **Arndt H**, Palitzsch KD, Anderson DC, Rusche J, Grisham MB, Granger DN. Leucocyte-endothelial cell adhesion in a model of intestinal inflammation. *Gut* 1995; **37**: 374-379
- 26 **Horie Y**, Wolf R, Miyasaka M, Anderson DC, Granger DN. Leukocyte adhesion and hepatic microvascular responses to intestinal ischemia/reperfusion in rats. *Gastroenterology* 1996; **111**: 666-673
- 27 **Levi M**, Ten Cate H, van der Poll T. Endothelium: interface between coagulation and inflammation. *Crit Care Med* 2002; **30**: S220-S224
- 28 **Souter PJ**, Thomas S, Hubbard AR, Poole S, Romisch J, Gray E. Antithrombin inhibits lipopolysaccharide-induced tissue factor and interleukin-6 production by mononuclear cells, human umbilical vein endothelial cells, and whole blood. *Crit Care Med* 2001; **29**: 134-139
- 29 **Neviere R**, Tournoy A, Mordon S, Marechal X, Song FL, Jourdain M, Fourrier F. Antithrombin reduces mesenteric venular leukocyte interactions and small intestine injury in endotoxemic rats. *Shock* 2001; **15**: 220-225

Science Editor Wang XL and Guo SY Language Editor Elsevier HK

Misperceptions among patients with chronic hepatitis B in Singapore

Chun-Tao Wai, Belinda Mak, Winnie Chua, Mei-Hua Tan, Seline Ng, Amelia Cheok, Mee-Lian Wong, Seng-Gee Lim

Chun-Tao Wai, Belinda Mak, Winnie Chua, Mei-Hua Tan, Seline Ng, Amelia Cheok, Seng-Gee Lim, Division of Gastroenterology, National University Hospital, Singapore

Mee-Lian Wong, Department of Community, Occupational, and Family Medicine, National University of Singapore, Singapore

Correspondence to: Dr. Chun-Tao Wai, Division of Gastroenterology, Department of Medicine, National University Hospital, 5 Lower Kent Ridge Road, Singapore 119074, Singapore. waict@nuh.com.sg
Telephone: +65-67724353 Fax: +65-67794112

Received: 2004-10-25 Accepted: 2004-12-08

Abstract

AIM: To identify the misperceptions among CHB patients, as well as to determine the factors associated with better knowledge.

METHODS: A telephone interview was conducted on 192 adult CHB patients, who earlier responded to an advertisement for free screening. The questionnaire included items about socio-demographic factors and a 14-item quiz on knowledge of general aspects, transmission, and management of HBV infection.

RESULTS: The mean knowledge score on HBV was 10.4/14. Common misperceptions included availability of treatment for HBV infection and early liver cancer, as well as on transmission. Having completed tertiary education was the only independent factor associated with a high knowledge score, after controlling other demographic factors.

CONCLUSION: More educational efforts should be focused on patients' misperceptions and target the less educated HBV carriers.

© 2005 The WJG Press and Elsevier Inc. All rights reserved.

Key words: Knowledge; Hepatitis B virus; Public health; Education

Wai CT, Mak B, Chua W, Tan MH, Ng S, Cheok A, Wong ML, Lim SG. Misperceptions among patients with chronic hepatitis B in Singapore. *World J Gastroenterol* 2005; 11 (32): 5002-5005

<http://www.wjgnet.com/1007-9327/11/5002.asp>

INTRODUCTION

HBV infection remains an important global health problem.

There are approximately 350 million people chronically infected with HBV worldwide. During the course of chronic HBV infection, an estimated 15-40% of HBV carriers would develop complications such as exacerbations of hepatitis, cirrhosis, liver failure, and hepatocellular carcinoma (HCC)^[1,2].

Singapore is a small, multi-racial nation in Southeast Asia with a population of four million, and racial distribution of 76% Chinese, 14% Malay, 8% Indian, and 2% others. HBV infection is an important disease in Singapore, where 4.1% of the general population are carriers of HBV^[3]. In Singapore, liver cirrhosis and its complications are the 10th commonest cause of death, and HCC is the 4th commonest cancer among Singaporean males^[4].

Only patients with chronic hepatitis B (CHB), elevated liver enzymes and high hepatitis B viral load are candidates for anti-viral treatment^[1,2,5]. As liver enzymes and viral replication may fluctuate during the prolonged course of CHB, regular measurement of liver panel and viral load is needed to identify suitable patients for antiviral therapy^[1,2,5]. In addition, regular surveillance for HCC may allow diagnosis of early lesions, which are potentially curable by resection or liver transplantation^[6,7]. To sum up, for the regular surveillance with liver panel and alpha-fetoprotein level, ultrasonography is important in the follow-up of patients with CHB to select suitable candidates for anti-viral therapy, and to diagnose complications early, for better treatment^[1,2,8-10]. However, compliance of surveillance among patients with CHB has not been evaluated. Our recent pilot study showed that about two-thirds of HBV carriers in Singapore are not on regular follow-up, and the reasons are unclear^[11].

Many hepatitis B carriers are not aware of the implications of their disease, and have numerous misperceptions. In one study among 320 Cambodian American women, the median score on their knowledge is only 4.8 out of a maximum of 12^[12]. In another similar study among 147 Chinese Canadian women, respondents correctly answered only 6.9 of the 12 questions^[13]. At multivariate analysis, fluency in spoken English and duration of education are independently associated with the level of knowledge about HBV of patients.

We hypothesize that the low compliance with follow-up among HBV carriers could be due to their lack of knowledge about HBV infection. Hence, in this study, our first objective was to identify the misperceptions among HBV carriers attending a free screening program in Singapore, as well as any particular group with poor knowledge of HBV, and our second objective was to correlate their knowledge of HBV with regular follow-up.

MATERIALS AND METHODS

Patients

A free screening program for adult HBV carriers was advertised in local newspapers in Chinese and English over a 4-wk period. Known HBV carriers were invited to come forward for a free screening. HBV carrier status of all subjects was confirmed by repeat testing of the hepatitis B surface antigen. The study subjects came from the community and included those not screened previously, or defaulted screening.

Six hundred and nineteen subjects responded and came forward for the free screening program. These subjects were then contacted and invited to take part in this study. All subjects gave informed consent to the study. Three hundred and ninety-eight subjects could not be contacted due to incorrect contact information. Two hundred and twenty-one subjects were contacted, 29 of them refused to take part in the study. Hence, 192 (86.9%) subjects of those who could be contacted were interviewed for the current study. A waiver for application was obtained from the Institutional Review Board of the National University Hospital but, all study subjects gave informed consent before taking part in the study.

Survey instrument

All subjects were interviewed through telephone, using a standard questionnaire by a team of bilingual (English and Chinese), hepatology-trained research nurses. The questionnaire contained questions on basic socio-demographic factors, and a 14-item quiz on general knowledge of HBV infection adapted from a previously validated questionnaire^[12,13] (Table 1). The survey was carried out in either Mandarin or English. Each interview lasted for about 20 min. Carriers of HBV who were seen by any doctor for monitoring of their liver status and surveillance of complications of CHB over the last 12 mo were considered to be on regular follow-up.

Data analysis

Data were expressed as mean \pm SE unless otherwise stated, and analyzed by SPSS v. 10.0 (SPSS Inc., Chicago, IL, USA). The main outcome variables were level of knowledge about HBV. Each question was answered as "Yes", "No", or "Do not know". A correct answer scored one point. An incorrect or "Do not know" answer scored zero point. A summary score of knowledge was computed by summing correct responses to the 14-item quiz. Hence, the maximum score for each subject was 14 and the minimum 0.

Total knowledge score was first analyzed as a continuous variable. Factors associated with total knowledge score, namely gender, age, ethnicity, education level, income level, family history of HCC, and hepatitis B, were analyzed by multiple linear regression to evaluate the independent factors associated with knowledge score.

In addition, the knowledge score was arbitrarily dichotomized as "high" (10 or higher) and "low" (9 or less), and analyzed as a categorical variable. Factors related to high knowledge scores were first analyzed by univariate analysis, where categorical and continuous variables were analyzed by Fisher's exact test or Mann-Whitney *U* test as

appropriate. Factors with $P < 0.10$ from univariate analysis were further analyzed by multivariate analysis using backward logistic regression to evaluate the significant independent factors associated with high knowledge scores.

Knowledge score between those with or without regular follow-up was compared by Kruskal-Wallis test. A two-tailed test with $P < 0.05$ was considered statistically significant.

RESULTS

Patient characteristics

One hundred and ninety-two HBV carriers, aged 43 ± 1 years, 148 (77%) male, and 184 (96%) Chinese, completed the survey. One hundred and thirty-five (70%) earned S \$ 2 000 (US \$ 1 100) or more monthly, and 64 (33%) had monthly income of S \$ 4 000 (US \$ 2 200) or more. One hundred and nine subjects (57%) completed tertiary (college) education, 76 (40%) secondary (up to Grade 12) education, and 7 (4%) primary (up to Grade 6) education. Sixty-seven subjects (35%) had a known family history of CHB and 35 (18%) had a known family history of HCC. One hundred and seven subjects (57%) were on regular follow-up for their CHB over the last 12 mo. None of the subjects consumed more than three drinks of alcohol per week.

Hepatitis B knowledge

Overall mean knowledge score was 10.4 ± 0.1 , out of a maximum of 14. More than 80% of study subjects were aware of that HBV was infectious and could cause long-term complications such as liver cirrhosis or HCC, and that they should not consume alcohol regularly (Table 1). More than 80% of subjects were also aware of the main modes of transmission such as childbirth, sexual activity, and sharing of needles.

However, many misperceptions existed. Only about one-third of them, knew that early liver cancer did not cause any symptom and treatment was available for CHB. Besides, half of the subjects were unaware of that HBV infection was not transmitted by sharing food, and 37% of the subjects thought that hepatitis B could be transmitted by taking seafood.

Table 1 Responses to hepatitis B knowledge questions ($n = 192$)

Statements (correct response)	Correct response (%)
General aspects of hepatitis B	
Hepatitis B is infectious? (Yes)	165 (86)
Hepatitis B causes liver cancer in the long run (Yes)	173 (90)
Hepatitis B causes liver cirrhosis in the long run (Yes)	168 (88)
Hepatitis B carriers can be recognized easily from their appearance (No)	143 (75)
Hepatitis B carriers can drink alcohol as much as non-carriers (No)	180 (94)
Management of hepatitis B	
Treatment is available for hepatitis B (Yes)	65 (34)
Early liver cancer causes symptoms (No)	62 (32)
Early liver cancer is curable (Yes)	133 (69)
My family members should be screened for hepatitis B (Yes)	185 (96)
Transmission of hepatitis B	
Hepatitis B transmits through sexual intercourse (Yes)	171 (89)
Hepatitis B transmits through sharing of needles (Yes)	179 (93)
Hepatitis B transmits through sharing of food (No)	96 (50)
Hepatitis B transmits through taking seafood (No)	120 (63)
Hepatitis B transmits through childbirth (Yes)	165 (86)

Factors associated with better knowledge

Knowledge score was first analyzed as a continuous variable. Multiple linear regression showed that having completed tertiary education was the only statistically significant factor associated with knowledge score ($P < 0.001$), after controlling for other potential confounding demographic factors.

Knowledge score was then analyzed as a categorical variable as "high" and "low" knowledge score. Overall, 139 (73%) subjects had high knowledge scores of 10 points or more. Univariate analysis revealed that subjects with high knowledge scores were significantly younger, and more likely to have received tertiary (college) education. Association of high knowledge with higher income reached borderline significance (Table 2). When these three factors were analyzed by logistic regression, having completed tertiary (college) education was the only independent factor associated with high knowledge scores. Those with tertiary (college) education were 3.3 times more likely (OR 3.30, 95%CI 1.4-7.6, $P = 0.005$) to have high knowledge score than those without tertiary (college) education.

Correlation between regular follow-up and knowledge score

No statistically significant difference in knowledge score was seen between those with and without regular follow-up (10.7 ± 0.2 vs 10.2 ± 0.4 , $P = 0.23$). Neither was there any difference in gender, age, income level, or educational level between the two groups.

DISCUSSION

One important finding of this study is that the mean knowledge score was reasonably good at 10.3 out of a maximum of 14. We also found that 139 (73%) of the subjects scored 10 or more, i.e., having a high knowledge score. Although it is difficult to compare the knowledge score in our population with the scores from prior studies, this may suggest that public health education in Singapore in the past has been generally successful.

However, we also identified many misperceptions among HBV carriers. To begin with, many HBV carriers were not aware of the benefits of regular surveillance for complications of HBV, as evidenced by the findings that many were not aware that treatment of HBV infection was available and were not aware of that early liver cancer was asymptomatic, but potentially curable. Secondly, although many HBV carriers were aware of the common modes of HBV transmission, and believed that HBV infection could

also be transmitted by sharing food or consuming seafood. Our findings are consistent with those by Taylor *et al.*^[12], and Thompson *et al.*^[13], where only 23.5% and 41% of their respondents thought that HBV infection can be spread by food. This highlights the need to improve the current public education program on hepatitis B.

Another important finding of our study is that patients with tertiary (college) education were more likely to have a high knowledge score. This is not surprising as patients with better education are more likely to have read or heard about HBV infection in schools or in the mass media. Besides, subjects with better education were more likely to understand the complexity of various aspects of HBV infection. Our study highlights the importance of targeting further public and patient education on those with less or no education.

One last important finding is that we found no difference in knowledge score between those with and without regular follow-up. This highlights the complexity of the issue of regular follow-up among patients with chronic illnesses^[14,15], and that factors other than knowledge influenced patient compliance with follow-up. Perhaps efforts from community, healthcare organizations, and patients are needed in improving the long-term compliance rate. Further studies are needed to identify factor(s) associated with better compliance in patients with chronic illnesses.

There are limitations in our study. Firstly, it is unclear to what extent our conclusions could be extended to HBV carriers in other geographical locations, where cultural backgrounds and educational level vary. Secondly, as we interviewed only those who responded initially to our advertisement for free HBV screening, it is possible that we could have selected a more health-conscious group of HBV carriers, who might have better knowledge of HBV. However, it should be noted that any new screening program would have a low uptake in the beginning. The strength of this study is that we were able to identify the educational needs of individuals who participated in our screening program and this has helped us achieve two objectives. Firstly, it provided us with a better understanding of the level of awareness and misperceptions among individuals, who were sufficiently motivated to participate in our screening program in the first place. This information would help us identify strategies to improve their compliance with regular screening. Secondly, this study has prepared us better for the next phase of our study, that is, to assess the level of knowledge and misperceptions among HBV carriers in the general population, which may be lower than the

Table 2 Factors associated with high and low scores on HBV knowledge

Factors	Low scores (≤ 9) $n = 53$	High scores (≥ 10) $n = 139$	Univariate analysis P	Multivariate analysis ¹ P
Age (yr)	46 \pm 1	41 \pm 1	0.002	0.066
Male (%)	39 (74)	109 (78)	0.57	
Chinese (%)	52 (98)	132 (97)	1.00	
Monthly income \geq S\$4 000 (%)	8 (15)	37 (27)	0.057	0.199
Family history of HBV (%)	19 (36)	48 (35)	0.87	
Family history of HCC (%)	11 (21)	24 (17)	0.68	
On regular follow-up (%)	61 (44)	78 (56)	0.91	
Tertiary educated (%)	17 (32)	92 (66)	<0.001	0.005

¹Multivariate analysis using multiple regression analysis.

participants in our present study. Notwithstanding the above limitations, we believe our study provides important findings for public health officials, as well as hepatologists, to improve their patient education programs particularly for individuals who have been motivated to participate in screening, to ensure that they would not default follow-up after their first screening appointments.

In conclusion, many misperceptions exist among HBV carriers who participated in a screening program in Singapore and HBV carriers with better education are more likely to know HBV better. Future patient and public health education efforts should focus on dispelling misperceptions and target HBV carriers with less education.

REFERENCES

- 1 **Lok AS**, McMahon BJ. Chronic hepatitis B. *Hepatology* 2001; **34**: 1225-1241
- 2 **de Franchis R**, Hadengue A, Lau G, Lavanchy D, Lok A, McIntyre N, Mele A, Paumgartner G, Pietrangelo A, Rodes J, Rosenberg W, Valla D. EASL Jury. EASL international consensus conference on hepatitis B. 13-14 september, 2002 Geneva Switzerland consensus statement (long version). *J Hepatol* 2003; **39**: S3-25
- 3 **James L**, Fong CW, Foong BH, Wee MK, Chow A, Shum E, Chew SK. Hepatitis B seroprevalence study 1999. *Singapore Med J* 2001; **42**: 420-424
- 4 Ministry of Health, Singapore. Statistics: Health facts Singapore 2002. <http://app.moh.gov.sg/sta/sta0202.asp#sta0202>. Accessed March 2004
- 5 **Wai CT**, Lok AS. Treatment of hepatitis B. *J Gastroenterol* 2002; **37**: 771-778
- 6 **Tang ZY**, Yang BH. Secondary prevention of hepatocellular carcinoma. *J Gastroenterol Hepatol* 1995; **10**: 683-690
- 7 **McMahon BJ**, Bulkow L, Harpster A, Snowball M, Lanier A, Sacco F, Dunaway E, Williams J. Screening for hepatocellular carcinoma in Alaska Natives infected with chronic hepatitis B: a 16-year population-based study. *Hepatology* 2000; **32**: 842-846
- 8 **Zoli M**, Magalotti D, Bianchi G, Gueli C, Marchesini G, Pisi E. Efficacy of a surveillance program for early detection of hepatocellular carcinoma. *Cancer* 1996; **78**: 977-985
- 9 **Oka H**, Kurioka N, Kim K, Kanno T, Kuroki T, Mizoguchi Y, Kobayashi K. Prospective study of early detection of hepatocellular carcinoma in patients with cirrhosis. *Hepatology* 1990; **12**: 680-687
- 10 Core working party for Asia-Pacific consensus on hepatitis B and C. Consensus statements on the prevention and management of hepatitis B and hepatitis C in the Asia-Pacific region. Core Working Party for Asia-Pacific Consensus on Hepatitis B and C. *J Gastroenterol Hepatol* 2000; **15**: 825-841
- 11 **Wai CT**, Mak B, Chua W, Lim SG. The majority of hepatitis B carriers are not on regular surveillance in Singapore. *Singapore Med J* 2004; **45**: 423-426
- 12 **Taylor VM**, Jackson JC, Chan N, Kuniyuki A, Yasui Y. Hepatitis B knowledge and practices among Cambodian American women in Seattle, Washington. *J Community Health* 2002; **27**: 151-163
- 13 **Thompson MJ**, Taylor VM, Yasui Y, Hislop TG, Jackson JC, Kuniyuki A, Teh C. Hepatitis B knowledge and practices among Chinese Canadian women in Vancouver, British Columbia. *Can J Public Health* 2003; **94**: 281-286
- 14 **Bodenheimer T**, Wagner EH, Grumbach K. Improving primary care for patients with chronic illness. *JAMA* 2002; **288**: 1775-1779
- 15 **Clark NM**. Management of chronic disease by patients. *Annu Rev Public Health* 2003; **24**: 289-313

Science Editor Wang XL and Guo SY Language Editor Elsevier HK

Pin1 overexpression in colorectal cancer and its correlation with aberrant β -catenin expression

Chang-Jae Kim, Yong-Gu Cho, Yong-Gyu Park, Suk-Woo Nam, Su-Young Kim, Sug-Hyung Lee, Nam-Jin Yoo, Jung-Young Lee, Won-Sang Park

Chang-Jae Kim, Yong-Gu Cho, Suk-Woo Nam, Su-Young Kim, Sug-Hyung Lee, Nam-Jin Yoo, Jung-Young Lee, Won-Sang Park, Department of Pathology, College of Medicine, The Catholic University of Korea, Seoul 137-701, South Korea
Yong-Gyu Park, Department of Statistics, College of Medicine, The Catholic University of Korea, Seoul 137-701, South Korea
Young-Mok Yang, Genetic Laboratory of Premedical Course, Kon-Kuk University College of Medicine, Chung-Ju, South Korea
Supported by the Korea Science and Engineering Foundation (KOSEF) through the Cell Death Disease Research Center at The Catholic University of Korea, No. R13-2002-005-01004-0
Correspondence to: Won-Sang Park, Department of Pathology, College of Medicine, The Catholic University of Korea, 505 Banpo-dong, Seocho-gu, Seoul 137-701, South Korea. wonsang@catholic.ac.kr
Telephone: +82-2-590-1192 Fax: +82-2-537-6586
Received: 2004-11-23 Accepted: 2005-01-05

Abstract

AIM: To investigate clinical significance of Pin1 and β -catenin expression in colorectal cancers and to demonstrate the relationship of their expression.

METHODS: The role of Pin1 and β -catenin protein in colorectal tumorigenesis and their clinicopathologic significance were analyzed by immunohistochemistry, and the correlation between Pin1 and β -catenin protein expressions was also studied in 124 patients with colorectal cancer who were surgically treated.

RESULTS: Normal colonic epithelium either failed to express or showed focal and weak expression of Pin1 and β -catenin. Overexpression of Pin1 and β -catenin protein was found in 23 (18.54%) and 50 (40.3%) of 124 colorectal cancers, respectively. Overexpression of both proteins was not related to the lymph node metastasis, tumor stage and survival period after excision. Survival analysis results indicated that tumor stage was a valuable predictor of survival. Interestingly, a significant correlation was found between Pin1 and β -catenin protein expression.

CONCLUSION: Overexpression of Pin1 and β -catenin may be closely related with the development and/or progression of colorectal carcinoma and further supports that Pin1 overexpression might contribute to the upregulation of β -catenin.

© 2005 The WJG Press and Elsevier Inc. All rights reserved.

Key words: Pin1; Immunohistochemistry; β -catenin; Survival

Kim CJ, Cho YG, Park YG, Nam SW, Kim SY, Lee SH, Yoo NJ, Lee JY, Park WS. Pin1 overexpression in colorectal cancer and its correlation with aberrant β -catenin expression. *World J Gastroenterol* 2005; 11(32): 5006-5009
<http://www.wjgnet.com/1007-9327/11/5006.asp>

INTRODUCTION

β -catenin is a multifunctional protein that plays an important role in the transduction of Wnt signals and in the intercellular adhesion by linking the cytoplasmic domain of cadherin^[1]. In general, the cytoplasmic level of β -catenin is kept low through interaction with a protein complex, comprised of adenomatous polyposis coli (APC), Axin, protein phosphatase 2A, and glycogen synthase kinase 3 β (GSK3 β). It is believed that this complex phosphorylates the β -catenin, thereby inducing ubiquitination-dependent proteolysis of β -catenin. Therefore, alterations of these genes cause accumulation of cytoplasmic β -catenin and nuclear translocation of β -catenin. After its translocation into the nucleus, β -catenin binds to members of the Tcf/Lef family thereby activating target genes, such as cyclin D1 and myc. In cancer cells, only one of these genes is mutated in a given tumor sample reflecting their role in a common pathway^[2]. For instance, colon tumor with mutations in APC has α wild-type β -catenin gene, and vice versa, any tumor with mutations in β -catenin is wild-type for APC.

Recently, it has been shown that Pin1 is overexpressed in some human malignancies and that its expression closely correlates with the level of cyclin D1 in human cancer^[3]. Pin1 is a peptidyl-prolyl cis-trans isomerase that isomerizes only phosphorylated serine/threonine residues preceding proline peptide bonds to regulate various cellular processes including cell division and transcription^[4-7]. Interestingly, Pin1 contributes to the upregulation of β -catenin in tumors such as breast cancer by inhibiting interaction between APC and β -catenin^[8]. Thus, this study aimed to elucidate, whether Pin1 and β -catenin expressions were involved in colorectal carcinogenesis and whether Pin1 expression contributed to aberrant β -catenin overexpression.

MATERIALS AND METHODS

Patients and specimens

One hundred and twenty-four patients with colorectal cancers from January 2001 to December 2002, were enrolled in this study. No patient had a family history of colorectal cancer and was treated with chemotherapy before tumor removal.

Tumor stage was classified according to Dukes' criteria. Thirteen patients were classified as Dukes' A, 47 as Dukes' B, 56 as Dukes' C and 8 as Dukes' D. The range of observation was 14-36 mo for the survivors. Of these, 15 patients showed relapse of cancer and 11 patients died of cancer during this time. Specimens collected from these patients were fixed by formalin and embedded in paraffin. Two pathologists screened histological sections and selected areas of the representative tumor cells. Three tissue cores (0.6 mm in diameter) were taken from each tumor sample and placed in a new recipient paraffin block using a commercially available microarray instrument (Beecher Instruments, Micro-Array Technologies, Silver Spring, MD, USA) according to established methods^[9]. One cylinder of normal colonic mucosa adjacent to each tumor was also transferred to the recipient block.

Immunohistochemistry for Pin1 and β -catenin

Primary polyclonal rabbit anti-Pin1 antibody (Oncogene Research Products, San Diego, CA, USA, dilution 1/100) and anti- β -catenin (Transduction Laboratories, Lexington, KY, USA) were used. Immunostaining was performed on microarray tissue sections with a tyramide signal amplification kit (NEN Life Science, Boston, MA, USA) for signal intensification. Antigen retrieval was performed by microwave heating in a citrate buffer (pH 6.0). Other procedures were performed as previously described^[10]. The reaction products were developed with diaminobenzidine (Sigma, St. Louis, MO, USA) and counterstained with hematoxylin. A negative control, using non-immune rabbit serum instead of the primary antisera, did not produce any staining (data not shown). Three pathologists independently reviewed the results. Immunoreactivities of both Pin1 and β -catenin were categorized into four groups: (1) negative, 0-5%; (2) low, 5-30%; (3) moderate, 30-50%; (4) high, \geq 50%. Since both

Pin1 and β -catenin expressions were negative or low in normal colonic mucosa, we considered moderate and high immunoreactivities as overexpression.

Statistical analysis

We used χ^2 test to analyze the correlation between clinicopathologic parameters of colorectal cancer and expressions of Pin1 and β -catenin, and the association between Pin1 and β -catenin expressions. $P < 0.05$ was considered statistically significant. The predictive value of clinical parameters for survival was evaluated using the Kaplan-Meier analysis.

RESULTS

Pin1 protein expression in colorectal cancer

One hundred and twenty-four colorectal carcinomas were screened for Pin1 protein expression. The expression was mainly negative or low in normal colonic mucosa. In the present study, overexpression of Pin1 was found in 23 (18.5%) of the 124 colorectal carcinomas, in which immunostaining was predominant in either the cytoplasm or the nuclei of tumor cells (Figure 1). Of these 23 colorectal carcinomas, 3 had high expression of Pin1 and 20 had moderate expression of Pin1. Positive staining was seen in 23.1% (3 of 13 cases) of stage A patients, 23.4% (11 of 47) of stage B patients, 12.5% (7 of 56) of stage C patients, and 25.0% (2 of 8) of stage D patients, respectively (Table 1). There was no significant correlation between overexpression of Pin1 and Dukes' stage. In addition, Pin1 expression was detected in 8 (13.6%) of 59 cases with lymph node metastasis and showed no significant correlation with lymph node metastasis. Univariate analysis showed that the expression of Pin1 in colorectal cancer was not related with survival period after excision, indicating that the presence of Pin1 staining was not a valuable predictor of survival.

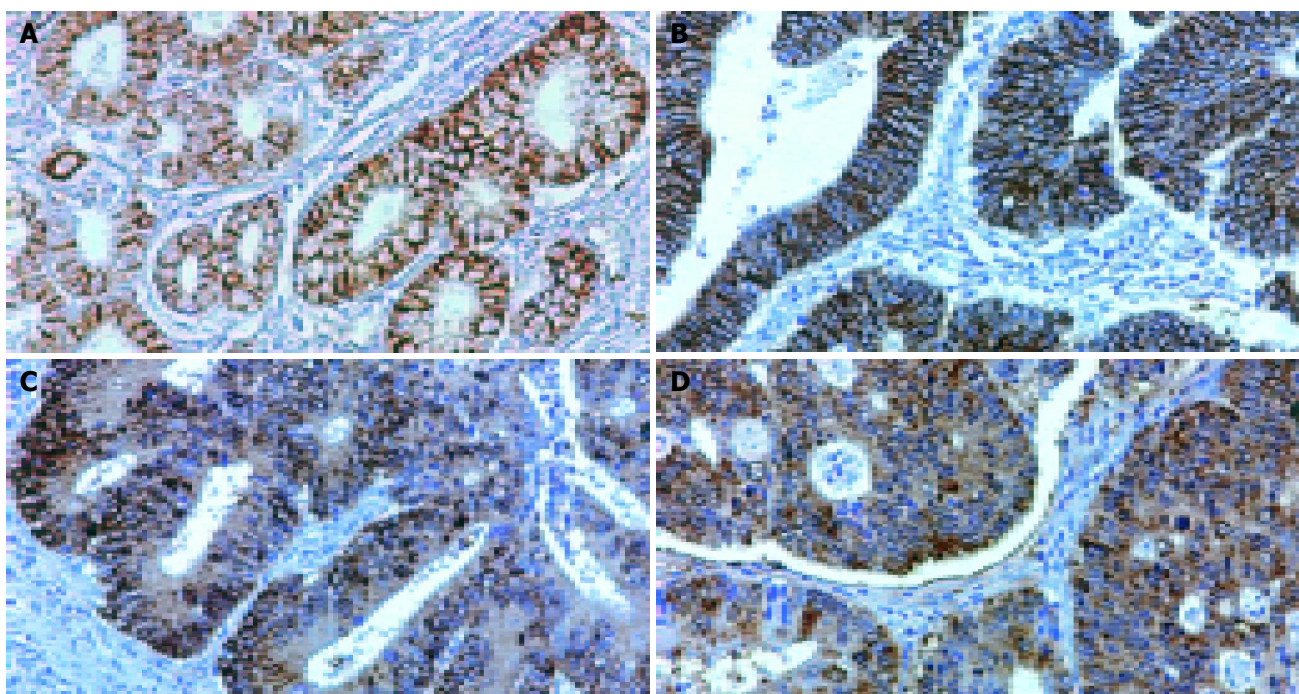


Figure 1 Expression of β -catenin and Pin1 proteins in normal colonic mucosa

(A) and cancer cells (C-D) (B and C, β -catenin; D, Pin1).

Table 1 Relationship between expression of Pin1 and β -catenin protein and clinicopathologic parameters

Groups	Pin1		Positive (%)	P	β -catenin		Positive (%)	P
	+	-			+	-		
Stage				0.4778				0.6774
A	3	10	23.1		6	7	46.2	
B	11	36	23.4		21	26	44.7	
C	7	49	12.5		21	35	37.5	
D	2	6	25.0		2	6	25.0	
L/N metastasis				0.2474				0.5114
+	8	51	13.6		22	37	37.3	
-	15	50	23.1		28	37	43.1	
Survival period				0.3312				0.5154
< 24 mo	3	7	30.0		5	5	50.0	
\geq 24 mo	20	94	17.5		45	69	15.8	
Pin1 protein								0.000004
+					19	4	82.6	
-					31	70	30.7	
Total	23	101	18.5		50	74	40.3	

L/N:lymphnode.

Expression of β -catenin protein

Expression of β -catenin protein was found on cell membrane in the normal colonic mucosa. The cancer cells demonstrated abnormal nuclear and cytoplasmic staining of β -catenin, whereas the membrane staining was negative or low in tumors (Figure 1). Overexpression was observed in 50 (40.3%) of 124 specimens. There was no significant correlation between β -catenin expression and clinicopathologic parameters, including lymph node metastasis, tumor stage and survival period after surgical resection (Table 1). Overall, only tumor stage was a significant predictor of survival, and lower stage patients had a longer survival as shown in log rank test ($P < 0.05$).

Correlation between Pin1 and β -catenin

Overexpression of Pin1 protein was detected in 19 of 50 colorectal cancers with aberrant expression of β -catenin protein. There was a significant positive correlation between the expressions of Pin1 and β -catenin ($P < 0.01$, Table 1).

DISCUSSION

Phosphorylation of proteins on serine/threonine residues preceding proline is a major regulatory mechanism in cell proliferation and transformation^[11,12]. The prolyl isomerase Pin1, catalyzes conformational changes in certain key proline-directed phosphorylation sites and functions as a pivotal catalyst for oncogenesis^[13]. Pin1 is overexpressed in many human tumors such as breast and prostate cancer^[14-16], and increases the transcriptional activity of c-Jun towards the cyclin D1 promoter^[3]. In the present study, we found that Pin1 protein levels in colorectal cancer cells were not positively correlated with any commonly used clinicopathologic parameters, such as tumor stage and lymph node metastasis. Additionally, univariate analysis demonstrated that there was no association between Pin1 expression and survival, suggesting that the Pin1 level might not a valuable prognostic marker for predicting the overall survival of colorectal cancer patients.

β -catenin is a multifunctional protein, and plays an

essential role in the transduction of Wnt signals. Cytosolic β -catenin is eliminated by APC-dependent proteasomal degradation pathways regulated by GSK3 β or p53-inducible Siah-1. Conditional degradation of β -catenin represents a central event of Wnt signaling pathway controlling cell fate and proliferation^[2]. Dysregulation of β -catenin turnover caused by genetic alterations of Wnt signaling pathway-related genes is implicated in cancers^[17]. Alterations of β -catenin expression have been documented in many malignancies, including breast cancer, gastric cancer, colonic and hepatocellular carcinomas^[18-21]. Additionally, overexpression of Pin1 can upregulate β -catenin in tumors, by inhibiting interaction between APC and β -catenin^[8]. We also found that β -catenin was abnormally expressed in 50 (40.3%) of 124 colorectal cancers. The expression was not related to clinical parameters and survival period after surgical excision. By comparing survival and clinicopathologic features, we found that only tumor stage was positively correlated with survival in log rank test ($P < 0.05$).

Interestingly, statistical analysis revealed a significant correlation between Pin1 overexpression and β -catenin expression, suggesting that Pin1 overexpression is significantly correlated with β -catenin expression in colorectal cancer and further supports, that aberrant Pin1 expression may be important for the upregulation of β -catenin expression.

REFERENCES

- 1 Peifer M, Polakis P. Wnt signaling in oncogenesis and embryogenesis—a look outside the nucleus. *Science* 2000; **287**: 1606-1609
- 2 Lustig B, Behrens J. The Wnt signaling pathway and its role in tumor development. *J Cancer Res Clin Oncol* 2003; **129**: 199-221
- 3 Wulf GM, Ryo A, Wulf GG, Lee SW, Niu T, Petkova V, Lu KP. Pin1 is overexpressed in breast cancer and cooperates with Ras signaling in increasing the transcriptional activity of c-Jun towards cyclin D1. *EMBO J* 2001; **20**: 3459-3472
- 4 Hunter T, Karin M. The regulation of transcription by phosphorylation. *Cell* 1992; **70**: 375-387
- 5 Lu KP, Hanes SD, Hunter T. A human peptidyl-prolyl isomerase essential for regulation of mitosis. *Nature* 1996; **380**: 544-547
- 6 Ranganathan R, Lu KP, Hunter T, Noel JP. Structural and

- functional analysis of the mitotic rotamase Pin1 suggests that substrate recognition is phosphorylation dependent. *Cell* 1997; **89**: 875-886
- 7 **Shen M**, Stukenberg PT, Kirschner MW, Lu KP. The essential mitotic peptidyl-prolyl isomerase Pin1 binds and regulates mitosis-specific phosphoproteins. *Genes Dev* 1998; **12**: 706-720
 - 8 **Ryo A**, Nakamura M, Wulf G, Liou YC, Lu KP. Pin1 regulates turnover and subcellular localization of β -catenin by inhibiting its interaction with APC. *Nat Cell Biol* 2001; **3**: 793-801
 - 9 **Kononen J**, Bubendorf L, Kallioniemi A, Barlund M, Schraml P, Leighton S, Torhorst J, Mihatsch MJ, Sauter G, Kallioniemi OP. Tissue microarrays for high-throughput molecular profiling of tumor specimens. *Nat Med* 1998; **4**: 844-847
 - 10 **Park WS**, Oh RR, Kim YS, Park JY, Shin MS, Lee HK, Lee SH, Yoo NJ, Lee JY. Absence of mutations in the kinase domain of the *Met* gene and frequent expression of Met and HGF/SF protein in primary gastric carcinomas. *APMIS* 2000; **108**: 195-200
 - 11 **Blume-Jensen P**, Hunter T. Oncogenic kinase signalling. *Nature* 2001; **411**: 355-365
 - 12 **Hanahan D**, Weinberg RA. The hallmarks of cancer. *Cell* 2000; **100**: 57-70
 - 13 **Lu KP**. Prolyl isomerase Pin1 as a molecular target for cancer diagnostics and therapeutics. *Cancer Cell* 2003; **4**: 175-180
 - 14 **Nakashima M**, Meirmanov S, Naruke Y, Kondo H, Saenko V, Rogounovitch T, Shimizu-Yoshida Y, Takamura N, Namba H, Ito M, Abrosimov A, Lushnikov E, Roumiantsev P, Tsyb A, Yamashita S, Sekine I. Cyclin D1 overexpression is thyroid tumours from a radio-contaminated area and its correlation with Pin1 and aberrant β -catenin expression. *J Pathol* 2004; **202**: 446-455
 - 15 **Bao L**, Kimzey A, Sauter G, Sowadski JM, Lu KP, Wang DG. Prevalent overexpression of prolyl isomerase Pin1 in human cancers. *Am J Pathol* 2004; **164**: 1727-1737
 - 16 **Ayala G**, Wang D, Wulf G, Frolov A, Li R, Sowadski J, Wheeler TM, Lu KP, Bao L. The prolyl isomerase Pin1 is a novel prognostic marker in human prostate cancer. *Cancer Res* 2003; **63**: 6244-6251
 - 17 **Kinzler KW**, Vogelstein B. Lessons from hereditary colorectal cancer. *Cell* 1996; **87**: 159-170
 - 18 **Bukholm IK**, Nesland JM, Borresen-Dale AL. Re-expression of E-cadherin, alpha-catenin and beta-catenin, but not of gamma-catenin, in metastatic tissue from breast cancer patients. *J Pathol* 2000; **190**: 15-19
 - 19 **Woo DK**, Kim HS, Lee HS, Kang YH, Yang HK, Kim WH. Altered expression and mutation of beta-catenin gene in gastric carcinomas and cell lines. *Int J Cancer* 2001; **95**: 108-113
 - 20 **Utsunomiya T**, Doki Y, Takemoto H, Shiozaki H, Yano M, Sekimoto M, Tamura S, Yasuda T, Fujiwara Y, Monden M. Correlation of beta-catenin and cyclin D1 expression in colon cancers. *Oncology* 2001; **61**: 226-233
 - 21 **Pang R**, Yuen J, Yuen MF, Lai CL, Lee TK, Man K, Poon RT, Fan ST, Wong CM, Ng IO, Kwong YL, Tse E. PIN1 overexpression and β -catenin gene mutations are distinct oncogenic events in human hepatocellular carcinoma. *Oncogene* 2004; **23**: 4182-4186

Effect of NCPB and VSPL on pain and quality of life in chronic pancreatitis patients

Andrzej Basinski, Tomasz Stefaniak, Ad Vingerhoets, Wojciech Makarewicz, Lukasz Kaska, Aleksander Stanek, Andrzej J. Lachinski, Zbigniew Sledzinski

Andrzej Basinski, Department of Emergency Medicine, Medical University of Gdansk, Poland

Tomasz Stefaniak, Wojciech Makarewicz, Lukasz Kaska, Aleksander Stanek, Andrzej J. Lachinski, Zbigniew Sledzinski, Department of General, Endocrine and Transplant Surgery, Medical University of Gdansk, Poland

Ad Vingerhoets, Department of Psychology and Health, and Research Institute for Psychology and Health, Tilburg University, the Netherlands

Correspondence to: Tomasz Stefaniak, MD, PhD, Department of General, Endocrine and Transplant Surgery, Medical University of Gdansk, 1 Debinki Str., Gdansk PL-80-211, Poland. wujstef@amg.gda.pl

Telephone: +48-583493805 Fax: +48-583492416

Received: 2004-10-19 Accepted: 2004-12-23

Abstract

AIM: To compare the effects of neurolytic celiac plexus block (NCPB) and videothoroscopic splanchnicectomy (VSPL) on pain and quality of life of chronic pancreatitis (CP) patients.

METHODS: Forty-eight small duct CP patients were treated invasively with NCPB ($n = 30$) or VSPL ($n = 18$) in two non-randomized, prospective, case-controlled protocols due to chronic pain syndrome, and compared to a control group who were treated conservatively ($n = 32$). Visual analog scales were used to assess pain and opioid consumption rate was evaluated. In addition, the quality of life was measured using QLQ C-30 for NCPB and FACIT for VSPL. Although both questionnaires covered similar problems, they could not be compared directly one with another. Therefore, the studies were compared by meta-analysis methodology.

RESULTS: Both procedures resulted in a significant positive effect on pain of CP patients. Opioids were withdrawn totally in 47.0% of NCPB and 36.4% of VSPL patients, and reduced in 53.0% and 45.4% of the respective patient groups. No reduction in opioid usage was observed in the control group. In addition, fatigue and emotional well-being showed improvements. Finally, NCPB demonstrated stronger positive effects on social support, which might possibly be attributed to earlier presentation of patients treated with NCPB.

CONCLUSION: Both invasive pain treatment methods are effective in CP patients with chronic pain.

Key words: Chronic pancreatitis; Pain; Neurolytic celiac plexus block; Videothoroscopic splanchnicectomy; Quality of life

Basinski A, Stefaniak T, Vingerhoets A, Makarewicz W, Kaska L, Stanek A, Lachinski AJ, Sledzinski Z. Effect of NCPB and VSPL on pain and quality of life in chronic pancreatitis patients. *World J Gastroenterol* 2005; 11(32): 5010-5014

<http://www.wjgnet.com/1007-9327/11/5010.asp>

INTRODUCTION

Pain is the most significant, frequent and difficult to treat symptom of chronic pancreatitis (CP). The pain is severe, persistent, excruciating and unbearable^[1-4]. It is often localized in the epigastrium, radiates to the left or more frequently to the right side, or to the lower part of the thoracic vertebral column or to the right scapula^[2-5]. The pain is often accompanied with nausea and vomiting. The underlying pathophysiological mechanisms of pain are still unknown.

Typical CP pain is associated with increased pancreatic duct pressure and caused by stimulation of specific nociceptors or sensing receptors^[3]. Currently, the most significant reason of pain in CP is considered to be the pressure of pancreatic fluid increased intraductally and within the pancreatic tissue. This may result in impaired outflow of pancreatic fluid and may also present as pancreatic pseudocysts (in cases of pancreatic duct rupture)^[1]. It can also be influenced by self-digestion of pancreatic ducts due to progressing inflammation and by inflammation of nerves involved in transfer of stimuli from the pancreas (pancreatitis associated neuritis)^[6].

Afferent fibers from the celiac region may enter the spinal cord at a different level from which the respective efferent fibers originate. Fibers of these bunches enter the gray matter and terminate within layers I and IV^[9]. There is no morphological or functional evidence for the existence of an indirect celiac projection in the layer II, contrary to the somatic projection found extensively in layers I and II^[7-9]. Thus, the distribution of celiac and somatic stimuli within the spinal cord is different. Nevertheless, the fact that visceral pain is sometimes associated with somatic structures and convergence of the stimuli from organs and somatic structures into sensory neurons may further initiate a sensation of somatic pain^[10].

It is generally acknowledged that the quality of life of CP patients significantly decreases due to severe and constant pain^[1,4]. Various methods, including invasive techniques, have been proposed to treat pain^[11]. The aim of the present study

was to compare the effect of two most frequently applied methods of treatment, NCPB and videothoroscopic splanchnicectomy (VSPL) on pain, opioid consumption rate and quality of life of CP patients.

MATERIALS AND METHODS

Patients

Two groups of small-duct CP patients were treated in two separate prospective, case-controlled studies with NCPB ($n = 30$) or VSPL ($n = 18$). In addition, a control group ($n = 32$) consisting of CP patients with chronic pain syndrome managed conservatively took part in this study.

The patients chose the procedure according to their needs (consumer approach – orientation towards the needs of patients).

All the procedures were performed by surgeons experienced in videoscopic surgery.

The demographic data of the three groups are presented in Table 1. No patient had structural lesions: pancreatic duct stricture, pseudocyst, or distal common bile duct stricture amenable to either endoscopic or surgical treatment. The inclusion criteria were a CP diagnosed by CT scan and endoscopic retrograde cholangiopancreatography, persistent pain for at least 3 mo, scoring at least 66.7% on the pain visual analog scale. Patients with pancreatic inflammatory tumors or pseudocysts were excluded from the study.

Measurement

Pain was measured using visual analog scales and quality of life of CP patients was assessed by well-validated EORTC, quality of life questionnaire QLQ C-30 and functional assessment of chronic illness therapy (FACIT). The control group completed both health-related quality of life measurements. The patients were assessed 2 d before the treatment, then followed up and reassessed after 2nd and 8th wk.

NCPB

The patients were fixed in the prone position with a slight bending forward. The lower margin of the 12th rib was marked on both sides of the body. After the superficial anesthesia with 1% lignocaine, the 20-G needle (10-12 cm) pierced into the point located 5-7 cm laterally from the midline on both sides just under the lower margin of the 12th rib, at the angle of 30-45 towards the trunk of L₁ and Th₁₂ vertebrae or the space between L₁ and Th₁₂ vertebrae. The canal of the needle was then additionally anesthetized with further 6-10 mL of 1% lignocaine. The needle was pierced into until the resistance of the bone was met. If this resistance was met at the level of 3-5 cm under the skin, it was assumed that the needle reached the vertebra and the needle was withdrawn and re-introduced in order to bypass above or below the vertebra towards its lateral surface.

The surface was achieved at the depth of 6-8 cm. Then, the needle was rotated 90 towards the vertebra and re-introduced with a continuous decrease of the angle of the introduction, aiming to slide on the lateral surface of the vertebra. When the needle bypassed the vertebra by 1-2 cm, and after reassuring that it was not located in the aorta or other major vessel, 20-30 mL of 50% ethanol with 5 mL of 1% lignocaine was injected into both sides.

VSPL

Because unilateral (preferably left-sided) splanchnicectomy was reported to be adequate in control of the intractable pancreatic pain^[12], all patients were given a left-sided intervention. General anesthesia was administered with single-bronchus intubation in every case. The patient was placed in the right lateral decubitus position with the left arm elevated at a 90° angle, and fixed with support-arms and bandages, and the table was then tilted 30° anteriorly in the longitudinal axis (thus, after induction of a pneumothorax, the lung would “fall away” from the costovertebral gutter). After desufflation of the lung, two trocars were inserted into the thorax: one (a 5-mm trocar) was placed in the fifth intercostal space in a medial axillary line for the camera, and the second (a 5-mm trocar) was placed in the seventh intercostal space in an anterior axillary line for the instruments. After identification of the splanchnic nerve, situated above the aorta on the left or above the azygos vein on the right, the parietal pleura was incised and the nerve together with its minor connecting branches, was prepared to a distance of 5-8 cm and then excised. After insufflation of the lung, the trocars were removed, a single chest tube was placed, and the wounds were closed according to surgical standards.

Statistical analysis

This study consisted of two separate, prospective, non-randomized, case-controlled experiments (NCPB *vs* control and VSPL *vs* control). By consequence, the statistical techniques applied in meta-analysis were employed, fixed-effects and effect sizes were calculated as the difference between the outcome means of the groups divided by the pooled standard deviations. An overall weighed effect size was obtained and presented with 95% confidence interval (95%CI). Results were tested for homogeneity using the Breslow-Day tests.

Parametric data were tested with *t* test, ANOVA, and non-parametric estimations were conducted with *U* Mann-Whitney and χ^2 tests. All analyses were performed using Statistica 6.0 software licensed to Medical University of Gdansk.

RESULTS

The raw data and univariate statistics for both protocols are shown in Figure 1.

Table 1 Socio-demographic data and initial medical information of all groups included in protocols 1 and 2 (mean±SD)

	Protocol 1 NCPB ($n = 30$)	Protocol 2 VSPL ($n = 18$)	Control ($n = 32$)
Age (yr)	49.9±7.8	47.3±5.0	52.3±6.6
Sex (M:F ratio)	3.01	3.51	3.34
Etiology (alcohol <i>vs</i> other ratio)	6.5	8.0	7.0
Period from the symptomatic onset of the disease	6.2±2.2	11.5±4.3	7.1±3.0

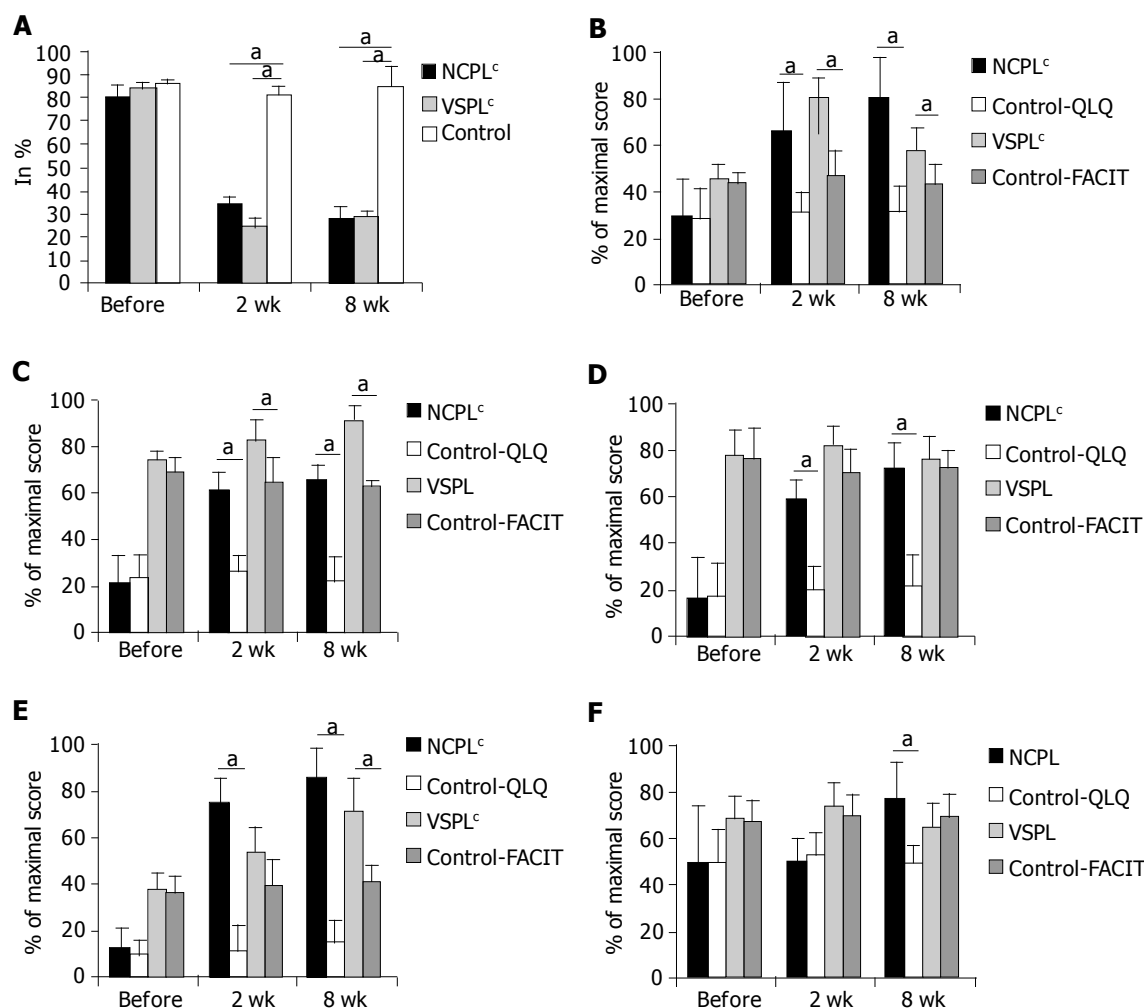


Figure 1 Results of pain and quality of life assessment in CP patients and controls. **A:** VAS-Pain; **B:** Physical well-being; **C:** Emotional well-being; **D:** Social support; **E:** Fatigue; **F:** Ailments characteristic for the illness. $^aP < 0.05$

t-test vs NCPB or VSPL group and corresponding control; $^aP < 0.05$ vs paired ANOVA. Results are shown as mean \pm SD.

In both groups of CP patients, the therapeutic intervention was beneficial (Table 2).

The effects were significant and very strong, especially concerning pain, as indicated on VAS scale. In order to control for possible regression to the mean effect, the mean effect sizes were calculated by comparison of the results after 2nd and 8th wk, not only to the pre-treatment baseline, but also to the results of the control group treated conservatively and evaluated at the corresponding periods of follow-up.

Opioids were administered to 17 patients (56.7%) in the NCPB group and to 11 patients (61.1%) in the VSPL group. In the control group, 18 patients (56.2%) were treated with opioids and this number was not altered during the follow-up. The initial frequency of opioid treatment did not differ between the groups. The opioids were withdrawn totally after invasive treatment in 8 (47%) NCPB patients, and in 4 (36.4%) VSPL patients, and the dosage was reduced in another 9 (53%) and 5 (45.4%) patients, respectively (no statistically significant difference). No changes were observed throughout the whole period of follow-up. In two remaining opioid-using patients (18.2%) after VSPL, no long-term opioid reduction could be achieved (Figure 2).

There was no mortality and no major morbidity. Orthostatic

hypotension was observed for 3 d in nine patients (30%) from NCPB group and in one patient (5.5%) from VSPL group. Diarrhea was resolved after symptomatic treatment for 14 d in four patients (13.3%) from the NCPB group. Intermittent intercostal pain was treated with paracetamol for 2 wk in four patients (22.2%) from VSPL group. In one of them (5.5%), intercostal nerve block had to be instituted. In one case, classic thoracotomy had to be performed due to massive adhesions (who was excluded from the study).

DISCUSSION

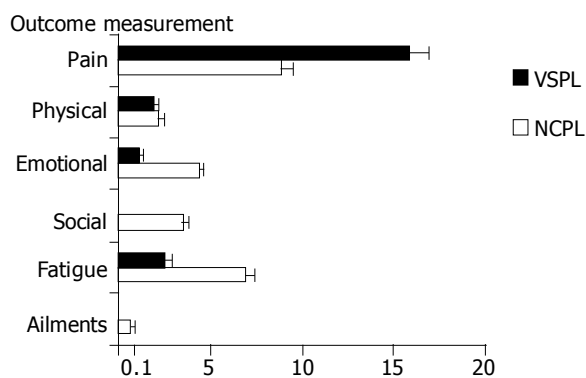
In the presented study, the effects of NCPB and VSPL on CP patients and controls were compared. As the methods for assessment of life quality differed in two protocols, the comparison was performed by meta-analytic approach. The reduction of pain was stronger in VSPL group than in NCPB group, but the effects in both groups were very potent.

The influence on physical well-being was slightly better in NCPB group, but did not differ statistically from the VSPL group. No improvement concerning ailments typical for the disease was noticed. This finding can be explained by the fact that the analgesic treatment cannot obviously affect the cause of the disease.

Table 2 Comparison of mean effects of both therapeutic interventions in CP patients

Therapy	Group size	Parameter	Mean effect	95% CI (min-max)
VSPL	18	Pain ^a	15.82	(14.68-16.96)
NCPL	30		8.89	(8.30-9.48)
VSPL	18	Physical well-being ^a	1.81	(1.57-2.06)
NCPL	30		2.19	(1.96-2.42)
VSPL	18	Emotional well-being ^a	1.12	(0.91-1.34)
NCPL	30		4.40	(4.07-4.73)
VSPL	18	Social support ^a	0.08	(-0.11-0.29)
NCPL	30		3.55	(3.27-3.84)
VSPL	18	Fatigue	2.52	(2.25-2.79)
NCPL	30		6.87	(6.39-7.34)
VSPL	18	Ailments typical for the illness ^a	0.05	(-0.14-0.26)
NCPL	30		0.64	(0.45-0.83)

The effects presented are mean effects of intervention after 2nd and 8th wk compared to the value measured before the therapy and after 2nd and 8th wk of follow-up compared to the control group ($n = 32$) treated conservatively and evaluated at the corresponding periods of time. ^a $P < 0.05$ vs others.

**Figure 2** Effect of VSPL and NCPB on pain of CP patients and controls. Bars show mean effect from two measurements.

Interestingly, the effect on social support and emotional well-being was significantly stronger in NCPB group than in VSPL group. Moreover, the effect of VSPL on social support was weak, while it was very strong after neurolysis. This may be explained by the fact, that this procedure is the first available treatment for the patients in the NCPB group, whereas the VSPL patients have already tried some other treatments, thus having longer history of chronic pain syndrome. Therefore, the decision to receive an invasive treatment is more intensely approved by the NCPB group and the improvement resulting from this treatment is very likely more appreciated emotionally by the patients.

Since conservative treatment of CP chronic pain syndrome is not always effective and may be associated with significant morbidity of iatrogenic opioid addiction, both at physical (suppression of immune function, chronic constipation, drowsiness, and fatigue^[13,14]) and psychological level (decrease in social support, depression, addiction behavior)^[14], an attention has been paid to more invasive methods for pain control.

In the present study, the reduction of opioid consumption was significant in both groups, which gives an optimistic perspective for minimizing the adverse effects of this group of drugs, especially in the chronic treatment. Nevertheless, in two patients treated with opioids for more than a year, VSPL did not result in decrease of the opioid consumption or withdrawal. As early as 3 d after the procedure, the patients

complained about persistent pain localized on the opposite side of the abdomen. The pain could only be alleviated by pethidine. As to date, no diagnostic or treatment guidelines for suspected iatrogenic opioid addiction are available, opioid analgesics were administered. It should be highlighted that administering opioids ought to be considered as the last resort and should only be applied, if any other method has failed. Since the life expectancy of CP patients is 10-20 years shorter than that of general population^[15], the adverse effects of iatrogenic opioid addiction are very likely to occur in these patients. In contrast, the life expectancy of pancreatic cancer rarely exceeds 12 mo^[16].

The pathogenesis of pain in CP still remains a mystery. The factors postulated in its genesis include the release of excessive oxygen-derived free radicals, tissue hypoxia and acidosis, inflammatory infiltration with influx of pain-transmitting substances into damaged nerve ends, and the development of pancreatic ductal and tissue fluid hypertension due to morphological changes of the pancreas^[1-5]. Di Sebastiano *et al.*^[6], reported that the possible additional relevant pancreatic pain pathology factors are ischemia as well as inflammatory and autoimmune reactions. Toma *et al.*^[17], described that expression of the neurotrophin nerve growth factor increased during the course of experimental acute pancreatitis in rats. In human CP, neurotrophin gene expression correlates with the intensity of pain^[18], so that pathogenesis could be speculated in acute phases of CP. Keith *et al.*^[19], proposed that neural and perineural alterations may be important in pain pathogenesis of CP, and concluded that pain severity correlates with duration of alcohol consumption, pancreatic calcification, and percentage of eosinophils in perineural inflammatory cell infiltrates, but not with duct dilatation.

Bockman *et al.*^[20], have provided evidence for an increase in both the number and diameter of pancreatic nerve fibers during the course of CP. In tissue specimens from patients suffering from CP, foci of chronic inflammatory cells are often found surrounding pancreatic nerves exhibiting a damaged perineurium and invasion by lymphocytes. These abnormalities might allow free access of inflammatory mediators or active pancreatic enzymes into nerves, generating and sustaining pain.

The pro-inflammatory cytokine, IL-8 is a well-known chemokine involved in leukocyte recruitment, and activation

of IL-8 release generates hyperalgesia by stimulation of post-ganglionic sympathetic neurones. A significant increase in IL-8 mRNA has been reported in CP tissue samples^[21]. Major sources of IL-8 are inflammatory cells present around enlarged nerves in the inflammatory foci. Thus, induction of IL-8 in immune cells might contribute to amplification of the inflammatory process in CP. The release of IL-8 from the remaining exocrine pancreatic parenchyma may indicate the intrinsic maintenance of the inflammatory response after the first damage to the pancreatic gland, thus sustaining progression and evolution of the disease^[6].

It has been recently suggested that differential epidural anesthesia might be beneficial for differentiating cases susceptible to further sympathetic pain treatment from those who are resistant to it^[22]. Moreover, we would add that the use of NCPB as a therapeutic and diagnostic procedure might be crucial for selecting patients for further VSPL treatment in case of the ailment recurrence. Thus, NCPB should be suggested as the first step of invasive analgetic therapy, as soon as the opioid treatment is needed. Vranken *et al.*^[23], have demonstrated that the efficacy of the second NCPB in CP is significantly lower than that of the first, and that the pain-free period is usually shorter. Therefore, when all the non-opioid methods of analgesia are exhausted, the second step would be left-sided VSPL. Due to rare but fairly significant complications following bilateral splanchnicectomy^[24,25], we would favor unilateral or bilateral non-simultaneous VSPL in CP patients. Only after both-sided VSPLs have been performed and additional NCPB is also attempted, use of opioids is justified in CP patients.

It should also be stressed that the present analysis covers a relatively short period of follow-up. Moreover, the use of two different quality of life measurements may be perceived as another drawback of the present study. Therefore, future studies should include randomization, uniform outcome assessment, and longer follow-up assessment.

REFERENCES

- 1 **Pitchumoni CS**. Pathogenesis and management of pain in chronic pancreatitis. *World J Gastroenterol* 2000; **6**: 490-496
- 2 **Witzigmann H**, Max D, Uhlmann D, Geissler F, Schwarz R, Ludwig S, Lohmann T, Caca K, Keim V, Tannapfel A, Hauss J. Outcome after duodenum-preserving pancreatic head resection is improved compared with classic Whipple procedure in the treatment of chronic pancreatitis. *Surgery* 2003; **134**: 53-62
- 3 **Di Sebastiano P**, Friess H, Di Mola FF, Innocenti P, Buchler MW. Mechanisms of pain in chronic pancreatitis. *Ann Ital Chir* 2000; **71**: 11-16
- 4 **Sohn TA**, Campbell KA, Pitt HA, Sauter PK, Coleman JA, Lillemo KD, Yeo CJ, Cameron JL. Quality of life and long-term survival after surgery for chronic pancreatitis. *J Gastrointest Surg* 2000; **4**: 355-364
- 5 **Sakorafas GH**, Anagnostopoulos G. Surgical management of chronic pancreatitis: current concepts and future perspectives. *Int Surg* 2003; **88**: 211-218
- 6 **Di Sebastiano P**, di Mola FF, Bockman DE, Friess H, Buchler MW. Chronic pancreatitis: the perspective of pain generation by neuroimmune interaction. *Gut* 2003; **52**: 907-911
- 7 **Gohlke F**, Janssen E, Leidel J, Heppelmann B, Eulert J. Histopathological findings in the proprioception of the shoulder joint. *Orthopade* 1998; **27**: 510-517
- 8 **de Leon-Casasola OA**. Critical evaluation of chemical neurolysis of the sympathetic axis for cancer pain. *Cancer Control* 2000; **7**: 142-148
- 9 **Cervero F**, Connell LA. Fine afferent fibers from viscera do not terminate in the substantia gelatinosa of the thoracic spinal cord. *Brain Res* 1984; **294**: 370-374
- 10 **Jänig W**, Morrison JF. Functional properties of spinal visceral afferents supplying abdominal and pelvic organs with special emphasis on visceral nociception. *Progr Brain Res* 1986; **67**: 87-92
- 11 **Ammori BJ**. Pancreatic surgery in the laparoscopic era. *JOP* 2003; **4**: 187-192
- 12 **Makarewicz W**, Stefaniak T, Kossakowska M, Basinski A, Suchorzewski M, Stanek A, Gruca ZB. Quality of life improvement after videothoroscopic splanchnicectomy in chronic pancreatitis patients: case control study. *World J Surg* 2003; **27**: 906-911
- 13 **Wong GY**, Schroeder DR, Carns PE, Wilson JL, Martin DP, Kinney MO, Mantilla CB, Warner DO. Effect of neurolytic celiac plexus block on pain relief, quality of life, and survival in patients with unresectable pancreatic cancer: a randomized controlled trial. *JAMA* 2004; **291**: 1092-1099
- 14 **Portnow JM**, Strassman HD. Medically induced drug addiction. *Int J Addict* 1985; **20**: 605-611
- 15 **Strate T**, Yekebas E, Knoefel WT, Bloechle C, Izbicki JR. Pathogenesis and the natural course of chronic pancreatitis. *Eur J Gastroenterol Hepatol* 2002; **14**: 929-934
- 16 **Liu SL**, Friess H, Kleeff J, Ji ZL, Buchler MW. Surgical approaches for resection of pancreatic cancer: an overview. *Hepatobiliary Pancreat Dis Int* 2002; **1**: 118-125
- 17 **Toma H**, Winston J, Micci MA, Shenoy M, Pasricha PJ. Nerve growth factor expression is up-regulated in the rat model of L-arginine-induced acute pancreatitis. *Gastroenterology* 2000; **119**: 1373-1381
- 18 **Friess H**, Zhu ZW, di Mola FF, Kulli C, Graber HU, Andren-Sandberg A, Zimmermann A, Korc M, Reinshagen M, Buchler MW. Nerve growth factor and its high affinity receptor in chronic pancreatitis. *Ann Surg* 1999; **230**: 615-624
- 19 **Keith RG**, Keshavjee SH, Kerényi NR. Neuropathology of chronic pancreatitis in humans. *Can J Surg* 1985; **28**: 207-211
- 20 **Bockman DE**, Buchler M, Malfertheiner P, Beger HG. Analysis of nerves in chronic pancreatitis. *Gastroenterology* 1988; **94**: 1459-1469
- 21 **Di Sebastiano P**, di Mola FF, Di Febbo C, Baccante G, Porreca E, Innocenti P, Friess H, Buchler MW. Expression of interleukin-8 (IL-8) and substance P in human chronic pancreatitis. *Gut* 2000; **47**: 423-428
- 22 **Bradley EL 3rd**, Bem J. Nerve blocks and neuroablative surgery for chronic pancreatitis. *World J Surg* 2003; **27**: 1241-1248
- 23 **Vranken JH**, Zuurmond WW, de Lange JJ. Increasing the efficacy of a celiac plexus block in patients with severe pancreatic cancer pain. *J Pain Symptom Manage* 2001; **22**: 966-977
- 24 **Howard TJ**, Swofford JB, Wagner DL, Sherman S, Lehman GA. Quality of life after bilateral thoracoscopic splanchnicectomy: long-term evaluation in patients with chronic pancreatitis. *J Gastrointest Surg* 2002; **6**: 845-852
- 25 **Buscher HC**, Jansen JB, van Dongen R, Bleichrodt RP, van Goor H. Long-term results of bilateral thoracoscopic splanchnicectomy in patients with chronic pancreatitis. *Br J Surg* 2002; **89**: 158-162

Alpha-fetoprotein expression is a potential prognostic marker in hepatocellular carcinoma

Dénes Görög, János Regöly-Mérei, Sándor Paku, László Kopper, Péter Nagy

Dénes Görög, Department of Transplantation and Surgery, Semmelweis University, Budapest, Hungary
János Regöly-Mérei, Third Department of Surgery, Semmelweis University, Budapest, Hungary
Sándor Paku, Joint Research Organization of the Hungarian Academy of Sciences and Semmelweis University, Budapest, Hungary

László Kopper, Péter Nagy, First Department of Pathology and Experimental Cancer Research, Semmelweis University, Budapest, Hungary

Supported by the National Science Foundation of Hungary, No. OTKA 42674

Correspondence to: Péter Nagy, First Department of Pathology and Experimental Cancer Research, Semmelweis University, Budapest, Üllői út 26, H-1086, Hungary. nagy@korp1.sote.hu
Telephone: +36-1-2661638 Fax: +36-1-3171074

Received: 2004-10-26 Accepted: 2004-12-20

fetoprotein expression is a potential prognostic marker in hepatocellular carcinoma. *World J Gastroenterol* 2005; 11(32): 5015-5018

<http://www.wjgnet.com/1007-9327/11/5015.asp>

INTRODUCTION

Alpha-fetoprotein (AFP) is one of the earliest recognized oncofetal markers^[1]. It is produced in large amount by the fetal liver, but its expression reduces sharply at birth. AFP is synthesized by most hepatoblastomas and approximately half of hepatocellular carcinomas (HCC), and widely used in differential diagnosis and follow-up of patients with liver tumors, but so far no correlation has been found between the clinical behavior and AFP production in HCC.

DNA microarray analysis may result in the discovery of new tumor markers and can re-evaluate the known tumor parameters. Two independent teams studied the gene expression profile of human HCC cell lines and divided the cell lines into two groups, based on their gene expression pattern. AFP expression is highly correlated with the molecular subtypes of HCC^[2,3]. This observation led us to study the AFP expression in HCC samples and to compare it with other immunophenotypic and clinical features of the tumor.

MATERIALS AND METHODS

Thirty-seven recently diagnosed HCC cases were collected. Formalin-fixed and paraffin-embedded tumor samples (19 needle biopsies and 18 resected tumors) were immunohistochemically stained. The primary antibodies used were: AFP: DAKO (A 0008), MLH-1: Bio PharMingen (554072), MSH-2: Bio PharMingen (556349), β -catenin: Sigma (C2206), CD44: R&D (BBA10), HNF-4: Santa Cruz (SC 6556), p53: DAKO (M 3566). The reaction was visualized using Vector Laboratories' Elite kit (Burlingame, CA, USA), DAB was used as a chromogen. Since AFP expression was frequently focal, all tumors were taken as positive when any reliable staining was detected. In case of p53 and β -catenin, tumors with at least 20% nuclear staining were deemed as positive. CD44 staining resulted in a more or less diffuse stromal reaction in positive cases. Tumor grade and histological subtype were evaluated on H&E-stained sections. Grading was done as previously described by Edmondson and Steiner^[4]. The tumors were classified histologically into pseudoglandular, trabecular, sheet-like, and mixed pattern groups. The clinical parameters studied were age and gender of the patients, the presence of cirrhosis and etiological factors (HCV, HBV, alcoholism, etc.).

Abstract

AIM: To characterize the alpha-fetoprotein (AFP) positive and negative hepatocellular carcinoma (HCC) samples.

METHODS: Thirty-seven paraffin-embedded human HCC samples were analyzed by immunohistochemistry for the following antigens: AFP, β -catenin, p53, CD44, MSH-2, MLH-1, and HNF-4. The tumors were divided into two groups based on the AFP expression. The immunophenotypic data and important clinical parameters were studied between the two groups.

RESULTS: Twenty-one of the thirty-seven examined HCCs were AFP positive. Seven with nuclear p53 staining were AFP positive, while seven tumors with nuclear β -catenin staining were AFP negative. CD44 staining and high histological tumor grade were more frequent among the AFP-positive HCCs. The other immunophenotypic and clinical parameters did not show statistically significant difference in their distribution between the AFP positive and negative samples.

CONCLUSION: AFP expression in HCC correlates with unfavorable prognostic factors, while nuclear β -catenin positivity is more common among the AFP-negative liver tumors. This observation supports the microarray data on *in vivo* human tumors.

© 2005 The WJG Press and Elsevier Inc. All rights reserved.

Key words: Hepatocellular carcinoma; Alpha-fetoprotein; p53; β -catenin; CD44

Görög D, Regöly-Mérei J, Paku S, Kopper L, Nagy P. Alpha-

Unfortunately, no serum AFP value was available for half of the patients; therefore, it was not included in our study. Since the majority of the cases were diagnosed in the last 2 years, their survival was not analyzed. Statistical analysis was done by χ^2 and Student's *t*-test.

The study protocol conformed to the ethical guidelines of the 1975 Declaration of Helsinki as reflected in *a priori* approval by the institution's guidelines (permission number: TUKEB 156/2003).

RESULTS

The tumors were divided into two groups, based on the AFP staining and other parameters. Twenty-one of the thirty-seven examined HCCs were AFP positive (Figure 1A), which was comparable to previous data in the literature. No correlation was found between the AFP staining and age/gender of the patients, etiological factors, presence or absence of cirrhosis, histological subtype of the tumor, MLH-1, MSH-2, HNF-4 staining (data not shown). However, four of the parameters showed statistically significant ($P < 0.05$) difference between the AFP positive and negative HCCs (Tables 1 and 2). Seven p53-positive tumors (Figure 1B) were positive for AFP, while seven nuclear β -catenin-positive tumors (Figure 1C) AFP negative. Nineteen of the twenty-one AFP-positive tumors were positive for CD44 (Figure 1D), while only 3 of the 17 AFP-negative tumors were positive for this adhesion molecule. Statistical comparison resulted in a significant difference between the tumor grades ($P < 0.05$). The AFP-positive tumors had a higher statistical value.

DISCUSSION

We compared the distribution of several parameters between AFP positive and negative HCCs and found that some of

Table 1 AFP negative cases

Casenumner	B-catenin ¹	p53 ¹	CD44 ²	grade
1	-	-	-	2
2	+	-	-	1
3	-	-	-	2
4	-	-	+	2
6	+	-	-	2
7	-	-	-	2
10	+	-	-	2
11	+	-	-	2
14	+	-	-	2
16	-	-	+	1
18	+	-	-	1
19	+	-	-	1
29	-	-	-	2
34	-	-	+	2
36	-	-	-	1
37	-	-	-	2
16 cases	7/16	0/16	3/16	

¹Positivity indicates more than 20% nuclear staining. ²Positivity indicates diffuse stromal staining.

them were significantly different between the two groups. All the p53-positive tumors were stained with AFP antibody and the CD44 positivity was also more common in this group.

β -catenin nuclear staining occurred exclusively in the AFP-negative tumors and the tumor grade was significantly lower in this group, which is in agreement with the reports of Kawai *et al.*^[2], and Lee and Thorgerirsson^[3]. There are some sporadic observations that AFP is more frequently expressed in poorly differentiated HCCs^[5-8].

We found that three unfavorable prognostic markers were correlated with positive AFP. Tumor grade is not as

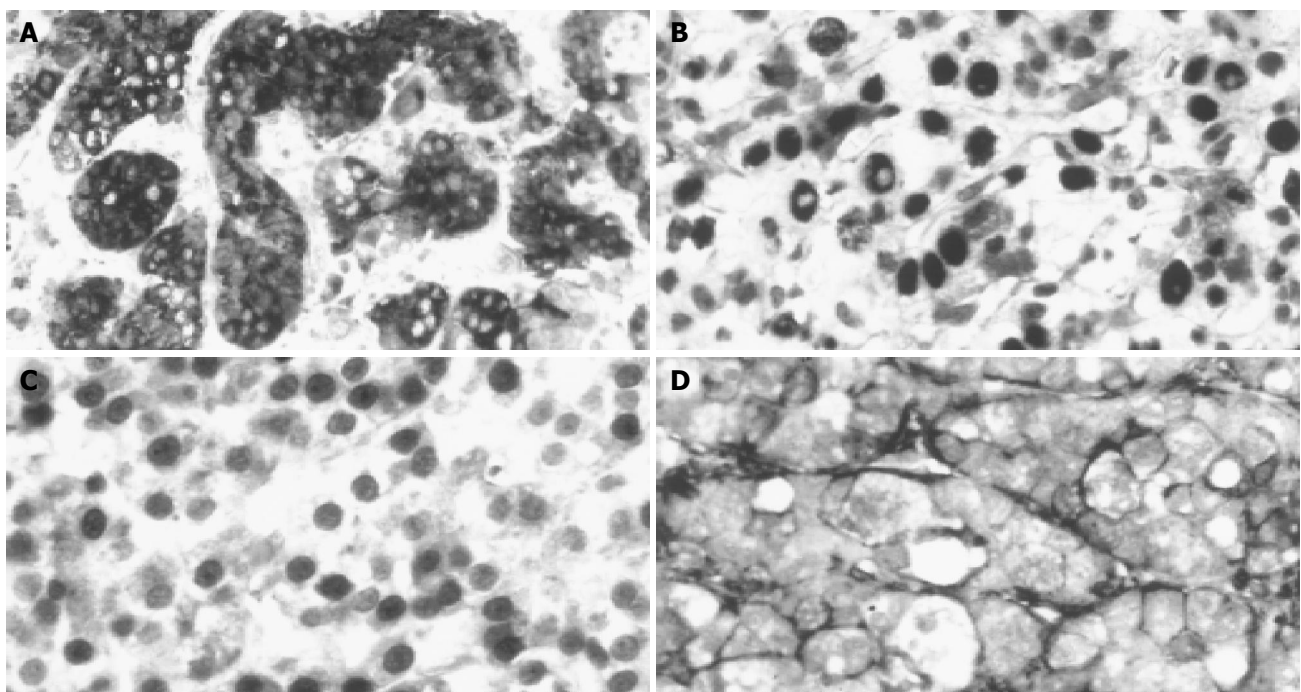


Figure 1 Immunohistochemical reactions on tumor specimens. **A:** Trabecular HCC, strong cytoplasmic AFP staining; **B:** Nuclear staining with p53 antibody in

tumor cells; **C:** β -Catenin nuclear staining in tumor cells; **D:** CD44 immunoreactivity in tumor stroma.

Table 2 AFP positive cases

Casenumber	B-catenin ¹	p53 ¹	CD44 ²	Grade
5	-	-	+	2
8	-	-	-	2
9	-	+	-	2
12	-	-	+	3
13	-	-	+	3
15	-	-	+	4
17	-	+	+	3
20	-	-	+	2
21	-	+	+	3
22	-	-	+	3
23	-	+	+	2
24	-	+	+	2
25	-	-	+	2
26	-	-	+	2
27	-	+	+	3
28	-	-	+	2
30	-	-	+	2
31	-	-	+	3
32	-	-	+	3
33	-	-	+	2
35	-	+	+	3
21 cases	0/21	7/21	19/21	

¹Positivity indicates more than 20% nuclear staining. ²Positivity indicates diffuse stromal staining.

meaningful in HCCs as in other tumors (e.g., prostate carcinoma), but shorter survival has been described in poorly differentiated tumors^[9]. Nuclear p53 staining indicates increased protein half-life, which is usually the consequence of point mutation. Therefore, we can assume that tumors with p53 nuclear staining carry p53 mutation. It is well documented that p53 mutation or nuclear accumulation is a valuable marker for predicting the poor prognosis of HCC patients^[10,11]. CD44, a widely distributed integral membrane protein, has been implicated in tumor invasion and development of metastasis. It was reported that upregulation of CD44 in liver tumors is associated with a shorter survival and p53 overexpression^[12,13].

β -catenin nuclear staining is observed in AFP-negative liver carcinomas. Nuclear accumulation of this protein indicates the increased activity of Wnt signal pathway^[14]. In cases of HCC, this is most frequently caused by β -catenin mutation^[15,16]. The significance of nuclear β -catenin positivity in HCC is controversial. Suzuki *et al.*^[17], have described nuclear expression in poorly differentiated tumors. Van Nhieu *et al.*^[18], reported that the higher proliferative index and poor outcome correlate with nuclear β -catenin-stained HCCs, but others could not confirm the role of β -catenin in the progression of HCC^[19]. In fact, Hsu *et al.*^[20], and Mao *et al.*^[21], have found that the nuclear expression of β -catenin is present in a subgroup of HCCs with a favorable prognosis. Laurent-Puig *et al.*^[22], demonstrated that nuclear β -catenin staining occurs in HCC with a low AFP serum level, but there is high chromosomal instability, frequent p53 mutations, and high AFP level in tumors without β -catenin mutation. A similar conclusion can be found in studies by Calvisi *et al.*^[23,24]. They suggested the existence of two major genetic pathways of neoplastic development in the liver. The first was characterized by disruption of

Wnt signaling, including β -catenin mutation and a low rate of loss of heterozygosity. The Wnt signaling is intact in the second group of tumors, but they could detect chromosomal instability in them. AFP expression was more common in the second group. Mao *et al.*^[21], also described that nuclear β -catenin expression is less frequently associated with serum AFP elevation. Unfortunately, the serum AFP values were not available in all the cases in our study, but our results had a close correlation with immunohistochemical staining.

Among the parameters we studied, only CD44 was detected in microarray experiments as differentially expressed between the AFP positive and negative HCC cell lines^[2]. This is not surprising, since the difference in p53 and β -catenin is not transcriptionally regulated.

In brief, the three clearly unfavorable prognostic markers of p53 nuclear staining, CD44 expression, and high grade are more common in AFP-producing HCCs, while one potentially favorable parameter, nuclear β -catenin staining occurs in AFP-negative tumors, indicating that AFP can be used as a prognostic marker in patients with liver tumors.

REFERENCES

- 1 **Taketa K.** Alpha-fetoprotein: re-evaluation in hepatology. *Hepatology* 1990; **12**: 1420-1432
- 2 **Kawai HF, Kaneko S, Honda M, Shirota Y, Kobayashi K.** α -fetoprotein-producing hepatoma cell lines share common expression profiles of genes in various categories demonstrated by cDNA microarray analysis. *Hepatology* 2001; **33**: 676-691
- 3 **Lee JS, Thorgeirsson SS.** Functional and genomic implications of global gene expression profiles in cell lines from human hepatocellular cancer. *Hepatology* 2002; **35**: 1134-1143
- 4 **Edmondson HA, Steiner PE.** Primary carcinoma of the liver: a study of 100 cases among 48,900 necropsies. *Cancer* 1954; **7**: 462-503
- 5 **Brumm C, Schulze C, Charels K, Morohoshi T, Klöppel G.** The significance of alpha fetoprotein and other tumor markers in differential immunohistochemistry of primary liver tumors. *Histopathology* 1989; **14**: 503-513
- 6 **Peng SY, Lai PL, Chu JS, Lee PH, Tsung PT, Chen DS, Hsu HC.** Expression and hypomethylation of alpha-fetoprotein gene in unicentric and multicentric human hepatocellular carcinomas. *Hepatology* 1993; **17**: 35-41
- 7 **Fujioka M, Nakashima Y, Nakashima O, Kojiro M.** Immunohistologic study on the expressions of α -fetoprotein and protein induced by vitamin K absence or antagonist II in surgically resected small hepatocellular carcinoma. *Hepatology* 2001; **34**: 1128-1134
- 8 **Tangkijvanich P, Anukularnkusol N, Suwangool P, Lertmaharit S, Hanvivatvong O, Kullavanijaya P, Poovorawan Y.** Clinical characteristics and prognosis of hepatocellular carcinoma: analysis based on alpha-fetoprotein levels. *J Clin Gastroenterol* 2000; **31**: 301-308
- 9 **Chedid A, Ryan LM, Dayal Y, Wolf BC, Falkson G.** Morphology and other prognostic factors of hepatocellular carcinoma. *Arch Pathol Lab Med* 1999; **123**: 524-528
- 10 **Sugo H, Takamori S, Kojima K, Beppu T, Futagawa S.** The significance of p53 mutations as an indicator of the biological behavior of recurrent hepatocellular carcinomas. *Surg Today* 1999; **29**: 849-855
- 11 **Heinze T, Jonas S, Karsten A, Neuhaus P.** Determination of the oncogenes p53 and c-ebr-B2 in the tumour cytosols of advanced hepatocellular carcinoma (HCC) and correlation to survival time. *Anticancer Res* 1999; **19**: 2501-2503
- 12 **Endo K, Terada T.** Protein expression of CD44 (standard and variant isoforms) in hepatocellular carcinoma: relationships with tumor grade, clinicopathologic parameters, p53 expression and patient survival. *J Hepatol* 2000; **32**: 78-84

- 13 **Washington K**, Telen MJ, Gottfried MR. Expression of cell adhesion molecule CD44 in primary tumors of the liver: an immunohistochemical study. *Liver* 1997; **17**: 17-23
- 14 **Funayama N**, Fagotto F, McCrea P, Gumbiner BM. Embryonic axis induction by the armadillo repeat domain of β -catenin: evidence for intracellular signaling. *J Cell Biol* 1995; **128**: 959-968
- 15 **Terris B**, Pineau P, Bregeaud L, Valla D, Belghiti J, Tiollais P, Degott C, Dejean A. Close correlation between beta-catenin gene alterations and nuclear accumulation of the protein in human hepatocellular carcinomas. *Oncogene* 1999; **18**: 6583-6588
- 16 **De La Coste A**, Romagnolo B, Billuart P, Renard CA, Buendia MA, Soubrane O, Fabre M, Chelly J, Beldjord C, Kahn A, Perret C. Somatic mutations of the b-catenin gene are frequent in mouse and human hepatocellular carcinomas. *Proc Natl Acad Sci USA* 1998; **95**: 8847-8851
- 17 **Suzuki T**, Yano H, Nakashima Y, Nakashima O, Kojiro M. Beta-catenin expression in hepatocellular carcinoma: a possible participation of beta-catenin in the dedifferentiation process. *J Gastroenterol Hepatol* 2002; **17**: 994-1000
- 18 **Van Nhieu JT**, Renard CA, Wei Y, Cherqui D, Zafrani ES, Buendia MA. Nuclear accumulation of mutated β -catenin in hepatocellular carcinoma is associated with increased cell proliferation. *Am J Pathol* 1999; **155**: 703-710
- 19 **Vona G**, Estepa L, Beroud C, Damotte D, Capron F, Nalpas B, Mineur A, Franco D, Lacour B, Pol S, Brechot C, Paterlini-Brechot P. Impact of cytomorphological detection of circulating tumor cells in patients with liver cancer. *Hepatology* 2004; **39**: 792-798
- 20 **Hsu HC**, Jeng YM, Mao TL, Chu JS, Lai PL, Peng SY. β -catenin mutations are associated with a subset of low-stage hepatocellular carcinoma negative for hepatitis B virus and with favourable prognosis. *Am J Pathol* 2000; **157**: 763-770
- 21 **Mao TL**, Chu JS, Jeng YM, Lai PL, Hsu HC. Expression of mutant nuclear β -catenin correlates with non-invasive hepatocellular carcinoma, absence of portal vein spread and good prognosis. *J Pathol* 2001; **193**: 95-101
- 22 **Laurent-Puig P**, Legoix P, Bluteau O, Belghiti J, Franco D, Binot F, Monges G, Thomas G, Bioulac-sage P, Zucman-Rossi J. Genetic alterations associated with hepatocellular carcinomas define distinct pathways of hepatocarcinogenesis. *Gastroenterology* 2001; **120**: 1763-1773
- 23 **Calvisi DF**, Factor VM, Loi R, Thorgeirsson SS. Activation of β -catenin hepatocarcinogenesis in transgenic mouse models: relationship to phenotype and tumor grade. *Cancer Res* 2001; **61**: 2085-2091
- 24 **Calvisi DF**, Factor VM, Ladu S, Conner EA, Thorgeirsson SS. Disruption of β -catenin pathway or genomic instability define two distinct categories of liver cancer in transgenic mice. *Gastroenterology* 2004; **126**: 1374-1386

Science Editor Wang XL and Guo SY Language Editor Elsevier HK

Replication of hepatitis B virus in primary duck hepatocytes transfected with linear viral DNA

Yun-Qing Yao, Ding-Feng Zhang, Ni Tang, Ai-Long Huang, Xiao-Yi Zou, Jiang-Feng Xiao, Yun Luo, Da-Zhi Zhang, Bo Wang, Wei-Ping Zhou, Hong Ren, Qi Liu, Shu-Hua Guo

Yun-Qing Yao, Xiao-Yi Zou, Jiang-Feng Xiao, Department of Infectious Diseases of the First Affiliated Hospital, Chongqing University of Medical Sciences, Chongqing 400016, China
Ding-Feng Zhang, Ni Tang, Ai-Long Huang, Yun Luo, Da-Zhi Zhang, Bo Wang, Wei-Ping Zhou, Hong Ren, Qi Liu, Shu-Hua Guo, Institute for Viral Hepatitis, Chongqing University of Medical Sciences, Chongqing 400010, China

Supported by the National Natural Science Foundation of China, No. 39670340, and the Applied Basic Research Programs of Science and Technology Commission Foundation of Chongqing, No. 20021889

Correspondence to: Dr. Yun-Qing Yao, Department of Infectious Diseases of the First Affiliated Hospital, Chongqing University of Medical Sciences, Chongqing 400016, China. cqyaoyunqing@126.com
Telephone: +86-23-66990741

Received: 2004-11-02 Accepted: 2004-12-26

© 2005 The WJG Press and Elsevier Inc. All rights reserved.

Key words: Hepatitis B virus; Replication; Expression; Primary duck hepatocytes

Yao YQ, Zhang DF, Tang N, Huang AL, Zou XY, Xiao JF, Luo Y, Zhang DZ, Wang B, Zhou WP, Ren H, Liu Q, Guo SH. Replication of hepatitis B virus in primary duck hepatocytes transfected with linear viral DNA. *World J Gastroenterol* 2005; 11(32): 5019-5021

<http://www.wjgnet.com/1007-9327/11/5019.asp>

Abstract

AIM: To explore the expression and replication of hepatitis B virus (HBV) DNA in primary duck hepatocytes (PDHs).

METHODS: Complete HBV genome was transfected into PDHs by electroporation (transfected group, 1.19×10^{12} copies of linear HBV DNA/ 1×10^7 PDHs). After 1-5 d of transfection, HBsAg and HBeAg in the supernatant and lysate of PDHs were measured with the IMX System. Meanwhile, replicative intermediates of HBV DNA were analyzed by Southern blotting and Dot blotting. PDHs electroporated were used as control group.

RESULTS: HBsAg in the hepatocyte lysates of transfected group was 15.24 (1 d), 14.55 (3 d) and 5.13 (5 d; P/N values, positive ≥ 2.1) respectively. HBeAg was negative (< 2.1). Both HBsAg and HBeAg were negative in the supernatant of transfected group. Dot blotting revealed that HBV DNA was strongly positive in the transfected group and negative in the control group. Southern blot analysis of intracellular total DNA indicated that there were relaxed circular (rc DNA), covalently closed circular (ccc DNA), and single-stranded (ss DNA) HBV DNA replicative intermediates in the transfected group, there was no integrated HBV DNA in the cellular genome. These parameters were negative in control group.

CONCLUSION: Expression and replication of HBV genes can occur in hepatocytes from non-mammalian species. HBV replication has no critical species-specificity, and yet hepatic-specific regulating factors in hepatocytes may be essential for viral replication.

INTRODUCTION

Hepatitis B is one of the fatal diseases all over the world, and its pathogenesis is still unclear and its therapy appears difficult too. In recent years, reports have revealed that hepatocytes were not only the target cells infected with hepatitis B virus (HBV) and destructed by activated cytotoxic T lymphocytes, but also the immune modulating cells activated by effector cells, and even take part in the process of HBV non-cytolytic clearance^[1,2]. In order to study interactions between HBV and hepatocytes, we established an *in vitro* model of primary culture hepatocytes from heterologous species transfected with linear HBV DNA. Since whether naked HBV DNA can replicate or express protein in non-human hepatocytes, and whether its replication process is similar to that in normal specific host are not reported, we transfected linear HBV DNA into primary duck hepatocytes (PDHs) to investigate the host-specific regulating role in the replication of HBV in hepatocytes from non-mammalian species.

MATERIALS AND METHODS

Isolation and culture of primary duck hepatocytes

Duck hepatitis B virus (DHBV) DNA and DHBsAg in duck serum were negative tested by Dot blot analysis and ELISA respectively. Hepatocytes were harvested from Chongqing ducks using an *in situ* collagenase perfusion technique^[3]. The ducks were injected into the peritoneal cavity pentobarbital sodium (30 mg/kg body weight) and heparin (100 IU/kg body weight), the abdomen of the animals was opened and the portal vein was exposed and cannulated. Then the liver was *in situ* perfused at 37 °C with calcium-free, Hanks' balanced salt solution (HBSS) for

10 min, then with 0.2 g/L collagenase type I in calcium-presenting HBSS for 15 min. The liver was removed and the cells were combed gently in tissue culture medium. Hepatocytes were centrifugated, washed, and separated from non-parenchymal cells by differential centrifugation at 50 g. Viability of hepatocytes detected by trypan blue exclusion (TBE) was about 90%, and the cells were counted.

Freshly isolated hepatocytes were transfected with linear HBV DNA, and then inoculated at a density of 3×10^6 cells per 25 cm² culture flask. Culture medium was composed of RPMI 1640 with insulin (100 IU/L), penicillin, streptomycin and 100 mL/L fetal bovine serum. Cultures were incubated at 37 °C in a humidified atmosphere containing 50 mL/L CO₂ and media were renewed every two days.

Extraction of linear HBV DNA

Plasmid pEcoB 6 containing two *EcoRI* copies of HBV genome in a head-to-tail arrangement was used to extract the linear HBV DNA. Extraction was carried out as previously described^[4]. Briefly, pEcoB 6 was digested by *EcoRI* at 37 °C for 2 h, then fractionated by electrophoresis on 1% agarose gel. The complete HBV DNA 3.2 kb fragment was extracted and quantified for transfection.

Transfection procedures

Transfection was performed as previously described^[5], electroporation conditions were optimized by Yao *et al.* In brief, 4 µg linear HBV DNA was added to 1×10^7 hepatocytes and electroporated for about 29 ms at 220 V and 950 µF of capacitance. After gene transfer, the cells were inoculated and cultured for 5 d. The electroporated hepatocytes were used as control.

Test for HBV-specific proteins

After 1-5 d of transfection, HBsAg and HBeAg in the supernatant and lysate of hepatocytes were identified using radioimmunoassay kits (Abbott Laboratories) according to the manufacturer's instructions. The HBsAg signal/noise (P/N ratio) >2.1 was considered positive.

DNA extraction from hepatocytes and HBV DNA replication analysis

Intracellular total DNA was extracted 2 d after transfection. Southern blotting was used to analyze replicative intermediates of HBV DNA. Dot blotting was used to test the total HBV DNA in hepatocytes from d 1 to 5 after transfection. All procedures were performed as previously described^[4].

RESULTS

Viral antigen production in transfected duck hepatocytes

Production of HBsAg and HBeAg was measured in culture supernatant and cell lysate was collected daily from transfected hepatocytes group. HBsAg in the lysate of transfected hepatocytes increased during the first 3 d following transfection, with HBsAg P/N value being around 15 (Table 1). HBsAg was negative in all culture supernatants of transfected hepatocytes. Both lysate and supernatant were negative for HBeAg. Both HBsAg and HBeAg in control group were negative.

Table 1 HBsAg values (P/N) in primary duck hepatocyte lysates

Time after transfection	1 d	3 d	5 d
Transfected group	15.24	14.55	5.13
Control group	1.01	0.93	1.38

DNA analysis of intracellular total DNA

Dot blotting revealed that total amount of HBV DNA in transfected hepatocytes was strongly positive from d 1 to 5 following transfection (Figure 1). Southern blot analysis of intracellular total DNA indicated that, there were relaxed circular (rc DNA), covalently closed circular (ccc DNA) and single-stranded (ss DNA) HBV DNA replicative intermediates in the transfected hepatocytes (Figure 2). There was no integrated viral DNA in the cellular genome.

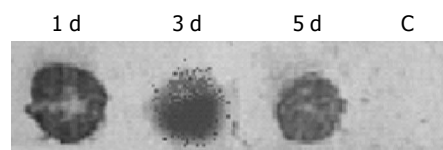


Figure 1 Dot blotting test of HBV DNA in transfection group. C: control group.

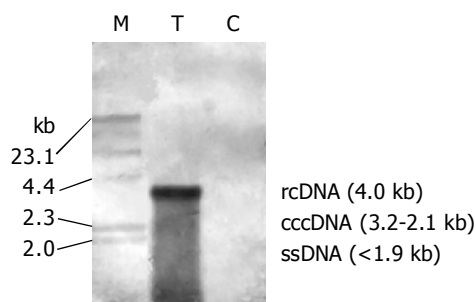


Figure 2 Southern blotting analysis of HBV DNA replication in transfected hepatocytes. M: marker of standard molecular weight; T: transfection group; C: control group.

DISCUSSION

DHBV *in vivo* and *in vitro* models have been used for the study of HBV infection and the evaluation of new anti-HBV strategies^[6-10]. However, until now, there is no report on the process of viral infection, the level of DNA replication and protein expression and the mechanisms of hepatitis B virus in hepatocytes from heterologous species. Whether naked HBV DNA can replicate or express protein in nonhuman hepatocytes, and whether its replication process is similar to that in normal specific host are still unclear. We transfected linear HBV DNA into non-mammalian hepatocytes, PDH to investigate the host-specific regulating role in the replication of HBV.

Our results indicate that naked DNA of HBV can effectively replicate in PDHs and its replicative intermediates include relaxed circular DNA, covalently closed circular DNA, single-stranded DNA, and non integrated viral DNA

in the cellular genome. The pattern of DNA replication of HBV is similar to that in normal permissive human cells and in liver of chimpanzee acutely infected with HBV^[11], which is the same as that of DHBV replication in liver of chronically infected duck^[12], and is further supported by the results of PDHs acutely or chronically infected with DHBV^[3,13]. Thus complete HBV genome effectively transfected into primary hepatocytes can efficiently replicate.

Our results also show that HBV can effectively express proteins in primary duck hepatocytes, such as HBsAg, with its P/N value peak being around 15.0 1-5 d after transfection. In our study, HBsAg was found only in the lysate of duck hepatocytes, but not in the supernatant of cultured hepatocytes, which can be explained that HBsAg is insufficient to excrete in outer media of hepatocytes, and unbalance between large, mediate and small proteins of HBsAg might also affect its secretion. Furthermore, it needs further study. No HBeAg was measured in the lysate or supernatant of duck hepatocytes, which might be related to two reasons. The first, is that in duck hepatocytes there is no sufficient translation activators essential for effective activation of HBV core gene promoter. Yu and Mertz^[14,15], found that HBV pre-C RNAs and pre-genome RNAs are separately regulated by two activators. The other reason is that shortly after expression, HBeAg is digested by lysozymes in duck hepatocyte plasma. The real causes need further study.

In conclusion, expression and replication of HBV genes can occur in hepatocytes from non-mammalian species, which strongly supports the idea that replication of HBV has no critical species-specificity, and hepatic-specific regulating factors in hepatocytes are essential for viral replication. Further more, the differences in inner environments of hepatocytes from different species affect and even determine the expressions of HBV genes and proteins.

REFERENCES

- 1 **Zhang DF.** To pursuit novel therapeutic approaches based on the mechanism of clearance of HBV infection. *Zhonghua Ganzangbing Zazhi* 2001; **9**: 196-202
- 2 **Yao Y, Zhang D.** Infection and replication of hepatitis B virus and its clearance mechanism: an overview. *Zhonghua Ganzangbing Zazhi* 2002; **10**: 398-400
- 3 **Yao Y, Tang N, Huang A.** Study on the replication of hepatitis B virus compared with that of duck hepatitis B virus in primary duck hepatocytes. *Zhonghua Yixue Zazhi* 2001; **81**: 1157-1161
- 4 **Yao YQ, Zhang DF, Luo Y, Zhang DZ, Huang AL, Wang B, Zhou WP, Ren H, Guo SH.** An *in vitro* model of hepatitis B virus gene replication and expression in primary rat hepatocytes transfected with circular viral DNA. *Zhonghua Ganzangbing Zazhi* 2002; **10**: 275-279
- 5 **Yao Y, Huang A, Tang N, Wang B, Zhang D.** Replication and transfection of hepatitis B virus DNA into primary duck hepatocytes. *Zhonghua Ganzangbing Zazhi* 2002; **10**: 34-36
- 6 **Zhang YY, Summers J.** Rapid production of neutralizing antibody leads to transient hepadnavirus infection. *J Virol* 2004; **78**: 1195-1201
- 7 **Seigneres B, Martin P, Werle B, Schorr O, Jamard C, Rimsky L, Trepo C, Zoulim F.** Effects of pyrimidine and purine analog combinations in the duck hepatitis B virus infection model. *Antimicrob Agents Chemother* 2003; **47**: 1842-1852
- 8 **Zoulim F, Berthillon P, Guerhier FL, Seigneres B, Germon S, Pichoud C, Cheng YC, Trepo C.** Animal models for the study of HBV infection and the evaluation of new anti-HBV strategies. *J Gastroenterol Hepatol* 2002; **17**: S460-463
- 9 **Tang H, McLachlan A.** Avian and Mammalian hepadnaviruses have distinct transcription factor requirements for viral replication. *J Virol* 2002; **76**: 7468-7472
- 10 **Delmas J, Schorr O, Jamard C, Gibbs C, Trepo C, Hantz O, Zoulim F.** Inhibitory effect of adefovir on viral DNA synthesis and covalently closed circular DNA formation in duck hepatitis B virus-infected hepatocytes *in vivo* and *in vitro*. *Antimicrob Agents Chemother* 2002; **46**: 425-433
- 11 **Guidotti LG, Rochford R, Chung J, Shapiro M, Purcell R, Chisari FV.** Viral clearance without destruction of infected cells during acute HBV infection. *Science* 1999; **284**: 825-829
- 12 **Ijichi K, Mitamura K, Ida S, Machida H, Shimada K.** *in vivo* antiviral effects of mismatched double-stranded RNA on duck 14 hepatitis B virus. *J Med Virol* 1994; **43**: 161-165
- 13 **Yao YQ, Zhang DF, Huang AL, Tang N, Wang B, Zhou WP, Ren H, Guo SH.** Study on the replication of Hepatitis B Virus in primary hepatocytes from heterogeneous species. *Zhonghua Ganzangbing Zazhi* 2004; **12**: 25-28
- 14 **Yu X, Mertz JE.** Promoters for synthesis of the pre-C and pregenomic mRNAs of human hepatitis B virus are genetically distinct and differentially regulated. *J Virol* 1996; **70**: 8719-8726
- 15 **Yu X, Mertz JE.** Distinct modes of regulation of transcription of hepatitis B virus by the nuclear receptors HNF4alpha and COUP-TF1. *J Virol* 2003; **77**: 2489-2499

Expression of early growth response factor-1 in rats with cerulein-induced acute pancreatitis and its significance

Lan-Bo Gong, Li He, Yang Liu, Xue-Qing Chen, Bo Jiang

Lan-Bo Gong, Yang Liu, Xue-Qing Chen, Bo Jiang, Department of Gastroenterology, Nanfang Hospital, Southern Medical University, Guangzhou 510515, Guangdong Province, China
Li He, Department of Gastroenterology, Second Affiliated Hospital of Shenyang Medical College, Shenyang 110002, Liaoning Province, China

Supported by the National Natural Science Foundation of China, No. 30370648

Correspondence to: Lan-Bo Gong, Department of Gastroenterology, Nanfang Hospital, Southern Medical University, Guangzhou 510515, Guangdong Province, China. lbgong@fimmu.com
Telephone: +86-20-61363222

Received: 2004-12-07 Accepted: 2005-01-26

Abstract

AIM: To observe the expressions of early growth response factor-1 (Egr-1) and tissue factor (TF) in rats with cerulein-induced acute pancreatitis and to explore its significance.

METHODS: A large dose of cerulein was used to create the experimental acute pancreatitis model in rats. The changes of Egr-1 mRNA and protein in rats were observed during 30 min to 4 h after the treatment and immunohistochemical method was used to observe the localized expression of Egr-1 in tissues. In addition to the mRNA expression of Egr-1 target gene, TF was also observed. A blank control group, and a bombesin-administered group were used for comparison.

RESULTS: After the stimulation of a large dose of cerulein, the rats showed typical inflammatory changes of acute pancreatitis. Thirty minutes after the stimulation, the mRNA expression of Egr-1 in the pancreatic tissue reached its peak and then declined, while the expression of Egr-1 protein reached its peak 2 h after the stimulation. Histologically, 2 h after the stimulation, almost all pancreatic acinar cells had the expression of Egr-1 protein, which was focused in the nuclei. The mRNA expression of TF occurred 1 h after the stimulation and gradually increased within 4 h. However, a large dose of bombesin only stimulated the pancreatic tissue to produce a little mRNA expression of Egr-1 and no mRNA expression of Egr-1 protein and TF.

CONCLUSION: Egr-1 as a pro-inflammatory transcription factor may play an important role in the pathogenesis of acute pancreatitis by modulating the expression of TF.

Key words: Growth response factor-1; Tissue factor; Acute pancreatitis; Cerulein; Bombesin

Gong LB, He L, Liu Y, Chen XQ, Jiang B. Expression of early growth response factor-1 in rats with cerulein-induced acute pancreatitis and its significance. *World J Gastroenterol* 2005; 11(32): 5022-5024

<http://www.wjgnet.com/1007-9327/11/5022.asp>

INTRODUCTION

Acute pancreatitis is a common disease with its severe case having a mortality of up to 25-40%, while its pathogenesis still remains unclear^[1,2]. The activation of pancreatic enzyme in acinar cells and its digestion of pancreatic tissues have been generally regarded as its trigger so far. However, recent studies on transcription factor, nuclear factor- κ B (NF κ B) and other cytokines showed that inflammatory cytokines play an important role in the pathogenesis of acute pancreatitis due to their inflammation-inducing properties^[3-7]. Early growth response factor-1 (Egr-1), also known as nerve growth factor-induced protein A, Krox-24 or Zif268, is a transcription factor -NF κ B^[8]. A recent study showed that Egr-1 may be an initial factor of inflammation^[9]. In our experiment, we studied the expression of Egr-1 in rats with cerulein-induced acute pancreatitis to understand its role in the pathogenesis of acute pancreatitis.

MATERIALS AND METHODS

Animal models

Following the procedures for construction of animal models^[3,6], cerulein was dissolved in normal saline. Then cerulein solution [20 μ g/(kg h)] was injected into abdominal cavity of male Wistar rats. After 4 h of the stimulation, a large dose of sodium pentobarbital was injected into the abdominal cavity of the rats, followed by incision of the thorax cavity to collect blood by a syringe needle; besides, a little lung tissue was harvested. Subsequently, an incision was made to open the abdominal cavity to expose the pancreatic tissue and a piece of pancreatic tissue was harvested and put into the pre-cooled neutral PBS (pH 7.4) with its fat removed. Pancreatic tissue was fixed in neutral 10% paraformaldehyde and cooled in liquid nitrogen and preserved at -70 °C. The blood was centrifuged for blood serum, which was then preserved at -70 °C.

Test for acute pancreatitis index

The acute pancreatitis indexes included serum amylase, tissue

myeloperoxidase (MPO) and percentage water content. The test procedures are described in our previous study^[6].

Western blotting

According to the method described in our previous study^[6], the cooled pancreatic tissue was homogenized and centrifuged with its supernatant for protein quantification. About 25 µg protein was added into each hole for PAGE-SDS gel electrophoresis, the product of which was then transferred to PVDF film for incubation with an antibody at -4 °C overnight. The immunoblotting protein band was detected using emission chemiluminescence kit. The film was scanned and saved as a digital image (Figure 1). The antibody used in our study was from Santa Cruz Company.

Quantitative polymerase chain reaction

The fresh pancreatic tissue was put into TRIzol (Invitrogen) for homogenate and then chloroform and isopropanol were added, followed by centrifugation of supernatant to obtain DNA by ethanol precipitation. The obtained DNA was then digested with DNA enzyme I and purified by RNA purification (Qiagen). Through qualification of RNA, RT kit (Promega) was used for transcription to obtain cDNA, which was then amplified by routine PCR. SYBR (Bio-Rad) dye was added and 27-32 cycles were amplified, the relative production was detected with quantitative PCR system. The result was shown in a ratio of the production to APRO. The primers used were Egr-1 (GenBank NM_012551) of sense: 5'CCCGTATGCTTGCCCTGTTGAGTC3' and antisense: 5'CCCGTTGAGGTGCTGAAGGAGTTG3' with PCR product of 548 bp and tissue factor (TF, GenBank U07619) of sense: 5'TGTTTCAGATAAGCGATAGA3' and antisense: 5'GTGCGAAGAAGCAGTAG3' with a PCR product of 482 bp as control, rat acidic ribosomal phosphoprotein (GenBank X15096) of sense: 5'CCGC-GGGAAGGCTGTGGTG3' and antisense: 5'AGGGC-CTGCTCTGTGATGTC3' with a PCR product of 492 bp as control.

Histology and immunohistochemistry

The tissue was processed routinely, dehydrated and paraffin-embedded, cut into 5-µm-thick sections and stained with hematoxylin and eosin. Then, the histological and morphological changes were observed under an optical microscope. During immunohistochemistry, the tissue

sections were routinely dewaxed and liquefied and rabbit Egr-1 antibody was added. Then, Egr-1 was detected.

Statistical analysis

The data were expressed as mean±SD and analyzed with SPSS 1.0 software package.

RESULTS

Large dose of cerulein-induced obvious acute pancreatitis and the pancreatic tissue had the manifestations of acute abscess, widened tissue interspace and obvious, swollen pancreatic acinar cells (Figure 1). The indexes for diagnosis of acute pancreatitis, including blood serum amylase, tissue MPO, and percentage of water content, significantly increased (Figure 2). Similar to the previous report^[10], bombesin failed to induce typical experimental acute pancreatitis. Large dose of bombesin induced only tissue edema, which was relatively milder than that induced by cerulein, amylase, and MPO increased with no statistical significance (Figure 2).

The expression of Egr-1 mRNA reached its peak 30 min after the injection of cerulein, which was 60 times higher than that in the control (Figure 3B). However, it significantly declined after 4 h. Correspondingly, the expression of Egr-1 protein occurred 2 h after injection and obviously declined after 4 h. Egr-1 protein expression occurred 2 h after the stimulation, and almost all acinar cells had the expression of Egr-1 protein, while the expression was locally stronger and the expression of Egr-1 was found in nuclei. The expression of TF was later than that of Egr-1. Obvious expression of TF mRNA was seen 1 h after the stimulation and peaked in 2-4 h (Figure 3A).

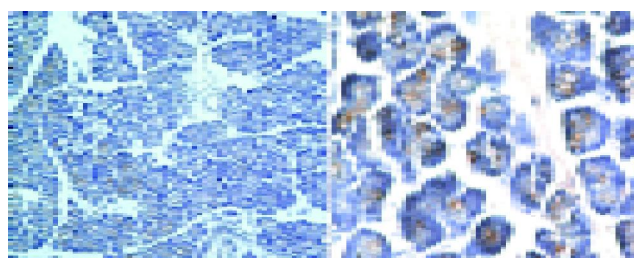


Figure 1 Immunohistochemistry of Egr-1 in rats with acute pancreatitis.

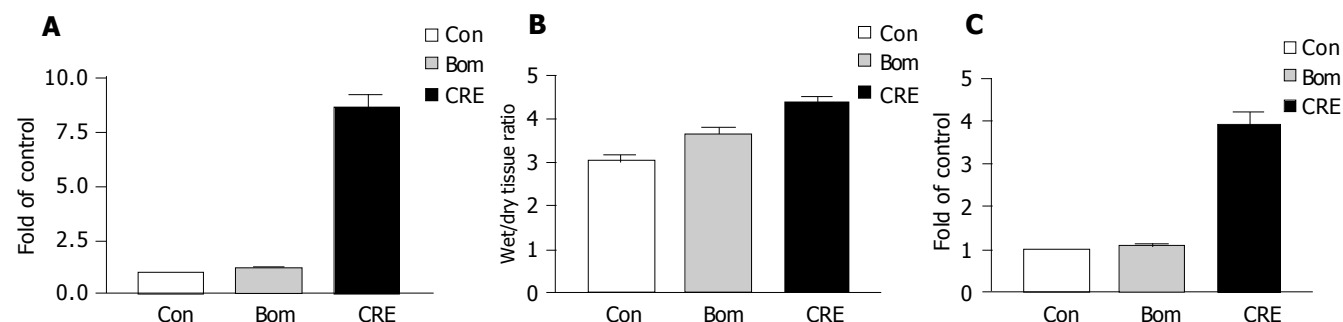


Figure 2 Effects of cerulein and bombesin on rat blood serum amylase (A), water content of pancreatic tissue (B), and MPO level (C). Con: control group;

Bom: bombesin control; CRE: cerulein group.

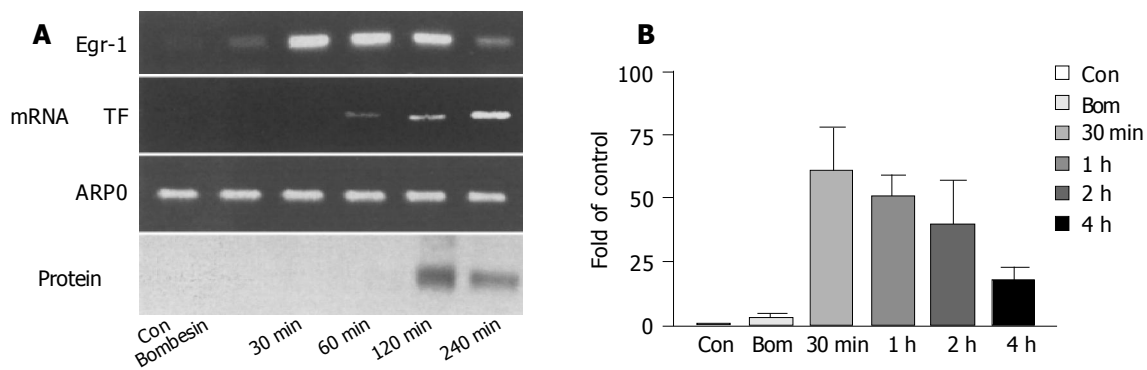


Figure 3 Expression of Egr-1 and TF in rats with acute pancreatitis (A) and

control (B). Con: control; Bom: bombesin control.

DISCUSSION

Recent studies have shown that Egr-1, as one of the transcription factors during the early stage of inflammation, can regulate the expression of multiple inflammatory factors, such as tumor necrosis factor, interleukin-2, transforming growth factor- β 1, intracellular adhesion molecule-1 (ICAM-1), and TF, and eradication of Egr-1 can protect lungs from injuries induced by ischemia and decrease the expression of tissue IL-1 β , IL-6, ICAM-1, MCP-1, TF, and PAI^[9]. However, the expression and function of Egr-1 in acute pancreatitis remain unclear.

In our study, during the early stage of acute pancreatitis induced by cerulein, Egr-1 demonstrated high expression in mRNA and protein. Its protein expression occurred 1 h after stimulation, peaked at 2 h, and lasted for at least 4 h. Egr-1 was found in nuclei 2 h after stimulation in our experiment, indicating that Egr-1 may play an important regulatory role during the early stage of acute pancreatitis. We also found that the expression of Egr-1 in acinar cells was locally distinct, which may be related to the property of Egr-1 that it is extremely easy to attenuate. Being different from cerulein, bombesin could not induce typical acute pancreatitis^[10] and did not increase blood serum amylase and tissue MPO level although bombesin could also induce mild edema of pancreatic tissue. Correspondingly, bombesin induced only trace expression of Egr-1 mRNA, but expression of protein could not be detected. The result further indicates, that the expression of Egr-1 plays a role in the pathogenesis of acute pancreatitis.

Previous studies have shown that during the initial and developmental process of acute pancreatitis, ischemia-reperfusion plays an important role^[11] and TF is an initial factor for coagulation, which can result in decrease of the tissue blood flow and ischemia^[8,9]. It was reported that TF is an important targeting factor of Egr-1, whose expression is modulated by Egr-1^[9]. Our study indicated that during the early stage of acute pancreatitis, TF also had high expression. However, compared to Egr-1, its expression was 1-2 h later. Therefore, we believe that during acute pancreatitis, Egr-1 may regulate the expression of TF and

trigger coagulation to induce ischemia of pancreatic tissue, thus aggravating the disease. Nevertheless, the detailed mechanism of TF during acute pancreatitis needs further studies.

In conclusion, Egr-1, as a pro-inflammatory transcription factor that may play an important role in the pathogenesis of acute pancreatitis.

REFERENCES

- 1 **Steer ML**. Pathobiology of experimental acute pancreatitis. *Yale J Biol Med* 1992; **65**: 421-430
- 2 **Lerch MM**, Gorelick FS. Early trypsinogen activation in acute pancreatitis. *Med Clin North Am* 2000; **84**: 549-563
- 3 **Gukovsky I**, Gukovskaya AS, Blinman TA, Zaninovic V, Pandol SJ. Early NF-kappaB activation is associated with hormone-induced pancreatitis. *Am J Physiol* 1998; **275**(6 Pt 1): G1402-G1414
- 4 **Grady T**, Liang P, Ernst SA, Logsdon CD. Chemokine gene expression in rat pancreatic acinar cells is an early event associated with acute pancreatitis. *Gastroenterology* 1997; **113**: 1996-1975
- 5 **Frossard JL**, Pastor CM, Hadengue A. Effect of hyperthermia on NF-kappaB binding activity in cerulein-induced acute pancreatitis. *Am J Physiol Gastrointest Liver Physiol* 2001; **280**: G1157-1162
- 6 **Chen X**, Ji B, Han B, Ernst SA, Simeone D, Logsdon CD. NF-kappaB activation in pancreas induces pancreatic and systemic inflammatory response. *Gastroenterology* 2002; **122**: 448-457
- 7 **Satoh A**, Shimosegawa T, Fujita M, Kimura K, Masamune A, Koizumi M, Toyota T. Inhibition of nuclear factor-kappaB activation improves the survival of rats with taurocholate pancreatitis. *Gut* 1999; **44**: 253-258
- 8 **Gashler A**, Sukhatme VP. Early growth response protein 1 (Egr-1): prototype of a zinc-finger family of transcription factors. *Prog Nucleic Acid Res Mol Biol* 1995; **50**: 191-224
- 9 **Yan SF**, Fujita T, Lu J, Okada K, Shan Zou Y, Mackman N, Pinsky DJ, Stern DM. Egr-1, a master switch coordinating upregulation of divergent gene families underlying ischemic stress. *Nat Med* 2000; **6**: 1355-1361
- 10 **Powers RE**, Grady T, Orchard JL, Gilrane TB. Different effects of hyperstimulation by similar classes of secretagogues on the exocrine pancreas. *Pancreas* 1993; **8**: 58-63
- 11 **Gullo L**, Cavicchi L, Tomassetti P, Spagnolo C, Freyrie A, D'Addato M. Effects of ischemia on the human pancreas.

Ca²⁺ cytochemical changes of hepatotoxicity caused by halothane and sevoflurane in enzyme-induced hypoxic rats

Wei-Feng Yu, Li-Qun Yang, Mai-Tao Zhou, Zhi-Qiang Liu, Quan Li

Wei-Feng Yu, Li-Qun Yang, Mai-Tao Zhou, Zhi-Qiang Liu, Quan Li, Department of Anesthesiology, Eastern Hepatobiliary Surgery Hospital, the Second Military Medical University, Shanghai 200438, China
Supported by Military Medical Science Found of China, No. 39400126

Correspondence to: Dr. Wei-Feng Yu, Department of Anesthesiology, Eastern Hepatobiliary Surgery Hospital, the Second Military Medical University, Shanghai 200438, China. yu1963@yahoo.com
Telephone: +86-21-25070783 Fax: +86-21-25070783
Received: 2004-10-30 Accepted: 2004-12-21

Abstract

AIM: To investigate the relation between hepatotoxicity of halothane and sevoflurane and altered hepatic calcium homeostasis in enzyme-induced hypoxic rats.

METHODS: Forty-eight rats were pretreated with phenobarbital and randomly divided into six groups (eight in each group) and exposed to O₂/N₂/1.2 MAC anesthetics for 1 h: normal control (NC), 21% O₂/79% N₂; hypoxic control (HC), 14% O₂/86% N₂; normal sevoflurane (NS), 21% O₂/N₂/1.2MAC sevoflurane; hypoxic sevoflurane (HS), 14% O₂/N₂/1.2MAC sevoflurane; normal halothane (NH) 21% O₂/79% N₂/1.2MAC halothane; hypoxic halothane (HH), 14% O₂/N₂/1.2MAC halothane. Liver specimens and blood were taken 24 h after exposure to calcium and determined by EDX microanalysis.

RESULTS: The liver of all rats given halothane (14% O₂) had extensive centrilobular necrosis and denaturation. Morphologic damage was accompanied with an increase in serum glutamic pyruvic transaminase. In groups NH and HH, more calcium was precipitated in cytoplasm and mitochondria.

CONCLUSION: These results suggest that halothane increases cytosolic Ca²⁺ concentration in hepatocytes. Elevation in Ca²⁺ concentration is implicated in the mechanism of halothane-induced hepatotoxicity. sevoflurane is less effective in affecting hepatic calcium homeostasis than halothane.

© 2005 The WJG Press and Elsevier Inc. All rights reserved.

Key words: Ca²⁺ cytochemistry; Hepatotoxicity; Calcium homeostasis; Halothane; Sevoflurane

Yu WF, Yang LQ, Zhou MT, Liu ZQ, Li Q. Ca²⁺ cytochemical changes of hepatotoxicity caused by halothane and

sevoflurane in enzyme-induced hypoxic rats. *World J Gastroenterol* 2005; 11(32): 5025-5028
<http://www.wjgnet.com/1007-9327/11/5025.asp>

INTRODUCTION

It is now recognized that two types of halothane-induced hepatic dysfunction exist^[1,2]. A mild sub-clinical form manifested by abnormal biochemical indices of hepatic function can be caused by toxic products of halothane metabolism, possibly determined by genetic factors, or by hepatic hypoxia, resulting from an imbalance between hepatic oxygen supply and demand. A much rarer, fulminant form may occur with severe necrosis, which may prove fatal^[3]. It is probable that this form results from an immune reaction: an oxidative metabolite binds covalently to liver proteins, producing a haptan, which in turn provokes immune reaction and formation of circulating antibody.

A major question being addressed in hepato-cellular injury is whether a unifying mechanism exists involving a loss of regulation of cellular Ca²⁺ levels. In this regard, alteration of Ca²⁺ homeostasis plays a major role in cell injury induced by a diversity of situations such as chemical intoxication and abnormal physiological states such as ischemia^[4,5].

Animal studies have provided evidence supporting a role for altered calcium fluxes in the mechanism of halothane-induced liver injury. In guinea pigs, hepatic calcium content increases significantly 24 h after exposure to halothane. Subsequent changes in liver calcium are proportional to the severity of liver necrosis, as determined morphologically^[6]. More recently it was shown that halothane, enflurane, and isoflurane stimulated dose-dependent release of radiolabeled calcium from internal calcium stores in isolated rat hepatocytes^[7]. Further evidence in support of the carcinogenic hypothesis of cell injury is offered by studies, in which the administration of a calcium channel blocker reduces hepatic necrosis in animals exposed to hepatotoxic agents, including halothane^[8]. For a better understanding of the mechanism of liver injury, attributing to halothane and sevoflurane hepatotoxicity, we used cytochemical methods to evaluate the changes of intracellular calcium and corresponding hepatic histopathological changes in enzyme-induced hypoxic rats.

MATERIALS AND METHODS

Animal model

The protocol was approved by the institutional Animal Care

and Use committee. Adult male Sprague-Dawley rats weighing 150-160 g were obtained from the Animal Center of the Second Military Medical University and maintained in a 12 h dark-light cycle. The animals had free access to water and diet of Wayne rodent food. To induce the hepatic microsomal drug-metabolizing enzymes, 48 animals were given phenobarbital (1 mg/mL) in their drinking water for 10 d prior to any experiment^[9].

For exposure to halothane and sevoflurane, animals were placed into 35 L plexiglass cages (g per cage). These animals were randomly divided into six groups and anesthetized for 1 h with O₂/N₂/1.2MAC anesthetic agents according to the following schedule: NC group was given 21% O₂/79% N₂; HC group 14% O₂/86% N₂; NNS group 21% O₂/79% N₂/1.2MAC sevoflurane; HS group 14% O₂/86% N₂/1.2MAC sevoflurane; NH group 21% O₂/79% N₂/1.2MAC halothane; HH group 14% O₂/86% N₂/1.2MAC halothane. Nitrogen and oxygen were delivered to the chamber by Dräger anesthetic machine at a flow rate of 4 L/min. The concentrations of O₂/CO₂, halothane, and sevoflurane in the chamber were monitored with a calibrated Capnormac Ultima.

After anesthesia or appropriate exposure, the animals were sent back into their metal cages and killed by decapitation, 24 h after anesthesia. Blood from the trunks was collected into dried beakers, and livers were rapidly removed and placed in chilled petridishes. Serum was separated from clotted blood, and assayed for ALT by automated methods in the Department of Clinical Chemistry. For histological examination, liver samples were collected into 10% PBS, fixed and mounted on paraffin blocks. Tissue sections were stained with hematoxylin and eosin, Gomori trichrome and a reticulin stain. Coded liver sections were examined without knowledge of the experimental details. The necrosis and denaturation of the slides of each section were quantitatively estimated as previously described^[10].

Calcium cytochemistry

A portion of the right anterior lobe was cut into 0.5 mm blocks. The specimens were treated in cold fixative consisting of 25% glutaraldehyde in 0.9 mol/L potassium oxalate adjusted to pH 7.4 with 1 mol/L potassium hydroxide. Sucrose was added to 1.4% final concentration. Fixation was done for 4 h at 4 °C. The specimens were subsequently kept in a cold mixture of 1% osmium tetroxide and 2% potassium pyroantimonate for 2 h, followed by osmium tetroxide and 1% potassium ferrocyanide for 1 h. Then, the specimens were rinsed for 15 min with distilled water adjusted to pH 10 with 1 mol/L potassium hydroxide, dehydrated in cold ethanol series, and routinely embedded in Epon-812 or Spur.

EDX microanalysis

The 100 nm thick sections for calcium cytochemistry, were left unstained and coated with carbon films in a vacuum evaporator. EDX microanalysis was performed under an analytical electron microscope (Hitachi-800) equipped with an energy-dispersive X-ray detecting system (EDAX, type 9 100/60). The acceleration voltage was 100 KV and the probe current was for 100 s and evaluation of the energy-

dispersive X-ray spectra was performed by a computer program^[11].

Statistical analysis

Data were expressed as mean±SE and analyzed by analysis of variance. Means were compared with Fisher's least significant difference test. *P*<0.05 was considered statistically significant.

RESULTS

Hepatotoxicity

Under conditions of hypoxia and induction of the microsomal enzymes, halothane anesthesia produced extensive hepatic injury. Within 24 h after exposure to halothane at 14% O₂, all the rats had many areas of hepatic necrosis radiating from the central veins. The necrosis and denaturation in HH group increased significantly as compared to the clusters of lymphocytes, histocytes and neutrophils, and often encircled by a layer of swollen hepatocytes containing single large vacuoles, strands of degenerating cytoplasm, and eccentric, intact pyknotic nuclei. Morphologic damage was accompanied with an increase in serum glutamic pyruvic transaminase (*P*<0.01, Table 1). No statistically significant histologic change was found in the following variables: normal control, hypoxic control, halothane anesthesia at 21% O₂, sevoflurane exposure at 21% O₂ (Figure 1).

Table 1 Serum ALT levels, and hepatic damage in enzyme-induced hypoxic rats (mean±SE)

Group	<i>n</i>	ALT (IU/L)	Hepatic damage
NC	8	56.12±20.88	0.145±0.043
HC	8	79.88±46.08	0.533±0.426
NS	8	58.31±23.12	0.576±0.106
HS	8	147.75±72.89	0.576±0.106
NH	8	142.15±78.19	0.614±0.433
HH	8	646.13±412.90 ^b	2.740±0.714 ^b

^b*P*<0.01 vs normal control.

Calcium cytochemistry

In NC and NS groups, calcium precipitation was located in nuclei with mitochondria and cytoplasm as fine particles. In HC and HS groups, intracellular calcium increased slightly. But after exposure to 21% O₂/ N₂/1.2MAC halothane or 14% O₂/ N₂/1.2MAC halothane, more and more calcium was precipitated in calcified cytoplasm and mitochondria. In HH group, a large amount of calcium deposition was found in cytoplasm and mitochondria (Figure 2).

EDX microanalysis

Qualitative analyses were performed in nuclei, mitochondria and cytoplasm. The characteristic emission of calcium (Kα) was observed. Neither sodium nor potassium was present. Semi-quantitative analyses were performed in mitochondria and cytoplasm. The calcium emission analyses are shown in Table 2. The amount of cellular calcium increased in HH group (*P*<0.01) and there was a positive linear correlation between the calcium in mitochondria and cytoplasm.

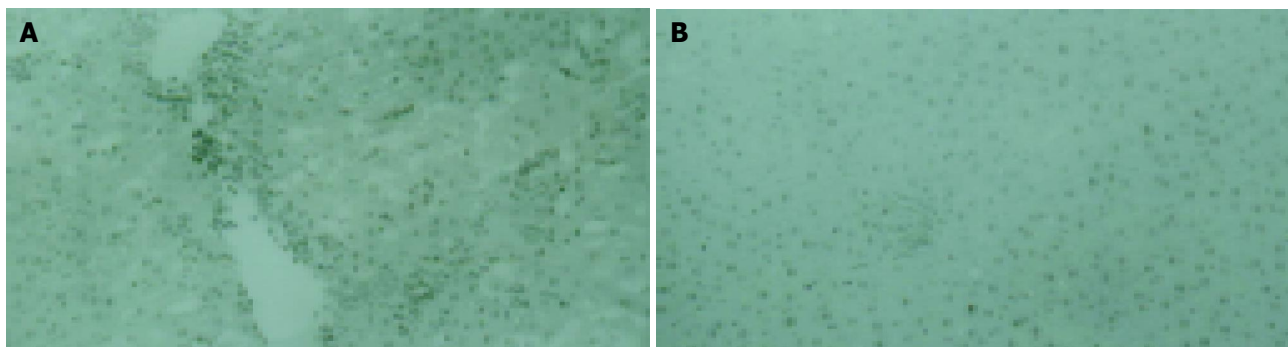


Figure 1 Morphological change in HH group (A) and NC group (B). ($\times 20\ 000$). A: The liver of rats anesthetized with 14% O₂/86% N₂/1.2MAC Halothane had extensive centrilobular necrosis and denaturation; B: There was

a increase in serum glutamic pyruvic transminase accompanying the morphologic damage, but no marked change was found in liver morphology inhaled with 21% O₂/79% N₂.

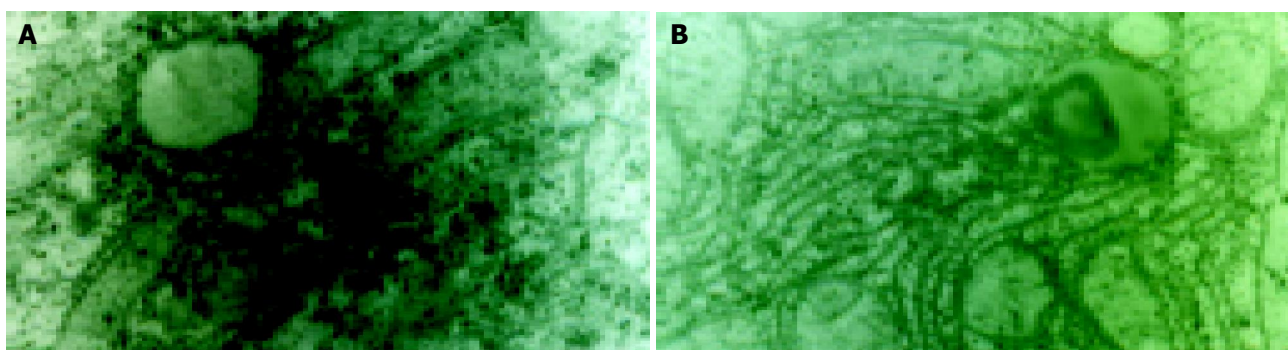


Figure 2 Hepatic Ca²⁺ cytochemical changes in HH group (A) and NC group (B). A: The liver of rats anesthetized with 14% O₂/86% N₂/1.2MAC. Halothane had a large amount of calcium deposition as shown in cytoplasm and

mitochondria; B: The liver of rats inhaled with 21% O₂/79% N₂, calcium precipitation was mainly located in nucleus, in mitochondria and cytoplasm as fine particles.

Table 2 Calcium content in mitochondria and cytoplasm (mean \pm SE)

Group	Ca ²⁺ (wt%)	
	Mitochondria	Cytoplasm
NC	3.14 \pm 1.08	3.44 \pm 1.28
HC	5.35 \pm 1.88	5.87 \pm 1.72
HS	5.25 \pm 1.61	5.49 \pm 1.32
HH	11.18 \pm 2.13 ^b	12.50 \pm 3.52 ^b

^bP<0.01 *vs* normal control group.

DISCUSSION

The principle of calcium cytochemical technique is to use potassium pyroantimonate to deposit intracellular cations and can contribute to the understanding of cellular cation redistribution resulting from physiologic and pathologic stimuli. Because the precipitation by potassium pyroantimonate of cations is nonspecific, careful choice of reaction conditions for calcium cytochemistry is very important, and it must be done in conjunction with analytical techniques such as X-ray analysis to ascertain whether other cations are deposited^[12]. When tissue is first fixed with glutaraldehyde and potassium pyroantimonate at low temperature (4 °C), better results can be acquired. Thus, the precipitation of calcium with cytochemical methods in combination with EDX microanalysis is valuable in investigating the mechanisms of hepatocellular injuries. Stereological methods provide

the means of efficiently producing quantitative data on the internal structure of organs, tissues, and cells. These methods can easily be applied to cytological work at the light or electron microscopy level of resolution^[13]. Although particular caution is indicated in avoiding systematic errors which may result from inadequate preparation, section thickness, etc, the results are generally very reliable.

Cytosolic Ca²⁺ concentration in hepatocytes may increase under hypoxic condition, which might be due to the changes of membrane functions, such as Ca²⁺-ATPase activity, Na⁺-Ca²⁺ exchange system^[14]. But cellular and mitochondrial calcium did not significantly increase in HC group. The causes are follows. (1) The degree of hypoxia (14% O₂) is not severe; (2) Hypoxia differs from ischemia, and the substances synthesizing ATP do not exhaust; (3) Ca²⁺-ATPase activity may partly recover 24 h after hypoxic exposure for 1 h.

It has been proposed that hepatic damage occurs secondary to the disruption of mechanism, which maintains cellular calcium homeostasis. A retrospective study showed that there is evidence that halothane can elevate cytosolic free Ca²⁺ by releasing calcium from internal calcium stores and uptaking calcium from extracellular medium^[15]. Recent work^[16] has demonstrated that loss of sarcoplasmic reticulum's Ca²⁺-ATPase activity by oxidizing agents, results direct oxidation of thiol groups on ATPase, but not lipid peroxidation. Halothane is also an oxidizing agent, but its mechanism underlying the increase of cytosolic Ca²⁺ is not

clear. Sevoflurane, an inhalation anesthetic agent, undergoes considerable less metabolism and less disturbed Ca^{2+} homeostasis than halothane, which may be relevant to its lesser hepatotoxicity^[17].

Cell injury due to loss of Ca^{2+} homeostasis correlates with blebbing of plasma membranes involving cytoskeletal proteins, Ca^{2+} ions and Ca^{2+} dependent proteases^[18]. The cytoskeletal protein is therefore expected to be a target for cytoplasmic calcium ions that promote changes in cell shape. Most of the known cytoskeletal receptors for calcium are associated with the actin filament system and these may be important in regulating many types of cell motility, including locomotion, phagocytosis, and secretion. Cytosolic free Ca^{2+} plays an increasingly important and fundamental role in the control of membrane permeability and cellular response to stimulation. Channel of discrete unitary conductance and selectivity activated by increased cytosolic free Ca^{2+} are responsible for K^+ efflux transfer and Na^+ influx, respectively. The elevation of mitochondrial Ca^{2+} influences mitochondrial respiration by changing activities of three matrix enzymes, pyruvate dehydrogenase, 2-oxoglutarate dehydrogenase and isocitrate dehydrogenase. Ca^{2+} activates proteases and endonucleases. Ca^{2+} enhances formation of active oxygen species, etc.

Sugimura *et al.*^[19], found that calcium channel blocking agent inhibits the production of radical intermediates during metabolism of halothane. These results suggest that calcium can activate the metabolism of halothane. Thus, we consider that the viscous circle of peroxidation activated by radical intermediates and elevation of cytosolic calcium may be the basis of halothane-induced hepatotoxicity under hypoxic internal environment.

REFERENCES

- 1 **Bond GR**. Hepatitis, rash and eosinophilia following trichloroethylene exposure: a case report and speculation on mechanistic similarity to halothane induced hepatitis. *J Toxicol Clin Toxicol* 1996; **34**: 461-466
- 2 **Kenna JG**. The molecular basis of halothane-induced hepatitis. *Biochem Soc Trans* 1991; **19**: 191-195
- 3 **El-Bassiouni EA**, Abo-Ollo MM, Helmy MH, Ismail S, Ramadan MI. Changes in the defense against free radicals in the liver and plasma of the dog during hypoxia and/or halothane anaesthesia. *Toxicology* 1998; **128**: 25-34
- 4 **Iaizzo PA**, Seewald MJ, Olsen R, Wedel DJ, Chapman DE, Berggren M, Eichinger HM, Powis G. Enhanced mobilization of intracellular Ca^{2+} induced by halothane in hepatocytes isolated from swine susceptible to malignant hyperthermia. *Anesthesiology* 1991; **74**: 531-538
- 5 **Frost L**, Prendergast D, Farrell G. Halothane hepatitis: damage to peripheral blood mononuclear cells produced by electrophilic drug metabolites is Ca^{2+} -dependent. *J Gastroenterol Hepatol* 1989; **4**: 1-9
- 6 **Frost L**, Mahoney J, Field J, Farrell GC. Impaired bile flow and disordered hepatic calcium homeostasis are early features of halothane-induced liver injury in guinea pigs. *Hepatology* 1996; **23**: 80-86
- 7 **Araki M**, Inaba H, Kon S, Imai M, Mizuguchi T. Effects of volatile anesthetics on the calcium ionophore A23187-mediated alterations in hepatic flow and metabolism in the perfused liver in fasted rats. *Acta Anaesthesiol Scand* 1997; **41**(1 Pt 1): 55-61
- 8 **Satorres J**, Perez-Mateo M, Mayol MJ, Esteban A, Graells ML. Protective effect of diltiazem against acetaminophen hepatotoxicity in mice. *Liver* 1995; **15**: 16-19
- 9 **Yamazoe Y**, Shimada M, Murayama N, Yamauchi K, Kato R. Alteration of hepatic drug metabolizing activities and contents of cytochrome P-450 isozymes by neonatal monosodium glutamate treatment. *Biochem Pharmacol* 1988; **37**: 1687-1691
- 10 **Baranska W**, Baran W, Skopinski P, Ziemba H. Morphometric analysis of satellite cells in rat skeletal muscles: soleus and extensor digitorum longus. *Acta Anat* 1997; **160**: 88-94
- 11 **Jonas L**, Fulda G, Kroning G, Merkord J, Nizze H. Electron microscopic detection of tin accumulation in biliopancreatic concretions after induction of chronic pancreatitis in rats by di-n-butyltin dichloride. *Ultrastruct Pathol* 2002; **26**: 89-98
- 12 **Musetti R**, Favali MA. Cytochemical localization of calcium and X-ray microanalysis of *Catharanthus roseus* L. infected with phytoplasmas. *Micron* 2003; **34**: 387-393
- 13 **Makita T**, Itagaki S, Ohokawa T. X-ray microanalysis and ultrastructural localization of cisplatin in liver and kidney of the rat. *Jpn J Cancer Res* 1985; **76**: 895-901
- 14 **Chang YJ**, Chang KJ. Calcium concentration in rat liver mitochondria during anoxic incubation. *J Formos Med Assoc* 2002; **101**: 136-143
- 15 **Byrne AM**, Lemasters JJ, Nieminen AL. Contribution of increased mitochondrial free Ca^{2+} to the mitochondrial permeability transition induced by tert-butylhydroperoxide in rat hepatocytes. *Hepatology* 1999; **29**: 1523-1531
- 16 **Favero TG**, Webb J, Papiez M, Fisher E, Trippichio RJ, Broide M, Abramson JJ. Hypochlorous acid modifies calcium release channel function from skeletal muscle sarcoplasmic reticulum. *J Appl Physiol* 2003; **94**: 1387-1394
- 17 **Johansson JS**, Zou H. Partitioning of four modern volatile general anesthetics into solvents that model buried amino acid side-chains. *Biophys Chem* 1999; **79**: 107-116
- 18 **Volbracht C**, Leist M, Nicotera P. ATP controls neuronal apoptosis triggered by microtubule breakdown or potassium deprivation. *Mol Med* 1999; **5**: 477-489
- 19 **Sugimura M**, Kitayama S, Morita K, Irifune M, Takarada T, Kawahara M, Dohi T. Effects of volatile and intravenous anesthetics on the uptake of GABA, glutamate and dopamine by their transporters heterologously expressed in COS cells and in rat brain synaptosomes. *Toxicol Lett* 2001; **123**: 69-76

Effect of *Helicobacter pylori* infection on gastric mucosal pathologic change and level of nitric oxide and nitric oxide synthase

Yong-Fu Wang, Chun-Lin Guo, Li-Zhen Zhao, Guo-An Yang, Peng Chen, Hong-Kun Wang

Yong-Fu Wang, Chun-Lin Guo, Li-Zhen Zhao, Guo -An Yang, Peng Chen, Hong-Kun Wang, First Hospital, Baotou Medical College, University of Science and Technology of Inner Mongolia, Baotou 014010, Inner Mongolia, China
Supported by the Science and Technology Committee of Baotou, China, No. 2000-26

Correspondence to: Dr. Yong-Fu Wang, Baotou Medical College, University of Science and Technology of Inner Mongolia, Baotou 014010, Inner Mongolia, China. wyf5168@hotmail.com
Telephone: +86-472-2178195 Fax: +86-472-2129235
Received: 2004-10-09 Accepted: 2004-12-21

Abstract

AIM: To investigate the level of nitric oxide (NO) and nitrous oxide synthase (NOS) enzyme and its effect on gastric mucosal pathologic change in patients infected with *Helicobacter pylori* (*H pylori*), and to study the pathogenic mechanism of *H pylori*.

METHODS: The mucosal tissues of gastric antrum were taken by endoscopy, then their pathology, *H pylori* and anti-CagA-IgG were determined. Fifty *H pylori* positive cases and 35 *H pylori* negative cases were randomly chosen. Serum level of NO and NOS was detected.

RESULTS: One hundred and seven cases (71.33%) were anti-CagA-IgG positive in 150 *H pylori* positive cases. The positive rate was higher especially in those with pre-neoplastic diseases, such as atrophy, intestinal metaplasia and dysplasia. The level of NO and NOS in positive group was higher than that in negative group, and apparently lower in active gastritis than in pre-neoplastic diseases such as atrophy, intestinal metaplasia and dysplasia.

CONCLUSION: *H pylori* is closely related with chronic gastric diseases, and type I *H pylori* may be the real factor for *H pylori*-related gastric diseases. Infection with *H pylori* can induce elevation of NOS, which produces NO.

© 2005 The WJG Press and Elsevier Inc. All rights reserved.

Key words: *Helicobacter pylori*; Nitric oxide; Nitric oxide synthase; Gastric mucosa; Pathology

Wang YF, Guo CL, Zhao LZ, Yang GA, Chen P, Wang HK. Effect of *Helicobacter pylori* infection on gastric mucosal pathologic change and level of nitric oxide and nitric oxide synthase. *World J Gastroenterol* 2005; 11(32): 5029-5031
<http://www.wjgnet.com/1007-9327/11/5029.asp>

INTRODUCTION

There is evidence that *Helicobacter pylori* (*H pylori*) is closely related with gastric carcinoma, and is considered as the first grade oncogene of gastric carcinoma by World Health Organization (WHO). *H pylori* infection correlates closely with gastric mucous pathology^[1-4].

NO is a medium produced in vessel endothelial cells or smooth muscle cells by NOS^[5,6]. As an inflammatory medium, NO plays an important role in the physical function and pathological process. Changes of NO in serum and tissue are related with damage to gastric mucosa and *H pylori* infection^[7-11].

This study aimed to investigate the changes of NO, NOS and the pathological transformation of gastric mucosa in patients infected with *H pylori*.

MATERIALS AND METHODS

Patients

Two hundred and eighty-two patients with chronic gastric disease were enrolled in this study. *H pylori* was detected by both rapid urease test and real-time fluorescent quantitative PCR in these patients. Anti-CagA-IgG was detected in the *H pylori* positive patients, the serum samples were collected from 50 *H pylori* positive patients and 35 *H pylori* negative patients for detection of NO and NOS.

Real-time fluorescent quantitative PCR

Real-time fluorescent quantitative PCR was performed with PCR kit (Da'an Gene Diagnosis Center, Guangzhou). Fluorescence was detected with a type DA620 fluorescent detector.

CagA *H pylori*-IgG

CagA *H pylori* IgG was detected according to the manufacturer's instructions (Shanghai Jingying Biology Corporation).

Measurement of NO and NOS

Because NO could be converted into NO₂⁻ and NO₃⁻ *in vivo*, nitrate reductase was used to deoxidize NO₃⁻ into NO₂⁻, and to determinate its concentration. NO and NOS were tested with the kits, (Nanjing Jiancheng Biology Corporation).

Statistical analysis

Data were presented as mean±SD and analyzed with SPSS software. Statistical analysis was performed using two-tailed Student's *t* test and χ^2 test. *P*<0.05 was considered statistically significant.

RESULTS

Relationship between *H pylori* infection and pathology

Among the 282 cases, *H pylori* was found in 150 cases, (53.19%), including 38.54% (37/96) in chronic superficial gastritis group, 51.26% (61/119) in atrophic gastritis group, 73.17% (30/41) in intestinal metaplasia group, and 84.62% (22/26) in dysplasia group. The *H pylori* positive rate in atrophic gastritis group was higher than that in chronic superficial gastritis group ($P < 0.05$), and significantly higher in intestinal metaplasia group and dysplasia group than that in chronic superficial gastritis group ($P < 0.01$, Table 1).

Table 1 *H pylori* positive rate in chronic gastric disease (%)

Group	n	<i>H pylori</i> positive	<i>H pylori</i> negative
CSG	96	37 (38.54)	59 (61.46)
CAG	119	61 (51.26) ^a	58 (48.74)
IM	41	30 (73.17) ^b	11 (26.83)
Dysplasia	26	22 (84.62) ^b	4 (15.38)
Total	282	150 (53.19)	132 (46.81)

^a $P < 0.05$, ^b $P < 0.01$ vs CSG.

Relationship between anti-CagA-IgG and pathology

The anti-CagA-IgG positive rate was 71.33% (107/150) in 150 *H pylori* positive patients, including 40.54% (15/37) in chronic superficial gastritis group, 75.41% (46/61) in atrophic gastritis group, 86.67% (26/30) in intestinal metaplasia group and 90.91% (20/22) in dysplasia group. The anti-CagA-IgG positive rate in chronic superficial gastritis group was significantly lower than that in the other three groups (Table 2).

Table 2 Positive rate of anti-CagA in 150 *H pylori* positive patients (%)

Group	CSG	CAG	IM	Dysplasia
n	37	61	30	22
Anti-CagA Positive (%)	15 (40.54) ^b	46 (75.41)	26 (86.67)	20 (90.91)

^b $P < 0.01$ vs Cag, IM, dysplasia.

Relationship between NO, NOS, and *H pylori* infection

The serum concentration of NO and NOS was 87.6 ± 16.1 $\mu\text{mol/L}$ and 51.4 ± 13.3 $\mu\text{mol/L}$ respectively in *H pylori* positive group, and 69.8 ± 19.4 $\mu\text{mol/L}$ and 35.2 ± 13.3 $\mu\text{mol/L}$ respectively in *H pylori* negative group (Table 3).

Table 3 Serum concentration of NO and NOS (mean \pm SD)

Group	n	NO ($\mu\text{mol/L}$)	NOS ($\mu\text{mol/L}$)
<i>H pylori</i> positive	50	87.6 ± 16.1 ^b	51.4 ± 13.3 ^b
<i>H pylori</i> negative	35	69.8 ± 19.4	35.2 ± 13.3

^b $P < 0.01$ vs *H pylori* negative group.

Relationship between NO, NOS, and pathology

The serum concentration of NO in chronic superficial

gastritis group was significantly lower than that in atrophic gastritis group, intestinal metaplasia group and dysplasia group ($P < 0.05$, Table 4).

Table 4 Serum concentration of NO in different pathological groups ($\mu\text{mol/L}$, mean \pm SD)

Group	<i>H pylori</i> positive		<i>H pylori</i> negative	
	n	Concentration	n	Concentration
CSG	16	80.0 ± 14.6 ^a	11	62.2 ± 16.9 ^a
CAG	25	95.4 ± 8.4	21	74.6 ± 19.2
IM	12	91.2 ± 13.9	4	75.5 ± 27.7
Dysplasia	9	95.3 ± 10.3	3	71.5 ± 19.6

^a $P < 0.05$ vs atrophic gastritis group, intestinal metaplasia group, and dysplasia group.

The serum concentration of NOS in chronic superficial gastritis group was significantly lower than that in atrophic gastritis group, intestinal metaplasia group and dysplasia group ($P < 0.05$), but there was no significant difference among the four groups (Table 5).

Table 5 Serum concentration of NOS in different pathological groups ($\mu\text{mol/L}$, mean \pm SD)

Group	<i>H pylori</i> positive		<i>H pylori</i> negative	
	n	Concentration	n	Concentration
CSG	16	38.0 ± 12.4 ^a	11	31.7 ± 9.4
CAG	25	57.6 ± 8.3	21	35.4 ± 13.0
IM	12	54.8 ± 8.3	4	26.1 ± 4.4
Dysplasia	9	59.6 ± 9.4	3	46.1 ± 22.9

^a $P < 0.05$ vs atrophic gastritis group, intestinal metaplasia group, and dysplasia group.

DISCUSSION

H pylori infection plays a leading role in the pathogenesis of chronic gastritis. Furthermore, *H pylori* infection is also a high risk factor for the development of gastric cancer [12]. *H pylori* can destroy gastric mucosa, leading to inflammation of gastric mucosa and digestive symptoms.

Our study showed that the *H pylori* positive rate in chronic superficial gastritis group was 38.54%, suggesting that *H pylori* is related to inflammation of gastric mucosa. Other factors may be involved in inflammation of gastric mucosa, such as pH value, mucus, glycoprotein. But in atrophic gastritis group, intestinal metaplasia group, and dysplasia group, the *H pylori* positive rate was 51.26%, 73.17% and 84.62%, respectively, indicating that *H pylori* infection has a close relationship with gastric pre-neoplastic diseases, such as atrophy, intestinal metaplasia, and dysplasia.

It was reported that *H pylori* has two types. Type I *H pylori* possesses high virulence energy producing cytotoxin-associated protein A and vacuole toxin, which are responsible for inflammatory response of gastric epithelial cells, and promotes cell proliferation and apoptosis [13,14]. Therefore, type I *H pylori* has a close relationship with development of gastric pre-neoplastic diseases [15-18]. Our study showed that

the pathological change of gastric mucosa was parallel with the anti-CagA-IgG positive rate. These observations support the hypothesis that type I *H pylori* infection is a high risk factor for the development of gastric pre-neoplastic diseases.

It has been proved that there are lots of NOS in smooth muscle cells and myenteric nerve plexus of stomach^[19], which are induced to produce endogenous NO by cytotoxins of *H pylori*. Moreover, a high pH value is beneficial for anaerobes to colonize in the stomach, and can degrade nitrate of food into nitrite. NO is regarded as an important inflammatory medium, related with acute and chronic inflammatory responses^[20-22]. But NO seems to have both beneficial and harmful effects on different stages of inflammation. In earlier period, NO can relieve mucosal inflammation and prevents cellular damage. However, it can prevent cellular apoptosis, induce mutation and contribute to the development of gastric pre-neoplastic diseases in later period^[23].

In this study, the levels of NO and NOS in chronic superficial gastritis group were significantly lower than those in pre-neoplastic diseases groups, such as atrophic gastritis group, intestinal metaplasia group, and dysplasia group in *H pylori* positive patients, but the condition existed not only in *H pylori* positive group, but also in *H pylori* negative group, suggesting that the serum level of NO induced by *H pylori* may be related with pre-neoplastic diseases. In *H pylori* negative patients, the levels of NOS had no difference in every pathological group, but the levels of NO were significantly higher in gastric pre-neoplastic disease groups, showing that other ways may stimulate the producing of NO besides *H pylori* in pre-neoplastic diseases. However, we believe that NO plays an important role in the development of pre-neoplastic diseases.

REFERENCES

- 1 **Sepulveda A**, Peterson LE, Shelton J, Gutierrez O, Graham DY. Histological patterns of gastritis in *H pylori*-infected individuals with a family history of gastric cancer. *Am J Gastroenterol* 2002; **97**: 1365-1370
- 2 **Nogueira C**, Figueiredo C, Carneiro F, Gomes AT, Barreira R, Figueira P, Salgado C, Belo L, Peixoto A, Bravo JC, Bravo LE, Realpe JL, Plaisier AP, Quint WG, Ruiz B, Correa P, van Doorn LJ. *Helicobacter pylori* genotypes may determine gastric histopathology. *Am J Pathol* 2001; **158**: 647-654
- 3 **Parsonnet J**, Friedman GD, Vandersteen DP, Chang Y, Vogelstein JH, Orentreich N, Sibley RK. *Helicobacter pylori* infection and the risk of gastric carcinoma. *N Engl J Med* 1991; **325**: 1127-1131
- 4 **Takeuchi K**, Ohno Y, Tsuzuki Y, Ando T, Sekihara M, Hara T, Kuwano H. *Helicobacter pylori* infection and early gastric cancer. *J Clin Gastroenterol* 2003; **36**: 321-324
- 5 **Antos D**, Enders G, Rieder G, Stolte M, Bayerdorffer E, Hatz RA. Inducible nitric oxide synthase expression before and after eradication of *Helicobacter pylori* in different forms of gastritis. *Immunol Med Microbiol* 2001; **30**: 127-131
- 6 **Yanaka A**, Muto H, Fukutomi H, Ito S, Silen W. Role of nitric oxide in restitution of injured guinea pig gastric mucosa *in vitro*. *Am J Physiol* 1995; **268** (6 Pt1): G933-942
- 7 **Bredt DS**, Hwang PM, Glatt CE, Lowenstein C, Reed RR, Snyder SH. Cloned and expressed nitric oxide synthase structurally resembles cytochrome P-450 reductase. *Nature* 1991; **351**: 714-718
- 8 **Lin HC**, Yang MC, Hou MC, Lee FY, Huang YT, Lin LF, Li SM, Hwang SJ, Wang SS, Tsai YT, Lee SD. Role of endotoxaemia in hyperdynamic circulation in rats with extrahepatic or intrahepatic portal hypertension. *J Gastroenterol Hepatol* 1996; **11**: 422-428
- 9 **Lin RS**, Lee FY, Lee SD, Tsai YT, Lin HC, Lu RH, Hsu WC, Huang CC, Wang SS, Lo KJ. Endotoxemia in patients with chronic liver diseases: relationship to severity of liver diseases, presence of esophageal varices, and hyperdynamic circulation. *J Hepatol* 1995; **22**: 165-172
- 10 **Albillos A**, de la Hera A, Gonzalez M, Moya JL, Calleja JL, Monserrat J, Ruiz-del-Arbol L, Alvarez-Mon M. Increased lipopolysaccharide binding protein in cirrhotic patients with marked immune and hemodynamic derangement. *Hepatology* 2003; **37**: 208-217
- 11 **Vallance P**, Moncada S. Hyperdynamic circulation in cirrhosis: a role for nitric oxide? *Lancet* 1991; **337**: 776-778
- 12 **Yao YL**, Zhang WD. The develop in research of nosogenetic factors of *H pylori*. *Shijie Huaren Xiaohua Zazhi* 2002; **10**: 455-458
- 13 **Telford JL**, Covacci A, Ghiara P, Montecucco C, Rappuoli R. Unravelling the pathogenic role of *Helicobacter pylori* in peptic ulcer: potential new therapies and vaccines. *Trends Biotechnol* 1994; **12**: 420-426
- 14 **Marchetti M**, Arico B, Burrioni D, Figura N, Rappuoli R, Ghiara P. Development of a mouse model of *Helicobacter pylori* infection that mimics human disease. *Science* 1995; **267**: 1655-1658
- 15 **Xiao S**, Liu W. More attention to the diversity of clinical outcome in *Helicobacter pylori*. *Zhonghua Neike Zazhi* 1999; **38**: 437-438
- 16 **Hu FL**, Zhou DY, Jia PQ. The basic and the clinical of *Helicobacter pylori* infection. 1th ed. *Beijing Technol Pub China* 2002: 172-176
- 17 **Zhang L**, Zhang LX, Zhang NX, Liu YG, Yan XJ, Han FC, Huo Y. The case control study of the relationship of *Helicobacter pylori* CagA and gastric carcinoma. *Shijie Huaren Xiaohua Zazhi* 2002; **10**: 593-594
- 18 **Yang WH**, Lin SR, Jin Z. The relationship of *Helicobacter pylori* nosogenetic factors and gastric mucosa pathology. *Zhonghua Xiaohua Zazhi* 2000; **1**: 56-57
- 19 **Stuehr DJ**, Marletta MA. Mammalian nitrate biosynthesis: mouse macrophages produce nitrate and nitrite in response to *Escherichia coli* lipopolysaccharide. *Proc Natl Acad Sci USA* 1985; **82**: 7738-7742
- 20 **Mannick EE**, Bravo LE, Zarama G, Realpe JL, Zhang XJ, Ruiz B, Fontham ET, Mera R, Miller MJ, Correa P. Inducible nitric oxide synthase, nitrosine and apoptosis in *Helicobacter pylori* gastritis. effect of a antibiotics and antioxidants. *Cancer Res* 1996; **56**: 3238-3243
- 21 **Akimoto M**, Hashimoto H, Shigemoto M, Yamashita K, Yokoyama I. Changes of nitric oxide and growth factors during gastric ulcer healing. *J Cardiovasc Pharmacol* 2000; **36**(5 Suppl 1): S282-S285
- 22 **Zhang X**, Ruiz B, Correa P, Miller MJ. Cellular dissociation of NF-kappaB and inducible nitric oxide synthase in *Helicobacter pylori* infection. *Free Radic Biol Med* 2000; **29**: 730-735
- 23 **Natanson C**, Hoffman WD, Suffredini AF, Eichacker PQ, Danner RL. A therapeutic target in sepsis. *Am Intern Med* 1994; **120**: 778-783

Expression and correlation of CD44v6, vascular endothelial growth factor, matrix metalloproteinase-2, and matrix metalloproteinase-9 in Krukenberg tumor

Ge Lou, Ying Gao, Xiao-Ming Ning, Qi-Fan Zhang

Ge Lou, Ying Gao, Xiao-Ming Ning, Qi-Fan Zhang, Tumor Hospital of Harbin Medical University, Harbin 150040, Heilongjiang Province, China

Supported by Foundation for Scholars Abroad of Ministry of Education of China, No. [2003]406, and Foundation of Heilongjiang Office of Education, No. 9551138

Correspondence to: Ge Lou, Department of Gynecology, Tumor Hospital of Harbin Medical University, Harbin 150040, Heilongjiang Province, China. dr-ig911@163.com

Telephone: +86-451-86677580-2133

Received: 2004-10-09 Accepted: 2004-12-09

carcinoma, gastric cancer, and Krukenberg tumor.

© 2005 The WJG Press and Elsevier Inc. All rights reserved.

Key words: CD44v6; VEGF; MMPs; Krukenberg tumor

Lou G, Gao Y, Ning XM, Zhang QF. Expression and correlation of CD44v6, vascular endothelial growth factor, matrix metalloproteinase-2, and matrix metalloproteinase-9 in Krukenberg tumor. *World J Gastroenterol* 2005; 11(32): 5032-5036

<http://www.wjgnet.com/1007-9327/11/5032.asp>

Abstract

AIM: To explore the expression and correlation of CD44v6, vascular endothelial growth factor (VEGF), matrix metalloproteinase (MMP)-2 and matrix metalloproteinase (MMP)-9 in Krukenberg and primary epithelial ovarian carcinoma.

METHODS: The expressions of CD44v6, VEGF, MMP-2 and MMP-9 were detected by immunohistochemical method in 20 cases of normal ovarian tissues, 38 cases of Krukenberg tumor and 45 cases of primary epithelial ovarian carcinoma.

RESULTS: The expression of CD44v6 (primary epithelial ovarian carcinoma tissue *vs* normal ovarian tissue: $\chi^2 = 4.516$, $P = 0.034$; Krukenberg tumor tissue *vs* normal ovarian tissue: $\chi^2 = 19.537$, $P = 0.001$) and VEGF (primary epithelial ovarian carcinoma tissue *vs* normal ovarian tissue: $P = 0.026$; Krukenberg tumor tissue *vs* normal ovarian tissue: $\chi^2 = 22.895$, $P = 0.001$) was significantly higher in primary epithelial ovarian carcinoma tissue and Krukenberg tumor tissue than in normal ovarian tissue. The positive expression rate of MMP-2 and MMP-9 was 0% in the normal ovarian tissue. The positive expression rate of CD44v6 ($\chi^2 = 10.398$, $P = 0.001$), VEGF ($\chi^2 = 13.149$, $P = 0.001$), MMP-2 ($\chi^2 = 33.668$, $P = 0.001$) and MMP-9 ($\chi^2 = 38.839$, $P = 0.001$) was remarkably higher in Krukenberg tumor than in primary epithelial ovarian carcinoma. The correlation of CD44v6, VEGF, MMP-2, and MMP-9 was observed in primary epithelial ovarian carcinoma and Krukenberg tumor.

CONCLUSION: CD44v6, VEGF, MMP-2, and MMP-9 are involved in ovarian carcinoma, gastric cancer and Krukenberg tumor. Detection of CD44v6, VEGF, MMP-2 and MMP-9 may contribute to the diagnosis of ovarian

INTRODUCTION

Gastric cancer is one of the common malignancies in gastrointestinal tract^[1-3]. Its metastasis rate is 64.2% in China^[4]. Krukenberg tumor is an ovary metastatic cancer from gastrointestinal cancer. Krukenberg tumor is highly malignant with a poor prognosis and its mechanism is not clear.

Invasion and metastasis are the leading biological characteristics of malignant tumor, and have a close relation with factors such as movement of tumor cells, apoptosis and metastasis-associated genes. VEGF is an important angiogenic factor, which may induce angiogenesis in tumor, and has a higher expression in tumor tissues, which is closely related with invasion and metastasis of tumor^[5-7]. CD44v6 is one of the numerous adhesive molecules and a transmembrane glycoprotein located on cell surface. It induces homing of lymphocytes and participates in adhesion between cells, influencing invasion and metastasis of tumor^[8-10]. MMP is one of the proteolytic enzymes and plays an important role in occurrence and development of tumor^[11-13].

MATERIALS AND METHODS

Patients and specimens

Patients were selected from Tumor Hospital of Harbin Medical University from 1992 to 2001. All patients were informed of the purpose of the study and gave their informed consent. Forty-five cases of primary epithelial ovarian carcinoma (15 cases of serious adenocarcinoma, 16 cases of mucous adenocarcinoma, and 14 cases of others pathologic types) and 35 cases of Krukenberg tumor were included in the study. All ovarian cancers had metastasis to other organs and all Krukenberg tumors came from gastric cancer. The age of the patients was 20-75 years, averaged

41 years. All cases were diagnosed by histology or cytology, and received no chemotherapy and radiotherapy before operation. Specimens were embedded in paraffin.

Reagents and method

Monoclonal antibody was purchased from Bossed Company of Wuhan. Immunohistochemical method was used to detect the expression of CD44v6, VEGF, and MMPs. Staining was performed following the manufacturer's instructions. The first antigen of negative control was replaced by PBS.

Determination criteria

The cells with unambiguous brown and yellow particles present in cytoplasm of tumor cells under optical microscope were defined as positive cells. Positive intensity was divided into three grades: weak positive (counting score was 1), strong positive (counting score was 3) and moderately positive (counting score was 2). At the same time, the number of positive cells was calculated. Zero to four grades represented the number of positive cells less than 5%, 5-25%, 26-50%, 51-75% and more than 75%, respectively. The last counting scores were intensity scores. If the product had one or more scores, it was positive. Otherwise, it was negative.

Statistical analysis

Analysis of variance was used to analyze the difference between groups. Data were analyzed by χ^2 test or Fisher's exact test. Correlation among variables was tested by Pearson of bivariate.

RESULTS

Expression of CD44v6, VEGF, MMP-2, and MMP-9 in ovarian carcinoma, Krukenberg tumor, and gastric carcinoma

Positively staining particles of Cd44v6 were mainly distributed in plasmalemma of tumor, some of which were expressed in cytoplasm (Figure 1A). Significant difference in positive expression was observed between normal ovarian tissue and primary epithelial ovarian carcinoma, Krukenberg tumor, and gastric carcinoma ($P < 0.05$). The positive expression of CD44v6 had no significant difference in ovarian carcinoma, ovarian mucous carcinoma and other carcinomas. No significant difference was found in moderately- and poorly-differentiated Krukenberg tumor.

Positive-staining particles of VEGF were mainly

distributed in cytoplasm (Figure 1B). The positive expression rate was higher in primary epithelial ovarian carcinoma, Krukenberg tumor, and gastric carcinoma than in normal ovarian tissue ($P < 0.05$). The positive expression rates of VEGF were 31.1% and 71.1% respectively for primary epithelial ovarian carcinoma and Krukenberg tumor ($P < 0.05$). No significant difference was found in ovarian carcinoma. No significant difference in positive expression rate was observed in moderately- and poorly-differentiated Krukenberg tumor.

Positive-staining particles of MMP-2 and MMP-9 were distributed in cytoplasm (Figures 1C and D). Positive expression rate of MMP-2 and MMP-9 was 0% in normal ovarian carcinoma (0/20). The positive expression rate of MMP-2 and MMP-9 was significantly higher in Krukenberg tumor, than in primary epithelial ovarian carcinoma ($P < 0.05$ for all of them). There was no relation between positive expression rate of MMPs and pathological types of primary epithelial ovarian carcinoma and between positive expression rate of MMPs and differentiation degree of Krukenberg tumor.

There was no significant difference in positive expression rate of VEGF, CD44v6, and MMP-2 between gastric carcinoma and Krukenberg tumor. The positive expression rate of MMP-9 was remarkably higher in Krukenberg tumor than in gastric carcinoma ($P < 0.05$). Obvious difference of positive expression rate of MMP-2 and MMP-9 was found in different differentiation degrees of gastric carcinoma. The positive expression rate was significantly higher in poorly-differentiated gastric carcinoma than in well- and moderately-differentiated gastric carcinoma ($P < 0.05$, Table 1).

Relation among expressions of CD44v6, VEGF, MMP-2, and MMP-9

Positive expression was graded by rank correlation method. The results indicated that there was a remarkable relation between positive expressions of VEGF and CD44v6, CD44v6 and MMP-2 and MMP-9, MMP-2, and MMP-9 (Table 2).

In primary epithelial ovarian carcinoma, there was a significant relation between expressions of CD44v6, VEGF, MMP-2, and MMP-9 (Table 3). VEGF *vs* MMP-9, and CD44v6 *vs* MMP-9.

The relation between variables was significant in gastric carcinoma (Table 4).

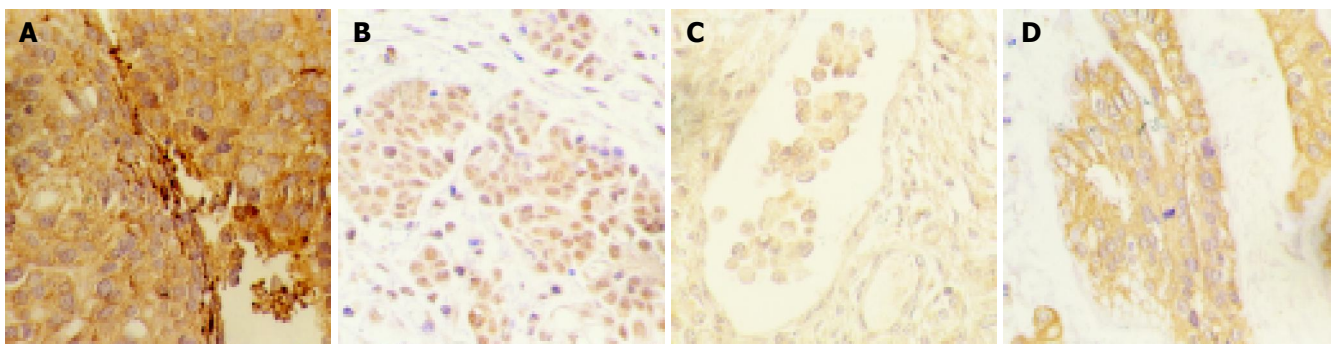


Figure 1 Expression of VEGF (A), CD44v6 (B), MMP-2 (C) and MMP-9 (D)

in Krukenberg tumor by immunohistochemical method.

Table 1 Expression of CD44v6, VEGF, MMP-2, and MMP-9 in epithelial ovarian carcinoma, Krukenberg tumor, and gastric carcinoma

	n	CD44v6		VEGF		MMP-2		MMP-9	
		n	%	n	%	n	%	n	%
Normal ovarian tissue	20	2	10.0	1	5.0	-		-	
Epithelial ovarian cancer	45	16	35.6	14	31.1	8	17.8	6	13.3
Serous adenocarcinoma	15	6	40.0	7	46.7	4	26.7	3	20.0
Mucous adenocarcinoma	16	4	25.0	3	18.8	2	12.5	2	12.5
Other types	14	6	42.9	4	28.6	2	14.3	1	7.1
Krukenberg tumor	38	27	71.1	27	71.1	31	81.6	31	81.6
Moderate differentiation	14	9	64.3	10	71.4	12	85.6	10	71.4
Poor differentiation	24	18	75.0	17	70.8	19	79.2	21	87.5
Gastric carcinoma	38	30	78.9	27	73.7	25	65.8	23	60.5
High and moderate differentiation	16	12	75.0	9	56.3	7	31.8	6	37.5
Poor differentiation	22	18	81.8	16	72.7	18	81.8	17	77.3

Table 2 Relation between expressions of CD44v6, VEGF, MMP-2, and MMP-9 in Krukenberg tumor

	CD44v6		MMP-2		MMP-9	
	r	P	r	P	r	P
VEGF	0.342	0.023	0.498	0.000	0.498	0.000
CD44v6			0.419	0.005	0.213	0.212
MMP-2					0.488	0.001

Table 3 Relation between expressions of CD44v6, VEGF, MMP-2, and MMP-9 in primary epithelial ovarian carcinoma

	CD44v6		MMP-2		MMP-9	
	r	P	r	P	r	P
VEGF	0.605	0.004	0.608	0.003	0.711	0.000
CD44v6			0.684	0.001	0.804	0.000
MMP-2					0.457	0.037

Table 4 Relation between expressions of CD44v6, VEGF, MMP-2, and MMP-9 in primary gastric carcinoma

	CD44v6		MMP-2		MMP-9	
	r	P	r	P	r	P
VEGF	0.366	0.046	0.246	0.378	0.385	0.035
CD44v6			0.456	0.011	0.200	0.475
MMP-2					0.439	0.015

DISCUSSION

CD44v6 is highly expressed in serum and tissues of ovarian carcinoma and correlates with development of ovarian carcinoma^[14,15]. In the present study, the expression of CD44v6 was significantly higher in primary epithelial ovarian carcinoma and Krukenberg tumor than in normal ovarian tissue ($P < 0.05$), suggesting that expression of CD44v6 is related with malignant behaviors of ovarian carcinoma. The high expression of CD44v6 correlates with formation, development and transfer of ovarian carcinoma.

CD44 plays an important role in regulation of progress and metastasis of primary gastric carcinoma. Our study found that there was a significant difference in positive expression rate of CD44 between primary epithelial ovarian

carcinoma and Krukenberg tumor ($P < 0.05$). The positive expression rate of CD44v6 was higher in primary gastric carcinoma (78.9%), indicating that higher expression of CD44v6 has a close correlation with metastasis of gastric carcinoma. It was reported that the positive expression rate of CD44v6 is 64-77% in gastric carcinoma tissue^[16-18]. Studies indicate that superfluous expression of CD44v6 correlates closely with occurrence, development, infiltration and metastasis of cancers.

VEGF is one of the agents accelerating the formation of blood vessels^[19-21], and has multiple functions after it binds to specific receptors of endothelial cell surface, indicating that the development, infiltration and metastasis of cancer is related with higher expression of CD44v6 in cancer^[5-7,22].

VEGF is highly expressed in serum and tissues of ovarian carcinoma^[23-28]. In the present study, the expression of VEGF was significantly higher in primary epithelial ovarian carcinoma and Krukenberg tumor than in normal ovarian tissue ($P < 0.05$), indicating that the occurrence, development and metastasis of ovarian carcinoma is closely related with high expression of VEGF.

It has been identified that tumor metastasis is accelerated by VEGF, which is highly expressed in gastric carcinoma. VEGF may be used as an index for poor prognosis of gastric carcinoma^[29-34]. The positive expression is significantly different between primary epithelial ovarian carcinoma and Krukenberg tumor ($P < 0.05$). There is no significant difference between mucous and mixed epithelial tumor and differentiation of Krukenberg tumor ($P > 0.05$). The expression of VEGF is higher in primary gastric cancer, suggesting that cancer metastasis may be accelerated by VEGF. It was reported that the expression of VEGF is higher in carcinoma of colon with metastasis, than in carcinoma of colon without metastasis^[35-38], suggesting that metastasis of colonic carcinoma is closely related with positive expression of VEGF.

MMPs play an important role among enzymes breaking the extracellular matrix. MMP-2 and MMP-9 are closely related with metastasis of tumor^[39-41]. Collagenase has enzymolysis not only for matrix component of cells, but also for main component of membrana basalis. The expression of collagenase increases obviously in tumor tissues, metastasis and serum^[42-44].

In this study, MMP-2 and MMP-9 were not expressed in ovarian normal tissue. The expression was low in primary epithelial ovarian carcinoma, the reasons might be that the samples were stored for a long time and the staining was not ideal. Expression of MMP-2 and MMP-9 was higher in malignant tumor tissues than in normal tissues. There was a significant difference in expression of MMP-2 and MMP-9 between Krukenberg tumor and normal tissue, and primary epithelial ovarian carcinoma and normal tissue ($P < 0.05$). The expression rate was higher in primary gastric cancer. The results indicate that invasion and metastasis of tumor are accelerated by MMP-2 and MMP-9, and MMP-2 and MMP-9 play an important role in the metastasis of gastric carcinoma. It was reported that invasion and metastasis of tumors are related to the expression of MMP-2 and MMP-9^[43,46]. High expression of MMP-2 and MMP-9 may be the molecular basis of invasion and metastasis of tumor cells. Invasion and metastasis are present, if there is overexpression of MMP-2 and MMP-9 in tumor tissue.

There was not a significant difference in MMP-2 expression between moderately- and poorly-differentiated Krukenberg tumor ($P > 0.05$), indicating that expression of MMP-2 is not related with tumor differentiation.

Tumor metastasis involves a series of complex processes. Many gene products take part in the process and play an important role in forming metastasis. The significant correlations were obtained between variables in primary epithelial ovarian carcinoma and Krukenberg tumor, but not in CD44v6 and MMP-9 in our study, indicating that the above-mentioned factors participate in tumor invasion and metastasis.

REFERENCES

- 1 Zhao GH, Li TC, Shi LH, Xia YB, Lu LM, Huang WB, Sun HL, Zhang YS. Relationship between inactivation of p16 gene and gastric carcinoma. *World J Gastroenterol* 2003; **9**: 905-909
- 2 Wang MW, Yang SB, Zhang ZQ, Zhu QF, Wang GS, Li H, Yao C, Wu BY, You WD. Gastroscopy follow-up study of pre-malignant gastric lesions in senile patients. *Shijie Huaren Xiaohua Zazhi* 2003; **11**: 1279-1281
- 3 Shen B, Zhu JS. Study progress of providing with blood and intervene chemotherapy by arteries. *Shijie Huaren Xiaohua Zazhi* 2003; **11**: 1425-1428
- 4 National gastric cancer pathology cooperation. Pathology study in 360 gastric cancer corpses examination. *Chin J Pathol* 1983; **12**: 124-128
- 5 Gerber HP, Ferrara N. The role of VEGF in normal and neoplastic hematopoiesis. *J Mol Med* 2003; **81**: 20-31
- 6 Vacca A, Ria R, Ribatti D, Semeraro F, Djonov V, Di Raimondo F, Dammacco F. A paracrine loop in the vascular endothelial growth factor pathway triggers tumor angiogenesis and growth in multiple myeloma. *Haematologica* 2003; **88**: 176-185
- 7 Conti CJ. Vascular endothelial growth factor: regulation in the mouse skin carcinogenesis model and use in antiangiogenesis cancer therapy. *Oncologist* 2002; **7**(Suppl 3): 4-11
- 8 Mi JQ, Zhang ZH, Shen MC. Significance of CD44v6 protein expression in gastric carcinoma and precancerous lesions. *Shijie Huaren Xiaohua Zazhi* 2000; **8**: 156-158
- 9 Junglin B, Menges M, Goebel R, Wittig BM, Weg-Remers S, Pistorius G, Schilling M, Bauer M, Konig J, Zeitz M, Stallmach A. Expression of CD44v6 has no prognostic value in patients with colorectal cancer. *Z Gastroenterol* 2002; **40**: 229-233
- 10 Morrin M, Delaney PV. CD44v6 is not relevant in colorectal tumour progression. *Int J Colorectal Dis* 2002; **17**: 30-36
- 11 Waas ET, Lomme RM, DeGroot J, Wobbes T, Hendriks T. Tissue levels of active matrix metalloproteinase-2 and -9 in colorectal cancer. *Br J Cancer* 2002; **86**: 1876-1883
- 12 Kuittinen O, Soini Y, Turpeenniemi-Hujanen T. Diverse role of MMP-2 and MMP-9 in the clinicopathological behavior of Hodgkin's lymphoma. *Eur J Haematol* 2002; **69**: 205-212
- 13 Jiang YS, Gao Y. Biologic characteristic of matrix metalloproteinase and its effects in soakage and metastasis of hepatic carcinoma. *Shijie Huaren Xiaohua Zazhi* 2000; **8**: 1403-1404
- 14 Li J, Liu J, Lu HO, Jiang Y, Guo L, Li H. Immunohistochemistry analysis of CD44 aberrance type in ovarian cancer. *Chin J Clin Oncol* 1998; **25**: 738-740
- 15 Wang J, Sui LH, Gao QY. Expression of transmembrane glycoprotein V6 and its signification in epithelia ovarian cancer. *Chin J Clin Obs Gynecol* 2001; **2**: 16-18
- 16 Cai Q, Lu HF, Sun MH, Du X, Fan YZ, Shi DR. Expression of CD44 v3 and v6 proteins in human colorectal carcinoma and its relevance with prognosis. *Shijie Huaren Xiaohua Zazhi* 2000; **8**: 1255-1258
- 17 Gu HP, Ni CR, Zhan RZ. Relationship of expressions of CD15, CD44v6 and nm23H1 mRNA with metastasis and prognosis of colon carcinoma. *Shijie Huaren Xiaohua Zazhi* 2000; **8**: 887-891
- 18 Yamaguchi A, Goi T, Yu J, Hirono Y, Ishida M, Iida A, Kimura T, Takeuchi K, Katayama K, Hirose K. Expression of CD44v6 in advanced gastric cancer and its relationship to hematogenous metastasis and longterm prognosis. *J Surg Oncol* 2002; **79**: 230-235
- 19 Giavazzi R, Sennino B, Coltrini D, Garofalo A, Dossi R, Ronca R, Tosatti MP, Presta M. Distinct role of fibroblast growth factor-2 and vascular endothelial growth factor on tumor growth and angiogenesis. *Am J Pathol* 2003; **162**: 1913-1926
- 20 Ferrara N. Role of vascular endothelial growth factor in physiologic and pathologic angiogenesis: therapeutic implications. *Semin Oncol* 2002; **29**(6 Suppl 16): 10-14
- 21 Bellamy WT. Expression of vascular endothelial growth factor and its receptors in multiple myeloma and other hematopoietic malignancies. *Semin Oncol* 2001; **28**: 551-559
- 22 Tarabozetti G, Poli M, Dossi R, Manenti L, Borsotti P, Faircloth GT, Brogginini M, D'Incalci M, Ribatti D, Giavazzi R. Antiangiogenic activity of apidine, a new agent of marine origin. *Br J Cancer* 2004; **90**: 2418-2424
- 23 Gadducci A, Viacava P, Cosio S, Cecchetti D, Fanelli G, Fanucchi A, Teti G, Genazzani AR. Vascular endothelial growth factor (VEGF) expression in primary tumors and peritoneal metastases from patients with advanced ovarian carcinoma. *Anticancer Res* 2003; **23**: 3001-3008
- 24 Ishikawa M, Kitayama J, Kazama S, Nagawa H. Expression of vascular endothelial growth factor C and D (VEGF-C and -D) is an important risk factor for lymphatic metastasis in undifferentiated early gastric carcinoma. *Jpn J Clin Oncol* 2003; **33**: 21-27
- 25 Kakeji Y, Koga T, Sumiyoshi Y, Shibahara K, Oda S, Maehara Y, Sugimachi K. Clinical significance of vascular endothelial growth factor expression in gastric cancer. *J Exp Clin Cancer Res* 2002; **21**: 125-129
- 26 Duan LX, Zhong DW, Hu FZ, Zhao H, Yang ZL, Yi W, Shu GS, Hua SW. Relationship between expression of VEGF, Flt1, bFGF and P53 and outcome in patients with gastric carcinoma. *Shijie Huaren Xiaohua Zazhi* 2004; **12**: 546-549
- 27 Zhang HT, Hu X. Relationship between VEGF and incursions and metastasis ingastric cancer. *Shijie Huaren Xiaohua Zazhi* 2003; **11**: 344-345
- 28 Li QM, Yu Q, Min CY. Expression of mutant P53 and VEGF in experimental gastric cancer in rats and the effect of decoction Weikang-ning. *Shijie Huaren Xiaohua Zazhi* 2003; **11**: 997-1000
- 29 Mao ZB, Xiao MB, Huang JF, Ni HB, Ni RZ, Wei Q, Zhang H. Expression of VEGF and its signification in serum of gastric cancer. *Shijie Huaren Xiaohua Zazhi* 2002; **10**: 1220-1221
- 30 Takahashi Y, Mai M. Significance of angiogenesis and clinical application of anti-angiogenesis. *Nihon Geka Gakkai Zasshi* 2001; **102**: 381-384
- 31 Kitadai Y, Amioka T, Haruma K, Tanaka S, Yoshihara M, Sumii K, Matsutani N, Yasui W, Chayama K. Clinicopatho-

- logical significance of vascular endothelial growth factor (VEGF)-C in human esophageal squamous cell carcinomas. *Int J Cancer* 2001; **93**: 662-666
- 32 **Linderholm BK**, Lindh B, Beckman L, Erlanson M, Edin K, Travelin B, Bergh J, Grankvist K, Henriksson R. Prognostic correlation of basic fibroblast growth factor and vascular endothelial growth factor in 1307 primary breast cancers. *Clin Breast Cancer* 2003; **4**: 340-347
- 33 **Liu F**, Zhang YJ. Roles of VEGF-C and its receptor Flt-4 in proliferation and metastasis of primary breast cancer. *Ai zheng* 2003; **22**: 1053-1056
- 34 **Yu CY**, Pam KF, Xing DY, Liang G, Tan W, Zhang L, Lin D. Correlation between a single nucleotide polymorphism in the matrix metalloproteinase-2 promoter and risk of lung cancer. *Cancer Res* 2002; **15**: 6430-6433
- 35 **Hao YD**, Zhao YW, Kong LF, Zhang YP. Chang of MMP-2 enzymologic activity in tissues of human hepatocellular cancer. *Shijie Huaren Xiaohua Zazhi* 2000; **8**: 952-953
- 36 **Ylisirnio S**, Hoyhtya M, Turpeenniemi-Hujanen T. Serum matrix metalloproteinases-2,-9 and tissue inhibitors of metalloproteinases-1,-2 in lung cancer-TIMP-1 as a prognostic marker. *Anticancer Res* 2000; **20**: 1311-1316
- 37 **Monig SP**, Baldus SE, Hennecken JK, Spiecker DB, Grass G, Schneider PM, Thiele J, Dienes HP, Holscher AH. Expression of MMP-2 is associated with progression and lymph node metastasis of gastric carcinoma. *Histopathology* 2001; **39**: 597-602
- 38 **Kabashima A**, Maehara Y, Kakeji Y, Baba H, Koga T, Sugimachi K. Clinicopathological features and overexpression of matrix metalloproteinases in intramucosal gastric carcinoma with lymph node metastasis. *Clin Cancer Res* 2000; **6**: 3581-3584
- 39 **Kabashima A**, Yan T, Sugimachi K, Tsuneyoshi M. Relationship between biologic behavior and phenotypic expression in intramucosal gastric carcinomas. *Hum Pathol* 2002; **33**: 80-86
- 40 **Cai H**, Kong ZR, Chen HM. Matrix metalloproteinase-2 and angiogenesis in gastric cancer. *Ai zheng* 2002; **21**: 25-28
- 41 **Hirvonen R**, Talvensaar-Mattila A, Paakko P, Turpeenniemi-Hujanen T. Matrix metalloproteinase-2 (MMP-2) in T (1-2) NO breast carcinoma. *Breast Cancer Res Treat* 2003; **77**: 85-91
- 42 **Takahashi Y**, Kitadai Y, Ellis LM, Bucana CD, Fidler IJ, Mai M. Multiparametric *in situ* mRNA hybridization analysis of gastric biopsies predicts lymph node metastasis in patients with gastric carcinoma. *Jpn J Cancer Res* 2002; **93**: 1258-1265
- 43 **Takahashi M**, Oka N, Naroda T, Nishitani MA, Kanda K, Kanayama HO, Kagawa S. Prognostic significance of matrix metalloproteinases-2 activation ratio in renal cell carcinoma. *Int J Urol* 2002; **9**: 531-538
- 44 **Matsuyama Y**, Takao S, Aikou T. Comparison of matrix metalloproteinase expression between primary tumors with or without liver metastasis in pancreatic and colorectal carcinomas. *J Surg Oncol* 2002; **80**: 105-110
- 45 **Liang YY**, Zhao T, He EST. Relationship between MMP-9, MMP-2 and metastasis of gastric cancer. *Chin J General Surg* 2000; **15**: 119
- 46 **Zhang CW**, Zou SC, Xu WJ, Zhao CS. Expression of MMP-9 and its clinical signification. *Zhongguo Weichang Waike Zazhi* 2000; **3**: 25-27

Science Editor Wang XL and Guo SY Language Editor Elsevier HK

Gene expression profiles in peripheral blood mononuclear cells of SARS patients

Shi-Yan Yu, Yun-Wen Hu, Xiao-Ying Liu, Wei Xiong, Zhi-Tong Zhou, Zheng-Hong Yuan

Shi-Yan Yu, Xiao-Ying Liu, Wei Xiong, Zheng-Hong Yuan, Key Laboratory of Medical Molecular Virology, Ministry of Education and Public Health, Shanghai Medical College of Fudan University, Shanghai 200032, China

Yun-Wen Hu, Zhi-Tong Zhou, Shanghai Public Health Center, Shanghai 201508, China

Supported by the Grants From Shanghai Commission of Science and Technology, Shanghai Bureau of Health, No. 024Y32 and the grants from the Sino-German Center for Research Promotion, No. GZ Nr. 239 (202/12)

Co-first-authors: Shi-Yan Yu and Yun-Wen Hu

Correspondence to: Zheng-Hong Yuan, Key Laboratory of Medical Molecular Virology, Ministry of Education and Public Health, Shanghai Medical College of Fudan University, Shanghai 200032, China. zhyuan@shmu.edu.cn

Telephone: +86-21-64161928 Fax: +86-21-64227201

Received: 2004-10-24 Accepted: 2004-12-21

Abstract

AIM: To investigate the role of inflammatory and anti-viral genes in the pathogenesis of SARS.

METHODS: cDNA microarrays were used to screen the gene expression profiles of peripheral blood mononuclear cells (PBMCs) in two SARS patients (one in the acute severe phase and the other in the convalescent phase) and a healthy donor. In addition, real-time qualitative PCR was also performed to verify the reproducibility of the microarray results. The data were further analyzed.

RESULTS: Many inflammatory and anti-viral genes were differentially expressed in SARS patients. Compared to the healthy control or the convalescent case, plenty of pro-inflammatory cytokines such as IL-1, TNF- α , IL-8, and MAPK signaling pathway were significantly upregulated in the acute severe case. However, anti-inflammatory agents such as IL-4 receptor, IL-13 receptor, IL-1Ra, and TNF- α -induced proteins 3 and 6 also increased dramatically in the acute severe case. On the contrary, a lot of IFN-stimulated genes like PKR, GBP-1 and 2, CXCL-10 and 11, and JAK/STAT signal pathway were downregulated in the acute severe case compared to the convalescent case.

CONCLUSION: Gene expression in SARS patients mirrors a host state of inflammation and anti-viral immunity at the transcription level, and understanding of gene expression profiles may make contribution to further studies of the SARS pathogenesis.

Key words: SARS pathogenesis; Gene expression profiles; cDNA microarray; Inflammation response; Innate anti-viral immunity

Yu SY, Hu YW, Liu XY, Xiong W, Zhou ZT, Yuan ZH. Gene expression profiles in peripheral blood mononuclear cells of SARS patients. *World J Gastroenterol* 2005; 11(32): 5037-5043
<http://www.wjgnet.com/1007-9327/11/5037.asp>

INTRODUCTION

A new contagious disease occurred in 2003^[1-3], which lasted for at least 6 mo and swept over 29 countries in the world, causing numerous deaths and triggering public panic^[4]. However, it took less than 2 mo to successfully identify the causative agent—a novel coronavirus^[3,5]. Meanwhile, investigation of the unique pathogenic mechanism of this disease is still challenging and intriguing. Clinical data suggest that it is an abnormal pathological reaction to pulmonary viral infection characterized by acute lung injury^[1,2,4,6] that determines the process of the symptoms. Acute lung injury is a multi-factorial, pathophysiological process involving cytokines and adhesion molecules, as well as inflammatory and immune cells^[6-8]. Many pro- and anti-inflammatory cytokines such as IL-1, TNF- α , IL-8, IL-4, and IL-10 have been demonstrated to play a pivotal role in the pathogenesis of acute lung injury and severe systemic inflammation^[6,8-11]. To determine the role of cytokines in the pathogenesis of SARS, immunological techniques such as RIA, ELISPOT, and ELISA have been employed to measure cytokine alterations in blood samples from SARS patients^[12-14]. Jones *et al.*^[12], reported that the number of IFN- γ , IL-2, IL-4, IL-10, and IL-12 secreting cells induced by T-cell activators is below normal in many or most patients, while the number of cells which are induced to produce IL-6 and TNF- α by T-cell or monocyte activators is higher than normal in many early SARS patients, and increases in some SARS patients during and after treatment. Wong *et al.*^[13], found that Th1 cytokine, inflammatory cytokines such as IL-1, IL-6, and IL-12 and chemokines such as IL-8, MCP-1, and IP-10 are increased. Furthermore, Zhang *et al.*^[14], revealed that there is a difference in relationship between IL6, IL-8, TGF- β concentration, and SARS severity (positive for IL-6, but negative for IL-8 and TGF- β). Although these studies have shown the evidence of activated Th1 cell-mediated immunity and the hyper-innate inflammatory response, the role of these cytokines in the pathogenesis of the severe systemic inflammation and the mechanisms underlying the pathogenesis of SARS need to be further studied.

Development of microarray technology has provided a powerful tool for study of the complicated biological process in cells and tissues. cDNA microarray is used to analyze the virus-host cell interactions, and improvements have been achieved in the diagnosis, treatment, and prevention of infectious diseases^[15]. Therefore, in this study, we used cDNA microarray to analyze the global gene expression profiles of peripheral blood mononuclear cells (PBMCs) from two SARS patients, one in the acute severe phase and the other in the convalescent phase. The results may make contribution to studies of the SARS pathogenesis.

MATERIALS AND METHODS

Patients

Shanghai Municipal Hospital for Infectious Diseases was the appointed hospital for SARS patients during the SARS outbreak in Shanghai area. A total of seven patients with SARS were accepted for treatment in this hospital from 2nd May to 20th August 2003. In this study, two SARS patients in different clinical courses were enrolled, one in the acute severe phase (1 wk after admission to hospital and died 1 d after blood samples were taken) and the other in the convalescent phase (about 1 mo after admission). After admission to the hospital, both patients received the standard treatment. Additional clinical information is summarized in Table 1.

Table 1 Clinical characteristics of two SARS patients

	P1	P2
Age (yr)	57	40
Gender	Male	Female
Body temperature (°C)	39.2	36.8
White cell count ($\times 10^9/L$)	13.30	4.67
Neutrophil ($\times 10^9/L$)	12.80	3.25
Lymphocyte ($\times 10^9/L$)	0.406	0.897
CD3 ⁺ (μL)	359	791
CD4 ⁺ CD3 ⁺ /CD3 ⁺ (%)	86	58
CD8 ⁺ CD3 ⁺ /CD3 ⁺ (%)	13	36
CD4 ⁺ CD8 ⁺ CD3 ⁺ /CD3 ⁺ (%)	4	2
CD4 ⁺ /CD8 ⁺	6.38	1.62
Monocyte ($\times 10^9/L$)	0.122	0.442
Eosinophil ($\times 10^9/L$)	0.004	0.033
Basophil ($\times 10^9/L$)	0.009	0.041
Outcome	Death	Rehabilitation

Blood samples and RNA isolation from peripheral blood mononuclear cells

Blood samples (5 mL each) were collected from two patients and a healthy donor with anticoagulant at bedside. PBMCs

in lymphocyte separation medium (Sigma, USA) were isolated. Total RNA was isolated using the TRIzol reagent (Invitrogen, USA) according to the manufacturer's instructions. After TRIzol purification, RNA was repurified by phenol-chloroform extraction and ethanol precipitation, and quantified by spectrophotometry. In addition, RNA samples were electrophoresed on 2.2 mol/L 0.7% agarose-formaldehyde gel and visualized by ethidium bromide staining to ensure that there was not overt RNA degradation.

Microarray hybridization and data analysis

Microarray hybridization was performed by Shanghai Genentech Company according to the standard Affymetrix protocol. In brief, RNA from two patients and a healthy control was converted to cDNA with SuperscriptTM II RT (Invitrogen, USA) and then to biotin-labeled cRNA with RNA transcript labeling kit (Affymetrix, USA). cRNA was cleaned up and qualified and then fragmented for hybridization. After hybridization to the human HG-U113A GeneChip containing approximately 13 000 unique genes or expression-signature tags (Affymetrix), the gene chips were automatically washed and stained with streptavidin-phycoerythrin by a fluidics system. After the chips were scanned with a GeneArray scanner (Hewlett-Packard, USA), gene transcript values were determined using algorithms in the Microarray Analysis Suite Software (5.0 version, Affymetrix). Each chip was scaled to an overall intensity of 1 500 to correct for minor differences in the overall chip hybridization intensity and to allow comparison between chips. Data were normalized to the average of the healthy control. The gene lists of two patients containing genes with $P < 0.05$ were put out in the style of Excel files.

Real-time quantitative PCR

Real-time quantitative PCR of cDNA samples from two patients and a healthy control was carried out in triplicate with the indicated primers (Table 2), at a volume of 20 μL using FastStart DNA Master SYBR Green I Mixture Kit[®] (Roche Diagnostics, USA) in a LightCycle[®] system (Roche Diagnostics, USA). Initial denaturing for 10 min at 95 °C was followed by 45 cycles at 95 °C for 10 s, at 55 °C for 15 s, and at 72 °C for 20 s. Detection of the fluorescent products was set at the last step of each cycle. To determine the specificity of amplification, melting curve analysis was applied to all final PCR products, after the cycling protocol. In addition, template-free negative controls were run with each gene specific primer. PCR for RNA products of three samples was performed in order to exclude genomic DNA contamination. The standard curve was prepared with a serial of dilutions of genomic cDNA from a GAPDH-containing plasmid. Results were representative of three independent experiments.

Table 2 Primer sequence used in real-time quantitative PCR analysis

Accession number	Description	Forward primer (5'→3')	Reverse primer (5'→3')
NM_000634	IL-8R α	GGAACGTGGTGTCTTCAGGG	CATCTAATGTCAGATTCGGGG
NM_003855	IL-18R1	GGGTATTACTCTCGGTGCA	CCATTTTCTCCCCGAACATCC
BC025925	GAPDH	GGTATCGTGGAAGGACTCATGAC	ATGCCAGTGAGCTTCCCGTTCAGC

RESULTS

Validation of microarray results

To verify the reproducibility of the microarray results, 2 genes (IL-8 receptor- α and IL-18 receptor-1) were selected and tested by real-time quantitative PCR. GAPDH was used as internal control to normalize the total RNA. The ratios of the signal intensity of specific genes to GAPDH, as well as their comparison to microarray results, are listed in Table 3. As shown in Table 3, the results of RT-PCR analysis were aligned with those from the microarray analysis, suggesting the creditability of our microarray results.

Table 3 Comparison of microarray and real-time quantitative PCR analysis on selected genes (mean \pm SD)

Gene description	Techniques	P1	P2
IL-8R α	Microarray	73.52	-
	Real-time qPCR	11.63 \pm 0.15	0.37 \pm 0.09
IL-18R1	Microarray	42.33	-
	Real-time qPCR	48.55 \pm 0.36	0.38 \pm 0.27

Global characteristics of gene expression in PBMCs of SARS patients

We uploaded the genes altered over 2.0-fold (at <http://www.mvlab-fudan.cn/part9.htm>) to Affymetrix online data analysis system (https://www.affymetrix.com/analysis/netaffx/batch_query.affx), and then got an illustration of hierarchical structure according to their biological process. The number of genes changed over 2.0-fold in two SARS patients is summarized in Table 4. Results showed that many genes including those for cell communication, cellular physiological process, death, metabolism, organismal physiological process, and response to stimulus changed significantly in both SARS patients. The number of genes changed in the acute severe case, was much higher than that in the convalescent case.

Table 4 Functional categories of over 2.0-fold-regulated genes in two SARS patients

Classification	P1	P2
Cell communication	802 (518 \uparrow 284 \downarrow)	288 (116 \uparrow 172 \downarrow)
Cell differentiation	65 (33 \uparrow 32 \downarrow)	24 (6 \uparrow 12 \downarrow)
Cellular physiological process	1 056 (645 \uparrow 411 \downarrow)	406 (188 \uparrow 218 \downarrow)
Coagulation	42 (25 \uparrow 17 \downarrow)	17 (6 \uparrow 11 \downarrow)
Development	316 (202 \uparrow 114 \downarrow)	132 (50 \uparrow 82 \downarrow)
Death	166 (116 \uparrow 50 \downarrow)	80 (45 \uparrow 35 \downarrow)
Extracellular structure organization and biogenesis	3 (1 \uparrow 2 \downarrow)	2 (2 \downarrow)
Homeostasis	30 (13 \uparrow 17 \downarrow)	11 (8 \uparrow 3 \downarrow)
Metabolism	1 497 (867 \uparrow 630 \downarrow)	512 (191 \uparrow 330 \downarrow)
Obsolete biological process	1 (1 \downarrow)	1 (1 \downarrow)
Organismal physiological process	467 (278 \uparrow 189 \downarrow)	198 (110 \uparrow 88 \downarrow)
Pathogenesis	1 (1 \uparrow)	2 (2 \uparrow)
Regulation of cell process	57 (57 \downarrow)	88 (48 \uparrow 40 \downarrow)
Response to stimulus	532 (317 \uparrow 215 \downarrow)	232 (124 \uparrow 108 \downarrow)
Viral life cycle	15 (7 \uparrow 8 \downarrow)	10 (5 \uparrow 5 \downarrow)
Behavior	14 (8 \uparrow 6 \downarrow)	6 (1 \uparrow 5 \downarrow)
Total	3 854 (2 273 \uparrow 1 581 \downarrow)	1 380 (527 \uparrow 853 \downarrow)

Differentially expressed genes involved in inflammation and immune response in SARS patients

In the light of a pivotal role in the pathogenesis of SARS, the genes involved in inflammation, immune response or anti-viral effect are categorized in Tables 5-7.

As shown in Table 5, the pro- and anti-inflammatory cytokine genes were differentially expressed in two patients. Compared to healthy control, the genes encoding IL-1, IL-8, TNF- α , and ICAM-1 increased by 3.73, 8.00, 17.15 and 17.15 folds respectively in the acute severe case. Type I IL-1 receptor, TNFRSF1A, IL-8 receptor, IL-18 receptor 1 also increased by 18.38, 4.00, 73.52/51.98, and 42.22 folds respectively in the acute severe case. However, all of them did not change in the convalescent case. In addition, many anti-inflammatory agents were also remarkably upregulated in the acute severe case. Inhibitors of IL-1 and TNF- α signal pathway such as type II IL-1 receptor, soluble type II IL-1 receptor, IL-1Ra, IRAK3, soluble IL-1 receptor accessory protein, TNFRSF10C, TNF- α -induced proteins 3 and 6 were upregulated by more than 10-folds in the acute severe case, but did not change or were expressed at low level in the convalescent case.

As shown in Table 6, in 21 IFN-related molecules, most of the IFN-related molecules except for IFNGRs and IFNAR1 were not upregulated in the severe case, but they were upregulated more than two-fold in the convalescent case. For the 12 chemokine-related genes detected in this microarray, RANTES (a marker of activated T cells) and CX3CR1 were strikingly downregulated in the acute severe case. Two viral RNA-recognized TLRs (TLR-3 and -7), especially TLR-7, were significantly downregulated in the acute severe case. The above results indicated that there was dysfunction of the innate immune responses in the acute severe case.

The altered genes which could play a vital role in the process of stress, inflammation, and immune response are summarized in Table 7. In comparison to the convalescent case, the JAK/STATs were suppressed in the acute severe case. The expression of STATs 1, 2, and 4 were not upregulated, while MAPKs were upregulated in the acute severe case as compared to the healthy control. Six out of seven components of MAPK signal cascade were upregulated.

DISCUSSION

As an emerging disease, attention has been paid to the high infectivity and virulence of SARS. In the course of the disease, the important observation is lymphopenia and the depletion of T-lymphocyte subsets in most SARS cases, indicating the immunity dysfunction in this readily-transmissible disease, particularly during its early phase^[7]. Another characteristic of the disease is acute lung injury accompanied with signs of the systemic inflammation, the duration and intensity of which are closely associated with the severity and prognosis of the disease^[1,2,4].

A typical feature of all inflammatory disorders is the excessive recruitment of leukocytes to the inflammation site, which is a well-orchestrated process involving several protein families, including pro-inflammatory cytokines, chemotactic cytokines, and adhesion molecules^[9,10]. This

Table 5 Differentially expressed genes encoding pro- and anti-inflammatory cytokines are involved in IL-1 and TNF- α signaling cassettes in two patients

GenBank access	Definition	P1	P2
Pro- and anti-inflammatory cytokines and receptors			
AF043337	IL-8	8.00	-2.46
NM_000634	IL-8 receptor, α	73.52	-
NM_001557	IL-8 receptor, β	51.98	4.29
NM_000575	IL-1, α	3.73	-
NM_000576	IL-1, β	6.50	11.31
NM_000877	IL-1 receptor, type I	18.38	-
NM_004633	IL-1 receptor, type II	362.04	3.84
U64094	Soluble type II IL-1 receptor	630.35	-
NM_003856	IL-1 receptor-like 1	11.31	3.25
U65590	IL-1 receptor antagonist IL-1Ra	14.93	-
AF051151	Toll/IL-1 receptor-like protein 3	14.93	-
NM_000418	IL-4 receptor	13.93	-
NM_000600	IL-6	-	3.03
NM_002184	IL-6 signal transducer gp130	-	-2.14
BC001903	IL-10 receptor, β	4.00	-
NM_004512	IL-11 receptor, α	-6.06	-2.30
NM_001560	IL-13 receptor, $\alpha 1$	3.25	-
U62858	IL-13 receptor	5.66	-
U81380.2	IL-13 receptor soluble form	4.29	-
NM_000585	IL-15	-3.03	2.00
NM_004513	IL-16	-	-2.83
NM_014339	IL-17 receptor	4.29	-
NM_003855	IL-18 receptor 1	42.22	-
NM_003853	IL-18 receptor accessory protein	19.70	-
AF269133	Novel interleukin receptor	-3.03	-
NM_004862	TNF- α	17.15	-
NM_001065	TNFRSF1A	4.00	-
NM_003841	TNFRSF10C	19.70	-
NM_000760	G-CSF 3 receptor	25.99	-
BC002635	GM-CSF 2 receptor, α , low-affinity	3.03	-
M64445	GM-CSF receptor	4.92	2.64
NM_002607	Platelet-derived growth factor α polypeptide	-2.46	-
NM_004347	Caspase 5	4.59	-
NM_000201	Intercellular adhesion molecule 1	17.15	-
NM_002162	Intercellular adhesion molecule 3	6.28	-
NM_003243	Transforming growth factor, β receptor III	-36.76	-4.59
NM_003242	Transforming growth factor, β receptor II	-	-2.30
NM_000358	Transforming growth factor, β -induced, 68 ku	-24.25	-
The genes involved in the IL-1 signaling pathway			
NM_007199	IL-1 receptor-associated kinase M	19.70	-
NM_002182	IL-1 receptor accessory protein	25.99	-
AF167343	Soluble IL-1 receptor accessory protein	55.72	-
M87507	IL-1 β convertase	3.25	-
U13698	IL-1- β converting enzyme isoform γ	3.03	-
U13699	IL-1- β converting enzyme isoform δ	-	2.14
U13700	IL-1- β converting enzyme isoform ϵ	2.64	-
The TNF signal downstream genes			
NM_004619	TNF receptor-associated factor 5	-	-2.00
NM_016614	TRAF and TNF receptor-associated protein	3.84	-2.30
NM_006290	TNF- α induced protein 3	5.66	-
NM_007115	TNF- α induced protein 6	45.25	4.92
AB034747	Small integral membrane protein of lysosome late endosome	7.46	-
U50062	RIP protein kinase	-	-2.00

process is resolved by anti-inflammatory cytokines such as IL-4, IL-10, IL-13, and TGF- β ^[10]. The well-known pro-inflammatory cytokines include IL-1 and TNF- α , which are induced as the signals by pattern recognition

receptors (like TLRs) and initiate activation of a series of signal transduction networks to release mediators, prompting inflammation and immunity^[10,16,17]. In our study, pro-inflammatory cytokines (like IL-1, IL-8, IL-17, IL-18, TNF- α

Table 6 Differentially expressed genes involved in immune regulation in two SARS cases

GenBank access	Definition	P1	P2
IFN and IFN-induced genes			
M29383	IFN- γ	-	2.14
NM_000416	IFN- γ receptor 1	4.59	-
NM_005534	IFN- γ receptor 2	3.84	-
NM_000629	IFN (α , β , and ω) receptor 1	4.29	-
NM_002198	IFN regulatory factor 1	-	3.84
NM_002460	IFN regulatory factor 4	-	-2.30
NM_004030	IFN regulatory factor 7	-	3.25
BC001356	IFN-induced protein 35	-	2.83
M34455	IFN- γ -inducible indoleamine 2,3-dioxygenase	-	5.66
NM_001548	IFN-induced protein with tetratricopeptide repeats 1	-	3.03
NM_001549	IFN-induced protein with tetratricopeptide repeats 4	-	6.06
NM_002053	Guanylate binding protein 1, IFN-inducible	-	3.03
NM_004120.2	Guanylate binding protein 2, IFN-inducible	-	3.73
NM_022873	IFN- α -inducible protein	-	6.50
NM_003641	IFN-induced transmembrane protein 1 (9-27)	-	2.30
NM_004509	IFN-induced protein 41	-	2.14
NM_005532	IFN- α inducible protein 27	-	14.93
NM_005101	IFN-stimulated protein, 15 ku	-	6.50
NM_006417	IFN-induced, hepatitis C-associated microtubular aggregate protein	-2.46	2.64
NM_002759	PKR	-	2.14
NM_002462	Mx1	-	2.14
Chemokines and receptors			
NM_001511	GRO1	55.72	-
NM_002993	Granulocyte chemotactic protein 2	3.73	-
NM_001565	CXCL10	-	14.93
AF030514	CXCL11	-	18.38
AJ224869	CXCR4	6.50	2.83
M21121	RANTES	-13.93	-
NM_001295	CCR1	3.84	-
NM_000648	CCR2	-9.19	-3.25
NM_001837	CCR3	-	6.50
NM_000579	CCR5	-3.25	-4.00
NM_001838	CCR7	-3.73	-2.64
U20350	CX ₃ CR1	-42.22	-
Toll-like receptors			
NM_003264	Toll-like receptor 2	8.00	-
NM_003265	Toll-like receptor 3	-3.25	-2.30
NM_003266	Toll-like receptor 4	3.73	-2.64
NM_016562	Toll-like receptor 7	-17.15	2.30

Table 7 Differentially expressed genes involving MAPK or JAK-STAT signaling pathways in two SARS cases

GenBank access	Definition	P1	P2
U35002	JNK2 β 1 protein kinase	-2.00	-2.14
U31601	JAK-3B	10.56	-
NM_007315	STAT-1	-	2.14
NM_005419	STAT-2	-	3.03
NM_003151	STAT-4	-2.30	-
NM_012448	STAT5B	8.57	-
AB005043	STAT induced STAT inhibitor 1	5.66	3.03
NM_003955	STAT induced STAT inhibitor 3	4.92	-
NM_002745	MAPK 1	4.00	-
NM_002748	MAPK 6	3.73	-
NM_001315	MAPK 14	9.19	-
NM_004759	MAPK-activated protein kinase 2	4.29	-
NM_003668	MAPK-activated protein kinase 5	-2.46	-
NM_001674	Activating transcription factor 3	2.46	5.27
NM_007348	Activating transcription factor 6	3.73	-

and etc.) were highly expressed in the acute severe case and lowly expressed in the convalescent case. Real-time quantitative PCR of empirically selected genes also showed that pro-inflammatory cytokines were highly expressed. These findings, as expected, are consistent with the clinical stage^[2,6,8], though individual variation and sensitivity of examination exist. In addition, anti-inflammatory agents (IL-4, 10, and 13 receptors) and agonists of IL-1 and TNF (type II IL-1 receptor, soluble IL-1 receptor, IL-1Ra, and TNF- α decoy receptor) increased dramatically in the acute severe case, which could constitute a negative feedback to robust inflammation or manifestations of systemic inflammation^[16,17]. But whether the alteration is associated with virus replication or interaction between the viral and cellular proteins is to be further elucidated.

Chemokines are also important cytokines involved in inflammation, dendritic cell maturation, neutrophil degranulation,

antibody class switching and T-cell activation^[18-20]. Furthermore, recent *in vitro* and *in vivo* findings support some members of chemokine system like CXCL9, CXCL10, and CXCL11 contribute to the resolution of viral infections^[19,20]. Unfortunately, transcripts of IFN-induced chemokines^[18,19] (RANTES, CXCL10, and CXCL11) were downregulated in the acute severe case, while inflammatory chemokines such as GRO-1, G-CSF3R, IL-8 and its receptors increased significantly. The expression profiles of chemokines as well as neutrophil predominance in white cells reflect rampant inflammation in the acute severe case^[8,9].

Although the acute severe case is treated with IFN- α , poor expression of IFN-stimulated genes^[21], TLR3, 7 and immune cell activation markers (CD antigens and MHC molecules, data not shown) may mirror the defect of host anti-viral immunity. Furthermore, some studies indicate that the activation of some pro-inflammatory cytokines such as IL-1, IL-6 or IL-8 signaling pathways interferes with the IFN signaling^[22-25], let alone the action of IL-4, IL-10 or IL-13^[9]. Outbreak of pro- and anti-inflammatory agents might interfere with the IFN signaling pathway, but direct interaction between coronavirus and IFN system cannot be excluded.

It is intriguing to find that, although the important genes involved in NF- κ B signaling pathway were not detected in our microarrays, JAK/STAT signaling pathway was suppressed, another important signaling pathway associated with production of inflammatory cytokines, the MAPK signaling pathway^[20,26,27], was upregulated in the acute severe case compared to the healthy control or convalescent case. It was reported that there are expression alterations in the MAPK pathway in different leukocytes from patients with SARS and virus infection and viral proteins exert effects on the MAPK signaling pathway in cell culture models^[27-29]. But the relationship between changes of three signaling pathways and the SARS process needs to be further studied.

In conclusion, our results may partially reveal the different expression patterns of inflammatory and immune genes and related signal pathways at different phases of SARS pathological process. The overexpressed pro- and anti-inflammatory cytokines may contribute to acute lung injury and imbalance of homeostasis especially in acute severe phase. Thus our results may hopefully make a contribution to further studies of the SARS pathogenesis.

REFERENCES

- Nie QH, Luo XD, Zhang JZ, Su Q. Current status of severe acute respiratory syndrome in China. *World J Gastroenterol* 2003; **9**: 1635-1645
- Peiris JS, Yuen KY, Osterhaus AD, Stohr K. The severe acute respiratory syndrome. *N Engl J Med* 2003; **349**: 2431-2441
- Rota PA, Oberste MS, Monroe SS, Nix WA, Campagnoli R, Icenogle JP, Penaranda S, Bankamp B, Maher K, Chen MH, Tong S, Tamin A, Lowe L, Frace M, DeRisi JL, Chen Q, Wang D, Erdman DD, Peret TC, Burns C, Ksiazek TG, Rollin PE, Sanchez A, Liffick S, Holloway B, Limor J, McCaustland K, Olsen-Rasmussen M, Fouchier R, Gunther S, Osterhaus AD, Drosten C, Pallansch MA, Anderson LJ, Bellini WJ. Characterization of a novel coronavirus associated with severe acute respiratory syndrome. *Science* 2003; **300**: 1394-1399
- Stadler K, Masignani V, Eickmann M, Becker S, Abrignani S, Klenk HD, Rappuoli R. SARS-beginning to understand a new virus. *Nat Rev Microbiol* 2003; **1**: 209-218
- Marra MA, Jones SJ, Astell CR, Holt RA, Brooks-Wilson A, Butterfield YS, Khattri J, Asano JK, Barber SA, Chan SY, Cloutier A, Coughlin SM, Freeman D, Girn N, Griffith OL, Leach SR, Mayo M, McDonald H, Montgomery SB, Pandoh PK, Petrescu AS, Robertson AG, Schein JE, Siddiqui A, Smailus DE, Stott JM, Yang GS, Plummer F, Andonov A, Artsob H, Bastien N, Bernard K, Booth TF, Bowness D, Czub M, Drebot M, Fernando L, Flick R, Garbutt M, Gray M, Grolla A, Jones S, Feldmann H, Meyers A, Kabani A, Li Y, Normand S, Stroher U, Tipples GA, Tyler S, Vogrig R, Ward D, Watson B, Brunham RC, Kraiden M, Petric M, Skowronski DM, Upton C, Roper RL. The genome sequence of the SARS-associated coronavirus. *Science* 2003; **300**: 1399-1404
- Bhatia M, Mochhala S. Role of inflammatory mediators in the pathophysiology of acute respiratory distress syndrome. *J Pathol* 2004; **202**: 145-156
- Wong RS, Wu A, To KF, Lee N, Lam CW, Wong CK, Chan PK, Ng MH, Yu LM, Hui DS, Tam JS, Cheng G, Sung JJ. Haematological manifestations in patients with severe acute respiratory syndrome: retrospective analysis. *BMJ* 2003; **326**: 1358-1362
- Hotchkiss RS, Karl IE. The pathophysiology and treatment of sepsis. *N Engl J Med* 2003; **348**: 138-150
- Nathan C. Points of control in inflammation. *Nature* 2002; **420**: 846-852
- Hanada T, Yoshimura A. Regulation of cytokine signaling and inflammation. *Cytokine Growth Factor Rev* 2002; **13**: 413-421
- Xu L, Yoon H, Zhao MQ, Liu J, Ramana CV, Enelow RI. Cutting edge: pulmonary immunopathology mediated by antigen-specific expression of TNF-alpha by anti-viral CD8⁺ T cells. *J Immunol* 2004; **173**: 721-725
- Jones BM, Ma ES, Peiris JS, Wong PC, Ho JC, Lam B, Lai KN, Tsang KW. Prolonged disturbances of *in vitro* cytokine production in patients with severe acute respiratory syndrome (SARS) treated with ribavirin and steroids. *Clin Exp Immunol* 2004; **135**: 467-473
- Wong CK, Lam CW, Wu AK, Ip WK, Lee NL, Chan IH, Lit LC, Hui DS, Chan MH, Chung SS, Sung JJ. Plasma inflammatory cytokines and chemokines in severe acute respiratory syndrome. *Clin Exp Immunol* 2004; **136**: 95-103
- Zhang Y, Li J, Zhan Y, Wu L, Yu X, Zhang W, Ye L, Xu S, Sun R, Wang Y, Lou J. Analysis of serum cytokines in patients with severe acute respiratory syndrome. *Infect Immun* 2004; **72**: 4410-4415
- Bryant PA, Venter D, Robins-Browne R, Curtis N. Chips with everything: DNA microarrays in infectious diseases. *Lancet Infect Dis* 2004; **4**: 100-111
- Auron PE. The interleukin 1 receptor: ligand interactions and signal transduction. *Cytokine Growth Factor Rev* 1998; **9**: 221-237
- Chung JY, Park YC, Ye H, Wu H. All TRAFs are not created equal: common and distinct molecular mechanisms of TRAF-mediated signaling transduction. *J Cell Sci* 2002; **115**(Pt 4): 679-688
- Luster AD. The role of chemokines in linking innate and adaptive immunity. *Curr Opin Immunol* 2002; **14**: 129-135
- Mahalingam S, Friedland JS, Heise MT, Rulli NE, Meanger J, Lidbury BA. Chemokines and viruses: friends or foes? *Trends Microbiol* 2003; **11**: 383-391
- Sen GC. Virus and infections. *Ann Rev Microbiol* 2001; **55**: 255-281
- de Veer MJ, Holko M, Frevel M, Walker E, Der S, Paranjape JM, Silverman RH, Williams BR. Functional classification of interferon-stimulated genes identified using microarrays. *J Leukoc Biol* 2001; **69**: 912-920
- Khabar KS, Al-Zoghaibi F, Al-Ahdal MN, Murayama T, Dhalla M, Mukaida N, Taha M, Al-Sedairy ST, Siddiqui Y, Kessie G, Matsushima K. The alpha chemokine, interleukin 8, inhibits the anti-viral action of interferon alpha. *J Exp Med*

- 1997; **186**: 1077-1085
- 23 **Nagabhushanam V**, Solache A, Ting LM, Escaron CJ, Zhang JY, Ernst JD. Innate inhibition of adaptive immunity: Mycobacterium tuberculosis-induced IL-6 inhibits macrophage responses to IFN-gamma. *J Immunol* 2003; **171**: 4750-4757
- 24 **Polyak SJ**, Khabar KS, Paschal DM, Ezelle HJ, Duverlie G, Barber GN, Levy DE, Mukaida N, Gretch DR. Hepatitis C virus nonstructural 5A protein induces interleukin-8, leading to partial inhibition of the interferon-induced anti-viral response. *J Virol* 2001; **75**: 6095-6106
- 25 **Tian Z**, Shen X, Feng H, Gao B. IL-1 beta Attenuates IFN-alpha beta -induced anti-viral activity and STAT1 activation in the liver: involvement of proteasome-dependent pathway. *J Immunol* 2000; **165**: 3959-3965
- 26 **Dong C**, Davis RJ, Flavell RA. MAP kinases in the immune response. *Annu Rev Immunol* 2002; **20**: 55-72
- 27 **Lee CH**, Chen RF, Liu JW, Yeh WT, Chang JC, Liu PM, Eng HL, Lin MC, Yang KD. Altered p38 mitogen-activated protein kinase expression in different leukocytes with increment of immunosuppressive mediators in patients with severe acute respiratory syndrome. *J Immunol* 2004; **172**: 7841-7847
- 28 **Mizutani T**, Fukushi S, Saijo M, Kurane I, Morikawa S. Importance of Akt signaling pathway for apoptosis in SARS-CoV-infected Vero E6 cells. *Virology* 2004; **327**: 169-174
- 29 **Mizutani T**, Fukushi S, Saijo M, Kurane I, Morikawa S. Phosphorylation of p38 MAPK and its downstream targets in SARS coronavirus-infected cells. *Biochem Biophys Res Commun* 2004; **319**: 1228-1234

Science Editor Wang XL and Guo SY Language Editor Elsevier HK

Inositol hexaphosphate-induced enhancement of natural killer cell activity correlates with suppression of colon carcinogenesis in rats

Zheng Zhang, Yang Song, Xiu-Li Wang

Zheng Zhang, Xiu-Li Wang, Department of Biochemistry and Molecular Biology, Qingdao University Medical College, Qingdao 266021, Shandong Province, China

Yang Song, Nutrition and Food Sanitation Institution, Qingdao University Medical College, Qingdao 266021, Shandong Province, China

Supported by the Health Bureau Foundation of Province Shandong, No. 1999CA2CBA2

Correspondence to: Yang Song, Nutrition and Food Sanitation Institution, Qingdao University Medical College, Qingdao 266021, Shandong Province, China. qdsongyang@126.com

Telephone: +86-532-2991029

Received: 2004-11-23 Accepted: 2005-01-26

suppression of colon carcinogenesis in rats. *World J Gastroenterol* 2005; 11(32): 5044-5046

<http://www.wjgnet.com/1007-9327/11/5044.asp>

INTRODUCTION

Inositol hexaphosphate (InsP₆) is a naturally occurring compound that has various chemical properties and biological activities^[1]. It is rich in matured plant seeds, particularly in cereals and legumes, and exists in nature as a salt with monovalent and divalent cations (Ca²⁺, Mg²⁺, and K⁺). It has the ability to chelate minerals such as iron, copper, zinc, cobalt, and manganese, most efficiently at neutral pH^[2-4].

InsP₆ has anti-neoplastic activity on a variety of experimental models of carcinogenesis, decreases serum cholesterol level, inhibits renal stone formation, and may find use in controlling myocardial damage following ischemia. Among these biological activities, anti-neoplastic activity is one of the most intriguing properties of InsP₆^[5,6].

The above facts need clinical trials in human colorectal cancer. It has been reported that intestinal lipodystrophy can be prevented by InsP₆ treatment^[7]. Recent studies demonstrate that InsP₆ inhibits experimental colon carcinogenesis in rats^[8-10]. There is a correlation between neoplastic diseases and depressed natural killer (NK) activity^[11]. There is evidence that NK cells are involved in the destruction and growth inhibition of tumor cells *in vivo*. This study aimed to study the effect of InsP₆ on blood NK cell activity in dimethylhydrazine (DMH)-induced colon tumor in rats.

MATERIALS AND METHODS

Animals and chemicals

Thirty-four-weeks old male Wistar rats (70-110 g) were purchased from Animal Center of Henan Medical University. After acclimatization for 1 wk, the experimental animals were randomly divided into control group and InsP₆ group (15 rats/group). Animals in the control group were fed with the basal diet and had regular access to drinking water. Rats in InsP₆ group were fed with the basal diet and had access to 2% sodium inositol hexaphosphate (purchased from Guangdong Qingyun Chemical Factory) solution. Basal diet was made by American Institute of Nutrition method.

Animals in both groups were given subcutaneous injections of DMH (from Sigma) dissolved in normal saline solution (20 mg/kg body wt) once a week for 20 wk. Body weight was measured and food consumption was recorded once a week. All surviving animals were killed under 4.3% trichloroaldehyde hydrate anesthesia after 21 wk.

Abstract

AIM: To investigate the anti-neoplastic effect of inositol hexaphosphate (InsP₆ or phytic acid) on dimethylhydrazine (DMH)-induced colon tumor in rats and its effect on blood natural killer (NK) cell activity.

METHODS: Healthy Wistar rats, 4 wk old, were divided into control group (fed with common food) and InsP₆ group (fed with common food+2% sodium inositol hexaphosphate in the drinking water), 15 rats in each group. Both groups were injected with 1,2-dimethylhydrazine subcutaneously (20 mg/kg body weight) once a week for 20 wk. Rats were killed after 21 wk. The whole large intestine was isolated to determine the general condition of tumors and to test blood NK cell activity by lactate-dehydrogenase-release assay.

RESULTS: Administration of InsP₆ significantly increased blood NK cell activity in DMH-induced colorectal tumor in rats. InsP₆ group had a smaller tumor size on average and a smaller number of tumors than the control group. Its mortality was also higher than that in control. However, the variables of body weight and tumor incidence were not significantly different between the two groups.

CONCLUSION: InsP₆ can increase blood NK cell activity in DMH-induced colon tumor in rats and inhibit tumor growth and metastasis in rats.

© 2005 The WJG Press and Elsevier Inc. All rights reserved.

Key words: Inositol hexaphosphate; Phytic acid; Natural killer cell activity; Colon cancer

Zhang Z, Song Y, Wang XL. Inositol hexaphosphate-induced enhancement of natural killer cell activity correlates with

Tissue processing

All animals (including rats that died before the end of experiment) were autopsied. The colons were removed, flushed with saline, opened along the longitudinal median axis. Macroscopically, the number of tumors in each colon was counted. Tumor width and length were measured with clippers. Simultaneously, peripheral blood was obtained from the abdominal aorta for testing NK cell activity.

Test of NK cell activity

Peripheral blood mononuclear cells (PBMCs) were separated by Ficoll-Hypaque density centrifugation from the collected blood. Lactate-dehydrogenase (LDH)-release assay was used to measure the NK cell activity. PBMCs were washed and suspended in complete RPMI-1640 medium, counted and diluted to 1.0×10^6 /mL. The amount of LDH released from the lysed target cells was determined for NK cell activity measurement. The NK-sensitive cell line K₅₆₂ (human erythroleukemia cell line, Shandong Medical Science Institute, Shandong, China) was used as the target cell. K₅₆₂ cells were washed with complete RPMI-1640 medium, counted and finally diluted to 1.0×10^5 /mL with the medium. An equal volume of K₅₆₂ cells and PBMCs was added to the wells of 96-round-bottomed microwell plates (the cell ratio of effector-to-target was 10:1). Each test was repeated in three wells. To ensure contact between cells, the plate was centrifuged at a low speed for 2 min. After 2-h incubation at 37 °C in a humidified atmosphere with 50 mL/L CO₂, the plate was centrifuged at 1 000 r/min for 5 min. The supernatant from each well (100 µL) was transferred into the corresponding wells of a 96-flat-bottomed microwell plate. Then 100 µL of lactic acid hydrogenase substrate mixture was added to each well. After 3 min, reactions were stopped by adding 50 µL of cold medium. Finally, a microtiter plate reader (Bio-Rad, MODE-550) was used for evaluation of changes in the absorbance at a wavelength of 490 nm. The release of LDH from K₅₆₂ cells was expressed as absorbance. The percentage of NK cell activity was calculated by the formula: NK cell activity = $(E-S)/(M-S) \times 100\%$, where *E* represents the experimental release of LDH activity from target cells incubated in the presence of PBMCs, *M* represents the maximum release of the LDH activity determined by lysing the target cells with 1% of NP40, and *S* is the spontaneous release of the LDH activity from target cells incubated in the absence of PBMCs.

Statistical analysis

Results were expressed as mean ± SD. Statistical analyses were performed with SPSS 9.0. The significance of differences in the average values between the two groups was analyzed using *t*-test. $P < 0.05$ was considered statistically significant.

RESULTS

During the initial period of the experiment, body weight of animals increased steadily in the first 20 wk. Then both groups began to lose their body weight. In addition, the animals consumed a less amount of food. The change in two groups had no difference (Figure 1).

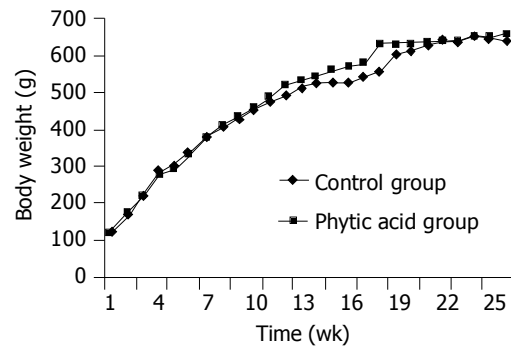


Figure 1 Body weight change of rats during feeding.

After DMH was injected for 10 wk, death occurred in rats of control group. By the end of the experiment, six rats died in the control group. Only one rat died in InsP₆ group. The difference in mortality was significant ($P < 0.01$, Table 1).

Table 1 Effect of InsP₆ on mortality of rats

Groups	Survival	Death	Mortality (%)
Control	9	6	40.0
InsP ₆	14	1	7.1 ^b

^b $P < 0.01$ vs control group.

Twelve rats had colon tumor in control group treated with DMH but not InsP₆. Tumors were found in 11 rats of InsP₆ group. The difference in tumor incidence was not significant ($P > 0.05$). But the number of tumors and their size were significantly less in InsP₆ group than in control group ($P < 0.05$, Table 2).

Table 2 Effect of InsP₆ on total large intestinal carcinomas (mean ± SD)

Groups	<i>n</i>	Incidence of tumor (%)	Average tumor number	Average sign of tumor (mm ³)
Control	15	80	4.1 ± 1.2	1 080.3 ± 463.4
InsP ₆	15	73	0.9 ± 0.2 ^b	123.6 ± 29.6 ^a

^a $P < 0.05$, ^b $P < 0.01$ vs control group.

Blood NK cell activity was reduced in the two groups after DMH treatment. But the blood NK cell activity was significantly higher in InsP₆ group than in control group ($P < 0.01$, Table 3).

Table 3 Effect of InsP₆ on blood NK cell activity (NK-A) (mean ± SD)

Group	<i>n</i>	NK-A (%)
Control	9	15.7 ± 1.2
InsP ₆	14	42.2 ± 1.1 ^b

^b $P < 0.01$ vs control group.

DISCUSSION

Diet composition is an important etiologic factor in colon

carcinogenesis and has a significant impact on colon cancer occurrence. InsP₆ is a dietary phytochemical present in cereals, soy, legumes, and fiber-rich foods^[12,13]. Epidemiological studies have shown that InsP₆ can inhibit the metastasis of tumor^[14-16]. But the anti-tumor mechanism of InsP₆ awaits further investigation.

Our study demonstrated that InsP₆ could significantly increase blood NK cell activity in DMH-induced colorectal cancer in rats ($P < 0.01$). The number and size of tumors were smaller in InsP₆ group than in control group ($P < 0.05$), indicating that InsP₆ can also inhibit tumor growth and metastasis in DMH-induced colorectal cancer in rats.

InsP₆ is degraded into lower polyphosphorylated forms of inositol (including InsP₁-InsP₅) by the enzyme meso-inositol hexaphosphate phosphohydrolase, and dephosphorylated by acid, acid phosphatase and intestinal alkaline phosphatase. When InsP₆ was administered to rats as a soluble form in drinking water, it is rapidly absorbed through the upper gastrointestinal tract and quickly distributed in various organs, most notably in liver, kidneys, and skeletal muscle^[17,18]. Among the lower polyphosphorylated forms of inositol, InsP₃ appears to act as a second messenger and promotes intracellular free calcium (Ca²⁺) release, which can induce proliferation of NK cells^[19] as well as the release of NK cell cytotoxicity factor (NKCF). NKCF can bind to target cells (tumor cells) which are subsequently lysed^[20]. Close contact between the plasma membrane of the two types of cells, affects the cytotoxic reaction. InsP₃ can also affect the membrane phosphatidyl inositol proteins, which may be important in attachment and subsequent fusion with the target cells, suggesting that InsP₆ mediates its chemopreventive and probably chemotherapeutic effect via InsP₃^[21,22].

Our data indicate that DMH depresses the NK cell activity, while InsP₆ significantly increases the NK cell activity and inhibits tumor growth, suggesting that changes in NK cell activity are related to progressive cancer growth^[23]. Since InsP₆ enhances the NK cell activity *in vivo*, it may have potential application in therapy of cancer and other diseases associated with depressed NK cytotoxicity.

REFERENCES

- 1 Singh RP, Sharma G, Mallikarjuna GU, Dhanalakshmi S, Agarwal C, Agarwal R. *In vivo* suppression of hormone-refractory prostate cancer growth by inositol hexaphosphate induction of insulin-like growth factor binding protein-3 and inhibition of vascular endothelial growth factor. *Clinical Cancer Res* 2004; **10** (1 Pt 1): 244-250
- 2 Singh A, Singh SP. Postnatal effect of smokeless tobacco on phytic acid or the butylated hydroxyanisole-modulated hepatic detoxication system and antioxidant defense mechanism in suckling neonates and lactating mice. *Cancer Lett* 1998; **122**: 151-156
- 3 Nickel KP, Belury MA. Inositol hexaphosphate reduces 12-O-tetradecanoylphorbol-13-acetate-induced ornithine decarboxylase independent of protein kinase C isoform expression in keratinocytes. *Cancer Lett* 1999; **140**: 105-111
- 4 Jenab M, Thompson LU. Phytic acid in wheat bran affects colon morphology, cell differentiation and apoptosis. *Carcinogenesis* 2000; **21**: 1547-1552
- 5 Singh RP, Agarwal C, Agarwal R. Inositol hexaphosphate inhibits growth, and induces G1 arrest and apoptotic death of prostate carcinoma DU145 cells: modulation of CDKI-CDK-cyclin and pRb-related protein-E2F complexes. *Carcinogenesis* 2003; **24**: 555-563
- 6 Midorikawa K, Murata M, Oikawa S, Hiraku Y, Kawanishi S. Protective effect of phytic acid on oxidative DNA damage with reference to cancer chemoprevention. *Biochem Biophys Res Comm* 2001; **288**: 552-557
- 7 Reddy BS. Role of dietary fiber in colon cancer: An overview. *Am J Med* 1999; **106**: 16S-19S
- 8 Singh A, Singh SP, Bamezai R. Modulatory influence of arecoline on the phytic acid-altered hepatic biotransformation system enzymes, sulfhydryl content and lipid peroxidation in a murine system. *Cancer Lett* 1997; **117**: 1-6
- 9 Alabaster O, Tang Z, Shivapurkar N. Dietary fiber and the chemopreventive modelation of colon carcinogenesis. *Mutation Res* 1996; **350**: 185-197
- 10 Takaba K, Hirose M, Yoshida Y, Kimura J, Ito N, Shirai T. Effects of *n*-tritiacontane-16, 18-dione, curcumin, chlorophyllin, dihydroguaiaretic acid, tannic acid and phytic acid on the initiation stage in a rat multi-organ carcinogenesis model. *Cancer Lett* 1997; **113**: 39-46
- 11 Shivapurkar N, Tang ZC, Frost A, Alabaster O. A rapid dual organ rat carcinogenesis bioassay for evaluating the chemoprevention of breast and colon cancer. *Cancer Lett* 1996; **100**: 169-179
- 12 Reddy BS, Hirose Y, Cohen LA, Simi B, Cooma I, Rao CV. Preventive potential of wheat bran fractions against experimental colon carcinogenesis: implications for human colon cancer prevention. *Cancer Res* 2000; **60**: 4792-4797
- 13 Ma Q, Hoper M, Halliday I, Rowlands BJ. Diet and experimental colorectal cancer. *Nutrition Res* 1996; **16**: 413-426
- 14 Weber G, Singhal RL, Prajda N, Yeh YA, Look KY, Sledge GW. Regulation of signal transduction. *Advan Enzyme Regul* 1995; **35**: 1-21
- 15 Baten A, Ullah A, Tomazic VJ, Shamsuddin AM. Inositol-phosphate induced enhancement of natural killer cell activity correlates with tumor suppression. *Carcinogenesis* 1989; **10**: 1595-1598
- 16 Shamsuddin AM, Ullah A, Chakravarthy AK. Inositol and inositol hexaphosphate suppress cell proliferation and tumor formation in CD-1 mice. *Carcinogenesis* 1989; **10**: 1461-1463
- 17 Sakamoto K, Venkatraman G, Shamsuddin AM. Growth inhibition and differentiation of HT-29 cells in vitro by inositol hexaphosphate(phytic acid). *Carcinogenesis* 1993; **14**: 1815-1819
- 18 Owen RW, Spiegelhalter B, Bartsch H. Generation of reactive oxygen species by the faecal matrix. *Gut* 2000; **46**: 225-232
- 19 Challa A, Rao DR, Reddy BS. Interactive suppression of aberrant crypt foci induced by azoxymethane in rat colon by phytic acid and green tea. *Carcinogenesis* 1997; **18**: 2023-2026
- 20 Thompson LU, Zhang L. Phytic acid and minerals: effect on early markers of risk for mammary and colon carcinogenesis. *Carcinogenesis* 1991; **12**: 2041-2045
- 21 Zi X, Singh RP, Agarwal R. Impairment of erbB1 receptor and fluid-phase endocytosis and associated mitogenic signaling by inositol hexaphosphate in human prostate carcinoma DU145 cells. *Carcinogenesis* 2000; **21**: 2225-2235
- 22 Vucenik I, Shamsuddin AM. Cancer Inhibition by Inositol Hexaphosphate (IP₆) and Inositol: From Laboratory to Clinic. *J Nutr* 2003; **133**: 3778S-3784S
- 23 Bode AM, Dong Z. Targeting signal transduction pathways by chemopreventive agents. *Mutation Res* 2004; **555**: 33-51

Level of proinsulin in association with cardiovascular risk factors and sleep snoring

En-Zhi Jia, Zhi-Jian Yang, Shi-Wei Chen, Guang-Yao Qi, Chun-Fa You, Jian-Feng Ma, Jing-Xin Zhang, Zhen-Zhen Wang, Wei-Chong Qian, Hai-Yan Wang, Wen-Zhu Ma

En-Zhi Jia, Zhi-Jian Yang, Zhen-Zhen Wang, Wei-Chong Qian, Hai-Yan Wang, Wen-Zhu Ma, Department of Cardiovascular Medicine, The First Affiliated Hospital of Nanjing Medical University, Nanjing 210029, Jiangsu Province, China
Shi-Wei Chen, Guang-Yao Qi, Chun-Fa You, The Disease Control Center of Pizhou City, Pizhou 221300, Jiangsu Province, China
Jian-Feng Ma, Department of Central Clinical Laboratory, The First Affiliated Hospital of Nanjing Medical University, Nanjing 210029, Jiangsu Province, China
Jing-Xin Zhang, Department of Nuclear Medicine, The First Affiliated Hospital of Nanjing Medical University, Nanjing 210029, Jiangsu Province, China
Supported by the National Natural Science Foundation of China, No. 30400173

Correspondence to: Dr. En-Zhi Jia, Department of Cardiovascular Medicine, The First Affiliated Hospital of Nanjing Medical University, Guangzhou Road 300, Nanjing 210029, Jiangsu Province, China. enzhijia@yahoo.com.cn

Received: 2004-11-08 Accepted: 2004-12-21

Abstract

AIM: To explore the relationship between the level of proinsulin with cardiovascular risk factors and sleep snoring.

METHODS: Based on the random stratified sampling principle, 1 193 Chinese residents in Pizhou City, Jiangsu Province (530 males and 663 females, aged 35-59 years with an average age of 46.69 years) were recruited. Their sleep snoring habits were investigated. Biotin-avidin based double mAbs ELISA was used to detect specific insulin and proinsulin, and a risk factor score was established to evaluate the individuals according to the number of their risk factors.

RESULTS: The results of Spearman correlation analysis and covariate ANOVA analysis after age and sex were controlled, indicated that not only the level of proinsulin ($r = 0.156$, $P = 0.000$, $F = 5.980$ $P = 0.000$), but also cardiovascular risk factors score ($r = 0.194$, $P = 0.000$, $F = 11.135$, $P = 0.000$) significantly associated with the frequency of sleep snoring, and the significant relationship between true insulin and frequency of sleep snoring was only shown in the covariate ANOVA analysis ($F = 2.868$, $P = 0.022$). The result of multivariate stepwise logistic regression after age, sex, body mass index, waist circumference and true insulin were controlled showed that proinsulin (division by interval of quartile) was an independent risk factor for sleep snoring (OR = 1.220, 95%CI: 1.085-1.373, $P = 0.001$).

CONCLUSION: The interaction of cardiovascular risk factors clustering, high proinsulin level and sleep breathing disorder may be a syndrome, which has not been recognized in human beings so far.

© 2005 The WJG Press and Elsevier Inc. All rights reserved.

Key words: True insulin; Proinsulin; Snoring; Epidemiology

Jia EZ, Yang ZJ, Chen SW, Qi GY, You CF, Ma JF, Zhang JX, Wang ZZ, Qian WC, Wang HY, Ma WZ. Level of proinsulin in association with cardiovascular risk factors and sleep snoring. *World J Gastroenterol* 2005; 11(32): 5047-5052

<http://www.wjgnet.com/1007-9327/11/5047.asp>

INTRODUCTION

Dyslipidemia, hypertension, hyperinsulinemia and obesity (special central obesity) have been recognized as potent risk factors for coronary heart disease in adults, the clustering of the above cardiovascular risk factors often occurs in adults, and the condition has been termed as syndrome X^[1], and insulin resistance emerges as a common pathogenetic denominator underlying the above risk factor clustering^[2]. Obstructive sleep apnea syndrome is associated with the increased cardiovascular and cerebrovascular morbidity. It is also recognized that many people with obstructive sleep apnea syndrome have features of the insulin resistance syndrome, and it is suggested that insulin resistance syndrome may actually include sleep apnea syndrome and could be better considered as syndrome Z^[3]. The level of circulating proinsulin (PI) has been recognized as a sensitive marker for the dysfunction of islet beta cells^[4], and several groups reported that proinsulin was more strongly associated with cardiovascular disease than true insulin^[5]. So far, few epidemiological studies have been focused on the relationship between true insulin vs proinsulin and cardiovascular risk factors clustering, and sleep breathing disorder. Although polysomnography is the definitive method for diagnosing sleep apnea syndrome, the costs of this method in combination with the high demand for accurate screening limits its utility in clinical practice and epidemiological studies. It has been proposed that snoring is a precursor to the development of obstructive sleep apnea syndrome. This theory is supported by retrospective studies in which patients reported snoring more loudly over the years, before they developed nocturnal respiratory pauses, which later became increasingly frequent^[6]. To explore the relationship between PI vs true insulin and

cardiovascular risk factors and sleep snoring, a population-based epidemiological investigation was conducted in Pizhou city, located in the mideastern part of China.

MATERIALS AND METHODS

Study subjects

From April 2001 to May 2001, a large cross-sectional, community-based epidemiological study was conducted. The subjects for the survey were adults aged between 35 and 59 years. A two-stage cluster-sampling scheme based on existing census divisions was used to randomly select four areas, each with a population from 300 to 350 subjects, and sample was stratified by sex and age group (5 years) to ensure representation of each part of the population. Among the 1 351 individuals investigated, the response rate was 88.5%, and the random sample and random-sample responder populations closely reflected the actual distribution of age group and sex in Pizhou area. Among 1 193 rural residents, there were 530 males (44.57%) and 663 females (55.43%), and their average age was 46.69 years. Signed informed consent was obtained from all participants and the study was approved by the Nanjing Medical University Ethics Review Committee.

Questionnaires and investigators

A standard questionnaire was adopted, and the investigators were students from Nanjing Medical University, who had received special training. The questionnaire included questions about occupation, height, weight, sleep habits, sleep quality, and frequency of disruptive snoring. The question concerning snoring was "How often do you snore loudly and disturbingly?" with the following response alternatives: 1 = never, 2 = seldom, 3 = sometimes, 4 = often, 5 = very often, and those who answered 2-5 were regarded as snorers.

Anthropometric measurements

Anthropometric measurements were performed after the participants had removed their shoes and upper garments and donned an examining gown. Each measurement was performed twice and the average was used in the analysis. Height was measured to the nearest 0.1 cm using a wall-mounted stadiometer. Weight was measured to the nearest 0.1 kg using a hospital balance beam scale. Body mass index (BMI) was calculated as weight (kg) divided by the square of height (m²). The waist circumference was measured to the nearest 0.5 cm at the point of narrowing between the umbilicus and xiphoid process (as viewed from behind) and the waist circumference was used as a judgment of upper-body adiposity. Blood pressure was measured in the right arm with the participant seated and the arm bared. Three readings were recorded for each individual, and the average of the three readings was defined as the subject's blood pressure.

Laboratory measurement

The 12-h fasting blood samples were drawn in the morning and the sera were stored at -70 °C immediately after centrifugation until being assayed. All laboratory measurements were conducted at the Central Clinical Laboratory in the

First Affiliated Hospital of Nanjing Medical University. Fasting blood glucose (FBG), fasting total cholesterol (TCH), fasting triglyceride (TG) and fasting high-density lipoprotein cholesterol (HDL-c) were determined by enzymatic procedures on an automated autoanalyzer (AU 2700 Olympus, 1st Chemical Ltd., Japan), and the source of reagents for the autoanalyzer was from 1st Chemical Ltd., Japan. The laboratory was monitored for precision and accuracy of glucose and lipid measurements by the agency's surveillance program. Measurements of agency-assigned quality control samples showed no consistent bias over time within or between surveys. Low-density lipoprotein cholesterol (LDL-c) was assessed by the Friedwald method^[7], and the concentration of LDL-c was calculated for each subject according to the following formula: $C_{LDL-c} = C_{PLASMA} - C_{HDL-c} - TG/5$.

Measurement of intact insulin and proinsulin

The intact insulin level was measured using a highly sensitive two-site sandwich ELISA^[8]. This assay method for insulin is based on the enzyme immunoassay principle and it is constructed as a sandwich immunoassay. Two monoclonal murine antibodies specific for insulin were employed. One of the antibodies (HUI-018), which binds to an epitope on one side of the insulin-molecule, was used for coating on the ELISA plate wells. The other antibody (OXI-005), which binds to another epitope on the other side of the insulin-molecule, was covalently bound to biotin. The biotin-antibody reagent and sample or calibrator were added to the precoated-wells followed by incubation. During incubation, a complex between plastic-surface, coated-antibody, insulin and the biotinylated-antibody was formed. This complex would not be removed by the washing procedure, which followed the incubation. After the wash, avidin-peroxidase was added. It bound to the biotin of the biotinylated-antibody and extended the complex with the enzyme peroxidase. The amount of enzyme was visualized by addition of the substrate peroxide and 3',3',5',5'-tetramethylbenzidine (TMB), which was converted to a soluble colored product. The developed color was proportional to the amount of insulin in the sample. The color-development progressed with time and it was interrupted after a fixed time by the addition of phosphoric acid. The color was stable and absorbance was measured in an ELISA-plate photometer. A calibrator curve was constructed based on the absorbance values and the insulin concentration in the serum samples could be found. The detection limit was 5.0 pmol/L. The specificity of the assay excluded intact, split (32-33) and des (31, 32) PI. There was some cross-reactivity with the less abundant split (65-66) PI (30%) and des (64, 65) PI (63%).

The PI level was measured in a similar manner using another sensitive two-site sandwich ELISA^[9]. The analysis for human PI is an enzyme immunoassay constructed as a sandwich immunoassay. Two monoclonal mouse antibodies were used: one with specificity for human C-peptide (PEP-001) was used for coating, the other antibody (HUI-001) with specificity for insulin was biotin labeled and acted as detecting antibody. The plasma samples were diluted 1:2 during analysis to eliminate the plasma effect. In the first reaction, after the samples were applied to the coated wells, PI in the samples would bind to the coating antibody. In the

second reaction, the bound PI was detected by the use of another mAb directed against human insulin and biotin labeled. In a third reaction, the amount of bound detecting antibody in the coating antibody-PI-detection antibody complex was visualized by the use of streptavidin-peroxidase that bound to the biotin label. Between each step, the plate was washed four times in a washing buffer in order to measure only the bound material. Finally, a substrate for the peroxidase (tetramethylbenzidine and H₂O₂) was applied to the wells resulting in color development proportional to the amount of peroxidase, i.e., PI present. The enzymatic reaction resulted in development of a blue color, which changed into yellow, when the reaction was stopped with H₃PO₄. The plate was read in an ELISA reader at 450 nm and the absorbance at 620 nm was subtracted. The detection limit in human serum was 0.25 pmol/L. There was no cross-reactivity with human insulin and human C-peptide. However, the four major PI conversion intermediates reacted at various proportions of 65-99%.

The between- and within-assay coefficients of variation were 6.8, 7.8% for true insulin respectively and 6.7, 7.8% for PI respectively. All measurements were performed in duplicate. The four mAbs including OXI-005, HUI-018, PEP-001 and HUI-001 were kind gifts from Novo Nordisk, Bagsvaerd, Denmark, and the standard samples of true insulin and PI were supplied by the Mercodia Company, Sweden. The ELISA-plate photometer (Bio-tek EL900, USA) and ELISA plate (NUNC company, Denmark) were employed in the assay.

Definition of risk factors

To investigate the relationship between the level of PI and cardiovascular risk factors clustering, we created a risk factor score to rank individuals according to the number of the risk factors at the time of the survey. The following risk factors and cut-off points were used to build up the risk factor scores: (1) hypertension was defined when systolic blood pressure (SBP) was ≥ 140 mmHg and/or diastolic blood pressure (DBP) ≥ 90 mmHg or taking anti-hypertensive drugs because of previous hypertension according to the 1999 WHO/ISH criteria^[10]; (2) hyperglycemia was diagnosed based on the FBG serum glucose ≥ 6.1 mmol/L according to the American Diabetes Association (ADA) criteria^[11] or having a history of diabetes mellitus; (3) hypercholesterolemia was defined as fasting TCH ≥ 5.20 mmol/L; (4) high LDL-c was defined as LDL-c ≥ 3.38 mmol/L; (5) low HDL-c was defined as HDL-c ≤ 1.04 mmol/L; (6) hypertriglyceridemia was defined as fasting TG ≥ 1.70 mmol/L^[12]; (7) overall overweight was considered as BMI ≥ 25.0 kg/m² according

to the WHO guideline^[13]; (8) visceral obesity was defined as waist circumference ≥ 85 cm in male and ≥ 80 cm in female^[14]. The final risk factor score varied from 0 to 5, with 0 meaning no exposure to these risk factors; one exposure to any one risk factor; 2-4 exposure to any combination of 2-4 risk factors respectively; five exposure to any combination of five or more than five risk factors simultaneously.

Statistical analysis

All data analyses were performed using statistical package for social science (SPSS for Windows, version 10.0, 1999, SPSS Inc, Chicago, IL, USA). Data of BMI, waist circumference, age and blood pressure were normally distributed parameters and presented as mean \pm SD, whereas skewed data including FBG, fasting lipid, fasting true insulin, and PI were logarithmically transformed before analysis and were expressed as median (quartile range).

RESULTS

Sex and age distribution of sleep snoring subjects

Tables 1 and 2 show sex and age distribution of sleep snoring in the population-based epidemiological study. The results indicated that the frequency of sleep snoring in males was significantly higher than in females ($\chi^2 = 68.227$, $P < 0.001$), and the frequency of sleep snoring significantly increased with the elevation of age ($\chi^2 = 44.465$, $P < 0.001$).

Table 1 Sex distribution of sleep snoring subjects

Snoring	Male	Female	Total
Never	265	481	746
Seldom	34	29	63
Sometimes	83	68	151
Often	59	39	98
Very often	89	46	135
Total	530	663	1193
Statistical parameter	$\chi^2 = 68.227$		$P < 0.001$

Spearman correlation analysis of sleep snoring with tested parameters

The results of Spearman correlation analysis (Table 3) indicated that the frequency of sleep snoring was significantly correlated with such parameters as BMI, waist circumference, SBP, DBP, fasting TCH, fasting TG, fasting LDL-c, PI, and risk factors score ($P < 0.01$). However, the significant correlation was not found between the frequency of sleep snoring and FBG, true insulin, and fasting HDL-c ($P > 0.05$).

Table 2 Age distribution of sleep snoring subjects

Snoring	35~	40~	45~	50~	55~	Total
Never	225	144	143	113	121	746
Seldom	17	5	9	14	18	63
Sometimes	39	18	31	28	35	151
Often	18	13	23	18	26	98
Very often	22	18	25	30	40	135
Total	321	198	231	203	240	1193
Statistical parameter			$\chi^2 = 44.465$	$P < 0.001$		

Table 3 Spearman correlation analysis of sleep snoring with tested parameters

Parameters	BMI	WC	SBP	DBP	FBG	CH
Correlation coefficient	0.177 ^b	0.268 ^b	0.211 ^b	0.191 ^b	0.027	0.126 ^b
Parameters	TG	HDL	LDL	TI	PI	RFS
Correlation coefficient	0.132 ^b	-0.043	0.108 ^b	0.050	0.156 ^b	0.194 ^b

^b $P < 0.01$ vs others. Abbreviations: BMI, body mass index; WC, waist circumference; SBP, systolic blood pressure; DBP, diastolic blood pressure; FBG, fasting blood glucose; CH, fasting total cholesterol; TG, fasting triglycerides; HDL, fasting high-density lipoprotein cholesterol; LDL, fasting low-density lipoprotein cholesterol; TI, true insulin; PI, proinsulin; RFS, risk factors score.

Analysis of covariate variance of sleep snoring with tested parameters

Table 4 summarizes the results of analysis of covariate variance of sleep snoring and its relevant parameters. In the analysis, age and sex were controlling variables; the frequency of sleep snoring was factor variable, and the parameters including BMI, waist circumference, SBP, DBP, FBG (logarithmically transformed value), TCH (logarithmically transformed value), TG (logarithmically transformed value), HDL (logarithmically transformed value), LDL (logarithmically transformed value), true insulin (logarithmically transformed value), PI (logarithmically transformed value), and risk factors score were employed as dependent variables, respectively. The results indicated that a significant difference in parameters including BMI, waist circumference, SBP, DBP, TCH, TG, true insulin, PI, and risk factors score was found among various sleep snoring groups respectively after controlling for age and sex, and significant difference was not found in FBG, HDL-c, LDL-c between different frequencies of sleep snoring groups.

Analysis of multivariate logistic regression with sleep snoring as an independent variable

The results of multivariate logistic regression analysis are shown in Table 5, in which the dependent variable was the frequency of sleep snoring (the never snoring was coded as 0, and the seldom, sometimes, often, and very often snoring was considered as sleep snoring and was coded as 1), and age stratum (age stratification was performed with 5-year age strata), sex (male was coded as 1, female as 0), BMI (group division by an interval of quartile), waist circumference (group division by an interval of quartile), true insulin (group division by an interval of quartile), and PI (group division by an interval of quartile) were employed as independent variables. In the analysis of multivariate logistic regression, the variables including sex, age, PI, and waist circumference were accepted by the final model, and BMI and true insulin were refused by the regression model. The final model suggested that male, age, PI, and waist circumference were risk factors for sleep snoring, and the OR (95%CI) for sex, age, PI, and waist circumference was 0.401 (0.311-0.518)

Table 4 Analysis of covariate variance with sleep snoring as factor variable, and age and sex as controlling variables

Parameters	Never	Seldom	Some-times	Often	Very often	F	P
BMI	23.49±2.83	24.08±2.89	24.14±2.84	24.56±3.66	25.32±3.47	16.335	0.000
WC	75.89±7.78	78.68±8.31	78.83±7.89	81.65±9.98	83.37±10.63	22.000	0.000
SBP	121.03±19.05	128.77±21.08	126.39±20.28	126.80±20.29	133.93±23.16	7.169	0.000
DBP	77.25±10.66	79.48±10.75	80.20±11.58	80.68±13.89	85.59±13.59	9.957	0.000
FBG	4.44 (4.06-4.89)	4.40 (4.17-4.80)	4.53 (4.12-4.93)	4.47 (4.08-4.81)	4.53 (4.07-4.88)	0.124	0.974
CH	3.95 (3.39-4.54)	4.25 (3.32-5.01)	4.09 (3.67-4.60)	4.00 (3.49-4.65)	4.34 (3.70-5.04)	2.580	0.007
TG	0.75 (0.55-1.08)	0.77 (0.59-1.22)	0.91 (0.62-1.31)	0.79 (0.61-1.33)	0.89 (0.63-1.59)	5.778	0.000
HDL	1.07 (0.89-1.28)	1.15 (0.93-1.31)	1.02 (0.83-1.23)	1.03 (0.80-1.28)	1.04 (0.83-1.29)	1.693	0.149
LDL	2.44 (2.02-2.85)	2.55 (2.03-3.10)	2.60 (2.19-3.10)	2.53 (2.13-2.96)	2.74 (2.19-3.21)	1.392	0.234
TI	4.81 (2.89-6.98)	4.69 (2.54-7.09)	5.11 (3.55-7.18)	5.13 (2.88-7.50)	5.06 (3.16-7.58)	2.868	0.022
PI	3.26 (1.92-5.11)	3.29 (1.77-5.19)	4.03 (2.46-6.49)	4.19 (2.22-6.09)	4.43 (2.72-7.18)	5.980	0.000
RFS	1.24±1.15	1.47±1.33	1.57±1.27	1.70±1.28	2.06±1.53	11.135	0.000

Abbreviations as in Table 3.

Table 5 Analysis of multivariate logistic regression with sleep snoring as an independent variable

Variable	B	S.E.	WALD	P	OR (95%CI)
Sex	-0.913	0.130	49.133	0.000	0.401 (0.311-0.518)
Age (yr)	0.223	0.044	25.762	0.000	1.249 (1.146-1.361)
Proinsulin	0.199	0.060	10.964	0.001	1.220 (1.085-1.373)
Waist circumference	0.335	0.062	29.504	0.000	1.398 (1.239-1.578)
Constant	-1.150	0.305	14.192	0.000	-

B, SE, and WALD were statistical parameters.

($P = 0.000$), 1.249 (1.146-1.361, $P = 0.000$), 1.220 (1.085-1.373) ($P = 0.001$), and 1.398 (1.239-1.578) ($P = 0.000$), respectively.

DISCUSSION

Snoring is the main symptom of obstructive sleep apnea syndrome, which is one of the most frequent sleep disorders affecting 2-4% of middle-aged white^[15] and Asian populations^[16]. A predominantly Chinese population-based epidemiological study was conducted in Singapore, in which, 220 people aged 30-60 years, were interviewed for their snoring habits, and 87.5% of loud habitual snorers had significant obstructive apneas on the polysomnogram and 72% of these apneics complained of excessive daytime sleepiness (EDS)^[17]. The results from a population-based study investigating the long-term outcome in men with snoring over a 10-year period suggest, that snoring is the preceding form of obstructive sleep apnea syndrome^[18]. PI is a multi-peptide with 86 amino acids and its molecular weight is 9 390. It is synthesized in the β -cells of the islets of Langerhans and is subsequently processed through enzymatic cleavage to form C-peptide and insulin^[19]. The biological activity of PI is very low (approximately 10% of insulin), and it is the major storage form of insulin. Under physiological conditions, only small amounts of intact and split PI (less than 3% of insulin) are co-secreted with insulin from the pancreatic β -cells^[4]. In the earlier studies, insulin concentration was measured with radioimmunoassay using polyclonal antibodies, which cross-reacted with largely inactive insulin precursor molecules such as PI and des-31, 32 PI, hence it was called immunoreactive insulin (IRI). These PI molecules can be distinguished from more biologically active true insulin molecules by using highly sensitive and specific, two site immunoassays based on monoclonal antibodies. Since it is rather common that sleep breathing disorder is accompanied with insulin resistance, it has been clinically considered that both of them are closely correlated and even syndrome Z was named for coexisting sleep breathing disorder and insulin resistance. So far the associated pathogenesis between sleep breathing disorder and insulin resistance has not been elucidated clearly. To explore the relationship between sleep snoring and true insulin *vs* PI, a population-based epidemiological investigation was conducted in Pizhou city located in the mideastern part of China.

The results from this study showed that the frequency of sleep snoring in males was significantly higher than those in females, and the frequency of sleep snoring significantly increased with age. Furthermore, the results of Spearman correlation analysis indicate that the frequency of sleep snoring was significantly correlated with the concentration of PI and risk factors score. Moreover, the results of analysis of covariate variance in which age and sex were controlling variables suggest that the frequency of sleep snoring was positively and significantly associated with the risk factors score, and this finding is in agreement with several previous studies^[3-5].

In the present study, the level of circulating PI was positively and significantly associated with the frequency of sleep

snoring in the analysis including Spearman correlation, covariate variance in which age and sex were controlling variables, and multivariate stepwise logistic regression in which age, sex, BMI, and true insulin were adjustment variables. To our knowledge, this finding is the first, from a Chinese population-based epidemiological study. Obesity is the accumulation of excessive fat in the body and plays a role in metabolic disorders and the mortality and morbidity of cardiovascular diseases. Obesity, especially the local obesity represented by increased waist circumference and neck circumference, is related to the narrowness of upper respiratory tract and can lead to sleep apnea and hypopnea, as well as hypoxia and hypercapnia^[20]. This study demonstrated that in the multivariate stepwise logistic regression analysis, when the obesity represented as BMI and local obesity represented by waist circumference entered in the final regression model, the waist circumference rather than BMI was accepted by the model. Thus, it could be concluded that visceral obesity rather than general obesity was the independent risk factor for sleep snoring. To date, the mechanism underlying the consistent and significant association between PI and sleep snoring is unknown. In insulin resistance atherosclerosis study (IRAS), it demonstrated that the visceral fat accumulation could result in the elevation of circulating PI level^[21], and the concentration of PI was independently correlated with fibrinogen, and plasminogen activator inhibitor type 1 (PAI-1)^[22]. The elevation of the activity of fibrinogen, and PAI-1 following the increase of PI level can lead to the disorder of homeostasis and finally result in the clustering of cardiovascular risk factors. The above finding may be one of the mechanisms for the association between PI, sleep snoring and cardiovascular risk factors clustering.

Our conclusions are that the frequency of sleep snoring which is the main symptom of obstructive sleep apnea syndrome is independently associated with the level of PI, and is associated with the clustering of cardiovascular risk factors. This might be the first study demonstrating a relationship between sleep breathing disorder, circulating PI level, and clustering of cardiovascular risk factors in healthy middle-aged subjects from the general Chinese population.

ACKNOWLEDGMENTS

Special thanks to Dr. Lennart Andersen, Dr. Jens Christian Wortmann, and Dr. Thomas Peter Dyrberg, from Novo Nordisk, Bagsvaerd, Denmark, for providing free monoclonal antibodies including OXI-005, HUI-018, PEP-001 and HUI-001.

REFERENCES

- 1 **Reaven GM.** Insulin resistance/compensatory hyperinsulinemia, essential hypertension, and cardiovascular disease. *J Clin Endocrinol Metab* 2003; **88**: 2399-2403
- 2 **Egan BM, Greene EL, Goodfriend TL.** Insulin resistance and cardiovascular disease. *Am J Hypertens* 2001; **14**: 116S-125S
- 3 **Wilcox I, McNamara SG, Collins FL, Grunstein RR, Sullivan CE.** "Syndrome Z": the interaction of sleep apnoea, vascular risk factors and heart disease. *Thorax* 1998; **53**: S25-28
- 4 **Roder ME, Porte D, Schwartz RS, Kahn SE.** Disproportionately elevated proinsulin levels reflect the degree of impaired

- B cell secretory capacity in patients with noninsulin-dependent diabetes mellitus. *J Clin Endocrinol Metab* 1998; **83**: 604-608
- 5 **Haffner SM**, Mykkanen L, Stern MP, Valdez RA, Heisserman JA, Bowsher RR. Relationship of proinsulin and insulin to cardiovascular risk factors in nondiabetic subjects. *Diabetes* 1993; **42**: 1297-1302
- 6 **Pendlebury ST**, Pepin JL, Veale D, Levy P. Natural evolution of moderate sleep apnoea syndrome: significant progression over a mean of 17 mo. *Thorax* 1997; **52**: 872-878
- 7 **Friedewald WT**, Levy RI, Fredrickson DS. Estimation of the concentration of low-density lipoprotein cholesterol in plasma, without use of the preparative ultracentrifuge. *Clin Chem* 1972; **18**: 499-502
- 8 **Andersen L**, Dinesen B, Jørgensen PN, Poulsen F, Roder ME. Enzyme immunoassay for intact human insulin in serum or plasma. *Clin Chem* 1993; **39**: 578-582
- 9 **Kjems LL**, Roder ME, Dinesen B, Hartling SG, Jørgensen PN, Binder C. Highly sensitive enzyme immunoassay of proinsulin immunoreactivity with use of two monoclonal antibodies. *Clin Chem* 1993; **39**: 2146-2150
- 10 Guidelines subcommittee of the WHO-ISH Mild Hypertension Liaison Committee. 1999 World health organization-international society of hypertension guidelines for the management of hypertension. *J Hypertension* 1999; **17**: 151-183
- 11 The expert committee on the diagnosis and classification of diabetes mellitus. Report of the expert committee on the diagnosis and classification of diabetes mellitus. *Diabetes Care* 2002; **25**(Suppl 1): S5-19
- 12 Expert panel on detection, evaluation, and treatment of high blood cholesterol in adults. Executive summary of the third report of national cholesterol education program(NCEP) expert panel on detection, evaluation, and treatment of high blood cholesterol in adults (adult treatment panel ?). *JAMA* 2001; **285**: 2486-2497
- 13 **Barreto SM**, Passos VM, Firmo JO, Guerra HL, Vidigal PG, Lima-Costa MF. Hypertension and clustering of cardiovascular risk factors in a community in Southeast Brazil-The Bambui Health and Ageing Study. *Arq Bras Cardiol* 2001; **77**: 576-581
- 14 **Zhou BF**, Wu YF, Zhao LC, Li L, Yang J, Li X. Relationship of central obesity to cardiovascular risk factors and their clustering in middle aged Chinese population. *Zhonghua Xinxue Guanbing Zazhi* 2001; **29**: 70-73
- 15 **Ohayon MM**, Guilleminault C, Priest RG, Caulet M. Snoring and breathing pauses during sleep: telephone interview survey of a United Kingdom population sample. *BMJ* 1997; **314**: 860-863
- 16 **Ulfberg J**, Carter N, Talback M, Edling C. Excessive daytime sleepiness at work and subjective work performance in the general population and among heavy snorers and patients with obstructive sleep apnea. *Chest* 1996; **110**: 659-663
- 17 **Puvanendran K**, Goh KL. From snoring to sleep apnea in a Singapore population. *Sleep Res Online* 1999; **2**: 11-14
- 18 **Lindberg E**, Elmasry A, Gislason T, Janson C, Bengtsson H, Hetta J, Nettelbladt M, Boman G. Evolution of sleep apnea syndrome in sleepy snorers. A population-based prospective study. *Am J Respir Crit Care Med* 1999; **159**: 2024-2027
- 19 **Davidson HW**, Rhodes CJ, Hutton JC. Interaorganellar Ca and pH control proinsulin cleavage in the pancreatic B-cell via two site-specific endopeptidases. *Nature* 1988; **333**: 93-96
- 20 **Coughlin S**, Calverley P, Wilding J. Sleep disordered breathing-a new component of syndrome X. *Obes Rev* 2001; **2**: 267-274
- 21 **Haffner SM**, D'Agostino R, Mykkanen L, Hales CN, Savage PJ, Bergman RN, O'Leary D, Rewers M, Selby J, Tracy R, Saad MF. Proinsulin and insulin concentrations in relation to carotid wall thickness: the insulin resistance atherosclerosis study. *Stroke* 1998; **29**: 1498-1503
- 22 **Festa A**, D'Agostino R Jr, Mykkanen L, Tracy RP, Zaccaro DJ, Hales CN, Haffner SM. Relative contribution of insulin and its precursors to Fibrinogen and PAI-1 in a large population with different states of glucose tolerance. *Arterioscler Thromb Vas Biol* 1999; **19**: 562-568

Effect of lactulose on establishment of a rat non-alcoholic steatohepatitis model

Jian-Gao Fan, Zheng-Jie Xu, Guo-Liang Wang

Jian-Gao Fan, Zheng-Jie Xu, Guo-Liang Wang, Department of Gastroenterology, Shanghai First People's Hospital, Jiaotong University, Shanghai 200080, China

Correspondence to: Professor Jian-Gao Fan, Department of Gastroenterology, Shanghai First People's Hospital, Jiaotong University, Shanghai 200080, China. fanjg@citiz.net

Telephone: +86-21-63240090 Fax: +86-21-63240825

Received: 2004-10-30 Accepted: 2004-12-21

Abstract

AIM: To explore the relationship between changes of intestinal environment and pathogenesis of non-alcoholic steatohepatitis (NASH).

METHODS: Forty-two Sprague-Dawley rats were randomly divided into model group ($n = 24$), treatment group ($n = 12$), and control group ($n = 6$). The rats of model and treatment groups were given high-fat diet, and those of the control group were given normal diet. Furthermore, the rats of treatment group were given lactulose after 8 wk of high-fat diet. Twelve rats of the model group were killed at 8 wk of high-fat diet. At the 16 wk the rats of treatment group, control group, and the rest of the model group were killed. The serum levels of aminotransferase were measured and the histology of livers was observed by H&E staining.

RESULTS: The livers of rats presented the pathological features of steatohepatitis with higher serum levels of alanine aminotransferase (ALT) and aspartate aminotransferase (AST) in the model group after 16 wk. Compared to the model group, the serum levels of ALT and AST in treatment group decreased significantly and were close to the normal group, and the hepatic inflammation scores also decreased markedly than those in the model group after 16 wk (5.83 ± 2.02 vs 3.63 ± 0.64 , $P < 0.05$), but were still higher than those in the model group after 8 wk (3.63 ± 0.64 vs 1.98 ± 0.90 , $P < 0.05$). However, the degree of hepatic steatosis had no changes in treatment group compared to the model group after 16 wk.

CONCLUSION: Lactulose could ameliorate the hepatic inflammation of rats with steatohepatitis induced by fat-rich diet, but could not completely prevent the development of steatohepatitis. It is suggested that intestinal environmental changes such as intestinal bacteria overgrowth, are one of the important factors in the pathogenesis of NASH.

© 2005 The WJG Press and Elsevier Inc. All rights reserved.

Key words: NASH; Lactulose; Intestinal environment

Fan JG, Xu ZJ, Wang GL. Effect of lactulose on establishment of a rat non-alcoholic steatohepatitis model. *World J Gastroenterol* 2005; 11(32): 5053-5056

<http://www.wjgnet.com/1007-9327/11/5053.asp>

INTRODUCTION

The pathogenesis of non-alcoholic steatohepatitis (NASH) remains unclear^[1-5]. Several studies have suggested that small intestine bacterial overgrowth might play a role in NASH^[6-9]. NASH is a common complication of jejuno-ileal bypass for morbid obesity^[10-12]. NASH has also been described in adults during total parenteral nutrition (TPN) and in multiple jejunal diverticulae with bacterial overgrowth in small intestine^[13,14]. However, evidence is insufficient to indicate that intestinal flora has much to do with the usually insidious process of NASH^[15-18]. Recently, it was reported that the prevalence of small intestine bacterial overgrowth is high in obese patients with NASH, as assessed by the 14C-D-xylose-lactulose breath test^[15], suggesting that intestinal environmental changes such as small intestine bacterial overgrowth and gut original endotoxemia may play an important role in the development of NASH. To further study the relationship between the change of intestinal environment and pathogenesis of NASH, we investigated the effect of lactulose on the establishment of a rat NASH model.

MATERIALS AND METHODS

Animals

Male Sprague-Dawley rats ($n = 42$) weighing 140-160 g were purchased from the Shanghai Experimental Animal Center (Shanghai, China), and housed in cages under standard conditions with free access to water. After being fed with standard rat chow for 1 wk, the animals were randomly divided into control, model, and treatment groups. The control group ($n = 6$) received normal diet, the model group ($n = 24$) and treatment group ($n = 12$) received fat-rich diet (normal diet plus 2% cholesterol and 10% lard). Eight weeks later, the treatment group was administered a solution of lactulose syrup (Solvay Pharma, China) instead of water. In general, the dose of lactulose syrup for adults was 45 mL/d. If the average weight of adults was 59 kg, the dose of lactulose liquid was 0.9 mL/(kg d). According to the dose of adults, rats might be given a 10-fold higher dose (3.7 mL/d). Livers and blood samples were collected from 12 rats of model group at the wk 8. At wk 16, samples were collected from other rats in three groups. In brief: after fasting and water deprivation for more than 12 h, the rats were weighed and

anesthetized with 1% pentobarbital by intraperitoneal injection. Then the blood samples were collected through abdominal aorta, the liver tissues were weighed and fixed in 40 g/L formaldehyde, embedded in paraffin.

Biochemical measurement

The serum levels of alanine aminotransferase (ALT), aspartate aminotransferase (AST), triglycerides (TG), and total cholesterol (TC) were measured using an automatic biochemical analytical system.

Serum endotoxin level

Serum endotoxin level was measured by chromogenic limulus amoebocyte lysate test in Shanghai Clinical Test Center, and the tubes without pyrogen were supplied by the center.

Hepatic histology

The liver tissue sections were stained with hematoxylin and eosin. Each section was assessed under 10×20 light microscopic fields and scored for the severity of steatosis and inflammation according to the following criteria: Steatosis was scored as: grade 0: no fat; grade 1: fatty hepatocytes occupying less than 33% of the hepatic parenchyma; grade 2: fatty hepatocytes occupying 34-66% of the hepatic parenchyma; and grade 3: fatty hepatocytes occupying more than 66% of the hepatic parenchyma. The diagnosis of fatty liver could be confirmed, when fatty hepatocytes occupying more than 33% of the hepatic parenchyma. Portal inflammation (P), intralobular inflammation (L), piecemeal necrosis (PN), and bridging hepatic necrosis (BN) had a score from 1 to 4 according to the pathologic severity. PN and BN had a greater correlation with the prognosis, the score was two times higher than P and L. The inflammation score was P+L+2PN+2BN.

Statistical analysis

All results were expressed as mean±SD. Statistical differences between means were determined by Student's *t* test. Rank sum test was used in enumeration of data. *P*<0.05 was considered statistically significant.

RESULTS

During the experiment, no rat died in three groups. In the treatment group, there were no marked increase in the volume of feces. The feces were soft. No significant difference was found in the body weights between model group and control group. But the ratio of the liver wet weight with the body weight in the model group increased significantly than that in the control group. In the treatment group, the body weights were lower than those in the model group at wk 16, and the ratio of the liver wet weight with the body weight (liver exponent, %) significantly decreased compared to that in the model group at wk 8 and 16 (Table 1).

Serum lipid

In model group, the serum level of TC was markedly higher than that in control group, but the serum level of TG was similar to that in control group. No significant difference in serum levels of TC between the model group and the treatment group, but the serum level of TG in the treatment group decreased markedly (Table 2).

Serum aminotransferase

The serum levels of ALT and AST in the model group had an increasing tendency at wk 8, but no significant difference was found between the model group and control group until wk 16. The serum levels of ALT and AST in treatment group decreased significantly, and almost became normal (Table 3).

Serum endotoxin level

The serum endotoxin level in portal vein was higher than that in abdominal aorta, both in model group and control group (*P*<0.05), but there was no significant difference in serum endotoxin level both in portal vein and in abdominal aorta between the two groups. Therefore, we did not measure the serum endotoxin level in treatment group (Table 4).

Hepatic histology

The livers of control group had normal morphology, while

Table 1 Rat body weight and the liver exponent (mean±SD)

Group	Time (wk)	<i>n</i>	Body weight (g)	Liver exponent (%)
Control	16	6	478.2±36.8	2.27±0.28
Model	8	12	425.8±26.7	3.37±0.05 ^b
	16	12	505.8±60.1	3.93±0.51 ^b
Treatment	16	12	433.3±58.2 ^a	2.96±0.24 ^a

^a*P*<0.05 vs model group; ^b*P*<0.01 vs control group.

Table 2 Serum lipid changes (mean±SD)

Group	Time (wk)	<i>n</i>	TG (mmol/L)	TC (mmol/L)
Control	16	6	0.83±0.20	1.10±0.18
Model	8	12	0.68±0.18	1.81±0.30 ^b
	16	12	0.83±0.22	2.00±0.38 ^b
Treatment	16	12	0.44±0.14 ^a	2.06±0.32

^a*P*<0.05 vs model group; ^b*P*<0.01 vs control group.

Table 3 Serum aminotransferase changes (mean±SD)

Group	Time (wk)	<i>n</i>	ALT (U/L)	AST (U/L)
Control	16	6	34.16±5.17	144.00±21.59
Model	8	12	64.54±40.54	224.45±54.07
	16	12	94.92±45.50 ^a	282.7±77.48 ^b
Treatment	16	12	47.8±11.0 ^c	133.7±26.5 ^d

^a*P*<0.05, ^b*P*<0.01 vs control group, ^c*P*<0.05, ^d*P*<0.01 vs model group.

Table 4 Rat blood endotoxin level (mean±SD)

Group	Time (wk)	<i>n</i>	Serum endotoxin level (EU/mL)	
			Portal vein	Abdominal aorta
Control	16	6	0.291±0.08	0.125±0.03
Model	8	12	0.264±0.07	0.089±0.02
	16	12	0.285±0.08	0.114±0.02
Treatment	16	12	-	-

the livers of model group and treatment group became yellow, dull, enlarged, fragile, and full. Microscopically, the livers of control group had no marked abnormality. At wk 8, the livers of model group were engorged with microvesicular and macrovesicular fat. Fatty liver could be diagnosed in 11 of 12 rats. Four out of twelve rats had mild intralobular inflammation. At wk 16, hepatic steatosis was much severe, and intralobular areas were infiltrated by mixed inflammatory cells in model group. These lesions were located mainly in zone 3 areas. Intralobular inflammation was more severe than portal inflammation. Some livers had several large areas of necrosis melted by focal intralobular inflammation. Two rats had hepatic piecemeal necrosis and three had bridging necrosis. In treatment group, the degree of hepatic steatosis slightly decreased, while the score of hepatic inflammation activity significantly decreased compared to those in model group. No hepatic piecemeal necrosis and bridging necrosis were found in treatment group (Tables 5 and 6).

DISCUSSION

The histological characteristics of NASH resemble those

of alcoholic steatohepatitis, suggesting that both diseases may have a similar pathogenesis and can benefit from similar therapies^[15-18]. Studies in alcohol-fed rodents have shown that intestinal bacteria, bacterial endotoxin, and endotoxin-inducible cytokine can modulate alcohol-induced liver damages including hepatic necrosis and fibrosis^[19,20]. Treatment with antibiotics and lactobacillus that inhibit production of endotoxin by the intestinal flora can significantly inhibit the development of steatohepatitis in alcohol-fed animals^[21,22].

Although the intestinal flora is known to play a critical role in the pathogenesis of alcohol-related liver disease, its role in NASH has been poorly understood. Surgical procedures (such as jejunio-ileal bypass) and TPN cause intestinal stasis and secondary bacterial overgrowth, accelerate the progression of fatty liver disease in obesity patients, suggesting that increased exposure to intestinal bacterial products may contribute to the pathogenesis of NASH^[1-3]. It has been reported that the prevalence of small intestinal bacterial overgrowth is high in patients with NASH^[15].

Lactulose could be fermented by colonic bacteria and turn into lactic acid and acetic acid, which can lower colonic

Table 5 Degree of hepatic steatosis in different groups

Group	Time (wk)	<i>n</i>	Degree of steatosis			
			-	+	++	+++
Control	16	6	6	0	0	0
Model	8	12	0	1	6	5
	16	12	0	0	1	11
Treatment	16	12	0	0	4	8

Table 6 Score of rat hepatic inflammation activity (mean±SD)

Group	Time (wk)	<i>n</i>	Score of inflammation activity
Control	16	6	0.66±0.76
Model	8	12	1.98±0.90
	16	12	5.83±2.02 ^b
Treatment	16	12	3.63±0.64 ^a

^a*P*<0.05 vs model group; ^b*P*<0.01 vs control group.

pH, diminish ammonia production and normalize intestinal transit; therefore, lactulose syrup can be used in treatment of hepatic encephalopathy. Lactulose promotes the growth of acidophilous lactobacilli, bifidobacteria, and Gram-positive bacteria, while inhibits Gram-negative bacteria and prevents gut-derived endotoxemia^[23]. In order to explore the relationship between the change of intestinal environmental and pathogenesis of NASH, we observed the effect of lactulose on NASH rats.

The treatment group was given lactulose after 8 wk of high-fat diet, when simple fatty liver developed in rats. The model group developed NASH after 16 wk, while treatment with lactulose for 8 wk improved both serum aminotransferase and hepatic inflammation. These results suggest that intestinal environmental changes, such as small intestinal bacterial overgrowth, increased intestinal permeability and subsequent gut-derived endotoxemia may play an important role in the development of NASH. Although the treatment group received lactulose for 8 wk, the hepatic inflammation scores were still higher than those in model group, indicating that lactulose can ameliorate hepatic inflammation, but cannot prevent NASH. Lactulose could not improve hepatic steatosis in treatment group, suggesting that the change of intestinal environment is not closely related to hepatic steatosis.

In our serial researches, we found that the serum endotoxin level in NASH rats were significantly elevated, when hepatic fibrosis occurred after 24 wk of high-fat diet. The serum endotoxin level in portal vein and peripheral vessels had no significant difference between model group and control group, but the serum endotoxin level in portal vein was markedly higher than that in peripheral vessels in both groups. These results suggest that SD rats might have mild endotoxemia. We also found that the expression of endotoxin receptors-CD14 and toll-like receptor 4 was upregulated in model group, suggesting that Kupffer cell sensitivity to endotoxin increases and low doses of endotoxin might injure liver. Oral administration of lactulose may improve hepatic inflammation of NASH rats by reducing serum endotoxin level in portal vein.

Furthermore, other bacterial products such as peptidoglycan-polysaccharide polymers rather than endotoxin, could stimulate Kupffer cells and injure liver, because bacterial species rather than aerobic Gram-negative bacteria such as *Escherichia coli* may play a role in the pathogenesis of small intestinal bacterial overgrowth^[23,24].

REFERENCES

- Hanley AJ, Williams K, Festa A, Wagenknecht LE, D'Agostino RB Jr, Kempf J, Zinman B, Haffner SM. Insulin resistance atherosclerosis study. Elevations in markers of liver injury and risk of type 2 diabetes: the insulin resistance atherosclerosis study. *Diabetes* 2004; **53**: 2623-2632
- Fassio E, Alvarez E, Dominguez N, Landeira G, Longo C. Natural history of nonalcoholic steatohepatitis: a longitudinal study of repeat liver biopsies. *Hepatology* 2004; **40**: 820-826
- Brunt EM. Nonalcoholic steatohepatitis. *Semin Liver Dis* 2004; **24**: 3-20
- Harrison SA, Torgerson S, Hayashi PH. The natural history of nonalcoholic fatty liver disease: a clinical histopathological study. *Am J Gastroenterol* 2003; **98**: 2042-2047
- Mofrad P, Contos MJ, Haque M, Sargeant C, Fisher RA, Luketic VA, Sterling RK, Shiffman ML, Stravitz RT, Sanyal AJ. Clinical and histologic spectrum of nonalcoholic fatty liver disease associated with normal ALT values. *Hepatology* 2003; **37**: 1286-1292
- Bugianesi E, Leone N, Vanni E, Marchesini G, Brunello F, Carucci P, Musso A, De Paolis P, Capussotti L, Salizzoni M, Rizzetto M. Expanding the natural history of nonalcoholic steatohepatitis: from cryptogenic cirrhosis to hepatocellular carcinoma. *Gastroenterology* 2002; **123**: 134-140
- Nakao K, Nakata K, Ohtsubo N, Maeda M, Moriuchi T, Ichikawa T, Hamasaki K, Kato Y, Eguchi K, Yukawa K, Ishii N. Association between nonalcoholic fatty liver, markers of obesity, and serum leptin level in young adults. *Am J Gastroenterol* 2002; **97**: 1796-1801
- Marchesini G, Brizi M, Bianchi G, Tomassetti S, Bugianesi E, Lenzi M, McCullough AJ, Natale S, Forlani G, Melchionda N. Nonalcoholic fatty liver disease: a feature of the metabolic syndrome. *Diabetes* 2001; **50**: 1844-1850
- Brunt EM. Nonalcoholic steatohepatitis: definition and pathology. *Semin Liver Dis* 2001; **21**: 3-16
- Chitturi S, Farrell GC. Etiopathogenesis of nonalcoholic steatohepatitis. *Semin Liver Dis* 2001; **21**: 27-41
- Corrodi P. Jejunoileal bypass: change in the flora of the small intestine and its clinical impact. *Rev Infect Dis* 1984; **6** (Suppl 1): S80-84
- Vanderhoof JA, Tuma DJ, Antonson DL, Sorrell MF. Effect of antibiotics in the prevention of jejunoileal bypass-induced liver dysfunction. *Digestion* 1982; **23**: 9-15
- Alverdy JC, Aoyo E, Moss GS. Total parenteral nutrition promotes bacterial translocation from the gut. *Surgery* 1988; **104**: 185-190
- Pappo I, Bercovier H, Berry EM, Haviv Y, Gallily R, Freund HR. Polymyxin B reduces total parenteral nutrition-associated hepatic steatosis by its antibacterial activity and by blocking deleterious effects of lipopolysaccharide. *J Parenter Enter Nutr* 1992; **16**: 529-532
- Wigg AJ, Roberts-Thomson IC, Dymock RB, McCarthy PJ, Grose RH, Cummins AG. The role of small intestinal bacterial overgrowth, intestinal permeability, endotoxaemia, and tumour necrosis factor alpha in the pathogenesis of non-alcoholic steatohepatitis. *Gut* 2001; **48**: 206-211
- Farrell GC. Is bacterial ash the flash that ignites NASH? *Gut* 2001; **48**: 148-149
- Nair S, Cope K, Risby TH, Diehl AM. Obesity and female gender increase breath ethanol concentration: potential implications for the pathogenesis of nonalcoholic steatohepatitis. *Am J Gastroenterol* 2001; **96**: 1200-1204
- Cope K, Risby T, Diehl AM. Increased gastrointestinal ethanol production in obese mice: implications for fatty liver disease pathogenesis. *Gastroenterology* 2000; **119**: 1340-1347
- Thurman RG. II. Alcoholic liver injury involves activation of Kupffer cells by endotoxin. *Am J Physiol* 1998; **275**(4 Pt 1): G605-611
- Thurman RG, Bradford BU, Iimuro Y, Knecht KT, Arteil GE, Yin M, Connor HD, Wall C, Raleigh JA, Frankenberg MV, Adachi Y, Forman DT, Brenner D, Kadiiska M, Mason RP. The role of gut-derived bacterial toxins and free radicals in alcohol-induced liver injury. *J Gastroenterol Hepatol* 1998; **13** (Suppl): S39-50
- Bode C, Schafer C, Fukui H, Bode JC. Effect of treatment with paromomycin on endotoxemia in patients with alcoholic liver disease—a double-blind, placebo-controlled trial. *Alcohol Clin Exp Res* 1997; **21**: 1367-1373
- Adachi Y, Moore LE, Bradford BU, Gao W, Thurman RG. Antibiotics prevent liver injury in rats following long-term exposure to ethanol. *Gastroenterology* 1995; **108**: 218-224
- Salminen S, Salminen E. Lactulose, lactic acid bacteria, intestinal microecology and mucosal protection. *Scand J Gastroenterol Suppl* 1997; **222**: 45-48
- Lichtman SN, Keku J, Schwab JH, Sartor RB. Hepatic injury associated with small bowel bacterial overgrowth in rats is prevented by metronidazole and tetracycline. *Gastroenterology* 1991; **100**: 513-519

Expression of cell cycle regulator p57^{kip2}, cyclinE protein and proliferating cell nuclear antigen in human pancreatic cancer: An immunohistochemical study

Hui Yue, Hui-Yong Jiang

Hui Yue, Institute for Digestive Medicine, Nanfang Hospital, Southern Medical University, Guangzhou 510515, Guangdong Province, China
Hui-Yong Jiang, Department of Pathology, Nanfang Hospital, Southern Medical University, Guangzhou 510515, Guangdong Province, China

Correspondence to: Dr. Hui Yue, Institute for Digestive Medicine, Nanfang Hospital, Southern Medical University, Guangzhou 510515, Guangdong Province, China. yh12070430@vip.sina.com
Telephone: +86-20-61641545 Fax: +86-20-61363220
Received: 2004-11-02 Accepted: 2004-12-21

Abstract

AIM: To investigate the effects of p57^{kip2}, cyclinE protein and proliferating cell nuclear antigen (PCNA) on occurrence and progression of human pancreatic cancer.

METHODS: The expression of p57^{kip2}, cyclinE protein and PCNA in tumor tissues and adjacent tissues from 32 patients with pancreatic cancer was detected by SP immunohistochemical technique.

RESULTS: The positive expression rate of p57^{kip2} protein in tumor tissues was 46.9%, which was lower than that in adjacent pancreatic tissues ($\chi^2 = 5.317$, $P < 0.05$). p57^{kip2} protein positive expression remarkably correlated with tumor cell differentiation ($P < 0.05$), but not with lymph node metastasis ($P > 0.05$). The positive expression rate of cyclinE protein in tumor tissues was 68.8%, which was higher than that in adjacent pancreatic tissues ($\chi^2 = 4.063$, $P < 0.05$). CyclinE protein positive expression significantly correlated with tumor cell differentiation and lymph node metastasis ($P < 0.05$). The positive expression rate of PCNA in the tumor tissues was 71.9%, which was higher than that in adjacent pancreatic tissues ($\chi^2 = 5.189$, $P < 0.05$). PCNA positive expression remarkably correlated with tumor cell differentiation and lymph node metastasis ($P < 0.05$).

CONCLUSION: The decreased expression of p57^{kip2} and/or overexpression of cyclinE protein and PCNA may contribute to the occurrence and progression of pancreatic cancer. p57^{kip2}, cyclinE protein, and PCNA play an important role in occurrence and progression of pancreatic cancer.

© 2005 The WJG Press and Elsevier Inc. All rights reserved.

Key words: p57^{kip2}; CyclinE; PCNA; Human pancreatic cancer

Yue H, Jiang HY. Expression of cell cycle regulator p57^{kip2},

cyclinE protein and proliferating cell nuclear antigen in human pancreatic cancer: An immunohistochemical study. *World J Gastroenterol* 2005; 11(32): 5057-5060

<http://www.wjgnet.com/1007-9327/11/5057.asp>

INTRODUCTION

Abnormality in mammalian cell cycle regulation is an important cause of cell proliferation and oncogenesis^[1]. Orderly progression of the cell cycle is controlled by a family of cyclins and cyclin-dependent kinases (CDKs), which are restrictively counterbalanced by CDK inhibitors (CDKIs)^[2]. Two distinct families of CDKIs, INK4, and CIP/KIP families, which regulate the activity of cyclin-CDK complexes, have been described^[3]. The CIP/KIP family, including p21, p27, and p57 proteins, harbors homologous CDK-binding domains or functions of cyclin-CDK complexes and causes the cell cycle to arrest in G₁ phase. CyclinE protein is a positive regulator of cell cycle, which promotes the transfer from G₁ to S phase. The expression of PCNA remarkably correlates with status of cell proliferation. There are few reports about the relationship between p57^{kip2} protein as negative factor of cell cycle regulation and pancreatic cancer. In this study, the expression of p57^{kip2}, cyclinE protein, and PCNA in pancreatic cancer tissues and adjacent tissues was detected by immunohistochemical technique to investigate the effects of p57^{kip2}, cyclinE protein, and PCNA on occurrence and progression of human pancreatic cancer.

MATERIALS AND METHODS

Patients and tumor samples

Thirty-two specimens of primary human pancreatic cancer were collected from pancreatic resection performed in the Department of General Surgery, General Hospital of Shenyang Military Command. There were 20 male and 12 female patients, with a mean age of 59.5 years (26-72 years). Nineteen patients had well-differentiated pancreatic cancer, 13 had moderately or poorly-differentiated pancreatic cancer, and 12 had lymph node metastasis. All patients were confirmed by clinicopathological diagnosis. These specimens were fixed in 10% buffered formalin and embedded in paraffin. All sections stained with hematoxylin and eosin were reviewed and kept for further studies.

Immunohistochemical study

Four-micrometer-thick sections from the tissues were cut for

immunohistochemical study. The expression of p57^{kip2}, cyclinE protein, and PCNA was assessed by SP immunohistochemical method using anti-human p57^{kip2} mAb (57P06), anti-human cyclinE protein mAb (13A3), anti-human PCNA mAb (PC10), and the UltraSensitive™ SP kit (kit-9720). Immunohistochemical staining for these proteins was then performed according to the UltraSensitive™ SP kit manual. All reagents were supplied by Maixin-Bio Co., Fuzhou, China. The cells with brown-yellow granules in the nuclei or cytoplasm were taken as positive. Five hundred cells on each slide were counted. The slides were classified as negative (-), positive (+), strong positive (++), and strongest positive (+++) according to the count of positive cells for p57^{kip2} and cyclinE proteins less than 10%, 10-25%, 25-50%, and more than 50%, respectively. The slides was distinguished as negative (-), and positive (+) when the count of positive cells were less than 50% and over 50% for PCNA respectively.

Statistical analysis

The χ^2 test and Fisher's exact test were used in the analysis by SAS system statistical software (release 6.12). $P < 0.05$ was considered statistically significant.

RESULTS

Expression of p57^{kip2} protein

The p57^{kip2} protein was located in the nuclei or cytoplasm of normal pancreatic cells and positive pancreatic cancer cells with brown-yellow granules (Figure 1A). The positive expression rate of p57^{kip2} protein in tumor tissues was 46.9%, which was lower than that in adjacent pancreatic tissues ($\chi^2 = 5.317$, $P < 0.05$). The positive expression rate of p57^{kip2} protein in the moderately or poorly differentiated tumor

tissues was 23.1%, which was lower than that in well-differentiated tumor tissues ($\chi^2 = 4.979$, $P < 0.05$). The positive expression rate of p57^{kip2} protein in lymph node metastasis group was 25.0%, which was lower than that in non-lymph node metastasis group ($P > 0.05$, Table 1).

Table 1 Expression of p57^{kip2} protein in pancreatic cancer tissues

Characteristics	p57 ^{kip2} protein expression				Rate (%)
	-	+	++	+++	
Tumor tissue	17	11	3	1	46.9 ^a
Well-differentiated	7	9	2	1	63.2 ^c
Moderately or poorly-differentiated	10	2	1	0	23.1 ^c
Lymph node metastasis	9	2	1	0	25.0 ^e
Non-lymphnode metastasis	8	9	2	1	60.0 ^e
Adjacent tissue	8	13	6	5	75.0 ^a

^a $P < 0.05$, ^c $P < 0.05$, ^e $P > 0.05$ vs others.

Expression of cyclinE protein

CyclinE protein was located in the nuclei or cytoplasm of normal pancreatic cells and positive pancreatic cancer cells with brown-yellow granules (Figure 1B). The positive expression rate of cyclinE protein in tumor tissues was 68.8%, which was higher than that in adjacent pancreatic tissues ($\chi^2 = 4.063$, $P < 0.05$). The positive expression rate of cyclinE protein in moderately or poorly differentiated tumor tissues was 84.6%, which was higher than that in well-differentiated tumor tissues ($\chi^2 = 5.128$, $P < 0.05$). The cyclinE protein positive expression rate in lymph node metastasis group was 91.7%, which was higher than that in non-lymph node metastasis group ($\chi^2 = 4.693$, $P < 0.05$, Table 2).

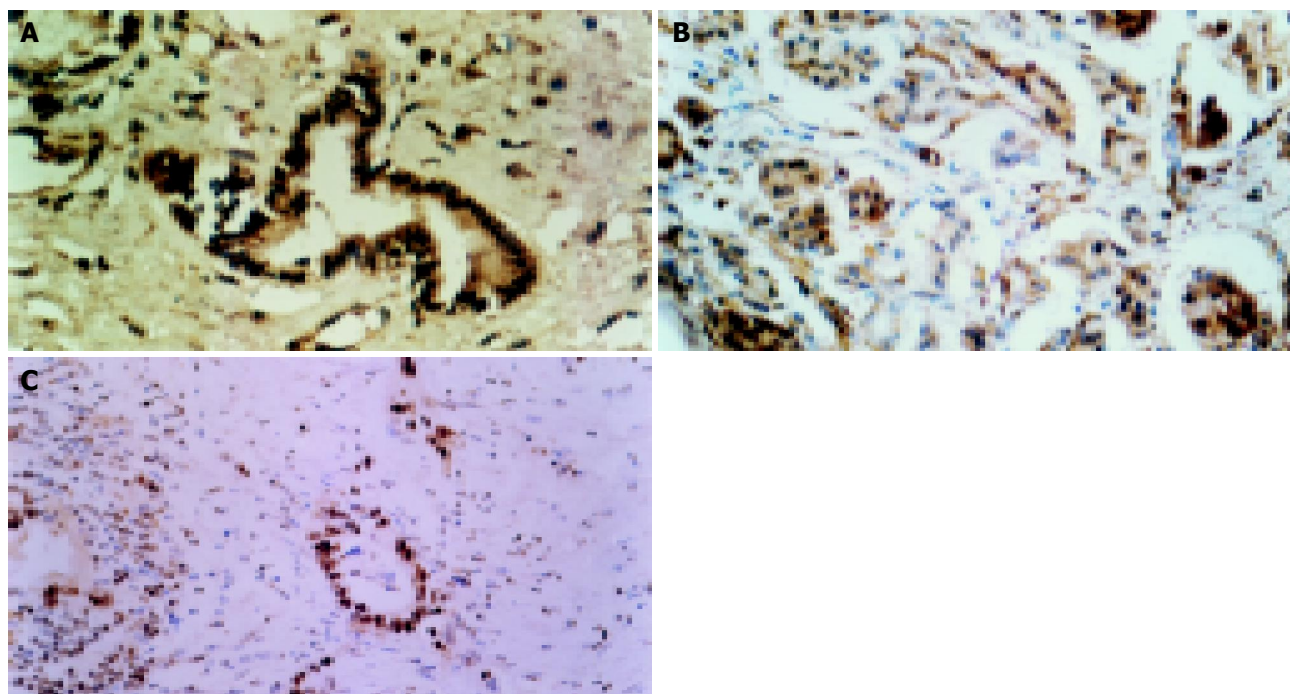


Figure 1 P57^{kip2} protein in well-differentiated pancreatic adenocarcinoma (A), cyclin E protein in poorly-differentiated pancreatic adenocarcinoma (B), and

PCNA protein in moderately-differentiated pancreatic adenocarcinoma (C).

Table 2 Expression of cyclinE protein in pancreatic cancer tissues

Characteristics	CyclinE protein expression				Rate (%)
	-	+	++	+++	
Tumor tissue	10	7	9	6	68.8 ^a
Well-differentiated	9	5	4	1	52.6 ^c
Moderately or poorly-differentiated	1	1	6	5	84.6 ^c
Lymph node metastasis	1	1	5	5	91.7 ^c
Non-lymph node metastasis	9	6	4	1	55.0 ^e
Adjacent tissue	18	6	8	0	43.8 ^a

^a $P < 0.05$, ^c $P < 0.05$, ^e $P < 0.05$ vs others.

Expression of PCNA

PCNA was located in the nuclei of normal pancreatic cells and positive pancreatic cancer cells with brown-yellow granules (Figure 1C). The positive expression rate of PCNA in tumor tissues was 71.9%, which was higher than that in adjacent pancreatic tissues ($\chi^2 = 5.189$, $P < 0.05$). The positive expression rate of PCNA in moderately or poorly differentiated tumor tissues was 92.3%, which was higher than that in well-differentiated tumor tissues ($\chi^2 = 4.522$, $P < 0.05$). The positive expression rate of PCNA in lymph node metastasis group was 100%, which was higher than that in non-lymph node metastasis group ($\chi^2 = 7.513$, $P < 0.05$, Table 3).

Table 3 Expression of PCNA in pancreatic cancer tissues

Characteristics	PCNA protein expression		
	-	+	Rate (%)
Tumor tissue	9	23	71.9 ^a
Well-differentiated	8	11	57.9 ^c
Moderately or poorly-differentiated	1	12	92.3 ^c
Lymph node metastasis	0	12	100 ^e
Non-lymph node metastasis	9	11	55.0 ^e
Adjacent tissue	18	14	43.8 ^a

^a $P < 0.05$, ^c $P < 0.05$, ^e $P < 0.05$ vs others.

Relationship between expression of p57^{kip2} and cyclinE proteins

The cyclinE protein positive expression rate in tumor tissues of the p57^{kip2} protein positive expression group and the p57^{kip2} protein negative expression was 60.0% and 76.5% respectively. There was no significant correlation between the two groups ($r = -0.11211$, $P > 0.05$, Table 4).

Table 4 Relationship between expression of p57^{kip2} and cyclinE proteins

p57 ^{kip2}	CyclinE protein expression				Rate (%)
	-	+	++	+++	
-	4	4	6	3	76.5
+	4	3	2	2	
++	2	0	0	1	60.0
+++	0	0	1	0	

DISCUSSION

Studies in recent years have shown that G₁ phase regulation is a complex procedure^[4-7]. p57^{kip2} gene is located in chromosome 11p15.5, and p57^{kip2} protein is a cell cycle inhibitor with molecular weight of 57 ku, which is included in the CIP/KIP family and similar to p21 and p27 proteins in functions^[8,9]. Lee *et al.*^[10], suggested that the tumor suppressor mechanism of p57^{kip2} protein may be integrated with cyclin-CDK complexes and makes cell cycle to arrest in the G₁ phase. Kondo *et al.*^[11], considered that paternal alleles of p57^{kip2} are imprinted, maternal alleles of p57^{kip2} are expressed in the normal status, loss of imprinting and imprinting mistakes of p57^{kip2} lead to a decrease at level of gene expression in tumors. Matsumoto *et al.*^[12], reported that p57^{kip2} protein positive expression rate is 43.3±3.2% in patients with esophageal squamous cell carcinoma. From then on, studies about p57^{kip2} protein expression in human colorectal carcinoma^[13], hepatocellular carcinoma^[14,15], prostate tumor^[16], neoplastic thyroid tissues^[17], epithelial ovarian tumor^[18], extrahepatic bile duct carcinoma and intrahepatic cholangiocellular carcinoma have been reported^[19,20], but few reports on the relationship between p57^{kip2} protein expression and pancreatic cancer are available^[21]. In this study, we found that the positive expression rate of p57^{kip2} protein in pancreatic cancer tissues was significantly lower than that in adjacent pancreatic tissues. The worse the cancer cell differentiation, the lower was the p57^{kip2} protein expression, and there was no correlation between the reduced expression of p57^{kip2} protein and lymph node metastasis. The results suggest that reduced expression of p57^{kip2} protein correlates with the occurrence and malignant degree of pancreatic cancer. CyclinE protein is a positive regulating factor in the cell cycle and promotes the genesis and progression of tumors^[22-24]. Our results suggest that overexpression of cyclinE is associated with the genesis and malignant degree, as well as lymph node metastasis of pancreatic cancer. PCNA is a δ -assistant factor of DNA synthetase, takes part in DNA biological synthesis and regulates cell cycle and cell proliferation by tetramer with cyclin, CDK and p21. Overexpression of PCNA is associated with a variety of tumors of digestive system including human colorectal cancer^[25], gastric cancer^[26], hepatocellular carcinoma^[27], pancreas tumor^[28,29]. The results in the present study suggest that overexpression of PCNA is associated with the occurrence and progression of pancreatic cancer, and malignant proliferation status of pancreatic cancer determined by expression of PCNA is of practical value. Our results suggest that cell proliferative activity is high for the negative or reduced expression of p57^{kip2} protein. Furthermore, p57^{kip2} protein plays a role in suppressing cell proliferation. Our findings are in accordance with the results of previous studies^[5].

In summary, decreased expression of p57^{kip2} and/or overexpression of cyclinE protein and PCNA might contribute to the occurrence and progression of pancreatic cancer. The p57^{kip2}, cyclinE protein, and PCNA might play an important role in occurrence and progression of pancreatic cancer.

REFERENCES

- 1 Clurman BE, Roberts JM. Cell cycle and cancer. *J Natl Cancer*

- Inst* 1995; **87**: 1499-1501
- 2 **Grana X**, Reddy EP. Cell cycle control in mammalian cells: role of cyclins, cyclin dependent kinase(CDKs), growth suppressor and cyclin dependent kinase inhibitors(CDKIs). *Oncogene* 1995; **11**: 211-219
 - 3 **Sherr CJ**. G₁ phase progression :cyclin on cue. *Cell* 1994; **79**: 551-555
 - 4 **Sherr CJ**. Cancer cell cycles. *Science* 1996; **274**: 1672-1677
 - 5 **Kamb A**. Cell-cycle regulators and cancer. *Trends Genet* 1995; **11**: 136-140
 - 6 **Hunter T**, Pines J. Cyclins and cancer II: CyclinD and CDK inhibitors come of age. *Cell* 1994; **79**: 573-582
 - 7 **Kamb A**, Gruis NA, Weaver-Feldhaus J, Liu Q, Harshman K, Tavitian SV, Stockent E, Day RS, Johon BE, Skolnick MH. A cell cycle regulator potentially involved in genesis of many tumor types. *Science* 1994; **264**: 436-440
 - 8 **Matsuoka S**, Edwards MC, Bai C, Parker S, Zhang P, Baldini A, Harper JW, Elledge SJ. p57^{KIP2} a structurally distinct member of the p2KIP1 cdk inhibitor family ,is a candidate tumor suppressor gene. *Genes Dev* 1995; **9**: 650-662
 - 9 **Orlow I**, Iavarone A, Crider-Miller SJ, Bonilla F, Latres E, Lee MH, Gerald WL, Massague J, Weissman BE, Cordon-Cardo C. Cyclin-dependent kinase inhibitor p57^{KIP2} in soft tissue sarcomas and wilms tumor. *Cancer Res* 1996; **56**: 1219-1221
 - 10 **Lee MH**, Reynisdottir I, Massague J. Cloning of p57^{KIP2}, a cyclin dependent kinase inhibitor with unique domain structure and tissue distribution. *Genes Dev* 1995; **9**: 639-649
 - 11 **Kondo M**, Matsuoka S, Uchida K, Osada H, Nagatake M, Takagi K, Harper JW, Takahashi T, Elledge SJ, Takahashi T. Selective maternal allele loss in human lung cancers of the maternally expressed p57^{KIP2} gene at 11p15.5. *Oncogen* 1996; **12**: 1365-1368
 - 12 **Matsumoto M**, Furihata M, Ohtsuki Y, Sasaguri S, Ogoshi S. Immunohistochemical characterization of p57^{KIP2} expression in human esophageal squamous cell carcinoma. *Anticancer Res* 2000; **20**: 1947-1952
 - 13 **Noura S**, Yamamoto H, Sekimoto M, Takemasa I, Miyake Y, Ikenaga M, Matsuura N, Monden M. Expression of second class of KIP protein p57^{KIP2} in human colorectal carcinoma. *Int J Oncol* 2001; **19**: 39-47
 - 14 **Ito Y**, Takeda T, Sakon M, Tsujimoto M, Monden M, Matsuura N. Expression of p57^{KIP2} protein in hepatocellular carcinoma. *Oncology* 2001; **61**: 221-225
 - 15 **Nakai S**, Masaki T, Shiratori Y, Ohgi T, Morishita A, Kurokohchi K, Watanabe S, Kuriyama S. Expression of p57^{KIP2} in hepatocellular carcinoma: relationship between tumor differentiation and patient survival. *Int J Oncol* 2002; **20**: 769-775
 - 16 **Schwarze SR**, Shi Y, Fu VX, Watson PA, Jarrard DF. Role of cyclin-dependent kinase inhibitors in the growth arrest at senescence in human prostate epithelial and uroepithelial cells. *Oncogen* 2001; **20**: 8184-8192
 - 17 **Ito Y**, Yoshida H, Nakano K, Kobayashi K, Yokozawa T, Hirai K, Matsuzuka F, Matura N, Kuma K, Miyauchi A. Expression of p57^{KIP2} protein in normal and neoplastic thyroid tissues. *Int J Mol Med* 2002; **9**: 373-376
 - 18 **Rosenberg E**, Demopoulos RI, Zeleniuch-Jacquotte A, Yee H, Sorich J, Speyer JL, Newcomb EW. Expression of cell cycle regulators p57(Kip2), cyclinD1, and cyclin E in epithelial ovarian tumors and survival. *Hum Pathol* 2001; **32**: 808-813
 - 19 **Ito Y**, Takeda T, Sasaki Y, Sakon M, Yamada T, Ishiguro S, Imaoka S, Tsujimoto M, Monden M, Matsuura N. Expression of p57/Kip2 protein in extrahepatic bile duct carcinoma and intrahepatic cholangiocellular carcinoma. *Liver* 2002; **22**: 145-149
 - 20 **Lee MH**, Yang HY. Negative regulators of cyclin-dependent kinases and their roles in cancers. *Cell Mol Life Sci* 2001; **58**: 1907-1922
 - 21 **Ito Y**, Takeda T, Wakasa K, Tsujimoto M, Matsuura N. Expression of p57/Kip2 protein in pancreatic adenocarcinoma. *Pancreas* 2001; **23**: 246-250
 - 22 **Keyomarsi K**, Tucker SL, Buchholz TA, Callister M, Ding Y, Hortobagyi GN, Bedrosian I, Knickerbocker C, Toyofuku W, Lowe M, Herliczek TW, Bacus SS. Cyclin E and survival in patients with breast cancer. *N Engl J Med* 2002; **347**: 1566-1575
 - 23 **Georgieva J**, Sinha P, Schandendorf D. Expression of cyclins and cyclin dependent kinases in human benign and malignant melanocytic lesions. *J Clin Pathol* 2001; **54**: 229-235
 - 24 **Oshita T**, Shigemasa K, Nagai N, Ohama K. p27, cyclin E, and CDK2 expression in normal and cancerous endometrium. *Int J Oncol* 2002; **21**: 737-743
 - 25 **Kunimoto Y**, Nakamura T, Ohno M, Kuroda Y. Relationship between immunohistochemical evaluation of thymidylate synthase and proliferating cell nuclear antigen labeling index in gastrointestinal carcinoma. *Oncol Rep* 2004; **12**: 1163-1167
 - 26 **Czyzewska J**, Guzinska-Ustymowicz K, Lebelt A, Zalewski B, Kemon A. Evaluation of proliferating makers Ki-67, PCNA in gastric cancers. *Rocz Akad Med Bialymst* 2004; **49** (Suppl1): 64-66
 - 27 **Tsuboi Y**, Ichida T, Sugitani S, Genda T, Inayoshi J, Takamura M, Matsuda Y, Nomoto M, Aoyagi Y. Overexpression of extracellular signal-regulated protein kinase and its correlation with proliferation in human hepatocellular carcinoma. *Liver Int* 2004; **24**: 432-436
 - 28 **Sato T**, Konishi K, Kimura H, Maeda K, Yabushita K, Tsuji M, Miwa A. Evaluation of PCNA, p53, K-ras, and LOH in endocrine pancreas tumors. *Hepatogastroenterology* 2000; **47**: 875-879
 - 29 **Niijima M**, Yamaguchi T, Ishihara T, Hara T, Kato K, Kondo F, Saisho H. Immunohistochemical analysis and in situ hybridization of cyclooxygenase-2 expression in intraductal papillary - mucinous tumors of the pancreas. *Cancer* 2002; **94**: 1565-1573

Pneumoscotum: A rare manifestation of perforation associated with therapeutic colonoscopy

Kuang-I Fu, Yasushi Sano, Shigeharu Kato, Takahiro Fujii, Masanori Sugito, Masato Ono, Norio Saito, Kiyotaka Kawashima, Shigeaki Yoshida, Takahiro Fujimori

Kuang-I Fu, Yasushi Sano, Shigeharu Kato, Takahiro Fujii, Shigeaki Yoshida, Division of Gastrointestinal Oncology and Digestive Endoscopy, National Cancer Center Hospital East, Kashiwa, Chiba 277-8577, Japan

Masanori Sugito, Masato Ono, Norio Saito, Kiyotaka Kawashima, Division of Surgery, National Cancer Center Hospital East, Kashiwa, Chiba 277-8577, Japan

Takahiro Fujimori, Department of Surgical and Molecular Pathology, Dokkyo University School of Medicine, 880 Kitakobaysashi, Mibu, Shimotuga, Tochigi 321-0293, Japan

Correspondence to: Kuang-I Fu, MD, Department of Surgical and Molecular Pathology, Dokkyo University School of Medicine, 880 Kitakobayashi, Mibu, Shimotuga, Tochigi, 321-0193, Japan. fukuangi@hotmail.com

Telephone: +81-282-86-1111 Fax: +81-282-86-5678

Received: 2004-12-31 Accepted: 2005-01-13

Abstract

Pneumoscotum is uncommon and also rarely reported as a complication associated with colonic perforation. A case of colonic perforation in delayed fashion associated with EMR, revealed by pneumoscotum, is reported and the associated literatures are reviewed. A 52-year-old male received piecemeal EMR for a laterally spreading tumor 35 mm in size in our hospital. He complained of enlargement of the scrotum and revisited our hospital the day after the procedure. A diagnosis of pneumoscotum was made, and as most such cases have been reported to be associated with pneumoperitoneum, colonic perforation was suspected. Free air but no fluid collection was found by abdominal computed tomography, and delayed colonic perforation was diagnosed. However, as there were no clinical signs of peritoneal irritation, conservative treatment was administered and the patient recovered uneventfully. Pneumoscotum could be a sign of colonic perforation after EMR, and treatment should be carefully chosen.

© 2005 The WJG Press and Elsevier Inc. All rights reserved.

Key words: Pneumoscotum; Colonic perforation; Endoscopic mucosal resection

Fu KI, Sano Y, Kato S, Fujii T, Sugito M, Ono M, Saito N, Kawashima K, Yoshida S, Fujimori T. Pneumoscotum: A rare manifestation of perforation associated with therapeutic colonoscopy. *World J Gastroenterol* 2005; 11(32): 5061-5063

<http://www.wjgnet.com/1007-9327/11/5061.asp>

INTRODUCTION

Endoscopic mucosal resection (EMR) is a well-established and non-invasive therapeutic procedure for colorectal neoplasm in the early stage. Although rare, various complications including hemorrhage and perforation have been reported. On the other hand, pneumoscotum is uncommon and it is generally a term used for the expression of the presence of gas within the scrotum^[1]. Although most cases are associated with pneumoperitoneum, there have only been two reported cases after colonoscopy. We report herein, a delayed colonic perforation revealed by a rare manifestation of pneumoscotum after EMR of a laterally spreading tumor in the descending colon.

CASE REPORT

A 52-year-old man underwent total colonoscopy because of a positive fecal occult blood test in our hospital. The colonoscopy showed a laterally spreading tumor with uneven nodules in the descending colon, of which the superficial margin was clear after chromoendoscopy using indigo-carmin dye spraying. (Figure 1A) Magnifying colonoscopy after indigo-carmin dye and crystal violet staining disclosed type IIIc and type IV pit patterns, therefore, this lesion was endoscopically diagnosed as an intra-mucosal carcinoma in an adenoma^[2]. Endoscopic mucosal resection (EMR) was attempted with a curative intent. Subsequently, for better elevation and identification of the submucosal layer, 20 mL of 10% glycerin (GLYCEOL[®]) containing a small amount of 0.4% indigo-carmin dye was injected into the submucosal layer^[3]. The lesion was well-elevated, and was resected with five fragments. After the EMR, magnifying observation revealed a small amount of residual tumor at the periphery, and argon plasma coagulation (APC) was performed for ablation. (Figure 1B) The argon plasma coagulator was used with setting at 2.0 L/min gas flow and with power of 50 W. To reduce the risk of perforation, APC was only applied to coagulate the edge of the EMR site and the duration of application was as short as 5 s. The patient did not complain of abdominal pain or fullness during or immediately after the therapeutic procedure, and no complication such as bleeding or perforation was identified during colonoscopy. The patient's education included no alcohol and no exercise for 1 wk after EMR. He was discharged 1 h after the procedure, uneventfully. However, he revisited our center the next day because of mild inguinal pain and an enlarged scrotum. Before admission, he had taken two meals including a dinner and a breakfast as usual. On admission, his vital

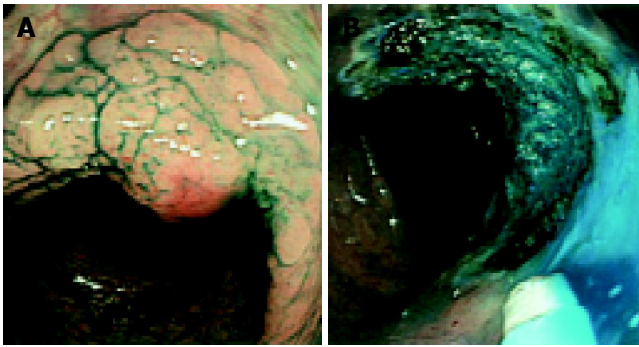


Figure 1 A: Colonoscopy after indigo-carmin dye spraying showed a laterally spreading tumor 35 mm in diameter in the descending colon; B: The ulcer after piecemeal EMR and APC revealed no active bleeding or perforation.



Figure 2 Upright abdominal X-p film showed free air in the sub-diaphragmatic space.

signs were within normal limits excluding mild fever, and physical examination disclosed only an enlarged but light scrotum, and no abdominal tenderness or muscular defense was found. Upright abdominal X-ray film showed free air in the left sub-diaphragm. (Figure 2) Computed tomography (CT) of the chest and abdomen revealed pneumopericardium, pneumoperitoneum and bilateral pneumoscrotum. (Figure 3) The laboratory data showed that WBC count was 12 000 and C-reactive protein was 58 mg/dL, respectively. Other data were within normal limitation. A diagnosis of colonic perforation in delayed fashion was made. After consultation with the surgeons, the patient was first treated medically under NPO; administration of antibiotics (cefmetazole sodium, 4 g/d) and subsequent hyperalimentation were carried out for 2 d. The fever and inguinal pain were relieved within 24 h. The pneumoscrotum resolved within 2 d, the resolution of the pneumoscrotum was judged by CT and physical examination and the symptoms of the patient. C-reactive protein levels decreased from 5.8 to 0.6 mg/dL in 4 d. The permission of oral intake was based on the clinical course, physical examination, laboratory data, and the patient's symptoms. Oral intake was started on the third day at hospital, and he was discharged uneventfully after five days of hospitalization. The removed specimen was histologically diagnosed as a tubular adenoma, with focal carcinoma limited to within the mucosal layer. No muscle layer was identified in the resected specimens.



Figure 3 Abdominal computed tomography disclosed free air in the scrotum.

DISCUSSION

Colonic perforation associated with therapeutic colonoscopy is uncommon, and the reported incidence ranges from 0.073% to 2.14%^[4-6]. It could occur immediately or in a delayed fashion. Most of the signs of colonic perforation are abdominal symptoms including peritonitis. However, our case presented pneumoscrotum as a sign of a colonic perforation after EMR in delayed fashion. Pneumoscrotum is a term, which implies the presence of air within the scrotum^[1]. Although pneumoscrotum associated with pneumomediastinum and subcutaneous emphysema, secondary to pneumothorax is a well-described entity, there have only been two reported cases following colonoscopy and both cases occurred immediately after the procedures^[7-11]. Our patient developed pneumoscrotum in a delayed fashion, which is different from the previous reports. The reason, why we diagnosed the perforation developed in delayed fashion is as follows, first, our patient did not complain of any symptoms related to colonic perforation during EMR or in the recovery room before discharge. Second, repeated review of the recorded video tape of the procedure also revealed no definite perforation. Therefore, the perforation was suggested to have developed in a delayed fashion to firstly create pneumoperitoneum, and the air then reached the scrotum and created pneumoscrotum, which presented as the first symptom and sign of colonic perforation.

Colonic perforation may be intraperitoneal or retroperitoneal, or both^[11]. Our case presented pneumoscrotum, pneumopericardium and pneumoperitoneum, which suggested that the perforation developed in the retroperitoneal space. That our case developed in a delayed fashion also supported that the perforation was retroperitoneal, as, compared to intraperitoneal perforation, retroperitoneal perforation is reported to be relatively painless and to become clear, some hours after the procedure. Furthermore, most cases presenting pneumoscrotum are associated with pneumoperitoneum, like ours^[12-14].

Our case was treated successfully without laparotomy, however, the choice of conservative or surgical treatment for iatrogenic colonic perforation remains controversial^[15-18]. The finding of air in the scrotal sac may be an early sign of a life-threatening condition, or may represent an incidental finding associated with more common benign conditions^[1]. It depends on the local air production or movement of air

from the peritoneal space. Local air production suggests gas gangrene or scrotal trauma, which is infectious and may be fatal, unless treated appropriately. On the other hand, movement of air from the peritoneal space is usually non-infectious and can be treated conservatively. The reported case of pneumoscotum secondary to colonic perforation in the retroperitoneal space following colonoscopy were successfully treated non-operatively^[10,11]. In this case, the choice of non-surgical treatment was based on the following: first, the patient's vital signs were stable; second, the abdominal pain was mild and localized; and third, the pneumoscotum was painless and the air was not locally produced but originated from the pneumoperitoneum. Additionally, and perhaps most important, no unexplained peritoneal fluid was found in the abdominal CT, which suggested no severe peritonitis. Therefore, in this case the pneumoscotum and pneumoperitoneum was finally judged to be non-infectious.

In conclusion, we report a case of colonic perforation occurring in delayed fashion after EMR, which was revealed by pneumoscotum. Although rare, colonoscopists should keep in mind that pneumoscotum could present as a sign of colonic perforation, and the choice of treatment should be chosen carefully.

REFERENCES

- 1 **Watson HS**, Klugo RC, Coffield KS. Pneumoscotum: report of two cases and review of mechanisms of its development. *Urology* 1992; **40**: 517-521
- 2 **Kato S**, Fujii T, Koba I, Sano Y, Fu KI, Parra-Blanco A, Tajiri H, Yoshida S, Rembacken B. Assessment of colorectal lesions using magnifying colonoscopy and mucosal dye spraying : Can significant lesions be distinguished. *Endoscopy* 2001; **33**: 306-310
- 3 **Torii A**, Sakai M, Kajiyama T, Kishimoto H, Kin G, Inoue K, Koizumi T, Ueda S, Okuma M. Endoscopic aspiration mucosectomy as curative endoscopic surgery; analysis of 24 cases of early gastric cancer. *Gastrointest Endosc* 1995; **42**: 475-479
- 4 **Ghazi A**, Grossman M. Complications of colonoscopy and polypectomy. *Surg Clin North Am* 1982; **62**: 889-896
- 5 **Heath B**, Rogers A, Taylor A, Lavergne J. Splenic rupture: an unusual complication of colonoscopy. *Am J Gastroenterol* 1994; **89**: 449-450
- 6 **Lo AY**, Beaton HL. Selective management of colonoscopic perforations. *J Am Coll Surg* 1994; **179**: 333-337
- 7 **Millmond SH**, Goldman SM. Pneumoscotum after spontaneous pneumothorax with air leak. *J Urol* 1991; **145**: 1271-1272
- 8 **Redman JF**, Pahls WL. Pneumoscotum following tracheal intubation. *J Urol* 1985; **133**: 1056-1057
- 9 **Archer GJ**. Pneumoscotum complicating pneumothorax and surgical emphysema. *Br J Urol* 1974; **46**: 343
- 10 **Fishman EK**, Goldman SM. Pneumoscotum after colonoscopy. *Urology* 1981; **18**: 171-172
- 11 **Humphreys F**, Hewetson KA, Dellipiani AW. Massive subcutaneous emphysema following colonoscopy. *Endoscopy* 1984; **16**: 160-161
- 12 **Bray JF**. Pneumoscotum with testicular delineation--a new sign of pneumoperitoneum. *Br J Radiol* 1982; **55**: 867-868
- 13 **Garcia C**, Markowitz RI. Pneumoperitoneum and pneumoscotum caused by gastric perforation. *Am J Perinatol* 1987; **4**: 75-77
- 14 **Coppes MJ**, Roukema JA, Bax NM. Scrotal pneumatocele: a rare phenomenon. *J Pediatr Surg* 1991; **26**: 1428-1429
- 15 **Mana F**, De Vogelaere K, Urban D. Iatrogenic perforation of the colon during diagnostic colonoscopy: endoscopic treatment with clips. *Gastrointest Endosc* 2001; **54**: 258-259
- 16 **Damore LJ**, Rantis PC, Vernava AM, Longo WE. Colonoscopic perforations. Etiology, diagnosis and management. *Dis Colon Rectum* 1996; **39**: 1308-1314
- 17 **Donckier V**, Andre R. Treatment of colon endoscopic perforations. *Acta Chir Belg* 1993; **93**: 60-62
- 18 **Kavin H**, Sinicrope F, Esker AH. Management of perforation of the colon at colonoscopy. *Am J Gastroenterol* 1992; **87**: 161-167

• CASE REPORT •

Recurrent thrombotic occlusion of a transjugular intrahepatic portosystemic stent-shunt due to activated protein C resistance

Elmar Siewert, Jan Salzmann, Edmund Purucker, Karl Schürmann, Siegfried Matern

Elmar Siewert, Jan Salzmann, Edmund Purucker, Siegfried Matern, Department of Internal Medicine III, Aachen University, Aachen, Germany

Karl Schürmann, Department of Diagnostic Radiology, Aachen University, Aachen, Germany

Correspondence to: Dr. Elmar Siewert, Pauwelsstr. 30, Department of Internal Medicine III, Aachen University, Aachen D-52074, Germany. siewert@rwth-aachen.de

Telephone: +49-241-8088634 Fax: +49-241-8082455

Received: 2004-12-30 Accepted: 2005-01-13

Abstract

The transjugular intrahepatic portosystemic stent-shunt (TIPS) has successfully been used in the management of refractory variceal bleeding and ascites in patients with portal hypertension. Major drawbacks are the induction of hepatic encephalopathy and shunt dysfunction. We present a 59-year-old woman with alcoholic liver cirrhosis who received a TIPS because of recurrent bleeding from esophageal varices. Stent occlusion occurred 4 mo after placement of the TIPS. Laboratory testing revealed resistance to activated protein C (APC). Combination therapy with low-dose enoxaparin and clopidogrel could not prevent her recurrent stent occlusion. Finally, therapy with high-dose enoxaparin was sufficient to prevent further shunt complications up to now (follow-up period of 1 year). In conclusion, early occlusion of a TIPS warrants testing for thrombophilia. If risk factors are confirmed, anticoagulation should be intensified. There are currently no evidence-based recommendations regarding the best available anticoagulant therapy and surveillance protocol for patients with TIPS.

© 2005 The WJG Press and Elsevier Inc. All rights reserved.

Key words: Transjugular intrahepatic portosystemic stent-shunt; Resistance to activated protein C; Factor V-Leiden; Thrombophilia; Thrombosis

Siewert E, Salzmann J, Purucker E, Schürmann K, Matern S. Recurrent thrombotic occlusion of a transjugular intrahepatic portosystemic stent-shunt due to activated protein C resistance. *World J Gastroenterol* 2005; 11(32): 5064-5067 <http://www.wjgnet.com/1007-9327/11/5064.asp>

INTRODUCTION

Cirrhosis, the common end stage of various chronic liver diseases, results from the necrosis of liver cells and increased

connective tissue production (fibrosis) with nodule formation. The distorted liver architecture interferes with liver function and blood flow, thereby producing the clinical features of impaired liver cell function and portal hypertension. When the portal vein pressure, which normally is around 7 mmHg, rises above 14 mmHg, splenomegaly, ascites and collaterals develop between the portal and systemic circulation^[1]. Ascites can be treated by diuretics and paracentesis, and esophago-gastric varices by β -blockers, vasoactive drugs (octreotide, terlipressin) and endoscopic procedures (variceal band ligation, sclerotherapy) respectively^[1]. Alternatively, a transjugular intrahepatic portosystemic stent-shunt (TIPS) which leads to portal decompression can be inserted by creation of a communication between a central hepatic vein and an intrahepatic branch of the portal vein. The idea of creating an intrahepatic shunt was first introduced more than 30 years ago^[2]. The use of an expandable metal stent was further developed in the 1980s. The relative ease with which the stent can be placed has led to the widespread use of TIPS for the treatment of many complications of portal hypertension (acute variceal hemorrhage, prevention of re-bleeding from varices, control of ascites, hepato-renal failure, hepato-pulmonary syndrome and hepatic hydrothorax^[3-7]), acute and chronic Budd-Chiari syndrome^[8] or portal vein thrombosis^[9-11]. We report a 59-year-old woman with alcoholic liver cirrhosis, who had recurrent TIPS occlusion after having received a TIPS because of variceal bleeding. Thrombophilia results from resistance to activated protein C (APC) and demands intensification of anticoagulant therapy, which prevents further stent dysfunction.

CASE REPORT

History and examination

Alcoholic liver cirrhosis (Child-Pugh class A) in a 59-year-old woman was complicated by recurrent hemorrhages from esophago-gastric varices. Finally, she was referred to our clinic with the request that a TIPS should be inserted. The past medical history was uneventful, except for an appendectomy at age 12, a hysterectomy because of intramural uterine fibroids and surgery for varicose veins. There was no history of venous thrombosis or embolism, but an episode of transient ischemic attack seemed to have occurred because the patient reported a brief episode of aphasia and weakness in her right arm, 3 years ago. She admitted alcohol dependence for a period of approximately 5 years.

Examination revealed that she was in slightly reduced general health condition and nutritional status with a

BMI of 20.8 kg/m² (58 kg, 1.67 m). There was neither lymphadenopathy nor jaundice nor edema. Some facial telangiectasia and spider naevi on the upper chest could be found, but no palmar erythema or other skin liver signs. Blood pressure was 115/60 mmHg, heart beats were regular at 74/min. Examination of the cardiovascular, respiratory, and abdominal systems was normal.

Blood tests and investigations

Routine laboratory testing revealed the following pathological parameters (normal range): hemoglobin 82 g/L (120-160 g/L), MCV 98 fL (<93 fL), platelets 104 000 G/L (150 000-350 000 G/L), aPTT (activated partial thromboplastin time) 46 s (28-45 s), INR 1.1 and Quick 75% (70-100%), CRP 25 mg/L (<5 mg/L), total protein 54 g/L (66-83 g/L), albumin 28 g/L (34-48 g/L), γ -globulins 22% (14-19%), total bilirubin 1.2 mg/dL (<1.1 mg/dL), γ -GT 120 U/L (<19 U/L), alkaline phosphatase 206 U/L (<180 U/L), pseudocholinesterase 2 127 U/L (>3 500 U/L). Serologically, there was no evidence for current or previous hepatitis A, B, or C.

On abdominal ultrasound, liver size was reduced to 9.6 cm in the right mid-clavicular line, the surface was irregular, the echogenicity enhanced. The spleen was enlarged to 15 cm×5 cm with no ascites. Color Doppler sonography demonstrated orthograde flow in the portal vein, but velocity was reduced to 4 cm/s on duplex sonography. Gastroscopy confirmed the fourth grade esophageal varices with scarring due to previous sclerotherapy, fundal gastric varices, and hypertensive gastropathy.

Treatment and follow-up

A TIPS (expandable metal Wallstent, Boston Scientific/Ratingen Germany, 10 mm in diameter) was inserted without any short-term complications. Post-interventionally, 75 mg of clopidogrel, an inhibitor of platelet aggregation, was taken orally once daily, and the patient was discharged from the hospital. The portocaval pressure gradient decreased from 24 to 7 mmHg. On an outpatient-visit 4 mo later, the patient was in good general health and asymptomatic, but color Doppler sonography and duplex sonography revealed thrombotic occlusion of the TIPS. Therefore, she was re-admitted to our hospital. Gastroscopy again found the fourth grade esophageal varices (Figure 1A). Shunt angiography verified TIPS occlusion (Figure 2A), and shunt revision was successfully performed (Figure 2B). Control gastroscopy confirmed excellent size reduction of the varices (Figure 1B). Additionally, screening laboratory testing for thrombophilia was initiated, and heterozygous factor V-Leiden resulting in resistance to APC was identified by PCR. Therefore, clopidogrel medication was supplemented with daily subcutaneous self-injections of 40 mg enoxaparin, a low molecular weight heparin. Intensified anticoagulation could not prevent the recurrent stent occlusion 2 mo after revision of the shunt, which became obvious on routine color Doppler examination after an additional 2 mo. Once again, TIPS revision was successfully performed. Due to repeated thrombosis, anticoagulant therapy was further intensified. In addition to clopidogrel, high-dose enoxaparin (60 mg twice daily s.c.) was initiated, which was sufficient to

prevent further shunt complications up to now, i.e. a follow-up period of 1 year.

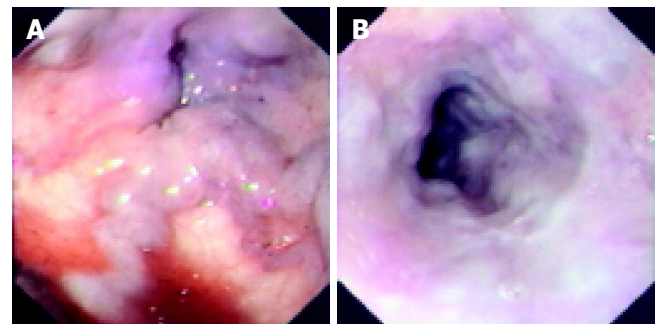


Figure 1 Esophageal varices before (A) and after (B) TIPS revision.

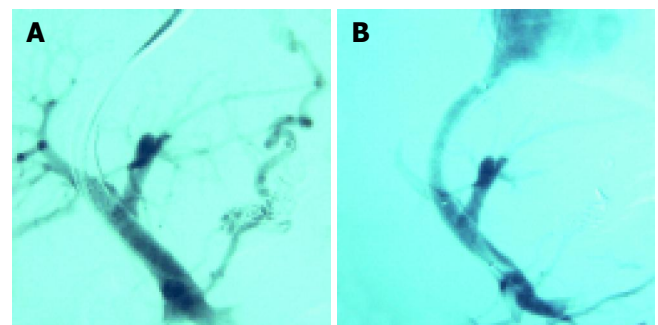


Figure 2 Shunt angiography before (A) and after (B) TIPS revision.

DISCUSSION

Though TIPS placement is used as a treatment modality for the complications of portal hypertension, only in the case of refractory ascites (four randomized controlled trials) and recurrent variceal hemorrhage, as in the patient presented here (12 randomized controlled trials), TIPS has been compared to other forms of therapy. The superiority of TIPS with regard to symptom control could be demonstrated, whereas insertion of a TIPS could not improve survival. TIPS is widely accepted as the main second-line treatment option for acute variceal hemorrhage not responding to other treatment options^[3-7,12,13].

On the one hand, TIPS is an elegant therapeutic procedure with a low (1-2%) procedure-related mortality^[4,5,7] thus offering the chance of taking a diagnostic transjugular liver biopsy in patients with advanced liver cirrhosis. Moreover, TIPS does not hamper or exclude future liver transplantation because normal anatomy of the extrahepatic vessels is preserved. Indeed, it can serve as a valuable bridging procedure to liver transplantation. On the other hand, placement of a TIPS can be complicated by substantial acute and chronic morbidity^[3,4,14] (Table 1). The major long-term drawback of TIPS besides the induction or worsening of hepatic encephalopathy^[15,16] is stent dysfunction due to occlusion or stenosis. Meta-analysis indicates that within 2 years of TIPS creation, re-intervention to re-establish or maintain the patency of the shunt is required in 70-90% of patients, and total occlusion occurs in 20-40% of patients.

Nevertheless the secondary or assisted patency rate during a 2- to 5-year follow-up period is between 72% and 91%^[3,16-20].

Stent occlusion during the first month after TIPS placement is mainly a consequence of shunt thrombosis, thereafter, shunt stenosis in most cases is the result of pseudointimal hyperplasia^[3-5,20]. We described a patient with repeated shunt thrombosis for a longer time period due to resistance to APC. Hence, in patients with recurrent thrombotic TIPS occlusion, hypercoagulopathy as a risk factor for shunt complications should be ruled out. APC resistance (or Factor V-Leiden) as a cause of familial thrombophilia was first described in 1993^[21]. A point mutation in the gene encoding factor V (G1691A) leads to a conformational change at the site, where factor Va is cleaved by APC and thereby inactivated. Prolonged activation of factor V results in hypercoagulopathy. Heterozygous factor V mutation carriers have a 5-10-fold increased risk of thromboembolic events, and in patients with homozygous factor V mutation, the risk shoots up further^[22,23]. Prevalence of the mutation is about 5% in the normal population, and inheritance follows an autosomal dominant manner. Other major causes of inherited and acquired thrombophilia which have to be excluded are listed in Table 2.

In the patient described here, escalation of anticoagulation combining the usually given inhibitors of platelet aggregation with low molecular weight heparin in therapeutic dosage was sufficient to prevent further shunt occlusions. However, no data are currently available on the optimal anticoagulant therapy to prevent shunt occlusion. When a TIPS is placed for the prevention of variceal re-bleeding, peri-interventional anticoagulation with heparin is recommended to reduce early shunt occlusion^[17]. Additional therapy with the inhibitors of platelet aggregation, ticlopidine and trapidil for 6 mo after initial intravenous heparin for 24 h significantly reduces the rate of TIPS stenosis^[24]. In a recent review article, the use of subcutaneous low-dose low molecular weight heparin for 4 wk, together with trapidil and ticlopidine for 12 mo^[3] is suggested. Higher dosage of heparin seems to be necessary in patients with thrombophilia, but in a controlled trial, phenprocoumon does not reduce the risk of early stent occlusion or later stent stenosis in patients without hypercoagulopathy^[25]. Moreover, since the risk of bleeding is significant in patients with cirrhosis, the use of oral anticoagulants with long half-lives is problematic. Alternatively, coated stents or drug-eluting stents can probably protect against shunt thrombosis, and preliminary results indicate that the rates of stent thrombosis and occlusion can be reduced^[26-30]. However, patients must be selected more carefully, because covered stents have a higher risk of hepatic encephalopathy^[31].

The high rates of shunt dysfunction with the resulting risk of re-bleeding ask for a surveillance program of TIPS patients. Unfortunately, follow-up protocols differ significantly between centers because the optimal regime is unknown. Duplex ultrasonography at intervals of 3-6 mo has been practiced in most studies exhibiting a sensitivity of 53-100% and a specificity of 62-98% in detecting shunt insufficiency^[3,4,17], although a recent study has reported a poorer sensitivity of only 35%^[32]. However, the finding of shunt dysfunction does not always make shunt revision

mandatory. When duplex sonography confirms TIPS occlusion or when the technique does not yield a clear result, an endoscopic re-evaluation is followed. Only when significant varices can be demonstrated, shunt angiography with measurement of the portal-venous pressure gradient is necessary and clearly discriminates whether radiological shunt revision is indicated or not.

In conclusion, TIPS is an elegant procedure which simultaneously serves as a diagnostic and therapeutic tool in patients with complications of portal hypertension. Shunt dysfunction by thrombosis or neointimal proliferation, the major complication besides worsening of hepatic encephalopathy, may be reduced temporarily by using inhibitors of thrombocyte aggregation and (low molecular weight) heparin. Repeated thrombotic TIPS occlusion is mostly due to thrombophilia, which requires more extensive laboratory testing to detect the underlying inherited or acquired coagulation disorder(s).

Table 1 Complications of TIPS

Acute complications	Chronic complications
Transcapsular puncture	Deterioration of liver function
Intrahepatic hematoma	New or worsened hepatic encephalopathy
Intraperitoneal bleed	TIPS dysfunction (thrombosis, stenosis)
Fistulae:	Hyperdynamic circulation and cardiac failure
Hemobilia	
Arterio-portal fistulae	
Malpuncture of other organs	
Portal vein thrombosis	
TIPS dislocation	
Infections and sepsis	
Hemolysis	
Contrast media-related complications:	
Allergic reactions	
Acute renal failure	
Cardiac arrhythmias/myocardial infarction	

Table 2 Causes of thrombophilia

Hereditary causes	Acquired causes
Resistance to APC = Factor V-Leiden (Factor V gene mutation G1691A)	Antiphospholipid syndrome
Prothrombin gene mutation (G20210A)	Lupus anticoagulant
Antithrombin III deficiency	Malignancy and myeloproliferative disorders
Hyperhomocysteinemia (MTHFR mutation)	Hyperviscosity (multiple myeloma)
Protein C deficiency	Cardiac failure and any type of shock
Protein S deficiency	Nephrotic syndrome
Dysfibrinogenemia	Liver cirrhosis
Increased factor VIII and PAI-1	Protein-losing enteropathy
Plasminogen deficiency	Chronic inflammatory bowel disease
tPA deficiency	Hemolytic uremic syndrome
	Thrombotic thrombocytopenic purpura
	Post-surgery, post-traumatic, immobilization
	Oral contraceptives and smoking
	Obesity
	Pregnancy
	Geriatric patients

REFERENCES

- 1 **Sherlock S**, Dooley J. Diseases of the liver and biliary system. 10th ed. Oxford: *Blackwell Sci Pub* 1997: 135-180
- 2 **Rosch J**, Hanafee W, Snow H, Barenfus M, Gray R. Transjugular intrahepatic portacaval shunt. An experimental work. *Am J Surg* 1971; **121**: 588-592
- 3 **Rossle M**, Grandt D. TIPS: an update. *Best Pract Res Clin Gastroenterol* 2004; **18**: 99-123
- 4 **Boyer TD**. Transjugular intrahepatic portosystemic shunt: current status. *Gastroenterology* 2003; **124**: 1700-1710
- 5 **Rosado B**, Kamath PS. Transjugular intrahepatic portosystemic shunts: an update. *Liver Transpl* 2003; **9**: 207-217
- 6 **McCashland TM**. Current use of transjugular intrahepatic portosystemic shunts. *Curr Gastroenterol Rep* 2003; **5**: 31-38
- 7 **Hassoun Z**, Pomier-Layrargues G. The transjugular intrahepatic portosystemic shunt in the treatment of portal hypertension. *Eur J Gastroenterol Hepatol* 2004; **16**: 1-4
- 8 **Menon KV**, Shah V, Kamath PS. The Budd-Chiari-Syndrome. *N Engl J Med* 2004; **350**: 578-585
- 9 **Jiang ZB**, Shan H, Shen XY, Huang MS, Li ZR, Zhu KS, Guan SH. Transjugular intrahepatic portosystemic shunt for palliative treatment of portal hypertension secondary to portal vein tumor thrombosis. *World J Gastroenterol* 2004; **10**: 1881-1844
- 10 **Bilbao JI**, Elorz M, Vivas I, Martinez-Cuesta A, Bastarrika G, Benito A. Transjugular intrahepatic portosystemic shunt (TIPS) in the treatment of venous symptomatic chronic portal thrombosis in non-cirrhotic patients. *Cardiovasc Intervent Radiol* 2004; **27**: 474-480
- 11 **Opitz T**, Buchwald AB, Lorf T, Awuah D, Ramadori G, Nolte W. The transjugular intrahepatic portosystemic stent-shunt (TIPS) as rescue therapy for complete Budd-Chiari syndrome and portal vein thrombosis. *Z Gastroenterol* 2003; **41**: 413-418
- 12 **Lata J**, Hulek P, Vanasek T. Management of acute variceal bleeding. *Dig Dis* 2003; **21**: 6-15
- 13 **Ferguson JW**, Tripathi D, Hayes PC. Review article: the management of acute variceal bleeding. *Aliment Pharmacol Ther* 2003; **18**: 253-262
- 14 **Kamath PS**, McKusick MA. Transvenous intrahepatic portosystemic shunts. *Gastroenterology* 1996; **111**: 1700-1705
- 15 **Luca A**, D'Amico G, La Galla R, Midiri M, Morabito A, Pagliaro L. TIPS for prevention of recurrent bleeding in patients with cirrhosis: meta-analysis of randomized clinical trials. *Radiology* 1999; **212**: 411-421
- 16 **Papatheodoridis GV**, Goulis J, Leandro G, Patch D, Burroughs AK. Transjugular intrahepatic portosystemic shunt compared with endoscopic treatment for prevention of variceal rebleeding: A meta-analysis. *Hepatology* 1999; **30**: 612-622
- 17 **Rossle M**, Siegerstetter V, Huber M, Ochs A. The first decade of the transjugular intrahepatic portosystemic shunt (TIPS): state of the art. *Liver* 1998; **18**: 73-89
- 18 **Tripathi D**, Helmy A, Macbeth K, Balata S, Lui HF, Stanley AJ, Redhead DN, Hayes PC. Ten years' follow-up of 472 patients following transjugular intrahepatic portosystemic stent-shunt insertion at a single centre. *Eur J Gastroenterol Hepatol* 2004; **16**: 9-18
- 19 **ter Borg PC**, Hollemans M, Van Buuren HR, Vleggaar FP, Groeneweg M, Hop WC, Lameris JS. Transjugular intrahepatic portosystemic shunts: long-term patency and clinical results in a patient cohort observed for 3-9 years. *Radiology* 2004; **231**: 537-545
- 20 **van Buuren HR**, ter Borg PC. Transjugular intrahepatic portosystemic shunt (TIPS): indications and long-term patency. *Scand J Gastroenterol Suppl* 2003; **239**: 100-104
- 21 **Dahlback B**, Carlsson M, Svensson PJ. Familial thrombophilia due to a previously unrecognized mechanism characterized by poor anticoagulant response to activated protein C: prediction of a cofactor to activated protein C. *Proc Natl Acad Sci USA* 1993; **90**: 1004-1008
- 22 **Ridker PM**, Miletich JP, Stampfer MJ, Goldhaber SZ, Lindpaintner K, Hennekens CH. Factor V Leiden and risks of recurrent idiopathic venous thromboembolism. *Circulation* 1995; **92**: 2800-2802
- 23 **Dulicek P**, Maly J, Safarova M. A prospective study of asymptomatic carriers of the factor V Leiden mutation to determine the incidence of venous thromboembolism. *Ann Intern Med* 2001; **135**: 322-327
- 24 **Siegerstetter V**, Huber M, Ochs A, Blum HE, Rossle M. Platelet aggregation and platelet-derived growth factor inhibition for prevention of insufficiency of the transjugular intrahepatic portosystemic shunt: a randomized study comparing trapidil plus ticlopidine with heparin treatment. *Hepatology* 1999; **29**: 33-38
- 25 **Sauer P**, Theilmann L, Herrmann S, Bruckner T, Roeren T, Richter G, Stremmel W, Stiehl A. Phenprocoumon for prevention of shunt occlusion after transjugular intrahepatic portosystemic stent shunt: a randomized trial. *Hepatology* 1996; **24**: 1433-1436
- 26 **Rossi P**, Salvatori FM, Fanelli F, Bezzi M, Marcelli G, Pepino D, Riggio O, Passariello R. Polytetrafluoroethylene-covered nitinol stent-graft for transjugular intrahepatic portosystemic shunt creation: 3-year experience. *Radiology* 2004; **231**: 820-830
- 27 **Charon JP**, Alaeddin FH, Pimpalwar SA, Fay DM, Olliff SP, Jackson RW, Edwards RD, Robertson IR, Rose JD, Moss JG. Results of a retrospective multicenter trial of the Viatorr expanded polytetrafluoroethylene-covered stent-graft for transjugular intrahepatic portosystemic shunt creation. *J Vasc Interv Radiol* 2004; **15**: 1219-1230
- 28 **Haskal ZJ**, Weintraub JL, Susman J. Recurrent TIPS thrombosis after polyethylene stent-graft use and salvage with polytetrafluoroethylene stent-grafts. *J Vasc Interv Radiol* 2002; **13**: 1255-1259
- 29 **Cejna M**, Peck-Radosavljevic M, Thurnher SA, Hittmair K, Schoder M, Lammer J. Creation of transjugular intrahepatic portosystemic shunts with stent-grafts: initial experiences with a polytetrafluoroethylene-covered nitinol endoprosthesis. *Radiology* 2001; **221**: 437-446
- 30 **Bureau C**, Garcia-Pagan JC, Otal P, Pomier-Layrargues G, Chabbert V, Cortez C, Perreault P, Peron JM, Abralde JG, Bouchard L, Bilbao JI, Bosch J, Rousseau H, Vinel JP. Improved clinical outcome using polytetrafluoroethylene-coated stents for TIPS: result of a randomized study. *Gastroenterology* 2004; **126**: 469-475
- 31 **Rossle M**, Mullen KD. Long-term patency is expected with covered TIPS stents: this effect may not always be desirable! *Hepatology* 2004; **40**: 495-497
- 32 **Owens CA**, Bartolone C, Warner DL, Aizenstein R, Hibblen J, Yaghamai B, Wiley TE, Layden TJ. The inaccuracy of duplex ultrasonography in predicting patency of transjugular intrahepatic portosystemic shunts. *Gastroenterology* 1998; **114**: 975-980

• CASE REPORT •

EUS diagnosis of ectopic opening of the common bile duct in the duodenal bulb: A case report

Miodrag Krstic, Bojan Stimec, Radmilo Krstic, Milenko Ugljesic, Sribislav Knezevic, Ivan Jovanovic

Miodrag Krstic, Radmilo Krstic, Milenko Ugljesic, Sribislav Knezevic, Ivan Jovanovic, Clinical Center of Serbia, Belgrade, Serbia and Montenegro
Bojan Stimec, Institute for Anatomy, School of Medicine, Belgrade, Serbia and Montenegro
Correspondence to: Miodrag Krstic, Clinical Center of Serbia, Clinic for Gastroenterology, 2 Koste Todorovica, Belgrade 11000, Serbia and Montenegro. misa@tehnicom.net
Telephone: +381-11-361-5575 Fax: +381-11-361-5575
Received: 2005-02-22 Accepted: 2005-04-09

Abstract

Among the various congenital anomalies of the biliary system, an ectopic opening of the common bile duct (CBD) in the duodenal bulb is extremely rare. ERCP is essential for diagnosing the anomaly. A 55-year-old male was admitted to hospital for severe right upper quadrant abdominal pain, followed by fever, chills, elevated body temperature and mild icterus. The diagnosis of ectopic opening of CBD in the duodenal bulb was established on endoscopic ultrasonography (EUS), which clearly demonstrated dilated CBD, with multiple stones and air in the lumen, draining into the bulb. A normal pancreatic duct, which did not drain into the bulb, was also observed. This finding was confirmed on ERCP and surgery. As far as we know, this is the first case of this anomaly diagnosed by EUS. Ectopic opening of the CBD in the duodenal bulb is not an incidental finding, but a pathologic condition which can be associated with clinical entities such as recurrent or intractable duodenal ulcer, recurrent biliary pain, choledocholithiasis or acute cholangitis. Endoscopic ultrasonography features allow preoperative diagnosis of this anomaly and can replace ERCP as a first diagnostic tool in such clinical circumstances. Embryology of the anomalies of the extrahepatic biliary tree has been also reviewed.

© 2005 The WJG Press and Elsevier Inc. All rights reserved.

Key words: Ectopic opening; Common bile duct; Congenital anomaly; Endoscopic ultrasound

Krstic M, Stimec B, Krstic R, Ugljesic M, Knezevic S, Jovanovic I. EUS diagnosis of ectopic opening of the common bile duct in the duodenal bulb: A case report. *World J Gastroenterol* 2005; 11(32): 5068-5071
<http://www.wjgnet.com/1007-9327/11/5068.asp>

INTRODUCTION

Among the various congenital anomalies of the biliary

system, an ectopic opening of the common bile duct (CBD) in the duodenal bulb is extremely rare. Until recently, there were only a few sporadic case reports of this anomaly in the literature worldwide^[1-3]. In 2003, Lee *et al.*, presented the largest study consisting of 18 Patients with this anomaly^[4]. In that study, as well as in case reports published elsewhere, the diagnosis of an ectopic opening of the CBD in the duodenal bulb was established on ERCP when: (1) an orifice was observed in the bulb by duodenoscopy or upper endoscopy, and the bile duct and/or the pancreatic duct were directly visualized radiographically, when contrast was injected via this opening; (2) there was direct drainage of the CBD into the duodenum on cholangiography; and (3) there was no evidence of a papilla-like structure in the second or third portion on duodenoscopic examination^[1-4]. However, ERCP is an invasive endoscopic procedure which is associated with significantly greater morbidity and mortality, when compared with either upper endoscopy or endoscopic ultrasonography (EUS)^[5]. Septic complications of ERCP can be life-threatening^[6]. Mortality rates for post-ERCP cholangitis vary from 10 to 16%^[7]. On the other hand, diagnostic EUS is a non-invasive endoscopic procedure with negligible rate of complications. We present, for the first time, a patient with ectopic opening of the CBD in duodenal bulb, diagnosed by EUS.

CASE REPORT

A 55-year-old male presented at the University Clinic for Gastroenterology on March 27, 2002, with severe right upper quadrant abdominal pain, followed by fever, chills, elevated body temperature (39.5 °C) and mild icterus. His history revealed two identical attacks in the previous 4 mo, which subsided with parenteral antibiotics at a local hospital. His body weight loss in the previous 6 mo was more than 10 kg. In 1998, he was operated on due to malignant melanoma and had a history of non-insulin dependent diabetes mellitus for the previous 4 years. On admission, physical examination revealed only mild tenderness in the upper abdomen followed by obscure jaundice. Routine biochemistry revealed cholestatic pattern: elevated alkaline phosphatase 149 U/L ($n < 70$ U/L), gamma glutamyl transpeptidase 404 U/L ($n < 35$ U/L), conjugated bilirubin 35 $\mu\text{mol/L}$ ($n < 11$ $\mu\text{mol/L}$) and ALT 88 U/L ($n < 23$ U/L). Abdominal ultrasonography performed at our hospital disclosed gall bladder with few small gallstones, dilatation of the common bile duct of more than 20 mm, with suspicious stones in the lumen, and a pseudotumor in the projection of the duodenal bulb. The computed tomography finding was unremarkable revealing

only discreet intrahepatic biliary dilatation in left liver lobe. Endoscopic examination of the duodenum disclosed bulbar deformity without ulcers and erosions, as well as a slit-like opening on the posterior bulbar wall from which bile flowed intermittently, especially when suction was applied with the endoscope (Figure 1). At that particular moment, our idea was that a spontaneous fistula, secondary to choledocholithiasis or ulcer disease had occurred in this patient. Endoscopic ultrasonography examination of the upper GI tract and biliary system (using radial 7.5/12 MHz switchable probe-Olympus device) was carried on. EUS exploration from the duodenal bulb with the 7.5 MHz radial probe clearly demonstrated dilated common bile duct with multiple stones and air in the lumen, draining in the duodenal bulb (Figures 2A and B). There were no EUS signs of fistula. The mild lobulation and inhomogeneity of pancreatic parenchyma was also documented, since the main pancreatic duct appeared non-dilated and unchanged and was not draining into the duodenal bulb (Figure 2C).



Figure 1 Endoscopic image: deformed duodenal bulb with slit-like opening (black arrow).

The final diagnosis of an ectopic opening of the CBD in the duodenal bulb was confirmed on ERCP, where markedly dilated biliary tree with stones was directly visualized radiographically on injection of contrast via the orifice observed previously in the bulb. Technically, it was especially demanding to cannulate the opening in the duodenal bulb blindly with duodenoscope placed horizontally in the stomach body (Figure 3A). At the end of this procedure, cannulation of the major duodenal papilla, which appeared regularly in the descending duodenum, disclosed the unchanged main pancreatic duct, making a loop in the head of pancreas (Figure 3B).

The patient underwent surgery including open cholecystectomy, bile duct exploration with subsequent extraction of biliary stones, and choledochenterostomy (Figure 4). On the 7th d after the operation, the patient was discharged from the hospital. Two years after the operation, he has been doing well and denied any symptoms.

DISCUSSION

The embryonic development of the liver and biliary tree begins late in the 3rd wk of intrauterine development, when a small hepatic diverticulum arises from the thickened area of endoderm (epithelium), at the junction of the foregut and the midgut^[8]. The cells of hepatic diverticulum penetrate the mesenchyma of the ventral mesogastrium, dividing into a ventral and a dorsal bud. The ventral bud (pars cystica) stays close to the free edge of the mesogastrium, and, after developing a lumen, forms the primitive gall bladder. The dorsal bud (pars hepatica) divides in turn to the left and right liver lobe primordia. As the liver and biliary tree develop inseparably, these primordia multiply to form an epithelial spongework or cords which come in close relation

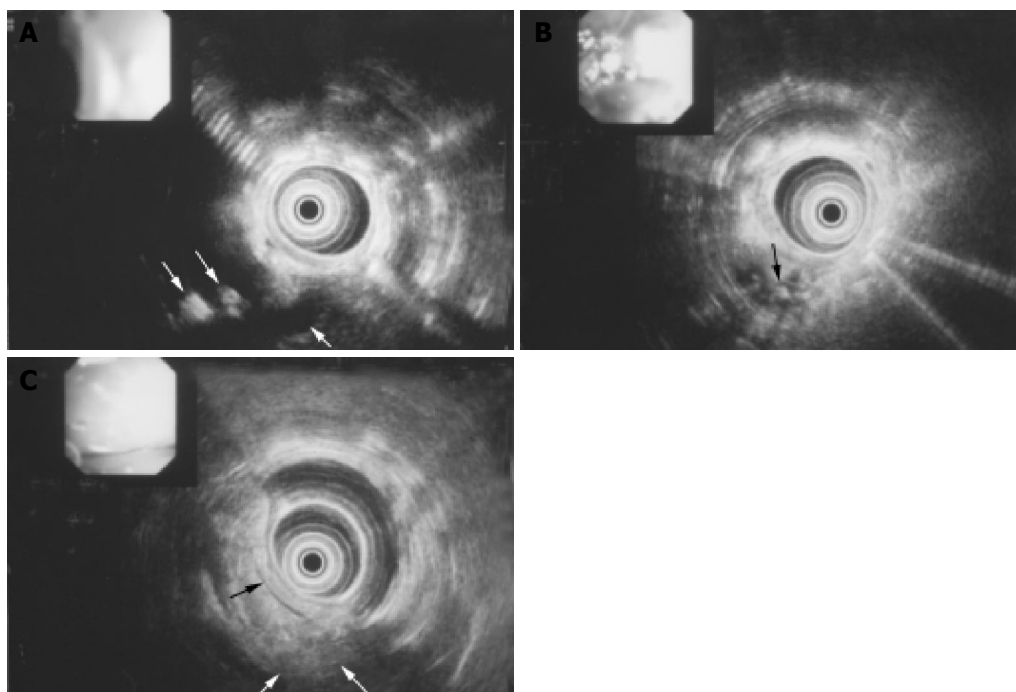


Figure 2 EUS image **A**: EUS image: dilated common bile duct (thick arrow) with stones and air (thin arrows) draining in the bulb; **B**: EUS image: dilated common

bile duct with stones (black arrow) in the lumen; **C**: EUS image: unchanged main pancreatic duct (black arrow) with parenchymal irregularity (white arrows).

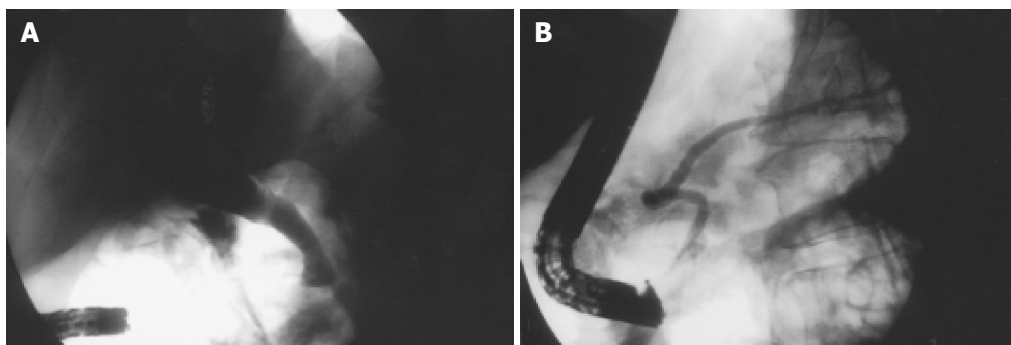


Figure 3 ERCP image. **A:** ERCP image: dilated biliary tree filled with stones cannulated from the duodenal bulb; **B:** ERCP image: the main pancreatic duct

making the loop in the pancreatic head.

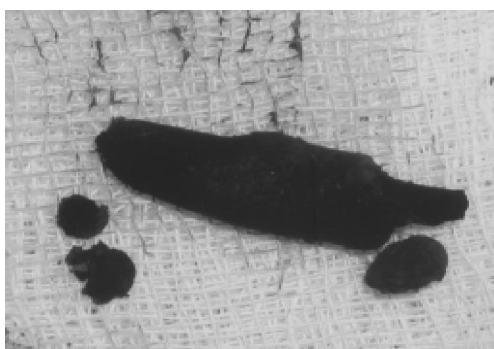


Figure 4 Extracted biliary stones.

to vitelline and umbilical veins. The stem of the hepatic primordium becomes the bile duct, its connection to the ventral bud forms the cystic duct, and the divisions of the dorsal bud become left and right hepatic ducts. Initially, the gall bladder is a hollow organ, but, as a result of proliferation of its epithelial lining, it becomes temporarily solid. The definite lumen develops by recanalization of the epithelium. The intra- and extrahepatic ducts also go through a solid and recanalization stage in their development. If their lumen fails to reopen, the ducts will appear as narrow, fibrous cords. Occasionally, such an atresia is limited to a small portion of the bile duct only. Another important feature of the bile duct development is rotation of the primitive duodenum 90° on its longer axis, which brings the bile duct dorsal to the upper limb of duodenum.

The development of duodenum, pancreas, and bile ducts has been wittily described as embryological “traffic jam”^[9]. In a case report of a complete absence of bile and pancreatic ducts in a newborn^[10], it has been postulated that there may be a genetic factor related to defects in the liver and pancreas. Like those genes themselves, their products are largely unknown, as are the interactions of the few products that have been identified^[8].

Variations in the extrahepatic duct topography, which extend from the complete absence of the CBD^[11], anomalous opening of the biliary tree^[12], through accessory hepatic ducts to duplications of the gall bladder or the bile duct, are thought to arise from the difference in extension and projection of the analage derived from the caudal hepatic bud.

The description of the development of liver, pancreas and connected duct systems provides no evidence that two extrahepatic ducts with separate openings into the gastrointestinal tract are stages in normal organogenesis^[13], so that the development of double common bile duct can be ascribed to disturbances in recanalization of the hepatic primordium. The accessory bile duct can open into various parts of the digestive tube-stomach^[14], all four portions of the duodenum, pancreatic duct, or can be only presented by a septum in the common bile duct^[15].

According to the above-mentioned criteria for diagnosing ectopic opening of CBD in the duodenal bulb^[4], in such cases there should be no evidence of a papilla-like structure in the lower duodenum. This is in contradiction to a previous report^[6], which permits the possibility of the pancreatic duct opening elsewhere in the duodenum, apart from the ectopic CBD. In our case, we clearly demonstrated an ectopic opening of CBD in the duodenal bulb, and, apart from it, the existence of a normal pancreatic duct opening through the papilla in the descending duodenum. Therefore, we hypothesize that the primary embryological event was the duplication of the common bile duct (double CBD). One of those ducts had an anomalous opening in the duodenal bulb, while the other took a normal course to join the pancreatic duct. The latter duct probably underwent atresia, which left the whole biliary drainage through the ectopically positioned duct. This is in accordance with the fact, that the pancreatic duct has been visualized in only 1/8 and 7/18 cases in the previous studies on ectopic opening of CBD into the duodenal bulb^[6,4]. Therefore, we suggest that the 3rd criterion concerning the papilla-like structure in the descending duodenum should be discarded.

An ectopic opening of the common bile duct in the duodenal bulb is extremely rare. The percentage of asymptomatic individuals is unknown, since there was no consistent autopsy study^[4]. Until recently there were only a few sporadic case reports of symptomatic anomaly^[1-3]. However, true incidence could be much higher than presently appreciated, as Lee *et al.* stressed recently^[4]. They concluded that ectopic opening of the CBD in the duodenal bulb is not an incidental finding, but a pathologic condition which can be associated with clinical entities such as recurrent or intractable duodenal ulcer, recurrent biliary pain, choledocholithiasis or acute cholangitis. Our patient had two episodes of acute cholangitis in regional hospitals before establishing correct diagnosis.

The same scenario took place in other studies, whereas anomaly was not diagnosed in any patient before referral to tertiary institutions, where the patients were evaluated^[16].

The diagnostic tools for such entities ranged from plain upper GI barium X-ray^[17], operative cholangiography^[1] to CT^[16], but ERCP is the “golden standard”. However, ERCP is an invasive endoscopic procedure, which is associated with a variety of possible complications^[18]. Some of them, like sepsis can be life-threatening^[6]. Mortality rate for post-ERCP cholangitis is very high, reaches even 16%^[7]. On the other hand, diagnostic EUS is a non-invasive endoscopic procedure with negligible rate of complications.

For the first time, we presented clear EUS features of this anomaly, which undoubtedly excluded other possibilities in differential diagnosis: fistula secondary to ulcer disease or choledocholithiasis or spontaneous biliodigestive fistula. Endoscopic ultrasonography features allow preoperative diagnosis of this anomaly and can replace ERCP as a first diagnostic tool in such clinical circumstances.

REFERENCES

- 1 **Lindner HH**, Pena VA, Ruggeri RA. A clinical and anatomical study of anomalous terminations of the common bile duct into the duodenum. *Ann Surg* 1976; **184**: 626-632
- 2 **Kubota T**, Fujioka T, Honda S, Suetsuna J, Matsunaga K, Terao H, Nasu M. The papilla of Vater emptying into the duodenal bulb. Report of two cases. *Jpn J Med* 1988; **27**: 79-82
- 3 **Doty J**, Hassall E, Fonkalsrud EW. Anomalous drainage of the common bile duct into the fourth portion of the duodenum. Clinical sequelae. *Arch Surg* 1985; **120**: 1077-1079
- 4 **Lee SS**, Kim MH, Lee SK, Kim KP, Kim HJ, Bae JS, Kim HJ, Seo DW, Ha HK, Kim JS, Kim CD, Chung JP, Min YI. Ectopic opening of the common bile duct in the duodenal bulb: clinical implications. *Gastrointest Endosc* 2003; **57**: 679-682
- 5 **Cotton PB**, Lehman G, Vennes J, Geenen JE, Russell RC, Meyers WC, Liguory C, Nickl N. Endoscopic sphincterotomy complications and their management: an attempt at consensus. *Gastrointest Endosc* 1991; **37**: 383-393
- 6 **Freeman ML**, DiSario JA, Nelson DB, Fennerty MB, Lee JG, Bjorkman DJ, Overby CS, Aas J, Ryan ME, Bochna GS, Shaw MJ, Snady HW, Erickson RV, Moore JP, Roel JP. Risk factors for post-ERCP pancreatitis: a prospective, multicenter study. *Gastrointest Endosc* 2001; **54**: 425-434
- 7 **Freeman ML**, Nelson DB, Sherman S, Haber GB, Herman ME, Dorsher PJ, Moore JP, Fennerty MB, Ryan ME, Shaw MJ, Lande JD, Pheley AM. Complications of endoscopic biliary sphincterotomy. *N Engl J Med* 1996; **335**: 909-918
- 8 **Knisely AS**. Biliary tract malformations. *Am J Med Genet A* 2003; **122**: 343-350
- 9 **Heij HA**, Niessen GJ. Annular pancreas associated with congenital absence of the gallbladder. *J Pediatr Surg* 1987; **22**: 1033
- 10 **Nakamura K**, Mitsubuchi H, Miyayama H, Yatsunami K, Ishimatsu J, Yamamoto T, Endo F. Complete absence of bile and pancreatic ducts in a newborn: a new entity of congenital anomaly in hepatopancreatic development. *J Hum Genet* 2003; **48**: 380-384
- 11 **Olsha O**, Steiner A, Rivkin LA, Sheinfeld A. Congenital absence of the anatomic common bile duct. Case report. *Acta Chir Scand* 1987; **153**: 387-390
- 12 **Rajnakova A**, Tan WT, Goh PM. Double papilla of Vater. A rare anatomic anomaly observed in endoscopic retrograde cholangiopancreatography. *Surg Laparosc Endosc* 1998; **8**: 345-348
- 13 **Teilm D**. Double common bile duct. Case report and review. *Endoscopy* 1986; **18**: 159-161
- 14 **Kanematsu M**, Imaeda T, Seki M, Goto H, Doi H, Shimokawa K. Accessory bile duct draining into the stomach: Case report and review. *Gastrointest Radiol* 1992; **17**: 27-30
- 15 **Yamashita K**, Oka Y, Urakami A, Iwamoto S, Tsunoda T, Eto T. Double common bile duct: A case report and a review of the Japanese literature. *Surgery* 2002; **131**: 676-681
- 16 **Lee HJ**, Ha HK, Kim MH, Jeong YK, Kim PN, Lee MG, Kim JS, Suh DJ, Lee SG, Min YI, Auh YH. ERCP and CT findings of ectopic drainage of the common bile duct into the duodenal bulb. *AJR Am J Roentgenol* 1997; **169**: 517-520
- 17 **Holz K**. Atypical orifice of the common bile duct during localization of the papilla Vateri on the rear wall of the duodenal bulb. *Fortschr Geb Rontgenstr Nuklearmed* 1970; **112**: 409-410
- 18 **Kohut M**, Nowak A, Nowakowska-Duiawa E, Marek T. Presence and density of common bile duct microlithiasis in acute biliary pancreatitis. *World J Gastroenterol* 2002; **8**: 558-561

Colonic duplication in adults: Report of two cases presenting with rectal bleeding

C Fotiadis, M Genetzakis, I Papandreou, EP Misiakos, E Agapitos, GC Zografos

C Fotiadis, I Papandreou, EP Misiakos, 3rd Department of Surgery, University of Athens, School of Medicine, Athens, Greece
M Genetzakis, GC Zografos, 1st Department of Propedeutic Surgery, University of Athens, School of Medicine, Hippokraton Hospital, Athens, Greece
E Agapitos, Department of Pathology, University of Athens, School of Medicine, Athens, Greece

Correspondence to: C Fotiadis, MD, Associate Professor of Surgery, University of Athens, 8 Tripoleos Street, Melissia, Athens 15127, Greece. costfot@yahoo.gr

Telephone: +11-30210-8034821 Fax: +11-30210-8133184

Received: 2004-10-19 Accepted: 2005-01-05

Abstract

Gastrointestinal duplication is an uncommon congenital abnormality in two-thirds of cases manifesting before the age of 2 years. Ileal duplication is common while colonic duplication, either cystic or tubular, is a rather unusual clinical entity that remains asymptomatic and undiagnosed in most cases. Mostly occurring in pediatric patients, colonic duplication is encountered in adults only in a few cases. This study reports two cases of colonic duplication in adults. Both cases presented with rectal bleeding on admission. The study was focused on clinical, imaging, histological, and therapeutical aspects of the presenting cases. Gastrografen enema established the diagnosis in both cases. The cystic structure and the adjacent part of the colon were excised en-block. The study implies that colonic duplication, though uncommon, should be included in the differential diagnosis of rectal bleeding.

© 2005 The WJG Press and Elsevier Inc. All rights reserved.

Key words: Colonic duplication; Gastrointestinal bleeding

Fotiadis C, Genetzakis M, Papandreou I, Misiakos EP, Agapitos E, Zografos GC. Colonic duplication in adults: Report of two cases presenting with rectal bleeding. *World J Gastroenterol* 2005; 11(32): 5072-5074

<http://www.wjgnet.com/1007-9327/11/5072.asp>

INTRODUCTION

Gastrointestinal duplication is an uncommon congenital abnormality^[1]. More than 80% of cases present before the age of 2 years as an acute abdomen or bowel obstruction and can occur anywhere throughout the alimentary tract^[1,2]. Ileum is the most common site for duplication, accounting for over 60% of cases^[4]. On the other hand, duplication of

the colon is a rare abnormality, accounting for 4-18% of all gastrointestinal duplications, often located in the cecum^[3,4]. A thorough review of the international literature since 1950, has revealed 83 cases of colonic duplications reported up-to-date.

Although intestinal duplications are considered to be benign lesions, mostly asymptomatic, they may result in significant morbidity and mortality, if left untreated^[5]. Indications for surgical intervention often arise in an acute setting, in the form of a complication. Specifically, patients with previously undetected duplications may present in the setting of bowel obstruction or severe gastrointestinal hemorrhage (i.e., ulcerating gastric mucosa within a duplication cyst)^[3]. If encountered incidentally, these lesions should be surgically addressed to avoid any future complication, including the possibility of malignant degeneration within the duplication cyst^[3,5].

The cases mentioned in the present article refer to patients manifesting bleeding of the lower gastrointestinal tract, which was finally proved as originating from the mucosa of a colonic duplication.

CASE REPORTS

Case 1

A 53-year-old male was admitted to our department with rectal bleeding. He claimed of stool mixed with blood, without pain or changes in bowel habits, 5 d prior to admission. The patient had a medical history of constipation, being treated with diet for more than 20 years. On admission, he was in a stable clinical condition, with normal vital signs and blood tests were within normal ranges. Rectal examination confirmed the presence of blood in the stools. Plain X-rays of the abdomen showed no particular findings.

Colonoscopy was performed showing only two small diverticula in the sigmoid colon, but could not reveal the site of bleeding. It was not possible for the right colon to be examined thoroughly, due to imperfect bowel cleansing. As a second step of the diagnostic procedure, radiographic colon imaging after gastrografen enema was performed. It showed a fistula in the middle of the ascending colon, communicating with a cystic formation approximately 2 cm×1 cm in dimension. Furthermore, a computerized tomography of the abdomen was performed, which confirmed the findings and a possible diagnosis of colonic duplication of ascending colon was concluded. A second colonoscopy detected the mucosa of the colonic duplication to be the origin of bleeding.

Excision of the cystic lesion was decided (Figure 1). It was resected en-block to the section of the ascending colon

and an end-to-end anastomosis of the colon was performed. Pathological examination of the resected lesion revealed a duplication cyst in the mesenteric border of the ascending colon, with normal intestinal mucosa lining its wall (Figure 2). Within the mucosa of the duplication, a site of angiodysplasia was detected as the origin of bleeding.

The patient had an uneventful postoperative course and was discharged on the 6th post-operative day. He remained asymptomatic ever since.



Figure 1 Surgical specimen including the ascending colon together with a duplication cyst attached to the mesenteric border of the colon.

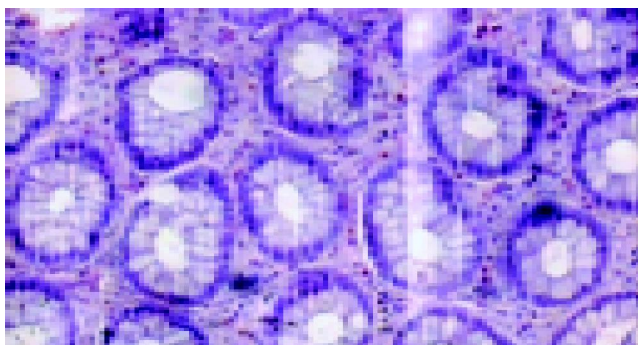


Figure 2 Normal intestinal mucosa of the cyst in the first case (HE ×125).

Case 2

A 45-year-old male was referred to our department claiming of fatigue and a 5-d history of bloody stools. Physical examination as well as blood investigations were entirely unremarkable. The patient was submitted to rectal examination as well as colonoscopy, which did not reveal any source of bleeding. The radiological imaging control using gastrografin enema showed a cystic formation of 0.5 cm×5 cm in size, located in the mesenteric border of the descending colon. This finding was confirmed by a second colonoscopy, which established the diagnosis of a colonic duplication.

A surgical intervention was decided in order to detect the site of bleeding, as well as to prevent any further complication of the cyst. The cystic lesion was resected en-block to the adjacent part of the colon (Figure 3) and an end-to-end anastomosis was performed. The cyst was confirmed to be a colonic duplication of normal colonic mucosa according to the pathologic study. Indeed, there

was a mucosal ulceration in the cystic cavity, probably representing the origin of bleeding. There was no immediate or delayed post-operative complication.



Figure 3 Surgical specimen in the second case including the descending colon with a duplication cyst adjacent to the colon.

DISCUSSION

Intestinal duplication is a congenital malformation, that occurs mostly in pediatric patients^{2,6}. It could be encountered anywhere throughout the gastrointestinal tract, from the mouth to the anus. Current nomenclature relies on the anatomic location of the duplication in relation to the normal intestinal tract and not on the histological features of the mucosal lining². Intestinal duplications are located in, or attached (share a common wall) to the wall of an adjacent part of the gastrointestinal tract and possess at least one exterior layer of smooth muscle and are lined with various types of gastrointestinal mucosa¹. Further characterization defines these abnormalities as either spherical or tubular. Rarely, complete duplication of the colon may be encountered⁷.

Approximately 75% of duplications have been reported to be located within the abdominal cavity. Jejunal and ileal lesions are the most commonly encountered (53%), while colonic lesions are found in 13% of cases. These lesions may be cystic (75%) or tubular (25%) in appearance and characteristically arise from the mesenteric border of the bowel^{5,6}. They may or may not have one or more direct communications with the adjacent part of the bowel across the common septum³. Non-communicating duplications typically contain clear alkaline fluid, except in cases in which gastric mucosa is present (25%) and acidic fluid is observed. In addition, non-activated pancreatic enzymes may also be observed in cases of ectopic pancreatic tissue within the duplication lesion³. In adults, either cystic or tubular duplication of the colon is a rare entity⁸.

Most colonic duplication cysts are asymptomatic and remain undiagnosed for years⁹. If symptomatic, they manifest with obstruction^{10,11}, bleeding¹⁰⁻¹³ or constipation⁸. Cystic duplications have been reported to cause obstruction of the colon as a result of direct compression, volvulus, or intussusception, whereas tubular duplications of the rectum have been described as having direct communication with the perineum^{3,13}. Although many duplications are diagnosed incidentally, most patients present with a combination of

pain and/or obstructive symptoms^[14,15]. These symptoms may be the direct effects of distension of the duplication or caused by compression of adjacent organs (including their associated blood supplies). In addition, abrupt hemorrhage with hemodynamic instability can be encountered in the case of a cyst, lined with mucosa that ulcerates and eventually erodes into adjacent organs and/or vessels^[3,13]. There are scattered reports of intestinal carcinomas found within duplication cysts^[14,16]. No significant difference in clinical presentation has been detected between communicating and non-communicating cysts^[3].

Histological analysis typically reveals at least one outer muscular layer with an inner gastrointestinal mucosal lining. The mucosal lining does not necessarily correspond to that of the adjacent normal intestine and may be comprised several different types of gastrointestinal mucosa^[2]. Because of the relative scarcity of such abnormalities, current literature consists mainly of small populations and case reports rather than any large single or multi-institutional series^[8-10,13].

The first patient reported in this study, presented with bleeding in the stools and constipation as his major complaints on admission, while the other one claimed of rectal bleeding. Abdominal X-rays in both cases showed no abnormal findings. The use of contrast material in the imaging control was necessary to discover the cysts. Ultrasonography could help in the diagnostic procedure^[17,18]. Colonoscopy and CT imaging could establish the diagnosis. Colonoscopic examination revealed a cystic formation, lined by normal intestinal mucosa, communicating with the colon. CT imaging showed a cystic mass attached to the colon.

Preoperative diagnosis of colonic duplication is often difficult. Symptoms usually include abdominal pain, often confusing colonic duplication with other more common diagnoses. Plain X-rays of the chest and abdomen should be routinely performed; however, because of the non-specificity of their results, it is difficult to make a pre-operative diagnosis on the basis of radiographic findings. Computerized tomography of the chest or abdomen is useful in establishing a diagnosis of alimentary tract duplication during the pre-operative workup and may be used to evaluate the synchronous lesions, once a single duplication is identified^[2,3]. Ultrasonography is also helpful in establishing a pre-operative diagnosis^[17,18].

Treatment is reserved for symptomatic cases and usually includes resection of the cyst and the neighboring part of the intestine^[11,13,19]. Complications related to surgical intervention are typically nonspecific and include post-operative bleeding, infection, and bowel obstruction^[3]. However, in patients with large tubular duplications, injury to the normal intestine with resultant short bowel syndrome must be considered^[3].

In most instances, cystic duplications can be completely excised. Resection of normal intestine must often accompany removal of the lesion, because of the intimate attachment of the common wall or because isolated resection of

the cyst would compromise blood flow to the adjacent intestinal segment^[3,11,13,19]. An alternative approach involving marsupialization of the cystic structure consists of a partial cystectomy combined with mucosal stripping of the remaining cyst wall to preserve normal anatomy^[3]. Although current literature does not specifically address the prognosis and outcome related to the diagnosis of alimentary tract duplications, the overall outcome is generally favorable^[2,3].

REFERENCES

- 1 **Macpherson RI**. Gastrointestinal tract duplications: clinical, pathologic, etiologic, and radiologic considerations. *Radiographics* 1993; **13**: 1063-1080
- 2 **O'Neil J, Rowe M**. Duplications of the gastrointestinal tract. In: *Essentials of Pediatric Surgery*. St. Louis, Mo. *Mosby Yearbook* 1995: 520-525
- 3 **Holcomb GW, Gheissari A, O'Neill JA, Shorter NA, Bishop HC**. Surgical management of alimentary tract duplications. *Ann Surg* 1989; **209**: 167-174
- 4 **Puligandla PS, Nguyen LT, St-Vil D, Flageole H, Bensoussan AL, Nguyen VH, Laberge JM**. Gastrointestinal duplications. *J Pediatr Surg* 2003; **38**: 740-744
- 5 **Chen CC, Yeh DC, Wu CC, Li MC, Kwan PC**. Huge cystic duplication of the ascending colon in adult. *Zhonghua Yixue Zazhi* 2001; **64**: 174-178
- 6 **Keramidas DC, Demetriades DM**. Total tubular duplication of the colon and distal ileum combined with transmesenteric hernia; surgical management and long-term results. *Eur J Pediatr Surg* 1996; **6**: 243-244
- 7 **Li L, Zhang J, Wang J, Wang Y, Chen R, Qin H**. Complete duplication of the colon: definitive management by resection of the duplication without the normal bowel. *Chin Med J* 2002; **115**: 779-781
- 8 **Pennehouat G, Houry S, Huguier M**. Sigmoid duplication in an adult. *J Chir* 1986; **123**: 169-170
- 9 **Favara BE, Franciosi RA, Akers DR**. Enteric duplications. Thirty-seven cases—a vascular theory of pathogenesis. *Am J Dis Child* 1971; **122**: 501-506
- 10 **Otter MI, Marks CG, Cook MG**. An unusual presentation of intestinal duplication with a literature review. *Dig Dis Sci* 1996; **41**: 627-629
- 11 **Van Elst F, Hubens A**. Duplication of the colon in the adult. *Acta Chir Belg* 1978; **77**: 335-342
- 12 **Bremer JL**. Diverticula and duplications of the intestinal tract. *Arch Pathol* 1944; **38**: 132-140
- 13 **Frittelli P, Costa G, Zanella L, Sguazzini G, Rossi FS, Frittelli P, Costa G, Zanella L, Sguazzini G, Rossi FS**. Intestinal duplication in the adult. A case report of colonic duplication and a review of the literature. *Chir Ital* 2002; **54**: 721-728
- 14 **Choong CK, Frizelle FA**. Giant colonic diverticulum: report of four cases and review of the literature. *Dis Colon Rectum* 1998; **41**: 1178-1185
- 15 **Salvador II, Modelli ME, Pereira CR**. Tubular duplication of the colon: a case report and review of the literature. *J Pediatr* 1996; **72**: 254-257
- 16 **Horie H, Iwasaki I, Takahashi H**. Carcinoid in a gastrointestinal duplication. *J Pediatr Surg* 1986; **21**: 902-904
- 17 **Kangaroo H, Sample WF, Hansen G, Robinson JS, Sarti D**. Ultrasonic evaluation of abdominal gastrointestinal tract duplication in children. *Radiology* 1979; **131**: 191-194
- 18 **Hayden CK**. Ultrasonography of the gastrointestinal tract in infants and children. *Abdom Imag* 1996; **21**: 9-20
- 19 **Robert J, Ambrosetti P, Widgren S, Rohner A**. Perforated tubular duplication of the sigmoid colon in adults. *Gastroenterol Clin Biol* 1990; **14**: 776-779

Difficulty with diagnosis of malignant pancreatic neoplasms coexisting with chronic pancreatitis

Ting-Kai Leung, Chi-Ming Lee, Fong-Chieh Wang, Hsin-Chi Chen, Hung-Jung Wang

Ting-Kai Leung, Chi-Ming Lee, Fong-Chieh Wang, Hsin-Chi Chen, Hung-Jung Wang, Department of Diagnostic Radiology, Taipei Medical University Hospital, Taiwan; Department of Internal Medicine, Taipei Medical University Hospital, Taiwan, China
Correspondence to: Chi-Ming Lee, Department of Diagnostic Radiology, Taipei Medical University Hospital, 252, Wu Hsing Street, Taipei 110, Taiwan, China. yyrubber2002@yahoo.com.tw
Telephone: +886-2-27372181-1131 Fax: +886-2-23780943
Received: 2005-03-12 Accepted: 2005-04-09

Abstract

Chronic pancreatitis is a relatively common disease. We encountered two different cases of belatedly demonstrated pancreatic carcinoma featuring underlying chronic pancreatitis. The first case was one that was highly suspected as that of a malignancy based upon imaging study, but unfortunately, it could not be confirmed by intra-operative cytology at that time. Following this, the surgeon elected to perform only conservative bypass surgery for obstructive biliary complication. Peritoneal carcinomatosis was later noted and the patient finally died. The second case, a malignant mucinous neoplasm, was falsely diagnosed as a pseudocyst, based upon the lesion's sonographic appearance and associated elevated serum amylase levels. After suffering repeated hemoptysis, the patient was found to exhibit lung metastasis and peritoneal seeding. We reviewed some of the literature, including those studies discussing chronic pancreatitis predisposing to a malignant change. These two case analyses illustrate clearly that the diagnosis for such conditions, which is simply based upon imagery or pathological considerations may end up being one of a mistaken malignancy. Some of our suggestions for the treatment of such malignancies as revealed herein include, total pancreatectomy for univocal mass lesion, and needle aspiration of lesion-contained tissue for amylase, CA199 and CEA levels for a suspicious cystic pancreatic mass.

© 2005 The WJG Press and Elsevier Inc. All rights reserved.

Key words: Mucinous cystic neoplasm; Pancreatic carcinoma; Pseudocyst; Pancreatic adenocarcinoma; Chronic pancreatitis

Leung TK, Lee CM, Wang FC, Chen HC, Wang HJ. Difficulty with diagnosis of malignant pancreatic neoplasms coexisting with chronic pancreatitis. *World J Gastroenterol* 2005; 11(32): 5075-5078

<http://www.wjgnet.com/1007-9327/11/5075.asp>

INTRODUCTION

We herein report on two cases of pancreatic malignancy, an adenocarcinoma and a mucinous cystadenocarcinoma, both of which featured an underlying chronic pancreatitis. The first case was incorrectly diagnosed initially, even though such diagnosis followed multiple-modality imagery studies and intra-operative frozen-section pathology. The second case was, initially, falsely diagnosed as a case of a pseudocyst that had missed the 'golden period' of opportunity for surgical treatment for this relatively non-aggressive malignant tumor. The true diagnosis for this case was made subsequent to the discovery of the widespread distribution of mucinous tumor cells to the lungs and peritoneum. In an attempt to improve our image-interpretation skills, and to provide some more-effective suggestions for clinicians as regards to the appropriate diagnostic procedures for future cases of a similar nature, we have discussed these cases and reviewed some of the related literature.

CASE REPORTS

Case 1

A 60-year-old female patient presented at our hospital, suffering from diabetes mellitus and chronic pancreatitis, and revealed a smoking habit of greater than 30 years. On one previous occasion, this patient was admitted to a local hospital on a complaint of chronic inflammation complicating post-inflammatory obstructive jaundice. Two years subsequent to this event, this patient suffered a relapse; she complained of abdominal fullness and poor appetite. Tea-colored urine and yellowish-colored skin were both noted, the patient was diagnosed with biliary obstruction, and her condition failed to improve following admission. The patient was then referred to our OPD for further evaluation, at which time her condition had progressed to one of general malaise and notable body-weight loss. Serum amylase, CA-199 and CEA levels were, respectively, 58 IU/L (normal <100), 1 387 U/mL (normal <37) and 5.75 ng/mL (normal <4.6). Endoscopic retrograde cholangiopancreatography (ERCP) was performed, but obviously not sufficiently and effectively, it only revealed pancreatic-duct dilatation and failed to provide appropriate visualization of the common bile duct (CBD). Subsequent enhanced CT and MRCP studies revealed dilatation of the CBD, IHD, and MPD, and an ill-defined, heterogeneous enhanced mass located in the uncinate process of the pancreatic head (Figure 1A). Our impression at that time was malignant pancreatic lesion complicating CBD obstruction. Surgical intervention was then conducted, it revealed the presence of a large, stony hard mass, measuring

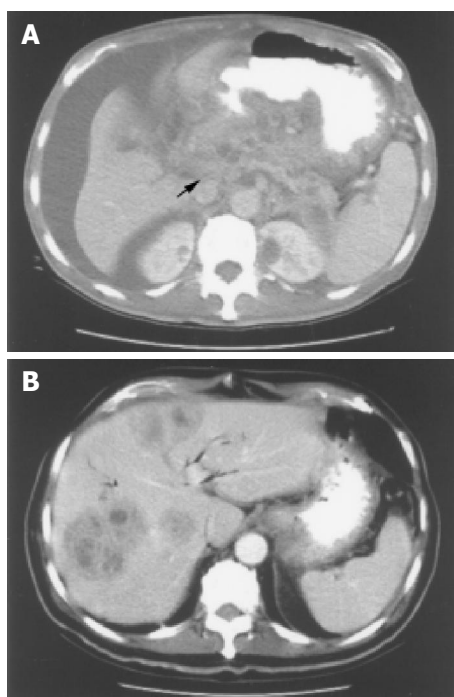


Figure 1 Enhanced CT scan shows extensive heterogenous mass (arrow) occupying at para-pancreatic region to be involved with adjacent gastric wall and para-ampullary region. Pancreatic duct dilatation is suggested and superior mesenteric vein thrombosis cannot be ruled out (A). multiple heterogenous hepatic lesions are demonstrated (B).

5-6 cm in diameter, located at the pancreatic head and being tightly adherent to the portal vein and the common hepatic artery. Further, we noted a 1.5 cm-diameter lymph node located along the superior mesenteric artery. A gall-bladder stone was also noted. Intra-operative frozen-sectioning of a needle biopsy from the pancreatic head and body revealed fibrosis and chronic inflammation with lymphocytic infiltration into the fibrotic stroma. Intralobular and perilobular fibrosis with atrophy of acini admixed with disorderly arranged islets were also seen, but no evidence of malignancy was apparent, a result that contrasted our initial impression. The patient then underwent a bypass surgery including cholecystectomy, choledochojejunostomy with Roux-en-Y and gastrojejunostomy. Two months later, this patient again presented at our hospital with similar symptoms to those detected at her previous admission, computed tomography (CT) revealing multiple heterogenous ill-defined hepatic tumors (Figure 1B). At this time, we strongly suspected metastatic lesions according to our past impressions of her condition, the past history of this patient, and the updated CT findings. Sonographically guided biopsy was conducted, but the subsequent histopathological report concluded that the lesion was a liver abscess. The patient was administered antibiotics and other supportive treatment. Her condition improved and remained stable for about 2 mo, following which, her condition deteriorated, and she was admitted again to our institution due to progressive abdominal distension, poor appetite and further body-weight loss. The patient's serum CA-199 level had elevated to 4 000 U/mL (normal <37). An abdominal CT scan was performed; it revealed a progressively enlarging heterogenous enhanced mass, located at the pancreatic body and tail

section. This pancreatic mass had also invaded the lesser sac of the stomach, there being direct invasion into the stomach. The pancreatic mass had also resulted in celiac-trunk encasement and the encirclement of the superior mesenteric vessels, with ascites being massive. A condition of pancreatitis superimposed onto malignant change and metastatic peritoneal seeding into the transverse mesocolon and sigmoid mesocolon was diagnosed. Pathological review finally confirmed intraperitoneal carcinomatosis due to the presence of an advanced pancreatic carcinoma, the patient expired about 5 mo later.

Case 2

This 62-year-old male patient featured chronic alcoholism over a period of more than 30 years. Chronic pancreatitis and liver cirrhosis were diagnosed for this patient and he was recommended regular OPD follow up. Slightly elevated serum amylase levels were recorded for this patient, and for approximately 3 mo, he suffered from intermittent abdominal fullness; diffuse dull pain and a general sensation of nausea. Sonographic evaluation revealed multiple pancreatic cystic lesions, ascites, splenomegaly and portal hypertension, with no evidence of tumor septation, loculation, no cystic-wall calcification, and no evidence of the presence of any soft-tissue masses. The initial diagnosis for this patient was chronic pancreatitis with associated pseudocyst formation, based upon the combined results of laboratory and sonographic investigations. Three months later, this patient's condition had, by-and-large, persisted, and upon presentation at our hospital for further evaluation, he was found to be suffering from hemoptysis. This patient's serum amylase, CA199 and CEA levels were reported as, respectively, 150 IU/L (normal <100), 3 841 U/mL (normal <37) and 9.79 ng/mL (normal <4.6). A chest X ray revealed hazy bilateral shadows over the lower lung fields. The patient underwent CT investigation, which revealed multiple cystic pancreatic masses (Figure 2A) confluent with contrast-enhanced soft-tissue components, the largest two masses measuring greater than 7.7 and 3.7 cm in diameter, these lesions arising from the pancreatic body and tail. Fluid distribution within the intraperitoneal and pelvic cavities was described, respectively, as extensive and moderate. CT investigation also revealed multiple foci of alveolar patches (Figure 2B) with a mean density of 10-15 HU. PET scanning was then performed, the results demonstrating multiple areas of FDG uptake including the posterior and bilateral aspects of the lower lungs, the middle-upper abdomen (pancreatic body featured irregular shapes) and the middle-lower abdomen. CT guided fine needle aspiration of the para-pancreatic cystic fluid [f] revealed normal level of amylase, but enormous elevation of CA-199 (32 000 001 U/mL) and CEA (43 000 ng/mL). CT guide biopsy for the lung patch also revealed mucinous adenocarcinoma metastasis. Combined with the results of images and the histopathological investigations, the presence of pancreatic mucinous adenocarcinoma complicated by lung and peritoneal seedings was confirmed.

DISCUSSION

Chronic pancreatitis may eventuate as a consequence of recurrent acute inflammation in the pancreas, such a condition

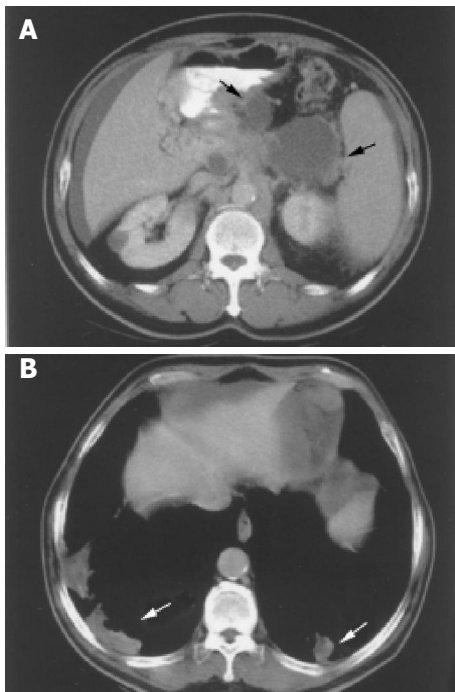


Figure 2 Enhanced CT scan shows multiple, non-enhanced, pancreatic cystic mass (straight and curved arrows) with soft tissue part (A), multiple, hypodense, alveolar patches at bilateral basal lung parenchyma (straight and curved arrows) (B).

often affecting neighboring structures and their functions. Typical image manifestations of chronic pancreatitis include pancreatic calcification on KUB, atrophic changes and/or the presence of coexistent focal hypertrophy, pseudocyst formation and a dilated pancreatic duct as detected by sonographic or CT investigation. ERCP may be used to demonstrate abnormalities of the main pancreatic duct as also secondary branches. Other possible imagery findings for chronic pancreatitis include fatty replacement, fibrotic changes complicating duodenal stenosis with outflow obstruction and long tapered stenoses of the distal common bile duct with biliary obstruction, aneurysms or pseudoaneurysms of the splanchnic arteries and splenic-vein thrombosis. The predisposing factors for pancreatic adenocarcinoma include chronic pancreatitis, diabetes mellitus, smoking and a potential underlying genetic risk^[1]. The pathophysiological and molecular events underlying chronic pancreatitis have been reported to predispose to the development of, or potentiate the growth of, pancreatic adenocarcinomas^[2]. Mutation of the codon 12 K-ras gene, tumor angiogenesis and microvascular proliferation are, reportedly, genetically-linked aberrations^[2] commonly associated with the development of pancreatic adenocarcinoma.

Discrimination between a well-differentiated pancreatic carcinoma^[3] and chronic fibrotizing pancreatitis is a challenge not only to the radiologist^[4], but also to the pathologist^[5,6]. As mentioned above, pancreatic adenocarcinoma and chronic pancreatitis may coexist, and a malignant tumor can develop as a complication of long-standing chronic pancreatitis. On the other hand, pancreatic carcinoma is frequently accompanied by chronic inflammation. The majority of adenocarcinomas induce a striking desmoplastic

stromal reaction within the pancreas, which may effectively mimic the macroscopic view of vigorous fibroblast proliferation. Microscopically, pancreatitis can be mistaken for pancreatic carcinoma, because the actively growing connective tissue associated with pancreatitis, tends to irregularly separate the existing pancreatic ducts. This continuous regenerative activity may lead to regressive atypia that resembles malignancy^[5]. A retrospective study of 5 837 previously histopathologically confirmed pancreatic carcinoma patients, reported little more than 0.5% false-positive results^[7]. In our opinion, for the first case described above, only total pancreatectomy with tissue sent for a precise histopathological examination, instead of frozen-section biopsy, could have increased the likelihood of arriving at a correct diagnosis.

Pseudocyst formation is present for about 30% of chronic pancreatitis cases, such lesions being a collection of pancreatic “juice” enclosed by a wall of fibrous or granulation tissue. Pseudocyst lesions of the pancreas tend to populate the majority of pancreatic cystic lesions. For our second case, however, the diagnostic challenge was to differentiate correctly between a cystic neoplasm and pseudocysts for the patient featuring underlying chronic pancreatitis. Patients who are afflicted with pseudocysts often reveal a history of acute or chronic pancreatitis, whilst most of those featuring cystic tumors lack such antecedent factors. The typical findings of a pseudocyst upon a CT scan, include the presence of a well-defined, non-epithelial, fibrous wall around the cyst lesion. Pseudocysts are typically round or ovoid in configuration and, apart from the assessment of pseudocysts by CT, pseudocysts can generally be identified by hypovascularity upon angiography; and the detection of a communication between the cyst and the pancreatic ductal system upon ERCP. On the other hand, MRI has its advantages over CT in the evaluation of pancreatic pseudocysts. T1W MRI with gadolinium could be more sensitive to demonstrate internal structure of cyst-like lesion, such as very thin septa, which may not be detected by enhanced CT scan. MRCP could help for ruling out of pseudocysts by determining whether they communicate with the pancreatic duct. Cystic neoplasm of the pancreas would appear to be rare, it constituting less than 4% of all pancreatic neoplasms^[8]. The features of a cystic neoplasm, as compared to a pseudocyst, include, for the former, the presence of septa, loculation, solid components and/or cystic-wall calcification. It would appear that sonography is not sufficiently reliable to unequivocally distinguish between pseudocysts and other cystic neoplasms of the pancreas. In our opinion, the early scheduling of abdominal CT subsequent to sonography having been completed for our second case, probably would have hastened the correct diagnosis for this patient. Moreover, analysis of cyst-contained fluid^[9,10], can also aid in the evaluation of cystic neoplasms, in that elevated fluid amylase levels are characteristic of over 95% of pseudocysts, and a normal serum amylase level can be used to exclude the presence of a pseudocyst. Fluid CEA levels can become elevated for a variety of cystic lesions including mucinous cystic neoplasm^[11], intra-ductal papillary mucinous tumors and some pseudocysts, but such levels are always low or normal for cases of serious cystadenoma. A summary of

the laboratory-elicited features of cystic fluid for the purposes of distinguishing between pancreatic cysts and the most-common type of cystic tumors is presented in Table 1.

Table 1 Laboratory features of cystic fluid in different cystic tumors of pancreas

	Pseudocyst	Serous cystadenoma	Mucinous cystadenoma	Mucinous cystadenocarcinoma
Amylase (normal <100 IU/L)	High	Low	Low	Low
CA 199 (normal <37 U/mL)	Low	Low	Intermediate	High
CEA (normal <4.6 ng/mL)	Low	Low	High	High

In conclusion, if an accurate diagnosis of suspicious pancreatic lesions for patients suffering from chronic pancreatitis is not able to be reached based upon appropriate imagery studies, we suggest fine-needle aspiration biopsy^[9] of cystic neoplasms for subsequent laboratory investigation, or, alternatively, wide resection of the pancreatic mass for a precise histopathological evaluation, rather than simple observation^[12].

REFERENCES

- Hall Pde L, Wilentz RE, de Klerk W, Bornman PP. Premalignant conditions of the pancreas. *Pathology* 2002; **34**: 504-517
- Banerjee SK, Zoubine MN, Mullick M, Weston AP, Cherian R, Campbell DR. Tumor angiogenesis in chronic pancreatitis and pancreatic adenocarcinoma: impact of K-ras mutations. *Pancreas* 2000; **20**: 248-255
- Machado MC, Montagnini AL, Machado MA, Falzoni R, Volpe P, Jukemura J, Abdo EE, Penteadó S, Bacchella T, Monteiro-Cunha JE. Cystic neoplasm diagnosed as pancreatic pseudocyst: report of 5 cases and review of the literature. *Rev Hosp Clin Fac Med Sao Paulo* 1994; **49**: 246-249
- Civello IM, Frontera D, Viola G, Maria G, Crucitti F. Cystic neoplasm mistaken for pancreatic pseudocyst. *Hepatogastroenterology* 1996; **43**: 967-970
- Zalatnai A. Pathologic diagnosis of pancreatic cancer-facts, pitfalls, challenges. *Oro Hetil* 2001; **142**: 1885-1890
- Nieman JL, Holmes FF. Accuracy of diagnosis of pancreatic cancer decreases with increasing age. *J Am Geriatr Soc* 1989; **37**: 97-100
- Alanen KA, Joensuu H. Long-term survival after pancreatic adenocarcinoma-often a misdiagnosis? *Br J Cancer* 1993; **68**: 1004-1005
- Bradley EL, Clements JL, Gonzalez AC. The natural history of pancreatic pseudocysts: a unified concept of management. *Am J Surg* 1979; **137**: 135-141
- Pinto MM, Kaye AD. Fine needle aspiration of cystic liver lesions. Cytologic examination and carcinoembryonic antigen assay of cyst contents. *Acta Cytol* 1989; **33**: 852-856
- Safi F, Schlosser W, Falkenreck S, Beger HG. Prognostic value of CA 19-9 serum course in pancreatic cancer. *Hepatogastroenterology* 1998; **45**: 253-259
- Buetow PC, Rao P, Thompson LD. From the Archives of the AFIP. Mucinous cystic neoplasms of the pancreas: radiologic-pathologic correlation. *Radiographics* 1998; **18**: 433-449
- Scott J, Martin I, Redhead D, Hammond P, Garden OJ. Mucinous cystic neoplasms of the pancreas: imaging features and diagnostic difficulties. *Clin Radiol* 2000; **55**: 187-192

Science Editor Guo SY Language Editor Elsevier HK

Sigmoid schwannoma: A rare case

Constantine I. Fotiadis, Ilias A. Kouerinis, Ioannis Papandreou, George C. Zografos, George Agapitos

Constantine I. Fotiadis, Ioannis Papandreou, George Agapitos, Third Department of Propaedeutic Surgery, University of Athens, Sotiria Hospital, Athens, Greece

Ilias A. Kouerinis, George C. Zografos, First Department of Propaedeutic Surgery, University of Athens, Hippokraton Hospital, Athens, Greece

Correspondence to: Ilias A. Kouerinis, 17 Kipselis Str., Athens 11257, Greece. ikouerinis@hotmail.com

Telephone: +30-6932-713171

Received: 2004-10-10 Accepted: 2004-12-01

Abstract

Schwannomas are rare tumors derived from the cells of Schwann that form the neural sheath. When located in the gastrointestinal tract, they constitute together with leiomyoma, leiomyoblastoma, and leiomyosarcoma, the gastrointestinal stromal tumors (GIST). Peripheral nerve sheath tumors represent 2-6% GIST with most common location, the stomach and the small intestine. Schwannomas of the colon and rectum are extremely rare and radical excision with wide margins is mandatory, due to their tendency to recur locally and become malignant, if left untreated. In the present study, we report a rare case of a sigmoid schwannoma, which was successfully treated in our department and reviewed the literature.

© 2005 The WJG Press and Elsevier Inc. All rights reserved.

Key words: Schwannoma; Rectum; GIST; Tumor; Prognosis; Treatment

Fotiadis CI, Kouerinis IA, Papandreou I, Zografos GC, Agapitos G. Sigmoid schwannoma: A rare case. *World J Gastroenterol* 2005; 11(32): 5079-5081

<http://www.wjgnet.com/1007-9327/11/5079.asp>

INTRODUCTION

Gastrointestinal stromal tumors (GIST) include a variety of primary mesenchymal tumors of the gastrointestinal tract such as leiomyoma, leiomyosarcoma, leiomyoblastoma, and schwannoma^[1]. They have recently been distinguished from each other on the basis of the tumor cell differentiation revealed by immunohistochemical studies^[2,3]. Besides the above-mentioned pathologies, the term GIST has been recently applied to mesenchymal tumors that represent neither typical leiomyoma nor schwannoma^[2,4].

It is well established that schwannomas appear more frequently in the stomach and the small intestine, while location in the colon or in the rectum is uncommon^[5,6].

Most of them are benign and asymptomatic; nevertheless, the possibility of malignant degeneration does exist and is directly related to the tumor dimensions. Radical surgical treatment is the gold standard in all cases, since the results of both chemotherapy and radiotherapy remain uncertain^[7].

CASE REPORT

A 55-year-old male patient was admitted to our department, with a chief complaint of intermittent rectal bleeding and diarrhea that had started 2 mo before admission. Physical findings and digital examination were undiagnostic, but laboratory tests disclosed red blood cell count: $3.2 \times 10^5/\text{mm}^3$, hemoglobin: 74 g/L, and hematocrit: 26.4%. Colonoscopy revealed a wide-based mass protruding from the posterior wall of sigmoid and multiple biopsies were taken from different parts of the tumor. Abdominal x-rays were negative for bowel obstruction, while CT scans proved no metastatic disease. Additionally, the serum levels of tumor markers including carcinoembryonic antigen and Ca 19-9 were within normal ranges. The diagnosis of schwannoma Antoni B type was set preoperatively based on the endoscopic biopsies and intraoperatively, segmental resection of the tumor with wide margins was performed (Figures 1A and B). Permanent sections with H&E confirmed the preoperative diagnosis (Figure 2). The patient recovered uneventfully and at 5 years following surgery, he was free of disease without receiving adjuvant therapy.

DISCUSSION

Schwannomas are mainly benign tumors derived from the cells of Schwann that form the neural sheath, which may become malignant, if left untreated^[8-10]. They can be located everywhere, but the most common type of benign schwannoma is the acoustic neuroma (VIII cranial nerve)^[11].

Malignant schwannomas usually come under the heading of soft tissue sarcomas and the gastrointestinal tract is one of the sites that such tumors can be found^[12]. In these cases they constitute together with leiomyoma, leiomyosarcoma, leiomyoblastoma, and another type with mixed characteristics between leiomyoma and schwannoma, the GIST^[13]. All of these primary mesenchymal tumors show a wide range of common histological and immunohistochemical characteristics^[2,14].

Peripheral nerve sheath tumors represent 2-6% of stromal tumors of the gastrointestinal tract^[3,4] but reports of solitary schwannomas of the rectum and colon are even more rare^[15]. They have almost the same incidence in men and women and a median age of presentation, 65 years of age^[4]. Their size may vary; a case of a rectal schwannoma with a diameter of 8 cm which was primarily misdiagnosed as a myogenic sarcoma has been reported^[2,5].

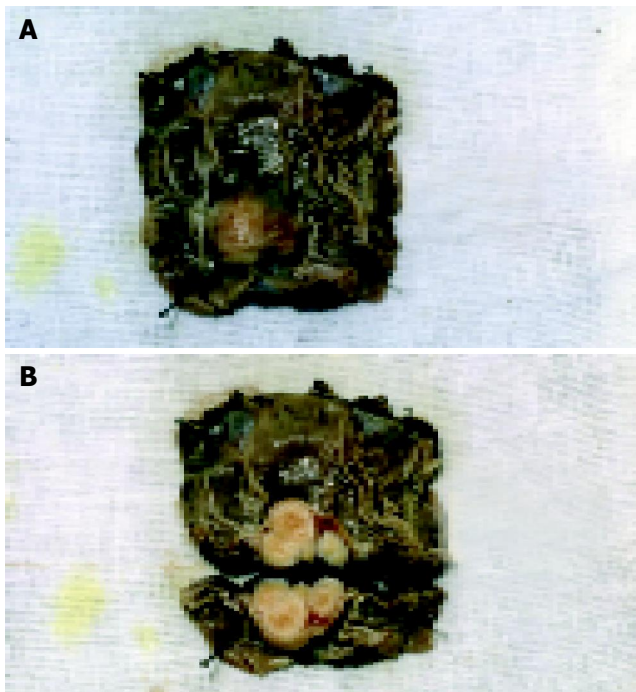


Figure 1 Macroscopic view of the sigmoid colon showed a well-circumscribed submucosal tumor (A). The cut surface of this tumor consisted of fibrotic and myxoid parts and was gray-yellowish in color (B).

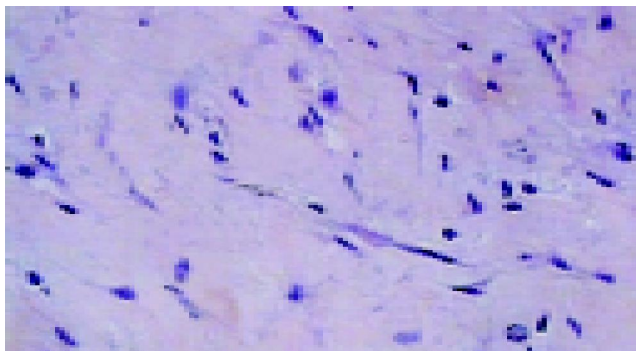


Figure 2 Microscopic view of a benign schwannoma (H&E×40). Compact spindle cells arranged in short bundles are seen.

Although, they usually grow very slowly and are asymptomatic, sometimes they may cause rectal bleeding, colonic obstruction, defecation disorders, and pain^[3,4]. It is very important to emphasize that rectal pain can also be the only symptom of intraspinal schwannomas which they often mislead the diagnosis to proctalgia fugax or rectal neuralgia^[15].

Two histologic types of schwannomas have been described; Antoni type A with densely packed spindle cells (Verocay bodies) and Antoni type B with loosely organized spindle cells (absence of Verocay bodies) in myxoid stroma^[3,4]. Immunology plays a central role to the diagnosis of schwannoma as in many other types of cancer^[16]. Strongly positive S-100 protein, low affinity, nerve growth factor receptor (P75), collagen IV, GFAP, CD34, and negative CD117, neurofilament protein, smooth muscle actin, and desmin, turn out to be supportive to the diagnosis of the benign tumor as a

schwannoma^[2,3,12]. Schwannomas may also appear in patients with Von Recklinghausen disease (NF I), although there is no evident connection between colorectal schwannomas and NF I^[17].

Radical excision with margins free of disease is the treatment of choice, since their response to both chemotherapy and radiotherapy remain uncertain^[4,18]. Nevertheless, despite aggressive surgical management, these tumors appear with a high rate of local recurrence and malignant degeneration. In such case's the treatment options are few and the prognosis is poor^[3,7,8].

The surgical approach depends on the tumor size and histologic features that mainly determine the prognosis. Preoperative imaging tests including abdominal x-rays, transanal 3D-ECHO, MRI, and CT scans can be very useful in the selection of patients for surgical treatment^[19]. Besides the commonly used surgical techniques, minimally invasive modalities can be performed too. In the transanal endoscopic microsurgery (TEM), the local excision is accomplished through a rectal expander^[20,21] with or without the use of an ultrasonically activated scalpel^[22]. Alternatively, in cases of the benign schwannomas located on the distal parts of the rectum, a transanal resection can be performed followed by recto-anal anastomosis^[21].

In conclusion, rectal schwannoma is a very rare tumor, whose diagnostic approach and treatment present certain gray areas. Nevertheless, it has become obvious that the preoperative histological identification of the tumor followed by a radical surgical resection is the cornerstone, which will determine the overall outcome.

REFERENCES

- 1 Prevot S, Bienvenu L, Vaillant JC, de Saint-Maur PP. Benign schwannoma of the digestive tract: a clinicopathologic and immunohistochemical study of five cases, including a case of esophageal tumor. *Am J Surg Pathol* 1999; **23**: 431-436
- 2 Miettinen M, Virolainen M. Gastrointestinal stromal tumors-value of CD34 antigen in their identification and separation from true leiomyomas and schwannomas. *Am J Surg Pathol* 1995; **19**: 207-216
- 3 Miettinen M, Shekitka KM, Sobin LH. Schwannomas in the colon and rectum. A clinicopathologic and immunohistochemical study of 20 cases. *Am J Surg Pathol* 2001; **25**: 846-855
- 4 Miettinen M, Sarlomo-Rikala M, Lasota J. Gastrointestinal stromal tumours. *Ann Chir Gynaecol* 1998; **87**: 278-281
- 5 Maciejewski A, Lange D, Wloch J. Case report of schwannoma of the rectum-Clinical and pathological contribution. *Med Sci Monit* 2000; **6**: 779-782
- 6 Bhardwaj K, Bal MS, Kumar P. Rectal schwannoma. *Indian J Gastroenterol* 2002; **21**: 116-117
- 7 Arcidiaco M, Uggeri G, Rumi A, Valenti L. Schwannoma of the rectum-Clinicotherapeutic study. *Minerva Chir* 1981; **36**: 267-272
- 8 Catania G, Puleo C, Cardi F, Catalano F, Iuppa A, Buffone A. Malignant schwannoma of rectum a clinical and pathological approach. *Chir Ital* 2001; **53**: 873-877
- 9 Kolodziejski LS, Dyczek ST, Pogodzinski M. Surgical management of retrorectal expanding tumors. *J Chir* 2004; **141**: 109-113
- 10 Reinbold WD, Hillemanns A, Seesko H, Jehn E. Malignant Schwannoma of the rectum. *Radiologe* 1996; **36**: 663-666
- 11 Darrouzet V, Martel J, Enee V, Bebear JP, Guerin J. Vestibular schwannoma surgery outcomes: our multidisciplinary experience in 400 cases over 17 years. *Laryngoscope* 2004; **114**: 681-688
- 12 Daimaru Y, Kido H, Hashimoto H, Enjoji M. Benign schwannoma

- of the gastrointestinal tract: a clinicopathologic and immunohistochemical study. *Hum Pathol* 1988; **19**: 257-264
- 13 **Shibata Y**, Ueda T, Seki H, Yagihashi N. GIST tumors of the rectum. *Eur J Gastroenterol Hepatol* 2001; **13**: 283-286
- 14 **Vorobev GI**, Odariuk TS, Shelygin IuA, Kapuller LL, Korniak BS, Tikhonov AA, Orlova LP. Differential diagnosis of non epithelial rectal neoplasms. *Khirurgiia* 1995: 45-50
- 15 **Kornel EE**, Vlahakos D. Intraspinal schwannoma presenting solely with rectal pain. *Neurosurgery* 1988; **22**: 417-419
- 16 **Kouerinis IA**, Zografos G, Tarassi KE, Athanasiades TH, Lontos M, Gorgoulis VG, Korkolis D, Konstandoulakis MM, Fotiadis CI, Androulakis G, Papasteriades CA. Human leukocyte antigens as genetic markers in Greek patients with sporadic pancreatic cancer. *Pancreas* 2004; **29**: 41-44
- 17 **Genna M**, Leopardi F, Fambri P, Postorino A. Neurogenic tumors of the anorectal region. *Ann Ital Chir* 1997; **68**: 351-353
- 18 **Pollock J**, Morgan D, Denobile J, Williams J. Adjuvant radiotherapy for gastrointestinal stromal tumor of the rectum. *Dig Dis Sci* 2001; **46**: 268-272
- 19 **Stroh C**, Manger T. Ultrasonnal diagnosis of rare retrorectal tumors. *Zentrabl Chir* 2003; **128**: 1075-1079
- 20 **Kakizoe S**, Kuwahara S, Kakizoe K, Kakizoe H, Kakizoe Y, Kakizoe T, Yamamoto O, Kakizoe S. Local excision of benign rectal schwannoma using rectal expander-assisted TEM. *Gastrointest Endosc* 1998; **48**: 90-92
- 21 **Porkovskii GA**, Eropkin PV, Shelygin IuA, Peresada IV. Transanal resection of the rectum. *Khirurgiia* 1994: 32-34
- 22 **Langer C**, Markus P, Liersch T, Fuzesi L, Becker H. Ultracision or high frequency knife in transanal and microsurgery TEM; advantages of a new procedure. *Surg Endosc* 2001; **15**: 513-517

Science Editor Wang XL and Guo SY Language Editor Elsevier HK

Prenatal diagnosis of choledochal cyst using magnetic resonance imaging: A case report

Alex Mun-Ching Wong, Yun-Chung Cheung, Yu-Hung Liu, Koon-Kwan Ng, Siu-Cheung Chan, Shu-Hang Ng

Alex Mun-Ching Wong, Yun-Chung Cheung, Koon-Kwan Ng, Siu-Cheung Chan, Shu-Hang Ng, Department of Diagnostic Radiology, Chang Gung Memorial Hospital, Kwei-Shan, Tao-Yuan, Taiwan, China

Yu-Hung Liu, Obstetrics and Gynecology, Chang Gung Memorial Hospital, 222, Mei Chin Road, Keelung, Taiwan, China

Correspondence to: Dr. Siu-Cheung Chan, Department of Diagnostic Radiology, Chang Gung Memorial Hospital, Kwei-Shan, Tao-Yuan, Taiwan, China. chan3015@ms27.hinet.net

Telephone: +886-3-3281544 Fax: +886-3-2702023

Received: 2005-02-24 Accepted: 2005-03-23

Abstract

Choledochal cysts are congenital anomalies of the biliary ducts, characterized by cystic dilatation of the ducts. Prenatal diagnosis of this anomaly using ultrasonography (US) has been well documented. Magnetic resonance imaging (MRI) has recently become an important complement to US in prenatal diagnosis of fetal anomalies. We herein report a patient in whom at 24 wk' gestation US suggested a right upper quadrant abdominal cyst and in whom at 26 wk' gestation MRI more clearly delineated the cyst and its surrounding structures and suggested a choledochal cyst, which was confirmed at postnatal surgery and histopathology.

© 2005 The WJG Press and Elsevier Inc. All rights reserved.

Key words: Choledochal cyst; Prenatal diagnosis; MRI

Wong AMC, Cheung YC, Liu YH, Ng KK, Chan SC, Ng SH. Prenatal diagnosis of choledochal cyst using magnetic resonance imaging: A case report. *World J Gastroenterol* 2005; 11(32): 5082-5083

<http://www.wjgnet.com/1007-9327/11/5082.asp>

INTRODUCTION

Choledochal cyst is characterized by a balloon-like dilatation of the extrahepatic duct, occasionally associated with dilatation of the intrahepatic ducts. Ultrasonography (US) remains the primary imaging modality for the evaluation of the fetus and can suggest the diagnosis of choledochal cyst, when a tubular structure is identified at the right upper quadrant abdomen^[1-4]. Magnetic resonance imaging (MRI) has evolved and has become an important complement to US, for more accurate and precise delineation and characterization of fetal anomalies. With recently developed ultrafast MR sequences such as half-Fourier, single-shot, turbo spin-echo

(HASTE), a single slice can be obtained in less than 400 ms^[5]. Many studies have shown the usefulness of these ultrafast MR scans in evaluating the fetus^[6-8]. Here, we report a case of choledochal cyst prenatally diagnosed by using US and MRI and confirmed by postnatal surgery and histopathology.

CASE REPORT

A 29-year-old woman, gravida 2, para 1, presented at our hospital at 24th wk' gestation for prenatal US surveillance. Fetal US showed an ovoid cystic lesion measuring 2.1 cm × 1.1 cm × 1.2 cm at the right upper quadrant abdomen. A choledochal cyst or an enteric cyst was impressed.

Two weeks later, a fetal MRI (Philips 1.5 T Intera; Erlangen, Germany) was performed to further evaluate the cyst using HASTE sequence (TR 10 ms; TE 100 ms; time of acquisition 12 s; flip angle 90°; field of view 280 mm × 250 mm; matrix 256 × 256). MRI showed a 1.3 cm × 1.2 cm × 2.7 cm, ellipsoid, homogeneous cystic lesion extending from the liver hilum posteriorly and inferomedially to the mid-abdomen (Figure 1). This lesion showed hypointensity on T1-weighted and hyperintensity on T2-weighted images. A more detailed anatomical relationship of the cyst to the gall bladder and the biliary tracts was shown. Type 1 choledochal cyst was tentatively diagnosed.

A female infant weighing 3 890 g was delivered at 39 wk with APGAR scores of 8 and 10 at 1 and 5 min, respectively. Postnatal US at 3 d of age showed further enlargement of the cyst. At 13 d of age, the cyst was excised and a Roux-en-Y hepatico-jejunostomy was performed. Histopathological examination confirmed the diagnosis of a choledochal cyst. The infant was discharged a week later with no jaundice noted thereafter.

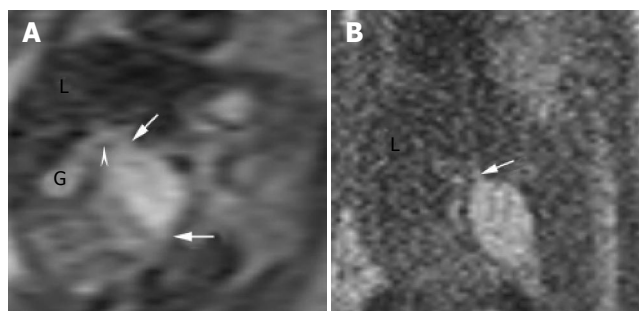


Figure 1 MRI performed at 26 wk' gestation using HASTE sequence. **A:** Coronal T2-weighted image showed the choledochal cyst, its tapered ends (arrows), its connection to the cystic duct (arrowhead), and its relationship to the gall bladder (G) and the liver (L); **B:** Sagittal T2-weighted image showed the posterior-inferior orientation of the choledochal cyst and its connection to the common hepatic duct (arrow).

DISCUSSION

Choledochal cysts are rare anomalies, characterized by cystic or fusiform dilatation of the intrahepatic and/or extrahepatic biliary tracts. These cysts have been classified into five major types^[9]. Cystic dilatation of the common bile duct (type 1 choledochal cyst) comprises 80-90% of the cysts. In affected newborns, about 70% had jaundice but only 25% had a palpable abdominal mass^[4]. Potential complications in untreated patients include recurrent cholangitis, pancreatitis, liver cirrhosis, portal hypertension, and malignant transformation^[10-12].

Ultrasonography is the primary imaging modality for evaluating the fetus due to its real-time display and non-invasiveness. In cases of choledochal cyst, tubular structures can be identified entering or leaving a right upper quadrant cyst^[1,2,4]. However, the choledochal cyst could be missed, if confused with the gall bladder and the umbilical vein. Other common cystic lesions, including hydronephrosis, duodenal duplication, intestinal atresia, mesenteric cyst, and ovarian cyst, may appear similar to a choledochal cyst.

Recent development of ultrafast MR imaging techniques has allowed MRI to become an important complement to US in fetal imaging^[5-8]. MRI offers superior soft tissue contrast, larger field of view, and is relatively operator independent. In our case, while the prenatal US showed a subhepatic cyst, the MRI showed additional findings of tapered ends of the cyst, its proximity to the liver hilum, its inferomedial orientation, and characteristic fluid-intensity of the cyst. Also, the relationship between the choledochal cyst, the cystic duct and the dilated gall bladder was clearly depicted. Concerning the differential diagnoses of a right upper quadrant cyst, an umbilical vein may be excluded by the lack of vascular flow void on MRI. Other common cystic lesions, including hydronephrosis, intestinal atresia, mesenteric cyst, and ovarian cyst have locations different from that of a choledochal cyst. Duodenal duplication may not be easily excluded, but it would be less likely to have tapered ends as a choledochal cyst^[13]. To our best knowledge, we found two reports of prenatal MRI investigation of choledochal cysts^[14,15]. However, the finding of tapered ends of the choledochal cyst, which may be specific to a biliary tract anomaly, was not emphasized in their reports.

In conclusion, owing to its excellent anatomical and contrast resolutions, MRI can clearly delineate a choledochal cyst and may be helpful in differential diagnosis of right upper quadrant cystic lesions. The additional information provided by prenatal MRI, which is complementary to US,

may be valuable for family counseling, and may help clinicians manage pregnancy and plan post-natal treatment earlier.

REFERENCES

- 1 **Elrad H**, Mayden KL, Ahart S, Giglia R, Gleicher N. Prenatal ultrasound diagnosis of choledochal cyst. *J Ultrasound Med* 1985; **4**: 553-555
- 2 **Frank JL**, Hill MC, Chirathivat S, Sfakianakis GN, Marchildon M. Antenatal observation of a choledochal cyst by sonography. *AJR Am J Roentgenol* 1981; **137**: 166-168
- 3 **Howell CG**, Templeton JM, Weiner S, Glassman M, Betts JM, Witzleben CL. Antenatal diagnosis and early surgery for choledochal cyst. *J Pediatr Surg* 1983; **18**: 387-393
- 4 **Bancroft JD**, Bucuvalas JC, Ryckman FC, Dudgeon DL, Saunders RC, Schwarz KB. Antenatal diagnosis of choledochal cyst. *J Pediatr Gastroenterol Nutr* 1994; **18**: 142-145
- 5 **Simon EM**, Goldstein RB, Coakley FV, Filly RA, Broderick KC, Musci TJ, Barkovich AJ. Fast MR imaging of fetal CNS anomalies in utero. *AJNR Am J Neuroradiol* 2000; **21**: 1688-1698
- 6 **Johnson IR**, Stehling MK, Blamire AM, Coxon RJ, Howseman AM, Chapman B, Ordidge RJ, Mansfield P, Symonds EM, Worthington BS. Study of internal structure of the human fetus in utero by echo-planar magnetic resonance imaging. *Am J Obstet Gynecol* 1990; **163**: 601-607
- 7 **Yamashita Y**, Namimoto T, Abe Y, Takahashi M, Iwamasa J, Miyazaki K, Okamura H. MR imaging of the fetus by a HASTE sequence. *AJR Am J Roentgenol* 1997; **168**: 513-519
- 8 **Quinn TM**, Hubbard AM, Adzick NS. Prenatal magnetic resonance imaging enhances fetal diagnosis. *J Pediatr Surg* 1998; **33**: 553-558
- 9 **Savader SJ**, Benenati JF, Venbrux AC, Mitchell SE, Widlus DM, Cameron JL, Osterman FA. Choledochal cysts: classification and cholangiographic appearance. *AJR Am J Roentgenol* 1991; **156**: 327-331
- 10 **Yamaguchi M**. Congenital choledochal cyst. Analysis of 1, 433 patients in the Japanese literature. *Am J Surg* 1980; **140**: 653-657
- 11 **Todani T**, Tabuchi K, Watanabe Y, Kobayashi T. Carcinoma arising in the wall of congenital bile duct cysts. *Cancer* 1979; **44**: 1134-1141
- 12 **Yoshida H**, Itai Y, Minami M, Kokubo T, Ohtomo K, Kuroda A. Biliary malignancies occurring in choledochal cysts. *Radiology* 1989; **173**: 389-392
- 13 **Wong AM**, Wong HF, Cheung YC, Wan YL, Ng KK, Kong MS. Duodenal duplication cyst: MRI features and the role of MR cholangiopancreatography in diagnosis. *Pediatr Radiol* 2002; **32**: 124-125
- 14 **Mackenzie TC**, Howell LJ, Flake AW, Adzick NS. The management of prenatally diagnosed choledochal cysts. *J Pediatr Surg* 2001; **36**: 1241-1243
- 15 **Chen CP**, Cheng SJ, Chang TY, Yeh LF, Lin YH, Wang W. Prenatal diagnosis of choledochal cyst using ultrasound and magnetic resonance imaging. *Ultrasound Obstet Gynecol* 2004; **23**: 93-94

• CASE REPORT •

Cystic lymphangioma of the jejunal mesentery in an adult: A case report

Chuang-Wei Chen, Sheng-Der Hsu, Chien-Hua Lin, Ming-Fang Cheng, Jyh-Cherng Yu

Chuang-Wei Chen, Sheng-Der Hsu, Chien-Hua Lin, Ming-Fang Cheng, Jyh-Cherng Yu, Division of General Surgery, Department of Surgery, Department of Pathology, Tri-Service General Hospital, Taipei, Taiwan, China

Correspondence to: Dr. Jyh-Cherng Yu, Division of General Surgery, Department of Surgery, Department of Pathology, Tri-Service General Hospital, National Defense Medical Center, 325, Section 2, Cheng-Gong Road, Neihu 114, Taipei, Taiwan, China. docallen.tw@yahoo.com.tw

Telephone: +886-2-87927191 Fax: +886-2-87927273

Received: 2005-03-03 Accepted: 2005-04-09

Abstract

We herein describe the case of a 27-year-old female, who presented with a large mass of the upper left abdominal cavity discovered incidentally, through an annual health examination. Preoperative studies including abdominal ultrasonography and magnetic resonance imaging were performed, but they could not accurately determine the nature of the tumor. At laparotomy, a large cystic tumor of the small bowel mesentery was found. Histopathologic examination diagnosed the tumor as a cystic lymphangioma. Although lymphangiomas are rare, especially in the abdomen of adults, they may sometimes present as acute abdomen, causing complications that require emergent surgery.

© 2005 The WJG Press and Elsevier Inc. All rights reserved.

Key words: Jejunum; Lymphangioma; Small bowel mesentery

Chen CW, Hsu SD, Lin CH, Cheng MF, Yu JC. Cystic lymphangioma of the jejunal mesentery in an adult: A case report. *World J Gastroenterol* 2005; 11(32): 5084-5086
<http://www.wjgnet.com/1007-9327/11/5084.asp>

INTRODUCTION

Lymphangiomas are rare benign tumors. They are preferentially located in the head, neck, and axilla in children. However, lymphangiomas in the peritoneal cavity are extremely rare, particularly in adults. This report describes a case of an adult with a large lymphangioma of the jejunal mesentery.

CASE REPORT

A 27-year-old female was referred to us on April 10, 2003 due to an intra-abdominal mass lesion found incidentally, during her annual health examination. Recently, she had begun to experience epigastralgia and abdominal fullness

especially after having meals. Her family and medical history were unremarkable. She had no history of previous abdominal surgery. On physical examination, a soft, non-tender mass was palpated in the upper left abdomen. Auscultation of the abdomen revealed normal bowel sounds. Laboratory data including tumor markers were within normal limits. A plain film of the abdomen showed several loops of small intestine without dilatation or air-fluid level. Abdominal ultrasonography revealed a large, multilocular, cystic mass with an obscure margin. MRI of the abdomen showed a large homogeneous mass measuring 16 cm×7 cm×5 cm in size with multiple enhancement septa by contrast medium. This lesion was located at the anterior aspect of the left kidney and descending colon, causing compression and stretching of the small bowel (Figure 1). A cystic neoplasm of the mesentery was considered.

At laparotomy, a yellowish cystic tumor with soft consistency was found in the mesentery of the jejunum, about 30 cm distal to Treitz's ligament. The tumor was not adhered to the wall of the intestine or adjacent organs. No ascites was seen in the peritoneal cavity, nor was there any dilatation or inflammatory change of the intestines or mesentery. With careful dissection of the mesenteric arteries, the tumor was resected completely without resection of the intestine. The specimen consisted of one piece of cystic tumor in the mesentery measuring 15 cm×8 cm×6 cm. Macroscopically, it was yellowish in color and soft in consistency (Figure 2). Microscopically, the sections showed numerous dilated lymphatic channels of varying sizes within loose fibroconnective tissue and a few disorganized bundles of smooth muscle present in the wall of the larger channels. Immunohistochemical stains were positive for Factor VIII and actin. The same cells did not react to cytokeratin. These findings were consistent with a cystic lymphangioma (Figure 3). The patient had an uneventful postoperative course, and no evidence of recurrence, 18 mo after the operation.

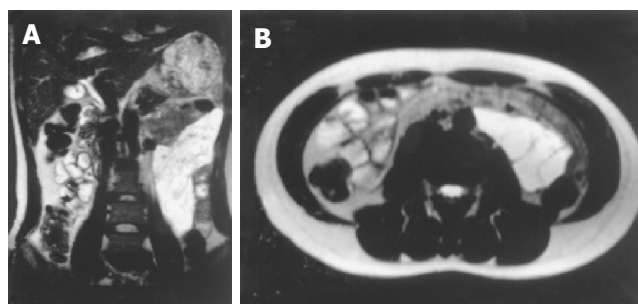


Figure 1 MRI of the abdomen showing a 16 cm×7 cm×5 cm homogenous multilocular tumor with enhancement by contrast medium (A and B).



Figure 2 Surgical findings (A-C). A large cystic tumor was located in the mesentery of the jejunum, causing compression and stretching of the small

bowel. The tumor was not adhered to the small intestine.

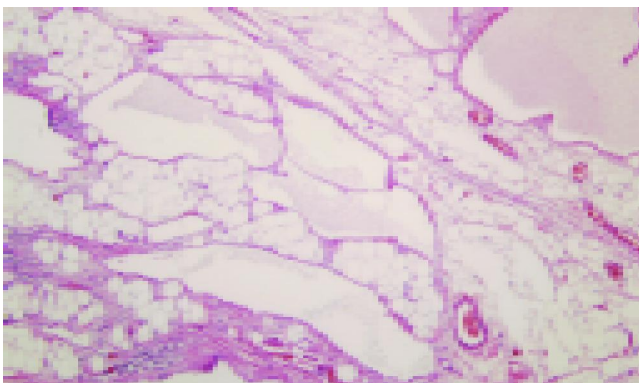


Figure 3 Histopathological results revealed that the mesenteric tumor contained numerous dilated lymphatic lumen of varying sizes lined by attenuated endothelial cells (H&E, ×100).

DISCUSSION

Lymphangiomas are uncommon and occur mainly in children; approximately 80-90% are diagnosed within the first few years of life and adult cases are rare^[1]. They are commonly found in the head, neck, and axillary region. However, isolated occurrence in the mesentery of the small intestine is encountered even less frequently, comprising less than 1% of all lymphangiomas^[2]. The most common location of such intraperitoneal lymphatic tumor appears to be the mesentery of the small bowel, accounting for 70% of all such tumors^[3,4].

The etiology of lymphangiomas is probably a congenital abnormality of the lymphatic system, causing sequestrations of lymphatic tissue during embryologic development^[2]. This theory would explain why lymphangiomas occur primarily in children. However, it is suggested that abdominal trauma, lymphatic obstruction, inflammatory process, surgery, or radiation therapy may lead to the secondary formation of such a tumor^[4,5]. Traditionally, lymphangiomas are classified as simple, cavernous, or cystic. The simple type is usually situated superficially in the skin and composed of small thin-walled lymphatic vessels. The cavernous type is composed of dilated lymphatic vessels and lymphoid stroma, and has a connection with spaces of various normal adjacent lymphatics. Lastly, the cystic type consists of lymphatic spaces of various sizes that contains fascicles of smooth muscle and collagen bundles, but has no connection with

adjacent normal lymphatics. However, cystic lymphangioma is not always clearly differentiated from cavernous type because the cystic type may also contain cavernous areas^[6].

Mesenteric lymphangiomas are usually asymptomatic until they enlarge. Abdominal pain and distention seem to be the most common symptoms, but the clinical presentation of mesenteric lymphangiomas varies^[7]. Although benign in nature, mesenteric lymphangiomas may cause significant morbidity or mortality due to their large size and critical location, when they compress the adjacent structures. In addition, complications such as secondary infection, rupture with hemorrhage, volvulus, or intestinal obstruction have all been reported^[8-11]. The ultrasonographic presentation of a mesenteric lymphangioma is described as a cystic lesion with multiple thin septa. On CT imaging, mesenteric lymphangiomas appear as a uni- or multilocular mass with enhancement of the wall and septum by contrast medium^[12]. These studies help to determine, if the tumor is cystic as well as its size and location, but they are insufficient to establish an accurate diagnosis preoperatively. One report suggested that fine needle aspiration of a milky fluid containing lymphoid cells could confirm a preoperative diagnosis of lymphangioma^[13].

Mesenteric lymphangiomas may behave in an aggressively invasive manner and grow to an enormous size. The optimal treatment is radical excision, even when asymptomatic. However, mesenteric lymphangiomas may cause complications such as infiltration of the intestine, or involvement of the main branch of mesenteric arteries or adjacent organs that necessitate segmental resection of the intestine. Sometimes radical resection might be technically impossible^[14]. Mesenteric lymphangiomas are very rare, but they can cause acute abdomen that requires an emergent surgery. Therefore, they should be included in the differential diagnosis of acute abdomen.

REFERENCES

- 1 **Hanagiri T**, Baba M, Shimabukuro T, Hashimoto M, Takemoto H, Inoue A, Sugitani A, Shirakusa T. Lymphangioma in the small intestine: Report of a case and review of the Japanese literature. *Surgery Today* 1992; **22**: 363-367
- 2 **Roisman I**, Manny J, Fields S, Shiloni E. Intra-abdominal lymphangioma. *Br J Surg* 1989; **76**: 485-489
- 3 **Chin S**, Kikuyama S, Hashimoto T, Tomita T, Hasegawa T, Ohno Y. Lymphangioma of the jejunal mesentery in an adult: a case report and a review of the Japanese literature. *Keio J Med* 1993; **42**: 41-43

- 4 **Hardin WJ**, Hardy JD. Mesenteric cysts. *Am J Surg* 1970; **119**: 640-645
- 5 **Daniel S**, Lazarevic B, Attia A. Lymphangioma of the mesentery of the jejunum: Report of a case and a brief review of the literature. *Am J Gastroenterol* 1983; **78**: 726-729
- 6 **Rieker RJ**, Quentmeier A, Weiss C, Kretzschmar U, Amann K, Mechtersheimer G, Blaker H, Herwart OF. Cystic lymphangioma of the small-bowel mesentery: case report and a review of the literature. *Pathol Oncol Res* 2000; **6**: 146-148
- 7 **Bliss DP**, Coffin CM, Bower RJ, Stockmann PT, Ternberg JL. Mesenteric cysts in children. *Surgery* 1994; **115**: 571-577
- 8 **Ricca RJ**. Infected mesenteric lymphangioma. *N Y State J Med* 1991; **91**: 359-361
- 9 **Porrás-Ramírez G**, Hernández-Herrera MH. Hemorrhage into mesenteric cyst following trauma as a cause of acute abdomen. *J Pediatr Surg* 1991; **26**: 847-848
- 10 **Yoon HK**, Han BK. Chronic midgut volvulus with mesenteric lymphangioma: a case report. *Pediatr Radiol* 1998; **28**: 611
- 11 **Troum S**, Solis MM. Mesenteric lymphangioma causing bowel obstruction in a child. *Southern Med J* 1996; **89**: 808-809
- 12 **Davidson AJ**, Hartman DS. Lymphangioma of the retroperitoneum. CT and sonographic characteristics. *Radiology* 1990; **175**: 507-510
- 13 **Sadola E**. Cystic lymphangioma of the jejunal mesentery in an adult. *J Clin Ultrasound* 1987; **15**: 542-543
- 14 **Melcher GA**, Ruedi T, Allemann J, Wust W. Cystic lymphangioma of the mesenteric root as a rare cause of acute abdomen. *Chirurg* 1995; **66**: 229-231

Science Editor Guo SY Language Editor Elsevier HK

Preoperative diagnosis of colonic angiolipoma: A case report

Yang-Yuan Chen, Maw-Soan Soon

Yang-Yuan Chen, Maw-Soan Soon, Division of Hepatogastroenterology, Changhua Christian Hospital, Changhua, Taiwan, China

Correspondence to: Yang-Yuan Chen, MD, Division of Hepatogastroenterology, Changhua Christian Hospital, 135 Nan-Siau Street, Changhua, Taiwan, China. yangyuan@cch.org.tw

Telephone: +886-4-7238595 Fax: +886-4-7289233

Received: 2004-11-23 Accepted: 2004-12-20

Abstract

Angiolipoma, a common benign tumor mostly seen in the subcutaneous tissue, is a rare pathological condition in the gastrointestinal tract that is usually diagnosed postoperatively. In this case report, an angiolipoma was diagnosed preoperatively by imaging (including CT scans, abdominal echo, barium enema, and colonoscopy). This pathology was confirmed postoperatively. Computed tomography scan, abdominal echo, and barium enema images were presented.

© 2005 The WJG Press and Elsevier Inc. All rights reserved.

Key words: Angiolipoma; Colon; Computed tomography; Sonography; Contrast barium enema

Chen YY, Soon MS. Preoperative diagnosis of colonic angiolipoma: A case report. *World J Gastroenterol* 2005; 11(32): 5087-5089

<http://www.wjgnet.com/1007-9327/11/5087.asp>

INTRODUCTION

Angiolipoma is a benign tumor, commonly occurring in the subcutaneous tissue and other locations, but is rarely found in the gastrointestinal tract. Histologically, it is comprised of adipose tissue and proliferative blood vessels. There have been three cases of colonic angiolipoma reported in the literature, which were all diagnosed postoperatively. This report presents the first preoperative diagnosis of colonic angiolipoma using a combination of colonoscopy, barium enema, abdominal echo, and CT scans. The diagnosis was confirmed postoperatively.

CASE REPORT

A 70-year-old male presented to Changhua Christian Hospital with a history of passing bloody stool once a day for 3 d. Additionally, the patient experienced abdominal distension and cramping pain for the past 7 d. Physical examination revealed mild anemia, abdominal obesity, no palpable mass,

and hyperactive bowel sounds. Full blood count showed Hb of 10.7 and Hct of 31.5, but otherwise normal results. Colonoscopy found a submucosal tumor with ulceration of 5 cm located in the transverse colon obstructing the lumen almost completely. Contrast barium enema also revealed a 5-cm submucosal tumor located at the transverse colon with nearly complete obstruction of the lumen (Figure 1). Abdominal echo showed a centrally hyperechoic dense tumor surrounded by hypoechoic density (Figure 2). Pre-contrast enhancement CT scan showed a mixed low density and isodensity tumor (Figure 3). Post-contrast enhancement scans showed a high-density tumor with a fat component (Figure 4).

Based on the combined findings, it was diagnosed as an angiolipoma and surgical segmental resection was carried out. The resected tumor was encapsulated by a thin layer of connective tissue arising from the submucosa. Histology showed that the tumor was comprised of mature adipose tissue and proliferative blood vessels (Figure 5). After 2 years of follow-up, the patient did not have any abnormalities.



Figure 1 Submucosal tumor with nearly complete obstruction shown in barium enema.

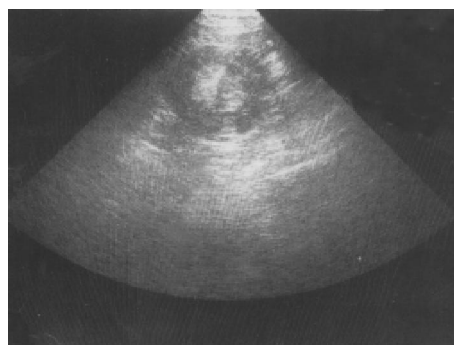


Figure 2 Centrally hyperechoic dense tumor surrounded by hypoechoic density shown by abdominal echo.

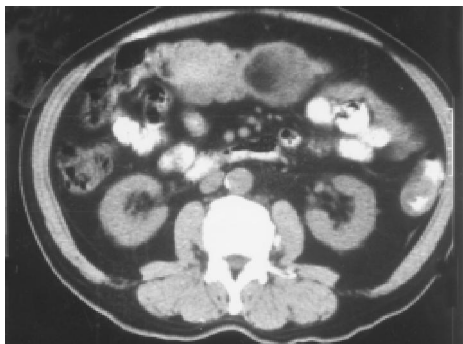


Figure 3 Mixed low and isodensity tumor shown by pre-contrast CT scan.



Figure 4 High-density tumor with a fat component shown by post-contrast CT.

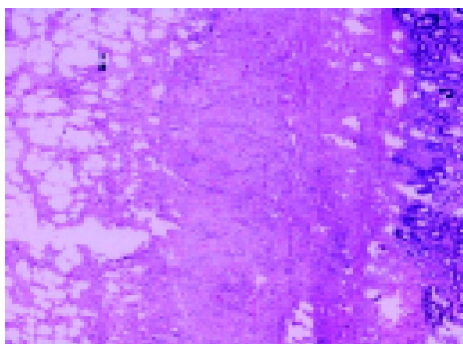


Figure 5 Photomicrograph of resection specimen.

DISCUSSION

Angioliipoma was first described in 1912 by Bowen. In 1960, Howard and Helwig described its clinical pathological characteristics, which are different from those of lipoma^[1]. Since then, angioliipoma has been regarded as a new entity. Angioliipoma is an encapsulated, subcutaneous tumor commonly occurring in young adults. It usually occurs in multiple locations on both the arms and trunk^[2,3]. Angioliipoma is usually painful. Histologically it is comprised of mature adipose tissue and proliferative vascular tissues. It can be classified as predominantly lipomatous- or angiomatous-type, based on the ratio of adipose tissue and vascular tissue composition.

A search of the current literature revealed only seven cases of angioliipoma in the gastrointestinal tract. Of these,

three cases had angioliipoma in the stomach^[4-6]. One angioliipoma was in the small intestine^[7] and three were reported to be in the colon^[8-10]. Two of the colonic angioliipomas were located at the ileocecal valve. One case had intussusception originally thought to be due to malignant tumor. Thus, the author emphasizes using histological pathology to diagnose this condition^[8]. In another case, the patient had right lower quadrant abdomen. Laparoscopy-assisted ileocecectomy is selected to remove the tumor^[9]. In the third case, the patient was asymptomatic, but had positive occult blood on routine medical examination. Double-contrast barium enema showed angioliipoma in the sigmoid colon, which was resected by colonoscopic polypectomy. The patient in this case report had lower gastrointestinal tract bleeding. Preoperative imaging allowed the diagnosis of angioliipoma, which was removed by segmentectomy.

None of the seven patients with gastrointestinal tract angioliipoma had preoperative abdominal echogram. Because the composition of angioliipoma can range from predominantly lipomatous to angiomatous type, echogram can vary from hyperechoic to hypoechoic density. In 1998, Mintz and Mengoni^[11] used sonography to diagnose breast angioliipoma, which showed homogeneously hyperechoic density under echogram. In this case report, the tumor was between the two types of angioliipoma, showing hyperechoic density centrally and hypoechoic density peripherally.

Computed tomography scan pattern depends on the composition of fat in the tumor. It can vary from a lipomatous type of tumor comprised totally of fat without post-contrast enhancement, which was thought to be lipoma preoperatively^[12], to a low-fat containing tumor, showing numerous small round density enhancements^[13,14]. In this case, diffuse high-density enhancement post-contrast was observed around the adipose tissue, which is consistent with the histological pattern.

In our case, contrast barium enema confirmed the submucosal tumor. Sonography showed hyperechoic density surrounded by hypoechoic density, and CT showed post-contrast fat containing mass, surrounded by high-density enhancement. The combination of these results allowed the tumor to be differentiated from lipoma, thus it could be diagnosed as an angioliipoma preoperatively.

Although management of colonic lipoma or angioliipoma is still controversial, endoscopic resection should not be used on sessile or broad-based lesions because of increased risk of bleeding or perforation. Urgent treatment should be given to those with intussusception, obstruction, or bleeding, as in this case. The tumor should then be removed, while the patient is still in the hospital. However, both lipoma and angioliipoma are benign tumors, thus colonic resection should be kept to a minimum when the tumor is removed^[9,10]. In this case, a small segmental resection was performed.

REFERENCES

- 1 Howard WR, Helwig EB. Angioliipoma. *Arch Dermatol* 1960; **82**: 924-931
- 2 Ackermano LV, Rosai J. Tumors of adipose tissue. In: Rosai J, editor: *Akerman's surgical pathology*. 8th ed Vol 12. St Louis: Mosby 1996: 2053-2060
- 3 Enzinger FM, Weiss SW. *Soft tissue tumors* 3rd ed. Benign

- lipomatous tumors, *St. Louis Mosby* 1995: 390
- 4 **Deridder PH**, Levin AJ, Katta JJ, Catto JA. Angioliipoma in the stomach as a case of chronic upper gastrointestinal bleeding. *Surg Endosc* 1989; **3**: 106-108
 - 5 **McGregor DH**, Kerley SW, McGregon MS. Gastric angioliipoma with chronic hemorrhage and severe anemia. *Am J M Sci* 1993; **305**: 229-235
 - 6 **Hunt J**, Tindal D. Solitary gastric Peutz-Jeghers polyp and angioliipoma presenting as acute hemorrhage. *Aust N Z J Surg* 1996; **66**: 713-715
 - 7 **Kaneko T**, Karasawa Y, Inada H, Tamura Y, Yamamura N, Iijima Y, Nagata A, Oohata T, Shirota H, Nakamura T, Hara E. An adult case of intussusception due to inverted Meckel's diverticulum accompanied by angioliipoma. *Nippon Shokakibyō Gakkai Zasshi* 1996; **93**: 260-265
 - 8 **Saroglia G**, Coverlizza S, Roatta L, Leil R, Fontana D. Angioliipoma of the cecum. *Minerva Chir* 1996; **51**: 59-62
 - 9 **Kato K**, Matsuda M, Onodera K, Sakata H, Kobayashi T, Kasai S. Angioliipoma of the colon with right lower quadrant abdominal pain. *Dig Surg* 1999; **16**: 441-444
 - 10 **Okuyama T**, Yoshida M, Watanabe M, Kinoshita Y, Harada Y. Angioliipoma of the colon diagnosed after endoscopic resection. *Gastrointestinal Endoscopy* 2002; **55**: 748-750
 - 11 **Mintz AD**, Mengoni P. Angioliipoma of the breast: sonographic appearance of two cases. *J Ultrasound Med* 1998; **17**: 67-69
 - 12 **Ferrozzi F**, Tognini G, Bova D, Pavone P. Lipomatous tumors of the stomach :CT Findings and differential diagnosis. *J Comput Assist Tomogr* 2002; **24**: 854-858
 - 13 **Biondetti PR**, Fiore D, Perin B, Ravasini R. Infiltrative angioliipoma of the thoracoabdominal wall. *J Comput Assist Tomogr* 1982; **6**: 847
 - 14 **Pfeil SA**, Weaver MG, Abdul- Karim FW, Yang P. Colonic lipomas: outcome of endoscopic removal. *Gastrointest Endosc* 1990; **36**: 435-438

Science Editor Wang XL and Guo SY Language Editor Elsevier HK

• ACKNOWLEDGMENTS •

Acknowledgments to Reviewers of *World Journal of Gastroenterology*

Many reviewers have contributed their expertise and time to the peer review, a critical process to ensure the quality of *World Journal of Gastroenterology*. The editors and authors of the articles submitted to the journal are grateful to the following reviewers for evaluating the articles (including those were published and those were rejected in this issue) during the last editing period of time.

Pierre Brissot, Professor

Liver Disease Unit And Inserm U-522, University Hospital Pontchaillou, 2, Rue Henri Le Guilloux, Rennes 35033, France

Zong-Jie Cui, Professor

Institute of Cell Biology, Beijing Normal University, Beijing 100875, China

Abdel-Rahman El-Zayadi, Professor

Department of Hepatology and Gastroenterology, Ain Shams University and Cairo Liver Center, 5, El-Gergawy St. Dokki, Giza 12311, Egypt

Kazuma Fujimoto, Professor

Department of Internal Medicine, Saga Medical School, Nabeshima, Saga, Saga 849-8501, Japan

Kazuhiro Hanazaki, M.D.

Department of Surgery, Shinonoi General Hospital, 666-1 Ai, Shinonoi, Nagano 388-8004, Japan

Naohiko Harada, PhD

Department of Gastroenterology, Fukuoka Higashi Medical Center, Chidori 1-1-1, Koga, Fukuoka 811-3195, Japan

Tetsuo Hayakawa, Emeritus Professor

Director general, Meijo Hospital, Meijo Hospital, Sannomaru 1-3-1, Naka-ku, Nagoya 460-0001, Japan

Ichiro Hirata, Professor

Internal Medicine II, Osaka Medical College, Takatsuki, Osaka 569-8686, Japan

Zhi-Qiang Huang, Professor

Abdominal Surgery Institute of General Hospital of PLA, Fuxing Road, Beijing 100853, China

Hiromi Ishibashi, Professor

Director General, Clinical Research Center, National Hospital Organization (NHO) Nagasaki Medical Center, Professor, Department of Hepatology, Nagasaki University Graduate School of Biomedical Sciences, Kubara 2-1001-1 Kubara Omura, Nagasaki 856-8562, Japan

Kei Ito, M.D.

Department of Gastroenterology, Sendai City Medical Center, 5-22-1, Tsurugaya, Miyagino-ku, Sendai City 983-0824, Japan

Rene Lambert, Professor

International Agency for Research on Cancer, 150 Cours Albert Thomas, Lyon 69372 cedex 8, France

Josep M Llovet, M.D.

Division of Liver Diseases.RM Transplantation Institute.Mount Sinai School of Medicine. Madison Ave 1425. 11F-70Box:1104, New York NY10029, United States

Osamu Matsui, Professor

Department of Radiology, Kanazawa University Graduate School of Medical Science, 13-1 Takara-machi, Kanazawa 920-8641, Japan

Chris Jacob Johan Mulder, Professor

VUMC, PO Box 7057, Amsterdam 1007, Netherlands

Hisato Nakajima, M.D.

Department of Gastroenterology and Hepatology, The Jikei University School of Medicine, 3-25-8, Nishi-Shinbashi, Minato-ku, Tokyo 105-8461, Japan

Bo-Rong Pan, Professor

Department of Oncology, Xijing Hospital, Fourth Military Medical University, No.1, F.8, Bldg 10, 97 Changying East Road, Xi'an 710032, Shaanxi Province, China

Miguel Perez-Mateo, Professor

Liver Unit, Hospital General Universitario Alicante, Pintor Baeza s/n, Alicante 03004, Spain

Jose Sahel, Professor

Hepato-gastroenterology, Hospital sainti Marevenite, I270 Boulevard AE Sainti Margrenise, Marseille 13009, France

Hidetsugu Saito, Assistant Professor

Department of Internal Medicine, Keio University, 35 Shinanomachi, Shinjuku-ku, Tokyo 1608582, Japan

Chifumi Sato, Professor

Department of Analytical Health Science, Tokyo Medical and Dental University, Graduate School of Health Sciences, 1-5-45 Yushima, Bunkyo-ku, Tokyo 113-8519, Japan

Kiichi Tamada, M.D.

Department of Gastroenterology, Jichi Medical School, 3311-1 Yakushiji, Minamikawachi, Kawachigun, Tochigi 329-0498, Japan

Paul Joseph Thuluvath, Professor

Department of Gastroenterology and Hepatology, The Johns Hopkins Hospital, 1830 E. Monument St, Baltimore MD 21205, United States

Shingo Tsuji, Professor

Department of Internal Medicine and Therapeutics, Osaka University Graduate School of Medicine(A8), 2-2 Yamadaoka, Suita, Osaka 565-0871, Japan